Journal of Pharmaceutical Sciences

JANUARY 1977

VOLUME 66 NUMBER 1

MARY H. FERGUSON
Editor

L. LUAN CORRIGAN
Assistant Editor

SHELLY ELLIOTT
Production Editor

JANET D. SHOFF
Copy Editor

EDWARD G. FELDMANN
Contributing Editor

SAMUEL W. GOLDSTEIN
Contributing Editor

LELAND J. ARNEY
Director of Publications

EDITORIAL ADVISORY BOARD

JOHN AUTIAN	HARRY B. KOSTENBAUDER
NORMAN R. FARNSWORTH	HERBERT A. LIEBERMAN
WILLIAM O. FOYE	DAVID E. MANN, JR.
WILLIAM J. JUSKO	GERALD J. PAPARIELLO

The *Journal of Pharmaceutical Sciences* is published monthly by the American Pharmaceutical Association at 2215 Constitution Ave., N.W., Washington, DC 20037. Second-class postage paid at Washington, D.C., and at additional mailing office.

All expressions of opinion and statements of supposed fact appearing in articles or editorials carried in this journal are published on the authority of the writer over whose name they appear and are not to be regarded as necessarily expressing the policies or views of the American Pharmaceutical Association.

Offices—Editorial, Advertising, and Subscription Offices: 2215 Constitution Ave., N.W., Washington, DC 20037. Printing Offices: 20th & Northampton Streets, Easton, PA 18042.

Annual Subscriptions—United States and foreign, industrial and government institutions $50, educational institutions $50, individuals *for personal use only* $30; single copies $5. All foreign subscriptions add $5 for postage. Subscription rates are subject to change without notice. Members of the American Pharmaceutical Association may elect to receive the *Journal of Pharmaceutical Sciences* as a part of their annual $60 (foreign $65) APhA membership dues.

Claims—Missing numbers will not be supplied if dues or subscriptions are in arrears for more than 60 days or if claims are received more than 60 days after the date of the issue, or if loss was due to failure to give notice of change of address. The Association cannot accept responsibility for foreign delivery when its records indicate shipment has been made.

Change of Address—Members and subscribers should notify at once both the Post Office and the American Pharmaceutical Association, 2215 Constitution Ave., N.W., Washington, DC 20037, of any change of address.

© Copyright 1977, American Pharmaceutical Association, 2215 Constitution Ave., N.W., Washington, DC 20037; all rights reserved.

THE "DUMB COPS" IMAGE

One day this past fall we were going through the daily Washington ritual of reviewing the current issue of the *Federal Register*—which is the principal means of keeping track of what is happening in the executive branch of government—when we spotted reference to a Presidential Proclamation which caught our eye. Specifically, the entry pertained to the designation of "Drug Abuse Prevention Week" and the thought struck us that this annual effort to promote means to control the problems of drug abuse was a bit later than usual this year.

Upon turning to the Proclamation in that issue of the *Federal Register*, the explanation became immediately clear. Although the Proclamation was signed by President Ford on October 18 and printed rather promptly in the *Federal Register* dated October 20, nevertheless, the week being so designated was indicated as beginning October 17. Normally, such Proclamations appear at least two weeks or so before the pertinent date and certainly not after the observance is to begin.

Those familiar with the operation of executive agencies will recognize that the tardiness here does not lie with the President, or the White House staff, or the *Federal Register* but, rather, with the particular agency having primary responsibility for the subject area. In this instance, we suspect that the fault lies with the Drug Enforcement Administration of the Department of Justice.

Whether or not DEA was responsible for this small flub, there is no question that the agency has been clearly at fault for a long string of other foul-ups and errors which, *in toto*, project the image of an inefficient, bungling agency.

When DEA was originally established some half-dozen years or so ago, a strong argument was made that responsibility for drug control involved scientific, medical, and other technical knowledge, which argues rather strongly that the agency should be placed within the U.S. Department of Health, Education, and Welfare rather than the Department of Justice. Others, however, argued vocally that drug abuse control basically is a regulatory and enforcement activity and, as such, the agency more properly should be made part of the Department of Justice where other federal investigative and police activities are primarily centralized.

In recent months, we have seen repeated instances where official notices, proposals, or finalized regulations issuing from DEA and published in the *Federal Register* have used terminology and nomenclature to describe the drugs involved which have been confusing, inconsistent, or otherwise inaccurate. In an effort to correct this problem, at our suggestion, the office of the United States Adopted Names (USAN) Council specifically communicated with the DEA and offered assistance in this regard. Not only did the DEA fail to take advantage of this offer but, in fact, actually repeated on at least two later dates the very error cited by the USAN Council office as an example of incorrect drug nomenclature being employed by the agency.

There are many dedicated and well-qualified professionals who serve in the DEA. Undoubtedly, the bureaucratic bungling of the agency such as that described above and which projects a "dumb cop" image is highly embarrassing to those professional staff members. What is particularly unfortunate, however, is that this problem is so unnecessary. It could be readily corrected if those responsible for determining general agency policy and direction were just a bit more sensitive to the need to exercise reasonable sophistication and care in the scientific and medically related aspects of their field of responsibility.

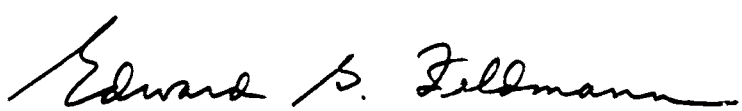

Journal of Pharmaceutical Sciences

JANUARY 1977

VOLUME 66 NUMBER 1

MARY H. FERGUSON
Editor

L. LUAN CORRIGAN
Assistant Editor

SHELLY ELLIOTT
Production Editor

JANET D. SHOFF
Copy Editor

EDWARD G. FELDMANN
Contributing Editor

SAMUEL W. GOLDSTEIN
Contributing Editor

LELAND J. ARNEY
Director of Publications

EDITORIAL ADVISORY BOARD

JOHN AUTIAN	HARRY B. KOSTENBAUDER
NORMAN R. FARNSWORTH	HERBERT A. LIEBERMAN
WILLIAM O. FOYE	DAVID E. MANN, JR.
WILLIAM J. JUSKO	GERALD J. PAPARIELLO

The *Journal of Pharmaceutical Sciences* is published monthly by the American Pharmaceutical Association at 2215 Constitution Ave., N.W., Washington, DC 20037. Second-class postage paid at Washington, D.C., and at additional mailing office.

All expressions of opinion and statements of supposed fact appearing in articles or editorials carried in this journal are published on the authority of the writer over whose name they appear and are not to be regarded as necessarily expressing the policies or views of the American Pharmaceutical Association.

Offices—Editorial, Advertising, and Subscription Offices: 2215 Constitution Ave., N.W., Washington, DC 20037. Printing Offices: 20th & Northampton Streets, Easton, PA 18042.

Annual Subscriptions—United States and foreign, industrial and government institutions $50, educational institutions $50, individuals *for personal use only* $30; single copies $5. All foreign subscriptions add $5 for postage. Subscription rates are subject to change without notice. Members of the American Pharmaceutical Association may elect to receive the *Journal of Pharmaceutical Sciences* as a part of their annual $60 (foreign $65) APhA membership dues.

Claims—Missing numbers will not be supplied if dues or subscriptions are in arrears for more than 60 days or if claims are received more than 60 days after the date of the issue, or if loss was due to failure to give notice of change of address. The Association cannot accept responsibility for foreign delivery when its records indicate shipment has been made.

Change of Address—Members and subscribers should notify at once both the Post Office and the American Pharmaceutical Association, 2215 Constitution Ave., N.W., Washington, DC 20037, of any change of address.

© Copyright 1977, American Pharmaceutical Association, 2215 Constitution Ave., N.W., Washington, DC 20037; all rights reserved.

THE "DUMB COPS" IMAGE

One day this past fall we were going through the daily Washington ritual of reviewing the current issue of the *Federal Register*—which is the principal means of keeping track of what is happening in the executive branch of government—when we spotted reference to a Presidential Proclamation which caught our eye. Specifically, the entry pertained to the designation of "Drug Abuse Prevention Week" and the thought struck us that this annual effort to promote means to control the problems of drug abuse was a bit later than usual this year.

Upon turning to the Proclamation in that issue of the *Federal Register*, the explanation became immediately clear. Although the Proclamation was signed by President Ford on October 18 and printed rather promptly in the *Federal Register* dated October 20, nevertheless, the week being so designated was indicated as beginning October 17. Normally, such Proclamations appear at least two weeks or so before the pertinent date and certainly not after the observance is to begin.

Those familiar with the operation of executive agencies will recognize that the tardiness here does not lie with the President, or the White House staff, or the *Federal Register* but, rather, with the particular agency having primary responsibility for the subject area. In this instance, we suspect that the fault lies with the Drug Enforcement Administration of the Department of Justice.

Whether or not DEA was responsible for this small flub, there is no question that the agency has been clearly at fault for a long string of other foul-ups and errors which, *in toto*, project the image of an inefficient, bungling agency.

When DEA was originally established some half-dozen years or so ago, a strong argument was made that responsibility for drug control involved scientific, medical, and other technical knowledge, which argues rather strongly that the agency should be placed within the U.S. Department of Health, Education, and Welfare rather than the Department of Justice. Others, however, argued vocally that drug abuse control basically is a regulatory and enforcement activity and, as such, the agency more properly should be made part of the Department of Justice where other federal investigative and police activities are primarily centralized.

In recent months, we have seen repeated instances where official notices, proposals, or finalized regulations issuing from DEA and published in the *Federal Register* have used terminology and nomenclature to describe the drugs involved which have been confusing, inconsistent, or otherwise inaccurate. In an effort to correct this problem, at our suggestion, the office of the United States Adopted Names (USAN) Council specifically communicated with the DEA and offered assistance in this regard. Not only did the DEA fail to take advantage of this offer but, in fact, actually repeated on at least two later dates the very error cited by the USAN Council office as an example of incorrect drug nomenclature being employed by the agency.

There are many dedicated and well-qualified professionals who serve in the DEA. Undoubtedly, the bureaucratic bungling of the agency such as that described above and which projects a "dumb cop" image is highly embarrassing to those professional staff members. What is particularly unfortunate, however, is that this problem is so unnecessary. It could be readily corrected if those responsible for determining general agency policy and direction were just a bit more sensitive to the need to exercise reasonable sophistication and care in the scientific and medically related aspects of their field of responsibility.

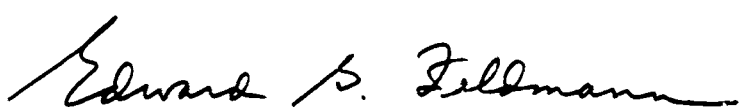

Drug Dosage Forms

Ecanow and Gold[1] incorrectly asserted that the Ocusert (pilocarpine) ocular therapeutic system is merely a dosage form delivery system containing a drug solution. They failed to make the distinction between a "dosage form" and a "controlled drug delivery system." The latter is a generic term for systems that go beyond conventional dosage forms in the sense that they are all specified by a drug delivery program—a predetermined rate and duration of drug delivery. The term "therapeutic system" is applied to controlled drug delivery systems that release a certain drug according to a temporal pattern designed for the therapy of a particular condition or disease state.

The therapeutic system functions according to this rate/duration program in automatic and uniform fashion. Moreover, the specification of rate and duration is based upon *in vitro* testing carried out under conditions that are predictive of the functioning of the therapeutic system *in vivo*. In contrast, a conventional dosage form is specified only by the weight or concentration of drug it contains. Thus, the distinction between dosage form and therapeutic system is clear from the labeling: the Ocusert system continuously delivers pilocarpine to the eye at either 20 or 40 μg/day for 1 week; an eyedrop solution contains pilocarpine in concentrations of 1, 2, 4, *etc.*, percent. The essential difference lies between the words "delivers" and "contains." The former labeling specifies function, and the latter only specifies general content of the bottle—not even the volume of the eyedrop is quantified.

We certainly agree with Ecanow and Gold that confusion can arise from ill-defined terminology. We propose, however, that the term "dosage form" be the broad description of pharmaceutical preparations intended for therapeutic use. This broad term encompasses various specific types of dosage forms such as tablets, capsules, suspensions, emulsions, solutions, semisolids, and controlled drug delivery systems. The drug delivery system can only be a specific entity (*e.g.*, a therapeutic system) if it is clearly distinguishable from other dosage types by definition, design, and function of the drug program.

"Dosage form delivery system," as proposed by Ecanow and Gold, would then be confined to the additional apparatus that may facilitate administration of dosage forms such as eyedroppers, syringes, and applicators. However, so restricted a meaning would create confusion and would be of dubious utility even when correctly employed.

Harriet Benson
William Mader
ALZA Corporation
Palo Alto, CA 94304

Received September 29, 1976.

[1] B. Ecanow and B. H. Gold, *J. Pharm. Sci.*, **65** (8), *viii (1976).*

Journal of Pharmaceutical Sciences

JANUARY 1977
VOLUME 66 NUMBER 1

REVIEW ARTICLE

Pharmaceutical Salts

STEPHEN M. BERGE *‡, LYLE D. BIGHLEY *, and DONALD C. MONKHOUSE ˣ

Keyphrases □ Pharmaceutical salts—general pharmacy, physicochemical properties, bioavailability, pharmaceutical properties, toxicology, review ■ Salts, pharmaceutical—general pharmacy, physicochemical properties, bioavailability, pharmaceutical properties, toxicology, review ■ Physicochemical properties—dissolution, solubility, stability, and organoleptic properties of pharmaceutical salts, review ■ Bioavailability—formulation effects, absorption alteration and pharmacokinetics of pharmaceutical salts, review □ Toxicology—pharmaceutical salts, review

CONTENTS

Potentially Useful Salts 2
Physicochemical Studies 4
Dissolution Rate 5
Solubility 7
Organoleptic Properties 8
Stability 9
Miscellaneous Properties 10
Bioavailability 10
Formulation Effects 11
Absorption Alteration 11
Pharmacokinetics 13
General Pharmacy 14
Pharmacological Effect 14
Dialysis 14
Miscellaneous 14
Toxicological Considerations 15
Toxicity of Salt Ion 15
Toxicity of Salt Form 15
Conclusions 16
References 16

The chemical, biological, physical, and economic characteristics of medicinal agents can be manipulated and, hence, often optimized by conversion to a salt form. Choosing the appropriate salt, however, can be a very difficult task, since each salt imparts unique properties to the parent compound.

Salt-forming agents are often chosen empirically. Of the many salts synthesized, the preferred form is selected by pharmaceutical chemists primarily on a practical basis: cost of raw materials, ease of crystallization, and percent yield. Other basic considerations include stability, hygroscopicity, and flowability of the resulting bulk drug. Unfortunately, there is no reliable way of predicting the influence of a particular salt species on the behavior of the parent compound. Furthermore, even after many salts of the same basic agent have been prepared, no efficient screening techniques exist to facilitate selection of the salt most likely to exhibit the desired pharmacokinetic, solubility, and formulation profiles.

Some decision-making models have, however, been developed to help predict salt performance. For example, Walkling and Appino (1) described two techniques, "decision analysis" and "potential problem analysis," and applied them to the selection of the most suitable derivative of an organic acid for development as a tablet. The derivatives considered were the free acid and the potassium, sodium, and calcium salts. Both techniques are based on the chemical, physical, and biological properties of these specific derivatives and offer a promising avenue for developing optimal salt forms.

Information on salts is widely dispersed throughout the pharmaceutical literature, much of which addresses the use of salt formation to prolong the release of the active component, thereby eliminating various undesirable drug properties (2–6). This review surveys literature of the last 25 years, emphasizing comparisons between the properties of different salt forms of the same compound. Included also is a discussion of potentially useful salt forms. Our purpose is twofold: to present an overview of the many different salts from which new drug candidates can be chosen and

Table I—FDA-Approved Commercially Marketed Salts

Anion	Percent[a]	Anion	Percent[a]
Acetate	1.26	Iodide	2.02
Benzenesulfonate	0.25	Isethionate[i]	0.88
Benzoate	0.51	Lactate	0.76
Bicarbonate	0.13	Lactobionate	0.13
Bitartrate	0.63	Malate	0.13
Bromide	4.68	Maleate	3.03
Calcium edetate	0.25	Mandelate	0.38
Camsylate[b]	0.25	Mesylate	2.02
Carbonate	0.38	Methylbromide	0.76
Chloride	4.17	Methylnitrate	0.38
Citrate	3.03	Methylsulfate	0.88
Dihydrochloride	0.51	Mucate	0.13
Edetate	0.25	Napsylate	0.25
Edisylate[c]	0.38	Nitrate	0.64
Estolate[d]	0.13	Pamoate (Embonate)	1.01
Esylate[e]	0.13	Pantothenate	0.25
Fumarate	0.25	Phosphate/diphosphate	3.16
Gluceptate[f]	0.18	Polygalacturonate	0.13
Gluconate	0.51	Salicylate	0.88
Glutamate	0.25	Stearate	0.25
Glycollylarsanilate[g]	0.13	Subacetate	0.38
Hexylresorcinate	0.13	Succinate	0.38
Hydrabamine[h]	0.25	Sulfate	7.46
Hydrobromide	1.90	Tannate	0.88
Hydrochloride	42.98	Tartrate	3.54
Hydroxynaphthoate	0.25	Teoclate[j]	0.13
		Triethiodide	0.13

Cation	Percent[a]	Cation	Percent[a]
Organic:		Metallic:	
Benzathine[k]	0.66	Aluminum	0.66
Chloroprocaine	0.33	Calcium	10.49
Choline	0.33	Lithium	1.64
Diethanolamine	0.98	Magnesium	1.31
Ethylenediamine	0.66	Potassium	10.82
Meglumine[l]	2.29	Sodium	61.97
Procaine	0.66	Zinc	2.95

[a] Percent is based on total number of anionic or cationic salts in use through 1974. [b] Camphorsulfonate. [c] 1,2-Ethanedisulfonate. [d] Lauryl sulfate. [e] Ethanesulfonate. [f] Glucoheptonate. [g] *p*-Glycollamidophenylarsonate. [h] *N,N'*-Di(dehydroabietyl)ethylenediamine. [i] 2-Hydroxyethanesulfonate. [j] 8-Chlorotheophyllinate. [k] *N,N'*-Dibenzylethylenediamine. [l] *N*-Methylglucamine.

to assemble data that will provide, for the student and practitioner alike, a rational basis for selecting a suitable salt form.

POTENTIALLY USEFUL SALTS

Salt formation is an acid–base reaction involving either a proton-transfer or neutralization reaction and is therefore controlled by factors influencing such reactions. Theoretically, every compound that exhibits acid or base characteristics can participate in salt formation. Particularly important is the relative strength of the acid or base—the acidity and basicity constants of the chemical species involved. These factors determine whether or not formation occurs and are a measure of the stability of the resulting salt.

The number of salt forms available to a chemist is large; surveys of patent literature show numerous new salts being synthesized annually. Various salts of the same compound often behave quite differently because of the physical, chemical, and thermodynamic properties they impart to the parent compound. For example, a salt's hydrophobicity and high crystal lattice energy can affect dissolution rate and, hence, bioavailability. Ideally, it would be desirable if one could predict how a pharmaceutical agent's properties would be affected by salt formation.

Tables I and II list all salts that were commercially marketed through 1974. The list was compiled from all agents listed in "Martindale The Extra Pharmacopoeia," 26th ed. (7). Table I categorizes all salt forms approved by the Food and Drug Administration (FDA), while Table II lists those not approved by the FDA but in use in other countries. (Only salts of organic compounds are considered because most drugs are organic substances.) The relative frequency with which each salt type has been used is calculated as a percentage, based on the total number of anionic or cationic salts in use through 1974. Because of simple availability and physiological reasons, the monoprotic hydrochlorides have been by far the most frequent choice of the available anionic salt-forming radicals, outnumbering the sulfates nearly six to one. For similar reasons, sodium has been the most predominant cation.

Knowledge that one salt form imparts greater water solubility, is less toxic, or slows dissolution rate would greatly benefit chemists and formulators. In some cases, such generalizations can be made. Miller and Heller (8) discussed some properties associated with specific classes of salt forms. They stated that, in general, salt combinations with monocarboxylic acids are insoluble in water and lend themselves to repository preparations, while those of dicarboxylic acids confer water solubility if one carboxylic group is left free. Pamoic acid, an aromatic dicarboxylic acid, is an exception since it is used as a means of obtaining prolonged action by forming slightly soluble salts with certain basic drugs. Saias *et al.* (9) reviewed the use of this salt form in preparing sustained-release preparations. More recently, latentiation of dihydrostreptomycin (10)

Table II—Non-FDA-Approved Commercially Marketed Salts

Anion	Percent[a]
Adipate	0.13
Alginate	0.13
Aminosalicylate	0.25
Anhydromethylenecitrate	0.13
Arecoline	0.13
Aspartate	0.25
Bisulfate	0.25
Butylbromide	0.13
Camphorate	0.13
Digluconate	0.13
Dihydrobromide	0.13
Disuccinate	0.13
Glycerophosphate	0.88
Hemisulfate	0.13
Hydrofluoride	0.13
Hydroiodide	0.25
Methylenebis(salicylate)	0.13
Napadisylate[b]	0.13
Oxalate	0.25
Pectinate	0.13
Persulfate	0.13
Phenylethylbarbiturate	0.13
Picrate	0.13
Propionate	0.13
Thiocyanate	0.13
Tosylate	0.13
Undecanoate	0.13
Cation	**Percent[a]**
Organic:	
Benethamine[c]	0.33
Clemizole[d]	0.33
Diethylamine	0.33
Piperazine	0.98
Tromethamine[e]	0.33
Metallic:	
Barium	0.33
Bismuth	0.98

[a] Percent is based on total number of anionic and cationic salts in use through 1974. [b] 1,5-Naphthalenedisulfonate. [c] *N*-Benzylphenethylamine. [d] 1-*p*-Chlorobenzyl-2-pyrrolidin-1′-ylmethylbenzimidazole. [e] Tris(hydroxymethyl)aminomethane.

using pamoic acid resulted in the formation of a delayed-action preparation. Numerous studies using pamoate salts are dispersed throughout the literature (11–15).

Alginic acid also has been used to prepare long-acting pharmaceuticals. Streptomycin alginate was prepared (16) and shown to be effective in sustained-release preparations. A striking example of a long-acting alginate salt is that of pilocarpine. When dispersed in sterile water and dried to a solid gel, this compound was found useful in the preparation of long-acting ophthalmic dosage forms (17). While liquid preparations of the alginate and hydrochloride salts possess similar miotic activity, studies showed that solid pilocarpine alginate flakes constricted pupil size more effectively and increased the duration of miosis significantly when compared with the liquid preparations. Solid dose pilocarpine may be more uniformly available, because it diffuses more slowly through the gel matrix which holds the drug in reserve. In contrast, drops of the commonly employed solution dosage form release the dose immediately to the conjunctival fluid.

Málek *et al.* (18) devised a unique way of prolonging action through salt formation; they showed that the distribution of several antibiotics could be markedly altered by merely preparing macromolecular salts. Since macromolecules and colloidal particles have an affinity for the lymphatic system, streptomycin, neomycin, viomycin, and streptothrycin were combined with high molecular weight compounds such as polyacrylic acids, sulfonic or phosphorylated polysaccharides, and polyuronic derivatives. Parenteral administration of these compounds produced low blood levels of the antibiotic for long periods, while lymph levels were high. (In comparison, streptomycin sulfate gave high blood levels but low lymph levels.) This alteration in distribution caused the streptomycin to prolong its passage through the body, since lymphatic circulation is quite slow.

The appropriate choice of a salt form has been found to reduce toxicity. It can be rationalized that any compound associated with the normal metabolism of food and drink must be essentially nontoxic. The approach of choosing organic radicals that are readily excreted or metabolized opened up a new class of substances from which to select a salt form. For example, certain salts of the strong base choline have proven to be considerably less toxic than their parent compound. The preparation and properties of choline salts of a series of theophylline derivatives were reported (19), and it was shown that choline theophyllinate possessed a greater LD_{50} than theophylline or its other salts (20). It was postulated that this agent would be less irritating to the GI tract than aminophylline, because "its basic constituent, choline, is an almost completely nontoxic substance of actual importance to the physiologic economy." This evidence led to the preparation of choline salicylate (21) as an attempt to reduce the GI disturbances associated with salicylate administration. Clinical studies indicated that choline salicylate elicited a lower incidence of GI distress, was tolerated in higher doses, and was of greater benefit to the patient than was acetylsalicylic acid (aspirin).

Amino acids and acid vitamins also have been used as salt-forming agents. Based on the evidence that coadministration of amino acids with aminoglycoside antibiotics reduced their toxicity, a series of amino acid salts of dihydrostreptomycin was prepared (22). In all but one case, the acute toxicities of these salts were lower than the toxicity of the sulfate. The ascorbate and pantothenate also were synthesized and shown to be less toxic than the sulfate. Of the salts prepared, the ascorbate had the highest LD_{50}.

The vitamins most commonly used for forming salts exhibiting reduced toxicity are ascorbic and pantothenic acids. Keller *et al.* (23) were the first to use pantothenic acid as a means of "detoxifying" the basic streptomyces antibiotics. Parenteral administration of the pantothenates of streptomycin and dihydrostreptomycin had a significantly reduced incidence of acute neurotoxicity in cats as compared with the sulfates. Subsequent studies (24–28) supported this finding and showed that the pantothenates of neomycin and viomycin also are less toxic. The ascorbate of oleandomycin was synthesized and its pharmacological properties were reported (29). Upon intramuscular injection in rats, it produced less irritation than the phosphate.

p-Acetamidobenzoic acid, an innocuous metabolite of folic acid present in normal blood and urine, has been used in preparing salts. In particular, it yields stable salts with amines that otherwise tend to form hygroscopic products with conventional acid components (30).

Often the salt form is chosen by determining a salt

component that will pharmacologically antagonize an unfavorable property or properties exhibited by the basic agent. Salts of *N*-cyclohexylsulfamic acid are an example of the practical application of this approach. *N*-Cyclohexylsulfamic acid salts, better known as cyclamates, have a characteristic sweet, pleasing taste. Although presently under investigation by the FDA for potentially carcinogenic properties, salts incorporating this compound can render unpleasant or bitter-tasting drugs acceptable. For example, the cyclamates of dextromethorphan and chlorpheniramine exhibit greatly improved bitterness thresholds compared to commonly occurring salts (31). Furthermore, their stability in aqueous solution was described as good when maintained at a pH not greater than 4.

N-Cyclohexylsulfamic acid salts of thiamine hydrochloride and lincomycin also have been synthesized. Thiamine *N*-cyclohexylsulfamate hydrochloride was reported to have a more pleasant taste than other thiamine salts while having an equal or greater stability (32). Lincomycin cyclamate, shown to possess an enhanced thermal stability over its hydrochloride, was prepared (33) to test the hypothesis that reduced lincomycin absorption in the presence of small quantities of cyclamates was due to a simple metathetic reaction. However, this assumption was found not to be true. An extensive study of the preparation and characterization of cyclamic acid salts of several widely used classes of drugs including antihistamines, antibiotics, antitussives, myospasmolytics, and local anesthetics was reported (34, 35).

Various salts of penicillin and basic amine compounds have been formulated in an effort to produce a long-acting, nonallergenic form of penicillin. Since antihistamines appear to mitigate the symptomatology of penicillin reactions in some patients, coadministration of the two has been advocated. The preparation of the benzhydralamine salt of penicillin was an attempt to produce a repository form of penicillin with antiallergic properties (36). Blood levels achieved with this salt were comparable to those of penicillin G potassium; however, its antiallergic properties were not evaluated. In fact, the investigators noted that antihistamines can actually cause sensitization at times and stated that "despite their occasionally favorable influence on the symptoms of penicillin sensitivity, they contribute directly to the potential of drug sensitivity when co-administered with penicillin."

Silver salts of sulfanilamide, penicillin, and other antibiotics have been prepared and represent cases where the species (ions) are complementary. When aqueous solutions of the salts were applied topically to burned tissue, they yielded the combined benefits of the oligodynamic action of silver and the advantages of the antibacterial agents (37).

The use of 8-substituted xanthines, particularly the 8-substituted theophyllines, as salt-forming agents was first reported in the preparation of a series of antihistamine salts (38–41). Synthesis of these xanthine salts was an attempt to find a drug to counteract the drowsiness caused by the antihistamines with the stimulant properties of the xanthines. When an electronegative group is introduced into the xanthine molecule at the 8-position, the electron-drawing capacity of the substituent results in the creation of an acidic hydrogen at position 7. Thus, these moderately strong acidic compounds can undergo salt formation with various organic bases.

The 8-halotheophyllines were the first group of xanthines studied as potential salt-forming agents. Since the report on the preparation of the 8-chlorotheophylline salt of diphenhydramine (42), synthesis of the 8-halotheophyllinates of a number of organic bases has been attempted. The 8-chlorotheophylline salts of quinine, ephedrine, and strychnine were prepared and characterized (43). These salts were less water soluble than the corresponding free alkaloidal bases. In a similar report, the 8-chlorotheophyllinates of three synthetic narcotics, meperidine, levorphanol, and metopon, were prepared (44).

Pharmacological and clinical studies involving the 8-bromotheophylline pyrilamine salt revealed the unusual diuretic properties associated with the 8-halotheophylline portion of the compound (45, 46). This finding initiated an investigation into the preparation of a soluble 8-bromotheophylline salt of high diuretic activity. With readily available amines, over 30 salts were synthesized and screened for diuretic activity (47). When tested against theophylline salts of the same amines, the 8-bromotheophyllinates showed greater activity in every case.

With the successful formation of 8-halotheophyllinates of organic bases, Morozowich and Bope (48) proposed that, if the halogen moiety was replaced with a more electronegative substituent such as a nitro group, a more acidic compound would be formed. Presumably, more stable salts would result and precipitation of the free xanthine derivative in the stomach would be less likely to occur. On this premise, they successfully prepared pharmacologically effective 8-nitrotheophyllinates of several pharmaceutically useful bases.

Duesel *et al.* (19), in their study of choline theophyllinate, prepared the 8-chloro-, 8-bromo-, and 8-nitrotheophylline salts of choline. Oral toxicity studies in mice showed that the LD_{50} of the 8-nitrotheophyllinate was much greater than that of either 8-halotheophylline. In fact, it remained nonlethal at doses as high as 5 g.

Polygalacturonic acid, a derivative of pectin, has been used to prepare quinidine salts exhibiting reduced toxicity (49, 50). The compound possesses special demulcent properties and inhibits mucosal irritation. The rationale for use of this agent is to reduce the ionic shock to the GI mucosa resulting from the flood of irritating ions liberated by rapid dissociation of the conventional inorganic quinidine salts. Studies have shown that it is four times less toxic orally than the sulfate. This difference was attributed to the slower release of quinidine from the polygalacturonate.

Other compounds reported to be potentially useful as pharmaceutical salt forms are listed in Table III.

PHYSICOCHEMICAL STUDIES

Biological activity of a drug molecule is influenced by two factors: its chemical structure and effect at a specific site and its ability to reach—and then be removed from—the site of action. Thus, a knowledge of the physicochemical properties of a compound that influence its absorption, distribution, metabolism, and excretion is essential for a complete understanding of the onset and duration of ac-

Table III—Potentially Useful Salt Forms of Pharmaceutical Agents

Salt-Forming Agent	Compound Modified	Modification	Reference
Acetylaminoacetic acid	Doxycycline	Solubility	51
N-Acetyl-L-asparagine	Erythromycin	Solubility, activity, stability	52
N-Acetylcystine	Doxycycline	Combined effect useful in pneumonia	53
Adamantoic acid	Alkylbiguanides	Prolonged action	54
Adipic acid	Piperazine	Stability, toxicity, organoleptic properties	55
N-Alkylsulfamates	Ampicillin	Absorption (oral)	56
	Lincomycin	Solubility	57
Anthraquinone-1,5-disulfonic acid	Cephalexin	Stability, absorption	58
Arabogalactan sulfate (arabino)	Various alkaloids	Prolonged action	59, 60
Arginine	Cephalosporins	Toxicity	61
	α-Sulfobenzylpenicillin	Stability, hygroscopicity, toxicity	62
Aspartate	Erythromycin	Solubility	63
Betaine	Tetracycline	Gastric absorption	64
Bis(2-carboxychromon-5-yloxy)alkanes	7-(Aminoalkyl)theophyllines	Activity, prolonged prophylactic effect	65
Carnitine	Metformin	Toxicity	66
4-Chloro-*m*-toluenesulfonic acid	Propoxyphene	Organoleptic properties	67
Decanoate	Heptaminol	Prolonged action	68
Diacetyl sulfate	Thiamine	Stability, hygroscopicity	69
Dibenzylethylenediamine	Ampicillin	Prolonged action	70, 71
Diethylamine	Cephalosporins	Reduced pain on injection	72
Diguaiacyl phosphate	Tetracycline	Activity	73
Dioctyl sulfosuccinate	Vincamine	Organoleptic properties	74
Embonic (pamoic) acid	Kanamycin	Toxicity	75
	2-Phenyl-3-methylmorpholine	Toxicity	76
Fructose 1,6-diphosphoric acid	Tetracycline	Solubility	77
	Erythromycin	Solubility	
Glucose 1-phosphoric acid, glucose 6-phosphoric acid	Tetracycline	Solubility	77
	Erythromycin	Solubility	
L-Glutamine	Erythromycin	Solubility, activity, stability	52
Hydroxynaphthoate	Bephenium	Toxicity	78
2-(4-Imidazolyl)ethylamine	Prostaglandin	Prolonged action	79
Isobutanolamine	Theophylline	Stability	80
Lauryl sulfate	Vincamine	Organoleptic properties	81
Lysine	α-Sulfobenzylpenicillin	Toxicity, stability, hygroscopicity	62
	Cephalosporins		61
Methanesulfonic acid	Pralidoxime (2-PAM)	Solubility	82
N-Methylglucamine	α-Sulfobenzylpenicillin	Toxicity, stability, hygroscopicity	62
	Cephalosporins	Reduced pain on injection	72
N-Methylpiperazine	Phenylbutazone	Toxicity, faster onset of action	83
Morpholine	Cephalosporins	Reduced pain on injection	72
2-Naphthalenesulfonic acid	Propoxyphene	Organoleptic properties	84
Octanoate	Heptaminol	Prolonged action	68
Probenecid	Pivampicillin	Organoleptic properties	85
Tannic acid	Various amines	Prolonged action	86, 87
Theobromine acetic acid	Propoxyphene	Activity	88
3,4,5-Trimethoxybenzoate	Tetracycline	Organoleptic properties	89
	Heptaminol	Prolonged action	68
Tromethamine	Aspirin	Absorption (oral)	90
	Dinoprost (prostaglandin $F_{2\alpha}$)	Physical state	91

tion, the relative toxicity, and the possible routes of administration (2).

In a review in 1960, Miller and Holland (92) stated that "different salts of the same drug rarely differ pharmacologically; the differences are usually based on the physical properties." In a subsequent review (93), Wagner expanded upon this statement, asserting that, although the nature of the biological responses elicited by a series of salts of the same parent compound may not differ appreciably, the intensities of response may differ markedly.

The salt form is known to influence a number of physicochemical properties of the parent compound including dissolution rate, solubility, stability, and hygroscopicity. These properties, in turn, affect the availability and formulation characteristics of the drug. Consequently, the pharmaceutical industry has systematically engaged in extensive preformulation studies of the physicochemical properties of each new drug entity to determine the most suitable form for drug formulation. Published information concerning such studies, however, is sparse. Preformulation studies have been outlined, and the influence of the salt form on the volatility and hygroscopicity of an agent under investigation was discussed (94).

In one such study, methylpyridinium-2-aldoxime (pralidoxime) salts were investigated (95). This study set out to prepare a salt with water solubility adequate to allow intramuscular injection of a low volume (2–3 ml) therapeutic dose. The original compound, the methiodide, had the disadvantages of limited aqueous solubility and high potential toxicity, since its high iodide content could result in iodism. On the basis of physiological compatibility, better water solubility, favorable stability, and relatively high percentage of oxime, the chloride salt of pralidoxime was selected for therapeutic administration; it was claimed that "the anion used to form the salt can confer physical properties of importance and significance for the formulation and administration of the compound" (95).

Some physicochemical properties of a series of mineral acid salts of lidocaine also were determined (96). While the hydrochloride and hydrobromide were more hygroscopic, they were more soluble in a number of solvents than the nitrate, perchlorate, phosphate, or sulfate salts.

Dissolution Rate—The dissolution rate of a pharmaceutical agent is of major importance to the formulator. In many cases, particularly with poorly soluble drugs, this characteristic best reflects the bioavailability of the com-

pound. As a rule, a pharmaceutical salt exhibits a higher dissolution rate than the corresponding conjugate acid or base at an equal pH, even though they may have the same equilibrium solubility. The explanation for this result lies in the processes that control dissolution.

Dissolution can be described by a diffusion layer model[1] in terms of an equation developed by Nernst and Brunner (97):

$$\frac{dW}{dt} = \frac{DS}{h}(C_s - C) \qquad \text{(Eq. 1)}$$

where W is the mass of the solute dissolved at time t, dW/dt is the rate of mass transfer per unit time, D is the solute molecule diffusion coefficient, S is the surface area of the dissolving solid, h is the diffusion layer thickness, C is the concentration of the drug in the bulk solution at time t, and C_s is the saturation solubility of the solute in the diffusion layer.

The driving force for dissolution in Eq. 1 is the difference between the saturation solubility of the drug and the concentration of the drug in the bulk fluid. If the drug is not rapidly absorbed after it dissolves, then C, the concentration in the bulk solution, approaches C_s and the dissolution rate is retarded. When this occurs, absorption is "absorption rate" limited (or "membrane transport" limited). If the absorption rate is rapid (or if the absorption mass transfer coefficient is much larger than DS/h of Eq. 1), however, C becomes negligible compared to C_s and dissolution occurs under "sink" conditions. Absorption is then said to be dissolution rate limited, which is what occurs with most poorly soluble drugs. In either case, an increase in C_s, as in salt formation, increases dissolution.

Salts often speed dissolution by effectively acting as their own buffers to alter the pH of the diffusion layer, thus increasing the solubility of the parent compound, C_s, in that layer over its inherent solubility at the pH of the dissolution medium. Hence, dissolution is controlled by solubility in the diffusion layer which, in turn, is determined by the pH of that layer. The influence of K_{sp} on the solubility term, C_s, and dissolution rate, should an accumulation of ions be allowed to occur, will be treated later.

Nelson (98), in a study of theophylline salts, was the first to show the correlation between diffusion layer pH and dissolution rate. The major impact that this study had on the pharmaceutical sciences was its conclusion that, if other factors remained constant, the dissolution rate of a compound determined the rate of buildup of blood levels with time and the maximum levels obtained. Those salts of the acidic theophylline with high diffusion layer pH's had greater *in vitro* dissolution rates than those exhibiting a lower diffusion layer pH. And, indeed, the rank order of dissolution rates correlated well with clinically determined blood levels. Presumably, the higher pH in the diffusion layer retards hydrolysis of the salt, thereby maintaining the anionic charge of the theophyllinate ion. This report led to many additional studies which illustrate the influence of the salt form on dissolution and the beneficial effects of changing nonionized drugs into salts.

Juncher and Raaschou (99) demonstrated that the rank order of peak blood levels of penicillin V, obtained upon administration of three different salts and the free acid, was the same as the rank order of their rates of dissolution *in vitro*. While the investigators ascribed these differences to the solubility properties of the salts, their experiments actually compared dissolution rates, not solubilities. The relative order of dissolution rates and mean maximal blood levels was: potassium salt > calcium salt > free acid > benzathine salt.

Nelson (100) determined dissolution rates for several weak acids and their sodium salts in media whose pH's represented GI fluids. In all cases, the sodium salt dissolved more rapidly than the free acid. This finding resolved the misconception that absorption of drugs is related only to solubility in the appropriate medium; rather, solubility affects absorption only to the extent that it affects dissolution rate. Absorption of drugs is a dynamic process, and the ultimate solubility of a drug in fluid at absorption sites is of limited consequence since absorption prevents the attainment of saturated solutions. Therefore, dissolution rate, more than solubility, influences absorption since it is a preceding process.

In two subsequent studies, Nelson and coworkers further illustrated the effects of changing nonionized drugs into salts. A report concerning tolbutamide (101), a weak acid, showed that the initial dissolution rate of tolbutamide sodium was approximately 5000 times more rapid than the free acid in acidic media and 300 times more rapid in neutral media. This difference, measured *in vitro*, reflected the differences observed between the free acid and the salt when administered to human subjects. Oral administration of tolbutamide sodium produced an immediate drop in blood sugar comparable to that produced by intravenous injection of the salt, while the slowly dissolving tolbutamide produced a smooth, sustained fall in blood sugar (102).

Correlation of urinary excretion rates and dissolution rates of tetracycline and some of its acid salts also was demonstrated by Nelson (103). The salts that exhibited greater *in vitro* dissolution rates showed greater urinary excretion rates, indicating more rapid absorption.

Benet (104), in a discussion of the biopharmaceutical basis for drug design, referred to the influence of the salt form on dissolution. He compared the dissolution rates of tetracycline and tolbutamide and their salts, as reported in the studies previously cited, and explained why the rates differ at the pH's exhibited by physiological fluids.

Although salt formation usually increases the dissolution rate of a drug, studies with aluminum acetylsalicylate (105, 106), warfarin sodium (107), and benzphetamine pamoate (108) showed that administration of the salt *slowed* dissolution of the drug and subsequent absorption compared to the nonionized form. This decrease appeared to result from precipitation of an insoluble particle or film on the surface of the tablet. Such a phenomenon decreases the effective surface area and prevents deaggregation of the particles. Theoretical considerations of the processes controlling dissolution of an acid salt of a base (108) and the sodium salt of a weak acid (109, 110) in reactive media have been discussed.

Tablet processing and various formulation factors can decrease the dissolution rate of a salt in human gastric juice over its nonionized form (111). Granulation and tableting caused the dissolution rate of phenobarbital sodium to

[1] The authors recognize the existence of other models; this one was chosen simply for illustrative purposes.

decrease but had the opposite effect on phenobarbital. Therefore, as a tablet dosage form, the dissolution rate of the sodium salt was slower than that of the free acid. These results were attributed to differences in the disintegrating properties of the tablets; in some instances, rapid dissolution may in fact be a problem for very soluble drugs.

Others have illustrated a phenomenon that decreases the dissolution rate of a salt below that of its nonionized form. Lin *et al.* (112) studied the relationship between salts and biological activity by dissolving three salts and the free base of an experimental antihypertensive in water, 0.1 *N* HCl, and pH 7.2 phosphate buffer. The dissolution rate of the monohydrochloride salt was lower than that of the free base in 0.1 *N* HCl and higher than the free base in both water and phosphate buffer. These authors ascribed this variation to the common ion effect and substantiated it experimentally. Although the biological activity of the monohydrochloride was greater than that of the free base, the implications of altered absorption characteristics on the activity of any other hydrochloride salt in GI fluids must be considered. Similar results also were reported for hydrochloride salts of some tetracyclines (113).

Some consideration must be given to the influence of salt formation on oral toxicity, which often reflects the relationship between the *in vivo* dissolution rate and the appearance of drug in the circulation (114, 115). Morozowich *et al.* (114) showed that the relative toxicities of a series of salts of a drug reflect the rate of absorption, providing the salt-forming agents themselves are relatively nontoxic. They stated that "when absorption is rate-limited by dissolution of the salt in the gastrointestinal tract, as will be the case with slowly soluble salts, the toxicity of a slowly dissolving salt will most probably be lower than that of a more rapidly dissolving salt." The implications of salt formation on toxicology will be discussed under *Toxicological Considerations.*

Several reviews dealt with the influence of the dissolution rate on drug availability and, in particular, salt effects (116, 117). Other reports illustrating the influence of salts and salt form on dissolution rate are listed in Table IV.

Solubility—Knowledge of the solubility characteristics of a pharmaceutical agent is essential, because solubility is usually an important factor in the pharmacokinetic profile, the chemical stability, and, ultimately, the formulation of the drug. As discussed previously, it is certainly a primary factor in controlling dissolution rates. The solubility of a compound depends basically upon the physical and chemical properties of the solute; *e.g.*, a lower melting point for a compound within a series reflects a decreased lattice energy, which would suggest a higher solubility. Solubility depends as well upon such elements as temperature, pressure, solvent properties (such as resulting pH), and, to a lesser extent, the state of subdivision of the solute.

An important solvent property which is often overlooked involves the common ion effect; in particular, hydrochloride salts of drugs often exhibit less than desirable solubility in gastric juice because of the abundance of chloride ions. The equilibrium involved is shown in Scheme I.

$$DH^+Cl^-_{(solid)} \overset{K_{sp}}{\rightleftharpoons} (DH^+)_{aq} + (Cl^-)_{aq}$$

Scheme I

Salt formation is perhaps one of the first approaches considered as a means of increasing a compound's water solubility. As with dissolution rates, however, salt formation does not always confer greater solubility. Liberally dispersed throughout the pharmaceutical literature are studies that compare the solubilities of different salt forms of the same compound with those of its free acid or base (Table IV). Selection of the salt form exhibiting the desired solubility properties is critical, since these properties often dictate the formulation characteristics of the drug.

Table IV—Additional References on Salt Form and Dissolution Rate

Topic	Reference
Dissolution rate of mixtures of weak acids and tribasic sodium phosphate	118
Physiological availability and *in vitro* dissolution characteristics of some solid dosage formulations of aminosalicylic acid and its salts	119
Biopharmaceutics, rate of dissolution: chronological bibliography	120
Biopharmaceutics: rate of dissolution *in vitro* and *in vivo*	121
Dissolution tests and interpretation of anomalies observed in the dissolution process of sulfaquinoxaline based on salt formation	122
Influence of the dissolution rate of lithium tablets on side effects	123
Dissolution kinetics of drugs in human gastric juice	124
Comparison of dissolution and absorption rates of different commercial aspirin tablets	125
In vitro dissolution rates of aminorex dosage forms and their correlation with *in vitro* availability	126

Phase solubility techniques were used to study the formation of complex salts of triamterene (127). The results indicated that the organic acid salts of basic drugs, such as amines, were more soluble in water than the corresponding inorganic (halide) salts. This consideration is important in the synthesis and selection of a salt form that will exhibit enhanced bioavailability and desirable formulation characteristics.

The hydrogen-ion concentration can significantly affect the solubility of a salt. Anderson (128) discussed the influence of pH on the solubility of pharmaceuticals. Mathematical relationships between pH and solubility of therapeutically useful weak acids and bases and their salts were given along with some considerations in the formulation of solutions of these particular agents.

An extensive study on the solubility interrelationships of the hydrochloride and free base of two pharmaceutically useful amines was reported (129). Mathematical equations describing the total solubility at an arbitrary pH in terms of the independent solubilities of the hydrochloride and free base species and the dissociation constant of the salt were derived and fitted to experimental data with good results. This report elucidated the point that, while the solubility of the amine hydrochloride generally sets the maximum obtainable concentration for a given amine, the solubility of the free base and the pKa determine the maximum pH at which formulation as a solution is possible (assuming that the desired concentration exceeds the free base solubility). Shifting the pH–solubility profile to higher pH values for formulation purposes may require increasing the solubility of the free base. This increase might be accomplished by using an appropriate cosolvent. Since the dissociation characteristics of carboxylic acids and other acidic organic species are similar to those of organic hydrochlorides, it is expected that the pH–solubility profiles

of these organic acids, although reversed, can be characterized theoretically using the same treatment.

Several reports showed that the structure of an organic salt-forming radical influences the solubility of the resulting salt. The water solubilities of 16 salts (carboxylates, sulfates, sulfamates, and phosphates) of the weak base erythromycin were dependent on the size of the alkyl group of the acid (130). In a study with *N*-alkylsulfamates of lincomycin (66), a similar phenomenon was observed: solubility of these salts decreased as the size of the alkyl group attached to the acidic function increased.

Senior (131), in a study on the formulation and properties of the antibacterial chlorhexidine, determined the water solubilities of 35 salts and the free base. He found that inorganic salts had remarkably low solubilities while those of the lower aliphatic acids proved to be somewhat more soluble. Hydroxylation of the acid increased solubility, since salt formation with polyhydroxy acids, particularly the sugar acids, conferred extensive water solubility to the molecule.

Several investigators reported the influence of the solubility of a drug on its formulation and subsequent availability from the dosage form. In a discussion of the preparation and formulation of epinephrine salts in an aerosol system using liquefied gas propellants, Sciarra *et al.* (132) pointed out that the solubility characteristics of the agent are important in two respects. First, the solubility of the therapeutically active ingredient in the various propellants is an important consideration if the product is to be used for either local action in the lungs or systemic therapy. Second, the solubility of the drug in extracellular fluids plays an important role in selection of the compound. The bitartrate, malate, maleate, and fumarate salts of epinephrine were prepared and subjected to solubility and stability studies. While all salts had similar partition coefficients, the solubility of the maleate in several propellants and its stability in formulated aerosols made it the drug form of choice.

Ephedrine hydrochloride was more rapidly released than the free base from theobroma oil suppositories containing different surfactants (133). This enhanced rate of release (dialysis) was ascribed primarily to the greater aqueous solubility of the hydrochloride, which solubilized faster from the oil-in-water emulsion, whereas the ephedrine alkaloid base tended to remain behind in the oil phase.

The solubility of the active ingredient in ointment bases can dramatically influence its diffusion properties. A study of salicylic acid and its sodium salt showed that the diffusion of both was very low from hydrophobic bases, whereas the solubility of the drug significantly affected the diffusion from hydrophilic bases. The more soluble sodium salicylate diffused much faster from these latter bases than did salicylic acid (134).

Additional references on the relationship of salt form and solubility are listed in Table V.

Table V—Additional References on Salt Form and Solubility

Topic	Reference
Influence of solubility on the rate of GI absorption of aspirin	135
Effect of dosage form upon the GI absorption rate of salicylates	136
Physical–chemical properties of polyene macrolide esters and their water-soluble salts	137
Isolation and reaction products of orotic acid and amines and their solubility in water	138
Solubility and stability of erythromycin salts	139
Studies on pharmaceutical preparations of orotic acid: water-soluble properties of orotic acid salts	140
Solubility of antibiotics in 24 solvents	141, 142
Solubility of antibiotics in 26 solvents	143

Organoleptic Properties—Modern medicine requires that a pharmaceutical formulation be efficacious, safe, stable, and acceptable to the patient. Of primary importance in the development of oral dosage forms is taste acceptability. This factor presents no major problems when the drug is to be administered as a tablet or a capsule and swallowed as a unit but is clearly a prominent factor in patient acceptability when it is to be administered as a liquid, chewable tablet, or lozenge.

Since taste is a chemical sense, a substance must be dissolved if it is to elicit a taste sensation—either by taking it as a solution or by its dissolving in the saliva. Therefore, one method used to minimize undesirable organoleptic properties of pharmaceuticals involves the preparation of a poorly soluble salt form of the drug such that the saturation concentration is less than the taste threshold.

Erythromycin estolate (lauryl sulfate) has approximately one-twelfth the solubility of the free base, is tasteless, and is useful in the formulation of oral suspensions (144). A study on erythromycin salts showed that the bitterness level was dependent on two properties: (*a*) the water solubility of the salt, which is dependent on the size of the alkyl group attached to the acid function; and (*b*) the strength of the acid used to form the salt, *i.e.*, the stability of the salt (130). The stearyl sulfamate salt possessed the most desirable organoleptic properties.

Many problems concerned with formulation and stability of topical and oral pharmaceuticals containing bacitracin have been overcome by incorporating bacitracin into the formulation as its zinc salt. One distinct advantage over the parent compound is its lack of taste, caused by its relative insolubility. Thus, it is the preferred drug form for preparations where taste is a factor (145). Taste panel evaluations of the comparative bitterness of bacitracin zinc and bacitracin indicate that the taste of the zinc salt is more easily masked and that the presence of a bitterness-masking adjuvant, such as sucrose, increases the bitterness threshold ratio differences between the two compounds even further (146).

Propoxyphene napsylate, nearly water insoluble, is only slightly bitter to the taste as compared to the highly water-soluble hydrochloride (147) and can be readily formulated into a flavored aqueous suspension. The taste of these suspensions can be improved significantly by the addition of a common ion (sodium or calcium napsylate) to depress solubility further.

A newer approach to the improvement of drug palatability has been to form insoluble salts with ion-exchange resins. Several investigators described and tested the practical application of this method (148–150). Spross *et al.* (149) outlined the conditions necessary for improving the palatability of a drug by adsorbing it onto an ion-exchange resin without appreciably modifying its pharmacological effects. They found that: (*a*) the degree of drug release from the ion-exchange adsorbate depends on the

equivalent quotient between the electrolytes in the surrounding fluid and the ionic drugs, (*b*) the amount of ions is far less in the saliva than in the gastric juice (the temporary electrolyte contents can be estimated at 0.05 mEq in the saliva and at 10 mEq in the gastric juice), and (*c*) the exchange rates should allow the equilibria to be attained within a fairly short period. Insoluble drug resinates formed between dextran gel[2] cation exchangers and several basic drugs were in many cases much more pleasant tasting than their parent compounds. Furthermore, release of the drug from the ion-exchange adsorbate was quite rapid and complete under conditions prevailing in the GI tract.

Similar findings were reported using a polymethacrylic acid ion-exchange resin (150). In addition, coating the adsorbate particles with a 4:1 ethylcellulose–hydroxypropyl methylcellulose mixture further reduced bitterness. While *in vitro* release from the uncoated resinate was rapid and complete, release from coated adsorbates varied with the extent of coating.

Another approach to improving the taste properties of pharmaceutical agents is to prepare a pleasant-tasting soluble salt of a poor-tasting parent drug. This approach often can be very difficult, however, since solubilization of the parent compound usually imparts its unpleasant taste to the preparation. Nevertheless, some success has been reported using the artificial sweeteners cyclamate sodium and saccharin.

As described earlier, formation of *N*-cyclohexylsulfamate salts of several drug substances has produced better tasting derivatives with enhanced solubility properties (31, 32). The physicochemical and toxicological properties of benzalkonium saccharinate and a series of saccharinates of other quaternary ammonium compounds were reported (151). While conventional quaternary ammonium compounds have a very bitter taste, their saccharin analogs are sweet.

Potassium salts frequently possess an unpleasant taste and a metallic aftertaste. The palatability of some potassium salts in flavored vehicles was reported (152); while the salts had similar taste thresholds at effective therapeutic levels, all potassium salts exhibited inferior palatability.

Table III includes several samples of other salts that exhibit an improved taste relative to their free acid or base forms.

Stability—The chemical and physical stability of a pharmaceutical must be known, because it can influence the choice of dosage form, the manufacturing and packaging, and the therapeutic efficacy of the final preparation. Systematic determination of the thermal stability, solution stability (at various pH's), and light sensitivity of a drug and its derivatives, both alone and in the presence of common additives, provides essential input toward selecting the most suitable derivative and dosage form.

Depending on the route of degradation, different salt forms impart different stability characteristics to the parent drug by various mechanisms. Most commonly used are sparingly soluble salts which, when used in the formulation of suspensions, reduce the amount of drug in solution and, hence, its degradation. Differences in hygroscopicity of several salts influence the stability of the drug in the dry state. In some cases, the salt-forming radical itself enhances the stability of the parent agent.

The stability of penicillin G and its salts has been widely studied due to the drug's therapeutic importance and its characteristic instability. Schwartz and Buckwalter (153) described some of the stability characteristics of this antibiotic, stating that, with present techniques, a solution of penicillin cannot be made stable for more than 2 weeks, even at refrigerator temperatures. They also discussed the use of suspensions of sparingly soluble amine salts in aqueous vehicles as a means of "allowing marketing of a 'ready-made' penicillin product." Procaine, benzathine, and hydrabamine salts are marketed, and their acceptable stability as aqueous suspensions is based mainly on their insolubility and the minimization of degradation in solution.

A theoretical treatment of the solubility of these salts was presented in which equations were derived for calculating the solubility as a function of pH and the pH of minimum solubility (154, 155). These equations are based on the mass action law and its relationship to the ionization constants of the amine and the penicillin and the solubility of the salt in water. Since the salt in solution is partially dissociated, further suppression of the solubility may be achieved by the common ion effect. Swintosky *et al.* (156) demonstrated this effect with penicillin G procaine by adding procaine hydrochloride to the preparation and further enhancing its stability. The 8-chlorotheophylline salt (or complex) of penicillin G was reported to be water soluble, yet stable in solution (157). Since 8-chlorotheophylline is acidic, it has been postulated that a buffer effect could account for the stabilization of this "salt."

While penicillin G procaine is more stable in aqueous vehicles, it is less thermally stable than the sodium or potassium salts, decomposing if heated much above 60°. The sodium and potassium salts are known to withstand heating up to 100° for 4 days with little loss in potency (158). This behavior might well be due to differences in melting points—*viz.*, 106° for penicillin G procaine and ~215° dec. for the potassium salt.

Since hydrolysis of penicillin is dependent on moisture content, preparations in which moisture is rigorously excluded are quite stable in the dry state. A study on the effect of moisture on penicillin salts found the calcium salt to be less hygroscopic than the sodium salt and, hence, more stable in moist atmospheres (159). Similarly, penicillin G potassium is also much less hygroscopic than penicillin G sodium and has become the preferred form for marketing in the dry state (160).

Several studies reported the relative stabilities of thiamine salts, particularly the hydrochloride and the mononitrate (161–163). The mononitrate is observed to be less hygroscopic and is accordingly much less water soluble than the hydrochloride. Investigations of various preparations including compressed tablets, multivitamin capsules, and dry-filled vitamin B complex capsules at various temperatures showed that the mononitrate was more stable than the hydrochloride (164, 165). The stabilities of numerous thiamine salts were studied in aqueous solution and in dry powder preparations with various excipients (166, 167). In aqueous solution, the resulting pH was the chief factor controlling hydrolysis and oxidative decomposition of thiamine salts; their stability as powder

[2] Sephadex.

preparations was related to their aqueous solubility, with the sparingly soluble salts being more stable (and presumably less hygroscopic).

An orally administered drug must be stable in acidic solution because it generally must pass intact through the acidic environment of the stomach if it is to exhibit therapeutic blood levels. The advantage of erythromycin estolate over the free base lies in its low solubility in gastric juice, which enables it to be administered with food without any decrease in attained blood levels. The salt is more stable in the stomach because it remains undissolved. Therefore, it retains its potency even when exposed to acidic environments for extended periods (144).

In a study on the preparation and characterization of lincomycin cyclamate (33), it was noted that the cyclamate salt had an enhanced thermal stability over the hydrochloride. In a subsequent report (168), differential thermal analysis and thermogravimetric analysis showed that while the hydrochloride easily undergoes thermal degradation, the cyclamate anion confers a considerably greater thermal stability on the lincomycin moiety.

Mullins and Macek (169) showed that the physical and chemical stability of the calcium salt of novobiocin makes it the form of choice for the formulation of a liquid preparation of the antibiotic. The amorphous calcium novobiocin salt proved to be tasteless, yet fully biologically active and perfectly stable in aqueous suspension. Neither the sodium salt nor the free acid is suitable; the sodium salt cannot be formulated in a liquid due to its chemical instability, while the crystalline free acid is not absorbed from the GI tract. Amorphous novobiocin is absorbed but is metastable in solution and slowly converts to the unabsorbed crystalline form.

Other reports of alterations in stability characteristics due to salt formation are listed in Table VI.

Miscellaneous Properties—The salt form has been reported to influence other physicochemical properties of a drug substance. Studies illustrating the effect of the salt-forming radical on surface tension, deaggregation behavior, and ion-pair extraction have appeared.

The influence of the anion on the absorption processes of two charged species, dextromethorphan and tetracycline, was studied in the rat stomach (186, 187). A linear relationship existed between the rate of absorption from buffer solutions of the anions under investigation and their surface tensions. Thus, the absorption process was related to the surface activity of the various salts and not to their lipid solubilities. This change of surface activity with the buffer (or salt) species is similar to the results reported in a study of the surface activity of various phenothiazine salts (188).

The antibacterial chlorhexidine possesses surface activity. A study of the colloidal properties of some chlorhexidine salts showed that the counterion can affect the critical micelle concentration of a surface-active agent, and this effect was usually associated with a change in micellar size (189).

The deaggregation behavior of a relatively insoluble acid and its sodium salt was studied, and deaggregation was postulated to be a possible rate-limiting step in the absorption of a drug from a dosage form (190). While no direct comparisons of the two forms were made, inspection of the data shows that the deaggregation rate of the salt was considerably more rapid than that of the free acid in equivalent dosage forms. Therefore, if absorption is dependent on the dissolution rate, which in turn is dependent on the deaggregation rate, the salt should produce the highest and earliest blood levels. On the other hand, it is possible that hygroscopic (and deliquescent) salts can absorb atmospheric moisture, cause a sticky surface, and inhibit deaggregation.

Table VI—Additional References on Salt Form and Stability

Topic	Reference
Stability of chlorhexidine solutions	170
Stability of chlorhexidine when autoclaved	171
Anhydrotetracycline and 4-epianhydrotetracycline in marketed tetracycline and aged tetracycline products	172
Solid-state stability of some crystalline vitamin A compounds	173
Physicochemical studies on the stability of penicillin salts	174
Light sensitivity of tetracyclines	175
Hygroscopic properties, thermostability, and solubility of oleandomycin salts	176
Stability of orotic acid and its amine salts in aqueous solution	177
Some factors influencing the stability of tablets (aspirin)	178
Stability of aqueous solutions of sodium aminosalicylate	179
Hygroscopic properties of various preparations of erythromycin	180
Physicochemical studies on the decomposition of aminosalicylic acid and its salts	181
Stabilities of aqueous solutions of 2-diethylaminoethyl-3-methyl-2-phenylvalerate hydrochloride and its methobromide	182
Investigation of some properties of penicillin G salts	183
Stability of ferrous iron tablets on storage	184
Stability of aspirin aluminum compounded with antacids	185

Higuchi and coworkers presented an extensive study on the physicochemical basis of the ion-pair extraction of pharmaceutical amines. Distribution ratios of dextromethorphan (191) and chlorpheniramine (192) between an organic layer and water were highly dependent on the concentration and nature of the anion present. Less hydrophilic anions yielded more readily extractable ion-pairs. A study of the thermodynamic properties, enthalpy, free energy, and entropy, involved in the extraction equilibria of dextromethorphan ion-pairs indicated that the entropy change associated with transfer of the different anions between phases is the main controlling factor in the extraction process (193).

BIOAVAILABILITY

Most drugs prescribed in the United States are administered in solid and polyphasic dosage forms. Consequently, dissolution of the drug must precede the absorption process. The simplest model that adequately describes this process is shown in Scheme II.

$$\text{solid drug} \xrightarrow[1]{\text{dissolution}} \text{dissolved drug} \xrightarrow[2]{\text{absorption}} \text{drug in circulation}$$

Scheme II

Since the dissolution rate is generally slow for drugs with poor solubility, Step 1 is frequently rate limiting in the overall absorption process. As a result, the onset, intensity, duration of pharmacological activity, and, hence, bioavailability are affected by changes in dissolution rate. As discussed previously, administering a salt of the parent drug often proves to be an effective means of altering dissolution rate and absorption.

Table VII—Additional References on Bioavailability and Formulation Effects

Topic	Reference
Effects of various substances on the absorption of tetracycline in rats	197
Effects of dosage form upon the GI absorption rate of salicylates	136
Determination of *in vivo* and *in vitro* release of theophylline aminoisobutanol in a prolonged-action system	198
Ion-exchange resin salts for oral therapy: carbinoxamine	199
Latentiation of dihydrostreptomycin by pamoate formation	10
Solid-state ophthalmic dosage systems in effecting prolonged release of pilocarpine in the cul-de-sac	17
Absorption of erythromycin: various pharmaceutical forms	200
Comparative study of the absorption of drugs from old and new rectal preparations	201

Formulation Effects—Choice of the salt form of a drug may have a pronounced effect on the formulation of the parent compound. For example, Fenton and Warren (194) found there was no release of medicament from proflavine cream BPC, a water-in-oil emulsion containing 0.1% proflavine as the hemisulfate salt. They also investigated the release of various salts of proflavine with aliphatic carboxylic acids from water-in-oil cream emulsions. Salts formed with the water-soluble, oil-insoluble "lower" acids, such as formic and acetic acids, showed very poor release from a water-in-oil cream. The "higher" acid salts (*e.g.*, *n*-valeric, caproic, cyclohexanecarboxylic, and caprylic) all showed increased diffusion from similar emulsions since these salts are soluble in both water and oil. Their release was even greater from oil-in-water emulsions, however, in agreement with their preferential oil solubility. The *n*-valerate salt provided the most effective water-in-oil cream. The primary factor responsible for diffusion of proflavine from a water-in-oil cream is the low hydrophilic–lipophilic balance conveyed to the salt by the acid. This finding illustrates the desirability of carefully selecting the salt anion of a cationic drug in lieu of the nature of the dosage form.

Studies of the effect of formulation on the bioavailability of warfarin sodium relative to warfarin yielded interesting results (107, 195). Absorption of warfarin upon administration of the sodium salt as a lactose-base tablet was no better than that from a similar formulation of the free acid. In fact, absorption was further depressed when the salt was formulated with starch instead of lactose. Later results indicated that the *in vitro* water dissolution rate of a warfarin sodium tablet was 350 times that of a slowly dissolving warfarin tablet formulation, yet the latter exhibited rapid and complete absorption *in vivo*. The virtual insolubility of warfarin in acidic gastric fluids precluded its absorption from the stomach. However, the strongly acidic medium was necessary for tablet disintegration, which, in turn, was critical for absorption. Following initial exposure to 0.1 *N* HCl, *in vitro* dissolution of the warfarin tablet in pH 7.4 buffer was 14 times faster than that of the sodium salt, a result that explained the otherwise contradictory *in vivo* blood level data. Therefore, absorption was ultimately dependent upon gastric emptying rate and gastric pH, as long as the formulation disintegrated properly in the stomach.

The rectal absorption of aspirin, aspirin aluminum, and calcium carbaspirin from several suppository bases was studied in dogs (196). The absorption of aspirin aluminum from either cocoa butter or a polyethylene glycol base was poor. While the maximum salicylate levels produced by aspirin and calcium carbaspirin from the cocoa butter base occurred at a later time than from the other bases studied, minimal plasma levels were exhibited by a polysorbate 61 base formulation. The highest peak and largest area under the blood level curve were seen with calcium carbaspirin in a vegetable fatty acid glyceride base. The poor absorption of aspirin aluminum from suppositories was not unexpected since it is poorly soluble. Furthermore, as pointed out for aspirin aluminum tablets (105, 106), an insoluble aluminum compound may form on the surface of the dissolving drug, further impeding its dissolution rate and bioavailability.

Additional references on bioavailability and formulation effects are given in Table VII.

Absorption Alteration—Several years ago, clinicians claimed that certain salts of theophylline were therapeutically preferable to other salts or to the free acid (202–204). For example, Schluger *et al.* (204) found higher blood theophylline levels after administering uncoated tablets of theophylline ethylenediamine than were observed with enteric-coated tablets of choline theophyllinate. These results were at variance with the *in vivo* work of Gagliani *et al.* (202), who found that the oral ingestion of choline theophyllinate produced significantly higher blood levels than the ethylenediamine salt. This apparent discrepancy could be explained by the formulation effects of tablet coating, *etc.*, which was not discussed in the work of Gagliani *et al.* In another study, a slightly more rapid rise in blood concentration and a greater area under the curve were observed with theophylline isopropanolamine than with theophylline ethylenediamine (203). It was suggested that the difference was a result of the greater water solubility of the isopropanolamine salt.

The *in vitro* dissolution rates of the choline and isopropanolamine salts of theophylline have been observed to be three to five times greater than the ethylenediamine salt, depending on the dissolution medium (98). It has been suggested that these differences in dissolution rate are consistent with, and offer an explanation for, the clinical results.

In a comparative study of the absorption of ampicillin trihydrate and ampicillin potassium following oral administration (205), the potassium salt yielded 37% higher peak levels and a larger area under the curve. Only 36% of the administered ampicillin trihydrate was absorbed while 53% of the potassium salt was absorbed. Determining the percentage of each drug eliminated in the urine showed that 39% was eliminated following administration of the trihydrate and 52% from the potassium salt. The entire difference between the two drug forms was accounted for in the initial 4 hr postadministration.

Several studies compared blood levels obtained with erythromycin and its salts and esters. Erythromycin estolate produced blood levels that were severalfold higher than those obtained with erythromycin base or erythromycin stearate (206–208). These differences were found to persist in the fasting as well as nonfasting subjects (207), indicating that food did not appreciably alter the absorption of erythromycin estolate when given under single or

multiple dosing (207). This finding is explained by the fact that this salt is acid stable and alkaline dissociable, permitting its passage through the acid of the stomach both in fasting and nonfasting subjects (209). Accordingly, the antibacterial activity remained essentially the same when this form of erythromycin was given, regardless of the state of fasting of the subject (209).

On first inspection, the higher serum levels attained with erythromycin estolate suggest that the salt form is more readily absorbed. Also critical to efficacy, however, is the volume of distribution of the drug, since extensive binding to plasma proteins can render a drug unavailable for activity at the biophase. Therefore, the significance of blood level data greatly depends on the measure of the free or unbound fraction of total antibiotics in the blood, which more directly indicates probable therapeutic benefit.

Wiegand and Chun (210) showed that, despite the higher blood levels attained with erythromycin estolate (after correction for half-life differences), the stearate salt produced seven times more free drug in serum than did the estolate salt. This finding explained the higher total tissue levels observed on administration of the stearate. They attributed the difference to a greater serum protein binding of the intact erythromycin estolate, proving that its higher serum levels did not necessarily reflect more efficient absorption.

Marked differences have been observed following oral administration of various salts of penicillin. Penicillin G potassium has been compared with penicillin G benzathine (benzethacil) (211, 212), penicillin G hydrabamine (213), penicillin V (214), penicillin G procaine (212), and penicillin G ammonium (215). As anticipated, penicillin G potassium produced higher and earlier blood levels than penicillin G benzathine (211, 212). Furthermore, tablets of penicillin G potassium buffered with sodium citrate yielded higher peak levels than unbuffered penicillin G potassium. While the absorption of buffered tablets was apparently not significantly affected by food intake, the unbuffered tablets yielded lower average levels and irregular absorption under similar conditions.

When penicillin G potassium was compared with penicillin G hydrabamine (213), a less soluble salt, blood levels similar to those produced by penicillin G benzathine were observed. When equivalent doses were administered, the penicillemia that occurred with penicillin G hydrabamine was only one-third or one-fourth as great and was of shorter duration than that produced by penicillin G potassium.

Budolfsen *et al.* (212) found that peak concentrations of penicillin G potassium were three to four times those obtained with penicillin G procaine and five to six times those of penicillin G benzathine, indicating a more rapid rate of absorption. The therapeutic action was related to the maximum concentration attained, but it also depended on the persistence of penicillemia, which was greater with penicillin G potassium than with the other two compounds. The authors suggested that the lower blood levels attained with the relatively insoluble penicillin G benzathine were caused by its destruction in the GI tract prior to absorption. This suggestion seems unlikely, however, since the drug should not degrade very rapidly as an undissolved suspension.

Because of its superior stability in gastric juice, penicillin V produces higher blood penicillin levels than corresponding doses of penicillin G. As a result, extensive investigations have been conducted with various salts of penicillin V (99, 214–220). For instance, tablets, capsules, and oral suspensions of penicillin V acid produced significantly higher blood concentrations than comparable penicillin G preparations (214). In the same study, the average serum levels produced by the benzathine salt of penicillin V were significantly higher than comparable doses of penicillin G benzathine for the first 4 hr but lower thereafter, again illustrating the value of using an insoluble salt to prolong blood levels of an acid-unstable compound. In another study (215), penicillin V acid was shown to produce higher and more prolonged plasma concentrations than either penicillin G potassium or ammonium, whose properties were comparable.

Plasma levels were correlated with dissolution rates of various forms of penicillin V (99). As solid dosage forms, the readily soluble potassium and calcium salts produced earlier and higher blood levels in fasting subjects than either the free acid or its benzathine salt. On the other hand, when the potassium and benzathine salts were administered orally as solutions, absorption was the same, implying that the poor solubility of the benzathine salt was responsible for the inferior blood levels obtained from its solid dosage forms. Other studies found that, while the potassium salt is 40% better absorbed than the free acid in fasting subjects, both forms produce therapeutic levels when administered with food (218).

Experiments with fistulated dogs indicated that penicillin V is absorbed primarily from the stomach. Therefore, it is not surprising that the potassium salt should show higher blood levels on oral administration since it is the most soluble salt in gastric pH (216). In accordance with this observation, it was also reported that the benzathine salt exhibited higher serum levels in patients with gastric achlorhydria (pernicious anemia) than in patients with normal gastric function (219). Differences in gastric emptying time may also explain this result.

Several studies compared the absorption of tetracycline and its salts (103, 221, 222). For example, serum concentrations in dogs and humans showed that a phosphate complex salt of tetracycline was absorbed more rapidly and gave higher blood levels during the first 6–8 hr than did tetracycline hydrochloride (221). The total amount of drug absorbed was about twice as great with the former compound.

Another study (222) suggested that tetracycline base produced higher blood levels than tetracycline hydrochloride. However, a subsequent investigation (223) showed that, in the absence of adjuvants or fillers, tetracycline hydrochloride and tetracycline base were absorbed equally well. Results obtained in this same study indicated that tetracycline hydrochloride encapsulated with citric acid produced higher serum concentrations than tetracycline hydrochloride mixed with hexametaphosphate or the phosphate complex salt of tetracycline.

In a study comparing urinary excretion rates and *in vitro* dissolution, the absorption of tetracycline and tetracycline phenolsulfonaphthaleinate was rate limited by their dissolution rates, whereas tetracycline hydrochloride absorption was rate limited by the absorption process itself (103).

Several lincomycin salts were studied for their comparative availability (224). In particular, the blood levels obtained with the relatively water-insoluble hexadecylsulfamate salt were compared to those of the hydrochloride following oral administration. Higher and extended whole blood and serum concentrations were obtained in mice, rats, and dogs with the hexadecylsulfamate. However, subcutaneously administered lincomycin did not produce significantly different fractions absorbed, regardless of which salt was administered. It is not known whether the greater area under the curve with oral administration of lincomycin hexadecylsulfamate is due to greater absorption from the GI tract, slower renal clearance, or greater enterohepatic circulations.

Salts of streptomycin, neomycin, viomycin, and streptothrycin have been formed with: (*a*) polyacrylic acids, (*b*) sulfonic or phosphorylated polysaccharides, and (*c*) natural polycarboxyl acids from a series of polyuronic substances and polysaccharide derivatives containing carboxyl groups (18). The report indicated that these salts were absorbed from the injection locus primarily by the lymph system. Blood levels from the salts were generally lower but were maintained for a longer time than the equivalent amount of antibiotic alone, and higher concentrations of longer duration may actually be produced in the lymphatic drainage.

The influence of salt formation on the onset and duration of pharmacological activity also was illustrated with tolbutamide and several of its salts (101). Following oral administration, the sodium salt produced a rapid decrease in blood sugar level followed by a rapid recovery. By contrast, the free acid of tolbutamide caused a slow and prolonged drop in blood sugar level, a preferred effect since the chance of hypoglycemic shock would be lessened. This finding also illustrates the often overriding influence of the actual disease state on the choice of drug form.

Additional references on the implications of salt formation on absorption are listed in Table VIII.

Pharmacokinetics—Because of the various new properties that are usually imposed on a compound by salt formation, the pharmacokinetics of the drug necessarily change as a function of these properties.

For example, a pharmacokinetic evaluation comparing ampicillin sodium and potassium with ampicillin trihydrate was performed after oral administration to beagle dogs (243). The absorption rate constants of the sodium and potassium salts, which were similar, proved significantly greater than the rate constant of ampicillin trihydrate, resulting in earlier, higher peak concentrations with two to three times higher serum concentrations during the 1st hr. Yet, any differences between the fraction absorbed for the three products were not statistically significant. Apparently, although dissolution of the ampicillin trihydrate was the rate-limiting step in its absorption, the overall extent of bioavailability remained unaffected.

An interesting study of the biliary excretion of erythromycin base and erythromycin estolate was reported (244). The biliary excretion of erythromycin base was high, while that of erythromycin estolate was much lower; preferential secretion of erythromycin in the bile could partially account for the lower serum levels exhibited by the base. However, the proportion of the ingested dose secreted in the bile was small, and the total amounts involved were not sufficient to account entirely for the differences in serum concentrations attained. Undoubtedly, the protein binding studies of Wiegand and Chun (210) (discussed under *Absorption Alteration*) more satisfactorily explain the difference in serum concentrations.

Table VIII—Additional References on Bioavailability and Absorption Alteration

Topic	Reference
Blood levels produced by three theophylline-containing elixirs	225
Naproxen oral absorption characteristics	226
Effect of food on absorption of a new form of erythromycin propionate	227
Effect of the anion on the absorption of tetracycline from the rat stomach	186
Blood levels following oral administration of different preparations of novobiocin	228
Absorption of iopanoic acid and its sodium salt	229
Oral absorption of secobarbital (quinalbarbitone) and its sodium salt	230
Absorption rate of barbiturates in humans	231
Morphine and atropine mucate	232
Excretion of bephenium salts in urine of human volunteers	233
Polymethylene bis(isothiuronium) salts: antituberculosis activity	234
Prolonged antitussive action of a resin-bound noscapine preparation	235
Pharmacology of sulfapyridine and sulfathiazole	236
Evaluation of plasma concentrations of propoxyphene utilizing a hybrid principal component analysis of variance technique: equimolar doses	237
Antrycide, a new trypanocidal drug	238
Pralidoxime methanesulfonate: plasma levels and pharmacokinetics after oral administration to humans	239
Intestinal absorption of pralidoxime and other aldoximes	240
Blood plasma levels and elimination of salts of pralidoxime (2-PAM) in humans after oral administration	241
Enhancement of GI absorption of a quaternary ammonium compound by trichloroacetate	242

Often, salt formation can be used to modify drug absorption and dose tolerance favorably. For example, aminosalicylic acid exhibits a short half-life and, therefore, requires large and frequent doses which may cause gastric irritation. Consequently, different chemical forms such as salts have been prepared (119, 245–247) to reduce the incidence of gastric irritation, increase absorption, and prolong blood levels.

Aminosalicylic acid is an interesting example in other ways; considerable confusion about this drug exists because many fail to recognize its nonlinear pharmacokinetics. Several definitive studies were reported regarding the absorption of the acid and its sodium, potassium, and calcium salts from solution, suspension, and tablet formulations (245, 246). Comparison of the relative bioavailabilities of aminosalicylic acid suspended in water and its salts dissolved in water showed that, while differences in rate of absorption were found to exist, absorption of both the acid and its salts was essentially complete. Absorption of the free acid from tablets reached only 77% of the dose, whereas that of the tableted salts was rapid and complete.

Regardless of formulation, the area under the plasma concentration–time curve of unmetabolized drug from free acid administration was less than that for the salts. This result was attributed to concentration-dependent metabolism during absorption: when the rate of absorption is high, the metabolic processes become saturated and more unmetabolized drug remains in the blood; conversely,

Table IX—Additional References on Bioavailability and Pharmacokinetics

Topic	Reference
Pharmacodynamics of fosfomycin (phosphonomycin) after intravenous administration to humans	248
Pharmacodynamics of phosphonomycin after oral administration to humans	249
Comparative studies on distribution, excretion, and metabolism of ^{3}H-hydroxyzine and its ^{14}C-methiodide in rats	250
Pharmacokinetics of ampicillin trihydrate, ampicillin sodium, and dicloxacillin sodium following intramuscular injection	251
Physiological disposition of fenoprofen in humans: pharmacokinetic comparison of calcium and sodium salts administered orally	252

when the absorption rate is low, as for the free acid, a higher percentage of drug is metabolized.

Additional references regarding bioavailability and pharmacokinetics are presented in Table IX.

GENERAL PHARMACY

Pharmacological Effect—Chlorpromazine hydrochloride and quaternary chlorpromazine chloride were investigated with respect to their effects on the central nervous system (CNS) (253). The quaternized compound was less potent and more toxic in rodents than the parent tertiary compound.

Naloxone, an effective opiate antagonist, is generally used as the hydrochloride salt; however, the drug has a very short duration of action. The mucate salt was prepared to extend its duration of action, since mucic acid is only slightly soluble in water (254). In a test on the blocking of morphine activity in mice, however, the mucate salt did not differ in duration from the hydrochloride. These investigators assumed the same receptor site for naloxone as for morphine and, since Heron's (232) work suggested that the receptor had a greater affinity for morphine mucate than for the free base, it also should have a greater affinity for naloxone mucate. The results disproved this hypothesis. Furthermore, this theory implies that intact salt reaches the receptor, which is highly unlikely, regardless of whether the drug is administered as a solution or as a suspension.

A series of salts of 9-aminoacridine and its derivatives was prepared and screened for antifungal and antibacterial activity (255–257). By using salts of fatty acids, the antifungal action was found to parallel the length of the carbon chain of the anion, with maximal activity occurring with acridine caproate, undecylate, and undecylenate (where undecylenic acid also exhibits some intrinsic antifungal activity) (255). This result appears reasonable, because these salts would be more lipid soluble and could be expected to pass through the cell wall of the infecting organism more readily, probably as an ion-pair.

The efficacy of bases or salts as topical anesthetics for relieving cutaneous itch, burning, and pain in unbroken skin has also been examined (258). In these experiments, itching and pricking were induced by an alternating current of low amperage and voltage applied to the skin or by exposure of the skin to UV light. Interestingly, aqueous solutions of salts of the local anesthetics did not alleviate itching or burning in any of the subjects, although saturated solutions of their bases in a mixture of water, 40% alcohol, and 10% glycerol were claimed to be effective. Such transport phenomena across the stratum corneum are often dependent on the polarity of the drug and vehicle and on the binding of the drug to keratin.

Table X—Additional References on General Pharmacy and Pharmacological Effect

Topic	Reference
Differential excretion of bromide and chloride ions and its role in bromide retention	259
Pharmacological study of calcium methionate	260
Synthesis and *in vitro* fungistatic evaluation of some *N*-substituted amides and amine salts of sorbic acid	261
Antiamebic studies on clamoxyquin [5-chloro-7-[[(3-diethylaminopropyl)amino]methyl]-8-quinolinol] *in vitro* and in experimentally infected animals	262
Adjunctive value of oral prophylaxis with the oximes pralidoxime (2-PAM) lactate and pralidoxime methanesulfonate to therapeutic administration of atropine in dogs poisoned by inhaled sarin vapor	263
Pralidoxime (2-hydroxyiminomethyl-*N*-methylpyridinium) methanesulfonate and atropine in the treatment of severe organophosphate poisoning	264
Efficacy and limitations of oxime–atropine treatment of organophosphorus anticholinesterase poisoning	265
Antitussive activity of enoxolone (glycyrrhetinic acid) and its derivatives	266
Pharmacological properties of glycyrrhetinic acid hydrogen succinate (disodium salt)	267
Ganglionic blocking activity of diastereomeric dimethylaminobornyl acetates and their methiodides	268
A new potent nonnarcotic antitussive, 1-methyl-3-[bis(2-thienyl)methylene]piperidine: pharmacology and clinical efficacy	269

Additional references on pharmacological effects can be found in Table X.

Dialysis—Dialysis through a cellophane membrane of the hydrochloride or sodium salts has been studied with several drugs (270). In many cases, it appeared that the ionic form of the drug was bound to the membrane whereas the nonionized form was not. Ephedrine hydrochloride presented an interesting example, however, since it dialyzed considerably faster than its corresponding base. It was theorized that the chloride ion dialyzed rapidly, enhancing the rate of dialysis of the ephedrine ion. Accordingly, when chloride ion was present on both sides of the membrane, the observed rate of dialysis for the ephedrine ion was comparable to the ephedrine base.

The diffusion of sodium chloride through a lipoprotein interface was very slow, especially if calcium chloride was present on both sides of the interface (271). In the presence of low concentrations of choline chloride or carbamylcholine chloride, the diffusion of sodium chloride is more rapid. Apparently, choline salts are able to increase the permeability of the lipoprotein to salts, which may relate to the physiological action of choline salts.

Miscellaneous—Release rates were determined for aminophylline, ephedrine alkaloid, and ephedrine hydrochloride from theobroma oil suppositories containing nonionic surfactants (133). While surfactants with hydrophilic–lipophilic balance (HLB) values less than 11 only minimally affected release rate, rates increased with surfactants of HLB values greater than 11. Under optimal conditions, aminophylline was faster than ephedrine hydrochloride which, in turn, was superior to the ephedrine base.

Willis and Banker (272) reported on the formation of polymer–drug salts as an approach to the physicochemical design of dosage forms. Poly(methyl vinyl ether/maleic

anhydride) salts of methapyrilene were prepared and tested with the free base for *in vitro* dissolution and dialysis. Their dissolution and dialysis rates were not appreciably different from the free drug or its hydrochloride salt. Various poly(methyl vinyl ether/maleic anhydride) hemiester salts of methapyrilene exhibited substantially slower release than the polymer ether salts, hydrochloride salt, or free base forms. Polymer–drug salts thus appear to have promise.

A series of metallic salts of edetic (ethylenediaminetetraacetic) acid were tested *in vitro* to determine their effect on blood coagulation (273). The results showed that only the dipotassium and disodium salts had any effect on coagulation. It was theorized that the lack of anticoagulant activity resulted from an almost complete suppression of ionization of the heavy metal salts.

Interesting research regarding the angina-preventive effect of some chromone-2-carboxylate salts showed a direct correlation between biological activity and pKa of the salt-forming amines (274).

Lin *et al.* (112) investigated the relationship between salt form and biological activity of a given antihypertensive. While the intrinsic dissolution rates of the dihydrochloride and disulfate salts were many fold greater than the monohydrochloride, the hypotensive potencies of the salts did not differ significantly from one another in an anesthetized dog study. Yet, when administered to renal hypertensive dogs, the dihydrochloride and disulfate salts produced greater hypotensive effects than did the monohydrochloride.

TOXICOLOGICAL CONSIDERATIONS

Toxicity of Salt Ion—Any discussion regarding the toxicity of salts of a drug must consider the pharmacological properties of the cation or anion used to form the salt as well as those of the free drug, since any of these may produce toxic effects. The toxicology of several ions that are commonly used to form salts and that are relevant to this review were discussed in depth (275).

Toxicity from ingestion of calcium salts of drugs is rare. If hypercalcemia occurs, however, calcium deposits in the kidney can bring on a reduction of renal function. The principal toxic effects of lithium also involve the kidneys. When small amounts of lithium are taken, no apparent damage occurs; yet large amounts of the metal can lead to irreversible damage. An apparent correlation was observed between lithium dosage and sodium intake (276). When lithium dosage was low or sodium intake was high, rats were able to excrete all lithium given and sustained a reversible polyuria. Conversely, if large amounts of lithium were administered to the rats or if their sodium intake was lowered, they incurred irreversible kidney damage. Ammonium ion, although it serves a major role in maintenance of the acid–base balance of the body, can be toxic in high concentrations and initiate CNS derangements.

Sulfate ions given orally tend to be minimally absorbed and may act as a laxative. The nitrate ion is irritating to the GI tract, causing nausea and gastric distress. Also, intestinal bacteria may convert the nitrate ion to nitrite which oxidizes hemoglobin to methemoglobin. The citrate ion, an intermediary in carbohydrate metabolism, can form a soluble complex with calcium which is poorly dissociable and rarely causes any toxic reactions. While tartrate ions are usually absorbed minimally from the GI tract, high concentrations reaching the circulation can cause renal damage.

Acetate and lactate ions are normal metabolites and appear to be well tolerated in relatively large amounts. Iodide and bromide ions can produce conditions known as iodism and bromidism, respectively. Bromide intoxication occurs quite frequently, since bromides are used as ingredients in some nonprescription preparations (277–280). Bromide is slowly excreted by the kidney (its half-life is 12 days) and tends to accumulate when taken for prolonged periods or when used by patients with decreased renal function (277).

Toxicity of Salt Form—Provided the salt-forming agents are nontoxic, the relative toxicities of a series of salts of a compound are often observed to reflect directly their absorption rates. For example, the toxicities of dibromide, dichloride, diiodide, and dimethylsulfate salts of quinapyramine[3], a trypanocidal drug, were determined (238). The sparingly soluble halogen salts were much less toxic subcutaneously or intramuscularly than the freely soluble dimethylsulfate, yet all salts showed about equal toxicity upon intravenous administration. The difference in toxicities obviously resulted from rapid absorption of the methylsulfate compared to the slowly absorbed, poorly soluble halogen salts. Similar reasoning has been used to explain the acute oral toxicity of propoxyphene hydrochloride in rodents, which is twice that of equimolar doses of the napsylate salt (281).

Several salts of benzphetamine and etryptamine were prepared as potential sustained-release formulations (114). The water solubility, *in vitro* dissolution rates at pH 1.0 and 7.2, and the median lethal times (LT_{50}) were determined for each salt. Both the LT_{50} and LD_{50} (determined on only a few salts) increased as the *in vitro* dissolution rate at pH 7.2 decreased. While dissolution at pH 1.0 did not correlate well with toxicity, the LT_{50}'s were inversely related to the square root of the dissolution rates at pH 7.2.

Toxicity studies comparing iopanoic acid, a cholecystographic contrast medium, with its sodium salt (115) showed that the salt form has 10-fold greater toxicity. The LD_{50}'s of the free acid and the salt were 22 and 2.32 g/kg, respectively. It was postulated that the free acid precipitated from the sodium salt upon its reaction with gastric hydrochloric acid. The fine, amorphous particles of precipitated acid had a greatly increased surface area and, therefore, dissolved more rapidly than even fine crystals of the free acid. The faster and more complete drug absorption then resulted in increased toxicity.

Salts exhibiting greater water solubility than their parent compounds or less soluble salts are not always more toxic. For example, various inorganic and organic ions were used to prepare salts of methyl pyridinium-2-aldoxime that would have greater water solubility and would eliminate undesirable side effects due to the iodide ion (95). Even though the aqueous solubility of the majority of these salts was many times greater than the iodide, their toxicity on a molar basis was not significantly different, with the exception of the dihydrogen phosphate salt which was 15%

[3] Aritrycide.

Table XI—Additional References on Toxicological Considerations

Topic	Reference
Toxicity and absorption of 2-sulfanilimidopyridine and its soluble sodium salt	285
Sorbic acid as a fungistatic agent for foods: harmlessness of sorbic acid as a dietary component	286
Toxicity and distribution of erythromycin	287
Further toxicological studies with erythromycin	288
Pharmacology and toxicology of erythromycin estolate	289
Erythromycin propionate (propionylerythromycin): a review of 20,525 case reports for side-effect data	290
New class of antibiotic salts of reduced toxicity	22
GI intolerance to oral iron preparations	291
Comparative toxicology of iron compounds	292
Influence of the dissolution rate of lithium tablets on side effect	123
Toxicity and tissue distribution studies on the hydrochloride, bismuth iodide complex, and a resinate of emetine	293
Bacitracin zinc in pharmaceutical preparations	145
New approach to quaternary ammonium compounds	151
Pharmacology of choline theophyllinate	294

more toxic. Further research with oximes revealed that other salts are also toxic (282).

GI bleeding is a common toxic effect of aspirin for a large percentage of the population. Consequently, a search was initiated for an aspirin derivative that would not induce GI blood loss (283). All compounds prepared, however, including the sodium and calcium salts, caused GI hemorrhage with a severity similar to aspirin.

Polyene antibiotics are potent antifungal agents but bear considerable toxicity. Even though the methyl ester hydrochlorides of these compounds are more soluble, they retain almost all of their antifungal activity and, more significantly, show a uniform decrease in toxicity compared to their parent compounds (284).

Additional references on toxicological considerations of salt formation are given in Table XI.

CONCLUSIONS

Salt formation is a means of altering the physical, chemical, and biological characteristics of a drug without modifying its chemical structure. Clearly, the salt form can have a dramatic influence on the overall properties of the parent compound. At present, selecting a salt form that exhibits the desired combination of properties is a difficult semiempirical choice. Pharmaceutical scientists now recognize these facts and are beginning to study the effects of different salt forms on the physicochemical properties, bioavailability, and toxicity of drug substances.

Although now only a few generalizations are available to predict the effect of particular salt forms on the characteristics of a drug, perhaps in time it will be possible to evolve increasingly more powerful generalizations regarding the effect of a salt on the properties of its parent compound. In addition, we predict that polymer–drug salts will have a revolutionary effect on future trends in drug therapy, particularly in the areas of reducing drug toxicity and in controlling the release profile of novel drug delivery systems.

REFERENCES

(1) D. Walkling and J. Appino, *Drug Cosmet. Ind.*, 112 (3), 39 (1973).

(2) N. J. Harper, *J. Med. Pharm. Chem.*, 1, 467 (1959).

(3) N. J. Harper, *Progr. Drug Res.*, 4, 221 (1962).

(4) K. Munzel, *ibid.*, **10**, 255 (1966).

(5) V. J. Stella, *Aust. J. Pharm. Sci.*, **NS2** (2), 57 (1973).

(6) A. A. Sinkula and S. H. Yalkowsky, *J. Pharm. Sci.*, **64**, 181 (1975).

(7) "Martindale The Extra Pharmacopoeia," 26th ed., Pharmaceutical Press, London, England, 1973.

(8) L. C. Miller and W. H. Heller, in "1974–75 Drugs of Choice," W. C. Modell, Ed., Mosby, St. Louis, Mo., p. 26.

(9) E. Saias, A. Jondet, and J. Phillipe, *Ann. Pharm. Fr.*, **27**, 557 (1969); through *Chem. Abstr.*, **72**, 125018e (1970).

(10) H. C. Caldwell, A. B. Rednick, G. C. Scott, G. J. Yakatan, and D. Ziv, *J. Pharm. Sci.*, **59**, 1689 (1970).

(11) G. R. Coatney, P. G. Contacos, and J. S. Lunn, *Am. J. Trop. Med. Hyg.*, **13**, 383 (1964).

(12) P. E. Thompson, B. J. Olsezewski, E. F. Elsager, and D. F. Worth, *ibid.*, **12**, 481 (1963).

(13) W. C. Miller, Jr., D. B. Marcotte, and L. McCurdy, *Curr. Ther. Res., Clin. Exp.*, **15**, 700 (1973).

(14) H. L. Goldberg and L. Nathan, *Psychosomatics*, **13**, 131 (1972).

(15) E. F. Elsager, *Ann. Rep. Med. Chem.*, **1965**, 137.

(16) H. A. M. El Shibini, M. Abdel Nasser, and M. M. Motawi, *Pharmazie*, **26**, 630 (1971).

(17) S. P. Loucas and H. M. Haddad, *J. Pharm. Sci.*, **61**, 985 (1972).

(18) P. Málek, J. Kolc, M. Herold, and J. Hoffman, in "Antibiotics Annual, 1957–1958," Medical Encyclopedia, New York, N.Y., 1958, p. 546.

(19) B. F. Duesel, H. Berman, and R. J. Schacter, *J. Am. Pharm. Assoc., Sci. Ed.*, **43**, 619 (1954).

(20) B. F. Duesel and T. I. Fand, *Int. Rec. Med. Gen. Pract. Clin.*, **167**, 245 (1954).

(21) R. H. Broh-Kahn, *ibid.*, **173**, 217 (1960).

(22) F. A. Alves, M. F. C. A. N. Graca, and H. L. Baptista, *Nature*, **181**, 182 (1958).

(23) H. Keller, W. Krüpe, H. Sous, and H. Mückter, *Arzneim.-Forsch.*, **5**, 170 (1955).

(24) *Ibid.*, **6**, 61 (1956).

(25) H. Keller, W. Krüpe, H. Sous, and H. Mückter, in "Antibiotics Annual, 1955–1956," Medical Encyclopedia, New York, N.Y., 1956, p. 35.

(26) A. C. Osterberg, J. J. Oleson, N. N. Yuda, C. E. Rauh, H. G. Parr, and L. W. Will, in "Antibiotics Annual, 1956–1957," Medical Encyclopedia, New York, N.Y., 1957, p. 564.

(27) R. Ducrot, O. Leau, and C. Coser, *Antibiot. Chemother.*, **6**, 404 (1956).

(28) R. S. Brigham and J. K. Nielsen, *ibid.*, **8**, 122 (1958).

(29) M. Khristov, *Khim.-Farmatsert. Zh.*, **11**, 19 (1972).

(30) A. Lasslo, C. Pfeiffer, and P. D. Waller, *J. Am. Pharm. Assoc., Sci. Ed.*, **48**, 345 (1959).

(31) J. A. Campbell and J. G. Slater, *J. Pharm. Sci.*, **51**, 931 (1962).

(32) J. A. Campbell, *ibid.*, **51**, 270 (1962).

(33) G. A. Neville and J. C. Ethier, *ibid.*, **60**, 497 (1971).

(34) T. Sciortino, *Boll. Chim. Farm.*, **105**, 223 (1966); through *Chem. Abstr.*, **65**, 622h (1966).

(35) *Ibid.*, **104**, 292 (1965); through *Chem. Abstr.*, **63**, 6783g (1965).

(36) W. P. Boger, S. C. Strickland, and J. M. Gylfe, *Antibiot. Med. Clin. Ther.*, **1**, 372 (1955).

(37) C. L. Fox, Jr., South African pat. 68 03, 461 (Oct. 31, 1968); through *Chem. Abstr.*, **71**, 33401a (1969).

(38) J. W. Cusic, U.S. pat. 2,499,058 (Feb. 28, 1950); through *Chem. Abstr.*, **44**, 4926g (1950).

(39) J. W. Cusic, U.S. pats. 2,534,235–2,534,247 (Dec. 19, 1950); through *Chem. Abstr.*, **46**, 527b–i (1952).

(40) J. W. Cusic, British pat. 677,798 (Aug. 20, 1952); through *Chem. Abstr.*, **48**, 4010a (1954).

(41) G. D. Searle Co., British pats. 683,645 (Dec. 3, 1952) and 683,236 (Nov. 26, 1952); through *Chem. Abstr.*, **48**, 2769b (1954).

(42) J. W. Cusic, *Science*, **109**, 574 (1949).

(43) M. L. Robinette and F. W. Bope, *J. Am. Pharm. Assoc., Sci. Ed.*, **44**, 32 (1955).

(44) D. J. Lamb and F. W. Bope, *ibid.*, **45**, 178 (1956).

(45) W. Bickers and M. Woods, *Tex. Rep. Biol. Med.*, **9**, 406 (1951).

(46) W. Bickers and M. Woods, *N. Engl. J. Med.*, **245** 453 (1951).
(47) J. M. Holbert, I. W. Grote, and H. Smith, *J. Am. Pharm. Assoc., Sci. Ed.*, **44**, 355 (1955).
(48) W. Morozowich and F. W. Bope, *ibid.*, **47**, 173 (1958).
(49) A. Halpern, N. Shaftel, and G. Schwartz, *Antibiot. Chemother.*, **9**, 97 (1959).
(50) A. Halpern, N. Shaftel, and A. J. Monte Bovi, *Am. J. Pharm.*, **130**, 190 (1958).
(51) P. A. Fernander, German Offen. 2,259,151 (June 7, 1973); through *Chem. Abstr.*, **79**, 53102x (1973).
(52) A. Reiner, German Offen. 2,330,380 (Jan. 31, 1974); through *Chem. Abstr.*, **80**, 100206b (1974).
(53) J. R. Blanco, F. J. U. Fernandez, and L. S. Vinals, German Offen. 2,144,679 (Dec. 21, 1972); through *Chem. Abstr.*, **78**, 71781b (1973).
(54) VEB Berlin-Chemie, German Offen. 2,316,721 (Dec. 20, 1973).
(55) M. T. Davies, J. Forrest, F. Hartley, and V. Petrow, *J. Pharm. Pharmacol.*, **6**, 707 (1954).
(56) Laboratorios Hosbon S. A., French Demande 2,138,498 (Feb. 9, 1973); through *Chem. Abstr.*, **79**, 83485s (1973).
(57) B. J. Magerlein, *J. Pharm. Sci.*, **54**, 1065 (1965).
(58) E. H. Massey, German Offen. 2,138,049 (Feb. 3, 1972); through *Chem. Abstr.*, **76**, 117507f (1972).
(59) R. Tixier, German Offen. 1,936,723 (May 14, 1970); through *Chem. Abstr.*, **73**, 28895b (1970).
(60) P. Wirth, German Offen. 2,117,902 (Nov. 4, 1971); through *Chem. Abstr.*, **76**, 46462z (1972).
(61) Takeda Chem. Ind. Ltd., German Offen. 2,332,878 (Jan. 17, 1974); through *Chem. Abstr.*, **80**, 96362v (1974).
(62) Takeda Chem. Ind. Ltd., German Offen. 2,332,840 (Jan. 17, 1974); through *Chem. Abstr.*, **80**, 87531x (1974).
(63) G. Fabrizio, U.S. pat. 3,764,595 (Oct. 9, 1973); through *Chem. Abstr.*, **80**, 6945k (1974) or *Chem. Abstr.*, **73**, 133984e (1970).
(64) Koniklijke Nederlandsche Gist en Spiritusfabriek, French pat. 2,126,443 (Oct. 6, 1972).
(65) R. Aries, French pat. 2,190,410 (Mar. 8, 1974).
(66) Otsuka Pharmaceutical Co., Ltd., Japanese pat. 71 03,600 (Jan. 28, 1971); through *Chem. Abstr.*, **75**, 40421t (1971).
(67) V. C. Stephens, U.S. pat. 3,728,379 (Apr. 17, 1973).
(68) Investigations Scientifiques Pharmaceutiques S. A., French Demande 2,097,064 (Apr. 7, 1972); through *Chem. Abstr.*, **77**, 168654e (1972).
(69) C. Jarowski, *Trans. N.Y. Acad. Sci., Ser. II*, **21**, 290 (1959).
(70) Andreu SA, West German pat. 2,237,267 (Feb. 1, 1973).
(71) E. N. Lazareva, L. A. Kovaleva, V. K. Vasil'evg, and P. S. Braginskaya, *Antibiotiki (Moscow)*, **14**, 813 (1969); through *Chem. Abstr.*, **71**, 111183x (1969).
(72) O. B. Ferno, T. O. E. Linderat, and B. Hansen, South African pat. 68 01,104 (July 12, 1968); through *Chem. Abstr.*, **70**, 60832c (1969).
(73) A. Allais and M. Paturet, French M. 5,309 (Sept. 25, 1967); through *Chem. Abstr.*, **71**, 64078e (1969).
(74) Cent. Ind. Pharmaceutique, French pat. 2,193,586 (Mar. 29, 1974).
(75) G. Guadagnini and F. Fabi, German Offen. 2,040,143 (Feb. 25, 1971); through *Chem. Abstr.*, **74**, 126005b (1971).
(76) Ciba-Geigy A.G., Canadian pat. 916,713 (Dec. 12, 1972).
(77) R. Ferrari, S. Magnaghi, and G. Ghielmetti, British pat. 1,205,441 (Sept. 16, 1970); through *Chem. Abstr.*, **73**, 133979e (1970).
(78) L. G. Goodwin, L. G. Jayewardene, and O. D. Standen, *Br. Med. J.*, **2**, 1572 (1958).
(79) A. Zaffaroni, U.S. pat. 3,708,492 (Jan. 2, 1973).
(80) F. K. Hansel, *Ann. Allergy*, **1**, 199 (1943).
(81) Cent. Ind. Pharmaceutique, French pat. 2,193,587 (Mar. 29, 1974).
(82) N. H. Creasey and A. L. Green, *J. Pharm. Pharmacol.*, **11**, 485 (1959).
(83) J. M. De Muylder, German Offen. 2,310,447 (Sept. 13, 1973); through *Chem. Abstr.*, **80**, 6982v (1974).
(84) V. C. Stephens, U.S. pat. 3,065,261 (1962).
(85) Merck & Co., Inc., West German pat. 2,256,538 (May 24, 1973).
(86) C. J. Cavallito and R. Jewell, *J. Am. Pharm. Assoc., Sci. Ed.*, **47**, 165 (1958).
(87) R. L. Kile, *Antibiot. Med. Clin. Ther.*, **5**, 578 (1958).
(88) Whitefin Holding S. A., Belgian pat. 793,548 (Apr. 16, 1973).
(89) Officina Therapeutica Italiana SRL, French pat. 2,099,449 (Mar. 17, 1972).
(90) J. Klosa, West German pat. 2,134,672 (Jan. 25, 1973); through *Chem. Abstr.*, **78**, 97334h (1973).
(91) T. J. Roseman and S. H. Yalkowsky, *J. Pharm. Sci.*, **62**, 1680 (1973).
(92) L. C. Miller and A. H. Holland, *Mod. Med.*, **28**, 312 (1960).
(93) J. G. Wagner, *J. Pharm. Sci.*, **50**, 359 (1961).
(94) T. H. Simons, abstracted from a paper presented at the APhA Academy of Pharmaceutical Sciences, Las Vegas meeting, Apr. 1967.
(95) A. A. Kondritzer, R. I. Ellin, and L. J. Edberg, *J. Pharm. Sci.*, **50**, 109 (1961).
(96) H. M. Koehler and J. J. Hefferren, *ibid.*, **53**, 1126 (1964).
(97) W. Nernst and E. Brunner, *Z. Phys. Chem.*, **47**, 52, 56 (1904).
(98) E. Nelson, *J. Am. Pharm. Assoc., Sci. Ed.*, **46**, 607 (1957).
(99) H. Juncher and F. Raaschou, *Antibiot. Med. Clin. Ther.*, **4**, 497 (1957).
(100) E. Nelson, *J. Am. Pharm. Assoc., Sci. Ed.*, **47**, 297 (1958).
(101) E. Nelson, E. L. Knoechel, W. E. Hamlin, and J. G. Wagner, *J. Pharm. Sci.*, **51**, 509 (1962).
(102) J. G. Wagner, *ibid.*, **50**, 375 (1961).
(103) E. Nelson, *J. Am. Pharm. Assoc., Sci. Ed.*, **48**, 96 (1959).
(104) L. Benet, in "Drug Design," vol. 4, E. Ariens, Ed., Academic, New York, N.Y., 1973, p. 1.
(105) G. Levy and B. A. Sahli, *J. Pharm. Sci.*, **51**, 58 (1962).
(106) G. Levy and J. A. Procknal, *ibid.*, **51**, 294 (1962).
(107) R. A. O'Reilly, E. Nelson, and G. Levy, *ibid.*, **55**, 435 (1966).
(108) W. I. Higuchi and W. E. Hamlin, *ibid.*, **52**, 575 (1963).
(109) W. I. Higuchi, N. A. Mir, A. P. Parker, and W. E. Hamlin, *ibid.*, **54**, 8 (1965).
(110) W. I. Higuchi, E. Nelson, and J. G. Wagner, *ibid.*, **53**, 333 (1964).
(111) S. Solvang and P. Finholt, *ibid.*, **59**, 49 (1970).
(112) S.-L. Lin, L. Lachman, C. J. Swartz, and C. F. Huebner, *ibid.*, **61**, 1418 (1972).
(113) S. Miyazaki, M. Nakano, and T. Arita, *Chem. Pharm. Bull.*, **23**, 1197 (1975).
(114) W. Morozowich, T. Chulski, W. E. Hamlin, P. M. Jones, J. I. Northam, A. Purmalis, and J. G. Wagner, *J. Pharm. Sci.*, **51**, 993 (1962).
(115) R. Peterhoff, *Acta Radiol.*, **46**, 719 (1956).
(116) G. Levy, *J. Mond. Pharm.*, **3**, 237 (1967).
(117) S. S. Davis, *Br. Med. J.*, **1**, 102 (1972).
(118) E. Nelson, *J. Am. Pharm. Assoc., Sci. Ed.*, **47**, 300 (1958).
(119) E. J. Middleton, H. S. Chang, and D. Cook, *Can. J. Pharm. Sci.*, **3**, 97 (1968).
(120) J. G. Wagner, *Drug Intell. Clin. Pharm.*, **4**, 17 (1970).
(121) *Ibid.*, **4**, 232 (1970).
(122) T. Paal and P. Regos, *Gyogyszereszet*, **17**, 59 (1973); through *Chem. Abstr.*, **78**, 128377f (1973).
(123) K. O. Borg, J. Jeppsson, and J. Sjögren, *Acta Pharm. Suec.*, **11**, 133 (1974).
(124) P. Finholt and S. Solvang, *J. Pharm. Sci.*, **57**, 1322 (1968).
(125) G. Levy, *ibid.*, **50**, 388 (1961).
(126) W. A. Cressman, C. A. Janicki, P. C. Johnson, J. T. Dolusio, and G. A. Braun, *ibid.*, **58**, 1516 (1969).
(127) L. W. Dittert, T. Higuchi, and D. R. Reese, *ibid.*, **53**, 1325 (1964).
(128) R. Anderson, *Aust. J. Pharm.*, **42**, 919 (1961).
(129) S. F. Kramer and G. L. Flynn, *J. Pharm. Sci.*, **61**, 1896 (1972).
(130) P. H. Jones, E. K. Rowley, A. L. Weiss, D. L. Bishop, and A. H. C. Chun, *ibid.*, **58**, 337 (1969).
(131) N. Senior, *J. Soc. Cosmet. Chem.*, **24**, 259 (1973).
(132) J. J. Sciarra, J. M. Patel, and A. L. Kapoor, *J. Pharm. Sci.*, **61**, 219 (1972).
(133) J. M. Plaxco, Jr., C. B. Free, Jr., and C. R. Rowland, *ibid.*, **56**, 809 (1967).
(134) J. Kucera and V. Veber, *Cesk. Dermatol.*, **41**, 229 (1966); through *Chem. Abstr.*, **65**, 18431e (1966).
(135) J. R. Leonards, *Clin. Pharmacol. Ther.*, **4**, 476 (1963).
(136) G. Levy, R. H. Gumtow, and J. M. Rutowski, *Can. Med. Assoc. J.*, **85**, 414 (1961).
(137) C. P. Schaffner and W. Mechlinski, *J. Antibiot. (Tokyo)*, **25**, 259 (1972).
(138) H. Nakatani, *Yakugaku Zasshi*, **83**, 6 (1963); through *Chem. Abstr.*, **58**, 11170e (1963).
(139) H.-C. Wang and P.-Y. Wang, *Yao Hsueh Hsueh Pao*, **13**, 63

(1966); through *Chem. Abstr.*, **65,** 5307b (1966).
(140) H. Nakatani, *Yakugaku Zasshi,* **84,** 1057 (1964).
(141) P. J. Weiss, M. L. Andrew, and W. W. Wright, *Antibiot. Chemother.*, **7,** 374 (1957).
(142) P. J. Weiss and M. L. Andrew, *ibid.*, **9,** 277 (1959).
(143) J. Marsh and P. J. Weiss, *J. Assoc. Offic. Anal. Chem.*, **50,** 457 (1967).
(144) V. C. Stephens, J. W. Conine, and H. W. Murphy, *J. Am. Pharm. Assoc., Sci. Ed.*, **48,** 620 (1959).
(145) H. M. Gross, *Drug Cosmet. Ind.*, **75,** 612 (1954).
(146) H. M. Gross, W. A. Johnson, and G. J. Lafferty, *J. Am. Pharm. Assoc., Sci. Ed.*, **45,** 447 (1956).
(147) C. M. Gruber, Jr., V. C. Stephens, and P. M. Terrill, *Toxicol. Appl. Pharmacol.*, **19,** 423 (1971).
(148) N. Brudney, *Can. J. Pharm.*, **92,** 245 (1959).
(149) B. Spross, M. Ryde, and B. Nyström, *Acta Pharm. Suec.*, **2,** 1 (1965).
(150) S. BoRodkin and D. P. Sundberg, *J. Pharm. Sci.*, **60,** 1523 (1971).
(151) W. J. Shibe, Jr., and D. H. Hanson, *Soap Chem. Spec.*, **40,** 83 (1964).
(152) G. E. Schumacher and W. J. Crowell, *Am. J. Hosp. Pharm.*, **21,** 226 (1964).
(153) M. A. Schwartz and F. H. Buckwalter, *J. Pharm. Sci.*, **51,** 1119 (1962).
(154) R. Brunner, *Monatsh. Chem.*, **86,** 767 (1955).
(155) R. Brunner and H. Margreiter, *ibid.*, **86,** 958 (1955).
(156) J. V. Swintosky, E. Rosen, M. J. Robinson, R. E. Chamberlain, and J. R. Guarini, *J. Am. Pharm. Assoc., Sci. Ed.*, **45,** 34 (1956).
(157) W. Storbeck, German pat. 971,830 (Apr. 2, 1959); through *Chem. Abstr.*, **55,** 4893d (1961).
(158) F. H. Buckwalter, *J. Am. Pharm. Assoc., Pract. Ed.*, **15,** 694 (1954).
(159) W. A. Woodward, *Q. J. Pharm. Pharmacol.*, **20,** 197 (1947).
(160) C. A. Johnson, in "Advances in Pharmaceutical Sciences," vol. 2, H. S. Bean, A. H. Beckett, and J. E. Carless, Eds., Academic, New York, N.Y., 1967, p. 227.
(161) A. Bojarski, D. Blitek, and B. Borkowski, *Diss. Pharm. Pharmacol.*, **19,** 297 (1967); through *Chem. Abstr.*, **67,** 102734t (1967).
(162) A. Bojarski, D. Blitek, and B. Borkowski, *Diss. Pharm.*, **17,** 345 (1965); through *Chem. Abstr.*, **64,** 4874c (1966).
(163) J. C. Bird and R. S. Shelton, *J. Am. Pharm. Assoc., Sci. Ed.*, **39,** 500 (1950).
(164) T. J. Macek, B. A. Feller, and E. J. Hanus, *ibid.*, **39,** 365 (1950).
(165) A. Taub, I. Katz, and M. Katz, *ibid.*, **38,** 119 (1949).
(166) R. Yamamoto, I. Takahashi, and M. Harada, *J. Pharm. Soc. Jpn.*, **76,** 853 (1956).
(167) R. Yamamoto, I. Takahashi, and K. Inazu, *ibid.*, **77,** 82 (1957).
(168) G. A. Nevill, J. C. Ethier, N. F. H. Bright, and R. H. Lake, *J. Assoc. Offic. Anal. Chem.*, **54,** 1200 (1971).
(169) J. D. Mullins and T. J. Macek, *J. Am. Pharm. Assoc., Sci. Ed.*, **49,** 245 (1960).
(170) R. R. Goodall, J. Goldman, and J. Woods, *Pharm. J.*, **200,** 33 (1968).
(171) J. Dolby, B. Gunnarsson, L. Kronberg, and H. Wikner, *Pharm. Acta Helv.*, **47,** 615 (1972).
(172) V. C. Walton, M. R. Howlett, and G. B. Selzer, *J. Pharm. Sci.*, **59,** 1160 (1970).
(173) J. K. Guillory and T. Higuchi, *ibid.*, **51,** 100 (1962).
(174) N. Narasimhachari and G. R. Rao, *Hind. Antibiot. Bull.*, **4,** 163 (1962); through *Chem. Abstr.*, **57,** 16758b (1962).
(175) D. Kodrnja and K. Weber, *Sci. Pharm.*, **39,** 34 (1971); through *Chem. Abstr.*, **75,** 40339x (1971).
(176) A. M. Nagle, E. I. Rodionovskaya, D. M. Trakhtenberg, and G. I. Kleiner, *Antibiotiki,* **12,** 420 (1967); through *Chem. Abstr.*, **67,** 76253p (1967).
(177) H. Nakatani, *Yakuzaiguku,* **23,** 75 (1963); through *Chem. Abstr.*, **59,** 12596h (1963).
(178) L. Kiss, B. Rozsondai, and T. Scholz, *Gyogyszereszet,* **8,** 341 (1964); through *Chem. Abstr.*, **62,** 405d (1965).
(179) D. Stefanescu, N. Tuchel, and V. Antonescu, *Farmacia (Bucharest),* **12,** 465 (1964); through *Chem. Abstr.*, **62,** 1520b (1965).
(180) M. G. Kostareva, *Antibiotiki (Moscow),* **16,** 312 (1972); through *Chem. Abstr.*, **75,** 40334s (1971).
(181) N. Tanaka and S. Takino, *Yakugaku Zasshi,* **82,** 329 (1962).
(182) H. Nogami, K. Kigasawa, N. Ikari, H. Ohtani, and M. Takayama, *ibid.*, **90,** 967 (1970).
(183) I. I. Inozemtseva, D. M. Trakhtenberg, and E. S. Zinatullina, *Antibiotiki,* **19,** 448 (1974); through *Chem. Abstr.*, **81,** 158634s (1974).
(184) H. Jalil and A. W. H. Daoud, *J. Fac. Med., Baghdad,* **9,** 175 (1967); through *Chem. Abstr.*, **69,** 54272h (1968).
(185) F. Kubo, K. Imaoka, and A. Kaneko, *Kyoritsu Yakka Daigaku Kenkyu Nempo,* **6/7,** 5 (1961/2); through *Chem. Abstr.*, **60,** 375d (1964).
(186) G. Fiese and J. Perrin, *J. Pharm. Sci.*, **58,** 599 (1969).
(187) J. Perrin and J. Vallner, *J. Pharm. Pharmacol.*, **22,** 758 (1970).
(188) G. Zografi and I. Zarenda, *Biochem. Pharmacol.*, **15,** 591 (1966).
(189) D. D. Heard and R. W. Ashworth, *J. Pharm. Pharmacol.*, **20,** 505 (1968).
(190) A. J. Aguiar, J. E. Zelmer, and A. W. Kinkel, *J. Pharm. Sci.*, **56,** 1243 (1967).
(191) T. Higuchi, A. Michaelis, T. Tan, and A. Hurwitz, *Anal. Chem.*, **39,** 979 (1967).
(192) T. Higuchi and K. Kato, *J. Pharm. Sci.*, **55,** 1080 (1966).
(193) A. F. Michaelis and T. Higuchi, *ibid.*, **58,** 201 (1969).
(194) A. H. Fenton and M. Warren, *Pharm. J.*, **188,** 5 (1962).
(195) R. A. O'Reilly, P. M. Aggeler, and L. S. Leong, *Thromb. Diath. Haemorrhag.*, **11,** 1 (1964).
(196) W. Lowenthal, J. F. Borzelleca, and C. D. Corder, Jr., *J. Pharm. Sci.*, **59,** 1353 (1970).
(197) E. H. Dearborn, J. T. Litchfield, Jr., H. J. Eisner, J. J. Corbett, and C. W. Dunnett, *Antibiot. Med. Clin. Ther.*, **4,** 627 (1957).
(198) L. L. Kaplan, *J. Pharm. Sci.*, **54,** 457 (1965).
(199) D. A. Schlichting, *ibid.*, **51,** 134 (1962).
(200) L. E. Josselyn, C. Endicott, and J. C. Sylvester, in "Antibiotics Annual, 1954–1955," Medical Encyclopedia, New York, N.Y., 1955, pp. 279–282.
(201) F. Neuwald and P. Ackad, *Am. J. Hosp. Pharm.*, **23,** 347 (1966).
(202) J. Gagliani, A. C. DeGraff, and H. S. Kupperman, *Int. Rec. Med. Gen. Pract. Clin.*, **167,** 251 (1954).
(203) A. E. Vivino, *J. Am. Pharm. Assoc., Sci. Ed.*, **43,** 234 (1954).
(204) J. Schluger, J. T. McGinn, and D. J. Hennessy, *Am. J. Med. Sci.*, **233,** 296 (1957).
(205) G. Hitzenberger and I. Jaschek, *Int. J. Clin. Pharmacol., Ther. Toxicol.*, **9,** 114 (1974).
(206) R. S. Griffith and H. R. Black, *Antibiot. Chemother.*, **12,** 398 (1962).
(207) R. S. Griffith and H. R. Black, *Am. J. Med. Sci.*, **247,** 69 (1964).
(208) S. M. Bell, *Med. J. Aust.*, **2,** 1280 (1971).
(209) R. S. Griffith, *Antibiot. Med. Clin. Ther.*, **7,** 320 (1960).
(210) R. G. Wiegand and A. H. C. Chun, *J. Pharm. Sci.*, **61,** 425 (1972).
(211) S. S. Wright, E. M. Purcell, E. H. Cass, and M. Finland, *J. Lab. Clin. Med.*, **42,** 417 (1953).
(212) S. E. Budolfsen, S. E. J. Hansen, and E. Rud, *Acta Pharmacol. Toxicol.*, **11,** 49 (1955).
(213) S. C. Strickland, J. M. Gylfe, and W. P. Boger, *Antibiot. Med. Clin. Ther.*, **1,** 388 (1955).
(214) L. E. Putnam, W. W. Wright, A. DeNunzio, and H. Welch, in "Antibiotics Annual, 1955–1956," Medical Encyclopedia, New York, N.Y., 1956, p. 483.
(215) W. P. Boger and S. C. Strickland, *Antibiot. Med. Clin. Ther.*, **4,** 452 (1957).
(216) C. C. Lee, R. O. Froman, R. C. Anderson, and K. K. Chen, *Antibiot. Chemother.*, **8,** 354 (1958).
(217) W. J. Kaipainen and P. Härkonen, *Scand. J. Clin. Lab. Invest.*, **8,** 18 (1956).
(218) F. B. Peck, Jr., and R. S. Griffith, in "Antibiotics Annual, 1957–1958," Medical Encyclopedia, New York, N.Y., 1958, pp. 1004–1011.
(219) J. Colquhoun, E. C. Scorer, G. Sandler, and G. M. Wilson, *Br. Med. J.*, **1,** 1451 (1957).
(220) W. W. Wright and H. Welch, *Antibiot. Med. Clin. Ther.*, **5,** 139 (1958).
(221) M. A. Kaplan, H. L. Dickison, K. A. Hubel, and F. H. Buckwalter, *ibid.*, **4,** 99 (1957).
(222) H. Welch, W. W. Wright, and A. Kirshbaum, *ibid.*, **4,** 293 (1957).

(223) W. M. Sweeney, S. M. Hardy, A. C. Dornbush, and J. M. Ruegsegger, *ibid.*, **4,** 642 (1957).
(224) C. Lewis, K. F. Stern, and J. E. Grady, *Antimicrob. Ag. Chemother.*, **1964,** 13.
(225) J. T. McGinn, *Curr. Ther. Res. Clin. Exp.*, **7,** 110 (1965).
(226) R. A. Runkel, K. S. Kraft, G. Boost, H. Sevelius, E. Forchielli, R. Hill, R. Magoun, J. B. Szakacs, and E. Segre, *Chem. Pharm. Bull.*, **20,** 1457 (1972).
(227) H. A. Hirsch, C. V. Pryles, and M. Finland, *Am. J. Med. Sci.*, **239,** 198 (1960).
(228) S. Fürész, *Antibiot. Chemother.*, **8,** 446 (1958).
(229) K. H. Holmdahl and H. Lodin, *Acta Radiol.*, **51,** 247 (1959).
(230) K. W. Anderson, *Arch. Int. Pharmacodyn. Ther.*, **147,** 171 (1964).
(231) J. Sjögren, L. Sölvell, and I. Karlsson, *Acta Med. Scand.*, **178,** 553 (1965).
(232) J. S. Heron, *Can. Med. Assoc. J.*, **72,** 302 (1955).
(233) E. W. Rogers, *Br. Med. J.*, **2,** 1576 (1958).
(234) A. C. Glasser and R. M. Doughty, *J. Pharm. Sci.*, **54,** 1055 (1965).
(235) O. Wulff, *ibid.*, **54,** 1058 (1965).
(236) O. W. Barlow and D. R. Climenko, *J. Am. Med. Assoc.*, **116,** 282 (1941).
(237) B. E. Rodda, N. E. Scholz, C. M. Gruber, Jr., and R. L. Wolen, *Toxicol. Appl. Pharmacol.*, **19,** 554 (1971).
(238) F. H. S. Curd and D. G. Davey, *Br. J. Pharmacol.*, **5,** 25 (1950).
(239) F. R. Sidell, W. A. Groff, and A. Kaminskis, *J. Pharm. Sci.*, **61,** 1136 (1972).
(240) R. R. Levine and G. M. Steinberg, *Nature*, **209,** 269 (1966).
(241) A. A. Kondritzer, P. Zvirblis, A. Goodman, and S. H. Paplanus, *J. Pharm. Sci.*, **57,** 1142 (1968).
(242) G. M. Irwin, H. B. Kostenbauder, L. W. Dittert, R. Staples, A. Misher, and J. V. Swintosky, *ibid.*, **58,** 313 (1969).
(243) B. E. Cabana, L. E. Willhite, and M. E. Bierwagen, *Antimicrob. Ag. Chemother.*, **1969,** 35.
(244) J. B. Hammond and R. S. Griffith, *Clin. Pharmacol. Ther.*, **2,** 308 (1961).
(245) S. H. Wan, P. J. Pentikainen, and D. L. Azarnoff, *J. Pharm. Sci.*, **63,** 708 (1974).
(246) S. H. Wan, P. Pentikainen, and D. L. Azarnoff, *J. Pharmacokinet. Biopharm.*, **2,** 1 (1974).
(247) R. V. Cohen, L. Molthan, and C. J. D. Zarafonetis, *Dis. Chest*, **30,** 418 (1956).
(248) E. L. Foltz and H. Wallick, *Antimicrob. Ag. Chemother.*, **1969,** 316.
(249) E. L. Foltz, H. Wallick, and C. Rosenblum, *ibid.*, **1969,** 322.
(250) S. F. Pong and C. L. Huang, *J. Pharm. Sci.*, **63,** 1527 (1974).
(251) J. T. Doluisio, J. C. LaPiana, and L. W. Dittert, *ibid.*, **60,** 715 (1971).
(252) A. Rubin, B. E. Rodda, P. Warrick, A. Ridolfo, and C. M. Gruber, *ibid.*, **60,** 1797 (1971).
(253) N. Watzman, A. A. Manian, H. Barry, III, and J. P. Buckley, *ibid.*, **57,** 2089 (1968).
(254) M. Jain, E. Bakutis, and J. C. Krantz, Jr., *Am. J. Pharm.*, **145,** 174 (1973).
(255) S. M. Viscia and D. C. Brodie, *J. Am. Pharm. Assoc., Sci. Ed.*, **43,** 52 (1954).
(256) G. R. Goetchius and C. A. Lawrence, *J. Lab. Clin. Med.*, **29,** 134 (1944).
(257) *Ibid.*, **30,** 145 (1945).
(258) H. Dalili and J. Adriani, *Clin. Pharmacol. Ther.*, **12,** 913 (1971).
(259) O. Bodansky and W. Modell, *J. Pharmacol. Exp. Ther.*, **73,** 51 (1941).
(260) G. V. Rossi, T. S. Miya, and L. D. Edwards, *J. Am. Pharm. Assoc., Sci. Ed.*, **45,** 47 (1956).
(261) L. W. Morgan, D. H. Cronk, and R. P. Knott, *J. Pharm. Sci.*, **58,** 942 (1969).
(262) P. E. Thompson, A. Bayles, P. McClay, and J. E. Meisenhelder, *J. Parasitol.*, **51,** 817 (1965).
(263) J. W. Crook, A. I. Goodman, J. L. Colbourn, P. Zvirblis, F. W. Oberst, and J. H. Wills, *J. Pharmacol. Exp. Ther.*, **136,** 397 (1962).
(264) D. R. Davies, A. L. Green, and G. L. Willey, *Br. J. Pharmacol.*, **14,** 5 (1959).
(265) J. F. O'Leary, A. M. Kunkel, and A. H. Jones, *J. Pharmacol. Exp. Ther.*, **132,** 50 (1961).
(266) D. M. Anderson and W. G. Smith, *J. Pharm. Pharmacol.*, **13,** 396 (1961).
(267) R. S. H. Finney and A. L. Tárnoky, *ibid.*, **12,** 49 (1960).
(268) G. H. Copper, D. M. Green, R. L. Rickard, and P. B. Thompson, *ibid.*, **23,** 662 (1971).
(269) Y. Kasé, T. Yulzono, T. Yamasaki, T. Yamada, S. Io, M. Tamiya, and I. Kondo, *Chem. Pharm. Bull.*, **7,** 372 (1959).
(270) A. Agren, *Acta Pharm. Suec.*, **5,** 37 (1968).
(271) L. Saunders, *J. Pharm. Pharmacol.*, **15,** 348 (1963).
(272) C. R. Willis, Jr., and G. S. Banker, *J. Pharm. Sci.*, **57,** 1598 (1968).
(273) R. Brendel, V. Swayne, R. Preston, J. M. Beiler, and G. J. Martin, *J. Am. Pharm. Assoc., Sci. Ed.*, **42,** 123 (1953).
(274) J. Couquelet, P. Bastide, J. B. Le Polles, and A. Paturet, *C. R. Soc. Biol.*, **164,** 329 (1970); through *Chem. Abstr.*, **74,** 21748t (1971).
(275) "The Pharmacological Basis of Therapeutics," 3rd ed., L. S. Goodman and A. Gilman, Eds., Macmillan, New York, N.Y., 1965, p. 741 and chaps. 37 and 38.
(276) M. Schou, *Acta Pharmacol. Toxicol.*, **15,** 70 (1958).
(277) G. Torosian, K. F. Finger, and R. B. Stewart, *Am. J. Hosp. Pharm.*, **30,** 716 (1973).
(278) M. W. P. Carney, *Lancet*, **2,** 523 (1971).
(279) J. A. Ewing and W. J. Grant, *South. Med. J.*, **58,** 148 (1965).
(280) R. B. Stewart, *Am. J. Hosp. Pharm.*, **30,** 85 (1973).
(281) J. L. Emerson, W. R. Gibson, and R. C. Anderson, *Toxicol. Appl. Pharmacol.*, **19,** 445 (1971).
(282) R. I. Ellin and J. H. Wills, *J. Pharm. Sci.*, **53,** 1143 (1964).
(283) P. H. N. Wood, E. A. Harvey-Smith, and A. St. J. Dixon, *Br. Med. J.*, **1,** 669 (1962).
(284) D. P. Bonner, W. Mechlinski, and C. P. Schaffner, *J. Antibiot. (Tokyo)*, **25,** 261 (1972).
(285) E. K. Marshall, Jr., A. C. Bratton, and J. T. Litchfield, Jr., *Science*, **88,** 597 (1938).
(286) H. J. Deuel, Jr., R. Alfin-Slater, C. S. Weil, and H. F. Smyth, Jr., *Food Res.*, **19,** 1 (1954).
(287) R. C. Anderson, P. N. Harris, and K. K. Chen, *J. Am. Pharm. Assoc., Sci. Ed.*, **41,** 555 (1952).
(288) *Ibid.*, **44,** 199 (1955).
(289) R. C. Anderson, C. C. Lee, H. M. Worth, and P. N. Harris, *ibid.*, **48,** 623 (1959).
(290) H. V. Kuder, *Clin. Pharmacol. Ther.*, **1,** 604 (1960).
(291) D. N. S. Kerr and S. Davidson, *Lancet*, **2,** 489 (1958).
(292) L. C. Weaver, R. W. Gardier, V. B. Robinson, and C. A. Bunde, *Am. J. Med. Sci.*, **241,** 296 (1961).
(293) K. J. Child, B. Davis, M. G. Dodds, and E. G. Tomich, *J. Pharm. Pharmacol.*, **16,** 65 (1964).
(294) R. J. Schachter, E. T. Kimura, G. M. Nowarra, and J. Mestern, *Int. Rec. Med. Gen. Pract. Clin.*, **167,** 248 (1954).

ACKNOWLEDGMENTS AND ADDRESSES

Received from *Central Research, Pfizer Inc., Groton, CT 06340.*
The authors thank Ms. L. Van Campen for assistance with the manuscript.
* College of Pharmacy, University of Iowa, Iowa City, IA 52242.
† 1974 Pfizer summer student in physical pharmacy.
ˣ To whom inquiries should be directed.

Separation and Analysis of Δ^9-Tetrahydrocannabinol in Biological Fluids by High-Pressure Liquid Chromatography and GLC

EDWARD R. GARRETT [x] and C. ANTHONY HUNT *

Abstract □ High-pressure liquid chromatographic (HPLC) systems were developed to separate quantitatively Δ^9-tetrahydrocannabinol from heptane-extractable lipoidal and other endogenous substances in biological fluids. These substances interfered with the quantitation by flame-ionization GLC of the unmodified compound and by electron-capture GLC of the pentafluorobenzoyl derivative. Reversed-phase HPLC elution, with 47% acetonitrile in water, and normal-phase HPLC with 25% chloroform in heptane separated Δ^9-tetrahydrocannabinol from 11-hydroxy-Δ^9-tetrahydrocannabinol and other monohydroxylated tetrahydrocannabinols. These systems also purified stock solutions of Δ^9-tetrahydrocannabinol from accompanying contaminants. The various monohydroxylated tetrahydrocannabinols were resolved from each other in the normal phase, 80% chloroform in heptane. The Δ^8- and Δ^9-tetrahydrocannabinols were separable in the normal phase with 5% tetrahydrofuran in hexane. The GLC analysis of pentafluorobenzoylated Δ^9-tetrahydrocannabinol had a sensitivity of 1 ng/ml of plasma, with an estimated 5% standard error with the developed extraction and GLC procedures. Radiochemical analysis of the HPLC-separated fraction had a sensitivity of 0.2 ng/ml of plasma, with an estimated 2% standard error. There was no significant difference between the liquid scintillation and electron-capture GLC assays of the HPLC-separated Δ^9-tetrahydrocannabinol obtained from the plasma of dogs administered the drug. Radiolabeled compounds can be added to plasma samples as internal standards to determine the recovery efficiencies of the several procedures in the analysis of unlabeled tetrahydrocannabinol.

Keyphrases □ Δ^9-Tetrahydrocannabinol—GLC and high-pressure liquid chromatographic analyses, biological fluids □ GLC—analysis, Δ^9-tetrahydrocannabinol in biological fluids □ High-pressure liquid chromatography—analysis, Δ^9-tetrahydrocannabinol in biological fluids

A GLC method for tetrahydrocannabinol in biological fluids was developed previously (1) and used electron-capture detection of the derived pentafluorobenzoylated tetrahydrocannabinol. It could readily detect 0.5 ng of tetrahydrocannabinol added to a 5.0-ml blood sample from a fasting dog. This sensitivity was only obtained when it was realized that tetrahydrocannabinol bound extensively (15–40%) to glass (1, 2) and rubber stoppers (2) and that the time-dependent degree of adsorption could be minimized by prior treatment of all glassware with an organic solution of a silyl reagent[1]. In the case of organic solutions, the tetrahydrocannabinol could be reincorporated from the glass into solution by vigorous shaking prior to any sampling.

The method's validity was demonstrated in the fasting dog with a low fat diet. Plasma levels down to 1 ng/ml of blood from 5-ml blood samples were monitored for 12 hr after the administration of 0.1 mg of pure tetrahydrocannabinol/kg (1). However, when the same method was applied to nonfasting animals, a significant increase in the GLC background from interfering plasma constituents was observed, particularly within 4 hr of feeding a previously fasted animal. The resultant minimal detectable quantity unfortunately increased to 5–10 ng/ml when a 5-ml blood sample was taken.

Since pharmacokinetic studies were contemplated in both dogs and humans over longer periods so that fasting would be impractical, such interferences were anticipated that would lower the analytical sensitivity. Thus, it was necessary to devise suitable separation and cleanup procedures prior to analysis to improve the sensitivity.

High-pressure liquid chromatography (HPLC) provided a powerful method of separation of drugs from their potential metabolites and from endogenous substances in biological fluids. While the classical on-line monitoring devices such as refractive index or UV spectrophotometry were too insensitive for direct assay at the plasma levels anticipated, the separated collected pertinent fractions were analyzed by analytical methods that provided the proper sensitivities. This paper presents HPLC techniques to separate tetrahydrocannabinol from various cannabinoids and interfering endogenous materials of biological fluids with subsequent analysis by various appropriate methods.

EXPERIMENTAL

Materials—Δ^9-Tetrahydrocannabinol[2], cannabinol[3], cannabidiol[4], 11-hydroxy-Δ^9-tetrahydrocannabinol[5], 8α-hydroxy-Δ^9-tetrahydrocannabinol[6], 8β-hydroxy-Δ^9-tetrahydrocannabinol[7], ^{3}H-11-hydroxy-Δ^9-tetrahydrocannabinol[8], and ^{14}C-Δ^9-tetrahydrocannabinol[9] were used.

Liquid Scintillation—Two different instruments were used. In one system[10], two of three channels were set specifically to read tritium and carbon-14. In the other system[11], all three channels were used. All samples were counted for 10 min with a blank inserted at the start of every 50 samples.

The degree of quench of each sample was estimated from the channel ratios of the sample and from known standards. When quench was indicated, it was calculated after addition of a ^{14}C-toluene or tritiated water standard. All samples were allowed to adapt to the dark, and this adaptation was checked by recounting selected samples.

[1] Rinsing glass for 30 min with a 1% (v/v) solution of Sil-Prep (Applied Sciences Laboratories, State College, PA 16801) in dichloromethane reduced adsorption to less than 5%. This rinsing was followed by a solvent rinse of dichloromethane and drying.

[2] Unless specified differently, obtained from the Department of Health, Education, and Welfare, Public Health Service, National Institute of Mental Health; Lot SSC-61591, 1 g/ml of ethanol.

[3] Lot NMH-IV-65c.

[4] Lot NMH-IV-65c.

[5] Lot DD-I-45A.

[6] Lot DD-I-61A.

[7] Lot RLH-III-39b.

[8] Lot SS-II-110A, 169.5 μCi/5 mg.

[9] Sample 3168-145-27, 3817 μCi/ml, R. T.I., Research Triangle Park, N.C.

[10] Model 3003, Packard Instruments, Downers Grove, Ill.

[11] Liquid scintillation system, Beckman Instruments, Fullerton, Calif.

GLC—A gas chromatograph[12], fitted with both ^{63}Ni- and flame-ionization detectors, was used. Detectors were maintained between 270 and 285°. The ^{63}Ni-detector had a separate nitrogen gas flow of 35 ml/min, and the glass columns were 30 cm or 1.8 m (6 ft) long (2.0 mm i.d.). The conditions were: column, 210–230°; injection port, 245°; 3% OV-225 on 100–120-mesh Gas Chrom Q or 3% OV-17 on 100–120-mesh Gas Chrom Q; nitrogen gas flow, 35–45 ml/min; standing current (^{63}Ni), 60–90% at 2×10^{-9}; and background noise, 2–3% at 1×10^{-10}.

HPLC—A chromatograph[13], equipped with a 6000-psi constant-flow pump, a 254-nm UV detector, and a differential refractometer detector, was used. The columns were either a low polarity 0.61-m (2-ft) × 0.3-cm (0.125-in.) Bondapak-C_{18} Corasil [with a $(CH_2)_{17}CH_3$ surface functionality], designed for reversed-phase chromatography, or a high polarity 30-cm μ-Porasil (with a SiOSiOH surface functionality), designed for normal-phase chromatography. All on-column injections were made under constant-flow conditions. Special high quality solvents[14] were used.

Extraction of ^{14}C-Δ^9-Tetrahydrocannabinol from Plasma—A 2-ml plasma sample containing the ^{14}C-Δ^9-tetrahydrocannabinol was transferred to a silylated 50-ml glass centrifuge tube. The pH was adjusted between 9.5 and 11.0 by addition of 0.1 *N* Na_2CO_3 (0.2–0.5 ml) prepared from water purified by HPLC using a clean Bondapak-C_{18} Corasil column. The final volume was adjusted to 2.5 ml by addition of water, and 15 ml of heptane[14] containing 1.5% isoamyl alcohol[14] was added. The tube was stoppered[15], shaken for 15 min, and centrifuged. It was not necessary to denature the plasma protein as described previously (1).

An aliquot (5–14 ml) of the organic layer to be used for HPLC was transferred to a glass centrifuge tube, and a second aliquot (0.5–1.0 ml) was transferred to a 20-ml glass liquid scintillation vial. Both vial and tube contents were dried under a stream of nitrogen in a water bath (50°).

Six milliliters of scintillation solution[16] was added to the vial contents, and the sample was analyzed by liquid scintillation spectroscopy. Samples with low counts (less than 400 cpm) were counted twice and averaged.

HPLC Separation of Δ^9-Tetrahydrocannabinol—The sides of the 5-ml tube were rinsed with 100 μl of ethanol, and the contents were dried again. The residue was dissolved in 15–21 μl of ethanol, and an aliquot (10–14 μl) was used for separation of Δ^9-tetrahydrocannabinol by the normal-phase HPLC system, which used a 20–25% chloroform in heptane solvent system at a constant flow rate (either 1.0 or 1.5 ml/min). The tetrahydrocannabinol fraction was collected over the predetermined collection range in a 5-ml tube and dried. The residue was dissolved in 0.5 ml of ethanol and stored in a freezer until time for derivatization and analysis by GLC with electron-capture detection.

After one to three injections of plasma extracts, it was necessary to remove from the column those components of the extract that had high affinities with the packing material. When normal-phase HPLC was used, the solvent system was changed to heptane, 4 ml of 10% heptane in tetrahydrofuran was injected, the flow rate was adjusted to 2 ml/min, and the heptane was replaced after 3 min by the original solvent system. No further injections were made until the system operated for 10 min at the original specifications.

The HPLC system was checked for reproducibility in collecting fractions of administered tetrahydrocannabinol prior to a series of injections on a given day. Known amounts of HPLC-purified ^{14}C-Δ^9-tetrahydrocannabinol were dissolved in 21 μl of ethanol, and 14 μl was injected in the chromatograph. The remainder of each sample was counted for total carbon-14. At the beginning of each series of HPLC collections, two reference standards of approximately 5 and 500 ng, each originally dissolved in 21 μl and of equal activity, were injected and collected as stated to assure that the collection range used was proper.

The collected fractions were counted for total carbon-14, and the collection efficiency was considered as the fraction injected recovered. It was shown previously (1) that Δ^9-tetrahydrocannabinol did not degrade significantly under the mild conditions of these analytical procedures (1–3). All glassware was silylated as described (1). It is possible to analyze eight samples/day, including the determination of the reproducibility of the HPLC system.

Derivatization of Samples for Sensitive Electron-Capture Detection (1)—Prior to GLC analysis, each stored sample was dried under a stream of nitrogen in a water bath (50°). One hour was a satisfactory drying time. The residue was dissolved in 0.1 ml of dry benzene. A 100 *M* excess of pyridine in benzene was added to the benzene solution of Δ^9-tetrahydrocannabinol. A 100 *M* excess of pentafluorobenzoyl chloride[17] in 5–20 μl of benzene was also added. The amounts were estimated from the known amount of radiolabeled tetrahydrocannabinol in the heptane extract. The tube was stoppered and allowed to stand for 15 min, and 100 μl of 0.1 *M* Na_2CO_3 was added. The mixture was shaken for 1 min on a vortex shaker and centrifuged.

The aqueous layer was removed, 200 μl of benzene was added, and the tube was centrifuged again. An aliquot, approximately 250 μl, of the benzene layer was transferred to a 5-ml centrifuge tube and dried under nitrogen in a water bath. The residue was dissolved in an appropriate volume, 0.2–2.0 ml, of toluene, usually containing 50 pg of cannabidiol pentafluorobenzoate (the internal standard)/ml. The optimum amount of internal standard to give an area ratio with tetrahydrocannabinol pentafluorobenzoate of about unity was predicted from the radiolabeled tetrahydrocannabinol concentration in the heptane extract of plasma. Aliquots of 0.5–1.5 μl of this final solution were analyzed by GLC.

Preparation of Internal Standard—Cannabidiol for use as the GLC internal standard was purified by injecting 1 mg into the normal-phase HPLC system with a 20% chloroform in heptane eluant. The central third of the peak was collected, dried, and dissolved in 10 ml of dry benzene. The concentration of the solution was determined by flame-ionization GLC (2, 3). Cannabidiol pentafluorobenzoate was prepared by adding 2 μl each of pyridine and pentafluorobenzoyl chloride to 1 ml of this solution. After 5 min, 1 ml of 0.1 *M* Na_2CO_3 was added, the solution was shaken for 1 min, and the organic layer was transferred to a 5-ml tube and dried.

The stable residue was dissolved in dry toluene to yield 50–500 pg/ml when needed for use as an internal standard. A given volume of this solution was analyzed by electron-capture GLC, and the area under the peak was determined. This approach provided a measure of the volume of internal standard solution necessary to add to the tetrahydrocannabinol sample to be analyzed to obtain the proper area ratio even without an exact knowledge of the internal standard concentration.

Preparation of Calibration Curves—Calibration curves of peak area ratios of drug to internal standard *versus* plasma concentration for monitoring plasma levels of tetrahydrocannabinol in pharmacokinetic studies were usually prepared from duplicate 2-ml plasma samples containing 1, 5, 10, 50, and 100 ng of ^{14}C-labeled or unlabeled Δ^9-tetrahydrocannabinol. After heptane extraction of the samples, normal-phase HPLC and electron-capture GLC assay of the derivatized material was effected.

The amount in the plasma sample could also be calculated from a calibration curve of the ratios of the peak area of the tetrahydrocannabinol pentafluorobenzoate prepared from pure tetrahydrocannabinol in toluene to that of the cannabidiol pentafluorobenzoate when the dilution, reconstitution, and separate efficiencies of the extraction and HPLC elution procedures were taken into account. The extraction efficiency was established for each batch of plasma by adding known amounts of ^{14}C-Δ^9-tetrahydrocannabinol to 2 ml of plasma and determining the fraction of the label recovered after extraction in 15 ml of heptane.

The HPLC eluant of the labeled Δ^9-tetrahydrocannabinol fraction was also collected in vials (20 ml), dried, and analyzed for total carbon-14, using liquid scintillation spectroscopy. The amount of tetrahydrocannabinol present was calculated from the known dilutions, reconstitutions, and evaluated efficiencies of the extraction and HPLC elution procedures.

Purification of Δ^9-Tetrahydrocannabinol by HPLC—Aliquots of the stock ^{14}C-Δ^9-tetrahydrocannabinol solutions were analyzed for radiolabel purity by HPLC with a reversed-phase column, using a 45 or 51% acetonitrile–water solvent system at a constant pressure below 3000 psi at a flow rate of 1.5 ml/min, or with the normal-phase column, using a 20 or 25% chloroform–heptane solvent system at a flow rate of 2.5 ml/min. The eluate was monitored for UV absorbance at 254 nm and collected in volumetric tubes at 0.5- or 1-ml intervals.

Each fraction was analyzed by GLC and by liquid scintillation counting for total carbon-14; its activity, corrected for background, was plotted against the cumulative volume for that fraction, defined as the volume eluted at a time after injection minus the "dead volume" of the system. The pooled volumes containing the separated ^{14}C-Δ^9-tetrahydro-

[12] Models 2100 and 20, Varian Aerograph, Walnut Creek, Calif.
[13] Model ALC 202, Waters Associates, Milford, Mass.
[14] Burdick and Jackson Laboratories, Muskegon, Mich.
[15] Kimble, polyethylene, Sargent-Welch, Birmingham, Ala.
[16] Handifluor, Mallinckrodt Chemical Works, St. Louis, Mo.
[17] PCR, Inc., Gainesville, Fla.

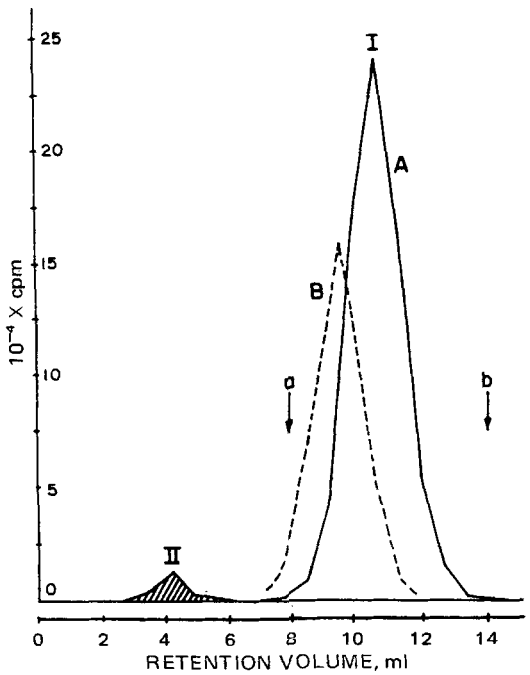

Figure 1—*Reversed-phase HPLC of stock* ^{14}C-Δ^9-*tetrahydrocannabinol. The total radioactivity per eluate fraction was plotted* versus *retention volume (curve A). Peak I is* ^{14}C-Δ^9-*tetrahydrocannabinol, and peak II is an unknown radioactive contaminant. Curve B is a plot of the mean UV detector response (arbitrary units)* versus *retention volume and is displaced relative to A by the solvent volume between the detector and the collection point. Collection between volumes* a *and* b *(peak retention volume ± 30%) for curve B recovered 92.5% of the radioactivity in this case. The column was Bondapack* C_{18}*; the eluant was 45% acetonitrile in water at 1.5 ml/min. Each fraction was corrected for background counts per minute.*

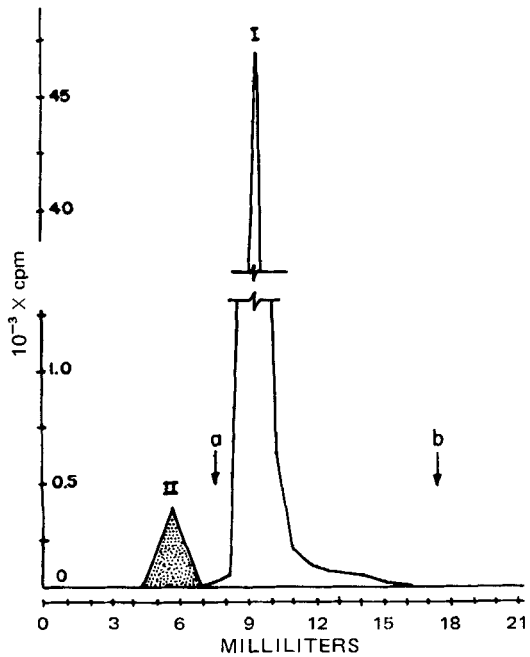

Figure 2—*Normal-phase HPLC of stock* ^{14}C-Δ^9-*tetrahydrocannabinol. The total activity per eluate fraction was plotted* versus *milliliters of eluate. Peak I is* ^{14}C-Δ^9-*tetrahydrocannabinol, and peak II is an unknown radioactive contaminant. Collection between volumes* a *and* b *recovered 97.5% of the radioactivity in this case. The column was μ-Porasil; the eluant was 20% chloroform in heptane at 2.5 ml/min. Each fraction was corrected for background counts per minute.*

cannabinol (peak I, Figs. 1 and 2), as evidenced by the observed single peak, contained the material used in the quantification of the efficiencies of the various separation and analytical methods.

Quantitation of Efficiency of HPLC Separation of Δ^9-Tetrahydrocannabinol—The described procedure was repeated on this purified material after the collected eluates containing the Δ^9-tetrahydrocannabinol fraction were dried under nitrogen at 50° and reconstituted in absolute ethanol to yield 2×10^4 cpm/μl. The fractions collected were analyzed for total carbon-14. Thus, a collection range for tetrahydrocannabinol was established that would contain at least 98% of the recoverable label. The eluates within this established collection range were analyzed for total carbon-14 when various aliquots of the purified ^{14}C-tetrahydrocannabinol in ethanol were injected on the two HPLC systems (Tables I and II). The effect of varying percentages of acetonitrile in the eluting solvent for the reversed phase was also studied (Fig. 3 and Table I). Similarly, an authentic sample of ^{3}H-11-hydroxy-Δ^9-tetrahydrocannabinol was purified, and its collection range for 98% recovery was determined for reversed-phase HPLC (Fig. 3).

The HPLC-purified ^{14}C-Δ^9-tetrahydrocannabinol, in known various amounts, was added to aliquots of fresh dog plasma to determine the efficiency of HPLC drug recovery from plasma. The tetrahydrocannabinol was extracted, the pertinent fraction of drug was collected on the HPLC system used, and the total carbon-14 activity of each collection was determined. A 45% acetonitrile–water solvent system was used in the reversed phase; a 20% chloroform–heptane solvent system was used in the normal phase.

As stated previously, it was necessary to remove components of the plasma extract that had high affinities with the packing material of the column after one to three injections of plasma. The cleanup procedure for normal-phase HPLC was given previously. When reversed-phase HPLC was used, 4 ml of 10% methanol in acetonitrile was injected or the eluant was changed to 100% acetonitrile, the flow rate was adjusted to 1 ml/min, and the flow rate was increased after 5 min to 3 ml/min for 3 min.

A 2-ml plasma sample was spiked with 400 ng of unlabeled Δ^9-tetrahydrocannabinol and 400 ng of 11-hydroxy-Δ^9-tetrahydrocannabinol, extracted, and prepared for HPLC. The sample was injected on

Table I—Recovery of Radioactivity of ^{14}C-Δ^9-Tetrahydrocannabinol[a] from Reversed-Phase HPLC

Eluting Solvent, % Acetonitrile in Water	n[b]	Average 10^{-4} cpm Injected[c]	Average 10^{-4} cpm Collected[d]	Average Recovery, %
51	2	4.006	3.813	95.18
	2	8.012	7.688	95.95
	2	12.018	11.86	98.7
	2	16.024	15.824	98.75
49	4	16.024	16.760	98.33
47	4	16.024	15.804	98.63
45	4	16.024	15.441	96.36
Overall average	20	—	—	97.57 ± 0.69[e]

[a] The stock solutions of the material had been purified previously by HPLC. [b] Numbers of replicates. [c] Injections of 2, 4, 6, or 8 μl were taken from the same ethanol solution of ^{14}C-Δ^9-tetrahydrocannabinol: 4×10^3 cpm/μg and 2.003×10^4 cpm/μl. [d] For each solvent, the collection range (Fig. 3) was constant. All samples were corrected for background counts. [e] Standard error of the mean where 3.07 is the standard deviation.

Table II—Recovery of Radioactivity of ^{14}C-Δ^9-Tetrahydrocannabinol[a] from Normal-Phase HPLC[b]

n[c]	Average 10^{-3} cpm Injected[c]	Average 10^{-3} cpm Collected[d]	Recovery[e], %
5	0.1420	0.1344	94.7 (6.58)
3	0.7110	0.689	97.04 (3.0)
3	1.423	1.377	96.82 (4.9)
2	14.29	13.615	95.88 (4.13)
2	71.02	69.77	98.27 (1.13)
3	142.06	137.81	97.05 (1.65)
	Total (n = 18)		96.32 ± 1.023[f]

[a] The stock solutions of the material had been purified previously by HPLC. [b] Eluting solvent was 25% chloroform in heptane. [c] Fifteen microliters of n replicates of each solution was injected. The specific activity of ^{14}C-Δ^9-tetrahydrocannabinol was 142 cpm/ng. [d] Each sample was corrected for background counts. [e] The parentheses contain standard deviations as percent of the mean. [f] Standard error of the mean where 4.23 is the standard deviation.

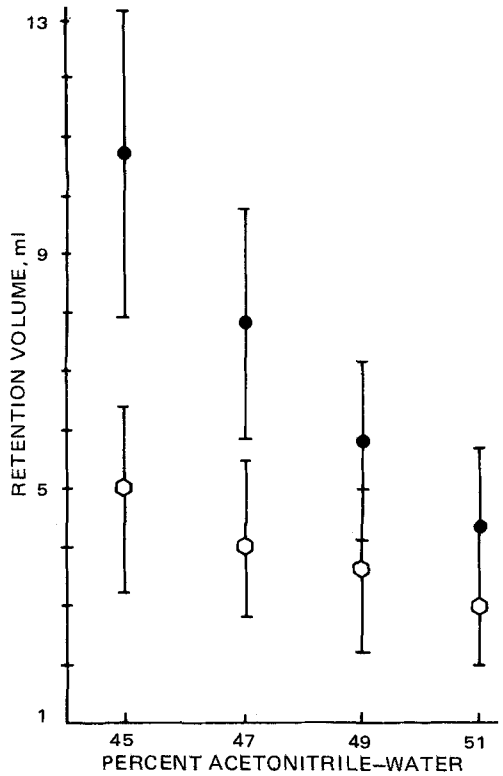

Figure 3—*Retention volumes for the peak amounts of Δ^9-tetrahydrocannabinol (●) and 11-hydroxy-Δ^9-tetrahydrocannabinol (○) for reversed-phase HPLC plotted* versus *solvent composition. Each point represents the mean peak retention volume for two determinations. The vertical bars represent the ranges of retention volumes that contained approximately 98% of the area under the plot of recovered radioactivity* versus *retention volume.*

the reversed-phase HPLC system, and the eluate was collected over the range for a 51% acetonitrile–water solvent system that would collect both compounds. The collected fraction was dried under nitrogen in a water bath (50°), reconstituted in 50 μl of chloroform, and analyzed by GLC, using flame ionization as previously described (2, 3).

Variability in Extraction, HPLC, and Electron-Capture GLC Analytical Procedures for Δ^9-Tetrahydrocannabinol in Plasma—The total error and the sources of error for such analyses were evaluated

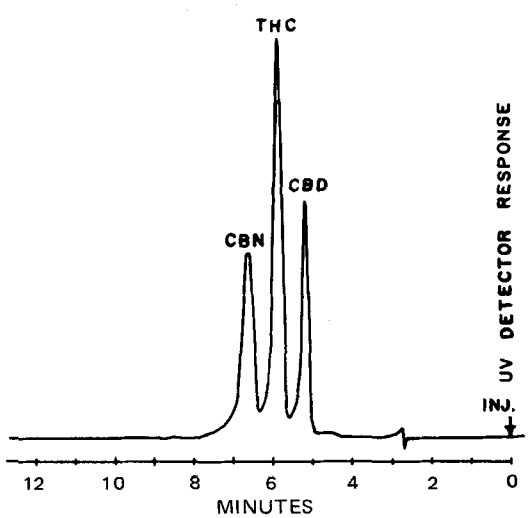

Figure 4—*Normal-phase HPLC separation of cannabinoids. The UV detector response (arbitrary units) was plotted* versus *retention time after injection (inj.) of a mixture of cannabidiol (CBD), Δ^9-tetrahydrocannabinol (THC), and cannabinol (CBN). The amounts of Δ^9-tetrahydrocannabinol and cannabidiol injected were approximately twice the amount of the cannabinol. The column was μ-Porasil; the eluant was 20% chloroform in heptane at 1.5 ml/min.*

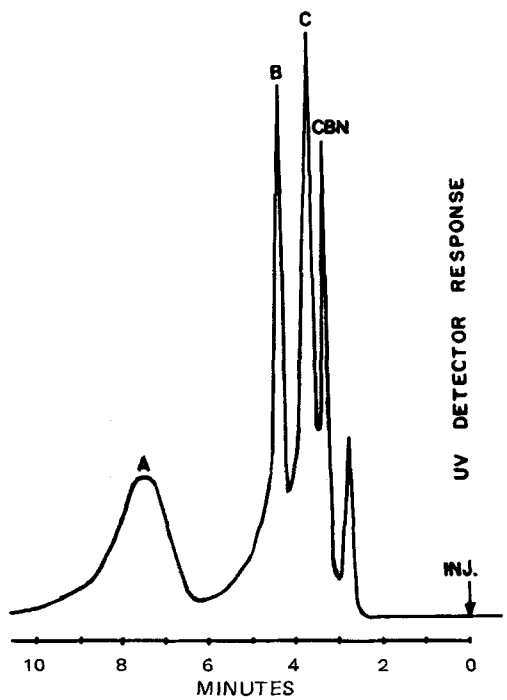

Figure 5—*Normal-phase HPLC separation of Δ^9-tetrahydrocannabinol metabolites. The UV detector response (arbitrary units) was plotted* versus *retention time after injection (inj.) of a mixture of cannabinol (CBN), 11-hydroxy-Δ^9-tetrahydrocannabinol (C), 8α-hydroxy-Δ^9-tetrahydrocannabinol (B), and 8β-hydroxy-Δ^9-tetrahydrocannabinol (A). The column was μ-Porasil; the eluant was 80% chloroform in heptane at 1.5 ml/min.*

for the overall analytical scheme in three separate experiments.

1. Each of three 9-ml plasma samples was spiked with 2.25, 22.5, or 225 ng of ^{14}C-Δ^9-tetrahydrocannabinol. Four 2-ml aliquots were removed from each sample, the tetrahydrocannabinol was extracted from each, and 14 of the 15 ml of the heptane extract was dried and analyzed for total carbon-14.

2. Three 9-ml plasma samples were prepared and extracted as already described. The tetrahydrocannabinol in the dried heptane extract was separated by normal-phase HPLC, and the tetrahydrocannabinol fraction was collected directly in counting vials and analyzed for total carbon-14.

3. Three 9-ml plasma samples were prepared as described, extracted, and separated by HPLC (normal phase). The proper eluant fraction was analyzed by GLC.

These three studies were carried out on different days and used fresh plasma from different dogs.

HPLC Separation of Δ^9-Tetrahydrocannabinol from Selected Cannabinoids and Metabolites—Normal-phase HPLC (20% chloroform in heptane) was tested for the degree of separation obtainable between cannabinol, cannabidiol, and tetrahydrocannabinol by injection of an aliquot of a mixture of the three cannabinoids at a flow rate of 1.5 ml/min. The compounds were monitored by UV detection. When an aliquot of a mixture of cannabinol and three monohydroxylated metabolites of tetrahydrocannabinol, 8α-hydroxy-Δ^9-tetrahydrocannabinol, 8β-hydroxy-Δ^9-tetrahydrocannabinol, and 11-hydroxy-Δ^9-tetrahydrocannabinol, was injected into the same HPLC system, no peaks for the three monohydroxy compounds were observed prior to 15 min. Thus, this system widely separated Δ^9-tetrahydrocannabinol, with its retention volume of 9 ml (Fig. 2), from these compounds. HPLC was obtained for the three metabolites in an 80% chloroform–heptane solvent system at a 1.5-ml/min flow rate. Δ^9-Tetrahydrocannabinol had a retention value equivalent to cannabinol in this system.

RESULTS AND DISCUSSION

Purification and Reproducibility of Collection from Injected Ethanolic Solutions of Δ^9-Tetrahydrocannabinol on HPLC—The ^{14}C-Δ^9-tetrahydrocannabinol used was reportedly[18] free of radiolabeled

[18] National Institutes of Health, personal communication in reference to Contract HSM-42-71-108.

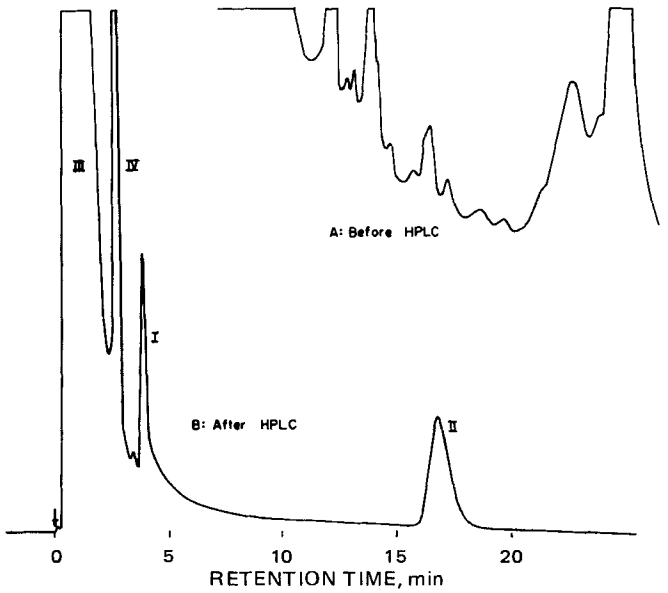

Figure 6—*Gas–liquid chromatograms (flame-ionization detection) of an extract of 2 ml of plasma containing Δ^9-tetrahydrocannabinol, I (200 ng/ml), and 11-hydroxy-Δ^9-tetrahydrocannabinol, II (200 ng/ml), before (A) and after (B) reversed-phase HPLC separation of both cannabinoids over a range of predetermined collection volumes (Fig. 1). One microliter of 18 μl of extract was injected into the gas chromatograph prior to HPLC (A). Ten microliters of 18 μl of the extract was injected into the liquid chromatograph, the collected fraction was reconstituted in 10 μl of chloroform, and 1 μl was injected into the gas chromatograph (B). Peak III is the solvent; peak IV is an unknown from plasma. For HPLC, the column was Corasil C_{18}; the eluant was 51% acetonitrile in water at 1.5 ml/min. For GLC, the column was 1.5 m (5 ft) × 2 mm, 1.9% OV-225 at 245°, with a nitrogen flow of 24 ml/min. An attenuation of 8×10^{-12} was used for both chromatograms. The initial baselines and injection times for both chromatograms are superimposed for comparison.*

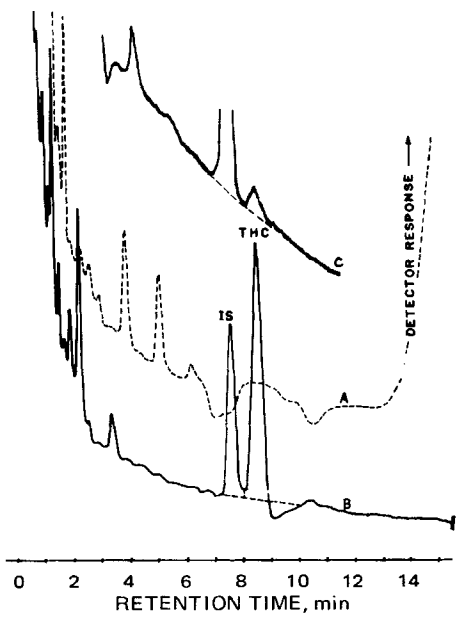

Figure 7—*GLC (electron-capture) analysis of derivatized samples. The chromatograms represent: (A) the injection of 1 of 300 μl from a derivatized extract of 2 ml of blank plasma without HPLC purification; (B) the injection of 1 of 200 μl of the final solution of derivatized compound, which was 70% of the total amount extracted from 2 ml of dog plasma containing 200 ng of Δ^9-tetrahydrocannabinol/ml, with extraction and normal-phase HPLC collection efficiencies of 91 and 95%, respectively; and (C) the injection of 1 of 200 μl from a derivatized extract of 2 ml of plasma containing 1.3 ng of Δ^9-tetrahydrocannabinol/ml. All other factors were the same as for chromatogram B. The peaks for the internal standard, cannabidiol pentafluorobenzoate (IS), and Δ^9-tetrahydrocannabinol pentafluorobenzoate (THC) are appropriately labeled. Typical estimated baselines are shown. The GLC conditions were: 1.8-m (6-ft) OV-17 column, 225°; detector, 280°; injector, 255°; nitrogen flow, 45 ml/min; and attenuations, 4×10^{-9} (A and B) and 8×10^{-10} (C).*

contaminants by TLC. However, reversed-phase HPLC (Fig. 1) revealed the presence of a labeled contaminant. The major peak, I, contained Δ^9-tetrahydrocannabinol (>96%) and Δ^8-tetrahydrocannabinol (≃3%), quantified by flame-ionization GLC (2, 3). A labeled contaminant was also found (Fig. 2) with a normal-phase column. The contaminant eluted prior to Δ^9-tetrahydrocannabinol in both cases. Since the more polar compounds elute first on reversed-phase HPLC whereas the least polar compounds elute first on normal-phase HPLC, the contaminants observed in the two systems probably were not the same. The contaminants were not analyzed further.

When the tetrahydrocannabinol under peak I (Figs. 1 and 2) was collected, dried, reconstituted in ethanol, and reanalyzed on the same HPLC system, only the single peak I was observed. All of the stock Δ^9-tetrahydrocannabinol used underwent this purification procedure. The percent of the total injected radioactivity under peak I recovered was 97.6 ± 0.7% (*SEM*) (Table I) in the reversed-phase system for the ranges of volumes collected (Figs. 1 and 3) and 96.3 ± 1.0% (Table II) for 1–1000 ng injected in the normal-phase system at a retention volume of 9.7 ml within the collection range of 7.3–16.2 ml (Fig. 2).

The fact that the retention volume of peak I and the appropriate collection ranges for 98% recovery of injected labeled tetrahydrocannabinol were sensitive to solvent composition (Fig. 3) necessitated the prior establishment of an appropriate collection range for each newly prepared batch of solvent by radiochemical analysis of the collected HPLC fractions of previously purified ^{14}C-Δ^9-tetrahydrocannabinol. The retention volume and the appropriate collection range increased with decreasing solvent polarity (less percent acetonitrile) due to peak spreading (Fig. 3).

The quality of the water used in the eluting solvent, acetonitrile–water, in reversed-phase HPLC was an important factor in maintaining the reproducibility of the percent radioactivity recovered for a given collection range. The UV detector clearly indicated that adsorbed contaminants in impure water could be eluted from a previously used column by 100% acetonitrile, a less polar solvent than the used mixed eluant. Additional evidence of these contaminants was demonstrated when the GLC background varied significantly when distilled water from various sources was collected after reversed-phase chromatography, extracted as if Δ^9-tetrahydrocannabinol were present, then treated by the derivatization procedure, and analyzed by electron-capture GLC.

HPLC Separation of Δ^9-Tetrahydrocannabinol from Selected Cannabinoids and Metabolites—Δ^9-Tetrahydrocannabinol, cannabinol, and cannabidiol were resolved by the normal-phase HPLC system (Fig. 4). If 98% of the Δ^9-tetrahydrocannabinol were to be collected after normal-phase HPLC in this system, the chosen range (Fig. 2) would also collect cannabinol and cannabidiol. The retention volumes of cannabinol and cannabidiol relative to Δ^9-tetrahydrocannabinol increased as the percent of chloroform in heptane increased.

The monohydroxylated metabolites had large retention volumes (>15 ml) on the normal-phase column when 20–25% chloroform in heptane was the solvent (Fig. 2) and could be completely separated from tetrahydrocannabinol on this system. They were resolved from each other with a more polar solvent, 80% chloroform in heptane (Fig. 5).

Δ^9-Tetrahydrocannabinol and 11-hydroxy-Δ^9-tetrahydrocannabinol were quantitatively separable on the reversed-phase HPLC system at 47% (or less) acetonitrile in water (Fig. 3). The collection efficiencies in the ranges given were 98% of the recoverable radioactivities of ^{3}H-11-hydroxy-Δ^9-tetrahydrocannabinol and ^{14}C-Δ^9-tetrahydrocannabinol.

Both Δ^8- and Δ^9-tetrahydrocannabinols were not readily resolvable in any of these systems. However, an HPLC system that readily resolved and separated these two compounds was 5% tetrahydrofuran in hexane on the normal-phase column at 0.5 ml/min, with retention volumes of 8.15 and 8.45 ml, respectively. The tetrahydrocannabinols collected under peak I (Figs. 1 and 2) could be further separated by this system.

Effect of HPLC Separation on GLC Analysis of Δ^9-Tetrahydrocannabinol in Plasma—An equal amount of Δ^9-tetrahydrocannabinol and 11-hydroxy-Δ^9-tetrahydrocannabinol in 2 ml of dog plasma was extracted and separated from a majority of the extracted components by reversed-phase HPLC. The reduction in potential contaminants from plasma observable on GLC was demonstrated by flame-ionization GLC analysis (2, 3) both before and after the HPLC treatment (Fig. 6).

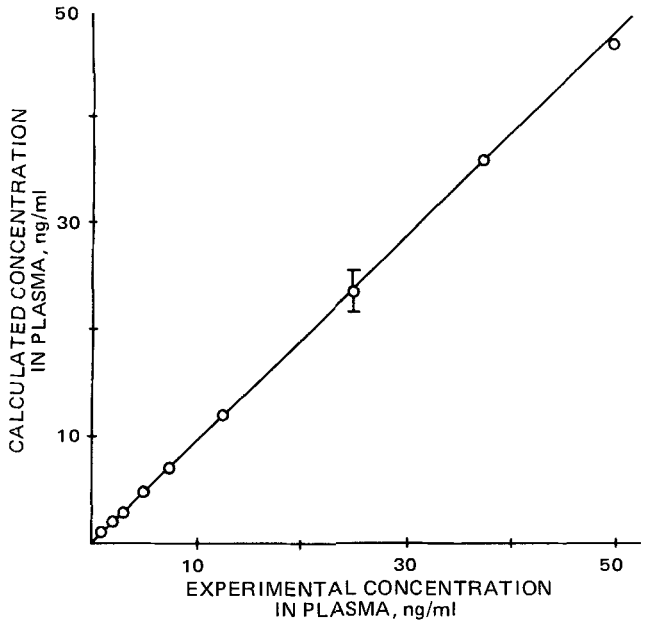

Figure 8—*Recovery of ^{14}C-Δ^9-tetrahydrocannabinol calculated as concentration in plasma corrected for an extraction efficiency of 91% against the experimentally prepared concentrations. The drug was extracted from plasma and collected over the proper volume range (Table I and Fig. 1) after reversed-phase HPLC with a 45% acetonitrile–water eluant. The collection was analyzed by liquid scintillation. The slope, 0.957, is the HPLC collection efficiency for Δ^9-tetrahydrocannabinol and was typical of the values obtained. The vertical bar is the range for ±1 SD (n = 4).*

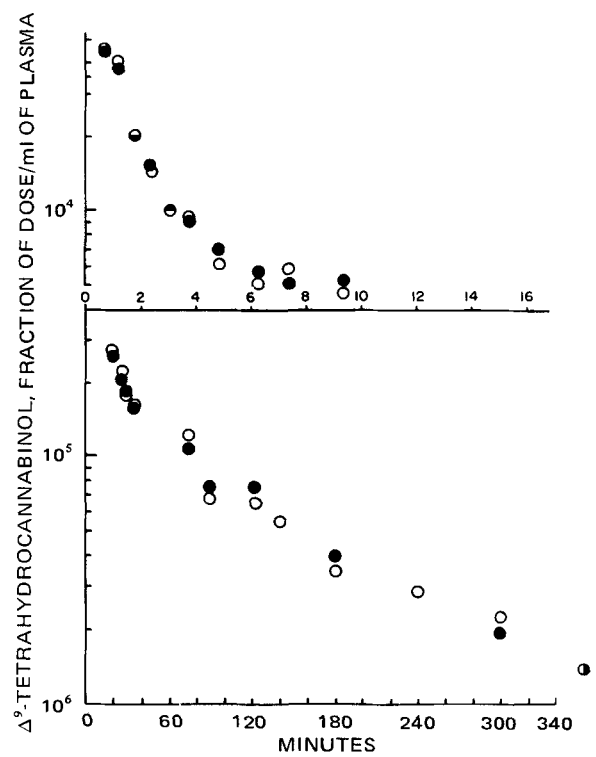

Figure 9—*Semilogarithmic plots of fraction of the Δ^9-tetrahydrocannabinol, 0.1-mg/kg dose/ml of plasma, against time for Dog A plotted from the liquid scintillation analysis of the total carbon-14 collected as Δ^9-tetrahydrocannabinol on normal-phase HPLC (○) and from the electron-capture GLC of the derivatized HPLC collected fraction (●). The values were corrected for the fractions of extracts and total collection range used.*

Normal-phase HPLC with 20% chloroform in heptane could separate Δ^9-tetrahydrocannabinol from monohydroxylated metabolites and 11-hydroxy-Δ^9-tetrahydrocannabinol. However, a minor overlap could be avoided by collecting the tetrahydrocannabinol in a slightly narrower volume range. The prior heptane extraction of alkalinized plasma separated these nonpolar constituents from any acidic metabolite. This separation of plasma extracts and normal-phase HPLC collection of volumes in the appropriate range resulted in a substantial reduction in GLC background from plasma components for derivatized Δ^9-tetrahydrocannabinol analyzed with electron-capture detection, as shown by a comparison of curves A and B or A and C in Fig. 7.

Plasma samples obtained from dogs administered Δ^9-tetrahydrocannabinol solutions intravenously were analyzed by electron-capture GLC in accordance with the modified procedures described here, including extraction, normal-phase HPLC separation, and derivatization, but no internal standard was added. These procedures would have included any cannabinol or cannabidiol in the HPLC collection volume range (Figs. 2 and 4) used. However, no peaks were seen at the retention times of cannabinol or cannabidiol pentafluorobenzoate, and no significant amounts of cannabinol or cannabidiol could be detected as metabolites of Δ^9-tetrahydrocannabinol in the dog. Thus, either compound, when purified, should serve as an appropriate internal standard in pharmacokinetic studies. However, since cannabinol has been reported as a minor metabolite (4–6), cannabidiol pentafluorobenzoate was chosen as the internal standard. Cannabinol is known to be a contaminant of degraded Δ^9-tetrahydrocannabinol (3).

The presented GLC methodology differed from the prior studies (1) in that the short 30-cm column of 3% OV-225 was supplanted by a longer OV-17-packed column to be consistent with the data in the literature accumulated for the resolution of the cannabinols (7–9).

Efficiency, Reproducibility, and Sensitivity of Radiochemical and Electron-Capture Assay of ^{14}C-Δ^9-Tetrahydrocannabinol in Dog Plasma—The heptane extraction efficiency from plasma was highly reproducible (Table III) over a wide range of plasma concentrations, 90.6 ± 0.7% (*SEM*).

The recovery of Δ^9-tetrahydrocannabinol from the heptane extract of dog plasma by normal-phase HPLC was reproducible (Table III) over the range of plasma concentrations studied. Equivalent overall recoveries (Table II) were obtained by both radiochemical analysis (83.7 ± 1.8% *SE*) and electron-capture GLC analysis (84.0 ± 4.9% *SE*) of the derivatized tetrahydrocannabinol (Fig. 7). Both methods permitted estimation of

Table III—Percent Recoveries[a] of ^{14}C-Δ^9-Tetrahydrocannabinol in the Heptane Extract of Plasma and in the Collection of the Proper Fraction of the Heptane Extract Separated by HPLC and the Overall Recovery after Both Extraction and HPLC Collection as Monitored by Both Electron-Capture GLC and Scintillation Analysis

^{14}C-Δ^9-Tetrahydrocannabinol[b], ng/2 ml of Plasma	Extracted by Heptane, %, Scintillation	Extract HPLC Collected[c], %		Overall Recovery[d], %	
		Scintillation	GLC	Scintillation	GLC
2.25	90.2 ± 4.7	93	92	84 ± 8	83 ± 32
22.5	90.8 ± 2.6	88	97	80 ± 6	88 ± 12
225	90.9 ± 8.5	97	89	88 ± 4	81 ± 7
Overall average ± *SE*	90.6 ± 0.7	92	93	84 ± 2	84 ± 5

[a] Given as the mean from four separate plasma samples ± *SD*. The scintillation analysis of recovered radioactivity was performed on a different set of four studies and on a different day than the electron-capture GLC analysis of the derivatized HPLC collection. [b] 142.47 cpm/ng. Two milliliters of plasma was extracted with 15 ml of heptane, and 14 ml was analyzed for total carbon-14. [c] Quotient divided by the extraction efficiency (0.91). Additional studies were conducted for 26 ng of ^{14}C-Δ^9-tetrahydrocannabinol/2 ml of plasma on 2 other days for four samples each, and the percents recovered on HPLC from the extract were 94 ± 4 and 92 ± 3% (*SE*), respectively. [d] Quotient of amount recovered corrected for volumes of extract used and amount added, which is the product of the extraction efficiency and the collection efficiency.

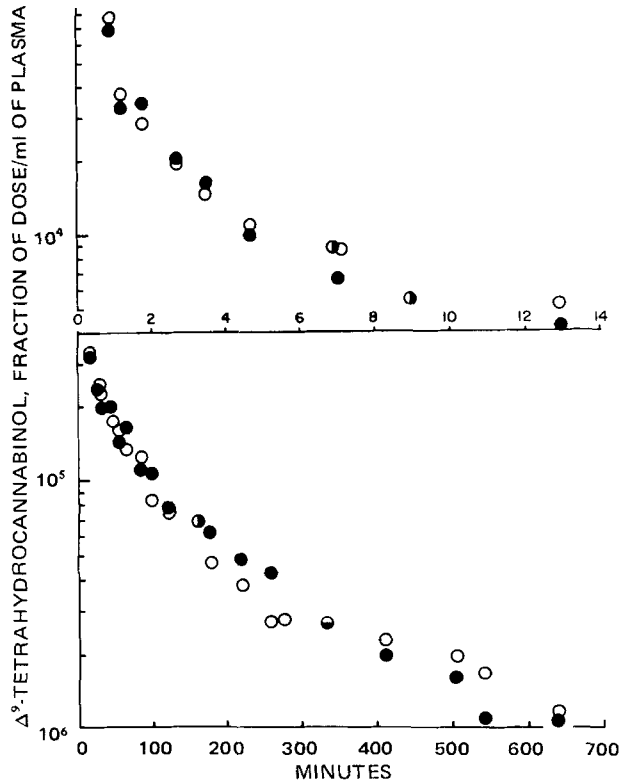

Figure 10—*Semilogarithmic plots of fraction of the Δ⁹-tetrahydrocannabinol, 2.0-mg/kg dose/ml of plasma, against time for Dog A plotted from the liquid scintillation analysis of the total carbon-14 collected as Δ⁹-tetrahydrocannabinol on normal-phase HPLC (○) and from the electron-capture GLC of the derivatized HPLC collected fraction (●). The values were corrected for the fractions of extracts and total collection range used.*

a 92.5% recovery of the amount in the heptane extract injected on normal-phase HPLC and collected in the chosen range.

The normal HPLC collection range was chosen to be slightly smaller than in the studies on ethanolic solutions of Δ⁹-tetrahydrocannabinol (Fig. 2 and Table II) since the procedure had to be modified to separate tetrahydrocannabinol from possible monohydroxylated or 11-hydroxy-Δ⁹-tetrahydrocannabinol metabolites in plasma. A slight overlap of their HPLC peak areas with Δ⁹-tetrahydrocannabinol would have occurred with the larger collection ranges.

A similar study of the reproducibility of collection of ^{14}C-Δ⁹-tetrahydrocannabinol in plasma assayed by liquid scintillation after extraction and reversed-phase HPLC was also conducted. The amounts recovered were proportional to the amounts injected (Fig. 8), and the HPLC recovery efficiency of the drug in the heptane extract was 95.7%.

Equivalency of Radiochemical Analyses of ^{14}C-Δ⁹-Tetrahydrocannabinol and GLC Electron-Capture Detection of Derivatized Material after Normal-Phase HPLC in Dog Plasma during Pharmacokinetic Studies—The plasma of a dog intravenously administered solutions of ^{14}C-Δ⁹-tetrahydrocannabinol was monitored with time after heptane extraction by both radiochemical analysis and electron-capture GLC of the derivative of the appropriately collected eluate fraction from normal-phase HPLC. Typical plots of the time course of the results from both methods are given in Figs. 9 and 10.

The procedures for GLC analysis gave a lower limit for quantitative analysis of tetrahydrocannabinol in plasma of approximately 1 ng/ml from twice the standard deviation (0.32 ng) obtained for the amount of tetrahydrocannabinol recovered from 2.25 ng in 2 ml of plasma (Table II). Similarly, the procedure for radiochemical analysis gave a lower limit of approximately 0.2 ng/ml from twice the standard deviation (0.084 ng). A statistical analysis of the apparent differences between the tetrahydrocannabinol assays at a given time from both analytical methods (Figs. 9 and 10) showed no significance. This finding demonstrated that all of the recovered radioactivity from the HPLC separation procedure could be assigned to the Δ⁹-tetrahydrocannabinol assayed specifically by electron-capture GLC. Thus, no significant amounts of radiolabeled metabolites were in the collected HPLC fractions.

It can be concluded that Δ⁹-tetrahydrocannabinol can be extracted from plasma and other biological fluids and that it can be separated on HPLC from the simultaneously extracted biologically endogenous materials and metabolites that would interfere with a chosen highly sensitive analytical method such as GLC. It is not necessary to collect all of the material to be analyzed; assurance that a reproducible or known fraction of the total material injected on HPLC is recovered is all that is necessary, since it is directly proportional to the total drug concentration. If unlabeled Δ⁹-tetrahydrocannabinol in a solution of plasma were analyzed, the calculated recovery of known amounts of labeled Δ⁹-tetrahydrocannabinol added either to plasma prior to extraction or to the heptane extract subsequent to extraction would permit calculation of the extraction and/or HPLC collection efficiencies for that particular biological sample. These known efficiencies would permit the calculation of the original plasma concentrations. If ^{14}C-Δ⁹-tetrahydrocannabinol were used in pharmacokinetic studies, extracted, and separated liquid chromatographically, ^{3}H-tetrahydrocannabinol could be used as the appropriate internal standard to monitor the recovery efficiencies.

REFERENCES

(1) E. R. Garrett and C. A. Hunt, *J. Pharm. Sci.*, **62**, 1211 (1973).

(2) *Ibid.*, **63**, 1056 (1974).

(3) E. R. Garrett and J. Tsau, *J. Pharm. Sci.*, **63**, 1563 (1974).

(4) N. K. McCallum, *J. Chromatogr. Sci.*, **11**, 509 (1973).

(5) N. K. McCallum, B. Yagen, S. Levy, and R. Mechoulam, *Experientia*, **31**, 520 (1975).

(6) M. Widman, M. Nordquist, S. Agurell, J. E. Lindgren, and F. Sandberg, *Biochem. Pharmacol.*, **23**, 163 (1974).

(7) R. S. Fetterman and C. E. Turner, *J. Pharm. Sci.*, **61**, 1476 (1972).

(8) C. E. Turner and K. Hadley, *ibid.*, **62**, 251, 1083 (1973).

(9) C. E. Turner, K. W. Hadley, J. Henry, and M. L. Mole, *ibid.*, **63**, 1872 (1974).

ACKNOWLEDGMENTS AND ADDRESSES

Received September 19, 1975, from the *College of Pharmacy, University of Florida, Gainesville, FL 32610.*

Accepted for publication March 8, 1976.

Abstracted in part from a dissertation submitted by C. A. Hunt to the Graduate School, University of Florida, in partial fulfillment of the Doctor of Philosophy degree requirements.

Supported in part by Grant DA-0073 from the National Institute of Mental Health, Bethesda, MD 20014.

The technical assistance of Mrs. Kathleen Eberst and the contributions of Hendryk Roseboom are gratefully acknowledged.

*Present address: School of Pharmacy, University of California, San Francisco, CA 94143.

[x] To whom inquiries should be directed.

Kinetics of Indomethacin Degradation I: Presence of Alkali

B. R. HAJRATWALA ˣ and J. E. DAWSON

Abstract □ The kinetics of indomethacin degradation were followed in alkaline aqueous solutions at various temperatures between 20.1 and 40.7°. The apparent first-order rate constants were evaluated from log absorbance *versus* time plots at λ_{max} 318 nm. The primary salt effect was positive. The rate constant–hydroxide-ion concentration profile was linear with a positive slope, suggesting the following rate law: $k_{obs} = k_1 [OH^-]$. The experimental data fit the proposed reaction of degradation, $I^- + OH^- \xrightarrow{k_1}$ products, where I^- = monodissociated indomethacin species. Activation energies and other related parameters were calculated from Arrhenius-type plots.

Keyphrases □ Indomethacin—degradation in alkaline aqueous solutions, various temperatures, kinetics, effect of ionic strength □ Degradation—indomethacin in alkaline aqueous solutions, various temperatures, kinetics, effect of ionic strength □ Kinetics—degradation of indomethacin in alkaline aqueous solutions, various temperatures, effect of ionic strength □ Anti-inflammatory agents—indomethacin, degradation in alkaline aqueous solutions, various temperatures, kinetics

Indomethacin [1-(4-chlorobenzoyl)-5-methoxy-2-methylindole-3-acetic acid, I] is a relatively new (1, 2) anti-inflammatory agent; it is not related to salicylates but is an acid. It is stable in neutral or slightly acidic media but is decomposed by strong alkali (3). Its physical properties, *e.g.*, solubility (4), polymorphism (5), and release rates from suppository bases (6, 7), have been reported, but its degradation kinetics have not.

The purposes of this investigation were to study the degradation of indomethacin in alkali, to establish the order of reaction, to study the effect of ionic strength, and to obtain an Arrhenius-type plot.

EXPERIMENTAL

Materials—All materials, including indomethacin[1], sodium hydroxide, and sodium chloride, were analytically pure grade. All-glass double-distilled water was used throughout.

Kinetic Studies—An accurately weighed quantity (~100 mg) of indomethacin was dissolved in 30 ml of 95% ethanol, and the volume was adjusted to 50 ml with water at 25°. The indomethacin solution, 0.1 *N* sodium hydroxide, and water were all kept at the temperature of the study. Mixtures of the indomethacin solution (2 ml), varying quantities of 0.1 *N* sodium hydroxide, and water to a final volume of 100 ml were immediately transferred to a quartz cell kept in a constant-temperature cell holder[2]. The initial concentration of indomethacin in the reaction cell was approximately 1.1×10^{-4} *M*.

Absorbance (against an appropriate blank) was recorded as a function of time at λ_{max} 318 nm. The pH was measured at the beginning and end of each run, and no significant change in pH was found. The absorbance data obtained were used to construct semilogarithmic plots of the function $(A_t - A_\infty)$ *versus* time, where A_t is the observed absorbance at time t, and A_∞ is the observed equilibrium absorbance value. Such plots are illustrated in Fig. 1, where the degradation behavior is observed to follow first-order kinetics. The apparent first-order rate constants, k_{obs} (Table I), were calculated using regression analysis (10 or more points). Correlation coefficients were between −0.993 and −0.999.

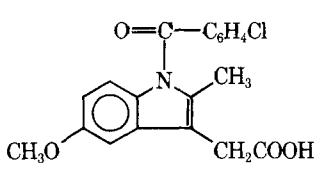

I

Effect of Ionic Strength—The effect of ionic strength was investigated at 25.8° in 0.005 *M* hydroxide-ion concentration adjusted to the ionic strengths of 0.045, 0.165, 0.505, and 1.00 and in 0.01 *M* hydroxide-ion concentration adjusted to the ionic strengths of 0.05, 0.17, 0.51, and 1.00. The ionic strength was adjusted by addition of sodium chloride (Fig. 2).

Effect of Hydroxide-Ion Concentration and Temperature—The study was carried out in various concentrations of hydroxide ion at 20.1, 25.8, 30.3, 35.1, and 40.7°.

Determination of pKa of Indomethacin—About 100 mg of indomethacin, accurately weighed, was dissolved in ethanol, and the volume was made up to 100 ml with water. The solutions were titrated potentiometrically (8) with 0.1 *M* KOH at 30°. The pKa's were calculated on a specially written Fortran program[3], using both Debye and Guntelberg activity coefficients (9). The difference between the pKa values calculated by the two methods was in all cases less than 0.002 unit. The pKa's reported are an average of 13 data points, with a range of ±0.05 unit.

RESULTS AND DISCUSSION

Figure 2 shows the effect of ionic strength. At both hydroxide-ion concentrations, there was a positive ionic strength effect with the slope of the line less than 1. At 0.005 and 0.01 *M* hydroxide-ion concentrations, the slopes of the line were 0.168 and 0.077, respectively. Since even model pharmaceutical systems by necessity are in concentration ranges above 0.01 ionic strength, it is not unusual to study pharmaceuticals at high ionic strength (10–12). This positive ionic strength effect suggests that the reaction of ions of like sign plays a role in the mechanism of indomethacin degradation (13).

Figure 3 shows the effect of varying hydroxide-ion concentrations on indomethacin degradation at various temperatures. The rate constant–hydroxide-ion concentration profile suggests a simple

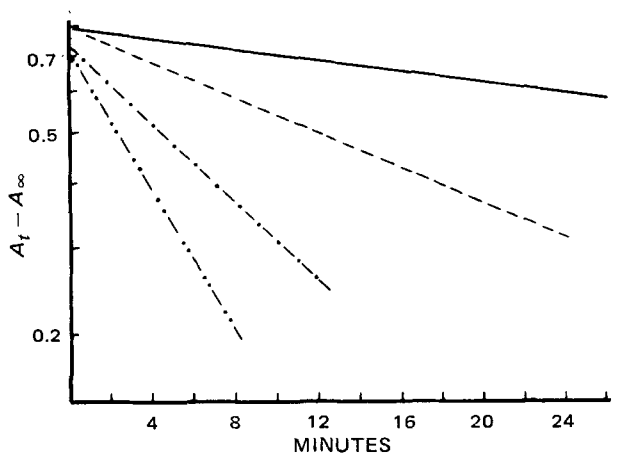

Figure 1—*Plot showing overall first-order character of indomethacin degradation at various hydroxide-ion concentrations* (M) *at 25.8°. Key: —, 0.001; - - -, 0.003; - · -, 0.006; and - · · -, 0.01. (Data were replotted from absorbance* versus *time recorder tracings.)*

[1] Lot L-590,229-00A108, Merck Sharp & Dohme, Rahway, N.J.
[2] Shimadzu spectrophotometer.
[3] Available on request from the authors.

Table I—Effect of Hydroxide-Ion Concentration on the Apparent First-Order Rate Constant, k_{obs}, for Indomethacin Degradation at Various Temperatures

	$k_{obs} \times 10^2$, min^{-1}				
[OH$^-$], M	20.1°	25.8°	30.3°	35.1°	40.7°
0.001	0.95 (0.86)[a]	1.34	1.74	2.16	2.83
0.002	2.15	3.04	3.84	5.32	6.51
0.003	3.26	4.48 (4.64)	5.91	8.05	10.12
0.004	4.45	6.25 (6.15)	8.00	11.03	13.70
0.005	5.78	7.53 (7.81)	9.96	13.66 (13.73)	17.38 (16.99)
0.0055	—	9.11	—	—	—
0.006	6.68	9.90 (9.83)	11.87	16.98	21.40
0.0065	—	10.73	—	18.13	—
0.007	—	10.75	15.20	19.20	—
0.0075	—	11.24	—	20.68	—
0.008	8.95 (9.18)	—	17.91 (17.46)	—	—
0.010	—	17.22 (17.06)	22.12 (21.03)	—	—

[a] Duplicate values are in parentheses.

mechanism. The reaction shown in Scheme I, where I^- is the monodissociated species of indomethacin, would give a rate constant–hydroxide-ion concentration profile that fits the experimental points well.

$$I^- + OH^- \xrightarrow{k_1} \text{products}$$
Scheme I

The overall velocity of the reaction is given by:

$$\frac{d[I]_T}{dt} = k_1[I^-][OH^-] \quad \text{(Eq. 1)}$$

and:

$$[I]_T = [I] + [I^-] \quad \text{(Eq. 2)}$$

where I = undissociated indomethacin species. The brackets signify molar concentrations of the appropriate species. Because of the overall first-order character of the reaction:

$$-\frac{d[I]_T}{dt} = k_{obs}[I]_T \quad \text{(Eq. 3)}$$

and:

$$K_a = \frac{K_w[I^-]}{[I][OH^-]} \quad \text{(Eq. 4)}$$

Combining these equations and substituting in Eq. 1 yield:

$$k_{obs} = \frac{k_1K_a[OH^-]^2}{[OH^-]K_a + K_w} \quad \text{(Eq. 5)}$$

The pKa for indomethacin was 6.02, 5.69, and 5.45 at 30° in 70, 60, and 50% ethanol in water, respectively. It was necessary to determine the pKa of indomethacin in the presence of ethanol because of its low solubility in water. Increasing concentrations of ethanol increase the pKa of weak acids, *e.g.*, sulfathiazole (14, 15), phenobarbital (16), and ascorbic acid (17). For the present study, for a weak acid such as indomethacin, $[OH^-]K_a \gg K_w$, where K_w is the ionic product for water. Thus, Eq. 5 reduces to:

$$k_{obs} = k_1[OH^-] \quad \text{(Eq. 6)}$$

Table II shows the values for k_1 at various temperatures together with standard errors of estimate and correlation coefficients.

The good agreement of the experimental data with Eq. 6 does not prove that Scheme I is correct but justifies its proposal. In considering the effect of hydroxide-ion concentration on the degradation of indomethacin in aqueous solution, Schemes I–VI are possible.

$$I^- + H^+ \xrightarrow{k_2} \text{products}$$
Scheme II

$$I^- \xrightarrow{k_3} \text{products}$$
Scheme III

$$I + OH^- \xrightarrow{k_4} \text{products}$$
Scheme IV

$$I + H^+ \xrightarrow{k_5} \text{products}$$
Scheme V

$$I \xrightarrow{k_6} \text{products}$$
Scheme VI

Schemes II and VI and III and IV are kinetically indistinguishable. On the basis of experimental results, Schemes II and V cannot be considered. If Schemes II (or VI) and V hold, the observed rate con-

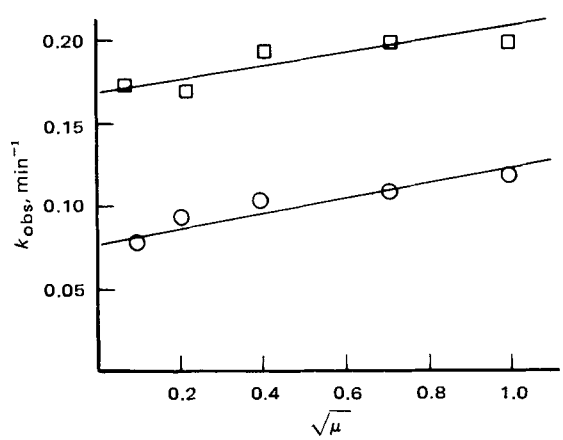

Figure 2—*Effect of ionic strength (μ) on the degradation of indomethacin at 25.8° in 0.005* M (○) *and 0.01* M (□) *hydroxide-ion concentrations.*

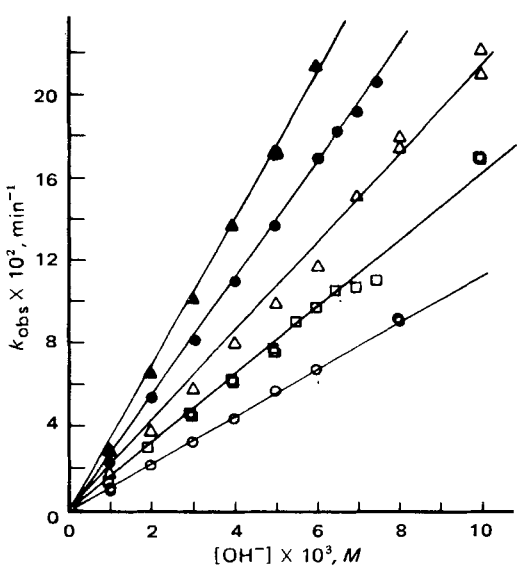

Figure 3—*Effect of varying concentrations of hydroxide ion on indomethacin degradation at various temperatures. Key:* ○, *20.1°;* □, *25.8°;* △, *30.3°;* ●, *35.1°; and* ▲, *40.7°.*

Table II—Second-Order Hydroxide-Ion Catalytic Rate Constant for Indomethacin Degradation at Various Temperatures

	20.1°	25.8°	30.3°	35.1°	40.7°
k_1, liter mole^{-1} min^{-1}	11.26	16.25	21.39	27.60	34.59
SE	0.1441	0.4967	0.5923	0.2655	0.4078
r	0.9995	0.9954	0.9976	0.9995	0.9994
n	9	16	11	10	7

Table III—Activation Energies and Other Parameters for Indomethacin Degradation in Aqueous Solution at 25° Obtained from Arrhenius-Type Plots

Hydroxide-Ion Concentration, *M*	E_a, kcal mole^{-1}	$\Delta H^{\ddagger}$, kcal mole^{-1}	$\Delta S^{\ddagger}$, cal mole^{-1} deg^{-1}	$\Delta F^{\ddagger}$, kcal mole^{-1}	$-r$	*n*
0.001	10.1	9.5	−35.2	20.1	0.995	6
0.002	10.0	9.4	−33.9	19.6	0.997	5
0.003	10.3	9.7	−32.3	19.3	0.998	6
0.004	10.2	9.6	−31.8	19.1	0.998	6
0.005	10.0	9.5	−32.0	19.0	0.996	8
0.006	10.3	9.7	−30.7	18.9	0.996	6
k_1	10.0	9.5	−21.4	15.8	0.997	5

stant would be inversely proportional to the hydroxide-ion concentration. If Scheme III (or IV) holds, the observed rate constant would be independent of the hydroxide-ion concentration. Thus, only Scheme I can be proposed.

The effect of temperature on the reaction rate can be expressed using the Arrhenius equation. As shown in Fig. 4, plots of log *k versus* $1/T$ yield a straight-line relationship at all hydroxide-ion concentrations used. Table III shows the activation energy values and other parameters calculated. The parallel slopes of the Arrhenius-type plots indicate that the mechanism of degradation is identical at all hydroxide-ion concentrations used.

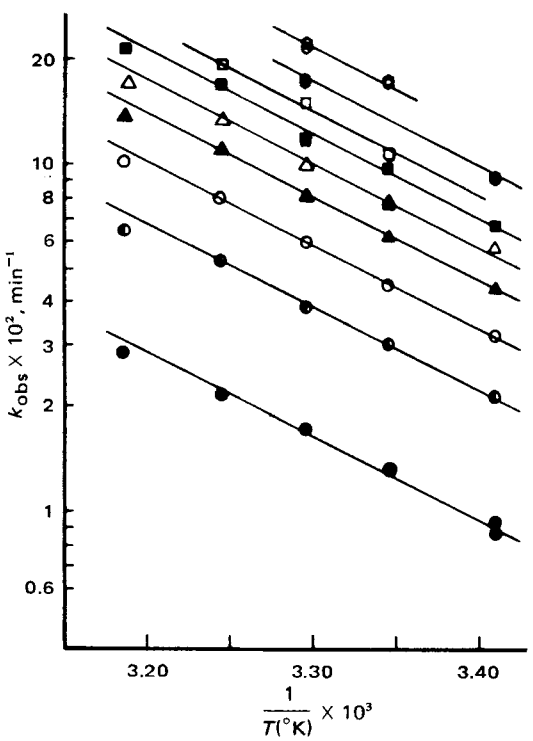

Figure 4—*Arrhenius plots showing temperature dependence of* k_{obs}, *the apparent first-order indomethacin degradation rate constant, at various hydroxide-ion concentrations* (M). *Key:* ○, *0.01;* ●, *0.008;* □, *0.007;* ■, *0.006;* △, *0.005;* ▲, *0.004;* ○, *0.003;* ◐, *0.002; and* ●, *0.001.*

REFERENCES

(1) T. Y. Shen, R. L. Ellis, T. B. Windholz, A. R. Matzuk, A. Rosegay, S. Lucas, B. E. Witzel, C. H. Stammer, A. N. Wilson, F. W. Holly, J. D. Willett, L. H. Sarett, W. J. Holtz, E. A. Risley, G. W. Nuss, and C. A. Winter, *J. Am. Chem. Soc.*, **85**, 488(1963).

(2) T. Y. Shen (to Merck & Co.), U.S. pat. 3,161,654 (1964).

(3) "The Merck Index," 8th ed., Merck & Co., Rahway, N.J., 1968, p. 566.

(4) H. Krasowska, L. Krowczynski, and E. Glab, *Diss. Pharm. Pharmacol.*, **24**, 623(1972).

(5) H. Yamamoto, *Chem. Pharm. Bull.*, **16**, 17(1968).

(6) L. P. J. Holt and C. F. Hawkins, *Br. Med. J.*, **1**, 1354(1965).

(7) H. P. M. Kerckhoffs and T. Huizinga, *Pharm. Weekbl.*, **102**, 1183(1967).

(8) A. Albert and E. P. Serjeant, "Ionization Constants of Acids and Bases," Butler and Tanner Ltd., London, England, 1962, p. 16.

(9) R. A. Robinson and R. H. Stokes, "Electrolyte Solutions," Butterworths, London, England, 1959, p. 231.

(10) P. Finholt, G. Jurgensen, and H. Kristiansen, *J. Pharm. Sci.*, **54**, 387(1965).

(11) J. Windheuser and T. Higuchi, *ibid.*, **51**, 354(1962).

(12) B. R. Hajratwala, *ibid.*, **64**, 45(1975).

(13) J. T. Carstensen, *ibid.*, **59**, 1140(1970).

(14) J. R. Stockton and C. R. Johnson, *J. Am. Chem. Soc.*, **33**, 383(1944).

(15) T. Higuchi, M. Gupta, and L. W. Busse, *J. Am. Pharm. Assoc., Sci. Ed.*, **42**, 157(1953).

(16) T. D. Edmonson and S. E. Goyan, *ibid.*, **47**, 810(1958).

(17) B. R. Hajratwala and P. Boonsaner, *Proc. Univ. Otago Med. Sch.*, **52**, 26(1974).

ACKNOWLEDGMENTS AND ADDRESSES

Received November 5, 1975, from the *Department of Pharmacy, University of Otago, Dunedin, New Zealand.*

Accepted for publication February 26, 1976.

Grateful acknowledgment is made to the New Zealand Medical Research Council for providing a Summer Student Scholarship to Mrs. J. E. Dawson.

[x] To whom inquiries should be directed.

Scattered Isergonic Profiles

JAMES J. ZIMMERMAN

Abstract □ Equations were developed for the geometric analysis of scatter in isergonic profiles as a function of vertical ($\Delta\Delta H$), horizontal ($\Delta\Delta S$), and perpendicular (d) distances from the error line. Sigma (σ^-) correlates with each of these quantities of the test series to produce statistics (F and r) identical to those for correlation with ΔG. The vertical distances, $\Delta\Delta H$, are shown to be identical to the substituent effect, $\delta\Delta G$; thus, it is concluded that the Hepler approach of implicating a solvation mechanism on the basis of ρ–σ correlations for these distances is not warranted. The uncertainty of points on the isergonic profile for the test series was determined using the joint confidence region ("error contour") approach. Statistical limits of the contour lengths overlapped extremely between members of the test series. To eliminate such overlap for series showing small ranges in substituent effects, extremely precise rate data would be required with N (number of data points) = 4 or 5 for the Arrhenius fits. A comparison between d values and the perpendicular half-widths ($w/2$) of the error contours resulted in $d > w/2$ for each member of the test series (excluding H), proving that scatter in the profile could not result from experimental error. A further comparison between differences in d, Δd, from suggested β lines for solvation and $w/2$ values showed that a β range as large as 45° could be included in the error contour widths of the test series. Since the average reaction temperature, $\overline{T}$, fell within this range, solvation effects could not be distinguished statistically from error effects.

Keyphrases □ Solvation isergonic profiles—geometric analysis of scatter as a function of vertical, horizontal, and perpendicular distances from error line □ Isergonic profiles, solvation—geometric analysis of scatter as a function of vertical, horizontal, and perpendicular distances from error line □ Reaction mechanisms—solvation isergonic profiles, geometric analysis of scatter as a function of vertical, horizontal, and perpendicular distances from error line

Attempts to demonstrate the usefulness of entropy–enthalpy (ΔH *versus* ΔS) profiles in augmenting the mechanistic descriptions of chemical reactions have been well documented (1). Recent publications attempted to extend them to enzyme reactions (2) and protein–small molecule interactions in general (3).

In many cases, ΔH *versus* ΔS profiles are linear; the slope of such profiles for either rate or equilibrium data yields β_i[1], the isergonic[2] temperature (1, 2), in accordance with:

$$\delta\Delta H = \beta_i\delta\Delta S \qquad \text{(Eq. 1)}$$

where δ = the Leffler–Grunwald operator for substituent or medium effects. The linearity of such profiles tends to confirm a common reaction mechanism for the members of a congeneric series, and the numerical value of β_i is potentially associated with a known reaction mechanism. Thus, a value of $\beta_i \simeq 280$°K is customarily associated with an aqueous solvation mechanism for a series (4).

Hepler (5) showed that Eq. 1 is one relationship obtained from an exact thermodynamic analysis of the Hammett equation (Eq. 2) when ΔH and ΔS are temperature independent:

$$\log (k_x/k_H) = \rho\sigma \qquad \text{(Eq. 2)}$$

where ρ = reaction constant, σ = substituent constant, and x and H refer to substituted and parent derivatives, respectively. As a result, congeneric series that obey Eq. 2 should also obey Eq. 1. However, some reaction series follow the Hammett relationship but their ΔH *versus* ΔS profiles are nonlinear or scattered (1). A rational explanation for the behavior of such series was discussed previously in terms of multiple interaction mechanisms and related compensation phenomena (1, 5).

THEORETICAL

Leffler–Grunwald Analysis of Scattered Isergonic Profiles—According to Leffler and Grunwald (1), the scatter in ΔH *versus* ΔS profiles may be explained in terms of multiple contributions to the observed enthalpies and entropies. For a model based on a two-interaction mechanism, the enthalpy and entropy expressions are given by:

$$\delta\Delta H = \delta\Delta H' + \delta\Delta H'' \qquad \text{(Eq. 3)}$$

$$\delta\Delta S = \delta\Delta S' + \delta\Delta S'' \qquad \text{(Eq. 4)}$$

where the superscripts, ′ and ″, refer to two different but additive types of substituent contributions (*e.g.*, resonance, inductive, steric, or solvation effects). These two contributions to the observed enthalpy and entropy would vary independently of one another for any given reaction series. Therefore, a plot of ΔH *versus* ΔS would not be expected to be linear. For the same reason, a plot of the Hammett equation (Eq. 2) would not be expected to be linear under these conditions.

On the other hand, when each of the two mechanisms is isergonically related (*i.e.*, $\delta\Delta H' = \beta'\delta\Delta S'$ and $\delta\Delta H'' = \beta''\delta\Delta S''$):

$$\delta\Delta H = \beta'\delta\Delta S' + \beta''\delta\Delta S'' \qquad \text{(Eq. 5)}$$

$$\delta\Delta S = \delta\Delta H'/\beta' + \delta\Delta H''/\beta'' \qquad \text{(Eq. 6)}$$

$$\delta\Delta G = [\beta' - T]\delta\Delta S' + [\beta'' - T]\delta\Delta S'' = [1 - (T/\beta')]\delta\Delta H' + [1 - (T/\beta'')]\delta\Delta H'' \qquad \text{(Eq. 7)}$$

From Eq. 7 it is apparent that for reactions run at $T = \beta'$ or $T = \beta''$, the free energy expression will be simpler by one interaction mechanism. The same, however, is not true for the observed enthalpy and entropy expressions (Eqs. 5 and 6), which remain complex independent of T when $\beta' \neq \beta''$ or $\beta' \gg \beta''$. In practice, then, it is possible to obtain linear Hammett plots even when the ΔH *versus* ΔS profile is scattered, provided that the reaction temperature is close to β' or β''.

Hepler Analysis of Scattered Isergonic Profiles—Hepler (4, 5) proposed a two-interaction model, which simplifies Eqs. 3 and 4 and permits the linearization of a scattered ΔH *versus* ΔS plot. According to the Hepler scheme, the prime and double-prime superscripts of Eqs. 3 and 4 refer to internal and external contributions of substituents, respectively. The internal contributions represent substituent interactions with the reaction center, and the environmental contributions represent substituent interactions with the solvent. By assuming an isergonic relationship for the environmental contributions and a negligible contribution from the internal entropy, Eq. 8 may be derived from Eqs. 3 and 4:

$$\delta\Delta H = \delta\Delta H' + \beta''\delta\Delta S \qquad \text{(Eq. 8)}$$

where β'' is the isergonic temperature for the solvation effect. The $\delta\Delta H'$ quantity, corresponding to the internal enthalpy contribution, may now be calculated from Eq. 8 using the experimentally observed values of $\delta\Delta H$ and $\delta\Delta S$ and letting $\beta'' = \overline{T}$, the average temperature for the determinations[3] (5, 6). The free energy expression for the Hepler scheme is given by:

$$\delta\Delta G = \delta\Delta H' + (\beta'' - T)\delta\Delta S \qquad \text{(Eq. 9)}$$

[1] The slope = $R\beta_i$ when Arrhenius parameters E_a and ln A are used for rate data.

[2] The general term isergonic is used here to include both isokinetic and isoequilibrium phenomena (Ref. 2).

[3] The reviewer of this manuscript appropriately commented that the Hepler scheme with 270° < β < 320° is specifically applicable to water and similar solvents. In other solvent systems, β'' for solvation may not necessarily approximate $\overline{T}$.

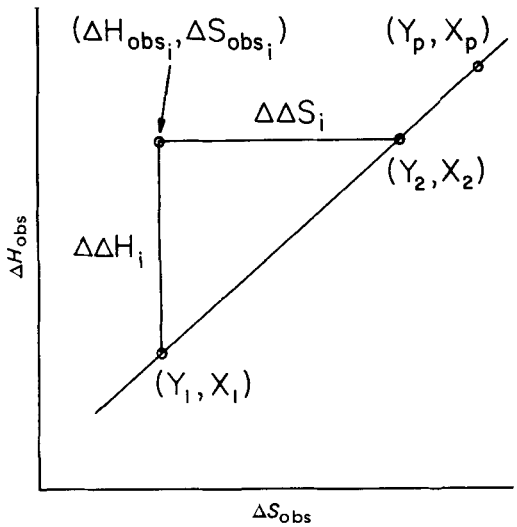

Figure 1—*Diagram showing the vertical* ($\Delta\Delta H_i$) *and horizontal* ($\Delta\Delta S_i$) *distances of point* (ΔH_{obs_i}, ΔS_{obs_i}) *from the error line,* $Y_i = \overline{T}X_i + b$.

Since thermodynamic parameters for reactions are normally reported for the average temperature of determination and since β'' equals $\overline{T}$ or follows it closely, the second term in Eq. 9 will equal zero in most cases; the calculated values of $\delta\Delta H'$ will equal $\delta\Delta G$. It is not surprising, therefore, that calculated $\delta\Delta H'$ values are linear in σ for series that obey the Hammett relationship (Eq. 2) (4, 7, 8).

Vertical and Horizontal Distances from Error Line—While the Hepler model is satisfying from a mechanistic point of view, the method has two serious drawbacks. First, $\overline{T}$ for the solvation effect is also equal to the error slope for any isergonic relationship. Second, the calculation of $\delta\Delta H'$ from Eq. 8 is identical to the method used in calculating $\delta\Delta G$ values for scatter about any isergonic line. Therefore, it is possible to obtain results identical to those of Hepler's without referring to a solvation mechanism merely by calculating the deviation in enthalpy or entropy from the error slope, $\overline{T}$.

The equations for an analysis based on distances from the error line may be formulated by reference to Fig. 1. The equation of the error line with a slope equal to $\overline{T}$ and drawn through the coordinates of the parent point (Y_p, X_p) is given by:

$$Y_i = \overline{T}X_i + b \qquad \text{(Eq. 10)}$$

where $b = \Delta H_{obs_p} - \overline{T}\Delta S_{obs_p}$ = free energy of parent compound, and Y_i and X_i represent ΔH_{obs} and ΔS_{obs} values for a given compound projected to the error line. The vertical distance of the observed point in the figure from the error line is given by the difference in ΔH_{obs_i} and Y_1 according to:

$$\Delta\Delta H_i = \Delta H_{obs_i} - \overline{T}\Delta S_{obs_i} - b \qquad \text{(Eq. 11)}$$

In a similar manner, the horizontal distance of the observed point from the error line is obtained as the difference between S_{obs_i} and X_2, which is equal to:

$$\Delta\Delta S_i = \Delta S_{obs_i} - (\Delta H_{obs_i}/\overline{T}) + b/\overline{T} \qquad \text{(Eq. 12)}$$

The corresponding free energy terms for the observed values calculated from the distances to the error line are obtained by substituting Eqs. 11 and 12 into the Gibbs free energy expression to obtain:

$$\Delta G_{obs_i} = \Delta\Delta H_i + b \qquad \text{(Eq. 13)}$$

and:

$$\Delta G_{obs_i} = -\overline{T}\Delta\Delta S_i + b \qquad \text{(Eq. 14)}$$

The values of $\Delta\Delta H_i$ of Eq. 11 and $\delta\Delta H'$ of Eq. 8 differ only by the constant b, which is equal to the free energy contribution of the parent compound. Furthermore, from Eqs. 13 and 14, it can be seen that the expression for ΔG_{obs_i} is given as a sum of two free energy terms: one for the parent compound (b) and one for the substituent ($\Delta\Delta H_i$ or $-\overline{T}\Delta\Delta S_i$). The vertical distance, $\Delta\Delta H_i$, or its counterpart on the horizontal axis, $-\overline{T}\Delta\Delta S_i$, simply yields the free energy contribution of the substituent symbolized by $\delta\Delta G$. Thus, series that obey the Hammett relationship (Eq. 2) will necessarily yield $\Delta\Delta H_i$ values that correlate with σ.

Lengths of Error Contours and Perpendicular Distances from β Line—The decision of whether to include any given member of a congeneric series within the classification of an assigned β value is arrived at by determining the error associated with that member on an isergonic profile. As stressed previously (1, 6), however, the uncertainty of any point on such a profile is not given by a rectangle with dimensions in standard errors for that point but instead by a region referred to as the error contour. The standard errors of ΔH and ΔS are appropriate when discussing either one of these two quantities independently of the other; but when both are considered jointly as in isergonic profiles, the correct uncertainty function is the joint confidence region (9). This region takes the shape of a highly eccentric ellipse when the variances of the two considered quantities differ widely and are strongly correlated. Such is the case for the least-squares estimates of the slope and intercept of Arrhenius plots from which ΔH and ΔS are derived.

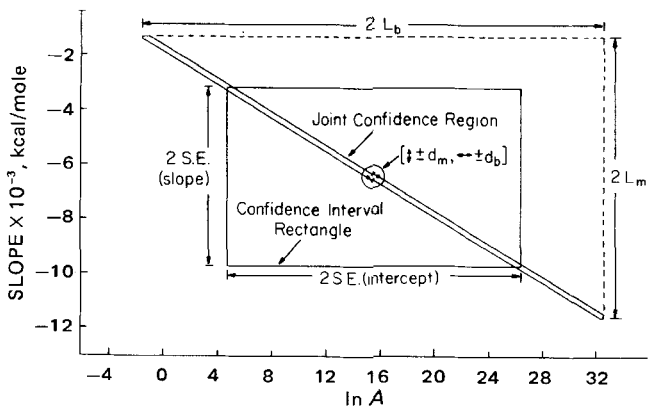

Figure 2—*Comparison of the joint confidence region (error contour) and confidence interval rectangle associated with the slope and intercept of the Arrhenius fit for the alkaline hydrolysis of phenyl benzoate.*

Mandel and Linnig (10) pointed out that a negative correlation exists between the errors in slope and intercept whenever the x values of the original data are positive. As a consequence, the upper part of the error ellipse tilts toward the ordinate in a plot of slope *versus* intercept[4]. The boundaries of this ellipse are determined by the standard error of estimate, s, for the least-squares analysis and by the $(F \text{ ratio})^{1/2}$ for the desired confidence level. Thus, at any desired confidence level, only values of the slope and intercept that fall within the boundaries of the ellipse are allowed on the basis of observed experimental error.

Mandel and Linnig (10) simplified the plotting of joint confidence regions by deriving a function that closely approximates the error ellipse from three sets of parallel tangents. These parallel lines can be plotted on graph paper with the aid of four constants (L_m, L_b, d_m, and d_b) describing the error function (see *Appendix* for equations). This method of ellipse construction was used to plot the joint error region associated with the slope and intercept of the Arrhenius fit for the alkaline hydrolyses of phenyl benzoates at 20, 30, and 35° (8). Figure 2 illustrates the extreme eccentricity of the error ellipse for this type of data as compared with the larger rectangular area based in the standrd errors of the slope and intercept.

Two important features arise out of the error ellipse analysis as applied to the interpretation of isergonic profiles. First, the lengths of the error regions determine whether two or more points lying along an isergonic line are potentially interchanged as a result of experimental error. Second, the widths, w, or thicknesses of the error regions determine which points of an isergonic profile belong to a given interaction line with slope = β. Both of these features can be utilized by plotting all individual error contours on an isergonic profile and then observing their distribution relative to either the least-squares line drawn through the data or the error line with a slope of $\overline{T}$.

Since the process of plotting error contours on graph paper is tedious and time consuming, even for the Mandel–Linnig projections, an alternative method for providing the same information is desirable. A comparison of the contour lengths projected along a given β line is easily accomplished by computing the value of (slope $\pm$ L_m) for each point and then visually inspecting the calculated limits for overlap between any

[4] A plot of $\Delta H^{\neq}$ *versus* $\Delta S^{\neq}$ for these data would yield an error ellipse with a positive slope because of the change in sign that occurs in converting the slope to $\Delta H^{\neq}$.

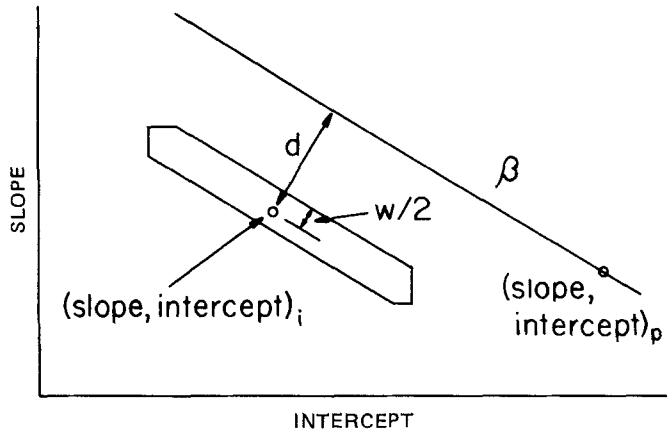

Figure 3—*Diagram showing the perpendicular distances* d (*distance from center of error ellipse to β line drawn through parent point*) *and* w/2 (*distance from center to ellipse boundary*).

points. These limits should not overlap if one wishes to gain statistical confidence in the relative positioning of points along the line.

The use of contour widths to interpret isergonic data requires a comparison between the perpendicular half-widths, $w/2$, of the contours and the respective perpendicular distances, d, from a given β line (Fig. 3). These distances may be calculated from Eq. 15 which, in general, gives the perpendicular distance, p, of any point from a given line (11):

$$p = (AX_i + BY_i + C)/(A^2 + B^2)^{1/2} \qquad \text{(Eq. 15)}$$

where X_i and Y_i are the coordinates of the point and where the equation for the line is given by $AX + BY + C = 0$, with X and Y representing the coordinates for a point on the line. The coefficients A, B, and C may be expressed in terms of the more usual slope–intercept form for a line, $Y = mX + b$, as follows: $A = -m$, $B = 1$, and $C = -b = -(Y - mX)$. For calculating the distance, d, in Fig. 3 from the line drawn through the parent point, these coefficients take on the values $A = -\beta$, $B = 1$, and $C = -[\text{slope}_p - \beta\ (\text{intercept}_p)]$. For calculating the distance, $w/2$, in the figure from the contour limit extending through a point with coordinates of $(\text{slope}_i + dm_i$ and $\text{intercept}_i)$, the coefficients take on the values $A = -L_m/L_b$, $B = 1$, and $C = -[(\text{slope}_i + dm_i) - L_m/L_b(\text{intercept}_i)]$[5]. A comparison between the values of d and $w/2$ for each point indicates whether the point belongs to the particular β line in question. Thus, a point may be rejected at the confidence level of its error contour when $d > w/2$.

RESULTS AND DISCUSSION

The data chosen for analysis are those of Washkuhn *et al.* (8) for the alkaline hydrolysis of 3- or 4-substituted phenyl benzoates (I), where X = 4-CH_3, H, 4-F, 4-Cl, 3-CN, 4-CN, or 4-NO_2. This congeneric series obeys the Hammett relationship (Eq. 2) but shows a scattered ΔH *versus* ΔS profile. Therefore, it is suitable for analysis using the equations given previously. The second-order rate constants, k_{OH}, for the series were reported as a function of temperature at 20, 25, 30, and 35° determined in 50% (v/v) acetonitrile–0.02 *M* phosphate buffer.

Activation Parameters—A preliminary graphical plot of the data showed a large systemic deviation of the rate constant at 25° for each member of the series. These displaced data points were tested for exclusion from further data analysis by determining the significance probability of the t value under such conditions (12). In all cases, the significance levels were considerably greater than 0.05, justifying a rejection of the null hypothesis. From these results and because of the large upward systemic displacement of each point, data at 25° were not included in calculating the parameters given in Table I. The slopes and intercepts of the Arrhenius plots based on data at 20, 30, and 35° were significant at least at the 0.05 level, except the intercept for the parent compound which was significant at the 0.10 level.

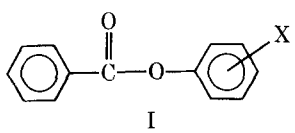

I

[5] From the *Appendix*, $L_m/L_b = (N/\Sigma X^2)^{1/2} = [N/\Sigma(1/T)^2]^{1/2}$ while $\overline{T} = (\Sigma T)/N$. The difference between these two quantities, however, is small ($\simeq$0.3°K) for the usual 20° temperature range used in collecting Arrhenius data.

Table I—Activation Parameters for the Alkaline Hydrolysis of Substituted Phenyl Benzoates[a]

Substituent (σ^-)[b]	$\Delta G^{\neq}$, kcal/mole	$\Delta H^{\neq}$, kcal/mole	$\Delta S^{\neq}$, cal/mole-deg
4-CH_3 (−0.17)	21.3	10.9	−34.8
H (0.00)	21.1	12.1	−29.7
4-F (0.062)	20.7	11.0	−32.4
4-Cl (0.226)	20.6	11.8	−29.3
3-CN (0.678)	19.9	10.3	−31.9
4-CN (1.00)	19.6	10.5	−30.2
4-NO_2 (1.27)	19.4	11.6	−25.8

[a] Activation parameters are based upon an initial linear least-squares fit of raw data (at 20, 30, and 35°) from Ref. 8 to the Arrhenius equation, where $\Delta H^{\neq} = E_a - RT$, $\Delta S^{\neq} = R\ [\ln k\overline{T} - \ln (k\overline{T}/h) + \Delta H^{\neq}/R\overline{T}]$, $\Delta G^{\neq} = \Delta H^{\neq} - \overline{T}\Delta S^{\neq}$ (before rounding off), and $\overline{T} = (\Sigma T)/N = 301.3$°K. [b] Values of σ^-, the Hammett constant for substituted phenols, were taken from Table 2-17 of Ref. 13.

Linear free energy and isergonic correlations for activation parameters of the phenyl benzoate series are given in Table II. Of the three parameters, only $\Delta G^{\neq}$ is a linear function of σ^- (Eq. 16). Furthermore, Eq. 19 shows that the isergonic profile is highly scattered. From the Leffler–Grunwald analysis given previously, nonlinearity observed with Eqs. 17–19 could be viewed in terms of multiple contributions to the observed enthalpies (Eqs. 3 and 4). When more than one mechanism contributes to ΔH, ΔS, or both, the separate contributions would not be expected to correlate with the same substituent parameter in either ΔH or ΔS, nor would a proportionality of effects be expected to exist between the mechanisms. Hence, the isergonic profile would be scattered.

Vertical and Horizontal Distances from β Line—The vertical ($\Delta\Delta H^{\neq}$) and horizontal ($\Delta\Delta S^{\neq}$) distances from the error slope (β = 301.3°) for the individual points on the isergonic profile (Table III) were calculated from the observed activation enthalpies and entropies before rounding off, using Eqs. 11 and 12, respectively. The vertical distance of each substituent from the error line is identical to its substituent effect, $\delta\Delta G^{\neq}$, in agreement with Eq. 13. Similarly, on the horizontal scale, $\delta\Delta G^{\neq}$ may be obtained as the product of $\Delta\Delta S^{\neq}$ times $-\overline{T}$, which is in agreement with Eq. 14.

Linear free energy correlations for the vertical and horizontal distances are presented in Table IV. For β = 301.3°, the resulting F ratios and correlation coefficients, r, are identical to those of Eq. 16 in Table II, demonstrating the redundancy between $\Delta G^{\neq}$, $\Delta\Delta H^{\neq}$, and $\Delta\Delta S^{\neq}$ as parameters for correlation with σ^-. Correlations based on $\Delta\Delta H^{\neq}$ and $\Delta\Delta S^{\neq}$ simply do not add any new information to the previously determined substituent effect based on $\Delta G^{\dagger}$ (Eq. 16).

Table IV also gives correlations for $\Delta\Delta H^{\neq}$ *versus* σ^- when β is varied using the values of $\Delta H^{\neq}$ and $\Delta S^{\neq}$ at 301.3°. The analysis demonstrates the effect upon F and r when β equals some value other than the error slope, $\overline{T}$. When β varies between 0 and 600°K, the correlation coefficient takes on values between −0.215 and −0.910, with a maximum appearing at β = 325°. For β = 0°, the resulting $\Delta\Delta H^{\neq}$ values equal $\delta\Delta H^{\neq}$; the resulting F and r values for the correlation are identical to those for Eq. 17 (Table II) based on $\Delta H^{\neq}$.

Values of β between 280 and 325° closely approximate the limits of β

Table II—Correlations for Activation Parameters[a]

Regression Equations[b] (n = 7)	S	F	r	Equation Number
$\Delta G^{\neq} = -1.33\sigma + 21.0$	0.136	175	−0.986	16
$\Delta H^{\neq} = -0.268\sigma + 11.3$	0.733	0	−0.215	17
$\Delta S^{\neq} = 3.53\sigma - 32.1$	2.27	4	−0.684	18
$\Delta H^{\neq} = 134\Delta S^{\neq} + 15{,}300$	625.0	2	−0.554	19

[a] n = number of data points used in linear least-squares fit; S = standard error of estimate; r = correlation coefficient; and F = F ratio (at the 90 and 95% confidence levels, F = 4.06 and 6.61, respectively, for 1,5 degrees of freedom). [b] Equations 16 and 17 are expressed in kcal/mole, Eq. 18 is expressed in cal/mole-deg, and Eq. 19 is expressed in cal/mole.

Table III—Comparison between Substituent Effects ($\delta\Delta G^{\neq}$) and Vertical ($\Delta\Delta H^{\neq}$) and Horizontal ($\Delta\Delta S^{\neq}$) Distances from the Error Slope, β = 301.3[a]

Substituent	$\delta\Delta G^{\neq}$, cal/mole	$\Delta\Delta H^{\neq}$, cal/mole	$\Delta\Delta S^{\neq}$, cal/mole-deg
4-CH_3	269	269	−0.894
H (none)	0	0	0
4-F	−324	−324	1.074
4-Cl	−483	−483	1.602
3-CN	−1143	−1143	3.792
4-CN	−1450	−1450	4.813
4-NO_2	−1669	−1669	5.538

[a] $\delta\Delta G = \Delta G_X^{\neq} - \Delta G_H^{\neq}$; $\Delta\Delta H^{\neq}$ and $\Delta\Delta S^{\neq}$ were calculated using Eqs. 11 and 12, respectively.

for aqueous solvation effects in phenols as suggested by Hepler ($270° < \beta < 320°$) (4). Within this range of β, the value of r for the $\Delta\Delta H^{\neq}$ *versus* σ^- correlations is observed to change only very slightly, and deviations in the slopes from $\overline{T}$ are not statistically significant even at the 50% level. Alternatively, it may be stated that values of β between 280 and 325°K for a proposed solvation mechanism could not be distinguished statistically from $\overline{T}$ falling within this temperature region.

Lengths of Error Contours—The constants L_m, L_b, d_m, and d_b were calculated for each member of the series, using the method of Mandel and Linnig (10) outlined in the *Appendix*. Based upon the values of L_m and the slope values for Arrhenius fits to the data, limits for lengths of error contours are given in Table V for the 90% confidence level. A visual inspection of these limits shows that each member of the series is overlapped to some extent by every other member of the series. If the individual data points for the present series fell upon a single isergonic line, $\beta = \overline{T}$, the result could only be attributed to experimental error.

The extreme overlap of error contours for this series is a function of: (*a*) the small number of data points, N, available for the Arrhenius fits; (*b*) the experimental error as reflected by S^2 (error variance); and (*c*) the narrow range of slope values (0.9 kcal/mole), which produces small differences between the individual members. The first two factors are included in the constant, K (Eq. A5), which determines the length of the error contour. If S^2 is maintained at the same level, simply increasing N for the Arrhenius fits would considerably reduce the lengths of the contours. Thus, lengths would be decreased by a factor of $[(F_{df} = 1)/(F_{df} = x)]^{1/2}$ for each additional increase in N above $N = 3$. For $N = 4$ and $N = 5$, the contour lengths decrease by factors of 2.35 and 3.01, respectively, at the 90% confidence level. For the present series, however, these decreases in contour lengths are not sufficient to eliminate their overlap because of the small differences between the slopes. Extremely precise data yielding very small values of S^2 would be required to remove the overlap.

Perpendicular Distances from β Line—As discussed under *Theoretical*, perpendicular distances represented by d and $w/2$ may be utilized to determine whether the individual members of a series belong to a given β line. These values for the present series are given in Table VI for variations in β and in significance levels. The perpendicular distances for the members of the series from the error line ($d_{301.3}$) is greater than their respective contour widths ($w/2$) measured perpendicularly to the contour boundary (Table VI). This comparison is good at both the 90 and 95% confidence levels. A similar comparison between d values measured from β = 280° and 325° and their respective $w/2$ values produces the same results.

Table IV—Correlations for Distances from the β-Line

β	Slope	Intercept	F	r
	Vertical Distances[a] ($\Delta\Delta H^{\neq}$ *versus* σ^-)			
0	−268	−839	0	−0.215
280	−1260	−153	118	−0.979
301.3	−1330	−102	175	−0.986
325	−1420	−43.6	211	−0.988
600	−2390	630.0	24	−0.910
	Horizontal Distances[a] ($\Delta\Delta S^{\neq}$ *versus* σ^-)			
301.3	4.42	0.337	175	0.986
	Perpendicular Distances (d *versus* σ^-)			
0	135	422	0	−0.215
280	2.26	0.276	118	0.979
301.3	2.23	0.170	175	0.986
325	2.19	0.0674	211	0.988
600	2.00	0.528	24	0.910

[a] The intercepts for vertical and horizontal distances are expressed in calories per mole and calories per mole-degree, respectively.

Table V—Limits for Lengths of Error Contours at 90% Confidence Level[a]

Substituent	Slope + L_m, kcal/mole	Slope − L_m, kcal/mole
4-CH_3	−4.64	−6.89
H (none)	−1.26	−11.6
4-F	−3.22	−8.44
4-Cl	−2.35	−10.1
3-CN	−3.23	−7.74
4-CN	−2.57	−8.60
4-NO_2	−4.55	−7.76

[a] Slope = $-(E_a/R)$, obtained from a linear least-squares fit of the data (at 20, 30, and 35°) to the Arrhenius equation. The L_m values were calculated from Eq. A1 (see *Appendix*). The F ratio = 49.5 for 2,1 degrees of freedom at the 0.90 level.

From the comparisons based on a β line of 301.3°, it is certain that the points do not fall along the error line or that the distribution of points on the isergonic profile is strongly affected by the correlation of error producing this line. The influence of a heavily weighted error slope would force the distribution of points along a slope of $\beta = \overline{T}$. This is not the case here since, from the previous $\Delta H^{\neq}$ *versus* $\Delta S^{\neq}$ correlation (Eq. 19), β = 134° and $r = -0.554$. Pure error would produce a perfect correlation between $\Delta H^{\neq}$ and $\Delta S^{\neq}$, with the resultant slope being equal to $\overline{T}$.

The Δd values given in Table VI provide a means of determining whether β = 301.3° is different from either β = 280° or β = 325°, the latter being close to the suggested limits for solvation effects in phenols (4). A comparison of either Δ^1 or Δ^2 (differences in d from either side of the error line) with the respective $w/2$ values for the 95% confidence level shows that the differences, Δd, fall within the error range of the perpendicular contour widths, $w/2$. The comparisons are approximately as good at the 90% confidence level. These results indicate that β = 301.3° cannot be distinguished from β = 280 or 325°.

The d values for each substituent at a given value of β follow a trend resembling its substituent effect (Table VI). Correlations between d and σ^- for values of β ranging between 0 and 600° are given in Table IV. The values of F and r obtained over the range of β for these correlations are identical to those values obtained for the correlation between $\Delta\Delta H^{\neq}$ and σ^- (Table IV). While a comparison between values of d and $w/2$ aids in the classification of β values, the absolute values of d identically parallel substituent effects ($\delta\Delta G^{\neq}$) and, therefore, provide no new information about substituent effects for the series.

CONCLUSIONS

The present analysis shows that the geometric distances of data points on an isergic profile, calculated either in the vertical ($\Delta\Delta H$), horizontal ($\Delta\Delta S$), or perpendicular (d) distances from the error slope, do not add any new information to a substituent effect analysis already based on ΔG. The vertical distances, $\Delta\Delta H$, are identical to the substituent effect $\delta\Delta G$; for series that obey the Hammett relationship (Eq. 2), these distances must correlate with σ^- regardless of the implication of a solvation mechanism. Thus, the use of the Hepler method (Eq. 8) to demonstrate a solvation effect in the scattered isergonic profile for series I would not be warranted. This conclusion does not deny the existence of a solvation mechanism for the series but does seriously question the Hepler approach for implicating the mechanism.

Statistically, the use of the joint confidence region (error contour) is the soundest way of analyzing the distribution of points on an isergonic profile. The method is simple and should routinely accompany such profiles appearing in the literature. The limits of the error contour lengths provide evidence of overlap between members of the series and, hence, dictate statistical uncertainty along the line. For series such as I, which do not show a wide variation in substituent effects, extremely precise rate data with N = 4 or 5 would be required to eliminate overlap between contours.

Leffler (6) suggested testing the randomness of the data along the isergonic line when overlap cannot be eliminated. Thus, points appearing

Table VI—Comparison between d and $w/2$ Values[a]

Substituent	d Values			Δd[b]		$w/2$ Values[c]	
	β = 280	β = 301.3	β = 325	Δ^1	Δ^2	CL = 0.90	CL = 0.95
4-CH_3	−0.290	−0.450	−0.604	0.154	0.160	0.078	0.157
H (none)	0	0	0	0	0	0.357	0.717
4-F	0.685	0.540	0.402	0.138	0.145	0.181	0.363
4-Cl	0.852	0.806	0.763	0.043	0.046	0.269	0.540
3-CN	2.140	1.908	1.686	0.222	0.232	0.156	0.314
4-CN	2.628	2.421	2.224	0.197	0.207	0.209	0.419
4-NO_2	2.849	2.787	2.727	0.060	0.062	0.111	0.223

[a] The d and $w/2$ values were calculated using Eq. 15 and the values of the coefficients A, B, and C described in the text. [b] Δ^1 and Δ^2 refer to the differences $(d_{301.3} - d_{325})$ and $(d_{280} - d_{301.3})$, respectively. [c] CL = confidence level.

along the line in an order that also follows their σ values could still represent a real effect. A comparison between the d and $w/2$ values provides a means of determining whether the points falling along an isergonic line differ statistically from those falling along another line such as the error line. For series such as I with scattered isergonic profiles, a result of $d > w/2$ simply proves that the scatter is not the result of experimental error.

A further comparison between differences in d, Δd, from various β lines and $w/2$ values provides a means of establishing a β range for the error contour. When using suggested β lines for solvation effects, this range for series I was approximately 45°. Since the average reaction temperature, $\overline{T}$, fell within this range, it must be concluded that solvation effects could not be distinguished statistically from error effects.

APPENDIX

Equations A1–A4 give the relationships for computing the four constants (L_m, L_b, d_m, and d_b) required in constructing the joint confidence region from three sets of parallel tangents (10):

$$L_m = K(N/\Delta)^{1/2} \quad \text{(Eq. A1)}$$

$$L_b = K(Q/\Delta)^{1/2} \quad \text{(Eq. A2)}$$

$$d_m = K[2W/Q(1 + W)]^{1/2} \quad \text{(Eq. A3)}$$

$$d_b = d_m(L_b/L_m) \quad \text{(Eq. A4)}$$

Definitions of the symbols appearing in these equations are further given by Eqs. A5–A8:

$$K = (2FS^2)^{1/2} \quad \text{(Eq. A5)}$$

$$\Delta = N\sum X^2 - (\sum X)^2 \quad \text{(Eq. A6)}$$

$$Q = \sum X^2 \quad \text{(Eq. A7)}$$

$$W = (N\sum X^2)^{1/2}/\sum X \quad \text{(Eq. A8)}$$

where F = F ratio for 2 and $N - 2$ degrees of freedom at the desired confidence level, S^2 = the error variance for the least-squares analysis, N = total number of data pairs, and X = X value for data pair.

The joint confidence region is constructed within a rectangle having the dimensions of $2L_m$ for the ordinate and $2L_b$ for the abscissa, as observed in Fig. 2. A diagonal line with a negative slope running from corner to corner through the rectangle forms the major axis of the simulated ellipse, thus producing a tilt slope of L_m/L_b. Plotted values $\pm d_m$ in the ordinate direction and $\pm d_b$ in the abscissa direction from the center of the rectangle form the guide points for drawing the two sloping major ellipse boundaries (Fig. 2).

REFERENCES

(1) J. E. Leffler and E. Grunwald, "Rates and Equilibrium of Organic Reactions," Wiley, New York, N.Y., 1963, chap. 9.

(2) R. L. Schowen, *J. Pharm. Sci.*, **56,** 931 (1967).

(3) R. Lumry and S. Rajender, *Biopolymers*, **9,** 1125 (1970).

(4) L. G. Hepler, *J. Am. Chem. Soc.*, **85,** 3089 (1963).

(5) L. G. Hepler, *Can. J. Chem.*, **49,** 2803 (1971).

(6) J. E. Leffler, *J. Org. Chem.*, **31,** 533 (1966).

(7) J. Zimmerman and S. J. Yau, *J. Pharm. Sci.*, **62,** 902 (1973).

(8) R. J. Washkuhn, V. I. Patel, and J. R. Robinson, *ibid.*, **60,** 736 (1971).

(9) N. R. Draper and H. Smith, "Applied Regression Analysis," Wiley, New York, N.Y., 1966, chap. 2.

(10) J. Mandel and F. J. Linnig, *Anal. Chem.*, **29,** 743 (1957).

(11) W. L. Hart, "Elements of Analytic Geometry," D. C. Heath, Boston, Mass., 1950, chap. 2.

(12) G. W. Snedecor and W. G. Cochran, "Statistical Methods," 6th ed., Iowa State University Press, Ames, Iowa, 1967, chap. 6.

(13) K. B. Wiberg, "Physical Organic Chemistry," Wiley, New York, N.Y., 1964, Part 2-8.

ACKNOWLEDGMENTS AND ADDRESSES

Received November 21, 1975, from the *Department of Pharmaceutics, School of Pharmacy, Temple University, Philadelphia, PA 19140.*

Accepted for publication March 1, 1976.

Effect of Lysine and Diethanolamine–Rutin on Blood Levels, Withdrawal Reaction, and Acute Toxicity of Ethanol in Mice

M. A. DORATO *, V. D. LYNCH, and C. O. WARD ˣ

Abstract □ The effects of L-lysine and diethanolamine–rutin on blood ethanol levels and withdrawal convulsions following a 4-day exposure to ethanol vapors were evaluated in 30–40-g male Swiss-Webster mice. The animals were exposed in groups, along with simultaneous controls, in a 34-liter dynamic Plexiglas exposure chamber. Blood was collected by retro-orbital puncture and analyzed enzymatically for ethanol. At the end of the inhalation period, convulsions on handling were scored over 24 hr. In addition, the effects of L-lysine and diethanolamine–rutin on blood ethanol levels and on acute ethanol toxicity following oral and intraperitoneal administration were evaluated. L-Lysine lowered blood ethanol levels following inhalation or oral administration of ethanol. Diethanolamine–rutin had no effect on blood ethanol levels. Both L-lysine and diethanolamine–rutin decreased the withdrawal reaction in dependent mice. L-Lysine increased the oral LD_{50} of ethanol, while diethanolamine–rutin decreased the intraperitoneal LD_{50} of ethanol.

Keyphrases □ Lysine—effect on blood levels, withdrawal reaction, and toxicity of ethanol, mice □ Diethanolamine–rutin—effect on blood levels, withdrawal reaction, and toxicity of ethanol, mice □ Ethanol—blood levels, withdrawal reaction, and toxicity, effect of lysine and diethanolamine–rutin, mice □ Blood levels—ethanol, effect of lysine and diethanolamine–rutin, mice □ Withdrawal reactions—ethanol, effect of lysine and diethanolamine–rutin, mice □ Toxicity—ethanol, effect of lysine and diethanolamine–rutin, mice □ α-Amino acids—lysine, effect on blood levels, withdrawal reaction, and toxicity of ethanol, mice □ Alcohols—ethanol, blood levels, withdrawal reaction, and toxicity, effect of lysine and diethanolamine–rutin, mice

Depletion of amino acids was reported to be characteristic in the development of delerium tremens following chronic alcohol ingestion (1). The prophylactic use of amino acids was accompanied by a high degree of success in forestalling delerium tremens in individuals whose low amino acid levels indicated their increased susceptibility (1). Specific amino acids, such as L-glutamine and L-lysine, also were effective in reducing or preventing ethanol toxicity (2–4).

BACKGROUND

Schiller (5) investigated the effects of amino acids (as a solution of protein hydrolysates[1]) on blood ethanol levels and the rate of disappearance of ethanol from the blood. The amino acids were administered intravenously and ethanol was administered orally to chronic alcoholics free of liver impairment. Ethanol-utilization curves showed that amino acids decreased blood ethanol levels and accelerated the rate of disappearance of ethanol from the blood (5). The specific amino acids in the mixture used by Schiller (5) could not be determined. Selected amino acids were effective in decreasing blood ethanol levels in dogs when administered orally simultaneously with ethanol (6). Certain amino acids possibly impede the absorption of orally administered ethanol by formation of a stable complex (7).

A significant reduction in the depressant action of ethanol (30% v/v) was reported following a 30-min pretreatment with L-lysine (2.5 g/kg ip or po) (3). The oral administration of L-lysine and ethanol resulted in the complete elimination of hypnotic effects. Administration of L-lysine and ethanol intraperitoneally resulted in a 65% reduction in ethanol sleeping time. Also, an increase in the LD_{50} of ethanol in rats was noted following treatment with L-lysine (3).

The interaction of ethanol or acetaldehyde, its major metabolite, with various biogenic amines is a possible cause of ethanol dependence following chronic administration (8–10). The presence of acetaldehyde may lead to localized increases in the concentrations of aromatic aldehydes in tissues rich in biogenic amines (9). Furthermore, these highly reactive aldehydes condense with their parent amines to yield a morphine-like benzyltetrahydroisoquinoline alkaloid (9). This effect was demonstrated *in vitro* using rat liver homogenates (8). Such condensation products were reported for dopamine (9), epinephrine, and norepinephrine (levarterenol) (10).

The coadministration of an excess reactive α-amino acid and ethanol might lead to a decrease in ethanol toxicity due to the combination of acetaldehyde with the amino acid (3).

Rutin-enhanced diethanolamine mixtures protected rats from the motor effects of ethanol, without affecting blood ethanol levels, *via* a weak agonist–antagonist action (11–13).

This study was undertaken to determine the extent to which L-lysine, a reactive α-amino acid, protects against ethanol toxicity and alters the ethanol-withdrawal reaction in dependent mice. In addition, because of the possible agonist–antagonist relationship of diethanolamine to ethanol, the effects of diethanolamine–rutin on the ethanol-withdrawal reaction and acute ethanol toxicity in mice were evaluated.

L-Lysine was chosen because of previous studies (3, 4) and because: (*a*) it has one of the fastest rates of reaction with acetaldehyde (14); (*b*) L-lysine levels of 0.57, 0.98, and 1.53 mg % were reported for patients with delerium tremens, recovered patients, and normal subjects, respectively (1); (*c*) L-lysine is the only essential α-amino acid having sufficient amino groups in nonzwitterionic form to interact with acetaldehyde (15); and (*d*) treatment with L-lysine significantly increased the LD_{50} of acetaldehyde[2].

EXPERIMENTAL

Production of Ethanol Dependence—Male Swiss-Webster mice[3], 30–40 g, were divided into four treatment groups of 10 mice each. These treatment groups were housed individually in 34-liter Plexiglas exposure chambers, along with simultaneous pH controls, for 4 days. Air was introduced into the chamber at the rate of 8 liters/min. The total air flow was split between two 1-liter erlenmeyer flasks (16); one flask contained ethanol (95%, USP) and the other remained empty. The air flow was joined again just before entering the chamber.

The relationship of air flow to chamber concentration is shown in Table I. A flowmeter in each line, between the air compressor pump and the flasks, allowed for control of the chamber ethanol levels. A chamber ethanol concentration of 11–15 mg/liter was appropriate in establishing ethanol dependence in mice over 4 days. The priming dose of ethanol (17) was not necessary if the chamber was allowed to reach equilibrium before introducing the mice (18). Therefore, the air flow through the chamber was begun approximately 20 hr before introducing the mice. During the exposure period, the chamber temperature varied from 24 to 27° and the relative humidity varied from 60 to 70%.

The test animals were removed from the chamber for a short period each day for administration of: Solution A, L-lysine[4] (20% w/v) prepared in a solution of protein hydrolysates[1], 1 g/kg po, pH 5.7; Solution B, L-lysine[4] (20% w/v) as an aqueous solution, 1 g/kg po twice daily,

[1] Aminosol, Abbott Laboratories, Chicago, Ill.

[2] Unpublished data.

[3] Camm Research Institute, Wayne, N.J.

[4] As the monohydrochloride salt, Sigma Chemical Co., St. Louis, Mo.

Table I—Relationship of Air Flow Split between Ethanol and Air Flasks to Chamber Ethanol Concentration

Air Flow through Ethanol Flask, liters/min	Air Flow through Air Flask, liters/min	Chamber Concentration, mg/liter
0.75	7.25	11
0.88	7.12	13
1.10	6.90	15
1.30	6.70	18
1.50	6.50	22

pH 5.7; protein hydrolysate[1], 9 ml/kg po, pH 5.7; or diethanolamine–rutin[5], 4.5 ml/kg po, pH 7.4.

In addition, each animal received pyrazole (34 mg/kg ip) for the maintenance of stable blood ethanol levels (19, 20). On Day 5, the animals were removed from the ethanol environment, and convulsions on handling were evaluated according to the method of Goldstein and Pal (19) over 24 hr.

pH Controls for Amino Acid and Diethanolamine–Rutin Treatments—A pH 5.7 phosphate buffer solution was administered orally to control groups exposed to ethanol vapors simultaneously with amino acid treatment groups. The control buffer was administered in volumes equivalent to the various amino acid treatments. Another pH 7.4 phosphate buffer was administered to the control group exposed simultaneously with the diethanolamine–rutin treatment group in a volume equivalent to that of the treatment. Each animal in the control groups received pyrazole, 34 mg/kg ip. The control groups were removed from the ethanol environment, and their withdrawal scores were evaluated simultaneously with the treatment groups (19).

Environmental Control—Ten animals were introduced into the exposure chamber and kept there for 4 days. The air flow was maintained at 8 liters/min. Ethanol, however, was not introduced into the chamber. The animals were removed for short periods each day for intubation. On Day 5, the animals were removed from the chamber, and convulsions on handling were evaluated (19).

Evaluation of Blood Ethanol Levels Resulting from Inhalation of Ethanol Vapors—Blood ethanol levels were measured enzymatically. Each day during the exposure period, three animals from the treated and control groups were randomly selected for blood sampling. The blood samples were obtained by retro-orbital puncture (21–23) before the administration of any treatment or control.

A volume of 0.25 ml of blood was collected from each animal, deproteinated, and added to the enzymatic reaction mixture[6] (24). After 30 min at room temperature, the fluorescence[7] of the mixture was measured at an absorption maximum of 340 nm and an emission maximum of 458 nm. This method is based on the natural fluorescence of the reduced diphosphopyridine nucleotide formed, since ethanol is metabolized by alcohol dehydrogenase to acetaldehyde (24). The reaction is pushed toward completion by the addition of semicarbazide (25). On Day 5, five animals from each group were chosen randomly for the blood ethanol analysis.

Determination of Chamber Ethanol Concentration—The chamber ethanol concentration also was determined enzymatically (24). Each day, a 1-ml sample of chamber air was withdrawn using a gastight syringe[8]. The sample was then injected into the headspace of a vial containing 3.5 ml of the enzymatic reaction mixture[6] (25). After 30 min at room temperature, the fluorescence[7] of the reaction mixture was measured (24). The sampling port was positioned to facilitate sampling at the respiratory level of the test animals (26). The chamber ethanol concentrations resulting from various rates of flow are shown in Table I.

Evaluation of Ethanol Intoxication—Before each exposure period, the animals were trained to maintain their balance on a rotating roller (10 rpm) for 1 min (27). This simple test was used each morning during the exposure period, before any treatment was administered, as an indication of the level of intoxication, tolerance, and loss of muscle control due to ethanol inhalation.

Effect of Amino Acids and Diethanolamine–Rutin on Acute Blood Ethanol Levels—Male Swiss-Webster mice, 30–40 g, were divided into 12 treatment groups of six mice each, with appropriate pH controls. The treatments were administered, as previously indicated, for 4 days. One hour after the last treatment on Day 4, ethanol was administered, 3 g/kg ip or 6 g/kg po. One treatment group received 6 g/kg po simultaneously with the last treatment. Blood was sampled 0.5 or 1 hr after the intraperitoneal or oral administration of ethanol, respectively. Blood was obtained by retro-orbital puncture (21–23) and analyzed enzymatically for ethanol (24, 25).

[5] Prepared according to Blum *et al.* (13).
[6] Sigma Chemical Co., St. Louis, Mo.
[7] Spectrofluorometer model 430, G. K. Turner Associates, Palo Alto, Calif.
[8] Precision Sampling Corp., Baton Rouge, La.

Table II—Mean Time on Rotating Roller during Ethanol Inhalation

Treatment	Mean Time, min ± *SD*	*p* Level[a] (Relative to Drug Control)	*p* Level[a] (Relative to Environmental Control)
Solution A	0.75 ± 0.17	NS	<0.05
Solution B	0.64 ± 0.22	NS	<0.01
Control	0.49 ± 0.29	—	<0.01
Protein hydrolysates	0.83 ± 0.13	NS	<0.05
Control	0.68 ± 0.21	—	<0.02
Diethanolamine–rutin	0.85 ± 0.14	NS	<0.05
Control	0.64 ± 0.24	—	<0.01
Environmental control	1.00 ± 0.00	—	—

[a] For significance, $p < 0.05$.

Effect of Amino Acids and Diethanolamine–Rutin on 24- and 72-hr LD_{50} of Ethanol—Male Swiss-Webster mice, 30–40 g, were divided into groups of 10 and treated as previously described for 4 days. One hour after the last treatment on Day 4, ethanol was administered (40% w/v) in graded doses of 1–5 g/kg ip and 5–11 g/kg po. The LD_{50} was calculated from the number dead at 24 and 72 hr by the log-probit method of Miller and Tainter (28).

Effect of Various Treatments and Controls on Weights of Mice Exposed to Ethanol Vapor—The subjects in the treatment and control groups were weighed each day. The mean weight of each group on Day 1 was taken as the base for comparison. Weight loss during the exposure period was recorded as percent of the starting weight.

RESULTS

No difference was found between treatment and control groups in their ability to maintain balance on a rotating roller (Table II). However, each treatment group maintained their balance for a longer time than the corresponding control.

None of the treatments used decreased blood ethanol levels after intraperitoneal administration (Table III). In those groups receiving ethanol orally, only the Solution A and Solution B treatments decreased the blood ethanol levels. This result was true for pretreatment as well as simultaneous administration (Table III).

Among the groups exposed to the inhalation of ethanol vapor, only the Solution A group showed a decrease in the daily mean blood ethanol levels (Table IV). However, both the Solution A and Solution B groups had blood ethanol levels below those of controls on Days 4 and 5 (Table IV).

The evaluation of convulsions on handling (19) during the withdrawal period showed that Solution A and diethanolamine–rutin groups had reduced mean withdrawal scores (Table V). The peak withdrawal score, the mean of the three highest consecutive scores, was reduced in the Solution A, Solution B, and diethanolamine–rutin groups (Table V). All treatment and control groups had peak withdrawal scores greater than the environmental control (Table V, $p < 0.001$). Peak withdrawal development, the mean of all scores up to the highest mean score for each group, was reduced in only the Solution A and diethanolamine–rutin groups (Table V).

The 24-hr oral LD_{50} of ethanol (40% w/v) was increased by Solutions A and B and protein hydrolysate (Table VI). The 72-hr oral LD_{50} of ethanol was increased only by Solutions A and B (Table VI). None of the various amino acid treatments affected either the 24- or 72-hr intraperitoneal LD_{50} of ethanol (Table VII).

The diethanolamine–rutin treatment did not affect the 24- or 72-hr oral LD_{50} of ethanol, nor did it affect the 24-hr intraperitoneal LD_{50} (Tables VI and VII). However, diethanolamine–rutin did decrease the 72-hr intraperitoneal LD_{50} of ethanol (Table VII).

Since weight loss can indicate toxicity, the mean percent weight

Table III—Effect of Amino Acids and Diethanolamine–Rutin on Blood Ethanol Levels[a]

Treatment	Blood Ethanol Levels, mg/ml ± *SD*					
	Pretreatment				Simultaneous	
	Intraperitoneal[b]	*p* Level[a]	Oral[c]	*p* Level[a]	Oral[d]	*p* Level[a]
Solution A	4.16 ± 0.57	>0.05	6.35 ± 1.03	<0.05	3.60 ± 0.58	<0.001
Control	4.06 ± 0.43	—	7.39 ± 0.42	—	6.98 ± 0.29	—
Solution B	4.67 ± 0.55	>0.05	6.93 ± 0.66	<0.02	5.20 ± 0.82	<0.02
Control	4.82 ± 0.48	—	7.63 ± 0.26	—	7.35 ± 1.56	—
Protein hydrolysate	3.70 ± 0.51	>0.05	5.25 ± 0.59	>0.05	5.98 ± 0.90	>0.05
Control	3.98 ± 0.48	—	5.82 ± 0.41	—	5.86 ± 0.38	—
Diethanolamine–rutin	4.10 ± 0.55	>0.05	6.29 ± 0.75	>0.05	7.72 ± 1.33	>0.05
Control	4.17 ± 0.41	—	5.85 ± 0.43	—	7.50 ± 0.93	—

[a] For significance, $p < 0.05$. [b] Ethanol, 3 g/kg ip, 1 hr following pretreatment; blood sampled 0.5 hr after ethanol. [c] Ethanol, 6 g/kg po, 1 hr following pretreatment; blood sampled 1 hr after ethanol. [d] Ethanol, 6 g/kg po, simultaneously with treatment; blood sampled in 1 hr.

Table IV—Effect of Amino Acids and Diethanolamine–Rutin on Blood Ethanol Levels Produced by Inhalation of Ethanol Vapors for 4 Days[a]

Treatment	Day 2, mg/ml	Day 3, mg/ml	Day 4, mg/ml	*p* Level[b]	Day 5, mg/ml	*p* Level[b]	5-Day Mean, mg/ml	*p* Level[a]
Solution A	1.70 ± 0.40	1.28 ± 0.52	1.40 ± 0.12	<0.05	1.46 ± 0.68	<0.02	1.46 ± 0.18	<0.05
Solution B	1.90 ± 0.55	1.33 ± 0.25	1.27 ± 0.12	<0.05	1.85 ± 0.48	<0.05	1.58 ± 0.33	>0.05
Control	2.00 ± 0.11	1.76 ± 0.57	2.40 ± 0.16	—	2.95 ± 1.03	—	2.28 ± 0.52	—
Protein hydrolysate	1.98 ± 0.35	1.42 ± 0.17	2.18 ± 0.37	>0.05	2.85 ± 0.67	>0.05	2.11 ± 0.51	>0.05
Control	2.04 ± 0.19	1.75 ± 0.12	2.55 ± 0.42	—	3.08 ± 0.26	—	2.35 ± 0.51	—
Diethanolamine–rutin	1.66 ± 0.23	1.87 ± 0.52	2.18 ± 0.27	>0.05	2.68 ± 0.38	>0.05	2.10 ± 0.37	>0.05
Control	1.66 ± 0.21	1.75 ± 0.31	2.14 ± 0.22	—	2.87 ± 0.39	—	2.11 ± 0.45	—

[a] Chamber concentration was 11–15 mg/liter. [b] For significance, $p < 0.05$.

loss of each treatment group was compared with the appropriate control (Table VIII). Only the diethanolamine–rutin group showed a lower mean percent weight loss. The weight loss in the diethanolamine–rutin group did not differ significantly from that resulting from pyrazole treatment alone. As expected, all groups showed weight loss when compared to the environmental control.

When the Solution A and Solution B treatments were compared, the Solution A group demonstrated a lower peak withdrawal score (0.95 ± 0.09 and 1.32 ± 0.12, respectively; $p < 0.02$). Also, simultaneous administration of ethanol (40% w/v) and amino acids orally resulted in lower blood ethanol levels for the Solution A group (3.60 ± 0.58 and 5.20 ± 0.82, respectively; $p < 0.01$). No difference in blood ethanol levels established by inhalation, nor in any other parameters except those mentioned, was noted between the Solution A and Solution B groups (Table IV).

DISCUSSION

Physical dependence on ethanol is rapidly established in rodents by inhalation techniques (16, 17, 19). To maintain adequate and stable blood ethanol levels, pyrazole, an inhibitor of alcohol dehydrogenase (20, 29), was necessary (16, 17, 19). A dose of 34 mg/kg ip (0.5 mmole/kg), rather than 68 mg/kg ip (1 mmole/kg) as previously reported (17, 19), was adequate (30). A 96-hr exposure at an ethanol concentration of 11–15 mg/liter produced a satisfactory, postalcohol, hyperexcitability reaction in mice. Beginning the air flow approximately 20 hr before introducing the animals to the chamber allowed for the elimination of a priming dose of ethanol (18).

The rotating roller test was used to evaluate the protection afforded by the various treatments against the muscular incoordination produced by ethanol (27) and to serve as an index of tolerance production. Since tolerance has been described as a homeostatic adjustment (31), a decrease followed by a gradual increase in the ability to stay on the rotating roller (10 rpm) would be expected. In fact, a rapid decline in balancing ability occurred during the first 2 days of ethanol inhalation. This decline was followed by a more gradual increase in balancing ability. Even though the mean time on the rotating roller was not significantly longer in the treated than control groups, the treated groups were consistent in maintaining balance for longer periods. This increase indicates a decrease in the intensity of ethanol effects in these groups.

Various amino acids hasten the disappearance of ethanol from the blood (5), resulting in lower blood ethanol levels. The Solution A and Solution B groups showed a decrease in blood ethanol levels following oral ethanol administration. This effect was seen with both the pretreatment with amino acids and the simultaneous administration of amino acids and ethanol. The protein hydrolysate treatment had no effect on blood ethanol levels. This result indicates the necessity of excess L-lysine (3). It was not expected that the diethanolamine–rutin treatment would affect blood ethanol levels by any route, or sequence, of administration[2], and no effect was found.

When ethanol was administered *via* inhalation, the Solution A group showed lower mean blood ethanol levels. The other treatments did not affect the mean blood ethanol levels. However, both the Solution A and the Solution B treatments lowered blood ethanol levels on Days 4 and 5. The rate of ethanol disappearance from the blood was increased by L-lysine[2] and by amino acids in general (5). An in-

Table V—Withdrawal Scores after 4-Day Exposure to Ethanol Vapors

Treatment	Mean Withdrawal Score ± *SD*	*p* Level[a]	Peak Withdrawal Score ± *SD*	*p* Level[a]	Peak Withdrawal Development ± *SD*	*p* Level[a]
Solution A	0.73 ± 0.27	<0.005	0.95 ± 0.09	<0.001	0.72 ± 0.31	<0.02
Solution B	0.94 ± 0.36	>0.05	1.32 ± 0.12	<0.001	0.98 ± 0.44	>0.05
Control	1.38 ± 0.58	—	1.94 ± 0.05	—	1.39 ± 0.68	—
Protein hydrolysate	0.78 ± 0.31	>0.05	1.08 ± 0.08	>0.05	0.84 ± 0.43	>0.05
Control	0.99 ± 0.36	—	1.22 ± 0.03	—	0.99 ± 0.42	—
Diethanolamine–rutin	0.73 ± 0.25	<0.05	1.00 ± 0.00	<0.001	0.79 ± 0.28	<0.05
Control	1.10 ± 0.39	—	1.48 ± 0.03	—	1.17 ± 0.43	—

[a] For significance, $p < 0.05$.

Table VI—Effect of Amino Acids and Diethanolamine–Rutin on the Acute Oral Toxicity of Ethanol

Treatment	24-hr LD_{50}, mg/kg ± SD	Confidence Limits (95%)	p Level[a]	72-hr LD_{50}, mg/kg ± SD	Confidence Limits (95%)	p Level[a]
Solution A	9500 ± 628.98	9026.17–9973.83	<0.05	8986 ± 592.61	8539.57–9432.43	<0.05
Solution B	9126 ± 215.67	8963.53–9288.47	<0.05	8746 ± 204.76	8591.75–8900.25	<0.05
Protein hydrolysate	9221 ± 448.25	8883.32–9558.68	<0.05	8127 ± 414.26	7814.92–8439.08	>0.05
Diethanolamine–rutin	7757 ± 864.57	7105.69–8408.31	>0.05	7747 ± 720.68	7214.09–8299.91	>0.05
Control	7484 ± 472.29	7128.21–7839.79	—	7484 ± 472.29	7128.21–7839.79	—

[a] For significance, $p < 0.05$.

Table VII—Effect of Amino Acids and Diethanolamine–Rutin on the Acute Intraperitoneal Toxicity of Ethanol

Treatment	24-hr LD_{50}, mg/kg ± SD	Confidence Limits (95%)	p Level[a]	72-hr LD_{50}, mg/kg ± SD	Confidence Limits (95%)	p Level[a]
Solution A	3742 ± 437.18	3412.66–4071.30	>0.05	3241 ± 358.92	2970.61–3511.39	>0.05
Solution B	3295 ± 309.27	3062.02–3527.98	>0.05	3000 ± 317.97	2760.47–3239.54	>0.05
Protein hydrolysate	3323 ± 532.18	2840.09–3641.91	>0.05	3000 ± 414.57	2687.69–3312.31	>0.05
Diethanolamine–rutin	3241 ± 532.18	2840.09–3641.91	>0.05	1732 ± 484.86	1366.74–2097.26	<0.05
Control	3241 ± 510.87	2856.14–3625.86	—	2876 ± 540.28	2695.91–3056.69	—

[a] For significance, $p < 0.05$.

crease in the rate of ethanol disappearance from the blood, developing over time, could account for the lower blood ethanol levels on the last 2 days of inhalation. This finding could also explain the lack of effect on blood ethanol levels following acute intraperitoneal administration of ethanol. The diethanolamine–rutin and protein hydrolysate treatments did not affect blood ethanol levels.

Differences in blood ethanol levels did not exist between Solutions A and B following ethanol inhalation or intraperitoneal or oral administration following a 1-hr pretreatment with the amino acid solutions. The lower blood ethanol level in the Solution A group following simultaneous oral administration with ethanol could be attributed to the additional reactive α-amino acids in the treatment.

Both Solutions A and B were expected to increase significantly the 24- and 72-hr oral LD_{50} of ethanol but not the 24- and 72-hr intraperitoneal LD_{50}. This was the case, but there was no difference between the two groups.

The diethanolamine–rutin treatment did not affect the 24- or 72-hr oral LD_{50} nor the 24-hr intraperitoneal LD_{50} of ethanol. However, the 72-hr intraperitoneal LD_{50} of ethanol was decreased by diethanolamine–rutin. Diethanolamine–rutin is a weak ethanol agonist, itself a central nervous system (CNS) depressant[2].

The protein hydrolysate treatment increased the 24-hr oral LD_{50} of ethanol. It did not, however, protect beyond this point. This result could be attributed to insufficient reactive α-amino acids, particularly L-lysine.

The acute and chronic effects of ethanol have been attributed to the augmentation, by ethanol and acetaldehyde, of tetrahydroisoquinoline alkaloid formation from biogenic amines (8, 9). It has been proposed that an increase in the steady-state level of one or more biogenic aldehydes, due to competitive inhibition of NAD-linked aldehyde dehydrogenase by acetaldehyde (9), could be responsible for the CNS effects related to ethanol (32).

L-Lysine decreases blood ethanol levels and accelerates its rate of disappearance from the blood. It also increases the LD_{50} of acetaldehyde (13) and forms a complex with acetaldehyde (3, 11). The formation of this complex could block, to some degree, the ability of acetaldehyde to inhibit NAD-linked aldehyde dehydrogenase, thereby decreasing the formation of tetrahydroisoquinoline derivatives and the pharmacological effects of ethanol. L-Lysine decreased ethanol sleeping time in rats (3). A decrease in alkaloid formation *per se* or in rate of formation could account for the decrease in the severity of the postalcohol hyperexcitability seen in dependent mice.

The Solution A treatment resulted in a decrease in mean withdrawal scores, peak withdrawal scores, and peak withdrawal development. The Solution B treatment resulted in a significant decrease in only the peak withdrawal, while treatment with protein hydrolysate had no effect. The Solution A treatment resulted in a lower peak withdrawal than did Solution B. This effect could be due to the additional reactive α-amino acids in the Solution A treatment.

Treatment with diethanolamine–rutin resulted in a reduction in mean withdrawal, peak withdrawal, and peak withdrawal development scores. However, no effect was seen on blood ethanol levels. Preliminary studies indicated a decreased rate of ethanol elimination following administration of diethanolamine–rutin[2].

Diethanolamine–rutin was proposed as a weak agonist–antagonist to ethanol[2]. However, the characteristic signs of ethanol withdrawal did not appear immediately after the administration of diethanolamine–rutin to dependent mice. Therefore, diethanolamine–rutin probably reduces the postalcohol hyperexcitability in mice by some other mechanism.

Chronic ethanol administration produced an increase in brain γ-aminobutyrate (33). Its inhibitory effects were implicated in the regulation of the depressant actions of ethanol (34, 35). A significant reduction in brain γ-aminobutyrate was reported to coincide with the maximum intensity of ethanol withdrawal scores in mice (30). The reduction in brain γ-aminobutyrate renders the subject more susceptible to postalcohol hyperexcitability (30). Since diethanolamine–rutin is also a CNS depressant[2], it too may increase brain γ-

Table VIII—Weight Loss of Animals Exposed to Ethanol Vapors for 4 Days

Treatment	Mean Weight Loss ± SD	p Level[a] (Relative to Drug Control)	p Level[a] (Relative to Pyrazole Control)	p Level[a] (Relative to Environmental Control)
Solution A	8.26 ± 1.74	>0.05	<0.01	<0.001
Solution B	10.59 ± 2.93	>0.05	<0.01	<0.001
Control	8.74 ± 2.49	—	<0.01	<0.001
Protein hydrolysate	5.68 ± 1.69	>0.05	<0.05	<0.001
Control	5.68 ± 2.85	—	>0.05	<0.01
Diethanolamine–rutin	5.37 ± 1.58	<0.05	>0.05	<0.001
Control	9.48 ± 2.76	—	<0.05	<0.001
Pyrazole control	3.26 ± 1.11	—	—	<0.001
Environmental control	0.00 ± 0.00	—	—	—

[a] For significance, $p < 0.05$.

aminobutyrate. In addition, its effect in slowing ethanol elimination from the blood[2] may cause a more gradual decline in brain γ-aminobutyrate during ethanol withdrawal, decreasing the intensity of the characteristic hyperexcitability.

Treatment with diethanolamine–rutin produced a peak withdrawal response at 5 hr, which remained constant for 3 hr. None of the other treatment groups showed a similar plateau in withdrawal responses. Possibly, brain γ-aminobutyrate was prevented from falling to levels low enough for maximal hyperexcitability to occur. Studies are in progress to determine this possibility.

SUMMARY AND CONCLUSIONS

The reactive α-amino acid, L-lysine, lowered blood ethanol levels when ethanol was administered orally or by inhalation. This decrease in blood ethanol could be the result of poor absorption or increased elimination. The withdrawal reaction, following ethanol inhalation in mice, was also reduced by L-lysine. L-Lysine possibly interferes with an acetaldehyde-mediated alkaloid formation from biogenic amines, thereby decreasing the degree of dependence on ethanol. The presence of additional reactive α-amino acids somewhat enhanced the effects of L-lysine.

Diethanolamine–rutin also reduced the ethanol withdrawal reaction in mice but had no effect on blood ethanol levels. It may prevent the fall in brain γ-aminobutyrate reported to accompany ethanol withdrawal convulsions by slowing the rate of ethanol elimination from the blood.

A relationship may exist between the formation of tetrahydroisoquinoline alkaloids and the increase in brain γ-aminobutyrate seen in ethanol-dependent mice. The increase in brain γ-aminobutyrate during ethanol administration and its subsequent decrease during withdrawal may cause postalcohol hyperexcitability in mice (30). The amino acid treatments seem to interfere with the acetaldehyde-dependent formation of these alkaloids. Diethanolamine–rutin seems to exert its effect by decreasing the rate of ethanol elimination, which then might prevent a significant decrease in brain γ-aminobutyrate during ethanol withdrawal.

REFERENCES

(1) A. Prigot, E. E. Corbin, A. Maynard, T. P. Ruden, and I. Hjelt-Harvey, *Q. J. Stud. Alcohol*, **23**, 390(1962).

(2) L. L. Rogers and R. B. Pelton, *ibid.*, **18**, 581(1957).

(3) C. O. Ward, C. A. LauCam, A. Tang, R. Breglia, and C. I. Jarowski, *Toxicol. Appl. Pharmacol.*, **22**, 422(1972).

(4) R. Breglia, C. O. Ward, and C. I. Jarowski, *J. Pharm. Sci.*, **62**, 45(1973).

(5) J. Schiller, *Arch. Neurol.*, **1**, 127(1959).

(6) E. Widmark, *Biochem. Z.*, **265**, 237(1938).

(7) *Ibid.*, **267**, 135(1938).

(8) V. E. Davis, M. J. Walsh, and Y. Yamanaka, *J. Pharmacol. Exp. Ther.*, **174**, 401(1970).

(9) V. E. Davis and M. J. Walsh, *Science*, **167**, 1005(1970).

(10) G. Cohen and M. Collins, *ibid.*, **167**, 1749(1970).

(11) V. J. Hoeflmayr and R. Fried, *Med. Ernaeh.*, **8**, 217(1967).

(12) I. Geller, N. D. Campbell, and K. Blum, *Res. Commun. Chem. Pathol. Pharmacol.*, **1**, 383(1970).

(13) K. Blum, J. E. Wallace, R. S. Rybach, and I. Geller, *Eur. J. Pharmacol.*, **19**, 218(1972).

(14) L. Rubert and F. S. Penaranda, *J. Polym. Sci.*, **12**, 337(1954).

(15) J. P. Greenstein and M. Winitz, "Chemistry of Amino Acids," Wiley, New York, N.Y., 1961, pp. 448, 449.

(16) S. W. French and J. R. Morris, *Res. Commun. Chem. Pathol. Pharmacol.*, **1**, 221(1972).

(17) B. Goldstein, *J. Pharmacol. Exp. Ther.*, **180**, 203(1972).

(18) S. D. Silver, *J. Lab. Clin. Med.*, **31**, 1153(1946).

(19) D. B. Goldstein and N. Pal, *Science*, **172**, 288(1972).

(20) D. B. Goldstein and N. Pal, *J. Pharmacol. Exp. Ther.*, **178**, 199(1971).

(21) D. A. Sorg and B. Buckner, *Proc. Soc. Exp. Biol. Med.*, **115**, 1131(1964).

(22) S. H. Stone, *Science*, **119**, 100(1954).

(23) V. Riley, *Proc. Soc. Exp. Biol. Med.*, **104**, 751(1960).

(24) W. A. Miller, Technical Report 8978, G. K. Turner Assoc., Palo Alto, Calif.

(25) Sigma Technical Bulletin No. 331-UV, Sigma Chemical Co., St. Louis, Mo., 1972.

(26) H. E. Swann, *Mod. Packag.*, **6**, 58(1972).

(27) N. W. Dunham and T. S. Miya, *J. Am. Pharm. Assoc., Sci. Ed.*, **46**, 208(1957).

(28) L. C. Miller and M. L. Tainter, *Proc. Soc. Exp. Biol. Med.*, **57**, 261(1944).

(29) L. Goldberg and U. Rydberg, *Biochem. Pharmacol.*, **18**, 1749(1969).

(30) G. J. Patel and H. Lal, *J. Pharmacol. Exp. Ther.*, **180**, 625(1973).

(31) A. Goldstein and D. B. Goldstein, *Assoc. Res. Nerv. Ment. Dis. Res. Publ.*, **16**, 265(1968).

(32) R. A. Dietrich and V. G. Erwin, *Fed. Proc.*, **34**, 1962(1975).

(33) I. Sutton and M. A. Simmons, *Biochem. Pharmacol.*, **22**, 1685(1973).

(34) R. J. Baldessarini and M. Karubuth, *Ann. Rev. Phys.*, **35**, 273(1973).

(35) H. M. Hakkinen and E. Kulonen, *J. Neurochem.*, **10**, 489(1963).

ACKNOWLEDGMENTS AND ADDRESSES

Received December 9, 1975, from the *Department of Pharmaceutical Sciences, College of Pharmacy and Allied Health Professions, St. John's University, Jamaica, NY 11439*

Accepted for publication February 26, 1976.

Presented at the APhA Academy of Pharmaceutical Sciences, Atlanta meeting, November 1975.

* Huntingdon Research Center, New City, NY 10956

[x] To whom inquiries should be directed. Present address: Huntingdon Research Center, New City, NY 10956

Simultaneous High-Pressure Liquid Chromatographic Determination of Niacin and Niacinamide in Multivitamin Preparations: Reversed-Phase, Ion-Pairing Approach

S. PAUL SOOD *, D. P. WITTMER ‡, S. A. ISMAIEL §, and W. G. HANEY ×

Abstract □ A high-pressure liquid chromatographic procedure for the simultaneous determination of niacin and niacinamide in multivitamin preparations was developed and evaluated. Reversed-phase liquid chromatography with dioctyl sodium sulfosuccinate in the mobile phase is utilized for the analysis. The accuracy and precision of the procedure were compared with those of the currently official procedure.

Keyphrases □ Niacin and niacinamide—simultaneous analysis, reversed-phase high-pressure liquid chromatography, multivitamin preparations □ High-pressure liquid chromatography, reversed phase—simultaneous analysis, niacin and niacinamide in multivitamin preparations □ Vitamins—niacin and niacinamide, simultaneous analysis, reversed-phase high-pressure liquid chromatography, multivitamin preparations

Currently, procedures for the determination of niacin and niacinamide in multivitamin preparations suffer from several disadvantages. An involved sample workup often is required (1, 2). Niacin is either ignored entirely in the determination (3) or included in the results as "niacinamide" due to hydrolysis of the sample prior to determination (4, 5). In addition, reagents required for analysis are often caustic and unstable.

These objections have been considerably reduced in procedures (6) where a solution of the vitamin product is chromatographed, the appropriate migration zones are eluted, and the eluate is determined spectrophotometrically. However, these procedures are somewhat tedious. Therefore, a related method for the simultaneous analysis of niacin and niacinamide, utilizing reversed-phase high-pressure liquid chromatography (HPLC), was developed and evaluated.

EXPERIMENTAL

Apparatus—A liquid chromatograph[1] equipped with a high-pressure pump and an injector was used, and effluents were monitored with the 254-nm detector. Peak areas were determined using an electronic digital integrator[2]. The column[3], 30 cm × 4 mm i.d. stainless steel, was packed with totally porous silica particles of 10-μm average size, chemically bonded to a monomolecular layer of octadecyltrichlorosilane. The flow rate was 2.5 ml/min.

Materials and Reagents—Niacin and niacinamide were obtained as USP reference standards. Dioctyl sodium sulfosuccinate, camphorsulfonic acid, and sodium hexanesulfonate were obtained from commercial suppliers and used as received. Commercial multivitamin preparations were obtained from local pharmacies.

Preparation of Mobile Phase—Solvent systems were prepared by dissolving the salt (2.0×10^{-3} *M*) in distilled water (300 ml), adjusting the pH to 2.5 with 10% formic acid solution, and combining the resulting solution with methanol (300 ml). The mobile phase was deaerated prior to use by the brief application of a vacuum.

Standard Solutions—Solutions of niacinamide in pH 6.0 phosphate buffer were prepared to contain 1.0, 2.0, 3.0, 4.0, 4.5, 5.0, 5.5, and 6.0 mg/100 ml. Niacin standard solutions were prepared to contain 0.5, 1.0, 1.5, 2.0, and 2.5 mg/100 ml.

Sample Solutions—The homogenized vitamin preparation (one dosage unit) was placed in a volumetric flask (100 ml) with pH 6.0 phosphate buffer (50.0 ml) and shaken for 5 min. Buffer was added to volume, the flask was shaken, and the particulate matter was allowed to settle. The sample was filtered when required, and the first 10–15 ml of filtrate was rejected. An aliquot of the remaining filtered solution was then diluted to a concentration of 2.5 mg/100 ml based on the label claim of niacinamide or 0.75 mg/100 ml based on the label claim of niacin.

Calibration Curves and Sample Analysis—Calibration curves were prepared by mixing niacinamide standard solutions (2.0 ml) with niacin solutions (2.0 ml) and injecting an aliquot (20 μl) of the mixture into the chromatographic system. Peak areas, determined using the digital integrator, were plotted against the analyte concentration for preparation of calibration curves.

Niacinamide and niacin were determined by injecting an aliquot (20 μl) of the sample solution, determining the resulting peak areas, and referring to the previously derived calibration curves.

RESULTS AND DISCUSSION

The complex matrixes in which the water-soluble vitamins are often found make chromatographic techniques a logical choice for their routine analysis. Of the quantitative chromatographic techniques, HPLC is particularly attractive since derivatives need not be formed prior to separation so sample preparation time may be reduced significantly. However, the choice of an appropriate stationary phase is critical in maximizing this advantage.

Methods using ion-exchange resins have been employed for separating niacin (7) from other constituents of vitamin products but suffer from poor reproducibility (8) and limited column life (9). Normal-phase chromatographic systems also may be used (10), but several constituents (*e.g.*, coloring and flavoring agents and diluents) are present in multivitamin preparations that are more polar than the vitamins. Methodologies based on these systems consequently require substantial sample workup or long analysis time.

Reversed-phase chromatographic systems appear to offer significant advantages in the determination of water-soluble vitamins in multivitamin preparations. Polar diluents, fillers, *etc.*, that dissolve in an aqueous dispersion of the multivitamin product elute at or near the solvent front while lipophilic constituents, such as the oil-soluble vitamins, have very limited solubility in the aqueous dispersion. Under such conditions, retention volumes are reproducible, column lifetimes are long (11), and sample preparation time is short. The latter advantage is not only important in terms of technician time but also in the precision of the method.

In such a chromatographic system, however, niacinamide and niacin have little affinity for the lipophilic stationary phase and also move through the system with the solvent front (Table I). However, it was shown previously (12) that addition of an appropriate salt to the mobile phase results in retention of ionic analytes in the reversed-phase system. For example, anionic analytes are retained in a reversed-phase system in which a small quantity of a lipophilic qua-

[1] ALC/GAS 202 equipped with an M6000 pump and a U6K injector, Waters Associates, Milford, Mass.
[2] Model 450, Varian Associates.
[3] μBondapak C_{18}, Waters Associates, Milford, Mass.

Table I—Retention Characteristics of Niacinamide and Niacin

Solute[a]	Niacin[b]	Niacinamide[b]
	1.8	1.8
Sodium heptanesulfonate	3.0	2.8
Sodium camphorsulfonate	6.2	5.6
Dioctyl sodium sulfosuccinate	10.5	9.0

[a] The salt (2×10^{-3} *M*) was dissolved in distilled water (300 ml), the pH was adjusted to 2.5 with 10% formic acid solution, and methanol (300 ml) was added. [b] Retention volume in milliliters with a flow rate of 3.0 ml/min.

ternary ammonium compound is added to the mobile phase. Conversely, cationic analytes in a mobile phase containing lipophilic sulfonate salts are dramatically retained when compared to the same systems not containing these salts. The advantages of such systems over ion-exchange procedures also were discussed (12).

In the current study, the pH of the aqueous component of the mobile phase was adjusted to 2.5, at which pH the heteronitrogens of niacin and niacinamide are protonated and carboxylate ionization (of niacin) is suppressed. Addition of the appropriate sulfonate salt to the mobile phase then results in retention of both niacin and niacinamide, with niacin less strongly retained because of its greater polarity. The retention characteristics of such ionic analytes in this system appear to be explicable in terms of the rate of formation and relative lipophilicity of the ion-pair formed within the system. This technique has been referred to as the reversed-phase, ion-pairing approach to HPLC; its use here allows sample preparation time to be held to a minimum.

By using this chromatographic system (Fig. 1), standard curves were prepared daily for 10 days. The standard deviations of the slope of the curve for niacinamide and niacin were 1.57 and 1.69%, respectively. The average correlation coefficient for niacinamide calibration curves was 0.996; for niacin, it was 0.998. The average *y*-intercepts

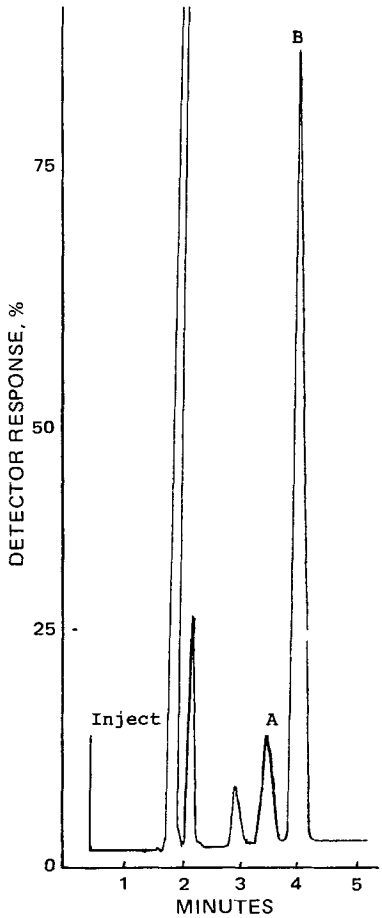

Figure 1—*Chromatographic trace of a multivitamin product found to contain niacin (A, 0.5 mg/dosage unit) and niacinamide (B, 9.3 mg/dosage unit).*

Table II—Analysis of Laboratory-Prepared Samples[a] by HPLC and the Cyanogen Bromide Procedure

	Niacin		Niacinamide		Total	
Sample	Amount Added, mg	Percent Recovered[b], HPLC	Amount Added, mg	Percent Recovered, HPLC	Amount Added, mg	Percent Recovered, USP
1	1.0	100.3 (1.46)	2.0	98.9 (1.55)	3.0	98.0 (3.14)
2	5.0	99.7 (1.74)	20.0	100.4 (1.76)	25.0	97.7 (2.46)
3	1.0	98.6 (1.85)	50.0	101.2 (1.94)	51.0	96.8 (3.44)
4	10.0	98.9 (1.40)	100.0	99.9 (1.63)	110.0	103.2 (2.16)
5	50.0	100.8 (1.21)	2.0	100.5 (1.40)	52.0	100.4 (2.96)
6	100.0	101.2 (1.81)	20.0	101.2 (1.84)	120.0	101.2 (2.84)
7	50.0	98.2 (1.64)	50.0	100.5 (1.77)	100.0	99.2 (3.10)

[a] Prepared according to the formula for decavitamin capsules USP. [b] Values in parentheses are percent standard deviation; $n = 8$.

Table III—Analysis of Niacinamide and Niacin in Multivitamin Products

				Amount Found[a]		
				Niacinamide		
Sample	Dosage Form	Labeled Components	Labeled Niacinamide, mg/Dosage Unit	USP	HPLC	Niacin[b], HPLC
1	Capsule	Nine vitamins, six minerals	100	101.6 (3.98)	94.5 (2.56)	5.4 (2.27)
2	Chewable tablet	Eight vitamins, artificial flavors, colors	10	103.4 (4.64)	97.6 (1.87)	3.2 (2.69)
3	Liquid	Eight vitamins, eight minerals, preservative, artificial flavors, colors	10	98.4 (3.60)	84.6 (2.20)	14.2 (2.90)
4	Drop	Eight vitamins	6	108.2 (3.14)	102.6 (1.94)	4.6 (2.20)
5	Capsule	Six vitamins	50	105.4 (3.90)	102.6 (2.27)	2.16 (1.86)
6	Tablet	Nine vitamins	50	99.8 (3.64)	96.4 (2.00)	5.46 (1.45)

[a] Percent of labeled amount (% *SD*); $n = 8$. [b] Expressed as percent of labeled niacinamide content.

were −3.24 integrator units for niacinamide and +4.70 integrator units for niacin. These data indicate that the procedure is amenable to use of a single-point standard.

The accuracy and precision of the proposed chromatographic procedure were investigated by analysis of laboratory-prepared samples (Table II), and results were compared with those of the USP procedure (4). In each case, the precision of the HPLC procedure was greater than that of the currently official procedure, and this result may be attributed to the less complicated sample workup required by the former. However, the two methods compared quite favorably in terms of the determination of the combined quantity of niacin and niacinamide.

Data regarding the suitability of the proposed procedure in the analysis of commercial multivitamin preparations are presented in Table III. Standard deviations of the HPLC procedure were again lower. Furthermore, niacinamide content, as determined by the proposed procedure, was less in each case. However, when the sum of niacinamide and niacin content was compared with that determined by the USP procedure, results were again comparable. Niacin was found in each sample examined, in quantities as high as 14.2% of the labeled niacinamide concentration.

This type of analysis is very attractive in terms of analysis time, since a trained technician can readily process 10 samples/hr with a minimum of active involvement. Column stability under these conditions of minimum sample preparation was a subject of concern initially. However, over 300 preparations have been processed with no change in the chromatographic characteristics of the system. This stability may be attributed in part to the small quantities of sample injected into the chromatographic system and in part to the daily flushing recommended by the column supplier.

In summary, the reversed-phase, ion-pairing approach to the simultaneous analysis of niacin and niacinamide appears to result in an accurate and precise procedure. These features, in combination with the simple sample preparation and short analysis time, should make the procedure attractive to pharmaceutical analysts. The application of this approach to the other water-soluble vitamins is currently under investigation.

REFERENCES

(1) A. Y. Taura, *J. Assoc. Offic. Anal. Chem.*, **57**, 910(1974).

(2) J. Lindquist and S. M. Farroha, *Analyst*, **100**, 377 (1975).

(3) J. Vessman and S. Stromberg, *J. Pharm. Sci.*, **64**, 311(1975).

(4) "The United States Pharmacopeia," 19th rev., Mack Publishing Co., Easton, Pa., 1975, p. 120.

(5) D. C. Egberg, R. H. Potter, and G. R. Honold, *J. Agr. Food Chem.*, **22**, 323(1974).

(6) S. A. Ismaiel and D. A. Yassa, *Analyst*, **1973**, 816.

(7) R. C. Williams, D. R. Baker, and J. A. Schmit, *J. Chromatogr. Sci.*, **11**, 618(1973).

(8) M. Singh, *J. Assoc. Offic. Anal. Chem.*, **57**, 219(1974).

(9) *Ibid.*, **57**, 358(1974).

(10) D. P. Wittmer and W. G. Haney, Jr., *J. Pharm. Sci.*, **63**, 588(1974).

(11) R. E. Huettemann and A. P. Shroff, *J. Chromatogr. Sci.*, **13**, 357(1975).

(12) D. P. Wittmer, N. O. Nuessle, and W. G. Haney, Jr., *Anal. Chem.*, **47**, 1422(1975).

ACKNOWLEDGMENTS AND ADDRESSES

Received September 25, 1975, from the *School of Pharmacy, University of Missouri–Kansas City, Kansas City, MO 64110*

Accepted for publication January 22, 1976.

* Present address: Marion Laboratories, Kansas City, MO 64112

‡ Present address: Waters Associates, Milford, MA 01757

§ Present address: Misr Company for Pharmaceutical Industries, Cairo, Egypt.

ˣ To whom inquiries should be directed (no reprints available).

Solubility Profiles and Thermodynamics of Parabens in Aliphatic Alcohols

KENNETH S. ALEXANDER *, JOHN W. MAUGER ‡, HAROLD PETERSEN, Jr. §, and ANTHONY N. PARUTA ˣ

Abstract □ The solubility of a series of compounds was determined in a wide polarity spectrum of normal aliphatic alcohols over a limited temperature range. The solutes chosen were the methyl through *n*-butyl *p*-hydroxybenzoates, several of these being useful preservatives. Solubility profiles were determined for these compounds, and the effect of temperature upon their solubility behavior was investigated. The solubility of the solutes is expressed in several concentration notations; mole fraction plots showed a variable twin peak array as a function of the dielectric constant for the solutes studied. Since heats of fusion were available and data were generated as a function of temperature, thermodynamic parameters for these systems could be calculated. The relationship of these parameters to multiple solubility peak array is discussed.

Keyphrases □ Parabens, alkyl—solubility and thermodynamics in aliphatic alcohols, effect of temperature □ Solubility—alkylparabens in aliphatic alcohols, effect of temperature □ Thermodynamics—alkylparabens in aliphatic alcohols, effect of temperature □ Alcohols, aliphatic—solvents for series of alkylparabens, effect of temperature □ Structure–activity relationships—alkylparabens, solubility and thermodynamics in aliphatic alcohols □ Antifungal agents—alkylparabens, solubility and thermodynamics in aliphatic alcohols

The effect of temperature upon the solubility of four normal alkyl *p*-hydroxybenzoates (parabens) was determined over a wide polarity spectrum of aliphatic alcohols from methanol to 1-decanol. The effect of decreasing polarity with an increase in size for the first four *n*-alkyl members for this ester series was also considered.

Previous solubility work (1–5) considered several of these compounds at ambient temperatures. It was believed that the extension of this work in pure solvents over a temperature range and polarity range would be instructive. Additionally, since several of these solutes gave multiple peak solubility isotherms, it was useful to determine if solubility was linear as a function of temperature. The temperature range used was 25–40° in four steps; the polarity range *via* dielectric constants was from 32 for methanol to eight for 1-decanol at 25°, utilizing seven in-

were −3.24 integrator units for niacinamide and +4.70 integrator units for niacin. These data indicate that the procedure is amenable to use of a single-point standard.

The accuracy and precision of the proposed chromatographic procedure were investigated by analysis of laboratory-prepared samples (Table II), and results were compared with those of the USP procedure (4). In each case, the precision of the HPLC procedure was greater than that of the currently official procedure, and this result may be attributed to the less complicated sample workup required by the former. However, the two methods compared quite favorably in terms of the determination of the combined quantity of niacin and niacinamide.

Data regarding the suitability of the proposed procedure in the analysis of commercial multivitamin preparations are presented in Table III. Standard deviations of the HPLC procedure were again lower. Furthermore, niacinamide content, as determined by the proposed procedure, was less in each case. However, when the sum of niacinamide and niacin content was compared with that determined by the USP procedure, results were again comparable. Niacin was found in each sample examined, in quantities as high as 14.2% of the labeled niacinamide concentration.

This type of analysis is very attractive in terms of analysis time, since a trained technician can readily process 10 samples/hr with a minimum of active involvement. Column stability under these conditions of minimum sample preparation was a subject of concern initially. However, over 300 preparations have been processed with no change in the chromatographic characteristics of the system. This stability may be attributed in part to the small quantities of sample injected into the chromatographic system and in part to the daily flushing recommended by the column supplier.

In summary, the reversed-phase, ion-pairing approach to the simultaneous analysis of niacin and niacinamide appears to result in an accurate and precise procedure. These features, in combination with the simple sample preparation and short analysis time, should make the procedure attractive to pharmaceutical analysts. The application of this approach to the other water-soluble vitamins is currently under investigation.

REFERENCES

(1) A. Y. Taura, *J. Assoc. Offic. Anal. Chem.*, **57**, 910(1974).

(2) J. Lindquist and S. M. Farroha, *Analyst*, **100**, 377 (1975).

(3) J. Vessman and S. Stromberg, *J. Pharm. Sci.*, **64**, 311(1975).

(4) "The United States Pharmacopeia," 19th rev., Mack Publishing Co., Easton, Pa., 1975, p. 120.

(5) D. C. Egberg, R. H. Potter, and G. R. Honold, *J. Agr. Food Chem.*, **22**, 323(1974).

(6) S. A. Ismaiel and D. A. Yassa, *Analyst*, **1973**, 816.

(7) R. C. Williams, D. R. Baker, and J. A. Schmit, *J. Chromatogr. Sci.*, **11**, 618(1973).

(8) M. Singh, *J. Assoc. Offic. Anal. Chem.*, **57**, 219(1974).

(9) *Ibid.*, **57**, 358(1974).

(10) D. P. Wittmer and W. G. Haney, Jr., *J. Pharm. Sci.*, **63**, 588(1974).

(11) R. E. Huettemann and A. P. Shroff, *J. Chromatogr. Sci.*, **13**, 357(1975).

(12) D. P. Wittmer, N. O. Nuessle, and W. G. Haney, Jr., *Anal. Chem.*, **47**, 1422(1975).

ACKNOWLEDGMENTS AND ADDRESSES

Received September 25, 1975, from the *School of Pharmacy, University of Missouri–Kansas City, Kansas City, MO 64110*

Accepted for publication January 22, 1976.

* Present address: Marion Laboratories, Kansas City, MO 64112

‡ Present address: Waters Associates, Milford, MA 01757

§ Present address: Misr Company for Pharmaceutical Industries, Cairo, Egypt.

ˣ To whom inquiries should be directed (no reprints available).

Solubility Profiles and Thermodynamics of Parabens in Aliphatic Alcohols

KENNETH S. ALEXANDER *, JOHN W. MAUGER ‡, HAROLD PETERSEN, Jr. §, and ANTHONY N. PARUTA ˣ

Abstract □ The solubility of a series of compounds was determined in a wide polarity spectrum of normal aliphatic alcohols over a limited temperature range. The solutes chosen were the methyl through *n*-butyl *p*-hydroxybenzoates, several of these being useful preservatives. Solubility profiles were determined for these compounds, and the effect of temperature upon their solubility behavior was investigated. The solubility of the solutes is expressed in several concentration notations; mole fraction plots showed a variable twin peak array as a function of the dielectric constant for the solutes studied. Since heats of fusion were available and data were generated as a function of temperature, thermodynamic parameters for these systems could be calculated. The relationship of these parameters to multiple solubility peak array is discussed.

Keyphrases □ Parabens, alkyl—solubility and thermodynamics in aliphatic alcohols, effect of temperature □ Solubility—alkylparabens in aliphatic alcohols, effect of temperature □ Thermodynamics—alkylparabens in aliphatic alcohols, effect of temperature □ Alcohols, aliphatic—solvents for series of alkylparabens, effect of temperature □ Structure–activity relationships—alkylparabens, solubility and thermodynamics in aliphatic alcohols □ Antifungal agents—alkylparabens, solubility and thermodynamics in aliphatic alcohols

The effect of temperature upon the solubility of four normal alkyl *p*-hydroxybenzoates (parabens) was determined over a wide polarity spectrum of aliphatic alcohols from methanol to 1-decanol. The effect of decreasing polarity with an increase in size for the first four *n*-alkyl members for this ester series was also considered.

Previous solubility work (1–5) considered several of these compounds at ambient temperatures. It was believed that the extension of this work in pure solvents over a temperature range and polarity range would be instructive. Additionally, since several of these solutes gave multiple peak solubility isotherms, it was useful to determine if solubility was linear as a function of temperature. The temperature range used was 25–40° in four steps; the polarity range *via* dielectric constants was from 32 for methanol to eight for 1-decanol at 25°, utilizing seven in-

Table I—Experimentally Determined Methylparaben Solubility Values

Solvent	25°		30°		35°		40°	
	Mole Fraction	mg/g	Mole Fraction	mg/g	Mole Fraction	mg/g	Mole Fraction	mg/g
Methanol	0.121	395.0	0.139	433.0	0.162	479.0	0.178	508.0
Ethanol	0.147	360.0	0.156	379.0	0.174	410.0	0.201	454.0
1-Propanol	0.138	295.0	0.152	309.0	0.180	355.0	0.199	383.0
1-Butanol	0.146	262.0	0.154	272.0	0.172	298.0	0.191	326.0
1-Hexanol	0.155	205.0	0.166	212.0	0.186	253.0	0.205	262.0
1-Octanol	0.111	147.0	0.151	172.0	0.166	188.0	0.172	195.0
1-Decanol	0.088	88.0	0.109	103.0	0.128	122.0	0.144	139.0

Table II—Experimentally Determined Ethylparaben Solubility Values

Solvent	25°		30°		35°		40°	
	Mole Fraction	mg/g	Mole Fraction	mg/g	Mole Fraction	mg/g	Mole Fraction	mg/g
Methanol	0.135	452.0	0.157	490.0	0.185	541.0	0.208	576.0
Ethanol	0.165	412.0	0.184	449.0	0.218	501.0	0.220	505.0
1-Propanol	0.176	362.0	0.188	388.0	0.216	429.0	0.229	447.0
1-Butanol	0.178	340.0	0.183	335.0	0.210	373.0	0.234	407.0
1-Hexanol	0.189	260.0	0.195	282.0	0.212	305.0	0.228	325.0
1-Octanol	0.156	207.0	0.183	222.0	0.204	246.0	0.226	271.0
1-Decanol	0.115	148.0	0.175	182.0	0.192	200.0	0.215	223.0

dividual solvents. The Hildebrand solubility parameter (6) was applied previously (2, 3) in a study of benzoic acid and alkyl esters of *p*-hydroxybenzoic acid; these solutes also were studied in binary mixtures (4, 5, 7) consisting of dioxane–water and ethanol–water.

A rather striking dichotomy appeared in contemporary work on solubility behavior (8–14). The excellent theoretical approach undertaken by Hildebrand and coworkers (15–22), referred to as the "solubility parameter" theory, certainly has much to offer in terms of the interpretation of solubility phenomena. Extension of this theory to systems of some pharmaceutical interest was undertaken by other investigators (23, 24). Work over the last decade has shown that a dielectric constant (dielectric requirement) approach has some validity. The Hildebrand approach only accounts for a monotonic isotherm or a single solubility maximum. This approach assumes a neat and smooth variation of molecular interactions such that an analytical solution can be formulated to approximate real behavior. A symmetrical isotherm can be expected from this theory and is quite reasonable, because the summed interactions are at a mathematical condition of constant differences.

Hildebrand, continuing elegant work in this area (18), was instrumental in shifting the thrust of past work from a dielectric constant approach to a more fundamental and theoretical thermodynamic approach. It now appears that the multiple solubility peak arrays observed for various solutes qualitatively resides in the nature of the systems and quantitatively resides in the values or magnitudes of the thermodynamic functions resulting from each individual system.

Therefore, this study deals with the thermodynamic parameters for various solutes in a series of normal aliphatic alcohols. Since heats of fusion were available (16), a theoretical ideal mole fraction solubility could be determined and compared with the actual mole fraction solubility. In this manner, the activity coefficients could be determined. The solubility of these solutes as a function of temperature would allow for the experimental determination of enthalpies and entropies of solution. A thermodynamic scheme for the interpretation of solubility behavior is presented. Excess free energy functions were calculated and utilized as a basis for multipeak solubility isotherms.

EXPERIMENTAL

Equipment—The following were used: a melting-point apparatus[1], a pH meter[2], a chemical oscillometer[3], a spectrophotometer[4], a temperature controller[5], and a refractometer[6].

Materials—The chemicals utilized were ethyl *p*-hydroxybenzoate (ethylparaben) and propyl *p*-hydroxybenzoate[7] (propylparaben); methanol[8], spectrograde; butyl *p*-hydroxybenzoate[9] (butylparaben); 1-propanol[10]; ethanol[11], absolute reagent quality; 1-butanol[12], analytical reagent; 1-hexanol and 1-octanol[13]; 1-decanol[14]; certified acetone[15], 99 mole % pure; certified benzene[16], 99 mole % pure; hydrochloric acid[17], certified pure reagent; and potassium chloride[18] USP. The purity of the alcohols was established by refractive indexes and dielectric constant measurements. Melting points were determined and were within 1° of literature values.

Method—Solubility was determined by the method described previously (1). The solubility of each solute was determined at least eight times for each solvent, and average values were taken. The experimental variation in solubility was about 2.5% in replicate samples for these solutes.

RESULTS AND DISCUSSION

The solubility of a series of solutes was determined in a chemically related series of solvents at various temperatures over 25–40° (Tables I–IV).

[1] Hoover 6406, A. H. Thomas Co., Philadelphia, Pa.
[2] Model 7401, Leeds and Northrup, Philadelphia, Pa.
[3] Model 5, E. H. Sargent and Co., Chicago, Ill.
[4] Cary model 16, Cary Instruments, Monrovia, Calif.
[5] Temptrol 150 tempunit, Precision Scientific Co., Chicago, Ill.
[6] Abbe 3L, Bausch & Lomb Optical Co., Rochester, N.Y.
[7] Lots EX 665 and PX 1910, respectively, Matheson, Coleman and Bell.
[8] Lot VMN, Mallinckrodt Chemical Works.
[9] U.S. Industrial Chemicals Co.
[10] Lot 35592, J. T. Baker Chemical Co.
[11] J. T. Baker Chemical Co.
[12] Lot TDY, Mallinckrodt Chemical Works.
[13] Lots 020251 and 22, respectively, Mallinckrodt Chemical Works.
[14] Lot 16, Matheson, Coleman and Bell.
[15] Lot 792902, Fisher Scientific Co.
[16] Lot 793869, Fisher Scientific Co.
[17] Lot E108262, Allied Chemical, General Chemical Division.
[18] Lot 8678, J. T. Baker Chemical Co.

Table III—Experimentally Determined Propylparaben Solubility Values

Solvent	25°		30°		35°		40°	
	Mole Fraction	mg/g	Mole Fraction	mg/g	Mole Fraction	mg/g	Mole Fraction	mg/g
Methanol	0.172	540.0	0.207	595.0	0.240	639.0	0.276	682.0
Ethanol	0.197	490.0	0.228	535.0	0.296	621.0	0.298	624.0
1-Propanol	0.198	436.0	0.236	478.0	0.273	527.0	0.298	557.0
1-Butanol	0.206	394.0	0.245	441.0	0.278	484.0	0.316	528.0
1-Hexanol	0.210	326.0	0.256	362.0	0.285	412.0	0.303	434.0
1-Octanol	0.200	266.0	0.228	290.0	0.271	339.0	0.298	370.0
1-Decanol	0.171	217.0	0.225	248.0	0.264	290.0	0.285	312.0

Table IV—Experimentally Determined Butylparaben Solubility Values

Solvent	25°		30°		35°		40°	
	Mole Fraction	mg/g	Mole Fraction	mg/g	Mole Fraction	mg/g	Mole Fraction	mg/g
Methanol	0.336	755.0	0.369	779.0	0.457	834.0	0.491	854.0
Ethanol	0.360	703.0	0.395	734.0	0.437	766.0	0.500	807.0
1-Propanol	0.355	647.0	0.402	682.0	0.458	729.0	0.502	763.0
1-Butanol	0.364	601.0	0.388	625.0	0.439	672.0	0.501	725.0
1-Hexanol	0.369	526.0	0.395	552.0	0.444	603.0	0.507	661.0
1-Octanol	0.331	457.0	0.379	476.0	0.440	539.0	0.497	595.0
1-Decanol	0.293	392.0	0.371	421.0	0.427	477.0	0.491	542.0

In Fig. 1, the solubility of the solutes is plotted as milligrams per gram of solution *versus* the carbon number in the aliphatic alcohol solvent series used. Typical nonlinear curves were generated in all cases; for each solute, the highest solubility occurred in methanol and decreased in value to 1-decanol. The order of solubility was the butyl ester > propyl ester > ethyl ester > methyl ester.

In Fig. 2, the solubility of the methyl *p*-hydroxybenzoate (methylparaben) as a typical solute is plotted in milligrams per gram of solution as a function of the temperature. The solubility increased linearly over the experimental temperature range utilized.

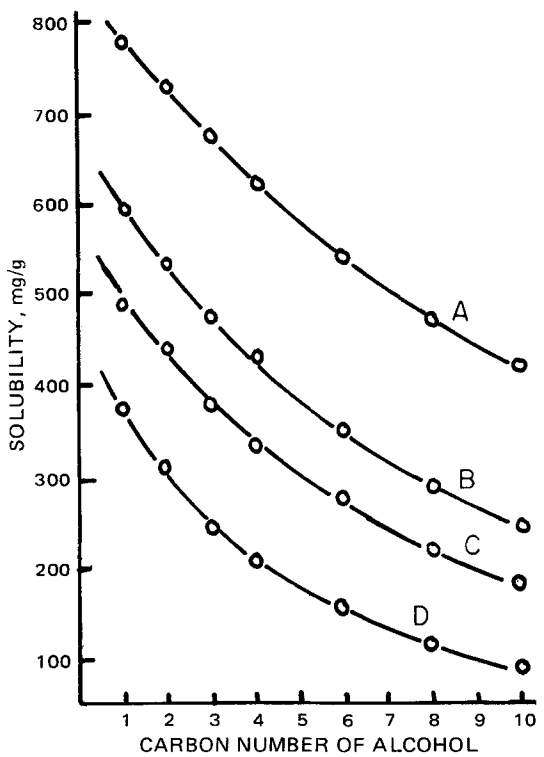

Figure 1—*Solubility of the noted substances in milligrams per gram of solution as a function of the carbon number of the alcohol used. Curve A = butyl* p*-hydroxybenzoate, curve B = propyl* p*-hydroxybenzoate, curve C = ethyl* p*-hydroxybenzoate, and curve D = methyl* p*-hydroxybenzoate.*

In Fig. 3, the solubility of methylparaben in milligrams per gram of solution is plotted as a function of the carbon number of the alcohol solvent at each of four temperatures. Nonlinear curves were observed with the typical incremental response of increased solubility with temperature.

In Fig. 4, the mole fraction solubility is plotted as a function of the dielectric constant of the solvents. For each compound, a twin peak array is observed possessing values of dielectric constants of about 10–13 and 19–22, as previously reported (1).

In Fig. 5, the mole fraction solubility profiles of methylparaben are plotted as a function of the dielectric constant of the alcohols at various temperatures. The dielectric constants vary and decrease over the 15° range of temperature used; however, these variations are about two to three units lower at 40° than at 25°. These solubility profiles are fairly consistent over this temperature range; each profile indicates a binary peak array, with the dielectric constant of maximum solubility showing fair consistency. The first maxima are found at a dielectric constant range of about 12–13.5, whereas the second maxima are found at 21–24.

It is felt that where the solubility maxima occur, these magnitudes of

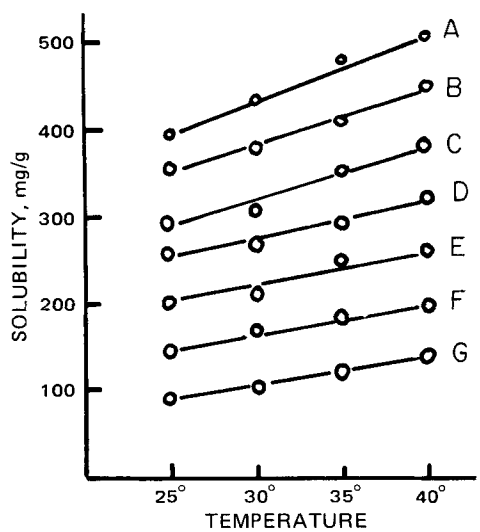

Figure 2—*Solubility of methyl* p*-hydroxybenzoate in the noted alcohol solvents as a function of temperature. Curve A = methanol, curve B = ethanol, curve C = 1-propanol, curve D = 1-butanol, curve E = 1-hexanol, curve F = 1-octanol, and curve G = 1-decanol.*

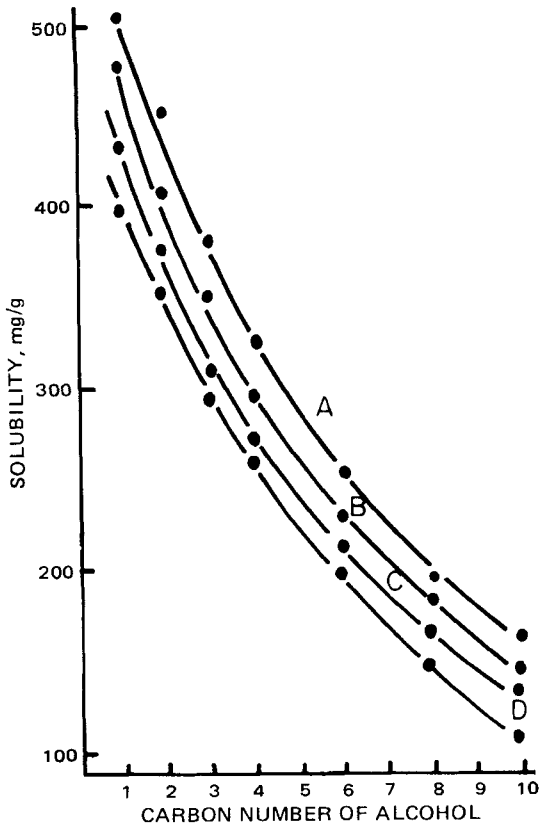

Figure 3—*Solubility of methyl* p-*hydroxybenzoate at various temperatures as a function of the carbon number of the alcohol solvents used. Curve A = 40°, curve B = 35°, curve C = 30°, and curve D = 25°.*

solubility are approaching ideal solubility values such that the excess free energy values at the maxima are approaching the ideal free energy values. It thus becomes desirable to differentiate "ideal" and "nonideal" solubility with a view of obtaining thermodynamic elements from literature

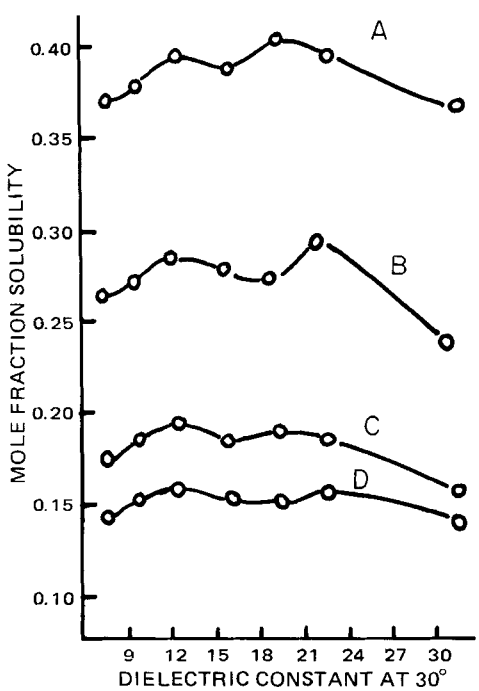

Figure 4—*Mole fraction solubility of the noted solutes as a function of the dielectric constants at 30° for the alcohol solvents used. Curve A = butyl* p-*hydroxybenzoate, curve B = propyl* p-*hydroxybenzoate, curve C = ethyl* p-*hydroxybenzoate, and curve D = methyl* p-*hydroxybenzoate.*

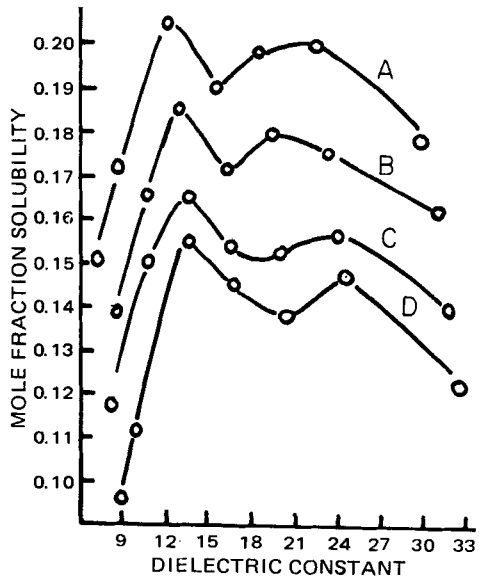

Figure 5—*Mole fraction solubility of methyl* p-*hydroxybenzoate as a function of the dielectric constants of the alcohol solvents used at four temperatures. Curve A = 40°, curve B = 35°, curve C = 30°, and curve D = 25°.*

and experimental data. Thus, ideal solubility can be calculated from ΔF_l values once the enthapy of fusion and entropy of fusion are known. These values can then be compared with those obtained experimentally. Thus, the ratio of the ideal solubility and the actual solubility can be used to determine activity coefficients for both the solute and the solvent. It is well known that the actual solubility is always less than ideal solubility. (The summation of two positive factors leads to a larger negative logarithm or a smaller X_2 value.) Thus, other determined elements, ideal solubility (X_2^i) and activity coefficients (γ_1 and γ_2), have been added to the existing list of thermodynamic elements: ΔH_f, ΔH_s, ΔS_f, and ΔS_s.

In summary, then, solubility can be expressed as a function of the energy change in the following manner: F_E (excess) = F_A (actual) − F_l (ideal) (1); therefore, as the excess energy approaches zero, the nonideal or actual solubility approaches the ideal solubility.

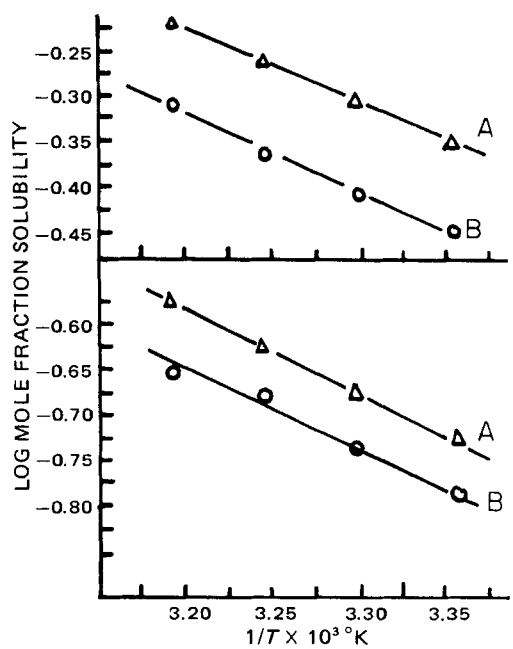

Figure 6—*Mole fraction solubility for ethyl* p-*hydroxybenzoate (lower figure) and butyl* p-*hydroxybenzoate (upper figure) as a function of reciprocal temperature (°K). The ideal curves (Δ, A) are from heat of fusion data, and the actual curves (O, B) are from experimental data.*

Table V—Literature and Calculated Thermodynamic Elements of the Solutes

Compound	ΔH_f, cal/mole[a]	T_M[a], °K	ΔS_f, cal/deg[b]	ΔF_I, cal/mole[c]	Ideal Mole Fraction Solubility[d] 25°	30°	35°	40°
Methylparaben	4352	398	11.04	1034	0.157	0.178	0.200	0.224
Ethylparaben	4243	388	11.02	926	0.189	0.213	0.239	0.267
Propylparaben	4026	369	10.9	716	0.272	0.304	0.339	0.376
Butylparaben	3737	341	11.02	415	0.450	0.500	0.553	0.610

[a] From Ref. 16. [b] From plot of log ideal mole fraction solubility *versus* $1/T$. [c] ΔF (ideal) = $\Delta H_f - T\,\Delta S_f$. [d] Calculated values.

Table VI—Calculated Solute Activity Coefficients

Temperature	Methanol	Ethanol	1-Propanol	1-Butanol	1-Hexanol	1-Octanol	1-Decanol
			Methylparaben				
25°	1.298	1.068	1.138	1.075	1.013	1.415	1.715
30°	1.284	1.141	1.175	1.156	1.072	1.190	1.633
35°	1.238	1.148	1.109	1.167	1.078	1.165	1.562
40°	1.257	1.113	1.126	1.172	1.212	1.305	1.555
			Ethylparaben				
25°	1.400	1.146	1.074	1.062	1.000	1.212	1.644
30°	1.361	1.156	1.132	1.163	1.094	1.164	1.221
35°	1.290	1.110	1.106	1.140	1.126	1.173	1.244
40°	1.286	1.212	1.168	1.141	1.170	1.183	1.244
			Propylparaben				
25°	1.582	1.381	1.374	1.321	1.295	1.360	1.591
30°	1.466	1.336	1.288	1.242	1.291	1.336	1.353
35°	1.414	1.149	1.241	1.218	1.191	1.253	1.203
40°	1.361	1.262	1.262	1.192	1.240	1.263	1.321
			Butylparaben				
25°	1.339	1.250	1.268	1.235	1.220	1.360	1.536
30°	1.354	1.265	1.243	1.290	1.268	1.321	1.347
35°	1.209	1.266	1.208	1.260	1.245	1.256	1.297
40°	1.244	1.220	1.215	1.217	1.204	1.229	1.243

Table VII—Calculated Solvent Activity Coefficients (γ_1)

Temperature	Methanol	Ethanol	1-Propanol	1-Butanol	1-Hexanol	1-Octanol	1-Decanol
			Methylparaben				
25°	0.959	0.988	0.978	0.987	0.998	0.948	0.930
30°	0.966	0.986	0.981	0.984	0.998	0.980	0.922
35°	0.954	0.969	0.976	0.966	0.982	0.959	0.917
40°	0.945	0.972	0.969	0.959	0.964	0.937	0.906
			Ethylparaben				
25°	0.938	0.972	0.984	0.987	1.000	0.961	0.917
30°	0.933	0.965	0.970	0.964	0.977	0.963	0.942
35°	0.934	0.973	0.971	0.963	0.966	0.956	0.942
40°	0.925	0.940	0.950	0.957	0.950	0.947	0.934
			Propylparaben				
25°	0.879	0.907	0.908	0.917	0.922	0.910	0.878
30°	0.878	0.901	0.911	0.922	0.911	0.901	0.898
35°	0.870	0.939	0.910	0.916	0.924	0.919	0.898
40°	0.862	0.889	0.889	0.912	0.896	0.889	0.872
			Butylparaben				
25°	0.813	0.844	0.837	0.850	0.856	0.807	0.764
30°	0.793	0.827	0.837	0.817	0.826	0.805	0.795
35°	0.824	0.794	0.825	0.797	0.804	0.799	0.780
40°	0.766	0.780	0.784	0.782	0.790	0.775	0.766

Table V presents literature values for the heat of fusion, ΔH_f, which were applied to calculate ideal mole fraction solubility values. The entropy of fusion, ΔS_f, presented can be obtained graphically from a plot of log X_2^i *versus* $1/T$. The ideal free energy change and the ideal mole fraction solubilities are also given for the four temperatures.

In Fig. 6, the ideal and actual mole fraction solubility for ethyl- and butylparaben are plotted *versus* reciprocal temperature. The ideal solubility, as expected, is greater than the actual solubility.

The rational activity coefficients for the solutes in a particular solvent with respect to temperature were calculated in the usual manner (Table VI). The rational activity coefficient for the solvent is given in like manner in Table VII. The error in the activity coefficients due to solubility variation is about ±0.005.

Tables VIII–XI give the thermodynamic elements that were determined graphically or by calculation. The legend for Table VIII applies to all subsequent tables. Inspection of the magnitude of excess free energy

Table VIII—Thermodynamic Elements Determined Graphically or by Calculation for Methylparaben when $\Delta H_f = 4352^a$, $\Delta S_f = 11.04^b$, and $\Delta F_I = 1034^c$

Solvent	ΔH_s, cal/mole[d]	ΔH_m, cal/mole[e]	ΔS_s, cal/deg[d]	ΔS_m, cal/deg[e]	ΔF_A, cal/mole[f]	ΔF_E, cal/mole[g]
Methanol	+4878	+526	12.17	+1.1	+1189	+155
Ethanol	+3894	−458	9.21	−1.8	+1102	+68
1-Propanol	+4714	+362	11.85	+0.8	+1122	+88
1-Butanol	+3384	−968	7.49	−3.5	+1114	+80
1-Hexanol	+2666	−1686	5.19	−5.8	+1093	+59
1-Octanol	+5244	+892	13.36	+2.3	+1194	+160
1-Decanol	+3066	−1566	5.39	−5.6	+1152	+118

[a] From Ref. 16. [b] Obtained from a plot of log ideal mole fraction solubility *versus* $1/T$. [c] $\Delta F_I = \Delta H_f - T\Delta S_f$. [d] Obtained from a plot of log mole fraction solubility *versus* $1/T$. [e] $\Delta H_m = \Delta H_s - \Delta H_f$; $\Delta S_m = \Delta S_s - \Delta S_f$. [f] $\Delta F_A = \Delta H_s - T\Delta S_s$. [g] $\Delta F_E = \Delta F_A - \Delta F_I$.

Table IX—Thermodynamic Elements Determined Graphically or by Calculation for Ethylparaben when $\Delta H_f = 4243^a$; $\Delta S_f = 11.02^b$, and $\Delta F_I = 926^c$

Solvent	ΔH_s, cal/mole[d]	ΔH_m, cal/mole[e]	ΔS_s, cal/deg[d]	ΔS_m, cal/deg[e]	ΔF_A, cal/mole[f]	ΔF_E, cal/mole[g]
Methanol	+5420	+1177	14.20	+3.2	+1115	+189
Ethanol	+3856	−387	9.38	−1.7	+993	+67
1-Propanol	+3428	−815	8.03	−3.0	+1012	+86
1-Butanol	+3545	−698	8.41	−2.6	+995	+69
1-Hexanol	+2415	−1828	4.76	−6.2	+972	+46
1-Octanol	+4514	+271	11.48	+0.5	+1034	+108
1-Decanol	+7346	+3103	20.52	+9.5	+1125	+199

[a] From Ref. 16. [b] Obtained from a plot of log ideal mole fraction solubility *versus* $1/T$. [c] $\Delta F_I = \Delta H_f - T\Delta S_f$. [d] Obtained from a plot of log mole fraction solubility *versus* $1/T$. [e] $\Delta H_m = \Delta H_s - \Delta H_f$; $\Delta S_m = \Delta S_s - \Delta S_f$. [f] $\Delta F_A = \Delta H_s - T\Delta S_s$. [g] $\Delta F_E = \Delta F_A - \Delta F_I$.

Table X—Thermodynamic Elements Determined Graphically or by Calculation for Propylparaben when $\Delta H_f = 4026^a$, $\Delta S_f = 10.86^b$, and $\Delta F_I = 716^c$

Solvent	ΔH_s, cal/mole[d]	ΔH_m, cal/mole[e]	ΔS_s, cal/deg[d]	ΔS_m, cal/deg[e]	ΔF_A, cal/mole[f]	ΔF_E, cal/mole[g]
Methanol	+5823	+1797	16.0	+5.1	+958	+242
Ethanol	+5592	+1566	15.6	+5.7	+879	+163
1-Propanol	+5102	+1076	13.9	+3.0	+880	+164
1-Butanol	+5232	+1206	14.4	+3.5	+931	+215
1-Hexanol	+4798	+772	13.0	+2.1	+852	+136
1-Octanol	+5078	+1052	13.8	+2.9	+905	+189
1-Decanol	+6295	+2269	17.7	+6.6	+930	+214

[a] From Ref. 16. [b] Obtained from a plot of log ideal mole fraction solubility *versus* $1/T$. [c] $\Delta F_I = \Delta H_f - T\Delta S_f$. [d] Obtained from a plot of log mole fraction solubility *versus* $1/T$. [e] $\Delta H_m = \Delta H_s - \Delta H_f$; $\Delta S_m = \Delta S_s - \Delta S_f$. [f] $\Delta F_A = \Delta H_s - T\Delta S_s$. [g] $\Delta F_E = \Delta F_I - \Delta F_A$.

Table XI—Thermodynamic Elements Determined Graphically or by Calculation for Butylparaben when $\Delta H_f = 3737^a$, $\Delta S_f = 11.02^b$, and $\Delta F_I = 415^c$

Solvent	ΔH_s, cal/mole[d]	ΔH_m, cal/mole[e]	ΔS_s, cal/deg[d]	ΔS_m, cal/deg[e]	ΔF_A, cal/mole[f]	ΔF_E, cal/mole[g]
Methanol	+5005	+1268	14.6	+3.6	579	+164
Ethanol	+4020	+283	11.4	+0.4	548	+138
1-Propanol	+4347	+610	12.5	+1.5	554	+133
1-Butanol	+4017	+280	11.4	+0.4	555	+140
1-Hexanol	+3959	+222	11.3	+0.3	546	+131
1-Octanol	+5077	+1340	14.8	+3.8	581	+166
1-Decanol	+6266	+2529	18.6	+7.6	616	+201

[a] From Ref. 16. [b] Obtained from a plot of log ideal mole fraction solubility *versus* $1/T$. [c] $\Delta F_I = \Delta H_f - T\Delta S_f$. [d] Obtained from a plot of log mole fraction solubility *versus* $1/T$. [e] $\Delta H_m = \Delta H_s - \Delta H_f$; $\Delta S_m = \Delta S_s - \Delta S_f$. [f] $\Delta F_A = \Delta H_s - T\Delta S_s$. [g] $\Delta F_E = \Delta F_I - \Delta F_A$.

of mixing (11) or ΔF_E for each solute shows that the values decrease to minima (approaching ideality) in the ethanol or propanol and hexanol solvents. This finding, of course, supports the concept of a multiple peak array from a thermodynamic point of view. Furthermore, heats of mixing changes were compensated for by entropy gain such that the free energy was reflective of a twin peak solubility array.

The twin peak array observed in the solubility spectrum shown in Fig. 5 is seen throughout the thermodynamic picture of the investigated compounds.

In Fig. 7, the entropy and corresponding enthalpy for methylparaben are plotted *versus* the carbon number of the alcohol solvent. The parallelism can easily be seen between these elements, leading to the excess free energy minimizing at carbon numbers 2 and 6. Any alteration in ΔH_s is also accompanied by a corresponding change in ΔS_s such that free energy remains consistent for any given system. Therefore, any increase in ΔH_s would be associated with an increase in ΔS_s (tending toward greater disorder or randomness).

Since ΔF_I is a fixed value for any solute regardless of the solvent, any system in which ΔF_A approaches ΔF_I will approach the ideal state. Hence, for any particular solute, there may be many combinations of values for ΔH_s and ΔS_s, depending upon the solvent employed, in which ΔF_A may approximate ΔF_I. In this study, the solutes dissolved in either

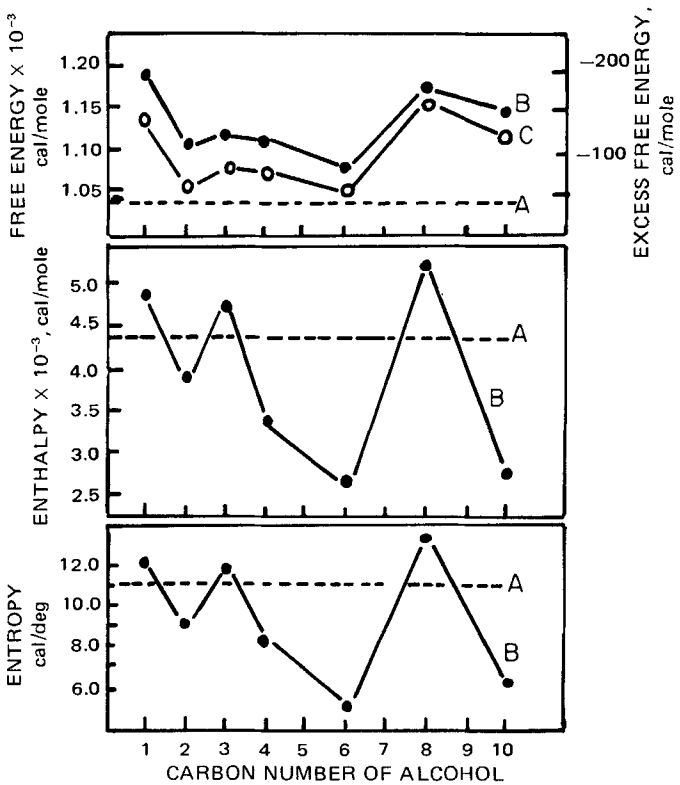

Figure 7—*Plot for methyl p-hydroxybenzoate illustrating the relationship for the entropy (curve A = entropy of fusion and curve B = entropy of solution), enthalpy (curve A = enthalpy of fusion and curve B = enthalpy of solution), and free energy [curve A = ideal free energy, curve B = actual free energy, and curve C = excess free energy (right-hand coordinates)]. Data were taken from Table VIII.*

ethanol or 1-propanol and 1-hexanol have their ΔF_A values approximating ΔF_I. This can be shown by the free energy determinations. However, since the excess free energy terms are based on mole fraction solubility, the emerging trends can be initially perceived by mere inspection of these data.

It has been established that the excess free energy is usually a small value, encompassing a range of 20–200 calories/mole. Since excess free energy is a function of both the mole fraction, which usually ranges from 0.1 to 0.3 for the solute, and the logarithm of the activity coefficient, which usually ranges from −0.75 to −0.9 for the solute and from 0.01 to 0.1 for the solvent, the small numbers obtained are not unexpected.

Thus, total inspection of the thermodynamic functions ΔH_s, ΔS_s, ΔH_m, and ΔF_E truly reveals a trend for a multipeak solubility array. Any solute that exhibits maxima in various solvents may be approaching ideal solubility at the individual maximum in the particular solubility profile.

The dielectric requirement of one peak is now felt to be related to the thermodynamics of the total system; hence, a multipeak system should signify that ideal solubility is being approximated in those particular solvent–solute systems.

REFERENCES

(1) A. N. Paruta, *J. Pharm. Sci.*, **55**, 1208 (1966).
(2) F. A. Restaino and A. N. Martin, *ibid.*, **53**, 636 (1964).
(3) S. A. Khalil and A. N. Martin, *ibid.*, **56**, 1225 (1967).
(4) A. N. Paruta, *ibid.*, **58**, 204 (1969).
(5) *Ibid.*, **58**, 364 (1969).
(6) H. Burrell, *Interchem. Rev.*, **14**, 3 (1955).
(7) A. N. Paruta, *J. Pharm. Sci.*, **58**, 216 (1969).
(8) A. N. Paruta, B. J. Sciarrone, and N. G. Lordi, *ibid.*, **53**, 463 (1964).
(9) *Ibid.*, **53**, 1349 (1964).
(10) A. N. Paruta and S. A. Irani, *J. Pharm. Sci.*, **55**, 1060 (1966).
(11) A. N. Paruta, *ibid.*, **53**, 636 (1964).
(12) A. N. Paruta, B. J. Sciarrone, and N. G. Lordi, *ibid.*, **54**, 1325 (1965).
(13) A. N. Paruta and S. A. Irani, *ibid.*, **54**, 1334 (1965).
(14) A. N. Paruta, *ibid.*, **56**, 1565 (1967).
(15) J. H. Hildebrand, *Chem. Rev.*, **44**, 37 (1949).
(16) J. H. Hildebrand and R. L. Scott, "Solubility of Non-electrolytes," 3rd ed., Reinhold, New York, N.Y., 1950, p. 427.
(17) J. H. Hildebrand and R. L. Scott, "Regular Solutions," Prentiss-Hall, Englewood Cliffs, N.J., 1962, p. 20.
(18) J. H. Hildebrand, R. L. Scott, and J. M. Pransnitz, "Regular and Related Solutions," Van Nostrand Reinhold, New York, N.Y., 1970, pp. 24, 47, 92.
(19) J. H. Hildebrand and H. A. Benesi, *J. Am. Chem. Soc.*, **70**, 3978 (1948).
(20) J. H. Hildebrand, *ibid.*, **41**, 1067 (1919).
(21) *Ibid.*, **56**, 995 (1934).
(22) J. H. Hildebrand and K. Shinoda, *J. Phys. Chem.*, **62**, 295 (1958).
(23) F. A. Restaino and A. N. Martin, *J. Pharm. Sci.*, **53**, 636 (1964).
(24) S. A. Kahlil and A. N. Martin, *ibid.*, **56**, 1225 (1967).

ACKNOWLEDGMENTS AND ADDRESSES

Received March 15, 1974, from the *College of Pharmacy, University of Rhode Island, Kingston, RI 02881.*

Accepted for publication January 12, 1976.

Abstracted in part from a dissertation submitted by K. S. Alexander to the Graduate School, University of Rhode Island, in partial fulfillment of the Doctor of Philosophy degree requirements.

* Present address: College of Pharmacy, University of Toledo, Toledo, OH 43606.

‡ Present address: School of Pharmacy, West Virginia University, Morgantown, WV 26506.

§ Department of Chemistry, University of Rhode Island, Kingston, RI 02881.

ˣ To whom inquiries should be directed.

Fluorocarbon Aerosol Propellants XI: Pharmacokinetics of Dichlorodifluoromethane in Dogs following Single and Multiple Dosing

SARFARAZ NIAZI and WIN L. CHIOU ˣ

Abstract □ A three-compartment open model was proposed for the disposition of dichlorodifluoromethane in dogs with average half-lives of 1.47, 7.95, and 58.5 min for the three disposition phases. This proposal is contrary to several studies that monitored blood levels for a shorter period. An analysis of the tissue compartment distribution following a single dose showed that about 1.5 hr was required to achieve pseudodistribution equilibration, following which more than 90% of the dose remaining in the body was retained in the tissue compartments. The pulmonary clearance and volumes of distribution were calculated considering the first-pass effect through the lungs. The volume of distribution after reaching pseudodistribution equilibrium was approximately 10 times the body weight in terms of the blood concentration, and about 68% of the propellant was cleared from the blood passing through the lungs in each cycle. Disposition of the propellant followed dose-independent kinetics after multiple dosing. No volatile metabolites were detected in the blood using GC.

Keyphrases □ Fluorocarbon aerosol propellants—dichlorodifluoromethane, single and multiple dosing, pharmacokinetic model proposed, dogs □ Aerosol propellants, fluorocarbon—dichlorodifluoromethane, single and multiple dosing, pharmacokinetic model proposed, dogs □ Dichlorodifluoromethane—single and multiple dosing, pharmacokinetic model proposed, dogs □ Pharmacokinetics—dichlorodifluoromethane, single and multiple dosing, three-compartment open model proposed, dogs □ Distribution—dichlorodifluoromethane, single and multiple dosing, pharmacokinetic model proposed, dogs

The toxicity aspects of fluorocarbon aerosol propellants reflected in their pharmacokinetics were reported recently (1–5). A similar approach is made here for the most commonly used fluorocarbon aerosol propellant, dichlorodifluoromethane, to show that this compound has a longer biological half-life than speculated and undergoes extensive distribution in body tissues. These findings may have bearing on the toxicity profile of this compound.

EXPERIMENTAL

Dichlorodifluoromethane[1] was administered intravenously in polyethylene glycol 400 solution to four male mongrel, unanesthetized, conditioned dogs, 16.8–20 kg. The doses of dichlorodifluoromethane administered ranged from 71 to 135 mg. Procedural details for the preparation of the dosage forms, animal preparation, single- and multiple-dose administrations, blood samples, and analysis of fluorocarbon in the blood samples were reported earlier (3, 4). The blood samples were analyzed as soon as possible to avoid any loss during storage (6). A duplicate study was performed on Dog 2976.

RESULTS AND DISCUSSION

Dosage Form and Route of Administration—The intravenous dosage form was selected to avoid the problems of biological availability in inhalation and oral administration (7–10). This mode of administration would be equivalent to inhalation (3, 4) if one considers that the intravenously administered fluorocarbon first passes through the lungs before being monitored in the blood. The fluorocarbon concentration profile in blood would, therefore, appear as if the fluorocarbon had been administered *via* inhalation, the customary route of its uptake.

Pharmacokinetic Model—In all instances, the blood concentration–time curves were characterized by three exponential equations, which can be represented as a three-compartment open model for the disposition of dichlorodifluoromethane (Fig. 1). The two compartments besides the central compartment can be described as the group of tissues with distinct affinity and capacity for dichlorodifluoromethane. The difference in the affinity may be due to solubility characteristics or to specific interactions such as protein binding or other complexations (11–15). A compartment can also be distinguished based on the blood supply to the tissues such as the vessel-rich group and the vessel-poor group (14, 16).

For further analysis of this model (Scheme I) to calculate various rate constants, a digital computer program was generated based on reported differential equation solutions (17).

The fraction of dose remaining in various pharmacokinetic compartments can be described in terms of hybrid constants (17):

$$X_1/X_0 = C_1e^{-b_1t} + C_2e^{-b_2t} + C_3e^{-b_3t} \quad \text{(Eq. 1)}$$

$$X_2/X_0 = C_{12}e^{-b_1t} + C_{22}e^{-b_2t} + C_{32}e^{-b_3t} \quad \text{(Eq. 2)}$$

$$X_3/X_0 = C_{13}e^{-b_1t} + C_{23}e^{-b_2t} + C_{33}e^{-b_3t} \quad \text{(Eq. 3)}$$

where X_1, X_2, and X_3 are the amounts of fluorocarbon present in different compartments; and X_0 is the dose that, in the model proposed, remains in the body after the first pass through the lungs, as described later.

The values of these pharmacokinetic parameters calculated for dichlorodifluoromethane are summarized in Table I.

Recently, Adir *et al.* (10) also proposed a pharmacokinetic model for this propellant, suggesting a two-compartment body distribution in dogs.

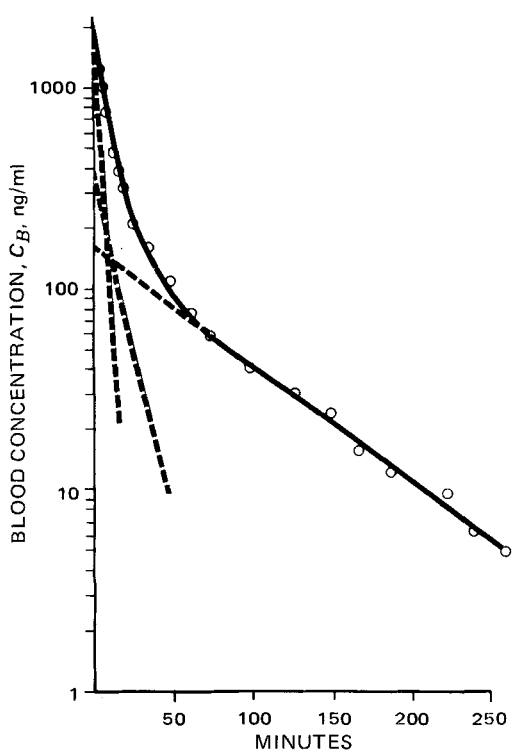

Figure 1—*Triexponential blood concentration decay following intravenous administration of 105.0 mg of dichlorodifluoromethane in 6.6 ml of polyethylene glycol 400 to a 19-kg dog:* $C_B = 1200e^{-0.227t} + 375e^{-0.079t} + 164e^{-0.016t}$

[1] E. I. du Pont De Nemours & Co., Wilmington, Del.

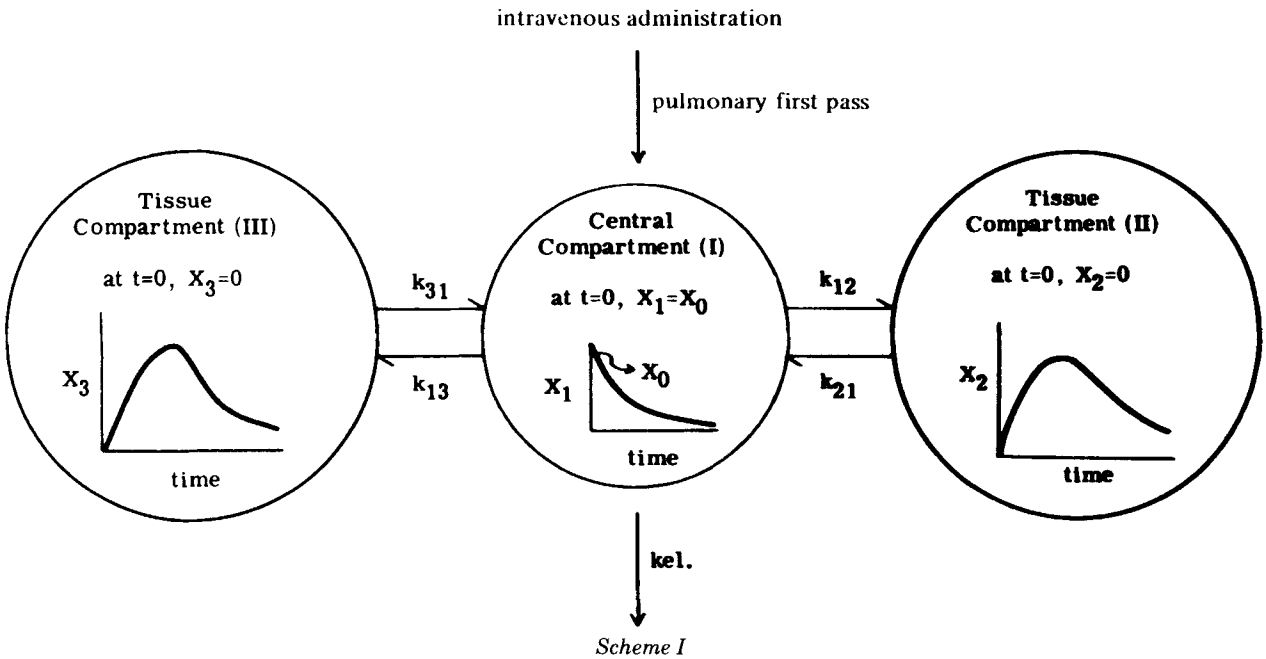

Scheme I

However, their study (10) monitored the blood levels following inhalation for only about 20–30 min, which does not allow for the elucidation of equilibration with the deeper tissue compartment. A comparison of initial and intermediate rate constants (b_1 and b_2 in Table I) shows good agreement with the values reported recently (10). For example, our average value of 0.60 min^{-1} for b_1 compared with 0.64 min^{-1} (10) and the value of 0.09 min^{-1} for b_2 compared with 0.07 min^{-1} (10). However, the actual values of these rate constants in the study of Adir *et al.* (10) will be higher if the deeper tissue compartment is "peeled off" from the observed blood concentrations.

Volume of Distribution and Pulmonary Clearance—In the present study, the dose administered is not the same as the dose made available to the body, since the total dose passes through the lungs where a significant fraction can be eliminated before it is distributed to the body. Therefore, an equation correcting for this first-pass effect was used to calculate the apparent volume of distribution following pseudodistribution equilibrium (3, 4, 18):

$$(V_d)_{b_3} = \frac{PFR \times D^0}{b_3(AUC \times PFR + D^0)} \qquad \text{(Eq. 4)}$$

where *PFR* is the pulmonary flow rate (~cardiac output), *AUC* is the total area under the blood concentration–time curve (extrapolated to time infinity), and D^0 is the dose administered. Equation 4, however, assumes that the pulmonary clearance is the only route of elimination for the compound. In the present study, no volatile metabolites could be detected from the blood sample by the GC analysis. Since the fluorocarbon studied in this investigation has been shown to be primarily eliminated intact from the lungs (19), Eq. 4 can be used as an approximation for the determination of the volume of distribution and pulmonary clearance (*PC*):

$$PC = (V_d)_{b_3}(b_3) \qquad \text{(Eq. 5)}$$

The fraction eliminated in each pass through the lungs, $(1 - f)$, can be calculated as:

$$(1 - f) = \frac{PC}{PFR} \qquad \text{(Eq. 6)}$$

Table II shows the values of the volume of distribution following pseudodistribution equilibrium to be almost 10 times the body weight. This finding indicates an extensive distribution of dichlorodifluoromethane to the body tissues. Recent findings on the binding of the propellant to human and bovine albumin (11) suggest that the propellant may be bound also to other tissue components. The possible high solubility in the fat tissue due to its lipophilic physical property also may contribute to the high apparent volume of distribution, as was found for trichloromonofluoromethane in dogs (3, 15) and chloroform in humans (20).

Table I—Pharmacokinetic Parameters of Dichlorodifluoromethane from Five Studies

Parameter[a]	Dog 3287	Dog 3288	Dog 3457	Dog 2976a	Dog 2976b
b_1	0.99	0.495	0.840	0.227	0.495
b_2	0.139	0.0894	0.0729	0.079	0.0792
b_3	0.0133	0.0103	0.0133	0.0157	0.009
C_1	0.967	0.920	0.843	0.690	0.904
C_2	0.0281	0.0763	0.134	0.216	0.0914
C_3	0.00445	0.00340	0.0231	0.0943	0.00452
C_{12}	−0.149	−0.242	−0.537	−0.261	−0.300
C_{22}	0.146	0.239	0.482	0.223	0.296
C_{32}	0.00379	0.00302	0.0548	0.0376	0.00509
C_{13}	−0.172	−0.0676	−0.0870	−0.170	−0.0772
C_{23}	−0.0400	−0.0348	−0.214	−0.208	−0.0549
C_{33}	0.212	0.102	0.301	0.378	0.132
K_{el}	0.661	0.328	0.218	0.0851	0.287
K_{21}	0.163	0.121	0.189	0.119	0.118
K_{31}	0.017	0.011	0.0198	0.0280	0.0104
K_{13}	0.173	0.0355	0.084	0.0492	0.0414
K_{12}	0.128	0.0984	0.415	0.0410	0.125
D^0b, mg	71	178	103	105	135
AUC^∞, μg/ml × min	15.6	16.5	16.0	20.4	18.10

[a] The units for all *b* and *k* values are minutes^{-1}. [b] $X_0 = (f)D^0$, where (f) is the fraction retained after the first pass through the lungs.

Table II—Volumes of Distribution and Clearance of Dichlorodifluoromethane

Dog	$(V_d)_{b_3}$, liters	V_c, liters	PC, liters/min	$(1-f)$, %
3287	135.5	2.73	1.81	60.21
3288	228.5	7.14	2.35	78.20
3457	153.4	9.37	2.04	68.17
2976a	120.3	22.25	1.89	63.14
2976b	237.7	7.45	2.14	71.31
Mean ± *SEM*	175.1 ± 24.3	9.79 ± 3.30	2.05 ± 0.09	68.21 ± 3.15

The average pulmonary clearance values show a clearance of 2.05 liters/min, corresponding to 68% clearance in each passage through the lungs. An error of this magnitude would have been made in the calculation of the volume of distribution had the correction due to the first-pass pulmonary effect not been made, as explained earlier.

The volume of the central compartment, from which the actual elimination takes place, can be calculated easily, since the clearance from the central compartment should be equal to the clearance from the body:

$$(V_d)_{b_3}(b_3) = (V_c)(K_{el}) \qquad \text{(Eq. 7)}$$

where K_{el} is the elimination rate constant from the central compartment. Table II also shows the values for the volumes of the central compartment. Smaller volumes as compared to the total volumes of distribution indicate the retention of a smaller fraction in the central compartment as compared to tissue compartments after the pseudodistribution phase.

Disposition Half-Lives—Table III shows the half-lives for three disposition phases of dichlorodifluoromethane. The terminal disposition half-lives reported here are much longer than those previously reported or speculated (7, 8, 10, 21–23).

The finding that dichlorodifluoromethane shows a multiexponential decay in the blood concentration can be utilized to study the elimination rate constant from the body and to evaluate the accumulation in the body following single or multiple exposures.

Retention following Single Intravenous Administration—Following administration of dichlorodifluoromethane through intravenous infusion, the concentration in the blood dropped sharply. Such an observation also was reported for fluorocarbons following their inhalation (10, 21–23). However, such sharp declines in blood concentrations do not necessarily follow a parallel loss of drug from the body (24). The amount of drug remaining in the body as a function of time can also be calculated using (24):

$$\text{fraction remaining in body} = \frac{(C_1/b_1)e^{-b_1t} + (C_2/b_2)e^{-b_2t} + (C_3/b_3)e^{-b_3t}}{(C_1/b_1) + (C_2/b_2) + (C_3/b_3)} \qquad \text{(Eq. 8)}$$

Figure 2 shows a plot of the amount of dichlorodifluoromethane remaining in the body and in various tissue compartments, as described previously. For example, the amount of dichlorodifluoromethane in the central compartment dropped to about 12% of the absorbed dose (dose after the pulmonary first pass) in 25 min, but about 45% of the absorbed dose was still present in the body.

Although the steady state was reached rather quickly, as indicated by arrows in Fig. 3, the ratio of the amount in tissue compartments over that in the central compartment continues increasing until attainment of the pseudodistribution equilibrium, which would take about 90 min. This finding is of importance because it was quite contrary to previous claims of fast elimination of fluorocarbons from the body (8, 21–23).

The total amount of the absorbed dose retained following pseudodistribution equilibrium is an important parameter, especially for extrapolating the single-dose study to multiple-dose studies. Table IV shows the retention of dichlorodifluoromethane in the tissue and central compartments after pseudodistribution equilibrium has been reached. The fraction of the fluorocarbon retained in the tissue compartments compared to that in the central compartment shows that more than 90% of the total amount present in the body is retained in tissue compartments.

Multiple-Dose Kinetics—The pharmacokinetic parameters calculated following single-dose administration (Table I) can be used to simulate multiple-dose kinetics. A typical study, such as the one with Dog 2976a, was used to generate[2] multiple-dose disposition curves. These curves were then superimposed on the experimental data obtained from two separate studies (Fig. 4). A good agreement between theoretical and experimental values provides the basis for the validity of the premise involved in the generation of multiple-dose curves that each dose decayed independently of the amount present in the body. In other words, dose-independent kinetics were operative for the disposition of this compound in the dose range studied.

Table III—Disposition Half-Lives of Dichlorodifluoromethane

Disposition Phase	Half-Life (Mean ± *SEM*), min (n = 5)
Initial	1.47 ± 0.42[a]
Intermediate	7.95 ± 0.79
Final	58.50 ± 5.99

[a] This value may be slightly different from the true value, because the experimental value would be influenced by the duration of the intravenous infusion.

Table IV—Average Retention ± *SEM* of Dichlorodifluoromethane at 200 min following Pseudodistribution Equilibrium in Various Compartments

Retention	$X_2 + X_3$ Compartments	X_1 Compartment
Percent of absorbed dose	1.88 ± 0.22	0.14 ± 0.07
Relative percent of total amount in body	93.0 ± 10.9	7.0 ± 3.5

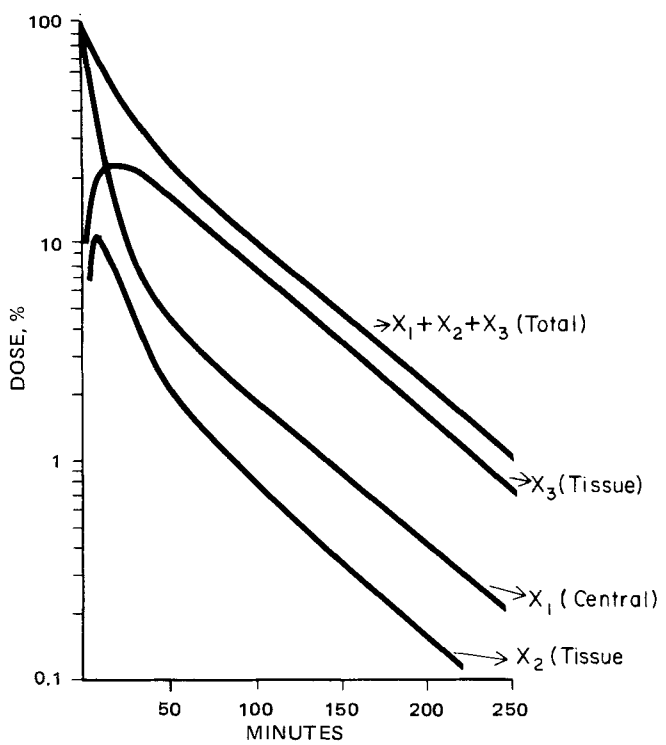

Figure 2—*Percent of absorbed dichlorodifluoromethane remaining in various body compartments based on a typical study (Dog 2976a).*

[2] IBM 370 computer at the University of Illinois Medical Center.

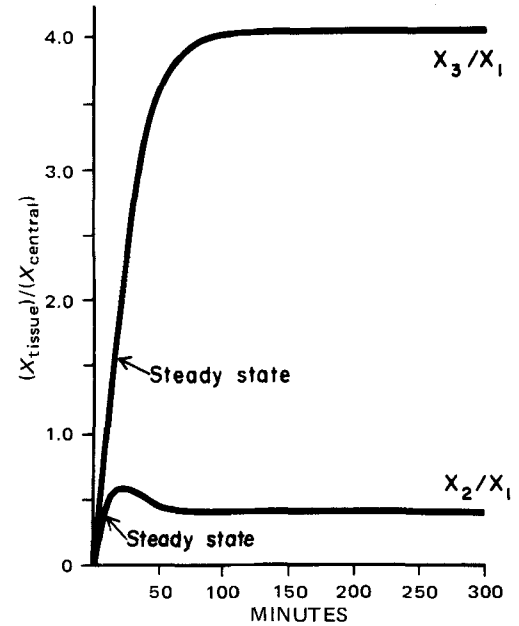

Figure 3—*Comparison of the relative amount of dichlorodifluoromethane remaining in tissue and central compartments based on a typical study (Dog 2976a).*

This approach allows the assessment of the accumulation of dichlorodifluoromethane in the tissue compartments during multiple exposures in the frequent use of commercial products containing fluorocarbon propellants. Figure 5 shows the calculated amount of dichlorodifluoromethane distributed to various tissue compartments following six doses. The magnitude of the problem of accumulation during multiple exposures to dichlorodifluoromethane is well emphasized in this study. For example, the total amount eventually accumulated in the tissues may well exceed the amount administered in one dose (Fig. 5).

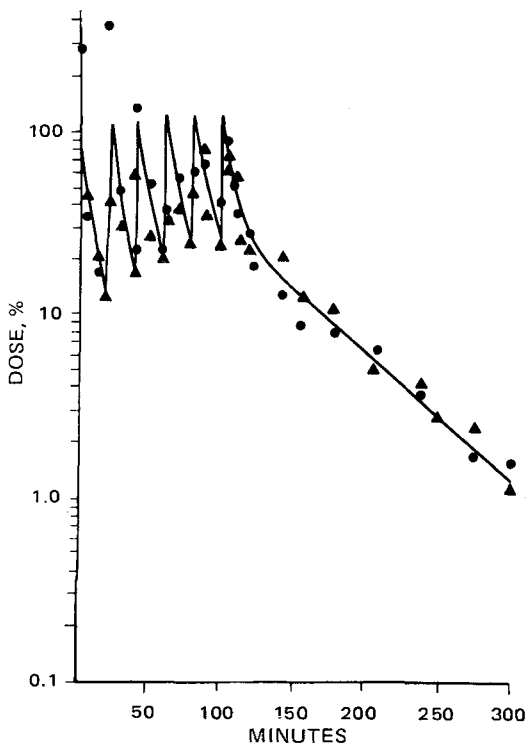

Figure 4—*Percent of absorbed dose remaining in the central compartment following six intravenous administrations of 74 (●) or 89 (▲) mg of dichlorodifluoromethane every 20 min. The solid curve represents the theoretical values based on a typical set of pharmacokinetic parameters obtained from a single-dose study (Dog 2976a).*

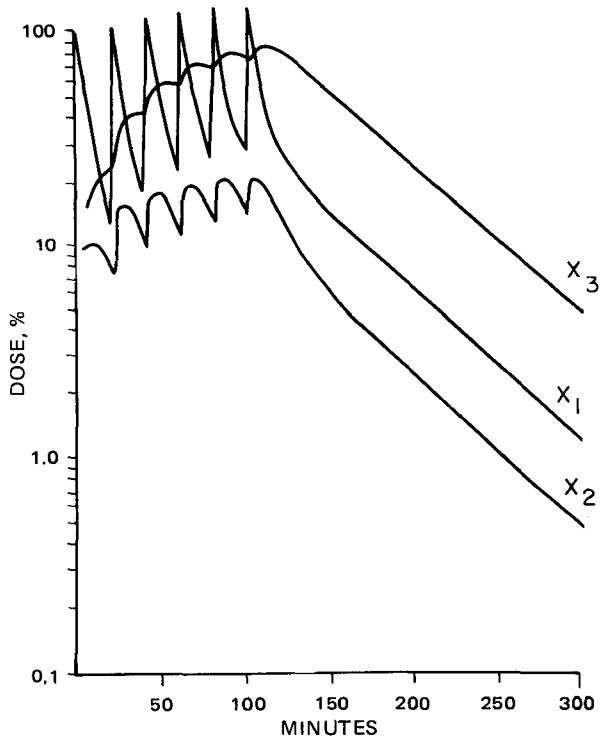

Figure 5—*Computer-generated curves for the distribution of dichlorodifluoromethane in various pharmacokinetic compartments following instantaneous absorption of six doses of 100 units each every 20 min. The pharmacokinetic parameters were obtained from a typical single-dose study (Dog 2976a).*

The toxicological aspects of the observations made here can be twofold. First, during excessive inhalation, it is possible that high tissue levels may be reached in spite of the high volatility of dichlorodifluoromethane. Sudden deaths reported following inhalation of aerosol packages can be attributed, at least in part, to the reaching of threshold toxic limits, although no such direct and reliable data have ever been reported. Second, the accumulation following multiple exposures can result in much higher deep tissue compartment levels than would be apparent from blood levels. Hence, the possibility of chronic toxicity cannot be ruled out entirely.

The toxicological implications of the use of aerosol packages containing fluorocarbon propellants and the environmental pollution hazard from these compounds are matters of controversy, but the data presented here warn against misleading toxicological interpretations that result from the application of erroneous pharmacokinetic principles.

REFERENCES

(1) W. L. Chiou, *J. Am. Med. Assoc.*, **227,** 658 (1974).
(2) *Ibid.*, **229,** 1722 (1974).
(3) S. Niazi and W. L. Chiou, *J. Pharm. Sci.*, **64,** 763 (1975).
(4) *Ibid.*, **65,** 60 (1976).
(5) C. T. Dollery, W. M. Faith, G. H. Draffan, G. Wise, H. Sahgoun, J. W. Paterson, and S. R. Walker, *Clin. Pharmacol. Ther.*, **15,** 59 (1974).
(6) W. L. Chiou and J. H. Hsiao, *J. Pharm. Sci.*, **63,** 1614 (1974).
(7) L. Shargel and R. Koss, *ibid.*, **61,** 1445 (1972).
(8) A. Azar, H. J. Trochimowicz, J. B. Terrill, and L. S. Mullin, *Am. Ind. Hyg. Assoc. J.*, **34,** 102 (1973).
(9) J. B. Terrill, *ibid.*, **33,** 736 (1972).
(10) J. Adir, D. A. Blake, and G. M. Mergner, *J. Clin. Pharmacol.*, **15,** 760 (1975).
(11) W. L. Chiou and J. H. Hsiao, *Res. Commun. Chem. Pathol. Pharmacol.*, **8,** 273 (1974).
(12) W. L. Chiou and J. H. Hsiao, *Pharmacology*, **13,** 128 (1975).
(13) W. L. Chiou and J. H. Hsiao, *J. Pharm. Sci.*, **64,** 1052 (1975).
(14) J. H. Hsiao and W. L. Chiou, *Pharmacology*, **12,** 303 (1974).
(15) K. Chang and W. L. Chiou, *J. Pharm. Sci.*, **65,** 55 (1976).
(16) M. Gibaldi, R. Nagashima, and G. Levy, *ibid.*, **58,** 193 (1969).

(17) A. Rescigno and G. Segre, "Drug and Tracer Kinetics," Blaisdell, New York, N.Y., 1966.
(18) W. L. Chiou, *Res. Commun. Chem. Pathol. Pharmacol.*, **7**, 679 (1974).
(19) A. Morgan, S. Black, and D. R. Belcher, *Int. J. Appl. Isotop.*, **23**, 285 (1972).
(20) W. L. Chiou, *J. Pharmacokinet. Biopharm.*, **3**, 193 (1975).
(21) C. T. Dollery, G. H. Draffan, D. S. Davies, F. M. William, and M. E. Conolly, *Lancet*, **1**, 1164 (1970).
(22) J. W. Paterson, M. F. Sudlow, and S. R. Walker, *ibid.*, **2**, 565 (1971).
(23) D. A. McClure, *Toxicol. Appl. Pharmacol.*, **22**, 221 (1972).
(24) W. L. Chiou, *J. Pharm. Pharmacol.*, **34**, 342 (1972).

ACKNOWLEDGMENTS AND ADDRESSES

Received October 22, 1975, from the *Department of Pharmacy, College of Pharmacy, University of Illinois at the Medical Center, Chicago, IL 60612.*

Accepted for publication February 26, 1976.

Abstracted in part from a dissertation submitted by S. Niazi to the Graduate College, University of Illinois at the Medical Center, in partial fulfillment of the Doctor of Philosophy degree requirements.

Supported in part by Food and Drug Administration Grant 1 R01 FD-00574-01 and in part by Public Health Service General Research Support Grant 1-501-RR05735-01.

[x] To whom inquiries should be directed.

Distribution and Pharmacokinetics of Triamterene in Rats

SEN T. KAU and B. V. RAMA SASTRY [x]

Abstract □ The tissue distribution of ^{14}C-triamterene was examined in the rat. After intravenous administration of ^{14}C-triamterene, high concentration ratios between tissues and blood were found in most tissues except the brain, fat, and testes. The maximal concentration of the drug was in the kidneys, liver, heart, lungs, and skeletal muscle within the first 20 min, when the maximal natriuresis was observed. No metabolite of triamterene was detected in these tissues. The pharmacokinetics of ^{14}C-triamterene also were investigated. The volume of distribution of the drug was greater in the central compartment (60% of the dose) than in the peripheral compartment (40%). The binding of the drug to skeletal muscle is responsible for the fraction of the dose in the peripheral compartment. Rate constants indicate that slow elimination of triamterene is related to its binding to tissue in the central compartment.

Keyphrases □ Triamterene—distribution and pharmacokinetics, radiochemical analysis, rats □ Drug distribution—triamterene, radiochemical analysis, rats □ Pharmacokinetics—triamterene, radiochemical analysis, rats □ Radiochemistry—analysis, triamterene distribution, rats □ Diuretic agents—triamterene, distribution and pharmacokinetics, radiochemical analysis, rats

Triamterene, in addition to its renal effects, significantly decreases the sodium content of cardiac and skeletal muscle without impairing the potassium content in the rat (1). Although an unusual tissue distribution of triamterene was reported in guinea pigs and baboons (2), its distribution in the rat has not been studied. Previous studies (3, 4) indicated that unchanged triamterene itself, rather than its metabolites, accounts for the observed changes of renal clearance of electrolytes.

It is not known whether the metabolism of triamterene in cardiac and skeletal muscle is similar to that in the kidneys in the rat. The contribution of the drug distributed in the tissue and of its metabolites to the total elimination of triamterene by humans and animals also is not known. The purpose of this study was to determine the tissue distribution and pharmacokinetics of triamterene in the rat to obtain a better understanding of the rate of distribution and elimination of triamterene and its extrarenal action.

EXPERIMENTAL

Animals and Materials—Male Sprague–Dawley rats[1], 200–250 g, were used. ^{14}C-Triamterene[2] (0.92 mCi/mmole) was used as supplied. It was found to be chemically pure by descending paper chromatography in two solvent systems, 1-butanol–acetic acid–water (4:1:1) and 2-propanol–water–ammonia (140:50:10), according to literature methods (4–6). A 4 × 4 countercurrent distribution of ^{14}C-triamterene between ethyl acetate (14 ml) and 0.1 *M* borate buffer at pH 10.00 (7 ml) showed that it behaved like a single compound (6–8).

Other commercially available chemical reagents were used.

Tissue Distribution—Rats were prepared for infusion as described previously (9), and ^{14}C-triamterene[3] (1, 2, or 4 mg/kg; 3.8 μCi/mg) was administered by intravenous infusion for 8 min at 0.5 ml/min/kg. Samples of blood and urine were collected 40 min after the beginning of the infusion, and the rat was then immediately decapitated. Submaxillary and thyroid glands, thymus, aorta, heart, lungs, liver, pancreas, spleen, adrenals, kidneys, ileum, biceps femoris, epididymal fat pads, testes, and brain were dissected, blotted, and weighed. The distribution of ^{14}C-triamterene and its metabolites was determined at 40 min, when the maximal potassium-sparing effect of triamterene was observed (3).

In a second series of experiments, a constant dose of ^{14}C-triamterene (2 mg/kg, 3.8 μCi/mg) was administered by infusion; the rats were sacrificed at intervals of 10, 20, 40, or 60 min thereafter. Plasma, liver, lung, heart, kidney, skeletal muscle (biceps femoris), and urine samples were collected.

The total carbon-14 in the tissues samples was measured[4]. About 200 mg of tissue was placed into a 20-ml glass counting vial. A 2-ml aliquot of liquid scintillation solute[5] was added, and the sample was shaken[6] at 50° until solubilized. To increase the counting efficiency of some heavily colored tissues (blood, liver, lungs, and spleen), 0.6 ml of benzoyl peroxide solution was added to the solubilized sample, and the mixture was shaken for an additional 0.5 hr to obtain a colorless solution.

To the solubilized tissues, 18 ml of counting solution[7] was added. The samples were cooled to 4° for 24 hr prior to counting. All samples were counted twice for 10 min. All data were converted to disintegrations per

[1] Holtzman, Inc., Madison, Wis.
[2] Smith Kline and French Laboratories, Inc.
[3] Triamterene was solublized in Solution A, containing inulin (0.15%), aminohippuric acid (0.2%), and ketamine (8 mg/kg/ml), with the aid of a few drops of 8.5% lactic acid and warming. The total volume administered was 4 ml/kg.
[4] Packard liquid scintillation counter.
[5] Soluene, Packard Instrument Co.
[6] Dubnoff metallic shaker.
[7] Phase Combing System, Amersham/Searle Corp.

(17) A. Rescigno and G. Segre, "Drug and Tracer Kinetics," Blaisdell, New York, N.Y., 1966.
(18) W. L. Chiou, *Res. Commun. Chem. Pathol. Pharmacol.*, **7**, 679 (1974).
(19) A. Morgan, S. Black, and D. R. Belcher, *Int. J. Appl. Isotop.*, **23**, 285 (1972).
(20) W. L. Chiou, *J. Pharmacokinet. Biopharm.*, **3**, 193 (1975).
(21) C. T. Dollery, G. H. Draffan, D. S. Davies, F. M. William, and M. E. Conolly, *Lancet*, **1**, 1164 (1970).
(22) J. W. Paterson, M. F. Sudlow, and S. R. Walker, *ibid.*, **2**, 565 (1971).
(23) D. A. McClure, *Toxicol. Appl. Pharmacol.*, **22**, 221 (1972).
(24) W. L. Chiou, *J. Pharm. Pharmacol.*, **34**, 342 (1972).

ACKNOWLEDGMENTS AND ADDRESSES

Received October 22, 1975, from the *Department of Pharmacy, College of Pharmacy, University of Illinois at the Medical Center, Chicago, IL 60612.*

Accepted for publication February 26, 1976.

Abstracted in part from a dissertation submitted by S. Niazi to the Graduate College, University of Illinois at the Medical Center, in partial fulfillment of the Doctor of Philosophy degree requirements.

Supported in part by Food and Drug Administration Grant 1 R01 FD-00574-01 and in part by Public Health Service General Research Support Grant 1-501-RR05735-01.

[x] To whom inquiries should be directed.

Distribution and Pharmacokinetics of Triamterene in Rats

SEN T. KAU and B. V. RAMA SASTRY [x]

Abstract □ The tissue distribution of ^{14}C-triamterene was examined in the rat. After intravenous administration of ^{14}C-triamterene, high concentration ratios between tissues and blood were found in most tissues except the brain, fat, and testes. The maximal concentration of the drug was in the kidneys, liver, heart, lungs, and skeletal muscle within the first 20 min, when the maximal natriuresis was observed. No metabolite of triamterene was detected in these tissues. The pharmacokinetics of ^{14}C-triamterene also were investigated. The volume of distribution of the drug was greater in the central compartment (60% of the dose) than in the peripheral compartment (40%). The binding of the drug to skeletal muscle is responsible for the fraction of the dose in the peripheral compartment. Rate constants indicate that slow elimination of triamterene is related to its binding to tissue in the central compartment.

Keyphrases □ Triamterene—distribution and pharmacokinetics, radiochemical analysis, rats □ Drug distribution—triamterene, radiochemical analysis, rats □ Pharmacokinetics—triamterene, radiochemical analysis, rats □ Radiochemistry—analysis, triamterene distribution, rats □ Diuretic agents—triamterene, distribution and pharmacokinetics, radiochemical analysis, rats

Triamterene, in addition to its renal effects, significantly decreases the sodium content of cardiac and skeletal muscle without impairing the potassium content in the rat (1). Although an unusual tissue distribution of triamterene was reported in guinea pigs and baboons (2), its distribution in the rat has not been studied. Previous studies (3, 4) indicated that unchanged triamterene itself, rather than its metabolites, accounts for the observed changes of renal clearance of electrolytes.

It is not known whether the metabolism of triamterene in cardiac and skeletal muscle is similar to that in the kidneys in the rat. The contribution of the drug distributed in the tissue and of its metabolites to the total elimination of triamterene by humans and animals also is not known. The purpose of this study was to determine the tissue distribution and pharmacokinetics of triamterene in the rat to obtain a better understanding of the rate of distribution and elimination of triamterene and its extrarenal action.

EXPERIMENTAL

Animals and Materials—Male Sprague–Dawley rats[1], 200–250 g, were used. ^{14}C-Triamterene[2] (0.92 mCi/mmole) was used as supplied. It was found to be chemically pure by descending paper chromatography in two solvent systems, 1-butanol–acetic acid–water (4:1:1) and 2-propanol–water–ammonia (140:50:10), according to literature methods (4–6). A 4 × 4 countercurrent distribution of ^{14}C-triamterene between ethyl acetate (14 ml) and 0.1 *M* borate buffer at pH 10.00 (7 ml) showed that it behaved like a single compound (6–8).

Other commercially available chemical reagents were used.

Tissue Distribution—Rats were prepared for infusion as described previously (9), and ^{14}C-triamterene[3] (1, 2, or 4 mg/kg; 3.8 μCi/mg) was administered by intravenous infusion for 8 min at 0.5 ml/min/kg. Samples of blood and urine were collected 40 min after the beginning of the infusion, and the rat was then immediately decapitated. Submaxillary and thyroid glands, thymus, aorta, heart, lungs, liver, pancreas, spleen, adrenals, kidneys, ileum, biceps femoris, epididymal fat pads, testes, and brain were dissected, blotted, and weighed. The distribution of ^{14}C-triamterene and its metabolites was determined at 40 min, when the maximal potassium-sparing effect of triamterene was observed (3).

In a second series of experiments, a constant dose of ^{14}C-triamterene (2 mg/kg, 3.8 μCi/mg) was administered by infusion; the rats were sacrificed at intervals of 10, 20, 40, or 60 min thereafter. Plasma, liver, lung, heart, kidney, skeletal muscle (biceps femoris), and urine samples were collected.

The total carbon-14 in the tissues samples was measured[4]. About 200 mg of tissue was placed into a 20-ml glass counting vial. A 2-ml aliquot of liquid scintillation solute[5] was added, and the sample was shaken[6] at 50° until solubilized. To increase the counting efficiency of some heavily colored tissues (blood, liver, lungs, and spleen), 0.6 ml of benzoyl peroxide solution was added to the solubilized sample, and the mixture was shaken for an additional 0.5 hr to obtain a colorless solution.

To the solubilized tissues, 18 ml of counting solution[7] was added. The samples were cooled to 4° for 24 hr prior to counting. All samples were counted twice for 10 min. All data were converted to disintegrations per

[1] Holtzman, Inc., Madison, Wis.
[2] Smith Kline and French Laboratories, Inc.
[3] Triamterene was solublized in Solution A, containing inulin (0.15%), aminohippuric acid (0.2%), and ketamine (8 mg/kg/ml), with the aid of a few drops of 8.5% lactic acid and warming. The total volume administered was 4 ml/kg.
[4] Packard liquid scintillation counter.
[5] Soluene, Packard Instrument Co.
[6] Dubnoff metallic shaker.
[7] Phase Combing System, Amersham/Searle Corp.

Table I—Distribution of Triamterene and Its Metabolites in Various Tissues[a]

Sample	4-mg/kg Dose			2-mg/kg Dose			1-mg/kg Dose		
	nCi/g[b]	T/B[c]	Found[d], %	nCi/g	T/B	Found, %	nCi/g	T/B	Found, %
Blood	4.26 ± 0.16	—	2.56 ± 0.09	2.20 ± 0.01	—	2.12 ± 0.13	1.10	—	2.28 ± 0.16
Submaxillary glands	24.38 ± 1.98	5.72	0.52 ± 0.04	11.07 ± 1.78	5.43	0.48 ± 0.07	7.16 ± 1.26	6.50	0.50 ± 0.08
Thyroid gland	16.42 ± 2.75	3.85	<0.01	8.54 ± 0.80	3.88	<0.01	6.12 ± 0.70	5.56	<0.01
Adrenal glands	23.69 ± 0.85	5.56	0.03	11.44 ± 1.13	5.20	0.03	6.75 ± 1.26	6.13	0.03
Thymus	15.82 ± 0.29	3.71	0.29	7.13 ± 0.68	3.23	0.26 ± 0.02	4.25 ± 0.36	3.86	0.25 ± 0.02
Spleen	13.53 ± 0.62	3.17	0.35 ± 0.01	6.86 ± 0.69	3.11	0.36 ± 0.03	4.24 ± 0.61	3.85	0.36 ± 0.05
Pancreas	16.61 ± 2.73	3.91	0.87 ± 0.14	8.58 ± 0.25	3.94	0.92 ± 0.02	4.80 ± 0.91	4.36	0.83 ± 0.15
Skeletal muscle	9.01 ± 1.10	2.11	40.95 ± 1.68	4.51 ± 0.61	2.05	36.66 ± 0.98	2.70 ± 0.10	2.45	33.79 ± 4.88
Intestine	8.18 ± 0.54	1.92	1.82 ± 0.01	4.32	1.96	1.96 ± 0.01	2.18	1.98	1.58 ± 0.05
Aorta	16.31 ± 1.17	3.83	—	6.79 ± 0.48	3.08	—	3.87 ± 0.15	3.51	—
Testes	2.87 ± 0.56	0.67	0.36 ± 0.07	1.39 ± 0.15	0.63	0.34 ± 0.03	0.72	0.65	0.30 ± 0.02
Brain	1.27	0.30	0.08	0.65	0.29	0.09	0.35	0.31	0.08
Fat	2.82	0.66	4.66 ± 0.26	0.91	0.41	3.24 ± 0.28	0.57	0.51	3.11 ± 0.46
Liver	17.05 ± 0.52	4.00	6.43 ± 0.19	10.18 ± 1.33	4.62	7.78 ± 1.02	5.56 ± 0.43	5.06	6.84 ± 2.05
Heart	10.41 ± 0.52	2.44	0.33 ± 0.01	4.69 ± 0.53	2.13	0.30 ± 0.03	2.71 ± 0.21	2.46	0.28 ± 0.02
Lungs	10.03 ± 0.74	2.35	0.45 ± 0.03	5.15 ± 0.76	3.24	0.47 ± 0.07	2.89 ± 0.45	2.62	0.42 ± 0.06
Kidneys	31.39 ± 3.61	7.36	2.97 ± 0.34	17.25 ± 1.64	7.82	2.41 ± 0.31	9.38 ± 1.41	8.53	2.90 ± 0.45
Urine	—	—	24.22 ± 2.59	—	—	23.38 ± 3.70	—	—	24.04 ± 2.86
Total recovery			86.89			82.71			77.59

[a] No metabolites of triamterene were detected in the liver, heart, lungs, kidneys, skeletal muscle, blood, or urine during these short-term studies (40 min after administration of triamterene). Each value is the mean ± *SE* from three rats. When the standard error is smaller than 0.01, it is not shown. [b] Nanocuries per gram of wet tissue. [c] Ratio of the mean value of the concentration in tissues (T) to that in the blood (B). About 50% of the ^{14}C-triamterene present in the blood was in the plasma. [d] Percentage dose was calculated on the basis of total ^{14}C-radioactivity in the whole tissue divided by the administered dose of ^{14}C-triamterene. Organ weights (except for total blood, total fat, and total muscle) were determined in each animal. It was not possible to determine total blood volume, total fat, and total muscle tissue within the same animal in which ^{14}C-triamterene distribution was determined. Therefore, estimated values (12–14) were used in the calculations: total blood, 6%; total fat, 16.5%; and total muscle, 45% of the body weight.

minute, using an automatic external standard and channels ratio technique. The remainder of each tissue was homogenized with 25 ml of aqueous acetone, the homogenate was centrifuged, and the aqueous acetone extract was separated and saved. The pellet was rehomogenized in 25 ml of aqueous acetone and centrifuged, and the supernate was combined with the original extract. After removal of the organic solvent by evaporation, the residue was dissolved in acetone and analyzed by paper chromatography and 4 × 4 countercurrent distribution as described previously (6–8). The procedure was repeated with each tissue.

Pharmacokinetics—Male rats were anesthetized with ketamine[8] (160 mg/kg ip). The femoral vein was cannulated with polyethylene tubing (PE 10) for the injection of ^{14}C-triamterene[9] (2 mg/kg, 3.8 μCi/mg). The femoral artery was cannulated with polyethylene tubing (PE 50) for collection of blood samples (0.3 ml for each) at timed intervals. In a second series of experiments, animals were maintained under light anesthesia with ether during cannulation of the femoral artery and vein. The rats received ^{14}C-triamterene after they recovered from the anesthesia in both series of experiments. Thereafter, blood samples were collected at timed intervals. The second series of experiments was used as a control to examine whether any postanesthetic effect of ketamine would influence the rate of distribution and elimination of triamterene in the first series.

Plasma samples were obtained after centrifuging whole blood samples, which were collected with heparinized syringes. The radioactivity in the samples of plasma was assayed according to the methods described in *Tissue Distribution*. The pharmacokinetic profile of ^{14}C-triamterene was determined in the plasma concentration–time curve, constructed according to the method described by Mayersohn and Gibaldi (10).

RESULTS

Tissue Distribution—In these short-term studies (60 min), no metabolite of triamterene was detected in the plasma, urine, or other tissues (liver, heart, lungs, kidneys, and skeletal muscle) analyzed by paper chromatography and countercurrent distribution. By comparison with the reference material, the single band at R_f 0.47 in 1-butanol–acetic acid–water or at R_f 0.42 in 2-propanol–water–ammonia was identified as unchanged triamterene in all tissues studied.

The distribution of the drug in various tissues after administration of different doses of ^{14}C-triamterene is shown in Table I. For most tissues, the concentration ratio between the tissue and the blood was greater than 1 (range of 1.80–8.53). The descending order of tissue and blood concentration ratios was: kidneys (7.36–8.53) > submaxillary glands > adrenal glands > liver > thyroid gland = pancreas > thymus > aorta = spleen > heart = lungs > diaphragm = biceps femoris > ileum. The ratio for brain was less than 1 (0.29–0.31). It was shown previously that there is a passive diffusion of triamterene into the brain across the blood–brain barrier, but it is actively transported out of the brain. This fact may explain partially the low tissue to blood ratio in the brain (11).

The same fraction of the drug was excreted in the urine irrespective of the size of the dose. The total amount of the drug in the organs was about 78–87% of the dose.

The tissue distribution of ^{14}C-triamterene as a function of time is shown in Fig. 1. The concentration of the drug reached a peak at 20 min in all tissues. The maximum concentration was in the renal tissue within the first 20 min, when the maximal natriuresis was also observed (3). The storehouse of the drug was the skeletal muscle, which contained about 39% of the dose at 20 min.

Pharmacokinetics—The pharmacokinetic profile of ^{14}C-triamterene in the rat was determined utilizing the data obtained following intravenous drug administration. The plasma concentration–time curve[10] of triamterene constructed from these data was biexponential (Fig. 2). The values of the parameters for the biexponential equation ($C_p = Ae^{-\alpha t} + Be^{-\beta t}$) are shown in Table II. The half-lives of the fast and slow components also were obtained. The two-compartment pharmacokinetic model was applied to this study, and its rate constants are shown in Table III.

DISCUSSION

Tissue Distribution—There are several interesting aspects to the distribution of ^{14}C-triamterene in the rat. After intravenous drug administration, the highest concentration was present in the kidneys at all timed intervals and dosage levels, whereas the largest fraction of the administered dose was deposited in the skeletal muscle. No metabolite was detected in these tissues. Therefore, the extensive accumulation of unchanged triamterene probably is responsible for its inhibitory action on sodium transport in skeletal muscle (1) as well as in kidneys (3).

A high concentration of the drug in all tissues analyzed, except the testes, brain, and fat, was maintained against a low concentration in the

[8] Bristol Laboratories.

[9] ^{14}C-Triamterene was suspended in 0.9% sodium chloride with a few drops of 8.5% lactic acid and warming until a clear solution was obtained.

[10] A nonlinear program was used for fitting the plasma concentration–time curve. The program was kindly provided by Dr. James Kao, Department of Chemistry, University of Georgia, Athens, Ga.

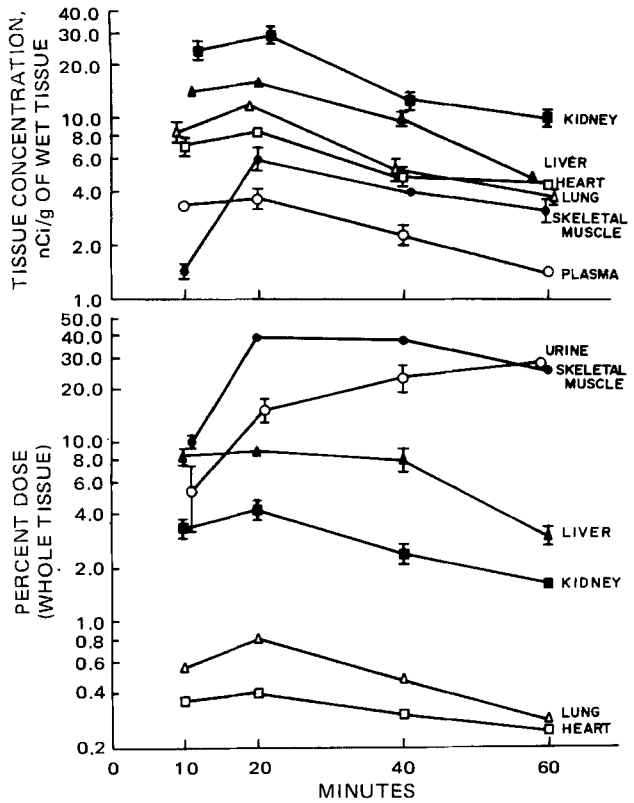

Figure 1—*Tissue distribution of ^{14}C-triamterene as a function of time. The upper panel indicates tissue concentration* versus *time; the lower panel shows percent dose* versus *time. The dose of ^{14}C-triamterene was 2 mg/kg iv. No metabolites of triamterene were detected in these tissues during the timed intervals. Each value is the mean ± SE from three rats. When the standard error is smaller than the dimension of the symbol, it is not shown.*

blood. Higher concentrations of triamterene were found inside dialysis bags in association with tissue homogenates (2). Therefore, the extensive accumulation of the drug in those tissues probably is a consequence of its binding by them.

Although the relationship of the tissue concentration of ^{14}C-triamterene to its effect on tissue electrolytes is not known, the data indicate that secretory (adrenal, submaxillary, and thyroid glands; liver; and kidneys) and lymphoid organs (thymus, spleen, and pancreas) accumulate the drug in higher concentrations than other tissues.

The highest concentration of the drug was found in the kidneys, liver, heart, lungs, and skeletal muscle within the first 20 min, when maximal

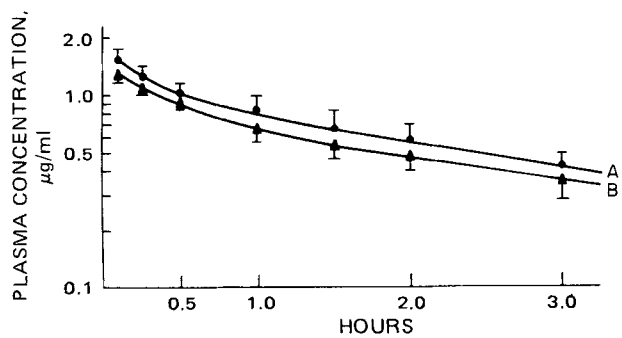

Figure 2—*Semilogarithmic plot of the plasma concentration of ^{14}C-radioactivity as a function of time after administration of ^{14}C-triamterene (2 mg/kg iv). Key: A (●), control group of animals that received light ether anesthesia during cannulation; and B (▲), group of animals that received ketamine instead of ether. Each point represents the mean ± SE for four animals in A and three animals in B. The plasma half-life of the fast component was 0.28 hr in A and 0.27 hr in B; the plasma half-life of the slow component was 2.77 hr in A and 2.78 hr in B. There was no significant difference between A and B in the plasma half-life of either the fast or slow component* ($p > 0.05$).

Table II—Values in the Equation[a] $C_p = Ae^{-\alpha t} + Be^{-\beta t}$ for Triamterene[b]

Parameter	Ketamine Anesthesia	Control[c]
A, μg/ml	0.68 ± 0.27	0.72 ± 0.17
α, hr^{-1}	2.61 ± 0.11	2.49 ± 0.22
B, μg/ml	0.79 ± 0.10	0.95 ± 0.14
β, hr^{-1}	0.25 ± 0.02	0.28 ± 0.03

[a] C_p is the drug concentration in the plasma at any time t, A and B are the ordinate axis intercepts, α is the fast disposition rate, and β is the slow disposition rate. [b] Each value is the mean ± SE for three rats in ketamine anesthesia and four rats in control experiments. [c] Control refers to the group of rats under light ether anesthesia during cannulation of the femoral artery and vein.

natriuresis was also observed (3). Since no metabolite of triamterene was detected in these tissues, there was a good correlation between the tissue concentration of the unchanged drug and its inhibitory effect on sodium transport. These data suggest that the extrarenal effect of triamterene on the tissue content of sodium deserves further investigation.

Pharmacokinetics—The rats were anesthetized with either ketamine or ether during surgery, and they received ^{14}C-triamterene only after they recovered from anesthesia. Although the pharmacology of ketamine is different from that of ether (5), the rate of distribution and elimination of triamterene was not significantly affected by any postanesthetic action of ketamine (Table III). Apparently, ketamine is as suitable as ether as an anesthetic agent in the pharmacokinetic study of triamterene.

The pharmacokinetic profile of triamterene was evaluated by the two-compartment open-model system (10). According to the biexponential plasma concentration–time curve of the drug, the first exponent is the fast disposition rate constant (α) and the second exponent is the slow disposition rate constant (β). The magnitudes of α and β indicate that triamterene ought to be distributed at a fairly rapid rate and be eliminated at a relatively slow rate. The ratio of β/k_{el} indicates that approximately two-thirds of the drug in the body would be in the central compartment available for elimination at any time.

The distribution volume of the drug was greater in the central compartment (*e.g.*, highly perfused tissues such as kidney and liver) than in the peripheral compartment (*e.g.*, poorly perfused tissues such as fat and muscle). These values reflect the high affinity of triamterene for binding substances in the central compartment. The result is well correlated with the present finding on the tissue distribution of ^{14}C-triamterene. A high drug concentration ratio between tissue and blood was found in kidney, liver, and other highly perfused tissues. Furthermore, the sum of the fractions of the dose found in skeletal muscle (37%), smooth muscle (2%), and fat (3%) was close to the value (38%) from pharmacokinetic studies in the peripheral compartment. Apparently, the high affinity of the drug

Table III—Distribution and Elimination Parameters of the Two-Compartment Open Model for Triamterene[a]

Parameter	Ketamine Anesthesia[b]	Control[b]
Distribution volume[c], ml		
V_c	311.1 ± 19.2	317.8 ± 64.2
V_p	175.5 ± 62.8	150.9 ± 17.5
V_d	486.7 ± 48.3	468.7 ± 74.4
Clearance[c], ml/min, C_t	2.27 ± 0.51	2.17 ± 0.39
Rate constants[d], hr^{-1}		
k_{12}	0.81 ± 0.18	0.79 ± 0.12
k_{21}	1.59 ± 0.03	1.56 ± 0.09
k_{el}	0.46 ± 0.13	0.46 ± 0.06
Constant ratio[e], β/k_{el}	0.61 ± 0.10	0.63 ± 0.05

[a] Each value is the mean ± SE as described in Table I. The evaluation of kinetic parameters was according to the methods described in Refs. 10 and 15. [b] Mean values for ketamine anesthesia and control were not significantly different in all parameters, $p > 0.05$ (calculated by the Student t test). Average weights of rats in ketamine and control groups were 210 and 230 g, respectively. [c] V_c = volume of central compartment, V_p = volume of peripheral compartment, V_d = total volume of distribution, and C_t = clearance of a drug from the central compartment. Distribution volume and clearance were calculated per rat. [d] The individual rate constants k_{12} and k_{21} reflect the rate of distribution into and out of the peripheral compartment from the central compartment; k_{el} is the sum of all rate constants governing the elimination process, including metabolism and urinary excretion. [e] Fraction of dose in the central compartment.

for skeletal muscle is responsible for its accumulation in the peripheral compartment.

The ratio of k_{21}/k_{12} ranged from 1.4 to 3.0, with a mean of 2.2, indicating that the drug returns rapidly from distribution sites for elimination from the body. However, the low k_{el}, with a mean of 0.46, indicates that the elimination of triamterene would not be as rapid as the ratio predicts. This situation could be related to the binding of the drug to tissue substances in the central compartment and to the ability of the rat to metabolize a limited amount of the drug (6). According to the plasma half-life of the slow component obtained in the present experiments, after intravenous administration of triamterene there will be a negligible concentration of the drug in the plasma within about five half-lives (13.9 hr).

In conclusion, the present observations illustrate the tissue binding property of triamterene in the rat. Although these data provide limited information about the nature of this property, they reveal the possibility of the effect of unchanged triamterene on the tissue content of sodium. A pharmacokinetic interpretation of the present study appears to be well correlated with the experimental results. Apparently, the tissue binding property of triamterene is an important factor in controlling its rate of distribution and elimination in the rat.

REFERENCES

(1) C. T. Spalding and V. D. Jones, *Proc. Soc. Exp. Biol. Med.*, **137**, 1297 (1971).

(2) P. G. Dayton, A. W. Pruitt, J. L. McNay, and J. Steinhorst, *Neuropharmacology*, **11**, 435 (1972).

(3) S. T. Kau, B. V. R. Sastry, J. D. Alvin, and M. T. Bush, *Pharmacologist*, **16**, 317 (1974).

(4) H. Herken, V. Neuhoff, and G. Senft, *Klin. Wochenschr.*, **43**, 960 (1965).

(5) K. Lehmann, *Arzneim.-Forsch.*, **15**, 812 (1965).

(6) S. T. Kau, B. V. R. Sastry, J. D. Alvin, and M. T. Bush, *Drug Metab. Dispos.*, **3**, 345 (1975).

(7) M. T. Bush and P. M. Densen, *Anal. Chem.*, **20**, 121 (1948).

(8) M. T. Bush and O. W. Post, *Anal. Biochem.*, **32**, 145 (1969).

(9) S. T. Kau, B. V. R. Sastry, and A. M. Michelakis, *Arch. Int. Pharmacodyn. Ther.*, **211**, 115 (1974).

(10) M. Mayersohn and M. Gibaldi, *Am. J. Pharm. Educ.*, **35**, 19 (1971).

(11) A. W. Pruitt, J. L. McNay, and P. G. Dayton, *Drug Metab. Dispos.*, **3**, 30 (1975).

(12) C. Long, "Biochemists' Handbook," Van Nostrand, Princeton, N.J., 1961.

(13) J. F. Manery, *Physiol. Rev.*, **34**, 334 (1954).

(14) J. F. Manery and A. B. Hastings, *J. Biol. Chem.*, **127**, 657 (1939).

(15) M. Gibaldi, R. Nagashima, and G. Levy, *J. Pharm. Sci.*, **58**, 193 (1969).

ACKNOWLEDGMENTS AND ADDRESSES

Received August 25, 1975, from the *Department of Pharmacology, Vanderbilt University School of Medicine, Nashville, TN 37232.*

Accepted for publication March 2, 1976.

S. T. Kau was supported by a predoctoral traineeship from the National Institutes of Health, Training Grant GM-00058, awarded by the National Institute of General Medical Sciences. B. V. Rama Sastry was supported in part by U.S. Public Health Service General Research Support Grant RR-05424.

The authors thank Dr. Glenn E. Ullyot of Smith Kline and French Laboratories, Philadelphia, Pa., for supplying ^{14}C-triamterene and a grant-in-aid.

[x] To whom inquiries should be directed.

Effect of Sodium Salicylate on Renal Elimination of a Quaternary Ammonium Compound

KISHOR A. DANDEKAR [*] and H. B. KOSTENBAUDER [x]

Abstract □ Administration of sodium salicylate inhibited elimination of the tetraethylammonium ion in rats. A two-compartment open model was used to describe plasma decline of tetraethylammonium bromide administered intravenously. The rate constant describing elimination from the central compartment was decreased by 25 and 40% in rats predosed with sodium salicylate at 30 and 50 mg/kg, respectively. Salicylate also enhanced the distribution of the tetraethylammonium ion to the peripheral compartment. Urinary excretion is the principal route of elimination for the tetraethylammonium ion, and studies of the effect of sodium salicylate on the uptake of the tetraethylammonium ion by rat renal cortical tissue indicated noncompetitive inhibition by salicylate.

Keyphrases □ Sodium salicylate—effect on renal elimination of tetraethylammonium bromide, rats □ Tetraethylammonium bromide—pharmacokinetic model, effect of sodium salicylate on renal elimination, rats □ Elimination, renal—tetraethylammonium bromide, effect of sodium salicylate, rats □ Pharmacokinetics—two-compartment open model for tetraethylammonium bromide, rats □ Quaternary ammonium compounds—tetraethylammonium bromide, pharmacokinetic model, effect of sodium salicylate on renal elimination, rats

Quaternary ammonium and other strongly basic compounds are actively secreted by the renal tubule. The secretory pathway for the basic compounds is similar, but not identical, to the anion transport mechanism. Both mechanisms are known to be saturable, specific, and subject to inhibition by structural analogs and antimetabolic compounds and to require energy for their operation. In general, tubular transport of basic compounds is not known to be inhibited by acidic compounds; conversely, the transport of acidic compounds is not known to be inhibited by basic compounds (1).

The recently reported, partly noncompetitive nature of the inhibition of *p*-aminohippurate tubular transport by salicylate (2) prompted investigation of the effect of salicylate on the renal tubular transport of a quaternary ammonium compound. The effect of sodium salicylate on renal elimination kinetics of the tetraethylammonium cation was investigated in *in vitro* and *in vivo* models. Rat renal cortical slice studies were used to determine the nature of the inhibitory effect of salicylate on the active uptake of the tetraethylammonium ion by cortical tissue. The significance of the salicylate effect on renal elimination of the ^{14}C-tetraethylammonium ion was then evaluated in pharmacokinetic studies in anesthetized rats.

for skeletal muscle is responsible for its accumulation in the peripheral compartment.

The ratio of k_{21}/k_{12} ranged from 1.4 to 3.0, with a mean of 2.2, indicating that the drug returns rapidly from distribution sites for elimination from the body. However, the low k_{el}, with a mean of 0.46, indicates that the elimination of triamterene would not be as rapid as the ratio predicts. This situation could be related to the binding of the drug to tissue substances in the central compartment and to the ability of the rat to metabolize a limited amount of the drug (6). According to the plasma half-life of the slow component obtained in the present experiments, after intravenous administration of triamterene there will be a negligible concentration of the drug in the plasma within about five half-lives (13.9 hr).

In conclusion, the present observations illustrate the tissue binding property of triamterene in the rat. Although these data provide limited information about the nature of this property, they reveal the possibility of the effect of unchanged triamterene on the tissue content of sodium. A pharmacokinetic interpretation of the present study appears to be well correlated with the experimental results. Apparently, the tissue binding property of triamterene is an important factor in controlling its rate of distribution and elimination in the rat.

REFERENCES

(1) C. T. Spalding and V. D. Jones, *Proc. Soc. Exp. Biol. Med.*, **137**, 1297 (1971).

(2) P. G. Dayton, A. W. Pruitt, J. L. McNay, and J. Steinhorst, *Neuropharmacology*, **11**, 435 (1972).

(3) S. T. Kau, B. V. R. Sastry, J. D. Alvin, and M. T. Bush, *Pharmacologist*, **16**, 317 (1974).

(4) H. Herken, V. Neuhoff, and G. Senft, *Klin. Wochenschr.*, **43**, 960 (1965).

(5) K. Lehmann, *Arzneim.-Forsch.*, **15**, 812 (1965).

(6) S. T. Kau, B. V. R. Sastry, J. D. Alvin, and M. T. Bush, *Drug Metab. Dispos.*, **3**, 345 (1975).

(7) M. T. Bush and P. M. Densen, *Anal. Chem.*, **20**, 121 (1948).

(8) M. T. Bush and O. W. Post, *Anal. Biochem.*, **32**, 145 (1969).

(9) S. T. Kau, B. V. R. Sastry, and A. M. Michelakis, *Arch. Int. Pharmacodyn. Ther.*, **211**, 115 (1974).

(10) M. Mayersohn and M. Gibaldi, *Am. J. Pharm. Educ.*, **35**, 19 (1971).

(11) A. W. Pruitt, J. L. McNay, and P. G. Dayton, *Drug Metab. Dispos.*, **3**, 30 (1975).

(12) C. Long, "Biochemists' Handbook," Van Nostrand, Princeton, N.J., 1961.

(13) J. F. Manery, *Physiol. Rev.*, **34**, 334 (1954).

(14) J. F. Manery and A. B. Hastings, *J. Biol. Chem.*, **127**, 657 (1939).

(15) M. Gibaldi, R. Nagashima, and G. Levy, *J. Pharm. Sci.*, **58**, 193 (1969).

ACKNOWLEDGMENTS AND ADDRESSES

Received August 25, 1975, from the *Department of Pharmacology, Vanderbilt University School of Medicine, Nashville, TN 37232.*

Accepted for publication March 2, 1976.

S. T. Kau was supported by a predoctoral traineeship from the National Institutes of Health, Training Grant GM-00058, awarded by the National Institute of General Medical Sciences. B. V. Rama Sastry was supported in part by U.S. Public Health Service General Research Support Grant RR-05424.

The authors thank Dr. Glenn E. Ullyot of Smith Kline and French Laboratories, Philadelphia, Pa., for supplying ^{14}C-triamterene and a grant-in-aid.

[x] To whom inquiries should be directed.

Effect of Sodium Salicylate on Renal Elimination of a Quaternary Ammonium Compound

KISHOR A. DANDEKAR [*] and H. B. KOSTENBAUDER [x]

Abstract □ Administration of sodium salicylate inhibited elimination of the tetraethylammonium ion in rats. A two-compartment open model was used to describe plasma decline of tetraethylammonium bromide administered intravenously. The rate constant describing elimination from the central compartment was decreased by 25 and 40% in rats predosed with sodium salicylate at 30 and 50 mg/kg, respectively. Salicylate also enhanced the distribution of the tetraethylammonium ion to the peripheral compartment. Urinary excretion is the principal route of elimination for the tetraethylammonium ion, and studies of the effect of sodium salicylate on the uptake of the tetraethylammonium ion by rat renal cortical tissue indicated noncompetitive inhibition by salicylate.

Keyphrases □ Sodium salicylate—effect on renal elimination of tetraethylammonium bromide, rats □ Tetraethylammonium bromide—pharmacokinetic model, effect of sodium salicylate on renal elimination, rats □ Elimination, renal—tetraethylammonium bromide, effect of sodium salicylate, rats □ Pharmacokinetics—two-compartment open model for tetraethylammonium bromide, rats □ Quaternary ammonium compounds—tetraethylammonium bromide, pharmacokinetic model, effect of sodium salicylate on renal elimination, rats

Quaternary ammonium and other strongly basic compounds are actively secreted by the renal tubule. The secretory pathway for the basic compounds is similar, but not identical, to the anion transport mechanism. Both mechanisms are known to be saturable, specific, and subject to inhibition by structural analogs and antimetabolic compounds and to require energy for their operation. In general, tubular transport of basic compounds is not known to be inhibited by acidic compounds; conversely, the transport of acidic compounds is not known to be inhibited by basic compounds (1).

The recently reported, partly noncompetitive nature of the inhibition of *p*-aminohippurate tubular transport by salicylate (2) prompted investigation of the effect of salicylate on the renal tubular transport of a quaternary ammonium compound. The effect of sodium salicylate on renal elimination kinetics of the tetraethylammonium cation was investigated in *in vitro* and *in vivo* models. Rat renal cortical slice studies were used to determine the nature of the inhibitory effect of salicylate on the active uptake of the tetraethylammonium ion by cortical tissue. The significance of the salicylate effect on renal elimination of the ^{14}C-tetraethylammonium ion was then evaluated in pharmacokinetic studies in anesthetized rats.

EXPERIMENTAL

Renal Cortical Slice Study—Male Sprague–Dawley rats, 200–300 g, were killed by decapitation. Kidneys were removed quickly by abdominal laparotomy. The kidneys were decapsulated and stored briefly (not more than 10 min) under ice-cold normal saline bubbled with 100% oxygen. After discarding the two surface slices, three cortical slices, approximately 0.3–0.4 mm in thickness, were cut from dorsal and ventral sides using a tissue slicer[1]. In each experiment, two or three animals were killed and the slices were pooled.

About 60–80 mg of tissue (two to three slices) was equilibrated with 3 ml of incubation medium under 100% oxygen for 5 min. ^{14}C-Tetraethylammonium bromide[2] (100 μCi/19.2 mg) was then added in a volume of 100 μl, and the flasks were incubated for 30 min with continuous shaking at 60 cpm. The period between animal decapitation and the beginning of the incubation was never more than 30 min. At the end of the incubation period, the flasks were chilled in an ice bath, the tissue slices were blotted lightly and weighed, and the ^{14}C-tetraethylammonium-ion content of the slices was determined by liquid scintillation counting.

The incubation medium was prepared as suggested by Robinson (3), except for the addition of 11 m*M* glucose. The optimum incubation period was determined by observing the uptake of the tetraethylammonium ion at the end of 5, 10, 20, 30, 50, and 60 min. This uptake was determined for initial tetraethylammonium bromide concentrations of 0.125, 0.250, 0.500, 1.00, and 2.00 m*M* in the presence and absence of 1 m*M* sodium salicylate. Each solution contained 0.075 μCi of the ^{14}C-tetraethylammonium ion.

Passive uptake of the tetraethylammonium ion by the renal tissue was determined in a separate experiment. Sodium cyanide (1 m*M*) was added to the salicylate-free medium, and nitrogen gas was used in place of oxygen. Ten flasks were used in this experiment.

Pharmacokinetic Studies—Male Sprague-Dawley rats, 420–580 g, were acclimatized to laboratory conditions for at least 2 days. The animals had free access to food and water until the experiments began. Rats were anesthetized with pentobarbital sodium[3], 50 mg/kg ip. The bile duct was cannulated after a small incision (about 1 cm) was made 1 cm below the sternum on the abdominal wall. The wound was sutured and kept covered with 4 × 4 gauze soaked in normal saline. The femoral vein was cannulated and provided with a three-way stopcock and a 5-ml disposable syringe filled with heparinized (10 units/ml) normal saline.

The surgical procedure was completed within 10 min after anesthesia, and 30 min was allowed between its completion and the administration of the intravenous dose of tetraethylammonium bromide. The rats were watched for uniform breathing, proper level of anesthesia, and unobstructed bile flow during this period. In the salicylate treatment experiments, 30 or 50 mg/kg iv of sodium salicylate was given immediately after completion of the surgical procedure. A 0.4-ml blood sample and a 10-min bile sample were collected during this period to serve as a blank or background determination in the analytical procedure.

At the end of 30 min, ^{14}C-tetraethylammonium bromide solution, 10 mg/kg iv, was administered over 20 sec. This injection contained 5 mg of total drug/ml and 3.0 μCi of ^{14}C-tetraethylammonium bromide/ml. The timer was started at the midpoint of the injection period. The dose was flushed into the circulation with about 0.4 ml of normal saline. The three-way stopcock and the 5-ml syringe were discarded, and a new 5-ml syringe containing fresh heparinized normal saline was connected directly to the venous cannula. This procedure prevented contamination of the first blood sample with the very high radioactivity of the dose.

Blood samples, 0.4 ml each, were withdrawn every 5 min for the first 40 min and then every 20 min for a total of 2 hr. The blood volume withdrawn was replaced by injecting 0.4 ml of heparinized normal saline after each withdrawal. Blood clotting in the cannula was avoided by maintaining heparinized normal saline in the cannula tubing between blood samples. The plasma was separated by centrifuging, and the plasma and bile samples were analyzed for carbon-14 radioactivity by scintillation counting immediately after the experiment.

Tetraethylammonium-Ion Partition Study—Five solutions, 5 ml each, containing 0.05 m*M* tetraethylammonium bromide and 0.5, 1.0, 1.5, 2.0, or 2.5 m*M* sodium salicylate were prepared in 0.1 *M* phosphate buffer (pH 7.4). Exactly 0.03 μCi of ^{14}C-tetraethylammonium bromide was added to each tube. Then 5 ml of chloroform was added to each tube, and the tubes were closed and gently rocked for 30 min. The tubes were then centrifuged to separate the two phases. Radioactivity in the aqueous phase, prior to and after partitioning, was determined by scintillation counting.

Table I—Results of Renal Cortical Slice Study

Tetraethylammonium Ion in Medium, m*M*	Micromoles of Tetraethylammonium Ion per Gram of Tissue per 30 min × 10[a]		
	Control (n = 4)	With Sodium Salicylate (1 m*M*) (n = 4)	With Sodium Cyanide (1 m*M*) under Nitrogen (n = 2)
0.125	3.8872 ± 0.7147	2.2731 ± 0.6674	0.9587 ± 0.0143
0.250	5.5133 ± 0.2124	3.9493 ± 0.4507	1.9150 ± 0.0640
0.500	9.4887 ± 1.4737	6.3751 ± 0.2024	3.8604 ± 0.0944
1.00	13.8346 ± 0.0648	10.1238 ± 1.2987	7.4922 ± 0.0371
2.00	20.3419 ± 3.3068	17.1054 ± 0.7102	14.8463[b]

[a] Mean ± *SD*. [b] n = 1.

Radioactivity in Renal Cortical Slices—After determination of tissue weight, renal cortical slices were dissolved in 15 ml of a toluene base scintillation cocktail with the aid of 1 ml of tissue solubilizer[4].

Each vial was counted for 10 min in a liquid scintillation counter[5] to determine the carbon-14 radioactivity. An appropriate quench curve was made by adding tissue to a constant amount of ^{14}C-tetraethylammonium bromide (5323 dpm/vial).

Radioactivity in Plasma and Bile—Exactly 100 μl of plasma was placed in the glass scintillation vials and mixed with 15 ml of scintillation fluid. Each vial was counted for 10 min in a scintillation counter. The quench curve made by adding various volumes (20–150 μl) of plasma but the same known amount of ^{14}C-tetraethylammonium bromide (2200 dpm/vial) allowed the exact determination of counting efficiency of the plasma samples.

Entire 10-min bile samples were used for determining the ^{14}C-tetraethylammonium ion in the bile. Addition of 2 ml of methanol to bile prior to mixing it with 15 ml of scintillation fluid improved the sample appearance and the counting efficiency.

Tetraethylammonium-Ion Uptake Calculations—The amount of tetraethylammonium ion in the tissue was expressed in terms of micromoles per gram of tissue. The active uptake of the tetraethylammonium ion was determined by subtracting the uptake in the presence of 1 m*M* potassium cyanide and a nitrogen atmosphere from the aerobic uptake. The active uptake was treated according to Michaelis–Menten kinetics.

Pharmacokinetic Calculations—The plasma tetraethylammonium-ion *versus* time profiles in all experiments were biexponential, suggesting that pharmacokinetic analysis would require minimally a two-compartment open model (4). The average plasma level–time profiles of four experiments done in each category, *i.e.*, control, with 30-mg/kg salicylate dose, and with 50-mg/kg salicylate dose, were determined. The mean plasma level–time data of each category of experiments were fitted to the following biexponential equation using the SAAM-23 digital computer program (5):

$$C = Ae^{-\alpha t} + Be^{-\beta t} \qquad \text{(Eq. 1)}$$

The constants A, B, α, and β, estimated by the computer fit, were then used to determine the individual rate constants and related volume parameters of the two-compartment open model (Scheme I) (4).

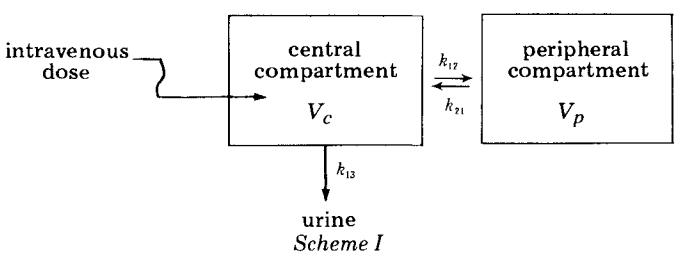

Scheme I

[1] Harvard Apparatus Co., Millis, MA 02054.
[2] New England Nuclear, Boston, Mass.
[3] Nembutal sodium, 50 mg/ml, Abbott Laboratories, North Chicago, Ill.
[4] Soluene-100, Packard Instrument Co., Downers Grove, Ill.
[5] Packard Tri-Carb scintillation spectrometer, model 3375, Packard Instrument Co., Downers Grove, Ill.

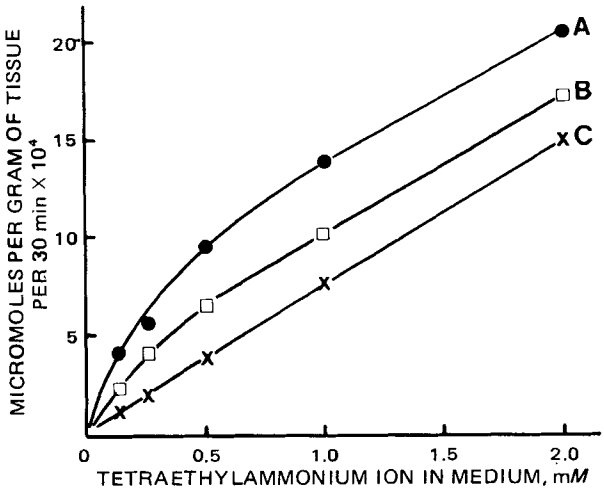

Figure 1—*Uptake of the tetraethylammonium ion by renal cortical slices. Key: A, control; B, in presence of 1 mM sodium salicylate; and C, under anaerobic conditions (nitrogen atmosphere) and with 1 mM sodium cyanide added to medium. Each data point represents the mean for the number of studies indicated in Table I.*

RESULTS AND DISCUSSION

Renal Cortical Slice Study—Data for the uptake of the tetraethylammonium ion by renal cortical tissue are presented in Table I. Maximum uptake occurred after 30 min of incubation. Tetraethylammonium-ion uptake in three categories of the experiments, *i.e.*, control, with 1 m*M* salicylate under proper physiological conditions, and in anaerobic conditions under nitrogen in the presence of 1 m*M* sodium cyanide, is illustrated in Fig. 1. The active uptake of the tetraethylammonium ion, with and without salicylate, is shown as a Woolf plot in Fig. 2.

Figure 1 clearly shows that the tetraethylammonium-ion active uptake by the cortical slices was a saturable process and obeyed Michaelis–Menten kinetics. The uptake of the tetraethylammonium ion in the presence of cyanide and nitrogen was the measure of passive diffusion of the tetraethylammonium ion into the cortical tissue and was a linear function of the concentration in the medium. The active oxygen and enzyme-dependent uptake, therefore, was determined by subtracting the passive uptake from the uptake determined in the presence of oxygen under proper physiological conditions. The Woolf plot of the active tetraethylammonium-ion uptake data (Fig. 2) indicates noncompetitive inhibition of the active uptake of the tetraethylammonium ion by salicylate. This result is in agreement with a generally accepted theory that an anionic drug does not compete with a cationic drug for tubular

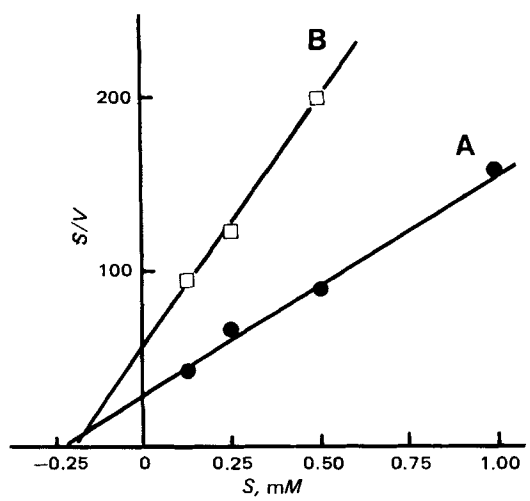

Figure 2—*Woolf plot of the active uptake of the tetraethylammonium ion by renal cortical slices; S is substrate concentration, and V is rate of uptake. Key: A, control, $V_{max} = 7.93 \times 10^{-4}$ mmole/g of tissue/30 min, and $K_m = 0.242$ mM; and B, in presence of 1 mM sodium salicylate, $V_{max} = 3.57 \times 10^{-4}$ mmole/g of tissue/30 min, and $K_m = 0.204$ mM. Data were derived from mean uptake reported in Table I.*

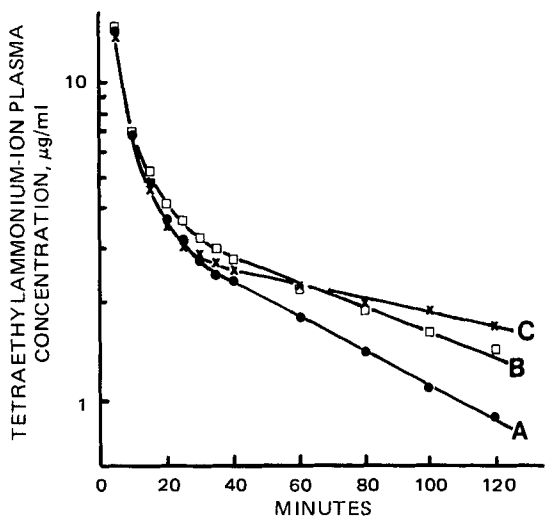

Figure 3—*Influence of salicylate on plasma decline of the ^{14}C-tetraethylammonium ion in rats following rapid intravenous injection of 10 mg of tetraethylammonium bromide/kg. Key: A, control; B, rats pretreated with 30 mg of sodium salicylate/kg; and C, rats pretreated with 50 mg of sodium salicylate/kg. Each data point is the mean for four animals in A and B and for three animals in C. The solid line is computer fit to Eq. 1.*

transport. Salicylate apparently did not cause the inhibition by acting as a competitive substrate but must have influenced tetraethylammonium-ion uptake by another mechanism.

Salicylate has been shown to be an uncoupler of oxidative phosphorylation, a subcellular biochemical process responsible for the synthesis of adenosine triphosphate (6). The exact mechanism of the salicylate effect on oxidative phosphorylation is not yet clearly defined (6). Salicylate also affects protein and amino acid metabolism in the body (7), which results in altered permeability of the cellular structure. Alteration of permeability of the cellular structure that constitutes a selective barrier could be the reason for the reduced uptake of the tetraethylammonium ion in the presence of salicylate.

Pharmacokinetic Study in Rats—After the inhibition of active tetraethylammonium-ion uptake by rat renal cortical slices was observed, the significance of the salicylate inhibition of tubular transport was assessed in single-injection pharmacokinetic studies in rats.

Biliary excretion of radioactive drug was examined as a possible route of extrarenal elimination of the tetraethylammonium ion. Biliary excretion of the tetraethylammonium ion was quantitated, but kinetic analysis suggested that less than 1% of the total elimination was taking place in bile.

The plasma level *versus* time data in each category of experiments, *i.e.*,

Table II—Pharmacokinetic Study of Tetraethylammonium Bromide (10 mg/kg iv) in Rats

	Plasma Tetraethylammonium Ion, μg/ml[a]		
Minutes	No Pretreatment ($n = 4$)	Pretreatment with 30 mg/kg iv Sodium Salicylate[b] ($n = 4$)	Pretreatment with 50 mg/kg iv Sodium Salicylate[c] ($n = 3$)
5	13.58 ± 1.22	14.15 ± 2.18	13.45 ± 1.05
10	7.00 ± 0.49	7.25 ± 0.93	6.63 ± 1.42
15	4.65 ± 0.38	5.02 ± 0.69	4.49 ± 0.69
20	3.57 ± 0.43	3.97 ± 0.58	3.43 ± 0.61
25	3.04 ± 0.42	3.54 ± 0.43	2.96 ± 0.61
30	2.64 ± 0.41	3.10 ± 0.54	2.76 ± 0.79
35	2.38 ± 0.40	2.89 ± 0.44	2.64 ± 0.83
40	2.32 ± 0.38	2.66 ± 0.52	2.44 ± 0.84
60	1.79 ± 0.25	2.17 ± 0.30	2.19 ± 0.75
80	1.40 ± 0.22	1.88 ± 0.30	1.96 ± 0.69
100	1.09 ± 0.21	1.60 ± 0.30	1.91 ± 0.65
120	0.89 ± 0.15	1.43 ± 0.17	1.69 ± 0.58

[a] Mean ± *SD*. [b] Plasma salicylate concentration of 10–12 mg %. [c] Plasma salicylate concentration of 16–18 mg %.

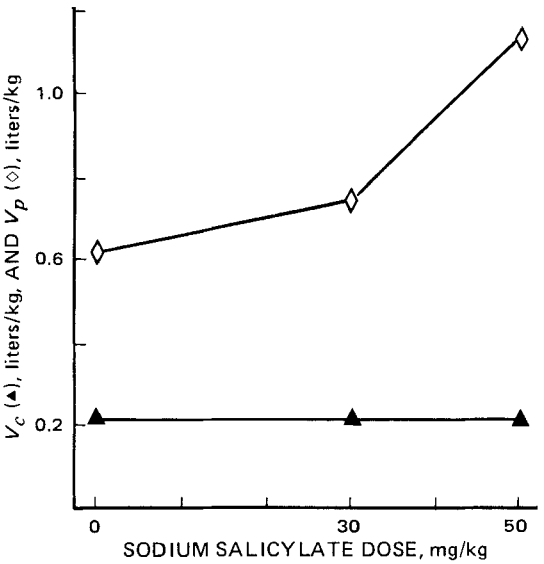

Figure 4—*Effect of sodium salicylate on the apparent volume of the central* (V_c) *and peripheral* (V_p) *compartments for the tetraethylammonium ion.*

control (four rats) and salicylate treatment at 30 (four rats) and 50 (three rats) mg/kg, are presented in Table II. The digital computer fit to mean plasma levels is illustrated in Fig. 3, and the pharmacokinetic parameters are given in Table III.

Salicylate treatments resulted in a significant decrease in the elimination rate constant, k_{13} (25 and 40% decrease compared to k_{13} in control experiments). This observation supports the results of the cortical slice study. Although it cannot be concluded whether tubular secretion, glomerular filtration, or tubular reabsorption was altered by salicylate, it appears that salicylate probably inhibited the active tubular secretion.

Besides the decrease in k_{13}, both k_{12} and k_{21} changed in the presence of salicylate. Increases in the volume of distribution and the ratio of k_{12}/k_{21} suggest enhanced distribution of the tetraethylammonium ion in the peripheral compartment. The apparent volume of the central compartment was unchanged by the salicylate treatment (Fig. 4).

Thus, in the present study, both elimination and distribution of the drug were altered by the salicylate treatment.

The actual amounts of the tetraethylammonium ion present in the peripheral compartment at various times in the three categories of experiments can be calculated by (8):

$$X_p = \frac{k_{12}(\text{dose})}{(\alpha - \beta)}(e^{-\beta t} - e^{-\alpha t}) \qquad \text{(Eq. 2)}$$

or they can be simulated using the CSMP (9) digital computer program. The amount of the tetraethylammonium ion in the peripheral compartment *versus* time data calculated by CSMP are shown graphically in Fig. 5.

Table III—Pharmacokinetic Parameters of Tetraethylammonium Ion

Parameter	Control	30 mg of Salicylate/kg	50 mg of Salicylate/kg
A, μg/ml	24.970 ±1.21	24.813 ±2.16	25.742 ±1.68
B, μg/ml	3.664 ±0.07	3.799 ±0.13	3.041 ±0.08
α, min^{-1}	0.1845 ±0.006	0.1796 ±0.011	0.1854 ±0.008
β, min^{-1}	0.0120 ±0.0003	0.0085 ±0.0005	0.0050 ±0.0004
k_{13}, min^{-1}	0.0649	0.0490	0.0385
k_{21}, min^{-1}	0.0340	0.0312	0.0240
k_{12}, min^{-1}	0.0975	0.1078	0.1278
k_{12}/k_{21}	2.8677	3.4551	5.3250
V_c, ml/kg	216.44	216.61	215.46
V_p, ml/kg	619.80	747.74	1144.72
V_{ss}, ml/kg	836.24	964.34	1360.18
V_{area}, ml/kg	1172.01	1245.09	1658.12

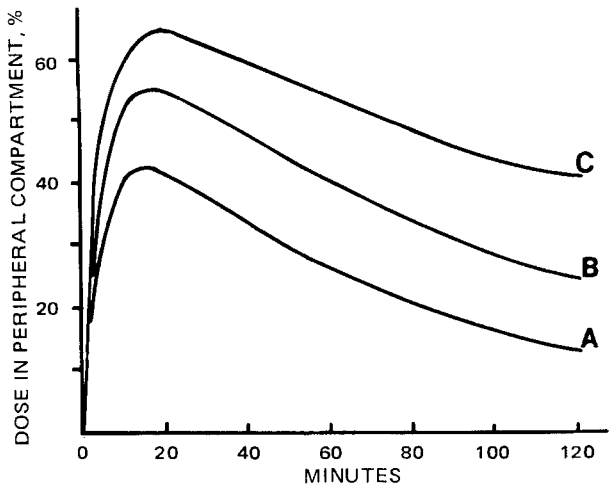

Figure 5—*Influence of sodium salicylate on the fraction of the tetraethylammonium dose in the peripheral compartment following rapid intravenous injection of tetraethylammonium bromide in rats. Key: A, control; B, pretreatment with 30 mg of sodium salicylate/kg; and C, pretreatment with 50 mg of sodium salicylate/kg.*

Tetraethylammonium ions are known to distribute only in extracellular space (10); penetration of the blood–brain barrier is limited. Pretreatment with salicylate resulted in enhanced distribution to peripheral tissues. An increased distribution could be taken as an opening of some barrier to tetraethylammonium-ion distribution somewhere outside the central compartment. Salicylate has various biochemical effects such as interference with protein and amino acid metabolism (7) and uncoupling of oxidative phosphorylation (11). Uncoupling agents are known to alter the selective barrier of the cellular membrane. Whether this alteration results primarily from the uncoupling action or its effects on protein metabolism is not clearly understood (12).

The results of a partition study suggest that there is no ion-pair formation between salicylate and the tetraethylammonium ion that would account for a change in *in vivo* distribution. The apparent partition coefficient of the tetraethylammonium ion between chloroform and pH 7.4 phosphate buffer in the presence of a 10–50 M excess of salicylate remained unchanged at 1.02×10^{-2}.

The most significant influence of the coadministration of salicylate on tetraethylammonium-ion pharmacokinetics was the increase in the amount of the tetraethylammonium ion in the peripheral compartment. This increase was a result of a decrease in k_{13} and an increase in the distribution of drug into the peripheral compartment. The amount of drug in the central compartment was essentially unchanged by salicylate administration. Therefore, the clinical significance of coadministration of salicylate with a quaternary ammonium drug such as tetraethylammonium bromide depends on whether pharmacological response to the drug most closely parallels the amount of drug in the central compartment or that in the peripheral compartment.

REFERENCES

(1) L. Peters, *Pharmacol. Rev.*, **12**, 1 (1960).

(2) K. A. Dandekar and H. B. Kostenbauder, *J. Pharm. Sci.*, in press.

(3) J. R. Robinson, *Biochem. J.*, **45**, 68 (1949).

(4) S. Riegelman, J. C. K. Loo, and M. Rowland, *J. Pharm. Sci.*, **57**, 117 (1968).

(5) M. Berman and M. F. Weiss, "User's Manual for SAAM," U.S. Public Health Service Publication 1703, U.S. Department of Health, Education, and Welfare, U.S. Government Printing Office, Washington, D.C., 1966.

(6) M. J. H. Smith and P. K. Smith, "The Salicylates: A Critical Bibliographic Review," Interscience, New York, N.Y., 1966, p. 58.

(7) *Ibid.*, p. 76.

(8) J. G. Wagner, "Biopharmaceutics and Relevant Pharmacokinetics," Drug Intelligence Publications, Hamilton, Ill., 1971, p. 295.

(9) "System/360 Continuous System Modeling Program," Program No. 360 A-CX-16X, 5th ed., IBM Corp., Technical Publications Department, White Plains, N.Y., 1972.

(10) "The Pharmacological Basis of Therapeutics," 4th ed., L. S. Goodman and A. Gilman, Eds., Macmillan, New York, N.Y., 1970, p. 597.

(11) T. M. Brody, *J. Pharmacol. Exp. Ther.*, 117, 39 (1956).
(12) "Drill's Pharmacology in Medicine," 3rd ed., J. R. DiPalma, Ed., McGraw-Hill, New York, N.Y., 1965, p. 294.

ACKNOWLEDGMENTS AND ADDRESSES

Received October 31, 1975, from the *College of Pharmacy, University of Kentucky, Lexington, KY 40506.*

Accepted for publication March 4, 1976.

Presented at the Basic Pharmaceutics Section, APhA Academy of Pharmaceutical Sciences, San Francisco meeting, April 1975.

Abstracted from a thesis submitted by K. A. Dandekar to the Graduate School, University of Kentucky, in partial fulfillment of the Doctor of Philosophy degree requirements.

* Present address: Wm. H. Rorer, Inc., Fort Washington, PA 19034.
x To whom inquiries should be directed.

Simultaneous Determination of 4-Nitroanisole, 4-Nitrophenol, and 4-Nitrocatechol by Phase-Sensitive ac Polarography

H. BURGSCHAT and K. J. NETTER x

Abstract □ Phase-sensitive ac polarography was applied to the simultaneous quantitative determination of 4-nitroanisole, 4-nitrophenol, and 4-nitrocatechol in alkaline solutions. Certain experimental precautions are necessary to determine each compound in the presence of the other two. Thus, 4-nitrocatechol is determined indirectly by forming a yellow ratio chelate with cupric ions, whereas 4-nitroanisole is determined directly by the reduction waves of the nitro group. For the determination of 4-nitrophenol, the interference by the simultaneously present 4-nitrocatechol must be eliminated by masking it by the addition of magnesium ions. The method described permits a qualitative and quantitative analysis of all three compounds in one solution since linear calibration curves are obtained.

Keyphrases ■ 4-Nitroanisole—polarographic analysis in presence of 4-nitrophenol and 4-nitrocatechol, alkaline solutions ■ 4-Nitrophenol—polarographic analysis in presence of 4-nitroanisole and 4-nitrocatechol, alkaline solutions ■ 4-Nitrocatechol—polarographic analysis in presence of 4-nitroanisole and 4-nitrocatechol, alkaline solutions □ Polarography—simultaneous analyses, 4-nitrophenol, 4-nitroanisole, and 4-nitrocatechol, alkaline solutions

Polarography is a common procedure in the analysis of aromatic nitro compounds of different character (1–3), because these compounds are easily reduced at the dropping mercury electrode. The mechanism of the electrode reaction was studied in aqueous solutions (4), and the mechanism of nitro derivative reduction was investigated in aprotic solvents (5, 6). More detailed studies with nitrophenol derivatives also were reported (7, 8).

From these studies, it follows that the nitro compounds can be quantitatively determined when analyzed independently. However, conditions become more complex when several nitro compounds are present. As expected (9), the peak potentials of such compounds are so close to each other that their peaks often overlap, and it is difficult to obtain qualitative and quantitative results without prior separation. Because of the inaccuracy of the results obtained by dc polarography (9), use of phase-sensitive ac polarography was suggested (10). This method allows a better interpretation of neighboring peaks. The logarithmic analysis for overlapping waves (11) is not feasible routinely.

In drug metabolism studies, 4-nitroanisole (I) was used as a model drug for demonstrating oxidative *O*-demethylation activity (12). More recently, the production of 4-nitrocatechol (III) was observed in microsomal suspensions after incubations of I or its main metabolic product, 4-nitrophenol (II) (13, 14). Compound III has an absorption maximum slightly different from that of II, the formation of which is usually recorded spectrophotometrically for 5–10 min at pH 7.85 as a routine kinetic method (15) to measure the initial velocity of the oxidative *O*-demethylation of I to II. Thus, III might interfere with the spectral recording of II formation during prolonged incubations[1].

Pharmacologically, it is desirable to determine these three compounds with the greatest possible simplicity and rapidity. The described experiments resulted in the development of a rapid ac polarographic method, allowing the simultaneous determination of these compounds[2]. In this connection, special emphasis is placed on the effects of pH variation in the polarographic base solution.

EXPERIMENTAL

Measurements were carried out using a phase-sensitive ac polarograph, as described previously (16), with an additional phase-sensitive rectifier.

An internal low frequency oscillator creates a frequency of 12 Hz, which is superimposed on the polarographic cell potential. The variable phase of the phase-sensitive rectifier was adjusted so that the capacitance current was largely eliminated. To avoid beat phenomena, a synchronization of the increase in drop size with the alternating current was necessary. Therefore, the internal low frequency was applied to the drop controller in the electrode stand[3]. The amplitude of the alternating current was 30 mv for all experiments.

The polarograms were recorded with an *xy*-recorder[4] after bubbling purified nitrogen through the solution for 2.5 min. The flow rate of mercury dropping into 0.1 *N* NaOH at a potential of −1.0 v was 3.24 mg/sec, and the drop time was 2.72 sec. With automatic drop control, it amounted to 0.69 sec at a reservoir height of 67 cm. All measurements were recorded *versus* a normal calomel electrode at 21 ± 1°. A commercially available pH meter[5] with a glass electrode was used after calibration

[1] P. Bergheim and K. J. Netter, unpublished results.
[2] The application of the polarographic determination to kinetic analyses in biological samples will be described later.
[3] Metrohm E 354, Herisau, Switzerland.
[4] Metrawatt AG, Nürnberg, Germany.
[5] Knick, Berlin, Germany.

(11) T. M. Brody, *J. Pharmacol. Exp. Ther.*, 117, 39 (1956).
(12) "Drill's Pharmacology in Medicine," 3rd ed., J. R. DiPalma, Ed., McGraw-Hill, New York, N.Y., 1965, p. 294.

ACKNOWLEDGMENTS AND ADDRESSES

Received October 31, 1975, from the *College of Pharmacy, University of Kentucky, Lexington, KY 40506.*

Accepted for publication March 4, 1976.

Presented at the Basic Pharmaceutics Section, APhA Academy of Pharmaceutical Sciences, San Francisco meeting, April 1975.

Abstracted from a thesis submitted by K. A. Dandekar to the Graduate School, University of Kentucky, in partial fulfillment of the Doctor of Philosophy degree requirements.

* Present address: Wm. H. Rorer, Inc., Fort Washington, PA 19034.
x To whom inquiries should be directed.

Simultaneous Determination of 4-Nitroanisole, 4-Nitrophenol, and 4-Nitrocatechol by Phase-Sensitive ac Polarography

H. BURGSCHAT and K. J. NETTER x

Abstract □ Phase-sensitive ac polarography was applied to the simultaneous quantitative determination of 4-nitroanisole, 4-nitrophenol, and 4-nitrocatechol in alkaline solutions. Certain experimental precautions are necessary to determine each compound in the presence of the other two. Thus, 4-nitrocatechol is determined indirectly by forming a yellow ratio chelate with cupric ions, whereas 4-nitroanisole is determined directly by the reduction waves of the nitro group. For the determination of 4-nitrophenol, the interference by the simultaneously present 4-nitrocatechol must be eliminated by masking it by the addition of magnesium ions. The method described permits a qualitative and quantitative analysis of all three compounds in one solution since linear calibration curves are obtained.

Keyphrases ■ 4-Nitroanisole—polarographic analysis in presence of 4-nitrophenol and 4-nitrocatechol, alkaline solutions ■ 4-Nitrophenol—polarographic analysis in presence of 4-nitroanisole and 4-nitrocatechol, alkaline solutions ■ 4-Nitrocatechol—polarographic analysis in presence of 4-nitroanisole and 4-nitrocatechol, alkaline solutions □ Polarography—simultaneous analyses, 4-nitrophenol, 4-nitroanisole, and 4-nitrocatechol, alkaline solutions

Polarography is a common procedure in the analysis of aromatic nitro compounds of different character (1–3), because these compounds are easily reduced at the dropping mercury electrode. The mechanism of the electrode reaction was studied in aqueous solutions (4), and the mechanism of nitro derivative reduction was investigated in aprotic solvents (5, 6). More detailed studies with nitrophenol derivatives also were reported (7, 8).

From these studies, it follows that the nitro compounds can be quantitatively determined when analyzed independently. However, conditions become more complex when several nitro compounds are present. As expected (9), the peak potentials of such compounds are so close to each other that their peaks often overlap, and it is difficult to obtain qualitative and quantitative results without prior separation. Because of the inaccuracy of the results obtained by dc polarography (9), use of phase-sensitive ac polarography was suggested (10). This method allows a better interpretation of neighboring peaks. The logarithmic analysis for overlapping waves (11) is not feasible routinely.

In drug metabolism studies, 4-nitroanisole (I) was used as a model drug for demonstrating oxidative *O*-demethylation activity (12). More recently, the production of 4-nitrocatechol (III) was observed in microsomal suspensions after incubations of I or its main metabolic product, 4-nitrophenol (II) (13, 14). Compound III has an absorption maximum slightly different from that of II, the formation of which is usually recorded spectrophotometrically for 5–10 min at pH 7.85 as a routine kinetic method (15) to measure the initial velocity of the oxidative *O*-demethylation of I to II. Thus, III might interfere with the spectral recording of II formation during prolonged incubations[1].

Pharmacologically, it is desirable to determine these three compounds with the greatest possible simplicity and rapidity. The described experiments resulted in the development of a rapid ac polarographic method, allowing the simultaneous determination of these compounds[2]. In this connection, special emphasis is placed on the effects of pH variation in the polarographic base solution.

EXPERIMENTAL

Measurements were carried out using a phase-sensitive ac polarograph, as described previously (16), with an additional phase-sensitive rectifier.

An internal low frequency oscillator creates a frequency of 12 Hz, which is superimposed on the polarographic cell potential. The variable phase of the phase-sensitive rectifier was adjusted so that the capacitance current was largely eliminated. To avoid beat phenomena, a synchronization of the increase in drop size with the alternating current was necessary. Therefore, the internal low frequency was applied to the drop controller in the electrode stand[3]. The amplitude of the alternating current was 30 mv for all experiments.

The polarograms were recorded with an *xy*-recorder[4] after bubbling purified nitrogen through the solution for 2.5 min. The flow rate of mercury dropping into 0.1 *N* NaOH at a potential of −1.0 v was 3.24 mg/sec, and the drop time was 2.72 sec. With automatic drop control, it amounted to 0.69 sec at a reservoir height of 67 cm. All measurements were recorded *versus* a normal calomel electrode at 21 ± 1°. A commercially available pH meter[5] with a glass electrode was used after calibration

[1] P. Bergheim and K. J. Netter, unpublished results.
[2] The application of the polarographic determination to kinetic analyses in biological samples will be described later.
[3] Metrohm E 354, Herisau, Switzerland.
[4] Metrawatt AG, Nürnberg, Germany.
[5] Knick, Berlin, Germany.

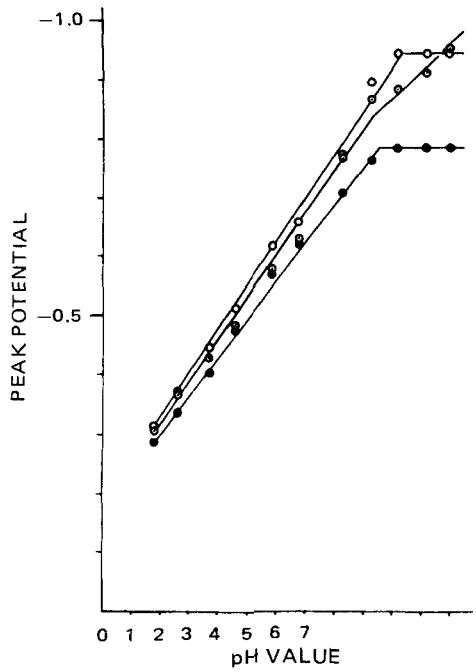

Figure 1—*The pH dependency of the peak potentials of I (●), II (○), and III (⊙). Concentration = 20 μM in Britton–Robinson buffer.*

with standard buffers[6]. All solvents and substances were of analytical grade and were not further purified.

RESULTS AND DISCUSSION

pH Dependency—Figure 1 shows the dependence of the peak potentials of I–III in Britton–Robinson buffer (17). The peak potentials exhibited a linear shift to more negative values with increasing pH; but at pH 9, the peak potentials for I and II became independent of pH. Similar results were obtained previously for nitroaniline (4). For III, however, the pH dependency persisted above pH 9 but showed a smaller increase. The shifts for the peak potentials per pH unit for I and II were 62 and 72 mv, respectively; for III, values of 68 mv below pH 9 and of 46 mv above pH 9 were found.

Further alkalinization above pH 12 by using 0.1 *N* NaOH instead of the buffer led to a further increase of the peak potential of III while the other two compounds showed a plateau. The values at pH 13 were −780 mv for I, −940 mv for II, and −1000 mv for III, showing that the second part of the curve for III in Fig. 1 was continued by 45 mv/pH unit. Therefore, 0.1 *N* NaOH (pH 13) was selected as a suitable medium for the quantitative and qualitative analyses of all three compounds.

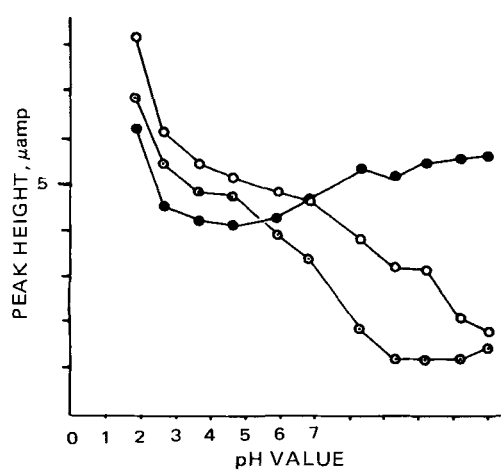

Figure 2—*The pH dependency of the peak heights of I (●), II (○), and III (⊙). Conditions were as in Fig. 1.*

[6] Merck, Darmstadt, Germany.

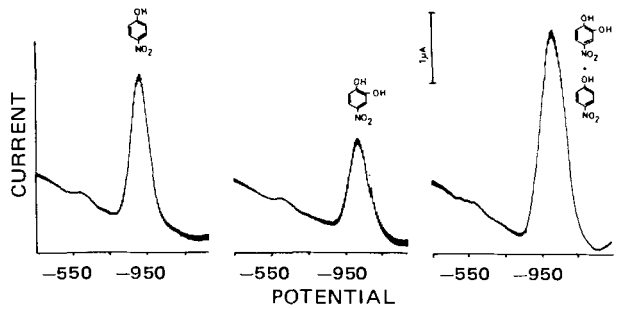

Figure 3—*Polarograms of II and III in 0.1 N NaOH. Key: left, polarogram of II (20 μM); middle, polarogram of III (20 μM); and right, polarogram of both phenols (each 20 μM).*

Not only the position of the peak potentials but also peak heights were influenced by an increase in pH. As shown in Fig. 2, the peak heights of II and III decreased with increasing pH. After an initial decrease, the peak height of I showed a slight increase above pH 4.5, which continued roughly until pH 12. In this region, it again reached the starting peak height of about pH 2.

The data in Fig. 1 show that, in the alkaline solution, I had a peak potential sufficiently different (about 160 mv) to allow a separate determination. The two phenols, however, did not possess peak potentials sufficiently apart from each other (Fig. 3), a fact that necessitated other means of determination. The left and middle polarograms of Fig. 3 represent the peaks of II and III in the base solution; the right one shows the effect of mixing both II and III. The result was a clear superposition of both peaks. The peak potentials and peak heights shown in the figures represent only the first observed reduction step of the nitro groups on the electrode surface. For II and III, this step was followed in alkaline solutions by a second reduction step in a more negative potential region located closely to the reduction of the sodium ion.

The second peaks (about −1.5 v) could not be quantitatively evaluated because of a lack of proportionality with concentration. This separation into two peaks, however, points to a different electrode mechanism for II and III in contrast to I, which did not show a reduction in peak height in alkaline solutions. This behavior is interpreted as representing two or four consecutive electron-transferring steps in II and III reduction (8, 18); in I, the transfer of all six electrons occurs in one step. Consequently, there is no second peak for I. For pH values below 7, however, all three substances seemed to be reduced by the same or a very similar mechanism.

Determination of II and III—*Indirect Determination of III in Presence of II*—In addition to the direct reduction of the nitro group, III can also indirectly be determined by utilizing the neighboring hydroxyl groups by the formation of a metal chelate (19–21).

Studies with a number of cations, *e.g.*, iron, copper, zinc, tin, cadmium, germanium, boron, aluminum, and magnesium, showed that only cupric and magnesium ions provided usable results in alkaline solution. On addition of cupric ions to the base solution containing III, the red color of III changed to yellow and a new peak at −540 mv appeared in the polarogram (Fig. 4, right). It was not obtained with cupric ions alone in the

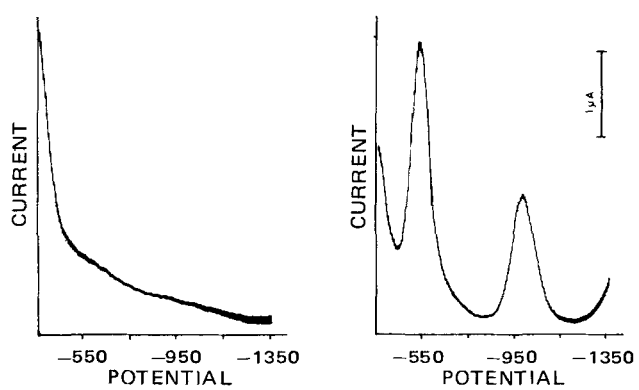

Figure 4—*Polarograms of III. Key: left, base current in 0.1 N NaOH in the presence of 5 μl of 1% $CuSO_4$ (final concentration of 40 μM); and right, polarogram of III (20 μM) under the same conditions. The peak at −540 mv represents chelate reduction, and the peak at −940 mv represents the first reduction step of the nitro group.*

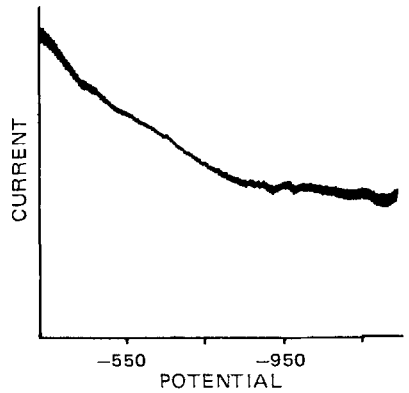

Figure 5—*Masking of III; polarogram after injection of 200 μl of 0.1 M $MgCl_2$ into the base solution containing III (20 μM).*

absence of III (Fig. 4, left). The reduction peaks of the nitro group appeared at the same potentials as mentioned previously.

Further experimentation revealed that only 0.5 mmole of cupric ions was necessary for the determination of 1 mmole of III, indicating that a 2:1 chelate had been formed. An increase in the cupric-ion concentration above this ratio had no effect on the peak height of III. Since it seemed desirable to have an excess of cupric ions, 5 μl of 1% $CuSO_4$ was added to 5 ml of the base solution (final concentration of 40 μ*M*). The relationship between the concentration of III and the respective peak heights of the "chelate peak" at −540 mv under these conditions was linear. The calibration curve was not influenced by the addition of I and II. A similar chelate with catechol and cupric ions was used for an indirect determination of catechol by atomic absorption spectrophotometry (21).

Determination of II in Presence of III—Magnesium ions showed an effect with III opposite to that of cupric ions. The addition of magnesium ions to the solution containing only III (Fig. 4, right) abolished the peaks of the chelate and of the nitro group reduction (Fig. 5). At the same time, the red color of III reappeared. In this case, the magnesium ion displaced the cupric ion in the chelate to form a more stable complex, which gave no polarographic signal in 0.1 *N* NaOH. The behavior of II in the presence of III is shown in Fig. 6. In the left polarogram, both phenols were present in a concentration of 20 μ*M*, each in 5 ml of base solution with 5 μl of 1% $CuSO_4$. The second peak at about −960 mv constitutes an overlapping mixture of the currents of two peaks as in Fig. 3 (right).

After adding 200 μl of 0.1 *M* $MgCl_2$ (Fig. 6, right), only the peak of II at −940 mv remained; the contribution by III disappeared. Experiments made with II alone under the same conditions in a volume of 5.2 ml (5.0 ml of 0.1 *N* NaOH and 0.2 ml of 0.1 *M* $MgCl_2$) gave a linear relationship between concentration and peak height. It is possible to determine II after "masking" III by the addition of magnesium ions.

Determination of I—As can be seen from Fig. 1, the peak potential of I in alkali was sufficiently different from those of the two phenols when measured in the absence of cupric ions. In their presence, there was no

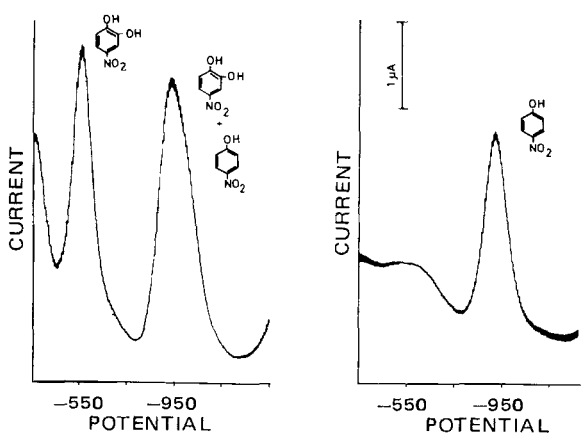

Figure 6—*Masking of III in the presence of II. Key: left, polarogram of both phenols (20 μM) in 0.1 N NaOH in the presence of 40 μM $CuSO_4$; and right, repeat polarogram of the same solution after addition of 200 μl of 0.1 M $MgCl_2$ (final volume of 5.2 ml). Only the peak of II remains in the right polarogram.*

Table I—Simultaneous Determination of I–III

Compound	Concentration Calculated, *M*	Concentration Found, *M*	Recovery, %
Concentration of I Was Varied and Concentrations of II and III Remained Constant			
I	2×10^{-6}	2.1×10^{-6}	105.0
II	2×10^{-5}	2×10^{-5}	100.0
III	2×10^{-5}	1.94×10^{-5}	97.0
I	4×10^{-6}	3.8×10^{-6}	95.0
II	2×10^{-5}	2×10^{-5}	100.0
III	2×10^{-5}	1.96×10^{-5}	98.0
I	6×10^{-6}	5.9×10^{-6}	98.3
II	2×10^{-5}	2×10^{-5}	100.0
III	2×10^{-5}	2.03×10^{-5}	101.5
I	8×10^{-6}	8.2×10^{-6}	102.5
II	2×10^{-5}	2.06×10^{-5}	103.0
III	2×10^{-5}	1.97×10^{-5}	98.5
I	1×10^{-6}	0.98×10^{-6}	98.0
II	2×10^{-5}	2.04×10^{-5}	102.0
III	2×10^{-5}	1.96×10^{-5}	98.0
Concentration of II Was Varied and Concentrations of I and III Remained Constant			
I	1×10^{-5}	0.97×10^{-5}	97.0
II	4×10^{-6}	4×10^{-6}	100.0
III	2×10^{-5}	1.94×10^{-5}	97.0
I	1×10^{-5}	0.98×10^{-5}	98.0
II	8×10^{-6}	7.8×10^{-6}	97.5
III	2×10^{-5}	2.02×10^{-5}	101.0
I	1×10^{-5}	0.97×10^{-5}	97.0
II	1.2×10^{-5}	1.18×10^{-5}	98.3
III	2×10^{-5}	1.96×10^{-5}	98.0
I	1×10^{-5}	0.98×10^{-5}	98.0
II	1.6×10^{-5}	1.6×10^{-5}	100.0
III	2×10^{-5}	1.98×10^{-5}	99.0
I	1×10^{-5}	0.99×10^{-5}	99.0
II	2×10^{-5}	1.95×10^{-5}	97.5
III	2×10^{-5}	2×10^{-5}	100.0
Concentration of III Was Varied and Concentrations of I and II Remained Constant			
I	1×10^{-5}	1.04×10^{-5}	104.0
II	2×10^{-5}	2.0×10^{-5}	100.0
III	4×10^{-6}	3.9×10^{-6}	97.5
I	1×10^{-5}	0.98×10^{-5}	98.0
II	2×10^{-5}	1.97×10^{-5}	98.5
III	8×10^{-6}	8.0×10^{-6}	100.0
I	1×10^{-5}	1×10^{-5}	100.0
II	2×10^{-5}	1.95×10^{-5}	97.5
III	1.2×10^{-5}	1.2×10^{-5}	100.0
I	1×10^{-5}	0.96×10^{-5}	96.4
II	2×10^{-5}	2.06×10^{-5}	103.0
III	1.6×10^{-5}	1.62×10^{-5}	101.25
I	1×10^{-5}	0.96×10^{-5}	96.4
II	2×10^{-5}	2.06×10^{-5}	103.0
III	2×10^{-5}	2.08×10^{-5}	104.0

interference from the newly formed chelate peak at −540 mv. The potential differences at pH 13 were 240 and 160 mv, as illustrated (in the presence of cupric ions) in Fig. 7 (left). The addition of magnesium ions did not affect the peak of I (Fig. 7, right), thereby allowing the quantitative evaluation of I in the presence of both II and III. Cupric ions, which are necessary for the routine estimation of III, had no influence on the peak height of I. Also, the subsequent addition of magnesium ions had only a negligible effect on the peak height of I.

Simultaneous Determination of I–III—In summary, the procedure for the polarographic estimation of the three nitro compounds is as follows. The compounds (0–250 nmoles) must be dissolved in 5 ml of 0.1 *N* NaOH in the polarographic vessel. Then 5 μl of 1% $CuSO_4$ in water is added by micropipet, and the vessel is gassed with purified nitrogen for 2.5 min. Recording of the polarogram yields curves of the type shown in Fig. 7 (left). The peak heights of these curves over the base current in

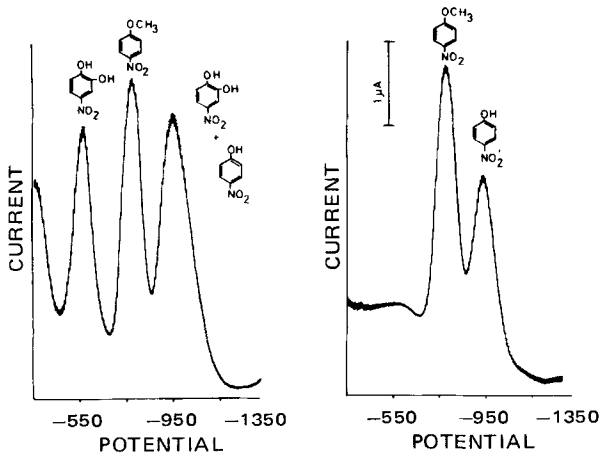

Figure 7—*Polarogram of I (10 μM), II (20 μM), and III (20 μM) in the presence of 40 μM $CuSO_4$. Key: left, before addition of magnesium ions; and right, after addition of magnesium ions.*

conjunction with calibration curves give direct measurements of III and I.

To determine II also, 200 μl of 0.1 *M* $MgCl_2$ is added to the same solution. Then this solution is bubbled again with nitrogen to achieve proper mixing and removal of the oxygen carried in during the manipulation. The newly taken polarogram (Fig. 7, right) shows peaks only for I and II, from which the concentration of II can be obtained by subtracting the base current. Theoretically, a second determination of I is possible from this second polarogram.

The accuracy of this method of determination for each substance in the presence of varying concentrations of the others is shown by the homogeneous and practically complete recovery rates given in Table I.

REFERENCES

(1) H. Buchowski and Z. Olemzpska, *Z. Anal. Chem.*, **172**, 439 (1960).

(2) H. Oelschläger, *Arch. Pharm.*, **296**, 7 (1963).

(3) H. G. Lordi, E. M. Cohen, and B. L. Taylor, *J. Am. Pharm. Assoc., Sci. Ed.*, **49**, 371 (1960).

(4) L. Holleck and H. Exner, *Z. Elektrochem.*, **56**, 46 (1952).

(5) G. Farnia, G. Mengoli, and E. Vianello, *Electroanal. Chem.*, **50**, 73 (1974).

(6) *Ibid.*, **57**, 191 (1974).

(7) T. Takahashi and H. Shirai, *Talanta*, **8**, 177 (1961).

(8) M. J. Astle and W. McConnell, *J. Am. Chem. Soc.*, **65**, 35 (1943).

(9) K. Honda and S. Kikuchi, *Bull. Chem. Soc. Jpn.*, **34**, 529 (1961).

(10) W. H. Reinmuth and D. E. Smith, *Anal. Chem.*, **33**, 964 (1961).

(11) J. Ruzic and M. Branica, *Electroanal. Chem. Interface Electrochem.*, **22**, 243 (1969).

(12) K. J. Netter, *Naunyn-Schmiedebergs Arch. Exp. Pathol. Pharmakol.*, **238**, 292 (1960).

(13) J. Daly, *J. Biochem. Pharmacol.*, **19**, 2379 (1970).

(14) J. Chrastil and J. T. Wilson, *J. Pharmacol. Exp. Ther.*, **193**, 631 (1975).

(15) K. J. Netter and G. Seidel, *ibid.*, **146**, 61 (1964).

(16) G. G. Willems and R. Neeb, *Z. Anal. Chem.*, **269**, 1 (1974).

(17) H. T. S. Britton and R. A. Robinson, *J. Chem. Soc., London*, **1931**, 1456.

(18) M. J. Astle and S. P. Stephenson, *J. Am. Chem. Soc.*, **65**, 2399 (1943).

(19) N. Konopik, *Monatsh. Chem.*, **91**, 717 (1960).

(20) J. Zelinka, M. Bartusek, and A. Okac, *Collect. Czech. Chem. Commun.*, **40**, 390 (1975).

(21) Y. Kidani, S. Uno, Y. Kato, and H. Koike, *Jpn. Anal.*, **23**, 740 (1974).

ACKNOWLEDGMENTS AND ADDRESSES

Received December 12, 1975, from the *Department of Pharmacology, Section on Toxicology, University of Mainz, D-6500 Mainz, West Germany.*

Accepted for publication March 5, 1976.

Supported by the Deutsche Forschungsgemeinschaft.

The authors thank Dr. G. Willems for the construction of the polarograph. The technical assistance of Mrs. Ursula Wulff is gratefully acknowledged.

[x] To whom inquiries should be directed.

Sustained-Release Applications of Montmorillonite Interaction with Amphetamine Sulfate

JAMES W. McGINITY [x] and JOHN L. LACH

Abstract □ Urinary recovery studies showed that montmorillonite significantly affects the initial therapeutic levels of amphetamine sulfate. The combination of a 1:20 drug–montmorillonite complex with pure drug in a 1:1 ratio, based on amphetamine content, resulted in recovery profiles resembling those obtained from prolonged-release dosage forms. The 1:20 complex, pure drug, and combination formulations showed comparable bioavailability after 48 hr.

Keyphrases □ Montmorillonite—effect on bioavailability of amphetamine sulfate, urinary recovery studies, applied to sustained-release dosage form □ Amphetamine sulfate—bioavailability, effect of montmorillonite, urinary recovery studies, applied to sustained-release dosage forms □ Urinary recovery studies—effect of montmorillonite on bioavailability of amphetamine sulfate, applied to sustained-release dosage form □ Dosage forms—sustained-release drug–clay complex, effect of montmorillonite on bioavailability of amphetamine sulfate □ Clays—montmorillonite, complex with amphetamine sulfate, effect on bioavailability □ Stimulants—amphetamine sulfate, effect of complexing with montmorillonite on bioavailability

The availability of a drug from a dosage form is dependent on both the rate and the completeness with which the drug is delivered to the absorption site in an absorbable form. In a recent review (1), excipients in solid dosage forms were shown to interact with various medicinals. Such drug–excipient interactions generally influence both the rate of drug absorption and the amount delivered unchanged to the general circulation.

An earlier publication (2) reported that cationic salts

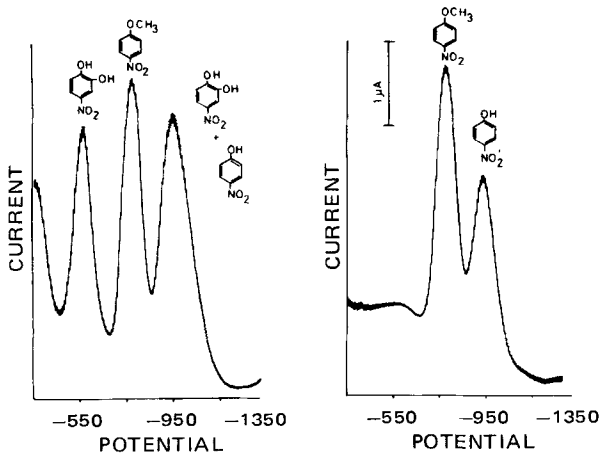

Figure 7—*Polarogram of I (10 μM), II (20 μM), and III (20 μM) in the presence of 40 μM $CuSO_4$. Key: left, before addition of magnesium ions; and right, after addition of magnesium ions.*

conjunction with calibration curves give direct measurements of III and I.

To determine II also, 200 μl of 0.1 *M* $MgCl_2$ is added to the same solution. Then this solution is bubbled again with nitrogen to achieve proper mixing and removal of the oxygen carried in during the manipulation. The newly taken polarogram (Fig. 7, right) shows peaks only for I and II, from which the concentration of II can be obtained by subtracting the base current. Theoretically, a second determination of I is possible from this second polarogram.

The accuracy of this method of determination for each substance in the presence of varying concentrations of the others is shown by the homogeneous and practically complete recovery rates given in Table I.

REFERENCES

(1) H. Buchowski and Z. Olemzpska, *Z. Anal. Chem.*, **172**, 439 (1960).

(2) H. Oelschläger, *Arch. Pharm.*, **296**, 7 (1963).

(3) H. G. Lordi, E. M. Cohen, and B. L. Taylor, *J. Am. Pharm. Assoc., Sci. Ed.*, **49**, 371 (1960).

(4) L. Holleck and H. Exner, *Z. Elektrochem.*, **56**, 46 (1952).

(5) G. Farnia, G. Mengoli, and E. Vianello, *Electroanal. Chem.*, **50**, 73 (1974).

(6) *Ibid.*, **57**, 191 (1974).

(7) T. Takahashi and H. Shirai, *Talanta*, **8**, 177 (1961).

(8) M. J. Astle and W. McConnell, *J. Am. Chem. Soc.*, **65**, 35 (1943).

(9) K. Honda and S. Kikuchi, *Bull. Chem. Soc. Jpn.*, **34**, 529 (1961).

(10) W. H. Reinmuth and D. E. Smith, *Anal. Chem.*, **33**, 964 (1961).

(11) J. Ruzic and M. Branica, *Electroanal. Chem. Interface Electrochem.*, **22**, 243 (1969).

(12) K. J. Netter, *Naunyn-Schmiedebergs Arch. Exp. Pathol. Pharmakol.*, **238**, 292 (1960).

(13) J. Daly, *J. Biochem. Pharmacol.*, **19**, 2379 (1970).

(14) J. Chrastil and J. T. Wilson, *J. Pharmacol. Exp. Ther.*, **193**, 631 (1975).

(15) K. J. Netter and G. Seidel, *ibid.*, **146**, 61 (1964).

(16) G. G. Willems and R. Neeb, *Z. Anal. Chem.*, **269**, 1 (1974).

(17) H. T. S. Britton and R. A. Robinson, *J. Chem. Soc., London*, **1931**, 1456.

(18) M. J. Astle and S. P. Stephenson, *J. Am. Chem. Soc.*, **65**, 2399 (1943).

(19) N. Konopik, *Monatsh. Chem.*, **91**, 717 (1960).

(20) J. Zelinka, M. Bartusek, and A. Okac, *Collect. Czech. Chem. Commun.*, **40**, 390 (1975).

(21) Y. Kidani, S. Uno, Y. Kato, and H. Koike, *Jpn. Anal.*, **23**, 740 (1974).

ACKNOWLEDGMENTS AND ADDRESSES

Received December 12, 1975, from the *Department of Pharmacology, Section on Toxicology, University of Mainz, D-6500 Mainz, West Germany.*

Accepted for publication March 5, 1976.

Supported by the Deutsche Forschungsgemeinschaft.

The authors thank Dr. G. Willems for the construction of the polarograph. The technical assistance of Mrs. Ursula Wulff is gratefully acknowledged.

[x] To whom inquiries should be directed.

Sustained-Release Applications of Montmorillonite Interaction with Amphetamine Sulfate

JAMES W. McGINITY [x] and JOHN L. LACH

Abstract □ Urinary recovery studies showed that montmorillonite significantly affects the initial therapeutic levels of amphetamine sulfate. The combination of a 1:20 drug–montmorillonite complex with pure drug in a 1:1 ratio, based on amphetamine content, resulted in recovery profiles resembling those obtained from prolonged-release dosage forms. The 1:20 complex, pure drug, and combination formulations showed comparable bioavailability after 48 hr.

Keyphrases □ Montmorillonite—effect on bioavailability of amphetamine sulfate, urinary recovery studies, applied to sustained-release dosage form □ Amphetamine sulfate—bioavailability, effect of montmorillonite, urinary recovery studies, applied to sustained-release dosage forms □ Urinary recovery studies—effect of montmorillonite on bioavailability of amphetamine sulfate, applied to sustained-release dosage form □ Dosage forms—sustained-release drug–clay complex, effect of montmorillonite on bioavailability of amphetamine sulfate □ Clays—montmorillonite, complex with amphetamine sulfate, effect on bioavailability □ Stimulants—amphetamine sulfate, effect of complexing with montmorillonite on bioavailability

The availability of a drug from a dosage form is dependent on both the rate and the completeness with which the drug is delivered to the absorption site in an absorbable form. In a recent review (1), excipients in solid dosage forms were shown to interact with various medicinals. Such drug–excipient interactions generally influence both the rate of drug absorption and the amount delivered unchanged to the general circulation.

An earlier publication (2) reported that cationic salts

Table I—Urine pH's for the Three Dosage Forms

Subject	Pure Drug		1:1 Combination, Drug–Complex		1:20 Drug–Montmorillonite Complex	
	0–10 hr	12–48 hr	0–10 hr	12–48 hr	0–10 hr	12–48 hr
1	6.25 ± 0.15	6.40 ± 0.20	6.35 ± 0.20	6.55 ± 0.25	6.25 ± 0.20	6.60 ± 0.20
2	6.35 ± 0.20	6.50 ± 0.25	6.00 ± 0.15	6.30 ± 0.25	6.20 ± 0.20	6.40 ± 0.25
3	6.05 ± 0.15	6.40 ± 0.20	5.95 ± 0.20	6.30 ± 0.35	6.20 ± 0.15	6.25 ± 0.35
4	6.20 ± 0.20	6.45 ± 0.25	6.35 ± 0.20	6.40 ± 0.25	6.15 ± 0.15	6.40 ± 0.25
5	6.65 ± 0.20	6.70 ± 0.20	6.55 ± 0.20	6.70 ± 0.25	6.89 ± 0.15	6.90 ± 0.25
6	6.50 ± 0.25	6.40 ± 0.30	6.40 ± 0.25	6.70 ± 0.25	6.35 ± 0.25	6.70 ± 0.20

of organic medicinals bind tenaciously to montmorillonite clay. Data *in vitro* demonstrated that the amount of drug released from the drug–clay complex was dependent on the amount of montmorillonite in the formulation.

The influence of montmorillonite in dosage forms containing diazepam (3) and tolbutamide (4) was evaluated clinically. The diazepam study showed that the clay hindered drug absorption; the opposite was true for tolbutamide. Montmorillonite reduced blood levels of dicumarol in dogs by 25% compared to blood levels following the administration of pure drug (5). However, warfarin sodium tablets containing montmorillonite released the drug much faster *in vitro* than did the best commercial tablets (6). These reports demonstrate the complexity of drug–clay interactions and indicate that the presence of montmorillonite in a dosage form may markedly influence drug effects.

The purpose of this investigation was to develop a sustained-release dosage form employing a drug–montmorillonite interaction. Amphetamine sulfate was the model drug chosen, and drug concentrations *in vivo* were followed *via* urinary recovery studies. Pure drug was compared with a 1:20 complex of drug and clay and a 1:1 combination of pure drug and complex. Previous studies *in vitro* (2) demonstrated that little drug was present in the uncomplexed form in the 1:20 formulation.

EXPERIMENTAL

Materials—Amphetamine sulfate[1], montmorillonite[2], anhydrous ether (analytical reagent), sodium hydroxide (analytical reagent), 0.5 *N* hydrochloric acid, pH 7.4 phosphate buffer, *p*-nitroaniline solution (0.69 g in 8.3 ml of concentrated hydrochloric acid, diluted to 100 ml with water and filtered), and 1.4% sodium nitrite aqueous solution were obtained commercially.

Trial Conditions—Six normal healthy subjects, one female and five males ranging in age from 23 to 26 years and weighing from 57 to 84 kg, were utilized. Subjects had no previous history of GI, liver, or kidney disease and did not require any medication on a regular basis. All subjects had undergone a physical examination for an earlier study (7) and were healthy.

The importance of maintaining an acidic urine to prevent reabsorption of amphetamine from the urine back into the blood was reported previously (8, 9). However, chemical acidosis was not induced by ammonium chloride administration for the following reasons: (*a*) huge doses of this substance are required to maintain the pH at 5, (*b*) it has been reported that up to 20% of subjects suffer emetic effects after taking ammonium chloride, (*c*) it was desired to maintain subjects in a normal physiological state, and (*d*) ammonium chloride would upset the release patterns *in vivo*, already established *in vitro*.

Breakfast, 1 hr before the test, consisted of cereal and milk. No food or liquids except water were taken during the first 4 hr following drug administration. Formulations were administered as powders with 100 ml of water and ingested at 8 am during a normal working day; thus, by being active and controlling diet and fluid intake (~200 ml of water/2 hr), a slightly acidic urine (Table I) was attained in the first 10 hr. This period was of major interest, because the maximum for urinary drug elimination would be attained during this interval.

Urine samples were collected every 2 hr for 16 hr and at 24, 36, and 48 hr. All subjects were given 15-mg doses of drug except Subject 3, who ingested 20-mg doses. The order of administration of the amphetamine formulations to the six subjects was randomized, and a washout period of at least 1 month was allowed before administering another formulation. Formulations containing the same amount of amphetamine were in three forms: pure drug, a 1:20 drug–montmorillonite complex (2), and a 1:1 combination of pure drug and complex.

Methods—The spectrophotometric assay developed and employed is similar to that of Alles and Wisegarver (10) but contains several modifications to improve sensitivity and reproducibility. Reproducibility from standard solutions of urine containing amphetamine sulfate was within ±2.5%. The colorimetric reaction used to assay amphetamine in the urine measures both amphetamine and the hydroxylated metabolite. However, in humans, less than 3% of the amphetamine is excreted as the hydroxylated metabolite (11), so interference was assumed to be minimal and fairly constant for a particular patient. In addition, the individual day-to-day variations in the blank for all patients fell within ±3.5%.

Steam Distillation Procedure—Ten milliliters of 5 *N* sodium hydroxide and 50 ml of double-distilled water were added to 50 ml of urine in an all-glass distillation apparatus and steam distilled. The distillate, 50–60 ml, was collected in a flask containing 2 ml of 1 *N* HCl immersed in an ice bath. The distillate was transferred to a separator and made alkaline with 0.5 ml of 5 *N* sodium hydroxide, and 50 ml of ether was added. The flask was shaken for 5 min, and the aqueous layer was separated and extracted with two additional aliquots of ether.

To the final ether extract, 10 ml of 0.5 *N* HCl was added to convert the extracted amphetamine to the acid salt. This flask was shaken for 5 min, and the aqueous acidic layer was transferred to the next flask where the shaking procedure was repeated. The aqueous portion was finally shaken with the first ether extract, which contained most of the drug. This extraction was repeated with another 10 ml of acid followed by 5 ml of distilled water to wash the ether layer. The extracts and washings were combined, and the pH was adjusted to 7.5 with dilute sodium hydroxide solution. The volume was adjusted to 50 ml with distilled water.

Colorimetric Determination—Two milliliters of pH 7.4 phosphate buffer was added to 10 ml of the 50-ml extract. At this point, the pH of the reaction mixture was 7.4 ± 0.1. Then 1 ml of the diazo reagent (10) was added. The solution was mixed and placed in a water bath at 37° for 30 min to allow the reaction to go to completion. The test tube was removed, and 0.5 ml of 5 *N* sodium hydroxide was added. The tube was lightly agitated and allowed to stand for 30 min. Urine collected from the patient during the day, prior to drug administration, was extracted and treated in the same manner and used as the reference sample.

The difference in absorbance between the sample and the blank was determined at 520 nm, and the concentration of amphetamine in the urine was calculated from a standard curve. The standard curve was prepared by adding a known quantity of drug to the urine and plotting absorbance *versus* quantity of drug. The drug solution replaced the distilled water, which was added to the urine prior to the steam distillation procedure. All readings were duplicated, and the average was plotted. An excellent linear correlation between ab-

[1] J. H. Walker and Co., Mount Vernon, N.Y.
[2] Veegum Regular, R. T. Vanderbilt Co., New York, N.Y.

Table II—Peak Urinary Excretion Rates of Amphetamine and Times of Peak Rates from 15-mg Doses of Amphetamine Sulfate

Subject	Peak Urinary Excretion Rate, mg/hr			Time of Peak, hr		
	Pure Drug	1:1 Combination of Pure Drug and 1:20 Complex	1:20 Complex	Pure Drug	1:1 Combination of Pure Drug and 1:20 Complex	1:20 Complex
1	1.19	0.66	0.97	2.0	6.0	7.1
2	0.74	0.57	0.74	1.3	3.8	5.0
3[a]	0.77	0.60	0.71	1.4	3.8	6.3
4	0.65	0.50	0.55	2.1	4.8	7.0
5	0.53	0.48	0.46	1.0	3.0	5.1
6	0.72	0.58	0.58	3.0	3.4	5.2
Mean	0.767	0.565	0.668	1.800	4.133	5.950
SD	0.224	0.066	0.181	0.724	1.093	0.973

[a] The 20-mg dose of amphetamine sulfate was administered.

sorbance and drug concentration was found, and the absorptivity value was 6250.

RESULTS AND DISCUSSION

The effect of montmorillonite in modifying the levels of orally administered cationic drugs was verified *in vivo*. For Subject 1, plots of the time course of drug excretion of pure drug, the 1:20 drug–montmorillonite complex, and the 1:1 combination of pure drug and complex are shown in Fig. 1. The smooth curves were fit by eye and drawn by hand. The peak excretion rates of amphetamine from the pure drug and the 1:20 complex occurred at 2.0 and 7.1 hr, respectivtly. This time difference of 5.1 hr was due primarily to the presence of montmorillonite in the sample, assuming all physiological conditions to be constant in both cases. Since the clay does not hydrate in acidic media, the influence of the montmorillonite on the gastric emptying rate would be minimal.

In vitro studies (2) demonstrated that, under acidic conditions, the uncomplexed moiety rapidly passed into solution, but drug complexed to the clay was bound so strongly that little was released in the medium. This slow release at low pH explains the initial low excretion rates for the 1:20 complex (Fig. 1). However, with the passage of the 1:20 complex down the GI tract, it appeared that drug was released from the complex for absorption. This phenomenon of increased bioavailability in alkaline media could not be illustrated *in vitro* due to problems in methodology; *i.e.*, when the drug–montmorillonite samples were added to alkaline buffer media, hydration of the montmorillonite occurred and the drug was released. If the drug was not removed, then readsorption of the drug onto the clay would occur. However, since the body is a perfect sink, the concentration of drug in the blood is negligible in comparison to the intestinal concentration. Thus, as the formulation passed from the stomach into the small intestine at a higher pH, more drug was released and absorbed before readsorption of the active substance back onto the clay could occur.

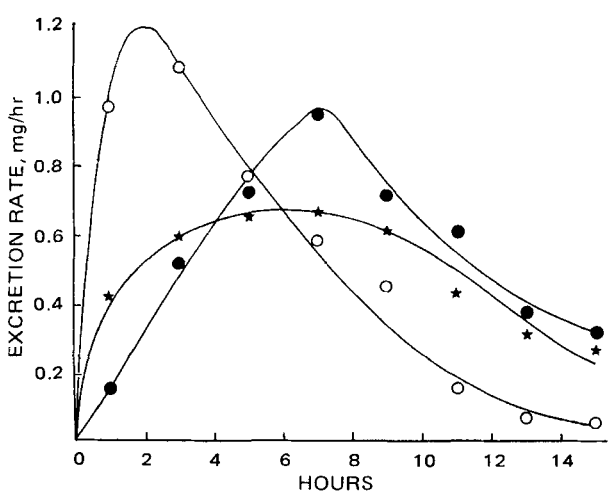

Figure 1—*Urine amphetamine levels following a single oral dose of amphetamine sulfate for Subject 1. Key: ○, 15 mg of drug alone; ★, 7.5 mg of drug–7.5 mg of drug as 1:20 complex; and ●, 15 mg of drug as 1:20 complex.*

Since it was shown *in vitro* that sodium chloride elutes drug from the drug–montmorillonite complex, and because of the high content of Na^+ ions in the intestinal juice, an increase in the concentration of free drug in solution also would be expected. Intestinal juice secreted at the rate of 0.7–3 liters/24 hr is rich in sodium ions (~140 mEq/liter). Because fresh liquid is continually being secreted, the elution rate of drug from the complex due to electrolyte effects would be expected to be greater *in vivo* than that found *in vitro*. The vacant sites on the clay left by the released drug would be occupied by the secreted cations and aid the absorption process. This would make readsorption of the amphetamine back onto the montmorillonite much more difficult and less likely to occur.

At the higher pH of the small intestine, amphetamine sulfate reverts to amphetamine, which is a nonpolar liquid. In such a physical state, this lipid-soluble substance may readily partition into the intestinal wall and be absorbed.

For Subject 1, the recovery curve (Fig. 1) for the combination sample containing 50% amphetamine sulfate and 50% as the 1:20 complex is typical of prolonged-action dosage forms. The peak excretion rate for the pure drug was 1.19 mg/hr, whereas the peak for the combination sample was only 0.66 mg/hr. By eliminating the peak levels seen with the pure drug, the incidence and intensity of possible side effects of the drug are reduced when amphetamine sulfate is administered as a combination of pure and complexed drug.

The peak excretion rates of amphetamine for each subject following the administration of the three test formulations appear in Table II. The time periods for the maxima to occur are also included. In all cases, the times for the peak excretion rates for the combination samples fell between the peak excretion rates for the pure drug and the 1:20 complex. The time period separating the peaks of these latter two samples varied from 2.2 hr for Subject 6 to 5.1 hr for Subject 1.

Montmorillonite affected the pharmacological response of the drug from all formulations. The stimulating effect of amphetamine in the complexed form reached its maximum effect several hours after drug administration. The peak response from the pure drug occurred within the 1st hr after administration. Due to the large doses of amphetamine sulfate administered, it was considered most unlikely that the hyperexcitability experienced by these subjects was psychological. Some subjects who suffered severe headaches from the pure and

Table III—Percent of Dose Recovered in Urine after 48 hr and the Bioavailability[a] of Amphetamine from the Combination Sample and Complex Compared to the Pure Drug for the 48-hr Period

Subject	Pure Drug	Combination	1:20 Complex
1	53	48 (91)	56 (105)
2	54	57 (105)	55 (102)
3	54	51 (94)	58 (107)
4	53	50 (94)	51 (96)
5	37	40 (108)	39 (105)
6	56	55 (98)	54 (96)
Mean	51.167	50.167	52.167
SD	7.026	5.981	6.853

[a] In parentheses and expressed as percentage.

complexed drug noticed a decrease in severity or no headache at all with the combination sample. This response can be explained from the recovery curve for the combination samples, since it was unlikely that development of tolerance to the stimulant occurred.

Table III shows the amount of amphetamine recovered in the urine over 48 hr and also the bioavailability of amphetamine from the complex and combination samples. When using the Student paired t test, no significant differences were seen in the bioavailability of amphetamine from all three formulations. However, excretion rates of amphetamine from the 1:20 complex were significantly different from the pure drug during the initial 4 hr.

In conclusion, the drug–excipient interaction between cationic drugs and montmorillonite clay can be employed successfully to prolong the action of such medicinals. The peak urinary excretion rate of amphetamine from the 1:20 drug–clay complex occurred at a much later time than the pure drug, indicating delayed absorption of amphetamine from the complex. In addition, the initial excretion rate of amphetamine from the complex was significantly lower than that of the pure drug. Finally, for all subjects, the bioavailability of the amphetamine from the 1:20 complex and the amphetamine–1:20 complex combination formulations over 48 hr was not significantly different from that of the pure drug.

REFERENCES

(1) D. C. Monkhouse and J. L. Lach, *Can. J. Pharm. Sci.*, **7**, 29(1972).

(2) J. W. McGinity and J. L. Lach, *J. Pharm. Sci*, **65**, 896(1976).

(3) K. Munzel, *Acta Pharmacol. Toxicol., Suppl. 3*, **29**, 81(1971).

(4) A. B. Varley, *J. Am. Med. Assoc.*, **206**, 1745(1968).

(5) M. J. Akers, J. L. Lach, and L. Fischer, *J. Pharm. Sci.*, **62**, 391(1973).

(6) J. G. Wagner, P. G. Welling, K. P. Lee, and J. E. Walker, *ibid.*, **60**, 666(1971).

(7) J. W. Bettis, J. L. Lach, and J. Hood, *Am. J. Hosp. Pharm.*, **30**, 240(1973).

(8) A. H. Beckett and M. Rowland, *J. Pharm. Pharmacol.*, **17**, 59(1965).

(9) A. H. Beckett, J. A. Salmon, and M. Mitchard, *ibid.*, **21**, 251(1969).

(10) G. A. Alles and B. B. Wisegarver, *Toxicol. Appl. Pharmacol.*, **3**, 678(1961).

(11) R. T. Williams, in "Fundamentals of Drug Metabolism and Drug Disposition," B. N. La Du, H. G. Mandel, and E. L. Way, Eds., Williams & Wilkins, Baltimore, Md., 1972, pp. 189–191.

ACKNOWLEDGMENTS AND ADDRESSES

Received June 19, 1975, from the *College of Pharmacy, University of Iowa, Iowa City, IA 52240*

Accepted for publication March 8, 1976.

[x] To whom inquiries should be directed. Present address: College of Pharmacy, University of Texas at Austin, Austin, TX 78712

Mass Screening and Confirmation of Codeine and Morphine in Urine by Radioimmunoassay–GLC

NARESH C. JAIN *‡[x], THOMAS C. SNEATH ‡, WAI J. LEUNG ‡, and ROBERT D. BUDD ‡

Abstract □ A rapid, sensitive, and specific procedure is described for the mass screening and confirmation of codeine and morphine in urine specimens. The method is sensitive to 0.5-μg/ml levels of both opiates in free and/or conjugate forms. The raw urine is screened directly by radioimmunoassay, which is reactive to both free and glucuronide forms of codeine and morphine. Specimens that are screened positive are confirmed by GLC using a flame-ionization detector. The opiates are analyzed as their acetyl derivatives on two different columns, OV-25 and Poly-A 103. This multiple approach eliminates false positives caused by interfering substances or structurally similar compounds present in the urine.

Keyphrases □ Codeine—radioimmunoassay–GLC analysis, human urine □ Morphine—radioimmunoassay–GLC analysis, human urine □ Radioimmunoassay–GLC—analysis, codeine and morphine in human urine □ GLC—analyis, codeine and morphine in human urine □ Opiates—codeine and morphine, radioimmunoassay–GLC analysis in human urine □ Narcotics—codeine and morphine, radioimmunoassay–GLC analysis in human urine

The widespread use and abuse of codeine, morphine, and heroin, which is largely metabolized to morphine (1), necessitate the development of large-scale procedures for the determination of codeine and morphine in urine samples. A large urine drug testing laboratory must have a sensitive and specific method that can rapidly separate "true negative" from "presumptive positive" specimens. It is equally important to have a fundamentally different confirmatory method that can independently and accurately confirm the presence of an opiate and, at the same time, identify the individual drug. The method should also give quantitative results when needed. Since codeine and morphine are primarily excreted in the urine as conjugates in the form of glucuronides (1, 2), the methods of analysis must be able to detect them in both forms.

BACKGROUND

Most laboratories use TLC to screen urine specimens for various drugs including codeine and morphine (3, 4). The technique is relatively inexpensive but, on a large scale, has many disadvantages such as poor sensitivity, inconsistency in R_f values, variations with humidity, subjectivity in data interpretation, and the requirement of hydrolysis to detect the opiate glucuronides. Although the reagents and equipment for radioimmunoassay are expensive, the consistency of results, ability to detect glucuronide forms, increased sensitivity, greater accuracy, and semiautomation of the method make it well worth the cost involved (5–8).

Since free opiates have poor sensitivity by GLC, a number of GLC procedures have been published to separate and identify their derivatives (9–11). Most methods use only one column, which provides no assurance of avoiding false positives from interfering peaks with retention times similar to the opiate derivatives on that particular column.

complexed drug noticed a decrease in severity or no headache at all with the combination sample. This response can be explained from the recovery curve for the combination samples, since it was unlikely that development of tolerance to the stimulant occurred.

Table III shows the amount of amphetamine recovered in the urine over 48 hr and also the bioavailability of amphetamine from the complex and combination samples. When using the Student paired t test, no significant differences were seen in the bioavailability of amphetamine from all three formulations. However, excretion rates of amphetamine from the 1:20 complex were significantly different from the pure drug during the initial 4 hr.

In conclusion, the drug–excipient interaction between cationic drugs and montmorillonite clay can be employed successfully to prolong the action of such medicinals. The peak urinary excretion rate of amphetamine from the 1:20 drug–clay complex occurred at a much later time than the pure drug, indicating delayed absorption of amphetamine from the complex. In addition, the initial excretion rate of amphetamine from the complex was significantly lower than that of the pure drug. Finally, for all subjects, the bioavailability of the amphetamine from the 1:20 complex and the amphetamine–1:20 complex combination formulations over 48 hr was not significantly different from that of the pure drug.

REFERENCES

(1) D. C. Monkhouse and J. L. Lach, *Can. J. Pharm. Sci.*, **7**, 29(1972).

(2) J. W. McGinity and J. L. Lach, *J. Pharm. Sci*, **65**, 896(1976).

(3) K. Munzel, *Acta Pharmacol. Toxicol., Suppl. 3*, **29**, 81(1971).

(4) A. B. Varley, *J. Am. Med. Assoc.*, **206**, 1745(1968).

(5) M. J. Akers, J. L. Lach, and L. Fischer, *J. Pharm. Sci.*, **62**, 391(1973).

(6) J. G. Wagner, P. G. Welling, K. P. Lee, and J. E. Walker, *ibid.*, **60**, 666(1971).

(7) J. W. Bettis, J. L. Lach, and J. Hood, *Am. J. Hosp. Pharm.*, **30**, 240(1973).

(8) A. H. Beckett and M. Rowland, *J. Pharm. Pharmacol.*, **17**, 59(1965).

(9) A. H. Beckett, J. A. Salmon, and M. Mitchard, *ibid.*, **21**, 251(1969).

(10) G. A. Alles and B. B. Wisegarver, *Toxicol. Appl. Pharmacol.*, **3**, 678(1961).

(11) R. T. Williams, in "Fundamentals of Drug Metabolism and Drug Disposition," B. N. La Du, H. G. Mandel, and E. L. Way, Eds., Williams & Wilkins, Baltimore, Md., 1972, pp. 189–191.

ACKNOWLEDGMENTS AND ADDRESSES

Received June 19, 1975, from the *College of Pharmacy, University of Iowa, Iowa City, IA 52240*

Accepted for publication March 8, 1976.

[x] To whom inquiries should be directed. Present address: College of Pharmacy, University of Texas at Austin, Austin, TX 78712

Mass Screening and Confirmation of Codeine and Morphine in Urine by Radioimmunoassay–GLC

NARESH C. JAIN *‡[x], THOMAS C. SNEATH ‡, WAI J. LEUNG ‡, and ROBERT D. BUDD ‡

Abstract □ A rapid, sensitive, and specific procedure is described for the mass screening and confirmation of codeine and morphine in urine specimens. The method is sensitive to 0.5-μg/ml levels of both opiates in free and/or conjugate forms. The raw urine is screened directly by radioimmunoassay, which is reactive to both free and glucuronide forms of codeine and morphine. Specimens that are screened positive are confirmed by GLC using a flame-ionization detector. The opiates are analyzed as their acetyl derivatives on two different columns, OV-25 and Poly-A 103. This multiple approach eliminates false positives caused by interfering substances or structurally similar compounds present in the urine.

Keyphrases □ Codeine—radioimmunoassay–GLC analysis, human urine □ Morphine—radioimmunoassay–GLC analysis, human urine □ Radioimmunoassay–GLC—analysis, codeine and morphine in human urine □ GLC—analyis, codeine and morphine in human urine □ Opiates—codeine and morphine, radioimmunoassay–GLC analysis in human urine □ Narcotics—codeine and morphine, radioimmunoassay–GLC analysis in human urine

The widespread use and abuse of codeine, morphine, and heroin, which is largely metabolized to morphine (1), necessitate the development of large-scale procedures for the determination of codeine and morphine in urine samples. A large urine drug testing laboratory must have a sensitive and specific method that can rapidly separate "true negative" from "presumptive positive" specimens. It is equally important to have a fundamentally different confirmatory method that can independently and accurately confirm the presence of an opiate and, at the same time, identify the individual drug. The method should also give quantitative results when needed. Since codeine and morphine are primarily excreted in the urine as conjugates in the form of glucuronides (1, 2), the methods of analysis must be able to detect them in both forms.

BACKGROUND

Most laboratories use TLC to screen urine specimens for various drugs including codeine and morphine (3, 4). The technique is relatively inexpensive but, on a large scale, has many disadvantages such as poor sensitivity, inconsistency in R_f values, variations with humidity, subjectivity in data interpretation, and the requirement of hydrolysis to detect the opiate glucuronides. Although the reagents and equipment for radioimmunoassay are expensive, the consistency of results, ability to detect glucuronide forms, increased sensitivity, greater accuracy, and semiautomation of the method make it well worth the cost involved (5–8).

Since free opiates have poor sensitivity by GLC, a number of GLC procedures have been published to separate and identify their derivatives (9–11). Most methods use only one column, which provides no assurance of avoiding false positives from interfering peaks with retention times similar to the opiate derivatives on that particular column.

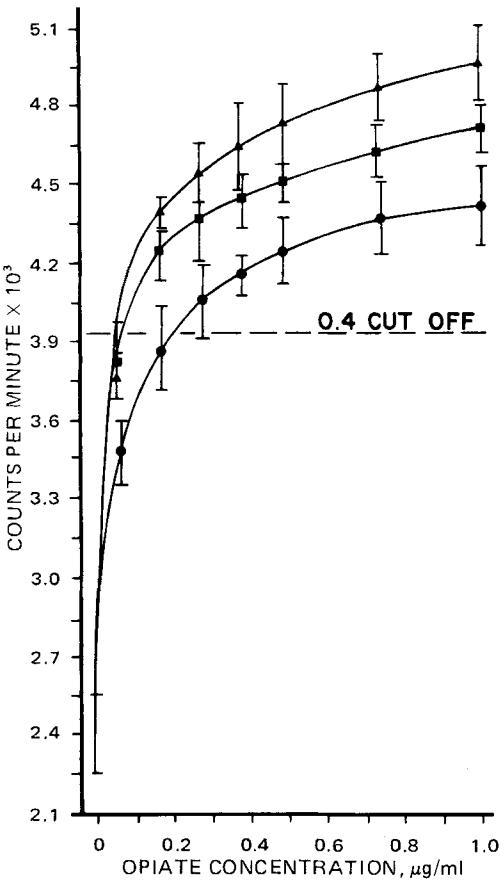

Figure 1—*Radioactive count curves for codeine (▲), morphine (●), and morphine glucuronide (■) with the morphine antibody. Standard deviations are included.*

This confirmation procedure is so designed that interfering substances are not reported as false positives. The opiates are analyzed as their acetyl derivatives on two quite different GLC columns: 3% OV-25 and 3% Poly-A 103. True positives must give the proper response on both columns.

Nalorphine is added to each urine specimen in the first step of extraction and is carried throughout the analytical process as an internal standard to ensure proper extraction and sample preparation. This procedure eliminates false negatives, allows accurate quantitation of positives, and assures correct results.

Several other opiates and drugs such as methadone, the primary metabolite of methadone (2-ethylidine-1,5-dimethyl-3,3-diphenylpyrrolidine), propoxyphene, norpropoxyphene, meperidine, apomorphine, dihydromorphine, hydrocodone, oxycodone, berberine (goldenseal), papaverine, and hydromorphine have been analyzed for possible interference with radioimmunoassay and/or GLC. With the procedure presented here, interference from any of these compounds is eliminated.

Table I—Relative Retention Times (RRT) of Acetylated Opiates and Other Drugs

Drug	Forms Acetyl Derivative[a]	RRT on 3% OV-25[b]	RRT on 3% Poly-A 103[c]
Codeine	Yes	0.50	0.46
Morphine	Yes	0.77	0.68
Nalorphine	Yes	1.00[d]	1.00[e]
Apomorphine	Yes	0.97	1.06
Dihydromorphine	Yes	0.82	0.91
Oxycodone	Yes	0.52	0.53
Hydromorphine	Yes	6.85	1.01[f]
Papaverine	No	1.86	2.35
Methadone	No	6.08	0.08
Methadone metabolite[g]	No	0.07	0.05
Propoxyphene	No	0.12	0.10
Norpropoxyphene	No	0.28	0.30[h]
Meperidine	No	0.03	0.03
Hydrocodone	Yes	0.49	0.60

[a] If "yes," relative retention times are for that derivative; if "no," relative retention times are for the parent drug. [b] Column temperature 250°; injector, 290°; detector, 300°; and carrier gas (nitrogen), 400 ml/min. [c] Column temperature, 230°; injector, 270°; detector, 280°; and carrier gas (nitrogen), 61 ml/min. [d] Retention time = 6.2 min. [e] Retention time = 7.3 min. [f] Second smaller peak with relative retention time of 0.70. [g] 2-Ethylidine-1,5-dimethyl-3,3-diphenylpyrrolidine. [h] Second smaller peak with retention time of 0.54.

EXPERIMENTAL

Materials—The following were obtained from commercial sources: morphine radioimmunoassay kit[1], ammonium sulfate[2], nalorphine hydrochloride[3], *tert*-butanol[2], chloroform[2], spectrograde chloroform[2], butyl acetate[2], dibasic potassium phosphate[2], potassium hydroxide[2], potassium carbonate[2], pyridine[2], anhydrous acetic anhydride[2], sodium hydroxide[2], hydrochloric acid[2], 3% Poly-A 103 on Gas Chrom Q[4] (100–120 mesh), and 3% OV-25 on HP Chrom W[5] (AW + DMCS) (80–100 mesh). All chemicals were reagent grade except as indicated.

Equipment—The following equipment was used: an automatic pipetting station[6], a centrifuge[7], a γ-scintillation counter with printer[8], a high-speed automatic pipet[9], 50-ml round-bottom centrifuge tubes with glass stoppers[10], 40-ml centrifuge tubes with tapered end[10], a dual-pen recorder[11], a gas chromatograph[12] equipped with dual flame-ionization detectors, and dual differential electrometers.

Radioimmunoassay Screening Procedure—The urine samples are screened for opiates using the Roche radioimmunoassay procedure (6) with slight modifications. Automatic pipetting stations are used for all dilutions; 0.40 ml of working reagent (morphine antigen–antibody 1:1) is added rather than 0.20 ml of each component separately.

A specimen is recorded as presumptive positive for opiates if its radioactive count is higher than the established cutoff value. The cutoff value is determined by checking all opiate controls run that day and selecting a level so that all 0.4-μg/ml controls of both opiates are detected. All specimens below the cutoff value are considered "negative." Specimens that give a radioactive count corresponding to 0.4 μg/ml or more of opiate are analyzed by GLC to confirm which particular drug is present.

GLC Confirmation Procedure—The urine samples screened positive by radioimmunoassay are confirmed as their acetylated derivatives by GLC using the procedure of Jain *et al.* (12).

Proper Sample Preparation—A peak for the internal standard (acetylated nalorphine) must appear on both GLC columns even when the specimen is negative for codeine and/or morphine. If the internal standard does not appear on a GLC column, the specimen has not been prepared properly and the procedure must be repeated.

Positive Specimen—A positive specimen for codeine and/or morphine must give the proper internal standard response and must produce acetylated codeine and/or morphine peaks of equal concentrations on both columns.

Negative Specimen—A negative specimen for codeine and/or morphine must give the proper internal standard response and must fail to give the proper acetylated codeine and/or morphine response on one or both GLC columns.

RESULTS AND DISCUSSION

The radioimmunoassay–GLC system is suitable for screening and confirming opiates in urine specimens on a large scale. The procedure can consistently detect 0.5-μg/ml levels of both free and conjugated forms of codeine and morphine.

The radioimmunoassay screening method is considered superior to other screening techniques, including TLC and the enzyme-multiplied

[1] Roche Diagnostics, Division of Hoffmann–La Roche, Nutley, N.J.
[2] Matheson, Coleman and Bell, Los Angeles, Calif.
[3] Merck Sharp and Dohme, West Point, Pa.
[4] Applied Science, State College, Pa.
[5] Varian Associates, Palo Alto, Calif.
[6] Model 24004, Micromedic Systems, Philadelphia, Pa.
[7] Model K with 418 head, International Equipment Co., Needham Heights, Mass.
[8] Model 5160, Packard Instrument Co., Los Angeles, Calif.
[9] Model 25004F, Micromedic Systems, Philadelphia, Pa.
[10] Corning Glass Works, Corning, N.Y.
[11] Model B2616 E, Soltec Corp., Encino, Calif.
[12] Model 2700, Varian Associates, Palo Alto, Calif.

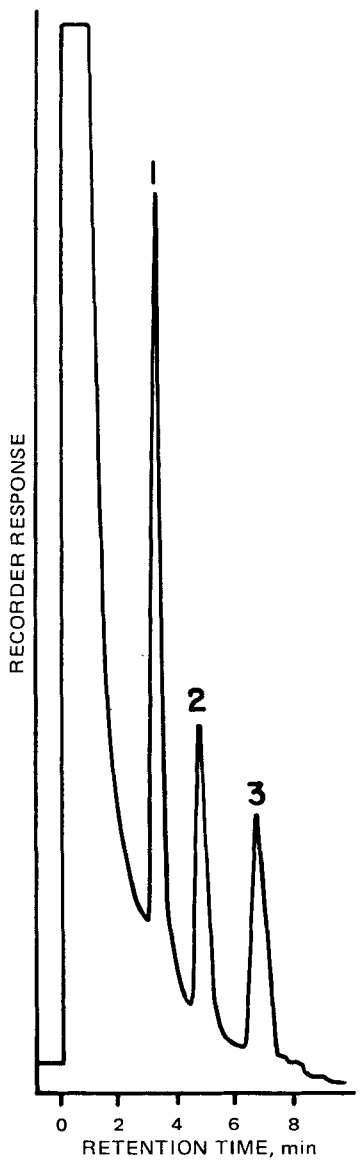

Figure 2—*Gas chromatogram of acetylated opiates on a 3% Poly-A 103 column (glass, 0.6 m × 2 mm). Operating conditions were: column, 230°; injector, 260°; and detector, 265°. Key: 1, codeine; 2, morphine; and 3, nalorphine.*

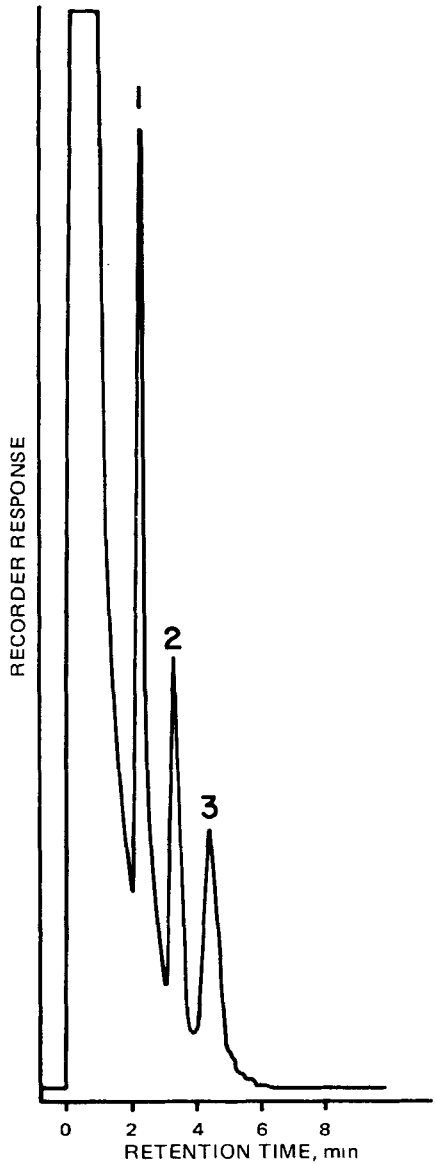

Figure 3—*Gas chromatogram of acetylated opiates on a 3% OV-25 column (glass, 0.9 m × 2 mm). Operating conditions were: column, 240°; injector, 280°; and detector, 285°. Key: 1, codeine; 2, morphine; and 3, nalorphine.*

immunoassay technique (13, 14). Both radioimmunoassay and the enzyme-multiplied immunoassay technique have much greater sensitivity, consistency, and accuracy of results than does TLC. They detect both free and glucuronide forms directly from raw urine and can be semiautomated so that one technician can screen many samples, depending upon the availability and type of equipment used. The radioimmunoassay antibody for opiates, however, is more sensitive than the enzyme-multiplied immunoassay technique reagents. For example, radioimmunoassay can detect morphine at a concentration of 0.1 μg/ml with greater than 99% accuracy (Fig. 1), whereas the enzyme-multiplied immunoassay technique requires a morphine concentration of 0.7 μg/ml to detect it 95% of the time (13, 14). The advantages of radioimmunoassay over other screening procedures make it preferable in spite of its increased cost.

As shown in Fig. 1, all of the opiates are not equally reactive to the radioimmunoassay antibody. As a result, the radioactive count cutoff value in radioimmunoassay must be based on the least reactive opiate to ensure that 0.5-μg/ml concentrations of all opiates of interest are detected. Contrary to earlier reports (6), morphine glucuronide is more reactive than free morphine to the opiate antibody.

Each specimen found positive by radioimmunoassay is confirmed by GLC. Since free opiates do not chromatograph well, codeine and morphine are confirmed by analyzing them as acetyl derivatives on two very different columns: OV-25 and Poly-A 103. The relative retention times of the opiates are presented in Table I. Figures 2 and 3 illustrate the clear separation obtained. The GLC confirmation method is designed so that, although the specimen is extracted only once, it is subjected to two parameters of analysis to obtain the most accurate and reliable results. This dual-column approach by GLC virtually eliminates false positive results. If GLC results for a sample require additional confirmation, the residue is spotted on a TLC plate[13], which is developed in ethyl acetate–acetone–concentrated ammonia (100:10:4). The R_f values for acetylated morphine, acetylated codeine, and acetylated nalorphine are 0.50, 0.65, and 0.83, respectively (15).

The use of nalorphine as an internal standard added at the beginning of the analysis not only allows the accurate quantitation of the opiates but also assures that samples are extracted properly. This procedure eliminates the possibility of reporting false negative results.

By using radioimmunoassay and both GLC columns, a series of spiked urine specimens containing varying concentrations of codeine, morphine, and morphine glucuronide, from 0.1 to 10 μg/ml of each, was analyzed. The data obtained showed above 99% accuracy at the 0.5-μg/ml level for each opiate. This error of less than 1% has always been due to borderline cases where a final result has been reported negative when, in fact, the sample

[13] Merck silica gel G, VWR Scientific, Los Angeles, Calif.

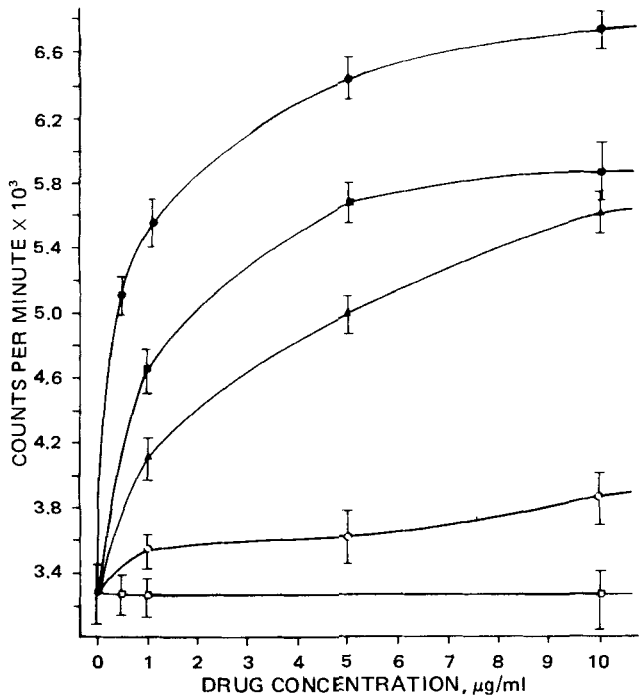

Figure 4—*Radioactive count curves for other drugs with the morphine antibody. Standard deviations are included. Key: ●, morphine; ■, dihydromorphine; ▲, heroin; ○, meperidine; and □, methadone, methadone metabolite, propoxyphene, norpropoxyphene, apomorphine, and papaverine.*

contained a very small amount of an opiate. These cases were detected by radioimmunoassay but, due to occasional variations in the extraction technique and flame-ionization detector response, the opiate gave a GLC response too small to be considered positive.

Urine samples spiked with various concentrations of methadone, methadone primary metabolite, propoxyphene, norpropoxyphene, apomorphine, dihydromorphine, hydrocodone, hydromorphine, heroin, papaverine, oxycodone, and berberine (goldenseal) also were tested. Heroin, dihydromorphine, hydromorphine, hydrocodone, oxycodone, and high concentrations of meperidine reacted with the radioimmunoassay opiate antibody (Fig. 4). All of these drugs could be differentiated from morphine, codeine, or nalorphine by the two GLC columns (Table I).

This radioimmunoassay–GLC method offers a sensitive and reliable confirmation procedure for ascertaining the presence or absence of codeine and morphine in urine on a large scale.

REFERENCES

(1) E. G. C. Clarke, "Isolation and Identification of Drugs," Pharmaceutical Press, London, England, 1969, pp. 164, 165, 269, 431, 432.

(2) J. T. Payte, J. E. Wallace, and K. Blum, *Curr. Ther. Res.*, **13**, 412 (1971).

(3) J. E. Wallace, J. D. Biggs, J. H. Meritt, H. E. Hamilton, and K. Blum, *J. Chromatogr.*, **71**, 135 (1972).

(4) J. Cochin and J. W. Daly, *Experientia*, **18**, 294 (1962).

(5) S. Spector and C. W. Parker, *Science*, **168**, 1347 (1970).

(6) "Abuscreen," Roche Diagnostics, Division of Hoffmann-La Roche, Nutley, N.J.

(7) S. J. Mulé, M. L. Bastos, and D. Jukofsky, *Clin. Chem.*, **20**, 243 (1974).

(8) S. J. Mulé, E. Whitlock, and D. Jukofsky, *ibid.*, **21**, 81 (1975).

(9) E. Schmezler, W. Yu, M. S. Hewitt, and I. J. Greenblatt, *J. Pharm. Sci.*, **55**, 155 (1966).

(10) J. E. Wallace, J. D. Briggs, and K. Blum, *Clin. Chem. Acta*, **36**, 85 (1972).

(11) F. Fish and W. D. Wilson, *J. Chromatogr.*, **40**, 164 (1969).

(12) N. C. Jain, R. D. Budd, and T. C. Sneath, in "CRC Methodology for Analytical Toxicology," I. Sunshine, Ed., CRC Press, Cleveland, Ohio, 1975, pp. 271–274.

(13) K. E. Rubenstein, R. S. Schneider, and E. F. Ullman, *Biochem. Biophys. Res. Commun.*, **47**, 846 (1972).

(14) "EMIT Opiate Assay," Syva Corp., Palo Alto, Calif., 1973.

(15) N. C. Jain, T. C. Sneath, R. D. Budd, and W. J. Leung, *Clin. Chem.*, **21**, 1486 (1975).

ACKNOWLEDGMENTS AND ADDRESSES

Received August 22, 1975, from the *Departments of Pharmacology and of Community Medicine and Public Health, University of Southern California Medical School, Los Angeles, CA 90033, and the ‡Rancho Los Amigos Hospital, Downey, CA 90242.

Accepted for publication March 10, 1976.

ˣ To whom inquiries should be directed (at Rancho Los Amigos Hospital).

Use of Rabbits for GI Drug Absorption Studies

TADAO MAEDA ˣ, HIROSHI TAKENAKA, YOSHIYA YAMAHIRA, and TAKESHI NOGUCHI

Abstract □ A novel procedure to control the stomach emptying rate in rabbits is presented. Rabbits were given a special solid diet for 1 week, and then the gastric contents were washed out with saline. Then the rabbits were muzzled to prevent coprophagy during the night. Fifty grams of special soft diet given to the "stomach-emptying-controlled" rabbit transferred exponentially from the stomach into the small intestine and almost disappeared from the stomach within 5 hr. Griseofulvin, indomethacin, or nalidixic acid was administered in a hard gelatin capsule or tablet, with subsequent feeding of a special soft diet. Good correlations were observed between the plasma level–time curves of these drugs in the stomach-emptying-controlled rabbits and in human subjects.

Keyphrases □ Absorption, GI—griseofulvin, indomethacin, and nalidixic acid, effect of stomach emptying rate, rabbits □ GI absorption—griseofulvin, indomethacin, and nalidixic acid, effect of stomach emptying rate, rabbits □ Stomach emptying rate—effect on GI absorption of griseofulvin, indomethacin, and nalidixic acid, rabbits □ Griseofulvin—GI absorption, effect of stomach emptying rate, rabbits □ Indomethacin—GI absorption, effect of stomach emptying rate, rabbits □ Nalidixic acid—GI absorption, effect of stomach emptying rate, rabbits

In the study of GI absorption of drugs, various *in vitro* or *in situ* methods have been widely used (1–4). From the physiological point of view, the experimental animal data obtained by these destructive or operative techniques have only limited value in predicting drug absorption characteristics in humans, although such data provide funda-

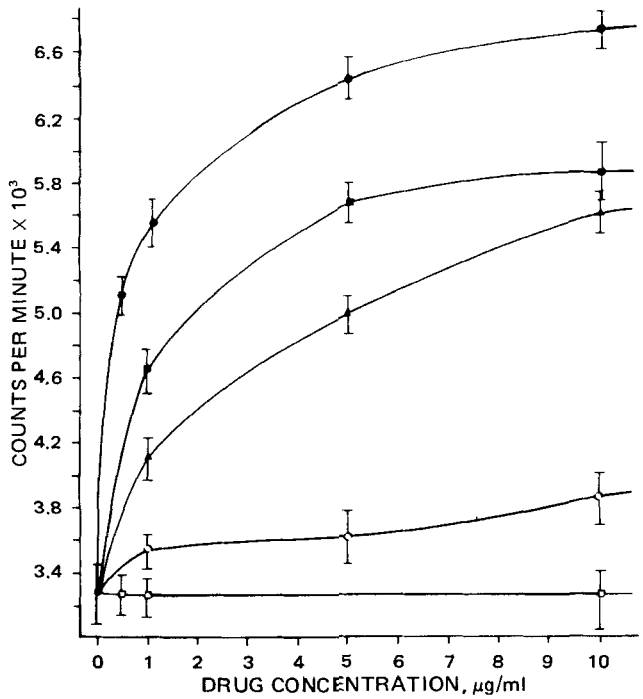

Figure 4—*Radioactive count curves for other drugs with the morphine antibody. Standard deviations are included. Key: ●, morphine; ■, dihydromorphine; ▲, heroin; ○, meperidine; and □, methadone, methadone metabolite, propoxyphene, norpropoxyphene, apomorphine, and papaverine.*

contained a very small amount of an opiate. These cases were detected by radioimmunoassay but, due to occasional variations in the extraction technique and flame-ionization detector response, the opiate gave a GLC response too small to be considered positive.

Urine samples spiked with various concentrations of methadone, methadone primary metabolite, propoxyphene, norpropoxyphene, apomorphine, dihydromorphine, hydrocodone, hydromorphine, heroin, papaverine, oxycodone, and berberine (goldenseal) also were tested. Heroin, dihydromorphine, hydromorphine, hydrocodone, oxycodone, and high concentrations of meperidine reacted with the radioimmunoassay opiate antibody (Fig. 4). All of these drugs could be differentiated from morphine, codeine, or nalorphine by the two GLC columns (Table I).

This radioimmunoassay–GLC method offers a sensitive and reliable confirmation procedure for ascertaining the presence or absence of codeine and morphine in urine on a large scale.

REFERENCES

(1) E. G. C. Clarke, "Isolation and Identification of Drugs," Pharmaceutical Press, London, England, 1969, pp. 164, 165, 269, 431, 432.

(2) J. T. Payte, J. E. Wallace, and K. Blum, *Curr. Ther. Res.*, **13**, 412 (1971).

(3) J. E. Wallace, J. D. Biggs, J. H. Meritt, H. E. Hamilton, and K. Blum, *J. Chromatogr.*, **71**, 135 (1972).

(4) J. Cochin and J. W. Daly, *Experientia*, **18**, 294 (1962).

(5) S. Spector and C. W. Parker, *Science*, **168**, 1347 (1970).

(6) "Abuscreen," Roche Diagnostics, Division of Hoffmann-La Roche, Nutley, N.J.

(7) S. J. Mulé, M. L. Bastos, and D. Jukofsky, *Clin. Chem.*, **20**, 243 (1974).

(8) S. J. Mulé, E. Whitlock, and D. Jukofsky, *ibid.*, **21**, 81 (1975).

(9) E. Schmezler, W. Yu, M. S. Hewitt, and I. J. Greenblatt, *J. Pharm. Sci.*, **55**, 155 (1966).

(10) J. E. Wallace, J. D. Briggs, and K. Blum, *Clin. Chem. Acta*, **36**, 85 (1972).

(11) F. Fish and W. D. Wilson, *J. Chromatogr.*, **40**, 164 (1969).

(12) N. C. Jain, R. D. Budd, and T. C. Sneath, in "CRC Methodology for Analytical Toxicology," I. Sunshine, Ed., CRC Press, Cleveland, Ohio, 1975, pp. 271–274.

(13) K. E. Rubenstein, R. S. Schneider, and E. F. Ullman, *Biochem. Biophys. Res. Commun.*, **47**, 846 (1972).

(14) "EMIT Opiate Assay," Syva Corp., Palo Alto, Calif., 1973.

(15) N. C. Jain, T. C. Sneath, R. D. Budd, and W. J. Leung, *Clin. Chem.*, **21**, 1486 (1975).

ACKNOWLEDGMENTS AND ADDRESSES

Received August 22, 1975, from the *Departments of Pharmacology and of Community Medicine and Public Health, University of Southern California Medical School, Los Angeles, CA 90033, and the ‡Rancho Los Amigos Hospital, Downey, CA 90242.

Accepted for publication March 10, 1976.

ˣ To whom inquiries should be directed (at Rancho Los Amigos Hospital).

Use of Rabbits for GI Drug Absorption Studies

TADAO MAEDA ˣ, HIROSHI TAKENAKA, YOSHIYA YAMAHIRA, and TAKESHI NOGUCHI

Abstract □ A novel procedure to control the stomach emptying rate in rabbits is presented. Rabbits were given a special solid diet for 1 week, and then the gastric contents were washed out with saline. Then the rabbits were muzzled to prevent coprophagy during the night. Fifty grams of special soft diet given to the "stomach-emptying-controlled" rabbit transferred exponentially from the stomach into the small intestine and almost disappeared from the stomach within 5 hr. Griseofulvin, indomethacin, or nalidixic acid was administered in a hard gelatin capsule or tablet, with subsequent feeding of a special soft diet. Good correlations were observed between the plasma level–time curves of these drugs in the stomach-emptying-controlled rabbits and in human subjects.

Keyphrases □ Absorption, GI—griseofulvin, indomethacin, and nalidixic acid, effect of stomach emptying rate, rabbits □ GI absorption—griseofulvin, indomethacin, and nalidixic acid, effect of stomach emptying rate, rabbits □ Stomach emptying rate—effect on GI absorption of griseofulvin, indomethacin, and nalidixic acid, rabbits □ Griseofulvin—GI absorption, effect of stomach emptying rate, rabbits □ Indomethacin—GI absorption, effect of stomach emptying rate, rabbits □ Nalidixic acid—GI absorption, effect of stomach emptying rate, rabbits

In the study of GI absorption of drugs, various *in vitro* or *in situ* methods have been widely used (1–4). From the physiological point of view, the experimental animal data obtained by these destructive or operative techniques have only limited value in predicting drug absorption characteristics in humans, although such data provide funda-

Table I—Composition of Solid Diet for Rabbits

Composition	Content, %	
	Commercial Solid Diet (Pellets)	Special Solid Diet (Pellets)
Crude fiber	17.5	3.9
Crude protein	18.6	21.4
Crude fat	3.4	3.5
Crude ash	10.4	4.5
Water content	5.1	6.0
Nitrogen-free extract	45.0	60.7

mentally useful information on drug absorption.

The principal purpose of this study was to clarify, by use of intact animals, the correlation of GI drug absorption of orally administered drugs between humans and animals so that the need for human trials in developing drugs and dosage forms of increased bioavailability can be minimized. Rabbits are often used for this purpose because of their low cost and ease in handling.

According to a relevant study (5), solid material remains in the rabbit stomach even after fasting for more than 24 hr. Moreover, the stomach emptying time of rabbits differs greatly from that of humans, whose stomachs usually empty within several hours following ingestion of food. Therefore, the rabbit is not a suitable animal for the evaluation of GI absorption characteristics of drugs, especially when stomach emptying is a limiting factor (5).

The present study was designed to examine the stomach emptying characteristics of rabbits and to establish a method for simulating the stomach emptying rate to that of humans so that rabbits could be used for studies of GI drug absorption.

EXPERIMENTAL

Materials—Two kinds of solid diet, commercial[1] and special[2], were used for the rabbits (Table I). The special solid diet was prepared by removing alfalfa from the commercial solid diet. A special soft diet was prepared by adding 60 parts of water to 40 parts of special solid diet. This mixture was left standing overnight in a cool place to swell and was then divided into required amounts and made into balls.

Both griseofulvin USP and indomethacin NF were micronized to less than 5 μm in size using a fluid energy mill[3] and capsulated in a hard gelatin capsule size No. 3. Nalidixic acid NF was milled to about 30 μm utilizing a pulverizer[4] and administered as a tablet. Each tablet contained 250 mg of nalidixic acid, 55 mg of lactose USP, 16 mg of calcium carboxymethylcellulose JP, 3.5 mg of starch USP, and 3.5 mg of magnesium stearate USP. The tablets met the USP disintegration test. The other chemicals were of reagent grade.

Procedure of Stomach-Emptying Control—White male rabbits, 2.4–3.4 kg, were fed the special solid diet in place of the commercial solid diet for 1 week of conditioning before the absorption study.

After being fasted overnight with water given freely, the rabbits were anesthetized by injection of 0.3–0.5 ml/kg of 5% pentobarbital sodium. A rubber stomach tube, 25 cm in length and 5 mm in external diameter with a large hole on the side of the tip, was inserted into the stomach, and 50–100 ml of warm saline (37°) was instilled. The fluid in the stomach was then withdrawn by suction with a syringe. This procedure was repeated until the fluid withdrawn hardly contained any solid material. The rabbits usually recovered from anesthesia within 2–3 hr.

After gastric lavage, the rabbits were allowed water *ad libitum* and were muzzled to prevent coprophagy during the night. On the following morning, the rabbits were given 200 g of the special soft diet and allowed water *ad libitum*. They were muzzled again at night until morning. These pretreated rabbits were called the "stomach-emptying-controlled" rabbits.

Table II—Effect of Diet and Muzzling on Stomach Emptying

Diet	Weight of Gastric Content[a], g	
	Coprophagy Not Restricted	Muzzled during the Night
Commercial pellet diet	97 ± 7.9	33 ± 4.5
Special soft diet	83 ± 6.5	34 ± 3.9

[a] Data represent average and *SE* for rabbits of each group.

Estimation of Coprophagy—Four groups, each consisting of three rabbits, 2.4–2.8 kg, were designated as Groups I-A, I-B, II-A, and II-B. The first two groups were fed 100 g of the commercial diet daily and allowed water *ad libitum* for 3 days. Group I-A was not restricted from coprophagy, while Group I-B was muzzled during the night. Similarly, Groups II-A and II-B were fed 250 g of the special soft diet daily and allowed water *ad libitum* for 3 days. Group II-A was allowed coprophagy, while Group II-B was muzzled during the night. On the morning of the 4th day, the rabbits were sacrificed. The stomach was removed, and the amount of gastric contents was determined by subtracting the weight of the gastric pouch from that of the total stomach.

In another experiment, the effect of muzzling on the amount of feces excreted was examined using stomach-emptying-controlled rabbits. Fifteen stomach-emptying-controlled rabbits, 2.5–3.0 kg, were divided equally into Groups A, B, and C. Each rabbit was housed separately in a cage with a double floor. The upper wire mesh floor was designed to allow feces to drop through so that they could be collected on the lower wire mesh floor. The experiment schedule employed was as follows.

Gastric lavage was performed for all rabbits at 11:00 am. Groups A and B were muzzled for 17 hr during the first period (4:00 pm–9:00 am), while Group C was not muzzled at all. Feces were weighed at the end of this first period. At the beginning of the second period of 7 hr (9:00 am–4:00 pm), every rabbit was fed with 200 g of soft special diet. Only Group A was then muzzled until 4:00 pm (for about 6 hr); Groups B and C were not muzzled. At the end of the second period (4:00 pm), feces excreted were weighed again for all rabbits. During the third period of 17 hr (4:00 pm–9:00 am), Groups A and B were muzzled but Group C was not muzzled. At the end of this period, feces were again weighed for all rabbits. Thus, the total muzzled period was 40 hr for Group A, 34 hr for Group B, and 0 hr for Group C.

Stomach Emptying of Special Soft Diet—Each of the 15 stomach-emptying-controlled rabbits, 2.5–2.7 kg, was fed 50 g of the special soft diet and was allowed water *ad libitum* until sacrifice. At 0.5, 1, 2, 3, and 5 hr after feeding, three rabbits were sacrificed.

The stomach was immediately removed, the contents of the stomach were centrifuged, and the precipitates were dried to constant weight *in vacuo* at 60°. The weight of the gastric residue was calculated on the basis of the weight of the special soft diet dried under the same condition.

Administration of Drugs—To each rabbit, an oral dose of 10 mg/kg of griseofulvin or indomethacin was administered in a capsule. An oral dose of 250 mg of nalidixic acid was administered as an intact tablet. Prior to administration of either the capsule or tablet, rabbits were secured to an animal board and the mouth was pried open with a wooden rod. Then the tongue was pulled out by rolling the wooden rod and pressed down so that the capsule or tablet could be easily placed on the radix linguae and pushed down with a rubber stomach tube to the esophagus. This administration was followed by feeding of 50 g of the special soft diet to the stomach-emptying-controlled rabbits and 20 g of commercial solid diet to the conventionally fasted rabbits. Rabbits not consuming this amount of diet within 5 min were excluded from further studies, being considered not to be in good health. During the blood sampling period, rabbits had free access to water but not to feed, and a blood specimen was drawn at the predetermined time for analysis.

In every drug administration experiment, two groups of five rabbits were used. One group was the stomach-emptying-controlled rabbits; the other group consisted of rabbits fed with commercial solid diet and then fasted but allowed water *ad libitum* for 24 hr prior to the experiment. Rabbits of the latter group are called the conventionally fasted rabbits.

Analytical Method and Equipment—Blood specimens obtained by

[1] Commercial solid diet CR-1, Nihon Clea Co., Aobadai 2-20-14, Meguro, Tokyo, Japan.
[2] Nihon Clea.
[3] GemT jet mill, Helme Chemicals Inc., Helmetta, NJ 08828.
[4] ECK atomizer, Fuji Paudal Corp., Joto-ku, Osaka, Japan.

Table III—Amount of Feces Excreted and Effect of Muzzling in Preventing Coprophagy

Group[b]	Amount of Feces Excreted[a], g: First Period (4 pm–9 am)	Second Period (9 am–4 pm)	Third Period (4 pm–9 am)	Total
A	4.3 ± 2.1	14.3 ± 3.2	14.1 ± 3.2	32.7 ± 4.1
B	4.9 ± 3.2	2.4 ± 0.6	16.8 ± 2.8	24.1 ± 2.7
C	0.2 ± 0.1	0.3 ± 0.1	0.3 ± 0.2	0.8 ± 0.2

[a] Data represent average and *SE* for rabbits of each group. [b] Group A rabbits were muzzled during the first, second, and third periods; Group B rabbits were muzzled during the first and third periods; and Group C rabbits were not muzzled at all.

cardiac puncture, using a heparinized syringe, were centrifuged to obtain plasma for analysis. Griseofulvin was extracted with ether from plasma and measured quantitatively by a gas chromatograph[5] equipped with a ^{63}Ni-electron-capture detector. Diazepam was used as an internal standard, and the method of Shah *et al.* (6) was followed.

The chromatographic column was a 1.5-m × 3-mm glass tube packed with 10% SE-30 on Chromosorb W AW DMCS. The column temperature was 270°, the injection port temperature was 300°, the detector block temperature was 310°, and the carrier gas (99.999% nitrogen) flow rate was 60 ml/min. Indomethacin in plasma was determined spectrofluorometrically[6], using a modification of the assay method of Hucker *et al.* (7). In this experiment, 0.01 *N* sodium hydroxide was used in place of 0.1 *N* sodium hydroxide, thus improving the analytical reproducibility in a low concentration of indomethacin. Nalidixic acid in plasma was spectrofluorometrically determined by the method of McChesney *et al.* (8).

RESULTS AND DISCUSSION

In considering stomach emptying of experimental animals, the effect of diet properties and the habit of coprophagy cannot be ignored. For laboratory animals, a solid pellet diet is convenient and popular. The refuse obtained during soybean-curd preparation[7], containing more than 60% water, has been widely used as rabbit feed in Japan. Rabbits do well on this food and require no water.

Preliminary experiments on stomach emptying of diet in the stomach-washed-out rabbits showed that the soybean curd refuse moved into the small intestine faster and more smoothly than the commercially available solid pellet diet. This result may be reasonably explained because the digestive function of the stomach is the formation of chyme and its transfer to the duodenum.

For these reasons, after gastric lavage the rabbits were fed the special soft diet resembling the soybean-curd refuse to satisfy the purpose of this study. Chiou *et al.* (5) reported that the stomachs of rabbits after fasting for 24 hr were almost as full as those of unfasted animals, although the rabbits were maintained on a wire mesh support which allowed feces to drop to the bottom of the cage, thus reducing coprophagy.

Two kinds of feces are excreted by rabbits: round and hard pellets, often seen in the cage, and soft pellets covered by a mucous material. During the night, rabbits take the latter directly from the anus and never take feces dropped on the floor (9, 10). Therefore, it was expected that the effective prevention of coprophagy would result in rather fast and smooth stomach-emptying of the rabbit gastric contents, although the quantitative estimation of coprophagy has not been reported. In this study, a muzzle was adopted for the rabbit to prevent the mouth from making a direct contact with the anus.

The effect of muzzling on the amount of gastric contents was examined (Tables II and III). The amount of the gastric contents of the nonmuzzled rabbits (Groups I-A and II-A) was about twice that of the muzzled rabbits, indicating that a fair amount of the contents was attributable to coprophagy (Table II).

Some soft fecal pellets, which were probably swallowed intact early in the morning, were found in the gastric contents of the nonmuzzled rabbits regardless of diet. The gastric contents of the muzzled rabbits were less solid in consistency but still contained hair, which might have retarded the stomach emptying of food. The amount of residual gastric

[5] Shimadzu GC-5APTFE.
[6] Hitachi MPF-2A.
[7] Okara.

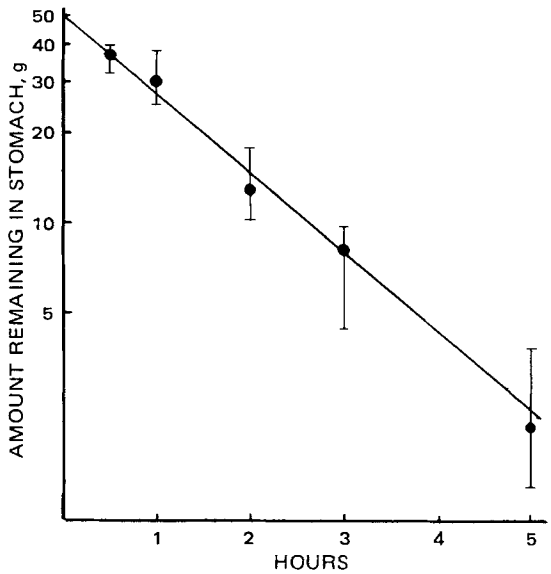

Figure 1—*Stomach emptying pattern of special soft diet (50 g) in the stomach-emptying-controlled rabbits. Each point represents the mean observation and the range on three rabbits.*

contents was not significantly affected by the type of diet. However, the gastric contents of rabbits fed the special solid diet were washed out more easily than those of rabbits fed the commercial solid diet. Therefore, the special solid diet was used during the conditioning period before performing GI absorption studies. In addition, gastric dissection confirmed that no solid material remained in the stomach when the gastric lavage procedure was employed.

The coprophagous amount and the gastric contents were examined using stomach-emptying-controlled rabbits. As shown in Table III, Group C rabbits, who were not restricted from coprophagy, hardly dropped any feces, even after ingesting 200 g of the special soft diet at the beginning of the second period. Group A rabbits, who were muzzled except during feeding time, excreted about 30 g of feces. It was reconfirmed that rabbits took feces directly from the anus as they were being excreted. Group B rabbits, who were not muzzled for several hours after feeding during the second period, ingested about 12 g of feces. This ingestion occurred during the daytime, although it had been believed to occur primarily at night. These findings demonstrate the strong physiological habit of coprophagy in rabbits, the difficulty of completely preventing coprophagy under customary conditions, and also the effectiveness of the muzzle.

After the third period, *i.e.*, after fasting for about 23 hr, all rabbits were sacrificed and the gastric contents of each group were examined. The stomachs of Group C rabbits were full of a wet mass as a result of coprophagy, although gastric lavage had been performed as in Groups A and B. For this reason, Group C was considered not suitable for GI absorption study. The stomachs of Group A rabbits were almost completely empty, and those of Group B contained some solid material, but the contents were so slurred that no difficulty would be expected in the transfer of the contents into the duodenum.

Stomach emptying in the stomach-emptying-controlled rabbits was estimated after feeding of 50 g of the special soft diet. Stomach emptying of diet appeared to be exponential in pattern (Fig. 1), and almost all ingested feed was transferred into the small intestine within 5 hr. This phenomenon is similar to the results of Hunt and Spurrell (11) with humans. The fact that such good semilogarithmic plots of amount were found with rabbits and resembled results with humans suggests that stomach emptying in these rabbits is sufficiently controlled for the GI absorption study of drugs with limited or regional solubility.

Griseofulvin is reported to be absorbed irregularly and incompletely from the GI tract because of its extremely low solubility (12). According to one study (13) on the GI absorption of this drug in rabbits, the blood level peaks occurred 6–11 hr after administration; in humans, the blood level peaks usually occurred approximately 2–3 hr after administration (14). However, Fig. 2 shows that the maximum plasma level was observed 2 hr after administration in the stomach-emptying-controlled rabbits.

Individual data of this experiment showed that the distribution of the plasma peak time observed from 1 to 2 hr after administration was characteristic in the stomach-emptying-controlled rabbits, while indi-

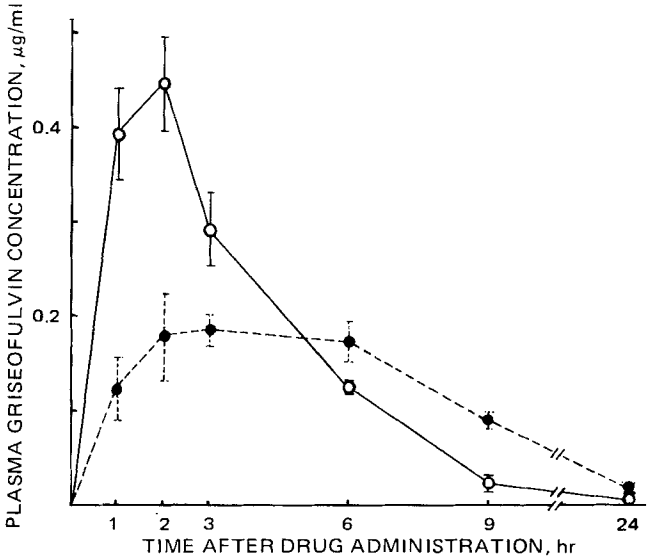

Figure 2—*Plasma levels of griseofulvin following oral administration of 10 mg/kg in the stomach-emptying-controlled rabbits (○) and rabbits fasted for 24 hr by the conventional method (●). Each point represents the mean observation ± SE on five rabbits.*

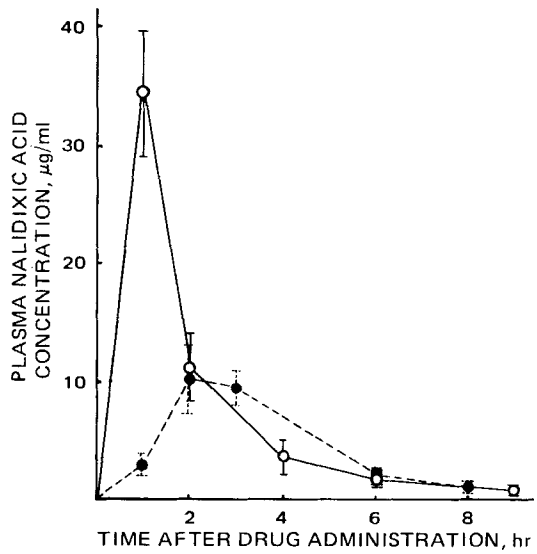

Figure 4—*Plasma levels of nalidixic acid following oral administration of 250 mg as a tablet to the stomach-emptying-controlled rabbits (○) and rabbits fasted for 24 hr by the conventional method (●). Each point represents the mean observation ± SE on five rabbits.*

vidual plasma peak time in the conventionally fasted rabbits ranged from 2 to 6 hr after administration. These results suggest that the slow and prolonged absorption of griseofulvin reported previously (13), after an oral dose of 150 mg/kg was administered as a suspension, was ascribable to an overdose and to the peculiarity of stomach emptying in rabbits, as pointed out in a later report (5).

Indomethacin absorption from the GI tract depends upon its holding time in the stomach and is retarded when stomach emptying is slow (15). The peak plasma level in the stomach-emptying-controlled rabbits prominently appeared in 1 hr, whereas slow absorption of the drug was observed in the conventionally fasted rabbits (Fig. 3). In the latter group, individual peak plasma time ranged from 2 to 5 hr after administration. The difference in the apparent absorption rates of indomethacin between the two groups of rabbits reflected the effect of the gastric emptying control procedure, because the water solubility of indomethacin is quite limited in the acidic pH range of the stomach (16). The fast absorption seen in the stomach-emptying-controlled rabbits is comparable to the

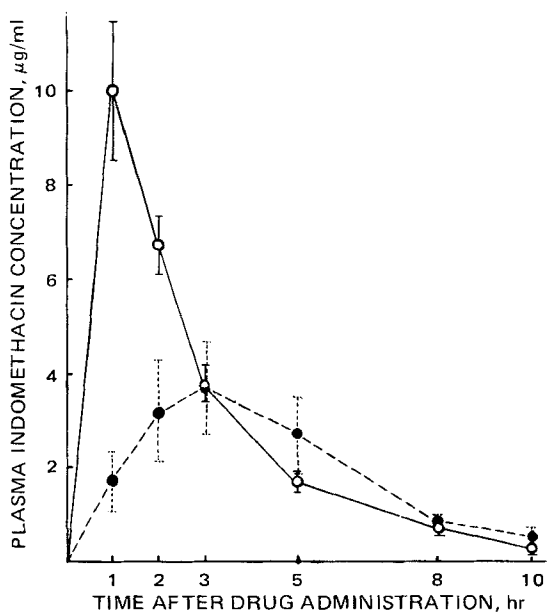

Figure 3—*Plasma levels of indomethacin following oral administration of 10 mg/kg in the stomach-emptying-controlled rabbits (○) and rabbits fasted for 24 hr by the conventional method (●). Each point represents the mean observation ± SE on five rabbits.*

results observed in humans whose peak plasma level occurred 1 hr after drug ingestion (7).

Plasma level curves in Fig. 4 demonstrate that absorption of nalidixic acid in the stomach-emptying-controlled rabbits was rapid. All individual plasma level curves showed a peak 1 hr after administration and the rapid disappearance of the drug from plasma thereafter, comparable to the results observed in humans (8). Individual peak plasma time in the conventionally fasted rabbits ranged from 2 to 6 hr.

Table IV summarizes the comparison of the individual peak plasma level, C_{max}, and its time of occurrence, t_{max}, following oral administration of griseofulvin, indomethacin, and nalidixic acid between two groups of rabbits. Fast and smooth transfer of drugs to the intestine in the stomach-emptying-controlled rabbits resulted in a statistically significant increase in the average C_{max} as compared to that in the conventionally fasted rabbits.

The t_{max} parameter also reflects the drug absorption rate. As mentioned previously, the individual t_{max} of the stomach-emptying-controlled rabbits for the three drugs was within 1–2 hr after drug administration while that of conventionally fasted rabbits ranged from 2 to 6 hr. Since the distribution range of individual t_{max} values differed between the two groups, it is quite obvious, even without statistical analysis, that the average t_{max} of the stomach-emptying-controlled rabbits was significantly less than that of the conventionally fasted rabbits.

The retardation and variation of drug absorption seen in the conventionally fasted rabbits are presumably due to the decrease and difference in the rate in which gastric contents transferred to the intestine, because

Table IV—Comparison of Peak Plasma Levels and Its Time of Occurrence following Oral Administration of Drug in Stomach-Emptying-Controlled and Conventionally Fasted Rabbits

Drug Administered (Dose)	Average of Individual Peak Plasma Level[a], C_{max}, μg/ml: Stomach-Emptying-Controlled Rabbits	Average of Individual Peak Plasma Level[a], C_{max}, μg/ml: Conventionally Fasted Rabbits	p Value[b]
Griseofulvin (10 mg/kg)	0.51 (1.6)	0.24 (3.4)	<0.01
Indomethacin (10 mg/kg)	10.47 (1.2)	5.48 (2.8)	<0.05
Nalidixic acid (250 mg/rabbit)	34.2 (1.0)	12.5 (3.2)	<0.01

[a] Numbers in parentheses are the averages of individual peak time (t_{max}, hr). [b] Determined by Student t test.

their stomachs should have been full of solid material as a result of coprophagy.

The data presented here show that the stomach-emptying-controlled rabbit can be a satisfactory model for evaluation of GI absorption characteristics of these drugs with limited or regional solubility.

CONCLUSION

Chiou *et al.* (5) concluded that the rabbit was not a useful animal for drug absorption studies because it was almost impossible to obtain an empty stomach in the rabbit by using the conventional fasting method and because the fasted state markedly prolonged the stomach emptying time. This conclusion has been very instructive to many investigators. However, in this study it was found possible to simulate the stomach emptying rate of rabbits to that of humans by taking adequate steps to empty the stomach and to feed the animals with a special soft diet. When the stomach emptying rate is controlled, the rabbit can be used as an animal model for predicting bioavailability of oral dosage for human subjects.

Results of bioavailability studies on oral dosage forms will be reported later.

REFERENCES

(1) T. H. Wilson and G. Wiseman, *J. Physiol.*, **123**, 116 (1954).

(2) L. S. Shanker, P. A. Shore, B. B. Brodie, and C. A. M. Hogben, *J. Pharmacol. Exp. Ther.*, **120**, 528 (1957).

(3) L. S. Shanker, D. J. Tocco, B. B. Brodie, and C. A. M. Hogben, *ibid.*, **123**, 81 (1958).

(4) S. Feldman, M. Salvino, and M. Gibaldi, *J. Pharm. Sci.*, **59**, 705 (1970).

(5) W. L. Chiou, S. Riegelman, and J. R. Amberg, *Chem. Pharm. Bull.*, **17**, 2170 (1969).

(6) V. P. Shah, S. Riegelman, and W. L. Epstein, *J. Pharm. Sci.*, **61**, 634 (1972).

(7) H. B. Hucker, A. G. Zacchei, S. V. Cox, D. A. Brodie, and N. H. R. Cantwell, *J. Pharmacol. Exp. Ther.*, **153**, 237 (1966).

(8) E. W. McChesney, E. J. Froelich, G. Y. Lesher, A. V. R. Crain, and D. Rosi, *Toxicol. Appl. Pharmacol.*, **6**, 292 (1964).

(9) C. E. Adams, "The UFAW Handbook on the Care and Management of Laboratory Animals," 4th ed., Churchill Livingstone, London, England, 1972, p. 167.

(10) K. W. Hagen, "The Biology of the Laboratory Rabbit," Academic, New York, N.Y., 1974, p. 33.

(11) J. N. Hunt and W. R. Spurrell, *J. Physiol.*, **113**, 157 (1951).

(12) C. Bedford, D. Busfield, K. J. Child, I. MacGregor, P. Sutherland, and E. G. Tomich, *Arch. Dermatol.*, **81**, 735 (1960).

(13) L. J. Fischer and S. Riegelman, *J. Pharm. Sci.*, **54**, 1571 (1965).

(14) M. Rowland, S. Riegelman, and W. L. Epstein, *ibid.*, **57**, 984 (1968).

(15) M. Moriyama, M. Saito, S. Awazu, M. Hanano, and H. Nogami, *Yakugaku Zasshi*, **91**, 1217 (1971).

(16) T. Fuwa, T. Iga, M. Hanano, H. Nogami, and M. Kashima, *ibid.*, **91**, 1223 (1971).

ACKNOWLEDGMENTS AND ADDRESSES

Received August 18, 1975, from the *Formulation Research Department, Pharmaceuticals Division, Sumitomo Chemical Co., Ltd., Kurakakiuchi 1-3-45, Ibaraki City, Osaka 567, Japan.*

Accepted for publication March 11, 1976.

Presented at the 94th Annual Meeting of the Pharmaceutical Society of Japan, Sendai, Japan, April 1974.

The authors thank Prof. H. Sezaki of Kyoto University for guidance and advice and Mr. Zenzo Harada for technical assistance.

[x] To whom inquiries should be directed.

Kinetics of Hydrolysis of Fenclorac

C. M. WON [x], J. J. ZALIPSKY, D. M. PATEL, and N. H. REAVEY-CANTWELL

Abstract □ The kinetics of hydrolysis of fenclorac were studied to determine its stability in aqueous solution at different pH's and temperatures. For this study, a stability-specific liquid chromatographic assay method was developed to separate fenclorac from its hydrolysis product, α-hydroxy-3-chloro-4-cyclohexylbenzeneacetic acid. The *k*–pH profile in the 0–12 pH range in various buffer solutions shows that fenclorac is stable in its undissociated form in strongly acidic media and is unstable in neutral and alkaline media. The instability of fenclorac in aqueous solution is proportional to the degree of ionization of the carboxyl group in the 1–4 pH range and is independent of pH above 4. The rate-determining step in the mechanism of hydrolysis of fenclorac involves ionization of the carbon–chlorine bond. The ionization is catalyzed by an intramolecular nucleophilic attack on the α-carbon by the dissociated carboxyl group, resulting in the formation of an unstable intermediate, a three-membered ring lactone. This unstable intermediate rapidly hydrolyzes to the final hydrolysis product. This mechanism is supported by experimental evidence such as the medium effect, positive salt effect, common ion effect, and substituent effect. Arrhenius parameters for the hydrolysis of fenclorac and its 3-nitro substituted analog were obtained.

Keyphrases □ Fenclorac—kinetics of hydrolysis, stability in aqueous solution, various pH's and temperatures, liquid chromatographic analysis □ Hydrolysis—fenclorac in aqueous solutions, kinetics, various pH's and temperatures, liquid chromatographic analysis □ Stability—fenclorac in aqueous solutions, various pH's and temperatures, liquid chromatographic analysis □ Liquid chromatography—analysis, fenclorac in aqueous solutions □ Anti-inflammatory agents—fenclorac, kinetics of hydrolysis, stability in aqueous solution, various pH's and temperatures, liquid chromatographic analysis

In the search for a new, nonsteroidal, anti-inflammatory compound for clinical utility, a series of substituted benzeneacetic acids was synthesized (1). Fenclorac (I) (α,3-dichloro-4-cyclohexylbenzeneacetic acid) diethylammonium salt exhibited promising anti-inflammatory activities. The anti-inflammatory activity of fenclorac was demonstrated in rats using the carrageenan paw edema assay[1].

A simple, sensitive analytical method was needed to follow the hydrolysis of relatively unstable fenclorac in

[1] G. Nuss *et al.*, to be published.

their stomachs should have been full of solid material as a result of coprophagy.

The data presented here show that the stomach-emptying-controlled rabbit can be a satisfactory model for evaluation of GI absorption characteristics of these drugs with limited or regional solubility.

CONCLUSION

Chiou *et al.* (5) concluded that the rabbit was not a useful animal for drug absorption studies because it was almost impossible to obtain an empty stomach in the rabbit by using the conventional fasting method and because the fasted state markedly prolonged the stomach emptying time. This conclusion has been very instructive to many investigators. However, in this study it was found possible to simulate the stomach emptying rate of rabbits to that of humans by taking adequate steps to empty the stomach and to feed the animals with a special soft diet. When the stomach emptying rate is controlled, the rabbit can be used as an animal model for predicting bioavailability of oral dosage for human subjects.

Results of bioavailability studies on oral dosage forms will be reported later.

REFERENCES

(1) T. H. Wilson and G. Wiseman, *J. Physiol.*, **123**, 116 (1954).

(2) L. S. Shanker, P. A. Shore, B. B. Brodie, and C. A. M. Hogben, *J. Pharmacol. Exp. Ther.*, **120**, 528 (1957).

(3) L. S. Shanker, D. J. Tocco, B. B. Brodie, and C. A. M. Hogben, *ibid.*, **123**, 81 (1958).

(4) S. Feldman, M. Salvino, and M. Gibaldi, *J. Pharm. Sci.*, **59**, 705 (1970).

(5) W. L. Chiou, S. Riegelman, and J. R. Amberg, *Chem. Pharm. Bull.*, **17**, 2170 (1969).

(6) V. P. Shah, S. Riegelman, and W. L. Epstein, *J. Pharm. Sci.*, **61**, 634 (1972).

(7) H. B. Hucker, A. G. Zacchei, S. V. Cox, D. A. Brodie, and N. H. R. Cantwell, *J. Pharmacol. Exp. Ther.*, **153**, 237 (1966).

(8) E. W. McChesney, E. J. Froelich, G. Y. Lesher, A. V. R. Crain, and D. Rosi, *Toxicol. Appl. Pharmacol.*, **6**, 292 (1964).

(9) C. E. Adams, "The UFAW Handbook on the Care and Management of Laboratory Animals," 4th ed., Churchill Livingstone, London, England, 1972, p. 167.

(10) K. W. Hagen, "The Biology of the Laboratory Rabbit," Academic, New York, N.Y., 1974, p. 33.

(11) J. N. Hunt and W. R. Spurrell, *J. Physiol.*, **113**, 157 (1951).

(12) C. Bedford, D. Busfield, K. J. Child, I. MacGregor, P. Sutherland, and E. G. Tomich, *Arch. Dermatol.*, **81**, 735 (1960).

(13) L. J. Fischer and S. Riegelman, *J. Pharm. Sci.*, **54**, 1571 (1965).

(14) M. Rowland, S. Riegelman, and W. L. Epstein, *ibid.*, **57**, 984 (1968).

(15) M. Moriyama, M. Saito, S. Awazu, M. Hanano, and H. Nogami, *Yakugaku Zasshi*, **91**, 1217 (1971).

(16) T. Fuwa, T. Iga, M. Hanano, H. Nogami, and M. Kashima, *ibid.*, **91**, 1223 (1971).

ACKNOWLEDGMENTS AND ADDRESSES

Received August 18, 1975, from the *Formulation Research Department, Pharmaceuticals Division, Sumitomo Chemical Co., Ltd., Kurakakiuchi 1-3-45, Ibaraki City, Osaka 567, Japan.*

Accepted for publication March 11, 1976.

Presented at the 94th Annual Meeting of the Pharmaceutical Society of Japan, Sendai, Japan, April 1974.

The authors thank Prof. H. Sezaki of Kyoto University for guidance and advice and Mr. Zenzo Harada for technical assistance.

[x] To whom inquiries should be directed.

Kinetics of Hydrolysis of Fenclorac

C. M. WON [x], J. J. ZALIPSKY, D. M. PATEL, and N. H. REAVEY-CANTWELL

Abstract □ The kinetics of hydrolysis of fenclorac were studied to determine its stability in aqueous solution at different pH's and temperatures. For this study, a stability-specific liquid chromatographic assay method was developed to separate fenclorac from its hydrolysis product, α-hydroxy-3-chloro-4-cyclohexylbenzeneacetic acid. The *k*–pH profile in the 0–12 pH range in various buffer solutions shows that fenclorac is stable in its undissociated form in strongly acidic media and is unstable in neutral and alkaline media. The instability of fenclorac in aqueous solution is proportional to the degree of ionization of the carboxyl group in the 1–4 pH range and is independent of pH above 4. The rate-determining step in the mechanism of hydrolysis of fenclorac involves ionization of the carbon–chlorine bond. The ionization is catalyzed by an intramolecular nucleophilic attack on the α-carbon by the dissociated carboxyl group, resulting in the formation of an unstable intermediate, a three-membered ring lactone. This unstable intermediate rapidly hydrolyzes to the final hydrolysis product. This mechanism is supported by experimental evidence such as the medium effect, positive salt effect, common ion effect, and substituent effect. Arrhenius parameters for the hydrolysis of fenclorac and its 3-nitro substituted analog were obtained.

Keyphrases □ Fenclorac—kinetics of hydrolysis, stability in aqueous solution, various pH's and temperatures, liquid chromatographic analysis □ Hydrolysis—fenclorac in aqueous solutions, kinetics, various pH's and temperatures, liquid chromatographic analysis □ Stability—fenclorac in aqueous solutions, various pH's and temperatures, liquid chromatographic analysis □ Liquid chromatography—analysis, fenclorac in aqueous solutions □ Anti-inflammatory agents—fenclorac, kinetics of hydrolysis, stability in aqueous solution, various pH's and temperatures, liquid chromatographic analysis

In the search for a new, nonsteroidal, anti-inflammatory compound for clinical utility, a series of substituted benzeneacetic acids was synthesized (1). Fenclorac (I) (α,3-dichloro-4-cyclohexylbenzeneacetic acid) diethylammonium salt exhibited promising anti-inflammatory activities. The anti-inflammatory activity of fenclorac was demonstrated in rats using the carrageenan paw edema assay[1].

A simple, sensitive analytical method was needed to follow the hydrolysis of relatively unstable fenclorac in

[1] G. Nuss *et al.*, to be published.

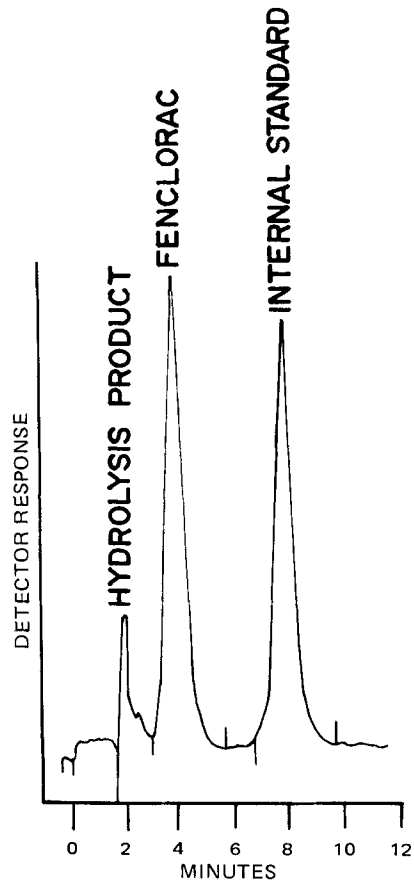

Figure 1—*Typical chromatogram of fenclorac, its hydrolysis product, α-hydroxy-3-chloro-4-cyclohexylbenzeneacetic acid, and the internal standard, triphenylethylene.*

aqueous solution. Previously reported methods for analysis of substituted aryl- and alkylphenoxyalkyl carboxylic acids, based on paper chromatographic separation and ion-pair formation with bromcresol green (2) and GLC assay (3), were not suitable. Therefore, a rapid stability-specific liquid chromatographic assay was developed for kinetic assay.

This report is concerned with the study of the kinetics and the mechanism of the hydrolysis of fenclorac in aqueous solution to utilize the basic information for pharmaceutical formulation design.

EXPERIMENTAL

Analytical Apparatus—A liquid chromatograph[2] equipped with a 254-nm UV detector and an electronic integrator[3] was used. The column was 50-cm × 7.9-mm (i.d.) stainless steel packed with chemically bonded octadecyl hydrocarbon on 30-μm porous silica[4].

Chromatographic Conditions—The solvent system was composed of methanol–water–acetic acid (50:36:14). The flow rate was 4.4 ml/min, and the pressure required to maintain this flow rate was 500 psi. The slightly different solvent systems used for α-chloro-4-cyclohexylbenzeneacetic acid and α-chloro-3-nitro-4-cyclohexylbenzeneacetic acid were methanol–water–acetic acid (54:40:6) and methanol–water–acetic acid (40:46:14), respectively.

Calibration Curve—Separate solutions containing 0.192, 0.384, 0.576, and 0.768 mg/ml of fenclorac standard and 36 μg/ml of internal standard, triphenylethylene[5], in methanol were injected into the column through a six-port injection valve with a loop capacity of 35 μl.

[2] Model 830, DuPont Instruments, Wilmington, Del.
[3] Model 3380A, Hewlett-Packard, Avondale, Pa.
[4] Permaphase ODS, DuPont Instruments, Wilmington, Del.
[5] Eastman Kodak, Rochester, N.Y.

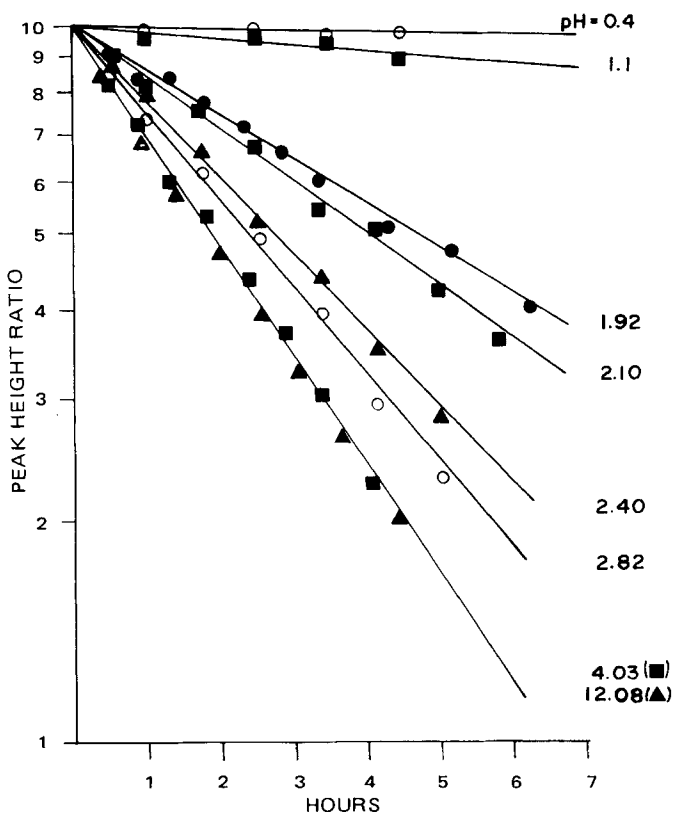

Figure 2—*Typical semilogarithmic plots of the ratio of the peak height of fenclorac to that of the internal standard, triphenylethylene, against time for the hydrolysis of fenclorac at 37.0° and the given pH.*

Kinetic Procedure—All kinetic experiments were performed at an ionic strength of 0.1 with sodium nitrate. Buffers employed were glycine (pH 2.1–2.8), formate (pH 3.3–4.0), acetate (pH 4.4), and carbonate (pH 10.1). An aliquot (0.8 ml) of a methanolic stock solution of fenclorac (50 mg/ml) was transferred into 100 ml of buffer solution equilibrated to the temperature under study. The low solubility of fenclorac in water at pH ≤ 4 necessitated the use of a stock solution of a lower concentration (1 mg/ml). The samples were withdrawn at various time intervals and analyzed as described.

Assay Procedure—Five milliliters of sample solution was cooled in an ice–water bath. An aliquot (4.0 ml) of the cooled sample was introduced into a vial with 4.0 ml of an internal standard solution. The internal standard solution contained 6 mg of triphenylethylene in 6 ml of acetic acid and 94 ml of methanol. The mixed sample was injected into the column through a six-port injection valve with a 35-μl capacity loop. A larger injection loop (1.39 ml) and a lower concentration of internal standard (1.2 μg/ml) were used for the sample solutions studied at pH ≤ 4.0.

RESULTS AND DISCUSSION

Liquid Chromatography—A typical liquid chromatogram of fenclorac (t_R = 4.6 min), its hydrolysis product (t_R = 2.4 min), and the internal standard (t_R = 9.7 min) is shown in Fig. 1. The plot of the ratio of peak height or area of fenclorac to that of internal standard *versus* the concentration of fenclorac showed a linear relationship between 0.192 and 0.768 mg/ml. The calibration curve had a mean slope of 1.945 mg^{-1},

Table I—Apparent First-Order Rate Constant in Hydrolysis of Fenclorac at 37.0° and pH 7.04 as a Function of Phosphate Buffer Anion, $[HPO_4^{2-}]$

$[HPO_4^{2-}]$, $M \times 10^{-2}$	10^4 k, sec^{-1}
1.4	1.15
2.8	1.13
7.0	1.11
11.2	1.11

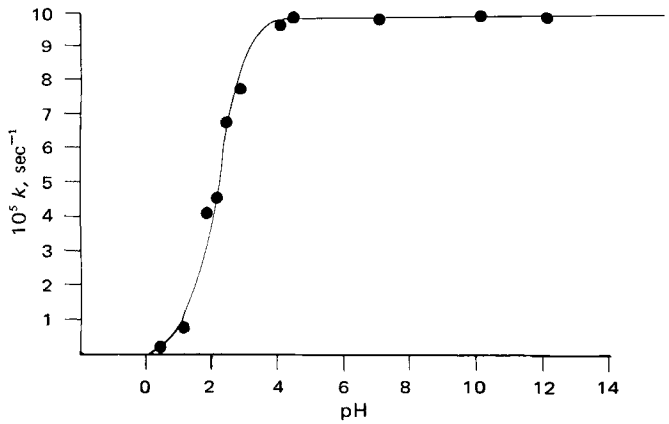

Figure 3—*The k–pH profile for the intramolecular nucleophilic catalysis in the hydrolysis of fenclorac in water (μ = 0.1) at 37.0°*

a mean Y-intercept of 0.014, and a mean correlation coefficient of 0.9998. These data indicate that the liquid chromatographic method can be used with a single-point standard.

Rate Constant—The apparent first-order rate constants were estimated from the slopes of appropriately plotted experimental data using:

$$\log R = \log R_0 - kt/2.303 \qquad \text{(Eq. 1)}$$

where R_0 was the initial ratio of peak height of fenclorac to that of the internal standard, and R was the ratio at any given time t. The reaction was irreversible, and no fenclorac peak was observed when the reaction went to completion. At any given pH, the semilogarithmic plots of the peak height ratio *versus* time showed linearity. Typical first-order plots at various pH values are given in Fig. 2. The hydrolysis of fenclorac was first order with respect to substrate over a 50-fold variation in initial concentration.

General Acid–Base Catalysis—The rate constants were independent of buffer concentration at constant pH and ionic strength when the phosphate buffer concentration was changed eightfold (Table I). This independence indicates that the hydrolysis is not due to the possible catalytic properties of the phosphate ions.

***k*–pH Profile**—The k–pH profile (Fig. 3) was constructed from the first-order rate constants and pH values at 37.0°. The first-order rate constant is independent of pH above 4 and is a sigmoid function of pH below 4. The hydrolysis rate is proportional to the degree of ionization of the carboxyl group, and the first-order rate constant for this system can be formulated as:

$$k = k_{AH}f_{AH} + k_Af_A \qquad \text{(Eq. 2a)}$$

$$k = \frac{k_{AH}[H^+] + k_AK_a}{[H^+] + K_a} \qquad \text{(Eq. 2b)}$$

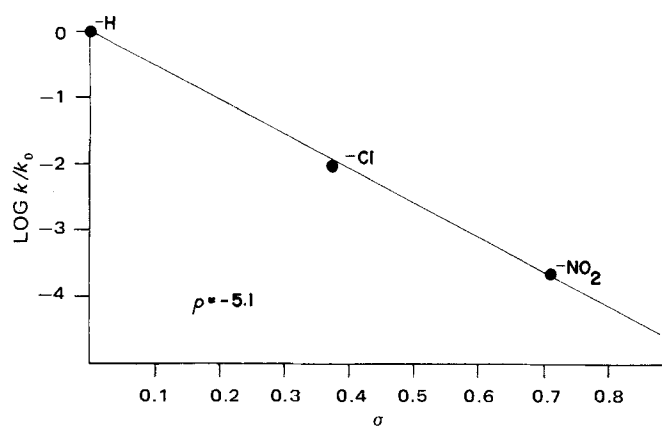

Figure 4—*Linear free energy relationship between the rates of hydrolysis of α-chloro-4-cyclohexylbenzeneacetic acid containing electron-withdrawing substituents and the Hammett substituent constants.*

Table II—Apparent First-Order Rate Constants in Hydrolysis of Fenclorac at 37.0° and pH 7.04 as a Function of Ionic Strength with Sodium Nitrate (k') and with Potassium Chloride (k), and Relative Rates of the Intermediate with Cl^- and Solvent (k_{Cl}/k_s)

μ	$10^5 k'$, sec^{-1}	$[Cl^-]$, M	$10^5 k$, sec^{-1}	k_{Cl}/k_s
0.096	9.86	0	9.86	—
0.446	11.7	0.35	10.2	0.42
0.846	13.6	0.75	10.5	0.39
1.596	14.4	1.50	11.1	0.20

where k_{AH} and k_A are the rate constants for the hydrolysis of undissociated and dissociated fenclorac, respectively; and f_{AH} and f_A are the fractions of undissociated and dissociated species, respectively. Since k_{AH} is negligible compared to k_A, Eq. 2*b* is reduced to:

$$k = \frac{k_AK_a}{[H^+] + K_a} \qquad \text{(Eq. 3)}$$

When $[H^+] \ll K_a$, Eq. 3 is reduced to $k = k_A$.

Thus, the k value becomes k_A when the rate constant is independent of pH above 4. The pKa value (pKa = 2.13) determined from the kinetic data using Eq. 3 agrees with that determined by the solubility method[6].

Salt and Common Ion Effects—The hydrolysis of fenclorac in phosphate buffer at pH 7.04 was tested for a salt effect using sodium nitrate up to an ionic strength of 1.596. An approximately 50% increase in the rate constant resulted by a change in ionic strength from 0.1 to 1.6 (Table II). A positive salt effect indicates generation of charge in the transition state, making the transition state more polar than the reactant. The first-order rate constant was not significantly increased when potassium chloride was used in place of sodium nitrate (Table II). The common ion effect, characteristic of an S_N1 reaction, can be taken into account by a reversible ionization mechanism (4) (Scheme I).

The apparent first-order rate constant, k, when the common ion effect is considered, is:

$$k = \frac{k'}{1 + (k_{Cl})/(k_s)[Cl^-]} \qquad \text{(Eq. 4)}$$

The ratio k_{Cl}/k_s (Table II) was estimated from the rate constants k' and k at a given ionic strength using sodium nitrate and potassium chloride, respectively.

Medium Effect—By changing the solvent from water to 50% aqueous methanol, the first-order rate constant for the hydrolysis of fenclorac at 50.0° and pH 5–12 decreased 6.5-fold ($k = 9.9 \times 10^{-5}$ sec^{-1}). The direction of the medium effect corresponds to that of a salt effect. This finding indicates that the solvent with greater polarity (water) stabilizes the transition state to the greater extent by solvation.

Substituent Effect—It was of interest to determine the electronic effect of different substituents (hydrogen and nitro) at the 3-position of the benzene ring on the hydrolysis rate of these analogs and to compare the effect with that of the 3-chloro substituent in fenclorac. The first-order rate constants were determined for fenclorac and the unsubstituted analog at pH 7.04 and 25.0°. The rate constant for the nitro substituent was extrapolated from its Arrhenius plot. The hydrolysis rate constants of the unsubstituted analog ($k = 1.67 \times 10^{-3}$ sec^{-1}) increased 100-fold from that of fenclorac, and that of the nitro-substituted analog ($k = 3.56 \times 10^{-7}$ sec^{-1}) decreased 50-fold. When the logarithm of k/k_0, where k_0 is the rate constant for the unsubstituted analog, was plotted against Hammett's σ-constants of the substituents, a linear relationship with $\rho = -5.1$ was obtained (Fig. 4). The reaction constant obtained was comparable to that of typical S_N1 reactions, *e.g.*, the solvolysis of 2-chloro-2-phenylpropane in 90% aqueous acetone with $\rho = -4.54$ (5).

From these data, it is seen that the different 3-substituents on the aromatic ring significantly affect the rate of hydrolysis. The large substit-

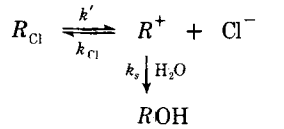

Scheme I

[6] B. Crugman *et al.*, Research Division, William H. Rorer Inc., personal communication.

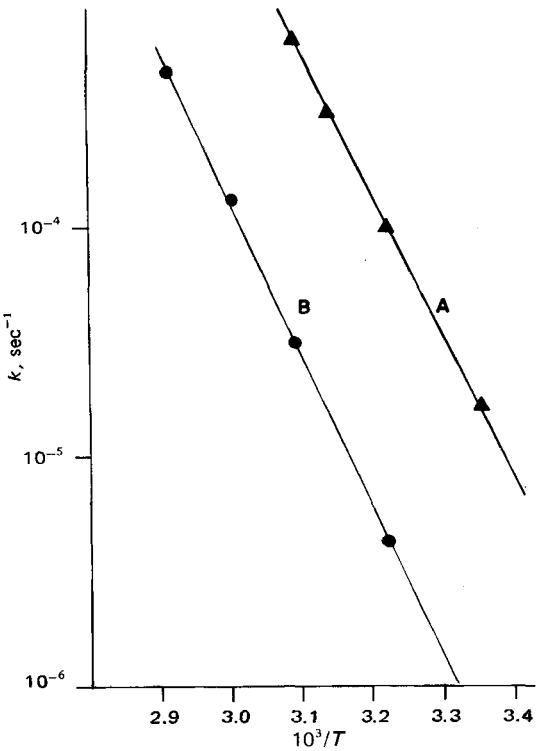

Figure 5—*Arrhenius plots for hydrolysis of fenclorac (A) and the 3-nitro-substituted analog (B).*

uent effect on the hydrolysis rate apparently is due to a change of the activation energy rather than the entropy of activation (Table III). This statement, however, is inconclusive, since the temperature dependence of the substituent effect was studied only for two compounds.

Rate Dependency on Temperature—The first-order rate constants were determined in phosphate buffer (pH 7.04) at four temperatures for fenclorac and the 3-nitro analog (Table III). The Arrhenius equation gives the quantitative relation of the rate constant and temperature. The logarithmic form of the equation is:

$$\log k = \frac{E_a}{2.303RT} + \log A \qquad \text{(Eq. 5)}$$

where E_a is the activation energy, and A is the frequency factor. The Arrhenius plots of the logarithms of the first-order rate constants *versus* $1/T$ are shown in Fig. 5. The Arrhenius parameters were calculated from the plots in accordance with Eq. 5. The values of E_a, log A, and $S^{\ddagger}$ (entropy of activation) are included in Table III.

Mechanism for Hydrolysis of Fenclorac—It has been well demonstrated (6–9) that α-bromopropionate hydrolyzes by the intramolecular displacement of bromine by the carboxyl anion and that the lactone formation follows the ionization of the carbon–bromine bond.

Table III—Apparent First-Order Rate Constants at Different Temperatures, Arrhenius Parameters, and Entropies of Activation for Hydrolysis of Fenclorac and the 3-Nitro-Substituted Analog at pH 7.04

	Fenclorac, 10^5 k, sec^{-1}	3-Nitro Analog, 10^5 k, sec^{-1}
Temperature		
25.0°	1.62	0.0356[a]
37.0°	9.95	0.273
45.0°	31.0	—
50.0°	65.7	3.07
60.0°	—	13.0
70.0°	—	47.2
E_a, kcal	28.3	33.0
log A	15.93	17.75
$S^{\ddagger}$, eu	6.2	10.4

[a] Extrapolated value.

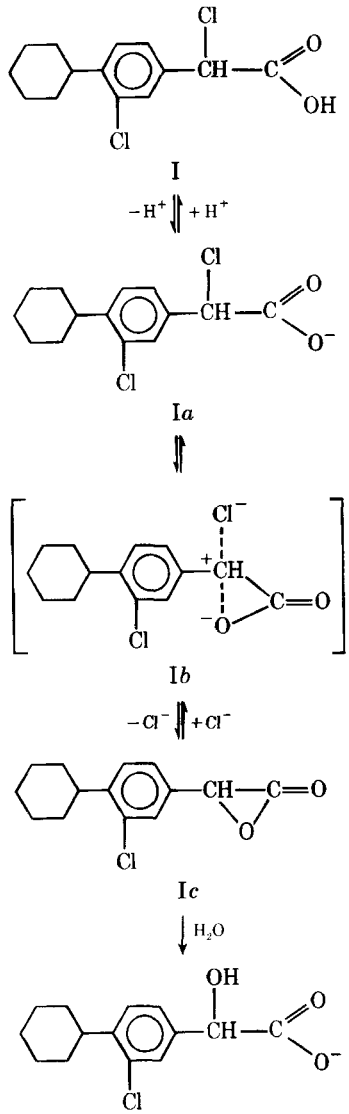

Scheme II

Scheme II is consistent with the proposed mechanism for the hydrolysis of fenclorac. The sequence explains the intramolecular catalysis of carboxyl anion in the ionization of the carbon–chlorine bond and the formation of an unstable intermediate, lactone.

Only the dissociated carboxyl anion participates in the intramolecular catalysis by nucleophilic attack on the α-carbon. The general base mechanism would be ruled out in the intramolecular catalysis, because no general acid–base catalysis was observed (Table I).

Since the increase in the rate constant was observed with an increasing salt concentration and polarity of the medium, it can be deduced that the transition state (Ib) has high ionic character (9). As the carbon–chlorine bond ionizes, a positive charge develops on the α-carbon, and the electron-withdrawing substituents destabilize the transition state by pulling electrons from already electron-deficient α-carbon and thus decrease the hydrolysis rate as shown by the substituent effect. The intermediate Ic, a three-membered ring lactone, would be trapped either by solvent water in the fast step to produce hydrolysis product Id or by added Cl^- to reverse the reaction as observed through the common ion effect.

REFERENCES

(1) J. Diamond and N. J. Santora, U.S. pat. 3,864,384 (1975).

(2) S. S. Adams and E. E. Cliffe, *J. Pharm. Pharmacol.*, **17**, 173 (1965).

(3) J. F. Nash, R. J. Bopp, and A. Rubin, *J. Pharm. Sci.*, **60**, 1062 (1971).

(4) J. Hine, "Physical Organic Chemistry," McGraw-Hill, New York,

N.Y., 1962, pp. 129–136.
(5) H. C. Brown and Y. Okamato, *J. Am. Chem. Soc.*, **80**, 4979 (1958).
(6) W. A. Cowdrey, E. D. Hughes, and C. K. Ingold, *J. Chem. Soc.*, **1937**, 1208.
(7) S. Winstein and H. J. Lucas, *J. Am. Chem. Soc.*, **61**, 1576 (1939).
(8) S. Winstein, *ibid.*, **61**, 1635 (1939).
(9) E. Grunwald and S. Winstein, *ibid.*, **70**, 841 (1948).

ACKNOWLEDGMENTS AND ADDRESSES

Received December 15, 1975, from the *Analytical and Physical Chemistry Department, Research Division, William H. Rorer, Inc., Fort Washington, PA 19034.*

Accepted for publication March 18, 1976.

The authors thank Dr. Sy-rong Sun for conducting preliminary studies.

[x] To whom inquiries should be directed.

Quantitative Determination of Amitriptyline and Its Principal Metabolite, Nortriptyline, by GLC–Chemical Ionization Mass Spectrometry

W. A. GARLAND

Abstract □ A quantitative GLC–mass spectrometry assay was developed for the determination of the tricyclic antidepressant amitriptyline and its desmethyl metabolite (nortriptyline) in human plasma. The assay utilizes selective ion detection to monitor in a GLC effluent the MH^+ molecular ions of amitriptyline and nortriptyline generated by isobutane chemical ionization. The procedure, which utilizes deuterated analogs of amitriptyline and nortriptyline as internal standards, requires 1 ml of plasma and can measure 1 ng/ml of amitriptyline and 0.5 ng/ml of nortriptyline. The curves relating the amounts of amitriptyline and nortriptyline added *versus* the amounts found over a 100-fold range of amitriptyline and nortriptyline concentrations are straight lines with intercepts of approximately zero and slopes of unity. Analyses of plasma samples from three subjects receiving 50 mg of amitriptyline orally, three times a day, gave an average plasma concentration of 115 ± 42 ng/ml for amitriptyline and 109 ± 20 ng/ml for nortriptyline. Similar analyses of the plasma of three subjects who had received a single 50-mg oral dose of amitriptyline showed an average maximum plasma concentration of 25 ± 10 ng/ml for amitriptyline and 10 ± 4 ng/ml for nortriptyline. Seventy-two hours after administration, the average plasma amitriptyline and nortriptyline levels were 3 ± 1 and 3 ± 2 ng/ml, respectively.

Keyphrases □ Amitriptyline—GLC–mass spectrometric analysis, human plasma □ Nortriptyline—GLC–mass spectrometric analysis, human plasma □ GLC–mass spectrometry—analyses, amitriptyline and nortriptyline in human plasma □ Antidepressants—amitriptyline and nortriptyline, GLC–mass spectrometric analyses, human plasma

Amitriptyline and nortriptyline are used extensively for treating psychic depression (1). Nortriptyline is also generated metabolically in humans from amitriptyline (2, 3). Indeed, it has been suggested that the action of amitriptyline is mediated through its nortriptyline metabolite (4). Therapeutically, these compounds are reported to be effective over a relatively narrow range of plasma concentrations (5), although large interindividual variations in plasma concentrations are observed with similar dosing schedules (6–8). In addition, there are conflicting reports concerning the relative amelioration of depression as a function of plasma amitriptyline and/or nortriptyline levels (5, 8, 9).

Research on problems associated with amitriptyline therapy has been hindered somewhat by the lack of a sufficiently sensitive and specific assay for determining low levels of amitriptyline in plasma, *e.g.*, no single-dose amitriptyline pharmacokinetic data are available. Two flame-ionization GC assays suitable only for determining "steady-state" plasma concentrations of amitriptyline and nortriptyline were described (10, 11). Both assays require 3–5 ml of plasma and have a sensitivity limit of 25 ng/ml.

Recently, a GC procedure using a nitrogen detector was reported (12). It has a quoted sensitivity of 5 ng/ml for amitriptyline and 10–15 ng/ml for nortriptyline (2 ml of plasma extracted), but it cannot determine nortriptyline in humans following a therapeutic single dose of amitriptyline. Furthermore, it is only marginally suitable for amitriptyline, since the typical maximum concentration of amitriptyline after a 50-mg dose is only 15–25 ng/ml.

An electron-capture GC method for the determination of the heptafluorobutyrate derivatives of nortriptyline and some of its metabolites was reported (13). This procedure requires 4 ml of plasma and has a reported sensitivity of 10 ng/ml.

This report describes a GLC–mass spectrometric assay requiring 1 ml of plasma that is capable of determining 1 ng/ml of amitriptyline and 0.5 ng/ml of nortriptyline. The method, which utilizes chemical ionization GLC–mass spectrometry (14) with isobutane functioning both as a reagent gas and GLC carrier gas, is suitable for measuring amitriptyline and nortriptyline in humans following single-dose amitriptyline administration. To obtain sufficient sensitivity, selective ion detection is used to monitor the MH^+ ion of both amitriptyline and either nortriptyline or the trifluoroacetyl derivative of nortriptyline. Known quantities of deuterated analogs of both amitriptyline and nortriptyline are added to the plasma as internal standards.

EXPERIMENTAL

Apparatus—A quadrupole mass filter system[1] and data system[2] were used in conjunction with the gas chromatograph[3]. The GLC column, 1.21 m (4 ft) × 2 mm i.d., was silanized and packed with 3% OV-17 on 100–

[1] Finnigan model 1015D.
[2] Finnigan model 6000.
[3] Finnigan model 9500.

N.Y., 1962, pp. 129–136.
(5) H. C. Brown and Y. Okamato, *J. Am. Chem. Soc.*, **80**, 4979 (1958).
(6) W. A. Cowdrey, E. D. Hughes, and C. K. Ingold, *J. Chem. Soc.*, **1937**, 1208.
(7) S. Winstein and H. J. Lucas, *J. Am. Chem. Soc.*, **61**, 1576 (1939).
(8) S. Winstein, *ibid.*, **61**, 1635 (1939).
(9) E. Grunwald and S. Winstein, *ibid.*, **70**, 841 (1948).

ACKNOWLEDGMENTS AND ADDRESSES

Received December 15, 1975, from the *Analytical and Physical Chemistry Department, Research Division, William H. Rorer, Inc., Fort Washington, PA 19034.*

Accepted for publication March 18, 1976.

The authors thank Dr. Sy-rong Sun for conducting preliminary studies.

[x] To whom inquiries should be directed.

Quantitative Determination of Amitriptyline and Its Principal Metabolite, Nortriptyline, by GLC–Chemical Ionization Mass Spectrometry

W. A. GARLAND

Abstract □ A quantitative GLC–mass spectrometry assay was developed for the determination of the tricyclic antidepressant amitriptyline and its desmethyl metabolite (nortriptyline) in human plasma. The assay utilizes selective ion detection to monitor in a GLC effluent the MH^+ molecular ions of amitriptyline and nortriptyline generated by isobutane chemical ionization. The procedure, which utilizes deuterated analogs of amitriptyline and nortriptyline as internal standards, requires 1 ml of plasma and can measure 1 ng/ml of amitriptyline and 0.5 ng/ml of nortriptyline. The curves relating the amounts of amitriptyline and nortriptyline added *versus* the amounts found over a 100-fold range of amitriptyline and nortriptyline concentrations are straight lines with intercepts of approximately zero and slopes of unity. Analyses of plasma samples from three subjects receiving 50 mg of amitriptyline orally, three times a day, gave an average plasma concentration of 115 ± 42 ng/ml for amitriptyline and 109 ± 20 ng/ml for nortriptyline. Similar analyses of the plasma of three subjects who had received a single 50-mg oral dose of amitriptyline showed an average maximum plasma concentration of 25 ± 10 ng/ml for amitriptyline and 10 ± 4 ng/ml for nortriptyline. Seventy-two hours after administration, the average plasma amitriptyline and nortriptyline levels were 3 ± 1 and 3 ± 2 ng/ml, respectively.

Keyphrases □ Amitriptyline—GLC–mass spectrometric analysis, human plasma □ Nortriptyline—GLC–mass spectrometric analysis, human plasma □ GLC–mass spectrometry—analyses, amitriptyline and nortriptyline in human plasma □ Antidepressants—amitriptyline and nortriptyline, GLC–mass spectrometric analyses, human plasma

Amitriptyline and nortriptyline are used extensively for treating psychic depression (1). Nortriptyline is also generated metabolically in humans from amitriptyline (2, 3). Indeed, it has been suggested that the action of amitriptyline is mediated through its nortriptyline metabolite (4). Therapeutically, these compounds are reported to be effective over a relatively narrow range of plasma concentrations (5), although large interindividual variations in plasma concentrations are observed with similar dosing schedules (6–8). In addition, there are conflicting reports concerning the relative amelioration of depression as a function of plasma amitriptyline and/or nortriptyline levels (5, 8, 9).

Research on problems associated with amitriptyline therapy has been hindered somewhat by the lack of a sufficiently sensitive and specific assay for determining low levels of amitriptyline in plasma, *e.g.*, no single-dose amitriptyline pharmacokinetic data are available. Two flame-ionization GC assays suitable only for determining "steady-state" plasma concentrations of amitriptyline and nortriptyline were described (10, 11). Both assays require 3–5 ml of plasma and have a sensitivity limit of 25 ng/ml.

Recently, a GC procedure using a nitrogen detector was reported (12). It has a quoted sensitivity of 5 ng/ml for amitriptyline and 10–15 ng/ml for nortriptyline (2 ml of plasma extracted), but it cannot determine nortriptyline in humans following a therapeutic single dose of amitriptyline. Furthermore, it is only marginally suitable for amitriptyline, since the typical maximum concentration of amitriptyline after a 50-mg dose is only 15–25 ng/ml.

An electron-capture GC method for the determination of the heptafluorobutyrate derivatives of nortriptyline and some of its metabolites was reported (13). This procedure requires 4 ml of plasma and has a reported sensitivity of 10 ng/ml.

This report describes a GLC–mass spectrometric assay requiring 1 ml of plasma that is capable of determining 1 ng/ml of amitriptyline and 0.5 ng/ml of nortriptyline. The method, which utilizes chemical ionization GLC–mass spectrometry (14) with isobutane functioning both as a reagent gas and GLC carrier gas, is suitable for measuring amitriptyline and nortriptyline in humans following single-dose amitriptyline administration. To obtain sufficient sensitivity, selective ion detection is used to monitor the MH^+ ion of both amitriptyline and either nortriptyline or the trifluoroacetyl derivative of nortriptyline. Known quantities of deuterated analogs of both amitriptyline and nortriptyline are added to the plasma as internal standards.

EXPERIMENTAL

Apparatus—A quadrupole mass filter system[1] and data system[2] were used in conjunction with the gas chromatograph[3]. The GLC column, 1.21 m (4 ft) × 2 mm i.d., was silanized and packed with 3% OV-17 on 100–

[1] Finnigan model 1015D.
[2] Finnigan model 6000.
[3] Finnigan model 9500.

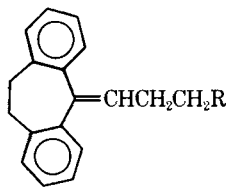

Ia: R = $N(CH_3)_2$—CH_3

Ib: R = $N(CH_3)_2$—CD_3

Ic: R = $N(CD_3)_2$—CD_3

IIa: R = $NHCH_3$

IIb: R = $NHCD_3$

IIc: R = $N(CH_3)$—$C(=O)CF_3$

IId: R = $N(CD_3)$—$C(=O)CF_3$

120-mesh Gas Chrom Q[4]. The column was conditioned at 325° with no flow for 3 hr and then at 275° overnight with a 20-ml/min helium flow.

Chromatographic conditions were: column oven, 230–240°; injection port, 275°; isobutane[5] gauge pressure, 1–3 lb/in.^{2}; and interface oven and glass-lined source reentrant tube, 250°. The column temperature and isobutane pressure were adjusted to provide an ion source pressure of 0.3–0.4 torr. Typical ion source settings were: ion volume + 8 v, ion repeller + 2 v, ion lens − 30 v, and filament − 150 v. The electron beam total emission was regulated at 800 μamp, while the source was operated without external heating (temperature 50°).

Materials—Nanograde quality *n*-hexane[6] and chloroform[6] and GLC quality trifluoroacetic anhydride[7] were used without further purification. Before each assay, hydrogen chloride gas was gently bubbled through 20 ml of chloroform in a 25-ml flask for 5 min. The flask was then capped, and this solution was used later to wash down the wall of the tubes used for evaporation of the plasma extraction solvent.

Stock solutions of amitriptyline (Ia), amitriptyline-d_3 (Ib), amitriptyline-d_6[8] (Ic), nortriptyline (IIa), and nortriptyline-d_3 (IIb) were made in distilled water using their respective hydrochloride salts, with all concentrations expressed in terms of the free base. Clinical control plasma[9] was used in the preparation of the amitriptyline and nortriptyline plasma standards.

Amitriptyline-d_3 and nortriptyline-d_3 were synthesized from nortriptyline and desmethylnortriptyline, respectively, using a published procedure (15). The relevant amine was treated with ethyl chlorocarbonate, and the resulting carbamate was reduced with lithium aluminum deuteride[10] at room temperature for no more than 8 hr. Both compounds showed satisfactory UV, IR, PMR, and mass spectral (electron and chemical ionization) properties. A selective ion detection analysis of amitriptyline-d_3 showed the presence of an ion equivalent to 3.03 ± 0.16% (n = 6) amitriptyline-d_0. A similar analysis of nortriptyline-d_3 showed the presence of an ion equivalent to 3.84 ± 0.17% (n = 6) nortriptyline-d_0. A selective ion detection analysis of amitriptyline-d_6 failed to detect any amitriptyline-d_0.

Tubes (15 ml)[11] with screw caps[12] were used for the plasma extractions; 5-ml glass-stoppered centrifuge tubes[13] were used for the final solvent evaporation. Pasteur pipets with hand-drawn constricted tips were utilized for all solution transfers. All glassware was soaked for 2 hr in a 0.1% solution of trimethylamine in methanol prior to use.

Assay Procedure—*Steady-State Plasma Concentrations*—One milliliter of plasma, 1.0 ml of internal standard solution (typically ~ 100 ng/ml of amitriptyline-d_3 and nortriptyline-d_3), 0.2 ml of 1 *M* H_2SO_4, and 5.0 ml of hexane were combined in a 15.0-ml test tube, and the mixture was shaken on a metabolic shaker–incubator[14] at 40 oscillations/min for 15 min. After centrifugation at 1000×*g*[15], the organic phase was removed and discarded. To the aqueous phase was then added 1.0 ml of 1.0 *M* NaOH and 5.0 ml of hexane. The mixture was then shaken and centrifuged, and the organic phase was transferred to a 5-ml centrifuge tube.

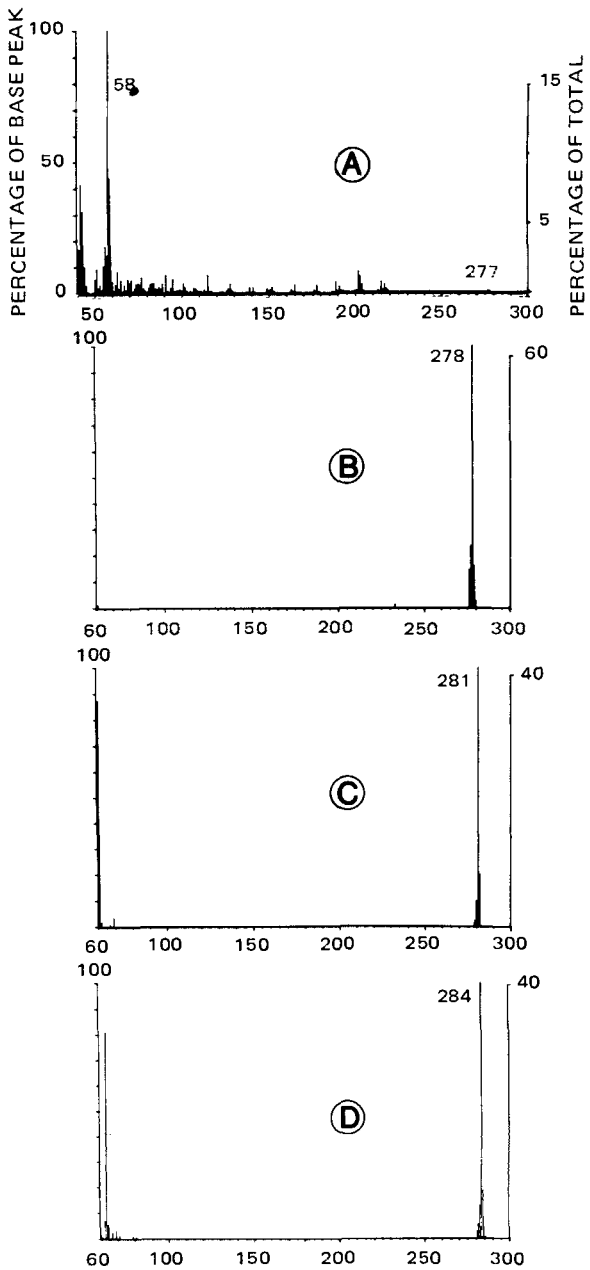

Figure 1—*Key: A, electron ionization (70 ev) mass spectrum of amitriptyline; B, isobutane (0.4 torr) chemical ionization mass spectrum of amitriptyline; C, isobutane (0.3 torr) mass spectrum of amitriptyline-*d_3*; and D, isobutane (0.6 torr) mass spectrum of amitriptyline-*d_6.

While the organic phase was being removed under a gentle stream of nitrogen at room temperature[16], another 5.0 ml of hexane was added to the aqueous phase, which was then shaken and centrifuged as before. This 5.0 ml was then transferred to the centrifuge tube, and the solvent was removed under nitrogen. The centrifuge tube wall was washed down first with 500 μl and then with 100 μl of hydrogen chloride (gas) treated chloroform. Following removal of this second chloroform wash, the residue was reconstituted in 30 μl of chloroform, and 10 μl was injected into the GLC–mass spectrometer.

Forty-five seconds after injection, the electron multiplier was turned on and the GLC flow divert valve was turned off, allowing the GLC effluent to enter the ion source. Fifty-five seconds after injection, the ion

[4] Applied Science Laboratories.
[5] Matheson, instrument purity.
[6] Mallinckrodt Chemicals.
[7] Pierce Chemicals.
[8] Synthesized by Dr. E. Kyburg, F. Hoffmann–La Roche & Co., Ltd., Basle, Switzerland.
[9] Hyland Laboratories.
[10] Stohler Isotopes, 99%D.
[11] Pyrex 9825.
[12] Lined with Teflon (du Pont).
[13] Pyrex 8084.
[14] Dubnoff, Scientific Glass Apparatus.
[15] Model HN-S, International Equipment Co.
[16] N-Evap, Organomation Associates.

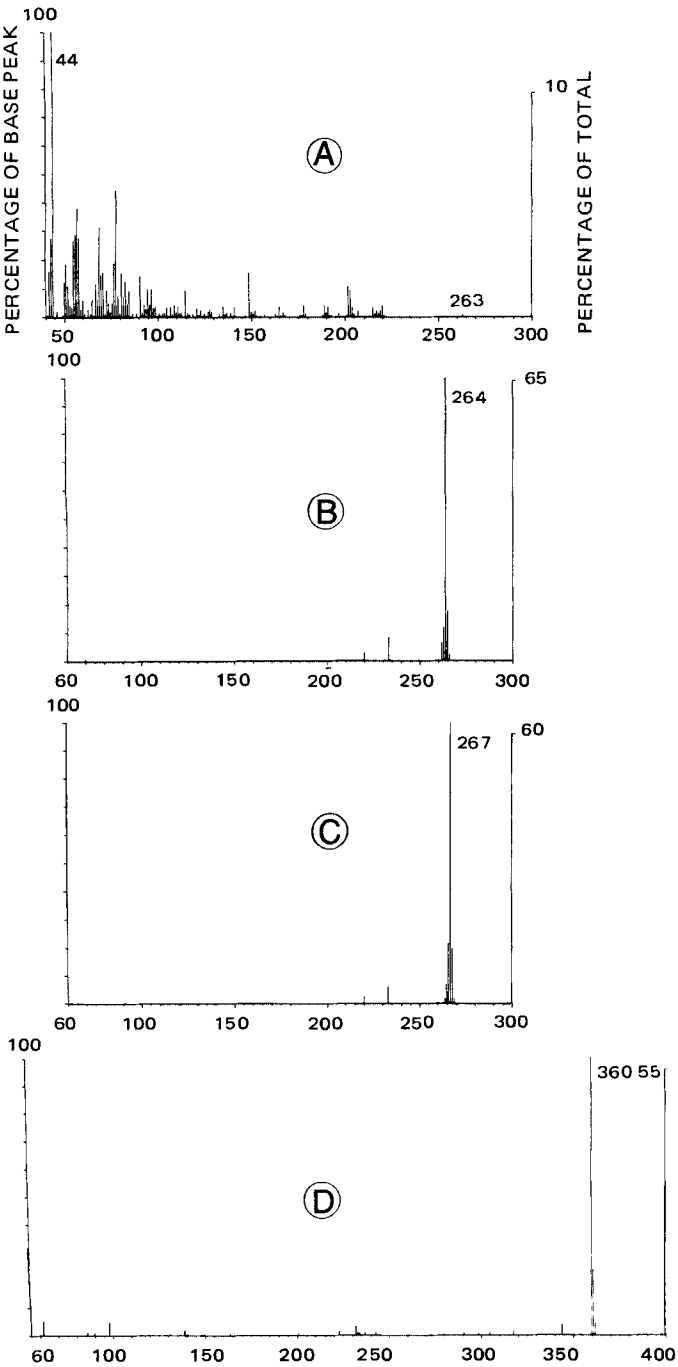

Figure 2—*Key: A, electron ionization (55 ev) mass spectrum of nortriptyline; B, isobutane (0.4 torr) chemical ionization mass spectrum of nortriptyline; C, isobutane (0.4 torr) chemical ionization mass spectrum of nortriptyline-*d_3*; and D, isobutane (0.6 torr) mass spectrum of the* N*-trifluoroacetyl derivative of nortriptyline.*

source supplies were turned on. Computer-controlled scanning and data collection were initiated another 5 sec later. Approximate retention times were 1.5 and 1.8 min for amitriptyline and nortriptyline, respectively. Three minutes after injection, the GLC flow divert valve was again turned on, the ion source supplies were turned off, and the computer data collection was halted.

Peak areas and preliminary concentrations were obtained using the software provided with the data system. Final concentrations were obtained by subtraction of the amount of either amitriptyline-d_0 or nortriptyline-d_0 present in the deuterated internal standards from the computer-calculated preliminary concentrations. The amounts of amitriptyline-d_0 and nortriptyline-d_0 in the d_3-labeled standards were periodically checked by selective ion analysis.

Single Amitriptyline Dose—The procedure followed was similar to

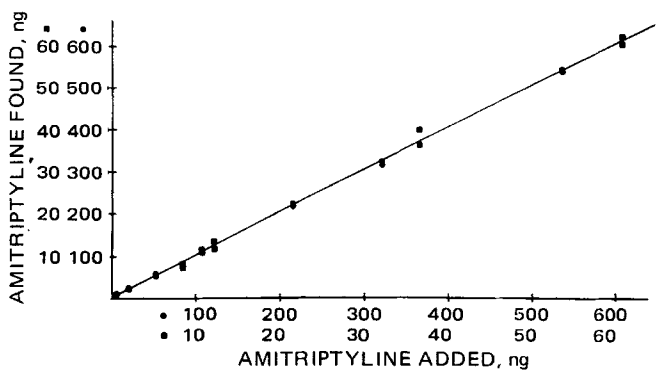

Figure 3—*Curve relating amount of amitriptyline added to clinical control plasma* versus *amount of amitriptyline found. Circles denote determinations using procedure described under* Experimental *for steady-state plasma amitriptyline* (m/e 278) *levels. For these samples, 122 ng/ml of amitriptyline-*d_3 (m/e 281) *was used as an internal standard. Squares denote determinations using the procedure described under* Experimental *for single-dose plasma amitriptyline levels. For these samples, 7.52 ng/ml of amitriptyline-*d_6 (m/e 284) *was used as an internal standard.*

that used with the steady-state plasma samples with the following three exceptions:

1. A lower internal standard concentration of approximately 20 ng/ml for both amitriptyline-d_6 and nortriptyline-d_3 was used. Amitriptyline-d_6 was usually used in preference to amitriptyline-d_3 in the single-dose assay, since the *m/e* 284 (amitriptyline-d_6) trace showed a significantly lower background signal at this concentration level as compared to that at *m/e* 281 (amitriptyline-d_3).
2. Fifty microliters of trifluoroacetic anhydride was added following the addition of the second hexane extract to the 5-ml centrifuge tube, and the solution was allowed to stand for 30 min before solvent evaporation.
3. The GLC flow divert valve was turned on again 4 min after sample injection. The retention time of *N*-trifluoroacetyl nortriptyline (IIc) and *N*-trifluoroacetyl nortriptyline-d_3 (II*d*) was 3.0 min.

Amitriptyline Single-Dose and Steady-State Human Plasma Samples—Plasma samples from normal adult volunteers were available from previous studies.

RESULTS AND DISCUSSION

A GLC–mass spectrometric assay for the heptafluorobutyrate derivative of nortriptyline was reported using conventional electron ionization and selective ion monitoring of the $M^+ - CH_3NHC(=O)C_3F_7$ fragment ion generated in the electron ionization mass spectrum (16). The quoted sensitivity for this assay is 1 ng/ml using 3 ml of plasma. Since amitriptyline cannot be easily derivatized, a similar electron ionization assay for this compound would require the monitoring of the relatively nonspecific *m/e* 58 ion found in the electron ionization mass spectrum of amitriptyline (Fig. 1A).

Isobutane chemical ionization, however, permits the monitoring of an ion (*m/e* 278) expressing information concerning amitriptyline's molecular weight (Fig. 1B). Similarly, this ionization technique also makes nortriptyline suitable for mass spectral analysis without prior derivatization (Figs. 2A and 2B). The maximum sensitivity obtainable, however, for the assay using underivatized nortriptyline was quite variable. Although this is of little consequence when determining steady-state plasma nortriptyline levels, it is significant when measuring the low nortriptyline levels found after single-dose amitriptyline administration. For low level determinations of nortriptyline, the *N*-trifluoroacetyl derivative had suitable chromatographic and mass spectral (Fig. 2D) properties.

Clinical control plasma subjected to the described procedure for steady-state plasma amitriptyline and nortriptyline levels showed no significant background ions at *m/e* 264, 267, 278, 281, or 284. If this same plasma is subjected to the procedure adopted for a single dose of amitriptyline, a noninterfering *m/e* 278 peak corresponding to a compound with a retention time longer than that of amitriptyline is sometimes observed.

Results obtained from the addition of known amounts of amitriptyline and nortriptyline to clinical control plasma followed by processing according to the described procedure can be seen in Figs. 3 and 4. A least-

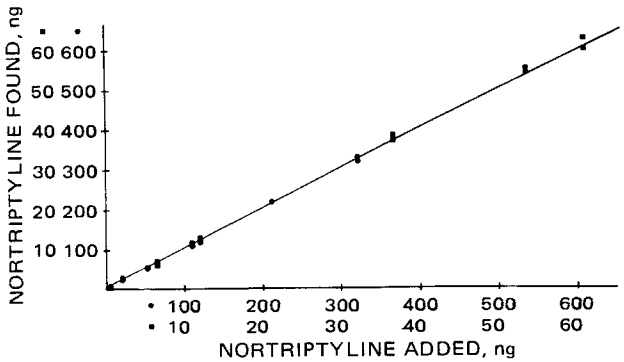

Figure 4—*Curve relating amount of nortriptyline added to clinical control plasma* versus *amount of nortriptyline found. Circles denote determinations using the procedure described under* Experimental *for steady-state plasma nortriptyline* (m/e *264*) *levels. For these samples, 108 ng/ml of nortriptyline-*d_3 (m/e *267*) *was used as an internal standard. Squares denote determinations using the procedure described under* Experimental *for single-dose plasma nortriptyline levels. For these samples, 4.61 ng/ml of nortriptyline-*d_3 *was used as an internal standard* [N-*trifluoroacetylnortriptyline-*d_3, m/e *363*].

squares analysis of the amitriptyline data (Fig. 3) gave a slope of 0.98 ± 0.01 and an intercept of 0.20 ± 0.23 ng. The corresponding curve (Fig. 4) for nortriptyline had a slope of 1.01 ± 0.01 and an intercept of 0.36 ± 0.20 ng. Thus, these data suggest that the extraction, mass spectrometry, and

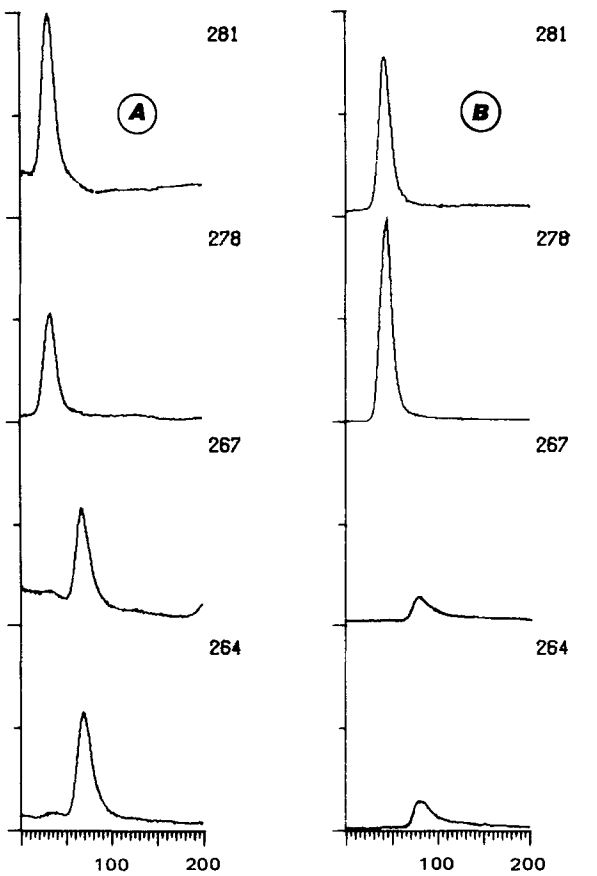

Figure 5—*Selective ion chromatograms for amitriptyline* (m/e *278*) *and nortriptyline* (m/e *264*). *Part A is for plasma obtained from Subject 1, 8 days after beginning oral 50-mg amitriptyline therapy three times a day. Internal standards amitriptyline-*d_3 (m/e *281*) *and nortriptyline-*d_3 (m/e *267*) *were present in concentrations of 122 and 104 ng/ml, respectively. The amitriptyline concentration was 64.2 ng/ml; the nortriptyline concentration was 100 ng/ml. Part B is the same as Part A except that the plasma is from Subject 3, 8 days after beginning amitriptyline therapy. The amitriptyline concentration was 124 ng/ml; the nortriptyline concentration was 87.1 ng/ml.*

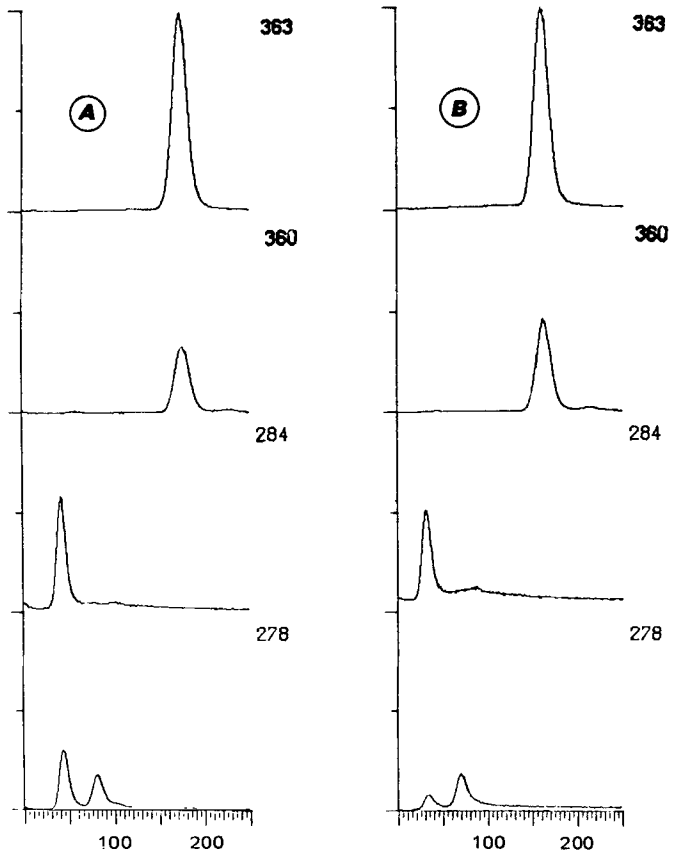

Figure 6—*Selective ion chromatograms for amitriptyline* (m/e *278*) *and* N-*trifluoroacetylnortriptyline* (m/e *360*). *Part A is for plasma obtained from Subject 6, 3 hr after oral administration of 50 mg of amitriptyline. Internal standards amitriptyline-*d_6 (m/e *284*) *and* N-*trifluoroacetylnortriptyline-*d_3 (m/e *360*) *were present in concentrations of 33.3 and 20.3 ng/ml, respectively. The amitriptyline concentration was 11.2 ng/ml; the nortriptyline concentration was 6.1 ng/ml. Part B is the same as Part A except 48 hr after amitriptyline administration. The amitriptyline concentration was 5.1 ng/ml; the nortriptyline concentration was 8.3 ng/ml.*

GLC characteristics of the labeled and unlabeled compounds are essentially identical.

Six samples containing 8.62 ng of amitriptyline plus 6.43 ng of nortriptyline were analyzed by the procedure for single-dose amitriptyline plasma levels using 7.52 ng/ml of amitriptyline-d_6 and 4.61 ng/ml of nortriptyline-d_3 as internal standards. The results ± *SD* for these samples were 8.03 ± 0.29 ng/ml for amitriptyline and 6.51 ± 0.23 ng/ml for nortriptyline. The recoveries ± *SD* for these samples, based on a comparison of the peak areas obtained by injecting known amounts of nortriptyline-d_3 and amitriptyline-d_6 into the GLC–mass spectrometer with those obtained from the internal standards carried through each assay, were 50 ± 26% for amitriptyline and 31 ± 10% for nortriptyline.

Six samples containing 53.9 ng of amitriptyline plus 53.6 ng of nortriptyline and six samples containing 539 ng of amitriptyline plus 536 ng of nortriptyline were analyzed by the procedure for steady-state levels, using 122 ng/ml of amitriptyline-d_3 and 104 ng/ml of nortriptyline-d_3 as internal standards. The results ± *SD* were 54.0 ± 0.5 ng/ml for amitriptyline and 52.8 ± 0.4 ng/ml for nortriptyline for the first set of samples and 547 ± 11 ng/ml for amitriptyline and 546 ± 10 ng/ml for nortriptyline for the second set. The recoveries ± *SD* for these 12 samples, based on a comparison of the peak areas obtained by injecting known amounts of amitriptyline-d_3 and nortriptyline-d_3 into the GLC–mass spectrometer with those obtained from the internal standards carried through each assay, were 80 ± 20% for amitriptyline and 65 ± 19% for nortriptyline.

The fairly wide range of recoveries observed for these 18 samples presumably is the result of considerable intersample variation in both extraction efficiencies and GLC column and glassware adsorption. These results further emphasize the importance of the stable isotope internal standards in ensuring accuracy.

Analyses for amitriptyline and nortriptyline in the plasma of three

Table I—Plasma Amitriptyline and Nortriptyline Levels (Nanograms per Milliliter) in Three Subjects Receiving Amitriptyline Therapy

Days after Beginning of Amitriptyline Therapy[a] (50 mg po Three Times a Day)	Subject 1		Subject 2		Subject 3	
	Amitriptyline	Nortriptyline	Amitriptyline	Nortriptyline	Amitriptyline	Nortriptyline
8	64.2 (63.0)[b]	100 (104)[b]	137	70.2	124	87.1
8.5	59.7 (56.1)	102 (99.4)	106	153	131	88.2
11	91.6 (86.2)	117 (116)	130	154	135	111
11.5	77.6 (74.3)	101 (102)	160	147	103	106
13	61.2 (59.8)	101 (102)	153	125	136	103
13.5	44.4 (40.4)	66.8 (67.3)	201	142	146	88.8
Average ± *SD*	66.5 ± 16.3 (63.3 ± 15.7)	98.1 ± 16.9 (98.3 ± 15.7)	148 ± 32	132 ± 32	129 ± 15	97.2 ± 12.7

[a] First blood sample on Days 8, 11, and 13 was taken immediately before the first dose of the day; the second blood sample was taken 1 hr after receiving the second dose. [b] Amitriptyline and nortriptyline levels obtained from a separate analysis of a 1-ml aliquot from the same plasma sample.

subjects receiving 50 mg of amitriptyline three times a day are presented in Table I. Excellent reproducibility of the duplicate analyses of the plasma samples from Subject 1 is seen, except for the amitriptyline levels calculated for the 13.5-day sample. The actual levels found are similar, if the difference in administered dose is considered, to those previously published (11, 17). Typical ion chromatograms from analyses of steady-state plasma samples can be seen in Fig. 5. In this figure, the substantial variation in nortriptyline and nortriptyline-d_3 recoveries from the two different samples (A and B) should be noted.

The results of single-dose administrations of 50 mg of amitriptyline can be seen in Table II. The maximum plasma amitriptyline levels ranged from 16 to 35 ng/ml in the three subjects. After 72 hr, the amitriptyline levels ranged from 2.3 to 4.4 ng/ml; nortriptyline levels ranged from 0.5 to 5.4 ng/ml. The drug half-lives for the three subjects, obtained using a least-squares analysis of the log amitriptyline concentration *versus* time data for the 8–72-hr plasma samples, were 35, 26, and 51 hr. These half-lives fall within the range (18–93 hr) previously found in 22 human subjects who had received a similar dose of nortriptyline (18). Typical ion chromatograms from an analysis of single-dose plasma samples can be seen in Fig. 6.

The sensitivity obtainable using this assay cannot be quoted in absolute terms but was found to be a function of both the condition of the ion source and quadrupole rod system and the amitriptyline and nortriptyline recoveries. With clean poles and ion source, an assay sensitivity of 1 ng/ml of amitriptyline and 0.5 ng/ml of nortriptyline is possible, provided the amitriptyline and nortriptyline recoveries for the particular samples are greater than 50%.

Table II—Plasma Amitriptyline and Nortriptyline Levels (Nanograms per Milliliter) in Three Subjects after Oral Administration of 50 mg of Amitriptyline

Hours after Administration	Subject 4		Subject 5		Subject 6	
	Amitriptyline	Nortriptyline	Amitriptyline	Nortriptyline	Amitriptyline	Nortriptyline
0	0	0	0	0	0	0
1	12.9	0.6	26.8	2.1	4.6	0
2	19.3	3.1	35.1	7.5	11.6	2.8
3	19.9	4.7	34.4	7.9	11.2	6.1
4	22.5	5.3	31.1	13.7	16.1	7.1
6	10.5	3.4	16.7	10.9	10.5	10.0
8	10.8	3.3	17.8	9.2	10.1	8.3
12	5.6	3.2	7.9	9.5	9.7	9.7
24	5.2	2.8	6.3	9.7	6.2	8.9
36	3.2	2.6	5.2	9.5	4.2	8.3
48	3.4	0.7	3.7	9.3	5.1	8.3
72	2.4	0.5	2.3	5.4	4.4	4.3

REFERENCES

(1) J. H. Biel and B. Bopp, in "Psychopharmacological Agents," M. Gordon, Ed., Academic, New York, N.Y., 1974, p. 283.

(2) H. B. Hucker, *Pharmacologist*, **4**, 171 (1962).

(3) E. Eschenhof and J. Rieder, *Arzneim.-Forsch.*, **19**, 957 (1969).

(4) M. H. Bickel and B. B. Brodie, *Int. J. Neuropharmacol.*, **3**, 611 (1964).

(5) M. Asberg, B. Cronholm, F. Sjoqvist, and D. Tuck, *Br. Med. J.*, **3**, 331 (1971).

(6) W. Hammer and F. Sjoqvist, *Life Sci.*, **6**, 1895 (1967).

(7) F. Sjoqvist, B. Alexanderson, M. Asberg, L. Bertilsson, O. Borga, B. Hamberger, and D. Tuck, *Acta Pharmacol. Toxicol., Suppl. 3*, **29**, 255 (1971).

(8) R. A. Braithwaite, R. Goulding, G. Theano, J. Bailey, and A. Coppen, *Lancet*, **1**, 1297 (1972).

(9) *Ibid.*, **1**, 556 (1973).

(10) H. B. Hucker and S. C. Stauffer, *J. Pharm. Sci.*, **63**, 296 (1974).

(11) R. A. Braithwaite and B. Widdop, *Clin. Chim. Acta*, **35**, 461 (1971).

(12) A. Jorgensen, *Acta Pharmacol. Toxicol.*, **36**, 79 (1975).

(13) O. Borga and M. Garle, *J. Chromatogr.*, **68**, 77 (1972).

(14) M. S. B. Munson, *Anal. Chem.*, **43**, 28A (1971).

(15) F. J. Marshall and R. E. McMahon, *J. Labelled Compd.*, **6**, 261 (1970).

(16) O. Borga, L. Palmer, A. Linnarsson, and B. Holmstedt, *Anal. Lett.*, **4**, 837 (1971).

(17) H. B. Hucker, S. C. Stauffer, F. G. Clayton, B. R. S. Nakra, and R. Gaind, *J. Clin. Pharmacol.*, **15**, 168 (1975).

(18) B. Alexanderson, *Eur. J. Clin. Pharmacol.*, **6**, 44 (1973).

ACKNOWLEDGMENTS AND ADDRESSES

Received November 17, 1975, from the *Department of Biochemistry and Drug Metabolism, Hoffmann-La Roche Inc., Nutley, NJ 07110.*

Accepted for publication March 10, 1976.

Vehicle Effects on Activity of an Anticonvulsant Compound

DILIP R. SANVORDEKER ˣ and JAMES BLOSS

Abstract □ The effect of several lipid and nonlipid pharmaceutical solvents on the *in vivo* activity of 1-diphenylmethyl-4-[(6-methyl-2-pyridyl)methyleneamino]piperazine (I) was evaluated in the mouse. The intensity of onset and the duration of anticonvulsant activity of the compound were affected depending on the type and form of liquid dosage preparation used. The rate of decline in anticonvulsant activity in the 80–20% response range followed apparent zero-order kinetics. A linear relationship between the observed ED_{50} and the concentration of sorbitol in the dosage form of I was observed. A reduction in the sorbitol content of the dosage form resulted in a proportional increase in the rapidity of onset and the duration of anticonvulsant activity of I. Emulsification restored both the onset and duration of pharmacological activity, which was virtually arrested when the compound was given orally as a solution in oil.

Keyphrases □ Piperazine, substituted—anticonvulsant activity after oral administration, effect of various solvents and dosage forms, mice □ Solvents, various—effect on anticonvulsant activity of a substituted piperazine after oral administration, mice □ Dosage forms, various—effect on anticonvulsant activity of a substituted piperazine after oral administration, mice □ Anticonvulsant activity—1-diphenylmethyl-4-[(6-methyl-2-pyridyl)methyleneamino]piperazine, effect of various solvents and dosage forms, oral administration, mice

To evaluate the pharmacological activity of a new compound, it is commonly dissolved in a suitable vehicle prior to administration to an animal. This approach is particularly useful for poorly water-soluble drugs, since the rate-limiting drug dissolution process is bypassed and penetration of the drug in solution across biological membranes is facilitated. Drugs with aqueous solubility at and below 0.15 mg/ml can pose potential absorption problems (1). To overcome such difficulties, the pharmaceutical scientist often uses water-miscible nonaqueous solvents that can be suitably blended with water and provide the desired solvency for the drug (2).

1-Diphenylmethyl -4- [(6-methyl -2- pyridyl)methyleneamino]piperazine[1] (I) is a potent anticonvulsant compound in animals (3). The saturation solubility of this compound at 37° is estimated to be less than 0.1 mg/ml. This study was designed to evaluate the effect of several lipid and nonlipid pharmaceutical solvents on the *in vivo* activity of I administered *via* the oral route.

EXPERIMENTAL

Materials—Corn oil[2], dimethylacetamide[3], 2,2-dimethyl-1,3-dioxolane-4-methanol[3], polyethylene glycol 400[3], poloxamer 237[4], sorbitol (70% solution[5]), polysorbate 80[3], propylene glycol[3], and normal saline[6] were used as supplied. Compound I[7] was supplied as the pure compound. The crystals of the compound were ground in a mortar and pestle to a fine powder prior to its use.

Preparation of Suspensions of I—Except for drug suspensions in sorbitol solution, an accurately weighed quantity of I was transferred to a 25-ml test tube. Normal saline[6], with and without 1.5 ml of a propylene glycol–polysorbate 80 (50:50 v/v) mixture as a wetting agent, was added to make suspensions of the compound in the 0.2–0.8-mg/ml range. The suspensions were thoroughly mixed with the aid of a portable homogenizer[8] for 5 min. Suspensions of I at the 0.8-mg/ml concentration in sorbitol solutions (7–70%) were prepared by adding a weighed amount of I to 200 ml of the vehicle followed by mixing and homogenizing[9] the suspensions. Prior to oral administration of the dose, all suspensions were shaken vigorously.

Preparation of Solutions of I—Compound I, 100 mg, was dissolved in a nonaqueous solvent. The final volume of this solution was made with distilled water to obtain 1 mg/ml of I in a cosolvent vehicle of a defined solvent composition. These stock solutions and blank vehicles of the same composition were used to prepare diluted solutions of I at 0.1–0.8-mg/ml concentrations.

Stock solutions of I in corn oil and in soya bean oil[2] were prepared by dissolving 100 mg of I in 100 ml of the oil. This solution was then used to prepare additional solutions at lower concentrations. All solutions were prepared fresh each day prior to testing pharmacological activity.

Preparation of Oil-in-Water Emulsions of I—Accurately weighed amounts of 50–500 mg of I were transferred to 100-ml volumetric flasks. The oil was added to make up the volume, and the flasks were placed on a steam bath for approximately 5 min. After cooling, 40 ml of the oil solution of I was transferred to a 250-ml glass container; the volume was increased to 200 ml with a 0.8% solution of a nonionic surfactant[4] in distilled water. The oil and water layers were then mixed and homogenized for 0.5 hr with a lab size homogenizer[9]. Emulsions without the compound were also prepared by this procedure.

For ED_{50} determinations, the emulsions were prepared 1 day prior to the experiment and stored in a refrigerator. All other studies were performed with emulsions prepared on the same day.

***In Vivo* Studies**—Male HAM/ICR mice[10], 20–30 g, were housed in 20.3 × 35.6-cm (8 × 14-in.) stainless steel cages (12 animals/cage) and maintained on a standard pellet diet and tap water prior to each experiment. All formulations of I were given at 0.1 ml/10 g of body weight by the intragastric (oral) route of administration. The electrical current for induction of seizures was generated by a commercially available apparatus[11].

Determination of ED_{50}—Liquid dosage forms of I and their blanks (without the compound) were tested for anticonvulsant activity according to the method of Swinyard *et al.* (4). Thirty minutes after administration of a dose to a group of 20 mice, each animal was challenged with a current of 50 mamp delivered *via* corneal electrodes. Except for 2,2-dimethyl-1,3-dioxolane-4-methanol solutions, this current was sufficient to induce hindlimb tonic extensor seizure in 100% of the control mice. All data were recorded as the number of mice protected per group of 20 animals dosed with a given dosage form. The ED_{50} values were calculated by the method of Litchfield and Wilcoxon (5).

Determination of Duration of Response to I—The method was essentially the same as described previously. Groups of 20 animals were dosed with 8.0 mg/kg of I in the dosage form. The animals were then challenged with electric shock every 0.5 hr up to 5 hr and then every hour up to 8 hr after dosing. The data were recorded as the ratio of animals protected to animals dosed.

RESULTS AND DISCUSSION

Figure 1 illustrates a log dose–response relationship for I administered intragastrically to mice in three different vehicles. The response to this compound followed a previously established semilogarithmic relationship

[1] SC-13504.
[2] Columbus Food Products, Chicago, Ill.
[3] Matheson, Coleman & Bell, Norwood, Ohio.
[4] Pluronic F-87, Wyandotte Chemical Co., Wyandotte, Mich.
[5] Searle & Co., San Juan, Puerto Rico; Emulsion Engineering Inc., Chicago, Ill.
[6] Baxter Laboratories, Morton Grove, Ill.
[7] Lots II-128B and G-136-3, Searle Laboratories, Chemical Development Group, Chicago, Ill.
[8] Model S63C, Tri-R Instruments, New York, N.Y.
[9] Model PCU-2, Polytron, Kinematika GmbH, Luzern, Switzerland.
[10] Charles River Mouse Farms & Co., Wilmington, Mass.
[11] Model 2-C, Hans Technical Associates, Palo Alto, Calif.

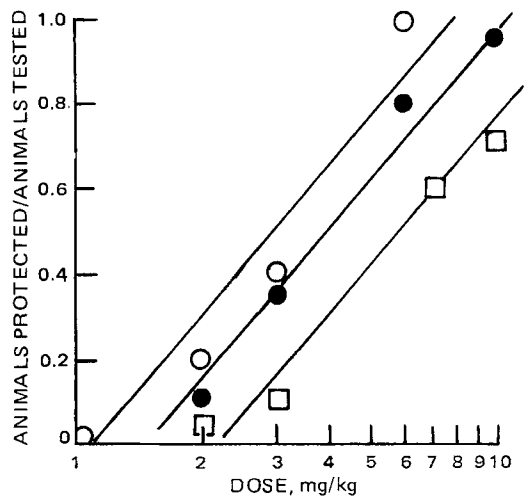

Figure 1—*Linear relationship between log dose and response to I in mice. Key: ○, suspension in saline; ●, solution in polyethylene glycol 400; and □, solution in dimethylacetamide–water (50:50 v/v).*

(6) describable by the following equation:

$$R = m \log D + e \qquad \text{(Eq. 1)}$$

where R is the intensity of the pharmacological response, D is the administered dose, m is the slope of the line illustrating the linear relationship, and e is the intercept on the x (dose) axis. From this plot, it is evident that administration of a solution of I in a water-miscible cosolvent such as dimethylacetamide results in a parallel shift of pharmacological response from lower doses to relatively higher doses.

A least-squares linear regression analysis of the log dose–response data in the 80–20% response range yielded 0.933–1.23 values for the slope. These values provide a good estimate for the free drug occupancy of the receptor sites in the biophase (7). This theoretical consideration implied that practically all of the free concentration of I available in the biophase occupied the receptor sites to provide the desired anticonvulsant response in mice. This observation agrees with the potency of this compound compared to that of its analogs at relatively low doses (1).

Table I lists the effect of several vehicles on the ED_{50} values of I estimated 0.5 hr after intragastric administration of the dosage form. Within 95% confidence limits, no difference was observed for the ED_{50} values estimated after administration of I as a suspension in normal saline and as a solution in polyethylene glycol 400. The apparent twofold increase in ED_{50} values observed for the dimethylacetamide solution is intriguing. Among the possibilities are interference with the bioavailability of I and competition at the receptor site, thus reducing the apparent efficacy by a twofold margin. The log dose–response plot demonstrates that, in the 6–10-mg/kg range, a maximal response was observed at 30 min after oral administration of the drug. With this information, subsequent studies on the duration of drug activity were conducted at the 8-mg/kg dose level to assess the effect of vehicles on this parameter.

Table I—Effect of Vehicles on the ED_{50} of I Estimated 30 min after Intragastric Dosing of Mice

Dosage Form	Vehicle Composition	ED_{50}, mg/kg (95% Confidence Limits)
Suspension	Normal saline	3.0 (2.7–3.7)
Solution	Polyethylene glycol 400–water (60:40 v/v)	3.7 (2.9–4.8)
Solution	Dimethylacetamide–water (50:50 v/v)	6.2 (4.7–8.2)
Solution	2,2-Dimethyl-1,3-dioxolane-4-methanol–water (50:50 v/v)	No effect; vehicle posesses convulsion-blocking activity
Solution	Corn oil	No effect
Emulsion	20% (v/v) corn oil in water emulsified with 0.8% surfactant solution	8.3 (7.9–9.4)

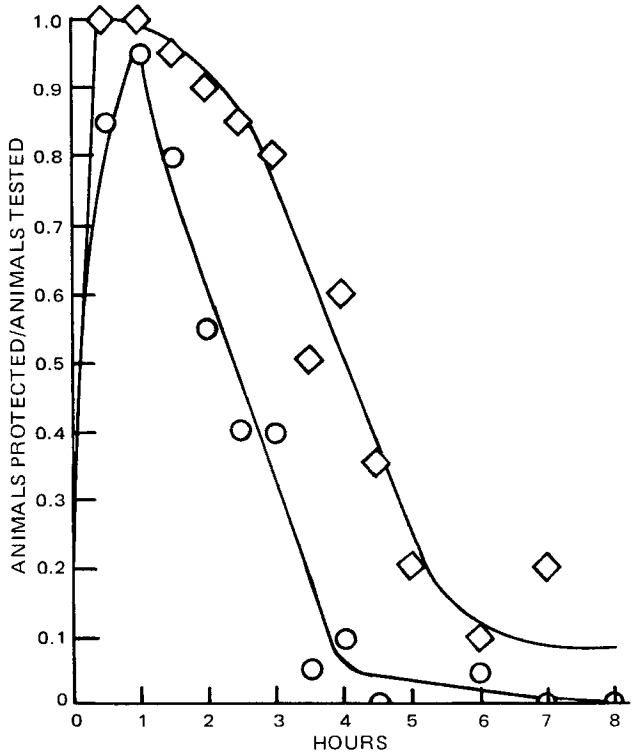

Figure 2—*Time course of pharmacological activity of I after oral administration of a suspension of I without (◇) and with (○) 0.8% surfactant solution in saline.*

Figure 2 illustrates a plot of the intensity, R, of the pharmacological activity of I monitored as a function of time following intragastric administration of an 8-mg/kg dose to mice. The decline in intensity of the anticonvulsant activity in the 80–20% range followed an apparent zero-order process. Since response to a drug is a function of the free drug concentration at the receptor site(s), this observation agrees with previously reported relationships (8–11). It is evident that inclusion of a surfactant (emulsifier) at the 0.8% concentration in the dosage form affects the duration of the anticonvulsant activity of I. However, the rate of decline in intensity of this response remains unaffected as evidenced from the slope of the plot.

The overall inference obtained from these observations is that the availability of the free concentration of I at the anticonvulsant receptor sites may be at a reduced level following its oral administration in the presence of a surfactant. Several investigators have shown that surfactants can affect the rate and extent of drug absorption across the GI tract (12–15). The surfactant solution used in the present study may have modified the extent of absorption of I; consequently, a reduction in the duration of its pharmacological activity can be expected.

Previous investigations (16) showed that absorption of drugs from oily solutions was significantly inhibited. The same authors (16) noted that with an oil-in-water emulsion system where a drug is in solution in the oil phase, the overall absorption rate is significantly large despite a high water-to-oil partitioning property of a drug. In recent years, it has been shown that administration of poorly water-soluble drugs as oil-in-water emulsion dosage forms allows extensive drug absorption as compared with other conventional dosage forms (17–20).

To assess this possibility, the relative pharmacological activity of I was evaluated after oral dosing of an oil-in-water emulsion and an oil solution. As illustrated in Fig. 3, the onset and duration of pharmacological activity of I achieved from an emulsion dosage form were comparable to that of the suspension without the surfactant (Fig. 2). Administration of the compound in a corn oil solution resulted in virtually total arrest of anticonvulsant activity in the mouse. Since the drug has been shown to be very lipophilic[12], it is likely that its transfer rate from large oil globules to intestinal fluid can be insignificant. Consequently, the rate and extent

[12] Lipophilicity of this compound was approximated on the basis of its high partition coefficient (P.C. heptane/pH 7.0 = 34.2). Partitioning data were generated by the Analytical Research Department.

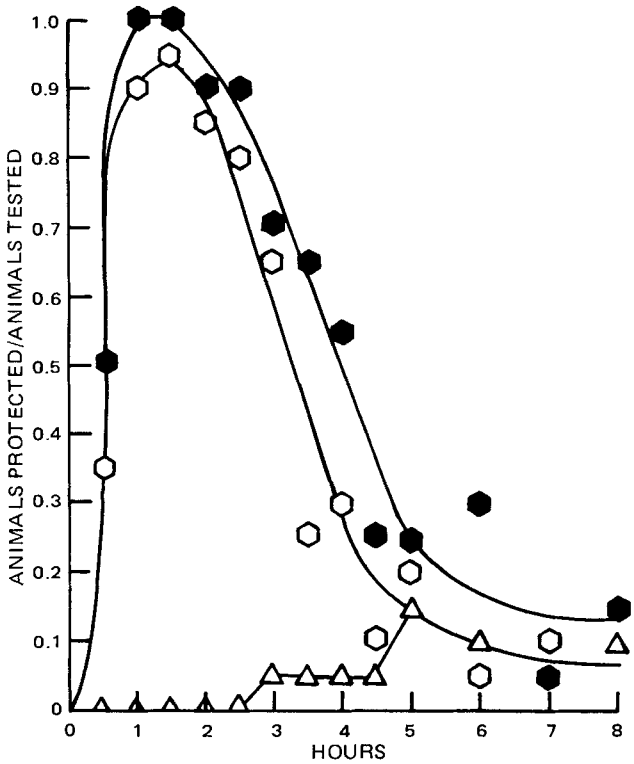

Figure 3—*Time course of pharmacological activity after oral administration of I as an emulsion with corn oil (●), an emulsion with soya bean oil (○), and a solution in corn oil (△).*

of absorption of I can be hindered by this rate-limiting factor. Hence, little or no anticonvulsant effect was observed.

Emulsification of oil in water results in an abundant increase in the surface area of oil, allowing a facile interfacial transport of the anticonvulsant compound from oil to the water phase of the luminal fluid. Under pseudo-sink conditions, rapid absorption of the compound across the intestinal membrane allowed a sufficient concentration to reach the receptor sites, and an optimal duration of anticonvulsant activity was observed.

The foregoing discussion is compatible with the theoretical (16, 21) and observed (17–20, 22) findings on drug delivery from emulsion dosage forms. The medium ED_{50} for a corn oil emulsion was estimated to be 8.3 mg/kg (Table I). It is evident from Fig. 3 that, at 30 min (the time for ED_{50} determination) after oral dosing of the emulsion dosage form, the intensity of the pharmacological response of I was only 50% as compared to the 100% intensity achieved with the drug suspension in normal saline. Thus, to achieve 100% activity at 30 min after dosing, a 16-mg/kg dose of I in the emulsion dosage form is needed. This dose was about 2.6 times higher than that of the suspension dosage form of I. The observed twofold difference between the ED_{50} values for the suspension and the emulsion dosage forms of I may be attributed to the rate-limiting transport of the compound from the oil phase to the aqueous (luminal fluid) phase from which its absorption across the GI tract occurs.

Figure 4 illustrates the effect of sorbitol content (percent w/v) on the apparent ED_{50} of I in mice. A multivariate regression analysis of these data showed that there was an apparent linear relationship (correlation coefficient $r = 0.96$ and residual variance $s^2 = 3.42$) between the observed ED_{50} and the sorbitol content of the dosage form. To test whether or not inclusion of sorbitol in the dosage form modifies the rapidity of onset as well as the duration of anticonvulsant activity of I in mice, experiments were conducted with a suspension dosage form of the compound with varying concentrations of sorbitol (Fig. 5).

The presence of 70% of sorbitol reduced the apparent pharmacological response by as much as 80%. As the concentration of sorbitol in the suspension dosage form was reduced, there was a proportional increase in the rapidity of onset and the duration of pharmacological activity. These results suggest that sorbitol modifies the availability of I for absorption. Animals dosed with distilled water and 70% sorbitol solution and then challenged 0.5 hr later with varying current levels showed no difference in seizure susceptibility. Thus, the possibility of sorbitol interference at the drug receptor sites was ruled out.

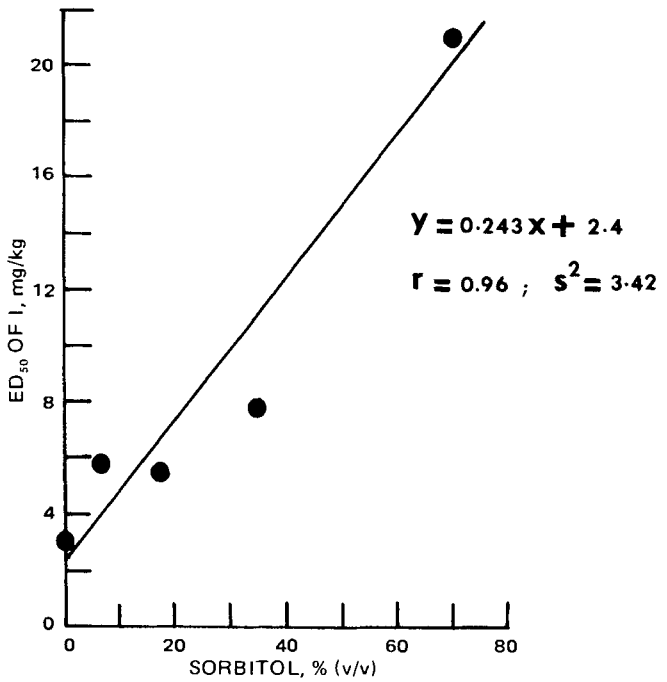

Figure 4—*Effect of sorbitol on the apparent ED_{50} of I in mice.*

Vogel *et al.* (23) reported on the effect of the osmolarity of the instillation fluid on the efficacy and toxicity of drugs given by the intraduodenal route. Administration of drug solutions made hypertonic with mannitol (10–15%) diminished both the efficacy and toxicity of atropine sulfate, pentobarbital sodium, and nicotine. It was concluded that transmucosal movement of fluid from the blood into the intestinal lumen interfered with drug absorption. This finding might explain our observations on the modification of anticonvulsant activity of I in mice in the presence of sorbitol.

Table II illustrates some pharmacokinetic parameters for the anticonvulsant activity of I measured after oral administration of several liquid dosage forms. The time required for peak response of I (T_{max}) showed a range of 0.5–1.5 hr. Emulsification of the drug solution in oil resulted in an increase in this parameter. Whereas the time required for 50% reduction in animal protection ($T_{0.5}$) ranged from 2.45 to 4.0 hr, the presence of a surfactant (emulsifier) at the 0.8% concentration resulted in an appreciable (1.6-fold) decrease in this parameter.

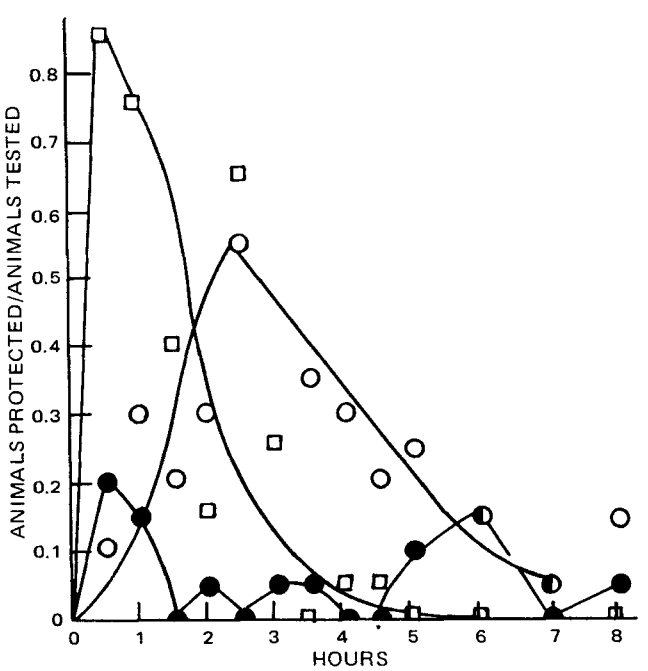

Figure 5—*Time course of pharmacological activity after oral administration of I with 7% (□), 35% (○), and 70% (●) sorbitol in water.*

Table II—Vehicle Effects on the Duration of Anticonvulsant Activity of I

Dosage Form	T_{max}, hr	$T_{0.5}$, hr	$\beta_{apparent}$, $(0.8-0.2)R$
Suspension in normal saline	0.5	4.0	0.265
Suspension in normal saline with 0.8% surfactant	1.0	2.45	0.27
Corn oil emulsion	1.0	3.8	0.26
Soya bean oil emulsion	1.5	3.25	0.24
Corn oil solution	0.5	Not observed	—
Polyethylene glycol (60% v/v) solution	0.5	2.8	0.12
Suspension in 70% sorbitol solution	0.5	Not observed	—

The negative slope, β, of the line (least-squares) drawn between the 80 and 20% response range of the time–response curve was virtually the same except for the polyethylene glycol 400 solutions. The observed constancy of the β-values supports the concept that the rate of decline of the pharmacological effect of a compound is independent of its total amount in the body. The apparent deviation of the β-value estimated for the polyethylene glycol 400 solution is intriguing and may be an artifact of the statistical analysis of the observed data. Binding of I to the polymer (polyethylene glycol 400) may have resulted in erratic absorption of this compound. This could contribute to fluctuations in drug availability at the receptor sites and, consequently, to a decrease in the β-value.

In conclusion, this study has shown that oral administration of I in different liquid dosage forms modified its anticonvulsant activity in mice. The intensity of onset and the duration of the pharmacological activity were affected depending on the liquid vehicle used.

REFERENCES

(1) D. J. Jallow and B. B. Brodie, *Pharmacology*, **8**, 21 (1972).

(2) A. J. Spiegel and M. M. Noseworthy, *J. Pharm. Sci.*, **52**, 917 (1963).

(3) C. R. Craig, *Arch. Int. Pharmacodyn. Ther.*, **165**, 328 (1967).

(4) E. A. Swinyard, W. C. Brown, and L. S. Goodman, *J. Pharmacol. Exp. Ther.*, **106**, 319 (1952).

(5) V. T. Litchfield, Jr., and F. Wilcoxon, *ibid.*, **96**, 99 (1949).

(6) L. K. Randolph and J. L. Cimmenera, in "Remington's Practice of Pharmacy," 12th ed., Mack Publishing Co., Easton, Pa., 1961, chap. 9.

(7) "Principles of Drug Action: The Basis of Pharmacology," 2nd ed., A. Goldstein, L. Aronow, and S. M. Kalman, Eds., Wiley, New York, N.Y., 1974, pp. 89–104.

(8) G. Levy, *J. Pharm. Sci.*, **53**, 342 (1964).

(9) G. Levy, *Br. J. Anaesth.*, **36**, 694 (1964).

(10) G. Levy, *Clin. Pharmacol. Ther.*, **7**, 362 (1966).

(11) G. Levy, *J. Pharm. Sci.*, **56**, 1687 (1967).

(12) S. Riegelman and W. J. Crowell, *J. Am. Pharm. Assoc., Sci. Ed.*, **47**, 115 (1958); *ibid.*, **47**, 125 (1958); *ibid.*, **47**, 127 (1958).

(13) S. S. Schneierson and D. Amsterdam, *Nature*, **182**, 56 (1958).

(14) G. Levy and R. H. Reuning, *J. Pharm. Sci.*, **53**, 1471 (1964).

(15) M. Gibaldi and S. Feldman, *ibid.*, **59**, 579 (1970).

(16) K. Kakemi, H. Sezaki, S. Muranishi, H. Ogata, and K. Giga, *Chem. Pharm. Bull.*, **20**, 715 (1972).

(17) J. G. Wagner, E. S. Gerard, and D. G. Kaiser, *Clin. Pharmacol. Ther.*, **7**, 610 (1966).

(18) R. H. Engel, S. J. Rigg, and M. J. Fahrenbach, *Nature*, **291**, 856 (1968).

(19) K. Kakemi, H. Sezaki, S. Muranishi, H. Ogata, and S. Isemura, *Chem. Pharm. Bull.*, **20**, 703 (1972).

(20) T. R. Bates and J. A. Sequeira, *J. Pharm. Sci.*, **64**, 793 (1975).

(21) S. A. Howard, M. A. Farvar, A. Suzuki, and W. I. Higuchi, *ibid.*, **58**, 1325 (1969); *ibid.*, **58**, 1330 (1969).

(22) A. Bikhazi and W. I. Higuchi, *Biochim. Biophys. Acta*, **233**, 676 (1971).

(23) G. Vogel, U. Becker, and M. Ulbritch, *Arzneim.-Forsch.*, **25**, 1037 (1975).

ACKNOWLEDGMENTS AND ADDRESSES

Received January 14, 1976, from the *Biopharmaceutics Group of the Product Development Department and the Division of CNS Pharmacology, Searle Laboratories, Chicago, IL 60680.*

Accepted for publication March 10, 1976.

The authors express their appreciation to Mrs. Melody Ferguson for technical assistance. Encouragement from Dr. H. Lambert and Dr. G. Clay was indispensable.

[x] To whom inquiries should be directed.

Use of Anemic Piglet to Assess Bioavailability of Iron from Oral Iron Preparations

A. P. INTOCCIA [x], S. S. WALKENSTEIN, R. W. WITTENDORF, R. C. HOPPE, and S. M. FREE

Abstract □ Except for methods using long-lived iron isotopes, there are no reliable means for assessing the bioavailability of iron from oral preparations in human subjects. Use of the anemic piglet as an alternative means was studied. When piglets were made anemic on a commercial milk diet and then dosed with solutions of 1, 2, and 5 mg/kg of ferrous sulfate/day, a dose-related recovery of hematocrit and hemoglobin levels resulted. The most sensitive dose range for use in a bioavailability study of iron was between 1 and 2 mg of iron/kg/day when using these parameters. A study carried out using this method indicated that the iron from a delayed-release capsule and from a ferrous sulfate solution was equally bioavailable. Hemoglobin and hematocrit recovery rates of the anemic piglet were shown to be reliable and sensitive indicators of the bioavailability of iron from various iron dosage forms.

Keyphrases □ Iron—bioavailability, ferrous sulfate delayed-release capsule compared to solution, piglets □ Ferrous sulfate—bioavailability, delayed-release capsule compared to solution, piglets □ Bioavailability—ferrous sulfate delayed-release capsule compared to solution, piglets □ Hematinics—ferrous sulfate, bioavailability, delayed-release capsule compared to solution, piglets

Absorption of iron from the GI tract is regulated by multiple factors, including the amount of iron stored in the body, the degree of hematopoietic activity present, and the amount of iron ingested. For example, an increase in iron absorption takes place if iron is fed orally (1). A study designed to measure the bioavailability of iron from different pharmaceutical iron preparations in human subjects would present many problems, since all of these regulatory factors

Table II—Vehicle Effects on the Duration of Anticonvulsant Activity of I

Dosage Form	T_{max}, hr	$T_{0.5}$, hr	$\beta_{apparent}$, $(0.8-0.2)R$
Suspension in normal saline	0.5	4.0	0.265
Suspension in normal saline with 0.8% surfactant	1.0	2.45	0.27
Corn oil emulsion	1.0	3.8	0.26
Soya bean oil emulsion	1.5	3.25	0.24
Corn oil solution	0.5	Not observed	—
Polyethylene glycol (60% v/v) solution	0.5	2.8	0.12
Suspension in 70% sorbitol solution	0.5	Not observed	—

The negative slope, β, of the line (least-squares) drawn between the 80 and 20% response range of the time–response curve was virtually the same except for the polyethylene glycol 400 solutions. The observed constancy of the β-values supports the concept that the rate of decline of the pharmacological effect of a compound is independent of its total amount in the body. The apparent deviation of the β-value estimated for the polyethylene glycol 400 solution is intriguing and may be an artifact of the statistical analysis of the observed data. Binding of I to the polymer (polyethylene glycol 400) may have resulted in erratic absorption of this compound. This could contribute to fluctuations in drug availability at the receptor sites and, consequently, to a decrease in the β-value.

In conclusion, this study has shown that oral administration of I in different liquid dosage forms modified its anticonvulsant activity in mice. The intensity of onset and the duration of the pharmacological activity were affected depending on the liquid vehicle used.

REFERENCES

(1) D. J. Jallow and B. B. Brodie, *Pharmacology*, **8**, 21 (1972).

(2) A. J. Spiegel and M. M. Noseworthy, *J. Pharm. Sci.*, **52**, 917 (1963).

(3) C. R. Craig, *Arch. Int. Pharmacodyn. Ther.*, **165**, 328 (1967).

(4) E. A. Swinyard, W. C. Brown, and L. S. Goodman, *J. Pharmacol. Exp. Ther.*, **106**, 319 (1952).

(5) V. T. Litchfield, Jr., and F. Wilcoxon, *ibid.*, **96**, 99 (1949).

(6) L. K. Randolph and J. L. Cimmenera, in "Remington's Practice of Pharmacy," 12th ed., Mack Publishing Co., Easton, Pa., 1961, chap. 9.

(7) "Principles of Drug Action: The Basis of Pharmacology," 2nd ed., A. Goldstein, L. Aronow, and S. M. Kalman, Eds., Wiley, New York, N.Y., 1974, pp. 89–104.

(8) G. Levy, *J. Pharm. Sci.*, **53**, 342 (1964).

(9) G. Levy, *Br. J. Anaesth.*, **36**, 694 (1964).

(10) G. Levy, *Clin. Pharmacol. Ther.*, **7**, 362 (1966).

(11) G. Levy, *J. Pharm. Sci.*, **56**, 1687 (1967).

(12) S. Riegelman and W. J. Crowell, *J. Am. Pharm. Assoc., Sci. Ed.*, **47**, 115 (1958); *ibid.*, **47**, 125 (1958); *ibid.*, **47**, 127 (1958).

(13) S. S. Schneierson and D. Amsterdam, *Nature*, **182**, 56 (1958).

(14) G. Levy and R. H. Reuning, *J. Pharm. Sci.*, **53**, 1471 (1964).

(15) M. Gibaldi and S. Feldman, *ibid.*, **59**, 579 (1970).

(16) K. Kakemi, H. Sezaki, S. Muranishi, H. Ogata, and K. Giga, *Chem. Pharm. Bull.*, **20**, 715 (1972).

(17) J. G. Wagner, E. S. Gerard, and D. G. Kaiser, *Clin. Pharmacol. Ther.*, **7**, 610 (1966).

(18) R. H. Engel, S. J. Rigg, and M. J. Fahrenbach, *Nature*, **291**, 856 (1968).

(19) K. Kakemi, H. Sezaki, S. Muranishi, H. Ogata, and S. Isemura, *Chem. Pharm. Bull.*, **20**, 703 (1972).

(20) T. R. Bates and J. A. Sequeira, *J. Pharm. Sci.*, **64**, 793 (1975).

(21) S. A. Howard, M. A. Farvar, A. Suzuki, and W. I. Higuchi, *ibid.*, **58**, 1325 (1969); *ibid.*, **58**, 1330 (1969).

(22) A. Bikhazi and W. I. Higuchi, *Biochim. Biophys. Acta*, **233**, 676 (1971).

(23) G. Vogel, U. Becker, and M. Ulbritch, *Arzneim.-Forsch.*, **25**, 1037 (1975).

ACKNOWLEDGMENTS AND ADDRESSES

Received January 14, 1976, from the *Biopharmaceutics Group of the Product Development Department and the Division of CNS Pharmacology, Searle Laboratories, Chicago, IL 60680.*

Accepted for publication March 10, 1976.

The authors express their appreciation to Mrs. Melody Ferguson for technical assistance. Encouragement from Dr. H. Lambert and Dr. G. Clay was indispensable.

[x] To whom inquiries should be directed.

Use of Anemic Piglet to Assess Bioavailability of Iron from Oral Iron Preparations

A. P. INTOCCIA [x], S. S. WALKENSTEIN, R. W. WITTENDORF, R. C. HOPPE, and S. M. FREE

Abstract □ Except for methods using long-lived iron isotopes, there are no reliable means for assessing the bioavailability of iron from oral preparations in human subjects. Use of the anemic piglet as an alternative means was studied. When piglets were made anemic on a commercial milk diet and then dosed with solutions of 1, 2, and 5 mg/kg of ferrous sulfate/day, a dose-related recovery of hematocrit and hemoglobin levels resulted. The most sensitive dose range for use in a bioavailability study of iron was between 1 and 2 mg of iron/kg/day when using these parameters. A study carried out using this method indicated that the iron from a delayed-release capsule and from a ferrous sulfate solution was equally bioavailable. Hemoglobin and hematocrit recovery rates of the anemic piglet were shown to be reliable and sensitive indicators of the bioavailability of iron from various iron dosage forms.

Keyphrases □ Iron—bioavailability, ferrous sulfate delayed-release capsule compared to solution, piglets □ Ferrous sulfate—bioavailability, delayed-release capsule compared to solution, piglets □ Bioavailability—ferrous sulfate delayed-release capsule compared to solution, piglets □ Hematinics—ferrous sulfate, bioavailability, delayed-release capsule compared to solution, piglets

Absorption of iron from the GI tract is regulated by multiple factors, including the amount of iron stored in the body, the degree of hematopoietic activity present, and the amount of iron ingested. For example, an increase in iron absorption takes place if iron is fed orally (1). A study designed to measure the bioavailability of iron from different pharmaceutical iron preparations in human subjects would present many problems, since all of these regulatory factors

would have to be controlled to the same extent in all subjects. With a double isotope technique, these problems were circumvented by using each subject as his own control (2, 3). With this technique, differences in iron absorption of various iron salts could be measured. The disadvantages of this method were that radioisotopes had to be used in human subjects and one of the isotopes, iron-55, has a half-life of 2.7 years.

Hemoglobin and/or red cell regeneration studies can be used as an indirect measure of iron bioavailability, but both require the rigid control of iron intake as well as the use of individuals depleted of body iron stores. These conditions are difficult to control in human subjects but can be readily achieved in animals. Several studies (4–6) indicated that suckling pigs rapidly become anemic if they are kept from ingesting soil and maintained solely on a milk diet. Furthermore, this anemia can be satisfactorily controlled by iron supplementation. Kolb (7), in a review of iron metabolism of various domesticated animals, showed that serum iron, iron binding capacity, and serum iron response to iron dosing in the pig is comparable to these parameters in humans. The data in this paper indicate that the anemic pig provides a reasonably alternative means of assessing iron bioavailability that is both reliable and sensitive.

EXPERIMENTAL

Littermate piglets, both male and female, from a crossbred dam (Chester White, Hampshire, Duroc) and a purebred Chester sire[1] were used. Animals were individually housed in galvanized steel monkey cages equipped with nursing bottle holders and rubber mesh floor padding. Room temperature was maintained between 27 and 30°.

A commercial modified milk product[2] at room temperature was placed in disposable-bag, plastic nursing bottles[3]. Piglets were encouraged to suckle by patient hand feeding during the first few days. During this time, the deciduous "needle" teeth were clipped from all animals. In the initial days of the study, it was sometimes necessary to feed this formula to reluctant feeders by stomach tube. The formula was eventually available to the piglets on an *ad libitum* basis.

Blood samples were taken from superficial abdominal skin veins (superficial epigastric) and occasionally, as animals grew older, from ear veins. Enough blood was taken to fill a No. 23, 25-mm disposable needle.

Hematocrit was determined in duplicate using a microhematocrit system[4]. Tubes were spun 4 min and read immediately.

Hemoglobin was measured using a disposable pipet kit[5]. After color development, samples were read on a spectrophotometer at 540 nm, and unknown samples were compared to a standard curve made from a certified cyanomethemoglobin standard[6].

The ferrous sulfate used was the reagent grade heptahydrate[7]. Solutions were made up fresh daily in distilled water. The delayed-release iron formulation used was a commercially available product[8]. The method used was as follows. Piglets, 5 days old, without prior iron supplementation, were fed a commercial modified milk product. When at least two piglets reached the desired level of anemia (approximately 6.5 g/100 ml of hemoglobin and 21% hematocrit) and remained at this level for 2 consecutive days, the animals were placed into the ferrous sulfate or the delayed-release capsule group. If three piglets became simultaneously available, the third animal was placed into a control (no iron) group. Where possible, paired animals of the same sex were used. The selection continued until all animals had been assigned to groups.

[1] H. Schick and Son, Kutztown, Pa.
[2] Similac infant formula, ready to feed, Ross Laboratories, Columbus, OH 43216.
[3] Playtex Ltd., Malton, Ontario, Canada.
[4] Drummond Scientific Co., Broomall, Pa.
[5] Unopette kit No. 5858, Becton Dickinson and Co., Rutherford, N.J.
[6] Hycel, Inc., Houston, Tex.
[7] Merck and Co., Rahway, N.J.
[8] Feosol Spansule Capsules, Smith Kline and French Laboratories, Philadelphia, PA 19101.

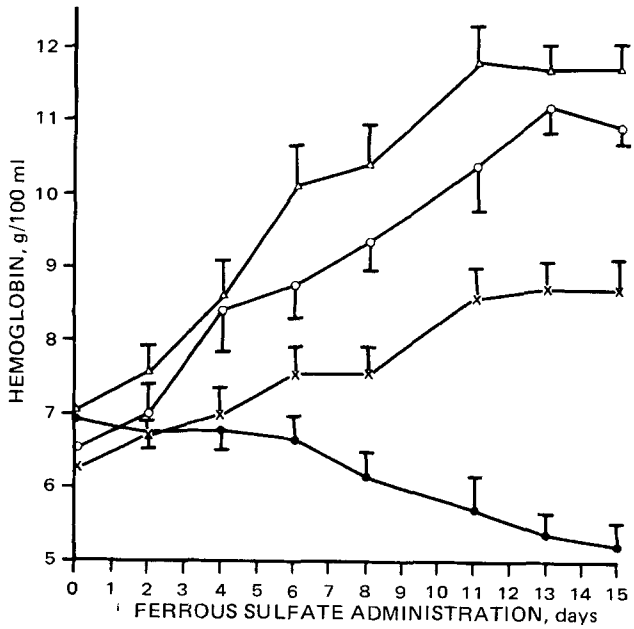

Figure 1—*Mean hemoglobin levels of anemic piglets following oral administration of various doses of iron administered as a ferrous sulfate solution. Each point represents the mean of six piglets* ± SEM. *Key:* △, *5 mg of iron/kg/day;* ○, *2 mg of iron/kg/day;* ×, *1 mg of iron/kg/day; and* ●, *controls (no iron).*

The animals were fed the iron doses daily and, based upon daily body weight, received doses of 1.5 mg of iron/kg as either ferrous sulfate solution or as the delayed-release capsule formulation. The capsule formulation was scaled individually to the weight of each piglet. Blood samples were taken on the 7th and 9th days of iron administration for measurement of both hemoglobin and hematocrit.

RESULTS

Preliminary Studies—To arrive at the final experimental design, preliminary studies had to be carried out to establish the optimum amount of iron for dosing, the iron dosing schedule, and the blood sampling periods necessary to provide a sensitive, comparative assessment of iron bioavailability.

To the uninitiated who desire to use the piglet as an experimental animal, an initial purchase of only two or three animals is suggested to enable laboratory personnel to become familiar with methods of handling, feeding, dosing, and bleeding these animals. With such a starter group, piglets under laboratory conditions were able to survive, grow, and, in the process, rapidly become anemic when fed a diet consisting solely of a commercial modified milk product. Oral administration of sufficient quantities of ferrous sulfate reversed the anemia, as measured by hematocrit and hemoglobin changes.

A second group of piglets was studied when only 24–48 hr old. Animals this age were obtained to avoid the possibility of their having been inadvertently dosed with iron by the supplier. However, an unbelievable amount of constant care was necessary to maintain this age piglet when away from the sow. During this study, one-third of the animals were lost, mostly from severe diarrhea and/or lack of appetite. A few preliminary dosing studies were carried out with the survivors.

When values of both hemoglobin and hematocrit indicated that the animals were anemic, single doses of iron as solutions of ferrous sulfate heptahydrate were administered. A single dose of 2, 10, or 20 mg/kg produced only small, inadequate responses in hematocrit and hemoglobin levels. However, chronic daily dosing of 1, 2, and 5 mg/kg showed promise of a dose–response in both hematocrit and hemoglobin levels. Chronic doses of 10 and 40 mg/kg caused hematocrit and hemoglobin values to rise no higher than did the 5-mg/kg doses. These data indicated that iron between 5 and 10 mg/kg exceeded the iron absorptive rate or the hemoglobin regeneration rate of the piglet and that the desirable dose range for a comparative bioavailability study was 1–5 mg/kg/day.

A third preliminary study was carried out to test this chronic dosing range for a dose–response and sensitivity as well as to determine if slightly older piglets would show an increased survival rate. Twenty-eight piglets were allowed to stay with the sow until 5 days old. These "older" piglets

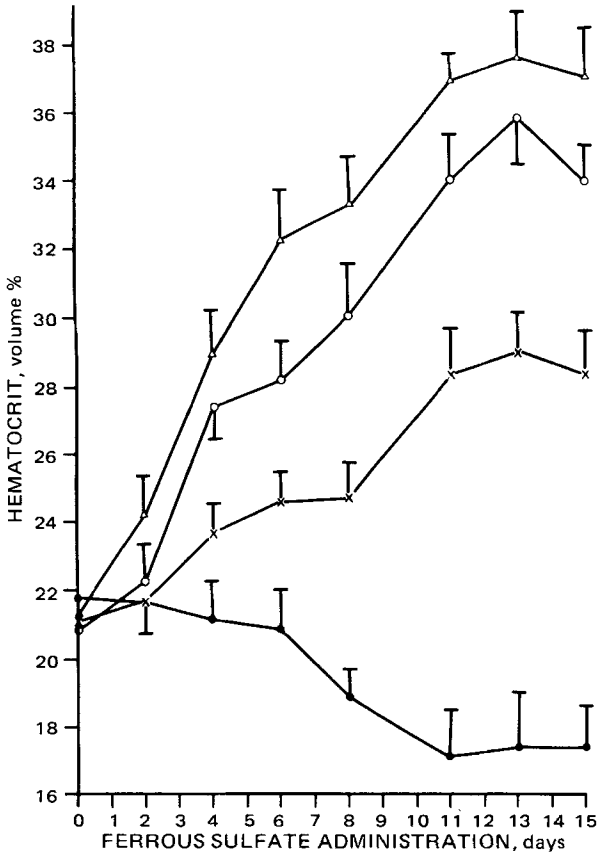

Figure 2—*Mean hematocrit values of anemic piglets following oral administration of various doses of iron administered daily as a ferrous sulfate solution. Each point represents the mean of six piglets* ± SEM. *Key:* Δ, *5 mg of iron/kg/day;* O, *2 mg of iron/kg/day;* ×, *1 mg of iron/kg/day; and* ●, *controls (no iron).*

were healthier and much easier to keep alive; only one of the 28 died. As groups of these piglets became anemic, they were placed into dose groups of 1, 2, and 5 mg of iron/kg. Animals were then dosed daily, and hematocrit and hemoglobin values were determined at frequent intervals.

Figures 1 and 2 show the results obtained. The control values indicated that piglets maintained on the low iron diet remained anemic during the entire experimental period. The data were analyzed statistically, and results are presented in Table I.

The dose of 1.5 mg of iron/kg was chosen for use in a subsequent iron bioavailability comparison study since it fell within the most sensitive detection range. Days 7 and 9 of a daily iron dosing regimen were chosen as hematocrit and hemoglobin measurement periods. Two measurement periods were chosen to assure that hemoglobin and hematocrit levels were monitored during a rising portion of the response curve and not during a plateau period. This criterion is important to establish because a plateau would indicate a maximized hemoglobin and hematocrit response to iron intake, rendering these parameters incapable of rapidly responding to varied levels of iron intake. Once this criterion was established, Day 7 and 9 values could be used individually or averaged for comparative iron bioavailability studies.

Comparison of Iron Bioavailability from Two Different Iron Dosage Forms—Based upon the preliminary studies, a comparative bioavailability study was carried out as outlined under *Experimental.* This study compared the bioavailability of iron from a delayed-release capsule form to similar doses of iron fed as a ferrous sulfate solution.

Thirteen pairs of pigs were assigned to the iron formulations along with six (no iron) controls for each group. Within a pair, both pigs were from the same litter and started on the iron formulation at the same time. Where possible, the same sex was studied as a pair. Table II reports the values obtained.

The results for Days 7 and 9 are reported individually to show that both hematocrit and hemoglobin values were changing in this interval. The differences obtained between Days 7 and 9 were statistically significant for both parameters, confirming that the study did not compare formulations when values were on or near a plateau. The average hemoglobin

Table I—Mean Values of Hematocrit and Hemoglobin following Daily Oral Administration of Iron as Ferrous Sulfate after Statistical Adjustment[a] and Testing for Significance

Iron Dose, mg/kg	Days of Chronic Iron Administration						
	2	4	6	8	11	13	15
	Hematocrit Averages[b], volume %						
1	22.44	23.99	25.25	24.84	27.78	28.07	27.49
2	21.83	27.35	27.69	31.31	34.62	36.36	34.54
5	23.99	28.72	32.22	32.92	37.12	38.10	37.46
	Significance of Hematocrit Averages[c]						
1 *versus* 5	---	**	**	**	**	**	**
2 *versus* 5	---	---	**	---	---	---	*
1 *versus* 2	---	*	---	**	**	**	**
	Hemoglobin Averages[b], g/100 ml						
1	7.11	7.03	7.70	7.53	8.40	8.48	8.44
2	6.88	8.35	8.70	9.49	11.40	11.25	11.07
5	7.30	8.55	10.09	10.37	11.95	11.99	12.02
	Significance of Hemoglobin Averages[c]						
1 *versus* 5	---	*	**	**	**	**	**
2 *versus* 5	---	---	*	---	---	---	**
1 *versus* 2	---	*	---	**	*	**	**

[a] Data adjusted by analysis with a multiple regression model that accounted for differences due to litter and starting baseline. Data prior to statistical adjustment are shown in Figs. 1 and 2. [b] Each value represents average of six piglets. [c] *, $p < 0.05$; **, $p < 0.01$; and ---, not significant.

values of 9.12 g/100 ml following the delayed-release capsule and 8.83 g/100 ml following ferrous sulfate solution were not significantly different. Therefore, one can conclude that the bioavailability of iron from the delayed-release capsule was equivalent to that of the ferrous sulfate solution.

Table II—Hemoglobin and Hematocrit Levels in Anemic Piglets following Daily Administration of 1.5 mg of Iron/kg as Either a Delayed-Release Capsule[a] or a Ferrous Sulfate Solution

	Delayed-Release Pelletized Iron Capsule[a]		Ferrous Sulfate Heptahydrate in Solution	
	Raw Data	Statistically Adjusted Data[b]	Raw Data	Statistically Adjusted Data[b]
	Average Hemoglobin[c], g/100 ml			
Controls (no iron)	5.72		5.47	
Day 7 levels	8.91	8.81	8.32	8.41
Day 9 levels	9.55	9.43	9.12	9.25
Average (Days 7 and 9)	9.23	9.12	8.72	8.83
	Average Hematocrit[c], volume %			
Controls (no iron)	19.4		19.1	
Day 7 levels	31.9	31.8	29.7	29.8
Day 9 levels	33.1	33.0	32.2	32.4
Average (Days 7 and 9)	32.5	32.4[d]	31.0	31.1

[a] Feosol Spansule Capsule, Smith Kline & French Laboratories. [b] To account for design variables and to adjust all results to a common baseline, all data were analyzed with a multiple regression model that accounted for differences due to litter and starting baselines. This produced the "adjusted means." Differences between Day 7 and 9 levels were significant in all cases. [c] All control values represent the mean of six piglets. All other values represent the mean of 13 piglets. [d] This value was significantly higher than hematocrit produced by ferrous sulfate administration, $p < 0.05$. Hemoglobin levels following either dose form were not significantly different. A difference of only 0.44 g of hemoglobin/100 ml would have been significant.

Comparison of hematocrits showed that average values obtained following the delayed-release capsule (32.4%) and following ferrous sulfate (31.1%) were statistically significant ($p < 0.05$). This finding indicated that the bioavailability of iron from the delayed-release capsule was equivalent to, and perhaps somewhat better than, ferrous sulfate solution when using hematocrit regeneration as an index of bioavailability. A difference of 1.2 hematocrit units (only 3.6% of the average hematocrit) would have been statistically significant. The careful selection of a dose of iron that was below the maximum capable of being absorbed by the gut and the regenerating capacity of the bone marrow was probably an important reason for the success of this approach to iron bioavailability methodology. The method demonstrated that delaying the release of iron in the pelletized iron preparations tested in no way impaired its bioavailability.

REFERENCES

(1) R. W. Beal, *Drugs*, **2**, 190 (1971).

(2) L. Hallberg, H. Brise, and L. Solwell, *Proc. VII Cong., Int. Soc. Hematol.*, **2**, 524 (1958).

(3) H. Brise and L. Hallberg, *Acta Med. Scand.*, **171**, 1, (1962).

(4) G. Matrone, E. L. Thomason, and C. R. Bunn, *J. Nutr.*, **72**, 459 (1960).

(5) J. Hannan, *Vet. Rec.*, **88**, 181 (1971).

(6) K. Furugouri, *J. Animal Sci.*, **34**, 421 (1972).

(7) E. Kolb, *Adv. Vet. Sci.*, **8**, 49 (1963).

ACKNOWLEDGMENTS AND ADDRESSES

Received August 25, 1975, from the *Research and Development Division, Smith Kline and French Laboratories, Philadelphia, PA 19101.*

Accepted for publication March 25, 1976.

The authors thank Carol Miller and James Swagzdis for their contributions, Gerald Joseph, Albert Bernstein, Sophronia Morgan, Louis Gutzait, and Warren Randolph for technical assistance, and Maryann Snyder for statistical analysis. The excellent advice and services of Drs. Dave and Diane Phelen, Mr. Thomas Flanagan, and Dr. Harry Green are also gratefully acknowledged.

[x] To whom inquiries should be directed.

Antibacterial Structure–Activity Relationships Obtained with Resistant Microorganisms I: Inhibition of R-Factor Resistant *Escherichia coli* by Tetracyclines

G. H. MILLER [x], H. L. SMITH, W. L. ROCK, and S. HEDBERG

Abstract □ Apparent partition coefficients and inhibitory activities against sensitive and resistant *Escherichia coli* were determined for 14 tetracyclines. The difference in the kinetics of inhibition of the two organisms is discussed in terms of their permeabilities. The partition coefficients were determined in an octanol–buffer system. Values for eight compounds were in general agreement with the literature; values for the remaining six compounds had not been reported previously. Growth of the organisms was determined by a single-point turbidimetric method in the presence and absence of tetracyclines. Inhibitory activities were obtained by a kinetic treatment. Derived rate constants for the sensitive organism were linearly related to antibiotic concentration. For the resistant organism and 12 compounds, the derived rate constants and antibiotic concentration were related in a manner typical of saturation kinetics. These inhibitory activities were related to the partition coefficients, while activities against the sensitive strain were not. These findings suggest that activity against the resistant strain is permeability controlled but that activity against the sensitive strain has a different rate-determining step.

Keyphrases □ Antibacterial activity—various tetracyclines, related to partition coefficients, resistant and sensitive microorganisms, structure–activity relationships □ Tetracyclines, various—antibacterial activity, related to partition coefficients, resistant and sensitive microorganisms, structure–activity relationships □ Partition coefficients—various tetracyclines, related to antibacterial activity, resistant and sensitive microorganisms □ *Escherichia coli*—resistant and sensitive, inhibition by various tetracyclines, related to partition coefficients, structure–activity relationships □ Structure–activity relationships—various tetracyclines, antibacterial activity, resistant and sensitive microorganisms

The development of safe, effective antimicrobial drugs has revolutionized medicine in the last 30 years. Unfortunately, microorganisms are highly versatile, and the brilliance of the chemotherapeutic achievement has been dimmed by the emergence of microbial strains resistant to these drugs. This emergence of resistant pathogens is becoming an increasingly important problem. In addition to limiting the use of antibiotics, two possible approaches to the problem would be to seek entirely new antibacterial agents and to modify existing chemotherapeutic agents. The latter approach has the advantage that derivatives of present chemotherapeutic agents are likely to retain the high benefit to risk ratios of the parent drugs.

The general mechanisms by which microorganisms may become resistant to antibiotics were summarized (1), and the one where drug modification might effectively overcome drug resistance is the loss of cell permeability to the drug. Changes in the physicochemical nature of a drug resulting in decreased or increased cell permeabilities were described for many systems (2).

Davies (3) stated that, as far as can be ascertained, all tetracycline-resistant strains obtained from clinical situations are resistant because they carry an R-factor. The nature of R-factor resistance to tetracyclines was investigated extensively and reviewed (4, 5). These studies indicate that tetracycline resistance is related to a decreased uptake of tetracyclines by resistant cells. Several investigators showed that cell-free protein-synthesizing systems from sensitive and resistant strains were equally inhibited by tetracyclines (6–8).

Escherichia coli accumulated oxytetracycline at high concentrations (9), and this accumulation was inhibited by azide and 2,4-dinitrophenol and was dependent upon the energy source in the medium. Similar observations

Comparison of hematocrits showed that average values obtained following the delayed-release capsule (32.4%) and following ferrous sulfate (31.1%) were statistically significant ($p < 0.05$). This finding indicated that the bioavailability of iron from the delayed-release capsule was equivalent to, and perhaps somewhat better than, ferrous sulfate solution when using hematocrit regeneration as an index of bioavailability. A difference of 1.2 hematocrit units (only 3.6% of the average hematocrit) would have been statistically significant. The careful selection of a dose of iron that was below the maximum capable of being absorbed by the gut and the regenerating capacity of the bone marrow was probably an important reason for the success of this approach to iron bioavailability methodology. The method demonstrated that delaying the release of iron in the pelletized iron preparations tested in no way impaired its bioavailability.

REFERENCES

(1) R. W. Beal, *Drugs*, **2**, 190 (1971).

(2) L. Hallberg, H. Brise, and L. Solwell, *Proc. VII Cong., Int. Soc. Hematol.*, **2**, 524 (1958).

(3) H. Brise and L. Hallberg, *Acta Med. Scand.*, **171**, 1, (1962).

(4) G. Matrone, E. L. Thomason, and C. R. Bunn, *J. Nutr.*, **72**, 459 (1960).

(5) J. Hannan, *Vet. Rec.*, **88**, 181 (1971).

(6) K. Furugouri, *J. Animal Sci.*, **34**, 421 (1972).

(7) E. Kolb, *Adv. Vet. Sci.*, **8**, 49 (1963).

ACKNOWLEDGMENTS AND ADDRESSES

Received August 25, 1975, from the *Research and Development Division, Smith Kline and French Laboratories, Philadelphia, PA 19101.*

Accepted for publication March 25, 1976.

The authors thank Carol Miller and James Swagzdis for their contributions, Gerald Joseph, Albert Bernstein, Sophronia Morgan, Louis Gutzait, and Warren Randolph for technical assistance, and Maryann Snyder for statistical analysis. The excellent advice and services of Drs. Dave and Diane Phelen, Mr. Thomas Flanagan, and Dr. Harry Green are also gratefully acknowledged.

[x] To whom inquiries should be directed.

Antibacterial Structure–Activity Relationships Obtained with Resistant Microorganisms I: Inhibition of R-Factor Resistant *Escherichia coli* by Tetracyclines

G. H. MILLER [x], H. L. SMITH, W. L. ROCK, and S. HEDBERG

Abstract □ Apparent partition coefficients and inhibitory activities against sensitive and resistant *Escherichia coli* were determined for 14 tetracyclines. The difference in the kinetics of inhibition of the two organisms is discussed in terms of their permeabilities. The partition coefficients were determined in an octanol–buffer system. Values for eight compounds were in general agreement with the literature; values for the remaining six compounds had not been reported previously. Growth of the organisms was determined by a single-point turbidimetric method in the presence and absence of tetracyclines. Inhibitory activities were obtained by a kinetic treatment. Derived rate constants for the sensitive organism were linearly related to antibiotic concentration. For the resistant organism and 12 compounds, the derived rate constants and antibiotic concentration were related in a manner typical of saturation kinetics. These inhibitory activities were related to the partition coefficients, while activities against the sensitive strain were not. These findings suggest that activity against the resistant strain is permeability controlled but that activity against the sensitive strain has a different rate-determining step.

Keyphrases □ Antibacterial activity—various tetracyclines, related to partition coefficients, resistant and sensitive microorganisms, structure–activity relationships □ Tetracyclines, various—antibacterial activity, related to partition coefficients, resistant and sensitive microorganisms, structure–activity relationships □ Partition coefficients—various tetracyclines, related to antibacterial activity, resistant and sensitive microorganisms □ *Escherichia coli*—resistant and sensitive, inhibition by various tetracyclines, related to partition coefficients, structure–activity relationships □ Structure–activity relationships—various tetracyclines, antibacterial activity, resistant and sensitive microorganisms

The development of safe, effective antimicrobial drugs has revolutionized medicine in the last 30 years. Unfortunately, microorganisms are highly versatile, and the brilliance of the chemotherapeutic achievement has been dimmed by the emergence of microbial strains resistant to these drugs. This emergence of resistant pathogens is becoming an increasingly important problem. In addition to limiting the use of antibiotics, two possible approaches to the problem would be to seek entirely new antibacterial agents and to modify existing chemotherapeutic agents. The latter approach has the advantage that derivatives of present chemotherapeutic agents are likely to retain the high benefit to risk ratios of the parent drugs.

The general mechanisms by which microorganisms may become resistant to antibiotics were summarized (1), and the one where drug modification might effectively overcome drug resistance is the loss of cell permeability to the drug. Changes in the physicochemical nature of a drug resulting in decreased or increased cell permeabilities were described for many systems (2).

Davies (3) stated that, as far as can be ascertained, all tetracycline-resistant strains obtained from clinical situations are resistant because they carry an R-factor. The nature of R-factor resistance to tetracyclines was investigated extensively and reviewed (4, 5). These studies indicate that tetracycline resistance is related to a decreased uptake of tetracyclines by resistant cells. Several investigators showed that cell-free protein-synthesizing systems from sensitive and resistant strains were equally inhibited by tetracyclines (6–8).

Escherichia coli accumulated oxytetracycline at high concentrations (9), and this accumulation was inhibited by azide and 2,4-dinitrophenol and was dependent upon the energy source in the medium. Similar observations

Table I—Partition Coefficients and Inhibitory Activities against Sensitive *E. coli* W (K_{sens}) and Resistant *E. coli* (K_R+)

Tetracycline	Partition Coefficients		Inhibitory Activities	
	Experimental	Lit. (22)	$K_{sens} \times 10^6$	$K_R + \times 10^6$
5a(6)-Anhydro-	6.0	—	0.12	0.108[a]
4-Dedimethylamino-	4.95	5.79	0.077	0.0208[a]
7-Dimethylamino-6-demethyl-6-deoxy-	1.47	1.48	0.25	0.6452
6-Demethyl-6-deoxy-	0.99	0.96	0.25	0.0714
9-Dimethylamino-6-demethyl-6-deoxy-	0.82	0.77	0.076	0.0222
7-Nitro-6-demethyl-6-deoxy-	0.78	—	1.45	0.0476
7-Chloro-	0.37	0.32	0.95	0.0125
7-Chloro-6-demethyl-	0.25	0.19	1.10	0.0057
9-Amino-6-demethyl-6-deoxy-	0.21	—	0.35	0.025
9-Nitro-6-demethyl-6-deoxy-	0.14	—	0.145	0.0030
5-Hydroxy-	0.12	0.087	0.65	0.0011
7-Amino-6-demethyl-6-deoxy-	0.09	—	0.19	0.0018
Unsubstituted	0.09	0.052	0.60	0.0018
5a(11)-Dehydro-7-chloro-	0.057	—	—	—[a]
7-Bromo-6-demethyl-6-deoxy-[b]	—	—	0.07	0.105
12a-Deoxy-[b]	—	—	0.0085	0.015[a]
4-Methiodide	—	0.01	0.0073	—

[a] These compounds had a linear relationship between tetracycline concentration and derived rate constants for growth of the resistant strain. [b] Samples of these compounds varied in the observed partition coefficients obtained at different wavelengths, so values for these compounds have not been used.

were reported with tetracycline and chlortetracycline at low concentrations (7). The resistance was associated with a marked decrease in the ability of *E. coli* to accumulate tetracyclines (7, 10–12). Similarly, Sompolinsky *et al.* (13) found a decreased uptake in resistant staphylococci, and Tseng and Bryan (14) noted decreased uptake of tetracycline in resistant *Pseudomonas* strains. The uptake of tetracycline by sensitive and resistant *E. coli* was correlated to the minimum inhibitory concentrations of the strains studied (15).

The exact mechanism of the uptake of tetracyclines by sensitive cells is not yet established. It was suggested that accumulation in *Staphylococcus aureus* follows saturation kinetics initially but that a multiplicity of sites becomes available at high antibiotic concentrations and antibiotic concentration becomes limiting (16). The uptake of tetracyclines by *E. coli* as a function of tetracycline concentration was reported to be biphasic (17). Resistance was suggested to be associated with a requirement for higher antibiotic concentrations before the second mode of accumulation became operative. However, Reynard and Nellis (18) were unable to find the initial phase of saturation kinetics in *E. coli*.

Regardless of the exact mechanism, tetracycline resistance probably is associated with a reduced ability to accumulate the antibiotic within the resistant cells. If this assumption is true, then alteration of the balance of water–lipid solubility of the antibiotics might lead to improved permeation by passive diffusion. As lipophilicity increased in a series of tetracycline derivatives, their activity against a tetracycline-resistant *S. aureus* increased (19). Furthermore, recent activity determinations (20) using various resistant *Staphylococcus* strains were also in general agreement with this principle. The present work extends these findings to R-factor resistant *E. coli* in a quantitative fashion.

EXPERIMENTAL

Materials—A tetracycline-sensitive *Escherichia coli* W (ATCC 9637) and a tetracycline-resistant *Escherichia coli* (ATCC 19215, recipient of an R-factor conferring multiple resistance to tetracycline, chloramphenicol, streptomycin, and sulfonamides) were used as test organisms. A high level of tetracycline resistance was induced in the R-factor strain by subculturing it in the presence of tetracycline (12). The culture broth was a high peptone medium buffered at pH 6.65 with potassium salts of phosphoric acid as previously described (21).

Samples of tetracycline, oxytetracycline, and chlortetracycline were purchased[1]; the remaining derivatives were supplied by the manufacturers[2]. Apparent partition coefficients were determined between a pH 6.6 phosphate buffer and 1-octanol[3]. Buffer solutions were prepared with the potassium salts of phosphoric acid and adjusted to an ionic strength of 0.1 *M* with sodium chloride. The water used in these solutions had been redistilled from an all-glass still[4].

Determination of Apparent Partition Coefficients of Tetracycline Analogs—A solution of the tetracycline under study was prepared in buffer saturated with octanol (buffer phase). Sufficient quantities of this solution were placed in 50-ml glass-stoppered centrifuge tubes so that the final concentration was 0.5 m*M* when the volume of solution was brought to 10 ml by the addition of buffer phase. Exactly 10 ml of octanol saturated with buffer (octanol phase) was added to each tube. Duplicate tubes were prepared for each tetracycline analog studied as well as blank tubes containing only buffer phase and octanol phase.

The capped tubes were mounted horizontally in a shaker[5] and vigorously shaken for 10 min. After centrifuging at 1500 rpm for 20 min, a sample of the buffer phase was carefully removed from each tube with a syringe equipped with a 15.2-cm (6-in.) 20-gauge needle. Aliquots of these samples as well as aliquots of the original tetracycline analog solutions were diluted with buffer phase and assayed spectrophotometrically[6]. Absorption measurements were made at wavelengths corresponding to the tetracycline peaks in the regions of 275 and 350 nm and at maxima and/or minima at about 250 and/or 450 nm, if they existed for the derivative. After correcting for blank readings, the absorbance values obtained at each wavelength for each sample and the absorbance values for its corresponding original solution were used to calculate the concentrations of tetracycline analog in both the buffer and octanol phases.

The apparent partition coefficients reported are average values obtained at all wavelengths studied (Table I). The agreement of partition coefficients obtained at several wavelengths for the tetracycline analogs is taken as an indication of their high degree of purity. Accordingly, the values obtained for two of the analogs studied are not reported since the apparent partition coefficients varied as a function of wavelength.

Inhibitory Activity Determinations with Tetracycline-Sensitive *E. coli* W—The inhibitory activities with the sensitive *E. coli* W were determined for tetracycline and its 15 analogs according to the following

[1] Calbiochem, La Jolla, CA 92037.

[2] The authors are grateful to Dr. James H. Boothe, Lederle Laboratories, Pearl River, N.Y., and Dr. Charles R. Stephens, Pfizer Laboratories, Groton, Conn., for assistance in providing the tetracycline analogs.

[3] Certified reagent grade, Fisher Scientific Co., Pittsburgh, PA 15238.

[4] Model AG-1a, Corning Glass Works, Corning, NY 14803.

[5] Dubnoff, Precision Scientific Co., Chicago, Ill.

[6] Gilford Instrument Laboratories, Oberlin, OH 44074.

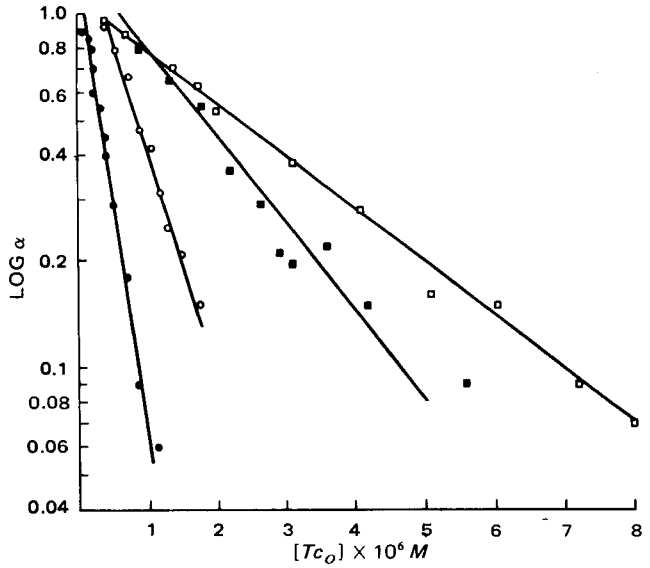

Figure 1—*Fractional activity against tetracycline sensitive* E. coli *W as a function of the concentration of tetracycline analogs. Key:* ●, *7-nitro-6-demethyl-6-deoxytetracycline;* ○, *oxytetracycline;* ■, *6-demethyl-6-deoxytetracycline; and* □, *9-nitro-6-demethyl-6-deoxytetracycline.*

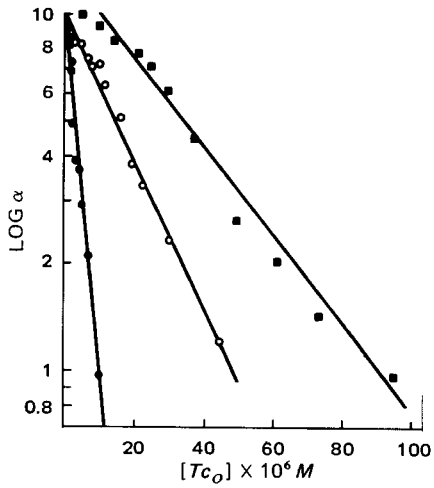

Figure 2—*Fractional activity against tetracycline-resistant* E. coli R^+ *as a function of the concentration of tetracycline analogs. Key:* ●, *5a(6)-anhydrotetracycline;* ○, *4-dedimethylaminotetracycline; and* ■, *12a-deoxytetracycline.*

procedure. Aliquots of a tetracycline analog solution were added to 3 ml of broth in sterile 6-ml capped tubes[7] so that a range of 12 tetracycline concentrations was obtained. Duplicate tubes were prepared and run for all analog concentrations. An overnight peptone broth culture of *E. coli* W was diluted with fresh broth so that a concentration of 1×10^7 *E. coli* W/ml was obtained when an aliquot (5, 10, or 20 μl) was added to each of the 24 tubes containing tetracycline and to two tubes without tetracycline.

The tubes were incubated for 3.5 hr at 37.5° in a constant-temperature water bath. Growth was stopped by the addition of 20 μl of formaldehyde solution. The turbidity of the cultures was determined[6] at 500 nm. The fractional activity, α, was calculated from the ratio of the turbidity of a culture grown in the presence of the tetracycline analog to that obtained for cultures without antibiotic. If one assumes that the turbidity of the cultures is proportional to the number of organisms per milliliter of culture and that growth of the cultures in the presence and absence of tetracyclines is first order in organisms per milliliter (21), then the logarithm of α is proportional to the difference in the growth rate constants in the presence (k_{app}) and absence (k_0) of antibiotic.

Inhibitory Activity Determinations with Tetracycline-Resistant *E. coli*—Inhibitory activities with the resistant *E. coli* were determined for tetracycline and its 14 analogs by the same procedure as that outlined for the sensitive organism except: (*a*) the overnight culture was 320 μ*M* in tetracycline, (*b*) the volume of the overnight culture added to the experimental cultures was between 100 and 300 μl, and (*c*) the time of incubation was 5 hr instead of 3.5 hr.

RESULTS AND DISCUSSION

Apparent Partition Coefficients of Tetracycline Analogs—Colaizzi and Klink (22) reported the apparent partition coefficients of a number of tetracycline analogs at several pH values, including 6.6. Their work was extended by determining the apparent partition coefficients of six compounds not available to those authors. In addition, the values reported by Colaizzi and Klink were verified for eight tetracycline analogs (Table I). The most lipophilic tetracycline analog studied was 5a(6)-anhydrotetracycline, with an apparent partition coefficient (K_p) of 6.0; the most hydrophilic studied was 5a(11)-dehydro-7-chlorotetracycline (K_p = 0.057). Agreement with reported values (22) was excellent except for the most hydrophilic derivatives (tetracycline and oxytetracycline), where the experimental error involved might be expected to be highest for procedures in which only the aqueous phase of the biphasic system is assayed.

As already mentioned, the agreement of apparent partition coefficients calculated at different wavelengths was excellent for the tetracyclines reported, indicating a high degree of purity. Two samples of 7-bromo-6-demethyl-6-deoxytetracycline were examined and showed considerable variation in the apparent partition coefficients calculated at the different wavelengths. Values for this compound as well as a similarly behaving sample of 12a-deoxytetracycline are not reported. The biological activity of these samples (Table I) is, however, similar to that reported (19).

Inhibitory Activities of Tetracycline Analogs against Sensitive *E. coli*—Initial estimates of the activities of the derivatives were made by plotting fractional activities, α, *versus* antibiotic concentration and estimating the concentration of antibiotic that would cause a 50% inhibition of growth. However, it became apparent that plots of log α *versus* antibiotic concentration were linear for all of the compounds studied with the tetracycline-sensitive organism, *E. coli* W (Fig. 1). This finding can be explained if it is assumed that the turbidity of the cultures is proportional to the number of cells per milliliter of culture (N) and that growth is first order for the period of incubation in N, both in the presence ($N = N_0 e^{k_{app} t}$) and absence ($N = N_0 e^{k_0 t}$) of antibiotic. Since N_0 is the same for both cultures, log α becomes equal to $2.3t(k_{app} - k_0)$. It was shown previously that for tetracycline inhibiting *E. coli* B/r (23) and for tetracycline analogs inhibiting *E. coli* W (21):

$$k_{app} = k_0 - K(Tc) \qquad \text{(Eq. 1)}$$

where (Tc) is the concentration of tetracycline analog, and K is a constant typical of the tetracycline analog. Rearrangement of Eq. 1 shows that a plot of log α *versus* (Tc) should be linear. The data suggest that these assumptions are true for all tetracycline derivatives studied with *E. coli* W. The negative slopes of such plots (Fig. 1) were evaluated, and the values obtained for each analog are listed as K_{sens} values in Table I. These activities were in substantial agreement with those previously published for these compounds and this organism but obtained by the more rigorous methods of bacterial growth kinetics (21). This agreement is shown by:

$$K_{sens} = -9.347 + 482.1\, K^I_{avg} \qquad r = 0.98\ n = 15 \qquad \text{(Eq. 2)}$$

where K^I_{avg} is the K of Eq. 1 obtained from kinetic measurements of cell division (total and viable), nucleic acid synthesis, and protein synthesis.

Inhibitory Activities of Tetracycline Analogs against Resistant *E. coli*—The *E. coli* employed was resistant to tetracycline to the extent that the concentration of tetracycline causing a 50% inhibition in growth in the test system was about 175 times greater than that necessary to inhibit *E. coli* W. In contrast to the results already described for *E. coli* W, plots of log α *versus* (Tc) were only linear for four tetracycline analogs (Fig. 2). In addition to the three compounds shown on this figure, 5a(11)-dehydro-7-chlorotetracycline also exhibited a linear relationship between log α and tetracycline concentration. Because of their extremely weak activity, it was not possible to determine the relationship between log α and tetracycline concentration for isochlortetracycline and tetracycline methiodide over a wide range of inhibition, but preliminary experiments indicated that they might also have a linear relationship. All

[7] Falcon, Oxnard, CA 93030.

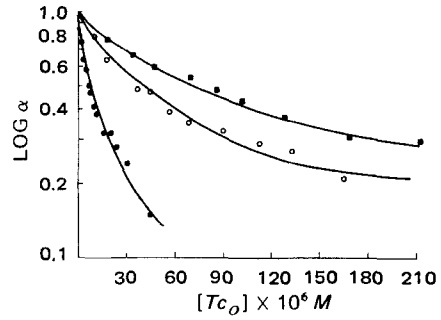

Figure 3—*Fractional activity against tetracycline-resistant* E. coli R^+ *as a function of the concentration of tetracycline analogs. Key:* ●, *6-demethyl-6-deoxytetracycline;* ○, *chlortetracycline; and* ■, *demeclocycline.*

of these compounds are unusual tetracyclines in that either their phenyl diketone moiety or their 4-dimethylamino moiety is modified. These moieties are usually considered to be essential for tetracycline-like activity. However, the activities of these compounds against sensitive *E. coli* W are correlatable with their physicochemical properties (24).

Plots of log α *versus* tetracycline concentration for the remaining 12 compounds studied were not linear, as shown for three of the compounds in Fig. 3. The curvature of these plots suggested that a data treatment typical of saturation kinetics would be useful. Plots of $-(1/\log \alpha)$ *versus* $1/(Tc)$ and of $-[(Tc)/\log \alpha]$ *versus* (Tc) were linear for these compounds. These plots would be expected to be linear if the assumptions given that allow log α to be related to $k_{app} - k_0$ are true and if the more complicated expression:

$$k_{app} = k_0 - K_a(Tc)/1 + K_b(Tc) \qquad \text{(Eq. 3)}$$

is applicable instead of Eq. 1. Such an expression has not been reported as being applicable to tetracycline activities, but similar expressions are known to apply to other antibacterial agents such as sulfonamides (25, 26), trimethoprim (26), and erythromycin (27) and to certain phases of lincomycin inhibition (27). Examples of the fit of the data to Eq. 3 are shown in Figs. 4 and 5. In general, the linearity of these lines is excellent considering the assumptions in the data treatment. Inhibitory activities, K_{R^+}, derived from the slopes and intercepts of the plots are given in Table I.

As might be expected, the activities against the sensitive strain were not related to the activities obtained with the resistant strain, as shown by:

$$K_{R^+} = 0.96 - 0.057\,K_{sens} \qquad r = -0.15 \quad n = 15 \qquad \text{(Eq. 4)}$$

Structure–activity relationships using activities obtained with sensitive strains (28, 29) would not be expected to be valid for resistant strains. Blackwood and English (19) suggested a qualitative relationship between activities obtained against a resistant *Staph. aureus* and lipophilicity. Our data show a quantitative relationship between tetracycline activity against the resistant *E. coli* and lipophilicity, as given in Eq. 5 and shown graphically in Fig. 6:

$$\log K_{R^+} = 1.98 + 1.74 \log K_p \qquad r = 0.918 \quad n = 11 \quad F_9^1 = 48.5 \qquad \text{(Eq. 5)}$$

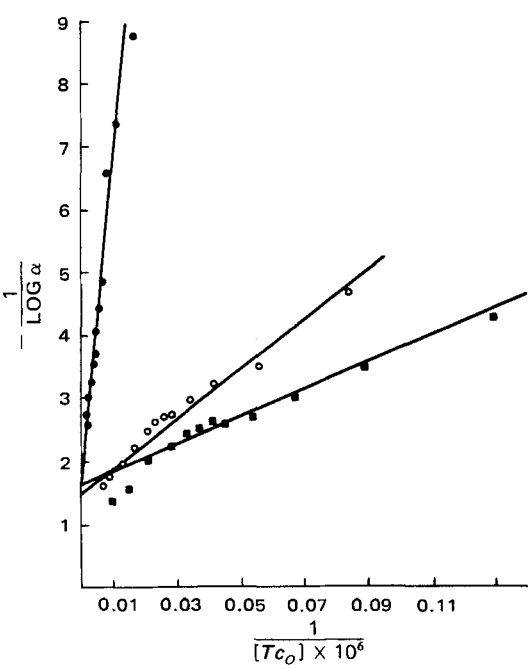

Figure 4—*Relationship between fractional activity against tetracycline-resistant* E. coli R^+ *and the concentration of tetracycline analogs. Key:* ●, *7-amino-6-demethyl-6-deoxytetracycline;* ○, *9-amino-6-demethyl-6-deoxytetracycline; and* ■, *7-nitro-6-demethyl-6-deoxytetracycline.*

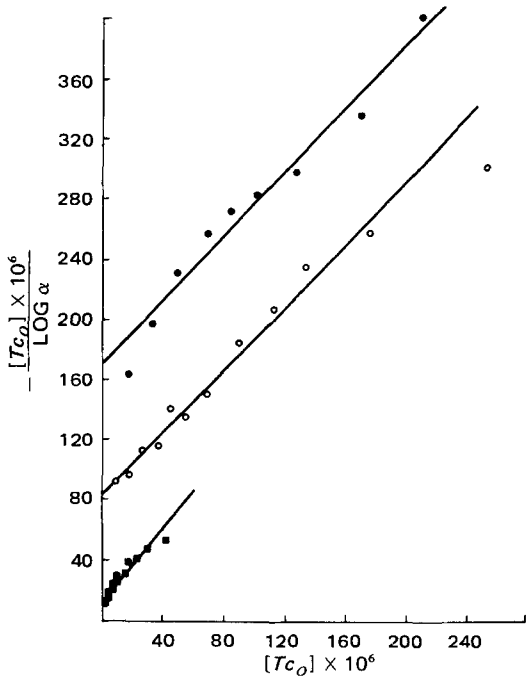

Figure 5—*Relationship between fractional activity against tetracycline-resistant* E. coli R^+ *and the concentration of tetracycline analogs. Key:* ●, *6-demethyl-6-deoxytetracycline;* ○, *chlortetracycline; and* ■, *demeclocycline.*

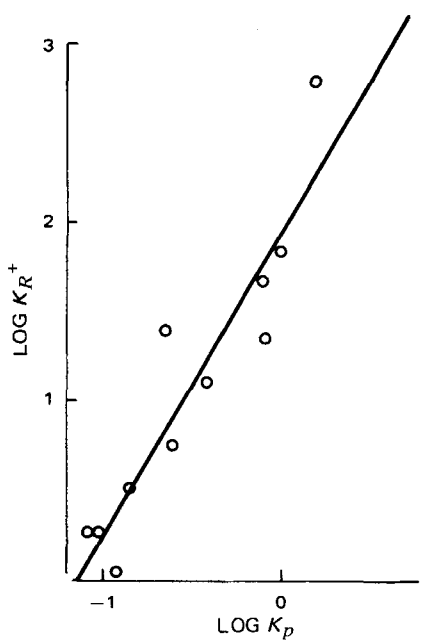

Figure 6—*Relationship of inhibitory activities against tetracycline-resistant* E. coli R^+ *and partition coefficients of tetracycline analogs.*

Inclusion of higher order terms in log K_p did not improve the fit of the data, nor did such expressions allow the fit of the compounds that were typified by a linear relationship between log α and tetracycline concentration. In addition, inclusion of several reported quantum mechanical parameters (24) for tetracyclines did not improve the fit of the data. The activities of the tetracycline antibiotics with intact phenyl diketone and 4-dimethylamino moieties against resistant *E. coli* probably are directly related to their lipophilicity. The compound that had the highest partition coefficient and the highest activity of those studied was 7-dimethylamino-6-demethyl-6-deoxytetracycline (minocycline).

Model of Tetracycline Inhibitory Activity—A reasonable explanation of the discussed structure–activity relationships may be derived from the model given by Garrett (30) or Peradejordi *et al.* (24). In this model, tetracycline outside the cell (Tc_o) is considered to permeate the cell wall (Tc_i) and then to react with a receptor reversibly in such a manner that growth is inhibited according to Schemes I and II:

$$Tc_o \underset{}{\overset{K_1}{\rightleftharpoons}} Tc_i$$

Scheme I

$$Tc_i + \text{receptor} \overset{K_2}{\rightleftharpoons} Tc_i\text{–receptor}$$

Scheme II

If one assumes that the generation of *E. coli* is related to the fraction of free receptors as given by:

$$dN/dt = k_o(1 - \theta)N \qquad \text{(Eq. 6)}$$

where θ is the fraction of receptors occupied by tetracyline, then Schemes I and II and Eq. 6 may be rearranged and related to the experimentally observed growth rate constant, k_{app}, as follows:

$$k_{app} - k_o = -\frac{k_o K_1 K_2 Tc_o}{1 + K_1 K_2 Tc_o} \qquad \text{(Eq. 7)}$$

Equation 7 is similar to Eq. 3, but K_a is now considered to be $k_o K_1 K_2$ and K_b is $K_1 K_2$.

The linear relationship between log α and tetracycline concentration found for *E. coli* W and for four tetracyclines with the resistant *E. coli* results when $K_1 K_2 Tc$ is less than 1. Under these conditions, the K_{sens} values reported are equal to $k_o K_1 K_2$.

In contrast, the complete expression is necessary to fit the data obtained for the 12 tetracyclines with normal phenyl diketone and 4-dimethylamino moieties against the resistant *E. coli*. The reported inhibitory activity, K_{R+}, would be equal to $K_1 K_2$ if this simple model is correct. Since the two activities are not related (Eq. 4) and since K_{R+} is related to the partition coefficients (Eq. 5), it seems logical that K_{sens} is controlled by K_2 and that K_{R+} is controlled by K_1. Thus, the resistance to tetracyclines is associated with a change in the rate-determining step from one involving the receptor to one involving permeation into the cell, consistent with previously published theories of tetracycline resistance (3).

The four compounds with abnormal phenyl diketone or 4-dimethylamino moieties are compounds with intrinsically low activities and, in two cases, very high apparent partition coefficients. Thus, for these compounds, K_2 continues to be the rate-controlling step in the inhibition of resistant *E. coli*.

REFERENCES

(1) B. D. Davis and W. K. Maas, *Proc. Nat. Acad. Sci.*, **38**, 775 (1952).

(2) C. Hansch, *Mol. Pharmacol.*, **5**, 333 (1969).

(3) J. Davies, *Ann. Rep. Med. Chem.*, **7**, 217 (1972).

(4) T. Watanabe, *Bacteriol. Rev.*, **27**, 87 (1963).

(5) J. S. Piton, *Ergebn. Physiol.*, **65**, 15 (1972).

(6) S. Okamoto and D. Mizuno, *J. Gen. Microbiol.*, **35**, 125 (1964).

(7) T. J. Franklin and A. Godfrey, *Biochem. J.*, **94**, 54 (1965).

(8) J. A. Last, K. Izaki, and J. F. Snell, *Can. J. Microbiol.*, **15**, 1077 (1969).

(9) K. Izaki and K. Arima, *J. Bacteriol.*, **89**, 1335 (1965).

(10) K. Izaki, K. Kiuchi, and K. Arima, *ibid.*, **91**, 628 (1966).

(11) T. J. Franklin, *Biochem. J.*, **105**, 371 (1967).

(12) T. J. Franklin and B. Higginson, *ibid.*, **116**, 287 (1970).

(13) D. Sompolinsky, Y. Zaidenzaig, R. Ziegler-Schlomowitz, and N. Abramova, *J. Gen. Microbiol.*, **62**, 351 (1970).

(14) J. T. Tseng and L. E. Bryan, *Antimicrob. Ag. Chemother.*, **3**, 638 (1973).

(15) A. M. Reynard, L. F. Nellis, and M. E. Beck, *Appl. Microbiol.*, **21**, 71 (1971).

(16) B. L. Hutchings, *Biochim. Biophys. Acta*, **174**, 734 (1969).

(17) J. R. De Zeeuw, *J. Bacteriol.*, **95**, 498 (1968).

(18) A. M. Reynard and L. F. Nellis, *Biochem. Biophys. Res. Commun.*, **48**, 1129 (1972).

(19) R. K. Blackwood and A. R. English, *Adv. Appl. Microbiol.*, **13**, 237 (1970).

(20) D. Sompolinsky and J. Krausz, *Antimicrob. Ag. Chemother.*, **4**, 237 (1973).

(21) G. H. Miller, S. A. Khalil, and A. N. Martin, *J. Pharm. Sci.*, **60**, 33 (1971).

(22) J. L. Colaizzi and P. R. Klink, *ibid.*, **58**, 1184 (1969).

(23) M. R. W. Brown and E. R. Garrett, *ibid.*, **53**, 179 (1964).

(24) F. Peradejordi, A. N. Martin, and A. Cammarata, *ibid.*, **60**, 576 (1971).

(25) E. R. Garrett and O. K. Wright, *ibid.*, **56**, 1576 (1967).

(26) J. K. Seydel, E. Wempe, G. H. Miller, and L. Miller, *Chemotherapy*, **17**, 217, (1972).

(27) E. R. Garrett, S. M. Heman-Ackah, and G. L. Perry, *J. Pharm. Sci.*, **59**, 1448 (1970).

(28) A. Cammarata, S. S. Yau, J. H. Collett, and A. N. Martin, *Mol. Pharmacol.*, **6**, 65 (1970).

(29) A. Cammarata and S. J. Yau, *J. Med. Chem.*, **13**, 94 (1970).

(30) E. R. Garrett, *Progr. Drug Res.*, **15**, 271 (1971).

ACKNOWLEDGMENTS AND ADDRESSES

Received August 23, 1974, from the *Departments of Pharmaceutical Chemistry and Pharmacy and Pharmaceutics, School of Pharmacy, Medical College of Virginia, Virginia Commonwealth University, Richmond, VA 23298.*

Accepted for publication March 19, 1976.

Presented at the Medicinal Chemistry Section, APhA Academy of Pharmaceutical Sciences, Chicago meeting, August 1974.

[x] To whom inquiries should be directed. Present address: Schering Corp., Bloomfield, NJ 07003.

Role of Neuronal and Extraneuronal Uptake in Responses of Rabbit Iris Dilator Muscle to Levarterenol and Phenylephrine

JAMES L. MATHENY, GERALD O. CARRIER, and RAYMOND P. AHLQUIST ˣ

Abstract □ The roles of neuronal and extraneuronal uptake mechanisms in the response of iris dilator muscles of rabbit to levarterenol (norepinephrine) and phenylephrine were investigated. Chemical denervation with 6-hydroxydopamine was used to eliminate neuronal uptake. Exposure to corticosterone prior to and during exposure to levarterenol or phenylephrine was used to assess the importance of extraneuronal uptake. Dose–response curves and ED_{50} values for levarterenol or phenylephrine in control and 6-hydroxydopamine-denervated tissues, both in the presence and absence of corticosterone, are shown. Curves illustrating the decay of tension on washout of levarterenol or phenylephrine from treated tissues were analyzed. 6-Hydroxydopamine denervation affected the response to levarterenol more than that to phenylephrine. Washout of both agonists was slower after 6-hydroxydopamine pretreatment, and washout of phenylephrine was more rapid when corticosterone was present. These data indicate that extraneuronal uptake in iris dilator muscles was more important in determining the response to phenylephrine than to levarterenol and that neuronal uptake was more important in determining tissue responsiveness to levarterenol than to phenylephrine.

Keyphrases □ Levarterenol—effect on iris dilator muscle response, roles of neuronal and extraneuronal uptake mechanisms, rabbits □ Phenylephrine—effect on iris dilator muscle response, roles of neuronal and extraneuronal uptake mechanisms, rabbits □ Neuronal and extraneuronal uptake mechanisms—roles in iris dilator muscle response, effect of levarterenol and phenylephrine, rabbits □ Iris dilator muscle response—effect of levarterenol and phenylephrine, roles of neuronal and extraneuronal uptake mechanisms, rabbits □ Adrenergic agents—levarterenol and phenylephrine, effect on iris dilator muscle response, roles of neuronal and extraneuronal uptake mechanisms, rabbits

Recent studies (1, 2) demonstrated the importance of extraneuronal uptake in the alteration of the action of adrenergic agonists in vascular smooth muscle. Earlier, the decline of muscle tension during washout of a stimulant drug was found to be a valid index of the decreasing concentration of the drug at its receptor sites (3, 4). Corticosterone blocked the uptake of adrenergic agonists into extraneuronal stores (5, 6), thus altering the time required to wash out the agonists.

6-Hydroxydopamine selectively destroys the adrenergic nerve terminals in many tissues. Since a recent study (7) demonstrated a virtually complete absence of adrenergic innervation of iris muscles of rabbits after treatment with 6-hydroxydopamine, the iris dilator muscle of the rabbit was selected for study. Chemical denervations by 6-hydroxydopamine and blockade of extraneuronal uptake with corticosterone were used to assess the role of various mechanisms in determining muscle responsiveness to α-adrenergic agonists.

EXPERIMENTAL

Materials—Albino rabbits of both sexes, approximately 1.5 kg, were stunned by a blow to the head and exsanguinated and the eyes were enucleated. Two strips of the iris dilator muscle of about 2 mm width were isolated from each eye by the method of Kern (8). The strips were then mounted in 25-ml baths containing a balanced salt solution of the following composition (micromolar): NaCl, 141.58; KCl, 5.40; $NaHCO_3$, 15.00; glucose, 11.00; NaH_2PO_4, 0.40; and $CaCl_2$, 2.10. The solution was aerated with a mixture of 97% oxygen and 3% carbon dioxide. The pH remained constant at 7.4 throughout the experiment after aeration with this gas mixture.

Strain-gauge transducers with microscale accessories were used to measure isometric contractions. Recordings were made of tension changes on an oscillographic recorder. Resting tension was adjusted to approximately 40 mg. Temperature was maintained at 37° using a heater-circulator.

Drugs—Solutions of drugs were prepared fresh in the balanced salt solution throughout the experiments. Levarterenol (norepinephrine), phenylephrine, corticosterone, and 6-hydroxydopamine were employed.

Procedure—Dose–response relationships were determined for levarterenol and phenylephrine using dose levels from 2.4×10^{-7} to 3.5×10^{-5} M and from 2×10^{-7} to 1×10^{-4} M, respectively, added in a cumulative fashion.

One eye of each animal was chemically denervated by administration of 200 μl of 2% (0.12 M) 6-hydroxydopamine subconjunctivally 24 hr prior to sacrifice. 6-Hydroxydopamine was prepared fresh in normal saline containing sodium bisulfite in equimolar concentration. The control eye was injected in the same manner with 200 μl of the sodium bisulfite solvent solution.

Some tissues, both control and denervated, were treated with 8.7×10^{-5} M corticosterone 10 min prior to exposure to the adrenergic agonists. Corticosterone was allowed to remain in the bath only as long as the agonist was present and was removed concurrently with the agonist. Corticosterone was first solubilized in absolute ethanol and then diluted to the final concentration with the balanced salt solution.

Washout curves were determined by exposing control, 6-hydroxydopamine-, and corticosterone-pretreated tissues to the agonists for 10 min. Tissues were initially washed twice and were then washed once every 5 min until they returned to the precontracted baseline level.

Data Analysis—The data were normalized by calculating tension responses as a percent of the maximum value obtained. Semilogarithmic plots represent the mean values of responses obtained for no less than eight tissues for each group. Means ± SE for various groups were calculated; data were compared using the Student t test for paired variables and considered significantly different when $p < 0.05$. The degree of supersensitivity was assessed by the ED_{50} values calculated from tension responses. A programmable calculator was used for all calculations in this study.

RESULTS

Preliminary results revealed no differences in dose–response curves or washout curves for nontreated iris dilator muscles as compared to those injected with the solvent solution for 6-hydroxydopamine. Therefore, muscles treated in this manner are referred to as controls.

Figure 1 illustrates dose–response relationships of iris dilator strips to levarterenol of both control and denervated tissues, obtained in the presence and absence of corticosterone. The dose–response curves for denervated tissues exhibited supersensitivity, as shown by the shift to the left. Also, a slight increase in sensitivity was seen in both control and denervated tissues when corticosterone was present during exposure to the agonist.

Dose–response relationships for phenylephrine in control and denervated tissues both in the presence and absence of corticosterone are illustrated in Fig. 2. The responses to phenylephrine suggested a slight supersensitivity of denervated tissues, but statistical analysis did not support this finding. Both control and denervated tissues appeared slightly more sensitive to phenylephrine when corticosterone was present

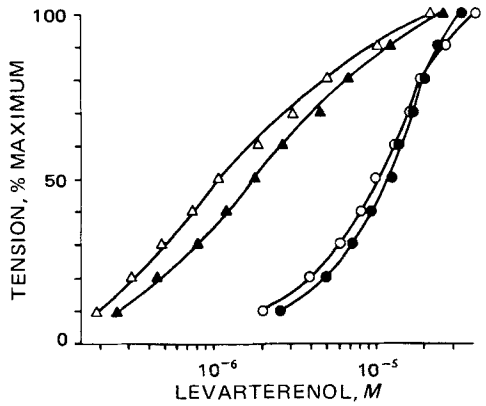

Figure 1—*Effect of 6-hydroxydopamine denervation and corticosterone blockade of extraneuronal uptake on the response of the rabbit iris dilator muscle to levarterenol. Key: ●, control; ○, control + corticosterone; ▲, denervated; and △, denervated + corticosterone. See text for* n *values and procedures of drug administration.*

before and during exposure to this agonist. Again, this finding was not supported by statistical analysis.

The ED_{50} values for levarterenol and phenylephrine on control and denervated iris dilator muscles, both in the presence and absence of corticosterone, are shown in Table I. Supersensitivity of denervated strips to levarterenol, but not to phenylephrine, was demonstrated by a significant decrease in the ED_{50} value for levarterenol as compared to the control value. Conversely, exposure of tissues to corticosterone prior to and during exposure to the agonists significantly decreased ED_{50} values for phenylephrine but not those for levarterenol.

Figure 3 shows tracings of typical response to, and washout of, levarterenol in control and denervated tissues. The marked prolongation of drug washout after chemical denervation is illustrated.

Figure 4 illustrates the washout of levarterenol (3.5×10^{-5} *M*) from control and denervated tissues in the presence and absence of corticosterone. Tension returned to the resting level significantly faster in control tissues ($t_{50\%}$ = 33 sec; time to 50% tension decay) than in denervated tissue ($t_{50\%}$ = 225 sec). The presence of corticosterone before and during exposure to levarterenol slightly increased the time required for washout in control ($t_{50\%}$ with corticosterone = 60 sec) and denervated ($t_{50\%}$ with corticosterone = 255 sec) strips.

The washout of phenylephrine (1×10^{-4} *M*) from control and denervated iris dilator muscle strips in the presence and absence of corticosterone is illustrated in Fig. 5. The washout of phenylephrine from denervated tissues ($t_{50\%}$ = 432 sec) was slower than from control tissues ($t_{50\%}$ = 177 sec), but this alteration was not as dramatic as the effect seen on levarterenol washout. Corticosterone had an effect on phenylephrine washout opposite to its effect on levarterenol washout. The washout times for phenylephrine decreased in both control ($t_{50\%}$ corticosterone = 139 sec) and denervated ($t_{50\%}$ corticosterone = 246 sec) tissues.

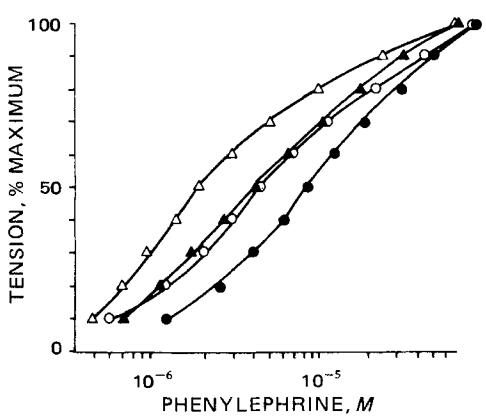

Figure 2—*Effect of 6-hydroxydopamine denervation and corticosterone blockade of extraneuronal uptake on the response of the rabbit iris dilator muscle to phenylephrine. Key: ●, control; ○, control + corticosterone; ▲, denervated; and △, denervated + corticosterone. See text for* n *values and procedures of drug administration.*

Table I—Effect of 6-Hydroxydopamine Denervation and Corticosterone Blockade of Extraneuronal Uptake on ED_{50} Values for Levarterenol and Phenylephrine on Rabbit Iris Dilator Muscle[a]

	Drug Concentration, × 10^6 *M*	
	Levarterenol	Phenylephrine
Control	21.0 ± 6.8	8.6 ± 1.9
Corticosterone	11.4 ± 0.9	3.9 ± 0.9[b]
Denervated	1.7 ± 0.7[b]	4.5 ± 1.3
Corticosterone	1.2 ± 0.4[b]	2.0 ± 0.5[b]

[a] See text for *n* values and methods of calculation. [b] Significantly different from control, $p < 0.05$.

DISCUSSION

Previous studies demonstrated that several factors are involved in the response of smooth muscle to adrenergic agents and that these factors also play a role in the decay of the response during washout of the agonists. The major factors involved are uptake by adrenergic neurons, enzymatic destruction by monoamine oxidase or catechol *O*-methyltransferase, and extraneuronal uptake.

The dose–response curves and ED_{50} values reported here for levarterenol for control and denervated tissues demonstrate the eminent importance of neuronal uptake and enzymatic (monoamine oxidase) mechanisms governing the response to this compound. The dose–response curves and ED_{50} values for phenylephrine were not altered to the same extent. This finding indicates that the neuronal uptake system of iris dilator muscle shows greater affinity for levarterenol than for phenylephrine. Support can be found for this conclusion in studies of the neuronal uptake process in other tissues (9, 10).

Corticosterone at the concentration used has been shown to block extraneuronal uptake of α-receptor agonists in other tissues (5, 6, 11). In this study, the dose–response curves and ED_{50} values for muscles treated with corticosterone suggest that extraneuronal uptake plays a more important role in determining the response to phenylephrine than to levarterenol.

The curves representing washout of agonists are sigmoid in nature and are believed to represent a valid measure of the amount of agonist present at the receptor site at any given time during washout (2). The agonist that is active at the receptor site may represent the agonist that originally interacted with the receptor or a fraction of agonist leaving some storage site such as an extraneuronal store. It is reasonable to suggest that the decline of tension upon washout of an adrenergic agonist is related to the sensitivity of that tissue to the agonist (*i.e.*, denervation-supersensitive tissues *versus* control tissues). Destruction of the adrenergic nerve terminals by 6-hydroxydopamine can potentially alter responses to agonists by two mechanisms. First, the neuronal uptake mechanism is totally absent, and second, the level of monoamine oxidase is decreased. Since corticosterone blocks extraneuronal uptake, the washout of compounds taken up into this store should be more rapid if it is blocked.

The washout of levarterenol is significantly prolonged in denervated tissues. This finding indicates that neuronal uptake and/or monoamine oxidase activity are important in the termination of its action. Levar-

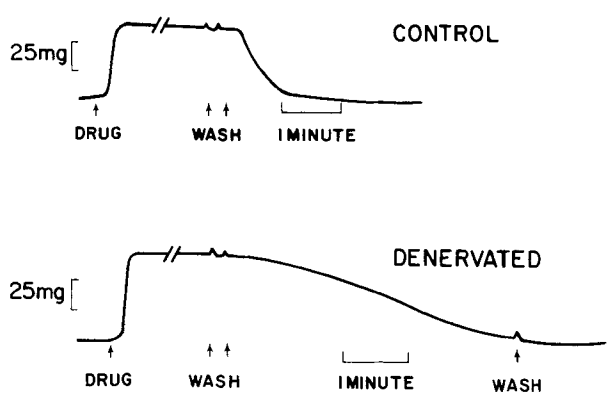

Figure 3—*Typical recording showing the effect of 6-hydroxydopamine denervation on the washout of levarterenol from the rabbit iris dilator muscle. Tissues were washed twice initially and then once every 5 min until baseline levels were reached.*

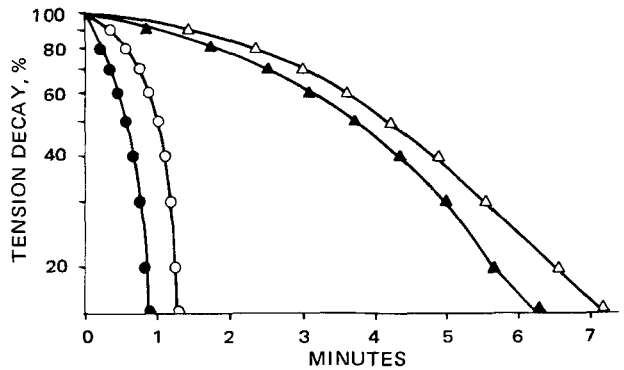

Figure 4—*Effect of 6-hydroxydopamine denervation and corticosterone blockade of extraneuronal uptake on washout of levarterenol from the rabbit iris dilator muscle. Key: ●, control; ○, control + corticosterone; ▲, denervated; and △, denervated + corticosterone. See text for* n *values and drug administration and removal protocol.*

terenol washout in tissues treated with corticosterone is slightly delayed. Thus, if extraneuronal stores are important in the termination of action of this compound, they are corticosterone insensitive in this tissue. Corticosterone-insensitive extraneuronal stores have been demonstrated (10). However, the slight but consistent delay in washout of levarterenol may be due merely to the slight shift in the ED_{50} of levarterenol under these conditions. Another possibility is that the destruction of levarterenol by catechol *O*-methyltransferase obscures the role played by extraneuronal uptake. Some support can be seen for this explanation in the data shown for washout of phenylephrine, which is not destroyed by

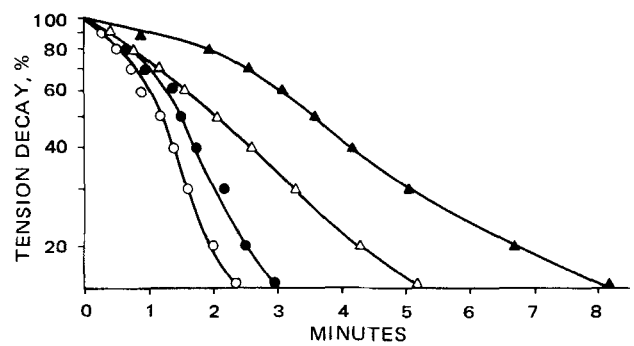

Figure 5—*Effect of 6-hydroxydopamine denervation and corticosterone blockade of extraneuronal uptake on washout of phenylephrine from the rabbit iris dilator muscle. Key: ●, control; ○, control + corticosterone; ▲, denervated; and △, denervated + corticosterone. See text for* n *values and drug administration and removal protocol.*

catechol *O*-methyltransferase.

The washout of phenylephrine from iris dilator muscle strips previously denervated with 6-hydroxydopamine was delayed as compared to control values, but not nearly so dramatically as was that of levarterenol. This finding again indicates that the affinity of the neuronal uptake mechanism is lower for phenylephrine than for levarterenol. The rate of washout of phenylephrine from corticosterone-treated tissues (both control and denervated) was more rapid than that of tissues not subjected to this treatment, indicating that extraneuronal uptake does play a role in the termination of the action of phenylephrine.

The data presented here support the view that extraneuronal uptake in iris dilator muscles from rabbits was more important in the determination of the response to phenylephrine than to levarterenol. Also, neuronal uptake was more important in determining the responsiveness to levarterenol than to phenylephrine. To clarify further the role of catechol *O*-methyltransferase and extraneuronal uptake in the termination of action of adrenergic agents in this tissue, experiments involving catechol *O*-methyltransferase inhibition and uptake of radioactively labeled compounds will be undertaken.

REFERENCES

(1) S. Kalsner, *Br. J. Pharmacol.*, **53**, 267 (1975).

(2) U. Trendelenburg, *Naunyn-Schmiedeberg's Arch. Pharmacol.*, **281**, 13 (1975).

(3) S. Kalsner and M. Nickerson, *J. Pharmacol. Exp. Ther.*, **163**, 1 (1968).

(4) S. Kalsner and M. Nickerson, *Can. J. Physiol. Pharmacol.*, **46**, 719 (1968).

(5) S. Kalsner, *Br. J. Pharmacol.*, **36**, 582 (1969).

(6) L. L. Iversen and P. J. Salt, *ibid.*, **40**, 528 (1970).

(7) M. G. Holland and J. L. Mims, III, *Invest. Ophthalmol.*, **10**, 120 (1971).

(8) R. Kern, *Arch. Klin. Exp. Ophthalmol.*, **180**, 231 (1970).

(9) U. S. V. Euler, in "Catecholamines," H. Blaschko and E. Muscholl, Eds., Springer-Verlag, New York, N.Y., 1972, p. 186.

(10) A. S. V. Burgen and L. L. Iversen, *Br. J. Pharmacol.*, **25**, 34 (1965).

(11) E. Eckert and M. Henseling, *Naunyn-Schmiedeberg's Arch. Pharmacol.*, **277**, R14 (1973).

ACKNOWLEDGMENTS AND ADDRESSES

Received November 28, 1975, from the *Department of Pharmacology, Medical College of Georgia, Augusta, GA 30902.*

Accepted for publication March 24, 1976.

Supported in part by U.S. Public Health Service Grants RR-05365-13 and AM-18424-01 and by a grant from Fight for Sight, Inc.

The technical assistance of Ms. J. Taylor is gratefully acknowledged.

[x] To whom inquiries should be directed.

Absorption, Distribution, and Excretion of ^{14}C-Meglumine in Rats and Dogs after Administration of ^{14}C-Meglumine Salicylate

JOEL F. HEEG *, GORDON S. BORN ˣ, WAYNE V. KESSLER, STANLEY M. SHAW, and WINTHROP E. LANGE ‡

Abstract □ Meglumine labeled with carbon-14 was administered orally as ^{14}C-meglumine salicylate to rats and dogs to study its distribution and excretion. The compound was incompletely absorbed; that which was absorbed was rapidly excreted in the urine. Peak blood levels were about 5–10 μg/ml in rats and 2–8 μg/ml in dogs. Tissue levels were negligible at the end of the experimental periods. No evidence for *N*-demethylation or oxidation to carbon dioxide was obtained.

Keyphrases □ ^{14}C-Meglumine—absorption, distribution, and excretion, rats and dogs □ Absorption—^{14}C-meglumine, rats and dogs □ Distribution—^{14}C-meglumine, rats and dogs □ Excretion—^{14}C-meglumine, rats and dogs □ Radiochemistry—analysis, ^{14}C-meglumine, tissues and biological fluids, rats and dogs

Several studies have been reported on the use of meglumine[1] (I) derivatives to increase the water solubility of certain pharmaceuticals, industrial chemicals, and X-ray contrast preparations (1–11). Meglumine salicylate is a promising new water-soluble salicylate compound. The absorption, distribution, and excretion of I have not been reported.

The synthesis of ^{14}C-labeled I was reported previously (12). Compound I was labeled with uniformly labeled ^{14}C-glucose to produce 1-deoxy-1-(methylamino)-D-[U-^{14}C]glucitol (I-G) and with ^{14}C-labeled methylamine to produce 1-deoxy-1-[^{14}C]methylamino-D-glucitol (I-M). These compounds were combined with equal molar amounts of salicylic acid and administered orally to I salicylate-primed and nonprimed rats and dogs to study distribution and excretion. The use of I with the ^{14}C-label in the two positions provided a means for determining whether I was metabolized by *N*-demethylation or glucose catabolism to carbon dioxide.

EXPERIMENTAL

Liquid Scintillation Counting—The liquid scintillation spectrometer was a three-channel, low temperature counter equipped with bialkali phototubes. Optimum counter settings were utilized. The scintillator consisted of 2,5-diphenyloxazole (0.4%) in an equal volume of toluene and 2-ethoxyethanol. The counting efficiency was determined by internal standardization with ring ^{14}C-labeled toluene.

Labeled Compounds—Compounds I-G and I-M were available from the syntheses reported previously (12). The specific activities measured for these compounds were used to determine the percentages of administered dose.

Animals—The rats were male Sprague–Dawley descendants[2], weighing 180–200 g except where noted. Registered male beagle dogs[3] were given a complete physical examination before the studies were initiated and were in good physical condition.

Sample Digestion Procedure—Tissue, blood, urine, bile, and fecal samples were prepared for liquid scintillation counting by a technique that was a slight modification of the acid digestion method of Mahin and Lofberg (13). This technique was similar to the method described by Bishara *et al.* (14) who used perchloric acid and hydrogen peroxide. Approximately 25–250 mg of the sample was placed in a counting vial. The amount of quenching after digestion of a sample dictated the amount of sample used for analysis. Perchloric acid (0.2 ml of 70%) was added, and the contents were mixed well to ensure thorough wetting of the sample. Hydrogen peroxide (0.2 ml of 30%) was added, and the contents were mixed.

The vials were capped, put in an oven at 70° for 30 min, and then cooled to room temperature. Another 0.5 ml of hydrogen peroxide was added, and the samples were bleached for another 30 min at 70°. The vials were again allowed to cool to room temperature, 15 ml of the scintillator was added, and the samples were mixed and counted. With the short periods of heating, there was no evidence of carbon-14 loss.

Triplicate samples (50 mg/organ and 25 mg for fecal material) for all animal studies were digested and analyzed for ^{14}C-activity. To ensure a homogeneous sample, the feces were prepared for counting by adding two to three times the sample weight of water and mixing with a stainless steel spatula in individual glass containers.

Duplicate 100–200-mg urine, bile, and blood samples were analyzed. The carcass of each rat was frozen in liquid nitrogen and then transferred to a blender. Five hundred milliliters of water was added, and the carcass was blended for about 10 min. Five aliquots, each weighing 200–250 mg, were digested. The GI tract was prepared in the same manner as the carcass, using 100 ml of water.

Dosage Preparation—*Rat Studies*—Aqueous solutions of I salicylate prepared from I-G and I-M with an equal molar amount of salicylic acid were employed for the rat studies. These solutions are referred to here as I-G salicylate and I-M salicylate. A solution containing unlabeled I salicylate was prepared for rats that were primed.

The volume of each solution administered was varied slightly for each rat to provide a 400-mg/kg dose of I salicylate. This volume was about 2 ml and contained about 5–6 μCi for the two solutions containing labeled compounds. All solutions were administered by oral intubation.

Dog Studies—The dry materials were placed in hard gelatin capsules for oral administration. Paralleling the rat studies, I-G salicylate, I-M salicylate, and unlabeled I salicylate capsules were prepared to provide each dog with a dose of 50 mg/kg of I salicylate. The amount of radioactivity in the labeled capsules was about 25 μCi.

Preliminary Experiments—Both labeled compounds, without and with salicylic acid, were used in preliminary studies in nonprimed rats. Although detectable amounts of activity were found in certain organs and tissues, no statistically significant ($p < 0.05$) amount of activity was found in any organ or tissue analyzed 24 hr after administration of either ^{14}C-labeled compound without salicylic acid. The addition of salicylic acid did not alter these findings.

Fecal excretion accounted for the largest portion of the administered dose, with renal excretion being second. Excretion of radioactivity *via* the lungs as respired ^{14}C-labeled carbon dioxide was measured by the method described by Meeks *et al.* (15). Respired ^{14}C-labeled carbon dioxide was minimal for both labeled compounds, representing 0.06–0.6% of the administered dose. This range was within the previously determined purity limits of the compounds.

Separation of the red blood cells from the plasma of heparinized whole blood, with subsequent washing of the cells five times with saline, revealed that the cells still contained greater than 33% of the total blood radioactivity 3 hr after administration. For this reason, whole blood was analyzed in the animal studies.

Distribution and Excretion Studies in Rats—A 5-day primed and nonprimed distribution and excretion study was conducted using 12 rats. These rats were divided equally into drug-primed and nonprimed groups. The drug-primed animals received unlabeled I salicylate daily for 7

[1] 1-Deoxy-1-(methylamino)-D-glucitol or *N*-methylglucamine.
[2] Laboratory Supply Co., Indianapolis, Ind.
[3] Ridglan Research Farms, Mt. Horeb, Wis.

Table I—Urinary and Fecal Excretion by Rats

Time[a]	^{14}C-Glucose-Labeled Meglumine		^{14}C-Methylamino-Labeled Meglumine	
	Urine	Feces	Urine	Feces
		Nonprimed		
8	6.28 ± 7.10[b]	2.56 ± 2.12	4.77 ± 1.33	3.17 ± 5.46
16	3.74 ± 2.53	23.23 ± 8.71	3.49 ± 2.03	29.53 ± 15.73
24	1.59 ± 1.20	14.00 ± 12.12	1.12 ± 0.41	19.58 ± 18.75
32	0.49 ± 0.38	21.46 ± 2.70	1.09 ± 0.55	15.02 ± 7.77
40	0.65 ± 0.63	10.08 ± 4.41	0.77 ± 0.52	11.94 ± 2.91
48	0.40 ± 0.38	5.37 ± 3.02	0.41 ± 0.26	3.91 ± 4.56
72	0.69 ± 0.75	5.07 ± 3.62	0.31 ± 0.26	1.12 ± 1.54
96	—[c]	—[c]	0.06 ± 0.04	0.09 ± 0.09
120	—[c]	—[c]	0.21 ± 0.25	0.03 ± 0.02
Total	13.84 ± 4.47	81.77 ± 4.66	12.23 ± 0.83	84.39 ± 1.94
		Primed		
8	3.62 ± 1.02	7.42 ± 6.54	2.47 ± 2.29	5.10 ± 8.81
16	1.73 ± 0.45	37.03 ± 18.15	2.20 ± 1.00	15.29 ± 21.00
24	1.44 ± 0.82	25.34 ± 16.48	1.52 ± 0.75	46.35 ± 23.26
32	0.39 ± 0.25	9.24 ± 0.53	0.50 ± 0.35	4.80 ± 4.53
40	0.37 ± 0.11	7.41 ± 4.22	0.25 ± 0.11	12.36 ± 5.92
48	0.19 ± 0.08	2.19 ± 1.71	0.11 ± 0.07	2.30 ± 1.37
72	0.26 ± 0.18	1.85 ± 1.42	0.12 ± 0.02	0.50 ± 0.24
96	0.09 ± 0.08	0.17 ± 0.21	0.06 ± 0.03	0.05 ± 0.35
120	0.04 ± 0.15	0.04 ± 0.38	0.05 ± 0.04	0.04 ± 0.05
Total	8.13 ± 1.75	90.69 ± 2.50	7.28 ± 3.81	86.79 ± 3.43

[a] Hours after administration. [b] Percentage of administered dose. Mean ± *SD* for three rats. [c] No sample taken.

consecutive days and were then divided into two groups of three animals each. One group was administered I-G salicylate; the other group received I-M salicylate. The nonprimed animals were similarly divided and treated.

The animals were housed in stainless steel metabolism cages with food and water provided *ad libitum*. Blood samples were taken by tail clip at 1, 2, 4, 8, 16, 24, 32, 40, 48, 72, and 120 hr after dosing. Feces and urine samples were collected 8, 16, 24, 32, 40, 48, 72, 96, and 120 hr after dosing.

After the 5-day period, the animals were sacrificed. The liver, kidneys, GI tract, GI tract contents, and remaining carcass were analyzed for ^{14}C-activity. Liver and kidneys were analyzed even though the preliminary studies showed nonsignificant activities. The cages housing the animals were washed and any residual activity was recovered. A materials balance was then conducted in an attempt to recover all of the radioactivity administered to each animal.

Rat Bile Duct Cannulation Study—Each of the two labeled compounds was used to determine biliary excretion. Four nonprimed rats, 325–350 g, were used. Two were dosed with I-G salicylate, and the remaining two received I-M salicylate. Immediately after dosing, the animals were anesthetized with pentobarbital sodium (45 mg/kg ip). An inhalation anesthetic[4] was also administered to control the level of anesthesia during surgery more effectively.

After cannulation of the bile duct, the polyethylene tubing[5] was brought out through the abdominal incision. The tubing was channeled under the skin to the right hindquarter and out an incision in the skin into a collection vial. After the incision was closed, the animal was placed on his stomach in a wire-mesh restraining cage.

Bile was collected beginning 1 hr after administration of the labeled compound, and samples were taken at 2, 3, 4, 6, 8, 12, and 24 hr after dosing. Duplicate 0.1–0.2-ml samples of bile were placed in scintillation vials, digested, and counted.

Five-Day Dog Distribution and Excretion Study—Four nonprimed dogs were used. Two received I-G salicylate, and the other two received I-M salicylate. After administration of the labeled compounds, the dogs were housed in steel cages and the urine and feces were collected. The animals were fed daily with a standard dry dog food[6]. Water was given *ad libitum* throughout the experimental period.

Blood samples were taken from each animal at 1, 2, 4, 8, 16, 24, 48, 72, 96, and 120 hr after dosing. At the end of the 5-day experimental period, the dog cages were washed and the amount of residual activity in the wash solutions was determined.

After termination of this nonprimed study, the dogs were rested for 10 days and then given complete physical examinations again. During the last 7 days of the recovery period, the animals were primed with daily doses of unlabeled I salicylate. After this priming period, the animals were again administered the labeled compounds as described previously; the urine, feces, and blood were collected at the same time intervals and analyzed.

Dog Gallbladder Cannulation Study—The bile ducts of two dogs were ligated as near the gallbladder as possible, and the bile was carefully removed from the gallbladder with a needle and syringe. An incision was made in the gallbladder just large enough to admit the end of a No. 16 French Foley indwelling catheter[7] (approximately 43.2 cm long), with a Luer inflation valve and a 5-ml balloon. The incision in the gallbladder was then closed, and the cannula was secured.

Eight milliliters of a solution of plaster of Paris was then injected into the Luer inflation valve, and the balloon portion of the catheter (within the gallbadder) was inflated. Approximately 15 cm of the catheter was brought out through the abdominal musculature, and the incision was sutured closed. The catheter was secured to the outside of the animal's body with surgical tape. An inflatable rubber collar[8] was placed around the dog's neck to prevent the animal from disturbing the catheter or the sutured area of his stomach. A plastic collection bag[9] was then positioned and secured between the front legs of the dog, the catheter was attached, and the bile was collected.

The rectal temperature of each animal was taken twice daily throughout the recovery and experimental periods. The temperature of each animal remained within normal limits at all times. Eight days after surgery, one dog was administered I-G salicylate and the other received I-M salicylate. Food and water were provided *ad libitum* throughout the experimental period. Bile was collected at 12, 24, 48, 72, 96, and 120 hr after administration of the labeled compounds.

At the end of the 5-day experimental period, the animals were sacrificed by intravenous administration of pentobarbital sodium. The following organs and tissues then were removed and frozen until analyzed: spleen, thymus, heart, kidneys, lungs, liver, adrenal, thyroid, pancreas, testes, muscle (hindleg), salivary gland, and epididymal and perirenal fat.

RESULTS

Table I shows the average percentage of the administered dose of each labeled compound and/or radioactive metabolite excreted at various time

[4] Metofane, Pitman-Moore Co., Division of Johnson & Johnson, New Brunswick, N.J.
[5] Intramedic, PE-10, Clay-Adams, Inc., New York, N.Y.
[6] Wayne Dog Food, Allied Mills, Inc., Chicago, Ill.
[7] Urogate, Abbott Laboratories, North Chicago, Ill.
[8] Davol, Inc., Providence, R.I.
[9] Bardic, Dispoz-a-Bag, C. R. Bard, Inc., Murray Hill, N.J.

Table II—Urinary and Fecal Excretion by Dogs

Time[a]	^{14}C-Glucose-Labeled Meglumine		^{14}C-Methylamino-Labeled Meglumine	
	Urine	Feces	Urine	Feces
		Nonprimed		
24	18.83 ± 0.86[b]	54.69 ± 11.60	22.87 ± 22.44	69.00 ± 19.66
48	3.60 ± 3.91	4.80 ± 4.90	1.21 ± 0.88	1.33 ± 0.92
72	0.55 ± 0.24	1.98 ± 2.47	0.26 ± 0.11	0.58 ± 0.60
96	0.21 ± 0.09	0.11 ± 0.07	0.16 ± 0.57	0.09 ± 0.11
120	0.10 ± 0.01	0.06 ± 0.01	0.06 ± 0.04	0.01 ± 0.01
Total	23.29 ± 3.39	61.64 ± 4.30	24.56 ± 23.53	71.01 ± 21.31
		Primed		
24	31.01 ± 6.95	23.28[c]	23.34[c]	61.11[c]
48	4.77 ± 2.18	35.52 ± 16.09	22.86 ± 28.57	26.27 ± 34.98
72	0.67 ± 0.06	1.88 ± 1.76	0.84 ± 0.11	0.26 ± 0.21
96	0.23 ± 0.01	0.27 ± 0.01	0.33 ± 0.01	0.07 ± 0.21
120	0.20 ± 0.05	0.11 ± 0.13	0.15 ± 0.04	0.11 ± 0.01
Total	36.88 ± 4.67	49.42 ± 1.53	35.85 ± 11.93	57.27 ± 8.40

[a] Hours after administration. [b] Percentage of administered dose. Mean ± *SD* for two dogs. [c] One dog did not urinate or did not defecate.

intervals in the urine and feces after oral administration in primed and nonprimed rats. The totals are also shown. The results indicate that excretion was nearly complete after 48 hr, and little difference was noted between urinary and fecal excretion of the glucose-labeled and methylamine-labeled compounds. Priming of the animals for 7 days prior to administration of the labeled compounds made little difference in the route or rate of excretion.

As in the preliminary study, the majority of the radioactivity was excreted in the feces and represented approximately 82–91% of the administered dose. Urinary excretion ranged from 7 to 14% of the administered dose. The total activity recovered, including that in the GI contents, the carcass, and the cage wash, ranged from about 94 to 99% of the administered activity.

The activities found in the GI contents and tract, liver, and kidneys were low and within the purity limits of the radiochemicals. This finding was also true with the carcass, which contained all of the remaining tissues and organs.

The radioactivity eliminated in the bile of rats was less than 0.1% of the administered dose for the 24-hr collection for both labeled compounds.

The urinary and fecal excretion of carbon-14 by primed and nonprimed dogs after oral administration of either I-G salicylate or I-M salicylate is shown in Table II. As was reported for the rat studies, the majority of the labeled compounds was excreted in the feces. This excretion was within the first 24-hr collection period except when the animal did not defecate.

The amount of feces excreted from nonprimed dogs was noticeably greater than from primed animals. Constipation is a possible side effect of salicylate therapy; thus, priming the animals for 7 consecutive days may have caused the decrease in fecal output by the primed animals. Concomitantly, more radioactivity was excreted in the feces of the nonprimed dogs as compared to the primed animals.

The tissue levels of I and/or radioactive metabolites in dogs were low. The muscle, which constitutes approximately 46% of live body weight (16), retained 0.1–0.2% of the administered dose after the 5-day period. Less than 0.1% of the administered dose was found in the fat of the animal. The remaining tissues analyzed showed negligible amounts of activity. All of these amounts were within the purity limits of the two labeled compounds.

Analysis of the biliary excretion data for the two dogs over the 5-day period revealed that no statistically significant ($p < 0.05$) amount of activity was detectable in any sample for either of the labeled compounds.

The peak blood levels for both rats and dogs occurred at 1–2 hr after administration. The level then slowly decreased throughout the experimental periods, with no apparent differences between the primed and nonprimed animals and between the two labeled compounds. Peak blood levels were about 5–10 μg/ml in the rats and 2–8 μg/ml in the dogs.

DISCUSSION

Blood levels of I in rats and dogs remained low, reaching a peak at about 1–2 hr after administration. Levels in other tissues were negligible in the rat and dog 5 days after administration. Thus, I was not retained in the body over a long period.

The feces were the major route of excretion for both animal species. Excretion in the feces was less in the dog than in the rat. Urinary excretion accounted for the remainder, with urinary levels being about three times higher in the dog than in the rat. Excretion by both routes in both species was nearly complete within 48 hr. Essentially no radioactivity was excreted in the bile of either the rat or dog.

Lack of biliary excretion and high fecal excretion indicated that I was poorly absorbed in both species. However, the higher urinary excretion in the dog indicated a greater absorption.

Priming of rats did not affect fecal or urinary excretion. The primed dogs did show a decrease in fecal excretion and a decrease in the total activity excreted in the feces. These decreases were probably due to the constipating effect of salicylates.

The lack of ^{14}C-labeled carbon dioxide excretion in the preliminary studies indicated that glucose catabolism to carbon dioxide did not occur. The similar behavior of both labeled compounds in all aspects studied suggested that *N*-demethylation did not occur.

REFERENCES

(1) E. H. Volwiler and E. E. Moore, U.S. pat. 2,161,114 (1939); through *Chem. Abstr.*, **33,** 7495 (1939).

(2) A. J. Guida and C. F. Peterson, *Am. Prof. Pharm.*, **18,** 196 (1953).

(3) C. F. Peterson and A. J. Guida, *J. Am. Pharm. Ass., Sci. Ed.*, **42,** 537 (1953).

(4) U. Laguzzi, British pat. 1,213,154 (1970); through *Chem. Abstr.*, **74,** 115891 (1971).

(5) J. K. J. Lim, H. O. Thompson, and C. Piantadosi, *J. Pharm. Sci.*, **53,** 1161 (1964).

(6) P. Mantovani and G. Ravasini, *Ateneo Parmense Sez. Suppl. 1,* **1969,** 69.

(7) H. L. Newmark and J. Berger, *J. Pharm. Sci.*, **59,** 1246 (1970).

(8) H. L. Newmark, J. Berger, and J. T. Carstensen, *ibid.*, **59,** 1249 (1970).

(9) A. Foldenauer, C. Meynen, and P. Boehm, *Deut. Med. Wochenschr.*, **92,** 745 (1967).

(10) S. Morishima, M. Takada, and Y. Yoichi, Japanese pat. 17,049 (1960); through *Chem. Abstr.*, **55,** P21495 (1961).

(11) R. N. Heslop and F. A. Waite, British pat. 927,404 (1963); through *Chem. Abstr.*, **60,** P1870 (1964).

(12) J. F. Heeg, G. S. Born, W. V. Kessler, S. M. Shaw, J. E. Christian, and W. E. Lange, *Can. J. Pharm. Sci.*, **10,** 75 (1975).

(13) D. T. Mahin and R. T. Lofberg, *Anal. Biochem.*, **16,** 500 (1966).

(14) R. H. Bishara, G. S. Born, and J. E. Christian, *J. Pharm. Sci.*, **61,** 1912 (1972).

(15) M. J. Meeks, R. R. Landolt, W. V. Kessler, and G. S. Born, *ibid.*, **60,** 482 (1971).

(16) "The Beagle as an Experimental Dog," A. C. Anderson and L. S. Good, Eds., Iowa University Press, Ames, Iowa, 1970, p. 83.

ACKNOWLEDGMENTS AND ADDRESSES

Received June 19, 1975, from the *Bionucleonics Department, School of Pharmacy and Pharmacal Sciences, Purdue University, West Lafayette, IN 47907.*

Accepted for publication March 15, 1976.

Supported in part by the Purdue Frederick Co., Norwalk, Conn., and by the U.S. Public Health Service, Bureau of Radiological Health, Training Grant 5-T01-RL-00064.

The authors thank Dr. Joseph L. Borowitz, Pharmacology Department, Purdue University, for his counsel in the surgical technique for the rat bile duct cannulation and Dr. Mark H. Engen, School of Veterinary Medicine, Purdue University, for conducting the bile duct cannulation in the dog.

* Present address: Pharmacokinetics/Metabolism Group, Dow Chemical, Midland, MI 48640.

‡ Present address: Purdue Frederick Co., Norwalk, CT 06856.

ˣ To whom inquiries should be directed.

Bioavailability and Activity of Topical Corticosteroids from a Novel Drug Delivery System, the Aerosol Quick-Break Foam

R. WOODFORD ˣ and B. W. BARRY

Abstract □ Experiments were conducted to: (*a*) compare the bioavailability of betamethasone benzoate in a quick-break aerosol foam and semisolid dosage forms, (*b*) compare the activity of betamethasone benzoate, betamethasone valerate, clobetasol propionate, triamcinolone acetonide, desonide, flumethasone pivalate, and hydrocortisone butyrate in foam concentrates, (*c*) assess steroid reservoir formation in skin, and (*d*) assess the effect of a natural moisturizer. Efficacy was determined by a graded response 6-hr occluded vasoconstriction test with subsequent reocclusion for reservoir demonstration. Moisturizer effect was assessed by a nonoccluded vasoconstriction test using "plain" and sodium 2-pyrrolidone-5-carboxylate-containing concentrates on arms pretreated with water or moisturizer. The activities of betamethasone benzoate concentrate, collapsed foam, ointment, and gel were similar and significantly better than the activity of the cream. Clobetasol propionate was significantly better than the other medicated concentrates, which were equivalent. Steroid-induced blanching decreased in the presence of a moisturizer.

Keyphrases □ Betamethasone benzoate—bioavailability and activity, quick-break aerosol foam and semisolid dosage forms, various corticosteroids in foam concentrates compared, effect of moisturizer □ Bioavailability—betamethasone benzoate, quick-break aerosol foam and semisolid dosage forms, effect of moisturizer □ Drug delivery systems—quick-break aerosol foam, betamethasone benzoate bioavailability and activity compared to semisolid dosage form, effect of moisturizer □ Aerosol foam, quick break—betamethasone benzoate bioavailability and activity compared to semisolid dosage form, effect of moisturizer □ Dosage forms—quick-break aerosol foam and semisolid, betamethasone benzoate bioavailability and activity compared, effect of moisturizer □ Moisturizers—effect on bioavailability and activity of betamethasone benzoate in quick-break aerosol foam and semisolid dosage forms □ Corticosteroids, topical—betamethasone benzoate, bioavailability and activity of quick-break aerosol foam and semisolid dosage forms, effect of moisturizer

Topical corticosteroid preparations are used widely to treat various dermatoses, and new formulations continue to be developed. While topical steroid aerosols have been advocated by dermatologists (1) and are commercially available, most new preparations are ointments, creams, or gels. Aerosols for clinical use are sprays or stable foams; although pharmaceutical quick-break foams offer possibilities (2), their medicinal application has apparently not been developed.

As a topical steroid dosage form, the quick-break aerosol foam offers the advantages of high activity (the steroid is in solution), ease of application, controlled dosage from a metering valve, economy in use, suitability for smooth or hairy skin, and reduced possibility of inhaling corticosteroid compared with aerosol sprays. Logical development involves devising suitable formulations and comparing them with current corticosteroid dosage forms.

This paper reports work performed to: (*a*) compare the activity and bioavailability of 0.025% (w/w) betamethasone benzoate formulated as an ointment, cream, gel, and quick-break aerosol foam, (*b*) compare the activity of 0.025% (w/w) betamethasone benzoate with that of other corticosteroids at the same concentration in quick-break foams, (*c*) assess steroid reservoir formation in the skin, and (*d*) assess the effect of sodium 2-pyrrolidone-5-carboxylate (a natural moisturizing factor) on the blanching response to steroid-containing quick-break foams.

The "activity" of a preparation is its ability to produce skin pallor (assumed to parallel anti-inflammatory activity), while the "bioavailability" of a formulation refers to the activity of a given corticosteroid in a particular base monitored as a function of time compared with this activity in different bases. Bioavailability is assessed from a pharmacological response rather than by measuring drug concentrations in tissues.

EXPERIMENTAL

Preparation of Quick-Break Foam—A nonionic emulsifying wax[1] is a suitable foaming agent for quick-break foams, especially in the presence of dichlorodifluoromethane and dichlorotetrafluoroethane. An aqueous–alcoholic system incorporating these ingredients produces excellent quick-break foams provided that the ethanol–water ratio lies between approximately 50:50 and 70:30 (3). Quick-break foams may also be prepared using propylene glycol–water mixtures. Twelve preliminary formulations were investigated consisting of various combinations of ethanol, propylene glycol, and water: ethanol, 56.5–13.0% (w/w); propylene glycol, 75.0–3.9% (w/w); and water, 27.0–0% (w/w).

Four basic formulations were developed, and from these the following preparation was selected as the most satisfactory: 0.025 g of betamethasone benzoate, 5.50 g of propylene glycol BP, 55.475 ml of dehydrated alcohol BP, 26.50 ml of purified water BP, 2.0 g of nonionic

[1] Polawax A31, Croda Chemicals Ltd., Goole, Yorks., United Kingdom.

ACKNOWLEDGMENTS AND ADDRESSES

Received June 19, 1975, from the *Bionucleonics Department, School of Pharmacy and Pharmacal Sciences, Purdue University, West Lafayette, IN 47907.*

Accepted for publication March 15, 1976.

Supported in part by the Purdue Frederick Co., Norwalk, Conn., and by the U.S. Public Health Service, Bureau of Radiological Health, Training Grant 5-T01-RL-00064.

The authors thank Dr. Joseph L. Borowitz, Pharmacology Department, Purdue University, for his counsel in the surgical technique for the rat bile duct cannulation and Dr. Mark H. Engen, School of Veterinary Medicine, Purdue University, for conducting the bile duct cannulation in the dog.

* Present address: Pharmacokinetics/Metabolism Group, Dow Chemical, Midland, MI 48640.

‡ Present address: Purdue Frederick Co., Norwalk, CT 06856.

ˣ To whom inquiries should be directed.

Bioavailability and Activity of Topical Corticosteroids from a Novel Drug Delivery System, the Aerosol Quick-Break Foam

R. WOODFORD ˣ and B. W. BARRY

Abstract □ Experiments were conducted to: (*a*) compare the bioavailability of betamethasone benzoate in a quick-break aerosol foam and semisolid dosage forms, (*b*) compare the activity of betamethasone benzoate, betamethasone valerate, clobetasol propionate, triamcinolone acetonide, desonide, flumethasone pivalate, and hydrocortisone butyrate in foam concentrates, (*c*) assess steroid reservoir formation in skin, and (*d*) assess the effect of a natural moisturizer. Efficacy was determined by a graded response 6-hr occluded vasoconstriction test with subsequent reocclusion for reservoir demonstration. Moisturizer effect was assessed by a nonoccluded vasoconstriction test using "plain" and sodium 2-pyrrolidone-5-carboxylate-containing concentrates on arms pretreated with water or moisturizer. The activities of betamethasone benzoate concentrate, collapsed foam, ointment, and gel were similar and significantly better than the activity of the cream. Clobetasol propionate was significantly better than the other medicated concentrates, which were equivalent. Steroid-induced blanching decreased in the presence of a moisturizer.

Keyphrases □ Betamethasone benzoate—bioavailability and activity, quick-break aerosol foam and semisolid dosage forms, various corticosteroids in foam concentrates compared, effect of moisturizer □ Bioavailability—betamethasone benzoate, quick-break aerosol foam and semisolid dosage forms, effect of moisturizer □ Drug delivery systems—quick-break aerosol foam, betamethasone benzoate bioavailability and activity compared to semisolid dosage form, effect of moisturizer □ Aerosol foam, quick break—betamethasone benzoate bioavailability and activity compared to semisolid dosage form, effect of moisturizer □ Dosage forms—quick-break aerosol foam and semisolid, betamethasone benzoate bioavailability and activity compared, effect of moisturizer □ Moisturizers—effect on bioavailability and activity of betamethasone benzoate in quick-break aerosol foam and semisolid dosage forms □ Corticosteroids, topical—betamethasone benzoate, bioavailability and activity of quick-break aerosol foam and semisolid dosage forms, effect of moisturizer

Topical corticosteroid preparations are used widely to treat various dermatoses, and new formulations continue to be developed. While topical steroid aerosols have been advocated by dermatologists (1) and are commercially available, most new preparations are ointments, creams, or gels. Aerosols for clinical use are sprays or stable foams; although pharmaceutical quick-break foams offer possibilities (2), their medicinal application has apparently not been developed.

As a topical steroid dosage form, the quick-break aerosol foam offers the advantages of high activity (the steroid is in solution), ease of application, controlled dosage from a metering valve, economy in use, suitability for smooth or hairy skin, and reduced possibility of inhaling corticosteroid compared with aerosol sprays. Logical development involves devising suitable formulations and comparing them with current corticosteroid dosage forms.

This paper reports work performed to: (*a*) compare the activity and bioavailability of 0.025% (w/w) betamethasone benzoate formulated as an ointment, cream, gel, and quick-break aerosol foam, (*b*) compare the activity of 0.025% (w/w) betamethasone benzoate with that of other corticosteroids at the same concentration in quick-break foams, (*c*) assess steroid reservoir formation in the skin, and (*d*) assess the effect of sodium 2-pyrrolidone-5-carboxylate (a natural moisturizing factor) on the blanching response to steroid-containing quick-break foams.

The "activity" of a preparation is its ability to produce skin pallor (assumed to parallel anti-inflammatory activity), while the "bioavailability" of a formulation refers to the activity of a given corticosteroid in a particular base monitored as a function of time compared with this activity in different bases. Bioavailability is assessed from a pharmacological response rather than by measuring drug concentrations in tissues.

EXPERIMENTAL

Preparation of Quick-Break Foam—A nonionic emulsifying wax[1] is a suitable foaming agent for quick-break foams, especially in the presence of dichlorodifluoromethane and dichlorotetrafluoroethane. An aqueous–alcoholic system incorporating these ingredients produces excellent quick-break foams provided that the ethanol–water ratio lies between approximately 50:50 and 70:30 (3). Quick-break foams may also be prepared using propylene glycol–water mixtures. Twelve preliminary formulations were investigated consisting of various combinations of ethanol, propylene glycol, and water: ethanol, 56.5–13.0% (w/w); propylene glycol, 75.0–3.9% (w/w); and water, 27.0–0% (w/w).

Four basic formulations were developed, and from these the following preparation was selected as the most satisfactory: 0.025 g of betamethasone benzoate, 5.50 g of propylene glycol BP, 55.475 ml of dehydrated alcohol BP, 26.50 ml of purified water BP, 2.0 g of nonionic

[1] Polawax A31, Croda Chemicals Ltd., Goole, Yorks., United Kingdom.

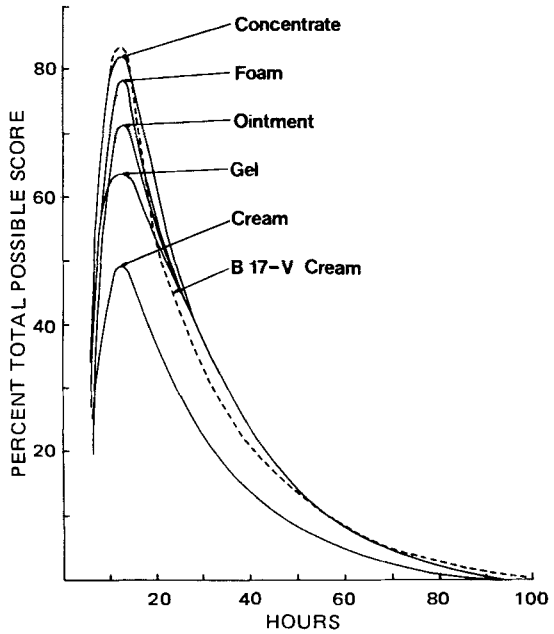

Figure 1—*Blanching response to betamethasone benzoate formulations containing 0.025% steroid and to 0.1% betamethasone valerate cream.*

emulsifying wax[1], 0.50 g of hydroxyethylcellulose[2], 4.0 g of dichlorodifluoromethane[3], and 6.0 g of dichlorotetrafluoroethane[4].

Water was added to the hydroxyethylcellulose with swirling. The mixture was gently heated to 60° until gelling commenced, and it was left to hydrate at room temperature for 1 hr with occasional swirling. Then propylene glycol was added with mixing. The corticosteroid was dissolved at room temperature in the alcohol, and this solution was added gradually with mixing. The nonionic emulsifying wax was added, and the system was warmed to approximately 60° with swirling until the wax dissolved. The homogeneous warm mixture was poured into a tin-plate aerosol container and cooled to below room temperature, and dichlorotetrafluoroethane was added. The valve system was crimped into place, and dichlorodifluoromethane was added *via* a transfer button.

Placebo formulations were prepared by replacing the steroid with dehydrated alcohol. Placebo foams were also produced using 5.0–6.0 g of a suitable mixture of hydrocarbons (propane, *n*-butane, and isobutane)[5] instead of the chlorofluorohydrocarbon propellent blend.

Assessment of Betamethasone Benzoate Formulations—Four formulations containing 0.025% (w/w) betamethasone benzoate were employed (quick-break foam, gel, cream, and ointment) together with the foam concentrate. A placebo foam and concentrate were also included. The carboxypolymethylene-based gel, oil-in-water cream, and white petrolatum-based ointment were used as received from the manufacturer[6].

Efficacy and bioavailability were assessed by a modified skin-blanching test (4, 5). Ten volunteers were selected without reference to their sex or steroid sensitivity. None had received topical corticosteroid therapy for at least 3 months prior to the study. Five milligrams of the semisolid preparations and 5 μl of the concentrates and expelled, collapsed foams were applied with reference to randomization charts to the washed flexor surface of each forearm. Application sites (7 × 7-mm areas punched out from double-sided polyethylene tape[7]) were occluded with polyester film[8] for 6 hr, the sites were washed with soap and water at skin temperature and dried, and readings were taken in a double-blind manner to provide data points for skin blanching at 6, 7, 8, 9, 12, 24, 32, 48, 72, 80, and 96 hr after application.

The degree of pallor was estimated on a 0–4 scale with half-point ratings (4). To assess steroid retention in the skin, the sites on selected volunteers were reoccluded with polyester film for 12 hr, 8 days after commencement of the experiment, and pallor was estimated 5 hr later when blanching was maximal.

Assessment of Steroid-Containing Concentrates—Seven corticosteroids (betamethasone benzoate, betamethasone valerate, clobetasol propionate, flumethasone pivalate, desonide, hydrocortisone 17-butyrate, and triamcinolone acetonide) were separately formulated as quick-break foam concentrates, and their activities were investigated as already described.

Assessment of Effect of Natural Moisturizing Factor—Five corticosteroids (betamethasone benzoate, betamethasone valerate, clobetasol propionate, flumethasone pivalate, and fluocinolone acetonide) were separately formulated in quick-break foam concentrates with and without 5% (w/w) of a 50% aqueous solution of sodium 2-pyrrolidone-5-carboxylate[9]. The "plain" concentrate contained 0.025 g of the corticosteroid, 5.0 g of propylene glycol BP, 55.475 ml of dehydrated alcohol BP, 25.0 ml of purified water BP, 2.0 g of nonionic emulsifying wax, and 0.50 g of hydroxyethylcellulose. The "moisturizing" concentrate was the same except that it contained 22.50 ml of purified water BP and 4.5 g of sodium 2-pyrrolidone-5-carboxylate (50% aqueous solution). The method of preparation was as previously described, the moisturizer being mixed with the hydrated hydroxyethylcellulose before the propylene glycol was added.

To accentuate any effect of the moisturizer, 0.7 ml of a 5% (w/w) aqueous solution of sodium 2-pyrrolidone-5-carboxylate was rubbed (3 min) into one arm of each of 10 volunteers twice a day for 7 days; the other arm was similarly treated with water as a control. A medical rubber finger-cot[10] was used, since experiments had shown that it was impermeable to water and sodium 2-pyrrolidone-5-carboxylate solutions. Five microliters of the plain and moisturizing concentrates were applied to each arm as described, and the polyethylene tape removed. The sites were left nonoccluded but protected by a perforated plastic guard for 6 hr (4) to avoid the hydrating effect of occlusion. Then the sites were washed and dried, and pallor was assessed as before.

In each blanching test, betamethasone valerate cream[11] was employed as a control "standard preparation" so that the results could be correlated with other investigations.

RESULTS AND DISCUSSION

Formulation of Quick-Break Foam—The quick-break foam easily rubbed into glabrous or hairy skin, leaving the site soft and not sticky. The hydroxyethylcellulose increased the viscosity of the liquid remaining after foam collapse, facilitating application to a limited area. During application, some ethanol evaporated, tending to increase the concentration and thermodynamic activity of the steroid in the solvent mixture and thus promoting percutaneous absorption; the propylene glycol minimized precipitation of medicament as the amount of alcohol decreased. Experiments on a placebo formulation, packed in a glass bottle fitted with a metering valve[12] and foam actuator, showed that an undisturbed 180 mg of foam (mean of 10 determinations, range of 178–183 mg) collapsed on the ventral surface of the forearm in 6.5 sec (mean of 10 determinations, range of 6.1–7.0 sec).

A can aged for 1 week at room temperature (17–20°) had a vapor pressure of 24 psig, as did a sample consisting of 90 g of concentrate and 5.8 g of a hydrocarbon propellent blend. Foams produced using chlorofluorocarbon propellents and hydrocarbon propellents usually appeared equally satisfactory, although the hydrocarbon-containing foams were more flammable. Because of their possible adverse effect on the ozone layer, the continued use of halogen-containing propellents has been criticized (6). A suitable mixture of hydrocarbons is a possible alternative propellent for a corticosteroid quick-break foam.

Betamethasone Benzoate Formulations—With each formulation, the results for all volunteers were expressed as a percentage of the total possible score at each time period. The method of calculation was as follows: maximum score per site = 4; for two arms, 4 × 2 = 8; for 10 volunteers, 8 × 10 = 80 (*e.g.*, 6-hr reading for quick-break foam, score of 25 out of a possible 80 = 31.3%). To relate the results obtained with the betamethasone benzoate formulations to those obtained with proprietary

[2] Cellosize QP-4400-L, Union Carbide U.K. Ltd., Rickmansworth, Herts., United Kingdom.
[3] Arcton 12, Imperial Chemical Industries Ltd., Runcorn, Cheshire, United Kingdom.
[4] Arcton 114, Imperial Chemical Industries Ltd., Runcorn, Cheshire, United Kingdom.
[5] Calor Aerosol Propellent, Calor Gas Co., Weybridge, Surrey, United Kingdom.
[6] William R. Warner & Co. Ltd., Eastleigh, Hants., United Kingdom.
[7] Blenderm, 3M Medical Products, London, United Kingdom.
[8] Melinex S 12 μm, Imperial Chemical Industries Ltd., Welwyn Garden City, Herts., United Kingdom.
[9] Ajidew N-50, Ajinomoto Co., Tokyo, Japan.
[10] London Rubber Products, London, United Kingdom.
[11] Betnovate cream, Glaxo Laboratories Ltd., Greenford, Middlesex, United Kingdom.
[12] 5883/5618 R valve, Bespak Industries Ltd., Cheshunt, Herts., United Kingdom.

Table I—Blanching Response to Betamethasone Benzoate Formulations Containing 0.025% (w/w) Steroid

Formulation	Area under Curve[a], % *TPS* × hr	Bioavailability[b]	Summed Percent Total Possible Score[c]	*Tm*/10 Mean Value[d]	$t_{1/2}$[e], hr	Percent Total Possible Score on Reocclusion[f]
Betamethasone benzoate concentrate	2350	1.0	392	5.58	13.1	45
Betamethasone benzoate foam	2180	0.93	381	5.50	12.4	45
Betamethasone benzoate ointment	2010	0.85	297	4.84	12.5	28
Betamethasone benzoate gel	2000	0.85	357	5.32	13.2	37
Betamethasone benzoate cream	1290	0.55	240	4.30	14.0	14
Betamethasone valerate cream, 0.1%	2140	—	393	5.58	14.0	24

[a] Obtained by planimetry of the blanching profile to three significant figures; *%TPS* = percent total possible score. [b] The bioavailability of a betamethasone benzoate preparation is the area under its blanching curve divided by the area under the curve of the concentrate (the most active formulation). [c] The percent total possible scores summed for all volunteers over all reading times. [d] The *Tm*/10 mean value is the square root transformation of sum of scores (*Tm*) divided by the number of volunteers (10). The minimum significance range value $k = 0.75$ ($p = 0.05$); *i.e.*, if the *Tm*/10 values of two formulations differ by more than 0.75, there is a significant difference between those formulations. [e] Apparent vasoconstriction half-life = $0.693/K_{vc}$. [f] Reoccluded for 12 hr, 8 days after commencement of the experiment.

preparations (4, 5), the percentages of total possible score values were multiplied by the value: summed percent total possible score value for betamethasone valerate cream in Ref. 4/summed percent total possible score value for betamethasone valerate cream in the betamethasone benzoate study. By this means, the results obtained in the present work were comparable with those reported previously.

Blanching profiles for the betamethasone preparations are shown in Fig. 1; experimental points were omitted for clarity but all lay on or near the curves as drawn. All preparations gave curves with a peak in the 12-hr region and a marked fall-off thereafter. The blanching profile for each formulation was a measure of its activity as a function of time, involving: (*a*) release of corticosteroid from the base, (*b*) penetration of the medicament through the epidermis into the dermis, (*c*) onset and duration of corticosteroid-induced pallor at the vascular region, and (*d*) decline of pharmacological response and elimination of drug from the site of action.

A single numerical parameter that takes account of these four factors is the area under the blanching curve; therefore, it is the parameter most suitable for comparing the bioavailability of steroids in various bases. When arranged in an area under the curve rank order, the aerosol concentrate and foam were superior to the other preparations (Table I). The comparative bioavailability of a formulation was obtained by dividing its area under the curve by that of the most active preparation (*i.e.*, the concentrate). The order was not identical to that based on a summed percentage of the total possible score relationship (*i.e.*, the percentage of the total possible scores summed for all time periods).

The scores for each volunteer were summed over all reading times and analyzed statistically as the nontransformed data and as each of five transformations (x^{-1}, $x^{-1/2}$, $\log x$, $x^{1/2}$, and x^2) (4). Tests for nonadditivity (7) indicated a preference for the square root transformation, and the analysis of variance was calculated using those values. The differences between the preparations were highly significant ($F = 8.36$, $p < 0.01$), while those between the volunteers were significant ($F = 2.21$, $p < 0.05$).

Calculation of the minimum significance range value k using the Student range test (8) permitted comparison of the betamethasone formulations. Significant differences between preparations occurred when their *Tm*/10 mean values (Table I) differed by a figure greater than the value of k. For example, the nonsignificance range for betamethasone benzoate concentration was $5.58 - 0.75 = 4.83$. Hence, the aerosol foam and concentrate were as active in the blanching test as the semisolid formulations with the exception of the betamethasone benzoate cream, which was significantly less active.

Linear plots of log percent total possible score against time over 24–72 hr permitted least-squares evaluation of the apparent vasoconstriction dissipation rate constant (K_{vc}) and the apparent vasoconstriction half-life ($t_{1/2}$) (9). The value of K_{vc} quantifies the disappearance of blanching arising from steroid biotransformation, homeostasis, vascular removal, diffusion from the site of action, and tachyphylaxis. The overall elimination process was described by apparent first-order kinetics, and the values of K_{vc}, $t_{1/2}$ (Table I), and the slope of the regression line equation were similar for all betamethasone formulations. Thus, the equation for the linear plots may be written as:

$$\ln (\%\ TPS) = \ln (\%\ TPS)_0 - K_{vc}t \qquad \text{(Eq. 1)}$$

where $\ln (\%\ TPS)_0$ represents the extrapolated value of the response at time $t = 0$. Regression line equations (for four points) to three significant figures were:

foam	$\ln (\%\ TPS) = 5.32 - 0.0560t$, $r = -0.999$
foam concentrate	$\ln (\%\ TPS) = 5.27 - 0.0529t$, $r = -1.00$
cream	$\ln (\%\ TPS) = 4.57 - 0.0494t$, $r = -0.997$
gel	$\ln (\%\ TPS) = 5.22 - 0.0524t$, $r = -0.997$
ointment	$\ln (\%\ TPS) = 5.31 - 0.0554t$, $r = -0.996$
betamethasone valerate cream	$\ln (\%\ TPS) = 5.01 - 0.0495t$, $r = -0.997$

These results indicated that the disappearance of betamethasone benzoate-induced pallor proceeded at a rate essentially independent of the nature of the vehicle. Furthermore, the replacement of the benzoate group by valerate at the 17-position had little apparent effect on the dissipation of blanching due to the betamethasone derivative.

Reocclusion of the application sites in two volunteers (for which, therefore, statistical analysis was inapplicable) permitted estimation of steroid retention in the stratum corneum. Obvious reservoirs were established with the foam and concentrate, while the least pallor on reocclusion was produced by betamethasone benzoate cream (Table I). Subsequent reocclusion showed that the presence of steroids in the skin could not be demonstrated after 12 days. The placebo concentrate and foam failed to blanch following 6 hr application or after reocclusion.

Steroid-Containing Concentrates—The blanching scores for the steroid-containing concentrates were expressed as percent total possible scores as already described, and blanching curves are shown in Figs. 2 and 3. In all cases, the shapes of the graphs were similar; Table II ranks the concentrates on an area under the blanching curve basis. As with the previous experiment, this listing was not identical to that based on summed percent total possible scores. Least-squares evaluation of linear plots of log percent total possible score against time over 24–72 hr (Figs. 2 and 3) showed that similar steroids (triamcinolone acetonide and desonide and betamethasone benzoate and betamethasone valerate) gave similar values of $t_{1/2}$ and K_{vc}. Regression line equations (for four points) to three significant figures for the medicated concentrates were:

clobetasol propionate	$\ln (\%\ TPS) = 5.02 - 0.0390t$, $r = -1.00$
flumethasone pivalate	$\ln (\%\ TPS) = 5.34 - 0.0596t$, $r = -1.00$
triamcinolone acetonide	$\ln (\%\ TPS) = 5.13 - 0.0463t$, $r = -0.999$
desonide	$\ln (\%\ TPS) = 5.12 - 0.0472t$, $r = -0.999$
hydrocortisone 17-butyrate	$\ln (\%\ TPS) = 5.61 - 0.0731t$, $r = -1.00$
betamethasone benzoate	$\ln (\%\ TPS) = 5.27 - 0.0529t$, $r = -0.999$
betamethasone valerate	$\ln (\%\ TPS) = 5.06 - 0.0530t$, $r = -1.00$
betamethasone valerate cream	$\ln (\%\ TPS) = 5.01 - 0.0497t$, $r = -1.00$

A ranking of steroid concentrates using $t_{1/2}$ values was similar to that based on area under the curve data (Table II).

Statistical analysis showed that the medicated concentrates were as effective in inducing pallor as the standard (betamethasone valerate cream) with the exception of that containing clobetasol propionate, which was significantly more active ($p < 0.05$). Similar steroid reservoirs were produced in the skin with all concentrates (Table II); subsequent reoc-

Table II—Blanching Response to Quick-Break Foam Concentrates Containing 0.025% (w/w) Steroid

Steroid or Formulation	Area under Curve[a], % *TPS* × hr	Summed Percent Total Possible Score[b]	*Tm*/10 Mean Value[c]	$t_{1/2}$[d], hr	Percent Total Possible Score on Reocclusion[e]
Clobetasol propionate	3070	568	6.74	17.8	28
Desonide	2610	441	5.89	14.7	24
Triamcinolone acetonide	2580	453	6.00	15.0	24
Betamethasone benzoate	2350	392	5.58	13.1	45
Flumethasone pivalate	2250	445	5.92	11.6	37
Betamethasone valerate	2020	409	5.70	13.1	34
Hydrocortisone 17-butyrate	1970	394	5.56	9.5	28
Betamethasone valerate cream, 0.1%	2140	393	5.58	13.9	24

[a] Obtained by planimetry of the blanching profile to three significant figures; *%TPS* = percent total possible score. [b] The percent total possible scores summed for all volunteers over all reading times. [c] The *Tm*/10 mean value is the square root transformation of sum of scores (*Tm*) divided by the number of volunteers (10). The minimum significance range value $k = 0.53$ ($p = 0.05$); *i.e.*, if the *Tm*/10 values of two formulations differ by more than 0.53, there is a significant difference between those formulations. [d] Apparent vasoconstriction half-life = $0.693/K_{VC}$. [e] Reoccluded for 12 hr, 8 days after commencement of the experiment.

clusion showed that the presence of medicament could not be demonstrated after 12 days with the exception of clobetasol propionate, which disappeared after 14 days.

The area under the blanching curve, summed percent total possible score, and percent total possible score on reocclusion values obtained with the foam concentrates were often higher than the values obtained previously with the corresponding commercial creams and ointments (4, 5), although the concentration of steroid in the semisolid formulations was usually two to four times greater than that of the concentrates. For flumethasone pivalate, the concentration of steroid in the ointment and cream was 0.02% (*i.e.*, approximately the same as that in the concentrate). However, the foam concentrate gave blanching values three to four times those of the commercial preparations, depending on the parameter employed (area under the curve or summed percent total possible score). No attempt was made to optimize fully the release and subsequent blanching activity of corticosteroid from each concentrate. It is thus possible that, by careful selection of the ethanol–propylene glycol–water ratio for each steroid (within the limits for quick-break foam production), a further enhanced vasoconstrictor efficacy for the concentrate could be achieved.

Assessment of Effect of Moisturizer—Hydration of the stratum corneum usually facilitates penetration of corticosteroid. To increase skin hydration, a moisturizer was employed both in the formulations and in pretreatment of the arms.

Steroid-induced blanching in the presence and absence of sodium 2-pyrrolidone-5-carboxylate is shown in Table III. Statistical examination by a three-way analysis of variance (10) followed by the Student range test showed significant differences ($p < 0.05$) between moisturizer- and water-treated arms for clobetasol propionate, fluocinolone acetonide, and betamethasone valerate, whereas only clobetasol propionate (the most potent steroid examined) showed a significant difference between concentrates with and without moisturizer on either arm.

The corticosteroids gave values that decreased in the order: control (moisturizer-free) concentrate on control (water-treated) arm > moisturizer-containing concentrate on control arm > control concentrate on moisturizer-treated arm > moisturizer-containing concentrate on moisturizer-treated arm. This sequence was surprising, and the reason

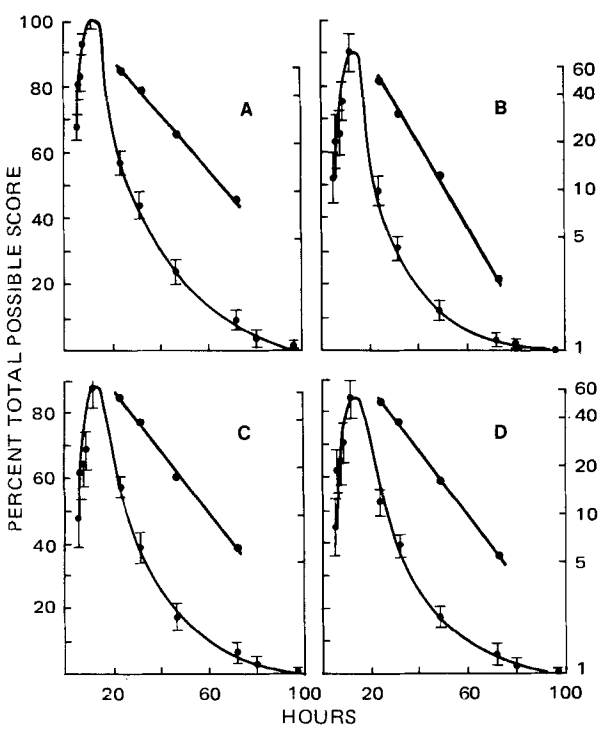

Figure 2—*Blanching response to quick-break foam concentrates containing 0.025% steroid. Curves are the arithmetic plots ± SEM; n = 10 (bar lines were omitted from occasional points for clarity). Straight lines are the percent total possible score logarithmic plots. Key: A, clobetasol propionate; B, flumethasone pivalate; C, triamcinolone acetonide; and D, desonide.*

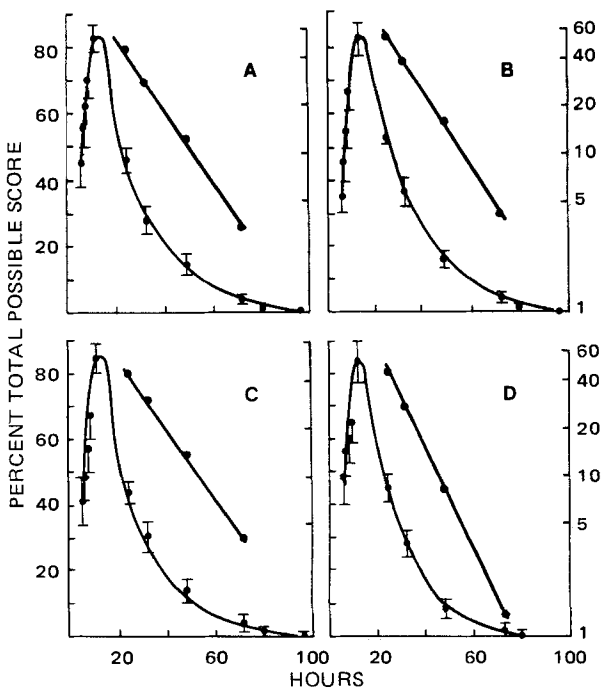

Figure 3—*Blanching response to quick-break foam concentrates containing 0.025% steroid and to 0.1% betamethasone valerate cream. Curves are the arithmetic plots ± SEM; n = 10 (bar lines were omitted from occasional points for clarity). Straight lines are the percent total possible score logarithmic plots. Key: A, betamethasone valerate; B, betamethasone benzoate; C, betamethasone valerate cream, 0.1%; and D, hydrocortisone 17-butyrate.*

Table III—Blanching Response to Quick-Break Foam Concentrates Containing 0.025% (w/w) Steroid in the Presence and Absence of Moisturizer[a]

	Tm/10 Mean Value[b]	
	Moisturizer-Treated Arm	Water-Treated Arm
Clobetasol propionate plus moisturizer	5.15	11.70
Fluocinolone acetonide plus moisturizer	1.70	6.90
Betamethasone valerate plus moisturizer	0.90	5.50
Betamethasone benzoate plus moisturizer	1.10	3.70
Flumethasone pivalate plus moisturizer	1.15	3.10
Clobetasol propionate	9.85	15.60
Fluocinolone acetonide	4.05	10.75
Betamethasone valerate	4.40	8.60
Betamethasone benzoate	3.25	6.90
Flumethasone pivalate	3.00	5.65

[a] Moisturizer was sodium 2-pyrrolidone-5-carboxylate, 5% (w/w) of concentrate. [b] Sum of scores (*Tm*) divided by number of volunteers (10). The minimum significance range value $k = 3.86$ ($p = 0.05$); *i.e.*, if two formulations differ by more than 3.86, there is a significant difference between those formulations. Betamethasone valerate cream, 0.1%, gave total scores of 38 (moisturizer-treated arm) and 78.5 (water-treated arm).

for the diminution of steroid-induced blanching in the presence of sodium 2-pyrrolidone-5-carboxylate remains unresolved. This result could have been due to the effects of moisturizer within the vehicle and/or within the skin.

For example, sodium 2-pyrrolidone-5-carboxylate may have increased the solubilities of the steroids in the vehicle and/or reduced their thermodynamic activities by complexation, thus lowering the skin–vehicle partition coefficients, with consequent reduction in flux through the skin. (Preliminary work[13] indicated that the water solubility of the parent steroid, hydrocortisone, increased approximately twofold in the presence of 2-pyrrolidone-5-carboxylic acid.) The moisturizer may have altered the diffusional properties of corticosteroid molecules in the skin (*e.g.*, by an effect on skin structure, by binding of water, or by complex formation with the steroid).

In addition, sodium 2-pyrrolidone-5-carboxylate may have had an effect on shunt diffusion; it was suggested[14] that if the corticosteroids penetrated significantly *via* the hair follicles and/or down the ducts of the sweat glands, lower blanching responses in the presence of moisturizer might have been caused by partial constriction of the shunt routes by sodium 2-pyrrolidone-5-carboxylate. To investigate this possibility for sweat glands, a 5% (w/w) aqueous solution of the moisturizer was rubbed into one side of the forehead of one volunteer twice a day for 7 days, the other side being similarly treated with water. After 1 week, the volunteer exercised vigorously to perspire. There was no apparent difference in sweating between the moisturizer-treated and control halves of the forehead. However, when the procedure was repeated using undiluted moisturizer (*i.e.*, 50% aqueous solution of sodium 2-pyrrolidone-5-carboxylate), there seemed to be some reduction in the sweat flow. These results indicate that large amounts of moisturizer may have some vehicle effect on shunt pathways. However, more sophisticated techniques are required to elucidate the reduction of corticosteroid-induced blanching in the presence of sodium 2-pyrrolidone-5-carboxylate.

The present work investigated the possible pharmaceutical use of an aerosol quick-break foam. The foam concentrate together with the propellent gave a homogeneous system at room temperature. When the product was discharged from the container, the propellent vaporized; the foaming agent (nonionic emulsifying wax) crystallized due to a loss of solubilizer (*i.e.*, propellent) and a reduction in temperature to below that at which the foaming agent deposited. The precipitation of the wax from solution produced a foam that collapsed on the skin as the wax redissolved at skin temperature, foam destruction being accelerated by shearing.

In use, the product is expelled onto a limited skin area; the resultant foam breakage brings the homogeneous liquid into intimate contact with the skin surface. The liquid may be rubbed into the skin to leave a site that is dry, soft, and not sticky. The present work indicates that quick-break foams containing corticosteroids are highly active preparations as assessed by the blanching test. Drug bioavailability is good, so the steroid is readily available to the skin from a controlled-dosage, esthetically attractive, economic preparation. It should be possible to modify the basic formulation to optimize release of drug or moisturizer or to control the breaking characteristics of the foam. The quick-break foam should be a suitable vehicle for a wide range of topical corticosteroids and may be a useful delivery system for other medicaments, offering the prospect of a sterile preparation that will remain so during use.

[13] A. Cripps, School of Pharmacy, Portsmouth Polytechnic, Portsmouth, Hants., United Kingdom, unpublished observations.

[14] B. Poulsen, Syntex Research, Palo Alto, Calif., personal communication.

REFERENCES

(1) H. I. Maibach and R. B. Stoughton, *Med. Clin. N. Am.*, **57**, 1253 (1973).

(2) J. J. Sciarra, *J. Pharm. Sci.*, **63**, 1815 (1974).

(3) J. F. L. Chester, *Soap Perfum. Cosmet.*, **40**, 393 (1967).

(4) B. W. Barry and R. Woodford, *Br. J. Dermatol.*, **91**, 323 (1974).

(5) *Ibid.*, **93**, 563 (1975).

(6) *Drug Cosmet. Ind.*, **116** (2), 36 (1975).

(7) H. L. Harter and M. D. Lum, Aeronautical Research Laboratories, USAF ARL 62-313, 1962, p. 1.

(8) A. Goldstein, "Biostatistics: An Introductory Text," Macmillan, New York, N.Y., 1964, p. 63.

(9) B. W. Barry and A. R. Brace, *J. Pharm. Pharmacol., Suppl.*, **26**, 67P (1974).

(10) K. A. Brownlee, "Statistical Theory and Methodology in Science and Engineering," Wiley, New York, N.Y., 1965, p. 504.

ACKNOWLEDGMENTS AND ADDRESSES

Received February 23, 1976, from the *School of Pharmacy, Portsmouth Polytechnic, King Henry I Street, Portsmouth, Hants. P01 2DZ, United Kingdom.*

Accepted for publication March 18, 1976.

Presented at the Basic Pharmaceutics Section, APhA Academy of Pharmaceutical Sciences, Atlanta meeting, November 1975.

The authors thank Mr. B. Tolman for assistance with the statistical analysis.

[x] To whom inquiries should be directed.

Polydisperse Particulate Solids Mixing and Segregation: Nonstationary Markov Chains

C. H. CHOU, J. R. JOHNSON *, and E. G. RIPPIE ˣ

Abstract □ The feasibility of analyzing interparticulate translocations within agitated beds of polydisperse particulate solids in terms of Markov chains was investigated. A binary mixture of spherical particles subjected to vertical sine wave vibration is shown to behave in accordance with a nonstationary Markov chain having singly stochastic transition matrixes. The transition probability elements of such matrixes, calculated from a knowledge of the initial and final occupancy vectors, agree with those estimated using tracer particles. With appropriate restrictions, the former method, based on the solution of simultaneous equations, permits a quantitative evaluation of particle mobilities throughout the bed.

Keyphrases □ Solids, polydisperse particulate—agitated beds, interparticulate translocations in terms of Markov chains □ Interparticulate translocations—polydisperse particulate solids, agitated beds, in terms of Markov chains □ Markov chains—polydisperse particulate solids, agitated beds, interparticulate translocations

The mixing of solid particles is a key step in many industrial and technical processes. Its pharmaceutical importance related to the manufacture of solid dosage forms is obvious, and the field of solids mixing has developed an extensive literature. Most of this literature deals with the statistical nature of the mixing process in its various forms, with the result that numerous degrees of mixedness (1) have been defined. These quantities are scalar and do not uniquely represent the composition tensors that would otherwise rigorously characterize the total state of mix. Such approaches, while of significant value in characterizing overall kinetic behavior (2), are necessarily incomplete.

A more comprehensive description of the translocations of particles within dynamic particulate beds can be achieved by the analysis of such systems in terms of stochastic theory. Some advantages of this approach are that both particle distributions and particle mobilities can be studied simultaneously and the processes of mixing and segregation can be examined in detail throughout the systems.

Oyama and Ayaki (3) considered the theoretical aspects of a Markov chain, having stationary transition matrixes, applied so as to describe the mixing of monodisperse particles, but they did not verify their results experimentally. The motion of monodisperse solids in a two-dimensional twin-shell mixer was studied, and the applicable stationary transition matrix of a Markov process was established by using single tracer particles (4). Good agreement was found between predicted and measured results using this technique.

The axial mixing of solid particles in a motionless mixer was studied in terms of a Markov chain (5). The transition probabilities were determined by measuring the distribution of tracer particles before and after passage of the bed through the mixer. Good agreement between experiment and theory was found for up to seven mixing passes, assuming the chain to be homogeneous.

The purpose of the present paper is to extend the application of Markov chains to polydisperse solids systems in which the transition matrixes are both nonstationary and singly stochastic. While such systems proceed to equilibrium states, these states represent nonuniform distributions of particles in general; the applicable Markov chains provide insight into the mixing–segregation process. The experimental system was selected to demonstrate the practical applicability of the theory and the experimental approach to polydisperse systems in general.

THEORY

Transition matrixes arising from Markov chains describing the mixing of monodisperse solids are, of necessity, stationary, since the magnitude of the elements representing the probabilities of particle movements from location to location are independent of local bed compositions. This condition is a result of the physical similarity of all particles in the system except for some superficial identifying feature of the tracer particles.

A further simplification results for such systems if, for purposes of analysis, the particulate mass is divided into cells containing equal numbers of particles. The transition matrix then becomes doubly stochastic, since both row and column sums are unity. For such finite, irreducible, aperiodic chains having doubly stochastic transition matrixes, it follows that all states become equally probable in the limit, and the system ultimately assumes a state of random mix. Since such systems are not subject to segregation, they can be mixed satisfactorily by any method, and their study is of somewhat limited practical utility.

Polydisperse particulate solids, in contrast, are subject to segregation; both mixing and segregation occur simultaneously when such systems are agitated. This result is a direct consequence of the fact that the motion of a given particle is affected significantly by the composition gradient it experiences in its immediate neighborhood. As mentioned previously, the transition matrixes of Markov chains applied to these systems are both nonstationary and singly stochastic. In the present paper, binary mixtures of spherical particles are subjected to vertical sine wave oscillation and the resultant particle translocations are analyzed.

A finite, discrete, first-order Markov chain is appropriate for processes where particles move among a finite number of imaginary cells within the bed over arbitrary time intervals and where the transition probabilities for movement depend solely on the state of the system and on the length of the time interval corresponding to a unit step. Mathematically, such a Markov chain can be expressed as the matrix product of a cell occupancy or distribution probability vector with a transition probability matrix. The resultant row vector represents the new occupancy or distribution probability following one or more steps in the chain. Thus:

$$a_i P_{ij} = a_j \qquad \text{(Eq. 1)}$$

where a_i denotes the ith occupancy or distribution probability vector for a system divided into n cells:

$$a_i = [a_1 a_2 \cdots a_n]_i \qquad \text{(Eq. 2)}$$

$$P_{ij} = \begin{bmatrix} p_{11}p_{12}\cdots p_{1n} \\ p_{21}p_{22}\cdots \\ \cdots \\ \cdots p_{kl}\cdots \\ \cdots \\ p_{n1}\cdots p_{nn} \end{bmatrix}_{ij} \qquad \text{(Eq. 3)}$$

P_{ij} is the transition matrix corresponding to the step(s) between the states that exist after steps i and j, respectively; p_{kl} is the probability of movement of a particle from cell k to cell l. Since the matrixes P_{ij} are nonstationary:

$$P_{a,a+2} = P_{a,a+1} P_{a+1,a+2} \neq P^2_{a,a+1} \qquad \text{(Eq. 4)}$$

From the definition of p_{kl}, it is apparent that $\Sigma_{l=1}^{n} p_{kl} = 1$ for all k whereas $\Sigma_{k=1}^{n} \neq 1$ in general. These relationships correspond to the singly stochastic condition.

With successive steps in the chain, $P_{i,i+1}$ approaches a limit having as an eigenvector the equilibrium occupancy or distribution vector and also having a corresponding eigenvalue of unity.

In the event the system is divided into cells of unequal volume, Eq. 1 must be written in the more general form:

$$a_i \Pi P_{ij} \Pi^{-1} = a_j \qquad \text{(Eq. 5)}$$

where:

$$\Pi = \begin{bmatrix} x_1 & 0 & . & . & . & 0 \\ 0 & x_2 & 0 & . & . & . \\ . & . & . & . & . & . \\ . & . & 0 & x_k & 0 & . \\ . & . & . & . & . & 0 \\ 0 & . & . & . & 0 & x_n \end{bmatrix} \qquad \text{(Eq. 6)}$$

and where x_k represents the relative volume of cell k. However, in the present paper, all cells are of the same volume so that Π and Π^{-1} cancel and Eq. 5 can be simplified to Eq. 1.

If it is assumed that the values of p_{kl} are unknown for a given step but that the corresponding initial and final occupancy vectors are known, then from the definition of p_{kl} it is apparent that n linear independent equations exist. Also, because the sum of the elements in any occupancy vector is a constant, an additional $n - 1$ linear independent equations can be written. That is, for a given step in the Markov chain under discussion, $2n - 1$ elements in the corresponding transition matrix can be determined from a knowledge of the states of the system before and after a given step. The remainder of the n^2 elements of the nth-order transition matrix either must be zero or must otherwise be known by some independent means. Unless this latter requirement is met, no unique solution can be found for Eq. 1.

It has been shown, by the experimental means discussed later, that all but $2n - 1$ of the n^2 elements p_{kl} of the transition matrix have negligible values and may be assumed to be zero for suitably short transition time intervals. The transition matrixes corresponding to these observations have the general form:

$$P_{ij} = \begin{bmatrix} p_{11} & 0 & . & . & . & 0 \\ p_{21} & p_{22} & 0 & . & . & . \\ 0 & p_{32} & p_{33} & 0 & . & . \\ . & 0 & p_{43} & p_{44} & 0 & . \\ . & . & . & . & . & . \\ 0 & . & . & 0 & p_{nn-1} & p_{nn} \end{bmatrix}_{ij} \qquad \text{(Eq. 7)}$$

The $2n - 1$ unknowns in P_{ij} can be determined from the solutions of the $2n - 1$ linear independent simultaneous equations, which have been shown to result from the stochastic condition of the transition matrix and from Eq. 1.

EXPERIMENTAL

A segmented brass cylinder, 2.54 cm i.d. and 30 cm in height, containing the particulate system under study was mounted vertically on a specially designed shaking device (2). This shaker imparted a vertical sinusoidal motion to the cylinder and was capable of precise adjustment of both the frequency and amplitude of the shaking motion.

The binary mixture used in this study was comprised of 112.5 g each of 2.38- and 5.56-mm chrome steel balls and was loaded into the cylinder in a randomly mixed state prior to each shaking sequence. A random mixture was achieved by the successive addition of mixtures of equal weights of both components in small increments of less than 8% of the total bed. The adequacy of this mixing method was verified by sampling.

The particulate bed was approximately 14 cm in depth and was permitted to expand freely during shaking. Shaking was conducted at a frequency of 17.08 Hz, with a peak to peak amplitude of 5.08 mm. Maximum expansion was estimated at 1–2 cm within each oscillation of the shaker.

Following agitation for various periods, the occupancy vectors of the bed were determined by sequentially removing the six 2.3-cm segments of the cylinder, one at a time, and noting the weight of the bed contained in each and the corresponding weight of the larger component. The fractional composition of each cell thus corresponded to the components a_j of the occupancy vector following agitation. The components a_i of the initial occupancy vector were taken as 0.5 where the bed was randomly mixed initially. Where the bed was partially segregated at the beginning of the transition time segment of interest, the components a_i were those found by measurement after independent runs of the proper duration. This procedure was necessary since the system was disrupted by the sampling method employed.

Table I—Transition Probability Elements for Tracer-Estimated and Computed Transition Matrixes

	0–5 sec		0–10 sec		0–15 sec	
p_{kl}	Estimated[a]	Computed[b]	Estimated	Computed	Estimated	Computed
p_{11}	1.000	1.000	1.000	1.000	1.000	1.000
p_{21}	0.229	0.198	0.338	0.272	0.474	0.324
p_{22}	0.771	0.802	0.662	0.728	0.526	0.676
p_{32}	0.263	0.296	0.504	0.564	0.560	0.631
p_{33}	0.737	0.704	0.496	0.436	0.440	0.369
p_{43}	0.303	0.288	0.582	0.620	0.729	0.847
p_{44}	0.697	0.712	0.418	0.380	0.271	0.153
p_{54}	0.155	0.238	0.557	0.578	0.807	0.851
p_{55}	0.845	0.762	0.443	0.422	0.193	0.149
p_{65}	0.092	0.136	0.428	0.423	0.521	0.600
p_{66}	0.908	0.864	0.572	0.577	0.479	0.400

[a] Elements estimated from the movements of tracer particles. [b] Elements computed from simultaneous equations.

Transition Matrixes Determined by Tracer Particles—One-sixth of both the large and small components were marked by being blued with a commercial cold process gun bluing solution. The randomly mixed bed was loaded into the segmented cylinder so that the marked particles were located within a given segment. After being vibrated for a predetermined period, the system was analyzed as previously described. The relative movement of the large and small marked components into cylinder segments other than those in which they were located originally corresponds to the transition probabilities p_{kl}. By repeated experiments in which the marked particles are placed in the various cylinder segments, it is possible to construct the transition matrix.

Transition Matrixes Determined by Solution of $2n - 1$ Simultaneous Equations—As discussed previously, Eq. 1 and the singly stochastic transition matrixes define $2n - 1$ linear independent equations whose coefficients correspond to the transition probability elements, p_{kl}, as indicated in Eq. 7. Sets of equations corresponding to various initial and final occupancy vectors were solved on a digital computer[1] using a double precision program based on the Gauss–Jordan method of condensed elimination with partial pivoting. This approach provides a convenient method of obtaining the transition matrixes for any component of a polydisperse mixture without the need for tedious multiple measurements of tagged particles.

RESULTS AND DISCUSSION

Transition matrixes for the large component were determined using tracer particles for transition time periods of 5, 10, 15, and 20 sec, beginning in each case with randomly mixed particulate beds. In no case were marked large particles found in bed segments below their initial location; however, after 20 sec of shaking some particles were found to have moved into the second segment above their original position. This latter movement corresponds to a transition giving rise to a positive value of $p_{k,k-2}$, where the six cylinder segments are serially numbered starting at the top. These results indicate that, for sufficiently short time intervals, transitions can be represented by matrixes of the type given in Eq. 7. However, as the system approaches its equilibrium state, other transitions become significant even for short time intervals. Results of the tracer particle studies are presented in Table I.

An indication of the accuracy of tracer-estimated transition matrixes can be obtained by comparing occupancy vectors computed from Eq. 1 with those obtained by direct bed analysis. Figure 1 displays bed compositions determined by direct measurement together with those predicted by Eq. 1. Errors are within probable statistical limits, and the accuracy permits prediction of the distribution of a component within approximately 3% based on total content. Correspondingly lower percent errors will result where samples contain larger numbers of particles due either to larger sample size or smaller average particle size.

[1] Control Data Corp. Cyber 74.

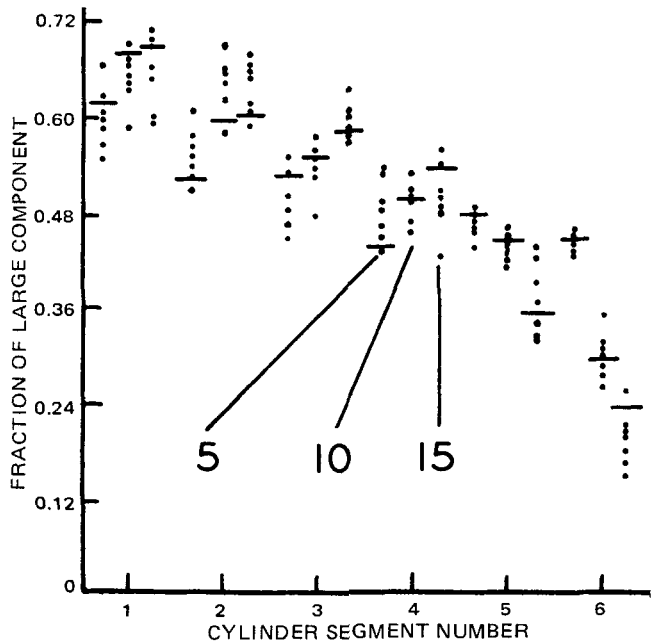

Figure 1—*Fraction of the large component as a function of bed location and time of agitation. Data are shown for 5-, 10-, and 15-sec periods of agitation for each of the six bed positions, numbered from the top. Points represent compositions by analysis, and lines represent calculated values based on the transition matrixes.*

Occupancy vectors, representing the averages of seven identical runs in each case, were used to compute transition matrixes corresponding to those determined by tracer methods. These are presented in Table I as a list of their component transition probability elements. Good agreement can be seen between transition probabilities determined by the two alternative methods used.

The average occupancy vectors were also used to compute P_{ij} for four successive 5-sec time intervals. The inequality expressed by Eq. 4 holds, and the chain is nonstationary (Table II).

Table II—Transition Probability Elements Computed for Successive 5-sec Time Intervals

p_{kl}	0–5 sec	5–10 sec	10–15 sec	15–20 sec
p_{11}	1.000	1.000	1.000	1.000
p_{21}	0.198	0.068	0.040	0.088
p_{22}	0.802	0.932	0.960	0.912
p_{32}	0.296	0.270	0.064	0.131
p_{33}	0.704	0.730	0.936	0.869
p_{43}	0.288	0.350	0.236	0.181
p_{44}	0.712	0.650	0.764	0.819
p_{54}	0.238	0.379	0.323	0.363
p_{55}	0.762	0.621	0.677	0.637
p_{65}	0.136	0.331	0.308	0.428
p_{66}	0.864	0.669	0.692	0.572

Mention should be made concerning the transition matrixes related to the movement of the second component. While it is true that the occupancy vectors of the first component uniquely define those of the second component, the same cannot be said of the respective transition matrixes. Experimentally, the blue 2.38-mm tracer balls had significantly greater mobility than the 5.56-mm balls. The smaller balls moved in both directions from their original locations, and their tracers could be found in as many as five segments after a single 5-sec period of agitation. Since more than $2n - 1$ transition probability elements were nonzero in this case, the transition matrixes could not be calculated from the occupancy vectors but could only be estimated *via* tracer particles.

CONCLUSIONS

The mixing and segregation that occur within vibrated polydisperse particulate beds can be studied as a nonstationary Markov chain. Transition matrixes corresponding to relatively short agitation time intervals can be satisfactorily computed from a knowledge of the initial and final occupancy vectors.

In a binary mixture, a single large particle moving into or out of a given cell does not uniquely imply a corresponding movement of either another single large particle or of several small particles. Hence, the transition matrix established for one component limits, but does not define, the transition matrix of the second component. This limitation is not serious, however, since the occupancy vectors of the two components are complementary. The general methods used in the present study can be applied to the analysis of movement of a given component in a complex polydisperse mixture regardless of the number of components.

The transition probability elements provide a quantitative indication of a given component's mobility as a function of time and location. It is particularly significant that the mechanisms responsible for the observed mobilities are not explicitly implied by the transition matrixes but are accurately manifested by them. Thus, the approach permits the *a posteriori* investigation of a variety of possible mechanistic models. The likelihood of wall effects in the system presented in this paper does not invalidate the analysis but can be investigated in depth using these methods.

REFERENCES

(1) L. T. Fan, S. J. Chen, and C. A. Watson, *Ind. Eng. Chem.*, **62**, 53 (1970).

(2) E. G. Rippie, M. D. Faiman, and M. K. Pramoda, *J. Pharm. Sci.*, **56**, 1523 (1967).

(3) Y. Oyama and K. Ayaki, *Kagaku Kogaku*, **20**, 148 (1956).

(4) I. Inoue and K. Yamaguchi, *Int. Chem. Eng.*, **10**, 490 (1970).

(5) S. J. Chen, L. T. Fan, and C. A. Watson, *AIChE J.*, **18**, 984 (1972).

ACKNOWLEDGMENTS AND ADDRESSES

Received December 19, 1975, from the *Department of Pharmaceutics, College of Pharmacy, University of Minnesota, Minneapolis, MN 55455.*

Accepted for publication March 19, 1976.

The authors wish to express their appreciation to Mr. E. Glenn Rippie for the computer programming associated with this research.

* Present address: Ayerst Laboratories, Rouses Point, NY 12979.

ˣ To whom inquiries should be directed.

Influence of Sunscreening Agents on Color Stability of Tablets Coated with Certified Dyes III: FD&C Yellow No. 6

B. R. HAJRATWALA [x] and A. J. HENNIG

Abstract □ The influence of a protective coating of six sunscreening agents (glyceryl *p*-aminobenzoate, benzocaine, cinoxate, homosalate, *n*-octyl salicylate, and amyl salicylate) upon the photostability of FD&C Yellow No. 6 used to color coat tablets was studied. The alcohol film-, modified sugar-, and film-coating methods were used to apply the sunscreening agents. Tablets were exposed to 1000 foot-candles of light for various times, after which reflectance measurements and visual observations were recorded. FD&C Yellow No. 6 did not follow the Kubelka–Munk equation. The order of relative stability was FD&C Yellow No. 6 > erythrosine sodium (FD&C Red No. 3) > FD&C Blue No. 1. The greatest protection against fading was afforded by benzocaine.

Keyphrases □ Sunscreening agents—effect on color stability of tablets coated with FD&C Yellow No. 6, various coating methods □ Color stability—tablets coated with FD&C Yellow No. 6, effect of sunscreening agents and various coating methods □ Stability, color—tablets coated with FD&C Yellow No. 6, effect of sunscreening agents and various coating methods □ Tablets—coated with FD&C Yellow No. 6, effect of sunscreening agents and various coating methods on color stability □ Dyes—FD&C Yellow No. 6 tablet coating, effect of sunscreening agents and various coating methods on color stability □ FD&C Yellow No. 6—tablet coating, effect of sunscreening agents and various coating methods on color stability

The influence of six sunscreening agents (salicylate, benzoate, and cinnamate types) on the color stability of tablets coated with erythrosine sodium (FD&C Red No. 3) and FD&C Blue No. 1 was reported previously (1, 2). Three different methods were developed for their application. For FD&C Red No. 3, the degree of protection was dependent not only upon the type of sunscreening agent but also upon the application method. For FD&C Blue No. 1, no sunscreening agent exhibited significant protective action.

The purposes of this study were to evaluate the influence of selected sunscreening agents on tablets coated with FD&C Yellow No. 6 and to predict the color shelflife of such coated tablets.

EXPERIMENTAL

Materials—The six sunscreening agents used were glyceryl *p*-aminobenzoate[1], benzocaine, cinoxate[2], homosalate, *n*-octyl salicylate, and amyl salicylate[3]. The dye was FD&C Yellow No. 6. All compounds were used as received without further purification.

Procedure—The preparation of tablets, the equipment, the method of regulating exposure to light, and the determination of the quantity of sunscreening agent per tablet were described previously (1).

Coating Procedure—Ten subcoats and 25 smoothing coats were applied to core tablets, in lots of 6 kg, using medium strength gelatin syrup and white subcoating dusting powder. After the tablets were completely dry, the color coating was applied. Plain coating syrup (170 g of sucrose and 100 ml of deionized water) and color syrup (0.300 g of dye in 100 ml of plain coating syrup) in the stated ratio were applied in the following order: nine coats of 25 ml each in 1:90 parts, nine coats of 30 ml each in 1:75 parts, nine coats of 32 ml each in 1:60 parts, six coats of 32 ml each in 1:20 parts, nine coats of 32 ml each in 1:10 parts, eight coats of 32 ml each in 1:4 parts, and 12 coats of 32 ml each in 1:1 parts of plain syrup and color syrup, respectively.

Application of Sunscreening Agents—Three coating techniques, alcohol film, modified sugar, and film, were used to apply the sunscreening agents to the color-coated tablets. Observations regarding the "wet" feel of tablets coated with glyceryl *p*-aminobenzoate, turbid solutions for the modified sugar-coating method, and mottled appearances of tablets coated with salicylates by the film-coating method were similar to those reported (1). The quantitative assessment of surface mottling of colored tablets as reported by Armstrong and March (3) was not performed, because it was beyond the scope of this study.

No change in hue occurred upon application of various sunscreening agents such as was reported with FD&C Red No. 3 upon the application of glyceryl *p*-aminobenzoate (1) and with FD&C Blue No. 1 upon the application of glyceryl *p*-aminobenzoate or benzocaine (2). However, a brilliant shine was obtained (even before polishing) with FD&C Yellow No. 6 upon the application of cinoxate or glyceryl *p*-aminobenzoate.

Measurement of Color Change—Adequate samples of each set of color-coated tablets were exposed to 1000 foot-candles of light and 26 ± 2° in a light cabinet. Samples were withdrawn at designated time intervals, and the reflectance of the tablets was measured using the transmittance scale. A spectrophotometer[4] and reflectance attachment unit (2) were used to measure the reflectance of individual tablets.

Measurements were made between 400 and 525 nm for each sample at appropriate wavelength intervals and at the maximum for the dye

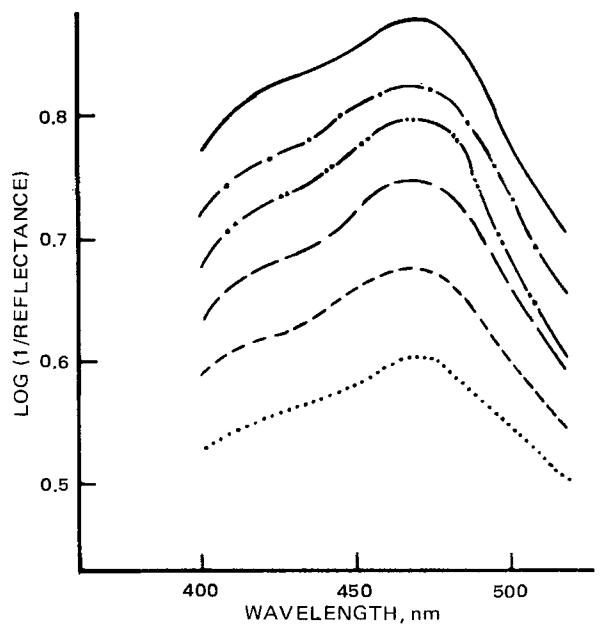

Figure 1—*Visible absorption spectra of control tablets color coated with FD&C Yellow No. 6 by film coating after intervals of storage under 1000 foot-candles of light. Key: —, initial; —·—, after 5 days; —··—, after 10 days; — —, after 20 days; - - - - -, after 30 days; and . . . . . , after 40 days.*

[1] Escalol-106, Van Dyke & Co.
[2] Giv-Tan-F, Sindar Co.
[3] Amyl Salicylate Extra, Fritsche Brother Inc.
[4] Beckman DU.

Table I—Log (1/Reflectance) Measurements of Tablets[a] Color Coated with FD&C Yellow No. 6 and Exposed to 1000 Foot-Candles of Light, with the Sunscreening Agent Applied by the Alcohol Film-Coating Method

	Log(1/Reflectance) after Exposure for				
Sunscreening Agent	Initial	8 Days	20 Days	40 Days	Initial −40 Days
Control	0.860	0.805	0.762	0.655	0.205
Glyceryl *p*-aminobenzoate	0.850	0.775	0.690	0.560	0.290
Benzocaine	0.840	0.825	0.772	0.635	0.205
Cinoxate	0.860	0.818	0.772	0.730	0.130
Homosalate	0.815	0.750	0.680	0.605	0.210
Homosalate (not polished)	0.885	0.745	0.705	0.652	0.233
n-Octyl salicylate	0.830	0.770	0.718	0.700	0.130
Amyl salicylate	0.825	0.770	0.718	0.700	0.125

[a] All tablets were polished except as noted.

Table II—Log (1/Reflectance) Measurements of Tablets Color Coated with FD&C Yellow No. 6 and Exposed to 1000 Foot-Candles of Light, with the Sunscreening Agent Applied by the Modified Sugar-Coating Method

	Log(1/Reflectance) after Exposure for				
Sunscreening Agent	Initial	8 Days	20 Days	40 Days	Initial −40 Days
Control	0.885	0.860	0.820	0.745	0.140
Glyceryl *p*-aminobenzoate	0.910	0.830	0.765	0.660	0.250
Benzocaine	0.910	0.830	0.765	0.660	0.250
Cinoxate	0.890	0.855	0.800	0.740	0.150
Homosalate	0.865	0.825	0.808	0.770	0.095
n-Octyl salicylate	0.885	0.860	0.815	0.745	0.140
Amyl salicylate	0.855	0.825	0.775	0.690	0.165
	0.920	0.818	0.818	0.752	0.168

(475 nm) (Fig 1). Color evaluation by visual observation was carried out as previously reported.

RESULTS AND DISCUSSION

The Kubelka–Munk equation:

$$\ln \theta_t = \ln \theta_t' - ktI \qquad \text{(Eq. 1)}$$

where $\theta_t = (1 - R)^2/2R$, R = reflectance at the absorbance maximum at time t, I = intensity in foot-candles, k = apparent first-order rate constant, and $\theta_t = \theta_t'$ at $t = 0$, conveniently describes the first-order degradation of various dyes, *e.g.*, FD&C Red No. 3 (1, 4) and FD&C Blue No. 1 (2). The data obtained for FD&C Yellow No. 6 plotted as log θ_t *versus* the product of time and intensity did not yield a straight line, indicating that the fading did not occur *via* a simple first-order process. The data were also plotted as $1/\theta_t$ *versus* the product of time and intensity; but this plot also failed to yield a straight line,

Table III—Log (1/Reflectance) Measurements of Tablets Color Coated with FD&C Yellow No. 6 and Exposed to 1000 Foot-Candles of Light, with the Sunscreening Agent Applied by the Film-Coating Method

	Log (1/Reflectance) after Exposure for				
Sunscreening Agent	Initial	8 Days	20 Days	40 Days	Initial − 40 Days
Control	0.880	0.814	0.748	0.605	0.275
Glyceryl *p*-aminobenzoate	0.905	0.870	0.710	0.620	0.285
Benzocaine	0.875	0.845	0.780	0.712	0.163
Cinoxate	0.860	0.845	0.790	0.690	0.170
Homosalate	0.810	0.838	0.715	0.660	0.150
n-Octyl salicylate	0.795	0.680	0.532	0.509	0.286
Amyl salicylate	0.700	0.675	0.600	0.572	0.128

Table IV—Summary of Visual Observations of Tablets Coated with FD&C Yellow No. 6 and Exposed to 1000 Foot-Candles of Light over 40 Days[a]

	Coating Type		
Sunscreening Agent	Alcohol Film	Modified Sugar	Film
Control	Noticeable fading objectionable within 30 days	1	3
Glyceryl *p*-aminobenzoate	3, S	2	2, S
Benzocaine	3	1	1
Cinoxate	2	1	1, S
Homosalate (not polished)	3	Not studied	Not studied
Homosalate	1	1	3A
n-Octyl salicylate	1	1	3A
Amyl salicylate	1	1	3A

[a] 1 = fading less than alcohol film control, 2 = fading similar to alcohol film control, 3 = fading greater than alcohol film control, 3A = fading greater than alcohol film control but with mottled appearance due to cracked film, and S = brilliant shine. All tablets were polished except as noted.

suggesting that the rate of fading did not follow a second-order equation either.

This failure to comply with the Kubelka–Munk equation prevents prediction of shelflife for color-coated tablets. However, it is possible, on the basis of reflectance measurements and visual observations, to assign an order of protection afforded by the sunscreening agents to FD&C Yellow No. 6. Reflectance measurements are reported for 0, 8, 20, and 40 days. Tables I–III show log (1/reflectance) measurements of various sets of color-coated tablets. These values are an average of two or three determinations. The range of these determinations generally varied between 0.005 and 0.010 unit [log (1/reflectance) was read off the absorbance scale]. Table IV summarizes visual observations.

Control—FD&C Yellow No. 6 exhibited sensitivity to the type of coating applied. The relative order of stability was modified sugar coating < alcohol film coating < film coating. In the absence of any

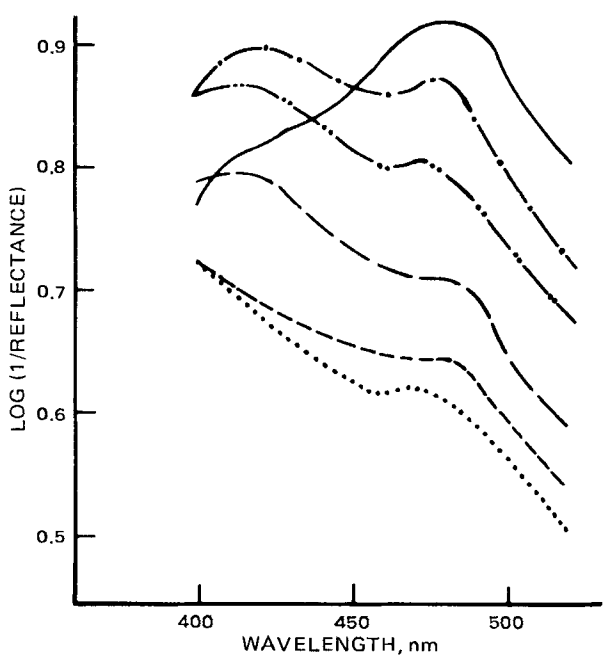

Figure 2—*Visible absorption spectra of tablets color coated with FD&C Yellow No. 6 with glyceryl* p*-aminobenzoate by film coating technique after intervals of storage under 1000 foot-candles of light. Key: —, initial; —·—, after 5 days; —··—, after 10 days; — —, after 20 days; - - - - -, after 30 days; and . . . . . , after 40 days.*

Table V—Visual Observations of Tablets Coated with Certified Dyes and Exposed to Varying Intensities of Light for up to 70 Days[a]

Days	750 Foot-Candles, Film Coating			1000 Foot-Candles, Sugar Coating		
	FD&C Yellow No. 6	FD&C Red No. 3	FD&C Blue No. 1	FD&C Yellow No. 6	FD&C Red No. 3	FD&C Blue No. 1
0—1	5	5	5	5	5	5
2—5	4	4	4	5	4	3
6—10	4	3	3	4	4	2
11—20	4	3	3	4	3	1
21—30	3	3	2	3	2	1
31—40	3	2	1	2	2	1
41—50	2	2	1	1	1	0
50—70	2	2	0	—	—	—

[a] 5 = no change, 4 = moderate change, 3 = noticeable change, 2 = poor stability, 1 = very poor stability, and 0=colorless. Material was condensed and retabulated from Ref. 5.

numerical values for rate constants or any other linear function, it is difficult to assign the relative order of stability of FD&C Yellow No. 6 with respect to FD&C Red No. 3 and FD&C Blue No. 1. Vaidya (5) assigned the following order: FD&C Yellow No. 6 > FD&C Red No. 3 > FD&C Blue No. 1 (Table V). The present findings are in general agreement with that order.

Glyceryl *p*-Aminobenzoate—FD&C Red No. 3 (1) and FD&C Blue No. 1 (2) both showed a distinct change of hue when tablets were coated by either the alcohol film-coating or the film-coating method. Although no change in hue was observed with any coating procedure in the present study, a different shade of yellow might have been produced that was not readily distinguishable by the eye. Tablets exhibited a brilliant shine (alcohol film- and film-coating method), which was retained even after 10 days of exposure to 1000 foot-candles of light. A chemical reaction between the dye and the glyceryl *p*-aminobenzoate apparently occurred, resulting in a slight shift in the maximum and a new peak at 420 nm (Fig. 2). No attempt was made to isolate the compound or to determine the reaction involved.

Benzocaine—The protective effect of the UV absorber, benzocaine, appeared most effective for FD&C Yellow No. 6 when applied as the modified sugar coat or the film coat.

Cinoxate—This compound appeared to have a distinct protective action on FD&C Yellow No. 6 when applied by the film-coating method. Only moderate fading occurred even after 40 days of exposure. A brilliant shine also was retained for up to 5 days of exposure at 1000 foot-candles of light.

Salicylates—Tablets coated with the salicylates by the film-coating method appeared mottled after 24 hr of drying due to cracking of the film. Compared to control tablets for each coating method, coating by the alcohol film method appeared to afford the best protection.

REFERENCES

(1) B. R. Hajratwala, *J. Pharm. Sci.*, **63**, 129(1974).

(2) *Ibid.*, **63**, 1927(1974).

(3) N. A. Armstrong and G. A. March, *J. Pharm. Sci.*, **63**, 126(1974).

(4) M. F. Everhard and F. W. Goodhart, *ibid.*, **52**, 281(1963).

(5) B. R. Vaidya, Ph.D. thesis, University of Colorado, Boulder, Colo., 1965.

ACKNOWLEDGMENTS AND ADDRESSES

Received May 28, 1975, from the *School of Pharmacy, University of Colorado, Boulder, CO 80302*

Accepted for publication February 13, 1976.

[x] To whom inquiries should be directed. Present address: Department of Pharmacy, University of Otago, Dunedin, New Zealand.

Quantitative Determination of Benzoic Acid and Salicylic Acid in Ointments by High-Pressure Liquid Chromatography

V. DAS GUPTA

Abstract □ Benzoic acid and salicylic acid in ointments were analyzed quantitatively by reversed-phase high-pressure liquid chromatography. Both benzoic and salicylic acids can be assayed in combinations directly without interference from each other or the ointment bases. The method is accurate, simple, and rapid. Excellent results were obtained with three commercial bases.

Keyphrases □ Benzoic acid—reversed-phase high-pressure liquid chromatographic analysis, pharmaceutical formulations containing salicylic acid □ Salicylic acid—reversed-phase high-pressure liquid chromatographic analysis, pharmaceutical formulations containing benzoic acid □ High-pressure liquid chromatography, reversed phase—analysis, benzoic and salicylic acids, pharmaceutical formulations □ Antifungal agents—benzoic acid, reversed-phase high-pressure liquid chromatographic analysis, pharmaceutical formulations □ Keratolytic agents—salicylic acid, reversed-phase high-pressure liquid chromatographic analysis, pharmaceutical formulations

The quantitative determination of benzoic acid (I) and salicylic acid (II) in ointments was reported (1). That method involved the determination of II by its reaction with ferric nitrate. Benzoic acid was determined by difference from the total acidity reading. Any error in the determination of II is carried over to results on I. The purpose of these investigations was to develop a direct, simple, and accurate method for the quantitative determinations of I and II in combinations.

EXPERIMENTAL

Chemicals and Reagents—All chemicals and reagents were ACS, USP, or NF grade and were used without further purification.

Apparatus—A high-pressure liquid chromatograph[1] equipped with a UV detector (254 nm) and recorder[2] was used.

Column—A very nonpolar packing material[3] consisting of a monomolecular layer of octadecyltrichlorosilane, permanently bonded by silicon–carbon bonds, and a 30-cm long × 4-mm i.d. column were used.

Chromatographic Conditions—The chromatographic solvent was 0.02 *M* KH_2PO_4 in 10% (v/v) methanol in water (pH adjusted[4] to 6.2 with ~0.1 *N* NaOH). The temperature was ambient, and the solvent flow rate was 2.0 ml/min (at an inlet pressure of approximately 1100 psig). The detector was set at a sensitivity of 0.16 absorbance unit full-scale, and the chart speed was 30.5 cm (12 in.)/hr.

Solutions—A standard solution of I (100.0 mg/250 ml) or II (50.0 mg/250 ml) or a combination of I and II was prepared by heating the acid(s) in 15 ml of approximately 0.1 *N* NaOH and 60 ml of water to almost boiling. The mixture was then cooled and brought to volume (250.0 ml).

Preparation of Ointments—Three lots of ointments were prepared by the trituration process. Lot A contained 3.0% of II by weight in white petrolatum; Lot B contained 6.0% of I and 3.0% of II in a cold cream[5]; Lot C contained the same ingredients as Lot B in a different base[6] (2).

Assay Procedure for Ointments—Weigh accurately about 1.667 g of the ointment, transfer it to a 150-ml beaker, and add 15 ml of the

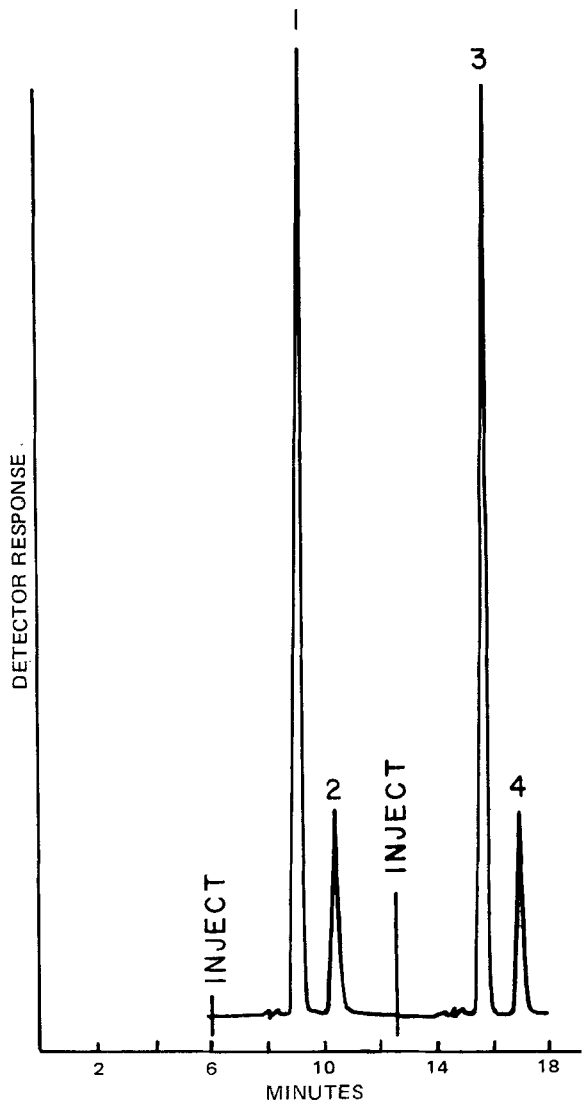

Figure 1—*Liquid chromatogram of I and II in combination (for conditions, see text). Peaks 1 and 2 are I and II from a standard solution, respectively; peaks 3 and 4 are I and II from an ointment sample, respectively.*

[1] Waters ALC 202 equipped with U6K universal chromatograph injector.
[2] Omniscribe 5213-12 equipped with an integrator.
[3] μBondapak-C18, Catalog No. 27324, Waters Associates.
[4] A Beckman Zeromatic SS-3 pH meter was used.
[5] The Upjohn Co., Kalamazoo, Mich. For ingredients, see Ref. 1.
[6] HEB base, Barnes-Hind Pharmaceuticals, Sunnyvale, Calif. For ingredients, see Ref. 2.

Table I—Assay Results[a] on Ointments

Ointment	Assay Results, % I	II
Lot A	0.0	99.6
Lot B	99.4	99.8
Lot C	97.9	99.2
Average deviation (based on six readings)	±2.1	±2.8

[a] Average of three.

0.1 *N* NaOH solution and 60 ml of water. Heat almost to boiling and cool until the base congeals at the top of the aqueous layer. Then decant and transfer the aqueous layer to a 250-ml volumetric flask, wash the beaker with small portions of water, and transfer the rinsings to a volumetric flask to bring the mixture to volume. Filter if necessary and inject 10–20 μl.

For comparison purposes, inject an identical volume of the appropriate standard solution after the assay sample is eluted.

Calculations—Since preliminary investigations indicated that the peak area of each ingredient was directly related to the concentration (range of 4–8 μg for I and of 2–4 μg for II), the results on I and II were calculated by direct comparison of the peak areas:

$$\frac{\text{corrected } A_a}{A_s} \times 100 = \text{percent of label claim} \qquad \text{(Eq. 1)}$$

where corrected A_a = peak area of the assay × (1.667/weight of sample in grams), and A_s = peak area of the standard solution.

A typical liquid chromatogram is shown in Fig. 1, and the assay results are presented in Table I.

DISCUSSION

The results (Table I) indicate that I and II in combinations can be assayed directly by high-pressure liquid chromatography. The separation of I from II is excellent (Fig. 1). The method is accurate, rapid, and simple. The three ointment bases used did not interfere with the assay; other bases may interfere. Any other base should be checked for interference by using the assay procedure on the plain base. It is necessary to run both the assay and the standard with the same lot of the chromatographic solvent, since slight differences in pH may change the area of the peak.

REFERENCES

(1) V. D. Gupta, *J. Pharm. Sci.*, **61**, 1625(1972).

(2) V. D. Gupta and A. N. Deleon, *Indian J. Hosp. Pharm.*, **10**, 141(1973).

ACKNOWLEDGMENTS AND ADDRESSES

Received October 28, 1975, from the *College of Pharmacy, University of Houston, Houston, TX 77004*

Accepted for publication February 13, 1976.

Effects of Aspirin and Acetaminophen on Fetal and Placental Growth in Rats

W. C. LUBAWY ˣ and R. J. BURRISS GARRETT

Abstract □ Aqueous suspensions of aspirin or acetaminophen (125 and 250 mg/kg/day) were administered orally to pregnant Sprague–Dawley rats on Days 8–19 of gestation. On gestation Day 20, each rat was sacrificed and the uterus was examined *in situ*. Each fetal–placental unit was resected and examined. Fetuses from rats given 125 or 250 mg/kg/day of aspirin were shorter and weighed less than those obtained from control rats. In animals receiving the higher dose of aspirin, the placentas were smaller and the number of fetal resorptions was increased. Acetaminophen (250 mg/kg/day) did not affect fetal length or weight or the incidence of resorptions. Acetaminophen interfered less with the normal growth of the rat fetus and placenta than did aspirin.

Keyphrases □ Aspirin—effects on fetal and placental growth, rats □ Acetaminophen—effects on fetal and placental growth, rats □ Fetal growth—effects of aspirin and acetaminophen, rats □ Placental growth—effects of aspirin and acetaminophen, rats

The antigonadal and antireproductive activities of the two most commonly used nonprescription analgesic drugs were reported previously. Chronic administration of acetaminophen to rats produced a decrease in testicular weight and impaired spermatogenesis (1). Also, chronic administration of acetaminophen significantly decreased fecundity in mice, but similar doses of aspirin were ineffective (2). Aspirin administration interfered with the rapid increase in ovarian size following hemicastration (3) and also caused embryotoxicity and teratogenecity in rats (4).

Many studies document the effects of salicylates on fetal growth and development (4–10); however, no studies are known that directly compare the effects of aspirin to those of acetaminophen. Since aspirin and acetaminophen may influence gonadal function, normal reproduction, and the growth of rapidly developing tissue, the effects of these widely used analgesics on fetal and placental growth were compared.

EXPERIMENTAL

Female Sprague–Dawley rats[1] were used. For gravid rats, the sperm-positive date indicated by the supplier was designated Day 0 of pregnancy. If allowed to progress to term, parturition occurred on Day 21. Animals were randomized, housed three or four to a wire mesh bottom cage, and fed rat chow[2] and water *ad libitum*.

From the 8th through the 19th day of gestation, groups of 21 sperm-positive rats were weighed and received aspirin[3] or acetaminophen[4] at 0, 125, or 250 mg/kg by gavage. Groups of nonmated female rats, comparable in age, were treated according to the same regimen. Each drug was suspended fresh daily in 0.5% methylcellulose with a homogenizer[5] at a concentration such that 1 ml was administered for every 200 g of body weight. Drugs were administered without anesthesia, since Kimmel *et al.* (5) observed abnormalities in offspring from rats anesthetized with ether.

[1] Holtzman Co., Madison, Wis.
[2] Purina.
[3] Merck and Co., Rahway, N.J.
[4] Provided by McNeil Laboratories, Fort Washington, Pa.
[5] Potter–Elvehjem.

Table I—Assay Results[a] on Ointments

Ointment	Assay Results, % I	II
Lot A	0.0	99.6
Lot B	99.4	99.8
Lot C	97.9	99.2
Average deviation (based on six readings)	±2.1	±2.8

[a] Average of three.

0.1 *N* NaOH solution and 60 ml of water. Heat almost to boiling and cool until the base congeals at the top of the aqueous layer. Then decant and transfer the aqueous layer to a 250-ml volumetric flask, wash the beaker with small portions of water, and transfer the rinsings to a volumetric flask to bring the mixture to volume. Filter if necessary and inject 10–20 μl.

For comparison purposes, inject an identical volume of the appropriate standard solution after the assay sample is eluted.

Calculations—Since preliminary investigations indicated that the peak area of each ingredient was directly related to the concentration (range of 4–8 μg for I and of 2–4 μg for II), the results on I and II were calculated by direct comparison of the peak areas:

$$\frac{\text{corrected } A_a}{A_s} \times 100 = \text{percent of label claim} \qquad \text{(Eq. 1)}$$

where corrected A_a = peak area of the assay × (1.667/weight of sample in grams), and A_s = peak area of the standard solution.

A typical liquid chromatogram is shown in Fig. 1, and the assay results are presented in Table I.

DISCUSSION

The results (Table I) indicate that I and II in combinations can be assayed directly by high-pressure liquid chromatography. The separation of I from II is excellent (Fig. 1). The method is accurate, rapid, and simple. The three ointment bases used did not interfere with the assay; other bases may interfere. Any other base should be checked for interference by using the assay procedure on the plain base. It is necessary to run both the assay and the standard with the same lot of the chromatographic solvent, since slight differences in pH may change the area of the peak.

REFERENCES

(1) V. D. Gupta, *J. Pharm. Sci.*, **61**, 1625(1972).

(2) V. D. Gupta and A. N. Deleon, *Indian J. Hosp. Pharm.*, **10**, 141(1973).

ACKNOWLEDGMENTS AND ADDRESSES

Received October 28, 1975, from the *College of Pharmacy, University of Houston, Houston, TX 77004*

Accepted for publication February 13, 1976.

Effects of Aspirin and Acetaminophen on Fetal and Placental Growth in Rats

W. C. LUBAWY ˣ and R. J. BURRISS GARRETT

Abstract □ Aqueous suspensions of aspirin or acetaminophen (125 and 250 mg/kg/day) were administered orally to pregnant Sprague–Dawley rats on Days 8–19 of gestation. On gestation Day 20, each rat was sacrificed and the uterus was examined *in situ*. Each fetal–placental unit was resected and examined. Fetuses from rats given 125 or 250 mg/kg/day of aspirin were shorter and weighed less than those obtained from control rats. In animals receiving the higher dose of aspirin, the placentas were smaller and the number of fetal resorptions was increased. Acetaminophen (250 mg/kg/day) did not affect fetal length or weight or the incidence of resorptions. Acetaminophen interfered less with the normal growth of the rat fetus and placenta than did aspirin.

Keyphrases □ Aspirin—effects on fetal and placental growth, rats □ Acetaminophen—effects on fetal and placental growth, rats □ Fetal growth—effects of aspirin and acetaminophen, rats □ Placental growth—effects of aspirin and acetaminophen, rats

The antigonadal and antireproductive activities of the two most commonly used nonprescription analgesic drugs were reported previously. Chronic administration of acetaminophen to rats produced a decrease in testicular weight and impaired spermatogenesis (1). Also, chronic administration of acetaminophen significantly decreased fecundity in mice, but similar doses of aspirin were ineffective (2). Aspirin administration interfered with the rapid increase in ovarian size following hemicastration (3) and also caused embryotoxicity and teratogenecity in rats (4).

Many studies document the effects of salicylates on fetal growth and development (4–10); however, no studies are known that directly compare the effects of aspirin to those of acetaminophen. Since aspirin and acetaminophen may influence gonadal function, normal reproduction, and the growth of rapidly developing tissue, the effects of these widely used analgesics on fetal and placental growth were compared.

EXPERIMENTAL

Female Sprague–Dawley rats[1] were used. For gravid rats, the sperm-positive date indicated by the supplier was designated Day 0 of pregnancy. If allowed to progress to term, parturition occurred on Day 21. Animals were randomized, housed three or four to a wire mesh bottom cage, and fed rat chow[2] and water *ad libitum*.

From the 8th through the 19th day of gestation, groups of 21 sperm-positive rats were weighed and received aspirin[3] or acetaminophen[4] at 0, 125, or 250 mg/kg by gavage. Groups of nonmated female rats, comparable in age, were treated according to the same regimen. Each drug was suspended fresh daily in 0.5% methylcellulose with a homogenizer[5] at a concentration such that 1 ml was administered for every 200 g of body weight. Drugs were administered without anesthesia, since Kimmel *et al.* (5) observed abnormalities in offspring from rats anesthetized with ether.

[1] Holtzman Co., Madison, Wis.
[2] Purina.
[3] Merck and Co., Rahway, N.J.
[4] Provided by McNeil Laboratories, Fort Washington, Pa.
[5] Potter–Elvehjem.

Table I—Effect of Aspirin and Acetaminophen on Weight Gain in Pregnant and Nonpregnant Rats[a]

Body Weight	Vehicle (0.5% Methylcellulose)	Aspirin (125 mg/kg/day)	Aspirin (250 mg/kg/day)	Acetaminophen (125 mg/kg/day)	Acetaminophen (250 mg/kg/day)
Nonpregnant rats:					
Initial weight[b], g	214.8 ± 5.4	212.3 ± 2.7	220.7 ± 6.4	219.9 ± 2.1	219.3 ± 3.3
Weight[b] after 12 days, g	242.2 ± 3.5	241.0 ± 2.5	238.0 ± 4.5	243.1 ± 3.5	236.4 ± 2.9
n	10	7	9	7	8
Pregnant rats:					
Initial weight[b], g	240.6 ± 4.6	238.7 ± 2.6	239.9 ± 4.7	240.5 ± 4.7	237.5 ± 4.4
Weight[b] after 12 days, g	332.6 ± 8.4	336.3 ± 4.9	298.9 ± 9.6[c]	320.4 ± 7.6	347.3 ± 4.8
n	18	21	15	17	16

[a] Drugs were administered by gavage once daily for 12 days. [b] Mean ± *SE*. [c] Differs from control at $p < 0.05$.

On Day 20 of gestation, the sperm-positive animals were sacrificed with ether overdosage. The uterus was examined *in situ* for implantation sites, and fetal viability was determined. Each fetal–placental unit was resected. The chorioallantoic placenta was dissected free of the fetus, and both were blotted and weighed. The length of each fetus was measured from crown to rump.

Continuous variables from fetuses and placentas grouped according to treatment were analyzed using an analysis of variance or a *t* statistic. Discrete variables were subjected to the Fisher Exact Probability Test or the χ-square test according to the criteria outlined by Siegel (11).

RESULTS

Among the nonpregnant rats, no significant differences occurred in average body weights between the various treatment groups and comparable controls at the end of the 12-day treatment period (Table I). Although the actual amount of weight gained during the experimental period by the high dose (250 mg/kg/day) aspirin-treated nonpregnant rats was approximately 10 g less than the average weight gain of the control animals, this difference was not statistically significant. Pregnant rats given aspirin at 250 mg/kg/day gained less weight than those receiving the vehicle, and some of this difference was probably due to the effect of the aspirin on the fetuses and placentas.

Data presented in Table II indicate some effects of aspirin and acetaminophen on fetal and placental development. Four of 17 pregnant rats given 125 mg/kg/day of acetaminophen and 12 of 15 pregnant rats given 250 mg/kg/day of aspirin had at least one resorption site. This incidence was statistically different from that seen in rats given the vehicle only in the aspirin-pretreated group. In this group, 44% of the fetuses were resorbed and the weight and length of the remaining fetuses were reduced. Furthermore, placental growth was depressed in these animals. Acetaminophen at a comparable dose level (250 mg/kg/day) did not affect fetal length, fetal weight, or placental weight.

In rats receiving 125 mg/kg/day of aspirin, fetal growth was depressed but placental weight was not influenced. The incidence of resorptions was not increased over control values. In contrast, 125 mg/kg/day of acetaminophen produced more resorptions than occurred in the control group, 16 *versus* 0%, respectively, and also shorter fetuses. At this dose, acetaminophen did not affect either fetal or placental weight.

DISCUSSION

After 12 days of drug administration, no difference resulted in the average body weight of vehicle-treated and analgesic-treated nonpregnant animals. Thus, it seems unlikely that the small fetal and placental sizes in the aspirin-treated rats resulted from reduced food consumption by the dam. This interpretation is only speculative, however, since the compounds may affect the appetite of pregnant rats differently than that of nonpregnant rats. Fetal growth inhibition produced by aspirin could be a result of some of the many biochemical actions of the salicylates such as altered protein synthesis (12–14). Other actions of the salicylates such as uncoupling oxidative phosphorylation (15) and interfering with prostaglandin synthesis (16) may also be involved.

In contrast to aspirin, acetaminophen had little effect on fetal and placental growth. Shorter fetuses did occur in pregnant rats receiving the lower dose of acetaminophen than in those receiving the high dose. No rigorous conclusions about these results should be drawn since the data were obtained from a single experiment. However, lack of a classical dose–response relationship has been reported for other actions of acetaminophen. Dikstein *et al.* (17) reported that doses of 2–10 mg/kg/day of acetaminophen produced a greater increase in the width of the female rat tibial epiphysial cartilage than did doses of 20 mg/kg/day.

As with all animal experiments, these results cannot be extrapolated to other species. Mechanisms involved in fetal development and teratogenesis are so complicated that any conclusions concerning the relative safety of each analgesic during human pregnancy must be drawn with caution. Women taking large doses of salicylates during pregnancy may have a more complicated delivery (18), but even daily

Table II—Effect of Aspirin and Acetaminophen on Placental Weight and Fetal Resorption, Viability, Weight, and Length

Parameter	Vehicle (0.5% Methylcellulose)	Aspirin (125 mg/kg/day)	Aspirin (250 mg/kg/day)	Acetaminophen (125 mg/kg/day)	Acetaminophen (250 mg/kg/day)
Number of pregnant rats	18	21	15	17	16
Number of implant sites	140	211	145	149	155
Number of resorption sites	0	3 (1%)	64 (44%)[a]	24 (16%)[a]	0
Number of viable fetuses	140	208	79	125	155
Number of rats with at least one resorption	0	3 (14%)	12 (80%)	4 (24%)	0
Average fetal weight, g[b]	3.86 ± 0.03	3.54 ± 0.03[a]	2.55 ± 0.06[a]	3.82 ± 0.04	3.89 ± 0.04
Average fetal length, cm[b]	3.73 ± 0.02	3.63 ± 0.02[a]	3.21 ± 0.03[a]	3.65 ± 0.01[a]	3.77 ± 0.02
Average placental weight, g[b]	0.63 ± 0.01	0.61 ± 0.01	0.52 ± 0.01[a]	0.64 ± 0.01	0.64 ± 0.01

[a] Differs from control at $p < 0.05$. [b] Mean ± *SE*.

doses of 6.5 g taken during an entire pregnancy have resulted in the birth of a normal healthy neonate (19). However, in an animal such as the rat in which a wide variety of compounds can affect fetal growth, acetaminophen in the doses used in this study seems to produce less of an adverse effect than does aspirin.

REFERENCES

(1) E. M. Boyd, *J. Clin. Pharmacol.*, **10**, 222(1970).

(2) H. N. Wright, *Toxicol. Appl. Pharmacol.*, **11**, 280(1967).

(3) M. Goldman and C. A. Poppens, *ibid.*, **24**, 159(1973).

(4) J. D. McColl, M. Globus, and S. Robinson, *ibid.*, **7**, 409(1965).

(5) C. A. Kimmel, J. G. Wilson, and H. J. Schumacher, *Teratology*, **4**, 15(1971).

(6) K. S. Larsson and H. Bostrom, *Acta Paediatr. Scand.*, **54**, 43(1965).

(7) S. C. Smith and I. W. Monie, *Teratology*, **2**, 1(1969).

(8) K. T. Szabo, S. M. Free, H. A. Birkhead, Y. J. Kange, E. Alston, and M. Henry, *Toxicol. Appl. Pharmacol.*, **19**, 371(1971).

(9) J. Warkany and E. Takacs, *Am. J. Pathol.*, **35**, 315(1959).

(10) E. Takacs and J. Warkany, *Teratology*, **1**, 109(1968).

(11) S. Siegel, "Non Parametric Statistics," McGraw-Hill, New York, N.Y., 1956, p. 110.

(12) R. D. Pawkins, B. J. Gould, and M. J. H. Smith, *Biochem. J.*, **99**, 702(1966).

(13) K. Janakidevi and M. J. H. Smith, *J. Pharm. Pharmacol.*, **22**, 51(1970).

(14) *Ibid.*, **22**, 249(1970).

(15) J. T. Miyahara and R. Karler, *Biochem. J.*, **97**, 194(1965).

(16) J. R. Vane, *Nature*, **231**, 232(1971).

(17) S. Dikstein, M. Grotto, V. Zor, M. Tamari, and F. G. Sulman, *J. Endocrinol.*, **36**, 257(1966).

(18) R. Lewis and J. Shulman, *Lancet*, **2**, 1159(1973).

(19) L. Garrettson, J. A. Procknal, and G. Levy, *Clin. Pharmacol. Ther.*, **17**, 98(1975).

ACKNOWLEDGMENTS AND ADDRESSES

Received November 8, 1974, from the *College of Pharmacy, University of Kentucky, Lexington, KY 40506*

Accepted for publication February 9, 1976.

Supported in part by University of Kentucky Research Committee Grant 201-12-83100-63039.

The authors acknowledge the assistance of Mr. Michael Chestnut, Mr. Douglas Droz, Ms. Kay Gaines, and Mr. John Triplett with the manipulative procedures.

[x] To whom inquiries should be directed.

Baeocystin in *Psilocybe semilanceata*

DAVID B. REPKE [*x] and DALE THOMAS LESLIE [‡]

Abstract □ Baeocystin and psilocybin were found in extracts of a variety of *Psilocybe semilanceata*. Psilocybin (but not baeocystin) was also detected in extracts of a related species, *Psilocybe pelliculosa*. Traces of psilocin were present in these two species. The structures of the isolated compounds were corroborated using mass spectrometry and UV spectroscopy.

Keyphrases □ Baeocystin—isolated from extracts of *Psilocybe semilanceata*, identified by mass spectrometry and UV spectroscopy □ Psilocybin—isolated from extracts of *Psilocybe semilanceata* and *P. pelliculosa*, identified by mass spectrometry and UV spectroscopy □ *Psilocybe semilanceata*—extracts of carpophores, baeocystin and psilocybin isolated, identified by mass spectrometry and UV spectroscopy

The genus *Psilocybe* contains many species with hallucinogenic properties (1). Their use for religious purposes in Mexico was first recorded 4 centuries ago (2). However, only in the last 35 years has serious study been devoted to this subject (3). In 1959, two active principles were isolated from several members of this genus (4): the 4-hydroxy-3-(2-dimethylaminoethyl)-indole (psilocin) and its corresponding phosphate ester (psilocybin). Since then psilocin and psilocybin have been detected in other members of *Psilocybe* and related genera (5).

Heim (6) suggested that the hallucinogenic mushroom described in a 16th century English report was *Psilocybe semilanceata* (Fr.) Kummer (Strophariaceae), considered the type species of the genus (7, 8). Investigators have verified the presence of psilocybin (but not psilocin) in several European collections of *P. semilanceata* (9–12).

The presence of the psilocybin analogs 4-phosphoryloxy-3-(2-methylaminoethyl)indole and its demethyl counterpart (baeocystin and norbaeocystin, respectively) have been reported only in *P. baeocystis* Singer and Smith (13). These compounds were not found in *P. attrobrunnea* (Lasch) Gillet, *P. pelliculosa* (Smith) Singer and Smith, *P. caerulipes* (Peck) Sacc., or *P. strictipes* Singer and Smith (14).

During investigations of the indole alkaloids of the genus *Psilocybe*, a compound with a mobility slightly slower than psilocybin was consistently detected on thin-layer chromatograms of extracts of a Pacific Northwest variety of *P. semilanceata*. This compound was observed in all collections of this species examined over several years.

EXPERIMENTAL[1]

Freeze-dried carpophores of *P. semilanceata*[2], 824 mg, were ground to a powder and extracted by shaking with methanol at room tem-

[1] TLC was carried out using 0.25- and 1.0-mm layers of silica gel GF on glass plates. The solvent system used was 1-propanol–5% ammonium hydroxide (5:2) (13). Mass spectra were obtained with an Atlas CH-4 spectrometer *via* direct inlet. The probe temperature was 300°, and the ion source potential was 70 ev. A Cary model 15 spectrophotometer was used to determine UV spectra.

[2] The collections are in the herbarium of the Escuela Nacional de Ciencias Biológicas, I. P. N., Mexico, D. F., Mexico, and some are also on deposit at the herbarium of the University of Michigan, Ann Arbor, Mich. Carpophores of *P. semilanceata* were collected in pastures at the following locations: Grays Harbor County, Wash., 1972–1975 [LESLIE 1351 (also at MICH), 1807 (also at MICH), 2426 (also at MICH), and 2647]; Jefferson County, Wash., 1973–1975 [LESLIE 1843 (also at MICH), 2409 (also at MICH), and 2664]; Randle, Wash., 1975 (LESLIE 2710); and Sixes, Ore., 1975 (LESLIE 2781). Collections of *P. pelliculosa* were found in forests on wood debris and sawdust in Grays Harbor County, Wash., 1973 (LESLIE 1822) and Maytown, Wash., 1975 (LESLIE 2758). The taxon, designated here as *P. semilanceata*, conforms to published descriptions of the European *P. semilanceata*, but some doubt remains concerning this specific placement which further study may clarify.

doses of 6.5 g taken during an entire pregnancy have resulted in the birth of a normal healthy neonate (19). However, in an animal such as the rat in which a wide variety of compounds can affect fetal growth, acetaminophen in the doses used in this study seems to produce less of an adverse effect than does aspirin.

REFERENCES

(1) E. M. Boyd, *J. Clin. Pharmacol.*, **10**, 222(1970).

(2) H. N. Wright, *Toxicol. Appl. Pharmacol.*, **11**, 280(1967).

(3) M. Goldman and C. A. Poppens, *ibid.*, **24**, 159(1973).

(4) J. D. McColl, M. Globus, and S. Robinson, *ibid.*, **7**, 409(1965).

(5) C. A. Kimmel, J. G. Wilson, and H. J. Schumacher, *Teratology*, **4**, 15(1971).

(6) K. S. Larsson and H. Bostrom, *Acta Paediatr. Scand.*, **54**, 43(1965).

(7) S. C. Smith and I. W. Monie, *Teratology*, **2**, 1(1969).

(8) K. T. Szabo, S. M. Free, H. A. Birkhead, Y. J. Kange, E. Alston, and M. Henry, *Toxicol. Appl. Pharmacol.*, **19**, 371(1971).

(9) J. Warkany and E. Takacs, *Am. J. Pathol.*, **35**, 315(1959).

(10) E. Takacs and J. Warkany, *Teratology*, **1**, 109(1968).

(11) S. Siegel, "Non Parametric Statistics," McGraw-Hill, New York, N.Y., 1956, p. 110.

(12) R. D. Pawkins, B. J. Gould, and M. J. H. Smith, *Biochem. J.*, **99**, 702(1966).

(13) K. Janakidevi and M. J. H. Smith, *J. Pharm. Pharmacol.*, **22**, 51(1970).

(14) *Ibid.*, **22**, 249(1970).

(15) J. T. Miyahara and R. Karler, *Biochem. J.*, **97**, 194(1965).

(16) J. R. Vane, *Nature*, **231**, 232(1971).

(17) S. Dikstein, M. Grotto, V. Zor, M. Tamari, and F. G. Sulman, *J. Endocrinol.*, **36**, 257(1966).

(18) R. Lewis and J. Shulman, *Lancet*, **2**, 1159(1973).

(19) L. Garrettson, J. A. Procknal, and G. Levy, *Clin. Pharmacol. Ther.*, **17**, 98(1975).

ACKNOWLEDGMENTS AND ADDRESSES

Received November 8, 1974, from the *College of Pharmacy, University of Kentucky, Lexington, KY 40506*

Accepted for publication February 9, 1976.

Supported in part by University of Kentucky Research Committee Grant 201-12-83100-63039.

The authors acknowledge the assistance of Mr. Michael Chestnut, Mr. Douglas Droz, Ms. Kay Gaines, and Mr. John Triplett with the manipulative procedures.

[x] To whom inquiries should be directed.

Baeocystin in *Psilocybe semilanceata*

DAVID B. REPKE [*x] and DALE THOMAS LESLIE [‡]

Abstract □ Baeocystin and psilocybin were found in extracts of a variety of *Psilocybe semilanceata*. Psilocybin (but not baeocystin) was also detected in extracts of a related species, *Psilocybe pelliculosa*. Traces of psilocin were present in these two species. The structures of the isolated compounds were corroborated using mass spectrometry and UV spectroscopy.

Keyphrases □ Baeocystin—isolated from extracts of *Psilocybe semilanceata*, identified by mass spectrometry and UV spectroscopy □ Psilocybin—isolated from extracts of *Psilocybe semilanceata* and *P. pelliculosa*, identified by mass spectrometry and UV spectroscopy □ *Psilocybe semilanceata*—extracts of carpophores, baeocystin and psilocybin isolated, identified by mass spectrometry and UV spectroscopy

The genus *Psilocybe* contains many species with hallucinogenic properties (1). Their use for religious purposes in Mexico was first recorded 4 centuries ago (2). However, only in the last 35 years has serious study been devoted to this subject (3). In 1959, two active principles were isolated from several members of this genus (4): the 4-hydroxy-3-(2-dimethylaminoethyl)-indole (psilocin) and its corresponding phosphate ester (psilocybin). Since then psilocin and psilocybin have been detected in other members of *Psilocybe* and related genera (5).

Heim (6) suggested that the hallucinogenic mushroom described in a 16th century English report was *Psilocybe semilanceata* (Fr.) Kummer (Strophariaceae), considered the type species of the genus (7, 8). Investigators have verified the presence of psilocybin (but not psilocin) in several European collections of *P. semilanceata* (9–12).

The presence of the psilocybin analogs 4-phosphoryloxy-3-(2-methylaminoethyl)indole and its demethyl counterpart (baeocystin and norbaeocystin, respectively) have been reported only in *P. baeocystis* Singer and Smith (13). These compounds were not found in *P. attrobrunnea* (Lasch) Gillet, *P. pelliculosa* (Smith) Singer and Smith, *P. caerulipes* (Peck) Sacc., or *P. strictipes* Singer and Smith (14).

During investigations of the indole alkaloids of the genus *Psilocybe*, a compound with a mobility slightly slower than psilocybin was consistently detected on thin-layer chromatograms of extracts of a Pacific Northwest variety of *P. semilanceata*. This compound was observed in all collections of this species examined over several years.

EXPERIMENTAL[1]

Freeze-dried carpophores of *P. semilanceata*[2], 824 mg, were ground to a powder and extracted by shaking with methanol at room tem-

[1] TLC was carried out using 0.25- and 1.0-mm layers of silica gel GF on glass plates. The solvent system used was 1-propanol–5% ammonium hydroxide (5:2) (13). Mass spectra were obtained with an Atlas CH-4 spectrometer *via* direct inlet. The probe temperature was 300°, and the ion source potential was 70 ev. A Cary model 15 spectrophotometer was used to determine UV spectra.

[2] The collections are in the herbarium of the Escuela Nacional de Ciencias Biológicas, I. P. N., Mexico, D. F., Mexico, and some are also on deposit at the herbarium of the University of Michigan, Ann Arbor, Mich. Carpophores of *P. semilanceata* were collected in pastures at the following locations: Grays Harbor County, Wash., 1972–1975 [LESLIE 1351 (also at MICH), 1807 (also at MICH), 2426 (also at MICH), and 2647]; Jefferson County, Wash., 1973–1975 [LESLIE 1843 (also at MICH), 2409 (also at MICH), and 2664]; Randle, Wash., 1975 (LESLIE 2710); and Sixes, Ore., 1975 (LESLIE 2781). Collections of *P. pelliculosa* were found in forests on wood debris and sawdust in Grays Harbor County, Wash., 1973 (LESLIE 1822) and Maytown, Wash., 1975 (LESLIE 2758). The taxon, designated here as *P. semilanceata*, conforms to published descriptions of the European *P. semilanceata*, but some doubt remains concerning this specific placement which further study may clarify.

perature for 20 hr. The mixture was filtered, and the solids were washed with methanol. The combined filtrate and washings were concentrated *in vacuo*. Analytical TLC of the extract (two developments) showed psilocybin (R_f 0.27) and the slower compound (R_f 0.22). Both spots exhibited the same dark-blue coloration when sprayed with 2% 4-dimethylaminobenzaldehyde in ethanol and exposed to hydrogen chloride vapors. Trace amounts of psilocin were also detected.

The concentrated residue was preparatively chromatographed on a 1.0-mm layer of silica gel in the described solvent system. A band containing the two components was removed from the plate, and the compounds were eluted with methanol containing 5% aqueous ammonia. The eluate was concentrated under reduced pressure, and the residue was rechromatographed on a 0.25-mm layer of silica gel to resolve the two components. Two developments in the propanol–ammonia system followed by elution of the bands afforded psilocybin (3 mg, 0.36%), mp 175–180° [lit. (15) mp 185–195°] and its slower-moving counterpart (1 mg, 0.12%), mp 245–248° [lit. (14) mp 254–258°]. Carpophores of *P. pelliculosa* were extracted in a similar manner to give 0.08% psilocybin. Traces of psilocin were also detected.

RESULTS AND DISCUSSION

The UV spectra of the two compounds were superimposable, with λ_{max} (methanol) 290 (ϵ 4000), 280 (sh)(5000), 268 (6300), and 222 (40,000) nm, typical of psilocybin (4). The mass spectra were consistent with published data for psilocybin (11) and baeocystin (13). Psilocybin showed peaks at *m/e* 204 (relative abundance, 19%), 160 (4), 159 (3), 146 (6), 130 (3), 117 (2), and 58 (100). Baeocystin showed peaks at 190 (8), 160 (4), 159 (4), 147 (16), 146 (14), 130 (4), 117 (5), and 44 (100).

Each compound exhibited typical fragmentations of 3-indolylethylamines (16), *e.g.*, a base peak arising from β-bond fission of the ethylamine side chain (psilocybin, *m/e* 58; and baeocystin, *m/e* 44). While neither compound showed a parent peak, both showed signals for the dephosphorylated species (psilocybin, *m/e* 204; and baeocystin, *m/e* 190). The concentration of psilocybin in *P. semilanceata* was consistent with isolated yields reported from European collections (9, 11).

In agreement with Leung and Paul (14), baeocystin was not detected in *P. pelliculosa*. Psilocybin (but not psilocin) has been reported previously in this species (17).

Preliminary investigations suggest the presence of baeocystin in other species and genera. In fact, Leung and Paul (13) and Benedict (18) suggested that baeocystin may have been the unidentified compound observed by Stein *et al.* (19) in a species of *Panaeolus*.

Pharmacological effects of the analogs of psilocybin have not been studied.

REFERENCES

(1) R. Heim and R. G. Wasson, "Les Champignons Hallucinogénes du Mexique," Museum National D'Histoire Naturelle, Paris, France, 1959.

(2) B. de Sahagún, "Florentine Codex, General History of New Spain," Books III and XI, A. J. O. Anderson and C. E. Dibble, Translators, University of Utah Press, Salt Lake City, Utah, 1970.

(3) R. G. Wasson, *Bot. Mus. Leafl. Harv. Univ.*, **20**, 25(1963).

(4) A. Hofmann, R. Heim, A. Brack, H. Kobel, A. Frey, H. Ott, T. Petrzilka, and F. Troxler, *Helv. Chim. Acta*, **42**, 1557(1959).

(5) R. E. Schultes and A. Hofmann, "The Botany and Chemistry of Hallucinogens," Charles C Thomas, Springfield, Ill., 1973, pp. 36–52.

(6) R. Heim, *Natur. Can.*, **98**, 415 (1971).

(7) R. Singer, "The Agaricales in Modern Taxonomy," 2nd ed., J. Cramer, Weinheim, Germany, 1962, p. 542.

(8) P. Konrad and A. Maublanc, "Révision des Hyménomycètes de France," Paul LeChevalier, Paris, France, 1937, p. 84.

(9) A. Hofmann, R. Heim, and H. Tscherter, *C. R. Acad. Sci.*, **257**, 10(1963).

(10) R. G. Benedict, V. E. Tyler, and R. Watling, *Lloydia*, **30**, 150(1967).

(11) P. G. Mantle and E. S. Waight, *Trans. Br. Mycol. Soc.*, **53**, 302(1969).

(12) M. Semerdzieva and F. Nerud, *Ceska Mykol.*, **27**, 42(1973).

(13) A. Y. Leung and A. G. Paul, *J. Pharm. Sci.*, **57**, 1667(1968).

(14) *Ibid.*, **56**, 146(1967).

(15) A. Hofmann, R. Heim, A. Brack, and H. Kobel, *Experientia*, **14**, 107(1958).

(16) H. Budzikiewicz, C. Djerassi, and D. H. Williams, "Structural Elucidation of Natural Products by Mass Spectrometry," vol. 1, Holden-Day, San Francisco, Calif., 1964, pp. 42–45.

(17) V. E. Tyler, *Lloydia*, **24**, 71(1961).

(18) R. G. Benedict, in "Microbial Toxins," S. Kadis, A. Ciegler, and S. J. Ajl, Eds., Academic, New York, N.Y., 1972, chap. 11.

(19) S. I. Stein, G. L. Closs, and N. W. Gabel, *Mycopathol. Mycol. App.*, **11**, 205(1959).

ACKNOWLEDGMENTS AND ADDRESSES

Received December 29, 1975, from **148-B West Dana Street, Mountain View, CA 94041*, and *‡104 Whitney Avenue, Los Gatos, CA 95030*

Accepted for publication May 28, 1976.

The authors thank Lornie Leslie and Jean Leslie for their help with this study and also Jerry Boydstein for assistance in collecting *P. pelliculosa* near Maytown, Wash.

ˣ To whom inquiries should be directed.

Simple Device for GLC Separations of Cannabinoids Using a Surface-Coated Open Tube Column without Stream Splitting

N. K. McCALLUM ˣ and E. R. CAIRNS

Abstract □ A simple device that allows the GLC analysis of greater than 10 μl of sample solution on capillary columns is described. The conditions necessary for application of this device to the quantitative analysis of cannabinoids are elaborated.

Keyphrases □ Cannabinoids—GLC analysis, device using a surface-coated open tube column □ GLC—analysis, cannabinoids, device using a surface-coated open tube column □ Marijuana—GLC analysis of constituents, device using a surface-coated open tube column

GLC is the method of choice for rapid qualitative and quantitative analysis of marijuana constituents. Much literature (1) is devoted to the use of this analytical technique with packed columns. Several investigators, however, reported problems with packed GLC columns for these analyses. Some long chain alkanes have similar re-

perature for 20 hr. The mixture was filtered, and the solids were washed with methanol. The combined filtrate and washings were concentrated *in vacuo*. Analytical TLC of the extract (two developments) showed psilocybin (R_f 0.27) and the slower compound (R_f 0.22). Both spots exhibited the same dark-blue coloration when sprayed with 2% 4-dimethylaminobenzaldehyde in ethanol and exposed to hydrogen chloride vapors. Trace amounts of psilocin were also detected.

The concentrated residue was preparatively chromatographed on a 1.0-mm layer of silica gel in the described solvent system. A band containing the two components was removed from the plate, and the compounds were eluted with methanol containing 5% aqueous ammonia. The eluate was concentrated under reduced pressure, and the residue was rechromatographed on a 0.25-mm layer of silica gel to resolve the two components. Two developments in the propanol–ammonia system followed by elution of the bands afforded psilocybin (3 mg, 0.36%), mp 175–180° [lit. (15) mp 185–195°] and its slower-moving counterpart (1 mg, 0.12%), mp 245–248° [lit. (14) mp 254–258°]. Carpophores of *P. pelliculosa* were extracted in a similar manner to give 0.08% psilocybin. Traces of psilocin were also detected.

RESULTS AND DISCUSSION

The UV spectra of the two compounds were superimposable, with λ_{max} (methanol) 290 (ϵ 4000), 280 (sh)(5000), 268 (6300), and 222 (40,000) nm, typical of psilocybin (4). The mass spectra were consistent with published data for psilocybin (11) and baeocystin (13). Psilocybin showed peaks at *m/e* 204 (relative abundance, 19%), 160 (4), 159 (3), 146 (6), 130 (3), 117 (2), and 58 (100). Baeocystin showed peaks at 190 (8), 160 (4), 159 (4), 147 (16), 146 (14), 130 (4), 117 (5), and 44 (100).

Each compound exhibited typical fragmentations of 3-indolylethylamines (16), *e.g.*, a base peak arising from β-bond fission of the ethylamine side chain (psilocybin, *m/e* 58; and baeocystin, *m/e* 44). While neither compound showed a parent peak, both showed signals for the dephosphorylated species (psilocybin, *m/e* 204; and baeocystin, *m/e* 190). The concentration of psilocybin in *P. semilanceata* was consistent with isolated yields reported from European collections (9, 11).

In agreement with Leung and Paul (14), baeocystin was not detected in *P. pelliculosa*. Psilocybin (but not psilocin) has been reported previously in this species (17).

Preliminary investigations suggest the presence of baeocystin in other species and genera. In fact, Leung and Paul (13) and Benedict (18) suggested that baeocystin may have been the unidentified compound observed by Stein *et al.* (19) in a species of *Panaeolus*.

Pharmacological effects of the analogs of psilocybin have not been studied.

REFERENCES

(1) R. Heim and R. G. Wasson, "Les Champignons Hallucinogénes du Mexique," Museum National D'Histoire Naturelle, Paris, France, 1959.

(2) B. de Sahagún, "Florentine Codex, General History of New Spain," Books III and XI, A. J. O. Anderson and C. E. Dibble, Translators, University of Utah Press, Salt Lake City, Utah, 1970.

(3) R. G. Wasson, *Bot. Mus. Leafl. Harv. Univ.*, **20**, 25(1963).

(4) A. Hofmann, R. Heim, A. Brack, H. Kobel, A. Frey, H. Ott, T. Petrzilka, and F. Troxler, *Helv. Chim. Acta*, **42**, 1557(1959).

(5) R. E. Schultes and A. Hofmann, "The Botany and Chemistry of Hallucinogens," Charles C Thomas, Springfield, Ill., 1973, pp. 36–52.

(6) R. Heim, *Natur. Can.*, **98**, 415 (1971).

(7) R. Singer, "The Agaricales in Modern Taxonomy," 2nd ed., J. Cramer, Weinheim, Germany, 1962, p. 542.

(8) P. Konrad and A. Maublanc, "Révision des Hyménomycètes de France," Paul LeChevalier, Paris, France, 1937, p. 84.

(9) A. Hofmann, R. Heim, and H. Tscherter, *C. R. Acad. Sci.*, **257**, 10(1963).

(10) R. G. Benedict, V. E. Tyler, and R. Watling, *Lloydia*, **30**, 150(1967).

(11) P. G. Mantle and E. S. Waight, *Trans. Br. Mycol. Soc.*, **53**, 302(1969).

(12) M. Semerdzieva and F. Nerud, *Ceska Mykol.*, **27**, 42(1973).

(13) A. Y. Leung and A. G. Paul, *J. Pharm. Sci.*, **57**, 1667(1968).

(14) *Ibid.*, **56**, 146(1967).

(15) A. Hofmann, R. Heim, A. Brack, and H. Kobel, *Experientia*, **14**, 107(1958).

(16) H. Budzikiewicz, C. Djerassi, and D. H. Williams, "Structural Elucidation of Natural Products by Mass Spectrometry," vol. 1, Holden-Day, San Francisco, Calif., 1964, pp. 42–45.

(17) V. E. Tyler, *Lloydia*, **24**, 71(1961).

(18) R. G. Benedict, in "Microbial Toxins," S. Kadis, A. Ciegler, and S. J. Ajl, Eds., Academic, New York, N.Y., 1972, chap. 11.

(19) S. I. Stein, G. L. Closs, and N. W. Gabel, *Mycopathol. Mycol. App.*, **11**, 205(1959).

ACKNOWLEDGMENTS AND ADDRESSES

Received December 29, 1975, from **148-B West Dana Street, Mountain View, CA 94041*, and *‡104 Whitney Avenue, Los Gatos, CA 95030*

Accepted for publication May 28, 1976.

The authors thank Lornie Leslie and Jean Leslie for their help with this study and also Jerry Boydstein for assistance in collecting *P. pelliculosa* near Maytown, Wash.

ˣ To whom inquiries should be directed.

Simple Device for GLC Separations of Cannabinoids Using a Surface-Coated Open Tube Column without Stream Splitting

N. K. McCALLUM ˣ and E. R. CAIRNS

Abstract □ A simple device that allows the GLC analysis of greater than 10 μl of sample solution on capillary columns is described. The conditions necessary for application of this device to the quantitative analysis of cannabinoids are elaborated.

Keyphrases □ Cannabinoids—GLC analysis, device using a surface-coated open tube column □ GLC—analysis, cannabinoids, device using a surface-coated open tube column □ Marijuana—GLC analysis of constituents, device using a surface-coated open tube column

GLC is the method of choice for rapid qualitative and quantitative analysis of marijuana constituents. Much literature (1) is devoted to the use of this analytical technique with packed columns. Several investigators, however, reported problems with packed GLC columns for these analyses. Some long chain alkanes have similar re-

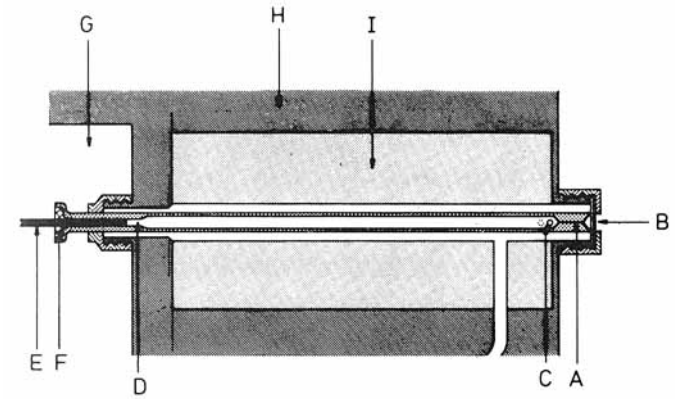

Figure 1—*Inlet port design. (See text.)*

tention times to cannabinoids and can interfere with their analyses (2). Similarly, the retention times of cannabichromene and cannabidiol are the same on most columns, and many reported analytical values for cannabidiol may be suspect for this reason (3).

Such analytical problems generally necessitate an extra analytical step, such as a preliminary chromatographic cleanup or derivatization. However, high-resolution GLC work (4) indicates that interferences by minor constituents are probably more the rule than the exception. Therefore, use of high-resolution capillary columns would be a simpler way of avoiding this problem.

DISCUSSION

Capillary columns have been used for the separation of the naturally occurring volatile terpenes (5) and cannabinoids (4, 6, 7) of *Cannabis*. Unfortunately, the use of capillary columns imposes severe restrictions on the volume of solutions that can be analyzed (0.1–1.0 μl, depending on the column diameter), so a stream splitter is generally used in conjunction with the injection system. Although stream splitters are adequate for qualitative analyses, they can introduce errors into quantitative work (8).

An alternative to the direct injection of very small quantities of solution for quantitative analysis was reported (9). This method allows the direct injection of larger quantities (usually ~0.3 μl) of the solution into an inlet port, designed so that the large amount of solvent vapor initially prevents migration of the sample components, concentrates them to 1% of the original length of the solvent plug, and allows them to be eluted after most solvent has disappeared. The theory of operation was discussed in detail (10).

The design of the inlet port is such that contact of solvent vapors with the septum is reduced to a minimum (solvent bleed from the septum being an important, undesirable factor), and all dead volumes are eliminated (9). A careful choice of solvents is also necessary to utilize the effect; the wrong solvent gives rise to broadened and misshapen peaks (10). Prolonged use of this system has not been found to affect the column life adversely (10).

The advantages of this system are clear: (*a*) utilization of the solvent to produce good resolution rather than complicated procedures to eliminate the solvent, (*b*) greatly improved sensitivity as a natural corollary to improved resolution and the injection of larger samples, and (*c*) strictly quantitative analyses without injection of very small volumes of solution. The disadvantages are designing and building the relatively complicated inlet port system and then finding the optimum solvent and conditions.

This paper presents an alternative, considerably simplified, all-glass system, which can be fabricated by most chemists of average glass-blowing ability. The described system was successfully used for the analysis of hydrocarbons and, in particular, cannabinoids.

EXPERIMENTAL

Inlet Port (Fig. 1)—The capillary (A) was chosen so that its inside diameter was a "snug" fit for the injection syringe needle and its end

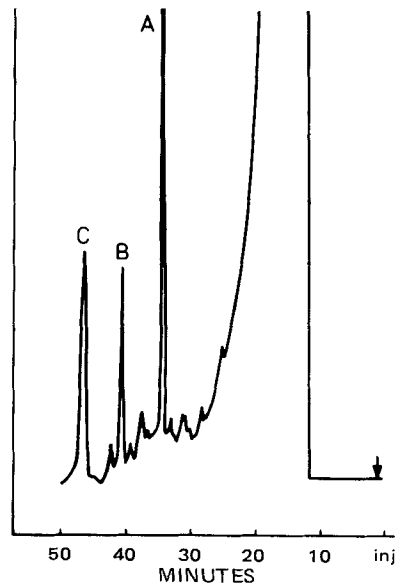

Figure 2—*Gas chromatogram of* Cannabis *sample in methyl laurate. Key: A, cannabidiol; B, Δ^9-tetrahydrocannabinol; and C, cannabinol.*

rested against the septum (B) to eliminate back-diffusion of solvent vapor. The carrier gas entered the system by two holes (C) at the base of the capillary.

The internal diameter of the exit (D) was 1.5 mm, providing an almost exact fit for the glass-lined steel tubing (E) leading to the column. The final seal at the exit was a cut-down, slightly compressed septum (F). Areas G, H, and I are the oven, oven wall, and inlet heater, respectively.

Capillary Column—The glass surface-coated open tube column[1] (70 m × 0.5 mm i.d.) was coated with SE-30, silanized, and deactivated. A "T" piece[1] for makeup gas was fitted at the exit of the capillary column, and connection with the detector port was by means of glass-lined steel tubing[1] to glass tubing (1.5 mm i.d.), using a septum for the final seal as was described for the inlet port.

Operation—A carrier gas flow of about 4 ml/min of helium was used. The makeup gas was nitrogen (~25 ml/min). A light petroleum *Cannabis* extract[2] was evaporated and taken up in the appropriate solvent to a concentration of about 0.1 mg/ml. The sample was then withdrawn completely into the barrel of the syringe, and the GLC[3] septum was penetrated to the full extent of the syringe needle (5–7 cm) and then released. After 2–3 sec, the plunger was withdrawn so that any solvent residues were taken back into the barrel of the syringe; then the syringe was withdrawn from the septum.

Sample sizes of 3 μl were taken when different solvents were being compared; 1–10-μl methyl laurate solutions were selected as the best solvents for these separations. The three major cannabinoids in the extracts (Fig. 2) were identified by comparison with authentic samples. Confirmation of these identities was provided by comparison of the derivatized and underivatized samples with authentic samples on conventional OV-1 and OV-225 columns.

RESULTS

The dimensions of the inlet system appear to have surprisingly little effect on efficiency. Vaporization chambers that were 15 cm × 1.5–3.5 mm i.d. were used and compared to 6-cm × 2.5–4-mm i.d. chambers used previously (9). The system is suitable for large sample sizes (up to 10 μl without sacrificing resolution), and differing dimensions of the oven wall and inlet heater for different models of gas chromatographs apparently present no problem for inlet design.

The suppliers of the capillary column determined its effective theoretical plates (N_{eff}) to be 43,000 for the C_{24} *n*-alkane in methylene chlo-

[1] Supplied by the Scientific Glass Engineering Pty. Ltd., N. Melbourne, Victoria, Australia 3051.

[2] A sample, identified and supplied by Mr. Peter D. Wilson of the Forensic Section, Chemistry Division, Department of Scientific and Industrial Research, Private Bag, Petone, New Zealand, is being held under Code No. AW 4520 by the Forensic Section.

[3] Tracor model 550 with flame-ionization detection.

ride (0.1 μl). When this inlet system was used with the C_{18} *n*-alkane in C_{12} *n*-alkane (5 μl), N_{eff} = 40,000 was obtained. However, GLC of cannabinoids in the higher alkanes produced very poor resolution with considerable peak tailing. Alternative solvents were tested (*e.g.*, *n*-alkanes up to C_{20}, branched chain alkanes up to C_{10}, higher boiling alkenes, alcohols, and ketones), and only fatty acid esters provided acceptable resolution. The best was methyl laurate, which yielded N_{eff} = 25,000 (Fig. 2).

The temperature of the inlet port is critical for good resolution. If the temperature is too low—by as little as 10–15°—no recognizable chromatogram will be achieved. Operating conditions for the cannabinoids in methyl laurate were: oven temperature, 230°; and inlet temperature, 250°.

The N_{eff} for cannabinoids is only 63% that achieved for alkanes. This reduction in efficiency apparently is due, at least in part, to support effects (11); the possibility exists that even more efficient separations of cannabinoids can be achieved with a different stationary phase in combination with another solvent. Different stationary phases may, of course, also provide more convenient elution orders to suit particular problems.

The main point to be noted is that the described device now permits the application of capillary columns (with its attendant 10-fold plus improvement in resolution over conventional columns) to cannabinoid analyses; this system should be of considerable use for biological as well as plant extracts. Other stationary phases and solvents possibly will be applicable to GLC of derivatized cannabinoids. This variety would allow further improvements in the sensitivity of detection of cannabinoids when utilizing electron-capture (12) and flame-ionization (13) detectors.

REFERENCES

(1) R. Mechoulam, N. K. McCallum, and S. Burstein, *Chem. Rev.*, **76**, 93 (1976).

(2) R. A. De Zeeuw, J. Wijsbeek, and T. Malingré, *J. Pharm. Pharmacol.*, **25**, 21 (1973).

(3) C. F. Turner and K. W. Hadley, *J. Pharm. Sci.*, **62**, 1083 (1973).

(4) J. Friedrich-Fiechtl and G. Spiteller, *Tetrahedron*, **31**, 479 (1975).

(5) C. A. L. Bercht, F. J. E. M. Küppers, R. J. J. C. Lousberg, C. A. Salemink, A. Baerheim Svendsen, and J. Karlsen, U.N. Document ST/SOA/SER, S/29, July 1971.

(6) M. Novotny and M. L. Lee, *Experientia*, **29**, 1038 (1973).

(7) D. C. Fenimore, R. R. Freeman, and P. R. Loy, *Anal. Chem.*, **45**, 2331 (1973).

(8) M. Verzele, M. Verstappe, P. Sandra, E. Van Luchene, and A. Vuye, *J. Chromatogr. Sci.*, **10**, 668 (1972).

(9) K. Grob and G. Grob, *Chromatographia*, **5**, 3 (1972).

(10) K. Grob and K. Grob, Jr., *J. Chromatogr.*, **94**, 53 (1974).

(11) Scientific Glass Engineering Pty. Ltd., GSC 2/74, N. Melbourne, Victoria, Australia 3051.

(12) E. R. Garrett and C. A. Hunt, *J. Pharm. Sci.*, **62**, 1211 (1973).

(13) N. K. McCallum *J. Chromatogr. Sci.*, **11**, 509 (1973).

ACKNOWLEDGMENTS AND ADDRESSES

Received August 27, 1975, from the *Chemistry Division, Department of Scientific and Industrial Research, Private Bag, Petone, New Zealand.*

Accepted for publication February 26, 1976.

The authors thank Professor R. Mechoulam, with whom this project originated.

[x] To whom inquiries should be directed.

Dihydralazine Sulfate Analysis Using 2-Methyl-3-nitropyridine-6-carboxaldehyde

A. F. YOUSSEF [x], S. A. IBRAHIM, and S. R. ELSHABOURI

Abstract □ A sensitive, selective colorimetric assay was developed for the quantitative analysis of dihydralazine sulfate. The method is based on the interaction of buffered (pH 4) dihydralazine sulfate with a methanolic solution of 2-methyl-3-nitropyridine-6-carboxaldehyde upon heating to give an orange color. This color can be quantified spectrophotometrically at 450 nm, with a lower limit of detection of 1 μg/ml. The color is stable for at least 24 hr. There is no interference from other drugs likely to be present along with dihydralazine sulfate and common excipients. The method was used successfully for the determination of dihydralazine sulfate in combination with other drugs in different commercial tablets. The developed method was applicable as a stability-indicating assay.

Keyphrases □ Dihydralazine sulfate—colorimetric analysis using 2-methyl-3-nitropyridine-6-carboxaldehyde, prepared samples □ Colorimetry—analysis, dihydralazine sulfate in prepared samples □ 2-Methyl-3-nitropyridine-6-carboxaldehyde—color reagent in analysis of dihydralazine sulfate in prepared samples □ Antihypertensive agents—dihydralazine sulfate, colorimetric analysis in prepared samples

Various methods for the analysis of dihydralazine sulfate (1,4-dihydrazinophthalazine) have been reported (1–11). The bromometric assay for pure dihydralazine sulfate used potassium dichromate (1) or potassium permanganate (2) as the titrant in the presence of potassium bromide. The dihydralazinebenzoic acid–bivalent metal complexes were estimated by titration with edetic acid (3, 4); the dihydralazine–copper thiocyanate complex was estimated by titration with silver nitrate (5).

The reported argentimetric procedures depend on either the estimation of excess silver nitrate added to the buffered solution of dihydralazine at pH 5–6 (6) or stoichiometric determination of metallic silver separated after the addition of ammoniacal silver nitrate (7). Direct potentiometric titration of pure dihydralazine sulfate and other hydrazine derivatives, using chloramine-T in an acidic medium, was reported (8). A coulometric method for dihydralazine, using electrolytically generated bromine, also was reported (9).

Colorimetric methods were developed for the estimation of dihydralazine sulfate in the pure form and in tablets, depending on the formation of a chromogenic product with ammonium molybdate (6) and ferric ion (10); the lower limits of detection were 70 and 150 μg, respectively. Also, a colorimetric method was reported

ride (0.1 μl). When this inlet system was used with the C_{18} *n*-alkane in C_{12} *n*-alkane (5 μl), N_{eff} = 40,000 was obtained. However, GLC of cannabinoids in the higher alkanes produced very poor resolution with considerable peak tailing. Alternative solvents were tested (*e.g.*, *n*-alkanes up to C_{20}, branched chain alkanes up to C_{10}, higher boiling alkenes, alcohols, and ketones), and only fatty acid esters provided acceptable resolution. The best was methyl laurate, which yielded N_{eff} = 25,000 (Fig. 2).

The temperature of the inlet port is critical for good resolution. If the temperature is too low—by as little as 10–15°—no recognizable chromatogram will be achieved. Operating conditions for the cannabinoids in methyl laurate were: oven temperature, 230°; and inlet temperature, 250°.

The N_{eff} for cannabinoids is only 63% that achieved for alkanes. This reduction in efficiency apparently is due, at least in part, to support effects (11); the possibility exists that even more efficient separations of cannabinoids can be achieved with a different stationary phase in combination with another solvent. Different stationary phases may, of course, also provide more convenient elution orders to suit particular problems.

The main point to be noted is that the described device now permits the application of capillary columns (with its attendant 10-fold plus improvement in resolution over conventional columns) to cannabinoid analyses; this system should be of considerable use for biological as well as plant extracts. Other stationary phases and solvents possibly will be applicable to GLC of derivatized cannabinoids. This variety would allow further improvements in the sensitivity of detection of cannabinoids when utilizing electron-capture (12) and flame-ionization (13) detectors.

REFERENCES

(1) R. Mechoulam, N. K. McCallum, and S. Burstein, *Chem. Rev.*, **76**, 93 (1976).

(2) R. A. De Zeeuw, J. Wijsbeek, and T. Malingré, *J. Pharm. Pharmacol.*, **25**, 21 (1973).

(3) C. F. Turner and K. W. Hadley, *J. Pharm. Sci.*, **62**, 1083 (1973).

(4) J. Friedrich-Fiechtl and G. Spiteller, *Tetrahedron*, **31**, 479 (1975).

(5) C. A. L. Bercht, F. J. E. M. Küppers, R. J. J. C. Lousberg, C. A. Salemink, A. Baerheim Svendsen, and J. Karlsen, U.N. Document ST/SOA/SER, S/29, July 1971.

(6) M. Novotny and M. L. Lee, *Experientia*, **29**, 1038 (1973).

(7) D. C. Fenimore, R. R. Freeman, and P. R. Loy, *Anal. Chem.*, **45**, 2331 (1973).

(8) M. Verzele, M. Verstappe, P. Sandra, E. Van Luchene, and A. Vuye, *J. Chromatogr. Sci.*, **10**, 668 (1972).

(9) K. Grob and G. Grob, *Chromatographia*, **5**, 3 (1972).

(10) K. Grob and K. Grob, Jr., *J. Chromatogr.*, **94**, 53 (1974).

(11) Scientific Glass Engineering Pty. Ltd., GSC 2/74, N. Melbourne, Victoria, Australia 3051.

(12) E. R. Garrett and C. A. Hunt, *J. Pharm. Sci.*, **62**, 1211 (1973).

(13) N. K. McCallum *J. Chromatogr. Sci.*, **11**, 509 (1973).

ACKNOWLEDGMENTS AND ADDRESSES

Received August 27, 1975, from the *Chemistry Division, Department of Scientific and Industrial Research, Private Bag, Petone, New Zealand.*

Accepted for publication February 26, 1976.

The authors thank Professor R. Mechoulam, with whom this project originated.

[x] To whom inquiries should be directed.

Dihydralazine Sulfate Analysis Using 2-Methyl-3-nitropyridine-6-carboxaldehyde

A. F. YOUSSEF [x], S. A. IBRAHIM, and S. R. ELSHABOURI

Abstract □ A sensitive, selective colorimetric assay was developed for the quantitative analysis of dihydralazine sulfate. The method is based on the interaction of buffered (pH 4) dihydralazine sulfate with a methanolic solution of 2-methyl-3-nitropyridine-6-carboxaldehyde upon heating to give an orange color. This color can be quantified spectrophotometrically at 450 nm, with a lower limit of detection of 1 μg/ml. The color is stable for at least 24 hr. There is no interference from other drugs likely to be present along with dihydralazine sulfate and common excipients. The method was used successfully for the determination of dihydralazine sulfate in combination with other drugs in different commercial tablets. The developed method was applicable as a stability-indicating assay.

Keyphrases □ Dihydralazine sulfate—colorimetric analysis using 2-methyl-3-nitropyridine-6-carboxaldehyde, prepared samples □ Colorimetry—analysis, dihydralazine sulfate in prepared samples □ 2-Methyl-3-nitropyridine-6-carboxaldehyde—color reagent in analysis of dihydralazine sulfate in prepared samples □ Antihypertensive agents—dihydralazine sulfate, colorimetric analysis in prepared samples

Various methods for the analysis of dihydralazine sulfate (1,4-dihydrazinophthalazine) have been reported (1–11). The bromometric assay for pure dihydralazine sulfate used potassium dichromate (1) or potassium permanganate (2) as the titrant in the presence of potassium bromide. The dihydralazinebenzoic acid–bivalent metal complexes were estimated by titration with edetic acid (3, 4); the dihydralazine–copper thiocyanate complex was estimated by titration with silver nitrate (5).

The reported argentimetric procedures depend on either the estimation of excess silver nitrate added to the buffered solution of dihydralazine at pH 5–6 (6) or stoichiometric determination of metallic silver separated after the addition of ammoniacal silver nitrate (7). Direct potentiometric titration of pure dihydralazine sulfate and other hydrazine derivatives, using chloramine-T in an acidic medium, was reported (8). A coulometric method for dihydralazine, using electrolytically generated bromine, also was reported (9).

Colorimetric methods were developed for the estimation of dihydralazine sulfate in the pure form and in tablets, depending on the formation of a chromogenic product with ammonium molybdate (6) and ferric ion (10); the lower limits of detection were 70 and 150 μg, respectively. Also, a colorimetric method was reported

Table I—Effect of pH on the Intensity of the Developed Color

pH	McIlvaine's Citric Acid–Phosphate Buffer, A^a	Acetic Acid–Sodium Acetate Buffer, A	Phosphate Buffer, A
2.20	0.410	—	—
3.00	0.680	—	—
3.45	—	0.075	—
3.60	0.680	—	—
3.72	—	0.670	—
3.80	0.690	—	—
4.00	0.780	—	—
4.05	—	0.760	—
4.20	0.720	—	—
4.27	—	0.710	—
4.40	0.710	—	—
4.45	—	0.680	—
4.99	—	0.660	—
5.00	0.660	—	—
6.00	Turbidity	—	0.380
7.00	Turbidity	—	0.270
8.00	Turbidity	—	0.160

$^a A$ = absorbance of solution containing 10 μg of dihydralazine sulfate/ml.

for the analysis of dihydralazine sulfate using 4,4′-dimethoxydiquinone as the chromogen-developing reagent.

It has been observed in these laboratories that 2-methyl-3-nitropyridine-6-carboxaldehyde interacts with hydrazine derivatives to form chromogenic products. The reaction can be quantified to be used as a simple analytical tool for selective estimation of hydrazine derivatives. This report describes the use of 2-methyl-3-nitropyridine-6-carboxaldehyde as a chromogenic reagent for sensitive and selective estimation of dihydralazine sulfate in the pure form and in combination with other drugs in commercial pharmaceutical formulations. The method also was investigated as a stability-indicating assay.

EXPERIMENTAL

Instrumentation—Spectra and absorbance measurements were made[1] using matched glass cells with 1-cm optical path.

Reagents and Chemicals—The color reagent (2-methyl-3-nitropyridine-6-carboxaldehyde) was prepared according to Banas and Skrowaczewska (12), bp_4 115°. Dihydralazine sulfate[2], hydrochlorothiazide, reserpine, glucose, sucrose, lactose, maize starch, gum acacia, and magnesium stearate were pharmaceutical grade and used as supplied. All solvents and other reagents were reagent grade.

Standard Solution of Dihydralazine Sulfate—Weigh accurately 10 mg of dihydralazine sulfate, transfer to a 10-ml volumetric flask, and dilute to volume with McIlvaine's citric acid–phosphate buffer (pH 4) (13).

Color Reagent—Weigh accurately 25 mg of 2-methyl-3-nitropyridine-6-carboxaldehyde, transfer to a 50-ml volumetric flask, and dissolve in, and dilute to volume with, methanol.

Preparation of Assay Solutions—*For Pure Dihydralazine Sulfate*—Use appropriate volumes of standard dihydralazine sulfate as the assay solution.

For Synthetic Mixture—Transfer an accurately weighed amount of the powdered synthetic mixture, equivalent to 1 mg of dihydralazine sulfate, to a 10-ml volumetric flask. Dissolve as completely as possible in, and dilute to volume with, McIlvaine's citric acid–phosphate buffer (pH 4). Filter and discard the first portion of the filtrate. The clear solution obtained is the assay solution.

For Tablets Containing Dihydralazine Sulfate—Weigh and powder 20 tablets. Transfer an accurately weighed quantity of the powder, equivalent to 10 mg of dihydralazine sulfate, to a 10-ml volumetric flask and proceed as for the synthetic mixture, starting from: "dissolve as completely . . . . "

Recovery Experiment—Add an accurately weighed amount of dihydralazine sulfate to an accurately weighed amount of the powdered tablets, equivalent to a known amount of dihydralazine sulfate, in a 10-ml volumetric flask and proceed as for the synthetic mixture, starting from: "dissolve as completely . . . . "

Development of Color—Into 10-ml volumetric flasks, each containing 1 ml of the color reagent, pipet 1 ml of the assay solution of appropriate dilution. Then heat on a boiling water bath for 5 min and cool. Dilute to volume with methanol and mix well. Determine the absorbance at 450 nm against the blank.

Application of Developed Method as Stability-Indicating Assay—Prepare a 0.1% solution of dihydralazine sulfate in McIlvaine's citric acid–phosphate buffer (pH 8). Titrate an aliquot of this solution with potassium iodate, using the NF XIII method (14). For the colorimetric assay, measure accurately suitable volumes of the prepared solution, make the appropriate dilution with McIlvaine's citric acid–phosphate buffer (pH 4), and carry out the assay as already described. Repeat the analysis by both methods after heating aliquots of the prepared solution on a boiling water bath for 15, 30, and 60 min.

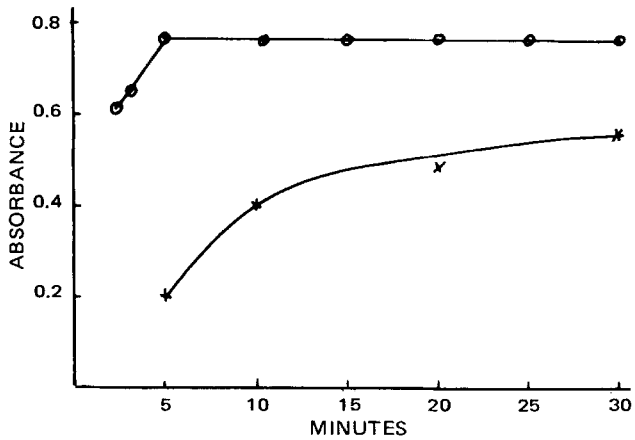

Figure 1—*Effect of the reaction time on the intensity of color. Key:* O, *at the temperature of the boiling water bath; and* ×, *at room temperature.*

RESULTS AND DISCUSSION

The interaction between hydrazino derivatives and aldehydes to yield the respective hydrazones is well known and reported to be acid or base catalyzed (15). Initial trials to react a methanolic solution of 2-methyl-3-nitropyridine-6-carboxaldehyde with dihydralazine sulfate in the presence of trichloroacetic acid failed to yield the chromogenic hydrazone, even upon heating in a boiling water bath for 1 hr.

Accordingly, a rigorous investigation was carried out to develop suitable conditions for color development. Different buffer systems of various constitution and pH were investigated.

When phosphate buffer was used (pH 6–8) (16), an orange-colored product developed with maximum absorption at 440 nm. The extinction of the colored product increased with a decrease in pH (Table I). By using McIlvaine's citric acid–phosphate buffer (pH 2.2–8), the intensity of the color production reached its maximum value at pH 4 (Table I) with an absorption peak at 450 nm and a broad absorption band extending from below 400 to 550 nm. The use of acetic acid–sodium acetate buffer (pH 4.05) (17) instead of McIlvaine's citric acid–phosphate buffer did not significantly affect color intensity or the λ_{max}. However, the McIlvaine's citric acid–phosphate buffer was tentatively chosen as the reaction medium because of the appreciable reduction in color development time compared with the acetate buffer.

Investigations were carried out to determine the solvent and reagent concentration that would give the highest color intensity. Solvents tested include methanol and ethanol. At reagent concentrations greater than 0.4 mg/ml, the intensity of color was only slightly de-

[1] Spekol spectrocolorimeter, Carl Zeiss Jena.
[2] Nepresol, Ciba.

Table II—Determination of Dihydralazine Sulfate in Presence of Reserpine, Hydrochlorothiazide, and Common Excipients

Substances Added[a]	Amount, mg	Recovery[b], %	SD
Reserpine	0.5	97.9	0.85
Hydrochlorothiazide	2.0	99.8	0.50
Glucose	20.0	95.6	0.37
Starch	20.0	100.6	0.58
Sucrose	20.0	99.9	0.45
Lactose	200.0	100.02	0.050
Magnesium stearate	20.0	97.1	0.057
Acacia	20.0	99.6	0.75
Mixture of all ingredients	—	99.1	1.20

[a] Per milligram of dihydralazine sulfate. [b] Average of four determinations.

pendent upon the reagent concentration. A concentration of 0.5 mg/ml was selected.

The reaction time was determined by following the color development at room temperature and at the temperature of a boiling water bath (Fig. 1). The results indicated that the 30-min interval was not sufficient to bring the color to maximum intensity. Under the same pH, a heating time interval of only 5 min was required to obtain the maximum color intensity, which remained stable for at least 24 hr. This asset is important for a quality control method and for a series of determinations. The color reaction product showed a broad absorption peak with a maximum at about 450 nm and an apparent molar absorptivity of 37.3×10^3.

Beer's law was obeyed ($r = 0.9997$) up to an initial dihydralazine sulfate concentration of 14 μg/ml ($A \approx 1.07$). A typical linear regression line had a slope of 0.078, an intercept of −0.028, and SS of 7.25×10^{-4}.

The specificity of the method for the determination of dihydralazine sulfate in the presence of several frequently encountered excipients, additives, and certain drugs, such as reserpine and hydrochlorothiazide, was investigated. A synthetic mixture was prepared by mixing a known amount of dihydralazine sulfate with an excipient or drug, each approximating sample weights of commercial tablets, and the assay was performed. The average recovery ranged from 97 to 100% (Table II). The relatively low percentage recovery obtained when glucose was the additive may be due to the partial reaction of dihydralazine with nonchromogenic aldose.

Different marketed dihydralazine tablets were satisfactorily analyzed by this method (Table III).

The preliminary stability study showed that solutions of dihydralazine in distilled water and in McIlvaine's citric acid–phosphate buffer below pH 7 were stable at room temperature for at least 48 hr, as shown by the constant readings of samples analyzed by the developed method and by the reference iodate method (14). Upon heating in a boiling water bath for 15 min, the color intensity decrease was not significant. However, a solution of dihydralazine in McIlvaine's citric acid–phosphate buffer (pH 8) acquired rapidly a yellow coloration, which was intensified by heating.

Table III—Determination of Dihydralazine Sulfate in Commercial Tablet Formulations

Formula[a]	Amount Claimed, mg	Amount Found[b], %	SD	Amount Added, mg	Recovery[b], %	SD
A	10	107	0.00	10	99.3	1.15
B	10	97.6	1.03	10	99.6	1.10

[a] A = reserpine, 0.1 mg; dihydralazine sulfate, 10 mg; hydrochlorothiazide, 10 mg; and excipients. B = reserpine, 0.1 mg; dihydralazine sulfate, 10 mg; and excipients. [b] Average of three determinations.

Table IV—Effect of Time on the Stability of Dihydralazine Sulfate Solution at pH 8

Minutes	Recovery[a], % Iodometric Method	Proposed Method
0	100.0	100.0
15	90.0	85.0
30	89.0	78.7
60	87.1	75.0

[a] Average of two determinations.

The degradation of dihydralazine sulfate at the temperature of the boiling water bath was followed by the colorimetric and iodometric methods at 15, 30, and 60 min. The rather low selectivity of the iodometric method was shown by the pattern of higher results obtained compared to the proposed method (Table IV). Any degradation product susceptible to oxidation by potassium iodate would probably interfere in the iodometric method, but the proposed method allows interaction only with the intact hydrazine moiety. Consequently, the proposed colorimetric method is more selective and can be recommended as a stability-indicating assay.

REFERENCES

(1) F. Jancik, B. Budesinsky, and J. Korbl, *Cesk. Farm.*, **9**, 304(1960).

(2) K. Kalinowski, *Farm. Pol.*, **21**, 914(1965); through *Chem. Abstr.*, **64**, 17359(1966).

(3) I. Grecu and E. Curea, *Farmacia (Bucharest)*, **13**, 527(1965); through *Anal. Abstr.*, **14**, 372(1967).

(4) I. Grecu and E. Curea, *Farmaco, Ed. Prat.*, **23**, 603(1968); through *Anal. Abstr.*, **18**, 1973(1970).

(5) I. Grecu and E. Curea, *Rev. Chim.*, **17**, 434(1966); through *Anal. Abstr.*, **14**, 6388(1967).

(6) *Ibid.*, **16**, 389(1965); through *Chem. Abstr.*, **64**, 11031(1966).

(7) R. Soliman and S. A. Belal, *J. Drug Res. Egypt*, **6**, 7(1974).

(8) S. Pinzauti, V. Dal Plaz, and E. La Porta, *J. Pharm. Sci.*, **63**, 1446(1974).

(9) Z. E. Kalinowsk, *Chem. Anal.*, **9**, 831(1964); through *Anal. Abstr.*, **13**, 933(1966).

(10) W. Kitzing, *Pharmazie*, **16**, 401(1961); through *Chem. Abstr.*, **62**, 403(1965).

(11) M. A. Eldawy, M. A. Elgendy, M. A. Abdelkader, and I. A. Ibrahim, "Abstracts," Fourth Arab Chemical Congress, Cairo, Apr. 1975, NIDOC, Egypt, p. 133.

(12) T. Banas and Z. Skrowaczewska, *Rocz. Chem.*, **43**, 739(1969).

(13) "Documenta Geigy Scientific Tables," 6th ed., J. R. Geigy, S. A., Basle, Switzerland, p. 314.

(14) "The National Formulary," 13th ed., Mack Publishing Co., Easton, Pa., 1970, p. 348.

(15) J. March, "Advanced Organic Chemistry. Reactions, Mechanisms, and Structure," McGraw-Hill, New York, N.Y., 1968, pp. 652, 653.

(16) "The United States Pharmacopeia," 18th rev., Mack Publishing Co., Easton, Pa., 1970, p. 939.

(17) A. I. Vogel, "Quantitative Inorganic Analysis," 3rd ed., Longmans, London, England, 1961, p. 35.

ACKNOWLEDGMENTS AND ADDRESSES

Received August 5, 1975, from the *Department of Pharmaceutical Chemistry and Pharmaceutics, Faculty of Pharmacy, University of Assiut, A.R. Egypt.*

Accepted for publication February 23, 1976.

[x] To whom inquiries should be directed.

Biological Effects of Cocaine Derivatives I: Improved Synthesis and Pharmacological Evaluation of Norcocaine

RONALD F. BORNE ˣ, JOHN A. BEDFORD, JUDITH L. BUELKE, CATHY B. CRAIG, THOMAS C. HARDIN, ARTHUR H. KIBBE, and MARVIN C. WILSON

Abstract □ An improved synthesis of norcocaine, a metabolite of cocaine, is reported. Following intravenous administration to a rhesus monkey, respiratory effects were similar to those observed following cocaine treatment. In addition, clonic convulsions, hypothermia, and mydriasis resulted. Norcocaine could be responsible for part of the pharmacological activity of cocaine.

Keyphrases □ Cocaine derivatives—norcocaine synthesized, pharmacological activity evaluated, monkeys □ Norcocaine—synthesized, pharmacological activity evaluated, monkeys □ Structure–activity relationships—norcocaine (cocaine derivative) synthesized, pharmacological activity evaluated, monkeys □ Narcotics, potential—norcocaine synthesized, pharmacological activity evaluated, monkeys

Great attention has been devoted recently to metabolic studies of the potent central nervous system (CNS) agent cocaine (I). Products resulting from ester hydrolysis have been known for some time (1–4), but only recently have *N*-demethylation products been reported (5–8). A recent study (9) regarding the pharmacological activity of norcocaine (II) prompted this examination of its *in vivo* effects. Previous syntheses of norcocaine entailed many steps and involved ester hydrolysis and reesterification procedures (*e.g.*, 10). A facile demethylation procedure was sought which would not result in ester hydrolysis. A report (11) on the synthesis of α-(±)-noracetylmethadol prompted this article.

DISCUSSION

The first attempt to synthesize norcocaine in a one-step synthesis from cocaine involved treating cocaine with potassium permanganate (10). Although some norcocaine was obtained, the product contained considerable amounts of cocaine. Attention was turned to the method of Abdel-Monem and Portoghese (12), which involved treating the *N*-methyl compound with phenyl chloroformate and hydrolysis of the resulting carbamate. Because carbamate hydrolysis requires strong alkaline conditions that would certainly hydrolyze both ester functions of cocaine, this reaction was attempted using benzyl chloroformate instead of phenyl chloroformate. The resulting benzyl carbamate probably could be cleaved under hydrogenolysis conditions that would not cause ester hydrolysis. Although many reaction conditions were employed, no reaction was observed between cocaine and benzyl chloroformate. Treating cocaine with diethyl azodicarboxylate (11) for 4 days in benzene at 50° gave, upon workup, a mixture of cocaine and norcocaine.

The method of Windholz and Johnston (13), as modified (11), was then explored (Scheme I). Norcocaine was obtained as the hydrochloride free of any contaminating cocaine based on data observed from TLC and GLC–mass spectral studies. Since the intermediate carbamate (III) is not purified before treatment with zinc dust, this approach constitutes a one-step synthesis of norcocaine from cocaine in quantities that should permit thorough pharmacological evaluation.

Preliminary evaluation of norcocaine hydrochloride in the rhesus monkey indicated potent CNS effects. Both cocaine and norcocaine produced a rapid increase in the respiratory rate of similar magnitude (Table I). On the basis of these preliminary data, norcocaine may be more potent with regard to this parameter since it produced a greater elevation in rate. However, the duration of this increase was shorter following norcocaine administration.

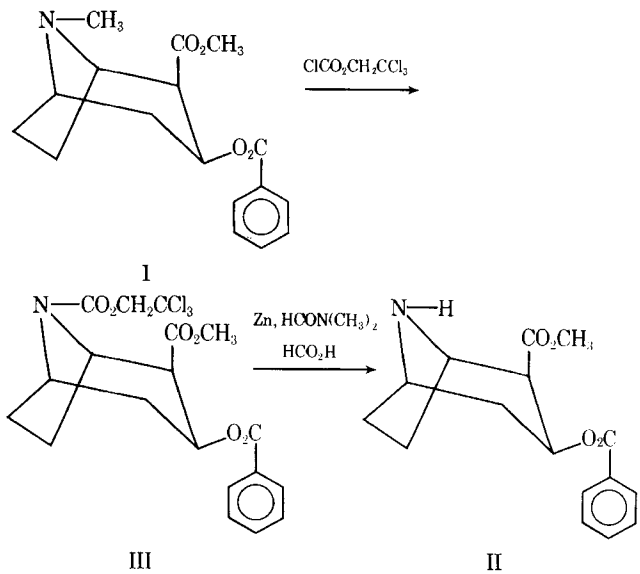

Scheme I

Within 1 min following the injection of norcocaine, clonic convulsions were observed. They occurred in a cyclical manner for the next 15 min. During this period, the interconvulsion interval increased from 5 sec to 1 min. However, the duration of each convulsive episode remained fairly constant, *i.e.*, 5–10 sec after an initial 45-sec convulsion. During the interconvulsion interval, respiration was shallow but rapid. Respiratory measures were determined during these intervals. The administration of cocaine produced a similar convulsive pattern. This effect began within 1 min following administration and was dissipated within 5 min.

Table I—Respiration and Temperature

	Cocaine Hydrochloride (4.5 mg/kg iv)		Norcocaine Hydrochloride (4.5 mg/kg iv)	
Minutes	Respiration per Minute	Temperature	Respiration per Minute	Temperature
Pre-15	28	38.2°	26	37°
Post-5	36	38°	36	37°
15	32	38°	50	37°
30	30	38°	34	36.8°
45	30	38.2°	36	36.5°
60	30	38.8°	36	36.5°
75	34	38.5°	34	35.5°
90	32	38.4°	30	35.5°
105	34	38.2°	22	35.7°
120	34	38.2°	24	36°
150	32	38.2°	20	36.1°
180	32	38.2°	20	36°
210	34	38°	46	35°
240	34	38.2°	22	35°

Although the convulsive pattern induced by these agents immediately after administration may have contributed to hyperventilation, this result is unlikely. Previous research in this laboratory indicated that respiratory depression is the more common result of convulsions induced with cocaine. Furthermore, with norcocaine, the duration of hyperventilation was much greater than that of the convulsive action. Additional data obtained in this laboratory demonstrate that substantial increases in respiration rate result from the administration of nonconvulsive doses of cocaine.

Cocaine increased body temperature by 0.6° 1 hr following treatment, but the effect was not statistically significant. This hyperthermic effect had dissipated within the next hour. Significant elevations in rectal temperature followed administration of cocaine to other subjects in this laboratory. The time course of this hyperthermic effect was identical to that in the present study.

Following treatment with norcocaine, body temperature significantly decreased within 45 min. This decrement in body temperature was still evident 4 hr posttreatment. Whether this hypothermia was the result of the longer convulsive action of norcocaine or whether it indicates a pharmacological difference between cocaine and norcocaine remains to be determined. It is unlikely that the convulsive pattern and duration that resulted from norcocaine administration would be reflected in temperature changes occurring 3.5 hr later. Hypothermia probably is the result of extensive vasodilation, a common toxic manifestation of local anesthetic agents. Norcocaine appears to resemble cocaine with respect to mydriatic action and enhancement of reactivity to stimuli.

These preliminary data, along with the *in vitro* results of Hawks *et al.* (9), suggest that norcocaine is a pharmacologically active metabolite of cocaine *in vivo*. More detailed pharmacological studies are currently being conducted.

EXPERIMENTAL[1]

Norcocaine (II)—Solutions of cocaine (7.2 g, 0.024 mole) in 50 ml of benzene and 2,2,2-trichloroethyl chloroformate (5.6 g, 0.027 mole) in 25 ml of benzene were combined, and the resulting solution was refluxed for 18 hr. The mixture was cooled to 5°, and 0.4 ml of formic acid was added. After stirring for an additional 30 min, 0.9 ml of triethylamine was added; the resulting mixture was stirred at room temperature for 1 hr. Water (50 ml) was added, and the mixture was extracted with ether (2 × 100 ml).

The organic extracts were combined, extracted with 250 ml of 5 *N* hydrochloric acid to remove any unreacted cocaine, dried over sodium sulfate, and evaporated to yield an oil whose IR and NMR spectra were consistent with Structure III. The oil was dissolved in dimethylformamide (25 ml) and cooled to 5°. Formic acid (2.0 g) was added, followed by the addition of zinc dust (3.6 g) in portions maintaining the temperature at 5°. After the zinc dust addition was complete, the mixture was stirred at room temperature for 18 hr. Then the mixture was filtered, and the filtrate was poured onto 100 g of crushed ice. The mixture was made strongly acidic in the cold with concentrated hydrochloric acid and extracted with ether (2 × 100 ml).

The acidic layer was recooled to 5°, made strongly alkaline with ammonium hydroxide, and extracted with ether (2 × 100 ml). The ether extracts were combined, dried over sodium sulfate, and evaporated to give a viscous oil. This oil gave one spot on TLC and one peak by GLC that differed from the R_f value and retention time, respectively, observed for cocaine. Trituration with petroleum ether gave a solid, mp 82–83°; NMR ($CDCl_3$): δ 3.03 (1H, s, NH, disappeared on addition of D_2O), 3.68 (3H, s, OCH_3), and 7.43–8.17 (5H, m, aromatic); $[\alpha]_D^{26}$ −41.0° (*c* 1, $CHCl_3$).

Anal.—Calc. for $C_{16}H_{19}NO_4$: C, 66.42; H, 6.62; N, 4.84. Found: C, 66.30; H, 6.62; N, 4.78.

The hydrochloride was prepared in the usual manner to give 4.4 g (56%) of II hydrochloride, mp 111–113°; *m/e* 289.

Pharmacological Methods—A male subadult rhesus monkey, surgically prepared with a chronic indwelling jugular catheter, was housed in a primate restraining chair[2] with free access to water. A rectal temperature probe was inserted on the day prior to drug administration, and respirometer bellows were attached on the morning of drug testing. Body temperature and respiratory rate and depth were continuously monitored for 15 min prior to drug administration. These parameters were recorded at 5 and 15 min postinjection, every 15 min thereafter until 2 hr posttreatment, and every 30 min for an additional 2 hr.

Drugs were dissolved in physiological saline and administered at approximately the same time of day *via* an intravenous catheter. Cocaine hydrochloride and norcocaine hydrochloride were administered at 6-week intervals at dose levels of 4.5 mg/kg.

REFERENCES

(1) H. Langeker and K. Lewitt, *Arch. Exp. Pathol. Pharmakol.*, **190,** 492(1938).

(2) L. A. Woods, F. G. McMahon, and M. H. Seevers, *J. Pharmacol. Exp. Ther.*, **101,** 200(1951).

(3) F. Fish and W. D. C. Wilson, *J. Pharm. Pharmacol.*, **21,** 135(1969).

(4) N. N. Valanju, M. M. Baden, S. N. Valanju, D. Mulligan, and S. K. Verma, *J. Chromatogr.*, **81,** 170(1973).

(5) J. Axelrod and J. Cochin, *J. Pharmacol. Exp. Ther.*, **121,** 107(1957).

(6) G. Werner, *Z. Physiol. Chem.*, **348,** 1151(1967).

(7) R. Ramos-Aliaga and J. Chiriboga, *Arch. Latinoam. Nutr.*, **20,** 415(1970).

(8) E. G. Leighty and A. F. Fentiman, *Res. Commun. Chem. Pathol. Pharmacol.*, **8,** 65(1974).

(9) R. L. Hawks, I. J. Kopin, R. W. Colburn, and N. B. Thoa, *Life Sci.*, **15,** 2189(1974).

(10) H. L. Schmidt and G. Werner, *Ann.*, **653,** 184(1962).

(11) R. N. Booher and A. Pohland, *J. Med. Chem.*, **18,** 266(1975).

(12) M. M. Abdel-Monem and P. S. Portoghese, *ibid.*, **15,** 208(1972).

(13) T. B. Windholz and D. B. R. Johnston, *Tetrahedron Lett.*, **1967,** 2555.

ACKNOWLEDGMENTS AND ADDRESSES

Received October 30, 1975, from the *School of Pharmacy, University of Mississippi, University, MS 38677*

Accepted for publication February 23, 1976.

Supported in part by the Research Institute of Pharmaceutical Sciences, University of Mississippi, and in part by Grant DA 01002-02 from the National Institute of Drug Abuse.

[x] To whom inquiries should be directed.

[1] Melting points were determined on a Thomas-Hoover Uni-Melt apparatus and are corrected. NMR spectra were determined on a Jeolco-C-60-HL spectrometer, using tetramethylsilane as the internal standard. The mass spectrum was determined on a DuPont model 21-492 mass spectrometer. TLC was performed on Eastman Chromagram silica gel sheets with fluorescent indicator, using benzene–ether (4:1) as the developing solvent. GLC was performed on a Hewlett-Packard model 52 chromatograph with a 3% OV-17 1.9-m × 0.3-cm (6-ft × 0.125-in.) column packed with Anachrom ABS. Microanalyses were carried out by Galbraith Laboratories, Knoxville, Tenn. Cocaine-free base was prepared from cocaine hydrochloride (Mallinckrodt Chemical Works) in the usual manner.

[2] Plas Labs.

NMR Determination of Trimethoprim and Sulfamethoxazole in Tablets and Powders

MARÍA R. RODRIGUEZ, MARÍA T. PIZZORNO, and SEM M. ALBONICO ˣ

Abstract □ An NMR spectroscopic method for the determination of mixtures of trimethoprim and sulfamethoxazole is described. Spectra are determined in dimethyl sulfoxide-d_6, containing 1,4-dinitrobenzene as an internal standard. Both synthetic mixtures and commercial formulations were assayed, and the results were compared to those obtained using the BP procedure.

Keyphrases □ Trimethoprim—NMR spectroscopic analysis, synthetic mixtures and commercial formulations containing sulfamethoxazole □ Sulfamethoxazole—NMR spectroscopic analysis, synthetic mixtures and commercial formulations containing trimethoprim □ NMR spectroscopy—analysis, trimethoprim and sulfamethoxazole, synthetic mixtures and commercial formulations □ Antibacterial agents—trimethoprim and sulfamethoxazole, NMR spectroscopic analysis, synthetic mixtures and commercial formulations

The chemotherapeutic activity of trimethoprim, 2,4-diamino-5-(3,4,5-trimethoxybenzyl)pyrimidine (I), resulting from its ability to inhibit dihydrofolate reductase is increased as much as 30–60-fold when combined with a sulfonamide (1). Owing to its synergism and pharmacokinetic similarity, the choice association is sulfamethoxazole (II) in a one to five relation (2).

Several methods are available to analyze I and its metabolites in biological fluids. One method requires oxidation and spectrophotofluorometric measuring of the trimethoxybenzoic acid formed (3, 4). The other procedure uses differential pulse polarography (5, 6) or TLC, followed by fluorescence determination (7).

Only a compendial procedure is known for the analysis of the mixture. The BP (8) describes an extraction procedure in an alkaline medium for I, followed by back-extraction with diluted acetic acid and spectrophotometric determination. For II, a simple Bratton–Marshall reaction using the aqueous solution is described.

The procedure for the analysis of mixtures of I and II proposed here uses ^{1}H-NMR spectroscopy. No isolation is required, and good quantitative results were obtained with known mixtures and commercial preparations (tablets and powders).

EXPERIMENTAL[1]

Materials—Standard trimethoprim (I) and sulfamethoxazole (II) were prepared by recrystallization from ethanol–water. 1,4-Dinitrobenzene[2] (III) was used as an internal standard after purification by sublimation, mp 173–174°, and dimethyl sulfoxide-d_6[2] (IV) was used as a solvent. Tetramethylsilane was the internal standard.

Samples—Tablets from two batches of each of the four brands (obtained locally) and two batches of the only pediatric powder available were used.

Procedure—Twenty tablets were weighed and powdered. A sample equivalent to 10 mg of I, 50 mg of II, and 30.0 mg of III was dissolved in 1 ml of IV in a 2-ml centrifuge tube. The tube was placed into a bath (70°)

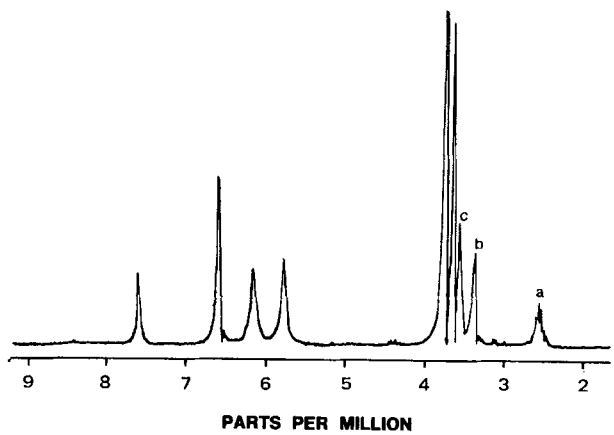

Figure 1—*NMR spectrum of trimethoprim in dimethyl sulfoxide-*d_6. *Key: a, solvent impurity; b, aromatic protons; and c, 4-methoxy group.*

for 2 min and centrifuged. About 0.4 ml of the solution was transferred to an NMR tube, and the spectrum was obtained.

The same procedure was used for the powdered tablets.

The amount of I was calculated as follows:

$$\frac{\text{mg of I}}{\text{tablets}} = \frac{EW_I}{EW_{III}} \times \frac{A_I}{A_{III}} \times \frac{\text{mg of III}}{W_s} \times \text{a.t.w.} \qquad \text{(Eq. 1)}$$

$$\frac{\text{mg of I}}{\text{100 g of powder}} = \frac{EW_I}{EW_{III}} \times \frac{A_I}{A_{III}} \times \frac{\text{mg of III}}{W_s} \times 100 \qquad \text{(Eq. 2)}$$

where EW_I is the molecular weight divided by the number of protons in the signal chosen, EW_{III} is the molecular weight of the internal standard divided by the number of protons in its signal, A_I is the integral value of the signal representing I, A_{III} is the integral value of the signal representing III, W_s is the weight of the sample in milligrams, and a.t.w. is the average tablet weight.

The amount of II was calculated by a similar procedure.

RESULTS AND DISCUSSION

The selection of a solvent and an internal standard is important in any NMR procedure. In this case, since the drugs, I and II, and the internal standard, III, are freely soluble in dimethyl sulfoxide, it is the solvent of

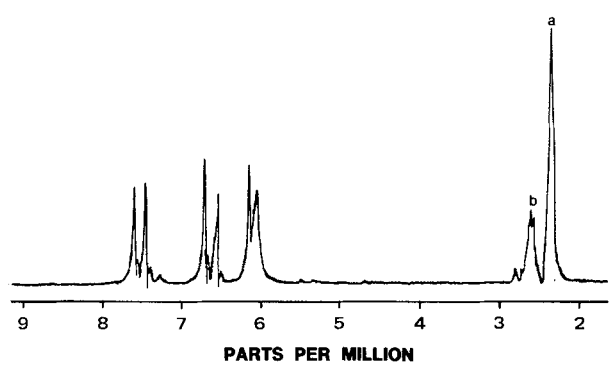

Figure 2—*NMR spectrum of sulfamethoxazole in dimethyl sulfoxide-*d_6. *Key: a, C-CH_3 group; and b, solvent impurity.*

[1] A Perkin-Elmer R-12 NMR spectrometer, 60 MHz, was used. All spectra were scanned at a probe temperature of 35°.

[2] Merck A. G., Darmstadt, Germany.

Table I—Determination of Sulfamethoxazole and Trimethoprim in Standard Mixtures by NMR

Standard Mixture	Internal Standard, mg	Sulfamethoxazole			Trimethoprim		
		Added, mg	Found, mg	Recovery, %	Added, mg	Found, mg	Recovery, %
1	30.0	50.0	50.7	101.4	10.0	10.1	100.0
2	50.0	50.0	50.0	100.0	10.0	9.87	98.7
3	30.0	60.0	60.2	100.3	12.0	12.10	100.8
4	30.0	50.0	49.5	99.0	10.0	9.95	99.5
5	20.0	50.0	49.6	99.2	10.0	9.91	99.1
6	50.0	50.0	50.0	100.0	10.0	10.10	101.0
7	30.0	50.0	50.4	100.8	10.0	10.00	100.0
8	30.0	40.0	40.4	101.0	8.0	8.08	101.0
			Average = 100.2 *SD* = 0.84			Average = 100.0 *SD* = 0.87	

Table II—Analysis of Dosage Forms by NMR and BP Methods

Sample	Sulfamethoxazole					Trimethoprim				
	Declared Dosage, mg/Unit	NMR		BP		Declared Dosage, mg/Unit	NMR		BP	
		mg/Unit	%	mg/Unit	%		mg/Unit	%	mg/Unit	%
A, Tablet	400.0	405.2	101.3	394.0	98.5	80.0	79.9	99.9	78.0	97.5
B, Tablet	400.0	395.2	98.8	388.0	97.0	80.0	80.8	101.0	79.4	99.2
C, Tablet	400.0	397.2	99.3	385.2	96.3	80.0	79.7	99.6	81.4	101.7
D, Tablet	400.0	396.0	99.0	404.8	101.2	80.0	79.8	99.8	80.0	100.0
E, Tablet	400.0	394.8	98.7	396.0	99.0	80.0	79.2	99.0	78.4	98.0
F, Tablet	400.0	396.8	99.2	393.2	98.3	80.0	80.2	100.2	77.2	96.5
G, Tablet	800.0	796.0	99.5	776.0	97.0	160.0	158.5	99.1	157.1	98.2
H, Tablet	800.0	808.0	101.0	813.6	101.7	160.0	157.6	98.5	155.2	97.0
I, Powder (mg/100 g)	4000.0	4020.0	100.5	3920.0	98.0	800.0	800.0	100.0	792.0	99.0
J, Powder (mg/100 g)	4000.0	3968.0	99.2	4016.0	100.4	800.0	792.0	99.0	808.0	101.0

choice. The use of IV offers the obvious advantage of adding no proton signals to the spectrum; its impurity appears at 2.5 ppm and it does not interfere with the signals chosen. Compound III provides a single signal at 8 ppm; it was used previously as an internal standard (9).

The signals chosen for the analysis were the singlet at 3.40 ppm due to the aromatic protons of I together with the singlet at 3.55 ppm due to the 4-methoxy group of I (Fig. 1), the singlet at 2.3 ppm due to the only C-CH_3 of II (Fig. 2), and the single signal given by III at 8 ppm.

The analysis of a group of known standard I and II mixtures by NMR is summarized in Table I. The method is both accurate and precise, with a mean (standard deviation) of 100.0 ± 0.87% for I and 100.2 ± 0.84% for II. The relative proportions of I and II to III (Table I) have no significant bearing on the accuracy of the determination for the ranges of proportions shown.

By applying this procedure to actual samples, eight commercial lots of tablets from four companies were studied (Fig. 3) together with two lots of the only pediatric powder available (Table II). One product (Samples E and F) also contained 50 mg of benzydamine hydrochloride/tablet. Benzydamine does not interfere in the method; with IV as a solvent, its peaks do not appear in the chosen region of the spectra.

The results are in good agreement with the declared dosages and with results obtained using the official BP (8) procedure (Table II). The NMR procedure has several distinct advantages over the official method.

NMR spectra of such binders as starch, lactose, methylcellulose, and povidone in dimethyl sulfoxide were obtained and examined. They did not interfere with the NMR analysis of I or II.

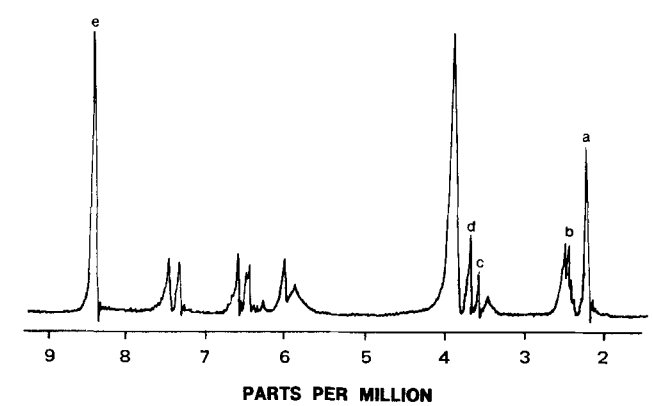

Figure 3—*NMR spectrum of a typical tablet analysis in dimethyl sulfoxide-d_6. Key: a, C-CH_3 group of II; b, solvent impurity; c, aromatic protons of I; d, 4-methoxy group of I; and e, single signal of III.*

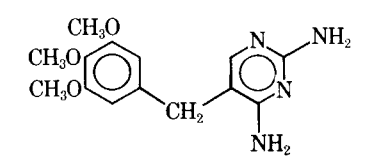

I

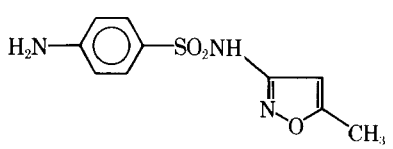

II

REFERENCES

(1) B. Reidberg, J. Herzog, and L. Weinstein, *Antimicrob. Ag. Chemother.*, **1966**, 424.

(2) S. R. M. Bushby and G. H. Hitchings, *Br. J. Pharmacol. Chemother.*, **33**, 72 (1968).

(3) D. E. Schwartz, B. A. Koechlin, and R. E. Weinfeld, *Chemotherapy (Suppl.)*, **14**, 22 (1969).

(4) S. A. Kaplan, R. E. Weinfeld, and T. L. Lee, *J. Pharm. Sci.*, **62**, 1865 (1973).

(5) M. A. Brooks, J. A. F. de Silva, and L. D'Arconte, *Anal. Chem.*, **45**, 263 (1973).

(6) M. A. Brooks, J. A. F. de Silva, and L. D'Arconte, *J. Pharm. Sci.*, **62**, 1395 (1973).
(7) C. Sigel and G. Michael, *J. Chromatogr.*, **80**, 111 (1973).
(8) "British Pharmacopoeia 1973," University Printing House, Cambridge, England, 1973, p. 128.
(9) P. Joseph-Nathan, M. A. Rodríguez, M. T. A. Ayala, and J. Padilla, *Rev. Soc. Quim. Mex.*, **15**, 175 (1971).

ACKNOWLEDGMENTS AND ADDRESSES

Received December 2, 1975, from the *Facultad de Farmacia y Bioquímica, Universidad de Buenos Aires, Junin 956, Buenos Aires, Argentina.*

Accepted for publication March 4, 1976.

[x] To whom inquiries should be directed.

Analysis of Homatropine Methylbromide Dosage Forms

S. HANNA [x], M. ROSEN, L. RASERO, and L. LACHMAN

Abstract □ A stability-indicating method of analysis for homatropine methylbromide in pharmaceutical formulations was developed. This method is based on the formation of a picric acid–quaternary ammonium complex, which is adsorbed on acid-washed diatomaceous earth in alkaline media followed by on-column chloroform extraction. The picrate complex is measured spectrophotometrically at 365 nm. The method was selective for homatropine methylbromide in that there was no interference from its major hydrolytic decomposition products, tropinium methylbromide and mandelic acid.

Keyphrases □ Homatropine methylbromide—spectrophotometric analysis, pharmaceutical formulations □ Spectrophotometry—analysis, homatropine methylbromide in pharmaceutical formulations □ Anticholinergic agents—homatropine methylbromide, spectrophotometric analysis in pharmaceutical formulations

Previously reported assay methods employed in the analysis of homatropine methylbromide dosage forms involved the precipitation of an insoluble salt of the methylhomatropine cation by anions such as the reineckate, silicotungstate, and tetraiodomercurate, followed by colorimetry (1) or turbidimetry (2, 3). Other colorimetric procedures involved chromogenesis with Dragendorff's reagent (4, 5) or measurement of the ferric hydroxamate complex (6). Analytical methods utilizing spectrophotometry (7, 8), TLC (9), and GLC (10, 11) also were reported. As previously discussed (12), these methods and official procedures (13) lack sensitivity, selectivity, or specificity or require additional washing or separation steps.

The stability-indicating assay procedure for homatropine methylbromide in syrups (12) is time consuming. This report presents a simple stability-indicating method, a modification of the method of Chin and Lach (14), for the assay of homatropine methylbromide dosage forms. The procedure was applied, with satisfactory results, to several commercial tablets, drops, and elixirs.

EXPERIMENTAL

Instruments—The recording spectrophotometer[1] had 1-cm cells and glass tubing columns[2], 200 × 25-mm o.d. with a tip 50 × 8-mm o.d. The columns were fitted with a small wad of glass wool at the bottom and top of the packing.

Materials and Reagents—The following were used: acid-washed diatomaceous earth[3]; homatropine methylbromide (NF reference standard); ammonium picrate reagent prepared by dissolving 11.2 g of picric acid[4] in 900 ml of distilled water, adding 6 ml of concentrated ammonia[4], and diluting to 1000.0 ml with distilled water; mandelic acid[4]; tropinium methylbromide[5]; and chloroform[4].

Standard Curve—A stock solution of homatropine methylbromide was prepared by dissolving 50.0 mg in 100 ml of distilled water. Further dilutions were made to obtain homatropine methylbromide standard solutions containing 0.125, 0.25, and 0.375 mg/ml. Two milliliters of stock and diluted standard solutions were each transferred into a 100-ml beaker containing 3.0 g of acid-washed diatomaceous earth, and 1.0 ml of ammonium picrate reagent was added. The mixture was mixed thoroughly and quantitatively transferred and packed into the glass column.

Elution was accomplished by immediately passing 17 × 5-ml portions of water-saturated chloroform at a flow rate of 7–9 ml/min, allowing each portion of eluant to run completely into the column before adding the next. The combined eluates were collected separately in 100-ml volumetric flasks and diluted to volume with chloroform. The absorbance of the standard solutions was measured in 1-cm absorption cells at 365 nm against chloroform as a blank.

Sample Procedure—*Tablets*—A number of tablets, equivalent to about 50 mg of homatropine methylbromide, were transferred to a 100-ml volumetric flask, and 75 ml of distilled water was added. The flask was shaken well for 30 min, and distilled water was added to the mark. The mixture was filtered through fluted filter paper, and the first 10 ml of filtrate was rejected. Two milliliters of the filtrate was pipetted into a 100-ml beaker, and the test was conducted as described under *Standard Curve*, beginning with "containing 3.0 g of acid-washed diatomaceous earth, ..."

Drops or Elixir—A volume of drops or elixir, equivalent to about 50 mg of homatropine methylbromide, was accurately measured and transferred to a 100-ml volumetric flask. Distilled water was added to the mark, and the contents were mixed well. Two milliliters was pipetted into a 100-ml beaker, and the test was conducted as described under *Standard Curve*, beginning with "containing 3.0 g of acid-washed diatomaceous earth, ..."

RESULTS AND DISCUSSION

This method, a modification of the one of Chin and Lach (14), is based on the reaction of picric acid with quaternary ammonium compounds in an alkaline medium to form a colored complex. The complex is adsorbed on acid-washed diatomaceous earth and measured spectrophotometrically after on-column extraction with water-saturated chloroform.

Under the experimental conditions, a linear relationship existed between the absorbance and concentration of homatropine methylbromide over the 0.25–1.0-mg/ml concentration range, with a correlation coefficient of 0.9996. Regression analysis showed that the regression equation was $y = 0.421x - 0.003$, with a standard error of the estimate of y on x

[1] Coleman-Hitachi model EPS-3T.
[2] SGA Scientific Inc., Bloomfield, N.J.
[3] Celite 545, Johns-Manville, Denver, Colo.
[4] Analytical grade, J. T. Baker.
[5] Endo Laboratories, Inc., Garden City, N.Y.

(6) M. A. Brooks, J. A. F. de Silva, and L. D'Arconte, *J. Pharm. Sci.*, **62**, 1395 (1973).
(7) C. Sigel and G. Michael, *J. Chromatogr.*, **80**, 111 (1973).
(8) "British Pharmacopoeia 1973," University Printing House, Cambridge, England, 1973, p. 128.
(9) P. Joseph-Nathan, M. A. Rodríguez, M. T. A. Ayala, and J. Padilla, *Rev. Soc. Quim. Mex.*, **15**, 175 (1971).

ACKNOWLEDGMENTS AND ADDRESSES

Received December 2, 1975, from the *Facultad de Farmacia y Bioquímica, Universidad de Buenos Aires, Junin 956, Buenos Aires, Argentina.*

Accepted for publication March 4, 1976.

[x] To whom inquiries should be directed.

Analysis of Homatropine Methylbromide Dosage Forms

S. HANNA [x], M. ROSEN, L. RASERO, and L. LACHMAN

Abstract □ A stability-indicating method of analysis for homatropine methylbromide in pharmaceutical formulations was developed. This method is based on the formation of a picric acid–quaternary ammonium complex, which is adsorbed on acid-washed diatomaceous earth in alkaline media followed by on-column chloroform extraction. The picrate complex is measured spectrophotometrically at 365 nm. The method was selective for homatropine methylbromide in that there was no interference from its major hydrolytic decomposition products, tropinium methylbromide and mandelic acid.

Keyphrases □ Homatropine methylbromide—spectrophotometric analysis, pharmaceutical formulations □ Spectrophotometry—analysis, homatropine methylbromide in pharmaceutical formulations □ Anticholinergic agents—homatropine methylbromide, spectrophotometric analysis in pharmaceutical formulations

Previously reported assay methods employed in the analysis of homatropine methylbromide dosage forms involved the precipitation of an insoluble salt of the methylhomatropine cation by anions such as the reineckate, silicotungstate, and tetraiodomercurate, followed by colorimetry (1) or turbidimetry (2, 3). Other colorimetric procedures involved chromogenesis with Dragendorff's reagent (4, 5) or measurement of the ferric hydroxamate complex (6). Analytical methods utilizing spectrophotometry (7, 8), TLC (9), and GLC (10, 11) also were reported. As previously discussed (12), these methods and official procedures (13) lack sensitivity, selectivity, or specificity or require additional washing or separation steps.

The stability-indicating assay procedure for homatropine methylbromide in syrups (12) is time consuming. This report presents a simple stability-indicating method, a modification of the method of Chin and Lach (14), for the assay of homatropine methylbromide dosage forms. The procedure was applied, with satisfactory results, to several commercial tablets, drops, and elixirs.

EXPERIMENTAL

Instruments—The recording spectrophotometer[1] had 1-cm cells and glass tubing columns[2], 200 × 25-mm o.d. with a tip 50 × 8-mm o.d. The columns were fitted with a small wad of glass wool at the bottom and top of the packing.

Materials and Reagents—The following were used: acid-washed diatomaceous earth[3]; homatropine methylbromide (NF reference standard); ammonium picrate reagent prepared by dissolving 11.2 g of picric acid[4] in 900 ml of distilled water, adding 6 ml of concentrated ammonia[4], and diluting to 1000.0 ml with distilled water; mandelic acid[4]; tropinium methylbromide[5]; and chloroform[4].

Standard Curve—A stock solution of homatropine methylbromide was prepared by dissolving 50.0 mg in 100 ml of distilled water. Further dilutions were made to obtain homatropine methylbromide standard solutions containing 0.125, 0.25, and 0.375 mg/ml. Two milliliters of stock and diluted standard solutions were each transferred into a 100-ml beaker containing 3.0 g of acid-washed diatomaceous earth, and 1.0 ml of ammonium picrate reagent was added. The mixture was mixed thoroughly and quantitatively transferred and packed into the glass column.

Elution was accomplished by immediately passing 17 × 5-ml portions of water-saturated chloroform at a flow rate of 7–9 ml/min, allowing each portion of eluant to run completely into the column before adding the next. The combined eluates were collected separately in 100-ml volumetric flasks and diluted to volume with chloroform. The absorbance of the standard solutions was measured in 1-cm absorption cells at 365 nm against chloroform as a blank.

Sample Procedure—*Tablets*—A number of tablets, equivalent to about 50 mg of homatropine methylbromide, were transferred to a 100-ml volumetric flask, and 75 ml of distilled water was added. The flask was shaken well for 30 min, and distilled water was added to the mark. The mixture was filtered through fluted filter paper, and the first 10 ml of filtrate was rejected. Two milliliters of the filtrate was pipetted into a 100-ml beaker, and the test was conducted as described under *Standard Curve*, beginning with "containing 3.0 g of acid-washed diatomaceous earth, ..."

Drops or Elixir—A volume of drops or elixir, equivalent to about 50 mg of homatropine methylbromide, was accurately measured and transferred to a 100-ml volumetric flask. Distilled water was added to the mark, and the contents were mixed well. Two milliliters was pipetted into a 100-ml beaker, and the test was conducted as described under *Standard Curve*, beginning with "containing 3.0 g of acid-washed diatomaceous earth, ..."

RESULTS AND DISCUSSION

This method, a modification of the one of Chin and Lach (14), is based on the reaction of picric acid with quaternary ammonium compounds in an alkaline medium to form a colored complex. The complex is adsorbed on acid-washed diatomaceous earth and measured spectrophotometrically after on-column extraction with water-saturated chloroform.

Under the experimental conditions, a linear relationship existed between the absorbance and concentration of homatropine methylbromide over the 0.25–1.0-mg/ml concentration range, with a correlation coefficient of 0.9996. Regression analysis showed that the regression equation was $y = 0.421x - 0.003$, with a standard error of the estimate of y on x

[1] Coleman-Hitachi model EPS-3T.
[2] SGA Scientific Inc., Bloomfield, N.J.
[3] Celite 545, Johns-Manville, Denver, Colo.
[4] Analytical grade, J. T. Baker.
[5] Endo Laboratories, Inc., Garden City, N.Y.

Table I—Reproducibility of Colored Complex of Replicate Homatropine Methylbromide Samples Containing 0.5 mg/ml

Solution	Absorbance
1	0.421
2	0.427
3	0.424
4	0.423
5	0.422
6	0.426
7	0.425
8	0.421
9	0.422
Average	0.423
CV	0.52%

of 0.005 and standard errors of the estimate of the intercept and slope of 0.05 and 0.84, respectively. The colored complex in chloroform was stable for at least 5 hr.

The precision of the assay procedure was determined by running replicate studies on nine 2.0-ml aliquots of a standard homatropine methylbromide solution containing 0.5 mg/ml. Each solution was assayed by the proposed procedure. The coefficient of variation for the nine replicate samples was 0.52% (Table I). A blank sample, containing tropinium methylbromide and mandelic acid equivalent to 100% hydrolytic degradation of homatropine methylbromide, assayed by the proposed procedure yielded no absorbance at 365 nm, demonstrating that the method is stability indicating.

Results obtained by applying the procedure to commercially available homatropine methylbromide dosage forms are presented in Table II. Comparison of the experimental data with those obtained using an ion-exchange method (12) shows a good correlation.

Table II—Results of Analysis of Commercially Available Homatropine Methylbromide Dosage Forms

Dosage Form	Amount Claimed, mg/Tablet or mg/ml	Percent of Claim Found[a]			
		Proposed Method	±*SD*	Ion-Exchange Method	±*SD*
Tablet[b]	5	98.4	0.47	98.5	0.14
Elixir[c]	1	99.6	0.36	98.8	0.30
Tablet[d]	5	97.8	0.58	97.5	0.88
Elixir[e]	1	101.0	0.71	101.2	1.90
Tablet[f]	5	95.1	0.11	95.1	0.23
Tablet[g]	2.5	91.3	0.83	91.9	0.46
Drops[h]	0.27	104.0	0.57	102.6	0.40
Tablet[i]	2.5	104.0	0.75	103.5	0.11

[a] Average of three assays. [b] Mesopin tablets, Endo Laboratories Pharm. [c] Mesopin elixir, Endo Laboratories Pharm. [d] Mesopin PB tablets, Endo Laboratories Pharm. [e] Mesopin PB elixir, Endo Laboratories Pharm. [f] Cholan V tablets, Pennwalt. [g] Cholan HMB tablets, Pennwalt. [h] Sedadrops, Merrell-National. [i] Gustase Plus tablets, Geriatric Pharmaceutical Corp.

REFERENCES

(1) F. J. Bandelin, *J. Am. Pharm. Assoc., Sci. Ed.*, **37**, 10 (1948).

(2) M. Margadida, F. Braga, and Baltazar, *Rev. Port. Farm.*, **13**, 145 (1963).

(3) R. H. Robinson, *J. Am. Pharm. Assoc., Sci. Ed.*, **41**, 392 (1952).

(4) S. Ahuja, D. Spiegel, and F. R. Brofazi, *J. Pharm. Sci.*, **59**, 417 (1970).

(5) *Ibid.*, **61**, 1631 (1972).

(6) J. A. Feldman and B. J. Robb, *J. Pharm. Sci.*, **59**, 1646 (1970).

(7) L. Chafetz, *ibid.*, **53**, 1192 (1964).

(8) L. Chafetz and R. E. Daly, *ibid.*, **57**, 1977 (1968).

(9) T. Bican-Fister, *J. Chromatog.*, **55**, 417 (1971).

(10) R. Achari and F. Newcombe, *Planta Med.*, **19**, 241 (1971).

(11) B. F. Garbowski, F. J. Softly, B. L. Chang, and W. G. Haney, Jr., *J. Pharm. Sci.*, **62**, 806 (1973).

(12) F. F. Cantwell, M. Domjan, and C. F. Hiskey, *ibid.*, **63**, 599 (1974).

(13) "The National Formulary," 14th ed., Mack Publishing Co., Easton, Pa., 1975, p. 320.

(14) T.-F. Chin and J. Lach, *J. Pharm. Sci.*, **54**, 1550 (1965).

ACKNOWLEDGMENTS AND ADDRESSES

Received November 10, 1975, from the *Quality Control Department, Endo Laboratories, Inc., Garden City, N.Y. (Subsidiary of E. I. du Pont de Nemours & Co.).*

Accepted for publication March 1, 1976.

[x] To whom inquiries should be directed.

Physical Form as a Determinant of Effect of Buffered Acetylsalicylate Formulations on GI Microbleeding

BARRIE M. PHILLIPS[x] and BLAZE T. PALERMO

Abstract □ During a 48-day period, 12 male dogs received four buffered sodium acetylsalicylate formulations, quantitatively virtually identical (a homogeneous disintegrating swallow tablet, a swallow tablet in which the sodium acetylsalicylate was contained in a dissolving core, an encapsulated powder, and an aqueous suspension), at 650-mg aspirin equivalent doses twice daily during four 7-day treatment periods (each preceded by a 5-day period of no treatment) in a complete changeover fashion. Mean daily fecal blood losses of 0.75, 1.37, 1.43, and 2.89 ml were observed in the 12 dogs during treatment with the aqueous suspension, the homogeneous tablet, the encapsulated powder, and the core tablet, respectively. These findings indicate that the physical form of buffered acetylsalicylate formulations is a critical factor in the effect of such formulations on GI microbleeding.

Keyphrases □ Sodium acetylsalicylate—buffered formulations, various dosage forms, effect on GI microbleeding, dogs □ Aspirin, sodium salt—buffered formulations, various dosage forms, effect on GI microbleeding, dogs □ GI microbleeding—buffered sodium acetylsalicylate, effect of various dosage forms, dogs □ Dosage forms—buffered sodium acetylsalicylate, effect on GI microbleeding, dogs □ Analgesics—sodium acetylsalicylate buffered formulations, various dosage forms, effect on GI microbleeding, dogs

Gastric mucosal irritation, reflected in increased fecal occult blood loss, is a common side effect of orally administered aspirin. Levy (1) suggested that the degree of gastric mucosal erosion following the oral administration of aspirin is related to two factors: the concentration of aspirin in solution and the duration of contact of the so-

Table I—Reproducibility of Colored Complex of Replicate Homatropine Methylbromide Samples Containing 0.5 mg/ml

Solution	Absorbance
1	0.421
2	0.427
3	0.424
4	0.423
5	0.422
6	0.426
7	0.425
8	0.421
9	0.422
Average	0.423
CV	0.52%

of 0.005 and standard errors of the estimate of the intercept and slope of 0.05 and 0.84, respectively. The colored complex in chloroform was stable for at least 5 hr.

The precision of the assay procedure was determined by running replicate studies on nine 2.0-ml aliquots of a standard homatropine methylbromide solution containing 0.5 mg/ml. Each solution was assayed by the proposed procedure. The coefficient of variation for the nine replicate samples was 0.52% (Table I). A blank sample, containing tropinium methylbromide and mandelic acid equivalent to 100% hydrolytic degradation of homatropine methylbromide, assayed by the proposed procedure yielded no absorbance at 365 nm, demonstrating that the method is stability indicating.

Results obtained by applying the procedure to commercially available homatropine methylbromide dosage forms are presented in Table II. Comparison of the experimental data with those obtained using an ion-exchange method (12) shows a good correlation.

Table II—Results of Analysis of Commercially Available Homatropine Methylbromide Dosage Forms

Dosage Form	Amount Claimed, mg/Tablet or mg/ml	Percent of Claim Found[a]			
		Proposed Method	±*SD*	Ion-Exchange Method	±*SD*
Tablet[b]	5	98.4	0.47	98.5	0.14
Elixir[c]	1	99.6	0.36	98.8	0.30
Tablet[d]	5	97.8	0.58	97.5	0.88
Elixir[e]	1	101.0	0.71	101.2	1.90
Tablet[f]	5	95.1	0.11	95.1	0.23
Tablet[g]	2.5	91.3	0.83	91.9	0.46
Drops[h]	0.27	104.0	0.57	102.6	0.40
Tablet[i]	2.5	104.0	0.75	103.5	0.11

[a] Average of three assays. [b] Mesopin tablets, Endo Laboratories Pharm. [c] Mesopin elixir, Endo Laboratories Pharm. [d] Mesopin PB tablets, Endo Laboratories Pharm. [e] Mesopin PB elixir, Endo Laboratories Pharm. [f] Cholan V tablets, Pennwalt. [g] Cholan HMB tablets, Pennwalt. [h] Sedadrops, Merrell-National. [i] Gustase Plus tablets, Geriatric Pharmaceutical Corp.

REFERENCES

(1) F. J. Bandelin, *J. Am. Pharm. Assoc., Sci. Ed.*, **37**, 10 (1948).

(2) M. Margadida, F. Braga, and Baltazar, *Rev. Port. Farm.*, **13**, 145 (1963).

(3) R. H. Robinson, *J. Am. Pharm. Assoc., Sci. Ed.*, **41**, 392 (1952).

(4) S. Ahuja, D. Spiegel, and F. R. Brofazi, *J. Pharm. Sci.*, **59**, 417 (1970).

(5) *Ibid.*, **61**, 1631 (1972).

(6) J. A. Feldman and B. J. Robb, *J. Pharm. Sci.*, **59**, 1646 (1970).

(7) L. Chafetz, *ibid.*, **53**, 1192 (1964).

(8) L. Chafetz and R. E. Daly, *ibid.*, **57**, 1977 (1968).

(9) T. Bican-Fister, *J. Chromatog.*, **55**, 417 (1971).

(10) R. Achari and F. Newcombe, *Planta Med.*, **19**, 241 (1971).

(11) B. F. Garbowski, F. J. Softly, B. L. Chang, and W. G. Haney, Jr., *J. Pharm. Sci.*, **62**, 806 (1973).

(12) F. F. Cantwell, M. Domjan, and C. F. Hiskey, *ibid.*, **63**, 599 (1974).

(13) "The National Formulary," 14th ed., Mack Publishing Co., Easton, Pa., 1975, p. 320.

(14) T.-F. Chin and J. Lach, *J. Pharm. Sci.*, **54**, 1550 (1965).

ACKNOWLEDGMENTS AND ADDRESSES

Received November 10, 1975, from the *Quality Control Department, Endo Laboratories, Inc., Garden City, N.Y. (Subsidiary of E. I. du Pont de Nemours & Co.).*

Accepted for publication March 1, 1976.

[x] To whom inquiries should be directed.

Physical Form as a Determinant of Effect of Buffered Acetylsalicylate Formulations on GI Microbleeding

BARRIE M. PHILLIPS[x] and BLAZE T. PALERMO

Abstract □ During a 48-day period, 12 male dogs received four buffered sodium acetylsalicylate formulations, quantitatively virtually identical (a homogeneous disintegrating swallow tablet, a swallow tablet in which the sodium acetylsalicylate was contained in a dissolving core, an encapsulated powder, and an aqueous suspension), at 650-mg aspirin equivalent doses twice daily during four 7-day treatment periods (each preceded by a 5-day period of no treatment) in a complete changeover fashion. Mean daily fecal blood losses of 0.75, 1.37, 1.43, and 2.89 ml were observed in the 12 dogs during treatment with the aqueous suspension, the homogeneous tablet, the encapsulated powder, and the core tablet, respectively. These findings indicate that the physical form of buffered acetylsalicylate formulations is a critical factor in the effect of such formulations on GI microbleeding.

Keyphrases □ Sodium acetylsalicylate—buffered formulations, various dosage forms, effect on GI microbleeding, dogs □ Aspirin, sodium salt—buffered formulations, various dosage forms, effect on GI microbleeding, dogs □ GI microbleeding—buffered sodium acetylsalicylate, effect of various dosage forms, dogs □ Dosage forms—buffered sodium acetylsalicylate, effect on GI microbleeding, dogs □ Analgesics—sodium acetylsalicylate buffered formulations, various dosage forms, effect on GI microbleeding, dogs

Gastric mucosal irritation, reflected in increased fecal occult blood loss, is a common side effect of orally administered aspirin. Levy (1) suggested that the degree of gastric mucosal erosion following the oral administration of aspirin is related to two factors: the concentration of aspirin in solution and the duration of contact of the so-

Table I—Description of the Buffered Sodium Acetylsalicylate[a] Formulations Employed

Formulation Code	Physical Form	Buffer Component, mg/Unit Dose			Calculated Excess Buffer Capacity, mEq
		Calcium Carbonate	Magnesium Carbonate	Tricalcium Phosphate	
A2	Aqueous suspension of powder[b]	215	182	48	8.98
B2	Encapsulated powder	215	182	48	8.98
C2	Homogeneous, disintegrating swallow tablet	246	211	—	6.77
D2	Dissolving core swallow tablet	215	182	48	8.98

[a] Unit doses of the four formulations contained 365 mg of sodium acetylsalicylate, equivalent to 325 mg of aspirin. [b] Aqueous suspensions were prepared just prior to administration. Powder equivalent to two unit doses was placed in a 150-ml beaker, 75 ml of distilled water was added, and the mixture was stirred manually for a time adequate to give a uniform suspension. The resulting suspension, followed by a 25-ml distilled water rinse, was administered by gavage.

lution with the mucosa. He noted that particles of solid aspirin adherent to the moist mucosal surface are surrounded by a saturated solution of aspirin; as dissolved unionized drug is absorbed into the mucosa, the solid particle acts as a reservoir and provides additional aspirin to the solution. Anderson (2) agreed with this view and noted that, with insoluble aspirin preparations, there was good correlation between the number of aspirin particles in the stomach and the number of focal erosions.

In recent years, Leonards and Levy (3–5) demonstrated conclusively that the effect of aspirin on the gastric mucosa can be minimized by administration of the analgesic either in dilute aqueous solution or as rapidly dissolving tablets buffered to maintain the acetylsalicylate in its ionized form. Phillips *et al.* (6) described a homogeneous swallow tablet formulation[1] containing sodium acetylsalicylate and 6.77 mEq excess base in the form of a nonabsorbable buffer system, which did not elicit GI microbleeding in humans; unfortunately, the formulation ultimately proved to be unstable. A second similar formulation[1] (containing more buffer), except that the sodium acetylsalicylate was contained in a dissolving core surrounded by the buffer ingredients, was prepared in an attempt to achieve adequate stability. While the second formulation proved to be stable, it also increased GI microbleeding significantly in humans[2].

It was hypothesized that the differential effect of the two formulations (C2 and D2, Table I) on GI microbleeding was attributable to the fact that the sodium acetylsalicylate component of the second formulation was contained in a surface-eroding, dissolving core. During the period following disintegration of the buffer shell, when the core is dissolving, the solid core may become adherent to the gastric mucosa. In that case, significant reconversion to the acid could take place.

The present study was undertaken to test this hypothesis; it illustrates the importance of physical form as a determinant of aspirin-induced GI microbleeding and supports the concepts of Leonards and Levy (3–5).

EXPERIMENTAL

Animals—Twelve male beagle dogs[3], 6.7–10.5 kg, were employed. The dogs were immunized previously against distemper and hepatitis and received a vermifuge on at least two occasions. The animals were caged individually and had free access to drinking water; approximately 300 g of dry food[4] was offered to each dog for 2 hr at about 10:00 am daily. Two weeks prior to the start of the experiment (Day −15), each dog received 50 μCi of ^{59}Fe-labeled ferrous sulfate[5] intravenously.

Sample Handling—GI blood loss was determined by measurement of the iron-59 content of 24-hr stool collections. Details regarding the collection, preparation, and counting of 24-hr stool and weekly whole blood samples and calculation of the whole blood content of 24-hr stool collections were described previously (7).

Acetylsalicylate Formulations—Four formulations (two swallow tablets, an encapsulated powder, and a powder suspended in water) were employed in the present study. They were coded at random for convenience and are described in Table I. Unit doses of the four formulations contained the equivalent of 325 mg of aspirin and had similar total buffer capacities.

Experimental Design—The dogs were assigned to three 4 × 4 Latin squares in such a manner as to place the lightest four in one square and the heaviest four in a second square. The four treatments were then assigned to rows within the squares in such a fashion as to balance the design to permit detection of residual effects of the treatments; the dogs were assigned at random to columns within the squares.

Study Days 0 through 5, 13 through 17, 25 through 29, and 37 through 41 were designated as control periods. Days 6 through 12, 18 through 24, 30 through 36, and 42 through 48 were designated as treatment periods. During these treatment times, two tablets (or the equivalent of two tablets as suspended or encapsulated powder) of the appropriate formulations were administered orally twice daily, at 8:00 am and 4:00 pm, in complete changeover fashion.

Statistics—The experimental observations were defined as the average daily fecal blood volume observed in each animal during each treatment period. Average daily fecal blood volumes observed in the 12 dogs during the four treatment periods were subjected to analysis of variance. When this analysis revealed that there were significant differences among the direct effects of the four treatments, the significance of differences between treatments was determined using the Student–Newman–Keuls test (8). Details regarding statistical evaluation of the data were described previously (6).

RESULTS

The average daily fecal blood losses observed in the 12 dogs during the four control and four treatment periods are summarized in Table II. The analysis of variance of the average daily fecal blood loss observed during the four treatment periods indicated that there were significant differences between the direct effects of the four treatments. The significance of differences between the means of average daily fecal blood loss observed during treatment with the four formulations is also summarized in Table II. The results indicate that the homogeneous tablet formulation C2 and the encapsulated powder B2 caused less GI microbleeding than the dissolving core tablet formulation D2 but more than the suspended powder A2.

The analysis of variance also revealed that there were: (*a*) significant differences between squares to which dogs had been assigned on the basis

[1] Prepared by the Pharmacy Research Department, Consumer Products Division, Miles Laboratories, Elkhart, IN 46514.
[2] Unpublished study.
[3] Obtained from Laboratory Research Enterprise, Kalamazoo, Mich. The dogs were maintained in an animal care facility fully accredited by the American Association for Laboratory Animal Care.
[4] Wayne Dog Krumettes, Allied Mills, Chicago, Ill.
[5] Lot 9601, New England Nuclear, Boston, Mass.

Table II—Summary of Average Daily Fecal Blood Loss Values

Dog	Average Daily Fecal Blood Loss, ml/Period in which Treatment was Administered							
	Control Period 1	A2	Control Period 2	B2	Control Period 3	C2	Control Period 4	D2
13	0.85	0.56/3	0.76	0.76/4	0.62	1.45/2	0.61	2.51/1
14	0.58	0.61/3	0.49	0.90/2	0.41	0.98/1	0.31	2.00/4
15	1.06	0.56/4	0.66	1.16/3	0.52	1.81/1	0.40	4.27/2
16	0.60	0.47/4	0.59	1.02/2	0.33	1.59/3	0.54	3.17/1
17	0.69	0.91/2	0.63	2.97/1	0.52	1.73/3	0.75	6.33/4
18	0.65	0.61/1	0.46	0.76/3	0.44	1.08/2	0.33	1.74/4
19	0.40	0.63/1	0.40	1.00/4	0.42	0.93/3	0.46	0.90/2
20	0.49	0.84/3	0.74	1.16/1	0.65	1.23/4	0.42	1.68/2
21	0.66	0.62/2	0.70	1.29/4	0.46	1.33/1	0.48	3.04/3
22	0.79	1.18/2	0.74	2.16/3	0.50	1.89/4	1.16	3.59/1
23	0.97	1.17/4	0.66	2.46/1	0.50	1.12/2	0.55	2.89/3
24	0.78	0.85/1	0.67	1.49/2	0.54	1.45/4	0.52	2.56/3
Mean	0.70	0.75[a]	0.62	1.43[b]	0.50	1.37[b]	0.54	2.89[c]
±*SE*	0.05	0.07	0.03	0.21	0.02	0.09	0.07	0.41

[a] Significantly ($p < 0.05$) different from B2, C2, and D2. [b] Significantly ($p < 0.05$) different from A2 and D2. [c] Significantly ($p < 0.05$) different from A2, B2, and C2.

of body weight, (*b*) no significant differences among periods, and (*c*) no significant residual effects of the treatments. The finding that there were significant differences between squares is consistent with the dose-dependent nature of aspirin-induced GI microbleeding in dogs (7), since all dogs received a fixed aspirin-equivalent dose regardless of body weight. Similarly, the finding of significant differences between dogs within squares is consistent with numerous reports indicating that the response of individuals to aspirin varies significantly.

DISCUSSION

These findings support the hypothesis that the differential effect of C2 and D2 tablets on the gastric mucosa is attributable to the sodium acetylsalicylate component of D2 being contained in a dissolving core. Of the four quantitatively similar, but physically different, formulations, only with D2, the dissolving core tablet, would significant reconversion of sodium acetylsalicylate to the unionized acid be expected to occur (if the dissolving sodium acetylsalicylate core became adherent to the gastric mucosa during tablet disintegration); D2 caused significantly more GI microbleeding than the other formulations. Therefore, the physical form of a buffered acetylsalicylate formulation is critical in the effect of such formulations on GI microbleeding.

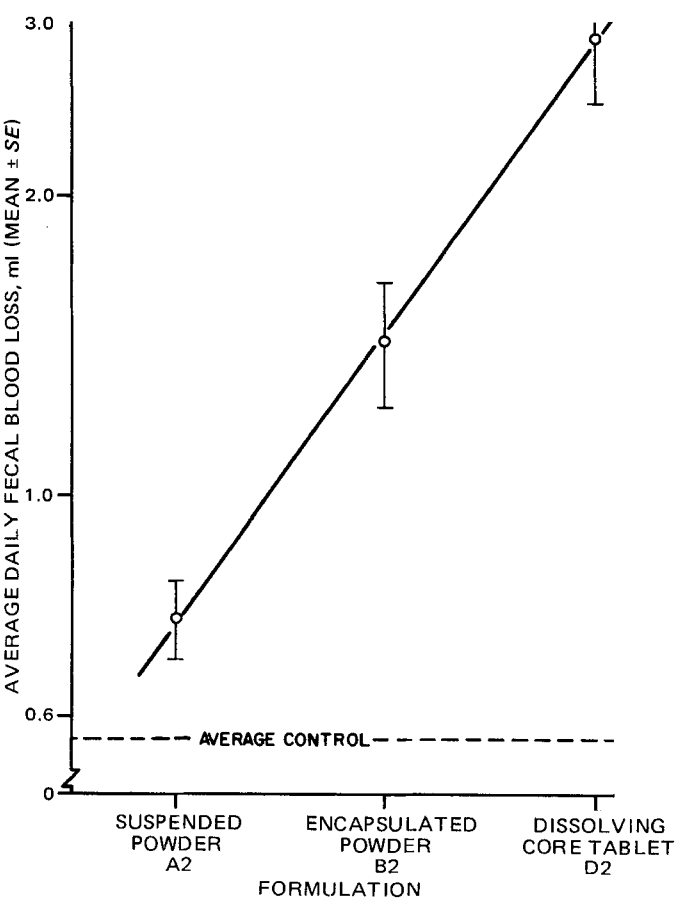

Figure 1—*Relationship of physical form to GI microbleeding.*

Aspirin, in the unionized form, must enter into the gastric mucosal cell to initiate gastric mucosal erosion. Therefore, the relationship of the physical form of a buffered sodium acetylsalicylate formulation to the GI microbleeding produced by the formulation is most likely attributable to the dissolution rate. In the case of a formulation with a rapid dissolution rate, there is little chance for reconversion of sodium acetylsalicylate to the acid; the converse is true for a formulation with a slow dissolution rate.

If it is assumed that the suspended (A2) and encapsulated (B2) powder formulations represent D2 tablet formulations with infinitely short dissolution and disintegration times, respectively (the fact that the encapsulated powder is not presented to the gastric mucosa until the capsule dissolves should be considered a form of delayed drug administration rather than delayed disintegration, since the material is completely disintegrated once presented to the mucosa), these results indicate clearly that a correlation exists between the rate of tablet dissolution and the effect on the gastric mucosa that is independent of total buffer capacity. Thus, a product with finite disintegration and solution times (D2) elicits significant GI microbleeding, while a product with an infinitely short disintegration time but a finite solution time (B2) causes significantly less microbleeding; a product with an infinitely short dissolution time (A2) causes even less microbleeding, despite the fact that all three formulations have similar total buffer capacities (Fig. 1). Almost certainly the fecal blood loss observed during treatment with A2 is not significantly greater than the control, although this possibility could not be tested statistically since no placebo was employed.

REFERENCES

(1) G. Levy, in "Salicylates," A. St. J. Dixon, B. K. Martin, M. J. H. Smith, and P. H. N. Wood, Eds., Little, Brown, Boston, Mass., 1963, p. 209.

(2) K. W. Anderson, in *ibid.*, p. 217.

(3) J. R. Leonards and G. Levy, *Clin. Pharmacol. Ther.*, **10**, 571 (1969).

(4) J. R. Leonards and G. Levy, *J. Pharm. Sci.*, **58**, 1277 (1969).

(5) J. R. Leonards and G. Levy, *Arch. Intern. Med.*, **129**, 457 (1972).

(6) B. M. Phillips, P. J. Kraus, J. L. Allen, and R. M. Buslee, *Toxicol. Appl. Pharmacol.*, **20**, 515 (1971).

(7) B. M. Phillips, *ibid.*, **24**, 182 (1973).

(8) R. R. Sokol and F. J. Rohlf, "Biometry," Freeman, San Francisco, Calif., 1969, p. 239.

ACKNOWLEDGMENTS AND ADDRESSES

Received January 28, 1974, from the *Toxicology Department, Corporate Research, and Pharmacy Research Department, Consumer Products Division, Miles Laboratories, Inc., Elkhart, IN 46514.*

Accepted for publication March 1, 1976.

The authors thank C. E. Myers and L. J. Baker for their expert technical assistance and J. L. Allen and T. Janakiraman for statistical analysis of the data.

ˣ To whom inquiries should be directed.

Quick Estimation of Kinetic Parameters for a Compartment with Exponential Absorption Rate and First-Order Elimination Rate

C. D. THRON

Abstract □ Two methods are presented for the quick estimation of kinetic parameters for a compartment with an exponential absorption rate and a first-order elimination rate. The first method is by direct computation from the observed levels of substance in the compartment at times t, $2t$, and $3t$, where t is arbitrary. The second method uses a numerical table to estimate the parameters from the observed peak level, the time of the peak level (or the time when the level rises to half of the peak level), and the time when the level has declined to half of its peak value. Some approximation equations also are given.

Keyphrases □ Kinetic parameters—compartment with exponential absorption rate and first-order elimination rate, two methods for quick estimation □ Pharmacokinetics—compartment with exponential absorption rate and first-order elimination rate, two methods for quick estimation of kinetic parameters

If the rate of absorption of a substance into an initially empty, well-stirred compartment declines exponentially with time and the rate of elimination is first order, then the quantity or concentration, y, of the substance in the compartment is a function of time, t, of the general form:

$$y = \frac{C(e^{-k_1 t} - e^{-k_2 t})}{k_2 - k_1} \qquad \text{(Eq. 1)}$$

where C, k_1, and k_2 are constants. The method usually recommended for estimating these constants from experimental data is a graphical procedure known as "peeling," "feathering," or the "method of residuals" (1, pp. 281–292), complemented by least-squares adjustment by computer (1, 2). The graphical procedure can be computerized, and these methods are entirely satisfactory if suitable computer programs and services are available. Without a computer, however, these methods are time consuming and are quite unwieldy for preliminary evaluation of data, rough comparison of published reports, and double-checking calculations.

This report describes methods of rapid, direct computation of C, k_1, and k_2 from experimental data; these methods may be useful for applications not requiring high accuracy or careful statistical weighting.

THEORY AND DISCUSSION

Estimation from y Values at t, $2t$, and $3t$—In principle, any three data points will determine the three parameters. In practice, however, the resulting three simultaneous equations cannot always be solved for the parameters. Therefore, direct computation of the parameters requires a suitable selection of data points.

Let t be any convenient time and let y_1, y_2, and y_3 be the observed levels at t, $2t$, and $3t$, respectively. Equation 1 gives:

$$y_j = \frac{C(e^{-k_1 jt} - e^{-k_2 jt})}{k_2 - k_1} \qquad \text{(Eq. 2)}$$

where $j = 1$, 2, or 3. For the solution of these three simultaneous equations, let:

$$r = +\sqrt{\frac{y_1 y_3}{y_2^2} - \frac{3}{4}} \qquad \text{(Eq. 3)}$$

Then:

$$k_1 = -\frac{1}{t}\log_e\left[\frac{y_2}{y_1}\left(\frac{1}{2} + r\right)\right] \qquad \text{(Eq. 4)}$$

$$k_2 = -\frac{1}{t}\log_e\left[\frac{y_2}{y_1}\left(\frac{1}{2} - r\right)\right] \qquad \text{(Eq. 5)}$$

and:

$$C = \frac{y_1^2(k_2 - k_1)}{2y_2 r} \qquad \text{(Eq. 6)}$$

The labeling of the constants k_1 and k_2 is entirely arbitrary. The conventions adopted here regarding the algebraic sign of r (Eqs. 3–5) assign the label k_2 to the larger of the two. If $r = 0$, then $k_1 = k_2 = k$ and Eq. 1 takes the limiting form:

$$y = Cte^{-kt} \qquad \text{(Eq. 7)}$$

If the quantity under the radical in Eq. 3 is negative, the data are inconsistent with the model underlying Eq. 1.

Equations 3–6 become simpler if t is selected on the rising limb of the y curve (Fig. 1) in such a way that $2t$ intercepts the falling limb at just the same level; *i.e.*, $y_2 = y_1$. Then the limiting case ($k_1 = k_2 = k$, Eq. 7) will have $y_3 = (\frac{3}{4})y_1$ (*cf.*, Eq. 3).

The use of Eqs. 3–6 may be illustrated by the example of Fig. 1. The steps for estimating the parameters are:

1. From the curve of Fig. 1, read the values of y at $t = 2$, 4, and 6: $y_1 = 1.85$, $y_2 = 1.43$, and $y_3 = 1.02$, respectively.
2. Compute $r = \sqrt{(1.85)(1.02)/(1.43)^2 - 0.75} = 0.416$ and $y_2/y_1 = 1.43/1.85 = 0.773$.
3. Compute $k_1 = -(\frac{1}{2})\log_e[0.773(0.5 + 0.416)] = 0.17$, $k_2 = -(\frac{1}{2})\log_e[0.773(0.5 - 0.416)] = 1.4$, and $C = fDk_a/V = (1.85)(1.4 - 0.17)/[2(0.773)(0.416)] = 3.5$.

Like any method of fitting the curve of Fig. 1, this analysis does not tell which of the two constants, k_1 (the smaller) or k_2 (the larger), is identified with k_a or k_e, nor does it evaluate the several factors of the coefficient C.

Estimation from Peak Level, y_m, Time of Peak Level, t_m, and Time of Decline to Half of Peak Level, t_{h_2}—Let y_m be the peak level, t_m be the time of the peak level, t_{h_1} be the time when the rising level first reaches $y_m/2$, and t_{h_2} be the time (after t_m) when the declining level reaches $y_m/2$ (Fig. 1). The theoretical equations (Eq. 1) for these ob-

ACKNOWLEDGMENTS AND ADDRESSES

Received January 28, 1974, from the *Toxicology Department, Corporate Research, and Pharmacy Research Department, Consumer Products Division, Miles Laboratories, Inc., Elkhart, IN 46514.*

Accepted for publication March 1, 1976.

The authors thank C. E. Myers and L. J. Baker for their expert technical assistance and J. L. Allen and T. Janakiraman for statistical analysis of the data.

ˣ To whom inquiries should be directed.

Quick Estimation of Kinetic Parameters for a Compartment with Exponential Absorption Rate and First-Order Elimination Rate

C. D. THRON

Abstract □ Two methods are presented for the quick estimation of kinetic parameters for a compartment with an exponential absorption rate and a first-order elimination rate. The first method is by direct computation from the observed levels of substance in the compartment at times t, $2t$, and $3t$, where t is arbitrary. The second method uses a numerical table to estimate the parameters from the observed peak level, the time of the peak level (or the time when the level rises to half of the peak level), and the time when the level has declined to half of its peak value. Some approximation equations also are given.

Keyphrases □ Kinetic parameters—compartment with exponential absorption rate and first-order elimination rate, two methods for quick estimation □ Pharmacokinetics—compartment with exponential absorption rate and first-order elimination rate, two methods for quick estimation of kinetic parameters

If the rate of absorption of a substance into an initially empty, well-stirred compartment declines exponentially with time and the rate of elimination is first order, then the quantity or concentration, y, of the substance in the compartment is a function of time, t, of the general form:

$$y = \frac{C(e^{-k_1 t} - e^{-k_2 t})}{k_2 - k_1} \qquad \text{(Eq. 1)}$$

where C, k_1, and k_2 are constants. The method usually recommended for estimating these constants from experimental data is a graphical procedure known as "peeling," "feathering," or the "method of residuals" (1, pp. 281–292), complemented by least-squares adjustment by computer (1, 2). The graphical procedure can be computerized, and these methods are entirely satisfactory if suitable computer programs and services are available. Without a computer, however, these methods are time consuming and are quite unwieldy for preliminary evaluation of data, rough comparison of published reports, and double-checking calculations.

This report describes methods of rapid, direct computation of C, k_1, and k_2 from experimental data; these methods may be useful for applications not requiring high accuracy or careful statistical weighting.

THEORY AND DISCUSSION

Estimation from y Values at t, $2t$, and $3t$—In principle, any three data points will determine the three parameters. In practice, however, the resulting three simultaneous equations cannot always be solved for the parameters. Therefore, direct computation of the parameters requires a suitable selection of data points.

Let t be any convenient time and let y_1, y_2, and y_3 be the observed levels at t, $2t$, and $3t$, respectively. Equation 1 gives:

$$y_j = \frac{C(e^{-k_1 jt} - e^{-k_2 jt})}{k_2 - k_1} \qquad \text{(Eq. 2)}$$

where $j = 1$, 2, or 3. For the solution of these three simultaneous equations, let:

$$r = +\sqrt{\frac{y_1 y_3}{y_2^2} - \frac{3}{4}} \qquad \text{(Eq. 3)}$$

Then:

$$k_1 = -\frac{1}{t}\log_e\left[\frac{y_2}{y_1}\left(\frac{1}{2} + r\right)\right] \qquad \text{(Eq. 4)}$$

$$k_2 = -\frac{1}{t}\log_e\left[\frac{y_2}{y_1}\left(\frac{1}{2} - r\right)\right] \qquad \text{(Eq. 5)}$$

and:

$$C = \frac{y_1^2(k_2 - k_1)}{2y_2 r} \qquad \text{(Eq. 6)}$$

The labeling of the constants k_1 and k_2 is entirely arbitrary. The conventions adopted here regarding the algebraic sign of r (Eqs. 3–5) assign the label k_2 to the larger of the two. If $r = 0$, then $k_1 = k_2 = k$ and Eq. 1 takes the limiting form:

$$y = Cte^{-kt} \qquad \text{(Eq. 7)}$$

If the quantity under the radical in Eq. 3 is negative, the data are inconsistent with the model underlying Eq. 1.

Equations 3–6 become simpler if t is selected on the rising limb of the y curve (Fig. 1) in such a way that $2t$ intercepts the falling limb at just the same level; *i.e.*, $y_2 = y_1$. Then the limiting case ($k_1 = k_2 = k$, Eq. 7) will have $y_3 = (\frac{3}{4})y_1$ (*cf.*, Eq. 3).

The use of Eqs. 3–6 may be illustrated by the example of Fig. 1. The steps for estimating the parameters are:

1. From the curve of Fig. 1, read the values of y at $t = 2$, 4, and 6: $y_1 = 1.85$, $y_2 = 1.43$, and $y_3 = 1.02$, respectively.
2. Compute $r = \sqrt{(1.85)(1.02)/(1.43)^2 - 0.75} = 0.416$ and $y_2/y_1 = 1.43/1.85 = 0.773$.
3. Compute $k_1 = -(\frac{1}{2})\log_e[0.773(0.5 + 0.416)] = 0.17$, $k_2 = -(\frac{1}{2})\log_e[0.773(0.5 - 0.416)] = 1.4$, and $C = fDk_a/V = (1.85)(1.4 - 0.17)/[2(0.773)(0.416)] = 3.5$.

Like any method of fitting the curve of Fig. 1, this analysis does not tell which of the two constants, k_1 (the smaller) or k_2 (the larger), is identified with k_a or k_e, nor does it evaluate the several factors of the coefficient C.

Estimation from Peak Level, y_m, Time of Peak Level, t_m, and Time of Decline to Half of Peak Level, t_{h_2}—Let y_m be the peak level, t_m be the time of the peak level, t_{h_1} be the time when the rising level first reaches $y_m/2$, and t_{h_2} be the time (after t_m) when the declining level reaches $y_m/2$ (Fig. 1). The theoretical equations (Eq. 1) for these ob-

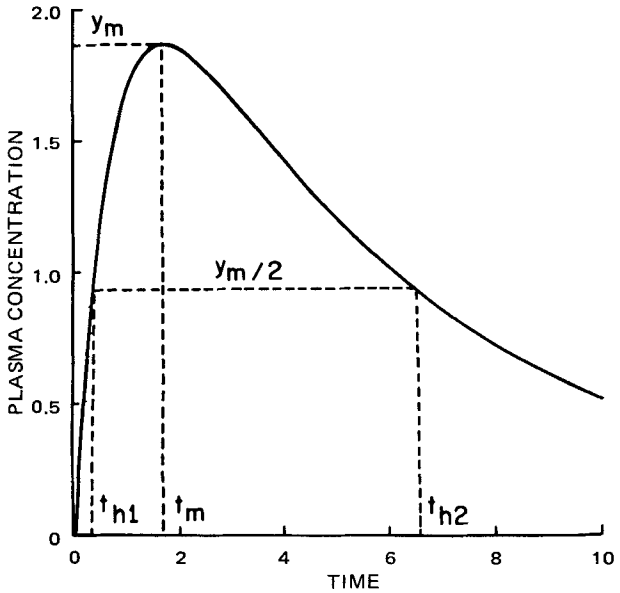

Figure 1—*Plasma concentration–time profile for a one-compartment system with absorption rate constant* $k_a = 1.4$, *elimination rate constant* $k_e = 0.17$, *volume of distribution* $V = 40$, *dose* $D = 100$, *and fraction absorbed* $f = 1$. *The plasma concentration* y *obeys the equation* $y = (fDk_a/V)[exp(-k_e t) - exp(-k_a t)]/(k_a - k_e)$, *where* t *is time* (cf., *Ref. 2, p. 292). The dashed lines indicate the peak level* y_m, *the time of the peak level* t_m, *the time* t_{h_1} *when the rising level first reaches* $y_m/2$, *and the time* t_{h_2} *when the declining level reaches* $y_m/2$.

servable values cannot be solved for the constants C, k_1, and k_2, so a numerical table is used (Table I). This table is based on the fact that if the value of the ratio t_{h_2}/t_m is known, the normalized parameters k_1/t_m, k_2/t_m, and Ct_m/y_m are entirely determined; from these values and the observed y_m and t_m, the constants k_1, k_2, and C are easily computed. The table also includes the ratio t_{h_2}/t_{h_1} in case the available value of t_m is more uncertain than that of t_{h_1}.

Computations for Table I were done as follows. Let $\kappa = k_2/k_1$. As before, the convention is adopted that $k_2 \geq k_1$ and, therefore, $\kappa \geq 1$. When $t = t_m$, $dy/dt = 0$ and Eqs. 1 and 7 give:

$$k_1 t_m = \frac{\log_e \kappa}{\kappa - 1} \qquad (k_1 \neq k_2) \qquad \text{(Eq. 8a)}$$

$$k_1 t_m = 1 \qquad (k_1 = k_2) \qquad \text{(Eq. 8b)}$$

and:

$$k_2 t_m = \kappa k_1 t_m \qquad \text{(Eq. 9)}$$

Equations 8a, 8b, and 9 are used to substitute for k_1 and k_2 in Eqs. 1 and 7 to obtain:

$$\frac{y}{y_m} = \frac{\kappa^{-(t/t_m)/(\kappa-1)} - \kappa^{-[\kappa(t/t_m)]/(\kappa-1)}}{\kappa^{-1/(\kappa-1)} - \kappa^{-\kappa/(\kappa-1)}} \qquad \text{(Eq. 10a)}$$

Table I—Normalized Parameters for a Compartment with Exponential Absorption and First-Order Elimination[a]

t_{h_2}/t_m	$k_1 t_m$	$k_2 t_m$	Ct_m/y_m	t_{h_2}/t_{h_1}
2.68[b]	1.000	1.00	2.72[c]	11.5[d]
2.70	0.840	1.18	2.73	11.7
2.75	0.726	1.34	2.76	12.0
2.80	0.657	1.45	2.79	12.3
2.85	0.607	1.53	2.82	12.6
2.90	0.567	1.61	2.84	12.9
2.95	0.534	1.68	2.87	13.3
3.00	0.505	1.74	2.89	13.6
3.10	0.459	1.86	2.94	14.2
3.20	0.422	1.95	2.98	14.8
3.30	0.392	2.04	3.02	15.5
3.40	0.367	2.12	3.06	16.1
3.50	0.345	2.20	3.10	16.7
3.60	0.326	2.26	3.14	17.4
3.70	0.309	2.33	3.17	18.0
3.80	0.294	2.39	3.20	18.7
3.90	0.281	2.44	3.24	19.3
4.00	0.269	2.50	3.27	20.0
4.10	0.258	2.55	3.30	20.6
4.20	0.248	2.60	3.33	21.3
4.30	0.239	2.64	3.36	22.0
4.40	0.230	2.69	3.38	22.6
4.50	0.222	2.73	3.41	23.3
4.60	0.215	2.77	3.44	24.0
4.70	0.208	2.81	3.46	24.7
4.80	0.202	2.85	3.49	25.3
4.90	0.196	2.89	3.51	26.0
5.00	0.190	2.92	3.53	26.7
5.20	0.180	2.99	3.58	28.1
5.40	0.171	3.06	3.62	29.5
5.60	0.162	3.12	3.67	30.9
5.80	0.155	3.18	3.71	32.3
6.00	0.148	3.23	3.75	33.7
6.20	0.142	3.28	3.78	35.1
6.40	0.136	3.34	3.82	36.6
6.60	0.131	3.38	3.86	38.0
6.80	0.126	3.43	3.89	39.5
7.00	0.121	3.48	3.92	41.0
7.20	0.117	3.52	3.96	42.4
7.40	0.113	3.56	3.99	43.9
7.60	0.110	3.60	4.02	45.4
7.80	0.106	3.64	4.05	46.9
8.00	0.103	3.68	4.08	48.4
8.20	0.100	3.71	4.11	50.0
8.40	0.0972	3.75	4.13	51.5
8.60	0.0945	3.78	4.16	53.0
8.80	0.0920	3.82	4.19	54.6
9.00	0.0896	3.85	4.21	56.1
9.20	0.0873	3.88	4.24	57.7
9.40	0.0851	3.91	4.26	59.2
9.60	0.0831	3.94	4.28	60.8
9.80	0.0811	3.97	4.31	62.4
10.00	0.0792	4.00	4.33	64.0
10.5	0.0749	4.07	4.39	67.9
11.0	0.0710	4.13	4.44	72.0
11.5	0.0676	4.20	4.49	76.0
12.0	0.0644	4.26	4.54	80.1
12.5	0.0615	4.31	4.58	84.2
13.0	0.0589	4.36	4.63	88.4
13.5	0.0565	4.42	4.67	92.6
14.0	0.0543	4.46	4.71	96.8
14.5	0.0522	4.51	4.75	101
15.0	0.0503	4.56	4.79	105
15.5	0.0485	4.60	4.83	110
16.0	0.0469	4.64	4.86	114
16.5	0.0453	4.68	4.90	118
17.0	0.0439	4.72	4.93	123
17.5	0.0426	4.76	4.97	127
18.0	0.0413	4.80	5.00	132
18.5	0.0401	4.83	5.03	136
19.0	0.0390	4.87	5.06	140
19.5	0.0379	4.90	5.09	145
20.0	0.0369	4.93	5.12	149
21.0	0.0350	5.00	5.17	159
22.0	0.0333	5.06	5.23	168
23.0	0.0318	5.11	5.28	177
24.0	0.0304	5.17	5.33	186
25.0	0.0291	5.22	5.37	196

[a] For values of t_{h_2}/t_m larger than those shown here, the following equations give estimates accurate to within 5%:

$$k_1 \simeq \frac{(\log_e 2)}{t_{h_2} - t_m} \qquad k_2 \simeq \frac{(\log_e 2)}{t_{h_1}} \qquad C \simeq k_2 y_m$$

If t_{h_1} is not available, $k_2 t_m$ can be estimated from the recursion equation $k_{2(i+1)}t_m = k_1 t_m - \log_e(k_1 t_m) + \log_e(k_{2i} t_m)$, where $k_{2i}t_m$ and $k_{2(i+1)}t_m$ are the ith and $(i+1)$th successive approximations to $k_2 t_m$, and a suitable starting estimate, $k_{21}t_m$, is $k_1 t_m - \log_e(k_1 t_m)$ or just $-\log_e(k_1 t_m)$. [b] The value is 2.67835. A value of t_{h_2}/t_m smaller than this is inconsistent with the model on which Eq. 1 is based. [c] 2.71828 = e. [d] The value is 11.54466.

$$\frac{y}{y_m} = \frac{\kappa^{-[(t/t_m)-1]/(\kappa-1)}\,(\kappa^{(t/t_m)} - 1)}{\kappa - 1} \qquad (\kappa \neq 1) \qquad \text{(Eq. 10}b\text{)}$$

$$\frac{y}{y_m} = (t/t_m)e^{-[(t/t_m)-1]} \qquad (\kappa = 1) \qquad \text{(Eq. 10}c\text{)}$$

Let $\theta_1 = t_{h_1}/t_m$ and $\theta_2 = t_{h_2}/t_m$; then, from Eqs. 10*b* and 10*c*:

$$\frac{1}{2} = \frac{\kappa^{-[\kappa(\theta-1)]/(\kappa-1)}(\kappa^{\theta} - 1)}{\kappa - 1} \qquad (\kappa \neq 1) \qquad \text{(Eq. 11}a\text{)}$$

$$\frac{1}{2} = \theta e^{-(\theta-1)} \qquad (\kappa = 1) \qquad \text{(Eq. 11}b\text{)}$$

for $\theta = \theta_1$ or θ_2. An iterative method [a one-dimensional modified version of the flexible simplex method described by Himmelblau (3)] was used to compute θ for a given κ or κ for a given θ from Eqs. 11*a* and 11*b*. (For a given κ, the algorithm employed converged either to θ_1 or θ_2, depending on the initial estimate.) For large κ and θ values, the computation of the right-hand side of Eqs. 11*a* and 11*b* produced intermediate values too large for the computer. To avoid these overflows, an alternative equation was used when κ was greater than 50 and θ was greater than 9:

$$\frac{1}{2} = \frac{\kappa^{(\kappa-\theta)/(\kappa-1)}}{\kappa - 1} \qquad \text{(Eq. 12)}$$

This equation is derived from Eqs. 11*a* and 11*b* by replacing the term $\kappa^{\theta} - 1$ by κ^{θ} and multiplying out the numerator.

Finally, Eqs. 8*a*, 8*b*, and 9 are used to substitute for k_1 and k_2 in Eqs. 1 and 7 to obtain:

$$\frac{Ct_m}{y_m} = \frac{\kappa^{\kappa/(\kappa-1)}\log_e \kappa}{\kappa - 1} \qquad (\kappa \neq 1) \qquad \text{(Eq. 13}a\text{)}$$

$$\frac{Ct_m}{y_m} = e \qquad (\kappa = 1) \qquad \text{(Eq. 13}b\text{)}$$

The use of Table I may be illustrated by the example of Fig. 1. The steps in estimating the parameters are:

1. From the curve of Fig. 1, read $t_m = 1.7$ and $y_m = 1.88$.
2. Compute $y_m/2 = 0.94$.
3. From the curve of Fig. 1, read $t_{h_2} = 6.5$ (where $y = 0.94$).
4. Compute $t_{h_2}/t_m = 3.8$.
5. From Table I, read $k_1 t_m = 0.294$, $k_2 t_m = 2.39$, and $Ct_m/y_m = 3.20$.
6. Compute $k_1 = 0.294/1.7 = 0.17$, $k_2 = 2.39/1.7 = 1.4$, and $C = fDk_a/V = (3.20)(1.88)/1.7 = 3.5$.

If t_{h_1} can be determined more accurately than t_m, the first four steps can be modified as follows:

1. From the curve of Fig. 1, read $y_m = 1.88$.
2. Compute $y_m/2 = 0.94$.
3. From the curve of Fig. 1, read $t_{h_1} = 0.35$ and $t_{h_2} = 6.5$.
4. Compute $t_{h_2}/t_{h_1} = 18.6$.

Since this value of t_{h_2}/t_{h_1} lies between the tabulated values, interpolation might be done. For most purposes, however, it is sufficiently accurate to take the normalized parameter values corresponding to the closest tabulated value of t_{h_2}/t_{h_1}, *i.e.*, 18.7.

The accuracy of this method is obviously limited by the accuracy of determination of t_m and t_{h_2} or t_{h_1}. These parameters, especially t_m and t_{h_1}, are likely to be quite inaccurately known when only a small number of data points are available, as is commonly the case. The values of k_1 and k_2 are especially uncertain when the ratio t_{h_2}/t_m is less than 3 or 3.5, because in this region the dependence of $k_1 t_m$ and $k_2 t_m$ on t_{h_2}/t_m is quite steep (Table I). These limitations on accuracy must be kept in mind when this method is used.

Approximation Equations—Attempts to find simple approximation equations for k_1, k_2, and C in terms of t_m, t_{h_1}, t_{h_2}, and y_m yielded only two that were both simple and reasonably accurate:

$$C = (\log_e 2)y_m/t_{h_1} = 0.693y_m/t_{h_1} \qquad \text{(Eq. 14)}$$

and:

$$k_1 = (\log_e 2)/(t_{h_2} - 1.5t_m) = 0.693/(t_{h_2} - 1.5t_m) \qquad \text{(Eq. 15)}$$

Equation 14 gives slightly high values, accurate to within 5% if $t_{h_2}/t_m > 4.7$ and to within 10% otherwise. Equation 15 gives values within ±5% if $t_{h_2}/t_m > 3.15$ and within 10% if $t_{h_2}/t_m > 2.95$; but for lower values of t_{h_2}/t_m, it gives values of k_1 that are as much as 41% too low.

Equation 15 may be convenient for estimating the elimination rate constant from plasma level–time curves following oral administration, assuming the elimination rate constant is smaller than the absorption rate constant. It is essentially the familiar equation for intravenous administration, $k_1 = (\log_e 2)/t_{h_2}$, corrected for gradual absorption by the term $-1.5t_m$.

The parameter k_2 can be estimated from k_1 and t_m by the recursion equation given in footnote *a* to Table I. Several iterations may be necessary if $k_1 t_m > 0.1$, and a programmable calculator is convenient for doing these calculations.

CONCLUSIONS

The described methods appear to be the best solutions to the problem of getting rough estimates of the parameters of Eq. 1 with minimum computation. These methods do not verify that the data in question do in fact obey Eq. 1; therefore, these methods could be misleading if applied to data that do not obey Eq. 1. If such misapplications are avoided, however, these methods may prove useful, especially for preliminary evaluation of data, rough comparison of published reports, and double-checking calculations.

REFERENCES

(1) M. Gibaldi and D. Perrier, "Pharmacokinetics," Dekker, New York, N.Y., 1975.

(2) J. G. Wagner, "Biopharmaceutics and Relevant Pharmacokinetics," Drug Intelligence Publications, Hamilton, Ill., 1971.

(3) D. M. Himmelblau, "Process Analysis by Statistical Methods," Wiley, New York, N.Y., 1970, pp. 181 ff.

ACKNOWLEDGMENTS AND ADDRESSES

Received January 12, 1976, from the *Department of Pharmacology and Toxicology, Dartmouth Medical School, Hanover, NH 03755.*

Accepted for publication March 8, 1976.

In Vitro Inhibition of Viral DNA Polymerase Activity by Litmomycin

MANOHAR L. SETHI

Abstract □ Litmomycin, an antibiotic isolated from *Streptomyces litmogenes*, is highly active against Gram-positive bacteria and possesses antitumor activity. It inhibited viral DNA polymerase activity *in vitro*. The amount of litmomycin required to cause 50% inhibition of enzyme activity was 80–100 μg (180–225 nmoles)/ml of reaction mixture. The enzyme inhibition was observed when polyriboadenylate–oligodeoxythymidylate, polydeoxyadenylate–oligodeoxythymidylate, polyribocytidylate–oligodeoxyguanylate, activated DNA, and 70S RNA were used as templates. Reaction kinetics and the mechanism of enzyme inhibition are discussed. The results suggest that litmomycin interacts with the template primer and not with the enzyme protein to stop the polymerization process.

Keyphrases □ Litmomycin—effect on viral DNA polymerase activity *in vitro*, reaction kinetics and mechanism □ Viral DNA polymerase—effect of litmomycin on *in vitro* activity, reaction kinetics and mechanism □ DNA polymerase, viral—effect of litmomycin on *in vitro* activity, reaction kinetics and mechanism □ Enzymes—viral DNA polymerase, effect of litmomycin on *in vitro* activity, reaction kinetics and mechanism □ Antibiotics—litmomycin, effect on viral DNA polymerase activity *in vitro*, reaction kinetics and mechanism

RNA-directed DNA polymerase (reverse transcriptase) is the unique enzyme found (1–4) in nucleocapsids of RNA tumor viruses. This enzyme is required for productive infection and transformation of normal cells by RNA tumor viruses (5–7). Recent publications (8–10) indicate that RNA tumor viruses are involved in at least some forms of human cancer (leukemia). Current evidence indicates that reverse transcriptase is required only to initiate, but not to maintain, the transformed state and the continuous production of new virus particles by these transformed cells (10, 11).

The relationship between the biochemical characteristics of reverse transcriptase from human acute leukemia cells and several RNA tumor viruses is well documented (12). In the event that RNA tumor viruses are involved in human cancer, reverse transcriptase is the important enzyme in the onset of oncogenesis (13). Therefore, specific inhibitors of reverse transcriptase might find use in the development of drugs for leukemia and cancer chemotherapy. In an effort to develop *in vitro* test systems for antiviral activity, an inhibition of reverse transcriptase activity by fagaronine was previously studied (14). This paper reports the effect of litmomycin on the purified protein fraction of reverse transcriptase from RNA tumor viruses.

Litmomycin (granaticin A[1]), an antibiotic isolated from a new *Streptomyces* species, *S. litmogenes* (15), is highly active against Gram-positive bacteria but has little or no activity against Gram-negative bacteria, mycobacterium, molds, and yeast (16). It has significant antitumor activity against P-388 lymphocytic leukemia in mice and cytotoxicity against KB cells (17).

[1] Granaticin B showed a distinct inhibition of various transplanted tumors in rodents after repeated intraperitoneal application (H. Bickel and K. Scheibli, Ciba-Geigy Ltd., Basel, Switzerland, personal communication).

EXPERIMENTAL

Materials—Purified DNA polymerase from avian myeloblastosis virus[2] had a specific activity of 10,108 units/mg and a protein content of 0.35 mg/ml. The enzyme was purified according to the published method (18). DNA polymerase from simian sarcoma virus type 1[3] was derived from tissue culture fluids of the SSV-1-NC-37 cell line and purified by the method described previously (14). It possessed an activity of 6.00 nmoles of thymidine monophosphate incorporation/30 min/ml. Purified DNA polymerase from Rauscher murine leukemia virus[4] propagated in the JLS-V9 cell line had an activity of 4.00 nmoles of thymidine monophosphate incorporation/30 min/ml. Viral 70S RNA[5] was obtained from Rauscher murine leukemia virus, which was purified by the published method (19).

The templates[6], polyriboadenylate–oligodeoxythymidylate (I), polydeoxyadenylate–oligodeoxythymidylate (II), and polyribocytidylate–oligodeoxyguanylate (III), were dissolved in a buffer containing 0.01 *M* tromethamine (IV) (pH 7.0), 0.10 m*M* ethylenediaminetetraacetic acid tetrasodium salt (V), and 0.10 *M* NaCl. ^{3}H-Thymidine triphosphate and ^{3}H-guanosine triphosphate (specific activity of 14 Ci/mmole[7]), unlabeled thymidine triphosphate[6], and guanosine triphosphate[6] were obtained commercially. Activated calf thymus DNA was prepared by incubating 4.50 mg of bovine serum albumin in 10 ml of buffer containing IV (0.05 *M*, pH 7.0) and 5.00 m*M* $MgCl_2$ with 0.01 mg of crystalline pancreatic deoxyribonuclease[8] for 15 min at 37°. It was chilled at 4°, further incubated at 70° for 5 min, and stored at 4°.

All other chemical reagents[9] were of analytical grade. Appropriate concentrations of litmomycin (mol. wt. 444) were made in dimethyl sulfoxide.

Viral DNA Polymerase Assay and Enzyme Inhibition—One hundred microliters of enzyme assay mixture contained 5.00 μmoles of IV (pH 7.30), 8.00 μmoles of potassium chloride, 0.10 μmole of manganese chloride, 0.50 μmole of dithiothreitol, 2.00 μmoles of ^{3}H-thymidine triphosphate (170 cpm/pmole), 20.00 μg of bovine serum albumin, 2.00 μg of I, 10% glycerol, and purified enzyme preparation. The reaction mixture was incubated at 37° for 30 min. The enzyme reaction was stopped by chilling at 4° and by the addition of V (25 μl, 0.10 *M*).

Each reaction mixture (100 μl) was uniformly spotted onto 2.50-cm filter paper[10] disks and kept at room temperature for 15 min. The filter paper disks were washed batchwise six times with 5% $Na_2HPO_4 \cdot 7H_2O$ (10 ml/filter paper disk), followed by two washings each of water and ethanol (10 ml/filter paper disk). Then these disks were dried, and the radioactivity incorporated into an acid-insoluble material was determined[11] in a toluene base scintillation fluid.

For testing the enzyme inhibition, two reaction mixtures (A and B) were prepared. Mixture A contained enzyme, buffer, and bovine serum albumin. Mixture B contained template, substrate, dithiothreitol, and glycerol. The final concentration of ingredients in Mixtures A and B (100 μl) was the same as mentioned previously. Appropriate concentrations of litmomycin were mixed with Mixture A and allowed to react for 10 min at 4° before Mixture B was added. Control assays contained an equivalent volume of dimethyl sulfoxide. The results were expressed as percent of control.

[2] Life Science Research Labs., St. Petersburg, Fla., through the courtesy of Dr. J. Beard. The enzyme preparation contained 3538 units of reverse transcriptase/ml (1 unit of enzyme activity is expressed as the incorporation of 1 nmole of deoxythymidine monophosphate into an acid-insoluble product in 10 min at 37°).
[3] Pfizer, Inc., Maywood, N.J.
[4] Bionetics Laboratory Products, Kensington, Md.
[5] Gift from Mr. Z. Salahuddin, Litton Bionetics Inc., Bethesda, Md.
[6] P.L. Biochemicals Inc., Milwaukee, Wis.
[7] Schwarz-Mann.
[8] Worthington Biochemicals Corp.
[9] Sigma Chemical Co., St. Louis, Mo.
[10] DE-81, Whatman.
[11] Unilux III liquid scintillation unit.

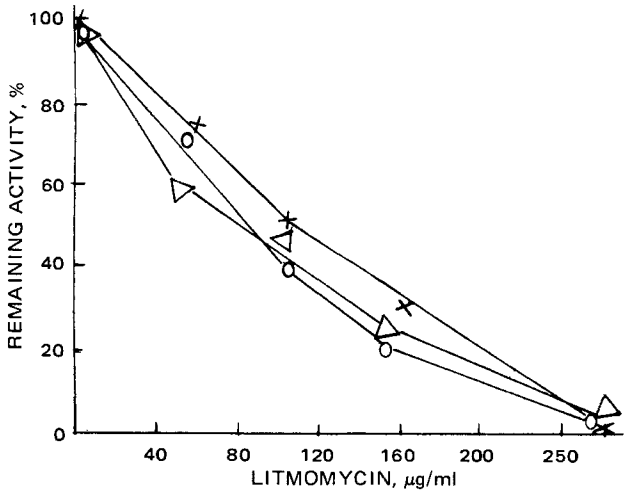

Figure 1—*Effect of litmomycin on the viral DNA polymerase activity. In a standard assay mixture (0.10 ml) containing 5 μl of avian myeloblastosis virus (○), 10 μl of simian sarcoma virus type 1 (△), or 10 μl of murine leukemia virus (×) DNA polymerase, different concentrations of litmomycin were added for enzyme inhibition.*

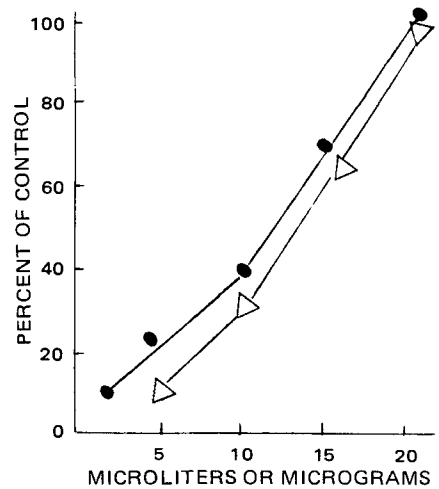

Figure 2—*Effect of increasing concentrations of avian myeloblastosis virus DNA polymerase and template primer on litmomycin-inhibited reaction mixture. The standard reaction mixture (0.10 ml) contained 5 μl of avian myeloblastosis virus DNA polymerase (△) or 2 μg of I (●). Twenty micrograms of litmomycin was used for each assay.*

RESULTS AND DISCUSSION

The inhibition of DNA polymerase activity from murine leukemia virus, simian sarcoma virus type 1, and avian myeloblastosis virus at increasing concentrations of litmomycin (0–240 μg/ml) was undertaken. The enzyme activity gradually declined when the litmomycin concentration in the reaction mixture was increased. The inhibition curves were very close and similar to each other (Fig. 1). Fifty percent inhibition of enzyme activity (ID_{50}) was obtained in the range of 80–100 μg (180–225 nmoles)/ml of the reaction mixture.

To explain the mode of enzyme inhibition, different template primers such as I, II, III, activated DNA, and 70S RNA were employed (Table I); different degrees of enzyme inhibition were obtained with different template primers. A high degree of enzyme inhibition in the presence of I or II, as compared to III, could be due to a strong binding affinity of litmomycin with adenine–thymine template primers. These results suggest that litmomycin did not interact with the enzyme protein. If litmomycin interacted with the enzyme, then the same degree of enzyme inhibition would have been observed regardless of the template primer used.

The interaction or competition of litmomycin with potassium chloride and ^{3}H-thymidine triphosphate or ^{3}H-guanosine triphosphate was not considered since they were present in the reaction mixture in eight- or 25-fold, respectively, in excess of the ID_{50} of the litmomycin concentration. The enzyme activity remained unchanged when the amount of manganese chloride in the assay mixture was increased (data not shown), indicating that the metal ions did not interact with the litmomycin. Therefore, litmomycin interacted with the template primers and not with the enzyme.

Effects of increasing concentrations of avian myeloblastosis virus DNA polymerase and template primer were observed on the litmomycin-inhibited reaction mixture to explain further the mechanism of enzyme inhibition. The enzyme activity of the litmomycin-inhibited reaction mixture was linearly restored when concentrations of I in the assay mixture were increased from 2 to 20 μg and the enzyme concentration was increased from 5 to 20 μl (Fig. 2). These results suggest that the enzyme–template–antibiotic complex in the reaction mixture was completely dissociated in the presence of excess template primers or the enzyme.

In the assay mentioned, litmomycin was added to the reaction mixture containing enzyme, template primer, metal ions, and substrate before incubation. The inhibitory effects of litmomycin were thus primarily directed to the free template primer and its complexes with the enzyme, substrate, and metal ions. In other assays where the enzyme molecule had already initiated the DNA synthesis, with subsequent elongation of polynucleotide chains, the effect of lit-

Table I—Effect of Different Template Primers on Avian Myeloblastosis Virus DNA Polymerase Inhibition by Litmomycin

Template Primer	Radioactive Substrate	Inhibition[a], %
I[b]	Thymidine triphosphate	80
II[b]	Thymidine triphosphate	86
III[c]	Deoxyguanosine triphosphate	15
Activated DNA[d]	Thymidine triphosphate	75
70S RNA[e]	Thymidine triphosphate	70

[a] Litmomycin, 20 μg/assay, was employed for each inhibition. [b] See standard assay conditions as specified in *Experimental* section. [c] Standard assay mixture contained 2 μg of this template primer and 2.0 nmoles of ^{3}H-deoxyguanosine triphosphate (370 cpm/mole). [d] Standard assay mixture contained 2.20 μg of activated DNA, 10 nmoles each of deoxyadenosine, deoxycytidine, and deoxyguanosine triphosphates, and 2.0 nmoles of ^{3}H-thymidine triphosphate. [e] In the standard assay conditions, 70S RNA (murine leukemia virus) with an optical density of 0.06 (260 nm) was used as the template.

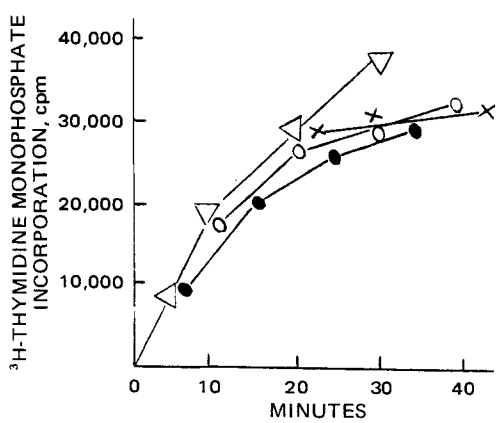

Figure 3—*Effect of addition of litmomycin at different time intervals during avian myeloblastosis virus DNA polymerase reaction. Two milliliters of standard assay mixture contained 100 μl of enzyme. The mixture was divided into four aliquots: A (0.60 ml), B (0.50 ml), C (0.50 ml), and D (0.40 ml). From A, a 0.10-ml sample was withdrawn at 0 min; A–D were incubated at 37°. One-tenth-milliliter samples from A (control, △) were withdrawn after 5, 10, 20, and 30 min of incubation. Litmomycin (250 μg/ml) was added after 5 (●), 10 (○), and 20 (×) min of incubation to B, C, and D, respectively. The enzyme activity was determined 1 min after the addition of litmomycin from the withdrawn samples (0.10 ml) at 10-min intervals.*

momycin was observed. Litmomycin was added to such a mixture at different time intervals during the reaction.

When litmomycin was added at 5 and 10 min after initiation of the polymerization reaction, the enzyme activity continued for about 20 min, comparable to the control. But when the litmomycin was added after 20 min, the enzyme activity stopped instantly, as indicated by the ^{3}H-thymidine monophosphate incorporation (Fig. 3). The results suggest that litmomycin did not inhibit the initial formation of an RNA–DNA hybrid but blocked the subsequent phase of the polymerization processes.

In conclusion, litmomycin inhibits DNA polymerase activity of RNA tumor viruses by interaction with (riboadenylate)$_n$–(deoxythymidylate)$_n$ or adenine–thymine bases and (ribocytidylate)$_n$–(deoxyguanylate)$_n$ or cytosine–guanine bases with a different degree of binding. It may be of interest to investigate the antiviral activity of litmomycin in cell culture.

REFERENCES

(1) H. M. Temin and S. Mizutani, *Nature*, **226**, 1211(1970).

(2) S. Spiegelman, A. Burny, M. R. Das, J. Keydar, J. Schlom, M. Travnicek, and K. Watson, *ibid.*, **227**, 563(1970).

(3) H. M. Temin and D. Baltimore, *Adv. Virus Res.*, **17**, 129(1972).

(4) P. Sarin and R. C. Gallo, in "International Review Science Series in Biochemistry," vol. 6, K. Burton, Ed., Butterworth and Medical and Technical Publishing Co., Oxford, England, 1974, chap. 8.

(5) M. M. Lieber, R. E. Benveniste, D. M. Livingston, and G. J. Todaro, *Science*, **182**, 59(1973).

(6) R. C. Gallo, *Nature*, **234**, 194(1971).

(7) H. M. Temin, *Cancer Res.*, **34**, 2835(1974).

(8) R. E. Gallagher and R. C. Gallo, *Science*, **187**, 250(1975).

(9) T. Mak, M. Aye, H. Messner, R. Sheinin, J. Till, and E. McCullough, *Br. J. Cancer*, **29**, 433(1974).

(10) R. C. Gallo, *Biomedicine*, **18**, 446(1973).

(11) H. Hanafusa and T. Hanafusa, *Virology*, **43**, 313(1971).

(12) P. S. Sarin, J. W. Abrell, and R. C. Gallo, "Control of Transcription," Plenum, New York, N.Y., 1974, pp. 345–353.

(13) R. C. Gallo, *Blood*, **39**, 117(1972).

(14) V. S. Sethi and M. L. Sethi, *Biochem. Biophys. Res. Commun.*, **63**, 1070(1975).

(15) P. Soong and A. A. Au, *Rep. Taiwan Sugar Exp. Stn.*, **29**, 33(1962).

(16) P. Soong, Y. Y. Jen, Y. S. Hsu, and A. A. Au, *ibid.*, **34**, 105(1974).

(17) G.-J. Chang, H. G. Floss, P. Soong, and C.-T. Chang, *Jpn. Antibiot. Res. Assoc.*, **28**, 156(1975).

(18) D. L. Kacian and S. Spiegelman, in "Methods in Enzymology," vol. 29E, L. Grossman and K. Moldave, Eds., Academic, New York, N.Y., 1973, p. 150.

(19) J. Bhattacharyya, M. Xuma, M. Reitz, P. S. Sarin, and R. C. Gallo, *Biochem. Biophys. Res. Commun.*, **54**, 324(1973).

ACKNOWLEDGMENTS AND ADDRESSES

Received November 10, 1975, from the *Department of Biomedicinal Chemistry, College of Pharmacy and Pharmacal Sciences, Howard University, Washington, DC 20059*

Accepted for publication March 4, 1976.

The author thanks Dr. H. G. Floss, Purdue University, for a gift sample of litmomycin. The arrangements made by Dr. Jack Gruber and Dr. M. A. Chirigos, National Institutes of Health, for the supply of reverse transcriptase are gratefully acknowledged. The technical help of Mr. Warren W. Schadt in the liquid scintillation counting is appreciated.

GLC Determination of Indoprofen in Plasma

ROBERT V. SMITH ˣ, DAVID W. HUMPHREY, and HENRY ESCALONA-CASTILLO

Abstract □ Implementation of human bioavailability studies with the analgesic indoprofen required a rapid, sensitive, and convenient assay in blood plasma. A procedure based on ether extraction of acidified plasma, derivatization with diazomethane, and GLC analysis using a 3% OV-1 column was sufficiently sensitive for measurement of plasma indoprofen concentrations in the 0.4–16-μg/ml range. An average recovery of 99.0 ± 7.6% (*SD*) was achieved when the pentanoic acid homolog was employed as an internal standard.

Keyphrases □ Indoprofen—GLC analysis, human plasma □ GLC—analysis, indoprofen in human plasma □ Analgesics—indoprofen, GLC analysis in human plasma

Indoprofen, *dl*-2-[4-(1-oxo-2-isoindolinyl)phenyl]propanoic acid (I), possesses promising analgesic and anti-inflammatory properties (1, 2). In humans, I reportedly appears unchanged in plasma (3). Furthermore, enantiomeric enrichment does not seem to be significant in humans (4). Implementation of human bioavailability studies in this laboratory required a rapid, sensitive, and convenient assay of I in blood plasma.

Two GLC methods were reported for the determination of I in plasma (4, 5). Both procedures employ a lengthy series of partition steps. In one (4), a trifluoroethyl ester

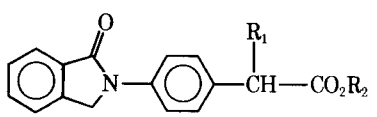

I: $R_1 = CH_3$, $R_2 = H$

II: $R_1 = CH_2CH_2CH_3$, $R_2 = H$

III: $R_1 = CH_3$, $R_2 = CH_3$

IV: $R_1 = CH_2CH_2CH_3$, $R_2 = CH_3$

is utilized after preparation with boron trifluoride–trifluoroethanol. The latter reagent is corrosive and difficult to eliminate prior to GLC development. The other method (5) involves preparation and resolution of a diastereomeric pair of amides obtained through reaction of I (as its acid chloride) with *l*-α-methylbenzylamine. While useful in evaluating *in vivo* enantiomeric interconversions, this procedure is not amenable to analyses of large numbers of samples because of its length.

A simplified assay based on a single ether extraction and GLC of I and the internal standard, *dl*-2-[4-(1-oxo-2-isoindolinyl)phenyl]pentanoic acid (II), as their methyl esters (III and IV) was developed and is the subject of this report.

momycin was observed. Litmomycin was added to such a mixture at different time intervals during the reaction.

When litmomycin was added at 5 and 10 min after initiation of the polymerization reaction, the enzyme activity continued for about 20 min, comparable to the control. But when the litmomycin was added after 20 min, the enzyme activity stopped instantly, as indicated by the ^{3}H-thymidine monophosphate incorporation (Fig. 3). The results suggest that litmomycin did not inhibit the initial formation of an RNA–DNA hybrid but blocked the subsequent phase of the polymerization processes.

In conclusion, litmomycin inhibits DNA polymerase activity of RNA tumor viruses by interaction with (riboadenylate)$_n$–(deoxythymidylate)$_n$ or adenine–thymine bases and (ribocytidylate)$_n$–(deoxyguanylate)$_n$ or cytosine–guanine bases with a different degree of binding. It may be of interest to investigate the antiviral activity of litmomycin in cell culture.

REFERENCES

(1) H. M. Temin and S. Mizutani, *Nature*, **226**, 1211(1970).

(2) S. Spiegelman, A. Burny, M. R. Das, J. Keydar, J. Schlom, M. Travnicek, and K. Watson, *ibid.*, **227**, 563(1970).

(3) H. M. Temin and D. Baltimore, *Adv. Virus Res.*, **17**, 129(1972).

(4) P. Sarin and R. C. Gallo, in "International Review Science Series in Biochemistry," vol. 6, K. Burton, Ed., Butterworth and Medical and Technical Publishing Co., Oxford, England, 1974, chap. 8.

(5) M. M. Lieber, R. E. Benveniste, D. M. Livingston, and G. J. Todaro, *Science*, **182**, 59(1973).

(6) R. C. Gallo, *Nature*, **234**, 194(1971).

(7) H. M. Temin, *Cancer Res.*, **34**, 2835(1974).

(8) R. E. Gallagher and R. C. Gallo, *Science*, **187**, 250(1975).

(9) T. Mak, M. Aye, H. Messner, R. Sheinin, J. Till, and E. McCullough, *Br. J. Cancer*, **29**, 433(1974).

(10) R. C. Gallo, *Biomedicine*, **18**, 446(1973).

(11) H. Hanafusa and T. Hanafusa, *Virology*, **43**, 313(1971).

(12) P. S. Sarin, J. W. Abrell, and R. C. Gallo, "Control of Transcription," Plenum, New York, N.Y., 1974, pp. 345–353.

(13) R. C. Gallo, *Blood*, **39**, 117(1972).

(14) V. S. Sethi and M. L. Sethi, *Biochem. Biophys. Res. Commun.*, **63**, 1070(1975).

(15) P. Soong and A. A. Au, *Rep. Taiwan Sugar Exp. Stn.*, **29**, 33(1962).

(16) P. Soong, Y. Y. Jen, Y. S. Hsu, and A. A. Au, *ibid.*, **34**, 105(1974).

(17) G.-J. Chang, H. G. Floss, P. Soong, and C.-T. Chang, *Jpn. Antibiot. Res. Assoc.*, **28**, 156(1975).

(18) D. L. Kacian and S. Spiegelman, in "Methods in Enzymology," vol. 29E, L. Grossman and K. Moldave, Eds., Academic, New York, N.Y., 1973, p. 150.

(19) J. Bhattacharyya, M. Xuma, M. Reitz, P. S. Sarin, and R. C. Gallo, *Biochem. Biophys. Res. Commun.*, **54**, 324(1973).

ACKNOWLEDGMENTS AND ADDRESSES

Received November 10, 1975, from the *Department of Biomedicinal Chemistry, College of Pharmacy and Pharmacal Sciences, Howard University, Washington, DC 20059*

Accepted for publication March 4, 1976.

The author thanks Dr. H. G. Floss, Purdue University, for a gift sample of litmomycin. The arrangements made by Dr. Jack Gruber and Dr. M. A. Chirigos, National Institutes of Health, for the supply of reverse transcriptase are gratefully acknowledged. The technical help of Mr. Warren W. Schadt in the liquid scintillation counting is appreciated.

GLC Determination of Indoprofen in Plasma

ROBERT V. SMITH ˣ, DAVID W. HUMPHREY, and HENRY ESCALONA-CASTILLO

Abstract □ Implementation of human bioavailability studies with the analgesic indoprofen required a rapid, sensitive, and convenient assay in blood plasma. A procedure based on ether extraction of acidified plasma, derivatization with diazomethane, and GLC analysis using a 3% OV-1 column was sufficiently sensitive for measurement of plasma indoprofen concentrations in the 0.4–16-μg/ml range. An average recovery of 99.0 ± 7.6% (*SD*) was achieved when the pentanoic acid homolog was employed as an internal standard.

Keyphrases □ Indoprofen—GLC analysis, human plasma □ GLC—analysis, indoprofen in human plasma □ Analgesics—indoprofen, GLC analysis in human plasma

Indoprofen, *dl*-2-[4-(1-oxo-2-isoindolinyl)phenyl]propanoic acid (I), possesses promising analgesic and anti-inflammatory properties (1, 2). In humans, I reportedly appears unchanged in plasma (3). Furthermore, enantiomeric enrichment does not seem to be significant in humans (4). Implementation of human bioavailability studies in this laboratory required a rapid, sensitive, and convenient assay of I in blood plasma.

Two GLC methods were reported for the determination of I in plasma (4, 5). Both procedures employ a lengthy series of partition steps. In one (4), a trifluoroethyl ester

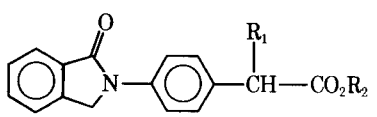

I: $R_1 = CH_3$, $R_2 = H$

II: $R_1 = CH_2CH_2CH_3$, $R_2 = H$

III: $R_1 = CH_3$, $R_2 = CH_3$

IV: $R_1 = CH_2CH_2CH_3$, $R_2 = CH_3$

is utilized after preparation with boron trifluoride–trifluoroethanol. The latter reagent is corrosive and difficult to eliminate prior to GLC development. The other method (5) involves preparation and resolution of a diastereomeric pair of amides obtained through reaction of I (as its acid chloride) with *l*-α-methylbenzylamine. While useful in evaluating *in vivo* enantiomeric interconversions, this procedure is not amenable to analyses of large numbers of samples because of its length.

A simplified assay based on a single ether extraction and GLC of I and the internal standard, *dl*-2-[4-(1-oxo-2-isoindolinyl)phenyl]pentanoic acid (II), as their methyl esters (III and IV) was developed and is the subject of this report.

EXPERIMENTAL

Reagents and Materials—Compounds I, II[1], and *N*-methyl-*N*-nitroso-*N'*-nitroguanidine[2] were used as obtained. All other solvents and reagents were analytical reagent grade. GLC columns were prepared with 3% OV-1 on acid-washed silanized Chromosorb W, 100–120 mesh[3].

Reference Methyl Esters—Compound I (1.01 g) was dissolved in 5 ml of methanol; 3 ml of 30% (w/w) boron trifluoride in methanol was added, and the resulting mixture was refluxed for 15 min. The reaction mixture was cooled, reduced to near dryness *in vacuo*, and shaken with 20 ml of water for 5 min. A white precipitate was collected by filtration, and the filtrate was extracted three times with 10 ml of ethyl acetate. The ethyl acetate extracts were combined with the previously collected precipitate, and the total product was crystallized from methanol–acetone (10:1) with a few drops of water to give 1.06 g (100%) of III as white plates, mp 120–122° [lit. (1) mp 124–126°]; mass spectrum, M^+ = 295; GLC, single peak, t_R (solvent front) = 2.87 min.

Compound II (1.00 g) was reacted in the same fashion. Crystallization from methanol–acetone (10:1) with a few drops of water gave 0.99 g (95%) of IV as white plates, mp 125–126°; mass spectrum, M^+ = 323; GLC, single peak, t_R (solvent front) = 4.22 min.

GLC System and Conditions—All chromatography was performed with U-shaped glass columns [0.61 m (2 ft) × 4 mm i.d.] packed with 3% OV-1 on acid-washed silanized Chromosorb W, 100–120 mesh[3]. All newly prepared columns were conditioned at 260° with carrier gas flowing (30 ml/min) for 12 hr. The columns were fitted into a gas chromatograph[4] equipped with dual flame-ionization detectors.

The chromatograph was operated under the following conditions: column and injection port temperature, 255°; detector temperature, 300°; carrier gas (nitrogen) flow, 30 ml/min; hydrogen and air flows, 40 and 300 ml/min, respectively; sensitivity (input attenuation), 10^2 (Mohm); and range, 8 (× 0.01 v). Injections were performed with a 10-μl syringe[5].

Diazomethane Reagent—*N*-Methyl-*N*-nitroso-*N'*-nitroguanidine (296 mg) was reacted with 4 ml of 2 *N* sodium hydroxide in a separator containing 40 ml of ether. The ether solution resulting was sufficient for derivatizing 10 samples and was prepared fresh daily.

Assay Procedure—All glassware was washed in detergent, soaked for 12 hr in alcoholic potassium hydroxide (1000 ml of ethanol added to 120 ml of water and 120 g of potassium hydroxide), thoroughly rinsed with water, silanized by rinsing with 2% trimethylchlorosilane in benzene, and dried at 100° for 15 min.

Preparation of Standards—To six blank plasma samples contained in 60-ml separators, add 2, 4, 6, 10, 12, and 20 μg of I along with 10 μg of II (contained in a total of 2 ml of methanol) and 4 ml of 0.1 *N* hydrochloric acid. Extract and analyze standards in the same manner as described for plasma samples.

Preparation of Samples—Place 2 ml of plasma in a glass-stoppered 60-ml separator and add 10 μg of II (in 2 ml of methanol), 4 ml of 0.1 *N* hydrochloric acid, and 40 ml of ether. Extract by shaking for 5 min and transfer the ether layer to a 50-ml conical flask; evaporate to dryness *in vacuo* at 40° with a rotary evaporator. Add 0.5 ml of methanol and 4 ml of ethereal diazomethane reagent and allow to react at room temperature for 15 min; quench the reaction (loss of yellow color and cessation of effervescence) by dropwise addition of ethyl acetate–acetic acid (10:1).

Reduce the final reaction mixture (~5 ml) in volume (to ~1 ml) *in vacuo* at 40° with a rotary evaporator; reduce the final volume to dryness under a stream of nitrogen at 25° to assure concentration of the residual solids in the tip of the conical flask. Redissolve the residue in 50 μl of ethyl acetate and inject 5 μl into the chromatograph.

Dilute samples that appear to contain greater than 8 μg of I/ml (from the initial GLC development) with an equal volume of ethyl acetate and chromatograph a 5-μl aliquot.

Calculations—The peak heights for III and IV are measured. Peak height ratios are obtained by dividing the peak height of III by the peak height of IV. Calibration curves are prepared by plotting peak height ratios from the standards *versus* the concentration of I in plasma, expressed as micrograms per milliliter. Values for unknown concentrations of I in sample plasma specimens are obtained by interpolation or calculated from the slope of the calibration curve. Once established, the standard curve need only be revalidated on a day-to-day basis with two or three standard samples.

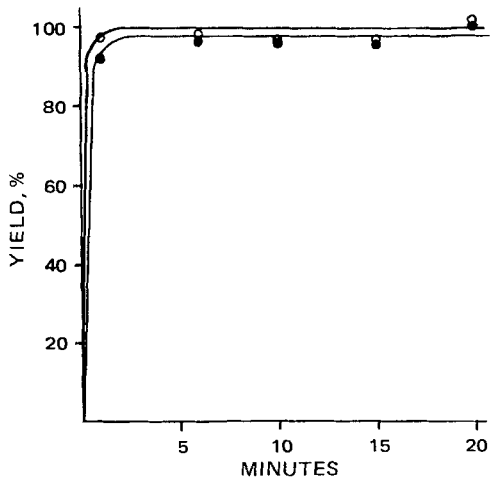

Figure 1—*Diazomethylation of I (●) and II (○).*

RESULTS AND DISCUSSION

Derivatization of I and II—GLC determination of I was initially attempted through use of its trifluoroethyl ester. The latter was reproducibly prepared in good yield through use of the boron trifluoride–trifluoroethanol reagent described previously (4). However, for biological samples containing low microgram amounts of I, it is necessary to eliminate the excess derivatization reagent completely prior to the GLC step, because the broad solvent peak produced by the latter obliterates the drug derivative. Unfortunately, reagent evaporation was not readily accomplished, apparently due to the poor volatility of alcohol–boron trifluoride mixtures[6].

Diazomethylation was studied as an alternative derivatization method[7]. When I and II were reacted with ethereal diazomethane at room temperature in the presence of approximately 10% methanol, essentially quantitative yields of methyl esters were rapidly formed (Fig. 1). Side reactions (6) and reagent polymerization (7) are potential problems with diazomethane. However, if methylation is catalyzed with methanol, these problems are reportedly minimized (7), as was evident in studies with I and II. An impurity appearing at the same retention time as III was observed when *N*-methyl-*N*-nitroso-*p*-toluenesulfonamide[8] was employed as a diazomethane-generating reagent. This apparent impurity was probably reagent derived since it did not appear when *N*-methyl-*N*-nitroso-*N'*-nitroguanidine was employed as indicated under *Experimental.*

Assay Selectivity—After confirming the reported high recovery of I and II from acidified aqueous solutions by extraction with ether (4, 5), the potential selectivity afforded by a single liquid–liquid extraction derivatization procedure was studied. Gas chromatograms resulting from this investigation are depicted in Fig. 2 and reveal no interfering peaks at the retention times for III and IV. Essentially identical chromatograms to those in Fig. 2 were produced when derivatized extracts from plasma samples of 10 different individuals were similarly treated.

Accuracy, Precision, and Convenience—Compounds I and II were added at levels of 1–10 μg/ml to 2-ml volumes of blank plasma samples. The spiked specimens were extracted with ether, and the latter extracts were derivatized and chromatographed according to the described procedure.

The peak heights of the resulting esters (III and IV) were compared to calibration curves prepared with authentic samples of III and IV. The absolute recoveries of I and II from plasma were 69.8% (n = 5) and 71.2% (n = 5), respectively. These results indicate that II could serve as a suitable internal standard for the determination of I.

Accordingly, blank plasma samples were spiked with 0.4–8-μg/ml concentrations of I and 5 μg/ml of II and analyzed using a standard curve prepared with triplicate standards equivalent to 0.4, 1.0, 3.0, 5.0, and 8.0 μg/ml of I in plasma (slope = 0.262; y-intercept essentially zero; r = 0.997). The accuracy and precision of these determinations are presented in Table I. The excellent recovery and acceptable reproducibility observed

[1] Adria Laboratories, Wilmington, Del.
[2] Aldrich Chemical Co., Milwaukee, Wis.
[3] Chromosorb W HP, Analabs, North Haven, Conn.
[4] Schimadzu GC-4BM, American Instrument Co., Silver Spring, Md.
[5] Hamilton 701 N.

[6] This was also found to be true when boron trifluoride–methanol was evaluated as a possible derivatization reagent.
[7] *N,O*-Bis(trimethylsilyl)acetamide was tried as a derivatization reagent. However, the trimethylsilyl esters of I and II did not chromatograph well.
[8] Diazald, Aldrich Chemical Co., Milwaukee, Wis.

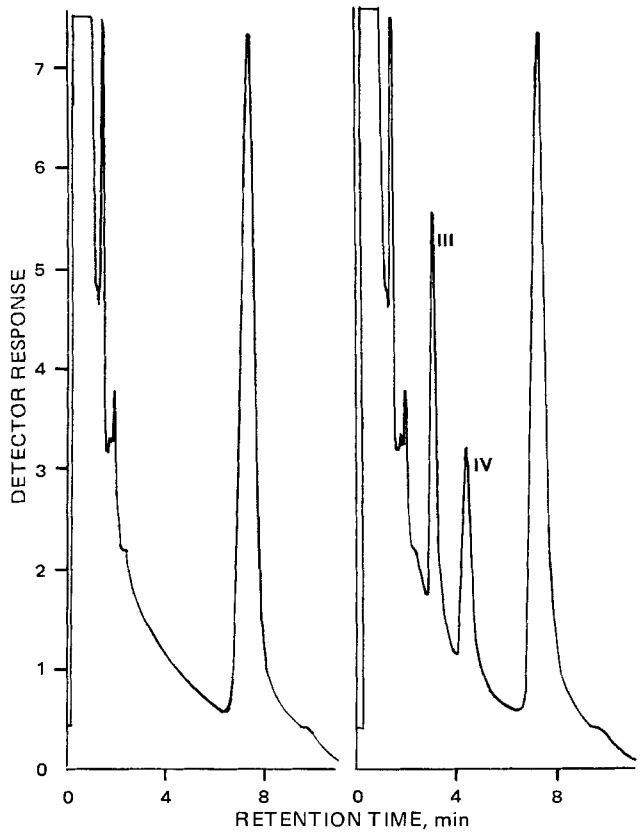

Figure 2—*Gas chromatograms of derivatized human plasma extracts. Key: left, normal plasma specimen; right, plasma specimen containing 6.6 μg of I/ml and 5.0 μg of II/ml; III, indoprofen methyl ester; and IV, internal standard methyl ester.*

provide good evidence for the utility of the developed method for plasma levels of I down to 0.4 μg/ml.

During routine analyses, it was found that a standard curve prepared on Day 1 (as described in *Experimental*) is validated day after day by simple comparison of results from two or three standard samples. In a recent series of determinations, for example, two to five (total = 13) standard samples were analyzed on 4 separate days over a 3-week period. After plotting the data from these determinations, a curve was produced with a slope of 0.269, an r of 0.999, and a y-intercept essentially equal to zero. These data are in excellent agreement with the parameters of the standard curve utilized in evaluating the accuracy and precision of the method and support the utility of the proposed method for routine determinations.

Table I—Accuracy and Precision of GLC Method for I

Concentration of I, μg/ml		
Added	Found	Recovery, %
0.4	0.40	100
0.4	0.41	103
1.0	0.82	82.0
1.0	1.00	100
1.0	1.12	112
3.0	2.65	88.3
3.0	2.99	99.7
3.0	3.08	103
5.0	4.55	91.0
5.0	5.06	101
5.0	5.36	107
8.0	7.55	94.4
8.0	7.73	96.6
8.0	8.16	102
8.0	8.39	105
Mean = 99.0% (n = 15)		
SD = ±7.6%		

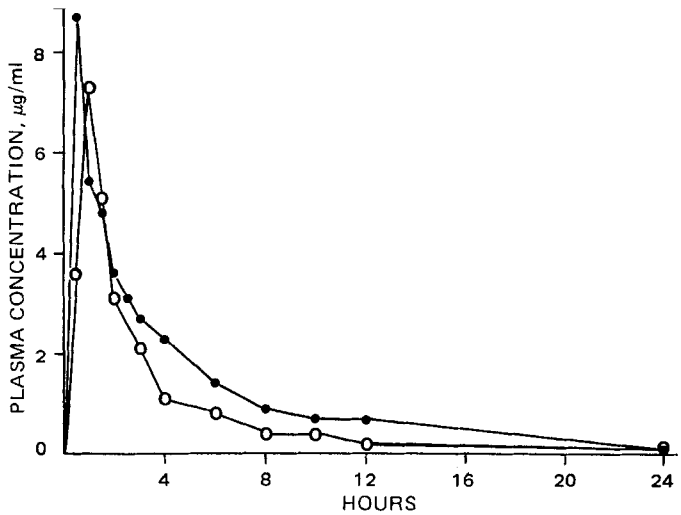

Figure 3—*Individual plasma levels of indoprofen following oral administration of single 100-mg capsules to two subjects as determined by the GLC method. Values less than 0.4 μg/ml are approximations only, since the method was not validated at concentrations below this level.*

The described method was devised as a convenient and more rapid procedure than those reported previously (4, 5). During ordinary usage, the described method permits analysis of 15 samples/one-worker day. This is a marked improvement over the 3–4 hr/sample required to assay I by the previously reported boron trifluoride–trifluoroethanol procedure (4), which is estimated to be the shorter of the two methods described in the literature (4, 5).

Plasma levels obtained in two patients administered single oral doses of 100 mg (capsules) of I were followed with the method described. Results of these analyses are presented in Fig. 3 and nicely parallel the findings published by Tosolini *et al.* (4).

REFERENCES

(1) G. Nannini, P. N. Giraldi, G. Molgora, G. Biasoli, F. Spinelli, W. Logemann, E. Dradi, G. Zanni, A. Buttinoni, and R. Tommasini, *Arzeim.-Forsch.*, **23**, 1090 (1973).

(2) A. Buttinoni, A. Cuttica, J. Franceschini, V. Mandelli, G. Orsini, N. Passerini, C. Turba, and R. Tommasini, *ibid.*, **23**, 1100 (1973).

(3) L. M. Fuccella, G. C. Coldaniga, E. Moro, V. Tamassia, G. P. Tosolini, and G. Valzelli, *Eur. J. Clin. Pharmacol.*, **6**, 256 (1973).

(4) G. P. Tosolini, A. Forgione, E. Moro, and V. Mandelli, *J. Chromatogr.*, **92**, 61 (1974).

(5) G. P. Tosolini, E. Moro, A. Forgione, M. Ranghieri, and V. Mandelli, *J. Pharm. Sci.*, **63**, 1072 (1974).

(6) M. L. Vorbech, L. R. Mattick, F. A. Lee, and C. S. Pederson, *Anal. Chem.*, **33**, 1513 (1961).

(7) H. Schlenk and J. L. Gellerman, *ibid.*, **32**, 1412 (1960).

ACKNOWLEDGMENTS AND ADDRESSES

Received December 22, 1975, from the *Drug Dynamics Institute, College of Pharmacy, University of Texas at Austin, Austin, TX 78712.*

Accepted for publication March 8, 1976.

Supported in part by a grant from Adria Laboratories, Wilmington, Del.

The authors are grateful to Ms. B. Diane Phillips for technical assistance.

[x] To whom inquiries should be directed.

Application of Salivary Concentration Data to Pharmacokinetic Studies with Antipyrine

PETER J. MEFFIN *x, ROGER L. WILLIAMS ‡, TERRENCE F. BLASCHKE ‡§, and MALCOLM ROWLAND *¶

Abstract □ The concentrations of antipyrine in plasma and saliva were equivalent in normal volunteers and in patients with acute viral hepatitis following oral doses of antipyrine. Estimates of clearance, volume of distribution, and half-life made from either plasma or saliva samples were not statistically different in these subjects. Differences in the disposition kinetics of antipyrine during the acute phase of viral hepatitis and on recovery were detected using either plasma or saliva samples.

Keyphrases □ Antipyrine—pharmacokinetics, normal subjects and hepatitis patients, plasma and saliva concentration data □ Pharmacokinetics—antipyrine, normal subjects and hepatitis patients, plasma and saliva concentration data □ Analgesics—antipyrine, pharmacokinetics, normal subjects and hepatitis patients, plasma and saliva concentration data

Antipyrine, used as an investigational marker of drug metabolism in humans, is thought to be metabolized in the liver; when given orally, less than 0.1% of the dose is excreted unchanged in the stool and less than 5% is excreted unchanged in the urine (1). The plasma half-life of antipyrine has small intrasubject variability (2–5) and has been correlated with genetic (2, 5, 6) and environmental (2, 3) factors, sex, and age (7). The antipyrine half-life or clearance also correlates with the half-life or clearance of phenylbutazone (4), phenytoin (8), and warfarin (9). However, no significant correlation was found between the antipyrine half-life and the half-life of amobarbital, glutethimide, or sulfinpyrazone (10). Because the many studies with antipyrine may eventuate in its use as a marker of drug metabolism, we decided to investigate the possibility that the disposition kinetics of antipyrine could be determined by studying the concentrations of antipyrine in saliva.

The concentrations of drugs in saliva have been used to determine the disposition kinetics of many drugs [*e.g.*, salicylate (11), theophylline (12), acetaminophen (13), digoxin (14), sulfonamides (15, 16), and tolbutamide (17)]. In humans, the concentration of antipyrine in saliva correlates with that in plasma (18).

Recently, two papers reported the equivalence of antipyrine concentrations in plasma and saliva and demonstrated the utility of salivary antipyrine measurements in estimating pharmacokinetic parameters in normal subjects and epileptic patients (19, 20). The present study confirmed these findings and extends the use of antipyrine salivary concentrations by demonstrating their validity in patients with acute viral hepatitis.

EXPERIMENTAL

Subjects and Treatment—Subjects 1 and 2 were normal, healthy, male volunteers who weighed 70.1 and 75 kg, respectively. Subjects 3 and 4 were studied during the acute phase of viral hepatitis (Studies 3A and 4A) and after recovery (Studies 3B and 4B); these latter studies took place 2–6 weeks after the initial study and after biochemical indexes of hepatic function had returned to normal. Subjects 3 and 4 weighed 51.0 and 60.5 kg, respectively.

Each subject fasted for approximately 12 hr before and 1 hr after ingesting 250 ml of an aqueous solution containing 1.0 g of antipyrine. During the first 8 hr, blood was drawn from a peripheral vein *via* an indwelling catheter; venipuncture was used thereafter. Heparin was used to prevent coagulation; plasma was obtained by centrifugation. Plasma samples were obtained prior to each dose for use as an analytical blank.

Saliva was collected at the same time that blood was drawn. If saliva flow was insufficient, the subjects chewed on a piece of plastic film[1] for 3 min; they then expectorated into a sampling container. Each saliva sample collected from Subjects 1 and 2 was weighed to determine the effect of saliva flow on antipyrine concentration. After each dose, the patients rinsed their mouths thoroughly before providing the first saliva sample. All plasma and saliva samples were frozen until they were analyzed.

Procedure—The following were added to a 15-ml tube fitted with a lined screw cap[1]: 0.5–2 ml of plasma or 0.5–2 g of saliva, both containing an estimated 1.0–30 μg of antipyrine; internal standard solution (10 μg of 4-bromoantipyrine[2] in 0.1 ml of water); and 7 ml of dichloromethane. The tube was then gently shaken by hand for 10 min and centrifuged. The organic phase was transferred carefully to a second 15-ml tube, which had a conical tip at its base, and the solvent was evaporated to dryness on a water bath at 45°. Immediately before injection into the gas chromatograph, 15 μl of distilled water was added to the tube and mixed gently.

Approximately 5 μl of water was injected into the gas chromatograph with a flame-ionization detector[3]. A glass column (1.8 m long and 0.32 cm o.d.), packed with a 3% OV-17 on 100–120-mesh Gas Chrom Q[4], was used. The injector port, fitted with a glass liner, was maintained at 150°; the oven was kept at 220°, and the detector was kept at 250°. The injector port liner was changed and the column was treated with a silylating agent[5] prior to each day's analyses.

Under these conditions, antipyrine and the internal standard had retention times of 1.6 and 3.5 min, respectively. Calibration curves, obtained by adding known amounts of antipyrine to samples of plasma and saliva and taking them through the analytical procedure, had an average coefficient of variation of 5.6% in the 1–30-μg range.

Data Analysis—A log-linear least-squares method was used to fit the data obtained in the postabsorptive period (usually those data obtained at times greater than 1 hr after dosing) to a straight line and thus to estimate the plasma and saliva half-life ($t_{1/2}$) values. Clearance was determined by dividing the dose by the area under the saliva and plasma concentration–time data sets (AUC) from zero to infinite time. The oral dose was assumed to be completely absorbed (21). The trapezoidal rule was used to determine the AUC. The area beyond the last data point was estimated by dividing the least-squares estimate of the concentration at that time by the elimination rate constant. The volume of distribution of antipyrine was determined using (22):

$$\text{volume of distribution} = \frac{\text{clearance} \times t_{1/2}}{0.693} \qquad \text{(Eq. 1)}$$

The correlation between plasma and saliva antipyrine concentrations was determined by standard regression analysis techniques. A paired t-test was used to compare the pharmacokinetic parameters in plasma to those in saliva for each individual.

RESULTS AND DISCUSSION

Comparison of Salivary and Plasma Concentrations—The results

[1] Teflon (du Pont).
[2] Melting point 110–113°.
[3] Model 1200, Varian, Palo Alto, Calif.
[4] Applied Science Laboratories, State College, Pa.
[5] Silyl-8, Pierce Chemical Co., Rockford, Ill.

Table I—Regression Analysis of Antipyrine Concentrations Measured in Saliva against Those Found in Plasma

Study	r	p
All data	0.958	<0.01
Study A data	0.967	<0.01
Nonstudy A data[a]	0.926	<0.01
Subject 1	0.909	<0.01
Subject 2	0.984	<0.01
Subject 3 (Studies A and B)	0.966	<0.01
Subject 4 (Studies A and B)	0.992	<0.01

[a] All data minus Study A data.

of the regression analysis of the plasma and saliva antipyrine concentrations are shown in Table I. As indicated, the correlation coefficients were all statistically significant.

Although the overall ratio between saliva and plasma concentrations was very close to 1, the correlation coefficients in Table I show that there was considerable scatter in the data. The major contribution to this scatter was probably analytical error. Because of the scatter, the ability to estimate plasma concentration from a single saliva antipyrine determination may err in the order of 20% at low antipyrine concentrations where analytical error is greatest. However, this limitation may not affect the use of saliva antipyrine concentrations in pharmacokinetic investigations involving multiple determinations.

These studies are in agreement with two recent reports which found no significant differences between saliva and plasma antipyrine concentrations in normal subjects (19, 20) and epileptic patients (19). When data from individuals with acute viral hepatitis were analyzed separately (Study A data, Table I), no apparent change in the correlations was observed, either for data obtained during disease or for the remaining analyses. This particular disease state apparently did not alter the ratio of saliva to plasma concentrations of antipyrine.

The influence of saliva flow on the ratio of antipyrine concentrations found in saliva to those found in plasma was examined by plotting this ratio *versus* the weight of saliva collected during 3 min (Fig. 1). The lack of correlation (r = 0.034) suggests that partitioning of antipyrine between saliva and plasma is independent of saliva flow.

Estimation of Pharmacokinetic Parameters—Table II shows the estimates of clearance, half-life, and volume of distribution for each study as calculated from saliva and plasma concentration–time data sets. No significant differences were noted between these estimates. Similar findings were reported recently (19, 20). The agreement in Table II is better than might have been anticipated, primarily because the multiple concentration data tend to average out analytical error. Salivary data could have been used to detect the difference in the pharmacokinetic parameters of Subject 4 during the acute phase of hepatitis (Study 4A, Fig. 2) and after the subject recovered (Study 4B, Fig. 2). It is in comparison studies of this sort that the use of salivary concentration will be most applicable. Saliva antipyrine concentration measurements have also been used to detect differences in antipyrine pharmacokinetic parameters in epileptic patients treated with anticonvulsants compared to those found in normal volunteers (19).

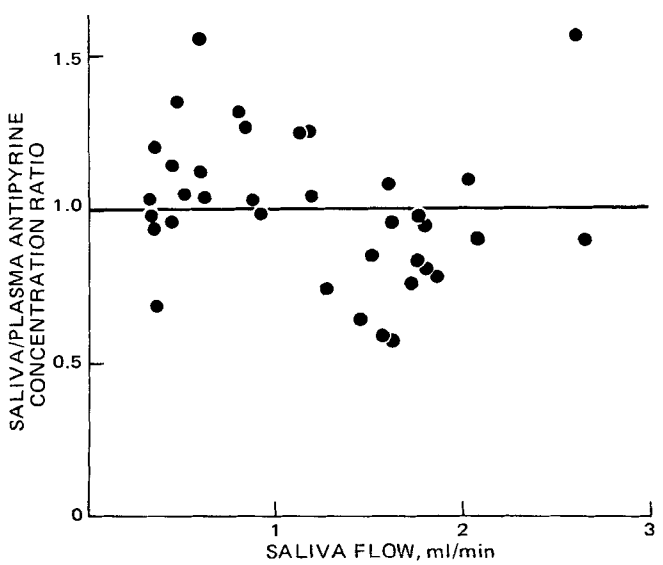

Figure 1—*Ratios of the concentrations of antipyrine in saliva to those in plasma* versus *the saliva flow during the 3-min collection period. The line would be obtained if the ratio were independent of plasma flow.*

Table II—Pharmacokinetic Parameters for Antipyrine Calculated from Saliva and Plasma Concentration–Time Data

	Clearance, ml/hr/kg		Volume of Distribution, liter/kg		Half-Life, hr	
Subject	Plasma	Saliva	Plasma	Saliva	Plasma	Saliva
1	38.8	38.2	0.71	0.64	12.7	11.6
2	34.1	40.2	0.60	0.60	12.1	10.3
3A	8.9	10.9	0.58	0.66	45.0	42.3
3B	58.0	50.8	0.80	0.63	9.4	8.6
4A	30.0	29.5	0.53	0.50	12.2	11.8
4B	45.9	48.5	0.49	0.54	7.5	7.8
Mean	36.0	36.6[a]	0.62	0.60[a]	16.5	15.4[a]

[a] These pairs of values were not significantly different.

Estimates of antipyrine clearance may effectively serve as a standard for evaluating the clearance of other drugs metabolized in the liver, although caution must be used in interpreting the results (23). The potential widespread clinical use of antipyrine clearance as an index of the capacity of the liver to metabolize drugs is enhanced because concentrations of antipyrine are equal in plasma and in saliva, because multiple saliva samples are easily obtained, and because determinations can be made by a simple GLC assay. If useful correlations between antipyrine clearance and the clearance of other drugs could be established, then the complete oral availability of antipyrine (21) and its low toxicity would make antipyrine a suitable test drug for individualizing doses of drugs that exhibit large intersubject variability in clearance. Data presented in this paper and elsewhere (19) indicate that it may prove possible to use saliva antipyrine concentration measurements to detect changes in pharmacokinetic parameters resulting from disease and coadministration of other drugs.

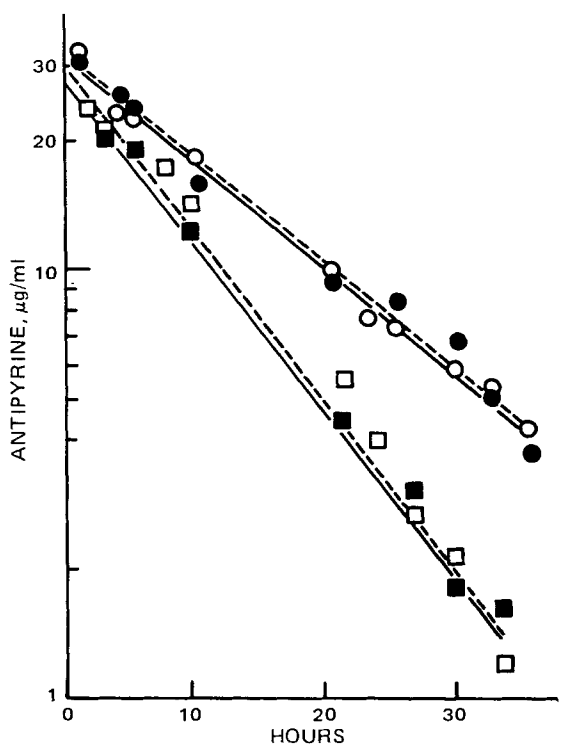

Figure 2—*Antipyrine concentrations in plasma (solid symbols, micrograms per milliliter) and in saliva (open symbols, micrograms per milliliter) at various times after a 1-g oral dose of antipyrine in Subject 4 during the acute phase of viral hepatitis (Study 4A, ○, ●) and after recovery (Study 4B, □, ■).*

REFERENCES

(1) B. B. Brodie and J. Axelrod, *J. Pharmacol. Exp. Ther.*, **98**, 97 (1950).

(2) E. S. Vesell, *Clin. Pharmacol. Ther.*, **16**, 135 (1974).

(3) B. Komodin, D. L. Azarnoff, and F. Sjoquist, *ibid.*, **10**, 638 (1969).

(4) D. S. Davies and S. S. Thorgeirsson, *Ann. N.Y. Acad. Sci.*, **179**, 411 (1971).

(5) E. S. Vesell and J. G. Page, *Science*, **161**, 72 (1968).

(6) E. S. Vesell and J. G. Page, *J. Clin. Invest.*, **48**, 2202 (1969).

(7) K. O'Malley, J. Crooks, E. Duke, and I. H. Stevenson, *Br. Med. J.*, **3**, 607 (1971).

(8) D. S. Davies, in "The Assessment of Drug Metabolism in Man—Methods and Clinical Applications," Abstracts of Symposium, Medical Sciences Institute, University of Dundee, Scotland, 1974.

(9) D. S. Hewick and J. McEwen, in *ibid.*

(10) D. Kadar, T. Inaba, L. Endrenyi, G. E. Johnson, and W. Kalow, *Clin. Pharmacol. Ther.*, **14**, 552 (1973).

(11) G. Graham and M. Rowland, *J. Pharm. Sci.* **61**, 1219 (1972).

(12) R. Koysooko, E. F. Ellis, and G. Levy, *Clin. Pharmacol. Ther.*, **15**, 454 (1974).

(13) J. P. Glynn and W. Bastain, *J. Pharm.*, **25**, 420 (1973).

(14) D. H. Huffman, *Clin. Pharmacol. Ther.*, **17**, 310 (1975).

(15) S. A. Killman and J. H. Thoysen, *Scand. J. Clin. Lab. Invest.*, **1**, 86 (1955).

(16) F. Rasmussen, *Acta Pharmacol. Toxicol.*, **21**, 11 (1964).

(17) S. B. Matin, S. H. Wan, and J. H. Karam, *Clin. Pharmacol. Ther.*, **16**, 1052 (1974).

(18) R. L. DeAngelis and R. M. Welch, *Fed. Proc.*, **33**, 534 (1974).

(19) R. M. Welch, R. L. DeAngelis, M. Wingfield, and T. W. Farmer, *Clin. Pharmacol. Ther.*, **18**, 249 (1975).

(20) E. S. Vesell, G. T. Passananti, P. A. Glenwright, and B. H. Dvorchik, *ibid.*, **18**, 259 (1975).

(21) P. B. Andreasen and E. S. Vesell, *ibid.*, **16**, 1059 (1974).

(22) M. Rowland, "Clinical Pharmacology: Basic Principles in Therapeutics," Macmillan, New York, N.Y., 1972, p. 44.

(23) E. S. Vesell, G. T. Passananti, and K. C. Aurori, *Pharmacology*, **13**, 101 (1975).

ACKNOWLEDGMENTS AND ADDRESSES

Received January 5, 1976, from the **Department of Pharmacy, School of Pharmacy, and the †Division of Clinical Pharmacology, Department of Medicine, University of California, San Francisco, CA 94143.*

Accepted for publication March 16, 1976.

Supported by National Institutes of Health Grants GM 16496, GM 01791, and GM 00001 and Training Grant GM 00728-13.

The authors thank Dr. Ronald Sawchuck for the 4-bromoantipyrine sample.

§ Present address: Division of Clinical Pharmacology, Stanford School of Medicine, Stanford, CA 93405. T. F. Blaschke is the recipient of a Faculty Development Award in Clinical Pharmacology from the Pharmaceutical Manufacturers Association Foundation.

¶ Present address: Department of Pharmacy, University of Manchester, Manchester, M13 9PL, England.

ˣ To whom inquiries should be directed. Present address: Division of Cardiology, Stanford School of Medicine, Stanford, CA 94305.

Application of a Convective Diffusion Model to Membrane Transport

K. G. NELSON * and A. C. SHAH ‡ˣ

Abstract □ Studies were carried out on the permeation rate of butamben through a dimethicone membrane. Under conditions of "aqueous diffusion layer control," the permeation rate was accurately described by a mathematical model based on convective diffusion theory. In accordance with the model, the rate of permeation from a saturated donor phase was shown to be equal to the rate of dissolution from a pure solid.

Keyphrases □ Diffusion, convective—model applied to permeation rate of butamben through dimethicone membrane □ Membrane transport—convective diffusion model applied to permeation rate of butamben through dimethicone membrane □ Permeation rate—butamben through dimethicone membrane, convective diffusion model □ Butamben—permeation rate through dimethicone membrane, convective diffusion model

One fundamental process that occurs during drug absorption is the transport of the active ingredient across various biological membranes. The study of membrane transport is thus of considerable interest, and the theoretical aspects of permeation models were recently reviewed (1).

In the model most frequently used to describe membrane transport, the membrane is considered to be in series with a stagnant or unstirred liquid diffusion layer on each side (2–5). For a liquid flowing past a surface, however, fluid flow occurs even at very small distances from the solid. Therefore, convective diffusion theory that accounts for fluid flow as well as diffusion should be applied (6). The differential equation of convective diffusion theory requires a mathematical description of the liquid flow past the dissolving surface. Although flow profiles are generally nonlinear, a constant velocity gradient can be assumed if the dissolving surface is relatively short (7, 8). Such a model recently was applied to describe drug dissolution into a moving liquid (9, 10). The purpose of this study was to evaluate the application of convective diffusion theory to membrane transport under conditions where transport across the dynamic liquid layer adjacent to the membrane is the rate-limiting step.

EXPERIMENTAL

The laminar flowcell was a modification of the dissolution cell described previously (10). The dissolution cell was adapted for membrane transport studies by constructing a donor compartment in the die such that the membrane would be positioned coplanar with the die surface. As shown in Fig. 1, the donor compartment consists of a cylindrical metal cup over which the membrane is positioned. When placed in the die as shown, the membrane made a watertight seal over the donor compartment. The donor compartment was stirred with a magnetic stirring bar.

The permeation rates were determined as follows using butamben as the permeating species. The donor cup was filled with an aqueous suspension of butamben and was mounted in the die with the membrane (thickness 0.025 cm) positioned as described. The membrane was prepared as described by Roseman (11). The die was placed in the flowcell, which was leveled and mounted on a vibration-free platform. Distilled

REFERENCES

(1) B. B. Brodie and J. Axelrod, *J. Pharmacol. Exp. Ther.*, **98**, 97 (1950).

(2) E. S. Vesell, *Clin. Pharmacol. Ther.*, **16**, 135 (1974).

(3) B. Komodin, D. L. Azarnoff, and F. Sjoquist, *ibid.*, **10**, 638 (1969).

(4) D. S. Davies and S. S. Thorgeirsson, *Ann. N.Y. Acad. Sci.*, **179**, 411 (1971).

(5) E. S. Vesell and J. G. Page, *Science*, **161**, 72 (1968).

(6) E. S. Vesell and J. G. Page, *J. Clin. Invest.*, **48**, 2202 (1969).

(7) K. O'Malley, J. Crooks, E. Duke, and I. H. Stevenson, *Br. Med. J.*, **3**, 607 (1971).

(8) D. S. Davies, in "The Assessment of Drug Metabolism in Man—Methods and Clinical Applications," Abstracts of Symposium, Medical Sciences Institute, University of Dundee, Scotland, 1974.

(9) D. S. Hewick and J. McEwen, in *ibid.*

(10) D. Kadar, T. Inaba, L. Endrenyi, G. E. Johnson, and W. Kalow, *Clin. Pharmacol. Ther.*, **14**, 552 (1973).

(11) G. Graham and M. Rowland, *J. Pharm. Sci.* **61**, 1219 (1972).

(12) R. Koysooko, E. F. Ellis, and G. Levy, *Clin. Pharmacol. Ther.*, **15**, 454 (1974).

(13) J. P. Glynn and W. Bastain, *J. Pharm.*, **25**, 420 (1973).

(14) D. H. Huffman, *Clin. Pharmacol. Ther.*, **17**, 310 (1975).

(15) S. A. Killman and J. H. Thoysen, *Scand. J. Clin. Lab. Invest.*, **1**, 86 (1955).

(16) F. Rasmussen, *Acta Pharmacol. Toxicol.*, **21**, 11 (1964).

(17) S. B. Matin, S. H. Wan, and J. H. Karam, *Clin. Pharmacol. Ther.*, **16**, 1052 (1974).

(18) R. L. DeAngelis and R. M. Welch, *Fed. Proc.*, **33**, 534 (1974).

(19) R. M. Welch, R. L. DeAngelis, M. Wingfield, and T. W. Farmer, *Clin. Pharmacol. Ther.*, **18**, 249 (1975).

(20) E. S. Vesell, G. T. Passananti, P. A. Glenwright, and B. H. Dvorchik, *ibid.*, **18**, 259 (1975).

(21) P. B. Andreasen and E. S. Vesell, *ibid.*, **16**, 1059 (1974).

(22) M. Rowland, "Clinical Pharmacology: Basic Principles in Therapeutics," Macmillan, New York, N.Y., 1972, p. 44.

(23) E. S. Vesell, G. T. Passananti, and K. C. Aurori, *Pharmacology*, **13**, 101 (1975).

ACKNOWLEDGMENTS AND ADDRESSES

Received January 5, 1976, from the **Department of Pharmacy, School of Pharmacy, and the †Division of Clinical Pharmacology, Department of Medicine, University of California, San Francisco, CA 94143.*

Accepted for publication March 16, 1976.

Supported by National Institutes of Health Grants GM 16496, GM 01791, and GM 00001 and Training Grant GM 00728-13.

The authors thank Dr. Ronald Sawchuck for the 4-bromoantipyrine sample.

§ Present address: Division of Clinical Pharmacology, Stanford School of Medicine, Stanford, CA 93405. T. F. Blaschke is the recipient of a Faculty Development Award in Clinical Pharmacology from the Pharmaceutical Manufacturers Association Foundation.

¶ Present address: Department of Pharmacy, University of Manchester, Manchester, M13 9PL, England.

ˣ To whom inquiries should be directed. Present address: Division of Cardiology, Stanford School of Medicine, Stanford, CA 94305.

Application of a Convective Diffusion Model to Membrane Transport

K. G. NELSON * and A. C. SHAH ‡ˣ

Abstract □ Studies were carried out on the permeation rate of butamben through a dimethicone membrane. Under conditions of "aqueous diffusion layer control," the permeation rate was accurately described by a mathematical model based on convective diffusion theory. In accordance with the model, the rate of permeation from a saturated donor phase was shown to be equal to the rate of dissolution from a pure solid.

Keyphrases □ Diffusion, convective—model applied to permeation rate of butamben through dimethicone membrane □ Membrane transport—convective diffusion model applied to permeation rate of butamben through dimethicone membrane □ Permeation rate—butamben through dimethicone membrane, convective diffusion model □ Butamben—permeation rate through dimethicone membrane, convective diffusion model

One fundamental process that occurs during drug absorption is the transport of the active ingredient across various biological membranes. The study of membrane transport is thus of considerable interest, and the theoretical aspects of permeation models were recently reviewed (1).

In the model most frequently used to describe membrane transport, the membrane is considered to be in series with a stagnant or unstirred liquid diffusion layer on each side (2–5). For a liquid flowing past a surface, however, fluid flow occurs even at very small distances from the solid. Therefore, convective diffusion theory that accounts for fluid flow as well as diffusion should be applied (6). The differential equation of convective diffusion theory requires a mathematical description of the liquid flow past the dissolving surface. Although flow profiles are generally nonlinear, a constant velocity gradient can be assumed if the dissolving surface is relatively short (7, 8). Such a model recently was applied to describe drug dissolution into a moving liquid (9, 10). The purpose of this study was to evaluate the application of convective diffusion theory to membrane transport under conditions where transport across the dynamic liquid layer adjacent to the membrane is the rate-limiting step.

EXPERIMENTAL

The laminar flowcell was a modification of the dissolution cell described previously (10). The dissolution cell was adapted for membrane transport studies by constructing a donor compartment in the die such that the membrane would be positioned coplanar with the die surface. As shown in Fig. 1, the donor compartment consists of a cylindrical metal cup over which the membrane is positioned. When placed in the die as shown, the membrane made a watertight seal over the donor compartment. The donor compartment was stirred with a magnetic stirring bar.

The permeation rates were determined as follows using butamben as the permeating species. The donor cup was filled with an aqueous suspension of butamben and was mounted in the die with the membrane (thickness 0.025 cm) positioned as described. The membrane was prepared as described by Roseman (11). The die was placed in the flowcell, which was leveled and mounted on a vibration-free platform. Distilled

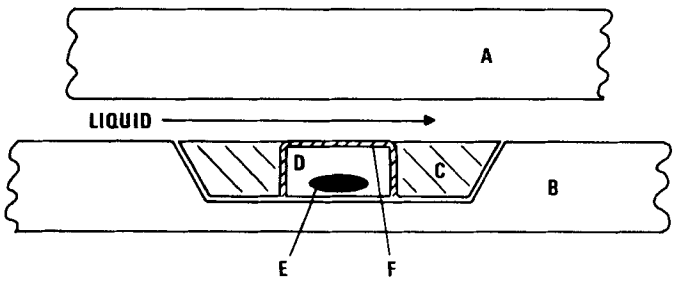

Figure 1—*Cross-sectional view of diffusion cell. Key: A, top plate; B, bottom plate; C, die; D, donor compartment; E, stirring bar; and F, membrane.*

water (25°) was pumped through the flowcell at a set flow rate with an infusion syringe pump[1], and the effluent was assayed spectrophotometrically[2] at 285 nm for the ester concentration. The ester concentration together with the flow rate permitted calculation of the permeation rate.

The permeation rate was studied as a function of the liquid flow rate and membrane area. The former was varied by changing the pump speed, while the latter was changed by using three donor cup–die assemblies with different radii (0.65, 1.0, and 1.25 cm).

RESULTS AND DISCUSSION

Figure 2 is a log–log plot of permeation rate *versus* flow rate. The initial rise followed by a plateau indicates that at low rates the permeation rate is influenced significantly by the transport in the liquid; at the higher flow rates, the major resistance to transport is offered by the membrane. The conditions corresponding to the former case are commonly called "diffusion layer control." Because the membrane offers only negligible resistance to permeation under these conditions, the aqueous concentration of solute at the interface between the membrane and the flowing liquid is equal to the concentration in the donor phase, which in this case is the solubility of the solute. Therefore, at low flow rates, the mathematical model describing the permeation rate should be the same as that used to describe the drug dissolution rate into a moving liquid (9, 10). The model, based on convective diffusion theory, gives the permeation rate, R, as:

$$R = 2.157 D^{2/3} C_0 \alpha^{1/3} r^{5/3} \qquad \text{(Eq. 1)}$$

where D is the diffusivity of the solute in water, C_0 is the solubility (or more generally the concentration of solute in the donor phase), α is the rate of shear over the membrane, and r is the radius of the membrane. The rate of shear immediately over the membrane is given by (10):

$$\alpha = \frac{6Q}{H^2 W} \qquad \text{(Eq. 2)}$$

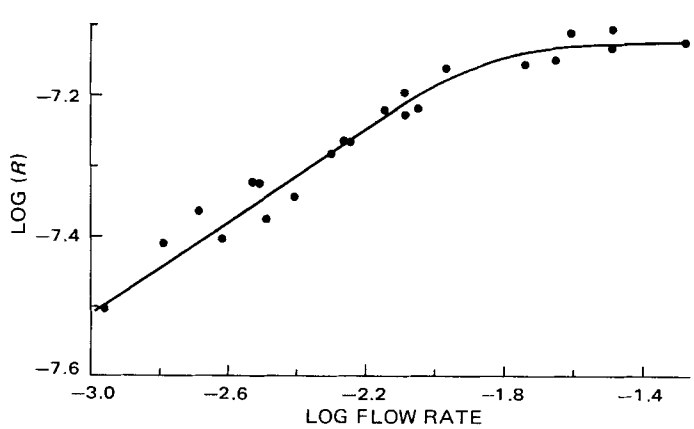

Figure 2—*Log–log plot of the permeation rate,* R, *as a function of the fluid flow rate.*

[1] Model 220, Sage Instruments, Cambridge, MA 02139.
[2] Zeiss recording spectrophotometer DMR 21, Oberkochen/Wuertt, West Germany.

Table I—Permeation Rate as a Function of Fluid Flow Rate

Flow Rate (Q) × 10^3, liters/min	Permeation Rate × 10^8, moles/min
1.00	3.126
1.60	3.880
2.05	4.328
2.38	3.934
2.92	4.740
3.03	4.692
3.24	4.180
3.92	4.497
5.00	5.176
5.50	5.455
5.68	5.400
7.17	5.985
8.12	6.405
8.25	5.886
8.83	6.033
10.70	6.827
18.20	6.967
22.00	7.044
24.30	7.752
32.25	7.295
32.50	7.840
52.50	7.490

where Q is the volumetric flow rate, and H and W are the height and width of the diffusion cell, respectively. Thus, Eqs. 1 and 2 would predict a straight line with a slope of one-third on a plot of log R *versus* log Q. In Fig. 2, a line with a slope of one-third is drawn through the data up to log $Q = -2.0$ to permit visual correlation between theory and experiment. The data are given in Table I, and a statistical analysis of the data up to log $Q = -2.0$ gives a least-squares slope of 0.297 (SD = 0.0215) with a correlation coefficient of 0.9626.

The permeation rate also was determined using the area of the membrane as a variable. Figure 3 shows a log–log plot of permeation rate *versus* membrane radius at a constant flow rate of 2.24 ml/min. The slope of this line is 1.66, which is in excellent agreement with the exponent of 5/3 on the radius in Eq. 1. These results indicate that, under conditions of diffusion layer control, the permeation rate is not directly proportional to area but to a somewhat reduced function of area ($r^{5/3}$) because of the interaction of diffusion and convection. Solute leaving the membrane near the upstream edge of the membrane enters liquid largely devoid of solute, whereas there is a buildup of solute further downstream. The model based on convective diffusion can quantitatively account for such phenomena.

A calculation of the permeation rate using Eqs. 1 and 2 further supports the applicability of the convective diffusion model. Independently determined values used for the calculation are: $D = 6 \times 10^{-6}$ cm^2 sec (12), $C = 9.4 \times 10^{-4} M$ (10), $r = 1.25$ cm, $H = 0.31$ cm, $W = 3.65$ cm, and $Q = 2.05$ ml/min. The permeation rate is calculated to be 4.88×10^{-8} mole/min, which corresponds quite well to the experimentally determined rate of 4.33×10^{-8} mole/min.

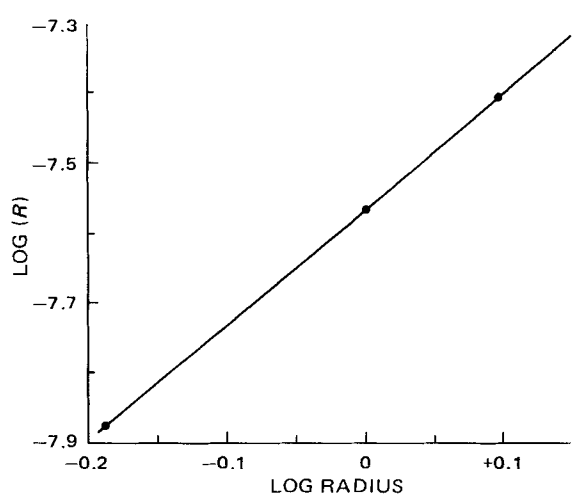

Figure 3—*Log–log plot of the permeation rate,* R, *as a function of the membrane radius.*

As in the studies on dissolution rates of drugs (9, 10), the model based on convective diffusion theory is able to describe quite accurately the membrane transport rate as a function of the physical–chemical parameters of the system. The convective diffusion model should apply to membrane transport for conditions intermediate between extremely low and high liquid flow rates. For the former conditions, as the flow approaches zero, it would be more appropriate to base a model on a nonsteady-state differential equation; for the latter, the transport is "membrane controlled" and has been thoroughly discussed (1).

REFERENCES

(1) G. L. Flynn, S. H. Yalkowsky, and T. J. Roseman, *J. Pharm. Sci.*, **63**, 479 (1974).

(2) S. B. Tuwiner, "Diffusion and Membrane Technology," Reinhold, New York, N.Y., 1962.

(3) O. H. LeBland, Jr., *J. Membr. Biol.*, **4**, 227 (1971).

(4) R. G. Stehle and W. I. Higuchi, *J. Pharm. Sci.*, **61**, 1922 (1972).

(5) E. G. Lovering and D. B. Black, *ibid.*, **63**, 1399 (1974).

(6) V. G. Levich, "Physiochemical Hydrodynamics," Prentice-Hall, Englewood Cliffs, N.J., 1962.

(7) R. B. Bird, W. E. Stewart, and E. N. Lightfoot, "Transport Phenomena," Wiley, New York, N.Y., 1960.

(8) H. Kramers and P. J. Kreyger, *Chem. Eng. Sci.*, **6**, 42 (1956).

(9) K. G. Nelson and A. C. Shah, *J. Pharm. Sci.*, **64**, 610 (1975).

(10) A. C. Shah and K. G. Nelson, *ibid.*, **64**, 1518 (1975).

(11) T. J. Roseman, *ibid.*, **61**, 46 (1972).

(12) G. L. Flynn and S. H. Yalkowsky, *ibid.*, **61**, 838 (1972).

ACKNOWLEDGMENTS AND ADDRESSES

Received October 17, 1975, from the *College of Pharmacy, University of Minnesota, Minneapolis, MN 55455, and [1]Pharmacy Research, The Upjohn Company, Kalamazoo, MI 49001.

Accepted for publication March 11, 1976.

The authors thank Dr. Theodore J. Roseman for providing membrane samples.

[x] To whom inquiries should be directed.

Quick Specific Assay for Aspirin

EDGAR E. THEIMER [x] and EMIL W. CIURCZAK

Abstract □ Use of the Schoenemann reaction for the assay of aspirin in pharmaceutical combinations is described.

Keyphrases □ Aspirin—colorimetric analysis using Schoenemann reaction, pharmaceutical combinations □ Colorimetry—analysis using Schoenemann reaction, aspirin in pharmaceutical combinations □ Analgesics—aspirin, colorimetric analysis using Schoenemann reaction, pharmaceutical combinations

Aspirin is often the most labile component in a combination-type analgesic compound. Therefore, its stability is often the initial concern in any formulation screening program. Preliminary screening of a large number of potential formulations can be arduous, since most current methods of analysis generally consist of several steps: extractions or column separations followed by UV, colorimetric, or GLC assay (1–4). The method proposed here is quite suited to large numbers of assays. It is straightforward and is not subject to interference from substances such as salicylic acid, caffeine, phenacetin, acetaminophen, and codeine. It is essentially a Schoenemann reaction with slight modifications (5, 6).

EXPERIMENTAL

Preparation of Sample—An amount of tablet granulation equivalent to 100 mg of aspirin is weighed into a 250-ml volumetric flask, and 200 ml of distilled water is added. The slurry is shaken for about 10 min; then the flask is diluted to volume with distilled water.

Standard—Aspirin, 0.4 mg/ml of water, is prepared freshly.

Equipment—A recording dual-beam spectrophotometer[1] was used at 455 nm with the recorder speed at 5 mm/min.

Reagents—*o*-Dianisidine hydrochloride[2] (3,3′-dimethoxybenzidine dihydrochloride) was obtained commercially[3]. Tribasic sodium phosphate, 3% hydrogen peroxide, and the various pharmaceuticals tested were all reagent or USP grade or good commercial grade. Acetone[4] was reagent spectrophotometric grade and was used without purification. Previous investigators warned that impure acetone leads to false results (5).

Assay—The reagents were mixed in the following order: 0.5 ml of *o*-dianisidine hydrochloride (0.5% aqueous solution), 3.0 ml of acetone, 1.0 ml of 3% hydrogen peroxide, 1.0 ml of standard, and 2.0 ml of 0.05 *M* tribasic sodium phosphate.

The maximum color developed was measured in a 1-cm cell against water in the reference beam of the spectrophotometer at 455 nm by recording absorbance as a function of time. The maximum always occurred within 5 min.

The entire procedure was repeated, substituting the sample solution for the standard.

The ratio of the maximum absorbances of sample and standard was used to calculate the amount of aspirin in the sample taken.

RESULTS AND DISCUSSION

Linearity—The maximum absorbance was determined for the standard over a concentration range from 0.1 to 1.6 mg/ml and found to be linear and directly proportional to concentration throughout this range.

Interferences—The specificity of the Schoenemann reaction for certain esters and anhydrides is well documented (8) and was confirmed by testing a wide range of pharmaceuticals likely to be present in aspirin formulations. Only salicylsalicylic acid interfered; it gave absorbance proportionate to its molar concentration when compared to aspirin. That is, the method should also be applicable to salicylsalicylic acid. Minor interference was noted with propylene glycol diacetate and acetylated mannitol.

Color of Blank—Initially, a reagent blank was routinely used in the reference beam during absorption scanning. However, it was unnecessary for aspirin samples, since the color change was negligible in the few minutes required to reach the maximum color of the sample.

Method Validation—The proposed method and a chromatographic method analogous to the NF procedure for aspirin, phenacetin, and caffeine tablets were used for the analysis of aspirin in stability samples of an experimental preparation containing aspirin, acetaminophen, and caffeine. The aspirin found (percent of label) with the chromatographic

[1] Cary model 15.

[2] *o*-Dianisidine is a derivative of benzidine, a common reagent used in blood analysis. Although there is evidence that it is less carcinogenic than benzidine (7), it should be handled with usual precautions against skin contact.

[3] Eastman Kodak Co.

[4] Matheson, Coleman and Bell.

As in the studies on dissolution rates of drugs (9, 10), the model based on convective diffusion theory is able to describe quite accurately the membrane transport rate as a function of the physical–chemical parameters of the system. The convective diffusion model should apply to membrane transport for conditions intermediate between extremely low and high liquid flow rates. For the former conditions, as the flow approaches zero, it would be more appropriate to base a model on a nonsteady-state differential equation; for the latter, the transport is "membrane controlled" and has been thoroughly discussed (1).

REFERENCES

(1) G. L. Flynn, S. H. Yalkowsky, and T. J. Roseman, *J. Pharm. Sci.*, **63**, 479 (1974).

(2) S. B. Tuwiner, "Diffusion and Membrane Technology," Reinhold, New York, N.Y., 1962.

(3) O. H. LeBland, Jr., *J. Membr. Biol.*, **4**, 227 (1971).

(4) R. G. Stehle and W. I. Higuchi, *J. Pharm. Sci.*, **61**, 1922 (1972).

(5) E. G. Lovering and D. B. Black, *ibid.*, **63**, 1399 (1974).

(6) V. G. Levich, "Physiochemical Hydrodynamics," Prentice-Hall, Englewood Cliffs, N.J., 1962.

(7) R. B. Bird, W. E. Stewart, and E. N. Lightfoot, "Transport Phenomena," Wiley, New York, N.Y., 1960.

(8) H. Kramers and P. J. Kreyger, *Chem. Eng. Sci.*, **6**, 42 (1956).

(9) K. G. Nelson and A. C. Shah, *J. Pharm. Sci.*, **64**, 610 (1975).

(10) A. C. Shah and K. G. Nelson, *ibid.*, **64**, 1518 (1975).

(11) T. J. Roseman, *ibid.*, **61**, 46 (1972).

(12) G. L. Flynn and S. H. Yalkowsky, *ibid.*, **61**, 838 (1972).

ACKNOWLEDGMENTS AND ADDRESSES

Received October 17, 1975, from the *College of Pharmacy, University of Minnesota, Minneapolis, MN 55455, and [1]Pharmacy Research, The Upjohn Company, Kalamazoo, MI 49001.

Accepted for publication March 11, 1976.

The authors thank Dr. Theodore J. Roseman for providing membrane samples.

[x] To whom inquiries should be directed.

Quick Specific Assay for Aspirin

EDGAR E. THEIMER [x] and EMIL W. CIURCZAK

Abstract □ Use of the Schoenemann reaction for the assay of aspirin in pharmaceutical combinations is described.

Keyphrases □ Aspirin—colorimetric analysis using Schoenemann reaction, pharmaceutical combinations □ Colorimetry—analysis using Schoenemann reaction, aspirin in pharmaceutical combinations □ Analgesics—aspirin, colorimetric analysis using Schoenemann reaction, pharmaceutical combinations

Aspirin is often the most labile component in a combination-type analgesic compound. Therefore, its stability is often the initial concern in any formulation screening program. Preliminary screening of a large number of potential formulations can be arduous, since most current methods of analysis generally consist of several steps: extractions or column separations followed by UV, colorimetric, or GLC assay (1–4). The method proposed here is quite suited to large numbers of assays. It is straightforward and is not subject to interference from substances such as salicylic acid, caffeine, phenacetin, acetaminophen, and codeine. It is essentially a Schoenemann reaction with slight modifications (5, 6).

EXPERIMENTAL

Preparation of Sample—An amount of tablet granulation equivalent to 100 mg of aspirin is weighed into a 250-ml volumetric flask, and 200 ml of distilled water is added. The slurry is shaken for about 10 min; then the flask is diluted to volume with distilled water.

Standard—Aspirin, 0.4 mg/ml of water, is prepared freshly.

Equipment—A recording dual-beam spectrophotometer[1] was used at 455 nm with the recorder speed at 5 mm/min.

Reagents—*o*-Dianisidine hydrochloride[2] (3,3′-dimethoxybenzidine dihydrochloride) was obtained commercially[3]. Tribasic sodium phosphate, 3% hydrogen peroxide, and the various pharmaceuticals tested were all reagent or USP grade or good commercial grade. Acetone[4] was reagent spectrophotometric grade and was used without purification. Previous investigators warned that impure acetone leads to false results (5).

Assay—The reagents were mixed in the following order: 0.5 ml of *o*-dianisidine hydrochloride (0.5% aqueous solution), 3.0 ml of acetone, 1.0 ml of 3% hydrogen peroxide, 1.0 ml of standard, and 2.0 ml of 0.05 *M* tribasic sodium phosphate.

The maximum color developed was measured in a 1-cm cell against water in the reference beam of the spectrophotometer at 455 nm by recording absorbance as a function of time. The maximum always occurred within 5 min.

The entire procedure was repeated, substituting the sample solution for the standard.

The ratio of the maximum absorbances of sample and standard was used to calculate the amount of aspirin in the sample taken.

RESULTS AND DISCUSSION

Linearity—The maximum absorbance was determined for the standard over a concentration range from 0.1 to 1.6 mg/ml and found to be linear and directly proportional to concentration throughout this range.

Interferences—The specificity of the Schoenemann reaction for certain esters and anhydrides is well documented (8) and was confirmed by testing a wide range of pharmaceuticals likely to be present in aspirin formulations. Only salicylsalicylic acid interfered; it gave absorbance proportionate to its molar concentration when compared to aspirin. That is, the method should also be applicable to salicylsalicylic acid. Minor interference was noted with propylene glycol diacetate and acetylated mannitol.

Color of Blank—Initially, a reagent blank was routinely used in the reference beam during absorption scanning. However, it was unnecessary for aspirin samples, since the color change was negligible in the few minutes required to reach the maximum color of the sample.

Method Validation—The proposed method and a chromatographic method analogous to the NF procedure for aspirin, phenacetin, and caffeine tablets were used for the analysis of aspirin in stability samples of an experimental preparation containing aspirin, acetaminophen, and caffeine. The aspirin found (percent of label) with the chromatographic

[1] Cary model 15.

[2] *o*-Dianisidine is a derivative of benzidine, a common reagent used in blood analysis. Although there is evidence that it is less carcinogenic than benzidine (7), it should be handled with usual precautions against skin contact.

[3] Eastman Kodak Co.

[4] Matheson, Coleman and Bell.

and proposed methods was 97.4 and 96.7%, respectively, for undegraded aspirin and 42.9 and 35.2%, respectively, for aspirin subjected to stress conditions. The comparison is satisfactory, especially if the method is used for screening purposes in formulation work.

REFERENCES

(1) "The National Formulary," 13th ed. Mack Publishing Co., Easton, Pa., 1970, p. 66.

(2) K. T. Koshy, *J. Pharm. Sci.*, **53**, 1280 (1964).

(3) J. Levine and J. D. Weber, *ibid.*, **57**, 631 (1968).

(4) C. A. Kelly, *ibid.*, **59**, 1053 (1970).

(5) B. Gehauf, J. Epstein, G. B. Wilson, B. Witten, S. Sass, V. E. Bauer, and W. H. C. Rueggeberg, *Anal. Chem.*, **29**, 278 (1957).

(6) J. S. Hanker, A. Gelberg, and B. Witten, *J. Am. Pharm. Assoc., Sci. Ed.*, **47**, 728 (1958).

(7) R. C. Garner, A. L. Wallpole, and F. L. Rose, *Cancer Lett.*, **1**, 39 (1975).

(8) D. J. Marsh and E. Neale, *J. Appl. Chem.*, **8**, 394 (June 1958).

ACKNOWLEDGMENTS AND ADDRESSES

Received February 18, 1975, from *Cooper Laboratories, Inc., Cedar Knolls, NJ 07927.*

Accepted for publication March 10, 1976.

[x] To whom inquiries should be directed.

Single-Dose Assay of Ferrous Ion in Pharmaceuticals

RICHARD JUNEAU

Abstract □ A method for the assay of the ferrous ion in hematinics or multivitamin tablets is described. The method is based on the spectrophotometric measurement of the chromophore produced by reacting the ferrous ion with the highly specific chelating agent ferrozine. The method is proposed as an alternative to the redox methods in the USP and NF.

Keyphrases □ Ferrous ion—spectrophotometric analysis, pharmaceutical formulations □ Iron—ferrous ion, spectrophotometric analysis, pharmaceutical formulations □ Spectrophotometry—analysis, ferrous ion in pharmaceutical formulations □ Hematinics—ferrous ion, spectrophotometric analysis in pharmaceutical formulations

The presence of the ferrous ion in many pharmaceutical preparations necessitates a rapid, economical, and sensitive method for its determination in pharmaceuticals. The official USP and NF methods primarily rely on the classical redox conversion of the ferrous to the ferric ion (1, 2). These redox methods are tedious and inaccurate due to difficult end-point visualization.

Other methods are available for the assay of iron-containing products, *e.g.*, atomic absorption spectrophotometry and X-ray emission spectrometry. However, these methods require involved sample preparation as well as sophisticated instrumentation (3, 4). This report describes a simple colorimetric procedure applicable to ferrous-containing pharmaceuticals such as hematinics and multiple-vitamin preparations with iron. The sensitivity is such that the method is ideal for single-dose assays.

The present method utilizes the reagent ferrozine, 3-(2-pyridyl)-5,6-bis(4-phenylsulfonic acid)-1,2,4-triazine disodium salt, a chelating agent highly specific for the ferrous ion. Although this compound is similar to the well-known chelating agent 2,4,6-tripyridyltriazine, previously used for iron assays of pharmaceuticals, it has the advantages of being significantly more water soluble, more sensitive, and possibly more economically feasible for repeated analyses (4, 5).

Ferrozine has been shown to react with the ferrous ion to yield a magenta-colored tris complex, *i.e.*, Fe-(ferrozine)$_3^{2+}$. This species forms completely in aqueous solution between pH 4 and 9 and exhibits a sharp peak with maximum absorbance at 562 nm (5). Interference studies showed that only monovalent copper and divalent cobalt formed colored species with ferrozine (5). Ferrozine was used in the determination of iron in municipal waters (5) and serum iron levels (6).

Table I—Stability of Iron–Ferrozine Complex

Hours after Mixing	Absorbance[a]	Absorbance[b]	Absorbance[c]
0.17	0.492	0.615	0.520
0.50	0.492	0.615	0.520
1.00	0.492	0.615	0.520
2.00	0.492	0.615	0.520
8.00	0.496	0.615	0.518
24.00	0.496	0.611	0.518
48.00	0.496	0.611	0.511

[a] Obtained from assay of ferrous fumarate tablet (Feostat, Westerfield Co.). [b] Obtained from assay of ferrous sulfate tablet (Feosol, Smith Kline and French). [c] Obtained from assay of analytical grade ferrous ammonium sulfate.

EXPERIMENTAL

Instrumentation—A double-beam spectrophotometer[1] and a pH meter[2] were used.

Reagents and Chemicals—The following ACS grade chemicals were used: sodium phosphate monohydrate, ascorbic acid, ferrous ammonium sulfate hexahydrate, acetic acid, and ferrozine[3]. Deionized water was obtained from a commercial deionizer[4] and was shown by conductance to contain not more than 0.25 ppm of dissolved ionic solids.

Color Reagent—Ferrozine, 125 mg, was placed in a 25-ml volumetric flask, and deionized water was added to volume. The solution should be protected from light.

Buffer Solution—Sodium phosphate, 6.25 g, and 12 mg of ascorbic acid were dissolved in 100 ml of deionized water. The pH of the resultant solution was adjusted to 5.3 by the dropwise addition of 10% sodium hydroxide.

Stock Solution of Ferrous Ammonium Sulfate—Ferrous ammonium sulfate, 615 mg, was placed in a 100-ml volumetric flask and brought to volume with deionized water.

Working Solution of Ferrous Ammonium Sulfate—For the working

[1] Beckman model 25 spectrophotometer.
[2] Coleman Metrion IV.
[3] Nutritional Biochemical Corp.
[4] Culligan deionizer.

and proposed methods was 97.4 and 96.7%, respectively, for undegraded aspirin and 42.9 and 35.2%, respectively, for aspirin subjected to stress conditions. The comparison is satisfactory, especially if the method is used for screening purposes in formulation work.

REFERENCES

(1) "The National Formulary," 13th ed. Mack Publishing Co., Easton, Pa., 1970, p. 66.

(2) K. T. Koshy, *J. Pharm. Sci.*, **53**, 1280 (1964).

(3) J. Levine and J. D. Weber, *ibid.*, **57**, 631 (1968).

(4) C. A. Kelly, *ibid.*, **59**, 1053 (1970).

(5) B. Gehauf, J. Epstein, G. B. Wilson, B. Witten, S. Sass, V. E. Bauer, and W. H. C. Rueggeberg, *Anal. Chem.*, **29**, 278 (1957).

(6) J. S. Hanker, A. Gelberg, and B. Witten, *J. Am. Pharm. Assoc., Sci. Ed.*, **47**, 728 (1958).

(7) R. C. Garner, A. L. Wallpole, and F. L. Rose, *Cancer Lett.*, **1**, 39 (1975).

(8) D. J. Marsh and E. Neale, *J. Appl. Chem.*, **8**, 394 (June 1958).

ACKNOWLEDGMENTS AND ADDRESSES

Received February 18, 1975, from *Cooper Laboratories, Inc., Cedar Knolls, NJ 07927.*

Accepted for publication March 10, 1976.

[x] To whom inquiries should be directed.

Single-Dose Assay of Ferrous Ion in Pharmaceuticals

RICHARD JUNEAU

Abstract □ A method for the assay of the ferrous ion in hematinics or multivitamin tablets is described. The method is based on the spectrophotometric measurement of the chromophore produced by reacting the ferrous ion with the highly specific chelating agent ferrozine. The method is proposed as an alternative to the redox methods in the USP and NF.

Keyphrases □ Ferrous ion—spectrophotometric analysis, pharmaceutical formulations □ Iron—ferrous ion, spectrophotometric analysis, pharmaceutical formulations □ Spectrophotometry—analysis, ferrous ion in pharmaceutical formulations □ Hematinics—ferrous ion, spectrophotometric analysis in pharmaceutical formulations

The presence of the ferrous ion in many pharmaceutical preparations necessitates a rapid, economical, and sensitive method for its determination in pharmaceuticals. The official USP and NF methods primarily rely on the classical redox conversion of the ferrous to the ferric ion (1, 2). These redox methods are tedious and inaccurate due to difficult end-point visualization.

Other methods are available for the assay of iron-containing products, *e.g.*, atomic absorption spectrophotometry and X-ray emission spectrometry. However, these methods require involved sample preparation as well as sophisticated instrumentation (3, 4). This report describes a simple colorimetric procedure applicable to ferrous-containing pharmaceuticals such as hematinics and multiple-vitamin preparations with iron. The sensitivity is such that the method is ideal for single-dose assays.

The present method utilizes the reagent ferrozine, 3-(2-pyridyl)-5,6-bis(4-phenylsulfonic acid)-1,2,4-triazine disodium salt, a chelating agent highly specific for the ferrous ion. Although this compound is similar to the well-known chelating agent 2,4,6-tripyridyltriazine, previously used for iron assays of pharmaceuticals, it has the advantages of being significantly more water soluble, more sensitive, and possibly more economically feasible for repeated analyses (4, 5).

Ferrozine has been shown to react with the ferrous ion to yield a magenta-colored tris complex, *i.e.*, Fe-(ferrozine)$_3^{2+}$. This species forms completely in aqueous solution between pH 4 and 9 and exhibits a sharp peak with maximum absorbance at 562 nm (5). Interference studies showed that only monovalent copper and divalent cobalt formed colored species with ferrozine (5). Ferrozine was used in the determination of iron in municipal waters (5) and serum iron levels (6).

Table I—Stability of Iron–Ferrozine Complex

Hours after Mixing	Absorbance[a]	Absorbance[b]	Absorbance[c]
0.17	0.492	0.615	0.520
0.50	0.492	0.615	0.520
1.00	0.492	0.615	0.520
2.00	0.492	0.615	0.520
8.00	0.496	0.615	0.518
24.00	0.496	0.611	0.518
48.00	0.496	0.611	0.511

[a] Obtained from assay of ferrous fumarate tablet (Feostat, Westerfield Co.). [b] Obtained from assay of ferrous sulfate tablet (Feosol, Smith Kline and French). [c] Obtained from assay of analytical grade ferrous ammonium sulfate.

EXPERIMENTAL

Instrumentation—A double-beam spectrophotometer[1] and a pH meter[2] were used.

Reagents and Chemicals—The following ACS grade chemicals were used: sodium phosphate monohydrate, ascorbic acid, ferrous ammonium sulfate hexahydrate, acetic acid, and ferrozine[3]. Deionized water was obtained from a commercial deionizer[4] and was shown by conductance to contain not more than 0.25 ppm of dissolved ionic solids.

Color Reagent—Ferrozine, 125 mg, was placed in a 25-ml volumetric flask, and deionized water was added to volume. The solution should be protected from light.

Buffer Solution—Sodium phosphate, 6.25 g, and 12 mg of ascorbic acid were dissolved in 100 ml of deionized water. The pH of the resultant solution was adjusted to 5.3 by the dropwise addition of 10% sodium hydroxide.

Stock Solution of Ferrous Ammonium Sulfate—Ferrous ammonium sulfate, 615 mg, was placed in a 100-ml volumetric flask and brought to volume with deionized water.

Working Solution of Ferrous Ammonium Sulfate—For the working

[1] Beckman model 25 spectrophotometer.
[2] Coleman Metrion IV.
[3] Nutritional Biochemical Corp.
[4] Culligan deionizer.

Table II—Assay Results of a Single Ferrous Sulfate Tablet[a]

Replication	Amount Found, mg	Percent Label
1	62.4	96.0
2	62.9	96.7
3	62.5	96.2
4	62.4	96.0

[a] Feosol tablets.

solution, 2.0 ml of the stock solution was placed in a 100-ml volumetric flask and brought to volume with deionized water.

Calibration Curve—Into separate 50-ml volumetric flasks were added 5.0, 4.0, 3.0, 2.0, or 1.0 ml of ferrous ammonium sulfate working solution, 2.0 ml of buffer solution, and 25 ml of deionized water. To these mixtures was added 1.0 ml of color reagent, and the mixtures were then brought to volume with deionized water. The solutions were allowed to stand with intermittent shaking for a minimum of 10 min, after which the solutions were read spectrophotometrically at 562 nm against a blank containing 2.0 ml of buffer solution and 1.0 ml of color reagent. (*Note:* Blanks did not give any visible color change upon addition of color reagent.)

Sample Preparation—*Solid Samples*—The tablet or contents of one capsule was placed in 100 ml of boiling deionized water containing 5 mg of ascorbic acid, and the mixture was boiled until complete dissolution occurred. The boiling mixture was then quantitatively filtered through a filter paper previously rinsed with several portions of boiling deionized water. After filtration, the residue on the filter paper was washed once with 50 ml of boiling deionized water followed by 100 ml of deionized water at room temperature. (If the sample contains ferrous fumarate, 100 ml of 0.1 *N* HCl should be used as the dissolution solvent.)

The mixture was then brought to volume. The final volume is variable and dependent on the labeled amount of iron. For example, if it is labeled 65 mg of elemental iron, the final volume may be 1 liter; if 33 mg of iron, then 500 ml; *etc.* One milliliter of this solution was then placed in a 50-ml volumetric flask, and the sample was prepared as were the solutions for the calibration curve and read against a blank prepared as described.

Liquid Samples—The liquid preparation (1.0 ml) was placed in a suitable volumetric flask (1 liter, 500 ml, *etc.*) and brought to volume with deionized water. Then 1.0 ml of this solution was placed in a 50-ml volumetric flask, and the sample was prepared as already described.

RESULTS AND DISCUSSION

A plot of absorbance *versus* concentration demonstrated that the Beer–Lambert law was obeyed over a wide concentration range as previously observed (5). Previous work indicated that an incubation step was needed for full color development (5, 6), but this step was shown to be unnecessary in these laboratories. Each calibration point of the Beer–Lambert plot was composed of three determinations. Two of these determinations utilized a 10-min incubation period at 40°; the third determination was allowed to stand at room temperature for this same period. Reading all three samples at room temperature gave readings that did not differ significantly, *i.e.*, a typical average deviation of 0.006 absorbance unit. Thus, it was only necessary to wait 10 min after mixing to obtain absorbance readings.

Once the color formed, it was stable almost indefinitely if kept at room temperature. Table I demonstrates the permanency of the chromophore produced. The data suggest that the permanency of color was not affected by product formulation, since iron from two different commercial formulations yielded colors as permanent as that obtained from analytical grade ferrous ammonium sulfate. The excellent stability of the chromophore offers distinct advantages when large numbers of assays must be performed since the chromophore can be produced and assayed at some later time without concern for stability. The instant and permanent color development was probably due to the fact that the concentration of ferrozine in the color reagent was well in excess of the required stoichiometric quantity.

Table III—Assay Results of a Single Multivitamin Tablet Containing Ferrous Fumarate[a]

Replication	Amount Found, mg	Percent Label
1	99.4	99.4
2	100.4	100.4
3	98.8	98.8
4	99.4	99.4

[a] Tabron.

Table IV—Assay Results Obtained from Synthetic Multiple-Tablet Composite Containing 33.04 mg of Iron per Tablet[a]

Sample	Iron per Tablet, mg	Recovery, %
1	33.31	100.8
2	33.10	100.2
3	33.25	100.6
4	33.31	100.8
5	33.21	100.5
6	33.35	100.9
7	33.25	100.6
8	33.15	100.3
9	33.15	100.3
10	33.20	100.5

[a] Prepared from ferrous ammonium sulfate and Clusivol tablets (Ayerst).

Tables II and III give typical results of replicated assays on a single tablet and demonstrate that the method gives values of relatively high precision. Initially, values were low for solid preparations containing ferrous fumarate. However, use of 0.1 *N* HCl for dissolution promoted the quantitative dissolution of the poorly soluble ferrous fumarate. The quantitativeness of the reaction with iron in pharmaceutical dosage forms was assured by adding ferrous ammonium sulfate to several iron-free multivitamin preparations of the solid or liquid type. In all cases, the iron content of these prepared samples was no less than 98.5% nor more than 101% of the amount added.

For example, the data in Table IV were obtained from a synthetic multiple-tablet composite. The composite was prepared by adding an accurately known amount of ferrous ammonium sulfate to 20 iron-free multivitamin tablets whose weight also was accurately known. The mixture was then thoroughly triturated, and approximately one-twentieth of the combined weight was used as a tablet sample. The data indicate that recovery and precision were excellent. It is assumed that the formulation characteristics of the spiked samples were comparable to the iron preparations assayed. This assumption appears to be valid, since assay of the iron-containing commercial products led to values very close to label claims.

Thus, the proposed method seems to offer several advantages over the present USP–NF method in terms of time, sensitivity, and convenience, especially when it is realized that one reagent suffices for all ferrous-containing products and that there are no interferences with tablet fillers, excipients, or colorants. The procedure should also have utility in automated assay methods.

REFERENCES

(1) "The United States Pharmacopeia," 19th rev., Mack Publishing Co., Easton, Pa., 1975, p. 196.

(2) "The National Formulary," 14th ed., Mack Publishing Co., Easton, Pa., 1975, p. 280.

(3) H. I. Tarlin and M. Batcholder, *J. Pharm. Sci.*, **59**, 1328 (1970).

(4) W. F. Beyer and K. G. Zipple, *ibid.*, **57**, 653 (1968).

(5) L. L. Stookley, *Anal. Chem.*, **42**, 779 (1970).

(6) J. P. Persijn, W. Van Der Slik, and A. Riethorst, *Clin. Chem. Acta*, **35**, 91 (1971).

ACKNOWLEDGMENTS AND ADDRESSES

Received October 9, 1975, from the *School of Pharmacy, Southwestern Oklahoma State University, Weatherford, OK 73096.*

Accepted for publication March 10, 1976.

High-Pressure Liquid Chromatographic Analysis of Drugs in Biological Fluids I: Warfarin

THORIR D. BJORNSSON *, TERRENCE F. BLASCHKE *, and PETER J. MEFFIN ‡x

Abstract □ A rapid, sensitive, and specific high-pressure liquid chromatographic (HPLC) method for the quantitative analysis of warfarin in plasma is described. The method involves a single solvent extraction of warfarin and the internal standard from acidified plasma, followed by evaporation and HPLC analysis. The method is sufficiently sensitive and accurate for most pharmacokinetic studies; concentrations between 0.1 and 4.0 μg/ml can be measured with a coefficient of variation of 2–5%. Known metabolites of warfarin do not interfere with the analysis.

Keyphrases □ Warfarin—high-pressure liquid chromatographic analysis, human plasma □ High-pressure liquid chromatography—analysis, warfarin in human plasma □ Anticoagulants—warfarin, high-pressure liquid chromatographic analysis, human plasma

Several methods have been reported for the analysis of warfarin in biological fluids, but each has some disadvantage in specificity, sensitivity, reproducibility, or convenience. One reported method (1) involves solvent extraction of warfarin from plasma with dichloroethane, followed by a buffer wash and back-extraction of warfarin into dilute sodium hydroxide solution. Concentration is calculated by UV absorbance at two wavelengths. A modification of this method (2) is still time consuming, since it requires several quantitative transfers. A fluorometric method (3) is rapid but gives consistently higher values than the more commonly used spectrophotometric methods. Thus, its specificity is in doubt. A TLC method for the analysis of warfarin and its metabolites also was described (4), but it is time consuming, making the analysis of a large number of samples difficult.

More recently, two GLC methods were described for the analysis of warfarin. One method (5) involves a complex solvent extraction, evaporation, and derivatization before GLC analysis, but it offers no apparent benefits over other methods. The other GLC method (6) is sensitive and can detect as little as 0.02 μg of warfarin/ml of plasma. The procedure, however, is complex and includes solvent extraction, evaporation, TLC, derivatization, and GLC analysis. In view of the commonly encountered therapeutic levels of warfarin of 1.5 ± 0.5 μg/ml, the added sensitivity of this method will be required in only a few types of investigations.

A high-pressure liquid chromatographic (HPLC) analysis of warfarin was described previously (7), but this report gave few details. Moreover, an internal standard was not used, thus necessitating quantitative transfer and sampling techniques, with their inherent inconveniences.

The method described in this paper is specific, accurate, and convenient, and it has sufficient sensitivity to measure accurately concentrations of warfarin as low as one-tenth of the normally encountered therapeutic levels in humans.

Table I—Statistics of Calibration Curves and Reproducibility

Day	Concentration Range, μg/ml	Number of Samples	Mean PHR[a]/ Micrograms of Warfarin	*SD*	Coefficient of Variation, %
		Calibration Curve Data			
1	0.1–4.0	13	1.456	0.065	4.5
2	0.1–4.0	9	1.352	0.068	5.0
3	0.1–4.0	6	1.465	0.067	4.6
4	0.1–4.0	6	1.405	0.106	7.5
5	0.1–4.0	5	1.464	0.046	3.1
6	0.1–4.0	5	1.349	0.046	3.4
7	0.1–4.0	5	1.329	0.077	5.8
		Averages	1.403	0.068	4.8
		Reproducibility at a Given Concentration			
8	0.5	5	1.468	0.058	4.0
9	1.0	10	1.534	0.026	1.7
10	2.0	5	1.495	0.051	3.4

[a] PHR = peak height ratio of warfarin to internal standard.

EXPERIMENTAL

Reagents and Materials—Warfarin[1] and *p*-chlorowarfarin[2] [3-(α-acetonyl-*p*-chlorobenzyl)-4-hydroxycoumarin] were used as supplied. Stock solutions of warfarin (2.0 mg/ml) and the internal standard (1.2 mg/ml) were prepared in methanol[3] and stored in the dark at 4°. Appropriate dilutions of these stock solutions with water were made weekly to produce working standards of 1.2 μg/100 μl for the internal standard and 0.1–4.0 μg/100 μl for warfarin.

Sample Preparation—Plasma, 0.2–1 ml, was placed in a screw-capped[4] centrifuge tube, and 100 μl of internal standard solution (containing 1.2 μg of *p*-chlorowarfarin), 0.5 ml of 0.5 *N* aqueous sulfuric acid[5], and 5 ml of ether[5] were added. The samples were extracted by mixing, using gentle hand tilting of the tubes for 10 min or using any method of gentle mechanical agitation, followed by centrifugation at 2500 rpm for 10 min to separate the organic and aqueous phases.

The lower aqueous phase was frozen by immersing the tube in a dry ice–acetone bath, and the organic phase was poured off into another tube having an elongated cone at its base of approximately 50-μl capacity. The organic solvent was evaporated to dryness in a water bath at 40–45°. The residue was dissolved in 25 μl of methanol[3] by washing the sides of the lowest part of the tube and its elongated cone several times with the aid of a 25-μl syringe. Then 15–20 μl of the methanol solution was injected into the chromatograph.

Chromatography—A high-pressure liquid chromatograph[6] fitted with a 25-cm long, 6.3-mm o.d., 2.2-mm i.d. reversed-phase column[7] was used. The detector was a variable wavelength spectrophotometer[8] with a 10-μl flowcell. Absorbance was measured at 308 nm, with 0.1 absorbance unit full scale and 2-nm slit width. One pump of the dual-pump gradient elution chromatograph contained methanol[3], and the other contained 0.5% acetic acid in distilled water. An isocratic 1:1 mixture of the two solvents was used. Although it was convenient to use two pumps operating under isocratic conditions, a 1:1 mixture of the two solvents in a single pump can be used.

[1] Sigma Chemical Co., St. Louis, Mo.
[2] Aldrich Chemical Co., Milwaukee, Wis.
[3] Spectroquality, MC & B Manufacturing Chemists, Norwood, Ohio.
[4] Lined with Teflon (du Pont).
[5] Analytical reagent, Mallinckrodt Chemical Works, St. Louis, Mo.
[6] Model 8500, Varian, Palo Alto, Calif.
[7] MicroPak CH-10, Varian, Palo Alto, Calif.
[8] Variscan, Varian, Palo Alto, Calif.

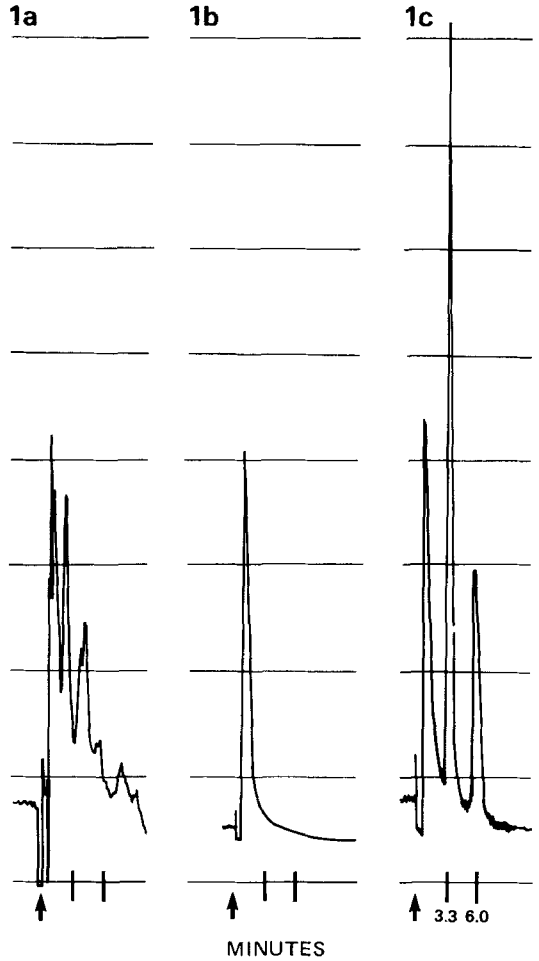

Figure 1—(a) *Chromatogram obtained when 1 ml of control plasma is extracted and absorbance is measured at 280 nm.* (b) *Chromatogram of the same control plasma with absorbance measured at 308 nm.* (c) *Typical chromatogram of plasma containing warfarin (2.0 μg/ml) and the internal standard. The marks on the chromatograms of control plasma correspond to the retention times of warfarin (3.3 min) and the internal standard (6.0 min). To improve visual clarity, only one tracing of the dual-pen recorder is shown.*

The flow rate of the solvent mixture was 60 ml/hr, with a column input pressure of 390–420 kg/cm^2 (374–408 atm). Chromatograms were recorded on a dual-pen recorder[9] with 0–50- and 0–100-mv spans.

Calibration and Accuracy—Calibration curves were constructed by adding known amounts of warfarin and internal standard to control plasma. The peak height ratio of warfarin to the internal standard was plotted against the amount of warfarin added. To calibrate the method and to determine its accuracy for each batch of unknown samples, standards of 0.1, 0.5, 1.0, 2.0, and 4.0 μg of warfarin were added to 1-ml samples of control plasma, which were assayed concurrently with the unknown samples. The peak height ratio of each standard was divided by the amount of warfarin added to give normalized peak height ratios. The mean normalized peak height ratio was used to calculate the amount of warfarin in unknown samples, and the standard deviation of the normalized peak height ratios was used to determine the accuracy of the method over the range of warfarin standards employed.

Reproducibility of the method was also studied by carrying replicate plasma samples containing 0.5, 1.0, and 2.0 μg of warfarin through the procedure. The effect of sample size on the method was investigated by adding 1 μg of warfarin to tubes containing different volumes of plasma, 0.2–2 ml, which were then assayed for warfarin. The volumes of internal standard solution, sulfuric acid, and ether were constant.

Plasma Level Study—A normal human male volunteer (weight 63.0 kg) was given 15 mg of warfarin sodium in aqueous solution after fasting for approximately 12 hr. Samples of venous blood (3 ml) were withdrawn

[9] Varian A-25, Varian, Palo Alto, Calif.

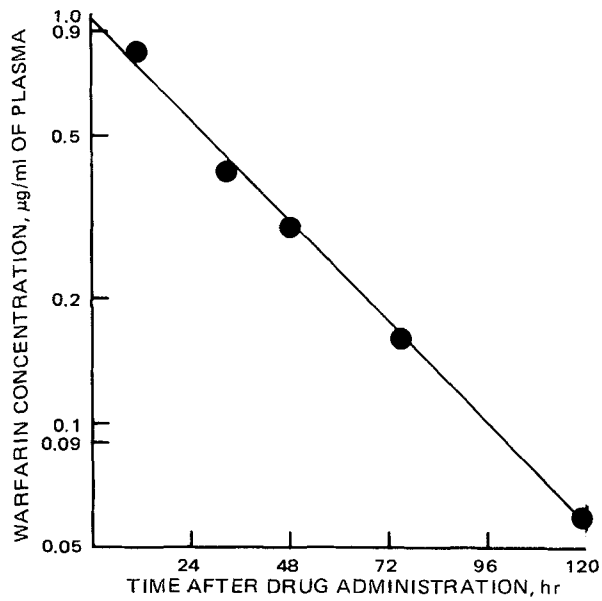

Figure 2—*Semilog plot of plasma warfarin levels in a male volunteer who received 15 mg of warfarin orally.*

by means of heparinized containers[10] prior to, and at intervals over 120 hr after, drug administration. The blood samples were centrifuged, and the plasma was transferred to glass containers; these containers were stored at −15° until analyzed.

RESULTS AND DISCUSSION

In preliminary work, ^{14}C-warfarin[11] was satisfactorily extracted from plasma acidified with dilute sulfuric acid by toluene, ether, isopentyl acetate, dichloroethane, and ethyl acetate. These solvents extracted 90–95% of warfarin from the plasma using a solvent to plasma ratio of 3:1. Although dichloroethane is used frequently, ether was selected for the extraction of warfarin from plasma for the following reasons. Ether has a lower specific gravity than water and has a low freezing point; thus it can be separated easily from the aqueous phase by freezing. It is readily evaporated and, because of its lower polarity, it is less likely to extract interfering compounds than dichloroethane.

Initially, absorbance was measured at 280 nm with a sensitive fixed-wavelength detector. At that wavelength, however, peaks interfering with both warfarin and the internal standard were present on chromatograms from control plasma (Fig. 1*a*). Extractions with various solvents and back-extraction of warfarin into 2.5 *N* sodium hydroxide solution failed to eliminate these peaks. The use of a UV absorbance detector at 308 nm eliminated these interfering peaks from the chromatograms and enabled the use of the simple extraction procedure described earlier. A chromatogram of control plasma sample (1 ml) obtained under these conditions is shown in Fig. 1*b*.

Although the use of a variable wavelength detector resulted in a loss in sensitivity compared to that possible with the fixed-wavelength detector due to differences in the energy output of the lamps, good reproducibility and accuracy were still attainable with 0.1 μg of warfarin. This lower limit is sufficient for most clinical and pharmacokinetic purposes. When using the chromatographic conditions previously described, the peaks corresponding to warfarin and the internal standard had retention times of 3.3 and 6.0 min, respectively. A typical chromatogram of a plasma sample containing 2.0 μg of warfarin/ml is shown in Fig. 1*c*.

There has been some controversy about the specificity of the nonchromatographic methods for the quantitative determination of warfarin in plasma (2, 4, 7–9). Lack of specificity in such analyses arises from variable blank values and the measurement of drug metabolites. Although not specifically investigated by some authors, it is probable that the chromatographic methods measure only unchanged warfarin.

The effect of known metabolites of warfarin on the assay was investigated by adding 6-hydroxy- and 7-hydroxywarfarin[11] and the ste-

[10] Vacutainers, V.W.R. Scientific, San Francisco, Calif.

[11] Provided by Dr. C. H. Schroeder, WARF Institute, Inc., Madison, Wis.

Table II—Comparison of Published Methods for the Analysis of Warfarin in Plasma

Reference	Method	Sensitivity, μg/ml	Specificity[a]	Reproducibility (Coefficient of Variation), %
1	Spectrophotometric	Not given	Questionable	9.9[b] (duplicates of mean 7.1 μg/ml)[c]
2	Spectrophotometric	0.1	Questionable	2.2[b] (replicates at 5 and 10 μg/ml)
3	Fluorometric	Not given	Nonspecific	1.0[b] (replicates at 5 μg/ml)
4	TLC–fluorometric	0.25	Specific	1.6 (replicates between 2 and 7 μg/ml)
5	GC	0.25	Specific	3.15 (replicates between 0.25 and 8.0 μg/ml)
6	TLC–GC	0.02	Specific	Not given
7	HPLC	Not given	Specific	2.0 (Not specified)
This method	HPLC	0.1	Specific	3.0 (replicates at 0.5, 1.0, and 2.0 μg/ml)

[a] See *Discussion*. [b] Value not reported but calculated by present authors from published data. [c] Comments in parentheses indicate the range of concentrations over which estimates of reproducibility were made.

reoisomeric alcohol metabolites[12] (10) to plasma samples, which were then taken through the procedure. These four metabolites all had retention times of 2 min or less under the conditions described and did not interfere with measurement of the peaks corresponding to warfarin or the internal standard. Since no peaks interfere with warfarin or the internal standard in blank plasma and the known metabolites of warfarin are well separated from the two peaks of analytical interest, it may be concluded that the method is specific for warfarin. Furthermore, plasma samples obtained in 18 patients receiving 50 different drugs were handled in a manner identical to that for samples known to contain warfarin, except that an internal standard was not added. Chromatograms of these samples showed no peaks that would interfere with the peaks of warfarin or the internal standard[13].

The average normalized peak height ratios obtained from seven calibration curves containing five or more data points had a mean coefficient of variation of 4.8% over approximately 3 months (Table I). This estimate of accuracy covers the entire range of the assay procedure, from 0.1 to 4.0 μg of warfarin/sample. Reproducibility studies using replicates of five samples of 0.5 μg of warfarin, 10 samples of 1.0 μg of warfarin, and five samples of 2.0 μg of warfarin/ml of plasma gave coefficients of variation of 4.0, 1.7, and 3.4%, respectively (Table I). Although these estimates of reproducibility for this method are larger than some estimates shown in Table II for other methods, most estimates for other methods were made at plasma warfarin concentrations in the upper range of therapeutic values or above. In contrast, the coefficients of variation presented in this paper were calculated at concentrations more commonly encountered in patients. Since it may be necessary to take variable volumes of plasma for warfarin measurement, the effect of plasma volume on the peak height ratio of warfarin to the internal standard was examined. Between the range of 0.2 and 2 ml, the peak height ratios were independent of the volume of plasma.

Application of the method to plasma level determinations in a normal human male volunteer is demonstrated in Fig. 2. The data are well described by a one-compartment open model, with $r = 0.998$ for a plot of log warfarin concentration *versus* time. The half-life of 29.5 hr and the volume of distribution of 0.25 liter/kg [assuming complete absorption (11)] are within the range of previously reported values (11). After this relatively small dose, it was possible to monitor plasma concentrations for four half-lives.

The HPLC method described here for the quantitative determination of warfarin in plasma is simpler and more rapid than other published methods with similar sensitivity or specificity (Table II). By using the techniques described, 30–40 samples can easily be assayed in a day. The method is not only convenient, but it is specific; and its accuracy and sensitivity are satisfactory for most pharmacokinetic studies.

[12] Provided by Dr. W. F. Trager, School of Pharmacy, University of Washington, Seattle, Wash.

[13] A list of these drugs is available upon request from the authors.

REFERENCES

(1) R. A. O'Reilly, P. M. Aggeler, M. S. Hoag, and L. Leong, *Thromb. Diath. Haemorrh.*, **8**, 82 (1962).

(2) P. G. Welling, K. P. Lee, U. Khanna, and J. G. Wagner, *J. Pharm. Sci.*, **59**, 1621 (1970).

(3) M. Corn and R. Berberich, *Clin. Chem.*, **13**, 126 (1967).

(4) R. J. Lewis, L. P. Ilnicki, and M. Carlstrom, *Biochem. Med.*, **4**, 376 (1970).

(5) K. K. Midha, I. J. McGilveray, and J. K. Cooper, *J. Pharm. Sci.*, **63**, 1725 (1974).

(6) D. G. Kaiser and R. S. Martin, *ibid.*, **63**, 1579 (1974).

(7) E. S. Vesell and C. A. Shively, *Science*, **184**, 466 (1974).

(8) R. J. Lewis, *J. Pharm. Sci.*, **60**, 1271 (1971).

(9) J. G. Wagner, *ibid.*, **60**, 1272 (1971).

(10) K. K. Chan, R. J. Lewis, and W. F. Trager, *J. Med. Chem.*, **15**, 1265 (1972).

(11) P. B. Andreasen and E. S. Vesell, *Clin. Pharmacol. Ther.*, **16**, 1059 (1974).

ACKNOWLEDGMENTS AND ADDRESSES

Received October 8, 1975, from the *Division of Clinical Pharmacology and the ‡Division of Cardiology, Department of Medicine, Stanford University School of Medicine, Stanford, CA 94305.

Accepted for publication March 18, 1976.

Supported in part by National Institutes of Health Grant GM 22209 and Program Project Grant 1-P01-HL-15833.

The authors acknowledge the generous gifts of the internal standard, warfarin metabolites, and ^{14}C-warfarin from David G. Kaiser, William F. Trager, and Collin H. Schroeder. T. D. Bjornsson is a recipient of a Merck Sharp & Dohme International Fellowship in Clinical Pharmacology. T. F. Blaschke is a recipient of a Faculty Development Award from the Pharmaceutical Manufacturers Association Foundation.

[x] To whom inquiries should be directed.

Comparative Pharmacokinetics of Coumarin Anticoagulants XXVIII: Predictive Identification of Rats with Relatively Steep Serum Warfarin Concentration–Anticoagulant Response Characteristics

Keyphrases □ Warfarin—serum concentration related to anticoagulant response characteristics, rats □ Anticoagulants—serum warfarin concentration related to response characteristics, rats □ Prothrombin complex synthesis—related to serum warfarin concentration, rats

To the Editor:

The coumarin anticoagulants produce their effect by inhibiting the synthesis of the vitamin K-dependent clotting factors. There is an essentially linear relationship between the degree of inhibition of the prothrombin complex synthesis rate, R_{syn}, and the logarithm of the plasma or serum concentration of warfarin and dicumarol in humans (1, 2) and rats (3, 4). The slope of a plot of R_{syn} *versus* log drug concentration is negative and was designated by the letter m in previous publications. Studies in humans showed pronounced and quite reproducible interindividual differences in m (1, 2).

One may assume that individuals with high m values are particularly likely to be subject to excessive or inadequate anticoagulation, with the attendant risks, since a small change in the drug concentration in these subjects causes a large change in the anticoagulant effect. It is impractical and probably unwise to determine m values directly in patients at the start of anticoagulant therapy since this approach requires administration of a very large dose (about 10 times larger than the usual therapeutic dose). Since the rat also exhibits pronounced interindividual differences in m, we used this animal as a model to explore the possibility of prospectively identifying "steep" responders to warfarin (*i.e.*, those with a high m value).

Ten male Sprague–Dawley rats received a single 0.6-mg/kg iv injection of ^{3}H-(*S*)-(−)-warfarin. Blood samples were collected periodically, and the concentration of warfarin and the prothrombin complex activity were determined in serum. A larger blood sample was obtained at the end of the experiment for determination of the serum free fraction of (*S*)-warfarin by equilibrium dialysis against pH 7.4 buffer containing 1.5 μg of (*S*)-warfarin/ml.

Another 10 rats received daily 0.083–0.098-mg/kg injections of (*S*)-warfarin for 13 days, the dose being adjusted to maintain a prothrombin complex activity of 30–40% of normal. On the 15th day, these rats received a single 0.6-mg/kg dose of (*S*)-warfarin, and studies were carried out as described in the previous paragraph.

The analytical procedures, the method for the determination of the serum free fraction of warfarin, and the calculations required to determine R_{syn} and m were described previously (1, 3). Separate experiments with a large dose of unlabeled (*S*)-(−)-warfarin and ^{3}H-(*S*)-(−)-warfarin, in which serum warfarin concentrations were determined both spectrophotometrically and by scintillation counting after extraction and TLC, demonstrated that the specific activity of the drug in serum remained constant with time after injection.

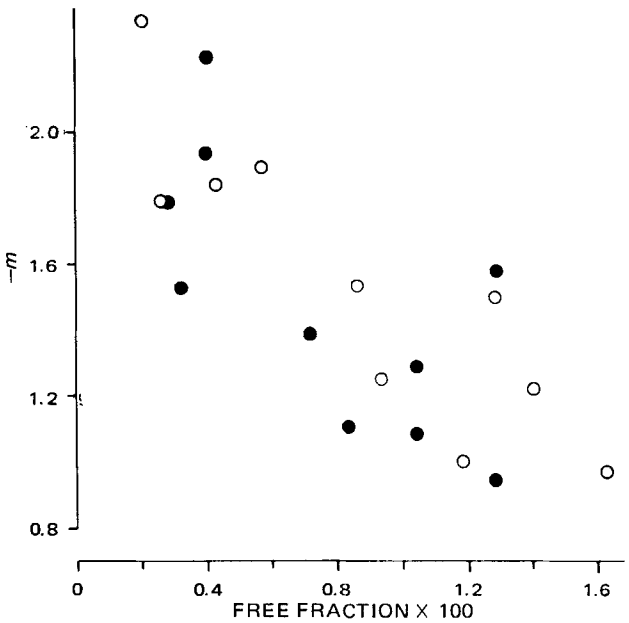

Figure 1—*Relationship between the slope of the relative anticoagulant effect–log warfarin concentration in the serum curve and the serum free fraction of* (S)-(−)-*warfarin in rats. Key:* ●, *acute dose; and* ○, *chronic dose.*

As shown in Fig. 1, m ranged from −0.939 to −2.33 and showed a statistically significant negative correlation with the serum free fraction value for warfarin ($r = -0.785$, $p < 0.001$). There was no apparent difference between acutely and chronically dosed animals. Thus, animals that showed the most extensive serum protein binding of warfarin also exhibited the steepest anticoagulant effect–log warfarin concentration curve. It is feasible, therefore, to identify predictively the steep responders to warfarin.

If the observations in rats can be confirmed in humans, it will be possible to identify, before institution of warfarin treatment, patients who have relatively steep anticoagulant effect–log serum warfarin concentration characteristics by taking a blood sample and determining the free fraction of warfarin in serum following *in vitro* addition of the drug. Previous studies showed more than fourfold differences in the serum free fraction of warfarin among 31 patients with cardiovascular disease who were being treated with warfarin (5).

(1) R. Nagashima, R. A. O'Reilly, and G. Levy, *Clin. Pharmacol. Ther.*, **10**, 22 (1969).

(2) R. A. O'Reilly and G. Levy, *ibid.*, **11**, 378 (1970).

(3) A. Yacobi, C.-M. Lai, and G. Levy, *J. Pharm. Sci.*, **64**, 1995 (1975).

(4) E. Jähnchen and G. Levy, *J. Pharmacol. Exp. Ther.*, **188**, 293 (1974).

(5) A. Yacobi, J. A. Udall, and G. Levy, *Clin. Pharmacol. Ther.*, **19**, 552 (1976).

Avraham Yacobi
Gerhard Levy [x]

Department of Pharmaceutics
School of Pharmacy
State University of New York at Buffalo
Buffalo, NY 14214

Received October 4, 1976.
Accepted for publication November 9, 1976.
Supported in part by Grant GM 20852 from the National Institute of General Medical Sciences, National Institutes of Health.
[x] To whom inquiries should be directed.

Estimation of Free Energy Change Associated with Conformational Transition of Proteins Showing Cooperative Binding Properties

Keyphrases □ Protein binding—log Q plot used to estimate free energy change associated with conformational transition □ Conformational transition—unbound to complexed proteins, log Q plot used to estimate free energy change □ Cooperative protein binding—log Q plot used to estimate free energy change associated with conformational transition □ Binding, cooperative protein—log Q plot used to estimate free energy change associated with conformational transition

To the Editor:

Sokoloski and Hoener (1) recently pointed out some corrections necessary in the use, as suggested by Ma *et al.* (2), of a log Q plot to determine protein–ligand affinity constants in systems where interaction between binding sites is indicated. These plots are usually used to calculate the relevant binding parameters following assumption of a model. However, in this article, we shall show that such plots can be used to evaluate a parameter that plays a key role in cooperative binding processes.

A protein–ligand system exhibiting positive interactions is used to illustrate the calculations. It is generally accepted, and supported by experimental evidence, that the protein must be able to assume at least two different conformations, depending upon the state of ligation (3, 4), for such cooperativity to occur. Let the conformation in the absence of ligand be the T conformation and that of the fully saturated protein be the R conformation. During ligation, the molecule changes its conformation from the T to the R form. Whether this process occurs stepwise or not is irrelevant to the current problem; Scheme I (where L is the ligand, n is the number of binding sites, and b is the experimentally observable ligation reaction) can be assumed to hold.

$$\begin{array}{ccc} T + nL & \overset{b}{\rightleftharpoons} & RL_n \\ {\scriptstyle a}\searrow & & \nearrow{\scriptstyle c} \\ & R + nL & \end{array}$$

Scheme I

The standard free energy change of this step can be considered to be composed of at least two other steps, namely the T to R conformational change as indicated by a and the binding of ligands to the R conformation as indicated by c in Scheme I. The standard free energy change, ΔF_a, of step a can be viewed as the driving force for cooperativity, its magnitude and variation with experimental conditions being important for understanding the molecular mechanism of cooperative effects. It is possible to estimate ΔF_a from a log Q plot as shown below.

The observed mean number of sites occupied is ν, so the fractional saturation, Y, is equal to ν/n, where n is the total number of binding sites. The free ligand concentration is x, allowing Q to be defined by (5):

$$\log Q = \log(Y/1 - Y) - \log x \qquad \text{(Eq. 1)}$$

where Q can be considered to be the apparent affinity constant at a given value of Y. In the case of a single site or of independent and equivalent sites, Q is a constant. Figure 1, constructed from the data of Tyuma *et al.* (6), illustrates the variation of log Q with Y when cooperativity occurs. If a model is assumed, then such a plot can be used to estimate successive binding constants. The method described in this article permits the evaluation of ΔF_a when suitable values for Y and x are available.

Wyman (7) showed that ΔF_b, the total standard free energy of ligand binding, is equal to $nRT \int_0^1 \ln x \, dY$. This true thermodynamic expression can be related to log Q as follows:

$$\int_0^1 \ln x \, dY = -\int_0^1 [\ln(Y/1 - Y) - \ln x] dY \qquad \text{(Eq. 2a)}$$

$$\int_0^1 \ln(Y/1 - Y) dY = 0 \qquad \text{(Eq. 2b)}$$

Therefore:

$$\Delta F_b = -nRT \int_0^1 \ln Q_b \, dY \qquad \text{(Eq. 3)}$$

where b indicates that Q is concerned with step b. A similar argument can be used to obtain:

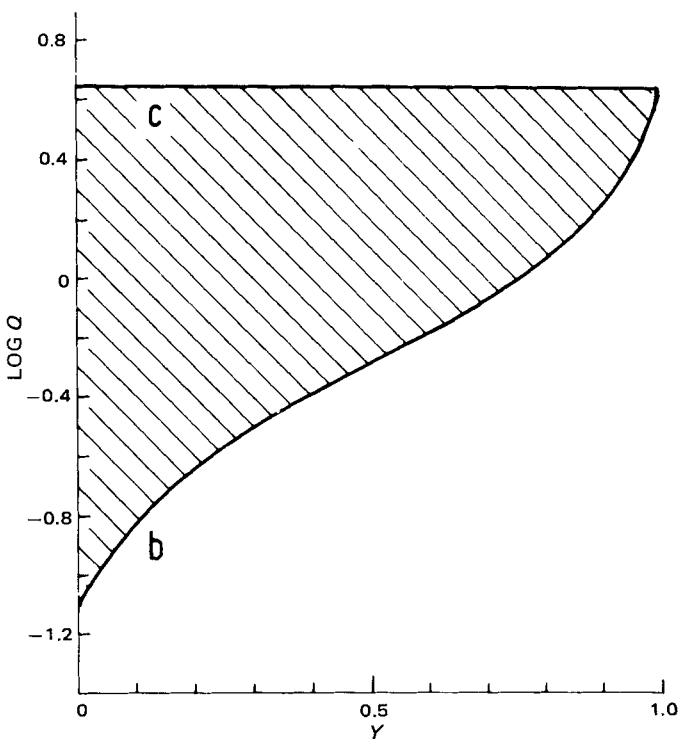

Figure 1—*Log Q plot of binding of oxygen to hemoglobin, calculated from the data in Ref. 6. In the calculation, partial oxygen pressure (in mm Hg) was used instead of molar oxygen concentration. Therefore, a conversion factor is involved in the calculation of* ΔF_b *or* ΔF_c *following the procedure outlined in the text. However, in the calculation of* ΔF_a, *this factor cancels out.*

Department of Pharmaceutics
School of Pharmacy
State University of New York at Buffalo
Buffalo, NY 14214

Received October 4, 1976.
Accepted for publication November 9, 1976.
Supported in part by Grant GM 20852 from the National Institute of General Medical Sciences, National Institutes of Health.
[x] To whom inquiries should be directed.

Estimation of Free Energy Change Associated with Conformational Transition of Proteins Showing Cooperative Binding Properties

Keyphrases □ Protein binding—log Q plot used to estimate free energy change associated with conformational transition □ Conformational transition—unbound to complexed proteins, log Q plot used to estimate free energy change □ Cooperative protein binding—log Q plot used to estimate free energy change associated with conformational transition □ Binding, cooperative protein—log Q plot used to estimate free energy change associated with conformational transition

To the Editor:

Sokoloski and Hoener (1) recently pointed out some corrections necessary in the use, as suggested by Ma *et al.* (2), of a log Q plot to determine protein–ligand affinity constants in systems where interaction between binding sites is indicated. These plots are usually used to calculate the relevant binding parameters following assumption of a model. However, in this article, we shall show that such plots can be used to evaluate a parameter that plays a key role in cooperative binding processes.

A protein–ligand system exhibiting positive interactions is used to illustrate the calculations. It is generally accepted, and supported by experimental evidence, that the protein must be able to assume at least two different conformations, depending upon the state of ligation (3, 4), for such cooperativity to occur. Let the conformation in the absence of ligand be the T conformation and that of the fully saturated protein be the R conformation. During ligation, the molecule changes its conformation from the T to the R form. Whether this process occurs stepwise or not is irrelevant to the current problem; Scheme I (where L is the ligand, n is the number of binding sites, and b is the experimentally observable ligation reaction) can be assumed to hold.

$$\begin{array}{ccc} T + nL & \overset{b}{\rightleftharpoons} & RL_n \\ {\scriptstyle a}\searrow & & \nearrow{\scriptstyle c} \\ & R + nL & \end{array}$$

Scheme I

The standard free energy change of this step can be considered to be composed of at least two other steps, namely the T to R conformational change as indicated by a and the binding of ligands to the R conformation as indicated by c in Scheme I. The standard free energy change, ΔF_a, of step a can be viewed as the driving force for cooperativity, its magnitude and variation with experimental conditions being important for understanding the molecular mechanism of cooperative effects. It is possible to estimate ΔF_a from a log Q plot as shown below.

The observed mean number of sites occupied is ν, so the fractional saturation, Y, is equal to ν/n, where n is the total number of binding sites. The free ligand concentration is x, allowing Q to be defined by (5):

$$\log Q = \log(Y/1 - Y) - \log x \qquad \text{(Eq. 1)}$$

where Q can be considered to be the apparent affinity constant at a given value of Y. In the case of a single site or of independent and equivalent sites, Q is a constant. Figure 1, constructed from the data of Tyuma *et al.* (6), illustrates the variation of log Q with Y when cooperativity occurs. If a model is assumed, then such a plot can be used to estimate successive binding constants. The method described in this article permits the evaluation of ΔF_a when suitable values for Y and x are available.

Wyman (7) showed that ΔF_b, the total standard free energy of ligand binding, is equal to $nRT \int_0^1 \ln x \, dY$. This true thermodynamic expression can be related to log Q as follows:

$$\int_0^1 \ln x \, dY = -\int_0^1 [\ln(Y/1 - Y) - \ln x] dY \qquad \text{(Eq. 2a)}$$

$$\int_0^1 \ln(Y/1 - Y) dY = 0 \qquad \text{(Eq. 2b)}$$

Therefore:

$$\Delta F_b = -nRT \int_0^1 \ln Q_b \, dY \qquad \text{(Eq. 3)}$$

where b indicates that Q is concerned with step b. A similar argument can be used to obtain:

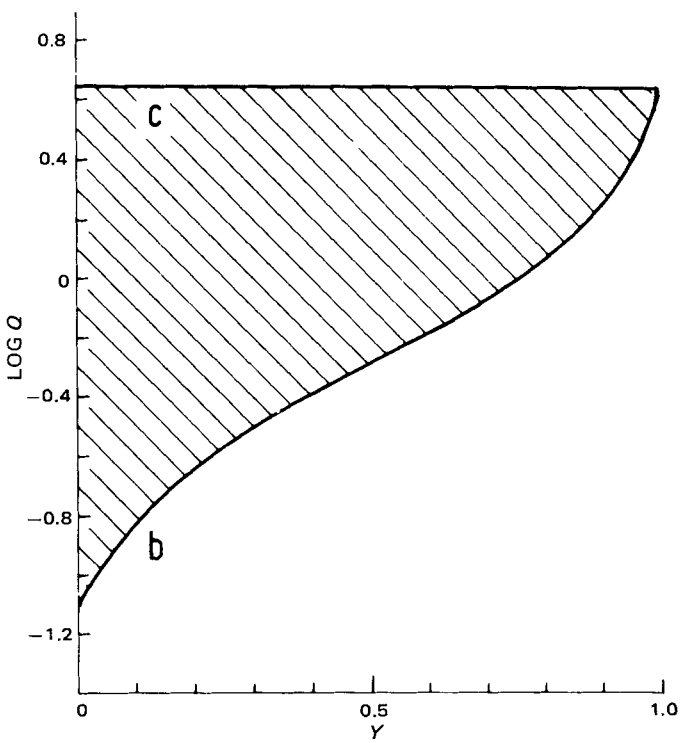

Figure 1—*Log Q plot of binding of oxygen to hemoglobin, calculated from the data in Ref. 6. In the calculation, partial oxygen pressure (in mm Hg) was used instead of molar oxygen concentration. Therefore, a conversion factor is involved in the calculation of* ΔF_b *or* ΔF_c *following the procedure outlined in the text. However, in the calculation of* ΔF_a, *this factor cancels out.*

$$\Delta F_c = -nRT \int_0^1 \ln Q_c \, dY \qquad \text{(Eq. 4)}$$

Therefore, as $\Delta F_a = \Delta F_b - \Delta F_c$:

$$\Delta F_a = 2.3nRT \int_0^1 (\log Q_c - \log Q_b) dY \qquad \text{(Eq. 5)}$$

In Fig. 1, curve b represents log Q_b, so the area under the curve multiplied by $-2.3nRT$ is equal to ΔF_b. However, Q_c cannot be obtained in a similar manner, because, in general, reaction c cannot be followed experimentally. A good approximation for log Q_c can be obtained, because all protein molecules are in the R state when Y approaches 1 so the limiting value of log Q_b and log Q_c must be the same. Therefore, an estimate of log Q_c can be obtained from Fig. 1, because line c should equal log Q_c when it is assumed that all sites are equal in the R state. This assumption immediately implies that, from Eq. 5, ΔF_a is equal to the shaded area of Fig. 1 multiplied by $2.3nRT$. In the figure, this area is equal to 5.0 kcal. From the figure, it can be seen that ΔF_a is always a positive quantity in a cooperative process, so the associated equilibrium constant is less than 1 or, in other words, the T conformation is highly favored in the absence of ligand.

This important result is obtained following the assumption that all sites in the R state are equal. A qualitative picture of the situation, when this assumption does not hold, can be obtained in the following way. All protein molecules are in the R state when Y approaches 1, so the limiting value of log Q_b when Y approaches 1 should form one point of the line representing log Q_c. However, when the binding sites are unequal, log Q_c is no longer equal to line c in Fig. 1. Log Q_c cannot lie below line c in Fig. 1, because this would indicate cooperativity in a molecule totally in the R state. Under these circumstances, log Q_c must lie somewhere above line c. This means that the true value of ΔF_a for nonidentical sites is higher than that obtained by applying the method for identical sites. Only when some specific model is assumed can the exact value of ΔF_a be calculated (8). It is obvious that dissimilarity of binding sites in the T state has no influence on the determination of ΔF_a.

(1) T. D. Sokoloski and B. Hoener, *J. Pharm. Sci.*, **64**, 1892 (1975).
(2) J. K. H. Ma, H. W. Jun, and L. A. Luzzi, *ibid.*, **62**, 2038 (1973).
(3) J. Monod, J. Wyman, and J. P. Changeux, *J. Mol. Biol.*, **12**, 88 (1965).
(4) D. E. Koshland, G. Nemethy, and P. Filmer, *Biochemistry*, **5**, 365 (1966).
(5) J. T. Edsall, C. Felsenfeld, D. S. Goodman, and F. R. N. Curd, *J. Am. Chem. Soc.*, **76**, 3054 (1954).
(6) I. Tyuma, K. Shimizu, and K. Imai, *Biochem. Biophys. Res. Commun.*, **43**, 423 (1971).
(7) J. Wyman, *Adv. Protein Chem.*, **19**, 223 (1964).
(8) L. H. M. Janssen and S. H. de Bruin, *Biophys. Chem.*, **1**, 130 (1973).

Lambert H. M. Janssen [x]
John H. Perrin *
School of Pharmacy
State University of Utrecht
Catharijnesingel 60
Utrecht, The Netherlands

Received July 26, 1976.
Accepted for publication October 8, 1976.

* Present address: College of Pharmacy, J. H. Miller Health Center, University of Florida, Gainesville, FL 32610.
[x] To whom inquiries should be directed.

BOOKS

REVIEWS

Topics in Infectious Diseases. Vol. 1. Drug Receptor Interactions in Antimicrobial Chemotherapy. Edited by J. DREWS and F. E. HAHN. Springer-Verlag, 175 Fifth Ave., New York, NY 10010, 1975. 314 pp. 17 × 24.5 cm. Price $19.40.

This book contains the papers presented at the Sandoz Symposium held in Vienna on September 4–6, 1974. It is divided into five general areas, *i.e.*, receptor hypothesis, DNA as a drug receptor, ribosomes as drug receptors, mode of action of chloramphenicol, and microbial enzymes as drug receptors, and includes papers that were contributed by 20 participants. The text of the book has 300 pages, 130 figures and illustrations, and 60 tables.

Drug–receptor interaction is the key to the effect and fate of a drug in the biological system. The authors exemplified the underlying mechanism of antibiotic–receptor interactions by systematically quantifying the relationship between physicochemical parameters and biological responses elicited by interactions of the drug with bioreceptors. Recent advances in research on binding sites of drug molecules to DNA and ribosomal subunits are presented.

The book offers a further insight into the mechanism of development of resistance in microorganisms and the role of plasmids in transmitting resistant genetic elements into the new cell line. Evidence has been produced demonstrating that there can be a surge of R factors in nonpathogenic enterobacteria which may be transferred to the pathogens such as *Shigellae* and *Salmonellae* due to the worldwide indiscriminate use of antibiotics. This is part of the endless race between medical science and microorganisms. The authors discussed the elimination of the genetic determinant elements from plasmids by binding DNA with a number of antibiotic as well as nonantibiotic agents. Enzyme inhibitory actions demonstrated by antibiotics and nonantibiotics suggest potential development of a bacterial enzyme inhibitor as an antimicrobial agent.

The authors suggest that when theory and knowledge of drug–receptor interactions are put into practice, a more ideal drug molecule with precise effect and anticipated mode of action may be designed with less time and expense.

Reviewed by Chian L. Huang
College of Pharmacy and Allied Health Professions
Wayne State University
Detroit, MI 48202

Medication Law and Behavior. By J. TYRONE GIBSON. Wiley, 605 Third Ave., New York, NY 10016, 1976. 407 pp. 16 × 23.5 cm. Price $15.95.

"The book is designed to help the reader learn more about the influence of medication law on the behavior of health care personnel who assist in providing medication and medication services." The author establishes this objective in the preface and in a highly readable style achieves it in the text.

Nonlawyers and those not in the health professions, as well as health professionals, can learn from reading this book. The book

$$\Delta F_c = -nRT \int_0^1 \ln Q_c \, dY \qquad \text{(Eq. 4)}$$

Therefore, as $\Delta F_a = \Delta F_b - \Delta F_c$:

$$\Delta F_a = 2.3nRT \int_0^1 (\log Q_c - \log Q_b) dY \qquad \text{(Eq. 5)}$$

In Fig. 1, curve b represents log Q_b, so the area under the curve multiplied by $-2.3nRT$ is equal to ΔF_b. However, Q_c cannot be obtained in a similar manner, because, in general, reaction c cannot be followed experimentally. A good approximation for log Q_c can be obtained, because all protein molecules are in the R state when Y approaches 1 so the limiting value of log Q_b and log Q_c must be the same. Therefore, an estimate of log Q_c can be obtained from Fig. 1, because line c should equal log Q_c when it is assumed that all sites are equal in the R state. This assumption immediately implies that, from Eq. 5, ΔF_a is equal to the shaded area of Fig. 1 multiplied by $2.3nRT$. In the figure, this area is equal to 5.0 kcal. From the figure, it can be seen that ΔF_a is always a positive quantity in a cooperative process, so the associated equilibrium constant is less than 1 or, in other words, the T conformation is highly favored in the absence of ligand.

This important result is obtained following the assumption that all sites in the R state are equal. A qualitative picture of the situation, when this assumption does not hold, can be obtained in the following way. All protein molecules are in the R state when Y approaches 1, so the limiting value of log Q_b when Y approaches 1 should form one point of the line representing log Q_c. However, when the binding sites are unequal, log Q_c is no longer equal to line c in Fig. 1. Log Q_c cannot lie below line c in Fig. 1, because this would indicate cooperativity in a molecule totally in the R state. Under these circumstances, log Q_c must lie somewhere above line c. This means that the true value of ΔF_a for nonidentical sites is higher than that obtained by applying the method for identical sites. Only when some specific model is assumed can the exact value of ΔF_a be calculated (8). It is obvious that dissimilarity of binding sites in the T state has no influence on the determination of ΔF_a.

(1) T. D. Sokoloski and B. Hoener, *J. Pharm. Sci.*, **64**, 1892 (1975).
(2) J. K. H. Ma, H. W. Jun, and L. A. Luzzi, *ibid.*, **62**, 2038 (1973).
(3) J. Monod, J. Wyman, and J. P. Changeux, *J. Mol. Biol.*, **12**, 88 (1965).
(4) D. E. Koshland, G. Nemethy, and P. Filmer, *Biochemistry*, **5**, 365 (1966).
(5) J. T. Edsall, C. Felsenfeld, D. S. Goodman, and F. R. N. Curd, *J. Am. Chem. Soc.*, **76**, 3054 (1954).
(6) I. Tyuma, K. Shimizu, and K. Imai, *Biochem. Biophys. Res. Commun.*, **43**, 423 (1971).
(7) J. Wyman, *Adv. Protein Chem.*, **19**, 223 (1964).
(8) L. H. M. Janssen and S. H. de Bruin, *Biophys. Chem.*, **1**, 130 (1973).

Lambert H. M. Janssen [x]
John H. Perrin *
School of Pharmacy
State University of Utrecht
Catharijnesingel 60
Utrecht, The Netherlands

Received July 26, 1976.
Accepted for publication October 8, 1976.

* Present address: College of Pharmacy, J. H. Miller Health Center, University of Florida, Gainesville, FL 32610.
[x] To whom inquiries should be directed.

BOOKS

REVIEWS

Topics in Infectious Diseases. Vol. 1. Drug Receptor Interactions in Antimicrobial Chemotherapy. Edited by J. DREWS and F. E. HAHN. Springer-Verlag, 175 Fifth Ave., New York, NY 10010, 1975. 314 pp. 17 × 24.5 cm. Price $19.40.

This book contains the papers presented at the Sandoz Symposium held in Vienna on September 4–6, 1974. It is divided into five general areas, *i.e.*, receptor hypothesis, DNA as a drug receptor, ribosomes as drug receptors, mode of action of chloramphenicol, and microbial enzymes as drug receptors, and includes papers that were contributed by 20 participants. The text of the book has 300 pages, 130 figures and illustrations, and 60 tables.

Drug–receptor interaction is the key to the effect and fate of a drug in the biological system. The authors exemplified the underlying mechanism of antibiotic–receptor interactions by systematically quantifying the relationship between physicochemical parameters and biological responses elicited by interactions of the drug with bioreceptors. Recent advances in research on binding sites of drug molecules to DNA and ribosomal subunits are presented.

The book offers a further insight into the mechanism of development of resistance in microorganisms and the role of plasmids in transmitting resistant genetic elements into the new cell line. Evidence has been produced demonstrating that there can be a surge of R factors in nonpathogenic enterobacteria which may be transferred to the pathogens such as *Shigellae* and *Salmonellae* due to the worldwide indiscriminate use of antibiotics. This is part of the endless race between medical science and microorganisms. The authors discussed the elimination of the genetic determinant elements from plasmids by binding DNA with a number of antibiotic as well as nonantibiotic agents. Enzyme inhibitory actions demonstrated by antibiotics and nonantibiotics suggest potential development of a bacterial enzyme inhibitor as an antimicrobial agent.

The authors suggest that when theory and knowledge of drug–receptor interactions are put into practice, a more ideal drug molecule with precise effect and anticipated mode of action may be designed with less time and expense.

Reviewed by Chian L. Huang
College of Pharmacy and Allied Health Professions
Wayne State University
Detroit, MI 48202

Medication Law and Behavior. By J. TYRONE GIBSON. Wiley, 605 Third Ave., New York, NY 10016, 1976. 407 pp. 16 × 23.5 cm. Price $15.95.

"The book is designed to help the reader learn more about the influence of medication law on the behavior of health care personnel who assist in providing medication and medication services." The author establishes this objective in the preface and in a highly readable style achieves it in the text.

Nonlawyers and those not in the health professions, as well as health professionals, can learn from reading this book. The book

$$\Delta F_c = -nRT \int_0^1 \ln Q_c \, dY \qquad \text{(Eq. 4)}$$

Therefore, as $\Delta F_a = \Delta F_b - \Delta F_c$:

$$\Delta F_a = 2.3nRT \int_0^1 (\log Q_c - \log Q_b) dY \qquad \text{(Eq. 5)}$$

In Fig. 1, curve b represents log Q_b, so the area under the curve multiplied by $-2.3nRT$ is equal to ΔF_b. However, Q_c cannot be obtained in a similar manner, because, in general, reaction c cannot be followed experimentally. A good approximation for log Q_c can be obtained, because all protein molecules are in the R state when Y approaches 1 so the limiting value of log Q_b and log Q_c must be the same. Therefore, an estimate of log Q_c can be obtained from Fig. 1, because line c should equal log Q_c when it is assumed that all sites are equal in the R state. This assumption immediately implies that, from Eq. 5, ΔF_a is equal to the shaded area of Fig. 1 multiplied by $2.3nRT$. In the figure, this area is equal to 5.0 kcal. From the figure, it can be seen that ΔF_a is always a positive quantity in a cooperative process, so the associated equilibrium constant is less than 1 or, in other words, the T conformation is highly favored in the absence of ligand.

This important result is obtained following the assumption that all sites in the R state are equal. A qualitative picture of the situation, when this assumption does not hold, can be obtained in the following way. All protein molecules are in the R state when Y approaches 1, so the limiting value of log Q_b when Y approaches 1 should form one point of the line representing log Q_c. However, when the binding sites are unequal, log Q_c is no longer equal to line c in Fig. 1. Log Q_c cannot lie below line c in Fig. 1, because this would indicate cooperativity in a molecule totally in the R state. Under these circumstances, log Q_c must lie somewhere above line c. This means that the true value of ΔF_a for nonidentical sites is higher than that obtained by applying the method for identical sites. Only when some specific model is assumed can the exact value of ΔF_a be calculated (8). It is obvious that dissimilarity of binding sites in the T state has no influence on the determination of ΔF_a.

(1) T. D. Sokoloski and B. Hoener, *J. Pharm. Sci.*, **64**, 1892 (1975).
(2) J. K. H. Ma, H. W. Jun, and L. A. Luzzi, *ibid.*, **62**, 2038 (1973).
(3) J. Monod, J. Wyman, and J. P. Changeux, *J. Mol. Biol.*, **12**, 88 (1965).
(4) D. E. Koshland, G. Nemethy, and P. Filmer, *Biochemistry*, **5**, 365 (1966).
(5) J. T. Edsall, C. Felsenfeld, D. S. Goodman, and F. R. N. Curd, *J. Am. Chem. Soc.*, **76**, 3054 (1954).
(6) I. Tyuma, K. Shimizu, and K. Imai, *Biochem. Biophys. Res. Commun.*, **43**, 423 (1971).
(7) J. Wyman, *Adv. Protein Chem.*, **19**, 223 (1964).
(8) L. H. M. Janssen and S. H. de Bruin, *Biophys. Chem.*, **1**, 130 (1973).

Lambert H. M. Janssen [x]
John H. Perrin *
School of Pharmacy
State University of Utrecht
Catharijnesingel 60
Utrecht, The Netherlands

Received July 26, 1976.
Accepted for publication October 8, 1976.

* Present address: College of Pharmacy, J. H. Miller Health Center, University of Florida, Gainesville, FL 32610.
[x] To whom inquiries should be directed.

BOOKS

REVIEWS

Topics in Infectious Diseases. Vol. 1. Drug Receptor Interactions in Antimicrobial Chemotherapy. Edited by J. DREWS and F. E. HAHN. Springer-Verlag, 175 Fifth Ave., New York, NY 10010, 1975. 314 pp. 17 × 24.5 cm. Price $19.40.

This book contains the papers presented at the Sandoz Symposium held in Vienna on September 4–6, 1974. It is divided into five general areas, *i.e.*, receptor hypothesis, DNA as a drug receptor, ribosomes as drug receptors, mode of action of chloramphenicol, and microbial enzymes as drug receptors, and includes papers that were contributed by 20 participants. The text of the book has 300 pages, 130 figures and illustrations, and 60 tables.

Drug–receptor interaction is the key to the effect and fate of a drug in the biological system. The authors exemplified the underlying mechanism of antibiotic–receptor interactions by systematically quantifying the relationship between physicochemical parameters and biological responses elicited by interactions of the drug with bioreceptors. Recent advances in research on binding sites of drug molecules to DNA and ribosomal subunits are presented.

The book offers a further insight into the mechanism of development of resistance in microorganisms and the role of plasmids in transmitting resistant genetic elements into the new cell line. Evidence has been produced demonstrating that there can be a surge of R factors in nonpathogenic enterobacteria which may be transferred to the pathogens such as *Shigellae* and *Salmonellae* due to the worldwide indiscriminate use of antibiotics. This is part of the endless race between medical science and microorganisms. The authors discussed the elimination of the genetic determinant elements from plasmids by binding DNA with a number of antibiotic as well as nonantibiotic agents. Enzyme inhibitory actions demonstrated by antibiotics and nonantibiotics suggest potential development of a bacterial enzyme inhibitor as an antimicrobial agent.

The authors suggest that when theory and knowledge of drug–receptor interactions are put into practice, a more ideal drug molecule with precise effect and anticipated mode of action may be designed with less time and expense.

Reviewed by Chian L. Huang
College of Pharmacy and Allied Health Professions
Wayne State University
Detroit, MI 48202

Medication Law and Behavior. By J. TYRONE GIBSON. Wiley, 605 Third Ave., New York, NY 10016, 1976. 407 pp. 16 × 23.5 cm. Price $15.95.

"The book is designed to help the reader learn more about the influence of medication law on the behavior of health care personnel who assist in providing medication and medication services." The author establishes this objective in the preface and in a highly readable style achieves it in the text.

Nonlawyers and those not in the health professions, as well as health professionals, can learn from reading this book. The book

provides a thorough review of medication law, particularly the Federal Food, Drug, and Cosmetic Act. However, it also considers such areas as professional practice acts and negligence.

The book, however, is not a text on pharmacy law. Rather, it relates the law to the behavior of people, primarily patients and providers of health care. For example, two chapters on the requirements of drug labeling are followed by a chapter on "How Drug Information is Used." The book deals not only with the legal controls on drug distribution but also with the behavioral aspects of why people take drugs (medication).

The book is well referenced and draws on legal citations, behavioral studies, and the clinical literature. The liberal use of figures and tables enhances the value of the book as a learning device. The book is unique in combining the legal aspects of medication with the behavioral aspects. It would be a valuable addition to the library of anyone involved in the drug use process.

Reviewed by Maven J. Myers
Philadelphia College of Pharmacy and Science
Philadelphia, PA 19104

Microencapsulation. Edited by J. R. NIXON. Dekker, 270 Madison Ave., New York, NY 10016, 1976. 215 pp. 16 × 23.5 cm. Price $19.50.

This book constitutes a collection of 17 papers delivered in London at the second international symposium on microencapsulation. The contributors to this hard-covered book are recognized international authorities in the field of microencapsulation.

In Chapter 1, the processes of coacervation, spray encapsulation, and nanoencapsulation are reviewed by P. Speiser. The intricacies of each method are well defined by the author, and applications are also given.

In Chapter 2, A. Watanabe and T. Hayashi describe gelatin–gum arabic coacervation, interfacial polymerization, and the preparation of multiwalled microcapsules. The authors describe the applications of microcapsules in the manufacture of carbonless copy paper, encapsulated perfume ink, and the image display panel, the latter employing the electrophoretic behavior of microcapsules. The chapter is well illustrated with several photographs and diagrams.

In Chapter 3, A. T. Florence and A. W. Jenkins deal with the assessment *in vitro* of microencapsulated drug systems utilized in sustained-release parenteral dosage forms. Drug dissolution, stability, and biodegradability are discussed. The paper is clearly written, well referenced, and illustrated with photographs.

T. M. S. Chang, in Chapter 4, reviews the vast amount of research and clinical applications of semipermeable microcapsules used as artificial cells. Professor Chang, being a leading world authority in this area, is amply qualified to handle this topic, and his paper is documented with 42 references. The applications of microcapsules to augment artificial kidney function are further discussed by R. E. Sparks *et al.* in Chapter 9.

A major problem in the microencapsulation of enzymes has been the loss of enzyme activity during the microencapsulation process. T. Kondo and N. Muramatsu suggest solutions to this problem in Chapter 5.

The use of microcapsules as food particles for marine particulate feeders is discussed by D. A. Jones and P. A. Gabbott in Chapter 6. A nylon coat for the microcapsules provided an indigestable wall to reduce bacterial contact with the enclosed diet. The authors also suggest another important use for microcapsules in the cultivation of marine organisms and that is to supply medicinal compounds, *e.g.*, antibiotics, to prevent or cure disease.

In Chapter 7, M. Calanchi describes several new dosage forms containing microcapsules prepared *via* coacervation. The author discusses the microencapsulation of antibiotics, aspirin, vitamin C, and steroids and suggests applications of the technique to improve drug stability, overcome incompatibilities, prolong the action of drugs, and conceal the bitter taste of medicinals. Further applications for microcapsules as drug delivery systems, particularly in topical dosage forms, are described in Chapter 10 by R. H. Sudekum.

In Chapter 8, G. C. Maggi and F. DiRoberto outline a method used to diagnose and monitor peripheral vascular disorders by employing encapsulated liquid crystal thermography. R. G. Arnold, in Chapter 11, reviews the many varied applications of microencapsulation and describes the sequence of events and procedures the FDA requires to approve a new microencapsulated animal drug product for marketing. This chapter should be of great interest to those interested in marketing such products. Further veterinary applications of microencapsulation are outlined in Chapter 12 by G. Rognoni.

V. de Sabata, in Chapter 13, reviews several published articles concerned with drug bioavailability from microencapsulated dosage forms. Chapter 14 should be of particular interest to the biologist. T. Kondo *et al.* describe the preparation and properties of artificial red blood cells containing hemoglobin solution.

Chapter 15, an excellent chapter by J. R. Nixon and B. R. Matthews, deals with the surface characteristics of gelatin coacervate microcapsules using scanning electron microscopy. Photographs of microcapsules prepared *via* alcohol coacervation and sodium sulfate coacervation procedures display definite surface properties, and these differences are discussed in the paper. Further physicochemical studies of microcapsules appear in Chapter 16. L. Nang and P. F. Carlier mathematically derive the wall diffusion coefficient and discuss its importance in evaluating microencapsulating methods and the optimization of a coacervation process.

In Chapter 17, the final chapter in the book, L. A. Luzzi reviews the applications, methods of preparation, and physicochemical properties of microcapsules. The chapter is well written and well referenced.

Discussions of some applications and methodologies, such as coacervation and interfacial polymerization, are redundant in the book; however, due to the multiple authorship, this repetition could be expected. The book contains an even balance of reviews and original research. It provides an insight to the science of microencapsulation and should stimulate new research ideas. The book is not only of interest to the pharmaceutical scientist but is also intended for pharmacologists, biologists, chemists, and veterinary scientists.

Reviewed by James W. McGinity
School of Pharmacy
Texas Southern University
Houston, TX 77004

Practical Pharmaceutical Chemistry. Third Edition—Part One. By A. H. BECKETT and J. B. STENLAKE. Humanities Press, Atlantic Highlands, NJ 07716, 1975. 370 pp. 16 × 24.5 cm. Price $25.00.

Two major additions and several minor revisions have been made in the third edition of this textbook. A new chapter on the registration and assessment of medicines in the United Kingdom has been added. The implications of the Medicines Act of 1968 and Good Manufacturing Practices published by HMSO in 1971 to the analysts and compilers of product applications is presented in a general manner. The treatment of general analytical procedures has been extended. This new chapter covers all important product types including tablets, capsules, suspensions, ointments, creams, pressurized aerosols, lozenges, suppositories, solutions, and mixtures as well as dissolution testing, sustained-release preparations, and particle-size control.

The subject matter is presented in 14 chapters. A limited theoretical treatment is presented, where pertinent, followed by practical examples which have been drawn from the British Pharmacopoeia and other sources. These examples are intended to serve as laboratory exercises.

The book is practical in every sense of the word. It covers primarily the classical methods of analysis, with discussion of the more sophisticated methods being reserved for Part 2. Although the style of presentation of determination of equivalent weights is somewhat different than this reviewer is accustomed to, it is very easy to follow. An insight into the chemistry of many of the limit tests as well as many of the monographs in the British Pharmacopoeia is provided. Of particular interest to this reviewer were the chapters on chemical purity and control, registration and assessment of medicines, and techniques of quantitative analysis. These chapters very basically cover the what, why, and how of quantitative analysis, something that is not infrequently overlooked in the education of analysts.

Reviewed by Robert E. Daly
Warner-Lambert Research Institute
Morris Plains, NJ 07950

provides a thorough review of medication law, particularly the Federal Food, Drug, and Cosmetic Act. However, it also considers such areas as professional practice acts and negligence.

The book, however, is not a text on pharmacy law. Rather, it relates the law to the behavior of people, primarily patients and providers of health care. For example, two chapters on the requirements of drug labeling are followed by a chapter on "How Drug Information is Used." The book deals not only with the legal controls on drug distribution but also with the behavioral aspects of why people take drugs (medication).

The book is well referenced and draws on legal citations, behavioral studies, and the clinical literature. The liberal use of figures and tables enhances the value of the book as a learning device. The book is unique in combining the legal aspects of medication with the behavioral aspects. It would be a valuable addition to the library of anyone involved in the drug use process.

Reviewed by Maven J. Myers
Philadelphia College of Pharmacy and Science
Philadelphia, PA 19104

Microencapsulation. Edited by J. R. NIXON. Dekker, 270 Madison Ave., New York, NY 10016, 1976. 215 pp. 16 × 23.5 cm. Price $19.50.

This book constitutes a collection of 17 papers delivered in London at the second international symposium on microencapsulation. The contributors to this hard-covered book are recognized international authorities in the field of microencapsulation.

In Chapter 1, the processes of coacervation, spray encapsulation, and nanoencapsulation are reviewed by P. Speiser. The intricacies of each method are well defined by the author, and applications are also given.

In Chapter 2, A. Watanabe and T. Hayashi describe gelatin–gum arabic coacervation, interfacial polymerization, and the preparation of multiwalled microcapsules. The authors describe the applications of microcapsules in the manufacture of carbonless copy paper, encapsulated perfume ink, and the image display panel, the latter employing the electrophoretic behavior of microcapsules. The chapter is well illustrated with several photographs and diagrams.

In Chapter 3, A. T. Florence and A. W. Jenkins deal with the assessment *in vitro* of microencapsulated drug systems utilized in sustained-release parenteral dosage forms. Drug dissolution, stability, and biodegradability are discussed. The paper is clearly written, well referenced, and illustrated with photographs.

T. M. S. Chang, in Chapter 4, reviews the vast amount of research and clinical applications of semipermeable microcapsules used as artificial cells. Professor Chang, being a leading world authority in this area, is amply qualified to handle this topic, and his paper is documented with 42 references. The applications of microcapsules to augment artificial kidney function are further discussed by R. E. Sparks *et al.* in Chapter 9.

A major problem in the microencapsulation of enzymes has been the loss of enzyme activity during the microencapsulation process. T. Kondo and N. Muramatsu suggest solutions to this problem in Chapter 5.

The use of microcapsules as food particles for marine particulate feeders is discussed by D. A. Jones and P. A. Gabbott in Chapter 6. A nylon coat for the microcapsules provided an indigestable wall to reduce bacterial contact with the enclosed diet. The authors also suggest another important use for microcapsules in the cultivation of marine organisms and that is to supply medicinal compounds, *e.g.*, antibiotics, to prevent or cure disease.

In Chapter 7, M. Calanchi describes several new dosage forms containing microcapsules prepared *via* coacervation. The author discusses the microencapsulation of antibiotics, aspirin, vitamin C, and steroids and suggests applications of the technique to improve drug stability, overcome incompatibilities, prolong the action of drugs, and conceal the bitter taste of medicinals. Further applications for microcapsules as drug delivery systems, particularly in topical dosage forms, are described in Chapter 10 by R. H. Sudekum.

In Chapter 8, G. C. Maggi and F. DiRoberto outline a method used to diagnose and monitor peripheral vascular disorders by employing encapsulated liquid crystal thermography. R. G. Arnold, in Chapter 11, reviews the many varied applications of microencapsulation and describes the sequence of events and procedures the FDA requires to approve a new microencapsulated animal drug product for marketing. This chapter should be of great interest to those interested in marketing such products. Further veterinary applications of microencapsulation are outlined in Chapter 12 by G. Rognoni.

V. de Sabata, in Chapter 13, reviews several published articles concerned with drug bioavailability from microencapsulated dosage forms. Chapter 14 should be of particular interest to the biologist. T. Kondo *et al.* describe the preparation and properties of artificial red blood cells containing hemoglobin solution.

Chapter 15, an excellent chapter by J. R. Nixon and B. R. Matthews, deals with the surface characteristics of gelatin coacervate microcapsules using scanning electron microscopy. Photographs of microcapsules prepared *via* alcohol coacervation and sodium sulfate coacervation procedures display definite surface properties, and these differences are discussed in the paper. Further physicochemical studies of microcapsules appear in Chapter 16. L. Nang and P. F. Carlier mathematically derive the wall diffusion coefficient and discuss its importance in evaluating microencapsulating methods and the optimization of a coacervation process.

In Chapter 17, the final chapter in the book, L. A. Luzzi reviews the applications, methods of preparation, and physicochemical properties of microcapsules. The chapter is well written and well referenced.

Discussions of some applications and methodologies, such as coacervation and interfacial polymerization, are redundant in the book; however, due to the multiple authorship, this repetition could be expected. The book contains an even balance of reviews and original research. It provides an insight to the science of microencapsulation and should stimulate new research ideas. The book is not only of interest to the pharmaceutical scientist but is also intended for pharmacologists, biologists, chemists, and veterinary scientists.

Reviewed by James W. McGinity
School of Pharmacy
Texas Southern University
Houston, TX 77004

Practical Pharmaceutical Chemistry. Third Edition—Part One. By A. H. BECKETT and J. B. STENLAKE. Humanities Press, Atlantic Highlands, NJ 07716, 1975. 370 pp. 16 × 24.5 cm. Price $25.00.

Two major additions and several minor revisions have been made in the third edition of this textbook. A new chapter on the registration and assessment of medicines in the United Kingdom has been added. The implications of the Medicines Act of 1968 and Good Manufacturing Practices published by HMSO in 1971 to the analysts and compilers of product applications is presented in a general manner. The treatment of general analytical procedures has been extended. This new chapter covers all important product types including tablets, capsules, suspensions, ointments, creams, pressurized aerosols, lozenges, suppositories, solutions, and mixtures as well as dissolution testing, sustained-release preparations, and particle-size control.

The subject matter is presented in 14 chapters. A limited theoretical treatment is presented, where pertinent, followed by practical examples which have been drawn from the British Pharmacopoeia and other sources. These examples are intended to serve as laboratory exercises.

The book is practical in every sense of the word. It covers primarily the classical methods of analysis, with discussion of the more sophisticated methods being reserved for Part 2. Although the style of presentation of determination of equivalent weights is somewhat different than this reviewer is accustomed to, it is very easy to follow. An insight into the chemistry of many of the limit tests as well as many of the monographs in the British Pharmacopoeia is provided. Of particular interest to this reviewer were the chapters on chemical purity and control, registration and assessment of medicines, and techniques of quantitative analysis. These chapters very basically cover the what, why, and how of quantitative analysis, something that is not infrequently overlooked in the education of analysts.

Reviewed by Robert E. Daly
Warner-Lambert Research Institute
Morris Plains, NJ 07950

provides a thorough review of medication law, particularly the Federal Food, Drug, and Cosmetic Act. However, it also considers such areas as professional practice acts and negligence.

The book, however, is not a text on pharmacy law. Rather, it relates the law to the behavior of people, primarily patients and providers of health care. For example, two chapters on the requirements of drug labeling are followed by a chapter on "How Drug Information is Used." The book deals not only with the legal controls on drug distribution but also with the behavioral aspects of why people take drugs (medication).

The book is well referenced and draws on legal citations, behavioral studies, and the clinical literature. The liberal use of figures and tables enhances the value of the book as a learning device. The book is unique in combining the legal aspects of medication with the behavioral aspects. It would be a valuable addition to the library of anyone involved in the drug use process.

Reviewed by Maven J. Myers
Philadelphia College of Pharmacy and Science
Philadelphia, PA 19104

Microencapsulation. Edited by J. R. NIXON. Dekker, 270 Madison Ave., New York, NY 10016, 1976. 215 pp. 16 × 23.5 cm. Price $19.50.

This book constitutes a collection of 17 papers delivered in London at the second international symposium on microencapsulation. The contributors to this hard-covered book are recognized international authorities in the field of microencapsulation.

In Chapter 1, the processes of coacervation, spray encapsulation, and nanoencapsulation are reviewed by P. Speiser. The intricacies of each method are well defined by the author, and applications are also given.

In Chapter 2, A. Watanabe and T. Hayashi describe gelatin–gum arabic coacervation, interfacial polymerization, and the preparation of multiwalled microcapsules. The authors describe the applications of microcapsules in the manufacture of carbonless copy paper, encapsulated perfume ink, and the image display panel, the latter employing the electrophoretic behavior of microcapsules. The chapter is well illustrated with several photographs and diagrams.

In Chapter 3, A. T. Florence and A. W. Jenkins deal with the assessment *in vitro* of microencapsulated drug systems utilized in sustained-release parenteral dosage forms. Drug dissolution, stability, and biodegradability are discussed. The paper is clearly written, well referenced, and illustrated with photographs.

T. M. S. Chang, in Chapter 4, reviews the vast amount of research and clinical applications of semipermeable microcapsules used as artificial cells. Professor Chang, being a leading world authority in this area, is amply qualified to handle this topic, and his paper is documented with 42 references. The applications of microcapsules to augment artificial kidney function are further discussed by R. E. Sparks *et al.* in Chapter 9.

A major problem in the microencapsulation of enzymes has been the loss of enzyme activity during the microencapsulation process. T. Kondo and N. Muramatsu suggest solutions to this problem in Chapter 5.

The use of microcapsules as food particles for marine particulate feeders is discussed by D. A. Jones and P. A. Gabbott in Chapter 6. A nylon coat for the microcapsules provided an indigestable wall to reduce bacterial contact with the enclosed diet. The authors also suggest another important use for microcapsules in the cultivation of marine organisms and that is to supply medicinal compounds, *e.g.*, antibiotics, to prevent or cure disease.

In Chapter 7, M. Calanchi describes several new dosage forms containing microcapsules prepared *via* coacervation. The author discusses the microencapsulation of antibiotics, aspirin, vitamin C, and steroids and suggests applications of the technique to improve drug stability, overcome incompatibilities, prolong the action of drugs, and conceal the bitter taste of medicinals. Further applications for microcapsules as drug delivery systems, particularly in topical dosage forms, are described in Chapter 10 by R. H. Sudekum.

In Chapter 8, G. C. Maggi and F. DiRoberto outline a method used to diagnose and monitor peripheral vascular disorders by employing encapsulated liquid crystal thermography. R. G. Arnold, in Chapter 11, reviews the many varied applications of microencapsulation and describes the sequence of events and procedures the FDA requires to approve a new microencapsulated animal drug product for marketing. This chapter should be of great interest to those interested in marketing such products. Further veterinary applications of microencapsulation are outlined in Chapter 12 by G. Rognoni.

V. de Sabata, in Chapter 13, reviews several published articles concerned with drug bioavailability from microencapsulated dosage forms. Chapter 14 should be of particular interest to the biologist. T. Kondo *et al.* describe the preparation and properties of artificial red blood cells containing hemoglobin solution.

Chapter 15, an excellent chapter by J. R. Nixon and B. R. Matthews, deals with the surface characteristics of gelatin coacervate microcapsules using scanning electron microscopy. Photographs of microcapsules prepared *via* alcohol coacervation and sodium sulfate coacervation procedures display definite surface properties, and these differences are discussed in the paper. Further physicochemical studies of microcapsules appear in Chapter 16. L. Nang and P. F. Carlier mathematically derive the wall diffusion coefficient and discuss its importance in evaluating microencapsulating methods and the optimization of a coacervation process.

In Chapter 17, the final chapter in the book, L. A. Luzzi reviews the applications, methods of preparation, and physicochemical properties of microcapsules. The chapter is well written and well referenced.

Discussions of some applications and methodologies, such as coacervation and interfacial polymerization, are redundant in the book; however, due to the multiple authorship, this repetition could be expected. The book contains an even balance of reviews and original research. It provides an insight to the science of microencapsulation and should stimulate new research ideas. The book is not only of interest to the pharmaceutical scientist but is also intended for pharmacologists, biologists, chemists, and veterinary scientists.

Reviewed by James W. McGinity
School of Pharmacy
Texas Southern University
Houston, TX 77004

Practical Pharmaceutical Chemistry. Third Edition—Part One. By A. H. BECKETT and J. B. STENLAKE. Humanities Press, Atlantic Highlands, NJ 07716, 1975. 370 pp. 16 × 24.5 cm. Price $25.00.

Two major additions and several minor revisions have been made in the third edition of this textbook. A new chapter on the registration and assessment of medicines in the United Kingdom has been added. The implications of the Medicines Act of 1968 and Good Manufacturing Practices published by HMSO in 1971 to the analysts and compilers of product applications is presented in a general manner. The treatment of general analytical procedures has been extended. This new chapter covers all important product types including tablets, capsules, suspensions, ointments, creams, pressurized aerosols, lozenges, suppositories, solutions, and mixtures as well as dissolution testing, sustained-release preparations, and particle-size control.

The subject matter is presented in 14 chapters. A limited theoretical treatment is presented, where pertinent, followed by practical examples which have been drawn from the British Pharmacopoeia and other sources. These examples are intended to serve as laboratory exercises.

The book is practical in every sense of the word. It covers primarily the classical methods of analysis, with discussion of the more sophisticated methods being reserved for Part 2. Although the style of presentation of determination of equivalent weights is somewhat different than this reviewer is accustomed to, it is very easy to follow. An insight into the chemistry of many of the limit tests as well as many of the monographs in the British Pharmacopoeia is provided. Of particular interest to this reviewer were the chapters on chemical purity and control, registration and assessment of medicines, and techniques of quantitative analysis. These chapters very basically cover the what, why, and how of quantitative analysis, something that is not infrequently overlooked in the education of analysts.

Reviewed by Robert E. Daly
Warner-Lambert Research Institute
Morris Plains, NJ 07950

Journal of Pharmaceutical Sciences

FEBRUARY 1977

VOLUME 66 NUMBER 2

MARY H. FERGUSON
Editor

L. LUAN CORRIGAN
Assistant Editor

SHELLY ELLIOTT
Production Editor

JANET D. SHOFF
Copy Editor

EDWARD G. FELDMANN
Contributing Editor

SAMUEL W. GOLDSTEIN
Contributing Editor

LELAND J. ARNEY
Director of Publications

EDITORIAL ADVISORY BOARD

JOHN AUTIAN	HARRY B. KOSTENBAUDER
NORMAN R. FARNSWORTH	HERBERT A. LIEBERMAN
WILLIAM O. FOYE	DAVID E. MANN, JR.
WILLIAM J. JUSKO	GERALD J. PAPARIELLO

The *Journal of Pharmaceutical Sciences* is published monthly by the American Pharmaceutical Association at 2215 Constitution Ave., N.W., Washington, DC 20037. Second-class postage paid at Washington, D.C., and at additional mailing office.

All expressions of opinion and statements of supposed fact appearing in articles or editorials carried in this journal are published on the authority of the writer over whose name they appear and are not to be regarded as necessarily expressing the policies or views of the American Pharmaceutical Association.

Offices—Editorial, Advertising, and Subscription Offices: 2215 Constitution Ave., N.W., Washington, DC 20037. Printing Offices: 20th & Northampton Streets, Easton, PA 18042.

Annual Subscriptions—United States and foreign, industrial and government institutions $50, educational institutions $50, individuals *for personal use only* $30; single copies $5. All foreign subscriptions add $5 for postage. Subscription rates are subject to change without notice. Members of the American Pharmaceutical Association may elect to receive the *Journal of Pharmaceutical Sciences* as a part of their annual $60 (foreign $65) APhA membership dues.

Claims—Missing numbers will not be supplied if dues or subscriptions are in arrears for more than 60 days or if claims are received more than 60 days after the date of the issue, or if loss was due to failure to give notice of change of address. The Association cannot accept responsibility for foreign delivery when its records indicate shipment has been made.

Change of Address—Members and subscribers should notify at once both the Post Office and the American Pharmaceutical Association, 2215 Constitution Ave., N.W., Washington, DC 20037, of any change of address.

© Copyright 1977, American Pharmaceutical Association, 2215 Constitution Ave., N.W., Washington, DC 20037; all rights reserved.

RELIABILITY OF SCIENTIFIC DATA

It is late Friday afternoon as this editorial is being written. In doing so, this writer has been reflecting on the numerous and varied occasions during this past week that he had occasion to make a judgment, or to base some decision, or otherwise to draw upon the research reports and laboratory findings of fellow scientists.

Just a few such examples might be mentioned by way of illustration: (*a*) we reviewed a draft monograph in APhA's Bioavailability series, (*b*) we examined in proof form a chapter for the new edition of the *OTC Drug Handbook*, (*c*) we assessed drafts of several abbreviated drug interaction monographs for the supplement that is now underway for *Evaluations of Drug Interactions*, (*d*) we provided advice and recommendations to a state government agency regarding inclusion of certain drugs in its state drug formulary, (*e*) we supplied information for inclusion in a background paper for one of the APhA policy committees, (*f*) we participated in the decision on whether a certain research report was sufficiently novel to warrant journal publication, and (*g*) we were involved in staff meetings, telephone inquiries, correspondence, and outside meetings too numerous to mention—all of which, in some way, involved a scientific component based upon somebody's research findings.

No matter how one views it, that is a lot of reliance on the findings and reports of others. And, we suspect, if our readers were to perform a similar exercise, many if not most of them would probably find that they have also depended very substantially on reports in the literature, personal communications, or other sources of information which have been drawn upon and utilized in carrying out their own activities.

Having said all this, what is our point? Simply put, it is that the workings of our whole scientific system rest on the fundamental assumption that scientists have integrity and that their reports can be accepted as being honest, factual, and reliable. Anything less will destroy the entire process and turn it into veritable shambles.

Fortunately, it has been exceedingly rare that scientists have violated this self-imposed code. In fact, in recent memory the only intellectually dishonest acts—in contrast to morally questionable research which is an entirely different matter—that come to mind were charges that certain people plagiarized the results of others to their own advantage, such as to complete requirements for a graduate degree. But as reprehensible as this practice may be, at least it did not introduce false and erroneous information into the body of scientific information.

People have observed that nothing is sacred any more. So perhaps it should not come as a surprise or disappointment that recent revelations have disclosed falsified, dishonest research reports. We refer to the recent disclosures by Food and Drug Administration spokesmen that data submitted to the agency to demonstrate the safety or efficacy of a number of drugs have been altered, "fudged," or otherwise falsified.

Although these deficient data have been submitted to FDA by pharmaceutical companies, in fairness to them it should be pointed out that for the most part the invalid data came from outside sources such as consulting laboratories. In accord with traditional scientific practice, the pertinent drug company innocently accepted the reports at face value and submitted them to the FDA as supporting documentation.

FDA Bureau of Drugs Director J. Richard Crout initially revealed the problem last fall in connection with agency action to review the approval of a new antiarthritic drug: *"We have learned that we cannot accept the test results submitted by drug sponsors on faith alone. Recent history has convinced us that we must look more closely at the validity and quality of the research done by industry."*

Subsequently, the FDA Commissioner has issued proposed new stringent regulations described in the press as an *"impressively detailed and sweeping Good Laboratory Practice code that would cover all labs carrying out preclinical studies intended to be submitted to the agency."* The new rules set forth standards for organization and personnel, buildings and facilities, equipment, testing facility operations, quality assurance, protocols, study implementation and conduct, recording and handling of data, and records and reports. Penalties for not following good laboratory practices range all the way to criminal prosecution.

In his preamble, the Commissioner cites several examples of problems which FDA staff have recently uncovered in the supporting data submitted by drug sponsors. Hence, corrective action clearly is needed.

However, we are grieved that this last bastion of honesty and reliability has fallen into question and disrepute. Until now, scientific research was virtually unregulated simply because it had never been felt necessary to impose regulations and controls. That has now all changed and, in the process, every scientist has lost an intangible little something. Perhaps this denouement is simply part of technical progress and the development of a more complex society. But still it leaves us just a little sad.

Edward G. Feldmann

Journal of Pharmaceutical Sciences

FEBRUARY 1977

VOLUME 66 NUMBER 2

MARY H. FERGUSON
Editor

L. LUAN CORRIGAN
Assistant Editor

SHELLY ELLIOTT
Production Editor

JANET D. SHOFF
Copy Editor

EDWARD G. FELDMANN
Contributing Editor

SAMUEL W. GOLDSTEIN
Contributing Editor

LELAND J. ARNEY
Director of Publications

EDITORIAL ADVISORY BOARD

JOHN AUTIAN	HARRY B. KOSTENBAUDER
NORMAN R. FARNSWORTH	HERBERT A. LIEBERMAN
WILLIAM O. FOYE	DAVID E. MANN, JR.
WILLIAM J. JUSKO	GERALD J. PAPARIELLO

The *Journal of Pharmaceutical Sciences* is published monthly by the American Pharmaceutical Association at 2215 Constitution Ave., N.W., Washington, DC 20037. Second-class postage paid at Washington, D.C., and at additional mailing office.

All expressions of opinion and statements of supposed fact appearing in articles or editorials carried in this journal are published on the authority of the writer over whose name they appear and are not to be regarded as necessarily expressing the policies or views of the American Pharmaceutical Association.

Offices—Editorial, Advertising, and Subscription Offices: 2215 Constitution Ave., N.W., Washington, DC 20037. Printing Offices: 20th & Northampton Streets, Easton, PA 18042.

Annual Subscriptions—United States and foreign, industrial and government institutions $50, educational institutions $50, individuals *for personal use only* $30; single copies $5. All foreign subscriptions add $5 for postage. Subscription rates are subject to change without notice. Members of the American Pharmaceutical Association may elect to receive the *Journal of Pharmaceutical Sciences* as a part of their annual $60 (foreign $65) APhA membership dues.

Claims—Missing numbers will not be supplied if dues or subscriptions are in arrears for more than 60 days or if claims are received more than 60 days after the date of the issue, or if loss was due to failure to give notice of change of address. The Association cannot accept responsibility for foreign delivery when its records indicate shipment has been made.

Change of Address—Members and subscribers should notify at once both the Post Office and the American Pharmaceutical Association, 2215 Constitution Ave., N.W., Washington, DC 20037, of any change of address.

© Copyright 1977, American Pharmaceutical Association, 2215 Constitution Ave., N.W., Washington, DC 20037; all rights reserved.

RELIABILITY OF SCIENTIFIC DATA

It is late Friday afternoon as this editorial is being written. In doing so, this writer has been reflecting on the numerous and varied occasions during this past week that he had occasion to make a judgment, or to base some decision, or otherwise to draw upon the research reports and laboratory findings of fellow scientists.

Just a few such examples might be mentioned by way of illustration: (*a*) we reviewed a draft monograph in APhA's Bioavailability series, (*b*) we examined in proof form a chapter for the new edition of the *OTC Drug Handbook*, (*c*) we assessed drafts of several abbreviated drug interaction monographs for the supplement that is now underway for *Evaluations of Drug Interactions*, (*d*) we provided advice and recommendations to a state government agency regarding inclusion of certain drugs in its state drug formulary, (*e*) we supplied information for inclusion in a background paper for one of the APhA policy committees, (*f*) we participated in the decision on whether a certain research report was sufficiently novel to warrant journal publication, and (*g*) we were involved in staff meetings, telephone inquiries, correspondence, and outside meetings too numerous to mention—all of which, in some way, involved a scientific component based upon somebody's research findings.

No matter how one views it, that is a lot of reliance on the findings and reports of others. And, we suspect, if our readers were to perform a similar exercise, many if not most of them would probably find that they have also depended very substantially on reports in the literature, personal communications, or other sources of information which have been drawn upon and utilized in carrying out their own activities.

Having said all this, what is our point? Simply put, it is that the workings of our whole scientific system rest on the fundamental assumption that scientists have integrity and that their reports can be accepted as being honest, factual, and reliable. Anything less will destroy the entire process and turn it into veritable shambles.

Fortunately, it has been exceedingly rare that scientists have violated this self-imposed code. In fact, in recent memory the only intellectually dishonest acts—in contrast to morally questionable research which is an entirely different matter—that come to mind were charges that certain people plagiarized the results of others to their own advantage, such as to complete requirements for a graduate degree. But as reprehensible as this practice may be, at least it did not introduce false and erroneous information into the body of scientific information.

People have observed that nothing is sacred any more. So perhaps it should not come as a surprise or disappointment that recent revelations have disclosed falsified, dishonest research reports. We refer to the recent disclosures by Food and Drug Administration spokesmen that data submitted to the agency to demonstrate the safety or efficacy of a number of drugs have been altered, "fudged," or otherwise falsified.

Although these deficient data have been submitted to FDA by pharmaceutical companies, in fairness to them it should be pointed out that for the most part the invalid data came from outside sources such as consulting laboratories. In accord with traditional scientific practice, the pertinent drug company innocently accepted the reports at face value and submitted them to the FDA as supporting documentation.

FDA Bureau of Drugs Director J. Richard Crout initially revealed the problem last fall in connection with agency action to review the approval of a new antiarthritic drug: *"We have learned that we cannot accept the test results submitted by drug sponsors on faith alone. Recent history has convinced us that we must look more closely at the validity and quality of the research done by industry."*

Subsequently, the FDA Commissioner has issued proposed new stringent regulations described in the press as an *"impressively detailed and sweeping Good Laboratory Practice code that would cover all labs carrying out preclinical studies intended to be submitted to the agency."* The new rules set forth standards for organization and personnel, buildings and facilities, equipment, testing facility operations, quality assurance, protocols, study implementation and conduct, recording and handling of data, and records and reports. Penalties for not following good laboratory practices range all the way to criminal prosecution.

In his preamble, the Commissioner cites several examples of problems which FDA staff have recently uncovered in the supporting data submitted by drug sponsors. Hence, corrective action clearly is needed.

However, we are grieved that this last bastion of honesty and reliability has fallen into question and disrepute. Until now, scientific research was virtually unregulated simply because it had never been felt necessary to impose regulations and controls. That has now all changed and, in the process, every scientist has lost an intangible little something. Perhaps this denouement is simply part of technical progress and the development of a more complex society. But still it leaves us just a little sad.

Edward G. Feldmann

Disintegration Test for Enteric-Coated Tablets

Enteric-coated dosage forms are intended to resist the release of their active ingredients in the acidic gastric fluid but to disintegrate and release their contents in the less acidic environment of the intestine. The official compendia recognize the use of enteric-coated dosage forms in situations where the drug may be destroyed or inactivated by the gastric juice or where it may irritate the gastric mucosa[1,2]. The compendia also recognize that such coatings are intended to delay the release of the medication until the dosage form passes through the stomach[1,2]. Therefore, the enteric coating must resist the release of its ingredient(s) in the stomach until gastric emptying can occur.

The official compendia specify disintegration test requirements for the enteric-coated tablet only, apparently because it is the only popular enteric-coated dosage form. The requirements of this disintegration test are met if the tablets show no evidence of disintegration, cracking, or softening in 1 hr in simulated gastric fluid TS maintained at 37 ± 2° but disintegrate completely in simulated intestinal fluid TS maintained at 37 ± 2° in a period equal to 2 hr plus the time limit specified in the individual monograph or, where only an enteric-coated tablet is recognized, for only the time specified in the monograph[3,4].

Thus, the test in its present form appears to fulfill the following two objectives: (*a*) prevent the disintegration, cracking, or softening of the tablets in 1 hr in the acidic environment, and (*b*) assure the disintegration of the tablets in the intestinal environment within a given period of time.

However, the test in its present form does not take into account the fact that the stomach residence time of enteric-coated tablets may not necessarily be 1 hr or less but may, in fact, vary greatly. For example, studies with various nondisintegrating solid dosage forms indicated an average residence time in the stomach ranging from 1.5 to 5.75 hr, with standard deviations of 50% from the mean[5,6]. Moreover, although the tablets may show no evidence of cracking (with the naked eye) or softening in the acidic gastric environment, they may be releasing their content(s) due to diffusion or leaching through the intact coating and/or small pores or minute cracks.

In a recent study dealing with commercially available enteric-coated sodium salicylate tablets[7], all products tested met the official test requirement but the coating on many of the products failed to prevent the release of sodium salicylate in the acidic environment. Recent evidence indicating that the local concentration of mucosal irritants at sites in contact with the tablets may be important and the fact that the enteric-coated tablet does not ensure safety from gastric toxicity[8] suggest that the present test requirement for the enteric-coated tablets may not be adequate.

Thus, to improve the performance of the disintegration test and enhance its validity, a more realistic test requirement should include "prevention of release" in the acidic environment as the primary objective.

P. L. Madan
H. Eisen
College of Pharmacy and Allied Health Professions
St. John's University
Jamaica, NY 11439

Received November 22, 1976.

[1] "The United States Pharmacopeia," 19th rev., Mack Publishing Co., Easton, Pa., 1975, p. 706.
[2] "The National Formulary," 14th ed., Mack Publishing Co., Easton, Pa., 1975, p. 941.
[3] *Ibid.*, p. 980.
[4] "The United States Pharmacopeia," 19th rev., Mack Publishing Co., Easton, Pa., 1975, p. 650.
[5] F. S. Bukey and M. Brew, *J. Am. Pharm. Assoc., Sci. Ed.*, **23**, 1217 (1934).
[6] R. H. Blythe, G. M. Grass, and D. R. MacDonnell, *Am. J. Pharm.*, **131**, 206 (1959).
[7] P. L. Madan and M. Minisci, *Drug Intel. Clin. Pharm.*, **10**, 588 (1976).
[8] R. J. Ferrand, J. H. Green, and C. Hawroth, *Br. Med. J.*, **3**, 85 (1975).

Journal of Pharmaceutical Sciences

FEBRUARY 1977
VOLUME 66 NUMBER 2

RESEARCH ARTICLES

Nucleophilic Addition of Bisulfite Ion to Prostaglandins E_2 and A_2: Implication in Aqueous Stability

M. J. CHO ˣ, W. C. KRUEGER, and T. O. OESTERLING

Abstract □ Evidence is presented to indicate that the bisulfite ion (HSO_3^-) adds across the C-9 carbonyl group of dinoprostone (prostaglandin E_2) and across the $\Delta^{10,11}$-bond of prostaglandin A_2. At room temperature, the apparent equilibrium constant, determined by phase solubility analysis, circular dichroism, UV spectroscopy, and partitioning, for the formation of the bisulfite adduct of dinoprostone is about 7.5 M^{-1} at neutral pH. From this result and a free energy relationship reported in the literature for the thermodynamics of nucleophilic addition to carbonyl groups, it is concluded that the chemical reactivity of the C-9 carbonyl group of dinoprostone is not high enough to improve aqueous stability through reversible one-step nucleophilic reactions. However, from a series of kinetic experiments, it is concluded that the equilibrium is extremely favorable for the formation of the bisulfite adduct of prostaglandin A_2 over pH 4–8 at room temperature. The second-order rate constant for the attack of sulfite ion (SO_3^{2-}) to prostaglandin A_2 is 1.75 $sec^{-1}\ M^{-1}$.

Keyphrases □ Prostaglandins—dinoprostone and prostaglandin A_2, nucleophilic addition of bisulfite ion, effect on aqueous stability □ Dinoprostone—nucleophilic addition of bisulfite ion, effect on aqueous stability □ Nucleophilic addition—bisulfite to dinoprostone and prostaglandin A_2, effect on aqueous stability □ Bisulfite ion—nucleophilic addition to dinoprostone and prostaglandin A_2, effect on aqueous stability □ Stability, aqueous—bisulfite adducts of dinoprostone and prostaglandin A_2

Prostaglandins are analogs of the parent 20-carbon prostanoic acid found in virtually all mammalian cells. After Bergström's pioneering work on the structural characterization and biosynthsis of prostaglandins (1), numerous articles have appeared defining the physiological role and total synthesis of prostaglandins (2). Recently, their general biology (3–5) and chemistry (6–8) were extensively reviewed.

BACKGROUND

Some of the naturally occurring E and F prostaglandins have found wide clinical application in human reproduction (9). In particular, dinoprostone (prostaglandin E_2) (I) has been successfully used for labor induction (10–12). However, the chemical instability of dinoprostone has limited the development of dosage forms, particularly those in aqueous solutions. The instability problem has resulted in a substantial challenge to the pharmaceutical scientist, and this work is part of a fundamental study aimed at exploring the utility of reversible chemical reactions in improving the stability of the E series prostaglandins.

As shown in Scheme I, dinoprostone, being a β-ketol, readily undergoes dehydration to produce prostaglandin A_2 (II) (13–18), which has a different spectrum of biological activity. In aqueous solutions, dinoprostone shows maximum stability at pH 3.5, but the half-life is only about 40 days at 25° (18); prostaglandin A_2, in turn, isomerizes to prostaglandin B_2 (III) in alkaline conditions. In addition to this major degradation reaction, the compound epimerizes at C-8 in the presence of general base (19), presumably because of the high acidity of the proton at C-8 (20). It also epimerizes at C-15 in acid, apparently because of the easy formation of a stable allylic cation at C-15 (21).

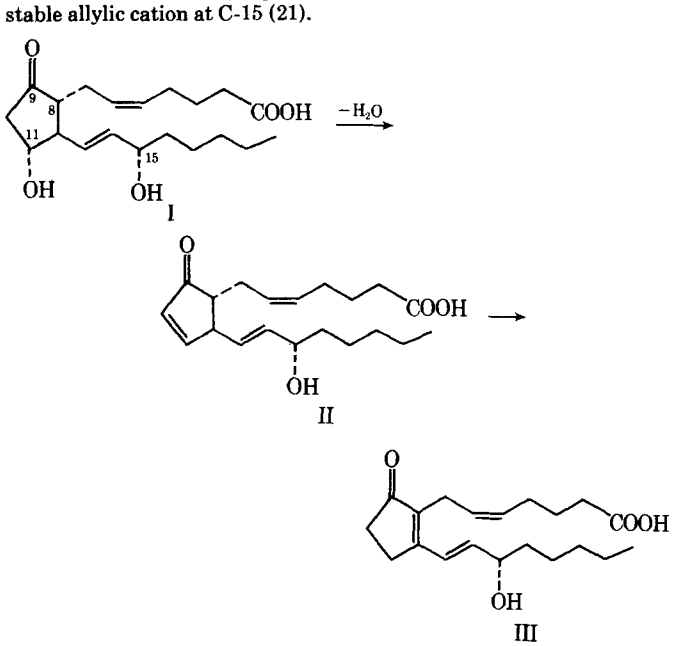

Scheme I

Kinetically, dinoprostone appears to undergo dehydration through the E1cB mechanism, with either the formation of enolate at C-9 or the expulsion of OH^- from C-11 as the rate-determining step. Although a thorough kinetic study has to be carried out to identify this proposed mechanism, it is strongly supported by a series of studies (22, 23) on the β-elimination reactions of β-oxy cyclic ketones with various leaving groups of pKa ranging from 5 to 16, including OH^-.

Thermodynamically, the fundamental driving force for the dehydration, which is practically irreversible, appears to be the reduction in free energy content derived from an extended conjugation present in prostaglandin A_2. Therefore, any reversible chemical reactions saturating the carbonyl group at C-9 of dinoprostone should enhance the overall stability through the relationships:

$$\frac{-d(\text{total dinoprostone})}{dt} = k(\text{free dinoprostone}) \qquad \text{(Eq. 1}a\text{)}$$

$$\frac{-d(\text{total dinoprostone})}{dt} = \frac{k}{1+K_{eq}}(\text{total dinoprostone}) \qquad \text{(Eq. 1}b\text{)}$$

where k is the apparent dehydration rate constant of dinoprostone, so long as the attainment of the reaction equilibrium is fast enough that it can be considered as an equilibrium reaction (with an equilibrium constant K_{eq}) prior to the dehydration of dinoprostone and the product of the reversible reaction is chemically stable.

The nucleophilic addition reaction of the bisulfite ion (HSO_3^-) to the carbonyl group at C-9 of dinoprostone was investigated to see if the reaction could be utilized to improve the aqueous stability of dinoprostone. Bisulfite was chosen, among many nucleophilic reagents, because it is relatively nontoxic and hence can be used in pharmaceutical formulations (24) and also because it is an extremely good nucleophile in a thermodynamic as well as a kinetic sense (25, 26). Thus, reactivity of bisulfite with dinoprostone can serve as a measure of the chemical reactivity (*i.e.*, electrophilicity) of the carbonyl group of C-9 of the E prostaglandins in general. The enone system present in prostaglandin A_2 was expected to be very susceptible to nucleophilic addition reactions, as frequently found in many Michael-type 1,4-additions (27). Therefore, it was necessary to study the extent of bisulfite addition to prostaglandin A_2 to draw a complete picture of an aqueous system of dinoprostone containing the nucleophilic reagent.

RESULTS AND DISCUSSION

Characterization of Reaction System—It is often difficult to identify chemically a facile equilibrium reaction, especially when the reaction product cannot be easily isolated. Consequently, various physical methods such as UV, IR, and NMR spectroscopic techniques are frequently employed, since in most cases the equilibrium condition is not to be disturbed.

In aqueous solutions, dinoprostone exhibits a negative circular dichroism band near 292 nm with $[\theta] = -1.35 \times 10^4$ due to the $n \rightarrow \pi^*$ transition of the C-9 carbonyl chromophore (5, 28). As shown in Fig. 1, the negative molar rotation was reduced in the presence of the bisulfite ion. At equilibrium, the reduction was a function of the total bisulfite concentration, indicating that the reaction was reversible in nature. If the reaction went to completion, the final spectrum would be independent of the total bisulfite concentration, unless its stoichiometric ratio to dinoprostone concentration was below 1:1.

The ketone carbonyl chromophore of dinoprostone absorbs UV energy very weakly ($\epsilon_{288} \sim 50$), so its absorption band is easily swamped by the bisulfite absorption at the bisulfite concentration level where the reaction can occur to a significant extent. Nevertheless, the absorption peak was significantly reduced upon addition of sodium bisulfite. As in the case of the circular dichroism spectrum, at equilibrium the decrease in absorbance at 288 nm was a function of the total bisulfite concentration. In identifying the reaction, attempts were also made to utilize the carbonyl stretching vibration at 1725 cm^{-1} (5.80 μm) in the IR spectrum of dinoprostone, the C-9 signal at 215.4 ppm (tetramethylsilane) in the ^{13}C-NMR spectrum of dinoprostone, and the quartet at 2.70 ppm due to the equatorial proton at C-10 in the PMR spectrum of dinoprostone. In all cases, supportive but inconclusive data were obtained, mainly because of the small magnitude of the equilibrium constant for the bisulfite adduct formation. From the results obtained from the spectroscopic studies together with the fact that cyclopentanone adds bisulfite (29), it was concluded that the bisulfite ion adds across the C-9 carbonyl group of prostaglandin E_2 in a reversible fashion (Scheme II). At present, the stereochemistry of the addition is not established.

A brief attempt was made to follow the kinetics of bisulfite addition to dinoprostone by monitoring the change in molar rotation at 292 nm,

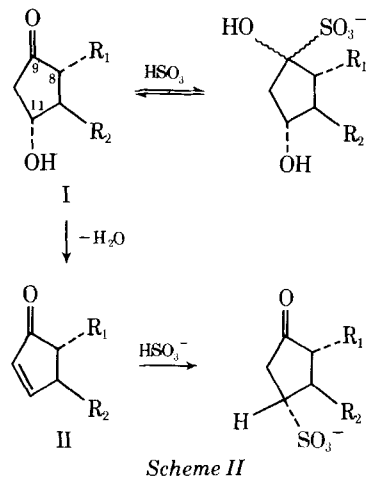

Scheme II

but no reliable data were obtained because the reaction occurred too rapidly. For example, the rotation at 292 nm of a 1.00-mg/ml solution of dinoprostone containing 0.692 mole of total bisulfite (spectrum C in Fig. 1) was identical after 4 and 20 min of the sample preparation. From this observation and the equilibrium constants measured, it was concluded that the bisulfite addition to dinoprostone is kinetically favorable, even though it is not so favorable thermodynamically.

The high reactivity of the enone system in prostaglandin A_2 is well exemplified by the easy formation of 11-substituted E prostaglandins from the reactions of nucleophiles with the A prostaglandins (28, 30). For instance, hydrogen peroxide adds to C-11 of prostaglandin A_2 to form eventually prostaglandin A_2 10,11-epoxide, an important intermediate in the process of converting prostaglandin A_2 to dinoprostone (31). According to the Sander and Jencks (32) γ-parameter, a measure of thermodynamic nucleophilicity originally derived from a series of reversible nucleophilic addition reactions across a carbonyl group, any nucleophiles of γ-value greater than that of hydrogen peroxide (−0.65) are expected to add to C-11 of prostaglandin A_2, as long as a proper reaction condition is provided. This hypothesis is based on the fact that the thermodynamics governing the nucleophilic addition across a carbonyl group were proved to predict the nucleophilic addition of the reactions across >C=N- (25) and >C=C< (26) bonds. However, no evidence can be found to support that water ($\gamma = -3.58$) adds to prostaglandin A_2 to form dinoprostone. In practice, dehydration of dinoprostone can be considered as an irreversible reaction. On the other hand, the addition of bisulfite ($\gamma = 4.02$)

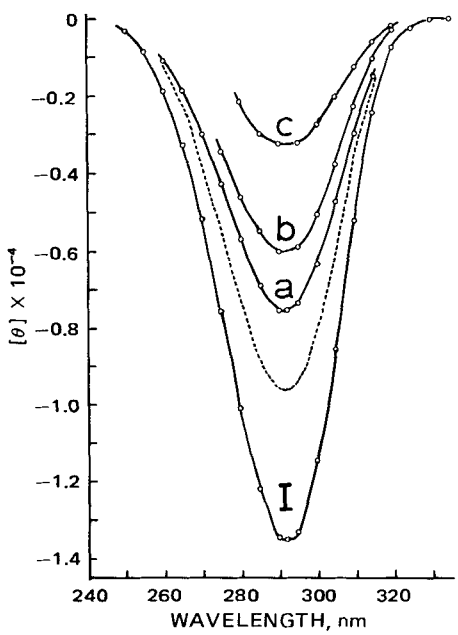

Figure 1—*Circular dichroism spectrum of dinoprostone (I) and its change in the presence of the bisulfite ion at 25°: dinoprostone = 1.00 mg/ml = 2.84 × 10⁻³ M in a phosphate buffer of pH 6.5. Total bisulfite concentrations were 1.042, 0.277, and 0.69 M for a, b, and c, respectively. For comparison, spectrum a in Fig. 2 is shown as a dotted line.*

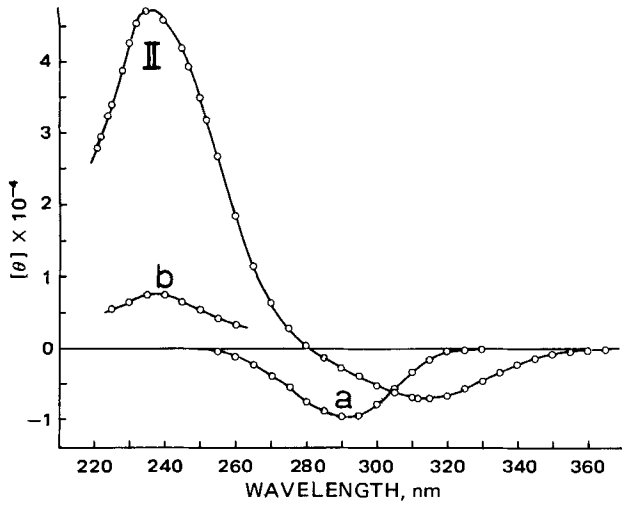

Figure 2—*Circular dichroism spectrum of prostaglandin A_2 (II) and its change in the presence of the bisulfite ion at 25°: prostaglandin A_2 = 0.02 mg/ml = 5.98 × 10^{-5} M in a phosphate buffer of pH 6.5 and I = 0.1 M. Total bisulfite concentrations were 5.38 × 10^{-3} and 2.99 × 10^{-3} M for a and b, respectively.*

to C-11 of prostaglandin A_2 was expected to be very favorable, and even the formation of the 9,11-bis derivative was considered to be possible.

The PMR spectrum of prostaglandin A_2 in deuterated bisulfite buffer of pD = 7.0 (pD = pH read on a meter + 0.4) (33) showed neither the two doublets at 7.6 ppm due to the proton at C-11 nor the two doublets at 6.2 ppm due to the proton at C-10, indicating that bisulfite either adds across the $\Delta^{10,11}$-bond or attacks at C-9 or both. However, the overall spectrum looked similar to that of dinoprostone. Especially at 2.9 ppm, where the equatorial proton at C-11 of dinoprostone was expected to show up as a quartet, poorly resolved but distinctive peaks were still observed, implying the presence of the proton at the carbon alpha to a carbonyl group.

That the C-9 carbonyl group of prostaglandin A_2 is intact in the presence of bisulfite, *i.e.*, that the 9,11-bis derivative is not formed, was also supported by the change in the circular dichroism spectrum of prostaglandin A_2 in the presence of bisulfite. As shown in Fig. 2, prostaglandin A_2 exhibits a strong positive band at 235 nm ($[\theta] = 4.72 \times 10^4$) and a negative band at 312 nm ($[\theta] = -0.69 \times 10^4$) due to the $\pi \rightarrow \pi^*$ and $n \rightarrow \pi^*$ transitions of the enone chromophore, respectively. When bisulfite was introduced to a prostaglandin A_2 solution, the spectrum underwent a hypsochromic shift of about 20 nm, and the final spectrum became similar to that of dinoprostone (Fig. 1). This type of spectral change arising from breaking a conjugated system is well known in circular dichroism spectroscopy (34).

The similarity of the final PMR and circular dichroism spectra of prostaglandin A_2 in the presence of bisulfite to those of dinoprostone unambiguously indicates that bisulfite adds across the $\Delta^{10,11}$-bond of prostaglandin A_2 (Scheme II). Because dinoprostone and the bisulfite adduct at C-11 of prostaglandin A_2 are similar to each other in chemical structure, a nearly identical spectroscopic behavior is expected. The possibility of forming the 9,11-bis derivative was ruled out not only by the presence of the C-9 carbonyl group at equilibrium, which was indicated by the PMR study, but also by the fact that only one molecule of bisulfite adds to the enone system in cortisone (35) and to the 1,4-dien-3-one system in dexamethasone (36). Formation of the bis derivative is probably hindered by the electrostatic repulsion between the negative charge on the sulfonate group at C-11 of the monoadduct and the oncoming second molecule of bisulfite.

According to Crabbé (28), various 11α-substituted derivatives of dinoprostone display a more negative Cotton effect with $[\theta] \sim -10{,}000$ at $\lambda_{max} \sim 298$ nm than their corresponding 11β-substituted derivatives. As shown by curve a in Fig. 2, the circular dichroism spectrum of the bisulfite adduct of prostaglandin A_2 is in accord with that of 11α-sulfonate. If this is the case, the stereochemistry involved in the nucleophilic attack at C-11 of prostaglandin A_2 appears to be sterically controlled by the β-side chain at C-12. The PMR study could have given additional information on the stereochemistry of the reaction if an accurate value of ^3J for the coupling of the protons at C-10 and C-11 of the adduct had been available. Such data would give an estimate of the dihedral angle between the deuterium

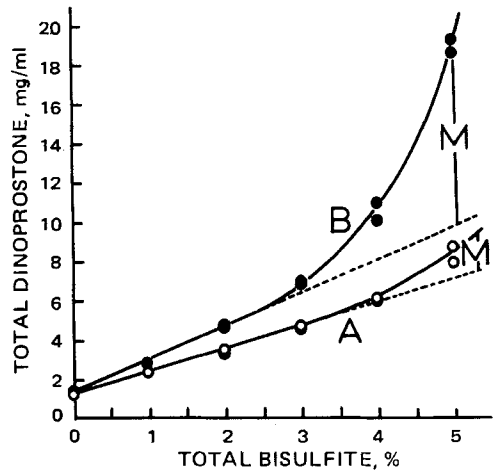

Figure 3—*Aqueous solubility of dinoprostone at 25° as a function of the total bisulfite concentration at pH 3 (A) and 4 (B). The portion showing deviation from linearity (M) indicates the contribution from the micelle formation.*

at C-10 and the sulfonate at C-11. However, as pointed out earlier, the resolution was unfortunately poor at about 3 ppm.

Measurement of Equilibrium Constant for Formation of Bisulfite Adduct of Dinoprostone—Of the many methods commonly employed in determining the equilibrium constant for a reversible reaction or complex formation, phase solubility analysis (37–40), UV and circular dichroism spectroscopic techniques (38, 39, 41), and the partition technique (39, 42) were chosen for the present study. The apparent equilibrium constant is defined as:

$$K = \frac{[ES]}{[E][S]} \qquad \text{(Eq. 2)}$$

where $[ES]$, $[E]$, and $[S]$ are the concentrations of all possible species of the adduct, dinoprostone, and bisulfite, respectively, at equilibrium.

In solubility analysis, if $K[E] \ll 1$, as in the present case ($\sim 10\ M^{-1} \times 2.8 \times 10^{-3}$), then the slope and the intercept of plots of $[E_T]$ *versus* $[S_T]$ become $K[E][S_T]$ and $[E]$, respectively (37, 38), where $[E]$ is the solubility of dinoprostone in the absence of bisulfite, and the subscript T refers to the total concentration of a given species. Therefore, the quantity obtained by dividing the slope by the intercept should be equal to K. However, as shown in Fig. 3, at both pH 3.0 and 4.0, positive deviations from the expected linearity were observed in the plot of $[E_T]$ *versus* $[S_T]$, starting at $[E_T]$ of about 6 mg/ml ($1.7 \times 10^{-3}\ M$). The equilibrium constants estimated from the initial straight lines in Fig. 3 are listed in Table I, together with those obtained by other methods.

The solubility behavior of dinoprostone shown in Fig. 3 can be best explained in terms of mixed micelle formation. The surface tension of a dinoprostone solution (20 mg/ml) at pH 4.0 in 5% bisulfite, measured by the drop-volume technique (43), was about 35 dynes/cm, which is very close to that of a typical surfactant solution (44); the surface tension of a blank solution without dinoprostone was 63 dynes/cm. This result is not surprising, because aqueous prostaglandin solutions are known to be surface active. For example, the dinoprostone-9-dihydro analog, *i.e.*, dinoprost (prostaglandin $F_{2\alpha}$), was reported to form micelles with a

Table I—Equilibrium Constant for the Formation of the Bisulfite Adduct of Dinoprostone at 25°

pH	K, M^{-1}	Method
3.0	10.4	Solubility
4.0	14.4	Solubility
4.9	6.8	UV
6.8	5.0	UV
7.6	2.0	UV
6.5	7.5[a]	Circular dichroism
3.0	5.7	Partition
4.2	6.7	Partition
5.5	8.7	Partition
6.4	10.1	Partition

[a] The most accurate value; see the text for the accuracy level.

critical micelle concentration (CMC) close to 0.02 M (7 mg/ml) (45). In this context, it is interesting that the deviations shown in Fig. 3 start at about 6 mg/ml. At present, the exact chemical composition of the micelle phase is not known.

Equilibrium constants also were calculated from differences in absorbance at 288 nm in the UV spectrum and in molar rotation at 292 nm in the circular dichroism spectrum (Fig. 1) between the buffered solutions of dinoprostone and the same solutions containing various amounts of bisulfite. The values of K calculated by an iterative procedure similar to the one described by Higuchi *et al.* (39) are listed in Table I.

One major assumption made in the partitioning experiment was that the bisulfite adduct of dinoprostone, being an ionic species under the experimental pH range, does not dissolve in the organic layer. Since dinoprostone is highly soluble in ethyl acetate and insoluble in hexane, the 1:1 (volume ratio) mixture of these two solvents was chosen as the organic layer to have an apparent partition coefficient of unity around pH 6. The values of K computed in a conventional manner (42) are collected in Table I. During the partitioning experiment, the apparent pKa of dinoprostone was obtained from a series of blank samples without bisulfite through the relationship:

$$PC' = \frac{(PC)[H^+]}{[H^+] + K_a} \qquad \text{(Eq. 3)}$$

where PC' and PC are the pH-dependent apparent partition coefficient and the intrinsic partition coefficient of neutral species of dinoprostone, respectively. From the data at pH around 5, a pKa value of 4.73 was obtained, which is somewhat lower than the values reported in the literature [5.32 in 85% aqueous ethanol (17), 5.00 (18), and 4.90 for dinoprost (45)].

Data given in Table I are approximately in ±20% error, except the K value obtained from the circular dichroism work, which is in ±5% error. Because of this large experimental error, the pH profile of the K value is not clearly revealed in the present study. As the pH approaches the pKa of the sulfonic acid in the adduct (pKa ~ 1.0), K is expected to decrease since HSO_3^-, a better leaving group than SO_3^{2-}, is formed on the adduct. On the other hand, in alkaline solutions, desulfonation is expected to occur, which is initiated by proton abstraction from the hydroxyl group at C-9 of the adduct. In fact, desulfonation occurring in acidic or alkaline conditions is widely used in purifying cyclic ketones (46).

Because of the low equilibrium constant (~7.5 M^{-1}) for the reaction of the bisulfite ion with dinoprostone, at least a 12.5% (1.2 M) sodium bisulfite solution is required to achieve a mere 10-fold increase in the aqueous stability of dinoprostone when the total concentration of dinoprostone is about 1 mg/ml (2.84×10^{-3} M). Under this condition, not only the toxicity but also the side reaction of the bisulfite ion with other functional groups in dinoprostone becomes troublesome. The side reaction observed is believed to be the substitution of the allylic hydroxyl group at C-15 by the bisulfite ion, since dinoprost, a dinoprostone 9-dihydro analog, also slowly reacts with the bisulfite ion when the latter is in a 100-fold excess of the former. Also, the related allylic system such as the benzylic hydroxyl group in epinephrine is known to undergo substitution with the bisulfite ion (47).

A patent was issued to a claim that the E prostaglandins can be stabilized by incorporation of bisulfite salts (48). Since the systems described in the patent were very rich in alcohol content (50% or sometimes up to 90%), the claimed stability might be the result of the change in the solvent composition rather than the reversible addition of the bisulfite ion to the prostaglandins.

Since the equilibrium constant is only about 7.5 M^{-1}, other nucleophiles known to be *thermodynamically* inferior to bisulfite (25, 32, 49) are not expected to add significantly to dinoprostone in aqueous solutions. Such a consideration of the linear free energy relationship governing the thermodynamics of nucleophilic addition to carbonyl groups appears to indicate that the chemical reactivity of the C-9 carbonyl group of dinoprostone is not high enough to be utilized in improving aqueous stability through reversible one-step nucleophilic reactions.

Kinetics of Bisulfite Addition of Prostaglandin A_2—Even though mathematical manipulation of the rate expression for a reversible reaction is generally more complicated than for an irreversible reaction, it is necessary to treat its kinetics by assuming that the reaction is reversible when it is not known whether the reaction can be considered practically irreversible or not. The reaction:

$$A + S \underset{k_{-1}}{\overset{k_2}{\rightleftharpoons}} AS$$

Scheme III

where A, S, and AS are all possible species of prostaglandin A_2, bisulfite, and the bisulfite adduct of prostaglandin A_2, respectively, can be schematically represented as:

$$A \underset{k_{-1}}{\overset{k_1}{\rightleftharpoons}} AS$$

Scheme IV

under pseudo-first-order kinetic conditions that can be established in the presence of a large excess of S over A, where $k_1 = k_2(S)$. The rate expression for Schemes III and IV becomes:

$$-\frac{d[A]}{dt} = k_2[A][S] - k_{-1}[AS] = k_1[A] - k_{-1}[AS] \qquad \text{(Eq. 4)}$$

One easy way to determine k_1, k_{-1}, and eventually the second-order rate constant k_2 is to follow the change in absorbance at a given wavelength accompanied by the reaction. Plots of log $(D - D_\infty)$ *versus* time t should result in a straight line where the slope is equal to $-(k_1 + k_{-1})/2.303$, where D and D_∞ are the absorbance at any t and at equilibrium, respectively. If k_{obs} is defined as the sum of k_1 and k_{-1}, then:

$$k_{obs} = k_1 + k_{-1} = k_2[S] + k_{-1} \qquad \text{(Eq. 5)}$$

Under a given reaction condition, k_{obs} is determined at various $[S]$ values, which must be at least 25 times excess over $[A]$ to ensure a pseudo-first-order kinetic condition. From the slope and the intercept of the plot of Eq. 5, k_2 and k_{-1} are obtained. Finally, the equilibrium constant can be obtained from:

$$K = \frac{k_2}{k_{-1}} \qquad \text{(Eq. 6)}$$

The absorption band at λ_{max} 220 nm with $\epsilon_{220} = 1.02 \times 10^4$ of prostaglandin A_2 gradually disappeared in the presence of bisulfite. Figure 4 shows typical plots of log $(D - D_\infty)$ *versus* t with varying concentrations of total bisulfite at pH 6.04. Linearity was observed at least over three $t_{1/2}$ periods. The lowest $[S_T]$ was still about 25 times in excess of the concentration of prostaglandin A_2. From the slopes, k_{obs} values were determined. Isolation of k_2 and k_{-1} from k_{obs} thus obtained is shown in Fig. 5 for all experimental pH values. Values of k_{obs} and k_2 estimated from k_{obs} are listed in Table II.

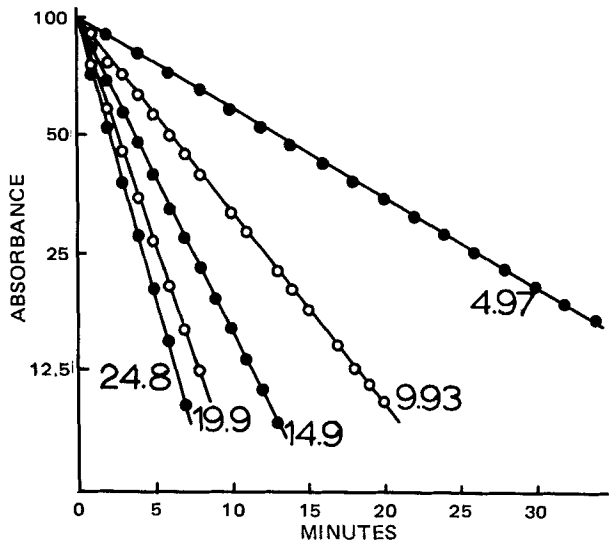

Figure 4—*Semilogarithmic plots against time of absorbance changes that occurred during bisulfite addition to prostaglandin A_2 in a phosphate buffer of pH 6.0 and I = 0.1 M at 25°. Experimental points were normalized to facilitate visual comparisons. Total absorbance changes were at least 0.5 absorbance unit. Prostaglandin A_2 = 2.12 × 10^{-4} M, and total bisulfite concentrations in 10^{-3} M are given on the figure.*

One interesting result indicated by Fig. 5 is the fact that the intercepts k_{-1} are all zero regardless of the pH; *i.e.*, the rate constant for the reverse adduct dissociation is extremely small. This would make the equilibrium constant K for the adduct formation very large over the experimental pH range. From this kinetic study, it is concluded that bisulfite adds across the $\Delta^{10,11}$-bond of prostaglandin A_2 practically in an irreversible fashion over a pH range of 4–8.

The pH dependence of k_2 (*i.e.*, the slope of Fig. 5) is better illustrated in Fig. 6. As pH increases, k_2 also increases, clearly indicating that the kinetically reactive species is SO_3^{2-} and that, under the experimental

Table II—Observed Pseudo-First-Order Rate Constant, k_{obs}, and Second-Order Rate Constant, k_2, for Bisulfite Addition to Prostaglandin A_2 at 24 ± 2°

pH	$[S_T] \times 10^3 M$	λ, nm	$k_{obs} \times 10^2$ min^{-1}	k_2 $min^{-1} M^{-1}$
4.98	11.87	232	1.99	1.43
	17.81	232	2.42	
	23.75	232	4.08	
	23.83	230	3.69	
	29.70	232	4.55	
	35.61	233	5.78	
	39.72	233.5	6.60	
	47.66	235	6.30	
	49.65	233.5	7.22	
5.47	9.93	232.5	4.15	4.05
	19.86	234	7.97	
	29.80	235	12.16	
6.04	4.97	232	5.44	12.00
	9.93	232	11.18	
	14.89	234.5	18.48	
	19.86	236.5	25.96	
	24.82	238	29.00	
6.50	5.93	240	21.7	28.98
	11.87	242	41.2	
	17.80	242	55.9	
	23.74	245	74.25	
	29.67	245	83.2	
7.05	4.97	237	25.7	55.5
	9.93	239	53.8	
	14.89	241	85.4	
7.97	4.97	232.5	46.8	94.0
	9.93	237	92.0	
	14.89	238.5	127.0[a]	

[a] Data not shown in Fig. 5.

conditions, the rate-determining step involves the attack of SO_3^{2-} at C-11. From a mechanistic point of view, protonation of C-10 can occur simultaneously (*i.e.*, 1,2-addition in a true sense) or the sulfite attack can lead to the formation of C-9 enolate (*i.e.*, 1,4-addition). But this point is not the concern of the present study. The reactivity of the $\Delta^{10,11}$-bond of prostaglandin A_2 should not be affected by the ionization of C-1 carboxylic acid (unless there is an unusual proximity field effect between C-1 and C-11). Therefore, when analyzing the pH profile of k_2, it is not necessary to assign a different reactivity to the free acid and to the carboxylate ion. Under this condition, the observed rate expression becomes:

$$\text{rate} = k_2[A][S] = k_2[A][SO_3^{2-}]\left(1 + \frac{[H^+]}{K_a}\right) \qquad \text{(Eq. 7)}$$

where K_a is the ionization constant of HSO_3^- (1.15×10^{-7} at $I = 0.1 M$). Since SO_3^{2-} is the kinetically reactive species, another rate expression is obtained:

$$\text{rate} = k_2^0[A][SO_3^{2-}] \qquad \text{(Eq. 8)}$$

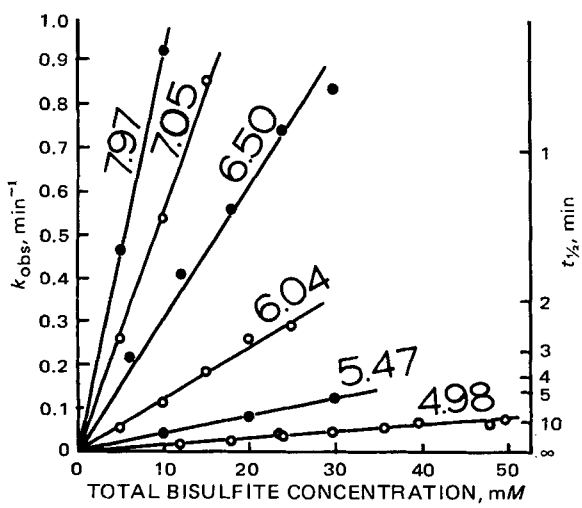

Figure 5—*Relationship of* $k_{obs} = k_2[S] + k_{-1}$ *for bisulfite addition to prostaglandin A_2 at 25° under pseudo-first-order kinetic conditions. The pH values are given on the figure.*

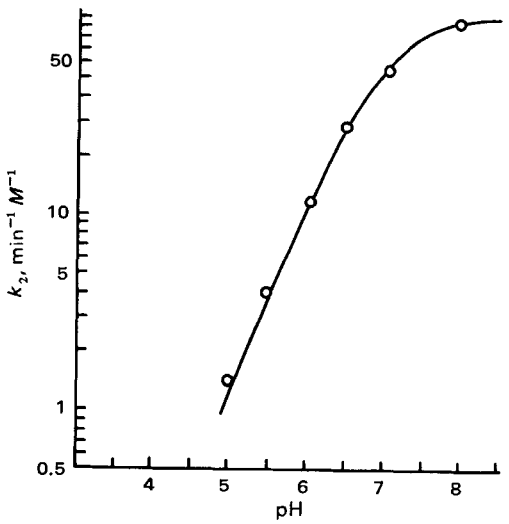

Figure 6—*Dependence on pH of the second-order rate constant,* k_2, *for the formation of the prostaglandin A_2 bisulfite adduct at 25°. The solid curve was theoretically generated using 105 min^{-1} M^{-1} as the value of the pH-independent second-order rate constant,* k_2^0, *for SO_3^{2-} attack on prostaglandin A_2.*

where k_2^0 is the pH-independent second-order rate constant specifically for SO_3^{2-} attack at C-11 of prostaglandin A_2. From Eqs. 7 and 8:

$$k_2 = k_2^0\left(1 + \frac{K_a}{K_a + [H^+]}\right) \qquad \text{(Eq. 9)}$$

By using four values of k_2 at pH > 6, the average k_2^0 of 1.75 $sec^{-1} M^{-1}$ (105 $min^{-1} M^{-1}$) was obtained. The solid curve on Fig. 6 was generated from this value of k_2^0 and Eq. 9. The small but significant (within the experimental accuracy) positive deviation of the experimental data from the theoretical pH profile observed at pH values below 5.5 is attributed to an extra kinetic contribution of HSO_3^- to k_2. The contribution of HSO_3^- is seldom reported as an additional kinetically reactive species; but at a sufficiently low pH range where the fractional concentration of HSO_3^- far exceeds that of SO_3^{2-}, its contribution to the observed rate constant can be clearly detected (25).

EXPERIMENTAL

Reagents and Apparatus—The following chemicals were used without further purification: dinoprostone[1], mol. wt. 352.46, mp 62–64°; prostaglandin A_2[1], mol. wt. 334.46, oily liquid at room temperature; dinoprost[1], mol. wt. 354.46, oily liquid at room temperature; and sodium bisulfite[2] (granular), analytical reagent. All other chemicals were of analytical reagent grade. Buffer systems used were the same as described previously (25). The spectroscopic data were obtained using commercially available instruments[3].

Procedure—The circular dichroism curves of Figs. 1 and 2 are expressed in terms of the molar ellipticity, $[\theta]$, in degrees centimeters[2] decimole^{-1}; $[\theta] = RM/100\,Cl$, where R = rotation (or ellipticity) in degrees, M = molecular weight, C = concentration in grams per milliliter, and l = path length in decimeters. The observed rotation was measured using 0.5-cm cells, except spectrum c. In each case, approximately 30 min passed after a sample solution was prepared when the rotation at 292 nm was measured. Because of the high concentration of bisulfite in Sample c, the noise–signal ratio was very high (dynode voltage was over 0.5 kv). Therefore, spectrum c was obtained using a 0.1-cm cell, and a fivefold increase in sensitivity was employed.

The circular dichroism spectra shown in Fig. 2 were constructed from the observed rotation measured using 1-cm cells for the λ range from 220 to 260 nm and 5-cm cells for the λ range from 250 to 400 nm. About 30 min elapsed after the sample solutions were prepared when the rotation at 285 and 235 was measured for both Samples a and b.

Throughout the phase solubility analysis and the partition experiment, the concentration of dinoprostone was determined by measuring absorbance at 283 nm after dinoprostone had been converted to prosta-

[1] The Upjohn Co.
[2] Mallinckrodt Chemical Co.
[3] Cary 14 spectrophotometer, Perkin-Elmer 621 IR grating spectrophotometer, Varian XL-100-15 spectrometer, and Cary 60 spectropolarimeter.

glandin B_2 in 1 *N* KOH: $\epsilon_{283} = 1.62 \times 10^4$. A quantitative conversion of dinoprostone to prostaglandin B_2 was obtained within 10 min at room temperature.

In phase solubility analysis, excess dinoprostone was added to each of 5-ml buffer solutions containing varying amounts of sodium bisulfite. Seven-milliliter capped[4] vials were used for both solubility and partition experiments. At equilibrium, attained by shaking the samples in a water bath of 25° for 20 hr, the vials were subjected to centrifugation. Undissolved dinoprostone formed an oily droplet at the bottom of the vials, and an aliquot of the supernate was taken out and diluted in 1 *N* KOH. At 25°, less than 2% of total dinoprostone is expected to degrade in 10 hr, since $k_{obs} \sim 10^{-3}$ hr^{-1} under the same conditions (18).

In partition experiments, 3.0 ml of a stock solution of dinoprostone in ethyl acetate–hexane (1:1), which had been saturated with water, and 3.0 ml of a buffer solution in a 7-ml vial were vigorously shaken for 5 hr in a water bath at 25°. At equilibrium, an aliquot of the organic solvent layer was withdrawn; dinoprostone was converted to prostaglandin B_2 after the solvent was evaporated under a nitrogen stream at room temperature. The aliquot from the aqueous layer was directly diluted with 1 *N* KOH.

The equilibrium constant determined by the UV spectrophotometric technique was not as accurate as that determined by circular dichroism spectroscopy, mainly because a wide range of bisulfite concentrations could not be employed. The absorbance of bisulfite solutions is a square (not linear) function of the bisulfite concentration (50).

Because of the UV absorption due to buffer components and bisulfite and other ionic species derived from it (50), the absorbance of λ_{max} of prostaglandin A_2 (220 nm) could not be used in the kinetic study of bisulfite addition to prostaglandin A_2. The results shown in Fig. 4 were, therefore, obtained by following the absorbance change at various wavelengths ranging from 230 to 254 nm (see Table II), using prostaglandin $A_2 = 2.12 \times 10^{-4}$ *M*. The lowest concentration of total bisulfite was about 5×10^{-3} *M*, which satisfies the pseudo-first-order kinetic condition. To protect the bisulfite solution from oxidation, usually a stock solution of about 0.1 *M* was prepared accurately in a deoxygenated buffer solution containing less than 0.5% of methanol as a free radical scavenger. This stock solution was diluted just prior to a kinetic run. To a spectrophotometer cell, 10 μl of stock solution of prostaglandin A_2 in methanol (10 mg/ml) was introduced, and 2.8 ml of a buffer solution containing bisulfite was rapidly added. The absorbance change at a given wavelength was then immediately followed using an identical solution without prostaglandin A_2 as a blank. The ionic strength of the reaction medium varied from 0.1 to about 0.2 *M*, and the temperature of the cell chamber was 24 ± 2°.

REFERENCES

(1) S. Bergström, *Science*, **157**, 382 (1967), and references cited therein.

(2) T. O. Oesterling, W. Morozowich, and T. J. Roseman, *J. Pharm. Sci.*, **61**, 1861 (1972).

(3) J. R. Weeks, *Ann. Rev. Pharmacol.*, **12**, 317 (1972).

(4) J. W. Hinman, *Ann. Rev. Biochem.*, **41**, 161 (1972).

(5) N. H. Andersen and P. W. Ramwell, *Arch. Intern. Med.*, **133**, 30 (1974).

(6) G. L. Bundy, *Ann. Rev. Med. Chem.*, **2**, 157 (1972).

(7) U. Axen, J. E. Pike, and W. P. Schneider, in "Progress in the Total Synthesis of Natural Products," vol. 1, J. W. ApSimon, Ed., Wiley, New York, N.Y., 1973.

(8) N. M. Weinshenker and N. H. Andersen, in "The Prostaglandins," vol. 1, P. W. Ramwell, Ed., Plenum, New York, N.Y., 1973.

(9) "The Prostaglandins: Clinical Applications in Human Reproduction," E. M. Southern, Ed., Futura Publishing, Mount Kisco, N.Y., 1972.

(10) G. A. Murnaghan, H. Lamki, and S. Rashid, *J. Obstet. Gynaecol. Br. Commonw.*, **81**, 141 (1974).

(11) A. W. F. Miller and D. S. Mack, *ibid.*, **81**, 706 (1974).

(12) M. G. Elder and M. Stone, *Prostaglandins*, **6**, 427 (1974).

(13) S. Bergström, in "Prostaglandins," Nobel Symposium 2, S. Bergström and B. Samuelsson, Eds., Interscience, New York, N.Y., 1967, p. 21.

(14) S. M. M. Karim, J. Devlin, and K. Hillier, *Eur. J. Pharmacol.*, **4**, 416 (1968).

(15) N. H. Andersen, *J. Lipid Res.*, **10**, 320 (1969).

(16) T. O. Oesterling, "Abstracts APhA Academy of Pharmaceutical Sciences," Washington, D.C., Apr. 1970, p. 44.

(17) D. C. Monkhouse, L. VanCampen, and A. J. Aguiar, *J. Pharm. Sci.*, **62**, 576 (1973).

(18) G. F. Thompson, J. M. Collins, and L. M. Schmalzried, *ibid.*, **62**, 1738 (1973).

(19) E. G. Daniels, W. C. Krueger, F. P. Kupiecki, J. E. Pike, and W. P. Schneider, *J. Am. Chem. Soc.*, **90**, 5894 (1968).

(20) R. P. Bell and P. W. Smith, *J. Chem. Soc. (B)*, **1966**, 241.

(21) J. E. Pike, F. H. Lincoln, and W. P. Schneider, *J. Org. Chem.*, **34**, 3552 (1969).

(22) L. R. Fedor and W. R. Glave, *J. Am. Chem. Soc.*, **93**, 985 (1971), and references cited therein.

(23) D. J. Hupe, M. C. R. Kendall, G. T. Sinner, and T. A. Spencer, *ibid.*, **95**, 2260 (1973).

(24) L. C. Schroeter, "Sulfur Dioxide," Pergamon, New York, N.Y., 1966, p. 273.

(25) M. J. Cho and I. H. Pitman, *J. Am. Chem. Soc.*, **96**, 1843 (1974), and references cited therein.

(26) I. H. Pitman, M. J. Cho, and G. S. Rork, *ibid.*, **96**, 1840 (1974).

(27) J. March, "Advanced Organic Chemistry; Reactions, Mechanisms, and Structure," McGraw-Hill, New York, N.Y., 1968, p. 568.

(28) P. Crabbé, *Tetrahedron*, **30**, 1979 (1974).

(29) P. Petrenko-Kritschenko and W. Kantscheff, *Chem. Ber.*, **39**, 1452 (1906); through Ref. 24, p. 105.

(30) C. V. Grudzinskas and M. J. Weiss, *Tetrahedron Lett.*, **1973**, 141.

(31) G. L. Bundy, F. H. Lincoln, N. Nelson, J. E. Pike, and W. P. Schneider, *Ann. N.Y. Acad. Sci.*, **180**, 76 (1971).

(32) E. G. Sander and W. P. Jencks, *J. Am. Chem. Soc.*, **90**, 6154 (1968).

(33) T. H. Fife and T. C. Bruice, *J. Phys. Chem.*, **65**, 1079 (1961).

(34) P. Crabbé, "Optical Rotatory Dispersion and Circular Dichroism in Organic Chemistry," Holden-Day, San Francisco, Calif., 1965, pp. 191–243.

(35) A. G. Long and L. J. Wyman (to Glaxo Labs), U.S. pat. 2,908,695 (Oct. 13, 1959); through Ref. 24, p. 111.

(36) G. S. Smith, L. M. Weinstock, F. E. Roberts, Jr., G. S. Brenner, A. M. Hoinowski, B. H. Arison, and A. W. Douglas, *J. Pharm. Sci.*, **61**, 708 (1972).

(37) T. Higuchi and K. A. Connors, in "Advances in Analytical Chemistry and Instrumentation," vol. 4, C. N. Reilley Ed., Interscience, New York, N.Y., 1965, pp. 117–212.

(38) K. A. Connors and J. A. Mollica, Jr., *J. Pharm. Sci.*, **55**, 772 (1966).

(39) T. Higuchi, J. H. Richards, S. S. Davis, A. Kimada, J. P. Hou, M. Nakano, N. I. Nakano, and I. H. Pitman, *ibid.*, **58**, 661 (1969).

(40) W. J. Mader, *Crit. Rev. Anal. Chem.*, **1**, 193 (1970).

(41) J. Meier and T. Higuchi, *J. Pharm. Sci.*, **54**, 1183 (1965).

(42) T. Higuchi and D. A. Zuck, *J. Am. Pharm. Assoc., Sci. Ed.*, **42**, 132 (1953).

(43) E. L. Rowe, *J. Pharm. Sci.*, **61**, 2630 (1972).

(44) B. A. Mulley, in "Advances in Pharmaceutical Sciences," vol. 1, H. S. Bean, A. H. Beckett, and J. E. Carless, Eds., Academic, New York, N.Y., 1964, pp. 86–194.

(45) T. J. Roseman and S. H. Yalkowsky, *J. Pharm. Sci.*, **62**, 1680 (1973).

(46) D. J. Pasto and C. R. Johnson, "Organic Structure Determination," Prentice-Hall, Englewood Cliffs, N.J., 1969, p. 393.

(47) T. Higuchi and L. C. Schroeter, *J. Am. Chem. Soc.*, **82**, 1904 (1960).

(48) D. C. Monkhouse (to Pfizer), U.S. pat. 3,851,052 (Nov. 26, 1974).

(49) J. Hine and R. W. Redding, *J. Org. Chem.*, **35**, 2769 (1970).

(50) D. W. A. Bourne, T. Higuchi, and I. H. Pitman, *J. Pharm. Sci.*, **63**, 865 (1974).

ACKNOWLEDGMENTS AND ADDRESSES

Received May 30, 1975, from *Pharmacy Research, The Upjohn Company, Kalamazoo, MI 49001.*

Accepted for publication April 14, 1976.

Thanks are expressed to Dr. W. Morozowich for valuable contributions, Mr. F. H. Lincoln for prostaglandin A_2 samples, and Ms. L. M. Pschigoda for assistance.

[x] To whom inquiries should be directed.

[4] Lined with Teflon (du Pont).

Plastic Flow during Compression of Directly Compressible Fillers and Its Effect on Tablet Strength

S. T. DAVID * and L. L. AUGSBURGER ˣ

Abstract □ The effects of the duration of the overall compression cycle and of the duration of the maximum compressive force on tablet strength were studied using an instrumented rotary tablet press. Various direct compression fillers were evaluated. Increasing the overall compression cycle duration to 10 sec resulted in significantly greater tablet tensile strengths with microcrystalline cellulose and compressible starch fillers but not with lactose or compressible sugar. Increasing the duration of the maximum compressive force to 20 sec significantly increased the tensile strength in all cases, but microcrystalline cellulose and compressible starch tablets were affected more than lactose or sugar tablets. The maximum compressive force decayed with time for all fillers but at a greater rate with microcrystalline cellulose and compressible starch. This behavior was attributed to differences in the extent of plastic flow. The decay curves were analyzed using the Maxwell model.

Keyphrases □ Tablets—plastic flow during formation, effect of duration of compression cycle and maximum compressive force on tensile strength □ Plastic flow—during tablet formation, effect of duration of compression cycle and maximum compressive force on tensile strength □ Compression cycle—tablet formation, effect of duration and maximum force on tablet tensile strength □ Dosage forms—tablets, effect of duration of compression cycle and maximum compressive force on tensile strength □ Tensile strength—tablets, effect of duration of compression cycle and maximum compressive force

In the mid-1950's, Train (1) formulated a hypothesis on the mechanics involved in tablet formation. The consolidation process was divided into stages. Stage I takes into account interparticulate slippage of the powder particles, which leads to a decrease in the relative volume of the compact. The formation of temporary struts, columns, and vaults due to the increased resistance of the powder to compression is manifested in Stage II. Failure of these structures, brought about by increasing the compression forces on the powder material, is obtained in Stage III. Here the structure failure is a result of the crushing of particles or plastic flow. In Stage IV, rebonding is taking place more quickly than particle fracture, and the decrease in the relative volume of the compact becomes quite small as compared to the former stages.

As stated by Train, one event reported to occur during the formation of tablets is plastic deformation, which results from the crushing or fracturing of particles or by plastic flow. Plastic flow in various materials has been evaluated by comparing their stress relaxation behavior under constant load (2, 3).

The purpose of this study was to investigate plastic flow, with particular reference to its effect on tablet tensile strength. Therefore, the effects of the duration of the total compression cycle and of the duration of the maximum compressive force on tablet strength were investigated. Directly compressible fillers were chosen, because there is much interest today in materials and formulas that permit the manufacture of tablets without the traditional and costly granulating step.

EXPERIMENTAL

Tablet Preparation—Tablets were prepared on a rotary tablet press[1], which had been instrumented with resistance strain gauges after the manner of Wray *et al.* (4) to monitor compression and ejection forces. The instrumentation of this machine was described in detail previously (5). Only a single station was used to help minimize tooling errors. The same circular, flat-faced punches and die, 1.588 cm in diameter, were used throughout the study.

Tablet weights were held constant at 750 mg, unless otherwise stated. When a lubricant was necessary, it was first prescreened through an 80-mesh screen to facilitate blending. Lubricated blends (500-g batches) were prepared by mixing in a 1.92-liter (2-qt) twin-shell blender[2] for 12 min, with the intensifier bar running for only the final 2 min. All tableting was conducted in a room where temperature and relative humidity were maintained at 26 ± 1° and 35 ± 5%, respectively.

Tablet Tensile Strength—Tablet tensile strength was determined from the force required to fracture tablets by diametral compression on a motorized tablet hardness tester[3]. Rather than report tablet strength as hardness (*i.e.*, fracture force), force readings were converted to tensile strength in the manner of Fell and Newton (6), because tensile strength is independent of tablet dimensions and is a measure of the strength of the "as compacted" material (7, 8). The equation used to compute tensile strength was:

$$\sigma_0 = \frac{2F}{\pi dt} \qquad \text{(Eq. 1)}$$

where σ_0 is the tensile strength, F is the force needed to cleave the tablet, d is the diameter of the tablet, and t is the tablet thickness. Care was taken to use only the fracture forces generated when tablets failed in tension, as evidenced by their uniform splitting into halves. Tablet dimensions were determined using an inch measure[4]. All tensile strengths reported are based on 10 determinations.

Effect of Duration of Compression Cycle—Compression cycle durations were varied from 0.09 to 10 sec for the following directly compressible materials: lactose[5] USP, direct compressible sugar[6] USP, microcrystalline cellulose[7] NF, and compressible starch[8] (pregelatinized starch USP). The first two materials each contained 0.50% magnesium stearate[9] USP as a lubricant to facilitate ejection of the compacts from the die cavity. In most cases, machine speed could be altered by making a mechanical adjustment to vary the time of the compression cycle; however, the 10-sec time was achieved by rotating the flywheel of the press manually at a relatively constant rate.

Ten tablets, representing each cycle duration, were evaluated for tensile strength (Table I). Increasing the duration of the compression cycle did not result in significantly different tensile strengths for the lactose or sugar tablets; however, the microcrystalline cellulose and compressible starch tablets were significantly stronger when the compression cycle was increased to 10 sec (5% level).

Effect of Duration of Maximum Compressive Force—The ef-

[1] Stokes model RB-2.
[2] Patterson-Kelly, Stroudsburg, Pa.
[3] Heberlein model 2E/106, series 7203, Key Industries, Farmingdale, N.Y.
[4] Model C815, Federal Products Corp., Wayne, Pa.
[5] Fast-Flo lactose, Foremost Dairies Inc., San Francisco, Calif.
[6] DiPac, Amstar Corp., Brooklyn, N.Y.
[7] Avicel PH101, F.M.C. Corp., American Viscose Division, Newark, Del.
[8] StaRx 1500 starch, A. E. Staley Manufacturing Co., Decatur, Ill.
[9] Ruger Chemical Co., New York, N.Y.

Table I—Effect of Duration of the Compression Cycle on Tablet Strength for a Few Directly Compressible Fillers

Filler	Compression Force, kg	Duration of Compression Cycle, sec	Tablet Tensile Strength kg/cm²	S[a]	t[b]
Compressible	938	0.11	10.0	0.72	—
lactose with 0.50%	938	0.13	10.2	0.68	0.639
magnesium stearate	938	10	10.1	0.70	0.314
Compressible	1619	0.11	11.6	0.69	—
sugar with 0.50%	1619	0.12	11.6	1.01	—
magnesium stearate	1619	10	11.6	0.50	—
Microcrystalline	203	0.10	13.6	0.51	—
cellulose	203	0.12	13.6	0.52	—
	203	10	14.2	0.69	2.21[c]
Compressible	643	0.10	8.0	0.32	—
starch	643	0.12	8.0	0.41	—
	643	10	8.7	0.50	3.72[c]

[a] Standard deviation, based on 10 determinations. [b] Student t statistic for difference comparing shortest cycle with each longer cycle. [c] Significant difference (5% level).

fect of the duration of the maximum compressive force on tablet tensile strength was examined using compressive forces required to make tablets of acceptable hardness. The same compressible materials used in the preceding study were again examined. The lactose and sugar contained 0.50% magnesium stearate.

Initially, samples were compressed utilizing a rotary tablet machine speed of 25 rpm where the duration of the compression force was less than 0.1 sec. Additional samples of the fillers were compressed on the same machine with the same maximum force but the duration of the force was prolonged. This change was accomplished by manually rotating the flywheel at approximately 0.5 rpm until the maximum compressive force was observed on a strip-chart recorder tracing. The position of the flywheel was held constant for 20 sec, and then the compressional force was released.

Tensile strengths were determined on 10 tablets produced on each run (Table II). Tablet strengths for these compacts increased significantly (5% level) in all cases when the duration of the maximum compressive force was increased to 20 sec.

Plastic Flow—In the previous experiment, increasing the duration of the maximum compressive force resulted in increased tablet tensile strength. However, of the four fillers tested, microcrystalline cellulose and compressible starch were affected to a markedly greater extent than compressible lactose and sugar. The compaction forces used in making these tablets were presumably in the range of Train's Stage III of compression, in which plastic flow and fracture take place. The differences could have been due to differences in the extent of plastic flow. To test this possibility, an experiment was designed to evaluate the role of plastic flow in the compaction of these materials.

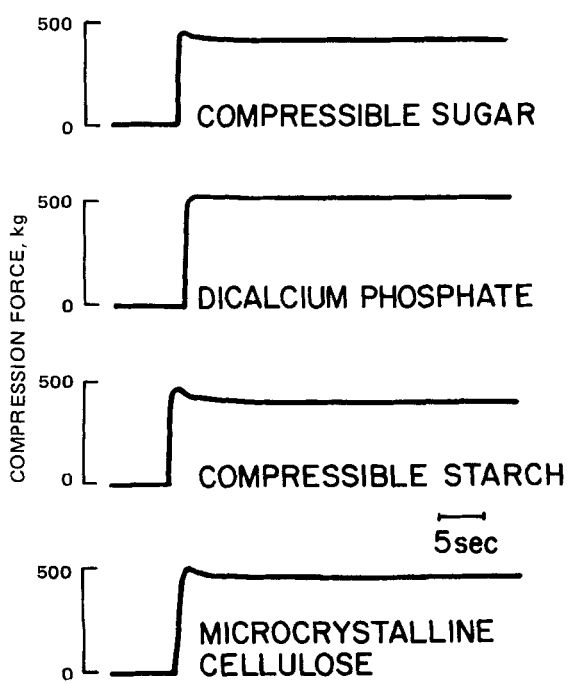

Figure 1—*Typical compression force decay curves.*

In the previous experiment, it was observed from the recorder tracings that during the extended times in which the compression cycle was halted at the point of maximum compressive force, this force tended to decay with time. This observation both supported the proposed role of plastic flow and suggested the instrumented rotary press as an experimental tool to evaluate this phenomenon. Thus, tablets were compressed manually on the instrumented rotary press by turning the flywheel by hand at an approximate rate of 0.5 rps until the maximum compressive force was observed on the recorder tracing. The flywheel was halted at this point, but the recorder was permitted to run, thus producing a continuous tracing of the compressive force.

Compressible starch, microcrystalline cellulose, dicalcium phosphate dihydrate[10] USP, and compressible sugar were evaluated. In all cases, maximum decay appeared to be reached within about 10 sec. The lactose used in the previous study was not used since a change had taken place in the material. Although microcrystalline cellulose and starch do not require a lubricant when tableted alone (9, 10), 0.30% magnesium stearate was added to each of the four fillers to keep the experimental conditions the same in all cases. Tablet weights for each blend were adjusted carefully to produce tablets with the same thickness of 0.300 ± 0.001 cm. Typical tracings appear in Fig. 1.

The data were treated in a manner similar to that of Shlanta and Milosovich (2). These substances were treated as materials showing both an elastic and a plastic nature during deformation. A linear, Hookean stress-strain relationship is combined in series with a linear, Newtonian viscous relationship to describe the material's behavior

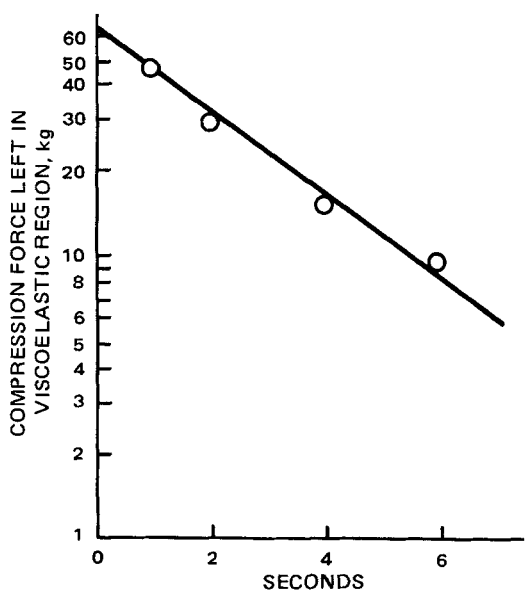

Figure 2—*Effect of time on the compression force observed for a compressible starch containing 0.30% magnesium stearate. Slope = 0.336 sec^{-1}. Intercept = 63 kg.*

[10] Unmilled, Stauffer Chemical Co., Chicago Heights, Ill.

Table II—Effect of Duration of the Maximum Compressive Force on Tablet Strength for a Few Directly Compressible Fillers

Filler	Compression Force, kg	Duration of Maximum Compressive Force, sec	Tablet Strength		
			kg/cm²	S^a	t^b
Compressible lactose with 0.50% magnesium stearate	826	<0.1	16.3	0.48	—
	826	20	18.8	0.77	8.71
Compressible sugar with 0.50% magnesium stearate	826	<0.1	10.0	0.42	—
	826	20	12.3	0.29	14.4
Microcrystalline cellulose	203	<0.1	13.6	0.62	—
	203	20	18.7	0.60	18.2
Compressible starch	643	<0.1	8.0	0.30	—
	643	20	18.8	0.44	63.5

[a] Standard deviation, based on 10 determinations. [b] Student t statistic comparing each pair. All differences are significant at the 5% level.

under real conditions. Thus, the plastic flow concept is treated mathematically as the Maxwell model under constant strain (11, 12), which involves combining one viscous parameter and one elastic parameter. The Hookean element is given by:

$$\sigma_1 = Ee_1 \qquad \text{(Eq. 2)}$$

From Newton's law of flow, the plastic or viscous relationship is:

$$\sigma_2 = n\frac{de_2}{dt} \qquad \text{(Eq. 3)}$$

where σ is the stress, e is the amount of powder constriction, de/dt is the rate of constriction with time, E is Young's modulus, and n is a viscosity coefficient. Since:

$$\sigma = \sigma_1 = \sigma_2 \qquad \text{(Eq. 4a)}$$

and:

$$e = e_1 + e_2 \qquad \text{(Eq. 4b)}$$

then:

$$\frac{de}{dt} = \frac{de_1}{dt} + \frac{de_2}{dt} = \frac{1}{E}\frac{d\sigma}{dt} + \frac{\sigma}{n} \qquad \text{(Eq. 4c)}$$

When a fixed constriction is applied to the powder mass at time t = 0 and held constant, one can express stress as a function of time. Therefore, de/dt is equal to zero so:

$$E^{-1}\frac{d\sigma}{dt} + \frac{\sigma}{n} = 0 \qquad \text{(Eq. 5a)}$$

and after integration:

$$\ln\frac{\sigma}{\sigma_0} = -Et/n \qquad \text{(Eq. 5b)}$$

or:

$$\Delta\sigma = \Delta\sigma_0 e^{-Et/n} \qquad \text{(Eq. 5c)}$$

The symbol Δ in front of the σ symbol represents the total range of compressive stresses located in the viscoelastic region in question. Since the area of contact between powder and punches was constant throughout, Eq. 5c becomes:

$$\Delta F = \Delta F_0 e^{-Et/n} \qquad \text{(Eq. 6)}$$

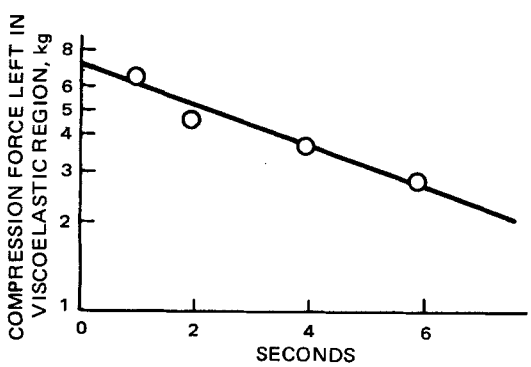

Figure 3—*Effect of time on the compression force observed for dibasic calcium phosphate containing 0.30% magnesium stearate. Slope = 0.182 sec^{-1}. Intercept = 7 kg.*

where ΔF is the amount of the compressional force left in the viscoelastic region at time t, and ΔF_0 is the total magnitude of this force at t = 0. Thus, according to Eq. 6, the decay of compression force with time from the continuous trace recordings can be treated as a first-order rate process. The logarithmic form of Eq. 6 is:

$$\ln \Delta F = \ln \Delta F_0 - kt \qquad \text{(Eq. 7)}$$

where the first-order rate constant, k, equals E/n and is the viscoelastic slope. Accordingly, compressive force data were obtained from tracings of the force decay curves of each filler. Data points were obtained and plotted in accordance with Eq. 7 on semilogarithmic paper. The first-order plots appear in Figs. 2–5. The data, including the first-order rate constants and the total magnitude of compression force decay, ΔF_0, appear in Table III. Results are based on three separate determinations for each filler.

RESULTS AND DISCUSSION

Although increasing the duration of the compression cycle did not result in statistically significant changes in the strength of the sugar or lactose tablets, the microcrystalline cellulose and starch tablets were significantly stronger (5% level) when a compression cycle of 10 sec was utilized (Table I). Plastic deformation results from fracture of particles and/or plastic flow. If plastic flow is an important factor affecting the compressibility of a substance, a prolongation of the compression cycle would be expected to increase the strength of tablets produced from such a substance, since more surface contact for interparticulate bonding would be produced through plastic flow.

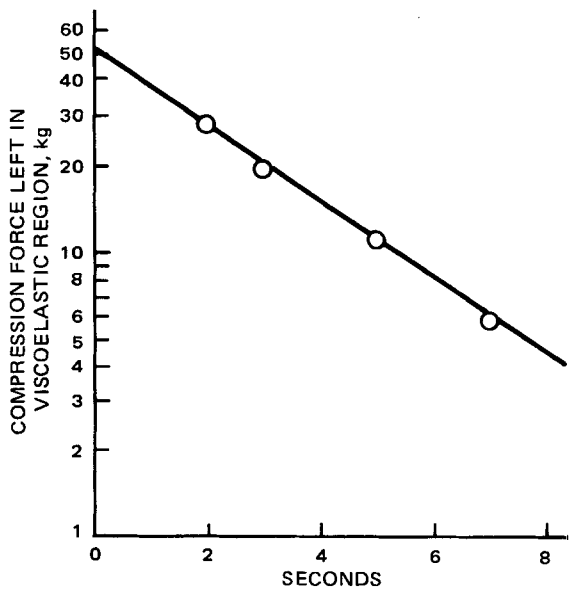

Figure 4—*Effect of time on the compression force observed for microcrystalline cellulose containing 0.30% magnesium stearate. Slope = 0.332 sec^{-1}. Intercept = 53 kg.*

Table III—Effect of Time on the Compression Force Observed for a Few Directly Compressible Fillers, All Containing 0.30% Magnesium Stearate

Filler	Seconds	Compression Force Observed, kg			Mean Viscoelastic Slope (k)	Mean Total Compression Force Lost in Viscoelastic Region, kg
Compressible starch	0	476	461	461	0.336	63
	1	454	441	432		
	2	439	425	419		
	4	425	417	406		
	6	419	412	403		
	12	412	403	394		
Microcrystalline cellulose	0	476	465	480	0.332	53
	1	463	454	463		
	2	450	441	450		
	3	441	436	443		
	5	432	425	436		
	7	425	421	432		
	12	421	416	425		
Compressible sugar	0	430	434	436	0.281	37
	1	425	423	425		
	2	410	414	414		
	3	406	410	410		
	5	403	404	406		
	7	401	402	403		
	12	392	399	397		
Dicalcium phosphate	0	529	507	531	0.182	7
	1	529	507	531		
	2	527	505	529		
	4	525	502	529		
	6	522	502	529		
	12	518	500	527		

To investigate further the role of the basic deformation properties of materials on compressibility, the effect of the duration of the maximum compressive force on tablet strength was examined. Increasing the duration of the maximum compressive force resulted in significantly greater tablet strengths in all cases (Table II). However, the differences appeared relatively greater with microcrystalline cellulose and compressible starch. These results, together with the findings of the experiment in which the overall compression cycle times were varied, give evidence that plastic flow may play a more important role in particle–particle bonding in the microcrystalline cellulose and starch tablets than in the lactose and compressible sugar tablets.

In the experiment in which the effect of the duration of the maximum compressive force on tablet tensile strength was studied, this compressive force decayed with time. As this result was no doubt due to plastic flow (3), this observation suggested that plastic flow data could be obtained by treating these compressive force decay curves viscoelastically using the Maxwell element. Accordingly, viscoelastic slopes, based on compressive force decay curves, were determined for compressible starch, microcrystalline cellulose, compressible sugar, and dicalcium phosphate. Dicalcium phosphate was included as an example of an inorganic compound.

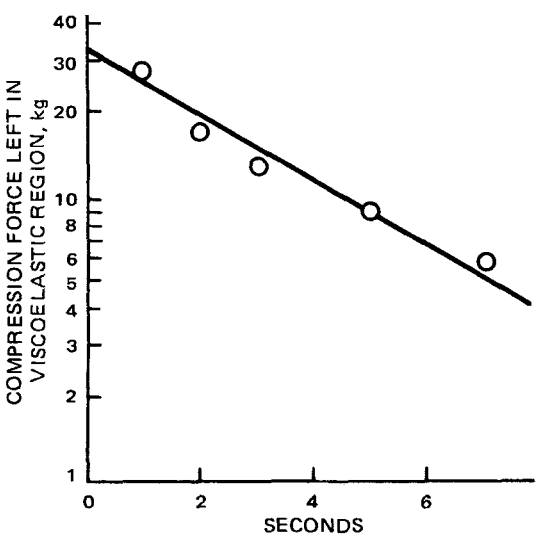

Figure 5—*Effect of time on the compression force observed for compressible sucrose containing 0.30% magnesium stearate. Slope = 0.281 sec^{-1}. Intercept = 37 kg.*

If the previous finding that plastic flow is more predominant in the compaction of compressible starch and microcrystalline cellulose and not as dominant in the compaction of sugar is correct, the viscoelastic slope, k, may be expected to be greater for the former two materials than for sugar. Furthermore, the total amount of compressive force decay, ΔF_0, should be less with sugar than with microcrystalline cellulose or compressible starch, as was found to be the case. The order of decreasing slopes and decreasing ΔF_0's (Figs. 2–5) is as follows: compressible starch > microcrystalline cellulose > compressible sugar > dicalcium phosphate. The viscoelastic plot for compressible sugar (Fig. 5) seems to deviate from linearity. One possible explanation is that, instead of a linear Newtonian element being applied, a nonlinear viscous relationship or a combination of the two may be involved.

The Maxwell element was used to determine the qualitative nature of polymers under stress, since it is generally unable to describe truly polymer properties quantitatively (11, 12). Vincent (12) pointed out that more complex models would be more suitable, but the behavior of the more complex models becomes "less easy to picture, as well as more difficult to analyze." However, since the Maxwell element is used to determine the qualitative behavior of polymers, the same treatment may be expected to help understand the important compressibility characteristics of various pharmaceutical materials during tablet compression. For example, Rees and Shotton (13) found that the tablet strength of sodium chloride tablets increased up to 100% or more 1 hr after tablet compression. This result was attributed to "stress relief of the crystals and interparticulate bonds" due to plastic flow. Therefore, a similar type of mathematical treatment, as described utilizing the Maxwell element, may become a useful tool in explaining unusual shifts in tablet hardness with time.

These results suggest that direct compression fillers can be classified according to their degree of plastic flow under compaction. Furthermore, these results help explain the phenomenon in which the compressibility of either microcrystalline cellulose or compressible starch is reduced to a much greater extent by the presence of lubricants than is observed with spray-dried lactose or sugar. It was suggested (5) that crystal fracture and the creation of new surfaces under compression may be more predominant factors in the bonding of tablets formed from lactose and sugar fillers than from microcrystalline cellulose or compressible starch. Thus, in the former cases, more new surfaces uncontaminated with lubricant would be formed which could participate essentially unhindered in bonding. Although plastic flow would be expected to increase the true area of contact

between particles, a lubricant initially present at particle surfaces would still exist at the interfaces formed by plastic flow where it could interfere with particle–particle bonding. The results of the present study help support this thesis, since microcrystalline cellulose and compressible starch appeared to exhibit a greater degree of plastic flow under compression than did sugar.

REFERENCES

(1) D. Train, *J. Pharm. Pharmacol.*, **8**, 745(1956).

(2) S. Shlanta and G. Milosovich, *J. Pharm. Sci.*, **53**, 562(1964).

(3) E. T. Cole, J. E. Rees, and J. A. Hersey, *Pharm. Acta Helv.*, **50**, 28(1975).

(4) P. W. Wray, J. G. Vincent, F. W. Moller, and G. J. Jackson, paper presented at the Industrial Pharmaceutical Section, APhA Academy of Pharmaceutical Sciences, Dallas meeting, Apr. 25–29, 1966.

(5) A. M. Salpekar and L. L. Augsburger, *J. Pharm. Sci.*, **63**, 298(1974).

(6) J. T. Fell and J. M. Newton, *ibid.*, **59**, 688(1970).

(7) J. M. Newton, G. Rowley, J. T. Fell, D. G. Peacock, and K. Ridgway, *J. Pharm. Pharmacol.*, **23**, 1955(1971).

(8) K. Ridgway, C. Lazarou, and E. E. Thorpe, *J. Pharm. Pharmacol.*, **24**, 265(1972).

(9) C. D. Fox, M. D. Richman, G. E. Reier, and R. Shangraw, *Drug Cosmet. Ind.*, **92**, 161(1963).

(10) K. W. Manudhane, A. M. Contractor, H. Y. Kim, and R. F. Shangraw, *J. Pharm. Sci.*, **58**, 616(1969).

(11) F. Rodriquez, "Principles of Polymer Systems," McGraw-Hill, New York, N.Y., 1970, pp. 201–218.

(12) P. I. Vincent, in "Physics of Plastics," Van Nostrand, Princeton, N.J., 1965, pp. 24–60.

(13) J. E. Rees and E. Shotton, *J. Pharm. Pharmacol.*, **22**, 175(1970).

ACKNOWLEDGMENTS AND ADDRESSES

Received April 25, 1975, from the *Department of Pharmacy (Pharmaceutics), School of Pharmacy, University of Maryland, Baltimore, MD 21201*

Accepted for publication March 1, 1976.

Presented at the Industrial Pharmaceutical Technology Section, APhA Academy of Pharmaceutical Sciences, New Orleans meeting, November 10–14, 1974.

Abstracted in part from a thesis submitted by S. T. David to the Graduate School, University of Maryland, in partial fulfillment of the Doctor of Philosophy degree requirements.

The authors thank Dr. Eugene E. Hamlow, Dr. Dana Brooke, and Mr. Benny Young of Meade Johnson Laboratories for their helpful advice and assistance in the preparation of this manuscript. They also gratefully acknowledge the assistance of Ms. Vickie J. Pforr in the preparation of this manuscript.

* American Foundation for Pharmaceutical Education Fellow, 1971–1973. Present address: Mead Johnson Research Center, Evansville, IN 47721

[x] To whom inquiries should be directed.

Zero-Order Drug Delivery System: Theory and Preliminary Testing

D. BROOKE [x] and R. J. WASHKUHN *

Abstract □ A new approach to zero-order drug delivery that includes geometric factors is described. An experimental device based on the theory was tested by following the release of stearic acid into ethanol. Three separate trials indicated that the solid was released *via* a zero-order process in a reproducible manner.

Keyphrases □ Drug delivery—zero-order system, geometric factors considered, experimental device tested □ Delivery, drug—zero-order system, geometric factors considered, experimental device tested □ Stearic acid—release into ethanol, zero-order drug delivery system, experimental device tested

Roseman and Higuchi (1) and, more recently, Roseman (2) treated the subject of drug release from silicone polymer matrixes containing suspended particulate drug. They developed equations for drug release from both planar and cylindrical surfaces (1). Roseman (2) showed that the fraction of drug release from a matrix with a planar surface was linear—not with time but with the square root of time. This finding confirmed an expectation published earlier (3). Roseman (2) also showed that the initial portion of a similar plot for a matrix of cylindrical shape was similar to that for the planar case. However, as more drug was released, the slope for the fraction *versus* square root of time plot decreased.

A study of these results indicates that polymer devices might be useful in dispensing drug to tissues or body cavities at fairly constant rates over reasonable periods of time. However, the ideal of a zero-order drug delivery system cannot be realized from planar or cylindrical devices of silicone polymer containing suspended particulate drug.

BACKGROUND

The planar case of a drug suspended in a polymer matrix fails as a zero-order drug delivery system because, as the drug is released, the boundary in the matrix at which drug dissolution occurs recedes from the surface from which the drug is released. The problem is one of a decreasing release rate due to an increasing drug diffusion path length within the matrix. For the cylindrical case, the situation is more complicated. Here, the diffusion path increases and the drug core within the matrix decreases in area.

The reduction of an effective dissolution surface, given a constant diffusion barrier, and its effect on drug dissolution, *e.g.*, from implants, are fairly well understood. In their derivation of the well-known "cube root law," Hixson and Crowell (4) showed an appreciation for the decreasing area of a single particle that maintained its shape during the dissolution process. Ballard and Nelson (5) related the rate of absorption from spherical implants to size. The same investigators (6) developed a graphical method of estimating the area of subcutaneously implanted cylindrical drug pellets.

More recently, Rippie and Johnson (7) attempted to regulate the dissolution behavior of drug pellets by controlling their geometry. However, their work involved dissolution in a turbulent flow, so that transport of the drug from the surface could not be considered limited to diffusion across a constant diffusion barrier.

between particles, a lubricant initially present at particle surfaces would still exist at the interfaces formed by plastic flow where it could interfere with particle–particle bonding. The results of the present study help support this thesis, since microcrystalline cellulose and compressible starch appeared to exhibit a greater degree of plastic flow under compression than did sugar.

REFERENCES

(1) D. Train, *J. Pharm. Pharmacol.*, **8**, 745(1956).

(2) S. Shlanta and G. Milosovich, *J. Pharm. Sci.*, **53**, 562(1964).

(3) E. T. Cole, J. E. Rees, and J. A. Hersey, *Pharm. Acta Helv.*, **50**, 28(1975).

(4) P. W. Wray, J. G. Vincent, F. W. Moller, and G. J. Jackson, paper presented at the Industrial Pharmaceutical Section, APhA Academy of Pharmaceutical Sciences, Dallas meeting, Apr. 25–29, 1966.

(5) A. M. Salpekar and L. L. Augsburger, *J. Pharm. Sci.*, **63**, 298(1974).

(6) J. T. Fell and J. M. Newton, *ibid.*, **59**, 688(1970).

(7) J. M. Newton, G. Rowley, J. T. Fell, D. G. Peacock, and K. Ridgway, *J. Pharm. Pharmacol.*, **23**, 1955(1971).

(8) K. Ridgway, C. Lazarou, and E. E. Thorpe, *J. Pharm. Pharmacol.*, **24**, 265(1972).

(9) C. D. Fox, M. D. Richman, G. E. Reier, and R. Shangraw, *Drug Cosmet. Ind.*, **92**, 161(1963).

(10) K. W. Manudhane, A. M. Contractor, H. Y. Kim, and R. F. Shangraw, *J. Pharm. Sci.*, **58**, 616(1969).

(11) F. Rodriquez, "Principles of Polymer Systems," McGraw-Hill, New York, N.Y., 1970, pp. 201–218.

(12) P. I. Vincent, in "Physics of Plastics," Van Nostrand, Princeton, N.J., 1965, pp. 24–60.

(13) J. E. Rees and E. Shotton, *J. Pharm. Pharmacol.*, **22**, 175(1970).

ACKNOWLEDGMENTS AND ADDRESSES

Received April 25, 1975, from the *Department of Pharmacy (Pharmaceutics), School of Pharmacy, University of Maryland, Baltimore, MD 21201*

Accepted for publication March 1, 1976.

Presented at the Industrial Pharmaceutical Technology Section, APhA Academy of Pharmaceutical Sciences, New Orleans meeting, November 10–14, 1974.

Abstracted in part from a thesis submitted by S. T. David to the Graduate School, University of Maryland, in partial fulfillment of the Doctor of Philosophy degree requirements.

The authors thank Dr. Eugene E. Hamlow, Dr. Dana Brooke, and Mr. Benny Young of Meade Johnson Laboratories for their helpful advice and assistance in the preparation of this manuscript. They also gratefully acknowledge the assistance of Ms. Vickie J. Pforr in the preparation of this manuscript.

* American Foundation for Pharmaceutical Education Fellow, 1971–1973. Present address: Mead Johnson Research Center, Evansville, IN 47721

[x] To whom inquiries should be directed.

Zero-Order Drug Delivery System: Theory and Preliminary Testing

D. BROOKE [x] and R. J. WASHKUHN *

Abstract □ A new approach to zero-order drug delivery that includes geometric factors is described. An experimental device based on the theory was tested by following the release of stearic acid into ethanol. Three separate trials indicated that the solid was released *via* a zero-order process in a reproducible manner.

Keyphrases □ Drug delivery—zero-order system, geometric factors considered, experimental device tested □ Delivery, drug—zero-order system, geometric factors considered, experimental device tested □ Stearic acid—release into ethanol, zero-order drug delivery system, experimental device tested

Roseman and Higuchi (1) and, more recently, Roseman (2) treated the subject of drug release from silicone polymer matrixes containing suspended particulate drug. They developed equations for drug release from both planar and cylindrical surfaces (1). Roseman (2) showed that the fraction of drug release from a matrix with a planar surface was linear—not with time but with the square root of time. This finding confirmed an expectation published earlier (3). Roseman (2) also showed that the initial portion of a similar plot for a matrix of cylindrical shape was similar to that for the planar case. However, as more drug was released, the slope for the fraction *versus* square root of time plot decreased.

A study of these results indicates that polymer devices might be useful in dispensing drug to tissues or body cavities at fairly constant rates over reasonable periods of time. However, the ideal of a zero-order drug delivery system cannot be realized from planar or cylindrical devices of silicone polymer containing suspended particulate drug.

BACKGROUND

The planar case of a drug suspended in a polymer matrix fails as a zero-order drug delivery system because, as the drug is released, the boundary in the matrix at which drug dissolution occurs recedes from the surface from which the drug is released. The problem is one of a decreasing release rate due to an increasing drug diffusion path length within the matrix. For the cylindrical case, the situation is more complicated. Here, the diffusion path increases and the drug core within the matrix decreases in area.

The reduction of an effective dissolution surface, given a constant diffusion barrier, and its effect on drug dissolution, *e.g.*, from implants, are fairly well understood. In their derivation of the well-known "cube root law," Hixson and Crowell (4) showed an appreciation for the decreasing area of a single particle that maintained its shape during the dissolution process. Ballard and Nelson (5) related the rate of absorption from spherical implants to size. The same investigators (6) developed a graphical method of estimating the area of subcutaneously implanted cylindrical drug pellets.

More recently, Rippie and Johnson (7) attempted to regulate the dissolution behavior of drug pellets by controlling their geometry. However, their work involved dissolution in a turbulent flow, so that transport of the drug from the surface could not be considered limited to diffusion across a constant diffusion barrier.

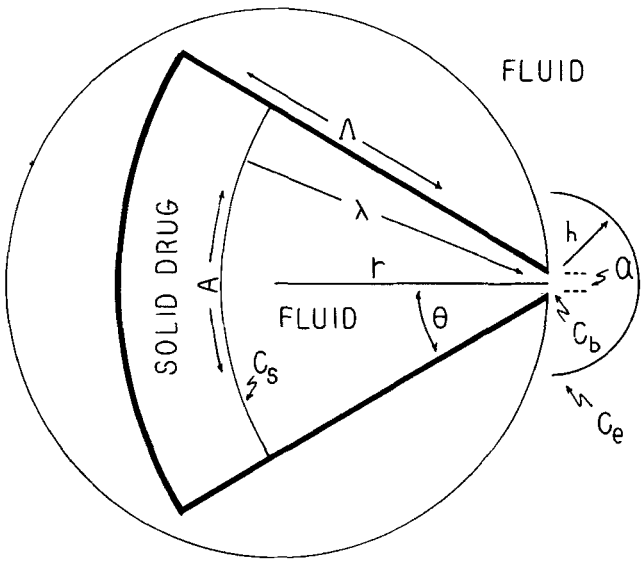

Figure 1—*Cross section of a zero-order drug delivery system containing solid drug. (See text.)*

This report details the theory for a drug delivery system that might be incorporated into implants or devices to be placed into body cavities or tissues. Under ideal conditions, this system should release drug *via* zero-order kinetics for virtually as long as it contains drug. The principle involves a particular geometry which, in turn, keeps a constant relationship between the drug diffusion path and the effective area of the dissolution boundary. The rigid device can be charged with a drug pellet or a suspension of drug in an aqueous gel, a waxy matrix, or a polymeric matrix. It is postulated that the principle described would be useful, not only in drug delivery systems, but as a means of experimentally defining physical parameters such as diffusion coefficients.

THEORETICAL

The essence of the drug delivery system described is a cavity of length L having a uniform cross section with geometric properties like those depicted in Fig. 1. Here, the bold lines describe the cross section of a cavity that might be found within a rigid cylinder having a base of radius r. The cavity communicates with the fluid in which the device is placed only through a narrow opening of width a, which runs the length of the device. In Fig. 1, this width is indicated by a pair of dashed lines. Although the opening must have a finite width, for theoretical purposes the width should be considered negligibly small. The cavity may be considered as a portion of a right circular cylinder of radius Λ and altitude L. Thus, in the ideal construction, the wall opposite the opening will be arcuate.

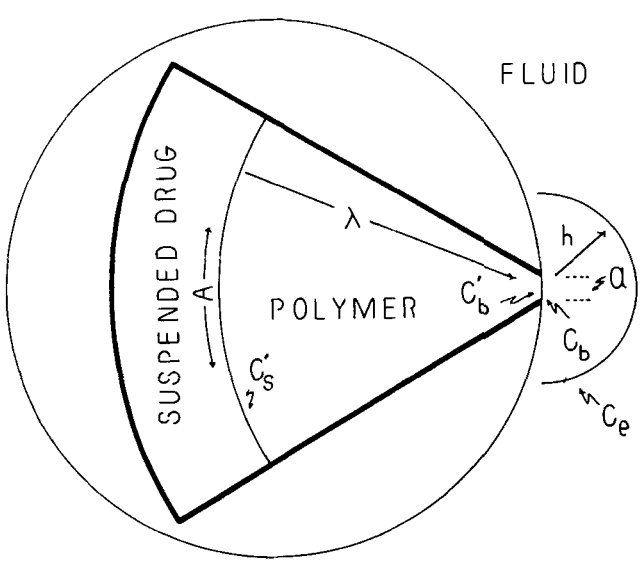

Figure 2—*Cross section of a zero-order device charged with a polymeric matrix containing suspended drug. (See text.)*

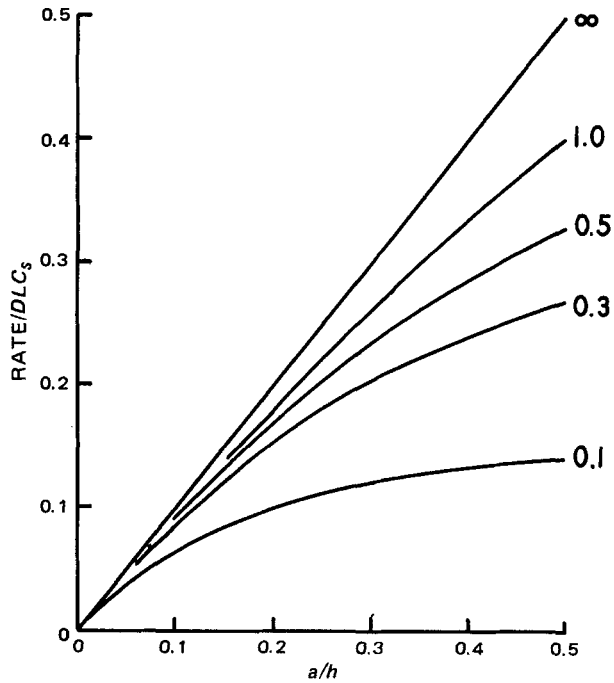

Figure 3—*Plot showing the interrelationships of a and θ in regard to release rate. The value for θ is indicated for each profile. (See text.)*

The device in Fig. 1 had been charged with a solid pellet of drug which dissolves isotropically. It is assumed that diffusion of drug out of the device and into the surrounding fluid is the rate-controlling process. In this case, about 60% of the initial charge has been released and fluid has diffused into the cavity. As drug continues to dissolve and diffuse from the curved surface through a distance, λ, to the opening, length A of the curve grows. It is clear from inspection that $A = 2\theta\lambda$ (for θ in radians). The fact that the relationship between the area of dissolving drug, AL, and the diffusion path length, λ, is a constant is the key to the zero-order performance of the device.

The rate equation describing the release of drug into the surrounding fluid can be derived by assuming that the rate of transport of drug to the opening of the device is equal to the rate of transport into the surrounding fluids. The concentration of drug at the dissolving surface is the solubility of drug, C_s, in the fluid. The concentration of drug at the opening is taken as C_b, and the concentration of drug at some distance, h, into the fluid is taken as C_e. The rate of transport of drug to the opening, R', is given in Eq. 1; the rate of transport away from the opening, R, is given in Eq. 2:

$$R' = \frac{DAL}{\lambda}(C_s - C_b) = 2D\theta L(C_s - C_b) \qquad \text{(Eq. 1)}$$

$$R = \frac{DaL}{h}(C_b - C_e) \qquad \text{(Eq. 2)}$$

Here, the diffusion coefficient for drug in fluid is indicated by D. By assuming that sink conditions prevail, *i.e.*, $C_e = 0$, and setting Eqs. 1 and 2 equal, it can be shown that the rate of drug release during steady state is described by:

$$R = \frac{2DaL\theta C_s}{a + 2\theta h} = \frac{DLC_s}{\frac{h}{a} + \frac{1}{2\theta}} \qquad \text{(Eq. 3)}$$

It is clear from Eq. 3 that, in a constant environment, *i.e.*, h constant, the release of drug occurs at a constant rate.

A different situation is shown in Fig. 2, where the cavity of a device has been filled with a suspension of drug in a polymeric matrix. The assumptions applied to this situation are those of Roseman and Higuchi (1). It is assumed that the total concentration of drug initially is large compared to the solubility of drug in the matrix, C_s'. It is assumed that steady-state conditions exist, that diffusion is the rate-controlling process, and that diffusion occurs through the matrix, not through pores.

The case depicted in Fig. 2 is one in which about 60% of the drug has been released, giving rise to a region depleted of solid drug particles. As drug dissolves at the boundary of the "zone of depletion," it must diffuse a distance, λ, to the opening where the concentration is C_b'. The rela-

Table I—Effect of a/h and θ on Rate × $100/DLC_s$

	θ						
a/h	0.1	0.3	0.5	0.7	1.0	3.0	∞
0.01	0.952	0.984	0.990	0.993	0.995	0.998	1.00
0.02	1.82	1.94	1.96	1.97	1.98	1.99	2.00
0.05	4.00	4.62	4.76	4.83	4.87	4.96	5.00
0.10	6.67	8.57	9.09	9.33	9.52	9.84	10.0
0.20	10.0	15.0	16.7	17.5	18.2	19.4	20.0
0.30	12.0	20.0	23.1	24.7	26.1	28.6	30.0
0.40	13.3	24.0	28.6	31.1	33.3	37.5	40.0
0.50	14.3	27.3	33.3	36.8	40.0	46.2	50.0

tionship between the area of the boundary where dissolution occurs, AL, and the diffusion path length, λ, is a constant since $A = 2\theta\lambda$. If the diffusion coefficient for drug in the matrix is D', the rate of transport of drug to the opening is given by:

$$R'' = \frac{D'AL}{\lambda}(C_s' - C_b') = 2D'\theta L(C_s' - C_b') \qquad \text{(Eq. 4)}$$

The rate of transport away from the opening is given by Eq. 2. By assuming that the partitioning of drug at the matrix–fluid interface can be described by a constant, K, such that:

$$K = C_b'/C_b = C_s'/C_s \qquad \text{(Eq. 5)}$$

it can be shown that the rate of drug release is given by:

$$R = \frac{DLC_s}{(h/a) + (D/D'K)(1/2\theta)} \qquad \text{(Eq. 6)}$$

The similarity between Eqs. 3 and 6 is obvious.

Equations 3 and 6 are derived for an ideal case wherein the opening is infinitely small (*i.e.*, $a \to 0$) but presents no barrier to diffusion of drug. In the real case, the zero-order phase develops only after the diffusion path length, λ, becomes significantly larger than the slit width, a. That is, a constant release rate occurs only after all points within the slit opening are approximately equidistant from any one point on the dissolution boundary, A. It should be obvious that in the initial portion of the drug release profile, where a has a small but real value and $\lambda \simeq 0$, the situation approximates the planar model of Roseman and Higuchi (1). Thus, in the real case, the rate of drug release is initially higher than that of the subsequent "zero-order" phase.

Equation 6 should also describe the release of drug from a device charged with a thixotropic aqueous suspension of drug. In that instance, D' would be the diffusion coefficient of drug in the suspension and K would, in a steady-state circumstance, have a value of unity.

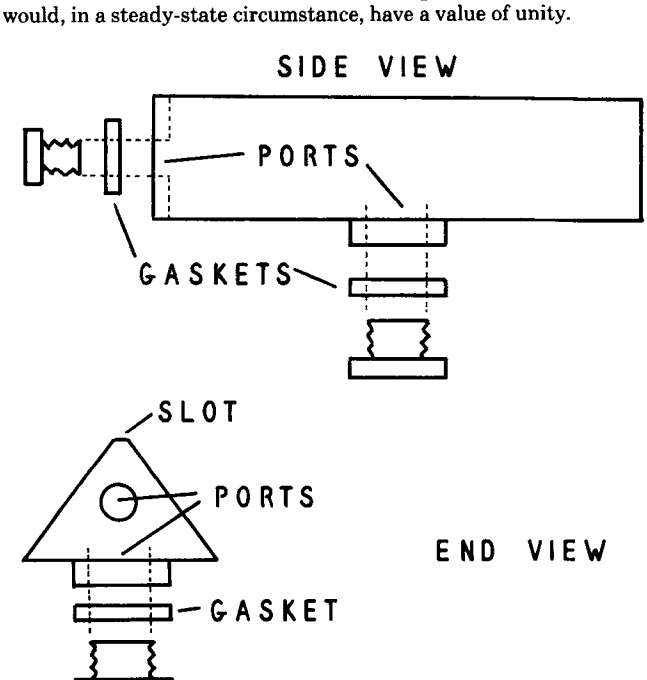

Figure 4—*Side and end views of an experimental stainless steel device used to test the zero-order theory.*

It is clear from Eqs. 3 and 6 that some latitudes prevail in the adjusting of the release rate through changes in a, θ, and L. The interrelationships of a and θ as concern the rate of release of drug from a cavity filled with solid material are depicted in Fig. 3 and Table I. Obviously, without specific knowledge of C_s, D, and h, exact values cannot be assigned. In general, however, the larger the values of a and θ, the larger is the rate. It is also clear from the equations that changes in the length, L, of the device result in proportionate changes in rate. Similar arguments hold for a cavity filled with a suspension of drug in a polymer.

Adjustments in the design parameters of a device might also prove useful in determining h and D. If one varies only the slit width, a, for a number of solid-filled cavities and plots the reciprocals of rates of release against $1/a$, a line with a slope of h/DLC_s and an intercept of $1/2\theta DLC_s$ is obtained. By dividing the slope by the intercept and multiplying by 2θ, one obtains a value for h. With a knowledge of C_s, θ, and L, one can calculate the diffusion coefficient, D, from the intercept value.

EXPERIMENTAL

The theory of the zero-order drug delivery system was tested experimentally by following the amount of stearic acid released from a device fabricated from stainless steel. The prism-shaped device used is illustrated in Fig. 4. Overall, it was 6.4 cm (2.5 in.) long, 2.54 cm (1.0 in.) wide at the base, and 1.6 cm (0.63 in.) high from the base to the slot. The sides, base, and one end were 18-gauge stainless steel. The other end was cut from 0.5-cm (3/16-in.) stainless steel and was drilled to provide a filling port which could be closed with a stainless steel bolt. All joints were silver soldered. A larger filling port was made in the base of the prism-like device by cutting a hole of appropriate size and soldering into place a stainless steel nut to be closed with a stainless steel bolt. Gaskets[1] were used at both filling ports. The slot width, a, was 0.08 cm (0.030 in.); the effective slot length, L, was 5.75 cm (2.263 in.). The angle, 2θ, was 80°.

For filling, the slot was covered with polyethylene and the device was inverted. Molten stearic acid[2] was added through the large port in increments. The device was rocked back and forth, and the portions were allowed to solidify after each addition. The device held approximately 9.5 g of stearic acid. After the port was closed, the polyethylene was removed carefully from the slit.

The release of stearic acid from the device into alcohol USP was followed by placing the device in the bottom of a double-walled beaker, 11.0 cm i.d., containing 1000 ml of alcohol. The port in the base and the bolt used to close it served as a pedestal for the device. The beaker was kept at 30°, and its contents were stirred with a three-blade propeller (radius of 2 cm and blade pitch of 30°) rotated at 50 rpm 2.5 cm below the surface. The distance between the top of the device and the propeller was 4.9 cm. A cover[1] with a hole for the stirrer and one for the sampling port was kept on the beaker.

Samples were withdrawn periodically. Alcohol at 30° was added to the beaker to maintain volume. The stearic acid concentration in the samples was estimated *via* an ion-pair extraction with methylene blue. A 5- or 10-ml aliquot of the ethanolic sample containing stearic acid was placed into a separator. A 50-ml volume of a 0.01 M pH 7.0 phosphate buffer containing 0.1% methylene blue (USP grade) and a 20-ml volume of redistilled reagent grade chloroform were added. If a 5-ml aliquot from the ethanolic sample was used, an additional 5 ml of alcohol was added. The separator was shaken, and the layers were allowed to separate. A 5-ml portion of the chloroform layer was diluted to 100 ml with methanol, and the density of the blue color was estimated at 640 nm against an appro-

[1] Teflon (du Pont).
[2] MC&B, SX950, 2733.

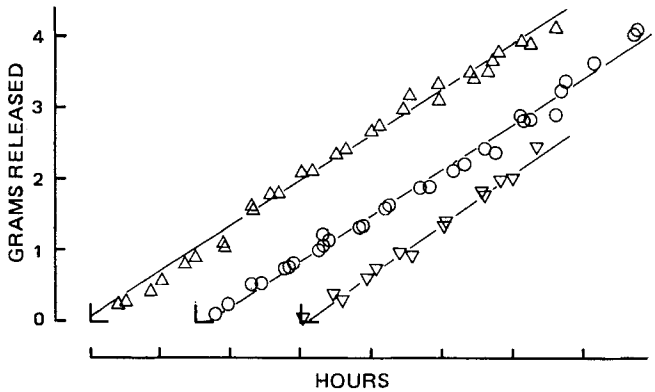

Figure 5—*Release of stearic acid* versus *time for three different trials [Trial I (○), Trial II (▽), and Trial III (△)]. The profiles are staggered for clarity, with the (0,0) point indicated by a right angle. Each division on the abscissa represents 50 hr. The lines for the profiles are the least-squares lines.*

priate blank. The blue color was stable after approximately 30 min. The absorbance was linearly dependent on the stearic acid in the sample.

RESULTS AND DISCUSSION

The cumulative release of stearic acid from the device tested for three different trials is shown in Fig. 5. The linear regression analysis for each trial is summarized in Table II. A survey of Table II shows that the coefficient of determination (r^2) was 0.99 in each case, indicating that the data were zero order. The variations in the slopes and intercepts do not appear to be great when it is understood that it was difficult to fill the device uniformly. Problems included the trapping of air bubbles in the melted stearic acid and a slight shrinkage of the melt on cooling. In the ideal case, there must be no penetration of fluid between the cavity wall and the fill. Shrinkage might have allowed spaces to form between the fill and the cavity wall.

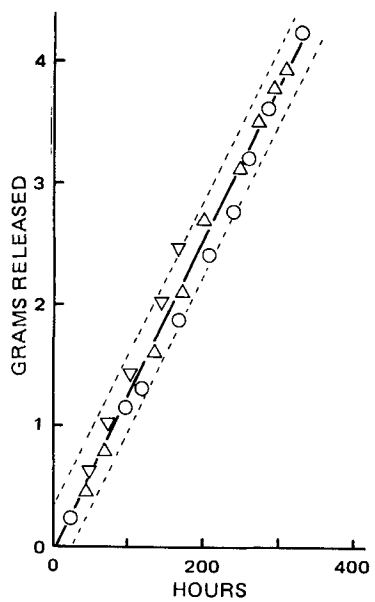

Figure 6—*Profile showing the amount of stearic acid released from the zero-order device. The regression line is based on a composite of all data from three trials, and the 95% confidence bounds are given as dashed lines. Selected points from Fig. 5 are shown. (See text.)*

Table II—Summary of Regression Analysis on Each Trial and on Composite of All Data

Parameter	Trial I	Trial II	Trial III	Composite Data
Release rate, mg/hr	12.73	14.24	12.89	12.72
SD (slope), mg/hr	0.23	0.41	0.24	0.18
r^2	0.990	0.990	0.991	0.985
Intercept, mg	−12.7	−48.3	+74.2	−21.9
SD (intercept), mg	44.5	41.3	47.2	33.1
n	32	14	30	76

Additionally, the theory requires that transport of solid within the cavity be diffusion controlled. If any currents arose in the fluid within the device during the experiment, then deviations from theory could occur. (Obviously this could not be a source of error in the case of a cavity filled with a polymeric matrix.)

It is calculated that the fabricated device, under ideal conditions, could release approximately 8.0 g of stearic acid at a zero-order rate. However, the trials were terminated after the release of 2.5–4.2 g when irregularities in the surface of the fill became obvious. The arcuate nature of the surface was always in evidence after a trial was terminated, but the surface did not show the perfect arc depicted in Fig. 1. Variations in the distance of the surface of the fill to the slot were also noted. Such variations, however, apparently "averaged out."

All data were collected under approximate "sink conditions" because the highest concentration of stearic acid achieved was about 0.4% compared to a solubility in ethanol of nearly 5% (8).

A summary of the regression analysis of a composite of all data for the three trials is given in Table II. The regression line and the 95% confidence bounds for single predicted values are shown in Fig. 6. Selected points from each individual trial are also given in Fig. 6 to illustrate the distribution of the data points.

Although the testing of the zero-order principle with stearic acid has been encouraging, a more critical approach will be necessary to validate the theory thoroughly. The filling of the device with a solid may prove to be more of an engineering problem than it is a pharmaceutical problem. A solid that is fused under high temperature and pressure in the process of filling the cavity should allow the most critical kind of test of the interrelationships of slit width, a, angle, 2θ, and length, L, of the device.

REFERENCES

(1) T. J. Roseman and W. I. Higuchi, *J. Pharm. Sci.*, **59**, 353 (1970).

(2) T. J. Roseman, *ibid.*, **61**, 46 (1972).

(3) T. Higuchi, *ibid.*, **52**, 1145 (1963).

(4) A. W. Hixson and J. H. Crowell, *Ind. Eng. Chem.*, **23**, 1002 (1931).

(5) B. E. Ballard and E. Nelson, *Arch. Int. Pharmacodyn. Ther.*, **123**, 206 (1961).

(6) B. E. Ballard and E. Nelson, *Am. J. Vet. Res.*, **23**, 678 (1962).

(7) E. G. Rippie and J. R. Johnson, *J. Pharm. Sci.*, **58**, 428 (1969).

(8) "The Merck Index," 8th ed., Merck and Co., Rahway, N.J., p. 980.

ACKNOWLEDGMENTS AND ADDRESSES

Received May 21, 1975, from *Pharmaceutical Product Development, Mead Johnson Research Center, Evansville, IN 47721.*

Accepted for publication February 9, 1976.

* Present address: Product Development Department, Arnar-Stone Laboratories, Mt. Prospect, IL 60056.

[x] To whom inquiries should be directed.

Analysis of Theoretical Behavior of a Proposed Zero-Order Drug Delivery System

R. A. LIPPER and W. I. HIGUCHI ˣ

Abstract □ An analysis of the theoretical behavior of a proposed zero-order drug delivery system is presented. Equations describing drug release with time are developed using a physically realistic model. The theory agrees well with experimental data and indicates that drug release from the device is nearly, although not rigorously, zero order.

Keyphrases □ Drug delivery—zero-order system, theoretical behavior, equations developed □ Delivery, drug—zero-order system, theoretical behavior, equations developed

Brooke and Washkuhn (1) presented the design of a drug delivery device, the unique geometry of which would, ideally, lead to zero-order release of its contents *via* dissolution from a solid pellet or diffusion from a suitable matrix. This ideal behavior depends in theory, however, on both the drug molecules and the opening through which they must pass having infinitely small dimensions. In this paper, the theoretical behavior of such a device modeled entirely with finite dimensions will be examined.

Discussion of prior work dealing with geometrical considerations in the determination of drug dissolution and release rates may be found in the previous paper (1).

THEORETICAL

The case to be treated here is that of a device charged with pure solid drug. It is assumed that dissolution takes place isotropically and that diffusion of drug out of the device is the rate-determining process. Similar equations could be derived for the case of drug being released from a polymer or other matrix.

The drug-containing cavity of the device in question (1) is essentially a sector of a right circular cylinder. Its cross section is shown in Fig. 1.

Let the center that defines the arc be outside the device and let the opening of the device be at radius n. The area of arcuate surface at diffusion path length s is then $2\theta L(s + n)$, where L is the length of the drug-filled cavity. The flux, J, at s is, therefore:

$$J = 2\theta LD(s + n)\frac{dC}{ds} \qquad \text{(Eq. 1)}$$

where D is the drug's diffusivity in the dissolution medium. The drug concentration at the dissolving surface is the solubility, C_s. The concentration at the opening is C_b; if sink conditions are assumed, the concentration at distance h into the bulk is zero. At steady state, integration of Eq. 1 from C_b to C_s and from zero to $\lambda - n$ yields:

$$J = \frac{2\theta LD(C_s - C_b)}{\ln\frac{\lambda}{n}} \qquad \text{(Eq. 2)}$$

Diffusion from the opening into the bulk is described by:

$$J = \frac{2\theta LDnC_b}{h} \qquad \text{(Eq. 3)}$$

Equation 3 treats the effective diffusion layer as the typical planar case rather than as radial diffusion from a point source. This treatment is justified if h is much less than the arc length at the opening. In any event, hydrodynamic conditions are important in determining release rate only at very early times when λ is of the order of magnitude of the opening arc length.

By solving for C_b in Eq. 3 in order to eliminate it from Eq. 2, the rate of drug release can be shown to be:

$$J = \frac{2\theta LDC_s}{\frac{h}{n} + \ln\frac{\lambda}{n}} \qquad \text{(Eq. 4)}$$

Given drug of density ρ, the mass dissolved at any time is:

$$M = (\lambda^2 - n^2)L\theta\rho \qquad \text{(Eq. 5)}$$

Integration of Eq. 4 after substituting for λ from Eq. 5 yields a relationship between mass dissolved and time:

$$\frac{\left(\frac{h}{n} - \frac{1}{2}\right)M + \left(\frac{M + L\theta\rho n^2}{2}\right)\ln\left(\frac{M}{L\theta\rho n^2} + 1\right)}{2\theta LDC_s} = t \qquad \text{(Eq. 6)}$$

If it is assumed that the mass in solution in the diffusion layer is negligible compared to the total drug mass, then:

$$M_r = M - M_d \qquad \text{(Eq. 7)}$$

where M_r is the mass released, and M_d is the mass dissolved within the device. At any given time:

$$M_d = \int_0^{\lambda - n} 2\theta L(s + n)C\,ds \qquad \text{(Eq. 8)}$$

where:

$$C = \frac{J}{2D\theta L}\ln\left(\frac{s + n}{\lambda}\right) + C_s \qquad \text{(Eq. 9)}$$

Following integration and the appropriate substitutions, Eq. 7 becomes:

$$M_r = (\lambda^2 - n^2)\left[L\theta\rho - L\theta C_s + \frac{L\theta C_s}{2\left(\frac{h}{n} + \ln\frac{\lambda}{n}\right)}\right] - \frac{L\theta C_s n^2}{\frac{h}{n} + \ln\frac{\lambda}{n}}\ln\frac{\lambda}{n} \qquad \text{(Eq. 10)}$$

and if Eq. 5 is substituted into Eq. 6, the following is obtained:

$$t = \frac{\left(\frac{h}{n} - \frac{1}{2}\right)(\lambda^2 - n^2)\rho + \lambda^2\rho\ln\frac{\lambda}{n}}{2DC_s} \qquad \text{(Eq. 11)}$$

Equations 10 and 11 relate λ to M_r and t, respectively. Thus, values for λ may be selected to generate M_r *versus* t data.

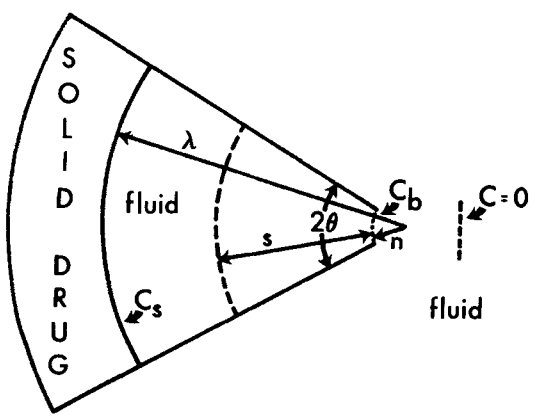

Figure 1—*Cross-sectional view of the device's drug-containing cavity, illustrating the case where the original charge of solid drug is partially dissolved. (See text.)*

RESULTS AND DISCUSSION

Equation 4 differs from the previously derived equation describing the idealized case (1) in that Eq. 4 contains a $\ln \lambda/n$ term. Since λ, the distance from the solid drug surface to the arc center, is time dependent, the flux expression derived here has a time dependence that was previously absent.

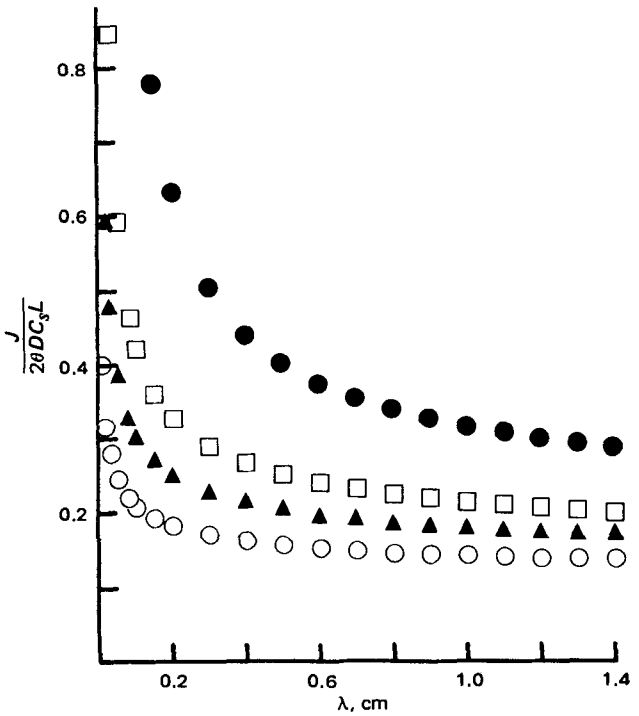

Figure 2—*Flux as a function of* λ *predicted by Eq. 4. The parameters used (in centimeters) are:* n = *0.050 and* h = *0.010* (●), n = *0.025 and* h = *0.025* (□), n = *0.010 and* h = *0.010* (▲), *and* n = *0.010 and* h = *0.025* (○).

Figure 2 shows the behavior of flux as a function of λ as predicted by Eq. 4, using four sets of reasonable parameters. In all cases, flux is initially high but quickly drops to a lower and nearly constant value. Thus, a small portion of the mass within the device would be released quickly, but by far the major portion would be released at a rate *approximating* zero order.

This point is further illustrated in Fig. 3 where the rate of change of flux with respect to λ is shown. The resulting family of curves clearly demonstrates the effect of diffusion layer thickness. For simplicity, λ and h are expressed as multiples of n, and $dJ/d\lambda$ is normalized by dividing by the initial $dJ/d\lambda$, i.e., when $\lambda/n = 1$. The rate of change of flux decreases markedly for $n \leq \lambda \lesssim 2n$; for $\lambda \gtrsim 2n$, the asymptotic approach to zero, *i.e.*, flux constant with λ, is obvious.

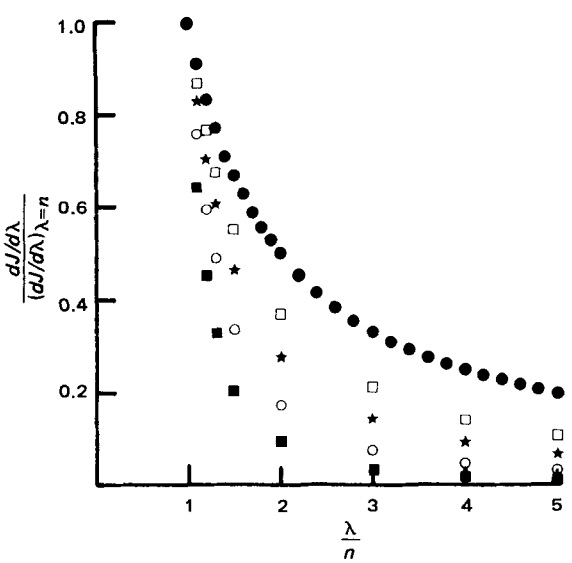

Figure 3—*Relative rate of change of flux with respect to* λ. *For simplicity,* λ *and* h *are expressed as multiples of* n, *such that* h = in *and* λ = jn. *The data shown are for* i = *0.5* (■), *1* (○), *2* (★), *and 4* (□) *and for the limiting right rectangular hyperbola as* i → ∞, i.e., *infinitely thick diffusion layer* (●).

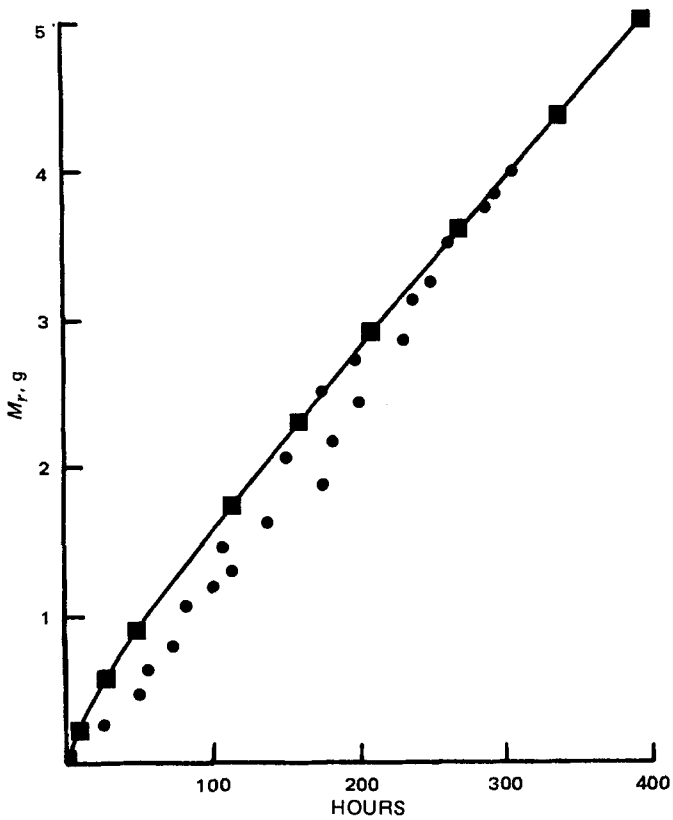

Figure 4—*Mass of stearic acid released with time as predicted by Eqs. 10 and 11* (■). *Experimental data* (●) *are from Ref. 1.*

Mass released *versus* time data were generated from Eqs. 10 and 11 to simulate the case experimentally tested by Brooke and Washkuhn (1), that of stearic acid being released into alcohol USP. The following parameters were used: $h = 100\ \mu m$, $n = 540\ \mu m$, $2\theta = 1.4$ radians, $L = 5.75$ cm, $C_s = 0.048$ g/cm^3 (2), and $\rho = 0.94$ g/cm^3 (3). A value for the only remaining parameter, diffusivity, was generated by forcing Eqs. 10 and 11 to yield the point $M_r = 5.07$ g at $t = 400$ hr from the previous paper's composite regression data (1). This leads to $D = 2.65 \times 10^{-5}$ cm^2/sec, which does not appear to be an unreasonable value (4, 5).

Figure 4 shows the resultant data. Good agreement is seen between the theoretically predicted release profile and the experimental data. Although systematic deviation from true zero order is apparent, the rapid approach to linearity is also evident. Indeed, a linear regression on the data for $t = 100$, 200, 300, and 400 hr gives $r^2 = 0.999$.

Although further experimental testing is certainly in order, it is thus concluded that the device examined here might exhibit release behavior that is nearly zero order and that, as such, it might be useful as a constant-rate drug delivery system.

REFERENCES

(1) D. Brooke and R. J. Washkuhn, *J. Pharm. Sci.*, **66**, 159 (1977).

(2) "The Merck Index," 8th ed., Merck and Co., Rahway, N.J., p. 980.

(3) "Handbook of Chemistry and Physics," 52nd ed., Chemical Rubber Co., Cleveland, Ohio, p. C-396.

(4) G. L. Flynn, S. H. Yalkowski, and T. J. Roseman, *J. Pharm. Sci.*, **63**, 502 (1974).

(5) K. C. Pratt and W. A. Wakeham, *Proc. Roy. Soc., Ser. A*, **336**, 339 (1974).

ACKNOWLEDGMENTS AND ADDRESSES

Received December 12, 1975, from the *College of Pharmacy, University of Michigan, Ann Arbor, MI 48109.*

Accepted for publication March 12, 1976.

[x] To whom inquiries should be directed.

Effect of Symmetrical Tetraalkylammonium Salts on Cloud Point of Nonionic Surfactants

HANS SCHOTT *x and SUK KYU HAN ‡

Abstract □ The salting in and salting out of the nonionic surfactant octoxynol NF by halides of ammonium and the four lowest symmetrical tetraalkylammonium cations were investigated by measuring their effect on the cloud point at various salt concentrations. The chloride anion tended to salt the surfactant out, lowering its cloud point. The iodide anion tended to salt it in, raising the cloud point, while the bromide ion had no pronounced effect. The ammonium and tetramethylammonium cations tended to lower the cloud point, the latter more extensively than the former. The tetraethylammonium cation had no pronounced effect, while the tetra-*n*-propylammonium and tetra-*n*-butylammonium cations tended to raise the cloud point, the latter more extensively than the former. The salt effect on the cloud point generally increased with increasing salt concentration. Tetramethylammonium chloride was the most efficient salt in lowering the cloud point (by 4° at the 0.10-molal level and by 20° at the 1.00-molal level), while tetrabutylammonium halides were the most efficient salts in raising the cloud point (by 18–19° at the 0.10-molal level for chloride and bromide). Cloud point increases were attributed to the formation of mixed micelles or to hydrotropy. The salting-out efficiency of tetramethylammonium chloride and bromide was ascribed to their ability to increase the structure of water.

Keyphrases □ Surfactants, nonionic—octoxynol, effect of tetraalkylammonium salts and ammonium halides on cloud point, various salt concentrations □ Octoxynol—effect of tetraalkylammonium salts and ammonium halides on cloud point, various salt concentrations □ Tetraalkylammonium salts—effect on cloud point of octoxynol, various salt concentrations □ Ammonium halides—effect on cloud point of octoxynol, various salt concentrations □ Cloud point—octoxynol, effect of tetraalkylammonium salts and ammonium halides, various salt concentrations

Two major trends were observed during a systematic investigation of the effect of inorganic cations on the cloud points of polyoxyethylated nonionic surfactants (1, 2). All polyvalent cations plus lithium form complexes with the ether oxygens of simple, model ethers like dioxane as well as with those of the polyoxyethylene moiety of nonionic surfactants. In this complex formation, which competes with the hydration of the cations, the flexible polyoxyethylene chains probably act as polydentate ligands (1, 2). The result is salting in of the surfactants, which manifests itself as an increase in cloud point. The reason that increases in this upper consolute temperature represent salting in is that they correspond to an increase in solubility, namely, an extension of the temperature range in which the nonionic surfactants exist in single-phase, undersaturated solutions (3).

The only inorganic cations incapable of forming complexes with the oxygen of ether groups or of water are sodium, potassium, ammonium, cesium, and, probably, rubidium. Their effect on nonionic surfactants is to lower the cloud points, salting them out (1, 2).

BACKGROUND

The cations of symmetrical tetraalkylammonium halides are of considerable physicochemical and biological interest. Their effect on the structure of water results in unusual behavior of their aqueous solutions such as peculiar activity and osmotic coefficients (4, 5) and conductance (6), high viscosity with large temperature coefficients (7), and unusual partial molal volumes (8–11).

Examples of tetraalkylammonium derivatives of biological importance are choline, found in lecithins and sphingomyelins; acetylcholine, crucial in the transmission of nerve impulses; and naturally occurring betaines including trimethylglycine. Examples of quaternary ammonium compounds with pharmacological activity include many alkaloidal salts and synthetic neuromuscular blocking drugs. An interesting type of interaction, pertinent to the present research, is supplied by the work of Belleau. The binding of tetraalkylammonium halides to the surfaces of acetylcholinesterase and of muscarinic and nicotinic receptors was shown to involve the structure of water in the vicinity of the receptor sites (12, 13).

The purpose of the present investigation was to examine the effect of tetraalkylammonium halides on the cloud point of a polyoxyethylated nonionic surfactant. It represents a logical sequence in our studies of the effect of the various categories of cations on cloud points and solubility of nonionic surfactants. Ether groups cannot act as ligands for tetraalkylammonium cations as they do for inorganic polyvalent cations. However, ion–dipole attraction (14) and hydrophobic interaction between the alkyl groups of the salts and the ethylene groups of the polyoxyethylene moiety of nonionic surfactants may take place.

Since the properties of symmetrical tetraalkylammonium halides strongly depend on the length of the alkyl groups (4–13), the number of carbon atoms per alkyl group was varied from zero (unsubstituted ammonium) to four.

The anion of the tetraalkylammonium halides was varied for two reasons. First, anions can enhance or reduce the structure of water. Structure-forming anions such as fluoride and chloride lower cloud points, salting the nonionic surfactants out, while structure-breaking anions such as iodide and thiocyanate have the opposite effect (2, 15). Second, large and poorly hydrated anions such as iodide are prone to ion-pairing, either of the usual electrostatic kind or "water structure enforced" (4–6).

Finally, there is the possibility of using the surfactant through its cloud point as a probe to obtain information on the structure and behavior of aqueous solutions of tetraalkylammonium salts.

EXPERIMENTAL

The nonionic surfactant employed was octoxynol NF[1], a branched octylphenol with an average of nine to 10 ethylene oxide units. It was selected because it is a monograph in the National Formulary and because it has been employed extensively in cloud point measurements (16), particularly when these were used as a criterion for salting in or out (1, 2). Its properties were given in Ref. 2 under Surfactant I.

The viscous liquid was dried over anhydrous calcium sulfate[2] to constant weight, losing less than 1% of moisture. The tetra-*n*-alkylammonium halides[3] were also dried to constant weight over anhydrous calcium sulfate. Sodium *m*-xylenesulfonate[4] was used as received. All other reagents were ACS reagent grade. Water was double distilled.

The procedures for preparing the ternary electrolyte–surfactant–water mixtures and for measuring cloud points were described previously (1). The surfactant concentration was 1.00% (w/w) based on the amount of water present, except for the hydrotrope experiments described in the *Appendix* where it was 2.00%. Such relatively small differences in surfactant concentration have no effect on the cloud point (17). Electrolyte concentrations are expressed as molality or as percent (w/w) based on the amount of water present in the mixtures.

RESULTS

The cloud point of octoxynol as a function of the concentration of the various electrolytes is listed in Table I.

[1] Triton X-100, Rohm & Haas Co.
[2] Drierite, W. A. Hammond Drierite Co., Xenia, Ohio.
[3] Tokyo Kasei Kogyo Co., Tokyo, Japan.
[4] Supplied as 2,4-dimethylbenzenesulfonic acid sodium salt, Eastman Organic Chemicals No. 2131.

Table I—Cloud Point of Octoxynol as a Function of the Concentration of Added Electrolytes[a]

Cation	Molality	Cloud Point for Anion: Chloride	Bromide	Iodide	Nitrate
Ammonium	0.10	60.8°	63.1°		62.7°
	0.20	60.0°	62.5°		63.2°
	0.50	56.9°	62.1°		63.1°
	1.00	52.3°	61.1°		63.0°
	1.50	48.8°	61.8°		61.5°
	2.00	46.5°	61.7°		59.7°
	3.00	—	—		54.5°
Tetramethyl-ammonium	0.10	60.5°	62.0°	65.3°	
	0.20	59.6°	61.5°	67.0°	
	0.50	53.2°	59.1°	70.4°	
	1.00	45.0°	55.3°	73.4°	
	1.50	37.8°	51.0°	—	
	2.00	31.0°	—	—	
Tetraethyl-ammonium	0.10	61.8°	63.0°	66.5°	
	0.20	61.0°	64.0°	69.1°	
	0.50	60.1°	65.2°	73.0°	
	1.00	57.4°	66.2°	78.5°	
	2.00	47.0°	61.8°	—	
Tetra-*n*-propyl-ammonium	0.10		67.3°	71.0°	
	0.20		72.8°	78.5°	
	0.50		87.5°	—	
Tetra-*n*-butyl-ammonium	0.05	73.5°	74.0°		
	0.10	83.0°	84.1°		

[a] Concentration of octoxynol was 1.00% (w/w) based on the weight of water. Its cloud point in the absence of electrolytes was 64.3°.

Effect of Anion—The anions are ranked in the following order of decreasing effectiveness for salting out (lowering the cloud point) or increasing effectiveness for salting in (raising the cloud point): chloride > nitrate ≅ bromide > iodide. This order is the same as the Hofmeister or lyotropic series (18), which was also followed by the anions of inorganic salts (1, 2, 15). The large, polarizable iodide ion is particularly effective in breaking the structure of water.

The destructuring of water increases the concentration of nonassociated water molecules. These molecules become available to hydrate the ether groups of the nonionic surfactant, increasing its solubility and raising its cloud point (1, 2). The effect of the anions on the cloud point is minor compared to the large effect of the cations.

Effect of Cation Size—The behavior of the electrolytes underwent profound changes as the number of carbon atoms per alkyl group was increased from zero to four. As is seen from Figs. 1–3, tetramethylammonium salts had the strongest salting-out efficiency. The chloride lowered the cloud point by more than 30° at the 2-molal level. Only the iodide raised the cloud point, because of the strong salting-in tendency of the anion.

The salts of ammonium and tetraethylammonium at low and intermediate concentrations produced moderate decreases or increases in cloud point, depending on the anion. Except for ammonium bromide and tetraethylammonium bromide, the tendency to lower or to raise the cloud point of octoxynol became stronger with an increasing concentration of the electrolyte. As the alkyl groups were increased to *n*-propyl and *n*-butyl, the salting-in effect became very pronounced. The 20° increase in cloud point produced by 0.10 molal tetrabutylammonium chloride and bromide was considerably greater than the increases produced by inorganic salts at comparable concentrations. A 20° increase in the cloud point of octoxynol required over 2 molal sulfuric or hydrochloric acid, over 3 molal cadmium or magnesium nitrate, 4 molal nickel nitrate, and nearly 6 molal calcium nitrate (1).

The salt effect of the tetraalkylammonium halides as a function of the number, p, of carbon atoms per alkyl group is illustrated in Fig. 4. The ammonium and tetramethylammonium salts lowered the cloud point, salting the surfactant out. The curves have a minimum for $p = 1$. As p increased beyond 2, the cloud point underwent steep increases. The tetrapropyl- and tetrabutylammonium cations were very effective at salting the surfactant in.

DISCUSSION

The influence of the chain length of the alkyl groups on the nature and magnitude of the salt effect must be attributed to more than one factor, because the effect changes from salting out for $p = 0$ and 1 to salting in for $p = 3$ and 4. Attempts to explain these observations in terms of existing theories of salt effects and water structure are made here.

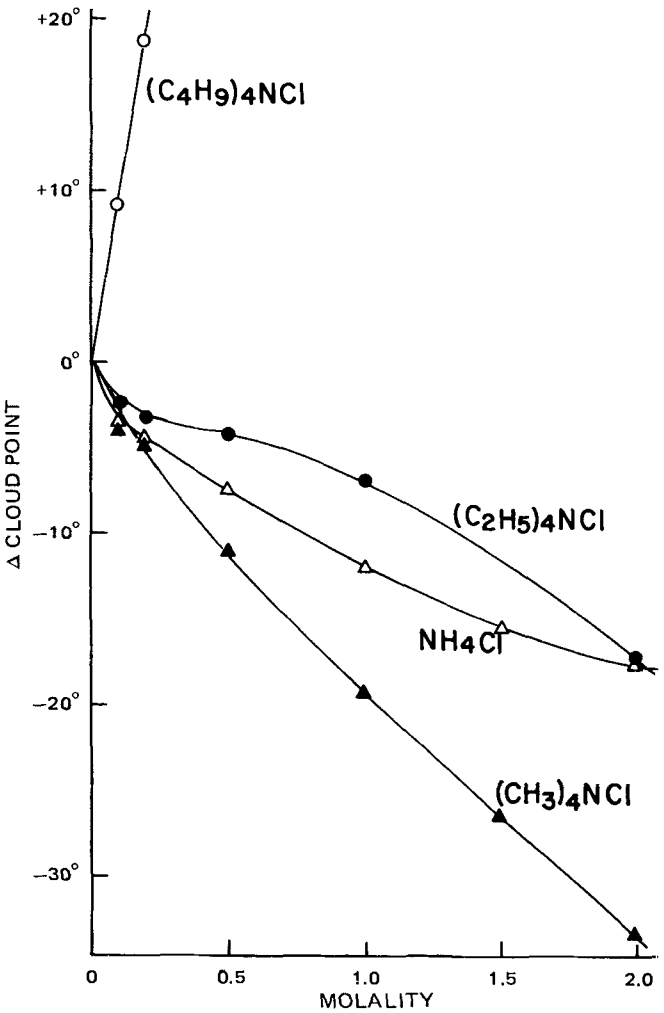

Figure 1—*Change in the cloud point of octoxynol as a function of the molal concentrations of added chlorides.*

Internal Pressure Theory—Long and McDevit (19) derived the following equation, which explains the effect of electrolytes on the solubility of nonelectrolytes in terms of internal pressure:

$$\ln \frac{S_n^o}{S_n} = \left[\frac{\bar{V}_n^o (V_e - \bar{V}_e^o)}{\beta RT} \right] C_e \qquad \text{(Eq. 1)}$$

The subscripts n and e designate the nonelectrolyte (*i.e.*, the nonionic surfactant) and electrolyte, respectively. The superscript o designates the property of the solute in water. Thus, S_n^o and S_n are the molar solubilities of the surfactant in water and in a solution containing C_e moles/liter of electrolyte, respectively; $\bar{V}^o$ represents partial molal volumes at infinite dilution; and V_e is the partial molal volume of the pure "liquid" electrolyte. The difference $(V_e - \bar{V}_e^o)$ represents the extent of electrostriction of water by the electrolyte. If $V_e > \bar{V}_e^o$, this difference is positive as is the logarithm of the ratio S_n^o/S_n. Hence, $S_n^o/S_n > 1$ and $S_n^o > S_n$. Physically, a positive $(V_e - \bar{V}_e^o)$ means that dissolution of the electrolyte produces a contraction in the volume of water. The solvent medium is compressed by the electrolyte, and the nonelectrolyte is squeezed out of solution or salted out.

The difference $(V_e - \bar{V}_e^o)$ was found to be negative for the three tetraalkylammonium bromides tested, namely, −10, −23, and −32 ml/mole for the tetramethyl-, tetraethyl-, and tetrapropylammonium bromides, respectively (20). These three salts loosen the solvent medium and should thereby increase the solubility of the nonelectrolyte, salting it in. This effect was observed with the nonpolar compound benzene (20). However, when the nonelectrolyte was the amphiphilic surfactant octoxynol, of the three salts only tetrapropylammonium bromide raised its cloud point, salting it in as predicted by the theory. Tetramethylammonium bromide salted it out, while tetraethylammonium bromide had no pronounced effect on the cloud point.

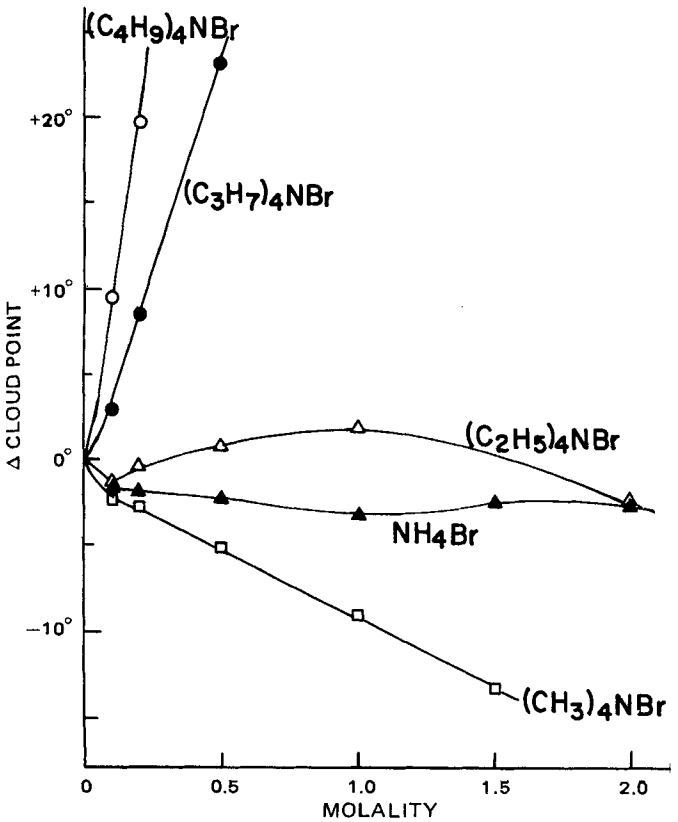

Figure 2—*Change in the cloud point of octoxynol as a function of the molal concentrations of added bromides.*

Thus, the internal pressure theory does not apply to the present situation, either because the nonelectrolyte is a large molecule or because it is a polar molecule (19). This finding represents a further limitation of the theory. Previously (2), it was found to fail because it did not take into account association between electrolytes and the nonelectrolyte by complex formation.

Effect of Alteration of Water Structure —Tetraalkylammonium salts are known to enhance the structure of water; the larger the alkyl groups, the greater is this effect (4). These hydrophobic groups do not attract or orient the water molecules in their immediate vicinity as strongly as does the next shell of water molecules, which surrounds the water molecules nearest to the hydrocarbon groups. Thus, the nearest water molecules are oriented and hydrogen bonded more strongly to the water molecules beyond them than would be the case if there were a strong counterattraction from the side of the hydrocarbon groups. This produces a tightening of the structure of the water surrounding these groups. Such an increase in water structure results in a large decrease in

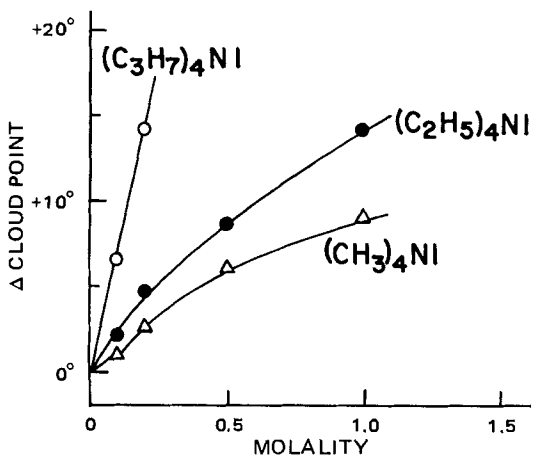

Figure 3—*Change in the cloud point of octoxynol as a function of the molal concentrations of added iodides.*

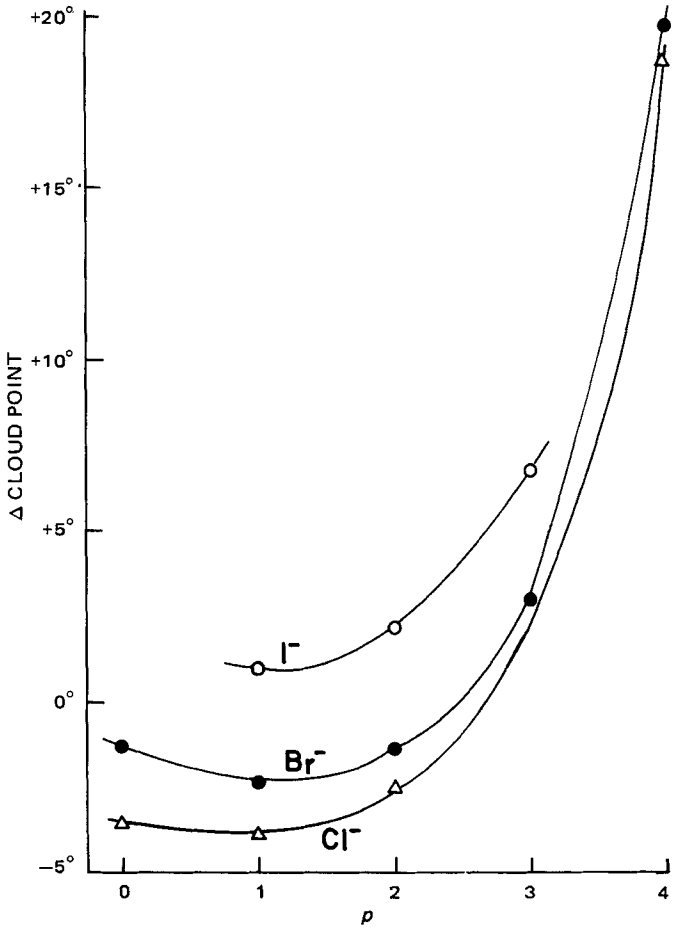

Figure 4—*Effect of chain length of the tetraalkylammonium ion on the cloud point of octoxynol at 0.10-molal electrolyte concentration;* p = *number of carbon atoms per alkyl group.*

entropy on dissolving a tetraalkylammonium salt in water compared with its dissolution in an unstructured organic solvent (4). Evidence of the enhanced water structure is the high viscosity and molal heat capacity of aqueous solutions of tetraalkylammonium halides (7).

As structure makers, tetraalkylammonium halides enhance the association among water molecules to the detriment of the hydration of the surfactant molecules. Thus, these electrolytes should salt the surfactant out. The observed increases in cloud point produced by the tetrapropyl- and tetrabutylammonium salts are in direct opposition to their structure-making activity. This finding indicates that a mechanism other than their effect on water structure is responsible for their salting-in or cloud point-raising ability. The new mechanism must be strong enough to overcome the effect of enhanced water structure formation by the tetrapropyl- and tetrabutylammonium ions, because this effect consists in reducing the solubility of nonelectrolytes or salting out. It is likely that at the cloud point temperature of 64° in the absence of electrolytes, the "icebergs" or "flickering clusters" (21) are largely melted or broken up. The tetrapropyl- and tetrabutylammonium salts boosted the cloud point to even higher temperatures, the latter above 80°, where these water structures cannot persist even in the presence of structure-making salts.

Electrolyte Association—Tetraalkylammonium halides reportedly associate in aqueous solution, either by cation–cation pairing (22) or by micelle formation (5, 23–25). The evidence for micellization is not supported by surface tension measurements (26) and could also be construed as indicating hydrotropy (27). The latter possibility is discussed in the *Appendix*. However, there is a strong likelihood that octoxynol and the tetraalkylammonium halides form mixed micelles, since the critical micelle concentration (CMC) of octoxynol is far below the 1.00% use level even at room temperature. Nonionic surfactants have a pronounced tendency to form mixed micelles with anionic (28) and cationic (29) surfactants at temperatures above the Krafft point of the ionic surfactants. The cloud points of the nonionic surfactants are considerably raised by comicellization (16, 30).

Of the four cations, ammonium salts do not form micelles. Tetramethylammonium bromide slightly increased the surface tension of water (26) in the manner of inorganic salts and is, therefore, also unlikely to associate into micelles. For the remaining tetraalkylammonium bromides, the decrease in surface tension with increasing salt concentration was steeper the larger their alkyl groups (26). This fact indicates that the tetrabutylammonium salts have the greatest tendency and the tetraethylammonium salts the least tendency toward forming micelles by themselves or mixed micelles with octoxynol. It corroborates the proposed concept of salting in of octoxynol through comicellization.

Ammonium and tetramethylammonium chloride and bromide salt octoxynol out because they are incapable of forming mixed micelles with it. The greater salting-out efficiency of tetramethylammonium salts compared to the corresponding ammonium salts may be due to their greater ability to increase the "ice-like" structure of water and/or to the smaller structure breaking caused by increasing temperatures in their presence. This assumption is corroborated by the observation that, in a group of salts including 15 different cations and eight anions, the tetramethylammonium ion had the largest negative activation energy for viscous flow of all the ions examined. These ions included barium and magnesium, the alkali metal cations and the halide anions, iodate, chlorate, hydroxyl, and sulfate. The ammonium ion had a small negative value. The activation energies of the higher tetraalkylammonium ions were positive and increased in the order tetraethyl-, tetrapropyl-, and tetrabutylammonium (7).

APPENDIX: EFFECT OF A HYDROTROPE ON CLOUD POINT

Hydrotropy is an increase in the water solubility of compounds of low intrinsic solubility by the addition of relatively large amounts of a second solute of high solubility. Such hydrotropic solubilizing agents, while amphiphilic in nature, are not surface active. They do not associate into micelles because their hydrophobic moiety is not large enough (27). Typical hydrotropes are alkali salts of benzene-, toluene-, xylene-, or cymenesulfonic acids and of benzoic, salicylic, or phthalic acids (27, 31, 32).

Even though hydrotropes are widely used as solubilizing or salting-in agents, their effect on the cloud point of polyoxyethylated nonionic surfactants has not been investigated. To examine the possibility that the salting-in action of the tetrapropyl- and tetrabutylammonium salts discussed may be one of hydrotropy, it became necessary to measure the effect of a typical hydrotrope on the cloud point of octoxynol to compare its direction and magnitude with those of the higher tetraalkylammonium salts.

The hydrotrope selected was sodium *m*-xylenesulfonate. The cloud points of solutions containing 2.00% (w/w) octoxynol at different hydrotrope concentrations were as follows: 64.7° in the absence of hydrotrope, 82.5° in the presence of 0.061 molal (1.25%) hydrotrope, 92.5° in the presence of 0.123 molal (2.50%) hydrotrope, and above 99° in the presence of 0.253 molal (5.00%) hydrotrope.

Interpolation places the cloud point of octoxynol in 0.10 molal sodium xylenesulfonate at 90°, compared to 83 and 84° in 0.10 molal tetrabutylammonium chloride and bromide, respectively (Table I). Sodium xylenesulfonate is more effective in raising the cloud point of the surfactant than the two tetrabutylammonium salts. If the trend of larger cloud point increases with increasing p values (Fig. 4) can be extrapolated, the tetrabutylammonium iodide or the tetrapentylammonium bromide would be more effective in salting the surfactant in than the anionic hydrotrope. The cloud point increases produced by the higher tetraalkylammonium salts and by a typical hydrotrope are thus of the same order of magnitude. Therefore, hydrotropy is another possible mechanism for the salting in of octoxynol by tetraalkylammonium salts instead of the formation of mixed micelles proposed.

The phenomenon of hydrotropy is poorly understood at the molecular level (27, 33). In our opinion, solutions of hydrotropes at the customary concentrated use levels contain patches that are largely oleophilic because of high local concentrations of aromatic groups. These hydrocarbon patches are not unlike the hydrocarbon cores of micelles but lack the precise boundaries of the latter. The formation of such patches with an increasing hydrotrope concentration is much more gradual than the sudden formation of micelles by surfactants once the CMC is exceeded. Nevertheless, the two phenomena may be so similar that the differences in the salting in of octoxynol by tetrapropyl- and tetrabutylammonium salts *via* mixed micelle formation and *via* hydrotropy are more semantic than based on physical reality. The higher tetraalkylammonium salts resemble some conventional hydrotropes in general composition (33). That the latter are usually anionic whereas the former are cationic is immaterial as far as their interaction with a nonionic surfactant is concerned.

REFERENCES

(1) H. Schott, *J. Colloid Interface Sci.*, **43,** 150 (1973).

(2) H. Schott and S. K. Han, *J. Pharm. Sci.*, **64,** 658 (1975).

(3) *Ibid.*, **65,** 979 (1976).

(4) R. M. Diamond, *J. Phys. Chem.*, **67,** 2513 (1963).

(5) S. Lindenbaum and G. E. Boyd, *ibid.*, **68,** 911 (1964).

(6) D. F. Evans and R. L. Kay, *ibid.*, **70,** 366 (1966).

(7) E. R. Nightingale, Jr., *ibid.*, **66,** 894 (1962).

(8) W.-Y. Wen and S. Saito, *ibid.*, **68,** 2639 (1964).

(9) B. E. Conway and R. E. Verrall, *ibid.*, **70,** 3952 (1966).

(10) F. J. Millero and W. Drost-Hansen, *ibid.*, **72,** 1758 (1968).

(11) A. LoSurdo and H. E. Wirth, *ibid.*, **76,** 1333 (1972).

(12) B. Belleau, in "Advances in Drug Research," vol. 2, N. J. Harper and A. B. Simmonds, Eds., Academic, New York, N.Y., 1965, pp. 104–118.

(13) B. Belleau and J. L. Lavoie, *Can. J. Biochem.*, **46,** 1397 (1968).

(14) J. B. Hyne, *J. Am. Chem. Soc.*, **85,** 304 (1963).

(15) M. J. Schick, *J. Colloid Interface Sci.*, **17,** 801 (1962).

(16) W. N. Maclay, *J. Colloid Sci.*, **11,** 272 (1956).

(17) H. Schott, *J. Pharm. Sci.*, **58,** 1443 (1969).

(18) J. W. McBain, "Colloid Science," D. C. Heath, Boston, Mass., 1950, chap. 9.

(19) F. A. Long and W. F. McDevit, *Chem. Rev.*, **51,** 119 (1952).

(20) N. C. Deno and C. H. Spink, *J. Phys. Chem.*, **67,** 1347 (1963).

(21) J. L. Kavanau, "Water and Solute–Water Interactions," Holden-Day, San Francisco, Calif., 1964.

(22) W.-Y. Wen and K. Nara, *J. Phys. Chem.*, **71,** 3907 (1967).

(23) H. E. Wirth, *ibid.*, **71,** 2922 (1967).

(24) H. E. Wirth and A. LoSurdo, *ibid.*, **72,** 751 (1968).

(25) A. LoSurdo and H. E. Wirth, *ibid.*, **76,** 130 (1972).

(26) K. Tamaki, *Bull. Chem. Soc. Jpn.*, **47,** 2764 (1974).

(27) M. E. L. McBain and E. Hutchinson, "Solubilization and Related Phenomena," Academic, New York, N.Y., 1955, chap. 6.

(28) H. Lange and K.-H. Beck, *Kolloid-Z. Z. Polym.*, **251,** 424 (1973).

(29) M. J. Schick, *J. Am. Oil Chem. Soc.*, **43,** 681 (1966).

(30) N. Charkhovskoy, *Bull. Soc. Chim. Belg.*, **65,** 474 (1956).

(31) H. S. Booth and H. E. Everson, *Ind. Eng. Chem.*, **41,** 2627 (1949).

(32) *Ibid.*, **42,** 1536 (1950).

(33) H. Rath, *Tenside*, **2,** 3 (1965).

ACKNOWLEDGMENTS AND ADDRESSES

Received August 19, 1975, from the *School of Pharmacy, Temple University, Philadelphia, PA 19140, and the ‡College of Pharmacy, Busan National University, Busan, Korea.

Accepted for publication March 18, 1976.

ˣ To whom inquiries should be directed.

Stereochemistry of Metabolism of Amphetamines: Use of (−)-α-Methoxy-α-(trifluoromethyl)phenylacetyl Chloride for GLC Resolution of Chiral Amines

JOSEPH GAL

Abstract □ Amphetamine and eight related compounds were reacted with the chiral acylating reagent (−)-α-methoxy-α-(trifluoromethyl)phenylacetyl chloride to obtain, in each case, two diastereomeric amide derivatives. GLC conditions were found for the separation of the diastereomers in seven of the nine cases studied. This procedure may be suitable for the resolution of amino acid enantiomers *via* the amide derivatives of the methyl esters. Secondary amines were not derivatized under the reaction conditions used. A correlation between absolute configuration and elution order of the diastereomeric amides was observed for five compounds. The chiral acylating reagent was used in the determination of the enantiomeric composition of 2,5-dimethoxy-4-methylamphetamine excreted in rat urine after intraperitoneal drug administration. The chiral acylating reagent is suitable for the determination of the optical composition of compounds extracted from biological fluids.

Keyphrases □ Amphetamine and related compounds—reacted with chiral acylating reagent, GLC separation of diastereomeric amide derivatives □ Chiral acylating reagents—(−)-α-methoxy-α-(trifluoromethyl)phenylacetyl chloride, reacted with amphetamine and related compounds, GLC separation of diastereomeric amide derivatives □ GLC—separation of diastereomeric amide derivatives of amphetamine and related compounds after reaction with chiral acylating reagent □ Stereochemistry—amphetamine and related compounds, reacted with chiral acylating reagent, GLC separation of diastereomeric amide derivatives □ Stimulants—amphetamine and related compounds, reacted with chiral acylating reagent, GLC separation of diastereomeric amide derivatives

While studying the stereochemistry of the metabolism of amphetamine (1-phenyl-2-aminopropane) derivatives, it was necessary to determine the enantiomeric compositions of several members of this class of compounds extracted in small amounts from biological fluids. A literature survey revealed that derivatization of an amphetamine with chiral acylating reagent I (1), II (2), or III (3), followed by GLC separation of the resulting diastereomeric amides, provides a sensitive analytical method for the determination of the enantiomeric composition of the parent amine extracted from a biological medium.

However, none of these compounds was deemed entirely satisfactory for this study. Compound I, an *l*-proline derivative, is easily racemized (1, 4), and commercial samples are contaminated with about 6–10% of the *d*-form. Attempts to achieve the resolution of *p*-methoxyamphetamine by derivatization with I failed, since five GLC bands were obtained when the reaction product was injected into the gas chromatograph. Others also reported (4) difficulties with I, although the reagent has been successfully used (5, 6).

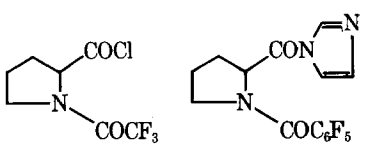

I

II

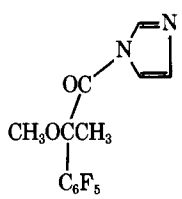

III

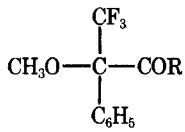

IV: R = OH
V: R = Cl

Compound II is highly suitable for electron-capture GLC due to the pentafluorophenyl group and has been employed with good results in the determination of the optical composition of a ring-substituted amphetamine derivative in metabolic studies (7). However, II provides poor GLC separation of the diastereomeric amides derived from amphetamine (2). Finally, III also appeared impractical since it must be synthesized *via* an elaborate route and its precursor carboxylic acid must be resolved (3). For these reasons, an alternative chiral reagent was sought.

Dale *et al.* (8) first reported the synthesis of α-methoxy-α-(trifluoromethyl)phenylacetic acid (IV) and its application to the determination of the enantiomeric purity of amines and alcohols by fluorine and proton NMR. Nichols *et al.* (4) extended the use of IV to the GLC determination of the enantiomeric purity of amphetamine derivatives prepared *via* a new asymmetric synthesis. Acid IV, lacking α-hydrogens, is highly resistant to racemization (8) and is commercially available in its resolved form[1]. In this paper, the applicability of IV to the GLC resolution of several amines of pharmacological interest is examined, and the suitability of this reagent for the determination of the enantiomeric composition of an amphetamine derivative excreted in rat urine is demonstrated.

EXPERIMENTAL

Materials—(*R,S*)- and (*S*)-Amphetamines[2] (VI), (*R,S*)- and (*R*)-*p*-hydroxyamphetamine[2] hydrobromides, (*R,S*)- and (*R*)-phenylalanine methyl ester[3] (VII) hydrochlorides, (*R,S*)- and (*S*)-α-methylbenzylamines[1] (VIII), (*R,S*)-*p*-chloroamphetamine[4] (IX) hydrochloride, (*R,S*)-β-phenylisopropylhydrazine[4] (X) hydrochloride, (*R,S*)-tranylcypromine[4] (XI) hydrochloride, and (*R,S*)-*p*-chlorophenylalanine[4] were obtained from commercial sources. (*R,S*)-*p*-Chlorophenylalanine methyl ester (XII) was prepared from the amino acid by the method of Brenner and Huber (9), using methanolic thionyl chloride. The treatment of (*R,S*)- and (*R*)-*p*-hydroxyamphetamines with diazomethane gave the corresponding *p*-methoxy compounds, (*R,S*)- and (*R*)-XIII. Samples of (*R,S*)- and (*R*)-2,5-dimethoxy-4-methylamphetamines (XIV) were donated[5].

The preparation (8) of V was carried out by refluxing for 50 hr a mixture of IV (1.0 g) and freshly distilled thionyl chloride (3 ml). The excess thionyl chloride was removed under reduced pressure (~30 mm), and the crude V was dissolved in 10 ml of 1,2-dichloroethane (XV). The solution

[1] Aldrich Chemical Co., Milwaukee, Wis.
[2] Smith Kline and French Laboratories, Philadelphia, Pa.
[3] Sigma Chemical Co., St. Louis, Mo.
[4] Regis Chemical Co., Morton Grove, Ill.
[5] Dr. Neal Castagnoli, Jr., School of Pharmacy, University of California, San Francisco, CA 94143.

Table I—GLC Data on Amides Derived from (—)-IV and Various Amines

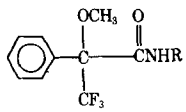

Amine Precursor	Retention Times of Diastereomers, min	Column Temperature	Resolution Factor[b]
VI	12.4[c], 14.0[d]	185°	1.4
XIII	12.5[c], 14.1[d]	210°	1.6
XIV	11.4[c], 13.6[d]	220°	2.3
IX	5.3, 6.0	210°	1.5
VII	11.6[d], 12.8[c]	206°	1.4
XII	8.4, 9.5	215°	1.5
VIII	13.4[c], 14.9[d]	175°	1.4

[a] See *Experimental* for GLC conditions. [b] See Ref. 11. Note that when the resolution factor = 1.0, the peak resolution is about 98% complete; when the resolution factor = 1.5, baseline separation (99.7%) is achieved. [c] From (*R*)-amine. [d] From (*S*)-amine.

was stored in a rubber-septum-capped bottle in a refrigerator. This reagent solution was used in the derivatizations.

Organic solvents used in the analytical procedures were of spectral quality grade.

GLC Analysis—GLC was carried out on two gas chromatographs[6,7], both equipped with flame-ionization detectors. System I[6], used to obtain the data in Table I and Fig. 1, consisted of a U-shaped glass column, 1.8 m × 0.2 cm i.d., packed with 3.0% phenyl methyl silicone[8] coated on acid-washed, dimethylchlorosilane-treated diatomite support[9]. The column temperatures used are given in Table I; the injector temperature was 250°, the detector temperature was 280°, and the nitrogen flow rate was 30 ml/min.

GLC System II[7], used for the analysis of XIV extracted from urine and derivatized with V, was performed using a coiled glass column of the same dimensions and containing the same packing as the column of System I. The nitrogen carrier gas rate was 20 ml/min. The ratios of diastereomeric amide derivatives of XIV were calculated from the area percent data of each peak provided by the instrument.

Mass Spectrometry—A quadrupole GLC–mass spectrometry system[10] was used with the GLC conditions given for GLC System II, except helium carrier gas was used at a flow rate of 50 ml/min.

Animal Procedures—Male Sprague–Dawley rats, 250–300 g, were given XIV hydrochloride (5 mg/kg ip) in saline or saline only. The animals were housed in individual metabolic cages with free access to food and water. Urine was collected for 24 hr.

Extraction, Purification, and Derivatization of XIV—To 4 ml of urine in a 20-ml screw-capped test tube were added 0.4 ml of 5 *N* NaOH and 6 ml of heptane. The mixture was shaken mechanically[11] for 15 min. After centrifugation for 10 min, 5 ml of heptane was transferred to a 12-ml conical screw-capped centrifuge tube containing 0.6 ml of 1 *N* HCl. The tubes were shaken for 10 min and centrifuged for 5 min. The heptane was aspirated and discarded.

One 500-μl aliquot of the acidic lower phase was removed with a micropipet and transferred to another conical centrifuge tube containing 1.2 ml of benzene and 0.2 ml of 5 *N* NaOH. After shaking for 15 min and centrifuging for 5 min, 1.0 ml of benzene was transferred to a 3-ml microcentrifuge tube[12], and the benzene was evaporated in a stream of nitrogen. To the residue were added 50 μl of the reagent solution of V and 10 μl of pyridine, and the mixture was swirled on a mixer[13] for 10 sec. The tube was then capped and heated at 70° for 30 min, followed by cooling in ice for 5 min.

The reaction mixture was treated with 1 ml of 1 *N* HCl, and the tube was shaken for 5 min and centrifuged for 5 min. The acidic upper layer was aspirated off and discarded, and 0.4 ml of 15% Na_2CO_3 was added to the tube. The tube was then shaken for 10 min and centrifuged for 10 min, followed by GLC analysis of the lower organic layer as described.

[6] Life Sciences gas chromatograph 2100, Varian Associates, Palo Alto, Calif.
[7] Gas chromatograph 5830, Hewlett-Packard, Palo Alto, Calif.
[8] OV-17, Applied Sciences Laboratories, State College, Pa.
[9] Gas Chrom Q, Applied Science Laboratories, State College, Pa.
[10] Model 5981A, Hewlett-Packard, Palo Alto, Calif.
[11] International bottle shaker, International Equipment Co., Boston, Mass.
[12] Microflex tube, Kontes Glass Co., Vineland, N.J.
[13] Vortex Genie, Scientific Industries, Springfield, Mass.

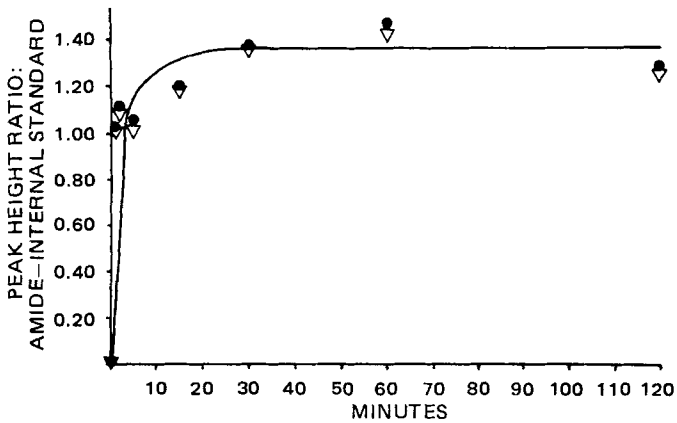

Figure 1—*Rates of formation of amides from V and (R)-VI (●) and (S)-VI (▽). See* Experimental *for reaction conditions and analytical procedure.*

Derivatization of Pure Compounds—The amine or amine salt (0.1–0.2 mg) in a conical screw-capped tube was treated with XV (50 μl), V reagent solution (50 μl), and pyridine (20 μl). The tube was heated in an oil bath at 70° for 30 min and then cooled in an ice bath. Hydrochloric acid (1 *N*, 1 ml) was added, and the tube was shaken mechanically for 5 min and centrifuged at 3000 rpm for 10 min. The aqueous acid layer was aspirated off, and 15% sodium carbonate solution (0.5 ml) and XV (100 μl) were added. The tube was shaken for 5 min and centrifuged for 10 min. The organic phase was then analyzed by GLC.

Rate of Formation of Derivatives—To a solution of (*R,S*)-amphetamine (2.0 mg) in 100 μl of XV was added 40 μl of dry pyridine. The solution was heated to 70°, 100 μl of the V reagent solution was added, and the stopwatch was started. At the appropriate times, a 25-μl aliquot was withdrawn and added to an ice-cold mixture containing 100 μl of XV, 1.0 ml of 1 *N* HCl, and 100 μl of a 10 m*M* solution of the internal standard, 1-methoxymethyl-3-methylphenobarbital (10).

The mixture was swirled for 15 sec and then frozen in dry ice–acetone until all of the time-point samples had been collected. The tubes were then shaken for 5 min and centrifuged for 10 min. The aqueous layer was aspirated off, 100 μl of 15% Na_2CO_3 solution was added, and the mixture was shaken for 5 min and centrifuged for 10 min. The organic layer was then analyzed by GLC.

RESULTS AND DISCUSSION

Acid IV was converted to V, its acid chloride (8), which could be used to acylate amines. The reaction (Scheme I) of V with racemic amphetamine at 70°, catalyzed by pyridine, was studied as a function of time (Fig. 1). The reaction was essentially complete in 30 min, and the product amides appeared to be stable under the reaction conditions. This short reaction time allows the use of the reagent in routine procedures where overnight reaction times (4) would be cumbersome.

Several amines (VI, VIII, IX, XI, XIII, and XIV), a hydrazine derivative (X), and two amino acid esters (VII and XII) were derivatized with V. The free base or a salt (*e.g.*, hydrochloride or sulfate) could be used in the acylation reaction with identical results. With two exceptions, the resulting diastereomeric amides[14] were well resolved by GLC (Table I). The identity of the product amides in Table I was confirmed by GLC–mass spectrometry. All amides gave a molecular ion[15].

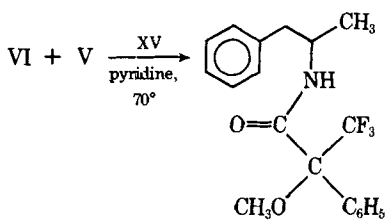

Scheme I

[14] All of the amides prepared were derived from (−)-IV.
[15] A detailed study of the mass spectral fragmentation of the amides prepared will be published.

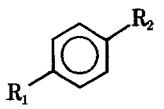

VI: R_1 = H, R_2 = $CH_2CH(NH_2)CH_3$
VII: R_1 = H, R_2 = $CH_2CH(NH_2)COOCH_3$
VIII: R_1 = H, R_2 = $CH(CH_3)NH_2$
IX: R_1 = Cl, R_2 = $CH_2CH(NH_2)CH_3$
X: R_1 = H, R_2 = $CH_2CH(NHNH_2)CH_3$
XI: R_1 = H, R_2 = *trans*-cyclo-$(C_3H_4)NH_2$
XII: R_1 = Cl, R_2 = $CH_2CH(NH_2)COOCH_3$
XIII: R_1 = OCH_3, R_2 = $CH_2CH(NH_2)CH_3$

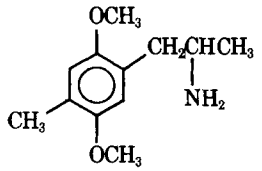

XIV

The successful resolution of the enantiomers of VII and XII indicates that V may be suitable for the resolution of amino acids (as their methyl esters), an area of considerable current interest (12). Two compounds, X and XI, gave diastereomeric amides that were not sufficiently resolved under the GLC conditions used, since only a slight "fork" at the top of the peak was observed in each case.

Attempts to derivatize secondary amines, *e.g.*, *N*-methylamphetamine, showed that the reaction of these amines with V was considerably slower than the reaction of primary amines. Under the reaction conditions used, secondary amines remained essentially underivatized.

Compounds VI–VIII, XIII, and XIV were available in their resolved form and, since their absolute configurations are known, the relationship between the elution order of their diastereomeric amide derivatives and absolute configuration could be examined. As seen from Table I, with one exception, the amides derived from the (*R*)-amines had shorter retention times than those from the corresponding (*S*)-amines, in agreement with the findings of Nichols *et al.* (4). The exception was VII, where the amide from (*S*)-VII eluted before the amide from (*R*)-VII. This finding is stereochemically logical, since (*S*)-VII and (*R*)-amphetamines have corresponding configurations, even though the configurational notations are opposite.

Among the desirable characteristics of a chiral reagent suitable for routine use in biological studies are: (*a*) ready availability in resolved form, (*b*) chemical stability and resistance to racemization, (*c*) simple derivatization procedure and workup, (*d*) good GLC resolution of the diastereomeric derivatives without unduly long retention times, and (*e*) high response of the derivatives to the GLC detector. While no chiral reagent has yet been developed that is superior in all of these considerations, the results described indicate that V offers distinct advantages over reagents I–III. In addition to the earlier mentioned ready availability and stability of V, this reagent was superior to I–III in providing better GLC resolution in cases where comparison could be made. For example, VI (5, 6), VII (13), and XIII (14) were derivatized with reagent I; VI, VIII, and XIV were resolved with II (2) and III (3). In these cases, V tended to give better resolution and/or shorter retention times. However, II and III gave derivatives with excellent electron-capture properties, most likely not equaled by those of V, which lacks the pentafluorophenyl group. This disadvantage of the derivatives of V may be partially overcome by using GLC–mass spectrometry in the selected-ion-monitoring mode, which provides extremely high sensitivity (15). Experiments in this direction are in progress.

By using a flame-ionization detector, the minimum detectable amount of V-derivatized (*R*)- or (*S*)-amphetamine was of the order of 1×10^{-13} mole/sec or 5 ng of sample injected.

The applicability of V to metabolic studies was tested by examining an aspect of the stereochemistry of the *in vivo* metabolism of XIV. The

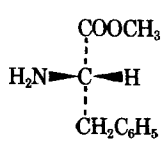

(*S*)-VII

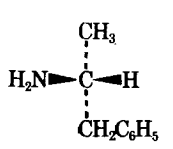

(*R*)-amphetamine

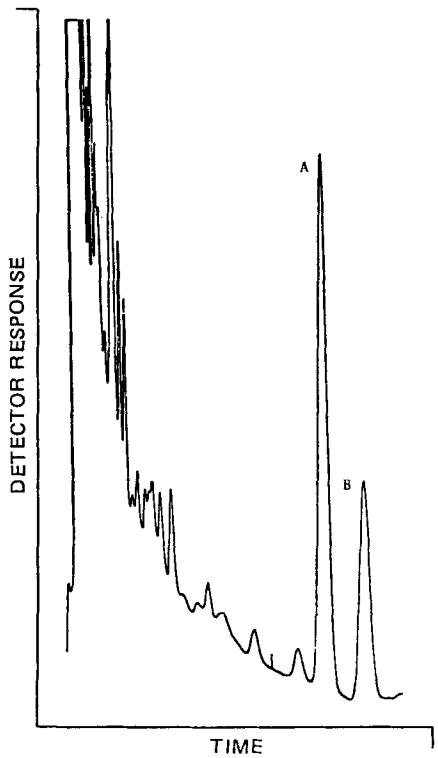

Figure 2—*Gas chromatogram of V-derivatized XIV extracted from rat urine. Key: A, derivative from* (R)*-XIV; and B, derivative from* (S)*-XIV. See* Experimental *for GLC conditions.*

metabolic fate of this compound, a potent psychotomimetic agent (16, 17), was studied in the rabbit (7, 18) and rat (19). Since the psychotomimetic activity of XIV resides in the (*R*)-enantiomer but not in the (*S*)-enantiomer (20), some investigators have paid special attention to the stereochemical aspects of its metabolism (7, 18). Thus, it was found (7) that the (*R*)/(*S*) ratio of unchanged XIV excreted in the 24-hr urine of rabbits administered racemic XIV was dose dependent and varied between 1.0 and 1.7.

Since the metabolism of XIV in the rabbit differs from that in the rat (7, 19), it seemed of interest to examine the stereochemistry of unchanged XIV excreted in the urine of rats. Racemic XIV hydrochloride (5 mg/kg ip) in saline was given to rats, and the urine was collected for 24 hr. Unchanged XIV was extracted from urine using a multistep procedure (21), which purifies and concentrates the amine before derivatization. Reaction with V was followed by GLC analysis. No peaks attributable to the amide derivatives of XIV were observed when the urine of the two animals given saline only was analyzed. The (*R*)/(*S*) ratio of XIV in the urine of three animals given the drug was 2.0, 2.1, and 1.3, respectively. Figure 2 shows a typical gas chromatogram of V-derivatized XIV extracted from rat urine.

The amount of unchanged XIV excreted was not determined, although it was reported (19) that 5% of a 5-mg/kg ip dose of racemic hydrochloride appeared as unchanged XIV in the 24-hr urine of rats. The magnitude of the (*R*)/(*S*) ratio of XIV found in rat urine is in the same direction as that observed in rabbits (7). However, at the 5-mg/kg dose level, the (*R*)/(*S*) ratio in rabbits was 1.0 and reached 1.7 only at 21 mg/kg (7).

Differences in pharmacological activity and in disposition between enantiomers of amphetamines and of related compounds are receiving considerable attention (7, 17, 22–24). Resolution of the optical isomers by GLC of diastereomeric derivatives may be useful in studying such differences. Compound V is an important addition to the list of chiral acylating agents (3, 25, 26) used for this purpose.

REFERENCES

(1) C. E. Wells, *J. Assoc. Offic. Anal. Chem.*, **53**, 113 (1970).

(2) S. B. Matin, M. Rowland, and N. Castagnoli, Jr., *J. Pharm. Sci.*, **62**, 821 (1973).

(3) L. R. Pohl and W. F. Trager, *J. Med. Chem.*, **16**, 475 (1973).

(4) D. E. Nichols, C. F. Barfknecht, D. B. Rusterholz, R. Benington, and R. D. Morin, *ibid.*, **16**, 480 (1973).

(5) L.-M. Gunne, *Biochem. Pharmacol.*, **16**, 863 (1967).
(6) E. Gordis, *ibid.*, **15**, 2124 (1966).
(7) S. B. Matin, P. S. Callery, J. S. Zweig, A. O'Brien, R. Rapoport, and N. Castagnoli, Jr., *J. Med. Chem.*, **17**, 877 (1974).
(8) J. A. Dale, D. L. Dull, and H. S. Mosher, *J. Org. Chem.*, **34**, 2543 (1969).
(9) M. Brenner and W. Huber, *Helv. Chim. Acta*, **36**, 1109 (1953).
(10) J. A. Vida, M. L. Hooker, and J. F. Reinhard, *J. Med. Chem.*, **16**, 602 (1973).
(11) H. McNair and E. J. Bonelli, "Basic Gas Chromatography," Varian Aerograph, Walnut Creek, Calif., 1969, p. 33.
(12) P. Husek and K. Macek, *J. Chromatogr.*, **113**, 139 (1975).
(13) J. W. Westley, B. Halpern, and G. L. Karger, *Anal. Chem.*, **40**, 2046 (1968).
(14) L.-M. Gunne and L. Galland, *Biochem. Pharmacol.*, **16**, 1374 (1967).
(15) D. J. Jenden and A. K. Cho, *Annu. Rev. Pharmacol.*, **13**, 371 (1972).
(16) S. H. Snyder, L. Faillace, and L. Hollister, *Science*, **158**, 669 (1967).
(17) M. B. Wallach, E. Friedman, and S. Gershon, *J. Pharmacol. Exp. Ther.*, **182**, 145 (1972).
(18) J. Gal, L. D. Gruenke, and N. Castagnoli, Jr., *J. Med. Chem.*, **18**, 683 (1975).
(19) B. T. Ho, V. Estevez, L. W. Tansey, L. F. Englert, P. J. Creaven, and W. M. McIsaac, *ibid.*, **14**, 153 (1971).
(20) A. T. Shulgin, *J. Pharm. Pharmacol.*, **25**, 271 (1973).
(21) A. K. Cho, B. Lindeke, B. J. Hodshon, and D. J. Jenden, *Anal. Chem.*, **45**, 570 (1973).
(22) H. C. Cheng, J. P. Long, D. E. Nichols, and C. F. Barfknecht, *J. Pharmacol. Exp. Ther.*, **188**, 114 (1974).
(23) H. Kreiskott and H. P. Hofmann, *Pharmakopsychiat./Neuro-Psychopharmakol.*, **8**, 136 (1975).
(24) J. A. Fuentes, M. A. Oleshansky, and N. H. Neff, *Biochem. Pharmacol.*, **24**, 1971 (1975).
(25) E. Gil-Av and D. Nurok, *Adv. Chromatogr.*, **10**, 99 (1974).
(26) M. T. Gilbert, J. D. Gilbert, and C. J. W. Brooks, *Biomed. Mass Spectrom.*, **1**, 274 (1974).

ACKNOWLEDGMENTS AND ADDRESSES

Received January 26, 1976, from the *Department of Pharmacology, School of Medicine, Center for the Health Sciences, University of California, Los Angeles, CA 90024.*

Accepted for publication March 3, 1976.

Supported by U.S. Public Health Service Contract ADM-45-74-178 and Grant DAO-1057.

The author is grateful to Professor Neal Castagnoli, Jr., School of Pharmacy, University of California, San Francisco, for generous samples of XIV. Thanks are also due to Professor A. K. Cho, Department of Pharmacology, University of California, Los Angeles, for his interest in this work. Assistance by Barbara J. Hodshon is greatly appreciated.

Present address: School of Pharmacy, University of Wisconsin, Madison, WI 53706.

Use of Microcapsules as Timed-Release Parenteral Dosage Form: Application as Radiopharmaceutical Imaging Agent

JOHN D. SCHEU *, GLEN J. SPERANDIO, STANLEY M. SHAW, ROBERT R. LANDOLT, and GARNET E. PECK ˣ

Abstract □ The development of a new type of parenteral dosage form is described. A system of microencapsulation was formulated which produced microcapsules containing a water-soluble core material. The basic microencapsulation system could be altered to produce microcapsules with varied timed-release characteristics. Tracer methodology was employed as a sensitive and versatile analytical tool for the development and evaluation of the microencapsulation system. The core material was labeled by neutron activation after microcapsule formulation, which eliminated the radiation hazard and contamination problems that could occur during formulation with a labeled core material. Both *in vitro* and *in vivo* testing showed that the release patterns of labeled core material could be altered and detected. The microcapsules developed have potential as a timed-release parenteral dosage form and as an organ-imaging radiopharmaceutical.

Keyphrases □ Microcapsules—formulated, potential as timed-release parenteral dosage form and organ-imaging radiopharmaceutical evaluated *in vitro* and *in vivo*, mice □ Dosage forms, parenteral—timed-release microcapsules formulated, evaluated *in vitro* and *in vivo*, mice □ Radiopharmaceuticals—timed-release microcapsules formulated, potential use in organ imaging evaluated, mice

A dependable parenteral timed-release dosage form would eliminate many problems associated with oral administration. The process of microencapsulation may hold the key to the ideal timed-release dosage form because of the smallness of the produced microcapsules and the various properties instilled into the microcapsules. However, such a dosage form must contain microcapsules with very precise properties.

The main objective of this investigation was to develop a microencapsulating system that utilized a water-soluble polymer as the chief capsule wall component and allowed for the encapsulation of a water-soluble material. Other desired characteristics included microcapsules from 1 to 20 μm in diameter and formulation flexibility allowing alterations in core release rates. Tracer methodology was selected as the analytical tool for evaluation of the microcapsules. A second objective was to produce radioactivity in the core material by neutron activation after formulation. *In vitro* and *in vivo* test procedures were derived to evaluate the microcapsules as a timed-release parenteral dosage form and as a radiopharmaceutical imaging agent.

EXPERIMENTAL

Basic Procedure—Coacervation was selected as the microencapsulation method after a review of other methods (1–16). The following general procedure (Table I) was used in preparing all microcapsules.

Forty milliliters of dioxane[1], analytical grade, was added to a 50-ml beaker. A 1.25-cm magnetic stirrer bar was placed in the beaker, which

[1] Mallinckrodt Chemical Works, St. Louis, Mo.

(5) L.-M. Gunne, *Biochem. Pharmacol.*, **16**, 863 (1967).
(6) E. Gordis, *ibid.*, **15**, 2124 (1966).
(7) S. B. Matin, P. S. Callery, J. S. Zweig, A. O'Brien, R. Rapoport, and N. Castagnoli, Jr., *J. Med. Chem.*, **17**, 877 (1974).
(8) J. A. Dale, D. L. Dull, and H. S. Mosher, *J. Org. Chem.*, **34**, 2543 (1969).
(9) M. Brenner and W. Huber, *Helv. Chim. Acta*, **36**, 1109 (1953).
(10) J. A. Vida, M. L. Hooker, and J. F. Reinhard, *J. Med. Chem.*, **16**, 602 (1973).
(11) H. McNair and E. J. Bonelli, "Basic Gas Chromatography," Varian Aerograph, Walnut Creek, Calif., 1969, p. 33.
(12) P. Husek and K. Macek, *J. Chromatogr.*, **113**, 139 (1975).
(13) J. W. Westley, B. Halpern, and G. L. Karger, *Anal. Chem.*, **40**, 2046 (1968).
(14) L.-M. Gunne and L. Galland, *Biochem. Pharmacol.*, **16**, 1374 (1967).
(15) D. J. Jenden and A. K. Cho, *Annu. Rev. Pharmacol.*, **13**, 371 (1972).
(16) S. H. Snyder, L. Faillace, and L. Hollister, *Science*, **158**, 669 (1967).
(17) M. B. Wallach, E. Friedman, and S. Gershon, *J. Pharmacol. Exp. Ther.*, **182**, 145 (1972).
(18) J. Gal, L. D. Gruenke, and N. Castagnoli, Jr., *J. Med. Chem.*, **18**, 683 (1975).
(19) B. T. Ho, V. Estevez, L. W. Tansey, L. F. Englert, P. J. Creaven, and W. M. McIsaac, *ibid.*, **14**, 153 (1971).
(20) A. T. Shulgin, *J. Pharm. Pharmacol.*, **25**, 271 (1973).
(21) A. K. Cho, B. Lindeke, B. J. Hodshon, and D. J. Jenden, *Anal. Chem.*, **45**, 570 (1973).
(22) H. C. Cheng, J. P. Long, D. E. Nichols, and C. F. Barfknecht, *J. Pharmacol. Exp. Ther.*, **188**, 114 (1974).
(23) H. Kreiskott and H. P. Hofmann, *Pharmakopsychiat./Neuro-Psychopharmakol.*, **8**, 136 (1975).
(24) J. A. Fuentes, M. A. Oleshansky, and N. H. Neff, *Biochem. Pharmacol.*, **24**, 1971 (1975).
(25) E. Gil-Av and D. Nurok, *Adv. Chromatogr.*, **10**, 99 (1974).
(26) M. T. Gilbert, J. D. Gilbert, and C. J. W. Brooks, *Biomed. Mass Spectrom.*, **1**, 274 (1974).

ACKNOWLEDGMENTS AND ADDRESSES

Received January 26, 1976, from the *Department of Pharmacology, School of Medicine, Center for the Health Sciences, University of California, Los Angeles, CA 90024.*

Accepted for publication March 3, 1976.

Supported by U.S. Public Health Service Contract ADM-45-74-178 and Grant DAO-1057.

The author is grateful to Professor Neal Castagnoli, Jr., School of Pharmacy, University of California, San Francisco, for generous samples of XIV. Thanks are also due to Professor A. K. Cho, Department of Pharmacology, University of California, Los Angeles, for his interest in this work. Assistance by Barbara J. Hodshon is greatly appreciated.

Present address: School of Pharmacy, University of Wisconsin, Madison, WI 53706.

Use of Microcapsules as Timed-Release Parenteral Dosage Form: Application as Radiopharmaceutical Imaging Agent

JOHN D. SCHEU *, GLEN J. SPERANDIO, STANLEY M. SHAW, ROBERT R. LANDOLT, and GARNET E. PECK ˣ

Abstract □ The development of a new type of parenteral dosage form is described. A system of microencapsulation was formulated which produced microcapsules containing a water-soluble core material. The basic microencapsulation system could be altered to produce microcapsules with varied timed-release characteristics. Tracer methodology was employed as a sensitive and versatile analytical tool for the development and evaluation of the microencapsulation system. The core material was labeled by neutron activation after microcapsule formulation, which eliminated the radiation hazard and contamination problems that could occur during formulation with a labeled core material. Both *in vitro* and *in vivo* testing showed that the release patterns of labeled core material could be altered and detected. The microcapsules developed have potential as a timed-release parenteral dosage form and as an organ-imaging radiopharmaceutical.

Keyphrases □ Microcapsules—formulated, potential as timed-release parenteral dosage form and organ-imaging radiopharmaceutical evaluated *in vitro* and *in vivo*, mice □ Dosage forms, parenteral—timed-release microcapsules formulated, evaluated *in vitro* and *in vivo*, mice □ Radiopharmaceuticals—timed-release microcapsules formulated, potential use in organ imaging evaluated, mice

A dependable parenteral timed-release dosage form would eliminate many problems associated with oral administration. The process of microencapsulation may hold the key to the ideal timed-release dosage form because of the smallness of the produced microcapsules and the various properties instilled into the microcapsules. However, such a dosage form must contain microcapsules with very precise properties.

The main objective of this investigation was to develop a microencapsulating system that utilized a water-soluble polymer as the chief capsule wall component and allowed for the encapsulation of a water-soluble material. Other desired characteristics included microcapsules from 1 to 20 μm in diameter and formulation flexibility allowing alterations in core release rates. Tracer methodology was selected as the analytical tool for evaluation of the microcapsules. A second objective was to produce radioactivity in the core material by neutron activation after formulation. *In vitro* and *in vivo* test procedures were derived to evaluate the microcapsules as a timed-release parenteral dosage form and as a radiopharmaceutical imaging agent.

EXPERIMENTAL

Basic Procedure—Coacervation was selected as the microencapsulation method after a review of other methods (1–16). The following general procedure (Table I) was used in preparing all microcapsules.

Forty milliliters of dioxane[1], analytical grade, was added to a 50-ml beaker. A 1.25-cm magnetic stirrer bar was placed in the beaker, which

[1] Mallinckrodt Chemical Works, St. Louis, Mo.

Table I—Formulations Used to Prepare Microcapsules for *In Vivo* Testing

Step	Formulation 1	2	3	4	5
Manufacturing media (dioxane), ml	40	40	40	40	40
Sphere former[a] (glycerin), ml	0.23	0.23	0.23	0.23	0.23
Mechanical step	—	—	—	—	—
Core material (gold sodium thiosulfate), mg	40	40	40	40	40
Polymer[a] (polyethyleneimine-18), ml	3	3	3	3	3
pH controlling agent[a], ml	0.06, sulfuric acid	0.14, hydrochloric acid	0.03, ammonium hydroxide	0.057, hydrochloric acid	0.07, hydrochloric acid
Anticlumping agent (ethylcellulose), ml	0.08	0.08	0.08	0.08	0.08
Hardening agent[a], ml	0.365, glutaraldehyde	0.22, glutaraldehyde	0.22, glutaraldehyde	0.22, glutaraldehyde	0.08, formaldehyde
Hardening process[a]	45 min, 65°	15 hr, 23°	20 min, 75°	20 min, 75°	20 min, 75°
Washing step	Dioxane	Dioxane	Dioxane	Dioxane	Dioxane
Washing step	Dioxane	Dioxane	Dioxane	Dioxane	Dioxane
Capsule drying	Steam bath	Steam bath	Steam bath	Steam bath	Steam bath

[a] Variable.

was then positioned on a stirrer hot plate and warmed to 35° (the time can vary). Glycerin USP was added and allowed to go into solution. Heating was terminated, and the magnetic stirrer was removed.

The beaker was then placed in an ultrasonic bath[2]. Micronized core material was added and dispersed by holding the beaker in the bath for 30 sec. When the core material was well dispersed, polyethyleneimine-18[3] solution was added, and the beaker was held in the ultrasonic bath for 15 more sec. The beaker was then removed from the ultrasonic bath, and a pH-controlling agent was added with light stirring.

After the mixture was allowed to stand for a desired length of time, ethylcellulose[4] solution was added with stirring. The ultrasonic bath was again used to disperse the microspheres. Glutaraldehyde[5] solution was added, and the beaker was left standing for 5 min. Then it was placed in a water bath at the desired temperature with moderate agitation for a desired time period. After the beaker was removed from the water bath, the contents were poured into a test tube and centrifuged. The top liquid was decanted off and replaced with fresh dioxane.

The microcapsules were redispersed in dioxane and left standing for 5 min. They were then centrifuged and washed with dioxane. After washing, the microcapsules were poured on a watch glass over a steam bath and allowed to dry. Microcapsules were recovered as a dry fine powder.

Core Material and Neutron Activation—Amaranth was used as the core material in the preliminary development of the microencapsulation system because it is a water-soluble colored material of a complex organic nature. These qualities simplified the microscopic examination of the effects of water on microcapsules. In the later stages of experimentation, gold sodium thiosulfate and sodium chloride were used as core materials. These three materials are water soluble, relatively nontoxic, and compatible with the microencapsulation system, and they can be micronized[6] to a particle size of 1–15 μm and labeled by exposure to a thermal neutron flux. The elemental gold-197 and sodium-23 contained in gold sodium thiosulfate and the sodium-23 in sodium chloride and amaranth were easily activated upon exposure to the thermal neutron flux of a reactor[7].

All samples to be activated in both the encapsulated and unencapsulated form were placed in polyethylene irradiation vials. The samples were then placed in a styrofoam container and lowered down a 10-cm diameter tube located at the face of the reactor core. The reactor was operated at a power level of 900 w, and the sample was irradiated for 60 min. The estimated fluence rate was 10^9 neutrons/cm^2/sec. After neutron exposure, the specific activity of samples was calculated.

Sample Counting—A sodium iodide scintillation crystal (25 × 27.5 cm) with a well[8] (10 × 20 cm) attached to a single-channel analyzer[9] was used in the detection of the γ-rays emitted by gold-198 and sodium-24, which were the respective radionuclides obtained from the activation of gold-197 and sodium-23. Differential counting was used for both nuclides to allow counting of one radionuclide in the presence of the other. Counting correction factors, applied as necessary, included coincidence loss, background, geometry, instrumentation efficiency, and radioactive decay.

Microcapsule Timed-Release Dosage Form *In Vitro* Testing Procedure—An *in vitro* test was designed to evaluate quantitatively the release rate of core material from microcapsules. The procedure allowed test fluid to contact the microcapsules and to leach out the core material contained inside. The core material, being radioactive and in solution, could be sampled and counted and the rate of release could be determined.

The *in vitro* test apparatus (Fig. 1) consisted of a constant-temperature water bath fabricated from a 10-cm deep plastic rectangular container supported by a wood platform. The platform was of sufficient height to allow a magnetic stirrer to be placed underneath. The plastic container was filled with water, which was circulated and kept at 3°. A 12.5-cm, 100-ml graduated cylinder containing a 1.88-cm magnetic stirring rod was placed in the center of the bath directly above the magnetic stirrer. The cylinder was filled with 100 ml of test fluid, which was isotonic sodium chloride solution at pH 7.4.

The *in vitro* test chamber consisted of a glass tube with a syringe on top and a filtering system on the lower portion. Microcapsules were placed within the chamber; the test fluid was drawn in and expelled through the filter, which retained all of the microcapsules. The chamber was supported by a ring stand with the lower portion of the chamber immersed in the test fluid in the graduated cylinder.

The test fluid was drawn into the chamber and expelled at set time intervals. One-milliliter samples of the test fluid in the cylinder were drawn for counting at the end of each expulsion from the test chamber. Then 1 ml of fresh test solution was added to the cylinder to maintain the volume. The procedure was repeated until the desired number of samples was obtained.

The samples were counted, and all necessary counting corrections were made. Based on the count rate of the samples, standards, and microcapsules prior to placement in the test chamber, the amount of core material removed from the microcapsules was determined.

Effect of Hardening Process on Microsphere Droplets—The basic formulation procedure was used to microencapsulate amaranth. During the hardening process, the microsphere droplets were exposed to 0.18 ml of glutaraldehyde at 60°. Samples of the microcapsules were removed after 1.5, 5, and 15 min of exposure and placed on separate glass slides, and a drop of isotonic sodium chloride solution at pH 7.4 was added.

Influence of pH on Dissolution Patterns—To investigate the effect

[2] Branson ultrasonic bath, Branson Instrument Co., Stamford, Conn.
[3] PEI, Dow Chemical Co., Midland, Mich.
[4] Ethocel, Hercules Inc., Wilmington, Del.
[5] Eastman Chemicals, Rochester, N.Y.
[6] Gem-T Risen Micronizer, Trost Co., Newton, Pa.
[7] RUR-I is a light water, graphite-moderated, swimming pool-type reactor fueled with enriched uranium-235 (Department of Nuclear Engineering, Purdue University, Lafayette, Ind.).
[8] Harshaw NaI(Tl) scintillation crystal detector, Harshaw Chemical Co., Cleveland, Ohio.
[9] Ortec Inc., Oak Ridge, Tenn.

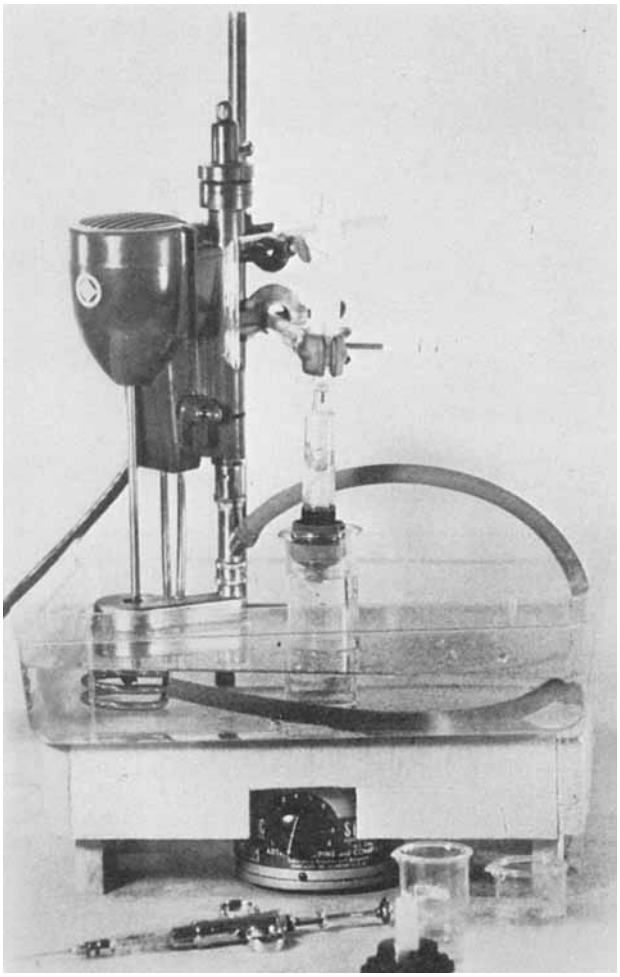

Figure 1—In vitro *test apparatus.*

of pH on the microcapsule properties, gold sodium thiosulfate was encapsulated using the basic formulation procedure except that the pH of the microencapsulating system was varied during the process. The pH was varied by the careful addition of 0.14 ml of hydrochloric acid stock solution[10] to one batch, 0.06 ml of sodium hydroxide stock solution[11] to a second batch, and no pH-controlling agent to the third batch. After the microcapsules were dried and collected, they were exposed to thermal neutrons, counted, and tested *in vitro* as described previously.

Influence of Test Fluid pH—To investigate the influence of test fluid pH on the release of gold-198, procedures similar to those in NF XIV (17) were followed. Two batches of microcapsules were prepared using the basic procedure, and neutron exposure and counting procedures were used as before. One batch was studied *in vitro* with a pH 5 test fluid while the other was placed in a test fluid of pH 7. When a dissolution plateau was reached, sodium hydroxide solution was added to change the pH of the test fluid to 8.

Screening of Microencapsulation Formulations—By using the basic formulation procedure and different combinations of materials, microcapsules were produced containing gold sodium thiosulfate. These microcapsules were exposed to thermal neutrons, counted, and subjected to *in vitro* testing as described previously. In evaluating the formulations, certain values were considered. The ratio between core material weight and encapsulation weight of the microcapsules and the percent of core material placed in the microencapsulated system were used to indicate microencapsulating system efficiency. The amount of core material released during *in vitro* testing within the first 15 min and the amount released at 120 min were important. Also, the difference between the two values was used as a basis for projecting *in vivo* release patterns from *in vitro* data.

[10] Hydrochloric acid stock solution was prepared by adding 0.8 ml of hydrochloric acid, reagent grade, to 29.2 ml of dioxane.

[11] Sodium hydroxide stock solution was prepared by adding 1 ml of 1 *M* NaOH solution, reagent grade, to 29 ml of dioxane.

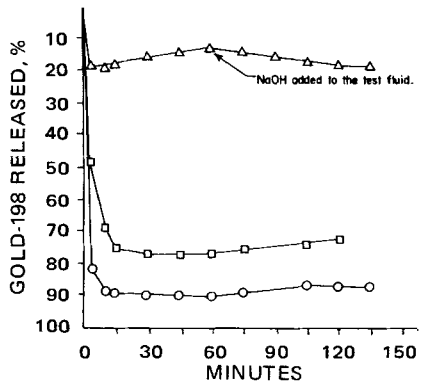

Figure 2—*Effect of the microencapsulation system pH on the release of gold-198. Key:* △, *hydrochloric acid added during microcapsule formation;* □, *no acid or base added during microcapsule formation; and* ○, *sodium hydroxide added during microcapsule formation.*

Five formulations (Table I) produced dissolution curves showing promise for use for either *in vivo* timed-release or radiopharmaceutical imaging studies.

Timed-Release Dosage Form *In Vivo* Testing Procedure—The *in vivo* testing was conducted to determine the levels of gold-198 in the blood and organs of a mouse after the injection of either unencapsulated or microencapsulated labeled gold sodium thiosulfate. The investigation consisted of injecting three groups of 21 mice[12] as follows. The first group was subcutaneously injected with unencapsulated labeled gold sodium thiosulfate. The second group was injected with microcapsules containing labeled gold sodium thiosulfate that had shown a relatively small release of gold-198 *in vitro* (Formulation 1, Table I). The third group was injected with microcapsules containing labeled gold sodium thiosulfate that had shown a timed-release pattern *in vitro* (Formulation 2, Table I).

The microcapsules and unencapsulated gold sodium thiosulfate were exposed to thermal neutrons, and the specific activity of each sample was calculated. The radioactive samples were suspended in a 50% glycerin–water for injection vehicle just prior to administration. To aid in microcapsule dispersion, 0.05 ml of polysorbate 80[13] was added to the injection vehicle. The mixtures were placed in an ultrasonic bath until good dispersion was observed.

Volumes of 0.25 ml of each material containing the same amount of either encapsulated or unencapsulated ^{198}Au-labeled gold sodium thiosulfate were injected subcutaneously behind the heads of 25–30-g mice, using a 1-ml tuberculin syringe fitted with a 26-gauge needle. At 2, 5, 8, 11, 16, 20, and 23 hr, three mice from each group were removed, and blood samples were obtained by means of ocular puncture. Blood was weighed according to the method of tares. The mice were sacrificed; their kidneys, lungs, livers, and spleens were removed, washed with saline, weighed, and stored individually. The remainder of the mouse, which was referred to as the carcass, was weighed and stored.

Each complete mouse was counted in the well detector after dissection by pooling the dissected parts of the mouse and the carcass. The count

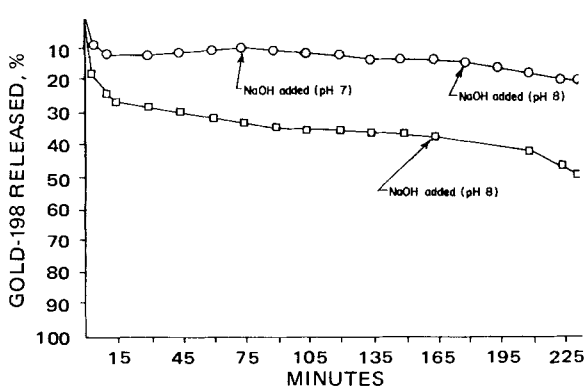

Figure 3—*Effect of test fluid pH on the release of gold-198. Key:* ○, *initial pH 5; and* □, *initial pH 7.*

[12] Cox Swiss male mice, Laboratory Supply, Indianapolis, Ind.

[13] Tween 80, ICI America, Inc., Wilmington, Del.

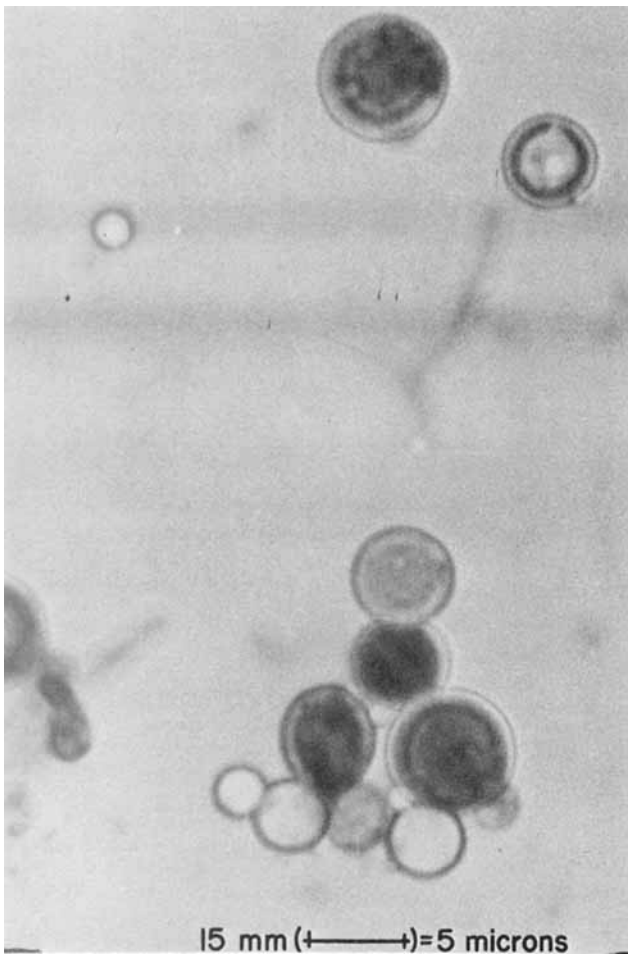

Figure 4—*Microcapsules with amaranth.*

rate of the pooled tissues was considered to represent 100% of the gold-198 activity. Organs were counted individually, and the percent of radioactivity in each organ was determined relative to the total mouse. The percent of activity per organ was divided by the milligram weight of the organ, with the resultant data referred to as the percent of total activity per milligram (% *Ta*/mg).

Radiopharmaceutical Imaging Agent *In Vivo* Testing Procedure—This test procedure was conducted to determine if Formulation 1 microcapsules (Table I), which exhibited low release of gold-198, had potential as imaging agents. The influence of microcapsule size on organ distribution was investigated.

Formulation 1 microcapsules were separated by scalping with nylon screens[14] into four size ranges: ≤5, 6–10, 11–15, and ≥16 μm. With a standard light microscope, the sizes were compared to reference pollen samples for verification of the scalping technique. No microcapsules exceeded 20 μm in diameter. Once the microcapsules were separated and dried, they were placed in separate 1-ml polyethylene vials and exposed to thermal neutrons. Unencapsulated gold sodium thiosulfate was also exposed. After exposure, the specific activity of each material was determined. The injection vehicle consisted of water for injection USP with 0.05 ml of polysorbate 80 added.

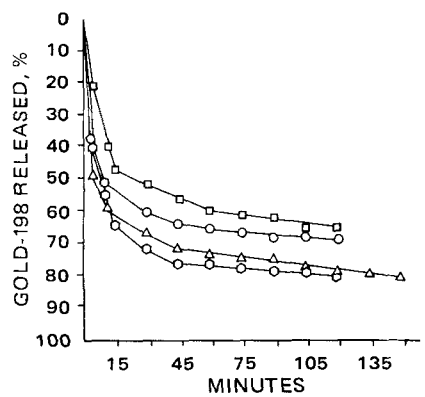

Figure 5—In vitro *release patterns of gold-198 from microcapsules. Key:* □, *Formulation 2;* ○, *Formulation 4;* △, *Formulation 5; and* ○, *Formulation 3.*

[14] Nitex nylon screen cloth, Kressilk Products, Inc., Des Plaines, Ill.

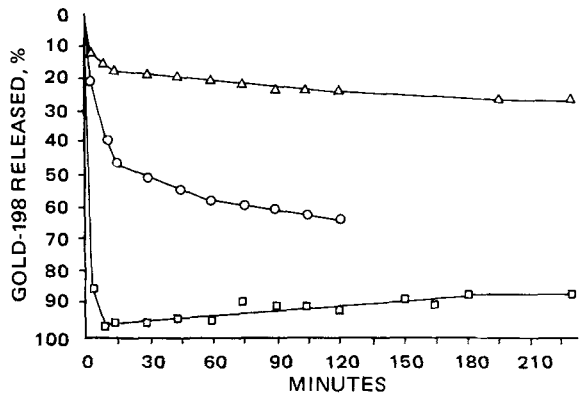

Figure 6—In vitro *release patterns in isotonic test fluid for timed-release dosage form samples later studied* in vivo. *Key:* △, *Formulation 1;* ○, *Formulation 2; and* □, *unencapsulated labeled gold sodium thiosulfate.*

With a 1-ml tuberculin syringe and a 27-gauge needle, 0.2 ml of suspension was injected intravenously into the tail vein of each mouse. Each group of animals consisted of seven mice. One group was injected with unencapsulated labeled gold sodium thiosulfate. A separate group was used for each size range of microcapsules. Two hours after injection, all mice were sacrificed. The liver, spleen, heart, lungs, and kidneys of each mouse were removed. The procedures of counting and calculation were identical to those utilized for testing the microcapsule timed-release dosage form.

RESULTS AND DISCUSSION

Changes in the basic formulation procedure influenced the microcapsules and their properties. Variables noted were: order of mixing of ingredients, temperature of the system during microcapsule formation, strength and type of acid used, the plasticizer, the hardening agent, the concentration, and the length of time microcapsules were hardened. These findings are consistent with those of earlier investigators (10).

The influence of pH during the encapsulation process is illustrated in Fig. 2. The dissolution curves show an alteration in the release of gold-198 activity resulting from variation in pH during this process. The labeled core material discussed throughout this section is based upon the gold-198 activity except where otherwise noted.

During the *in vitro* testing of the microcapsules prepared with hydrochloric acid, sodium hydroxide solution was added after a plateau in gold-198 release occurred (Fig. 2). An immediate increase in activity was noticed in the test fluid, indicating that the test fluid pH influenced the

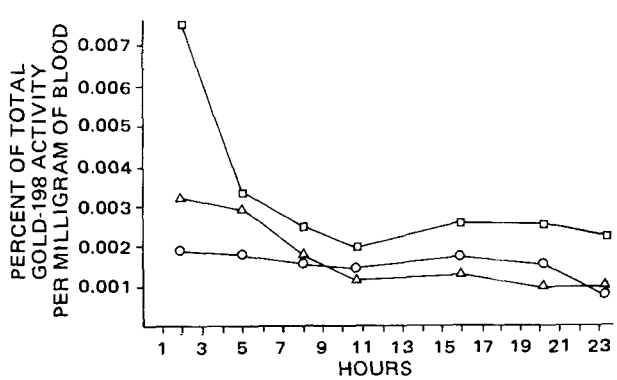

Figure 7—*Gold-198 blood concentration from timed-release study. Key:* □, *unencapsulated labeled gold sodium thiosulfate;* ○, *Formulation 2; and* △, *Formulation 1.*

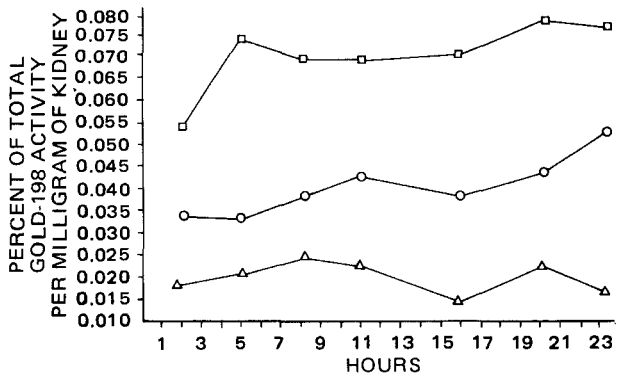

Figure 8—*Gold-198 kidney concentration from timed-release study. Key: □, unencapsulated labeled gold sodium thiosulfate; ○, Formulation 2; and △, Formulation 1.*

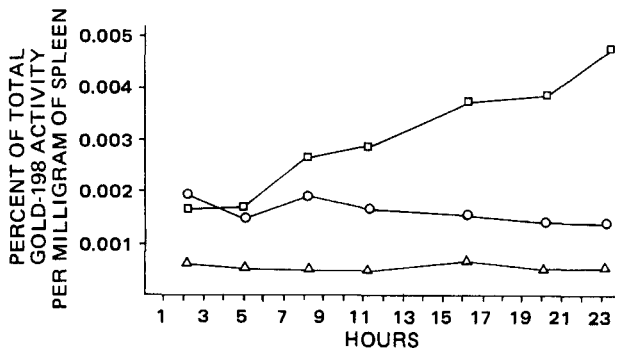

Figure 10—*Gold-198 spleen concentration from timed-release study. Key: □, unencapsulated labeled gold sodium thiosulfate; ○, Formulation 2; and △, Formulation 1.*

release of gold-198. The observation was confirmed with additional experimentation. More gold-198 was released from microcapsules in a test fluid of pH 7 than of pH 5 (Fig. 3). The addition of sodium hydroxide solution increased the release of gold-198 after a plateau was reached.

Microscopic examination of microcapsules containing amaranth was used to study the influence of the hardening process on core release. As the time of exposure to the hardening agent was increased, diffusion of the amaranth through the microcapsules decreased. Amaranth was used to aid in defining the hardening process. Figure 4 is representative of microcapsules produced throughout the investigation.

After extensive investigation, five formulations produced dissolution curves showing promise for use as either *in vivo* timed-release agents or radiopharmaceutical imaging agents. The formulations are listed in Table I, and dissolution curves are illustrated in Figs. 5 and 6. The apparent loss in activity by the unencapsulated sample with time (Fig. 6) could be eliminated by the addition of unlabeled gold sodium thiosulfate. This phenomenon was probably due to the adsorption of the labeled material of high specific activity by the test chamber.

The dissolution curves showed that the basic microencapsulation formulation could be altered to produce microcapsules with differing timed-release characteristics. A rather extensive release of gold-198 was attained with Formulations 2–5 in contrast to a limited gold-198 release from Formulation 1. The maximum release of gold-198 was variable among Formulations 2–5. Representative aliquots of formulations prepared for *in vivo* experimentation were subjected to *in vitro* testing. Dissolution curves for the samples are presented in Fig. 6. The release patterns showed that Formulation 1 microcapsules inhibited the release of the labeled core material more than Formulation 2 microcapsules. The dissolution rate for unencapsulated labeled core material was much greater than exhibited by the microcapsules.

***In Vivo* Timed-Release Dosage Form Study**—The percent of total activity per milligram (% *Ta*/mg) of organ, carcass, and blood was calculated for samples obtained during the *in vivo* study. The data, presented as mean values for each group of three mice sacrificed at a particular time period (Figs. 7–12), were subjected to statistical examination. A Burr–Foster test was employed to determine homogeneity of variance of the means; a two-way analysis of variance also was applied, followed by a Newman–Keuls test for comparison of the means.

The results of the statistical analysis showed that the three lines in each figure (Figs. 7–12) were statistically different and distinct from each other at the 95% confidence level. The unencapsulated labeled gold sodium thiosulfate produced the highest activity levels in the blood, kidneys, lungs, spleen, and liver; the least amount of activity remained in the carcass, indicating an extensive removal of the unencapsulated labeled compound from the site of injection. Formulation 1 microcapsules provided the lowest tissue activity levels and resulted in the highest amount of labeled gold sodium thiosulfate remaining at the site of injection. Gold-198 release exhibited by Formulation 2 microcapsules fell between the two extremes shown by unencapsulated gold sodium thiosulfate and Formulation 1 microcapsules. The timed-release data from the *in vivo* study correlated with the data generated by the dissolution curves.

Statistically, there was no evidence at the 95% confidence level that the three lines within each figure (Figs. 7–12) were anything but parallel to each other. If present, differences in slopes were not observed statistically because of the variance error in the data resulting from the small number of animals per time interval and the short duration of the *in vivo* study.

***In Vivo* Radiopharmaceutical Imaging Agent Study**—The data for this phase of the investigation were subjected to statistical examination as in the timed-release phase. The data are presented as a mean value per organ per micrometer particle-size range in Fig. 13.

The gold-198 level in the lungs of animals receiving microcapsules of ≤5, 6–10, and 11–15 μm was statistically greater at the 95% confidence level than the activity present in the lungs of mice receiving unencapsulated labeled gold sodium thiosulfate. The largest lung uptake was observed with 11–15-μm microcapsules. The microcapsules exhibited localization properties favorable for a radiopharmaceutical lung-imaging agent.

No consistent statistical differences were found between the microcapsules of differing micrometer ranges and the unencapsulated labeled gold sodium thiosulfate for the carcass, spleen, kidneys, liver, and heart. The data may reflect the high level of free gold-198 produced in the process of separating the microcapsules into size ranges.

The *in vivo* data only illustrate the applicability of the basic microcapsule formulation for the production of a radiopharmaceutical imaging agent. Extensive experimentation must be conducted to ascertain the true potential of the microcapsules.

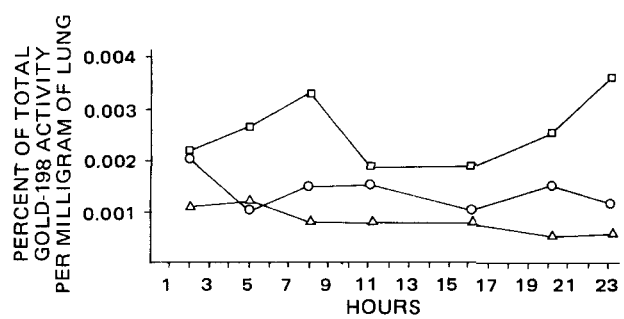

Figure 9—*Gold-198 lung concentration from timed-release study. Key: □, unencapsulated labeled gold sodium thiosulfate; ○, Formulation 2; and △, Formulation 1.*

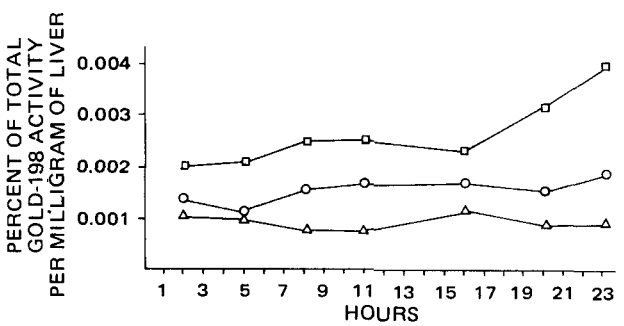

Figure 11—*Gold-198 liver concentration from timed-release study. Key: □, unencapsulated labeled gold sodium thiosulfate; ○, Formulation 2; and △, Formulation 1.*

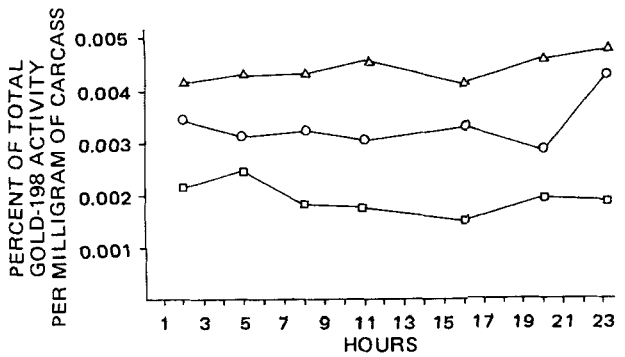

Figure 12—*Gold-198 carcass concentration from timed-release study. Key:* □, *unencapsulated labeled gold sodium thiosulfate;* ○, *Formulation 2; and* △, *Formulation 1.*

SUMMARY AND CONCLUSIONS

A new method of preparing parenteral dosage forms was developed. A system of microencapsulation was formulated that produced microcapsules containing a water-soluble core material. The microcapsules ranged in size from 1 to 20 μm and could be collected as a fine powder. The basic microencapsulation system allowed for many variable changes which affected the properties of the microcapsules. Only a few of these variables and their effects on the microcapsules were studied. Although a great deal of research on this microencapsulation system still must be accomplished, a basic workable process was developed which can serve as a model for further study for parenteral application.

Neutron activation of the microencapsulated core material proved to be an efficient and convenient procedure for producing a radioactive core material. Contamination problems that would occur if the core material was labeled during formulation were avoided. The radioactivity was used as a sensitive and versatile analytical tool in evaluating the microencapsulation system and the properties of the microcapsules.

An *in vitro* test for ascertaining the properties of the microcapsules was developed and proved to be sensitive and reproducible. The test was designed to evaluate the applicability of the labeled microcapsules produced in the study as a timed-release dosage form and as a radiopharmaceutical.

In vitro and *in vivo* experimentation showed that release patterns of labeled core material could be altered by the formulation process. A direct correlation in release patterns was found for microcapsules studied *in vitro* and *in vivo*. The data showed that the basic microencapsulation system developed in this investigation has potential as a timed-release parenteral dosage form.

Microcapsules containing labeled gold sodium thiosulfate concentrated in the lungs after intravenous injection. The potential of the basic microencapsulation system as an *in vivo* diagnostic radiopharmaceutical was illustrated. Further testing is needed to demonstrate the total potential of this microcapsule in the parenteral field.

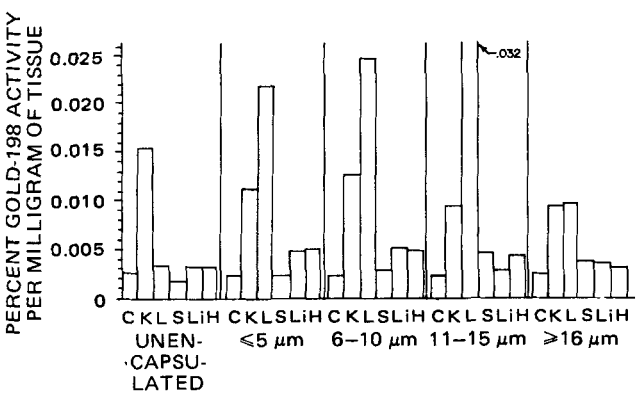

Figure 13—*Gold-198 organ distribution from radiopharmaceutical study. Key: C, carcass; K, kidneys; L, lungs; S, spleen; Li, liver; and H, heart.*

REFERENCES

(1) J. A. Herbig, "Encyclopedia of Chemical Technology," vol. 13, 2nd ed., Interscience New York, N.Y. 1967, pp. 437, 451–455.

(2) G. R. Somerville, Jr. (to The Southwest Research Institute), U.S. pat. 3,015,128 (Aug. 18, 1960).

(3) C. F. Raley, W. J. Burkett, and J. S. Swearingen, U.S. pat. 2,766,478 (Oct. 16, 1956).

(4) D. E. Wurster (to Wisconsin Alumni Research Foundation), U.S. pat. 2,648,609 (Aug. 11, 1953).

(5) D. E. Wurster (to Wisconsin Alumni Research Foundation), U.S. pat. 2,799,241 (Feb. 6, 1953).

(6) D. E. Wurster, *J. Am. Pharm. Assoc., Sci. Ed.*, **48**, 451 (1959).

(7) L. A. Luzzi, *J. Pharm. Sci.*, **59**, 1368 (1970).

(8) H. G. Bungenburg de Jong, in "Colloid Science II," H. R. Kruyt, Ed., Elsevier, New York, N.Y., 1949, pp. 243–487.

(9) B. K. Green and L. Scheicher (to National Cash Register Co.), U.S. pat. 2,809,457 (July 23, 1957).

(10) M. W. Ranney, "Microencapsulation Technology," Noyes Development Corp., Park Ridge, N.J., 1960.

(11) R. E. Phares and G. J. Sperandio, *J. Pharm. Sci.*, **53**, 515 (1964).

(12) J. D. La Mothe, Ph.D. thesis, Purdue University, West Lafayette, Ind., 1968.

(13) L. D. Tolle, Ph.D. thesis, Purdue University, West Lafayette, Ind., 1966.

(14) T. M. S. Chang, F. C. MacIntosh, and S. G. Mason, *Can. J. Physiol. Pharmacol.*, **44**, 115 (1965).

(15) T. M. S. Chang, L. J. Johnson, and O. J. Ransome, *ibid.*, **45**, 705 (1967).

(16) J. Whitmore, Ph.D. thesis, University of Florida, Gainsville, Fla., 1966.

(17) "The National Formulary," 14th ed., Mack Publishing Co., Easton, Pa., 1975, p. 985.

ACKNOWLEDGMENTS AND ADDRESSES

Received January 13, 1976, from the *School of Pharmacy and Pharmacal Sciences, Purdue University, West Lafayette, IN 47907.*

Accepted for publication March 23, 1976.

J. D. Scheu was a fellow of the American Foundation for Pharmaceutical Education.

* Present address: Department of Nuclear Pharmacy, University Hospital, Ohio State University, Columbus, OH 43210.

[x] To whom inquiries should be directed.

Interpretation of Plasma Concentration–Time Curves after Oral Dosing

ROBERT A. RONFELD *x **and LESLIE Z. BENET** ‡

Abstract □ The pharmacokinetic information obtained after oral administration is examined using the two-compartment model. Data were obtained by simulation and experimentally by administering sulfisoxazole by an exponential infusion to rabbits. When the absorption rate constant is allowed to approach α, a typical two-compartment oral absorption curve is obtained, which is described by a triexponential equation. However, if the absorption rate constant approaches E_2 (the sum of the elimination rate constants out of the peripheral compartment), the data are adequately fit by a one-compartment model, with the calculated absorption rate equal to α. The relative error in using a one-compartment model to calculate absorption rate constants for two-compartment data is also evaluated.

Keyphrases □ Pharmacokinetics—interpretation of plasma concentration–time curves after oral administration of sulfisoxazole, rabbits □ Absorption rate constants—data fitted to one- and two-compartment models, relative error evaluated, oral administration of sulfisoxazole, rabbits □ Oral administration—sulfisoxazole, interpretation of plasma concentration–time curves, rabbits □ Sulfisoxazole—oral administration, interpretation of plasma concentration–time curves, rabbits □ Antibacterial agents—sulfisoxazole, oral administration, interpretation of plasma concentration–time curves, rabbits

One major problem confronting the drug industry is the correlation of *in vitro* dissolution studies with *in vivo* absorption measurements for oral dosage forms. Information can be gained about the pharmacokinetics of a drug and the relative efficacy of its oral dosage forms from oral plasma concentration–time curves where no data exist describing the drug disposition after intravenous administration. Although it would always be better to have intravenous data in humans, regulations and therapeutic considerations often dictate situations where this kind of data is not available even for drugs in current clinical use. The present work describes a situation where completely invalid measurements of absorption rates would be obtained if previous intravenous measurements had not been made.

The determination of absorption rate constants that depend on the model used to describe the disposition kinetics of the drug after an intravenous dose has been the subject of several publications. Most absorption calculations have been made using a one- or two-compartment body model. The Wagner–Nelson method (1) has been used for drugs seemingly described by the one-compartment model, and the Loo–Riegelman method (2) has been used for those following kinetics consistent with the two-compartment model. The representative equations for the one- (Eq. 1) and two-compartment (Eq. 2) models are:

$$C_p = \frac{k_{a1}FD}{V_d(k_{a1} - k_d)}(e^{-k_d t} - e^{-k_{a1}t}) \qquad \text{(Eq. 1)}$$

and:

$$C_p = \frac{k_{a2}FD}{V_1}\left[\frac{(E_2 - k_{a2})}{(\alpha - k_{a2})(\beta - k_{a2})}e^{-k_{a2}t} + \frac{(E_2 - \alpha)}{(\beta - \alpha)(k_{a2} - \alpha)}e^{-\alpha t} + \frac{(E_2 - \beta)}{(\alpha - \beta)(k_{a2} - \beta)}e^{-\beta t}\right] \qquad \text{(Eq. 2)}$$

where:

C_p = plasma concentration
FD = available dose
k_{a1} = absorption rate constant, one-compartment body model
k_{a2} = absorption rate constant, two-compartment body model
k_d = elimination rate constant, one-compartment body model
E_2 = sum of the exit (or micro) rate constants out of Compartment 2 in a two-compartment model
α, β = disposition (or macro) constants describing distribution and elimination in a two-compartment model
V_d, V_c = volumes of distribution for a one-compartment model and central compartment of a two-compartment model, respectively.

The term "flip-flop model" has been used recently to illustrate the nonuniqueness of any concentration–time curve believed to describe first-order input and disposition from a one-compartment pharmacokinetic model, since the slow rate constant may be attributed to *either* absorption or elimination and the fast rate constant may be attributed to the alternate. Therefore, it is impossible to tell from a single curve (following an oral dose) whether the terminal half-life is due to absorption or elimination. The two-compartment model is somewhat more unique in that it does take on characteristic shapes depending on the relative size of the absorption rate constant with respect to α, β, or E_2.

In this study, generated curves are used to illustrate characteristic shapes and to compare one- and two-compartment analyses. In addition, representative curves were obtained experimentally in the rabbit, using sulfisoxazole [N^1-(3,4-dimethyl-5-isoxazolyl)sulfanilamide]. Oral absorption was simulated experimentally with a logarithmic infusion.

EXPERIMENTAL

The left and right marginal ear veins of 4-kg rabbits were cannulated[1], one ear being used for chronic sampling and the other ear for drug administration. One-milliliter blood samples were taken at frequent intervals and analyzed according to the Bratton–Marshall method (3). Initially, the drug was administered as a bolus injection, and the disposition parameters were calculated from the plasma concentration–time curve.

Subsequent experiments were run in which oral absorption was simulated by administering the drug by a first-order intravenous infusion, accomplished by exponential dilution of a drug solution with the apparatus represented in Fig. 1. A 5–10-ml disposable syringe (pictured) on the left was fixed at a constant volume, while a 50-100-ml syringe in a Harvard syringe pump determined the flow and constantly diluted the

[1] Intracath catheter sets.

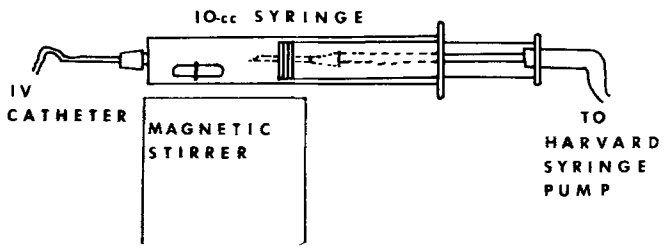

Figure 1—*Apparatus used to administer first-order infusions intravenously.*

contents in the small syringe with dextrose (5%). A magnetic stirring bar was activated in the small syringe to ensure proper mixing. Any first-order infusion rate can be obtained by proper selection of the infusion rate in milliliters per minute on the Harvard infusion pump and the appropriate fixed volume of the small syringe.

The value of the simulated first-order absorption rate constant is equal to the zero-order infusion rate (maintained with the infusion pump) divided by the fixed volume in the small syringe. Each infusion was continued until at least 97% of the dose was administered. Both the experimental sulfisoxazole data and the generated data were fit on a digital computer[2] using the nonlinear least-squares fitting program NONLIN (4).

RESULTS AND DISCUSSION

Analysis of oral data can be very inexact, since oral absorption often adds more than one variable to the intravenous data even though the data appear to be fit adequately by addition of a single exponential term and an availability constant. However, this "smoothed" interpretation of the absorption process may include variations due to nonlinearities in dosage form release and dissolution of the drug, first-pass effects and decreased physiological availability, stomach emptying, biliary recycling, blood flow to the GI tract, and other problems of non-first-order absorption related to distribution into and diffusion through the GI membrane. However, despite the complexity of the absorption process, there are numerous examples of oral absorption being adequately described by a single first-order process. This may be due to the lack of sufficient blood level data to model the absorption process precisely or to the fact that one of these processes becomes rate limiting, thereby simplifying the absorption mechanism into a process that may be described by a single exponential term.

A single first-order absorption process, commonly used in pharmacokinetic modeling, is assumed for the remainder of this discussion. If absorption can be represented by a first-order process, then, in the case of the two-compartment model, the shape of the blood level curve can

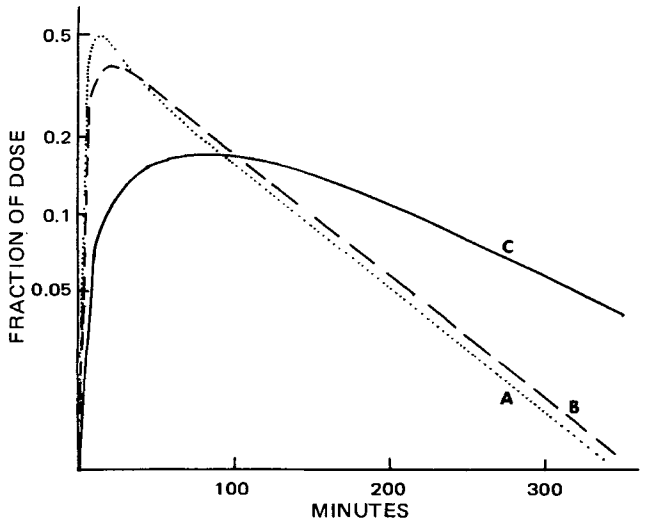

Figure 2—*Blood level curves for two-compartment model following first-order absorption. Key: A,* $k_{a2} \simeq \alpha$; *B,* $k_{a2} \simeq E_2$; *and C,* $k_{a2} \simeq \beta$.

[2] IBM 360/50.

Table I—Comparison of One-Compartment Analysis of Two-Compartment-Generated Data

Case	Two Compartment[a], k_{a2}, hr^{-1}	One Compartment	
		k_{a1}, hr^{-1}	k_d, hr^{-1}
A	7.2	25.9	0.83
D	5.4	14.1	0.76
B	3.6	7.54	0.67
E	1.8	2.58	0.61
C	0.6	1.10	0.40

[a] The two-compartment rate constants were $\alpha = 7.46\ hr^{-1}$, $\beta = 0.67\ hr^{-1}$, and $E_2 = 3.57\ hr^{-1}$.

be indicative of the relative size of the absorption rate constant. Figure 2 illustrates three blood level curves, generated using the same two-compartment rate constants (given in the left-hand side of Table I) and differing only in the absorption rate constants following oral dosing. Curve A is characterized by a "nose," which can be visualized by extrapolating back the log-linear line and having a convex curve lie above it. Curve A is generally thought to be characteristic of a two-compartment model, whereas curve B is often representative of a one-compartment model.

Curve A in Fig. 2 is an example of a case where the absorption rate constant approached α ($k_{a2} = 7.2$, $\alpha = 7.46$). When referring to Eq. 2, it is important to realize that although two of the exponentials are almost equal to each other, this triexponential equation does not simplify to a biexponential equation. This predominant nose is characteristic of a two-compartment model when k_{a2} is larger than E_2 and approaching or larger than α. However, based on oral data alone, it is not possible to predict whether the larger rate constant in the triexponential equation describing this curve should be assigned to k_{a2} or α.

Curve B of Fig. 2 illustrates a curve apparently following a one-compartment model. Actually, this curve was generated with the two-compartment equation and the rate constants given in the left-hand side of Table I, but with k_{a2} very nearly equal to E_2 ($k_{a2} = 3.6$, $E_2 = 3.57$). This curve could be perfectly fit to a one-compartment model. The slow rate constant could be correctly assigned to β. However, the fast rate constant, regardless of whether it was obtained by the method of residuals or by a computer fit, would not be equal to the absorption rate constant k_{a2} but rather equal to α. This result can be explained quite easily by referring to Eq. 2. As k_{a2} approaches E_2, the coefficient of the exponential term describing absorption approaches zero.

Curves A and B in Fig. 2 could present a perplexing problem if they resulted from the administration of two different dosage forms of the same drug. That is, both dosage forms seem to be equally available (from a comparison of areas under the curves) and to have the same slow rate of disposition from the body (both curves are parallel and log linear after 1 hr). However, dosage form B appears to follow a one-compartment body model and dosage form A follows a two-compartment body model. And, if each set of data is treated by the seemingly appropriate model, the absorption rates calculated would almost be equal.

Curve C in Fig. 2 is an example of a case where k_{a2} is allowed to approach β ($k_{a2} = 0.6$, $\beta = 0.67$). Here, it appears that the data could be fit by either a one- or two-compartment model, depending upon the number and preciseness of the data points. Even though this curve is described by a triexponential equation, it will not have the characteristic nose of curve A. If the oral blood curve is of this form, it is not possible to make a unique assignment of the slow rate constant to either β or k_{a2} when only a single oral data curve is available.

Even though the investigator may fit oral data to the seemingly appropriate model, significant errors may occur when interpreting and comparing the absorption rate constants. In cases such as these, inconsistencies between the relative absorption rate constants and relative times of peak concentration may arise. Time of peak concentration should be a reliable relative measurement since it is model independent. That is, from the peak times in Fig. 2, the investigator should know that the absorption rate constant for curve A is greater than that for curve B, which is greater than that for curve C. However, due to experimental error, it is often difficult to define the peak time precisely. In addition, any lag time greatly influences the peak time and may invalidate comparisons between different dosage forms based upon peak time measurements.

Similar data obtained experimentally for sulfisoxazole are pictured in Fig. 3. The parameters obtained after an intravenous dose (curve A)

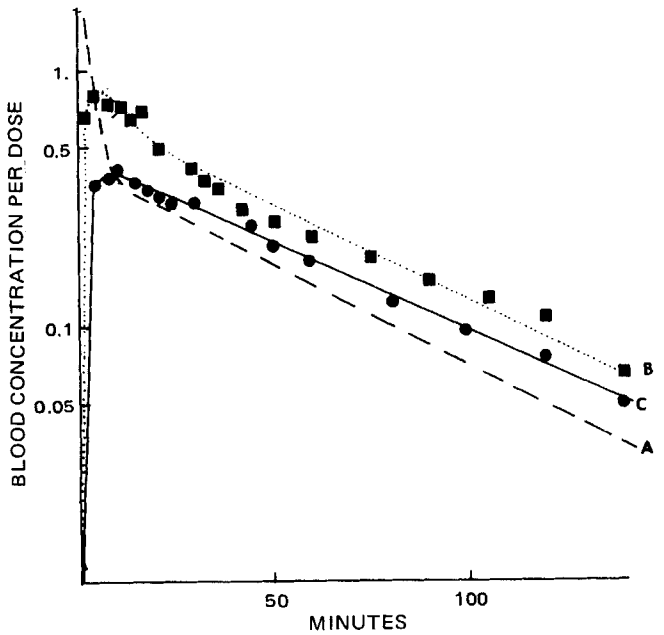

Figure 3—*Blood sulfisoxazole levels in the rabbit following intravenous administration as a bolus and as two different first-order infusions. Key: A, intravenous bolus; B,* $k_{a2} = 0.16$*; and C,* $k_{a2} = 0.08$.

were $\alpha = 0.45$, $\beta = 0.018$, and $E_2 = 0.11$. Curve B, the result of a first-order infusion (with a rate constant of 0.16), is obviously two-compartment data and was fit to Eq. 2. The computer-fitted parameters for curve B were equal to the intravenous disposition parameters and the actual absorption rate constant (0.16). Curve C appears to be one-compartment data and was fit to Eq. 1, resulting in fitted values of $k_{a1} = 0.47$ and $k_d = 0.016$. These values are approximately equal to the α and β obtained with the intravenous data. The actual k_a in this case was 0.08, a value less than E_2. Without the intravenous curve, there would be an apparent inconsistency to these data. Curve B has a characteristic nose, yielding an absorption rate constant of either 0.45 or 0.16 since the investigator cannot distinguish between k_{a2} and α. The apparent one-compartment data (curve C), in which absorption appears to be slightly slower on the basis of the peak time comparisons, yields an absorption rate constant of 0.47.

Wagner and Metzler (5) showed that simulated two-compartment blood level data can often be fit with minimal error to a one-compartment model. Table I gives the results from computer fitting the two-compartment data illustrated in Fig. 2 (A, B, and C) and two intermediate absorption rate constants (D and E) to a biexponential equation (Eq. 1). The best-fit absorption and elimination rate constants for the one-compartment model are listed. Although the computer-fitted absorption rate constants yield marked overestimates of the real absorption rate constants, the relative order of these fitted constants agrees with the relative order of the real absorption constants. In the case where k_{a2} approaches E_2, the computed absorption rate constant, k_{a1}, approaches α.

Wagner (6) suggested that even in cases where the one-compartment fit is poor, the ratio of the absorption rate constants calculated for two dosage forms using one-compartment analyses would be a good approximation of the actual ratio of the absorption rate constants. Such a comparison was made using the values in Table I. Table II gives the ratios of the fitted or determined absorption constants using a one-compartment model (k_{a1x}/k_{a1y}) in comparison to the ratio of the actual absorption constants (k_{a2x}/k_{a2y}), followed by a column giving the percent error found in the computer-fitted ratio with respect to the actual ratio. Although the percent error is quite large in some cases, an evaluation of the relative rank merits of different dosage forms can be accurately determined with one-compartment fits, as pointed out by Wagner (6).

SUMMARY

The present work analyzes the information that may be obtained concerning the pharmacokinetics of drug absorption from oral plasma concentration–time curves when no data exist describing drug disposition after intravenous administration. All examples used here describe the absorption process by a single rate constant, although this constant may represent the best fit to limited data for a very complex multistep process.

Sulfisoxazole, a drug following two-compartment kinetics after an intravenous bolus, is infused logarithmically into male rabbits at absorption rates approximately equal to values found for α, β, and E_2 (data determined from intravenous bolus data) in addition to rates between and above these values. When the absorption rate approaches α, the data points yield a curve consistent with the usual two-compartment oral absorption picture where a relatively fast absorption rate constant gives a large hump or nose in the early part of the curve. However, when the absorption rate is close to E_2, the data are best fit by a one-compartment model. Yet, the "absorption rate" calculated from these data will, in fact, be α and will often overestimate the absorption rate constant by more than a factor of 2.

This error in assigning the α-value as the absorption rate constant will occur no matter what calculation method is utilized if no data from other experiments are available (*e.g.*, intravenous studies or studies with drug delivery systems having a markedly different absorption rate). Data points measured after low absorption rates (close to β) will appear to follow a one-compartment model. Although the percent error in calculation of the absorption rate constant may be relatively large, evaluation of the relative rank order of absorption rates will be correct even when the one-compartment model is chosen instead of the correct two-compartment model.

Table II—Comparison of Actual Absorption Rate Constant Ratios for Two-Compartment Data with Ratios Obtained when Data Are Analyzed According to a One-Compartment Model, Utilizing Input and Output Values Given in Table I

k_{a2x}	k_{a2y}	Input Ratio, k_{a2x}/k_{a2y}	Output Ratio, k_{a1x}/k_{a1y}	Error, %
7.2	5.4	1.33	1.84	38.3
7.2	3.6	2.00	3.44	72.0
7.2	1.8	4.00	10.04	151.0
7.2	0.6	12.00	23.55	96.3
5.4	3.6	1.50	1.87	24.7
5.4	1.8	3.00	5.47	82.2
5.4	0.6	9.00	12.82	42.4
3.6	1.8	2.00	2.92	46.1
3.6	0.6	6.00	6.85	14.2
1.8	0.6	3.00	2.34	−21.8

REFERENCES

(1) J. G. Wagner and E. Nelson, *J. Pharm. Sci.*, **52**, 610 (1963).

(2) J. C. K. Loo and S. Riegelman, *ibid.*, **57**, 918 (1968).

(3) A. C. Bratton and E. K. Marshall, *J. Biol. Chem.*, **128**, 537 (1939).

(4) C. Metzler, "A User's Manual for NONLIN," Upjohn Co., Kalamazoo, Mich., Nov. 25, 1969.

(5) J. G. Wagner and C. M. Metzler, *J. Pharm. Sci.*, **58**, 87 (1969).

(6) J. G. Wagner, *ibid.*, **59**, 1049 (1970).

ACKNOWLEDGMENTS AND ADDRESSES

Received September 25, 1975, from the *School of Pharmacy, University of Connecticut, Storrs, CT 06268, and the ‡Department of Pharmacy, School of Pharmacy, University of California, San Francisco, CA 94143.

Accepted for publication March 24, 1976.

Presented in part at the Basic Pharmaceutics Section, APhA Academy of Pharmaceutical Sciences, San Francisco meeting, March 1971.

Supported in part by Program Project Grant GM 16496 and Training Grant GM 00728 from the National Institutes of Health. Dr. Ronfeld is grateful for the support he received as a Fellow of the American Foundation for Pharmaceutical Education and as an NIH Predoctoral Fellow.

ˣ To whom inquiries should be directed. Present address: Astra Pharmaceutical Products, Framingham, MA 01701.

Quantitative Estimation of Particulate Matter in Pharmaceutical Preparations Intended for Intravenous Administration

ANWAR B. BIKHAZI ˣ, JOANNIS A. SHIATIS, and AMIN F. HADDAD

Abstract □ A fast, reproducible, economical, and dependable automated counter method is recommended for the quality control of pharmaceutical preparations intended for intravenous administration. The USP gives no specifications on the limitations of particulate matter in intravenous products, while the BP specifies limitations on intravenous solutions of more than 500-ml volume. Out of 15 different marketed products, few passed the BP specifications. The microscopically identifiable particles included starch, cellulose fibers, glass, rubber, lacquer flakes, carbon black, and metal shavings. The proposed quality control method introduces a modification to the BP specifications. The method includes a standard log–log plot obtainable from a least-squares line fit to the data of the marketed products showing minimal particle contamination. The standard plot is compared to the experimental data obtained from any other product and, accordingly, it is decided whether the product is acceptable or not.

Keyphrases □ Particles—automated counter analysis, intravenous pharmaceutical preparations, proposed as quality control method □ Intravenous dosage forms—automated counter particle analysis proposed as quality control method □ Dosage forms—intravenous pharmaceutical preparations, automated counter particle analysis, proposed as quality control method □ Automated counter—particle analysis, intravenous pharmaceutical preparations, proposed as quality control method

The presence of particulate matter in parenteral preparations for intravenous administration gave rise to three important questions: the nature and origin of particulate matter (1–4), the hazards produced by these particles (5–12), and quality control of such products. Recent investigations (13–23) in this area have not covered quality control. The present work resulted in a quality control method for the analysis of particulate matter in any intravenous preparation.

EXPERIMENTAL

Sample Analysis—An automated counter[1] was employed. The test solutions were placed in carefully washed beakers to eliminate the possibility of contamination. The particulate matter concentrations in the tested products were small enough to allow the particles to pass through the aperture one at a time.

Calibration of Counter—According to a rough estimate of the particle-size distribution of the tested solution, a 30-, 50-, 70-, or 100-μm aperture tube opening was installed into the machine. Standard monosized calibration materials with a size range between 5 and 20% of the aperture diameter were used to estimate the calibration factor, K, calculated by:

$$K = \frac{D}{\sqrt[3]{t}} \qquad \text{(Eq. 1)}$$

where D is the particle diameter, and t is the threshold value setting on the machine.

Materials such as polyvinyl toluene latex (D = 1.87 μm), polystyrene divinyl benzene latex (D = 5.02 μm), and puff ball spores[1] (D = 3.36 μm) were used for calibration of the machine. The particles were dispersed in a particle-free normal saline solution (see *Preparation of Particle-Free Control Stocks*) in a beaker and placed on the counter stand for counting. The desired dilution of the calibration material was used such that at low threshold (t) settings, the machine was counting at a low coincidence factor.

Standard calibration curves were obtained from a plot of the number of particles oversize *versus* threshold. The threshold corresponding to 50% of the number of particles oversize was taken to be proportional to the volume of a sphere whose average diameter was that of the calibration material. The calibration factor, K, was then calculated from Eq. 1. During experimentation, the machine was occasionally recalibrated.

Preparation of Particle-Free Control Stocks—A particle-free stock solution for control experiments was prepared as follows. Nine grams of sodium chloride[2] was dissolved in 1000 ml of distilled water. A stainless filter holder[3] adapted with a 47-mm, 0.45-μm membrane filter[3] and attached to a vacuum flask was used for the filtration. This procedure resulted in the filtration of particulate matter whose diameter exceeded 0.45 μm. The filtrate was refiltered through a newly installed filter until it was almost particle free, as checked microscopically and by the automated counter.

Part of the freshly prepared particle-free stock was used to fill the reservoir of the machine to avoid leakage of particulate matter from the reservoir during flushing of the inner part of the aperture tube. Another part of the particle-free stock solution served to run the baseline control experiments for a particle-free solution. The control study was run in exactly the same manner as the study of the marketed products. The solution was poured into a clean beaker and then placed on the automated counter stand. Aluminum foil was placed around the stand to eliminate electrical noise pickup from the environment. The aperture tube and the outer electrode were then dipped into the solution, and the counts were taken at different thresholds. The counts obtained at specified thresholds from the control stock were considered as background counts and, therefore, were subtracted from the corresponding threshold counts when the marketed products were being counted for adulterated particles. During the experiments, the solution in the beaker was constantly stirred by a stirrer attached to the counter. The rest of the particle-free stock solution was used as a suspending fluid for the calibration material.

Testing Marketed Products for Particulate Matter—Three types of marketed products intended for intravenous administration were studied. First, intravenous infusion fluids packed in plastic bags and in glass containers with lacquered and nonlacquered rubber stoppers were chosen. Products containing an electrically conductive liquid were directly used in the counting process; those containing a nonconductive liquid, such as 5% dextrose solution, were diluted in a 1:1 ratio with 4% particle-free sodium chloride solution.

Second, plastic bags employed for blood collection in blood banks were selected. They contained anticoagulant citrate dextrose solution. Since the label stated that they should be made up to 500 ml with blood, they were diluted in a 1:4 ratio with 0.9% particle-free sodium chloride solution.

Third, powdered unexpired antibiotic products (some of them lyophilized), packed in glass containers with rubber-like stoppers, were randomly selected from the market. These products were dissolved in 250 ml of particle-free normal saline solution, exactly as recommended by the manufacturers.

All of the products were tested for particulate matter utilizing the automated counter and microscopy for possible particle identification. Each container was lightly shaken before opening to assure uniform distribution of particles. A sample of 200 ml was then placed into a very clean beaker for counting. The procedure followed was exactly the same as that described in the previous sections.

Flocculation Experiments—Flocculation experiments were done to study the particle-size distribution of flocculated and deflocculated systems and to correlate the results with those obtained using the mar-

[1] Coulter counter model A, Coulter Electronics, Hialeah, Fla.; puff ball spores were also obtained from Coulter Electronics.

[2] Sodium chloride crystals G.R., E. Merck, Darmstadt, W. Germany.

[3] Millipore Corp., Bedford, MA 01730.

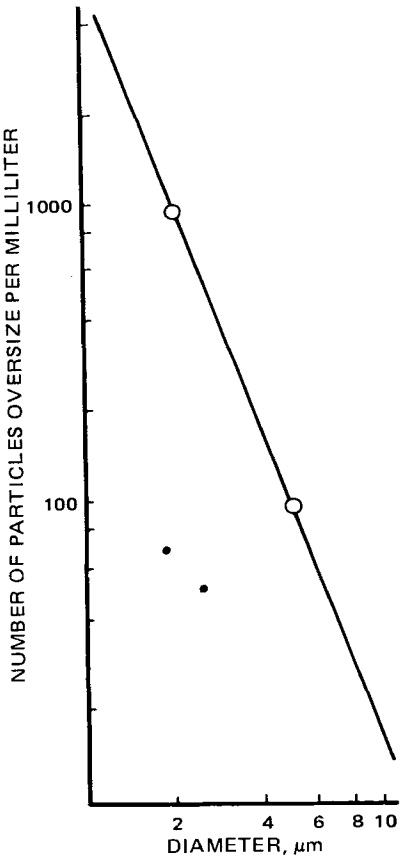

Figure 1—*Logarithmic plot of log (number of particles oversize per milliliter) versus log (diameter) for the extrapolated BP specification.*

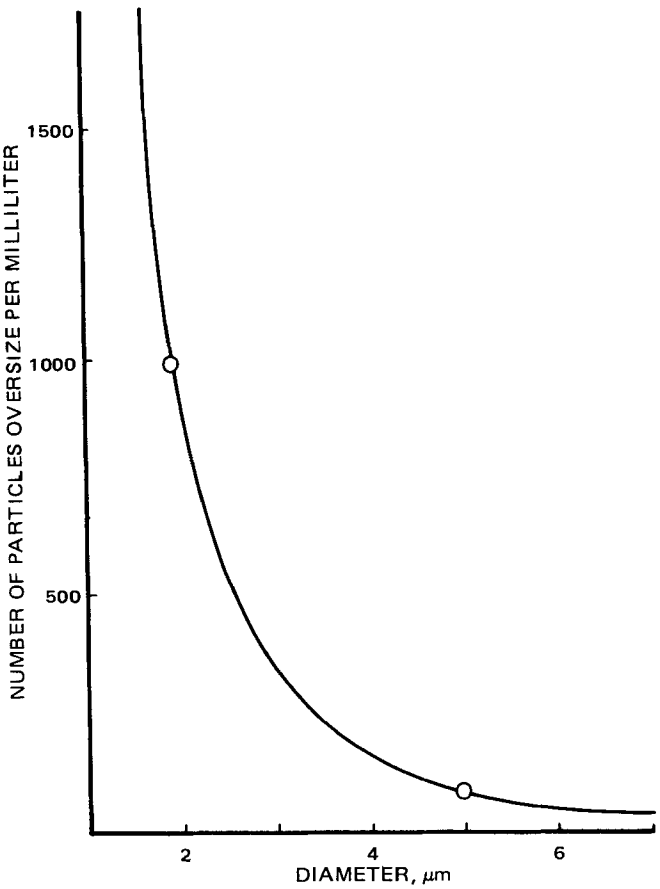

Figure 2—*Rectangular coordinate plot of log (number of particles oversize per milliliter) versus log (diameter) for the extrapolated BP specification.*

keted products. A 0.9% particle-free sodium chloride solution was prepared as described under *Preparation of Particle-Free Stock Solutions.* A small quantity of puff ball spores (D = 3.36 μm) was suspended in 100 ml of this solution with the aid of 2 ml of 1% aqueous dioctyl sodium sulfosuccinate[4] solution. This served as a nonflocculated suspension stock. Then 35 ml of this nonflocculated suspension stock was diluted to 250 ml with particle-free normal saline solution, resulting in a nonflocculated suspension sample for counting. To another 35-ml sample, 10 drops of saturated magnesium chloride[5] solution were added, providing the counterion effect for flocculation. The suspension was then made up to 250 ml with particle-free normal saline solution.

These solutions were gently shaken and left to sediment for a few days. At the time of counting, the suspension was shaken and counted by the automated counter.

Microscopic Identification of Particulate Matter—A 13-mm membrane filter[3] (0.45-μm pore size) adapted to a filter holder[3] was used for the collection of particulate matter. A 10-ml syringe was fitted to the filter holder, and the sample containing particulate matter was poured into the syringe. A vacuum flask attached with a rubber tube to the end of the filter holder was used for the filtration of the solution. The particulate matter was collected on the filter. A filter through which particle-free normal saline solution was filtered was used as a control. The filter was carefully removed from the filter holder, placed in a petri dish, dried in an oven, and then mounted on a slide.

To use transmitted polarized light, it is necessary to make the filter transparent by immersing it in a liquid of the same refractive index as that of the filter. Immersion oil[6] with a refractive index of 1.515 was used. Several drops were placed on a clean glass slide, and the filter was lowered onto the oil drops and allowed to soak up the oil. A scrupulously clean cover glass was placed over the filter. Subsequently, the mounted filters were systematically scanned with a polarizing microscope so that the entire 13-mm diameter filtration area was observed. Finally, a photomicrograph was taken for each sample, using a camera attached to a polarizing microscope[7].

Calculations and Treatment of Data—Groves (14) reported the following log–log relationship between the number of particles oversize *versus* diameter:

$$\log_{10}N = a + k \log_{10}D \qquad \text{(Eq. 2)}$$

Furthermore, the BP reported the following on the limit test of intravenous solutions of more than 500-ml volume: "The mean counts of particles per 1.0 ml do not exceed 1000 equal to or greater than 2 μm and 100 equal to or greater than 5 μm" (24). Application of Eq. 2 to the BP specification would result in a two-point plot on log–log graph paper, namely the points (2, 1000) and (5, 100). The equation of the straight line joining these two points was then deduced to be:

$$\log_{10}N = \log_{10} 5630 - 2.5 \log_{10}D \qquad \text{(Eq. 3)}$$

where N is the number of particles oversize, and D is the diameter. Figure 1 shows the log–log plot of the BP recommendation using Eq. 3. Also, Eq. 3 can be simplified into the following relationship:

$$N = \frac{5630}{D^{2.5}} = \frac{a}{D^b} \qquad \text{(Eq. 4)}$$

Equation 4 is an exponential (to the base D) type of relationship that would fit with any automated counter data when the value of a is 5630 and that of b is 2.5. A rectangular coordinate plot of Eq. 4 is shown in Fig. 2.

RESULTS

The results are presented as graphs. Particulate matter identification and measurement are presented in Table I, which was formulated from the photomicrographs taken of these samples. Because of lack of space, photomicrographs were not included.

[4] Aerosol OT.
[5] E. Merck, Darmstadt, W. Germany.
[6] Cargille type B, Bausch & Lomb Inc., Rochester, N.Y.
[7] Reichert Photo-Automatic, Wien Austria, A1171 Vienna, Austria.

Table I—Compilation of Some Identifiable Particles in the Marketed Products with Their Approximate Sizes[a]

Product[b]	Particles Identified and Size
1H	Rubber (2–100 μm), carbon black (1–5 μm), pigments (1–5 μm), calcium carbonate crystals (2 μm), cellulose fibers (up to 100 μm), glass (5–10 μm), starch grains (10 μm), *etc.*
1G	Carbon black (1–5 μm), starch grains (15 μm), unidentified particles (1–3 μm), *etc.*
1P	Rubber (5–40 μm), carbon black (1–5 μm), lacquer coating (5–100 μm), pigments (3 μm), calcium carbonate crystals (2 μm), *etc.*
1AL	Carbon black (1–5 μm), pigments (1–5 μm), calcium carbonate crystals (2 μm), lacquer flakes (5–50 μm), rubber (5–50 μm), starch grains (8 μm), metal shavings (5 μm), *etc.*
1S	Unidentified particles (1–2 μm), few particle contaminants
2AL	Carbon black (1–10 μm), starch grains (8–15 μm), lacquer flakes (20 μm), rubber (5–100 μm), unidentified particles (1–5 μm), *etc.*
2G	Carbon black (1–3 μm), unidentified particles (1–5 μm), *etc.*
3AL	Carbon black (1–5 μm), pigments (1–3 μm), rubber (5–50 μm), starch grains (15 μm), fibers (100 μm), *etc.*
3G	Unidentified particles (1–3 μm), few particle contaminants
4G	Unidentified particles (1–5 μm)
1E	Unidentified particles (1–5 μm)
1B	Carbon black (1–5 μm), starch grains (10–50 μm), fibers (100 μm), unidentified particles (1–5 μm), *etc.*
4AL	Starch grains (25 μm), carbon black (1–10 μm), fibers (up to 100 μm), unidentified particles (1–4 μm), *etc.*
1A	Unidentified particles (1–5 μm)
2A	Fibers (up to 120 μm), carbon black (1–10 μm), unidentified particles (1–5 μm), *etc.*

[a] Particles identified with help of Ref. 25. [b] For type of formulation, check Figs. 3–14. The letter H after a number signifies a product manufactured by a local hospital in Lebanon. The letter P designates a local Lebanese product, G designates a German product, S designates a Swiss product, B designates a Belgian product, and E designates an Egyptian product. The letter A signifies a United States product, and AL indicates a product manufactured by a United States company under license in a European or Middle Eastern country.

Cumulative Size Distribution in Solutions Intended for Intravenous Administration—Figures 3 and 4 are representative plots on rectangular and logarithmic coordinates for particulate matter in Products 1AL, 1P, and 1S. Similarly, Figs. 5 and 6 are representative rectangular and logarithmic plots for data obtained for Products 1H and 1G. In both plots, a profile was drawn of data obtained on particulate matter existing in the filtrate of Product 1H after filtration through a 0.45-μm membrane filter.

Figures 7 and 8 represent data for Products 2AL and 2G, while Figs. 9 and 10 represent data for anticoagulant citrate dextrose solutions of Products 4G and 1E. Figures 3–10 include a comparison between the results of the marketed products and the smooth curves obtained from the extrapolated BP specifications as already described.

Cumulative Size Distribution in Powdered Antibiotic Products Intended for Intravenous Administration—The dilutions of these products were already discussed. Figures 11 and 12 represent rectangular and logarithmic plots for particulate matter in Products 1B and 4AL containing ampicillin sodium. Figures 13 and 14 are similar plots for Products 1A and 2A for cephapirin sodium and cephalothin sodium, respectively. The smooth curves appearing in Figs. 11–14 are the extrapolated BP limit test plots. The BP does not mention any limit test for the quality control of adulterated particles in antibiotic products.

Cumulative Size Distribution in Deflocculated and Flocculated Puff Ball Spores—Figures 15 and 16 represent typical rectangular and logarithmic plots on deflocculated and flocculated systems. The plots show the monosized distribution in the deflocculated systems and the deviation from monosized distribution in flocculated systems. Similar deviations resulted in the data obtained for some marketed products as shown in Figs. 5–12 and 14.

Microscopic Identification of Particulate Matter in Marketed Products—Table I represents a compilation of most of the identifiable particles, with their approximate sizes, in the tested products.

DISCUSSION

A thorough literature survey revealed that previous findings concerning quantifying and identifying particulate matter in intravenous solutions did not result in substantial recommendations for quality control. There appeared to be agreement that particulate matter in intravenous products was hazardous to patients and that the pharmacopeias should include specific and strict recommendations for its limitations.

Proposed Analysis of Results on Basis of BP Specifications—The advantages of this method of analysis based on the extrapolated BP specifications, as described under *Experimental*, are that it is fast, reproducible, economical, and dependable for the quality control of pharmaceutical preparations intended for intravenous administration. As previously reported, the particle-size distribution of the particulate matter in an intravenous infusion under storage may change with time due to particle aggregation or deaggregation. The BP has given only two specific particle numbers with their corresponding sizes, with no mention of possible aggregation or deaggregation.

The proposed analysis, based on the extrapolated BP limitations, gives a whole range of size distributions, permitting quality control personnel to check possible particle flocculation or deflocculation instantaneously. This check is in addition to a general analysis of the particle-size distribution in the products. A simple comparison analysis was needed. To support this method, Figs. 15 and 16 showed the general trend of the curve for flocculated and deflocculated systems. Any deviation from this curve due to flocculation would result from a change in the particle-size distribution. Therefore, in an intravenous product, any behavior similar to that of these plots could be explained on the basis of particle aggregation or deaggregation.

Recommendations—Some drug companies have been able to produce products for intravenous administration in which the particulate matter is far below BP limitations. Some marketed products, especially the powdered antibiotic products, far exceed the proposed limitations. The comparison of the results obtained in this work with the BP specifications for powdered antibiotic and blood bank bag products was done to show the importance of limitations for the quality control of these pharmaceutical preparations.

Recommendation I—The following model is proposed for all products manufactured for intravenous administration. This model is very arbitrary and flexible and is not mentioned as a replacement for any limitations proposed by a pharmacopeia. The emphasis is directed toward a similar applicability in any quality control laboratory.

Since the particle-size analysis of some marketed products showed low particle contamination and since any limit test is arbitrary, the best products (1G, 1S, and 3G) were used to set out the proposed limit test. The number of particles oversize per 1.0 ml *versus* diameter was plotted on log–log paper (Fig. 17). The best straight line through all points was drawn utilizing the method of least squares (26). The following is the equation of the straight line obtained as a result of the least-squares line method:

$$\ln N = \ln 225 - 1.80 \ln D \qquad \text{(Eq. 5)}$$

where N is the number of particles oversize per 1.0 ml, -1.8 is the slope of the line, D is the particle diameter, and 225 is the intercept when $D = 1$ μm. Equation 5 can be reduced to:

$$N = \frac{225}{D^{1.80}} \qquad \text{(Eq. 6)}$$

A plot of N *versus* D of Eq. 5 on rectangular coordinates is shown in Fig. 18.

The best least-squares line fit shown in Fig. 17 was used in this work as the basis for the proposed limitations. However, some products had particle contaminants (as seen in Fig. 17) that did not pass the specifications. To take this into account, it was suggested that a line be drawn parallel to the least-squares line and that products (1S, 1G, and 3G) fitting this line be considered acceptable. This procedure also took into account flocculated systems where the size distribution caused a change in the linearity of the plot (Fig. 16). The straight line passed through the points (1, 700), (2, 200), (3, 100), and (5, 40). The following is the equation of the straight line passing through these points:

$$\ln N = \ln 700 - 1.80 \ln D \qquad \text{(Eq. 7)}$$

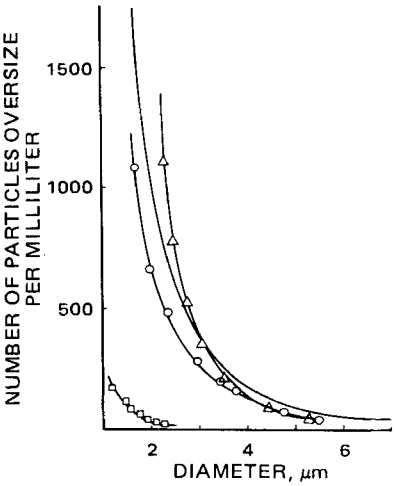

Figure 3—*Cumulative particle-size distribution in 0.9% sodium chloride solutions for injection. Key: △, Product 1AL packed in 500-ml glass containers with lacquer-coated rubber stopper; ○, Product 1P packed in 1-liter glass containers with lacquer-coated rubber stopper; □, Product 1S packed in 500-ml plastic bags; and smooth curve, BP specification.*

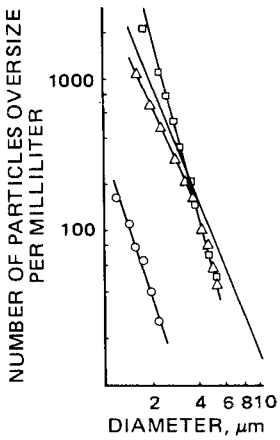

Figure 4—*Logarithmic plot of cumulative particle-size distribution in 0.9% sodium chloride solutions for injection. Key: □, Product 1AL; △, Product 1P; ○, Product 1S; and smooth curve, BP specification.*

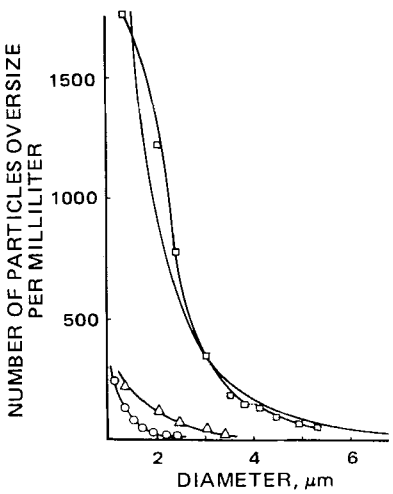

Figure 5—*Cumulative particle-size distribution in 0.9% sodium chloride solutions for injection. Key: □, Product 1H packed in 1-liter glass containers with rubber stopper; △, Product 1H after filtration through a 0.45-μm filter; ○, Product 1G packed in 500-ml plastic bags; and smooth curve, BP specification.*

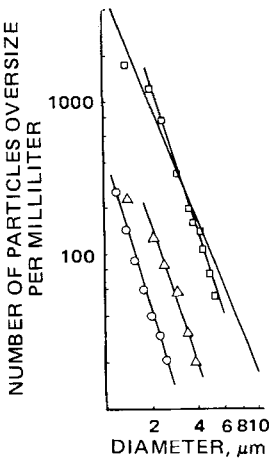

Figure 6—*Logarithmic plot of cumulative particle-size distribution in 0.9% sodium chloride solutions for injection. Key: □, Product 1H; △, Product 1H after filtration; ○, Product 1G; and smooth curve, BP specification.*

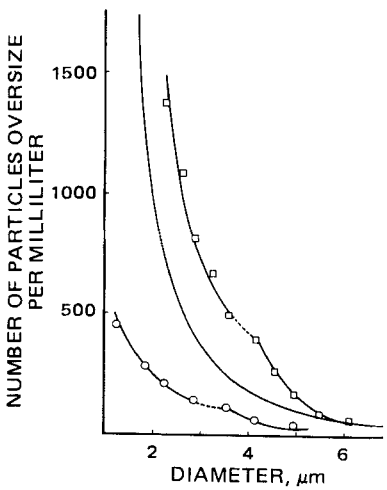

Figure 7—*Cumulative particle-size distribution in 5% dextrose solutions for injection. Key: □, Product 2AL packed in 500-ml glass containers with lacquer-coated rubber stopper; ○, Product 2G packed in 500-ml plastic bags; and smooth curve, BP specification.*

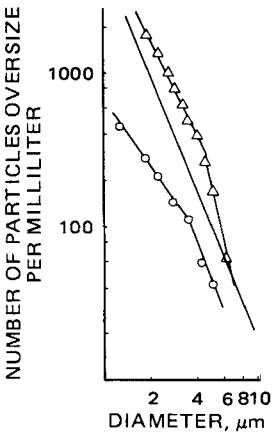

Figure 8—*Logarithmic plot of cumulative particle-size distribution in 5% dextrose solutions for injection. Key: △, Product 2AL; ○, Product 2G; and smooth curve, BP specification.*

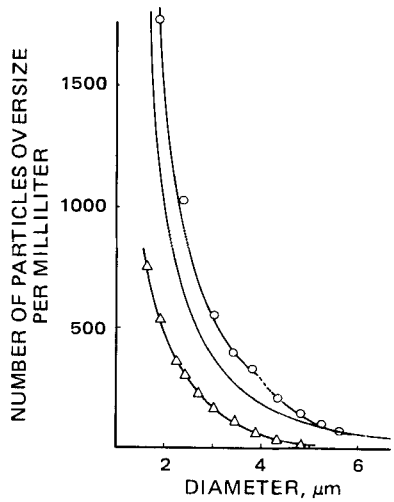

Figure 9—*Cumulative particle-size distribution in anticoagulant citrate dextrose solutions intended for blood collection. Key: ○, Product 4G packed in 500-ml plastic bags; △, Product 1E packed in 500-ml plastic bags; and smooth curve, BP specification.*

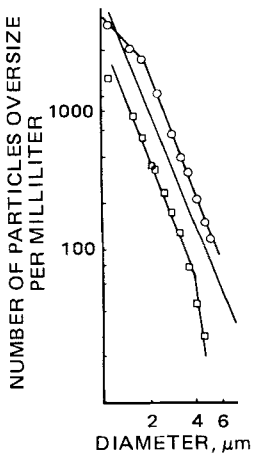

Figure 10—*Logarithmic plot of cumulative particle-size distribution in anticoagulant citrate dextrose solutions intended for blood collection. Key: ○, Product 4G; □, Product 1E; and smooth curve, BP specification.*

Therefore, the proposed limitations should be: "For any product intended for intravenous administration, regardless of its volume, the average counts per 1.0 ml of five to 10 samples should not be more than 700 equal to or greater than 1 μm, 200 equal to or greater than 2 μm, 100 equal to or greater than 3 μm, and 40 equal to or greater than 5 μm."

The plots in Figs. 17 and 18 can be used as standard curves for the quality control of any product intended for intravenous administration, utilizing for counting an electronic counting device that can count the cumulative number of particles in a solution. Five to 10 products from the production line could be randomly picked up and sent to the quality control laboratory. By using a precalibrated counting device with an aperture tube of 30, 50, or 70 μm and counting the number of particles oversize *versus* particle diameter, a similar plot could be drawn. Comparison of the standard plots (Figs. 17 and 18) to the experimentally obtained plot will indicate whether the product is acceptable or not. Such a quality control method will take only a few minutes, provided the machine is kept clean, precalibrated, and ready for use. The handling and maintenance of the machine should not be more difficult than for any equipment utilized in a quality control laboratory.

Recommendation I has the disadvantage that large particles may not be counted by the counter. Microscopic analysis could concurrently be done on the product. This does not mean that microscopic analysis, which is very tedious and time consuming, is a better tool.

Recommendation II—Figures 5 and 6 present the cumulative size distribution of particulate matter when Product 1H was filtered through a 0.45-μm membrane filter. It appeared obvious that the number of particle contaminants was far below the BP specification. Therefore, filtration prior to administration of the product was recommended as an efficient method of removing particulate matter. This could be accomplished by using an in-line final filtration device.

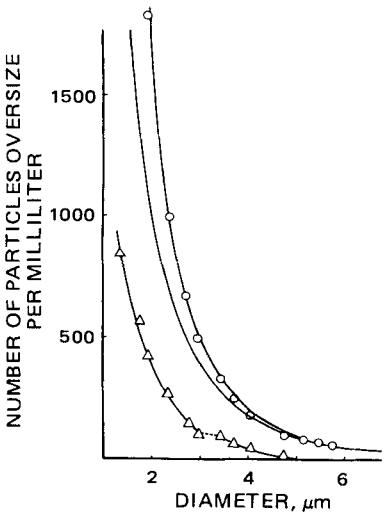

Figure 11—*Cumulative particle-size distribution in injection vials containing ampicillin sodium. Key: ○, Product 1B in 500-mg ampicillin sodium vials; △, Product 4AL in 1-g ampicillin sodium vials; and smooth curve, BP specification.*

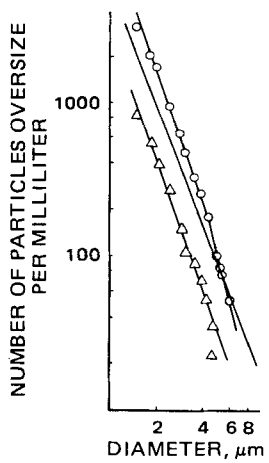

Figure 12—*Logarithmic plot of cumulative particle-size distribution in injection vials containing ampicillin sodium. Key: ○, Product 1B; △, Product 4AL; and smooth curve, BP specification.*

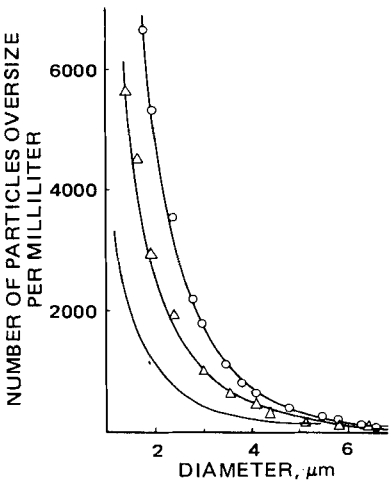

Figure 13—*Cumulative particle-size distribution in injection vials containing cephalothin sodium. Key: △, Product 2A in 1-g cephalothin sodium vials; ○, Product 1A in 500-mg cephapirin sodium vials; and smooth curve, BP specification.*

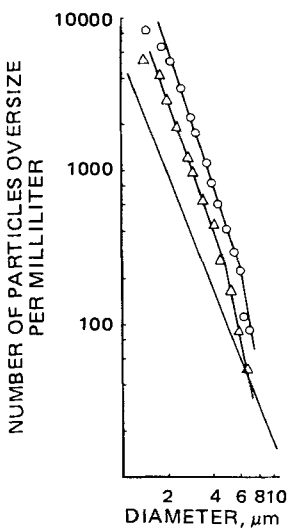

Figure 14—*Logarithmic plot of cumulative particle-size distribution in injection vials containing cephalothin sodium. Key: △, Product 2A; ○, Product 1A; and smooth curve, BP specification.*

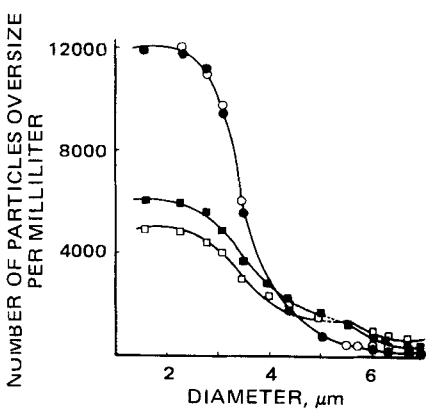

Figure 15—*Cumulative particle-size distribution in flocculated and deflocculated suspensions. Key: ●, deflocculated Suspension A (counts taken after 1 day); ○, deflocculated Suspension B (counts taken after 2 days); ■, flocculated Suspension A; and □, flocculated Suspension B.*

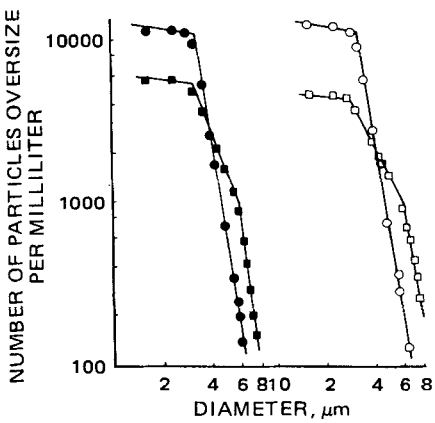

Figure 16—*Logarithmic plot of cumulative particle-size distribution in flocculated and deflocculated suspensions. Key: ●, deflocculated Suspension A; ○, deflocculated Suspension B; ■, flocculated Suspension A; and □, flocculated Suspension B.*

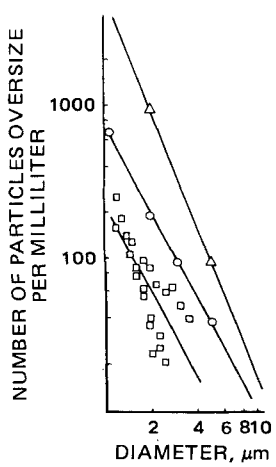

Figure 17—*Cumulative particle-size distribution indicating the least-squares line fit through data points of Products 1G, 1S, and 3G. Key: □, data points for Products 1G, 1S, and 3G; smooth curve, least-squares line; ○, proposed specification; and △, BP specification.*

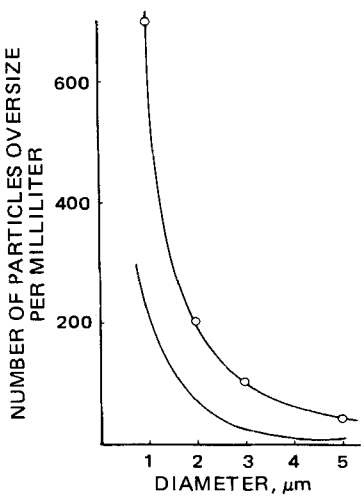

Figure 18—*Plot of number of particles oversize* versus *diameter. Key: smooth curve, least-squares line; and ○, proposed specification to fit* $N = 225/D^{1.8}$.

REFERENCES

(1) E. O. Krueger and T. H. Riggs, *Bull. Parenteral Drug Assoc.*, **22**, 99 (1968).

(2) J. M. Garvan and B. W. Gunner, *Med. J. Austr.*, **50**(2), 140 (1963).

(3) *Ibid.*, **51**(2), 1 (1964).

(4) R. G. Draftz and J. Craf, *Bull. Parenteral Drug Assoc.*, **28**, 35 (1974).

(5) J. S. Dunn, *Q. J. Med.*, **13**, 192 (1920).

(6) L. V. Gardmer and D. E. Cummings, *J. Ind. Hygiene Toxicol.*, **13**, 112 (1931).

(7) J. H. Brewer and J. H. F. Dunning, *J. Am. Pharm. Assoc., Sci. Ed.*, **36**, 287 (1947).

(8) W. E. Stehbeus and H. W. Flory, *Q. J. Exp. Physiol.*, **45**, 252 (1960).

(9) J. D. Lockhardt, in "Proceedings F.D.A. Symposium on Safety of Large Volume Parenteral Solutions," Washington, D.C., July 28–29, 1966.

(10) A. M. Jonas, in *ibid.*

(11) R. V. Moseley and D. B. Doty, *Ann. Surg.*, **171**, 336 (1970).

(12) J. M. Garvan and B. W. Gunner, *Br. J. Clin. Pract.*, **25**, 119 (1971).

(13) J. Vessey and C. E. Kendall, *Analyst*, **91**, 273 (1966).

(14) M. J. Groves, *ibid.*, **94**, 992 (1969).

(15) C. E. Kendall, *Ann. N.Y. Acad. Sci.*, **158**, 640 (1968).

(16) W. L. Nicholson, C. J. Maggiore, and I. J. Selicoff, *Science*, **177**, 171 (1972).

(17) J. Y. Masuda and J. H. Beckerman, *Am. J. Hosp. Pharm.*, **30**, 72 (1973).

(18) G. H. Hopkins and R. W. Young, *Bull. Parenteral Drug Assoc.*, **28**, 15 (1974).

(19) M. J. Groves, *Pharm. J.*, **213**, 581 (1974).

(20) L. Ernerot, *Acta Pharm. Suec.*, **11**, 1 (1974).

(21) R. J. Whitlow, J. E. Needham, and L. A. Luzzi, *J. Pharm. Sci.*, **63**, 1610 (1974).

(22) H. F. Hammer, *Bull. Parenteral Drug Assoc.*, **28**, 205 (1974).

(23) J. Y. Masuda and J. H. Beckerman, *Am. J. Hosp. Pharm.*, **31**, 1189 (1974).

(24) "British Pharmacopoeia 1973," Her Majesty's Stationary Office, London, England, 1973.

(25) W. C. McCrone, R. G. Draftz, and J. G. Delly, "The Particle Atlas," Ann Arbor Science Publishers, Ann Arbor, Mich., 1967.

(26) J. A. Shiatis, M. S. thesis, American University of Beirut, Beirut, Lebanon, 1975.

ACKNOWLEDGMENTS AND ADDRESSES

Received December 9, 1975, from the *School of Pharmacy, American University of Beirut, Beirut, Lebanon.*

Accepted for publication April 5, 1976.

Supported in part by a grant from the University Medical Research Fund, American University of Beirut, Beirut, Lebanon.

[x] To whom inquiries should be directed.

Oxidation Photosensitized by Tetracyclines

JOY ANNE WIEBE and DOUGLAS E. MOORE [x]

Abstract □ Irradiation with 365-nm UV light of aerated aqueous solutions of tetracycline gives rise to oxygen uptake when the pH of the solution is above 7.5. The kinetics of the reaction were followed using a polarographic oxygen electrode at a range of pH values for seven currently prescribed tetracyclines. Variation of tetracycline concentration, UV light intensity, and temperature showed the characteristics normally associated with a sensitized photo-oxygenation mechanism rather than a free-radical process. Copper(II) ions inhibited the photo-oxidation of tetracycline, apparently by complex formation. The tetracyclines were tested for photosensitizing capability with oxidizable acceptors. In aqueous solution, no photosensitizing effect could be seen, but methanol solutions of 2,5-dimethylfuran and *dl*-limonene were oxidized at considerably increased rates when small amounts of tetracyclines were present. This observation has implications for the mechanism of *in vivo* photosensitivity reactions that occur when tetracyclines are taken internally.

Keyphrases □ Tetracyclines, various—photosensitized oxidation, reaction kinetics followed using polarographic oxygen electrode, effect of pH and copper(II) ions □ Photosensitized oxidation—various tetracyclines, reaction kinetics followed using polarographic oxygen electrode, effect of pH and copper(II) ions □ Oxidation, photosensitized—various tetracyclines, reaction kinetics followed using polarographic oxygen electrode, effect of pH and copper(II) ions □ Polarography—determination, rate of oxygen uptake by solutions of various tetracyclines irradiated with UV light, effect of pH and copper(II) ions □ Antibacterial agents—various tetracyclines, photosensitized oxidation, reaction kinetics followed using polarographic oxygen electrode, effect of pH and copper(II) ions

Photosensitivity reactions have been reported for the tetracyclines after exposure of the patient to strong sunlight (1). The phenomenon of "photodynamic action" has been recognized since 1900, when it was discovered that microorganisms can be killed when exposed to light in the presence of oxygen and sensitizing dyes (2). The basic mechanism is the photosensitized oxidation of the adsorbate or substrate by molecular oxygen (3, 4). All tetracycline antibiotics have a strong absorption in the near UV region at about 365 nm, the first requirement for a sensitizer of photodynamic action.

Little information is available, however, concerning the reactions of tetracyclines following absorption of UV light. Chlortetracycline, tetracycline, and oxytetracycline lost significant antibiotic potency when irradiated with visible light in solution with riboflavin, which probably acted as a photosensitizer (5). Leeson and Weidenheimer (6) reinvestigated this system at pH 4.5 and concluded that the loss of tetracycline activity could be suppressed by the addition of ascorbic acid. Thus, an oxidative pathway was implied for degradation of tetracycline after irradiation.

This paper reports a more detailed study of the photooxidation of seven currently prescribed tetracyclines, together with some experiments that indicate that the tetracyclines can act as photosensitizers for the oxidation of suitable acceptor molecules.

EXPERIMENTAL

Samples of tetracycline[1] (I), oxytetracycline[1], doxycycline[1], metha-

[1] Pfizer Laboratories.

REFERENCES

(1) E. O. Krueger and T. H. Riggs, *Bull. Parenteral Drug Assoc.*, **22**, 99 (1968).

(2) J. M. Garvan and B. W. Gunner, *Med. J. Austr.*, **50**(2), 140 (1963).

(3) *Ibid.*, **51**(2), 1 (1964).

(4) R. G. Draftz and J. Craf, *Bull. Parenteral Drug Assoc.*, **28**, 35 (1974).

(5) J. S. Dunn, *Q. J. Med.*, **13**, 192 (1920).

(6) L. V. Gardmer and D. E. Cummings, *J. Ind. Hygiene Toxicol.*, **13**, 112 (1931).

(7) J. H. Brewer and J. H. F. Dunning, *J. Am. Pharm. Assoc., Sci. Ed.*, **36**, 287 (1947).

(8) W. E. Stehbeus and H. W. Flory, *Q. J. Exp. Physiol.*, **45**, 252 (1960).

(9) J. D. Lockhardt, in "Proceedings F.D.A. Symposium on Safety of Large Volume Parenteral Solutions," Washington, D.C., July 28–29, 1966.

(10) A. M. Jonas, in *ibid.*

(11) R. V. Moseley and D. B. Doty, *Ann. Surg.*, **171**, 336 (1970).

(12) J. M. Garvan and B. W. Gunner, *Br. J. Clin. Pract.*, **25**, 119 (1971).

(13) J. Vessey and C. E. Kendall, *Analyst*, **91**, 273 (1966).

(14) M. J. Groves, *ibid.*, **94**, 992 (1969).

(15) C. E. Kendall, *Ann. N.Y. Acad. Sci.*, **158**, 640 (1968).

(16) W. L. Nicholson, C. J. Maggiore, and I. J. Selicoff, *Science*, **177**, 171 (1972).

(17) J. Y. Masuda and J. H. Beckerman, *Am. J. Hosp. Pharm.*, **30**, 72 (1973).

(18) G. H. Hopkins and R. W. Young, *Bull. Parenteral Drug Assoc.*, **28**, 15 (1974).

(19) M. J. Groves, *Pharm. J.*, **213**, 581 (1974).

(20) L. Ernerot, *Acta Pharm. Suec.*, **11**, 1 (1974).

(21) R. J. Whitlow, J. E. Needham, and L. A. Luzzi, *J. Pharm. Sci.*, **63**, 1610 (1974).

(22) H. F. Hammer, *Bull. Parenteral Drug Assoc.*, **28**, 205 (1974).

(23) J. Y. Masuda and J. H. Beckerman, *Am. J. Hosp. Pharm.*, **31**, 1189 (1974).

(24) "British Pharmacopoeia 1973," Her Majesty's Stationary Office, London, England, 1973.

(25) W. C. McCrone, R. G. Draftz, and J. G. Delly, "The Particle Atlas," Ann Arbor Science Publishers, Ann Arbor, Mich., 1967.

(26) J. A. Shiatis, M. S. thesis, American University of Beirut, Beirut, Lebanon, 1975.

ACKNOWLEDGMENTS AND ADDRESSES

Received December 9, 1975, from the *School of Pharmacy, American University of Beirut, Beirut, Lebanon.*

Accepted for publication April 5, 1976.

Supported in part by a grant from the University Medical Research Fund, American University of Beirut, Beirut, Lebanon.

[x] To whom inquiries should be directed.

Oxidation Photosensitized by Tetracyclines

JOY ANNE WIEBE and DOUGLAS E. MOORE [x]

Abstract □ Irradiation with 365-nm UV light of aerated aqueous solutions of tetracycline gives rise to oxygen uptake when the pH of the solution is above 7.5. The kinetics of the reaction were followed using a polarographic oxygen electrode at a range of pH values for seven currently prescribed tetracyclines. Variation of tetracycline concentration, UV light intensity, and temperature showed the characteristics normally associated with a sensitized photo-oxygenation mechanism rather than a free-radical process. Copper(II) ions inhibited the photo-oxidation of tetracycline, apparently by complex formation. The tetracyclines were tested for photosensitizing capability with oxidizable acceptors. In aqueous solution, no photosensitizing effect could be seen, but methanol solutions of 2,5-dimethylfuran and *dl*-limonene were oxidized at considerably increased rates when small amounts of tetracyclines were present. This observation has implications for the mechanism of *in vivo* photosensitivity reactions that occur when tetracyclines are taken internally.

Keyphrases □ Tetracyclines, various—photosensitized oxidation, reaction kinetics followed using polarographic oxygen electrode, effect of pH and copper(II) ions □ Photosensitized oxidation—various tetracyclines, reaction kinetics followed using polarographic oxygen electrode, effect of pH and copper(II) ions □ Oxidation, photosensitized—various tetracyclines, reaction kinetics followed using polarographic oxygen electrode, effect of pH and copper(II) ions □ Polarography—determination, rate of oxygen uptake by solutions of various tetracyclines irradiated with UV light, effect of pH and copper(II) ions □ Antibacterial agents—various tetracyclines, photosensitized oxidation, reaction kinetics followed using polarographic oxygen electrode, effect of pH and copper(II) ions

Photosensitivity reactions have been reported for the tetracyclines after exposure of the patient to strong sunlight (1). The phenomenon of "photodynamic action" has been recognized since 1900, when it was discovered that microorganisms can be killed when exposed to light in the presence of oxygen and sensitizing dyes (2). The basic mechanism is the photosensitized oxidation of the adsorbate or substrate by molecular oxygen (3, 4). All tetracycline antibiotics have a strong absorption in the near UV region at about 365 nm, the first requirement for a sensitizer of photodynamic action.

Little information is available, however, concerning the reactions of tetracyclines following absorption of UV light. Chlortetracycline, tetracycline, and oxytetracycline lost significant antibiotic potency when irradiated with visible light in solution with riboflavin, which probably acted as a photosensitizer (5). Leeson and Weidenheimer (6) reinvestigated this system at pH 4.5 and concluded that the loss of tetracycline activity could be suppressed by the addition of ascorbic acid. Thus, an oxidative pathway was implied for degradation of tetracycline after irradiation.

This paper reports a more detailed study of the photooxidation of seven currently prescribed tetracyclines, together with some experiments that indicate that the tetracyclines can act as photosensitizers for the oxidation of suitable acceptor molecules.

EXPERIMENTAL

Samples of tetracycline[1] (I), oxytetracycline[1], doxycycline[1], metha-

[1] Pfizer Laboratories.

Table I—Initial Rate of Oxygen Uptake by Irradiated Tetracycline Solutions at pH 9.0 and 30°

[Tetracycline], $M \times 10^4$	Initial Rate[a], moles/liter/min $\times 10^6$	Transmittance[b] at 373 nm, %
0.5	1.7 ± 0.2	17.8
1.0	3.5 ± 0.1	3.2
1.5	5.3 ± 0.3	<0.01
3.0	5.8 ± 0.2	<0.01
5.0	5.8 ± 0.2	<0.01
6.0	5.7 ± 0.3	<0.01
10.0	5.4 ± 0.2	<0.01

[a] Mean of at least three determinations from initial slope of P_{O_2} recorder trace. [b] Calculated for 1-cm path length and molar absorptivity of $1.5 \times 10^4 M^{-1}$ cm^{-1} at pH 9.0.

cycline[1], chlortetracycline[2], demeclocycline[2], and minocycline[2] of the purest grade available commercially were used without further purification. The absorbance ratio method of McCormick *et al.* (7) showed that the purity of tetracycline, oxytetracycline, and chlortetracycline was at least 99%.

Rates of oxygen uptake by solutions irradiated by UV light were determined using the polarographic oxygen electrode apparatus described previously (8). In the procedure used, 2 ml of freshly prepared solution of I in buffer was mixed with 200 ml of air-saturated buffer solution before filling the reaction vessel. Buffers (0.05 *M*) were prepared in double-distilled water using analytical grade materials as follows: pH 4.0–4.9, acetate; pH 6.0–8.4, phosphate; pH 9.0, tromethamine; and pH 10.0–10.8, carbonate.

For experiments in which the tetracyclines were tested as photosensitizers, benzyl alcohol[3], benzaldehyde[3], *dl*-limonene[4], and 2,5-dimethylfuran[5] were purified by distilling twice under high vacuum in an all-glass apparatus at room temperature. Sodium xanthine[6], α-tocopherol[6], *dl*-tyrosine[6], and *l*-phenylalanine[6] were used as received. Limonene, dimethylfuran, and α-tocopherol are almost insoluble in aqueous systems, so experiments with these compounds were performed in methanol solution.

The rate data were recorded with the oxygen electrode operating successfully in methanol, although it was designed for operation in aqueous phases only (9). The validity of oxygen uptake data measured in methanol solution was verified by experiments with benzaldehyde for which the mechanism is known (8). Moreover, the stability of the oxygen electrode and the reproducibility of readings were greatly improved in methanol solutions; this finding may be attributed to the greater concentration of oxygen in air-saturated methanol ($2.06 \times 10^{-3} M$) compared to air-saturated water ($2.35 \times 10^{-4} M$) at 30° (10).

RESULTS

Preliminary Measurements with Tetracycline—The rate of oxygen uptake by UV-irradiated I in solution was examined over pH 4.0–10.8. No significant oxygen uptake occurred below pH 8, although there were changes in absorbance[7] at pH 4 and 5 in the 240–280-nm range, corresponding to epimerization (11). The loss of antibiotic activity of irradiated I reported (6) at pH 4.5 is thus largely due to epimerization, which occurs only between pH 2 and 6 (11).

During irradiation at pH 9.0, oxygen consumption was accompanied by color change of the solution from yellow to pink, red, or brown (depending on the extent of oxidation), with the appearance of a broad absorption centered at 530 nm. The absorbance decreased at 373 nm, which is the λ_{max} for I at pH 9.0, and disappeared completely if irradiation was continued. There was no absorption in the 400–450-nm region, indicating that neither acid degradation product (12) (anhydrotetracycline or epianhydrotetracycline) was formed during photo-oxidation. The oxygen uptake from irradiated I solutions continued (at a much reduced rate) after the lamp had been switched off, indicating that the product(s) of I photo-oxidation are labile. Analysis of these solutions with iodine immediately after irradiation produced no evidence of peroxides.

[2] Lederle Laboratories.
[3] British Drug Houses, Poole, England.
[4] Eastman Kodak, Rochester, N.Y.
[5] Fluka AG, Switzerland.
[6] Nutritional Biochemicals Corp., Cleveland, Ohio.
[7] Varian Techtron model 635 UV-visible spectrophotometer.

Table II—Effect of Edetate Disodium and Copper(II) Ions on Tetracycline Photo-Oxidation at pH 9.0 and 30°[a]

[Edetate Disodium], $M \times 10^5$	[Cu^{2+}], $M \times 10^5$	Initial Rate, moles of Oxygen/liter/min $\times 10^6$
0	0	3.5 ± 0.1
10	0	3.5 ± 0.2
0	1.0	2.2 ± 0.1
0	2.5	1.46 ± 0.10
0	5.0	1.17 ± 0.10
0	40	0.1 ± 0.1

[a] [Tetracycline] = $10^{-4} M$ in all experiments.

Correlation of the amount of oxygen consumed with the depletion of I, as indicated by the spectral change at 373 nm, established that 1.06 ± 0.08 moles of oxygen reacted per mole of I. These experiments were performed at two concentrations of I; to keep secondary reactions to a minimum, irradiation was continued until no more than 15% of the dissolved oxygen was consumed.

To test for general acid or base catalysis by the buffer components, a characteristic of the epimerization reaction (7), the irradiation of I was performed at pH 9.0 in: (*a*) 0.05 *M* tromethamine buffer, (*b*) 0.05 *M* carbonate buffer, and (*c*) unbuffered solution adjusted to pH 9.0 with 1 *M* NaOH solution. After 20 min of irradiation, the pH of the unbuffered solution had fallen to 8.6 but the initial rate of oxygen uptake was the same for all three solutions, indicating that there is no participation by the buffers in the reaction nor any effect of ionic strength.

Temperature variation over 25–40° showed that the reaction rate was independent of temperature. The incident light intensity was varied as previously described (8), and the reaction rate was directly dependent. Both these observations are characteristic of a primary photochemical process rather than a free radical chain mechanism (13).

Variation of Tetracycline Concentration—Table I shows the measured initial rate of oxygen uptake as the I concentration was varied from 5×10^{-5} to $10^{-3} M$. Straight-line (*i.e.*, zero-order) recorder traces of oxygen pressure (P_{o_2}) *versus* time were obtained for $[I] \geq 10^{-4} M$. Below $10^{-4} M$, the traces were curved, but straight lines were obtained for plots of log P_{o_2} *versus* time. The solubility of oxygen in dilute buffer is $2.35 \times 10^{-4} M$ (10), so I concentration was rate limiting here and the rate can be said to be first order in I concentration. At the lower I concentrations, the rate was proportional to [I]; above $3 \times 10^{-4} M$, the light intensity was the limiting factor, as indicated by the percent transmittance values given in Table I. This effect also was observed previously (5, 6).

Effect of Edetate Disodium and Copper on Tetracycline Photo-Oxidation—It is well known that traces of metal ions catalyze radical chain oxidation (14) and that I complexes with many metal ions (15). The experiments summarized in Table II showed that the addition of edetate disodium to the buffer had no effect on the photo-oxidation rate, indicating that there are no accelerating effects of trace metal ions. The addition of copper(II) ions, however, led to a decrease in rate, indicating that complexed I is not susceptible to photo-oxidation. The fact that a complex was formed was indicated by a shift in the absorption maximum of I from 373 to 405 nm. The absorbance of the complex at 365 nm (the wavelength of maximum output of the UV lamp) remained sufficient to initiate photo-oxidation, provided that the complex was susceptible.

Comparative Study of Seven Tetracyclines—The initial rates of photo-oxidation for seven tetracyclines at a range of pH values are recorded in Table III. Minocycline showed little reactivity under the present conditions; methacycline also reacted more slowly than the other five tetracyclines. In general, the reaction rate was at a minimum at neutral pH and increased as the alkalinity of the solution was raised. Doxycycline showed a maximum oxidation rate at pH 9.0, while tetracycline exhibited a similar maximum at pH 10.0.

The UV spectral changes described earlier for tetracycline were observed for the other members of the group, the extent of the change in the 360–380-nm peak being directly proportional to the oxygen uptake. Chlortetracycline alone had a significant dark reaction, not involving oxygen uptake but involving a 10% reduction in absorbance of the 380-nm peak at pH 9.0 in 1 hr, the time course of the photo-oxidation reaction. Hughes and Wilson (16) showed that isochlortetracycline forms upon heating alkaline solutions of chlortetracycline while other tetracyclines are less labile in this respect.

Tetracyclines as Photosensitizers—The fact that I is the primary UV-absorbing species for its own photo-oxidation suggests that it may

Table III—Initial Rates of Photo-Oxidation of Tetracyclines at 30° and Various pH Values

Compound	Concentration, $\times 10^4 M$	Initial Rate[a] of Oxygen Uptake (moles/liter/min $\times 10^6$) at pH 6.0	pH 7.0	pH 8.0	pH 9.0	pH 10.0	pH 10.8
Tetracycline	0.5	0	0.23	0.82	1.72	2.08	1.67
	2.0	0	0.24	1.40	5.3	6.2	4.4
Oxytetracycline	0.5	0	0.10	0.60	1.44	1.76	—
	2.0	0	0.24	1.35	3.1	4.2	—
Chlortetracycline	0.5	0	0.32	1.02	1.70	1.84	—
	2.0	0	0.89	1.6	3.3	4.2	—
Demeclocycline	0.5	0	0.22	0.8	1.33	2.22	—
	2.0	0	0.55	1.3	2.32	4.1	—
Doxycycline	0.5	0	0.66	1.4	1.68	1.12	—
	2.5	0	0.82	3.1	4.3	1.96	—
Methacycline	0.5	0	0.20	0.32	0.51	0.82	—
	2.0	0	0.32	0.73	1.20	1.32	—
Minocycline	0.5	0	<0.1	0.14	0.20	0.30	—
	2.0	0	<0.1	0.18	0.32	0.40	—

[a] Mean of three determinations from initial slope of P_{O_2} recorder trace.

be capable of sensitizing the photo-oxidation of other molecules. Various concentrations (10^{-5}–10^{-4} M) of I were tested for sensitizing capability with the following systems:

System 1—Benzyl alcohol or benzaldehyde (2×10^{-2} M) in aqueous solution at pH 4.0 and 9.0, as representative of compounds susceptible to free radical oxidation (8).

System 2—Xanthine, phenylalanine, or tyrosine (10^{-2} M) in aqueous solutions at pH 6.0 and 8.0. Both purines (17) and aromatic amino acids (18) undergo sensitized photo-oxidation in alkaline solution.

System 3—α-Tocopherol (2×10^{-2} M), a natural antioxidant that undergoes both free radical autoxidation (19) and dye-sensitized photo-oxidation (20) in methanol solution.

System 4—2,5-Dimethylfuran or *dl*-limonene in methanol solution. These agents were used (21, 22) previously as model compounds in dye-sensitized photo-oxygenations and chemical oxygenations to test for the participation of singlet molecular oxygen.

For Systems 1–3, the oxygen uptake upon irradiation was very slight and corresponded to that recorded in control experiments with I or substrate alone. Dimethylfuran and limonene, however, were oxidized significantly in the presence of all tetracyclines except minocycline (Table IV). A 10-fold change in [I] produced less than double the rate of limonene oxidation, while the doubling of doxycycline increased the rate of dimethylfuran oxidation by only 6%. Also, the absorbance of the reaction mixtures at 370 nm decreased by only about 2%, and the tetracyclines by themselves in methanol did not absorb measurable amounts of oxygen in the time course of the irradiation (1 hr). These observations establish the role of the tetracyclines as photosensitizers.

Table IV—Photo-Oxidation of Limonene and 2,5-Dimethylfuran in Methanol Solution Sensitized by Tetracyclines at 30°

Sensitizer	Concentration $\times 10^4 M$	Substrate Concentration, M	Rate of Oxygen Uptake, moles/liter/min $\times 10^6$
	Limonene		
None	—	0.062	0.2
Tetracycline	0.1	0.062	1.8
Tetracycline	1.0	0.062	3.2
Oxytetracycline	1.0	0.062	2.1
Doxycycline	1.0	0.062	2.4
Chlortetracycline	1.0	0.062	3.8
Demeclocycline	1.0	0.062	3.7
Methacycline	1.0	0.062	2.6
Minocycline	1.0	0.062	0.5
	2,5-Dimethylfuran		
None	—	0.038	<0.2
Tetracycline	0.5	0.038	3.4
Tetracycline	0.5	0.055	4.2
Tetracycline	0.5	0.104	7.5
Oxytetracycline	0.5	0.055	2.7
Doxycycline	0.5	0.055	2.0
Doxycycline	1.0	0.055	2.2
Chlortetracycline	0.5	0.055	3.5
Demeclocycline	0.5	0.055	3.6
Methacycline	0.5	0.055	2.8
Minocycline	0.5	0.055	1.2

DISCUSSION

The major kinetic characteristics observed for the photo-oxidation of I in aqueous alkaline solution may be summarized as follows: (*a*) dependence on [I] only at low concentrations, (*b*) direct dependence on incident light intensity, (*c*) independence of temperature, and (*d*) use of oxygen in a 1:1 stoichiometry with I. These are the characteristics of a photosensitized oxygen addition or photo-oxygenation process (2) rather than of a free radical chain mechanism such as occurs with benzaldehyde (8).

The structures of the tetracyclines in this study are given in Table V together with the known pKa values. While it is difficult to correlate differences in structure with the differences in photo-oxidative reactivity, the rate variation with pH is clearly related to the state of ionization of the tetracyclines in mildly alkaline solution and is similar to the pH profile observed for the photo-oxidation of several aromatic amino acids (18). The pKa values are attributed (23) respectively to the tricarbonyl system of ring A (pK_1), the dimethylammonium function of ring A (pK_2), and the phenolic β-diketone system in the C-10–11–12 region (pK_3). From the pKa values, I is said to exist as a zwitterion at neutral pH and increasingly as the monoanion as the pH is raised above 8. On this basis, the monoanion would appear to be the reactive species.

The photo-oxidation reaction is accompanied by a loss of the absorption peak at about 370 nm, which is due to the chromophore grouping in the BCD ring (7, 24) containing the ionizable system corresponding to pK_3. The dissociation of this group is essentially unaffected by the 7-chloro substitution, but it is not known whether the different substituents

Table V—Structures and pKa Values of Tetracyclines

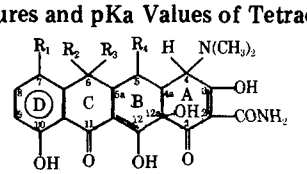

Name	R_1	R_2	R_3	R_4	pK_1	pK_2	pK_3	Reference
Tetracycline	H	CH_3	OH	H	3.30	7.68	9.69	23
Chlortetracycline	Cl	CH_3	OH	H	3.30	7.44	9.27	23
Oxytetracycline	H	CH_3	OH	OH	3.27	7.32	9.11	23
Doxycycline	H	CH_3	H	OH	3.4	7.7	9.7	30
Demeclocycline	Cl	H	OH	H	3.30	7.16	9.25	31
Methacycline	H	—CH_2—		OH	—	—	—	—
Minocycline	$N(CH_3)_2$	H	H	H	—	—	—	—

in methacycline and minocycline cause a significant alteration in the pK value and, therefore, the concentration of the monoanion. There is no marked difference in the absorption peak at 370 nm for all tetracyclines studied here.

The addition of copper(II) ions shifts the 370-nm absorption to longer wavelength and renders the complex stable to photo-oxidation at pH 9.0. This tends to implicate the C-10–11–12 grouping as the binding site for metal ions. Mitscher *et al.* (24) concluded, from optical rotatory dispersion studies, that chelation occurred first in the BCD ring and then in the A ring as the pH was raised above 10. Williamson and Everett (25) recently suggested, on the basis of NMR studies in dimethyl sulfoxide, that the tricarbonylmethane function of ring A is the chelating group, but the solvent difference may give rise to a different binding behavior.

The decreased rate of photo-oxidation above pH 10.0 for I and pH 9.0 for doxycycline are not easily attributable to the decrease in the concentration of the monoanion in solution; if the monoanion is the only oxidizable species of I, the maximum rate should occur at pH 8–9, where its concentration would be at a maximum on the basis of the pK values.

The demonstration that the tetracyclines are capable of acting as photosensitizers for the oxygenation of suitable acceptor molecules has relevance to the photosensitivity reactions observed following the ingestion of I and its analogs. Dimethylfuran and limonene are acceptors (A) of energy transferred from $^1O_2$, the excited singlet molecular oxygen (21). This implies that excited I is capable of interacting with $^3O_2$ (ground-state triplet oxygen) to give singlet oxygen according to Scheme I.

$$(I) \xrightarrow{h\nu} (I)^*$$

$$(I)^* + {}^3O_2({}^3\textstyle\sum_g^-) \rightarrow (I) + {}^1O_2({}^1\Delta_g)$$

$$^1O_2 + A \rightarrow AO_2$$

Scheme I

This phenomenon has been principally studied using dyes that absorb in the visible region, such as methylene blue or rose bengal, since the energy difference between the triplet oxygen ground state and the singlet excited state is only 92 kJ (22 kcal), which corresponds to a wavelength of 1270 nm (21). It also usually requires that the dye pass to the excited triplet state, which has a longer lifetime in which to effect the energy transfer.

Foote (26) stated that if the oxidation proceeds purely through singlet oxygen as an intermediate, it should produce the same rate for all acceptors at constant sensitizer and oxygen concentrations. Thus, the similarity in rates observed with limonene and dimethylfuran is in agreement with this concept. No photosensitizing capability of I could be demonstrated in aqueous solution, so it is clear that the acceptor or substrate molecule and solvent medium have to be specifically matched to the sensitizer for greatest efficiency. Young *et al.* (27) suggested that the lifetime of singlet oxygen in photosensitized oxidations increases as the polarity decreases. This aspect could not be tested, since the amino acids and purines are insufficiently soluble in methanol and limonene and dimethylfuran are insoluble in water.

Reports of *in vivo* photosensitivity have implicated demeclocycline more frequently than the other members of the group (28, 29). The results in Table IV indicate some differences in photosensitizing efficiency, with demeclocycline, chlortetracycline, and tetracycline being the most efficient. The relative inactivity of minocycline is due to a shift of the λ_{max} in methanol solution to 345 nm, so that its molar absorptivity at 365 nm is approximately half that of the other tetracyclines. The investigation is continuing with systems that can be related more closely to the skin.

REFERENCES

(1) E. Stempel and R. Stempel, *J. Am. Pharm. Assoc.*, **NS13,** 200 (1973).

(2) H. H. Seliger and W. D. McElroy, "Light: Physical and Biological Action," Academic, New York, N.Y., 1965, p. 324.

(3) J. D. Spikes and R. Straight, *Ann. Rev. Phys. Chem.*, **18,** 409 (1967).

(4) R. P. Wayne, "Photochemistry," Butterworths, London, England, 1970, p. 190.

(5) J. Dony-Crotteux, *J. Pharm. Belg.*, **12,** 179 (1957).

(6) L. J. Leeson and J. F. Weidenheimer, *J. Pharm. Sci.*, **58,** 355 (1969).

(7) J. R. D. McCormick, S. M. Fox, L. L. Smith, B. A. Bitler, V. E. Origoni, W. H. Muller, R. Winterbottom, and A. P. Doerschuk, *J. Am. Chem. Soc.*, **79,** 2849 (1957).

(8) D. E. Moore, *J. Pharm. Sci.*, **65,** 1447 (1976).

(9) L. C. Clark, *Trans. Am. Soc. Artif. Intern. Organs*, **2,** 41 (1956).

(10) *Int. Crit. Tables*, **3,** 262 (1928).

(11) D. A. Hussar, P. J. Niebergall, E. T. Sugita, and J. T. Doluisio, *J. Pharm. Pharmacol.*, **20,** 539 (1968).

(12) K. D. Schlecht and C. W. Frank, *J. Pharm. Sci.*, **62,** 258 (1973).

(13) J. G. Calvert and J. N. Pitts, Jr., "Photochemistry," Wiley, New York, N.Y., 1966, pp. 645, 651.

(14) J. E. Carless and J. R. Nixon, *J. Pharm. Pharmacol.*, **9,** 963 (1957).

(15) J. T. Doluisio and A. N. Martin, *J. Med. Chem.*, **6,** 16, 20 (1963).

(16) D. W. Hughes and W. L. Wilson, *Can. J. Pharm. Sci.*, **8,** 67 (1973).

(17) M. I. Simon and H. Van Vunakis, *Arch. Biochem. Biophys.*, **105,** 197 (1964).

(18) C. Hasselman and G. Laustrait, *Photochem. Photobiol.*, **17,** 275 (1973).

(19) A. S. Csallany, M. Chui, and H. H. Draper, *Lipids*, **5,** 63 (1970).

(20) G. W. Grams and R. M. Inglett, *ibid.*, **7,** 442 (1972).

(21) C. S. Foote, *Acc. Chem. Res.*, **1,** 104 (1968).

(22) K. Gollnick and G. O. Schenck, *Pure Appl. Chem.*, **9,** 507 (1964).

(23) C. R. Stephens, K. Murai, K. J. Brunings, and R. B. Woodward, *J. Am. Chem. Soc.*, **78,** 4155 (1956).

(24) L. A. Mitscher, A. C. Bonacci, and T. D. Sokoloski, *Antimicrob. Ag. Chemother.*, **1968,** 78.

(25) D. E. Williamson and G. W. Everett, Jr., *J. Am. Chem. Soc.*, **97,** 2397 (1975).

(26) C. S. Foote, *Science*, **162,** 963 (1968).

(27) R. H. Young, K. Wehrly, and R. L. Martin, *J. Am. Chem. Soc.*, **93,** 5774 (1971).

(28) A. Marten, in "Side Effects of Drugs," vol. 6, L. Meyler and A. Herxheimer, Eds., Excerpta Medica Foundation, Amsterdam, The Netherlands, 1968, p. 280.

(29) W. P. Coleman and V. J. Derbes, in "Drug Induced Clinical Toxicity," F. G. McMahon, Ed., Futura Publishing, Mount Kisco, N.Y., 1974, p. 126.

(30) C. R. Stephens, K. Murai, H. H. Rennhard, L. H. Conover, and K. J. Brunings, *J. Am. Chem. Soc.*, **80,** 5324 (1958).

(31) L. Z. Benet and J. E. Goyan, *J. Pharm. Sci.*, **54,** 983 (1965).

ACKNOWLEDGMENTS AND ADDRESSES

Received December 29, 1975, from the *Department of Pharmacy, University of Sydney, Sydney 2006, Australia.*

Accepted for publication March 24, 1976.

Presented at the Australian Pharmaceutical Science Association, National Seminar, Melbourne, November 1975.

Samples of tetracyclines were donated by Pfizer Laboratories and Lederle Laboratories.

J. A. Wiebe acknowledges support from the Australian Commonwealth Scholarship Scheme.

[x] To whom inquiries should be directed. Present address (until August 1977): Section of Biochemistry and Molecular Biology, Cornell University, Ithaca, NY 14853.

Identification of Nonpolar Methotrimeprazine Metabolites in Plasma and Urine by GLC–Mass Spectrometry

SVEIN G. DAHL *x and MATS GARLE ‡

Abstract □ Two metabolites of methotrimeprazine, the sulfoxide and the demethylated analog, were identified in extracts from patient plasma by combined GLC–mass spectrometry. Methotrimeprazine and its sulfoxide had similar mass spectra but different GLC retention times. In addition to the metabolites found in plasma, two other metabolites, the didesmethyl analog and the monodesmethyl sulfoxide, were identified in a urine extract.

Keyphrases □ Methotrimeprazine and metabolites—GLC–mass spectral analysis, human plasma and urine □ GLC–mass spectrometry—analysis, methotrimeprazine and four metabolites, human plasma and urine □ Phenothiazines—methotrimeprazine and four metabolites, GLC–mass spectral analysis, human plasma and urine □ Analgesics—methotrimeprazine and four metabolites, GLC–mass spectral analysis, human plasma and urine

Information about plasma levels of the phenothiazine drug methotrimeprazine[1] (I) and a metabolite (IV) recently was published (1). The biological half-life of I appeared similar to that of its congener chlorpromazine (2), and the apparent volume of distribution (V_β or $V_{d,area}$) appeared somewhat larger. A striking observation was that the plasma levels of the sulfoxide (IV) were about twice as high as the levels of I after oral drug administration. *In vitro* studies later demonstrated that IV must be considered pharmacologically active with regard to cardiac effects, differing in this respect from the corresponding metabolite of chlorpromazine (3).

The plasma levels of I and IV were measured by a GLC method based on flame-ionization detection (4), and the probable identity of the extracted compounds with I and IV was shown by their GLC retention times. The present study was carried out to ascertain the identity of the compounds extracted from plasma by combined GLC–mass spectrometry. A urine extract was analyzed by the same procedure to verify that the metabolites excreted were identical to the corresponding reference compounds.

The molecular formulas of I and its monodesmethyl (II), didesmethyl (III), sulfoxide (IV), and monodesmethyl sulfoxide (V) metabolites are shown in Scheme I.

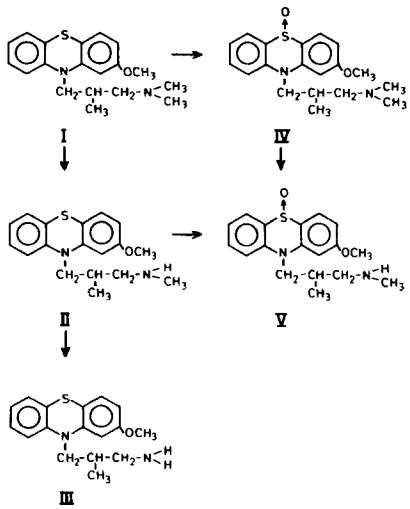

Scheme I

EXPERIMENTAL

Standard Solutions—Reference samples were supplied by various companies[2,3]. Compounds I, III, and IV were dissolved in heptane containing 1.5% isopentyl alcohol; the bases of II and V were extracted from 0.5 ml of 5% NaOH into 10 ml of the same heptane–isopentyl alcohol mixture.

Blood and Urine Sampling—Blood and urine were collected from four somatically healthy psychiatric patients treated with I tablets for at least 4 weeks, without any additional medication. Subjects 1 and 2 were females, 49 and 43 years old, respectively; Subjects 3 and 4 were males, 46 and 38 years old, respectively. Blood samples were collected 3 and 5 hr after the morning dose and immediately centrifuged, and the plasma was frozen and kept at −24°. Urine was collected before and 5 hr after the morning dose and kept at −24° until analyzed.

Extraction and GLC—The plasma concentrations of I and IV were determined by a GLC method (4) prior to the GLC–mass spectral analysis. The urine concentrations of I, II, and IV were determined by the same procedure but without the internal standard, using peak heights for quantitation.

The plasma and urine extracts analyzed by GLC–mass spectrometry were obtained by the same extraction procedure. For each patient, two 4.5–6-ml aliquots of the plasma sample containing the highest sulfoxide concentrations (Table I) were extracted simultaneously, and the organic phases from the two aliquots of plasma were combined before evaporation to dryness. A 6-ml aliquot of urine from Subject 1, collected 5 hr after the morning dose, was extracted by the same procedure.

GLC–Mass Spectrometry—The evaporated extracts from plasma or urine were dissolved in 10 μl of heptane containing 20% isopentyl alcohol, and 4 μl of this solution was analyzed on a computerized GLC–mass spectrometer[4] (5). The gas chromatograph was equipped with a 120-cm silanized glass column, 2 mm i.d., packed with 3% OV-17 on 80–100-mesh Gas Chrom Q. The injector and column temperatures were 255 and 242°, respectively; the flow rate of helium carrier gas was 30 ml/min. The ionizing potential, trap current, and accelerating voltage were 20 ev, 60 μamp, and 3.5 kv, respectively; the temperatures of the separator and ion source were 270 and 290°, respectively.

Mass spectra were obtained by repetitive scanning over the mass range of *m/e* 10–500 every 2.9 sec and stored in the external memory of the computer. The scan speed was 0.8 sec/spectrum. Gas chromatograms showing total ion current as a function of scan number and mass chromatograms showing the intensity of particular ions as a function of scan number were later generated by the computer.

RESULTS

Reference Samples—The relative retention times of I, II, III, IV, and V were 1, 1.25, 1.40, 3.95, and 4.70, respectively, in the GLC system connected to the mass spectrometer.

Mass spectra of reference samples of I, II, and IV are shown in Fig. 1. The mass spectrum of IV, which was similar to that of I, contained only traces (relative intensity 0.2%) of the molecular ion (*m/e* 344). The base

[1] Known as levomepromazine in Europe.
[2] Société des Usines Chimiques Rhône-Poulenc, 94, Vitry-sur-Seine, France.
[3] AB Mekos, Helsingborg, Sweden.
[4] LKB 9000, LKB, Stockholm, Sweden.

Table I—Dosages and Concentrations of Methotrimeprazine and Metabolites in Plasma 3 and 5 hr after, and in Urine before (0 hr) and 5 hr after, Administration of the Morning Dose

Subject	I Dose, mg		Plasma Concentration, ng/ml				Urine Concentration, ng/ml					
			I		IV		I		II		IV	
	Morning	Evening	3 hr	5 hr	3 hr	5 hr	0 hr	5 hr	0 hr	5 hr	0 hr	5 hr
1	100	200	59	36	257	163	135	432	220	850	4,510	4081
2	200	200	141	135	231	336	500	—	555	—	10,594	—
3	175	175	76	66	389	237	175	371	345	857	5,359	7714
4	100	200	51	61	208	353	84	125	128	150	4,414	2120

peak in both mass spectra had mass number 58, corresponding to the dimethylaminomethylene group at the end of the side chain. The most abundant ion in both mass spectra was the molecular ion of I (*m/e* 328).

The molecular ion of II (*m/e* 314) was the most abundant peak in its mass spectrum. The mass spectra of II and its sulfoxide (V) were similar, like the mass spectra of I and IV. The predominant peaks in the mass spectrum of V had the following mass numbers (and relative intensities): 44 (14%), 58 (20%), 229 (96%), 242 (61%), 269 (36%), 312 (27%), and 314 (100%).

The predominant peaks in the mass spectrum of the reference sample of III were at 228 (41%), 242 (70%), 269 (18%), 300 (100%), and 314 (13%). The ion of mass 314 probably arises from contamination with II in the reference sample, since the molecular weight of III is only 300.

Plasma and Urine Extracts—The concentrations of I and IV in plasma and of I, II, and IV in urine are given in Table I.

Figure 2 shows computer-generated mass chromatograms of ions with mass numbers 314 and 328, obtained after injection of a plasma extract. The chromatogram of mass number 328 contained two peaks with retention times similar to those of I and IV, while the chromatogram of mass number 314 contained one peak with a retention time similar to that of II. The mass spectra corresponding to the peak intensities in the mass chromatograms shown in Fig. 2 are shown in Fig. 3.

The total ion current gas chromatograms of plasma extracts from all subjects showed three peaks with retention times similar to I, II, and IV. The mass numbers and relative intensities of the predominant peaks in the corresponding mass spectra are summarized in Table II.

Figure 4 shows mass chromatograms of ions with mass 314, 300, and 328, obtained from a urine extract. The *m/e* 314 mass chromatogram contained two peaks with maximum intensities obtained in scan numbers 230 and 300, corresponding to the retention times of II and V. The mass spectrum recorded in scan number 230 was similar to the mass spectrum of II (Fig. 1). The predominant peaks in the mass spectrum recorded in scan number 300 had the following mass numbers (and relative intensities): 58 (100%), 229 (72%), 242 (52%), 269 (28%), and 314 (77%).

The *m/e* 300 mass chromatogram showed one small peak with peak intensity obtained in scan number 232, corresponding to the retention time of III. The predominant peaks in the mass spectrum recorded in scan number 232 had the following mass numbers (and relative intensities): 44 (25%), 86 (12%), 229 (74%), 242 (45%), 269 (17%), 300 (10%), and 314 (100%).

The *m/e* 328 mass chromatogram (Fig. 4) contained two peaks with retention times similar to I and IV. The mass spectra recorded in scan numbers 225 and 300 were similar to the mass spectra of I and IV shown in Fig. 1.

It was previously reported that peaks from two unidentified substances appeared in the flame-ionization gas chromatograms of samples extracted

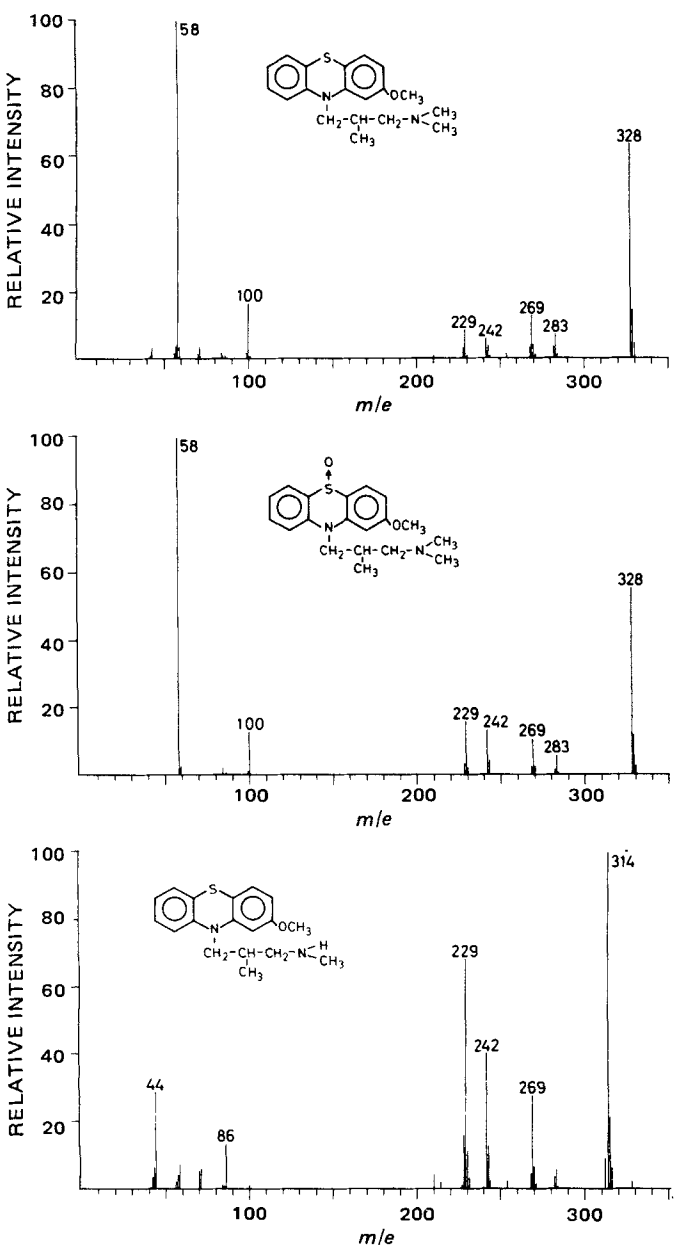

Figure 1—*Mass spectra of I, IV, and II obtained after injection of 1 μg of each compound from organic standard solutions.*

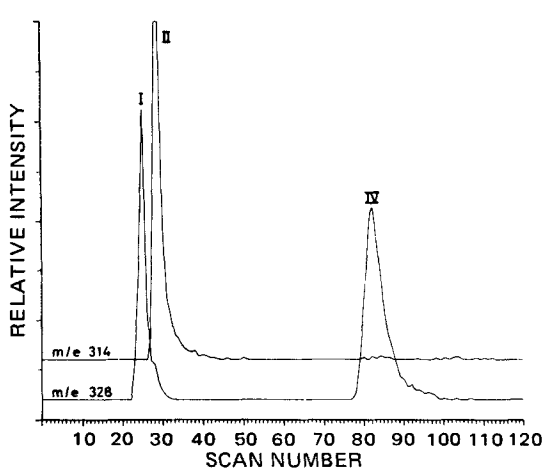

Figure 2—*Mass chromatograms obtained from an extract of 11.3 ml of plasma from Subject 1, collected 3 hr after administration of the morning dose.*

Table II—Predominant Peaks in Mass Spectra from Plasma Extracts

Subject	Mass Number (Relative Intensity, %) RRT[a] 1.0	RRT 1.25	RRT 3.95
1	58 (100), 328 (50), 43 (18), 100 (18)	314 (100), 229 (61), 242 (36), 44 (29)	58 (100), 328 (63), 100 (15), 229 (13)
2	58 (100), 328 (54), 100 (15), 229 (10)	314 (100), 229 (64), 242 (37), 269 (27)	58 (100), 328 (73), 229 (34), 242 (15)
3	58 (100), 328 (53), 100 (16), 229 (9)	314 (100), 229 (65), 242 (40), 44 (25)	58 (100), 328 (55), 229 (17), 100 (14)
4	58 (100), 42 (64), 328 (58), 71 (49), 100 (24)	314 (100), 44 (88), 72 (65), 229 (53)	58 (100), 328 (54), 229 (16), 207 (15)
	I[b]	II[b]	IV[b]
	58 (100), 328 (64), 100 (17), 269 (13)	314 (100), 229 (68), 242 (40), 44 (29), 269 (27)	58 (100), 328 (56), 229 (15), 242 (13), 100 (12)

[a] RRT = relative retention time. [b] Reference sample.

from plasma by this procedure (4). The mass spectrum of the one with the shortest retention time on the OV-17 column showed relatively high intensities of ions with mass numbers 149, 167, and 279, indicating that this compound was the commonly used plasticizer bis(2-ethylhexyl) phthalate (6).

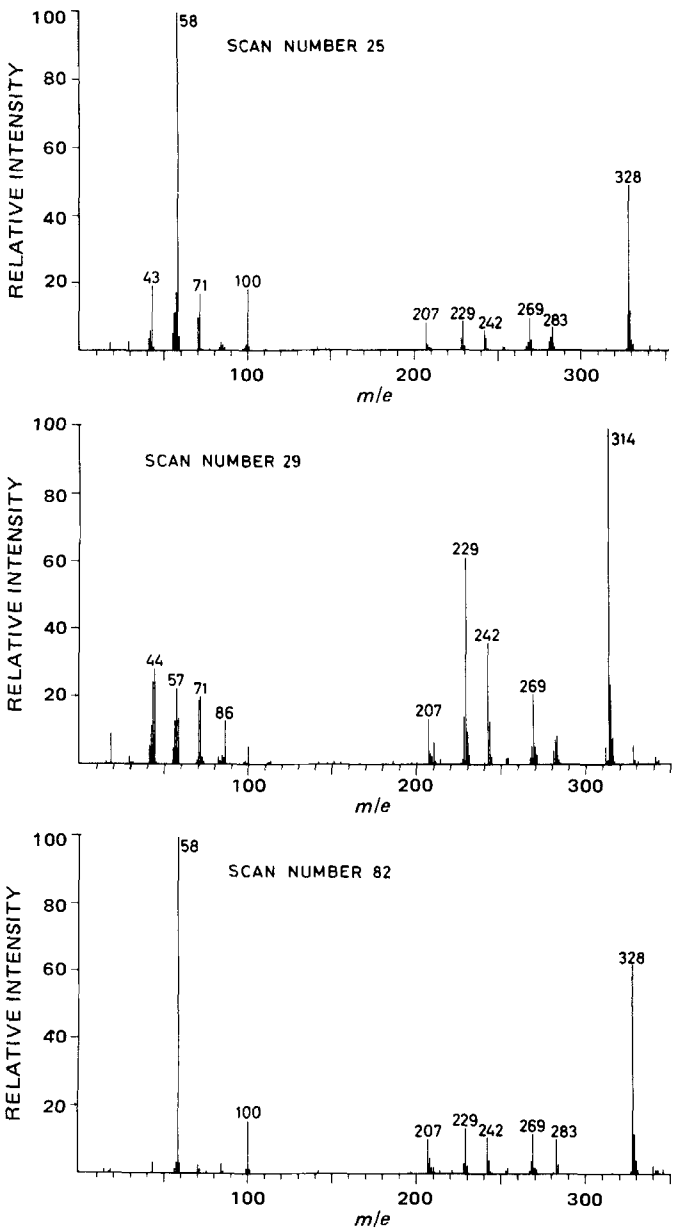

Figure 3—*Mass spectra obtained from the same sample as the mass chromatograms shown in Fig. 2.*

DISCUSSION

The 70-ev mass spectra of chlorpromazine sulfoxide and promazine sulfoxide were reported to contain an ion of mass corresponding to the dimethylamino side chain less two hydrogen atoms, which was absent from the mass spectra of the parent drugs (7). It was later reported that the two hydrogen atoms were eliminated from the methylene group in the middle of the side chain (8). In methotrimeprazine, one of these hydrogen atoms is substituted by a methyl group; no ion of mass corresponding to the side chain less one or two hydrogen atoms was seen in the mass spectra of I and IV, which were similar (Fig. 1).

It was reported previously that the 70-ev mass spectrum of IV, obtained by using a direct inlet system at 150°, showed a relatively high intensity of the molecular ion (*m/e* 344) and was distinguishable from the mass spectrum of I by the absence of ions with mass numbers 100 and 149 (9). The absence of the molecular ion of IV in the mass spectrum shown in Fig. 1 might have been due to reduction of the sulfoxide in the molecule separator, which was kept at 270°. A 70-ev mass spectrum of IV, recorded under otherwise the same conditions, was similar to the 20-ev mass spectrum and showed a relative intensity of the molecular ion of 0.9%.

The blood and urine samples were collected from patients receiving relatively large doses of I (Table I) and at the times of the day when the highest concentrations of I, II, and IV were expected. The method used for assay of I, II, and IV in urine was less accurate than the original procedure for I and IV in plasma, since no internal standard was used. Nevertheless, the results were sufficiently accurate for the scaling of the mass spectrometric analysis.

Several different components supposed to be conjugated metabolites of I were found previously in urine from psychiatric patients (10). Relatively polar components like glucuronides or hydroxylated metabolites of I are not, however, likely to be extracted by the present procedure. Compounds I, II, and IV previously were identified and quantitated in human urine (9), and the results given in Table I are in good agreement with the previously reported concentrations.

The peak in the *m/e* 300 mass chromatogram shown in Fig. 4 was not resolved from the peak of II (*m/e* 314), which had a much higher intensity;

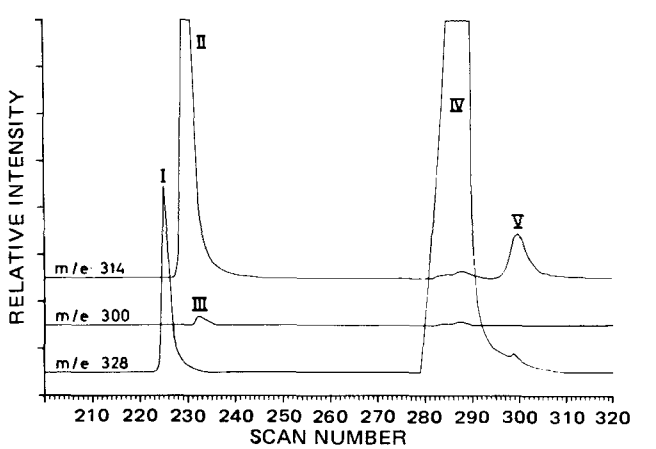

Figure 4—*Mass chromatograms obtained from an extract of 6 ml of urine from Subject 1, collected 5 hr after administration of the morning dose.*

therefore, the mass spectrum recorded in scan number 232 was similar mainly to that of II. Since the mass spectra of reference samples of I and II contained no ion with mass number 300, which was the base peak in the mass spectrum of III, the peak in the *m/e* 300 mass chromatogram still indicates that the urine contained III, although in apparently low concentration compared to I, II, and IV. The total recoveries of III and V by the extraction procedure were, however, not determined and may have been lower than the recoveries of I, II, and IV.

The mass spectrum recorded in scan number 300 was similar to the mass spectrum of V, confirming that the urine also contained this metabolite.

It may be concluded from the data given in Table II that all plasma extracts analyzed by combined GLC–mass spectrometry contained I, II, and IV. Some additional peaks of relatively high intensities, originating from the background, appeared in the mass spectra of plasma extracts from Subject 4.

In vitro studies indicated that IV must be considered pharmacologically active with regard to cardiac effects, while chlorpromazine sulfoxide possesses much less activity (3). The chlorpromazine (11–13) and promazine (14) metabolites analogous to II have proved pharmacologically active in different biological systems, and it seems reasonable that II should also possess significant pharmacological activity. Therefore, it would be desirable to have a sufficiently sensitive and specific method for quantitation of I and both of its nonpolar metabolites, II and IV, in plasma.

REFERENCES

(1) S. G. Dahl, *Clin. Pharmacol. Ther.*, **19**, 435 (1976).

(2) J. D. Maxwell, M. Carella, J. D. Parkes, R. Williams, G. P. Mould, and S. H. Curry, *Clin. Sci.*, **43**, 143 (1972).

(3) S. G. Dahl and H. Refsum, *Eur. J. Pharmacol.*, **37**, 241 (1976).

(4) S. G. Dahl and S. Jacobsen, *J. Pharm. Sci.*, **65**, 1329 (1976).

(5) B. Hedfjell and R. Ryhage, *Anal. Chem.*, **47**, 666 (1975).

(6) K. Biemann, "Mass Spectrometry, Organic Chemical Applications," McGraw-Hill, New York, N.Y., 1962, p. 170.

(7) L. G. Brookes, M. A. Holmes, I. S. Forrest, V. A. Bacon, A. M. Duffield, and M. D. Solomon, *Agressologie*, **12**, 333 (1971).

(8) A. M. Duffield, in "The Phenothiazines and Structurally Related Drugs," I. S. Forrest, C. J. Carr, and E. Usdin, Eds., Raven, New York, N.Y., 1974, p. 111.

(9) A. De Leenheer and A. Heyndrickx, *J. Pharm. Sci.*, **61**, 914 (1972).

(10) L.-G. Allgén, L. Hellström, and C. J. Sant'Orp, *Acta Psychiatr. Scand., Suppl.*, **39**, 169, 366 (1963).

(11) H. Nybäck and G. Sedvall, *Psychopharmacologia*, **26**, 155 (1972).

(12) H. S. Posner, E. Hearst, W. L. Taylor, and G. J. Cosmides, *J. Pharmacol. Exp. Ther.*, **137**, 84 (1962).

(13) S. Lal and T. L. Sourkes, *Eur. J. Pharmacol.*, **17**, 283 (1972).

(14) H. Rieger and J. Krieglstein, *Psychopharmacologia*, **39**, 163 (1974).

ACKNOWLEDGMENTS AND ADDRESSES

Received January 19, 1976, from the **Institute of Pharmacology, University of Oslo, Blindern, Oslo 3, Norway,* and the *‡Department of Clinical Pharmacology, Karolinska Institutet, Huddinge University Hospital, Huddinge, Sweden.*

Accepted for publication March 24, 1976.

Supported by Grant B 0106.4033 from the Royal Norwegian Council for Science and Industrial Research.

The plasma and urine samples were obtained from patients at Gaustad Hospital, Oslo, with the approval of Dr. S. Sigfusson and Dr. O. Prestegarden. The authors also thank Miss T. Morsund and Mrs. E. Rystad for technical assistance and Rhône-Poulenc and Mekos for providing reference samples.

ˣ To whom inquiries should be directed. Present address: Institute of Medical Biology, University of Tromsø, 9000 Tromsø, Norway.

Potential Long Acting Opiate Antagonists: Preparation, Pharmacological Activity, and Opiate–Receptor Binding of *N*-Substituted 2′-Hydroxy-5-methyl-9α-propyl-6,7-benzomorphans

KENNER C. RICE *, WERNER A. KLEE ‡, MARIO D. ACETO §, HENRY H. SWAIN ¶, and ARTHUR E. JACOBSON *ˣ

Abstract □ A homologous series of *N*-substituted 2′-hydroxy-5-methyl-9α-propyl-6,7-benzomorphans (hydrogen to octyl inclusive, allyl, and cyclopropylmethyl) was prepared. In contradistinction to the normetazocine, normorphine, and (−)-3-hydroxymorphinan series, the *N*-pentyl and *N*-hexyl derivatives do not have the analgesic potency of the parent *N*-methyl compound; instead, they are narcotic antagonists with a long duration of action. All of the *N*-substituted 9α-propylbenzomorphans, except for methyl, heptyl, and octyl, have antagonist activity. The receptor binding constants of the *N*-alkyl compounds are uniformly two- to threefold lower than those of the *N*-substituted normetazocines.

Keyphrases □ Opiate antagonists, potential—various *N*-substituted benzomorphans synthesized, pharmacological activity and opiate–receptor binding evaluated □ Benzomorphans, *N*-substituted—synthesized, pharmacological activity and opiate–receptor binding evaluated □ Structure–activity relationships—various *N*-substituted benzomorphans synthesized, pharmacological activity and opiate–receptor binding evaluated □ Binding, opiate–receptor—various *N*-substituted benzomorphans evaluated

Narcotic analgesics based on fused ring systems, such as the 6,7-benzomorphans and the more complex morphinans and morphines, have commonly been converted to antagonists by modification of the *N*-substituent (1, 2) [classically by replacing the *N*-methyl with allyl (3), cyclopropylmethyl (1), or propyl (1)]. Many antagonists prepared in this manner are highly potent and some are used clinically (2). Most antagonists studied have only a short duration of action, for reasons that are not exactly clear. Long duration of action is a useful property in treating opiate overdosage and in some addiction treatment programs.

therefore, the mass spectrum recorded in scan number 232 was similar mainly to that of II. Since the mass spectra of reference samples of I and II contained no ion with mass number 300, which was the base peak in the mass spectrum of III, the peak in the *m/e* 300 mass chromatogram still indicates that the urine contained III, although in apparently low concentration compared to I, II, and IV. The total recoveries of III and V by the extraction procedure were, however, not determined and may have been lower than the recoveries of I, II, and IV.

The mass spectrum recorded in scan number 300 was similar to the mass spectrum of V, confirming that the urine also contained this metabolite.

It may be concluded from the data given in Table II that all plasma extracts analyzed by combined GLC–mass spectrometry contained I, II, and IV. Some additional peaks of relatively high intensities, originating from the background, appeared in the mass spectra of plasma extracts from Subject 4.

In vitro studies indicated that IV must be considered pharmacologically active with regard to cardiac effects, while chlorpromazine sulfoxide possesses much less activity (3). The chlorpromazine (11–13) and promazine (14) metabolites analogous to II have proved pharmacologically active in different biological systems, and it seems reasonable that II should also possess significant pharmacological activity. Therefore, it would be desirable to have a sufficiently sensitive and specific method for quantitation of I and both of its nonpolar metabolites, II and IV, in plasma.

REFERENCES

(1) S. G. Dahl, *Clin. Pharmacol. Ther.*, **19**, 435 (1976).

(2) J. D. Maxwell, M. Carella, J. D. Parkes, R. Williams, G. P. Mould, and S. H. Curry, *Clin. Sci.*, **43**, 143 (1972).

(3) S. G. Dahl and H. Refsum, *Eur. J. Pharmacol.*, **37**, 241 (1976).

(4) S. G. Dahl and S. Jacobsen, *J. Pharm. Sci.*, **65**, 1329 (1976).

(5) B. Hedfjell and R. Ryhage, *Anal. Chem.*, **47**, 666 (1975).

(6) K. Biemann, "Mass Spectrometry, Organic Chemical Applications," McGraw-Hill, New York, N.Y., 1962, p. 170.

(7) L. G. Brookes, M. A. Holmes, I. S. Forrest, V. A. Bacon, A. M. Duffield, and M. D. Solomon, *Agressologie*, **12**, 333 (1971).

(8) A. M. Duffield, in "The Phenothiazines and Structurally Related Drugs," I. S. Forrest, C. J. Carr, and E. Usdin, Eds., Raven, New York, N.Y., 1974, p. 111.

(9) A. De Leenheer and A. Heyndrickx, *J. Pharm. Sci.*, **61**, 914 (1972).

(10) L.-G. Allgén, L. Hellström, and C. J. Sant'Orp, *Acta Psychiatr. Scand., Suppl.*, **39**, 169, 366 (1963).

(11) H. Nybäck and G. Sedvall, *Psychopharmacologia*, **26**, 155 (1972).

(12) H. S. Posner, E. Hearst, W. L. Taylor, and G. J. Cosmides, *J. Pharmacol. Exp. Ther.*, **137**, 84 (1962).

(13) S. Lal and T. L. Sourkes, *Eur. J. Pharmacol.*, **17**, 283 (1972).

(14) H. Rieger and J. Krieglstein, *Psychopharmacologia*, **39**, 163 (1974).

ACKNOWLEDGMENTS AND ADDRESSES

Received January 19, 1976, from the **Institute of Pharmacology, University of Oslo, Blindern, Oslo 3, Norway,* and the *‡Department of Clinical Pharmacology, Karolinska Institutet, Huddinge University Hospital, Huddinge, Sweden.*

Accepted for publication March 24, 1976.

Supported by Grant B 0106.4033 from the Royal Norwegian Council for Science and Industrial Research.

The plasma and urine samples were obtained from patients at Gaustad Hospital, Oslo, with the approval of Dr. S. Sigfusson and Dr. O. Prestegarden. The authors also thank Miss T. Morsund and Mrs. E. Rystad for technical assistance and Rhône-Poulenc and Mekos for providing reference samples.

ˣ To whom inquiries should be directed. Present address: Institute of Medical Biology, University of Tromsø, 9000 Tromsø, Norway.

Potential Long Acting Opiate Antagonists: Preparation, Pharmacological Activity, and Opiate–Receptor Binding of *N*-Substituted 2′-Hydroxy-5-methyl-9α-propyl-6,7-benzomorphans

KENNER C. RICE *, WERNER A. KLEE ‡, MARIO D. ACETO §, HENRY H. SWAIN ¶, and ARTHUR E. JACOBSON *ˣ

Abstract □ A homologous series of *N*-substituted 2′-hydroxy-5-methyl-9α-propyl-6,7-benzomorphans (hydrogen to octyl inclusive, allyl, and cyclopropylmethyl) was prepared. In contradistinction to the normetazocine, normorphine, and (−)-3-hydroxymorphinan series, the *N*-pentyl and *N*-hexyl derivatives do not have the analgesic potency of the parent *N*-methyl compound; instead, they are narcotic antagonists with a long duration of action. All of the *N*-substituted 9α-propylbenzomorphans, except for methyl, heptyl, and octyl, have antagonist activity. The receptor binding constants of the *N*-alkyl compounds are uniformly two- to threefold lower than those of the *N*-substituted normetazocines.

Keyphrases □ Opiate antagonists, potential—various *N*-substituted benzomorphans synthesized, pharmacological activity and opiate–receptor binding evaluated □ Benzomorphans, *N*-substituted—synthesized, pharmacological activity and opiate–receptor binding evaluated □ Structure–activity relationships—various *N*-substituted benzomorphans synthesized, pharmacological activity and opiate–receptor binding evaluated □ Binding, opiate–receptor—various *N*-substituted benzomorphans evaluated

Narcotic analgesics based on fused ring systems, such as the 6,7-benzomorphans and the more complex morphinans and morphines, have commonly been converted to antagonists by modification of the *N*-substituent (1, 2) [classically by replacing the *N*-methyl with allyl (3), cyclopropylmethyl (1), or propyl (1)]. Many antagonists prepared in this manner are highly potent and some are used clinically (2). Most antagonists studied have only a short duration of action, for reasons that are not exactly clear. Long duration of action is a useful property in treating opiate overdosage and in some addiction treatment programs.

Table I—Data for *N*-Substituted 2′-Hydroxy-5-methyl-9α-propyl-6,7-norbenzomorphans

N-Substituent	Salt Form	Melting Point	Yield, %	Method	Recrystallization Solvent	Empirical Formula	Analysis, %	
							Calc.	Found
H	—	—	—[a]	—	—	—	—	—
H	Hemioxalate monohydrate	287–288° dec.	90	—	Ethanol–water	$C_{34}H_{48}N_2O_6 \cdot H_2O$	C 68.20 H 8.42 N 4.68	68.22 8.70 4.74
Ethyl	—	238.5–240°	—[b]	A	2-Methoxyethanol	$C_{18}H_{27}NO$	C 79.07 H 9.95 N 5.12	79.13 10.16 5.09
Ethyl	Oxalate	217–219° dec.	88		Ethanol	$C_{20}H_{29}NO_5$	C 66.09 H 8.04 N 3.85	66.21 7.84 3.75
Propyl	—	182–184°	92	A	2-Propanol	$C_{19}H_{29}NO$	C 79.39 H 10.17 N 4.87	79.51 10.43 4.77
Propyl	Oxalate monohydrate	108–110°	—[c]		Water	$C_{21}H_{31}NO_5 \cdot H_2O$	C 63.77 H 8.41 N 3.54	63.95 8.34 3.50
Butyl	—	144.5–146°	—[b]	A	Acetonitrile–ethanol	$C_{20}H_{31}NO$	C 79.67 H 10.37 N 4.65	79.87 10.48 4.57
Butyl	Oxalate	138–141° dec.	97		Acetone–methanol	$C_{22}H_{33}NO_5$	C 67.49 H 8.50 N 3.58	67.45 8.57 3.70
Pentyl	—	138.5–140.5°	—[b]	A	Acetonitrile–ethanol	$C_{21}H_{33}NO$	C 79.94 H 10.54 N 4.44	79.86 10.24 4.35
Pentyl	Oxalate	147–150° dec.	91		Acetone–methanol	$C_{23}H_{35}NO_5$	C 68.12 H 8.70 N 3.45	68.12 8.40 3.43
Hexyl	—	131–132°	—[b]	A	Isopropyl ether	$C_{22}H_{35}NO$	C 80.19 H 10.71 N 4.25	80.14 10.74 4.13
Hexyl	Oxalate	120–122° dec.	92		Ethanol	$C_{24}H_{37}NO_5$	C 68.70 H 8.89 N 3.34	68.45 8.94 3.20
Heptyl	—	97.5–98.5°	—[b]	A	Heptane	$C_{23}H_{37}NO$	C 80.14 H 10.86 N 4.08	80.20 10.88 3.88
Heptyl	Oxalate	140.5–142.5° dec.	95		Acetone–methanol	$C_{25}H_{39}NO_5$	C 69.25 H 9.07 N 3.23	68.85 9.23 3.12
Octyl	—	—[d]	—[b]	A	—	$C_{24}H_{39}NO$	—	—
Octyl	Oxalate	182.5–184° dec.	92		Acetone–methanol	$C_{26}H_{41}NO_5$	C 69.76 H 9.23 N 3.13	69.80 9.39 3.04
Allyl	—	208.5–210.5°	—[b]	A	2-Methoxyethanol	$C_{19}H_{27}NO$	C 79.95 H 9.54 N 4.91	80.08 9.82 4.81
Allyl	Oxalate	221.5–223.5° dec.	88		Acetone–methanol	$C_{21}H_{29}NO_5$	C 67.18 H 7.79 N 3.73	67.37 7.84 3.57
Cyclopropylmethyl	—	198.5–200.5°	—[b]	B	Ethanol	$C_{20}H_{27}NO$	C 80.22 H 9.76 N 4.68	79.96 9.95 4.46
Cyclopropylmethyl	Oxalate	163–165° dec.	88		Ethanol	$C_{22}H_{31}NO_5$	C 67.84 H 8.02 N 3.60	67.45 8.04 3.68

[a] See Ref. 18. [b] Isolated as oxalate. [c] As purified free base. [d] Syrup, not analyzed.

BACKGROUND

This paper explores the effects of replacing a methyl group with a propyl group at the 9α-position of a benzomorphan. This simple substitution has led to a series of compounds with dramatic changes in biological activity. Of particular interest is the fact that some of these compounds are relatively pure antagonists with a long duration of action. Also interesting is the fact that the *N*-pentyl derivative, which in the normetazocine, normorphine, and 3-hydroxymorphinan series is approximately equipotent with the methyl derivative as an agonist, is devoid of analgesic activity in 2′-hydroxy-5-methyl-9α-propyl-6,7-norbenzomorphan.

In the metazocine series (I), replacement of the *N*-methyl (I*b*) by saturated alkyl moieties (4, 5) from ethyl to butyl (I*c*–I*e*) caused a diminution or loss of analgesic activity and a concurrent gain in narcotic antagonist activity (6), which was maximal with the *N*-propyl (I*d*) derivative (7). The *N*-ethyl compound (I*c*) (8, 9) was a weak agonist and a longer lasting but less potent antagonist than nalorphine with a steeper dose–response curve (9). The *N*-butyl derivative (I*e*) (7) had 0.2 times the antagonist potency and the same duration of action as nalorphine, and it had little analgesic activity, as measured by the Eddy hot-plate (10, 11) and Nilsen (12) assays.

When a five- or six-carbon side chain was introduced to form the *N*-pentyl (I*f*) or *N*-hexyl (I*g*) compounds, the potent analgesia associated with the parent *N*-methyl compound, metazocine (I*b*), was restored. A slight lessening of agonist potency was noted in I*g* (13). Although I*f* and, presumably, I*g* did not have the high physical dependence capacity associated with morphine, the *N*-pentyl did show a low physical dependence capacity, similar to metazocine, in single-dose suppression tests and in nonwithdrawn monkeys (14). These physical dependence capacity data are presently being reinvestigated.

A similar fluctuation of analgesic potency was noted in the comparable homologous normorphine (15) and (−)-3-hydroxymorphinan (16) series. Maximal analgesic potency was noted with the *N*-methyl and *N*-pentyl compounds in these series; the analgesic potency of the *N*-hexyl compound decreased a little. A considerable loss of analgesic potency was

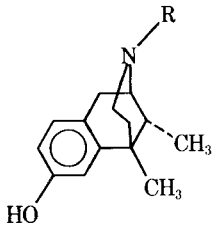

Ia: R = H
Ib: R = CH_3
Ic: R = C_2H_5
Id: R = C_3H_7
Ie: R = C_4H_9
If: R = C_5H_{11}
Ig: R = C_6H_{13}

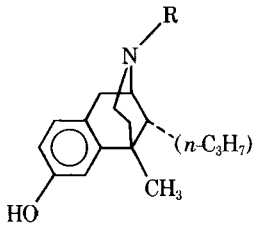

IIa: R = H
IIb: R = CH_3
IIc: R = C_2H_5
IId: R = C_3H_7
IIe: R = C_4H_9
IIf: R = C_5H_{11}
IIg: R = C_6H_{13}
IIh: R = C_7H_{15}
IIi: R = C_8H_{17}
IIj: R = $CH_2CH{=}CH_2$
IIk: R = CH_2—▽

noted with the *N*-ethyl and *N*-butyl derivatives. Thus, a binodal curve for analgesic activity could be used to describe the variation in potency in each of the three homologous series of compounds.

From the morphine data, a hypothesis was generated (17) which could be reformulated to say that compounds with narcotic antagonist activity have a saturated, aliphatic, three-carbon side chain on the nitrogen atom or the structural components of an allyl group. Potent analgesics with the physical dependence capacity of the opiate type are usually obtainable from methyl, pentyl, or hexyl substituents.

Since only these three groups of structurally rigid analgesics had been examined in this way, and the hypothesis certainly appeared to be valid for them, it was of interest to see whether it could be verified using a fourth homologous series prepared from a different benzomorphan, 2′-hydroxy-5-methyl-9α-propyl-6,7-norbenzomorphan (IIa). Thus, the methyl to octyl, allyl, and cyclopropylmethyl derivatives (IIb–IIj) of this benzomorphan were prepared by known methods (1, 13, 18).

EXPERIMENTAL[1]

Method A: 2-Alkyl-2′-hydroxy-5-methyl-9α-propyl-6,7-benzomorphans—A mixture of IIa (737 mg, 3.0 mmoles) (18), the appropriate alkyl iodide (allyl bromide for IIj) (3.1 mmoles), anhydrous potassium carbonate (1.0 g, 7.25 mmoles), and dry dimethylformamide (10 ml) was heated at 100–110° for 2.5 hr with stirring. After cooling, the inorganic material was filtered and washed with chloroform, and the filtrate and washings were evaporated *in vacuo*. The residue was dissolved in chloroform, washed with water, and dried (sodium sulfate).

Evaporation of the solvent left a residue, which was dissolved in acetone (15 ml) and treated with oxalic acid (288 mg, 3.2 mmoles) in acetone (5 ml). The crystalline acid oxalate salt that separated was collected, washed with acetone, and dried. Treatment of a methanol–water solution of the oxalate with 12 *M* ammonium hydroxide and extraction of the resulting oil into chloroform, drying (sodium sulfate), and evaporation of the solvent gave the purified base, which was recrystallized from the appropriate solvent for analysis (Table I).

Method B: 2-Cyclopropylmethyl-2′-hydroxy-5-methyl-9α-propyl-6,7-benzomorphan (IIk) Oxalate—A solution of cyclopropylcarbonyl chloride (1.0 g, 9.6 mmoles) in chloroform (5 ml) was added dropwise to a slurry of IIa (18) (737 mg, 3.0 mmoles) in dry pyridine (15 ml) maintained at 5–10°. When the addition was completed, stirring was continued at 5–10° until the solid dissolved and then at 25° for an additional 1 hr. The solution was evaporated to a semisolid, chloroform (70 ml) was added, and the solution was washed successively with water (50 ml), 1 *N* hydrochloric acid (50 ml), and brine (30 ml).

The chloroform solution was dried (sodium sulfate) and evaporated to give a syrupy, crude *O,N*-dicyclopropylcarbonyl derivative (1.265 g). This material was added to a slurry of lithium aluminum hydride (900 mg, 23.8 mmoles) in dry tetrahydrofuran (100 ml), and the mixture was refluxed overnight (stirring). After cooling, 12 *M* ammonium hydroxide (8 ml) was slowly added. The mixture was stirred for 1.0 hr, the tetrahydrofuran was decanted from the semisolid inorganic material and evaporated, the residue was dissolved in chloroform (100 ml), washed with water (50 ml), and dried (sodium sulfate), and the solvent was removed *in vacuo*. The residual base was dissolved in acetone (15 ml) and treated with oxalic acid (300 mg, 3.33 mmoles) in acetone (5 ml). The resulting crystalline salt was filtered, washed with acetone, and dried to give 991 mg of IIk. Recrystallization from 95% ethanol gave pure material (Table I).

[1] Melting points were determined in open capillary tubes using a Thomas-Hoover apparatus and are corrected. Microanalyses were performed by the Laboratory of Chemistry's Section of Microanalytical Services and Instrumentation. IR (Perkin-Elmer 257) and NMR (Varian A-60) spectra were consistent with the assigned structures. Mass spectra of the free bases were obtained using a Hitachi Perkin-Elmer RMU6E spectrometer (70 ev); each spectrum was consistent with the assigned structure and showed the expected molecular ion.

Table II—Pharmacological Activities of the *N*-Substituted 2′-Hydroxy-5-methyl-9α-propyl-6,7-norbenzomorphans

N-Substituent	ED_{50}[a]	ED_{50}[b]	EC_{50}[c]	PDC[d]
H (IIa)	—[e,f]	—[e,g]	50	None
Methyl[h] (IIb)	1.61 (1.03–2.52)	1.8 (1.3–2.6)	10	Low
Ethyl (IIc)	17.5 (9.7–31.6)	—[e,g]	60	None
Propyl (IId)	—[e,i]	—[j]	8	None
Butyl (IIe)	—[e,k]	—[e,g]	20	None
Pentyl (IIf)	—[e,l]	—[j]	30	None
Hexyl (IIg)	4.8 (3.4–6.7)	8.6 (5.5–13.4)	30	None
Heptyl (IIh)	50.8 (24.4–90.9)	—	90	None
Octyl (IIi)	—[m]	—	200	None
Allyl (IIj)	—[n]	—	1.3	None
Cyclopropylmethyl (IIk)	—[n]	7.2 (4.0–13.0)	5	None
Morphine hydrochloride	1.2 (0.9–1.3)	0.8 (0.6–1.2)	3	High
Nalorphine hydrochloride	36.4 (27.2–48.7)	4.8 (2.1–11.0)	1.5	None

[a] Eddy hot-plate assay (95% *SE* limits, as obtained by probit analysis, in milligrams per kilogram), subcutaneous injection in mice using oxalate salts. See Refs. 10 and 11. [b] Nilsen assay (95% *SE* limits, as obtained by probit analysis, in milligrams per kilogram), subcutaneous injection in mice using oxalate salts. See Ref. 12. [c] Binding constant, n*M*. See Ref. 20. [d] Physical dependence capacity, single-dose suppression or nonwithdrawn monkeys. See Ref. 6. [e] Insufficient data for probit analysis due to poor dose–response relationship or toxicity. [f] Six out of 10 mice were affected at 50 mg/kg. [g] Three out of 10 mice were affected at 20 mg/kg. [h] K. C. Rice, A. E. Jacobson, and E. L. May, *J. Med. Chem.*, 18, 854 (1975). [i] Toxic at 20 mg/kg (convulsions). [j] Inactive at 20 mg/kg. [k] Five out of 10 mice were affected at 20 mg/kg; toxic at 50 mg/kg (convulsions). [l] Toxic at 10 mg/kg (convulsions). [m] Inactive at 100 mg/kg. [n] Inactive at 50 mg/kg.

RESULTS AND DISCUSSION

The homologous series prepared from 2′-hydroxy-5-methyl-9α-propyl-6,7-norbenzomorphan did not follow the described biological patterns established by the normetazocines, morphines, and (−)-3-hydroxymorphinans. Analgesic potency dropped considerably in the *N*-ethyl (IIc) and *N*-butyl (IIe) compounds, as compared with the *N*-methyl (IIb), and did not return with the introduction of *N*-pentyl (IIf) into the molecule (Table II). The *N*-ethyl to *N*-hexyl (IIc–IIg) derivatives all appeared to have narcotic antagonist activity (Table III). Both agonist and antagonist activities disappeared in the *N*-heptyl (IIh) and *N*-octyl (IIi) compounds.

The unsubstituted benzomorphan, a secondary amine (IIa), had no antagonist activity (Table III). Benzomorphans unsubstituted on the nitrogen atom generally do not display antagonist behavior in monkeys. Normetazocine (Ia), normorphine, norketobemidone, and norbemidone have been shown to have a weak antagonist component in their pharmacological profile by their actions on the narcotic receptor in the guinea pig ileum (19). A strong agonist component in the pharmacological activity of IIa has been shown by an adenylate cyclase assay[2].

As the number of carbon atoms on the nitrogen increased, the duration of action of the compound as an antagonist also increased (Table III). The *N*-ethyl compound had a moderate duration of antagonist action (Table III). The *N*-propyl compound had a very long duration. Compound IIe was less potent than nalorphine but longer lasting. Compound IIf had a rapid onset and long duration of action as an antagonist. Compound

Table III—Summary of Data Obtained from Monkey Studies

N-Substituent	Test[a] / Dose Range[b]	Duration of Antagonist Action[c]	Comments
H (II*a*)	SDS / 5.0–10.0	—	Did not substitute for morphine and exacerbated withdrawal reaction only slightly
	NW / 10.0–20.0	—	Did not precipitate withdrawal; only a slight increase in respiration
Methyl (II*b*)	SDS / 1.5–6.0	—	Nondose-related reduction in withdrawal signs; did not substitute for morphine
Ethyl (II*c*)	SDS / 2.0–8.0	—	Nondose-related reduction in withdrawal signs; did not exacerbate withdrawal reaction
	NW / 4.0–32.0	1.5	Precipitated withdrawal; quick onset (0–30 min) and moderate duration of action
Propyl (II*d*)	SDS / 0.5–2.0	>3*c*	Did not substitute for morphine and appeared to exacerbate withdrawal; long duration of action
Butyl (II*e*)	SDS / 5.0	—	Increase in severity of abstinence signs
	NW / 1.25–5.0	10	Precipitation of moderate to severe abstinence; very long duration of action
Pentyl (II*f*)	SDS / 3.0–12.0	—	Did not substitute for morphine; severe withdrawal in one-third animals at highest dose
	NW / 4.0–32.0	2.5	Precipitated withdrawal; rapid onset (0–30 min) and long duration of action
Hexyl (II*g*)	SDS / 3.0–12.0	>3*c*	Did not substitute for morphine in the dose range tested and appeared to exacerbate withdrawal reaction; very long duration of action
Heptyl (II*h*)	SDS / 10.0	—	Neither suppresses nor precipitates abstinence syndrome
Octyl (II*i*)	SDS / 10.0	—	No alteration of signs of morphine abstinence
Allyl (II*j*)	SDS / 0.5–1.0	—	Increase in severity of abstinence signs
	NW / 0.125–2.0	10	Possible precipitation of abstinence signs at low doses; precipitation of severe, very long lasting abstinence at high doses
Cyclopropylmethyl (II*k*)	SDS / 0.5	—	Prompt intensification of signs of morphine abstinence
	NW / 0.03–1.25	0.5–1.5	Precipitation of mild abstinence signs at the low doses; severe abstinence signs at highest dose
Naloxone or nalorphine	NW / 0.5	0.5–1.5	Precipitated intense withdrawal reactions; rapid onset (0–30 min) and short to moderate duration of action

[a] SDS is single-dose suppression; NW is nonwithdrawn (see Ref. 6). [b] Milligrams per kilogram, subcutaneous injection, oxalate salts. [c] In hours. The duration of action ascertained by NW studies can be directly compared with nalorphine and naloxone data; SDS test data do not have reference standards (see Ref. 6) and can only be compared with other SDS results.

II*g* was a little different in that it had a slow onset and a very long duration of antagonist action. The *N*-allyl (II*j*) and *N*-cyclopropylmethyl (II*k*) compounds were potent, long acting antagonists.

The binding constants of these homologous compounds to rat brain homogenates known to contain receptors to the narcotic analgesics and their antagonists, as determined by standard techniques (13, 20), are presented in Table II. There appears to be a qualitative agreement between these binding constants and overall *in vivo* activity (analgesic or agonist-antagonist). There can be, of course, no quantitative fit to these data since antagonist activity has not been quantified, and only a few of the compounds show analgesic activity *in vivo* by either the hot-plate or Nilsen assay. However, it is thought that they all have an agonist component. This possible agonist activity will be examined in the future using the guinea pig ileum (21) and adenylate cyclase (22) assays.

There is less variation in the binding constants of the homologous normetazocine series (13) than with II*b*–II*j*. The *N*-unsubstituted normetazocine had a binding constant (EC_{50}) of 50; the *N*-ethyl had an EC_{50} of 20. The *N*-methyl, *N*-propyl, *N*-butyl, *N*-pentyl, and *N*-hexyl normetazocines all had EC_{50} values between 5 and 10. Thus, introduction of the 9α-propyl substituent increases the selectivity with which the opiate receptor recognizes different *N*-alkyl substituents. In all cases, however, binding of the 9α-propyl *N*-alkyl-substituted compounds was two- to threefold weaker than the corresponding 9α-methyl derivatives.

The 9α-alkyl group has been shown to be conformationally oriented toward the aromatic ring (away from the nitrogen atom) (23). The upfield position of those protons in the NMR spectra, as compared with the protons on a 9β-alkyl group, is due to the shielding influence of the aromatic ring (23). The introduction of a larger group in that area, such as a 9α-propyl group, may interfere with the fit of the flat phenolic region to a receptor, a fit that was previously postulated to be of importance to the interaction of the structurally rigid analgesics to the receptor (24).

This sterically generated interference could conceivably alter a conformational fit and, thus, cause a different pharmacological response.

Within the benzomorphans, it is unusual to find a statistically good fit between binding constants and *in vivo* analgesic activity[2]. The only series in which such correlations have been achieved are the structurally less rigid homologous ketobemidones (25), the benzazocines (13), and prodines (26). Evidently, the homologous ketobemidones had predominantly analgesic activity; only a few had an antagonist component in their pharmacological activity, and those were relatively weak antagonists. Thus, pharmacological activity could be closely approximated by analgesic potency with homologous ketobemidones, and analgesic activity was shown to be directly related to their binding constants (26). Unfortunately, homologous benzomorphans do not have pharmacological activity that is predominantly related to an accurately measurable analgesic potency. As has been seen, many *N*-substituted 9α-propylbenzomorphans are long acting antagonists, a pharmacological activity difficult to quantify in monkeys. Even if this activity could be quantified, as it might be using the guinea pig ileum assay procedure, pharmacokinetic factors, such as transport to the active site and metabolism, could complicate a correlation between *in vivo* pharmacological activity and *in vitro* binding constants.

A simple modification of the 9α-position in the benzomorphan molecule converted potent agonists (the *N*-pentyl- and *N*-hexylnormetazocines) to long acting antagonists (the *N*-pentyl- and *N*-hexyl-9α-propylbenzomorphans). The 9α-alkyl moiety has never before been implicated in the change of the pharmacological profile of a benzomorphan. This change, from potent agonist to narcotic antagonist, was thought to be caused only by the *N*-substituent. Further variation of the 9α-alkyl substituent to produce benzomorphans with bulkier and more hydrophobic groups in this position may be worthy of investigation to obtain even longer acting antagonists and to provide more clues to the nature of receptor interactions leading to antagonist activity.

REFERENCES

(1) S. Archer, N. F. Albertson, L. S. Harris, A. K. Pierson, and J. G. Bird, *J. Med. Chem.*, **7**, 123 (1964).

(2) A. E. Jacobson, in "Chemical and Biological Aspects of Drug Dependence," S. J. Mule and H. Brill, Eds., CRC Press, Cleveland, Ohio, 1972, pp. 101–118.

(3) M. Gordon, J. J. Lafferty, D. H. Tedeschi, N. B. Eddy, and E. L. May, *Nature*, **192**, 1089 (1962).

(4) J. H. Ager and E. L. May, *J. Org. Chem.*, **25**, 984 (1960).

(5) B. C. Joshi, C. F. Chignell, and E. L. May, *J. Med. Chem.*, **8**, 694 (1965).

(6) Committee on Problems of Drug Dependence, *Bull. Narc.*, **XXV** (2), 25 (1973).

(7) J. E. Villarreal and M. H. Seevers, "Addendum 7 to the Proceedings of the Committee on Problems of Drug Dependence," National Academy of Sciences, Washington, D.C., 1972, p. 1044.

(8) H. H. Swain and M. H. Seevers, "Addendum to the Proceedings of the Committee on Problems of Drug Dependence," National Academy of Sciences, Washington, D.C., 1975.

(9) M. D. Aceto, L. S. Harris, W. L. Dewey, and R. L. Balster, *ibid.*

(10) N. B. Eddy and D. Leimbach, *J. Pharmacol. Exp. Ther.*, **107**, 385 (1953).

(11) A. E. Jacobson and E. L. May, *J. Med. Chem.*, **8**, 563 (1965) (see Ref. 9 therein).

(12) T. D. Perrine, L. Atwell, I. B. Tice, A. E. Jacobson, and E. L. May, *J. Pharm. Sci.*, **61**, 86 (1972).

(13) M. E. Rogers, H. H. Ong, E. L. May, and W. A. Klee, *J. Med. Chem.*, **18**, 1036 (1975).

(14) G. A. Deneau and M. H. Seevers, "Addendum 1 to the Proceedings of the Committee on Drug Addiction and Narcotics," National Academy of Sciences, Washington, D.C., 1960.

(15) C. A. Winter, P. D. Orahovats, and E. G. Lehman, *Arch. Int. Pharmacodyn. Ther.*, **110**, 186 (1957).

(16) J. Hellerbach, H. Bessendorf, B. Pellmont, and O. Schnider, "Synthetic Analgesics, Part II-A, Morphinans," Pergamon Press, Oxford, England, 1966.

(17) R. L. Clark, A. A. Pessolano, J. Weijlard, and K. Pfister, III, *J. Am. Chem. Soc.*, **75**, 4963 (1953).

(18) K. C. Rice, *J. Org. Chem.*, **40**, 1850 (1975).

(19) H. W. Kosterlitz and A. A. Waterfield, *Ann. Rev. Pharmacol.*, **15**, 29 (1975).

(20) W. A. Klee and R. A. Streaty, *Nature (London)*, **248**, 61 (1974).

(21) H. W. Kosterlitz and A. J. Watt, *Br. J. Pharmacol.*, **33**, 266 (1968).

(22) S. K. Sharma, M. Nierenberg, and W. A. Klee, *Proc. Nat. Acad. Sci. USA*, **72**, 590 (1975).

(23) S. E. Fullerton, E. L. May, and E. D. Becker, *J. Org. Chem.*, **27**, 2144 (1962).

(24) A. H. Beckett and A. F. Casy, *J. Pharm. Pharmacol.*, **6**, 986 (1954).

(25) R. S. Wilson, M. E. Rogers, C. B. Pert, and S. H. Snyder, *J. Med. Chem.*, **18**, 240 (1975).

(26) M. A. Iorio, A. F. Casy, E. L. May, and W. A. Klee, Proceedings of the Budapest Pharmacology Congress, Academia Kiado, Budapest, Hungary, 1975.

[2] W. A. Klee, unpublished data, 1975.

ACKNOWLEDGMENTS AND ADDRESSES

Received January 23, 1976, from the *Medicinal Chemistry Section, *Laboratory of Chemistry, National Institute of Arthritis, Metabolism, and Digestive Diseases, National Institutes of Health, Bethesda, MD 20014,* the ‡*Laboratory of General and Comparative Biochemistry, National Institute of Mental Health, Bethesda, MD 20014,* the §*Department of Pharmacology, Medical College of Virginia, Virginia Commonwealth University, Richmond, VA 23298,* and the ¶*Department of Pharmacology, University of Michigan, Ann Arbor, MI 48104.*

Accepted for publication April 5, 1976.

The authors thank Mrs. Louise Atwell (NIAMDD) for the analgesic data and Dr. L. Harris (Medical College of Virginia) and Dr. E. L. May, (NIAMDD) for their counsel.

ˣ To whom inquiries should be directed.

High-Performance Liquid Chromatographic Determination of Diethylpropion Hydrochloride in Tablets: Isolation and Identification of Two Decomposition Products

MILDA J. WALTERS and STEPHEN M. WALTERS ˣ

Abstract □ A rapid assay was developed for diethylpropion hydrochloride tablets using high-performance liquid chromatography (HPLC) with UV detection. This technique provided separation of the drug from other UV-absorbing components present as the result of decomposition. A major decomposition product detected by HPLC in extracts of tablets and of the cotton filler from a tablet bottle was collected from the column effluents. This product was subsequently identified as 1-phenyl-1,2-propanedione, a highly volatile compound. A second decomposition product, isolated from decomposed drug by distillation from alkaline solution, was identified as diethylamine, apparently present as the hydrochloride salt. GLC, UV, IR, NMR, and mass spectrometry were used to confirm the identity of the decomposition products. HPLC assay results compared favorably with results of the NF assay; the latter procedure separates the drug from 1-phenyl-1,2-propanedione *via* liquid–liquid extraction.

Keyphrases □ Diethylpropion hydrochloride—high-performance liquid chromatographic analysis in tablets, identification of two decomposition products □ High-performance liquid chromatography—analysis, diethylpropion hydrochloride in tablets, identification of two decomposition products □ Anorectic agents—diethylpropion hydrochloride, high-performance liquid chromatographic analysis in tablets, identification of two decomposition products □ Decomposition products—of diethylpropion hydrochloride, identification, high-performance liquid chromatographic analysis in tablets

Diethylpropion has been reported to be an effective anorectic agent (1–3). A GLC method for the analysis of diethylpropion and its basic metabolites in urine was described previously (4). The metabolites investigated in that study (4) and in a later study (5) consisted of amino ketones and amino alcohols formed by *N*-dealkylation and keto reduction. Another study (6) detected 23 metabolic products of diethylpropion in human urine, of which 21 were identified. Two major products remained unidentified.

The investigation of possible decomposition of diethylpropion hydrochloride (I) in tablets was prompted by a disparity in analytical results obtained during the assay of several samples. Results obtained by the NF UV spectrophotometric procedure (7) were significantly lower than the monograph requirements. However, assays of extracts of these samples by perchloric acid titration gave results near the labeled amounts. Therefore, it was assumed that molecular dissociation had occurred, leaving the diethylamine group (reactant with perchloric acid) separated at some point from the remaining UV-absorbing portion. This assumption was further evidenced by the discovery of a yellow, highly volatile, UV-absorbing material in the cotton filler of a freshly opened bottle of tablets.

A high-pressure liquid chromatography (HPLC)–UV detection method was developed to provide a relatively rapid assay of I in tablets. It provided an additional advantage of isolating I from other UV-absorbing components present as the result of decomposition. GLC, UV, IR, NMR, and mass spectrometry were subsequently used to identify two decomposition products, 1-phenyl-1,2-propanedione (II) and diethylamine as the hydrochloride (III).

A report of the formation of II as a product of I has not been found, and the mechanism involved remains to be elucidated. The formation of diethylamine, in addition to ethylamine, acetaldehyde, and propiophenone, was reported as a result of photo- (254 nm) and radium-irradiation of aqueous and methanolic solutions of I (8).

EXPERIMENTAL

Instrumentation—*HPLC*—The liquid chromatograph[1] was equipped with a variable wavelength spectrophotometric detector[2] and a 2.6-mm i.d. × 50-cm stainless steel column containing a chemically bonded octadecylsilane on silica (13 ± 5 μm particle size) reversed-phase packing[3]. The detector wavelength was set at 255 nm, and the sensitivity was adjusted to produce a peak height of approximately 100 mm for 1.25 μg of I on a 50-mv recorder[4].

Two mobile solvent systems were used: A, a mixture containing 70% acetonitrile, 10% methanol, and 20% aqueous 0.1% ammonium carbonate; and B, a mixture containing 35% acetonitrile, 5% methanol, and 60% aqueous 0.1% ammonium carbonate. The flow rate was 1.0 ml/min, and elutions were made at ambient temperature. The retention volumes (V_R's) of I and II were 5.2 and 2.7 ml, respectively, using System B. The V_R of the internal standard, procaine hydrochloride, was 10.5 ml using System A for the quantitation of I.

GLC—A gas chromatograph[5] equipped with a flame-ionization detector was used. Compound II was chromatographed on a 2-mm × 1.83-m (6-ft) glass column packed with 16% DC 200 on Chromosorb WHP (80–100 mesh), with injector, column, and detector temperatures at 200, 100, and 250°, respectively. The helium carrier gas flow was 90 ml/min, and the detector sensitivity was 8×10^{-10} amp/mv. The retention time of II was 7.4 min.

Compound III was chromatographed on a 2-mm × 1.83-m (6-ft) glass column packed with 20% Carbowax 20M on Chromosorb WHP (80–100 mesh), with injector, column, and detector temperatures at 150, 60, and 250°, respectively. The helium carrier gas flow rate was 24 ml/min, and the detector sensitivity was 8×10^{-9} amp/mv. The retention time of III was 1 min.

IR—The IR spectrum of neat II was obtained[6] between sodium chloride plates, scanning from 2.5 to 16 μm. The spectrum of III was obtained[7] in the vapor phase in a 10-cm gas cell, scanning from 2 to 14 μm.

UV—The UV spectra of I and II were obtained[8] using 1-cm cells, scanning from 350 to 200 nm.

NMR—The NMR spectrum of II was obtained[9] in deuterated chloroform, scanning from 0 to 9 ppm.

Mass Spectrometry—The mass spectrum of II was obtained on a magnetic deflection mass spectrometer[10]. The sample was introduced *via* the liquid–solid direct insertion probe and ionized at a potential of 70 ev.

HPLC Determination of I in Tablets—A portion of finely ground

[1] Perkin-Elmer model 1220.
[2] Perkin-Elmer model LC-55.
[3] ODS SIL-X-1, Perkin-Elmer Corp., Norwalk, CT 06856.
[4] Leeds & Northrup Speedomax X/L 680.
[5] Perkin-Elmer model 990.
[6] Beckman model IR 20.
[7] Perkin-Elmer model 21.
[8] Cary model 118.
[9] Perkin-Elmer model R12B.
[10] Hitachi Perkin-Elmer model RMS-4.

Table I—Assays of Drug Substance and Commercial 25-mg Tablets[1]: Comparison of Titrimetric, NF, and HPLC Methods

Sample	Diethylpropion Hydrochloride, % of Labeled Amount Found		
	Titrimetric	NF	HPLC
A (tablets)	101.0	88.6	—
B (tablets)	96.8	86.2	—
C (tablets)	—	82.4	81.7[a]
D (tablets)	—	80.8	83.6[a]
E (tablets)	96.8	97.2	96.3 ± 0.53[b]
F (drug substance)	98.9	98.9	99.9

[a] Average of three determinations. [b] Average ± *SD* of six determinations.

tablet composite equivalent to 25 mg of I was weighed into a 50-ml volumetric flask, and 25 ml of methanol was added. The flask was placed in an ultrasonic bath[11] for 10 min, and then the solution was diluted to volume with methanol. The solution was filtered through fast filter paper, the first 10 ml of filtrate was discarded, and a 2-ml aliquot was mixed with 2.0 ml of procaine hydrochloride internal standard solution (2 mg/ml in methanol). A standard solution of I was prepared by mixing 2.0 ml of a stock solution (0.5 mg/ml in methanol) with 2.0 ml of internal standard solution.

Five-microliter injections of these solutions were made into the liquid chromatograph using mobile Solvent System A. When the peak height ratios (*PHR*) of I to the internal standard were reproducible within ±1% of the average for at least three consecutive injections of the standard

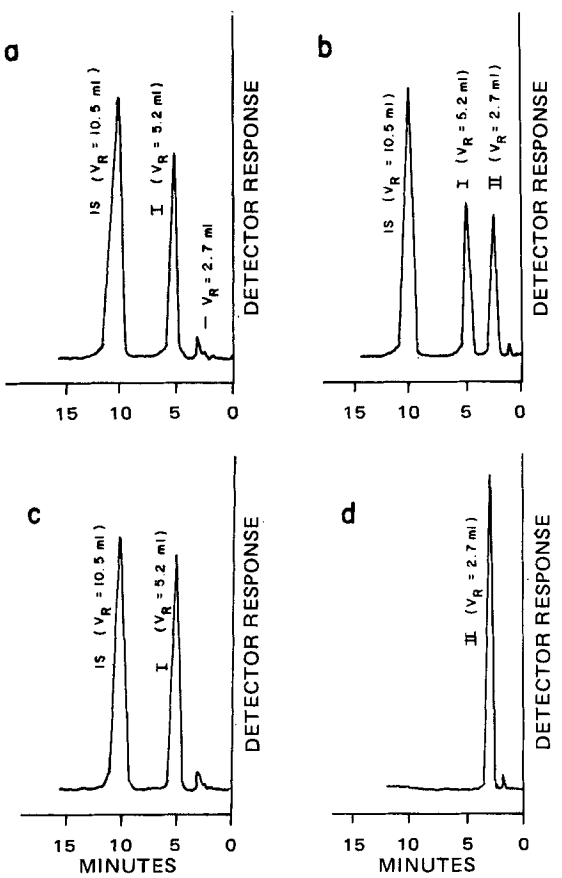

Figure 1—*HPLC separation of diethylpropion hydrochloride (I), decomposition product 1-phenyl-1,2-propanedione (II), and internal standard procaine hydrochloride (IS). Chromatograms are: a, an extract of a freshly prepared composite of undecomposed tablets; b, an extract of an aged, decomposed tablet composite; c, a standard solution of I; and d, an extract of yellow material from a cotton filler removed from a tablet bottle.*

[11] Bransonic 32, Branson Instruments Co., Shelton, CT 06484.

Table II—Effects of Elevated Temperature and Humidity on Diethylpropion Hydrochloride Assay Results

Sample	Conditions			Percent of Labeled Amount Found[a]	Method
	Temperature	Humidity	Hours		
D (tablets)	50°	Dry	48	98.0	HPLC
	50°	Dry	144	96.0	HPLC
	50°	Dry	744	88.8	HPLC
	50°	Humid	72	74.4	NF
				84.4	Titrimetric
	50°	Humid	960	52.4	NF
				82.4	Titrimetric
E (drug substance)	50°	Humid	36	94.7	HPLC
	50°	Humid	528	90.0	NF
				105.0	Titrimetric

[a] All results are corrected for weight increases due to absorption of water.

solution, alternate sample and standard injections were made and the concentration of I in the tablets was calculated as:

$$\frac{PHR_{spl}}{PHR_{std}} \times \text{standard concentration, mg/ml} \times \text{dilution of sample (50 ml)} \times \frac{\text{average tablet weight, g}}{\text{weight of sample, g}} = \frac{\text{mg of I}}{\text{tablet}} \quad \text{(Eq. 1)}$$

Titrimetric Determination of I in Tablets—A portion of tablet composite equivalent to 200 mg of I was weighed and transferred into a separator containing 25 ml of water. The solution was made alkaline with 0.1 *N* NaOH and extracted with three 50-ml portions of chloroform. The extracts were filtered through a funnel containing a cotton plug covered with 5 g of anhydrous sodium sulfate. To the filtrate was added 25 ml of acetic acid, and the solution was titrated with 0.1 *N* perchloric acid in acetic acid, using 2 drops of gentian violet solution (10 mg/ml in acetic acid) as indicator.

Isolation of II from Tablets and Cotton Fillers—The yellow substance found in the cotton fillers in the tablet bottles and a portion of an aged tablet composite were both extracted with methanol, concentrated, and injected into the liquid chromatograph. Retention volumes were measured and compared using both Solvent Systems A and B. Fractions of the eluant corresponding to the equal retention volumes of the major peak in the cotton extract chromatogram and of the extraneous peak in the tablet extract chromatogram were collected from System B. UV spectrophotometric measurements were made directly on the collected eluants. The eluants were then extracted into pentane and concentrated by evaporation for GLC, IR, and mass spectrometric analyses. The volatility of the collected material proved to be a problem in isolating sufficient amounts for IR and mass spectrometric analyses. A satisfactory mass spectrum of the cotton extract only was obtained.

Accelerated Production of II—In an attempt to collect larger amounts of this unknown component for further analysis, accelerated degradation of I (drug substance) was performed. The most efficient method found was to place 1–2 g of the drug substance in an erlenmeyer flask with 1–2 ml of water, connecting the flask to a distilling adapter with the tip immersed in distilled water contained in a second erlenmeyer flask, and placing the first flask on a steam bath while maintaining the second flask near room temperature. After collecting the volatile product in this manner over 3–4 days, the unknown component was isolated from the water solution by extraction into pentane; very careful evaporation of the solvent yielded a yellow liquid residue.

Stability Study on Tablets and Drug Substance—A limited study of the effects of elevated temperature and humidity on the stability of I in both tablet and drug substance form was performed. Portions of previously assayed samples were weighed into small beakers. Some portions were subjected to an elevated temperature condition by placing them in an oven at 50°. The remaining portions were subjected to humid, elevated temperature conditions by placing them in a large beaker containing a smaller beaker of water, covering the large beaker with aluminum foil, and placing it in an oven at 50°.

The samples were assayed at various times by the NF or HPLC method, and some were assayed by the titrimetric method as well. All results were corrected for weight increases due to water absorption.

Isolation of III from Decomposed Drug Substance—To a portion

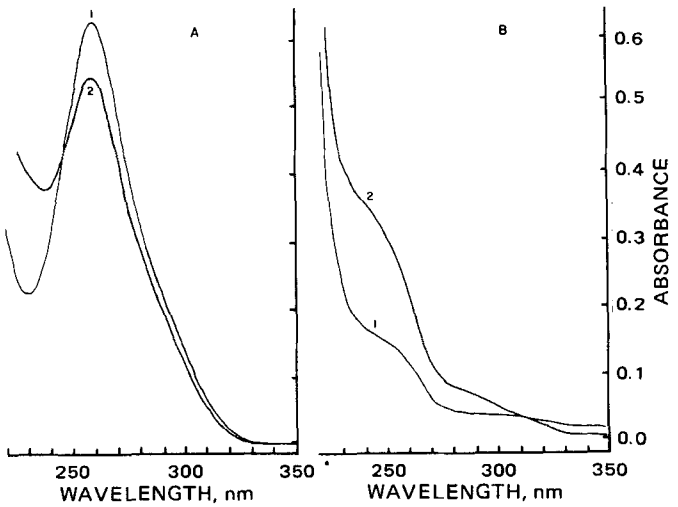

Figure 2—*UV spectra of (1) 1-phenyl-1,2-propanedione reference material and (2) isolated decomposition product II. A shows spectra obtained in water, and B shows spectra obtained after addition of sodium hydroxide.*

(~0.5 g) of decomposed drug substance remaining from the stability study was added 10 ml of 1 *N* NaOH. This solution was distilled from a microdistillation apparatus[12] by placing the distilling flask on a steam bath until several drops (~0.5 ml) of distillate were collected.

A portion of the aqueous distillate was extracted with chloroform for GLC analysis. Another portion was placed in a gas cell and warmed briefly to induce vaporization just prior to obtaining the IR spectrum.

RESULTS AND DISCUSSION

The assumption that partial decomposition of I in tablets had occurred *via* molecular dissociation of the amine group and the UV chromophore, with a rearrangement of the latter to a volatile compound, is evidenced by the comparative results of the titrimetric and NF or HPLC assays (Table I). This assumption was further evidenced by the finding of a foreign, UV-active, yellow material in a cotton filler, which was examined immediately upon removal from a bottle of tablets.

The volatile decomposition product exhibited UV activity with maximum absorbance near that of I. Thus, the agreement of results between the NF and the specific HPLC assays suggests that the volatile decomposition product (II) had escaped entirely from the tablet samples prior to performing the NF assays or that isolation of I from any remaining residues of II occurred in the liquid–liquid extraction steps of the NF procedure. A subsequent investigation found that the latter would occur.

The results of the limited stability study (Table II) indicate a significantly faster rate of decomposition with increased humidity, suggesting that hydrolysis may be involved in the process.

The relative values obtained by the NF and titrimetric assays of the decomposed samples again reflect the loss of UV-absorbing material in the decomposition process.

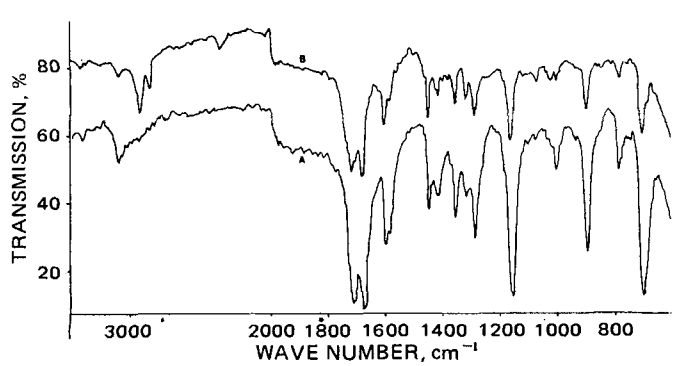

Figure 3—*IR spectra of (A) 1-phenyl-1,2-propanedione reference material and (B) isolated decomposition product II.*

[12] Ace Glass Inc., Vineland, N.J.

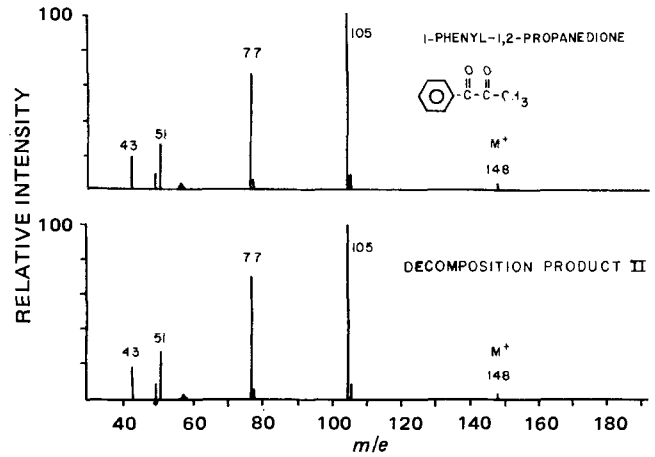

Figure 4—*Mass spectra of 1-phenyl-1,2-propanedione reference material and isolated decomposition product II.*

Typical liquid chromatograms obtained using Solvent System A are shown in Fig. 1. The aged tablet composite chromatogram contains an extraneous peak with the same V_R as the peak seen in the cotton filler chromatogram. This peak is absent in the standard and fresh composite chromatograms.

The liquid chromatograms obtained for the aged tablet composite and the cotton filler using Solvent System B also show an extraneous peak in the former with the same V_R as the peak seen in the latter. The use of this solvent system provided a larger V_R than did System A for the extraneous peak, with greater resolution from minor unknown peaks (probably decomposition by-products), thus permitting greater selectivity in the fraction collection process.

Subsequent HPLC analysis of the laboratory-produced decomposition product resulted in chromatograms similar to those of the cotton filler extract for both solvent systems.

The gas chromatograms and UV spectra showed identical characteristics for the laboratory-produced material and the collected HPLC fractions of the cotton filler and aged tablet composite extracts. The UV spectra consisted of a single maximum at about 255 nm when scanned in methanol or water, but it changed to a shoulder after addition of sodium hydroxide (Fig. 2).

The mass spectra of the laboratory-produced material and the collected fraction of the cotton extract showed identical fragmentation patterns, with a molecular ion peak at *m/e* 148 and major peaks at *m/e* 105, 77, 51, and 43.

The IR spectrum of the laboratory-produced material showed a double carbonyl band in the 1700-cm^{-1} region. A lack of bands in the 3500–

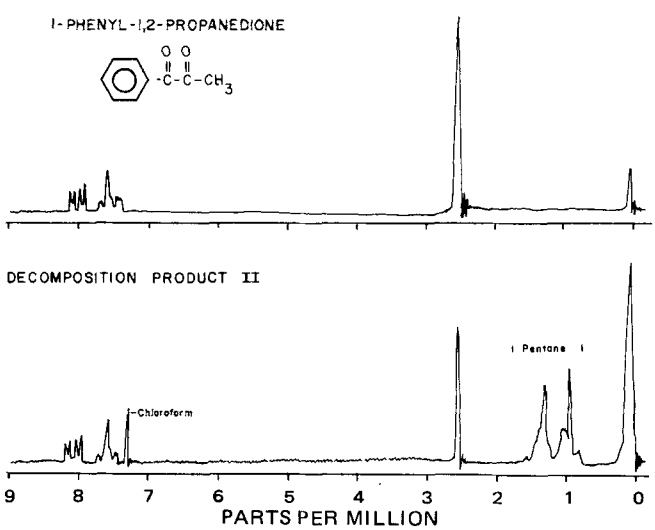

Figure 5—*NMR spectra of 1-phenyl-1,2-propanedione reference material and isolated decomposition product II.*

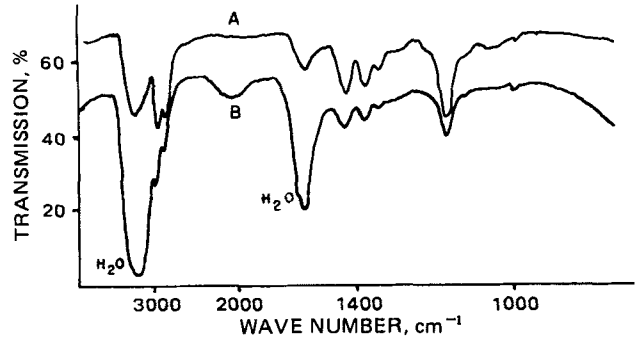

Figure 6—*IR spectra of (A) diethylamine reagent and (B) isolated decomposition product III.*

3000-cm^{-1} region indicated the absence of hydroxyl and primary or secondary amine groups.

The mass and IR spectra provided sufficient evidence for the elucidation of the structure of II. This compound was available commercially[13] and was purchased to serve as a reference material. The UV spectra of this reference material were nearly identical to those of the laboratory-produced decomposition product (Fig. 2). However, some background absorbance was apparent in the latter.

The IR and mass spectra of these two materials appeared identical (Figs. 3 and 4). The NMR spectra (Fig. 5) were also identical, with the exception of pentane peaks in the spectrum of the laboratory-produced material due to a residue remaining from the extraction step. A peak due to a chloroform impurity in the deuterated solvent was also visible in this spectrum because of the higher instrument gain used.

Gas and liquid chromatograms subsequently obtained for the reference material showed peaks identical to those of the previously unknown component. The chromatographic and spectral data combined with the identical physical characteristics of the cotton filler extract, the laboratory-produced material, and the reference material provided convincing evidence that II was formed as a major decomposition product of I.

Prior to the distillation of III from decomposed drug substance, the latter material was tested and found positive for secondary amines by the NF monograph test. The identity of III as a second decomposition product was then established by comparison of the gas chromatogram and the IR spectrum of the distillate with those of the diethylamine reagent[14]. Water was added to the latter prior to vaporization in the IR cell to simulate better its effect on the isolate spectrum (Fig. 6).

The distillate of an alkaline solution of undecomposed drug substance was found to contain no diethylamine, thus eliminating the suspicion that the latter may have been formed during the isolation procedure.

The route of decomposition from I to II and III has not been satisfactorily elucidated at this time and is apparently quite complex. However, it has been demonstrated that this type of decomposition has occurred in commercial tablet products and that it is accelerated by the presence of moisture.

The NF monograph assay procedure is specific for I in the presence of II, since it was found that II is retained in the sodium hydroxide solution while I is extracted into chloroform. However, the content uniformity procedure involves the direct UV determination of filtered hydrochloric acid solutions of the tablets. Since II was found to have considerable absorptivity and a maximum at 257 nm in this solvent, its presence in tablets could be expected to increase significantly the absorbance readings of their solutions, leading to inaccurately high results.

REFERENCES

(1) O. T. Bolding, *Curr. Ther. Res. Clin. Exp.*, **16**, 40 (1974).

(2) Y. K. Sedat and J. Reddy, *ibid.*, **16**, 398 (1974).

(3) D. E. Carney and E. D. Tweddell, *Med. J. Aust.*, **1**, 13 (1975).

(4) B. Testa and A. H. Beckett, *J. Chromatogr.*, **71**, 39 (1972).

(5) D. Mihailova, A. Rosen, B. Testa, and A. H. Beckett, *J. Pharm. Pharmacol.*, **26**, 711 (1974).

(6) E. C. Schreiber, B. H. Min, A. V. Zeiger, and J. F. Lang, *J. Pharmacol. Exp. Ther.*, **159**, 372 (1968).

(7) "The National Formulary," 14th ed., Mack Publishing Co., Easton, Pa., 1975, pp. 204, 205.

(8) K. G. Weidmann, A. Wolf, and J. Reisch, *Arch. Pharm.*, **306**, 954 (1973).

ACKNOWLEDGMENTS AND ADDRESSES

Received December 15, 1975, from the *Food and Drug Administration, Department of Health, Education, and Welfare, Detroit, MI 48207.*

Accepted for publication March 25, 1976.

The authors thank Russell J. Ayers, FDA, Detroit District, for assistance in performing the mass spectral analyses and Dr. Eric B. Sheinen, Pharmaceutical Research and Testing Laboratory, FDA, Washington, D.C., for assistance in the NMR spectral analyses.

[x] To whom inquiries should be directed.

[13] Aldrich Chemical Co., Milwaukee, WI 53233.

[14] MC/B Manufacturing Chemists, Norwood, OH 45212.

Identification of Diacetylmorphine Metabolites in Humans

S. Y. YEH[x], R. L. McQUINN, and C. W. GORODETZKY

Abstract □ With the techniques of column chromatography, TLC, and GLC, morphine, 6-acetylmorphine, normorphine, morphine 3-glucuronide, 6-acetylmorphine 3-glucuronide, and normorphine glucuronide were identified as metabolites of diacetylmorphine (heroin) in the urine of humans administered 10 mg iv/70 kg body weight.

Keyphrases □ Diacetylmorphine—metabolites identified using TLC, GLC, and column chromatography, human urine □ Metabolites—diacetylmorphine, identified using TLC, GLC, and column chromatography, human urine □ TLC—identification, diacetylmorphine metabolites, human urine □ GLC—identification, diacetylmorphine metabolites, human urine □ Column chromatography—identification, diacetylmorphine metabolites, human urine □ Narcotics—diacetylmorphine, metabolites identified using TLC, GLC, and column chromatography, human urine

Studies in laboratory animals *in vitro* and *in vivo* indicated that diacetylmorphine (heroin) (I) was rapidly metabolized first to 6-acetylmorphine and then to morphine (1–5). In humans, diacetylmorphine was excreted in the urine mainly as morphine (6, 7). Approximately 50–60% of I administered to heroin addicts was excreted in the urine as conjugated morphine and 7% as free morphine (8, 9). In addition to free and conjugated morphine, small

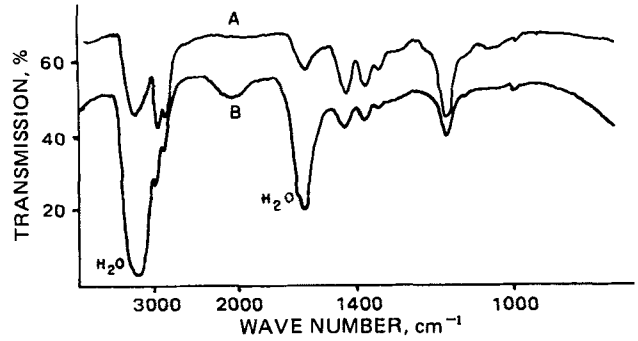

Figure 6—*IR spectra of (A) diethylamine reagent and (B) isolated decomposition product III.*

3000-cm^{-1} region indicated the absence of hydroxyl and primary or secondary amine groups.

The mass and IR spectra provided sufficient evidence for the elucidation of the structure of II. This compound was available commercially[13] and was purchased to serve as a reference material. The UV spectra of this reference material were nearly identical to those of the laboratory-produced decomposition product (Fig. 2). However, some background absorbance was apparent in the latter.

The IR and mass spectra of these two materials appeared identical (Figs. 3 and 4). The NMR spectra (Fig. 5) were also identical, with the exception of pentane peaks in the spectrum of the laboratory-produced material due to a residue remaining from the extraction step. A peak due to a chloroform impurity in the deuterated solvent was also visible in this spectrum because of the higher instrument gain used.

Gas and liquid chromatograms subsequently obtained for the reference material showed peaks identical to those of the previously unknown component. The chromatographic and spectral data combined with the identical physical characteristics of the cotton filler extract, the laboratory-produced material, and the reference material provided convincing evidence that II was formed as a major decomposition product of I.

Prior to the distillation of III from decomposed drug substance, the latter material was tested and found positive for secondary amines by the NF monograph test. The identity of III as a second decomposition product was then established by comparison of the gas chromatogram and the IR spectrum of the distillate with those of the diethylamine reagent[14]. Water was added to the latter prior to vaporization in the IR cell to simulate better its effect on the isolate spectrum (Fig. 6).

The distillate of an alkaline solution of undecomposed drug substance was found to contain no diethylamine, thus eliminating the suspicion that the latter may have been formed during the isolation procedure.

The route of decomposition from I to II and III has not been satisfactorily elucidated at this time and is apparently quite complex. However, it has been demonstrated that this type of decomposition has occurred in commercial tablet products and that it is accelerated by the presence of moisture.

The NF monograph assay procedure is specific for I in the presence of II, since it was found that II is retained in the sodium hydroxide solution while I is extracted into chloroform. However, the content uniformity procedure involves the direct UV determination of filtered hydrochloric acid solutions of the tablets. Since II was found to have considerable absorptivity and a maximum at 257 nm in this solvent, its presence in tablets could be expected to increase significantly the absorbance readings of their solutions, leading to inaccurately high results.

REFERENCES

(1) O. T. Bolding, *Curr. Ther. Res. Clin. Exp.*, **16**, 40 (1974).

(2) Y. K. Sedat and J. Reddy, *ibid.*, **16**, 398 (1974).

(3) D. E. Carney and E. D. Tweddell, *Med. J. Aust.*, **1**, 13 (1975).

(4) B. Testa and A. H. Beckett, *J. Chromatogr.*, **71**, 39 (1972).

(5) D. Mihailova, A. Rosen, B. Testa, and A. H. Beckett, *J. Pharm. Pharmacol.*, **26**, 711 (1974).

(6) E. C. Schreiber, B. H. Min, A. V. Zeiger, and J. F. Lang, *J. Pharmacol. Exp. Ther.*, **159**, 372 (1968).

(7) "The National Formulary," 14th ed., Mack Publishing Co., Easton, Pa., 1975, pp. 204, 205.

(8) K. G. Weidmann, A. Wolf, and J. Reisch, *Arch. Pharm.*, **306**, 954 (1973).

ACKNOWLEDGMENTS AND ADDRESSES

Received December 15, 1975, from the *Food and Drug Administration, Department of Health, Education, and Welfare, Detroit, MI 48207.*

Accepted for publication March 25, 1976.

The authors thank Russell J. Ayers, FDA, Detroit District, for assistance in performing the mass spectral analyses and Dr. Eric B. Sheinen, Pharmaceutical Research and Testing Laboratory, FDA, Washington, D.C., for assistance in the NMR spectral analyses.

[x] To whom inquiries should be directed.

[13] Aldrich Chemical Co., Milwaukee, WI 53233.

[14] MC/B Manufacturing Chemists, Norwood, OH 45212.

Identification of Diacetylmorphine Metabolites in Humans

S. Y. YEH[x], R. L. McQUINN, and C. W. GORODETZKY

Abstract □ With the techniques of column chromatography, TLC, and GLC, morphine, 6-acetylmorphine, normorphine, morphine 3-glucuronide, 6-acetylmorphine 3-glucuronide, and normorphine glucuronide were identified as metabolites of diacetylmorphine (heroin) in the urine of humans administered 10 mg iv/70 kg body weight.

Keyphrases □ Diacetylmorphine—metabolites identified using TLC, GLC, and column chromatography, human urine □ Metabolites—diacetylmorphine, identified using TLC, GLC, and column chromatography, human urine □ TLC—identification, diacetylmorphine metabolites, human urine □ GLC—identification, diacetylmorphine metabolites, human urine □ Column chromatography—identification, diacetylmorphine metabolites, human urine □ Narcotics—diacetylmorphine, metabolites identified using TLC, GLC, and column chromatography, human urine

Studies in laboratory animals *in vitro* and *in vivo* indicated that diacetylmorphine (heroin) (I) was rapidly metabolized first to 6-acetylmorphine and then to morphine (1–5). In humans, diacetylmorphine was excreted in the urine mainly as morphine (6, 7). Approximately 50–60% of I administered to heroin addicts was excreted in the urine as conjugated morphine and 7% as free morphine (8, 9). In addition to free and conjugated morphine, small

amounts of I and free 6-acetylmorphine were observed in the urine of humans infused with a large dose of I intravenously (10). Morphine ethereal sulfate, free and conjugated normorphine, morphine 6-glucuronide, and dihydromorphinone could also be metabolites of I, since these substances have been identified as morphine metabolites in humans and laboratory animals (11–19). The present article reports the identification of I metabolites in humans following intravenous administration of a single 10-mg dose.

EXPERIMENTAL

Materials—Diacetylmorphine hydrochloride [free of contaminant when determined by TLC (20) but shown to contain about 5% 6-acetylmorphine as determined by GLC], 6-acetylmorphine hydrochloride, and normorphine hydrochloride were obtained[1]. Morphine sulfate and codeine phosphate were commercial products. Morphine 3-glucuronide and morphine 3-ethereal sulfate were isolated, respectively, from the urine of dogs and cats administered morphine (14, 21). Normorphine 3-glucuronide was isolated from the urine of dogs administered normorphine hydrochloride (22).

Methods—Twelve healthy, postaddict, male, federal prisoner volunteers, with an average age of 36 years and an average body weight of 77 kg, were administered 10 mg iv of I/70 kg body weight. Urine collections were made before drug administration and at intervals of 2, 4, 6, 8, 16, and 24 hr and *ad libitum* following drug administration. The urine was frozen after collection.

Extraction of I Metabolites—The method for extraction and determination of I metabolites was described previously (23).

Glucuronic Acid Determination—The content of glucuronic acid in the conjugated metabolites was determined according to the procedure of Dische (24).

Hydrolysis of Conjugated Metabolites: Acid Hydrolysis—Conjugated metabolites were hydrolyzed by autoclaving the sample in 2.2 *N* HCl [20% (v/v) concentrated hydrochloric acid] in a steam-jacketed autoclave at 6.8 kg of pressure and 115° for 30 min. After cooling, the sample was adjusted to about pH 10 and then extracted and silylated for GLC determination according to the procedure described (11, 23). Under these conditions, 6-acetylmorphine and its conjugates were hydrolyzed to morphine. Identical samples without hydrolysis were used as controls.

Hydrolysis of Conjugated Metabolites: Enzymatic Hydrolysis—Samples were adjusted to pH 7, buffered with 1.0 ml of 0.1 *M* phosphate buffer at pH 6.8, and incubated with 5 mg of β-glucuronidase[2] (type II bacterial powder, 170 Fishmen units/mg and no sulfatase activity) and 2 drops of chloroform at 37° for 4 hr (for hydrolysis of 6-acetylmorphine conjugate) or 18 hr (for hydrolysis of morphine and normorphine conjugates). Samples incubated without enzyme were used as the control. After incubation, the sample was adjusted to pH 8.5 (for extraction of 6-acetylmorphine and morphine) or pH ~10 (for extraction of normorphine and morphine) and then extracted and silylated for GLC determination according to the described procedure (11, 23).

TLC—TLC was performed with either instant TLC silica gel sheets[3] or linear preadsorbent TLC silica gel plates[4]. With the instant TLC silica gel sheets, samples were spotted 2.54 cm (1 in.) above the edge. The chromatogram was developed with 1-butanol–acetic acid–water (35:3:10). With the linear TLC silica gel plates, aliquots of unknown samples along with authentic samples were spotted on the preadsorbent section. The chromatogram was developed with ethyl acetate–methanol–ammonium hydroxide (17:2:1), and the R_f values were calculated using the beginning of the silica gel section as the origin. All chromatograms were visualized by spraying with iodoplatinate reagent[5].

GLC—A gas chromatograph[6] equipped with dual flame-ionization detectors and dual columns was used. A 0.9-m (3-ft) × 2-mm glass column (Column 1) was packed with 3% OV-17 coated on Gas Chrom Q (60–80 mesh). A 1.5-m (5-ft) × 2-mm stainless steel column (Column 2) was packed with 3% SE-30 coated on Varaport (100–200 mesh). The temperatures of the injector and detector were set at 255 and 295°, respectively; gas flow rates were 30 ml/min for nitrogen and hydrogen and 300–400 ml/min for compressed dried air.

Derivatization—An aliquot of the sample was placed in an acylation tube and evaporated to dryness under a stream of nitrogen in a water bath at about 60°. The residue was derivated to make silyl, trifluoroacetyl, acetyl, or propionyl derivatives. Silylated derivatives were prepared by heating the residue with 50 μl of 25% trimethylsilylimidazole in pyridine[7] at 90–95° for 1 hr. Trifluoroacetyl derivatives were prepared by heating the residue with 0.2 ml of trifluoroacetic anhydride at 60–70° for 0.5 hr. Acetyl derivatives were made by heating the residue with 0.2 ml of acetic anhydride and 0.1 ml of pyridine at 60–70° for 0.5 hr. Propionyl derivatives were prepared by heating the residue with 0.2 ml of propionic anhydride (glass redistilled) and 0.1 ml of pyridine at 60–70° for 0.5 hr. The excess anhydride and pyridine were removed by evaporation, and the residue was reconstituted with 50 μl of ethyl acetate. One microliter of the solution was injected into the gas chromatograph.

GLC–Mass Spectrometry— The chemical ionization mass spectral data were obtained[8] using a glass column [1.5 m (5 ft) × 2 mm] packed with 3% SE-30 coated on Gas Chrom Q. Methane was used as the carrier gas as well as the chemical ionization reagent gas in the ion source. The column, injector, and ion source temperatures were 240, 250, and 100°, respectively. The electron energy was 80 ev, and ion repeller voltage was 3 v.

Isolation with Column Chromatography—The urine samples collected during the 0–16-hr period from 10 subjects were pooled, centrifuged to remove insoluble substances, and chromatographed with a resin[9] column. Two hundred milliliters of the urine was passed, at a flow rate of about 2–4 ml/min, through the column (2.1 × 40 cm) previously washed with acetone, methanol, and water. The column then was washed with 150 ml of distilled water and eluted with 250 ml of methanol. The first 100 ml of washing was discarded, and the second 50 ml of washing was combined with the eluate. The eluate was evaporated to dryness under vacuum in a rotary evaporator in a water bath between 40 and 50° (all evaporation was done in the same manner). The residue was triturated with methanol and yielded methanol-soluble and insoluble (water-soluble) fractions.

Methanol-Soluble (Free Base Drug) Fraction—The methanol-soluble fraction was evaporated to dryness. The residue was dissolved with 15 ml of 10% acetic acid solution and extracted three times with 15 ml of *n*-butyl chloride to remove such substances as nicotine and caffeine. Morphine, I, and acetylmorphine were not extracted under these circumstances. The aqueous phase, after extraction with *n*-butyl chloride, was adjusted to pH 4.5 with 1 *N* NaOH and extracted with 15 ml of chloroform three times to attempt to extract I. After extraction with chloroform, the aqueous phase was adjusted to pH 8.5 with 1 *N* NaOH and extracted three times with 15 ml of 1,2-dichloroethane containing 30% (v/v) 2-propanol.

After extraction, the aqueous phase was again evaporated to dryness and triturated with methanol. The methanol-soluble portion was combined with the extract of 1,2-dichloroethane containing 30% 2-propanol. The methanol-insoluble portion was discarded. The extracts of *n*-butyl chloride, chloroform, and 1,2-dichloroethane containing 30% 2-propanol were separately pooled and evaporated to dryness, and the residues were dissolved with 1 ml of *n*-butyl chloride, chloroform, and ethyl acetate, respectively.

RESULTS

Aliquots of the extracts of *n*-butyl chloride, chloroform, and 1,2-dichloroethane containing 30% 2-propanol were chromatographed on linear TLC silica gel plates with ethyl acetate–methanol–ammonium hydroxide (17:2:1) as the developing solvent. The chromatogram of the extract of *n*-butyl chloride showed two spots with R_f 0.35 and 0.8. The retention time of the peaks of the extract did not correspond to any hypothesized possible I metabolite. The chromatogram of the chloroform extract showed three spots with R_f 0.43 (morphine), 0.8 (to be identified), and 0.9 (6-acetylmorphine and I). The chromatogram of the 1,2-dichloroethane containing 30% 2-propanol extract showed three spots with R_f 0.23 (normorphine), 0.43, and 0.9.

Preparative TLC of the chloroform extract was performed on two large

[1] Courtesy of Dr. E. L. May, National Institutes of Health.
[2] Sigma Chemical Co., St. Louis, Mo.
[3] Gelman Instrument Co., Ann Arbor, Mich.
[4] Quantum Industries, Fairfield, N.J.
[5] Consisting of 0.25 g of chloroplatinic acid and 5 g of potassium iodide/100 ml of water.
[6] Varian Aerograph, Series 2700.
[7] Tri-Sil-Z, Pierce Chemical Co., Rockford, Ill.
[8] Model 3300 GLC–mass spectrometer equipped with a model 6000 interactive data system, Finnigan, Sunnyvale, Calif.
[9] Amberlite XAD-2, a styrene–divinyl benzene copolymer, Rohm & Haas, Philadelphia, Pa.

Table I—GLC Retention Time (Minutes) of Diacetylmorphine Metabolites and Standards

Sample	Trifluoroacetyl Derivative	Trimethylsilyl Derivative	
	3% OV-17, 210°	3% OV-17, 220°	3% OV-17, 230°
6-Acetylmorphine hydrochloride	6.9	—	7.1
Codeine phosphate	5.8	—	—
Morphine sulfate	3.8	7.4	4.3
Norcodeine hydrochloride	9.1	—	—
Normorphine hydrochloride	6.2	8.8	—
Methanol-soluble fraction separated on TLC[a]			
R_f 0.23	3.8, 6.2	7.4, 8.8	—
R_f 0.40	3.8	7.4	—
R_f 0.9	6.9	—	7.1

[a] Linear TLC silica gel plate using ethyl acetate–methanol–ammonium hydroxide (17:2:1).

Table II—R_f Values of Diacetylmorphine Metabolites and Standards

Sample	Linear TLC Silica Gel Plate	Instant TLC Silica Gel Sheet
Authentic samples		
6-Acetylmorphine hydrochloride	0.90	0.9
Diacetylmorphine hydrochloride	0.90	0.9
Morphine sulfate	0.40	0.9
Normorphine hydrochloride	0.20	0.8
Morphine 3-glucuronide	—	0.40
Morphine 3-ethereal sulfate	—	0.65
Normorphine 3-glucuronide	—	0.66
Acetylcodeine	0.84	—
Codeine	0.67	—
Norcodeine	0.47	—
Codeine 6-glucuronide	—	0.60
Metabolites		
Methanol-soluble fraction		
n-Butyl chloride extract	0.35, 0.80	—
Chloroform extract	0.40, 0.80, 0.87	—
1,2-Dichloroethane–2-propanol extract	0.23, 0.40, 0.90	—
Methanol-insoluble fraction	—	0.03, 0.40, 0.76, 0.90

plates (20 × 20 cm), and preparative TLC of the 1,2-dichloroethane–2-propanol extract was performed on one plate. A section of the chromatogram was sprayed with iodoplatinate reagent. The zones corresponding to the iodoplatinate-positive regions and to R_f 0.7 (where codeine would be expected) were horizontally scraped off and eluted with methanol. The eluate was concentrated and aliquots were derivatized and determined by GLC. The identity of metabolites with R_f 0.23, 0.4, and 0.9 was further supported as normorphine, morphine, and 6-acetylmorphine, respectively, by cochromatography with authentic samples and by GLC (Table I).

Compound I was not detected in the eluate obtained from the region with R_f 0.9. The retention time of the peaks of the eluate with R_f 0.8 did not correspond to any hypothesized possible I metabolite. Norcodeine and codeine were not detected in the eluate obtained from the zone with R_f 0.4 and 0.7.

Methanol-Insoluble Fraction—The chromatogram of the methanol-insoluble (water-soluble) fraction on an instant TLC silica gel sheet developed with 1-butanol–acetic acid–water (35:3:10) showed four iodoplatinate-positive spots with R_f 0.03, 0.4, 0.76, and 0.9 (Table II). Preparative TLC was performed on 10 instant TLC silica gel sheets (20 × 20 cm), and a section of the chromatogram was sprayed with iodoplatinate reagent. The zones corresponding to the iodoplatinate-positive spots were horizontally cut off and eluted with warm water. The material located at R_f 0.9 was eluted first with methanol and then with water. In addition, the iodoplatinate-negative regions with R_f 0.5 and 0.6 (corresponding to R_f values of morphine 6-glucuronide and morphine 3-ethereal sulfate) were isolated and eluted with water. It was thought that these metabolites could be present in small amounts, too low to show positive with iodoplatinate.

The metabolite with R_f 0.03 was hydrolyzed to yield morphine. Since this metabolite could have been due to morphine 3-glucuronide, held back by an impurity, it was rechromatographed. The chromatogram again showed one spot with R_f 0.03. The metabolite with R_f 0.03 was negative with the phenolic test and hydrolyzed with β-glucuronidase or with acid to yield morphine. This metabolite appears to be a polar morphine metabolite, but its identity has not yet been determined.

The metabolite with R_f 0.4 was negative with the phenolic test, positive with the glucuronic acid test, and hydrolyzed with β-glucuronidase or with acid to give morphine. Cochromatography of this metabolite with authentic morphine 3-glucuronide showed a single spot. Therefore, this metabolite was identified as morphine 3-glucuronide.

The metabolite with R_f 0.76 was positive with the glucuronic acid test and hydrolyzed with β-glucuronidase to yield 6-acetylmorphine and normorphine. These metabolites were tentatively identified as 6-acetylmorphine 3-glucuronide and normorphine glucuronide, respectively.

The material with R_f 0.9, corresponding to the R_f of free morphine and 6-acetylmorphine, showed peaks of morphine and 6-acetylmorphine on GLC. The concentration of morphine and 6-acetylmorphine did not significantly increase after enzymatic hydrolysis, suggesting that the compound was in the free form. Other peaks were also observed but did not correspond to those of any known I metabolites.

The eluate obtained from the iodoplatinate-negative region with R_f 0.5–0.6 was concentrated and passed through a neutral alumina column (1.0 × 2.5 cm). The column was eluted with 100 ml of water. The eluate was concentrated to about 1.5 ml and rechromatographed on one instant TLC silica gel sheet (20 × 20 cm), using 1-butanol–acetic acid–water (35:3:10) as the developing solvent. After a section of the chromatogram was sprayed with iodoplatinate reagent, a faint spot with R_f 0.5 was clearly distinguished from the spot of morphine 3-glucuronide (0.4) and codeine 6-glucuronide (0.6). The zone corresponding to R_f 0.5 was cut off and eluted with water, and the eluate was concentrated. The eluate was positive with the Folin–Ciocalteu phenolic test and with a glucuronic test. After hydrolysis with β-glucuronidase, the metabolite yielded morphine. The content of glucuronic acid in the eluate was determined according to the described procedure (24), and the content of morphine was determined by GLC. The ratio of morphine to glucuronic acid was about 1:1. These data suggest this metabolite to be morphine 6-glucuronide.

Identification of Normorphine by GLC–Mass Spectrometry—The chemical ionization mass spectral data of a sample (as the acetyl derivative) showed a peak with a retention time and mass fragmentation spectrum [with mass at *m/e* 398 (M − 1) and 338 (M − acetic acid + 1)] identical with those of authentic triacetylnormorphine (Fig. 1).

Search for Dihydromorphinone as Possible Metabolite of I—Aliquots (200 ml) of the first 8-hr urine from two subjects were acid hydrolyzed, buffered at pH ~10, and extracted with chloroform instead of 1,2-dichloroethane containing 30% 2-propanol according to a described triple-extraction procedure (11). The organic phase was concentrated and applied along with authentic samples to an aluminum oxide 1B plate[10]. The chromatogram was developed using the lower phase of the solvent mixture of chloroform–methanol–water–acetic acid (20:10:20:2) (19). A section of the plate was sprayed with iodoplatinate, and a spot corresponding to morphine was observed; no dihydromorphinone spot was seen. The presence of normorphine was inconclusive because of an impurity masking the spot.

The zones corresponding to normorphine (R_f 0.03), morphine (0.23), and dihydromorphinone (0.38) were separately scraped off and eluted with methanol. Aliquots of the eluate were evaporated to dryness, and the residues were made into propionyl derivatives. One microliter of the reconstituted solution was injected into Column 2 with an oven temperature at 240°. Peaks corresponding to normorphine (R_t 22) and morphine (7.2) were observed in the eluate. The dihydromorphinone peak (R_t 4.9) was not observed. A detailed procedure for the determination of dihydromorphinone as a morphine metabolite will be published later.

DISCUSSION

Free morphine, 6-acetylmorphine, free normorphine, morphine 3-glucuronide, morphine 6-glucoronide, 6-acetylmorphine 3-glucuronide,

[10] J. T. Baker, Phillipsburg, N.J.

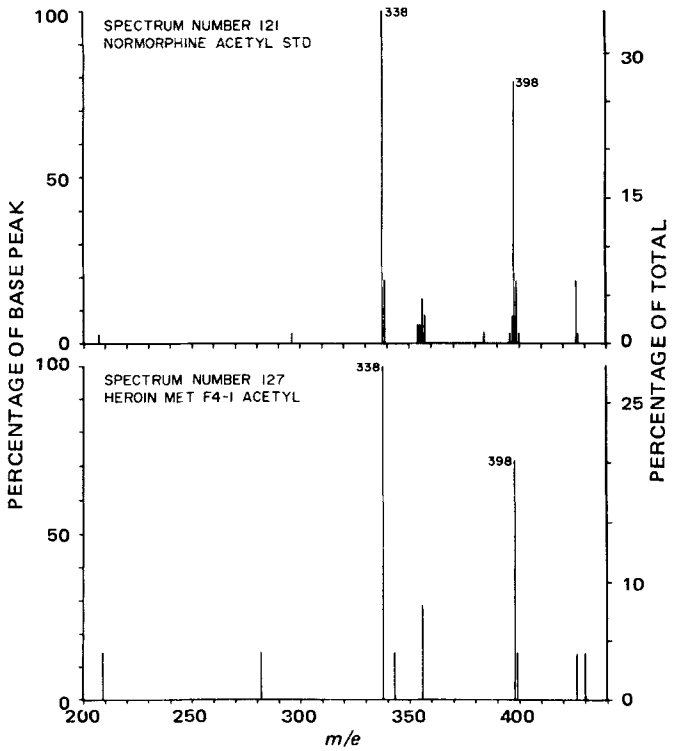

Figure 1—*GLC–mass spectrometric analysis of acetylated normorphine and the peak corresponding to acetylated normorphine of the extract of 5 ml of urine collected 0–8 hr from Subject F administered 10 mg of diacetylmorphine hydrochloride.*

and normorphine glucuronide were found as metabolites of I in human urine. Morphine 3-glucuronide was the major metabolite, accounting for approximately 50% of the administered dose. Free morphine accounted for about 7%, and the remaining metabolites were present in a magnitude of less than 5%. The quantitative studies on metabolism of I in humans will be published elsewhere (25).

Since heroin is deacetylated to 6-acetylmorphine and then to morphine (2, 3, 5), it seems likely that the 6-acetylmorphine present in the administered dose was deacetylated to morphine *in vivo* and the 6-acetylmorphine found in the urine was a minor I metabolite. However, the possibility could not be ruled out that it was an autohydrolysis product of I excreted in the urine or that it occurred during the process of extraction.

An attempt to isolate 6-acetylmorphine 3-glucuronide was unsuccessful because of the small amount of material and the labile acetyl group. The existence of 6-acetylmorphine 3-glucuronide could be further illustrated by incubation of the eluate obtained from the resin[9]. The eluate was evaporated to dryness and reconstituted with water prior to incubation with β-glucuronidase. The amount of 6-acetylmorphine was increased about twofold after incubation, while morphine increased five- to sixfold as compared to that without incubation.

In the present study, normorphine glucuronide together with 6-acetylmorphine 3-glucuronide was located at R_f 0.76. An attempt to isolate normorphine glucuronide was unsuccessful because of the small amount of material.

Codeine and norcodeine were not observed as metabolites of I in the present studies, although they have been reported as metabolites of morphine in humans (26, 27). The existence of codeine and norcodeine as metabolites of morphine in humans has been questioned (28, 29). The sensitivity of the present GLC method could detect 0.5 μg of codeine, 1.0 μg of norcodeine, and 5 μg of dihydromorphinone. Dihydromorphinone has been reported as a morphine metabolite in the rat chronically administered morphine but was not observed in the present study. This result could be due to a species difference.

The chromatograms of the extract of *n*-butyl chloride on a linear TLC silica gel plate, developed with ethyl acetate–methanol–ammonium hydroxide (17:2:1), showed spots with R_f 0.35 and 0.8. These spots were probably due to nicotine and caffeine and their metabolites. A chromatographic study on the urine from cigarette smokers and coffee drinkers was described previously (30).

REFERENCES

(1) G. Rizzott, *Bull. Soc. Ital. Biol. Spec.*, **9**, 507 (1934); through *Chem. Abstr.*, **29**, 225 (1934).

(2) C. I. Wright, *J. Pharmacol. Exp. Ther.*, **71**, 164 (1941).

(3) E. L. Way, J. W. Kemp, J. M. Young, and D. R. Grassetti, *ibid.*, **129**, 144 (1960).

(4) E. L. Way, J. M. Young, and J. W. Kemp, *Bull. Narc.*, **17**(1), 15 (1965).

(5) G. L. Cohn, J. A. Cramer, and H. D. Kleber, *Proc. Soc. Exp. Biol. Med.*, **144**, 351 (1973).

(6) T. M. Shen, *J. Chin. Pharm. Assoc.*, **1**, 124 (1936); through *Chem. Abstr.*, **31**, 730 (1937).

(7) F. W. Oberst, *J. Pharmacol. Exp. Ther.*, **73**, 401 (1941).

(8) *Ibid.*, **79**, 266 (1943).

(9) P. N. Mo and E. L. Way, *J. Pharmacol. Exp. Ther.*, **154**, 142 (1966).

(10) H. W. Elliott, K. D. Parker, J. A. Wright, and N. Nomof, *Clin. Pharmacol. Ther.*, **12**, 806 (1971).

(11) S. Y. Yeh, *J. Pharmacol. Exp. Ther.*, **192**, 201 (1975).

(12) J. M. Fujimoto and V. B. Haarstad, *ibid.*, **165**, 45 (1969).

(13) D. G. May, J. M. Fujimoto, and C. E. Inturrisi, *ibid.*, **157**, 626 (1967).

(14) S. Y. Yeh, H. I. Chevnov, and L. A. Woods, *J. Pharm. Sci.*, **60**, 469 (1971).

(15) H. Yoshimura, K. Oguri, and H. Tsukamoto, *Biochem. Pharmacol.*, **18**, 279 (1968).

(16) A. L. Misra, S. Y. Yeh, and L. A. Woods, *ibid.*, **19**, 1536 (1970).

(17) H. Yoshimura, M. A. Mori, K. Oguri, and H. Tsukamoto, *ibid.*, **19**, 2353 (1970).

(18) K. Oguri, S. Ida, H. Yoshimura, and H. Tsukamoto, *Chem. Pharm. Bull.*, **18**, 2414 (1970).

(19) A. Klutch, *Drug Metab. Disp.*, **2**, 23 (1974).

(20) G. R. Nakamura, *J. Assoc. Offic. Anal. Chem.*, **49**, 1086 (1966).

(21) S. Y. Yeh and L. A. Woods, *J. Pharmacol. Exp. Ther.*, **173**, 21 (1970).

(22) S. Y. Yeh, *Fed. Proc.*, **34**, 814 (1975).

(23) S. Y. Yeh and R. L. McQuinn, *J. Pharm. Sci.*, **64**, 1237 (1975).

(24) Z. Dische, *J. Biol. Chem.*, **167**, 189 (1947).

(25) S. Y. Yeh, C. W. Gorodetzky, and R. L. McQuinn, *J. Pharmacol. Exp. Ther.*, **196**, 249 (1976).

(26) U. Boerner and S. Abbott, *Experientia*, **29**, 180 (1973).

(27) U. Boerner, R. L. Roe, and C. E. Becker, *J. Pharm. Pharmacol.*, **26**, 393 (1974).

(28) S. Y. Yeh, *Experientia*, **30**, 265 (1974).

(29) S. Y. Yeh, *J. Pharm. Pharmacol.*, **27**, 214 (1975).

(30) S. Y. Yeh, *J. Pharm. Sci.*, **62**, 1827 (1973).

ACKNOWLEDGMENTS AND ADDRESSES

Received June 30, 1975, from the *National Institute on Drug Abuse, Division of Research, Addiction Research Center, Lexington, KY 40511 (U.S. Department of Health, Education, and Welfare Public Health Service, Alcohol, Drug Abuse, and Mental Health Administration).*

Accepted for publication April 14, 1976.

The authors thank Dr. E. J. Cone for the mass spectrum of acetylnormorphine.

[x] To whom inquiries should be directed.

Kinetic Spectrophotometric Study of Effect of Triazolopyrazines on *p*-Benzoquinone Complexes

G. H. MOXON and M. A. SLIFKIN ˣ

Abstract □ The effect of adding triazolopyrazines to a *p*-benzoquinone–proline system and a *p*-benzoquinone–histamine system was studied by observing the kinetics of the spectral changes and analyzing the results using digital simulation methods. Below 35°, the major effect was that the triazolopyrazine competed with the electron donors for the acceptors to form complexes. Above 35°, there was predominantly a chemical interaction between the triazolopyrazine and the acceptors. A separate experiment showed that the triazolopyrazine interacted with *p*-benzoquinone to form a complex initially but that a chemical interaction took place later.

Keyphrases □ *p*-Benzoquinone complexes—with proline and histamine, effect of various triazolopyrazines, kinetic spectrophotometric study □ Triazolopyrazines, substituted—effect on complexes of *p*-benzoquinone with proline and histamine, kinetic spectrophotometric study □ Complexes—*p*-benzoquinone with proline and histamine, effect of various triazolopyrazines, kinetic spectrophotometric study □ Spectrophotometry—kinetic study, effect of triazolopyrazines on complexes of *p*-benzoquinone with proline and histamine □ Structure–activity relationships—various triazolopyrazines, effect on complexes of *p*-benzoquinone with proline and histamine

The spectral properties of some nitrogen heterocyclic drugs, some triazolopyrazines, and a triazolopyrimidine (1) have been studied, as has the effect of these drugs on the potentiation of the reversal of metachromasia of a toluidine blue–heparin complex in the presence of amino acids (2). It was suggested that the triazolopyrazines might function as electron donors, competing with both the dye and amino acids for acceptor sites on the dye. The electron-donating properties of some of these drugs have now been studied by observing the interaction directly with the electron acceptor *p*-benzoquinone and by observing the effect of the drugs on systems of *p*-benzoquinone with the electron acceptors histamine and proline.

Both systems were studied extensively by the method of time-dependent spectrophotometry under various temperature, solvent, and pH conditions. The curves were analyzed using digital simulation methods (3, 4). Furthermore, since some of these heterocyclic drugs have antiasthmatic activity, their interaction with a histamine system might have medicinal interest. The alteration of a reaction rate by the complexing of one reactant in a two-molecule system with an added third compound has been studied (5, 6) and is a very useful technique where the interaction between the added third compound and either interactant is weak or is not shown clearly by the techniques in use.

EXPERIMENTAL

Histamine, *p*-benzoquinone, and proline were obtained and purified as described previously (3, 4). 3-Amino-6-methyl-8-propyl-*s*-triazolo[4,3-*a*]pyrazine (I), 3-acetamido-5-methyl-8-*n*-propyl-*s*-triazolo[4,3-*a*]pyrazine (II), 3-acetamido-6-methyl-8-*n*-propyl-*s*-triazolo[4,3-*a*]pyrazine (III), and 2-amino-5-*n*-propyl-*s*-triazolo[2,3-*c*]-pyrimidine (IV) were used as supplied[1]. (Their structures are shown in Fig. 1 of Ref. 1.) The experimental methods and techniques were described previously (3, 4).

[1] Courtesy of ICI Pharmaceutical Division.

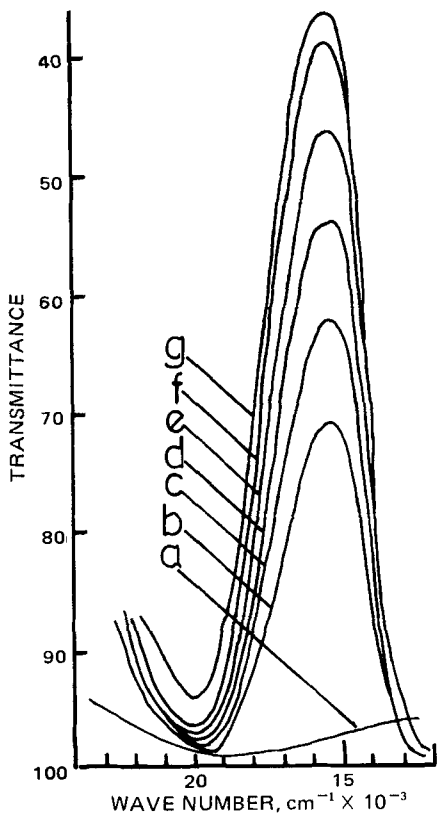

Figure 1—*Development of peak at 15,200 cm^{-1} (658 nm) attributed to the I (2 × 10^{-2} M)-p-benzoquinone (2 × 10^{-4} M) complex at 25° in pH 7 phosphate buffer. Readings were at: (a) zero time, (b) 6 days, (c) 7 days, (d) 8 days, (e) 9 days, (f) 10 days, and (g) 15 days.*

RESULTS AND DISCUSSION

Interaction of I with p-Benzoquinone—The effect of I with *p*-benzoquinone in phosphate buffer was studied first. Figure 1 shows the spectrum obtained in a mixed solution of the drug and quinone in pH 7 phosphate buffer. The effect of drug concentration on the development of the absorption spectrum is illustrated in Fig. 2. The shape of the curve is indicative of the formation of more than one species (7) and indicates that the interaction is of the form:

$$A \underset{k_2}{\overset{k_1}{\rightleftharpoons}} B \xrightarrow{k_3} C$$

The observed peak at 15,200 cm^{-1} (658 nm) corresponds not to the immediate product of the interaction but to some subsequent reaction product (*C*), as evidenced by the initial induction period and the shape of its growth curve.

Figure 3 shows the effect of temperature on the absorption band at 15,200 cm^{-1} (658 nm). Increasing the temperature from 25 to 55° resulted in a marginal increase in the intensity which was not reversible. This behavior indicates a chemical interaction and not a complexing mechanism. The initial reaction between the drug and the quinone, which was not observable spectroscopically, probably is the formation of a reversible complex, since many organic amines and amides are known to form complexes with quinones and then chemical products (3, 8).

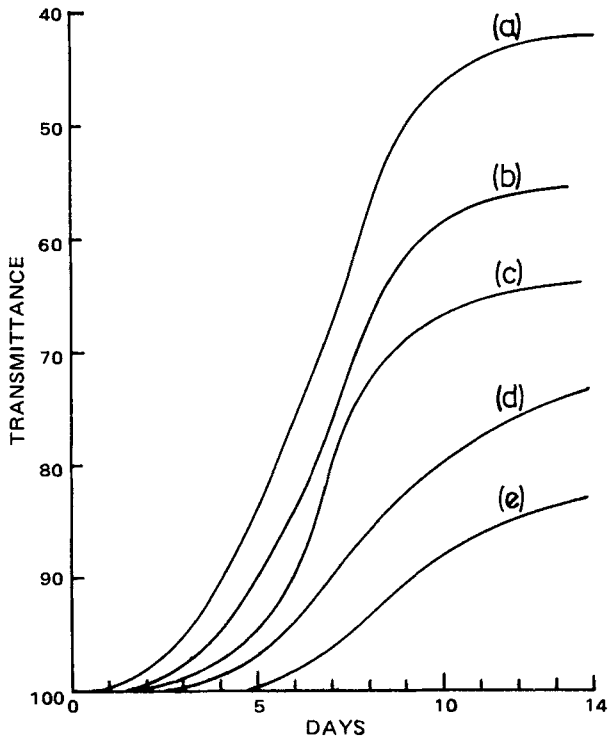

Figure 2—*Effect of I concentration on the development of the 15,200-cm^{-1} (658-nm) peak of the* p*-benzoquinone–I complex at 25° in pH 7 phosphate buffer. Key: a, 2 × 10^{-2} M; b, 10^{-2} M; c, 7 × 10^{-3} M; d, 4 × 10^{-3} M; and e, 10^{-3} M.*

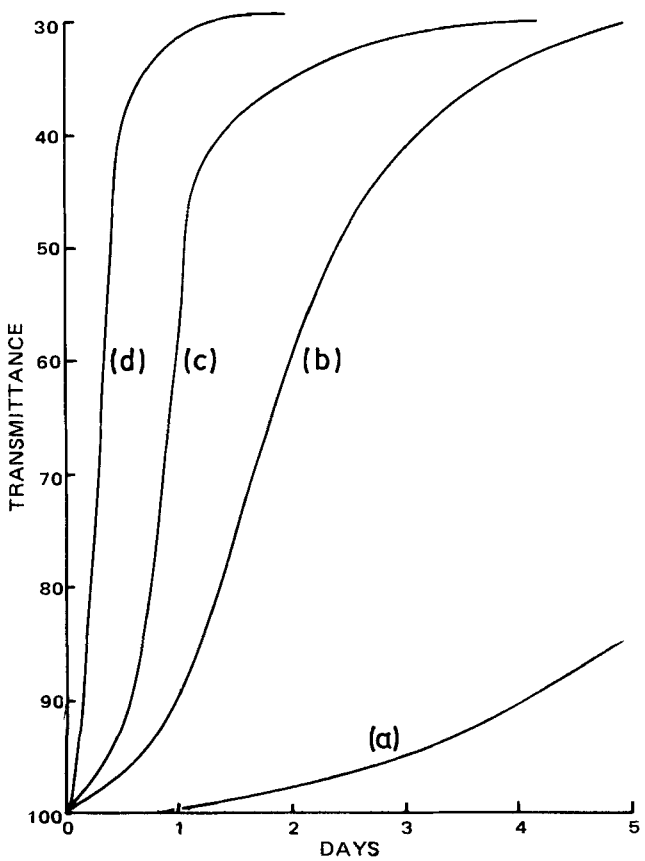

Figure 3—*Effect of temperature on the development of the 15,200-cm^{-1} (658-nm) peak of the* p*-benzoquinone–I complex in pH 7 phosphate buffer. Key: a, 25°; b, 35°; c, 45°; and d, 55°.*

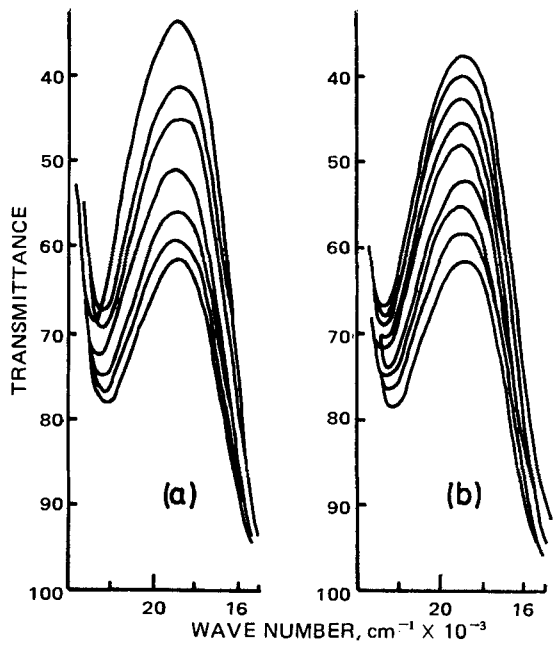

Figure 4—*Effect of I (2 × 10^{-2} M) on the absorption band at 18,800 cm^{-1} (532 nm) ascribed to the* p*-benzoquinone (2 × 10^{-4} M)–proline (7 × 10^{-2} M) complex in pH 7 phosphate buffer at 55°. Key: a, peak decreasing with time (0, 7, 10, 15, 20, 25, and 35 min); and b, peak increasing with time (35, 50, 60, 70, 85, 100, 120, 150, and 180 min).*

Interaction of I and Proline with *p*-Benzoquinone—To clarify the interactions of this termolecular system, three separate sets of experiments were performed. In Experiment A, both proline and I were added more or less simultaneously to the quinone. Experiment B concerned the effect of adding proline to a solution to which I had been added to the quinone several hours previously. Experiment C examined the effect of adding I to a solution in which a proline–quinone complex equilibrium had been established.

Experiment A—The addition of proline and I to the *p*-benzoquinone solution caused changes in absorption that were identical to those caused when proline alone was added to the quinone (4). Compound I can be dissolved in *p*-benzoquinone for up to 4 hr before adding proline without affecting the rate of formation of the proline–quinone complex.

Experiment B—When I was added to *p*-benzoquinone and allowed to stand for many hours, a band at 15,200 cm^{-1} (658 nm) gradually formed. The addition of proline to the solution in which this band was fully formed had no effect whatsoever. Old solutions of proline and quinone also gave rise to a similar band, preceded by the formation of a proline–quinone complex (4).

Experiment C—The addition of proline to *p*-benzoquinone resulted in the formation of a reversible complex with maximum absorption at 18,800 cm^{-1} (532 nm). After many hours, this absorption slowly decreased and was replaced by an absorption at 15,200 cm^{-1} (658 nm), belonging to some later formed reaction product (4). The addition of I to a solution

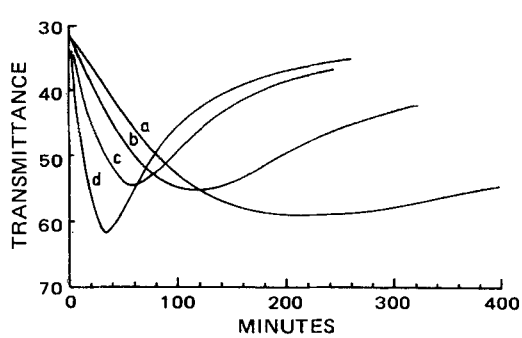

Figure 5—*Effect of varying concentration of I on changes in the proline–*p*-benzoquinone complex as measured by the absorption band at 18,800 cm^{-1} (532 nm) in phosphate buffer at pH 7 and 55°. Key: a, 10^{-3} M; b, 4 × 10^{-3} M; c, 10^{-2} M; and d, 2 × 10^{-2} M.*

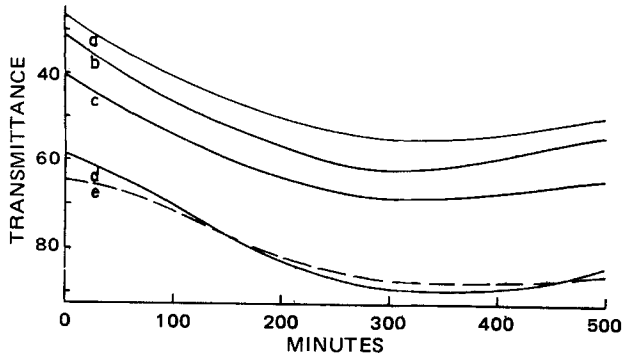

Figure 6—*Effect of I (2×10^{-2} M) on the absorption band at 18,800 cm^{-1} (532 nm) formed by mixing, at pH 7 and 25°, 2×10^{-4} M p-benzoquinone and the following concentrations of proline: (a) 4×10^{-1} M, (b) 7×10^{-2} M, (c) 1.5×10^{-2} M, (d) 2×10^{-4} M, and (e) 10^{-4} M.*

of *p*-benzoquinone and proline in which the complex absorbing at 18,800 cm^{-1} (532 nm) was fully formed but had not begun to decompose to give the absorption at 15,200 cm^{-1} (658 nm) gave some surprising changes. There was an initial slow decrease in the absorption at 18,800 cm^{-1} (532 nm) followed by an increase in the absorbance back toward the initial absorbance (Fig. 4).

Figures 5 and 6 show the effect of varying the drug and proline concentrations. As the drug concentration increased, so did the rate of its interaction with the proline–quinone system. From Fig. 6 it can be deduced that the concentration of proline does not affect the initial interaction rate—only the rate at which the absorption peak regains its equilibrium value.

Figure 7 shows the effect of temperature on the interaction of the drug on the quinone–proline system. As expected, raising the temperature caused an increase in the rate of interaction for both the decrease and later increase of the complex. The higher the temperature above 35°, the greater was the effect of temperature on the decrease of the complex as compared with the later increase. This trend was reversed below 35°. A similar effect was noted later with the histamine–quinone system.

From these experiments, it can be concluded that:

1. Compound I does not interfere with the initial complexing reaction between proline and the quinone.

2. There is a very slow chemical interaction between I and quinone with a large induction time, showing that intermediates are produced before the final product absorbing at 15,200 cm^{-1} (658 nm). This final product may be a disubstituted quinone (9).

3. A reaction between I and the proline–quinone complex leads to a decrease in the concentration of the complex.

Presumably there is competition for complexing with the quinone between I and proline. However, at a later time, the concentration of the complex returns to its original value with proline alone due to either an increase in the proline available for complexing or a decrease in drug. The proline exists mainly in its zwitterionic form at pH 7, but interaction is *via* the neutral amino form. At these pH's, this form is present only in about 1 part in 1000 (4). Similarly, the drug exists mainly in its ionized form at pH 7 (1), although some unionized form is present. This system

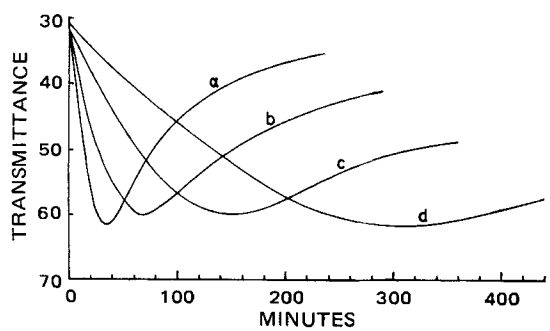

Figure 7—*Effect of I (2×10^{-2} M) on the absorption band at 18,800 cm^{-1} (532 nm) formed by mixing proline (7×10^{-2} M) with p-benzoquinone (2×10^{-4} M) at 25° in pH 7 phosphate buffer. Key: a, 55°; b, 45°; c, 35°; and d, 25°.*

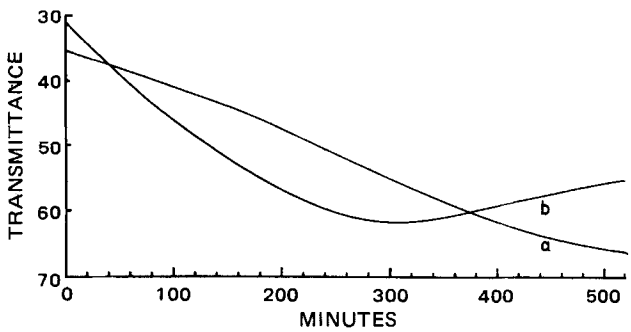

Figure 8—*Effect of I (2×10^{-2} M) on the absorption at 18,800 cm^{-1} (532 nm) of the proline (7×10^{-2} M)–p-benzoquinone (2×10^{-4} M) complex in phosphate buffer at 25°. Key: a, pH 8.0; and b, pH 7.0.*

is obviously very complicated; the various equilibria producing complexing forms of proline and drug are interdependent. Thus, either the shift of the equilibrium to produce more unionized proline or to produce less unionized drug would explain the results, the latter seeming more suitable.

Another explanation for the slow recovery of the proline–quinone complex concentration is the removal of drug by dimerization, although there is not any evidence for this, or by some other chemical reaction. However, at this stage of the interaction, the quinone is not removed from solution, as seen by the return of the complex absorption to its initial value at temperatures less than 35°. Only at higher temperatures is quinone removed from the solution and the complex does not regain its initial value with time. These various reactions are summarized in Scheme I.

It was previously observed that an increase in pH leads to a considerable apparent increase in the reaction rate between proline and *p*-benzoquinone (4). Therefore, the interaction of the drug with the proline–quinone system at pH 8 also was investigated (Fig. 8). There was the decrease of the band associated with the complex but no subsequent increase as at pH 7. The binding between the drug and *p*-benzoquinone at pH 8 apparently is stronger than that between proline and *p*-benzoquinone. Thus, pH is a strong determining factor in the interaction of this termolecular system. The effect of the drug on the hydroxyproline–quinone system is similar to that described for proline, but the reaction rates are slightly different.

Figure 9 shows the effect of some related drugs (II–IV) on the proline–quinone complex. Compound IV, a triazolopyrimidine, had only a marginal effect; the other drugs, all triazolopyrazines, had a marked effect, albeit in different ways. Among the triazolopyrazines, only I exhibited the reversal in the downward trend of the complex concentration at pH 7. None of these drugs other than I showed any spectroscopic evidence of an interaction with *p*-benzoquinone alone, although II and III obviously interacted with the proline–*p*-benzoquinone system (Fig. 9).

There is now a body of evidence showing that amines and amides, especially biological amines and amides in the unionized form, complex with quinones and other charge acceptors (3, 4, 8). If the drugs interact in a similar manner, then this interaction explains the rather slow forward reaction times; at the pH values used, the amines or amides are mainly in the ionized XNH_3^+ or XNH_2^+ form, so the effective concentration of XNH_2 or XNH is quite low.

Interaction of I with Histamine–*p*-Benzoquinone Complex—In the presence of I, there was a change in both the apparent rate constants

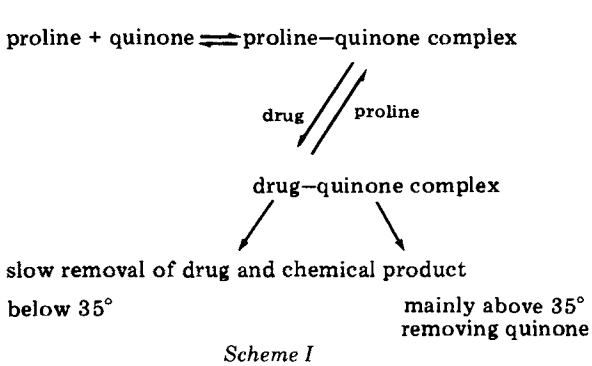

Scheme I

Table I—Apparent and Corrected Rate Constants for the Interactions of Histamine with *p*-Benzoquinone in the Presence of I in pH 7 Phosphate Buffer[a]

k_1, M^{-1} min^{-1}	k_2, min^{-1}	k_3, min^{-1}	$\frac{k_1}{k_2}$, M^{-1}	Temperature
1.51×10^{-2} (8.4)	4.53×10^{-4}	2.72×10^{-6}	33.3 (18,700)	25°
4.37×10^{-2} (1.26×10)	3.52×10^{-3}	6.77×10^{-5}	12.4 (3570)	35°
1.19×10^{-1} (2.07×10)	2.63×10^{-2}	1.21×10^{-3}	4.5 (784)	45°
2.87×10^{-1} (2.92×10)	1.02×10^{-1}	7.57×10^{-3}	2.8 (286)	55°

[a] Data in parentheses are corrected for histamine concentration only and not for I.

and the thermodynamic parameters of the histamine–quinone complex (Tables I and II). The effect of the drug was greater the longer it was dissolved in quinone solution prior to the addition of histamine, confirming that the drug interacts slowly with the quinone, forming a chemical compound. After 24 hr, almost all quinone had interacted with the drug, as evidenced by the negligible reaction with histamine if added after this time. On the other hand, there was no evidence of the 15,200 cm^{-1} (658 nm) peak at this time.

The data in Table I can be compared with the data for the interaction of histamine with *p*-benzoquinone alone given in Tables 1 and 2 of Ref. 3[2]. The data in Table I are compatible with a competitive reaction between the drug and the histamine for complexing with *p*-benzoquinone. There was a decrease in the apparent interaction rate between histamine and the *p*-benzoquinone in the presence of the drug at lower temperatures. However, at higher temperatures, there was an apparent increase in the interaction rate of histamine, showing that a more complicated set of interactions occurred in the presence of the drug at these elevated temperatures. A similar effect of temperature was already noticed for the interaction of the drug with the proline–*p*-benzoquinone system (4). Presumably, at the higher temperatures, the chemical interactions become significantly large compared to the complexing mechanism that predominates at the lower temperatures.

Obviously, any rate constants derived for the interaction of the drug with the *p*-benzoquinone from these termolecular systems will contain a contribution from the irreversible chemical interactions. The apparent rate constants for the drug–quinone complex derived from these data, assuming a simple competition between the drug and histamine, are:

$$k_1 = 1.04 \times 10^{-2} \text{ liter mole}^{-1} \text{ min}^{-1} \quad \text{(Eq. 1)}$$

$$k_2 = 7.28 \times 10^{-4} \text{ min}^{-1} \quad \text{(Eq. 2)}$$

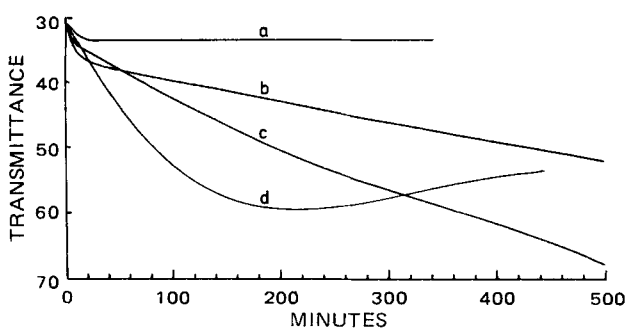

Figure 9—*Effect of different drugs (10^{-3} M) on the absorption at 18,800 cm^{-1} (532 nm) of the proline (7×10^{-2} M)-p-benzoquinone (2×10^{-4} M) complex in pH 7 phosphate buffer at 25°. Key: a, IV; b, III; c, II; and d, I.*

[2] Due to a mistake in the computer printout, all values of k_1, k_2, and k_3 in Ref. 3 should be multiplied by 10^5. Other parameters are not affected.

Table II—Apparent and Corrected Thermodynamic Data for the Interaction of Histamine with *p*-Benzoquinone in the Presence of I in pH 7 Phosphate Buffer[a]

	ΔH	ΔS	ΔG	E_A
k_1	18.3 (6.6)	−36.6 (−31.2)	29.2 (15.9)	18.9 (7.2)
k_2	34.6	11.4	31.2	35.2
k_3	50.9	56	34.2	51.5
$\frac{k_1}{k_2}$	−16.3 (−28)	−48.0 (42.6)	−2.0 (15.3)	

[a] Data in parentheses are corrected for histamine concentration only and not for I. H = enthalpy, S = entropy, G = free energy, and E_A = activation energy; all parameters are in kilocalories mole^{-1} except entropy which is in entropy units.

with $k_1/k_2 = 14.3\ M^{-1}$, and:

$$k_3 = 2.05 \times 10^{-5} \text{ min}^{-1} \quad \text{(Eq. 3)}$$

all at 25°. Since the ionization constant of the drug is unknown, it is not possible to give corrected data. The thermodynamic data in Table II are averaged out over the temperature range and again must contain substantial contributions from the irreversible chemical interactions.

CONCLUSIONS

The addition of certain heterocyclic nitrogen compounds to solutions of the electron-acceptor *p*-benzoquinone causes no change in the absorption spectrum in the near UV and visible regions. The only exception is I, which shows very slow changes after a long induction period. However, the addition of these compounds to solutions containing electron donors and acceptors has marked spectral effects which demonstrate that these compounds do initially complex with electron acceptors and later form chemical compounds with them. At temperatures below 35°, the interaction is due to some form of complexing; at higher temperatures, irreversible chemical reactions between the drugs and acceptors occur quite rapidly. This study illustrates the utility of using termolecular systems to characterize reactions that cannot be characterized by observing directly the interactions between the compounds and the acceptors. The pH effects suggest that these amines and amides interact in their neutral form—not the ionic form that predominates at the pH's studied.

REFERENCES

(1) G. H. Moxon and M. A. Slifkin, *Spectrochim. Acta*, **28A**, 2419 (1972).

(2) G. H. Moxon and M. A. Slifkin, *Biochim. Biophys. Acta*, **304**, 693 (1973).

(3) *Ibid.*, **286**, 98 (1972).

(4) G. H. Moxon and M. A. Slifkin, *J. Chem. Soc. Perkin II*, **1972**, 1159.

(5) J. T. Overbeek, C. J. Wink, and H. Deenstra, *Rec. Trav. Chim.*, **74**, 69 (1955).

(6) D. E. Guttman and D. Brooke, *J. Pharm. Sci.*, **52**, 941 (1963).

(7) T. R. Crossley and M. A. Slifkin, in "Progress in Reaction Kinetics," vol. 5, G. Porter, Ed., Pergamon, Oxford, England, 1970, p. 409.

(8) M. A. Slifkin, "Charge Transfer Interactions of Biomolecules," Academic, London, England, 1971.

(9) R. Foster, N. Kulevsky, and D. S. Wanigasekera, *J. Chem. Soc. Perkin*, **1974**, 1318.

ACKNOWLEDGMENTS AND ADDRESSES

Received July 28, 1975, from the *Department of Pure and Applied Physics, University of Salford, Salford M5 4WT, England.*

Accepted for publication April 19, 1976.

Sponsored by ICI (Pharmaceutical Division).

G. H. Moxon acknowledges tenure of an SRC research studentship. The SP 700 spectrophotometer was a gift of the Medical Research Council to M. A. Slifkin.

[x] To whom inquiries should be directed.

Protein Binding of Benz[a]anthracene and Benzo[a]pyrene

JOSEPH K. H. MA ˣ, PETER P. FU, and LOUIS A. LUZZI

Abstract □ Fluorometric studies on the binding of benz[a]anthracene and benzo[a]pyrene to human serum albumin are described. The protein molecule appears to have one binding site for the hydrocarbons, but all of the sites on the protein are not fully occupied even in relatively large hydrocarbon concentrations. Equilibrium studies showed that both hydrocarbons bind to the protein to the same extent. Evidence for the energy transfer from the tryptophan residue of the protein to bound hydrocarbons is examined. By using Förster's theory, the mean distance between the tryptophan residue and bound ligand was found to be 15.2 Å for benz[a]anthracene and 19.6 Å for benzo[a]pyrene. It is concluded that the two hydrocarbons may bind to the same general area on the protein molecule near the tryptophan residue but at different sites. The structural differences of the hydrocarbons, which may greatly affect their orientations on the protein molecule, affect mainly the selection of the binding site rather than the binding equilibrium.

Keyphrases □ Benz[a]anthracene—binding to human serum albumin, fluorometric analysis □ Benzo[a]pyrene—binding to human serum albumin, fluorometric analysis □ Binding, protein—benz[a]anthracene and benzo[a]pyrene to human serum albumin, fluorometric analysis □ Fluorometry—binding of benz[a]anthracene and benzo[a]pyrene to human serum albumin □ Hydrocarbons—benz[a]anthracene and benzo[a]pyrene, binding to human serum albumin, fluorometric analysis □ Carcinogens—benz[a]anthracene and benzo[a]pyrene, binding to human serum albumin, fluorometric analysis

Carcinogenic hydrocarbons are biologically active but chemically inert. Because of the aromatic system, these hydrocarbons are capable of forming complexes with macromolecules *via* hydrophobic stacking forces. The hydrophobic interaction is not uncommon in biological systems. For example, a nucleic acid possesses profound hydrophobic stacking interaction between its bases (1, 2), and the binding of protein to nucleic acid involves the stacking interaction between the tryptophan residues of the protein and the nucleic acid bases (3, 4).

The hydrophobic binding of the carcinogenic hydrocarbons with proteins or other macromolecules is important for several reasons. Carcinogenesis may be initiated by the covalent binding of the carcinogens with cell constituents (5–7). Therefore, the hydrophobic binding represents the initial step toward carcinogenesis. Transport of the carcinogens to active receptor sites and the activation of parent carcinogens are also necessary for chemical reaction.

Furthermore, because of the extensive, delocalized π-electron system, these hydrocarbons can be easily activated into long-lived free radicals (8), which may efficiently form covalent bonds with macromolecules if a strong hydrophobic stacking interaction occurs. Therefore, binding information such as the nature of the binding sites on the macromolecule should help in understanding the mechanism of carcinogenic action. Besides the plausible involvement of carcinogenesis, the interaction of these hydrocarbons with macromolecules may result in other serious biological effects yet to be known, since such binding may effectively change the conformations of the macromolecules and, consequently, alter the precision of their physiological functions.

The carcinogenicity of the polycyclic aromatic hydrocarbons is sensitive to trivial structural changes. For example, 7,12-dimethylbenz[a]anthracene is the most potent of the known chemical carcinogens, whereas 7,12-diethylbenz[a]anthracene does not evoke cancer; benz[a]anthracene is only a weak carcinogen, whereas benzo[a]pyrene is strongly carcinogenic. The structural differences may have a profound effect on the orientation of these compounds on a macromolecule, resulting in binding at different sites. Thus, the measurement of binding affinity alone is insufficient for the correlation of binding with biological effects.

Fluorescence spectroscopy is one of the most useful tools for energy transfer studies. In a protein interaction, the tryptophan residue of the protein may transfer its electronic energy to a bound ligand if, among other conditions, the two units are closely located on the macromolecule. The energy transfer data permit calculation of the mean distance between the energy donor and the acceptor, which can be used to differentiate the binding sites for compounds with similar structures.

This study was an attempt to provide additional insight into the interaction of carcinogenic hydrocarbons with proteins. By using the fluorescence technique, studies were made on the binding of benz[a]anthracene and benzo[a]pyrene to human serum albumin. Emphasis was placed on the nature and quantitative aspects of the binding and the difference in binding between benz[a]anthracene and benzo[a]pyrene.

EXPERIMENTAL

Materials—Benz[a]anthracene[1], benzo[a]pyrene[1], L-tryptophan[2], crystalline human serum albumin[3], and soluble ribonucleic acid from liver[4] were purchased from commercial sources. Further purification of benz[a]anthracene and benzo[a]pyrene was made by recrystallization from methanol. The solvents were spectroscopic grade, and all other chemicals were reagent grade.

Instruments and Methods—Fluorescence measurements were made with a spectrophotofluorometer[5] equipped with a 150-w xenon lamp and a 1P21 photomultiplier tube. Fluorescence spectra were recorded with an *x–y* recorder[6]. The entrance slit of the excitation light and the exit slit of the fluorescence emission were 4 and 5 mm, respectively. Absorption spectra and measurements were made with a UV–visible spectrophotometer[7]. Except in the solvent and pH studies, all measurements were carried out in pH 7 phosphate buffer (0.5 *M*). The temperature was controlled at 25 ± 0.5°.

Human serum albumin was freeze dried to constant weight before use. The concentration of the protein was calculated with a molecular weight of 69,000. The concentrations of benz[a]anthracene and benzo[a]pyrene used were 10^{-7}–10^{-5} *M*; microliter amounts of stock solution (10^{-3} or 10^{-4} *M* in acetone) were transferred, using microsyringes, into a fluorescence cell containing 2 or 3 ml of a protein or other solution.

Binding Studies—The binding of benz[a]anthracene and benzo-

[1] Eastman Kodak Co.
[2] Nutritional Biochemicals Corp.
[3] Lot 5868, Nutritional Biochemicals Corp.
[4] Lot 9020, Nutritional Biochemicals Corp.
[5] Aminco-Bowman, American Instrument Co., Silver Spring, Md.
[6] Omnigraphic, Houston Instrument, Bellaire, Tex.
[7] Cary 118, model C, Varian Instrument Division, Palo Alto, Calif.

Table I—Fluorescence Data of 10^{-6} *M* Benz[*a*]anthracene and Benzo[*a*]pyrene in Various Solvents

Solvent	Benz[*a*]anthracene			Benzo[*a*]pyrene		
	A[a]	B[b]	C[c]	A	B	C
pH 7 Phosphate buffer	300	410	5	310	420	2
	300	500	15	310	505	10
	372	500	20	393	505	13
Methanol	288	403	54	300	420	80
	342	403	18	382	420	115
Acetone	350	403	18	384	420	118
Cyclohexane	288	403	59	300	420	85
	342	403	18	384	420	122

[a] Excitation maximum in nanometers. [b] Emission maximum in nanometers. [c] Relative fluorescence intensity of the emission.

[*a*]pyrene to human serum albumin was determined by the Scatchard equation:

$$\overline{V}/D_f = nK - \overline{V}K \qquad \text{(Eq. 1)}$$

where D represents the hydrocarbons, D_f is the concentration of unbound D, $\overline{V}$ is the ratio of bound D per protein concentration, n is the number of binding sites on the protein, and K is the binding constant. The values of $\overline{V}$ and D_f were measured by fluorescence quenching titration (9). In this method, a protein solution is titrated with successive additions of D, and the quenching of the native fluorescence of the protein is recorded after each addition. The quenched fluorescence, expressed as a percentage of the initial fluorescence of the protein, is then plotted as a function of the concentration ratio of D and the protein.

The method requires titration curves at several protein concentrations. Above a certain protein concentration, the titration curves are superimposable since D is all bound. This superimposed curve represents the degree of quenching as a function of $\overline{V}$. In a solution of lower protein concentration, D is only partially bound, and $\overline{V}$ is equal to the concentration ratio on the superimposed curve at the same degree of quenching.

The quenching of the fluorescence of human serum albumin by benz[*a*]anthracene and benzo[*a*]pyrene was measured at the emission wavelength of 348 nm with the excitation at 280 nm. The binding constants were calculated for solutions containing 2.5×10^{-6} *M* human serum albumin and varying concentrations of the hydrocarbons in the 5×10^{-7}–6×10^{-6} *M* range. The high protein concentration, in which the hydrocarbons were all bound, was 2.5×10^{-5} *M*.

Energy Transfer Theory—The quenching of the fluorescence of human serum albumin by benz[*a*]anthracene and benzo[*a*]pyrene, like that observed in other protein interactions (10, 11), is due to energy transfer from the excited-state tryptophan residue (energy donor) to the bound ligand (energy acceptor). The energy transfer information allows calculation of the mean distance, R, between the donor and acceptor by the equation (12):

$$X/(1 - X) = (R_0/R)^6 \qquad \text{(Eq. 2)}$$

where X is the fraction of the absorbed photons transferred, and R_0 is the characteristic distance at which the probability of energy transfer is equal to the probability of fluorescence. The degree of energy transfer may be measured by the degree of quenching of the protein fluorescence.

According to Förster's theory (13):

$$R_0 = (1.69 \times 10^{-33}\, \tau J_v / r^2 \bar{v}_0^2)^{1/6} \text{ cm} \qquad \text{(Eq. 3)}$$

where τ is the fluorescence lifetime of the donor in the absence of transfer, r is the refractive index of the solvent, $\bar{v}_0$ is the mean of the wave numbers of maximum absorption of the acceptor and the emission of the donor, and J_v is the overlap integral. To determine $\bar{v}_0$ and J_v, Eq. 4 may be used:

$$J_v = \int_0^\infty E(v)F(v)dv \qquad \text{(Eq. 4)}$$

where $E(v)$ is the molar absorptivity of the acceptor, and $F(v)$ is the molar emission coefficient of the donor. The molar emission function, $F(v)$, represents the photospectral distribution of the fluorescence in units dependent on $F(v)$ at maximum emission being equal to the molar absorptivity of the donor. By redrawing the absorption and emission data of the acceptor and donor in terms of the wave number scale, J_v and $\bar{v}_0$ can be determined by graphical integration.

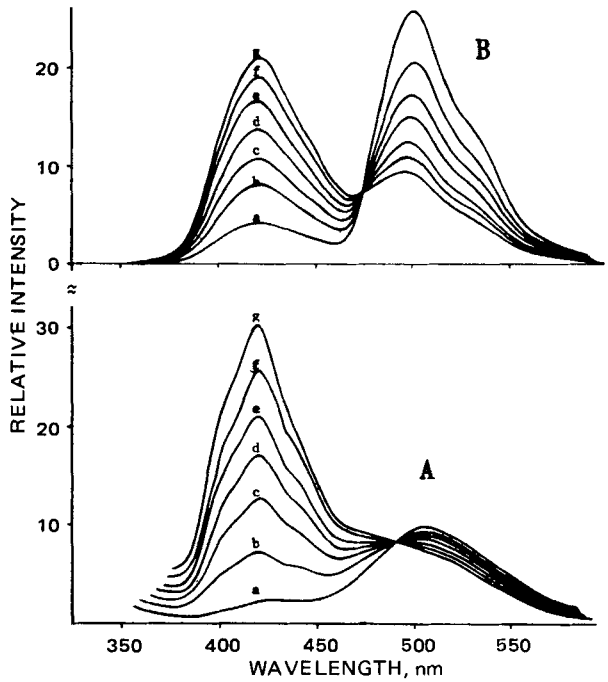

Figure 1—*Effect of human serum albumin on the fluorescence spectrum of (A) 10^{-6} M benzo[a]pyrene (excited at 310 nm) and (B) 10^{-6} M benz[a]anthracene (excited at 300 nm) in pH 7 buffer. The concentration of the protein (a to g) was 0–3 × 10^{-6} M with an increment of 0.5 × 10^{-6} M. In B, a polarizing film was used in the emission slit slide to diminish the protein fluorescence.*

RESULTS

The fluorescence data of 10^{-6} *M* benz[*a*]anthracene (I) and of benzo[*a*]pyrene (II) measured in various solvents are shown in Table I. In pH 7 phosphate buffer, the emission maxima of the hydrocarbons were found to be in two regions: the A region bands at 500 and 505 nm for I and II, respectively, and the relatively weak fluorescence bands in the B region at 395–420 nm. In organic solvents, the A region bands were diminished and strong fluorescence bands were found in the B region. Despite the spectral difference as observed in aqueous and organic solvents, the emission maxima of the hydrocarbons did not shift according to the solvent polarity. The spectra obtained in cyclohexane and in methanol were almost identical. Thus, the spectral change cannot be explained by the dipole–dipole interaction theory (14). Except in acetone, two excitation maxima were observed for the hydrocarbons. Acetone was able to eliminate the short wavelength excitation bands (320 nm or shorter) of many fluorescent compounds. For example, salicylic acid was fluorescent in water when excited at 300 nm but nonfluorescent in acetone when excited at any wavelength.

Figure 1A shows the effect of human serum albumin on the fluorescence spectrum of benzo[*a*]pyrene in pH 7 buffer. The excitation wavelength was set at 310 nm. The binding of the hydrocarbon to the protein was clearly indicated by the spectral change and the appearance of an isosbestic point, indicating the existence of two species in the solution, *i.e.*, the bound and unbound benzo[*a*]pyrenes. The spectra of the enhanced B region fluorescence were similar to those observed in organic solvents.

The effect of human serum albumin on the fluorescence spectrum of benz[*a*]anthracene, excited at 300 nm, at neutral pH is shown in Fig. 1B. Since the excitation wavelength was quite close to that of the protein fluorescence, interference of the B region fluorescence of the hydrocarbon by the fluorescence of the protein was expected. To eliminate the interference, the spectra of Fig. 1B were recorded using a polarizing film in the emission slit slide. Although the B region fluorescence spectrum was slightly changed and shifted toward longer wavelength, the effect of the protein on the spectrum of the hydrocarbon clearly indicated the binding.

The enhancement of the B region fluorescence of the hydrocarbons by the protein was stronger in high pH than in low pH solutions. Below pH 4, where most serum albumins undergo molecular unfolding (9), no significant enhancement was observed. These results suggest a strong interaction between the protein and the hydrocarbons in basic solution,

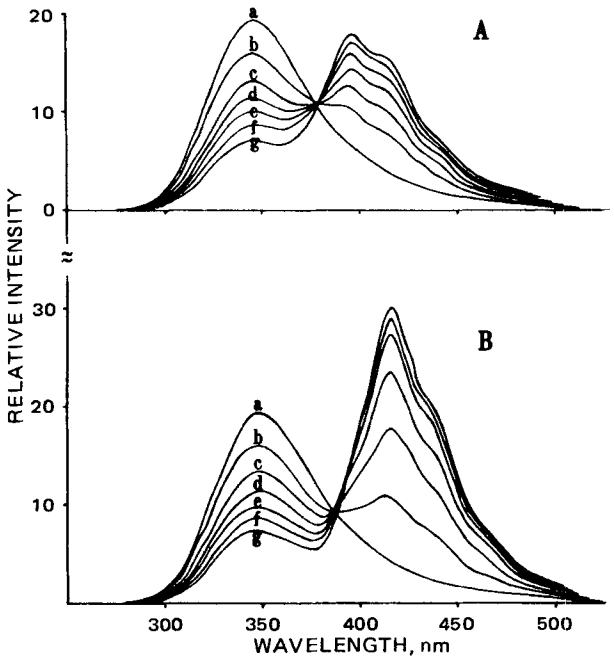

Figure 2—*Effect of benz[a]anthracene (A) and benzo[a]pyrene (B) on the fluorescence spectrum of 2.5 × 10^{-5} M human serum albumin (excited at 310 nm) at neutral pH. The concentration of the hydrocarbons (a to g) was 0–3 × 10^{-6} M with an increment of 0.5 × 10^{-6} M.*

presumably due to a conformational change of the protein upon changing pH. The fluorescence of the hydrocarbons was not affected by solution pH.

Figure 2 shows the effect of I and II on the fluorescence spectrum of human serum albumin at neutral pH. The excitation wavelength was set at 280 nm. The quenching of the protein fluorescence was again accompanied by the enhancement of the B region fluorescence.

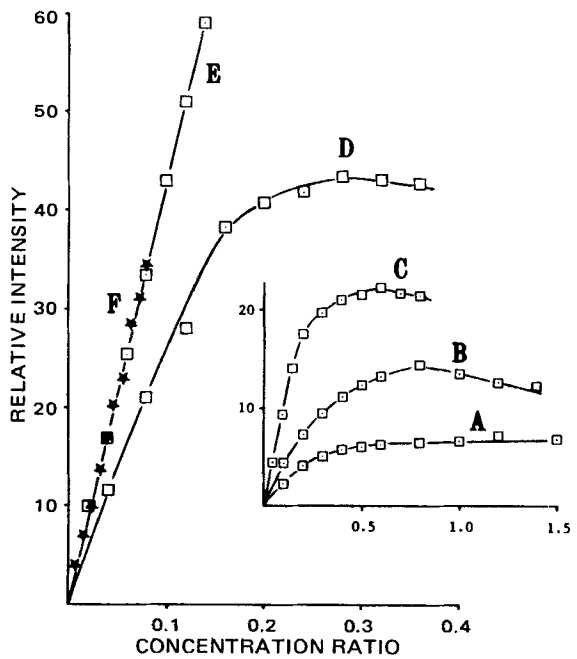

Figure 3—*Plots of the fluorescence enhancement at 420 nm (excited at 310 nm) for benzo[a]pyrene as a function of the concentration ratio of benzo[a]pyrene and human serum albumin at several protein concentration levels. The protein concentrations were: A, 1.25 × 10^{-6} M; B, 2.5 × 10^{-6} M; C, 5 × 10^{-6} M; D, 1.25 × 10^{-5} M; E, 2.5 × 10^{-5} M; and F, 5 × 10^{-5} M. The data were obtained by titrating the protein solutions in pH 7 buffer with successive additions of benzo[a]pyrene. Corrections of the residue fluorescence of the protein and the hydrocarbon were made before the plot.*

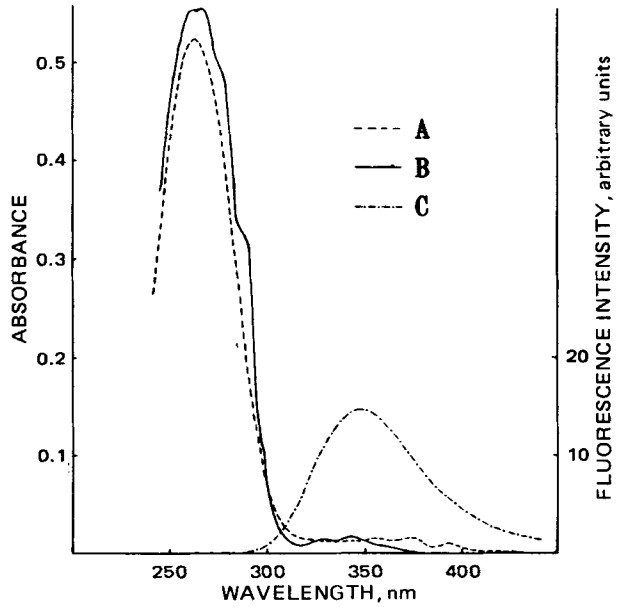

Figure 4—*(A) Absorption spectrum of 2 × 10^{-6} M benz[a]anthracene. (B) Absorption spectrum of 2 × 10^{-6} M benz[a]anthracene in the presence of 2.5 × 10^{-5} M human serum albumin. The same amount of protein was also present in the reference cell. In this spectrum, the hydrocarbon is all bound. (C) Fluorescence spectrum of 2.5 × 10^{-5} M human serum albumin (excited at 280 nm). All solutions were prepared in pH 7 phosphate buffer.*

Figure 3 shows the plots of the fluorescence enhancement at 420 nm *versus* the concentration ratio of benzo[a]pyrene and the protein at several protein concentration levels. Corrections of the residue fluorescence of the protein and benzo[a]pyrene were made prior to the plots. In curve A, where the protein concentration was 1.25 × 10^{-6} *M*, the titration curve plateaued when the concentration ratio was one or larger. This finding suggests that the protein molecule has one binding site for benzo[a]pyrene. The same is true for benz[a]anthracene. At higher protein concentrations, the fluorescence enhancement reached a maximum with the concentration ratio well less than one. Further addition of benzo[a]pyrene led to fluorescence quenching.

Although the reason for the quenching is not clear, the results suggest that the binding sites of the protein are not fully occupied by the hydrocarbon at high protein concentrations. This result is possible since, at high concentrations, the protein molecules tend to self-associate and the binding of hydrocarbon may even aid in the association by forming complexes with more than one protein molecule. When the protein concentration was 2.5 × 10^{-5} *M* or larger, the hydrocarbon in the concentration range shown in Fig. 5 was all bound. This result is indicated by the superimposed straight-line plot and by the absence of the A region fluorescence. Similar results were obtained for benz[a]anthracene.

To elucidate the enhancement of B region fluorescence by the protein, similar studies were made with tryptophan and soluble ribonucleic acid. Tryptophan also can induce the B region fluorescence of the hydrocarbons, but the concentration of tryptophan has to be much larger than that of the protein containing one tryptophan residue per molecule. On the other hand, the addition of soluble ribonucleic acid did not enhance the B region fluorescence; instead, the fluorescence of the hydrocarbons was strongly quenched by an interaction with nucleic acid. These results suggest that the B region fluorescence in protein interaction is due to energy transfer from the tryptophan residue to bound hydrocarbons. The absence of the B region fluorescence in the nucleic acid interaction may be attributed to the lack of an energy donor in the nucleic acid molecule.

A prerequisite for energy transfer is that the absorption spectrum of the energy acceptor must overlap the fluorescence spectrum of the donor. Figures 4 and 5 show that this prerequisite is met in the binding of the hydrocarbons to human serum albumin. In binding with the protein, the visible absorption bands of the hydrocarbons shifted toward high energy or shorter wavelength. The difference spectra of bound hydrocarbons (spectrum B of Figs. 4 and 5), in which the protein absorption was canceled using a double-beam technique, exhibited shoulder bands in the 280–300-nm region, indicating the involvement of the tryptophan residue

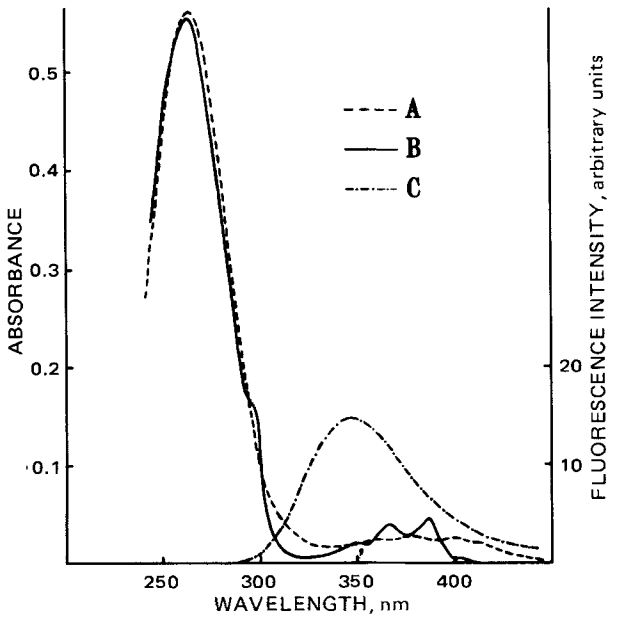

Figure 5—*(A) Absorption spectrum of 2 × 10^{-6} M benzo[a]pyrene. (B) Absorption spectrum of 2 × 10^{-6} M benzo[a]pyrene in the presence of 2.5 × 10^{-5} M human serum albumin. In this solution, the hydrocarbon is all bound. The protein absorption is canceled using a double-beam method. (C) Fluorescence spectrum of 2.5 × 10^{-5} M human serum albumin. All solutions were prepared in pH 7 phosphate buffer.*

in the binding. This finding is particularly true for benz[a]anthracene, whose binding site may be in the vicinity of the tryptophan residue.

The energy transfer data for the binding of I and II to human serum albumin are shown in Table II. The characteristic distances, R_0, were 25.9 and 32.0 Å for I and II, respectively, and were calculated from the following data: r = 1.36, τ = 2.64 nsec, $\bar{\nu}_0$ = 2.90 × 10^4 cm^{-1} for I and 2.72 × 10^4 cm^{-1} for II, and J_ν = 1.05 × 10^{11} cm^3-$mmole^{-2}$ for I and 3.25 × 10^{11} cm^3-$mmole^{-2}$ for II. The value of τ was calculated from the equation: $\tau = Q\tau_n/P$, where Q is the quantum yield of human serum albumin; τ_n is the natural fluorescence lifetime of tryptophan, which was taken to be 12 nsec (15); and P is the fraction of protein absorption due to the tryptophan residue, which was reported to be 19.5% for human serum albumin (16).

The quantum yield of human serum albumin in pH 7 phosphate buffer was determined by comparison of the emission peak areas of the protein and the tryptophan solutions of equal absorbance at 280 nm. The quantum yield of tryptophan was taken to be 0.13 (17). The values of $\bar{\nu}_0$ and J_ν were graphically determined, according to Eq. 4, by redrawing the data of Figs. 4 and 5 in terms of the wave number scale. The unit of the molar emission function, $F(\nu)$, was set so that $F(\nu)$ at maximum emission was equal to 0.59 × 10^4 cm^2-$mmole^{-1}$, the molar absorptivity of tryptophan at 280 nm in pH 7 phosphate buffer. Although the characteristic distance, R_0, calculated in this manner is an approximation because of the complicated protein system, the results show the difference in binding sites for the two hydrocarbons.

Figure 6 shows the fluorescence quenching titrations of human serum albumin with I and II. The data were obtained by titrating the protein solutions with successive additions of the hydrocarbons, with the excitation and emission wavelengths set at 280 and 348 nm, respectively. In a high protein concentration (2.5 × 10^{-5} M), about 95% of the protein fluorescence was quenched as a result of energy transfer. According to Eq. 2, the mean distances between the tryptophan residue of the protein and bound hydrocarbons were 15.2 and 19.6 Å for I and II, respectively.

Table II—Energy Transfer Data for the Binding of Benz[a]anthracene and Benzo[a]pyrene to Human Serum Albumin

	J_ν, cm^3-$mmole^{-2}$	R_0, Å	R, Å	K^a, M^{-1}
Benz[a]anthracene	1.05 × 10^{11}	25.9	15.2	1.56 × 10^5
Benzo[a]pyrene	3.25 × 10^{11}	32.0	19.6	1.46 × 10^5

[a] Binding constant.

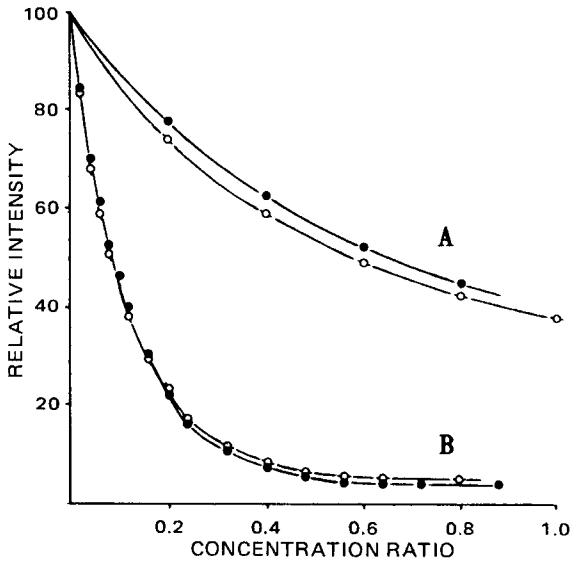

Figure 6—*Quenching of the fluorescence of human serum albumin by benz[a]anthracene and benzo[a]pyrene. The quenched fluorescence is plotted as a function of the concentration ratio of the hydrocarbons and the protein. Key: ●, benz[a]anthracene; ○, benzo[a]pyrene; A, 2.5 × 10^{-6} M protein concentration; and B, 2.5 × 10^{-5} M protein concentration.*

The Scatchard plots for the binding of I and II to human serum albumin are shown in Fig. 7. In a protein solution of 2.5 × 10^{-6} M, the number of binding sites was 0.5 for both compounds. The binding constants for I and II were 1.56 × 10^5 and 1.46 × 10^5 M^{-1}, respectively. Despite the structural difference of the two hydrocarbons, their binding affinities to the protein were approximately equal. In view of the energy transfer and binding data, it is concluded that the two hydrocarbons bind in the same general area on the protein molecule but at different sites. The structural factor, which may greatly affect the orientations of the hydrocarbons on the protein molecule, affects mainly the energy transfer distance rather than the binding equilibrium.

DISCUSSION

The quenching of the fluorescence of human serum albumin by benz[a]anthracene and benzo[a]pyrene, as well as the strong enhancement of the B region fluorescence of the hydrocarbons, indicates the transfer of electronic energy from the tryptophan residue to bound ligands. The conditions necessary for energy transfer are: (*a*) the donor must be a fluorescent group with a sufficiently long lifetime, (*b*) the absorption spectrum of the acceptor must overlap the emission spectrum of the donor, (*c*) the relative orientations of the oscillators must permit a strong interaction, and (*d*) the donor and the acceptor must be within a certain distance for a given efficiency of energy transfer (18). The results of the present study are in excellent agreement with these conditions.

As shown in Figs. 4 and 5, the protein fluorescence band strongly ov-

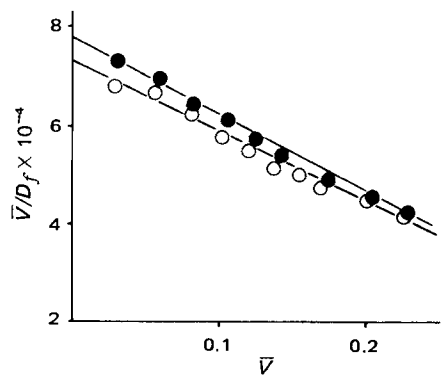

Figure 7—*Scatchard plots for the binding of benz[a]anthracene (●) and benzo[a]pyrene (○) to 2.5 × 10^{-6} M human serum albumin at neutral pH.*

erlapped the absorption bands of the hydrocarbons. The absorption spectra of the protein-bound hydrocarbons exhibited shoulder bands in the 280–300-nm region, indicating the involvement of the tryptophan residue in the interaction. The strong enhancement of the B region fluorescence for the hydrocarbons in binding with the protein represents a transition resulting from an energy transfer process because the binding of these compounds with soluble ribonucleic acid, a macromolecule without an energy donor, does not induce the B region fluorescence.

Excluding the fact of energy transfer, the fluorescence of the hydrocarbons is strongly quenched by interacting with the protein and soluble ribonucleic acid. This result probably indicates a stacking interaction between the hydrocarbon and the aromatic moieties of the macromolecules. The association of fluorescence quenching with stacking interactions was reported previously. For example, the binding of protein to nucleic acid always results in strong quenching of the protein fluorescence, which has been shown to be due to the stacking interaction between the tryptophan residues and the nucleic acid bases (3, 4). In a fluorescence study of compounds in which an indole group is connected to nucleic acid bases by a three- or four-atom bridge, Mutai *et al.* (19) showed that the stacked form, in contrast to the fluorescent unstacked form, is nearly nonfluorescent. Benz[*a*]anthracene and benzo[*a*]pyrene are planar molecules. In binding with nucleic acid, benzo[*a*]pyrene intercalates with the nucleic acid bases (8). In protein interactions, it is possible that the binding allows plane parallelism between the tryptophan residue and the hydrocarbon and, therefore, results in fluorescence quenching of both units.

The fact that only bound benz[*a*]anthracene and benzo[*a*]pyrene can receive energy is indicated by the fluorescence studies of tryptophan with the hydrocarbons. Human serum albumin has one tryptophan residue per molecule. However, the addition of tryptophan, in the same concentration range as that of the protein (Fig. 1), does not induce the B region fluorescence. Only in high tryptophan concentrations do the spectra of the hydrocarbons become similar to those observed in protein solutions, since the two units are then close enough for the efficiency of energy transfer. These results suggest that the binding sites for the hydrocarbons are quite close to the tryptophan residue and that the hydrocarbons are favorably oriented with the tryptophan residue to permit interaction and energy transfer. The small R value for benz[*a*]anthracene indeed suggests that the binding site is in the vicinity of the tryptophan residue.

The energy transfer information is important in understanding the interaction of carcinogenic hydrocarbons with proteins. Benz[*a*]anthracene and benzo[*a*]pyrene interact with human serum albumin to approximately the same extent as indicated by the binding constants. This is expected since these compounds are chemically inert and the binding is of a hydrophobic nature. The difference in structure of the two would probably make little difference in their binding affinities. The difference in ring structure, however, may have a profound effect on their orientations on the protein molecule. Conclusions based on binding strength alone could be misleading. Benzo[*a*]pyrene is strongly carcinogenic, whereas benz[*a*]anthracene is not. While the binding constants of the two suggest similar binding, their protein binding sites are distinguished by energy transfer data.

REFERENCES

(1) S. I. Chan, M. P. Schweizer, P. O. P. Ts'o, and G. K. Helmkamp, *J. Am. Chem. Soc.*, **86**, 4182 (1964).

(2) M. P. Schweizer, A. D. Broom, P. O. P. Ts'o, and D. P. Hollis, *ibid.*, **90**, 1042 (1968).

(3) J. G. Farrelly, J. W. Longworth, and M. P. Stulberg, *J. Biol. Chem.*, **246**, 1266 (1971).

(4) C. Helene, F. Brun, and M. Yaniv, *J. Mol. Biol.*, **58**, 349 (1971).

(5) W. M. Baird, A. Dipple, P. L. Grover, P. Sims, and P. Brookes, *Cancer Res.*, **33**, 2386 (1973).

(6) P. Brookes and P. D. Lawley, *Nature (London)*, **200**, 781 (1964).

(7) M. Duncan, P. Brookes, and A. Dipple, *Int. J. Cancer*, **4**, 813 (1969).

(8) P. O. P. Ts'o, S. A. Lesko, and R. S. Umans, in "Physico-Chemical Mechanisms of Carcinogenesis," Proceedings of an International Symposium in Jerusalem, Oct. 1968, E. D. Bergmann and B. Pullman, Eds., Israel Academy of Sciences and Humanities, Jerusalem, Israel, 1969, p. 106.

(9) C. F. Chignell, "Methods in Pharmacology," vol. 2, Appleton-Century-Crofts, Meredith Corp., New York, N.Y., 1972, p. 57.

(10) R. F. Steiner, J. Roth, and J. Robbins, *J. Biol. Chem.*, **241**, 560 (1966).

(11) R. F. Chen and J. C. Kernohan, *ibid.*, **242**, 5813 (1967).

(12) T. Förster, *Ann. Phys. (Leipzig)*, **2**, 55 (1948).

(13) T. Förster, "Fluoreszenz Organischer Verbindungen," Vandenhoeck und Rupprecht, Gottingen, Germany, 1951, p. 85.

(14) E. Lippert, *Z. Elektrochem.*, **61**, 962 (1957).

(15) G. Weber, in "Light and Life," W. D. McElroy and B. Glass, Eds., Johns Hopkins, Baltimore, Md., 1961, p. 82.

(16) W. J. Teale, *Biochem. J.*, **76**, 381 (1960).

(17) R. F. Chen, *Anal. Lett.*, **1**, 35 (1967).

(18) I. Z. Steinberg, *Ann. Rev. Biochem.*, **40**, 83 (1971).

(19) K. Mutai, B. A. Gruber, and N. J. Leonard, *J. Am. Chem. Soc.*, **97**, 4095 (1975).

ACKNOWLEDGMENTS AND ADDRESSES

Received February 17, 1976, from the *School of Pharmacy, West Virginia University, Morgantown, WV 26506.*

Accepted for publication April 14, 1976.

[x] To whom inquiries should be directed.

Rapid Sensitive Fluorometric Analysis of Cephalosporin Antibiotics

A. B. C. YU [*], C. H. NIGHTINGALE [‡], and D. R. FLANAGAN [x]

Abstract □ A rapid and sensitive fluorometric analysis for cephalosporins, which can also be applied to penicillins, is presented. The method involves reaction with 0.1 *N* sodium hydroxide at 100°, producing stable fluorescent products. This method was applied to cephalexin and ampicillin with detection at concentrations as low as 0.01 μg/ml.

Keyphrases □ Cephalosporins, various—fluorometric analysis, commercial samples in aqueous solutions □ Fluorometry—analysis, various cephalosporins, commercial samples in aqueous solutions □ Antibacterials—various cephalosporins, fluorometric analysis, commercial samples in aqueous solutions

Several methods for the quantitative measurement of cephalosporins in aqueous solution have been described. They utilize such techniques as microbiological assay (1), GLC (2), formol titration (3), colorimetry (4–7), liquid chromatography (8, 9), iodometry (4, 10), reaction with hydroxylamine (4), and polarography (11). The nonmi-

erlapped the absorption bands of the hydrocarbons. The absorption spectra of the protein-bound hydrocarbons exhibited shoulder bands in the 280–300-nm region, indicating the involvement of the tryptophan residue in the interaction. The strong enhancement of the B region fluorescence for the hydrocarbons in binding with the protein represents a transition resulting from an energy transfer process because the binding of these compounds with soluble ribonucleic acid, a macromolecule without an energy donor, does not induce the B region fluorescence.

Excluding the fact of energy transfer, the fluorescence of the hydrocarbons is strongly quenched by interacting with the protein and soluble ribonucleic acid. This result probably indicates a stacking interaction between the hydrocarbon and the aromatic moieties of the macromolecules. The association of fluorescence quenching with stacking interactions was reported previously. For example, the binding of protein to nucleic acid always results in strong quenching of the protein fluorescence, which has been shown to be due to the stacking interaction between the tryptophan residues and the nucleic acid bases (3, 4). In a fluorescence study of compounds in which an indole group is connected to nucleic acid bases by a three- or four-atom bridge, Mutai *et al.* (19) showed that the stacked form, in contrast to the fluorescent unstacked form, is nearly nonfluorescent. Benz[*a*]anthracene and benzo[*a*]pyrene are planar molecules. In binding with nucleic acid, benzo[*a*]pyrene intercalates with the nucleic acid bases (8). In protein interactions, it is possible that the binding allows plane parallelism between the tryptophan residue and the hydrocarbon and, therefore, results in fluorescence quenching of both units.

The fact that only bound benz[*a*]anthracene and benzo[*a*]pyrene can receive energy is indicated by the fluorescence studies of tryptophan with the hydrocarbons. Human serum albumin has one tryptophan residue per molecule. However, the addition of tryptophan, in the same concentration range as that of the protein (Fig. 1), does not induce the B region fluorescence. Only in high tryptophan concentrations do the spectra of the hydrocarbons become similar to those observed in protein solutions, since the two units are then close enough for the efficiency of energy transfer. These results suggest that the binding sites for the hydrocarbons are quite close to the tryptophan residue and that the hydrocarbons are favorably oriented with the tryptophan residue to permit interaction and energy transfer. The small R value for benz[*a*]anthracene indeed suggests that the binding site is in the vicinity of the tryptophan residue.

The energy transfer information is important in understanding the interaction of carcinogenic hydrocarbons with proteins. Benz[*a*]anthracene and benzo[*a*]pyrene interact with human serum albumin to approximately the same extent as indicated by the binding constants. This is expected since these compounds are chemically inert and the binding is of a hydrophobic nature. The difference in structure of the two would probably make little difference in their binding affinities. The difference in ring structure, however, may have a profound effect on their orientations on the protein molecule. Conclusions based on binding strength alone could be misleading. Benzo[*a*]pyrene is strongly carcinogenic, whereas benz[*a*]anthracene is not. While the binding constants of the two suggest similar binding, their protein binding sites are distinguished by energy transfer data.

REFERENCES

(1) S. I. Chan, M. P. Schweizer, P. O. P. Ts'o, and G. K. Helmkamp, *J. Am. Chem. Soc.*, **86**, 4182 (1964).

(2) M. P. Schweizer, A. D. Broom, P. O. P. Ts'o, and D. P. Hollis, *ibid.*, **90**, 1042 (1968).

(3) J. G. Farrelly, J. W. Longworth, and M. P. Stulberg, *J. Biol. Chem.*, **246**, 1266 (1971).

(4) C. Helene, F. Brun, and M. Yaniv, *J. Mol. Biol.*, **58**, 349 (1971).

(5) W. M. Baird, A. Dipple, P. L. Grover, P. Sims, and P. Brookes, *Cancer Res.*, **33**, 2386 (1973).

(6) P. Brookes and P. D. Lawley, *Nature (London)*, **200**, 781 (1964).

(7) M. Duncan, P. Brookes, and A. Dipple, *Int. J. Cancer*, **4**, 813 (1969).

(8) P. O. P. Ts'o, S. A. Lesko, and R. S. Umans, in "Physico-Chemical Mechanisms of Carcinogenesis," Proceedings of an International Symposium in Jerusalem, Oct. 1968, E. D. Bergmann and B. Pullman, Eds., Israel Academy of Sciences and Humanities, Jerusalem, Israel, 1969, p. 106.

(9) C. F. Chignell, "Methods in Pharmacology," vol. 2, Appleton-Century-Crofts, Meredith Corp., New York, N.Y., 1972, p. 57.

(10) R. F. Steiner, J. Roth, and J. Robbins, *J. Biol. Chem.*, **241**, 560 (1966).

(11) R. F. Chen and J. C. Kernohan, *ibid.*, **242**, 5813 (1967).

(12) T. Förster, *Ann. Phys. (Leipzig)*, **2**, 55 (1948).

(13) T. Förster, "Fluoreszenz Organischer Verbindungen," Vandenhoeck und Rupprecht, Gottingen, Germany, 1951, p. 85.

(14) E. Lippert, *Z. Elektrochem.*, **61**, 962 (1957).

(15) G. Weber, in "Light and Life," W. D. McElroy and B. Glass, Eds., Johns Hopkins, Baltimore, Md., 1961, p. 82.

(16) W. J. Teale, *Biochem. J.*, **76**, 381 (1960).

(17) R. F. Chen, *Anal. Lett.*, **1**, 35 (1967).

(18) I. Z. Steinberg, *Ann. Rev. Biochem.*, **40**, 83 (1971).

(19) K. Mutai, B. A. Gruber, and N. J. Leonard, *J. Am. Chem. Soc.*, **97**, 4095 (1975).

ACKNOWLEDGMENTS AND ADDRESSES

Received February 17, 1976, from the *School of Pharmacy, West Virginia University, Morgantown, WV 26506.*

Accepted for publication April 14, 1976.

[x] To whom inquiries should be directed.

Rapid Sensitive Fluorometric Analysis of Cephalosporin Antibiotics

A. B. C. YU [*], C. H. NIGHTINGALE [‡], and D. R. FLANAGAN [x]

Abstract □ A rapid and sensitive fluorometric analysis for cephalosporins, which can also be applied to penicillins, is presented. The method involves reaction with 0.1 *N* sodium hydroxide at 100°, producing stable fluorescent products. This method was applied to cephalexin and ampicillin with detection at concentrations as low as 0.01 μg/ml.

Keyphrases □ Cephalosporins, various—fluorometric analysis, commercial samples in aqueous solutions □ Fluorometry—analysis, various cephalosporins, commercial samples in aqueous solutions □ Antibacterials—various cephalosporins, fluorometric analysis, commercial samples in aqueous solutions

Several methods for the quantitative measurement of cephalosporins in aqueous solution have been described. They utilize such techniques as microbiological assay (1), GLC (2), formol titration (3), colorimetry (4–7), liquid chromatography (8, 9), iodometry (4, 10), reaction with hydroxylamine (4), and polarography (11). The nonmi-

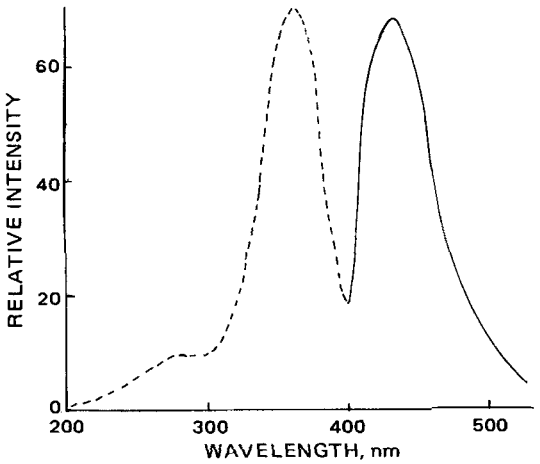

Figure 1—*Fluorescence spectra of caphalothin (1 μg/ml) after reaction at 100° for 75 min in 0.1 N NaOH. Key: - - -, excitation; and —, emission.*

crobiological methods cited are not generally used routinely for analysis of biological samples because of limited sensitivity or, if sensitive enough, because they are less practical than microbiological assays.

This report describes a fluorometric analysis that is simple, rapid, and sensitive enough to be useful for determining cephalosporin levels in biological samples. This same procedure can be applied to ampicillin, amoxicillin, penicillin G, and possibly other penicillins.

EXPERIMENTAL

Samples of cephalothin[1], desacetyl cephalothin[1], cephalexin[1], cephaloglycin[1], cefamandole[1], cefazolin[2], ampicillin[3], amoxicillin[4], and penicillin G[1] were used as received. Stock solutions containing 100 μg/ml of drug in distilled water were freshly prepared prior to use. The stock solution was appropriately diluted with sodium hydroxide solution (various concentrations), and the resulting solutions were sealed in capped[5] culture tubes and heated at various temperatures to produce fluorescent products. After heating in a water bath, the samples were cooled under cold tap water and the fluorescence was measured with a scanning[6] or filter[7] fluorometer.

Separation of the fluorescent products was accomplished with TLC using silica gel precoated plates[8]. The plates were developed for 1.5 hr in chloroform–acetone–acetic acid (50:50:7) and visualized with a UV viewing box.

Standard curves for cephalexin and ampicillin in bovine serum were made using a modification of the extraction procedure described by Jusko (12). This procedure involves adding 0.5 ml of 10% trichloroacetic acid and 0.5 ml of water to 1.0 ml of serum containing drug, mixing for 1 min, and centrifuging at 5000×*g* for 5 min. The supernate (1.3 ml) is mixed with 0.4 ml of 1.0 *N* NaOH and then heated to form fluorescent products as described. After cooling, 0.5 ml of 1 *N* HCl and 8 ml of chloroform–acetone (1:1) are added; the solution is shaken for 15 min and centrifuged at 2000×*g* for 2 min. The organic layer (5 ml) is shaken with 2 ml of 0.1 *N* NaOH for 15 min and centrifuged at 2000×*g* for 2 min. The fluorescence of the aqueous layer is then measured and compared to similarly prepared standards.

RESULTS AND DISCUSSION

Cephalothin—Assay conditions were optimized with cephalothin and then applied with minor variations to other cephalosporins and penicillins. The fluorescence of cephalosporins depends upon their reaction with sodium hydroxide at elevated temperatures. The reaction conditions varied to optimize fluorescence included the sodium hydroxide concentration, the reaction temperature, and the reaction time.

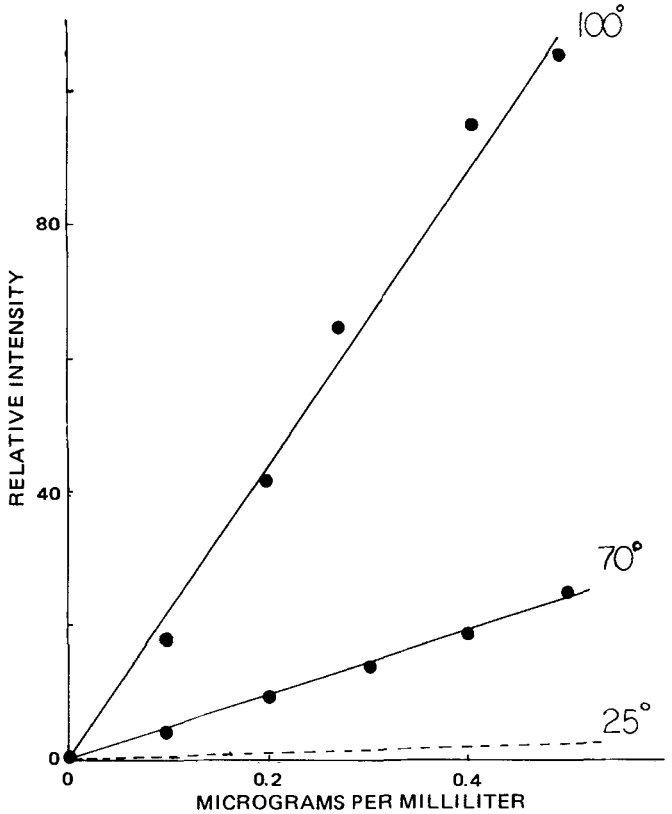

Figure 2—*Effect of temperature on the fluorescence of cephalothin standards reacted in 0.1 N NaOH at 100, 70, and 25° for 75, 240, and 1380 min, respectively. Dashed line is an extrapolation from a linear curve made at concentrations of 1.0–10 μg/ml. Reaction times are optimized for each temperature.*

Figure 1 shows the fluorescence spectrum of a 1-μg/ml solution of cephalothin after reaction at 100° for 75 min in 0.1 *N* NaOH. Figure 2 shows the fluorescence of cephalothin standards reacted in 0.1 *N* NaOH at 100, 70, and 25° for 75, 240, and 1380 min, respectively; 100° was the optimum reaction temperature. At lower reaction temperatures, even at much longer reaction times, the fluorescence intensity did not approach that obtained at 100°. Therefore, all further studies were conducted at 100°.

The effect of sodium hydroxide concentration upon fluorescence is shown in Fig. 3. When 1.0 μg of cephalothin/ml was reacted with 0.1 *N* NaOH, a higher fluorescence was obtained compared to reaction with 0.5 or 1.0 *N* NaOH. At least 75 min was required for maximal fluorescence

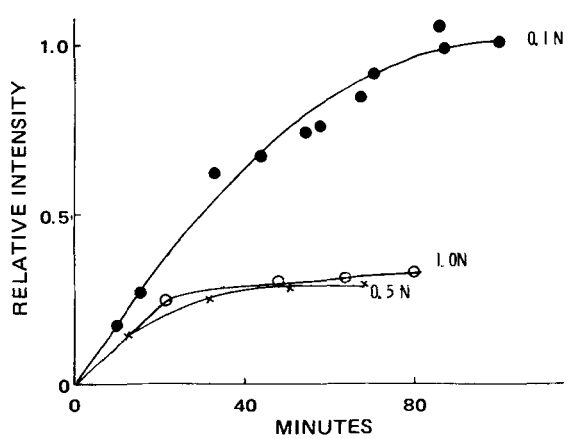

Figure 3—*Effect of sodium hydroxide concentration on the fluorescence of cephalothin (1 μg/ml) reacted at 100°.*

[1] Eli Lilly & Co., Indianapolis, Ind.
[2] Smith Kline and French Laboratories, Philadelphia, Pa.
[3] Bristol Laboratories, Syracuse, N.Y.
[4] Beecham-Massengill, Nashville, Tenn.
[5] Lined with Teflon (du Pont).
[6] Aminco-Bowman SPF spectrophotofluorometer, American Instrument Co., Silver Spring, Md.
[7] Turner model 111 filter fluorometer, Turner Associates, Palo Alto, Calif.
[8] F-254, Brinkmann Instruments, Inc., Westbury, N.Y.

Table I—Relative Fluorescent Intensities and Reaction Conditions for Various Cephalosporins

Compound	Reaction Conditions at 100°	Excitation (Ex), Emission (Em)	Relative Intensity
Cephalothin	0.1 *N* NaOH, 75 min	360 Ex 435 Em	1
Desacetyl cephalothin	0.1 *N* NaOH, 75 min	360 Ex 435 Em	0.33
Cephaloridine	0.1 *N* NaOH, 2.5 hr	360 Ex 435 Em	2.5
Cefazolin	0.05 *N* NaOH, 35 min	330 Ex 415 Em	0.14
Cephaloglycin	0.1 *N* NaOH, 30 min	342 Ex 430 Em	0.45
Cephalexin	0.1 *N* NaOH, 30 min	340 Ex 425 Em	0.55
Cefamandole	0.1 *N* NaOH, 12 hr	310 Ex 390 Em	0.03

to develop in 0.1 *N* NaOH, while only half that time was required for 0.5 or 1.0 *N* NaOH. If assay sensitivity is not as important as rapidity of assay, the higher sodium hydroxide concentrations may be more advantageous.

After maximal fluorescence was attained with 0.1 *N* NaOH, longer reaction times up to 2.5 hr did not affect the fluorescence, indicating fairly stable products. Sodium hydroxide concentrations as low as 0.05 *N* did not significantly alter the fluorescence from that observed with 0.1 *N* NaOH. Cephalothin standards exhibited linear fluorescence from 0.05 up to 5 μg/ml. Linearity may extend beyond concentrations of 5 μg/ml, but such experiments were not performed.

Other Cephalosporins—Table I and Fig. 4 summarize the fluorescence results for various cephalosporins. The fluorescence properties of the alkaline reaction products varied from one cephalosporin to another with respect to excitation and emission maxima, the degree of fluorescence, and optimum reaction time. Minor variations in excitation and emission wavelengths can be ignored if a filter fluorometer[7] is used with specific excitation[9] and emission[10] filters. A filter fluorometer does not alter the detection limits of the assay and may be more convenient.

Since reaction conditions were not completely optimized for each cephalosporin (except reaction time), the fluorescence possibly could be increased by altering the sodium hydroxide concentration or reaction temperature for each cephalosporin. In general, detectable fluorescence was obtained at 0.05 μg/ml (except for cefamandole) and linearity extended to 0.5–1.0 μg/ml or above. Certainly, this assay is applicable in nonlinear regions by comparison with actual standard curves.

Penicillins—Fluorescence was observed with penicillin G, ampicillin, and amoxicillin when subjected to the same reaction conditions producing fluorescence with cephalosporins. Penicillin G was only weakly fluorescent compared to cephalothin, requiring concentrations above 10 μg/ml to obtain detectable fluorescence after reaction times over 3 hr. The fluorescence obtained, though, confirms an earlier observation that a fluorescent product is produced from penicillin G when subjected to alkaline degradation conditions (13).

Ampicillin and amoxicillin were much more fluorescent than cephalothin after reaction in 0.1 *N* NaOH. Ampicillin standards exhibited linear fluorescence down to concentrations as low as 0.005 μg/ml. Comparison with the results of Jusko (12) is difficult, but the limits he suggested (0.01–20 μg/ml) for his fluorescent assay indicate that the sodium hydroxide reaction is of approximately the same sensitivity. Jusko obtained maximal fluorescence in pH 2 reaction solutions at 75° and observed much reduced (~10-fold) fluorescence when alkaline conditions up to pH 9 were employed.

This study indicates that the reaction profile for ampicillin may have two pH maxima (pH 2 and 13) or that entirely different products are obtained under extremely alkaline conditions compared to acidic conditions. This latter possibility is quite likely, since penicillin G and cephalothin were nonfluorescent after reaction under acidic conditions but fluorescent after reaction under high temperature and high pH conditions.

Fluorescent Products—The literature on cephalosporins gives no hint to possible fluorescent products under extremely alkaline conditions.

[9] Corning 7-60.
[10] Combination of Wratten 2A and 47B.

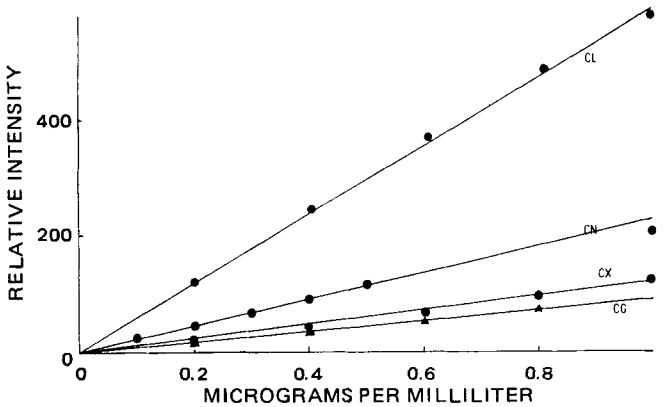

Figure 4—*Fluorescence of cephalosporin standards reacted with sodium hydroxide according to the conditions shown in Table I. Key: CL, cephaloridine; CN, cephalothin; CX, cephalexin; and CG, cephaloglycin.*

Alkaline degradation studies on cephradine, which is structurally similar to cephalexin, indicate the formation of a diketopiperazine product (14) similar to the structure Jusko (12) proposed for the fluorescent product obtained by acidic hydrolysis of ampicillin. Neither of these products would account for the fluorescence of penicillin G or cephalosporins without the α-aminobenzyl side chain.

The thin-layer chromatograms of the final reaction solutions for a number of cephalosporins after heating with 0.1 *N* NaOH for 1 hr are shown in Fig. 5. In each case, except for cefamandole and cefazolin, at least two fluorescent spots were obtained, one with a high R_f value and one with a low R_f value. Cephalexin also gave two fluorescent spots with intermediate R_f values. At this time, the nature of these fluorescent products is speculative. Nevertheless, further investigation of the relationship between cephalosporin and penicillin degradation products is warranted.

It has been observed that penicillenic acid-type compounds and oxazolones, in general, are not obtained from cephalosporins (15). This may be true under the reaction conditions studied to date. However, under the high temperature and extreme alkaline conditions employed in our studies, such degradation pathways possibly may become preferred or at least comparable in rate to other pathways. Oxazolone production could account for the general fluorescence obtained from cephalosporins and penicillins of varying side chains. The various degrees of fluorescence could also be explained on the basis of faster parallel pathways for certain cephalosporins (*i.e.*, cefamandole) leading to a greater proportion of nonfluorescent products than fluorescent products. Studies are in progress to elucidate these fluorescent species.

Fluorescence in Biological Fluids—To assess the utility of this fluorometric method for the analysis of biological samples, cephalexin and ampicillin standards were prepared in serum and treated as described previously, and their fluorescence intensity was measured. Although the fluorescence intensity was reduced compared to aqueous samples, linearity was obtained over the concentration range studied (0.05–10.0 μg/ml).

It is expected that other cephalosporins could be treated similarly or

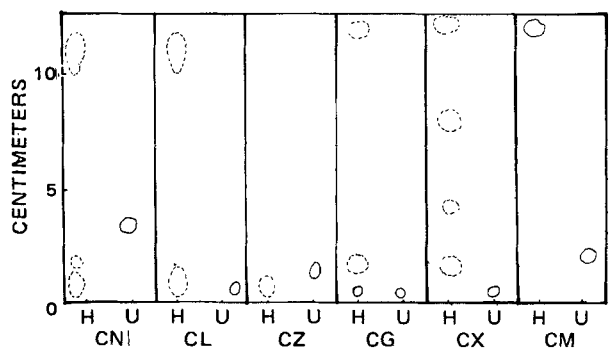

Figure 5—*Chromatogram of hydrolyzed (H) and unhydrolyzed (U) cephalosporins. Dotted lines indicate fluorescence under long UV light. Key: CN, cephalothin; CL, cephalexin; CZ, cefazolin; CG, cephaloglycin; CX, cephalexin; and CM, cefamandole.*

extracted and then reacted with sodium hydroxide to give sufficient fluorescence for detection in serum or tissue samples.

REFERENCES

(1) J. V. Bennett, J. L. Brodie, E. J. Benner, and W. M. M. Kirby, *Appl. Microbiol.*, 14, 170 (1966).

(2) P. W. Mullen, G. E. Maner, and J. A. Tooth, *Res. Commun. Chem. Pathol. Pharmacol.*, 7, 86 (1974).

(3) F. Moll and H. Doker, *Arch. Pharm. Berl.*, **305**, 548 (1972).

(4) "Code of Federal Regulations," 38, 31505 (1973).

(5) E. H. Flynn, "Cephalosporins and Penicillins. Chemistry and Biology," Academic, New York, N.Y., 1972, p. 615.

(6) J. Kirschbaum, *J. Pharm. Sci.*, **63**, 923 (1974).

(7) L. P. Marrelli, *ibid.*, **61**, 1647 (1972).

(8) M. J. Cooper, M. W. Anders, and B. L. Mirkin, *Drug Metab. Dispos.*, 1, 659 (1973).

(9) "Analytical Profiles of Drug Substances," vol. 4, K. Florey, Ed., Academic, New York, N.Y., 1974, p. 19.

(10) "British Pharmacopoeia," Pharmaceutical Press, London, England, 1973, p. 88.

(11) "Analytical Profiles of Drug Substances," vol. 1, K. Florey, Ed., Academic, New York, N.Y., 1972, p. 335.

(12) W. J. Jusko, *J. Pharm. Sci.*, **60**, 728 (1971).

(13) H. T. Clarke, J. R. Johnson, and R. Robinson, "The Chemistry of Penicillin," Princeton University Press, Princeton, N.J., 1949, p. 67.

(14) A. Cohen, P. T. Funke, and M. S. Puar, *J. Pharm. Sci.*, **62**, 1559 (1973).

(15) J. D'A. Jeffrey, E. P. Abraham, and G. G. F. Newton, *Biochem. J.*, **75**, 216 (1960).

ACKNOWLEDGMENTS AND ADDRESSES

Received February 25, 1976, from the *School of Pharmacy, University of Connecticut, Storrs, CT 06268.*

Accepted for publication April 23, 1976.

The authors thank Mr. Ronald Goldberg for technical assistance.

* Present address: College of Pharmacy and Allied Health Professions, Northeastern University, Boston, MA 02115.

‡ Present address: School of Pharmacy, State University of New York at Buffalo, Buffalo, NY 14214.

ˣ To whom inquiries should be directed.

Vaginal Drug Absorption in Rhesus Monkeys I: Development of Methodology

E. OWADA, C. R. BEHL, S. S. HWANG, L. SUHARDJA, G. L. FLYNN, N. F. H. HO, and W. I. HIGUCHI ˣ

Abstract □ Earlier reports from these laboratories described a procedure for determining vaginal drug absorption in the rabbit based upon a perfusion system, and data on the vaginal absorption of the straight-chain aliphatic alcohols and carboxylic acids were given. These studies have been extended to the rhesus monkey. Rib-cage-type cells were designed for intravaginal insertion through the vulval orifice and to fit the specific dimensions of the monkey vagina. The general design of the cell was similar to that used in the rabbit vaginal absorption studies. The perfusion system was checked by using ^{3}H-polyethylene glycol 4000, and no significant leaks from the cell were found. The absorption of the alcohols followed first-order kinetics. The computed apparent permeability coefficients for the alcohols were of comparable magnitude to those previously reported for the rabbit vaginal membrane.

Keyphrases □ Absorption, vaginal—various straight-chain aliphatic alcohols, perfusion system designed, rhesus monkeys □ Vaginal absorption—various straight-chain aliphatic alcohols, perfusion system designed, rhesus monkeys □ Perfusion systems—vaginal drug absorption, various straight-chain aliphatic alcohols, rhesus monkeys □ Alcohols, straight-chain aliphatic, various—vaginal absorption, perfusion system, rhesus monkeys

Research efforts in these laboratories have been based upon the premise that the pivotal event in regional or systemic therapy *via* the vaginal absorption route may be drug transport across the vaginal membrane. A method was described (1) for evaluating drug absorption in the vagina, using the rabbit doe as a prototype animal. A rib-cage-type cell, which provided a closed absorption compartment in the vaginal tract, was designed and surgically implanted. Drug absorption was determined by perfusing the drug solution through this system.

In subsequent reports, the absorption of straight-chain aliphatic alcohols (2) and aliphatic carboxylic acids (3) was described. The data agreed with a physical model involving a diffusion layer in series with a membrane consisting of two parallel pathways: a lipoidal pathway and an aqueous "pore" pathway. The surface pH of the rabbit vaginal membrane under the conditions prevailing during the experiments could be well approximated by the pH of the bulk lumenal solution (4).

The rabbit doe was chosen for these studies because it does not exhibit an estrous cycle and the vaginal tissues exhibit a constancy in their histological, biochemical, and physiological properties not seen with other rodents and most other mammals (5). The lack of a sexual cycle in the rabbit was expected to provide minimum variability in the membrane permeability behavior (1–4).

In the human female, however, the secretion of estrogenic hormones in the ovarian cycle induces cyclic changes in the histology, biochemistry, and physiology of the vaginal tissues; therefore, the vaginal membrane might exhibit a corresponding cyclic barrier behavior. Thus, the rationale for the present investigation was to extend the studies to a sexually cyclical animal, closely approximating the human female with regard to ovarian-induced membrane changes. The Macaques rhesus species of the higher primates was selected. The rhesus has an ovarian cycle of approximately 28 days, as does the human female. It is widely believed by researchers in the fertility area that the rhesus and human reproductive systems are functionally similar in that they have comparable anatomy and phys-

extracted and then reacted with sodium hydroxide to give sufficient fluorescence for detection in serum or tissue samples.

REFERENCES

(1) J. V. Bennett, J. L. Brodie, E. J. Benner, and W. M. M. Kirby, *Appl. Microbiol.*, 14, 170 (1966).

(2) P. W. Mullen, G. E. Maner, and J. A. Tooth, *Res. Commun. Chem. Pathol. Pharmacol.*, 7, 86 (1974).

(3) F. Moll and H. Doker, *Arch. Pharm. Berl.*, **305**, 548 (1972).

(4) "Code of Federal Regulations," 38, 31505 (1973).

(5) E. H. Flynn, "Cephalosporins and Penicillins. Chemistry and Biology," Academic, New York, N.Y., 1972, p. 615.

(6) J. Kirschbaum, *J. Pharm. Sci.*, **63**, 923 (1974).

(7) L. P. Marrelli, *ibid.*, **61**, 1647 (1972).

(8) M. J. Cooper, M. W. Anders, and B. L. Mirkin, *Drug Metab. Dispos.*, 1, 659 (1973).

(9) "Analytical Profiles of Drug Substances," vol. 4, K. Florey, Ed., Academic, New York, N.Y., 1974, p. 19.

(10) "British Pharmacopoeia," Pharmaceutical Press, London, England, 1973, p. 88.

(11) "Analytical Profiles of Drug Substances," vol. 1, K. Florey, Ed., Academic, New York, N.Y., 1972, p. 335.

(12) W. J. Jusko, *J. Pharm. Sci.*, **60**, 728 (1971).

(13) H. T. Clarke, J. R. Johnson, and R. Robinson, "The Chemistry of Penicillin," Princeton University Press, Princeton, N.J., 1949, p. 67.

(14) A. Cohen, P. T. Funke, and M. S. Puar, *J. Pharm. Sci.*, **62**, 1559 (1973).

(15) J. D'A. Jeffrey, E. P. Abraham, and G. G. F. Newton, *Biochem. J.*, **75**, 216 (1960).

ACKNOWLEDGMENTS AND ADDRESSES

Received February 25, 1976, from the *School of Pharmacy, University of Connecticut, Storrs, CT 06268.*

Accepted for publication April 23, 1976.

The authors thank Mr. Ronald Goldberg for technical assistance.

* Present address: College of Pharmacy and Allied Health Professions, Northeastern University, Boston, MA 02115.

‡ Present address: School of Pharmacy, State University of New York at Buffalo, Buffalo, NY 14214.

ˣ To whom inquiries should be directed.

Vaginal Drug Absorption in Rhesus Monkeys I: Development of Methodology

E. OWADA, C. R. BEHL, S. S. HWANG, L. SUHARDJA, G. L. FLYNN, N. F. H. HO, and W. I. HIGUCHI ˣ

Abstract □ Earlier reports from these laboratories described a procedure for determining vaginal drug absorption in the rabbit based upon a perfusion system, and data on the vaginal absorption of the straight-chain aliphatic alcohols and carboxylic acids were given. These studies have been extended to the rhesus monkey. Rib-cage-type cells were designed for intravaginal insertion through the vulval orifice and to fit the specific dimensions of the monkey vagina. The general design of the cell was similar to that used in the rabbit vaginal absorption studies. The perfusion system was checked by using ^{3}H-polyethylene glycol 4000, and no significant leaks from the cell were found. The absorption of the alcohols followed first-order kinetics. The computed apparent permeability coefficients for the alcohols were of comparable magnitude to those previously reported for the rabbit vaginal membrane.

Keyphrases □ Absorption, vaginal—various straight-chain aliphatic alcohols, perfusion system designed, rhesus monkeys □ Vaginal absorption—various straight-chain aliphatic alcohols, perfusion system designed, rhesus monkeys □ Perfusion systems—vaginal drug absorption, various straight-chain aliphatic alcohols, rhesus monkeys □ Alcohols, straight-chain aliphatic, various—vaginal absorption, perfusion system, rhesus monkeys

Research efforts in these laboratories have been based upon the premise that the pivotal event in regional or systemic therapy *via* the vaginal absorption route may be drug transport across the vaginal membrane. A method was described (1) for evaluating drug absorption in the vagina, using the rabbit doe as a prototype animal. A rib-cage-type cell, which provided a closed absorption compartment in the vaginal tract, was designed and surgically implanted. Drug absorption was determined by perfusing the drug solution through this system.

In subsequent reports, the absorption of straight-chain aliphatic alcohols (2) and aliphatic carboxylic acids (3) was described. The data agreed with a physical model involving a diffusion layer in series with a membrane consisting of two parallel pathways: a lipoidal pathway and an aqueous "pore" pathway. The surface pH of the rabbit vaginal membrane under the conditions prevailing during the experiments could be well approximated by the pH of the bulk lumenal solution (4).

The rabbit doe was chosen for these studies because it does not exhibit an estrous cycle and the vaginal tissues exhibit a constancy in their histological, biochemical, and physiological properties not seen with other rodents and most other mammals (5). The lack of a sexual cycle in the rabbit was expected to provide minimum variability in the membrane permeability behavior (1–4).

In the human female, however, the secretion of estrogenic hormones in the ovarian cycle induces cyclic changes in the histology, biochemistry, and physiology of the vaginal tissues; therefore, the vaginal membrane might exhibit a corresponding cyclic barrier behavior. Thus, the rationale for the present investigation was to extend the studies to a sexually cyclical animal, closely approximating the human female with regard to ovarian-induced membrane changes. The Macaques rhesus species of the higher primates was selected. The rhesus has an ovarian cycle of approximately 28 days, as does the human female. It is widely believed by researchers in the fertility area that the rhesus and human reproductive systems are functionally similar in that they have comparable anatomy and phys-

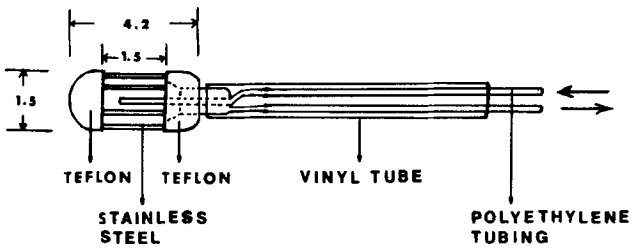

Figure 1—*Drawing of a typical rib-cage cell, which is inserted into the vagina of the monkey through the vulval orifice (all dimensions are given in centimeters for the medium size cell).*

iology (6). Therefore, the female rhesus is believed to provide an excellent model for the human female.

The purpose of the present report is to describe a method for the determination of the vaginal membrane permeability using the female rhesus monkey and straight-chain aliphatic alcohols as model compounds.

EXPERIMENTAL

Animals—Mature female Macaques rhesus monkeys (4–9 years old and 4–6 kg) known to have menstrual cycles were employed. Their vaginal tracts ranged from 1.3 to 1.7 cm in diameter and were approximately 4 cm in length. The animals were maintained under regular animal health care in an air conditioned building (25°) with free access to water and a normal diet.

The condition of the monkeys was monitored by visual examination throughout the studies. The overall procedure did not appear to affect the appetite or temperament of the animals, nor was there any significant change in body weight. Vaginal examinations revealed no vaginal infections due to the inserted rib-cage cell in any monkey.

Materials—All materials were used without further purification. A liquid scintillator was prepared by dissolving 18 g of 2,5-diphenyloxazole[1] and 300 g of naphthalene[2] in 3 liters of dioxane[2]. The buffer solution of

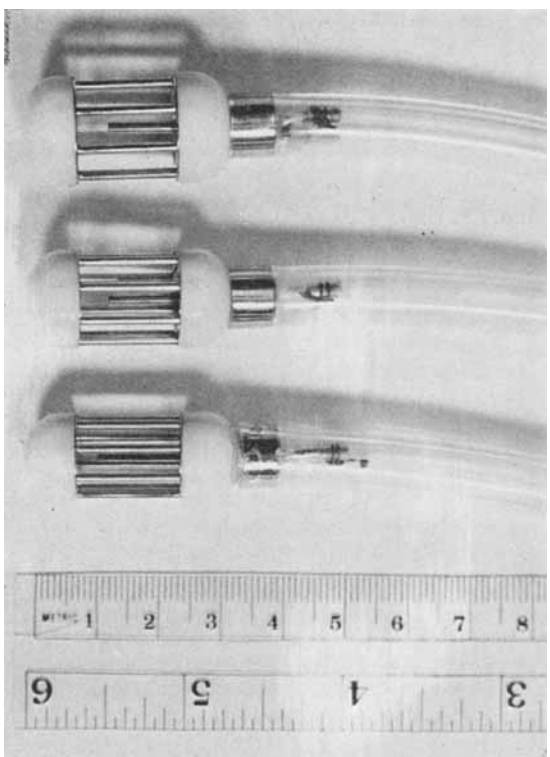

Figure 2—*Photograph of three rib-cage cells.*

[1] Isolab Inc., Akron, Ohio.
[2] Matheson, Coleman and Bell, Norwood, Ohio.

Table I—Dimensions of the Three Rib-Cage Cells Designed for Intravaginal Insertion

Cell	Length of Stainless Steel Rods, cm	Diameter of Ends, cm	Volume within Cage, ml	Surface Area, cm^2
Small	1.53	1.30	1.83	6.10
Medium	1.53	1.50	2.43	7.03
Large	1.53	1.70	3.13	7.98

pH 6.0 was prepared by dissolving 13.8 g of monobasic sodium phosphate[2] in 16.0 ml of 1.0 *N* sodium hydroxide[3] and adding distilled water to give a final volume of 1 liter. The buffer solution was then made isotonic by adding sodium chloride[3].

Design of Rib-Cage Cell—The rib-cage cell was designed to fit the vaginal dimensions of the monkey in such a way as to provide a constant volume and surface area in the absorption compartment (Fig. 1). The general design was similar to that used in the rabbit vaginal absorption studies (1). The cell was constructed with two smooth endings[4] connected by eight stainless steel rods. The stainless steel inlet and outlet for the perfusate were installed through one ending from which polyethylene tubes were led through vinyl tubing, for protection and convenient handling, to the rest of the perfusion system.

The dimensions of the cells were adjusted to fit each specific monkey, and the cell was constructed so it could be inserted through the vulval orifice without difficulty. The dimensions of three such cells (Fig. 2) are presented in Table I.

Perfusion System and General Procedure—The perfusion system consisted of two sections (Fig. 3). The first included the rib-cage cell, which was intravaginally inserted. The second section, external to the animal, consisted of a rotating and reciprocating pump[5] and a constant-temperature solution reservoir. The entire perfusion path in the system was glass tubing and stainless steel, except for the connections, which were polyethylene tubing[6]. A washing device and drain flasks were connected through two three-way stopcocks to the reservoir. During the experiments, the two sections were securely attached to provide a closed system for perfusion.

The monkeys were anesthetized by administering approximately 20 mg/kg im of ketamine hydrochloride[7]. The level of anesthetization was maintained by administering additional doses of ketamine every 0.5 hr.

The monkey was positioned on an operating table with the dorsal side up. The rib-cage cell was inserted into the monkey's vagina with care and connected by tubing to the rest of the perfusion system (Fig. 4). A sodium chloride irrigation solution was passed through the vagina for approximately 15 min at a flow rate of 20 ml/min to remove any exfoliated cells and other debris and secretions. Then the saline was replaced by the

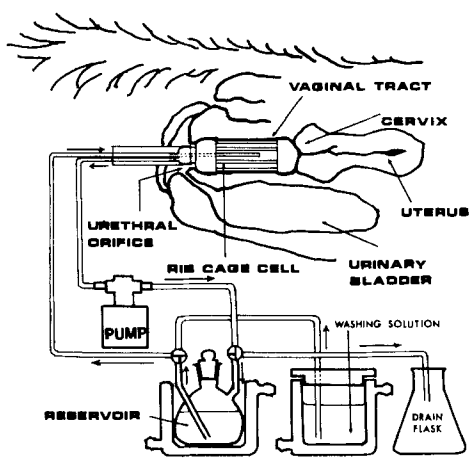

Figure 3—*Diagram of the perfusion system.*

[3] Mallinckrodt Chemical Works, St. Louis, Mo.
[4] Teflon (du Pont).
[5] FMI lab pump, model RRP 2G 150, Fluid Metering Inc., Oyster Bay, N.Y.
[6] Intramedic PE 205, Clay Adams, Division of Becton, Dickinson & Co., Parsippany, NJ 07054.
[7] Vetalar, Parke-Davis and Co., Detroit, Mich.

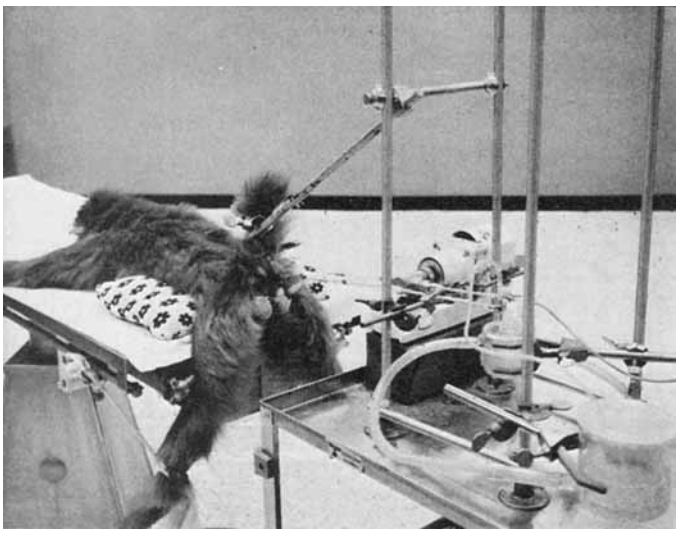

Figure 4—*Entire setup under typical experimental conditions.*

buffer solution used in the experiments, warmed to 37°, and the washing was continued for an additional 5 min. The washings were not circulated but were collected and discarded.

Independently, 5 ml of a perfusate concentrate solution was placed in the reservoir at the perfusion system, which could be isolated from the rib-cage cell and lines leading to it by a set of stopcocks. Upon completion of the rinsing procedure, the contents of the reservoir were introduced into the perfusion circuit, which contained about 10 ml of additional buffer in the cell and lines, *via* the stopcocks. This manipulation also formed a closed perfusion loop consisting of a total volume of approximately 15 ml in the reservoir, tubing, and rib-cage cell. This procedure was employed in studies checking the tightness of fit of the cell using radiolabeled polyethylene glycol 4000 (I) and in the permeation studies using the alcohols.

In all experiments, the flow rate through the pump was 20 ml/min. In order that the solution in the system would be mixed well, a 10-min period was allowed before the first sample was withdrawn. Further samples were withdrawn at 10-min intervals up to 80 min. At the end of a perfusion run, the solution was washed out with isotonic saline introduced into the system *via* the three-way stopcocks (polyethylene glycol 4000) or quantitatively collected (alcohols). In the polyethylene glycol 4000 experiments, the wash was collected and a mass balance on the radiolabeled compound was obtained after bringing the wash volume up to 250 ml. The residual I concentration was determined radioisotopically by using a liquid scintillation counter[8].

In the experiment with I, its perfusate concentration was 2.5×10^{-4} *M*. Initial concentrations were 5×10^{-6}, 4.8×10^{-5}, and 4.1×10^{-5} *M* for ^{3}H-methanol, ^{14}C-1-butanol, and ^{14}C-1-octanol, respectively. ^{3}H-Methanol was used as a reference permeant, and its absorption was followed simultaneously with that of the ^{14}C-labeled alcohols using a dual-label analytical procedure (2).

RESULTS AND DISCUSSION

Tightness of Rib-Cage Cell—The experiments with ^{3}H-I were aimed at assessing whether the cell was leakproof as used and whether there was

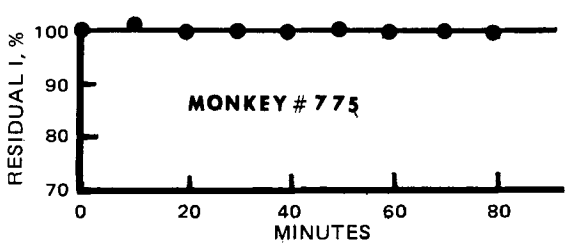

Figure 5—*Typical plot of change in concentration of I as a function of perfusion time.*

[8] Model LS 200, Beckman Instruments, Inc., Scientific and Process Instruments Division, Fullerton, Calif.

Table II—Percent Recovery Values for Polyethylene Glycol 4000 Obtained with the Three Rib-Cage Cells

Monkey	Cell Used	I Recovered, %
775	Small	90.2
774	Medium	90.3
788	Large	91.1

a significant or measurable amount of water gained or lost during the experiment. Compound I, being a large and very polar molecule, is essentially unabsorbed. Its constancy in concentration over the lifetime of a typical run coupled with total recovery is adequate evidence of the absence of *in situ* leakage. Gradual increases in the concentration of I coupled with its total recovery would suggest water absorption. Constancy of concentration without total recovery would suggest leakage.

The percent residual I values were plotted as a function of the perfusion time. A typical plot is shown in Fig. 5. The data generally indicated no significant water flux across the vaginal membrane. The computed values of I recovery (Table II) indicated no significant leakage from the cell.

Absorption of Alcohols—The primary purpose of these experiments was to assess the utility of the perfusion procedure and system for measuring vaginal permeability. Consequently, in these experiments, the periodicity of the vaginal cycle, which is presumed to affect vaginal permeability, was neglected. Rather, each run constituted an absolute test of the procedure; first-order absorption patterns previously seen in the rabbit work were expected and sought.

The logarithm of the percent residual alcohol concentrations was plotted as a function of the perfusion time (Figs. 6 and 7). The linear relationship obtained on a semilogarithmic scale indicates that the drug disappearance followed a first-order pattern. The rate of disappearance can thus be expressed by:

$$\frac{dC_b}{dt} = -K_u C_b \qquad \text{(Eq. 1)}$$

$$K_u = \frac{A}{V} P_{app} \qquad \text{(Eq. 2)}$$

where C_b is the concentration of the drug in the bulk solution, K_u is the first-order rate constant, A is the effective surface area of the vaginal membrane exposed to the drug solution and is dependent on the geo-

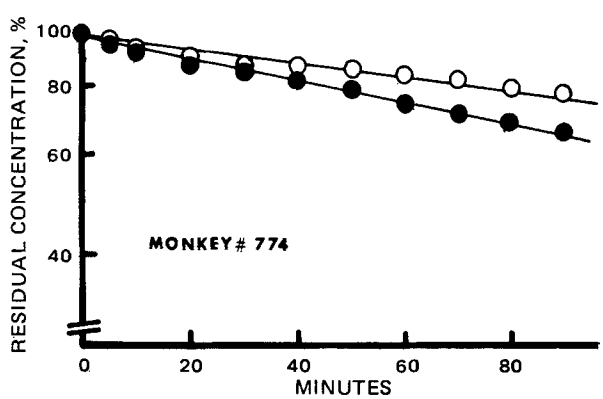

Figure 6—*Typical plots of the change in the concentrations of methanol and 1-butanol in the sampling reservoir as a function of perfusion time.*

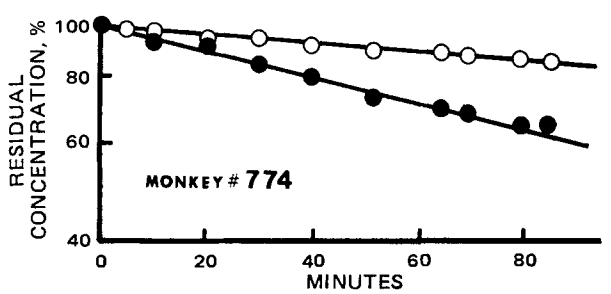

Figure 7—*Typical plots of the change in the concentrations of methanol and 1-octanol in the sampling reservoir as a function of perfusion time.*

Table III—Apparent Permeability Coefficient, P_{app}, Determined for the Vaginal Absorption of the Alcohols

Monkey	$P_{app} \times 10^4$, cm/sec		
	Methanol	1-Butanol	1-Octanol
774	0.80	1.44	2.18
775	1.16	1.77	3.52
778	0.75	0.96	2.85

metrical surface area of the cell used, V is the total volume of the drug solution, and P_{app} is the apparent permeability coefficient. The ratio of the surface area to the volume depended upon the cell employed.

The results of some typical P_{app} determinations are summarized in Table III. As can be seen, the values increased from methanol through octanol for all monkeys used. This finding is in qualitative accord with the results obtained in the rabbit vaginal absorption studies. Furthermore, the P_{app} values for the monkey were approximately of the same order of magnitude as those obtained with the rabbit system (2). However, since these experiments were carried out with little regard for the menstrual cycle effects, the results in Table III mainly represent a demonstration of the feasibility of the experiments. A rather systematic study of the menstrual cycle effects, that is, the influence of the phase of the cycle and the influence of the alkyl chain length as a function of the menstrual cycle, will be reported[9] (7).

In separate experiments, as was found in the rabbit studies, there were no significant losses of the alcohols in the perfusion system through, for example, adsorption when the rib-cage cell was bypassed.

[9] Presented at the APhA Academy of Pharmaceutical Sciences, New Orleans meeting, Apr. 1976 (abstract 54).

In conclusion, this study has shown that a relatively simple procedure involving perfusion and a special cell inserted into the vagina may be used to carry out vaginal membrane permeability experiments in the rhesus monkey. The procedure should be well suited for determining vaginal membrane permeability coefficients over a wide range of conditions, especially as a function of the menstrual cycle employing, wherever possible, the particular monkey as its own control.

REFERENCES

(1) T. Yotsuyanagi, A. Molokhia, S. Hwang, N. F. H. Ho, G. L. Flynn, and W. I. Higuchi, *J. Pharm. Sci.*, **64**, 71 (1975).

(2) S. Hwang, E. Owada, T. Yotsuyanagi, L. Suhardja, N. F. H. Ho, G. L. Flynn, and W. I. Higuchi, *ibid.*, **65**, 1574 (1976).

(3) S. Hwang, E. Owada, L. Suhardja, N. F. H. Ho, G. L. Flynn, and W. I. Higuchi, *ibid.*, in press.

(4) *Ibid.*, in press.

(5) L. P. Bengtsson, *Acta Endocrinol., Suppl.*, **13**, 11 (1953).

(6) C. G. Hartman, *Endocrinology*, **25**, 670 (1939).

(7) E. Owada, C. R. Behl, Y. Kurono, S. S. Hwang, G. L. Flynn, N. F. H. Ho, and W. I. Higuchi, *Obstet. Gynecol.*, in press.

ACKNOWLEDGMENTS AND ADDRESSES

Received February 12, 1976, from the *College of Pharmacy, University of Michigan, Ann Arbor, MI 48109.*

Accepted for publication March 31, 1976.

Supported by the National Institute of Child Health and Human Development, Bethesda, Md. (Contract NO1-HD-3-2740).

The authors thank Dr. T. J. Roseman, Dr. K. T. Kirton, and Dr. F. H. Schadewald for helpful comments on the feasibility of the reported method.

[x] To whom inquiries should be directed.

Aqueous Chamber Drug Distribution Volume Measurement in Rabbits

JOSEPH M. CONRAD and JOSEPH R. ROBINSON [x]

Abstract □ A method was developed for aqueous chamber drug distribution volume measurement in the albino rabbit, and the apparent volume of distribution was determined for inulin, pilocarpine alkaloid, and 1-hexanoic acid. The method consists of injecting a suitable concentration of drug, in an appropriate volume of fluid, into the anterior chamber of the eye and monitoring the decline in drug concentration as a function of time by periodic sampling of the aqueous humor. Graphical analysis of the resulting data yields both the apparent volume of distribution and the turnover rate constant of the aqueous humor. The technique does traumatize the eye, causing formation of plasmoid aqueous, which does not interfere with the apparent drug distribution volume measurement or the determination of aqueous humor turnover. Inulin was used to determine the physiological aqueous volume, 287 μl, in good agreement with literature values. The turnover rate constant was 0.016 min^{-1}, also in good agreement with literature values. The apparent volume of distribution for pilocarpine alkaloid was 575 μl in albino eyes and 760 μl in pigmented irides; for 1-hexanoic acid in albino eyes, it was 760 μl. For pilocarpine alkaloid, literature citations on the fraction of dose absorbed have been based on an assumed apparent volume of distribution of 250–300 μl. Therefore, a factor of two error has been introduced when using albino eyes and a factor of almost three has been introduced when using pigmented eyes. The implication of the apparent volume of distribution for pilocarpine in its ocular disposition is discussed, as is the unexpected observation that pilocarpine alkaloid apparently inhibits formation of plasmoid aqueous and follows one-compartment kinetics during these studies. It is shown that the one-compartment kinetics for pilocarpine are due to its biological activity in the aqueous chamber.

Keyphrases □ Drug distribution—aqueous chamber drug volume, inulin, pilocarpine, and 1-hexanoic acid, rabbit eyes □ Inulin—aqueous chamber volume of distribution, rabbit eyes □ Pilocarpine—aqueous chamber volume of distribution, rabbit eyes □ 1-Hexanoic acid—aqueous chamber volume of distribution, rabbit eyes □ Ocular volumes of distribution—aqueous chamber, pilocarpine, inulin, and 1-hexanoic acid, rabbit eyes

To make meaningful quantitative statements about the bioavailability of an ophthalmic preparation, it is necessary to know the apparent volume of distribution for that drug in the eye. At present, the ophthalmic literature contains statements on the bioavailability of topically applied ocular drugs that are based, at best, only on an approximation to the actual aqueous humor volume, ignoring all other factors, and, at worst, on poorly controlled clinical studies

Table III—Apparent Permeability Coefficient, P_{app}, Determined for the Vaginal Absorption of the Alcohols

Monkey	$P_{app} \times 10^4$, cm/sec		
	Methanol	1-Butanol	1-Octanol
774	0.80	1.44	2.18
775	1.16	1.77	3.52
778	0.75	0.96	2.85

metrical surface area of the cell used, V is the total volume of the drug solution, and P_{app} is the apparent permeability coefficient. The ratio of the surface area to the volume depended upon the cell employed.

The results of some typical P_{app} determinations are summarized in Table III. As can be seen, the values increased from methanol through octanol for all monkeys used. This finding is in qualitative accord with the results obtained in the rabbit vaginal absorption studies. Furthermore, the P_{app} values for the monkey were approximately of the same order of magnitude as those obtained with the rabbit system (2). However, since these experiments were carried out with little regard for the menstrual cycle effects, the results in Table III mainly represent a demonstration of the feasibility of the experiments. A rather systematic study of the menstrual cycle effects, that is, the influence of the phase of the cycle and the influence of the alkyl chain length as a function of the menstrual cycle, will be reported[9] (7).

In separate experiments, as was found in the rabbit studies, there were no significant losses of the alcohols in the perfusion system through, for example, adsorption when the rib-cage cell was bypassed.

[9] Presented at the APhA Academy of Pharmaceutical Sciences, New Orleans meeting, Apr. 1976 (abstract 54).

In conclusion, this study has shown that a relatively simple procedure involving perfusion and a special cell inserted into the vagina may be used to carry out vaginal membrane permeability experiments in the rhesus monkey. The procedure should be well suited for determining vaginal membrane permeability coefficients over a wide range of conditions, especially as a function of the menstrual cycle employing, wherever possible, the particular monkey as its own control.

REFERENCES

(1) T. Yotsuyanagi, A. Molokhia, S. Hwang, N. F. H. Ho, G. L. Flynn, and W. I. Higuchi, *J. Pharm. Sci.*, **64**, 71 (1975).

(2) S. Hwang, E. Owada, T. Yotsuyanagi, L. Suhardja, N. F. H. Ho, G. L. Flynn, and W. I. Higuchi, *ibid.*, **65**, 1574 (1976).

(3) S. Hwang, E. Owada, L. Suhardja, N. F. H. Ho, G. L. Flynn, and W. I. Higuchi, *ibid.*, in press.

(4) *Ibid.*, in press.

(5) L. P. Bengtsson, *Acta Endocrinol., Suppl.*, **13**, 11 (1953).

(6) C. G. Hartman, *Endocrinology*, **25**, 670 (1939).

(7) E. Owada, C. R. Behl, Y. Kurono, S. S. Hwang, G. L. Flynn, N. F. H. Ho, and W. I. Higuchi, *Obstet. Gynecol.*, in press.

ACKNOWLEDGMENTS AND ADDRESSES

Received February 12, 1976, from the *College of Pharmacy, University of Michigan, Ann Arbor, MI 48109.*

Accepted for publication March 31, 1976.

Supported by the National Institute of Child Health and Human Development, Bethesda, Md. (Contract NO1-HD-3-2740).

The authors thank Dr. T. J. Roseman, Dr. K. T. Kirton, and Dr. F. H. Schadewald for helpful comments on the feasibility of the reported method.

[x] To whom inquiries should be directed.

Aqueous Chamber Drug Distribution Volume Measurement in Rabbits

JOSEPH M. CONRAD and JOSEPH R. ROBINSON [x]

Abstract □ A method was developed for aqueous chamber drug distribution volume measurement in the albino rabbit, and the apparent volume of distribution was determined for inulin, pilocarpine alkaloid, and 1-hexanoic acid. The method consists of injecting a suitable concentration of drug, in an appropriate volume of fluid, into the anterior chamber of the eye and monitoring the decline in drug concentration as a function of time by periodic sampling of the aqueous humor. Graphical analysis of the resulting data yields both the apparent volume of distribution and the turnover rate constant of the aqueous humor. The technique does traumatize the eye, causing formation of plasmoid aqueous, which does not interfere with the apparent drug distribution volume measurement or the determination of aqueous humor turnover. Inulin was used to determine the physiological aqueous volume, 287 μl, in good agreement with literature values. The turnover rate constant was 0.016 min^{-1}, also in good agreement with literature values. The apparent volume of distribution for pilocarpine alkaloid was 575 μl in albino eyes and 760 μl in pigmented irides; for 1-hexanoic acid in albino eyes, it was 760 μl. For pilocarpine alkaloid, literature citations on the fraction of dose absorbed have been based on an assumed apparent volume of distribution of 250–300 μl. Therefore, a factor of two error has been introduced when using albino eyes and a factor of almost three has been introduced when using pigmented eyes. The implication of the apparent volume of distribution for pilocarpine in its ocular disposition is discussed, as is the unexpected observation that pilocarpine alkaloid apparently inhibits formation of plasmoid aqueous and follows one-compartment kinetics during these studies. It is shown that the one-compartment kinetics for pilocarpine are due to its biological activity in the aqueous chamber.

Keyphrases □ Drug distribution—aqueous chamber drug volume, inulin, pilocarpine, and 1-hexanoic acid, rabbit eyes □ Inulin—aqueous chamber volume of distribution, rabbit eyes □ Pilocarpine—aqueous chamber volume of distribution, rabbit eyes □ 1-Hexanoic acid—aqueous chamber volume of distribution, rabbit eyes □ Ocular volumes of distribution—aqueous chamber, pilocarpine, inulin, and 1-hexanoic acid, rabbit eyes

To make meaningful quantitative statements about the bioavailability of an ophthalmic preparation, it is necessary to know the apparent volume of distribution for that drug in the eye. At present, the ophthalmic literature contains statements on the bioavailability of topically applied ocular drugs that are based, at best, only on an approximation to the actual aqueous humor volume, ignoring all other factors, and, at worst, on poorly controlled clinical studies

(1–4). The present study was designed to establish procedures for obtaining ocular volumes of distribution in the anterior and posterior chambers of the eye, to provide an accurate value for aqueous humor volume, and to determine the apparent volume of distribution of some typical ophthalmic drugs.

BACKGROUND

The apparent volume of distribution for ocular drugs can be used to provide insight on drug disposition if a physiological basis for the actual volume is provided, *i.e.*, if the ocular tissue volume is known. Significant deviations from the physiological volume for a determined apparent volume of distribution would be helpful in a mechanistic understanding of a drug's disposition.

Reported values for the physiological volume of the aqueous humor in rabbits have been derived primarily from paracentesis studies where the anterior chamber was aspirated and the volume was determined. Such values, however, may be in error since they may not measure the aqueous humor in the posterior chamber or fluid adhering to the walls of the anterior chamber. The aqueous humor contained in and on these structures is not measurable *via* normal aspiration techniques. Moreover, the iris and ciliary body are relatively porous structures containing aqueous humor that probably will not be removed *via* paracentesis.

Apparently, there are no reports on the apparent volumes of distribution for ocular drugs. For situations requiring an apparent volume of distribution, *e.g.*, determination of the fraction of dose absorbed, it is common practice to assume a 250–300-μl volume, irrespective of the drug under study.

Without an accurate value for the apparent volume of distribution of a drug in the eye, it is still possible to make statements regarding the percent of an applied dose that crosses the cornea to the aqueous humor. However, these values are only estimates and do not consider many parameters that can affect the bioavailability of a particular drug, *e.g.*, protein binding, partitioning into tissues, and poor mixing. By determining a precise value for the apparent distribution volume, it is possible to calculate accurately the fraction of dose absorbed. Armed with this information, it is possible to modify the size of the dose, the frequency of dosing, the vehicle for the dose, *etc.*, and to gauge the improvement in drug bioavailability due to these manipulations. In addition, the apparent volume of distribution for a drug can be used as an initial probe in the design of mechanistic studies of drug disposition.

An additional parameter, important to the disposition of a drug in the aqueous chamber, is aqueous humor turnover, since drug can be rapidly eliminated by the inflow and outflow of the aqueous humor. Removal of drug *via* this route is influenced by distribution equilibria of the drug in the aqueous chambers. Hence, the terminal elimination portion of the aqueous humor drug concentration–time profile can be used to estimate the importance of aqueous humor turnover, as well as distribution, on drug elimination.

Physiological turnover rates have been determined by various invasive and noninvasive techniques in several animal species (5–9). The results derived from the present method compare well with previously reported values. The salient feature of the described method is that it allows calculation of both the rate of aqueous humor turnover and the apparent volume of distribution for the drug from a single experimental technique. Other methods, both invasive and noninvasive, do not have the capability of determining the apparent volume of distribution, since they are mainly either continuous perfusions of the anterior chamber or intravenous injections of tracer material that appears in the eye after penetration of the blood–aqueous barrier *via* the animal's circulatory system (5–14). Thus, these methods do not provide for extrapolating drug concentration–time data to zero time, which is a necessary feature in developing a procedure to obtain the apparent volume of distribution for a drug.

EXPERIMENTAL

Materials—Male, albino, and mixed breed dark iride rabbits[1], 1.8–2.4 kg, were maintained on a regular diet with no restrictions on food or water intake.

^{14}C-Inulin[2] dry powder, specific activity 2.47 μCi/mg, was used as received. ^{3}H-Pilocarpine alkaloid[2] alcoholic solution, specific activity 2.4 mCi/mg, was purified by vacuum distillation (15) prior to use. The purification of pilocarpine was carried out immediately before each experimental run to minimize tritium exchange with the solvent. ^{14}C-1-Hexanoic acid[3], sodium salt aqueous solution, specific activity 10 mCi/mmole, was used as received. ^{14}C-Inulin and ^{14}C-1-hexanoic acid were 99% chromatographically pure. All other chemicals were either reagent or analytical grade.

Methods—*Preparation of ^{14}C-Inulin Solution*—^{14}C-Inulin was dissolved in water so that a concentration of 2×10^{-5} *M* was obtained. Since this concentration represents the limit of aqueous solubility for inulin, no "cold" (nonlabeled) inulin was added to the solution. This concentration corresponds to 0.1 μg of inulin/μl of solution. In the study employing an inulin–pilocarpine solution, radioactive inulin, 2×10^{-5} *M*, was added to a 1×10^{-4} *M* cold pilocarpine solution.

Preparation of ^{3}H-Pilocarpine Solution—Earlier work established a peak aqueous humor drug level of approximately 1×10^{-4} *M* from topical application of a 1×10^{-2} *M* solution of pilocarpine (16). Since the present study involved direct injection of drug into the anterior chamber, 1×10^{-4} *M* pilocarpine was used. The alcoholic solution of ^{3}H-pilocarpine alkaloid was evaporated to dryness. To the evaporated ^{3}H-pilocarpine was added 5 ml of 1×10^{-4} *M* cold pilocarpine alkaloid in aqueous solution. The addition of ^{3}H-pilocarpine alkaloid was small enough to have no appreciable effect on the molarity of the final solution. The solution concentration corresponded to 2.08 μg of pilocarpine alkaloid/μl.

Preparation of ^{14}C-1-Hexanoic Acid Solution—From the aqueous solution of the sodium salt, 50-μl samples were diluted to 3 ml with water to produce a solution that was 1.67×10^{-4} *M* in ^{14}C-1-hexanoic acid. Therefore, the solution for injection corresponded to 1.94×10^{-2} μg of hexanoic acid/μl.

Aqueous Humor Drug Concentration–Time Profile—Rabbits were anesthetized by intraperitoneal injection of pentobarbital sodium solution followed by phenobarbital sodium solution (17). Due to variations in response to the anesthetic doses, some animals had to be titrated with additional anesthetic until no head movements and/or blink responses were present. Also, for time points beyond 30 min, an intravenous infusion of a phenobarbital sodium solution was administered periodically to maintain anesthesia.

Anesthetized animals were then placed in wooden restraining boxes which maintained the normal upright posture for the animal. About 10 min prior to dosing, each eye received 1 drop of 0.5% tetracaine hydrochloride solution[4]. Due to the manipulations required, each rabbit was used for two different time points. For example, the left eye was dosed 10 min after the right eye so that at the end of 20 min the right eye yielded a 20-min point while the left eye yielded a 10-min point. To eliminate any right to left or left to right bias, the next rabbit was dosed so that the left eye yielded the 20-min point while the right eye yielded the 10-min point. For the later time points of 60 min and beyond, the same time point could be obtained from both eyes since the entire procedure of refilling the syringes, injecting the drug solution, and positioning the delivery apparatus on the wooden blocks took approximately 1 min, and this period introduced a potential error of only 1.67% in a 60-min time point. Moreover, this error was averaged out by reversing the order of dosing in the next rabbit.

Once the anesthetized animal was positioned in the restraining box and the topical anesthetic was applied, measured volumes of drug solution (5, 10, or 20 μl) were accurately administered to each rabbit eye *via* a microliter syringe[5]. The syringe was fitted with a modified vein infusion set[6] prefilled with the drug solution. The modification consisted of shortening the tubing length from the normal 30 cm to approximately 3 cm. This change was made to minimize drug solution loss and to make the delivery apparatus more manageable. Once the needle of the infusion set had punctured the cornea and was in position in the anterior chamber, the appropriate dose was delivered from the syringe. To prevent leakage of the aqueous humor fluid, the 3-cm tubing was then clamped off with Kelly forceps and the tubing was cut just behind the clamp. The clamp was then supported on a wooden block so that its weight would not pull on the punctured cornea and produce leakage at the entrance point of the needle into the cornea.

The clamp assured no loss of aqueous humor due to positive pressure outflow caused by the intraocular pressure. The small amount of tubing

[1] Klubertanz, Edgerton, Wis.
[2] New England Nuclear, Boston, Mass.
[3] ICN, Chemical and Radioisotope Division, Irvine, Calif.
[4] Pontocaine, Winthrop Laboratories, New York, N.Y.
[5] Hamilton 705, Hamilton Co., Reno, Nev.
[6] Miniset, Travenol Laboratories, Deerfield, Ill.

Table I—Pharmacokinetic Parameters Obtained *via* Anterior Chamber Injection of Various Drugs

Drug	Dose, μl	Amount of Drug per Dose, μg	C_0, μg/ml	Apparent V_d, μl	Turnover Rate Constant, k, min^{-1}
Inulin[a]	5	0.5	1.75	286	0.018
	10	1.0	3.40	294	0.011
	20	2.0	7.15	280	0.020
				Average 287	Average 0.016
Pilocarpine[b]	10	0.2083	0.36	579	0.060
	20	0.4165	0.73	571	0.058
				Average 575	Average 0.059
Pilocarpine[c]	10	0.2083	0.27	760	0.066
1-Hexanoic acid[a]	10	0.1937	0.26	745	0.019
	20	0.3874	0.50	775	0.015
				Average 760	Average 0.017

[a] Analyzed by apparent two-compartment open model. The turnover rate constant was determined from the terminal portion of the line. [b] Analyzed by apparent one-compartment open model. [c] In dark iride rabbits. The turnover rate constant was determined from the initial portion of the line.

remaining, 1.5 cm, and the supported clamp allowed the rabbit some head movement without danger of dislodging the needle.

At the end of the designated time periods, 5, 10, 15, 20, 30, and 60 min, the rabbit was sacrificed by rapid marginal ear vein injection of an overdose of phenobarbital sodium. The 90- and 120-min time points were obtained only with the ^{14}C-inulin at the 20-μl volume. The aqueous humor was aspirated from each eye using a 1-ml tuberculin syringe fitted with a 27-gauge, 1.27-cm needle. Aqueous humor samples, 100 μl, were quantitatively transferred to scintillation counting vials[7] containing 5 ml of a scintillation cocktail[8]. Samples were then stored in the dark at room temperature for a minimum of 48 hr prior to counting to eliminate error due to chemiluminescence. Ten-minute counts of each sample were made using a liquid scintillation spectrometer[9]. The final count for each sample, corrected for background, was then converted to a microgram of drug per milliliter of aqueous humor basis by standardization techniques to facilitate analysis and interpretation of results.

A minimum of 10 eyes was used for each data point, with the exception of the 60-min point for pilocarpine in albino rabbits where four eyes were used; no animal was used more than once. Mean values and standard errors of the mean were determined from the pooled data at each time point. The concentration–time profiles were least-squares fit to the one- or two-compartment model.

RESULTS

Inulin has been employed in the past to measure renal clearance values. Since it does not readily penetrate tissues and is not bound to protein to any measurable extent, it was considered ideal for such clearance measurements because it is eliminated solely by glomerular filtration. These same properties make inulin an attractive probe for measuring the physiological aqueous humor volume. In addition, tissues surrounding the aqueous chamber, *i.e.*, iris and ciliary body, are porous and should allow free movement of the relatively small inulin molecule so that all resident aqueous humor is detected. These assumptions are borne out by experimentation. Assay of ocular tissues surrounding the anterior chamber, *i.e.*, cornea, ciliary body, iris, vitreous humor, and lens, shows that inulin is not absorbed and/or adsorbed onto these tissues. Thus, the only means of exit for inulin from the anterior chamber is by normal aqueous humor drainage.

Figure 1 shows the aqueous humor inulin concentration–time profile for three different injected volumes (5, 10, and 20 μl). Different volumes were employed to determine the influence of instilled volumes on the apparent volume of distribution and apparent aqueous humor turnover as well as to check on the proposed mechanism for inulin removal, *i.e.*, to explain the shape of the drug concentration–time profile. The drug concentration–time profiles were analyzed as an apparent two-compartment open model[10], with the initial portion of the curve attributed to an effect due to injection of a volume above that of the normal resident volume and the terminal portion due to normal aqueous humor turnover.

An analogy can be made between this system and instilling a volume of drug into the precorneal portion of the eye (18). In the precorneal portion, an instilled solution is diluted by resident tears, the tear–drug solution then rapidly drains from the eye until the volume is back to the normal resident volume, and, finally, tear turnover accounts for most of the remaining drug removal. In the aqueous chamber, the injected inulin mixes with resident aqueous humor and drains from this area until a normal volume is achieved, at which point aqueous humor turnover is responsible for additional removal. Thus, the initial portion of the inulin profile is attributed to rapid removal of drug simply because a volume has been injected. The increasing slopes of these lines with an increasing volume support this proposal. The terminal portion of the profile corresponds to aqueous humor turnover. Since no distribution of inulin into aqueous chamber tissues occurs, the terminal slope can be directly related to aqueous humor turnover.

After graphical analysis and extrapolation to time zero, the volume of distribution of the aqueous humor can be calculated in the usual manner. These values for the three volumes are presented in Table I along with the turnover rate constants obtained from the terminal portion of the curves. The physiological volume of distribution, *i.e.*, true aqueous humor volume, and the turnover rate constant derived from these measurements agree very well with those reported for rabbits using other techniques (5, 19).

The problem of plasmoid aqueous formation due to trauma has been well documented for the rabbit (20–22). Any trauma such as inflammation or puncture of the globe of the eye leads to a breakdown on the blood–

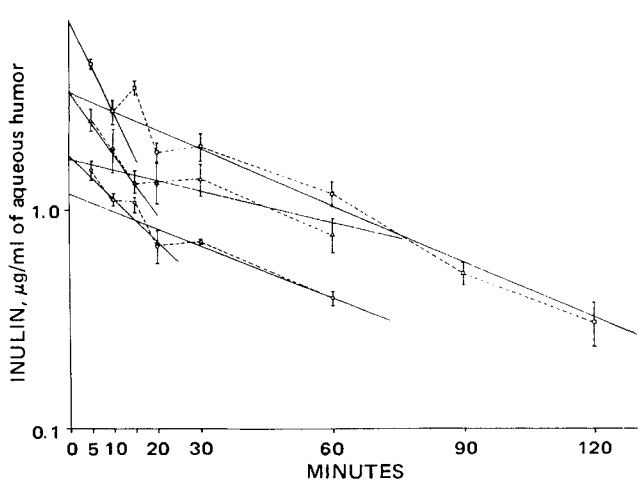

Figure 1—*Aqueous humor drug concentrations following intracameral injection of 2 × 10^{-5} M inulin solutions in albino rabbits. Error bars represent the standard error of the mean. Where no error bars are drawn, the standard error was smaller than the symbol used. Solid lines are best-fit lines. Dotted lines connect the mean value at each time point. Key: ○, 5 μl injected; △, 10 μl injected; and □, 20 μl injected.*

[7] Mini-vial, Research Products International Corp., Elk Grove Village, Ill.
[8] Aquasol.
[9] Packard model 2002, Packard Instrument Co., Downers Grove, Ill.
[10] The term compartment is used in a very loose sense throughout this article. With inulin, only the aqueous chamber is involved, *i.e.*, one compartment, and the biphasic concentration–time profile is simply a fast volume-dependent removal of drug followed by a slower removal.

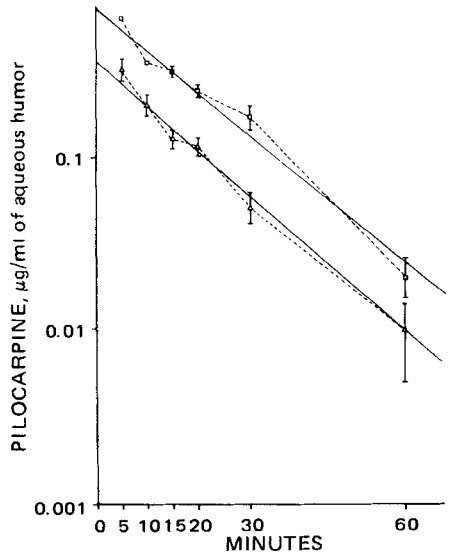

Figure 2—*Aqueous humor drug concentrations following intracameral injection of 1 × 10^{-4} M pilocarpine solutions in albino rabbits. Error bars represent the standard error of the mean. Where no error bars are drawn, the standard error was smaller than the symbol used. Solid lines are best-fit lines. Dotted lines connect the mean value at each time point. Key: △, 10 μl injected; and □, 20 μl injected.*

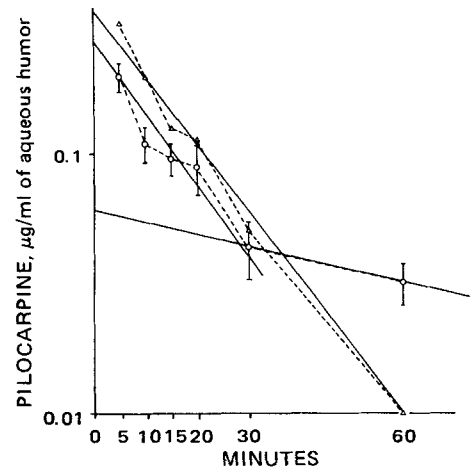

Figure 3—*Comparison of aqueous humor drug concentrations following intracameral injection of 1 × 10^{-4} M pilocarpine solutions in albino and pigmented iride rabbits. Error bars represent the standard error of the mean. Error bars were deleted from the albino rabbit data to facilitate comparisons. Solid lines are best-fit lines. Dotted lines connect the mean value at each time point. Key: △, 10 μl injected in albino rabbits; and ○, 10 μl injected in pigmented rabbits.*

aqueous barrier with a concomitant rise in the protein content of the aqueous humor. In the inulin study, plasmoid formation was visually observed at the 30-min time point and beyond. Plasmoid formation results in an extremely viscous aqueous humor, which is difficult to aspirate into the tuberculin syringe. It appears as a transparent semisolid, gel-like substance which undergoes shear thinning with repeated uptake and discharge through the syringe needle.

Formation of plasmoid aqueous in the rabbit occurs with very mild trauma, whereas the human eye seems much more resistant to its formation (23). Since plasmoid aqueous does not appear to affect vision, at least in the human eye, and the calculated turnover rate constant of the aqueous humor from the present study agrees well with that of normal aqueous humor in rabbits, its formation does not appear to be a cause for concern in the present study. Apparently, the rabbit eye makes all necessary accommodative changes to compensate for the more viscous plasmoid aqueous. Plasmoid aqueous formation is, of course, a reversible process; in a relatively short period, *i.e.*, a few hours, a normal aqueous humor is again formed.

Figure 2 shows the aqueous humor drug concentration–time profile for pilocarpine, and Table I shows the apparent volume of distribution and turnover rate constant for pilocarpine derived from graphical analysis of the data. From the data in Table I, it is clear that the apparent volume of distribution for pilocarpine is twice that of the physiological volume and the turnover rate constant is significantly greater than the normal value. The larger volume of distribution can be attributed to the fact that pilocarpine is somewhat protein bound, can and does penetrate ocular tissues, and may be bound to tissue surfaces (4, 24–27)[11].

Because protein contained in the aqueous humor leaves the eye during the normal removal of the aqueous humor, the present method is unable to discern whether or not a drug is highly bound to protein, as can be done with the traditional drug volume of distribution in the blood. However, the method can discern tissue penetration and binding of drugs to ocular tissue surfaces, as was shown clearly in the study of pilocarpine in dark iride rabbits (Fig. 3). The apparent volume of distribution for pilocarpine was 760 μl, considerably larger than the 575 μl determined in albino rabbits. For comparative purposes, Fig. 3 includes the albino rabbit data for pilocarpine. The decline in drug concentration between pigmented and nonpigmented animals was parallel. However, the 60-min point was considerably different between the pigmented and nonpigmented animals. No explanation for this difference is offered, but it is important to recognize that the data from albino rabbits are based on only four eyes with a large standard error and that the radioactive counts at this level are uncomfortably low. Thus, we have less confidence in this point as compared to others.

The shape of the drug concentration–time profile for pilocarpine was considerably different than that of inulin. A biphasic curve was not observed over the time course of the study, and the slope of the line yielded a rate constant considerably greater than physiological turnover of the aqueous humor. A suggested explanation for this behavior is related to the pharmacological effect of pilocarpine. It is well known that pilocarpine exerts various pharmacological effects in the eye, such as decreased anterior chamber depth (28) and an influence on aqueous humor turnover (9, 29–30). These effects were absent with inulin as well as with 1-hexanoic acid, and both of these compounds showed the expected biphasic appearance. In support of the idea that this finding is not an artifact of the present technique, it was observed that the 1st hr or so beyond the peak of the aqueous humor pilocarpine–time profile, from topically applied drug, also showed an increased rate of removal over and above physiological turnover[11].

As an alternative explanation for the data, it is possible that the apparent one-compartment profile for pilocarpine represents a nonsteady-state distribution into other tissues, which would invalidate this approach for pilocarpine apparent volume of distribution measurement. However, other data[11] do not support this thesis; therefore, a pharmacological effect is offered as a reasonable explanation. As added support for a pharmacological effect explanation, a study was undertaken where inulin and pilocarpine were injected together and the decline in inulin concentration was monitored as a function of time. If a pharmacological effect from pilocarpine occurs, it would be expected that the decline in inulin concentration, when an inulin–pilocarpine solution is injected, would be more rapid and perhaps follow different kinetics than when inulin is administered by itself.

Figure 4 shows the results of this study as well as the data for inulin and pilocarpine. Inulin did indeed leave the aqueous chamber at a more rapid rate when pilocarpine was present. Although there are insufficient data to draw a firm conclusion, it appears that the inulin–pilocarpine data closely parallel the pilocarpine elimination line, and it is considerably different than the inulin line by itself.

When pilocarpine was injected into the anterior chamber, no plasmoid aqueous humor was observed up to 60 min postinjection while with inulin and 1-hexanoic acid, a plasmoid aqueous formed readily.

Figure 5 presents the aqueous humor drug concentration–time profile for 1-hexanoic acid. This compound, of course, is not used in ophthalmic therapy. However, because it is a medium chain-length fatty acid, it can be expected to penetrate tissues readily and to have a relatively large apparent volume of distribution. As indicated in Table I, its apparent volume of distribution was approximately 2.5 times larger than the true physiological volume of distribution obtained in the inulin study.

Graphical analysis of the 1-hexanoic acid data yielded an apparent two-compartment open model with the same volume effect initially as that shown for inulin. The break points in the curves for the two volumes followed the same pattern established for inulin, and this finding lends credibility to the volume effect argument.

[11] M. C. Makoid, University of Wisconsin, Madison, Wis., unpublished data.

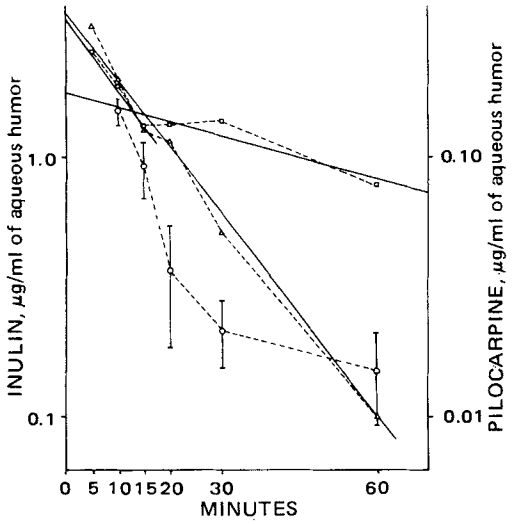

Figure 4—*Comparison of aqueous humor drug concentrations following intracameral injection of 10 μl of 2 × 10^{-5} M inulin solutions (□), 1 × 10^{-4} M pilocarpine solutions (△), or 2 × 10^{-5} M inulin in 1 × 10^{-4} M cold pilocarpine solutions (○) in albino rabbits. Error bars represent the standard error of the mean. Error bars were deleted from the 2 × 10^{-5} M inulin and from the 1 × 10^{-4} M pilocarpine data to facilitate comparisons. Solid lines are best-fit lines. Dotted lines connect the mean value at each time point.*

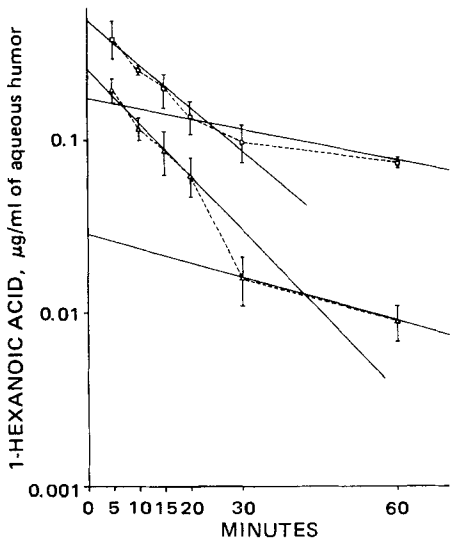

Figure 5—*Aqueous humor drug concentrations following intracameral injection of 1.67 × 10^{-4} M 1-hexanoic acid solutions in albino rabbits. Error bars represent the standard error of the mean. Where no error bars are drawn, the standard error was smaller than the symbol used. Solid lines are best-fit lines. Dotted lines connect the mean value at each time point. Key: △, 10 μl injected; and □, 20 μl injected.*

Another feature of the apparent two-compartment open model used to describe the inulin and 1-hexanoic acid data is that the turnover rate constant obtained after curve stripping of the initial phase of the curves, *i.e.*, that portion attributed to the volume effect, agrees reasonably well with the turnover rate constant found for pilocarpine in that study. This result indicates that the volume effect is qualitatively similar to the pharmacological effect produced by pilocarpine.

DISCUSSION

A primary consideration of this study was the development of a technique for systematically measuring the apparent volume of distribution of ophthalmic drugs. The method itself is obviously unrealistic for human use, since it involves puncturing the cornea and direct injection of drug solution into the anterior chamber. However, the insights gained from animal studies are useful in providing initial estimates of ocular behavior in humans. For example, since the rabbit eye is similar in size and gross morphology to the human eye, a drug's apparent volume of distribution measured in rabbits is expected to approximate that of human eyes.

The described method has limitations. As mentioned previously, protein binding will not be detected *per se*, because the movement of drug bound to protein will be indistinguishable from free drug movement. Both bound and free drug leave the chamber *via* normal aqueous humor drainage, and the present technique cannot distinguish free and bound drug.

A second limitation is that the drug must be in an aqueous vehicle. Since it is injected into a small confined aqueous milieu, an oil-soluble drug in an oily vehicle could precipitate in the anterior chamber and block the aqueous humor drainage pathways or the oil vehicle could cause a physical blockade to drainage.

Based on the previous discussion, relative to the effect of injected volume on the pharmacokinetic profile, it is clear that there should be constraints on the volume employed. Too large a volume may result in possible tissue damage so that an upper limit is placed on the accommodative mechanism of the rabbit eye. A small volume is limited by the reproducibility of repetitive injections. It is suggested that the 10-μl volume be used on a routine basis, because the 5-μl volume requires considerable skill for reproducibility and the 20-μl volume might generate damage to the eye, particularly if small rabbits are employed. However, if solubility problems or assay limitations are encountered, the 20-μl volume can be employed; in fact, a 30-μl volume can be used. Studies using 30 μl were also conducted for inulin, and the results (not reported here) from these studies are consistent with the reported volumes.

One concern with the proposed experimental technique was that having the test animal under general anesthesia throughout the experiment might decrease the rate of aqueous humor formation and removal (6, 31). Results, namely that physiological turnover rates of the aqueous humor were determined from the inulin and 1-hexanoic acid data, indicate that this reduction or stoppage does not occur in the rabbit under anesthesia.

Several additional observations made during this study require further comment. As noted earlier, the trauma of intracameral injection and increased volumes in the chamber due to injection caused the formation of plasmoid aqueous within 30 min postinjection of inulin and 1-hexanoic acid. At first glance, it would seem likely that this more viscous, proteinaceous aqueous humor should not leave the anterior chamber very easily, thus leading to a slow turnover rate. This is obviously not the case. Two possible mechanisms can explain this finding. Either the rabbit's trabecular meshwork expands to accommodate the plasmoid aqueous or a microdiffusion effect removes the more fluid portions of the plasmoid, leaving behind a "matrix" of highly viscous protein plasmoid aqueous which is subsequently removed at a slower rate.

If increased accommodation is the method of plasmoid aqueous removal, this process is easily reversible since, upon removal of the cause of plasmoid aqueous, the rabbit aqueous humor returns to normal within a matter of a few hours (32). The accommodation must be throughout the anterior and posterior chambers because, not only does the viscous plasmoid leave at a normal rate, it must form and enter the posterior chamber at a normal rate to maintain a constant turnover rate (20, 32).

The second possibility, a microdiffusion effect, would involve formation and destruction of a protein matrix with relatively free flow of the aqueous humor in and through this matrix. If this microdiffusion mechanism is operative, it presents an interesting form of sustained release for any highly protein-bound drug. The drug would be bound to the protein matrix, which should prolong its residence time in the aqueous chamber. These possible mechanisms for plasmoid aqueous removal are interesting and require additional work. However, the most important factor relative to the proposed technique is that plasmoid aqueous formation does not interfere with the apparent volume of distribution determination.

The pilocarpine and 1-hexanoic acid data were intriguing from several points of view. As noted in Table I, the apparent volume of distribution for pilocarpine in the aqueous humor was 575 μl, and the concentration–time data fit a monoexponential curve with an apparent first-order rate constant of 0.059 min^{-1}. The apparent volume of distribution was twice the physiological volume, which was attributed to sorption of the drug into and onto tissues lining the aqueous chamber (4, 24–27)[11]. Since published studies on the fraction of dose absorbed for pilocarpine have relied on an assumed volume of distribution of 250–300 μl, these values probably are off by a factor of two for albino rabbits and by a factor of almost three for pigmented rabbits. The more important point is that other drugs, as illustrated by 1-hexanoic acid, could have much larger

apparent volumes of distribution and be off by factors of three, four, or greater.

In defense of the proposed mechanism for the increased turnover rate constant due to pilocarpine, *i.e.*, a pharmacological effect, a comparison of these results in rabbits with those obtained in humans (33) for topically applied pilocarpine is in order. Yoshida and Mishima (33) found that the rate constant for normal aqueous turnover in humans was 0.7 hr^{-1} while that following topical dosing with pilocarpine was 0.27 hr^{-1}. In the present study, the normal aqueous turnover in rabbits was 0.72 hr^{-1} while the turnover following pilocarpine injection was 4.2 hr^{-1}. It would appear that these data are in conflict. However, it should be kept in mind that topical dosing leads to a reservoir effect in the corneal epithelium (34) so that, at later times, the turnover of pilocarpine appears slower than it actually is. As pilocarpine leaves the aqueous chamber, more drug is being fed in to maintain a level of drug in the aqueous chamber that falls less rapidly than would occur if the reservoir was absent. Application of drug through direct injection bypasses the reservoir effect of the corneal epithelium and generates a more rapid removal of the aqueous humor, in keeping with what one would intuitively expect for a glaucoma drug. Over the time course of these studies, pilocarpine apparently is unable to penetrate the corneal epithelium from direct injection so there is no reservoir effect. Recent evidence (4, 24)[11] demonstrates that pilocarpine disposition from the aqueous humor is quite complex and does not follow a simple one- or two-compartment model.

From the results of this pilocarpine study in albino and pigmented animals, it is clear that the method can discern binding. Thus, the earlier noted differences in pilocarpine uptake in heavily pigmented animal eyes (4, 25) as well as humans (26) have been borne out in an *in vivo* experiment and support the need for more drug to treat glaucoma in heavily pigmented eyes.

1-Hexanoic acid data were biphasic, with the terminal portion of the curve having an apparent rate constant of 0.017 min^{-1}, in agreement with normal aqueous humor turnover. One would intuitively expect that the elimination of a drug that distributes extensively into aqueous chamber tissues would be influenced by this distribution and that, therefore, the terminal portion of the 1-hexanoic acid curve should probably not correspond to normal turnover. One can speculate that drug taken up by tissue is removed from the aqueous chamber by absorption into the general circulation or perhaps that the drug is irreversibly bound to tissue or in some manner degraded.

REFERENCES

(1) H. K. Von Muller, O. Hockwin, and O. Kleifeld, *Graefes Arch. Ophthalmol.*, **162,** 107 (1960).

(2) J. E. Harris, in "Symposium on Ocular Therapy," J. H. Leopold, Ed., C. V. Mosby, St. Louis, Mo., 1968, p. 99.

(3) C. F. Asseff, R. L. Weisman, S. M. Podos, and B. Becker, *Am. J. Ophthalmol.*, **75,** 212 (1973).

(4) R. Lazare and M. Horlington, *Exp. Eye Res.*, **21,** 281 (1975).

(5) V. E. Kinsey and D. V. N. Reddy, in "The Rabbit in Eye Research," J. H. Prince, Ed., Charles C Thomas, Springfield, Ill., 1964, p. 235.

(6) S. J. Cevario and F. J. Macri, *Invest. Ophthalmol.*, **13,** 384 (1974).

(7) F. J. Macri and J. O'Rourke, *Arch. Ophthalmol.*, **83,** 741 (1970).

(8) F. J. Macri, R. Dixon, and D. P. Rall, *Invest. Ophthalmol.*, **5,** 386 (1966).

(9) J. Edwards, V. L. Hallman, and E. S. Perkins, *Exp. Eye Res.*, **6,** 316 (1967).

(10) F. J. Macri, *Arch. Ophthalmol.*, **78,** 629 (1967).

(11) W. W. Oppelt, *Invest. Ophthalmol.*, **6,** 76 (1967).

(12) F. J. Marci, R. L. Dixon, and D. P. Rall, *ibid.*, **4,** 927 (1965).

(13) J. K. Lauber, J. E. Boyd, and T. A. S. Boyd, *Exp. Eye Res.*, **13,** 77 (1972).

(14) E. Barany and V. E. Kinsey, *Am. J. Ophthalmol.*, **32,** 177 (1949).

(15) S. S. Chrai and J. R. Robinson, *ibid.*, **77,** 735 (1974).

(16) T. F. Patton and J. R. Robinson, *J. Pharm. Sci.*, **64,** 1312 (1975).

(17) T. J. Mikkelson, S. S. Chrai, and J. R. Robinson, *ibid.*, **62,** 1648 (1973).

(18) S. S. Chrai, T. F. Patton, A. Mehta, and J. R. Robinson, *ibid.*, **62,** 1112 (1973).

(19) D. M. Maurice, *Am. J. Ophthalmol.*, **47,** 361 (1958).

(20) W. G. Unger, D. F. Cole, and B. Hammond, *Exp. Eye Res.*, **20,** 255 (1975).

(21) M. de Vincentiis, *J. Physiol.*, **146,** 252 (1959).

(22) H. Davson and C. B. Weld, *Am. J. Physiol.*, **134,** 1 (1941).

(23) F. H. Adler, "Physiology of the Eye," C. V. Mosby Co., St. Louis, Mo., 1965, pp. 96–143.

(24) L. Sendelbeck, D. Moore, and J. Urquhart, *Am. J. Ophthalmol.*, **80,** 274 (1975).

(25) J. S. Lyons and D. L. Krohn, *ibid.*, **75,** 885 (1973).

(26) L. S. Harris and M. A. Galin, *ibid.*, **72,** 923 (1971).

(27) D. A. Newsome and R. Stern, *ibid.*, **77,** 918 (1974).

(28) D. H. Abramson, D. J. Coleman, M. Forbes, and L. A. Franzen, *Arch. Ophthalmol.*, **87,** 615 (1972).

(29) P. P. Ellis, *Surv. Ophthalmol.*, **16,** 165 (1971).

(30) L. S. Harris, T. W. Mittag, and M. A. Galin, *Arch. Ophthalmol.*, **86,** 1 (1971).

(31) B. Becker, T. Krupin, and S. M. Podos, *Am. J. Ophthalmol.*, **70,** 686 (1970).

(32) H. Davson, in "The Eye," vol. I, 2nd ed., Academic, London, England, 1969, pp. 67–186.

(33) S. Yoshida and S. Mishima, *Jpn. J. Ophthalmol.*, **19,** 121 (1975).

(34) J. W. Sieg and J. R. Robinson, *J. Pharm. Sci.*, **65,** 1816 (1976).

ACKNOWLEDGMENTS AND ADDRESSES

Received February 26, 1976, from the *School of Pharmacy, University of Wisconsin, Madison, WI 53706.*

Accepted for publication April 15, 1976.

Supported by Allergan Pharmaceuticals, Irvine, CA 92664, and Grant EY-01332 from the National Institutes of Health.

[x] To whom inquiries should be directed.

Biological Distribution of Chemical Analogs of Fatty Acids and Long Chain Hydrocarbons Containing a Strong Chelating Agent

STEPHEN M. KARESH *, WILLIAM C. ECKELMAN *‡x, and RICHARD C. REBA *‡

Abstract □ The pharmaceutical preparation, chromatography, and biological distribution of a series of new chemical analogs of palmitic acid and diethylenetriaminepentaacetic acid, ethylenediaminetetraacetic acid, or diethylenetriamine are described. The biological distribution in rabbits 30 min after intravenous administration of these ^{99m}Tc-labeled and ^{57}Co-labeled derivatives was compared to the biological distribution of the parent compound, ^{3}H-palmitic acid. The average myocardial uptake for these compounds was 0.04%/g, compared to 0.15%/g for palmitic acid. The heart to blood ratio at 30 min reached a maximum of 3:1 for the best physiological analog of palmitic acid, compared to an average of 30:1 for palmitic acid. Although none of these analogs appears to be clinically useful, their production methods might be applicable to the synthesis of new compounds that might increase the specificity of radiopharmaceuticals.

Keyphrases □ Fatty acid analogs, ^{99m}Tc- and ^{57}Co-labeled—containing chelating agents, biological distribution, compared to ^{3}H-palmitic acid, rabbits □ Distribution, biological—^{99m}Tc- and ^{57}Co-labeled fatty acid analogs containing chelating agents, compared to ^{3}H-palmitic acid, rabbits □ Radiochemistry—technetium Tc 99m as label for fatty acid analogs containing chelating agents, biological distribution, compared to ^{3}H-palmitic acid, rabbits □ Technetium Tc 99m—label for fatty acids containing chelating agents, biological distribution, compared to ^{3}H-palmitic acid, rabbits

Of the conveniently available radionuclides, technetium Tc 99m has the best physical characteristics for external imaging; however, poor chemical properties have limited its use as a label for biological molecules. The weak chelate ion characteristics of technetium Tc 99m in aqueous solution are such that many organic compounds have been only nominally labeled with it. For example, for such molecules as tetracycline (1) and the carbohydrates (2), the chelating strength of the functional groups on the molecule itself is apparently too weak to assure the integrity of the chelate *in vivo*.

The preparation of derivatives may be a means of producing radiopharmaceuticals with better metal binding properties but similar biological properties. Specifically, a biologic molecule covalently bound to a strong chelating group should then bind technetium Tc 99m more strongly than the biologic molecule itself. Simple polyaminopolycarboxylic acids like diethylenetriaminepentaacetic acid (I) have been shown to bind technetium Tc 99m so that it is distributed and excreted in vertebrates in a manner similar to that of ^{14}C-labeled I (3). Compound I, therefore, seems to be a useful chelating agent to bind to interesting biologic molecules.

The fatty acids are a class of compounds known to localize in the myocardium. By combining long chain fatty acids with I-like compounds (strong chelating agents to carry the ^{99m}Tc-label for other cations), new compounds were obtained (4). This paper describes the pharmaceutical preparation, chromatography, and relative distribution at 30 min of this series of compounds designed as myocardial imaging agents.

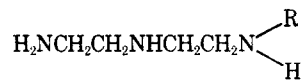

II: R = $C_{12}H_{25}$
III: R = $C_{16}H_{33}$
IV: R = $C_{18}H_{37}$
V: R = $(CH_2)_6CH{=}CH(CH_2)_7COOH$

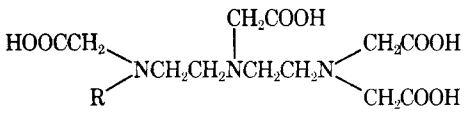

VI: R = $C_{12}H_{25}$
VII: R = $C_{16}H_{33}$
VIII: R = $C_{18}H_{37}$
IX: R = $(CH_2)_6CH{=}CH(CH_2)_7COOH$

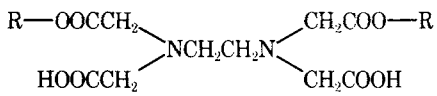

X: R = $C_{16}H_{33}$
XII: R = $C_{18}H_{37}$
XIII: R = $C_{14}H_{28}COOH$
XIV: R = $C_{15}H_{30}COOH$

EXPERIMENTAL

Synthesis, Purification, and Characterization of New Compounds—The synthesis, purification, and physical characterization of II–X and XII–XIV were published previously (4).

Preparation of Radioactive Compound—The tin chelates of VII, IX, X, and XIV were prepared in a nitrogen atmosphere. Twenty-five milligrams of stannous chloride dihydrate was placed in a 100-ml serum vial, and the vial was nitrogen purged and sealed. Three milliliters of nitrogen-purged absolute ethanol was then added by syringe, and the vial was shaken. To the vial was added 1.25 ml of a hot nitrogen-purged ethanol solution of the chelating agent (150 mg/ml, pH 4), and the mixture was shaken vigorosly. Then a nitrogen-purged ethanol–water solution was added so that the final volume was 100 ml and the resulting ethanol concentration was 20% by volume.

After the solution cooled to room temperature, it was filtered through a 0.22-μm filter. Then 2 ml of ^{99m}Tc-labeled sodium pertechnetate was added to 2 ml of the tin chelate solution. In every case, the reduced technetium bound to the chelating agent. Chromatography data showed no evidence of either $^{99m}TcO_4^-$ or ^{99m}Tc-labeled technetium stannous oxide for all of the compounds (Table I). Potentiometric titration of an aliquot of the tin chelate solution was performed for each preparation using a glass electrode[1] and standard iodine solution prior to addition of the $^{99m}TcO_4^-$ to the tin chelate solution.

The cobalt-57 chelates of IV, VII, IX, X, and XIV were prepared by heating alcoholic solutions of ^{57}Co-labeled cobalt chloride and the chelating agent in sealed serum vials for 1 hr at 100°. Labeling of each compound with cobalt-57 was verified by paper chromatography or TLC, using ^{57}Co-labeled cobalt chloride as a reference standard (Table I). Cobalt chelates were preferred for preliminary studies because of the stable oxidation state of cobalt(III).

[1] Corning platinum combination electrode.

Table I—Summary of Chromatography Data for Radiolabeled Chelates

Compound	Chromatography System	R_f Values: Cobalt-57 Chelates	R_f Values: Cobalt-57 Control
	Cobalt-57 Chelates		
IV	Cellulose, chloroform–methanol (5:1, v/v)	0.89	0.12
IV	Cellulose, 0.9% NaCl	0.00	0.92
IV	Cellulose, ethanol	0.75	0.00
VII	Cellulose, 0.9% NaCl	0.00	0.92
VII	Cellulose, ethanol	0.92	0.00
IX	Cellulose, 0.9% NaCl	0.42	0.92
IX	Cellulose, ethanol	0.86	0.00
X	Cellulose, 0.9% NaCl	0.00	0.92
X	Cellulose, ethanol	0.86	0.00
XIV	Cellulose, 0.9% NaCl	0.00	0.92
XIV	Cellulose, ethanol	0.85	0.00
	^{3}H-Labeled Chelating Agents	**R_f Values**	
V	Silica gel G, 50% 2-propanol	0.77	
V	Silica gel G, 10% ammonium acetate–ethanol (1:1, v/v)	0.46	
VII	Silica gel G, 0.1 *N* NaOH–methanol (1:1, v/v)	0.77	
IX	Silica gel G, 0.1 *N* NaOH–methanol (1:1, v/v)	0.60	
XIV	Silica gel G, 0.1 *N* NaOH–methanol (1:1, v/v)	0.83	
XIV	Cellulose, ethanol	0.91	
		R_f Values or Elution Volume	
	Technetium Tc 99m Chelates	**Technetium Tc 99m Chelate**	**TcO_4^- Control**
VII	Sephadex LH-20, methanol	34 ml	58 ml
VII	Sephadex C-25, 0.9% NaCl	V.V.[a]	34 ml
VII	Paper, methanol–0.1 *N* NaOH (1:1, v/v)	0.63	0.75
VII	Sephadex G-75, 0.9% NaCl	V.V.	54 ml
VII	Sephadex G-100, 0.9% NaCl	V.V., 36 ml	55 ml
VII	Sephadex G-150, 0.9% NaCl	V.V., 35 ml	58 ml
VII	Sephadex G-200, 0.9% NaCl	V.V.	60 ml
IX	Sephadex LH-20, methanol	V.V.	38 ml
X	Paper, 0.9% NaCl	0.50	0.75
XIV	Sephadex LH-20, methanol	V.V.	37 ml

[a] Void volume.

Table II—Biodistribution (Percent Dose per Gram) of Radiolabeled Compounds in Rabbits[a]

Compound	IV	V	VII	VII	VIII	IX
Chelating agent, μg	7	10	125	10	100	10
Isotope	^{57}Co	^{3}H	^{99m}Tc	^{3}H	^{57}Co	^{57}Co
Solvent	50% ethanol	Ammonium acetate–ethanol[b]	25% HSA[c]	Ethanol	Ethanol	0.9% NaCl
Heart	0.03 ± 0.01	0.05 ± 0.007	0.06 ± 0.01	0.03 ± 0.00	0.04 ± 0.005	0.05 ± 0.01
Lungs	0.08 ± 0.03	0.03 ± 0.007	0.10 ± 0.01	0.15 ± 0.06	0.45 ± 0.23	0.11 ± 0.03
Liver	0.12 ± 0.007	0.16 ± 0.08	0.75 ± 0.46	0.15 ± 0.02	0.38 ± 0.05	0.54 ± 0.16
Muscle	—	0.02 ± 0.007	—	0.03 ± 0.006	0.02 ± 0.005	0.03 ± 0.006
Blood	0.07 ± 0.03	0.08 ± 0.04	0.24 ± 0.11	0.03 ± 0.01	0.03 ± 0.009	0.03 ± 0.01

Compound	IX	IX	IX	IX
Chelating agent, μg	800	10	10	10
Isotope	^{3}H	^{3}H	^{57}Co	^{57}Co
Solvent	0.9% NaCl	Ethanol	Ethanol	HSA
Heart	0.12 ± 0.04	0.03 ± 0.01	0.03 ± 0.006	0.03 ± 0.006
Lungs	0.09 ± 0.08	0.07 ± 0.01	0.27 ± 0.007	0.14 ± 0.01
Liver	0.20 ± 0.11	0.06 ± 0.02	0.56 ± 0.23	0.19 ± 0.04
Muscle	0.04 ± 0.03	0.03 ± 0.01	0.01 ± 0.002	0.02 ± 0.006
Blood	0.07 ± 0.006	0.02 ± 0.006	0.04 ± 0.02	0.01 ± 0.01

Compound	X	X	XIV	XIV
Chelating agent, μg	100	100	500	100
Isotope	^{57}Co	^{99m}Tc	^{99m}Tc	^{3}H
Solvent	Ethanol	50% Ethanol	50% Ethanol	Ethanol
Heart	0.04 ± 0.009	0.03 ± 0.01	0.03 ± 0.007	0.05 ± 0.04
Lungs	1.52 ± 0.30	0.32 ± 0.20	0.12 ± 0.0002	0.18 ± 0.07
Liver	0.23 ± 0.04	0.27 ± 0.007	0.28 ± 0.09	0.09 ± 0.02
Muscle	0.01 ± 0.0009	0.003 ± 0.002	0.01 ± 0.00	0.03 ± 0.006
Blood	0.06 ± 0.01	0.08 ± 0.02	0.08 ± 0.03	0.01 ± 0.005

[a] Blanks in table indicate that particular organ was not assayed. Each value in Table II represents the average for three rabbits. [b] Ten percent aqueous ammonium acetate and absolute ethanol (1:1, v/v). [c] Fraction V human serum albumin.

Table III—Biodistribution (Percent Dose per Gram) of ^{3}H-Palmitic Acid in Rabbits[a]

Diet	Normal	Normal	Dextrose[b]	Dextrose	16-hr Fast	16-hr Fast	Normal	Normal	Normal
Palmitic acid, μg	7	7	7	700	7	700	7	7	7
Sacrifice time, hr	0.5	0.5	0.5	0.5	0.5	0.5	0.5	1.0	2.0
Solvent for injection	HSA[c]	PBS[d]	Absolute ethanol	Absolute ethanol	Absolute ethanol	Absolute ethanol	Absolute ethanol	Absolute ethanol	Absolute ethanol
Heart	0.15 ± 0.05	0.03 ± 0.007	0.21 ± 0.06	0.18 ± 0.00	0.11 ± 0.07	0.08 ± 0.03	0.24 ± 0.13	0.19 ± 0.10	0.05 ± 0.02
Lungs	0.13 ± 0.08	1.64 ± 0.71	0.20 ± 0.11	0.16 ± 0.18	0.28 ± 0.05	0.35 ± 0.03	0.29 ± 0.17	0.05 ± 0.04	0.17 ± 0.03
Liver	0.14 ± 0.04	0.33 ± 0.11	0.26 ± 0.15	0.18 ± 0.13	0.30 ± 0.12	0.23 ± 0.06	0.28 ± 0.17	0.12 ± 0.07	0.16 ± 0.007
Spleen	0.26 ± 0.04	0.62 ± 0.05	0.18 ± 0.18	0.19 ± 0.04	0.08 ± 0.05	0.07 ± 0.01	—	—	—
Skeletal muscle	0.02 ± 0.01	0.00	0.04 ± 0.00	0.01 ± 0.008	0.01 ± 0.006	0.01 ± 0.006	0.01 ± 0.00	0.02 ± 0.06	0.02 ± 0.01
Blood	0.005 ± 0.05	0.02 ± 0.006	0.01 ± 0.007	0.02 ± 0.00	0.003 ± 0.001	0.01 ± 0.007	0.005 ± 0.001	0.05 ± 0.00	0.006 ± 0.03

[a] Female New Zealand White rabbits, 2.5–3.5 kg, were used. Each value in Table III represents the average for three rabbits. Blanks in table indicate that particular organ was not assayed. [b] With 250 ml of 10% dextrose in place of drinking water the night before and 1 ml iv of 50% dextrose 10 min prior to injection. [c] Fraction V human serum albumin, fatty acid free (Miles Laboratories). [d] Phosphate-buffered saline, pH 7.4.

Compounds V and IX were labeled with tritium by catalytic reduction, using tritium gas[2] and palladium-on-charcoal catalyst[2]. Compounds VII and XIV were labeled with tritium by Wilzbach bombardment with tritium gas over 2 weeks. All tritiated compounds were purified by suitable preparative thin-layer methods and were redissolved in absolute ethanol. 9,10-^{3}H-Palmitic acid[2] was used as a reference standard for biodistribution studies, since this simple long chain fatty acid is known (5, 6) to localize in, and be metabolized by, normal myocardium in humans.

Chromatography of Radiolabeled Chelates and Chelating Agents—Paper chromatography[3], TLC on silica gel glass plates[4] or cellulose plates[5], and column chromatography on 1 × 30-cm cross-linked polysaccharide columns[6] were performed (Table I). Tritium counting of scraped sections from radiochromatograms was performed using a liquid scintillation counter; the channels-ratio method was used for quench correction. All strips containing γ-emitting isotopes were cut and counted in a sodium iodide crystal scintillation counter. In most cases, two systems are presented for verification of the degree of labeling.

Thirty-Minute Biodistribution Studies—Male New Zealand White rabbits, 2–4 kg, were used for each distribution study. After purification by preparative chromatography, 0.10 ml (~10 μCi) was injected into the marginal ear vein of the rabbit. The animal was sacrificed 30 min postinjection, unless otherwise specified. A midline incision was made, and the heart, lungs, liver, spleen, and kidneys were removed, as well as samples of skeletal muscle, perirenal fat, urine, and blood.

For each whole organ or tissue sample containing a tritium-labeled compound, one 25–50-mg sample of each type of tissue from each animal was removed, weighed (±0.01 mg), digested in 0.5 ml of 5 *N* NaOH overnight, bleached with 2 drops of hydrogen peroxide, and finally suspended in 10 ml of scintillation fluid[2]. After 4-day dark-adaption and cooling, each sample was counted for 40 min (at ≥5000 counts/sample) in a liquid scintillation counter. All data are reported in terms of percent administered dose per organ and percent administered dose per gram of organ.

Table II summarizes the tissue concentrations for the various labeled compounds and specifies the experimental conditions of the biodistribution study. Ethanol, saline, and dilute human serum albumin were used as solvents to determine if the insolubility of the fatty acid derivatives is a factor in the distribution. The dose of the chelating agent was varied to study the possibility of the saturation of the transport mechanism. Fasted animals received water *ad libitum*. The dextrose diet consisted of the normal pellet diet plus 10% dextrose solution instead of water and 1 ml of 50% dextrose injected intravenously 10 min before injection of the compound. The distribution with time was studied for ^{3}H-palmitic acid.

In a preliminary experiment, the cobalt-57 chelate of IX was studied in two 18–20-kg mongrel dogs with experimentally induced infarcts. The infarcts were induced by ligation of the anterior descending branch of the left coronary artery just distal to the origin of the circumflex branch. This procedure produced an area of ischemia in the apical region of the left ventricle, which was evident by ECG. The radiopharmaceutical was injected intravenously 30 min after sudden and complete ligation. The animal was killed 30 min after injection, and the heart was immediately excised and divided into the left and right ventricles and the interventricular septum. Each part was then further subdivided, and the radioactivity was counted.

RESULTS AND CONCLUSIONS

Chromatographic studies of the radiolabeled derivatives in the appropriate system (Table I) indicate that the technetium Tc 99m or cobalt-57 was quantitatively bound to the new derivative. However, the results presented in Tables II and III show a significantly lower ($p \leq 0.05$) concentration in the myocardium for all chelates tested than for palmitic acid, the reference standard. Approximately 0.04%/g of the administered dose localized in the entire heart, compared to 0.15%/g for ^{3}H-labeled palmitic acid. The generally high degree of localization of these compounds in the liver (~20–30%) was approximately the same as that for palmitic acid. There was no evidence of particle formation in the chromatographic studies of the original chelate.

A significant percentage of the injected dose of most of these synthetic compounds remained in the intravascular space (15–25% of the admin-

[2] New England Nuclear, Boston, Mass.
[3] Whatman No. 1 paper, Whatman Inc., Clifton, N.J.
[4] E. M. Laboratories, Elmsford, N.Y.
[5] J. T. Baker Chemical Co., Phillipsburg, N.J.
[6] Sephadex, Pharmacia Fine Chemicals, Piscataway, N.J.

istered dose) at the 30-min observation point. This finding compares with an average of about 3% remaining in the blood at 30 min for palmitic acid. Heart–blood ratios for palmitic acid on a per gram basis were in the range of from a 30:1 to 40:1; for the metal chelates the concentration was always less than 3:1, thus making it impossible to differentiate myocardium from blood.

The high blood concentration may be due to the fact that these compounds are more tightly bound to serum albumin so that the transport of fatty acid derivatives across the cell membrane into the intracellular fluids is reduced. The greater difference in polarity between a simple fatty acid, *e.g.*, palmitic acid, and fatty acid derivatives (*i.e.*, IX) could affect the localization of the labeled compound. Compounds containing a diethylenetriamine chelating group also showed slow blood clearance.

The 30-min distribution was chosen to screen this series of compounds rapidly. Because the palmitic acid does not concentrate in an infarct but does concentrate in the normal myocardia, the 30-min myocardia to blood ratio is the important factor and should indicate if the compound may be useful.

The results of the distribution of the labeled IX in dogs with experimentally induced infarcts revealed that an average accumulation of 0.94% of the injected dose was localized in the heart, 16.6% was in the liver, and 2.7% was in the lungs and that 3.8% remained in the intravascular compartment at 30 min. The infarct contained less than half of the radioactivity found in adjacent normal myocardium.

The chemical analogs described here are not sufficient biological analogs to act as tracers for fatty acid metabolism in the myocardium. However, this approach of preparing drug derivatives should lead to more specific radiopharmaceuticals and will be pursued using other biologic molecules.

REFERENCES

(1) M. K. Dewanjee, C. Fliegle, S. Treves, and M. A. Davis, *J. Nucl. Med.*, **13**, 427 (1972).

(2) B. Persson and S. E. Strand, "Radiopharmaceutical and Labeled Compounds," vol. I, International Atomic Energy Agency, Vienna, Austria, 1973, p. 169.

(3) J. F. Klopper, W. Hauser, H. L. Atkins, *et al.*, *J. Nucl. Med.*, **13**, 107 (1972).

(4) W. C. Eckelman, S. M. Karesh, and R. C. Reba, *J. Pharm. Sci.*, **64**, 704 (1975).

(5) J. G. Bragdon and R. Gordon, Jr., *J. Clin. Invest.*, **37**, 574 (1958).

(6) C. L. Malmendier, *ibid.*, **41**, 185 (1962).

ACKNOWLEDGMENTS AND ADDRESSES

Received August 4, 1975, from the *Department of Nuclear Medicine, Washington Hospital Center, Washington, DC 20010, and the ‡Department of Radiology, George Washington University, Washington, DC 20037.

Accepted for publication March 29, 1976.

Adapted from a dissertation to be submitted by S. M. Karesh to the Graduate School, University of Maryland, in partial fulfillment of the Doctor of Philosophy degree requirements.

Supported in part by the Research Foundation of the Washington Hospital Center, the Women's Auxiliary of the Washington Hospital Center, and National Institutes of Health Grant R01 HL 19127.

ˣ To whom inquiries should be directed (at George Washington University).

Chemical Ionization Mass Spectra of Phenothiazine Derivatives and Their Oxygenated Analogs

ARMEN P. MELIKIAN *ˣ, NORMAN W. FLYNN ‡, FREDERICK PETTY ‡, and JOSEPH D. WANDER ‡§

Abstract □ Twenty-nine derivatives of phenothiazine formed relatively stable ions by proton capture under conditions of chemical ionization, using methane or isobutane as reagent gas. Fragments of generally low abundance formed by simple bond cleavage in the trimethylene portion of the side chain and by loss of water or hydrogen halide. Mass spectra obtained from pyrolyzates of amine salts and from the corresponding free bases were essentially identical.

Keyphrases □ Chemical ionization mass spectrometry—various phenothiazines and oxygenated analogs □ Phenothiazines, various—and oxygenated analogs, chemical ionization mass spectra □ Mass spectrometry, chemical ionization—various phenothiazines and oxygenated analogs

Phenothiazines have dominated the interest of researchers in many diverse areas since the discovery that they exert profound effects upon the central nervous system, and a wealth of information pertaining to pharmacological action, therapeutic applications, and biotransformation pathways has been accumulated (1, 2). Some of the vicissitudes encountered in assaying phenothiazine compounds and their metabolites in biological fluids were summarized by Usdin (3).

Elucidation of the mechanisms of action and metabolic conversion and evaluation of the relationship of plasma concentrations of these drugs to their clinical efficacy became possible only after analytical procedures possessing adequate sensitivity and specificity had been developed. A recent monograph outlining many aspects of current research efforts in the area of phenothiazine derivatives describes three approaches to mass spectrometric identification of promazine, chlorpromazine, and several oxygenated homologs (4–6). Whereas electron-impact mass spectrometry has made significant contributions to the biomedical and pharmaceutical sciences over the years, application of chemical ionization mass spectrometry to these areas represents a fairly recent development (7). Finkle *et al.* (8) reported chemical ionization (methane) mass spectra of pharmaceutical agents, including some phenothiazines, and their metabolites as part of a broad program for rapid identification of the contents of body fluids in patients suspected to be intoxicated by a drug overdose.

As part of a continuing program of developing applications of chemical ionization GC–mass spectrometry in neurochemistry (9, 10), the chemical ionization mass spectra for 29 derivatives of phenothiazine were investigated including the tranquilizing agents chlorpromazine (VII), promazine (XV), promethazine (XVI), prochlorperazine (XVIII), trifluoperazine (XXII), perphenazine

istered dose) at the 30-min observation point. This finding compares with an average of about 3% remaining in the blood at 30 min for palmitic acid. Heart–blood ratios for palmitic acid on a per gram basis were in the range of from a 30:1 to 40:1; for the metal chelates the concentration was always less than 3:1, thus making it impossible to differentiate myocardium from blood.

The high blood concentration may be due to the fact that these compounds are more tightly bound to serum albumin so that the transport of fatty acid derivatives across the cell membrane into the intracellular fluids is reduced. The greater difference in polarity between a simple fatty acid, *e.g.*, palmitic acid, and fatty acid derivatives (*i.e.*, IX) could affect the localization of the labeled compound. Compounds containing a diethylenetriamine chelating group also showed slow blood clearance.

The 30-min distribution was chosen to screen this series of compounds rapidly. Because the palmitic acid does not concentrate in an infarct but does concentrate in the normal myocardia, the 30-min myocardia to blood ratio is the important factor and should indicate if the compound may be useful.

The results of the distribution of the labeled IX in dogs with experimentally induced infarcts revealed that an average accumulation of 0.94% of the injected dose was localized in the heart, 16.6% was in the liver, and 2.7% was in the lungs and that 3.8% remained in the intravascular compartment at 30 min. The infarct contained less than half of the radioactivity found in adjacent normal myocardium.

The chemical analogs described here are not sufficient biological analogs to act as tracers for fatty acid metabolism in the myocardium. However, this approach of preparing drug derivatives should lead to more specific radiopharmaceuticals and will be pursued using other biologic molecules.

REFERENCES

(1) M. K. Dewanjee, C. Fliegle, S. Treves, and M. A. Davis, *J. Nucl. Med.*, **13**, 427 (1972).

(2) B. Persson and S. E. Strand, "Radiopharmaceutical and Labeled Compounds," vol. I, International Atomic Energy Agency, Vienna, Austria, 1973, p. 169.

(3) J. F. Klopper, W. Hauser, H. L. Atkins, *et al.*, *J. Nucl. Med.*, **13**, 107 (1972).

(4) W. C. Eckelman, S. M. Karesh, and R. C. Reba, *J. Pharm. Sci.*, **64**, 704 (1975).

(5) J. G. Bragdon and R. Gordon, Jr., *J. Clin. Invest.*, **37**, 574 (1958).

(6) C. L. Malmendier, *ibid.*, **41**, 185 (1962).

ACKNOWLEDGMENTS AND ADDRESSES

Received August 4, 1975, from the *Department of Nuclear Medicine, Washington Hospital Center, Washington, DC 20010, and the ‡Department of Radiology, George Washington University, Washington, DC 20037.

Accepted for publication March 29, 1976.

Adapted from a dissertation to be submitted by S. M. Karesh to the Graduate School, University of Maryland, in partial fulfillment of the Doctor of Philosophy degree requirements.

Supported in part by the Research Foundation of the Washington Hospital Center, the Women's Auxiliary of the Washington Hospital Center, and National Institutes of Health Grant R01 HL 19127.

ˣ To whom inquiries should be directed (at George Washington University).

Chemical Ionization Mass Spectra of Phenothiazine Derivatives and Their Oxygenated Analogs

ARMEN P. MELIKIAN *ˣ, NORMAN W. FLYNN ‡, FREDERICK PETTY ‡, and JOSEPH D. WANDER ‡§

Abstract □ Twenty-nine derivatives of phenothiazine formed relatively stable ions by proton capture under conditions of chemical ionization, using methane or isobutane as reagent gas. Fragments of generally low abundance formed by simple bond cleavage in the trimethylene portion of the side chain and by loss of water or hydrogen halide. Mass spectra obtained from pyrolyzates of amine salts and from the corresponding free bases were essentially identical.

Keyphrases □ Chemical ionization mass spectrometry—various phenothiazines and oxygenated analogs □ Phenothiazines, various—and oxygenated analogs, chemical ionization mass spectra □ Mass spectrometry, chemical ionization—various phenothiazines and oxygenated analogs

Phenothiazines have dominated the interest of researchers in many diverse areas since the discovery that they exert profound effects upon the central nervous system, and a wealth of information pertaining to pharmacological action, therapeutic applications, and biotransformation pathways has been accumulated (1, 2). Some of the vicissitudes encountered in assaying phenothiazine compounds and their metabolites in biological fluids were summarized by Usdin (3).

Elucidation of the mechanisms of action and metabolic conversion and evaluation of the relationship of plasma concentrations of these drugs to their clinical efficacy became possible only after analytical procedures possessing adequate sensitivity and specificity had been developed. A recent monograph outlining many aspects of current research efforts in the area of phenothiazine derivatives describes three approaches to mass spectrometric identification of promazine, chlorpromazine, and several oxygenated homologs (4–6). Whereas electron-impact mass spectrometry has made significant contributions to the biomedical and pharmaceutical sciences over the years, application of chemical ionization mass spectrometry to these areas represents a fairly recent development (7). Finkle *et al.* (8) reported chemical ionization (methane) mass spectra of pharmaceutical agents, including some phenothiazines, and their metabolites as part of a broad program for rapid identification of the contents of body fluids in patients suspected to be intoxicated by a drug overdose.

As part of a continuing program of developing applications of chemical ionization GC–mass spectrometry in neurochemistry (9, 10), the chemical ionization mass spectra for 29 derivatives of phenothiazine were investigated including the tranquilizing agents chlorpromazine (VII), promazine (XV), promethazine (XVI), prochlorperazine (XVIII), trifluoperazine (XXII), perphenazine

Table I—Phenothiazine Derivatives

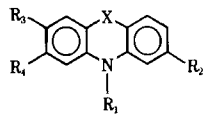

Compound	R_1[a]	R_2	R_3	R_4	X	Mol. Wt.
I	H	Cl	H	H	S	249
II	$(CH_2)_2CO_2H$	Cl	H	H	S	305
III	$(CH_2)_3NH_2$	Cl	H	H	S	290
IV	$(CH_2)_3NHCH_3$	Cl	H	H	S	304
V	$(CH_2)_3\overset{O}{\uparrow}NHCH_3$	Cl	OH	H	S	320
VI	$(CH_2)_3N(CH_3)_2$	Cl	H	H	S	334
VIa	$CH_2CH{=}CH_2$	Cl	H	H	S	273
VII	$(CH_2)_3N(CH_3)_2$	Cl	H	H	S	318
VIII	$(CH_2)_3N(CH_3)_2$	Cl	H	H	S→O	334
IX	$(CH_2)_3N(CH_3)_2$	Cl	OH	H	S	334
X	$(CH_2)_3N(CH_3)_2$	Cl	OH	H	S→O	350
XI	$(CH_2)_3N(CH_3)_2$	Cl	H	OH	S	334
XII	$(CH_2)_3N(CH_3)_2$	Cl	OH	OH	S	350
XIII	$(CH_2)_3N(CH_3)_2$	Cl	$OCOCH_3$	$OCOCH_3$	S	434
XIV	$(CH_2)_3N(CH_3)_2$	CF_3	OH	H	S	368
XV	$(CH_2)_3N(CH_3)_2$	H	H	H	S	284
XVI	$CH_2CH(CH_3)N(CH_3)_2$	H	H	H	S	284
XVII	$CH_2CH(CH_3)N(CH_3)_2$	H	H	H	S→O	300
XVIII	$(CH_2)_3C_4H_8N_2CH_3$	Cl	H	H	S	373
XIX	$(CH_2)_3C_4H_8N_2CH_3$	Cl	OH	H	S	389
XX	$(CH_2)_3C_4H_8N_2CH_3$	Cl	H	OH	S	389
XXI	$(CH_2)_3C_4H_8N_2CH_3$	Cl	OH	OH	S	405
XXII	$(CH_2)_3C_4H_8N_2CH_3$	CF_3	H	H	S	407
XXIII	$(CH_2)_3C_4H_8N_2CH_3$	CF_3	H	H	S→O	423
XXIV	$(CH_2)_3C_4H_8N_2(CH_2)_2OH$	Cl	H	H	S	403
XXV	$(CH_2)_3C_4H_8N_2(CH_2)_2OH$	Cl	OH	H	S	419
XXVI	$(CH_2)_3C_4H_8N_2(CH_2)_2OH$	Cl	OH	OH	S	435
XXVII	$(CH_2)_3C_4H_8N_2(CH_2)_2OH$	CF_3	H	H	S	437
XXVIII	$(CH_2)_3C_4H_8N_2(CH_2)_2OH$	CF_3	OH	H	S	453
XXIX	$(CH_2)_3C_4H_8N_2(CH_2)_2OH$	$COCH_3$	H	H	S	411

[a] $C_4H_8N_2$ is equivalent to —N⟨ ⟩N—.

(XXIV), fluphenazine (XXVII), and acetophenazine (XXIX), together with 21 possible or known (4, 6) metabolites (Table I) of these and related drugs.

EXPERIMENTAL

Chemical ionization mass spectra were obtained using a quadrupole mass spectrometer[1] interfaced to an interactive data system[2]. Source pressures were maintained at 1 (methane) or 0.8 (isobutane) Torr. These pressures were found, by observing the spectrum of the reagent gas, to afford optimal conditions for chemical ionization in the instrument. The source temperature was 110–130°. Samples (1 ± 0.5 μg) were placed in glass capillary tubes (5 mm long × 1 mm i.d.) and introduced through a vacuum lock into the source by a direct-insertion probe, which was then gradually heated above 300° to effect volatilization.

Tabulated intensities are expressed as the percent of the intensity of the base peak; satellite peaks due to isotopes present in natural abundance are not included, although characteristic satellite clusters facilitated the identification of some ions at unit resolution. Compounds XIII, XVIII, and XXIX were introduced into the mass spectrometer as bimaleate salts; the remainder of the compounds were examined as hydrochlorides.

RESULTS AND DISCUSSION

Relative intensities of prominent peaks larger than *m/e* 100 in the chemical ionization mass spectra of I–XXIX are given in Table II; separate determinations are presented using methane or isobutane as the reactant gas. Although these values were obtained for the hydrochloride or bimaleate salts of amines subjected to pyrolysis in the region proximate to the source of the mass spectrometer, essentially identical results were found using the free bases of VII, VIII, XVIII, XXII, XXIII, XXVII, and XXIX; an intense peak at *m/e* 117 (MH^+ of maleic acid) was observed for derivatives (XIII, XVIII, and XXIX) introduced as bimaleate salts.

In all chemical ionization (isobutane) spectra and in all but a few of the chemical ionization (methane) spectra, the base peak was the intact, protonated molecular ion (MH^+); intensity of the MH^+ ion exceeded 50% of the base peak in the spectra of XX and XXI. The failure of VI to afford a prominent MH^+ ion is a consequence of spontaneous degradation of VI (prior to ionization) by the Cope-elimination process (11) illustrated in Scheme I. The MH^+ ion of the resulting *N*-allyl derivative (VIa) was the base peak in the spectrum under both chemical ionization conditions. In general, the usual satellite pattern of hydrocarbon-capture ions [M + $C_2H_5^+$ and M + $C_3H_5^+$ for chemical ionization (methane) and M + $C_4H_9^+$ for chemical ionization (isobutane)] was present to confirm the molecular weight indicated by the MH^+ ion.

Apparent molecular ions (M^+) were found one mass number below the MH^+ ion in these spectra. Although the precise abundance of the M^+ ion varied somewhat between determinations for a given compound, the value was generally >30% of the base peak for all derivatives except the sul-

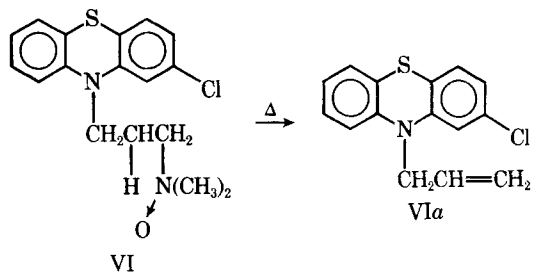

Scheme I

[1] Model 3200, Finnigan Corp., Sunnyvale, Calif.
[2] Model 6000, Finnigan Corp., Sunnyvale, Calif.

Table II—The *m/e* and Relative Intensity Values of Characteristic Ions in the Chemical Ionization (Methane and Isobutane) Mass Spectra of Phenothiazine Derivatives I–XXIX

Compound	Chemical Ionization Condition	MH^+	M^+	$M+C_2H_5^+$	$M+C_3H_5^+$	$M+C_4H_9^+$	MH^+-H_2O	MH^+-34	MH^+-HX	Ion B	Ion A	Ion D	Ion C	Other
I	CH_4[a]	250 (100)[b]	249 (55)	278 (1)	—	—	232 (12)	216 (7)[c]	214 (40)	—	—	—	—	—
	C_4H_{10}	(100)	(75)	—	—	306 (2)	(<1)	(1)	(<1)	—	—	—	—	—
II	CH_4	306 (100)	305 (85)	334 (8)	—	—	288(<1)	272 (5)	270 (10)	246 (45)	232 (36)	—	—	—
	C_4H_{10}	(100)	(85)	—	—	362 (11)	(<1)	(10)	—	(8)	(11)	—	—	—
III	CH_4	291 (100)	290 (90)	319 (11)	331 (2)	—	—	257(<1)	255 (32)	246 (12)	232 (5)	—	—	274 (10)
	C_4H_{10}	(100)	(35)	—	—	347 (10)	—	—	—	(2)	(2)	—	—	—
IV	CH_4	305 (100)	304 (65)	333 (9)	345(<1)	—	—	271 (8)	269 (6)	246 (5)	232 (3)	—	—	—
	C_4H_{10}	(100)	(35)	—	—	361 (9)	—	(9)	—	(<1)	(<1)	—	—	—
V	CH_4	321 (100)	320 (75)	349 (9)	361 (1)	—	303 (8)	287 (1)	285 (10)	262 (6)	248 (6)	—	—	—
	C_4H_{10}	(100)	(35)	—	—	377 (12)	—	(<1)	—	(1)	(2)	—	—	—
VI	CH_4	335 (<1)	—	—	—	—	—	—	—	—	—	—	—	—
		274[d] (100)	273 (70)	302 (11)	314 (1)	—	—	240 (6)	238 (70)	246 (4)	232 (40)	—	—	233 (45)[e]
	C_4H_{10}	335 (1)	—	—	—	—	—	—	—	—	—	—	—	—
		274[d] (100)	273 (65)	—	—	330 (20)	—	(1)	(<1)	(2)	(12)	—	—	233 (45)[e]
VII	CH_4	319 (100)	318 (90)	347 (8)	359 (4)	—	—	285 (4)	283 (3)	246 (2)	232 (5)	—	—	—
	C_4H_{10}	(100)	(20)	—	—	375 (7)	—	(11)	—	(<1)	(<1)	—	—	—
VIII	CH_4	335 (100)	334 (15)	363 (12)	375 (3)	—	—	301 (1)	299 (7)	262 (<1)	248 (1)	—	—	—[f]
	C_4H_{10}	(100)	(9)	—	—	391 (2)	—	(1)	—	—	—	—	—	—[f]
IX	CH_4	335 (100)	334 (60)	363 (8)	375 (1)	—	317 (8)	301 (<1)	299 (5)	262 (3)	248 (1)	—	—	—
	C_4H_{10}	(100)	(40)	—	—	391 (13)	—	(<1)	—	(<1)	(<1)	—	—	—
X	CH_4	351 (100)	350 (15)	379 (10)	391 (3)	—	333 (5)	317 (2)	315 (8)	278 (<1)	264 (1)	—	—	—[g]
	C_4H_{10}	(100)	(5)	—	—	407 (3)	(3)	(5)	(<1)	(<1)	(1)	—	—	—[g]
XI	CH_4	335 (100)	334 (65)	363 (10)	375 (2)	—	—	301 (1)	299 (8)	262 (2)	248 (2)	—	—	—
	C_4H_{10}	(100)	(40)	—	—	391 (16)	—	(<1)	(<1)	(<1)	(<1)	—	—	—
XII	CH_4	351 (100)	350 (80)	379 (15)	—	—	—	318 (<1)	316 (5)	278 (4)	264 (3)	—	—	—
	C_4H_{10}	(100)	(45)	—	—	407 (8)	—	(<1)	—	(<1)	(<1)	—	—	—
XIII	CH_4	435 (100)	434 (80)	463 (7)	—	—	—	—	—	—	—	—	—	—[h]
	C_4H_{10}	(100)	(35)	—	—	491 (1)	—	—	—	—	—	—	—	—[h]
XIV	CH_4	369 (100)	368 (80)	397 (3)	—	—	351 (3)	—	349 (14)	296 (3)	282 (2)	—	—	—
	C_4H_{10}	(100)	(55)	—	—	425 (2)	—	—	—	(2)	(1)	—	—	—
XV	CH_4	285 (100)	284 (80)	313 (4)	—	—	—	—	—	212 (8)	198 (7)	—	—	—
	C_4H_{10}	(100)	(35)	—	—	341 (5)	—	—	—	(1)	(1)	—	—	—
XVI	CH_4	285 (100)	284 (90)	313 (7)	—	—	—	—	—	212 (9)	198 (57)	—	—	240 (30)
	C_4H_{10}	(100)	(20)	—	—	341 (5)	—	—	—	(4)	(2)	—	—	—
XVII	CH_4	301 (100)	300 (5)	329 (3)	341 (1)	—	—	—	—	—	214 (1)	—	—	285 (2)
		—	—	—	—	—	—	—	—	—	—	—	—	256 (8)
		—	—	—	—	—	—	—	—	—	—	—	—	212 (2)
		—	—	—	—	—	—	—	—	—	—	—	—	198 (2)[i]
	C_4H_{10}	301 (100)	300 (15)	—	—	357 (2)	—	—	—	—	214 (3)	—	—	341 (1)
		—	—	—	—	—	—	—	—	—	—	—	—	285 (7)
		—	—	—	—	—	—	—	—	—	—	—	—	256 (7)
		—	—	—	—	—	—	—	—	—	—	—	—	212 (2)
		—	—	—	—	—	—	—	—	—	—	—	—	198 (2)[i]

Table II—*Continued*

Compound	Chemical Ionization Condition	MH^+	M^+	$M + C_2H_5^+$	$M + C_3H_5^+$	$M + C_4H_9^+$	$MH^+ - H_2O$	$MH^+ - 34$	$MH^+ - HX$	Ion B	Ion A	Ion D	Ion C	Other
XVIII	CH_4	374 (100)	373 (70)	402 (8)	414 (<1)	—	—	340 (5)	338 (9)	246 (2)	232 (1)	141 (9)	113 (17)	—
	C_4H_{10}	(100)	(20)	—	—	430 (6)	—	(10)	(<1)	(1)	(<1)	(6)	(10)	—
XIX	CH_4	390 (100)	389 (45)	418 (12)	430 (1)	—	—	356 (1)	354 (16)	262 (2)	248 (2)	141 (22)	113 (37)	—
	C_4H_{10}	(100)	(40)	—	—	446 (11)	—	(1)	(<1)	(<1)	(<1)	(7)	(9)	—
XX	CH_4	390 (100)	389 (90)	418 (4)	—	—	—	—	354 (9)	262 (1)	248 (1)	141 (100)	113 (160)	—
	C_4H_{10}	(100)	(45)	—	—	446 (8)	—	356 (2)	(<1)	(<1)	(<1)	(20)	(27)	—
XXI	CH_4	406 (100)	405 (25)	—	—	—	—	372 (5)	370 (3)	278 (2)	264 (3)	141 (140)	113 (170)	—
	C_4H_{10}	(100)	(40)	—	—	462 (6)	—	(1)	—	(<1)	(2)	(14)	(22)	—
XXII	CH_4	408 (100)	407 (75)	436 (9)	448 (2)	—	—	—	388 (35)	280 (2)	266 (3)	141 (5)	113 (12)	—
	C_4H_{10}	(100)	(20)	—	—	464 (3)	—	—	—	(1)	(12)	(7)	(9)	—
XXIII	CH_4	424 (100)	423 (10)	452 (17)	464 (4)	—	—	—	404 (25)	296 (<1)	282 (<1)	141 (10)	113 (18)	436 (2)
		—	—	—	—	—	—	—	—	—	—	—	—	408 (23)
		—	—	—	—	—	—	—	—	—	—	—	—	388 (7)
		—	—	—	—	—	—	—	—	—	—	—	—	280 (4)
		—	—	—	—	—	—	—	—	—	—	—	—	266 (2)[i]
	C_4H_{10}	424 (100)	423 (5)	—	—	480 (2)	—	—	—	—	—	141 (4)	113 (6)	464 (2)
		—	—	—	—	—	—	—	—	—	—	—	—	408 (11)
		—	—	—	—	—	—	—	—	—	—	—	—	280 (1)
		—	—	—	—	—	—	—	—	—	—	—	—	266 (<1)[i]
XXIV	CH_4	404 (100)	403 (50)	432 (8)	444 (2)	—	386 (6)	370 (2)	368 (5)	246 (5)	232 (2)	171 (7)	143 (9)	—
	C_4H_{10}	(100)	(15)	—	—	460 (14)	(1)	(2)	(<1)	(1)	(<1)	(1)	(2)	—
XXV	CH_4	420 (100)	419 (80)	448 (7)	—	—	402 (6)	386 (1)	384 (4)	262 (15)	248 (9)	171 (31)	143 (40)	—
	C_4H_{10}	(100)	(35)	—	—	476 (7)	(1)	—	—	(2)	(1)	(11)	(12)	—
XXVI	CH_4	436 (100)	435 (30)	464 (12)	478 (2)	—	418 (7)	402 (20)	400 (10)	278 (3)	264 (10)	171 (27)	143 (37)	430 (2)
		—	—	—	—	—	—	—	—	—	—	—	—	131 (100)
		—	—	—	—	—	—	—	—	—	—	—	—	113 (42)
	C_4H_{10}	436 (18)	435 (40)	—	—	492 (2)	—	402 (3)	—	278 (1)	264 (29)	171 (13)	143 (15)	—
XXVII	CH_4	438 (100)	437 (35)	466 (14)	478 (2)	—	—	—	418 (27)	280 (6)	266 (3)	171 (7)	143 (16)	420 (9)
		—	—	—	—	—	—	—	—	—	—	—	—	258 (12)
	C_4H_{10}	438 (100)	437 (15)	—	—	494 (14)	—	—	—	280 (3)	266 (1)	171 (3)	143 (5)	420 (2)
		—	—	—	—	—	—	—	—	—	—	—	—	258 (3)
XXVIII	CH_4	454 (100)	453 (50)	482 (7)	494 (1)	—	436 (8)	—	434 (15)	296 (9)	282 (3)	171 (5)	143 (4)	414 (6)
	C_4H_{10}	(100)	(35)	—	—	—	(2)	—	—	(5)	(2)	(7)	(13)	422 (3)
XXIX	CH_4	412 (100)	411 (20)	430 (8)	442 (1)	—	394 (4)	—	—	254 (2)	240 (1)	171 (4)	143 (9)	—
	C_4H_{10}	(100)	(15)	—	—	468 (10)	(1)	—	—	(2)	(<1)	(3)	(5)	—

[a] CH_4 = chemical ionization (methane), and C_4H_{10} = chemical ionization (isobutane). [b] The *m/e* ratio of the ion (intensity of the ion expressed as the percent of the intensity of the MH^+ ion). [c] Possibly due to unchlorinated contaminants. [d] The tertiary *N*-oxide VI undergoes virtually complete degradation by a Cope reaction (Scheme I) preceding or concurrent with vaporization, affording the *N*-allyl derivative VI*a*. [e] Probably arising by loss of C_3H_4 from the allyl substituent. [f] Compound VII is present as a contaminant. [g] Compound IX is present as a contaminant. [h] Compound XII and its monoacetate appear to be present as contaminants. [i] Compound XVI is present as a contaminant. [j] Compound XXII is present as a contaminant.

foxides VIII, X, XVII, and XXIII, the latter affording M^+ ions having <15% relative abundance. The variations in the abundance of this ion are not surprising because plausible processes leading to its formation (including charge transfer to M, loss of H· from MH^+, and direct ionization by electron impact) are sensitive to slight variations in temperature, pressure, and chemical entities in and near the source.

Fragmentation processes involving the trimethylene bridge appeared to be common to the spectra of II–V, VII–XV, and XVIII–XXIX (phenothiazine–$CH_2CH_2CH_2$–base) and to XVI and XVII, producing weak ions that corresponded in mass to the (substituted) phenothiazin-10-yl nucleus (Ion A) and to its methylene homolog (Ion B). Generally more abundant ions, corresponding in mass to the terminal methylene unit plus the attached aliphatic nitrogen atom and its substituents (Ion C, CH_2–base or CH_3CH–base) and to the ethylene homolog (Ion D, C_3H_6–base), were observed at *m/e* 113 and 141 (XVIII–XXIII) or 143 and 171 (XXIV–XXIX), respectively. Although the corresponding ions in the spectra of III–XVIII had *m/e* values <100 and were, therefore, not measured in this study, the chemical ionization (methane) mass spectra of XII and two other hydroxylated homologs of XII were found (6) to exhibit prominent ions at *m/e* 58 and 86, corresponding to $[CH_2N(CH_3)_2]^+$ and $[C_3H_6N(CH_3)_2]^+$, respectively, in accord with the idea that these form by processes general for compounds of this type.

Molecules in this study having polar substituents (halogen or hydroxyl groups) also generally appeared to undergo loss of a hydrogen atom plus the substituent from the MH^+ species. Fragments resulting from such processes were relatively abundant in the chemical ionization (methane) spectra but minor or not observed in the corresponding chemical ionization (isobutane) spectra. The derivatives of 2-chlorophenothiazine (I–XII, XVIII–XXI, and XXIV–XXVI) also exhibited an $MH^+ - 34$ ion that did not have a satellite ion heavier by two mass numbers; this resulted from contamination by the respective halogen-free homologs.

In summary, derivatives of phenothiazine generally form very stable MH^+ and M^+ ions under conditions of chemical ionization. Although no simple correlation is obvious to account for the variations in relative intensity of fragment ions formed by different compounds in this study, decomposition appears to be limited mainly to cleavage of exocyclic carbon–carbon single bonds, plus loss of water or hydrogen halide in appropriately substituted derivatives. The prominence of these stable proton-capture ions in the chemical ionization spectra affords a measurable property that is not only characteristic of a given drug or metabolite but also exquisitely sensitive for its detection. These two conditions suggest that selective ion monitoring techniques (12) in conjunction with chemical ionization are potentially useful for bioanalytical studies of phenothiazines.

REFERENCES

(1) Second International Symposium on Phenothiazines, *Agressologie*, **9**, 1 (1968).

(2) "The Phenothiazines and Structurally Related Drugs," I. S. Forrest, C. J. Carr, and E. Usdin, Eds., Raven, New York, N.Y., 1974.

(3) E. Usdin, in "Critical Reviews in Clinical Laboratory Science," vol. 2, Chemical Rubber Co., Cleveland, Ohio, 1971, pp. 347–391.

(4) A. M. Duffield, in "The Phenothiazines and Structurally Related Drugs," I. S. Forrest, C. J. Carr, and E. Usdin, Eds., Raven, New York, N.Y., 1974, p. 111.

(5) D. E. Green, in *ibid.*, p. 119.

(6) J. C. Craig, W. A. Garland, L. D. Gruenke, L. R. Kray, and K. A. M. Walker, in *ibid.*, p. 405.

(7) G. P. Arsenault, in "Biochemical Applications of Mass Spectrometry," G. R. Waller, Ed., Wiley–Interscience, New York, N.Y., 1972, p. 817.

(8) B. Finkle, F. L. Foltz, and D. Taylor, *J. Chromatogr. Sci.*, **12**, 304 (1974).

(9) F. Petty, J. G. Wood, H. N. Tucker, S. V. Molinary, J. D. Wander, and N. Flynn, *Neurosci. Abstr.*, **1**, 366 (1975).

(10) F. Petty, H. N. Tucker, S. V. Molinary, N. W. Flynn, and J. D. Wander, *Clin. Chim. Acta*, **66**, 111 (1976).

(11) J. C. Craig, N. Y. Mary, and S. K. Roy, *Anal. Chem.*, **36**, 1142 (1964).

(12) B. Holmstedt and L. Palmér, *Adv. Biochem. Psychopharmacol.*, **7**, 1 (1973).

ACKNOWLEDGMENTS AND ADDRESSES

Received January 9, 1976, from the **Department of Medicinal Chemistry, the ‡Charles B. Stout Neuroscience Laboratory, and the §Department of Biochemistry, University of Tennessee Center for the Health Sciences, Memphis, TN 38163.*

Accepted for publication March 29, 1976.

Supported in part by U.S. Public Health Service Grant RR 05423 and by the Charles B. Stout Memorial Fund. Upgrading of the mass spectrometer was accomplished with funds from the Memphis Regional Medical Program.

Sincere gratitude for generous gifts of the compounds used in the study is extended to Dr. A. A. Manian of the National Institute of Mental Health, Psychopharmacology Research Branch, Rockville, MD 20852 (I–VI, IX–XIV, XIX–XXI, XXIII, XXV, XXVI, and XXVIII); to Wyeth Laboratories, Philadelphia, Pa. (XV–XVII); to E. R. Squibb and Sons, Princeton, N.J. (XXVII); to Smith Kline and French Laboratories, Philadelphia, Pa. (VII, VIII, XVIII, and XXII); and to Schering Corp., Kenilworth, N.J. (XXIV, XXVII, and XXIX).

ˣ To whom inquiries should be directed. Present address: Drug Metabolism Department, Warner-Lambert Research Institute, Morris Plains, NJ 07950.

Possible Antineoplastic Agents II

A. U. DE ˣ and D. PAL

Abstract □ Various glutarimide derivatives were synthesized, and some showed significant activity against Ehrlich ascites carcinoma in Swiss albino mice.

Keyphrases □ Glutarimides, substituted—various derivatives synthesized, antineoplastic activity evaluated, mice □ Antineoplastic activity, potential—substituted glutarimides synthesized and screened, mice □ Structure–activity relationships—various substituted glutarimides synthesized and screened for antineoplastic activity in mice

Synthesis of a few glutarimide analogs of the types 2-phthalimidoglutarimide (thalidomide) (I) and 3-phenylglutarimide (II) and their biological evaluation in Ehrlich ascites carcinoma were reported previously (1). Meanwhile, more derivatives of I and II were synthesized and evaluated biologically according to the same procedures (1) (Table I).

In the previous article (1), the rationale behind the projected synthesis of these glutarimides (I and II) and others with some structural variations (II*a*–II*l*, III, and IV) was discussed. These structural changes were designed to determine the effects of electron-repelling or electron-

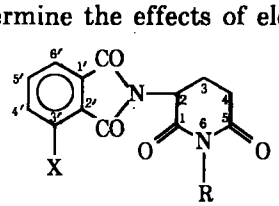

I

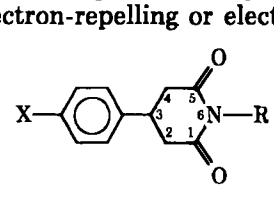

II

foxides VIII, X, XVII, and XXIII, the latter affording M^+ ions having <15% relative abundance. The variations in the abundance of this ion are not surprising because plausible processes leading to its formation (including charge transfer to M, loss of H· from MH^+, and direct ionization by electron impact) are sensitive to slight variations in temperature, pressure, and chemical entities in and near the source.

Fragmentation processes involving the trimethylene bridge appeared to be common to the spectra of II–V, VII–XV, and XVIII–XXIX (phenothiazine–$CH_2CH_2CH_2$–base) and to XVI and XVII, producing weak ions that corresponded in mass to the (substituted) phenothiazin-10-yl nucleus (Ion A) and to its methylene homolog (Ion B). Generally more abundant ions, corresponding in mass to the terminal methylene unit plus the attached aliphatic nitrogen atom and its substituents (Ion C, CH_2–base or CH_3CH–base) and to the ethylene homolog (Ion D, C_3H_6–base), were observed at *m/e* 113 and 141 (XVIII–XXIII) or 143 and 171 (XXIV–XXIX), respectively. Although the corresponding ions in the spectra of III–XVIII had *m/e* values <100 and were, therefore, not measured in this study, the chemical ionization (methane) mass spectra of XII and two other hydroxylated homologs of XII were found (6) to exhibit prominent ions at *m/e* 58 and 86, corresponding to $[CH_2N(CH_3)_2]^+$ and $[C_3H_6N(CH_3)_2]^+$, respectively, in accord with the idea that these form by processes general for compounds of this type.

Molecules in this study having polar substituents (halogen or hydroxyl groups) also generally appeared to undergo loss of a hydrogen atom plus the substituent from the MH^+ species. Fragments resulting from such processes were relatively abundant in the chemical ionization (methane) spectra but minor or not observed in the corresponding chemical ionization (isobutane) spectra. The derivatives of 2-chlorophenothiazine (I–XII, XVIII–XXI, and XXIV–XXVI) also exhibited an $MH^+ - 34$ ion that did not have a satellite ion heavier by two mass numbers; this resulted from contamination by the respective halogen-free homologs.

In summary, derivatives of phenothiazine generally form very stable MH^+ and M^+ ions under conditions of chemical ionization. Although no simple correlation is obvious to account for the variations in relative intensity of fragment ions formed by different compounds in this study, decomposition appears to be limited mainly to cleavage of exocyclic carbon–carbon single bonds, plus loss of water or hydrogen halide in appropriately substituted derivatives. The prominence of these stable proton-capture ions in the chemical ionization spectra affords a measurable property that is not only characteristic of a given drug or metabolite but also exquisitely sensitive for its detection. These two conditions suggest that selective ion monitoring techniques (12) in conjunction with chemical ionization are potentially useful for bioanalytical studies of phenothiazines.

REFERENCES

(1) Second International Symposium on Phenothiazines, *Agressologie*, **9**, 1 (1968).

(2) "The Phenothiazines and Structurally Related Drugs," I. S. Forrest, C. J. Carr, and E. Usdin, Eds., Raven, New York, N.Y., 1974.

(3) E. Usdin, in "Critical Reviews in Clinical Laboratory Science," vol. 2, Chemical Rubber Co., Cleveland, Ohio, 1971, pp. 347–391.

(4) A. M. Duffield, in "The Phenothiazines and Structurally Related Drugs," I. S. Forrest, C. J. Carr, and E. Usdin, Eds., Raven, New York, N.Y., 1974, p. 111.

(5) D. E. Green, in *ibid.*, p. 119.

(6) J. C. Craig, W. A. Garland, L. D. Gruenke, L. R. Kray, and K. A. M. Walker, in *ibid.*, p. 405.

(7) G. P. Arsenault, in "Biochemical Applications of Mass Spectrometry," G. R. Waller, Ed., Wiley–Interscience, New York, N.Y., 1972, p. 817.

(8) B. Finkle, F. L. Foltz, and D. Taylor, *J. Chromatogr. Sci.*, **12**, 304 (1974).

(9) F. Petty, J. G. Wood, H. N. Tucker, S. V. Molinary, J. D. Wander, and N. Flynn, *Neurosci. Abstr.*, **1**, 366 (1975).

(10) F. Petty, H. N. Tucker, S. V. Molinary, N. W. Flynn, and J. D. Wander, *Clin. Chim. Acta*, **66**, 111 (1976).

(11) J. C. Craig, N. Y. Mary, and S. K. Roy, *Anal. Chem.*, **36**, 1142 (1964).

(12) B. Holmstedt and L. Palmér, *Adv. Biochem. Psychopharmacol.*, **7**, 1 (1973).

ACKNOWLEDGMENTS AND ADDRESSES

Received January 9, 1976, from the **Department of Medicinal Chemistry, the ‡Charles B. Stout Neuroscience Laboratory, and the §Department of Biochemistry, University of Tennessee Center for the Health Sciences, Memphis, TN 38163.*

Accepted for publication March 29, 1976.

Supported in part by U.S. Public Health Service Grant RR 05423 and by the Charles B. Stout Memorial Fund. Upgrading of the mass spectrometer was accomplished with funds from the Memphis Regional Medical Program.

Sincere gratitude for generous gifts of the compounds used in the study is extended to Dr. A. A. Manian of the National Institute of Mental Health, Psychopharmacology Research Branch, Rockville, MD 20852 (I–VI, IX–XIV, XIX–XXI, XXIII, XXV, XXVI, and XXVIII); to Wyeth Laboratories, Philadelphia, Pa. (XV–XVII); to E. R. Squibb and Sons, Princeton, N.J. (XXVII); to Smith Kline and French Laboratories, Philadelphia, Pa. (VII, VIII, XVIII, and XXII); and to Schering Corp., Kenilworth, N.J. (XXIV, XXVII, and XXIX).

ˣ To whom inquiries should be directed. Present address: Drug Metabolism Department, Warner-Lambert Research Institute, Morris Plains, NJ 07950.

Possible Antineoplastic Agents II

A. U. DE ˣ and D. PAL

Abstract □ Various glutarimide derivatives were synthesized, and some showed significant activity against Ehrlich ascites carcinoma in Swiss albino mice.

Keyphrases □ Glutarimides, substituted—various derivatives synthesized, antineoplastic activity evaluated, mice □ Antineoplastic activity, potential—substituted glutarimides synthesized and screened, mice □ Structure–activity relationships—various substituted glutarimides synthesized and screened for antineoplastic activity in mice

Synthesis of a few glutarimide analogs of the types 2-phthalimidoglutarimide (thalidomide) (I) and 3-phenylglutarimide (II) and their biological evaluation in Ehrlich ascites carcinoma were reported previously (1). Meanwhile, more derivatives of I and II were synthesized and evaluated biologically according to the same procedures (1) (Table I).

In the previous article (1), the rationale behind the projected synthesis of these glutarimides (I and II) and others with some structural variations (II*a*–II*l*, III, and IV) was discussed. These structural changes were designed to determine the effects of electron-repelling or electron-

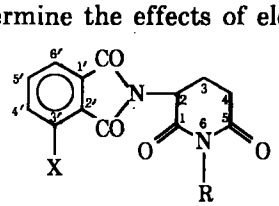

I

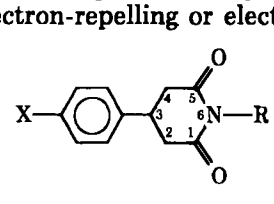

II

attracting groups on carcinolytic activity. The inclusion of a sulfonamide moiety in either the cyclic or noncyclic parts of the glutarimide analogs was utilized to evaluate antineoplastic effects. Synthesis and biological evaluation of 6-substituted 3-*p*-methoxyphenylglutarimides (IIc–II*l*), 2-benzenesulfinocarboximidoglutarimide (III) and 2-*p*-substituted benzenesulfonamidoglutarimides (IV) have been accomplished. The *p*-acetamido derivative (IV*c*) was selected with the hope that it might be hydrolyzed *in vivo* to the therapeutically active sulfanilamido derivative.

DISCUSSION

Chemistry—Treatment of 3-*p*-methoxyphenylglutaric anhydride (2) with appropriate amines furnished the described imides (IIc–II*l*) (3). Possible formation of the diamides was ruled out by elemental analyses and IR spectra.

Reaction between saccharin sodium and 2-bromoglutarimide (4) in the presence of dimethylformamide resulted in the desired imide (III), as confirmed by elemental analysis and IR spectra.

Interaction of potassium benzenesulfonamides and 2-bromoglutarimide in dimethylformamide or water did not give the desired imides (IV*a*–IV*c*) because the anionic parts of the benzenesulfonamides, acting as strong bases, brought about the β-elimination-type reaction. Hence, 2-benzenesulfonamidoglutaric acids (5) were either converted to the corresponding dichlorides with thionyl chloride or to the diethyl esters to avoid any acid hydrolysis of the *p*-acetamido group by thionyl chloride. Interaction of these dichlorides and diesters with ammonia led to the diamides. These compounds were heated in the presence of refluxing nitrobenzene, with liberation of ammonia, to provide the desired imides (IV*a*–IV*c*).

Biological Activity (6)—Antineoplastic potency was evaluated against Ehrlich ascites carcinoma in Swiss albino mice according to the procedure described previously (1, 7) (Table I). In the present case also, both test and control groups contained five animals. The compounds were administered at a dose level of 50 mg/kg ip in buffered saline (pH 7.2); both the cell count and weight of ascitic fluid were regarded as activity parameters. Mitomycin at 1 mg/kg ip in buffered saline was used as a standard. Compounds I*a*, II*f*, and IV*a* showed significant activity.

Structure–Activity Relationships—Although a systematic interpretation has not been attempted, some logical deductions can be made after examination of the observed antineoplastic potency of the compounds listed in this article as well as in a previous one (1). In the 2-phthalimidoglutarimide series (I*a*–I*d*), an alkyl or aryl substituent at the 6-position and an electronegative substituent like a nitro group in the benzene ring separately increased the activity. But an aralkyl or cycloalkyl group at the 6-position or the simultaneous combination of a nitro group at the 3-position and an alkyl group such as hexyl at the 6-position had the reverse effect.

In the 3-phenylglutarimides (II*a*–II*l*), introduction of an alkyl substituent at the 6-position and an electron-donating group such as methoxyl at the *para*-position of the benzene ring increased the activity. Aliphatic substituents such as ethyl, *n*-propyl, *n*-butyl, *n*-pentyl, and *n*-hexyl at the 6-position increased the activity, which reached a maximum when the substituent was *n*-propyl. Cycloalkyl, aralkyl, and aryl groups had the opposite effect.

In the sulfonamidoglutarimides (III and IV*a*–IV*c*), incorporation of the sulfonamide group in a ring structure tended to decrease the activity more than when it was in a straight chain; significant activity was observed in the latter case. Introduction of an electron-donating group such as methyl at the *para*-position of the benzene ring did not improve the activity, while an acetamido group decreased the activity considerably. However, the most significant feature is that all the glutarimide derivatives had higher activity than the glutarimide itself.

EXPERIMENTAL[1]

6-Substituted 3-*p*-Methoxyphenylglutarimides (IIc–II*l*)—A mixture of 3-*p*-methoxyphenylglutaric anhydride (1 mole) and the appropriate amine (1 mole) was heated in a sealed tube on an oil bath at 180° for 8 hr. The reaction mass was washed with sodium bicarbonate solution and crystallized from dilute ethanol after charcoal treatment (Table I).

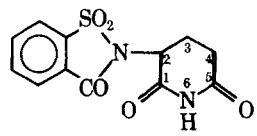

III

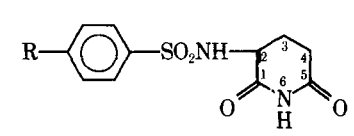

IV

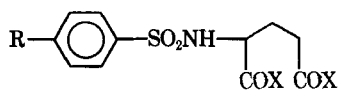

V*a*: R = H, X = Cl
V*b*: R = CH_3, X = Cl
V*c*: R = $NHCOCH_3$, X = OC_2H_5
V*d*: R = H, X = NH_2
V*e*: R = CH_3, X = NH_2
V*f*: R = $NHCOCH_3$, X = NH_2

6-Methyl-3-*p*-methoxyphenylglutarimide (II*d*) showed the characteristic carbonyl stretching frequency at 1675 cm^{-1} and no amino stretching frequency, the absence of which ruled out the possibility of diamide structure formation.

2-Benzenesulfinocarboximidoglutarimide (III)—A mixture of 2-bromoglutarimide (2 g), saccharin sodium (2.2 g), and dimethylformamide (20 ml) was stirred at room temperature for 10 hr until a negative Beilstein test was observed. Dimethylformamide was removed as completely as possible by distillation under reduced pressure in an oil bath, and the residual colored mass was washed with a little water to remove the excess saccharin sodium. The desired imide (III) was obtained by crystallization from dilute ethanol with charcoal treatment. Its physical characteristics are recorded in Table I.

Compound III showed characteristic sulfonyl stretching frequencies at 1165 and 1330 cm^{-1}, a carbonyl stretching frequency at 1705 cm^{-1}, and an amino stretching frequency at 3120 cm^{-1}.

2-*p*-Substituted Benzenesulfonamidoglutaryl Dichlorides (V*a* and V*b*)—A mixture of the diacids (10 mmoles) and thionyl chloride (15 ml) was refluxed on a steam bath until hydrogen chloride evolution ceased. Excess thionyl chloride was exhaustively removed, first by distillation under reduced pressure and then by adding 3 × 10 ml of benzene to the mass with subsequent removal by distillation. The acid chlorides solidified on cooling and were sufficiently pure for the next step. Compound V*a* had a melting point of 95–97°; the melting point of V*b* was 58–60°.

Diethyl 2-*p*-Acetamidobenzenesulfonamidoglutarate (V*c*)—A mixture of 2-*p*-acetamidobenzenesulfonamidoglutaric acid (6 g), absolute ethanol (25 ml), and sulfuric acid (specific gravity 1.84; 0.36 ml) was refluxed for 8 hr and worked up in the usual way. Compound V*c* had a melting point of 104–106°.

2-*p*-Substituted Benzenesulfonamidoglutaricdiamides (V*d*–V*f*)—The acid dichlorides (V*a* and V*b*, 5 g) were slowly basified with liquor ammonia (20 ml) under cooling in an ice bath to give the crude diamides (V*d* and V*e*). Compounds V*d* and V*e* were then crystallized from dilute ethanol after charcoal treatment to yield the pure product. The diethyl ester (V*c*, 2 g) and liquor ammonia (10 ml) were heated in a sealed tube in a steam bath for 8 hr to yield the crude diamide (V*f*), which was crystallized from dilute ethanol with charcoal treatment. Compound V*d* had a melting point of 214–216°, V*e* had a melting point of 219–221°, and V*f* had a melting point of 231–233°.

2-*p*-Substituted Benzenesulfonamidoglutarimides (IV*a*–IV*c*)—Mixtures of the diamides (V*d*–V*f*, 2 g) and nitrobenzene (10 ml) were refluxed on an oil bath until ammonia evolution ceased. The reaction mass then was cooled and diluted with benzene or petroleum ether (bp 60–80°) to yield the crude imides. These compounds were purified by crystallization from dilute ethanol after charcoal treatment as glistening needles. Their physical characteristics are recorded in Table I.

2-Benzenesulfonamidoglutarimide (IV*a*) showed sulfonyl stretching frequencies at 1165 and 1340 cm^{-1}, a carbonyl stretching frequency at 1650 cm^{-1}, and an amino stretching frequency at 3500 cm^{-1}. 2-*p*-Toluenesulfonamidoglutarimide (IV*b*) showed sulfonyl stretching frequencies at 1165 and 1346 cm^{-1}, a carbonyl stretching frequency at 1655 cm^{-1}, and an amino stretching frequency at 3505 cm^{-1}. 2-*p*-Acetamidobenzenesulfonamidoglutarimide (IV*c*) showed sulfonyl

[1] Melting points were recorded with a Gallenkamp instrument and are uncorrected. IR spectra were recorded in potassium bromide pellets using a Perkin-Elmer spectrophotometer, Infracord model 137.

Table I—Physical Characteristics and Antineoplastic Activity of Some Glutarimides

Compound	R	X	Yield, %	Melting Point	Formula	Analysis, %		Antineoplastic Activity[a]	
						Calc.	Found	Inhibition of Ascitic Cells, %	Inhibition of Ascitic Fluid, %
I*a*	Phenyl	H	60	158–160°	$C_{19}H_{14}N_2O_4$	C 68.26 H 4.19 N 8.38	67.91 4.47 8.49	87.31	98.40
I*b*	Benzyl	H	62	176–178°	$C_{20}H_{16}N_2O_4$	C 68.97 H 4.60 N 8.05	69.27 4.84 8.42	100.00[b]	84.00
I*c*	Cyclohexyl	H	64	108–110°	$C_{19}H_{20}N_2O_4$	C 67.06 H 5.88 N 8.24	67.37 6.24 7.95	47.60	43.99
I*d*	*n*-Hexyl	3′-NO_2	55	182–184°	$C_{19}H_{21}N_3O_6$	C 58.91 H 5.43 N 10.85	58.72 5.03 11.22	15.72	64.07
II*a*	Benzyl	H	73	94–96°	$C_{18}H_{17}NO_2$	C 77.42 H 6.09 N 5.02	77.37 5.84 5.29	100.00[b]	80.64
II*b*	Cyclohexyl	H	60	204–206°	$C_{17}H_{21}NO_2$	C 75.28 H 7.75 N 5.17	74.89 8.02 5.18	85.55	80.64
II*c*	H	OCH_3	70	169–171°	$C_{12}H_{13}NO_3$	C 65.75 H 5.94 N 6.39	65.79 6.29 6.44	33.39	30.00
II*d*	Methyl	OCH_3	69	115–117°	$C_{13}H_{15}NO_3$	C 66.95 H 6.44 N 6.01	67.13 6.70 6.19	44.96	60.00
II*e*	Ethyl	OCH_3	64	113–115°	$C_{14}H_{17}NO_3$	C 68.02 H 6.88 N 5.67	67.87 6.94 5.32	63.03	97.33
II*f*	*n*-Propyl	OCH_3	62	75–77°	$C_{15}H_{19}NO_3$	C 68.97 H 7.28 N 5.36	69.11 7.02 4.98	100.00[c]	100.00[c]
II*g*	*n*-Butyl	OCH_3	60	81–83°	$C_{16}H_{21}NO_3$	C 69.82 H 7.64 N 5.09	69.89 8.01 5.33	28.50	92.31
II*h*	*n*-Pentyl	OCH_3	58	52–54°	$C_{17}H_{23}NO_3$	C 70.59 H 7.96 N 4.84	70.32 7.57 5.17	76.48	92.31
II*i*	*n*-Hexyl	OCH_3	65	96–98°	$C_{18}H_{25}NO_3$	C 71.29 H 8.25 N 4.62	71.38 8.16 4.41	62.94	91.77
II*j*	Phenyl	OCH_3	75	158–160°	$C_{18}H_{17}NO_3$	C 73.22 H 5.76 N 4.75	73.61 6.07 4.66	76.08	84.00
II*k*	Benzyl	OCH_3	73	80–82°	$C_{19}H_{19}NO_3$	C 73.79 H 6.15 N 4.53	73.69 6.27 4.72	66.41	88.89
II*l*	Cyclohexyl	OCH_3	55	218–220°	$C_{18}H_{23}NO_3$	C 71.76 H 7.64 N 4.65	71.95 7.37 5.00	26.87	58.82
III	—	—	51	254–256°	$C_{12}H_{10}N_2O_5S$	C 48.98 H 3.40 N 9.52	48.62 3.36 9.89	5.61	34.12
IV*a*	H	—	55	190–192°	$C_{11}H_{12}N_2O_4S$	C 49.25 H 4.48 N 10.45	49.29 4.53 10.19	100.00[c]	100.00[c]
IV*b*	Methyl	—	53	192–194°	$C_{12}H_{14}N_2O_4S$	C 51.06 H 4.97 N 9.93	50.73 5.12 10.17	84.45	88.39
IV*c*	Acetamido	—	51	238–240° dec.	$C_{13}H_{15}N_3O_5S$	C 48.00 H 4.62 N 12.92	48.25 5.02 12.67	57.34	48.58

[a] Mitomycin at a dose level of 1 mg/kg was used as standard showing 100% inhibition of ascitic cell and ascitic fluid. [b] Ascitic fluid could not be drawn by a syringe. [c] Ascitic fluid did not form.

stretching frequencies at 1160 and 1340 cm^{-1}, a carbonyl stretching frequency at 1680 cm^{-1}, and an amino stretching frequency at 3405 cm^{-1}.

REFERENCES

(1) A. U. De and D. Pal, *J. Pharm. Sci.*, **64**, 262 (1975).

(2) W. T. Smith, Jr., and J. W. Ryan, *J. Org. Chem.*, **26**, 3857 (1961).

(3) E. C. Kornfeld, R. G. Jones, and T. V. Parke, *J. Am. Chem. Soc.*, **71**, 150 (1949).

(4) S. Ose, Y. Yoshimura, and T. Saheki, Japanese pat. 5277 (May 17, 1960); through *Chem. Abstr.*, **55**, 572f (1961).

(5) C. R. Harington and R. C. G. Moggridge, *J. Chem. Soc.*, **1940**, 706.

(6) V. M. Rosenoer, in "Experimental Chemotherapy," vol. IV, R. J. Schnitzer and F. Hawking, Eds., Academic, New York, N.Y., 1966, pp. 9–72.

(7) A. U. De and B. P. Saha, *J. Pharm. Sci.*, **64**, 249 (1975).

ACKNOWLEDGMENTS AND ADDRESSES

Received March 12, 1975, from the *Department of Pharmacy, Jadavpur University, Calcutta-32, India.*

Accepted for publication March 15, 1976.

D. Pal thanks the University Grants Commission, New Delhi, India, for a Senior Research Fellowship.

[x] To whom inquiries should be directed.

Radioimmunoassay of the Anticonvulsant Agent Clonazepam

W. R. DIXON [x], R. L. YOUNG, R. NING, and A. LIEBMAN

Abstract □ A simple and specific radioimmunoassay was developed for the determination of the anticonvulsant agent clonazepam directly in plasma without extraction. Antibodies to clonazepam were produced in rabbits after immunization with an immunogen prepared by covalently linking the 3-hemisuccinyloxy derivative of clonazepam to bovine serum albumin. When employing ^{3}H-clonazepam as the tracer, the radioimmunoassay has a limit of sensitivity of 5 ng/ml using a 0.1-ml sample of plasma. The antibodies exhibited a high degree of specificity for clonazepam; no cross-reactivity was observed with its 7-amino and 7-acetylamino metabolites nor with a number of other widely prescribed anticonvulsant agents that might be administered in conjunction with clonazepam. Satisfactory agreement was obtained for the plasma levels of clonazepam in humans when samples were assayed by the radioimmunoassay and an established electron-capture GC technique. By virtue of its simplicity, the radioimmunoassay offers a distinct advantage to the clinician for monitoring plasma clonazepam levels and the compliance of patients undergoing anticonvulsant therapy with the drug.

Keyphrases □ Clonazepam—radioimmunoassay, human plasma □ Radioimmunoassay—clonazepam, human plasma □ Anticonvulsants—clonazepam, radioimmunoassay, human plasma

Clonazepam (I) is a member of the 1,4-benzodiazepine class of compounds which has recently been found to be clinically effective in controlling minor motor seizures (petit mal) in humans (1–4). Studies on the pharmacokinetics and metabolism of the drug also have been reported (5–7).

At the present time, only electron-capture GC methods have been reported for the determination of the nanogram levels of clonazepam that exist in the plasma of subjects undergoing anticonvulsant therapy (8–10). These electron-capture–GC methods have a limit of sensitivity in the order of 1 ng of clonazepam/ml of plasma using a 2-ml sample. However, apart from requiring skilled technical operation, these techniques are time consuming and thereby restrictive for the routine analysis of the numerous samples obtained during clinical studies.

The present report concerns the development of a specific and rapid radioimmunoassay for clonazepam in plasma. This assay allows the clinician to relate therapeutic response to plasma levels of the drug in individual patients.

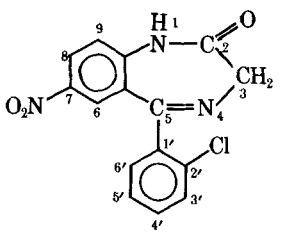

I

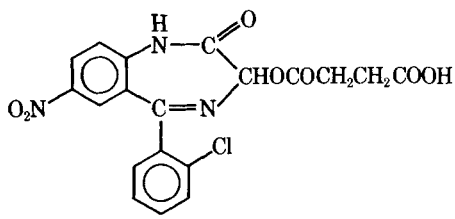

II

EXPERIMENTAL

Tritium-Labeled Clonazepam—^{3}H-Clonazepam was prepared by tritium exchange using dimethylformamide–tritiated water (specific activity 100 Ci/g). The product was purified by silica gel column chromatography, yielding material with a specific activity of 4.23 mCi/mg. This method of introducing tritium probably provided exchange mainly at the C-3 position.

Preparation of Immunogen—The 3-hemisuccinyloxy derivative of clonazepam (II) was covalently coupled to bovine serum albumin using the mixed anhydride procedure of Erlanger *et al.* (11). After successive dialysis against dioxane–water (1:1), 0.05 *M* borate buffer (pH 9), and water, the immunogen was isolated by lyophilization.

On the basis of its absorbance at 365 nm in 0.1 *N* NaOH against a standard solution of II mixed with albumin, it was estimated that the immunogen consisted of 35 moles of II covalently coupled to 1 mole of albumin.

Antibody Production—Two New Zealand White female rabbits were immunized intradermally at multiple sites with 1 mg of the immunogen as an emulsion in Freund's complete adjuvant as previously described (12). The animals were then boosted intravenously with 50 μg of immunogen at monthly intervals, and serum was harvested 10–14 days after each administration. Both rabbits produced satisfactory titers of antibodies to clonazepam within 3 months following the initial immunization, and their serum was pooled. At a 1:2000 dilution, 1 ml of diluted serum bound approximately 60% of the ^{3}H-clonazepam used for the assay.

stretching frequencies at 1160 and 1340 cm^{-1}, a carbonyl stretching frequency at 1680 cm^{-1}, and an amino stretching frequency at 3405 cm^{-1}.

REFERENCES

(1) A. U. De and D. Pal, *J. Pharm. Sci.*, **64**, 262 (1975).

(2) W. T. Smith, Jr., and J. W. Ryan, *J. Org. Chem.*, **26**, 3857 (1961).

(3) E. C. Kornfeld, R. G. Jones, and T. V. Parke, *J. Am. Chem. Soc.*, **71**, 150 (1949).

(4) S. Ose, Y. Yoshimura, and T. Saheki, Japanese pat. 5277 (May 17, 1960); through *Chem. Abstr.*, **55**, 572f (1961).

(5) C. R. Harington and R. C. G. Moggridge, *J. Chem. Soc.*, **1940**, 706.

(6) V. M. Rosenoer, in "Experimental Chemotherapy," vol. IV, R. J. Schnitzer and F. Hawking, Eds., Academic, New York, N.Y., 1966, pp. 9–72.

(7) A. U. De and B. P. Saha, *J. Pharm. Sci.*, **64**, 249 (1975).

ACKNOWLEDGMENTS AND ADDRESSES

Received March 12, 1975, from the *Department of Pharmacy, Jadavpur University, Calcutta-32, India.*

Accepted for publication March 15, 1976.

D. Pal thanks the University Grants Commission, New Delhi, India, for a Senior Research Fellowship.

[x] To whom inquiries should be directed.

Radioimmunoassay of the Anticonvulsant Agent Clonazepam

W. R. DIXON [x], R. L. YOUNG, R. NING, and A. LIEBMAN

Abstract □ A simple and specific radioimmunoassay was developed for the determination of the anticonvulsant agent clonazepam directly in plasma without extraction. Antibodies to clonazepam were produced in rabbits after immunization with an immunogen prepared by covalently linking the 3-hemisuccinyloxy derivative of clonazepam to bovine serum albumin. When employing ^{3}H-clonazepam as the tracer, the radioimmunoassay has a limit of sensitivity of 5 ng/ml using a 0.1-ml sample of plasma. The antibodies exhibited a high degree of specificity for clonazepam; no cross-reactivity was observed with its 7-amino and 7-acetylamino metabolites nor with a number of other widely prescribed anticonvulsant agents that might be administered in conjunction with clonazepam. Satisfactory agreement was obtained for the plasma levels of clonazepam in humans when samples were assayed by the radioimmunoassay and an established electron-capture GC technique. By virtue of its simplicity, the radioimmunoassay offers a distinct advantage to the clinician for monitoring plasma clonazepam levels and the compliance of patients undergoing anticonvulsant therapy with the drug.

Keyphrases □ Clonazepam—radioimmunoassay, human plasma □ Radioimmunoassay—clonazepam, human plasma □ Anticonvulsants—clonazepam, radioimmunoassay, human plasma

Clonazepam (I) is a member of the 1,4-benzodiazepine class of compounds which has recently been found to be clinically effective in controlling minor motor seizures (petit mal) in humans (1–4). Studies on the pharmacokinetics and metabolism of the drug also have been reported (5–7).

At the present time, only electron-capture GC methods have been reported for the determination of the nanogram levels of clonazepam that exist in the plasma of subjects undergoing anticonvulsant therapy (8–10). These electron-capture–GC methods have a limit of sensitivity in the order of 1 ng of clonazepam/ml of plasma using a 2-ml sample. However, apart from requiring skilled technical operation, these techniques are time consuming and thereby restrictive for the routine analysis of the numerous samples obtained during clinical studies.

The present report concerns the development of a specific and rapid radioimmunoassay for clonazepam in plasma. This assay allows the clinician to relate therapeutic response to plasma levels of the drug in individual patients.

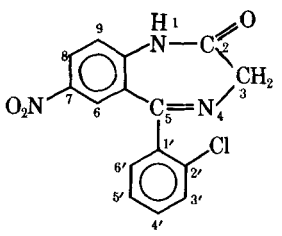

I

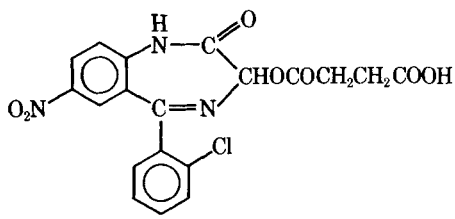

II

EXPERIMENTAL

Tritium-Labeled Clonazepam—^{3}H-Clonazepam was prepared by tritium exchange using dimethylformamide–tritiated water (specific activity 100 Ci/g). The product was purified by silica gel column chromatography, yielding material with a specific activity of 4.23 mCi/mg. This method of introducing tritium probably provided exchange mainly at the C-3 position.

Preparation of Immunogen—The 3-hemisuccinyloxy derivative of clonazepam (II) was covalently coupled to bovine serum albumin using the mixed anhydride procedure of Erlanger *et al.* (11). After successive dialysis against dioxane–water (1:1), 0.05 *M* borate buffer (pH 9), and water, the immunogen was isolated by lyophilization.

On the basis of its absorbance at 365 nm in 0.1 *N* NaOH against a standard solution of II mixed with albumin, it was estimated that the immunogen consisted of 35 moles of II covalently coupled to 1 mole of albumin.

Antibody Production—Two New Zealand White female rabbits were immunized intradermally at multiple sites with 1 mg of the immunogen as an emulsion in Freund's complete adjuvant as previously described (12). The animals were then boosted intravenously with 50 μg of immunogen at monthly intervals, and serum was harvested 10–14 days after each administration. Both rabbits produced satisfactory titers of antibodies to clonazepam within 3 months following the initial immunization, and their serum was pooled. At a 1:2000 dilution, 1 ml of diluted serum bound approximately 60% of the ^{3}H-clonazepam used for the assay.

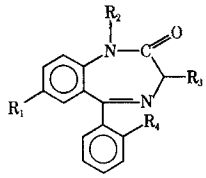

Table I—Cross-Reactivity of Substituted 1,4-Benzodiazepines

Compound	R_1	R_2	R_3	R_4	Cross-Reactivity, %[a]
Clonazepam	NO_2	H	H	Cl	100
Clonazepam 3-hydroxy derivative	NO_2	H	OH	Cl	24
Nitrazepam	NO_2	H	H	H	3.2
III	Cl	H	H	Cl	1.4
Oxazepam	Cl	H	OH	H	0.3
Desmethyldiazepam	Cl	H	H	H	0.06
Clonazepam 7-amino derivative	NH_2	H	H	Cl	0.04
Nitrazepam 7-amino derivative	NH_2	H	H	H	0.02
IV	H	H	H	Cl	0.02
Clonazepam 7-acetylamino derivative	CH_3CONH	H	H	Cl	<0.01
V	CH_3CONH	H	OH	Cl	<0.01
Diazepam	Cl	CH_3	H	H	<0.01

[a] Percentage cross-reactivity is defined as $100\ x/y$, where x is the mass of unlabeled clonazepam and y is the mass of competitor required to produce 50% inhibition of binding of ^{3}H-clonazepam by the antiserum.

Radioimmunoassay Procedure—The following stock solutions were prepared for the assay: standard solutions of 5, 10, 20, 50, 100, and 200 ng of clonazepam/ml of assay buffer (sodium phosphate, 0.01 *M*, pH 7.4, containing 0.9% sodium chloride); a solution of ^{3}H-clonazepam in buffer, 25,000 cpm/ml; and antiserum diluted 1:800 with buffer and containing 0.01% sodium azide. All stock solutions were stored at 4°.

To perform the assay, 0.1 ml of control plasma was added to 0.1 ml of each clonazepam standard in a 12 × 75-mm disposable tube to generate a calibration curve. Appropriate controls were included by adding the control plasma to 0.1 ml of buffer alone. Each unknown plasma sample (0.1 ml) was added to tubes containing 0.1 ml of buffer. Then 0.4 ml (10,000 cpm) of the ^{3}H-clonazepam solution followed by 0.4 ml of the diluted antiserum was added, and the contents (1.0 ml) of each tube were mixed and allowed to stand at room temperature for 30 min. Saturated ammonium sulfate (1 ml) was added to precipitate the globulin-bound ^{3}H-clonazepam and, after mixing, the tubes were allowed to stand for 15 min at 0° in a refrigerated centrifuge and were then centrifuged at 3000 rpm for 30 min.

Each supernate, containing the unbound ^{3}H-clonazepam, was decanted into a counting vial, and 10 ml of toluene scintillator[1] was added. The vials were then placed in a covered vial tray and shaken for 5 min on a reciprocating shaker with the tray in the vertical position. In this way, the ^{3}H-clonazepam was quantitatively extracted into the toluene scintillator. The samples were assayed for ^{3}H-activity in a liquid scintillation counter.

All samples including the standards, unknowns, and controls were assayed in duplicate, and the average of the tritium counts was used for calculation of percentage inhibition of binding (12). Quantitation of unknown samples was accomplished by interpolation from a logit–log plot of the percentage inhibition of binding *versus* the concentration of each standard (13).

RESULTS AND DISCUSSION

Sensitivity and Precision of Radioimmunoassay—Linearization of the calibration curve was obtained by plotting the percentage inhibition of binding of the ^{3}H-clonazepam *versus* the concentration of unlabeled clonazepam on logit–log transformation graph paper[2]. An almost perfect straight line was obtained in the range of 0.5–20 ng of unlabeled clonazepam added. The calibration lines obtained using 0.02, 0.05, and 0.1 ml of plasma were virtually superimposable. In repeated assays, the percentage inhibition of binding by 0.5 ng of clonazepam always exceeded 10%. However, since 0.1 ml of plasma was routinely assayed, the working limit of sensitivity was actually 5 ng/ml. This sensitivity is adequate for routine clinical determination of clonazepam (4).

The accuracy and intraassay precision of the radioimmunoassay were determined by the addition of 10, 50, and 100 ng of clonazepam to separate 1.0-ml aliquots of a clonazepam-free plasma pool obtained from 20 patients receiving other anticonvulsants. Six 0.1-ml replicates of each of the three concentrations were assayed. The mean values and coefficients of variation obtained were 9.62 ± 7.1, 49.7 ± 5.2, and 99.7 ng/ml ± 4.9%, respectively. The interassay precision was determined by assaying unknown samples from four different subjects who had received 5–29 mg of clonazepam/day in conjunction with other anticonvulsants. The samples were stored at 4° and assayed on five different occasions over 2 weeks. The mean values for clonazepam and the coefficients of variation were 21.4 ± 4.2, 36 ± 2, 69.6 ± 2.4, and 625 ng/ml ± 4%. The sample with a mean value of 625 ng/ml was diluted 1:10 with control plasma prior to analysis.

The foregoing data, apart from showing adequate intra- and interassay precision for routine clinical analysis, indicate no decomposition of clonazepam in plasma when stored at 4°.

Specificity—In designing the radioimmunoassay for clonazepam, several points were considered regarding a suitable hapten. As in any radioimmunoassay procedure, antibody specificity was of the utmost importance. In the case of clonazepam, this specificity centered on the ability of the antibodies to recognize clonazepam alone in the presence of its known major metabolites in plasma: the 7- amino and 7-acetylamino derivatives (5). Recent studies[3] (7) have shown that the 7-amino metabolite is present in plasma in almost equal concentration to clonazepam on chronic administration. The 7-acetylamino metabolite appears to be present in considerably lower concentrations (9). Another consideration was that other benzodiazepines might be administered concomitantly to subjects receiving clonazepam. For these reasons, II was chosen as a possible hapten to fulfill the specificity requirements of the antibodies. By coupling at the C-3 position to the protein, the 7-nitro and 2′-chloro groups are relatively free to act as antigenic determinants.

To determine which functional groups on the hapten influenced the specificity of the antibodies obtained to clonazepam, various benzodiazepines with different substituents in the 1-, 2′-, 3-, and 7-positions were examined for their extent of cross-reactivity. The greatest cross-reactivity (24%) occurred with the 3-hydroxy derivative of clonazepam (Table I). This is not surprising, since the hapten was coupled to the protein at the C-3 position. Although the 3-hydroxy derivative of clonazepam has been isolated as a conjugated metabolite of clonazepam in urine (5), it has not been detected in plasma.

Nitrazepam, which differs from clonazepam by the absence of the 2′-chloro group, showed only 3.2% cross-reactivity. This result illustrates the effect of the 2′-chloro group on the immunogen as an antigenic determinant. However, when rabbits were immunized with an albumin conjugate of the 3-hemisuccinyloxy derivative of nitrazepam, the resulting antibodies recognized both nitrazepam and clonazepam almost equally well[3]. The most significant lack of cross-reactivity was observed with compounds that did not have a nitro group but had some other substituent at the 7-position. The latter included the 7-amino and 7-acetylamino metabolites of clonazepam, which showed 0.04 and <0.01% cross-reactivity, respectively.

[1] Omnifluor, New England Nuclear Corp., Boston, MA 02118.
[2] TEAM, Box 25, Tamworth, NH 03886.

[3] Data on file, Hoffmann–La Roche Inc., Nutley, NJ 07110.

Table II—Specificity of the Radioimmunoassay for Clonazepam in Plasma Containing 20 ng of Clonazepam/ml in the Presence of High Concentrations of Various Potential Competitors

Competitor	Competitor Concentration, ng/ml	Clonazepam Found, ng/ml
Clonazepam 7-amino derivative	10,000	21
Diazepam	10,000	19
Desmethyldiazepam	10,000	23
Acetazolamide	20,000	19
Phenytoin	50,000	20
Phenobarbital	50,000	19
Primidone	50,000	20
Ethosuximide	100,000	21
Trimethadione	100,000	21

To evaluate further the specificity of the radioimmunoassay in the clinical situation, several drugs commonly used for seizure control that might be administered with clonazepam were checked for their possible interference. Control plasma containing 20 ng of clonazepam/ml was used as the reference standard, and aliquots were spiked with each compound listed in Table II. The concentration of each potential competitor added was judged to be greater than the concentration that might be encountered in plasma during routine seizure control therapy.

Each sample was assayed for clonazepam, and Table II shows the percent response for clonazepam in the presence of each compound studied as compared to the control sample containing 20 ng/ml of clonazepam alone (100% response). No competitor, including the 7-amino metabolite of clonazepam, which was in a 500–5000-fold excess, caused any serious error in the clonazepam determination, and it is unlikely that a false positive reaction would be encountered. These studies are further substantiated when one considers the almost quantitative response previously obtained for clonazepam when added to the pool of plasma from patients receiving other anticonvulsants. In the latter instance, the plasma pool contained all anticonvulsants listed in Table II and their respective plasma metabolites.

Comparison of Radioimmunoassay with Electron-Capture GC Determination of Clonazepam—Sixteen plasma samples, obtained from subjects receiving clonazepam either alone or with concomitant anticonvulsants, were assayed for clonazepam using the radioimmunoassay and the electron-capture GC method[4] of de Silva *et al.* (8). The joint determinations were subjected to straight-line analysis by the method of Wald (14) using a 95% confidence ellipse[5]. The fitted intercept and slope (−0.56 and 0.94, respectively) were not significantly different from 0 and 1 over a range of 7–130 ng of clonazepam/ml. This result shows that the radioimmunoassay can measure clonazepam as precisely as the electron-capture GC method.

Plasma Clonazepam Levels during Routine Anticonvulsant Therapy—To obtain data regarding the range of plasma levels of clonazepam *versus* dose that might be encountered during routine anticonvulsant therapy, plasma samples from subjects who had received various doses of clonazepam in conjunction with other anticonvulsants were assayed by the radioimmunoassay. Figure 1 shows the steady-state plasma levels of clonazepam *versus* dose for 15 subjects, each of whom had been treated chronically with at least two different doses of the drug. Each subject was also receiving concomitantly at least one anticonvulsant listed in Table II, and 10 subjects were receiving two or three of the latter anticonvulsants in various combinations. There was as much as a fivefold variation in the plasma levels at steady state with the same chronic dose

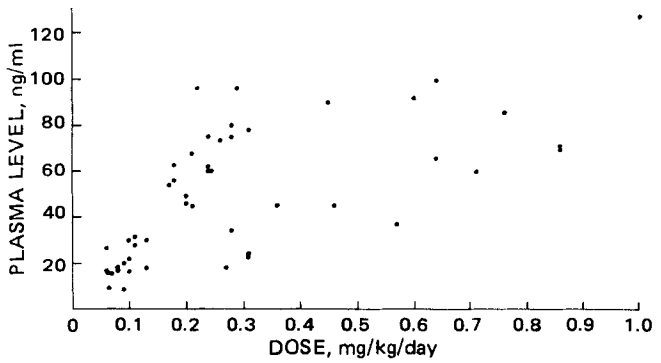

Figure 1—*Steady-state plasma levels of clonazepam in 15 subjects, each of whom had been treated chronically with at least two different doses of the drug.*

of clonazepam. Several factors probably contributed to this result. First, it was not known at what time the blood samples were drawn relative to the time the patient took the last dose of clonazepam. Although the half-life of clonazepam ranges from 19 to 39 hr, somewhat elevated plasma levels would exist for a few hours following each dose (6). Second, every patient was receiving concomitant anticonvulsants, and their effect on the disposition of clonazepam is unknown. Third, the compliance of each patient for the prescribed dosage regimen was unknown.

Although there is undoubtedly some correlation between plasma level and dose, no attempt has been made to define it statistically in this instance since such a definition could be misleading in view of the lack of controlled experimental conditions. The data, however, realistically illustrate the range of plasma clonazepam levels that may be encountered in the clinical situation.

REFERENCES

(1) R. Kruse, *Epilepsia*, **12**, 179 (1971).

(2) H. Gastant, J. Courjon, R. Poire, and M. Weber, *ibid.*, **12**, 197 (1971).

(3) H. Hooshmand, *ibid.*, **12**, 287 (1971).

(4) C. Y. Huang, J. G. McLeod, D. Sampson, and W. J. Hensley, *Med. J. Aust.*, **2**, 5 (1974).

(5) E. Eschenhof, *Arzneim.-Forsch.*, **23**, 390 (1974).

(6) S. A. Kaplan, K. Alexander, M. L. Jack, C. V. Puglisi, J. A. F. de Silva, T. L. Lee, and R. E. Weinfeld, *J. Pharm. Sci.*, **63**, 527 (1974).

(7) O. Sjo, E. F. Hvidberg, J. Naestoft, and M. Lund, *Eur. J. Clin. Pharmacol.*, **8**, 249 (1975).

(8) J. A. F. de Silva, C. V. Puglisi, and N. Munno, *J. Pharm. Sci.*, **63**, 520 (1974).

(9) J. Naestaft and N. E. Larkin, *J. Chromatogr.*, **93**, 113 (1974).

(10) J. A. F. de Silva and I. Bekersky, *ibid.*, **99**, 447 (1974).

(11) B. F. Erlanger, F. Borek, S. M. Beiser, and S. Lieberman, *J. Biol. Chem.*, **234**, 1090 (1959).

(12) W. R. Dixon, J. Earley, and E. Postma, *J. Pharm. Sci.*, **64**, 937 (1975).

(13) W. R. Dixon, R. L. Young, A. Holazo, M. L. Jack, R. E. Weinfeld, K. Alexander, A. Liebman, and S. A. Kaplan, *ibid.*, **65**, 701 (1976).

(14) M. Kendall and S. Stuart, "The Advanced Theory of Statistics," vol. 2, Hafner, New York, N.Y., 1961, pp. 397–405.

ACKNOWLEDGMENTS AND ADDRESSES

Received January 19, 1976, from the *Department of Biochemistry and Drug Metabolism and the Chemical Research Division, Hoffmann-La Roche Inc., Nutley, NJ 07110.*

Accepted for publication April 23, 1976.

[x] To whom inquiries should be directed.

[4] Electron-capture GC analyses were carried out by Dr. H. Kupferberg, National Institutes of Health, Bethesda, Md., and Mr. C. Puglisi, Hoffmann-La Roche Inc., Nutley, NJ 07110.

[5] Statistical analyses were performed by Mr. T. Lewinson, Hoffmann-La Roche Inc., Nutley, NJ 07110.

Effects of Long-Term Exposure to Environmental Levels of Polychlorinated Biphenyls on Pharmacokinetics of Pentobarbital in Rats

C. K. CHU, V. J. STELLA ˣ, J. V. BRUCKNER *, and W. D. JIANG *

Abstract □ The pharmacokinetics of pentobarbital, 30 mg/kg iv, were studied in untreated rats and rats pretreated with 1, 5, and 25 ppm of polychlorinated biphenyls in food for up to 140 days. Environmental contaminants may contribute to variations in metabolic rates of drugs by causing enzyme induction. The objective of this work was to quantitate the effects of environmental levels of the contaminant and enzyme inducer, a polychlorinated biphenyl, on the pharmacokinetics of pentobarbital, a drug whose primary elimination route is liver metabolism. The pharmacokinetics of pentobarbital in rats could be fit to a biexponential equation of the type $C_p = Ae^{-\alpha t} + Be^{-\beta t}$. After 35 days of pretreatment, only the 25-ppm-treated rats showed any significant acceleration of pentobarbital elimination. At the 70- and 140-day samplings, both the 5- and 25-ppm pretreatments showed significant acceleration of pentobarbital elimination. There were no significant effects on A, α, B, and V_d for any pretreatment. The β-values for the 25-ppm-pretreated rats reached a constant value from the 35-day pretreatment period onward. A calculation of total body clearance suggested that pentobarbital elimination in those rats had approached portal blood flow rate-limited metabolism.

Keyphrases □ Biphenyls, polychlorinated—effects on pharmacokinetics of pentobarbital, rats □ Pharmacokinetics—pentobarbital, effects of polychlorinated biphenyls, rats □ Pentobarbital—pharmacokinetics, effects of polychlorinated biphenyls, rats □ Contaminants, environmental—polychlorinated biphenyls, effects on pharmacokinetics of pentobarbital, rats □ Sedatives—pentobarbital, pharmacokinetics, effects of polychlorinated biphenyls, rats

Polychlorinated biphenyls have become a major environmental contaminant because of their extreme stability and lipophilicity (1–4). Polychlorinated biphenyls have been found in human tissues (5), and an outbreak of chloracne in Japan (6) has been attributed to their accumulation in tissue. Adverse effects on reproduction in rats (7) and monkeys (8) have also been associated with polychlorinated biphenyl ingestion. Polychlorinated biphenyls induce the activity of the hepatic mixed-function oxidase system (1, 4, 9–14), and several studies showed that polychlorinated biphenyl-treated animals have enlarged livers (10, 15). However, most previous studies were carried out on animals pretreated with high levels of polychlorinated biphenyls over a relatively short time.

Rational drug therapy requires an understanding of the pharmacokinetics of drug substances and the effects that dietary, genetic, and environmental factors, as well as disease states, have on pharmacokinetics. The pharmacokinetics of pentobarbital in rats *per se* have been studied (16, 17). The objective of this study was to quantitate the effects of environmental levels of polychlorinated biphenyls on the pharmacokinetics of pentobarbital, a drug whose primary elimination route is liver metabolism (17).

This report appears to be the first to present a full pharmacokinetic study of the effects of an environmental contaminant on the distribution and elimination kinetics of a drug. The study deals with the effect of exposure to a commercial polychlorinated biphenyl for up to 140 days. The pharmacokinetics were studied in control groups and groups exposed to three different levels of polychlorinated biphenyls[1]. The three levels were 1, 5, and 25 ppm in food, representing submaximum, maximum, and above maximum Food and Drug Administration (FDA) and Environmental Protection Agency (EPA) recommended allowable limits in most food products (18), respectively.

EXPERIMENTAL

Male, Sprague–Dawley rats[2], ~100 g, were housed in stainless steel cages in groups of three or four. Tap water was available *ad libitum*. The rats were fed standard powdered laboratory rat chow diet[3] for 1 week before a special diet was started. The animals were divided into four groups and were fed the lab chow in powdered form containing 0, 1, 5, or 25 ppm of the polychlorinated biphenyl.

The powdered diet was prepared by dissolving appropriate quantities of polychlorinated biphenyl in acetone and mixing this solution thoroughly with a small amount of ground chow. After allowing the acetone to evaporate, this contaminated chow was mixed by geometric dilution with increasing amounts of ground chow until the desired concentrations of polychlorinated biphenyl were achieved.

Four rats from each group were studied at the end of each period (35, 70, and 140 days). Each rat received 30 mg/kg iv of pentobarbital sodium *via* the dorsal vein of the penis. Blood sampling from the tail vein was started immediately after drug administration. About 250 μl of blood was collected in a heparinized microcapillary tube at specified timed intervals (Table I). The time required for the animal to regain its righting reflex was also noted. The blood was immediately centrifuged; the plasma was removed, placed into a test tube, and kept frozen until analyzed. All plasma samples were analyzed within 1 month (19).

The plasma concentration was analyzed using GC. This method was a modification of the procedure of Ehrnebo *et al.* (20). To each 100-μl plasma sample, 25 μl of internal standard (80 μg/ml of secobarbital sodium in methanol) and 0.1 ml of 0.05 *N* sodium hydroxide were added. The mixture was extracted with 1.0 ml of water-saturated ether on a mixer[4] for about 1 min. After centrifugation, the organic phase was discarded. The aqueous phase was then acidified with 1.0 ml of 4 *M* monobasic sodium phosphate and reextracted with 1.0 ml of water-saturated ether. The ether extract was then evaporated to dryness under nitrogen.

Just before injection into the chromatograph, 25 μl of 0.2 *M* trimethylanilinium hydroxide[5] was added and the sample was agitated in a mixer. An aliquot of 1.5–3.5 μl of this mixture was then injected into a gas chromatograph[6] equipped with a flame-ionization detector. The column of choice was a 1.83-m (6-ft) × 0.31-cm (0.125-in.) U-shaped glass column[7] packed with 3% OV-1 on 100–120-mesh Gas Chrom Q[8]. The following conditions were used: injector temperature, 250°; column temperature, 130°; detector temperature, 240°; nitrogen flow, 50 ml/min; hydrogen flow, 40 ml/min; and compressed air (19–23% O_2, 77–81% N_2) flow, 365 ml/min. The sensitivity was 10^{-12} amp/mv. The described procedure was used for plasma samples containing known amounts of

[1] Aroclor 1254 containing 54% (w/w) of chlorine, lot KA601, Monsanto Chemical Co., St. Louis, Mo.
[2] ARS/Sprague–Dawley, Madison, Wis.
[3] Wayne Lab-Blox, Allied Mills Inc., Chicago, Ill.
[4] Vortex Genie, Scientific Products, McGraw Park, Ill.
[5] Supelco, Inc., Supelco Park, Bellefonte, Pa.
[6] Varian Aerograph model 2100, Walnut Creek, Calif.
[7] Supelcoport, Supelco, Inc., Supelco Park, Bellefonte, Pa.
[8] Applied Sciences Labs, State College, Pa.

Table I—Plasma Sampling Times in the Study of Pentobarbital Pharmacokinetics in Rats Pretreated over Various Time Intervals with Polychlorinated Biphenyls

Days of Treatment	Sampling Time, min									
35	0	5	10	15	30	60	90	120	—	—
70	5	10	15	20	30	45	60	75	90	—
140	2	3	5	10	15	20	30	45	60	75[a]

[a] The 75-min sample was omitted for 5- and 25-ppm groups.

pentobarbital and secobarbital to produce a standard curve of the area under the peak *versus* the pentobarbital concentration (5–50 μg/ml of plasma).

The pharmacokinetics of pentobarbital in rats were fit to a two-compartment model (21) previously (16, 17). This model predicts that the data for plasma pentobarbital levels *versus* time in rats after rapid intravenous injection should show a biexponential decay. The decay curve should be described by:

$$C_p = Ae^{-\alpha t} + Be^{-\beta t} \quad \text{(Eq. 1)}$$

where C_p is the plasma level at any time t, and A, α, B, and β are parameters which were described adequately by others (21). If only a single exponential decay is noted because of the sampling schedule or because of a rapid distribution phase, then the plasma concentration *versus* time curve will be given by:

$$C_p = Be^{-\beta t} \quad \text{(Eq. 2)}$$

In the present case, for the 35- and 70-day pretreatments, the data were fit to a one-compartment model (Eq. 2) because plasma sampling times were started too late to fit the data to a two-compartment model. Therefore, the postdistribution data for each 35- and 70-day-pretreated animal were fit to Eq. 2 utilizing the simplex method of fitting[9] (22). This approach helped generate appropriate values of β and B from which the volume of distribution extrapolated (23), $V_{d(ext)}$, and total body clearance (24), Cl_{TB}, could be calculated from Eqs. 3 and 4, respectively:

$$V_{d(ext)} = \frac{\text{dose}}{B} \quad \text{(Eq. 3)}$$

$$Cl_{TB} = \beta V_{d(ext)} \quad \text{(Eq. 4)}$$

The mean values for all calculated parameters for each pretreatment were determined and statistically compared to the same parameters for the control group using the standard Student t test. The mean values of β and B were then used to generate lines to describe the plasma pentobarbital level *versus* time curves for each group.

For the 140-day-pretreated rats, plasma samples at 2 and 3 min as well as other plasma samples (Table I) did allow the fit of the data to a two-compartment model using the simplex method of fitting (22). The mean values for A, α, B, and β as well as values for $V_{d(ext)}$, $V_{d(area)}$, and Cl_{TB} were calculated for each animal in each pretreatment. The value of $V_{d(area)}$ was calculated using:

$$V_{d(area)} = \frac{\text{dose}}{\beta\left(\frac{A}{\alpha} + \frac{B}{\beta}\right)} \quad \text{(Eq. 5)}$$

These values were compared, using the Student t test, to the same parameter for the control animals. The mean values of A, α, B, and β were then used to generate lines representing the mean plasma levels *versus* time decay curves for pentobarbital in rats pretreated over 140 days with 0, 1, 5, and 25 ppm of polychlorinated biphenyl. The plasma pentobarbital concentration at the righting reflex time for each animal was determined by substituting the righting reflex time for that animal into the equation describing the plasma level *versus* time curve for that animal.

RESULTS AND DISCUSSION

Based on the study of Lin *et al.* (16), plasma samples for pentobarbital determination for both the 35- and 70-day-pretreated rats were begun at 5 min postdosing with 30 mg of pentobarbital sodium/kg (27.22 mg of pentobarbital acid/kg). Unfortunately, this time proved to be too late

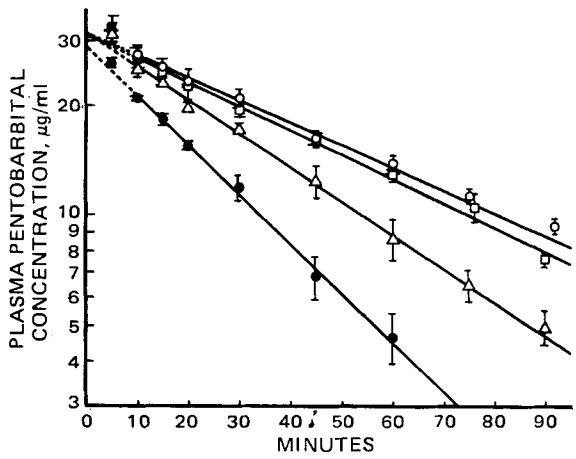

Figure 1—*Time courses of plasma concentration ± SE of pentobarbital in rats pretreated over 70 days at 1 (□), 5 (△), and 25 (●) ppm of polychlorinated biphenyls in food and in a control group of rats (○) after administration of pentobarbital sodium (30 mg/kg iv). Each point is the mean of four animals. Lines are generated utilizing pharmacokinetic parameters in Table III.*

to observe the distribution phase of the pentobarbital decay curve. Figure 1 shows the plasma level *versus* time plots for pentobarbital decay in the 70-day-pretreated rats. The solid lines are drawn by a fit to Eq. 2 utilizing the mean values of B and β for each group.

Tables II and III summarize the pharmacokinetic parameters for pentobarbital determined for the 35- and 70-day polychlorinated biphenyl-pretreated rats compared to the same parameters for the control groups. The only parameters affected by the polychlorinated biphenyl pretreatments to any significant extent were those directly related to β, the total body elimination rate constant.

At the 35-day pretreatment, β for the 1-ppm-pretreated rats was significantly smaller than β for the control and 5-ppm-pretreated rats. The cause of this apparent inhibition is unknown. There was a significant catalysis of pentobarbital elimination at 35 days in the 25-ppm-pretreated animals.

With the 70-day-pretreated animals, both the 5- and 25-ppm-pretreated animals showed a significant catalysis in pentobarbital total body elimination compared to the elimination in the control and 1-ppm-pretreated groups. These results are consistent with the shorter sleeping time in the 5- and 25-ppm-pretreated animals *versus* the controls and 1-ppm-pretreated animals.

Figure 2 shows the plasma level *versus* time plots for pentobarbital decay in the 140-day-pretreated animals. The data had been fit to a two-compartment model. Table IV summarizes the pharmacokinetic parameters for these animals. The only parameters affected by the polychlorinated biphenyl pretreatments to any statistically significant extent were those directly related to β, the total body elimination rate constant. Both the 5- and 25-ppm-pretreated animals showed a significant catalysis of pentobarbital elimination, total body clearance, and sleeping time.

A number of other observations can be made. The righting times were directly related to the plasma concentration of pentobarbital (~15 μg/ml). The β and Cl_{TB} for the 25-ppm-pretreated animals remained constant from the 35-day sampling period onward, and a similar observation can be made for the 5-ppm-pretreated animals when the results for the 70- and 140-day pretreatments are compared.

The clearance of any compound from the body whose primary mode of elimination is liver metabolism can be given by:

$$Cl_{TB} = QE \quad \text{(Eq. 6)}$$

where Q is the portal blood flow rate, and E is the extraction ratio for the liver. Literature values of Q for rats are 60 (25) and 42 (26) ml/min/kg and 1.2 ml/min/g (27) of liver. Since liver to body weights for the rats were determined[10] in the present study, the clearance value of 1.2 ml/min/g

[9] The program was developed by Dr. W. White and various graduate students of the Department of Pharmaceutical Chemistry, University of Kansas. The program was run on a Hewlett-Packard model 2100 computer. For copies of the program and further information, contact Dr. W. White.

[10] Independent *in vitro* metabolism studies were carried out on paired animals receiving the same diet and pretreated over the same time interval as the animals used in the present study. Liver weights as percent of total body weight were determined. An average liver weight of 3.75% of total body weight was used. This value of 3.75% is the percent liver weight of 25-ppm-pretreated animals. The percent liver weight for the 0-, 1-, and 5-ppm-treated animals was 3.41%.

Table II—Pharmacokinetic Parameters[a] of the Disposition of Pentobarbital in Rats Pretreated at Three Different Levels of Polychlorinated Biphenyls over 35 Days

Parameter	Pretreatment Level			
	Control	1 ppm	5 ppm	25 ppm
$\beta \pm SEM^b$, min^{-1}	0.017 ± 0.001	0.013 ± 0.001 ($p < 0.0125$)[c]	0.016 ± 0.002 (NS)	0.033 ± 0.001 ($p < 0.0025$)[c]
$t_{1/2} \pm SEM^b$, min	40.5 ± 2.1	52.4 ± 3.4 ($p < 0.0125$)[c]	39.9 ± 4.6 (NS)	20.8 ± 0.4 ($p < 0.0025$)[c]
$V_{d(ext)} \pm SEM^b$, liters/kg	0.84 ± 0.06	0.88 ± 0.05 (NS)	0.88 ± 0.03 (NS)	0.97 ± 0.02 (NS)
$Cl_{TB} \pm SEM^b$, ml/min/kg	14.3 ± 0.8	11.7 ± 0.7 ($p < 0.05$)[c]	15.7 ± 1.3 (NS)	32.5 ± 1.2 ($p < 0.0025$)[c]
Righting reflex $\pm SEM^b$, min	49.5 ± 3.9	50.7 ± 5.6 (NS)	51.5 ± 2.7 (NS)	20.2 ± 2.3 ($p < 0.0025$)[c]
C_p at righting reflex time $\pm SEM^b$, μg/ml	13.9 ± 0.9	16.0 ± 1.6 (NS)	12.5 ± 1.3 (NS)	15.2 ± 1.0 (NS)
Weight of rat $\pm SEM^b$, g	296 ± 6	272 ± 11	311 ± 10	287 ± 7

[a] Mean of four rats, except that there were only three rats in the 1- and 25-ppm groups. [b] Mean value ± *SE* of the mean. [c] Results are significantly different from the control group of animals at the level indicated.

Table III—Pharmacokinetic Parameters of the Disposition of Pentobarbital in Rats Pretreated at Three Different Levels of Polychlorinated Biphenyls over 70 Days

Parameter	Pretreatment Level			
	Control	1 ppm	5 ppm	25 ppm
$\beta \pm SEM^a$, min^{-1}	0.014 ± 0.001	0.015 ± 0.001 (NS)	0.021 ± 0.002 ($p < 0.0025$)[b]	0.031 ± 0.002 ($p < 0.0005$)
$t_{1/2} \pm SEM^a$, min	50.5 ± 1.0	48.4 ± 3.2 (NS)	33.7 ± 3.0 ($p < 0.0025$)[b]	22.8 ± 1.9 ($p < 0.0005$)[b]
$V_{d(ext)} \pm SEM^a$, liters/kg	0.88 ± 0.05	0.88 ± 0.04 (NS)	0.88 ± 0.05 (NS)	0.94 ± 0.02 (NS)
$Cl_{TB} \pm SEM^a$, ml/min/kg	12.1 ± 0.6	12.7 ± 0.8 (NS)	18.2 ± 1.0 ($p < 0.0025$)[b]	29.2 ± 1.8 ($p < 0.0005$)[b]
Righting reflex $\pm SEM^a$, min	51.7 ± 1.7	46.5 ± 1.8 ($p < 0.05$)[b]	35.7 ± 2.9 ($p < 0.0025$)[b]	22.7 ± 2.0 ($p < 0.0005$)[b]
C_p at righting reflex time $\pm SEM^a$, μg/ml	15.6 ± 1.1	15.9 ± 0.9 (NS)	15.0 ± 1.2 (NS)	14.6 ± 0.6 (NS)
Weight of rat $\pm SEM^a$, g	372 ± 17	374 ± 10	379 ± 6	367 ± 16

[a] Mean value ± *SE* of the mean. [b] Results are significantly different from the control group of animals at the level indicated.

Table IV—Pharmacokinetic Parameters of the Disposition of Pentobarbital in Rats Pretreated at Three Different Levels of Polychlorinated Biphenyls over 140 Days

Parameter	Pretreatment Level			
	Control	1 ppm	5 ppm	25 ppm
$\beta \pm SEM^a$, min^{-1}	0.016 ± 0.001	0.015 ± 0.002 (NS)	0.021 ± 0.001 ($p < 0.01$)[b]	0.031 ± 0.002 ($p < 0.0005$)[b]
$t_{1/2} \pm SEM^a$, min	43.7 ± 2.9	47.4 ± 5.9 (NS)	33.2 ± 1.3 ($p < 0.01$)[b]	22.3 ± 1.5 ($p < 0.0005$)[b]
$V_{d(ext)} \pm SEM^a$, liters/kg	0.89 ± 0.04	0.85 ± 0.05 (NS)	0.85 ± 0.03 (NS)	0.99 ± 0.10 (NS)
$V_{d(area)} \pm SEM^a$, liters/kg	0.73 ± 0.15	0.82 ± 0.05 (NS)	0.81 ± 0.03 (NS)	0.92 ± 0.07 (NS)
$Cl_{TB} \pm SEM^a$, ml/min/kg	13.1 ± 1.0	12.7 ± 0.8 (NS)	17.7 ± 1.0 ($p < 0.01$)[b]	30.7 ± 2.1 ($p < 0.0005$)[b]
Righting reflex $\pm SEM^a$, min	48.3 ± 4.8	49.5 ± 3.6 (NS)	38.0 ± 2.5 (NS)	25.0 ± 1.9 ($p < 0.01$)[b]
C_p at righting reflex time $\pm SEM^a$, μg/ml	15.2 ± 1.6	15.4 ± 0.8 (NS)	14.7 ± 1.2 (NS)	13.0 ± 0.9 (NS)
$A \pm SEM^a$, μg/ml	40.6 ± 18.7	35.2 ± 11.5 (NS)	43.2 ± 14.3 (NS)	38.7 ± 25.9 (NS)
$\alpha \pm SEM^a$, min^{-1}	0.69 ± 0.19	0.47 ± 0.14 (NS)	0.69 ± 0.19 (NS)	0.54 ± 0.16 (NS)
$B \pm SEM^a$, μg/ml	31.5 ± 1.5	32.5 ± 2.0 (NS)	32.5 ± 1.5 (NS)	28.4 ± 2.6 (NS)
Weight of rat $\pm SEM^a$, g	434 ± 7	447 ± 6	414 ± 8	422 ± 12

[a] Mean value ± *SE* of the mean. [b] Results are significantly different from the control group of animals at the level indicated.

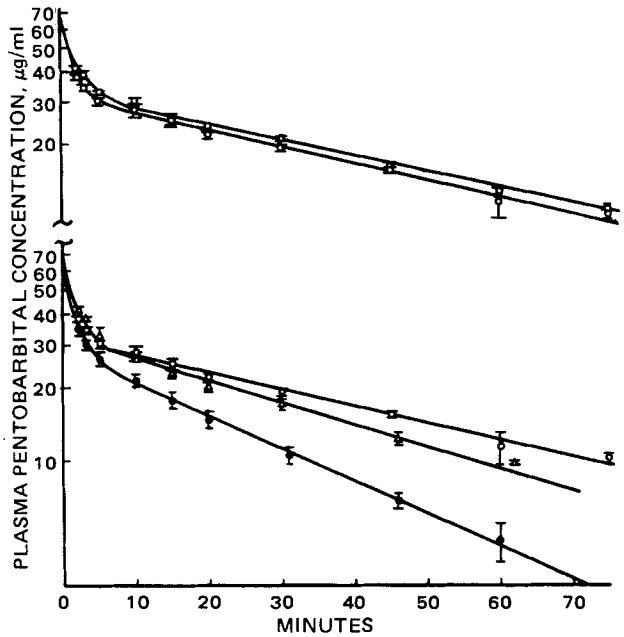

Figure 2—*Time courses of plasma concentration ± SE of pentobarbital in rats pretreated over 140 days at 1 (□), 5 (△), and 25 (●) ppm of polychlorinated biphenyls in food and in a control group of rats (○) after administration of pentobarbital sodium (30 mg/kg iv). Each point is the mean of four animals. Lines are generated utilizing pharmacokinetic parameters in Table IV.*

of liver translates to approximately 45 ml/min/kg. This value was then used for further calculations. Total body clearance in the 25-ppm-pretreated animals was calculated to be approximately 30 ml/min/kg. The extraction constant for the liver is then 0.67. This figure is only approximate in that the potential effect of enzyme induction on liver blood flow was not corrected for.

It is obvious, therefore, that two possible conditions can explain the constant pentobarbital clearance value for the 25-ppm-pretreated rats between 35 and 140 days: (*a*) the extraction constant reached a constant value and this constant value was a function of the amount of liver enzyme inducer, and/or (*b*) the clearance approached portal blood flow rate-limited metabolism. The second explanation is not totally valid in that an extraction constant of >0.8 is usually taken as portal blood flow rate-limited metabolism (28). The fact that a constant clearance was also seen in the 5-ppm-pretreated animals (70- and 140-day pretreatment) is more consistent with the first explanation that a constant E value was reached. Mechanistically, this can be explained by the hypothesis that the liver simply synthesized sufficient microsomal enzyme to prevent accumulation of the contaminant. Residues of polychlorinated biphenyls in body tissues of rats have been demonstrated to remain relatively constant on long-term feeding of similar dietary levels of polychlorinated biphenyls (29). The 1-ppm pretreatment with the polychlorinated biphenyl appeared to have no significant long-term effects on pentobarbital pharmacokinetics, suggesting that a critical mass of contaminant was needed to produce liver microsomal enzyme stimulation; *i.e.*, normal liver enzyme levels were capable of handling the 1 ppm of polychlorinated biphenyl.

Obviously, it is impossible to carry out controlled experiments of the effects of low levels of polychlorinated biphenyls on human liver microsomal enzyme activity. The FDA and EPA currently allow an upper limit of 5 ppm of polychlorinated biphenyls in most food substances (18). The present study demonstrated that 5 ppm of a polychlorinated biphenyl in food can, over a period greater than 35 days, induce liver microsomal metabolism of pentobarbital in rats as measured by the shorter half-lives of pentobarbital. At 5 and 25 ppm, the polychlorinated biphenyl stimulated pentobarbital elimination as measured by increased β and Cl_{TB} values, decreased half-lives, and shorter righting reflex times. The polychlorinated biphenyl did not significantly affect the distribution kinetics or the volume of distribution of pentobarbital, suggesting strongly that its primary effect was to induce liver metabolism *via* enzyme stimulation[10].

REFERENCES

(1) R. W. Riseborough, P. Rieche, D. B. Peakall, S. G. Herman, and M. N. Kirven, *Nature (London)*, **220**, 1098 (1968).

(2) S. Jensen, *New Sci.*, **32**, 612 (1966).

(3) F. J. Biros, A. C. Walker, and A. Medberg, *Bull. Environ. Contam. Toxicol.*, **5**, 317 (1970).

(4) J. L. Lincer and D. B. Peakall, *Nature*, **228**, 783 (1970).

(5) A. R. Yobbs, *Environ. Health Perspect.*, **1**, 79 (1972).

(6) M. Kuratsune, T. Yoshimura, J. Matuszaka, and A. Yamguchi, *ibid.*, **1**, 119 (1972).

(7) R. E. Linder, T. B. Gaines, and R. D. Kimbrough, *Food Cosmet. Toxicol.*, **12**, 63 (1974).

(8) J. R. Allen, L. A. Carstens, and D. A. Barsotti, *Toxicol. Appl. Pharmacol.*, **30**, 440 (1974).

(9) C. L. Litterst, T. M. Farber, A. M. Baker, and E. J. VanLoon, *ibid.*, **23**, 112 (1972).

(10) D. R. Bickers, L. C. Harber, A. Kappas, and A. P. Alvares, *Res. Commun. Chem. Pathol. Pharmacol.*, **3**, 505 (1972).

(11) D. C. Villeneuve, D. L. Grant, W. E. J. Philips, M. L. Clark, and D. J. Clegg, *Bull. Environ. Contam. Toxicol.*, **6**, 120 (1971).

(12) J. V. Bruckner, K. L. Khanna, and H. H. Cornish, *Toxicol. Appl. Pharmacol.*, **24**, 434 (1973).

(13) *Ibid.*, **28**, 189 (1974).

(14) J. V. Bruckner, K. L. Khanna, and H. H. Cornish, *Food Cosmet. Toxicol.*, **12**, 323 (1974).

(15) D. C. Grant, W. E. J. Philips, and D. C. Villeneuve, *Bull. Environ. Contam. Toxicol.*, **6**, 102 (1971).

(16) Y. J. Lin, S. Awazu, M. Hanano, and H. Nogami, *Chem. Pharm. Bull.*, **21**, 2749 (1973).

(17) F. W. Ossenberg, M. Peignoux, D. Bourdiau, and J. P. Benhamou, *J. Pharmacol. Exp. Ther.*, **194**, 111 (1975).

(18) *Federal Register*, **39**, 42727 (Dec. 6, 1974).

(19) R. B. Smith, L. W. Dittert, W. O. Griffen, Jr., and J. T. Doluisio, *J. Pharmacokinet. Biopharm.*, **1**, 5 (1973).

(20) M. Ehrnebo, S. Agurell, and L. O. Boreus, *Eur. J. Clin. Pharmacol.*, **4**, 191 (1972).

(21) J. G. Wagner, "Fundamentals of Clinical Pharmacokinetics," Drug Intelligence Publications, Hamilton, Ill., 1975, pp. 57–127.

(22) S. N. Deming and S. L. Morgan, *Anal. Chem.*, **45**, 278A (1973).

(23) S. Riegelman, J. Loo, and M. Rowland, *J. Pharm. Sci.*, **57**, 128 (1968).

(24) M. Rowland, *ibid.*, **61**, 70 (1972).

(25) J. Grayson and D. Mendel, "Physiology of the Splanchnic Circulation," Williams & Wilkins, Baltimore, Md., 1965, p. 74.

(26) S. S. Steiner and C. E. Mueller, *Circulation Res.*, **14**, 99 (1961).

(27) E. L. Dobson and H. B. Jones, *Acta Med. Scand.*, **144**, 34, Suppl. 273 (1952).

(28) G. R. Wilkinson, *Ann. Rev. Pharmacol.*, **15**, 11 (1975).

(29) D. L. Grant, C. A. Moodie, and W. E. J. Philips, *Environ. Physiol. Biochem.*, **4**, 214 (1974).

ACKNOWLEDGMENTS AND ADDRESSES

Received March 5, 1976, from the *Departments of Pharmaceutical Chemistry and Pharmacology and Toxicology, School of Pharmacy, University of Kansas, Lawrence, KS 66045.*

Accepted for publication April 26, 1976.

Presented at the Basic Pharmaceutics Section, APhA Academy of Pharmaceutical Sciences, New Orleans meeting, April 1976.

Supported by University of Kansas General Research Funds and an HSAA award to V. J. Stella and J. V. Bruckner.

* Present address: Department of Pharmacology, Medical School, University of Texas Health Science Center at Houston, Houston, TX 77030.

ˣ To whom inquiries should be directed (at the Department of Pharmaceutical Chemistry).

Pharmacokinetics of β-Methyldigoxin in Healthy Humans I: Intravenous Studies

PETER H. HINDERLING *, EDWARD R. GARRETT ˣ, and RONALD C. WESTER ‡

Abstract □ The pharmacokinetics of intravenously administered solutions of 0.30- and 0.60-mg bolus doses of ^{3}H-β-methyldigoxin, labeled in the 12α-position, were dose independent. Individual radioactivities assignable to the parent drug and specifically identified metabolites after TLC separation were followed in the plasma, urine, and feces. A sum of four exponentials described the plasma β-methyldigoxin data with apparent half-lives of 0.04, 0.33, 3.5, and 41 hr. β-Methyldigoxin was 10% plasma protein bound and had a red blood cell–plasma water partition coefficient of 0.9. The only significant metabolite observed in plasma was digoxin, although glucuronides and sulfates of β-methyldigoxin, digoxin, and digoxigenin also were observed in urine. As much as 92 ± 3% of the dose was excreted by all processes by 144 hr. Of this amount, renal excretion accounted for fractions that were 0.47 unchanged, 0.35 digoxin, and 0.058 water-soluble metabolites. The fraction in the feces was 0.13. The urine flow independent renal clearances of β-methyldigoxin and derived digoxin were 59 and 206 ml/min, respectively. The metabolism was a relatively fast process. The terminal pseudo-steady-state elimination of β-methyldigoxin with a half-life of 41 hr was reached 27 hr after drug administration and was primarily dependent on the slow release of sequestered or distributed drug from the tissues into the central compartment. The drug and metabolite levels in plasma and urine were consistent with analog computer fitting to the proposed pharmacokinetic multicompartmental model.

Keyphrases □ β-Methyldigoxin—intravenous, pharmacokinetics in humans, radiochemical–TLC study □ Pharmacokinetics—intravenous β-methyldigoxin, humans, radiochemical–TLC study □ Radiochemistry–TLC—study of pharmacokinetics of intravenous β-methyldigoxin in humans □ Cardiac glycosides—β-methyldigoxin, intravenous, pharmacokinetics in humans, radiochemical–TLC study

Frequently used methods for the assay of digoxin glycosides, radioimmunoassay (1) and liquid scintillation spectrophotometry (2–4) of labeled drug, are not specific for the parent compounds *per se* and measure drug plus metabolites. Their only valid use in pharmacokinetics or bioavailability studies is after proper separation of the drug and its metabolites or if the metabolic route of disposition is negligible. An argument could be made for those clinical circumstances where the sum of cardioactive drug and metabolites could be correlated with observed cardial or extracardial pharmacodynamic parameters.

Pharmacokinetic and bioavailability studies of glycosides with specific analyses of the parent drug and metabolites in plasma and urine as functions of the dose, formulation, and route of administration are needed. Apparently, no published studies demonstrate the linearity of the area under blood level–time curves (*AUC*) with the administered dose of digoxin-like drugs, a necessary prerequisite for the use of *AUC* as a criterion of bioavailability. The studies that did attempt to separate such drugs from their metabolites prior to assay by such nonspecific methods were limited. Column chromatographic (2, 3) and extraction (4) procedures were used to separate the labeled parent drug and metabolite. However, none of these papers clearly showed quantifications based on evaluated extraction efficiencies, nor did they demonstrate specific identifications of parent drug and metabolites in plasma or urine.

The present studies were conducted to determine the time course of radiolabeled ^{3}H-β-methyldigoxin (medigoxin) and its identified metabolites, separated and analyzed individually after both oral and intravenous administration at two dosage levels in the same individual, and to establish valid pharmacokinetic models and their parameters. This paper considers the pharmacokinetics of β-methyldigoxin after intravenous administration.

EXPERIMENTAL

Materials—The following were used: ^{3}H-β-methyldigoxin[1], digoxin[1], digoxigenin bisdigitoxoside[1], digoxigenin monodigitoxoside[1], and digoxigenin[1]. ^{3}H-β-Methyldigoxin was synthesized with the label in the 12α-position according to the method of von Wartburg *et al.* (5) and had a specific activity of 431 μCi/mg. β-Glucuronidase[2] and aryl sulfatase[3] were used for the enzymatic hydrolysis of conjugated metabolites. All organic solvents were analytical grade.

Commercially available scintillation fluids[4,5], solubilizer[6], dioxane, and a scintillation fluid prepared as described previously (6) were used for radioactivity counting. Heparin sodium[7] was used to prevent coagulation.

Heparinized blood and plasma with known protein fractions were obtained from healthy volunteers[8] who had no prior drug intake.

Criteria for Volunteer Selection—Seven healthy male Caucasian volunteers[9] between 21 and 25 years of age were selected. An individual was considered healthy when there was no history of problems with the cardiovascular system, kidneys, liver, blood, GI tract, and endocrine organs and no prostatic hypertrophy, drug addiction, and alcoholism. The volunteers had a normal status, ECG, blood pressure, and X-ray (chest).

The following initial laboratory checkup was performed on each volunteer: complete blood count (hematocrit included), sedimentation rate, serum electrophoresis, creatinine clearance, urinalysis, bilirubin, serum glutamic oxaloacetic transaminase, serum glutamic pyruvic transaminase, alkaline phosphatase, and serum electrolytes (sodium, potassium, calcium, and inorganic phosphate). The following tests were repeated prior to the second, third, and fourth studies on each individual to determine toxic drug effects or clinical changes due to the experimental procedures: complete blood count (hematocrit included), sedimentation rate, serum electrophoresis, serum creatinine, and serum electrolytes.

Pharmacokinetic Procedures—Four diffferent studies were performed in each of the seven volunteers; 0.30- and 0.60-mg doses in solution were administered both orally and intravenously. A total of 28 studies was conducted with an incomplete Latin-square design. Intervals of 3 weeks were maintained between studies in a subject to exclude any possible enzyme induction due to repeated drug administration. The volunteers were supine during the first 24 hr after drug administration. Later they were ambulant, although no exercise was allowed.

The individuals were fasted 12 hr before drug administration in both the intravenous and oral experiments. After drug administration, the

[1] Boehringer & Co., Mannheim, West Germany.
[2] Ketodase, Warner-Chilcott Laboratories, Morris Plains, N.J.
[3] Calbiochem, San Diego, Calif.
[4] Scintillar, Mallinckrodt Chemical Works, St. Louis, Mo.
[5] Spectrafluor, Amersham-Searle, Arlington Heights, Ill.
[6] Bio-Solv, Beckman Instruments, Fullerton, Calif.
[7] Heparin sodium injection USP, The Upjohn Co., Kalamazoo, Mich.
[8] Blood Bank, Shands Teaching Hospital and Clinics, Gainesville, Fla.
[9] Informed consent was obtained from all volunteers, and the experimental protocol was approved by both the Committee for Protection of Human Subjects and the Clinical Research Advisory Committee, Health Center, University of Florida.

volunteers fasted 8 hr. Within the first 24 hr after drug administration, food intake was restricted to fluids, *e.g.*, soups, milk shakes, and other beverages. The caloric intake was balanced in all studies to maintain constant weight. The daily fluid intake was fixed at 2500 ml/24 hr. Neither beverages nor food containing caffeine or other diuretically effective substances were allowed.

Three hours prior to drug administration, the volunteers were given water (10 ml/kg). One hour before the drug was given, a butterfly needle[10] was placed in a cubital vein. A constant drip of 0.45% sodium chloride[11], 1.7 ml/min in the oral experiments and 1.5 ml/min in the intravenous experiments, was started immediately through the butterfly needle. In the intravenous experiments, a catheter[12] was placed in the cubital vein on the other side and a constant drip of 0.9% sodium chloride (2.0 ml/min) was started immediately through the catheter. Both infusion solutions contained heparin[7], 1000 I.U./1000 ml, to prevent coagulation. Both the butterfly needle and the catheter were removed 11 hr after drug administration. Later blood samples were taken by venipuncture.

The freshly prepared solutions in 0.9% sodium chloride were assayed. They were intravenously administered at a constant rate for 1 min through the catheter, which was immediately flushed with 20 ml of 0.9% sodium chloride.

Blood (6 ml) was taken within 10 sec at 0, 1.5, 2, 2.5, 3.5, 7, 10, 15, 30, 45, 60, and 90 min and at 2, 3, 5, 7, 9, 11, 15, 20, 24, 36, 48, 60, 72, 84, 96, 120, and 144 hr after intravenous drug administration through the butterfly needle with syringes using a three-way stopcock[13]. An initial 2 ml of blood was discarded. The samples were immediately transferred to glass tubes[14] containing 12 mg of edetate disodium to prevent coagulation. After centrifugation at 1500 rpm for 20 min within 1 hr after sampling, the plasma was transferred to storage tubes and then frozen until assayed.

Total volumes of urine were obtained for the following collection periods: −3–0, 0–2, 2–4, 4–6, 6–8, 8–10, 10–12, 12–18, 18–24, 24–48, 48–72, 72–96, 96–120, and 120–144 hr. The pH was monitored, and aliquots were transferred to storage containers and frozen until assayed. Total feces were collected for the following collection periods: −12–0, 0–24, 24–48, 48–72, 72–96, 96–120, and 120–144 hr; the samples were frozen until assayed.

Analytical Procedures—The ^{3}H-β-methyldigoxin had a specific activity of 431 μCi/mg. Its purity was investigated in three different TLC systems: A, acetone–chloroform (4:6) on silica gel; B, ethyl acetate–formic acid (98:2) developed three times on basic alumina; and C, chloroform–ethanol–acetic acid–water (91.0:7.5:1.0:0.5) on basic alumina. Quantities and identities of the separable contaminants were determined by thin-layer scraping, elution of the material, and radioactivity counting in a liquid scintillation counter[15]. Corrections were made for background and efficiency using the channels ratio method (7).

When the ^{3}H-β-methyldigoxin used in the pharmacokinetic studies was chromatographed, the developed TLC spot assignable to the ^{3}H-β-methyldigoxin retained 97.6% (System A), 83.7% (System B), and 84.6% (System C) of the total radioactivity spotted in the three thin-layer systems used. It was concluded that 0.837 of the material represented ^{3}H-β-methyldigoxin, and this fraction of the total radioactivity was considered as the dose of β-methyldigoxin. The TLC separable contaminants assignable to digoxigenin monodigitoxoside (3.3%), digoxigenin (2.5%), digoxin (1.6%), and digitoxin and digoxigenin bisdigitoxoside (<1.0%) retained the percentages of the total radioactivity designated.

Since TLC System A was the least sensitive, only Systems B and C (with 250-μm basic alumina[16]-coated glass plates in activated chambers) were used in all other TLC studies on plasma and urine composition. The compounds were visualized by spraying with 50% aqueous sulfuric acid and heating the plates at 110° for 10 min. For the detection of the individual radioactive compounds, 4-mm bands of alumina were scraped from the plates using a zonal scraper[17]; the radioactivity in each zone was determined by liquid scintillation spectrophotometry using a prepared scintillation fluid (6). The radioactivity distribution pattern was then plotted by a computer plotter programmed to give the total radioactivity eluted from the plates, the number of radioactivity peaks, their R_f values, and the percentage of radioactivity in each peak. The efficiency of this process, 46.3 ± 1.3%, was determined by counting the scrapings of known spotted amounts. Corrections were made for the individual extractability of each compound.

For the determination of total radioactivity in plasma and urine, the samples were thawed and shaken, and 100- and 500-μl replicates were pipetted into vials containing 10 ml of scintillation fluid. In three of the seven investigated volunteers, total radioactivity was determined in the feces. Fecal samples were freeze dried and the dry powder was mixed thoroughly. Weighed aliquots were then combusted[18] to tritiated water, which was added to 10 ml of scintillation fluid and counted.

Aliquots of plasma (0.5–3.0 ml) were acidified to pH 4–5 with 10% HCl and extracted twice with three times the volume of ethyl acetate. The extracts were swirled over anhydrous sodium sulfate and decanted, and the solution was concentrated to dryness under nitrogen and then redissolved in 95% methanol (0.1 ml). Aliquots of the resultant solutions were then spotted on thin-layer plates, which were developed with Solvent Systems B and C. Sequential plasma samples with low radioactivity counts were pooled before extraction and TLC, and the weighted average of their sample times was taken as representative.

The extraction efficiencies into ethyl acetate of plasma samples spiked with various compounds were: β-methyldigoxin, 74.6 ± 0.7%; digoxin, 77.0 ± 1.6%; digoxigenin bisdigitoxoside, 74.3 ± 1.0%; digoxigenin monodigitoxoside, 85.5 ± 3.0%; and digoxigenin, 76.0 ± 1.0%.

Aliquots of urine (5 ml) were acidified with 10% HCl to pH 4–5 and extracted three times with equal volumes of chloroform. Each chloroform extract was swirled over anhydrous sodium sulfate, decanted, concentrated to dryness under nitrogen, and then redissolved in 95% methanol (0.1 ml). Aliquots of the resultant solutions were then spotted on thin-layer plates, which were developed with Solvent Systems B and C.

The aqueous phase was further analyzed in all urine samples in the 0.6-mg oral experiments of three volunteers. Aliquots of urine (5 ml) (Scheme I) were acidified with 10% HCl to pH 4–5 and extracted three times with equal volumes of chloroform to give chloroform extracts, C_1, which contained β-methyldigoxin and the less polar metabolites. The aqueous eluate, A_1 (pH 5.0), was incubated for at least 12 hr with 1.0 ml (5000 Fishmann units) of β-glucuronidase/ml of eluate. Extraction of A_1 with chloroform generated the chloroform eluate, C_2, which was chromatographed, and the generated aqueous eluate, A_2 (pH 5.0), was incubated with 0.1 ml of aryl sulfatase (5000 Whitehead units) for at least 12 hr.

After a third chloroform extraction of A_2, the newly generated aqueous eluate, A_3 (pH 5.0), was incubated with 1.0 ml of β-glucuronidase for at least 12 hr to assure complete enzymatic hydrolysis. The generated chloroform eluate, C_3, was subjected to TLC. After a final chloroform extraction of A_3, the generated aqueous eluate, A_4, was also chromatographed. The chloroform eluate, C_4, was not processed further, since it did not contain any radioactivity. Each chloroform extract was swirled over anhydrous sodium sulfate, decanted, concentrated to dryness under nitrogen, and assayed for percent recovery.

Recoveries of the compounds from urine spiked with specific radiolabeled compounds were, in the chloroform and residual water layer, respectively: β-methyldigoxin, 96.6 ± 1.5 + 2.1 ± 0.3 = 98.7%; digoxin, 100.9 ± 1.5 + 1.9 ± 0.3 = 102.8%; digoxigenin bisdigitoxoside, 104.2 ± 0.9 + 3.2 ± 0.8 = 107.4%; digoxigenin monodigitoxoside, 76.8 ± 2.7 + 18.9 ± 1.0 = 95.7%; and digoxigenin, 69.9 ± 1.8 + 31.6 ± 0.5 = 101.5%.

The β-methyldigoxin and metabolites in the extracts of plasma and urine were identified by admixing known standards with the extracts and separating in Systems B and C. The scrapings that corresponded to the R_f values were eluted with 95% methanol and definitely identified by three consecutive recrystallizations to constant specific activity (8) with standard deviations of less than ±4%. The metabolites in plasma and urine whose extraction efficiencies and recoveries were studied were checked by this procedure.

The extent of tritiated water formation was checked in urine by distillation (9). Equal aliquots of five total volumes of urine collected between 0 and 10 hr after 0.3 mg po was administered to one volunteer were combined and distilled. Distillate aliquots were assayed for tritiated water and compared with aliquots of water serving as controls. Triplicates (0.1 ml) of each were added to 10 ml of scintillation fluid and counted. Only 0.035% of the total radioactivity excreted was tritiated water. This amount was considered as a measure of negligible tritium exchange of labeled β-methyldigoxin with body water.

Protein Binding of β-Methyldigoxin—Plasma was equilibrated with chromatographically pure β-methyldigoxin (TLC System B) for 0.5 hr

[10] Abbott Laboratories, North Chicago, Ill.
[11] Baxter Laboratories, Division of Travenol Laboratories, Morton Grove, Ill.
[12] Intracath, Deseret Pharmaceutical Co., Sandy, Utah.
[13] Tomac, American Hospital Supply, Evanston, Ill.
[14] Vacutainer, Becton-Dickinson, Rutherford, N.J.
[15] Mark II, Searle Analytic Inc., Des Plaines, Ill.
[16] Woelm, Waters Associates, Framingham, Mass.
[17] Snyder-Kimble, Analabs Inc., North Haven, Conn.
[18] Tri-Carb oxidizer, Packard Instruments Co., Downers Grove, Ill.

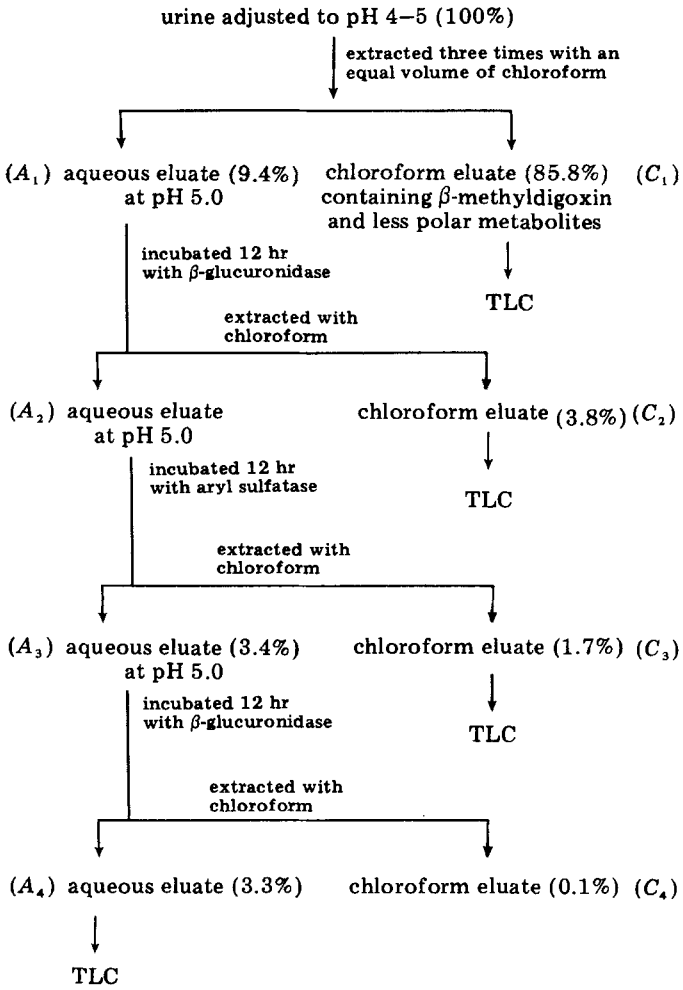

Scheme I—Isolation scheme for separation of metabolites of ^{3}H-β-methyldigoxin in urine. Typical percentages of total radioactivity in each fraction are given in parentheses.

and filtered at 1200 rpm for 18–20 min in a centrifuge[19] through two to four high flux cone membranes[20]. Half-filtration was preferred, since complete filtration of plasma might trap and inhibit the free passage of other soluble plasma components (10–12). Total drug concentration (bound and unbound) in the plasma prior to filtration and the free drug concentration in the plasma water of the filtrate were determined by liquid scintillation spectrophotometry.

The protein binding of β-methyldigoxin was investigated at five pharmacokinetically observed concentrations between 0.49 and 76.0 ng/ml at 25–29°, pH 7.32–7.34, in the fresh human plasma of two healthy fasted volunteers with no prior drug intake. The total protein content and the protein fractions of the two plasmas were determined (13).

The concentration-dependent membrane binding of β-methyldigoxin was compensated for by presaturating the cones. Several prior half-filtrations of 3–4 min of plasma water spiked with drug of the same concentration as the plasma were half-filtered through the cone. Only those membranes that yielded greater than 85% recovery of plasma water concentration and less than 5% variability in two consecutive filtrations were used.

Red Blood Cell–Plasma Water Partition Coefficient of β-Methyldigoxin—Centrifugally separated red blood cells were washed twice with sterile isotonic sodium chloride solution, recentrifuged, and suspended in plasma water obtained by ultrafiltration. Chromatographically pure β-methyldigoxin (TLC System B) was added to prepare 45.2-, 5.53-, and 2.90-ng/ml concentrations in the presence and absence of unlabeled digoxin at the pharmacokinetically anticipated 31 and 42% of these concentrations. Aliquots were centrifuged, and their plasma water concentrations were assayed at 6, 10, and 16 min. The reproducibility of the hematocrits[21] after each sampling demonstrated thorough mixing of the red blood cell–plasma water suspensions.

The partition coefficient was also determined in whole blood with 8.3–47.8 ng/ml of radiolabeled β-methyldigoxin sampled from three volunteers shortly after intravenous administration when minimum metabolites were present. The plasma water concentrations were assayed after separation by centrifugation at 1500 rpm for 15 min. The concentrated red blood cells after two consecutive centrifugations at 2500 rpm for 20 min had hematocrits of 0.80–0.90 and were hemolyzed at −4°. The ghost cells were removed by centrifugation, and radioactivity was analyzed in the hemolysate.

RESULTS AND DISCUSSION[22]

Protein Binding of β-Methyldigoxin—The percent of drug bound to protein was calculated from:

$$f = \frac{100([A_p] - [A_p{}^u])}{[A_p]} = \frac{100[A_p{}^b]}{[A_p]} \qquad \text{(Eq. 1)}$$

where $[A_p]$, $[A_p{}^u]$, and $[A_p{}^b]$ are the concentrations of total, free, and bound drug in plasma, respectively. The value of $[A_p]$ was measured in plasma after the drug was added and before ultrafiltrations were performed.

The average f values for the parenthetical total plasma concentrations of drug, $[A_p]$, were 10.9% (76.0 ng/ml), 7.6% (30.4 ng/ml), 9.9% (6.00 ng/ml), 10.2% (2.40 ng/ml), and 11.4% (0.49 ng/ml), with an overall mean of 9.8 ± 1.1% for the concentration-independent protein binding of β-methyldigoxin. This amount is close to the 14% value of Dengler *et al.* (14) from equilibrium dialysis of radiolabeled drug in human plasma. Both do not agree with the reported 28.8% of Kramer *et al.* (15), obtained by dual closed-loop dialysis. By using their reported equation (15) to calculate protein binding, a value of 15% was obtained.

Red Cell Partitioning of β-Methyldigoxin—The red cell–plasma partition coefficient, D, of a drug has been defined as the ratio of the total drug concentration in the erythrocytes, $[A_{RBC}]$, to the free or unbound concentration of drug in plasma, $[A_p{}^u]$ (16):

$$D = [A_{RBC}]/[A_p{}^u] \qquad \text{(Eq. 2)}$$

The $[A_p{}^u]$ was calculated from $[A_p{}^u] = (1 - f)[A_p]$, with $f = 0.10$ for blood and $f = 0$ for red blood cell suspensions in plasma water.

The average D values obtained for the parenthetical concentrations in whole blood were: 0.86 ± 0.05 (45.0 ng/ml), 0.93 ± 0.04 (30.0 ng/ml), 0.91 ± 0.04 (20.0 ng/ml), and 0.87 ± 0.05 (10.0 ng/ml). Similar D values resulted with red blood cell–plasma water suspensions: 0.84 ± 0.04 (45.2 ng/ml) and 1.03 ± 0.06 (5.5 ng/ml). Therefore, D is invariant with changing concentrations of β-methyldigoxin. The drug equilibrated rapidly between red blood cells and plasma water, at least in the first sample that was taken 6 min after drug addition. The addition of digoxin to give molar ratios of 2.4 and 3.20 of β-methyldigoxin to digoxin had no effect on the rate or the extent of partitioning in red blood cells: 0.91 ± 0.02 (5.53 ng of β-methyldigoxin/ml–2.27 ng of digoxin/ml) and 1.11 ± 0.03 (5.53 ng of β-methyldigoxin/ml–1.73 ng of digoxin/ml).

Plasma Pharmacokinetics of ^{3}H-β-Methyldigoxin after Intravenous Administration—The concentrations of plasma β-methyldigoxin and digoxin were determined in three subjects at the two different dose levels for intravenous and oral administrations. They were calculated from the fraction of the total radioactivity of the TLC plate that could be assigned to the radioactivities of their respective spots. The fractions bound to plasma proteins were taken as 0.10 and 0.25 (17), respectively.

The concentrations of unbound β-methyldigoxin, $[A_p{}^u]$, in plasma were fitted against time by "feathering," the method of residuals (Figs. 1 and 2):

$$[A_p{}^u] = A_1'e^{-\alpha_1 t} + A_2'e^{-\alpha_2 t} + B'e^{-\beta t} + C'e^{-\gamma t} \qquad \text{(Eq. 3)}$$

The evaluated parameters for the various studies are given in Table I.

[19] Clay Adams Co., New York, N.Y.
[20] Amicon Corp., Lexington, Mass.

[21] Microhematocrit centrifuge model MB, International Equipment Co., Needham Heights, Mass.; tubes, Yankee, Clay Adams Division of Becton-Dickinson & Co., Parsippany, N.J.; microcapillary reader, International Equipment Co., Needham Heights, Mass.

[22] The plus and minus values for such mean values given in the text refer to the standard error, $\sigma/\sqrt{n}$, of such means, where σ is the standard deviation given in Table I and n is the number of values considered and was 6 unless otherwise specified.

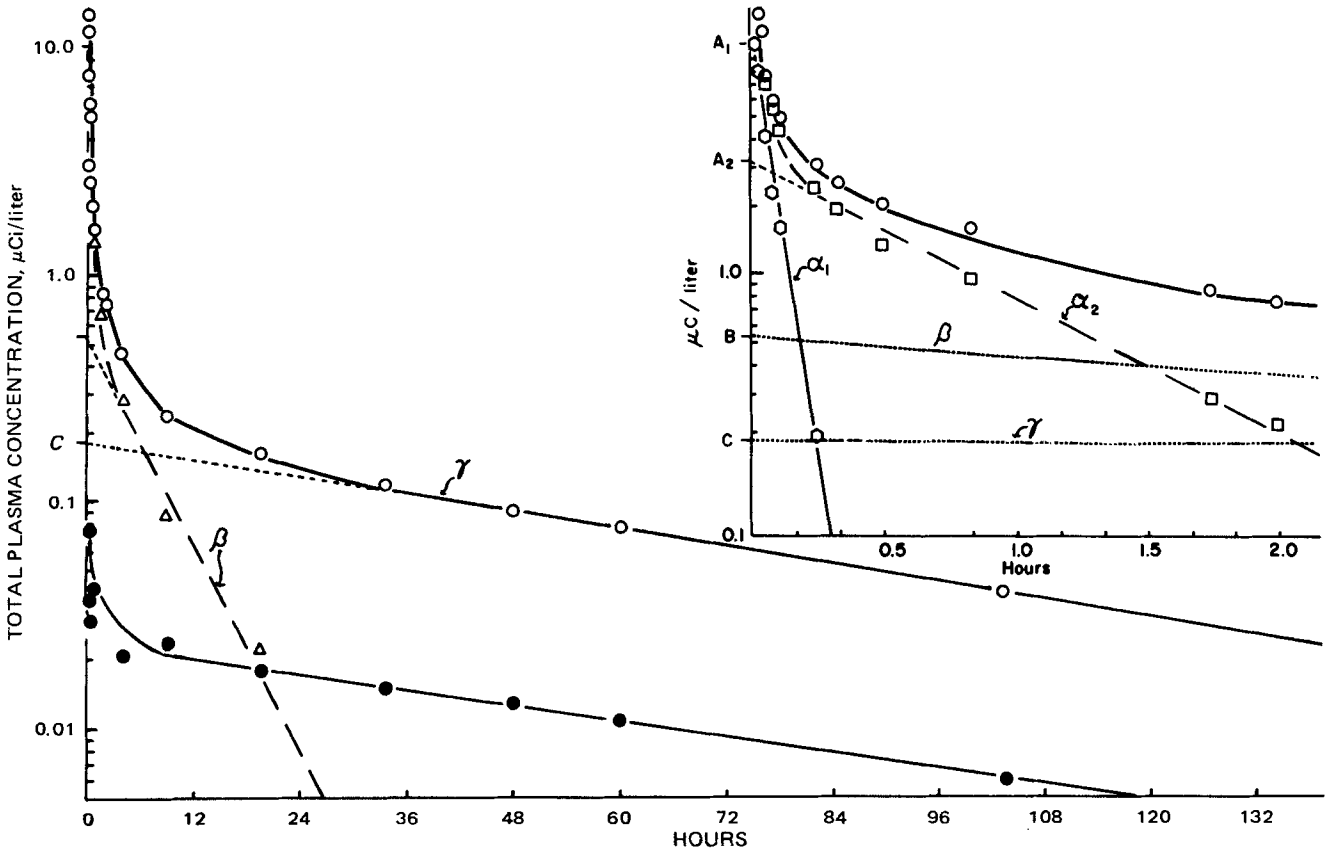

Figure 1—*Typical semilogarithmic plots of plasma β-methyldigoxin (○) and digoxin (●) concentrations, [A_p], against time for intravenous administration: 113.8 μCi = 264 μg of ^{3}H-β-methyldigoxin to Subject C. The inset is a plot of the initial β-methyldigoxin data on an expanded time axis. The data were treated by the method of residuals to obtain the parameters of* $[A_p] = A_1e^{-\alpha_1 t} + A_2e^{-\alpha_2 t} + Be^{-\beta t} + Ce^{-\gamma t}$, *where the data points* △ *represent* $[A_p] - Ce^{-\gamma t} = A_1e^{-\alpha_1 t} + A_2e^{-\alpha_2 t} + Be^{-\beta t}$, □ *represent* $[A_p] - Be^{-\beta t} - CE^{-\gamma t} = A_1e^{-\alpha_1 t} + A_2e^{-\alpha_2 t}$, *and* ○ *represent* $[A_p] - A_2e^{-\alpha_2 t} - Be^{-\beta t} - Ce^{-\gamma t} = A_1e^{-\alpha_1 t}$, *so that the straight lines that fit the terminal semilogarithmically plotted data have slopes* $\gamma/2.303$, $\beta/2.303$, $\alpha_2/2.303$, *and* $\alpha_1/2.303$ *and intercepts log C, log B, log* A_2, *and log* A_1, *respectively.*

Attempts to fit with a linear sum of only three exponentials consistently underestimated plasma data in the 3–30-hr time interval (Fig. 2).

The apparent volumes of distribution of the central compartment, $V_p{}^u$, referenced to the unbound drug in the plasma were estimated (16) from the individual $[A_p{}^u]_0$, 8.4 ± 1.9% of the dose per liter of plasma calculated at $t = 0$ from Eq. 3 and the intravenously administered dose, D = 100%:

$$V_p{}^u = D/[A_p{}^u]_0 \qquad \text{(Eq. 4)}$$

In 65% of the intravenous experiments, the plasma sample value taken at 90 sec after the start of the 1-min drug infusion was less than that taken at 120 sec. In some cases, the plasma maximum was not reached until 180 or 300 sec (Fig. 2). Thus, the injection and sampling sites could not be considered as being in the same kinetic compartment, and simultaneous penetration into and distribution from the central compartment must be postulated. The apparent volumes of distribution, $V_p{}^u$, as estimated by application of Eqs. 3 and 4, would be overestimated in these cases; large variability existed in the estimates of α_1 and A_1'.

The $V_p{}^u$ values were reasonably consistent within an individual for the two dose levels (Table I). If the α_1 phase, with its inherent variability in parameter estimations, were excluded, the apparent volume of distribution, $(V_p{}^u)'$, estimated on the premise that α_1 is infinite and A_1' is zero in Eq. 3 to produce an $[A_p{}^u]_0'$ value for Eq. 4, represented the volume of a central compartment larger than $V_p{}^u$. These volumes, $(V_p{}^u)'$ = 38.5 ± 3.7 liters, were remarkably consistent among individuals for all doses (Table I).

Plasma Pharmacokinetics of Digoxin after ^{3}H-β-Methyldigoxin Administration—Digoxin was the only metabolite of β-methyldigoxin found in significant concentrations in plasma, with a peak of 0.15 ± 0.03% of the dose per liter of plasma at 32.3 ± 7.0 min after intravenous administration of ^{3}H-β-methyldigoxin (Figs. 1–3). The plasma digoxin levels decreased subsequently by processes that could be described by the sum of two exponentials: a β-phase, $\beta = 0.68 \pm 0.21$ hr^{-1}, and a slower terminal γ-phase, $\gamma = 0.012 \pm 0.001$ hr^{-1}, that was reasonably linear in log plasma concentration–time and log digoxin to be excreted in urine–time plots (Figs. 1–3). Obviously, these values do not fully characterize the pure pharmacokinetic parameters since digoxin is being simultaneously formed from β-methyldigoxin.

When the concentration of total radioactivity in the plasma was plotted against time, a small anomalous increase in the plasma level with a subsequent decrease was consistently observed between 18 and 24 hr after both oral and intravenous administrations. This result could indicate enterohepatic circulation consistent with the observations of Doherty *et al.* (18) for digoxin. The time at which this increase occurred was consistent with such absorption being effected in the lower small intestine but was not of sufficient magnitude to perturb greatly the pharmacokinetic analyses.

Excretion Pharmacokinetics—The total radioactivity excreted in a time interval was the product of the concentration, microcuries per liter or gram, and the volume of urine or weight of feces collected. The amounts of ^{3}H-β-methyldigoxin and its individual metabolites excreted in the urine were calculated from the respective fractions of total radioactivity assignable to each on TLC analysis for the same three subjects for which β-methyldigoxin and digoxin had been analyzed in plasma. These amounts of materials in urine, U_t, were plotted cumulatively as the percent of dose against time (Fig. 4) to estimate the total recovery, U_∞, and were reasonably superimposable for all doses.

The semilogarithmic plots of the amounts of drug or metabolite not yet excreted in the urine, ln $(U_\infty - U_t)$, and the rate of excretion, ln $\Delta U/\Delta t$, against time (Figs. 3 and 5) exhibited the apparent terminal phases observed previously in the plasma (Figs. 1 and 2).

The percentages of the ^{3}H-β-methyldigoxin dose renally excreted as β-methyldigoxin, digoxin, and water-soluble metabolites are given in Table I. The percentages of the total administered radioactivity renally and totally (renal plus fecal) excreted also are given.

There were no apparent dose-dependent pharmacokinetics. When the plasma concentrations and cumulative urine content of β-methyldigoxin and digoxin were plotted against time in terms of the percent of the

Table I—Parameters for Intravenously Administered ^{3}H-β-Methyldigoxin Pharmacokinetics by Graphical Methods

Parameter	Subject A (66.3 kg, 169 cm, 1.76 m² Surface Area)		Subject B (71.3 kg, 179 cm, 1.89 m² Surface Area)		Subject C (67.4 kg, 166 cm, 1.75 m² Surface Area)		Average ± *SD*
D, dose, μg	294	589	273	633	264	631	
α_1, hr^{-1} [a]	13.9	9.2	16.7	8.3	15.1	33.3	16.1 ± 9.1
α_2, hr^{-1} [a]	2.8	1.7	2.4	1.7	1.5	2.7	2.1 ± 0.6
$10^2\beta$, hr^{-1} [a], intravenous, plasma (urine)	17 (23)	17 (28)	16 (23)	31 (28)	18 (28)	11 (35)	18 ± 7 (28 ± 4)
$10^3\gamma$, hr^{-1}, intravenous, plasma (urine)	16 (22)	16 (22)	18 (19)	20 (22)	15 (20)	19 (20)	17.3 ± 2.0 (20.8 ± 1.3)
A_1, % of dose/liter of plasma [a]	1.85	1.42	6.12	4.62	7.90	12.14	5.68 ± 4.02
A_2 [a]	1.78	2.02	1.76	1.35	2.53	3.44	2.15 ± 0.74
B [a]	0.57	0.50	0.33	0.53	0.43	0.45	0.47 ± 0.09
C [a]	0.12	0.12	0.09	0.12	0.15	0.14	0.12 ± 0.02
$V_p{}^u$, liters [b]	23.1	24.6	12.0	15.1	9.1	6.2	15.0 ± 7.5
$(V_p{}^u)'$, liters [c]	40.5	37.7	45.9	50.0	32.2	24.7	38.5 ± 9.2
10^2 area/*D*, hr/liter [d]	14.6	18.5	8.9	10.3	16.8	16.4	14.3 ± 3.8
Clearances, ml/min							
$(Cl_p{}^u)_{tot}$ [e]	114	90	187	162	99	102	126 ± 39
$(Cl_p{}^u)_r$ [f]	53	50	82	79	52	40	59 ± 17
$(Cl_p{}^u)_{mg}$ [g]	61	40	105	83	47	62	66 ± 24
$V^u_{pD_{ss}}$, liters [h]	427	338	621	486	396	321	432 ± 111
Percent of β-methyldigoxin dose, *D*, in urine from							
$10^2\ U^{BMD}_{\infty}/D$ [i]	43.8	44.4	55.1	46.4	51.0	40.4	46.9 ± 5.3
$10^2 U^{BMD}_{144\ hr}/D$ [j]	39.1	41.6	50.5	43.4	46.5	38.1	43.2 ± 4.7
$10^2\ U^{DIG}_{144\ hr}/D$ [k]	36.7	30.5	34.2	28.8	37.0	22.7	31.7 ± 5.5
$10^2\ U^{H_2O}_{144\cdot hr}/D$ [l]	5.9	5.9	3.2	5.0	3.4	8.3	5.3 ± 1.9
Recovery of administered radioactivity at 144 hr [m]							
Fecal, %	12.6	12.3	11.7	13.1	8.7	12.2	11.8 ± 1.6
Fecal + urinary, %	84.0	83.0	87.1	83.1	89.1	88.2	85.8 ± 2.7
144-hr recovery of β-methyldigoxin dose, %	94	90	100	90	96	81	91.8 ± 6.5

[a] Parameters of the sum of exponentials to express the unbound β-methyldigoxin concentration in percent of dose per liter of plasma: $10^2[A_p{}^u]/D = A_1e^{-\alpha_1 t} + A_2e^{-\alpha_2 t} + Be^{-\beta t} + Ce^{-\gamma t}$, where $[A_p{}^u]$ is the concentration in micrograms per liter at time *t*. Values were obtained by the method of residuals (35) from urine or plasma. [b] Estimated apparent volume of distribution of the central compartment referenced to unbound β-methyldigoxin in plasma from $D/[A_p{}^u]_0 = 10^2/(A_1 + A_2 + B + C)$ for $t = 0$ in equation of footnote *a*, where $[A_p{}^u]_0$ estimates the concentration of drug in plasma at zero time. [c] Estimated apparent volume of distribution of the equilibrated combined α-compartments from $D/[A_p{}^u]_0' = 10^2/(A_1 + B + C)$ from $t = 0$ in equation of footnote *a*, where $[A_p{}^u]_0'$ estimates the concentration of drug in plasma at zero time on assumption of instantaneous equilibration in the α_1- and α_2-compartments. [d] Determined by graphical integration of the area in micrograms-hour per liter under the unbound β-methyldigoxin plasma concentration–time curve; the area is divided by the administered dose in micrograms. [e] Total clearance from dose, *D*, divided by the area under the unbound plasma concentration–time plots. [f] Renal clearance from slope of plots of renal elimination rates of β-methyldigoxin, $\Delta U/\Delta t$, against plasma concentrations of unbound drug. [g] Metabolic clearance from the difference of total and renal clearances, $(Cl_p{}^u)_{tot} - (Cl_p{}^u)_r$. [h] Estimated equilibrated apparent volume of distribution during the psuedo-steady state or γ-phase, $(Cl_p{}^u)_{tot}/\gamma$. [i] Calculated from the micrograms of β-methyldigoxin renally excreted at infinite time, U^{BMD}_{∞}, which was estimated by adding to the amount excreted at 144 hr that amount that would have been excreted for five more half-lives if the slope of the natural logarithm of the excretory rate, ln $\Delta U/\Delta t$, against time was a constant, $-\gamma$. [j] Calculated from the micrograms of β-methyldigoxin renally excreted at 144 hr, $U^{BMD}_{144\ hr}$. [k] Calculated from the micrograms of β-methyldigoxin equivalent of the digoxin renally excreted at 144 hr, $U^{DIG}_{144\ hr}$. [l] Calculated from the micrograms of β-methyldigoxin equivalent of water-soluble metabolites renally excreted at 144 hr, $U^{H_2O}_{144\ hr}$. [m] Percent of total radioactivity administered excreted by 144 hr by specified route(s). [n] Percent of dose of β-methyldigoxin excreted by 144 hr renally as unchanged drug, digoxin, and water-soluble metabolites plus fecal excretion.

^{3}H-β-methyldigoxin dose per liter of plasma and the percent of dose, respectively, for the two dose levels of ^{3}H-β-methyldigoxin, the curves were superimposable (Fig. 4).

It can be estimated (Table I) that 92 ± 2.7% of the intravenous ^{3}H-β-methyldigoxin dose was eliminated by all processes at 144 hr. Of this percent, renal excretion accounted for fractions that were 0.470 unchanged, 0.345 digoxin, and 0.058 water-soluble metabolites. The fraction in the feces was 0.127. As will be justified later, the biliary excretion of unchanged β-methyldigoxin was negligible. The biliary excretion of digoxin has been estimated as 0.16 of its renal excretion (18). Thus, the fraction of digoxin formed from the dose of ^{3}H-β-methyldigoxin was estimated on the premise of negligible enterohepatic reabsorption as 0.16 (0.345) + 0.345 = 0.40. The fraction of the other metabolites of β-methyldigoxin would then be 0.127 [fecal] − 0.16 (0.345) [biliary digoxin] + 0.058 [urinary water solubles] = 0.130, of which 0.67 (0.058) = 0.039 would be renally excreted sulfates and glucuronide conjugates of β-methyldigoxin.

Clearances of β-Methyldigoxin—Total clearances of plasma-unbound β-methyldigoxin $(Cl_p{}^u)_{tot}$ of 126 ± 4 ml/min were estimated from the areas (Table I) under the plasma unbound concentration–time curves extrapolated to infinite time on the presumption of terminal first-order decay of plasma levels. Total clearance does not necessarily imply pharmacodynamic inactivation, since it includes the metabolic clearance of β-methyldigoxin where pharmacodynamically active digoxin is the major metabolite. There was no dose dependency. Thus:

$$(Cl_p{}^u)_{tot} = fD/\text{area} \qquad \text{(Eq. 5)}$$

where *D* = administered dose, and *f* = 1 for intravenously administered β-methyldigoxin.

The renal clearances of β-methyldigoxin, $(Cl_p{}^u)_r$, were determined from the slopes of plots (Fig. 6) of the rates of urinary excretion, $\Delta U/\Delta t$, against the plasma concentrations of unbound drug, $[A_p{}^u]$, taken at the midtime of the urine collection period. There was no apparent dose dependency (Table I). The average renal clearance was 59 ± 7 ml/min. The renal clearances appeared to be independent of urine flow between 0.9 and 5.5 ml/min and of urinary pH between 5.5 and 7.4. Literature values of renal clearances corrected for protein binding were 73 ml/min based

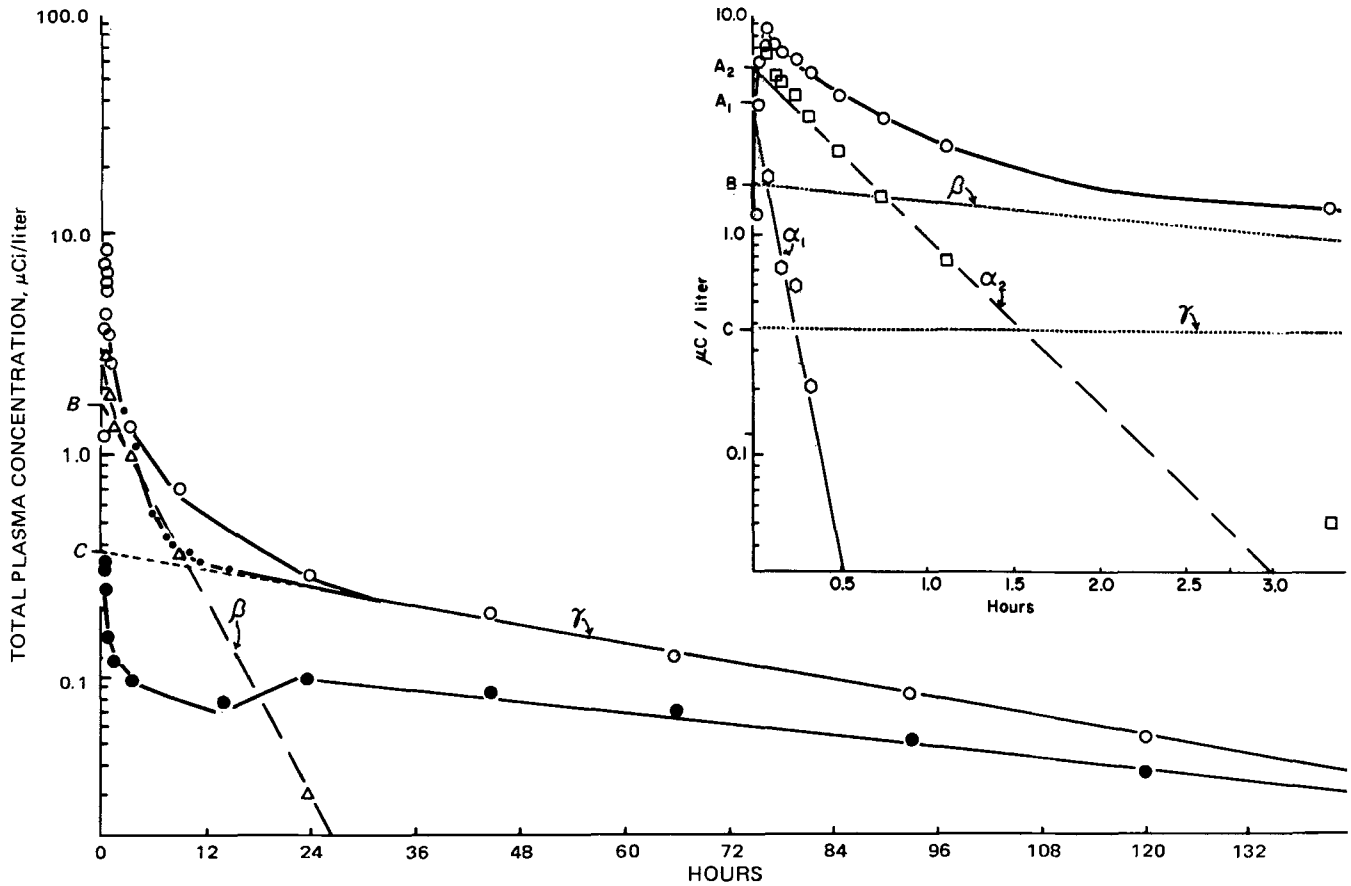

Figure 2—*Typical semilogarithmic plots of plasma β-methyldigoxin (○) and digoxin (●) concentrations, [A_p], against time for intravenous administration: 254.1 μCi = 589 μg of ^{3}H-β-methyldigoxin to Subject A. The various lines and symbols obtained by the method of residuals are as specified in Fig. 1. The dotted segment (·····) between 3 and 24 hr represents the best fit if [A_p] was the sum of only three exponentials. In this subject, there was a time delay in obtaining the maximum plasma concentration of β-methyldigoxin after intravenous administration.*

on total radioactivity (19) and 84 ml/min based on radioimmunoassay (20). These latter values overestimate the true renal clearance of β-methyldigoxin because they are modified by the simultaneous clearance of the major metabolite, digoxin, which is significantly higher than that of the parent drug.

The fraction of the total radioactivity administered intravenously that was fecally excreted in the first 48 hr was 0.083 ± 0.012 (n = 3) and agreed with the data of Abshagen *et al.* (21) for the fraction of total radioactivity excreted biliary. These investigators obtained the value of 0.105 ± 0.027 (n = 3) for the fraction of total radioactivity administered intravenously as tritiated β-methyldigoxin that appeared in the bile within 48 hr from patients with biliary tract disease in whom a biliary cannula was inserted. The average biliary clearance, $(Cl_p{}^u)_G$, of unbound β-methyldigoxin was estimated from the quotient of the average rates, dG/dt, of biliary excretion of β-methyldigoxin for the three patients given in the literature (21), dG/dt = 0.32, 0.032, and 0.0092% of the total dose of radioactivity excreted per hour during 0–4-, 4–24-, and 24–48-hr intervals, respectively, and the average plasma concentrations of unbound drug, $[A_p{}^u]$ = 2.21, 0.187, and 0.066% of the dose of unbound β-methyldigoxin per liter of plasma at the 2-, 14-, and 36-hr midpoints of these intervals in the three subjects of this present study who were given the drug intravenously. The respective individual quotients, $(Cl_p{}^u)_G = dG/dt/[A_p{}^u]$, were 0.145, 0.171, and 0.135 liter/hr and averaged 2.5 ± 0.2 ml/min (n = 3).

Since this biliary clearance would make a negligible contribution to the total clearance, the average metabolic clearance of unbound β-methyldigoxin, $(Cl_p{}^u)_m$ = 66 ± 10 (intravenous), was determined only from the differences between the total and renal clearances (Table I). If β-methyldigoxin metabolism occurs only in the liver and the average hepatic plasma flow is 800 ml/min (22), the metabolic efficiency is 66/800 = 0.083.

The endogenous creatinine clearances were normal (23) and were 129 ± 6 ml/min (n = 7), corrected for a body surface of 1.73 m^2 (n = 7) at urine flows of 1.2 ± 0.2 ml/min. The ratio of the renal clearance of β-methyldigoxin to creatinine was 0.42 ± 0.02 and implies an excess of tubular reabsorption for β-methyldigoxin.

Clearances of Digoxin after Intravenous ^{3}H-β-Methyldigoxin Administration—The average renal clearance, $(Cl_p{}^u)_r$ = 222 ± 32 ml/min (n = 5), of plasma-unbound digoxin was determined by the method described previously for β-methyldigoxin (Fig. 6) and can be compared with the values calculated for unbound digoxin of 163 (24), 133 (25), 120 (26), and 205 (27) in normal subjects. However, these estimates were based on total radioactivity or immunoassay rather than pure di-

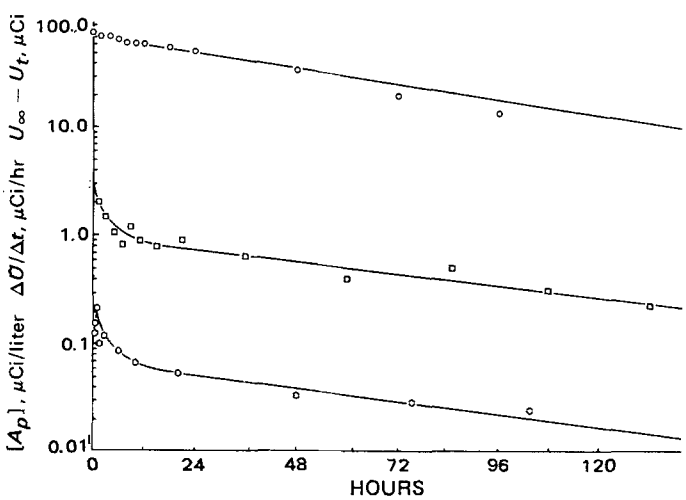

Figure 3—*Typical semilogarithmic plots of plasma concentrations of digoxin, [A_p] (○); amounts of digoxin yet to be excreted, $U_\infty - U_t$ (○); and rates of urinary excretion of digoxin, $\Delta U/\Delta t$ (□), against time for intravenous administration: 272.8 μCi = 633 μg of ^{3}H-β-methyldigoxin to Subject A.*

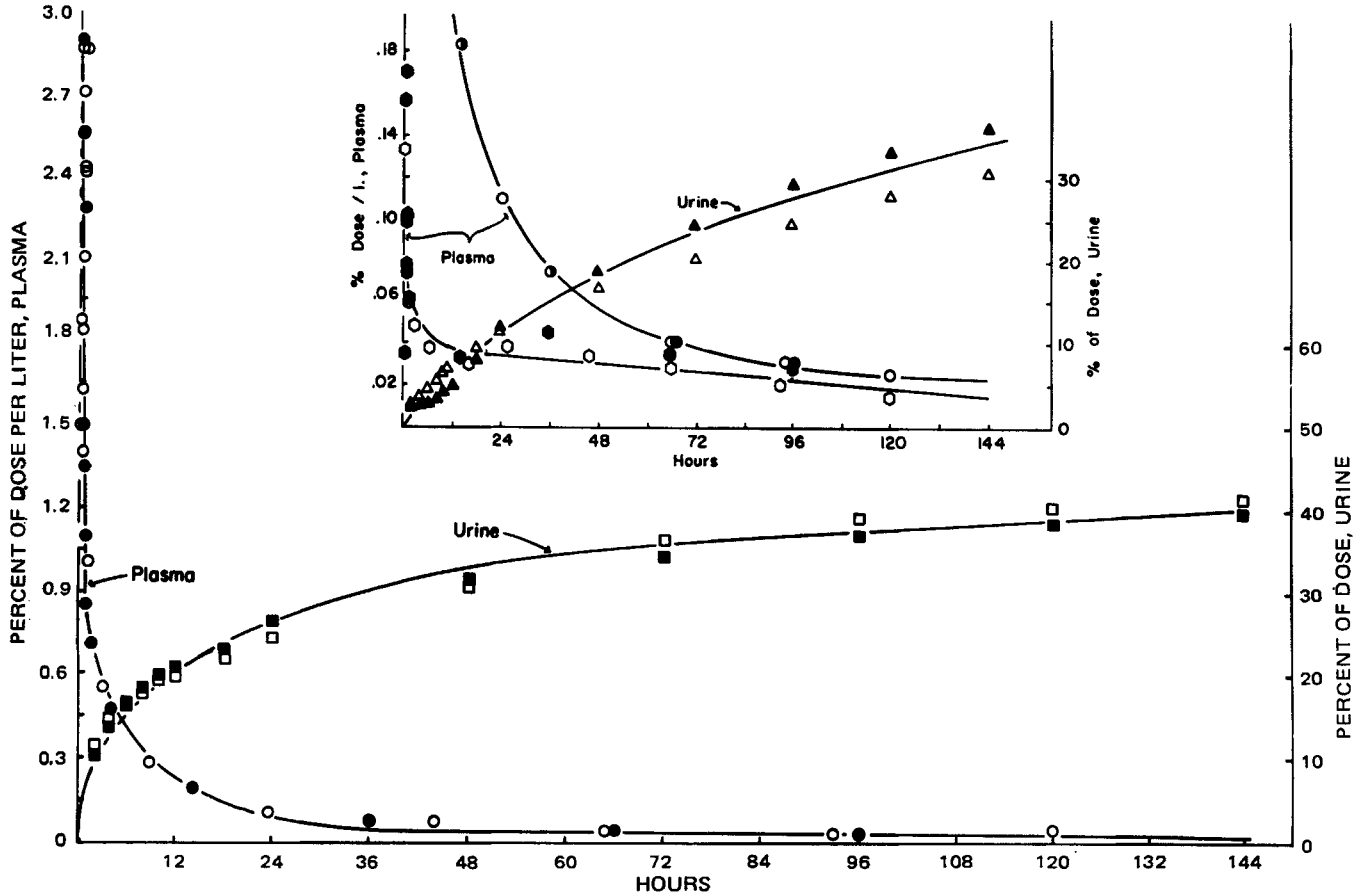

Figure 4—*Typical plasma concentrations and cumulative urine excretions in percent of β-methyldigoxin dose per liter of plasma and percent of dose, respectively, against time for intravenous administration: 126.7 μCi = 294 μg (open symbols) and 254.1 μCi = 590 μg (solid symbols) of ^{3}H-β-methyldigoxin to Subject A. Key: ○, ●, plasma levels of β-methyldigoxin; □, ■, urinary amounts of β-methyldigoxin; ○, ● (inset), plasma levels of digoxin; and △, ▲ (inset), urinary amounts of digoxin.*

goxin in plasma and underestimated the renal clearance when the plasma values were not corrected for metabolites, particularly if the metabolites had a smaller volume of distribution than digoxin. The urine flows in these studies were not specified. Evidence for urine flow dependency of the renal clearance of digoxin was reported (28). In these studies, the renal clearance of the metabolite appeared to be independent of urine flow between 0.9 and 5.5 ml/min and of urinary pH between 5.5 and 7.4.

An alternative rationale for the apparent discrepancy between the renal clearance values is a pharmacokinetic interaction between β-methyldigoxin and digoxin. β-Methyldigoxin could alter the renal clearance of digoxin by increasing its volume of distribution and/or its rate constant

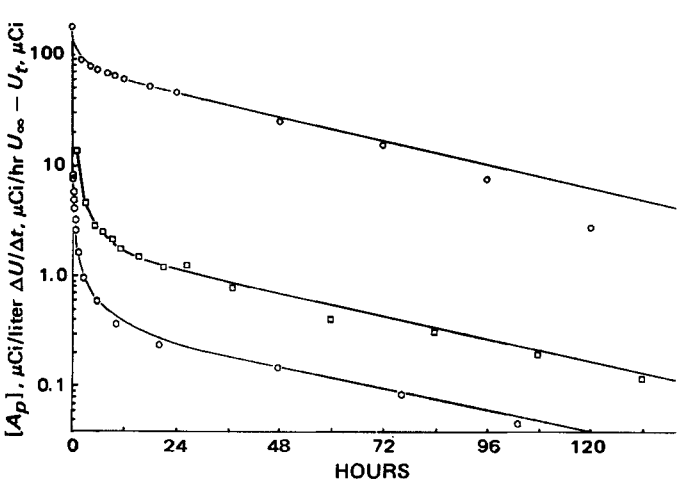

Figure 5—*Typical semilogarithmic plots of plasma concentrations of β-methyldigoxin, [A_p] (○); amounts of β-methyldigoxin yet to be excreted, $U_\infty - U_t$ (○); and rates of urinary excretion of unchanged drug, $\Delta U/\Delta t$ (□), against time after intravenous administration: 272.8 μCi = 633 μg of ^{3}H-β-methyldigoxin to Subject B.*

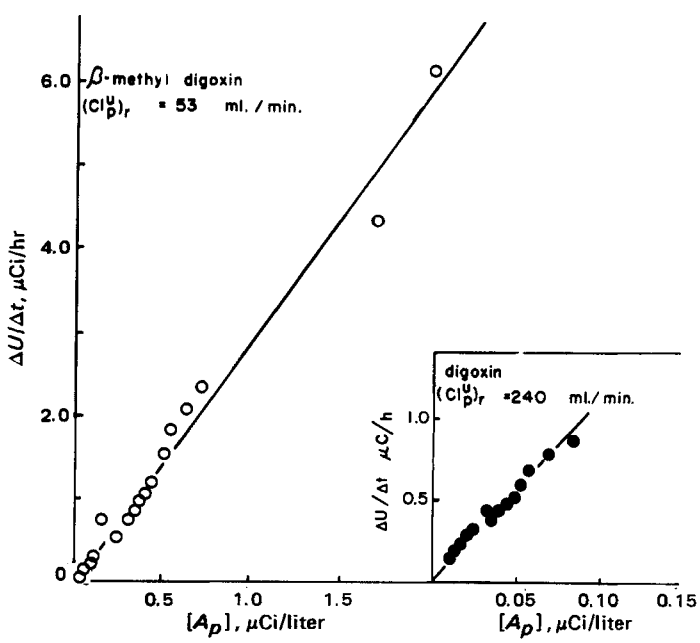

Figure 6—*Typical renal clearance plots for β-methyldigoxin and digoxin (inset) after ^{3}H-β-methyldigoxin intravenous administration of 126.7 μCi = 294 μg and 117.5 μCi = 272.6 μg to Subjects A and B, respectively. The renal clearances, (Cl$_p^u$)$_r$, of unbound drug were obtained by multiplying the slopes by the respective fractions of drug unbound to plasma protein.*

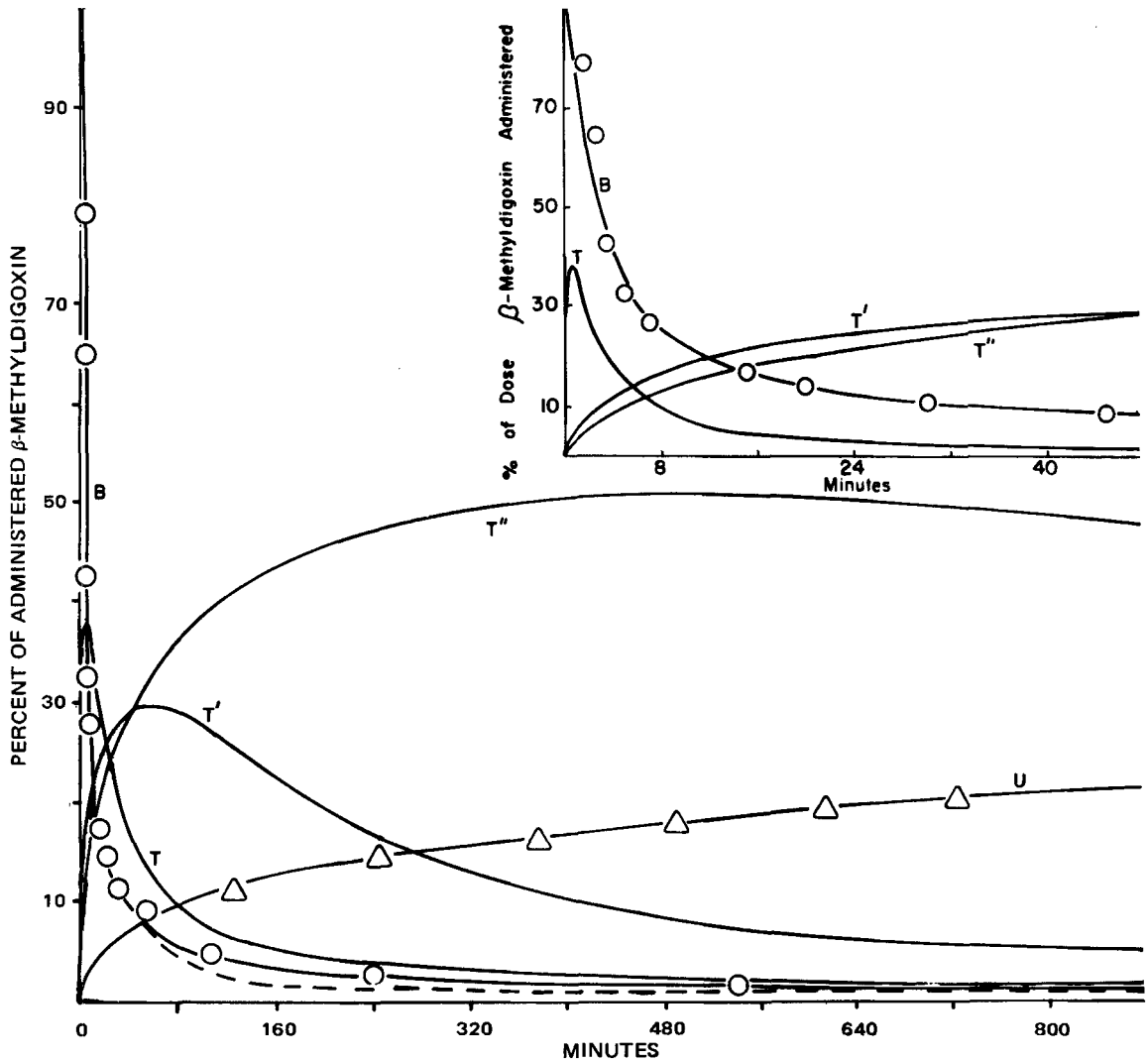

Figure 7—*Typical analog computer fitting of plasma water (unbound drug),* B (○), *and urine,* U (△), *data of β-methyldigoxin to the four-compartment body model for the 0.3-mg iv administration to Subject C over 13 hr with the parameters of Table II. The amounts of drug in various tissues* T, T′, *and* T″ *are generated in terms of percent of administered dose where the concentration of drug at zero time is taken as 100%. The inset is for an expanded time scale and shows the fit for the early plasma data. The dashed line represents the best attempt to fit the plasma data to a three-compartment body model.*

of elimination. The latter would imply saturable renal elimination of digoxin, but the renal clearances for digoxin were constant over wide ranges of plasma concentration ratios of β-methyldigoxin to digoxin (Fig. 6).

A more plausible rationale is to postulate renal metabolism of β-methyldigoxin to digoxin, which could account for the apparent discrepancy between the apparent renal clearances of digoxin observed when the drug *per se* or β-methyldigoxin was administered.

The biliary clearances of plasma-unbound digoxin were determined by the method described previously for β-methyldigoxin. The average rates, dG/dt, of biliary excretion of digoxin for the three patients given in the literature (21) were dG/dt = 0.188, 0.052, and 0.029% of the total dose of radioactivity excreted per hour during 0–4-, 4–24-, and 24–48-hr intervals, respectively. The average plasma concentrations of unbound digoxin were $[A_p{}^u]$ = 0.070, 0.026, and 0.016% of the dose of ^{3}H-β-methyldigoxin per liter of plasma at the 2-, 14-, and 36-hr midpoints of these intervals in the three subjects of this present study who were given ^{3}H-β-methyldigoxin intravenously. The respective individual quotients for the biliary clearance of digoxin, $(Cl_p{}^u)_G = dG/dt/[A_p{}^u]$, were 2.69, 2.00, and 1.83 liters/hr and averaged 36 ± 4 ml/min (n = 3). The ratio of these estimates of biliary and renal clearances of digoxin is 0.16, which agrees well with the ratio of drug biliary excreted to drug renally excreted of 0.16 obtained by Doherty *et al.* (18).

The total clearances of digoxin were also calculated from Eq. 5 from the areas up to the 144 hr studied, where the average area divided by the dose was 0.025 ± 0.005 hr/liter (n = 5) for the area under the plasma unbound concentration–time curves of digoxin for intravenously administered ^{3}H-β-methyldigoxin. However, the f in Eq. 5 is that fraction of the dose, D, of intravenously administered ^{3}H-β-methyldigoxin that is transformed to digoxin in 144 hr. It can be estimated from the ratio of the metabolic clearance, $(Cl_p{}^u)_m$, of β-methyldigoxin to its renal clearance, $(Cl_p{}^u)_r$, which is equal to the ratio of metabolites formed to renally excreted unchanged β-methyldigoxin. Thus, the average fraction transformed to metabolites is:

$$f = (U_{144}^{BMD}/D)(Cl_p{}^u)_m/(Cl_p{}^u)_r = 0.48 \pm 0.05 \qquad \text{(Eq. 6)}$$

where U_{144}^{BMD}/D is the fraction of ^{3}H-β-methyldigoxin dose renally excreted unchanged at 144 hr. To be completely rigorous, the fraction of β-methyldigoxin that is biliary excreted or changed to other metabolites than digoxin (such as conjugates of β-methyldigoxin) should be subtracted from f. It can be estimated from the experimentally determined composition of the water-soluble metabolite fraction of urine and the biliary excretion (29) that this amount comprises only 0.09 of the total ^{3}H-β-methyldigoxin dose; a better estimate of f is 0.39 ± 0.05, which agrees well with the previous estimates of 0.40 from the excretion pharmacokinetics.

The total clearance of digoxin was estimated as 290 ± 73 ml/min (n = 5). Subtraction of an estimated renal clearance of 222 ± 32 ml/min (n = 5) and a biliary clearance of 36 ml/min implies that the metabolic clearance of digoxin is 34 ± 16 ml/min. If digoxin metabolism occurs only in the liver, the metabolic efficiency is 34/800 = 0.043. Total and extrarenal unbound digoxin clearances of 277 and 72 ml/min, respectively,

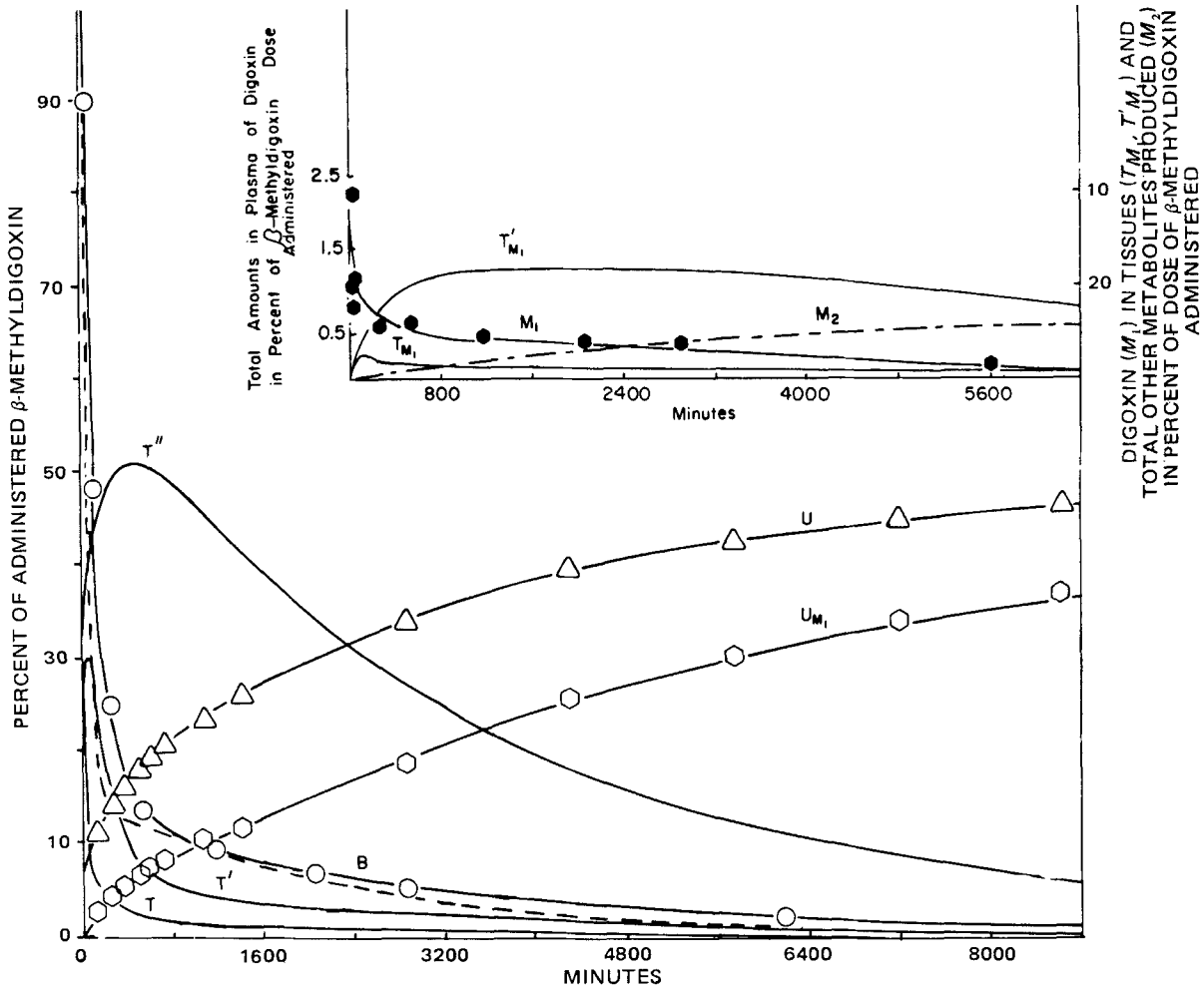

Figure 8—*Typical analog computer fitting of plasma water (unbound drug), B (○), and urine, U (△), data of β-methyldigoxin for the four-compartment body model for the 0.3-mg iv administration to Subject C over the complete time of the study. The digoxin (○) urine values, U_{M_1}, are fitted, and the amounts of drug in various tissues T, T′, and T″ are generated in terms of percent of administered dose where the concentration of drug at zero time is taken as 100%. The plasma β-methyldigoxin values (○) are shown multiplied by a factor of 10. The inset demonstrates the fitting to the total plasma data of formed digoxin, M_1 (●), in accordance with the necessary three-compartment body model (left scale); the amounts of digoxin in the various tissues are generated (T_{M_1} and T'_{M_1}) (right scale). The amounts of other metabolites, M_2, produced are also shown in the inset (right scale). The dashed line represents the best attempt to fit the plasma β-methyldigoxin data to a three-compartment body model.*

were reported for digoxin administration (27), in agreement with the values of this study.

The ratio of the renal clearance of digoxin to creatine was 1.52 ± 0.10 (n = 5) and implies an excess of tubular secretion in addition to glomerular filtration. Evidence for the tubular secretion of digoxin was reported previously (27, 30).

Pharmacokinetic Models for Intravenously Administered ^{3}H-β-Methyldigoxin and Digoxin and Their Fitting by Analog Computer—The model with the minimum number of compartments consistent with the experimental data was sought. The four-compartment body model postulated for plasma β-methyldigoxin levels with time by graphical analysis was challenged by both digital[23] and analog computation. A three-compartment body model (Scheme II) failed consistently to fit the terminal portion of the data (Figs. 1, 2, 4, 7, and 8) by both computer methods. Residual plots (31) showed definite trends about the mean with the three-compartment body model but random distribution with the four-compartment body model (Scheme III) to confirm the latter; typical best fits on this premise are given in Figs. 7 and 8.

Similar procedures were used in analog computer fitting of the digoxin metabolite, M_1, generated from β-methyldigoxin. A two-compartment body model (Scheme IV) failed consistently to fit the initial plasma data of the metabolite, M_1, and a three-compartment body model (Scheme V) was preferred (Fig. 7). This result agrees with the findings of Kramer *et al.* (32), who obtained better overall fits with a three- than with a two-compartment body model for digoxin on digoxin administration.

Typical computer programs and details were given previously (16). The initial conditions were placed on the central compartment, B, to obtain the initial drug concentration, $[A_p{}^u]_0$, from the best analog computer fit to Scheme III of the unbound plasma concentrations of β-methyldigoxin against time (Figs. 7 and 8). This voltage was considered as 100% of the drug in the central compartment that contained the plasma and associated fluids on the assumption of instantaneous mixing.

The cumulative urinary excreted amounts of the parent drug and metabolite, M_1, in microcuric-equivalent metabolite were plotted in terms of percent of dose administered. The simultaneous analog computer fitting of the plasma and urine data generated drug and metabolite amounts in the peripheral tissues and the total body, respectively, with time. Good and consistent fits were obtained with the four-compartment body model for the parent drug in plasma and urine and with the three-compartment body model for M_1 in urine. A typical fitting is shown in Figs. 7 and 8. The experimental plasma data of digoxin metabolite M_1 showed greater variability. Sets of microscopic rate constants that gave the best analog computer fittings to a four-compartment body model and the derived apparent volumes of distribution are given in Table II. The route of M_1 to bile M_1 in Scheme V was omitted in the analog computer fitting; therefore, $k_{M_1M_2}$ in the program and Table II was actually $k_{M_1M_2} + k_{M_1\,\text{bile}}$, which overestimates the former by 12% since the biliary clearance of digoxin is this percent of its total clearance.

Significance of Apparent Volumes of Distribution—The apparent

[23] Nonlinear regression program, Wang calculator 720, typewriter 702, Wang Laboratories, Tewksbury, MA 01876.

Table II—Parameters[a] for ^{3}H-β-Methyldigoxin and Digoxin Pharmacokinetics on Intravenous Administration Obtained by Analog Computer Fitting

Parameter	Subject A (66.3 kg, 169 cm, 1.79 m² Surface Area)		Subject B (71.3 kg, 179 cm, 1.89 m² Surface Area)		Subject C (67.4 kg, 166 cm, 1.75 m² Surface Area)		Averages ± *SD*
D, dose, μg	294	589	273	633	264	631	—
$10^4\ k_{BT}$, sec^{-1}	23.9	22.6	21.8	24.4	25.2	21.7	23.3 ± 1.4
$10^4\ k_{TB}$	15.4	26.1	12.2	11.9	16.0	11.3	15.5 ± 5.6
$10^4\ k_{BT'}$	7.85	6.05	5.27	5.91	7.17	6.91	6.53 ± 0.95
$10^4\ k_{T'B}$	1.78	3.15	0.766	1.18	1.64	1.67	1.70 ± 0.81
$10^4\ k_{BT''}$	1.49	2.10	3.14	3.43	5.45	3.84	3.24 ± 1.39
$10^4\ k_{T''B}$	0.109	0.146	0.185	0.125	0.156	0.115	0.139 ± 0.029
$10^4\ k_{BU}$	0.771	0.635	1.12	1.16	1.37	1.63	1.11 ± 0.37
$10^4\ k_{BM}$	1.08	0.776	0.906	1.30	1.38	2.38	1.30 ± 0.57
$10^4\ k_{MT}$	13.0	14.1	7.75	7.95	7.37	12.9	10.5 ± 3.1
$10^4\ k_{TM}$	13.0	7.81	3.40	4.23	2.62	2.41	5.58 ± 4.13
$10^4\ k_{MT'}$	11.4	11.0	5.58	6.12	5.15	11.10	8.38 ± 3.04
$10^4\ k_{T'M}$	0.130	0.109	0.198	0.135	0.151	0.0833	0.134 ± 0.0390
$10^4\ k_{M_1U}$	3.01	3.83	2.50	1.82	2.59	1.86	2.60 ± 0.76
$10^4\ (k_{M_1M_2} + k_{M_1\text{bile}})$[b]	0.615	1.54	0.260	0.703	0.474	1.15	0.79 ± 0.47
$(V_p{}^u)_{\text{BMD}}$, liters[c]	13.6	15.2	15.1	11.8	7.0	7.0	11.6 ± 3.8
$(V_{pT}{}^u)_{\text{BMD}}$[d]	21.0	13.2	27.0	24.1	12.0	13.5	16.9 ± 6.2
$(V^u_{pT'})_{\text{BMD}}$[d]	59.9	29.3	103.8	58.9	30.7	29.1	56.8 ± 26.2
$(V^u_{pT''})_{\text{BMD}}$[d]	186	219	256	322	245	234	244 ± 46
$(V_{pD}{}^u)_{\text{BMD}}$[e]	280	277	402	417	295	284	326 ± 65
$(V^u_{pD_{ps}})_{\text{BMD}}$[f]	514	458	757	676	566	573	570 ± 128
$(V_p)_{\text{DIG}}$[g]	9.38	10.3	22.1	74.6	32.8	14.9	27.3 ± 24.7
$(V_D)_{\text{DIG}}$[h]	838	1058	695	3596	1241	2079	1585 ± 1099

[a] Values for the microscopic rate constants in second^{-1} of distribution and elimination were obtained from the best simultaneous analog computer fits of the plasma and urine data in accordance with Schemes III and V. [b] The value is 112% of $k_{M_1M_2}$, since the biliary clearance of digoxin is 12% of its total clearances. [c] Values for the apparent volumes of distribution of the central compartment referenced to unbound β-methyldigoxin in plasma were calculated from the estimate of $[A_p{}^u]_0$ obtained from the initial conditions placed on B to give the best analog computer fit of the plasma data according to Scheme III, where $V_p{}^u = [A_p{}^u]_0/\text{dose}$. [d] The volumes of distribution for β-methyldigoxin at steady state for the different tissue compartments were calculated from $V_{pT}{}^u = V_p{}^u(k_{BT}/k_{TB})$, $V^u_{pT'} = V_p{}^u(k_{BT'}/k_{TB})$, and $V^u_{pT''} = V_p{}^u(k_{BT''}/k_{T''B})$. [e] The values of the overall steady-state volume of distribution for β-methyldigoxin were calculated (35) from $V_p{}^u[1 + (k_{BT}/k_{TB}) + (k_{BT'}/k_{T'B}) + (k_{BT''}/k_{T''B})]$. [f] The values of the overall pseudo-steady-state volume of distribution (36) for β-methyldigoxin were calculated from $(\text{Cl}_p{}^u)_{\text{tot}}/\gamma$, where $(\text{Cl}_p{}^u)_{\text{tot}} = (k_{BM} + k_{BU})V_p{}^u$ on the presumption that this value is $\gamma V^u_{pD_{ps}}$ in the terminal pseudo-steady state. The value of γ was estimated from the terminal slope of the semilog plot of the terminal analog computer fit of the plasma data. [g] Values for the apparent volume of distribution of the central compartment referenced to total (bound and unbound) digoxin in plasma were obtained from the best analog computer fit of the data for a three-compartment body model. [h] The values of the overall steady-state volumes of distribution of digoxin were calculated (35) from $(V_p)_{\text{DIG}}[1 + (k_{MT}/k_{TM}) + (k_{MT'}/k_{T'M})]$. The mean value is 1182 ± 542 if the anomalous 3596 of Subject B is excluded.

volume of distribution, $V_p{}^u$, of the central compartment referenced to unbound β-methyldigoxin in the plasma is 15 ± 3 liters by graphical methods (Table I) and 12 ± 2 liters by analog computer fitting (Table II). This amount is approximately the 15-liter extracellular body water of a young man (22).

The overall volumes of distribution at steady state (Table II) of β-methyldigoxin, $(V_{pD}{}^u)_{\text{BMD}} = 326 \pm 27$ liters, and digoxin, $(V_D)_{\text{DIG}} = 1182 \pm 245$ liters ($n = 5$) if one anomalous value of 3596 liters is excluded, are larger than the total body water volume of 40 liters (22) and imply significant binding to and/or partitioning into tissues. A similar mean $(V_D)_{\text{DIG}}$ for digoxin of 800 liters can be calculated from the data obtained in healthy volunteers after digoxin administration by Kramer *et al.* (32). The overall volume of distribution at pseudo-steady state of β-methyldigoxin is significantly larger than the overall volume of distribution at steady state for β-methyldigoxin ($V^u_{D_{ps}} = 1.75 \times V^u_{D_{ss}}$). This result is a normal consequence of the kinetic properties of a slowly equilibrating deep compartment, T'', of large capacity (33) and implies that, after administration of a single dose of β-methyldigoxin, a relatively larger fraction of the dose in the body is in the tissue compartment than after chronic dosing with steady-state conditions.

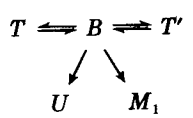

Scheme II

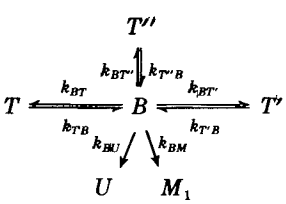

Scheme III

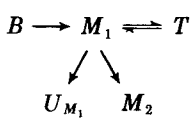

Scheme IV

Criteria for Determination of Terminal Half-Lives of β-Methyldigoxin Disposition—The magnitudes of the microscopic rate constants of equilibration for the shallow compartments T and T' (Scheme III), imply that these are relatively rapidly equilibrating with the central compartment and that the model ultimately degenerates to a two-compartment body model consisting of a new "central compartment," B +

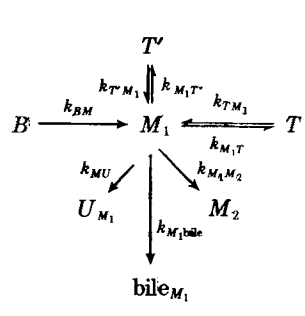

Scheme V

Table III—Data for Estimates of "True" Renal Clearances of 0.6-mg Doses, D, of β-Methyldigoxin on Premise of Renal Metabolism

Subject	$Cl_{app\ BMD}$[a]	$(U_{BMD})144\ hr/D$[b]	$(U_{DIG})144\ hr/D$[b]	AUC_{DIG}/D[c]
A	50	0.416	0.305	1.808×10^{-3}
B	79	0.434	0.288	0.923×10^{-3}
C	40	0.381	0.227	1.178×10^{-3}
Mean ± *SD*	56 ± 20	0.410 ± 0.027	0.273 ± 0.041	$1.30 \pm 0.46 \times 10^{-3}$

[a] Obtained from slopes of plots of the rates of urinary excretion of β-methyldigoxin against unbound plasma concentrations at the midtime of the urine collection interval. [b] Fractions of total dose excreted into urine at 144 hr. The individual doses are given in Table I. [c] Areas under the plasma concentrations of plasma unbound digoxin concentrations with time are expressed as micrograms per milliliter per minute.

$T + T'$, and the peripheral compartment, T''. It is practical and useful to ascertain the time of pseudo-steady-state equilibration between this new central compartment and the tissue, T'', so that the terminal slopes, $-\gamma$, of the natural logarithm of the plasma level against time can be considered as constant and truly representative of the overall half-life of drug elimination from the body, a constant of importance in the prediction of blood level on chronic administration.

Representative analog computation (Subject B, 0.6 mg iv of ^{3}H-β-methyldigoxin) using the appropriate pharmacokinetic parameters (Table II) showed that changes in the ratios, r, of the amounts in the peripheral compartment to the amounts in this new central compartment:

$$r = T''/(B + T + T') = T''/C \qquad \text{(Eq. 7)}$$

were relatively small, <7.5%, 1600 min after drug administration and that the semilogarithmic plot of plasma level, $[A_p{}^u]$, against time of slope $-\gamma$ was reasonably linear after that time.

Thus, Eq. 7 for the expression of plasma level of β-methyldigoxin as a sum of exponentials can be reduced to two exponentials:

$$[A_p{}^u] = A'e^{-\alpha' t} + C'e^{-\gamma t} \qquad \text{(Eq. 8)}$$

where after 1600 min the term $A'e^{-\alpha' t}$ should become negligible. It was stated previously (34) that the final pseudo-steady state would be achieved for all practical purposes when, as applied to this case of β-methyldigoxin, the fractional contribution, $f_{\alpha'}$, of the α' term to the total plasma concentration of Eq. 8 is:

$$f_{\alpha'} = A'e^{-\alpha' t}/(A'e^{-\alpha' t} + C'e^{-\gamma t}) < 0.01 \qquad \text{(Eq. 9)}$$

The amounts of drug in the $C = B + T + T'$, T'', and $E = U + M$ compartment were generated on the analog computer for the four-compartment body model of Scheme III using the parameters listed in Table II for Subject B at the 633-μg dose (0.6 mg). The generated data were then fit by analog computation to the degenerated two-compartment body model (Scheme VI).

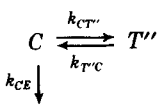

Scheme VI

The values of $k_{CT''} = 3.72 \times 10^{-5}\ sec^{-1}$, $k_{T''C} = 1.18 \times 10^{-5}\ sec^{-1}$, and $k_{C,E} = 2.85 \times 10^{-5}\ sec^{-1}$ fit the C, T'', and E compartments generated from the four-compartment body model of Scheme III excellently after 1600 min with the same terminal half-life of 42 hr. The ratios, r (Eq. 7), generated by the parameters of the two-compartment body model were definitely coincidental with those generated by the parameters of the four-compartment body model after 4000 min at 5.18; r was 5.17 compared to 5.10 at 2200 min and 5.10 compared to 4.90 at 1600 min for the two- and four-compartment body models, respectively. The $f_{\alpha'}$ was less than 0.01 (Eq. 9) subsequent to this 1600 min.

Valid estimates of the overall half-life of β-methyldigoxin must be based on satisfactory numbers of points adequately placed in time at least 1600 min or 27 hr after drug administration. This fact casts doubts on the validity of estimates of half-lives of all digoxin-type drugs based on plasma levels obtained within the 1st day after acute drug administration.

Effect of Renal Metabolism on Apparent Renal Clearances of a Drug and Its Metabolite—If a drug is metabolized by the liver *and* the kidney, the apparent renal clearances of both the drug and the metabolite are erroneous and the renal clearances of the metabolite derived from the administered drug and the metabolite administered *per se* differ significantly.

A model for both liver and kidney metabolism of β-methyldigoxin to digoxin from β-methyldigoxin content (B) in the central compartment is given in Scheme VII, where M_B is the amount of digoxin metabolite from hepatic metabolism, M_K is the amount of digoxin metabolite in the kidney that results from renal metabolism, and U_{DIG} and U'_{DIG} are the amounts of digoxin in the urine that result from the hepatic and renal processes, respectively. The area under a plasma level–time curve, AUC, can be related to the amount of drug provided to the body, D, and the total clearance, Cl_{tot}, of that drug provided that all elimination processes are first order (33). Thus, the AUC for digoxin on digoxin administration is:

$$AUC_{DIG} = D_{DIG}/(Cl_{tot})_{DIG} \qquad \text{(Eq. 10)}$$

where:

$$(Cl_{tot})_{DIG} = (Cl_{met})_{DIG} + (Cl_G)_{DIG} + (Cl_{ren})_{DIG} \qquad \text{(Eq. 11)}$$

and the amount of digoxin ultimately renally excreted, $(U_{DIG})_\infty$, from the amount in the body can be estimated from the fraction of the total clearance that is due to renal clearance:

$$(U_{DIG})_\infty = \frac{(Cl_{ren})_{DIG}}{(Cl_{tot})_{DIG}} D_{DIG} \qquad \text{(Eq. 12)}$$

Combination of Eqs. 10 and 12 gives:

$$(U_{DIG})_\infty = (Cl_{ren})_{DIG}\, AUC_{DIG} \qquad \text{(Eq. 13)}$$

This equation also represents the amount of digoxin at infinite time appearing in the urine as a consequence of the renal clearance of digoxin produced by the hepatic metabolism of β-methyldigoxin.

Thus, the difference between the total digoxin excreted into the urine, $(U_{DIG})_{tot}$, and the value from Eq. 13 represents that amount of digoxin, $(U'_{DIG})_\infty$, that could be a product of renally metabolized β-methyldigoxin:

$$(U'_{DIG})_\infty = (U_{DIG})_{tot} - (U_{DIG})_\infty = (U_{DIG})_{tot} - (Cl_{ren})_{DIG} AUC_{DIG} \qquad \text{(Eq. 14)}$$

The ratio of the true renal clearance of β-methyldigoxin, $Cl_{true\ BMD}$, to its apparent renal clearance, $Cl_{app\ BMD}$, is equal to the ratio of the sum of the ultimate amount of β-methyldigoxin excreted in the urine, $(U_{BMD})_\infty$, and the ultimate amount of digoxin excreted in the urine that was formed from renal metabolism of the β-methyldigoxin filtered and secreted into the kidney, $(U'_{DIG})_\infty$, to the ultimate amount of β-methyl-

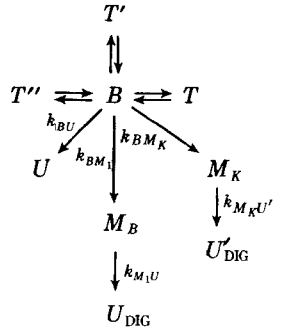

Scheme VII

digoxin excreted:

$$\frac{Cl_{true\ BMD}}{Cl_{app\ BMD}} = \frac{(U_{BMD})_\infty + (U_{DIG})_\infty}{(U_{BMD})_\infty} \quad \text{(Eq. 15)}$$

Thus, on consideration of Eqs. 14 and 15 with appropriate rearrangement:

$$Cl_{true\ BMD} = Cl_{app\ BMD}\left[\frac{(U_{BMD})_\infty + (U_{DIG})_{tot} - (Cl_{ren})_{DIG}AUC_{DIG}}{(U_{BMD})_\infty}\right] \quad \text{(Eq. 16)}$$

and if renal metabolism of β-methyldigoxin does exist, its true renal clearance can be calculated from the experimental values (Table III) of its apparent renal clearance, $Cl_{app\ BMD}$, appropriate values of the renal clearance of digoxin obtained on digoxin administration *per se*, $(Cl_{ren})_{DIG}$, and the area under the plasma digoxin level–time curve on intravenous β-methyldigoxin administration, AUC_{DIG}. The amounts of β-methyldigoxin and digoxin excreted into the urine at 144 hr on intravenous β-methyldigoxin administration were considered to be estimates of $(U_{BMD})_\infty$ and $(U_{DIG})_\infty$, respectively (Table III).

When the renal clearance of unbound digoxin, $(Cl_{ren})_{DIG}$, on digoxin administration was taken as 205 ml/min, close to the 222 value obtained in these studies and the average for all values on bolus and infusion digoxin administration given in the literature (27) after correction for protein binding, the calculated "true" renal clearance of β-methyldigoxin (Eq. 16) was equal to its apparent renal clearance, 56 ml/min. When $(Cl_{ren})_{DIG}$ was taken as 120 (26), 133 (25), and 163 (24) ml/min, the true renal clearances of β-methyldigoxin were 72, 70, and 64 ml/min, respectively, to suggest respective renal metabolisms of 16, 14, and 8 ml/min. Only if a true renal clearance for digoxin of 78 ml/min could be postulated would the true renal clearance of β-methyldigoxin be the same as this value.

REFERENCES

(1) R. G. Stoll, M. S. Christensen, E. Sakmar, and J. G. Wagner, *Res. Commun. Chem. Pathol. Pharmacol.*, **4**, 503 (1972).

(2) J. E. Doherty, W. M. Perkins, and G. K. Mitchell, *Arch. Intern. Med.*, **108**, 87 (1961).

(3) F. I. Marcus, G. Kapadia, and G. G. Kapadia, *J. Pharmacol. Exp. Ther.*, **145**, 203 (1964).

(4) H. J. Dengler, G. Bodem, and K. Wirth, *Arzneim.-Forsch.*, **23**, 64 (1973).

(5) A. von Wartburg, F. Kalberer, and J. Rutschmann, *Biochem. Pharmacol.*, **14**, 1883 (1965).

(6) F. Snyder, *Anal. Biochem.*, **9**, 183 (1964).

(7) L. A. Baillie, *Int. J. Appl. Radiat. Isotopes*, **8**, 1 (1960).

(8) L. R. Axelrod, C. Matthijssen, J. W. Goldzieher, and J. E. Pulliam, *Acta Endocrinol., Suppl.*, **49**, 99 (1969).

(9) H. Werbin, I. L. Chaikoff, and M. R. Imada, *Proc. Soc. Exp. Biol. Med.*, **102**, 8 (1959).

(10) A. Grollman, *J. Gen. Physiol.*, **9**, 813 (1926).

(11) A. Goldstein, *Pharmacol. Rev.*, **1**, 102 (1949).

(12) M. C. Meyer and D. E. Guttman, *J. Pharm. Sci.*, **57**, 895 (1968).

(13) J. Savory, M. G. Heintges, and R. G. Sobel, *Clin. Chem.*, **17**, 301 (1971).

(14) H. J. Dengler, G. Bodem, and K. Wirth, *Cardiovasc. Res., VI, World Congr. Cardiol.*, **1970**, 119.

(15) P. Kramer, E. Köthe, J. Saul, and F. Scheler, *Eur. J. Clin. Invest.*, **4**, 53 (1974).

(16) E. R. Garrett and H. J. Lambert, *J. Pharm. Sci.*, **62**, 550 (1973).

(17) E. E. Ohnhaus, P. Spring, and L. Dettli, *Eur. J. Clin. Pharmacol.*, **5**, 34 (1972).

(18) J. E. Doherty, W. J. Flanigan, M. L. Murphy, R. T. Bulloch, G. L. Dalrymple, O. W. Beard, and W. M. Perkins, *Circulation*, **42**, 867 (1970).

(19) P. Kramer and F. Scheller, *Dtsch. Med. Wochenschr.*, **97**, 1485 (1972).

(20) R. Haasis, D. Larbig, and K. O. Kleck, *Klin. Wochenschr.*, **53**, 529 (1975).

(21) H. Abshagen, M. Rennekamp, R. Küchler, and N. Rietbrock, *Eur. J. Clin. Pharmacol.*, **7**, 177 (1974).

(22) A. C. Guyton, "Textbook of Medical Physiology," 5th ed., Saunders, Philadelphia, Pa., 1968, pp. 325, 422.

(23) G. J. Tobias, R. F. McLaughlin, Jr., and J. Hopper, Jr., *N. Engl. Med. J.*, **266**, 317 (1962).

(24) G. A. Ewy, G. G. Kapadia, L. Yao, M. Lullin, and F. I. Marcus, *Circulation*, **39**, 449 (1969).

(25) P. M. Bloom and W. B. Nelp, *Am. J. Med. Sci.*, **44**, 133 (1966).

(26) J. E. Doherty and W. M. Perkins, *Am. Heart J.*, **63**, 528 (1962).

(27) J. R. Koup, D. J. Greenblatt, W. J. Jusko, T. W. Smith, and J. Koch-Weser, *J. Pharmacokinet. Biopharm.*, **3**, 181 (1975).

(28) H. Halkin, L. B. Sheiner, C. C. Peck, and K. L. Melmon, *Clin. Pharmacol. Ther.*, **17**, 385 (1975).

(29) N. Rietbrock and U. Abshagen, *Dtsch. Med. Wochschr.*, **98**, 117 (1973).

(30) E. Steiness, *Circulation*, **50**, 103 (1974).

(31) C. Daniel and F. S. Wood, "Fitting Equations to Data," Wiley-Interscience, New York, N.Y., 1971, p. 27.

(32) W. G. Kramer, R. P. Lewis, T. C. Cobb, W. F. Forester, Jr., J. A. Visconti, L. A. Wanke, H. G. Boxenbaum, and R. M. Reuning, *J. Pharmacokinet. Biopharm.*, **2**, 299 (1974).

(33) E. R. Garrett, in "Klinische Pharmakologie und Pharmakotherapie," Kuemmerle H. P., E. R. Garrett and K. M. Spitzy, Eds., Urban & Schwarzenberg, München, West Germany, 1971, p. 38.

(34) P. H. Hinderling and E. R. Garrett, *J. Pharmacokinet. Biopharm.*, **4**, 199 (1976).

(35) D. S. Riggs, in "The Mathematical Approach to Physiological Problems," Williams & Wilkins, Baltimore, Md., 1963, pp. 146, 193.

(36) R. Nagashima, G. Levy, and R. A. O'Reilly, *J. Pharm. Sci.*, **57**, 1888 (1968).

ACKNOWLEDGMENTS AND ADDRESSES

Received December 19, 1975, from *The Beehive, College of Pharmacy, University of Florida, Gainesville, FL 32610.*

Accepted for publication May 6, 1976.

Supported in part by Grant NIH-RR-82 from the National Institutes of Health, Bethesda, Md., and by an unrestricted grant from Searle Laboratories, Skokie, Ill.

The authors thank the nursing staff of the Clinical Research Center, Shands Hospital, University of Florida, for their assistance in performing the clinical studies.

* Present address: Biozentrum, Der Universitat Basel, 4056 Basel, Switzerland.

‡ Searle Laboratories, Skokie, Ill.

ˣ To whom inquiries should be directed.

Prediction of Tableting Problems such as Capping and Sticking: Theoretical Calculations

SHUN-ICHI NAITO *x, KEIJI MASUI *, and TAMOTSU SHIRAKI ‡

Abstract □ Tabletability factors were developed through the use of an automated tabletability tester, and the applicability of these factors to actual manufacturing procedures was tested by the large-scale manufacturing of tablets. Use of this approach does not require knowledge of the tablet's physical properties, *e.g.*, moisture content, porosity, particle size, fluidity, and angle of repose.

Keyphrases □ Tablet formulation—prediction factors developed, applied to manufacturing procedures □ Powdered materials—capacity for tablet formulation, prediction factors developed, applied to manufacturing procedures □ Dosage forms—tablets, formulation prediction factors developed, applied to manufacturing procedures

A tabletability tester, a device used to measure the passive pressure of a lower punch and the degree of binding between the punch face and the surface of a tablet (1), was previously proposed to predict the capacity of a powdered material to form a "good" or "bad" tablet. From the direct compression of common tablet ingredients (2) with a tabletability tester, four factors were found to be critical in the making of a good tablet: (*a*) the pressure of a loaded upper punch, (*b*) the passive pressure of a lower punch, (*c*) the force of the lower punch to extrude a tablet, and (*d*) the slipping force of the tablet surface.

The observed values of these four factors were difficult to reproduce due to the lack of consistency in manual determinations. Therefore, a fully automatic tabletability tester was developed to measure the four tabletability factors. The principles of the compression fixture and the sizes of the upper punches, lower punches, and dies are identical to those described previously (1, 2).

EXPERIMENTAL

Apparatus—The compression fixture used to determine the slipping force (*SF*), the passive pressure of the lower punch (*R*), the pressure of the loaded upper punch (*U*), and the force needed to extrude a tablet by the lower punch (*E*) were essentially the same as described previously (2), but the current fixture was automated by adding an electrical mechanism.

The values of *R*, *U*, and *E* were measured by using strain gauges[1] (type S-104, resistance 119.3Ω, gauge factor 1.92); *SF* was measured by using a U-gauge (type UT, capacity 1 kg, resistance 119.30Ω, gauge factor 1.92). The actual procedure of determining the slipping force was described previously (2), but the principle is as follows. When the upper plunger of the tablet machine strikes the head of the upper punch at a constant pressure and the striking is stopped, a split die is removed and the upper plunger is pulled out. The strain gauge is activated electrically and pushes the knob attached to the upper punch. The upper punch is supported by both a ball-bearing ring and a nonskid ring. Deformation of the strain gauge is recorded on a chart. Thus, the slipping force between the punch face and the tablet surface can be determined. The tablet held in the die does not rotate while the upper punch is rotated on the tablet surface. Presumably, the binding force between the tablet side and the die wall is larger than the slipping force because *E* is in kilograms and *SF* is in grams.

The cross section of the automatic tabletability tester is illustrated in Fig. 1. Since an important feature of the tester is the device used to measure the slipping force (2), a stereogram of this device is depicted in Fig. 2. Figure 2 clarifies the independent position of the upper punch (relative to the position) when the slipping force is measured.

Table I—Formulas of Materials Compressed into Test Tablets

Material	Composition
1	Mixture[a,b]
4	Calcium cellulose gluconate[c,d]
5	Magnesium oxide–aluminum oxide–silicon dioxide[e,f] (1:1:2)
6	Magnesium, oxide–aluminum oxide–silicon dioxide[g,f] (1:1:2)
10	Microcrystalline cellulose[h,i]
12	Dibasic calcium phosphate, anhydrous[j]
13	Dibasic calcium phosphate, anhydrous light[j]
14	Dibasic calcium phosphate, anhydrous, heavy[j]
15	Magnesium silicate, JP
19	Aluminum silicate, synthetic, JP
24	Aluminum hydroxide, anhydrous[j]
29	Aluminum hydroxide gel–magnesium hydroxide[j,l]
31	Dibasic calcium phosphate[j,m]
32	Magnesium oxide–aluminum oxide–silicon dioxide (1:1:2), neutral fine particles[f,n]
33	Magnesium oxide–aluminum oxide–silicon dioxide (1:1:2), fine particles[f,o]
34	Magnesium oxide–aluminum oxide–silicon dioxide (1:1:2), superfine particles[f,p]
39	Magnesium silicate[j]
40	Aluminum silicate, synthetic[j]
42	50% Lactose–19.5% potato starch–15% microcrystalline cellulose–15% synthetic aluminum silicate– 0.5% calcium stearate

[a] Per-filler. [b] Froint Sangyo Co. Ltd., Tokyo, Japan. [c] ECG 505. [d] Gotoku Yakuhin Kogyo Co. Ltd., Tokyo, Japan. [e] Neusilin S_1. [f] Fuji Kagaku Kogyo Co. Ltd., Toyama, Japan. [g] Neusilin SG_1. [h] Avicel. [i] Asahi Kasei Kogyo Co. Ltd., Tokyo, Japan. [j] Kyowa Kagaku Kogyo Co. Ltd., Tokyo, Japan. [l] Sanalmin A. [m] Licamit U-100. [n] Neusilin SG_2. [o] Neusilin SG_3. [p] Neusilin S_2.

Materials—The pharmaceutical materials were simple compounds or mixtures widely used as tablet additives in direct tableting (Table I). The materials and their numbers are identical to those used in previous experiments (2) so that the new data can be easily compared with data from the manual hand process.

A tablet hardness tester[2] was also used.

Calculations—When pressure is loaded on a powder housed in a cylinder (and the stress distribution due to the dead load of a powder itself is neglected), the vertical stress distribution in the powder layer may be shown by Eq. 1 as presented by Train and Lewis (3):

$$P/P_0 = \exp\left(-\frac{4\mu\beta h}{D}\right) \qquad \text{(Eq. 1)}$$

where P is the vertical load, h is the upper limit of the lower punch (the depth of the powder layer when compressed), D is the diameter of the cylinder, μ is the friction coefficient of the cylinder wall, β is the ratio of horizontal pressure to P, and P_0 is the loaded pressure at $h = 0$.

From Fig. 3*b*, the following equation can be derived using Eq. 1:

$$R/U = \exp\left(-\frac{4\mu'\beta'h'}{D}\right) \qquad \text{(Eq. 2)}$$

where:

$$\mu'\beta' = \frac{D(\ln U - \ln R)}{4h'} \qquad \text{(Eq. 3)}$$

and R is the passive pressure of the lower punch, U is the pressure of a loaded upper punch, and μ' and β' correspond to μ and β in Eq. 1 in the powder layer between the surfaces b and c.

[1] Shinko Tsushin Co.

[2] Monsanto.

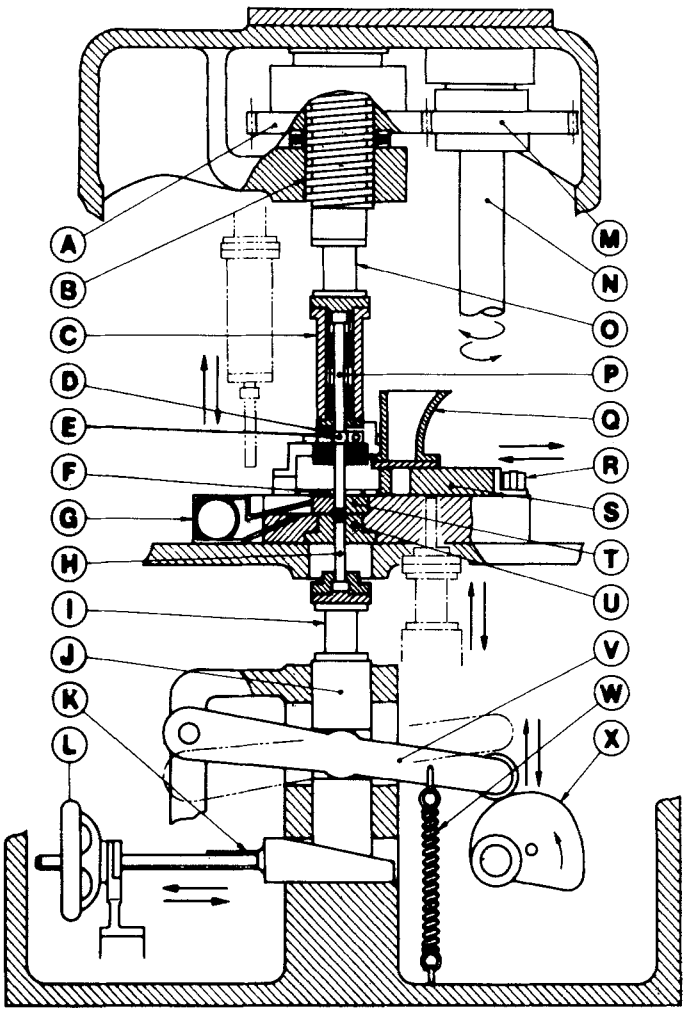

Figure 1—*Cross section of the main parts of the automatic tabletability tester. Key: A, pressure gear; B, piston; C, needle-bearing case; D, strain gauge for recording the slipping force; E, holder for the upper punch when the slipping force is measured; F, adjustment plate for the split die; G, exhaust pipe for the powder, H, lower punch; I, strain gauge for recording the force of the lower punch, J, adjustment liner for adjusting the filling depth of the powder; K, adjustment table for changing the filling depth of the powder; L, adjustment handle for controlling the quantity of the powder; M, vertical shaft gear; N, interlocker for upper punch; O, strain gauge for recording the force of the upper punch; P, upper punch; Q, hopper for powder; R, lever of feed-shoe; S, shuttle feed-shoe; T, split die; U, die base; V, push-up lever; W, spring for push-up lever; and X, push-up cam for the lower punch. The broken line illustrates a hypothetical scheme.*

Train and Lewis (3) stated that β does not show a constant value even in the same powder layer at different positions. However, if $\mu'\beta'$ is constant for the same powder in a range that is not yet known, the $\mu'\beta'$ obtained from Eq. 3 can be used for the calculation of U_1 and U_2 in Fig. 3c:

$$\ln U_1 = \ln U - \frac{4\mu'\beta' h_1}{D} \qquad \text{(Eq. 4)}$$

$$\ln U_2 = \ln R + \frac{4\mu'\beta' h_2}{D} \qquad \text{(Eq. 5)}$$

Adding Eqs. 4 and 5 yields:

$$\ln U_1 + \ln U_2 = \ln U + \ln R - \frac{4\mu'\beta'(h_1 - h_2)}{D} \qquad \text{(Eq. 6a)}$$

$$\ln U_1 U_2 = \ln UR - \frac{4\mu'\beta'(h_1 - h_2)}{D} \qquad \text{(Eq. 6b)}$$

when $h_1 = h_2$, $\ln U_1 U_2 = \ln UR$, and, logically, $U_1 = U_2$. Therefore, if $U_1 = U_2 = U_c$, the following simple relationships can be derived:

$$U_c^2 = UR \qquad \text{(Eq. 7a)}$$

$$U_c = \sqrt{UR} = K_V \qquad \text{(Eq. 7b)}$$

The pressure K_V obtained involves the pressure at the center layer of a formed tablet; K_V can be calculated without knowing the value of $\mu'\beta'$. Since K_V is concerned with vertical stress distribution, K_V should be called a "vertical factor."

In Fig. 3a, P is the pressure set mechanically at surface a. If the upper punch moves from surface a to surface b, P at surface a changes to U at surface b. Accordingly, $\mu\beta$ of a powder confined between surfaces a and b should differ from a powder confined between surfaces b and c. The former product is designated $\mu''\beta''$, and the latter is designated $\mu'\beta'$. Equations 8–12 are derived theoretically:

$$\ln U = \ln P - \frac{4h\mu''\beta''}{D} \qquad \text{(Eq. 8)}$$

$$\mu''\beta'' = \frac{D(\ln P - \ln U)}{4h} \qquad \text{(Eq. 9)}$$

$$\ln R = \ln U - \frac{4h'\mu'\beta'}{D} \qquad \text{(Eq. 10)}$$

$$\mu'\beta' = \frac{D(\ln U - \ln R)}{4h'} \qquad \text{(Eq. 11)}$$

$$\mu''\beta''/\mu'\beta' = \frac{h'(\ln P - \ln U)}{h(\ln U - \ln R)} = K_H \qquad \text{(Eq. 12)}$$

The value of K_H represents the horizontal stress distribution at the surface of a formed tablet. Since K_H is concerned with horizontal stress distribution, this value is termed a horizontal factor to contrast with K_V, the vertical factor.

It is of particular interest to ascertain whether the capacity of a material or a mixture to form a good or bad tablet (especially with respect to capping and/or sticking) could be manifested in either K_H or K_V. The ability of a powder to form a tablet is subject not only to vertical and horizontal pressure transmissions but also to the nature of the tablet surface and tablet hardness. Therefore, it is desirable to use the term "tabletability factors" for the prediction of tableting problems. This general term consists of K_H, K_V, SF (1), and tablet hardness. The significance of the surface factor is to predict the behavior of the surface

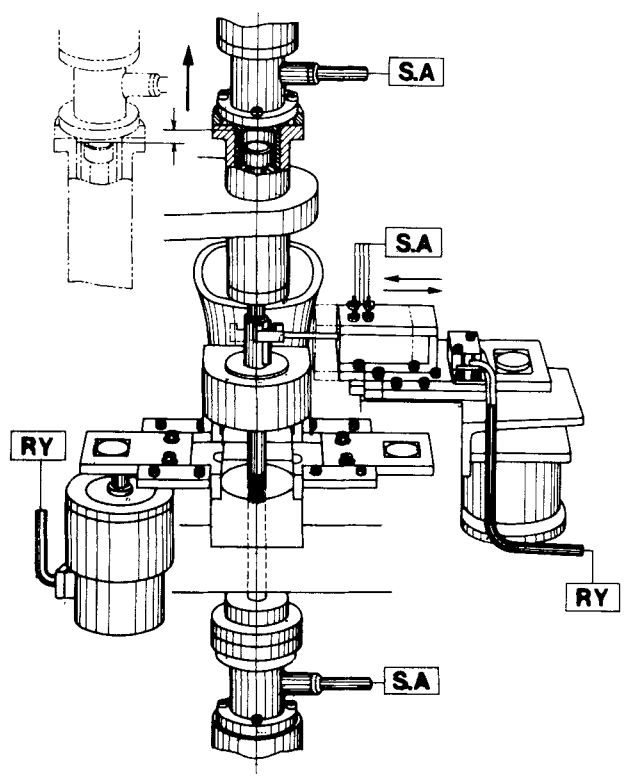

Figure 2—*Stereogram of the main parts for measuring slipping force. Key: S.A, strain amplifier; and RY, relay. The broken lines show a hypothetical scheme.*

Table II—Data on Tabletability Factors: Passive Pressure of Lower Punch, Lower Punch Force to Extrude a Tablet, Pressure of Upper Punch Loaded, and Slipping Force[a]

Material	R	E	U	SF		
				First	Second	Third
			Filling Depth 18 mm			
1	1400 ± 41	200 ± 0	1868 ± 46	122 ± 5	102 ± 4	102 ± 4
4	1100 ± 63	240 ± 25	1780 ± 49	OS	OS	OS
5	640 ± 25	120 ± 0	810 ± 49	OS	OS	OS
10	560 ± 21	100 ± 0	784 ± 14	126 ± 8	112 ± 9	104 ± 8
12	530 ± 74	120 ± 16	670 ± 107	OS	OS	OS
14	2100 ± 45	423 ± 10	OS	OS	OS	OS
19	890 ± 33	—	1096 ± 53	164 ± 4	141 ± 4	142 ± 5
29	606 ± 12	184 ± 4	788 ± 23	OS	OS	OS
39	1204 ± 4	—	1842 ± 16	OS	OS	OS
40	830 ± 20	292 ± 5	1450 ± 18	OS	OS	OS
42	2380 ± 20	OS	OS	OS	OS	OS
			Filling Depth 22 mm			
1	570 ± 12	494 ± 15	1438 ± 17			
5	300 ± 0	194 ± 3	496 ± 4			
6	216 ± 4	184 ± 4	640 ± 47			
10	128 ± 8	92 ± 5	77 ± 4			
12	384 ± 29	110 ± 12	718 ± 76			
13	364 ± 17	232 ± 19	816 ± 34			
14	920 ± 46	748 ± 64	2432 ± 94			
15	414 ± 18	384 ± 8	740 ± 8			
19	1044 ± 33	542 ± 27	2110 ± 89			
24	782 ± 12	495 ± 5	1600 ± 8			
29	188 ± 5	106 ± 4	304 ± 4			
31	390 ± 6	705 ± 5	1480 ± 20			
32	396 ± 4	302 ± 2	918 ± 9			
33	418 ± 5	356 ± 13	1056 ± 43			
34	364 ± 12	210 ± 10	860 ± 17			
39	618 ± 9	512 ± 16	1560 ± 21			
40	416 ± 4	384 ± 4	1202 ± 7			
42	630 ± 12	362 ± 5	1320 ± 9			
			Filling Depth 26 mm			
1	196 ± 4	208 ± 5	640 ± 14	83 ± 1	81 ± 3	81 ± 2
4	458 ± 18	398 ± 5	1280 ± 16	100 ± 4	87 ± 3	84 ± 4
5	96 ± 4	82 ± 7	220 ± 8	87 ± 2	80 ± 4	79 ± 3
6	200 ± 0	200 ± 0	500 ± 6	108 ± 4	104 ± 4	101 ± 3
10	34 ± 4	88 ± 5	162 ± 7	99 ± 4	92 ± 4	92 ± 4
12	100 ± 0	110 ± 10	248 ± 15	86 ± 4	80 ± 3	77 ± 1
13	80 ± 0	56 ± 6	192 ± 5	86 ± 7	82 ± 9	80 ± 10
14	162 ± 2	200 ± 0	752 ± 18	139 ± 3	125 ± 4	115 ± 7
15	300 ± 0	284 ± 16	672 ± 10	100 ± 0	89 ± 1	89 ± 1
19	208 ± 5	196 ± 4	564 ± 18	69 ± 3	83 ± 4	85 ± 2
24	100 ± 0	100 ± 0	296 ± 4	52 ± 4	44 ± 3	43 ± 3
29	56 ± 2	46 ± 4	186 ± 4	OS	OS	OS
31	250 ± 0	700 ± 0	1275 ± 25	—	—	—
32	200 ± 0	100 ± 0	584 ± 6	OS	OS	OS
33	202 ± 2	200 ± 0	856 ± 10	OS	OS	OS
34	200 ± 0	192 ± 5	444 ± 13	OS	OS	OS
39	300 ± 0	448 ± 17	880 ± 10	120 ± 6	144 ± 3	139 ± 6
40	380 ± 3	574 ± 6	1100 ± 0	OS	188 ± 5	186 ± 4
42	208 ± 4	196 ± 7	446 ± 19	106 ± 4	96 ± 2	90 ± 2

[a] All values are the mean of five experiments ±SE. Material numbers are the same as given in a previous paper (2). R = passive pressure of the lower punch in kilograms, E = force to extrude a tablet from the lower punch in kilograms, U = pressure of the loaded upper punch in kilograms, SF = slipping force of the tablet surface in grams [first, second, and third observations (1)], and OS = off scale.

between the upper punch and the surface of a tablet when a powder is compressed. As mentioned earlier (1, 2), if major tableting problems are attributed to sticking, the differences between the first, second, and third observations of the surface factors and their standard errors are relatively large.

RESULTS AND DISCUSSION

The purpose of the present work was to discover what properties of a material contribute to the formation of a good or bad tablet without knowing the physical properties of the material (*e.g.*, moisture content, porosity, particle size, fluidity, and angle of repose), and other independent factors (*e.g.*, tablet thickness and tablet size).

Presumably, these results demonstrate that the capping and/or sticking tendency of a material during tableting could be predicted primarily from data from tabletability factors. The constant values established for the tabletability tester were P = 2000 kg, h = 15.5 mm, and D = 10 mm. The passive pressure data of the loaded upper punch are shown in Tables II and III. Data for tabletability factors are shown in Table IV.

Although the force applied to the lower punch to extrude a tablet is not included in the calculation for tabletability factors *per se*, this force may serve to provide some general guidelines concerning the operation of a tableting machine. An extremely low force may result in a tendency toward capping, and an extremely high force may cause physical damage to the machine from the high binding tendency. Empirically, it was found that when more than 500 kg of pressure was required to extrude tablets (at a die depth of 22 mm), the likelihood of some damage to the machine was high.

Although these studies were only preliminary, the results suggest that tabletability factors may prove to be useful for the prediction of some tableting problems. The following interpretations of the data obtained from this study are proposed.

Table III—Tabletability and Other Factors[a]

Material	K_V	K_H	TT	TH
		Filling Depth 18 mm		
1	1617	0.10	5.44	>12
4	1399	0.30	9.94	—
5	720	1.33	4.64	4.9
10	663	1.14	5.24	>12
12	596	1.62	4.64	<2
29	691	1.23	4.64	4.2
40	1097	0.26	5.69	>12
		Filling Depth 22 mm		
1	905	0.29	10.04	>12
5	345	3.70	8.54	5.0
6	372	0.69	8.74	5.2
10	156	3.96	8.79	5.5
12	525	1.09	8.79	<2
13	545	0.68	8.34	<2
14	1496	−0.12	8.34	<2
15	553	1.05	8.34	5.0
19	1484	−0.06	9.69	12.0
24	1119	0.20	8.64	9.0
29	239	2.63	8.84	5.5
31	760	0.35	13.34	4.2
32	603	0.67	9.24	11.0
33	664	0.54	9.69	8.0
34	560	0.65	8.74	9.2
39	982	0.18	8.84	5.0
40	707	0.34	9.19	11.2
42	912	0.43	9.54	11.8

[a] All values are the mean of five experiments ±SE. Material numbers are the same as given in a previous paper (2). K_V = vertical factor; K_H = horizontal factor; TT = tablet thickness in millimeters; and TH = tablet hardness in kilograms, measured by a Monsanto tablet hardness tester.

Data in Tables II and III—Even though the poor fluidity of a material may have caused relatively large standard errors, comparisons of the present results with earlier data (2) show that the standard errors of observed values were diminished by using a fully automated tabletability tester instead of a manually operated one.

To compare the data, a standard material should be chosen and, ideally, its characteristics should take into account good compressibility, good formation, and the appearance of the tablet surface. Material 1 was selected as the standard since it came closest to meeting these criteria and included characteristics such as good lubricity and compressibility without apparent capping or sticking when incorporated as an excipient in a tablet. Material 1 consisted of a combination product whose formulation is a company trade secret. Hereafter, unless otherwise indicated, discussions of the data are based on a comparison between Material 1, the standard, and all other materials.

When the die whose filling depth (the lower limit of the lower punch) was 18 mm was used, only seven out of 19 materials gave complete data, *i.e.*, values for R as well as E and U. Materials for which only incomplete data could be obtained caused mechanical problems with the tabletability tester. For example, when Materials 19 and 39 were introduced, the force needed to extrude tablets by the lower punch registered zero. The reason for this reading was traced by observation to the fugacity of the powdered material outside of the die which flew about in all directions.

Another problem centered around the sticking tendencies of Materials 6, 13–15, 24, 31–34, and 42. An alarm bell was activated and the tester shut down automatically any time the pressure of the loaded upper punch exceeded 2500 kg. All of these materials caused a shut down at one time or another and made it impossible to obtain the mean of five consecutive and continuous tableting operations. The powders adhered heavily to the upper punch face, and the distance between the upper and lower punch faces was constantly lessened. Because of this phenomenon, the pressure of the loaded upper punch was increased during each successive operation, causing the alarm to ring and halting all operations and measurements. Since the reason for this occurrence was unknown, data for the dies with filling depths of 18 and 22 mm could not be used to predict tabletability.

However, the surface factor data obtained when using the die with a filling depth of 22 mm in a large-scale operation were better predictors of problems between the upper punch face and the tablet surface than the data obtained when using the other dies with filling depths of 18 and 26 mm. When slipping force is measured in the field to predict surface-sticking problems, a combination of high pressure and a die depth of 22 mm apparently is preferable to a combination of a more moderate pressure and a die depth of 26 mm. A powder that exhibited a very high surface factor, *i.e.*, an "off scale" powder or a powder that requires a force greater than the upper range of the instrument[3] (1), showed a strong tendency to stick to the face of the upper punch.

The fact that dies of different depths must be selected according to the directions of the forces or factors measured is an indication that when a powder is compressed, its various properties are changed and it no longer maintains the original physical relationships and proportions between those properties.

Table IV—Data obtained with a die depth of 26 mm showed no contradictions such as a negative value for K_H. To interpret the data, four assumptions were made:

1. An adequate value of the vertical factor, K_V, should exist for the formation of a good tablet from a powder. A material having a small K_V cannot be compressed into tablet form due to the poor transmittance of pressure.
2. An adequate value of the horizontal factor, K_H, should exist for the formation of a good tablet from a powder. Generally, the horizontal factor is considered to be the ratio of the compression stress of a powder occupying an upper space in a die (from surface a to b in Fig. 3*a*) to that of a powder occupying a lower space in a die (from surface b to c). Obviously, these two stress distributions must be different from each other. On the one hand, if a material has a relatively small K_H, the pressure of an upper punch can easily reach the surface of a tablet being compressed. However, if a material shows a large K_H, the pressure of an upper punch cannot reach the surface of a tablet effectively. An ideal K_H value is around 1.0.
3. The logical interrelationship between K_V and K_H is when: (*a*) K_V is large and K_H is small (capping would take place between the hard layer on the top and the tablet body below) and (*b*) K_V is small and K_H is large (capping would take place between the soft layer on the top surface of a tablet and its body) (Fig. 4).
4. The balance between the horizontal factor, K_H, and the vertical factor, K_V, can govern the tabletability of a powder. By definition, a good balance is reached when a powder could be compressed into a tablet with uniform compactness throughout its layers, but the numerical values of such a condition are still unknown. However, it should be possible to attain a numerical balance experimentally by repeated trials of many different kinds of materials and by a comparison of results from large-scale tablet manufacturing operations.

If these assumptions are applied, it is easier to understand the reasons for the capping problems encountered in industry. In addition, these assumptions indicate that a favorable balance of vertical and horizontal components in tableting is normally difficult to attain in large-scale production. It makes little difference if the values for K_H or K_V are large or small, as long as a suitable ratio or balance is maintained between the two components. This concept also takes into account the reality that, in a tableting operation, the production of acceptable thin tablets is easier than the production of acceptable thick ones.

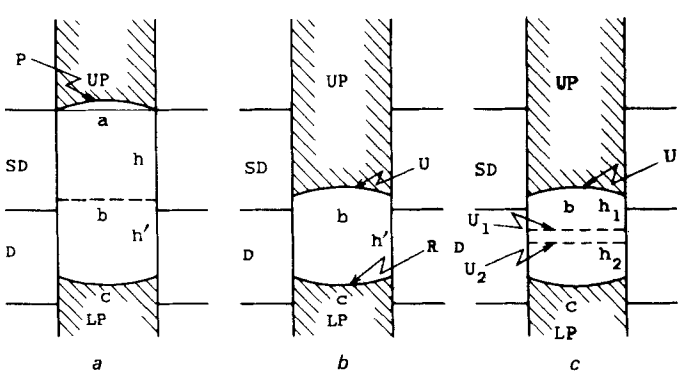

Figure 3—*Compression process. Key: UP, upper punch; LP, lower punch; SD, split die; D, die;* a, *top surface of the split die;* b, *lowest limit of the upper punch;* c, *lowest limit of the lower punch;* P, U, *and* R, *pressures at surfaces a, b, and c, respectively;* h *and* h′, *distances between surfaces a and b and surfaces b and c, respectively; and* h_1 *and* h_2, *distances between surfaces b and c, respectively.*

[3] Visigraph.

Table IV—Tabletability Factors for the Prediction of the Tabletability of a Powder[a]

Material	TT	TH	K_V^{26}	K_H^{26}	SF^{22} First	SF^{22} Second	SF^{22} Third
1	12.59	9.8	354	0.90	112 ± 4	118 ± 10	120 ± 11
4	14.84	<2	766	0.58	—	—	—
5	11.74	5.0	145	2.19	OS	OS	OS
6	11.84	12.0	316	1.27	OS	OS	OS
10	11.74	2.0	74	1.32	72 ± 2	72 ± 2	72 ± 2
12	11.34	0	157	1.78	OS	OS	OS
13	11.74	0	124	2.20	OS	OS	OS
14	11.64	<2	349	0.52	158 ± 8	147 ± 6	144 ± 7
15	11.84	4.5	449	1.13	OS	OS	OS
19	11.84	5.5	343	1.06	148 ± 6	144 ± 7	144 ± 7
24	11.74	3.0	172	1.45	OS	OS	OS
29	10.84	<2	102	1.41	OS	OS	OS
31	15.34	5.0	565	0.40	OS	OS	OS
32	11.74	7.5	342	0.95	OS	OS	OS
33	11.44	8.0	416	0.46	OS	OS	OS
34	11.34	9.0	298	1.46	OS	OS	OS
39	11.64	<2	514	0.62	128 ± 3	111 ± 5	107 ± 4
40	11.84	7.0	647	0.47	190 ± 3	178 ± 8	176 ± 9
42	11.74	3.2	305	1.62	68 ± 3	63 ± 3	62 ± 3

[a] All values are the mean of five experiments ±SE. TT = tablet thickness in millimeters (filling depth 26 mm), TH = tablet hardness in kilograms (filling depth 26 mm), K_V^{26} = vertical factor (filling depth 26 mm), K_H^{26} = horizontal factor (filling depth 26 mm), and SF^{22} = surface factor in grams (filling depth 22 mm).

In this discussion, the compressibility of a powder was based on the balance of the two factors during tableting. However, some materials rated high on the tabletability factor but could not be compressed into a tablet because of their poor binding characteristics. In these cases, results can be justified by measuring tablet hardness.

The substances used in the present experiment were primarily tablet additives. Therefore, few of the substances could be compressed to form good tablets in actual production practice[4]. The results of the experiment were categorized and analyzed as follows.

Material Compressed into Good Tablets by Using the Tabletability Tester, Not on a Large-Scale Manufacturing Basis (Table IV)—Material 1 was compressed to form a good tablet (tablet hardness = 8.2 kg). Materials 15 and 19 exhibited a K_V^{26} and K_H^{26} similar to those of Material 1, but the SF^{22} of Material 15 was "off scale" and could not be compressed into an acceptable tablet. Material 19 was compressed into a tablet (hardness ≅ 1.0 kg), but its SF^{22} was somewhat scattered.

Material 5 exhibited a small K_V^{26} and a large K_H^{26}, but it produced a good tablet. This result could be explained on the basis of Assumption 4; *i.e.*, it could have attained a suitable balance between K_V and K_H. Otherwise, Material 5, whose SF^{22} was off scale, showed a strong sticking tendency to the face of the upper punch and could not be compressed regularly into good tablets under regular production procedures.

The results with Material 24 were similar to those of Material 5. Material 24 could be made into good tablets by using the tabletability tester, for possibly the same reasons as with Material 5, but its SF^{22} was also off scale; it could not be compressed into good tablets under regular production conditions because of sticking and cracking. The reason for cracking may be due to the relatively smaller K_H^{26} value when compared to that of Material 5; the K_H of No. 24 was not strong enough to form a thicker, harder layer to prevent cracking.

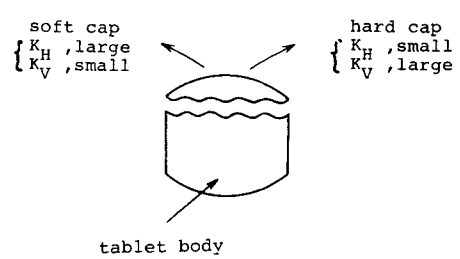

Figure 4—*Diagram of capping.*

[4] Tablet machine RT-S15-H, Kikusui Seisakusho Co., Kyoto, Japan. This machine had an 8-mm (5/16-in.) diameter standard-faced punch and die system, a tableting speed of 15 rpm, and an upper limit of the lower punch of 7.5 mm. When a powder was tabletable, about 30 kg of the powder was tableted continuously.

Material Compressed to Form Good Tablets on a Large-Scale Manufacturing Basis—Material 4 had a small K_H^{26} and a large K_V^{26} with a good balance between them. Although the SF^{22} of Material 4 was not measured, it was possible to make a good tablet, especially when relatively thin tablets were produced. The hardness of the tablets averaged about 7.8 kg (in actual tablet manufacturing).

Material 10 had a large K_H^{26} and a small K_V^{26}, but the balance between these factors allowed it to be compressed into a good tablet. The SF^{22} of Material 10 was somewhat scattered, and the lubricity of the tablet surface was poorer than others. The hardness of a tablet produced in actual tablet manufacturing was about 2.2 kg, but it was possible to make good tablets, especially when thin tablets were required.

Tableting problems arising from large-scale production procedures included the definite capping of tablets from Materials 6, 12–14, 29, 31, 33, 34, 39, 40, and 42. These materials exhibited K_H^{26} values that had both small and large variances from the ideal value of 1.0. Furthermore, there was strong adherence of Materials 5, 6, 12, 13, 15, 29, and 31–34 to the face of the upper punch after capping. All of these materials had an SF^{22} that was off scale. A creaking sound was also heard between the die and the lower punch when introducing Materials 14, 19, 24, 31, and 39. All of these materials required more than 500 kg of pressure to extrude the tablets.

The present investigation demonstrated the possibility of using tabletability factors to predict some tableting problems. It may be surmised that when a given powder sample exhibits a large K_V^{26}, it may be desirable to mix in a powder with a small K_V^{26} or K_H^{26}. Changes in K_V and K_H under these mixed powder conditions will be investigated at a later time.

In conclusion, it should be reiterated that the purposes of this study were to find a practical use for data obtained from a tabletability tester and to predict tableting problems. It was not intended to provide a detailed theoretical discussion of the data obtained. Further treatment of the theoretical considerations of the compression of powder-like materials can be found in Ref. 4. Although the present work was undertaken to obtain practical information from compression data, a major question still remains as to the final definition of the horizontal factor, since $\mu''\beta''$ in Eqs. 8 and 9 has no theoretical basis at all. The use of the horizontal factor seems to be helpful in predicting tableting problems when a powder is compressed into tablets in a large-scale operation instead of a tabletability tester. Therefore, further evaluation of this factor as a practical method for predicting tableting problems in a large-scale manufacturing procedure is still necessary.

REFERENCES

(1) S. Naito and K. Nakamichi, *Chem. Pharm. Bull.*, **17**, 2507 (1969).

(2) S. Naito, I. Shimizu, and S. Iwaki, *ibid.*, **19**, 1949 (1971).

(3) D. Train and C. J. Lewis, *Trans. Inst. Chem. Eng.*, **35**, 258 (1957).

(4) S. Bessho, S. Tomioka, and S. Ito, *Yakugaku Zasshi*, **99**, 686 (1972).

ACKNOWLEDGMENTS AND ADDRESSES

Received April 1, 1975, from the *Kyoto College of Pharmacy, Yamashina Misasagi, Higashiyama-ku, Kyoto 607, Japan, and the ‡Kikusui Seisakusho Co. Ltd., Nishinokyo Minamikamiaicho, Nakagyo-ku, Kyoto 604, Japan.

Accepted for publication April 29, 1976.

The authors are indebted to Mr. Yasuo Shimada, the President of Kikusui Seisakusho Co. Ltd., for encouragement and trial manufacturing of a fully automatic tabletability tester. They are also grateful to Masao Takada, Giichiro Kowada, Toyojiro Koyama, and Masami Yuge of the same company for cooperation.

ˣ To whom inquiries should be directed.

Indolizine Derivatives with Biological Activity I: *N'*-Substituted Hydrazides of Indolizine-2-carboxylic Acid

MARIO CARDELLINI ˣ, FRANCESCO CLAUDI, MARIO GRIFANTINI, UGO GULINI, and SANTE MARTELLI

Abstract □ The synthesis and antimonoamine oxidase activity of some *N'*-substituted hydrazides of indolizine-2-carboxylic acid are described. They all inhibit monoamine oxidase and are more active than iproniazid. The structure–activity relationships also are discussed.

Keyphrases □ Indolizine-2-carboxylic acid hydrazides—synthesized, screened for effect on monoamine oxidase activity □ Hydrazides, *N'*-substituted—of indolizine-2-carboxylic acid synthesized, screened for effect on monoamine oxidase activity □ Monoamine oxidase activity—effect of various *N'*-substituted hydrazides of indolizine-2-carboxylic acid □ Structure–activity relationships—*N'*-substituted hydrazides of indolizine-2-carboxylic acid screened for effect on monoamine oxidase activity

Numerous *N'*-substituted hydrazides of indolecarboxylic acids have been synthesized in recent years as potential psychotherapeutic agents, and their inhibiting activity on monoamine oxidase has been tested *in vitro* (1, 2). The fundamental characteristic of such derivatives, some of which have proved to be intensely active, is the association in a single compound of a functional group with known antimonoamine oxidase activity, such as the hydrazide group, and the indole system. The indole system is present in various natural and synthetic compounds distinguished by psychotropic properties. The present paper reports the synthesis and study of the antimonoamine oxidase activity of a series of *N'*-substituted hydrazides of indolizine-2-carboxylic acid, which are analogs of the indole derivatives.

There are few literature reports on analogs of biologically active indole derivatives in which indole is replaced by indolizine. 1-Indolizinylalanine (3) has been prepared as a potential tryptophan antimetabolite; 1-indolizineacetic acid (4), an analog of 3-indoleacetic acid, has shown moderate auxinic activity; and numerous alkylindolizines (5), arylindolizines (6), and alkylaminoalkylindolizines (7, 8) have been synthesized and shown to influence the central nervous system.

Some 1-indolizineacetic acids (9, 10) possess analgesic and anti-inflammatory activity. Several indolizine analogs of indoxole (11, 12), a well-known anti-inflammatory agent, were synthesized recently.

CHEMISTRY

The *N'*-substituted hydrazides of indolizine-2-carboxylic acid (XV–XXVI) were synthesized according to Scheme I. On treatment with hydrazine hydrate, methyl indolizine-2-carboxylate (I), obtained by esterification of the corresponding acid (13) with methanol, gave indolizine-2-carboxylic acid hydrazide (II). The latter, by reaction with aldehydes and ketones, yielded the corresponding hydrazones, which were reduced with sodium borohydride.

It is not possible to perform the reduction of benzylidenehydrazide (IX) by this method. It was performed with lithium aluminum hydride or with hydrogen in the presence of palladium-on-charcoal and traces of acetic acid. At the end of each reduction, the IR spectrum of the product obtained indicated that the characteristic band of the C=N group of the initial hydrazones had disappeared.

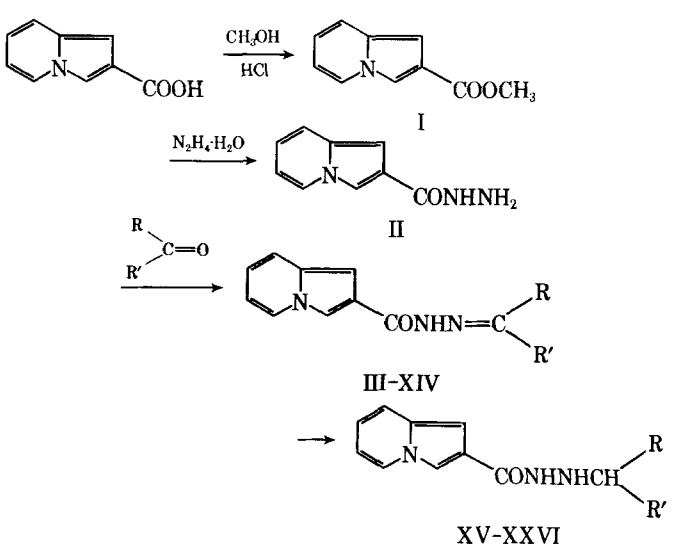

Scheme I

(4) S. Bessho, S. Tomioka, and S. Ito, *Yakugaku Zasshi*, **99**, 686 (1972).

ACKNOWLEDGMENTS AND ADDRESSES

Received April 1, 1975, from the *Kyoto College of Pharmacy, Yamashina Misasagi, Higashiyama-ku, Kyoto 607, Japan, and the ‡Kikusui Seisakusho Co. Ltd., Nishinokyo Minamikamiaicho, Nakagyo-ku, Kyoto 604, Japan.

Accepted for publication April 29, 1976.

The authors are indebted to Mr. Yasuo Shimada, the President of Kikusui Seisakusho Co. Ltd., for encouragement and trial manufacturing of a fully automatic tabletability tester. They are also grateful to Masao Takada, Giichiro Kowada, Toyojiro Koyama, and Masami Yuge of the same company for cooperation.

ˣ To whom inquiries should be directed.

Indolizine Derivatives with Biological Activity I: *N'*-Substituted Hydrazides of Indolizine-2-carboxylic Acid

MARIO CARDELLINI ˣ, FRANCESCO CLAUDI, MARIO GRIFANTINI, UGO GULINI, and SANTE MARTELLI

Abstract □ The synthesis and antimonoamine oxidase activity of some *N'*-substituted hydrazides of indolizine-2-carboxylic acid are described. They all inhibit monoamine oxidase and are more active than iproniazid. The structure–activity relationships also are discussed.

Keyphrases □ Indolizine-2-carboxylic acid hydrazides—synthesized, screened for effect on monoamine oxidase activity □ Hydrazides, *N'*-substituted—of indolizine-2-carboxylic acid synthesized, screened for effect on monoamine oxidase activity □ Monoamine oxidase activity—effect of various *N'*-substituted hydrazides of indolizine-2-carboxylic acid □ Structure–activity relationships—*N'*-substituted hydrazides of indolizine-2-carboxylic acid screened for effect on monoamine oxidase activity

Numerous *N'*-substituted hydrazides of indolecarboxylic acids have been synthesized in recent years as potential psychotherapeutic agents, and their inhibiting activity on monoamine oxidase has been tested *in vitro* (1, 2). The fundamental characteristic of such derivatives, some of which have proved to be intensely active, is the association in a single compound of a functional group with known antimonoamine oxidase activity, such as the hydrazide group, and the indole system. The indole system is present in various natural and synthetic compounds distinguished by psychotropic properties. The present paper reports the synthesis and study of the antimonoamine oxidase activity of a series of *N'*-substituted hydrazides of indolizine-2-carboxylic acid, which are analogs of the indole derivatives.

There are few literature reports on analogs of biologically active indole derivatives in which indole is replaced by indolizine. 1-Indolizinylalanine (3) has been prepared as a potential tryptophan antimetabolite; 1-indolizineacetic acid (4), an analog of 3-indoleacetic acid, has shown moderate auxinic activity; and numerous alkylindolizines (5), arylindolizines (6), and alkylaminoalkylindolizines (7, 8) have been synthesized and shown to influence the central nervous system.

Some 1-indolizineacetic acids (9, 10) possess analgesic and anti-inflammatory activity. Several indolizine analogs of indoxole (11, 12), a well-known anti-inflammatory agent, were synthesized recently.

CHEMISTRY

The *N'*-substituted hydrazides of indolizine-2-carboxylic acid (XV–XXVI) were synthesized according to Scheme I. On treatment with hydrazine hydrate, methyl indolizine-2-carboxylate (I), obtained by esterification of the corresponding acid (13) with methanol, gave indolizine-2-carboxylic acid hydrazide (II). The latter, by reaction with aldehydes and ketones, yielded the corresponding hydrazones, which were reduced with sodium borohydride.

It is not possible to perform the reduction of benzylidenehydrazide (IX) by this method. It was performed with lithium aluminum hydride or with hydrogen in the presence of palladium-on-charcoal and traces of acetic acid. At the end of each reduction, the IR spectrum of the product obtained indicated that the characteristic band of the C=N group of the initial hydrazones had disappeared.

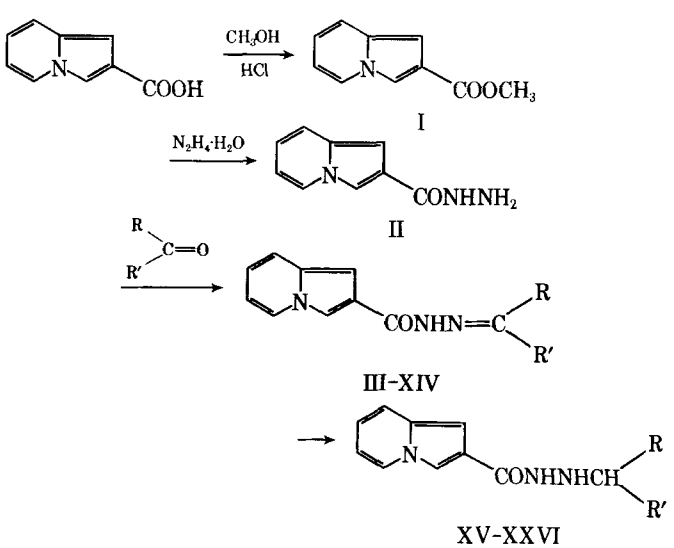

Scheme I

Table I—*N'*-Alkyl- and *N'*-Arylalkylhydrazides of Indolizine-2-carboxylic Acid and Their Monoamine Oxidase Inhibitory Activity

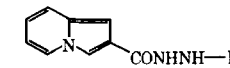

Compound	R	Reaction Solvent[a]	Extraction Solvent[a]	Melting Point, Recrystallization Solvent	Yield, %	Melting Point, Hydrochloride	I_{50}	X[b]	Molecular Formula	Analysis, %		Analysis[c], Hydrochloride, %	
										Calc.	Found	Calc.	Found
Iproniazid[d]		—	—	—	—	—	7.24×10^{-4}	1	—	—		—	
II	H	—	—	167–168°, E	74	228–230°	1.24×10^{-5}	58.2	$C_9H_9N_3O$	C 61.70 H 5.18 N 23.99	61.92 5.42 23.71	C 51.07 H 4.76 N 19.85	51.02 4.61 19.91
XV	CH_2CH_3	E–D (3:1)	G	128–130°, B	57	224–226°	1.44×10^{-4}	5	$C_{11}H_{13}N_3O$	C 65.00 H 6.45 N 20.68	65.07 6.63 20.95	C 55.15 H 5.88 N 17.53	55.38 6.09 17.62
XVI	$CH_2CH_2CH_3$	H	A	107–109°, E	70	218–220°	1.77×10^{-4}	4	$C_{12}H_{15}N_3O$	C 66.34 H 6.96 N 19.34	66.57 7.07 19.68	C 56.80 H 6.35 N 16.56	57.02 6.51 16.82
XVII	$CH_2CH_2CH_2CH_3$	H	A	96–98°, E	70	208–210°	2.18×10^{-4}	3.3	$C_{13}H_{17}N_3O$	C 67.50 H 7.41 N 18.17	67.71 7.16 18.47	C 58.31 H 6.77 N 15.69	58.59 6.52 15.81
XVIII		H	G	114–115°, E	60	228–230°	1.60×10^{-4}	4.5	$C_{13}H_{17}N_3O$	C 67.50 H 7.41 N 18.17	67.64 7.42 17.98	C 58.31 H 6.77 N 15.69	58.56 6.83 15.63
XIX		E–H (1:1)	G	151–152°, F	90	228–230°	1.52×10^{-4}	4.7	$C_{14}H_{17}N_3O$	C 69.11 H 7.04 N 17.27	69.13 7.10 17.32	C 60.1. H 6.48 N 15.02	60.05 6.42 15.06
XX	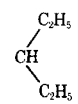	H	G	127–128°, E	80	230–231°	2.5×10^{-4}	2.89	$C_{14}H_{19}N_3O$	C 68.54 H 7.81 N 17.13	68.83 7.64 17.28	C 59.67 H 7.15 N 12.58	59.82 7.21 12.72
XXI	$CH_2C_6H_5$	—	—	150–152°, E	54	224–226°	4.6×10^{-5}	15.7	$C_{16}H_{15}N_3O$	C 72.43 H 5.70 N 15.84	72.73 5.72 15.86	C 63.67 H 5.34 N 13.92	63.54 5.41 13.79
XXII		E–H (1:1)	G	176–177°, E	73	230–232°	1.73×10^{-4}	4.17	$C_{17}H_{17}N_3O$	C 73.09 H 6.13 N 15.04	72.74 6.18 14.96	C 64.65 H 5.75 N 13.30	64.62 6.01 13.06
XXIII	$CH_2C_6H_4p\text{-}CH_3$	E–H (1:1)	A	176–178°, E	55	222–224°	9.82×10^{-5}	7.37	$C_{17}H_{17}N_3O$	C 73.09 H 6.13 N 15.04	73.29 6.38 15.24	C 64.65 H 5.75 N 13.30	64.41 5.93 13.19
XXIV		H–D (14:1)	G	133–134°, E	75	208–210°	1.27×10^{-4}	5.67	$C_{18}H_{19}N_3O$	C 73.69 H 6.53 N 14.33	73.83 6.55 14.48	C 65.54 H 6.11 N 12.74	65.42 6.02 12.88
XXV	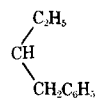	H–D (7:1)	G	131–132°, E	80	215–218°	1.13×10^{-4}	6.39	$C_{19}H_{21}N_3O$	C 74.24 H 6.89 N 13.67	74.65 6.79 13.94	C 66.36 H 6.44 N 12.22	66.28 6.19 12.03
XXVI	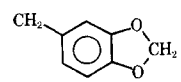	H–E (1:1)	C	155–158°, E	35	216–218°	1.77×10^{-5}	40.8	$C_{17}H_{15}N_3O_3$	C 66.01 H 4.89 N 13.59	66.15 5.04 13.72	C 59.04 H 4.66 N 12.15	59.15 4.85 11.81

[a] A = ethyl acetate, B = benzene, C = methylene chloride, D = dioxane, E = ethanol, F = anhydrous ethanol, G = ethyl ether, and H = methanol. [b] X = I_{50}iproniazid/I_{50}compound. [c] Monohydrochlorides. [d] *N'*-Isonicotinoyl-*N'*-isopropylhydrazine.

Table II—*N'*-Alkylidene- and *N'*-Arylalkylidenehydrazines of Indolizine-2-carboxylic Acid

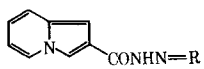

Compound	R	Recrystallization Solvent	Melting Point	Reaction Time (hr)/ Reaction Temperature	Yield, %	Molecular Formula	Analysis, %	
							Calc.	Found
III	$CHCH_3$	Methanol	167–169°	4/20°	87	$C_{11}H_{11}N_3O$	C 65.67 H 5.51 N 20.88	65.85 5.65 21.08
IV	$CHCH_2CH_3$	Ethanol	150–153°	4/40°	70	$C_{12}H_{13}N_3O$	C 66.95 H 6.09 N 19.52	67.01 6.19 19.75
V	$CHCH_2CH_2CH_3$	Ethanol	146–148°	2/50°	89	$C_{13}H_{15}N_3O$	C 68.10 H 6.59 N 18.33	67.95 6.65 18.29
VI		Ethanol	141–142°	5/45°	89	$C_{13}H_{15}N_3O$	C 68.10 H 6.59 N 18.33	68.44 6.75 18.29
VII		Ethanol	160–161°	4/Reflux	80	$C_{14}H_{15}N_3O$	C 69.69 H 6.27 N 17.42	69.46 6.24 17.23
VIII		Ethanol	131–132°	5/Reflux	77	$C_{14}H_{17}N_3O$	C 69.11 H 7.04 N 17.27	69.00 7.01 17.23
IX		Ethanol	224–226°	1/20°	75	$C_{16}H_{13}N_3O$	C 72.98 H 4.98 N 15.96	72.71 4.87 16.21
X		Tetrahydrofuran	210–212°	3/20°	82	$C_{17}H_{15}N_3O$	C 73.63 H 5.45 N 15.15	73.84 5.44 15.15
XI	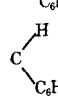	Ethanol	210–212°	5/20°	77	$C_{17}H_{15}N_3O$	C 73.63 H 5.45 N 15.15	73.82 5.45 15.30
XII		Ethanol	176–177°	15/20°	75	$C_{18}H_{17}N_3O$	C 74.20 H 5.88 N 14.42	74.28 5.73 14.48
XIII	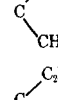	Ethanol	141–142°	1/Reflux	92	$C_{19}H_{19}N_3O$	C 74.73 H 6.27 N 13.76	75.03 6.45 14.05
XIV		Ethanol	196–197°	3/20°	75	$C_{17}H_{13}N_3O_3$	C 66.44 H 4.26 N 13.68	66.09 4.32 13.48

EXPERIMENTAL[1]

Methyl Indolizine-2-carboxylate (I)—Indolizine-2-carboxylic acid (0.2 mole) (13) was added to 500 ml of methanol saturated with dry hydrogen chloride gas. The mixture was refluxed for 6 hr, and hydrogen chloride gas was bubbled through the solution. The solvent was then eliminated under vacuum, and the residue was extracted with hot *n*-hexane. Evaporation of the *n*-hexane gave a solid, which was crystallized from ethanol, yielding 80%, mp 96–97° [lit. (13) mp 97–99°].

Hydrazide of Indolizine-2-carboxylic Acid (II)—Hydrazine hydrate (85%) (1.06 moles) was added to a solution of 0.14 mole of I in 260 ml of methanol, and the mixture was refluxed for 6 hr. Cooling led to the precipitation of a solid which was washed with water and crystallized; IR (ν_{max}): 1660, 1620 (C=O), 3290, and 3200 (NH) cm^{-1} (Table I).

***N'*-Alkylidene- and *N'*-Arylalkylidenehydrazides of Indolizine-2-carboxylic Acid (III–XIV)**—The appropriate aldehyde or ketone (0.006 mole) was added to a solution of 0.005 mole of II in 40 ml of methanol. The mixture was stirred at room temperature or was heated for various times. With 3,4-methylenedioxybenzaldehyde and the ketones, the reaction was promoted by the addition of 0.005 mole of acetic acid. The products precipitated directly on cooling or by concentration of the solution and were subsequently crystallized; IR (ν_{max}): 3120–3390 (NH), 1630–1655 (C=O), and 1600–1630 (C=N) cm^{-1} (Table II).

***N'*-Alkyl- and *N'*-Arylalkylhydrazides of Indolizine-2-carboxylic Acid (XV–XXVI)**—With stirring at 0°, 0.020–0.10 mole of sodium borohydride was slowly added to 0.021 mole of one compound, III–XIV, dissolved in the minimum amount of solvent. At the end of the addition, the mixture was stirred for 5 hr and the solvent was evaporated under vacuum. The residue was treated with water and extracted with a suitable solvent. The organic solution was dried over sodium sulfate, and the solvent was eliminated under reduced pressure. The residue was crystallized; IR (ν_{max}): 3200–3290 (NH) and 1620–1660 (C=O) cm^{-1} (Table I).

***N'*-Benzylhydrazide of Indolizine-2-carboxylic Acid (XXI)**—*Method A*—The benzylidenehydrazide IX (0.0046 mole) in 50 ml of anhydrous tetrahydrofuran was added to a suspension of 0.021 mole of lithium aluminum hydride in 20 ml of anhydrous tetrahydrofuran. The mixture was refluxed for 2.5 hr and then stirred overnight at room temperature. Excess lithium aluminum hydride was destroyed with water-saturated ether. The mixture was filtered, the solvent was evaporated under vacuum, and the residue was crystallized.

Method B—A suspension of 0.0038 mole of IX in 200 ml of absolute ethanol and 30 ml of dioxane containing 0.1 g of 10% palladium-on-charcoal and a few drops of acetic acid was hydrogenated at 1.5 atm and 60°. When the theoretical amount of hydrogen had been consumed, the suspension was filtered while hot. The solvent was evaporated under vacuum, and the residue was crystallized, yielding 45%.

Hydrochlorides of *N'*-Alkyl- and *N'*-Arylalkylhydrazides of Indolizine-2-carboxylic Acid—Dry hydrochloric acid was bubbled through a solution of 0.005 mole of one of the hydrazides, XV–XXVI, in the minimum amount of absolute ethanol. The hydrochlorides precipitated directly or on the addition of anhydrous ether and were crystallized from absolute ethanol (Table I).

Antimonoamine Oxidase Activity *In Vitro*—The enzyme was prepared from pig plasma by a reported method (14). For the tests of

[1] Melting points were determined with a Büchi apparatus and are not corrected. IR spectra were taken in mineral oil using a Perkin-Elmer 257 spectrophotometer.

enzyme activity and inhibition, the protein extract derived from stage II (precipitation with 35–55% ammonium sulfate) was used. The monoamine oxidase activity of the enzyme, determined by the method of Zeller *et al.* (15), was followed at 253 nm[2] at 37° and pH 7.2, and the values of ΔE/min during the first 10 min of the reaction were calculated. The reaction mixture consisted of 40 μl of 4.29×10^{-3} *M* 3-iodobenzylamine, 20 μl of protein solution (1.6 mg), 1500 μl of 0.1 *M* sodium phosphate buffer (pH 7.2), and double-distilled water to a final volume of 2000 μl. The same reaction mixture not containing the substrate was used as the reference sample.

The inhibition tests were performed (15) using the described mixture and keeping the concentrations of the components and the final volume constant while varying only the inhibitor concentration, both in the reference solution and the test solution. The I_{50} values (inhibitor molar concentration producing 50% inhibition) were calculated graphically.

Some water-insoluble compounds were added to the reaction mixture in dioxane solution. The dioxane concentration in the reaction mixture was less than 3%. To determine the I_{50} values, the inhibition due to the dioxane was taken into account, since this solvent has a weak inhibiting effect on enzymatic activity. Compounds XV–XVIII were added to the reaction mixture as hydrochlorides, while the others were used in the form of the free bases dissolved in dioxane because of the low solubility of the hydrochlorides in the aqueous solution and in dioxane.

RESULTS AND DISCUSSION

All tested compounds proved to be about three to 58 times more active than iproniazid in the inhibition of monoamine oxidase (Table I). In addition, their activity was distinctly greater than that of the corresponding hydrazides of indole-2-carboxylic and indole-3-carboxylic acids tested on an enzyme from calf liver with iproniazid as the standard. Hence, the displacement of the nitrogen from the 1-position of the indole to the bridge 4-position of indolizine leads, at least in the cases studied, to an enhancement of activity.

The unsubstituted hydrazide was most active. In general, the activity was greater in the series containing arylalkyl groups on the *N'*-nitrogen of the hydrazide chain than in the series with simple alkyl chains.

In the first series, one of the most active compounds was the benzyl derivative (XXI). Compounds XXII and XXIII, with a methyl substituent on the benzyl methylene group or on the benzene ring, were less active than the parent compound; XXVI, with a methylbenzodioxole substituent, was more active. The α-methyl- and α-ethyl-β-phenylethyl homologs (XXIV and XXV) were also more active than the α-methylbenzyl derivative (XXII).

In the second series, the activity decreased with an increase in the length of the chain (XV–XVII). However, with the same number of carbon atoms, branching (XVII *versus* XVIII) and replacement of the alkyl group by the corresponding cycloalkyl group (XIX *versus* XX) appeared to have a positive influence.

[2] Zeiss PMQ II spectrophotometer.

REFERENCES

(1) A. Alemany, M. Bernabé, C. Elorriaga, E. Fernandez Alvarez, M. Lora-Tamayo, and O. Nieto, *Bull. Soc. Chim. Fr.*, **1966**, 2486.

(2) A. Alemany, E. Fernandez Alvarez, and R. Hernandez Sanchez, *An. Real Soc. Espan. Fis. Quim.*, **71**, 88 (1975). *Ibid.*, **71**, 406 (1975).

(3) J. A. Carbon and S. Brehm, *J. Org. Chem.*, **26**, 3376 (1961).

(4) M. Cardellini, S. Ottolino, and P. Tafaro, *Ann. Chim. (Rome)*, **58**, 1206 (1968).

(5) T. Hirosawa, *Jpn. J. Med. Sci. IV. Pharmacol.*, **11** (2/3), *Proc. Jpn. Pharmacol. Soc.*, **12**, 218 (1938); through *Chem. Abstr.*, **34**, 7425 (1940).

(6) V. S. Venturella, *J. Pharm. Sci.*, **52**, 868 (1963). *Ibid.*, **53**, 107 (1964). *Ibid.*, **53**, 1166 (1964).

(7) W. B. Harrell and R. F. Doerge, *ibid.*, **56**, 225 (1967). *Ibid.*, **56**, 1200 (1967). *Ibid.*, **57**, 1989 (1968).

(8) L. A. Walter and P. Margolis, *J. Med. Chem.*, **10**, 498 (1967).

(9) J. H. C. Nayler, British pat. 1,174,124 (Dec. 10, 1969); through *Chem. Abstr.*, **72**, 55285 (1970).

(10) C. Casagrande, A. Invernizzi, R. Ferrini, and G. Miragoli, *Farmaco, Ed. Sci.*, **26**, 1059 (1971).

(11) K. R. Kallay and R. F. Doerge, *J. Pharm. Sci.*, **61**, 949 (1972).

(12) J. Szmuszkovicz, E. M. Glenn, R. V. Heinzelman, J. B. Hester, Jr., and G. A. Youngdale, *J. Med. Chem.*, **9**, 527 (1966).

(13) E. T. Borrows and D. O. Holland, *J. Chem. Soc.*, **1947**, 672.

(14) "Methods in Enzymology," vol. 17, part B, S. P. Colowick and N. O. Kaplan, Eds., Academic, New York, N.Y., 1971, p. 682.

(15) V. Zeller, G. Ramachander, and E. A. Zeller, *J. Med. Chem.*, **8**, 440 (1965).

ACKNOWLEDGMENTS AND ADDRESSES

Received October 21, 1975, from the *Istituto di Chimica Farmaceutica e di Chimica Organica, Università di Camerino, 62032 Camerino (MC), Italia.*

Accepted for publication April 16, 1976.

Supported by a grant from the Consiglio Nazionale delle Ricerche (CNR), Rome, Italy.

[x] To whom inquiries should be directed.

Synthesis and Anticancer Screening of 2-Indolyl 5-(1,2,3,6-Tetrahydropyridyl) Ketones

RICHARD J. SUNDBERG ˣ, D. EUGENE REARICK, and HENRY F. RUSSELL

Abstract □ Several derivatives of 2-indolyl 5-(1,2,3,6-tetrahydropyridyl) ketone with various substituents on the pyridine nitrogen and with or without a benzenesulfonyl group on the indole nitrogen were synthesized and characterized by spectroscopic and analytical data. Only one showed erratic but confirmed activity in the P-388 screen. The other derivatives were inactive in the L-1210 leukemia screen.

Keyphrases □ 2-Indolyl 5-pyridyl ketone derivatives—synthesized, screened for cytotoxic activity □ Cytotoxic activity—various 2-indolyl 5-pyridyl ketone derivatives screened □ Structure–activity relationships—various 2-indolyl 5-pyridyl ketone derivatives screened for cytotoxic activity

An intermediate from a program to prepare biologically active indole derivatives submitted for anticancer screening was 1-benzenesulfonyl-2-indolyl 5-[1,2,3,6-tetrahydro-1-(2-oxo-2-ethoxyethyl)pyridyl] ketone (IV*a*). Since this compound showed erratic but confirmed activity in the mouse P-388 leukemia screen, several analogs were prepared.

DISCUSSION

The starting material for each compound was 1-benzenesulfonyl-2-indolyl 5-pyridyl ketone (II), which is obtained efficiently in two steps from 1-benzenesulfonyl-2-lithioindole (1) (Scheme I). Alkylation of II with alkyl bromides followed by catalytic reduction gives analogs of IV with various substituents at the pyridine nitrogen. The partial reduction of 3-acylpyridines is a well-documented procedure that owes its success to the resistance to reduction of the residual vinylogous amide unit (2). Analogs lacking the 1-benzenesulfonyl substituent were prepared by hydrolytic cleavage of the 1-benzenesulfonyl substituent from I prior to alkylation (1). The yields in the alkylation step were good in each case. The yields in the reduction step were lower and are given in Table I.

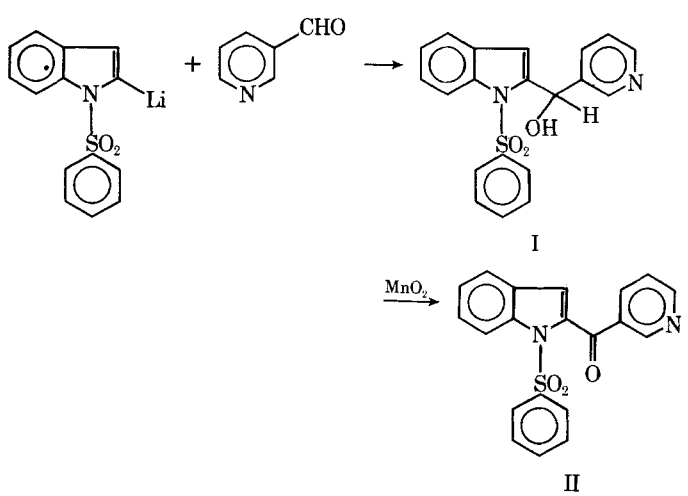

Scheme I

PMR, UV, and mass spectral data were indicative of the assigned structures. The PMR and UV data are given in Table II. All tetrahydropyridines exhibited a characteristic set of two broadened triplets at δ 2.5 ± 0.2 and 3.2 ± 0.1, attributable to the C-4 and C-2 methylene groups, respectively. The C-3 methylene signal appeared as a broader multiplet at about 2 ppm. There is some uncertainty about the assignment of the vinyl proton at C-6. It probably appears as the signal at 6.2–6.8 ppm observed in each spectrum. An alternative assignment for this peak would be the indole 3-proton, but this proton usually is found in the aromatic multiplet when the indole ring carries a carbonyl substituent as in the present case.

The only chemical complication noted in the preparation of these compounds was in the reduction of III*d*. Concomitant reduction of the ketone group in the *N*-phenacyl substituent occurred, giving the carbinol (IV*e*). The reduction products were usually contaminated with unidentified colored impurities and were best purified by preliminary chromatography on silica gel followed by crystallization. Some products had the troublesome property of forming nonstoichiometric solvates, but satisfactory analyses were obtained by drying at the melting point immediately prior to combustion analysis. The pyridinium salts were also troublesome in this regard and tended to form methanol solvates. Analytical data are given in Table III.

No analog of IV*a* showed significant activity. Compounds I, II, III*h*, IV*c*, and IV*e*–IV*g* were inactive in the L-1210 mouse leukemia screen in the 100–400-mg/kg dose range. Compound IV*b* was inactive in the P-388 leukemia screen, and III*g* and IV*c* showed no cytotoxicity in KB cell culture.

EXPERIMENTAL

Alkylations—The pyridyl ketone and a slight excess (~10%) of the appropriate halide were dissolved in acetonitrile (~2 ml/mmole) and

Table I—Yields and Melting Points of Synthesized 2-Indolyl 5-Pyridyl and 5-(1,2,3,6-Tetrahydropyridyl) Ketones

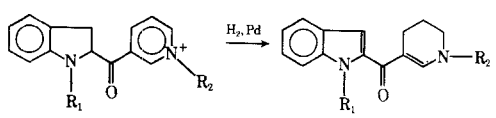

Compound	R_1	R_2	Yield, %	Melting Point
III*a*	$C_6H_5SO_2$	$-CH_2CO_2C_2H_5$	98	—[a]
IV*a*	$C_6H_5SO_2$	$-CH_2CO_2C_2H_5$	33	157–158°
III*b*	H	$-CH_2CO_2C_2H_5$	90	—[a]
IV*b*	H	$-CH_2CO_2C_2H_5$	29	126–128°
III*c*	H	$C_6H_5C(=O)CH_2-$	95	253–255°
IV*c*	H	$C_6H_5C(=O)CH_2-$	26	194–196.5°
III*d*	$C_6H_5SO_2$	$C_6H_5C(=O)CH_2-$	95	225–227°
IV*e*	$C_6H_5SO_2$	$C_6H_5CHOHCH_2-$	20	158–159°
III*f*	$C_6H_5SO_2$	$-CH_2CH_2CH_2OH$	75	186–187°
IV*f*	$C_6H_5SO_2$	$-CH_2CH_2CH_2OH$	28	164–165°
III*g*	$C_6H_5SO_2$	$CH_3OC_6H_4(C=O)CH_2-$	100	161–162°
IV*g*	$C_6H_5SO_2$	$CH_3OC_6H_4(C=O)CH_2-$	55	107–109°
III*h*	H	$CH_3OC_6H_4(C=O)CH_2-$	91	253–255°

[a] Not extensively purified.

Table II—UV–Visible Absorption and PMR Spectral Data of 2-Indolyl 5-(1,2,3,6-Tetrahydropyridyl) Ketones

Compound	UV–Visible Data[a]	PMR Spectral Data[b]
	1-Benzenesulfonylindoles	
IV*a*	250 (1.51 × 10^4), 320 (2.63 × 10^4)	1.25 (t, 3), 1.95 (2, m), 2.55 (t, 2), 3.20 (t, 2), 3.75 (s, 2), 4.10 (q, 2), 6.55 (s, 1), 7.05–8.30 (m, 10)
IV*e*	265 (1.40 × 10^4), 332 (2.75 × 10^4)	1.8 (m, 2), 2.40 (t, 2), 3.21 (m, 5), 4.70 (m, 1), 6.19 (s, 1), 7.02 (s, 1), 7.0–8.3 (m, 14)
IV*f*	265 (1.23 × 10^4), 329 (2.70 × 10^4)	1.5–2.0 (m, 4), 2.48 (t, 2), 3.15 (m, 4), 3.55 (t, 2), 6.55 (s, 1), 7.0–8.2 (m, 9)
IV*g*	273 (2.38 × 10^4), 329 (2.88 × 10^4)	2.0 (m, 2), 2.58 (t, 2), 3.21 (t, 2), 3.82 (s, 3), 4.46 (s, 2), 6.59, (1, s), 6.87 (d, 2), 7.0–8.3 (m, 12)
	Unsubstituted Indoles	
IV*b*	232 sh (1.07 × 10^4), 260 sh (5.10 × 10^3), 300 (1.29 × 10^4), 355 (2.14 × 10^4)	1.25 (t, 2), 1.7–2.1 (m, 2), 2.61 (t, 2), 3.20 (t, 2), 3.85 (s, 2), 4.17 (q, 2), 6.80 (d, $J \sim 2$ Hz, 1) 7.0–7.7 (m, 4), 10.4 (s, 1)
IV*c*	245 (2.00 × 10^4), 310 sh (1.44 × 10^4), 358 (2.37 × 10^4)	2.02 (m, 2), 2.63 (t, 2), 3.20 (t, 2), 4.53 (s, 2), 6.76 (d, $J \sim$ 2 Hz, 1), 7.0–8.0 (m, 10), 10.0 (s,1)

[a] For absolute ethanol solutions; the wavelengths (in nanometers) of maxima or distinct shoulders (sh) and absorptivities are given. [b] For deuterochloroform solutions~50 mg/ml; chemical shifts are relative to the internal standard, tetramethylsilane, and coupling constants are given in hertz.

heated to reflux overnight under nitrogen. The pyridinium salts precipitated and were isolated by filtration. With III*f*, addition of ether was necessary to effect precipitation. The salts were recrystallized from methanol.

Reductions—The pyridinium salts were suspended or dissolved in ethanol. For the unsubstituted indoles, about 2 mmoles of triethylamine was added per millimole of pyridinium salt. A palladium-on-carbon catalyst was used, and the reductions were carried out at atmospheric pressure, usually overnight. The solutions were filtered and evaporated to dryness. The residue was dissolved in chloroform, and the solution was washed with aqueous sodium bicarbonate solution. The solvent was then evaporated, and the residue was chromatographed on silica gel using chloroform containing 0.5% methanol for elution. Pure fractions were combined and crystallized from chloroform or ethyl acetate.

Table III—Analytical Data

	Calc.			Found		
	C	H	N	C	H	N
IV*a*	63.21	5.35	6.19	63.63	5.43	6.10
IV*b*	69.21	6.45	8.97	69.09	6.50	8.87
III*c*	62.72	4.07	6.65	62.46	4.15	6.62
IV*c*	76.72	5.85	8.13	76.75	5.90	8.13
III*d*	59.90	3.77	4.99	59.85	3.78	5.02
IV*e*	69.12	5.39	5.76	69.00	5.42	5.73
III*f*	55.09	4.22	5.59	54.77	4.34	5.70
IV*f*	65.07	5.70	6.60	65.14	5.76	6.55
III*g*[a]	57.79	4.36	4.49	57.76	4.37	4.56
IV*g*	67.69	5.09	5.44	67.44	5.22	5.07
III*h*	61.20	4.24	6.20	60.97	4.19	6.21

[a] Calculated analysis is for methanol solvate.

REFERENCES

(1) R. J. Sundberg and H. F. Russell, *J. Org. Chem.*, **38**, 3324 (1973).

(2) E. Wenkert, *Accounts Chem. Res.*, **1**, 78 (1968); E. Wenkert, K. G. Dave and F. Haglid, *J. Amer. Chem. Soc.*, **87**, 5461 (1965); E. Wenkert, K. G. Dave, F. Haglid, R. G. Lewis, T. Oishi, R. V. Stevens, and M. Terashima, *J. Org. Chem.*, **33**, 747 (1968).

ACKNOWLEDGMENTS AND ADDRESSES

Received December 17, 1975, from the *Department of Chemistry, University of Virginia, Charlottesville, VA 22901.*

Accepted for publication March 23, 1976.

Supported by Grant 12940 from the National Institutes of Health.

[x] To whom inquiries should be directed.

Rapid Determination of Nitroglycerin Volatility Using Thermogravimetric Analysis

H. GUCLUYILDIZ ˣ, F. W. GOODHART, and F. C. NINGER

Abstract □ The effect of selected tablet components on the volatility of nitroglycerin from compressed sublingual tablets was studied by thermogravimetric analysis. The results, confirmed by chemical analyses, showed that nitroglycerin volatility is significantly reduced by the use of povidone USP and microcrystalline cellulose NF in tablet formulations. In general, the stabilizing effect of these materials was dependent on the presence and the concentration of each other. These studies demonstrated the utility of thermogravimetric analysis as a rapid and reliable means of screening nitroglycerin formulations for stability purposes.

Keyphrases □ Nitroglycerin—volatility, effect of various tablet components, thermogravimetric determination □ Volatility—nitroglycerin, effect of various tablet components, thermogravimetric determination □ Thermogravimetry—determination, effect of various tablet components on nitroglycerin volatility □ Tablets—nitroglycerin, effect of various tablet components on volatility, thermogravimetric determination □ Vasodilators, coronary—nitroglycerin, volatility, effect of various tablet components, thermogravimetric determination

In recent years considerable attention has been focused on nitroglycerin stability. Several investigators have conducted extensive research to improve the volatility and, thus, content uniformity of nitroglycerin tablets (1–9). It is now well established that nitroglycerin stability can best be improved by reformulation of conventional molded tablets rather than by modifications in packaging materials. One approach toward this end has been the inclusion of various macromolecular substances in tablet formulations (3–7, 9).

From the experimental standpoint, the dependency of nitroglycerin stability in tablet formulations has been studied using extreme conditions of storage, *i.e.*, completely exposing the tablets to air or to high vacuum, followed by chemical analysis of individual tablets. While studies of this type are of fundamental value in development work, they are generally time consuming when a large number of formulations is investigated.

Therefore, as an alternative procedure, thermogravimetric analysis was explored for its utility in screening various nitroglycerin formulations. It was found that thermogravimetric analysis affords a rapid and reliable means of evaluating the influence of various tablet components on the volatility of nitroglycerin. This report describes preliminary studies which ultimately led to the development of a stabilized compressed nitroglycerin tablet (9).

EXPERIMENTAL

Tablet Preparation—Nitroglycerin tablets, containing 0.6 mg of drug in each 30-mg tablet, were prepared using nitroglycerin spirit (9.1% w/v), alcohol USP, lactose (anhydrous) USP, starch USP, microcrystalline cellulose[1] NF, and calcium stearate NF. The diluent mixture was granulated with a solution or dispersion of a binder in nitroglycerin spirit and alcohol USP. When necessary, a small amount of water was employed to aid dispersion of the binder.

Ethylcellulose[2], povidone USP[3], hydroxypropyl methylcellulose[4], and gelatin USP were used as binders and were added to each formulation at a ratio of 1:2 with respect to nitroglycerin. The amount of starch was maintained constant (25%) while, in later experiments, microcrystalline cellulose and povidone were included at various levels to determine the stabilizing effects of these materials. The wet granulated product after drying at 30–35° was mixed with the lubricant and compressed into 0.40-cm tablets.

Thermogravimetric Studies—The volatility of nitroglycerin from tablets was studied by following the change in sample weight as a function of time under isothermal conditions. Two tablets representing each formulation were placed into the pan of the thermogravimetric analyzer[5] previously equilibrated at the desired temperature. The instrument was operated at a sensitivity of 0.2 mg/2.54 cm (1 in.). A stream of nitrogen gas was passed through the furnace containing the sample at a constant flow rate of 20 ml/min to remove the gaseous products evolved during the experiment.

Generally, after 1.5 hr of treatment at 80°, sufficient weight loss was observed for comparison of relative stability. However, in later experiments, it was necessary to extend the tests over 4 hr to permit adequate opportunity for volatilization of nitroglycerin.

Nitroglycerin Assay—To compare and confirm the volatility of nitroglycerin by thermogravimetric analysis, samples of each formulation were subjected to individual tablet assay before and after the thermogravimetric analysis treatment using the spectrophotometric method of Bell (10).

RESULTS AND DISCUSSION

The results of nitroglycerin volatility from various tablet formulations are summarized in Fig. 1 and Table I. Figure 1 depicts typical thermograms, which are of two general types. The first type, represented by curves A and B, shows linearity over the entire thermogram. These linear thermograms correspond to formulations prepared from anhydrous materials, so the weight loss observed can be totally attributed to the volatility of nitroglycerin.

The second type (curves C–G and placebo) is characterized by a sudden change in sample weight during the initial stage of the experiment but later exhibits the same general linearity as the first type. These thermograms are associated with tablets prepared from excipients containing water, *e.g.*, starch. It can be seen from Fig. 1 that the placebo tablets containing lactose and starch exhibited a similar pattern of weight loss in the first 10 min of the thermogravimetric analysis.

In duplicate determinations, the initial portions of the thermograms exhibited slight variations in the amount of weight loss, apparently due to minor differences in the water content of different samples, but reproducibility was excellent for the remaining linear portions of the curves. From these results, it can be assumed that the initial weight loss is almost entirely due to the evaporation of water and, for practical purposes, can be omitted from consideration. Therefore, the volatility of nitroglycerin is taken as the loss in sample weight after the first 10 min of the thermogravimetric analysis.

From the data in Table I, it can be seen that nitroglycerin volatility in different formulations as determined by thermogravimetric analysis showed an acceptable level of agreement with chemical assay results. Table I also shows that tablets containing povidone had a significant reduction in the loss of nitroglycerin. Formulations containing gelatin, on the other hand, exhibited similar stability as the tablets containing no binder. The addition of hydroxypropyl methylcellulose or ethylcellulose caused some improvement in tablet stability but not to a significant extent.

[1] Avicel PH-102, American Viscous Division of FMC Corp.

[2] Ethocel, 100 cps, Hercules Inc.
[3] Plasdone K 29-32, General Aniline and Film Corp.
[4] Methocel, 60 HG 50 cps, Dow Chemical Co.
[5] DuPont model 950 analyzer with model 900 console.

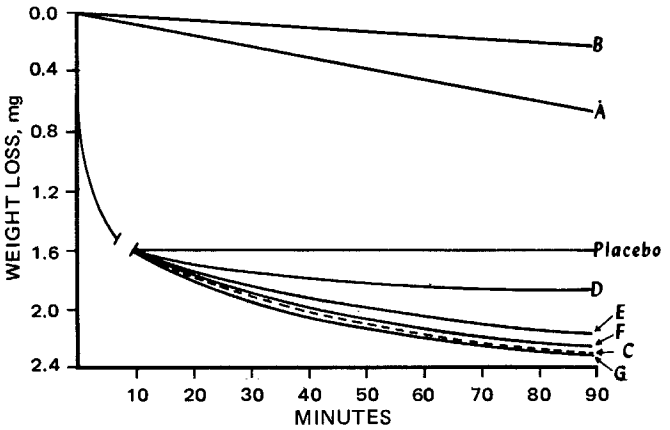

Figure 1—*Typical thermograms of nitroglycerin tablets containing various binders. See Table I for details.*

These preliminary experiments prompted the use of povidone as a stabilizing agent in the formulation of a compressed sublingual nitroglycerin tablet. Additional stability screening experiments were then designed to examine further the effect of various concentration ratios of povidone along with an additional stabilizer, *i.e.*, microcrystalline cellulose (11).

Figure 2 summarizes the volatility of nitroglycerin tablets prepared with three different concentrations of microcrystalline cellulose and povidone at various ratios with respect to nitroglycerin. The samples were subjected to thermogravimetric analysis at 80° for 4 hr. This figure illustrates the stabilizing effect of povidone and shows that better nitroglycerin stability was achieved as the level of povidone was increased in each formulation. This result can best be seen with formulations containing no microcrystalline cellulose, where addition of povidone at a 1:4 ratio resulted in a retention of 86% of the original potency during the test period as compared to 10% for tablets without povidone. The retention of nitroglycerin content in formulations prepared with 50% microcrystalline cellulose was also increased from 81 to 92% by inclusion of povidone at a 1:4 ratio.

Figure 2 also demonstrates the effect of microcrystalline cellulose in reducing the volatility of nitroglycerin. Since this material possesses

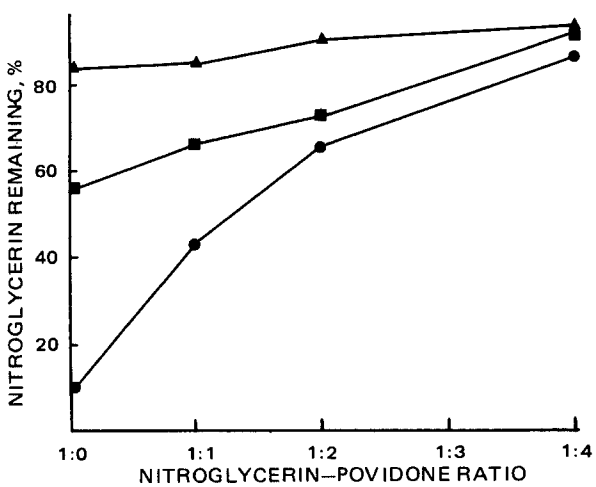

Figure 2—*Volatility of nitroglycerin tablets as a function of the nitroglycerin–povidone ratio. These tablets were prepared with different concentrations of microcrystalline cellulose. Key: ●, 0%; ■, 25%; and ▲, 50%.*

Table I—Comparison of Thermogravimetric and Chemical Analyses for the Volatility of Nitroglycerin Tablets

Formulation		Nitroglycerin Remaining, %	
Designation	Composition[a]	Thermogravimetric Method	Chemical Method
A	Lactose	54	51
B	Lactose, povidone	84	83
C	Lactose, starch	25	23
D	Lactose, starch, povidone	84	82
E	Lactose, starch, hydroxypropyl methylcellulose	45	42
F	Lactose, starch, ethylcellulose	34	30
G	Lactose, starch, gelatin	25	22

[a] Each tablet also contained 0.6 mg of nitroglycerin.

excellent compression characteristics, judicious selection of its concentration along with that of povidone allows the formulation of compressed nitroglycerin tablets with optimum stability as well as disintegration and bioavailability properties (9).

The studies reported here clearly show the utility of thermogravimetric analysis as a simple, rapid, and reliable means to investigate the volatility of nitroglycerin formulations. This method also permits the selection of accelerated test conditions which can be controlled precisely. The volatility of nitroglycerin can be studied from one or two tablets, thereby eliminating the migration of the drug from tablet to tablet during accelerated stability studies. By the use of thermogravimetric analysis, potentially stable formulations can be selected in a short period; and, finally, by the use of thermogravimetric analysis at various temperatures, the kinetics of nitroglycerin volatility from tablets may be studied.

REFERENCES

(1) B. A. Edelman, A. M. Contractor, and R. F. Shangraw, *J. Am. Pharm. Assoc.*, **NS11**, 30 (1971).

(2) R. F. Shangraw and A. M. Contractor, *ibid.*, **NS12**, 633 (1972).

(3) S. A. Fusari, *J. Pharm. Sci.*, **62**, 122 (1973).

(4) *Ibid.*, **62**, 2012 (1973).

(5) British pat. 1,343,374 (Jan. 9, 1974).

(6) S. A. Fusari and L. M. Lueck, U.S. pat. 3,789,119 (Jan. 29, 1974).

(7) H. Fung, S. K. Yap, and C. T. Rhodes, *J. Pharm. Sci.*, **63**, 1811 (1974).

(8) B. Dorsch and R. Shangraw, *Am. J. Hosp. Pharm.*, **32**, 795 (1975).

(9) F. W. Goodhart, H. Gucluyildiz, R. E. Daly, L. Chafetz, and F. C. Ninger, *J. Pharm. Sci.*, **65**, 1466 (1976).

(10) F. K. Bell, *ibid.*, **53**, 752 (1964).

(11) M. D. Richman, C. D. Fox, and R. F. Shangraw, *ibid.*, **54**, 447 (1965).

ACKNOWLEDGMENTS AND ADDRESSES

Received December 31, 1975, from the *Pharmaceutical Research and Development Laboratory, Warner-Lambert Research Institute, Morris Plains, NJ 07950.*

Accepted for publication March 16, 1976.

The authors appreciate the technical assistance of Mr. R. Phillips in the preparation of tablet samples.

[x] To whom inquiries should be directed.

Bioavailability of Digoxin in a New Soluble Pharmaceutical Formulation in Capsules

P. GHIRARDI ˣ, G. CATENAZZO *, O. MANTERO *, G. C. MEROTTI, and A. MARZO

Abstract □ The *in vitro* dissolution and the bioavailability of two pharmaceutical formulations of digoxin were compared, one being a common commercial tablet form and the other a solution of the glycoside in soft gelatin capsules. Digoxin capsules dissolved more readily *in vitro* and showed higher bioavailability than digoxin tablets in both dogs and humans. In dogs, the capsules and tablets were compared with an elixir of digoxin, which possesses complete bioavailability. The better bioavailability of digoxin capsules as compared with tablets may be explained by the fact that this formulation contains the cardiac glycoside in a solution.

Keyphrases □ Digoxin—*in vitro* dissolution and bioavailability, commercial tablets and soft gelatin capsules, dogs and humans □ Dissolution, *in vitro*—digoxin, commercial tablets and soft gelatin capsules compared □ Bioavailability—digoxin, commercial tablets and soft gelatin capsules compared, dogs and humans □ Cardiotonic agents—digoxin, *in vitro* dissolution and bioavailability, commercial tablets and soft gelatin capsules compared, dogs and humans □ Dosage forms—digoxin tablets and soft gelatin capsules, *in vitro* dissolution and bioavailability, dogs and humans

Several investigators (1–8) have reported marked differences in the bioavailability of digoxin tablets among different products of the glycoside or different batches of the same product. In addition, a lack of digoxin content uniformity was observed in the same tablet preparations, varying from 28 to 148% (9). To control this problem, the Food and Drug Administration standardized an analytical monitoring program (10) to ensure that individual tablets of digoxin do not differ significantly in glycoside content.

The best bioavailability of digoxin is achieved when the glycoside is administered in a solution or in the form of an elixir (11, 12). This paper reports a comparative study of the composition, *in vitro* dissolution, and bioavailability in dogs and humans of two pharmaceutical formulations of digoxin, a commercial tablet[1] and soft gelatin capsules containing the glycoside in a dissolved form[2].

EXPERIMENTAL

Digoxin Tablets and Capsules—Both capsules and tablets contained 250 μg of the glycoside and were from the same batch. The capsules also contained 1.500 mg of *N,N*-dimethylacetamide and 139.250 mg of polyethylene glycol 400.

Tablets and capsules were assayed for glycoside content according to Italian F.U. 1972 (13). The capsules contained 102% ± 0.35 (*SE*) of glycoside; this value is marginally higher than the 97% ± 0.35 (*SE*) found in the tablets.

Dissolution Rate—The dissolution rate of both tablets and capsules of digoxin was investigated *in vitro* according to the "paddle water" (distilled water) and "paddle acid" [0.6% (v/v) HCl] methods (14). Five hundred milliliters of distilled water or 0.6% HCl and a digoxin tablet or capsule were placed in a 1000-ml flask, thermostated at 37°, and stirred at 50 ± 2 rpm. After 15 or 60 min, a sample was taken from the flask. Digoxin was extracted and determined by the spectrophotofluorometric method. Evaluation of dissolution rates was made using the Student *t* test for independent data (Table I).

Bioavailability in Dogs—Four mongrel dogs, 16–18 kg, received the digoxin tablets during a single trial, followed 10 days later by the capsules and 10 days later by a digoxin elixir.

All dogs received 250 μg of the glycoside in each of the three formulations. The digoxin elixir contained 50 μg/ml of the glycoside in propylene glycol–95% ethanol–water [10:2.5:112.5 (v/v/v)]. Venous blood samples were taken from each dog at 0, 7.5, 15, 30, 45, 60, 90, 120, and 240 min. Plasma digoxin levels were determined by the radioimmunoassay method of Smith *et al.* (15)[3].

The statistical comparison of results was processed using an analysis of variance for all three preparations, followed by a Tukey test for specific pairs (Table II).

Bioavailability in Humans—The investigation was carried out on six healthy volunteers (58–82 kg and 36–70 years of age). Each subject received two digoxin capsules (500 μg) and two digoxin tablets (500 μg). The two administrations were carried out with a crossover design at an interval of 10 days.

The statistical comparison of capsules and tablets was made using the Student *t* test for paired observations.

Venous blood samples were taken from each patient at 0, 15, 30, 45, 60, 120, and 240 min. Plasma digoxin levels were determined as described previously.

Blood samples in both dogs and human subjects were taken over 4 hr, on the basis of reported observations (16–18). These reports concluded that areas under the plasma level–time curves (*AUC*) correlate well for the first 5 hr with areas obtained after longer sampling times, indicating that extended sampling may not be necessary for digoxin studies.

RESULTS

With the paddle water method, both digoxin tablets and capsules dissolved almost entirely in 15 min. Standard errors with digoxin tablets were two to three times higher than with digoxin capsules. With the paddle acid method, the degree of dissolution of digoxin tablets after 15 min was about 70% of the values obtained in the same time with capsules ($p < 0.001$); after 60 min, both the capsules and tablets dissolved almost entirely and to a similar degree (Table I).

In the dog, the digoxin solution showed the best bioavailability in terms of plasma levels of the glycoside, followed by the capsules and tablets (Table II). Average peak times were the earliest (22 min) with the solution, followed by the capsules (45 min) and tablets (52 min). A difference of $p < 0.05$ existed between the solution and capsules, and a difference of $p < 0.01$ existed between the solution and tablets. A comparison between the capsules and tablets gave a statistically insignificant p value. Peak concentrations were highest with the solution, followed by the capsules and tablets. For the solution–tablet comparison, $p < 0.01$; tablet–capsule and solution–capsule comparisons did not give any statistically significant p value.

The area under the plasma level–time curve, evaluated by the trapezoidal rule from 0 to 240 min, showed the highest value with the solution, followed by the capsules and tablets. A statistical comparison gave the following values: solution–capsules and solution–tablets, $p < 0.01$. Tablet–capsule comparisons did not give a statistically significant p. The differences found in bioavailability between the capsules and solution of digoxin might be explained in part by the much higher concentration in the capsules than in the solution.

In human subjects, the best bioavailability was found with the capsules, which is in accord with previous findings with dogs. The peak times were longer with the tablets than with the capsules ($p > 0.05$), the peak con-

[1] Lanoxin, lot 4 B 16.
[2] Eudigox, lot 2019, Simes S.p.A.
[3] Kits for radioimmunoassay determination were supplied by Sorin S.p.A., Saluggia, Italy.

Table I—Dissolution Rate of Digoxin Tablets[a] and Capsules[a] in Paddle Water and in Paddle Acid Methods after 15 and 60 min[b]

	15 min		60 min	
	Digoxin Tablets	Digoxin Capsules	Digoxin Tablets	Digoxin Capsules
Paddle water method	88.33 ± 4.39[b]	91.50 ± 1.43	89.50 ± 5.05	95.67 ± 2.64
Paddle acid method	64.83 ± 3.62[c]	93.50 ± 3.14[c]	95.50 ± 1.86	95.17 ± 2.10

[a] $n = 6$. [b] Mean values ± *SE* in percent of digoxin dissolved. [c] $p < 0.001$ for the comparison of 64.83 with 93.50. The p value was evaluated with the Student t test.

Table II—Peak Plasma Concentration, Peak Time, and *AUC* in Four Dogs after Administration of Digoxin Solution (250 μg), Digoxin Capsules (250 μg), and Digoxin Tablets (250 μg)

	Peak Plasma Concentration, ng/ml			Peak Time, min			*AUC*, ng/ml/min		
Dog	Solution	Capsules	Tablets	Solution	Capsules	Tablets	Solution	Capsules	Tablets
1	4.5	2.9	1.4	30	60	45	592	267	167
2	5.0	4.4	1.6	30	45	60	508	273	219
3	3.8	3.2	2.5	15	30	45	461	324	262
4	3.2	2.3	1.8	15	45	60	340	209	180
Mean ± *SE*	4.1 ±0.4	3.2 ±0.4	1.8 ±0.2	22 ±4	45 ±6	52 ±4	475 ±53	268 ±23	207 ±21
Analysis of variance									
F ratio		9.847			9.750			15.689	
p		<0.01			<0.01			<0.01	
p value obtained with Tukey method									
Solution *versus* capsules		>0.05			<0.05			<0.01	
Solution *versus* tablets		<0.01			<0.01			<0.01	
Capsules *versus* tablets		>0.05			>0.05			>0.05	

centration was higher with the capsules (4.5 ng/ml) than with the tablets (2.2 ng/ml) ($p < 0.02$), and the *AUC* was higher with the capsules than the tablets ($p < 0.05$) (Table III).

DISCUSSION

The area under the plasma level–time curve is a useful parameter and allows the relative bioavailability of the oral formulation of a drug to be evaluated as a percentage related to an intravenous or oral solution of the same drug.

According to this method, several investigators (16, 17, 19) obtained a relative bioavailability of the tablets (of the same commercial type as those investigated here) of around 56–58%, assuming 100% values after intravenous solution, and of around 70%, assuming 100% values after oral solution.

From these data on the dog, it is possible to calculate a relative bioavailability of 56.5% for capsules and 44% for tablets. These values are a little lower than those obtained previously (16, 17, 19). However, dogs may absorb digoxin at a different rate from humans. In effect, the mean peak time with capsules was 45 min in dogs and 72 min in humans; with tablets, it was 52 min in dogs and 95 min in humans. For human subjects, all three parameters (peak plasma concentration, peak time, and *AUC*) agree with the data on the dog concerning the better bioavailability with the capsules than with the tablets.

Table III—Peak Plasma Concentration, Peak Time, and *AUC* in Six Human Volunteers after Administration of Digoxin Capsules (500 μg) and Digoxin Tablets (500 μg)

	Peak Plasma Concentration, ng/ml		Peak Time, min		*AUC*, ng/ml/min	
Subject	Capsules	Tablets	Capsules	Tablets	Capsules	Tablets
1	5.4	1.7	45	45	534	224
2	4.8	1.0	45	120	861	90
3	2.9	2.5	120	120	279	270
4	6.3	2.6	60	120	622	234
5	4.7	3.2	45	45	496	283
6	3.2	2.5	120	120	570	255
Mean	4.5	2.2	72	95	560	226
± *SE*	±0.5	±0.3	±15	±16	±77	±29
p[a]	<0.02		>0.05		<0.05	

[a] Evaluated with the Student t test for paired observations.

The problem of drug bioavailability as a whole is serious. Digoxin possesses an unfavorable therapeutic index, which requires optimum absorption from an oral pharmaceutical preparation. A digoxin product with poor or incomplete absorption could cause a poor or incomplete effect on myocardial contractility. However, it is undesirable to adjust dosage of an incompletely absorbed digoxin product because it may be associated with individual variability in enteral absorption related principally to the GI transit rate. It is also undesirable to adjust dosage in patients being treated with other drugs (*e.g.*, metoclopramide) (20). None of the digoxin tablet preparations available possesses total bioavailability, as does the solution or elixir (11, 12). The preparation of digoxin in soft gelatin capsules, containing a solution of the drug, dissolved faster *in vitro* and possessed better bioavailability in the dog and human subjects than did the preparation in tablets.

Some clinical trials (21–23) showed an earlier, more intense, and longer lasting effect with digoxin capsules than with tablets in terms of heart rate and polycardiographic measurements in both healthy subjects and in patients suffering from heart failure, thus confirming the greater efficacy of the capsules.

These data, obtained from both human subjects and dogs, agree with the recent results of Mallis *et al.* (24). They found better bioavailability with a digoxin solution in capsules than with tablets in human subjects. The results of this investigation also demonstrate that dogs are a valid model for testing experimental digoxin formulations.

REFERENCES

(1) J. Lindenbaum, M. H. Mellow, M. O. Blackstone, and U. P. Butler, *N. Engl. J. Med.*, **285**, 1344 (1971).

(2) P. F. Binnion and M. McDermott, *Lancet*, **2**, 592 (1972).

(3) T. R. D. Shaw, M. R. Howard, and J. Hamer, *ibid.*, **2**, 303 (1972).

(4) A. Bertler, A. Redfors, S. Medin, and L. Nyberg, *ibid.*, **2**, 708 (1972).
(5) V. Manninen, J. Melin, and G. Hartel, *ibid.*, **2**, 934 (1971).
(6) E. Steiness, V. Christensen, and H. Johansen, *Clin. Pharmacol. Ther.*, **14**, 949 (1973).
(7) A. J. Dunning, E. J. Buurke, J. C. Roos, A. C. A. Paalman, and H. H. van Rooy, *Ned. Tydschr. Geneesk.*, **117**, 1809 (1973).
(8) J. Lindenbaum, *Pharmacol. Rev.*, **25**, 229 (1973).
(9) M. C. B. Van Oudtshoorn, *Lancet*, **2**, 1153 (1972).
(10) *Federal Register*, **39** (15), 2471 (1974).
(11) D. H. Huffman and D. L. Azarnoff, *J. Am. Med. Assoc.*, **222**, 957 (1972).
(12) D. J. Greenblatt, D. W. Duhme, J. Koch-Weser, and T. W. Smith, *N. Engl. J. Med.*, **289**, 651 (1973).
(13) F. U., 8th ed., vol. 3, Istituto Poligrafico dello Stato Ed., Rome, Italy, 1972, p. 94.
(14) *Federal Register*, **39** (15), 2478 (1974).
(15) T. W. Smith, V. P. Butler, and E. Haber, *N. Engl. J. Med.*, **281**, 1212 (1969).
(16) J. G. Wagner, M. Christensen, E. Sakmar, D. Blair, J. D. Yates, P. W. Willis, A. J. Sedman, and R. G. Stoll, *J. Am. Med. Assoc.*, **224**, 199 (1973).
(17) P. R. Klink, R. I. Poust, J. L. Colaizzi, and R. H. McDonald, *J. Pharm. Sci.*, **63**, 1231 (1974).
(18) J. L. Colaizzi and J. G. Wagner, *J. Am. Pharm. Assoc.*, **NS 15**, 43 (1975).
(19) D. H. Huffman and C. V. Manion, *Clin. Pharmacol. Ther.*, **15**, 310 (1974).
(20) G. Levy and M. Gibaldi, *Circulation*, **49**, 391 (1974).
(21) G. Catenazzo, P. Ghirardi, O. Mantero, and G. Gianfranceschi, *Gazz. Med. Ital.*, **133**, 37 (1974).
(22) E. Astorri, D. Assanelli, G. Bianchi, and B. Colla, *Boll. Soc. Ital. Cardiol.*, in press.
(23) S. Lusena and A. Fontana, *Prog. Med.*, **31**, 28 (1975).
(24) I. G. Mallis, D. H. Schmidt, and J. Lindenbaum, *Clin. Pharmacol. Ther.*, **18**, 761 (1975).

ACKNOWLEDGMENTS AND ADDRESSES

Received May 27, 1975, from the *Institute of Biological Chemistry, School of Medicine, State University, 20100 Milan, Italy.*

Accepted for publication March 16, 1976.

The authors thank Simes S.p.A. for providing Eudigox capsules and Dr. Gandolfi of Sorin S.p.A. for providing kits for digoxin radioimmunoassay.

* Vergani Division of the Ospedale Maggiore "Ca Granda," Milan, Italy.

[x] To whom inquiries should be directed.

Cardiovascular and Neuromuscular Effects of Dimethyl Sulfoxide in Anesthetized Rabbits

FLOYD R. DOMER [x], DAVID M. CHIHAL, and H. CECIL CHARLES

Abstract □ In rabbits anesthetized with pentobarbital, the carotid arterial blood pressure and bilateral contractions of the gastrocnemius muscles due to electrical stimulation of the sciatic nerves were recorded. Intravenous administration of up to 1 ml of dimethyl sulfoxide/kg caused profound hypotension and eventually failure of neuromuscular transmission. Caution must be used in considering dimethyl sulfoxide as a solvent for drug administration.

Keyphrases □ Dimethyl sulfoxide—intravenous administration, cardiovascular and neuromuscular effects, anesthetized rabbits □ Toxicity—dimethyl sulfoxide, intravenous administration, anesthetized rabbits □ Cardiovascular system—effects of intravenous administration of dimethyl sulfoxide, anesthetized rabbits □ Nerve impulse transmission—effects of intravenous administration of dimethyl sulfoxide, anesthetized rabbits

Previous reports demonstrated that dimethyl sulfoxide (I) has blocking activity at the neuromuscular junction *in vitro*. These studies ranged from depression of the guinea pig phrenic nerve diaphragm (1) to partial reversal of tubocurarine blockade in the frog sartorius nerve-muscle preparation (2) to a shift in the dose–response curve with acetylcholine in the chicken biventer cervicis muscular preparation (3). *In vivo* reports of the effects of I include the slow infusion of a 40% solution intravenously in unanesthetized rabbits; this dose (19.2 g/kg) resulted in a 12-mm Hg rise in arterial blood pressure and then bradycardia, which continued until death at 92 min (4). In unanesthetized cats, the LD_{50} for I was approximately 4 g/kg (5), but it was less than 0.4 g/kg in anesthetized cats (6). These findings imply that central nervous system (CNS) depression would have an appreciable effect on the toxicity caused by I.

EXPERIMENTAL

The present experiments were occasioned by the need to have a solvent for some bisquaternary ammonium water-insoluble compounds. Since the compounds were found to have sufficient solubility in I, its effect in one biological preparation to be used for the evaluation of the activity of the bisquaternary compounds was studied.

Albino rabbits, 2.2–2.5 kg, were anesthetized with pentobarbital sodium, 30 mg/kg, administered into the marginal ear vein. The right carotid artery and jugular vein were cannulated to permit the recording of the blood pressure *via* a pressure transducer and the administration of drugs, respectively. The trachea was cannulated, and the respiratory activity was monitored with a transducer connected to a polygraph. The sciatic nerve of each leg was cut proximally, and the distal stump was placed on an electrode connected to a stimulator. The Achilles tendon was cut at its insertion and attached to a transducer. The right leg was stimulated with supramaximal voltage at 1 Hz, and the left leg was stimulated at 0.1 Hz. Doses of I, 0.1, 0.5, and 1.0 ml/kg iv, were given.

RESULTS AND DISCUSSION

The lowest dose caused the diastolic blood pressure to decrease initially about 25 mm Hg. It returned to the control level within 25 min. There was an associated decrease of 50% in the force of contraction of the leg being stimulated at the faster rate. There was no appreciable change in the response occurring on the side being stimulated at the slower rate or in respiration.

When the 0.5-ml/kg dose of I was administered, there was a rapid decrease of 55 mm Hg in diastolic pressure, which returned to the control level within 1 min. Subsequently, there was a second decrease of 35 mm Hg in pressure, which was maximal at 3 min and returned to the control

(4) A. Bertler, A. Redfors, S. Medin, and L. Nyberg, *ibid.*, **2**, 708 (1972).
(5) V. Manninen, J. Melin, and G. Hartel, *ibid.*, **2**, 934 (1971).
(6) E. Steiness, V. Christensen, and H. Johansen, *Clin. Pharmacol. Ther.*, **14**, 949 (1973).
(7) A. J. Dunning, E. J. Buurke, J. C. Roos, A. C. A. Paalman, and H. H. van Rooy, *Ned. Tydschr. Geneesk.*, **117**, 1809 (1973).
(8) J. Lindenbaum, *Pharmacol. Rev.*, **25**, 229 (1973).
(9) M. C. B. Van Oudtshoorn, *Lancet*, **2**, 1153 (1972).
(10) *Federal Register*, **39** (15), 2471 (1974).
(11) D. H. Huffman and D. L. Azarnoff, *J. Am. Med. Assoc.*, **222**, 957 (1972).
(12) D. J. Greenblatt, D. W. Duhme, J. Koch-Weser, and T. W. Smith, *N. Engl. J. Med.*, **289**, 651 (1973).
(13) F. U., 8th ed., vol. 3, Istituto Poligrafico dello Stato Ed., Rome, Italy, 1972, p. 94.
(14) *Federal Register*, **39** (15), 2478 (1974).
(15) T. W. Smith, V. P. Butler, and E. Haber, *N. Engl. J. Med.*, **281**, 1212 (1969).
(16) J. G. Wagner, M. Christensen, E. Sakmar, D. Blair, J. D. Yates, P. W. Willis, A. J. Sedman, and R. G. Stoll, *J. Am. Med. Assoc.*, **224**, 199 (1973).
(17) P. R. Klink, R. I. Poust, J. L. Colaizzi, and R. H. McDonald, *J. Pharm. Sci.*, **63**, 1231 (1974).
(18) J. L. Colaizzi and J. G. Wagner, *J. Am. Pharm. Assoc.*, **NS 15**, 43 (1975).
(19) D. H. Huffman and C. V. Manion, *Clin. Pharmacol. Ther.*, **15**, 310 (1974).
(20) G. Levy and M. Gibaldi, *Circulation*, **49**, 391 (1974).
(21) G. Catenazzo, P. Ghirardi, O. Mantero, and G. Gianfranceschi, *Gazz. Med. Ital.*, **133**, 37 (1974).
(22) E. Astorri, D. Assanelli, G. Bianchi, and B. Colla, *Boll. Soc. Ital. Cardiol.*, in press.
(23) S. Lusena and A. Fontana, *Prog. Med.*, **31**, 28 (1975).
(24) I. G. Mallis, D. H. Schmidt, and J. Lindenbaum, *Clin. Pharmacol. Ther.*, **18**, 761 (1975).

ACKNOWLEDGMENTS AND ADDRESSES

Received May 27, 1975, from the *Institute of Biological Chemistry, School of Medicine, State University, 20100 Milan, Italy.*

Accepted for publication March 16, 1976.

The authors thank Simes S.p.A. for providing Eudigox capsules and Dr. Gandolfi of Sorin S.p.A. for providing kits for digoxin radioimmunoassay.

* Vergani Division of the Ospedale Maggiore "Ca Granda," Milan, Italy.

[x] To whom inquiries should be directed.

Cardiovascular and Neuromuscular Effects of Dimethyl Sulfoxide in Anesthetized Rabbits

FLOYD R. DOMER [x], DAVID M. CHIHAL, and H. CECIL CHARLES

Abstract □ In rabbits anesthetized with pentobarbital, the carotid arterial blood pressure and bilateral contractions of the gastrocnemius muscles due to electrical stimulation of the sciatic nerves were recorded. Intravenous administration of up to 1 ml of dimethyl sulfoxide/kg caused profound hypotension and eventually failure of neuromuscular transmission. Caution must be used in considering dimethyl sulfoxide as a solvent for drug administration.

Keyphrases □ Dimethyl sulfoxide—intravenous administration, cardiovascular and neuromuscular effects, anesthetized rabbits □ Toxicity—dimethyl sulfoxide, intravenous administration, anesthetized rabbits □ Cardiovascular system—effects of intravenous administration of dimethyl sulfoxide, anesthetized rabbits □ Nerve impulse transmission—effects of intravenous administration of dimethyl sulfoxide, anesthetized rabbits

Previous reports demonstrated that dimethyl sulfoxide (I) has blocking activity at the neuromuscular junction *in vitro*. These studies ranged from depression of the guinea pig phrenic nerve diaphragm (1) to partial reversal of tubocurarine blockade in the frog sartorius nerve-muscle preparation (2) to a shift in the dose–response curve with acetylcholine in the chicken biventer cervicis muscular preparation (3). *In vivo* reports of the effects of I include the slow infusion of a 40% solution intravenously in unanesthetized rabbits; this dose (19.2 g/kg) resulted in a 12-mm Hg rise in arterial blood pressure and then bradycardia, which continued until death at 92 min (4). In unanesthetized cats, the LD_{50} for I was approximately 4 g/kg (5), but it was less than 0.4 g/kg in anesthetized cats (6). These findings imply that central nervous system (CNS) depression would have an appreciable effect on the toxicity caused by I.

EXPERIMENTAL

The present experiments were occasioned by the need to have a solvent for some bisquaternary ammonium water-insoluble compounds. Since the compounds were found to have sufficient solubility in I, its effect in one biological preparation to be used for the evaluation of the activity of the bisquaternary compounds was studied.

Albino rabbits, 2.2–2.5 kg, were anesthetized with pentobarbital sodium, 30 mg/kg, administered into the marginal ear vein. The right carotid artery and jugular vein were cannulated to permit the recording of the blood pressure *via* a pressure transducer and the administration of drugs, respectively. The trachea was cannulated, and the respiratory activity was monitored with a transducer connected to a polygraph. The sciatic nerve of each leg was cut proximally, and the distal stump was placed on an electrode connected to a stimulator. The Achilles tendon was cut at its insertion and attached to a transducer. The right leg was stimulated with supramaximal voltage at 1 Hz, and the left leg was stimulated at 0.1 Hz. Doses of I, 0.1, 0.5, and 1.0 ml/kg iv, were given.

RESULTS AND DISCUSSION

The lowest dose caused the diastolic blood pressure to decrease initially about 25 mm Hg. It returned to the control level within 25 min. There was an associated decrease of 50% in the force of contraction of the leg being stimulated at the faster rate. There was no appreciable change in the response occurring on the side being stimulated at the slower rate or in respiration.

When the 0.5-ml/kg dose of I was administered, there was a rapid decrease of 55 mm Hg in diastolic pressure, which returned to the control level within 1 min. Subsequently, there was a second decrease of 35 mm Hg in pressure, which was maximal at 3 min and returned to the control

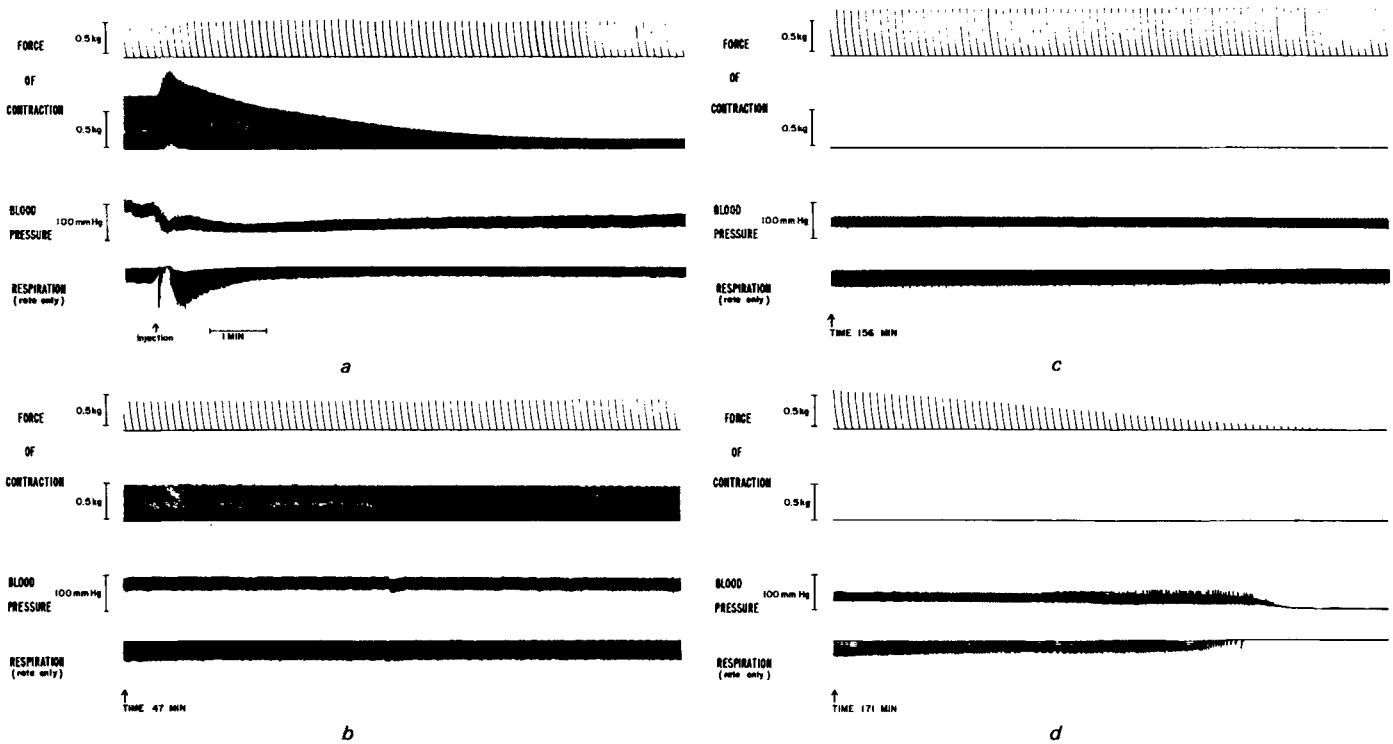

Figure 1—*Effect of dimethyl sulfoxide (1 ml/kg) on force of contraction, blood pressure, and respiration rate in anesthetized rabbits.*

level at 22 min. The leg being stimulated at the faster rate exhibited a 3–7% decrease in the force of contraction during the 1st min. After returning to the control intensity of contraction, there was a secondary decrease to a maximum of 31% at 6 min, which returned to the control level at about the same time as the blood pressure.

When the 1.0-ml/kg dose was administered, there was a rapid decrease of 55 mm Hg in diastolic pressure (Fig. 1*a*) during the 1st min. At 47 min (Fig. 1*b*), the blood pressure was still 20 mm Hg less than it had been prior to the injection. Thereafter, the blood pressure decreased progressively and the animal died at 179 min. The neuromuscular activity was initially decreased 83% at about 10 min. Subsequently, the force of contraction returned to 70% of control at 47 min (Fig. 1*b*). A secondary blockade developed, which became 100% by 156 min (Fig. 1*c*). The animal died 23 min later (Fig. 1*d*).

The profound effects upon the cardiovascular system are in agreement with a recent report (7) indicating that I caused a profound negative chronotropic effect. The effect on the force of myocardial contraction was variable and was thought to be dependent upon the efficiency of filling of the ventricles prior to each beat. The profound, sustained hypotension may have embarrassed the neuromuscular function too.

The fact that such profound effects were found in anesthetized rabbits with a total dose of 1.6 ml/kg of I is rather striking when compared to the infused dose of 19.2 g/kg required to kill unanesthetized rabbits (4). A similar enhancing effect of anesthesia on toxicity of I was found in cats (5, 6). This finding indicates that CNS depression caused by general anesthetics potentiates the toxic effects of I.

These results characterize the profound effects of I on both the cardiovascular and neuromuscular systems of the rabbit. They severely restrict its possible utility as a solvent for *in vivo* studies of poorly water-soluble compounds.

REFERENCES

(1) W. M. Sams, Jr., N. V. Carroll, and P. L. Crantz, *Proc. Soc. Exp. Biol. Med.*, **122**, 103 (1966).

(2) M. H. Evans and P. J. Jaggard, *Br. J. Pharmacol.*, **49**, 651 (1973).

(3) A. Gandiha and I. G. Marshall, *J. Pharm. Pharmacol.*, **24**, 417 (1972).

(4) F. M. E. Caujolle, D. H. Caujolle, S. B. Cros, and M.-M. J. Calvet, *Ann. N.Y. Acad. Sci.*, **141**, 110 (1967).

(5) E. R. Smith, Z. Hadidian, and M. M. Mason, *ibid.*, **141**, 96 (1967).

(6) V. Distefano and J. J. Klahn, *Toxicol. Appl. Pharmacol.*, **7**, 660 (1965).

(7) M. Shlafer and A. M. Karow, Jr., *Ann. N.Y. Acad. Sci.*, **243**, 110 (1975).

ACKNOWLEDGMENTS AND ADDRESSES

Received January 30, 1976, from the *Department of Pharmacology, School of Medicine, Tulane University, New Orleans, LA 70112.*

Accepted for publication March 29, 1976.

Supported in part by Grant 5 R01 NS11580 from the National Institutes of Health.

[x] To whom inquiries should be directed.

Biological Disposition of Rigid Analogs of Amphetamine

RAY W. FULLER[x], JOHN C. BAKER, and BRYAN B. MOLLOY

Abstract □ Tissue levels of amphetamine and of amphetamine analogs with a rigid conformation (2-aminoindan, 2-aminotetralin, and 2-aminobenzocycloheptene) were measured in rats by a spectrofluorometric method involving the reaction of the primary amine group with fluorescamine. All drugs were concentrated in tissues, the order of distribution being lungs > kidneys > liver = spleen = brain > muscle > fat = heart > blood. In brain, amphetamine and 2-aminoindan were present mostly in the supernatant fraction after high speed centrifugation of brain homogenates; the two higher molecular weight drugs were present at slightly greater concentrations in the particulate fraction. All four drugs disappeared from rat brain with half-lives of 1–2 hr. Iprindole pretreatment increased drug levels in brain and prolonged the half-lives by two- to threefold. The data suggest that the biological disposition of the rigid analogs resembles generally that of amphetamine and that all of the drugs are probably metabolized by ring hydroxylation in the rat.

Keyphrases □ Amphetamine and analogs—with rigid conformation, biological disposition, spectrofluorometric analysis in rat tissues, effect of pretreatment with iprindole □ Distribution, biological—amphetamine and analogs with rigid conformation, spectrofluorometric analysis in rat tissues, effect of pretreatment with iprindole □ Spectrofluorometry—analysis, amphetamine and analogs with rigid conformation, rat tissues □ Iprindole—pretreatment, effect on biological disposition of amphetamine and analogs with rigid conformations, rats □ Stimulants, central—amphetamine and analogs with rigid conformation, biological disposition, rats

Among drugs acting on the central nervous system, amphetamine has been one of the most widely investigated. Numerous structural derivatives of amphetamine have been synthesized and studied, including amphetamine analogs having a rigid conformation due to a bridge between the α-carbon and the ring. For instance, hydroxylated and methoxylated 2-aminotetralins have been of interest because of their relationship to psychotomimetic drugs such as mescaline (1, 2). 2-Aminoindans and 2-aminotetralins have been evaluated as potential antiparkinsonism drugs based on their structural similarity to dopamine (3, 4). Effects of these rigid analogs on monoamine metabolism *in vivo* and on monoamine oxidase *in vitro* have been reported (5, 6).

This paper deals with three rigid analogs of amphetamine (I), in which the α-carbon is connected to the *ortho*-position of the ring directly (2-aminoindan, II) or through one (2-aminotetralin, III) or two (2-aminobenzocycloheptene, IV) methylene units. Much is known about the metabolism and biological disposition of amphetamine in various animal species. This study compares some fundamental pharmacokinetic parameters of these rigid analogs of amphetamine in rats, including their levels in tissues and rates of disappearance from brain.

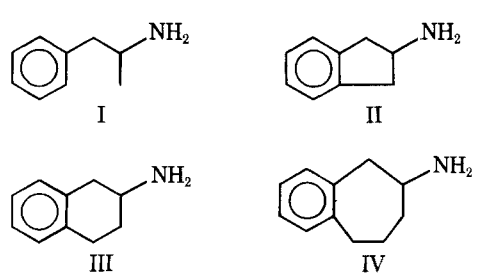

Table I—Subcellular Distribution of Amphetamine and Rigid Analogs in Rat Brain[a]

Drug	Drug Level in Brain, nmoles/g: Particulate (P)	Supernate (S)	Ratio, P/S
I	44 ± 7	75 ± 7	0.6
II	51 ± 1	90 ± 3	0.6
III	67 ± 1	62 ± 5	1.1
IV	61 ± 7	49 ± 2	1.2

[a] Drugs were injected at 0.1 mmole/kg ip 1 hr before the rats were killed. Brain homogenates (in 2.5 m*M* sucrose) were centrifuged for 30 min at 100,000×*g*. Drug levels were measured both in particulate and supernatant fractions.

EXPERIMENTAL

dl-Amphetamine hemisulfate was used as purchased[1]. The derivatives of amphetamine were synthesized[2] as hydrochloride or hemisulfate salts. All were racemic mixtures. The drugs were injected intraperitoneally in aqueous solution into male Wistar rats[3] weighing about 150 g. The rats were maintained in a room with controlled lighting and temperature and with food and water available *ad libitum*. After they were treated with drugs, the rats were killed by decapitation. Tissues were quickly removed and frozen on dry ice and then stored frozen prior to analysis.

Drug levels were measured spectrofluorometrically[4] by a previously described method (7) after extraction and reaction with fluorescamine. All data are expressed as mean values with standard errors for five rats per group. Comparisons between groups were made by the Student *t* test.

RESULTS AND DISCUSSION

The three rigid analogs of amphetamine reacted with fluorescamine to form fluorophores with characteristics similar to those of the fluorophore produced by amphetamine, *i.e.*, with maximum excitation at 390 nm and maximum emission at 490 nm. Standard curves over a 30–90-nmoles/ml concentration range established fluorescent intensity to be linearly proportional to concentration. The standard curves were similar for all four amines, so reaction with fluorescamine provided a sensitive means for assaying tissue levels of these drugs.

Figure 1 shows the distribution of the drugs in various tissues 1 hr after injection of equimolar doses. All compounds were highly concentrated in tissues, with blood levels of the drugs (not shown) being very low (about half of the levels shown for heart). The general pattern of tissue distribution was similar for the four drugs. For instance, drug levels in lung were higher in all cases than in any other tissue. Drug levels in skeletal muscle were low, and drug levels in epididymal fat and heart were even lower for all four drugs.

Some differences in relative drug levels were noticed in the remaining tissues. Compound II was present in most tissues at higher levels than amphetamine or the other derivatives with a rigid conformation. Levels of all rigid analogs tended to be higher in brain than those of amphetamine. Levels of III and IV were at least as high in brain as in liver or spleen. The ratio of drug levels in brain–skeletal muscle progressively increased with size of the drug molecule (1.3 for I, 2.0 for II, 3.2 for III, and 3.9 for IV). These differences suggest that the larger bicyclic compounds have a greater relative affinity for brain than does amphetamine.

The subcellular distribution of the drugs in brain homogenates subjected to centrifugation at 100,000×*g* is shown in Table I. As reported

[1] Chemicals Procurement Laboratories, College Park, N.Y.
[2] In the Lilly Research Laboratories.
[3] Harlan Industries, Cumberland, Ind.
[4] Aminco-Bowman spectrophotofluorometer.

Table II—Drug Levels and Half-Lives of Rigid Analogs of Amphetamine in Brains of Control Rats and Rats Treated with Iprindole to Inhibit Aromatic Hydroxylation

Drug	Iprindole	Drug Level in Brain, nmoles/g				Half-Life, hr
		1 hr	2 hr	3 hr	4 hr	
I	–	84 ± 6	49 ± 10	39 ± 4	18 ± 3	1.4
	+	109 ± 9[a]	103 ± 9[a]	83 ± 8[a]	65 ± 5[a]	3.9[a]
II	–	148 ± 6	110 ± 7	78 ± 6	44 ± 6	1.7
	+	136 ± 4	111 ± 3	91 ± 6	73 ± 4[a]	3.3[a]
III	–	120 ± 7	69 ± 8	52 ± 8	25 ± 4	1.3
	+	133 ± 9	103 ± 7[a]	87 ± 5[a]	71 ± 3[a]	3.6[a]
IV	–	100 ± 7	55 ± 4	26 ± 4	16 ± 5	1.0
	+	120 ± 7	89 ± 2[a]	78 ± 3[a]	81 ± 3[a]	3.3[a]

[a] Significant difference from corresponding group without iprindole, $p < 0.05$. Drugs were injected at zero time at a dose of 0.1 mmole/kg ip; some rats had been pretreated 1 hr earlier with iprindole (10 mg/kg ip).

previously (8), about two-thirds of the amphetamine (I) in brain was recovered in the supernatant fraction. The same distribution was found for II, but III and IV were present in the particulate fraction at slightly higher concentrations than in the supernatant fraction. This distribution may reflect, at least in part, the lipophilic character of the drug molecule, since halogenated derivatives of amphetamine have high particulate–supernatant ratios (8).

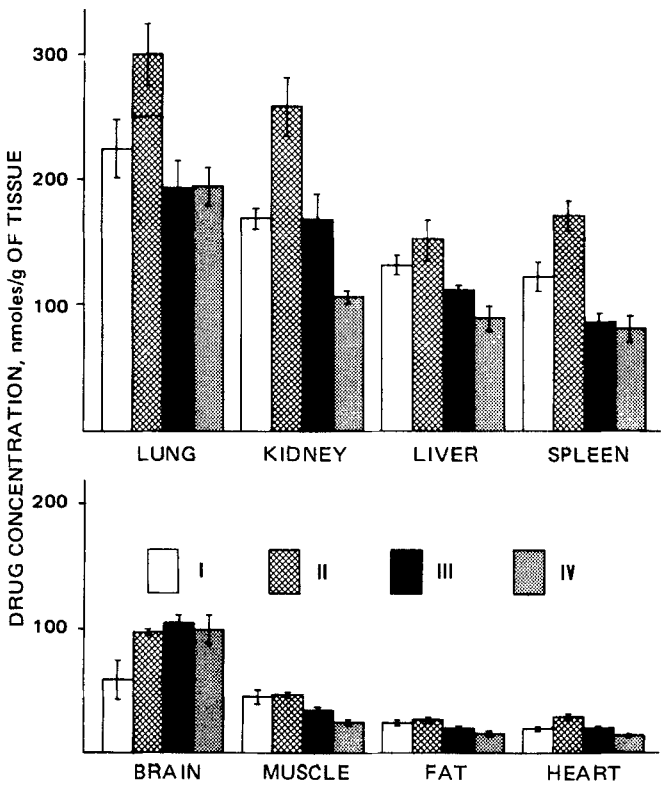

Figure 1—*Tissue distribution of amphetamine and rigid analogs in various organs of the rat. Drugs were injected at 0.1 mmole/kg ip 1 hr before the rats were killed.*

Drug levels in brain at four different times are shown in Table II. From semilogarithmic plots of drug levels *versus* time, half-life values of all four drugs were calculated to be between 1 and 2 hr. In rats pretreated with iprindole, an inhibitor of the aromatic hydroxylation of amphetamine (9), half-lives were increased two- to threefold. This finding constitutes indirect evidence that all of these drugs are metabolized by aromatic hydroxylation in the rat.

REFERENCES

(1) J. P. Green, K. P. Dressler, and N. Khazan, *Life Sci.*, **12**, 475 (1973).

(2) C. F. Barfknecht, D. E. Nichols, D. B. Rusterholz, J. P. Long, J. A. Engelbrecht, J. M. Beaton, R. J. Bradley, and D. C. Dyer, *J. Med. Chem.*, **16**, 804 (1973).

(3) Y. C. Martin, C. H. Jarboe, R. A. Krause, K. R. Lynn, D. Dunnigan, and J. B. Holland, *ibid.*, **16**, 147 (1973).

(4) J. D. McDermed, G. M. McKenzie, and A. P. Phillips, *ibid.*, **18**, 362 (1975).

(5) P. A. Crooks, H. J. Little, and J. M. H. Rees, *J. Pharm. Pharmacol.*, **25**, P124 (1973).

(6) Y. C. Martin, J. B. Holland, C. H. Jarboe, and N. Plotnikoff, *J. Med. Chem.*, **17**, 409 (1974).

(7) R. W. Fuller, K. W. Perry, J. C. Baker, C. J. Parli, N. Lee, W. A. Day, and B. B. Molloy, *Biochem. Pharmacol.*, **23**, 3267 (1974).

(8) R. W. Fuller and C. W. Hines, *J. Pharm. Sci.*, **56**, 302 (1967).

(9) J. J. Freeman and F. Sulser, *J. Pharmacol. Exp. Ther.*, **183**, 307 (1972).

ACKNOWLEDGMENTS AND ADDRESSES

Received January 15, 1976, from *Lilly Research Laboratories, Division of Eli Lilly and Company, Indianapolis, IN 46206.*

Accepted for publication March 29, 1976.

[x] To whom inquiries should be directed.

Rapid Acetylation of a Dihydroxy Compound by 4-(Dimethylamino)pyridine Catalysis: Application to GLC Determination of Clindamycin Palmitate Hydrochloride

ENGLEBERT L. ROWE ˣ **and SUSAN M. MACHKOVECH** *

Abstract □ The acetylation of clindamycin palmitate hydrochloride, preparatory to GLC assay, was accelerated greatly by the use of 4-(dimethylamino)pyridine as a catalyst. The reaction time was reduced from 2.5 hr at 100° using pyridine and acetic anhydride to 30 min or less at ambient temperature upon addition of excess catalyst.

Keyphrases □ Clindamycin palmitate hydrochloride—GLC analysis after acetylation catalyzed by 4-(dimethylamino)pyridine □ 4-(Dimethylamino)pyridine—catalyst for acetylation of clindamycin palmitate hydrochloride preparatory to GLC assay □ GLC—analysis, clindamycin palmitate hydrochloride, after acetylation catalyzed by 4-(dimethylamino)pyridine □ Dihydroxy compounds—clindamycin palmitate hydrochloride, GLC analysis after acetylation catalyzed by 4-(dimethylamino)pyridine □ Antibacterials—clindamycin palmitate hydrochloride, GLC analysis after acetylation catalyzed by 4-(dimethylamino)pyridine

The acetylation of clindamycin palmitate hydrochloride (I) for GLC assay is catalyzed by the use of pyridine, which also acts as a solvent for the reaction (1). Pyridine forms an intermediate with acetic anhydride, acetylpyridinium ion (2), which then reacts with the hydroxyl groups at the 3- and 4-positions of clindamycin palmitate hydrochloride. The reaction requires 2.5 hr at 100° for completion.

4-(Dimethylamino)pyridine (II) recently was reported to be a much better catalyst than pyridine for various acylations (2, 3). The present study compares the rate of acetylation of I in pyridine in both the presence and absence of II.

EXPERIMENTAL

Materials—All materials were analytical reagent grade.

GLC Conditions—A gas chromatograph[1] equipped with a flame-ionization detector and an electronic integrator[2] was used. The glass U-shaped column, 3 mm × 60 cm, was packed with 1% SE-54 on Gas Chrom Q (100–120 mesh). The column was conditioned for 1 week at 295° under low helium flow. The operating temperatures were: column, 275°; detector, 290°; and flash heater, off. Helium was used as the carrier gas at about 60 ml/min. One microliter of sample was injected, and the attenuation was adjusted to give peak heights averaging about 50% of the chart heights.

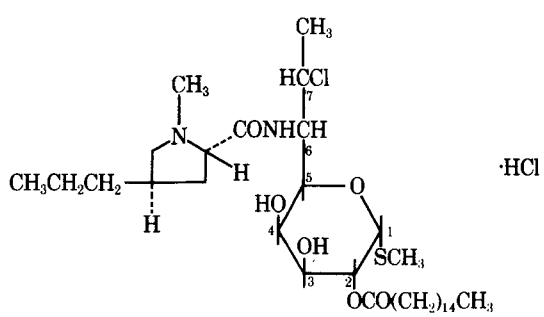

I

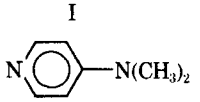

II

Internal Standard Solution—A solution of trilaurin in chloroform was used at a concentration of 5 mg/ml.

Procedure—About 75 mg of I was accurately weighed and dissolved in 5 ml of double-distilled water. One milliliter of 30% sodium carbonate solution and 5 ml of internal standard were added, and the solution was shaken vigorously for 10 min and centrifuged to form distinct layers. The aqueous layer was aspirated off, and 1-ml portions of the chloroform layer were transferred to 15-ml centrifuge tubes. One milliliter of acetic anhydride and 1 ml of pyridine were added to the tubes, and the tubes were stoppered and allowed to react at the appropriate temperature.

In the standard method, the reaction was carried out in an oven at 95° and sampled at various intervals. In the modified method, II was dissolved in pyridine at a concentration of 15 mg/ml. One milliliter of this solution (instead of pure pyridine) was used for the acylation medium. The tubes were held at ambient temperature (23–26°) and sampled for GLC injection at various times.

RESULTS AND DISCUSSION

The progress of acetylation of I using II as a catalyst at room temperature is compared to the pyridine-catalyzed reaction at 95° in Fig. 1. The GLC peak for diacetylated I becomes sharper as the reaction progresses. The disappearing peak on the tailing edge of the main peak is the 3-monoacetate ester of I. It was reported (4) that the 3-hydroxy group is the least sterically hindered hydroxyl group in the lincomycin[3] molecule

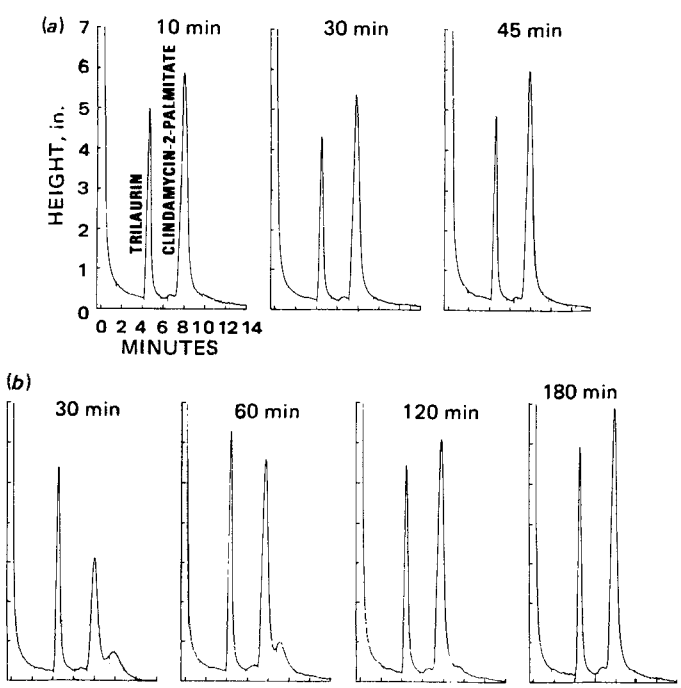

Figure 1—*Gas chromatograms illustrating the acetylation of I. Key: a, 4-(dimethylamino)pyridine added to pyridine, reaction at room temperature; and b, pyridine alone, reaction at 95°.*

[1] F & M model 402.

[2] Infotronics model CRS-104.

[3] Clindamycin is the 7-deoxy-7-(*S*)-chloro analog of lincomycin.

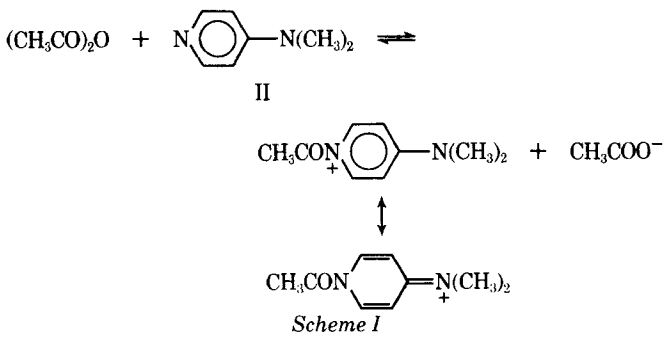

Scheme I

and, therefore, the most reactive. The 4-hydroxy group reacts more slowly and is the controlling factor in the diacetylation of I. The shoulder on the leading edge, always present even in highly purified lots of I, is the acetate esters of clindamycin B-2-palmitate (the 4′-ethyl analog of I) and clindamycin 3-palmitate, as indicated by Brown (1). In practice, this latter peak is not integrated with the main peak.

The acetylation reaction, using II as a catalyst, was virtually complete within 30 min at ambient temperature (Fig. 1*a*). In the absence of II, the reaction was not complete until well after 2 hr at 95° (Fig. 1*b*).

The quantitative GLC data are given in Table I. Clearly, the two procedures differed considerably in their reaction rates. Even after 26 hr, the peak area ratio for the II-catalyzed reaction was still at the plateau value without significant change.

The complete acetylation of I is a two-step reaction as already described. Acetylation of the more labile 3-hydroxy group is fast, so the reaction is controlled primarily by the second acetylation of the 4-hydroxy group. The rate of reaction is dependent on the concentrations of I, II, pyridine, and acetic anhydride. Since the latter three reagents are present in large excess compared to I, they can be considered constant. Therefore, the reaction can be approximated by the simple first-order expression:

$$-\frac{d[I]}{dt} = k_{obs}[I] \qquad \text{(Eq. 1)}$$

In integrated form, expressing concentration in percent:

$$\log \frac{100[I]}{[I_0]} = \log 100 - k_{obs}t \qquad \text{(Eq. 2)}$$

where $[I_0]$ is the initial concentration of I, and [I] is the concentration at time t.

In Fig. 2, the data are plotted according to Eq. 2. The slopes differ by a factor of about nine. In other words, even with a temperature difference of 70°, the room temperature reaction using II as a catalyst was about nine times faster than the pyridine-catalyzed reaction at 95°. If the temperatures were equal, the differences would be several orders of magnitude. Connors and Albert (2) found that the rate constant using II was 2×10^4 greater than that of the corresponding pyridine-catalyzed acetylation of 2-propanol at 54°.

The intercepts from least-squares regression analysis of the data are considerably less than 100%, as can be seen from Fig. 2. This result is due to the stepwise nature of the acetylation, which is better represented by two consecutive first-order reactions rather than by a single first-order reaction. If sufficient early time points were available, it would be apparent that there is a steep slope initially which would intersect the y-axis at about 100%.

The mechanism of the catalytic action of pyridine involves formation of an intermediate with acetic anhydride. The acetylpyridinium ion then undergoes nucleophilic attack by the hydroxy group. There is spectroscopic evidence that the acetylpyridinium ion has a very small stability constant because its presence is almost undetectable (5). Connors and Albert (2) suggested that the intermediate formed by II has enhanced stability due to the resonance forms made possible by the dimethylamino group (Scheme I).

The modified assay was applied to other 2-acyl esters of clindamycin ranging in chain length from 10 to 18 carbon atoms. The reaction rates were about equal to the palmitate, requiring no more than 30 min at ambient temperature in any case. Compound II should prove to be a versatile catalyst for acylation of other hydroxy compounds being prepared for GLC analysis.

Table I—Comparison of Two Procedures for Acetylation of I (GLC Assay)

Acetylation Procedure	Minutes	Sample	Peak Area Ratio	Average
Pyridine, 95°	30	1	1.476	1.249
		2	1.022	
	60	1	1.640	1.548
		2	1.512	
		2	1.492	
	120	1	1.894	1.917
		1	1.963	
		2	1.917	
		2	1.895	
	180	1	2.038	2.024
		2	2.009	
II in pyridine, room temperature	10	1	1.694	1.822
		2	2.002	
		2	1.771	
	30	1	2.050	2.120
		2	2.214	
		2	2.096	
	45	1	1.988	2.116
		2	2.227	
		2	2.134	
	60	1	1.971	2.065
		2	2.160	
	75	1	2.054	2.099
		1	2.092	
		2	2.152	
	90	1	2.093	2.108
		2	2.122	
	120	1	2.050	2.050
	26 hr	1	2.130	2.130

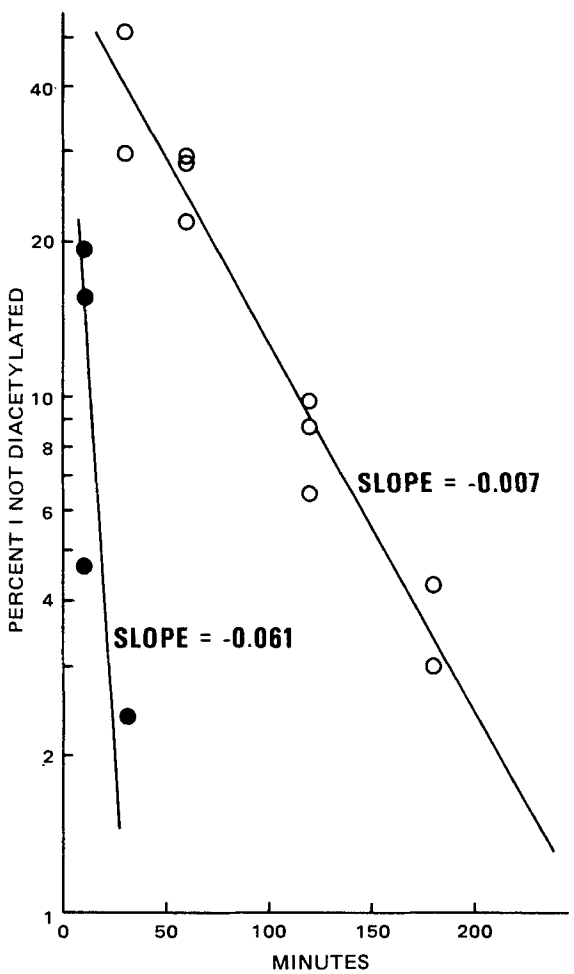

Figure 2—*Pseudo-first-order plot of acetylation of I by acetic anhydride. Key:* ○, *pyridine only, reaction at 95°; and* ●, *4-(dimethylamino)pyridine added to pyridine (15 mg/ml), reaction at room temperature.*

REFERENCES

(1) L. W. Brown, *J. Pharm. Sci.*, **63**, 1597 (1974).

(2) K. A. Connors and K. S. Albert, *ibid.*, **62**, 845 (1973).

(3) W. Steglich and G. Höfle, *Angew. Chem., Int. Ed.*, **8**, 981 (1969).

(4) W. Morozowich, F. A. MacKellar, and C. Lewis, presented at APhA Academy of Pharmaceutical Sciences, Washington meeting, Apr. 1970.

(5) G. H. Schenk, P. Wines, and C. Mojzis, *Anal. Chem.*, **36**, 914 (1964).

ACKNOWLEDGMENTS AND ADDRESSES

Received January 21, 1976, from *Pharmacy Research, The Upjohn Company, Kalamazoo, MI 49001.*

Accepted for publication March 29, 1976.

The authors are grateful to Mr. E. J. Kubiak at The Upjohn Co. for providing materials and advice on column conditioning and assay parameters and to Dr. W. Morozowich for suggestions and consultations.

* Present address: School of Pharmacy, University of Michigan, Ann Arbor, MI 48104.

ˣ To whom inquiries should be directed.

Tissue Distribution of ^{3}H-Canrenoate Potassium in Rabbits

A. MICHAELS FINN, R. BROWN, and W. SADÉE ˣ

Abstract □ Plasma and various organ concentrations of canrenone, canrenoate, and total ^{3}H-activity were measured following single doses of 20 mg of ^{3}H-canrenoate/kg iv to rabbits. Organs studied included heart, lungs, brain, kidneys, liver, adrenal glands, and spleen. Canrenoate was shown to be in rapid equilibrium with canrenone. Both were eliminated from plasma and other tissues with a half-life of about 1 hr. Plasma concentrations of both drugs were equal as early as 10 min after intravenous drug administration. Canrenone was concentrated about 10-fold in organ tissues when compared to plasma, while no such preferential uptake was found with canrenoate. Total ^{3}H-activity declined slowly in all tissues with a half-life of approximately 15 hr, indicating extensive metabolism and metabolite retention in the rabbit.

Keyphrases □ Canrenoate potassium—tissue distribution and metabolism, radiochemical study, rabbits □ Distribution, tissue—canrenoate potassium, radiochemical study, rabbits □ Metabolism—canrenoate potassium, radiochemical study, rabbits □ Radiochemistry—study of tissue distribution and metabolism, canrenoate potassium, rabbits □ Aldosterone antagonists—canrenoate potassium, tissue distribution and metabolism, radiochemical study, rabbits

The antimineralocorticoid compounds spironolactone[1] (I) and canrenoate potassium (III) are useful diuretic agents (1). Spironolactone is rapidly metabolized *via* a 7α-thiol derivative (2) to canrenone (II), a major metabolite, which exists in enzymatic equilibrium with III (Scheme I). The pharmacokinetics of I–III were investigated in rats (3), dogs (4), and humans (5, 6). Data on the kinetic disposition and further metabolism of II and III are scant (2, 7). Large differences between the tissue distribution of the lipophilic II and the water-soluble III can be expected and should be considered in the interpretation of plasma II and III levels. In this study, the tissue distribution of III potassium was investigated in rabbits.

EXPERIMENTAL

Chemicals—Pure crystalline samples of I and III were used[2], and II was prepared from III as previously described (8). ^{3}H-Canrenoate potassium[3], with a specific activity of 860 μCi/mg, was purified by solvent extraction (8) and TLC[4] in dichloromethane–methanol (8:2) prior to use. All reagents and chemicals were spectroquality.

Analytical Procedures—The fluorometric determination of II and III was performed as described previously (9). This method was specific for II and III in the presence of all other metabolites of III (8). Tritium measurements were performed by liquid scintillation counting as described previously (8). Efficiency was measured by the channels ratio method.

Rabbit Protocols—*Serial Blood Sampling*—Female New Zealand White rabbits, 2–2.5 kg, were used. Each rabbit was prepared for blood sampling by insertion of a polyethylene 50 catheter about 4 cm into an ear artery. Doses of 5, 10, and 20 mg of III/kg in aqueous solution were given by venous injections into the opposite ear. Blood samples of 2 ml each were taken with heparinized syringes at appropriate time intervals and centrifuged, and the plasma was frozen for subsequent analysis.

Tissue Analysis—Doses of 20 mg of ^{3}H-III/kg, with a specific activity of 0.2–0.5 μCi/mg, were given intravenously into an ear vein. Rabbits were sacrificed by decapitation at the following times after drug administration: 5, 10, 20, 30, 60, and 90 min and 2, 4, 8, 16, and 32 hr. One animal was used per time interval, with the exception of the 2-hr experiments where three animals were used.

Blood was collected by exsanguination from the abdominal aorta. The heart, lungs, brain, kidneys, liver, adrenal glands, and spleen were re-

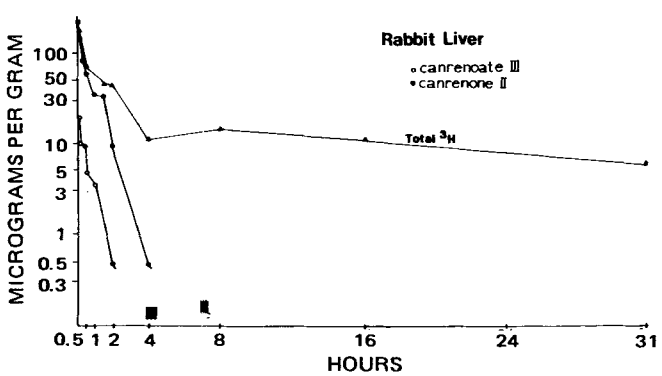

Figure 1—*Concentrations of total ^{3}H-radioactivity measured by liquid scintillation counting and concentrations of II and III measured by a specific fluorescence assay in rabbit liver.*

[1] Aldactone, Searle and Co.

[2] Boehringer Mannheim G.M.b.H.

[3] G. D. Searle and Co.

[4] Silica gel K C F254 Merck plates were used.

REFERENCES

(1) L. W. Brown, *J. Pharm. Sci.*, **63**, 1597 (1974).

(2) K. A. Connors and K. S. Albert, *ibid.*, **62**, 845 (1973).

(3) W. Steglich and G. Höfle, *Angew. Chem., Int. Ed.*, **8**, 981 (1969).

(4) W. Morozowich, F. A. MacKellar, and C. Lewis, presented at APhA Academy of Pharmaceutical Sciences, Washington meeting, Apr. 1970.

(5) G. H. Schenk, P. Wines, and C. Mojzis, *Anal. Chem.*, **36**, 914 (1964).

ACKNOWLEDGMENTS AND ADDRESSES

Received January 21, 1976, from *Pharmacy Research, The Upjohn Company, Kalamazoo, MI 49001.*

Accepted for publication March 29, 1976.

The authors are grateful to Mr. E. J. Kubiak at The Upjohn Co. for providing materials and advice on column conditioning and assay parameters and to Dr. W. Morozowich for suggestions and consultations.

* Present address: School of Pharmacy, University of Michigan, Ann Arbor, MI 48104.

ˣ To whom inquiries should be directed.

Tissue Distribution of ^{3}H-Canrenoate Potassium in Rabbits

A. MICHAELS FINN, R. BROWN, and W. SADÉE ˣ

Abstract □ Plasma and various organ concentrations of canrenone, canrenoate, and total ^{3}H-activity were measured following single doses of 20 mg of ^{3}H-canrenoate/kg iv to rabbits. Organs studied included heart, lungs, brain, kidneys, liver, adrenal glands, and spleen. Canrenoate was shown to be in rapid equilibrium with canrenone. Both were eliminated from plasma and other tissues with a half-life of about 1 hr. Plasma concentrations of both drugs were equal as early as 10 min after intravenous drug administration. Canrenone was concentrated about 10-fold in organ tissues when compared to plasma, while no such preferential uptake was found with canrenoate. Total ^{3}H-activity declined slowly in all tissues with a half-life of approximately 15 hr, indicating extensive metabolism and metabolite retention in the rabbit.

Keyphrases □ Canrenoate potassium—tissue distribution and metabolism, radiochemical study, rabbits □ Distribution, tissue—canrenoate potassium, radiochemical study, rabbits □ Metabolism—canrenoate potassium, radiochemical study, rabbits □ Radiochemistry—study of tissue distribution and metabolism, canrenoate potassium, rabbits □ Aldosterone antagonists—canrenoate potassium, tissue distribution and metabolism, radiochemical study, rabbits

The antimineralocorticoid compounds spironolactone[1] (I) and canrenoate potassium (III) are useful diuretic agents (1). Spironolactone is rapidly metabolized *via* a 7α-thiol derivative (2) to canrenone (II), a major metabolite, which exists in enzymatic equilibrium with III (Scheme I). The pharmacokinetics of I–III were investigated in rats (3), dogs (4), and humans (5, 6). Data on the kinetic disposition and further metabolism of II and III are scant (2, 7). Large differences between the tissue distribution of the lipophilic II and the water-soluble III can be expected and should be considered in the interpretation of plasma II and III levels. In this study, the tissue distribution of III potassium was investigated in rabbits.

EXPERIMENTAL

Chemicals—Pure crystalline samples of I and III were used[2], and II was prepared from III as previously described (8). ^{3}H-Canrenoate potassium[3], with a specific activity of 860 μCi/mg, was purified by solvent extraction (8) and TLC[4] in dichloromethane–methanol (8:2) prior to use. All reagents and chemicals were spectroquality.

Analytical Procedures—The fluorometric determination of II and III was performed as described previously (9). This method was specific for II and III in the presence of all other metabolites of III (8). Tritium measurements were performed by liquid scintillation counting as described previously (8). Efficiency was measured by the channels ratio method.

Rabbit Protocols—*Serial Blood Sampling*—Female New Zealand White rabbits, 2–2.5 kg, were used. Each rabbit was prepared for blood sampling by insertion of a polyethylene 50 catheter about 4 cm into an ear artery. Doses of 5, 10, and 20 mg of III/kg in aqueous solution were given by venous injections into the opposite ear. Blood samples of 2 ml each were taken with heparinized syringes at appropriate time intervals and centrifuged, and the plasma was frozen for subsequent analysis.

Tissue Analysis—Doses of 20 mg of ^{3}H-III/kg, with a specific activity of 0.2–0.5 μCi/mg, were given intravenously into an ear vein. Rabbits were sacrificed by decapitation at the following times after drug administration: 5, 10, 20, 30, 60, and 90 min and 2, 4, 8, 16, and 32 hr. One animal was used per time interval, with the exception of the 2-hr experiments where three animals were used.

Blood was collected by exsanguination from the abdominal aorta. The heart, lungs, brain, kidneys, liver, adrenal glands, and spleen were re-

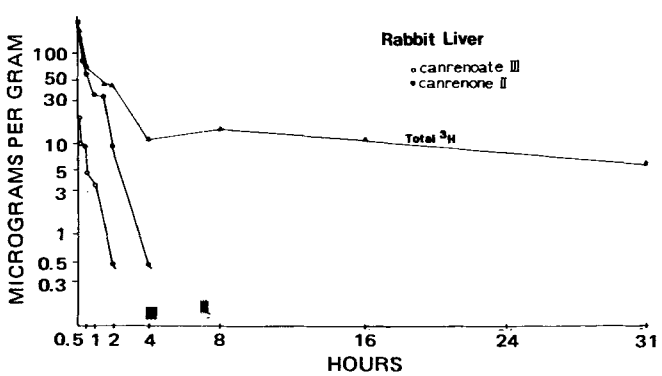

Figure 1—*Concentrations of total ^{3}H-radioactivity measured by liquid scintillation counting and concentrations of II and III measured by a specific fluorescence assay in rabbit liver.*

[1] Aldactone, Searle and Co.

[2] Boehringer Mannheim G.M.b.H.

[3] G. D. Searle and Co.

[4] Silica gel K C F254 Merck plates were used.

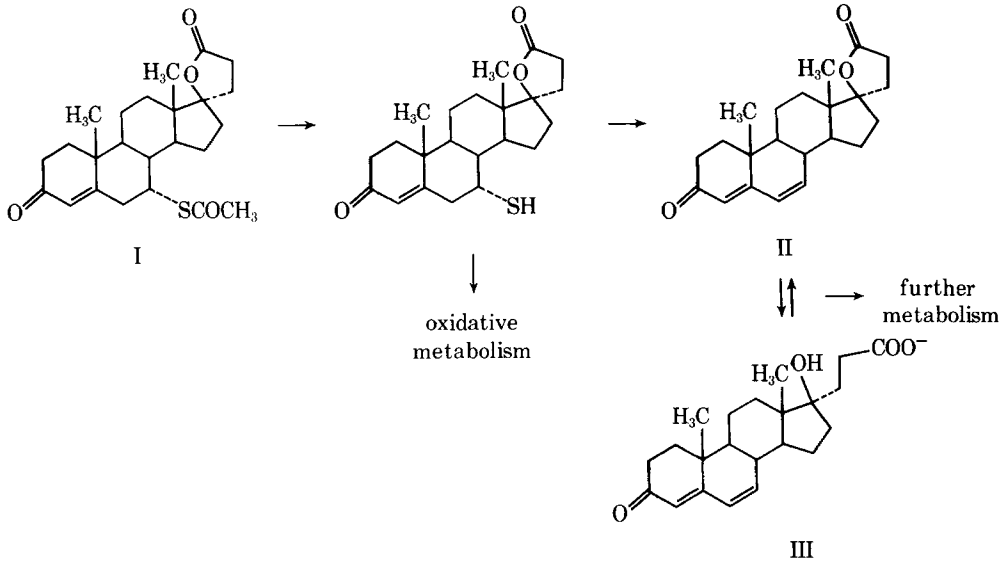

Scheme I—Metabolic pathways of the spirolactones

moved. Tissue samples were homogenized using a tissue homogenizer in a fivefold volume of methanol. After centrifugation at 2000 rpm, the supernate was removed and the tissue pellet was washed with methanol and kept at 20° for further analysis. The supernate (0.3 ml) or 0.1 ml of plasma was placed in a counting vial, and ^{3}H-counts were determined by scintillation counting or measured fluorometrically for II and III.

Tissue pellets were analyzed to measure the extraction yield by methanol homogenization. Liquefaction of the methanol and water-washed pellet was achieved using a tissue solubilizer[5], and an aliquot of the total volume was counted in 10 ml of counting solution[6]. Pellet extractibility was quantitative in all tissues, since all counts were found in the supernate. ^{3}H-Activity was not significantly accounted for by ^{3}H-water following possible ^{3}H-exchange from ^{3}H-III or its metabolites, since the ^{3}H-activity of the supernates was the same when measured directly and following evaporation to dryness.

RESULTS AND DISCUSSION

Plasma concentration *versus* time curves of II and III were obtained by serial blood sampling after 5, 10, and 20 mg of III/kg iv. Equilibrium between II and III was obtained as early as 10 min following administration of III. The plasma elimination half-life was about 1 hr, which is much faster than that observed in other species (2, 4, 5), and was unchanged at all dose levels studied. Following increased doses, proportionally increased plasma levels with the same elimination half-life demonstrated linear first-order disposition kinetics. A dose of 20 mg of III/kg was selected for all subsequent studies.

Figure 1 shows measurements of total radioactivity and of II and III

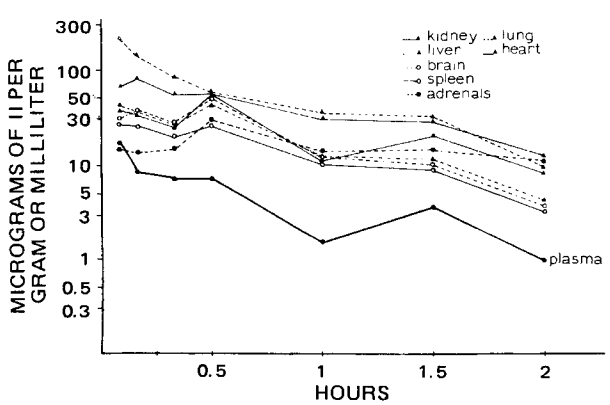

Figure 2—*Plasma and organ concentrations of II.*

[5] NCS, Amersham/Searle Corp.
[6] Aquasol, New England Nuclear.

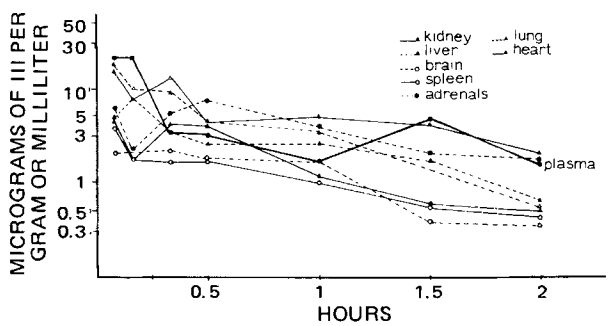

Figure 3—*Plasma and organ concentrations of III.*

measured by a specific fluorescence assay in rabbit liver tissue. Liver appears to show a high uptake of II and not III, even at the earliest time point of 10 min after a dose of III potassium where II accounts for most of the radioactivity. This result indicates a rapid conversion of III to II. The high concentration and slow elimination of ^{3}H-activity suggest extensive metabolism.

Figure 2 shows II levels in plasma and all tissues analyzed. Canrenone is rapidly taken up and concentrated in tissues, by a factor of 10 compared to plasma. The large differences in II concentration after 10 min in various tissues may be attributed in part to perfusion differences of the various organs. Levels of III in plasma and tissues (Fig. 3) are similar in order of magnitude, indicating a lower tissue affinity of III when compared to II.

To examine the variability between animals, three animals were analyzed at the 2-hr time point. All other points are represented by single-animal experiments. Table I shows the averaged values and ranges for the 2-hr experiments in rabbit plasma and liver.

Plasma concentrations of II represent a larger amount of this metabolite in the body when compared to plasma levels of III. Therefore, it seems justified to consider II as a major metabolite upon which pharmacokinetic studies such as bioavailability should be based. This result

Table I—Levels of Canrenone (II) and Canrenoate (III) in Plasma and Liver at 2 hr following Administration of ^{3}H-III to Three Rabbits

	Mean (Range)		
	Total ^{3}H-Activity	II	III
Plasma, μg/ml	18 (12–25)	1.16 (0.6–1.48)	1.3 (0.36–1.76)
Liver, g	68 (35–119)	10 (4–16)	1 (0.6–1.2)

can probably also be applied to species other than the rabbit. However, extensive transformation to metabolites of unknown structures and pharmacological activity appears to occur, which will be discussed in a separate report.

REFERENCES

(1) C. M. Kagawa, D. J. Bouska, M. L. Anderson, and W. F. Krol, *Arch. Int. Pharmacodyn. Ther.*, **149**, 8 (1964).

(2) W. Sadée, U. Abshangen, C. Finn, and N. Rietbrock, *Arch. Pharmacol.*, **283**, 303 (1974).

(3) C. M. Kagawa, D. J. Bouska, and M. L. Anderson, *Proc. Soc. Exp. Biol. Med.*, **115**, 837 (1964).

(4) W. Sadée, S. Riegelman, and D. C. Jones, *J. Pharm. Sci.*, **61**, 1129 (1972).

(5) W. Sadée, M. Dagcioglu, and R. Schröder, *J. Pharmacol. Exp. Ther.*, **185**, 686 (1973).

(6) A. Karim, R. E. Ranney, and H. I. Maibach, *J. Pharm. Sci.*, **60**, 708 (1971).

(7) A. Karim and E. A. Brown, *Steroids*, **20**, 18 (1972).

(8) W. Sadée, A. M. Finn, P. Schmiedek, and A. Baethmann, *ibid.*, **25**, 301 (1975).

(9) W. Sadée, M. Dagcioglu, and S. Riegelman, *J. Pharm. Sci.*, **61**, 1126 (1972).

ACKNOWLEDGMENTS AND ADDRESSES

Received January 21, 1976, from the *University of California, School of Pharmacy, San Francisco, CA 94143.*

Accepted for publication April 15, 1976.

Supported in part by Grants GM 16496 and GM 001 from the National Institute of General Medical Sciences, National Institutes of Health, Bethesda, MD 20014.

[x] To whom inquiries should be directed.

Synthesis and Biological Activity of a Novel Analog of Nitrofurantoin

RALPH L. WHITE [x], STANLEY E. BURROUS, and THOMAS J. SCHWAN

Abstract □ The synthesis of 5-hydroxy-1-[[(5-nitro-2-furanyl)methylene]amino]-2,4-imidazolidinedione is described, and its antibacterial activity is reported.

Keyphrases □ Nitrofurantoin analog—synthesized, screened for antibacterial activity □ 2,4-Imidazolidinedione, substituted—synthesized, screened for antibacterial activity □ Antibacterial activity—substituted 2,4-imidazolidinedione evaluated

Because of the continuing interest (1–3) in the chemotherapeutic properties of 1-[[(5-nitro-2-furanyl)methylene]amino]-2,4-imidazolidinediones, the 5-hydroxy analog of nitrofurantoin[1] was prepared by utilizing the general preparative route to 5-hydroxy-1-(substituted amino)-2,4-imidazolidinediones (4, 5).

DISCUSSION

The synthesis of the desired 5-hydroxy-1-[[(5-nitro-2-furanyl)methylene]amino]-2,4-imidazolidinedione (I) (5) required catalytic reduction of 1-[(phenylmethylene)amino]imidazolidinetrione (II) to yield 1-amino-5-hydroxy-2,4-imidazolidinedione (III). Compound III was not isolated but was trapped with 1,1′-biphenyl-4-carboxaldehyde (IV) to yield 1-[[[(1,1′-biphenyl)-4-yl]methylene]amino]-5-hydroxy-2,4-imidazolidinedione (V). Exchange on the 1-amino-5-hydroxyimidazolidinedione moiety of V was accomplished by stirring V and 5-nitro-2-furancarboxaldehyde (VI) in the presence of an acid catalyst, which yielded the desired product I (Scheme I).

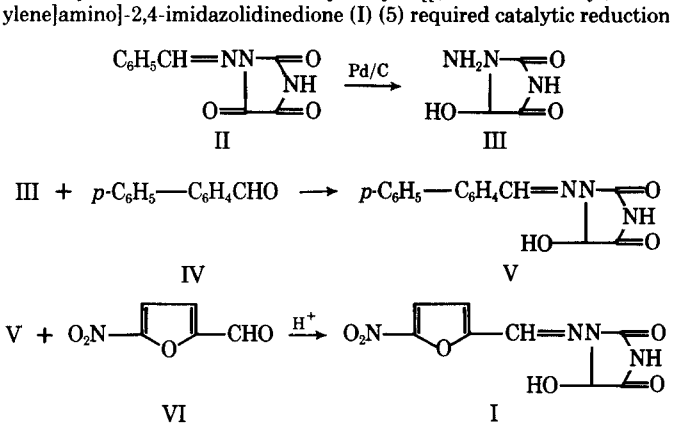

Scheme I

Evidence supporting reduction of II at the 5-oxo group to give a 5-hydroxy-1-substituted 2,4-imidazolidinedione was found by comparing the NMR spectrum of I with spectra of nitrofurantoin (VII) and its isomer 3-[[(5-nitro-2-furanyl)methylene]amino]-2,4-imidazolidinedione (VIII) (6). The NH signal of I is at 11.5 ppm, the N_3H signal of VII occurs at 11.2 ppm, and the N_1H signal of VIII is at 8.57 ppm, indicative of a N_3H proton for I rather than an N_1H proton. These NMR data confirm that I is a 5-hydroxy-1-(substituted amino)-2,4-imidazolidinedione and not a 5-hydroxy-3-(substituted amino)-2,4-imidazolidinedione. The structure of I is thus a 5-hydroxy-substituted nitrofurantoin.

Compound I was tested for antibacterial activity against eight bacterial species in a standard broth dilution assay and had good activity against

Table I—Serial Dilution Method for I and Nitrofurantoin[a]

Organism	MIC, μg/ml I	MIC, μg/ml Nitrofurantoin
Staphylococcus aureus (Mi-12)	50	12.5
Escherichia coli (Es-90)	12.5	6.2
Salmonella typhosa (SaD-13)	25	6.2
Aerobacter aerogenes (Ae-6)	>100	100
Pseudomonas aeruginosa (Ps-44)	>100	>200
Shigella flexneri (Sh-378)	25	12.5
Proteus mirabilis (Pr-91)	>100	200
Hemophilus vaginalis (He-127)	3.1	1.5

[a] Activities are given in MIC values (minimum inhibitory concentrations).

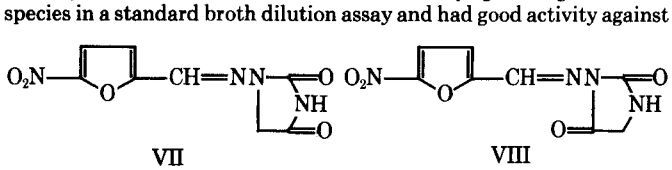

VII VIII

[1] Furadantin, Eaton Laboratories, Division of Morton-Norwich Products, Inc.

can probably also be applied to species other than the rabbit. However, extensive transformation to metabolites of unknown structures and pharmacological activity appears to occur, which will be discussed in a separate report.

REFERENCES

(1) C. M. Kagawa, D. J. Bouska, M. L. Anderson, and W. F. Krol, *Arch. Int. Pharmacodyn. Ther.*, **149**, 8 (1964).

(2) W. Sadée, U. Abshangen, C. Finn, and N. Rietbrock, *Arch. Pharmacol.*, **283**, 303 (1974).

(3) C. M. Kagawa, D. J. Bouska, and M. L. Anderson, *Proc. Soc. Exp. Biol. Med.*, **115**, 837 (1964).

(4) W. Sadée, S. Riegelman, and D. C. Jones, *J. Pharm. Sci.*, **61**, 1129 (1972).

(5) W. Sadée, M. Dagcioglu, and R. Schröder, *J. Pharmacol. Exp. Ther.*, **185**, 686 (1973).

(6) A. Karim, R. E. Ranney, and H. I. Maibach, *J. Pharm. Sci.*, **60**, 708 (1971).

(7) A. Karim and E. A. Brown, *Steroids*, **20**, 18 (1972).

(8) W. Sadée, A. M. Finn, P. Schmiedek, and A. Baethmann, *ibid.*, **25**, 301 (1975).

(9) W. Sadée, M. Dagcioglu, and S. Riegelman, *J. Pharm. Sci.*, **61**, 1126 (1972).

ACKNOWLEDGMENTS AND ADDRESSES

Received January 21, 1976, from the *University of California, School of Pharmacy, San Francisco, CA 94143.*

Accepted for publication April 15, 1976.

Supported in part by Grants GM 16496 and GM 001 from the National Institute of General Medical Sciences, National Institutes of Health, Bethesda, MD 20014.

[x] To whom inquiries should be directed.

Synthesis and Biological Activity of a Novel Analog of Nitrofurantoin

RALPH L. WHITE [x], STANLEY E. BURROUS, and THOMAS J. SCHWAN

Abstract □ The synthesis of 5-hydroxy-1-[[(5-nitro-2-furanyl)methylene]amino]-2,4-imidazolidinedione is described, and its antibacterial activity is reported.

Keyphrases □ Nitrofurantoin analog—synthesized, screened for antibacterial activity □ 2,4-Imidazolidinedione, substituted—synthesized, screened for antibacterial activity □ Antibacterial activity—substituted 2,4-imidazolidinedione evaluated

Because of the continuing interest (1–3) in the chemotherapeutic properties of 1-[[(5-nitro-2-furanyl)methylene]amino]-2,4-imidazolidinediones, the 5-hydroxy analog of nitrofurantoin[1] was prepared by utilizing the general preparative route to 5-hydroxy-1-(substituted amino)-2,4-imidazolidinediones (4, 5).

DISCUSSION

The synthesis of the desired 5-hydroxy-1-[[(5-nitro-2-furanyl)methylene]amino]-2,4-imidazolidinedione (I) (5) required catalytic reduction of 1-[(phenylmethylene)amino]imidazolidinetrione (II) to yield 1-amino-5-hydroxy-2,4-imidazolidinedione (III). Compound III was not isolated but was trapped with 1,1′-biphenyl-4-carboxaldehyde (IV) to yield 1-[[[(1,1′-biphenyl)-4-yl]methylene]amino]-5-hydroxy-2,4-imidazolidinedione (V). Exchange on the 1-amino-5-hydroxyimidazolidinedione moiety of V was accomplished by stirring V and 5-nitro-2-furancarboxaldehyde (VI) in the presence of an acid catalyst, which yielded the desired product I (Scheme I).

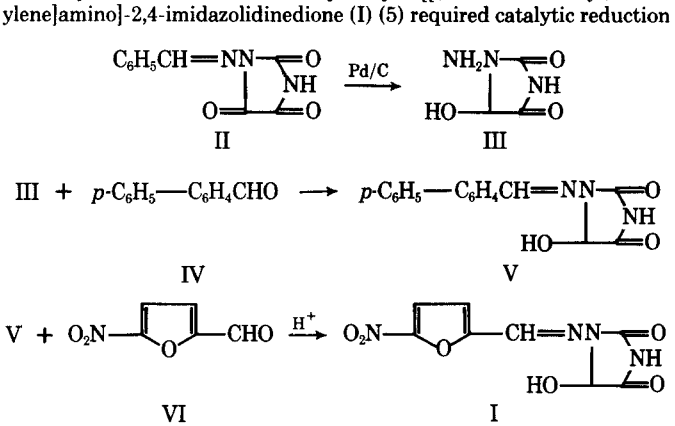

Scheme I

Evidence supporting reduction of II at the 5-oxo group to give a 5-hydroxy-1-substituted 2,4-imidazolidinedione was found by comparing the NMR spectrum of I with spectra of nitrofurantoin (VII) and its isomer 3-[[(5-nitro-2-furanyl)methylene]amino]-2,4-imidazolidinedione (VIII) (6). The NH signal of I is at 11.5 ppm, the N_3H signal of VII occurs at 11.2 ppm, and the N_1H signal of VIII is at 8.57 ppm, indicative of a N_3H proton for I rather than an N_1H proton. These NMR data confirm that I is a 5-hydroxy-1-(substituted amino)-2,4-imidazolidinedione and not a 5-hydroxy-3-(substituted amino)-2,4-imidazolidinedione. The structure of I is thus a 5-hydroxy-substituted nitrofurantoin.

Compound I was tested for antibacterial activity against eight bacterial species in a standard broth dilution assay and had good activity against

Table I—Serial Dilution Method for I and Nitrofurantoin[a]

Organism	MIC, μg/ml I	MIC, μg/ml Nitrofurantoin
Staphylococcus aureus (Mi-12)	50	12.5
Escherichia coli (Es-90)	12.5	6.2
Salmonella typhosa (SaD-13)	25	6.2
Aerobacter aerogenes (Ae-6)	>100	100
Pseudomonas aeruginosa (Ps-44)	>100	>200
Shigella flexneri (Sh-378)	25	12.5
Proteus mirabilis (Pr-91)	>100	200
Hemophilus vaginalis (He-127)	3.1	1.5

[a] Activities are given in MIC values (minimum inhibitory concentrations).

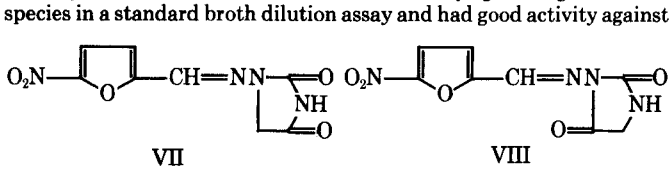

VII VIII

[1] Furadantin, Eaton Laboratories, Division of Morton-Norwich Products, Inc.

Table II—Serial Dilution Method for the Urine of Rats Dosed with I[a]

Collection Interval, Hours after Dosing	*Escherichia coli* (Es-90)	*Proteus mirabilis* (Pr-91)	*Aerobacter aerogenes* (Ae-6)	*Pseudomonas aeruginosa* (Ps-44)
0—4	48	48	<6	<6
4—8	<6	<6	<6	<6

[a] Activities are given in RID values (reciprocal of the highest inhibitory dilution).

all organisms tested except *Aerobacter aerogenes, Pseudomonas aeruginosa,* and *Proteus mirabilis* in a standard minimum inhibitory concentration (MIC) serial dilution test (Table I). Antibacterial activity of nitrofurantoin was measured by the serial dilution method to have a direct comparison of MIC values in the same species. Nitrofurantoin exhibited better general antibacterial activity than I for the bacteria tested. MIC values for nitrofurantoin against various bacterial species also may be found in the literature (7, 8).

Urine collected in 0.1 *N* HCl from rats fasted overnight prior to receiving a single oral dose (30 mg/kg) of I was evaluated for antibacterial activity in a broth dilution assay (Table II) (9). Rats dosed with I excreted urine having excellent antibacterial activity against *Escherichia coli* and *P. mirabilis* (Table II). The *in vivo* antibacterial activity was measured in a standardized rat unilateral pyelonephritis model (Table III) (10); efficacy against *E. coli* and *P. mirabilis* was apparent. The estimated oral 72-hr LD_{50} for I in mice was 668 mg/kg. Urine from rats or dogs fed nitrofurantoin (VII) contained no detectable I, and urine from rats fed I contained no detectable VII, as indicated by TLC with three different solvent systems [(*a*) 1-butanol–ethanol–ammonium hydroxide, (*b*) ethyl acetate–hydrochloric acid, and (*c*) 1-butanol–ethanol–acetic acid] on nitromethane extracts (pH 2.0) of appropriate urines and standards, internal standards, control urines, and spent, extracted urines.

EXPERIMENTAL[2]

1-[[[(1,1′-Biphenyl)-4-yl]methylene]amino] -5-hydroxy-2,4-imidazolidinedione (V)—In each of two 2-liter reduction vessels were placed 1-(benzylideneamino)imidazolidinetrione (87 g, 0.40 mole) (1), palladium-on-charcoal (5% with 50% water, 20 g), and methanol (500 ml). The mixtures were reduced on a Parr apparatus until about 95% of the theoretical three equivalents of hydrogen was taken up (24 hr). The combined reduction mixtures were filtered, and the insoluble residue was rinsed with methanol (600 ml). The combined methanolic solution was made acidic with concentrated hydrochloric acid, and then 1,1′-biphenyl-4-carboxaldehyde (73 g, 0.40 mole) was added. The mixture was stirred for 2 hr, and the resulting solid was collected (21 g, 28% yield). A sample was recrystallized from absolute ethanol, mp 224–225°.

Anal.—Calc. for $C_{16}H_{13}N_3O_3$: C, 65.08; H, 4.44; N, 14.23. Found: C, 65.19; H, 4.52; N, 14.10.

5-Hydroxy-1-[[(5-nitro-2-furanyl)methylene]amino]-2,4-imidazolidinedione (I)—In tetrahydrofuran (500 ml) were placed V (20 g, 0.070 mole), VI (11 g, 0.080 mole), and concentrated hydrochloric acid (5 ml). The solution was refluxed for 1 hr and concentrated under reduced pressure to a yellow solid. Benzene (100 ml) was added, and the mixture was again concentrated to a solid. The solid was stirred for 30 min with anhydrous ether (400 ml), and the mixture was filtered to yield the desired product I (15 g, 88% yield). Recrystallization of a sample from acetonitrile gave the white product, mp 213–214°; NMR: δ 5.68 (d, 1H, CH, J = 10 Hz, s after exchange), 7.18 (d, 1H, furan CH, J = 4 Hz), 7.47 (d, 1H, OH, J = 10 Hz, exchange), 7.75 (d, 1H, furan CH, J = 4 Hz), 8.18 (s, 1H, azomethine CH), and 11.5 (broad s, 1H, NH, exchange).

Anal.—Calc. for $C_8H_6N_4O_6$: C, 37.80; H, 2.38; N, 22.05. Found: C, 37.77; H, 2.35; N, 22.00.

NMR Spectrum of Nitrofurantoin (VII)—Signals were observed at δ 4.40 (s, 2H, CH), 7.15 (d, 1H, furan CH, J = 4 Hz), 7.78 (d, 1H, furan CH, J = 4 Hz), 7.82 (s, 1H, azomethine CH), and 11.2 (broad s, 1H, NH, exchange).

NMR Spectrum of 3-[[(5-Nitro-2-furanyl)methylene]amino]-2,4-imidazolidinedione (VIII)—The synthesis of this compound was reported previously (6); NMR: δ 4.10 (s, 2H, CH), 7.33 (d, 1H, furan CH, J = 4 Hz), 7.66 (d, 1H, furan CH, J = 4 Hz), 8.57 (s, 1H, NH, exchange), and 9.51 (s, 1H, azomethine CH).

[2] A Varian Associates A-60A instrument was used for NMR spectra, which were run in dimethyl sulfoxide-d_6 with tetramethylsilane as the internal standard. Melting points were determined in open capillary tubes with a Mel-Temp melting-point apparatus and are uncorrected.

Table III—Standard Rat Bacterial Pyelonephritis Efficacy[a]

Organism	Treated	Untreated
Escherichia coli (Es-90)	2.6	4.9
Proteus mirabilis (Pr-91)	3.8	4.8
Aerobacter aerogenes (Ae-6)	4.5	5.2
Klebsiella pneumoniae (Kl-10)	4.9	5.5

[a] Activities are expressed as the $\log_{10}$ of the geometric mean of the viable bacterial titers of the infected kidneys from 10 rats (per group) dosed 10 mg/kg twice daily for 14 days with I.

REFERENCES

(1) R. E. Bambury, H. K. Yaktin, and K. K. Wyckoff, *J. Heterocycl. Chem.*, **5**, 95 (1968).

(2) W. Hoyle and E. P. Roberts, *J. Med. Chem.*, **16**, 709 (1973).

(3) E. B. Akerblom, *ibid.*, **17**, 609 (1974).

(4) R. L. White and T. J. Schwan, *J. Pharm. Sci.*, **65**, 135 (1976).

(5) T. J. Schwan and R. L. White, Jr., U.S. pat. 3,748,326 (1973).

(6) G. C. Wright, J. G. Michels, and C. F. Spencer, *J. Med. Chem.*, **12**, 379 (1969).

(7) H. E. Paul and M. F. Paul, in "Experimental Chemotherapy," vol. II, R. J. Schnitzer and F. Hawking, Eds., Academic, New York, N.Y., 1964, p. 315.

(8) "Antibiotics and Chemotherapy," 4th ed., L. P. Garrod, H. P. Lambert, and F. O'Grady, Eds., Churchill Livingstone, London, England, 1973, p. 43.

(9) S. E. Burrous, R. Freedman, R. E. Chamberlain, and R. P. Basson, *Appl. Microbiol.*, **20**, 598 (1970).

(10) S. E. Burrous and J. B. Cawein, *ibid.*, **18**, 448 (1969).

ACKNOWLEDGMENTS AND ADDRESSES

Received June 16, 1975, from *Norwich Pharmacal Company, Division of Morton-Norwich Products, Inc., Norwich, NY 13815.*

Accepted for publication April 12, 1976.

[x] To whom inquiries should be directed.

Survival of Pleomorphic Sarcoma-37 Transplanted Virgin Female DBA/2J Mice: Effects Produced by High Blood Glucose Levels Alone and in Combination with Drugs

RONALD E. ORTH ˣ, HOWARD J. SWIDLER, and MILO S. ZARAKOV

Abstract □ Procedures for producing, monitoring, and maintaining 3-hr 400–500-mg % whole blood glucose levels in Sarcoma-37 (S-37) transplanted virgin female inbred DBA/2J mice are described. Aqueous infused 40% (w/v) dextrose was evaluated as a potential therapeutic factor. The effects of procedural variations on treatment survival and longevity are discussed. One hundred percent infusion safety and 25% increased longevity over nontreated transplanted mice were achieved. Doxorubicin and/or dacarbazine were also evaluated when administered prior to the dextrose infusion. Doxorubicin followed by intravenous dextrose increased survivor longevity by 37%, but this combination was unsafe at the drug dosages employed. A large dose of dacarbazine was safe and effective alone but unsafe when given prior to the infusion, although the survivors lived 29% longer than the untreated transplanted controls. Both drugs were marginally effective, but safe, when given together. When given together prior to the infusion, only 87% survived the treatment. The survivors lived 6 days longer than the controls.

Keyphrases □ Blood glucose—high levels, alone and with doxorubicin or dacarbazine, effect on survival of tumor-transplanted mice □ Dextrose infusion—alone and with doxorubicin or dacarbazine, effect on survival of tumor-transplanted mice □ Doxorubicin—combined with high blood glucose levels, effect on survival of tumor-transplanted mice □ Dacarbazine—combined with high blood glucose levels, effect on survival of tumor-transplanted mice □ Antineoplastics—doxorubicin and dacarbazine, alone and with high blood glucose levels, mice

The selectively higher aerobic glycolytic rate noted in cancerous tissue as opposed to normal tissue was reported by Warburg in 1930 (1). This finding is controversial (2), although it has been demonstrated (3, 4) that dextrose levels of 400 mg/100 ml of whole blood cause a pH differential of as much as 1 unit to exist only a few millimeters apart in normal *versus* malignant tissues of the same organ. Tumor remissions were reported following the maintenance of hyperacidic tumor tissue (5).

Cancerous mice, stabilized at 400-mg % blood glucose levels, exhibit slower tumor growth, more remissions, and greater longevity than untreated mice (6). Maintenance of 400-mg % dextrose-induced hyperglycemia assures equilibration between tissues and high target tissue acidity. Although the pH of both tumor and normal tissues drops, the acidity of the former is greatest. Lysosomal enzymes, more active at lower pH's, catabolize the malignant tissue preferentially. The less acidic normal tissue provides a poorer substrate for the lysozymes, and the "self-destruction" stops according to this hypothesis.

It was suggested (6) that a "triggering attack" by one or more agents be employed in addition to dextrose infusion, since higher remission rates are desirable. X-Irradiation, massive doses of vitamin A, and cell cycle-specific or nonspecific antineoplastic agents disrupt the DNA and/or protein synthetic sequence, weakening lysosomal and cellular membranes. In theory, the application of several membrane-weakening agents with different mechanisms of action, given together, could produce additive, if not synergistic, beneficial results.

This study was designed to: (*a*) create an easily duplicated procedure for producing, monitoring, and maintaining safe 3-hr 400–500-mg % whole blood glucose levels in Sarcoma-37[1] (S-37) transplanted DBA/2J mice; (*b*) determine whether a causal relationship exists between this treatment and mouse longevity; and (*c*) evaluate whether doxorubicin (I) and/or dacarbazine (II), administered prior to the dextrose infusion, alter safety and longevity results. This investigation utilized known active mouse (7) and human (8) antisarcoma agents I and II. Tumor size, shape, and growth characteristics were observed.

EXPERIMENTAL

The following materials were used: genetically standardized inbred strains of virgin female DBA/2J mice with in-host S-37 transplanted tumors[2]; an infusion pump with variable rate settings and interchangeable holders for different syringe capacities[3], syringes[4]; polyethylene tubing[5]; 26-gauge 12.7-mm hypodermic needles[6]; a reflectance colorimeter[7]; glucose oxidase reagent strips[8]; capillary tubes (1.12–1.17 mm i.d.); I and II[9]; 40 % (w/v) aqueous dextrose; aqueous pentobarbital sodium, 32 mg/10 ml; and normal saline.

Virgin female DBA/2J mice, 15–20 g, were transplanted with 1 mm^3 of vascular S-37 tumor tissue[10]. They were treated 6 days later; chemotherapeutic agents were administered 15 min prior to anesthesia. Compound I was administered subcutaneously, II was given intraperitoneally, and 80 mg of pentobarbital sodium/kg was given with an oral syringe. Anesthetized mice were secured, and the tails were immobilized.

An infusion pump syringe holder was adapted to contain six 1-ml syringes. Each syringe was connected to 1 m of polyethylene tubing by a 26-gauge 12.7-mm needle. Another needle of the same size was broken near the syringe adaptor end, and this end was fitted into the far end of the tubing. The beveled end of the needle was then inserted into the mouse tail vein. The six syringes, prefilled to 0.5 mg with 40 % (w/v) aqueous dextrose, were activated at a slow setting (No. 19-21) on the pump.

Postorbital venous blood samples were periodically taken with a capillary tube. Blood glucose levels were determined by comparing the glucose oxidase strip color with chart standards (Cage 2 in Table I) or by reading the strip in a reflectance colorimeter (Cages 3–9 and 13 in Table I). Levels of 450 mg % were usually obtained in 60 ± 15 min (~0.2 ml of infusate). The infusion was discontinued at this time, and blood sampling was continued for another 2 hr. If the level fell below the desired 400 mg %, the infusion was reinstated. To prevent blinding the mice, no more than three samples were taken from behind either eye. A limit of four samples per mouse prevented too great a reduction in blood volume.

The dextrose original method (Cage 2) involved a 1:2 blood to saline

[1] R. E. Orth, unpublished data.
[2] Jackson Laboratories, Bar Harbor, ME 04609.
[3] Model 975, Harvard Apparatus Co., Millis, MA 02054.
[4] Plastipak disposable sterile tuberculin syringe 5602, 1 ml-TB, Becton-Dickinson and Co., Rutherford, NJ 07070.
[5] PE 20 (7407), Intramedic, Animal Tested Medical Formulation, Clay Adams Co., Parsippany, NJ 07064.
[6] B-D Yale hypodermic needle, Luer-lok hub, sterile, disposable, *stainless steel* cannula, Becton-Dickinson and Co., Rutherford, NJ 07070.
[7] Reflectance meter, Ames Co., Elkhart, IN 46514.
[8] Dextrostix, Ames Co., Elkhart, IN 46514.
[9] Doxorubicin (NSC 123,127) was supplied as the hydrochloride in 10-mg vials, and dacarbazine (NSC 45,388) was packaged in vials of 100 mg (Division of Cancer Treatment, National Cancer Institute, National Institutes of Health, Bethesda, MD 20014).
[10] Macerated S-37 tumor obtained from 7-day serial transplants.

Table I—Hyperglycemic and Drug Treatment of S-37 Transplanted DBA/2J Mice

Cage	Treatment	Fraction Surviving Treatment[a]	Longevity beyond Transplant Date[b]
1	Controls[c]	78/78	26.3 ± 1.8
2	Dextrose original method	48/62	26.1 ± 2.3[d]
3	Dextrose first modification	19/19	28.1 ± 1.3[d]
4	Dextrose second modification	16/16	31.2 ± 2.6
5	Dextrose third modification	36/36	32.8 ± 2.2
6	Dextrose second modification plus I, 5 mg/kg sc	8/16	36.0 ± 5.6
7	Dextrose second modification plus I, 2.5 mg/kg sc	11/16	35.9 ± 10.8
8	Dextrose second modification plus II, 200 mg/kg ip	12/16	33.8 ± 0.3
9	Dextrose second modification plus II, 100 mg/kg ip	16/16	30.2 ± 6.3
10	Isotonic saline plus I, 5 mg/kg sc	12/12	30.1 ± 2.6
11	Isotonic saline plus II, 200 mg/kg ip	12/12	31.5 ± 2.6
12	Isotonic saline plus I, 2.5 mg/kg sc plus II, 100 mg/kg ip	16/16	28.5 ± 2.3
13	Dextrose second modification plus I, 2.5 mg/kg sc plus II, 100 mg/kg ip	14/16	32.1 ± 2.4

[a] Includes deaths occurring within 24 hr of treatment. [b] The mean and the standard error of the mean in days surviving transplantation with 95% confidence. [c] Obtained from Cages 2–13 following transplantation prior to treatment. [d] Insignificant change in longevity from control values of Cage 1 (Student two-tailed t test with 95% confidence).

dilution and then placement of this mixture on the glucose oxidase reagent strip 1 min before washing and reading. The results were compared with a color chart on the reagent strip container. Data collected by reading the strips in a reflectance colorimeter were obtained by the dextrose first modification procedure (Cage 3). These mice were infused with aqueous dextrose immediately upon immobilization while still unconscious. This method required no dilution of the fresh venous blood samples, since readings up to 1000 mg % were possible using the expanded scale of the colorimeter. The dextrose second modification procedure (Cage 4) introduced a time lapse between immobilization and treatment. Therapy was commenced only when the mice were conscious.

These first three procedures rely on tail vein intravenous aqueous dextrose administration. The dextrose third modification (Cage 5) varied from the second modification procedure only by the route of administration. The intraperitoneal method was adopted in this latter infusion technique. The control mice (Cage 1) were anesthetized, secured, and infused with 0.2 ml of isotonic saline for 1 hr. The dextrose second modification method was utilized in all combination therapy with drugs.

RESULTS AND DISCUSSION

Untreated control mice lived 26.3 days beyond the S-37 tumor transplantation date (Cage 1). Twenty-three percent of the mice subjected to the dextrose original method died during treatment (Cage 2). The longevity for survivors in Cage 2 was about the same as for the Cage 1 controls. This dextrose monitoring procedure, employing a blood–saline dilution technique coupled with naked eye reagent strip color comparison with chart standards, was ineffective. The technique yielded false low values, resulting in extremely high actual blood glucose levels. More accurate assessments of undiluted blood glucose concentrations were obtained with the three following procedural modifications. An expanded scale reflectance colorimeter was utilized in which readings up to 1000 mg % were possible.

The dextrose first modification procedure (Cage 3) differed from the original method only by utilization of the colorimeter. Mice were unconscious at the time the infusion was initiated in both procedures. A safe treatment (100% survival) and a small but insignificant increase in longevity were observed. If, as in the dextrose second modification procedure (Cage 4), the sugar infusion was commenced only after the animal regained consciousness, the treatment yielded a safe and a significant 5-day increase in life expectancy over the control group.

The last variation of the infusion procedure was administration of the 40% (w/v) aqueous dextrose intraperitoneally (Cage 5). This dextrose third modification method resulted in a 100% safe treatment and a significant 6-day increase in longevity over the controls.

Obtaining and maintaining 400–500-mg % blood glucose levels was more difficult intraperitoneally than intravenously. The longevity differences obtained by these two procedures were statistically insignificant. Therefore, the more easily regulated intravenous dextrose second modification method is preferred and was used with drug therapy (Cages 6–9 and 13).

A 5-mg/kg sc dose of I (Cage 10) was safe and effected a significant 4-day increase in transplanted mouse lifespan. When I was given with infused dextrose, the treatment was unsafe, but the survivors of either 2.5 (Cage 6) or 5 (Cage 7) mg/kg lived 10 days longer than the controls. Although hyperglycemic treatment with I yielded significant longevity increases, the great deviations from the mean longevity and poor treatment survival rates did not favor adoption of this therapy.

A 200-mg/kg ip dose of II (Cage 11) was safe and resulted in a significant 5-day increase in longevity over the controls. If this same dose of II was administered with the dextrose treatment (Cage 8), the 75% surviving lived 7 days longer than did the control animals. By reducing the dose of II to 100 mg/kg prior to infusion with dextrose (Cage 9), survival was assured but therapy was minimally effective.

Given together, I and II provided safe but marginally effective therapy for the S-37 transplanted mice (Cage 12). However, when hyperglycemic treatment was added to the regimen (Cage 13), the mice survived an additional 6 days. Unfortunately, 12% of the mice died during treatment.

"Selective survival" may account, in whole or in part, for the increased longevity noted for mice given I and/or II during unsafe treatments (Cages 6–8 and 13). A toxic treatment may selectively kill the weakest mice, allowing the stronger animals to survive and live longer lives. The 26-day longevity values noted for both the controls and the unsafe dextrose original method survivors may provide evidence that conflicts with the selective survival concept.

SUMMARY

Safe procedures for producing, monitoring, and maintaining 3-hr 400–500-mg % whole blood glucose levels in S-37 transplanted virgin female inbred DBA/2J mice were achieved (Cages 3–5). Sarcoma-37 transplanted mouse longevity was significantly increased following a 100% safe treatment with a single incident of: 40% dextrose infusion (Cages 4 and 5), 5 mg/kg sc of I (Cage 10), 200 mg/kg ip of II (Cage 11), or 2.5 mg/kg sc of I with 100 mg/kg ip of II (Cage 12). Combinations of I and/or II with the dextrose may be less than 100% safe, but survivor longevity is increased (Cages 6–8 and 13).

REFERENCES

(1) O. Warburg, "The Metabolism of Tumors," 1st ed., Constable, London, England, 1930.

(2) G. M. Hahn, *Cancer Res.*, **34**, 3117 (1974).

(3) M. von Adrenne, *Vortr. Heidelberger Krebsforschungszentru*, **24**, 9 (1965).

(4) M. von Ardenne, R. A. Chaplain, and O. Prokop, *Dtsch. Gesundheitswes.*, **24**, 1589 (1969).

(5) M. von Ardenne, "Advances in Pharmacology and Chemotherapy," vol. 10, Academic, New York, N.Y., 1972, pp. 341–347.

(6) M. von Ardenne, "Theoretische und Experimentelle Grundlagen der Krebs-Mehr-Schritt-Therapie," 2nd ed., vols. I and II, VEB Verlag Volk u. Gesundheit, Berlin, Germany, 1971.

(7) F. M. Schabel, Jr., "Pharmacological Basis of Cancer Chemotherapy," Williams & Wilkins, Baltimore, Md., 1975, pp. 595–623.

(8) J. A. Gottlieb, L. H. Baker, J. M. Quagliana, J. K. Luce, J. P. Whitcar, J. G. Sinkovics, S. E. Rivkin, R. Brownlee, and E. Frei, III, *Cancer*, **30**, 1632 (1972).

ACKNOWLEDGMENTS AND ADDRESSES

Received August 8, 1975, from the *Department of Pharmaceutical Sciences, College of Pharmacy, University of Arizona, Tucson, AZ 85721.*

Accepted for publication April 23, 1976.

Supported by the University of Arizona Foundation, the University of Arizona Vice President for Research, and the Pharmacy College Overhead Allocation.

[x] To whom inquiries should be directed.

New and Simple Method for Determination of 2-(3-Benzoylphenyl)propionic Acid in Body Fluid

R. BALLERINI, A. CAMBI, and P. DEL SOLDATO ˣ

Abstract □ A simple, fast, sensitive, and reliable method for the determination of 2-(3-benzoylphenyl)propionic acid in biological fluid is described. The method is based on a quantitative ether extraction of plasma samples followed by TLC separation, spot visualization and elution, and determination at 255 nm. The acid is detectable in amounts as low as 1 μg.

Keyphrases □ 2-(3-Benzoylphenyl)propionic acid—TLC analysis, plasma, rats □ TLC—analysis, 2-(3-benzoylphenyl)propionic acid, plasma, rats □ Analgesic agents—2-(3-benzoylphenyl)propionic acid, TLC analysis, plasma, rats

GC, polarographic, and colorimetric methods (1) have been used to determine the concentration of 2-(3-benzoylphenyl)propionic acid (I), a recently synthesized compound with analgesic and anti-inflammatory properties (2), in body fluids. Unfortunately, these methods are complicated, unreliable, time consuming, nonspecific, and not sufficiently sensitive. Furthermore, they are limited to the determination of I in the urine and require rather expensive instrumentation.

The thin-layer method described in this paper overcomes most of these limitations.

EXPERIMENTAL

Reagents and Materials—Compound I was synthesized and characterized by means of IR, NMR, UV, and TLC techniques[1]. All solvents were analytical reagent grade[2], and the developing solvent, ether–benzene–1-butanol–methanol (85:8:6:1), was prepared fresh daily. Silica gel plates[3], 250 μm thick, were activated at 105° for 1 hr.

Instrumentation—A UV lamp[4] (250 nm), a prism spectrophotometer[5], and 1-cm quartz microcells[6] were used.

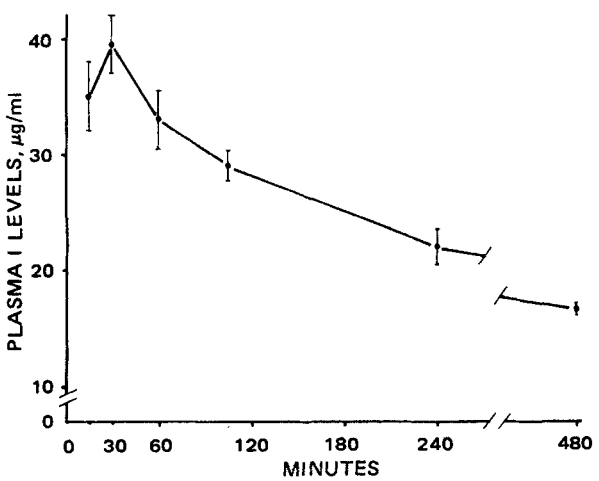

Figure 1—*Concentration of I in plasma of male rats at different time intervals after oral administration of 25 mg/kg.*

[1] Chemical Department, Menarini Laboratories, Florence, Italy.
[2] Merck.
[3] Merck 60 F 254.
[4] Mineral light UVS 11.
[5] Beckman DB.
[6] Hellma 108/2 QS.

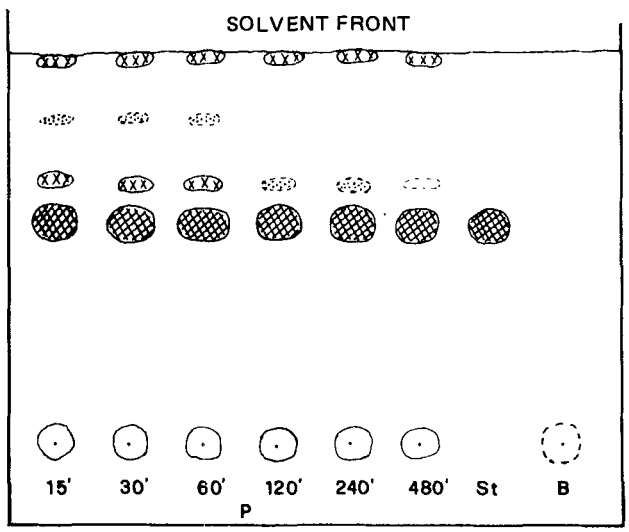

Figure 2—*Thin-layer chromatogram of I. Key: B, 0.1 ml of plasma from untreated rats; St, 0.1 ml of I (250 μg/ml in 96% ethanol); and P, plasma sample obtained at different time intervals from I-treated rats (25 mg/kg po).*

Preparation of Standards—Compound I was dissolved in 96% ethanol. Aliquots equivalent to 2.5, 7.5, 10, and 12.5 μg were placed in glass-stoppered centrifuge tubes and evaporated to dryness under a gentle stream of nitrogen. Then 0.25 ml of plasma from untreated rats was added to each tube and mixed well. These standards and the appropriate blanks were handled in the same manner as the plasma specimens.

Preparation of Samples—Plasma (0.25 ml) from treated animals, 10 ml of water, and 1 ml of 1 *N* HCl were introduced into a 100-ml separator.

Compound I was extracted with three 40-ml portions of ether. The standards and the appropriate blanks were handled in a similar manner. The pooled extracts were washed with 20 ml of 0.1 *N* HCl and 20 ml of water, dried on sodium sulfate, and flash evaporated to a volume of about 5 ml. This final amount as well as the successive ether washes was transferred to a glass-stoppered centrifuge tube and evaporated to dryness under a gentle stream of nitrogen.

TLC—Each sample was taken up in 0.2 ml of ethanol, and 100-μl aliquots were spotted 2 cm from the edge of the chromatographic plate. Aliquots equivalent to 1.25, 2.5, 5, and 6.25 μg of I standard ethanolic solution were likewise spotted on the plate.

The chromatograms were developed in an ascending system of ether–benzene–1-butanol–methanol (85:8:6:1) in a saturated atmosphere. After 30 min the solvent front was marked, plates were dried, and I spots were visualized by exposure to the UV lamp. These areas were scraped into glass-stoppered centrifuge tubes, eluted with 1.5 ml of ethanol, and shaken every 5 min for 30 min. A similar spotless area (blank) was also scraped off and subjected to the identical procedure. The test tubes were then centrifuged at 4000 rpm for 10 min, and the relative absorbance of the supernates was measured at 255 nm against a blank.

Calculation—Calibration curves were prepared by plotting absorbance at 255 nm against known concentrations of I in plasma or 96% ethanol. Values for unknown concentrations of I in plasma specimens were calculated from the slope of the standard curve.

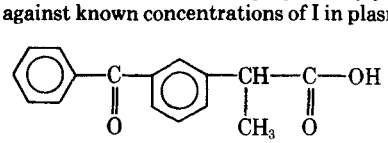

I

Table I—Recovery of I Added to Rat Plasma or 96% Ethanol

Amount of I Added to Plasma or 96% Ethanol, μg/ml	Amount Recovered from Plasma, μg/ml	Recovery, %	Amount Recovered from 96% Ethanol, μg/ml	Recovery, %
2.50	2.24	89.6	2.30	92.0
	2.28	91.2	2.28	91.0
	2.30	92.0	2.26	90.0
	2.29	91.6	2.28	91.0
	2.31	92.6	2.30	92.0
	2.30	92.0	2.27	90.0
7.50	6.80	90.7	6.90	92.0
	6.60	88.0	6.60	88.0
	6.75	90.9	6.80	90.7
	6.90	92.0	6.80	90.7
	6.90	92.0	6.70	89.3
	6.70	89.3	6.90	92.0
10	9.10	91.0	9.00	90.0
	9.15	91.5	8.80	88.0
	9.15	91.5	9.15	91.5
	9.12	91.2	9.10	91.0
	8.90	89.0	8.80	88.0
	9.10	91.0	8.90	89.0
		Mean ± *SD* = 90.95 ± 1.22		Mean ± *SD* = 90.35 ± 1.41

Drug Administration to Rats—Male Wistar albino rats, 300–330 g, were divided into six groups of six or seven animals each. Compound I was suspended in an aqueous vehicle consisting of 0.9% sodium chloride, 0.4% polysorbate 80, 0.5% carboxymethylcellulose sodium, and 0.9% benzyl alcohol and administered by gavage at a dose of 25 mg/kg in a constant volume of 5 ml/kg.

Blood samples were obtained by cardiac puncture by means of a heparinized syringe at time intervals ranging from 15 min up to 8 hr after drug administration. Plasma samples were obtained by centrifugation at 2000 rpm for approximately 10 min.

Table II—Precision Data from Determinations in Plasma[a]

Sample	Concentration of I at 15 min, μg/ml	Concentration of I at 480 min, μg/ml
Mean	16.5	38.4
SD	0.45	1.21
RSD	2.75	3.15

[a] Reproducibility limits are $RL = \bar{X} \pm RSD.t_{38;0.05} = \bar{X} \pm 6.01\%$ of $\bar{X}$.

RESULTS AND DISCUSSION

Known amounts of I were added either to plasma or 96% ethanol. The percentage recovery of I from plasma was identical to that from the alcoholic solution spotted directly on the plate (Table I), with an accuracy index of 100%. This method is adequately specific, since it was unaffected by endogenous substances. The values relative to plasma concentration at different time intervals after oral administration of 25 mg/kg of I to male rats are shown in Fig. 1.

Preliminary chromatograms of I added to plasma indicated that recoveries of 90 ± 1.2% were obtained following an elution time of 30 min. Prolongation of the elution time (up to 5 hr) did not improve recovery. Compound I has an R_f value of 0.75 (Fig. 2). No attempt was made to identify the chemical nature of the substances (metabolites) with an R_f greater than that of I. Due to a sufficiently high molar absorptivity ($E^{1\%}_{1cm}$ in 96% ethanol or plasma at 255 nm is 640), I can be determined in an amount as low as 1 μg.

To assess the precision of the procedure, 20 determinations were carried out on two plasma samples obtained at 15 and 480 min following I administration (Table II). The relative mean standard deviation was 2.95% and the reproducibility limits were ±6.01%.

The time required to determine the concentration of I in plasma varies according to number of samples, *i.e*, about 3 hr for one sample and 1 day for six samples.

The described method is fast and reliable and does not require expensive instrumentation. Furthermore, it is sensitive enough for the determination of unaltered I in the biological fluids of both experimental animals and humans.

REFERENCES

(1) P. Populaire, B. Terlain, S. Pascal, B. Decovelaere, G. Lebreton, A. Renard, and J. P. Thomas, *Ann. Pharm. Fr.*, **31**, 11, 679 (1973).

(2) L. Julou, J. C. Guyonnet, R. Ducrot, C. Garret, M. C. Bardone, G. Maignan, and J. Pasquet, *J. Pharmacol. (Paris)*, **2**, 259 (1971).

ACKNOWLEDGMENTS AND ADDRESSES

Received December 24, 1975, from the *Laboratorio Chimico Farmaceutico "A. Menarini," Via Sette Santi, 3, 50131 Firenze, Italy.*

Accepted for publication April 13, 1976.

The authors are indebted to Professor A. Meli for interest and advice.

[x] To whom inquiries should be directed.

Water as a Nonpolar Partition Medium

H. TAKRURI *§, B. ECANOW *‡x, and R. BALAGOT *‡

Abstract □ Coacervates have been suggested as models for cytoplasm since cytoplasm is also essentially an aqueous phase of water–protein–colloid complexes. This study on partition coefficient properties made use of coacervate phases as the nonpolar phases in equilibrium with polar water phases. The partition coefficients of four barbiturates were obtained, and their values correlated with those reported in the literature for systems using organic solvents as the nonpolar medium. These values also correlated with reported values for the absorption ranking of the barbiturates in the rat colon. The partition coefficients of theobromine and theophylline in gelatin–benzalkonium chloride coacervate systems were also found to correlate with the partition values reported in the literature for heptane–water and chloroform–water systems. It is suggested that coacervate systems form a more realistic model for studying and predicting the absorption characteristics of drugs than do conventional organic solvent–water systems.

Keyphrases □ Partition coefficients—various barbiturates and xanthines, coacervates as nonpolar phases in equilibrium with polar water phases □ Barbiturates, various—partition coefficients, coacervates as nonpolar phases in equilibrium with polar water phases □ Xanthines, various—partition coefficients, coacervates as nonpolar phases in equilibrium with polar water phases □ Coacervates—nonpolar phases in equilibrium with polar water phases, partition coefficients, various barbiturates and xanthines

Meyer (1) and Overton (2) showed a correlation between anesthetic drug activity and the partition coefficient, *i.e.*, the ratio of drug solubility in a lipoid phase to its solubility in a water phase. For the lipoid phase, olive oil, corn oil, chloroform, and a spectrum of nonpolar organic solvents have been used. Water can act as a nonpolar solvent when it is bound to various molecules (proteins, surface-active agents, *etc.*) to form a liquid that is insoluble in a regular or bulk liquid water. This nonpolar structured water complex is referred to as a coacervate. Coacervates have been suggested as models for cytoplasm since cytoplasm is also essentially an aqueous phase of water–protein–colloid complexes (3, 4).

This report considers the use of a coacervate system as the nonpolar phase in equilibrium with a normal water phase.

BACKGROUND

The partition coefficients of four barbiturates were obtained, and the values were compared to those reported in the literature using an organic nonpolar medium (5). Schanker (5) studied the absorption of barbiturates from the rat colon and compared the percent absorption with the partition coefficients of the free acids in chloroform–water systems. The reported percent absorption values are compared here with the partition coefficient values of the barbiturate salts in a coacervate–water system.

The partition coefficients of theobromine and theophylline in gelatin–benzalkonium chloride coacervate systems were obtained and compared to those reported for heptane–water and chloroform–water systems (6). Comparisons were also made to percent drug absorption in the rat colon as reported in the literature (6).

The rationale for attempting to correlate partition coefficients of compounds with reported values for percent absorption is as follows. Since coacervates, regardless of their composition and pH, are complex aqueous colloidal systems, it is expected that they bear more resemblance in overall properties to protoplasm than do lipids and lipid-like solvents such as chloroform and heptane. Any correlation between interactions of compounds with coacervates, as evidenced by preferential uptake or exclusion, and absorption profiles of these compounds can be considered to support the hypothesis that complex coacervates systems (not necessarily the systems considered in this work) can be considered as models for protoplasm. It is obvious that barbiturates are not appreciably ionized at physiological pH. However, since the properties and interactions of the salts reflect, in some ways, the properties of the parent compounds, it is not unreasonable to attempt correlation of salt–coacervate interactions with absorption characteristics.

EXPERIMENTAL

Preparations of Coacervate System—In 15-ml graduated tubes, 3.0 ml of a 10% gelatin solution, 2.0 ml of a 5% benzalkonium chloride solution, and sufficient 0.1 *N* sodium hydroxide were added to give a pH above 9. This solution was diluted to 15 ml with distilled water. The tubes were stoppered, mixed vigorously, and left undisturbed for 24 hr at 37°. Complete separation of two aqueous phases occurred. The bottom layer was the coacervate and contained most of the colloidal material.

Assay of Drug by Difference—The concentration of the barbiturates used in this study was determined spectrophotometrically. The concentration of the compound in the coacervate was determined from the difference between the total amount in the system and the amount spectrophotometrically found in the equilibrium liquid. The sodium salts of barbital, phenobarbital, pentobarbital, and secobarbital were studied at 37°. The concentration of the salts in equilibrium liquid was determined at 240 nm, using a 0.2 *M* borate buffer (pH 9.6) as the diluting solvent and a total system concentration of 200 mg %.

Partitioning of theophylline and theobromine was studied at 37°. Theophylline dilutions were prepared in a potassium chloride–sodium hydroxide buffer of pH 12 and measured at 275 nm. The same solvent was used for theobromine, which was measured at 274 nm. The partition coefficients (P.C.) were obtained at 50 and 100 mg %, and the average values are reported in Table I.

RESULTS AND DISCUSSION

The partitioning patterns of barbiturate salts are shown in Fig. 1. Barbital sodium showed the least uptake in coacervates. At concentrations higher than 100 mg %, it exerted a suppressive action on coacervation as evidenced by a decrease in the volume of the coacervate layer. At a concentration of 200 mg %, the compound was distributed equally between the two phases.

Barbital sodium did not show a precipitation–resolubilization interaction with benzalkonium chloride, which explains its weak affinity for coacervates. The partitioning isotherms for the sodium salts of phenobarbital, pentobarbital, and secobarbital showed a strong affinity of these salts toward coacervates and the dependence of this affinity on the concentration of the salt.

Schanker (5) studied the absorption of barbiturates from the rat colon and compared the percent absorption with the partition coefficient of the free acids in chloroform–water systems. Figure 2 shows the correlation between the percent absorption and the partition coefficient of the barbiturate salts in gelatin–benzalkonium chloride systems. The averages of the partition coefficients at the four highest concentrations studied

Table I—Partition Coefficient Studies of Theophylline and Theobromine[a]

Compound	Percent Absorbed	Partition Coefficients: Heptane–Water	Chloroform–Water	Coacervates
Theophylline	30	0.02	0.3	3.32
Theobromine	22	0.002	0.4	2.37

[a] The data, with the exception of the partition coefficients in coacervates, are from Ref. 6.

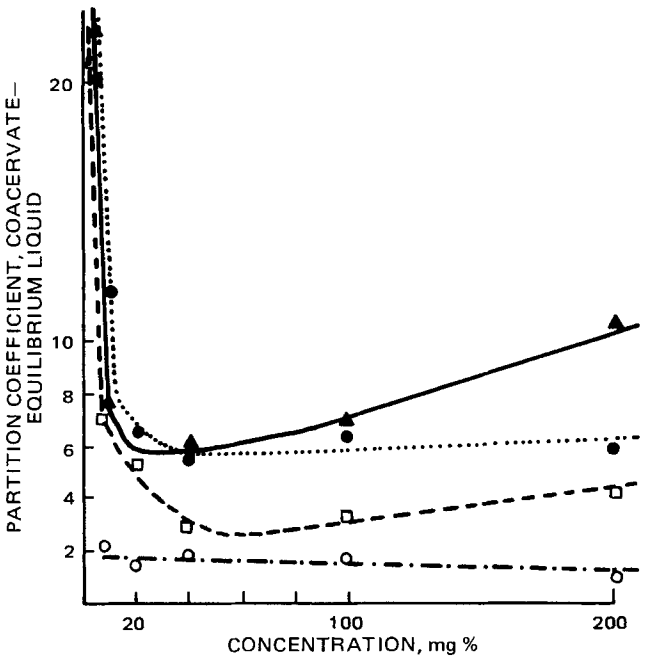

Figure 1—*Partitioning of barbiturate salts in gelatin–benzalkonium chloride system at 37°. Key: ▲—▲, secobarbital sodium; ●·····●, pentobarbital sodium; □- - -□, phenobarbital sodium; and O----O, barbital sodium.*

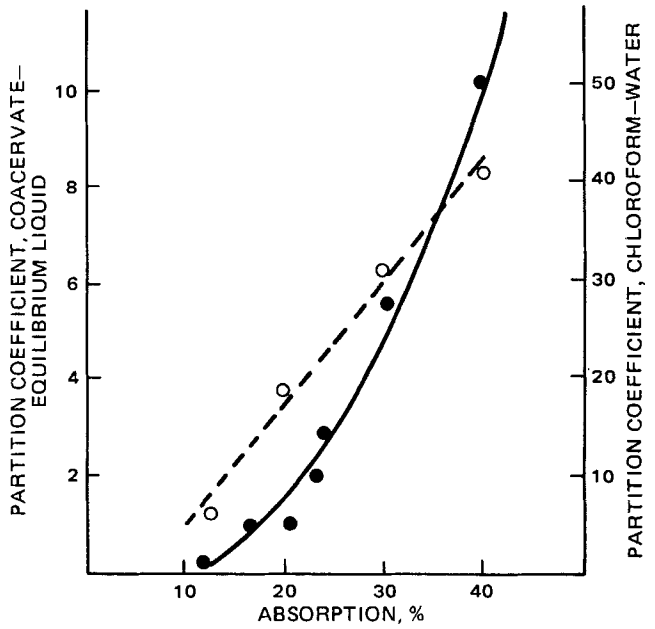

Figure 2—*Correlation of the partition coefficients of barbiturate salts with percent absorption from the rat colon. Data for percent absorption and chloroform–water partition coefficients are from Schanker (5). Key: O- - -O, partition coefficient, coacervate–equilibrium liquid, of barbiturate salts; and ●—●, partition coefficient, chloroform–water, of free acids.*

(20–200 mg %) were plotted *versus* the percent absorption as reported by Schanker. The choice of these average values was arbitrary and based on the assumption that the average partition coefficient over a wide concentration range was more representative of the intrinsic affinity between the coacervate and the barbiturate salt and tended to cancel the effects of any secondary interactions between the compound and the components of the coacervate.

Table I shows the intestinal absorption of theobromine and theophylline in relation to their partition coefficients in heptane–water, chloroform–water, and gelatin–benzalkonium chloride systems. It is obvious that there exists a better correlation between the percent absorption and the partitioning in coacervates than between the absorption and the partitioning in nonpolar organic solvents.

These coacervates are particularly useful for studying partitioning of water-soluble salts of insoluble weak acids between coacervates and their equilibrium liquids. The hypothesis underlying these studies is that the differences between the "hydrophobicity" of these anions will be manifested in their affinity (*i.e.*, partitioning) for structured water in the coacervate phase.

There is a clear correlation between variables in the experiments using barbiturates and xanthines, suggesting that coacervates of this type might serve as biological models for studying and predicting the absorption characteristics of drugs.

The purpose of benzalkonium chloride is to act as a coacervating agent in the system. The gelatin used has an isoelectric point of 8.2. Above this pH, gelatin is negatively charged and, under the proper conditions, forms true complex coacervates with benzalkonium chloride. Most of the studies on coacervation of gelatin with, for example, acacia involved gelatin of a lower isoelectric point and the pH of coacervates was, generally, on the acid side. At the time of these studies, true complex coacervation between a high isoelectric point gelatin and other ingredients, particularly surface-active agents, had not been reported in the literature.

REFERENCES

(1) H. H. Meyer, *Arch. Exp. Pathol. Pharmakol.*, **42**, 109 (1899).

(2) E. Overton, "Studien uber die Narkose Sugleich ein Beitrag zur Allgemeinen Pharmakologic," G. Fischer, Jena, E. Germany, 1901.

(3) A. I. Oparin, in "Origins of Prebiological Systems and of their Molecular Matrices," S. W. Fox, Ed., Academic, New York, N.Y., 1965.

(4) B. Ecanow and H. L. Klawans, "Models of Human Neurological Diseases," Excerpta Medica, Amsterdam, The Netherlands, 1974, pp. 253, 284.

(5) L. S. Schanker, *J. Pharmacol. Exp. Ther.*, **126**, 283 (1959).

(6) C. A. Hogben, D. H. Tocco, B. B. Brodie, and L. S. Schanker, *ibid.*, **125**, 275 (1959).

ACKNOWLEDGMENTS AND ADDRESSES

Received December 30, 1974, from the *College of Pharmacy, University of Illinois at the Medical Center, Chicago, IL 60612 and the [1] *Hines Veterans Administration Hospital, Hines, IL 60153.

Accepted for publication April 5, 1976.

[§] Present address: Eli Lilly and Co., Indianapolis, Ind.

[x] To whom inquiries should be directed (at the University of Illinois).

Chemistry and Pharmacology of Homologs of 6-Acetyl- and 3,6-Diacetylmorphine

EVERETTE L. MAY and ARTHUR E. JACOBSON ˣ

Abstract □ 3,6-Diformyl- and 3,6-dipropanoylmorphine and 6-formyl- and 6-propanoylmorphine were prepared to obtain longer acting, heroin-like compounds. The 6-acylated compounds were more potent than heroin subcutaneously and were orally effective, and their duration of action was at least two to three times greater than that of heroin in monkey species.

Keyphrases □ Morphine derivatives, various—synthesized, analgesic activity evaluated, monkeys □ Analgesic activity—various morphine derivatives, monkeys □ Structure–activity relationships—various morphine derivatives, analgesic activity evaluated, monkeys

For some time, there has been an interest in heroin-like compounds whose duration of action would be greater than that of heroin (3,6-diacetylmorphine, I). Goldstein (1), for example, recently suggested a provocative procedure for rehabilitating "hard-core" addicts who resist contemporary methods of treatment. One early step that might lead to the complete withdrawal of narcotics would entail the use of a longer acting heroin. As potential agents for this phase of treatment, higher and lower homologs of I, the 3,6-diformyl (II), 3,6-dipropanoyl (III), 6-formyl (V), and 6-propanoyl (VI) derivatives were prepared. The chemistry and pharmacology of I–VI and 3-acetylmorphine (VII) are described here and some stability data are presented.

3,6-Diformylmorphine (II) was prepared from morphine hydrate and excess formic–acetic anhydride (2) at 15–25°. If pyridine was used as a solvent, 6-formylmorphine (V) resulted. Excess propanoic anhydride and morphine at 100° gave 3,6-dipropanoylmorphine (III) (3). Anhydrous morphine, potassium carbonate, and 1.2 *M* equivalents of propanoic anhydride (reflux temperature) produced 6-propanoylmorphine (VI). Finally, 3-acetylmorphine (VII) was synthesized by the method of Welsh (4) for pharmacology and stability comparisons.

EXPERIMENTAL[1]

3,6-Diformylmorphine (II)—To 60 ml of acetic anhydride (ice cooled and stirred) was added dropwise (5–10 min) 25 ml of 97% formic acid (5). The mixture was warmed slowly to 50–55°, where it was kept for 15–20 min. To 25 ml of this solution was added (ice cooling) 5.0 g of morphine monohydrate so that the temperature did not rise above 15°. The solution was then treated with an additional 5 ml of the acetic anhydride–acetic acid mixture.

Stirring was continued at room temperature (21–24°) for 24 hr, after which another 25-ml portion of the formylating mixture was added during 5 min. The solution was left at 21–24° for an additional 70 hr and then evaporated to dryness *in vacuo*. The residue was dissolved in ice water; after 20 min, methylene chloride and then 10% Na_2CO_3 were added to pH 9 (at 10–12°). The dried (sodium sulfate) methylene chloride layer was evaporated to dryness *in vacuo*. The residue was dissolved in 50–70 ml of boiling acetone, from which II crystallized on cooling to 0°, yielding 4.5 g, mp 170° (gas evolution) and 212–215° dec.

Anal.—Calc. for $C_{19}H_{19}NO_5$: C, 66.84; H, 5.61; N, 4.00. Found: C, 66.64; H, 5.58; N, 4.10.

The hydrochloride salt (from acetone–hydrogen chloride gas) was dried at 65°, mp 210–211° (froth).

Anal.—Calc. for $C_{19}H_{20}ClNO_4 \cdot 0.5H_2O$: C, 58.98; H, 5.47; Cl, 9.16; N, 3.62. Found: C, 58.93; H, 5.53; Cl, 9.04; N, 3.40.

6-Formylmorphine (V)—Formic acid (90 ml) and 40 ml of acetic anhydride (5) were mixed at 0° and then kept at 50–55° for 15 min. The solution was cooled to 0° (stirring) and treated dropwise (at 0°) with 7.4 g of morphine monohydrate in 50 ml of pyridine. The mixture was kept at 25° for 65–70 hr, poured into ice water, and treated with 100 ml of methylene chloride and 20% Na_2CO_3 to pH 9. The organic layer and one methylene chloride extract of the aqueous layer were combined, dried (magnesium sulfate), and evaporated to dryness *in vacuo*. Trituration of the 9.1 g of residue in acetone gave, after cooling to 0°, 5.4 g of V, mp 208–215° dec.

Anal.—Calc. for $C_{18}H_{19}NO_4$: C, 68.99; H, 6.11; N, 4.47. Found: C, 69.03; H, 6.07; N, 4.29.

The hydrochloride salt (from acetone–hydrogen chloride gas) melted at 265–267° dec.

Anal.—Calc. for $C_{18}H_{20}ClNO_4$: C, 61.80; H, 5.76; Cl, 10.14; N, 4.00. Found: C, 61.44; H, 5.93; Cl, 10.05; N, 3.84.

3,6-Dipropanoylmorphine (III)—Morphine (2.0 g) and 5.0 ml of propanoic anhydride were kept on the steam bath for 4 hr, cooled to room temperature, and treated with water. After 1 hr, the clear solution was partitioned between ether and 10% KOH (ice cooling). The ether was washed once with water, dried over sodium sulfate, and evaporated. The hydrochloride salt (3) (from ether–hydrogen chloride gas) weighed 2.6 g (87%). After a recrystallization from ethyl acetate, it melted at 150–155° (froth).

In another run, 0.25 g of crude III, obtained as described, was dissolved in acetone and treated with 0.08 g of sulfamic acid in 0.5 ml of water. Further dilution with acetone gave 0.3 g of the sulfamate salt of III, mp 190–191° if the capillary tube was inserted in a bath preheated to 185–188°. Otherwise, the sample became brown at 175° and did not melt even at 200°.

Anal.—Calc. for $C_{23}H_{30}N_2O_8$: C, 55.85; H, 6.11; N, 5.67. Found: C, 56.13; H, 5.91; N, 5.78.

6-Propanoylmorphine (VI) Hydrochloride—Morphine (2.9 g of anhydrous base) and 50 ml of acetone (dried over molecular sieve) were stirred and refluxed together while 1.6 ml (1.2 equivalents) of propanoic anhydride in 10 ml of dry acetone was added during 1 hr. The mixture was refluxed for 4–5 hr and evaporated to dryness *in vacuo*. The residue was treated with cold water, ether, and excess potassium carbonate. The ether was dried (sodium sulfate) to give 3.3 g of base which, as determined by TLC analysis [chloroform–methanol–ammonium hydroxide (85:14:1)] on silica gel, consisted of about 97% of VI and 2–3% of III. It was dissolved in acetone–ether (3:1) and treated (to pH 4–5) with hydrogen chloride gas to give (ice cooling) 2.2 g of VI hydrochloride, which was dissolved in 140 ml of boiling acetone. The solution was concentrated to 45–50 ml

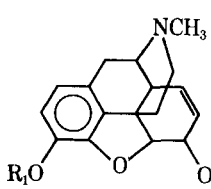

I: $R_1 = R_2 = COCH_3$
II: $R_1 = R_2 = CHO$
III: $R_1 = R_2 = COC_2H_5$
IV: $R_1 = H$, $R_2 = COCH_3$
V: $R_1 = H$, $R_2 = CHO$
VI: $R_1 = H$, $R_2 = COC_2H_5$
VII: $R_1 = COCH_3$, $R_2 = H$

[1] Melting points (uncorrected) were taken on a Fisher-Johns apparatus or by capillary (SGA Melt-Meter). IR (Perkin-Elmer 257), NMR (Varian A60 or HA 100 with tetramethylsilane as internal standard) and mass spectra (Hitachi Perkin-Elmer RMU6E, at 70 ev) were consistent with assigned structures. Analytical results are from the Section on Microanalytical Services and Instrumentation of this Laboratory.

Table I—Pharmacological Properties of *O*-Acylmorphines

Morphine Derivatives[a]	ED_{50}, mg/kg[b]	PDC[c]	Duration of Action, hr (Monkeys)
I	0.5 (0.4–0.6)	High (1.0)[d]	3–4
II	0.6 (0.5–0.8)	—[e]	—
III	0.3 (0.2–0.4)	High (0.8)[d]	3–4
IV	0.5 (0.4–0.6)	High (1.0)[d]	—[f]
V	0.3 (0.2–0.4)	High (1.6)[d]	12
VI	0.3 (0.2–0.4)	Medium high (2.0)[d]	>6
VII[g]	1.3 (1.2–1.5)	High (2.0)[d]	3
Morphine[a]	1.2 (0.9–1.3)	High (3.0)[d]	6

[a] Subcutaneously administered as hydrochloride salts, unless otherwise noted, to mice. [b] Determined by the hot-plate method (6, 7). Numbers in parentheses are the 95% *SE* limits, as obtained by probit analysis. [c] Physical dependence capacity as determined in monkeys (8, 9). [d] Equivalence to 3 mg/kg of morphine sulfate. [e] Too unstable to test in monkeys. [f] Of shorter duration than morphine. [g] Sulfamate salt.

(to the appearance of crystals) and cooled finally to 0° for 1 hr to give 1.8 g, mp 155–165°.

Anal.—Calc. for $C_{20}H_{24}ClNO_4 \cdot 0.5H_2O$: C, 62.07; H, 6.47; Cl, 9.16; N, 3.62. Found: C, 61.70; H, 6.43; Cl, 9.18; N, 3.29.

RESULTS AND DISCUSSION

As seen in Table I, the 3,6-diformyl (II), 3,6-dipropanoyl (III), and 6-propanoyl (VI) derivatives were comparable to heroin (I) and 6-acetylmorphine (IV) in analgesic potency and were three to four times as potent as morphine (6, 7). 3-Acetylmorphine (VII) sulfamate (4) was nearly identical in potency to morphine. As expected, all had good capacity to sustain morphine dependence in monkeys (8, 9) with a wide variation in duration of action. Superiority in this respect was shown by V (12 hr) and VI (>6 hr), both longer acting than morphine, heroin, or 6-acetylmorphine[2].

The mode of action of the 6-acylated compounds, V and VI, is not known. Like 6-acetylmorphine, they are probably metabolized to morphine (10), albeit less rapidly. Their duration of action for analgesia (mice) was much longer than that for heroin but similar to morphine. Their considerably longer action than heroin and even morphine in higher animals (monkeys) may be more indicative of their behavior in humans.

The oral activity of V and VI (in mice) was relatively good (ED_{50} 11.6 and 7.4 mg/kg, respectively). Thus, V and VI would appear to be the most interesting compounds of this group for further study as possible maintenance drugs or in detoxification therapy. The diformyl compound (II) was too unstable to be tested in monkeys.

Qualitatively, the order of stability of these compounds in the salt form noted in Table I appeared to be: 3,6-diacetyl ≅ 3,6-dipropanoyl > 6-propanoyl ≅ 6-acetyl ≅ 3-acetyl > 6-formyl > 3,6-diformyl derivatives at 25°. This order seems to be at variance with the durations of action in supporting morphine dependence in monkeys. The impression is given by these qualitative studies that the acylmorphines (as salts), except II, are more stable in aqueous solution than is generally believed.

[2] Extracted from Addenda to the Proceedings of several meetings of the Committee on Problems of Drug Dependence in early to mid-1950's.

REFERENCES

(1) A. Goldstein, *Arch. Gen. Psychiat.*, in press.

(2) L. Krimen, in Organic Syntheses, vol. 50, R. Breslow, Ed., Wiley, New York, N.Y.

(3) H. Emile, *Helv. Chim. Acta*, **13**, 1035 (1930).

(4) L. H. Welsh, *J. Org. Chem.*, **19**, 1409 (1954).

(5) K. Miyatake, A. Okano, K. Hoji, T. Miki, and A. Sakashita, *Chem. Pharm. Bull.*, **9**, 524 (1961).

(6) N. B. Eddy and D. Leimbach, *J. Pharmacol. Exp. Ther.*, **107**, 385 (1953).

(7) A. E. Jacobson and E. L. May, *J. Med. Chem.*, **8**, 563 (1965).

(8) Committee on Problems of Drug Dependence, "Bulletin on Narcotics," vol. XXV, no. 2, National Academy of Sciences, Washington, D.C., 1972, p. 25.

(9) H. H. Swain and M. H. Seevers, "Addendum to the Proceedings of the Thirty-Seventh Meeting of the Committee on Problems of Drug Dependence," National Academy of Sciences, Washington, D.C., 1975.

(10) E. L. Way, J. W. Kemp, J. M. Young, and D. R. Grasetti, *J. Pharmacol. Exp. Ther.*, **129**, 144 (1960).

ACKNOWLEDGMENTS AND ADDRESSES

Received October 21, 1975, from the *Section on Medicinal Chemistry, Laboratory of Chemistry, National Institute of Arthritis, Metabolism and Digestive Diseases, National Institutes of Health, Bethesda, MD 20014.*

Accepted for publication March 23, 1976.

The stimulus for this research came from Dr. Bert La Du, Department of Pharmacology, University of Michigan, who first suggested the preparation of 3,6-diformylmorphine, a lower homolog of heroin.

[x] To whom inquiries should be directed.

Liquid Chromatography in Pharmaceutical Analysis VI: Determination of Dantrolene Sodium in a Dosage Form

S. J. SAXENA, I. L. HONIGBERG [x], J. T. STEWART, G. R. KEENE, and J. J. VALLNER

Abstract □ Operating conditions are described for the qualitative and quantitative determination of dantrolene sodium by high-pressure liquid chromatography. A 10-μm porous silica column was employed, using carbon tetrachloride–dimethylformamide (90:10) as the mobile phase. The flow rate was 2.0 ml/min (1800 psig), and the peaks were detected at 375 nm. The analysis of a dosage form can be carried out within 30 min with an accuracy of 3.1%. The results agree favorably with those obtained with a modified spectrophotofluorometric method.

Keyphrases □ Dantrolene sodium—high-pressure liquid chromatographic analysis, commercial dosage forms □ High-pressure liquid chromatography—analysis, dantrolene sodium, commercial dosage forms □ Relaxants, skeletal muscle—dantrolene sodium, high-pressure liquid chromatographic analysis, commercial dosage forms

Dantrolene sodium, 1-[[5-(*p*-nitrophenyl)furfurylidene]amino]hydantoin sodium salt hydrate, was first reported by Snyder *et al.* (1) as a representative of a new class of muscle relaxants which apparently acts directly on the skeletal muscle.

Previous reported analyses of dantrolene sodium include spectrophotofluorometry (2, 3), differential pulse polarography (4), and a colorimetric procedure for qualitative

Table I—Pharmacological Properties of *O*-Acylmorphines

Morphine Derivatives[a]	ED_{50}, mg/kg[b]	PDC[c]	Duration of Action, hr (Monkeys)
I	0.5 (0.4–0.6)	High (1.0)[d]	3–4
II	0.6 (0.5–0.8)	—[e]	—
III	0.3 (0.2–0.4)	High (0.8)[d]	3–4
IV	0.5 (0.4–0.6)	High (1.0)[d]	—[f]
V	0.3 (0.2–0.4)	High (1.6)[d]	12
VI	0.3 (0.2–0.4)	Medium high (2.0)[d]	>6
VII[g]	1.3 (1.2–1.5)	High (2.0)[d]	3
Morphine[a]	1.2 (0.9–1.3)	High (3.0)[d]	6

[a] Subcutaneously administered as hydrochloride salts, unless otherwise noted, to mice. [b] Determined by the hot-plate method (6, 7). Numbers in parentheses are the 95% *SE* limits, as obtained by probit analysis. [c] Physical dependence capacity as determined in monkeys (8, 9). [d] Equivalence to 3 mg/kg of morphine sulfate. [e] Too unstable to test in monkeys. [f] Of shorter duration than morphine. [g] Sulfamate salt.

(to the appearance of crystals) and cooled finally to 0° for 1 hr to give 1.8 g, mp 155–165°.

Anal.—Calc. for $C_{20}H_{24}ClNO_4 \cdot 0.5H_2O$: C, 62.07; H, 6.47; Cl, 9.16; N, 3.62. Found: C, 61.70; H, 6.43; Cl, 9.18; N, 3.29.

RESULTS AND DISCUSSION

As seen in Table I, the 3,6-diformyl (II), 3,6-dipropanoyl (III), and 6-propanoyl (VI) derivatives were comparable to heroin (I) and 6-acetylmorphine (IV) in analgesic potency and were three to four times as potent as morphine (6, 7). 3-Acetylmorphine (VII) sulfamate (4) was nearly identical in potency to morphine. As expected, all had good capacity to sustain morphine dependence in monkeys (8, 9) with a wide variation in duration of action. Superiority in this respect was shown by V (12 hr) and VI (>6 hr), both longer acting than morphine, heroin, or 6-acetylmorphine[2].

The mode of action of the 6-acylated compounds, V and VI, is not known. Like 6-acetylmorphine, they are probably metabolized to morphine (10), albeit less rapidly. Their duration of action for analgesia (mice) was much longer than that for heroin but similar to morphine. Their considerably longer action than heroin and even morphine in higher animals (monkeys) may be more indicative of their behavior in humans.

The oral activity of V and VI (in mice) was relatively good (ED_{50} 11.6 and 7.4 mg/kg, respectively). Thus, V and VI would appear to be the most interesting compounds of this group for further study as possible maintenance drugs or in detoxification therapy. The diformyl compound (II) was too unstable to be tested in monkeys.

Qualitatively, the order of stability of these compounds in the salt form noted in Table I appeared to be: 3,6-diacetyl ≅ 3,6-dipropanoyl > 6-propanoyl ≅ 6-acetyl ≅ 3-acetyl > 6-formyl > 3,6-diformyl derivatives at 25°. This order seems to be at variance with the durations of action in supporting morphine dependence in monkeys. The impression is given by these qualitative studies that the acylmorphines (as salts), except II, are more stable in aqueous solution than is generally believed.

[2] Extracted from Addenda to the Proceedings of several meetings of the Committee on Problems of Drug Dependence in early to mid-1950's.

REFERENCES

(1) A. Goldstein, *Arch. Gen. Psychiat.*, in press.

(2) L. Krimen, in Organic Syntheses, vol. 50, R. Breslow, Ed., Wiley, New York, N.Y.

(3) H. Emile, *Helv. Chim. Acta*, **13**, 1035 (1930).

(4) L. H. Welsh, *J. Org. Chem.*, **19**, 1409 (1954).

(5) K. Miyatake, A. Okano, K. Hoji, T. Miki, and A. Sakashita, *Chem. Pharm. Bull.*, **9**, 524 (1961).

(6) N. B. Eddy and D. Leimbach, *J. Pharmacol. Exp. Ther.*, **107**, 385 (1953).

(7) A. E. Jacobson and E. L. May, *J. Med. Chem.*, **8**, 563 (1965).

(8) Committee on Problems of Drug Dependence, "Bulletin on Narcotics," vol. XXV, no. 2, National Academy of Sciences, Washington, D.C., 1972, p. 25.

(9) H. H. Swain and M. H. Seevers, "Addendum to the Proceedings of the Thirty-Seventh Meeting of the Committee on Problems of Drug Dependence," National Academy of Sciences, Washington, D.C., 1975.

(10) E. L. Way, J. W. Kemp, J. M. Young, and D. R. Grasetti, *J. Pharmacol. Exp. Ther.*, **129**, 144 (1960).

ACKNOWLEDGMENTS AND ADDRESSES

Received October 21, 1975, from the *Section on Medicinal Chemistry, Laboratory of Chemistry, National Institute of Arthritis, Metabolism and Digestive Diseases, National Institutes of Health, Bethesda, MD 20014.*

Accepted for publication March 23, 1976.

The stimulus for this research came from Dr. Bert La Du, Department of Pharmacology, University of Michigan, who first suggested the preparation of 3,6-diformylmorphine, a lower homolog of heroin.

[x] To whom inquiries should be directed.

Liquid Chromatography in Pharmaceutical Analysis VI: Determination of Dantrolene Sodium in a Dosage Form

S. J. SAXENA, I. L. HONIGBERG [x], J. T. STEWART, G. R. KEENE, and J. J. VALLNER

Abstract □ Operating conditions are described for the qualitative and quantitative determination of dantrolene sodium by high-pressure liquid chromatography. A 10-μm porous silica column was employed, using carbon tetrachloride–dimethylformamide (90:10) as the mobile phase. The flow rate was 2.0 ml/min (1800 psig), and the peaks were detected at 375 nm. The analysis of a dosage form can be carried out within 30 min with an accuracy of 3.1%. The results agree favorably with those obtained with a modified spectrophotofluorometric method.

Keyphrases □ Dantrolene sodium—high-pressure liquid chromatographic analysis, commercial dosage forms □ High-pressure liquid chromatography—analysis, dantrolene sodium, commercial dosage forms □ Relaxants, skeletal muscle—dantrolene sodium, high-pressure liquid chromatographic analysis, commercial dosage forms

Dantrolene sodium, 1-[[5-(*p*-nitrophenyl)furfurylidene]amino]hydantoin sodium salt hydrate, was first reported by Snyder *et al.* (1) as a representative of a new class of muscle relaxants which apparently acts directly on the skeletal muscle.

Previous reported analyses of dantrolene sodium include spectrophotofluorometry (2, 3), differential pulse polarography (4), and a colorimetric procedure for qualitative

Table I—Calibration Data for Standard Drug Solutions

Analytical Method	Initial Concentration of Dantrolene Sodium, mg/ml	Observed Results	Slope	Intercept	$r \pm s_{yx}$[a]
HPLC	0.2	1.1192 ± 0.0010[b]			
	0.5	2.8129 ± 0.0100	0.5362	0.0795	0.9997 ± 0.0369
	1.0	5.4219 ± 0.0099			
Spectrophotofluorometric	0.2	28.5[c]			
	0.5	55.0	8.9439	10.4847	0.9999 ± 0.1458
	1.0	100.0			

[a] r is the correlation coefficient determined from linear regression analysis, and s_{yx} is the sample standard deviation, also from regression analysis. [b] The D/IS ratio is based on four replicate injections of standard solution. The table value is the mean ± *SD*. The D/IS is the ratio of the integrated area of the drug at some concentration to the integrated area of furil at a concentration of 4 mg/ml. [c] Arbitrary fluorescence units.

determination (5). Although the use of liquid chromatography *via* a reversed-phase process has been successful with various drugs (6–8), the limited solubility of dantrolene sodium in polar mobile phases has precluded use of this technique. This paper reports the conversion of the drug to its free acid followed by extraction, chromatographic separation, and quantification using adsorption chromatography. The analysis of dosage forms can be performed within 30 min. The results of the high-pressure liquid chromatographic (HPLC) procedure are compared to those of a spectrophotofluorometric method, modified from that reported by Hollifield and Conklin (3).

EXPERIMENTAL

Reagents and Chemicals—A powdered sample of dantrolene sodium[1] was used; chemicals and reagent grade solvents were obtained commercially and used as received. The chromatographic solvents, carbon tetrachloride and dimethylformamide, were filtered through a 0.5-μm filter[2] prior to use. The pH of a 0.5 *M* aqueous solution of dimethylformamide was consistently 6.8 ± 0.1.

Mobile Phase—The mobile phase consisted of carbon tetrachloride–dimethylformamide (90:10) and was used after degassing.

Internal Standard Solution—The stock internal standard solution (20 mg/ml) was prepared by dissolving powdered furil[3] in water-saturated 1-butanol–chloroform (30:70). It was filtered through a 5.0-μm filter[4] before use.

Standard Solution for Calibration Curve—A stock solution of dantrolene sodium was prepared by dissolving 25 mg of dantrolene sodium powder in 5 ml of dimethylformamide in a 25-ml volumetric flask. The solution was then diluted to 25 ml with distilled water to yield a solution of 1 mg/ml.

Determination of Calibration Curve—Accurately pipetted volumes of 2.0, 5.0, and 10.0 ml of the dantrolene sodium stock solution were each placed in a 60-ml separator. Where necessary, the volume of each solution was adjusted to 10 ml with distilled water. Then 5.0 ml of 2 *N* HCl solution was added to each separator to precipitate dantrolene. The aqueous solutions were extracted with 2 × 10-ml portions of 1-butanol–chloroform (30:70), and the organic layer from each separator was separated and transferred to 25-ml volumetric flasks.

The volume of each flask was then adjusted to 25 ml with additional organic solvent, and the organic extract was filtered through a 5.0-μm filter[4]. Four milliliters of the filtered extract was pipetted into a 5-ml volumetric flask followed by the addition of 1 ml of the internal standard stock solution. Twenty microliters of each solution was injected into the chromatograph.

Determination of Percent Extraction of Dantrolene Sodium—A solution of dantrolene[5] (0.0522 mg/ml) was prepared in 1-butanol–chloroform (30:70). Four milliliters was pipetted into a 5-ml volumetric flask, 1 ml of internal standard solution was added, and the solution was chromatographed. The ratio of the dantrolene peak area to the area of the internal standard (D/IS) was compared with the D/IS ratio obtained by a theoretically equivalent amount of dantrolene free acid, extracted from dantrolene sodium, which was prepared as follows. Two milligrams of dantrolene sodium was dissolved in 10 ml of water, converted to dantrolene, and extracted into 3 × 10-ml portions of 1-butanol–chloroform (30:70) to give a solution with a theoretical dantrolene concentration of 0.0522 mg/ml. Four milliliters of this solution was pipetted into a 5-ml volumetric flask, 1 ml of internal standard solution was added, and the solution was chromatographed.

Determination of Dantrolene Sodium in Dosage Form—The contents of two 25-mg capsules[6] were quantitatively transferred to separate 50-ml volumetric flasks with the aid of a small amount of distilled water. The contents were dissolved in 10 ml of dimethylformamide and

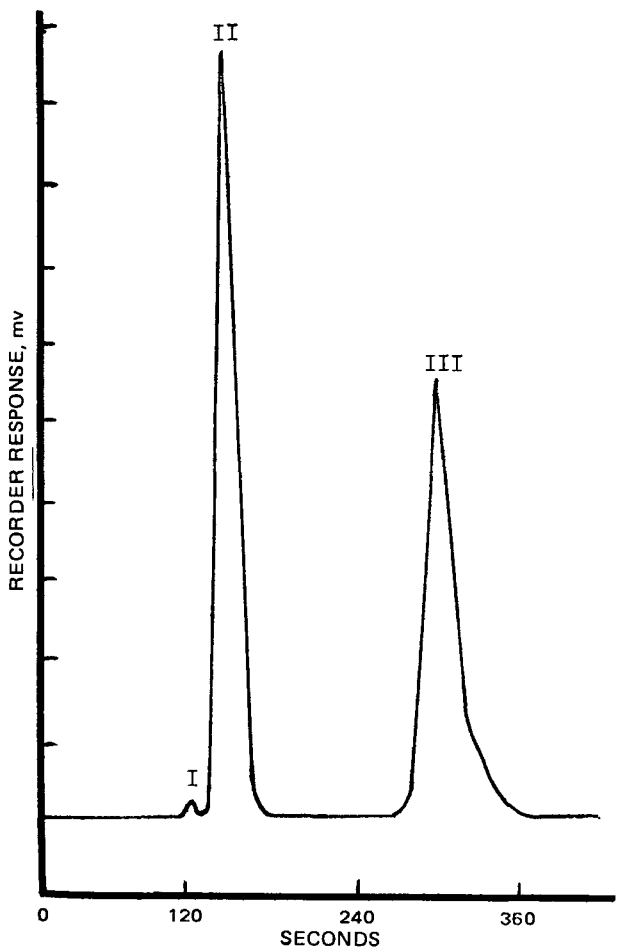

Figure 1—*Typical chromatogram of dantrolene sodium using a porous silica column (room temperature) at a flow rate of 2.0 ml/min. Mobile phase was carbon tetrachloride–dimethylformamide (90:10). Key: I, solvent front; II, furil (internal standard); and III, dantrolene.*

[1] Courtesy of Eaton Laboratories, Norwich, N.Y.
[2] Catalog No. FHL PO 4700, Millipore Corp., Bedford, Mass.
[3] Catalog No. 2040, Eastman Organic Chemicals, Rochester, N.Y.
[4] Catalog No. LSWF01300, Millipore Corp., Bedford, Mass.
[5] Free acid, courtesy of Eaton Laboratories.
[6] Dantrium, Eaton Laboratories, Norwich, N.Y.

Table II—Determination of Dantrolene Sodium in Dosage Form[a]

Capsule	Labeled Amount, mg	Percent Found	
		HPLC[b]	Spectrophotofluorometric Method[c]
1	25	98.50 ± 1.66[d]	100.28 ± 0.73[d]
2	25	104.15 ± 1.17	106.03 ± 0.90

[a] There was no significant difference between the HPLC results and the fluorometric results at the $p = 0.01$ level. [b] Based on four replicate injections. [c] Based on three replicate determinations. [d] Confidence limits at $p = 0.05$.

diluted to volume with distilled water. The solutions were then filtered[7]. Ten milliliters of the filtrate was transferred to a 60-ml separator, acidified, extracted, and analyzed as described under *Determination of Calibration Curve*.

Conditions for Chromatographic Quantification—The liquid chromatograph was equipped with a pump[8], a variable wavelength detector[9], an integrator with digital printout[10], and a column containing a porous silica packing[11]. The degassed mobile phase was pumped through the column at a flow rate of 2.0 ml/min (1800 psig) at room temperature (23 ± 2°) until a stable baseline was obtained. Replicate 20-μl injections of sample and standard solutions were made using a 25-μl syringe[12]. The chart recorder provided a record of drug elution from the column as peaks on a chromatogram. The peaks were detected at 375 nm. In all cases, the solute was measured by digital integration of the peak area.

Determination of Dantrolene Sodium by Fluorescence—One milliliter of the 1-butanol–chloroform extract from both the calibration curve and the dosage form was added to a 100-ml volumetric flask and diluted to volume with 1-butanol–chloroform (30:70). The fluorescence was measured in a spectrophotofluorometer[13] with the following operating parameters: slit width for excitation and emission, 5 nm; sensitivity, 3.0; excitation wavelength, 395 nm; and emission wavelength, 575 nm. By using the fine sensitivity control, the recorder was set to read full scale (100 units) for the 1-butanol–chloroform solution containing the highest concentration of dantrolene. Measurements for the standard and dosage form were made respective to this arbitrary setting.

RESULTS AND DISCUSSION

Studies on the dosage form of dantrolene sodium showed that dantrolene free acid could be precipitated in acidic media between pH 2.5 and 4.0 using 2 *N* HCl. The free acid was then extracted into 1-butanol–chloroform with a percent extraction of 90.97 ± 0.14 as compared to the theoretical amount of known dantrolene free acid. When injected into the chromatograph, dantrolene was eluted within 6 min (Fig. 1). Furil was found to be a suitable internal standard. Although furil and dantrolene have absorption maxima at 305 and 395 nm, respectively, an intermediate wavelength of 375 nm was selected to obtain the sensitivity necessary to detect both components.

Standard solutions of dantrolene sodium were chromatographed using the microsilica column. The area under the curve for each peak on the chromatogram was digitally integrated. The ratio of the dantrolene peak area to the area of the internal standard was calculated for each chromatogram. A linear regression analysis of the data at three concentrations of dantrolene sodium gave the results shown in Table I. The calibration data for the fluorometric method are also listed.

Dantrolene sodium in a commercial dosage form was dissolved, extracted, and chromatographed in a manner analogous to the standard solutions, and the D/IS ratio was calculated. The constants (slope and intercept) from the linear regression equation shown in Table II were used to solve for drug concentration [D/IS = (slope × concentration) + intercept]; a programmable calculator[14] was used. The same extraction solutions were analyzed fluorometrically after appropriate dilutions.

The data in Table II demonstrate the quantitative results obtained for the dosage form. The utility of HPLC in the analysis of dantrolene sodium is clearly indicated, and the results agree favorably with those obtained with the spectrophotofluorometric method.

With various concentrations of dantrolene sodium as unknowns, the accuracy of the overall chromatographic procedure was shown to be 3.1%.

REFERENCES

(1) H. R. Snyder, Jr., C. S. Davis, R. K. Bickerton, and R. P. Halliday, *J. Med. Chem.*, **10**, 807 (1967).

(2) R. D. Hollifield and J. D. Conklin, *Arch. Int. Pharmacodyn. Ther.*, **174**, 333 (1968).

(3) R. D. Hollifield and J. D. Conklin, *J. Pharm. Sci.*, **62**, 271 (1973).

(4) P. L. Cox, J. P. Heotis, D. Polin, and G. M. Rose, *ibid.*, **58**, 987 (1969).

(5) J. D. Conklin and R. J. Sobers, *ibid.*, **62**, 1024 (1973).

(6) I. L. Honigberg, J. T. Stewart, and A. P. Smith, *ibid.*, **63**, 766 (1974).

(7) I. L. Honigberg, J. T. Stewart, A. P. Smith, R. D. Plunkett, and D. W. Hester, *ibid.*, **63**, 1762 (1974).

(8) I. L. Honigberg, J. T. Stewart, A. P. Smith, and D. W. Hester, *ibid.*, **64**, 1201 (1975).

ACKNOWLEDGMENTS AND ADDRESSES

Received February 6, 1976, from the *Department of Medicinal Chemistry and the Department of Pharmacy, School of Pharmacy, University of Georgia, Athens, GA 30602.*

Accepted for publication April 2, 1976.

[x] To whom inquiries should be directed.

[7] Whatman No. 1 filter paper, W.&R. Balston, Ltd., England.

[8] Waters Associates liquid chromatograph, model ALC/GPC 201, equipped with an M-6000 pump.

[9] Perkin-Elmer model LC-55 UV-visible.

[10] Infotronics integrator, model CRS-204.

[11] Waters packed 10-μm μPorasil column, 4 mm i.d. × 30 cm.

[12] Model B-110, Precision Sampling Corp., Baton Rouge, La.

[13] Perkin-Elmer model MPF-4.

[14] Olivetti-Underwood programma No. 101.

Effect of Chloroquine Adsorption on Acid Reactivity of Magnesium Trisilicate

SALEH A. H. KHALIL

Abstract □ Due to the adsorption of chloroquine by magnesium trisilicate, both the BP acid absorption test and the rate of hydrochloric acid uptake, as monitored by pH measurements, were significantly reduced. This reduction was dependent on the amount of chloroquine adsorbed, since multilayer adsorption produced relatively more suppressive effects than did monolayer adsorption. The presence of adsorbed chloroquine also decreased the amounts of magnesium released in an acid medium. The inhibition of the antacid property due to chloroquine adsorption may be attributed to the occupation of the reactive sites of the antacid surface by chloroquine and to a reduction of the surface area of the antacid due to flocculation of the particles.

Keyphrases □ Chloroquine—adsorption by magnesium trisilicate, effect on acid reactivity □ Magnesium trisilicate—adsorption of chloroquine, effect on acid reactivity □ Adsorption, drug—chloroquine by magnesium trisilicate, effect on acid reactivity □ Acid reactivity—magnesium trisilicate, effect of adsorption of chloroquine □ Antacids—magnesium trisilicate, adsorption of chloroquine, effect on acid reactivity □ Antimalarial agents—chloroquine, adsorption by magnesium trisilicate, effect on acid reactivity

Few reports have appeared on the effects of drug adsorption on the surface properties of the adsorbents. However, protective colloids and surfactants adsorbed at liquid–solid interfaces are known to inhibit crystal growth (1, 2) and polymorphic conversion of drugs (3). The adsorption of some certified dyes resulted in the inhibition of single crystal dissolution of a number of pharmaceuticals (4, 5). In recent years, the adsorption of some drugs by magnesium trisilicate was reported (6, 7), but no detailed studies appear to have been made concerning the effect of drug adsorption on the antacid efficacy.

The present work examines the influence of chloroquine adsorption on the acid reactivity of magnesium trisilicate as measured by both the BP acid absorption test and the rate of hydrochloric acid uptake. Measurements of flocculation and determination of the amounts of magnesium released were also made before and after chloroquine adsorption by magnesium trisilicate.

EXPERIMENTAL

Materials—Magnesium trisilicate powder BP[1] of 11.2-nm mean surface–volume diameter and chloroquine phosphate powder BP[2] were used.

Methods—*Adsorption Experiments*—These experiments were carried out at 37 ± 0.2° by adding aqueous solutions of chloroquine phosphate (100 ml) of appropriate concentrations to a series of weighed quantities (1 g) of magnesium trisilicate. The glass-stoppered flasks were shaken in an oscillating water bath (25 ± 2 strokes/min) until completely equilibrated (6 hr). After centrifugation at 2000 rpm for 3 min, the supernate was suitably diluted with 0.01 *N* HCl and the chloroquine concentration was determined spectrophotometrically[3] at 329 nm.

Acid Absorption Test—The BP procedure (8) was adopted using magnesium trisilicate before and after chloroquine adsorption. The results were expressed as the volume of 0.05 *N* HCl absorbed by 1 g of magnesium trisilicate. To study the effect of chloroquine adsorption on the acid absorption test, the antacid after the adsorption experiment was centrifuged and the residue, equivalent to 0.3 g of magnesium trisilicate, was tested.

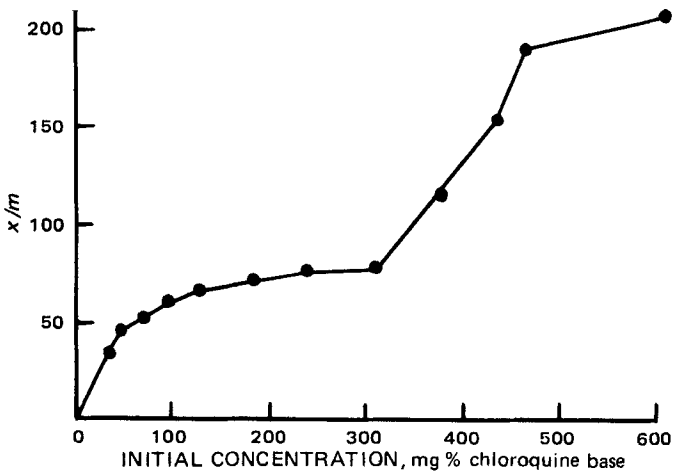

Figure 1—*Adsorption of chloroquine by 1% (w/v) magnesium trisilicate at 37 ± 0.2° (pH of the medium was 9.6).*

Rate of Hydrochloric Acid Uptake—The rate was determined at 37 ± 0.2° by monitoring the pH changes produced after the addition of 340 ml of 0.02 *N* HCl to 1 g of magnesium trisilicate. The apparatus and procedure adopted were as reported previously (9). To study the effect of chloroquine adsorption on the rate of hydrochloric acid uptake, the residue, equivalent to 1 g of the antacid remaining after the adsorption run, was used.

Determination of Magnesium Release—The amounts of magnesium

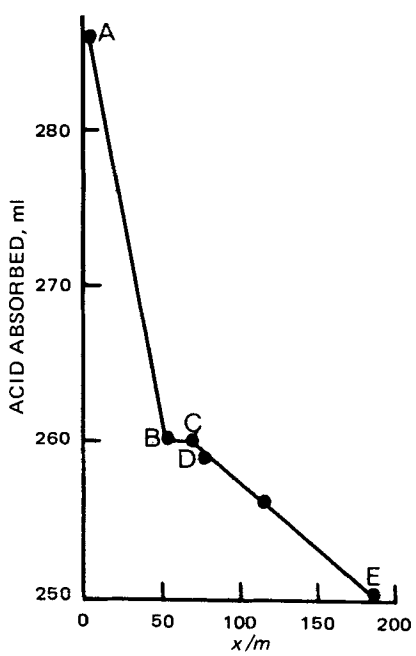

Figure 2—*Effect of amount of chloroquine adsorbed on the volume of 0.05 N HCl absorbed by 1 g of magnesium trisilicate (x/m) as measured by the BP acid absorption test.*

[1] Evans Medical Ltd., England.
[2] May & Baker, England.
[3] Unicam SP 500 Series 2.

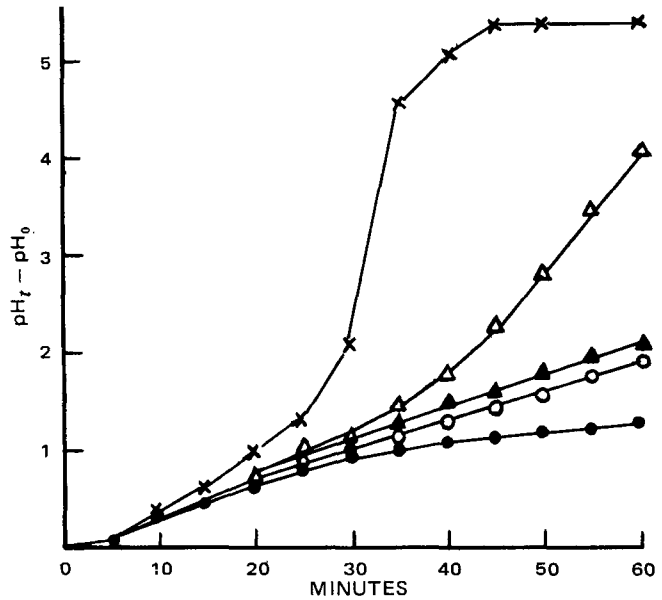

Figure 3—*The pH change* versus *time curves for magnesium trisilicate before chloroquine adsorption* (×) *and after adsorption of the following amounts of chloroquine (in milligrams per gram):* △, *68.2;* ▲, *75.9;* ○, *112.0; and* ●, *183.5.*

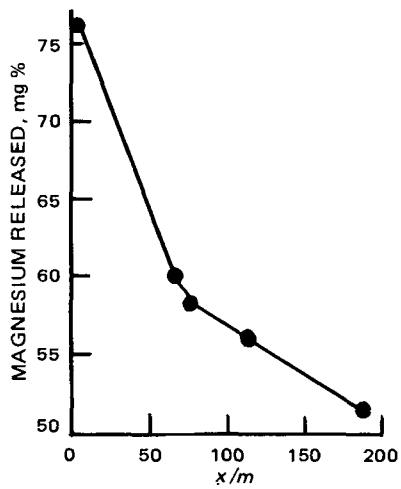

Figure 4—*Effect of amount of chloroquine adsorbed on the amount of magnesium released after 1 hr under the conditions of the BP acid absorption test.*

released after 1 hr under the conditions of the rate of hydrochloric acid uptake were determined by titrating an aliquot of the supernate with 0.05 *M* disodium ethylenediaminetetraacetate. A mordant black mixture was used as the indicator. Interference due to the released chloroquine was negligible.

Turbidity Measurements—A nephelometer[4] was used to measure, at 25°, the turbidity of the supernate sampled from the suspension after 10 min from a depth of 5 cm. The suspension was prepared by dispersing the residue (equivalent to 0.3 g of magnesium trisilicate) obtained after the adsorption experiment in 100 ml of water in a stoppered glass measure.

RESULTS AND DISCUSSION

Figure 1 shows the adsorption plot of chloroquine (where *x/m* is milligrams of chloroquine adsorbed per gram) on magnesium trisilicate (1% w/v) at pH 9.6[5]. At initial chloroquine concentrations below 300 mg %, the adsorption data fitted a Langmuir plot within the monolayer adsorption region; at higher drug concentrations, multilayer adsorption occurred. In the present study, the acid reactivity of magnesium trisilicate was tested before and after adsorbing varying amounts of chloroquine. Figure 2 shows the results of the BP acid absorption test. The adsorption of chloroquine on magnesium trisilicate resulted in a reduction of the volume of 0.05 *N* HCl absorbed by 1 g of the antacid. After an initial decrease from 282.2 to 260.1 ml (line AB, Fig. 2), an increase in the amount of chloroquine adsorbed within the region of monolayer adsorption (BCD) did not produce any significant reduction in the volume of the acid. Multilayer adsorption of chloroquine, however, produced a further decrease (line DE).

Measurements of the rate of hydrochloric acid uptake were made by monitoring the pH changes over 1 hr. The results shown in Fig. 3 illustrate a gradual suppression of the rate of acid uptake as the amount of chloroquine adsorbed was increased. At an *x/m* value of 183.5 mg/g, the acid reactivity decreased to 24.1%, calculated by comparing the pH changes 1 hr before and after adsorption. Determinations of the amounts of magnesium released under acidic conditions showed a gradual decrease due to chloroquine adsorption (Fig. 4). As a result of the adsorption, the antacid particles flocculated. Consequently, the turbidity percentages of the supernate decreased to 53.1, 41.6, and 40.3 for *x/m* values of 68.2, 75.9, and 112.0 mg/g, respectively.

The results suggest that the acid reactivity of magnesium trisilicate was suppressed due to chloroquine adsorption. This finding was evidenced by the acid absorption test where the volume of 0.05 *N* HCl consumed by 1 g of the antacid decreased from 282.2 ml to between 260.1 and 250.3 ml (Fig. 2). The suppressive effect of chloroquine adsorption of the acid reactivity was also reflected in the rate of hydrochloric acid uptake (Fig. 3). In the absence of adsorption, the pH change recorded after 1 hr was 5.4 units. Due to the adsorption of 183.5 mg of chloroquine, however, the pH value did not change by more than 1.3 units.

Since chloroquine has pKa values of 8.4 and 10.8, the ionization percentages at pH 9.6 (of the adsorption medium) would be 5.9 and 94.1, respectively. Therefore, the monoprotonated form probably is mainly involved in the adsorption. The mechanism suggested is probably electrostatic attraction between the negatively charged silicate surface and the monoprotonated form of chloroquine. As a result, neutralization of the charges occurred, as evidenced by the flocculation of the system. Since the reactive sites on the antacid were occupied by chloroquine, both the volume of the acid absorbed by 1 g of the antacid and the rate of acid uptake were reduced. Also, the amounts of magnesium released decreased as the amount of chloroquine adsorbed was increased, probably due to the "blocking" of the dissolution sites on the surface. The suppression of the acid reactivity may have been due to the decreased surface area of the flocculated antacid. The latter was, however, a direct effect of chloroquine adsorption.

In conclusion, the interaction between chloroquine and magnesium trisilicate not only resulted in the adsorption of the antimalarial drug (possibly altering its bioavailability) but also reduced the acid reactivity of magnesium trisilicate.

[4] Corning EEL, Evans Electroselenium Ltd., Essex, England.

[5] At this pH, no precipitation of chloroquine occurs since it is monoprotonated (pKa values of 8.4 and 10.8).

REFERENCES

(1) D. J. Allen, G. Milosovich, and A. M. Mattocks, *J. Pharm. Sci.*, **54,** 383 (1965).

(2) J. E. Carless and A. A. Foster, *J. Pharm. Pharmacol.*, **18,** 697 (1966).

(3) E. R. Ebian, M. A. Moustafa, S. A. Khalil, and M. M. Motawi, *ibid.*, **25,** 13 (1973).

(4) J. Piccolo and R. Tawashi, *J. Pharm. Sci.*, **59,** 56 (1970).

(5) *Ibid.*, **60,** 59 (1971).

(6) S. El-Masry and S. a. H. Khalil, *J. Pharm. Pharmacol.*, **26,** 243 (1974).

(7) S. A. H. Khalil, *ibid.*, **26,** 961 (1974).

(8) "British Pharmacopoeia 1973," Her Majesty's Stationery Office, London, England, 1973, p. 276.

(9) Y. Kawashima and H. Takenaka, *J. Pharm. Sci.*, **63,** 1546 (1974).

ACKNOWLEDGMENTS AND ADDRESSES

Received November 19, 1975, from the *Department of Pharmacy and Pharmacology, College of Medical Sciences, University of Benin, Benin City, Nigeria.*

Accepted for publication March 18, 1976.

Present address: Department of Pharmaceutics, Faculty of Pharmacy, Alexandria University, Alexandria, Egypt.

Hydrazones of Isoniazid for Colorimetric Analysis

P. R. SHAH and R. R. RAJE ˣ

Abstract □ Two sensitive color reactions of isoniazid are described. They are based on the formation of hydrazone Schiff bases when isoniazid is reacted with 4-nitrobenzaldehyde or pyridoxal. Linear curves were obtained with both reagents when absorbance values were plotted against concentrations.

Keyphrases □ Isoniazid—colorimetric analysis, hydrazones formed with 4-nitrobenzaldehyde or pyridoxal, prepared samples □ Colorimetry—analysis, isoniazid, hydrazones formed with 4-nitrobenzaldehyde or pyridoxal, prepared samples □ Antitubercular agents—isoniazid, colorimetric analysis, hydrazones formed with 4-nitrobenzaldehyde or pyridoxal, prepared samples □ Hydrazones—formed by reaction of isoniazid and 4-nitrobenzaldehyde or pyridoxal, colorimetric analysis

The USP XVIII (1) assay for isoniazid is based on iodometry. Some earlier reported spectrophotometric estimation methods involving color reactions due to Schiff base formation entailed reactions of isoniazid with benzaldehyde (2), vanillin (3), and 4-(dimethylamino)benzaldehyde (4). This report describes two color reactions based on the formation of yellow hydrazone Schiff bases when isoniazid is treated with 4-nitrobenzaldehyde or pyridoxal. Linear curves are obtained with both reagents by measuring the color intensities and plotting the absorbance values against graded concentrations of isoniazid.

EXPERIMENTAL

Reagents and Chemicals—The following were used: 4-nitrobenzaldehyde solution, 0.4% (w/v), prepared by dissolving 4-nitrobenzaldehyde[1] (analytical reagent) in ethyl alcohol; pyridoxal hydrochloride solution, 0.25% (w/v), prepared by dissolving pyridoxal hydrochloride[2] (analytical reagent) in distilled water; and 1 *N* sodium hydroxide solution, prepared by dissolving sodium hydroxide[3] (analytical reagent) in distilled water.

Standard Solution of Isoniazid—Isoniazid[4] was dissolved in distilled water to give a 1-mg/ml solution.

Determination of Wavelength of Maximum Absorption—*Method A*—A 2.0-ml quantity of the standard solution of isoniazid (1 mg/ml) and 1.0 ml of 4-nitrobenzaldehyde solution (0.4% w/v) were mixed; after 10 min, the mixture was brought to volume (25 ml) with 1 *N* sodium hydroxide solution. After shaking the mixture well and allowing it to stand for 75 min, the yellow solution was scanned in the visible range using a spectrophotometer[5]. A broad peak was recorded between 409 and 430 nm. A blue filter (range of 400–530 nm) and a photoelectric colorimeter[6] were used for further analyses.

Method B—A 2.0-ml quantity of the standard solution of isoniazid (1 mg/ml), 6.0 ml of distilled water, and 2.0 ml of pyridoxal hydrochloride solution (0.25% w/v) were mixed in a glass-stoppered cylinder. After allowing the mixture to stand for 90 min, the yellow solution was scanned in the visible range using a spectrophotometer[5]. Although a well-defined peak could not be recorded, the maximum absorption was observed at 400 nm. The same blue filter and photoelectric colorimeter used in Method A were used for further analyses.

Colorimetric Analysis with Graded Concentrations of Isoniazid—4-Nitrobenzaldehyde solution, 1.0 ml (0.4% w/v), was added to each of seven volumetric flasks (25 ml) containing the standard solution of isoniazid as shown in Table I and treated as described for Method A. Similarly, 2.0 ml of pyridoxal hydrochloride solution (0.25% w/v) was added to each of five glass-stoppered cylinders (10 ml) containing the standard solution of isoniazid, diluted to volume with distilled water, and treated as described for Method B (Table II).

[1] B. D. H., England.
[2] E. Merck, Darmstadt, West Germany.
[3] Sarabhai M. Chemicals, Baroda, India.
[4] Pharmacopeial grade, Chemopharma Pvt. Ltd., Bombay, India.
[5] Beckman model DB.
[6] Systronix, type 101, Serial No. 149.

DISCUSSION

The results given in Tables I and II indicate that the color reactions were sensitive at low concentrations of isoniazid and gave linear absorbance *versus* concentration curves with both chromogenic reagents. Color development in the isoniazid and 4-nitrobenzaldehyde system requires an alkaline medium.

Table I—Concentration *versus* Absorbance for Isoniazid–4-Nitrobenzaldehyde Solutions

Number	Quantity of Standard Solution of Isoniazid, ml	Concentration of Isoniazid, mg/ml	Absorbance
1	1.5	0.06	0.190
2	1.75	0.07	0.210
3	2.0	0.08	0.230
4	2.25	0.09	0.250
5	2.5	0.10	0.270
6	2.75	0.11	0.290
7	3.0	0.12	0.310

Table II—Concentration *versus* Absorbance for Isoniazid–Pyridoxal Solutions

Number	Quantity of Standard Solution of Isoniazid, ml	Final Concentration of Isoniazid, mg/ml	Absorbance
1	1.0	0.10	0.110
2	1.5	0.15	0.140
3	2.0	0.20	0.170
4	2.5	0.25	0.200
5	3.0	0.30	0.230

Both color reactions can be used for the estimation of isoniazid in pharmaceutical formulations. Examination of one commercial tablet preparation of isoniazid using both procedures afforded results comparable to those obtained by the USP XVIII procedure.

The hydrazone formed in the case of pyridoxal hydrochloride might conceivably be of therapeutic value in that it might not cause vitamin B_6 deficiency. In addition, it might possess lower toxicity and enhanced antituberculous activity when compared with isoniazid, as was reported for similar hydrazone compounds (5–7). The conversion of hydrazide to hydrazone apparently effectuates no loss in antituberculous activity.

REFERENCES

(1) "The United States Pharmacopeia," 18th rev., Mack Publishing Co., Easton, Pa., 1970, p. 349.
(2) L. H. Welsh, *J. Assoc. Offic. Agr. Chem.*, **40**, 807(1957).
(3) E. N. Deeb, *Drug Stand.*, **22**, 194(1954).
(4) G. Machek, *Sci. Pharm.*, **24**, 11(1956).
(5) R. R. Ross, *J. Am. Med. Assoc.*, **168**, 273(1958).
(6) J. M. Robson and F. M. Sullivan, *Pharmacol. Rev.*, **15**, 169(1963).
(7) S. D. Rubbo, J. Edgar, and G. Vaughan, *Am. Rev. Tuberc. Pulm. Dis.*, **76**, 331(1957).

ACKNOWLEDGMENTS AND ADDRESSES

Received August 25, 1975, from *K.M.K. College of Pharmacy, Ulhasnagar-3, District Thana, India.*

Accepted for publication April 2, 1976.

Adapted in part from a paper submitted by P. R. Shah to the University of Bombay, Bombay, India, in partial fulfillment of the Bachelor of Pharmacy degree requirements.

[x] To whom inquiries should be directed. Present address: M.S.T. Laboratories, University of Tennessee Center for Health Sciences, Memphis, TN 38163.

Rapid Near IR Spectrophotometric Determination of Meprobamate in Pharmaceutical Preparations

ALFRED F. ZAPPALA [x] and ALEX POST

Abstract □ A rapid near IR spectrophotometric method was developed for determining meprobamate in tablets, sustained-release capsules, suspensions, and injectables. The absorbance of a chloroform solution of the drug is obtained at about 1.96 μm for quantitation. Assay of nine commercial products from four different manufacturers gave results ranging from 97 to 104% of label claim. Coefficients of variation of 0.7 and 1.3% were obtained on the tablets and a sustained-release product, respectively.

Keyphrases □ Meprobamate—IR spectrophotometric analysis, commercial dosage forms □ IR spectrophotometry—analysis, meprobamate, commercial dosage forms □ Sedatives—meprobamate, IR spectrophotometric analysis, commercial dosage forms

Since the USP XVIII (1) titrimetric procedure for determining meprobamate in tablets is lengthy and somewhat cumbersome, a rapid and easy-to-handle method is needed. A significant step toward this goal was taken by Sherken (2), who spectrophotometrically scanned chloroform solutions of the drug from 3.00 to 2.80 μm and utilized the absorbance at 2.91 μm to obtain the meprobamate concentration. This wavelength is characteristic of the symmetric stretching band of the primary amine group of meprobamate. However, for this procedure to be applicable, it was of paramount importance that the chloroform be freed of the stabilizer, alcohol. Therefore, extraction of the chloroform with water, followed by column chromatography through two tandem columns of activated alumina, was necessary.

Since the commencement of this work, USP XIX (3) adopted a colorimetric method for the assay of meprobamate in tablets. This method is sensitive and fairly rapid. However, the pH of the reagents must be carefully controlled and the acidified phenol reagent must be added carefully to decompose completely any chlorinating solution retained on the neck of the volumetric flask.

Because of the difficulties with these methods, a more rapid and facile procedure was desired that would be applicable to tablets and other dosage forms. The described near IR method is more rapid and does not suffer from the critical requirements of the other methods. Purification of the chloroform solution is not required since the alcohol does not interfere with the absorbance at 1.958 μm used to quantitate meprobamate. This band is subject to fewer interferences than the one at 2.91 μm (4). That the primary amine combination band at 1.958 μm is significantly weaker than the one at 2.91 μm also does not present any detection problem. High sensitivity is not of concern, because the levels of meprobamate in pharmaceutical preparations are generally high.

Table I—Comparison of Results Obtained on Commercial Products[a]

Sample	Label Claim, mg	Near IR Found, mg	Near IR Label Claim, %	USP XIX Found, mg	USP XIX Label Claim, %
1 (Tablet)	400	408	102.0	388	97.0
2 (Tablet)	400	403	100.8	393	98.3
3 (Tablet[b])	400	402	100.5	402	100.5
4 (Tablet)	200	205	102.5	200	100.0
5 (Tablet)	400	415	103.8	404	101.0
6 (Injectable[c])	400	394	98.6	400	100.0
7 (Capsule[d])	200	200	100.0	200	100.0
8 (Capsule[e])	300	295	98.3	355	118.0
9 (Suspension)	200	194	97.0	—	—
Mean			100.4[f]		99.5[g]

[a] Values reported are the average of duplicate assays. [b] Film-coated tablet. [c] Intramuscular injectable. [d] Sustained-release capsule. [e] Sustained-release capsule containing 15 mg of dextroamphetamine sulfate. [f] Samples 1–9. [g] Samples 1–7.

EXPERIMENTAL

Apparatus—A recording spectrophotometer equipped with an IR source[1] and matching 5-cm silica cells were used.

Reagents—Chloroform (reagent grade) and a standard solution of meprobamate (NF XIV), 3.0–4.0 mg/ml in chloroform, were used.

Sample Preparation—*Tablets*—Determine the average tablet weight of not less than 20 tablets. Reduce the tablets to a fine powder and accurately weigh a portion, equivalent to 300–400 mg of meprobamate, into a 100-ml volumetric flask. Add about 70 ml of chloroform to the flask and shake for 15–20 min. Dilute to volume with chloroform and filter through paper[2], discarding the first 15–20 ml.

Sustained-Release Capsules—Determine the average net fill of not less than 20 capsules. Shake the contents to obtain a representative sample. Triturate an accurately weighed sample, equivalent to 300–400 mg of meprobamate; transfer it to a 100-ml volumetric flask with the aid of about 70 ml of chloroform and shake for 15–20 min. Dilute to volume with chloroform and filter as described for tablets.

Suspensions—Shake the sample for several minutes so that a representative sample aliquot can be removed. With a "to contain" pipet, transfer an aliquot equivalent to about 400 mg of meprobamate to a separator. Rinse the pipet thoroughly with distilled water into the separator and add water, if necessary, to obtain a volume of about 30 ml.

[1] Cary model 14.

[2] Whatman No. 1.

ACKNOWLEDGMENTS AND ADDRESSES

Received August 25, 1975, from *K.M.K. College of Pharmacy, Ulhasnagar-3, District Thana, India.*

Accepted for publication April 2, 1976.

Adapted in part from a paper submitted by P. R. Shah to the University of Bombay, Bombay, India, in partial fulfillment of the Bachelor of Pharmacy degree requirements.

[x] To whom inquiries should be directed. Present address: M.S.T. Laboratories, University of Tennessee Center for Health Sciences, Memphis, TN 38163.

Rapid Near IR Spectrophotometric Determination of Meprobamate in Pharmaceutical Preparations

ALFRED F. ZAPPALA [x] and ALEX POST

Abstract □ A rapid near IR spectrophotometric method was developed for determining meprobamate in tablets, sustained-release capsules, suspensions, and injectables. The absorbance of a chloroform solution of the drug is obtained at about 1.96 μm for quantitation. Assay of nine commercial products from four different manufacturers gave results ranging from 97 to 104% of label claim. Coefficients of variation of 0.7 and 1.3% were obtained on the tablets and a sustained-release product, respectively.

Keyphrases □ Meprobamate—IR spectrophotometric analysis, commercial dosage forms □ IR spectrophotometry—analysis, meprobamate, commercial dosage forms □ Sedatives—meprobamate, IR spectrophotometric analysis, commercial dosage forms

Since the USP XVIII (1) titrimetric procedure for determining meprobamate in tablets is lengthy and somewhat cumbersome, a rapid and easy-to-handle method is needed. A significant step toward this goal was taken by Sherken (2), who spectrophotometrically scanned chloroform solutions of the drug from 3.00 to 2.80 μm and utilized the absorbance at 2.91 μm to obtain the meprobamate concentration. This wavelength is characteristic of the symmetric stretching band of the primary amine group of meprobamate. However, for this procedure to be applicable, it was of paramount importance that the chloroform be freed of the stabilizer, alcohol. Therefore, extraction of the chloroform with water, followed by column chromatography through two tandem columns of activated alumina, was necessary.

Since the commencement of this work, USP XIX (3) adopted a colorimetric method for the assay of meprobamate in tablets. This method is sensitive and fairly rapid. However, the pH of the reagents must be carefully controlled and the acidified phenol reagent must be added carefully to decompose completely any chlorinating solution retained on the neck of the volumetric flask.

Because of the difficulties with these methods, a more rapid and facile procedure was desired that would be applicable to tablets and other dosage forms. The described near IR method is more rapid and does not suffer from the critical requirements of the other methods. Purification of the chloroform solution is not required since the alcohol does not interfere with the absorbance at 1.958 μm used to quantitate meprobamate. This band is subject to fewer interferences than the one at 2.91 μm (4). That the primary amine combination band at 1.958 μm is significantly weaker than the one at 2.91 μm also does not present any detection problem. High sensitivity is not of concern, because the levels of meprobamate in pharmaceutical preparations are generally high.

Table I—Comparison of Results Obtained on Commercial Products[a]

Sample	Label Claim, mg	Near IR Found, mg	Near IR Label Claim, %	USP XIX Found, mg	USP XIX Label Claim, %
1 (Tablet)	400	408	102.0	388	97.0
2 (Tablet)	400	403	100.8	393	98.3
3 (Tablet[b])	400	402	100.5	402	100.5
4 (Tablet)	200	205	102.5	200	100.0
5 (Tablet)	400	415	103.8	404	101.0
6 (Injectable[c])	400	394	98.6	400	100.0
7 (Capsule[d])	200	200	100.0	200	100.0
8 (Capsule[e])	300	295	98.3	355	118.0
9 (Suspension)	200	194	97.0	—	—
Mean			100.4[f]		99.5[g]

[a] Values reported are the average of duplicate assays. [b] Film-coated tablet. [c] Intramuscular injectable. [d] Sustained-release capsule. [e] Sustained-release capsule containing 15 mg of dextroamphetamine sulfate. [f] Samples 1–9. [g] Samples 1–7.

EXPERIMENTAL

Apparatus—A recording spectrophotometer equipped with an IR source[1] and matching 5-cm silica cells were used.

Reagents—Chloroform (reagent grade) and a standard solution of meprobamate (NF XIV), 3.0–4.0 mg/ml in chloroform, were used.

Sample Preparation—*Tablets*—Determine the average tablet weight of not less than 20 tablets. Reduce the tablets to a fine powder and accurately weigh a portion, equivalent to 300–400 mg of meprobamate, into a 100-ml volumetric flask. Add about 70 ml of chloroform to the flask and shake for 15–20 min. Dilute to volume with chloroform and filter through paper[2], discarding the first 15–20 ml.

Sustained-Release Capsules—Determine the average net fill of not less than 20 capsules. Shake the contents to obtain a representative sample. Triturate an accurately weighed sample, equivalent to 300–400 mg of meprobamate; transfer it to a 100-ml volumetric flask with the aid of about 70 ml of chloroform and shake for 15–20 min. Dilute to volume with chloroform and filter as described for tablets.

Suspensions—Shake the sample for several minutes so that a representative sample aliquot can be removed. With a "to contain" pipet, transfer an aliquot equivalent to about 400 mg of meprobamate to a separator. Rinse the pipet thoroughly with distilled water into the separator and add water, if necessary, to obtain a volume of about 30 ml.

[1] Cary model 14.

[2] Whatman No. 1.

Table II—Results of Precision Study on Sample 5

Determination	Amount Found, mg	
	Near IR	USP XIX
1	415	395
2	415	396
3	413	408
4	413	404
5	416	399
6	422	401
7	416	403
8	410	405
9	415	412
10	415	414
Mean	415	404
SD	3.1	6.3
CV	0.7	1.5

Extract with three 30-ml portions of chloroform, collecting the chloroform extracts in a 100-ml volumetric flask after filtering through a small amount of anhydrous sodium sulfate. Then dilute to volume with chloroform and mix well. Accurately weigh about 400 mg of meprobamate standard material into a separator, suspend the material in about 30 ml of water, and similarly extract with chloroform.

Injectables—Combine the contents of several ampuls and transfer an aliquot, equivalent to about 400 mg of meprobamate, to a separator. Add about 25 ml of distilled water and extract with chloroform as described for suspensions. Prepare a placebo solution containing the same amount of polyethylene glycol 400 as is found in the commercial ampul preparation. In addition, accurately prepare a standard of about 400 mg of meprobamate dissolved in the placebo solution and then extract as described for suspensions.

Assay Procedure—*Tablets, Sustained-Release Capsules, and Suspensions*—Balance the instrument at 2.00 μm with chloroform in both cells and then scan to 1.93 μm to establish the baseline. Record the spectra of the prepared samples and standard solutions *versus* chloroform over the same range (Fig. 1). Draw a line connecting the points on the curve at 1.945 and 1.980 μm. Obtain the absorbance difference (ΔA) between the absorbance maximum at about 1.958 μm and at the same point on the line drawn.

Injectables—Balance the instrument at 2.00 μm with the extracted placebo in both cells and then scan to 1.93 μm to establish the baseline. Record the spectra of the standard and ampul extracts *versus* the placebo extract over the same range.

Calculations—Calculate the quantity of meprobamate using:

$$\frac{\Delta A \times f \times d \times c}{s} = \text{mg meprobamate/capsule or tablet} \quad \text{(Eq. 1)}$$

or:

$$\frac{\Delta A \times f \times d}{v} = \text{mg meprobamate/ml of suspension or injectable} \quad \text{(Eq. 2)}$$

where ΔA = absorbance difference at 1.958 μm, f = standard factor in milligrams of meprobamate per milliliter per ΔA, d = dilution volume, c = average capsule fill or tablet weight in grams, s = sample weight in grams, and v = sample aliquot in milliliters.

RESULTS AND DISCUSSION

A series of standard solutions ranging from 2.0 to 7.0 mg/ml was analyzed, and adherence to Beer's law was observed. Nine commercial samples of meprobamate products from four different manufacturers were assayed by the near IR method and the USP XIX method (Table I). The near IR method can be successfully applied to various dosage forms including a combination product. A precision study, based on 10 separate determinations of a tablet preparation, was performed using both the near IR method and the USP XIX method (Table II).

When a suspension was assayed by the USP XIX colorimetric method, very low and widely scattered results were obtained. Similarly, when the same suspension was assayed by the USP XVIII titrimetric method, low results were obtained. During the hydrolysis step in the latter procedure, the suspension darkened to such an extent that the detection of the colorimetric end-point of the subsequent titration became extremely difficult.

When an intramuscular injectable was first assayed by the near IR method used to assay suspensions, it was immediately apparent that the spectra were distorted. The gross distortion was due to the large amount of polyethylene glycol 400 in the formulation (400 mg of meprobamate/5 ml of a 65% solution of polyethylene glycol 400). This problem was circumvented by "blanking out" this interference as already described. However, since the amount of polyethylene glycol 400 might vary by as much as ±10% of the label declaration, an experiment was performed to determine the effect of such a variation on the assay. The meprobamate extracted from a 65% polyethylene glycol 400 solution, when assayed against extracted placebos containing 58 and 72% polyethylene glycol 400, yielded recoveries of 99.7 and 101.0%, respectively. Thus, the proposed method is unaffected by variable amounts of polyethylene glycol 400. The results of the near IR method compare favorably with those obtained by the USP XIX method (Table I).

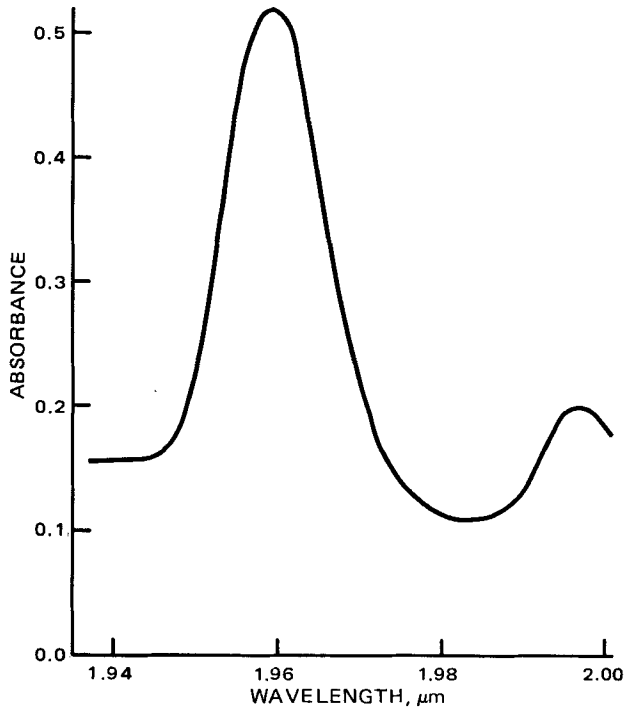

Figure 1—*Near IR absorption spectrum of meprobamate (4.17 mg/ml) in chloroform (5-cm cells).*

The product containing meprobamate in combination with dextroamphetamine gave a high result when assayed by the USP XIX procedure (Table I). This high value was partially due to dextroamphetamine reacting with the reagents. The dye used in the capsule also contributed to the high result. In contrast, dextroamphetamine and the dye did not cause any interference with the determination of meprobamate in this combination product by the near IR method.

REFERENCES

(1) "The United States Pharmacopeia," 18th rev., Mack Publishing Co., Easton, Pa., 1970, p. 402.

(2) S. Sherken, *J. Assoc. Offic. Anal. Chem.*, **51**, 616 (1968).

(3) "The United States Pharmacopeia," 19th rev., Mack Publishing Co., Easton, Pa., 1975, p. 305.

(4) N. B. Colthup, L. H. Daly, and S. E. Wiberley, "Introduction to Infrared and Raman Spectroscopy," Academic, New York, N.Y., 1964, p. 327.

ACKNOWLEDGMENTS AND ADDRESSES

Received November 12, 1975, from the *Analytical and Physical Chemistry Laboratories, Planning and Operations, Pharmaceutical Research and Development, Smith Kline and French Laboratories Division, SmithKline Corporation, Philadelphia, PA 19101.*

Accepted for publication April 15, 1976.

Appreciation is expressed to Dr. Walter W. Holl for technical assistance.

[x] To whom inquiries should be directed.

pH Partition Behavior of Ampicillin

Keyphrases □ Partition coefficients—ampicillin in aqueous buffer–octanol systems, effect of pH □ Ampicillin—partition coefficients in aqueous buffer–octanol systems, effect of pH □ pH—effect on partition coefficients of ampicillin in aqueous buffer–octanol systems □ Antibacterials—ampicillin, partition coefficients in aqueous buffer–octanol systems, effect of pH

To the Editor:

The pH partition behavior of the ampholytic β-lactam antibiotics ampicillin, cephalexin, and cephaloglycin was previously studied in aqueous buffer–1-octanol and aqueous buffer–1-butanol systems (1). The results obtained for ampicillin in both systems appeared to indicate that the anion was the partitioning species. Over the pH 4.9–7.9 range, apparent partition coefficients increased with pH. Apparent partition coefficient values for ampicillin in aqueous octanol were calculated after spectrophotometric analysis of only the aqueous phase and ranged from 0.18 to 0.31. These values were nearly an order of magnitude greater than the apparent partition coefficient values reported for ampicillin in water–ethyl acetate (2). In contrast, the partition coefficient values for penicillin G in water–octanol or water–ethyl acetate only differed by a factor of about 1.5 (3). The purpose of this study was to obtain reproducible partition coefficient values for ampicillin based on analyses of both the aqueous and organic phases.

Buffered solutions of ampicillin were prepared at 2 mg/ml. Twenty milliliters of both the buffer and octanol were pipetted into a container suitable for shaking. In some cases, each phase was presaturated with the other. The samples were shaken[1] mechanically for 20 min at 200–300 cpm and then centrifuged.

The octanol phase was withdrawn and transferred to a separator, where any carried-over aqueous phase was separated and discarded. Then the octanol was extracted with one 20-ml and two 10-ml portions of pH 5.2 buffer containing copper sulfate (4). These buffer portions were combined and diluted to volume in a 50-ml volumetric flask using the prepared pH 5.2 buffer. This solution was analyzed to determine the organic phase concentrations.

The aqueous phase was analyzed after dilution of a 0.3-ml aliquot with pH 5.2 buffer containing copper sulfate to 25 ml in a volumetric flask.

Analysis was by a copper catalyst procedure (4) in which the absorbance difference between the maximum near 320 nm and the baseline at 390 nm was determined from a spectrophotometric[2] recording. The concentration of each solution was calculated using a calibration curve obtained with standard solutions. Total recovered ampicillin was calculated by summing the amounts found in each solvent phase. Recovery was 100 ± 5% for the samples handled by one chemist. A slightly broader variation was noted for samples handled by another chemist.

Table I—Aqueous Buffer–Octanol Apparent Partition Coefficient Values for Ampicillin at 25°

pH	Apparent Partition Coefficient × 10^3	n
3.0	8.3	2
5.0	7.4	2
	6.2[a]	2
7.0	7.4[a]	2
	8.2	10
7.2	8.0	3
7.9	8.2	2
	6.4	2

[a] Determinations made by a second chemist.

The apparent partition coefficient was calculated by dividing the organic phase concentration by the aqueous phase concentration:

$$\text{partition coefficient} = \frac{[\text{ampicillin}]_{\text{octanol}}}{[\text{ampicillin}]_{\text{water}}} \qquad \text{(Eq. 1)}$$

The results obtained in the pH 3.0–7.9 range at 25° are shown in Table I. Contrary to previous reports, no change in the apparent partition coefficient with pH was observed.

Temperature may affect the observed partition coefficient values. However, for ampicillin in aqueous buffer–octanol systems at 25 and 37°, differences were insignificant. At pH 5.1 and 7.0 at 37°, the apparent partition coefficients were 8.3×10^{-3} and 7.3×10^{-3}, respectively, based on two determinations at each pH.

The precision and accuracy of the analytical procedure for each phase were determined, and the apparent partition coefficients were calculated. First, a spiked octanol solution, extracted with buffer as previously described, gave a mean total recovery (n = 6) of 95.5% with a range of 92.8–97.6% and a coefficient of variation of 2.0%. After partitioning, the coefficient of variation values of 0.97 and 21% were obtained for aqueous phase and organic phase concentrations, respectively. Thus, determination of the apparent partition coefficient values gave a coefficient of variation of 21% too. These values were calculated for duplicate determinations on 5 consecutive days. The poor precision probably resulted from poor phase separation, which has the greatest effect on the determination of the organic phase concentration. Therefore, a significant variation in the apparent partition coefficient value resulted.

Other factors evaluated included the time of mixing and presaturation of each phase with the other. Neither mixing time in the 10–160-min range nor presaturation of phases appeared to affect the results.

The results indicate that the extent of ampicillin partitioning in aqueous buffer–octanol systems is significantly less than had been reported earlier and is apparently unaffected by pH in the 3.0–7.9 range.

[1] Eberback Co., Ann Arbor, Mich.
[2] Cary model 14 or Perkin-Elmer model 402.

(1) E. D. Purich, J. L. Colaizzi, and R. I. Poust, *J. Pharm. Sci.*, **62**, 545 (1973).

(2) J. P. Hou and J. W. Poole, *ibid.*, **58**, 1510 (1969).
(3) A. Leo, C. Hansch, and D. Elkins, *Chem. Rev.*, **71**, 604 (1971).
(4) J. Smith, G. Degrey, and V. Patel, *Analyst*, **92**, 247 (1967).

C. F. Carney
A. R. Hurwitz [x]

Pharmacy Research and Development
Ayerst Laboratories, Inc.
Rouses Point, NY 12979

Received September 7, 1976.
Accepted for publication November 9, 1976.
[x] To whom inquiries should be directed.

BOOKS

REVIEWS

The *Catharanthus* Alkaloids. Edited by W. I. TAYLOR and N. R. FARNSWORTH. Dekker, 270 Madison Ave., New York, NY 10016, 1975. 323 pp. 16 × 32.5 cm. Price $29.50.

This valuable book for students, teachers, researchers, and clinicians interested in the pharmacognosy of the *Catharanthus* alkaloids opens with a concise and significant introduction by Gordon H. Svoboda, in which he outlines the history and discovery of the outstanding alkaloid pair, vinblastine and vincristine. Dr. Svoboda, responsible for much of this research, reviews the scientific and medical aspects of these and other *Catharanthus* alkaloids in terms of their biological specificity and their relative clinical merit.

The book includes chapters dealing with the following topics: a Synopsis of the Genus *Catharanthus* (William T. Stearn, British Museum), the Photochemistry and Pharmacology of *Catharanthus roseus* (G. H. Svoboda and D. A. Blake), the Phytochemistry of the Minor *Catharanthus* Species (M. Tin-Wa and N. R. Farnsworth), Structure Elucidation and Chemistry of the Bis *Catharanthus* Alkaloids (D. J. Abrahams), the Biosynthesis of *Catharanthus* Alkaloids (R. J. Parry), and Tissue Culture Studies of *Catharanthus roseus* (David P. Carew). The final chapters, dealing with Biochemistry (William A. Creasey) and the Clinical Aspects of the Dimeric *Catharanthus* Alkaloids (R. C. DeConti and W. A. Creasey), comprehensively and thoroughly review these important topics.

The book is well organized; tables, figures, and text are of professional quality; and, in spite of the many botanical terms used, the number of misprints is remarkably small, a rare exception being a twice misspelled catharanthine (I) (p. 128).

The total amount of multidisciplinary information contained in this monograph is considerable. The book, therefore, constitutes a valuable reference work for diverse professionals needing reliable information. The authors all have worked extensively in their various specialties, thus endowing the book with an authoritative quality. In particular, the chapter on clinical effects of vinblastine and vincristine as well as other alkaloids of lesser efficacy summarizes the relative and specific clinical activity in a clear and comprehensive manner. For researchers not having easy access to detailed medical literature in this area, this chapter by DeConti and Creasey constitutes a good source for reliable information on clinical usages of currently available oncolytic *Catharanthus* alkaloids.

The only regret felt during the reading of various chapters, especially those dealing with topics presently in an active state of investigation, is in the time lag during writing and publication. Few references beyond 1972 are included in most chapters. Much excellent work during the following years thus remains unmentioned through no fault of authors or publishers.

In summary, the editors have made an excellent selection of topics and authors. The resulting book summarizes available information on this important class of alkaloids in a most readable and reliable manner. The book is heartily recommended for readers wanting to become acquainted or reacquainted with the chemistry or biology of these complex herbal products of outstanding medicinal value.

Reviewed by Koert Gerzon
Chemical Research Division
Lilly Research Laboratories
Indianapolis, IN 46206

Pro-drugs as Novel Drug Delivery Systems. Edited by T. HIGUCHI and V. STELLA. American Chemical Society, 1155 16th Street, N.W., Washington, DC 20036, 1975. 245 pp. 16 × 24 cm. Price $13.50.

This volume is a collection of papers presented during a symposium on prodrugs held in Atlantic City, September 10, 1974, under the sponsorship of the ACS Division of Medicinal Chemistry. The book consists of six sections. The first section, which constitutes approximately half of the volume, is a review of the basic concepts and approaches to the design of prodrugs. The second section covers applications of the prodrug approach to antibiotics. The remainder of the volume describes, in the form of research papers, chemical and biological studies on prodrug candidates performed in the laboratories of the authors. These chapters deal with prodrugs of phenytoin (diphenylhydantoin) and epinephrine and with the use of prodrugs in the formulation of cytotoxic agents for parenteral administration.

Although the enzymatic and some biological aspects, which are important in the design of new prodrugs, are not discussed, this book represents an excellent compilation of data on the subject. The extensive bibliography, particularly of the first two sections, and the excellent examples selected to illustrate the chemical approaches to the problem of drug delivery should make this volume a valuable addition to the library of every researcher in this field.

The book is easily readable and is recommended to graduate students and faculty of both chemistry and pharmacy. The material described in this book by the authors, who are experts in this field, ought to stimulate greatly the thinking of those who are seeking new ideas in the application of chemistry to biology and pharmacy.

Reviewed by George A. Digenis
College of Pharmacy
University of Kentucky
Lexington, KY 40506

The Effect of Disease States on Drug Pharmacokinetics. Edited by LESLIE Z. BENET. American Pharmaceutical Association, 2215 Constitution Ave. N.W., Washington, DC 20037, 1976. 252 pp. 15.5 × 23 cm. Price $9.25 (APhA Member Rate, $6.50).

"The Effect of Disease States on Drug Pharmacokinetics" is a collection of the papers presented at the April 1976 symposium sponsored by the Academy of Pharmaceutical Sciences of the American Pharmaceutical Association. The 29 contributors to this symposium are among the most prominent researchers in the field of clinical pharmacokinetics.

The introduction is a general orientation to the subject and a brief discussion of various possible approaches to the investigation of potential pharmacokinetic changes. The book is divided into four parts, each of which contains one chapter that discusses the subtopic in general and one or more chapters that deal with specific examples.

In the first section, Body Perfusion, Chapter 2 presents an overview of pharmacokinetics in disease states that modify blood flow and organ perfusion. Chapter 3 deals specifically with the effects of cardiac failure on GI absorption.

(2) J. P. Hou and J. W. Poole, *ibid.*, **58**, 1510 (1969).
(3) A. Leo, C. Hansch, and D. Elkins, *Chem. Rev.*, **71**, 604 (1971).
(4) J. Smith, G. Degrey, and V. Patel, *Analyst*, **92**, 247 (1967).

C. F. Carney
A. R. Hurwitz [x]

Pharmacy Research and Development
Ayerst Laboratories, Inc.
Rouses Point, NY 12979

Received September 7, 1976.
Accepted for publication November 9, 1976.
[x] To whom inquiries should be directed.

BOOKS

REVIEWS

The *Catharanthus* Alkaloids. Edited by W. I. TAYLOR and N. R. FARNSWORTH. Dekker, 270 Madison Ave., New York, NY 10016, 1975. 323 pp. 16 × 32.5 cm. Price $29.50.

This valuable book for students, teachers, researchers, and clinicians interested in the pharmacognosy of the *Catharanthus* alkaloids opens with a concise and significant introduction by Gordon H. Svoboda, in which he outlines the history and discovery of the outstanding alkaloid pair, vinblastine and vincristine. Dr. Svoboda, responsible for much of this research, reviews the scientific and medical aspects of these and other *Catharanthus* alkaloids in terms of their biological specificity and their relative clinical merit.

The book includes chapters dealing with the following topics: a Synopsis of the Genus *Catharanthus* (William T. Stearn, British Museum), the Photochemistry and Pharmacology of *Catharanthus roseus* (G. H. Svoboda and D. A. Blake), the Phytochemistry of the Minor *Catharanthus* Species (M. Tin-Wa and N. R. Farnsworth), Structure Elucidation and Chemistry of the Bis *Catharanthus* Alkaloids (D. J. Abrahams), the Biosynthesis of *Catharanthus* Alkaloids (R. J. Parry), and Tissue Culture Studies of *Catharanthus roseus* (David P. Carew). The final chapters, dealing with Biochemistry (William A. Creasey) and the Clinical Aspects of the Dimeric *Catharanthus* Alkaloids (R. C. DeConti and W. A. Creasey), comprehensively and thoroughly review these important topics.

The book is well organized; tables, figures, and text are of professional quality; and, in spite of the many botanical terms used, the number of misprints is remarkably small, a rare exception being a twice misspelled catharanthine (I) (p. 128).

The total amount of multidisciplinary information contained in this monograph is considerable. The book, therefore, constitutes a valuable reference work for diverse professionals needing reliable information. The authors all have worked extensively in their various specialties, thus endowing the book with an authoritative quality. In particular, the chapter on clinical effects of vinblastine and vincristine as well as other alkaloids of lesser efficacy summarizes the relative and specific clinical activity in a clear and comprehensive manner. For researchers not having easy access to detailed medical literature in this area, this chapter by DeConti and Creasey constitutes a good source for reliable information on clinical usages of currently available oncolytic *Catharanthus* alkaloids.

The only regret felt during the reading of various chapters, especially those dealing with topics presently in an active state of investigation, is in the time lag during writing and publication. Few references beyond 1972 are included in most chapters. Much excellent work during the following years thus remains unmentioned through no fault of authors or publishers.

In summary, the editors have made an excellent selection of topics and authors. The resulting book summarizes available information on this important class of alkaloids in a most readable and reliable manner. The book is heartily recommended for readers wanting to become acquainted or reacquainted with the chemistry or biology of these complex herbal products of outstanding medicinal value.

Reviewed by Koert Gerzon
Chemical Research Division
Lilly Research Laboratories
Indianapolis, IN 46206

Pro-drugs as Novel Drug Delivery Systems. Edited by T. HIGUCHI and V. STELLA. American Chemical Society, 1155 16th Street, N.W., Washington, DC 20036, 1975. 245 pp. 16 × 24 cm. Price $13.50.

This volume is a collection of papers presented during a symposium on prodrugs held in Atlantic City, September 10, 1974, under the sponsorship of the ACS Division of Medicinal Chemistry. The book consists of six sections. The first section, which constitutes approximately half of the volume, is a review of the basic concepts and approaches to the design of prodrugs. The second section covers applications of the prodrug approach to antibiotics. The remainder of the volume describes, in the form of research papers, chemical and biological studies on prodrug candidates performed in the laboratories of the authors. These chapters deal with prodrugs of phenytoin (diphenylhydantoin) and epinephrine and with the use of prodrugs in the formulation of cytotoxic agents for parenteral administration.

Although the enzymatic and some biological aspects, which are important in the design of new prodrugs, are not discussed, this book represents an excellent compilation of data on the subject. The extensive bibliography, particularly of the first two sections, and the excellent examples selected to illustrate the chemical approaches to the problem of drug delivery should make this volume a valuable addition to the library of every researcher in this field.

The book is easily readable and is recommended to graduate students and faculty of both chemistry and pharmacy. The material described in this book by the authors, who are experts in this field, ought to stimulate greatly the thinking of those who are seeking new ideas in the application of chemistry to biology and pharmacy.

Reviewed by George A. Digenis
College of Pharmacy
University of Kentucky
Lexington, KY 40506

The Effect of Disease States on Drug Pharmacokinetics. Edited by LESLIE Z. BENET. American Pharmaceutical Association, 2215 Constitution Ave. N.W., Washington, DC 20037, 1976. 252 pp. 15.5 × 23 cm. Price $9.25 (APhA Member Rate, $6.50).

"The Effect of Disease States on Drug Pharmacokinetics" is a collection of the papers presented at the April 1976 symposium sponsored by the Academy of Pharmaceutical Sciences of the American Pharmaceutical Association. The 29 contributors to this symposium are among the most prominent researchers in the field of clinical pharmacokinetics.

The introduction is a general orientation to the subject and a brief discussion of various possible approaches to the investigation of potential pharmacokinetic changes. The book is divided into four parts, each of which contains one chapter that discusses the subtopic in general and one or more chapters that deal with specific examples.

In the first section, Body Perfusion, Chapter 2 presents an overview of pharmacokinetics in disease states that modify blood flow and organ perfusion. Chapter 3 deals specifically with the effects of cardiac failure on GI absorption.

(2) J. P. Hou and J. W. Poole, *ibid.*, **58**, 1510 (1969).
(3) A. Leo, C. Hansch, and D. Elkins, *Chem. Rev.*, **71**, 604 (1971).
(4) J. Smith, G. Degrey, and V. Patel, *Analyst*, **92**, 247 (1967).

C. F. Carney
A. R. Hurwitz [x]

Pharmacy Research and Development
Ayerst Laboratories, Inc.
Rouses Point, NY 12979

Received September 7, 1976.
Accepted for publication November 9, 1976.
[x] To whom inquiries should be directed.

BOOKS

REVIEWS

The *Catharanthus* Alkaloids. Edited by W. I. TAYLOR and N. R. FARNSWORTH. Dekker, 270 Madison Ave., New York, NY 10016, 1975. 323 pp. 16 × 32.5 cm. Price $29.50.

This valuable book for students, teachers, researchers, and clinicians interested in the pharmacognosy of the *Catharanthus* alkaloids opens with a concise and significant introduction by Gordon H. Svoboda, in which he outlines the history and discovery of the outstanding alkaloid pair, vinblastine and vincristine. Dr. Svoboda, responsible for much of this research, reviews the scientific and medical aspects of these and other *Catharanthus* alkaloids in terms of their biological specificity and their relative clinical merit.

The book includes chapters dealing with the following topics: a Synopsis of the Genus *Catharanthus* (William T. Stearn, British Museum), the Photochemistry and Pharmacology of *Catharanthus roseus* (G. H. Svoboda and D. A. Blake), the Phytochemistry of the Minor *Catharanthus* Species (M. Tin-Wa and N. R. Farnsworth), Structure Elucidation and Chemistry of the Bis *Catharanthus* Alkaloids (D. J. Abrahams), the Biosynthesis of *Catharanthus* Alkaloids (R. J. Parry), and Tissue Culture Studies of *Catharanthus roseus* (David P. Carew). The final chapters, dealing with Biochemistry (William A. Creasey) and the Clinical Aspects of the Dimeric *Catharanthus* Alkaloids (R. C. DeConti and W. A. Creasey), comprehensively and thoroughly review these important topics.

The book is well organized; tables, figures, and text are of professional quality; and, in spite of the many botanical terms used, the number of misprints is remarkably small, a rare exception being a twice misspelled catharanthine (I) (p. 128).

The total amount of multidisciplinary information contained in this monograph is considerable. The book, therefore, constitutes a valuable reference work for diverse professionals needing reliable information. The authors all have worked extensively in their various specialties, thus endowing the book with an authoritative quality. In particular, the chapter on clinical effects of vinblastine and vincristine as well as other alkaloids of lesser efficacy summarizes the relative and specific clinical activity in a clear and comprehensive manner. For researchers not having easy access to detailed medical literature in this area, this chapter by DeConti and Creasey constitutes a good source for reliable information on clinical usages of currently available oncolytic *Catharanthus* alkaloids.

The only regret felt during the reading of various chapters, especially those dealing with topics presently in an active state of investigation, is in the time lag during writing and publication. Few references beyond 1972 are included in most chapters. Much excellent work during the following years thus remains unmentioned through no fault of authors or publishers.

In summary, the editors have made an excellent selection of topics and authors. The resulting book summarizes available information on this important class of alkaloids in a most readable and reliable manner. The book is heartily recommended for readers wanting to become acquainted or reacquainted with the chemistry or biology of these complex herbal products of outstanding medicinal value.

Reviewed by Koert Gerzon
Chemical Research Division
Lilly Research Laboratories
Indianapolis, IN 46206

Pro-drugs as Novel Drug Delivery Systems. Edited by T. HIGUCHI and V. STELLA. American Chemical Society, 1155 16th Street, N.W., Washington, DC 20036, 1975. 245 pp. 16 × 24 cm. Price $13.50.

This volume is a collection of papers presented during a symposium on prodrugs held in Atlantic City, September 10, 1974, under the sponsorship of the ACS Division of Medicinal Chemistry. The book consists of six sections. The first section, which constitutes approximately half of the volume, is a review of the basic concepts and approaches to the design of prodrugs. The second section covers applications of the prodrug approach to antibiotics. The remainder of the volume describes, in the form of research papers, chemical and biological studies on prodrug candidates performed in the laboratories of the authors. These chapters deal with prodrugs of phenytoin (diphenylhydantoin) and epinephrine and with the use of prodrugs in the formulation of cytotoxic agents for parenteral administration.

Although the enzymatic and some biological aspects, which are important in the design of new prodrugs, are not discussed, this book represents an excellent compilation of data on the subject. The extensive bibliography, particularly of the first two sections, and the excellent examples selected to illustrate the chemical approaches to the problem of drug delivery should make this volume a valuable addition to the library of every researcher in this field.

The book is easily readable and is recommended to graduate students and faculty of both chemistry and pharmacy. The material described in this book by the authors, who are experts in this field, ought to stimulate greatly the thinking of those who are seeking new ideas in the application of chemistry to biology and pharmacy.

Reviewed by George A. Digenis
College of Pharmacy
University of Kentucky
Lexington, KY 40506

The Effect of Disease States on Drug Pharmacokinetics. Edited by LESLIE Z. BENET. American Pharmaceutical Association, 2215 Constitution Ave. N.W., Washington, DC 20037, 1976. 252 pp. 15.5 × 23 cm. Price $9.25 (APhA Member Rate, $6.50).

"The Effect of Disease States on Drug Pharmacokinetics" is a collection of the papers presented at the April 1976 symposium sponsored by the Academy of Pharmaceutical Sciences of the American Pharmaceutical Association. The 29 contributors to this symposium are among the most prominent researchers in the field of clinical pharmacokinetics.

The introduction is a general orientation to the subject and a brief discussion of various possible approaches to the investigation of potential pharmacokinetic changes. The book is divided into four parts, each of which contains one chapter that discusses the subtopic in general and one or more chapters that deal with specific examples.

In the first section, Body Perfusion, Chapter 2 presents an overview of pharmacokinetics in disease states that modify blood flow and organ perfusion. Chapter 3 deals specifically with the effects of cardiac failure on GI absorption.

(2) J. P. Hou and J. W. Poole, *ibid.*, **58**, 1510 (1969).
(3) A. Leo, C. Hansch, and D. Elkins, *Chem. Rev.*, **71**, 604 (1971).
(4) J. Smith, G. Degrey, and V. Patel, *Analyst*, **92**, 247 (1967).

C. F. Carney
A. R. Hurwitz [x]

Pharmacy Research and Development
Ayerst Laboratories, Inc.
Rouses Point, NY 12979

Received September 7, 1976.
Accepted for publication November 9, 1976.
[x] To whom inquiries should be directed.

BOOKS

REVIEWS

The *Catharanthus* Alkaloids. Edited by W. I. TAYLOR and N. R. FARNSWORTH. Dekker, 270 Madison Ave., New York, NY 10016, 1975. 323 pp. 16 × 32.5 cm. Price $29.50.

This valuable book for students, teachers, researchers, and clinicians interested in the pharmacognosy of the *Catharanthus* alkaloids opens with a concise and significant introduction by Gordon H. Svoboda, in which he outlines the history and discovery of the outstanding alkaloid pair, vinblastine and vincristine. Dr. Svoboda, responsible for much of this research, reviews the scientific and medical aspects of these and other *Catharanthus* alkaloids in terms of their biological specificity and their relative clinical merit.

The book includes chapters dealing with the following topics: a Synopsis of the Genus *Catharanthus* (William T. Stearn, British Museum), the Photochemistry and Pharmacology of *Catharanthus roseus* (G. H. Svoboda and D. A. Blake), the Phytochemistry of the Minor *Catharanthus* Species (M. Tin-Wa and N. R. Farnsworth), Structure Elucidation and Chemistry of the Bis *Catharanthus* Alkaloids (D. J. Abrahams), the Biosynthesis of *Catharanthus* Alkaloids (R. J. Parry), and Tissue Culture Studies of *Catharanthus roseus* (David P. Carew). The final chapters, dealing with Biochemistry (William A. Creasey) and the Clinical Aspects of the Dimeric *Catharanthus* Alkaloids (R. C. DeConti and W. A. Creasey), comprehensively and thoroughly review these important topics.

The book is well organized; tables, figures, and text are of professional quality; and, in spite of the many botanical terms used, the number of misprints is remarkably small, a rare exception being a twice misspelled catharanthine (I) (p. 128).

The total amount of multidisciplinary information contained in this monograph is considerable. The book, therefore, constitutes a valuable reference work for diverse professionals needing reliable information. The authors all have worked extensively in their various specialties, thus endowing the book with an authoritative quality. In particular, the chapter on clinical effects of vinblastine and vincristine as well as other alkaloids of lesser efficacy summarizes the relative and specific clinical activity in a clear and comprehensive manner. For researchers not having easy access to detailed medical literature in this area, this chapter by DeConti and Creasey constitutes a good source for reliable information on clinical usages of currently available oncolytic *Catharanthus* alkaloids.

The only regret felt during the reading of various chapters, especially those dealing with topics presently in an active state of investigation, is in the time lag during writing and publication. Few references beyond 1972 are included in most chapters. Much excellent work during the following years thus remains unmentioned through no fault of authors or publishers.

In summary, the editors have made an excellent selection of topics and authors. The resulting book summarizes available information on this important class of alkaloids in a most readable and reliable manner. The book is heartily recommended for readers wanting to become acquainted or reacquainted with the chemistry or biology of these complex herbal products of outstanding medicinal value.

Reviewed by Koert Gerzon
Chemical Research Division
Lilly Research Laboratories
Indianapolis, IN 46206

Pro-drugs as Novel Drug Delivery Systems. Edited by T. HIGUCHI and V. STELLA. American Chemical Society, 1155 16th Street, N.W., Washington, DC 20036, 1975. 245 pp. 16 × 24 cm. Price $13.50.

This volume is a collection of papers presented during a symposium on prodrugs held in Atlantic City, September 10, 1974, under the sponsorship of the ACS Division of Medicinal Chemistry. The book consists of six sections. The first section, which constitutes approximately half of the volume, is a review of the basic concepts and approaches to the design of prodrugs. The second section covers applications of the prodrug approach to antibiotics. The remainder of the volume describes, in the form of research papers, chemical and biological studies on prodrug candidates performed in the laboratories of the authors. These chapters deal with prodrugs of phenytoin (diphenylhydantoin) and epinephrine and with the use of prodrugs in the formulation of cytotoxic agents for parenteral administration.

Although the enzymatic and some biological aspects, which are important in the design of new prodrugs, are not discussed, this book represents an excellent compilation of data on the subject. The extensive bibliography, particularly of the first two sections, and the excellent examples selected to illustrate the chemical approaches to the problem of drug delivery should make this volume a valuable addition to the library of every researcher in this field.

The book is easily readable and is recommended to graduate students and faculty of both chemistry and pharmacy. The material described in this book by the authors, who are experts in this field, ought to stimulate greatly the thinking of those who are seeking new ideas in the application of chemistry to biology and pharmacy.

Reviewed by George A. Digenis
College of Pharmacy
University of Kentucky
Lexington, KY 40506

The Effect of Disease States on Drug Pharmacokinetics. Edited by LESLIE Z. BENET. American Pharmaceutical Association, 2215 Constitution Ave. N.W., Washington, DC 20037, 1976. 252 pp. 15.5 × 23 cm. Price $9.25 (APhA Member Rate, $6.50).

"The Effect of Disease States on Drug Pharmacokinetics" is a collection of the papers presented at the April 1976 symposium sponsored by the Academy of Pharmaceutical Sciences of the American Pharmaceutical Association. The 29 contributors to this symposium are among the most prominent researchers in the field of clinical pharmacokinetics.

The introduction is a general orientation to the subject and a brief discussion of various possible approaches to the investigation of potential pharmacokinetic changes. The book is divided into four parts, each of which contains one chapter that discusses the subtopic in general and one or more chapters that deal with specific examples.

In the first section, Body Perfusion, Chapter 2 presents an overview of pharmacokinetics in disease states that modify blood flow and organ perfusion. Chapter 3 deals specifically with the effects of cardiac failure on GI absorption.

Hepatic and Metabolic Function is the subject of the second section, which includes Chapters 4–6. A comprehensive review of drug kinetics in patients with hepatic dysfunction is presented in Chapter 4. The effect of chronic liver disease on hepatic clearance is examined in Chapter 5, and Chapter 6 is a description of the kinetics of a single drug, carbamazepine, in a particular disease state, epilepsy.

The third section, Protein Binding, contains, in Chapter 7, a survey of disease-induced changes in drug-binding components and factors that alter drug–protein binding. Chapter 8 reviews the effects of uremia, bacterial infections, and cardiopulmonary bypass on serum protein binding. The clinical implications of interindividual differences of plasma protein binding, specifically for warfarin, phenytoin, and bilirubin, are discussed in Chapter 9.

Renal Function, the final section, is the area in which the most progress has been made in evaluating effects of disease states on drug kinetics. Chapter 10 presents a broad consideration of the field and a tabular compilation that may be used in adjusting drug dosage for compounds influenced by changes in renal function. The influence of renal disease on the elimination of procainamide and the accumulation of *N*-acetylprocainamide is described in Chapter 11. Finally, in Chapter 12, the effect of changes in renal function on gentamicin kinetics is discussed.

This book should be of particular value to students and researchers in the field of clinical pharmacokinetics, as well as practitioners and professionals in allied fields.

Staff Review

Practical Pharmaceutical Chemistry. Third Edition–Part Two. By A. H. BECKETT and J. B. STENLAKE. Humanities Press, Atlantic Highlands, NJ 07716, 1976. 552 pp. 16 × 24 cm. Price $37.50.

The present volume is an attempt to provide to students the benefit of numerous developments in practical pharmaceutical chemistry since the book was first written (1970). This resulted in an increase in the length of the volume by 127 pages, a figure that gives some idea of the new matter incorporated in the present edition.

This edition again opens with a chapter on "General Physical Methods," which covers some of the general topics in physics including molecular weight, refractometry, optical activity, and viscosity. These topics, systematically presented in concise form, lay the groundwork for subsequent chapters. It would be invidious to single out any chapter for special mention because the book covers such a wide variety of topics. These topics include analysis of drugs, measurement of electromotive force and pH, conductometric titrations, polarography, chromatography, spectrophotometry, flame photometry, and atomic absorption spectroscopy, spectrofluorometry, IR, NMR, mass spectrometry, and radiochemical techniques. These topics provide a sound basic knowledge to chemistry and pharmacy students.

The organization of this edition is identical to the previous edition. In addition to the material covered in the previous edition, this edition has given more detailed coverage to flame photometry, atomic absorption, and GC–mass spectrometric systems and has incorporated excellent introductions to, and practical applications of, circular dichroism spectra, thermal methods of analysis, coulometry, and high pressure liquid chromatography. The sections on NMR have been extended to include lanthanide shift reagents, ^{13}C-NMR spectroscopy, fourier transform NMR, and an introduction to internuclear double resonance and nuclear overhauser effect. The chapter on radiochemical techniques includes additional practical experiments with radionuclide generators and the use of radioimmunoassay techniques. All chapters of the book are sufficiently illustrated with diagrams, experiments (none in chapters on NMR and mass spectrometry), cognate experiments, and references. At the end of certain chapters, the authors provide a list of recommended books for additional study.

Overall, this is a lucid book presented in the style employed by Arthur I. Vogel, the author of "Practical Organic Chemistry." It is the opinion of this reviewer and his associates that this edition will not only stimulate the interest of chemistry and pharmacy students but will also assist in enhancing their knowledge.

Reviewed by S. D. Jolad
Division of Pharmaceutical Chemistry
College of Pharmacy
University of Arizona
Tucson, AZ 85721

NOTICES

Dictionnaire Pratique De Pharmacologie Clinique. By Y. TOUITOU and L. PERLEMUTER. Masson et cie, 120 bd Saint-Germain, 75280 Paris 6, France, 1976. 1204 pp. 15 × 21 cm. Price 167 F.

Receptors and Recognition. Vol. 1 Series A. Edited by P. CUATRECASAS and M. F. GREAVES. Wiley, 605 Third Ave., New York, NY 10016, 1976. 175 pp. 16 × 24 cm. Price $24.00.

Arzneiformenlehre. Ein Lehrbuch für Pharmazeuten. By PAUL HEINZ LIST *et al.* Wissenschaftliche Verlagsgesellschaft mbH., 7000 Stuttgart 1, P.O. Box 40, Germany, 1976. 514 pp. 17 × 24.5 cm. Price DM 62.—.

Carbohydrate Chemistry. Vol. 8. Edited by J. S. BRIMACOMBE *et al.* The Chemical Society, Blackhorse Road, Letchworth, Herts. SG6 1HN, England, 1976. 485 pp. 14 × 22 cm. Price $66.00. May be obtained from Special Issue Sales, American Chemical Society, 1155 Sixteenth St., N.W., Washington, DC 20036.

Innovative Medical-Psychiatric Therapies. Edited by RICHARD M. SUINN and RICHARD G. WEIGEL. University Park Press, Baltimore, MD 21202, 1976. xvi + 302 pp. 16.5 × 23.5 cm. Price $19.50.

Reviews of Physiology, Biochemistry and Pharmacology. Vol. 74. (The Role of Cyclic Nucleotides in Central Synaptic Function; Renal Transport of Amino Acids). Springer-Verlag, 175 Fifth Ave., New York, NY 10010, 1975. 200 pp. 17 × 25 cm. Price $39.80.

Biosynthesis. Vol. 4. Edited by J. D. BU'LOCK *et al.* The Chemical Society, Burlington House, London, W1V 0BN, England, 1976. 274 pp. 14 × 22 cm. Price $44.00.

Dental Practitioners' Formulary 1976–78. The British Medical Association, Tavistock Square, London, WC1H 9JP and The Pharmaceutical Press, 17 Bloomsbury Square, London WC1A 2NN, England, 1976. 64 pp. 15.5 × 9.5 cm. Price £ 0.55.

Handbook of Ocular Toxicity. By MARVIN B. SMITH. Publishing Sciences Group Inc., 162 Great Rd., Acton, MA 01720, 1976. 525 pp. 16 × 24 cm. Price $20.00.

British National Formulary 1976–78. The British Medical Association, Tavistock Square, London, WC1H 9JP and The Pharmaceutical Press, 17 Bloomsbury Square, London WC1A 2NN, England, 1976. 422 pp. 16.5 × 10.5 cm. Price £ 1.55.

Thiamine. Edited by CLARK J. GUBLER, MOTONORI FUJIWARA, and PIERRE M. DREYFUSS. Wiley, 605 Third Ave., New York, NY 10016, 1976. 393 pp. 16 × 23.5 cm. Price $27.00.

Contemporary Organic Chemistry. By MARION H. O'LEARY. McGraw-Hill Book Co., 1221 Avenue of the Americas, New York, NY 10020, 1975. 396 pp. 16.5 × 24 cm. Price $13.95.

Visceral Muscle. Its Structure and Function. By HENRY HUDDART and STEPHEN HUNT. Halsted, 605 Third Ave., New York, NY 10016, 1976. 181 pp. 15 × 21 cm. Price $13.95.

Biochemical Fluorescence: Concepts. Vol. 2. Edited by RAYMOND F. CHEN and HAROLD EDELHOCH. Dekker, 270 Madison Ave., New York, NY 10016, 1976. 944 pp. 16 × 24 cm. Price $38.00.

The Heroin Epidemics. A Study of Heroin Use in the United States, 1965–1975. By LEON GIBSON HUNT and CARL D. CHAMBERS. Halsted, 605 Third Ave., New York, NY 10016, 1976. 145 pp. 16 × 23.5 cm. Price $12.95.

Immunopharmacology. Edited by MARVIN E. ROSENTHALE and HERBERT C. MANSMANN, Jr. Halsted, 605 Third Ave., New York, NY 10016, 1976. 332 pp. 15.5 × 23.5 cm. Price $25.00.

Hormones, Behavior and Psychopathology. Edited by EDWARD J. SACHAR. Raven, 1140 Avenue of the Americas, New York, NY 10036, 1976. 307 pp. 16 × 24.5 cm. Price $24.00.

Hepatic and Metabolic Function is the subject of the second section, which includes Chapters 4–6. A comprehensive review of drug kinetics in patients with hepatic dysfunction is presented in Chapter 4. The effect of chronic liver disease on hepatic clearance is examined in Chapter 5, and Chapter 6 is a description of the kinetics of a single drug, carbamazepine, in a particular disease state, epilepsy.

The third section, Protein Binding, contains, in Chapter 7, a survey of disease-induced changes in drug-binding components and factors that alter drug–protein binding. Chapter 8 reviews the effects of uremia, bacterial infections, and cardiopulmonary bypass on serum protein binding. The clinical implications of interindividual differences of plasma protein binding, specifically for warfarin, phenytoin, and bilirubin, are discussed in Chapter 9.

Renal Function, the final section, is the area in which the most progress has been made in evaluating effects of disease states on drug kinetics. Chapter 10 presents a broad consideration of the field and a tabular compilation that may be used in adjusting drug dosage for compounds influenced by changes in renal function. The influence of renal disease on the elimination of procainamide and the accumulation of *N*-acetylprocainamide is described in Chapter 11. Finally, in Chapter 12, the effect of changes in renal function on gentamicin kinetics is discussed.

This book should be of particular value to students and researchers in the field of clinical pharmacokinetics, as well as practitioners and professionals in allied fields.

Staff Review

Practical Pharmaceutical Chemistry. Third Edition–Part Two. By A. H. BECKETT and J. B. STENLAKE. Humanities Press, Atlantic Highlands, NJ 07716, 1976. 552 pp. 16 × 24 cm. Price $37.50.

The present volume is an attempt to provide to students the benefit of numerous developments in practical pharmaceutical chemistry since the book was first written (1970). This resulted in an increase in the length of the volume by 127 pages, a figure that gives some idea of the new matter incorporated in the present edition.

This edition again opens with a chapter on "General Physical Methods," which covers some of the general topics in physics including molecular weight, refractometry, optical activity, and viscosity. These topics, systematically presented in concise form, lay the groundwork for subsequent chapters. It would be invidious to single out any chapter for special mention because the book covers such a wide variety of topics. These topics include analysis of drugs, measurement of electromotive force and pH, conductometric titrations, polarography, chromatography, spectrophotometry, flame photometry, and atomic absorption spectroscopy, spectrofluorometry, IR, NMR, mass spectrometry, and radiochemical techniques. These topics provide a sound basic knowledge to chemistry and pharmacy students.

The organization of this edition is identical to the previous edition. In addition to the material covered in the previous edition, this edition has given more detailed coverage to flame photometry, atomic absorption, and GC–mass spectrometric systems and has incorporated excellent introductions to, and practical applications of, circular dichroism spectra, thermal methods of analysis, coulometry, and high pressure liquid chromatography. The sections on NMR have been extended to include lanthanide shift reagents, ^{13}C-NMR spectroscopy, fourier transform NMR, and an introduction to internuclear double resonance and nuclear overhauser effect. The chapter on radiochemical techniques includes additional practical experiments with radionuclide generators and the use of radioimmunoassay techniques. All chapters of the book are sufficiently illustrated with diagrams, experiments (none in chapters on NMR and mass spectrometry), cognate experiments, and references. At the end of certain chapters, the authors provide a list of recommended books for additional study.

Overall, this is a lucid book presented in the style employed by Arthur I. Vogel, the author of "Practical Organic Chemistry." It is the opinion of this reviewer and his associates that this edition will not only stimulate the interest of chemistry and pharmacy students but will also assist in enhancing their knowledge.

Reviewed by S. D. Jolad
Division of Pharmaceutical Chemistry
College of Pharmacy
University of Arizona
Tucson, AZ 85721

NOTICES

Dictionnaire Pratique De Pharmacologie Clinique. By Y. TOUITOU and L. PERLEMUTER. Masson et cie, 120 bd Saint-Germain, 75280 Paris 6, France, 1976. 1204 pp. 15 × 21 cm. Price 167 F.

Receptors and Recognition. Vol. 1 Series A. Edited by P. CUATRECASAS and M. F. GREAVES. Wiley, 605 Third Ave., New York, NY 10016, 1976. 175 pp. 16 × 24 cm. Price $24.00.

Arzneiformenlehre. Ein Lehrbuch für Pharmazeuten. By PAUL HEINZ LIST *et al.* Wissenschaftliche Verlagsgesellschaft mbH., 7000 Stuttgart 1, P.O. Box 40, Germany, 1976. 514 pp. 17 × 24.5 cm. Price DM 62.—.

Carbohydrate Chemistry. Vol. 8. Edited by J. S. BRIMACOMBE *et al.* The Chemical Society, Blackhorse Road, Letchworth, Herts. SG6 1HN, England, 1976. 485 pp. 14 × 22 cm. Price $66.00. May be obtained from Special Issue Sales, American Chemical Society, 1155 Sixteenth St., N.W., Washington, DC 20036.

Innovative Medical-Psychiatric Therapies. Edited by RICHARD M. SUINN and RICHARD G. WEIGEL. University Park Press, Baltimore, MD 21202, 1976. xvi + 302 pp. 16.5 × 23.5 cm. Price $19.50.

Reviews of Physiology, Biochemistry and Pharmacology. Vol. 74. (The Role of Cyclic Nucleotides in Central Synaptic Function; Renal Transport of Amino Acids). Springer-Verlag, 175 Fifth Ave., New York, NY 10010, 1975. 200 pp. 17 × 25 cm. Price $39.80.

Biosynthesis. Vol. 4. Edited by J. D. BU'LOCK *et al.* The Chemical Society, Burlington House, London, W1V 0BN, England, 1976. 274 pp. 14 × 22 cm. Price $44.00.

Dental Practitioners' Formulary 1976–78. The British Medical Association, Tavistock Square, London, WC1H 9JP and The Pharmaceutical Press, 17 Bloomsbury Square, London WC1A 2NN, England, 1976. 64 pp. 15.5 × 9.5 cm. Price £ 0.55.

Handbook of Ocular Toxicity. By MARVIN B. SMITH. Publishing Sciences Group Inc., 162 Great Rd., Acton, MA 01720, 1976. 525 pp. 16 × 24 cm. Price $20.00.

British National Formulary 1976–78. The British Medical Association, Tavistock Square, London, WC1H 9JP and The Pharmaceutical Press, 17 Bloomsbury Square, London WC1A 2NN, England, 1976. 422 pp. 16.5 × 10.5 cm. Price £ 1.55.

Thiamine. Edited by CLARK J. GUBLER, MOTONORI FUJIWARA, and PIERRE M. DREYFUSS. Wiley, 605 Third Ave., New York, NY 10016, 1976. 393 pp. 16 × 23.5 cm. Price $27.00.

Contemporary Organic Chemistry. By MARION H. O'LEARY. McGraw-Hill Book Co., 1221 Avenue of the Americas, New York, NY 10020, 1975. 396 pp. 16.5 × 24 cm. Price $13.95.

Visceral Muscle. Its Structure and Function. By HENRY HUDDART and STEPHEN HUNT. Halsted, 605 Third Ave., New York, NY 10016, 1976. 181 pp. 15 × 21 cm. Price $13.95.

Biochemical Fluorescence: Concepts. Vol. 2. Edited by RAYMOND F. CHEN and HAROLD EDELHOCH. Dekker, 270 Madison Ave., New York, NY 10016, 1976. 944 pp. 16 × 24 cm. Price $38.00.

The Heroin Epidemics. A Study of Heroin Use in the United States, 1965–1975. By LEON GIBSON HUNT and CARL D. CHAMBERS. Halsted, 605 Third Ave., New York, NY 10016, 1976. 145 pp. 16 × 23.5 cm. Price $12.95.

Immunopharmacology. Edited by MARVIN E. ROSENTHALE and HERBERT C. MANSMANN, Jr. Halsted, 605 Third Ave., New York, NY 10016, 1976. 332 pp. 15.5 × 23.5 cm. Price $25.00.

Hormones, Behavior and Psychopathology. Edited by EDWARD J. SACHAR. Raven, 1140 Avenue of the Americas, New York, NY 10036, 1976. 307 pp. 16 × 24.5 cm. Price $24.00.

Hepatic and Metabolic Function is the subject of the second section, which includes Chapters 4–6. A comprehensive review of drug kinetics in patients with hepatic dysfunction is presented in Chapter 4. The effect of chronic liver disease on hepatic clearance is examined in Chapter 5, and Chapter 6 is a description of the kinetics of a single drug, carbamazepine, in a particular disease state, epilepsy.

The third section, Protein Binding, contains, in Chapter 7, a survey of disease-induced changes in drug-binding components and factors that alter drug–protein binding. Chapter 8 reviews the effects of uremia, bacterial infections, and cardiopulmonary bypass on serum protein binding. The clinical implications of interindividual differences of plasma protein binding, specifically for warfarin, phenytoin, and bilirubin, are discussed in Chapter 9.

Renal Function, the final section, is the area in which the most progress has been made in evaluating effects of disease states on drug kinetics. Chapter 10 presents a broad consideration of the field and a tabular compilation that may be used in adjusting drug dosage for compounds influenced by changes in renal function. The influence of renal disease on the elimination of procainamide and the accumulation of *N*-acetylprocainamide is described in Chapter 11. Finally, in Chapter 12, the effect of changes in renal function on gentamicin kinetics is discussed.

This book should be of particular value to students and researchers in the field of clinical pharmacokinetics, as well as practitioners and professionals in allied fields.

Staff Review

Practical Pharmaceutical Chemistry. Third Edition–Part Two. By A. H. BECKETT and J. B. STENLAKE. Humanities Press, Atlantic Highlands, NJ 07716, 1976. 552 pp. 16 × 24 cm. Price $37.50.

The present volume is an attempt to provide to students the benefit of numerous developments in practical pharmaceutical chemistry since the book was first written (1970). This resulted in an increase in the length of the volume by 127 pages, a figure that gives some idea of the new matter incorporated in the present edition.

This edition again opens with a chapter on "General Physical Methods," which covers some of the general topics in physics including molecular weight, refractometry, optical activity, and viscosity. These topics, systematically presented in concise form, lay the groundwork for subsequent chapters. It would be invidious to single out any chapter for special mention because the book covers such a wide variety of topics. These topics include analysis of drugs, measurement of electromotive force and pH, conductometric titrations, polarography, chromatography, spectrophotometry, flame photometry, and atomic absorption spectroscopy, spectrofluorometry, IR, NMR, mass spectrometry, and radiochemical techniques. These topics provide a sound basic knowledge to chemistry and pharmacy students.

The organization of this edition is identical to the previous edition. In addition to the material covered in the previous edition, this edition has given more detailed coverage to flame photometry, atomic absorption, and GC–mass spectrometric systems and has incorporated excellent introductions to, and practical applications of, circular dichroism spectra, thermal methods of analysis, coulometry, and high pressure liquid chromatography. The sections on NMR have been extended to include lanthanide shift reagents, ^{13}C-NMR spectroscopy, fourier transform NMR, and an introduction to internuclear double resonance and nuclear overhauser effect. The chapter on radiochemical techniques includes additional practical experiments with radionuclide generators and the use of radioimmunoassay techniques. All chapters of the book are sufficiently illustrated with diagrams, experiments (none in chapters on NMR and mass spectrometry), cognate experiments, and references. At the end of certain chapters, the authors provide a list of recommended books for additional study.

Overall, this is a lucid book presented in the style employed by Arthur I. Vogel, the author of "Practical Organic Chemistry." It is the opinion of this reviewer and his associates that this edition will not only stimulate the interest of chemistry and pharmacy students but will also assist in enhancing their knowledge.

Reviewed by S. D. Jolad
Division of Pharmaceutical Chemistry
College of Pharmacy
University of Arizona
Tucson, AZ 85721

NOTICES

Dictionnaire Pratique De Pharmacologie Clinique. By Y. TOUITOU and L. PERLEMUTER. Masson et cie, 120 bd Saint-Germain, 75280 Paris 6, France, 1976. 1204 pp. 15 × 21 cm. Price 167 F.

Receptors and Recognition. Vol. 1 Series A. Edited by P. CUATRECASAS and M. F. GREAVES. Wiley, 605 Third Ave., New York, NY 10016, 1976. 175 pp. 16 × 24 cm. Price $24.00.

Arzneiformenlehre. Ein Lehrbuch für Pharmazeuten. By PAUL HEINZ LIST *et al.* Wissenschaftliche Verlagsgesellschaft mbH., 7000 Stuttgart 1, P.O. Box 40, Germany, 1976. 514 pp. 17 × 24.5 cm. Price DM 62.—.

Carbohydrate Chemistry. Vol. 8. Edited by J. S. BRIMACOMBE *et al.* The Chemical Society, Blackhorse Road, Letchworth, Herts. SG6 1HN, England, 1976. 485 pp. 14 × 22 cm. Price $66.00. May be obtained from Special Issue Sales, American Chemical Society, 1155 Sixteenth St., N.W., Washington, DC 20036.

Innovative Medical-Psychiatric Therapies. Edited by RICHARD M. SUINN and RICHARD G. WEIGEL. University Park Press, Baltimore, MD 21202, 1976. xvi + 302 pp. 16.5 × 23.5 cm. Price $19.50.

Reviews of Physiology, Biochemistry and Pharmacology. Vol. 74. (The Role of Cyclic Nucleotides in Central Synaptic Function; Renal Transport of Amino Acids). Springer-Verlag, 175 Fifth Ave., New York, NY 10010, 1975. 200 pp. 17 × 25 cm. Price $39.80.

Biosynthesis. Vol. 4. Edited by J. D. BU'LOCK *et al.* The Chemical Society, Burlington House, London, W1V 0BN, England, 1976. 274 pp. 14 × 22 cm. Price $44.00.

Dental Practitioners' Formulary 1976–78. The British Medical Association, Tavistock Square, London, WC1H 9JP and The Pharmaceutical Press, 17 Bloomsbury Square, London WC1A 2NN, England, 1976. 64 pp. 15.5 × 9.5 cm. Price £ 0.55.

Handbook of Ocular Toxicity. By MARVIN B. SMITH. Publishing Sciences Group Inc., 162 Great Rd., Acton, MA 01720, 1976. 525 pp. 16 × 24 cm. Price $20.00.

British National Formulary 1976–78. The British Medical Association, Tavistock Square, London, WC1H 9JP and The Pharmaceutical Press, 17 Bloomsbury Square, London WC1A 2NN, England, 1976. 422 pp. 16.5 × 10.5 cm. Price £ 1.55.

Thiamine. Edited by CLARK J. GUBLER, MOTONORI FUJIWARA, and PIERRE M. DREYFUSS. Wiley, 605 Third Ave., New York, NY 10016, 1976. 393 pp. 16 × 23.5 cm. Price $27.00.

Contemporary Organic Chemistry. By MARION H. O'LEARY. McGraw-Hill Book Co., 1221 Avenue of the Americas, New York, NY 10020, 1975. 396 pp. 16.5 × 24 cm. Price $13.95.

Visceral Muscle. Its Structure and Function. By HENRY HUDDART and STEPHEN HUNT. Halsted, 605 Third Ave., New York, NY 10016, 1976. 181 pp. 15 × 21 cm. Price $13.95.

Biochemical Fluorescence: Concepts. Vol. 2. Edited by RAYMOND F. CHEN and HAROLD EDELHOCH. Dekker, 270 Madison Ave., New York, NY 10016, 1976. 944 pp. 16 × 24 cm. Price $38.00.

The Heroin Epidemics. A Study of Heroin Use in the United States, 1965–1975. By LEON GIBSON HUNT and CARL D. CHAMBERS. Halsted, 605 Third Ave., New York, NY 10016, 1976. 145 pp. 16 × 23.5 cm. Price $12.95.

Immunopharmacology. Edited by MARVIN E. ROSENTHALE and HERBERT C. MANSMANN, Jr. Halsted, 605 Third Ave., New York, NY 10016, 1976. 332 pp. 15.5 × 23.5 cm. Price $25.00.

Hormones, Behavior and Psychopathology. Edited by EDWARD J. SACHAR. Raven, 1140 Avenue of the Americas, New York, NY 10036, 1976. 307 pp. 16 × 24.5 cm. Price $24.00.

Journal of Pharmaceutical Sciences

MARCH 1977

VOLUME 66 NUMBER 3

MARY H. FERGUSON
Editor

L. LUAN CORRIGAN
Assistant Editor

SHELLY ELLIOTT
Production Editor

JANET D. SHOFF
Copy Editor

EDWARD G. FELDMANN
Contributing Editor

SAMUEL W. GOLDSTEIN
Contributing Editor

LELAND J. ARNEY
Director of Publications

EDITORIAL ADVISORY BOARD

JOHN AUTIAN
HARRY B. KOSTENBAUDER
NORMAN R. FARNSWORTH
HERBERT A. LIEBERMAN
WILLIAM O. FOYE
DAVID E. MANN, JR.
WILLIAM J. JUSKO
GERALD J. PAPARIELLO

The *Journal of Pharmaceutical Sciences* is published monthly by the American Pharmaceutical Association at 2215 Constitution Ave., N.W., Washington, DC 20037. Second-class postage paid at Washington, D.C., and at additional mailing office.

All expressions of opinion and statements of supposed fact appearing in articles or editorials carried in this journal are published on the authority of the writer over whose name they appear and are not to be regarded as necessarily expressing the policies or views of the American Pharmaceutical Association.

Offices—Editorial, Advertising, and Subscription Offices: 2215 Constitution Ave., N.W., Washington, DC 20037. Printing Offices: 20th & Northampton Streets, Easton, PA 18042.

Annual Subscriptions—United States and foreign, industrial and government institutions $50, educational institutions $50, individuals *for personal use only* $30; single copies $5. All foreign subscriptions add $5 for postage. Subscription rates are subject to change without notice. Members of the American Pharmaceutical Association may elect to receive the *Journal of Pharmaceutical Sciences* as a part of their annual $60 (foreign $65) APhA membership dues.

Claims—Missing numbers will not be supplied if dues or subscriptions are in arrears for more than 60 days or if claims are received more than 60 days after the date of the issue, or if loss was due to failure to give notice of change of address. The Association cannot accept responsibility for foreign delivery when its records indicate shipment has been made.

Change of Address—Members and subscribers should notify at once both the Post Office and the American Pharmaceutical Association, 2215 Constitution Ave., N.W., Washington, DC 20037, of any change of address.

© Copyright 1977, American Pharmaceutical Association, 2215 Constitution Ave., N.W., Washington, DC 20037; all rights reserved.

HOW MUCH IS "ENOUGH"?

For the past year or two, articles, speeches, testimony, and assorted other means of communication have been rife with comment and opinion to the effect that either additional regulation is needed in the area of drug discovery and introduction or, conversely, that already drug discovery and introduction are subjected to excessive regulation.

On the one side, those who advocate additional legal controls present persuasive arguments based upon statistics showing significant toxicity, adverse reactions, and related harmful effects associated with a particular drug which often come to light only after its widespread or long-term use. On the other hand, opponents to further regulation present equally persuasive arguments that already drug innovation has been inhibited, a so-called "drug lag" has developed, and patients are presently being denied the benefit of important new drug discoveries, all due to what they regard as the excessively restrictive current regulations which delay or prevent new drug marketing approval.

It is, of course, just such differences of viewpoint which are said "to make a horse race." All of this reminds us of an anecdote which may or may not have basis in fact but certainly is pertinent. We were told that the river which ran through a small rural town was closed to swimming by the local health department on grounds that it was polluted and a menace to health. The town leaders went to extensive effort to correct the problem and to clean up their river. But when they then requested the health department to open the river to swimming, their request was again denied—this time with the explanation that the river constituted the source of the local drinking water supply and it would be unsanitary, therefore, to permit swimming!

Whether or not such an incident actually occurred, we do know for a fact that rather comparable incidents repeatedly have happened in the area of drug standards. For example, on many occasions, critics from the drug industry have alleged that official compendia specifications were insufficient to assure an aspect of drug quality whether it be potency, identity, bioavailability, stability, or some other related characteristic. Subsequently, the compendia proposed adoption of either a new or more stringent specification in order to remedy the alleged deficiency. Not uncommonly, such proposals then met with objection from the very same critics on grounds that such test requirements were excessive, or would contribute prohibitively to manufacturing costs, or even that the proposed requirements were too "severe" because their own products could not meet the new standard!

It is well to recognize that the genesis of any proposed new law or regulation generally can be traced back to some sort of abuse or problem. For example, the Good Laboratory Practice regulations which were discussed in our February editorial were the direct result of falsified test data submitted to FDA in support of certain New Drug Applications. Consequently, as a general observation, most disinterested parties would tend to feel that society and government must impose regulatory controls to avoid problems or to prevent repeated abuses.

Our view tends to concur but, at the same time, we also recognize that such regulations must be reasonable and properly tempered to avoid excessive restrictions which will unduly inhibit and discourage future research by destroying legitimate incentives. Drug regulation is particularly susceptible to "overkill," and care must be exercised to avoid a result which might be even more disastrous than the problem it is intended to control.

Edward G. Feldmann

Journal of Pharmaceutical Sciences

MARCH 1977
VOLUME 66 NUMBER 3

RESEARCH ARTICLES

Predictive Conversion of *In Vitro* Drug Dissolution Data into *In Vivo* Drug Response *versus* Time Profiles Exemplified for Plasma Levels of Warfarin

VICTOR F. SMOLEN ˣ **and RANDALL J. ERB**

Abstract □ A mathematical approach to computing the *in vivo* drug response profiles (such as plasma level, pharmacological response, and urinary recovery *versus* time curves) corresponding to observed *in vitro* dissolution of drug dosage form *versus* time profiles is described. The method is exemplified for warfarin tablets, for which observed *in vivo* plasma level profiles are compared to corresponding predicted profiles computed from *in vitro* dissolution data. The potential of the method is demonstrated; approaches to its improvement, as well as its limitations, are discussed.

Keyphrases □ Drug response profiles, *in vivo*—plasma warfarin levels, predicted from *in vitro* dissolution data □ Dissolution data, *in vitro*—predictive conversion into *in vivo* drug response–time profiles, plasma warfarin levels □ Warfarin—plasma levels predicted from *in vitro* dissolution data

Even seemingly trivial changes in the formulation and manufacture of drug products can significantly alter the dynamics of a drug's release from its dosage form and, consequently, affect its therapeutic performance. The growing number of multisource drugs resulting from the expiration of patents is increasing the importance of this problem. It is not feasible to perform routinely the extensive *in vivo* bioavailability testing of drug products necessary to ensure their bioequivalency. Consequently, considerable efforts have been expended to develop and apply *in vitro* drug release tests that are rapid, convenient, and reliable in reflecting the *in vivo* behavior of drug dosage forms. Such tests have to varying degrees been successful in providing results that correlate with *in vivo* bioavailability (1).

Recently, a systematic, control engineering approach to developing drug dissolution tests that are optimally predictive of the entire time course of *in vivo* drug product performance was described (2, 3). Suggestions also were made concerning the manner in which *in vitro* tests may be improved to reflect *in vivo* behavior better (4–6). By properly adjusting the conditions under which drug product dissolution testing is performed, it is sometimes possible to achieve a linear, multiple-point relationship between the time variation of the amount of drug dissolved from dosage forms *in vitro* and analogous amounts absorbed *in vivo* (4); such relationships were successfully demonstrated (7–10). In such cases, it was shown that the time course of *in vivo* pharmacological effects can be computed from *in vitro* dissolution data under certain conditions (4).

Despite such possibilities for handling *in vitro* dissolution data, relationships between the results of *in vitro* drug product dissolution testing and *in vivo* bioavailability are most commonly reported as single-point correlations. For example, the amounts of drug dissolved *in vitro* after a given time are correlated with the amounts absorbed *in vivo* or the plasma levels of the drug observed at the same or other times after dosing (11); times for a percentage of the drug to be dissolved *in vitro* are related to time or rates at which the drug is available *in vivo* (12). It would obviously be of greater utility to correlate or predict the entirety of *in vivo* drug response profiles, *i.e.*, plasma, urinary recovery rate, and/or pharmacological response, *versus* time curves with *in vitro* results and in this manner maximize the amount of information obtainable from drug dissolution testing data.

With drugs such as warfarin, which have a long half-life and are chronically administered, the extent of the drug's bioavailability from its dosage forms is clinically more important than the rates at which it reaches the systemic circulation. However, in addition to not taking full ad-

vantage of all the *in vivo* and *in vitro* kinetic data collected in bioavailability and dissolution experiments, single-point *in vivo* to *in vitro* data correlations can be misinterpreted and misleading as tacit indicators of the extent of drug bioavailability.

For example, in a single-point correlation of average warfarin dissolved from tablets in 1 hr to *in vivo* plasma levels observed after 1 hr (11), a tablet designated A was shown to be approximately 6% dissolved *in vitro* and to elicit a plasma level of 1.11 μg/ml. A second tablet, D, was only about 3% dissolved and yielded a 1-hr plasma level of 0.58 μg/ml. The implication of such linearly correlated results is that Tablet D and other tablets having similar *in vitro* dissolution behavior are only approximately 50% as bioavailable as Tablet A in their dissolution behavior. Actually, however, the areas under the plasma curves reveal Tablet D to have an extent of bioavailability that is 1.08 times that of Tablet A.

This report presents a relatively simple mathematical approach which, under certain described conditions (3, 13, 14), allows the conversion of *in vitro* drug dissolution time curves into *in vivo* drug response *versus* time profiles. The method and its limitations are exemplified using plasma drug levels and dissolution data for warfarin reported by Wagner *et al.* (11).

THEORETICAL

Background and Assumptions—Linear systems theory (15) can be implemented to develop a mathematical relationship which, for a defined set of *in vitro* and *in vivo* experimental conditions, allows *in vitro* drug product dissolution *versus* time data to be transformed into computationally predicted or simulated *in vivo* drug response *versus* time profiles. This is feasible to accomplish provided that the dynamics of the system behavior can be presumed linear, *i.e.*, the following assumptions and conditions apply:

1. The *in vitro* and *in vivo* kinetic processes remain qualitatively the same for all of the different dosage formulations tested.

2. All kinetic processes can be described as linear, or at least approximated as linear, in the sense that the superposition principle (16) applies over an operational range of interest. *In vivo*, both the preabsorption dynamics of the drug's release from its dosage forms and the subsequent systemic absorption into the blood, as well as its disposition and elimination from the body, are required to be dose independent and nonsaturable, *i.e.*, linear. In practice, it may be sufficient that the *in vivo* system approximates linearity over the range of difference seen between the dosage forms tested. However, as commonly heard, it is not necessary that the *in vivo* bioavailability of the drug be rate limited only by its dissolution from its dosage forms. However, the *in vivo* absorption, as well as any presystemic metabolism of the drug in the gut lumen, wall, or liver, must be linear and describable by proportional rate constants that are time invariant. In other words, drug absorption occurring by site specific, facilitated, or active transport, as well as the involvement of saturable metabolic processes, could vitiate the approach, depending upon the magnitude of the effects.

It is emphasized, however, that the *in vitro* time course of dissolution rates or extents of release of the drug from its dosage form can theoretically have any type of kinetic behavior provided that the apparatus and conditions of the *in vitro* dissolution test are such that the experimentally recorded drug dissolution rate or extent *versus* time profiles are direct reflections of drug release into the dissolution media or are consistently related to it by first- or higher order lag times (transfer function) (13). However, in the extreme case where a drug dissolves so slowly that its dissolution time exceeds its transit time in the GI tract, *in vitro* dissolution curves that are run to completion will obviously predict a greater *in vivo* bioavailability than would actually be observed; conceivably, this result could be at least approximately corrected for by truncating *in vitro* dissolution experiments after a time *in vitro* that is known to exceed a correspondingly proportional time *in vivo* at which further absorption of the drug no longer proceeds. The other extreme of instantaneous drug release, as is accomplished by administering a solution of the drug, merely represents an impulse input to the GI contents (2, 13, 14) and poses no theoretical difficulties.

3. No specific chemical or biochemical effects are operative with any dosage form being tested that are not operative with the rest. The operation of such biologically specific factors can be introduced if the drug forms soluble, nonabsorbable complexes with excipients in the formulations or if such excipients alter the barrier properties of the GI mucosa through which the drug must pass to be systemically absorbed. Such biological occurrences obviously could not be easily detected or taken into account by *in vitro* testing results unless they consistently occurred in all dosage forms (3).

General Computational Procedure—With the described assumptions and limitations in mind, the application of linear systems, transfer function, analysis provides the mathematical means to relate and predict *in vivo* drug response profiles, symbolized as $Q_B(t)$, from *in vitro* dissolution rate *versus* time profiles, presently symbolized as $\dot{A}(t)_D$, once a weighting function, $G_{BD}(t)$ [or transfer function, $G_{BD}(s)$, as defined in the complex frequency domain] is established. A function, f, is converted from the time domain, $f(t)$, into the complex frequency domain, $F(s)$, by taking its Laplace transform, as defined by:

$$F(s) = \int_0^\infty f(t)e^{-st}\,dt \qquad \text{(Eq. 1)}$$

The advantage of working in the s domain relative to the time, t, domain, is that the mathematical operations of convolution and deconvolution necessary in the time domain to compute output functions from input functions and vice versa are replaced by multiplication and division, respectively. For the present purposes, there are two such input–output transfer function relationships to consider, one for the *in vitro* system and another for the *in vivo* system. The *in vivo* response to an oral dosage form would be given by Eq. 2:

$$Q_B(s) = G_B(s)\dot{A}(s)_G \qquad \text{(Eq. 2)}$$

where $\dot{A}(s)_G$ is the Laplace transform of the time curve which describes the *in vivo* rate of drug release into the GI contents and, therefore, represents the *in vivo* input function (14); $\dot{A}(s)_G$ has an *in vitro* counterpart, $\dot{A}(s)_D$, which describes the rates of dissolution *in vitro*. For example, $\dot{A}(s)_D$ for a flow-through dissolution apparatus (3) would be given by Eq. 3:

$$\dot{A}(s)_D = \dot{V}C(s) \qquad \text{(Eq. 3)}$$

where $\dot{V}(t)$ is the flow rate through the dissolution cell, and $C(t)$ is the concentration in the stream; $C(t)$ can be continuously monitored using a spectrophotometer equipped with a flowcell. The flow rate is usually kept constant.

The transfer function for a linear system(s) that is generally applicable to relating *any* input is defined and obtained in the Laplace domain as the ratio of any *known* output function from the system to the corresponding *known* input function that caused the output. If $\dot{A}(s)_{G,r}$ and $\dot{A}(s)_{D,r}$ are known for any reference dosage form, r, for which the assumptions of linearity apply to both the *in vivo* and *in vitro* systems, they can be considered as input and output functions, respectively, and interrelated by the transfer function defined by:

$$\frac{\dot{A}(s)_{G,r}}{\dot{A}(s)_{D,r}} = G(s)_{DG,r} \qquad \text{(Eq. 4)}$$

Once $G(s)_{DG,r}$ is known, it can be used to compute *in vivo* response profiles, $Q_B(s)_i$, for any ith dosage form using *in vitro* determined dissolution input functions and:

$$Q_B(s)_i = G(s)_B G(s)_{DG}\dot{A}(s)_{D,i} \qquad \text{(Eq. 5)}$$

In practice, it is computationally expeditious to treat *in vitro* dissolution data as the output, $Q_D(s)$, relating it directly to the *in vivo* output, as shown in Eq. 6:

$$\frac{Q_B(s)_r}{Q_D(s)_r} = G(s)_{BD,r} \qquad \text{(Eq. 6)}$$

This equation defines a transfer function, $G(s)_{BD,r}$, based upon data from a reference dosage form, r.

For any other dosage forms that do not violate the assumptions on which this treatment is based, the *in vivo* response profile will be given by Eq. 7 using the *in vitro* dissolution data results observed for the ith dosage form:

$$Q_B(s)_i = G(s)_{BD,r}Q_D(s)_i \qquad \text{(Eq. 7)}$$

The two approaches obviously yield the same results. The relationship between *in vitro* dissolution and *in vivo* absorption dynamics is now

implicit in $G(s)_{BD,r}$. The conditions of the *in vitro* test must, of course, be maintained while testing each dosage form. Obviously, if the dissolution test does not yield at least some type of single-point correlations, such as between the time for 50% of the drug to dissolve *in vitro* and the time for 50% of the drug to be absorbed *in vivo*, it probably cannot provide results from which entire plasma levels, urinary recovery rates, and/or pharmacological response *versus* time profiles can be predicted.

The computational operations of deconvolution (Eq. 6) and convolution (Eq. 7) can be performed by various methods. Some methods used in pharmacokinetics were described previously (13, 14, 17, 18), and all of the various techniques generally used in engineering practice were recently reviewed (17). Such computations may rapidly and conveniently be performed using a Fourier analyzer[1] computer, as was implemented to obtain the results described in the present report. However, such specialized equipment is expensive and not very common. Therefore, a computational scheme for convolution–deconvolution appropriate for analog computers is presented in the *Appendix*. The same results are obtainable from the analog computer approach, which is presented here merely as a convenience to investigators without access to a Fourier analyzer.

EXPERIMENTAL

***In Vitro* Dissolution and *In Vivo* Plasma Curve Data**—The *in vitro* and *in vivo* data for warfarin treated in this study were abstracted from a report by Wagner *et al.* (11). Four dose treatments using four different dosage forms (Tablets A[2], B[3], C[4], and D[5]) were studied by these authors. Panels of six and 12 human volunteers were used in two separate studies. In the first study, six subjects received 25-mg dose treatments of Tablet B. In the second study, 12 subjects received 10-mg doses of Tablets A, C, and D. Plasma samples were periodically collected from the volunteers and assayed for the drug.

Dissolution testing of the tablets was performed using a paddle-agitated, three-necked, round-bottom flask, in which individual tablets were initially exposed to 900 ml of 0.1 *N* HCl for 30 min followed by the addition of 100 ml of strong phosphate buffer. The buffer instantaneously raised the pH to 7.5 ± 0.1 for the remainder of the dissolution test. The amounts of warfarin dissolved from the tablets as a function of time were determined by circulating the dissolution medium through a flowcell in a spectrophotometer. The tablets used were reported to have been assayed for their drug content using the official USP XVIII method.

Data Treatment—The average data reported by Wagner *et al.* (11) for each dose treatment were used to perform the described computations. Tablet C, administered as two 5-mg tablets, was selected as the reference dosage form from which data were used to determine the *in vitro* input → *in vivo* output transfer function, $G(s)_{DB,r}$; $G(s)_{DB,r}$ was subsequently used to compute plasma level *versus* time profiles for Tablets A (two 5-mg tablets), D (two 5-mg tablets), and B (one 25-mg tablet).

To obtain data points at discrete, constant time intervals, as needed for subsequent convolution and deconvolution computations, the *in vivo* plasma level data for Tablet B were fitted to multiexponential expressions of the form $y = \Sigma_{i=1}^{n} A_i e^{-m_i t}$. An iteratively converging, least-squares, digital computer program, which performs log peeling and derives initial estimates for the equation parameters (A_i's and m_i's), was used to perform the fitting. This program, called MULTIFIT, was developed in this laboratory (19). By using the fitted equations, data points were interpolatively generated at 2-hr intervals for up to 96 hr.

The *in vitro* dissolution test data, reported as cumulative amounts of drug dissolved *versus* time profiles, were incomplete in that the testing was prematurely discontinued before all of the drug in the tablets was dissolved. Consequently, an equation of the form $Q_D(t)_\% = 100\,(1 - e^{-kt})$, where $Q_D(t)_\%$ is the percent of the drug dissolved at time t, was fitted by linear least-squares regression to the data reported by Wagner *et al.* (11); the symbol k represents an apparent first-order dissolution rate constant.

This curve fitting was performed to allow the extrapolation of the *in vitro* dissolution curves to 100% to account for all of the drug contained in the tablets; values generated by the fitted equations were only used to obtain data points lying beyond the times at which the experimental data were truncated. Before these times, the *in vitro* data were directly estimated at 5-min intervals from the dissolution curves reported previously (11).

Convolution—The convolution and deconvolution computations were made with the use of a Fourier analyzer[1]. The system performs discrete Fourier transformation of time data and arithmetical operations on functions in the frequency domain. The Fourier transform of a time function as defined by Eq. 8 has similar properties to its Laplace transform:

$$\mathcal{F}f(t) = \int_0^\infty f(t)e^{-j\omega t}\,dt \qquad \text{(Eq. 8)}$$

$$\mathcal{F}f(t) = F(\omega) \qquad \text{(Eq. 9)}$$

In Eqs. 8 and 9, $j = \sqrt{-1}$ and ω is frequency. In the Laplace complex frequency domain, transformation of time functions yields, instead of ω, functions of a complex number, $s = \sigma + j\omega$. The σ is a real part added as a convergence factor; it allows transformation of some functions that otherwise cannot be Fourier transformed (20). For present purposes, the use of Fourier transforms can be considered equivalent to Laplace transforms. The Fourier analyzer-computer system obtains discrete finite transforms of time data using the algorithm defined by:

$$f(m\,\Delta f) = \Delta t \sum_{N=0}^{N-1} f(n\,\Delta t)e^{-j2\pi mn\,\Delta\omega\,\Delta t} \qquad \text{(Eq. 10)}$$

where Δt is the time interval between data points, $f(n\,\Delta t)$ is the measured value of the data point, ω is the frequency in Hertz, N is the number of data points, and m and n are integers denoting the multiple discrete time and frequency values.

The computations were performed on the Fourier analyzer using a data block size of 256 channels. The Fourier transform of the *in vivo* data was taken using data points at 2-hr intervals for up to 96 hr. *In vitro* data points were spaced 5 min apart for up to 1280 min. The transfer function, $G(s)_{DB,r}$ [more accurately symbolized as $G(\omega)_{DB,r}$] was obtained for Tablet C data by complex division in the frequency domain as the ratio $Q_B(\omega)_c/Q_D(\omega)_c$. Fourier-transformed *in vitro* data for any particular tablet was then multiplied by the transfer function, $G(\omega)_{DB,c}$, to obtain the Fourier transform of the *in vivo* plasma level curve which was to be computationally predicted for that tablet. The result was then multiplied by a scale factor which appropriately adjusted the gain of the transfer function as needed in accordance with the actual assayed amount of drug contained in the tablet(s). The inverse Fourier transform of this result then provided the computational prediction of the *in vivo* plasma drug level *versus* time profiles for the dosage form.

The scale factor (*SF*) for dose treatments with Tablet A was 9.88 mg/8.9 mg = 1.02; for Tablet D, the *SF* was 9.40 mg/8.94 mg = 1.05; for Tablet B, the *SF* was 23.9 mg/8.94 mg = 2.67. The *SF* values are calculated using reported assay results (11) for drug content in the tablets rather than with nominal values. The *SF* values are needed to normalize the transfer function first to unit, 1-mg, doses of the drug and then to adjust the magnitude of each $Q(t)_{D,i}$ to correspond to the actual amount of drug input to the system.

The computational steps followed to convert *in vitro* drug dissolution curves into their corresponding plasma level curves are summarized in Scheme I.

$$\text{Step 1: } Q_B(t)_r \xrightarrow{\text{FT}} Q_B(\omega)_r$$

$$\text{Step 2: } Q_D(t)_r \xrightarrow{\text{FT}} Q_D(\omega)_r$$

$$\text{Step 3: } Q_D(t)_i \xrightarrow{\text{FT}} Q_D(\omega)_i$$

$$\text{Step 4: } Q_B(\omega)_i = \frac{Q_B(\omega)_r}{Q_D(\omega)_r} Q_D(\omega)_i SF = G_{DB}(\omega)Q(\omega)_i SF$$

$$\text{Step 5: } Q_B(\omega)_i \xrightarrow{\text{IFT}} Q_B(t)_i$$

Scheme I—Summary of stepwise computational procedure implemented on a Fourier analyzer to obtain the conversion of in vitro *drug product dissolution curves into* in vivo *plasma level curves. The subscript* r *corresponds to the reference dosage form from which the transfer function is obtained. FT and IFT refer to Fourier and inverse Fourier transformations, respectively.* $Q_B(t)_i$ *and* $Q_D(t)_i$ *symbolize biological response and dissolution profiles for an* ith *dosage form, and* $Q_B(\omega)_i$ *and* $Q_D(\omega)_i$ *refer to their Fourier transforms.*

[1] Hewlett-Packard 5451B, Santa Clara, Calif.
[2] Coumadin sodium, 5 mg, Endo Laboratories.
[3] Coumadin sodium, 25 mg, Endo Laboratories.
[4] Athrombin-K, 5 mg, Purdue Frederick.
[5] Panwarfin sodium, 5 mg, Abbott Laboratories.

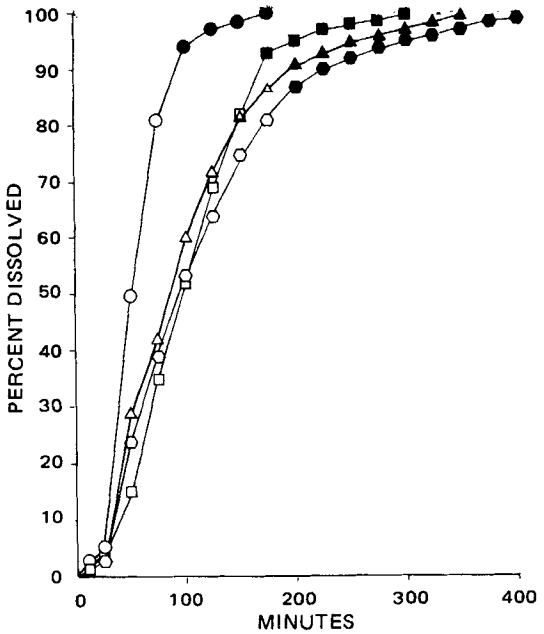

Figure 1—In vitro *dissolution curves plotted as percent warfarin dissolved for Tablets A (○), B (□), C (△), and D (○). Extrapolated values (●, ■, ▲, and ●), indicated on the latter part of the curves, resulted from fitting the earlier observed points to the equation* $Q_D(t)_c = 100(1 - e^{-kt})$, *where* $Q_D(t)_c$ *is the percent drug dissolved and K is a constant.*

RESULTS

Exponential Curve Fitting to *In Vitro* and *In Vivo* Data—Figure 1 presents the linear least-squares fits of the *in vitro* dissolution data results reported by Wagner *et al.* (11) to curves described by the equation $Q_D(t)_\infty = 100(1 - e^{-kt})$. The early observed data points on the time curve, indicated by the open symbols, were used to obtain a least-squares value for the apparent first-order dissolution rate constant, k, by fitting them to a linearized form of the equation given by $\log_e[1 - Q_D(t)_\infty/100] - kt$, where $Q_D(t)$ is the percent of the drug dissolved at any time, t. Linear correlation coefficients for comparisons of data points computed from the fitted equation with corresponding observed values were 0.96, 0.95, 0.98, and 0.99 for Tablets A, B, C, and D, respectively. Therefore, the assumed first-order dissolution of the tablets described by the fitted equations was satisfactory and could be used to estimate data points extrapolatively for dissolution curves beyond the times at which the dissolution tests were prematurely terminated. The solid symbols in Fig. 1 represent such values estimated with the use of the fitted equations.

The curve in Fig. 2 is a plot of the least-squares multiexponential fit obtained to the *in vivo* plasma level data observed for Tablet C. The data

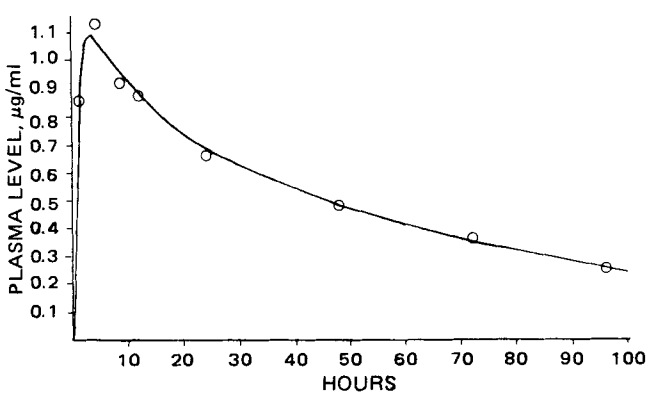

Figure 2—*Time variation of averaged plasma warfarin levels observed following dosing of 12 human subjects with two 5-mg tablets (Tablet C). The convolution of this curve with the* in vitro *dissolution profile shown in Fig. 1 for Tablet C provided the weighting function,* $G_{DB}(t)_c$ *(shown in Fig. 3), used for the computational prediction of plasma curves from* in vitro *data.*

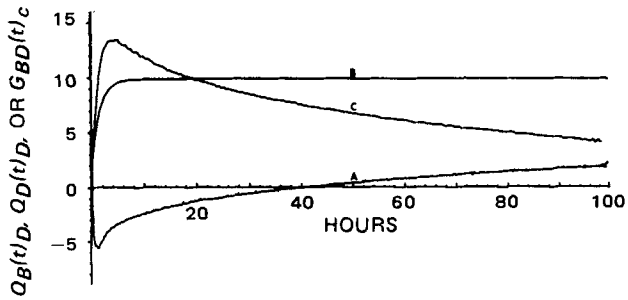

Figure 3—*Computer-constructed time curves exemplifying the functions used to predict* in vivo *plasma curves computationally from* in vitro *dissolution data for Tablet D. Curve A represents the weighting function,* $G_{BD}(t)_c$, *derived from the deconvolution of the* in vitro *dissolution profile,* $Q_D(t)_c$ *(percent dissolved), with the observed* in vivo *plasma curve,* $Q_B(t)_c$ *(micrograms per milliliter), for the reference dosage form, C.* $G_{BD}(t)_c$ *was convolved with the* in vitro *dissolution profile,* $Q_D(t)_D$ *(curve B, with the ordinate* $\times 10^{-1}$*), to obtain the computationally predicted plasma curve,* $Q_B(t)_D$ *(curve C, with the ordinate* $\times 10^{-1}$*).*

were abstracted from Wagner *et al.* (11). The equation for the curve is given by:

$$Q_B(t)_c = 0.91e^{-0.0133t} + 0.36e^{-0.1200t} - 1.27e^{-1.261t} \quad \text{(Eq. 11)}$$

The sum of squares of deviations from the fitted curve is 0.04917. The curve provides a satisfactory representation of the observed data points.

Comparisons of Computed and Observed Plasma Curves—As already discussed, the Fourier transforms of the curve in Fig. 2 and the dissolution curve for Tablet C in Fig. 1 were deconvolved to provide the transfer function, $G_{DB}(\omega)_c$. A computer-constructed plot of the resulting inverse Fourier transform of $G_{DB}(\omega)_c$, *i.e.*, the weighting function $G_{DB}(t)_c$, is presented in Fig. 3. Mathematically, a weighting function is usually defined as the transient time response of a system to an impulse, *i.e.*, Dirac delta function (21) input. However, as a consequence of defining the cumulative warfarin dissolution profiles, $Q_D(t)_i$ [rather than using rates of dissolution, $\dot{Q}_D(t)_i$] as the inputs into the hypothetical linear system that converts *in vitro* data into *in vivo* plasma curves, the weighting function in this case is the derivative of the impulse response, *i.e.*, the doublet response (21). This fact accounts for its values being negative and lying in the fourth quadrant.

The cumulative drug dissolution profiles were chosen as the input function in order to use data for the predictive computations that were as close to those that were experimentally observed as possible. Exemplary results for Tablet D are also shown in Fig. 3, which presents a comparison of the forms of $G_{DB}(t)_c$ with $Q_D(t)_D$ (curve B) with which it is convolved to obtain the computationally predicted plasma curve, $Q_B(t)_D$, for Tablet D (curve C).

The transfer function, $G_{DB}(\omega)_c$, was consistently employed (Scheme I) to obtain the computationally predicted *in vivo* plasma curves for Tablet A (10-mg), D (10-mg), and B (25-mg) dose treatments shown in Figs. 4, 5, and 6, respectively. The computed plasma curves can be directly

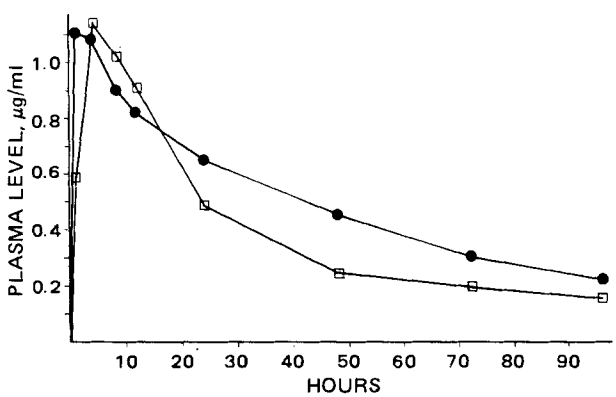

Figure 4—*Comparison of a computationally predicted (□) plasma warfarin curve for Tablet A (two 5 mg), calculated from the results of* in vitro *drug dissolution testing, with the average plasma curve (●) observed in an* in vivo *study of 12 human subjects (11).*

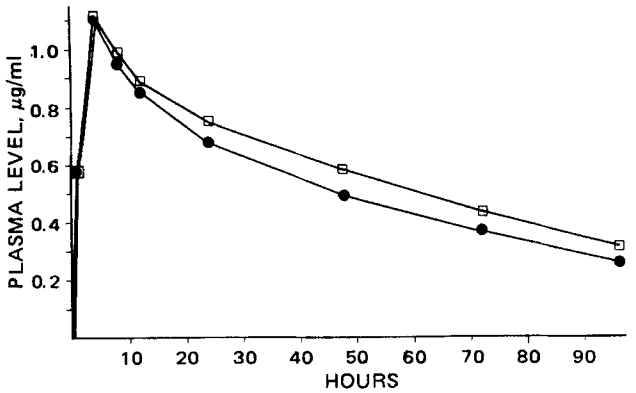

Figure 5—*Comparison of a computationally predicted* (□) *plasma warfarin curve for Tablet D (two 5 mg), calculated from the results of* in vitro *dissolution testing, with the average plasma curve* (●) *observed in an* in vivo *study of 12 human subjects (11).*

compared to the *in vivo* observed average curves, which are in each case plotted on the same coordinates.

Figure 6 contains an additional curve resulting from a correction of the computed curve for the incomplete absorption of only 84% of the administered dose. The corrected curve more closely resembles the observed data points. Without the *a priori* knowledge that the extent of warfarin bioavailability from Tablet B is only 84% of that obtained from Tablet C, the computed plasma curve obviously overestimates the *in vivo* drug absorption efficiency of Tablet B. In each case, as shown in Figs. 4–6, the points plotted on the predicted plasma curves were computed from the results of the convolutions at the same time at which blood sampling was performed *in vivo*; this procedure allowed a direct comparison of each computationally predicted point with its *in vivo* observed counterpart.

The results of plotting each observed plasma level data point as a function of its *in vitro*, computationally predicted, counterpart are shown in Fig. 7. The straight line in Fig. 7 is drawn through the origin with a slope of unity. If the data were exact and the correspondence between the *in vivo* and *in vitro* predicted data points was perfect, all points plotted in Fig. 7 would obviously fall exactly on this line. The largest discrepancies are seen at the upper end of the line for Tablet B for which *in vitro* predicted data points left uncorrected for incomplete *in vivo* absorption were used in constructing the plot.

The relatively excellent linear correlations of the *in vitro* predicted and *in vivo* observed data seen in Fig. 7 can be contrasted to the comparatively poor linear relationship seen between the *in vitro* and *in vivo* data plotted in Fig. 8. In this case, the *in vivo* plasma levels observed for each dosage form were merely plotted as a function of the corresponding rates of percent dissolved *in vitro* [*i.e.*, $\dot{Q}_D(t)_{\%,i}$] occurring at times ap-

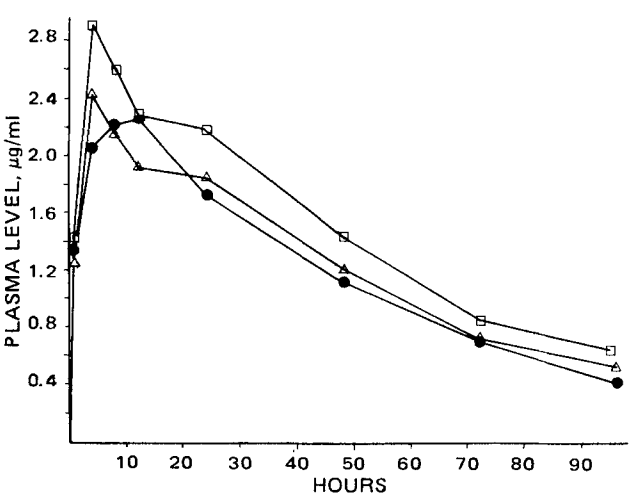

Figure 6—*Comparisons of computationally predicted* [*uncorrected* (□) *and corrected* (△) *for an incomplete, 84%,* in vivo *absorption*] *plasma warfarin curves for Tablet B (one 25 mg), calculated from the results of* in vitro *drug dissolution testing, with the average plasma curve* (●) *observed in an* in vivo *study of six human subjects (11).*

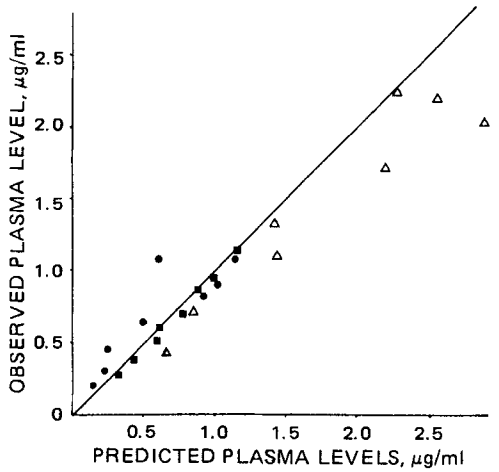

Figure 7—*Linear plot comparison of computationally predicted plasma warfarin levels for Tablets A (two 5 mg,* ●), *B (one 25 mg,* △), *and D (two 5 mg,* ■) *with plasma levels observed at corresponding times in an* in vivo *study (11). The computations were made using data from the same panel of 12 subjects used to study Tablets A and D; data for B were obtained in another study with six human volunteers.*

propriately scaled to correspond to the *in vivo* plasma curves. The scale factor of $\frac{1}{15}$ aligns the *in vitro* and *in vivo* curves on the time axis and is based on the relative times for dissolution to be virtually completed as compared to the return of plasma drug levels to zero; the relative time scales involved can be seen in Fig. 3 for the plot of $Q_D(t)_D$ and $Q_B(t)_D$, respectively.

The $Q_D(t)_i$ values at each time corresponding to an observed plasma level were calculated using the derivative of the equations providing the linear least-squares fits to the *in vitro* drug dissolution profiles shown in Fig. 1; *i.e.*, the values were obtained from $Q_D(t)_{\%,i} = 100k_i e^{-k_i t/15}$, where k_i is the least-squares, apparent dissolution rate constant for the ith dosage form. As was the case in Fig. 7, the straight line in Fig. 8 is again drawn through the origin with a slope of unity. The systematic deviations of the points from this line are quite apparent.

The linear correlations of *in vitro* predicted to *in vivo* observed plasma levels shown in Fig. 6 are summarily described in Table I. The Pearson, r, linear regression coefficients indicate that the calculated plasma level curves are highly correlated with the actual *in vivo* observed plasma levels. A perfect correspondence between computed and observed plasma levels would provide least-squares values of 1.00 for the slopes, zero for the intercepts, and 1.00 for the linear regression coefficients. The ratios of the areas under the calculated and observed plasma curves are also

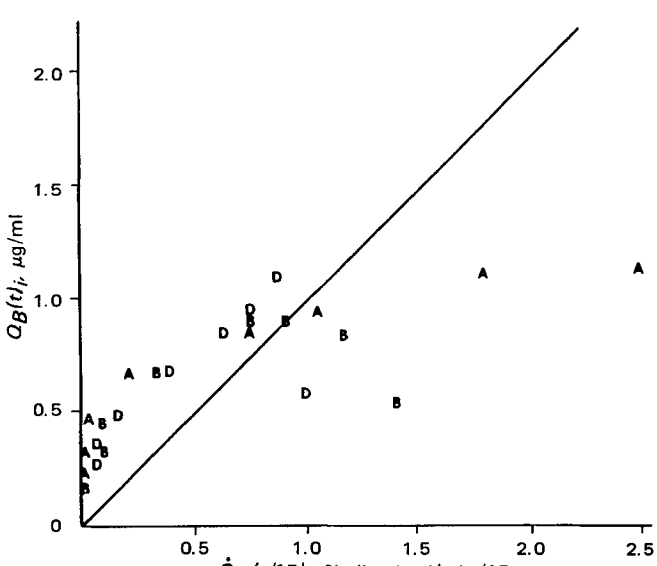

Figure 8—*Linear plot comparison of* in vitro *dissolution rates,* $Q_D(t/15)_i$, *for Tablets A (two 5 mg), D (two 5 mg), and B (one 25 mg) to corresponding* in vivo *observed plasma levels,* $Q_B(t)_i$. *(See text.)*

Table I—Results of Comparisons of Plasma Warfarin Levels for Different Dose Treatments, which were Computationally Predicted from *In Vitro* Dissolution Data with Corresponding *In Vivo* Observed Plasma Levels

Dose Treatment	Statistical Parameters[a]				
	a^a	b^a	r^b	p^b	Computed AUC^c / Observed AUC
Tablet A (10 mg)	0.74	0.26	0.85	0.01	0.79
Tablet D (10 mg)	1.04	−0.08	0.99	0.001	1.11
Tablet B (25 mg)	0.80	0.05	0.95	0.001	1.23
Tablet B (25 mg) X 0.84	0.96	0.03	0.95	0.001	1.04

[a] Linear regression line of best fit: $y = ax + b$. [b] Pearson r, the linear least-squares regression coefficient, and its probability level, p, for the computationally predicted *in vivo* plasma levels compared to corresponding observed *in vivo* plasma levels. [c] Ratios of the areas under the *in vivo* curves (AUC) from 0 to 90 hr for the computed and actual plasma levels.

listed in Table I to provide an indication of the fidelity with which the computations can predict the extent of drug bioavailability from the tablets.

DISCUSSION

A comparison of the two types of linear correlations (Figs. 7 and 8) of *in vitro* data derived from dissolution testing with *in vivo* plasma levels clearly justifies the added computational effort required to obtain computationally predicted plasma curves in assessing the bioavailability behavior of drug dosage forms from *in vitro* studies. Figure 8 was constructed using *in vitro* dissolution rates that proceed through a maximum and decay with time in a manner analogous to plasma level curves, which they obviously resemble much more than cumulative amount *versus* time curves; the latter proceed to a plateau at 100% dissolved. Because of their at least superficial resemblance to plasma curves, dissolution rates rather than extents were chosen for the correlations to make them appear as good as possible and comparable to those in Fig. 7.

As expected, and as confirmed by Fig. 8, multiple-point correlations of dissolution rates with plasma levels are obviously nonlinear. This is the case even when the dissolution rates are properly time scaled. Therefore, the direct use of *in vitro* dissolution data provide, at least in the present case for warfarin, a poor predictor of *in vivo* drug product performance. In contrast, the use of *in vitro* predicted plasma levels obtained by the computational conversion of observed *in vitro* dissolution data provides a theoretically rational, meaningful, and more reliable means of judging the *in vivo* behavior of drug products from the results of *in vitro* dissolution testing. However, the limitations of even this method, as exemplified by the discrepancies in Table I, must be kept in mind.

Deviations of predicted from observed *in vivo* results can be attributed to violations of any or all of the assumptions on which the linear systems treatment of the data is based. Unfortunately, linear systems theory provides the only generally applicable means of converting *in vitro* dissolution profiles into predicted *in vivo* drug response profiles. Any attempts to improve the relationships through the use of nonlinear modeling approaches require some knowledge of the specific mechanisms operating in any given case to produce the observed or suspected nonlinear systems behavior. Such information is commonly unavailable. If it were available, its applicability to any particular drug formulation might not be known *a priori*; consequently, its usefulness in predicting *in vivo* bioavailability behavior would be vitiated. Therefore, despite its shortcomings, the presently implemented linear systems method of computationally predicting *in vivo* drug performance represents the best, generally applicable, approach to converting *in vitro* data into *in vivo* drug response profiles that is likely to be devised.

Considering the many assumptions involved in the linear systems, transfer function, approach applied in this study, the predictions obtained are quite good and generally fall close to the observed *in vivo* data. The results (Figs. 4–6) are quite successful in predicting two out of three of the plasma level curves for the drug from *in vitro* dissolution profiles. Direct comparisons of the data points obtained from computationally predicted plasma profiles with their corresponding experimentally observed *in vivo* plasma curves in all cases provided linear correlation probabilities of $p \geq 0.01$ or 0.001 (Table I), indicating that the shapes of the computed and *in vivo* plasma curves over time were nearly the same.

As expected, however, differences in the extent of *in vivo* bioavailability cannot always be predicted, as was the case for Tablet B. This treatment, relative to the others, was only 84% bioavailable, even though its dissolution *versus* time profile was well within the range reported for the other tablets. This particular discrepancy may at least in part be attributable to the *in vivo* data for Tablet B having been obtained from a separate study involving a panel of six subjects whereas the other *in vivo* data came from a different panel of 12 subjects. Treatment B also consisted of a single 25-mg tablet as opposed to the other dose treatments being comprised of 10-mg doses (two 5-mg tablets). In any event, results obtained for Tablet B exemplify a limitation of all *in vitro* dissolution testing in being incapable of predicting exceptions to previously observed correlations. Although this limitation may be minimized by judiciously selecting the design of the dissolution apparatus and systematically optimizing the process conditions of the dissolution testing (3), it cannot be always entirely eliminated.

As demonstrated by the results of the present study, the *in vitro* computational predictions of *in vivo* bioavailability may be expected to have the greatest fidelity for dosage formulations that are the most similar to the reference dosage form from which the transfer function is obtained. Therefore, for dosage formulations with the same nominal dose content and of qualitatively equal composition, predictions of the *in vivo* drug response profile for the same panel of subjects from which the *in vivo* data for the reference dosage form were obtained can probably be made with an often acceptable degree of fidelity. This would particularly be the case in quality control testing for *in vivo* significance of batch-to-batch variations. Obviously, in all cases, consistency in the process variables of the test, such as the geometry of the apparatus, the dissolution medium composition, and agitation, must be maintained. Ideally, dissolution testing should be performed with a flexible method using process variables that have been systematically optimized to provide directly drug dissolution profiles that are predictive, within predetermined confidence levels, of *in vivo* drug response profiles (3). A new control engineering approach to accomplish such systematic optimization of drug dissolution testing methodologies was described previously (3).

Although optimized dissolution testing methods are always to be preferred, the predictive estimates of *in vivo* drug product performance obtained by the methods and apparatus commonly used (20) may conceivably be improved and expanded through the incorporation of data from an increasing number of dosage formulations into the transfer function as such additional data become available. For this purpose, the *in vitro* data must always be obtained using the same dissolution test conditions; however, *in vivo* data would generally be obtained with different panels of human subjects. The simplest approach would be to combine transfer functions obtained for different drug formulations into an average.

For example, in the present case, an average transfer function obtained for Tablets A, C, and D, *i.e.*, $\overline{G}_{DB}(s)_{A,C,D}$, would likely improve the prediction of plasma level curves for other dose treatments resembling A, C, and D. However, each individual, $G_{DB}(s)_i$, transfer function could not be expected to produce predictions with equal fidelity. Therefore, it is reasonable to weight the contribution of each individual transfer function on the basis of its predictive capability. Such a weighted average transfer function for different formulations could be defined by Eq. 12:

$$\overline{G}_{DB}(s) = \sum_{i=1}^{N} W_i G_{DB}(s)_i \qquad \text{(Eq. 12)}$$

where $W_i (\Sigma_{i=i}^{N} W_i = 1)$ represents the weight factors for the transfer functions derived from data observed for each ith drug formulation.

A weighting scheme that might be used to obtain W_i values could be based on the ability of the ith transfer function to predict the plasma curves observed for the other $N - 1$ dosage forms contributing to the average, as expressed by:

$$W_i = \frac{\sum_{J=1 \neq i}^{N-1} \sum_{q=1}^{K} (P_{\text{pred}} - P_{\text{obs}})_q^{-2}}{\sum_{i=1}^{N} \sum_{J=1 \neq i}^{N-1} \sum_{q=1}^{K} (P_{\text{pred}} - P_{\text{obs}})_q^{-2}} \qquad \text{(Eq. 13)}$$

where P_{pred} and P_{obs} represent computationally predicted and observed data points corresponding to the qth sampling time, respectively; and K is the total number of data points sampled for the ith dosage form. The W_i defined by Eq. 13 emphasizes the predictive capability of each $G_{DB}(s)_i$. Weighting for variability of the *in vivo* data for each dosage form contributing to the average transfer function is attenuated by the predictive capability of the transfer function and is, therefore, implicit in

the value of each W_i. By using this scheme or some alternative one, transfer functions for predicting *in vivo* temporal drug response behavior could be continuously updated as new data from additional dosage forms become available.

SUMMARY AND CONCLUSIONS

Single-point correlations of *in vitro* drug dissolution behavior with *in vivo* bioavailability results for different drug dosage forms do not take advantage of all of the observed data and can have serious shortcomings with regard to their significance and interpretation. Therefore, a mathematical, linear systems, approach to computationally predicting *in vivo* drug response *versus* time curves [such as plasma levels, pharmacological responses (22), and urinary recovery rates] from observed *in vitro* drug product dissolution time curves was developed and exemplified with data for four different dosage forms of warfarin (11).

Despite the linearity assumption implicit in the use of the approach, the method was verified by the surprisingly good computational predictions of *in vivo* plasma curves, which were produced for two of the dosage forms (A and D). The discrepancy observed for a third dosage form was in part attributed to the *in vivo* data being obtained on a different panel of human subjects and to the administered dosage being 0.84 times that of the others. This result exemplified the general inability of *in vitro* testing to predict differences in extents of bioavailability that are likely attributable to specific biological mechanisms whose operation was relatively insignificant or absent in contributing to the bioavailability behavior of other dosage forms for which relatively accurate predictions or correlations are observed.

Systematically optimized *in vitro* dissolution testing conditions based on the ability of the test to predict *in vivo* drug response behavior (3) are recommended whenever practical. Alternatively, an approach to continuously upgrading the reliability and applicability of the transfer function used to predict *in vivo* drug product response curves computationally from the results of commonly employed testing methodologies is suggested. However, the usefulness of the described approach remains to be demonstrated in actual practice.

APPENDIX: ANALOG COMPUTER METHOD FOR CONVOLUTION AND DECONVOLUTION

The operations of deconvolution (Eq. 6) and convolution (Eq. 7) can be performed with an analog computer. Although curve fitting can also be done with an analog computer, it can most readily be accomplished with a digital computer using programs such as MULTIFIT (19), MBDX-85, or PLTEST (17) to obtain a multiexponential fit of observed *in vitro* data points to:

$$Q_D(t)_r = \sum_{1=i}^{n} A_i e^{-m_i t} \qquad \text{(Eq. A1)}$$

The A_i and m_i equation parameters are then used to set the potentiometers in an analog computer circuit, which is appropriate for performing deconvolution. An analog electrical signal representing the $G_B(t)_r$ function, against which $Q_D(t)_r$ is to be deconvolved to obtain $G_{DB}(t)_r$, can be produced using a variable diode function generator. Alternatively, $G_{DB}(t)$ can be obtained directly on a digital computer using the PLTEST program (17, 23). The PLTEST program, as developed in this laboratory, is recommended because it will accept properly interpolated $Q_D(t)_r$ and $Q_B(t)_r$ observed data and perform their deconvolution to provide $Q_{DB}(t)_r$ in the form of a multiexponential expression, which it derives from curve fitting a Bode diagram generated by the program.

The analog computer approach for performing convolution described here can be modified to accomplish deconvolution, as will be shown later. However, convolution is required to obtain $Q_B(t)_i$ by convolving $Q_D(t)_i$ against $G_{DB}(t)_r$, which has been fitted with a sum of exponentials expression. The approach is developed for biexponential fits to $G_{DB}(t)_r$ [*i.e.*, $G_{DB}(t)_r = A_i e^{-m_i t} + A_2 e^{-m_2 t}$]. A similar derivation for third- or higher order systems does not involve any new principles.

For a second-order system, the ratio of biological plasma level output to *in vitro* dissolution input is given in the Laplace domain by Eqs. A2–A4 for an ith dosage form:

$$\frac{Q_B(s)_i}{Q_D(s)_i} = G_{DB}(s)_r \qquad \text{(Eq. A2)}$$

$$\frac{Q_B(s)_i}{Q_D(s)_i} = \frac{A_1}{m_1 + s} + \frac{A_2}{m_2 + s} \qquad \text{(Eq. A3)}$$

$$\frac{Q_B(s)_i}{Q_D(s)_i} = \frac{A_1 m_1 + A_2 m_2 + (A_1 + A_2)s}{s^2 + (m_1 + m_2)s + (m_1 m_2)} \qquad \text{(Eq. A4)}$$

Dividing the numerator and denominator by s^2 and substituting $\alpha = A_1 m_1 + A_2 m_2$ into Eq. A4 yield:

$$\frac{Q_B(s)_i}{Q_D(s)_i} = \frac{(A_1 + A_2)s^{-1} + \alpha s^{-2}}{1 + (m_1 + m_2)s^{-1} + (m_1 m_2)s^{-2}} \qquad \text{(Eq. A5)}$$

A variable, $R(s)$, is now defined by Eqs. A6 and A7:

$$R(s) = \frac{Q_D(s)_i}{1 + (m_1 + m_2)s^{-1} + (m_1 m_2)s^{-2}} \qquad \text{(Eq. A6)}$$

$$R(s) = \frac{Q_B(s)}{(A_1 + A_2)s^{-1} + \alpha s^{-2}} \qquad \text{(Eq. A7)}$$

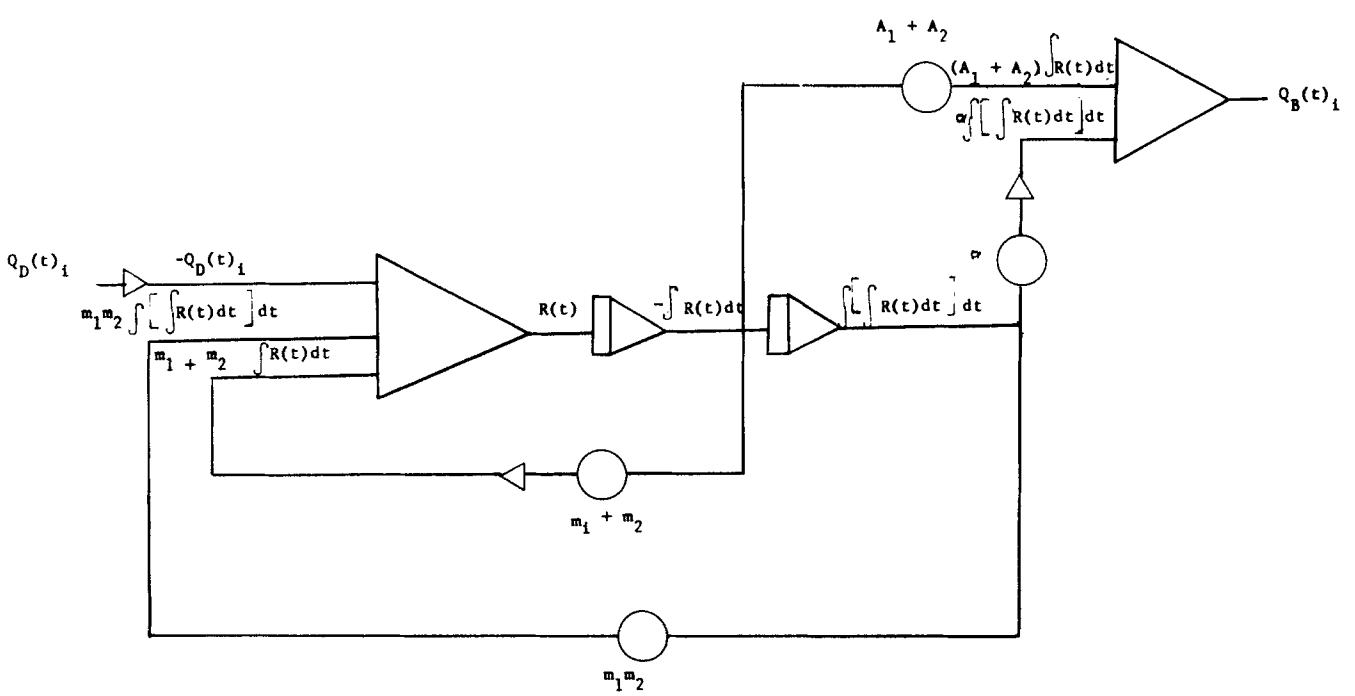

Figure 9—*Circuit diagram showing solution of Eq. A11 to give* $Q_B(t)$, *using* R(t) *and its integrals.*

Equations A6 and A7 are rearranged to yield Eqs. A8 and A10 in the Laplace domain and Eqs. A9 and A11 in the time domain:

$$R(s) = Q_D(s)_i - (m_1 + m_2)s^{-1}R(s) - (m_1m_2)s^{-2}R(s) \quad \text{(Eq. A8)}$$

$$R(t) = Q_D(t)_i - (m_1 + m_2)\int R(t)\,dt - m_1m_2\int [\int R(t)\,dt]\,dt \quad \text{(Eq. A9)}$$

$$Q_B(s)_i = (A_1 + A_2)s^{-1}R(s) + \alpha s^{-2}R(s) \quad \text{(Eq. A10)}$$

$$Q_B(t)_i = (A_1 + A_2)\int R(t) + \alpha\int [\int R(t)\,dt]\,dt \quad \text{(Eq. A11)}$$

Equation A9 is solved on the analog computer to give $R(t)$; Eq. A11 is then solved to give $Q_B(t)$ using $R(t)$ and its integrals as shown by the circuit diagram in Fig. 9.

A similar approach can be applied to solve for input functions by rearranging Eqs. A6 and A7 to give $R(s)$ and the input function and solving these on the analog computer. Therefore, both convolution and deconvolution can be performed by this general approach which, when modified in this manner, can also be used to deconvolve $Q_D(t)_r$ against $Q_B(t)_r$ to obtain $G_{DB}(t)_r$.

REFERENCES

(1) S. A. Kaplan, in "Dissolution Technology," L. F. Leeson and J. T. Carstensen, Eds., APhA Academy of Pharmaceutical Sciences, Washington, D.C., 1974, pp. 163–187.

(2) V. F. Smolen, P. B. Kuehn, and E. J. Williams, *Drug Develop. Commun.*, **2**, 143 (1975).

(3) V. F. Smolen and W. A. Weigand, *J. Pharm. Sci.*, **65**, 1718 (1976).

(4) V. F. Smolen, *ibid.*, **60**, 878 (1971).

(5) V. F. Smolen, *Hosp. Pharm.*, **4**, 14 (1969).

(6) W. Brownell, S. Riegelman, and W. J. Mader, "Committee Report on Drug Dissolution Methodology," APhA Academy of Pharmaceutical Sciences, Washington, D.C., 1968.

(7) G. Levy and L. E. Hollister, *J. Pharm. Sci.*, **58**, 1368 (1969).

(8) G. Levy, *ibid.*, **52**, 1039 (1963).

(9) M. Gibaldi and H. Weintraub, *ibid.*, **58**, 1368 (1969).

(10) H. Weintraub and M. Gibaldi, *ibid.*, **59**, 1792 (1970).

(11) J. G. Wagner, P. G. Welling, P. L. Kwang, and I. E. Walker, *ibid.*, **60**, 666 (1971).

(12) W. A. Cressman, C. A. Janicki, P. C. Johnson, J. T. Doluisio, and G. A. Braun, *ibid.*, **58**, 1516 (1969).

(13) V. F. Smolen, *J. Pharmacokinet. Biopharm.*, **4**, 337 (1976).

(14) *Ibid.*, **4**, 355 (1976).

(15) D. S. Riggs, "Control Theory and Physiological Feedback Mechanisms," Williams & Wilkins, Baltimore, Md., 1970, pp. 23–26.

(16) *Ibid.*, pp. 91–97.

(17) E. R. Rodeman and J. T. P. Yao, "Structural Identification—Literature Review," NSF Technical Report Ce-STR-73-3, School of Civil Engineering, Purdue University, West Lafayette, Ind., 1973.

(18) C. D. McGillem and G. R. Cooper, "Continuous and Discrete Signal and System Analysis," preliminary ed., School of Electrical Engineering, Purdue University, West Lafayette, Ind., 1971, pp. 6–1 ff.

(19) R. D. Schoenwald, Ph.D. thesis, Purdue University, West Lafayette, Ind., 1971, p. 313.

(20) M. Pernarowski, in "Dissolution Technology," L. F. Leeson and J. T. Carstensen, Eds., APhA, Academy of Pharmaceutical Sciences, Washington, D.C., 1974, pp. 58–105.

(21) C. D. McGillem and G. R. Cooper, "Continuous and Discrete Signal and System Analysis," preliminary ed., School of Electrical Engineering, Purdue University, West Lafayette, Ind., 1971, pp. 3–43 ff.

(22) V. F. Smolen, E. J. Williams, and P. B. Kuehn, *Can. J. Pharm. Sci.*, **10**, 95 (1975).

(23) P. B. Kuehn, Ph.D. thesis, Purdue University, West Lafayette, Ind., 1974.

ACKNOWLEDGMENTS AND ADDRESSES

Received March 12, 1976, from the *Interdisciplinary Drug Engineering and Assessment Laboratory and the Department of Industrial and Physical Pharmacy, School of Pharmacy and Pharmacal Sciences, Purdue University, West Lafayette, IN 47907.*

Accepted for publication May 4, 1976.

[x] To whom inquiries should be directed.

Pattern Recognition II: Investigation of Structure–Activity Relationships

GOVIND K. MENON and ARTHUR CAMMARATA [x]

Abstract □ A simple form of pattern recognition is successfully used to classify a set of structurally diverse therapeutic agents. By using only organic structural information, the major pharmacological classes present were correctly identified and the pharmacologically unrelated compounds were separated out. One technique of factor analysis—principal component analysis—is shown to be readily adaptable in preprocessing the data. Simple graphical representation of the results enables their direct interpretation.

Keyphrases □ Structure–activity relationships—determined using pattern recognition methods of analysis, various drugs □ Pattern recognition—analysis methods used to determine therapeutic classes of various drugs □ Factor analysis techniques—used to determine therapeutic classes of various drugs

The application of pattern recognition methods in solving chemical problems has provided the incentive for considerable research within the past few years (1–6). Recently, these methods have been applied in the development of new biological agents due to their capacity to analyze rapidly large stores of accumulated information and to detect substances worthy of further investigation (7–10). In other words, the techniques can be directed toward establishing structural specificity in biological action, providing rationales in selecting substances for biological assay, and identifying pharmacophoric patterns of molecular substitution (1).

Several detailed accounts describe the various pattern recognition techniques (11–14), but a brief conceptual summary follows. Pattern recognition involves the detection and recognition of regularities or invariant properties among accumulated (often large) sets of measurements, the purpose being to provide a basis for new hypotheses. For example, consider an attempt to derive a

Equations A6 and A7 are rearranged to yield Eqs. A8 and A10 in the Laplace domain and Eqs. A9 and A11 in the time domain:

$$R(s) = Q_D(s)_i - (m_1 + m_2)s^{-1}R(s) - (m_1m_2)s^{-2}R(s) \quad \text{(Eq. A8)}$$

$$R(t) = Q_D(t)_i - (m_1 + m_2)\int R(t)\,dt - m_1m_2\int [\int R(t)\,dt]\,dt \quad \text{(Eq. A9)}$$

$$Q_B(s)_i = (A_1 + A_2)s^{-1}R(s) + \alpha s^{-2}R(s) \quad \text{(Eq. A10)}$$

$$Q_B(t)_i = (A_1 + A_2)\int R(t) + \alpha\int [\int R(t)\,dt]\,dt \quad \text{(Eq. A11)}$$

Equation A9 is solved on the analog computer to give $R(t)$; Eq. A11 is then solved to give $Q_B(t)$ using $R(t)$ and its integrals as shown by the circuit diagram in Fig. 9.

A similar approach can be applied to solve for input functions by rearranging Eqs. A6 and A7 to give $R(s)$ and the input function and solving these on the analog computer. Therefore, both convolution and deconvolution can be performed by this general approach which, when modified in this manner, can also be used to deconvolve $Q_D(t)_r$ against $Q_B(t)_r$ to obtain $G_{DB}(t)_r$.

REFERENCES

(1) S. A. Kaplan, in "Dissolution Technology," L. F. Leeson and J. T. Carstensen, Eds., APhA Academy of Pharmaceutical Sciences, Washington, D.C., 1974, pp. 163–187.

(2) V. F. Smolen, P. B. Kuehn, and E. J. Williams, *Drug Develop. Commun.*, **2**, 143 (1975).

(3) V. F. Smolen and W. A. Weigand, *J. Pharm. Sci.*, **65**, 1718 (1976).

(4) V. F. Smolen, *ibid.*, **60**, 878 (1971).

(5) V. F. Smolen, *Hosp. Pharm.*, **4**, 14 (1969).

(6) W. Brownell, S. Riegelman, and W. J. Mader, "Committee Report on Drug Dissolution Methodology," APhA Academy of Pharmaceutical Sciences, Washington, D.C., 1968.

(7) G. Levy and L. E. Hollister, *J. Pharm. Sci.*, **58**, 1368 (1969).

(8) G. Levy, *ibid.*, **52**, 1039 (1963).

(9) M. Gibaldi and H. Weintraub, *ibid.*, **58**, 1368 (1969).

(10) H. Weintraub and M. Gibaldi, *ibid.*, **59**, 1792 (1970).

(11) J. G. Wagner, P. G. Welling, P. L. Kwang, and I. E. Walker, *ibid.*, **60**, 666 (1971).

(12) W. A. Cressman, C. A. Janicki, P. C. Johnson, J. T. Doluisio, and G. A. Braun, *ibid.*, **58**, 1516 (1969).

(13) V. F. Smolen, *J. Pharmacokinet. Biopharm.*, **4**, 337 (1976).

(14) *Ibid.*, **4**, 355 (1976).

(15) D. S. Riggs, "Control Theory and Physiological Feedback Mechanisms," Williams & Wilkins, Baltimore, Md., 1970, pp. 23–26.

(16) *Ibid.*, pp. 91–97.

(17) E. R. Rodeman and J. T. P. Yao, "Structural Identification—Literature Review," NSF Technical Report Ce-STR-73-3, School of Civil Engineering, Purdue University, West Lafayette, Ind., 1973.

(18) C. D. McGillem and G. R. Cooper, "Continuous and Discrete Signal and System Analysis," preliminary ed., School of Electrical Engineering, Purdue University, West Lafayette, Ind., 1971, pp. 6–1 ff.

(19) R. D. Schoenwald, Ph.D. thesis, Purdue University, West Lafayette, Ind., 1971, p. 313.

(20) M. Pernarowski, in "Dissolution Technology," L. F. Leeson and J. T. Carstensen, Eds., APhA, Academy of Pharmaceutical Sciences, Washington, D.C., 1974, pp. 58–105.

(21) C. D. McGillem and G. R. Cooper, "Continuous and Discrete Signal and System Analysis," preliminary ed., School of Electrical Engineering, Purdue University, West Lafayette, Ind., 1971, pp. 3–43 ff.

(22) V. F. Smolen, E. J. Williams, and P. B. Kuehn, *Can. J. Pharm. Sci.*, **10**, 95 (1975).

(23) P. B. Kuehn, Ph.D. thesis, Purdue University, West Lafayette, Ind., 1974.

ACKNOWLEDGMENTS AND ADDRESSES

Received March 12, 1976, from the *Interdisciplinary Drug Engineering and Assessment Laboratory and the Department of Industrial and Physical Pharmacy, School of Pharmacy and Pharmacal Sciences, Purdue University, West Lafayette, IN 47907.*

Accepted for publication May 4, 1976.

[x] To whom inquiries should be directed.

Pattern Recognition II: Investigation of Structure–Activity Relationships

GOVIND K. MENON and ARTHUR CAMMARATA [x]

Abstract □ A simple form of pattern recognition is successfully used to classify a set of structurally diverse therapeutic agents. By using only organic structural information, the major pharmacological classes present were correctly identified and the pharmacologically unrelated compounds were separated out. One technique of factor analysis—principal component analysis—is shown to be readily adaptable in preprocessing the data. Simple graphical representation of the results enables their direct interpretation.

Keyphrases □ Structure–activity relationships—determined using pattern recognition methods of analysis, various drugs □ Pattern recognition—analysis methods used to determine therapeutic classes of various drugs □ Factor analysis techniques—used to determine therapeutic classes of various drugs

The application of pattern recognition methods in solving chemical problems has provided the incentive for considerable research within the past few years (1–6). Recently, these methods have been applied in the development of new biological agents due to their capacity to analyze rapidly large stores of accumulated information and to detect substances worthy of further investigation (7–10). In other words, the techniques can be directed toward establishing structural specificity in biological action, providing rationales in selecting substances for biological assay, and identifying pharmacophoric patterns of molecular substitution (1).

Several detailed accounts describe the various pattern recognition techniques (11–14), but a brief conceptual summary follows. Pattern recognition involves the detection and recognition of regularities or invariant properties among accumulated (often large) sets of measurements, the purpose being to provide a basis for new hypotheses. For example, consider an attempt to derive a

structure–activity relationship. If the relationship of structure to activity is to be developed from a basis involving a small number of structurally diverse compounds or from a large number of structurally similar compounds, then a visual examination is often sufficient. However, if a large number of structurally diverse compounds is involved, visual examination of the data to arrive at a structure–activity relationship is cumbersome if not impossible. Pattern recognition methods then can be employed to advantage.

A few reports in the recent literature describe the application of pattern recognition techniques in the investigation of structure–activity relationships (7–10). These have been concerned with two specific areas: classification of sedatives and tranquilizers (7, 9) and prediction of the activity of potential anticancer agents (8, 10). Although these investigations have been fairly successful, criticism (15, 16) has been directed at some studies (10, 17) that employed these methods in deriving structure–activity relationships. Misleading relationships have been shown to result due to the improper choice of compounds in the data set and to inappropriate structural representation. The approach taken in this article attempts to overcome these problems and, with proper researcher–computer interaction, should provide a simple and consistent means of deriving structure–activity relationships.

In a nonvisual approach to establish the structure–activity relationships, representation of molecular structures in numerical terms is necessary. Coding of molecular structures is thus a key step. Most biological effects may be readily measured and coded, and compounds possessing similar activity are readily identified. However, coding of organic structural groups or features is not as simple. In previous reports, augmented atom fragment (8), substructural fragment (18), and heteropath (9) representations were adopted in molecular structural coding. Several disadvantages are inherent in such procedures, however, especially in the identification of structure–activity relationships: (*a*) molecular structural information is lost by considering fragments of molecules independently of each other, (*b*) several such molecular discriminators may have to be specified in the representation of a given compound, (*c*) redundant codings may have to be included to distinguish between different compounds satisfactorily, and (*d*) interpretation of results in terms of structural prototypes is extremely difficult.

One method associated with pattern recognition, factor analysis, is readily applicable to structure–activity studies (19). Weiner and Weiner (19) used the method directly in deriving structure–activity relationships and obtained readily interpretable results. However, factor analysis is also adaptable as the preprocessing step of a pattern recognition procedure, and this approach is taken in this paper.

Briefly, the method requires that one view molecular structures in a manner consistent with the way medicinal chemists have done in proposing candidate compounds. To retain molecular bonding information, all molecular structures of the data set are superposed upon each other *in a chemically consistent manner.* Major discriminating features between the molecules are then identified. These molecular discriminators are coded so as to distinguish between bioisosteric atoms or groups (20). Following such representation, a factor analytical procedure is applied to reduce the dimensionality of the data matrix. Only a few molecular features need to be specified to classify correctly the compounds of the data set into the pharmacologically distinct categories present.

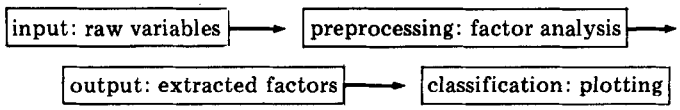

Scheme I

BASIS OF APPROACH

The basic operations of pattern recognition as applied in this work may be represented as shown in Scheme I. Coding of molecular structures comprising the data set leads to their numerical representation in terms of a discrete number of variables (the input). The input data are then operated on, or preprocessed, to reduce the number of variables required to represent the data, *i.e.*, to reduce the dimensionality. The preprocessing method adopted in this work is principal component analysis, which is but one of the several factor analytical methods available (21–25).

Classification of the output from the preprocessing step is performed next. This step may be done by mathematical techniques such as cluster analysis (26, 27) and discriminant analysis (28) or with the aid of "learning machines" (13, 29–31). In this paper, however, classification is done graphically to provide a clearer conceptual understanding and to point out the parallelism that exists between the classical and pattern recognition approaches for deriving structure–activity relationships. Several detailed accounts in the literature describe the theory and application of various factor analysis techniques (22–25), and only a brief discussion is presented in this article.

A set of M molecules comprising a given data set is coded so as to be represented by N molecular groups or features, giving rise to an $M \times N$ data matrix. This matrix is then used to construct an $N \times N$ correlation matrix. This correlation matrix is next operated on by a factor analytical procedure to extract factors, *i.e.*, to reduce the dimensionality. The two most commonly used methods are principal component analysis and common factor analysis. In principal component analysis (22, 23), one seeks to transform the variables of the data set into a linearly independent set of component variables consisting of the original variables. When N molecular features are chosen as independent variables, then N linear combinations are needed to account for all of the variance in the data. However, in some cases, fewer linear combinations (in comparison with the number of variables in the data matrix) suffice to account for a large proportion of the variance within the data. These may then be used to represent the data and, since these linear combinations are defined to be orthogonal to one another, a reduction in dimensionality is achieved.

In common factor analysis, however, the assumption is made that the variables in a data matrix may be influenced to varying degrees by properties common to *all* variables (*common* variance) and by properties unique to only a few variables (*unique* variance). In other words, every variable selected to represent a specific molecular feature is regarded as reflecting a common set of physical attributes for the majority of compounds in the data set and a unique set of physical attributes for others. Identification is sought of those variables that reflect common physical attributes for the majority of compounds in the data set; all other compounds are treated as unique. The method thus holds the promise of providing some insight regarding the mechanisms leading to major and minor pharmacological actions of drugs. Although some advances have been made in the application of common factor analysis to physiological studies such as olfaction (32), principal component analysis is more readily adaptable in the investigation of structure–activity relationships and is the method used here.

THEORY

The basis for a principal component analysis may be placed in perspective by considering an attempt to transform a multiple regression into a simple linear one. In a multiple regression model, one seeks to relate the biological activities, A, for M compounds to N variables, X, in the

Table I—Pharmacological Classification and Therapeutic Use of Compounds Studied

Compound	Drug	Pharmacological Classification	Therapeutic Use
I	Levarterenol	α-Agonist	Antihypotensive, vasoconstrictor
II	Methoxamine	α-Agonist	Antiarrhythmic, antihypotensive
III	Metaraminol	α-Agonist	Antihypotensive
IV	Ethylnorepinephrine	β-Agonist	Bronchodilator
V	Phenylpropanolamine	α-Agonist, CNS stimulant	Nasal decongestant, anorexiant
VI	Amphetamine	CNS stimulant	Antidepressant, minimal brain dysfunction, anorexiant, narcolepsy
VII	Chlorphentermine	CNS stimulant	Anorexiant
VIII	Phentermine	CNS stimulant	Anorexiant
IX	Hydroxyamphetamine	α-Agonist	Antihypotensive
X	Methyldopa	CNS agent	Antihypertensive
XI	Levodopa	CNS agent	Antiparkinsonian
XII	Epinephrine	α,β-Agonist	Antihypotensive, bronchodilator, decongestant, antiarrhythmic
XIII	Methoxyphenamine	β-Agonist	Bronchodilator
XIV	Phenylephrine	α-Agonist	Decongestant, antihypotensive
XV	Ephedrine	α-Agonist, CNS stimulant	Antihypotensive, decongestant, bronchodilator, antiarrhythmic
XVI	Methamphetamine	CNS stimulant	Anorexiant, minimal brain dysfunction, antidepressant, narcolepsy
XVII	Mephentermine	CNS stimulant, α-agonist	Antihypotensive
XVIII	Propylhexedrine	α-Agonist	Nasal decongestant
XIX	Phenmetrazine	CNS stimulant	Anorexiant
XX	Phendimetrazine	CNS stimulant	Anorexiant
XXI	Isoproterenol	β-Agonist	Antiarrhythmic, bronchodilator
XXII	Isoxsuprine	β-Agonist	Peripheral vascular disease
XXIII	Nylidrin	β-Agonist	Peripheral vascular disease
XXIV	Propranolol	β-Antagonist	Antiarrhythmic, antihypertensive
XXV	Benzphetamine	CNS stimulant	Anorexiant
XXVI	Diethylpropion	CNS stimulant	Anorexiant
XXVII	Phenoxybenzamine	α-Antagonist	Peripheral vascular disease, antihypertensive
XXVIII	Acetylcholine	Parasympathomimetic	Miotic
XXIX	Succinylcholine	Myoneural blocker, parasympathomimetic	Muscle relaxant
XXX	Methacholine	Parasympathomimetic	Glaucoma
XXXI	Carbachol	Parasympathomimetic	Glaucoma, miotic
XXXII	Bethanechol	Parasympathomimetic	Intestinal relaxant
XXXIII	Pilocarpine	Parasympathomimetic	Glaucoma
XXXIV	Ambenonium	Anticholinesterase	Myasthenia gravis
XXXV	Edrophonium	Anticholinesterase	Myasthenia gravis
XXXVI	Physostigmine	Anticholinesterase	Glaucoma, myasthenia gravis
XXXVII	Neostigmine	Anticholinesterase	Myasthenia gravis
XXXVIII	Demecarium	Anticholinesterase	Glaucoma
XXXIX	Pyridostigmine	Anticholinesterase	Myasthenia gravis

form of a linear combination:

$$Ai = b_1X_{1i} + b_2X_{2i} + b_3X_{3i} + \ldots + b_NX_{Ni} + \mu \qquad i = 1, 2, \ldots, M \quad \text{(Eq. 1)}$$

However, in evaluating the least-squares estimates of the b coefficients, the values of the coefficients are necessarily a function of the covariance between the independent variables, X, as well as of the covariance between the biological activities and the independent variables. One may thus seek to account for the covariance between X prior to attempting a regression analysis.

In making this attempt, a transformed variable, T, may be defined as a linear combination of the independent variables, X:

$$Ti = m_1X_{1i} + m_2X_{2i} + m_3X_{3i} + \ldots + m_NX_{Ni} \qquad i = 1, 2, \ldots, M \quad \text{(Eq. 2)}$$

This equation is fundamental to all factor analysis procedures (principal component analysis in this case). In the simple case where only three independent variables are involved, Eq. 2 is written as:

$$Ti = m_1X_{1i} + m_2X_{2i} + m_3X_{3i} \qquad i = 1, 2, \ldots, M \quad \text{(Eq. 3)}$$

Squaring both sides of Eq. 3 yields:

$$\sum_i Ti^2 = \sum_i (m_1X_{1i} + m_2X_{2i} + m_3X_{3i})^2 \quad \text{(Eq. 4)}$$

where $\sum_i$ indicates that the summation is over all compounds (1 to M) unless otherwise specified. For convenience of mathematical manipulation, u is defined by the expression:

$$u = \sum_i Ti^2 \quad \text{(Eq. 5)}$$

so that:

$$u = \sum_i (m_1X_{1i} + m_2X_{2i} + m_3X_{3i})^2 \quad \text{(Eq. 6)}$$

The coefficients m_1, m_2, and m_3 may be defined to be orthogonal; *i.e.*, they are subject to the conditional equation:

$$v = m_1^2 + m_2^2 + m_3^2 - 1 = 0 \quad \text{(Eq. 7)}$$

(v is introduced for mathematical convenience). Minimization of the coefficients of Eq. 6 under the restraint imposed by Eq. 7 can be accomplished with the aid of Lagrangian multipliers (33). Differentiation with respect to each coefficient thus leads to:

$$\frac{\partial u}{\partial m_1} - \lambda \frac{\partial v}{\partial m_1} = 0 \quad \text{(Eq. 8a)}$$

$$\frac{\partial u}{\partial m_2} - \lambda \frac{\partial v}{\partial m_2} = 0 \quad \text{(Eq. 8b)}$$

$$\frac{\partial u}{\partial m_3} - \lambda \frac{v}{\partial m_3} = 0 \quad \text{(Eq. 8c)}$$

Evaluation of Eqs. 8a–8c provides the set of relationships that may be written in matrix formalism as:

$$\begin{vmatrix} \sum X_1^2 - \lambda & \sum X_1X_2 & \sum X_1X_3 \\ \sum X_2X_1 & \sum X_2^2 - \lambda & \sum X_2X_3 \\ \sum X_3X_1 & \sum X_3X_2 & \sum X_3^2 - \lambda \end{vmatrix} \begin{vmatrix} m_1 \\ m_2 \\ m_3 \end{vmatrix} = 0 \quad \text{(Eq. 9)}$$

In Eq. 9, the matrix involving the independent variables is a covariance matrix. However, a technical problem arises in such cases as a consequence of the relative magnitudes of the values used to represent the

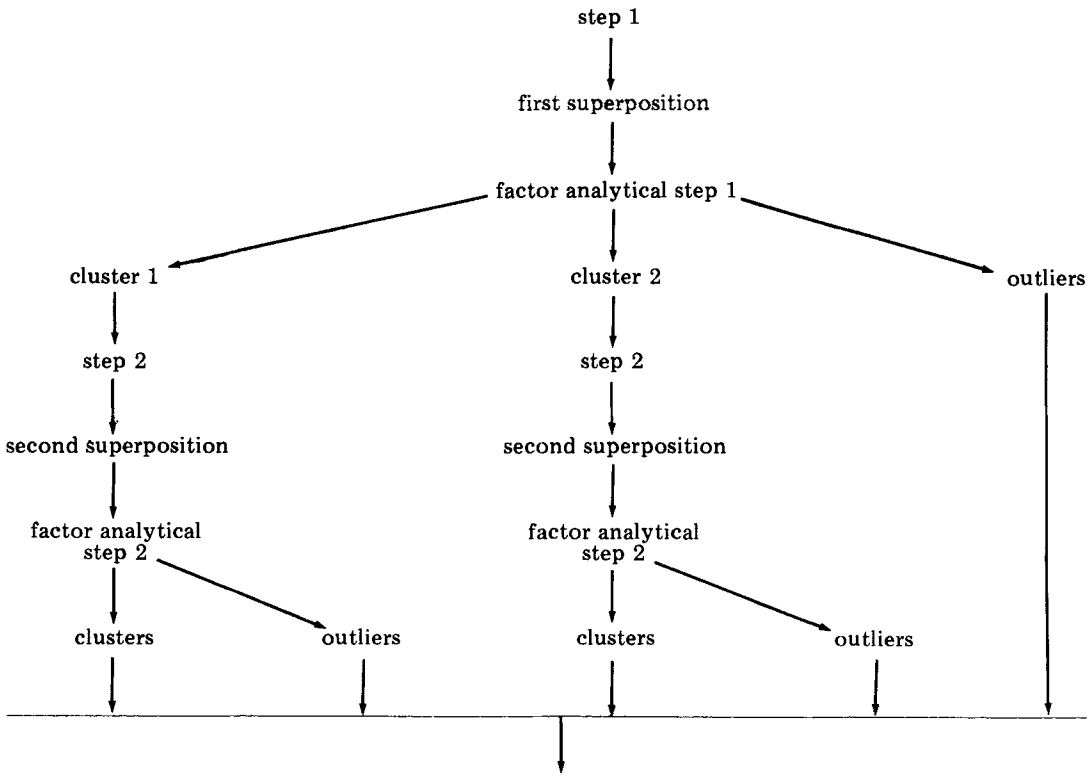

Scheme II

independent variables. Variables that are numerically greater in a data matrix will lead to covariances of a numerically large magnitude; therefore, these variables will be designated, artificially, as the more important contributors in a given linear combination. The potential for an artifact of this type in Fujita–Iwasa–Hansch (34) analyses has been pointed out (35). Autoscaling of variables is a means of avoiding this problem (13). Autoscaling involves the use of correlation coefficients in the place of covariances when establishing normal equations such as is represented by Eq. 9. The elements of a correlation matrix are defined by the relationship:

$$r_{rs} = \frac{\sum_i (X_{ri} - \overline{X}_r)(X_{si} - \overline{X}_s)}{\sqrt{\sum_i (X_{ri} - \overline{X}_r)^2 \sum_i (X_{si} - \overline{X}_s)^2}} \qquad \text{(Eq. 10)}$$

where r and s designate the variables whose intercorrelation is being evaluated. Equation 9 may thus be rewritten as:

$$\begin{vmatrix} r_{11} - \lambda & r_{12} & r_{13} \\ r_{21} & r_{22} - \lambda & r_{23} \\ r_{31} & r_{32} & r_{33} - \lambda \end{vmatrix} \begin{vmatrix} \beta_1 \\ \beta_2 \\ \beta_3 \end{vmatrix} = 0 \qquad \text{(Eq. 11)}$$

The β coefficients of Eq. 11 are related to the m coefficients of Eq. 9 by the expression:

$$m_k = \beta_k \lambda^{1/2} \qquad \text{(Eq. 12)}$$

By using correlation coefficients, any one of the elements of the correlation matrix can vary only between ±1 and 0, so no element of the matrix is overweighted.

The solutions for Eq. 11 can be obtained by first determining the eigenvalues, λ_i, which characterize the correlation matrix. As many eigenvalues will be obtained as there are variables in the data matrix. For each eigenvalue, an associated set of eigenvectors, T_i, is obtained.

A relative measure of the information content of the linear combinations T_i is provided by the magnitudes of the associated eigenvalues. The total variance explained by one or more of the eigenvalues is given by the expression:

$$\text{fraction "explained" variance} = \frac{\sum_{i=1}^{L} \lambda i}{N} \qquad \text{(Eq. 13)}$$

where L is the number of eigenvalues selected, and N is the number of variables in the data matrix. It is apparent that all of the eigenvalues taken together represent the data exactly; *i.e.*, the fraction of explained variance is 1. However, in some cases it may be sufficient to choose only a few high value eigenvectors so that only a predetermined fraction of the variance in the data is explained. Thus, one may choose those high value eigenvectors that explain greater than 0.95 of the data, as is often the case in physicochemical applications, or one may choose to work with an approximated form of the data matrix, selecting only those eigenvectors whose associated eigenvalues are equal to 1 or greater (23). The latter approach is taken in this paper, because fewer numbers of eigenvectors are required to represent the data graphically and because such an approximation is quite adequate for the present purposes.

Principal component analysis presents a means by which optimization procedures involving regression methods such as Fujita–Iwasa–Hansch analyses (34) can be made less prone to error due to intercorrelation between variables. Correlation analysis utilizing principal component analysis as a preprocessing method would thus be based on the multiple regression model in the form:

$$Ai = \sum_{t=1}^{K} C_t T_{ti} + \mu \qquad i = 1, 2, \ldots, M \qquad \text{(Eq. 14)}$$

where the K orthogonal variables, T, explain the major proportion of the variance in the data. An interface thus exists between pattern recognition techniques and the more widely used quantitative structure–activity methods.

METHOD

The 39 drugs comprising the data set are listed in Table I along with their known pharmacological classifications (36) and therapeutic uses (37). They consist of various pharmacological types, including α- and β-adrenergic agents, cholinergic agents, and central nervous system (CNS) stimulants. The study was directed toward separating these compounds into the distinct pharmacological groups they are known to fall into and to separate out the unrelated compounds.

Scheme II is an example of a two-step pattern recognition procedure as followed in this work. In the first step, a preliminary factor analysis is performed to separate broadly the entire data set. Classification is then accomplished by plotting the output from the preprocessing step. Clusters

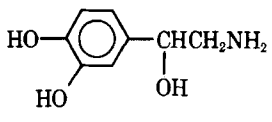

I

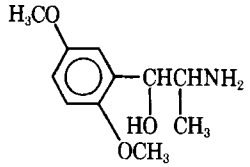

II

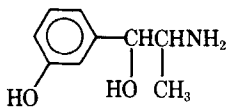

III

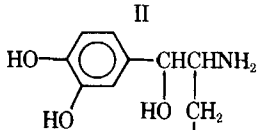

IV

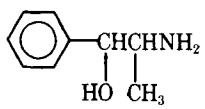

V

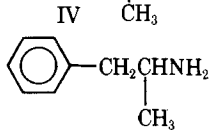

VI

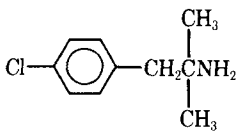

VII

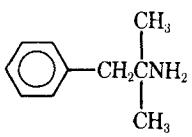

VIII

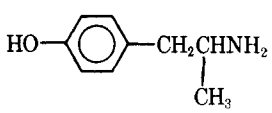

IX

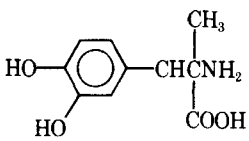

X

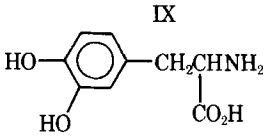

XI

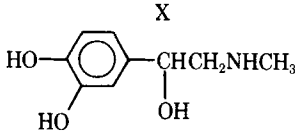

XII

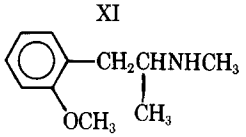

XIII

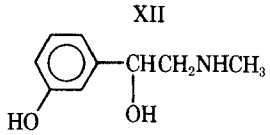

XIV

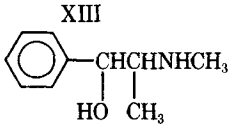

XV

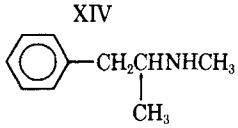

XVI

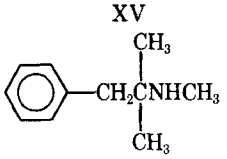

XVII

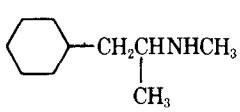

XVIII

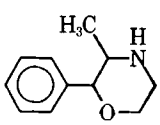

XIX

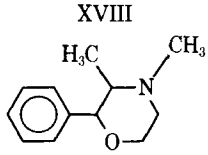

XX

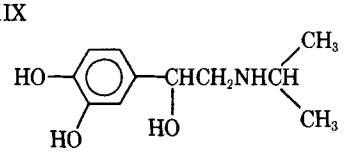

XXI

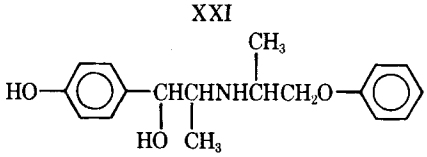

XXII

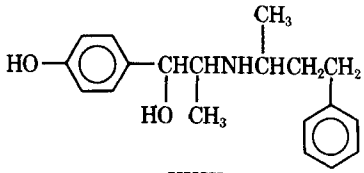

XXIII

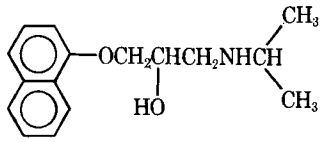

XXIV

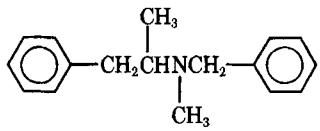

XXV

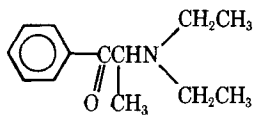

XXVI

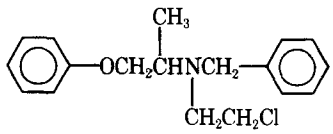

XXVII

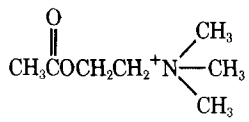

XXVIII

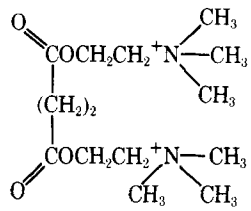

XXIX

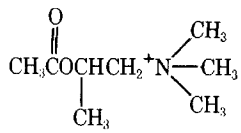

XXX

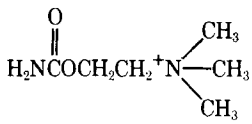

XXXI

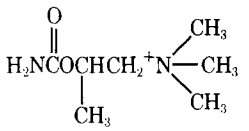

XXXII

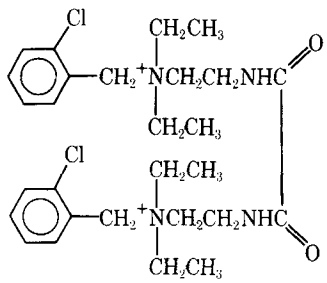

XXXIII

XXXIV

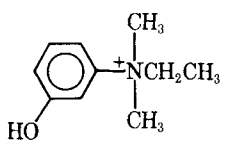

XXXV

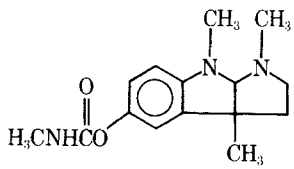

XXXVI

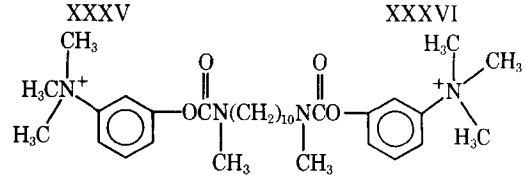

XXXVIII

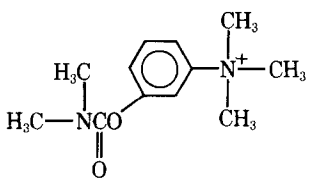

XXXVII

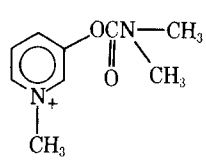

XXXIX

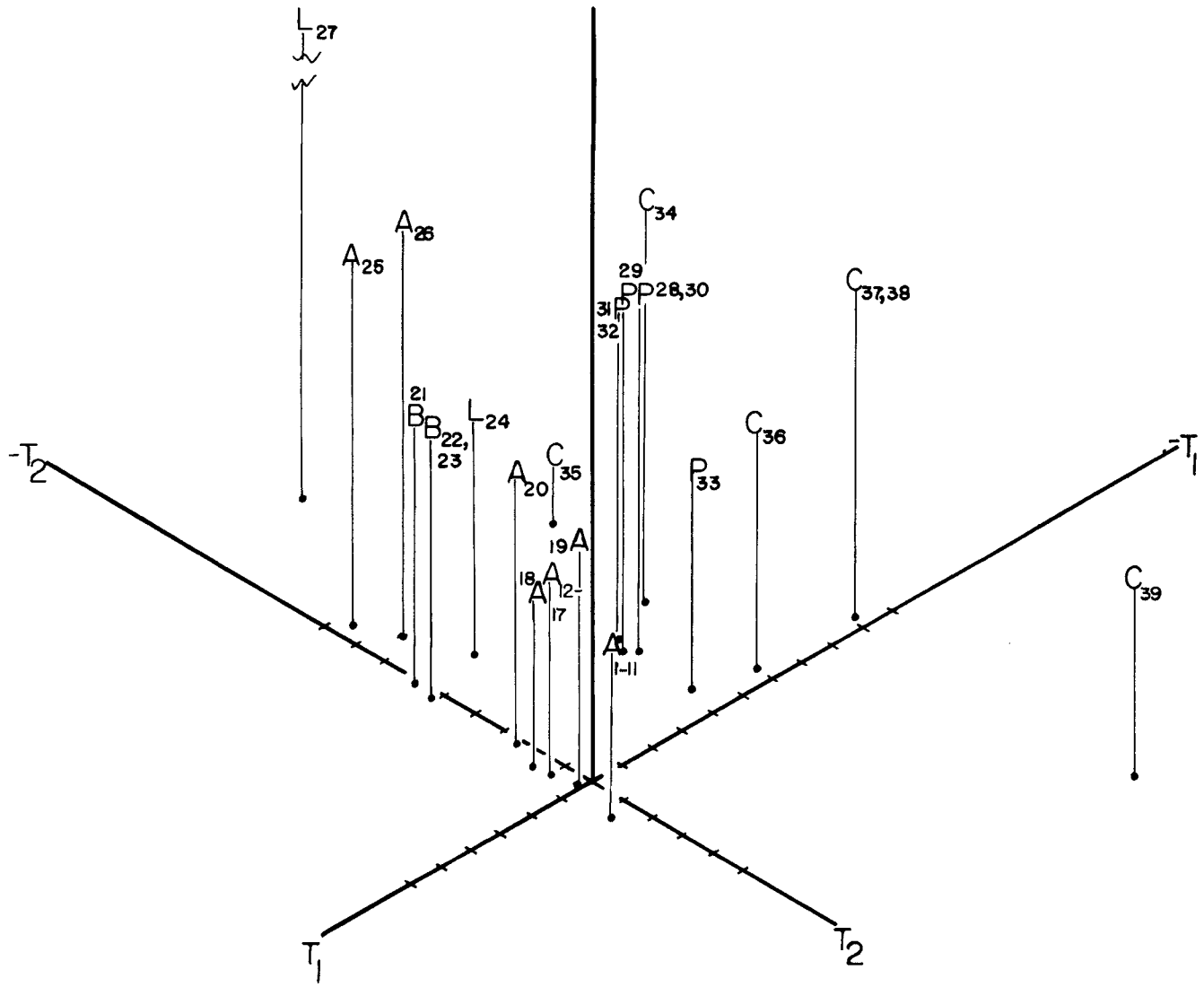

Figure 1—*Three-dimensional plot of factor coordinates from factor analytical step 1. A = α-adrenergic or CNS agent, B = β-adrenergic agent, C = anticholinesterase, L = adrenergic blocker, and P = parasympathomimetic. (Arabic numbers correspond to the roman numerals for the compounds used in the text.)*

so obtained are then factor analyzed separately to yield smaller clusters. Such a sequential procedure has two distinct advantages: (*a*) only a few discriminating features need to be specified in each step, and (*b*) since only a few discriminators are included in the data matrix, easily interpretable results are obtained, the solutions being in two or three dimensions.

Step 1—*Superpositioning of Structures*—Since only variant molecular features are included in the basic equation (Eq. 2), all of the compounds of the data set must first be superimposed to generate the simplest possible superposed structure or "superstructure." This composite structure is so designed that all molecules of the data set can be superposed on it in a consistent manner. This is a key step of the procedure adopted here, since the complexity of the final results depends on the complexity of the superposed structure chosen. This structure has no molecular significance; it is only a geometrical construction. It may be described as a hypothetical parent structure for all compounds of the data set.

In the present case, examination of the structures of I–XXXIX shows a wide variation of structural types. The task of superimposition of all these structures is considerably simplified if representative structures are selected from among structurally related compounds. In the given data set, one might pick XXI, XXIV, XXVII, XXXIII, and XXXVI as being representatives. All of these structures have the common feature X—$(C)_n$—N, where X may be a carboxylic acid derivative or aromatic ring, *n* is the number of carbon atoms intervening, and the amine nitrogen N may be variously substituted. The superposition of the molecules is achieved by superposing the X groups and the N groups while, at the same time, carefully accounting for the length of the carbon chain between them (XL).

In the case of phenethylamines like isoproterenol (XXI) and amphetamine (VI), the aromatic ring is superposed on ring X (see Structure XL), the carbon atom joined to the ethylamine group being placed on position 2. The two-carbon chain is superposed on 4 and 11; the isopropylamino group is on N, 5, and 6; and all other positions (7, 8, 9, 10, 12, 13) are nonexistent. For a molecule like acetylcholine, the carbonyl group is superposable on 2 and 3, the esteratic methyl group on 1, the ether oxygen on 4, the two-carbon chain on 9 and 11, and the trimethylammonium function on N, 5, 6, and 7. Positions 8, 10, 12, and 13 are absent

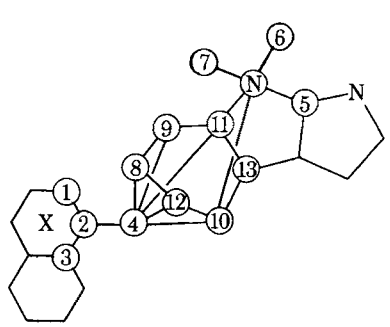

XL

Table II—Molecule-Feature Matrix

Compound	Position[a] 1	2	3	4	5	6	7	8	9	10	11	12	13
I	C_r	C_r	C_r	C_a	H	H	—	—	—	—	C_a	—	—
II	C_r	C_r	C_r	C_a	H	H	—	—	—	—	C_a	—	—
III	C_r	C_r	C_r	C_a	H	H	—	—	—	—	C_a	—	—
IV	C_r	C_r	C_r	C_a	H	H	—	—	—	—	C_a	—	—
V	C_r	C_r	C_r	C_a	H	H	—	—	—	—	C_a	—	—
VI	C_r	C_r	C_r	C_a	H	H	—	—	—	—	C_a	—	—
VII	C_r	C_r	C_r	C_a	H	H	—	—	—	—	C_a	—	—
VIII	C_r	C_r	C_r	C_a	H	H	—	—	—	—	C_a	—	—
IX	C_r	C_r	C_r	C_a	H	H	—	—	—	—	C_a	—	—
X	C_r	C_r	C_r	C_a	H	H	—	—	—	—	C_a	—	—
XI	C_r	C_r	C_r	C_a	H	H	—	—	—	—	C_a	—	—
XII	C_r	C_r	C_r	C_a	H	CH_3	—	—	—	—	C_a	—	—
XIII	C_r	C_r	C_r	C_a	H	CH_3	—	—	—	—	C_a	—	—
XIV	C_r	C_r	C_r	C_a	H	CH_3	—	—	—	—	C_a	—	—
XV	C_r	C_r	C_r	C_a	H	CH_3	—	—	—	—	C_a	—	—
XVI	C_r	C_r	C_r	C_a	H	CH_3	—	—	—	—	C_a	—	—
XVII	C_r	C_r	C_r	C_a	H	CH_3	—	—	—	—	C_a	—	—
XVIII	C_a	C_a	C_a	C_a	H	CH_3	—	—	—	—	C_a	—	—
XIX	C_r	C_r	C_r	C_a	CH_2	H	—	—	—	—	C_a	—	—
XX	C_r	C_r	C_r	C_a	CH_2	$CH(CH_3)_2$	—	—	—	—	C_a	—	—
XXI	C_r	C_r	C_r	C_a	H	$CH(CH_3)CH(CH_3)_2$	—	—	—	—	C_a	—	—
XXII	C_r	C_r	C_r	C_a	H	$CH(CH_2OC_6H_5)CH_3$	—	—	—	—	C_a	—	—
XXIII	C_r	C_r	C_r	C_a	H	$CH(CH_2CH_2C_6H_5)CH_3$	—	—	—	—	C_a	—	—
XXIV	C_r	C_r	C_r	O	H	$CH(CH_3)_2$	—	C_a	C_a	—	C_a	—	—
XXV	C_r	C_r	C_r	C_a	CH_3	$CH_2C_6H_5$	—	—	—	—	C_a	—	—
XXVI	C_r	C_r	C_r	C_a	CH_2CH_3	CH_2CH_3	—	—	—	—	C_a	—	—
XXVII	C_r	C_r	C_r	O	CH_2CH_2Cl	$CH_2C_6H_5$	—	—	—	—	C_a	—	—
XXVIII	CH_3	C_o	=O	O	CH_3	CH_3	CH_3	—	C_a	—	C_a	—	—
XXIX	CH_2	C_o	=O	O	CH_3	CH_3	CH_3	—	C_a	—	C_a	—	—
XXX	CH_3	C_o	=O	O	CH_3	CH_3	CH_3	—	C_a	—	C_a	—	—
XXXI	NH_2	C_o	=O	O	CH_3	CH_3	CH_3	—	C_a	—	C_a	—	—
XXXII	NH_2	C_o	=O	O	CH_3	CH_3	CH_3	—	C_a	—	C_a	—	—
XXXIII	CH	C_o	=O	O	HC=	CH_3	—	C_a	C_a	—	C_a	C_a	—
XXXIV	CONH	C_o	=O	NH	CH_2	CH_2CH_3	CH_2CH_3	—	C_a	—	C_a	—	—
XXXV	—	H	—	O	CH_3	CH_2CH_3	CH_2CH_3	C_r	C_r	C_r	C_r	C_r	C_r
XXXVI	$NHCH_3$	C_o	=O	O	CH	CH_3	—	C_r	C_r	C_r	C_r	C_r	C_r
XXXVII	$N(CH_3)_2$	C_o	=O	O	CH_3	CH_3	CH_3	C_r	C_r	C_r	C_r	C_r	C_r
XXXVIII	$N(CH_3)_2$	C_o	=O	O	CH_3	CH_3	CH_3	C_r	C_r	C_r	C_r	C_r	C_r
XXXIX	$N(CH_3)_2$	C_o	=O	O	—	—	CH_3	C_r	C_r	C_r	C_r	C_r	—

[a] C_r = aromatic carbon atom, C_a = aliphatic carbon atom, and C_o = carbonyl carbon atom.

in this case. For compounds like neostigmine or physostigmine, the ester or amide group is treated just as for acetylcholine; the aromatic ring is superposed on the six-membered ring formed by positions 8, 9, 11, 13, 10, and 12. If the esteratic group is *para* to the amine function, then the former is linked to the aromatic ring by the 4–12 bond; if the esteratic group is *meta* to the aromatic ring, it is linked to the latter by the 4–10 bond.

Two of the molecules of the data set, pilocarpine (XXXIII) and pyridostigmine (XXXIX), are structurally distinct from the rest; they may be superposed on Structure XL as follows. The ester group of pilocarpine is treated just as for acetylcholine; the four-carbon chain between the ester group and the amine function is superposable on positions 12, 8, 9, and 11. The superpositioning of the nitrogen-containing rings is apparent from the figure. In the case of pyridostigimine, the pyridine ring is superposed on N, 11, 9, 12, and 10. Position 4 (ether oxygen) is linked to 12 to represent the *meta*-substitution.

All other structures are similarly superposable; Table II shows exactly how each compound was treated.

Selection of Discriminators—Discriminators are groups, bonds, or other functionalities that serve to distinguish between compounds of a data set. When a wide variety of structural types are being studied, the number of variables in the data matrix will be inordinately large if *all* structural differences are designated as discriminators. Therefore, it is desirable to specify the minimum number of discriminators required to differentiate between the compounds of the data set.

In the present study, more than one factor analytical step is to be applied (Scheme II). In the first step, only a broad classification is sought, so only major structural differences need be specified while selecting discriminators. Thus, fine distinctions such as aromatic or aliphatic substitution patterns may be ignored while major distinctions such as those between aromatic and aliphatic groups should be specified. On this basis, positions 1–13 of XL may be chosen as discriminators. However, closer examination of Structures I–XXXIX and of Table II shows that positions 11–13 are not major discriminators; they represent only two variations in structure (aromatic or aliphatic carbon atoms). Furthermore, these positions are equally well represented by others, *e.g.*, 12 and 13 by

Table III—Descriptor Code for Designating Discriminator Groups

Group[a]	Atomic/Structural Constant	Code
Cl	5.84	1.00
C_r	3.37	0.58
C_a	2.59	0.44
H	1.03	0.18
CH_3	5.65	0.97
CH_2CH_3	10.30	1.76
CH_2	4.65	0.80
$CH(CH_3)_2$	14.98	2.57
$CHCH_3$	13.95[b]	2.39
CH_2		
$CH_2(C_r)_3$[c]	16.81[b]	2.88
CH	3.62	0.62
NH_2	4.44	0.76
$NHCH_3$	9.06[b]	1.55
$N(CH_3)_2$	13.68[b]	2.34
CONH	8.01[b]	1.37
C_o	0.79[b]	0.13
=O	3.81[b]	0.65
O	1.76	0.30
NH	3.62	0.62
=CH	1.82[b]	0.31
CH_2CH_2Cl	15.14[b]	2.59
OH_a[d]	2.55	0.44
OH_p[e]	3.55	0.60
OCH_3	7.41	1.26
COOH	7.23	1.24

[a] C_r = aromatic carbon, C_o = carbonyl carbon, and C_a = aliphatic carbon. [b] Value was calculated. [c] Only the aromatic carbon attached to the methylene group and the two *ortho*-carbon atoms were included to be consistent in designating discriminators; the value of 16.81 was calculated using the molar refraction value for the benzene ring (38). [d] Aliphatic hydroxyl group. [e] Phenolic hydroxyl group.

8 for all compounds [except for pilocarpine (XXXIII) and pyridostigmine (XXXIX), which are in any case different from the other compounds of the data set]. Similarly, position 11 is represented by position 4 in I–XXVII and by position 9 in XXVIII–XXXIX. Positions 11–13 may therefore be ignored.

Designation of Discriminators: Coding—The discriminators selected are designated in numerical terms by a descriptor code. One has to choose a property of the groups that can adequately represent and distinguish between them. It is seen that many of the substituents involved are bioisosteric, *e.g.*, $COOCH_3$, $CONH_2$, and $CON(CH_3)_2$. Since it is generally true that classical isosteric groups have similar molar refractivities, molar refraction values were used in the coding (38). The molar refraction value of chlorine (5.84) was selected as standard, and all other codes were determined relatively. The molar refraction values used and the descriptor codes adopted are given in Table III. Several molar refraction values were calculated by using the additive-constitutive property.

With the codes given in Table III, the molecule-discriminator data matrix shown in Table IV was constructed. Comparison of Structures I–XXXIX with XL and of Tables II–IV will indicate exactly how each compound of the data set was numerically designated.

Preprocessing: Factor Analytical Step 1—By using the coded molecule-discriminator data matrix of Table IV, the correlation matrix shown in Table V was constructed (as described under *Theory*). The solution of Eq. 13 gave three eigenvalues whose values were greater than unity. These values, together with the associated eigenvectors, are given in Table VI. The three eigenvalues chosen explain $(4.87 + 1.61 + 1.32)/10 = 0.78$ of the variance. This value is not very high, but only major classification patterns are sought in this part of the analysis. That an explained variance of 78% is sufficient for the present purposes is obvious upon examination of the clustering pattern obtained (Fig. 1).

Classification: Plotting—By using the eigenvectors associated with the three eigenvalues, three factor coordinates, t_1, t_2, and t_3, were calculated for each compound of the data set. The points were then plotted by simple solid geometrical construction (Fig. 1). After plotting each point, its associated biological activity was used to label it in the distri-

Table IV—Coded Molecule-Feature Data Matrix

Compound	Position									
	1	2	3	4	5	6	7	8	9	10
I	0.58	0.58	0.58	0.44	0.18	0.18	0.00	0.00	0.00	0.00
II	0.58	0.58	0.58	0.44	0.18	0.18	0.00	0.00	0.00	0.00
III	0.58	0.58	0.58	0.44	0.18	0.18	0.00	0.00	0.00	0.00
IV	0.58	0.58	0.58	0.44	0.18	0.18	0.00	0.00	0.00	0.00
V	0.58	0.58	0.58	0.44	0.18	0.18	0.00	0.00	0.00	0.00
VI	0.58	0.58	0.58	0.44	0.18	0.18	0.00	0.00	0.00	0.00
VII	0.58	0.58	0.58	0.44	0.18	0.18	0.00	0.00	0.00	0.00
VIII	0.58	0.58	0.58	0.44	0.18	0.18	0.00	0.00	0.00	0.00
IX	0.58	0.58	0.58	0.44	0.18	0.18	0.00	0.00	0.00	0.00
X	0.58	0.58	0.58	0.44	0.18	0.18	0.00	0.00	0.00	0.00
XI	0.58	0.58	0.58	0.44	0.18	0.18	0.00	0.00	0.00	0.00
XII	0.58	0.58	0.58	0.44	0.18	0.97	0.00	0.00	0.00	0.00
XIII	0.58	0.58	0.58	0.44	0.18	0.97	0.00	0.00	0.00	0.00
XIV	0.58	0.58	0.58	0.44	0.18	0.97	0.00	0.00	0.00	0.00
XV	0.58	0.58	0.58	0.44	0.18	0.97	0.00	0.00	0.00	0.00
XVI	0.58	0.58	0.58	0.44	0.18	0.97	0.00	0.00	0.00	0.00
XVII	0.58	0.58	0.58	0.44	0.18	0.97	0.00	0.00	0.00	0.00
XVIII	0.44	0.44	0.44	0.44	0.18	0.97	0.00	0.00	0.00	0.00
XIX	0.58	0.58	0.58	0.44	0.80	0.18	0.00	0.00	0.00	0.00
XX	0.58	0.58	0.58	0.44	0.80	0.97	0.00	0.00	0.00	0.00
XXI	0.58	0.58	0.58	0.44	0.18	2.57	0.00	0.00	0.00	0.00
XXII	0.58	0.58	0.58	0.44	0.18	2.39	0.00	0.00	0.00	0.00
XXIII	0.58	0.58	0.58	0.44	0.18	2.39	0.00	0.00	0.00	0.00
XXIV	0.58	0.58	0.58	0.30	0.18	2.57	0.00	0.44	0.44	0.00
XXV	0.58	0.58	0.58	0.44	0.97	2.88	0.00	0.00	0.00	0.00
XXVI	0.58	0.58	0.58	0.44	1.76	1.76	0.00	0.00	0.00	0.00
XXVII	0.58	0.58	0.58	0.30	2.59	2.88	0.00	0.00	0.44	0.00
XXVIII	0.97	0.13	0.65	0.30	0.97	0.97	0.97	0.00	0.44	0.00
XXIX	0.80	0.13	0.65	0.30	0.97	0.97	0.97	0.00	0.44	0.00
XXX	0.97	0.13	0.65	0.30	0.97	0.97	0.97	0.00	0.44	0.00
XXXI	0.76	0.13	0.65	0.30	0.97	0.97	0.97	0.00	0.44	0.00
XXXII	0.76	0.13	0.65	0.30	0.97	0.97	0.97	0.00	0.44	0.00
XXXIII	0.62	0.13	0.65	0.30	0.31	0.97	0.00	0.44	0.44	0.00
XXXIV	1.37	0.13	0.65	0.62	0.80	1.76	1.76	0.58	0.58	0.58
XXXV	0.00	0.18	0.00	0.30	0.97	1.76	1.76	0.58	0.58	0.58
XXXVI	1.55	0.13	0.65	0.30	0.62	0.97	0.00	0.58	0.58	0.58
XXXVII	2.34	0.13	0.65	0.30	0.97	0.97	0.97	0.58	0.58	0.58
XXXVIII	2.34	0.13	0.65	0.30	0.97	0.97	0.97	0.58	0.58	0.58
XXXIX	2.34	0.13	0.65	0.30	0.00	0.00	0.97	0.58	0.58	0.58

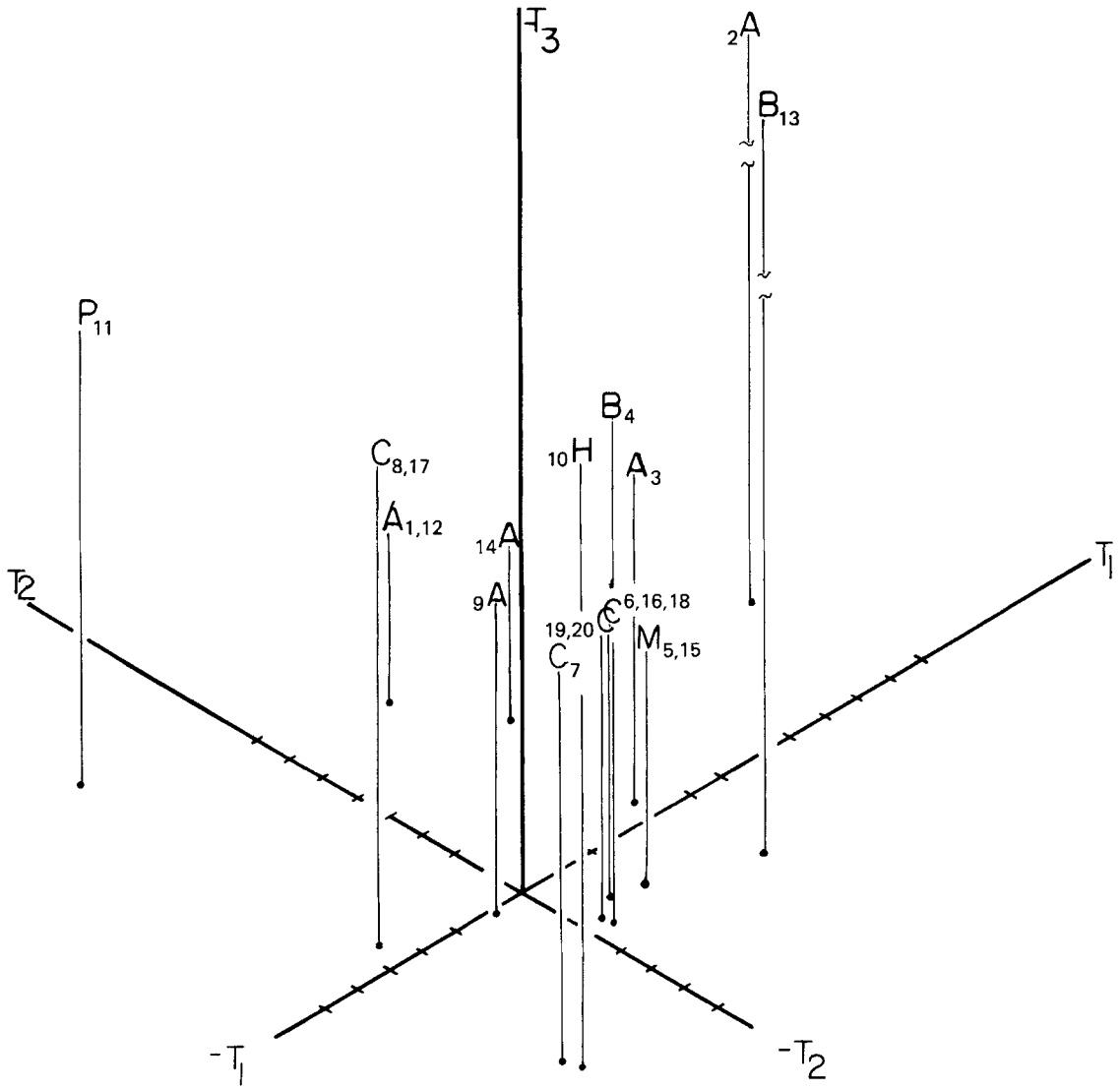

Figure 2—*Three-dimensional plot of factor coordinates from factor analytical step 2. A = α-adrenergic agonist, B = β-adrenergic agonist, C = CNS stimulant, H = antihypertensive, M = mixed-acting agent (α-adrenergic agonist and CNS stimulant), and P = antiparkinsonian. (Arabic numbers correspond to the roman numerals for the compounds used in the text.)*

bution (B for β-adrenergic agent, P for parasympathomimetic, C for anticholinesterase, A for α-adrenergic or CNS agent, and L for adrenergic blocker). Examination of Fig. 1 shows distinct patterns in the distribution. Adrenergics and cholinergics are well separated, and the β-agonists form a well-resolved cluster. The parasympathomimetics form a distinct cluster compared to the scattered distribution of the anticholinesterases. Phenoxybenzamine (XXVII), the only α-blocker, is far removed from the rest of the data set; propranolol (XXIV), the only β-blocker, is removed from, but close to, the β-agonists.

Pilocarpine (XXXIII) appears to occupy an ambiguous position; however, this compound is structurally and pharmacologically quite different from the rest so it can be regarded as well resolved. Only two compounds, ethylnorepinephrine (IV) and methoxyphenamine (XIII), are not properly classified. They are found within the cluster of α-adrenergic and CNS agents (these agents are primarily β-adrenergic agonists). However, they are well resolved after the second factor analytical step, when fine substitution patterns are considered.

Step 2—The distribution pattern of Fig. 1 indicates that, although the major pharmacological classes have been correctly identified and well separated, further separation is desirable among the adrenergic and CNS agents. The group of 20 compounds clustering around the T_3 axis (I–XX, Fig. 1) is fairly large and is subjected to another analysis. The list of

Table V—Correlation Matrix for Factor Analytical Step 1

Position	Position									
	1	2	3	4	5	6	7	8	9	10
1	1.000	−0.605	0.460	−0.352	0.130	−0.115	0.445	0.616	0.611	0.705
2		1.000	−0.107	0.626	−0.329	0.002	−0.822	−0.564	−0.891	−0.560
3			1.000	−0.007	−0.008	−0.143	−0.178	−0.177	0.034	−0.229
4				1.000	−0.394	−0.103	−0.358	−0.607	−0.763	−0.502
5					1.000	0.445	0.359	0.067	0.472	0.134
6						1.000	0.079	0.063	0.191	−0.037
7							1.000	0.382	0.754	0.477
8								1.000	0.722	0.886
9									1.000	0.649
10										1.000

Table VI—Eigenvalues and Associated Eigenvectors for Step 1

	Eigenvalue I = 4.87	Eigenvalue II = 1.61	Eigenvalue III = 1.32
β_1	−0.33[a]	0.39	0.22
β_2	0.40	−0.03	−0.14
β_3	0.00	0.38	0.74
β_4	0.34	0.10	−0.04
β_5	−0.19	−0.51	0.35
β_6	−0.05	−0.60	0.12
β_7	−0.34	−0.13	0.00
β_8	−0.37	0.13	−0.34
β_9	−0.43	−0.09	0.09
β_{10}	−0.37	0.16	−0.35

[a] Values are the associated eigenvector coefficients.

compounds is given in Table VII, which also includes the molecule-feature matrix. The distinction in this case (compared to Step 1, Table III) is that fine substitution patterns are taken into account.

By following the same operational procedures outlined earlier, a composite superstructure for all of the molecules of the data set was generated (XLI). Structure XLI is considerably simplified from Structure XL, since only a limited data set is involved and preliminary separation has already been effected.

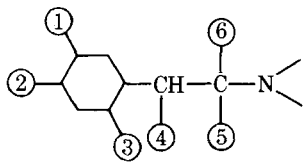

XLI

By using the molecule-feature data matrix shown in Table VII, the coded molecule-discriminator matrix was constructed as explained earlier, using the coding given in Table III. Upon factor analyzing the data matrix, three eigenvalues with magnitudes greater than one were obtained; these values, together with their associated eigenvectors, are given in Table VIII. The three eigenvalues together explain 75% of the variance.

The factor coordinates of each compound were obtained as described earlier, and the three-dimensional plot is shown in Fig. 2. The adrenergic agents are well separated from the CNS agents. The two β-adrenergic agents present, ethylnorepinephrine (IV) and methoxyphenamine (XIII), are well resolved. The mixed acting agents, ephedrine (XV) and phenylpropanolamine (V), occupy a position between the α-adrenergic and CNS stimulant agents. This is also characteristic of their pharmacological action, because they have both types of activity. Methyldopa (X) and levodopa (XI) occupy distinct positions, reflecting their characteristically different pharmacological activities.

Table VII—Molecule-Feature Matrix for Factor Analytical Step 2

Compound	Position 1	2	3	4	5	6
I	OH_p[a]	OH_p	H	OH_l[b]	H	H
II	OCH_3	H	OCH_3	OH_l	H	H
III	OH_p	H	H	OH_l	H	CH_3
IV	OH_p	OH_p	H	OH_l	H	CH_2 CH_3
V	H	H	H	OH_l	H	CH_3
VI	H	H	H	H	H	CH_3
VII	H	Cl	H	H	CH_3	CH_3
VIII	H	H	H	H	CH_3	CH_3
IX	H	OH_p	H	H	H	CH_3
X	OH_p	OH_p	H	H	COOH	CH_3
XI	OH_p	OH_p	H	H	COOH	H
XII	OH_p	OH_p	H	OH_l	H	H
XIII	H	H	OCH_3	H	H	CH_3
XIV	OH_p	H	H	OH_l	H	H
XV	H	H	H	OH_l	H	CH_3
XVI	H	H	H	H	H	CH_3
XVII	H	H	H	H	CH_3	CH_3
XVIII	H	H	H	H	H	CH_3
XIX	H	H	H	O	H	CH_3
XX	H	H	H	O	H	CH_3

[a] Phenolic hydroxyl. [b] Aliphatic hydroxyl.

Table VIII—Eigenvalues and Associated Eigenvectors for Step 2

	Eigenvalue I = 1.96	Eigenvalue II = 1.54	Eigenvalue III = 1.10
β_1	0.43[a]	0.52	−0.30
β_2	−0.29	0.55	0.00
β_3	0.37	−0.06	−0.76
β_4	0.57	0.18	0.38
β_5	−0.51	0.35	−0.32
β_6	−0.06	−0.51	−0.30

[a] Values are the associated eigenvector coefficients.

CONCLUSIONS

When dealing with a large number of structurally diverse compounds, a likely problem with the method adopted here is incorrect structural superposition. Attempts to overcome this difficulty are underway.

To researchers accustomed to setting a cutoff level of 0.95 or greater for experimental accuracy, the approximation of 0.75 may not be satisfying. However, a highly accurate reproduction of the data is not essential here; only an approximation of the data is sought so that the major distinctions between the elements of the data set can readily be identified. Furthermore, graphical representation of the results, which is possible by such an approach, is directly interpretable and is conceptually simpler than the mathematical methods available.

To summarize, a simple factor analytical approach was successfully applied to classify a set of 39 therapeutic agents using organic structural information. The major pharmacological groups present were correctly identified and separated. Pharmacologically unrelated compounds such as levodopa (an antiparkinsonian) and methyldopa (an antihypertensive) were separated out. Inspection of the clusters indicated some degree of order; for example, ephedrine and phenylpropanolamine occupied the border region between α-adrenergic agents and CNS stimulant agents. The results show that factor analysis can be employed advantageously as the preprocessing step of a pattern recognition scheme in the investigation of structure–activity relationships.

REFERENCES

(1) A. Cammarata and G. K. Menon, *J. Med. Chem.*, **19**, 739 (1976).

(2) T. L. Isenhour and P. C. Jurs, *Anal. Chem.*, **43**, 20A (1971).

(3) B. R. Kowalski and C. F. Bender, *J. Am. Chem. Soc.*, **94**, 5632 (1972).

(4) B. R. Kowalski, *Anal. Chem.*, **47**, 1152A (1975).

(5) D. R. Preuss and P. C. Jurs, *ibid.*, **46**, 520 (1974).

(6) J. B. Justice and T. L. Isenhour, *ibid.*, **46**, 223 (1974).

(7) K. C. Chu, *ibid.*, **46**, 1181 (1974).

(8) K. C. Chu, R. J. Feldmann, M. B. Shapiro, G. F. Hazard, Jr., and R. I. Geran, *J. Med. Chem.*, **18**, 539 (1975).

(9) A. J. Stuper and P. C. Jurs, *J. Am. Chem. Soc.*, **97**, 182 (1975).

(10) B. R. Kowalski and C. F. Bender, *ibid.*, **96**, 916 (1974).

(11) H. C. Andrews, "Introduction to Mathematical Techniques in Pattern Recognition," Wiley–Interscience, New York, N.Y., 1972.

(12) W. S. Meisel, "Computer Oriented Approaches to Pattern Recognition," Wiley–Interscience, New York, N.Y., 1972.

(13) P. C. Jurs and T. L. Isenhour, "Chemical Applications of Pattern Recognition," Wiley–Interscience, New York, N.Y., 1975.

(14) C. Chen, "Statistical Pattern Recognition," Hayden Book Co., Rochelle Park, N.J., 1973.

(15) R. J. Mathews, *J. Am. Chem. Soc.*, **97**, 935 (1975).

(16) C. L. Perrin, *Science*, **183**, 551 (1974).

(17) K. H. Ting, R. C. T. Lee, G. W. A. Milne, M. Shapiro, and A. M. Guarino, *ibid.*, **180**, 417 (1973).

(18) R. D. Cramer, III, G. Redl, and C. E. Berkoff, *J. Med. Chem.*, **17**, 533 (1974).

(19) M. L. Weiner and P. H. Weiner, *ibid.*, **16**, 655 (1973).

(20) H. L. Friedman, *Symp. Chem. Biol. Correl., 1st Nat. Res. Council Publ.*, **206**, 296 (1951).

(21) L. L. Thurstone, "Multiple Factor Analysis," University of Chi-

cago Press, Chicago, Ill., 1947.
(22) S. A. Mulaik, "The Foundations of Factor Analysis," McGraw-Hill, New York, N.Y., 1972.
(23) J. E. Overall and C. J. Klett, "Applied Multivariate Analysis," McGraw-Hill, New York, N.Y., 1972.
(24) L. L. Thurstone, "The Vectors of the Mind," University of Chicago Press, Chicago, Ill., 1935.
(25) N. R. Bohidar, F. A. Restaino, and J. B. Schwartz, *J. Pharm. Sci.*, **64**, 966 (1975).
(26) C. Hansch, S. H. Unger, and A. B. Forsythe, *J. Med. Chem.*, **16**, 1217 (1973).
(27) S. R. Heller, C. L. Chang, and K. C. Chu, *Anal. Chem.*, **46**, 951 (1974).
(28) F. K. Kawahara, J. F. Santner, and E. C. Julian, *ibid.*, **46**, 266 (1974).
(29) N. J. Nilsson, "Learning Machines," McGraw-Hill, New York, N.Y., 1965.
(30) P. C. Jurs, B. R. Kowalski, T. L. Isenhour, and C. N. Reilley, *Anal. Chem.*, **41**, 690 (1969).
(31) B. R. Kowalski, P. C. Jurs, T. L. Isenhour, and C. N. Reilley, *ibid.*, **41**, 695 (1969).
(32) S. S. Schiffman, *Science*, **185**, 112 (1974).
(33) A. E. Taylor, "Advanced Calculus," Blaisdell, New York, N.Y., 1965.
(34) T. Fujita, J. Iwasa, and C. Hansch, *J. Med. Chem.*, **8**, 150 (1965).
(35) A. Cammarata, *ibid.*, **10**, 525 (1967).
(36) "Medicinal Chemistry," vol. II, 3rd ed., A. Burger, Ed., Wiley–Interscience, New York, N.Y., 1970.
(37) "AMA Drug Evaluations," 2nd ed., Publishing Sciences Group, Acton, Mass., 1973.
(38) A. I. Vogel, "Elementary Practical Organic Chemistry Part 2: Qualitative Organic Analysis," 2nd ed., Wiley, New York, N.Y., 1966.

ACKNOWLEDGMENTS AND ADDRESSES

Received December 23, 1975, from the *School of Pharmacy, Temple University, Philadelphia, PA 19140.*

Accepted for publication April 23, 1976.

The support provided G. K. Menon through a Temple University Graduate Fellowship is gratefully acknowledged.

[x] To whom inquiries should be directed.

Pharmacokinetics of β-Methyldigoxin in Healthy Humans II: Oral Studies and Bioavailability

PETER H. HINDERLING [*], EDWARD R. GARRETT [x], and RONALD C. WESTER [‡]

Abstract □ The pharmacokinetics of orally administered aqueous ^{3}H-β-methyldigoxin solutions were studied at two dose levels, 0.3 and 0.6 mg, in healthy human subjects. The drug and its metabolites were specifically assayed in biological fluids and compared with results after intravenous doses to the same subjects. No significant dose dependency was observed. The apparent half-life of absorption was 16 ± 6 min (*SEM*). Digoxin was the only metabolite observed in the plasma and comprised 28.6 ± 3.7% of the dose in the urine. ^{3}H-β-Methyldigoxin, renally excreted unchanged, comprised 25.7 ± 1.7% (*SEM*). Water-soluble metabolites in the urine comprised 9.0 ± 1.8%. Fecal and urinary excretion accounted for 85% of the dose at 144 hr. The oral absorption of unchanged ^{3}H-β-methyldigoxin from solution was 59 ± 6% by area under the curve methods and 60 ± 4% by renal excretion. A total of 73% of the dose in the solution was absorbed as β-methyldigoxin and digoxin. First-pass metabolism prior to absorption was largely prehepatic and assignable to GI degradation; 21.9 ± 2.8% was degraded with 12.8 ± 4.0% to digoxin and 9.1 ± 4.0% to water-soluble metabolites. From 14 to 18% of the administered oral dose did not reach the systemic circulation. Analog computer fitting of plasma and urine levels of drug and digoxin was consistent with the first-pass premise with a delayed absorption of GI-generated digoxin and other metabolites. There were no significant differences between the oral absorption of a tablet formulation and the solution. Orally administered β-methyldigoxin solution delivered 97% cardioactivity as itself and digoxin with respect to an equivalent amount of intravenously administered digoxin. This value contrasts to the 140% delivered by intravenously administered β-methyldigoxin on the premise of pharmacodynamic equivalence of systemically appearing digoxin and β-methyldigoxin. Literature reports on the oral bioavailability of solutions and solid dosage forms of digoxin were critically reviewed, but no reliable comparison of the extent and reproducibility of oral absorption of cardioactive agents from administered digoxin or β-methyldigoxin could be made from the widely variable digoxin studies with nonspecific assays.

Keyphrases □ β-Methyldigoxin—oral, pharmacokinetics and bioavailability in humans, radiochemical–TLC study □ Pharmacokinetics—oral β-methyldigoxin, humans, radiochemical–TLC study □ Bioavailability—oral β-methyldigoxin, humans, radiochemical–TLC study □ Radiochemistry–TLC—study of pharmacokinetics and bioavailability of oral β-methyldigoxin in humans □ Cardiac glycosides—β-methyldigoxin, oral, pharmacokinetics and bioavailability in humans, radiochemical–TLC study

Semisynthetic derivatives of digoxin (Ia) such as β-methyldigoxin (Ib), a methyl ether of digoxin, and β-acetyldigoxin (Ic), an acetyl ester of digoxin, have been claimed to have higher intrinsic rate constants and efficiencies of absorption than digoxin in animals and in humans (1–14). Presumably, the rationale for their preferred usage is that a completely absorbed compound has the most consistent bioavailability in multiple dosage regimens. This is a valid approach, since glycosides have a narrow therapeutic range (15–18) and the occurrence of toxic manifestations in patients undergoing chronic therapy is 7–20% (19). Whereas β-acetyldigoxin was extensively metabolized or degraded before reaching the systemic circulation (20), β-methyldigoxin was claimed to

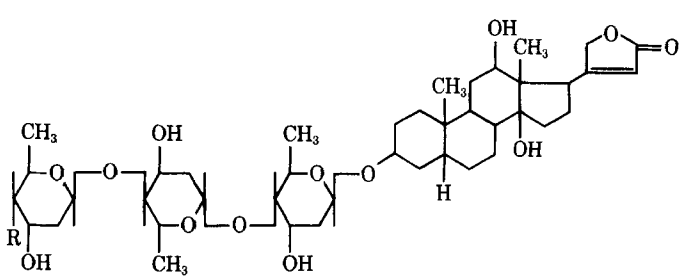

Ia: R = OH
Ib: R = OCH_3 Ic: R = $OCCH_3$

cago Press, Chicago, Ill., 1947.
(22) S. A. Mulaik, "The Foundations of Factor Analysis," McGraw-Hill, New York, N.Y., 1972.
(23) J. E. Overall and C. J. Klett, "Applied Multivariate Analysis," McGraw-Hill, New York, N.Y., 1972.
(24) L. L. Thurstone, "The Vectors of the Mind," University of Chicago Press, Chicago, Ill., 1935.
(25) N. R. Bohidar, F. A. Restaino, and J. B. Schwartz, *J. Pharm. Sci.*, **64**, 966 (1975).
(26) C. Hansch, S. H. Unger, and A. B. Forsythe, *J. Med. Chem.*, **16**, 1217 (1973).
(27) S. R. Heller, C. L. Chang, and K. C. Chu, *Anal. Chem.*, **46**, 951 (1974).
(28) F. K. Kawahara, J. F. Santner, and E. C. Julian, *ibid.*, **46**, 266 (1974).
(29) N. J. Nilsson, "Learning Machines," McGraw-Hill, New York, N.Y., 1965.
(30) P. C. Jurs, B. R. Kowalski, T. L. Isenhour, and C. N. Reilley, *Anal. Chem.*, **41**, 690 (1969).
(31) B. R. Kowalski, P. C. Jurs, T. L. Isenhour, and C. N. Reilley, *ibid.*, **41**, 695 (1969).
(32) S. S. Schiffman, *Science*, **185**, 112 (1974).
(33) A. E. Taylor, "Advanced Calculus," Blaisdell, New York, N.Y., 1965.
(34) T. Fujita, J. Iwasa, and C. Hansch, *J. Med. Chem.*, **8**, 150 (1965).
(35) A. Cammarata, *ibid.*, **10**, 525 (1967).
(36) "Medicinal Chemistry," vol. II, 3rd ed., A. Burger, Ed., Wiley–Interscience, New York, N.Y., 1970.
(37) "AMA Drug Evaluations," 2nd ed., Publishing Sciences Group, Acton, Mass., 1973.
(38) A. I. Vogel, "Elementary Practical Organic Chemistry Part 2: Qualitative Organic Analysis," 2nd ed., Wiley, New York, N.Y., 1966.

ACKNOWLEDGMENTS AND ADDRESSES

Received December 23, 1975, from the *School of Pharmacy, Temple University, Philadelphia, PA 19140.*

Accepted for publication April 23, 1976.

The support provided G. K. Menon through a Temple University Graduate Fellowship is gratefully acknowledged.

[x] To whom inquiries should be directed.

Pharmacokinetics of β-Methyldigoxin in Healthy Humans II: Oral Studies and Bioavailability

PETER H. HINDERLING [*], EDWARD R. GARRETT [x], and RONALD C. WESTER [‡]

Abstract □ The pharmacokinetics of orally administered aqueous ^{3}H-β-methyldigoxin solutions were studied at two dose levels, 0.3 and 0.6 mg, in healthy human subjects. The drug and its metabolites were specifically assayed in biological fluids and compared with results after intravenous doses to the same subjects. No significant dose dependency was observed. The apparent half-life of absorption was 16 ± 6 min (*SEM*). Digoxin was the only metabolite observed in the plasma and comprised 28.6 ± 3.7% of the dose in the urine. ^{3}H-β-Methyldigoxin, renally excreted unchanged, comprised 25.7 ± 1.7% (*SEM*). Water-soluble metabolites in the urine comprised 9.0 ± 1.8%. Fecal and urinary excretion accounted for 85% of the dose at 144 hr. The oral absorption of unchanged ^{3}H-β-methyldigoxin from solution was 59 ± 6% by area under the curve methods and 60 ± 4% by renal excretion. A total of 73% of the dose in the solution was absorbed as β-methyldigoxin and digoxin. First-pass metabolism prior to absorption was largely prehepatic and assignable to GI degradation; 21.9 ± 2.8% was degraded with 12.8 ± 4.0% to digoxin and 9.1 ± 4.0% to water-soluble metabolites. From 14 to 18% of the administered oral dose did not reach the systemic circulation. Analog computer fitting of plasma and urine levels of drug and digoxin was consistent with the first-pass premise with a delayed absorption of GI-generated digoxin and other metabolites. There were no significant differences between the oral absorption of a tablet formulation and the solution. Orally administered β-methyldigoxin solution delivered 97% cardioactivity as itself and digoxin with respect to an equivalent amount of intravenously administered digoxin. This value contrasts to the 140% delivered by intravenously administered β-methyldigoxin on the premise of pharmacodynamic equivalence of systemically appearing digoxin and β-methyldigoxin. Literature reports on the oral bioavailability of solutions and solid dosage forms of digoxin were critically reviewed, but no reliable comparison of the extent and reproducibility of oral absorption of cardioactive agents from administered digoxin or β-methyldigoxin could be made from the widely variable digoxin studies with nonspecific assays.

Keyphrases □ β-Methyldigoxin—oral, pharmacokinetics and bioavailability in humans, radiochemical–TLC study □ Pharmacokinetics—oral β-methyldigoxin, humans, radiochemical–TLC study □ Bioavailability—oral β-methyldigoxin, humans, radiochemical–TLC study □ Radiochemistry–TLC—study of pharmacokinetics and bioavailability of oral β-methyldigoxin in humans □ Cardiac glycosides—β-methyldigoxin, oral, pharmacokinetics and bioavailability in humans, radiochemical–TLC study

Semisynthetic derivatives of digoxin (Ia) such as β-methyldigoxin (Ib), a methyl ether of digoxin, and β-acetyldigoxin (Ic), an acetyl ester of digoxin, have been claimed to have higher intrinsic rate constants and efficiencies of absorption than digoxin in animals and in humans (1–14). Presumably, the rationale for their preferred usage is that a completely absorbed compound has the most consistent bioavailability in multiple dosage regimens. This is a valid approach, since glycosides have a narrow therapeutic range (15–18) and the occurrence of toxic manifestations in patients undergoing chronic therapy is 7–20% (19). Whereas β-acetyldigoxin was extensively metabolized or degraded before reaching the systemic circulation (20), β-methyldigoxin was claimed to

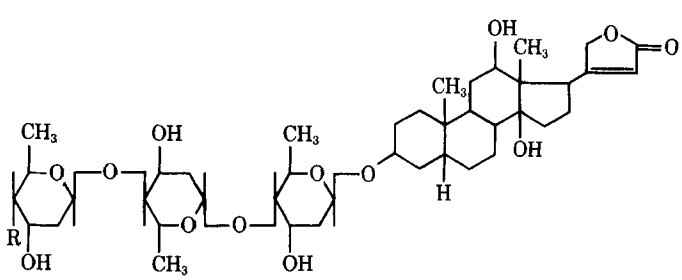

Ia: R = OH
Ib: R = OCH_3 Ic: R = $OCCH_3$

Table I—Parameters for Orally Administered β-Methyldigoxin Pharmacokinetics by Graphical Methods

Parameter	Subject A (66.3 kg, 169 cm, 1.76 m² surface area)		Subject B (71.3 kg, 179 cm, 1.89 m² surface area)		Subject C (67.4 kg, 166 cm, 1.75 m² surface area)		Average ± SD
D, dose, μg	284	604	271	588	278	621	
k_a, hr^{-1} [a]	3.0	13.9	4.6	2.6	0.92	3.8	4.8 ± 4.6
10^2 area/D, hr/liter po (iv) [b]	6.1 (14.6)	7.6 (18.5)	6.6 (8.9)	7.4 (10.3)	9.6 (16.8)	11.3 (16.4)	8.1 ± 2.0 (14.3 ± 3.8) [m]
Clearances, ml/min							
$(Cl_p^u)_{tot}$ [c]	113	90	173	178	99	99	125 ± 40 (125 ± 40) [m]
$(Cl_p^u)_r$ [d]	62	46	99	63	44	42	59 ± 22 (59 ± 17) [m]
$(Cl_p^u)_m$ [e]	51	44	74	115	55	57	66 ± 22 (66 ± 24) [m]
Percent of β-methyldigoxin dose, D, in urine from							
$10^2\ U_{\infty}^{BMD}/D$ [f]	26.7	24.6	37.3	29.0	24.0	26.3	28.0 ± 4.9 (46.9 ± 5.3) [m]
$10^2\ U_{144\ hr}^{BMD}/D$ [g]	23.7	22.9	33.8	27.1	22.9	23.7	25.7 ± 4.3 (43.2 ± 4.7) [m]
$10^2\ U_{144\ hr}^{DIG}/D$ [h]	29.1	28.4	45.3	24.1	18.6	26.2	28.6 ± 9.0 (31.7 ± 5.5) [m]
$10^2\ U_{144\ hr}^{H_2O}/D$ [i]	9.9	12.3	4.7	6.4	14.2	6.3	9.0 ± 3.8 (5.3 ± 1.9) [m]
Absorption efficiency from [j]:							
areas, f_1	0.42	0.41	0.74	0.72	0.57	0.69	0.59 ± 0.15
U_{∞}^{BMD}	0.61	0.55	0.68	0.63	0.47	0.65	0.60 ± 0.08
$U_{144\ hr}^{BMD}$	0.61	0.57	0.67	0.62	0.50	0.62	0.60 ± 0.06
$U_{144\ hr}^{DIG}$	0.79	0.93	1.32	0.84	0.56	1.15	0.92 ± 0.29
$U_{144\ hr}^{H_2O}$	1.7	2.1	1.2	1.3	4.2	0.75	1.9 ± 1.2
Recovery of administered radioactivity at 144 hr [k]:							
Fecal, %	14.3	38.8	19.3	24.6	32.5	20.6	25.9 ± 8.1 (11.8 ± 1.6) [m]
Fecal + urinary, %	74.4	97.2	92.1	76.3	88.2	81.1	84.9 ± 9.1 (85.8 ± 2.7) [m]
144-hr recovery of β-methyldigoxin dose, % [l]	82	102	103	82	89	76	89.0 ± 11.2 (91.8 ± 6.5) [m]

[a] Apparent first-order rate constant of absorption of β-methyldigoxin from method of residuals on oral administration. [b] Determined by graphical integration of the area in micrograms-hour per liter under plasma unbound β-methyldigoxin concentration–time curve; this area is divided by the administered dose in micrograms. The parenthetical values were from the intravenous studies (25). [c] Total clearance from f_1D/area under plasma unbound concentration–time plots, where f_1 is the absorption efficiency from the ratio of the areas per unit dose for oral to intravenous administration. [d] Renal clearance from slope of plots of renal elimination rates of β-methyldigoxin, $\Delta U/\Delta t$, against plasma concentrations of unbound drug. [e] Metabolic clearance from the difference of total and renal clearances, $(Cl_p^u)_{tot} - (Cl_p^u)_r$. [f] Calculated from the micrograms of β-methyldigoxin renally excreted at infinite time, U_{∞}^{BMD}, which was estimated from adding to the amount excreted at 144 hr the amount that would have been excreted for five more half-lives if the slope of the natural logarithm of the excretory rate, $\ln \Delta U/\Delta t$, against time was a constant, $-\gamma$. [g] Calculated from the micrograms of β-methyldigoxin renally excreted at 144 hr, $U_{144\ hr}^{BMD}$. [h] Calculated from the micrograms of β-methyldigoxin equivalent of the digoxin renally excreted at 144 hr, $U_{144\ hr}^{DIG}$. [i] Calculated from the micrograms of β-methyldigoxin equivalent of water-soluble metabolites renally excreted at 144 hr, $U_{144\ hr}^{H_2O}$. [j] Value from oral administration divided by pertinent value from intravenous administration (25) for each subject. [k] Percent of total radioactivity administered excreted by 144 hr by specified route(s). [l] Percent of dose of β-methyldigoxin excreted by 144 hr renally as unchanged drug, digoxin, and water-soluble metabolite plus fecal excretion. [m] Parenthetical values were obtained from intravenous studies (25).

have a higher absorption efficiency than digoxin and β-acetyldigoxin on intraduodenal application in guinea pigs (3) and absorption efficiencies of 75–100% in humans (4–10).

These conclusions were based on pharmacodynamic cardiovascular parameters (4–6, 10) and the total radioactivity in plasma and/or excreted in urine after oral and intravenous administration (7, 8). Both methods do not give the intrinsic bioavailability of β-methyldigoxin, since the contributions of digoxin activity or the production of active or labeled metabolites prior to absorption cannot be excluded. Radioimmunoassay is a highly sensitive assay for cardiac glycosides (21, 22) and is applicable for the assay of the sum of β-methyldigoxin and its derived metabolites in biological fluids (22–24). It suffers from the same limitations as total radioactivity.

The pharmacokinetics of intravenously administered ^{3}H-β-methyldigoxin and its derived metabolites were considered previously (25). The present studies were conducted with the same subjects to determine the time course and bioavailability of ^{3}H-β-methyldigoxin and its metabolites, analyzed separately, at two dosage levels after oral administration.

EXPERIMENTAL

Details of the materials and analytical procedures used and the general pharmacokinetic procedures and design were given previously (25). The assayed solutions of 0.30- and 0.60-mg doses of ^{3}H-β-methyldigoxin in 0.9% saline solution were administered orally to the subjects (25) by a syringe with immediate swallowing to avoid sublingual or buccal absorption. A 40-ml water rinse was swallowed immediately. Blood (6 ml) was taken within 10 sec at 0, 2.5, 5, 10, 15, 20, 30, 45, 60, and 90 min and at 2, 3, 5, 7, 9, 11, 15, 20, 24, 36, 48, 60, 72, 84, 96, 120, and 144 hr after the oral drug administration through the butterfly needle with syringes; procedures were as described previously (25). The urine was collected

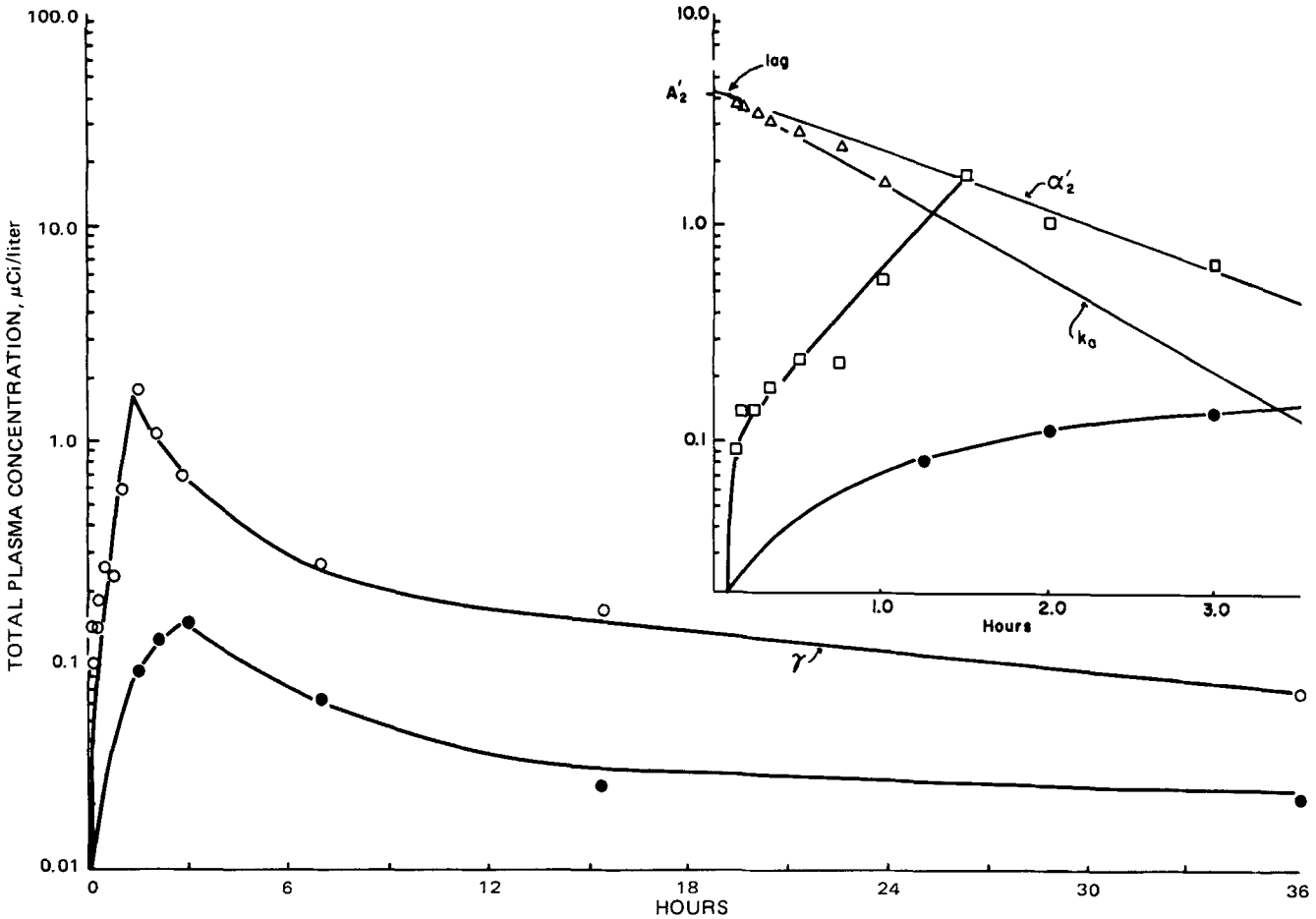

Figure 1—*Typical semilogarithmic plots of plasma β-methyldigoxin (○) and digoxin (●) concentrations, [A_p], against time for oral administration: 120.1 μCi = 278 μg of β-methyldigoxin in aqueous solution to Subject C. The insert is a plot of the plasma β-methyldigoxin (□) and digoxin (●) concentrations on an expanded time axis. The data were treated by the method of residuals by extrapolating the α_2-phase to time zero and plotting semilogarithmically the difference (△) of the antilogarithms of the extrapolated line and the plasma concentrations against time on the assumption that the absorption process was concluded during the α_2'-phase. The slope, $-k_a/2.303$, of this line permits estimation of the apparent first-order absorption rate constant, k_a. The lag time was estimated from the intersection of the extrapolated α_2-phase and the plot of the differences.*

and assayed as described in the intravenous studies (25). The subjects[1] were prostrate during the first 24 hr after drug administration.

In addition to the solutions, a tablet formulation of ^{3}H-β-methyldigoxin was administered to six of the seven volunteers. Five tablets (0.1 mg/tablet) with 100 ml of water were swallowed immediately, and biological fluids were sampled up to 24 hr after tablet administration as in the oral studies on solutions.

RESULTS AND DISCUSSION[2]

Plasma Pharmacokinetics of ^{3}H-β-Methyldigoxin after Oral Administration—The α_2-, β-, and γ-phases with pharmacokinetic constants similar to those of intravenous administration (25) were observed for ^{3}H-β-methyldigoxin. These phases were preceded by a rapid absorption phase, characterized by an apparent first-order absorption rate constant, k_a (Table I and Fig. 1). Peak plasma concentrations for total drug of 1.1 ±.0.1% of the dose/liter of plasma were reached at 50 ± 9 min after administration. The fact that these values were markedly consistent among doses, 1.14 ± 0.17 at 300 μg and 1.11 ± 0.15 at 600 μg (n = 3), was strongly indicative of a first-order absorption process. The rate constant, k_a, was obtained by "feathering" after excluding lag times of 9.4 ± 1.5 min. The α_2-phase of the semilogarithmic plot was extrapolated to zero time, and k_a was estimated from the linear slope of the differences of the antilogarithm of the extrapolated line and the plasma concentration against time (Fig. 1, insert) to give an apparent half-life of absorption of 16 ± 6 min.

The lack of dose dependency was evident by the superimposability of plots at various doses for the percent of dose per liter of plasma against time (Fig. 2).

Digoxin was the only metabolite observed in the plasma and peaked at 90 ± 24 min after oral administration of ^{3}H-β-methyldigoxin (Fig. 1), in contrast to the 32.3 ± 7.0 min observed after intravenous administration (25).

The apparent overall rate constant of elimination, γ, for the pseudo-steady state after equilibration among tissues, 19.3 ± 1.6 × 10^{-3} hr^{-1}, obtained from the slope of the semilogarithmic plot of plasma ^{3}H-β-methyldigoxin concentration against time, was not significantly different from the 17.3 ± 0.8 × 10^{-3} hr^{-1} value obtained after intravenous administration (25).

Urine Pharmacokinetics—The amounts of β-methyldigoxin cumulatively excreted in urine were plotted as percent of dose against time (Fig. 2) to estimate the total recovery and were reasonably superimposable for all doses. The apparent rate constant, γ, for the terminal phase of drug elimination in the urine, 20.5 ± 0.6 × 10^{-3} hr^{-1}, obtained from the slope of the natural logarithm of the amount yet to be excreted, $\ln(U_\infty - U)$ against time, was not significantly different from the 20.8 ± 0.5 × 10^{-3} hr^{-1} value obtained after intravenous administration (25).

The percentages of the ^{3}H-β-methyldigoxin dose renally excreted by 144 hr as β-methyldigoxin, digoxin, and water-soluble metabolites were 25.7 ± 1.7, 28.6 ± 3.7, and 9.0 ± 1.8 (Table I), respectively, in contrast to the intravenous values of 43.2 ± 1.9, 31.7 ± 2.2, and 5.3 ± 0.8, respectively (25).

The water-soluble metabolites in an 18-hr urine collection after oral administration were composed of glucuronides (42.4 ± 14.2%), sulfates

[1] Informed consent was obtained from all subjects. The protocol was approved by the Committee for Protection of Human Subjects and the Clinical Research Committee, J. Hillis Miller Health Center, University of Florida.

[2] The plus and minus values for mean values given in the text refer to the standard error, $\sigma/\sqrt{n}$, of such means, where σ is the standard deviation given in the tables of this paper or Ref. 25, and n is the number of values considered (6 unless otherwise specified).

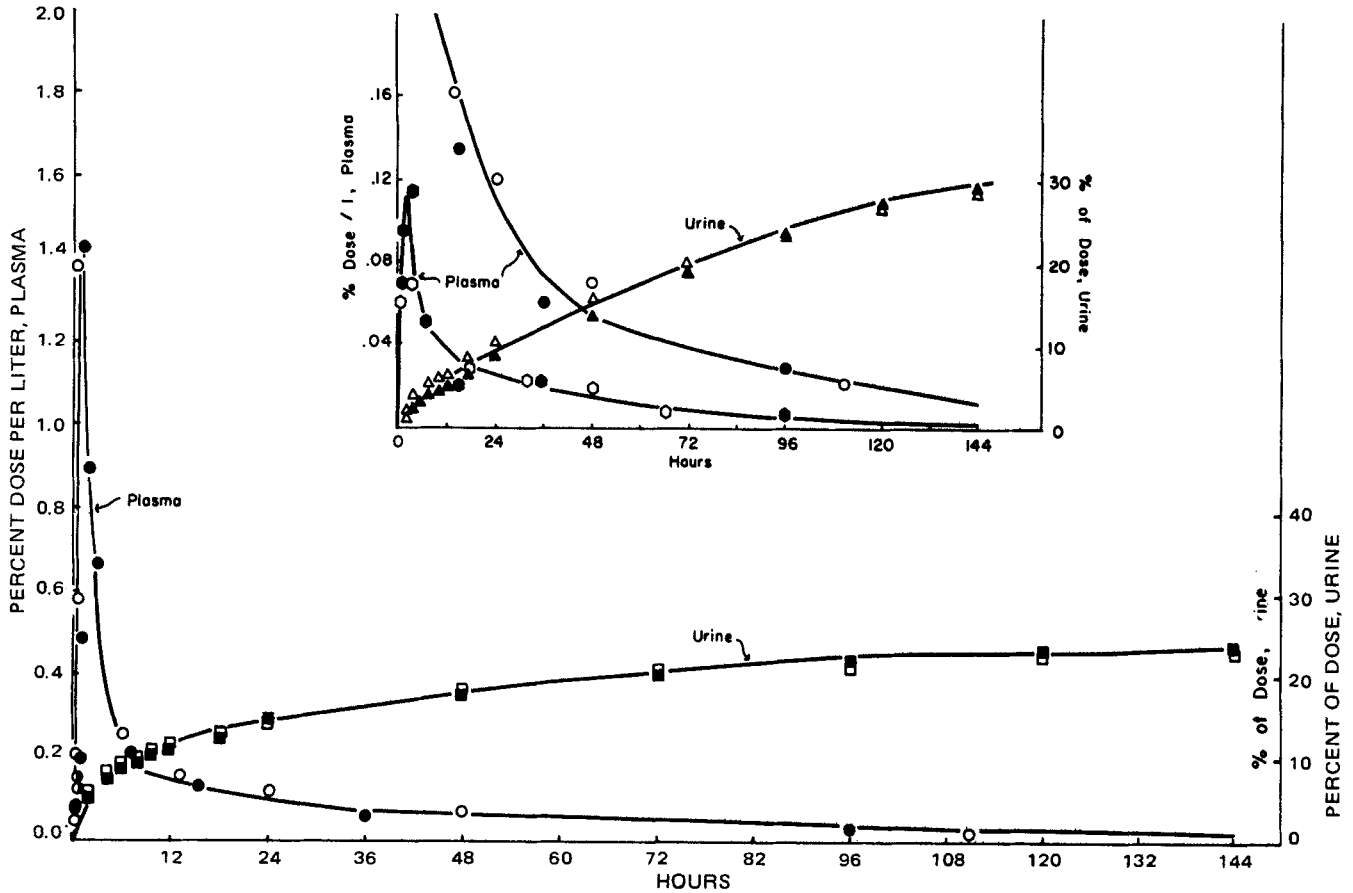

Figure 2—*Typical plasma concentrations and cumulative urine excretions in percent of β-methyldigoxin dose per liter of plasma and of dose, respectively, against time for oral solution administration: 126.7 μCi = 294 μg (open symbols) and 254.1 μCi = 590 μg (solid symbols) of β-methyldigoxin to Subject A. Key: ○, ●, plasma β-methyldigoxin levels; □, ■, urinary β-methyldigoxin amounts; ○, ● (inset), plasma digoxin levels; and △, ▲ (inset), urinary digoxin amounts.*

(24.6 ± 8.2%), and unidentifiable metabolites (33.6 ± 7.6%) (all $n = 3$). The percent compositions of these two fractions of glucuronide and sulfate conjugates were 82.4 ± 2.8 and 67.3 ± 9.8% with β-methyldigoxin, respectively, 8.6 ± 2.5 and 23.3 ± 9.6% with digoxin, respectively, and 9.0 ± 6.5 and 9.5 ± 1.2% with digoxigenin, respectively (all $n = 3$).

The percentages of the administered total radioactivity renally excreted as total radioactivity at 144 hr were 70.3 ± 1.2%, intravenous (25), and 57.7 ± 1.7%, oral ($n = 14$). The percentages of the administered total radioactivity fecally excreted as total radioactivity at 144 hr were 11.8 ± 0.6%, intravenous (25), and 25.9 ± 3.3%, oral. The combined urinary and fecally recovered amounts of total radioactivity at 144 hr were 85.8 ± 1.1%, intravenous (25), and 84.9 ± 3.%, oral, of the total radioactivity administered.

Clearances—The total clearances of unbound ^{3}H-β-methyldigoxin were calculated from:

$$(Cl_p{}^u)_{tot} = fD_{po}/area_{po} \qquad \text{(Eq. 1)}$$

where D_{po} is the orally administered dose. The area was determined under the plasma unbound concentration–time curves extrapolated to infinite time; f, the fraction of dose absorbed, was calculated from:

$$f = \frac{area_{po}}{D_{po}} \Big/ \frac{area_{iv}}{D_{iv}} \qquad \text{(Eq. 2)}$$

The areas and dose, D_{iv}, after intravenous administration to the same individual were given previously (25). Total clearance does not necessarily imply pharmacodynamic inactivation, since it includes the metabolic clearance of β-methyldigoxin where pharmacodynamically active digoxin is the major metabolite.

The total clearances of unbound β-methyldigoxin were the same after oral administration (Table I) as after intravenous administration (25). The average renal (59 ± 9 ml/min) and metabolic (66 ± 9 ml/min) clearances after oral administration were the same as those after intravenous administration, 59 ± 7 and 66 ± 10 ml/min, respectively (25). All clearances for a given individual were similar, whatever the mode of administration (Table I and Ref. 25).

The renal clearance of plasma-unbound digoxin after oral administration of ^{3}H-β-methyldigoxin was 159 ± 8 ml/min ($n = 2$) and was significantly less than that after intravenous administration, 222 ± 32 ml/min ($n = 5$).

The renal clearance of the water-soluble metabolite fraction taken as an entity can be estimated from the observed rates of renal elimination, $\Delta U/\Delta t$ (Fig. 3), obtained in these studies at the respective plasma levels,

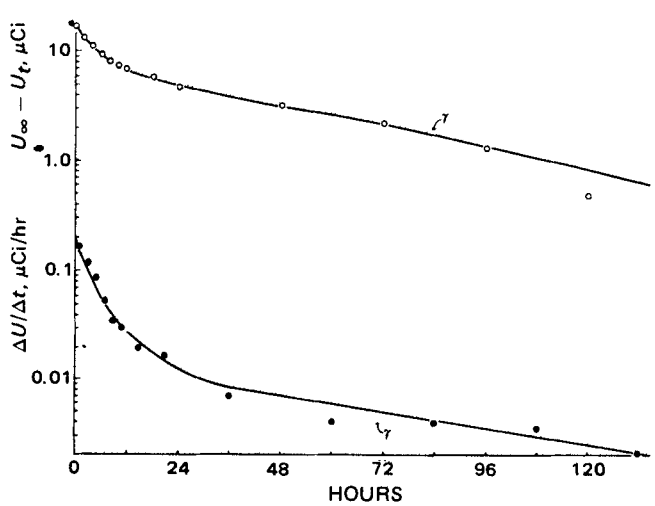

Figure 3—*Typical semilogarithmic plots of amounts of water-soluble metabolites yet to be excreted, $U_\infty - U_t$ (○), and rates of urinary excretion of water-soluble metabolites, ΔU/Δt (●), against time after oral administration: 120.1 μCi = 279 μg of β-methyldigoxin to Subject C with an apparent terminal half-life of 40 hr.*

Table II—Estimates of First-Pass Metabolism on Oral Administration

Parameter	Subject A (66.3 kg, 169 cm, 1.76 m² surface area)		Subject B (71.3 kg, 179 cm, 189 m² surface area)		Subject C (67.4 kg, 166 cm, 175 m² surface area)		Average ± *SD*
D, dose, μg	284	604	271	588	278	621	
$10^2\ U^{DIG}_{144\ hr}/D$							
Actual[a]	29.1	28.4	45.3	24.1	18.6	26.2	28.6 ± 9.0
Predicted[b]	22.4	17.4	22.9	17.9	18.5	14.1	18.9 ± 3.3
$10^2\ U^{H_2O}_{144\ hr}/D$							
Actual[c]	9.9	12.3	4.7	6.4	14.2	6.3	9.0 ± 3.8
Predicted[d]	3.6	3.4	2.1	3.1	1.7	5.2	3.2 ± 1.2
Percent of dose metabolized on first pass and excreted in urine:							
Digoxin[e], $10^2\ (U_{DIG}/D)_{first\ pass}$	6.7	11.0	22.4	6.2	0.1	12.1	9.8 ± 7.5
H_2O solubles[e], $10^2\ (U_{WS}/D)_{first\ pass}$	6.3	8.9	2.6	3.3	12.5	1.1	5.8 ± 4.3
Percent of dose metabolized to digoxin on first pass[f], $10^2(E_{DIG}/D)_{first\ pass}$	8.8	14.4	29.3	8.1	0.1	15.8	12.8 ± 9.8
Percent of dose metabolized to water solubles on first pass[g], $10^2\ (E_{WS}/D)_{first\ pass}$	10.5	14.4	—	4.7	25.0	—	9.1 ± 9.7
Total percent of dose metabolized on first pass[h], $[10^2\ (E_{DIG} + E_{WS})/D]_{first\ pass}$	19.3 (20.7)	28.8 (14.5)	29.3 (26.0)	12.8 (15.2)	25.1 (20.3)	15.8 (20.9)	21.9 ± 6.9 (19.6 ± 4.2)

[a] Calculated from the micrograms of β-methyldigoxin equivalent of the digoxin renally excreted at 144 hr, $U^{DIG}_{144\ hr}$, after oral administration of a dose of β-methyldigoxin, *D*, in micrograms. [b] Calculated from the product of the absorption efficiency of β-methyldigoxin (determined from the ratio of β-methyldigoxin renally excreted 144 hr after oral and intravenous administration) and the percent of the dose renally excreted as digoxin 144 hr after intravenous administration (Table I). [c] Calculated from the micrograms of β-methyldigoxin equivalent of the water-soluble metabolites renally excreted at 144 hr, $U^{H_2O}_{144\ hr}$, after oral administration of a dose of β-methyldigoxin, *D*, in micrograms. [d] Calculated from the product of the absorption efficiency of β-methyldigoxin [based on $U^{BMD}_{144\ hr}$ (po)/$U^{BMD}_{144\ hr}$ (iv) values of Table I] and the percent of the dose renally excreted as water-soluble metabolites 144 hr after intravenous administration. [e] Difference between actual and predicted values. [f] Amount of digoxin as percent of the dose formed on first pass, $10^2\ (E_{DIG}/D)_{first\ pass}$, can be estimated from the percent dose metabolized on first pass that is excreted in the urine, $10^2\ (U_{DIG}/D)_{first\ pass}$, *i.e.*, $10^2\ (E_{DIG}/D)_{first\ pass} = 10^2\ (U_{DIG}/D)_{first\ pass} \times (Cl_{DIG})_{tot}/(Cl_{DIG})_{ren}$, where the values for $(Cl_{DIG})_{tot}$ = 290 ml/min and $(Cl_{DIG})_{ren}$ = 222 ml/min were taken from the values obtained in the intravenous studies. An alternative method of estimation, on the premise that only digoxin is significantly formed on first pass and that all water solubles are derived from systemic digoxin and excreted in urine, is from $10^2\ (E_{DIG}/D)'_{first\ pass} = 10^2\ (U_{WS}/D)_{first\ pass} \times (Cl_{DIG})_{tot}/(Cl_{DIG})_{met}$, where $(Cl_{DIG})_{tot}$ = 290 ml/min and $(Cl_{DIG})_{met}$ = 68 ml/min. These $10^2\ (E_{DIG}/D)'_{first\ pass}$ values averaged 25 ± 18 (*SD*), larger than the averaged estimate of $10^2\ (E_{DIG}/D)_{first\ pass}$ = 12.2 ± 9.8 (*SD*). Although the standard deviations were large, it was concluded that water-soluble metabolites probably were not formed on first pass. [g] The total amount of water-soluble metabolites as a percent of dose, $10^2\ (E_{WS}/D)_{first\ pass}$, may be calculated from $10^2\ (U_{WS}/D)_{first\ pass} \times (Cl_{WS})_{tot}/(Cl_{WS})_{ren} - 10^2(E_{DIG}/D)_{first\ pass} \times (Cl_{DIG})_{met}/(Cl_{DIG})_{tot}$, where the latter term containing a ratio of the digoxin clearances of 0.234 corrects for water-soluble metabolites produced that result from the additional digoxin available systemically on first pass. The ratio of the water-soluble clearances in the first term on the right (the term that estimates the total amount of water solubles produced from that renally excreted) is taken as 2, since the data of Abshagen *et al.* (43) demonstrated relatively equal amounts of water solubles eliminated in the bile and urine on β-methyldigoxin administration. [h] The parenthetical values give the analog computer estimates of the total first-pass metabolism calculated from the ratio $k_{GIGI'}/(k_{GIGI'} + k_{GIB})$ (Scheme I).

$[A_p]$, of water-soluble metabolites obtained from the data of Rietbrock and Abshagen (26), where both sets of data were obtained after oral administration. No significant plasma levels of water-soluble metabolites were obtained in our studies. The average rates of renal elimination in the three subjects were 1.03, 1.16, 0.56, 0.41, and 0.27% of the total dose of radioactivity excreted per hour during 0–2-, 2–4-, 4–6-, 6–8-, and 8–10-hr intervals, respectively. The average plasma concentrations of water-soluble metabolites were 0.061, 0.070, 0.039, 0.023, and 0.013% of the dose of radioactivity per liter of plasma at 1, 3, 5, 7, and 9 hr, respectively, in the studies of Rietbrock and Abshagen (26). The respective individual quotients for the renal clearance of water-soluble metabolites, $(Cl^{H_2O}_p)_r = dU/dt/[A_p]$, were 17.0, 16.6, 14.4, 17.8, and 20.8 liters/hr and averaged 288 ± 17 ml/min.

The ratio of the renal clearance of water-soluble metabolites to creatinine clearance was 2.1 ± 0.1, indicating an excess of tubular secretion in addition to glomerular filtration.

An apparent linear terminal γ-phase with an average half-life of 36 hr was obtained from the semilogarithmic plots of $\Delta U/\Delta t$ and $U_\infty - Ut$ *versus* time for the water-soluble metabolites (Fig. 3). The slopes of these plots were similar to those observed for the terminal elimination γ-phase of the parent drug (40 hr). This terminal phase of the water-soluble metabolite fraction probably is dependent on its formation rather than its elimination, and the rate-limiting step probably is the rate of return of the parent drug from its deepest compartment, T'', with the overall rate constant of elimination of the water-soluble metabolites being a much faster process.

Absorption Efficiency and Evidence for First-Pass Metabolism—When the plasma concentrations and cumulative urine content of ^{3}H-β-methyldigoxin and digoxin were plotted against time in terms of the percent of the β-methyldigoxin dose per liter of plasma and the percent of dose, respectively, for the two dose levels of ^{3}H-β-methyldigoxin, the curves were superimposable for intravenous (25) and oral (Fig. 2) administration. Thus, the pharmacokinetics of β-methyldigoxin are dose independent, and the Dost principle (27) of corresponding areas is applicable to determine the degree of absorption. The areas (Table I) under the plasma concentration–time curves were estimated by graphical integration.

For the β-methyldigoxin curves, the area after oral absorption was 59 ± 6% of the area after intravenous administration and agreed with the fact that 60 ± 4% of the amount of β-methyldigoxin renally excreted at 144 hr and at infinite time after intravenous administration was renally excreted after oral administration. For the concentration of total radioactivity in plasma against time curves, the area after oral absorption was 76 ± 2% (n = 13) of the area after intravenous administration and was independent of dose. The amount of total radioactivity renally excreted after oral administration in 144 hr was 83 ± 3% (n = 14) of the amount renally excreted after intravenous administration. The relative percent renally excreted, oral–intravenous, did not reach reasonable constancy until after 24 hr, the minimum time that can be used for preliminary estimations of bioavailability.

This discrepancy between apparent oral absorption efficiencies from β-methyldigoxin and total radioactivity data indicates that ^{3}H-β-methyldigoxin was metabolized prior to its arrival in the systemic circulation, a first-pass phenomenon (28). This result is confirmed by the fact that apparent absorption efficiencies calculated from urinary excretion data (Table I) for digoxin (0.92 ± 0.12) and water-soluble me-

Table III—Parameters for β-Methyldigoxin Pharmacokinetics on Oral Administration Obtained by Analog Computer Fitting to Scheme I

Parameter	Subject A (66.3 kg, 169 cm, 1.76 m² surface area)		Subject B (71.3 kg, 179 cm, 1.89 m² surface area)		Subject C (67.4 kg, 166 cm, 1.75 m² surface area)		Average ± SD
D, dose, μg	284	604	271	588	278	621	—
$10^4\ k_{BT}$, sec^{-1} [a]	23.3	23.2	23.4	23.4	20.2	30.5	23.3 ± 0.1
$10^4\ k_{TB}$ [a]	15.1	20.8	12.3	12.3	13.4	11.2	15.1 ± 4.0
$10^4\ k_{BT'}$ [a]	7.71	6.97	5.62	5.62	5.53	7.18	6.43 ± 0.96
$10^4\ k_{T'B}$ [a]	1.79	2.46	0.979	0.979	1.08	0.947	1.37 ± 0.62
$10^4\ k_{BT''}$ [a]	3.44	1.79	3.30	3.30	4.76	4.80	3.57 ± 1.12
$10^4\ k_{T''B}$ [a]	0.120	0.135	0.125	0.125	0.141	0.146	0.132 ± 0.010
$10^4\ k_{BU}$ [a]	0.865	0.599	1.16	0.880	0.979	0.979	0.910 ± 0.19
$10^4\ k_{BM}$ [a]	1.18	1.03	0.469	0.870	1.63	1.43	1.10 ± 0.41
$10^4\ k_{M_1T}$ [b]	13.5	13.5	7.72	7.75	15.1	13.8	11.9 ± 3.3
$10^4\ k_{TM_1}$ [b]	10.4	12.5	3.78	3.80	7.66	2.55	6.78 ± 4.05
$10^4\ k_{M_1T'}$ [b]	11.1	13.4	5.77	5.75	8.38	8.45	8.81 ± 3.01
$10^4\ k_{T'M_1}$ [b]	0.156	0.146	0.177	0.162	0.120	0.162	0.154 ± 0.019
$10^4\ k_{M_1U}$ [b]	2.65	2.46	1.37	2.53	1.45	2.10	2.09 ± 0.56
$10^4\ (k_{M_1M_2} + k_{M_1\ \text{bile}})$ [b]	0.438	1.12	0.474	1.29	2.09	1.44	1.14 ± 0.63
$10^4\ k_{GIB}$ [b]	9.16	6.41	10.4	5.76	1.33	5.73	6.46 ± 3.16
$10^4\ k_{GIGI}$ [b]	2.39	1.09	3.64	1.03	0.339	1.51	1.67 ± 1.18
$10^4\ k_{GI'M_1}$ [b]	0.276	0.859	0.714	0.766	0.938	0.766	0.720 ± 0.23
V_p [u], liters [c]	14.5	14.5	13.4	13.4	7.02	7.02	11.7 ± 3.6
$(V_p)_{DIG}$ [d]	15.2	15.8	28.0	10.5	14.9	16.0	16.7 ± 5.9
$(V_D)_{DIG}$ [e]	1121	1479	997	404	1088	935	1004 ± 350
Absorption lag time, min [f]	24	8	8	17	7	8	12.0 ± 7.0

[a] Values for the microscopic rate constants of distribution and elimination were slightly modified to obtain the best fit from those obtained from the best analog computer fits of the plasma and urine data after intravenous administration (25). [b] Obtained from the best analog computer fit of the oral data with consideration of a lag time and a first-pass effect. The k_{GIB} corresponds to the intrinsic rate constant of absorption of unchanged drug absorbed. Its value is not expected to be coincident with the k_a value in Table I. The value for the latter was obtained by feathering and corresponds to the sum of the intrinsic rate constant and parallel first-order rate constant for the loss of the drug from the GI tract by other processes than absorption of unchanged drug. The value for $k_{M_1M_2} + k_{M_1\ \text{bile}}$ is 112% of $k_{M_1M_2}$, since the biliary clearance of digoxin is 12% of its total clearance (25). [c] Average values for both intravenous doses for the apparent volumes of distribution of the central compartment referenced to unbound drug in plasma were obtained from the best analog computer fit of the intravenous plasma data according to a four-compartment body model. The values of the volume of distribution of the central compartment in the oral experiments were postulated to be the same as in the intravenous experiments. [d] Values for the apparent volume of distribution of the central compartment referenced to total (bound and unbound) digoxin in plasma were obtained from the best analog computer fit of the data according to a three-compartment body model. [e] The value of the overall steady-state volume of distribution of digoxin was calculated (44) from $(V_p)_{DIG}[1 + (k_{MT'}/k_{TM}) + (k_{MT'}/k_{T'M})]$. [f] Determined from the best analog computer fits of the oral plasma data under the presumption of a first-pass phenomenon.

tabolite (1.9 ± 0.8) renal excretion were greatly in excess of the absorption efficiency of β-methyldigoxin (0.60). The area under the less precise plasma digoxin level–time curves after oral absorption of ^{3}H-β-methyldigoxin was 84 ± 10% of that area after intravenous administration and was confirmatory. A more detailed analysis of this first-pass phenomenon is given in Table II and indicates that 21.9 ± 2.8% (or 19.6 ± 1.7% by analog computer fitting) of the orally administered dose was metabolized in the GI lumen, gut wall, and/or the liver prior to absorption: 12.8 ± 4.0% to digoxin and 9.1 ± 4.0% (n = 4) to water-soluble metabolites.

Both digoxin and water-soluble metabolites probably are formed during the first pass and reach the systemic circulation. The extent of this total 22% first-pass metabolism in light of an estimated metabolic efficiency for β-methyldigoxin of 8% (25) implies a significant prehepatic first-pass metabolism. The former value, taken with the 60% absorption of β-methyldigoxin as such, implies that 18% does not reach the systemic circulation. The difference between the fecal recoveries of radioactivity between oral and intravenous administration, 25.9 ± 3.3 − 11.8 ± 0.7 = 14.1% (Table I), provides an alternative and similar estimate of the amount of material that does not reach the systemic circulation as β-methyldigoxin, digoxin, or other metabolites after oral administration. This amount may be an overestimate if the first-pass phenomenon after oral administration produces metabolites that are preferentially biliary excreted.

Evidence for an acid-catalyzed degradation of β-methyldigoxin *in vitro* and *in vivo* was given by Beerman (29), who determined individual radioactivities aspirated from the GI contents of volunteers administered labeled drug in polyethylene glycol. Non-β-methyldigoxin products were 28 and 15% of the total radioactivity in the gastric and duodenal aspirates, respectively, 10–15 min after drug administration. Their parameters of β-methyldigoxin absorption were similar to those found in this study; lag times were ~10 min, and peak concentrations occurred at ~50 min. β-Methyldigoxin incubated at pH 1.0 for 1 hr degraded 70% to digoxin, digoxigenin, and mono- and bisdigoxigenin digitoxosides. However, these three latter potential metabolites did not comprise any significant portion of the dose (<1%). The implication that the extent of the first-pass phenomenon may be a consequence of GI retention time was not confirmed by any apparent correlation with lag time for the studies in Table II.

Total radioactivities were measured in plasma and urine for 24 hr after administration of ^{3}H-β-methyldigoxin tablets. Peak plasma concentrations of 0.78 ± 0.17% of the administered radioactivity per liter were observed at 94 ± 21 min after administration. The corresponding value for the solutions given orally were 0.89 ± 0.11 at 72 ± 13 min (n = 11) after administration. A lag period of 15.8 ± 2.0 min between administration and the start of absorption was observed with the tablets compared to a lag period of 6.7 ± 1.6 min (n = 11) with the oral solutions; the latter was of the magnitude of the 5-min gastric emptying time of fluids in fasting individuals (30).

The ratios of the areas under the plasma concentration–time curves and the urinary excreted amounts of total radioactivity in 24 hr, corrected for the dose, were used to estimate the bioavailability of the tablets with respect to the solutions. They were 0.56 ± 0.05 and 0.92 ± 0.06 in plasma and urine, respectively, for tablets relative to the intravenous solutions and 0.87 ± 0.03 and 1.02 ± 0.05 in plasma and urine, respectively, for tablets relative to oral solutions. These findings indicate relatively complete absorption of β-methyldigoxin from the tablets relative to the solutions.

Pharmacokinetic Models for Orally Administered Solutions of β-Methyldigoxin and Digoxin and Their Fitting by Analog Computer—The existence of a first-pass metabolism of β-methyldigoxin was indicated by the fact that a greater percentage of the dose was excreted after oral administration relative to intravenous administration as the metabolite digoxin, M_1, and as the water-soluble metabolites, M_2 (Table II). The four-compartment body model for β-methyldigoxin and the three-compartment body model for the metabolite digoxin, developed previously for the intravenous case (25), were modified by adding a GI compartment to which the drug was administered with first-order absorption of β-methyldigoxin to the central compartment with rate constant k_{GIB} and with first-order generation of digoxin, M_1, with rate constant k_{GIM_1} to the central compartment of digoxin, M_1. Attempted analog computer fitting of the orally administered plasma β-methyldigoxin data to this model, using the microscopic rate constants obtained by fitting the intravenous data, consistently predicted initial plasma concentrations and urinary excreted amounts of digoxin greater than those actually observed. When this model was modified to include a first-pass metabolism directly to water-soluble metabolites in their

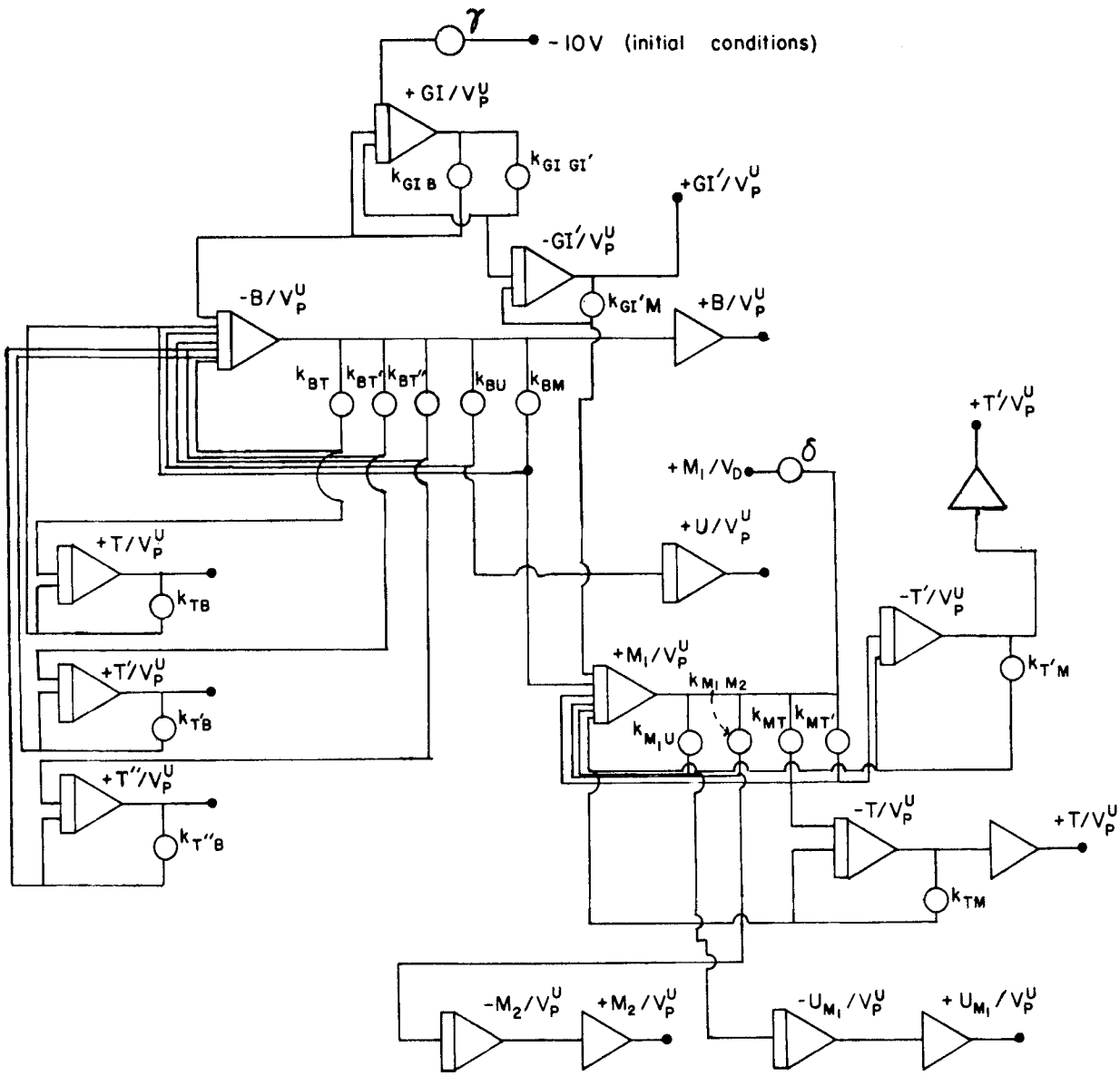

Figure 4—*Analog computer program to fit simultaneously the model of Scheme I to the experimental plasma and urine data where* $k_{GI'M_2}$ *is omitted and only* M_2 *as* $M_2/V_p{}^u$ *is generated. The route of* M_1 *to bile*$_{M_1}$ *is also omitted. Thus,* $k_{M_1M_2}$ *in the program and Table III was actually* $k_{M_1M_2} + k_{M_1 bile}$*, which overestimated the former by 12% since the biliary clearance of digoxin was estimated to be 36 ml/min out of a total clearance of 290 ml/min for digoxin in the intravenous studies* (25).

central compartment, the predicted cumulative terminal urinary amounts of digoxin generated by the analog computer were consistently lower than those actually observed.

These facts can be rationalized by postulating a delayed absorption of GI-generated digoxin, M_1, and/or water-soluble metabolites, M_2. Two alternative models are given in Scheme I, with and without the pathway indicated by the dashed line of rate constant $k_{GI'M_2}$. These models presume a significantly retarded production and absorption of GI-produced digoxin, $GI'M_1$, which is consistent with the literature reports (31) that digoxin is absorbed in the lower part of the small intestine and would be characterized by first-order rate constants $k_{GI,GI'}$ and $k_{GI'M_1}$, respectively. The plasma β-methyldigoxin and digoxin experimental values in concentration per liter were fitted to Scheme I (omitting the pathways characterized by $k_{GI'M_2}$ and k_{M_1bile}) by the analog computer program of Fig. 4. Concomitantly, the data for amounts of drug and metabolites in urine divided by the apparent volume of distribution of the central compartment for β-methyldigoxin, $(V_p{}^u)_{BMD}$, obtained in the intravenous studies were fitted.

Initial estimates of the amount of β-methyldigoxin absorbed either as drug or metabolites were made from the urinary recovery of unchanged drug and metabolites after multiplying by their respective ratios of total clearance to renal clearance. However, the initial condition, placed on

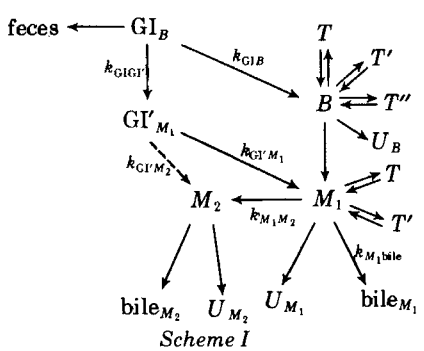

Scheme I

the GI_B compartment representing the dose, D, of ^{3}H-β-methyldigoxin that was actually absorbed as drug or metabolites [divided by this apparent volume of distribution $D/(V_p{}^u)_{BMD}$], was varied to give the best fit of the model since it cannot be presumed that the total dose, either as drug or metabolites, was transferred to the body. The $GI_B \rightarrow$ feces in Scheme I represents the route of fecal elimination of the total dose of ^{3}H-β-methyldigoxin not absorbed as drug or metabolite.

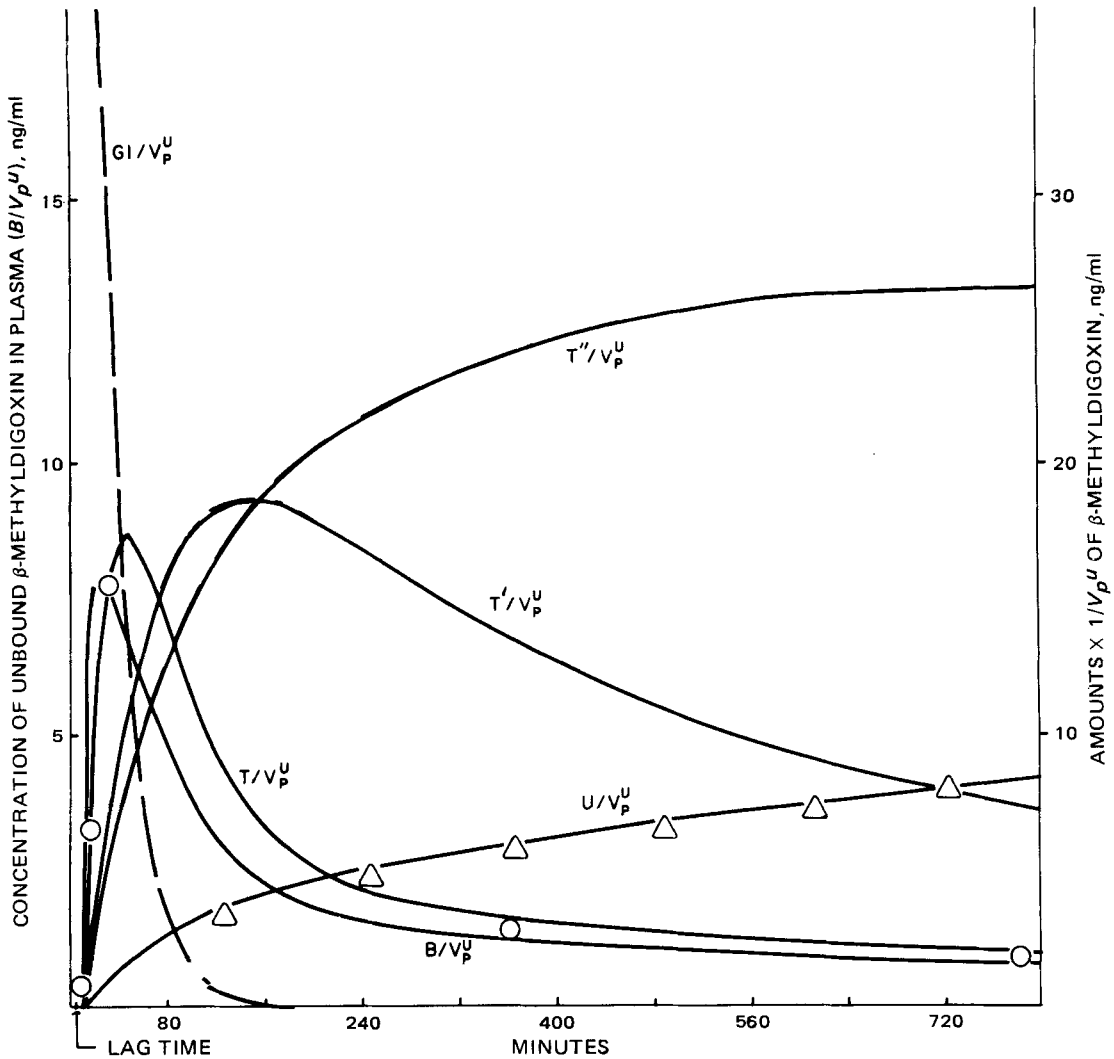

Figure 5—*Typical analog computer fitting of plasma water (unbound drug) concentration (O, left scale) and urine (Δ, right scale) data of β-methyldigoxin for 0.6-mg oral solution administration to Subject C over 13 hr in accordance with a four-compartment body model and a first-pass effect. All data are given as per milliliter of the volume of distribution of the central compartment referenced to unbound β-methyldigoxin, and the apparent concentrations of drug in the various tissues (GI, T, T′, and T″) and urine (U) (right scale) are generated with the parameters of Table III.*

The simultaneous analog computer fitting of the plasma and urine generated drug and metabolite amounts in peripheral tissues, urine, and the GI tract in terms of arbitrary concentrations (*i.e.*, amounts divided by $V_p{}^u$). The generated plasma concentrations of the metabolite $M_1/(V_p{}^u)_{BMD}$ were multiplied by a constant $\delta = (V_p{}^u)_{BMD}/(V_p)_{DIG}$ to fit best the plotted metabolite $M_1/(V_p)_{DIG}$ data so that the apparent volume of distribution, $(V_p)_{DIG}$, of M_1 could be calculated from the obtained values of δ. Lag times of absorption, 8–24 min, had to be assumed to fit best the first portion of the β-methyldigoxin data. Good fits always were obtained for the drug concentration in plasma and urine and the apparent concentration of M_1 in urine—*viz.*, $U_{BMD}/(V_p{}^u)_{BMD}$ and $U_{M_1}/(V_p{}^u)_{BMD}$; typical examples are given in Figs. 5 and 6. Only minor adjustments in the values of the microscopic rate constants found in the intravenous experiments were necessary to give optimal fits of the oral data. Their values are given in Table III.

Comparisons of Bioavailabilities of Orally Administered β-Methyldigoxin and Orally Administered Digoxin—The intrinsic bioavailability of unchanged ^{3}H-β-methyldigoxin after oral administration of solutions with respect to intravenous administration was 59.5 ± 3.3% (n = 12), evaluated by both renal excretion and areas under the unbound plasma level–time curves (Table I). The values ranged from 41 to 74% among all subjects, although urinary excretion estimates ranged only from 50 to 67% and, if one value was discarded, from 57 to 67%. However, this finding does not completely characterize the pharmacodynamic availability of such oral solutions since cardioactive digoxin is formed systemically (25, 32) from β-methyldigoxin and from first-pass prehepatic and hepatic metabolism of orally administered β-methyldigoxin (Table II). It was estimated previously (25) that the fraction of digoxin formed from the systemic β-methyldigoxin was 40% of the intravenously administered dose (34.5% renally eliminated and 5.5% biliary excreted). Thus, 0.40 × 60 = 24% is the amount of the total oral dose of ^{3}H-β-methyldigoxin absorbed as such that delivers digoxin to the body. The cardioactive digoxin formed by the first pass that reaches the systemic circulation as such (Table II) was 12.8 ± 4.0%. A total of 60 + 13 = 73% of digoxin plus β-methyldigoxin is absorbed.

However, the total systemic bioavailability of these cardioactive agents, digoxin plus β-methyldigoxin, on the premise of pharmacodynamic equivalence and similar terminal overall elimination rates of ~40 hr half-life, would be 60% (as β-methyldigoxin delivered directly) +24% (as digoxin derived from systemic β-methyldigoxin) + 13% (as digoxin derived from first-pass transformation of β-methyldigoxin prior to absorption) = 97%. On the same premise of pharmacodynamic equivalency of β-methyldigoxin and digoxin, intravenous β-methyldigoxin would deliver 100% (as β-methyldigoxin) + 40% (as digoxin derived from systemic β-methyldigoxin) = 140% of an equivalent dose of intravenously administered digoxin. Thus, the oral pharmacodynamic bioavailability of β-methyldigoxin relative to its intravenous administration would be 97/140 = 69%, where the oral pharmacodynamic bioavailability of β-methyldigoxin relative to equimolar intravenously administered digoxin, on the premise of equimolar pharmacodynamic equivalency, is 97%. These calculations were based on the presumption that the metabolites other than digoxin did not possess cardioactivity.

The proper comparison of the relative bioavailabilities of orally administered β-methyldigoxin and orally administered digoxin should be

Table IV—Critical Evaluations of Solution and Solid Dosage Form Oral Bioavailabilities of Digoxin Referenced to Intravenous Administration from Major Studies in the Literature

Reference	Oral Vehicle	Assay	Mean Estimated Absorption Efficiency, %	Method of Evaluation	Comments	Dose, mg	t_{max} (approx), min	$C_{max,po}$, % Dose/Liter of Plasma
33[a]	Ethanol, 95%	Total radioactivity	85[b]	Fecal excretion represents unabsorbed material, 7 days	Fecal excretion method criticized in Refs. 31 and 36 and herein; intravenous and oral population differed, > 20 subjects; total excretion in urine and stools; 49% oral and 85% intravenous	1.0, 2.0	70	—
			46[b]	Oral–intravenous, relative urinary excretion[c], 7 days				
31	Polyethylene glycol solution	Radioactivity of separated digoxin	50[b]	Intestinal aspirates	Based on oral studies only, five subjects	0.25	60	—
35	5% Dextrose solution	Radioimmunoassay	80[b]	Oral–intravenous, relative area under curve, 0–96 hr	Two subjects	0.50	30	0.75
37	40% Propylene glycol–10% ethanol	Radioimmunoassay	100, 93[b,c]	Oral–intravenous, relative urinary excretion, 10 days	Only 57% of intravenous dose recovered in urine of four subjects, well below other reported values	0.50	90	0.70
39	40% Propylene glycol–10% ethanol	Radioimmunoassay	81, 87[c,d] (50–115% range for 0.125 mg) 68, 61[c,d] (53–89% range for 0.25 mg)	Oral–intravenous, relative area under 0–24 hr curve for daily chronic dose	Gross inconsistencies of bioavailability estimates within the five or six subjects from different methods; apparent dose dependency by area and steady-state serum digoxin methods	0.125, 0.25 daily	60	—
			94, 96[c,d] (69–116% range for 0.125 mg) 82, 88[c,d] (71–122% range for 0.25 mg)	Oral–intravenous, relative mean steady-state serum levels				
			83, 87[c,d] (48–126% range)	Oral–intravenous, relative urinary excretion in 24 hrs				
36	5% Propylene glycol–10% ethanol	Radioimmunoassay	78[b]	Oral–intravenous, area under curve, 0–80 hr	—	1.0	75	0.70
			75[b] (57–96% range)	Oral–intravenous, relative urinary excretion, 12 days				
35	Tablet[e]	Radioimmunoassay	57	Oral–intravenous, relative area under curve, 0–96 hr	Two subjects, 70% bioavailability relative to oral solution	0.50	—	0.30 (0.15 and 0.44)
37	Tablet[e]	Radioimmunoassay	70[b] (49–80% range)	Oral–intravenous, relative urinary excretion, 10 days	Only 57% of intravenous dose recovered in urine of four subjects, well below other reported values, 78% bioavailability relative to oral solution	0.50	100	0.38
			62[b] (48–80% range)	Oral–intravenous, relative area under curve				

39	Tablet[e]	Radioimmunoassay	58, 61[c,d] (50–80% range) 64, 87[c,d] (49–111% range)	Oral–intravenous, relative area under 0–24-hr curve; 100% bioavailability[c] relative to oral solution Oral–intravenous, relative urinary excretion in 24 hr; 100%[c] bioavailability relative to oral solution	Gross inconsistencies of bioavailability estimates within the five or six subjects from different methods	0.25 daily	60	—
			65, 69[c,d]	Oral–intravenous, relative mean steady-state serum levels; 78% bioavailability relative to oral solution				
36	Tablet[e]	Radioimmunoassay	64[b] 63[b] (44–82% range)	Oral–intravenous, area under curve, 0–80 hr Oral–intravenous, relative urinary excretion, 12 days	82% bioavailability relative to oral solution 84% bioavailability relative to oral solution	1.0–1.5	75	0.36
40	Capsule	Total radioactivity	79.8 ± 3.7[b]	Oral–intravenous, relative area under 0–∞-hr curves		0.25	75	0.84
			80.2 ± 8.8[b]	Oral–intravenous, relative urinary excretion				
41	Not cited	Total radioactivity	69.7 ± 7.0	Oral–intravenous, relative urinary excretion, 0–96 hr			75	

[a] And references therein. [b] Acute administration. [c] Evaluated from data given in reference. [d] Daily chronic administration; data evaluated at last 2–3 days of 14-day dosing. [e] Presumably standard Lanoxin tablets.

based on crossover studies of specifically quantified separated drug and metabolites monitored in the same subjects where the results from intravenous administration of both drugs are used as relative standards. An alternative is to compare such independent studies on each drug. Surprisingly, no bioavailability comparisons of digoxin oral solutions and intravenous administrations have been attempted with specific assays of drug and metabolites in the same subjects. In general, estimates of absorption efficiency of digoxin in the literature were made by nonspecific methods using total radioactivity or radioimmunoassay.

Beerman *et al.* (31) were especially critical of a claim (33) for 85% oral absorption from a solution with different subject populations. The claim was based on the assumption that the fecal excretion of radioactivity within 5 days represented unabsorbed material since the total recovery in urine and feces averaged only 49% within 7 days. They suggested that polar metabolites may have been lost on chloroform extraction of fecal radioactivity and that digoxin decomposition before absorption was not considered. The criticism (31) of this paper (33) appears justified. The renally excreted percent of administered tritiated digoxin in Table 2 of Ref. 33 showed that the apparent bioavailability of an orally administered solution to that intravenously administered for more than 20 subjects was 100 × 34% (po)/74% (iv) = 46%, a far cry from the 85% estimated.

The urinary excretion of intravenously administered tritiated digoxin in six other patients, with biliary fistula and bile from the T-tube completely collected, was 58.5% of the dose, indicative of a minimum of 100 × {[74% (iv) − 59% (iv, fistula)]/74% (iv)} = 20% enterohepatic recirculation of digoxin. The presumption would be the same made by Doherty *et al.* (33) that the two populations, with and without bile collection, were similar. A direct measurement of biliary excretion was 8.1 ± 1.4% (*SEM*), which was significantly less then the 20% estimated. However, since 1.3 ± 0.4% (*SEM*) fecal excretion was observed with the biliary collection, it was obvious that the T-tube was not completely effective and that the 7–8% estimate (33) of enterohepatic recycling was an underestimate. The fecal excretion of non-biliary-cannulated subjects on intravenous administration was reported as 11.3 (33) and 14.8% (34). Beerman *et al.* (31) demonstrated significant decomposition of orally administered digoxin in the GI tract and claimed that absorption of intact digoxin administered in water solution was approximately 50%.

Wagner *et al.* (35) were critical of their own estimate of 80% oral bioavailability as digoxin of a 5% dextrose solution relative to intravenous bioavailability as performed in two subjects, 78.3 and 82.0%, respectively. Areas under the radioimmunoassay plasma level–time curves were used for evaluation; it was admitted that any gastroenterohepatically formed metabolites, as by first pass, would have led to overestimation. It was also stated that the use of total radioactivity and radioimmunoassay methods make extensive pharmacokinetic analysis tenuous.

Johnson *et al.* (36), who also used radioimmunoassay, studied intravenous and oral solution absorption of digoxin in eight volunteers. They estimated that oral absorption from an elixir was 78% of the intravenous absorption by the area under the curve method and 75% by urinary excretion, with the latter ranging from 57 to 96% in different subjects. This was admittedly not digoxin *per se*. The absorption of digoxin from tablets[3] relative to intravenous administration varied between 44 and 82% in different subjects with a mean of 64%. These authors were also critical of the previously mentioned claim of 85% relative absorption (33) and a similar claim of high relative absorption (37) of a 40% propylene glycol solution. In the latter case, the stated percentage urinary excretion of injected digoxin by radioimmunoassay was well below other reported values; other investigators could only claim 65% relative absorption for such an elixir (38).

When steady-state procedures were used to estimate the relative bioavailability by the authors that had previously claimed high absorption (37), the absolute bioavailability of a digoxin solution relative to intravenous bioavailability was only radioimmunologically estimated as either 77 or 87%, depending on the magnitude of the oral dose (39). However, when the bioavailability estimates within an individual by the different methods used are compared, gross inconsistencies become apparent and cast suspicion on the averaged estimates. All of these radioimmunoassay studies can be criticized for their nonspecificity. In addition, Huffman *et al.* (39), who studied apparent dose dependency, claimed that the area under the curve after oral digoxin solution administration was not proportional to dose. If true, this finding signifies that such a method for estimating relative bioavailability is not valid for digoxin.

Estimates of oral absorption efficiencies, relative to intravenous administration in the same subjects, with presumably optimumly bioa-

[3] Lanoxin.

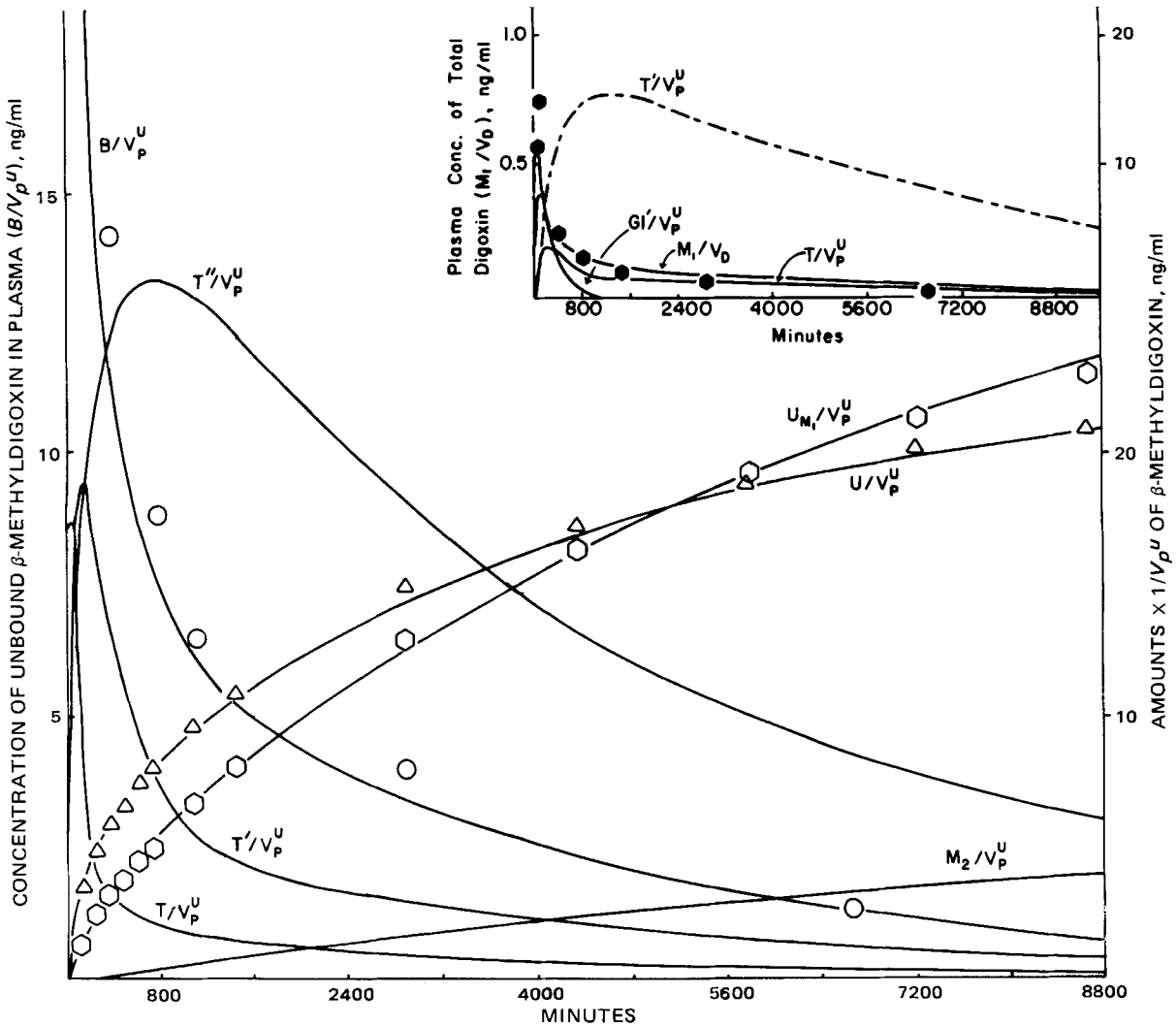

Figure 6—*Typical analog computer fitting of plasma water (unbound drug) concentration (○, left scale) and urine (△) data of β-methyldigoxin and (○) digoxin (right scale) for 0.6-mg oral solution administration to Subject C over the full time scale of 144 hr. All data are given as per milliliter of the volume of distribution of the central compartment referenced to unbound β-methyldigoxin, except for the plasma digoxin data (●) in the inset which are given as the observed concentration in terms of its own volume of distribution, V_D. The apparent concentrations of β-methyldigoxin in its various tissues (T, T′, and T″) and GI tract (GI′), M_2 in the body, and digoxin in its tissues (T and T′) are generated (right scale) with the parameters of Table III.*

vailable tablets where radioimmunoassay was used, included 57% by area methods (35) and 62% (39) and 64% (36) by urinary excretion. In one instance of total radioactivity measurements, the estimate for oral absorption efficiency of solid dosage forms compared to intravenous administration was 80.2 ± 8.8% for digoxin (40). In another, based on 96-hr urine collections, the estimates were 69.7 ± 7% for digoxin and 90.7 ± 13.1% for β-methyldigoxin (41). However, the fact that no digoxin was found in these urines (41) as a β-methyldigoxin metabolite is confusing in light of our consistent recovery of approximately equivalent amounts of ^{3}H-digoxin and ^{3}H-β-methyldigoxin in urine after ^{3}H-β-methyldigoxin administration (Table I).

A critical summary of the best estimates of absolute bioavailability of oral digoxin solution and solid dosage forms relative to intravenous administration is given in Table IV.

The appearance of a peak plasma concentration for orally administered digoxin solutions of 0.70–0.75% of total dose/liter of plasma by total assay methods at about 60–90 min (Table IV) is not inconsistent with the oral solution absorption data of β-methyldigoxin based on total radioactivity with a peak plasma level of 0.89 ± 0.11% at 72 ± 13 min and a lag time of 6.7 ± 1.6 min (n = 11). The tablet data for β-methyldigoxin showed comparable values of 0.78 ± 0.17% at 94 ± 21 min with a lag time of 15.8 ± 2.0 min but were significantly greater than the 0.37% values shown in several cases for administered digoxin tablets (36, 37).

In summary, oral absorption of digoxin from solutions and tablets varies widely with the individual (Table IV), consistent with the arguments that GI or other prehepatic degradations are the determining processes in digoxin bioavailability. Specific analytical procedures have not been generally attempted for digoxin. Thus, mean bioavailability estimates of oral solutions of digoxin assayed by methods nonspecific for digoxin relative to intravenous administration range from 50 to 93% (Table IV). Comparatively, the radioactivity absorbed for β-methyldigoxin solutions was 76 ± 2% by the area method and 83 ± 3% by urinary excretion at 144 hr compared to intravenous administration. β-Methyldigoxin plus its derived metabolite digoxin had a systemic bioavailability of 59.5 ± 3.3% as β-methyldigoxin and 12.8 ± 4.0% as digoxin for a total of 72% relative to intravenous administration in these studies using specific analysis.

It is difficult to state conclusively that β-methyldigoxin was more effectively and reproducibly absorbed than digoxin administered *per se* on oral administration based on this evidence because of the obvious difficulty in appraising the digoxin studies in the literature. Such a decision can only be made if proper crossover intravenous and oral solution studies of β-methyldigoxin and digoxin are made in the same subjects using specific analyses of the separated drug and metabolites.

However, there are suggestions of advantages of β-methyldigoxin relative to digoxin. β-Methyldigoxin apparently delivers more cardioactive agent per mole administered than digoxin. In these studies, there was more consistency in measured oral bioavailability among and within individuals (Table I) than had been indicated for digoxin (36, 39). If this finding indicates that β-methyldigoxin has a more reproducible

availability within and among individuals, it is clinically significant. The tablet studied had a bioavailability equivalent to that of the oral solution by the criteria used. Although a pilot-plant production lot rather than a normal production lot was used, the study indicates that a tablet of β-methyldigoxin can be made that is equivalent to an oral solution, something that cannot be said for digoxin.

There are several possible rationales as to why β-methyldigoxin may have properties that could favor it over digoxin. The observed 11-fold greater water solubility[4] of β-methyldigoxin (46 mg/100 ml at pH 7.5 and 22°) over digoxin (4 mg/100 ml) implies the relatively greater rate of dissolution of β-methyldigoxin. On the premise that the dissolution rate from solid dosage forms is the limiting step in glycoside availability from tablets, this property should favor β-methyldigoxin. The fact that β-methyldigoxin, notwithstanding its greater aqueous solubility, is a less polar compound than digoxin (42) and has a higher partition coefficient into chloroform—*viz.*, 85.1 to digoxin's 9.4 (41), implies that its penetration of the lipid-like GI wall may be more facile than digoxin and thus abet a more reproducible and possibly more complete absorption (3).

REFERENCES

(1) H. Czerwek, K. Hardebeck, F. Kaiser, W. Schaumann, and A. Wohlfarth-Ribbentrop, *Arzneim.-Forsch.*, **21**, 231 (1971).

(2) W. Schaumann and R. Wegerle, *ibid.*, **21**, 225 (1971).

(3) W. Schaumann, F. Zielske, K. Kohler, and K. Koch, *Naunyn-Schmiedebergs Arch. Pharmacol.*, **272**, 32 (1972).

(4) E. König and A. Ohly, *Med. Klin.*, **65**, 296 (1970).

(5) M. Storz, *Med. Welt*, **21**, 2066 (1970).

(6) P. Ghabussi, K. D. Krämer, and H. Hochrein, *Med. Klin.*, **69**, 802 (1974).

(7) D. Larbig, F. Scheler, H. J. Schmidt, G. Betzien, and B. Kaufmann, *Klin. Wochenschr.*, **49**, 604 (1971).

(8) P. U. Carbonin, P. Zecchi, F. Bellocci, S. Ruffa, and F. Loperdifo, Atti del XXXII Congresso della Società Italiana di Cardiologia, Taormina, May 1971.

(9) H. Rennekamp, C. Rennekamp, U. Abshagen, K. V. Bergmann, and N. Rietbrock, *Naunyn-Schmiedebergs Arch. Pharmacol.*, **273**, 172 (1972).

(10) W. Doering, E. König, D. Kronski, and D. Hall, *Dtsch. Med. Wochenschr.*, **98**, 2274 (1973).

(11) A. Färber and W. Riedel, *Muench. Med. Wochenschr.*, **III**, 721 (1966).

(12) J. Grauwiler, W. R. Schalch, and M. Zaeschler, *Schweiz. Med. Wochenschr.*, **96**, 1381 (1966).

(13) E. F. Hueber, *Wien. Klin. Wochenschr.*, **77**, 912 (1965).

(14) E. F. Hueber, *Wien. Med. Wochenschr.*, **117**, 713 (1967).

(15) "The Pharmacological Basis of Therapeutics," 3rd ed., L. S. Goodman and A. Gilman, Eds., Hamilton, New York, N.Y., 1965, p. 681.

(16) T. W. Smith, V. P. Butler, and E. Haber, *N. Engl. J. Med.*, **281**, 1212 (1969).

(17) D. C. Evered and C. Chapman, *Br. Heart J.*, **33**, 540 (1971).

(18) G. A. Beller, T. W. Smith, W. H. Abelman, E. Maher, and W. B. Hood, *N. Engl. J. Med.*, **284**, 989 (1971).

(19) G. Bodem and H. J. Gilfrich, *Klin. Wochenschr.*, **51**, 57 (1973).

(20) A. Ruiz-Torres and H. Burmeister, *ibid.*, **50**, 191 (1972).

(21) V. P. Butler and J. P. Chen, *Proc. Nat. Acad. Sci. USA*, **57**, 71 (1967).

(22) R. G. Stoll, M. S. Christensen, E. Sakmar, D. Blair, and J. G. Wagner, *Res. Commun. Chem. Pathol. Pharmacol.*, **4**, 503 (1972).

(23) D. Larbig and K. Kochsiek, *Dtsch. Med. Wochenschr.*, **97**, 1310 (1972).

(24) G. Härtel, V. Manninen, J. Melin, and A. Apajalahti, *Ann. Clin. Res.*, **5**, 87 (1973).

(25) P. H. Hinderling, E. R. Garrett, and R. C. Wester, *J. Pharm. Sci.* **66**, 242 (1977).

(26) N. Rietbrock and U. Abshagen, *Dtsch. Med. Wochenschr.*, **98**, 117 (1973).

(27) F. M. Dost, "Grundlagen der Pharmakokinetik," Georg Thieme Verlag, Stuttgart, Germany, 1953, p. 155.

(28) J. G. Wagner, "Fundamentals of Clinical Pharmacokinetics," 1st ed., Drug Intelligence Publications, Hamilton, Ill., 1975, p. 4.

(29) B. Beerman, *Eur. J. Clin. Pharmacol.*, **5**, 28 (1972).

(30) J. G. Wagner, "Biopharmacuetics and Relevant Pharmacokinetics," 1st ed., Drug Intelligence Publications, Hamilton, Ill., 1971, p. 4.

(31) B. Beerman, K. Hellström, and A. Rosén, *Clin. Sci.*, **43**, 507 (1972).

(32) H. Rennekamp, C. Rennekamp, U. Abshagen, K. v. Bergmann, and N. Rietbrock, *Naunyn-Schmiedebergs Arch. Pharmacol.*, **272**, 454 (1972).

(33) J. E. Doherty, W. J. Flanigan, M. L. Murphy, R. T. Bulloch, G. L. Dalrymple, O. W. Beard, and W. M. Perkins, *Circulation*, **42**, 867 (1970).

(34) F. I. Marcus, G. J. Kapadia, and G. G. Kapadia, *J. Pharmacol. Exp. Ther.*, **145**, 203 (1964).

(35) J. G. Wagner, M. Christensen, E. Sakmar, D. Blair, J. D. Yates, P. W. Willis, A. J. Sedman, and R. G. Stoll, *J. Am. Med. Assoc.*, **224**, 199 (1973).

(36) B. F. Johnson, C. Bye, and S. Lader, *Postgrad. Med. J., Suppl, 6*, **50**, 62 (1974).

(37) D. M. Huffmann and D. L. Azarnoff, *J. Am. Med. Assoc.*, **222**, 957 (1972).

(38) D. J. Greenblatt, D. W. Duhme, J. Koch-Weser, and T. W. Smith, *N. Engl. J. Med.*, **289**, 651 (1973).

(39) D. M. Huffman, C. V. Manion, and D. L. Azarnoff, *Clin. Pharmacol. Ther.*, **16**, 310 (1974).

(40) M. J. Dengler, G. Bodem, and K. Wirth, *Arzneim.-Forsch.*, **23**, 64 (1973).

(41) K. Wirth, G. Boden, and H. J. Dengler, in "Aktuelle Digitalis Problems," R. Schroeder and K. Greeff, Eds., Urban and Schwarzenberg, Munich, Germany, 1972, pp. 51–61.

(42) W. Schaumann, *Ther. Woche*, **23**, 35 (1973).

(43) U. Abshagen, H. Rennekamp, R. Küchler, and N. Rietbrock, *Eur. J. Clin. Pharmacol.*, **7**, 177 (1974).

(44) D. S. Riggs, in "The Mathematical Approach to Physiological Problems," Williams & Wilkins, Baltimore, Md., 1963, p. 197.

[4] W. Schaumann, Boehringer-Mannheim, Germany, personal communication.

ACKNOWLEDGMENTS AND ADDRESSES

Received January 8, 1976, from *The Beehive, College of Pharmacy, University of Florida, Gainesville, FL 32610.*

Accepted for publication May 10, 1976.

Supported in part by Grant NIH-RR-82 from the National Institutes of Health, Bethesda, Md., and by an unrestricted grant from Searle Laboratories, Skokie, Ill.

The authors thank the nursing staff of the Clinical Research Center, Shands Hospital, University of Florida, for their assistance in performing the clinical studies.

* Present address: Biozentrum, Der Universität Basel, 4056 Basel, Switzerland.

‡ Searle Laboratories, Skokie, Ill.

ˣ To whom inquiries should be directed.

Pharmacokinetics of β-Methyldigoxin in Healthy Humans III: Pharmacodynamic Correlations

PETER H. HINDERLING * and EDWARD R. GARRETT ˣ

Abstract □ Significant decreases in left ventricular ejection time and heart rate were observed after the oral and intravenous administration of β-methyldigoxin. The time course of this action correlated with the time course of β-methyldigoxin and its active metabolite, digoxin, in their deepest pharmacokinetic compartments and not with their plasma levels. This pharmacodynamic activity peaked (decrease of 6.3% at 0.6 mg iv and 3.5% at 0.3 mg iv; decrease of 3.8% at 0.6 mg po and 4.5% at 0.3 mg po) at about 10 hr, concomitantly with the amounts of β-methyldigoxin in its deepest compartment and showed a terminal half-life equivalent to the 41 hr for β-methyldigoxin. The relative peak heights and area under the ejection time–time curves indicated a linear dose–response relationship on intravenous administration and an effect greater than that reported for larger amounts of digoxin. The time course of heart rate action correlated (8.3 and 12.5% decreases with 0.3 and 0.6 mg iv, respectively; 6.5 and 9.5% decreases with 0.3 and 0.6 mg po, respectively) with the time course of β-methyldigoxin and its metabolite digoxin in shallower pharmacokinetic compartments (peaks at ~80 min intravenously and 135 min orally), and significant effects had disappeared by 10 hr after drug administration. This finding indicated that the biophases differ for ejection time and heart rate action. Mean arterial blood pressure could not be correlated with the time course of drug, although a small consistent decrease (4–8%) was observed from 22 to 72 hr after drug administration.

Keyphrases □ β-Methyldigoxin—oral and intravenous, effect on left ventricular ejection time and heart rate correlated with pharmacokinetic parameters, humans □ Pharmacokinetics—β-methyldigoxin, oral and intravenous, correlated with effect on left ventricular ejection time and heart rate, humans □ Pharmacodynamics—β-methyldigoxin, oral and intravenous, effect on left ventricular ejection time and heart rate correlated with pharmacokinetic parameters, humans □ Cardiac glycosides—β-methyldigoxin, oral and intravenous, effect on left ventricular ejection time and heart rate correlated with pharmacokinetic parameters, humans

Cardiac glycosides have been shown to exert positive inotropic and negative chronotropic effects both in patients with congestive heart failure (1, 2) and in healthy subjects (3–5). Effects on the left ventricular performance are reflected in shortening of the left ventricular ejection time interval (LVET) when corrected for the heart rate. Noninvasive methods can monitor glycoside effects on these cardiovascular parameters (6).

Few attempts have been made to correlate simultaneously measured pharmacokinetics and pharmacodynamics of glycosides (7, 8). In many cases, both the parent drug and some of its metabolites are pharmacologically active (9). The availability of a specific assay is mandatory to correlate specifically the observed effects and the individual kinetics of the parent drug and its active metabolites. Such correlations may lead to the proper characterization of the biophases of drug and metabolite action.

β-Methyldigoxin undergoes significant metabolism to active metabolites such as digoxin in humans (10, 11) and has demonstrated positive inotropic and negative chronotropic effects in patients with congestive heart failure and in healthy subjects (12, 13). The purposes of these studies were to monitor such pharmacodynamic parameters with time in normal volunteers administered 0.3 and 0.6 mg of β-methyldigoxin both orally and intravenously and to relate these effects with the previously evaluated pharmacokinetics of the drug and its metabolites (11, 14).

EXPERIMENTAL[1]

The left ventricular ejection time derived from the external carotid pulse[2] and the heart rates[3] were simultaneously recorded on a three-channel recorder[4] (paper speed of 50 mm/min). The left ventricular ejection time was measured from the beginning of the upstroke to the trough of the incisura (2). The heart rate was calculated from the quotient 60/(average RR interval) of at least 10 consecutive beats (3). Besides the standard ECG, a vector ECG was recorded on a three-channel recorder[5]. The blood pressure was measured according to Korotkov, using an inflatable cuff connected to a mercury manometer on the left a brachialis. The diastolic blood pressure was measured during phase 5.

For all measurements, each individual was in a prostrate position. The subjects were prostrate during the first 24 hr after β-methyldigoxin administration and then were ambulant. They were in a prostrate position for at least 30 min prior to and during measurements taken between 24 and 144 hr after drug administration. Details of the concomitant pharmacokinetic studies on β-methyldigoxin were given previously (11, 14).

Sufficient control values were taken in each study prior to drug administration before and after the placement of the needle and the catheter. The carotid arterial pulse and the ECG's were taken continuously up to 30 min, at 5-min intervals up to 60 min, at 15-min intervals up to 4 hr, at 30-min intervals up to 11 hr, and then at 12-hr intervals up to 72 hr after drug administration. In some experiments, the measurements were expanded to 132 hr.

The left ventricular ejection time values were determined in Subjects A–F. Subject G was excluded because the beginning of the upstroke could not be defined clearly in his carotid pulse recordings. The experimentally determined values were normalized (3) for the heart rate, HR:

$$\text{LVETI} = \text{LVET} + 0.0016 \times \text{HR} \qquad \text{(Eq. 1)}$$

where LVETI is the left ventricular ejection time index. The stroke volume, SV, was calculated (2) for the control period from:

$$\text{SV} = \frac{\text{LVETI} - 0.266 + (0.0017 \times 82)}{0.0017} \qquad \text{(Eq. 2)}$$

and the cardiac output, CO, for the control period was calculated from:

$$\text{CO} = \text{SV} \times \text{HR} \qquad \text{(Eq. 3)}$$

The LVETI values were expressed as percent of the control values taken prior to drug administration (Table I).

The blood pressure was measured in Subjects A–G at 5-min intervals up to 30 min, at 15-min intervals up to 4 hr, at 30-min intervals up to 11 hr, and then at 12-hr intervals up to 72 hr after drug administration. The mean arterial blood pressure was calculated by adding to the diastolic pressure one-third of the difference between the experimental systolic and diastolic pressures (15). The cardiac outputs measured during the control period before drug administration ranged between 5390 and 6257 ml/min in all four studies and all individuals and were normal (16).

[1] The volunteers were informed orally and in writing of any and all potential risks and of the experimental protocol prior to the studies; verbal consent and written consent were obtained. The human experimentation, radioactive substance, and clinical research committees of the Health Center, University of Florida, reviewed and approved the research protocol prior to the studies. A physician was in attendance during the studies.

[2] Pulse wave pickup, Hewlett-Packard Co., Palo Alto, Calif.

[3] Standard-ECG, Lead II, Hewlett-Packard Co., Palo Alto, Calif.

[4] Hewlett-Packard Co., Palo Alto, Calif.

[5] Marquetter patient transmitter, Marquette Electronics, Milwaukee, Wis.

Table I—Control Values of LVETI, RR Interval, and Heart Rate prior to Drug Administration

LVETI, sec	Subject	Number of Measurements	RR Interval (±*SD*), sec	Average Heart Rate
0.410 ± 0.0062	D	8	1.122 ± 0.368	53
0.392 ± 0.0063	E	8	0.962 ± 0.098	62
0.389 ± 0.0061	F	8	1.083 ± 0.108	55
0.395 ± 0.0059	G	8	1.111 ± 0.106	54
0.408 ± 0.0032	A	8	1.062 ± 0.060	57
0.403 ± 0.0090	B	8	1.134 ± 0.075	53
0.400 ± 0.010		48	1.079 ± 0.099	56

RESULTS AND DISCUSSION

Tolerance of β-Methyldigoxin—No systematic changes were found in the clinical laboratory data obtained in the subjects prior to each of the four administrations of β-methyldigoxin (11, 14). In particular, the serum sodium and potassium concentrations, reportedly critical (16) for the myocardial glycoside uptake and effect, were within the normal range for all subjects and all studies. The administered β-methyldigoxin was well tolerated at the two dosage levels (0.6 and 0.3 mg) and by both the oral and intravenous routes. No adverse cardiac effects were observed.

Pharmacodynamic Action on Left Ventricular Ejection Time of β-Methyldigoxin and Digoxin on β-Methyldigoxin Administration—The LVETI and RR values obtained for each volunteer during the control period prior to oral and intravenous administration of drug at two dosage levels are listed in Table I. The LVETI values for all subjects were within the normal range of 0.395 ± 0.017 for healthy male adults (6). Plots of the percent LVETI decrease against time, averaged for all subjects, showed a maximal decrease at 10–22 hr after both dosages of β-methyldigoxin administered intravenously or orally (Figs. 1 and 2).

The subsequently decreasing effect on the LVETI was observable for the 132-hr (0.6 mg iv) and 72-hr periods of observation (0.3 mg iv, 0.6 and 0.3 mg po), respectively.

Reuning *et al.* (8) stated that the percent LVETI decrease observed with time by Shapiro *et al.* (7) can be best correlated with tissue levels of digoxin generated by the analog computer from plasma levels on the basis of a two-compartment body model for digoxin. The pharmacokinetics of both β-methyldigoxin and the active main metabolite, digoxin, have to be considered to correlate the magnitude and time course of the LVETI effect on β-methyldigoxin administration.

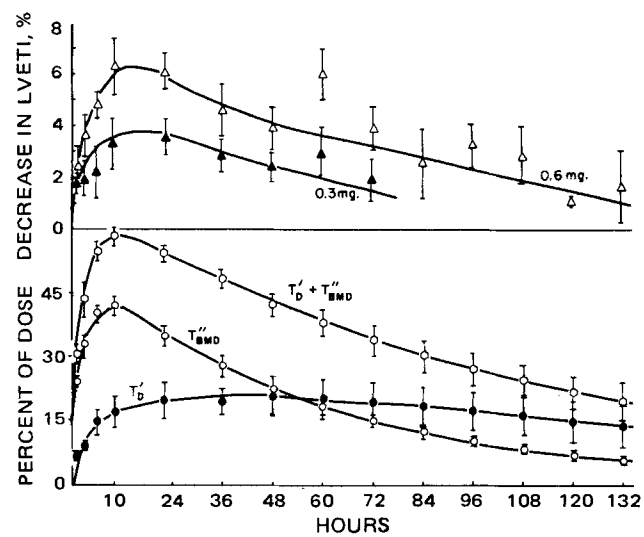

Figure 1—*Apparent correlation between the mean percent LVETI decrease at 0.3 (▲) and 0.6 (△) mg of β-methyldigoxin (BMD) and the mean amounts of β-methyldigoxin (○) and digoxin (●) in their respective deepest tissues, T_{BMD}'' and T_D', and in their sum (○) in percent of the administered intravenous dose of β-methyldigoxin as a function of time. The LVETI values obtained prior to drug administration served as controls. The vertical bars indicate ±1 SEM of the means. The amounts in the tissues were generated by the analog computer from the best fits of the experimental plasma and urine data for all studies. They are given as percent of dose and are valid for both dose levels since the intravenous pharmacokinetics were independent of dose (11).*

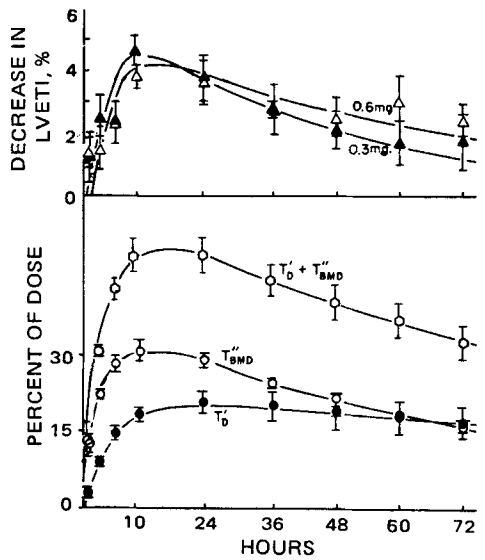

Figure 2—*Apparent correlation between the mean percent LVETI decrease at 0.3 (▲) and 0.6 (△) mg of β-methyldigoxin and the mean amounts of β-methyldigoxin (○) and digoxin (●) in their respective deepest tissues, T_{BMD}'' and T_D', and in their sum (○) in percent of the administered oral dose of β-methyldigoxin as a function of time. The LVETI values obtained prior to drug administration served as controls. The vertical bars indicate ±1 SEM of the means. The amounts in the tissues were generated by the analog computer from the best fits of the experimental plasma and urine data for all studies. They are given as percent of dose and are valid for both dose levels since the oral pharmacokinetics were independent of dose (14).*

Statistically significant negative linear correlations existed between the averaged LVETI effect and both the averaged amounts of parent drug in its deepest compartment, T_{BMD}'', and the averaged amounts of digoxin in its deepest compartment, T_D', for both modes of administration and both dose levels (Table II, Scheme I, and Figs. 1 and 2). The amounts of β-methyldigoxin and digoxin in these tissues as percent of the dose were generated by the analog computer from the best fit of the experimental data in plasma and urine (11, 14). No such correlations could exist between the LVETI effect and the amounts of drug in the other tissues or plasma since the maxima of the former (Figs. 1 and 2) occurred well after the maximum values of the latter (11, 14). The peak amounts of the sum of β-methyldigoxin in the moderately deep tissues, T_{BMD}' and T_D, occurred at 80 and 135 min for intravenous (Figs. 3 and 4) and oral (Fig. 5) administration, respectively. The peak amounts in the plasma and shallower tissues such as T_{BMD} occurred much earlier (Fig. 5) (11, 14). The assumption of a linear relationship between drug content in the deepest tissues and its effect on ventricular performance during the time course of both cannot be excluded.

The peak effect of the averaged LVETI decrease occurred at 10–22 hr after drug administration for both dosage levels and routes (Figs. 1 and 2). The β-methyldigoxin amounts in T_{BMD}'' peaked at 10–12 hr after intravenous administration and at 13 hr after oral administration. The

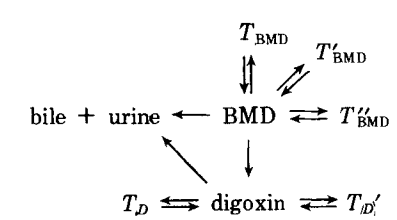

Scheme I—Simplified pharmacokinetic model for the distribution of β-methyldigoxin from its central compartment to its successively deeper tissues in the order T_{BMD}, T_{BMD}' and T_{BMD}'' and for the distribution of metabolically generated digoxin to its successively deeper tissues in the order T_D and T_D'.

Table II—Correlations[a] between Amounts[b] of β-Methyldigoxin and Digoxin in Their Respective Tissue Compartments and the LVETI and Heart Rate Change

Dose, mg	Modes of Administration	LVETI *versus* T''_{BMD}	LVETI *versus* T_D'	Heart Rate *versus* T'_{BMD}	Heart Rate *versus* T_D
0.6	Intravenous	$r = -0.86, p \leq 0.01$	$r = -0.41, p \leq 0.20$	$r = -0.84, p \leq 0.01$	$r = -0.85, p \leq 0.01$
0.3	Intravenous	$r = -0.41, p \leq 0.50$	$r = -0.76, p \leq 0.02$	$r = -0.83, p \leq 0.01$	$r = -0.82, p \leq 0.01$
0.6	Oral	$r = -0.72. p \leq 0.05$	$r = -0.85, p \leq 0.01$	$r = -0.63, p \leq 0.10$	$r = -0.40, p \leq 0.10$
0.3	Oral	$r = -0.87, p \leq 0.01$	$r = -0.51, p \leq 0.20$	$r = -0.63, p \leq 0.01$	$r = -0.47, p \leq 0.05$

[a] r is the correlation coefficient, and p is the probability of estimate that the correlation is random. [b] As percent of β-methyldigoxin dose.

amounts of digoxin in T_D' were at maximum considerably later, at 34 or 43 hr after intravenous administration and at 20–29 hr after oral administration (11, 14).

Maximum decreases of the LVETI of 5.6 and 7.2% were reported in healthy volunteers by 6 hr after 1.6 and 1.0 mg iv of digoxin, respectively (5, 7). After 3.2 mg po of digoxin, a maximum decrease of 4.7% was reported at 12–24 hr after dosing (5). These values are not inconsistent with what was observed herein for β-methyldigoxin: maximum decreases of LVETI of 6.3 and 3.5% at about 10 hr after 0.6 and 0.3 mg iv of β-methyldigoxin, respectively. It may even imply a greater potency for the β-methyldigoxin over digoxin at equivalent doses, consistent with the fact that intravenously administered β-methyldigoxin delivers 140% more cardioactive material than an equivalent dose of digoxin (14).

A linear dose–LVETI effect relationship was indicated for deslanoside (5). In the intravenous studies reported here, the maxima (6.3% for 0.6 mg and 3.5% for 0.3 mg of β-methyldigoxin) and areas under the effect–time curves up to 72 hr (364% hr for 0.6 mg and 197% hr for 0.3 mg of β-methyldigoxin) were proportional to the dose. This finding is indicative of a linear dose–effect relationship. In the oral studies, the observed maxima (3.8% for 0.6 mg and 4.5% for 0.3 mg) and areas under the effect–time curve up to 72 hr (205% hr for 0.6 mg and 192% hr for 0.3 mg of β-methyldigoxin) were practically the same for both dose levels. However, the variability in the effect data was larger in the oral studies.

Calculations of the bioavailability of the two oral dosages of β-methyldigoxin relative to the respective intravenous dose from the areas under the LVETI effect–time curves, with admittedly high variability, gave values of 60 and 100% for 0.6 and 0.3 mg, respectively. It was shown previously (14) for both doses that an orally administered β-methyldigoxin solution delivered 70% of the cardioactivity of an equivalent intravenous dose on the presumption that the drug and its metabolite, digoxin, had equivalent cardioactivity in the body.

Pharmacodynamic Action on Heart Rate of β-Methyldigoxin and Digoxin on β-Methyldigoxin Administration—Plots of the percent heart rate decrease against time, averaged for all subjects, showed significant decreases after drug administration with apparent maximal decreases of 8.3% at 150 min and 12.2% at 80 min for 0.3- and 0.6-mg iv doses, respectively, indicative of a dose dependency (Fig. 3). The amounts of β-methyldigoxin in compartment T'_{BMD} and of digoxin in T_D both peaked at approximately 80 min after intravenous administration of β-methyldigoxin (Figs. 3 and 4). After oral administration of β-methyldigoxin, maximal amounts were reached at about 135 min for β-methyldigoxin in T'_{BMD} and at 155 min for digoxin in T_D (Fig. 5), where maximal heart rate decreases were 6.5 and 9.5% at 90–120 and 90 min for 0.3- and 0.6-mg po doses, respectively. The variabilities in the data were too great to conclude dose dependence on oral administration.

Statistically significant linear negative correlations existed between percent heart rate effect and amounts in percent of the dose of β-methyldigoxin in its moderately deep compartment, T'_{BMD}, and of digoxin in its shallower compartment, T_D, for both modes of administration and both dose levels of β-methyldigoxin (Table II and Figs. 3–5) but not with the amounts in the deep compartments, T''_{BMD} and T_D' (Fig. 4).

The possibility that the observed decrease in heart rate is a procedural effect cannot be rigorously excluded since no placebo experiments were performed. However, similar significant decreases in heart rate in healthy volunteers were attributed to such glycosides (5).

Maximum heart rate decreases of 16% at 20–120 min and of 15% at 240

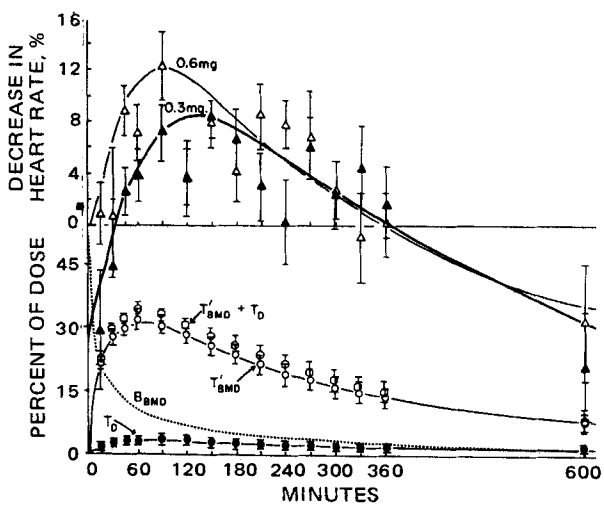

Figure 3—*Apparent correlation between the mean percent heart rate decrease at 0.3 (▲) and 0.6 (△) mg of β-methyldigoxin and the mean amounts of β-methyldigoxin (○) and digoxin (●) in their respective moderately deep tissues, T'_{BMD} and T_D, and in their sum (○) in percent of the administered intravenous dose of β-methyldigoxin as a function of time. The heart rate values obtained prior to drug administration served as controls. The vertical bars indicate ±1 SEM of the means. The amounts in the tissues were generated by the analog computer from the best fits of the experimental plasma and urine data for all studies. They are given as percent of dose and are valid for both dose levels since the intravenous pharmacokinetics were independent of dose (11). The dashed line shows the mean of the analog computer-fitted amounts of β-methyldigoxin in the central compartment, B_{BMD}, in percent of β-methyldigoxin administered as a function of time for comparison.*

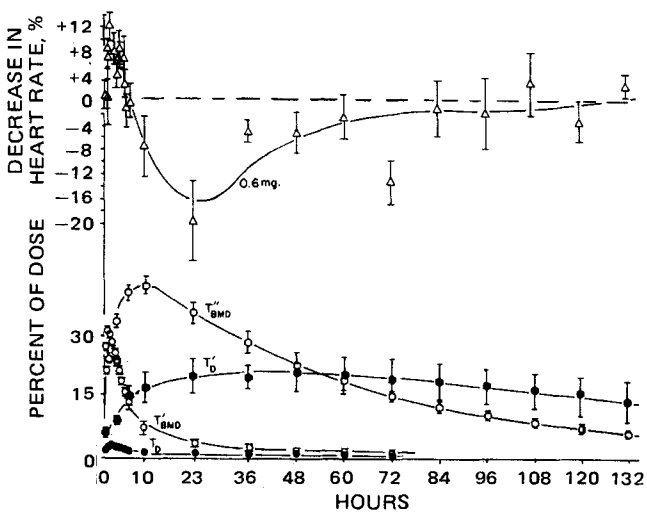

Figure 4—*Apparent correlation between the mean percent heart rate decreases at 0.6 mg (△) of β-methyldigoxin over 132 hr and the mean amounts of β-methyldigoxin (○) and digoxin (●) in their respective moderately deep tissues, T'_{BMD} and T_D, and in their sum (○) in percent of the administered intravenous dose of β-methyldigoxin as a function of time. The heart rate values obtained prior to drug administration served as controls. The vertical bars indicate ±1 SEM of the means. The amounts in the tissues were generated by the analog computer from the best fits of the experimental plasma and urine data for all studies and are given as the percent of the dose. The time course of the mean amounts of β-methyldigoxin (○) and digoxin (●) in their respective deepest compartments, T''_{BMD} and T_D', are shown for comparison in terms of the percent of administered dose. The increase in heart rate at 22 hr and subsequently is attributed to the fact that the previously prostrate patients became ambulatory at that time.*

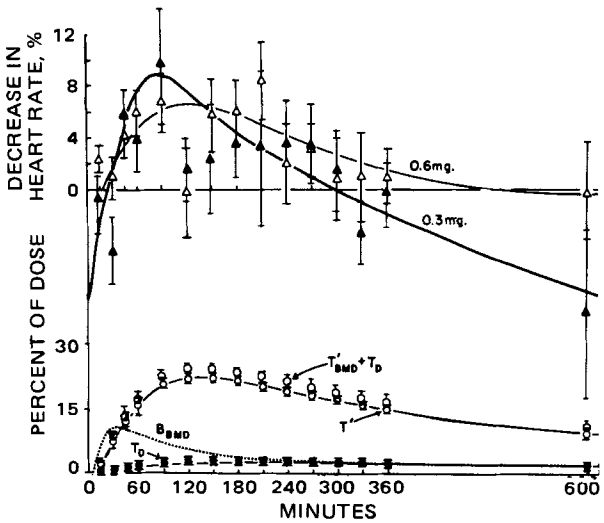

Figure 5—*Apparent correlation between the mean percent heart rate decreases at 0.3 (▲) and 0.6 (△) mg of β-methyldigoxin and the mean amounts of β-methyldigoxin (○) and digoxin (●) in their respective moderately deep tissues, T'_{BMD} and T_D, and in their sum (○) in percent of the administered oral dose of β-methyldigoxin as a function of time. The heart rate values obtained prior to drug administration served as controls. The vertical bars indicate ±1 SEM of the means. The amounts in the tissues were generated by the analog computer from the best fits of the experimental plasma and urine data for all studies. They are given as percent of dose and are valid for both dose levels since the oral pharmacokinetics were independent of dose (14). The dashed line shows the mean of the analog computer-fitted amounts of β-methyldigoxin in the central compartment, B_{BMD}, in percent of β-methyldigoxin administered as a function of time for comparison.*

min were reported after 1.6 mg iv and 3.25 mg po of digoxin, respectively (17, 18); intravenous injection of a placebo led to a maximal 3.3% heart rate decrease in these subjects. Maximal decreases in heart rate at 60–150 min were also observed in patients with coronary heart disease that were given 0.6 mg iv of β-methyldigoxin (19), consistent with our results.

Possible Differences in Apparent Biophases—The time course of this apparent negative chronotropic effect observed from heart rate measurements was remarkably different from the time course of the positive inotropic effect observed from LVETI measurements after β-methyldigoxin administration. Therefore, these two receptor site-containing biophases are kinetically different.

The mean arterial blood pressure was averaged for all subjects and showed a small, but consistent, decrease of 4–8%, 22–72 hr after administration for both doses and both modes of administration and was probably a procedural effect. The mean arterial blood pressure showed no consistent pattern, and the changes were small (±4%) during the first 22 hr.

REFERENCES

(1) "The Pharmacological Basis of Therapeutics," 3rd ed., L. S. Goodman and A. Gilman, Eds., Hamilton, New York, N.Y., 1965, pp. 668, 673.

(2) A. M. Weissler, R. G. Peeler, and W. H. Roehll, *Am. Heart J.*, **62**, 367 (1961).

(3) A. M. Weissler, W. G. Gamel, H. E. Grode, S. Cohen, and C. D. Schoenfeld, *Circulation*, **29**, 721 (1964).

(4) E. Braunwald, R. D. Bloodwell, L. I. Goldberg, and A. G. Morrow, *J. Clin. Invest.*, **40**, 52 (1961).

(5) A. M. Weissler, J. R. Snyder, C. D. Schoenfeld, and S. Cohen, *Am. J. Cardiol.*, **17**, 768 (1966).

(6) A. M. Weissler, L. C. Harris, and G. D. White, *J. Appl. Physiol.*, **18**, 919 (1963).

(7) W. Shapiro, K. Narahara, and K. Taubert, *Circulation*, **42**, 1065 (1970).

(8) R. H. Reuning, R. A. Sams, and R. E. Notari, *J. Clin. Pharmacol.*, **13**, 127 (1973).

(9) H. Lüllmann and T. Peters, *Eur. J. Pharmacol.*, **14**, 204 (1971).

(10) N. Rietbrook, C. Rennekamp, H. Rennekamp, K. v. Bergmann, and U. Abshagen, *Naunyn-Schmiedeberg's Arch. Pharmacol.*, **272**, 450 (1972).

(11) P. H. Hinderling, E. R. Garrett, and R. C. Wester, *J. Pharm. Sci.*, **66**, 242 (1977).

(12) R. Eberl, *Med. Klin.*, **67**, 849 (1972).

(13) R. Haasis, D. Larbig, and K. O. Klenk, *Klin. Wochenschr.*, **53**, 529 (1973).

(14) P. H. Hinderling, E. R. Garrett, and R. C. Wester, *J. Pharm. Sci.*, **66**, 314 (1977).

(15) D. S. Riggs, "The Mathematical Approach to Physiological Problems," Williams & Wilkins, Baltimore, Md., 1963, p. 8.

(16) A. C. Guyton, "Textbook of Medical Physiology," Saunders, Philadelphia, Pa., 1968, p. 337.

(17) G. A. Langer, *Circulation*, **44**, 180 (1972).

(18) K. E. Cohn, R. E. Kleiger, and D. C. Harrison, *Circ. Res.*, **20**, 473 (1967).

(19) W. Doering, T. König, D. Kronski, and D. Hull, *Dtsch. Med. Wochenschr.*, **98**, 2274 (1973).

ACKNOWLEDGMENTS AND ADDRESSES

Received January 8, 1976, from *The Beehive, College of Pharmacy, University of Florida, Gainesville, FL 32610.*

Accepted for publication March 31, 1976.

Supported in part by Grant NIH-RR-82 from the National Institutes of Health, Bethesda, Md., and by an unrestricted grant from Searle Laboratories, Skokie, Ill.

The authors thank the nursing staff of the Clinical Research Center, Shands Hospital, University of Florida, for their assistance in performing the clinical studies.

* Present address: Biozentrum, Der Universität Basel, 4056 Basel, Switzerland.

ˣ To whom inquiries should be directed.

Stability of (Pyrrolidone-5-hydroxamato)iron(III) Chelates

M. PEĆAR †, N. KUJUNDŽIĆ ˣ, and J. PAZMAN

Abstract □ Overall stability constants of mono-, bis-, and tris(pyrrolidone-5-hydroxamato)iron(III) chelates were determined in aqueous solutions at 25° as log β_I = 1.49, log β_{II} = 1.55, and log β_{III} = 0.21, respectively, where $\beta_I = [Fe(C_5H_7O_3N_2)^{2+}][H^+]/[Fe^{3+}][HC_5H_7O_3N_2]$, $\beta_{II} = [Fe(C_5H_7O_3N_2)_2^+][H^+]^2/[Fe^{3+}][HC_5H_7O_3N_2]^2$, and $\beta_{III} = [Fe(C_5H_7O_3N_2)_3][H^+]^3/[Fe^{3+}][HC_5H_7O_3N_2]^3$. Stability constants of all three chelates were determined potentiometrically in the 3.00–3.23 pH region. The stability constant of the mono chelate also was determined spectrophotometrically at 25° as log β_I = 1.52 by measuring absorbance at 500 nm (absorbance maximum), where the molar absorptivity was ϵ = 1124 liters/(mole cm). Biological implications of hydroxamic acid-containing compounds are discussed.

Keyphrases □ (Pyrrolidone-5-hydroxamato)iron(III)—mono, bis, and tris chelates, stability constants determined in aqueous solutions □ Iron(III) chelates—mono, bis, and tris, with pyrrolidone-5-hydroxamic acid, stability constants in aqueous solutions □ Chelates—pyrrolidone-5-hydroxamic acid with iron(III), mono, bis, and tris, stability constants in aqueous solutions □ Hydroxamic acid derivatives—(pyrrolidone-5-hydroxamato)iron(III) mono, bis, and tris chelates, stability constants in aqueous solutions □ Stability constants—mono-, bis-, and tris(pyrrolidone-5-hydroxamato)iron(III) chelates in aqueous solutions

The role of the hydroxamic acid-containing compounds in living systems has become a lively issue since they are constituents of antibiotics, growth factors, tumor inhibitors, cell division factors, and pigments and are intimately associated with iron transport phenomena (1–7). A striking feature of hydroxamic acids is the ability to form coordination compounds with the pronounced preference for iron(III) (1). There is much interest in the hydroxamic acid–iron(III) chelates (6, 8–12). The paucity of data on heterocyclic aminohydroxamic acids and their iron(III) complexes necessitated the selection of pyrrolidone-5-hydroxamic acid and their iron(III) chelates as a model system for the nitrogen heteropentacyclic hydroxamic acids and their complexes.

A previous paper (12) described the coordination ability of pyrrolidone-5-hydroxamic acid to bind ferric ion, forming a mixture of mono, bis, and tris chelates from which the tris(pyrrolidone-5-hydroxamato)iron(III) complex was isolated and characterized.

This paper reports results related to the thermodynamic stability of mono, bis, and tris chelates in aqueous solutions. In a solution containing iron(III) ions and a bidentate pyrrolidone-5-hydroxamic acid, the system at equilibrium may be described by Schemes I–IV and Eqs. 1–4, where K_a is the acidity constant and the stepwise equilibrium constants are K_I, K_{II}, and K_{III} (12).

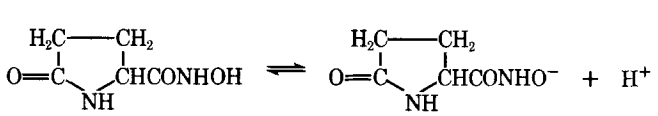

Scheme I

$$K_a = \frac{[C_5H_7O_3N_2^-][H^+]}{[HC_5H_7O_3N_2]} \qquad \text{(Eq. 1)}$$

$$Fe^{3+} + HC_5H_7O_3N_2 \rightleftharpoons Fe(C_5H_7O_3N_2)^{2+} + H^+$$

Scheme II

$$K_I = \frac{[Fe(C_5H_7O_3N_2)^{2+}][H^+]}{[Fe^{3+}][HC_5H_7O_3N_2]} \qquad \text{(Eq. 2)}$$

$$Fe(C_5H_7O_3N_2)^{2+} + HC_5H_7O_3N_2 \rightleftharpoons Fe(C_5H_7O_3N_2)_2^+ + H^+$$

Scheme III

$$K_{II} = \frac{[Fe(C_5H_7O_3N_2)_2^+][H^+]}{[Fe(C_5H_7O_3N_2)^{2+}][HC_5H_7O_3N_2]} \qquad \text{(Eq. 3)}$$

$$Fe(C_5H_7O_3N_2)_2^+ + HC_5H_7O_3N_2 \rightleftharpoons Fe(C_5H_7O_3N_2)_3 + H^+$$

Scheme IV

$$K_{III} = \frac{[Fe(C_5H_7O_3N_2)_3][H^+]}{[Fe(C_5H_7O_3N_2)_2^+][HC_5H_7O_3N_2]} \qquad \text{(Eq. 4)}$$

The overall β and stepwise stability constants K are related by the familiar expressions:

$$\beta_I = K_I \qquad \text{(Eq. 5a)}$$

$$\beta_{II} = K_I K_{II} \qquad \text{(Eq. 5b)}$$

$$\beta_{III} = K_I K_{II} K_{III} \qquad \text{(Eq. 5c)}$$

Constants $\beta_{1,2,3}$ and $K_{1,2,3}$ are defined by:

$$\beta_1 = \beta_I K_a^{-1} \qquad \text{(Eq. 6a)}$$

$$\beta_2 = \beta_{II} K_a^{-2} \qquad \text{(Eq. 6b)}$$

$$\beta_3 = \beta_{III} K_a^{-3} \qquad \text{(Eq. 6c)}$$

$$K_1 = K_I K_a^{-1} \qquad \text{(Eq. 7a)}$$

$$K_2 = K_{II} K_a^{-1} \qquad \text{(Eq. 7b)}$$

$$K_3 = K_{III} K_a^{-1} \qquad \text{(Eq. 7c)}$$

EXPERIMENTAL

Chemicals—The preparation of pyrrolidone-5-hydroxamic acid and its iron(III) coordination compounds was described previously (12). The iron(II) solutions were prepared *in situ* by catalytic hydrogenation of iron(III) over palladium-on-carbon. All experiments involving iron(II) ions were performed under nitrogen. All other chemicals were reagent grade, and water was distilled from aqueous acidified potassium permanganate solution and stored in glass[1] containers.

Physical Measurements[2]—The potentiometric method (13, 14) involving nucleophilic potentiometric titration of iron(III) chelates was initially applied to the determination of the stability constants. The method was abandoned because reasonable results could not be obtained; the examined chelates were too stable for this method. The stability constants of mono, bis, and tris chelates were obtained by the potentiometric method in addition to the spectrophotometric method, which could be used only for mono chelate. In spectrophotometric and potentiometric experiments, the pH was adjusted to a constant value by hydrochloric acid or sodium hydroxide solution.

Redox potential measurements of iron(II)–iron(III) solutions were used to calculate the concentration of the free iron(III) ions at low pH, since iron(II)–hydroxamate complexes cannot be formed below pH 6 and the interfering base hydrolysis takes place above pH 8 (15, 16). In a typical redox potential measurement, the iron(II)–iron(III) solution was added to a pyrrolidone-5-hydroxamic acid solution, giving 50 ml of 2.064×10^{-4} *M* Fe^{3+} and 2.064×10^{-4} *M* Fe^{2+}. The total concentration of the pyrrolidone-5-hydroxamic acid was $1–6 \times 10^{-3}$ *M*. Ionic strength was maintained at 0.1 by potassium chloride.

[1] Pyrex.

[2] The pH and potentiometric determinations were performed with a MA 5701 ISKRA pH meter and a Radiometer SRB2c/ABU 1b/TTA3 titrigraph. Visible spectra were obtained with a Opton PMQ II single-beam spectrophotometer and a Cary model 16K recording spectrophotometer equipped with quartz cells.

Table I—Stability Constant of Mono(pyrrolidone-5-hydroxamato)iron(III) Chelate from Absorbance Measurements at 500 nm and Ionic Strength 0.1 (Sodium Chloride), Using 1-cm Quartz Cells[a]

Experiment	pH	Absorbance, nm	$[H^+] \times 10^4$	$[Fe(C_5H_7O_3N_2)^{2+}] \times 10^4$	$[Fe^{3+}] \times 10^4 = [HC_5H_7O_3N_2] \times 10^4$	K_I	log K_I
1	1.90	0.260	126	2.31	2.69	40.2	1.60
2	2.43	0.353	57.2	3.14	1.86	33.8	1.53
3	2.49	0.371	32.4	3.30	1.70	37.0	1.57
4	2.70	0.398	20.0	3.54	1.46	33.2	1.52
5	2.78	0.409	16.6	3.64	1.36	32.7	1.51
6	2.95	0.414	11.2	3.68	1.32	23.7	1.37
7	3.19	0.424	6.46	3.77	1.23	16.1	1.21
8	3.33	0.388	4.68	3.45	1.55	6.7	0.83

[a] Total concentrations of pyrrolidone-5-hydroxamic acid and of iron(III) ions were kept equal at 5×10^{-4} *M*. K_I was calculated from Eq. 2.

RESULTS AND DISCUSSION

Spectrophotometric Determination of Stability Constant of Mono(pyrrolidone-5-hydroxamato)iron(III) Complex—The behavior of the iron(III)–pyrrolidone-5-hydroxamic acid solution depicted by Schemes I–IV was described recently (12). In view of the interference of bis and tris chelates, only the stability constant of the mono chelate can be determined spectrophotometrically, if the pH is sufficiently low and there is an excess of iron(III) over hydroxamic acid. The visible spectrum of the mono(pyrrolidone-5-hydroxamato)iron(III) complex shows the maximum absorption at 500 nm with a molar absorptivity of ϵ_{max} 500 nm = 1124 liters/(mole cm). The quantitative conversion of pyrrolidone-5-hydroxamic acid to the mono chelate is illustrated in Fig. 1. The necessary data for the calculation of K_I (Eqs. 2 and 5*a*–5*c*) are given in Table I. The concentration of $Fe(C_5H_7O_3N_2)^{2+}$ was determined spectrophotometrically, the concentration of H^+ was obtained from the measured pH, and the concentrations of iron(III) and pyrrolidone-5-hydroxamic acid were calculated from:

$$[\text{iron(III)}] = [\text{iron(III)}]_{total} - [Fe(C_5H_7O_3N_2)^{2+}] \quad \text{(Eq. 8)}$$

and:

$$[HC_5H_7O_3N_2] = [HC_5H_7O_3N_2]_{total} - [Fe(C_5H_7O_3N_2)^{2+}] \quad \text{(Eq. 9)}$$

respectively. It was assumed that there is no appreciable amount of the $C_5H_7O_3N_2^-$ anion below pH 3 due to the low acidity of pyrrolidone-5-hydroxamic acid [pKa = 8.65 (12)]. Both good constancy and reproducibility of K_I values in the pH 1.90–2.95 region were observed, and K_I = 33.4 (or log K_I = 1.52) was calculated as the arithmetic mean of the six values. At the higher pH value of 2.95, there was a decrease in K_I due to interfering reactions, such as base hydrolysis of iron(III) ions.

Potentiometric Determination of Stability Constants of Mono-, Bis-, and Tris(pyrrolidone-5-hydroxamato)iron(III) Complexes—The procedure for the determination of the stability constants of mono, bis, and tris iron(III) chelates was essentially the Schwarzenbach method (16). According to Schemes II–IV, the total concentration of iron(III), Fe_T, in solutions containing pyrrolidone-5-hydroxamic acid and iron(III) ions at low pH is:

$$Fe_T = [Fe^{3+}] + [Fe(C_5H_7O_3N_2)^{2+}] + [Fe(C_5H_7O_3N_2)_2^+] + [Fe(C_5H_7O_3N_2)_3] \quad \text{(Eq. 10)}$$

Equation 10 can be rearranged to Eq. 11:

$$Fe_T/[Fe^{3+}] = \alpha = 1 + \beta_I^*[HC_5H_7O_3N_2] + \beta_{II}^*[HC_5H_7O_3N_2]^2 + \beta_{III}^*[HC_5H_7O_3N_2]^3 \quad \text{(Eq. 11)}$$

where:

$$\beta_I^* = [Fe(C_5H_7O_3N_2)^{2+}]/([Fe^{3+}][HC_5H_7O_3N_2]) \quad \text{(Eq. 12a)}$$

$$\beta_{II}^* = [Fe(C_5H_7O_3N_2)_2^+]/([Fe^{3+}][HC_5H_7O_3N_2]^2) \quad \text{(Eq. 12b)}$$

$$\beta_{III}^* = [Fe(C_5H_7O_3N_2)_3]/([Fe^{3+}][HC_5H_7O_3N_2]^3) \quad \text{(Eq. 12c)}$$

The function F_1 is defined by:

$$F_1 = (\alpha - 1)/[HC_5H_7O_3N_2] = \beta_I^* + \beta_{II}^*[HC_5H_7O_3N_2] + \beta_{III}^*[HC_5H_7O_3N_2]^2 \quad \text{(Eq. 13)}$$

Equation 14 can be similarly obtained for the total concentration of the pyrrolidone-5-hydroxamic acid moiety $C_5H_7O_3N_{2T}$:

$$C_5H_7O_3N_{2T} = [HC_5H_7O_3N_2] + [Fe(C_5H_7O_3N_2)^{2+}] + 2[Fe(C_5H_7O_3N_2)_2^+] + 3[Fe(C_5H_7O_3N_2)_3] \quad \text{(Eq. 14)}$$

The concentration of the free $C_5H_7O_3N_2^-$ anion can be neglected because of low K_a and pH values. Furthermore, a good starting approximation can be made, $[HC_5H_7O_3N_2] = C_5H_7O_3N_{2T}$, in Eq. 14 if there is a sufficient excess of $C_5H_7O_3N_{2T}$ over Fe_T as in these experiments.

By plotting F_1 *versus* $[HC_5H_7O_3N_2]$, one obtains, according to Eq. 13, β_I^* as an intercept, since $F_1 = \beta_I^*$ when $[HC_5H_7O_3N_2] = 0$.

Another approximation, $\beta_{III}^*[HC_5H_7O_3N_2]^2 = 0$, can be made for very small values of $[HC_5H_7O_3N_2]$. Under this condition, quadratic Eq. 13 is reduced to:

$$F_1 = \beta_I^* + \beta_{II}^*[HC_5H_7O_3N_2] \quad \text{(Eq. 15)}$$

with the slope being equal to β_{II}^*.

Another rearrangement of Eq. 13 leads to:

$$F_2 = (F_1 - \beta_I^*)/[HC_5H_7O_3N_2] = \beta_{II}^* + \beta_{III}^*[HC_5H_7O_3N_2] \quad \text{(Eq. 16)}$$

with β_{II}^* as an intercept and β_{III}^* as a slope.

Similarly, the third function, F_3, can be obtained from:

$$F_3 = (F_2 - \beta_{II}^*)/[HC_5H_7O_3N_2] = \beta_{III}^* = \text{constant} \quad \text{(Eq. 17)}$$

In this procedure, one starts by plotting F_1 *versus* $[HC_5H_7O_3N_2]$, which gives diagrams such as those shown in Figs. 2 and 3. The F_1 in Eq. 13 is easily calculated from the known starting concentrations of Fe_T and $C_5H_7O_3N_{2T}$ and the concentration of the free Fe^{3+} ions determined from the redox potential. Depending on the experimental conditions, such as pH, three types of diagrams are possible (Figs. 2 and 3). Figure 2 shows that F_1 at pH 1.59 does not depend on $[HC_5H_7O_3N_2]$, indicating the reduction of Eq. 13 to the form $F_1 = \beta_I^*$ and, therefore, $\beta_{II}^* = 0$ and $\beta_{III}^* = 0$. It follows from Eqs. 12*b* and 12*c* that $[Fe(C_5H_7O_3N_2)_2^+]$ and $[Fe(C_5H_7O_3N_2)_3]$ are also zero under these conditions and that only the mono chelate is formed at pH 1.59.

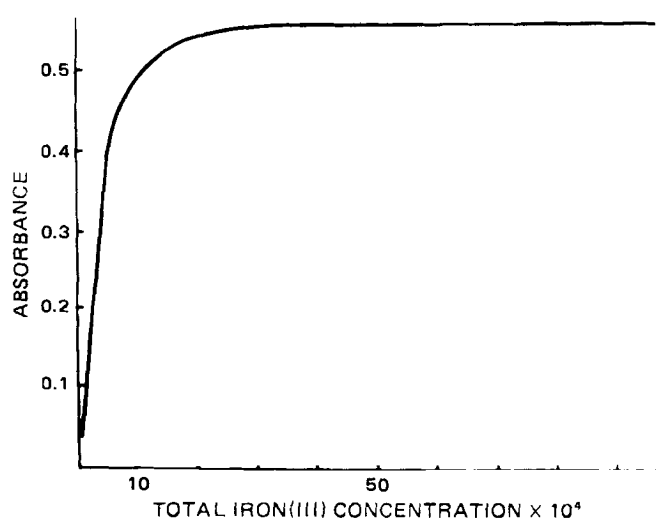

Figure 1—*Spectrophotometric titration of 5 × 10⁻⁴ M pyrrolidone-5-hydroxamic acid by iron(III) solution at 500 nm, pH 2.0, and ionic strength 0.1 (sodium chloride), using 1-cm quartz cells.*

Table II—Overall Stability Constants, β

pH	$\beta_I^* \times 10^{-3}$	$\beta_I \times 10^{-1}$	log β_I	β_{II}^*	$\beta_{II} \times 10^{-1}$	log β_{II}	β_{III}^*	β_{III}	log β_{III}
1.59	1.3	3.34	1.52	—	—	—	—	—	—
1.83	2.3	3.40	1.53	2.0×10^5	4.37	1.64	—	—	—
2.21	5.3	3.26	1.51	9.1×10^5	3.46	1.54	—	—	—
3.00	25.0	2.50	1.40	2.2×10^7	2.20	1.34	1.0×10^9	1.00	0.00
3.23	50.0	2.94	1.47	1.2×10^3	4.15	1.62	2.05×10^{10}	4.18	0.62
Mean	—	3.09	—	—	3.55	—	—	2.59	—
Log	—	1.49	—	—	1.55	—	—	0.41	—

Linear dependence of F_1 on $[HC_5H_7O_3N_2]$ is found at pH 1.83 and 2.21 (Fig. 2), indicating reduction of Eq. 13 to Eq. 15. Therefore, in this case, $\beta_{III}^* = 0$ and, from Eq. 12*c*, $[Fe(C_5H_7O_3N_2)_3] = 0$. This result is explained by the presence of both mono and bis, but not tris, chelates at pH 1.83 and 2.21. The β_I^* is always easily obtained from the intercept of F_1, and function F_2 may be calculated from Eq. 16. Figure 2 illustrates no dependence of F_2 on $[HC_5H_7O_3N_2]$, because Eq. 16 is reduced to the form $F_2 = \beta_{II}^*$, indicating an absence of the tris chelate.

The formation of all three chelates requires the nonlinear dependence of F_1 on $[HC_5H_7O_3N_2]$; furthermore, Eq. 13 must hold as is seen in Fig. 3 at pH 3.00. The nonlinear dependence is not pronounced in Fig. 3 at pH 3.23, probably due to the insufficiently high concentration of pyrrolidone-5-hydroxamic acid. In Fig. 3, β_I^* at pH 3.00 and 3.23 is obtained from the intercept of F_1, where $[HC_6H_7O_3N_2] = 0$, thus enabling the plotting of F_2 *versus* $[HC_5H_7O_3N_2]$ according to Eq. 16. The resulting straight line is used to obtain β_{II}^* from the intercept as well as to plot F_3 *versus* $[HC_5H_7O_3N_2]$ to get β_{III}^* from the intercept at pH 3.00 and 3.23. Equation 17 requires no dependence of F_3 on pyrrolidone-5-hydroxamic acid when all three chelates are present in solution (illustrated in Fig. 3 for pH 3.00). Deviation of F_3 at pH 3.23 from the expected horizontal line is negligible and due to experimental error.

This procedure yields only approximate values of β_I^*, β_{II}^*, and β_{III}^*. Therefore, only approximate values of $[Fe(C_5H_7O_3N_2)^{2+}]$, $[Fe(C_5H_7O_3N_2)_2^+]$, and $[Fe(C_5H_7O_3N_2)_3]$ can be obtained from Eqs. 12*a*, 12*b*, and 12*c*, respectively, and inserted in Eq. 14. However, Eq. 14 yields a more accurate value for $[HC_5H_7O_3N_2]$, which is again introduced in Eqs. 13, 16, and 17, giving more accurate values of β_I^*, β_{II}^*, and β_{III}^*. The procedure is to be repeated until the starting Eq. 10 is satisfied.

By following this procedure, the data for β_I^*, β_{II}^*, and β_{III}^* were obtained (Tables II and III). Figures 2 and 3 represent the corresponding diagrams. The overall stability constants, β, are calculated from β^* by the simple relations $\beta_I = \beta_I^*[H^+]$, $\beta_{II} = \beta_{II}^*[H^+]^2$, and $\beta_{III} = \beta_{III}^*[H^+]^3$. All other constants such as K_I, K_{II}, K_{III}, K_1, K_2, K_3, β_1, β_2, and β_3 are easily calculated from Eqs. 5*a*–5*c*, 6*a*–6*c*, and 7*a*–7*c*. They are listed in Table III to show the great influence of the hydrogen ion on various forms of the stability constants of chelates because of the rather high pKa value.

In this procedure, the best accuracy is expected in the determination of β_I^*; less accuracy is expected for β_{II}^*, and the least accuracy is expected for β_{III}^*. The value of $\beta_I^* = 1.3 \times 10^3$ obtained from Fig. 2 at pH 1.59 is substantiated by the excellent agreement between the calculated value of $Fe_T = 2.066 \times 10^{-4}$ *M* from Eq. 10 as an average of six determinations and the used analytical concentration of $Fe_T = 2.064 \times 10^{-4}$ *M*. The lower accuracy of β_{II}^* and β_{III}^* in the system at pH 3.23 in Fig. 3 results in less agreement between analytical and calculated values of Fe_T, 2.064×10^{-4}

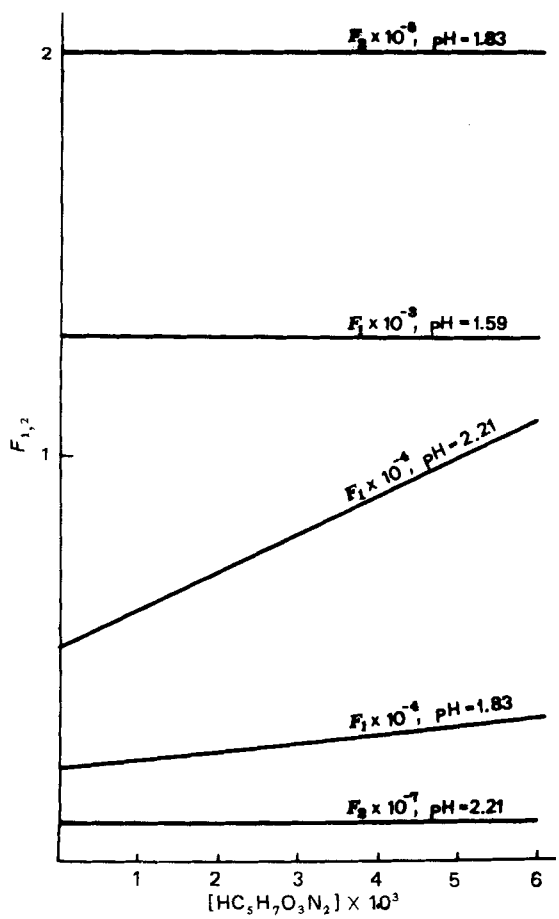

Figure 2—*Dependence of* F_1 *and* F_2 *on* $[HC_5H_7O_3N_2]$ *at pH 1.59, 1.83, and 2.21. Intercepts of* F_1 *at pH 1.59, 1.83, and 2.21 give* β_I^* *of* 1.3×10^3, 0.23×10^4, *and* 0.53×10^4, *respectively. Intercepts of* F_2 *at pH 1.83 and 2.21 give* β_{II}^* *of* 2.0×10^5 *and* 0.091×10^7, *respectively. For details, see text.*

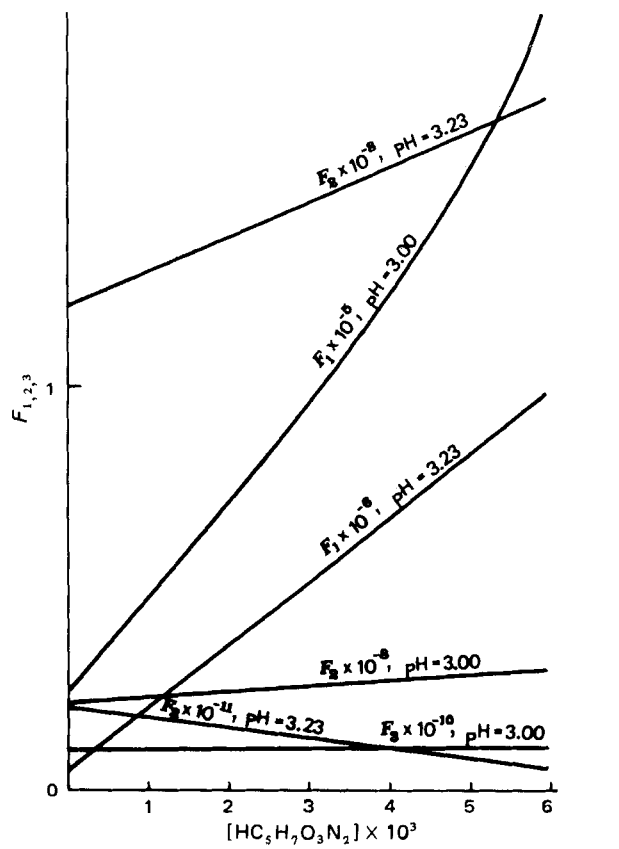

Figure 3—*Dependence of* F_1, F_2, *and* F_3 *on* $[HC_5H_7O_3N_2]$ *at pH 3.00 and 3.23. Intercepts of* F_1 *at pH 3.00 and 3.23 give* β_I^* *of* 0.25×10^5 *and* 0.05×10^6, *respectively. Intercepts of* F_2 *at pH 3.00 and 3.23 give* β_{II}^* *of* 0.22×10^8 *and* 1.2×10^8, *respectively. Intercepts of* F_3 *at pH 3.00 and 3.23 give* β_{III}^* *of* 0.1×10^{10} *and* 0.205×10^{11}, *respectively. For details, see text.*

Table III—Stability Constants of (Pyrrolidone-5-hydroxamato)iron(III)[a]

Index	K	log K	β	log β
I	3.09×10^{1}	1.49	3.09×10^{1}	1.49
II	1.15×10^{0}	0.06	3.55×10^{1}	1.55
III	4.57×10^{-2}	−1.34	1.62×10^{0}	0.41
1	1.38×10^{10}	10.14	1.38×10^{10}	10.14
2	5.13×10^{8}	8.71	7.08×10^{18}	18.85
3	2.04×10^{7}	7.31	1.44×10^{26}	26.16

[a] Chelates were calculated from Eqs. 5a–5c, 6a–6c, 7a–7c, and Table II and are expressed as K_{I}, K_{II}, K_{III}, K_{1}, K_{2}, K_{3}, β_{I}, β_{II}, β_{III}, β_{1}, β_{2}, and β_{3}.

M and 2.168×10^{-4} M, respectively. The agreement is significantly improved by rejecting one extreme value of Fe_T, which gives the calculated average value of 2.075×10^{-4} M. The precision decreases in the order $\beta_{I} > \beta_{II} > \beta_{III}$ (Table II). The value of log β_{I} (= log K_{I}) = 1.49 is in excellent agreement with the spectrophotometrically obtained value of log β_{I} = 1.52.

Overall stability constants of related iron(III) hydroxamates are listed in Table IV. The decrease in stability when going from benzohydroxamic to pyrrolidone-5-hydroxamic acid chelates of iron(III) is larger than may be expected from the increase in acidity in the same direction. Some other factors must be involved such as the interference by chelating iron(III) *via* carbonyl and imine groups of the pyrrolidone ring.

The stability of (pyrrolidone-5-hydroxamato)iron(III) chelates is important for the behavior of these complexes in living systems. There is an indication that hydroxamic acid-containing compounds are constituents of siderophilin, the iron-binding β-pseudoglobulin of human plasma (17), and of ferritin (18). It is obvious that the higher the stability of hydroxamic acid–iron(III) chelates, the easier is iron transport and the better is iron resorption at various biological pH's. Iron-containing hydroxamic acids have been patented as metalotherapeutics (5). (Pyrrolidone-5-hydroxamato)iron(III) chelates may be considered as possible metalotherapeutics in view of their stability and the presence of the pyrrolidone ring, which, like povidone, is used as a substitute for blood plasma (7) and also shows a mitostimulating effect (19).

Table IV—Comparison of Stabilities of Iron(III) Hydroxamines

Acid	pKa	log β_3
Acetohydroxamic	9.37[a]	28.30[a]
Benzohydroxamic	8.79[a]	27.83[a]
Pyrrolidone-5-hydroxamic	8.65[b]	26.36[c]

[a] From Ref. 16. [b] From Ref. 12. [c] This work.

REFERENCES

(1) H. Maehr, *Pure Appl. Chem.*, **28**, 603 (1971).
(2) J. B. Neilands, *Struct. Bonding*, **1**, 59 (1966).
(3) O. Mikeš and J. Turkova, *Chem. Listy*, **58**, 65 (1964).
(4) J. B. Neilands, *Science*, **156**, 1443 (1967).
(5) E. Bayer, Swiss pat. 440, 314 (Cl.C. 07f) (Dec. 29, 1967).
(6) R. T. Coutts, *Can. J. Pharm. Sci.*, **2** (1), 2 (1967).
(7) C. R. Noller, "Chemistry of Organic Compounds," Saunders, Philadelphia, Pa., 1961.
(8) D. H. Biggs, R. T. Coutts, M. L. Selley, and G. A. Towill, *J. Pharm. Sci.*, **61**, 1739 (1972).
(9) J. W. Munson and K. A. Connors, *ibid.*, **61**, 211 (1972).
(10) R. E. Notari, *ibid.*, **58**, 1069 (1969).
(11) R. E. Notari and J. W. Munson, *ibid.*, **58**, 1060 (1969).
(12) M. Pećar, N. Kujundžić, B. Mlinarević, D. Čerina, B. Horvat, and M. Verić, *ibid.*, **64**, 970 (1975).
(13) T. M. Beck, "Chemistry of Complex Equilibria," Akadémiai Kiadó, Budapest, Hungary, 1970, p. 131.
(14) A. N. Martin, "Physical Pharmacy," Lea & Febiger, Philadelphia, Pa., 1960, pp. 395–428.
(15) M. Pećar, N. Kujundžić, and J. Pazman, 2nd International Symposium on Analytical Chemistry, Ljubljana, Yugoslavia, 1972.
(16) G. Schwarzenbach and K. Schwarzenbach, *Helv. Chim. Acta*, **46**, 1390 (1963).
(17) S. Fiala and D. Burk, *Arch. Biochem.*, **20**, 172 (1949).
(18) H. N. Munro and J. W. Drysdale, *Fed. Proc.*, **29**, 1469 (1970).
(19) N. Kujundžić, L. Butula, and M. Pećar, *Bull. Sci. Sect. A Yougosl.*, **1975**, 65.

ACKNOWLEDGMENTS AND ADDRESSES

Received July 9, 1975, from the *Faculty of Pharmacy and Biochemistry, University of Zagreb, Zagreb, Yugoslavia.*

Accepted for publication April 23, 1976.

Supported by the Republic Foundation for Scientific Work of the Croatia.

The authors are grateful to the Alexander von Humboldt Foundation for the Opton PMQ II spectrophotometer.

M. Pećar was the recipient of a fellowship from the Foundation at the Max Planck Institute for Medical Research, Heidelberg.

† Deceased.

ˣ To whom inquiries should be directed.

Methods for Evaluating Hermetic Closures for Screw-Capped Bottles

R. D. CILENTO

Abstract □ With the described method, a large number of sealed bottles can be tested to determine their effectiveness, integrity, and reliability in preserving an inert atmosphere. The method consists of placing milligram quantities of dry ice into the bottles, capping them, and periodically weighing them on an analytical balance; leaky bottles are detected by a loss in weight. This method can be applied to test a large number of bottles with a minimum of effort and manpower and without complicated instrumentation. The data presented are highly reproducible and correlate well with data from other methods and with the physical defects of the bottles.

Keyphrases □ Seals, hermetic—testing method developed for large numbers of screw-capped bottles □ Bottles, screw capped—method of testing hermetic seals developed for large numbers □ Technology, pharmaceutical—method of testing hermetic seals of large numbers of screw-capped bottles developed

By definition, hermetic containers are impervious to air and any other gas under ordinary conditions of handling. For the primary container of a drug to qualify as hermetic, it must be leakproof; *i.e.*, no gases or vapors must be capable of entering it or escaping from it.

A product is hermetically sealed to protect it from con-

Table III—Stability Constants of (Pyrrolidone-5-hydroxamato)iron(III)[a]

Index	K	log K	β	log β
I	3.09×10^{1}	1.49	3.09×10^{1}	1.49
II	1.15×10^{0}	0.06	3.55×10^{1}	1.55
III	4.57×10^{-2}	−1.34	1.62×10^{0}	0.41
1	1.38×10^{10}	10.14	1.38×10^{10}	10.14
2	5.13×10^{8}	8.71	7.08×10^{18}	18.85
3	2.04×10^{7}	7.31	1.44×10^{26}	26.16

[a] Chelates were calculated from Eqs. 5a–5c, 6a–6c, 7a–7c, and Table II and are expressed as K_{I}, K_{II}, K_{III}, K_{1}, K_{2}, K_{3}, β_{I}, β_{II}, β_{III}, β_{1}, β_{2}, and β_{3}.

M and 2.168×10^{-4} M, respectively. The agreement is significantly improved by rejecting one extreme value of Fe_T, which gives the calculated average value of 2.075×10^{-4} M. The precision decreases in the order $\beta_{I} > \beta_{II} > \beta_{III}$ (Table II). The value of log β_{I} (= log K_{I}) = 1.49 is in excellent agreement with the spectrophotometrically obtained value of log β_{I} = 1.52.

Overall stability constants of related iron(III) hydroxamates are listed in Table IV. The decrease in stability when going from benzohydroxamic to pyrrolidone-5-hydroxamic acid chelates of iron(III) is larger than may be expected from the increase in acidity in the same direction. Some other factors must be involved such as the interference by chelating iron(III) *via* carbonyl and imine groups of the pyrrolidone ring.

The stability of (pyrrolidone-5-hydroxamato)iron(III) chelates is important for the behavior of these complexes in living systems. There is an indication that hydroxamic acid-containing compounds are constituents of siderophilin, the iron-binding β-pseudoglobulin of human plasma (17), and of ferritin (18). It is obvious that the higher the stability of hydroxamic acid–iron(III) chelates, the easier is iron transport and the better is iron resorption at various biological pH's. Iron-containing hydroxamic acids have been patented as metalotherapeutics (5). (Pyrrolidone-5-hydroxamato)iron(III) chelates may be considered as possible metalotherapeutics in view of their stability and the presence of the pyrrolidone ring, which, like povidone, is used as a substitute for blood plasma (7) and also shows a mitostimulating effect (19).

Table IV—Comparison of Stabilities of Iron(III) Hydroxamines

Acid	pKa	log β_3
Acetohydroxamic	9.37[a]	28.30[a]
Benzohydroxamic	8.79[a]	27.83[a]
Pyrrolidone-5-hydroxamic	8.65[b]	26.36[c]

[a] From Ref. 16. [b] From Ref. 12. [c] This work.

REFERENCES

(1) H. Maehr, *Pure Appl. Chem.*, **28**, 603 (1971).
(2) J. B. Neilands, *Struct. Bonding*, **1**, 59 (1966).
(3) O. Mikeš and J. Turkova, *Chem. Listy*, **58**, 65 (1964).
(4) J. B. Neilands, *Science*, **156**, 1443 (1967).
(5) E. Bayer, Swiss pat. 440, 314 (Cl.C. 07f) (Dec. 29, 1967).
(6) R. T. Coutts, *Can. J. Pharm. Sci.*, **2** (1), 2 (1967).
(7) C. R. Noller, "Chemistry of Organic Compounds," Saunders, Philadelphia, Pa., 1961.
(8) D. H. Biggs, R. T. Coutts, M. L. Selley, and G. A. Towill, *J. Pharm. Sci.*, **61**, 1739 (1972).
(9) J. W. Munson and K. A. Connors, *ibid.*, **61**, 211 (1972).
(10) R. E. Notari, *ibid.*, **58**, 1069 (1969).
(11) R. E. Notari and J. W. Munson, *ibid.*, **58**, 1060 (1969).
(12) M. Pećar, N. Kujundžić, B. Mlinarević, D. Čerina, B. Horvat, and M. Verić, *ibid.*, **64**, 970 (1975).
(13) T. M. Beck, "Chemistry of Complex Equilibria," Akadémiai Kiadó, Budapest, Hungary, 1970, p. 131.
(14) A. N. Martin, "Physical Pharmacy," Lea & Febiger, Philadelphia, Pa., 1960, pp. 395–428.
(15) M. Pećar, N. Kujundžić, and J. Pazman, 2nd International Symposium on Analytical Chemistry, Ljubljana, Yugoslavia, 1972.
(16) G. Schwarzenbach and K. Schwarzenbach, *Helv. Chim. Acta*, **46**, 1390 (1963).
(17) S. Fiala and D. Burk, *Arch. Biochem.*, **20**, 172 (1949).
(18) H. N. Munro and J. W. Drysdale, *Fed. Proc.*, **29**, 1469 (1970).
(19) N. Kujundžić, L. Butula, and M. Pećar, *Bull. Sci. Sect. A Yougosl.*, **1975**, 65.

ACKNOWLEDGMENTS AND ADDRESSES

Received July 9, 1975, from the *Faculty of Pharmacy and Biochemistry, University of Zagreb, Zagreb, Yugoslavia.*

Accepted for publication April 23, 1976.

Supported by the Republic Foundation for Scientific Work of the Croatia.

The authors are grateful to the Alexander von Humboldt Foundation for the Opton PMQ II spectrophotometer.

M. Pećar was the recipient of a fellowship from the Foundation at the Max Planck Institute for Medical Research, Heidelberg.

† Deceased.

ˣ To whom inquiries should be directed.

Methods for Evaluating Hermetic Closures for Screw-Capped Bottles

R. D. CILENTO

Abstract □ With the described method, a large number of sealed bottles can be tested to determine their effectiveness, integrity, and reliability in preserving an inert atmosphere. The method consists of placing milligram quantities of dry ice into the bottles, capping them, and periodically weighing them on an analytical balance; leaky bottles are detected by a loss in weight. This method can be applied to test a large number of bottles with a minimum of effort and manpower and without complicated instrumentation. The data presented are highly reproducible and correlate well with data from other methods and with the physical defects of the bottles.

Keyphrases □ Seals, hermetic—testing method developed for large numbers of screw-capped bottles □ Bottles, screw capped—method of testing hermetic seals developed for large numbers □ Technology, pharmaceutical—method of testing hermetic seals of large numbers of screw-capped bottles developed

By definition, hermetic containers are impervious to air and any other gas under ordinary conditions of handling. For the primary container of a drug to qualify as hermetic, it must be leakproof; *i.e.*, no gases or vapors must be capable of entering it or escaping from it.

A product is hermetically sealed to protect it from con-

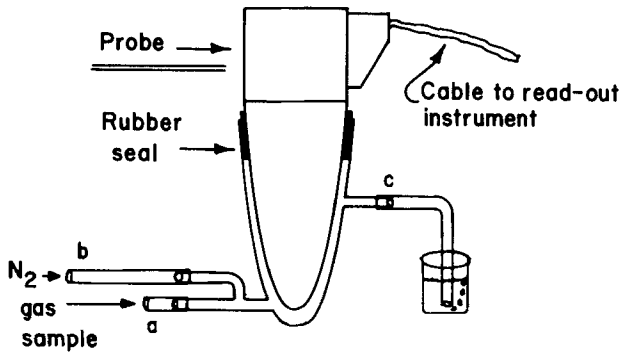

Figure 1—*Oxygen analyzer glass cell.*

tact with components of the atmosphere that may cause it to deteriorate, *e.g.*, oxygen or water vapor, or to prevent its volatile components from escaping. The need for this practice is well documented (1–17).

A review of the work done in the field of inert-gas flushing of containers has revealed an extensive effort dedicated to the development of procedures for purging primary containers (13, 15, 18) and to measurement of the effectiveness of these procedures (14, 15, 19–22). What seems to be lacking, however, is information on methods for studying the effectiveness of screw-capped bottles in preserving an inert atmosphere within them throughout their shelflife. Such methods could be subdivided into two categories: (*a*) testing the efficacy of components (in particular, seals and seal materials), and (*b*) testing the impermeability of the assembled system.

Much published work exists for the first category (3, 5, 9, 23–28). In the second category, methods have been reported for testing plastic bottles (29), single-dose pouches (28), and ampuls; but no effective, simple, fast, precise method has been reported for testing screw-capped glass bottles. It is not enough to demonstrate that seal materials are impervious to moisture or oxygen; their effectiveness must be demonstrated after they have been applied as finished closures.

This paper presents a method by which a large number of sealed bottles can be tested for determination of the most effective seal and for the cause of malfunctioning of a container, *e.g.*, the bottle, the seal, the cap, or the assembling operation. The results should provide guidance in developing necessary controls or precautions.

EXPERIMENTAL

Equipment—A vacuum chamber (20 × 20 × 30 cm), an analytical balance[1], a spring torque tester[2], a pressure vessel (a cylindrical 110-liter tank), and an oxygen analyzer[3] were used.

Materials Tested—The bottle[4] size was 100 ml with beaded glass lips, 38 mm. Standard metal screw caps matched the bottle size and finish. The liners were polyvinyl chloride, 0.7-mm thick solid disks.

Test Methods—The following test methods were developed to study the efficacy and reliability of closure systems.

Test 1: Vacuum Chamber—A number of bottles are capped at a specified torque and placed into the vacuum chamber for 4 hr. The vacuum is quickly broken, and each bottle is immediately placed, cap down, in a tray containing enough water to keep the cap entirely submerged. The bottle is vented by holding the cap with a pair of pliers or similar device and twisting the bottom of the bottle. Any bottle that had been evacuated through a leaky closure will be partially or totally filled with water.

Test 2: Dry Ice—Immediately after a chip or two of crushed dry ice has been placed into a tared bottle, the bottle is capped at a specified torque and then weighed to the nearest milligram on the analytical balance. The amount of dry ice placed in each bottle should produce enough gaseous carbon dioxide to give a pressure of 40.000–70.000 Nm^{-2} (6–10 psi). The amount varies with bottle size, *i.e.*, about 50 mg for a 25-ml bottle, 150 mg for a 100-ml bottle, and 250 mg for a 200-ml bottle.

A leak-free bottle prepared in this way maintains its weight indefinitely. A leaky bottle starts losing weight immediately and, depending on the magnitude of the defect, loses 70–80% of the carbon dioxide gas within minutes, hours, or days; the remainder of the gas diffuses out more slowly. If a perfectly sealed bottle is opened months later, the hissing sound of the escaping gas under pressure is still audible. A skilled technician can prepare more than 30 sample bottles/hr.

Test 3: Oxygen Diffusion—Each bottle is flooded with nitrogen and capped at a specified torque. The bottles are held for 1–4 days in a pressure vessel that has been flooded with oxygen. Oxygen is maintained in the vessel under a positive pressure, being permitted to flow in continuously and to bubble out through a vent tube. At the end of the storage period, the bottles are tested for oxygen content.

Nitrogen flooding of the bottles is accomplished in either of two ways.

1. The bottles are first evacuated in the vacuum chamber, and then the vacuum is broken with nitrogen. While nitrogen is still flowing, the cap is screwed on each bottle fingertip tight. A specified torque is applied to the cap as soon as the bottle has been removed from the chamber. Precautions must be taken to avoid introducing air into the bottle during capping.

2. The procedure of blowing nitrogen into open bottles is not as effective as is the use of the vacuum chamber, but it is much faster and, if properly controlled, can yield very reproducible results. The four critical factors in the control of this procedure are the nitrogen velocity, time, position of the nitrogen-delivery tube with respect to the neck of the bottle, and mode of application of the cap. The optimum conditions for each size and shape of the bottle must be determined experimentally.

Procedure 1 can produce bottles containing less than 2% oxygen, whereas Procedure 2 produces bottles containing 2–5% oxygen.

The oxygen content of the bottles is determined by use of the oxygen analyzer, which can be adapted to receive a gas sample by mounting a specially built glass cell on its probe (Fig. 1). The cell is purged with a stream of nitrogen through intake line b; as soon as the instrument reads zero, this line is closed and a 5-ml gas sample is introduced *via* syringe through line a. The instrument response is practically immediate. The instrument is calibrated by introducing samples of known oxygen composition; a straight-line relationship exists between sample composition and meter readings, with the curve passing through the zero point. The method can be used to measure accurately oxygen concentrations of 0–60 ± 0.5%. Concurrent testing of several samples proved this method to be as accurate and reproducible as a GC assay.

To obtain a gas sample, a hole is made in the cap of the bottle with an awl; a 5-ml sample of gas is withdrawn into a syringe through a hypodermic needle fitted with a rubber flange at its base. The gas is then immediately injected into the cell of the instrument. The main advantage of this method is the speed with which a large number of samples can be tested (a skilled technician can test more than 30 samples/hr) with results immediately determined from a standardized graph; its main disadvantage is the large sample of gas (5 ml) needed.

RESULTS AND DISCUSSION

The described test methods were used to determine the most effective closure system for screw-capped glass bottles. The three methods were developed concurrently, but only the dry ice method was used extensively in the screening and concluding phases of the study. The oxygen-diffusion method was used only to confirm the results of systems that had passed the dry ice test once the validity of the dry ice method had been demonstrated by good correlation between these two methods. The vacuum chamber method, developed early in the program, produced results that correlated with those of the other methods, but its use was discontinued after the superiority of the dry ice method had been demonstrated.

The data in Table I show that a good correlation exists between results obtained by the dry ice and oxygen-diffusion tests. Leakage of Bottles 1, 4, 7, 12, 15, 16, 18, and 19 was demonstrated by the dry ice test and confirmed by the oxygen-diffusion test. The data in Table II confirm the

[1] Sartorius type 2472, 200-g range, 0.0001-g sensitivity.
[2] Owens-Illinois Glass Co.
[3] Model 300, Weston & Stack, Inc.
[4] GCMI glass finish No. 400.

Table I—Determination of Leakage of Bottles[a] by Dry Ice and Oxygen Diffusion Tests

Bottle	Dry Ice Test, Weight Loss, %				Oxygen Diffusion Test, Oxygen Content, %
	First Run		Second Run		
	18 hr	42 hr	20 hr	44 hr	
1	54	66	77	76	7.0
2	0	6	0	0	3.0
3	0	2	0	0	2.5
4	58	67	46	57	4.5
5	0	0	0	0	2.5
6	5	8	0	0	2.0
7	27	40	46	55	9.0
8	0	2	0	0	2.5
9	12	24	7	10	2.5
10	0	0	0	0	2.0
11	0	0	0	0	2.0
12	68	69	78	76	15.5
13	0	5	0	0	2.5
14	22	34	3	7	2.5
15	77	72	81	82	13.5
16	79	75	72	74	15.5
17	0	3	0	0	2.0
18	35	54	57	68	7.5
19	27	39	11	22	>60
20	2	5	0	0	2.0
21	24	39	7	11	2.0
22	0	0	0	0	2.0
23	28	42	5	7	2.0
24	0	0	0	0	2.5
25	0	0	0	0	2.5

[a] Bottles were picked at random from the same lot of the supplier. In this experiment, the caps were applied with torques of 2.2 ± 0.2 mN.

results shown in Table I and also show that leakage could be corrected by increasing the torque applied to the caps. In this experiment, carried out with the same set of bottles used earlier (Table I), the effect of torque on the efficacy of the closure system was studied. The caps were applied at torques of 1.65–1.85, 2.50–2.75, and >2.75 mN. For the low and intermediate levels of torque, the caps were twisted to the prescribed torque and quickly released; for the high torque level, the caps were twisted to the limit of the torque tester and held so for 5 sec. For the three levels of torque, 50, 20, and 0% of the bottles had lost weight after 4, 24, and 96 hr, respectively. The complete integrity of the seal for bottles in the third group must be attributed both to the magnitude of the torque (>2.75 mN) and to the duration of its application.

The results of the first two experiments demonstrated that the set of bottles tested included highly defective, moderately defective, and perfect specimens. The third experiment sought to discover the nature of the defect. The initial assumption of the cause of leakage was a lack of flatness of the bottle lip. To test this hypothesis, a vacuum device (Fig. 2) to measure the flatness of the bottle lip was built. The testing procedure consisted of connecting the device to a source of vacuum, placing the Plexiglas plate on the bottle, and reading the gauge. The results were highly reproducible and are assumed to be an accurate measure of the degree of flatness of the lip of the bottle, the highest reading being obtained for a bottle with a perfectly flat lip (Table III).

The results of this experiment, however, showed no correlation with the results of the first two experiments. For example, Bottles 15 and 16, which were among the worst leakers, showed the highest readings; on the other hand, Bottles 11 and 22, which did not leak, showed very low readings. It was concluded that the lack of flatness of the bottle lip was not responsible for the leak. At this point, the bottles were closely inspected with a magnifying glass and a stereoscopic microscope; most of them showed thin, smooth grooves across the lip (Fig. 3). All grooves were

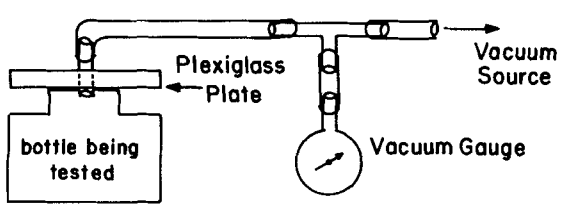

Figure 2—*Vacuum testing device.*

Table II—Relationship between Leakage[a] and Put on Torque (P.O.T.) Applied to Caps

Bottle	P.O.T., mN, Weight Loss, %		
	1.65–1.85[b]	2.50–2.75[c]	>2.75[d]
1	5.5	0	0
2	0	0	0
3	0	0	0
4	61	59	0
5	0	0	0
6	0	0	0
7	66	0	0
8	0	0	0
9	9	0	0
10	0	0	0
11	0	0	0
12	77	15	0
13	0	0	0
14	19	0	0
15	76	76	0
16	84	85	0
17	19	0	0
18	18	0	0
19	69	41	0
20	0	0	0
21	39	0	0
22	0	0	0
23	48	0	0
24	0	0	0
25	0	0	0

[a] As measured by the dry ice test. [b] Determined at 4 hr from initial dry ice charge. [c] Determined at 24 hr. [d] Determined at 96 hr.

ranked on an arbitrary scale (from 0 = no grooves to 10 = widest).

The results showed that bottles lacking grooves or having grooves of minimal width had not leaked under any of the conditions shown in Table II. The five bottles that leaked after the caps had been applied with a torque of 2.50–2.75 mN showed grooves rated between 4 and 7. One bottle (26) that had, in another experiment, leaked even after it had been capped with a maximum torque showed a groove much larger than any other found. Grooves ranked 3, 6, 7, and 10 on this scale were later shown, by microscopic comparison with hairs of known diameter, to have widths of 50, 75, 100, and 200 μm, respectively.

Table III—Determination of Defects of Bottle Lip

Bottle	Vacuum Device[a], Nm^{-2}	Groove Size Estimate	
		Rank Order[b]	Microscope[c]
1	53.2	4	—
2	62.2	1	—
3	48.6	1	—
4	30.5	4	—
5	66.0	2	—
6	64.2	2	—
7	56.5	4	—
8	56.8	0	—
9	60.8	3	—
10	50.0	0	—
11	36.2	0	—
12	26.4	7	100
13	66.8	0	—
14	67.8	3	—
15	75.5	6	75
16	75.5	7	—
17	53.2	3	50
18	73.7	3	—
19	60.0	5	—
20	54.0	1	—
21	48.4	3	—
22	48.6	1	—
23	59.2	3	—
24	49.0	1	—
25	56.8	1	—
26	39.0	10	200

[a] Average of two measurements taken 90° apart. [b] Estimates by three persons, averaged to closest whole number. [c] By matching against hairs of known diameters.

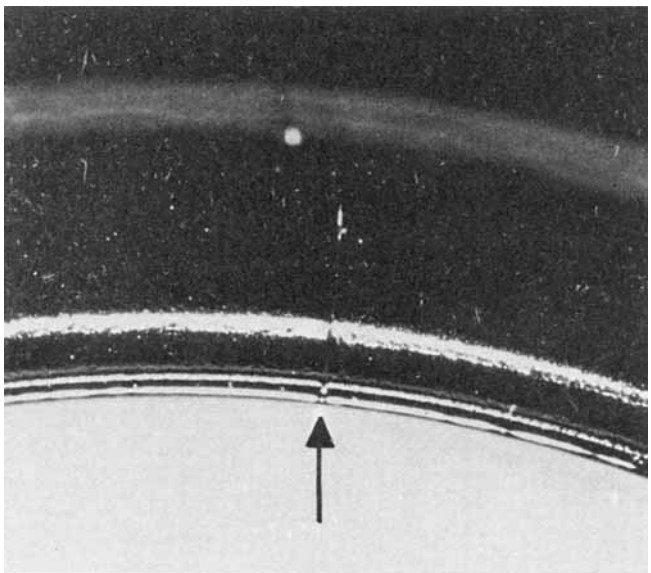

Figure 3—*Groove defect (at approximately 10×) (photograph courtesy of R. Walton)*

The dry ice test method was also used to evaluate a variety of liner seals. To compensate for the groove defects in bottle lips, polyvinyl chloride foam liners required an application torque as great as that required for polyvinyl chloride solid liners. Moreover, wax-coated laminates were inferior to polyvinyl chloride, and pressure-sensitive seals[5], applied with an acceptable torque, were more effective than the other liner seals.

SUMMARY AND CONCLUSIONS

A dry ice method has proved very useful for testing the effectiveness of screw-capped bottles in preserving an inert atmosphere within them. The method permits the testing of a large number of samples with a minimum of effort; it utilizes uncomplicated equipment and is simple to apply. The results are highly reproducible and correlate well with those of the oxygen-diffusion method and with the physical defects of the system.

This method is specifically designed to test the assembled package, but it can be used to test components or procedures. By its use, various seals were evaluated. Polyvinyl chloride proved to be an excellent sealing material which compensates very well for out-of-flat defects, but it requires too great a torque to be useful in compensating for the groove defects.

The method can be used by packaging engineers to develop and evaluate closure systems and procedures and by quality-control units for routine spot checks of container materials or for extensive tests of questionable shipments.

REFERENCES

(1) E. O. Krueger, *Drug Cosmet. Ind.*, **99**, 79 (1966).

(2) N. E. Webb, presented at the Symposium on Pharmaceutical Packaging, APhA Academy of Pharmaceutical Sciences, Miami Beach, Fla., May 6, 1968.

(3) H. G. Garman, *ibid.*

(4) "Code of Federal Regulations," Title 21, Part 133.

(5) T. L. Grimes, "Packaging Evaluation Programs for Pharmaceuticals," Report F-7018, Packaging Institute, New York, N.Y., 1970.

(6) J. F. Wranko, "Quality Control on the Packaging Line," Report F-6843, Packaging Institute, New York, N .Y., 1968.

(7) E. O. Krueger, "Controlling Quality of Incoming Materials," Report F-6621, Packaging Institute, New York, N.Y., 1966.

(8) J. M. Jackson and J. F. Carroll, "Materials Testing *vs.* Food Package Performance: A Dilemma," Report F-6928, Packaging Institute, New York, N.Y., 1969.

(9) S. M. Blaug, E. Hickman, and J. L. Lach, *J. Am. Pharm. Assoc., Sci. Ed.*, **47**, 54 (1958).

(10) U. Kesselring and I. Kapetanidis, *Pharm. Acta Helv.*, **41**, 428 (1966).

(11) Z. Sykulska and M. Gariska, *Acta Pol. Pharm.*, **22**, 133 (1965).

(12) Z. Sykulska and J. W. Sosnowska, *Farm. Pol.*, **22**, 510 (1966).

(13) O. Warts and P. Wessberg, *Farm. Tid.*, **77**, 905 (1967).

(14) L. F. Cullen and G. J. Papariello, *J. Pharm. Sci.*, **59**, 94 (1970).

(15) M. Brown and L. J. Leeson, *ibid.*, **58**, 242 (1969).

(16) J. A. Satkowski, "Outgoing Quality Control for Pharmaceutical and Device Packaging Materials," Report T-7021, Packaging Institute, New York, N.Y., 1970.

(17) E. L. Meyers, presented at the Seminar on Quality Control Procedures, University of Wisconsin, Madison, Wis., Aug. 1965.

(18) M. Brown and L. J. Leeson, presented at the Eastern Regional Meeting, APhA Academy of Pharmaceutical Sciences, Oct. 6, 1967.

(19) D. F. Percival and R. L. Anderson, "Control by Chromatography," Report F-6632, Packaging Institute, New York, N.Y., 1966.

(20) F. C. Wheeler, *Bull. Parenteral Drug Assoc.*, **18**, 23 (1964).

(21) V. Spiebler, *Mod. Packag.*, **45**, 46 (1972).

(22) W. L. McKenzie and C. H. Athanasiou, *Bull. Parenteral Drug Assoc.*, **25** (3), 106 (1971).

(23) N. J. Lopapa, "Accelerated Storage Testing," Report F-7028, Packaging Institute, New York, N.Y., 1970.

(24) E. E. Kennedy, "Standards of Quality in the Drug and Pharmaceutical Industry," Report F-6619, Packaging Institute, New York, N.Y., 1966.

(25) M. J. Gluckman and H. O. Ranger, "Development and Design of an Automatic High Speed Water Vapor Transmission Test Device," Report F-6419, Packaging Institute, New York, N.Y., 1964.

(26) R. H. Thomas, "Testing Primary Containers," Report F-6959, Packaging Institute, New York, N.Y., 1969.

(27) "Test of Water Vapor Transmission in Screw Cap Closures," Test Procedures PI Closures 1t-51, Packaging Institute, New York, N.Y. 1951.

(28) R. McFedries and J. E. Samuels, presented at the Symposium on Pharmaceutical Packaging, APhA Academy of Pharmaceutical Sciences, Miami Beach, Fla., May 6, 1968.

(29) C. A. Speas, "A New Method of Measuring Oxygen Permeation in Plastic Containers," Report F-6638, Packaging Institute, New York, N.Y., 1966.

[5] Type PLXV-PS, supplied by F. Gutmann & Co., Brooklyn, N.Y. (Its surface is covered with a soft, rubbery, adhesive material.)

ACKNOWLEDGMENTS AND ADDRESSES

Received December 17, 1975, from the *Department of Pharmaceutical Research & Development, Squibb Institute for Medical Research, New Brunswick, NJ 08903.*

Accepted for publication May 5, 1976.

Presented at the APhA Academy of Pharmaceutical Sciences, Atlanta meeting, November 1975.

Convective Diffusional Analysis for Drug Transport through a Tubular Polymeric Membrane

D. R. FLANAGAN *x **and S. H. YALKOWSKY** ‡

Abstract □ The transport of three *p*-aminobenzoate esters (ethyl, butyl, and hexyl) through a tubular dimethyl polysiloxane membrane into a flowing liquid was investigated. The tubular configuration permits the exact determination of the convective diffusional contribution to membrane transport with models that account for fluid hydrodynamics. The observed transport behavior ranged from complete convective diffusion control for the hexyl ester to complete membrane control for the ethyl ester; the butyl ester exhibited a change in control with flow rate. The implications of convective diffusional considerations to intestinal absorption and dissolution studies are discussed.

Keyphrases □ Diffusion—three *p*-aminobenzoate esters through tubular dimethyl polysiloxane membrane into a flowing liquid □ Transport, drug—three *p*-aminobenzoate esters through tubular dimethyl polysiloxane membrane into a flowing liquid □ Membrane permeation—three *p*-aminobenzoate esters through tubular dimethyl polysiloxane membrane into a flowing liquid

Most studies on the transport of drugs through model membranes (1–3) have utilized transport systems with reproducible hydrodynamics and maximal surface-to-volume ratios. The stagnant diffusion layer or film model has been applied as a convenient tool for the interpretation of diffusional resistances in or on either side of the model membranes. The convenience and wide application of this model have led to the implication that it accurately reflects physical reality (4), but its limitations have been known for some time, particularly its weakness in predicting convective influences on mass transfer without use of empirical relationships (5).

By changing the experimental design for membrane transport studies, it will be shown that the convective diffusional contributions to mass transfer can be exactly determined with models that are more accurate pictures of physical reality. The experimental design utilizes a tubular membrane with an aqueous solution flowing at a constant rate through the tube. Such a system can be assembled easily and inexpensively to provide the advantages of previous systems plus the added advantage of being able to determine exactly the aqueous convective diffusional contribution to the overall transport rate. These studies also have important implications for intestinal absorption and dissolution studies.

THEORY

For an experimental design in which a flowing liquid is taking up solute from a tube wall, several models predict the extent of solute uptake under various convective conditions. The first type of convective condition may be termed plug flow (Fig. 1*a*), in which there is no velocity gradient in the flowing liquid. In this model, all liquid in the tube moves at a constant velocity, V_0, and the solute is taken up from the wall as the liquid flows through the tube. For a tube of a particular length, L, a constant solute concentration, C_{av}, is expected to be flowing out of the end if the flow rate is held constant. The differential equation describing the mass transfer due to convection and diffusion for this situation is:

$$V_0 \frac{\partial c}{\partial z} = D \frac{1}{r} \frac{\partial}{\partial r}\left(r \frac{\partial c}{\partial r}\right) \qquad \text{(Eq. 1)}$$

where $\partial c/\partial z$ = longitudinal concentration gradient, D = diffusion coefficient, r = radius, and $\partial c/\partial r$ = radial concentration gradient.

Equation 1 equates the convective contribution, $V_0(\partial c/\partial z)$, to the diffusional contribution:

$$D \frac{1}{r} \frac{\partial}{\partial r}\left(r \frac{\partial c}{\partial r}\right)$$

at steady state. This differential equation can be solved for the boundary conditions $C = 0$ at $z = 0$ for all r and $C = C_s$ (solute solubility in liquid at $r = R$, the inner radius of tube for all z) to give:

$$C_{av}/C_s = 1 - 4 \sum_{n=1}^{\infty} \frac{1}{\alpha_n} \exp\left(\frac{-\alpha_n DL}{V_0 R^2}\right) \qquad \text{(Eq. 2)}$$

where the α_n's are roots for the Bessel function, $J_0(r) = 0$. Equation 2 is an exact expression for C_{av} in terms of measurable quantities (C_s, D, L, V_0, and R) for systems adhering to the previously mentioned flow and boundary conditions.

A second, more physically realistic model is one in which the liquid velocity profile is not flat but parabolic (Fig. 1*b*). A parabolic velocity profile is in accordance with the prediction of the Navier–Stokes equations for laminar fluid flow in a tube (6). For this parabolic model, the fluid velocity is not a constant, V_0, but varies parabolically across the tube and can be characterized by a maximum velocity, V_{max}, or an average velocity, V_{av}. The differential equation describing mass transfer with a parabolic velocity profile is:

$$V_{max}\left[1 - \left(\frac{r}{R}\right)^2\right] \frac{\partial c}{\partial z} = D \frac{1}{r} \frac{\partial}{\partial r}\left(r \frac{\partial c}{\partial r}\right) \qquad \text{(Eq. 3)}$$

Equation 3 is identical to Eq. 1 for the diffusive contribution while differing in the convective term, which defines the flow conditions. A solution to Eq. 3 can be obtained numerically (7) with the same boundary conditions for Eq. 1 and takes the form:

$$C_{av}/C_0 = 1 - \sum_{n=1}^{\infty} a_n \exp\left(-\frac{b_n DL}{V_{av} R^2}\right) \qquad \text{(Eq. 4)}$$

where a_n and b_n are constants that have been determined numerically up to $n = 11$ (7). As in the plug flow model (Eq. 2), Eq. 4 for parabolic flow is an exact expression for C_{av} in terms of measurable quantities.

A third model involves parabolic flow with the added constraint that the solute concentration gradient does not penetrate to a great distance into the flowing fluid (8). Therefore, the diffusing solute is subjected to a velocity gradient that is essentially linear. With this assumption, the convective term in the differential equation for mass transfer becomes $V_{max}[2(R - r)/R]$, with $r \simeq R$ rather than the convective term given on the left-hand side of Eq. 3. The mass transfer differential equation thus becomes:

$$V_{max} 2 \frac{(R - r)}{R} \frac{\partial c}{\partial z} = D \frac{1}{r} \frac{\partial}{\partial r}\left(r \frac{\partial c}{\partial r}\right) \qquad \text{(Eq. 5)}$$

Again, the diffusive expression in Eq. 5 is identical to that in the previous models, with the difference being the convective expression. The solution to Eq. 5 becomes:

$$C_{av}/C_s = 2.53 \left(\frac{DL}{V_{av} R^2}\right)^{2/3} \qquad \text{(Eq. 6)}$$

This third model can be considered an asymptotic solution of the parabolic model, which is applicable when $DL/V_{av}R^2$ is small. Since Eq. 6 does not involve a power series or the need to evaluate constants (a_n and b_n) numerically, it is easier to handle mathematically than Eq. 4 within its limits of applicability. All of these models are similar in explicitly accounting for the increase in solute concentration as fluid travels down the tube, which continuously reduces the concentration gradient and diffusional flux, and differ only in their treatment of the convective contribution.

An inspection of Eqs. 2, 4, and 6 shows that the dimensionless term $DL/V_{av}R^2$ (for plug flow $V_0 = V_{av}$) is common to each and can be considered as a single variable, Z. Figure 2 shows a log–log plot of C_{av}/C_s predicted by the three models *versus* the variable Z. Graphically, it can be seen that the parabolic model (Eq. 4) and its asymptotic solution (Eq. 6) approach each other as Z decreases. The plug flow model (Eq. 2) gives

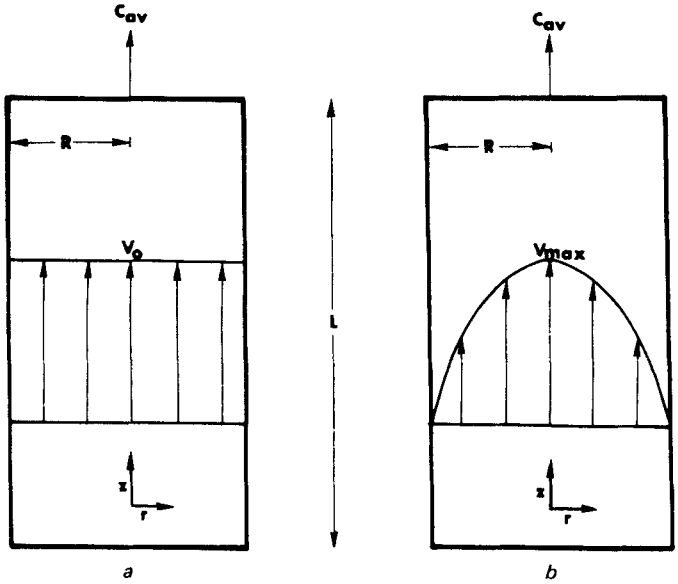

Figure 1—*Velocity profiles for liquid flow in a tube. Key:* a, *plug flow; and* b, *parabolic flow.*

the highest prediction of C_{av}/C_s throughout, with a limiting slope of 0.5 at low Z.

To evaluate the applicability of these models to experimental data, one must obtain steady-state values of C_{av} (effux concentration from the tube) for constant liquid flow rates in a tube of known diameter and length. By using the diffusion coefficient, D, and the solubility, C_s, of the solute in the liquid, the appropriate Z value and the ratio C_{av}/C_s can be calculated for each flow rate. The agreement of these model predictions can then be graphically compared with experimental data. Such comparisons of these models with experiment were conducted for solid tubes dissolving into flowing aqueous media (9).

For the application of convective diffusion models to membrane systems, an expansion of these equations is required to include a contribution due to membrane permeability. Under limiting conditions where membrane permeability is much higher than the mass transfer rate through the flowing fluid, the previously derived models can be applied without modification. Such limiting conditions imply that experimental studies on systems adhering exactly to Eq. 2, 4, or 6 would characterize only the convective diffusional properties of the solute in the flowing liquid and not the permeability of the membrane. At the opposite extreme, limiting conditions can be approached at which the membrane transport resistance is much higher than the convective diffusional resistance of the solute in the flowing liquid. At this limit, the effluent concentration, C_{av}, decreases linearly with flow rate. Between these limits, the transport behavior of a tubular membrane system exhibits varying contributions of membrane and convective diffusion control.

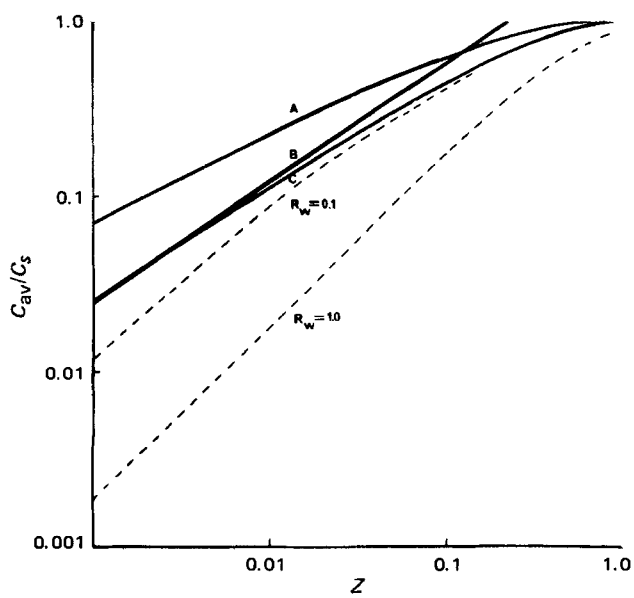

Figure 2—*Log–log plot of* C_{av}/C_s *versus* Z *for plug flow (A), parabolic asymptote (B), parabolic flow (C), and parabolic flow with wall resistance (- - -).*

Table I—Physical Constants for *p*-Aminobenzoate Esters

Compound	Membrane–Water Partition Coefficient[a]	Aqueous Diffusion Coefficient[b], $cm^2/sec \times 10^6$	Membrane Diffusion Coefficient[a], $cm^2/sec \times 10^6$
Ethyl ester	0.33	6.4	2.7
Butyl ester	3.90	6.0	2.7
Hexyl ester	46.90	5.7	2.7

[a] From Ref. 3. [b] Calculated from equations given in Ref. 15.

This behavior, of course, is not unique to tubular membrane systems. However, in this case the convective diffusional contribution in the flowing liquid is explicit and can be determined exactly without resort to semiempirical methods. The transport characteristics of liquids flowing with a parabolic velocity gradient in tubular systems with a contribution from wall resistance were treated analytically for heat transfer (10) and extended to mass transfer systems (11, 12). The treatment for mass transfer utilizes a wall resistance term, R_w, given by:

$$R_w = \frac{D_{aq}}{D_m P} \ln\left(\frac{\text{o.d.}}{\text{i.d.}}\right) \qquad \text{(Eq. 7)}$$

where D_m = membrane diffusion coefficient, D_{aq} = aqueous (liquid) diffusion coefficient, P = partition coefficient (membrane/aqueous), o.d. = outer tube diameter, and i.d. = inner tube diameter.

Figure 2 (dashed curves) shows the deviations from the parabolic model for selected values of R_w. As R_w increases, the effluent concentration, C_{av}, decreases at a particular Z value; as Z varies, the influence of a particular value of R_w on C_{av} also varies. At low Z, a particular R_w causes larger deviations from convective diffusion control than at high Z where the contribution can be small or negligible.

EXPERIMENTAL

Materials—The ethyl (benzocaine), butyl (butamben), and hexyl esters of *p*-aminobenzoic acid were obtained commercially[1] (ethyl and butyl) or synthesized (hexyl) (3). Table I includes the physical constants for these esters required for evaluating the transport data according to the theoretical equations. Medical grade silicone tubing[2] (dimethyl polysiloxane) was used in 1-m lengths with an inside diameter of 1.47 mm and an outside diameter of 1.96 mm. Deionized water was used throughout.

Analytical Procedures—All analyses for *p*-aminobenzoate esters were conducted spectrophotometrically[3] at 285 nm.

Membrane Transport Systems—The two experimental transport configurations differed from each other only by the degree of curvature of the tubing. The tubing was either threaded through stainless steel paper clips soldered to a circular stainless steel rod and mounted in a 18.95-liter (5-gallon) covered stainless steel container or suspended straight in a polyethylene-lined trough.

In both configurations, the silicone tubing was completely immersed in deionized water saturated with excess solid ester. High agitation of the saturated reservoir solution outside the tubing was maintained in the stainless steel container by a 10-cm magnetic stirring bar rotated at 600 rpm and in the trough with three magnetic stirrers and two overhead stirrers placed along its length. High agitation was required to maintain saturation and to minimize transport resistance in the reservoir solution. Temperature was ambient (23–25°). Slight variations in temperature were compensated for by measuring the saturation concentration, C_s, at regular intervals during each study.

The silicone tubing, immersed in the saturated ester solution, was attached to either a two-stage syringe pump[4] or a reciprocating pump[5] with polyethylene and stainless steel tubing. The pump was connected to a supply of deionized water, which was pumped through the tubing at a

[1] Ethyl *p*-aminobenzoate from Eastman; butyl *p*-aminobenzoate from Matheson, Coleman and Bell.
[2] Silastic, Dow Corning, Midland, Mich.
[3] Beckman DB or Zeiss DMR21 recording spectrophotometer.
[4] Model 220, Sage Instruments, Cambridge, Mass.
[5] Single stream type B, Zenith Products, West Newton, Mass.

constant flow rate. Samples of the effluent solution were collected and assayed for the concentration, C_{av}, of ester at each flow rate.

RESULTS AND DISCUSSION

Figure 3 shows the results of transport studies carried out with the hexyl, butyl, and ethyl esters. It is quite apparent that the plug flow model (Eq. 2) is not applicable to any of the systems. This result was not unexpected, since plug flow is not applicable to Newtonian liquids under laminar flow conditions in a tube. The parabolic model (and its asymptotic solution at low Z) is apparently applicable to hexyl ester throughout the range of Z values studied, while butyl and ethyl esters exhibited varying degrees of negative deviations from the parabolic model.

For hexyl *p*-aminobenzoate (Fig. 3), the parabolic model fits the data well enough to confirm that the convective diffusional contribution to mass transfer can be predicted with a high degree of accuracy. All of the constants (D_{aq}, L, V_{av}, C_s, R, a_n, and b_n) found in Eq. 4 were independently obtained and used to calculate Z and the theoretical curve. Therefore, once C_{av} was determined at a particular V_{av}, no empirical fitting or correction was required to obtain the observed correlation between theory and experiment found in Fig. 3. One must be cautious, however, in interpreting these data with regard to the membrane transport of hexyl *p*-aminobenzoate through dimethyl polysiloxane, because, in fact, only the convective diffusional contribution to mass transfer was characterized.

Without the butyl and ethyl ester studies as a comparison, little can be said about the permeability characteristics of the hexyl ester through dimethyl polysiloxane, except that it is much higher than the convective diffusional resistance in the flowing liquid. Thus, the transport rate of a solute such as hexyl *p*-aminobenzoate in this tubular membrane system is completely governed by the bulk hydrodynamics of the system and not the membrane permeability. Such behavior is not unexpected, in general, and was demonstrated in similar transport systems (12). The value of these observations on hexyl *p*-aminobenzoate lies in the fact that the convective diffusional contribution can be calculated *a priori* with the aforementioned parameters and equations and compared with experimental results.

For a convective diffusion-controlled system, close control is required over the experimental conditions to obtain reproducible results. In the case of the hexyl ester (Fig. 3), when the circular tube configuration was employed, C_{av}/C_s values (open points) were consistently higher than predicted by theory, particularly at low Z (high flow rate). This positive deviation arose from secondary flows in the flowing liquid due to centrifugal forces which increase with flow rate (13). This effect essentially increases the convective contribution to mass transfer, allowing the liquid to take up more solute from the wall than would be predicted under purely laminar flow conditions. These secondary flows do not significantly affect the butyl and ethyl ester studies because both are in at least partial membrane control at Z values (<0.1) where the centrifugal effect becomes important. Twisting the tubing into irregular configurations induces turbulent flow conditions which gives rise to even greater positive deviations from theory than are observed with the circular configuration.

Butyl *p*-aminobenzoate (Fig. 3) exhibited the same adherence to the parabolic model as the hexyl ester at large Z (low flow rates) but deviated negatively at small Z (high flow rates). Such behavior indicates that, at low flow rates, butyl *p*-aminobenzoate transport is purely convective diffusion controlled but that membrane transport resistance becomes limiting at high flow rates. As can be seen from Fig. 3 at the lowest Z values studied, the log–log plot of C_{av}/C_s *versus* Z is linear with a slope of approximately 1, indicating that the system is completely membrane controlled. This graphical characteristic allows the differentiation of complete convective diffusion control and membrane control in a laminar flow tubular membrane system; the former exhibits a slope of two-thirds for a log–log plot of C_{av}/C_s *versus* Z, while the latter gives a slope of 1.

The transition region over which the type of transport control changes depends upon the solute, membrane properties, and hydrodynamic conditions. Comparison of the butyl and hexyl esters shows that the important physicochemical difference lies in their membrane–water partition coefficients, P. There is approximately a 10-fold difference in the partition coefficients of the butyl and hexyl esters (Table I), which would predict an order of magnitude lower membrane permeability for butyl *p*-aminobenzoate compared to hexyl *p*-aminobenzoate. With lower membrane permeability, the butyl ester begins to show membrane control at $C_{av}/C_s \simeq 0.1$; it can be estimated that the hexyl ester would begin to exhibit membrane control at $C_{av} \simeq 0.01$, which is above the range of flow rates used.

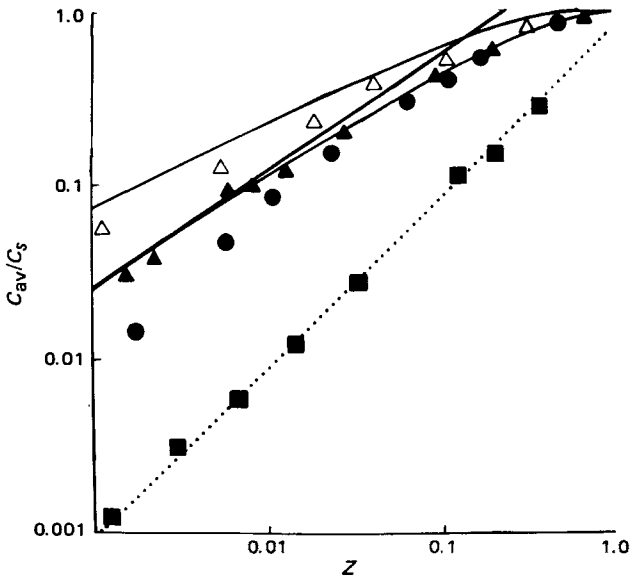

Figure 3—*Log–log plot of* C_{av}/C_s versus Z *for* p-*aminobenzoate esters. Key:* ▲, *hexyl ester (straight tube configuration);* △, *hexyl ester (curved tube configuration);* ●, *butyl ester;* ■, *ethyl ester;* —, *theoretical predictions as labeled in Fig. 2; and . . ., plot of Eq. 9 for the ethyl ester.*

By comparing the data obtained for butyl *p*-aminobenzoate to the predictions in Fig. 2, a value for R_w of 0.1–0.2 can be estimated. With values of D_m, D_{aq}, and P in Table I and the tubing dimensions, R_w was determined to be 0.15 using Eq. 7. Such a correlation between experiment and theory under membrane-controlled conditions further supports the utility of tubular membrane systems for determining the relative importance of membrane permeability and convective diffusion to overall transport rates.

The results for ethyl *p*-aminobenzoate (Fig. 3), in contrast to the previous two esters, fall significantly below theoretical convective diffusion predictions. Throughout the range of flow rates studied, the ethyl ester remained in essentially complete membrane control. Studies at very low flow rates (not shown) indicate that ethyl *p*-aminobenzoate approaches $C_{av}/C_s = 1$ at $Z > 1$. Using values for D_m, D_{aq}, and P found in Table I for the ethyl ester with Eq. 7 leads to a predicted R_w of 2.08, which indicates that membrane resistance is high and that convective diffusion is unimportant to mass transfer over the range of flow rates studied. As with the butyl ester at low Z, the log–log plot of C_{av}/C_s *versus* Z for the ethyl ester exhibits a slope of 1, indicating that the solute flux through the membrane is constant and maximal and that changes in C_{av}/C_s with Z only reflect a change in throughput of liquid.

Under complete membrane control, the transport rate is independent of hydrodynamics (laminar or turbulent flow). As a test of this independence, Eq. 8 (14), which predicts the flux, F, through a cylindrical wall at steady state with the inner wall at zero concentration and the outer wall in contact with a saturated solution, was employed:

$$F = \frac{2\pi D_m P C_s}{\ln (\text{o.d./i.d.})} \qquad \text{(Eq. 8)}$$

Since F is the flux per unit length, multiplying by the tube length, L, dividing by the volume flow rate, f, and rearranging give:

$$\frac{C_{av}}{C_s} = \frac{2\pi D_m P L}{f \ln(\text{o.d./i.d.})} \qquad \text{(Eq. 9)}$$

Using the parameters from Table I and the tubing dimensions gives $C_{av}/C_s = 0.116/f$, which is plotted in Fig. 3 (dotted line). Such a close correlation between the experimental C_{av}/C_s values and Eq. 9 confirms the independence of ethyl *p*-aminobenzoate transport from hydrodynamics, since no account is taken of the type of convection in obtaining Eq. 9. Thus, the flowing fluid serves only to carry the ethyl ester from the inner tubing wall and provides no detectable resistance to solute transport.

With the three *p*-aminobenzoate esters chosen for study, three typical transport patterns were demonstrated: the extremes of complete membrane (ethyl ester) and complete convective diffusion (hexyl ester) control and a change in transport control with flow rate (butyl ester). The ability to calculate accurately, *a priori*, the influence of hydrodynamics is unattainable by other experimental designs. These studies, of course, do not detract from previous membrane transport work in which stagnant

liquid diffusion layers were employed in the theoretical analysis (1, 3). Rather, this work demonstrates that such diffusion layers are in reality convenient "fictions," which need not be invoked with certain experimental designs. Certainly, the concept of aqueous diffusion layers has been instrumental in the understanding of membrane transport processes, but too much credence has been given to their actual existence.

Biological analogies to these polymeric tube transport studies are the isolated perfusion and *in situ* techniques for intestinal absorption. An isolated intestinal segment suspended as nearly straight as possible would serve as a means for determining the luminal convective diffusion contribution to intestinal transport. For an *in situ* intestinal system, definite bends in the intestine would induce secondary flows or turbulence, which would require that absorption data be carefully analyzed for the demarcation between convective diffusion control and membrane control. With the ability to determine accurately the luminal contribution to overall intestinal transport, absorption models can be established on a firmer physical basis. Without the need for semiempirical approaches to obtain diffusion layer or stagnant film permeability coefficients, the elucidation of membrane transport characteristics should be facilitated.

Furthermore, the tube configuration is of value pharmaceutically for obtaining the intrinsic dissolution rates of solids (9). Solid tubes, obtained by various methods, can be infused with dissolution media and the efflux concentrations can be measured as a function of flow rate. From such information, the presence or absence of surface or other kinetic barriers can be determined by comparison of efflux concentrations with the theoretical predictions for pure convective diffusion control.

REFERENCES

(1) R. G. Stehle and W. I. Higuchi, *J. Pharm. Sci.*, **61**, 1922, 1931 (1972).

(2) E. R. Garrett and P. B. Chemburkar, *ibid.*, **57**, 944, 949; 1401 (1968).

(3) G. L. Flynn and S. H. Yalkowsky, *ibid.*, **61**, 838 (1972).

(4) N. Lakshminarayanaiah, "Transport Phenomena in Membranes," Academic, New York, N.Y., 1969.

(5) V. G. Levich, "Physicochemical Hydrodynamics," Prentice-Hall, Englewood Cliffs, N.J., 1962, pp. 40–46.

(6) J. G. Knudsen and D. L. Katz, "Fluid Dynamics and Heat Transfer," McGraw-Hill, New York, N.Y., 1958, pp. 82–87.

(7) G. M. Brown, *A.I.Ch.E.J.*, **6**, 179 (1960).

(8) V. G. Levich, "Physicochemical Hydrodynamics," Prentice-Hall, Englewood Cliffs, N.J., 1962, p. 115.

(9) W. H. Linton and T. K. Sherwood, *Chem. Eng. Progr.*, **46**, 258 (1950).

(10) J. Schenk and J. M. Dumoré, *Appl. Sci. Res.*, **A4**, 39 (1954).

(11) R. G. Buckles, E. W. Merrill, and E. R. Gilliland, *A.I.Ch.E.J.*, **14**, 703 (1968).

(12) R. E. Collingham, P. L. Blackshear, and E. R. G. Eckert, *Chem. Eng. Progr. Symp. Ser. 102*, **66**, 141 (1970).

(13) Y. Mori and W. Nakayama, *Int. J. Heat Mass Transfer*, **10**, 681 (1967).

(14) M. H. Jacobs, "Diffusion Processes," Springer-Verlag, New York, N.Y., 1967, p. 120.

(15) G. L. Flynn, S. H. Yalkowsky, and T. J. Roseman, *J. Pharm. Sci.*, **63**, 479 (1974).

ACKNOWLEDGMENTS AND ADDRESSES

Received February 9, 1976, from the *School of Pharmacy, University of Connecticut, Storrs, CT 06268, and the ‡Pharmacy Research Unit, The Upjohn Company, Kalamazoo, MI 49001.

Accepted for publication May 5, 1976.

Support for this study in the form of a Summer Visiting Professorship from The Upjohn Co. is gratefully acknowledged by D. R. Flanagan.

ˣ To whom inquiries should be directed.

Quantitative Determination of Phenacetin and Its Metabolite Acetaminophen by GLC–Chemical Ionization Mass Spectrometry

W. A. GARLAND *ˣ, K. C. HSIAO ‡, E. J. PANTUCK ‡, and A. H. CONNEY *

Abstract □ A quantitative GLC–mass spectrometric procedure was developed for the determination of phenacetin and its *O*-desethyl metabolite, acetaminophen, in human plasma. The assay utilizes selective ion detection to monitor, in a GLC effluent, the MH^+ molecular ions of both phenacetin and the methyl derivative of acetaminophen, *p*-acetanisidine, generated by isobutane chemical ionization. Deuterated analogs of phenacetin and acetaminophen, phenacetin-d_3 and acetaminophen-d_3, respectively, are added to the plasma before extraction to serve as internal standards. To determine phenacetin and unconjugated acetaminophen, 1.0 ml of plasma is extracted with 5 ml of benzene–dichloroethane (7:3). The extraction solvent is removed, and the residue is methylated with diazomethane. The solution is again evaporated to dryness, and the residue is reconstituted in ethyl acetate. A portion of this solution is then analyzed by GLC–mass spectrometry, with the mass spectrometer set to monitor *m/e* 166 (*p*-acetanisidine), 169 (*p*-acetanisidine-d_3), 180 (phenacetin), and 183 (phenacetin-d_3). To determine total acetaminophen, 0.1 ml of plasma is treated with a mixture of β-glucuronidase and sulfatase, extracted with ethyl acetate, methylated, and analyzed by GLC–mass spectrometry. The procedure has a sensitivity limit of 1 ng of phenacetin/ml and 0.1 μg of acetaminophen/ml. The curves relating the amount of phenacetin and acetaminophen added *versus* the amount of phenacetin and acetaminophen found for 12 known phenacetin concentrations over the 9.9–246.6-ng/ml range and for 16 known acetaminophen concentrations over the 0.52–13.10-μg/ml range are straight lines with intercepts of nearly zero and with slopes of unity. Analyses of six separate plasma samples, each containing 25 ng of phenacetin/ml and 1.31 μg of acetaminophen/ml, had a precision of ±1 ng/ml for phenacetin and ±0.08 μg/ml for acetaminophen.

Keyphrases □ Phenacetin—GLC–mass spectrometric analysis, human plasma □ Acetaminophen—GLC–mass spectrometric analysis, human plasma □ GLC–mass spectrometry—analyses, phenacetin and acetaminophen, human plasma □ Analgesics—phenacetin and acetaminophen, GLC–mass spectrometric analysis, human plasma

Various nonspecific spectrophotometric (1–5) procedures or time-consuming liquid (6, 7), paper (8, 9), or thin-layer (10–12) chromatographic procedures have been developed to measure the analgesic phenacetin (I) and its analgesic biotransformation product, acetaminophen (II), in human plasma. The published GLC procedures for these compounds have a detection limit of 50 ng/ml (13–15). While this sensitivity is suitable for the measurement of

liquid diffusion layers were employed in the theoretical analysis (1, 3). Rather, this work demonstrates that such diffusion layers are in reality convenient "fictions," which need not be invoked with certain experimental designs. Certainly, the concept of aqueous diffusion layers has been instrumental in the understanding of membrane transport processes, but too much credence has been given to their actual existence.

Biological analogies to these polymeric tube transport studies are the isolated perfusion and *in situ* techniques for intestinal absorption. An isolated intestinal segment suspended as nearly straight as possible would serve as a means for determining the luminal convective diffusion contribution to intestinal transport. For an *in situ* intestinal system, definite bends in the intestine would induce secondary flows or turbulence, which would require that absorption data be carefully analyzed for the demarcation between convective diffusion control and membrane control. With the ability to determine accurately the luminal contribution to overall intestinal transport, absorption models can be established on a firmer physical basis. Without the need for semiempirical approaches to obtain diffusion layer or stagnant film permeability coefficients, the elucidation of membrane transport characteristics should be facilitated.

Furthermore, the tube configuration is of value pharmaceutically for obtaining the intrinsic dissolution rates of solids (9). Solid tubes, obtained by various methods, can be infused with dissolution media and the efflux concentrations can be measured as a function of flow rate. From such information, the presence or absence of surface or other kinetic barriers can be determined by comparison of efflux concentrations with the theoretical predictions for pure convective diffusion control.

REFERENCES

(1) R. G. Stehle and W. I. Higuchi, *J. Pharm. Sci.*, **61**, 1922, 1931 (1972).

(2) E. R. Garrett and P. B. Chemburkar, *ibid.*, **57**, 944, 949; 1401 (1968).

(3) G. L. Flynn and S. H. Yalkowsky, *ibid.*, **61**, 838 (1972).

(4) N. Lakshminarayanaiah, "Transport Phenomena in Membranes," Academic, New York, N.Y., 1969.

(5) V. G. Levich, "Physicochemical Hydrodynamics," Prentice-Hall, Englewood Cliffs, N.J., 1962, pp. 40–46.

(6) J. G. Knudsen and D. L. Katz, "Fluid Dynamics and Heat Transfer," McGraw-Hill, New York, N.Y., 1958, pp. 82–87.

(7) G. M. Brown, *A.I.Ch.E.J.*, **6**, 179 (1960).

(8) V. G. Levich, "Physicochemical Hydrodynamics," Prentice-Hall, Englewood Cliffs, N.J., 1962, p. 115.

(9) W. H. Linton and T. K. Sherwood, *Chem. Eng. Progr.*, **46**, 258 (1950).

(10) J. Schenk and J. M. Dumoré, *Appl. Sci. Res.*, **A4**, 39 (1954).

(11) R. G. Buckles, E. W. Merrill, and E. R. Gilliland, *A.I.Ch.E.J.*, **14**, 703 (1968).

(12) R. E. Collingham, P. L. Blackshear, and E. R. G. Eckert, *Chem. Eng. Progr. Symp. Ser. 102*, **66**, 141 (1970).

(13) Y. Mori and W. Nakayama, *Int. J. Heat Mass Transfer*, **10**, 681 (1967).

(14) M. H. Jacobs, "Diffusion Processes," Springer-Verlag, New York, N.Y., 1967, p. 120.

(15) G. L. Flynn, S. H. Yalkowsky, and T. J. Roseman, *J. Pharm. Sci.*, **63**, 479 (1974).

ACKNOWLEDGMENTS AND ADDRESSES

Received February 9, 1976, from the *School of Pharmacy, University of Connecticut, Storrs, CT 06268, and the ‡Pharmacy Research Unit, The Upjohn Company, Kalamazoo, MI 49001.

Accepted for publication May 5, 1976.

Support for this study in the form of a Summer Visiting Professorship from The Upjohn Co. is gratefully acknowledged by D. R. Flanagan.

ˣ To whom inquiries should be directed.

Quantitative Determination of Phenacetin and Its Metabolite Acetaminophen by GLC–Chemical Ionization Mass Spectrometry

W. A. GARLAND *ˣ, K. C. HSIAO ‡, E. J. PANTUCK ‡, and A. H. CONNEY *

Abstract □ A quantitative GLC–mass spectrometric procedure was developed for the determination of phenacetin and its *O*-desethyl metabolite, acetaminophen, in human plasma. The assay utilizes selective ion detection to monitor, in a GLC effluent, the MH^+ molecular ions of both phenacetin and the methyl derivative of acetaminophen, *p*-acetanisidine, generated by isobutane chemical ionization. Deuterated analogs of phenacetin and acetaminophen, phenacetin-d_3 and acetaminophen-d_3, respectively, are added to the plasma before extraction to serve as internal standards. To determine phenacetin and unconjugated acetaminophen, 1.0 ml of plasma is extracted with 5 ml of benzene–dichloroethane (7:3). The extraction solvent is removed, and the residue is methylated with diazomethane. The solution is again evaporated to dryness, and the residue is reconstituted in ethyl acetate. A portion of this solution is then analyzed by GLC–mass spectrometry, with the mass spectrometer set to monitor *m/e* 166 (*p*-acetanisidine), 169 (*p*-acetanisidine-d_3), 180 (phenacetin), and 183 (phenacetin-d_3). To determine total acetaminophen, 0.1 ml of plasma is treated with a mixture of β-glucuronidase and sulfatase, extracted with ethyl acetate, methylated, and analyzed by GLC–mass spectrometry. The procedure has a sensitivity limit of 1 ng of phenacetin/ml and 0.1 μg of acetaminophen/ml. The curves relating the amount of phenacetin and acetaminophen added *versus* the amount of phenacetin and acetaminophen found for 12 known phenacetin concentrations over the 9.9–246.6-ng/ml range and for 16 known acetaminophen concentrations over the 0.52–13.10-μg/ml range are straight lines with intercepts of nearly zero and with slopes of unity. Analyses of six separate plasma samples, each containing 25 ng of phenacetin/ml and 1.31 μg of acetaminophen/ml, had a precision of ±1 ng/ml for phenacetin and ±0.08 μg/ml for acetaminophen.

Keyphrases □ Phenacetin—GLC–mass spectrometric analysis, human plasma □ Acetaminophen—GLC–mass spectrometric analysis, human plasma □ GLC–mass spectrometry—analyses, phenacetin and acetaminophen, human plasma □ Analgesics—phenacetin and acetaminophen, GLC–mass spectrometric analysis, human plasma

Various nonspecific spectrophotometric (1–5) procedures or time-consuming liquid (6, 7), paper (8, 9), or thin-layer (10–12) chromatographic procedures have been developed to measure the analgesic phenacetin (I) and its analgesic biotransformation product, acetaminophen (II), in human plasma. The published GLC procedures for these compounds have a detection limit of 50 ng/ml (13–15). While this sensitivity is suitable for the measurement of

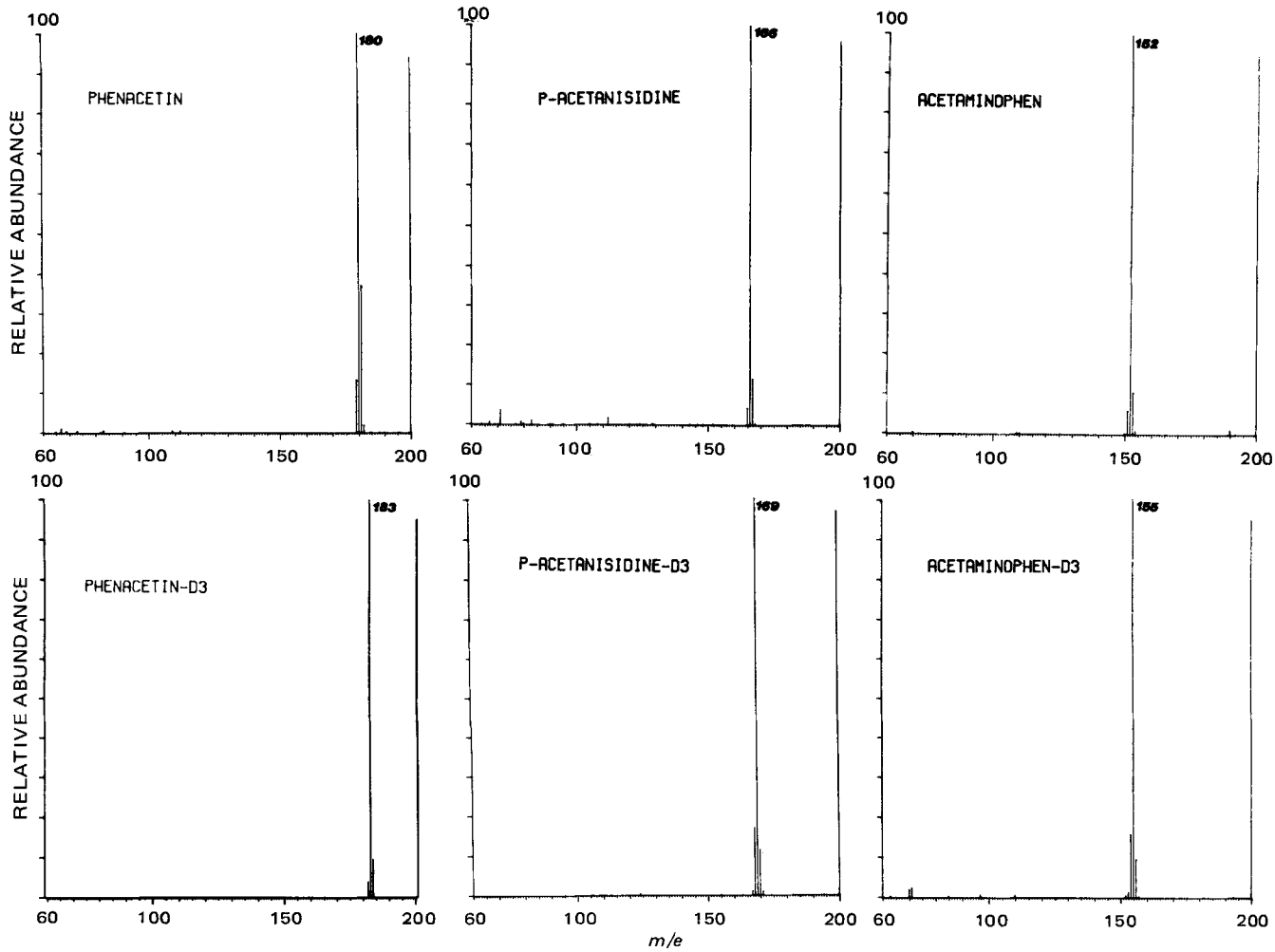

Figure 1—*Isobutane mass spectra of phenacetin, p-acetanisidine, acetaminophen, and their deuterated analogs.*

acetaminophen, it permits the determination of phenacetin concentrations in normal subjects for only a few hours after oral administration of a therapeutic phenacetin dose and is insufficient for phenacetin determinations in many subjects with induced drug-metabolizing capabilities (16, 17).

This report describes a GLC–mass spectrometric assay that requires 1.1 ml of plasma and is capable of determining 1 ng of phenacetin/ml and 0.1 μg of unconjugated and conjugated acetaminophen/ml. The method utilizes chemical ionization (18) GLC–mass spectrometry, with isobutane functioning both as a reagent and GLC carrier gas. To obtain sufficient sensitivity, selective ion detection is used to monitor the MH^+ ion of both phenacetin and the methyl derivative of acetaminophen, *p*-acetanisidine (III). Deuterated analogs of phenacetin and acetaminophen, phenacetin-d_3 (IV) and acetaminophen-d_3 (V), respectively, are added to the plasma as internal standards.

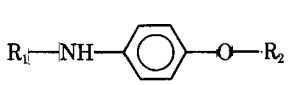

I: $R_1 = CH_3CO$, $R_2 = CH_2CH_3$
II: $R_1 = CH_3CO$, $R_2 = H$
III: $R_1 = CH_3CO$, $R_2 = CH_3$
IV: $R_1 = CH_3CO$, $R_2 = CH_2CD_3$
V: $R_1 = CD_3CO$, $R_2 = H$
VI: $R_1 = CD_3CO$, $R_2 = CH_3$

EXPERIMENTAL

Apparatus—A quadrupole mass filter[1] and data system[2] were used in conjunction with a gas chromatograph[3]. The GLC column, 1.21 m (4 ft) × 2 mm i.d., was silanized, packed with 3% OV-17 on 100–120-mesh Gas Chrom Q[4], and conditioned at 325° with no flow for 3 hr and then at 275° overnight with a 20-ml/min helium flow. The chromatographic conditions were: column oven, 180–195°; injection port, 300°; isobutane[5] pressure, 0.45–1.36 kg (1–3 lb)/in.^{2}; and interface oven and glass-lined source reentrant tube, 250°. Typical ion source settings were: ion volume, +8 v; ion repeller, +2 v; lens, −30 v; and filament, −110 v with the electron beam total emission regulated at 800 μamp. Column temperature and isobutane pressure were adjusted to provide an ion source pressure of 0.4 torr. The source was operated without external heating (temperature approximately 50°).

Materials—Nanograde quality benzene[6], methanol[6], and ethyl acetate[6] and spectrograde quality 1,2-dichloroethane[7] were used without further purification. Before each assay, ethereal diazomethane (50 ml) was prepared according to Arnt's (19) decanting procedure and dried over anhydrous sodium sulfate.

Tubes (15 ml)[8] equipped with screw caps[9] were used for the plasma extractions, and glass-stoppered centrifuge tubes (5 ml)[10] were used for the final solvent evaporation.

Phenacetin-d_3—A mixture of 4-hydroxyacetanilide (5.0 g, 32 mmoles),

[1] Finnigan model 1015D.
[2] Finnigan model 6000.
[3] Finnigan model 9500.
[4] Applied Science Laboratories.
[5] Matheson, instrument purity.
[6] Mallinckrodt Chemicals.
[7] Fisher Scientific.
[8] Pyrex 9825.
[9] Lined with Teflon (du Pont).
[10] Pyrex 8084.

potassium carbonate (2.8 g, 20 mmoles), ethyl iodide-d_3 (3 ml, 35 mmoles)[11], and acetone (20 ml) was refluxed for 20 hr (20). The solution was cooled, transferred to a separator, and combined with water (20 ml), chloroform (75 ml), and 10% potassium hydroxide (5 ml). The chloroform extract was washed twice with 10% potassium hydroxide (10 ml), the chloroform was removed, and the resulting gum was crystallized from methanol–water to yield 3.85 g (21 mmoles, 66%) of phenacetin-d_3, mp (uncorrected) 131–132° [lit. (21) mp (phenacetin) 134–135°].

The UV (methanol) and IR (potassium bromide) spectra were identical to those of authentic phenacetin, while the PMR[12] spectrum (deuterochloroform) differed from that of phenacetin only by the lack of the triplet at 1.4 ppm. A precise mass determination[13] of the *m/e* 182 molecular ion in the electron ionization mass spectrum gave 182.1137 ($C_{10}H_{10}D_3N_1O_2$ = 182.1135). A selective ion detection analysis of this compound using the developed GLC–mass spectrometric procedure showed the presence of less than 0.5% phenacetin-d_0.

p-Hydroxyacetanilide-d_3—*p*-Hydroxyaniline (535 mg, 5 mmoles), 12 *M* HCl (71 μl), deuterium oxide (8.43 ml)[11], 0.2 *M* sodium acetate (5 ml), acetic anhydride-d_6 (510 mg, 468 μl, 5 mmoles)[11], and ether (10 ml) were combined in a 25-ml separator. The mixture was gently shaken every 5 min for 1 hr (8). Then the aqueous layer was removed, and the ether was extracted with 0.5 *M* potassium hydroxide (3 × 5 ml) and discarded. The combined alkaline extracts were then acidified to pH 1 and extracted with ethyl acetate (3 × 10 ml). The residue remaining after removal of the ethyl acetate was recrystallized from water to yield 387 mg (2.56 mmoles, 51%) of the title compound, mp (uncorrected) 166–168° [lit. (22) mp (acetaminophen) 169–170°].

The UV (ethanol) and IR (potassium bromide) spectra were identical to those of acetaminophen, while the PMR spectrum (deuterochloroform) differed from that of acetaminophen only by the lack of the three-proton singlet at 2.07 ppm. A precise mass determination[13] of the *m/e* 154 molecular ion in the electron ionization mass spectrum gave 154.0841 ($C_8H_6D_3NO_2$ = 154.0821). A selective ion detection analysis of this compound using the described GLC–mass spectrometric procedure showed the presence of less than 0.5% *p*-hydroxyacetanilide-d_0.

Mass Spectrometry—The isobutane chemical ionization mass spectra of phenacetin, phenacetin-d_3, acetaminophen, acetaminophen-d_3, acetanisidine, and acetanisidine-d_3 can be seen in Fig. 1. The spectra are quite simple, consisting principally of MH^+ molecular ions, and were obtained at 0.4 torr by the separate injections of 10 μg of each compound into the GLC–mass spectrometer with the electron multiplier run at low gain to deemphasize background ions resulting from column bleed.

If both phenacetin and acetaminophen were to be determined, the mass spectrometer was set to monitor the MH^+ molecular ions at *m/e* 166 (acetanisidine), 169 (acetanisidine-d_3), 180 (phenacetin), and 183 (phenacetin-d_3). To measure only acetaminophen, the instrument was set to monitor *m/e* 166 and 169.

Assay Procedure—*Phenacetin and Unconjugated Acetaminophen (Procedure A)*—To 1.0 ml of plasma in a 15-ml tube was added 1.0 ml of internal standard solution containing 25–300 ng of phenacetin-d_3/ml and 2.5 μg of acetaminophen-d_3/ml. The resulting solution was allowed to stand for 2 hr. Then 5 ml of benzene–1,2-dichloroethane (7:3) was added, and the mixture was shaken[14] for 20 min. After centrifugation[15] for 20 min at 150×*g*, 4.0 ml of the organic layer was transferred to a 5-ml centrifuge tube. The extraction solvent was then removed at 30° under a gentle stream of nitrogen[16].

The resulting residue was dissolved in 0.5 ml of methanol and treated with 0.5 ml of a diazomethane–ether solution. This mixture was vortexed[17] and allowed to stand for 2 hr. The solvents were removed under a stream of nitrogen, and the residue was reconstituted in 30 μl of ethyl acetate. Depending on the expected phenacetin and acetaminophen concentrations, between 0.5 and 5 μl was injected into the gas–liquid chromatograph.

Thirty seconds after injection, the electron multiplier was turned on and the GLC divert valve was turned off, allowing the GLC effluent to enter the ion source. Forty-five seconds after injection, the ion source supplies were turned on; 15 sec later, computer-controlled scanning and data collection were initiated. Approximate retention times were: *p*-acetanisidine, 1.8 min; and phenacetin, 2.3 min. Three minutes after injection, the GLC divert valve was turned on, the ion source supplies were turned off, and the computer data collection was halted.

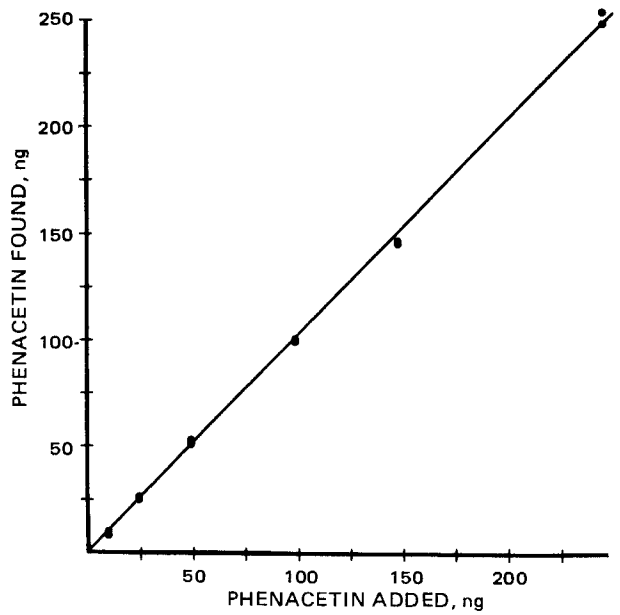

Figure 2—*Curve relating amount of phenacetin added to 1 ml of human control plasma* versus *amount of phenacetin found using Procedure A for two separate analyses at each of six different concentrations. The concentration of the phenacetin-*d_3 *internal standard was 50.5 ng/ml.*

To determine the phenacetin concentration, the area of the *m/e* 180 (phenacetin) peak was divided by that of the *m/e* 183 (phenacetin-d_3) peak and the ratio was multiplied by that of the phenacetin-d_3 concentration. A similar procedure was followed for acetaminophen, except peak heights instead of peak area were used.

Total Acetaminophen (Procedure B)—Plasma (0.1 ml), a β-glucuronidase–sulfatase mixture[18] (0.1 ml), 0.2 *M* sodium acetate pH 5.0 buffer (1 ml), distilled water (0.6 ml), and 0.5 μg of acetaminophen-d_3/ml (1 ml) were incubated with shaking[19] for 16 hr at 37°. The mixture was extracted for 20 min with 8 ml of ethyl acetate and centrifuged at 150×*g* for 15 min. A portion (5 ml) of the organic phase was removed and evaporated to dryness under nitrogen.

The residue was methylated and reconstituted in 30 μl of ethyl acetate, and 1 μl of the solution was injected into the GLC–mass spectrometer. The GLC and mass spectrometric parameters were identical to those used in Procedure A, except the mass spectrometer was set to monitor only *m/e* 166 and 169.

Samples—Plasma standards were prepared by the addition of known amounts of phenacetin and acetaminophen to human control plasma[20].

A 72-kg white male received an oral dose of phenacetin (900 mg)[21] as a fine powder followed by water (300 ml). A heparinized whole blood sample was drawn just before dosing and then every hour for 8 hr. The blood was centrifuged for 20 min at 150×*g*, and the plasma was removed for analysis.

RESULTS AND DISCUSSION

To measure phenacetin and unconjugated acetaminophen, 1 ml of plasma was extracted with benzene–1,2-dichloroethane (7:3). Recoveries for this extraction procedure (Procedure A), determined from a comparison of the peak areas of the internal standards obtained from six separate analyses with the areas from the injection of known amounts of diazomethane-treated phenacetin-d_3 and acetaminophen-d_3, were 95 ± 8% for phenacetin and 0.91 ± 0.12% for acetaminophen. This 104-fold greater extraction of phenacetin permitted both compounds to be determined from a single injection in spite of the commonly observed 100–1000-fold greater plasma acetaminophen concentration.

To determine total acetaminophen, 0.1 ml of plasma was treated with a β-glucuronidase–sulfatase mixture[18] and the acetaminophen was ex-

[11] Stohler Isotopes.
[12] Varian HA-100.
[13] CEC 21-110.
[14] International bottle shaker, International Equipment Corp.
[15] International centrifuge model K.
[16] N-Evap, Organomation Associates.
[17] Vortex Genie, Scientific Industries.
[18] Glusulase, Endo Laboratories Inc.
[19] Lab-Line, No. 3581.
[20] Hyland Laboratories.
[21] Eli Lilly, Indianapolis, Ind.

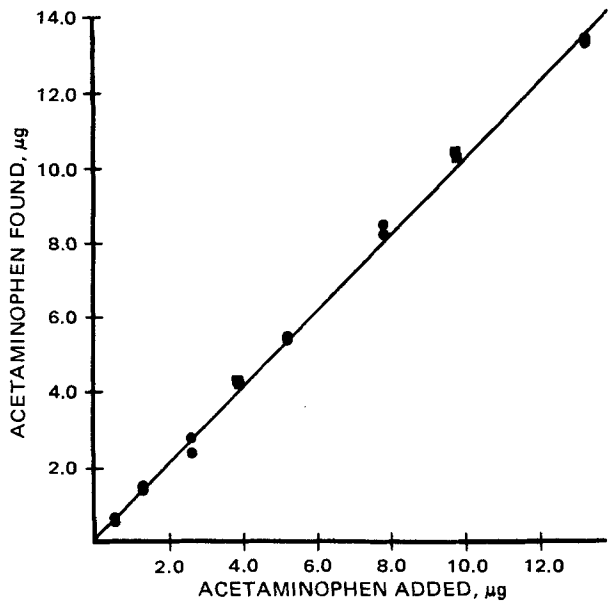

Figure 3—*Curve relating amount of acetaminophen added to 1 ml of human control plasma* versus *amount of acetaminophen found for two separate analyses at each of eight different concentrations. Circles are analyses using Procedure A with 2.52 μg of acetaminophen-d_3/ml used as the internal standard. Squares are determinations using Procedure B with 5.00 μg of acetaminophen-d_3/ml used as the internal standard.*

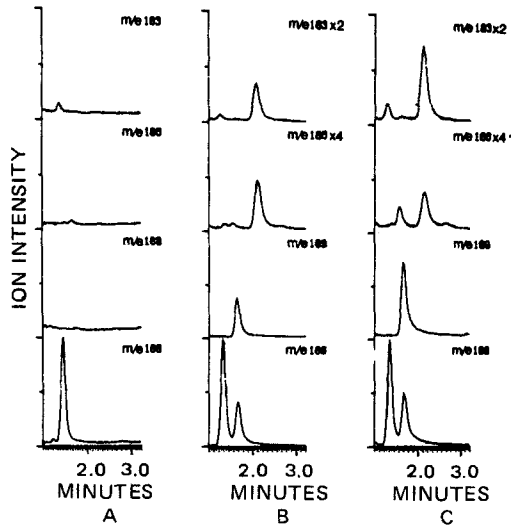

Figure 4—*Typical ion chromatograms from the determination by Procedure A of phenacetin and acetaminophen in a subject who had received an oral dose of 900 mg of phenacetin. Key: A, plasma blank, zero time; B, 6 hr after dosing, phenacetin* (m/e *180*) = *17 ng/ml, phenacetin-d_3* (m/e *183*) = *25.3 ng/ml, acetaminophen* (m/e *166*) = *2.51 μg/ml, and acetaminophen-d_3* (m/e *169*) = *2.52 μg/ml; and C, 8 hr after dosing, phenacetin = 6.1 ng/ml, phenacetin-d_3 = 25.3 ng/ml, acetaminophen = 1.62 μg/ml, and acetaminophen-d_3 = 2.52 μg/ml. For the purpose of display, ion tracings at* m/e *183 and 180 in B and C were multiplied by factors of two and four, respectively.*

tracted into ethyl acetate. The acetaminophen recovery for this extraction procedure (Procedure B), determined from a comparison of the peak heights of the internal standards for six separate analyses with the heights from the injection of known amounts of diazomethane-treated acetaminophen-d_3, was 89 ± 18%. Conjugated acetaminophen was calculated from the difference between the acetaminophen levels determined by Procedures A and B.

Both total acetaminophen and phenacetin can be simultaneously determined by preceding Procedure A with enzyme[18] treatment. The plasma blank, however, for phenacetin (*m/e* 180 and 183) after enzyme[18] treatment shows a number of small background ions that interfere with the accurate determination of low phenacetin levels (<5 ng/ml). In addition, the enzyme[18] treatment releases some compounds with prominent *m/e* 180 or 183 ions but with longer retention times than phenacetin. Thus, if phenacetin is to be determined in this manner, the sample injections must be spaced at least 20 min apart to ensure specificity. When using Procedure A, however, a sample can be injected every 3 min.

Human control plasma subjected to either Procedure A or B showed no significant background ions at *m/e* 169, 180, and 183. With Procedure A, a peak with a retention time shorter than that of acetaminophen was observed at *m/e* 166; ions with retention times both shorter and longer than acetaminophen were observed with Procedure B. Because of these background ions, peak heights—not peak areas—were used for the quantification of acetaminophen.

Neither phenacetin-d_3 nor acetaminophen-d_3 showed any isotope exchange when subjected to Procedure A or B.

Results obtained from the addition of known amounts of phenacetin and acetaminophen to human control plasma followed by processing according to Procedure A can be seen in Figs. 2 and 3. A least-squares analysis of the results for 12 phenacetin standards (Fig. 2) gave a slope of 0.999 ± 0.001 and an intercept of 0.304 ± 1.00 ng. The phenacetin-d_3 internal standard concentration for these analyses was 50.5 ng/ml. The corresponding curves (Fig. 3) for 12 acetaminophen standards analyzed by Procedure A and four acetaminophen standards analyzed by Procedure B gave a slope of 1.02 ± 0.015 and an intercept of 0.102 ± 0.103 ng. The acetaminophen-d_3 internal standard concentration for these analyses was 2.52 μg/ml with Procedure A and 5.00 μg/ml with Procedure B. Thus, these data suggest that the extraction, mass spectral, and GLC characteristics of the labeled and unlabeled compounds and their reactivity toward diazomethane are essentially identical.

To determine assay precision, six separate samples of control plasma, each containing 24.7 ng of phenacetin/ml and 1.31 μg of acetamino-

Table I—Plasma Levels of Phenacetin and Acetaminophen (Unconjugated, Conjugated, and Total) in a 72-kg White Male at Various Intervals after Oral Administration of 900 mg of Phenacetin[a]

Hours	Phenacetin, ng/ml	Acetaminophen, μg/ml		
		Unconjugated	Conjugated	Total
0	—[b]	—[b]	—	—[b]
1	264	5.6	2.1	7.7
2	167	6.8	6.4	13.1
3	115	6.4	7.8	14.2
4	69	5.2	9.9	15.1
5	61	4.1	8.1	12.1
6	17	2.5	9.2	11.7
7	10	2.0	9.7	11.6
8	6.1	1.6	9.3	11.0

[a] Phenacetin and unconjugated acetaminophen were determined using Procedure A; total acetaminophen was determined using Procedure B. Conjugated acetaminophen is the difference between that determined by Procedures A and B. [b] Not measurable.

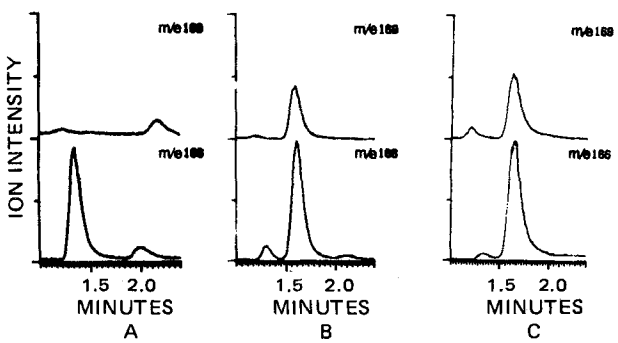

Figure 5—*Typical ion chromatograms from the determination by Procedure B of acetaminophen in a subject who had received an oral dose of 900 mg of phenacetin. Key: A, Subject 1 plasma blank, zero time; B, 6 hr after dosing, acetaminophen* (m/e *166*) = *11.7 μg/ml and acetaminophen-d_3* (m/e *169*) = *5.0 μg/ml; and C, 8 hr after dosing, acetaminophen = 11.0 μg/ml and acetaminophen-d_3 = 5.0 μg/ml. Chromatogram A is normalized to the value of the background ions at* m/e *166 which elute before* p-*acetanisidine. The intensity of these ions relative to* p-*acetanisidine in an actual assay can be seen in B and C.*

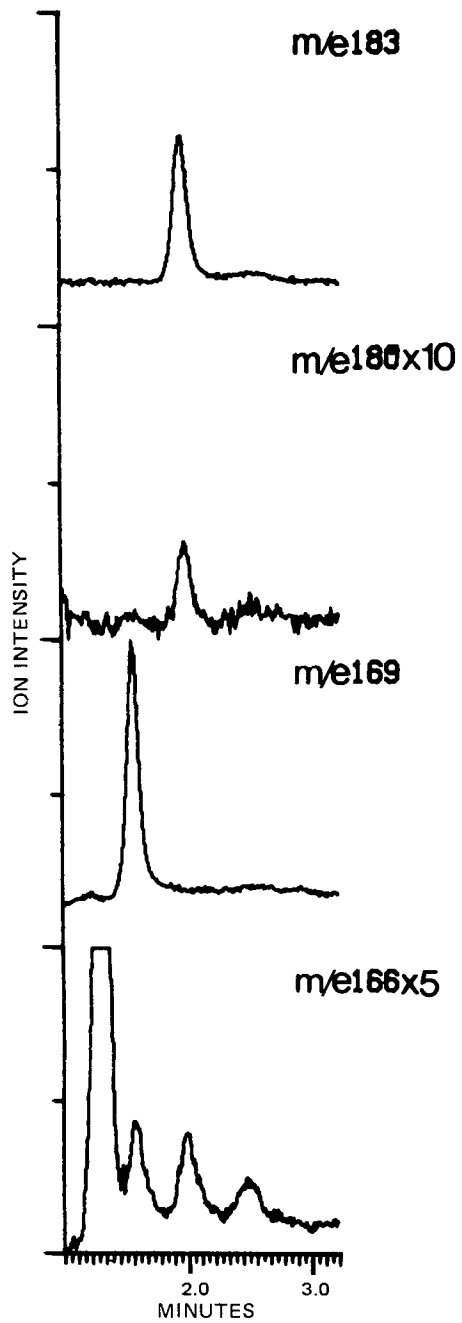

Figure 6—*Analysis of 1 ml of plasma containing 1 ng of phenacetin* (m/e *180*) *and 0.100 μg of* p-*acetanisidine* (m/e *166*) *by Procedure A. Phenacetin-*d_3 (m/e *183*) *and* p-*acetanisidine-*d_3 (m/e *169*) *internal standards were present in concentrations of 25.3 ng/ml and 2.52 μg/ml, respectively. For the purpose of display, the ion tracing at* m/e = *166 was multiplied by five while that at* m/e *180 was multiplied by a factor of 10.*

phen/ml, were analyzed using Procedure A. The average phenacetin concentration of these samples was determined to be 24.6 ± 1.0 ng/ml, while the average concentration of acetaminophen was 1.36 ± 0.08 μg/ml.

The phenacetin and unconjugated, conjugated, and total acetaminophen plasma levels for a subject who had received a 900-mg oral dose of phenacetin are reported in Table I. Typical ion chromatograms from this analysis can be seen in Figs. 4 and 5. After dosing, the phenacetin (264 ng/ml) and unconjugated acetaminophen (6.76 μg/ml) concentrations peaked at 1 and 2 hr, respectively, while the conjugated acetaminophen reached an 8–10-μg/ml plateau after 3 hr.

A least-squares analysis of the log concentration *versus* time curve for the 0–8-hr phenacetin concentrations in plasma gave a 1.3-hr elimination half-life; a similar analysis of the 3–8-hr unconjugated acetaminophen levels gave a 2.4-hr disappearance half-life. These half-lives were similar to those previously reported (23) for phenacetin and acetaminophen. Plasma levels of total acetaminophen for this subject decreased very slowly.

The sensitivity of this assay for phenacetin and acetaminophen is a function of the condition of the ion source and quadrupole rods. An analysis of a 1-ng of phenacetin/ml and a 100-ng of acetaminophen/ml plasma standard can be seen in Fig. 6. This ion chromatogram was the 113th obtained following ion source and quadrupole rod cleaning. Seven out of the available 30 μl was injected into the GLC–mass spectrometer. Both the phenacetin and acetaminophen ion peaks still had a signal-to-noise ratio greater than 5:1.

This sensitivity, while required to measure phenacetin in subjects with induced drug-metabolizing capabilities (17), should also be useful in determining basic pharmacokinetic data in humans after administration of a 300-mg therapeutic (24) phenacetin oral dose. Studies to determine the plasma concentration–time profile for phenacetin have typically required a higher than therapeutic phenacetin dose of between 1000 and 1800 mg to obtain measurable plasma levels over a sufficient timespan (23, 25–27).

REFERENCES

(1) B. B. Brodie and J. Axelrod, *J. Pharmacol. Exp. Ther.*, **94**, 22 (1948).

(2) *Ibid.*, **97**, 58 (1949).

(3) R. M. Welch and A. H. Conney, *Clin. Chem.*, **11**, 1064 (1965).

(4) J. I. Routh, N. A. Shane, E. G. Arredondo, and W. D. Paul, *ibid.*, **14**, 882 (1968).

(5) J. Knepil, *Clin. Chim. Acta*, **52**, 369 (1974).

(6) C. A. Burtis, W. C. Butts, and W. T. Rainey, *Am. J. Clin. Pathol.*, **53**, 769 (1970).

(7) J. E. Mrochek, S. Katz, W. H. Christie, and S. R. Dinsmore, *Clin. Chem.*, **20**, 1086 (1974).

(8) R. L. Smith and J. A. Timbrell, *Xenobiotica*, **4**, 489 (1974).

(9) D. J. Jollow, S. S. Thorgeirsson, W. Z. Potter, M. Hashimoto, and J. R. Mitchell, *Pharmacology*, **12**, 251 (1974).

(10) H. Buch, K. Pfleger, and W. Rudiger, *Z. Klin. Chem.*, **5**, 119 (1967).

(11) H. Buch, H. Hauser, K. Pfleger, and W Rudiger, *ibid.*, **4**, 288 (1966).

(12) A. Klutch and M. Bordun, *J. Pharm. Sci.*, **57**, 524 (1968).

(13) J. Grove, *J. Chromatogr.*, **59**, 289 (1971).

(14) L. F. Prescott, *J. Pharm. Pharmacol.*, **23**, 111 (1971).

(15) B. H. Thomas and B. B. Coldwell, *ibid.*, **24**, 243 (1972).

(16) E. J. Pantuck, R. Kuntzman, and A. H. Conney, *Science*, **175**, 1248 (1972).

(17) E. J. Pantuck, K.-C. Hsiao, A. Maggio, K. Nakamura, R. Kuntzman, and A. H. Conney, *Clin. Pharmacol. Ther.*, **15**, 9 (1974).

(18) M. S. B. Munson, *Anal. Chem.*, **43**, 28A (1971).

(19) F. Arnt, *Org. Syn., Coll. Vol. 2*, **1943**, 461.

(20) C. F. Allen and J. W. Gates, *Org. Syn., Coll. Vol. 3*, **1955**, 140.

(21) "The Merck Index," 8th ed., Merck and Co. Inc., Rahway, N.J., 1968, p. 8.

(22) *Ibid.*, p. 5.

(23) L. F. Prescott, M. Sansur, W. Levin, and A. H. Conney, *Clin. Pharmacol. Ther.*, **9**, 605 (1968).

(24) "The Pharmacological Basis of Therapeutics," L. S. Goodman and A. Gilman, Eds., 4th ed., Macmillan, New York, N.Y., 1968, p. 331.

(25) J. Raaflaub and U. C. Dubach, *Eur. J. Clin. Pharmacol.*, **8**, 261 (1975).

(26) C. A. Shively and E. S. Vesell, *Clin. Pharmacol. Ther.*, **18**, 413 (1975).

(27) L. F. Prescott, R. F. Steel, and W. R. Ferrier, *ibid.*, **11**, 496 (1970).

ACKNOWLEDGMENTS AND ADDRESSES

Received March 25, 1976, from the *Department of Biochemistry and Drug Metabolism, Hoffmann–La Roche Inc., Nutley, NJ 07110, and the ‡Department of Anesthesiology, College of Physicians and Surgeons, Columbia University, New York, NY 10032.

Accepted for publication April 28, 1976.

ˣ To whom inquiries should be directed.

Pharmacokinetics of Ampicillin and Methoxymethyl Ester of Hetacillin in Dogs

TORBEN B. KJAER *, PETER G. WELLING ‡, and PAUL O. MADSEN *x

Abstract □ Concentrations of ampicillin and the methoxymethyl ester of hetacillin were measured in plasma, prostatic fluid, and spinal fluid of dogs receiving ampicillin or the hetacillin ester by continuous intravenous infusion. The ratios of ampicillin in prostatic fluid relative to plasma levels were higher after dosing with the hetacillin ester. Pharmacokinetic parameter values were consistent with urinary excretion characteristics. Ready diffusion of the ester across biological membranes may facilitate eradication of pathogenic organisms in prostatic and spinal fluids.

Keyphrases □ Ampicillin—pharmacokinetics, plasma, prostatic fluid, and spinal fluid levels, dogs □ Hetacillin methoxymethyl ester—pharmacokinetics, plasma, prostatic fluid, and spinal fluid levels, dogs □ Pharmacokinetics—ampicillin and hetacillin methoxymethyl ester, plasma, prostatic fluid, and spinal fluid levels, dogs □ Antibacterials—ampicillin and hetacillin methoxymethyl ester, pharmacokinetics, plasma, prostatic fluid, and spinal fluid levels, dogs □ Distribution, drug—ampicillin and hetacillin methoxymethyl ester, plasma, prostatic fluid, and spinal fluid levels, dogs

The methoxymethyl ester of hetacillin[1] (I) is a new lipophilic prodrug of ampicillin, with distribution and kinetic properties different from other ampicillin precursors (1, 2). These properties include rapid absorption from the GI tract and extensive distribution into body tissues, particularly prostatic and central nervous system (CNS) tissue. The hetacillin ester appears to be absorbed after oral doses largely as the intact ester. Once absorbed, the ester undergoes hydrolysis in the blood and other tissues and body fluids to yield ultimately free ampicillin. Distribution characteristics of the unchanged ester and ampicillin are functions of the relative rates of tissue uptake and enzymatic and chemical hydrolyses.

The entry of ampicillin and the hetacillin ester into prostatic fluid and tissue of dogs during continuous intravenous infusion was described previously (2). The purposes of the present study were to examine these data from a pharmacokinetic point of view and to describe the tissue distribution characteristics of the hetacillin ester after continuous intravenous infusion in dogs.

EXPERIMENTAL

Full details regarding animal preparation, dosing, sampling, and assay procedures were given elsewhere (2). In summary, eight male beagle dogs, 17–21 kg, were anesthetized with intravenous thiopental sodium[2] and ventilated with air on a respirator. Three dogs received ampicillin sodium[3]

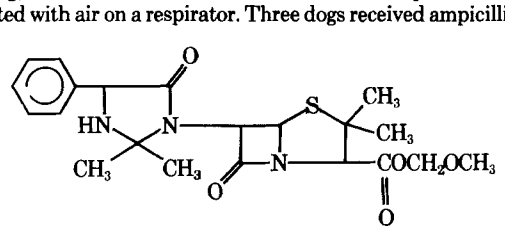

I

[1] BL-P1761.
[2] Pentothal sodium, Abbott.
[3] Polycillin-N, Bristol Laboratories, Syracuse, N.Y.

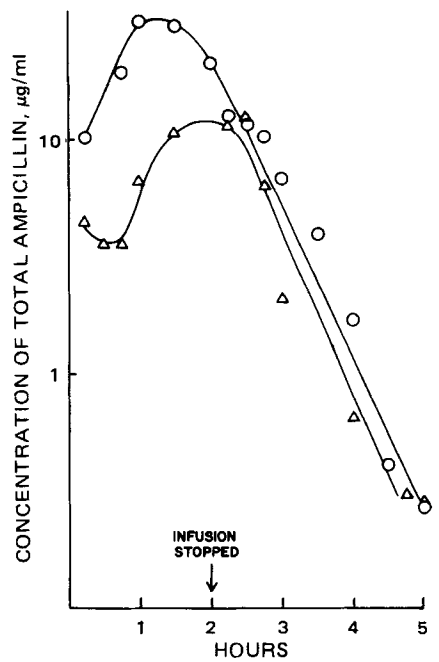

Figure 1—*Concentration of total ampicillin activity in plasma (○) and prostatic fluid (△) during and after infusion of the hetacillin ester (Dog 10).*

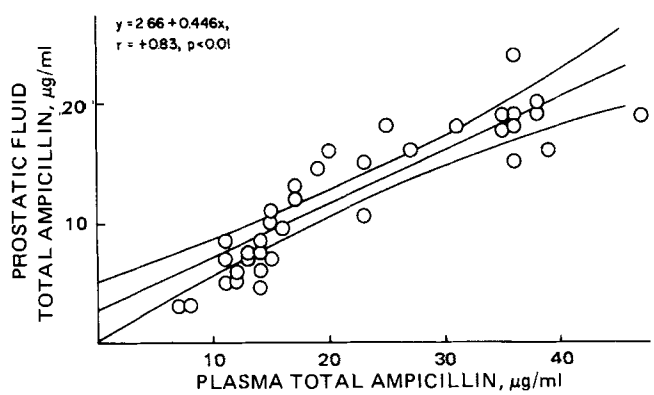

Figure 2—*Linear regression with 95% confidence limits of total ampicillin concentration in prostatic fluid against total ampicillin concentration in plasma during hetacillin ester infusion.*

as an initial bolus injection of 3 (Dogs 1 and 2) and 10 (Dog 3) mg/kg and then as a constant infusion into a femoral vein in sterile lactated Ringer's solution at a rate of 10 mg/kg/hr for 4 hr. The infusion was started simultaneously with the bolus injection. Five dogs (Dogs 4–8) were similarly treated with the hetacillin ester[4], receiving a bolus injection of 1.8 mg of ampicillin equivalents/kg followed by a constant infusion of 10 mg/kg/hr iv.

All dogs were sacrificed after a 4-hr infusion. Two other dogs (Dogs 9 and 10) were similarly infused with the hetacillin ester for 2 hr, and plasma and prostatic or spinal fluid were obtained both during and fol-

[4] Sterile bottles containing 50 mg of ampicillin equivalents/bottle, Bristol Laboratories.

Table I—Plasma and Prostatic Fluid Levels of Ampicillin during Infusion of Ampicillin

Dog		Concentration, μg/ml							
		30 min	60 min	90 min	120 min	150 min	180 min	210 min	240 min
1	Plasma	50	38	33	31	29	—[a]	23	18
	Prostatic fluid	0.5	1.0	1.0	1.2	0.9	1.1	1.0	0.2
	Prostatic fluid / Plasma	0.01	0.03	0.03	0.04	0.03	–	0.04	0.01
2	Plasma	22	25	17	23	–	30	18	19
	Prostatic fluid	0.3	0.5	0.7	0.8	1.1	0.7	0.9	0.8
	Prostatic fluid / Plasma	0.01	0.02	0.04	0.03	–	0.02	0.05	0.04
3	Plasma	19	24	23	26	–	38	33	23
	Prostatic fluid	0.2	0.2	1.9	1.4	0.9	1.9	2.0	2.2
	Prostatic fluid / Plasma	0.01	0.01	0.08	0.05	–	0.05	0.06	0.10

[a]Not determined.

lowing the infusion. Infusion bottles containing the hetacillin ester were kept in ice water, and fresh solutions were prepared hourly to minimize ester hydrolysis during administration.

Prostatic fluid was obtained by urethral intubation in the perineum just distal to the prostate gland. Urine was collected by cannulation of both ureters, thus preventing contamination of prostatic fluid with urine. The vas deferens was ligated. Prostatic fluid secretion was stimulated by constant infusion of pilocarpine, 0.25 mg/kg/hr iv for 4 hr.

Blood samples were collected from a femoral artery in heparinized tubes at 30-min intervals, and plasma was separated. Prostatic fluid was collected at hourly intervals in vessels contained in an ice bath. Spinal fluid was obtained by suboccipital puncture. All samples were deep frozen immediately after collection until assayed.

Assays for free ampicillin and the unhydrolyzed hetacillin ester were carried out by a disk diffusion method, using *Sarcina lutea* (ATCC 9341) as the test organism as described previously (2). Renal clearances were calculated from hourly urinary excretion of ampicillin or the hetacillin ester during the 2nd, 3rd, and 4th hr of infusion.

RESULTS

Concentrations of ampicillin in plasma and prostatic fluid from the ampicillin infusion and urinary excretion details are given in Tables I and II. Average plasma and prostatic fluid concentrations of ampicillin and the hetacillin ester and urinary excretion details are given in Tables III and IV.

As shown in Tables I and III, the ratio of prostatic fluid to plasma ampicillin varied from 0.1 to 0.01 during ampicillin infusion, with prostatic fluid levels ranging from 0.2 to 2.2 μg/ml. However, during hetacillin ester infusion, mean prostatic fluid levels of ampicillin ranged from 2.2 to 7.4 μg/ml, increasing from the infusion time; the ratios of prostatic fluid to plasma ampicillin were considerably increased to about 0.4.

It can be seen from Tables II and IV that the concentrations of ampicillin in urine were lower after hetacillin ester infusion but were still very high compared to plasma levels. Approximately one-half of the infused ampicillin was recovered unchanged in urine, and renal clearance was 40–80 ml/min. During hetacillin ester infusion, recovery of ampicillin in urine was considerably reduced. However, the renal clearances, except from Dogs 5 and 6 which were atypically low, were similar to those resulting from ampicillin infusion (38–74 ml/min). These values are similar to those reported previously (3). The renal clearance of the hetacillin ester was essentially zero, confirming the quantitative hydrolysis and metabolism of this agent *in vivo*.

Table II—Urinary Excretion of Ampicillin during Infusion of Ampicillin

Dog	Urine Concentration, mg/ml	Urine Volume, ml	4-hr Recovery, % of Dose	Renal Clearance, ml/min
1	4.23 (3.95)[a]	214	44.7	65.1 (25.2)[a]
2	2.44 (1.53)	252	50.1	84.8 (33.1)
3	2.86 (2.08)	157	46.3	40.7 (8.9)

[a]Mean and standard deviation from three 1-hr collections.

Spinal fluid levels of ampicillin and the hetacillin ester were obtained in Dogs 4–7 at the end of the infusion period and in Dogs 8 and 9 at 30–60-min intervals during infusion. The mean 4-hr values for ampicillin and the hetacillin ester were 11.0 ± 8.1 and 2.6 ± 1.7 μg/ml, respectively, which were both about one-third the respective plasma levels.

In Dog 8, spinal fluid concentrations of total ampicillin activity at 30, 90, 120, 180, and 240 min during infusion were 4, 12, 19, 20, and 26.5 μg/ml, respectively. In Dog 9, spinal fluid levels of total ampicillin at 30, 60, 90, and 120 min during infusion were 0.0, 1.2, 3.4, and 4.2 μg/ml, respectively. Thus, in both dogs, there appeared to be an accumulation of the antibiotic in spinal fluid during the infusion while plasma levels remained constant. Furthermore, ampicillin appeared to be cleared from spinal fluid very slowly because the levels of ampicillin in Dog 9 remained constant during 90 min postinfusion while plasma levels decreased from 3.6 to 0.8 μg/ml.

The relative rates of loss of total ampicillin activity (ampicillin plus the hetacillin ester) from plasma and prostatic fluid were determined in Dog 10 by repeated sampling during 3 hr following a 2-hr infusion of the hetacillin ester. The similarity of the rates of decline is indicated in Fig. 1. The calculated elimination half-lives in plasma and prostatic fluid were 0.46 and 0.45 hr, respectively. The linear relationship between the various combined ester and ampicillin concentrations in prostatic and spinal fluids and plasma during infusion is illustrated in Figs. 2 and 3.

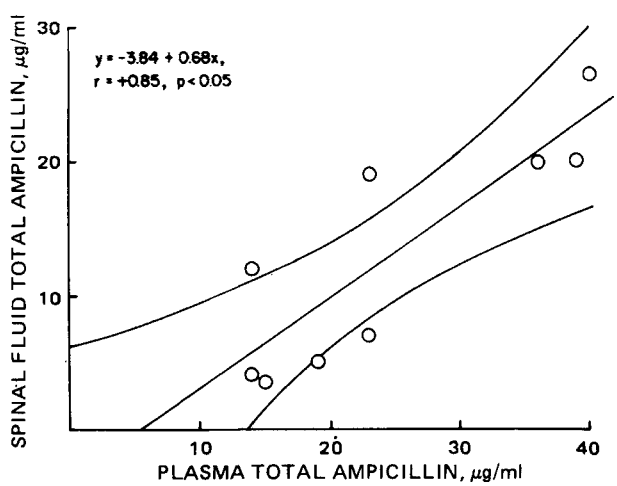

Figure 3—*Linear regression with 95% confidence limits of total ampicillin concentration in spinal fluid against total ampicillin concentration in plasma during hetacillin ester infusion.*

Table III—Mean Plasma and Prostatic Fluid Levels of Ampicillin and Hetacillin Ester during Infusion of Hetacillin Ester in Five Dogs

	Concentration, μg/ml							
	30 min	60 min	90 min	120 min	150 min	180 min	210 min	240 min
Plasma ampicillin	8.2 (4.7)[a]	11.6 (5.5)	12.4 (6.5)	16.0 (7.9)	17.0 (7.9)	22.6 (12.1)	22.2 (6.1)	20.0 (8.2)
Plasma hetacillin ester	5.0 (3.3)	5.0 (3.0)	5.2 (2.8)	5.8 (2.2)	6.6 (3.5)	5.2 (4.9)	7.0 (2.9)	6.4 (3.2)
Prostatic fluid ampicillin	2.2 (2.7)	3.1 (2.8)	2.6 (0.5)	5.6 (3.2)	6.7 (2.3)	5.9 (2.1)	6.2 (2.7)	7.4 (3.1)
Prostatic fluid hetacillin ester	4.6 (3.1)	6.3 (2.5)	5.8 (1.9)	7.2 (2.2)	6.4 (3.5)	8.2 (3.4)	8.3 (4.1)	8.8 (4.2)
Prostatic / Plasma ampicillin	0.23 (0.13)	0.24 (0.10)	0.28 (0.06)	0.39 (0.05)	0.42 (0.15)	0.34 (0.08)	0.31 (0.07)	0.43 (0.15)
Prostatic / Plasma hetacillin ester	0.82 (0.32)	1.50 (0.81)	1.51 (0.34)	1.53 (0.46)	1.00 (0.29)	2.70 (2.0)	1.21 (0.42)	1.51 (0.5)

[a] Mean and standard deviation from three 1-hr collections.

Table IV—Urinary Excretion of Ampicillin and Hetacillin Ester after Infusion of Hetacillin Ester

Dog		Urine Concentration, mg/ml	Urine Volume, ml	4-hr Recovery, % of Dose	Renal Clearance, ml/min
4	Ampicillin	1.17 (0.28)[a]	122	22.7	74.3 (3.9)
	Hetacillin ester	4.5 (0.6)[b]		0.1	1.0 (0.3)
5[c]	Ampicillin	0.71 (0.45)	91	7.9	20.0[d]
	Hetacillin ester	3.7 (1.5)		0.02	0.21 (0.17)
6	Ampicillin	0.70 (0.59)	218	14.3	40.8 (14.0)
	Hetacillin ester	4.5 (2.6)		0.1	0.5 (0.15)
7	Ampicillin	0.40 (0.27)	268	11.6	38.1 (15.3)
	Hetacillin ester	2.3 (0.5)		0.07	0.61 (0.34)
8[c]	Ampicillin	2.03[d]	30	6.1	21.8[d]
	Hetacillin ester	2.5		0.02	0.18

[a] Mean and standard deviation from three 1-hr collections. [b] Urinary concentration of the hetacillin ester is expressed in micrograms per milliliter in all cases. [c] Dogs 5 and 8 developed slow heart rates and low blood pressures due to pilocarpine and were generally in poor condition during the experiment. Renal excretion in these animals was low. [d] Only two collections.

DISCUSSION

If it is assumed that the hetacillin ester obeys apparent one-compartment model kinetics, plasma data during infusion of the ester can be described by Scheme I. In this model, concentration of ester in plasma at the steady state, C_{ss}, is given by (4):

$$C_{ss} = k_0/VK \qquad \text{(Eq. 1)}$$

where k_0 is the zero-order infusion rate constant, K is the apparent first-order rate constant for loss of the ester by all processes, and V is the ester distribution volume in the body. The product VK is the ester plasma clearance (5).

With the plasma concentrations in Table III and known infusion rates, plasma clearances of the ester for Dogs 4, 5, 6, 7, and 8 were 1087, 321, 529, 833, and 457 ml/min, respectively. The values contrast with the almost negligible renal clearances of unchanged ester.

The distribution volume of the hetacillin ester was reported to be approximately 85% of body weight (1). Substituting this value into Eq. 1 and using the relationship $t_{1/2} = \ln 2/K$ yielded a hetacillin ester half-life of 0.34 ± 0.18 hr. This value is identical to that reported for the *in vitro* degradation of the hetacillin ester in dog serum (2).

The overall ratio of ampicillin renal clearance to creatinine clearance in Dogs 1–8 was 1.31 ± 0.55, indicating some renal tubular secretion. This secretion is not as extensive as that usually observed in humans (6) but may have been influenced to some extent by the experimental conditions and surgical procedures.

The relationship between prostatic and spinal fluid levels and plasma levels of ampicillin during hetacillin ester infusion suggests that the lipophilic ester is transported readily into these fluids and that hydrolysis occurs subsequently. It is evident that drug levels in spinal and prostatic fluids can be predicted with reasonable accuracy from observed plasma levels, at least during continuous dosing. Although prostatic fluid levels of ampicillin decline with plasma levels, the antibiotic may stay within spinal fluid for longer periods.

The ability of the hetacillin ester to penetrate spinal and prostatic fluids may prove of considerable use in the eradication of pathogenic organisms resident in these sites which have been relatively inaccessible to the penicillins.

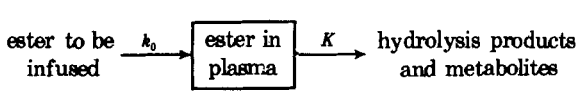

Scheme I—One-compartment open model with zero-order absorption

REFERENCES

(1) "Disposition and Safety Evaluation Studies on BL-P1761," Bristol Laboratories, Syracuse, N.Y., Jan. 1974.

(2) T. B. Kjaer and P. O. Madsen, *Invest. Urol.*, **14**, 57 (1976).

(3) B. E. Cabana, L. E. Willhite, and M. E. Bierwagen, *Antimicrob. Ag. Chemother.*, **1969**, 35 (1970).

(4) J. G. Wagner, "Biopharmaceutics and Relevant Pharmacokinetics," Drug Intelligence Publications, Hamilton, Ill., 1971.

(5) P. G. Welling, W. A. Craig, G. L. Amidon, and C. M. Kunin, *Clin. Pharmacol. Ther.*, **15**, 344 (1974).

(6) L. W. Dittert, W. O. Griffin, J. C. LaPiana, F. J. Shainfeld, and J. T. Doluisio, *Antimicrob. Ag. Chemother.*, **1969**, 42 (1970).

ACKNOWLEDGMENTS AND ADDRESSES

Received December 8, 1975, from the *Section of Urology, Veterans Administration Hospital, Department of Surgery, School of Medicine, Madison, WI 53705, and the [‡]School of Pharmacy, University of Wisconsin, Madison, WI 53706.

Accepted for publication May 5, 1976.

[x] To whom inquiries should be directed.

Serum Lipid-Lowering Properties of 6-Chloro-9-[2-(6-methyl-3-pyridyl)ethyl]-1,2,3,4-tetrahydrocarbazole-2-carboxylic Acid

COLIN DALTON ˣ and WILLIAM R. POOL

Abstract □ 6-Chloro-9-[2-(6-methyl-3-pyridyl)ethyl]-1,2,3,4-tetrahydrocarbazole-2-carboxylic acid hydrochloride lowered serum cholesterol, triglyceride, phospholipid, and free fatty acid levels in normal rats. The compound appeared to have a low toxicity and to be well tolerated in mice, adult and neonatal rats, and rabbits. At hypolipidemic doses, it caused a slight hepatomegaly associated with an increase in liver phospholipid and protein content. Liver *N*-demethylase and catalase activities were increased by the drug treatment. This acid had no *in vitro* antilipolytic activity and did not affect serum desmosterol–cholesterol ratios. The results indicate that it has a mechanism of action similar to clofibrate.

Keyphrases □ Tetrahydrocarbazole, substituted—effect on serum lipid levels in rats, toxicity in rats, mice, and rabbits □ Lipid levels, serum—effect of substituted tetrahydrocarbazole, rats □ Toxicity—substituted tetrahydrocarbazole, rats, mice, and rabbits □ Antihyperlipidemic activity—substituted tetrahydrocarbazole evaluated, rats

Interest in pharmacological agents that lower blood lipid levels is primarily based upon data that implicate elevated blood lipid levels in the etiology of coronary disease. Clofibrate[1], ethyl 2-(4-chlorophenoxy)-2-methylpropanoate, is currently marketed as an active hypolipidemic agent. It is being extensively tested in an international primary prevention trial of ischemic heart disease (1) and for its long-term influence on morbidity and mortality in patients with a history of clinical heart disease (2). This report concerns a new compound, 6-chloro-9-[2-(6-methyl-3-pyridyl)ethyl] -1,2,3,4 -tetrahydrocarbazole- 2-carboxylic acid hydrochloride (I) (3), which is structurally unrelated to clofibrate but has serum lipid-lowering properties.

EXPERIMENTAL

Treatment of Animals—Male albino rats[2], 180–200 g, were housed in individual stainless steel cages with wire screen bottoms. The cages were maintained at 23°. All animals were allowed food[3] and tap water *ad libitum*.

Drugs were suspended or dissolved in an aqueous suspending vehicle (sodium chloride, 9 g/liter; carboxymethylcellulose, 5 g/liter; polysorbate 80, 3.9 g/liter; and benzyl alcohol, 8.6 ml/liter, in distilled water) and administered at the doses indicated in 5 ml of vehicle/kg. Control rats received an equal volume of the vehicle. Routes and times of drug administration are given under *Results*.

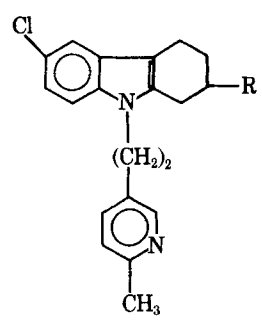

I: R = COOH
II: R = CH_2OH

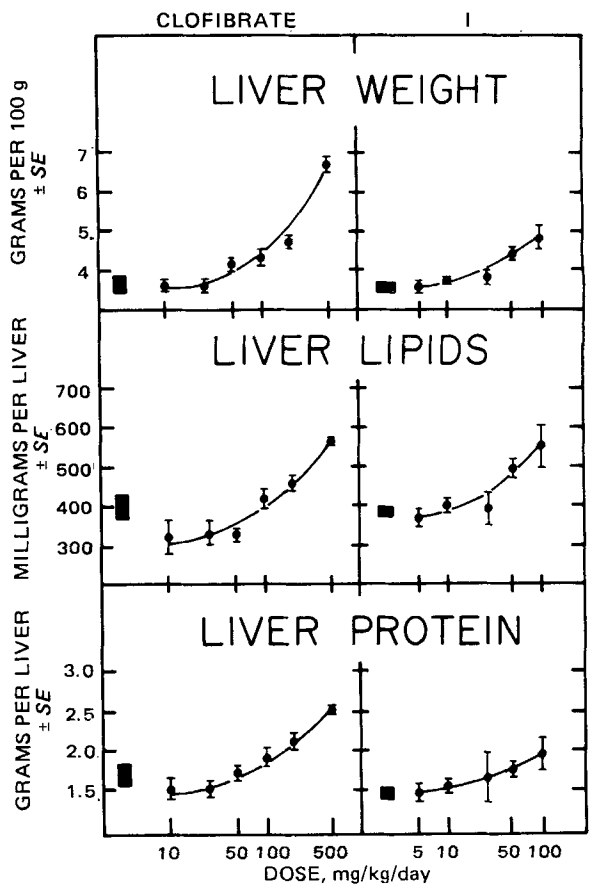

Figure 1—*Effect of hypolipidemic agents on rat liver weight and liver lipid and protein content. Key:* ■, *control.*

The animals were fasted overnight and sacrificed by decapitation. Body, liver, adrenal, and epididymal fat pad weights were recorded. Separate portions of liver were used for the preparation of subcellular fractions, analysis of lipids, and determination of *N*-demethylase activity.

Hypertriglyceridemic Rats—The test compounds were suspended in 5% gum acacia solution and administered orally for 11 days by intubation each day, except on the weekend when the compounds were administered as a dietary admix. Six animals were used for each dose level. Two groups of 10 control animals each were untreated. A 10% fructose solution was substituted for normal drinking water for the last 20 hr of the test. One control group continued to receive normal drinking water. On Day 12, the animals were sacrificed for serum triglyceride determination (4).

Preparation of Subcellular Fractions—A 10% liver homogenate in 0.25 *M* sucrose was prepared using six strokes of a motor-driven glass–plastic[4] homogenizer at 4°. Mitochondria were isolated according to the method of Schneider (5). Samples were centrifuged[5] at 800×*g* at

[1] Atromid-S, Ayerst Laboratories, New York, N.Y.
[2] Charles River Breeding Laboratories.
[3] Pelleted Purina Rat Chow.
[4] Teflon (du Pont).
[5] International refrigerated centrifuge model PR-6.

Table I—Effect of I on Rat Serum Lipid Content[a]

Dose, mg/kg/day	Cholesterol, mg % ± *SE*	Triglycerides, mg % ± *SE*	Phospholipids, mg % ± *SE*	Free Fatty Acids, μEq/liter ± *SE*
0	77 ± 3	79 ± 10	118 ± 5	819 ± 26
50	60 ± 5*	48 ± 8*	83 ± 3***	650 ± 29**
100	60 ± 5*	47 ± 10*	90 ± 6**	607 ± 25***

[a] The significance of the difference between the treated and the control groups is designated by the *p* values: * <0.05, ** <0.01, and *** <0.001; *n* = six to 12 rats per group.

Table II—Effect of I on Rat Body and Organ Weight

Dose, mg/kg/day	Increase in Body Weight, g ± *SE*	Adrenal Weight, mg ± *SE*	Fat Pad Weight, g ± *SE*	Liver Weight, g ± *SE*
0	59.4 ± 2.1	46 ± 3	1.5 ± 0.09	9.1 ± 0.2
50	56.5 ± 7.5	43 ± 2	1.3 ± 0.16	10.8 ± 0.7
100	60.1 ± 5.2	45 ± 2	1.2 ± 0.12	11.7 ± 0.6[a]

[a] The significance of the difference between the treated and the control groups is designated by the *p* value: <0.01.

Table III—Acute Toxicity of I

Species	Route of Administration	LD_{50} ± *SE* mg/kg
Mice	Oral	13,000 ± 1120
Mice	Intraperitoneal	410 ± 20
Mice	Subcutaneous	>2000
Adult rats	Oral	>4000
Neonatal rats	Oral	3700 ± 240
Rabbits	Oral	880 ± 200

Table IV—Effect of I on Serum Triglyceride Levels in Hypertriglyceridemic Rats

Dose, mg/kg po	Serum Triglycerides, mg % ± *SE*	Change from Control, %
Control	223 ± 10	—
1	244 ± 23	+9
20	193 ± 12	−13
50	185 ± 25	−17
100	151 ± 11[a]	−32

[a] $p < 0.01$.

2° for 10 min to remove nuclei and unbroken cells. The supernate was collected, and the residue was washed twice with isotonic sucrose. Washes were combined with the supernate, and the residue was discarded. The combined supernates were then centrifuged[6] at 8500×*g* at 2° for 10 min to sediment the mitochondria. The supernate was collected and the mitochondrial pellet was washed twice with isotonic sucrose.

Microsomes were prepared by centrifuging[7] the combined supernates from the mitochondrial fraction of 105,000×*g* at 2° for 75 min. The mitochondrial and microsomal pellets were resuspended in isotonic sucrose and rehomogenized gently with a glass–plastic[4] homogenizer to a final tissue equivalent of 150 mg/ml.

Analytical Procedures—Serum was analyzed for cholesterol (6), triglycerides (4), phospholipids (7), and free fatty acids (8). The protein content of the fractions was determined by the biuret reaction conducted on an automated analyzer[8]. Lipids were extracted with chloroform–methanol (2:1 v/v), using a modification of the Folch *et al.* procedure (9), determined gravimetrically, and analyzed for phospholipid content (7).

Determination of Hepatic *N*-Demethylase Activity—A 20% liver homogenate in 0.01 *M* phosphate buffer containing 1.15% KCl was prepared by homogenizing in a high speed blender[9] three times for 10 sec each. The homogenate was centrifuged[10] in 50-ml polyethylene tubes at 10,000×*g* for 30 min at 2°, and the supernate was removed with a syringe and either analyzed immediately or frozen overnight. *N*-Demethylase activity was assayed using an automated adaptation (10) of the method of Axelrod (11), utilizing ethylmorphine as the substrate.

GLC of Sterols—Aliquots of rat serum were saponified with 0.5 *N* ethanolic potassium hydroxide by heating for 5 min at 90°, and water was added after cooling. The nonsaponifiable fraction was extracted four times with 3 ml of petroleum ether (bp 30–60°), and cholestane was added to the extracts as an internal standard. The extracts were combined, brought to dryness at 70° under nitrogen flow, and dissolved in 0.1 ml of chloroform[11].

Isothermal GLC was performed on a gas chromatograph equipped with flame-ionization detectors using a 1.8-m (6-ft) × 4-mm glass column, 3% OV-17 on Gas Chrom Q, at 240° with a helium carrier flow rate of 90 ml/min. All peak area measurements were made in triplicate by polar planimetry and were quantitated by internal standardization with cholestane (12).

***In Vitro* Lipolytic Activity**—An isolated fat cell suspension was prepared according to Rodbell (13) and incubated in plastic vials in a total volume of 1 ml of Krebs–Ringer bicarbonate buffer (pH 7.4) containing 4% bovine plasma albumin. Theophylline (5×10^{-4} *M*) or levarterenol (5×10^{-7} *M*) was used to stimulate lipolysis. Compound I was dissolved in ethanol and added to yield the concentrations indicated. The control samples were incubated with an equal volume of ethanol. The cell suspension was incubated for 1 hr at 37°. The reaction was terminated, and glycerol was extracted by the addition of 4 ml of water to the incubation vial followed by mechanical shaking for 5 min.

The aqueous extract was used directly for the enzymatic glycerol analysis (14). Separate aliquots of the fat cell suspension were taken for triglyceride analysis (4), and the results were expressed as micromoles of glycerol released per gram of triglyceride per hour.

Catalase Determination—Livers from freshly sacrificed rats were homogenized in a glass–plastic[4] homogenizer at 4° with 1.25 m*M* phosphate buffer. The homogenate was allowed to stand for 30 min at 4°, rehomogenized, and adjusted to a final volume of 50 ml. The absorbance at 240 nm was measured[12] at room temperature. A 0.01-ml aliquot of the liver homogenate was added to 3 ml of hydrogen peroxide–phosphate buffer, and the time required for a decrease in absorbance from 0.55 to 0.50 was determined.

Catalase activity is expressed as units per milligram of wet weight of liver. A catalase unit is defined as the amount of enzyme that liberates half of the peroxide oxygen from a hydrogen peroxide solution of any concentration in 100 sec at 25° (15).

Acute Toxicity—CF-1 mice (17–25 g), Wistar-strain adult (130–175 g) and neonatal (6–9 g) rats, and albino rabbits (1.9–2.7 kg) were used. Compound I was ground in a mortar and suspended in 5% gum acacia solution or aqueous suspending vehicle and was administered orally, intraperitoneally, or subcutaneously. Eight to 10 animals were used per

[6] Sorvall automatic refrigerated centrifuge model RC2-B.
[7] Beckman model L-2 ultracentrifuge.
[8] Technicon Corp. methodology N-14-b.
[9] Waring.
[10] Sorvall centrifuge with SS-34 head.
[11] M.C.B. spectroquality.
[12] Beckman DU spectrophotometer.

Table V—Effect of Hypolipidemic Drugs on Liver Lipid Content[a]

	Cholesterol		Triglycerides		Phospholipids	
	mg/g	mg/Liver	mg/g	mg/Liver	mg/g	mg/Liver
Control	4.1 ± 0.4	36 ± 1	5.9 ± 0.8	52 ± 8	31 ± 1	278 ± 1
Clofibrate	2.9 ± 0.1**	34 ± 2	5.7 ± 1.4	68 ± 17	35 ± 1	406 ± 2*
I	3.6 ± 0.1**	39 ± 1	3.8 ± 0.4**	42 ± 5	35 ± 3	380 ± 2**

[a] The significance of the difference between the treated and the control groups is designated by the p values: * <0.01, and ** <0.001.

dose level. The animals were observed for 5 days, and total mortality was reported. The LD_{50} was calculated by the method of Miller and Tainter (16). Some of the treated neonates were missing and were presumed to have been cannibalized after dying. The missing rats were counted as dead rats in calculating the LD_{50}.

The statistical significance of the data was determined by the Student t test and is designated as a p value.

RESULTS

Oral administration of I for 2 weeks to rats lowered serum concentrations of cholesterol, triglycerides, phospholipids, and free fatty acids (Table I). Maximum lipid lowering was observed after dosing with 50 mg/kg, and no further decrease was found at 100 mg/kg. Rats treated with I gained weight at the same rate as placebo controls, indicating that appetite was not affected and that the drug was well tolerated (Table II). Drug-tested rats looked and behaved like normal, healthy animals.

Acute toxicity determinations in mice, rats, and rabbits indicated that I had low oral, intraperitoneal, and subcutaneous toxicity (Table III). The high LD_{50} ratio for oral *versus* intraperitoneal routes of administration indicated a low bioavailability for high oral doses of I. Such decreased absorption after large oral dosage may explain the apparent lack of a dose–response curve for serum lipid lowering. A female dog receiving the compound in gelatin capsules tolerated oral doses up to 320 mg/kg without symptoms. Normal hematological and serum clinical chemical values were observed in this dog[13].

The low toxicity during 2 weeks of drug administration was corroborated by normal adrenal and epididymal fat pad weights (Table II). In common with other hypolipidemic agents (17), I increased rat liver weight (Table II). Compound I also caused a dose-related decrease in serum triglyceride levels in rats made hypertriglyceridemic by adding fructose to their drinking water (Table IV).

Compound I was studied in comparison with clofibrate to compare their mechanisms of action. Both compounds caused a dose-related increase in liver weight and in liver lipid and protein content (Fig. 1). Examination of the composition of the liver from rats treated with various hypolipidemic agents revealed no change in DNA or water content, indicating that neither hyperplasia nor edema could explain the liver enlargement (17). Significant increases in liver RNA were found. Analysis of the different lipid classes in the hepatomegalic livers, induced by two hypolipidemic drugs, revealed an apparent decrease in cholesterol and triglyceride concentrations when expressed on a milligrams per gram of liver basis. However, this result represented no change in the total cholesterol or triglyceride content of the liver (Table V). Liver phospholipid content was strikingly increased in clofibrate- and I-treated rats.

It was of interest to determine the subcellular localization of the changes in liver composition. Oral administration of 250 mg/kg of clofi-

Table VI—Effect of Hypolipidemic Agents on Liver Microsomal *N*-Demethylase Activity[a]

Dose, mg/kg/day	*N*-Demethylase Activity, μmoles/g/min	
	I	Clofibrate
0	7.4 ± 0.5	5.9 ± 0.9
10	9.8 ± 1.0	6.4 ± 1.1
25	11.2 ± 0.5	7.9 ± 1.9
100	11.6 ± 0.9*	9.1 ± 1.1
200	—	14.0 ± 0.8**

[a] The significance of the difference due to the drugs is designated by the p values: * <0.01, and ** <0.001.

Table VII—Effect of Hypolipidemic Drugs on Serum Cholesterol and Desmosterol Composition

Treatment	Dose, mg/kg/day	Cholesterol, %	Desmosterol, %
Control	—	99+	Trace
Triparanol	50	38.9	61.1
I	50	95.1	4.9
Clofibrate	250	99+	Trace

Table VIII—Effect of I and Clofibrate on Liver Catalase Activity[a]

Drug	Dose, mg/kg	Catalase Activity, units/mg
Control	—	6.1 ± 0.4
I	100	10.0 ± 1.1*
Clofibrate	350	7.2 ± 0.4**

[a] The significance of the difference due to drugs is designated by the p values: * <0.05, and ** <0.01.

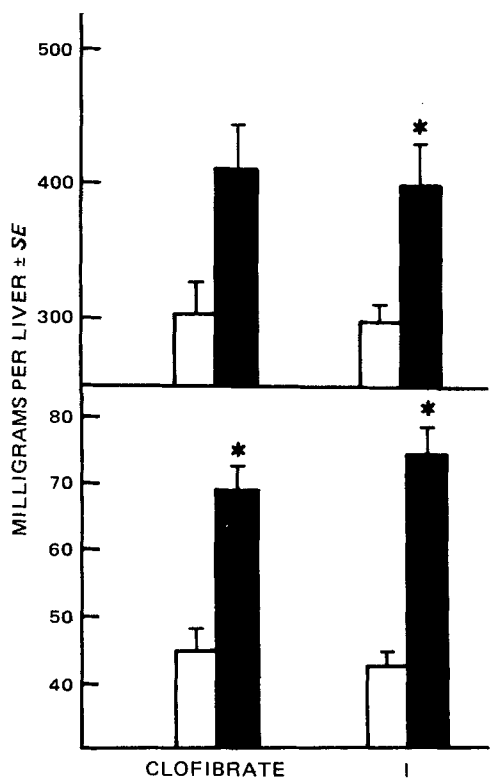

Figure 2—*Effect of chronic administration of hypolipidemic agents on liver mitochondrial protein (top) and phospholipid content (bottom). The significance of the difference between the treated and the control groups, designated by the *, was a p value of <0.05. Key: □, control; and ■, treated.*

[13] Data on file, Hoffmann–La Roche.

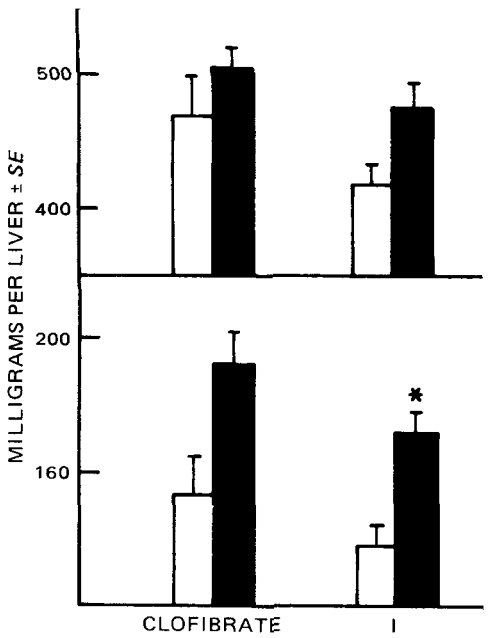

Figure 3—*Effect of chronic administration of antihyperlipidemic drugs on liver microsomal protein (top) and phospholipid content (bottom). The significance of the difference between the treated and the control groups, designated by the *, was a p value of <0.05. Key: □, control; and ■, treated.*

brate or 50 mg/kg of I for 9 days increased rat liver mitochondrial phospholipid and protein content (Fig. 2). A slight, but not statistically significant, increase in liver microsomal protein and phospholipid content was also obtained in rats treated with clofibrate (250 mg/kg/day), and a significant increase in microsomal phospholipid content was found upon treatment with I (50 mg/kg/day) (Fig. 3). Both agents induced liver microsomal drug-metabolizing enzymes, as shown by the ability of these enzymes to *N*-demethylate a test substrate, ethylmorphine (Table VI).

Triparanol, an effective lipid-lowering drug in experimental animals, is known to interfere with cholesterol synthesis by blocking the enzymatic step immediately prior to cholesterol formation, thus leading to an accumulation of desmosterol. During comparative tests, I and clofibrate had only minimal effects on serum desmosterol–cholesterol ratios, whereas serum sterols derived from triparanol-treated rats contained approximately 60% desmosterol (Table VII).

One characteristic finding in animals that have ingested clofibrate is a reversible increase in liver size, accompanied by the appearance of numerous microbodies (peroxisomes) detectable with an electron microscope (18, 19). The enzyme, catalase, is a useful peroxisome marker, since it is a major constituent of peroxisomes. Increased catalase activity in clofibrate-treated rats correlated with an increase in the number of microbodies. An increase in liver size and increased catalase activity were confirmed in clofibrate-treated rats and also found in I-treated rats (Table VIII).

Incubation of I at different concentrations had no effect on the basal rate of glycerol release from rat-isolated fat cells and did not alter the increased rates of glycerol release induced by incubation with optimal concentrations of levarterenol (0.5 μM) or theophylline (0.5 mM) (Table IX).

Table IX—Effect of I on Basal, Levarterenol, and Theophylline-Induced Lipolysis in Isolated Fat Cells

Drug	Lipolysis, μmoles of Glycerol/g of Fat Cells/hr ± *SE*		
	Control	I (1 mM)	I (0.1 mM)
	7.7 ± 0.2	7.8 ± 0.1	7.8 ± 0.8
Levarterenol, 0.5 μM	8.9 ± 0.2	9.6 ± 0.2	9.7 ± 0.1
Theophylline, 0.5 mM	21.5 ± 0.8	22.0 ± 0.5	24.1 ± 1.0

DISCUSSION

Data presented here demonstrate that I is an effective serum lipid-lowering compound in normal and hypertriglyceridemic rats. The effect of I on serum lipids resembles that of clofibrate (20), lifibrate[14] (III) (21), and nafenopin[15] (IV) (22). The chemical structure of I is quite different from III and IV, both of which structurally resemble clofibrate. All four compounds, however, have similar lipid-lowering activities. Serum lipid lowering occurred after a 50-mg/kg po regimen of I, III, or IV, whereas a 250-mg/kg regimen of clofibrate was required for consistent lipid-lowering activity (17). The low toxicity gives I a high therapeutic index so that I might be considered as a possible prophylactic agent for the prevention of hyperlipidemic "risk factor" of atherosclerosis.

Compound I was selected as one of many substituted tetrahydrocarbazoles with hypolipidemic activity (3) and studied in detail. Its analog, 6-chloro-9-[2-(2-methyl-5-pyridyl)ethyl]-1,2,3,4-tetrahydrocarbazole-2-methanol hydrochloride (II), showed similar marked hypolipidemic activity to I in rats[13]. Spectrofluorometric methods for the detection of I and II in biological systems were developed (23) and applied to a biopharmaceutical and pharmacokinetic evaluation of these substituted tetrahydrocarbazoles[16].

Many explanations have been offered for the serum lipid-lowering mechanism of clofibrate. These include an enhancement of thyroid hormone activity produced by competition for binding sites on plasma proteins (24), inhibition of cholesterol (25) and fatty acid (26) biosynthesis, increased hepatic cholesterol oxidation (27), decreased rates of release of hepatic lipoproteins (28), increased peripheral removal of lipoproteins (29), and increased neutral sterol excretion (30). More recently, Dalton *et al.* (17), in attempting to explain the mechanism of action of clofibrate, proposed that the demand for new membrane constituents by the livers of drug-treated animals restricts the production of triglycerides in order to favor that of phospholipids. Thus, the formation and transport of triglyceride-rich lipoproteins into circulating blood are reduced.

The observation that I had only minimal effects on the normal serum cholesterol–desmosterol ratio indicates that the cholesterol-lowering mechanism of action of I does not concern inhibition of the terminal stage of cholesterol biosynthesis. In this regard, it differs from triparanol and is, therefore, unlikely to give rise to an undesirable accumulation of desmosterol after chronic administration. These experiments, however, would not detect an effect of I on earlier stages of cholesterol biosynthesis.

It has been suggested (31, 32) that inhibition of free fatty acid mobilization could be indirectly responsible for serum lipid lowering in experimental animals. Compound I had no direct lipolytic or antilipolytic activity in isolated rat fat cells, indicating that the cholesterol-lowering mechanism of this compound is probably not associated with an inhibition of free fatty acid mobilization. An indirect inhibition of mobilization of free fatty acids was also ruled out, since an acute depletion of free fatty acids was not observed in fasted rats following drug administration.

An increase in liver size and the number of liver microbodies was reported in experimental animals treated with clofibrate (18, 19). Rats treated with I or clofibrate had both increased liver sizes and catalase activities, an enzyme specifically associated with peroxisomes. However, electron microscope studies to detect changes in liver peroxisomal numbers were not completed. In addition, chronic administration of either I or clofibrate caused an accumulation of phospholipids and protein but not of triglycerides or cholesterol in the liver. This result is in agreement with the findings of others with clofibrate (20, 33, 34) and clearly separates this hepatomegalic condition from the pathological types of fatty liver that have high levels of triglyceride and cholesterol esters associated in fat droplets. The increased amounts of phospholipids and proteins are probably associated with membranes of subcellular organelles. Upon cessation of drug administration, the hepatomegaly and ultrastructural changes induced by clofibrate were readily reversible (18, 19, 35).

These data might indicate that the primary event after administration of either clofibrate or I is an induction of enzyme protein resulting from

[14] SaH 42-348, Sandoz Pharmaceuticals, East Hanover, N.J.
[15] Su-13437, Ciba Pharmaceutical Co., Summit, N.J.

[16] S. A. Kaplan, D. E. Maynard, A. Maggio, V. Mattaliano, C. Abruzzo, and S. Cotler, to be published.

a functional enlargement of the liver. The induction of rat liver microsomal enzymes after clofibrate and I treatment is in agreement with a similar observation in rats treated with clofibrate and III (36). Clofibrate and I also increased mitochondrial protein and phospholipid content, effects that are difficult to link with drug metabolism. Our observation, however, is consistent with the increase in number (37) and protein content of the mitochondria (38) produced after clofibrate administration. These intracellular structural changes and the broad influence of clofibrate and related drugs on mitochondrial enzyme activity (39–41) are difficult to explain but may be related to the protein binding capacity of these drugs (33).

REFERENCES

(1) M. F. Oliver, in "Atherosclerosis: Proceedings of the 2nd International Symposium," R. J. Jones, Ed., Springer-Verlag, New York, N.Y., 1970, p. 582.

(2) J. Stamler, in *ibid.*, p. 586.

(3) L. Berger and A. J. Corraz, U.S. pat. 3,862,953 (Jan. 28, 1975).

(4) G. Kessler and H. Lederer, in "Automation in Analytical Chemistry," L. T. Skeggs, Jr., Ed., Mediad, New York, N.Y., 1966, p. 341.

(5) W. Schneider, *J. Biol. Chem.*, **176,** 259 (1948).

(6) W. D. Block, K. J. Jarrett, and J. B. Levine, in "Automation in Analytical Chemistry," L. T. Skeggs, Jr., Ed., Mediad, New York, N.Y., 1966, p. 345.

(7) R. Whitely and H. Alburn, *Ann. N. Y. Acad. Sci.*, **130,** 634 (1965).

(8) C. Dalton and C. Kowalski, *Clin. Chem.*, **13,** 744 (1967).

(9) J. Folch, M. Lees, and G. H. S. Stanley, *J. Biol. Chem.*, **226,** 497 (1957).

(10) C. Dalton and D. DiSalvo, *Technicon Quart.*, **3,** 20 (1972).

(11) J. Axelrod, *J. Pharmacol. Exp. Ther.*, **117,** 322 (1956).

(12) P. C. Barbato, G. R. Umbreit, and R. J. Leibrand, "Applications Laboratory Report 1005," Hewlett-Packard, Avondale, Pa., 1966, p. 1.

(13) M. Rodbell, *J. Biol. Chem.*, **239,** 375 (1964).

(14) J. P. Mallon and C. Dalton, *Anal. Biochem.*, **40,** 174 (1971).

(15) H. Luck, in "Methods of Enzymatic Analysis," H. U. Bergmeyer, Ed., Academic, New York, N.Y., 1965, p. 885.

(16) L. C. Miller and M. L. Tainter, *Proc. Soc. Exp. Biol. Med.*, **57,** 261 (1944).

(17) C. Dalton, W. C. Hope, H. R. Hope, and H. Sheppard, *Biochem. Pharmacol.*, **23,** 685 (1974).

(18) D. Svoboda and D. Azarnoff, *J. Biol. Chem.*, **30,** 442 (1966).

(19) D. Svoboda, H. Grady, and D. Azarnoff, *J. Cell Biol.*, **35,** 127 (1967).

(20) M. M. Best and C. H. Duncan, *J. Lab. Clin. Med.*, **64,** 634 (1964).

(21) A. R. Timms, L. A. Kelly, R. S. Ho, and J. H. Trapold, *Biochem. Pharmacol.*, **18,** 1861 (1969).

(22) R. Hess and W. L. Bencze, *Experientia*, **24,** 418 (1968).

(23) J. A. F. de Silva, N. Strojny, F. Rubio, J. C. Meyer, and B. A. Koechlin, *J. Pharm. Sci.*, **66,** 353 (1977).

(24) J. M. Thorp, *J. Atheroscler. Res.*, **3,** 351 (1963).

(25) D. R. Avoy, E. A. Swyryd, and R. G. Gould, *J. Lipid Res.*, **6,** 369 (1965).

(26) M. E. Maragoudakis, *J. Biol. Chem.*, **244,** 5005 (1969).

(27) D. Kritchevsky and S. A. Tepper, *Fed. Proc.*, **27,** 822 (1968).

(28) R. G. Gould, E. A. Swyryd, D. Avoy, and B. Coan, "Progress in Biochemical Pharmacology," vol. 2, D. Steinberg, Ed., S. Karger, New York, N.Y., 1967, p. 345.

(29) W. G. Ryan and T. B. Schwartz, *J. Lab. Clin. Med.*, **64,** 1001 (1964).

(30) S. M. Grundy, E. A. Ahrens, G. Salen, and E. Quintao, *J. Clin. Invest.*, **48,** 33a (1969).

(31) L. A. Carlson and E. R. Nye, *Acta Med. Scand.*, **179,** 453 (1966).

(32) C. Dalton, C. Kowalski, J. Mallon, and C. Marschhaus, *J. Atheroscler. Res.*, **8,** 265 (1968).

(33) J. M. Thorp and W. S. Waring, *Nature*, **194,** 948 (1962).

(34) R. G. Gould, E. A. Swyryd, B. J. Coan, and D. R. Avoy, *J. Atheroscler. Res.*, **6,** 555 (1966).

(35) R. Hess, W. Straubli, and W. Reiss, *Nature*, **208,** 856 (1965).

(36) R. A. Salvador, S. Haber, S. Atkins, B. W. Gommi, and R. M. Welch, *Life Sci.*, **9,** 397 (1970).

(37) G. E. Paget, *J. Atheroscler. Res.*, **3,** 729 (1963).

(38) C. K. R. Kurup, H. N. Aithal, and T. Ramasarma, *Biochem. J.*, **116,** 773 (1970).

(39) D. S. Platt and B. L. Cockrill, *Biochem. Pharmacol.*, **15,** 927 (1966).

(40) *Ibid.*, **16,** 2257 (1967).

(41) U. Schacht and E. Granzer, *Biochem. Pharmacol.*, **19,** 2963 (1970).

ACKNOWLEDGMENTS AND ADDRESSES

Received March 1, 1976, from the *Departments of Pharmacology and Toxicology, Roche Research Center, Hoffmann-La Roche Inc., Nutley, NJ 07110.*

Accepted for publication May 18, 1976.

The authors thank Dr. L. O. Randall for support, Mr. L. Berger for chemical analogs, and Robert Scism, Diane DiSalvo, William C. Hope, Theordore C. Van Trabert, Janie B. Quinn, Dorothy Hane, and Helen Reich for assistance.

[x] To whom inquiries should be directed.

Spectrofluorometric Determination of Substituted Tetrahydrocarbazoles by a Methylene Blue Sensitized Photolytic Reaction

J. ARTHUR F. de SILVA [x], NORMAN STROJNY, FELIX RUBIO, JOHN C. MEYER, and BERNARD A. KOECHLIN

Abstract □ A spectrofluorometric method was developed for the determination of 6-chloro-9-[2-(2-methyl-5-pyridyl)ethyl]-1,2,3,4-tetrahydrocarbazole-2-methanol hydrochloride and its carboxylic acid analog in blood and urine. It involves extraction of both compounds at neutral pH, either from blood into ethyl acetate (the residue of which is dissolved in ether) or from urine directly into ether. Both the alcohol and the acid are separated from each other by selective extraction into acid or base, respectively, and then reextracted into ether from the respective aqueous medium by appropriate pH adjustment. The residues of the ether extracts containing the compounds are dissolved separately in 0.25 *N* NH_4OH. Methylene blue is added to all samples, which are then exposed to UV energy for 15 min to produce the fluorophores. The fluorescence of the solutions is read at 370 nm, with excitation at 340 nm. The linear range of quantitation of both compounds is 0.02–10 μg each/ml of final solution. The method was applied to the determination of blood levels and urinary excretion of the alcohol and its acid metabolite in a dog.

Keyphrases □ Tetrahydrocarbazoles, substituted—spectrofluorometric analysis, human blood and urine □ Spectrofluorometry—analysis, various substituted tetrahydrocarbazoles, human blood and urine □ Photolytic reactions—substituted tetrahydrocarbazoles sensitized with methylene blue, spectrofluorometric analysis, human blood and urine □ Antihyperlipidemic agents, potential—various substituted tetrahydrocarbazoles, spectrofluorometric analysis, human blood and urine

Compounds containing the indole moiety have been extensively studied because of their anti-inflammatory (1–4), analgesic, and hallucinogenic (5–7) properties, their inhibition of monoamine oxidase (8), and their cardiovascular effects (5). The compound 6-chloro-9-[2-(2-methyl-5-pyridyl)ethyl]-1,2,3,4-tetrahydrocarbazole-2-methanol (I) hydrochloride and its 2-carboxylic acid analog (II) hydrochloride were synthesized (9) and are of clinical interest, because they have shown marked hypolipidemic activity in animals (10).

Spectrofluorometric analysis of catecholamines (levarterenol and epinephrine) as their trihydroxyindole derivatives has led to the use of condensation reactions to produce fluorescent derivatives. Condensation reactions have been used to determine: (*a*) catecholamines that condense with formaldehyde to form highly fluorescent 3,4-dihydroisoquinolines (11), (*b*) 5-hydroxytryptamine by condensation with *o*-phthalaldehyde as the phthalimidine derivatives (12) and with ninhydrin as the β-carboline derivative (13), (*c*) indole-3-acetic acid by condensation with acetic anhydride (catalyzed with boron trifluoride) as the highly fluorescent indolo-α-pyrone derivative (14), and (*d*) tryptophan by photolytic condensation with acetic acid, using methylene blue as a "sensitizer," to yield highly fluorescent β-carboline derivatives (15, 16).

A spectrofluorometric assay was developed for the quantitation of I and II in blood and urine based on a photolytic reaction of the tetrahydrocarbazole to produce a fluorophore of strong intrinsic fluorescence. The reaction is performed in an alkaline medium catalyzed by methylene blue used as a sensitizer. The overall recovery of both compounds from blood and urine is 90 ± 5.0%. The assay is specific for each compound by virtue of the differential extraction procedure used and has a sensitivity limit of 0.10–0.20 μg/ml of blood or urine using a 2-ml specimen/assay and a sample to blank fluorescence ratio of 2:1 as the limit of detectability.

The method was applied to the determination of the blood levels of I and the urinary excretion of I and its metabolite, II, in a dog following a single intravenous dose of 10 mg/kg.

EXPERIMENTAL

Standard Solutions—Compound I hydrochloride, mol. wt. 391.34, mp 191–193°, and Compound II hydrochloride, mol. wt. 405.33, mp 218.5–220° (pharmaceutical grade purity >98%), are the analytical standards required.

Dissolve 11.02 mg of I hydrochloride and 11.00 mg of II hydrochloride equivalent to 10 mg of the respective free base or acid separately in 100 ml of methanol to give stock solutions containing 100 μg of free base/ml. Dilute 1 ml of each stock solution separately in 10 ml of methanol to give working solutions containing 10 μg/ml, suitable aliquots of which are added to blood or urine as internal standards for the determination of percent recovery. Prepare all solutions in amber actinic volumetric flasks and store in a refrigerator.

Instrument—The spectrofluorometer[1] used was equipped with a 150-w xenon arc energy source[2] and photomultiplier[3]. It was used with the 10-nm slit arrangement in all four positions, with the instrument energy adjusted for maximum sensitivity using a Pyrex reference rod and a standard solution of the compound(s) to be analyzed.

Reagents—All reagents were analytical reagent grade (ACS) and were used without further purification; all aqueous solutions were made in distilled deionized water. These solutions included 1.0 *M* (pH 7.0) phosphate buffer, 2 *N* HCl, 0.5 and 10.0 *N* NaOH, 0.25 *N* NH_4OH, and 0.025% methylene blue[4] (USP grade dissolved in water). Ethyl acetate[5] (spectrograde), ether[5] (absolute) from a freshly opened can, chloroform[6], and formaldehyde[7] (37%) were the other reagents used.

Assay in Blood—To 50-ml glass-stoppered centrifuge tubes, add 2 ml of whole blood, 2.0 ml of 1.0 *M* pH 7 buffer, 1.5 g of potassium chloride, and 10 ml of ethyl acetate. Stopper[8] the tubes and extract by shaking for 10 min on a reciprocating shaker. Centrifuge the samples at 0–5° in a refrigerated centrifuge at 2000 rpm for 10 min and transfer the supernate to another 50-ml centrifuge tube. Along with the samples, process a 2-ml specimen of control blood and three 2-ml specimens of control blood to which 0.5, 2.5, and 5.0 μg of I and II (0.05, 0.25, and 0.5 ml of the respective working solutions evaporated to dryness at 40–50° under nitrogen) are added as internal standards.

Repeat the extraction with another 10 ml of ethyl acetate, combine the extracts, and evaporate to dryness under nitrogen in a 60° water bath. Dissolve the residues in 15 ml of ether. Add 5 ml of 0.5 *N* NaOH to the

[1] Model Mark I, Farrand Optical Co., Mount Vernon, N.Y. The spectrofluorometer was equipped with a specially selected high UV energy source and photomultiplier.
[2] Hanovia lamp, Engelhardt Industries, Newark, N.J.
[3] RCA 1-P-28 (lumen output >10).
[4] Eastman Chemical Co.
[5] Mallinckrodt Chemical Co.
[6] Fisher Scientific Co.
[7] Allied Chemical Co.
[8] Teflon stoppers (du Pont).

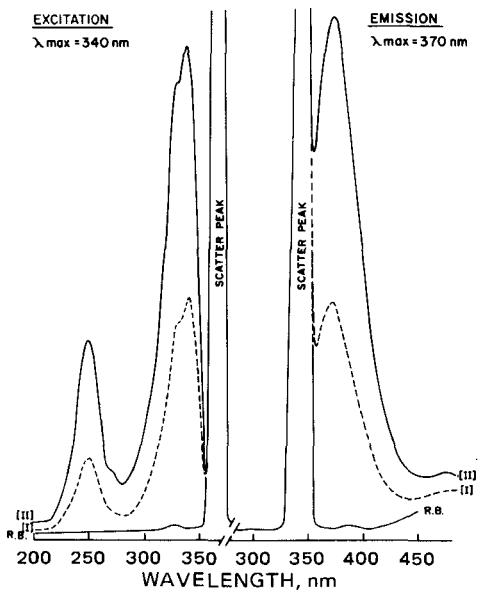

Figure 1—*Excitation and emission spectra of the photochemically produced fluorophores of I and II determined at room temperature for equivalent concentrations of 5 μg/ml.*

ether phase, extract by shaking, centrifuge, and transfer the supernatant ether quantitatively into another 50-ml tube. Wash the sodium hydroxide solution with 10 ml of ether by shaking, centrifuge, and combine the ether wash with the original ether extract. The sodium hydroxide phase contains the carboxylic acid (II) while the ether supernate contains the alcohol (I).

Add 5 ml of 2 *N* HCl to the ether extract containing I and shake for 10 min. Then centrifuge, aspirate, and discard the ether layer. Wash the acid phase containing I with another 10-ml portion of ether, shake, centrifuge, and aspirate off the ether as before. Neutralize the acid with 1.0 ml of 10 *N* NaOH, add 5 ml of 1.0 *M* pH 7.0 phosphate buffer, and extract with 2 × 10-ml aliquots of ether by shaking for 10 min per extraction. Centrifuge and then combine the ether extracts in another 50-ml centrifuge tube.

Evaporate the ether extracts containing I to dryness and dissolve the residues in 5 ml of 0.25 *N* NH_4OH. Add 0.1 ml of 0.025% methylene blue solution to each series containing I and II, and mix well on a Vortex action supermixer. Expose all samples to UV energy[9] for exactly 15 min, placing the tubes in a single row approximately 30.5 cm (12 in.) in front of the lamp. After irradiation, to the sample series containing I *only*, immediately add 0.25 ml of formaldehyde to reduce the excess methylene blue reagent to stop any further autocatalyzed photochemical reaction. The final solution is turquoise blue in color, and its fluorescence is read directly. The blue color does not apparently affect the fluorescence reading of I, since the fluorescence due to the reagent blank is quite low. Wash the sample series containing II, which are reddish purple in color, with 5 ml of chloroform to remove the colored material from the sodium hydroxide phase, resulting in a colorless solution containing the fluorophore of II.

The fluorescence of all solutions is read in a 1-cm path quartz cell at 370 nm, with excitation at 340 nm (Fig. 1).

Calculations—Correct all sample readings for their respective control (blank) reading and calculate the concentrations of I and II in the unknowns by interpolation of the fluorescence readings from their respective internal standard curves. The percent recovery from blood or urine is determined by direct comparison of the fluorescence of known amounts of the internal standards against that of similar concentrations of the external standards processed along with the samples to standardize the process of fluorophore formation. The percent recovery of the internal standards should be determined routinely as a check on the reproducibility of the method.

Assay in Urine—To 5 ml of urine in a 50-ml erlenmeyer flask (adjusted approximately to pH 5.5 with 1 *N* HCl), add 5 ml of 0.2 *M* (pH 5.5) acetate buffer and 200 μl of the glucuronidase–sulfatase preparation[10] (2% by volume). Along with the unknowns, process 3 × 5-ml specimens of control urine containing internal standards of I and II added in the same concentrations as in the blood assay.

Incubate all samples at 37° for 2 hr in an incubation shaker[11]. Cool to room temperature and transfer the specimens to 50-ml centrifuge tubes. Titrate the specimen to pH 7.0 with 2 *N* NaOH, add 5 ml of 1.0 *M* (pH 7.0) phosphate buffer and 5.0 g of potassium chloride, and extract with 2 × 10-ml aliquots of ether by shaking for 10 min on a reciprocating shaker. Centrifuge the samples for 10 min (at 0–5° in a refrigerated centrifuge) at 2000 rpm and combine the ether extracts in another 50-ml centrifuge tube. Process the samples from this point using the differential extraction procedure described for blood.

RESULTS AND DISCUSSION

The intense fluorescence of carbazole and polynuclear carbazoles was used in their quantitation in the nanogram range (17). Therefore, the fluorometric analysis of the tetrahydrocarbazoles (I and II) by chemical oxidation to their aromatized carbazole derivatives was investigated. Several oxidation reactions were attempted but did not yield a suitable fluorophore.

A photochemical reaction using methylene blue as a catalytic sensitizer, reported for the formation of highly fluorescent β-carbolines (15, 16), was investigated and gave the most reproducible and optimal yields of a fluorophore for both I and II.

Methylene blue is highly soluble in water, yielding a deep-blue solution (λ_{max} 609 and 668 nm). The free base can be quantitatively extracted into organic solvents (chloroform) at alkaline pH. This fact was used to advantage in the analysis of II in that the reagent was extracted, resulting in a colorless solution of 0.5 *N* NaOH containing the fluorophore of II. This "cleanup" step is not possible in the analysis of I, since both the reagent and the fluorophore are coextracted into organic solvents.

The presence of the methylene blue reagent in the analysis of I appears to catalyze the further reaction of I or its fluorophore, since the fluorescence readings increased on standing, resulting in poor reproducibility, especially in 0.5 *N* NaOH. Formaldehyde was used to oxidize the excess methylene blue to a turquoise blue-colored product, which stabilized the fluorophore of I. The absorption maximum of this colored product (350–400 nm) apparently absorbs sufficient UV energy during fluorometric analysis (excitation of 340 and emission of 370 nm) to quench the fluorescence of I compared to that of II where the methylene blue reagent has been removed.

This fact is seen in the spectra of the photochemical products of the two compounds (Fig. 1) for equivalent concentrations of 5 μg/ml of each. The peak heights of the excitation–emission spectra of I were about half those of II, both determined at the same instrument settings. This difference was probably due to a quenching effect and/or to the fact that the fluorophore of I is chemically different from that of II (Schemes I and II). The fluorescence of the two reaction products, however, was linear with concentration over 0.10–5.0 μg/ml of final solution, with excitation at 340 nm and emission at 370 nm for each compound (Fig. 1).

Characterization of Fluorophores of I and II—Characterization of the reaction products of I and II was attempted following their separation by TLC. Compounds I and II (100 μg of each) were reacted separately as previously described. The reaction products of I were extracted into ether from the reaction medium (0.25 *N* NH_4OH) following neutralization with 1 *N* HCl and pH adjustment with 1 *M* pH 7.0 buffer. The reaction products of II were extracted into ethyl acetate–1-butanol (80:20) following acidification of the reaction medium (0.5 *N* NaOH) with 2 *N* HCl and pH adjustment to 5.5 with 1 *M* phosphate buffer.

The respective organic solvent extracts were evaporated to about 100 μl, transferred quantitatively onto silica gel chromatoplates[12], and developed to 15 cm in acetone–ammonium hydroxide (90:10). In the respective extracts, I migrated with R_f Ω 0.9; its reaction product had R_f Ω 0.7, while II had R_f Ω 0.2 and its reaction product had R_f Ω 0.3. The respective reaction products were eluted from the silica gel into ethanol and then examined by UV absorption, fluorescence, and phosphorescence emission spectrophotometry.

The UV spectra of the authentic compounds in methanol showed a major band at 235–237 nm with minor bands at 265 and 290 nm. Fol-

[9] Pyro-Lux R-57 lamp (Luxor Corp., New York, N.Y.), contained in an aluminum foil-lined reflector box of sufficient size [61 × 61 × 61 cm (2 × 2 × 2 ft)] for adequate ventilation.

[10] Glusulase enzyme preparation containing 100,000 units of glucuronidase and 50,000 units of sulfatase/ml, Endo Laboratories, Garden City, N.Y.

[11] Dubnoff, GCA/Precision Scientific, Chicago, Ill.

[12] E. Merck F_{254} silica gel G, 60-μm particle size, 250-μm bed thickness, Brinkmann Instruments, Westbury, N.Y.

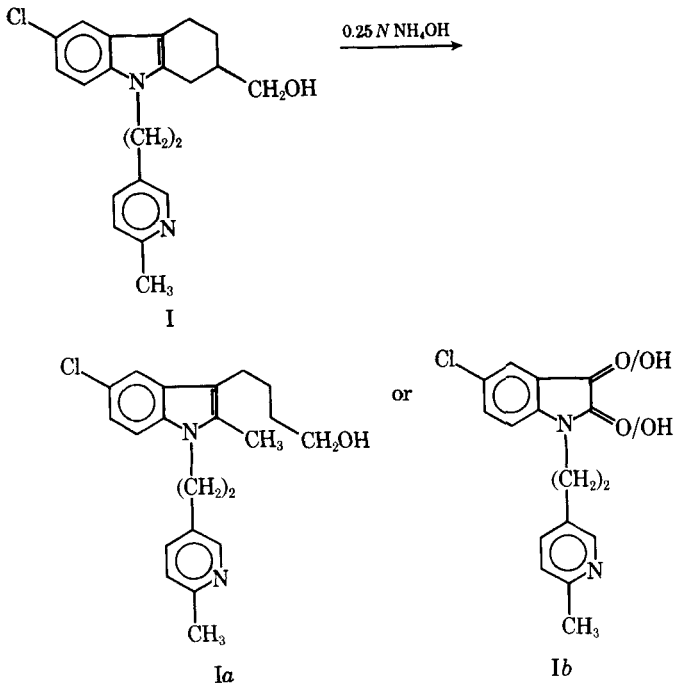

Scheme I

lowing photochemical reaction, the spectrum of I showed a bathochromic shift to 258 nm with secondary peaks at 330 and 343 nm, respectively. The spectrum of II also showed a similar bathochromic shift to longer wavelengths, with the major band at 250 nm and minor bands at 308, 330, and 345 nm. These UV spectral changes indicated major structural changes.

The fluorescence spectra of the reaction products of I and II (5 μg/ml) at room temperature (Fig. 1) were practically identical. Both exhibited excitation maxima at 250 and 340 nm and a broad emission maximum at 370 nm; the excitation bands corresponded fairly well with the UV absorption maxima of the reaction products.

Further insight into the character of these products was sought from a comparison of their phosphorescence spectra (77° K) in ethanol (18) with those of I and II. The spectra showed characteristic differences, permitting certain structural deductions by reference to spectra of known analogous compounds (19). The phosphorescence spectra of unreacted authentic I (Fig. 2A) and II (Fig. 3A) were almost identical, with excitation–emission maxima at 305 and 455 nm, respectively. The excitation spectra of both reaction products possessed considerable fine structure. The spectrum of I (Fig. 2A) had excitation maxima at 250, 330, and 345 nm (major bands); that of II (Fig. 3A) had maxima at 250, 315 (major bands), 340, 350, 365, and 380 nm, indicating a higher degree of aromaticity.

The emission spectrum of the reaction product of I showed a hypsochromic shift to a single maximum at 445 nm; that of II showed a similar

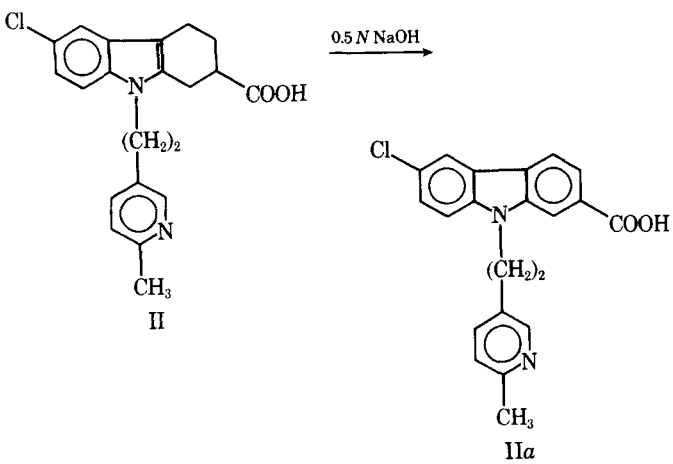

Scheme II

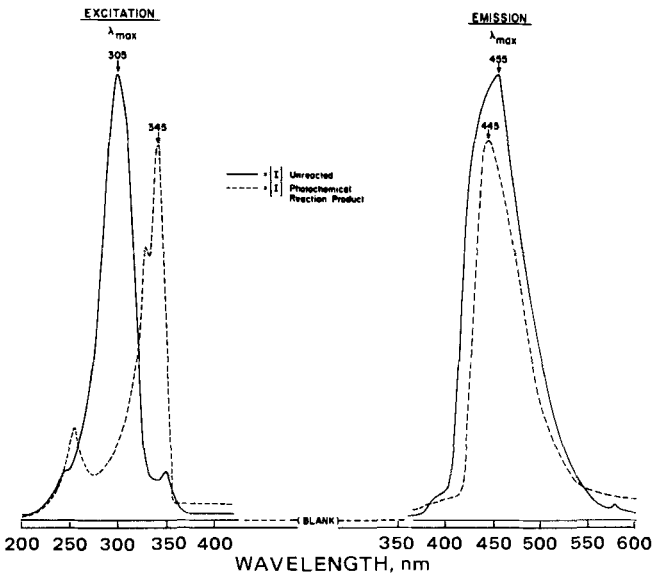

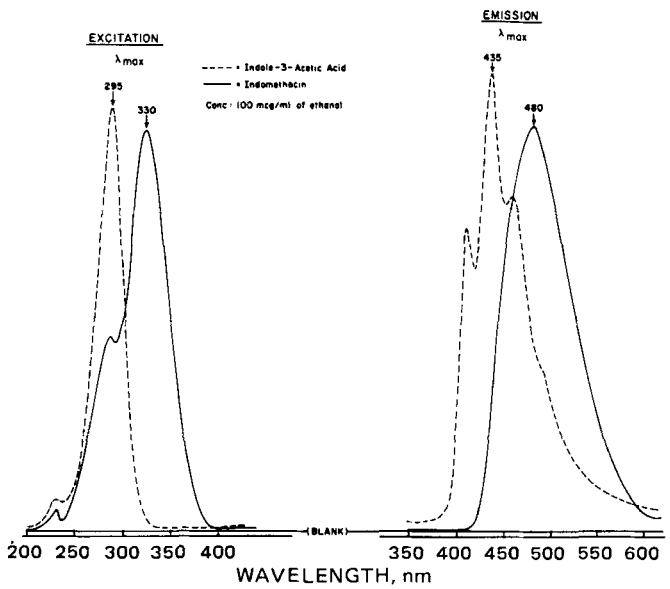

Figure 2—*Phosphorescence spectra in ethanol (77° K) of (top) authentic I and its photochemical reaction product and (bottom) indole acetic acid and indomethacin.*

shift, with a characteristic doublet at 440 and 450 nm of approximately equal intensity. The striking differences in the phosphorescence spectra suggested marked structural differences in the respective reaction products.

The phosphorescence excitation–emission spectrum of the reaction product of I (Fig. 2A) exhibited maxima at 345 and 445 nm, respectively. The absence of a high degree of fine structure suggests that it is not a carbazole derivative. The phosphorescence spectral characteristics were fairly similar to that of indomethacin, whose excitation–emission maxima were at 330 and 480 nm, respectively (also with very little fine structure). Indole-3-acetic acid (III), whose excitation–emission maxima were at 295 and 435 nm, respectively, showed a more complex emission spectrum (Fig. 2B) (20) than either indomethacin (IV) or the reaction product of I. This result was probably due to a reduction of the aromaticity of the indole ring in indomethacin and in the reaction product of I because of the electron-withdrawing effects of the *p*-chlorobenzoyl group in the former and the *p*-methyl-3-pyridylethyl group in the latter, which are attached to the indole nitrogen.

These similarities suggest that the tetrahydrocarbazole ring has either been partially cleaved, resulting in a product structurally similar to indomethacin (Scheme I, Ia), or totally cleaved with possible concomitant oxidation of the indole ring to an indoxyl derivative (Scheme I, Ib). The formation of such an indole or indoxyl derivative could also lead to further

Table I—Luminescence Properties of I and II, Their Photochemical Reaction Products, and the Analogous Carbazole, V, as a Reference Compound

Compound	Fluorescence (25°) Excitation/ Emission Maxima, nm	Intensity, $TM^a/\mu g/ml$	Sensitivity Limit, $\mu g/ml$	Phosphorescence (77° K) Excitation/ Emission Maxima, nm	Intensity, $TM/\mu g/ml$	Sensitivity Limit, $\mu g/ml$
I	—	Nil 100 $\mu g/ml$	>100 $\mu g/ml$	302/455	10	10.0
I Reaction product	340/370	250	0.2	345/445	Ω 300	0.5[b]
II	—	Nil	>100 $\mu g/ml$	305/450	10	10.0
II Reaction product	340/370	550	0.1	305/445	Ω 450	0.5[b]
V	310/400	1250	0.02	312/445, 475	4100	0.001

[a] Fluorescence (TM) units = transmittance (T) × meter multiplier factor (M). [b] Phosphorescence of the reaction products of I and II was approximately corrected for reaction efficiency, extraction efficiency, and efficiency of TLC elution.

reaction under the photolytic conditions to form other condensation products which would be difficult to isolate (21).

The phosphorescence excitation–emission spectrum of the reaction product of II (Fig. 3A) was similar in its fine structure to that of 6-chloro-2-carbazolecarboxylic acid (V) (Fig. 3B). The excitation spectrum of the reaction product of II and V exhibited similar fine structure with multiple peaks at 250, 300, 315 (major bands), 340, 350, and 365 nm. The emission spectra of the reaction product of II and V exhibited a characteristic doublet with maxima at 430 and 445 nm for II and 445 and 475 nm for V. The similarities in the spectral characteristics of the photochemical reaction product of II to those of V and of other known carbazoles (17, 18, 22) strongly suggest that it is a carbazole derivative (Scheme II, II*a*). Attempts to characterize these products further by electron-impact mass spectrometry were unsuccessful due to the poor fragmentation patterns obtained.

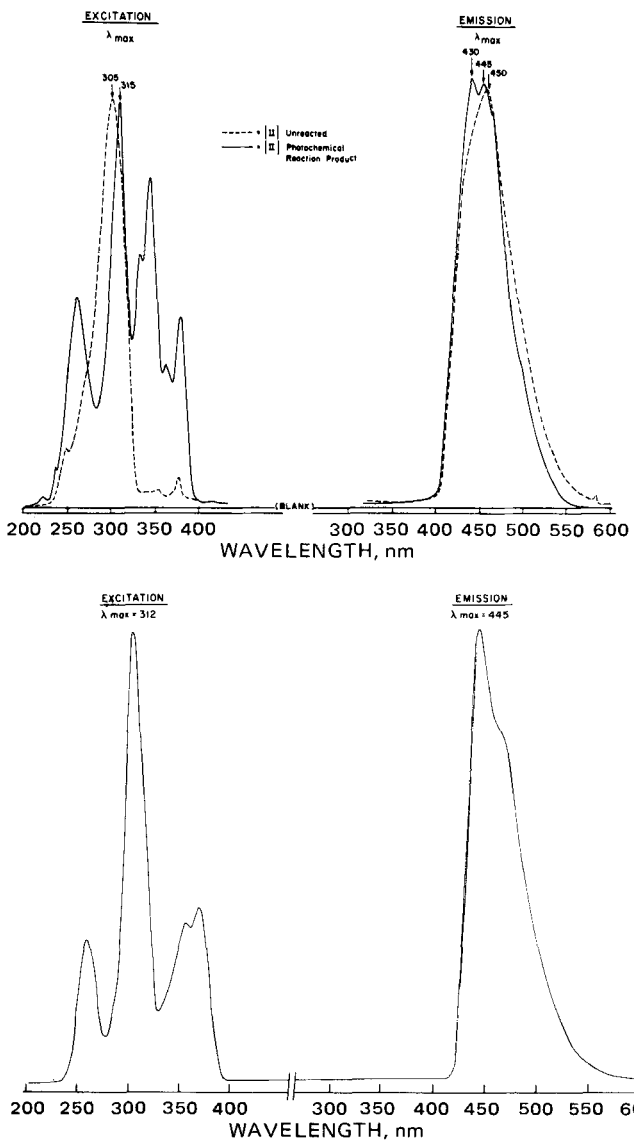

Figure 3—*Phosphorescence spectra in ethanol (77° K) of (top) authentic II and its photochemical reaction product compared with that of (bottom) V, a 9-unsubstituted analog. (Attenuation = 3×.)*

The relative sensitivities of the luminescence properties of I, II, their photochemical reaction products, and the analogous carbazole (V) are given in Table I. Compounds I and II had no measurable fluorescence at room temperature, whereas their intrinsic phosphorescence provided detection limits of 10 μg for I and 0.5–1.0 μg for II and can also be used to analytical advantage where high sensitivity is not a requirement.

Assay Specificity—Preliminary studies in the dog indicated that the carboxylic acid analog, II, is not a major metabolite. Compound I is excreted as a glucuronide conjugate in the urine and feces[13]. However, the presence of small amounts of II in blood or urine would impair the accuracy of the assay for I if it is not resolved from it, because of the relatively high fluorescence yield of its photochemical reaction product.

The spectrofluorometric assay is specific for each compound due to the differential extraction procedure used to separate the two compounds prior to photochemical irradiation and quantitation. The overall recovery of I hydrochloride or II hydrochloride added to blood or urine in the concentration range of 0.10–10.0 $\mu g/ml$ is of the order of 90 ± 5.0% (SD). The sensitivity limits of the assay for I and II are 0.15–0.20 and 0.10–0.15 $\mu g/ml$, respectively, of blood or urine using a 2-ml specimen per assay and a sample–blank fluorescence ratio of 2:1 as the limit of quantitation.

Applications to Biological Specimens—The blood levels and urinary excretion of I and II (produced as a metabolite) were determined in a pilot study in a dog following administration of a single 10-mg/kg iv dose of

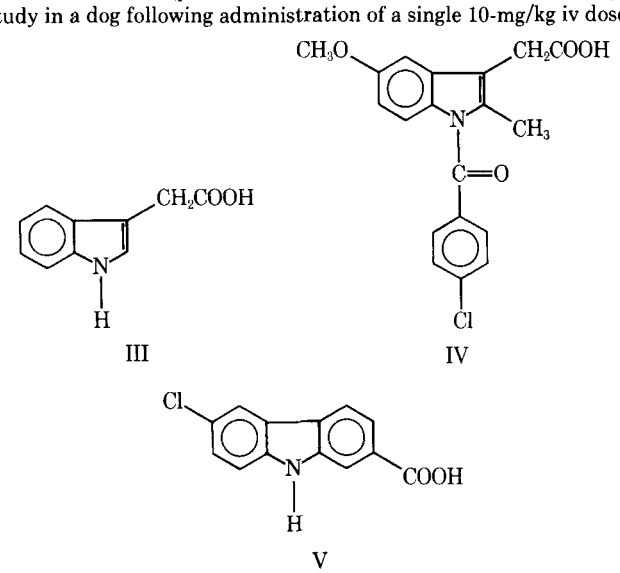

[13] S. A. Kaplan, D. E. Maynard, A. Maggio, V. Mattaliano, C. Abruzzo, and S. Cotler, to be published.

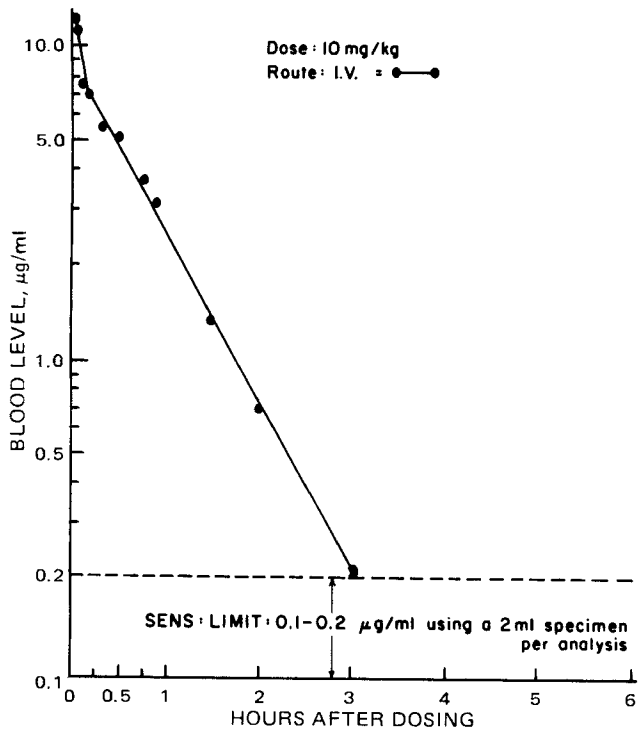

Figure 4—*Blood level curves of I in a dog following the administration of a single 10-mg/kg iv dose of I hydrochloride.*

I hydrochloride. The blood levels of the intact drug I (Fig. 4) showed a biphasic fall-off pattern with an apparent half-life of elimination of about 30 min. Urinary excretion of the parent drug accounted for only 0.1% of the administered dose, present mainly as a glucuronide–sulfate conjugate. No measurable levels of II were seen in either the blood or urine. The utility of the assay was demonstrated in the evaluation of the biopharmaceutic and pharmacokinetic profile of the drug in the dog[13].

REFERENCES

(1) H. J. Sanders, *Chem. Eng. News*, **Aug. 12, 1968,** 46.

(2) R. E. Harman, M. A. P. Meisinger, G. E. Davis, and F. A. Kuehl, *J. Pharmacol. Exp. Ther.*, **143,** 215 (1964).

(3) H. B. Hucker, A. G. Zacchei, S. V. Cox, D. A. Brodie, and N. H. R. Cantwell, *ibid.*, **153,** 237 (1966).

(4) D. E. Duggan, A. F. Hogans, K. C. Kwan, and F. G. McMahon, *ibid.*, **181,** 563 (1972).

(5) T. A. Slotkin, V. di Stefano, and W. Y. W. Au, *ibid.*, **173,** 26 (1970).

(6) T. A. Slotkin and V. di Stefano, *Biochem. Pharmacol.*, **19,** 125 (1970).

(7) T. A. Slotkin and V. di Stefano, *J. Pharmacol. Exp. Ther.*, **174,** 456 (1970).

(8) B. T. Ho, W. M. McIssac, and K. E. Walker, *J. Pharm. Sci.*, **57,** 1364 (1968).

(9) L. Berger and A. J. Corraz, U.S. pat. 3,862,953 (Jan. 28, 1975) and U.S. pat. 3,896,145 (July 22, 1975).

(10) C. Dalton and W. R. Pool, *J. Pharm. Sci.*, **66,** 348 (1977).

(11) H. Corradi and N. A. Hillarp, *Helv. Chim. Acta*, **46,** 2425 (1963).

(12) R. P. Maickel and F. P. Miller, *Anal. Chem.*, **38,** 1937 (1966).

(13) W. B. Quay, *J. Pharm. Sci.*, **57,** 1568 (1968).

(14) A. Stoessl and M. A. Venis, *Anal. Biochem.*, **34,** 344 (1970).

(15) G. Jori, G. Galiazzo, and G. Gannari, *Photochem. Photobiol.*, **9,** 179 (1969).

(16) G. Cauzzo and G. Jori, *J. Org. Chem.*, **37,** 1429 (1972).

(17) M. Zander "Phosphorimetry—The Application of Phosphorescence to the Analysis of Organic Compounds," Academic, New York, N.Y., 1968, pp. 95–106, 158–194.

(18) J. A. F. de Silva, N. Strojny, and K. Stika, *Anal. Chem.*, **48,** 144 (1976).

(19) J. N. Bridges and R. T. Williams, *Biochem. J.*, **107,** 225 (1968).

(20) W. A. Remers, in "Indoles," part I, W. J. Houlihan, Ed., in "The Chemistry of Heterocyclic Compounds," A. Weissberger and E. C. Taylor, Eds., Wiley, New York, N.Y., 1972, pp. 19–33.

(21) R. J. Sundberg, "The Chemistry of Indoles," in "Organic Chemistry," A. T. Blomquist, Ed., Academic, New York, N.Y., 1970, pp. 282–315.

(22) N. Strojny and J. A. F. de Silva, *J. Chromatogr. Sci.*, **13,** 583 (1975).

ACKNOWLEDGMENTS AND ADDRESSES

Received March 1, 1976, from the *Department of Biochemistry and Drug Metabolism, Hoffmann-La Roche Inc., Nutley, NJ 07110.*

Accepted for publication May 18, 1976.

The authors thank Mr. L. Berger of the Chemical Research Division for the authentic standards and chemical analogs and Mr. R. McGlynn for the drawings.

[x] To whom inquiries should be directed.

Oxidative Reactions of Hydroxylated Chlorpromazine Metabolites

RICHARD L. McCREERY

Abstract □ The oxidation pathways of two hydroxylated chlorpromazine metabolites were investigated using modern electrochemical techniques. Upon oxidation, the 7-hydroxy derivative of chlorpromazine rapidly reacts to form the 7,8-dihydroxy derivative and a substituted quinone. The oxidation potentials for both compounds were determined in the pH 3–8 range. The importance of these redox reactions and potentials to the pharmacology of the materials is discussed.

Keyphrases □ Chlorpromazine metabolites—oxidation pathways, electrochemical study, pH 3–8 □ Oxidation pathways—hydroxylated chlorpromazine metabolites, electrochemical study, pH 3–8 □ Electrochemistry—study of oxidation pathways of hydroxylated chlorpromazine metabolites □ Tranquilizers—chlorpromazine metabolites, electrochemical study of oxidation pathways

The widespread use of phenothiazine derivatives in the treatment of mental illness has inspired a large amount of research on their chemical properties and reactions. Of relevance to the present discussion are studies of the importance of redox reactions to the metabolism and mode of action of chlorpromazine and related neuroleptic drugs.

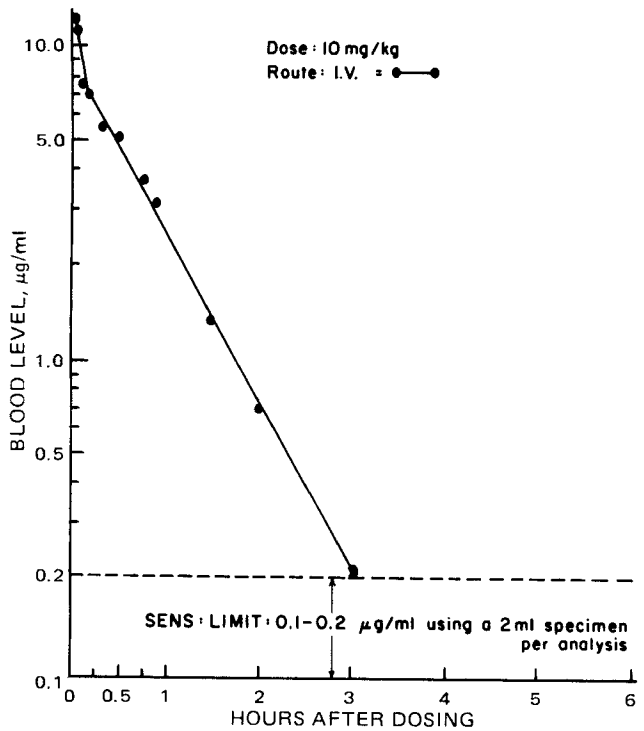

Figure 4—*Blood level curves of I in a dog following the administration of a single 10-mg/kg iv dose of I hydrochloride.*

I hydrochloride. The blood levels of the intact drug I (Fig. 4) showed a biphasic fall-off pattern with an apparent half-life of elimination of about 30 min. Urinary excretion of the parent drug accounted for only 0.1% of the administered dose, present mainly as a glucuronide–sulfate conjugate. No measurable levels of II were seen in either the blood or urine. The utility of the assay was demonstrated in the evaluation of the biopharmaceutic and pharmacokinetic profile of the drug in the dog[13].

REFERENCES

(1) H. J. Sanders, *Chem. Eng. News*, **Aug. 12, 1968,** 46.

(2) R. E. Harman, M. A. P. Meisinger, G. E. Davis, and F. A. Kuehl, *J. Pharmacol. Exp. Ther.*, **143,** 215 (1964).

(3) H. B. Hucker, A. G. Zacchei, S. V. Cox, D. A. Brodie, and N. H. R. Cantwell, *ibid.*, **153,** 237 (1966).

(4) D. E. Duggan, A. F. Hogans, K. C. Kwan, and F. G. McMahon, *ibid.*, **181,** 563 (1972).

(5) T. A. Slotkin, V. di Stefano, and W. Y. W. Au, *ibid.*, **173,** 26 (1970).

(6) T. A. Slotkin and V. di Stefano, *Biochem. Pharmacol.*, **19,** 125 (1970).

(7) T. A. Slotkin and V. di Stefano, *J. Pharmacol. Exp. Ther.*, **174,** 456 (1970).

(8) B. T. Ho, W. M. McIssac, and K. E. Walker, *J. Pharm. Sci.*, **57,** 1364 (1968).

(9) L. Berger and A. J. Corraz, U.S. pat. 3,862,953 (Jan. 28, 1975) and U.S. pat. 3,896,145 (July 22, 1975).

(10) C. Dalton and W. R. Pool, *J. Pharm. Sci.*, **66,** 348 (1977).

(11) H. Corradi and N. A. Hillarp, *Helv. Chim. Acta*, **46,** 2425 (1963).

(12) R. P. Maickel and F. P. Miller, *Anal. Chem.*, **38,** 1937 (1966).

(13) W. B. Quay, *J. Pharm. Sci.*, **57,** 1568 (1968).

(14) A. Stoessl and M. A. Venis, *Anal. Biochem.*, **34,** 344 (1970).

(15) G. Jori, G. Galiazzo, and G. Gannari, *Photochem. Photobiol.*, **9,** 179 (1969).

(16) G. Cauzzo and G. Jori, *J. Org. Chem.*, **37,** 1429 (1972).

(17) M. Zander "Phosphorimetry—The Application of Phosphorescence to the Analysis of Organic Compounds," Academic, New York, N.Y., 1968, pp. 95–106, 158–194.

(18) J. A. F. de Silva, N. Strojny, and K. Stika, *Anal. Chem.*, **48,** 144 (1976).

(19) J. N. Bridges and R. T. Williams, *Biochem. J.*, **107,** 225 (1968).

(20) W. A. Remers, in "Indoles," part I, W. J. Houlihan, Ed., in "The Chemistry of Heterocyclic Compounds," A. Weissberger and E. C. Taylor, Eds., Wiley, New York, N.Y., 1972, pp. 19–33.

(21) R. J. Sundberg, "The Chemistry of Indoles," in "Organic Chemistry," A. T. Blomquist, Ed., Academic, New York, N.Y., 1970, pp. 282–315.

(22) N. Strojny and J. A. F. de Silva, *J. Chromatogr. Sci.*, **13,** 583 (1975).

ACKNOWLEDGMENTS AND ADDRESSES

Received March 1, 1976, from the *Department of Biochemistry and Drug Metabolism, Hoffmann-La Roche Inc., Nutley, NJ 07110.*

Accepted for publication May 18, 1976.

The authors thank Mr. L. Berger of the Chemical Research Division for the authentic standards and chemical analogs and Mr. R. McGlynn for the drawings.

[x] To whom inquiries should be directed.

Oxidative Reactions of Hydroxylated Chlorpromazine Metabolites

RICHARD L. McCREERY

Abstract □ The oxidation pathways of two hydroxylated chlorpromazine metabolites were investigated using modern electrochemical techniques. Upon oxidation, the 7-hydroxy derivative of chlorpromazine rapidly reacts to form the 7,8-dihydroxy derivative and a substituted quinone. The oxidation potentials for both compounds were determined in the pH 3–8 range. The importance of these redox reactions and potentials to the pharmacology of the materials is discussed.

Keyphrases □ Chlorpromazine metabolites—oxidation pathways, electrochemical study, pH 3–8 □ Oxidation pathways—hydroxylated chlorpromazine metabolites, electrochemical study, pH 3–8 □ Electrochemistry—study of oxidation pathways of hydroxylated chlorpromazine metabolites □ Tranquilizers—chlorpromazine metabolites, electrochemical study of oxidation pathways

The widespread use of phenothiazine derivatives in the treatment of mental illness has inspired a large amount of research on their chemical properties and reactions. Of relevance to the present discussion are studies of the importance of redox reactions to the metabolism and mode of action of chlorpromazine and related neuroleptic drugs.

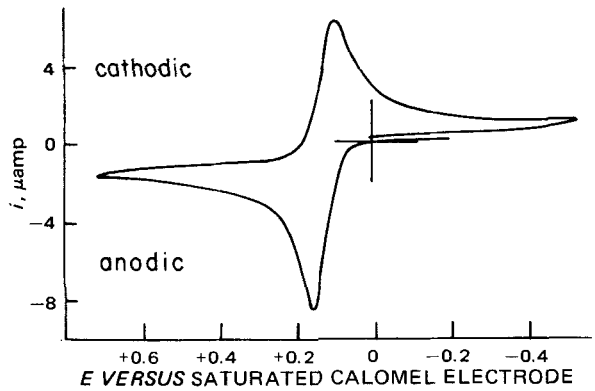

Figure 1—*Cyclic voltammogram of 5 × 10^{-4} M II in pH 4 McIlvaine buffer (carbon paste electrode; scan rate = 0.10 v/sec).*

The one-electron oxidation product of chlorpromazine, its cation radical, has been associated with membrane interactions that may be responsible for the drug's effect (1), and the radical has been suggested as a metabolic intermediate in the formation of chlorpromazine sulfoxide and hydroxylated chlorpromazine metabolites (2).

BACKGROUND

More recent investigations involved the importance of two hydroxylated metabolites of chlorpromazine to the beneficial and toxic effects of chlorpromazine therapy. The 7-hydroxy derivative of chlorpromazine (I) has pharmacological effects comparable to chlorpromazine in animal tests and has been suggested as the active form of the drug in neuroleptic therapy (3). In addition, the 7-hydroxy compound has been associated with the corneal opacity and skin pigmentation that occur in 5–25% of the patients receiving chlorpromazine chronically (4, 5). The 7,8-dihydroxy derivative of chlorpromazine (II) is also a metabolite of chlorpromazine in humans (6) and is a strong candidate for an agent producing toxic side effects. It also causes corneal opacity in rabbits (5) and has pronounced effects on mitochondrial membranes (7) and Na^+–K^+-dependent adenosine triphosphatase (8).

It is important to consider the possible role of oxidation in the metabolism and side effects of chlorpromazine. Oxidation of II by molecular oxygen produces hydrogen peroxide, the superoxide ion, and hydroxyl radicals (9). Heikkila *et al.* (9) suggested that this oxidation and the accompanying generation of reactive species are responsible for the neurotoxicity of the dihydroxy compound. In addition, it has been proposed that oxidation and polymerization of II result in the purple pigmentation of the skin or corneal opacity observed in chronic chlorpromazine patients. A further effect of II may be degeneration of nerve tissue, similar to that caused by 6-hydroxydopamine. The mechanism of neurotoxicity of the 6-hydroxy derivative of dopamine remains an active subject of research, but the ease of oxidation is important for its effects. Information about the oxidation potential of II would be useful in appraising its possible chemical similarity to the 6-hydroxy derivative of dopamine.

Although photoxidation of I has been associated with skin pigmentation, the reaction is not well characterized (4). The mushroom tyrosinase-catalyzed oxidation of I generates the dihydroxy derivative, as shown by UV and electron spin resonance spectra (10).

The work described here was undertaken to clarify the oxidative reactions of chlorpromazine, I, and II in solutions near physiological pH. Hopefully, information about oxidation potentials and reaction mechanisms will clarify the role of hydroxylated chlorpromazine metabolites in the toxic and beneficial effects of chlorpromazine therapy. The electrochemical results show that II is oxidized at a potential near that of the 6-hydroxy derivative of dopamine and that the product is stable on the time scale used here. Compound I rapidly undergoes further reaction upon oxidation to yield II and a quinone intermediate. The results provide an overall picture of the oxidation pathways of these compounds consistent with previously reported observations.

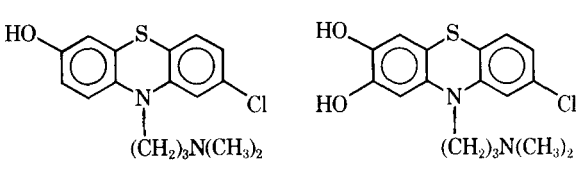

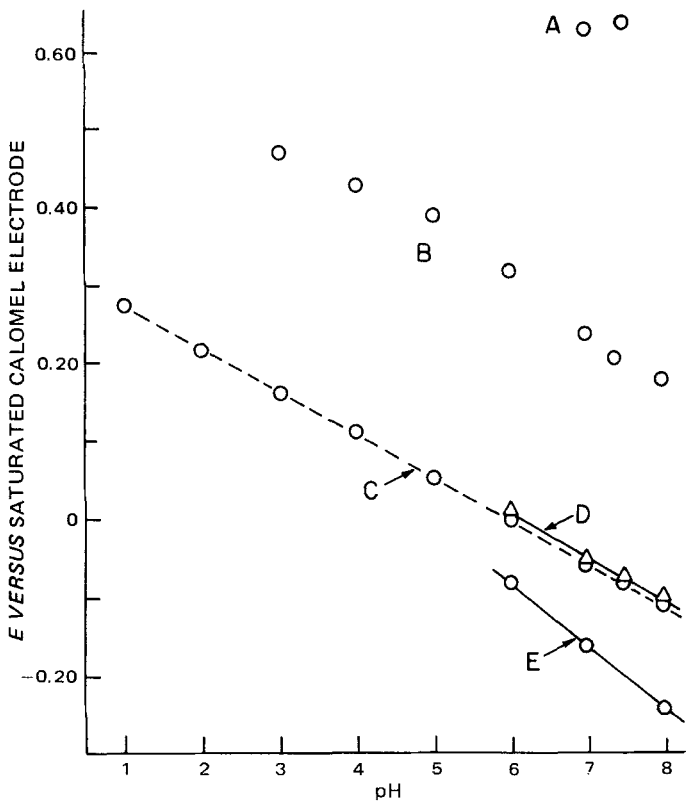

Figure 2—*Potential* versus *pH profiles for chlorpromazine and two hydroxylated metabolites. Key: A, $E_{p/2}$ for chlorpromazine; B, $E_{p/2}$ for I; C, $E_{p/2}$ for II; D, $E^{o'}$ for II; and E, $E^{o'}$ for dopamine 6-hydroxy derivative. Voltammograms were obtained using a carbon paste electrode. $E^{o'}$ values are midpoint potentials for titrations with the ferricyanide ion using a platinum indicator electrode.*

EXPERIMENTAL

All voltammetric experiments with scan rates below 0.5 v/sec were performed with an operational amplifier potentiostat of conventional design (11). A 27.9 × 35.5-cm (11 × 14-in.) *x–y* recorder was used to record slow scan voltammograms. Large-scale electrolysis was performed using a more powerful potentiostat based on a 50-w power amplifier. A 25.4-cm (10-in.) strip-chart recorder was used to record electrolysis current. High speed (above 0.5 v/sec) voltammograms were performed with a fast rising potentiostat interfaced to a laboratory scale minicomputer. The system allowed control of high speed experiments, with sampling of current occurring at a maximum rate of 200 kHz. The resultant voltammograms were displayed on an *x–y* oscilloscope monitor.

Electrochemical cell design was conventional and utilized a carbon paste working electrode, platinum wire auxiliary electrode, and saturated calomel reference electrode (12). To avoid any question about electrode fouling from electrolysis products, a new carbon paste surface was prepared for each voltammetric scan. To conserve the supply of phenothiazine derivatives, cell volume was limited to 1.5 ml; typical experiments consumed 400–600 μg of electroactive material. McIlvaine buffers made from 0.2 *M* Na_2HPO_4 and 0.1 *M* citric acid were utilized in the pH 3–8 range. Phosphate buffer, 0.2 *M*, at pH 2 and 0.1 *M* HCl were used below pH 3. In many cases, phenothiazines were dissolved with a few drops of 10^{-3} *M* HCl before addition of the buffer solutions.

Chlorpromazine hydrochloride[1], I[2], and III[2] were used without further purification.

[1] Courtesy of Dr. R. N. Adams, University of Kansas.
[2] Courtesy of Dr. A. A. Manian, Psychopharmacology Research Branch, National Institutes of Health.

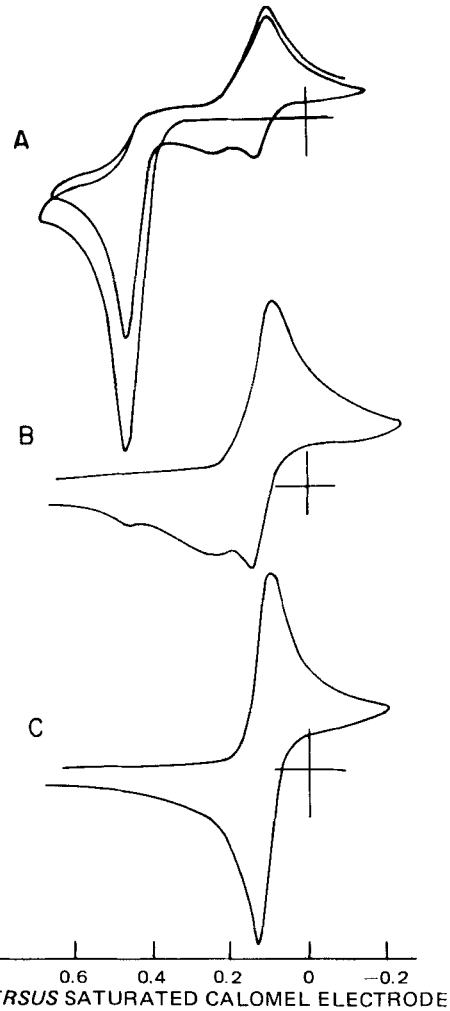

Figure 3—*Voltammograms before and during the coulometric oxidation of 554 μg of I in 3 ml of pH 4 McIlvaine buffer. Key: A, before electrolysis was initiated* (n = *0); B,* n = *3.2; and C,* n = *4.02.*

RESULTS

The electrochemistry of II was the simplest of the three compounds studied. Figure 1 shows the nearly reversible, well-defined voltammetric wave of II at pH 4. A similar wave was observed from pH 1 to 8, with the only effect of pH being a shift in the oxidation potential. Figure 2 includes a graph of the half-peak potential of the anodic wave *versus* pH. The plot is linear from pH 1 to 8, with a slope of 0.056 v/pH unit, indicating that the number of protons and electrons involved in the oxidation process is equal. The linearity of the pH profile for II below pH 4 was unexpected, since the reported value for the pKa of the thiazine nitrogen is 3.4 (13). Unless the pKa for the thiazine nitrogen is the same for both the oxidized and reduced forms of II, one would expect a change in slope in the $E_{p/2}$ *versus* pH profile in the region of pH 3.4.

After considering the pKa's of diphenylamine (0.79) and the 3-hydroxy derivative of phenothiazine (−2) (14), one has reason to doubt the published value of 3.4. The inconsistency may arise from the possibility that the value of 3.4 represents the titration of free hydrogen ions rather than the protonated thiazine nitrogen, in light of the fact that the investigators reporting that value started with a 10^{-3} *M* solution of II. Potentiometric titrations of II with ferricyanide yielded an average *n* value of 1.93 electrons per molecule in the pH 6–8 region. Titrations below pH 6 were not possible because the redox potential of ferricyanide is too low. The $E^{o'}$ values derived from these titrations are also plotted in Fig. 2. Coulometry of II at a carbon cloth electrode confirmed the value of two electrons per molecule for the oxidation. The UV–visible spectra of oxidized material agree well with those published by Grover *et al.* (10), with peaks at 262 and 508 nm. The molecular implications of these bands were discussed previously (15).

A cyclic voltammogram of I at pH 4 is shown in Fig. 3A. The voltammograms in the pH 3–8 range were qualitatively similar, with the only

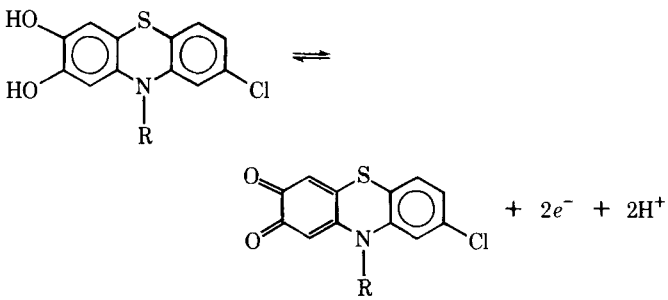

Scheme I

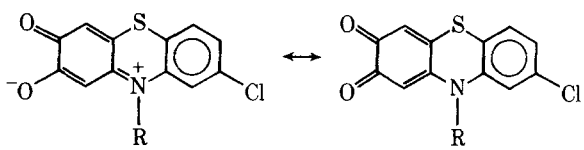

Scheme II

change being in the positions and magnitudes of the peaks. Figure 2 shows a plot of the half-peak potential for the major anodic peak as a function of pH. The cathodic peak shifted with pH in a fashion identical to the dihydroxy derivative. Since the oxidation of I is chemically irreversible, no attempt was made to titrate it potentiometrically. Coulometry of I at pH 4 consumed 4.04 electrons per molecule. Changes in the voltammograms that occurred during coulometry are shown in Fig. 3. Voltammogram A was performed before electrolysis was started at +0.6 v *versus* the saturated calomel electrode. After about three electrons per molecule were passed (*n* = 3.20), voltammogram B was taken; C was taken when *n* = 4.02. The UV–visible spectra and voltammetry of the electrolysis product were identical to those of oxidized II at all pH's, with UV–visible peaks at 262 and 508 nm. Reduction of the electrolysis product at −0.2 v *versus* the saturated calomel electrode consumed between 1.7 and 1.9 electrons per molecule of original I.

The voltammetric oxidation of chlorpromazine itself was studied briefly for comparison. Figure 4A is a voltammogram of chlorpromazine hydrochloride in pH 6 McIlvaine buffer at a scan rate of 0.1 v/sec. The oxidation potential was pH independent, with a value for the half-peak potential of +0.65 v *versus* the saturated calomel electrode. The absence of a reverse (reduction) wave indicates that the product of the oxidation was unstable under these conditions. At the fast scan rate of 10 v/sec (Fig. 4B), a reverse wave was apparent, indicating that the oxidized material had not had time to react to an electroinactive material. The nature and kinetics of the reactions of the oxidized form are presently under study, but an estimate of the half-life of the oxidized material from these data is 10 msec.

Table I summarizes the electrochemical data for the three compounds studied. All potentials are referred to the saturated calomel electrode; to determine the potential referred to the normal hydrogen electrode, 0.246 v must be added.

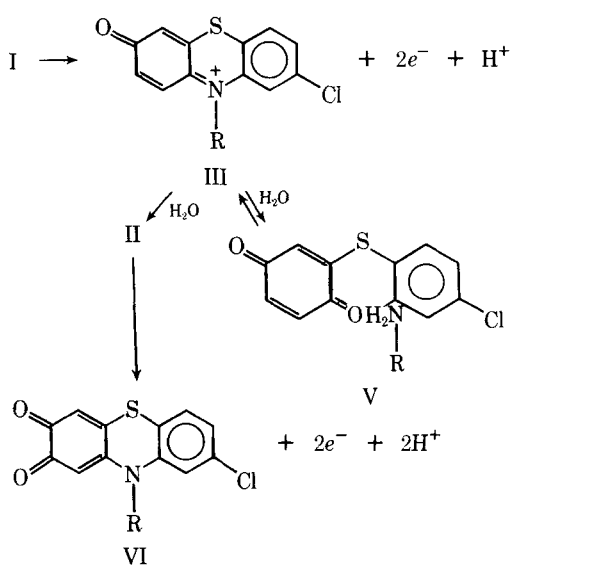

Scheme III

Table I—Half-Peak and Midpoint Potentials for Chlorpromazine Derivatives

Compound	pH 6	pH 7	pH 7.4	pH 8	Method[a]
Chlorpromazine	—	0.63	0.64	—	A
I	0.322	0.242	0.210	0.181	A
II	−0.002	−0.060	−0.080	−0.105	A
II	0.010	−0.051	−0.074	−0.103	B
6-Hydroxy derivative of dopamine[b]	−0.078	−0.160	—	−0.240	B

[a] A = potential when the current equals half the peak current for the anodic (oxidation) wave, and B = $E^{o'}$ for potentiometric titration (potential at half-titration point). [b] Data from Ref. 21.

DISCUSSION

The results of potentiometric titrations, coulometry, and voltammetry indicate that the oxidation of II is an uncomplicated two-electron process, with an accompanying loss of two hydrogen ions [Scheme I, R = $(CH_2)_3N^+H(CH_3)_2$]. Although the product of the oxidation is shown here as an *ortho*-quinone, it has been pointed out that it has some zwitterionic character due to the quinone–imine resonance form (15) (Scheme II).

For an ideal, reversible, voltammogram, the formal redox potential, $E^{o'}$, for the system is the potential when the current equals 85% of the peak current (16). Since all studied systems yielded quasireversible waves, $E^{o'}$ cannot be determined accurately from the waves. The half-peak potential, $E_{p/2}$, is a useful indication of the ease of oxidation and can be used for observations of trends and for purposes of comparison. In the case of II, it can be seen that $E_{p/2}$ and $E^{o'}$ are equal to within 10 mv.

The $E_{p/2}$ *versus* pH profile for I is nonlinear, probably due to the complex nature of the followup reactions occurring immediately after oxidation. These reactions distort the voltammetric wave, and the pH dependence is unpredictable. Due to the instability of oxidized I, potentiometric titrations were not attempted. However, for reasons discussed already, $E_{p/2}$ is a good approximation for the redox potential. The observations are consistent with the oxidation mechanism shown in Scheme III.

This mechanism is supported by the following evidence. The complete oxidation of I liberates four electrons per molecule of starting material. The product is voltammetrically and spectroscopically indistinguishable from oxidized II quinone (VI). An intermediate is observed during oxidation, which is not present after four electrons have been passed, and which has a voltammogram consistent with Structure V. The electrolysis of I occurs in two distinct phases: a rapid, initial oxidation corresponding to the consumption of I to form V and VI and a slower phase corresponding to the cyclization of V back to III and eventual complete generation of VI. The oxidation slows down when approximately three electrons have been passed per molecule of I. The reduction of the final oxidation product required 1.7–1.9 electrons per molecule. Although the suggested mechanism predicts a value of 2.0 electrons, slow degradation of the quinone might account for the low values.

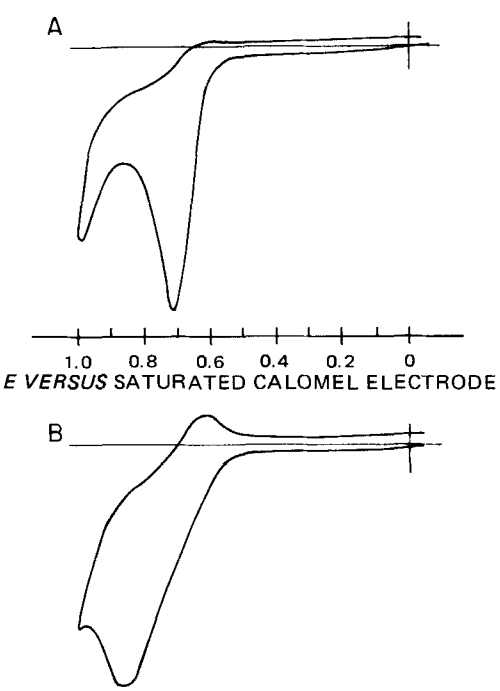

Figure 4—*Voltammograms of chlorpromazine in pH 6 McIlvaine buffer (carbon paste electrode). Key: A, scan rate = 0.1 v/sec; and B, scan rate = 10 v/sec.*

$$IV \longrightarrow IV^+ + e^-$$
$$\downarrow$$
$$IV^{2+} + e^-$$

Scheme IV

Although several reports have been published on the electrochemical oxidation of chlorpromazine in acidic media (17–19), the author is unaware of any studies near physiological pH. Figure 4 indicates that the product of the oxidation rapidly degrades to an electroinactive product, probably the sulfoxide. At a fast scan rate, the reduction of the initial product can be observed, since the product has insufficient time to degrade completely. The distortion of the oxidation wave could be caused by two distinct phenomena: adsorption of the chlorpromazine (IV) on the electrode or splitting of the wave into two one-electron oxidations (Scheme IV). Two waves are not observed at slow scan rates, since the dication rapidly degrades to the sulfoxide, shifting the disproportionation equilibrium toward the dication and resulting in a single peak at the potential of the first oxidation. Further studies are being carried out to clarify this process.

The important conclusions that can be drawn from these results are the mechanism of oxidation of I and the relative oxidation potentials of the three chlorpromazine derivatives studied. Of the molecules studied, II oxidizes at the lowest potential, near that of the 6-hydroxy derivative of dopamine (Fig. 2). The 6-amino derivative of dopamine, another cytotoxic agent, has an oxidation potential of −0.135 v *versus* the saturated calomel electrode at pH 7.4 (20), which is even closer to the dihydroxy derivative. The importance of oxidation to cytotoxic action remains unconfirmed, but the similarity of II to the catecholamine derivatives is obvious in this respect.

Although I is more difficult to oxidize, its immediate oxidation product (III) is unstable near physiological pH. Compound III can hydrolyze to the quinone (V) or hydroxylate to II and eventually oxidize to II quinone (VI). The hydrolysis of III to form V is reversible in these experiments, but interactions of V with tissue components must be considered when examining I pharmacology. Since both degradative reactions of III are fast, even slow oxidation of I would result in formation of both V and VI. The pH dependence of these reactions and the interactions of the products with tissue components are subjects of current study.

REFERENCES

(1) I. S. Forrest and D. E. Green, *J. Forensic Sci.*, **17**, 592 (1972).

(2) L. H. Piette, G. Bulow, and I. S. Forrest, *Psychopharmacol. Serv. Cent. Bull.*, **2**, 46 (1962).

(3) J. P. Buckley, M. L. Steenberg, H. Barry, and A. A. Manian, *J. Pharm. Sci.*, **62**, 712 (1973).

(4) T. L. Perry, C. F. A. Culling, K. Berry, and S. Hansen, *Science*, **146**, 82 (1964).

(5) H. R. Adams, A. A. Manian, M. L. Steenberg, and J. P. Buckley, in "The Phenothiazines and Structurally Related Drugs," I. S. Forrest, C. J. Carr, and E. Usdin, Eds., Raven, New York, N.Y., 1974, p. 281.

(6) P. Turano, W. J. Turner, and D. Donato, in *ibid.*, p. 315.

(7) S. A. Tjioe, A. A. Manian, and J. J. O'Neill, *Biochem. Biophys. Res. Commun.*, **48**, 212 (1972).

(8) T. Akera, S. I. Baskin, T. Tobin, T. M. Brody, and A. A. Manian, in "The Phenothiazines and Structurally Related Drugs," I. S. Forrest,

C. J. Carr, and E. Usdin, Eds., Raven, New York, N.Y., 1974, p. 633.
(9) R. E. Heikkila, G. Cohen, and A. A. Manian, *Biochem. Pharmacol.*, **24**, 363 (1975).
(10) T. A. Grover, L. H. Piette, and A. A. Manian, in "The Phenothiazines and Structurally Related Drugs," I. S. Forrest, C. J. Carr, and E. Usdin, Eds., Raven, New York, N.Y., 1974, p. 561.
(11) R. L. McCreery, R. J. Dreiling, and R. N. Adams, *Brain Res.*, **73**, 23 (1974).
(12) R. N. Adams, "Electrochemistry at Solid Electrodes," Marcel Dekker, New York, N.Y., 1969.
(13) K. S. Rajan, A. A. Manian, J. M. Davis, and A. Skripkus, in "The Phenothiazines and Structurally Related Drugs," I. S. Forrest, C. J. Carr, and E. Usdin, Eds., Raven, New York, N.Y., 1974, p. 571.
(14) L. Michaelis and S. Granick, *J. Am. Chem. Soc.*, **64**, 1861 (1942).
(15) A. Zirnis, J. Suzuki, J. W. Daly, and A. A. Manian, *J. Heterocycl. Chem.*, **12**, 239 (1975).
(16) R. S. Nicholson and I. Shain, *Anal. Chem.*, **36**, 715 (1964).
(17) F. H. Merkle and C. A. Discher, *J. Pharm. Sci.*, **53**, 620 (1964).
(18) G. J. Patriarche and J. J. Lingane, *Anal. Chim. Acta*, **49**, 25 (1970).
(19) P. Kabasakalian and J. McGlotten, *Anal. Chem.*, **31**, 431 (1959).
(20) C. L. Blank, R. L. McCreery, R. M. Wightman, W. Chey, R. N. Adams, J. R. Reid, and E. E. Smissman, *J. Med. Chem.*, **19**, 178 (1976).
(21) R. L. McCreery, Ph.D. thesis, University of Kansas, Lawrence, Kans., 1974.

ACKNOWLEDGMENTS AND ADDRESSES

Received December 24, 1975, from the *Department of Chemistry, Ohio State University, Columbus, OH 43210.*

Accepted for publication May 5, 1976.

The author gratefully acknowledges the support of this work by the Research Corporation through a Cottrell Research Grant. Helpful discussions with Dr. A. A. Manian and Dr. John S. Swenton were appreciated.

GI Drug Absorption in Rats Exposed to Cobalt-60 γ-Radiation I: Extent of Absorption

MICHAEL E. BRADY * and WILLIAM L. HAYTON ˣ

Abstract □ The extent of absorption of sulfanilamide, bretylium tosylate, sulfisoxazole acetyl, and riboflavin was determined in rats exposed to 850 rad of cobalt-60 γ-radiation or sham irradiated. The drugs were administered orally at 1 or 5 days postirradiation, and the amount of drug excreted in the urine was used as the measure of absorption. Following intravenous drug administration, there was no difference between irradiated and control animals in the amount of drug excreted in the urine. At 1 day postirradiation, the absorption of sulfanilamide and bretylium was not affected by radiation; the absorption of sulfisoxazole acetyl and riboflavin was increased. The fraction of sulfanilamide excreted in the urine as N^4-conjugate was increased at 1 day postirradiation. At 5 days postirradiation, there was no detectable difference between irradiated and control animals in the extent of drug absorption. The effects of radiation on the extent of absorption of orally administered drugs were most pronounced immediately following irradiation. Irradiation apparently does not affect the absorption of drugs that are normally well absorbed or poorly absorbed due to slow transport across the GI mucosa. Following irradiation, there may be an increase in the extent of absorption of drugs that are poorly absorbed due to low aqueous solubility or that are absorbed by a saturable transport mechanism.

Keyphrases □ Absorption, GI—various drugs, effect of cobalt-60 γ-radiation, rats □ Radiation, gamma—effect on GI absorption of various drugs, rats □ Sulfanilamide—GI absorption, effect of cobalt-60 γ-radiation, rats □ Bretylium tosylate—GI absorption, effect of cobalt-60 γ-radiation, rats □ Sulfisoxazole acetyl—GI absorption, effect of cobalt-60 γ-radiation, rats □ Riboflavin—GI absorption, effect of cobalt-60 γ-radiation, rats

Patients exposed to ionizing radiation for the treatment of cancer commonly receive drugs during or following radiation therapy. When the GI tract is involved in radiation therapy, its structure and function may be altered for several days. Such alterations may affect the bioavailability of orally administered drugs.

The potential mechanisms by which radiation may alter drug absorption were explored by studying the absorption of several drugs in rats that were exposed to cobalt-60 γ-radiation. The drugs used were chosen so that the absorption rate of each drug was controlled by a different step in the overall process of absorption (Table I). Experiments were performed to assess the effects of radiation on the rate and extent of absorption of each drug and on the permeability of the intestinal mucosa. The studies on the extent of drug absorption are presented here; the other studies are reported elsewhere (1, 2).

BACKGROUND

Following oral administration, the rate and extent of absorption of many drugs are determined by one or more of the following steps: dissolution in the lumen of the GI tract, transport across the GI epithelium, and gastric emptying (3, 4). The primary rate-controlling step (or steps) in the absorption of a particular drug depends on dosage formulation and on the physicochemical properties of the drug; *e.g.*, the solubility in water affects the rate of solution, and the oil/water partition coefficient affects epithelial permeability. Since drugs with low solubility in water tend to dissolve slowly following oral administration, dissolution is usually the step that controls the absorption rate of poorly water-soluble drugs. As water solubility increases, the dissolution rate increases, but the permeability of the intestinal epithelium tends to decrease due to the lipophilic nature of this barrier. The rate-controlling step in the absorption of very polar drugs is the transport of the dissolved drug across the intestinal epithelium.

The rate of gastric emptying may determine the rate of drug absorption since most drugs tend to be absorbed more rapidly from the intestine than from the stomach. For drugs that are absorbed by a saturable transport process in the intestine, slowed gastric emptying may enhance absorption by maintaining a low concentration of drug at the site of absorption for

C. J. Carr, and E. Usdin, Eds., Raven, New York, N.Y., 1974, p. 633.
(9) R. E. Heikkila, G. Cohen, and A. A. Manian, *Biochem. Pharmacol.*, **24**, 363 (1975).
(10) T. A. Grover, L. H. Piette, and A. A. Manian, in "The Phenothiazines and Structurally Related Drugs," I. S. Forrest, C. J. Carr, and E. Usdin, Eds., Raven, New York, N.Y., 1974, p. 561.
(11) R. L. McCreery, R. J. Dreiling, and R. N. Adams, *Brain Res.*, **73**, 23 (1974).
(12) R. N. Adams, "Electrochemistry at Solid Electrodes," Marcel Dekker, New York, N.Y., 1969.
(13) K. S. Rajan, A. A. Manian, J. M. Davis, and A. Skripkus, in "The Phenothiazines and Structurally Related Drugs," I. S. Forrest, C. J. Carr, and E. Usdin, Eds., Raven, New York, N.Y., 1974, p. 571.
(14) L. Michaelis and S. Granick, *J. Am. Chem. Soc.*, **64**, 1861 (1942).
(15) A. Zirnis, J. Suzuki, J. W. Daly, and A. A. Manian, *J. Heterocycl. Chem.*, **12**, 239 (1975).
(16) R. S. Nicholson and I. Shain, *Anal. Chem.*, **36**, 715 (1964).
(17) F. H. Merkle and C. A. Discher, *J. Pharm. Sci.*, **53**, 620 (1964).
(18) G. J. Patriarche and J. J. Lingane, *Anal. Chim. Acta*, **49**, 25 (1970).
(19) P. Kabasakalian and J. McGlotten, *Anal. Chem.*, **31**, 431 (1959).
(20) C. L. Blank, R. L. McCreery, R. M. Wightman, W. Chey, R. N. Adams, J. R. Reid, and E. E. Smissman, *J. Med. Chem.*, **19**, 178 (1976).
(21) R. L. McCreery, Ph.D. thesis, University of Kansas, Lawrence, Kans., 1974.

ACKNOWLEDGMENTS AND ADDRESSES

Received December 24, 1975, from the *Department of Chemistry, Ohio State University, Columbus, OH 43210.*

Accepted for publication May 5, 1976.

The author gratefully acknowledges the support of this work by the Research Corporation through a Cottrell Research Grant. Helpful discussions with Dr. A. A. Manian and Dr. John S. Swenton were appreciated.

GI Drug Absorption in Rats Exposed to Cobalt-60 γ-Radiation I: Extent of Absorption

MICHAEL E. BRADY * and WILLIAM L. HAYTON ˣ

Abstract □ The extent of absorption of sulfanilamide, bretylium tosylate, sulfisoxazole acetyl, and riboflavin was determined in rats exposed to 850 rad of cobalt-60 γ-radiation or sham irradiated. The drugs were administered orally at 1 or 5 days postirradiation, and the amount of drug excreted in the urine was used as the measure of absorption. Following intravenous drug administration, there was no difference between irradiated and control animals in the amount of drug excreted in the urine. At 1 day postirradiation, the absorption of sulfanilamide and bretylium was not affected by radiation; the absorption of sulfisoxazole acetyl and riboflavin was increased. The fraction of sulfanilamide excreted in the urine as N^4-conjugate was increased at 1 day postirradiation. At 5 days postirradiation, there was no detectable difference between irradiated and control animals in the extent of drug absorption. The effects of radiation on the extent of absorption of orally administered drugs were most pronounced immediately following irradiation. Irradiation apparently does not affect the absorption of drugs that are normally well absorbed or poorly absorbed due to slow transport across the GI mucosa. Following irradiation, there may be an increase in the extent of absorption of drugs that are poorly absorbed due to low aqueous solubility or that are absorbed by a saturable transport mechanism.

Keyphrases □ Absorption, GI—various drugs, effect of cobalt-60 γ-radiation, rats □ Radiation, gamma—effect on GI absorption of various drugs, rats □ Sulfanilamide—GI absorption, effect of cobalt-60 γ-radiation, rats □ Bretylium tosylate—GI absorption, effect of cobalt-60 γ-radiation, rats □ Sulfisoxazole acetyl—GI absorption, effect of cobalt-60 γ-radiation, rats □ Riboflavin—GI absorption, effect of cobalt-60 γ-radiation, rats

Patients exposed to ionizing radiation for the treatment of cancer commonly receive drugs during or following radiation therapy. When the GI tract is involved in radiation therapy, its structure and function may be altered for several days. Such alterations may affect the bioavailability of orally administered drugs.

The potential mechanisms by which radiation may alter drug absorption were explored by studying the absorption of several drugs in rats that were exposed to cobalt-60 γ-radiation. The drugs used were chosen so that the absorption rate of each drug was controlled by a different step in the overall process of absorption (Table I). Experiments were performed to assess the effects of radiation on the rate and extent of absorption of each drug and on the permeability of the intestinal mucosa. The studies on the extent of drug absorption are presented here; the other studies are reported elsewhere (1, 2).

BACKGROUND

Following oral administration, the rate and extent of absorption of many drugs are determined by one or more of the following steps: dissolution in the lumen of the GI tract, transport across the GI epithelium, and gastric emptying (3, 4). The primary rate-controlling step (or steps) in the absorption of a particular drug depends on dosage formulation and on the physicochemical properties of the drug; *e.g.*, the solubility in water affects the rate of solution, and the oil/water partition coefficient affects epithelial permeability. Since drugs with low solubility in water tend to dissolve slowly following oral administration, dissolution is usually the step that controls the absorption rate of poorly water-soluble drugs. As water solubility increases, the dissolution rate increases, but the permeability of the intestinal epithelium tends to decrease due to the lipophilic nature of this barrier. The rate-controlling step in the absorption of very polar drugs is the transport of the dissolved drug across the intestinal epithelium.

The rate of gastric emptying may determine the rate of drug absorption since most drugs tend to be absorbed more rapidly from the intestine than from the stomach. For drugs that are absorbed by a saturable transport process in the intestine, slowed gastric emptying may enhance absorption by maintaining a low concentration of drug at the site of absorption for

Table I—Drugs Selected for Study

Drug and Dosage Form	Physicochemical and Biological Properties	Probable Rate-Limiting Step in Absorption
Sulfanilamide suspension	Relatively high aqueous solubility, high oil/water partition coefficient, normally well absorbed	Gastric emptying
Bretylium tosylate solution	Ionized, high aqueous solubility, low oil/water partition coefficient, not well absorbed due to low mucosal permeability	Mucosal permeability
Sulfisoxazole acetyl suspension	Low aqueous solubility, high oil/water partition coefficient, not well absorbed due to slow dissolution	Dissolution
Riboflavin solution	Low aqueous solubility, low oil/water partition coefficient, may be absorbed in part by a capacity-limited mechanism	Mucosal permeability

a prolonged time. In addition, changes in intestinal motility may affect the absorption of drugs that dissolve slowly or are absorbed slowly by altering the time available for dissolution or absorption.

Exposure of the GI tract to ionizing radiation could alter bioavailability by altering the normal rates of the primary rate-controlling steps, particularly transfer across the GI epithelium, and GI motility. The normally rapid rate of cell division in the intestinal epithelium is slowed following irradiation, resulting in villi that are abnormal in size and shape (5). In addition, the mass of the epithelium decreases following irradiation, *e.g.*, 50% in mice exposed to 600 rad (6). In rodents, the maximal change in the structure of the epithelium occurs 4–6 days postirradiation (5, 7). A decrease in the surface area of the intestinal mucosa could significantly reduce the absorption of drugs that slowly cross the normal intestinal epithelium. The impaired absorption of digoxin in a human (8) and slowed absorption of diazepam and aminobenzoic acid in rats[1] following irradiation may have resulted from a reduction in the capacity of the intestinal epithelium to absorb these drugs.

Both gastric emptying and intestinal motility are altered following irradiation of the gut. Radiation-induced changes in GI motility depend on the dose of radiation and are greatest immediately following irradiation. Slowed gastric emptying was shown to be the major cause of the reduced rate of absorption of sulfadiazine and quinine observed in irradiated mice and rats (9). Following irradiation, both an increase and a decrease in the motility of the rat small intestine, as reflected by the rate of intestinal transit of a nonabsorbed marker, have been reported. The intestinal transit rate increased in irradiated animals following intraduodenal administration of the marker (10) but decreased following intragastric administration. The greatest reduction in transit rate occurred in the middle segment of the intestine (11).

Other mechanisms by which irradiation of the GI tract could alter absorption include an alteration in blood flow to the intestine (12, 13) and inactivation of carriers associated with transport across the intestinal epithelium (14–16).

EXPERIMENTAL

Materials—Sulfisoxazole acetyl[2], bretylium tosylate[3], riboflavin[4], and sulfanilamide[5] were used as received. ^{14}C-Riboflavin[6] was dissolved in a pH 5.0 aqueous buffer and stored at 5° in an opaque container. The labeled radiochemical purity of ^{14}C-riboflavin was 99%; it was verified periodically by TLC on silica gel G-coated plates developed with either methanol–benzene–acetone–acetic acid (20:70:5:5) or pyridine–acetic acid–water (20:2:80). Methylcellulose 4000, polyethylene glycol 400[7], 2,2′,4,4′,6,6′-hexanitrodiphenylamine[8] (dipicrylamine), sodium nitrite[9], sulfamic acid[9], and *N*-(1-naphthyl)ethylenediamine dihydrochloride[4] were used as received. All other reagents and solvents were reagent grade.

Irradiation Procedure—A 7000-Ci cobalt-60 source, stored in a lead chamber at the bottom of a bulk shielding reactor pool, was used to irradiate rats. Animals were placed in a Plexiglas restraining cage, rotated at 20 rpm, and lowered down a watertight sample tube to a position near the source of radiation. To irradiate animals, the source was elevated automatically from its storage chamber.

The dose of radiation was checked regularly with an ionization-type dosimeter[10], and the sample-to-source distance was adjusted to maintain a dose of 850 ± 42 rad delivered over 5.0 min. Sham-irradiated animals were manipulated as were irradiated animals, except that the source of radiation remained in its storage chamber.

The level of radiation in the sample tube when the source was shielded was less than 1 rad/hr.

Bioavailability Studies—Experiments were conducted on the 1st and 5th days postirradiation to maximize the potential effects of radiation on gastric emptying (9, 17, 18) and intestinal epithelial permeability (19–21), respectively. Equal numbers of irradiated and sham-irradiated male Sprague–Dawley rats (170–250 g) were fasted for 16–20 hr prior to and for 3 hr following drug administration. Drug was administered at the same time of day either intravenously *via* the penile vein or orally by gastric intubation. Animals were anesthetized lightly with ether to facilitate drug administration.

After drug administration, animals were housed individually in metabolism cages[11] which permitted quantitative separation of urine and feces. The room in which the animals were housed was maintained at 16° and lighted 9 hr followed by 15 hr of darkness per day. Urine was collected until the drug and metabolites were no longer excreted. Each urine sample was combined with a distilled water rinse of the lower section of the metabolism cage and was stored at −20° until assayed.

Sulfanilamide, 200 mg/kg, and sulfisoxazole acetyl, 100 mg/kg, were administered orally suspended in 8.0 ml of 0.5% methylcellulose solution/kg. Identical doses of the sulfonamides were dissolved in 2.0 ml of polyethylene glycol 400–water (9:1)/kg and administered intravenously. Prior to administration, suspensions were agitated for 24 hr at room temperature and sonicated. Riboflavin, 0.8 and 4.0 mg/kg, was given orally and intravenously in 12.0- and 1.6-ml/kg doses, respectively; the intravenous solutions contained 200 mg of niacinamide[12]/ml. ^{14}C-Riboflavin was diluted with unlabeled riboflavin to a specific activity of approximately 0.5 mCi/g. Bretylium tosylate was administered orally, 30 mg/kg, and intravenously, 5 mg/kg, dissolved in 8.0 and 2.0 ml of water/kg, respectively.

Analytical Methods—Free (unconjugated) and total (free + N^4-conjugated) sulfanilamide and sulfisoxazole acetyl were determined in urine by a colorimetric method[13] involving extraction of the free drug with ethyl acetate and acid hydrolysis for total drug (22). Sulfisoxazole acetyl was measured as sulfisoxazole and converted on a molar basis to equivalent amounts of sulfisoxazole acetyl. Radioactivity was determined by liquid scintillation spectrometry[14]; ^{14}C-toluene was used as an internal standard to correct for quenching. Bretylium was analyzed by a spectrophotometric method[13] involving ion-pair extraction of drug from urine (23).

Recovery of sulfanilamide and sulfisoxazole acetyl from urine was greater than 95%; urine blanks of free and total sulfonamides were 0.25 and 0.31 mg/day, respectively. Recovery of bretylium and ^{14}C-riboflavin from urine was 101 and 97%, respectively; urine blanks of both were negligible.

[1] Z. Fendrick, Charles University, Hradec Kralove, Czechoslovakia, personal communication.
[2] Donated by Hoffmann–La Roche, Nutley, N.J.
[3] Donated by Burroughs Wellcome Co., Research Triangle Park, N.C.
[4] Eastman Organic Chemicals, Rochester, N.Y.
[5] Sigma Chemical Co., St. Louis, Mo.
[6] Amersham/Searle, Arlington Heights, Ill.
[7] Ruger Chemical Co., Irvington, N.Y.
[8] Aldrich Chemical Co., Milwaukee, Wis.
[9] J. T. Baker Chemical Co., Phillipsburg, N.J.
[10] Landsverk Roentgen meter, Landsverk Co., Glendale, Calif.
[11] Model HB-11M with HB-66 food tunnel, Hoeltge, Inc., Cincinnati, Ohio.
[12] Riboflavin and niacinamide 1-ml ampul, Eli Lilly and Co., Indianapolis, Ind.
[13] Beckman DU (Beckman Instruments, Fullerton, Calif.) with a Gilford model 2000 multiple sample recorder (Gilford Instrument Laboratories, Oberlin, Ohio).
[14] Packard Tri-Carb model 3320, Packard Instrument Co., Downers Grove, Ill.

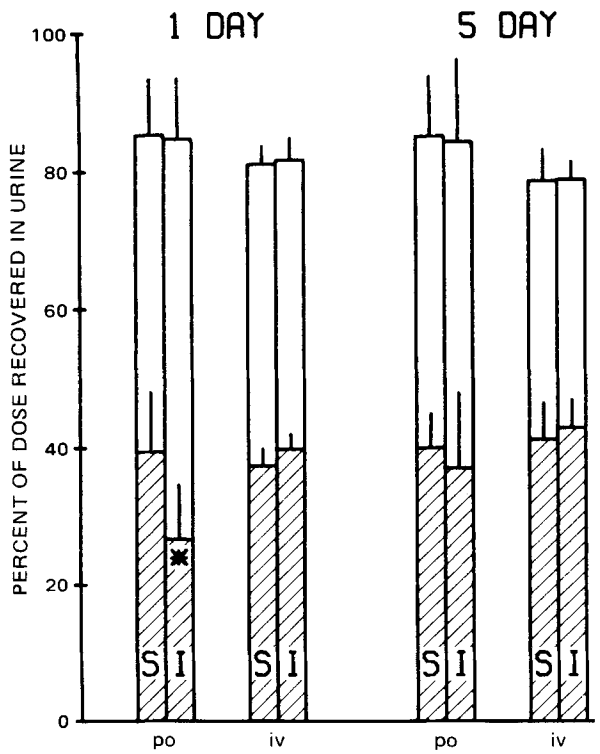

Figure 1—*Recovery of sulfanilamide in the urine of rats exposed to 850 rad of γ-radiation (I) or sham irradiated (S) 1 or 5 days before administration of 200 mg/kg. Each bar represents the mean of five or more animals, the vertical line in the center of each bar indicates 1* SD, *and the * indicates that recovery was significantly different (p < 0.01) from the corresponding S group. The hatched and open portions of each bar represent non-*N^4*-conjugated and* N^4*-conjugated sulfanilamide, respectively.*

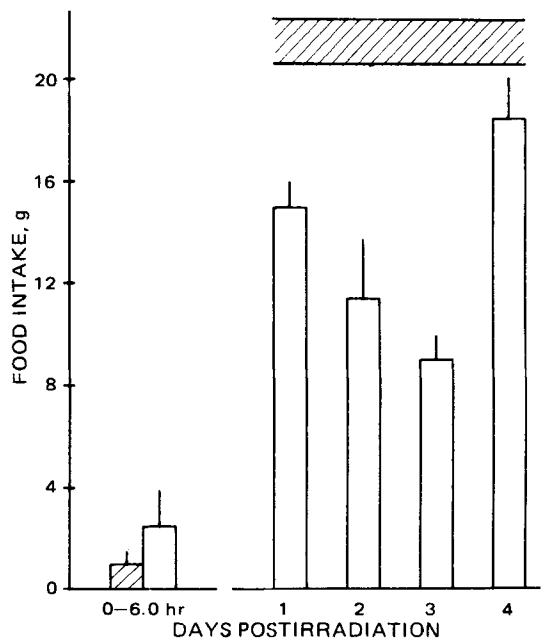

Figure 2—*Food intake in rats following exposure to 850 rad of γ-radiation (open bars) or sham irradiation (hatched bars). Each vertical bar represents the mean of 10 or more animals, and the vertical line in the center of each bar indicates 1* SD. *The horizontal bar represents the mean daily food intake of 10 or more sham-irradiated animals* ± SE.

RESULTS AND DISCUSSION

Sulfanilamide—Similar recoveries of sulfanilamide in the urine following oral and intravenous administration (Fig. 1) indicate that the orally administered drug was absorbed completely, as reported by others (24, 25). Following intravenous administration, neither the total recovery of the drug in the urine nor the fraction excreted in the urine as N^4-conjugate was affected significantly by prior irradiation of the animals (Fig. 1). Other studies in mice and rats found that serum and whole blood levels following intravenous or intraperitoneal administration of certain sulfonamides were not affected by prior irradiation (9, 26). Thus, the differences between irradiated and sham-irradiated animals in the urinary recovery of sulfanilamide administered orally reflect the effects of radiation on the absorption of sulfanilamide rather than on the distribution or elimination of the drug.

The lack of effect of radiation on the extent of metabolism of sulfanilamide *in vivo* is interesting in view of *in vitro* drug metabolism studies with homogenates of liver from irradiated rats. In these studies, prior whole-body exposure to γ-radiation induced a subsequent decrease in microsomal enzyme activity at 3–5 days postirradiation for several drugs (27, 28), including sulfanilamide (29). Recent pharmacokinetic analyses showed that *in vitro* studies of drug metabolism do not necessarily provide information about the intrinsic capacity of liver tissue to metabolize drugs (30, 31). Apparently, the *in vivo* rate of metabolism of sulfanilamide

Table II—Recovery of Sulfanilamide in Urine following Oral Administration[a] of 200 mg/kg to Rats Fasted Postirradiation

	Percent of Dose Recovered[c]	
Treatment[b]	Unconjugated	Total
Sham	40.9 ± 4.84	80.3 ± 6.29
850 rad	29.5 ± 10.2[d]	78.7 ± 11.1

[a] Administered as a suspension in 0.5% aqueous methylcellulose. [b] Rats were exposed to 850 rad of cobalt-60 γ-radiation or sham irradiated 1 day before sulfanilamide administration. Following irradiation, animals were not allowed food. [c] Mean of five animals ± *SD*. [d] Significantly different from sham ($p < 0.05$).

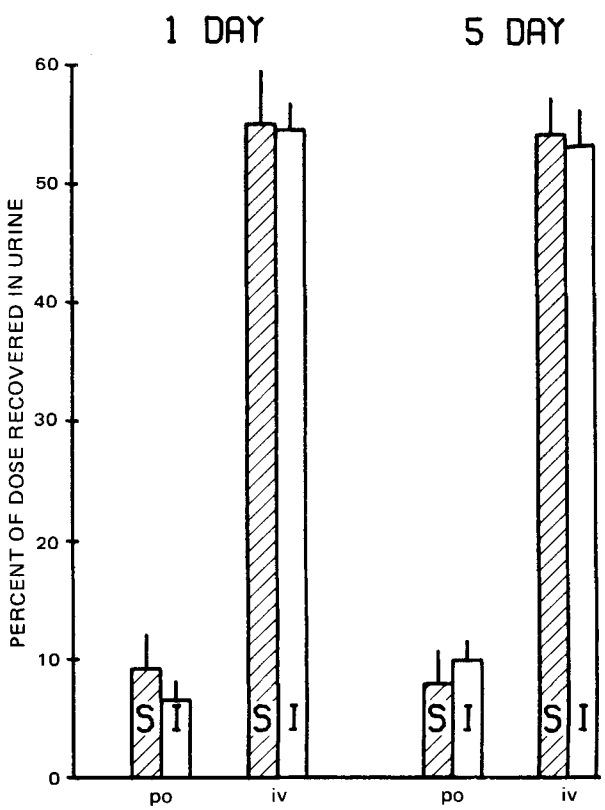

Figure 3—*Recovery of bretylium in the urine of rats exposed to 850 rad of γ-radiation (I) or sham irradiated (S) 1 or 5 days before administration of 30 mg/kg po or 5 mg/kg iv of bretylium tosylate. Each bar represents the mean of five animals, and the vertical line in the center of each bar indicates 1* SD.

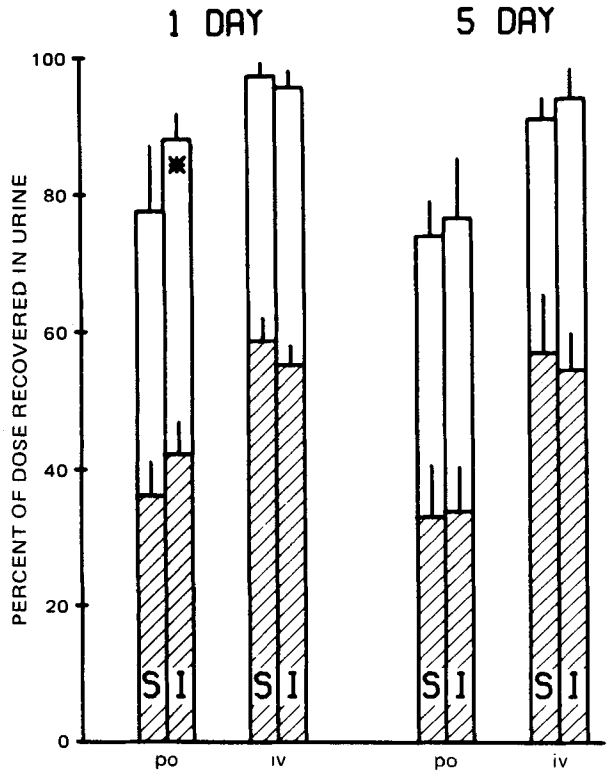

Figure 4—*Recovery of sulfisoxazole acetyl in the urine of rats exposed to 850 rad of γ-radiation (I) or sham irradiated (S) 1 or 5 days before administration of 100 mg/kg. Each bar represents the mean of five animals, the vertical line in the center of each bar indicates 1* SD, *and the * indicates that recovery was significantly different ($p < 0.05$) from the corresponding S group. The hatched and open portions of each bar represent non- N^4-conjugated and N^4-conjugated sulfisoxazole acetyl, respectively.*

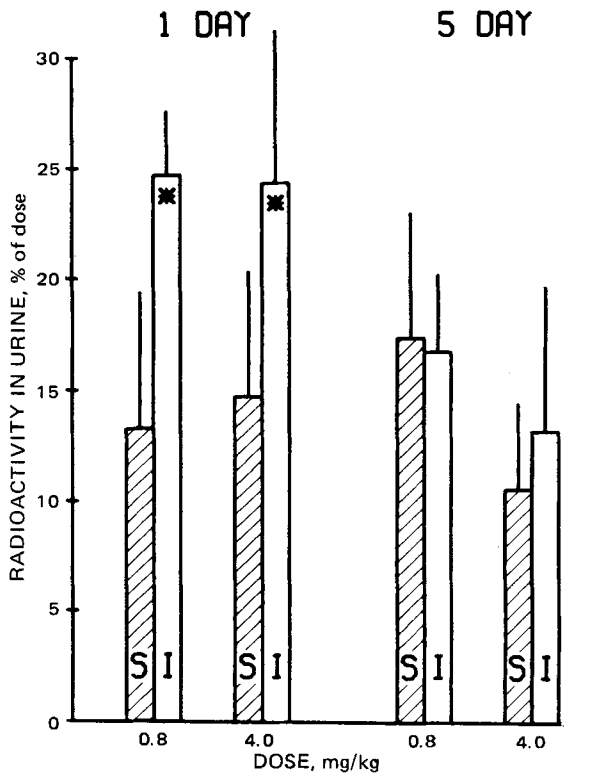

Figure 5—*Recovery of radioactivity in the urine of rats exposed to 850 rad of γ-radiation (I) or sham irradiated (S) 1 or 5 days before oral administration of 0.8 or 4.0 mg of ^{14}C-riboflavin/kg. Each bar represents the mean of six animals, the vertical line in the center of each bar indicates 1* SD, *and the * indicates that recovery was significantly different ($p < 0.05$) from the corresponding S group.*

is not controlled by the intrinsic metabolic capacity of the liver; changes in this capacity, as indicated by *in vitro* microsomal enzyme studies, do not result in changes in the *in vivo* rate of elimination or extent of metabolism of the drug.

Exposure of rats to 850 rad of γ-radiation 1 or 5 days prior to oral administration of sulfanilamide did not affect the total urinary recovery of the drug and its metabolites (Fig. 1). At 1 day postirradiation, however, the fraction of sulfanilamide excreted as metabolite increased significantly; this increase was not evident at 5 days postirradiation. Since the extent of metabolism of intravenously administered sulfanilamide was not affected by prior irradiation of the animals, the observed increase in the extent of metabolism of orally administered sulfanilamide apparently occurs before the drug reaches the systemic circulation. Whole-body irradiation is known to cause a subsequent transient reduction in the rate of gastric emptying (1, 32). The increased residence time of sulfanilamide in the stomachs of irradiated animals compared to controls may have resulted in metabolism of part of the dose prior to absorption. Both the gastric emptying rate (1) and the extent of metabolism of sulfanilamide (Fig. 1) returned to control values by 5 days postirradiation.

Following irradiation, rats alter their pattern of food consumption (6). In this study, food consumption was increased immediately following irradiation but reduced on Days 1–4 postirradiation (Fig. 2). In addition, the stomach at 1 day postirradiation was markedly distended by food following an overnight fast. By 5 days postirradiation, both food intake and the amount of food in the stomach were similar in irradiated and control animals.

To determine whether differences in food consumption between irradiated and control animals affected sulfanilamide absorption, the experiment was repeated with animals that were fasted from the time of irradiation or sham irradiation to 3 hr after drug administration. The results (Table II) were similar to the results of the study shown in Fig. 1. Thus, the effect of radiation on sulfanilamide absorption at 1 day postirradiation is apparently not due to a radiation-induced alteration in food consumption.

Bretylium—Following oral administration, the urinary recovery of bretylium was less than 20% of the recovery following intravenous administration (Fig. 3). This comparatively low recovery indicates that bretylium was poorly absorbed, probably due to low permeability of the GI epithelium to this ionized compound. The urinary recovery of intravenously administered bretylium was not affected by prior irradiation of the animals (Fig. 3). Thus, differences between irradiated and sham-irradiated animals in the urinary recovery of bretylium indicate the effect of prior irradiation on the absorption of orally administered bretylium.

Because bretylium is poorly absorbed following oral administration, the extent of drug absorption was anticipated to be sensitive to radiation-induced alterations in the permeability of the GI mucosa. At both 1 and 5 days postirradiation, the absorption of bretylium by irradiated rats was not significantly different from drug absorption by sham-irradiated animals (Fig. 3). There is evidence that the rate of small intestinal transit is increased in rats at 1 day postirradiation (10). Such an increase would reduce the time available for bretylium absorption, possibly explaining the tendency toward decreased absorption at 1 day postirradiation (Fig. 3). The extensive histological changes occurring in the small intestinal epithelium following irradiation (5, 33) probably do not affect significantly the capacity of the intestine to absorb bretylium.

Sulfisoxazole Acetyl—Following intravenous administration of sulfisoxazole acetyl, neither the total urinary recovery of the drug nor the fraction excreted unchanged was affected by prior irradiation of the animals (Fig. 4). In addition, irradiation did not affect significantly the extent of metabolism of sulfisoxazole acetyl (Fig. 4). As shown previously (34), the urinary recovery of orally administered sulfisoxazole acetyl was significantly lower than after intravenous administration, indicating incomplete absorption (Fig. 4). The low oral bioavailability was presumably due to the low aqueous solubility of the drug.

At 1 day postirradiation, the extent of sulfisoxazole acetyl absorption was significantly greater in irradiated animals than in sham-irradiated controls (Fig. 4). Since the sulfisoxazole acetyl absorption is dissolution rate limited (1, 34), the reduced rate of gastric emptying in irradiated animals apparently allows additional time for dissolution of sulfisoxazole acetyl and, therefore, increases absorption. At 5 days postirradiation, both the gastric emptying rate (1) and the extent of sulfisoxazole acetyl absorption (Fig. 4) were not significantly different from control values.

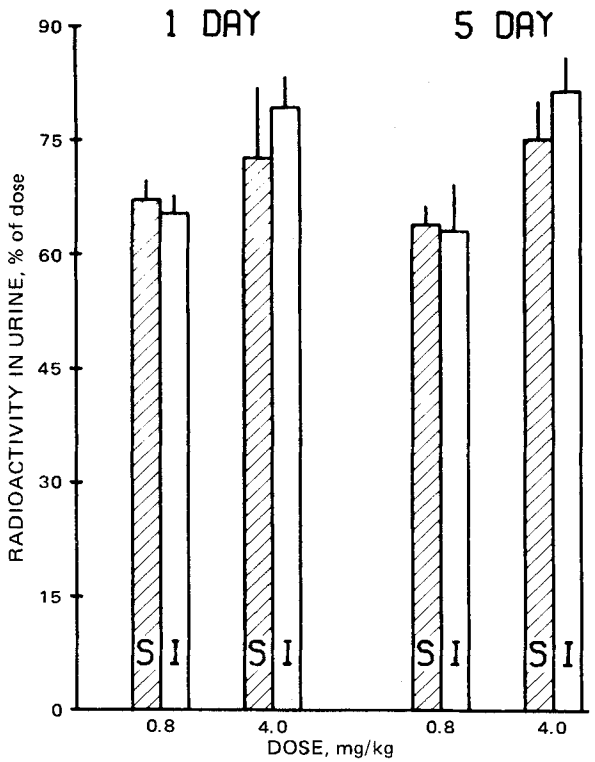

Figure 6—*Recovery of radioactivity in the urine of rats exposed to 850 rad of γ-radiation (I) or sham irradiated (S) 1 or 5 days before intravenous administration of 0.8 or 4.0 mg of ^{14}C-riboflavin/kg. Each bar represents the mean of six animals, and the vertical line in the center of each bar indicates 1* SD.

Riboflavin—The low recovery of radioactivity in the urine following oral administration of ^{14}C-riboflavin (Fig. 5) compared to intravenous administration (Fig. 6) indicates that riboflavin was not completely absorbed. The absorption of the vitamin in rats is probably limited by its low oil/water partition coefficient and low solubility in water.

Irradiation had a negligible effect on the excretion of riboflavin following intravenous administration of either 0.8 or 4.0 mg/kg (Fig. 6). However, irradiated animals receiving riboflavin orally at 1 day postirradiation excreted 70–85% more radioactivity than controls (Fig. 5). A similar increase in the bioavailability of orally administered riboflavin was reported in humans pretreated with propantheline to reduce the rate of gastric emptying (35). Delayed gastric emptying in humans apparently increased absorption by prolonging the contact of the vitamin with a capacity-limited mechanism for absorption. Although capacity-limited absorption of riboflavin has not been found in rats (36 and references therein), a reduction in the gastric emptying rate could increase the bioavailability of a passively absorbed drug as was reported for phenolsulfonphthalein (37).

The recovery of radioactivity (percent of dose) in urine following intravenous administration of riboflavin increased with dose (Fig. 6). This dose-dependent increase may be due to saturable tubular reabsorption in the kidney (38) or to saturable tissue binding (36). The urinary recovery of riboflavin following oral and intraperitoneal administration decreases as the dose is increased, apparently because of a nonlinear biliary excretion mechanism (36, 39).

In summary, there was no detectable difference between irradiated and sham-irradiated animals in the extent of drug absorption at 5 days postirradiation. At 1 day postirradiation, the extent of sulfisoxazole acetyl and riboflavin absorption was increased significantly while sulfanilamide and bretylium tosylate absorption was not affected. The extent of metabolism of sulfanilamide was increased at 1 day postirradiation.

REFERENCES

(1) M. E. Brady and W. L. Hayton, *J. Pharm. Sci.*, **66**, 366 (1977).

(2) *Ibid.*, in press.

(3) T. R. Bates and M. Gibaldi, in "Current Concepts in the Pharmaceutical Sciences: Biopharmaceutics," J. Swarbrick, Ed., Lea & Febiger, Philadelphia, Pa., 1970, chap. 2.

(4) L. Z. Benet, in "Drug Design," vol. 4, E. J. Ariens, Ed., Academic, New York, N.Y., 1973, chap. 1.

(5) K. E. Carr and P. G. Toner, *Virchows Arch. B*, **11**, 201 (1972).

(6) A. D. Perris, E. L. Jervis, and D. H. Smyth, *Radiat. Res.*, **28**, 13 (1966).

(7) R. F. Hagemann and S. Lesher, *Br. J. Radiol.*, **44**, 599 (1971).

(8) W. J. Jusko, D. R. Conti, A. Molson, P. Kuritzky, J. Giller, and R. Schultz, *J. Am. Med. Assoc.*, **230**, 1554 (1974).

(9) A. Hurwitz and J. Doull, *Radiat. Res.*, **59**, 606 (1974).

(10) R. W. Summers, T. H. Kent, and J. W. Osborne, *Gastroenterology*, **59**, 731 (1970).

(11) G. E. Sagan and F. W. Lengemann, *Radiat. Res.*, **53**, 480 (1973).

(12) G. Janossy, *Acta Med. Acad. Sci. Hung.*, **26**, 13 (1969).

(13) J. Kabal, S. J. Baum, and L. J. Parkhurst, *Radiat. Res.*, **50**, 528 (1972).

(14) V. P. Bond, *Am. J. Clin. Nutr.*, **12**, 194 (1963).

(15) A. D. Perris, *Radiat. Res.*, **34**, 523 (1968).

(16) M. F. Sullivan, *Am. J. Physiol.*, **201**, 1013 (1961).

(17) R. D. Goodman, A. E. Lewis, and E. A. Schuck, *ibid.*, **169**, 242 (1952).

(18) M. N. Swift, S. T. Taketa, and V. P. Bond, *ibid.*, **182**, 479 (1955).

(19) W. L. Hayton, *J. Pharm. Sci.*, **63**, 645 (1974).

(20) M. J. Mattila, S. Takki, and L. R. Holsti, *Arzneim.-Forsch.*, **18**, 889 (1968).

(21) M. J. Mattila, L. R. Holsti, V. M. K. Venho, and S. Takki, *ibid.*, **20**, 533 (1970).

(22) J. Rieder, *Chemotherapy*, **17**, 1 (1972).

(23) C. D. Johnson and J. P. Revill, *Acta Pharmacol. Toxicol.*, **27**, 404 (1972).

(24) J. W. Bridges, Ph.D. thesis, University of London; through R. T. Williams, *Fed. Prac. Fed. Am. Soc. Exp. Biol.*, **26**, 1029 (1967).

(25) E. Sögen, *Acta Pharmacol. Toxicol.*, **22**, 19 (1965).

(26) H. Krysicka-Doczka, A. Danysz, T. Koter, and K. Wierzba, *Strahlentherapie*, **147**, 634 (1974).

(27) J. C. A. Knott and E. D. Wills, *Radiat. Res.*, **53**, 65 (1973).

(28) O. Yukawa and T. Nakazawa, *ibid.*, **58**, 101 (1974).

(29) H. K. Hanel and I. Wilian-Ulrich, *Int. J. Radiat. Biol.*, **1**, 366 (1959).

(30) D. Perrier and M. Gibaldi, *J. Pharmacol. Exp. Ther.*, **191**, 17 (1974).

(31) G. R. Wilkinson and D. G. Shand, *Clin. Pharmacol. Ther.*, **18**, 377 (1975).

(32) V. Chmelar, V. Grossmann, I. M. Hais, and F. Deml, *Radiat. Res.*, **37**, 627 (1969).

(33) H. R. Withers, *Cancer*, **28**, 75 (1971).

(34) D. C. Bloedow and W. L. Hayton, *J. Pharm. Sci.*, **65**, 328 (1976).

(35) G. Levy, M. Gibaldi, and J. A. Procknal, *ibid.*, **61**, 798 (1972).

(36) J. E. Axelson and M. Gibaldi, *ibid.*, **61**, 404 (1972).

(37) J. J. Ashley and G. Levy, *ibid.*, **62**, 688 (1973).

(38) W. J. Jusko and G. Levy, *ibid.*, **59**, 765 (1970).

(39) H. Nogami, M. Hanano, S. Awazu, and T. Iga, *Chem. Pharm. Bull.*, **18**, 228 (1970).

ACKNOWLEDGMENTS AND ADDRESSES

Received March 24, 1976, from the *College of Pharmacy, Washington State University, Pullman, WA 99164.*

Accepted for publication May 12, 1976.

Presented in part at the Basic Pharmaceutics Section, APhA Academy of Pharmaceutical Sciences, San Francisco meeting, April 1975.

Abstracted from a dissertation submitted by M. E. Brady to Washington State University in partial fulfillment of the Doctor of Philosophy degree requirements.

Supported in part by funds provided for biological and medical research by Washington State University Initiative Measure No. 171.

The authors appreciate the gifts of sulfisoxazole acetyl provided by Dr. W. E. Scott, Research Division, Hoffmann–La Roche Inc., and bretylium tosylate provided by Dr. R. A. Maxwell, Burroughs Wellcome Co.

* AFPE Paul M. Scott Memorial Fellow. Present address: College of Pharmacy, University of Cincinnati, Cincinnati, OH 45221.

ˣ To whom inquiries should be directed.

GI Drug Absorption in Rats Exposed to Cobalt-60 γ-Radiation II: *In Vivo* Rate of Absorption

MICHAEL E. BRADY * **and WILLIAM L. HAYTON** ˣ

Abstract □ The rate of absorption of sulfanilamide, bretylium tosylate, sulfisoxazole acetyl, and riboflavin was studied in rats exposed to 850 rad of cobalt-60 γ-radiation either 1 or 5 days before oral drug administration. Polyethylene glycol 4000 was administered with sulfanilamide; its distribution along the GI tract indicated that the gastric emptying rate was reduced threefold at 1 day postirradiation but returned to normal at 5 days postirradiation; the small intestinal transit rate was not detectably altered by irradiation. At 1 day postirradiation, there was a marked decrease in the absorption rate of sulfanilamide, a smaller, although significant, decrease in the absorption rate of sulfisoxazole acetyl and bretylium, and an increase in the absorption rate of riboflavin. At 5 days postirradiation, the drug absorption rate was normal. The changes in the absorption rate of the drugs were due to a radiation-induced reduction in the gastric emptying rate; the permeability of the GI epithelium did not appear to be affected by radiation. The results indicate that, immediately following irradiation, a marked reduction in the gastric emptying rate causes a pronounced reduction in the absorption rate of rapidly absorbed drugs, a less pronounced reduction in the absorption rate of drugs that are absorbed slowly because of slow dissolution or slow diffusion across the GI epithelium, and an increase in the absorption rate of drugs that are absorbed by a saturable mechanism provided the mechanism is not impaired by irradiation.

Keyphrases □ Absorption, GI—various drugs, effect of cobalt-60 γ-radiation, rats □ Radiation, gamma—effect on GI absorption of various drugs, rats □ Sulfanilamide—GI absorption, effect of cobalt-60 γ-radiation, rats □ Bretylium tosylate—GI absorption, effect of cobalt-60 γ-radiation, rats □ Sulfisoxazole acetyl—GI absorption, effect of cobalt-60 γ-radiation, rats □ Riboflavin—GI absorption, effect of cobalt-60 γ-radiation, rats

The results of a previous study (1) showed that prior exposure of rats to cobalt-60 γ-radiation may significantly alter the absorption pattern of orally administered drugs. In irradiated animals, the extent of absorption of sulfisoxazole acetyl and riboflavin was increased compared to control animals. Irradiation did not have a detectable effect on the extent of absorption of bretylium tosylate or sulfanilamide, although the extent of metabolism of sulfanilamide was significantly increased in irradiated animals.

While the previous study dealt with the effects of ionizing radiation on the extent of drug absorption, radiation-induced changes in GI structure and motility may also affect the rate of drug absorption. To explore this possibility, the *in vivo* absorption rate of sulfanilamide, bretylium tosylate, sulfisoxazole acetyl, and riboflavin was studied in irradiated and sham-irradiated rats.

EXPERIMENTAL

Materials—The drugs and reagents used were described previously (*1*). 1,2-^{14}C-Polyethylene glycol 4000[1] (specific activity 0.3 mCi/g) was dissolved in water and stored at 5° in an opaque container.

Absorption Rate—Male Sprague–Dawley rats, 170–250 g, were irradiated or sham irradiated as described previously (1). At 1 or 5 days postirradiation, 8.0 ml/kg of a water–propylene glycol (1:1) solution of sulfanilamide (200 mg/kg) and ^{14}C-polyethylene glycol (4.0 mg/kg) was administered by gastric intubation (2) to animals that had been fasted overnight. Equal numbers of irradiated and sham-irradiated animals were used each time an experiment was performed.

At 0.5, 1.0, 2.0, and 6.0 hr after dosing, the animals were sacrificed by exposing the head to microwave radiation[2] for 15 sec (3, 4). Blood was immediately removed by cardiac puncture, and the GI tract was excised and separated into five portions: stomach, small intestine divided into three segments of equal length, and the caecum and colon. The intestinal segments and serum separated by centrifugation from clotted blood were frozen until assayed.

In similar studies, 8.0 ml/kg of an aqueous sulfisoxazole acetyl suspension (100 mg/kg), a bretylium tosylate solution (30 mg/kg), or 12 ml/kg of an aqueous riboflavin solution (0.80 mg/kg, 0.12 μCi/ml) was administered by gastric intubation; polyethylene glycol 4000 was not present. At 0.5 or 2.0 hr after dosing, the animals were sacrificed; the GI tract and a sample of serum were removed and frozen until analysis.

Analytical Methods—Each portion of the GI tract was homogenized[3], and the amount of drug or radioactivity in the homogenate and serum was assayed by methods described previously (1). Radioactivity was not detected in serum following administration of ^{14}C-polyethylene glycol or ^{14}C-riboflavin. Recovery of radioactivity from homogenates containing ^{14}C-riboflavin or ^{14}C-polyethylene glycol was greater than 94%; chemiluminescence was not a problem since homogenate blanks were negligible.

Mean recoveries of bretylium tosylate, free sulfanilamide, and total sulfisoxazole acetyl from GI homogenates were 96, 96, and 101%, respectively. Blank values of free sulfanilamide from homogenates of the stomach, small intestine, and caecum and colon were 0.32, 0.22, and 0.64 mg, respectively. Blank values of total sulfisoxazole acetyl from stomach and intestinal homogenates were 0.10 and 0.56 mg, respectively; bretylium blank values were negligible. Recovery of free sulfanilamide and sulfisoxazole acetyl from serum was nearly 100% with serum blanks of 8.6 and 6.1 μg/ml, respectively.

RESULTS AND DISCUSSION

At 1 day postirradiation, the distribution of orally administered polyethylene glycol, a nonabsorbable marker (5), along the GI tract of irradiated animals was quite different from that of the controls (Figs. 1 and 2, respectively). The most notable difference in distribution was the increased level of polyethylene glycol in the stomachs of irradiated animals, indicating that prior irradiation reduced the gastric emptying rate as reported by others (6, 7). In both irradiated and control animals, the gastric emptying of polyethylene glycol followed apparent first-order kinetics with half-lives of 3.4 and 0.8 hr, respectively. At 5 days postirradiation, the GI distribution of polyethylene glycol was not altered appreciably by irradiation. Since the distribution appeared similar to that in Fig. 2 for both groups of animals, it is not shown.

Small intestinal transit times for polyethylene glycol were calculated by a method described previously (8). No radiation-induced change in the motility of the small intestine was detected. This finding agrees with previous studies in which a nonabsorbable marker was administered to the stomach (6, 9). However, when the marker was administered intraduodenally, the small intestinal transit rate was increased in irradiated rats (10). Since this latter study was not complicated by the effects of radiation on gastric emptying, it may be a more sensitive measure of the effects of radiation on intestinal motility than studies that involved gastric administration of the marker.

The recovery of polyethylene glycol from the GI tract of both irradiated and control animals was nearly complete (>90%) at all times up to 6 hr following its administration (Table I). Thus, the very low permeability of the GI epithelium to large, polar molecules is not altered by prior irradiation of the epithelium, even though marked anatomical and phys-

[1] New England Nuclear, Boston, Mass.

[2] Toshiba electronic oven model ER-625BT, Toshiba American, Inc., Flushing, N.Y.

[3] Sorvall Omni-Mixer, Ivan Sorvall, Inc., Newtown, Conn.

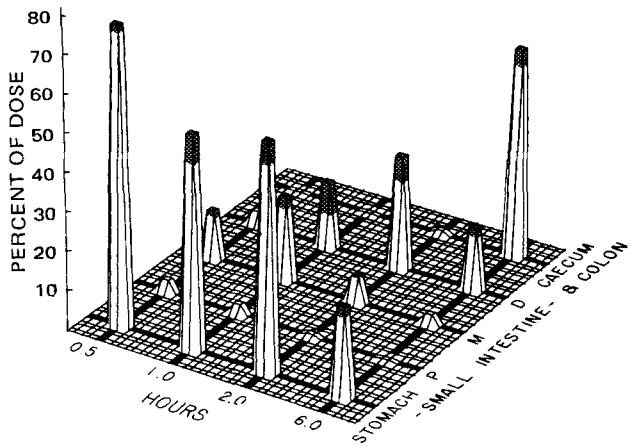

Figure 1—*Distribution of polyethylene glycol 4000 along the GI tract following its oral administration to rats exposed to 850 rad of cobalt-60 γ-radiation 1 day previously. Each bar represents the mean of six animals; stippling represents 1* SE. *P, M, and D are the proximal, middle, and distal thirds of the small intestine, respectively.*

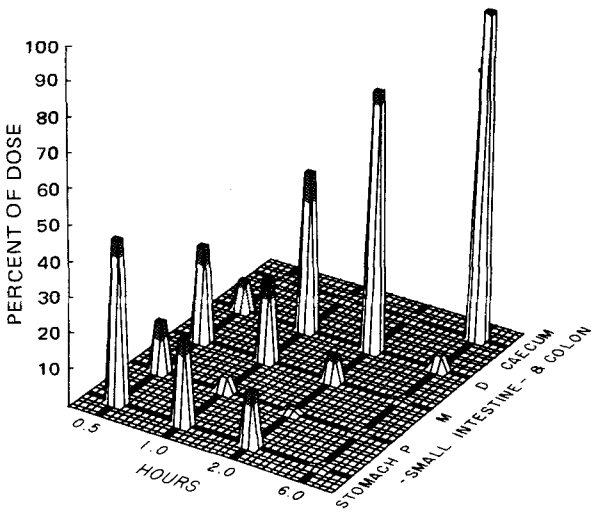

Figure 2—*Same as Fig. 1 except that the rats were sham irradiated.*

iological changes are manifest for several days following irradiation (11, 12).

Sulfanilamide was administered simultaneously with polyethylene glycol; its distribution along the GI tract at 1 day postirradiation is shown in Figs. 3 and 4 for irradiated and control animals, respectively. In both groups, less than 10% of the administered drug was recovered below the level of the stomach at any time. In addition, sulfanilamide disappeared from the stomach at the same rate as polyethylene glycol 4000 (Fig. 5). Since polyethylene glycol 4000 was not absorbed, sulfanilamide apparently was not absorbed from the stomach. The intestine is the primary site for absorption of sulfanilamide, and gastric emptying is the rate-controlling step in the absorption of this drug.

Table I—Recovery of Polyethylene Glycol from GI Tract following Oral Administration to Irradiated and Sham-Irradiated Rats

Time after Dosing, hr	Percent of Dose Recovered[a]			
	1 Day Postirradiation		5 Days Postirradiation	
	Sham	850 rad	Sham	850 rad
0.5	94.4 ± 2.23	96.0 ± 4.46	102.3 ± 7.72	91.7 ± 4.35
1.0	92.9 ± 5.22	94.6 ± 2.28	94.2 ± 3.38	104.4 ± 11.25
2.0	94.6 ± 1.62	96.7 ± 4.40	94.1 ± 2.00	103.2 ± 4.28
6.0	94.0 ± 2.81	91.7 ± 2.57	100.5 ± 5.18	92.7 ± 2.42
Mean	94.0 ± 0.76	94.8 ± 2.22	97.8 ± 4.25	98.2 ± 6.73

[a] Mean of six animals ± *SD*.

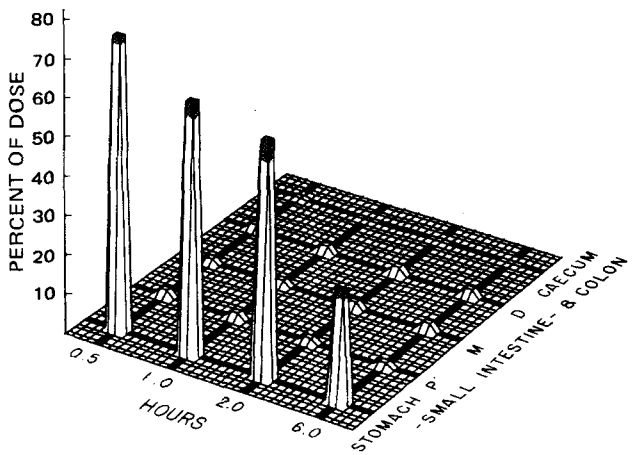

Figure 3—*Distribution of sulfanilamide along the GI tract following oral administration of 200 mg/kg to rats exposed to 850 rad of cobalt-60 γ-radiation 1 day previously. Each bar represents the mean of six animals; stippling represents 1* SE. *P, M, and D are proximal, middle, and distal thirds of the small intestine, respectively.*

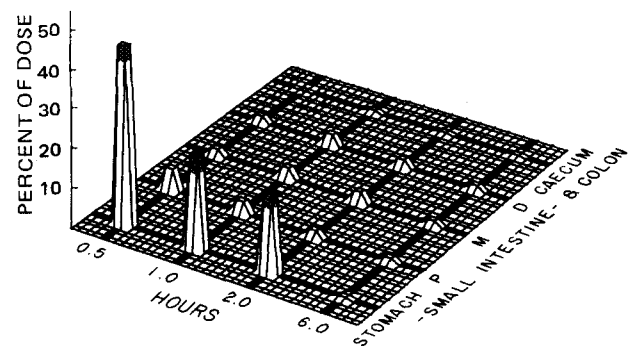

Figure 4—*Same as Fig. 3 except that the rats were sham irradiated.*

The reduced rate of absorption of sulfanilamide in irradiated animals at 1 day postirradiation is apparent in Figs. 3 and 4. The relatively slow absorption of sulfanilamide is also evident in the serum concentration–time curve of sulfanilamide; the serum level was threefold higher in control animals than in the irradiated group (Fig. 6). The linear relationship between serum concentrations of sulfanilamide and the amount of drug absorbed for both irradiated and control animals indicates that

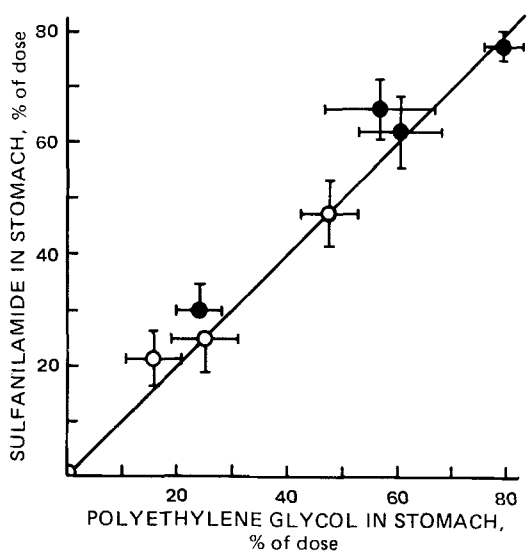

Figure 5—*Relationship between the recoveries of sulfanilamide and polyethylene glycol from the rat stomach at various times following their oral administration 1 day postirradiation. Key: ●, irradiated (850 rad); and ○, sham irradiated. Each point represents the mean of six animals, and lines indicate ± 1* SE.

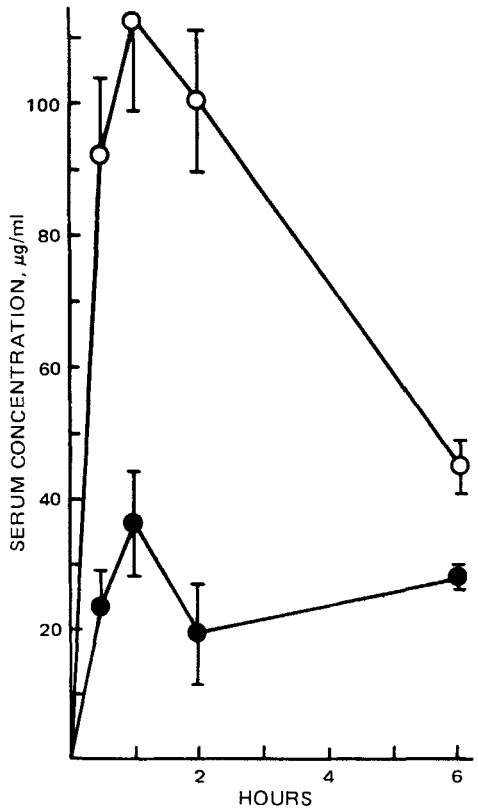

Figure 6—*Serum levels of sulfanilamide in rats following oral administration of 200 mg/kg 1 day postirradiation. Key: ●, irradiated (850 rad); and ○, sham irradiated. Each point represents the mean of six animals; bars indicate ± 1 SE.*

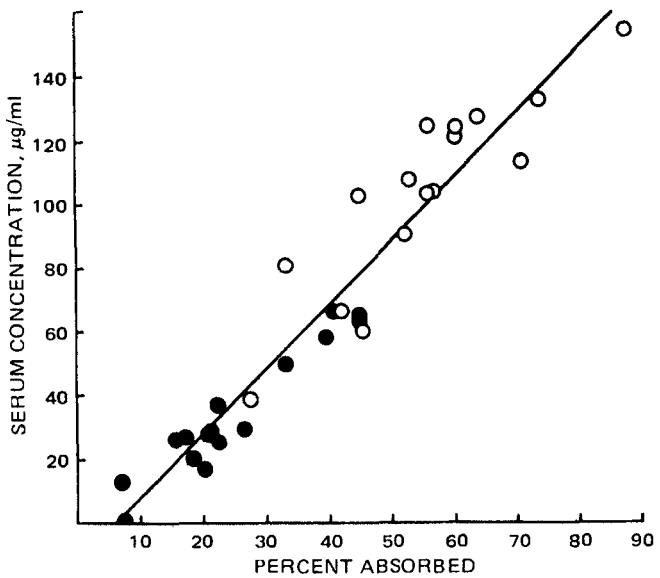

Figure 7—*Serum levels of sulfanilamide in rats and corresponding percent of dose absorbed at 0.5 and 1.0 hr following oral administration of 200 mg/kg 1 day postirradiation. Key: ●, irradiated (850 rad); and ○, sham irradiated.*

differences in serum levels were due solely to differences in the absorption rate (Fig. 7); distribution and elimination of the drug following absorption were apparently not affected by irradiation with 850 rad.

Immediately following irradiation, irradiated animals consume considerably more food than sham-irradiated animals (1). The stomachs of irradiated animals were greatly distended at 1 day postirradiation, even following an overnight fast. To determine whether food in the stomachs of irradiated animals caused the reduced absorption rate of sulfanilamide, the experiment was performed with animals that were not permitted food following irradiation. The sulfanilamide absorption rate remained significantly lower in the irradiated animals (Table II), indicating that these differences between irradiated and sham-irradiated animals were not due to differences in food consumption.

In agreement with the studies on polyethylene glycol 4000 and sulfanilamide, the gastric emptying rate of bretylium tosylate in irradiated animals was significantly reduced at 1 day postirradiation compared to sham-irradiated animals (Table III). This difference was not apparent at 5 days postirradiation. High levels of bretylium in the intestine indicate that the rate-controlling step in the absorption of this drug is diffusion across the GI mucosa to the blood rather than gastric emptying. Radiation-induced slowing of the gastric emptying rate, therefore, did not markedly reduce the bretylium absorption rate (Table III) as it did for sulfanilamide. The tendency for the absorption rate of bretylium to be reduced in irradiated animals is probably due both to a reduced rate of gastric emptying and a reduced mucosal permeability. The absorption rate of bretylium is probably more rapid from the intestine than the stomach, and both *in vitro* and *in situ* studies indicate that irradiation may cause a subsequent reduction in the permeability of the GI mucosa (13–15). Bretylium concentrations in serum were below the sensitivity of the analytical procedure, 5 μg/0.5 ml of serum.

The gastric emptying rate and the absorption rate of sulfisoxazole acetyl were reduced significantly in irradiated animals compared to the sham-irradiated group at 1 day postirradiation, but no detectable difference between the two groups was observed at 5 days postirradiation (Table IV). The reduced rate of drug absorption in irradiated animals compared to controls was also apparent from the significantly lower concentration of the drug in serum at 1 day postirradiation (Table IV).

Sulfisoxazole acetyl is absorbed more rapidly than sulfanilamide from solution by the rat small intestine (15). The relatively high level of sulfisoxazole acetyl in the intestine following its oral administration as a suspension indicates that the rate-controlling step in the absorption of this drug is dissolution. Although the absorption rate of sulfisoxazole acetyl is reduced in irradiated animals, the extent of absorption is increased (1), apparently because the reduced rate of GI transit allows more time for the drug to dissolve.

The gastric emptying rate of riboflavin was decreased in irradiated animals at 1 day postirradiation. In accord with previous studies, it appeared normal by 5 days postirradiation (Table V). The riboflavin level in the intestine was quite high. Since the vitamin was administered in solution, the rate-controlling step in the absorption process is apparently transport across the intestinal epithelium, in a manner similar to bretylium absorption. In contrast to the absorption of bretylium, however, the absorption rate of riboflavin was significantly *greater* in irradiated than in sham-irradiated animals. A possible explanation for this difference is that riboflavin is absorbed by a saturable process at a specific site in the proximal small intestine (16 and references cited therein) while the

Table II—Sulfanilamide in Serum and GI Tract following Oral Administration[a] of 200 mg/kg to Rats Fasted Postirradiation

Time after Dosing, hr	Treatment[b]	Serum Concentration[c,d], μg/ml	Percent of Dose Recovered[c]		Percent Absorbed[c,e]
			Stomach	Intestine	
0.5	Sham	105.0 ± 23.7	40.3 ± 10.9	6.33 ± 2.11	53.2 ± 12.9
0.5	850 rad	44.1 ± 23.8[f]	67.4 ± 15.3[f]	4.69 ± 1.95	27.9 ± 16.9[f]
2.0	Sham	117.0 ± 12.0	14.4 ± 9.12	5.29 ± 1.81	80.3 ± 8.01
2.0	850 rad	51.7 ± 14.9[f]	49.2 ± 11.7[f]	3.27 ± 0.99	47.5 ± 11.2[f]

[a] Administered as a solution in water–propylene glycol (1:1). [b] Rats were exposed to 850 rad of cobalt-60 γ-radiation or sham irradiated 1 day before administration of sulfanilamide. [c] Mean of five animals ± *SD*. [d] Non-N^4-conjugated. [e] Difference between dose and recovery from the stomach and intestine. [f] Significantly different ($p < 0.05$) from corresponding sham-irradiated animals.

Table III—Bretylium Tosylate in GI Tract following Oral Administration[a] of 30 mg/kg to Rats

Time after Treatment, days	Time after Dosing, hr	Treatment[b]	Percent of Dose Recovered[c]		Percent Absorbed[c,d]
			Stomach	Intestine	
1	0.5	Sham	38.8 ± 4.43	55.8 ± 13.4	8.7 ± 9.4
1	0.5	850 rad	69.6 ± 6.02[e]	25.4 ± 2.64[e]	5.0 ± 4.0
1	2.0	Sham	2.13 ± 1.46	85.5 ± 4.65	12.3 ± 4.40
1	2.0	850 rad	39.9 ± 7.37[e]	54.2 ± 8.03[e]	6.0 ± 3.4[e]
5	0.5	Sham	42.0 ± 12.0	47.5 ± 13.2	10.5 ± 8.22
5	0.5	850 rad	44.4 ± 10.8	46.5 ± 8.03	9.1 ± 6.6
5	2.0	Sham	1.63 ± 1.24	81.4 ± 6.20	16.8 ± 6.11
5	2.0	850 rad	4.73 ± 0.47[e]	84.8 ± 4.38	10.4 ± 4.38

[a] Administered as a solution in water. [b] Rats were exposed to 850 rad of cobalt-60 γ-radiation or sham irradiated 1 or 5 days before administration of bretylium tosylate. [c] Mean of five animals ± *SD*. [d] Difference between dose and recovery from the stomach and intestine. [e] Significantly different ($p < 0.05$) from corresponding sham-irradiated animals.

Table IV—Sulfisoxazole Acetyl in Serum and GI Tract following Oral Administration[a] of 100 mg/kg to Rats

Time after Treatment, days	Time after Dosing, hr	Treatment[b]	Serum Concentration[c,d], μg/ml	Percent of Dose Recovered[c,e]		Percent Absorbed[c,f]
				Stomach	Intestine	
1	0.5	Sham	62.9 ± 10.8	40.0 ± 9.94	35.3 ± 8.41	26.0 ± 9.39
1	0.5	850 rad	48.7 ± 7.58[g]	74.4 ± 5.93[g]	22.5 ± 6.31[g]	4.1 ± 4.9[g]
1	2.0	Sham	163.0 ± 19.8	16.0 ± 5.73	47.4 ± 7.67	36.6 ± 2.80
1	2.0	850 rad	97.5 ± 13.3[g]	70.7 ± 7.63[g]	11.8 ± 4.01[g]	17.4 ± 4.31[g]
5	0.5	Sham	58.7 ± 25.6	43.8 ± 8.31	39.3 ± 12.4	16.8 ± 13.0
5	0.5	850 rad	46.4 ± 21.4	48.1 ± 4.24	30.7 ± 12.6	21.2 ± 10.9
5	2.0	Sham	161.0 ± 11.4	10.9 ± 3.37	54.4 ± 3.88	34.8 ± 4.87
5	2.0	850 rad	155.0 ± 20.3	19.4 ± 7.56[g]	43.0 ± 7.55[g]	37.6 ± 7.58

[a] Administered as a suspension in water containing 0.5% methylcellulose. [b] Rats were exposed to 850 rad of cobalt-60 γ-radiation or sham irradiated 1 or 5 days before administration of sulfisoxazole acetyl. [c] Mean of five animals ± *SD*. [d] Non-N^4-conjugated sulfisoxazole acetyl. [e] Total sulfisoxazole acetyl and sulfisoxazole. [f] Difference between dose and recovery from the stomach and intestine. [g] Significantly different ($p < 0.05$) from corresponding sham-irradiated animals.

Table V—Riboflavin in GI Tract following Oral Administration[a] of 0.8 mg/kg to Rats

Time after Treatment, days	Time after Dosing, hr	Treatment[b]	Percent of Dose Recovered[c]		Percent Absorbed[c,d]
			Stomach	Intestine	
1	0.5	Sham	44.1 ± 14.9	51.2 ± 11.8	4.6 ± 4.5
1	0.5	850 rad	67.3 ± 10.7[e]	26.8 ± 18.7[e]	8.9 ± 5.4
1	2.0	Sham	0.69 ± 0.26	93.3 ± 7.44	7.3 ± 5.0
1	2.0	850 rad	39.0 ± 22.8[e]	45.0 ± 28.9[e]	16.0 ± 6.49[e]
5	0.5	Sham	29.4 ± 13.1	64.1 ± 9.60	6.5 ± 6.2
5	0.5	850 rad	36.7 ± 16.4	66.5 ± 24.2	2.4 ± 2.4
5	2.0	Sham	2.54 ± 2.98	88.2 ± 4.93	9.3 ± 3.1
5	2.0	850 rad	2.76 ± 3.28	85.0 ± 5.13	12.1 ± 5.33

[a] Administered as a solution in water. [b] Rats were exposed to 850 rad of cobalt-60 γ-radiation or sham irradiated 1 or 5 days before administration of riboflavin. [c] Mean of five animals ± *SD*. [d] Difference between dose and recovery from the stomach and intestine. [e] Significantly different ($p < 0.05$) from corresponding sham-irradiated animals.

absorption of bretylium is not saturable. Slow release of riboflavin from the stomach of irradiated animals at 1 day postirradiation presents the vitamin to the absorption site at a relatively low concentration for a relatively long time. This increased time of contact allows a greater fraction of the dose to be absorbed. The *in vivo* extent of riboflavin absorption was also increased in irradiated rats at 1 day postirradiation (1).

An alternative explanation for the radiation-induced increase in riboflavin absorption is that riboflavin is absorbed more rapidly from the stomach than from the intestine, and slowed gastric emptying thereby increases the absorption rate. In view of the very slow absorption of practically all drugs from the stomach compared to the intestine, this latter mechanism is not likely.

With regard to the drug absorption rate, the primary effect of irradiation is the marked reduction in the gastric emptying rate immediately following irradiation. The slowed gastric emptying appears to be a normal response to intestinal injury in the rat (17). By 5 days postirradiation, the gastric emptying rate had returned to normal.

The net effect on the drug absorption rate of a reduction in the gastric emptying rate depends partly on the drug. Irradiation markedly slows the absorption rate of drugs that are rapidly absorbed from the intestine; it causes a less pronounced reduction in the absorption rate of drugs that are slowly absorbed from the intestine, whether slow absorption is due to low mucosal permeability or low dissolution rate. The drug absorption rate may be increased for drugs that are absorbed by a saturable, relatively low capacity mechanism.

In this study, the effect of radiation on the permeability of the GI mucosa appeared to be negligible, although the large reduction in the rate of gastric emptying may have masked a change in mucosal permeability. To explore further the possible effects of radiation on the permeability of the intestinal mucosa, the effects of radiation on the rate of drug absorption from solution by the *in situ* rat intestine were determined and will be reported elsewhere (15).

REFERENCES

(1) M. E. Brady and W. L. Hayton, *J. Pharm. Sci.*, **66**, 361 (1977).

(2) D. C. Bloedow and W. L. Hayton, *ibid.*, **65**, 328 (1976).

(3) W. B. Stavinoha, B. Peplke, and P. W. Smith, *Pharmacologist*, **12**, 257 (1970).

(4) M. J. Schmidt, D. E. Schmidt, and G. A. Robinson, *Science*, **173**, 1142 (1971).

(5) A. B. French, I. F. Brown, C. J. Good, and G. M. McLeod, *Am. J.*

Dig. Dis., **13**, 558 (1968).
(6) R. D. Goodman, A. E. Lewis, and E. A. Schuck, *Am. J. Physiol.*, **169**, 242 (1952).
(7) M. S. Swift, S. T. Taketa, and V. P. Bond, *ibid.*, **182**, 479 (1955).
(8) P. C. Reynell and G. H. Spray, *J. Physiol.*, **131**, 452 (1956).
(9) D. C. Jones and D. J. Kimeldorf, *Radiat. Res.*, **11**, 832 (1959).
(10) R. W. Summers, T. H. Kent, and J. W. Osborne, *Gastroenterology*, **59**, 731 (1970).
(11) K. E. Carr and P. G. Toner, *Virchows Arch. B*, **11**, 201 (1972).
(12) H. R. Withers, *Cancer*, **28**, 75 (1971).
(13) M. J. Mattila, S. Takki, and L. R. Holsti, *Arzneim.-Forsch.*, **18**, 889 (1968).
(14) M. J. Mattila, L. R. Holsti, V. M. K. Venho, and S. Takki, *ibid.*, **20**, 533 (1970).
(15) M. E. Brady and W. L. Hayton, *J. Pharm. Sci.*, in press.
(16) G. Levy, M. Gibaldi, and J. A. Procknal, *ibid.*, **61**, 798 (1972).
(17) T. H. Kent, B. Cannon, J. Reynolds, and J. W. Osborne, *Gastroenterology*, **69**, 1246 (1975).

ACKNOWLEDGMENTS AND ADDRESSES

Received March 24, 1976, from the *College of Pharmacy, Washington State University, Pullman, WA 99164.*

Accepted for publication May 12, 1976.

Presented in part at the Basic Pharmaceutics Section, APhA Academy of Pharmaceutical Sciences, San Francisco meeting, April 1975.

Abstracted from a dissertation submitted by M. E. Brady to Washington State University in partial fulfillment of the Doctor of Philosophy degree requirements.

Supported in part by funds provided for biological and medical research by Washington State University Initiative Measure No. 171.

The authors appreciate the gifts of sulfisoxazole acetyl provided by Dr. W. E. Scott, Research Division, Hoffmann–La Roche Inc., and bretylium tosylate provided by Dr. R. A. Maxwell, Burroughs Wellcome Co.

* AFPE Paul M. Scott Memorial Fellow. Present address: College of Pharmacy, University of Cincinnati, Cincinnati, OH 45221.

[x] To whom inquiries should be directed.

Application of Gluconolactone in Direct Tablet Compression

S. S. NASIR [x], L. O. WILKEN, Jr., and BEHROZE AKHTAR

Abstract □ Gluconolactone was evaluated as an excipient for tablets prepared by direct compression using various drugs known to be difficult to compress. The physical properties of the tablets were evaluated after compression and after storage and were satisfactory. Comparative studies were conducted between gluconolactone and anhydrous lactose, a common direct compression diluent, for development of static charges during blending, flow, drug distribution, drug stratification, color distribution, compressibility, and preservation against mold growth. Gluconolactone possesses those properties necessary to produce high quality tablets by the direct compression process. Separate powdered mixtures of aspirin USP with gluconolactone, anhydrous lactose, spray-dried lactose, mannitol, and sorbitol were stored at various humidities and temperatures for specified periods and tested for the integrity of aspirin. Gluconolactone contributed least to the degradation of the drug as compared to other excipients studied. A preliminary *in vivo* study also was conducted on the bioavailability of aspirin from separate and similar mixtures with gluconolactone, anhydrous lactose, and starch. Gluconolactone did not show any inhibitory effect on aspirin absorption.

Keyphrases □ Gluconolactone—excipient in directly compressed tablets of various drugs, effect on physical characteristics □ Excipients—gluconolactone in directly compressed tablets of various drugs, effect on physical characteristics □ Tablets, direct compression—various drugs, gluconolactone as excipient, effect on physical characteristics □ Dosage forms—directly compressed tablets of various drugs, gluconolactone as excipient, effect on physical characteristics

In terms of economics and stability, the direct compression process offers distinct advantages over other methods used in the manufacture of compressed tablets. During the last decade, considerable interest has been shown in this process. Excipients such as spray-dried lactose (1), microcrystalline cellulose (2), fused mannitol (3), calcium phosphate (4), dextrose (5), amylose (6), anhydrous lactose (7), and directly compressible starch (8) have been studied for their ability to aid in the preparation of compressed tablets. The use of these materials had certain limitations including the difference in particle size and bulk density leading to stratification, the excipients to drug ratio necessary to effect compression, the requirement of an optimum amount of moisture, incompatibility with the drugs, the development of static charges during processing, and cost.

Table I—Properties of Gluconolactone (I) and Anhydrous Lactose

Property	I	Anhydrous Lactose
Solubility in water at 25°, g/ml	0.59	0.2
Particle-size distribution[a] of commercial powders used, % retained		
20 mesh	0.0010	0.00257
30 mesh	0.0450	0.02318
40 mesh	3.4000	0.21894
60 mesh	3.8975	4.6623
80 mesh	4.0525	11.9391
100 mesh	4.250	14.90907
Flow properties, angle of repose		
Plain	26° 23′	22° 43′
With 1% magnesium stearate	23° 50′	20° 12′

[a] A total of 84.354% of I and 64.246% of anhydrous lactose passed through the 100-mesh sieve.

Due to these factors, evaluation of new excipients is warranted. Preliminary experiments with gluconolactone (D-glucono-1,5-lactone, I) indicated considerable potential as an excipient in direct compression; therefore, a thorough study was undertaken.

Compound I was used previously in pharmaceuticals as a stabilizer for multivitamins (9) and tetracycline (10). It is prepared by the oxidation of glucose with bromine water (11) or by oxidation of glucose in *Acetobacter suboxydans* (12). Compound I has a sweet taste and is highly soluble in water (59 g/100 ml); it is slowly hydrolyzed by water to gluconic acid. The calcium and ferrous salts of this acid are

Dig. Dis., **13**, 558 (1968).
(6) R. D. Goodman, A. E. Lewis, and E. A. Schuck, *Am. J. Physiol.*, **169**, 242 (1952).
(7) M. S. Swift, S. T. Taketa, and V. P. Bond, *ibid.*, **182**, 479 (1955).
(8) P. C. Reynell and G. H. Spray, *J. Physiol.*, **131**, 452 (1956).
(9) D. C. Jones and D. J. Kimeldorf, *Radiat. Res.*, **11**, 832 (1959).
(10) R. W. Summers, T. H. Kent, and J. W. Osborne, *Gastroenterology*, **59**, 731 (1970).
(11) K. E. Carr and P. G. Toner, *Virchows Arch. B*, **11**, 201 (1972).
(12) H. R. Withers, *Cancer*, **28**, 75 (1971).
(13) M. J. Mattila, S. Takki, and L. R. Holsti, *Arzneim.-Forsch.*, **18**, 889 (1968).
(14) M. J. Mattila, L. R. Holsti, V. M. K. Venho, and S. Takki, *ibid.*, **20**, 533 (1970).
(15) M. E. Brady and W. L. Hayton, *J. Pharm. Sci.*, in press.
(16) G. Levy, M. Gibaldi, and J. A. Procknal, *ibid.*, **61**, 798 (1972).
(17) T. H. Kent, B. Cannon, J. Reynolds, and J. W. Osborne, *Gastroenterology*, **69**, 1246 (1975).

ACKNOWLEDGMENTS AND ADDRESSES

Received March 24, 1976, from the *College of Pharmacy, Washington State University, Pullman, WA 99164.*

Accepted for publication May 12, 1976.

Presented in part at the Basic Pharmaceutics Section, APhA Academy of Pharmaceutical Sciences, San Francisco meeting, April 1975.

Abstracted from a dissertation submitted by M. E. Brady to Washington State University in partial fulfillment of the Doctor of Philosophy degree requirements.

Supported in part by funds provided for biological and medical research by Washington State University Initiative Measure No. 171.

The authors appreciate the gifts of sulfisoxazole acetyl provided by Dr. W. E. Scott, Research Division, Hoffmann–La Roche Inc., and bretylium tosylate provided by Dr. R. A. Maxwell, Burroughs Wellcome Co.

* AFPE Paul M. Scott Memorial Fellow. Present address: College of Pharmacy, University of Cincinnati, Cincinnati, OH 45221.

[x] To whom inquiries should be directed.

Application of Gluconolactone in Direct Tablet Compression

S. S. NASIR [x], L. O. WILKEN, Jr., and BEHROZE AKHTAR

Abstract □ Gluconolactone was evaluated as an excipient for tablets prepared by direct compression using various drugs known to be difficult to compress. The physical properties of the tablets were evaluated after compression and after storage and were satisfactory. Comparative studies were conducted between gluconolactone and anhydrous lactose, a common direct compression diluent, for development of static charges during blending, flow, drug distribution, drug stratification, color distribution, compressibility, and preservation against mold growth. Gluconolactone possesses those properties necessary to produce high quality tablets by the direct compression process. Separate powdered mixtures of aspirin USP with gluconolactone, anhydrous lactose, spray-dried lactose, mannitol, and sorbitol were stored at various humidities and temperatures for specified periods and tested for the integrity of aspirin. Gluconolactone contributed least to the degradation of the drug as compared to other excipients studied. A preliminary *in vivo* study also was conducted on the bioavailability of aspirin from separate and similar mixtures with gluconolactone, anhydrous lactose, and starch. Gluconolactone did not show any inhibitory effect on aspirin absorption.

Keyphrases □ Gluconolactone—excipient in directly compressed tablets of various drugs, effect on physical characteristics □ Excipients—gluconolactone in directly compressed tablets of various drugs, effect on physical characteristics □ Tablets, direct compression—various drugs, gluconolactone as excipient, effect on physical characteristics □ Dosage forms—directly compressed tablets of various drugs, gluconolactone as excipient, effect on physical characteristics

In terms of economics and stability, the direct compression process offers distinct advantages over other methods used in the manufacture of compressed tablets. During the last decade, considerable interest has been shown in this process. Excipients such as spray-dried lactose (1), microcrystalline cellulose (2), fused mannitol (3), calcium phosphate (4), dextrose (5), amylose (6), anhydrous lactose (7), and directly compressible starch (8) have been studied for their ability to aid in the preparation of compressed tablets. The use of these materials had certain limitations including the difference in particle size and bulk density leading to stratification, the excipients to drug ratio necessary to effect compression, the requirement of an optimum amount of moisture, incompatibility with the drugs, the development of static charges during processing, and cost.

Table I—Properties of Gluconolactone (I) and Anhydrous Lactose

Property	I	Anhydrous Lactose
Solubility in water at 25°, g/ml	0.59	0.2
Particle-size distribution[a] of commercial powders used, % retained		
20 mesh	0.0010	0.00257
30 mesh	0.0450	0.02318
40 mesh	3.4000	0.21894
60 mesh	3.8975	4.6623
80 mesh	4.0525	11.9391
100 mesh	4.250	14.90907
Flow properties, angle of repose		
Plain	26° 23′	22° 43′
With 1% magnesium stearate	23° 50′	20° 12′

[a] A total of 84.354% of I and 64.246% of anhydrous lactose passed through the 100-mesh sieve.

Due to these factors, evaluation of new excipients is warranted. Preliminary experiments with gluconolactone (D-glucono-1,5-lactone, I) indicated considerable potential as an excipient in direct compression; therefore, a thorough study was undertaken.

Compound I was used previously in pharmaceuticals as a stabilizer for multivitamins (9) and tetracycline (10). It is prepared by the oxidation of glucose with bromine water (11) or by oxidation of glucose in *Acetobacter suboxydans* (12). Compound I has a sweet taste and is highly soluble in water (59 g/100 ml); it is slowly hydrolyzed by water to gluconic acid. The calcium and ferrous salts of this acid are

Table II—Physical Properties of Tablets Prepared with Gluconolactone (I) Formulations

Tablet Formula	Hardness[a], kg ± *SD*		Friability, %		Thickness, mm ± *SD*	Weight, mg ± *SD*	Disintegration Time, min ± *SD* at 37°	
	Initial	6 Months of Storage	Initial	6 Months of Storage			Initial	6 Months of Storage
Plain I tablets, Batch 1 I, 497.7 mg Methylcellulose (1500 cps), 63 mg Dried starch, 63 mg Magnesium stearate, 6.3 mg 9.5-mm deep concave punches and dies	6.670 ± 0.830	7.900 ± 0.464	0.45	0.43	5.63 ± 0.83	628.00 ± 9.520	Water: 2.22 ± 0.23 SGF[b]: 2.13 ± 0.56 SIF[c]: 6.01 ± 0.42	Water: 4.39 ± 0.489 SGF: 4.11 ± 0.48 SIF: 6.20 ± 0.11
Plain I tablets, Batch 2 I, 560.7 mg Methylcellulose (1500 cps), 63 mg Magnesium stearate, 6.3 mg 11.1-mm standard concave punches and dies	8.700 ± 0.100	8.840 ± 0.744	0.31	0.31	6.50 ± 0.057	630.00 ± 16.570	Water: 3.55 ± 0.33 SGF: 6.57 ± 1.26 SIF: 6.91 ± 0.73	Water: 5.39 ± 0.487 SGF: 7.30 ± 1.24 SIF: 7.1 ± 0.48
Plain I tablets, Batch 3 I, 560.7 mg Methylcellulose (1500 cps), 31.5 mg Dried starch, 31.5 mg Magnesium stearate, 6.3 mg 11.1-mm standard concave punches and dies	6.040 ± 0.850	5.500 ± 0.964	0.43	0.48	5.60 ± 0.058	623.00 ± 6.570	Water: 4.17 ± 0.43 SGF: 5.22 ± 0.31 SIF: 7.4 ± 0.8	Water: 6.02 ± 0.42 SGF: 6.55 ± 0.38 SIF: 8.2 ± 1.7
Ferrous sulfate tablets Ferrous sulfate (anhydrous), 149 mg I, 360 mg Methylcellulose (1500 cps), 40 mg Magnesium stearate, 11 mg 9.5-mm deep concave punches and dies	5.150 ± 0.657	5.240 ± 0.363	0.65	0.64	5.50 ± 0.033	559.00 ± 9.23	Water: 9.30 ± 0.810	Water: 8.53 ± 0.508
Phenobarbital tablets Phenobarbital, 30 mg I, 160 mg Methylcellulose (1500 cps), 40 mg Magnesium stearate, 1.25 mg Stearic acid, 3.75 mg 7.9-mm standard concave punches and dies	6.400 ± 0.917	5.400 ± 0.487	0.25	0.28	4.10 ± 0.00	243.00 ± 9.24	Water: 6.03 ± 1.28	Water: 7.77 ± 1.09
Sodium chloride tablets Sodium chloride, 600 mg I, 540 mg Methylcellulose (1500 cps), 60 mg Magnesium stearate, 12 mg 12.7-mm flat-faced punches and dies	5.20 ± 0.341	6.37 ± 1.31	0.050	0.045	6.26 ± 0.051	1211.00 ± 36.20	Water: 6.28 ± 0.350	Water: 9.36 ± 0.546
Ephedrine hydrochloride tablets Ephedrine hydrochloride, 30 mg I, 135 mg Methylcellulose, 15 mg Stearic acid, 3 mg Magnesium stearate, 2 mg 7.9-mm standard concave punches and dies	4.60 ± 1.22	4.77 ± 0.535	0.30	0.35	3.62 ± 0.103	195.00 ± 20.0	Water: 11.30 ± 0.18	Water: 6.79 ± 0.909

(continued)

Table II—(*Continued*)

Tablet Formula	Hardness[a], kg ± *SD*		Friability, %		Thickness, mm ± *SD*	Weight, mg ± *SD*	Disintegration Time, min ± *SD* at 37°	
	Initial	6 Months of Storage	Initial	6 Months of Storage			Initial	6 Months of Storage
Isoniazid tablets Isoniazid, 50 mg I, 260 mg Methylcellulose (1500 cps), 40 mg Magnesium stearate, 7 mg 7.9-mm standard concave, punches and dies	5.25 ± 0.485	5.93 ± 0.574	0.41	0.39	5.45 ± 0.097	354.00 ± 7.24	Water: 8.32 ± 0.50	Water: 14.01 ± 0.350
Methenamine tablets Methenamine, 250 mg I, 150 mg Methylcellulose (1500 cps), 25 mg Magnesium stearate, 4.4 mg Stearic acid, 8.6 mg 11.1-mm standard concave punches and dies	6.15 ± 0.885	6.11 ± 0.769	0.41	0.47	4.64 ± 0.097	445.00 ± 11.0	Water: 6.25 ± 0.78	Water: 6.22 ± 0.814
Ascorbic acid tablets Ascorbic acid, 300 mg I, 240 mg Methylcellulose (1500 cps), 80 mg Magnesium stearate, 6 mg Stearic acid, 12 mg 11.1-mm standard concave punches and dies	6.55 ± 1.26	5.830 ± 0.799	0.81	0.75	6.640 ± 0.135	633.00 ± 14.80	Water: 16.00 ± 0.00	Water: 19.04 ± 1.29
Sulfathiazole tablets Sulfathiazole, 500 mg I, 360 mg Methylcellulose (1500 cps), 45 mg Dried starch, 45 mg Magnesium stearate, 4.8 mg Stearic acid, 19.2 mg 12.7-mm flat-faced beveled-edge punches and dies	6.80 ± 0.809	6.97 ± 1.139	0.40	0.45	5.900 ± 0.087	967.00 ± 22.17	Water: 25.00 ± 4.73	Water: 24.23 ± 3.57
Ferrous gluconate tablets Ferrous gluconate, 300 mg I, 270 mg Methylcellulose (1500 cps), 30 mg Magnesium stearate, 6 mg Stearic acid, 12 mg 11.1-mm standard concave punches and dies	11.00 ± 1.80	8.860 ± 1.153	0.68	0.72	5.90 ± 0.10	627.00 ± 10.15	Water: 9.77 ± 3.47	Water: 12.13 ± 2.156
Calcium lactate tablets Calcium lactate, 300 mg I, 240 mg Methylcellulose (1500 cps) 60 mg Magnesium stearate, 6 mg Stearic acid, 12 mg 11.1-mm standard concave punches and dies	13.30 ± 1.26	2.190 ± 0.378	0.71	0.10	6.50 ± 0.124	616.00 ± 20.28	Water: 15.60 ± 3.22	Water: 18.32 ± 3.11

Aspirin tablets Aspirin, 150 mg I, 360 mg Methylcellulose (1500 cps), 40 mg Dried starch, 40 mg Magnesium stearate, 6 mg 11.1-mm standard concave punches	5.50 ± 0.687	5.73 ± 0.448	0.78	0.68	5.70 ± 0.141	607.00 ± 19.09	Water: 3.88 ± 0.799	Water: 5.92 ± 1.012
Riboflavin tablets Riboflavin, 5 mg I, 90 mg Methylcellulose (1500 cps), 10 mg Magnesium stearate, 1 mg 6.3-mm deep concave punches and dies	2.40 ± 0.394	2.73 ± 0.495	0.22	0.31	3.37 ± 0.105	108.00 ± 2.90	Water: 5.38 ± 0.56	Water: 7.93 ± 0.661
Multivitamins and mineral tablets Vitamin A, 5000 USP units Vitamin D, 400 USP units Thiamine, 2 mg Riboflavin, 3 mg Niacinamide, 20 mg Ascorbic acid, 50 mg Pyridoxine, 1 mg Cyanocobalamin, 1 μg Calcium pantothenate, 1 mg Ferrous sulfate, 18 mg Copper sulfate, 1 mg Magnesium oxide, 5 mg Magnesium citrate, 1 mg Zinc chloride, 1.5 mg I, 180 mg Methylcellulose (1500 cps), 20 mg Magnesium stearate, 3 mg Stearic acid, 6 mg 9.5-mm deep concave punches and dies	4.95 ± 1.01	4.00 ± 0.512	0.35	0.40	4.38 ± 0.103	312 ± 5.0	Water: 5.78 ± 1.60	Water: 7.30 ± 0.973
Aminosalicylic acid tablets Aminosalicylic acid, 250 mg I, 320 mg Methylcellulose (1500 cps), 80 mg Magnesium stearate, 6 mg Stearic acid, 14 mg 11.1-mm standard concave punches and dies	6.55 ± 1.26	—	0.85	—	6.64 ± 0.135	700.00 ± 22.90	Water: 16.0 ± 1.5	—
Digitalis tablets Digitalis, 50 mg I, 400 mg Methylcellulose (1500 cps), 80 mg Magnesium stearate, 10.6 mg 9.5-mm deep concave punches and dies	5.40 ± 0.817	6.26 ± 0.375	0.78	0.73	5.81 ± 0.316	526.00 ± 9.92	Water: 11.33 ± 0.18	Water: 15.41 ± 0.47

[a] Stokes tester. [b] SGF = simulated gastric fluid. [c] SIF = simulated intestinal fluid.

Table III—Estimation of Sticking of Powders during Blending

Drug	Weight per 500 ml of Powder, g	Amount Retained, g ± *SD*	Percent Retained
I	336.8	3.8 ± 0.12	1.13
Anhydrous lactose	361.0	4.3 ± 0.10	1.19
Spray-dried lactose	318.0	0.8 ± 0.03	0.25

commonly administered orally in large doses for the effect of the cations.

EXPERIMENTAL

Particle-Size Analysis—The particle-size distribution of I was determined with a testing sieve shaker[1] using stainless steel U.S. standard sieve series in 20-, 30-, 40-, 60-, 80-, and 100-mesh sizes. A 200-g sample was tested in the sieve shaker for 10 min.

Moisture Content—The moisture content of I was determined on a moisture determination balance[2]. The test was continued until three consecutive readings at 3-min intervals were constant.

Flow Pattern of I—The flow properties of I were estimated by determination of the angle of repose without and with 1% magnesium stearate by a described procedure (13). Flow properties of anhydrous lactose also were studied by the same method for comparison.

Development of Static Charges during Blending—A plastic V-shaped container with a volume of 848 ml and a smooth inner surface was used. The container was dried at 45° for 12 hr, cooled to room temperature in a desiccator, and filled with 500 ml of the specified powder of known weight. The V-shaped container with the material was then rotated[3] at 36 rpm for 15 min. Then the material was immediately poured out gently, without disturbing the powder sticking to the container, and weighed. The weight of the sticking material was then calculated. The environmental working conditions for the test were maintained at 29° and a relative humidity of 42%.

Tablet Preparation—Five thousand tablets of I and 5000 tablets each of I in combination with the following drugs were prepared: ferrous sulfate, phenobarbital, sodium chloride, ephedrine hydrochloride, isoniazid, methenamine, ascorbic acid, sulfathiazole, ferrous gluconate, calcium lactate, aspirin, riboflavin, multivitamins with minerals, aminosalicylic acid, and powdered digitalis.

Appropriate changes in the formulas were made to establish minimum quantities of I and other essential ingredients required to produce satisfactory tablets. All tablets were prepared on a four-station press[4] at 300 tablets/min using various types and sizes of punches and dies, with the exception of riboflavin and multivitamin tablets which were compressed on a single-punch press[5] at 60 tablets/min. The resulting tablets were

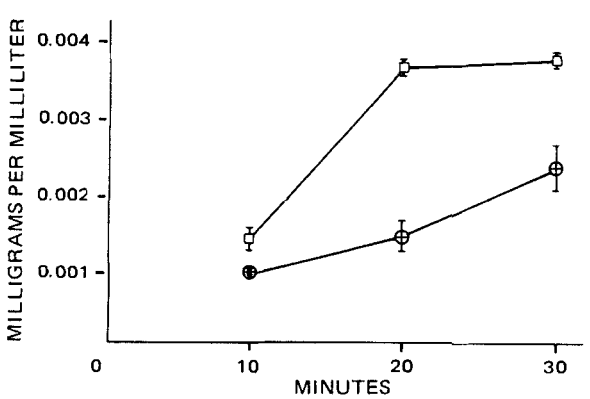

Figure 1—In vitro *dissolution rates of aspirin tablets. Key:* ⊕, *tablets with anhydrous lactose; and* □, *tablets with I.*

[1] Ro-Tap, W. S. Tyler Co.
[2] Model 6010, Ohaus Scale Corp., Union, N.J.
[3] Erweka motor drive model Ku-1, Chemical and Pharmaceutical Industry Co.
[4] Colton model 204, Cherry-Burrell Corp.
[5] Stokes model F-1.

Table IV—Color Distribution in Powder Mixture[a]

Amaranth Concentration, mg/0.1 g ± *SD*		
I	Anhydrous Lactose	Spray-Dried Lactose
0.439 ± 0.001	0.475 ± 0.007	0.590 ± 0.005

[a] Powder formula was I, anhydrous lactose, or spray-dried lactose, 345.23 mg, and amaranth, 18.97 mg.

evaluated for the following properties:

1. Hardness[6].
2. Thickness—Thickness was measured by means of a vernier caliper graduated in millimeters.
3. Weight—Tablets were randomly collected during compression, and groups of 20 tablets from those collected were weighed individually. The weight variation was then calculated.
4. Friability—Friability was ascertained with a friabilator[7] using a 4-min cycle and at least 20 tablets or a minimum 6.0-g tablet sample.
5. Disintegration Time—Disintegration time of all tablets in water at 37° was determined by means of a USP XVIII apparatus using disks. Disintegration time of plain I tablets was also determined in simulated gastric fluid USP without pepsin and simulated intestinal fluid USP without pancreatin using the same apparatus and procedure.

Drug Stratification—Sufficient I to make 5000 tablets was mixed with the specified drug and other essential ingredients in a blender[8] for 5 min. Then a specified quantity of magnesium stearate was added and mixed for an additional 5 min.

Six samples were collected from different portions of mixed powder and analyzed for the drug content.

The mixed powder was collected in a hopper, a six-mesh stainless steel screen was fixed at the bottom of the hopper, and the hopper was then attached to a sieve shaker[9] and vibrated at a constant speed until all of the powder passed through the screen into a container. Six samples were withdrawn from different portions of the powder and analyzed for drug concentration.

The remaining powder, without further mixing, was compressed into tablets on a four-station press[4] at 300 tablets/min. Six 20-tablet samples were tested for drug distribution. Tablets of sulfathiazole, riboflavin, and aspirin were prepared and studied for drug distribution and stratification. Sulfathiazole and riboflavin were assayed by the USP XIV procedure and a described procedure (14), respectively.

Aspirin tablets were assayed by the following method. A sample of 20 tablets was powdered. A portion of this powder, equivalent to 300 mg of

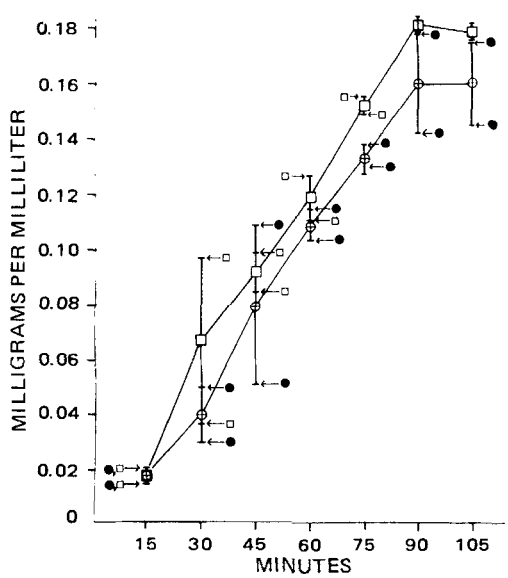

Figure 2—In vitro *dissolution rates of ferrous sulfate tablets. Key:* ⊕, *tablets with anhydrous lactose; and* □, *tablets with I.*

[6] Stokes hardness tester.
[7] Roche.
[8] Model LB4575, Patterson Kelley Co.
[9] Erweka type VT, Chemical and Pharmaceutical Industry Co.

Table V—Color Distribution in Tablets

Tablet Formula	I				Anhydrous Lactose				Spray-Dried Lactose			
	Weight, mg ± *SD*	Thickness, mm ± *SD*	Hardness[a], kg ± *SD*	Amaranth Concentration, mg/0.1 g ± *SD*	Weight, mg ± *SD*	Thickness, mm ± *SD*	Hardness[a], kg ± *SD*	Amaranth Concentration, mg/0.1 g ± *SD*	Weight, mg ± *SD*	Thickness, mm ± *SD*	Hardness[a], kg ± *SD*	Amaranth Concentration, mg/0.1 g ± *SD*
I, anhydrous lactose, or spray-dried lactose, 345.23 mg Amaranth, 18.97 mg Methylcellulose, 92.00 mg Magnesium stearate, 4.60 mg	456.700 ±4.120	6.120 ±0.040	5.750 ±0.490	0.428 ±0.001	461.200 ±0.694	7.040 ±0.120	7.350 ±1.330	0.363 ±0.002	463.000 ±6.113	6.390 ±0.060	5.800 ±0.590	0.422 ±0.005

[a] Stokes tester.

Table VI—Drug Distribution in Powder Mixtures and Compressed Tablets

Tablet Formula	Milligrams of Drug per Tablet	Powder Mixtures				Tablets							
		I		Anhydrous Lactose		I				Anhydrous Lactose			
		Blending Drug Concentration, mg ± *SD*	Sieving, Drug Concentration, mg ± *SD*	Blending, Drug Concentration, mg ± *SD*	Sieving, Drug Concentration, mg ± *SD*	Weight, mg ± *SD*	Thickness, mm ± *SD*	Hardness[a], kg ± *SD*	Drug Concentration per Tablet, mg ± *SD*	Weight, mg ± *SD*	Thickness, mm ± *SD*	Hardness[a], kg ± *SD*	Drug Concentration per Tablet, mg ± *SD*
Sulfathiazole tablets I or anhydrous lactose, 360 mg Methylcellulose, 45 mg Starch, 45 mg Magnesium stearate, 4.15 mg Stearic acid, 19 mg 12.7-mm flat-faced beveled-edge punches and dies	500.00	499.90 ±8.20	498.48 ±6.47	498.28 ±4.13	494.75 ±17.30	1086.90 ±29.04	6.58 ±0.14	5.14 ±0.47	503.19 ±5.67	1030.00 ±24.29	6.27 ±0.12	11.19 ±1.07	502.06 ±2.24
Riboflavin tablets I or anhydrous lactose, 265 mg Methylcellulose, 60 mg Magnesium stearate, 3 mg 8.7-mm standard concave punches and dies	5.00	5.60 ±0.42	5.57 ±0.79	5.60 ±0.75	5.58 ±1.24	311.55 ±8.82	4.77 ±0.20	7.40 ±1.68	4.78 ±0.21	324.98 ±5.69	4.90 ±0.70	8.25 ±1.80	4.74 ±0.52
Aspirin tablets I or anhydrous lactose, 235 mg Magnesium stearate, 5 mg 11.9-mm standard concave punches and dies	300.00	297.46 ±3.56	297.25 ±3.47	297.00 ±3.49	307.33 ±10.20	663.00 ±14.41	6.14 ±1.50	2.45 ±0.83	298.23 ±2.37	617.00 ±11.47	6.28 ±0.15	1.55 ±0.19	299.27 ±2.75

[a] Stokes tester.

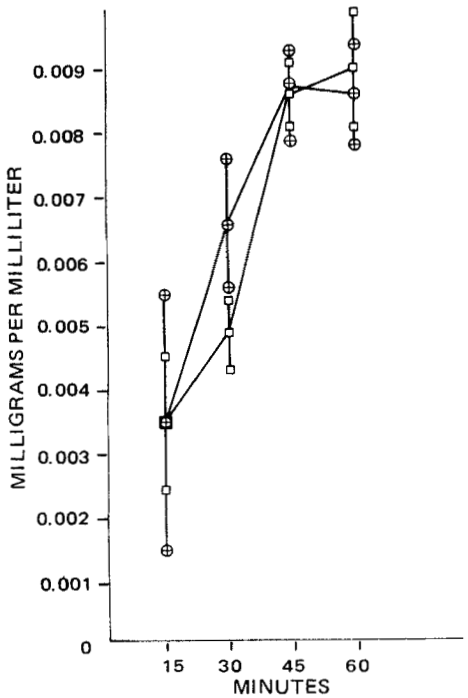

Figure 3—In vitro *dissolution rates of phenobarbital tablets. Key:* ⊕, *tablets with anhydrous lactose; and* □, *tablets with I.*

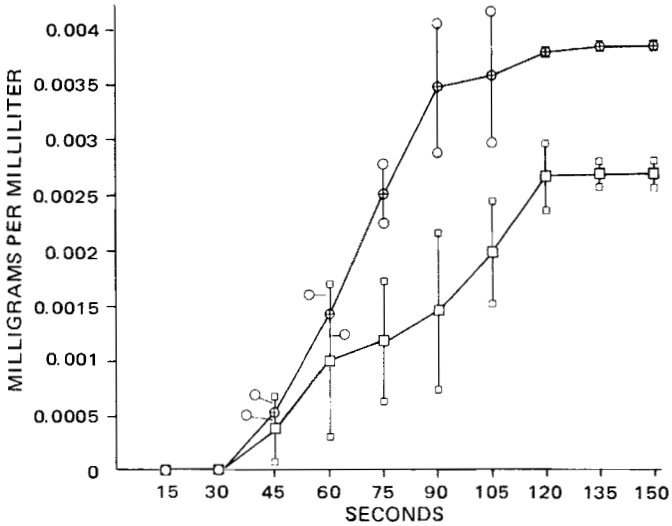

Figure 4—In vitro *dissolution rates of benzoic acid tablets. Key:* ⊕, *tablets with anhydrous lactose; and* □, *tablets with I.*

aspirin, was weighed accurately, mixed with 60 ml of ether, stirred for 5 min, and then filtered to remove the excipients. Then 45 ml of water and 5 ml of 95% alcohol were added to the filtrate, and the filtrate was heated to remove the ether. The resulting solution was assayed according to a described procedure (15). For comparison, anhydrous lactose was evaluated for drug stratification by the same procedure using the same drugs.

Color Distribution—To study the color uniformity in I tablets, 0.5% amaranth USP was used as a source of color. A specified quantity of amaranth was mixed with a portion of I, added to the remainder of the lactone in a blender[8], and mixed for 15 min. The intensifier was turned on at 5-min intervals for 15 sec. Six random samples were withdrawn from the mixture and assayed for amaranth spectrophotometrically at 385 nm.

Specified quantities of methylcellulose, 1500 cps, and magnesium

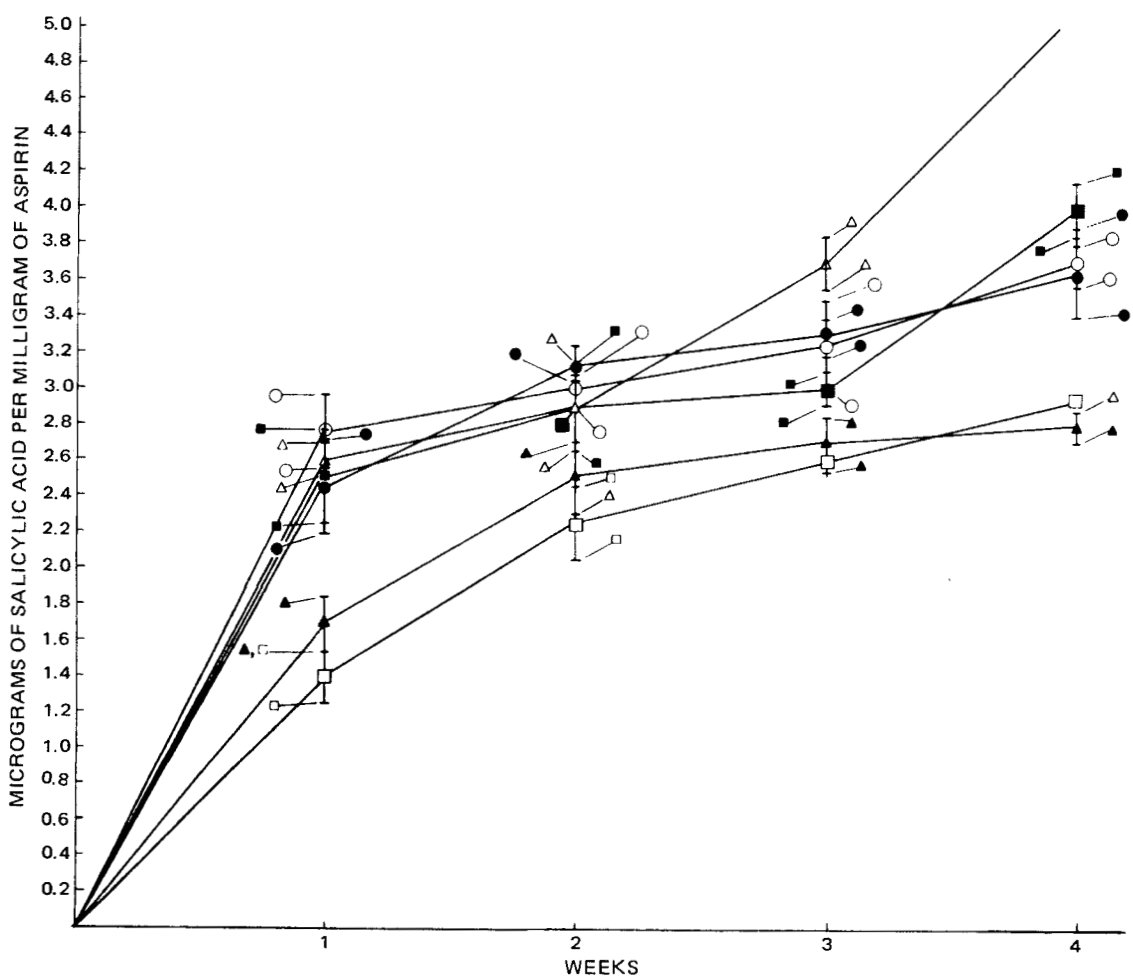

Figure 5—*Stability of aspirin with various diluents at 52% relative humidity. Key:* ○, *anhydrous lactose;* □, *I;* △, *sorbitol;* ■, *mannitol;* ●, *spray-dried lactose; and* ▲, *aspirin.*

Table VII—Physical Properties of Tablets Used for Dissolution Studies

Tablet	Hardness[a], kg ± *SD*		Thickness, mm ± *SD*		Weight, mg ± *SD*	
	Anhydrous Lactose	I	Anhydrous Lactose	I	Anhydrous Lactose	I
Aspirin	1.55 ± 0.19	1.45 ± 0.83	6.28 ± 0.15	6.14 ± 0.15	616.60 ± 11.47	663.00 ± 14.41
Benzoic acid	5.08 ± 0.52	5.90 ± 0.46	6.49 ± 0.07	6.13 ± 0.05	423.70 ± 7.20	413.70 ± 9.77
Ferrous sulfate	11.25 ± 0.78	11.03 ± 0.87	6.65 ± 0.07	6.04 ± 0.13	572.30 ± 14.21	552.25 ± 24.86
Phenobarbital	3.90 ± 0.93	4.70 ± 0.43	3.73 ± 0.04	3.74 ± 0.05	111.30 ± 1.13	116.45 ± 2.62

[a] Stokes tester.

stearate were added to the amaranth–I mixture and compressed on a four-station rotary press; 5000 such tablets were prepared. Six 20-tablet random samples were collected and assayed for amaranth by this procedure. Anhydrous and spray-dried lactose also were studied for color distribution by the same procedure as described for I. Finished tablets were stored at room temperature for 6 months and observed for color changes.

Dissolution Studies—To investigate the effect of I on tablet dissolution, phenobarbital, benzoic acid, aspirin, and ferrous sulfate were selected as representative drugs. Tablets of these drugs were prepared with I and anhydrous lactose as excipients. Attempts were made to maintain equal weight and hardness for similar tablets.

Dissolution rates of these tablets were determined in water at 37° with the USP XVIII dissolution apparatus. Samples were withdrawn at specified intervals and assayed for drug concentration. Phenobarbital was assayed according to a described procedure (16). Similarly, benzoic acid (17) and aspirin (18) were analyzed by reported procedures. Ferrous sulfate was assayed by the following procedure.

To each 1-ml sample were added 1 ml of hydrogen peroxide and 5 ml of a reagent consisting of 5.835 mg of sodium salicylate, 200 mg of mercuric chloride, and 0.6 ml of 1 *N* hydrochloric acid dissolved in water. The resulting solution was assayed spectrophotometrically at 540 nm.

Mold Growth—Tablets of phenobarbital, ferrous sulfate, and aspirin prepared with I and anhydrous lactose for dissolution studies and plain tablets of I from Batch 1 were stored at 95% relative humidity at room temperature for 2 months and observed for mold growth.

Effect of I on Stability of Moisture-Sensitive Drugs—Aspirin was selected as a representative drug, and anhydrous lactose, spray-dried lactose, mannitol, and sorbitol were selected as excipients for comparison with I.

Aspirin, 6 g, and 59 g of each excipient were mixed separately. Six samples of each type were prepared and stored at 52 and 81% relative humidity and 50 and 60°. These samples were assayed at 1-week intervals for 4 weeks for free salicylic acid content by a reported procedure (19). These mixtures also were stored at room temperature for 3 months and then assayed for free salicylic acid by the same procedure.

Preliminary Bioavailability Assessment—To obtain some rudimentary information about the influence of I on drug absorption, a comparative *in vivo* study was conducted on aspirin absorption from separate combinations with I, anhydrous lactose, and starch. Each dose consisted of 50 mg of aspirin mixed with 50 mg of I or anhydrous lactose and with 12.5 mg of starch.

Each combination was studied on a group of six male rabbits, approximately 3 kg. Each dose, in a No. 2 gelatin capsule, was administered

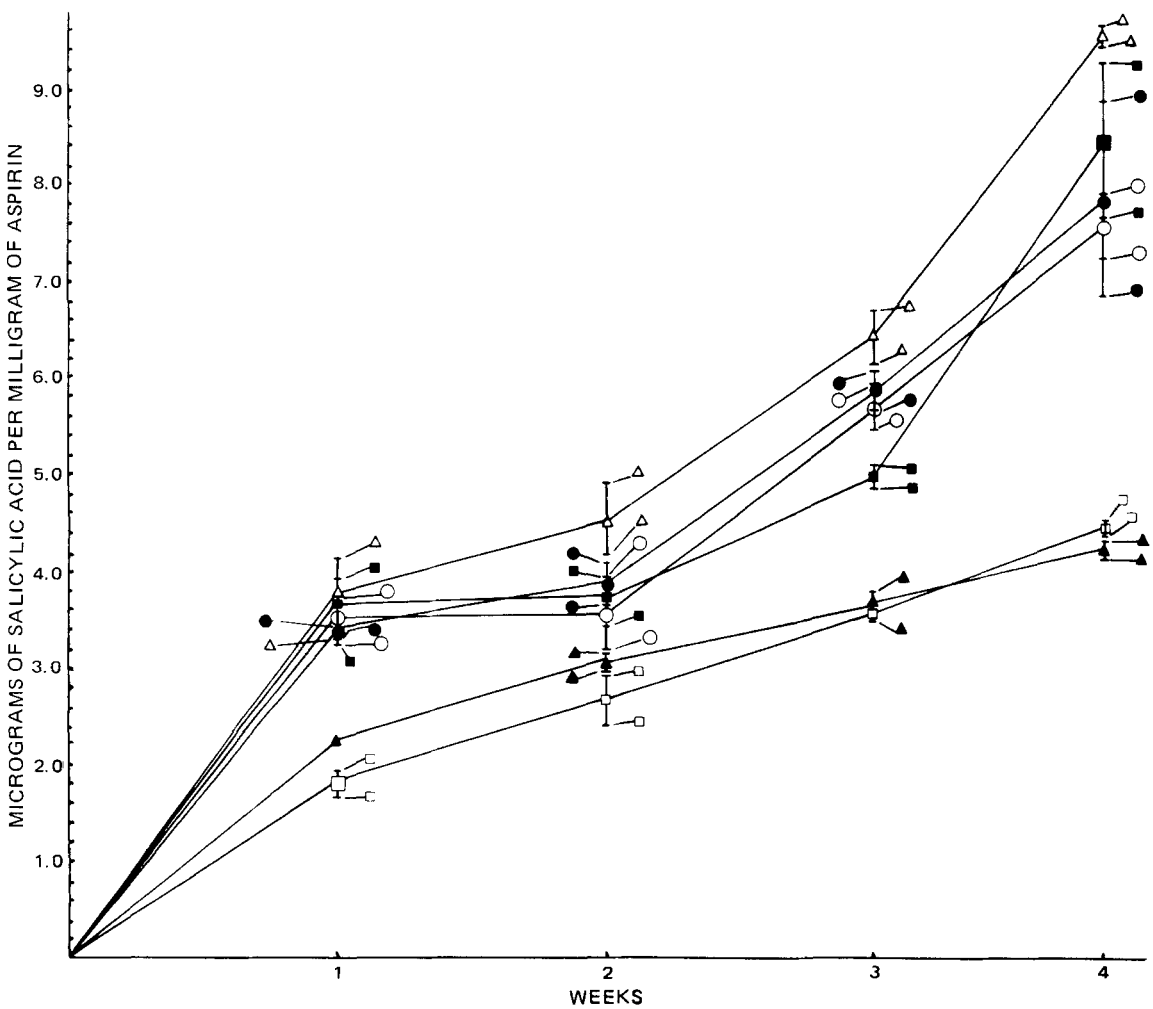

Figure 6—*Stability of aspirin with various diluents at 81% relative humidity. Key, ○, anhydrous lactose; □, I; △, sorbitol; ■, mannitol; ●, spray-dried lactose; and ▲, pure aspirin.*

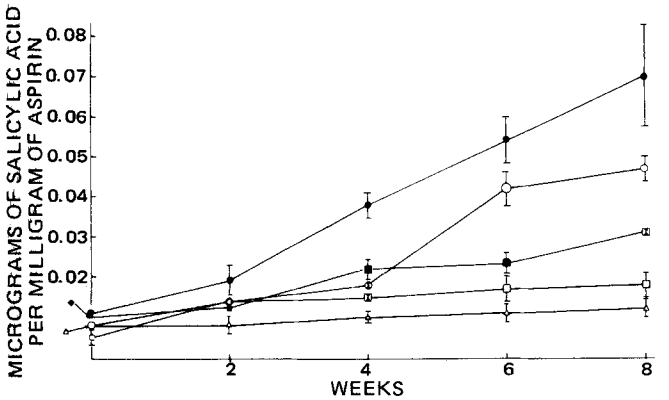

Figure 7—*Stability of aspirin with various diluents at 50°. Key: ○, anhydrous lactose; □, I; △, pure aspirin; ■, mannitol; and ●, spray-dried lactose.*

orally to a rabbit. Blood samples were taken at 0, 30, 60, 90, 120, 150, 210, 270, and 330 min from the ear marginal vein and assayed for salicylic acid by a reported procedure (20).

RESULTS AND DISCUSSION

Most particles of I are finer than 100 mesh. This particle-size distribution is advantageous for tableting (Table I) because most drugs formulated as tablets fall in a fine particle-size range. Due to the similarity in particle size, the drugs can be blended with the excipient more easily, and stratification and separation can be avoided at the compression stage.

Compound I has only 0.5% moisture, which can be an advantage in the preparation of compressed tablets of drugs that decompose by hydrolysis and of drugs whose deterioration or interaction with other drugs is accelerated by moisture.

Compound I has a higher angle of repose than anhydrous lactose (Table I). This property does not seem disadvantageous, because the flow of I in the tablet press did not differ from that of anhydrous lactose. Pharmaceutically acceptable tablets of various drugs with different properties and amounts per tablet were prepared with I (Table II). After 6 months of storage at room temperature, the tablets did not show any undesirable changes in hardness, friability, and disintegration time, with the exception of calcium lactate tablets, the hardness of which decreased considerably.

The disintegration time and hardness of sodium chloride and ferrous sulfate tablets did not increase considerably. Undesirable increases are expected in conventionally prepared tablets of these salts.

Since the aminosalicylic acid tablets were not coated, no attempt was made to evaluate their physical properties on storage. Properties of ascorbic acid, sulfathiazole, aspirin, and aminosalicylic acid tablets prepared with I indicate that this excipient can be used successfully with

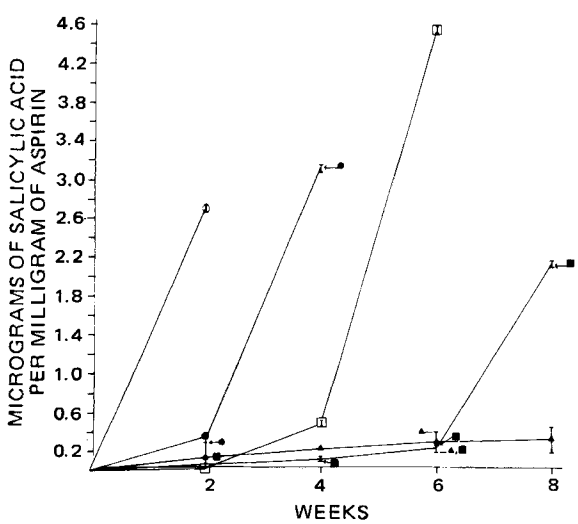

Figure 8—*Stability of aspirin with various diluents at 60°. Key: ○, anhydrous lactose; □, I; ■, mannitol; ●, spray-dried lactose; and ▲, pure aspirin.*

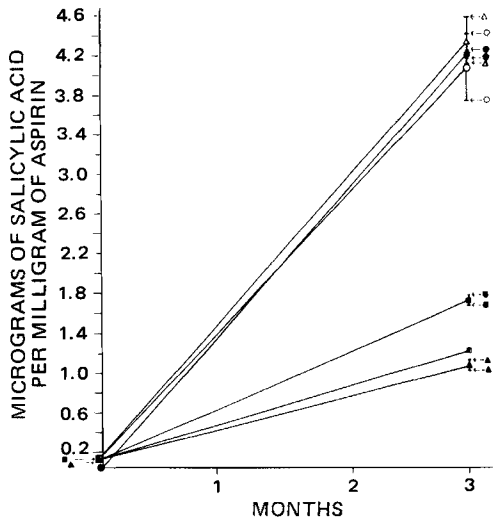

Figure 9—*Stability of aspirin with various diluents after 3 months of storage at room temperature. Key: ●, spray-dried lactose; ○, anhydrous lactose; ■, mannitol; □, I; ▲, aspirin; and △, sorbitol.*

these materials. The amount of I required depends on the amount and inherent compression properties of the drug.

In the test for estimation of sticking of a material to a surface due to static charges (Table III), the amounts of anhydrous lactose lost were approximately 0.05% less and 0.91% more than those lost with I and spray-dried lactose, respectively. Less sticking of spray-dried lactose was probably due to its larger particle size. In addition to production of static charges, the loss of material in this test can be attributed to the shape and size of particles and the number of fines in the powder.

In the color distribution studies with amaranth, the dye was more uniformly distributed in I than anhydrous lactose and spray-dried lactose; the deviations between samples assayed for amaranth concentration were less with I compared to the other two materials (Tables IV and V).

Similar results were obtained from tablets compressed from these powders. Color distribution was most uniform in tablets with I, followed closely by anhydrous lactose tablets. Mottling was predominant in spray-dried lactose tablets. None of these tablets showed any signs of fading after 6 months of storage.

Sulfathiazole, riboflavin, and aspirin were selected for drug stratification studies. The quantity of each drug was such that it represented a certain drug to excipient ratio.

In all cases, the drug distribution at blending, sieving, and compression stages was well within acceptable limits, both with I and anhydrous lactose, but anhydrous lactose had considerably higher deviation at the sieving stage as compared to I. The uniform distribution of a small quantity of riboflavin in a large quantity of I shows that this material also can be used for making tablets with small quantities of drugs by the direct compression process (Table VI).

A comparative dissolution rate study was conducted between tablets prepared with I and anhydrous lactose. Aspirin, ferrous sulfate, phenobarbital, and benzoic acid were studied. Similar tablets of these drugs were prepared with each excipient and tested for dissolution. Properties of these tablets are shown in Table VII. Aspirin and ferrous sulfate tablets

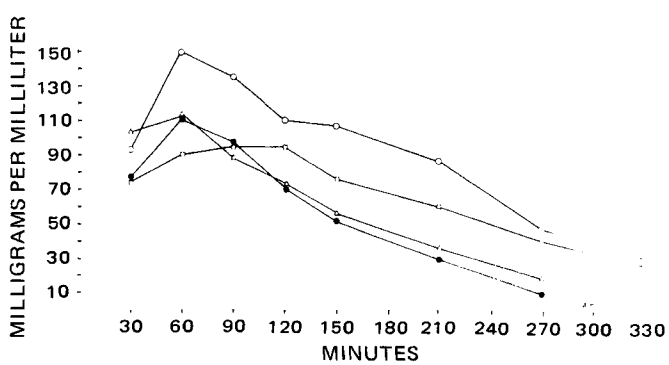

Figure 10—*In vivo bioavailability of aspirin from tablets with various diluents. Key: ○, lactose; □, I; △, starch; and ●, pure aspirin.*

prepared with I had faster dissolution than the tablets with anhydrous lactose. The dissolution rate of phenobarbital tablets with anhydrous lactose was higher than that of tablets with I. This result may be due to the greater hardness of tablets with I. This hardness was needed to produce satisfactory tablets. The dissolution rate of benzoic acid tablets with I was considerably less than that of tablets made with anhydrous lactose. This finding can be attributed to a further decrease in dissolution medium pH due to the hydrolysis of I to gluconic acid. The results of the dissolution studies are shown in Figs. 1–4.

Aspirin, ferrous sulfate, and phenobarbital tablets prepared with I, anhydrous lactose, and spray-dried lactose and plain tablets of I were stored at 95% relative humidity for 2 months. Mold growth was observed on aspirin tablets and phenobarbital tablets prepared with anhydrous lactose and spray-dried lactose, respectively. None of the tablets prepared with I showed any signs of mold growth.

A comparative study was conducted at various humidity and temperature conditions on the stability of aspirin in a mixture with I and other excipients such as anhydrous lactose, spray-dried lactose, mannitol, and sorbitol. Aspirin hydrolyzed less when mixed with I as compared to other excipients (Figs. 5–9). Mannitol, which is an excellent excipient for moisture-sensitive drugs due to its water-repellent properties (21), contributed more to the hydrolysis of aspirin as compared to I.

No attempt was made to study aspirin–sorbitol mixtures at higher temperatures because a preliminary investigation showed excessive hydrolysis of aspirin in such mixtures.

These results on the stability of aspirin indicate that I probably takes up the environmental moisture for its own hydrolysis into gluconic acid, thereby preventing the hydrolysis of aspirin. A similar mechanism is expected for the stability of other drugs that deteriorate in moisture. A detailed study on this aspect is being conducted.

A preliminary *in vivo* bioavailability study was conducted to obtain information on the effect of I on drug absorption. The results shown in Fig. 10 do not indicate any inhibitory effect of I on aspirin absorption. Detailed bioavailability studies are being conducted on various drugs in combination with I using different test animals. Compound I and anhydrous lactose seem to prolong blood aspirin levels for a greater period as compared to pure aspirin and aspirin–starch mixtures.

Compound I merits serious consideration for use as a direct compression excipient. It can effect compression of problem drugs at relatively low concentrations and yields tablets possessing desired characteristics for pharmaceutical use. The enhancement of stability of moisture-sensitive drugs with I is an additional advantage.

REFERENCES

(1) W. C. Gunsel and L. Lachman, *J. Pharm. Sci.*, **52**, 178 (1963).

(2) C. D. Fox, M. D. Richman, G. E. Reiner, and R. Shangraw, *Drug Cosmet. Ind.*, **92**, 161 (1963).

(3) J. L. Kanig, *J. Pharm. Sci.*, **53**, 188 (1964).

(4) P. Ranchordas and J. H. Wiley, U.S. pat. 3,134,719 (1964).

(5) R. N. Duvall, K. T. Koshy, and R. E. Dashiell, *J. Pharm. Sci.*, **54**, 1196 (1965).

(6) K. C. Kwan and G. Milosovich, *ibid.*, **55**, 340 (1966).

(7) N. H. Batuyios, *ibid.*, **55**, 727 (1966).

(8) K. S. Manudhane, A. M. Contractor, and H. Y. Kim, *ibid.*, **58**, 616 (1969).

(9) C. J. Kern and H. W. DelVecchio, U.S. pat. 2,491,452 (1948).

(10) J. A. Hill and G. N. Cyr, U.S. pat. 3,106,512 (1963).

(11) I. Pigman, *Res. Natl. Bur. Stand.*, **10**, 337 (1933).

(12) C. King, *Biochem. J.*, **68**, 31 (1958).

(13) E. Nelson, *J. Am. Pharm. Assoc., Sci. Ed.*, **44**, 435 (1955).

(14) M. Z. Barakat and N. Badron, *J. Pharm. Pharmacol.*, **3**, 501 (1951).

(15) T. Higuchi, "Pharmaceutical Analysis," Interscience, New York, N.Y., 1961, p. 18.

(16) J. T. Jacob and E. M. Plein, *J. Pharm. Sci.*, **57**, 798 (1968).

(17) M. Gibaldi and S. Feldman, *ibid.*, **56**, 1238 (1967).

(18) G. Levy and B. A. Haynes, *N. Engl. J. Med.*, **262**, 1053 (1960).

(19) L. J. Edwards, D. N. Gore, H. D. C. Rapson, and M. P. Taylor, *J. Pharm. Pharmacol.*, **7**, 892 (1955).

(20) F. Trinder, *Biochem. J.*, **57**, 301 (1954).

(21) R. G. Doust and M. J. Lynch, *Drug Cosmet. Ind.*, **93**, 26 (1963).

ACKNOWLEDGMENTS AND ADDRESSES

Received May 12, 1975, from the *Industrial Pharmacy Laboratories, School of Pharmacy, Auburn University, Auburn, AL 36830.*

Accepted for publication May 10, 1976.

Presented at the Industrial Pharmaceutical Technology Section, APhA Academy of Pharmaceutical Sciences, San Francisco meeting, April 1975.

[x] To whom inquiries should be directed. Present address: Aspro-Nicholas (Pakistan) Limited, C/36, Estate Avenue, S.I.T.E., Karachi, Pakistan.

Electrochemical Analysis of the Cephalosporin Cefamandole Nafate

EUGENE C. RICKARD [x] and GARY G. COOKE

Abstract □ The polarographic assays for cefamandole sodium and its formyl ester, cefamandole nafate, are described. Controlled potential coulometry is used as an absolute method for the assignment of purity of these compounds without the need for a reference material. The precision, accuracy, and selectivity of these assays were better than for the microbiological autoturbidimetric and automated iodometric assays. NMR, TLC, GC, and polarography are used to detect and quantitate likely impurities and degradation products.

Keyphrases □ Cefamandole nafate—polarographic analysis, prepared samples □ Polarography—analysis, cefamandole nafate, prepared samples □ Antibacterials—cefamandole nafate, polarographic analysis, prepared samples

Cefamandole (I) has *in vitro* activity against various Gram-positive and Gram-negative bacteria (1–3). A formyl ester, cefamandole nafate (II), was prepared for use in the clinical formulation because it can be purified in a crystalline form having good long-term stability. The ester is hydrolyzed rapidly to cefamandole *in vivo* (4) or in basic aqueous solution (5). Title 21 of the Code of Federal Regulations, Part 442, Cepha Antibiotics, generally provides for both microbiological and chemical assay procedures for cephalosporin antibiotics. However, the microbiological assay results are considered conclusive even though this assay is not specific for any one compound. This paper focuses on the additional tests necessary to characterize completely antibiotic materials such as cefamandole and cefamandole nafate.

Electrochemical techniques are uniquely suited for the assay of compounds containing reducible or oxidizable functions. These include the cephalosporin antibiotics

prepared with I had faster dissolution than the tablets with anhydrous lactose. The dissolution rate of phenobarbital tablets with anhydrous lactose was higher than that of tablets with I. This result may be due to the greater hardness of tablets with I. This hardness was needed to produce satisfactory tablets. The dissolution rate of benzoic acid tablets with I was considerably less than that of tablets made with anhydrous lactose. This finding can be attributed to a further decrease in dissolution medium pH due to the hydrolysis of I to gluconic acid. The results of the dissolution studies are shown in Figs. 1–4.

Aspirin, ferrous sulfate, and phenobarbital tablets prepared with I, anhydrous lactose, and spray-dried lactose and plain tablets of I were stored at 95% relative humidity for 2 months. Mold growth was observed on aspirin tablets and phenobarbital tablets prepared with anhydrous lactose and spray-dried lactose, respectively. None of the tablets prepared with I showed any signs of mold growth.

A comparative study was conducted at various humidity and temperature conditions on the stability of aspirin in a mixture with I and other excipients such as anhydrous lactose, spray-dried lactose, mannitol, and sorbitol. Aspirin hydrolyzed less when mixed with I as compared to other excipients (Figs. 5–9). Mannitol, which is an excellent excipient for moisture-sensitive drugs due to its water-repellent properties (21), contributed more to the hydrolysis of aspirin as compared to I.

No attempt was made to study aspirin–sorbitol mixtures at higher temperatures because a preliminary investigation showed excessive hydrolysis of aspirin in such mixtures.

These results on the stability of aspirin indicate that I probably takes up the environmental moisture for its own hydrolysis into gluconic acid, thereby preventing the hydrolysis of aspirin. A similar mechanism is expected for the stability of other drugs that deteriorate in moisture. A detailed study on this aspect is being conducted.

A preliminary *in vivo* bioavailability study was conducted to obtain information on the effect of I on drug absorption. The results shown in Fig. 10 do not indicate any inhibitory effect of I on aspirin absorption. Detailed bioavailability studies are being conducted on various drugs in combination with I using different test animals. Compound I and anhydrous lactose seem to prolong blood aspirin levels for a greater period as compared to pure aspirin and aspirin–starch mixtures.

Compound I merits serious consideration for use as a direct compression excipient. It can effect compression of problem drugs at relatively low concentrations and yields tablets possessing desired characteristics for pharmaceutical use. The enhancement of stability of moisture-sensitive drugs with I is an additional advantage.

REFERENCES

(1) W. C. Gunsel and L. Lachman, *J. Pharm. Sci.*, **52**, 178 (1963).

(2) C. D. Fox, M. D. Richman, G. E. Reiner, and R. Shangraw, *Drug Cosmet. Ind.*, **92**, 161 (1963).

(3) J. L. Kanig, *J. Pharm. Sci.*, **53**, 188 (1964).

(4) P. Ranchordas and J. H. Wiley, U.S. pat. 3,134,719 (1964).

(5) R. N. Duvall, K. T. Koshy, and R. E. Dashiell, *J. Pharm. Sci.*, **54**, 1196 (1965).

(6) K. C. Kwan and G. Milosovich, *ibid.*, **55**, 340 (1966).

(7) N. H. Batuyios, *ibid.*, **55**, 727 (1966).

(8) K. S. Manudhane, A. M. Contractor, and H. Y. Kim, *ibid.*, **58**, 616 (1969).

(9) C. J. Kern and H. W. DelVecchio, U.S. pat. 2,491,452 (1948).

(10) J. A. Hill and G. N. Cyr, U.S. pat. 3,106,512 (1963).

(11) I. Pigman, *Res. Natl. Bur. Stand.*, **10**, 337 (1933).

(12) C. King, *Biochem. J.*, **68**, 31 (1958).

(13) E. Nelson, *J. Am. Pharm. Assoc., Sci. Ed.*, **44**, 435 (1955).

(14) M. Z. Barakat and N. Badron, *J. Pharm. Pharmacol.*, **3**, 501 (1951).

(15) T. Higuchi, "Pharmaceutical Analysis," Interscience, New York, N.Y., 1961, p. 18.

(16) J. T. Jacob and E. M. Plein, *J. Pharm. Sci.*, **57**, 798 (1968).

(17) M. Gibaldi and S. Feldman, *ibid.*, **56**, 1238 (1967).

(18) G. Levy and B. A. Haynes, *N. Engl. J. Med.*, **262**, 1053 (1960).

(19) L. J. Edwards, D. N. Gore, H. D. C. Rapson, and M. P. Taylor, *J. Pharm. Pharmacol.*, **7**, 892 (1955).

(20) F. Trinder, *Biochem. J.*, **57**, 301 (1954).

(21) R. G. Doust and M. J. Lynch, *Drug Cosmet. Ind.*, **93**, 26 (1963).

ACKNOWLEDGMENTS AND ADDRESSES

Received May 12, 1975, from the *Industrial Pharmacy Laboratories, School of Pharmacy, Auburn University, Auburn, AL 36830.*

Accepted for publication May 10, 1976.

Presented at the Industrial Pharmaceutical Technology Section, APhA Academy of Pharmaceutical Sciences, San Francisco meeting, April 1975.

[x] To whom inquiries should be directed. Present address: Aspro-Nicholas (Pakistan) Limited, C/36, Estate Avenue, S.I.T.E., Karachi, Pakistan.

Electrochemical Analysis of the Cephalosporin Cefamandole Nafate

EUGENE C. RICKARD [x] and GARY G. COOKE

Abstract □ The polarographic assays for cefamandole sodium and its formyl ester, cefamandole nafate, are described. Controlled potential coulometry is used as an absolute method for the assignment of purity of these compounds without the need for a reference material. The precision, accuracy, and selectivity of these assays were better than for the microbiological autoturbidimetric and automated iodometric assays. NMR, TLC, GC, and polarography are used to detect and quantitate likely impurities and degradation products.

Keyphrases □ Cefamandole nafate—polarographic analysis, prepared samples □ Polarography—analysis, cefamandole nafate, prepared samples □ Antibacterials—cefamandole nafate, polarographic analysis, prepared samples

Cefamandole (I) has *in vitro* activity against various Gram-positive and Gram-negative bacteria (1–3). A formyl ester, cefamandole nafate (II), was prepared for use in the clinical formulation because it can be purified in a crystalline form having good long-term stability. The ester is hydrolyzed rapidly to cefamandole *in vivo* (4) or in basic aqueous solution (5). Title 21 of the Code of Federal Regulations, Part 442, Cepha Antibiotics, generally provides for both microbiological and chemical assay procedures for cephalosporin antibiotics. However, the microbiological assay results are considered conclusive even though this assay is not specific for any one compound. This paper focuses on the additional tests necessary to characterize completely antibiotic materials such as cefamandole and cefamandole nafate.

Electrochemical techniques are uniquely suited for the assay of compounds containing reducible or oxidizable functions. These include the cephalosporin antibiotics

having a thioether linkage to a substituent at the 3-cephem position. Specifically, cefamandole and cefamandole nafate are easily reduced at the dropping mercury electrode.

This paper reports the polarographic reduction characteristics of these compounds and describes the use of polarography in analytical control and stability procedures. Controlled potential coulometry is proposed as an absolute method for purity evaluation. The purities obtained from these two electrochemical techniques are evaluated by comparison with the microbiological autoturbidimetric and automated iodometric assays. Finally, the effect of impurities on each assay technique is presented. Electrochemical techniques were found to be less affected by impurities than other assay techniques. The use of NMR, TLC, GC, and polarography to monitor the types and levels of impurities also is discussed.

EXPERIMENTAL

Apparatus—Polarograms were recorded using a three-electrode polarograph[1]. Either a natural drop time dropping mercury electrode or a mechanically controlled drop time of 1 sec was used. Potential scan rates were 1 or 2 mv/sec. Instantaneous currents were measured. Electronic damping was not used. The three-compartment, water-jacketed polarographic cell was thermostated at the desired temperature (20–25°). The cell compartments were separated by medium-porosity sintered-glass disks and 4% agar–potassium chloride salt bridges. A saturated calomel reference electrode (SCE) and a 1-cm^2 platinum foil counter electrode were used. Water-saturated nitrogen was used for deaeration of the sample solutions.

A potentiostat[2] with current-to-voltage converter was used for coulometry. The current-to-voltage converter output was integrated electronically using an operational amplifier circuit constructed with a differential input, low drift, chopper-stabilized operational amplifier[3]. The integrator-calibrated time constant was 10.73/sec. The coulometric cell consisted of a 40-mm (diameter) × 45-mm Pyrex weighing bottle fitted with a rubber stopper containing the appropriate cell connections.

The working electrode was a 12.6-cm^2 stirred mercury pool. A magnetic stirrer was used for agitation. A 4-cm^2 platinum foil or wire counter electrode was separated from the working electrode compartment by a medium-porosity sintered-glass disk. The saturated calomel reference electrode was double isolated from the cell through a two-compartment salt bridge having sintered-glass disks. To exclude oxygen, a continuous stream of nitrogen was bubbled through the solution from a 10-mm, medium-porosity, fritted-disk immersion filter.

NMR spectra[4] were acquired from 99.7% deuterium oxide solutions, except for IV where solubility dictated the use of deuterated dimethyl sulfoxide. Sodium 3-(trimethylsilyl)propanesulfonate was used as the zero delta standard. All spectra were obtained at the equilibrium probe temperature.

Procedure—Solutions for polarography were prepared by weighing approximately 5 mg (measured to 0.01 mg) of sample into a 25-ml volumetric flask, dissolving in water, adding buffer, and diluting to volume. No surfactants were used for analytical investigations. The pH of this solution was measured. An aliquot was transferred to the polarographic cell and deaerated, and the polarogram was recorded. The diffusion current, i_d, and half-wave potentials, $E_{1/2}$, were measured by the usual procedures (6).

Coulometric solutions were prepared in deionized water at a nominal concentration of 5 mg/ml. Aliquots (5 ml) were pipetted into the coulometric cell containing the supporting electrolyte preelectrolyzed at the electrolysis potential. The number of coulombs consumed during electrolysis was determined using the calibrated time constant of the integrator, its output voltage (measured to 1 mv), and the current range of the potentiostat.

[1] Beckman Instruments Electroscan 30 operated with a natural drop time dropping mercury electrode, or Princeton Applied Research Corp. model 174A polarograph with a mechanically controlled 1-sec drop time operated in the "sampled dc" mode.

[2] Princeton Applied Research Corp. model 173 with model 176 current-to-voltage converter.

[3] Burr Brown model 3355.

[4] Varian T-60A spectrometer.

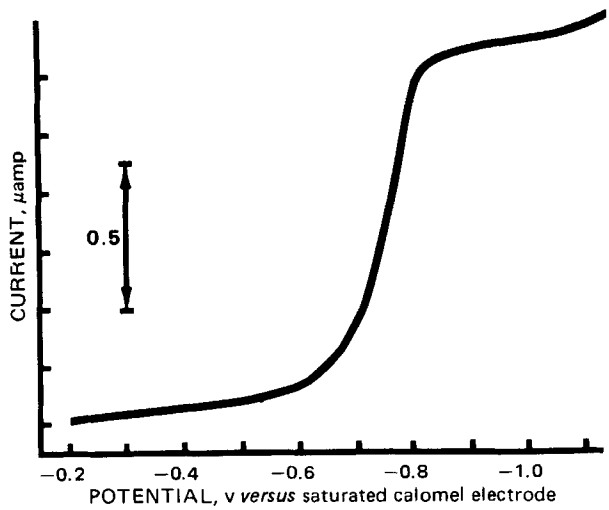

Figure 1—*Polarogram of 0.4 m*M *cefamandole nafate in pH 2.3 McIlvaine buffer.*

The total number of coulombs was corrected for the residual current observed after the electrolysis by integration of the residual current. This residual current was higher in the presence of the electrolysis products than in the preelectrolyzed electrolyte. The purity was calculated by comparison to the theoretical charge that should have been transferred for the amount of sample. These calculations were performed using:

$$Q\text{ (observed)} = RC \times V\text{ (out)} \times \text{sensitivity} \quad \text{(Eq. 1)}$$

$$Q\text{ (net)} = Q\text{ (observed)} - Q\text{ (correction)} \quad \text{(Eq. 2)}$$

$$Q\text{ (theory)} = \text{sample weight, mg} \times n \times F/\text{MW} \quad \text{(Eq. 3)}$$

$$\text{purity, \%} = Q\text{ (net)} \times 100/Q\text{ (theory)} \quad \text{(Eq. 4)}$$

where Q is charge in millicoulombs; RC is the integrator time constant per second; V (out) is integrator output voltage; sensitivity is the current-to-voltage sensitivity in milliamperes per volt; n is the number of electrons transferred per species; F is Faraday's constant, 96,500 mcoulombs/mEq; and MW is molecular weight in milligrams per mmole. Analytical results were obtained using an electrode potential of −0.875 v *versus* the saturated calomel reference electrode.

Electrochemical buffer solutions were prepared using reagent grade chemicals and were checked for contamination from electroactive impurities in the potential region of interest. Phosphate–citrate–potassium chloride 0.5 *M* constant ionic strength buffers were used unless otherwise stated.

The best NMR results were obtained when special attention was given to instrument adjustment. Optimization of spin rate, spectrum amplitude, and phasing was crucial. A spin rate of 45–50 rps prevented interference from spinning side bands. For best precision, the α-phenylmethine resonance amplitude was adjusted to full scale. Proper phasing was necessary for accurate measurements of peak heights. Spectra were acquired on 200-mg/ml solutions.

Thin-layer chromatograms were obtained using a 250-μg sample loading from an aqueous solution on silica gel plates[5]. The developing solvent was ethyl acetate–acetone–acetic acid–water (5:2:1:1). Chromatographic zones were examined by either shortwave UV light (254 nm) or after exposure to iodine vapors.

RESULTS

Polarography—Cefamandole and cefamandole nafate each gave a two-electron reduction wave at the dropping mercury electrode (Fig. 1). The transfer of two electrons was apparent from the coulometric results and by comparison of the observed diffusion current with that observed from compounds having known two-electron reductions (7). The polarographic wave corresponded to the reductive cleavage of the thioether linkage at position 3 of the cephalosporin (7). It exhibited a maximum of the first kind (8) at concentrations greater than 0.2 m*M* when the capillary drop time was 1 sec. When surfactant[6] or surface-active impurities were present, the maximum was suppressed.

[5] Merck precoated 0.25-mm silica gel 60 F-254 TLC plates.

[6] Triton X-100.

Table I—Concentration and pH Dependence of Polarographic Waves[a]

Cefamandole				Cefamandole Nafate			
pH	Concentration, m*M*	$E_{1/2}$, v *versus* SCE	i_d/C^b, μamp/m*M*	pH	Concentration, m*M*	$E_{1/2}$, v *versus* SCE	i_d/C^b, μamp/m*M*
0.67[c]	0.395	−0.749	4.15	0.60[c]	0.336	−0.744	3.98
1.60[c]	0.370	−0.776	4.03	1.66[c]	0.340	−0.769	4.01
2.29	0.202	−0.716	3.94	2.43	0.174	−0.698	3.88
2.29	0.387	−0.755	3.92	2.43	0.351	−0.750	3.85
2.29	0.395	−0.755	3.98	2.43	0.375	−0.744	3.89
2.29	0.772	−0.802	4.17	2.43	0.7079	−0.786	3.99
2.29	1.942	−0.859	4.01	2.43	1.136	−0.823	4.08
2.29	4.10	−0.902	3.99	2.43	1.676	−0.851	3.96
2.29	7.90	−0.959	4.00	2.43	3.572	−0.900	3.90
3.30	0.364	−0.798	3.92	3.31	0.353	−0.792	3.86
4.72	0.347	−0.880	3.96	4.49	0.347	−0.860	4.09
5.57[d]	0.377	−0.971	3.98	5.38[d]	0.340	−0.951	3.80
7.19	0.419	−1.122	4.58	6.91	0.344	−1.092	4.72

[a] Data were obtained using a capillary with $m^{2/3}\,t^{1/6}$ of 1.382, open circuit, 1 *M* KCl, 1-sec mechanically controlled drop time. All supporting electrolytes were 0.5 *M* constant ionic strength McIlvaine buffers except as noted. [b] i_d = 3.991 (±0.010 *SD*) *C* + 0.0234 (±0.034 *SD*) and 3.902 (±0.031 *SD*) *C* + 0.058 (±0.052 *SD*) least-squares calculation for data obtained in pH 2.3 buffer. Instantaneous currents measured at the half-wave potential are reported. [c] Hydrochloric acid, 0.32 and 0.2 *M* ionic strength for pH 0.67 and 1.60, respectively. [d] Acetic acid—acetate, 0.7 *M* ionic strength.

Plots of $\log i/(i_d - i)$ *versus* *E* of the polarograms were nonlinear at all concentrations investigated. At very low concentrations such as 2×10^{-5} *M*, the logarithmic plots became nearly linear. The limiting current was proportional to concentration and to the square root of the corrected mercury column height. It had a temperature coefficient of approximately +0.8%/degree at 25°. These observations indicate that the limiting current was diffusion controlled.

The half-wave potentials of cefamandole and cefamandole nafate were complex functions of pH and concentration (Table I), as was previously observed for related compounds (7, 9). In the pH 0.6–2.3 range, $E_{1/2}$ was generally independent of pH. In contrast, a shift of $E_{1/2}$ with pH was observed from pH 2.3 to 7. The carboxylate pKa of these compounds was about 2.6–2.9 as determined by aqueous titration or 3.0 as determined by spectrophotometry. The diffusion current normalized with respect to concentration was approximately independent of pH at or below pH 5.8 and nearly equal for both compounds (diffusion current constant, *I*, equals 2.89). The half-wave potential was dependent upon concentration. This variation is reported in Table I, but it was impossible to measure "true" values of $E_{1/2}$ when maxima were present (concentrations above 0.2 m*M*).

The precision obtained for the normalized diffusion current in the pH 2.3 supporting electrolyte for individually weighed samples of identical material was 1.1% (n = 12). Thus, for the comparison of a sample to a standard reference material, a relative standard deviation of 1.6% may be expected. Decreases in the diffusion current of approximately 0.4%/hr (3.1% in 7 hr and 9.2% in 24 hr) were observed. Therefore, all polarograms were acquired on freshly prepared solutions.

Compounds III–VIII were not polarographically reducible under the assay conditions. However, 1-methyl-5-mercapto-1,2,3,4-tetrazole sodium salt (VII) can be oxidized at either platinum or mercury electrodes. At the platinum electrode, the oxidation product of thiols is the disulfide. However, the oxidation product of thiols at a mercury electrode is the mercurous salt (10).

Table II—Comparison of Purity Assays[a]

	Cefamandole Sodium			Cefamandole Nafate		
Assay Ratio	n	Result	*SD*	n	Result	*SD*
Polarography—microbiological	4	0.999	0.022	32	1.018	0.035
Polarography—iodometric	4	1.002	0.012	34	0.991	0.029
Coulometry—microbiological	7	1.003	0.004	15	1.045	0.034
Coulometry—iodometric	6	0.989	0.006	9	0.990	0.026
Coulometry—polarography	19	1.006	0.022	7	0.974	0.038

[a] See text for explanation of assay procedures.

Comparison of Polarographic with Microbiological and Iodometric Assays—The relative purities of raw material lots of cefamandole sodium and cefamandole nafate determined by the polarographic, microbiological, and iodometric techniques are compared in Table II. All assays used a common cefamandole reference material. The polarographic assay was performed as already described. The microbiological turbidimetric assay measured the inhibition of growth of *Staphylococcus aureus* (ATCC 9144). The assay precision is about 2–4% as measured by relative standard deviation. The automated iodometric titration measured the increase in iodine uptake by the β-lactam following alkaline hydrolysis (11). The relative standard deviation for this assay is 1–2%.

The polarographic purity results were in excellent agreement with the purities determined by the other assay techniques. The observed ratio of assay results was less than 1 *SD* from unity for both cefamandole and cefamandole nafate (Table II).

Controlled Potential Coulometry—When the anode and cathode compartments of the coulometric cell were separated, a two-electron reductive cleavage of the thioether bond was obtained. This arrangement corresponded to the normal experimental one. If the anode were located in the main portion of the cell, then the 1-methyl-5-mercapto-1,2,3,4-tetrazole formed at the mercury pool cathode would be transported to the platinum anode and oxidized to the corresponding disulfide. Under these conditions, a net three-electron transfer would be observed.

Analytical data were obtained using a cell with separated anode and cathode compartments. Plots of the logarithm of the current *versus* time were not linear, indicating that the reduction was not a simple electron transfer. This result was consistent with previous observations (7).

The products of the controlled potential coulometric reduction of cefamandole were examined by TLC and polarography. TLC indicated the presence of two major, one minor, and several trace zones. The retention factors for the major zones corresponded to the tetrazole derivative (VII) and VI. The minor zone retention factor correlated with 7-D-mandelamidocephalosporanic acid (mandelic acid form of III). The only identified trace zone appeared to be V. The amount of free VII as measured by polarography was greater than 80% of the amount expected for quantitative formation of this compound.

Comparison of Coulometry with Other Assay Techniques—The relative purities obtained for raw material lots of cefamandole and cefamandole nafate using the coulometric, microbiological, and iodometric assays are given in Table II. A comparison of the coulometric and polarographic assays is included also.

The coulometric assay results were in good agreement with results obtained by the other techniques. However, the ratio of the coulometric assay to the microbiological assay was more than 1 *SD* from unity for cefamandole nafate. This result may be explained by the relatively small number of samples from which the comparison was made. Moreover, the difference probably partially resulted from the nature of the microbiological assay for cefamandole nafate. For this assay, the sample is hydrolyzed to cefamandole in a sodium carbonate solution at room temperature and then is compared to a standard of cefamandole. In contrast, the polarographic and iodometric assays of cefamandole nafate use a standard lot of cefamandole nafate for the comparison. Thus, the mi-

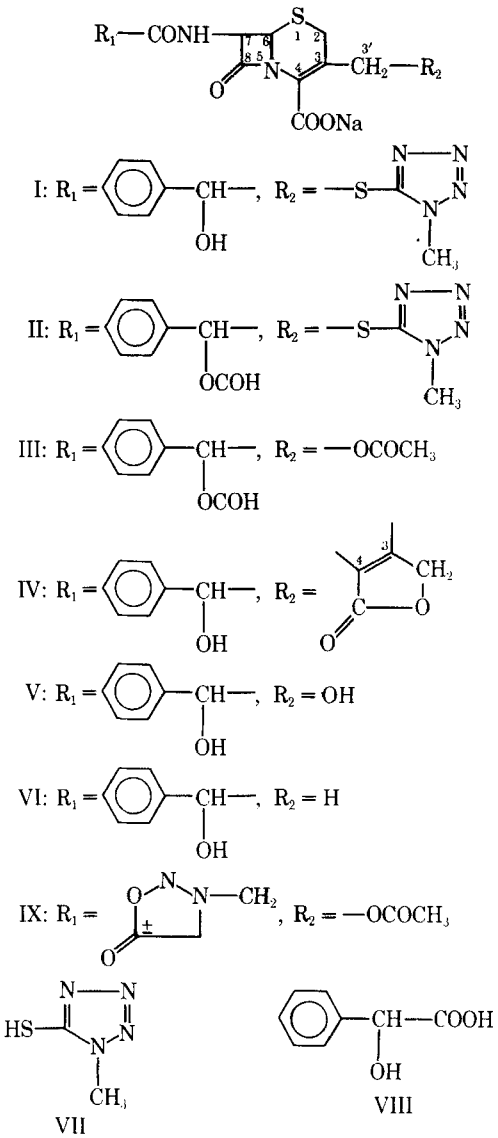

crobiological assay for cefamandole nafate uses a different reference material and a more complicated procedure than do the chemical assays. The coulometric assay does not need a reference material.

NMR—Spectra of I–V are shown in Fig. 2. The spectrum of IV obtained in dimethyl sulfoxide exhibits the expected solvent shifts when compared to the other compounds. The assigned chemical shift values are listed in Table III.

Significant spectral differences occurred between compounds in the areas of δ 5.2–6.2 and 2.05. The α-phenylmethine resonance shifts from the region of δ 5.25 in mandelic acid derivatives to the δ 6.2 region in compounds containing the formyl ester of mandelic acid. This shift

Table III—60-MHz NMR Chemical Shift Values (δ)

Proton	Compound I	II	III	IV[a]	V	VI	VIII
α-Mandeloyl-formyl	—	8.33	8.28	—	—	—	—
Phenyl	7.45	7.43	7.50	7.37	7.45	7.47	7.52
α-Phenylmethine	5.25	6.20	6.20	5.08	5.25	5.25	5.37
C-7	5.60	5.63	5.63	5.83	5.60	5.55	—
C-6	5.05	4.97	4.95	5.08	5.07	5.00	—
3′-Methylene	4.17	4.17	4.83	5.03	4.22	1.92	—
N-Methyl	3.97	3.95	—	—	—	—	—
C-2	3.50	3.40	3.28	3.75	3.45	3.38	—
3′-Acetoxy	—	—	2.07	—	—	—	—

[a] Deuteratated dimethyl sulfoxide.

Figure 2—*The 60-MHz NMR spectra of (A) I, (B) II, (C) III, (D) IV (in dimethyl sulfoxide), and (E) V.*

provides a convenient means of detecting substances containing the mandelic acid functionality (*e.g.*, I and IV–VI) in cefamandole nafate. Accurate measurements for the amounts of these compounds in cefamandole nafate were possible by comparing the height of the δ 5.25 peak to the sum of the heights of the peaks at δ 5.25 and 6.2. The detection level was 2 mole %, and a linear calibration curve was obtained for samples spiked with known amounts of impurities. The slope of the calibration curve was unity when the observed ratio was plotted *versus* mole percent added.

Cefamandole and cefamandole nafate had no resonances upfield of δ 2.5. Trace solvent peaks were occasionally observed such as acetone at δ 2.2 and acetates at δ 2.0. However, impurities containing an acetoxy function such as III had a very sharp resonance at δ 2.05. This resonance provided a positive indication of their presence. A quantitative measure of the mole ratio of these compounds was obtained by comparison of the acetoxy peak height to the α-phenylmethine peak height (δ 6.2). The detection level was about 1 mole % of acetoxy compounds, and the calibration curve was linear with a slope of one when the acetoxy peak height was normalized to one proton.

TLC—TLC was used to identify impurities, degradation products, and the products of the electrochemical reduction. It also provided a rough estimate of the levels of these substances. The relative retention factors for this series of compounds are given in Table IV. With a 250-μg plate loading, generally 1% of a substance was visible on the developed plate. However, D-mandelic acid was not visible except above the 10% impurity level.

DISCUSSION

The initial description of the electrochemistry of cephalosporins was given by Jones *et al.* (9). Those investigators (9) and Hall (7) used the

Table IV—TLC Data

Compound	R_f	Detection Limit[a], %
I	0.46	1
II	0.52	—
III	0.58	1
IV	0.82	1
V	0.34	1
VI	0.66	1
VII	0.92	1
VIII	0.74	~10

[a] Detection limit using a 250-μg sample of cefamandole nafate.

polarographic reduction wave for quantitative assays. Controlled potential electrolysis has been used to obtain n values (7) and for electrosynthesis (12) but not for quantitative analysis. We found that, under appropriate conditions, cefamandole and cefamandole nafate may be quantitatively reduced at a mercury pool electrode at a controlled potential.

Hall (7) was able to identify explicitly the functional group that undergoes reduction in cephaloridine, cephalothin, cephalosporin C, and IX, a cephalosporin similar to cefamandole. In all cases, the substituent at the 3-position was reductively eliminated in a two-electron, irreversible polarographic wave. The initial reduction products probably were the free, protonated 3-position substituent and the anion radical of the cephalosporin nucleus. In aqueous solutions, the anion radical immediately reacted with a proton donor such as the hydronium ion or the supporting electrolyte components. Typical products reported (7, 12) were the 3-methylenecepham derivatives, which were easily isomerized to the corresponding 3-deacetoxycephalosporanic acid derivatives such as VI[7]. These observations are consistent with the partial identification of the coulometric reduction products described.

The shift of the polarographic half-wave potential observed with pH indicated involvement of hydronium ions in the reduction mechanism. This potential shift is between 50 and 90 mv cathodic per pH unit but is apparently not linear with pH.

Cyclic voltammetry was used to elucidate the mechanism of this reaction. The qualitative features—no anodic peak at scan rates up to 5 v/sec, approximately constant current function (peak current/square root of scan rate) at low scan rates, and a cathodic shift of reduction peak potentials with increasing scan rate—were in agreement with a chemical reaction following charge transfer (13). However, the large effects due to adsorption of impurities, uncompensated potential drops, and variation of parameters with concentration prevented any detailed correlation of experimental results with theoretical expectations. It can, however, be assumed that the 1-methyl-5-mercapto-1,2,3,4-tetrazole is eliminated and then protonated. Simultaneously, the cephalosporin nucleus moiety undergoes successive chemical reactions, probably involving the solvent. Thus, the products of the electrochemical reaction are quickly removed and unavailable for an electrochemical reoxidation step except at extremely short times. These chemical reactions account for the irreversible electrochemical reduction observed on the experimentally accessible time scale.

The data presented indicate that polarography and controlled potential coulometry are useful assay techniques for purity determinations on raw material samples of cefamandole and cefamandole nafate. The electrochemical assay results were essentially identical to the microbiological and iodometric assay results. However, a good analytical assay also must be selective or essentially free from interferences. The various assay techniques were examined to determine what effect impurities or degradation products had on each technique.

The most likely impurity in cefamandole nafate is III. This impurity occurs when the acetoxy group is not displaced by the substituted tetrazole in the synthetic sequence. In solution, cefamandole nafate is hydrolyzed by an alkaline-catalyzed reaction (5). Cefamandole nafate and any cefamandole formed by hydrolysis respond essentially identically in the chemical assay procedures. The degradation of cefamandole or cefamandole nafate then follows one of two possible sequences according to the pH of its environment. These sequences were reviewed for a general cephalosporin (7) and studied for these particular compounds[8].

In acidic media, cefamandole initially loses the substituted tetrazole to give the hydroxymethyl compound, V, and VII. Compound V rapidly dehydrates to form the α,β-unsaturated lactone, IV. Under extremely harsh conditions, mandelic acid (VIII) is cleaved and the cephalosporin nucleus is destroyed. In basic media, the substituted tetrazole is initially lost also. At prolonged times or high temperatures in basic media, the mandelic acid substituent is cleaved and the β-lactam ring is opened[8]. Therefore, III–V, VII, and VIII can be present in aged cefamandole nafate as either initial impurities or degradation products. The polarographic assay for cefamandole or cefamandole nafate, which measures the thioether linkage, will not have interference from these compounds and can be considered a selective assay technique.

In the microbiological assay, any compound that inhibited the growth of the test organism was a positive assay interference. In general, compounds with an intact cephalosporin nucleus exhibited some activity. Compounds III–V interfered with the microbiological assay. Compound III had the highest activity of these interferences. The iodometric assay is based on the reaction at the β-lactam. The likely impurities and degradation products III–V interfered with this assay.

Even though the electrochemical assays were very selective, the presence of large amounts of impurities, especially if they were surface active, tended to distort the polarographic wave and make it irreproducible. This problem was not a major concern until the contaminant content was more than 20–30%. In controlled potential coulometry, none of the known contaminants interfered directly. At high levels of impurity (10–20%), a decrease in precision was noted. The greatest value of the coulometric technique was in the evaluation of relatively pure raw materials such as the establishment of an analytical reference standard material. This reference material was then used to assay material by a precise, selective technique such as polarography.

In addition to a selective, precise assay, one needs a thorough screen for impurities and methods of quantitating detected contaminants. NMR, TLC, GC, and polarography are useful. The use of NMR for the initial evaluation of impurities and for monitoring the extent of degradation was discussed. TLC was used to detect the presence of cefamandole and III–V and VII in cefamandole nafate with an approximate sensitivity level of 1–3%. Mandelic acid may be determined by a separate GC assay if necessary. The free substituted tetrazole (VII) can be measured using the polarographic oxidation wave.

SUMMARY

Both cefamandole and its formyl ester, cefamandole nafate, can be assayed by two electrochemical methods. Dropping mercury electrode polarography was used to determine the purity of the samples by comparison to a reference material of known purity. Controlled potential coulometry was used as an absolute measure of the purity of these compounds without the need for a reference material. These techniques utilize reductive cleavage of the thiotetrazole substituent at the 3-position.

With pure raw material, the results from the electrochemical assays are essentially identical to the purity results obtained with the microbiological autoturbidimetric and automated iodometric assays. The precision of the electrochemical assays is better than the microbiological assay and comparable to the iodometric assay.

For raw material samples containing typical impurities or degradation products, polarography is the most selective of the three types of purity assays. NMR, TLC, GC, and polarography are used for the detection and quantitative measurement of compounds that could interfere with the various assay procedures.

REFERENCES

(1) W. E. Wick and D. A. Preston, *Antimicrob. Ag. Chemother.*, **1**, 221 (1972).

(2) H. Neu, *ibid.*, **6**, 177 (1974).

(3) R. B. Krammer, D. A. Preston, and J. R. Turner, in "Abstracts 9th International Congress of Chemotherapy," London, England, 1975.

(4) J. S. Wold, R. R. Joost, H. R. Black, and K. E. Briscoe, in *ibid.*

(5) J. M. Indelicato, W. L. Wilham, and B. J. Cerimele, *J. Pharm. Sci.*, **65**, 1175 (1976).

(6) L. Meites, "Polarographic Techniques," 2nd ed., Interscience, New York, N.Y., 1965, chaps. 3–5.

(7) D. A. Hall, *J. Pharm. Sci.*, **62**, 980 (1973).

(8) L. Meites, "Polarographic Techniques," 2nd ed., Interscience, New York, N.Y., 1965, chap. 6.

(9) I. F. Jones, J. E. Page, and C. T. Rhodes, *J. Pharm. Pharmacol., Suppl.*, **20**, 45S (1968).

(10) I. M. Kolthoff and J. J. Lingane, "Polarography," 2nd ed., vol. II, Interscience, New York, N.Y., 1952, chap. XLIII.

(11) L. P. Marrelli, in "Cephalosporins and Penicillins," E. H. Flynn, Ed., Academic, New York, N.Y., 1972, chap. 14.

(12) M. Ochiai, O. Aki. A. Morimoto, T. Okada, K. Shinozaki, and Y. Asahi, *Tetrahedron Lett.*, **23**, 2341 (1972), and *J. Chem. Soc., Perkin I*, **1974**, 258.

(13) R. S. Nicholson and I. Shain, *Anal. Chem.*, **36**, 706 (1964).

ACKNOWLEDGMENTS AND ADDRESSES

Received November 24, 1975, from the *Lilly Research Laboratories, Eli Lilly and Company, Indianapolis, IN 46206.*

[7] D. A. Hall, Eli Lilly and Co., Indianapolis, IN 46206, personal communication.

[8] A. Dinner, R. J. Templeton, and A. D. Kossoy, Eli Lilly and Co., Indianapolis, IN 46206, personal communication.

Accepted for publication May 12, 1976.
Presented in part at the Second Federation of Analytical Chemistry and Spectroscopy Societies, October 1975.
The authors thank Dr. C. Ryan and Dr. J. M. Greene for preparation of compounds. They also thank Dr. J. K. Frischmann, Dr. D. A. Hall, and Dr. R. E. Schirmer for helpful discussions and P. A. Farb for assistance.
[x] To whom inquiries should be directed.

Electron-Capture GLC Determination of Nanogram to Picogram Amounts of Isosorbide Dinitrate

J. O. MALBICA [x], K. MONSON, K. NEILSON, and R. SPRISSLER

Abstract □ A GLC method for the determination of plasma isosorbide dinitrate using electron-capture detection is described. The organic nitrates are especially suited for electron-capture detection if the detector temperature is optimized for maximum sensitivity, *e.g.*, 175°. Proper maintenance of the detector and column assures reproducible data in the low nanogram range. The extraction procedure described is simple, efficient, and expedient for processing large numbers of samples. The method was used to study plasma levels in four human volunteers after a single dose of a 5-mg chewable isosorbide dinitrate tablet. Concentration levels of isosorbide dinitrate as low as 0.5 ng/ml of plasma can be measured by this procedure.

Keyphrases □ Isosorbide dinitrate—electron-capture GLC analysis, human plasma □ GLC, electron capture—analysis, isosorbide dinitrate, human plasma □ Vasodilators, coronary—isosorbide dinitrate, electron-capture GLC analysis, human plasma

The low dosage of isosorbide dinitrate sufficient for pharmacological effectiveness results in low circulating blood levels of the drug, and difficulties exist in assaying for low nanogram to picogram amounts. Previously described GLC methods (1, 2) were either laborious or not sensitive enough to follow rapidly declining blood levels of isosorbide dinitrate.

Since only limited data are available on the blood levels of isosorbide dinitrate following administration of therapeutic doses, a method was needed that would allow reliable estimations of blood isosorbide dinitrate levels in the low nanogram to picogram range using conventional electron-capture GLC instrumentation. This report describes an assay method for isosorbide dinitrate that is expedient, sensitive, and reproducible for routinely handling large numbers of samples.

EXPERIMENTAL

Reagents and Materials—Benzene[1] and ethyl acetate[1] were glass-distilled reagent grade solvents. Anhydrous sodium sulfate[2] was reagent grade, ACS certified. Charcoal-treated paper disks[3], 6.5-mm diameter, were made with a paper punch-out.

One hundred grams of anhydrous sodium sulfate powder was washed with benzene for 20 min, allowed to air dry, and then placed in an oven at 100° until needed.

The charcoal-treated paper disks were similarly washed in benzene. Excess benzene was removed, and the paper disks were allowed to air dry. The disks were stored in an air-tight container until required.

Isosorbide dinitrate[4] and isoidide dinitrate[4] were purified by recrystallization from ethanol.

Plasma Level Study—Isosorbide dinitrate was administered to four healthy volunteers (one male, age 34; three females, ages 23, 25, and 27); each received a 5-mg chewable isosorbide dinitrate tablet[5]. Blood, 10 ml, was drawn from the cubital vein into a heparinized tube from each subject 0, 15, 30, 60, 120, and 180 min following isosorbide dinitrate administration. The blood was immediately centrifuged at 3000 rpm in an angular head clinical centrifuge[6] for 15 min. The plasma was collected and stored at −10° prior to analysis.

Extraction of Isosorbide Dinitrate—Five-milliliter aliquots of benzene were added to a 15.0-ml graduated conical centrifuge tube containing 1.0 ml of plasma spiked with 10 ng of isoidide dinitrate as an internal standard. The tube was mixed on a vortex[7] for 1 min and centrifuged at 2000 rpm to separate the phases. Then the benzene phase was carefully removed to another 15-ml centrifuge tube. A 0.5-g portion of benzene-washed sodium sulfate and three benzene-washed charcoal-treated paper disks were added to the benzene extract.

The tube and its contents were again vortexed for 15 sec and centrifuged as previously described. As much of the benzene layer as possible was carefully removed to another centrifuge tube and dried completely under a nitrogen stream (using an in-line activated silica gel desiccant filter). To each residue was added 100 μl of ethyl acetate just prior to injection. Samples to be analyzed at a later time, *i.e.*, up to 24 hr, were stored, covered tightly, and protected from light.

Electron-Capture GLC Detection—The prepared GLC samples were analyzed using a gas chromatograph[8] equipped with a ^{63}Ni-electron-capture detector. A glass column (120 cm × 4 mm i.d.) was packed with 3% QF-1 on Gas Chrom Q, 100–200 mesh. The injection port and oven temperatures were maintained at 210 and 150°, respectively. The detector was set at 175° and operated with a pulse interval of 150 μsec. The flow rate of the carrier gas, argon with 5% methane, was 95 ml/min. Under these conditions, the retention times of isoidide dinitrate and isosorbide dinitrate were 2.0 and 3.0 min, respectively. The injection volume was 5 μl, and the injection was performed in duplicate.

Calculations—A stock solution of isosorbide dinitrate in absolute ethyl alcohol (1 μg/ml) was used to spike plasma in the 5–75-ng/ml range. A stock solution of isosorbide dinitrate (0.5 μg/ml) was used to spike plasma in the 0–5-ng/ml range. The samples were likewise spiked with 10 ng of isoidide dinitrate as an internal standard. A response factor (peak area ratio) was calculated for the standard. The concentration of isosorbide dinitrate in the samples was determined from the standard's response factor.

Extraction Efficiency—The overall recovery of isosorbide dinitrate by the described extraction procedure was determined by spiking plasma

[1] Burdick-Jackson Labs., Bodman Chemicals, Narberth, Pa.
[2] J. T. Baker Chemical Co., Phillipsburg, N.J.
[3] S & S charcoal-treated filter paper No. 505.
[4] Stuart Pharmaceutical Division, ICI United States Inc.
[5] Sorbitrate, Stuart Pharmaceutical Division, ICI United States Inc.
[6] International Equipment Co., Needham, Pa.
[7] Vortex Genie, Fisher Scientific.
[8] Hewlett-Packard HP 7620A.

Accepted for publication May 12, 1976.
Presented in part at the Second Federation of Analytical Chemistry and Spectroscopy Societies, October 1975.
The authors thank Dr. C. Ryan and Dr. J. M. Greene for preparation of compounds. They also thank Dr. J. K. Frischmann, Dr. D. A. Hall, and Dr. R. E. Schirmer for helpful discussions and P. A. Farb for assistance.
[x] To whom inquiries should be directed.

Electron-Capture GLC Determination of Nanogram to Picogram Amounts of Isosorbide Dinitrate

J. O. MALBICA [x], K. MONSON, K. NEILSON, and R. SPRISSLER

Abstract □ A GLC method for the determination of plasma isosorbide dinitrate using electron-capture detection is described. The organic nitrates are especially suited for electron-capture detection if the detector temperature is optimized for maximum sensitivity, *e.g.*, 175°. Proper maintenance of the detector and column assures reproducible data in the low nanogram range. The extraction procedure described is simple, efficient, and expedient for processing large numbers of samples. The method was used to study plasma levels in four human volunteers after a single dose of a 5-mg chewable isosorbide dinitrate tablet. Concentration levels of isosorbide dinitrate as low as 0.5 ng/ml of plasma can be measured by this procedure.

Keyphrases □ Isosorbide dinitrate—electron-capture GLC analysis, human plasma □ GLC, electron capture—analysis, isosorbide dinitrate, human plasma □ Vasodilators, coronary—isosorbide dinitrate, electron-capture GLC analysis, human plasma

The low dosage of isosorbide dinitrate sufficient for pharmacological effectiveness results in low circulating blood levels of the drug, and difficulties exist in assaying for low nanogram to picogram amounts. Previously described GLC methods (1, 2) were either laborious or not sensitive enough to follow rapidly declining blood levels of isosorbide dinitrate.

Since only limited data are available on the blood levels of isosorbide dinitrate following administration of therapeutic doses, a method was needed that would allow reliable estimations of blood isosorbide dinitrate levels in the low nanogram to picogram range using conventional electron-capture GLC instrumentation. This report describes an assay method for isosorbide dinitrate that is expedient, sensitive, and reproducible for routinely handling large numbers of samples.

EXPERIMENTAL

Reagents and Materials—Benzene[1] and ethyl acetate[1] were glass-distilled reagent grade solvents. Anhydrous sodium sulfate[2] was reagent grade, ACS certified. Charcoal-treated paper disks[3], 6.5-mm diameter, were made with a paper punch-out.

One hundred grams of anhydrous sodium sulfate powder was washed with benzene for 20 min, allowed to air dry, and then placed in an oven at 100° until needed.

The charcoal-treated paper disks were similarly washed in benzene. Excess benzene was removed, and the paper disks were allowed to air dry. The disks were stored in an air-tight container until required.

Isosorbide dinitrate[4] and isoidide dinitrate[4] were purified by recrystallization from ethanol.

Plasma Level Study—Isosorbide dinitrate was administered to four healthy volunteers (one male, age 34; three females, ages 23, 25, and 27); each received a 5-mg chewable isosorbide dinitrate tablet[5]. Blood, 10 ml, was drawn from the cubital vein into a heparinized tube from each subject 0, 15, 30, 60, 120, and 180 min following isosorbide dinitrate administration. The blood was immediately centrifuged at 3000 rpm in an angular head clinical centrifuge[6] for 15 min. The plasma was collected and stored at −10° prior to analysis.

Extraction of Isosorbide Dinitrate—Five-milliliter aliquots of benzene were added to a 15.0-ml graduated conical centrifuge tube containing 1.0 ml of plasma spiked with 10 ng of isoidide dinitrate as an internal standard. The tube was mixed on a vortex[7] for 1 min and centrifuged at 2000 rpm to separate the phases. Then the benzene phase was carefully removed to another 15-ml centrifuge tube. A 0.5-g portion of benzene-washed sodium sulfate and three benzene-washed charcoal-treated paper disks were added to the benzene extract.

The tube and its contents were again vortexed for 15 sec and centrifuged as previously described. As much of the benzene layer as possible was carefully removed to another centrifuge tube and dried completely under a nitrogen stream (using an in-line activated silica gel desiccant filter). To each residue was added 100 μl of ethyl acetate just prior to injection. Samples to be analyzed at a later time, *i.e.*, up to 24 hr, were stored, covered tightly, and protected from light.

Electron-Capture GLC Detection—The prepared GLC samples were analyzed using a gas chromatograph[8] equipped with a ^{63}Ni-electron-capture detector. A glass column (120 cm × 4 mm i.d.) was packed with 3% QF-1 on Gas Chrom Q, 100–200 mesh. The injection port and oven temperatures were maintained at 210 and 150°, respectively. The detector was set at 175° and operated with a pulse interval of 150 μsec. The flow rate of the carrier gas, argon with 5% methane, was 95 ml/min. Under these conditions, the retention times of isoidide dinitrate and isosorbide dinitrate were 2.0 and 3.0 min, respectively. The injection volume was 5 μl, and the injection was performed in duplicate.

Calculations—A stock solution of isosorbide dinitrate in absolute ethyl alcohol (1 μg/ml) was used to spike plasma in the 5–75-ng/ml range. A stock solution of isosorbide dinitrate (0.5 μg/ml) was used to spike plasma in the 0–5-ng/ml range. The samples were likewise spiked with 10 ng of isoidide dinitrate as an internal standard. A response factor (peak area ratio) was calculated for the standard. The concentration of isosorbide dinitrate in the samples was determined from the standard's response factor.

Extraction Efficiency—The overall recovery of isosorbide dinitrate by the described extraction procedure was determined by spiking plasma

[1] Burdick-Jackson Labs., Bodman Chemicals, Narberth, Pa.
[2] J. T. Baker Chemical Co., Phillipsburg, N.J.
[3] S & S charcoal-treated filter paper No. 505.
[4] Stuart Pharmaceutical Division, ICI United States Inc.
[5] Sorbitrate, Stuart Pharmaceutical Division, ICI United States Inc.
[6] International Equipment Co., Needham, Pa.
[7] Vortex Genie, Fisher Scientific.
[8] Hewlett-Packard HP 7620A.

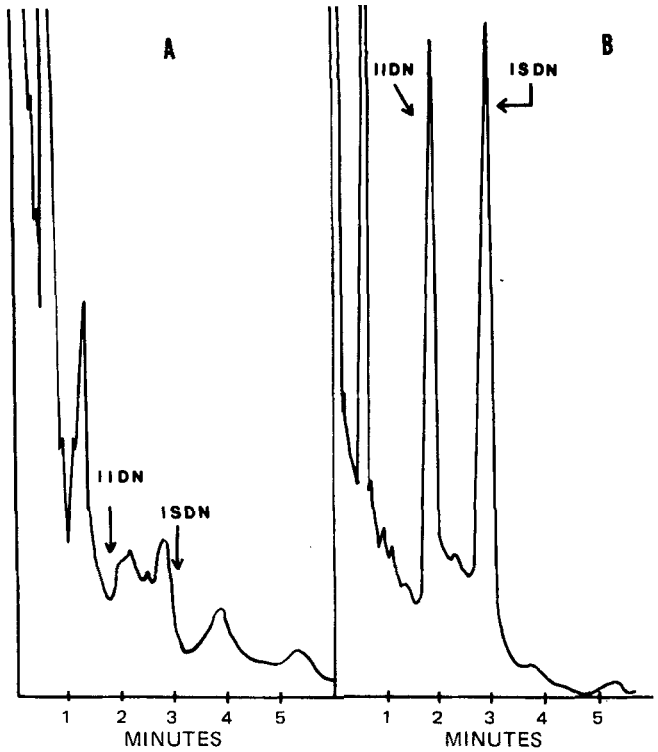

Figure 1—*Typical gas chromatograms obtained from blank plasma (A) and plasma containing 15 ng of isosorbide dinitrate/ml (B). Key: ISDN, isosorbide dinitrate; and IIDN, isoidide dinitrate.*

samples in triplicate with 20 μl of ^{14}C-isosorbide dinitrate (18 μCi/mg, 4.5 μg/ml). Likewise, a triplicate set of plasma samples was spiked with 5 and 10 μl of ^{14}C-isosorbide dinitrate solution (18 μCi/mg, 0.45 μg/ml). The samples were extracted as previously described and dried under nitrogen. The residue was dissolved in 1.5 ml of ethyl acetate, and 1.0 ml was counted to determine the ^{14}C-isosorbide dinitrate content. The recovered ^{14}C-isosorbide dinitrate was compared with the actual amount of ^{14}C-isosorbide dinitrate added.

RESULTS AND DISCUSSION

A typical gas chromatogram of isosorbide dinitrate extracted from plasma is shown in Fig. 1B; the chromatogram obtained from blank plasma is shown in Fig. 1A. The lower limit of detection was 0.5 ng/ml and was reproducible under the experimental conditions.

Table I—Response Ratios[a] (Day-to-Day Variations in the Mean)

Isosorbide Dinitrate Concentration, ng/ml of Plasma	Day 1		Day 2		Day 3	
	Mean[b]	CV[c]	Mean	CV	Mean	CV
1	0.10 ± 0.02	17	0.11 ± 0.05	49	0.08 ± 0.01	11
3	0.19 ± 0.03	15	0.14 ± 0.07	49	0.15 ± 0.01	6
5	0.26 ± 0.03	14	0.25 ± 0.05	19	0.21 ± 0.08	38
10	0.45 ± 0.07	16	0.39 ± 0.13	33	0.50 ± 0.18	40
25	1.05 ± 0.17	16	1.02 ± 0.17	17	0.96 ± 0.10	10
50	2.01 ± 0.21	10	1.94 ± 0.09	5	2.12 ± 0.14	7
75	3.35 ± 0.19	6	2.64 ± 0.27	10	3.14 ± 0.15	5

[a] The area of isosorbide dinitrate was divided by the area of isoidide dinitrate. [b] Mean ± *SD* based on a quadruplicate plasma run for each concentration value. [c] *CV* = coefficient of variation = (σ/mean) × 100.

Table II—Effect of Electron-Capture Detector Temperature on Peak Height for a Total of 4 ng of Isosorbide Dinitrate Injected onto the Column

Detector Temperature	Peak Height, cm
170°	4.178
175°	4.882
180°	4.545
185°	4.415
197°	4.512
210°	3.388
227°	3.041

Table III—Human Plasma Levels of Isosorbide Dinitrate after Administration of a 5-mg Chewable Isosorbide Dinitrate Tablet

Subject (Sex, Age)	Plasma Isosorbide Dinitrate Level, ng/ml					
	0	15 min	30 min	60 min	120 min	180 min
F.B. (M, 34)	N.D.[a]	2.4	1.9	0.9	N.D.	N.D.
J.F. (F, 23)	N.D.	5.6	2.8	1.4	N.D.	N.D.
K.M. (F, 27)	N.D.	5.3	1.2	0.6	N.D.	N.D.
K.N. (F, 25)	N.D.	3.7	2.6	N.D.	N.D.	N.D.
Total	N.D.	4.3 ± 1.3	2.1 ± 0.6	0.7 ± 0.4	N.D.	N.D.

[a] N.D. = not detected.

The results from quadruplicate runs on plasma spiked with varying amounts of isosorbide dinitrate are summarized in Table I where the day-to-day mean, standard deviation, and coefficient of variation are given. The overall coefficient of variation of the procedure in the 1–75-ng/ml range was less than 20% except in the 1–10-ng/ml range where, as expected, it sometimes increased with decreasing concentration.

A plot of the response ratio *versus* concentration showed that the described procedure was reproducible from day to day and that linearity was established throughout the 0–75-ng/ml range.

Isosorbide dinitrate was stable when stored frozen in plasma up to 1 week. Isosorbide dinitrate can be extracted from plasma and stored as the dry residue for at least 24 hr.

To obtain maximum sensitivity for the GLC measurement of isosorbide dinitrate, the optimal detector response with temperature was determined (Table II). The detector produced the maximum response for a given quantity of isosorbide dinitrate (4 ng) in the 175–200° temperature range. It is suggested that the optimal electron-capture detector temperature be determined for each GLC unit. The detector temperature was raised to 350° overnight to eliminate the accumulation of any plasma-derived components as a result of operating at a lower temperature during the assay.

Priming the column was essential to achieve high sensitivity. Several 1-μl injections of an isosorbide dinitrate solution (10 ng/ml) were made until a constant peak height for isosorbide dinitrate in the chromatogram was obtained.

After a period of weeks, as a result of numerous injections, a gradual

Table IV—Overall Recovery of ^{14}C-Isosorbide Dinitrate Added to Human Plasma

Isosorbide Dinitrate, ng/ml	Disintegrations per Minute Added	Disintegrations per Minute Recovered	Recovery, % ± *SD*
2.2	99	81	81.8
2.2	99	79	79.8
2.2	99	78	78.8
		Average	80.1 ± 1.2
4.5	192	147	76.6
4.5	192	141	73.4
4.5	192	144	75.0
		Average	75.0 ± 1.3
90.0	3621	2752	76.0
90.0	3621	2754	76.1
90.0	3621	2732	75.4
		Average	75.8 ± 0.3

loss in sensitivity was observed as well as the appearance of interfering peaks in the chromatogram. At this time, a new column was installed and primed.

The isosorbide dinitrate human plasma levels following a 5-mg dose of chewable isosorbide dinitrate were highest at 15 min after administration in all four subjects (Table III). No isosorbide dinitrate levels were detectable at 120 min or more after administration.

The overall recovery of ^{14}C-isosorbide dinitrate in the 2.2–90-ng/ml concentration range is shown in Table IV. The recovery of 75–80% was independent of concentration.

Previous attempts to quantitate isosorbide 2-mononitrate and isosorbide 5-mononitrate in the same concentration range as isosorbide dinitrate were unsuccessful. Certain plasma components that appeared in the benzene extract from time to time interfered with the determination of the mononitrates of isosorbide dinitrate.

REFERENCES

(1) M. T. Rosseel and M. G. Bogaert, *J. Pharm. Sci.*, **62**, 754 (1973).

(2) P. A. Sherbar, M. Marcus, and S. I. Kleinberg, *Enzymol. Biol. Clin.*, **10**, 365 (1969).

ACKNOWLEDGMENTS AND ADDRESSES

Received December 5, 1975, from the *Biomedical Research Department, Stuart Pharmaceutical Division, ICI United States Inc., Wilmington, DE 19897.*

Accepted for publication May 10, 1976.

The authors thank Mr. R. Lenkiewicz and Dr. R. Kwok for their support in the early phase of this study.

[x] To whom inquiries should be directed.

Potency of Synthetic Luteinizing Hormone Releasing Hormone Preparations in Rat Anterior Pituitary Cell Cultures

W. C. DERMODY [x], C. A. PASTUSHOK, R. SAKOWSKI, J. W. VAITKUS, and J. R. REEL

Abstract □ Selected synthetic luteinizing hormone releasing hormone preparations were assayed, and their potencies were determined relative to one sample utilizing primary cultures of enzymatically dispersed rat anterior pituitary cells. Preliminary cell culture experiments indicated that luteinizing hormone releasing hormone had to be in constant contact with cells for continued luteinizing hormone secretion. Luteinizing hormone levels in media reached a maximum concentration after 4 hr of continuous luteinizing hormone releasing hormone exposure. Cell culture bioassay was selected over the bioassay employing chronically ovariectomized steroid-blocked rats due to greater sensitivity and economy. The assay of each luteinizing hormone releasing hormone preparation was replicated four to seven times. Preparations from several companies were less potent ($p < 0.05$) than the reference product. Contaminants were disclosed by TLC in preparations with potencies lower than the reference product.

Keyphrases □ Luteinizing hormone releasing hormone—various synthetic preparations analyzed by TLC and radioimmunoassay, potencies determined, rat anterior pituitary cells □ TLC—analysis, luteinizing hormone releasing hormone, various synthetic preparations □ Radioimmunoassay—analysis, luteinizing hormone releasing hormone, various synthetic preparations □ Hormones—luteinizing hormone releasing hormone, various synthetic preparations analyzed by TLC and radioimmunoassay, potencies determined, rat anterior pituitary cells

Although luteinizing hormone releasing hormone has been synthesized in many laboratories, no potency comparisons of various synthetic preparations have been published. However, it was reported that luteinizing hormone releasing hormone, synthesized by several laboratories (1–3), exhibited biological activity equivalent to an isolated natural porcine luteinizing hormone releasing hormone preparation[1]. These results were obtained utilizing either short-term incubations of minced pituitary tissue or ovariectomized estrogen–progesterone-blocked rats. This report presents potency comparisons of various synthetic luteinizing hormone releasing hormone preparations assayed with cultures of rat anterior pituitary cells.

EXPERIMENTAL

Various synthetic luteinizing hormone releasing hormone preparations (Samples 1–6[2–6]) were obtained commercially. These preparations were compared to Sample 7[7] luteinizing hormone releasing hormone.

The reference product (Sample 7) was prepared by fragment condensation and purified by partition chromatography[8] with 1-butanol[9]–acetic acid–water (4:1:5, upper phase). The major fraction from the partition column was homogeneous in the following TLC systems on silica gel 60 F-254 glass plates[10]: System 1, chloroform–methanol–water (45:45:10); System 2, chloroform–methanol–water–acetic acid (60:45:10:1); System 3, chloroform–methanol–32% acetic acid (60:45:20); System 4, 1-butanol–acetone–water–acetic acid–5% ammonium hydroxide (45:15:20:10:10); System 5, 2-propanol–1 *M* acetic acid (2:1); System 6, 1-butanol–acetic acid–water (upper phase) (4:1:5); System 7, pyridine–ethyl acetate–acetic acid–water (5:5:1:3); and System 8, 1-butanol–pyridine–acetic acid–water (30:20:6:24).

The reference product corresponded to 89% peptide content (1.4 acetate salt, 3.5 hydrates) with a molecular weight of 1329.6 and $[\alpha]_D^{25} - 55.8°$ (c, 1 in 1% CH_3CO_2H)[11].

Molecular weights and peptide contents (Table I) of comparative luteinizing hormone releasing hormone preparations were obtained from package inserts or the company of origin. Peptide content varied from 80 to 88%. The purity of these preparations was examined using TLC System 2. Preliminary experiments indicated that System 2 was superior

[1] AVS 77-35, 215-269.

[2] Sample 1, lot 208052, and Sample 2, lot 221040, Spectrum Medical Industries, Torrance, Calif.

[3] Sample 3, lot A0402, Beckman Instruments, Palo Alto, Calif.

[4] Sample 4, lot 4562, Bachem, Marina Del Rey, Calif.

[5] Sample 5, lot 19-192AL, Abbott Laboratories, North Chicago, Ill.

[6] Sample 6, lot SY-1, Sankyo Co., Tokyo, 140 Japan.

[7] Sample 7, lot 10746 X71A, Parke, Davis & Co., Ann Arbor, Mich.

[8] Sephadex G-25 coarse, Pharmacia Fine Chemicals, Piscataway, N.J.

[9] All analytical reagents, Mallinckrodt, St. Louis, Mo.

[10] EM Laboratories, Elmsford, N.Y.

[11] Model 141, Perkin-Elmer Corp., Norwalk, Conn.

loss in sensitivity was observed as well as the appearance of interfering peaks in the chromatogram. At this time, a new column was installed and primed.

The isosorbide dinitrate human plasma levels following a 5-mg dose of chewable isosorbide dinitrate were highest at 15 min after administration in all four subjects (Table III). No isosorbide dinitrate levels were detectable at 120 min or more after administration.

The overall recovery of ^{14}C-isosorbide dinitrate in the 2.2–90-ng/ml concentration range is shown in Table IV. The recovery of 75–80% was independent of concentration.

Previous attempts to quantitate isosorbide 2-mononitrate and isosorbide 5-mononitrate in the same concentration range as isosorbide dinitrate were unsuccessful. Certain plasma components that appeared in the benzene extract from time to time interfered with the determination of the mononitrates of isosorbide dinitrate.

REFERENCES

(1) M. T. Rosseel and M. G. Bogaert, *J. Pharm. Sci.*, **62**, 754 (1973).

(2) P. A. Sherbar, M. Marcus, and S. I. Kleinberg, *Enzymol. Biol. Clin.*, **10**, 365 (1969).

ACKNOWLEDGMENTS AND ADDRESSES

Received December 5, 1975, from the *Biomedical Research Department, Stuart Pharmaceutical Division, ICI United States Inc., Wilmington, DE 19897.*

Accepted for publication May 10, 1976.

The authors thank Mr. R. Lenkiewicz and Dr. R. Kwok for their support in the early phase of this study.

[x] To whom inquiries should be directed.

Potency of Synthetic Luteinizing Hormone Releasing Hormone Preparations in Rat Anterior Pituitary Cell Cultures

W. C. DERMODY [x], C. A. PASTUSHOK, R. SAKOWSKI, J. W. VAITKUS, and J. R. REEL

Abstract □ Selected synthetic luteinizing hormone releasing hormone preparations were assayed, and their potencies were determined relative to one sample utilizing primary cultures of enzymatically dispersed rat anterior pituitary cells. Preliminary cell culture experiments indicated that luteinizing hormone releasing hormone had to be in constant contact with cells for continued luteinizing hormone secretion. Luteinizing hormone levels in media reached a maximum concentration after 4 hr of continuous luteinizing hormone releasing hormone exposure. Cell culture bioassay was selected over the bioassay employing chronically ovariectomized steroid-blocked rats due to greater sensitivity and economy. The assay of each luteinizing hormone releasing hormone preparation was replicated four to seven times. Preparations from several companies were less potent ($p < 0.05$) than the reference product. Contaminants were disclosed by TLC in preparations with potencies lower than the reference product.

Keyphrases □ Luteinizing hormone releasing hormone—various synthetic preparations analyzed by TLC and radioimmunoassay, potencies determined, rat anterior pituitary cells □ TLC—analysis, luteinizing hormone releasing hormone, various synthetic preparations □ Radioimmunoassay—analysis, luteinizing hormone releasing hormone, various synthetic preparations □ Hormones—luteinizing hormone releasing hormone, various synthetic preparations analyzed by TLC and radioimmunoassay, potencies determined, rat anterior pituitary cells

Although luteinizing hormone releasing hormone has been synthesized in many laboratories, no potency comparisons of various synthetic preparations have been published. However, it was reported that luteinizing hormone releasing hormone, synthesized by several laboratories (1–3), exhibited biological activity equivalent to an isolated natural porcine luteinizing hormone releasing hormone preparation[1]. These results were obtained utilizing either short-term incubations of minced pituitary tissue or ovariectomized estrogen–progesterone-blocked rats. This report presents potency comparisons of various synthetic luteinizing hormone releasing hormone preparations assayed with cultures of rat anterior pituitary cells.

EXPERIMENTAL

Various synthetic luteinizing hormone releasing hormone preparations (Samples 1–6[2–6]) were obtained commercially. These preparations were compared to Sample 7[7] luteinizing hormone releasing hormone.

The reference product (Sample 7) was prepared by fragment condensation and purified by partition chromatography[8] with 1-butanol[9]–acetic acid–water (4:1:5, upper phase). The major fraction from the partition column was homogeneous in the following TLC systems on silica gel 60 F-254 glass plates[10]: System 1, chloroform–methanol–water (45:45:10); System 2, chloroform–methanol–water–acetic acid (60:45:10:1); System 3, chloroform–methanol–32% acetic acid (60:45:20); System 4, 1-butanol–acetone–water–acetic acid–5% ammonium hydroxide (45:15:20:10:10); System 5, 2-propanol–1 *M* acetic acid (2:1); System 6, 1-butanol–acetic acid–water (upper phase) (4:1:5); System 7, pyridine–ethyl acetate–acetic acid–water (5:5:1:3); and System 8, 1-butanol–pyridine–acetic acid–water (30:20:6:24).

The reference product corresponded to 89% peptide content (1.4 acetate salt, 3.5 hydrates) with a molecular weight of 1329.6 and $[\alpha]_D^{25} - 55.8°$ (c, 1 in 1% CH_3CO_2H)[11].

Molecular weights and peptide contents (Table I) of comparative luteinizing hormone releasing hormone preparations were obtained from package inserts or the company of origin. Peptide content varied from 80 to 88%. The purity of these preparations was examined using TLC System 2. Preliminary experiments indicated that System 2 was superior

[1] AVS 77-35, 215-269.

[2] Sample 1, lot 208052, and Sample 2, lot 221040, Spectrum Medical Industries, Torrance, Calif.

[3] Sample 3, lot A0402, Beckman Instruments, Palo Alto, Calif.

[4] Sample 4, lot 4562, Bachem, Marina Del Rey, Calif.

[5] Sample 5, lot 19-192AL, Abbott Laboratories, North Chicago, Ill.

[6] Sample 6, lot SY-1, Sankyo Co., Tokyo, 140 Japan.

[7] Sample 7, lot 10746 X71A, Parke, Davis & Co., Ann Arbor, Mich.

[8] Sephadex G-25 coarse, Pharmacia Fine Chemicals, Piscataway, N.J.

[9] All analytical reagents, Mallinckrodt, St. Louis, Mo.

[10] EM Laboratories, Elmsford, N.Y.

[11] Model 141, Perkin-Elmer Corp., Norwalk, Conn.

Table I—*In Vitro* Potency of Commercial Synthetic Luteinizing Hormone Releasing Hormone Preparations[a]

Preparation	Slope ± 95% *CL*[b]	Relative Potency	95% Fiducial Limits	λ[c]
Samples 1 and 2, mol. wt. = 1338, 88% peptide	37.1 ± 6.0	0.35[d]	0.31–0.39	0.95
	40.5 ± 5.7	0.29[d]	0.23–0.37	0.52
	27.5 ± 3.9	0.73[e]	0.57–0.95	0.92
	51.0 ± 12.3	0.50[d]	0.41–0.62	0.64
	72.6 ± 25.1	0.75[e]	0.55–0.94	0.85
	47.9 ± 10.5	0.44[d]	0.36–0.54	0.72
	38.7 ± 9.3	0.36[d]	0.27–0.48	0.67
	Average ± *SEM*[f]	0.489 ± 0.070		
Sample 3, 80% peptide	38.4 ± 2.5	0.45[d]	0.42–0.49	0.73
	46.6 ± 13.8	0.66[d]	0.53–0.82	0.89
	43.7 ± 11.2	0.72[d]	0.61–0.85	0.82
	53.3 ± 31.9	0.44[d]	0.35–0.55	0.99
	42.5 ± 6.9	0.60[d]	0.52–0.70	0.87
	54.0 ± 8.0	0.56[d]	0.47–0.67	0.89
	Average ± *SEM*	0.572 ± 0.046		
Sample 4, mol. wt. = 1338, 88% peptide	44.9 ± 9.7	0.54[d]	0.42–0.71	0.55
	31.0 ± 6.2	0.60[d]	0.46–0.77	0.87
	45.7 ± 13.4	0.73[d]	0.59–0.90	0.95
	24.8 ± 13.4	0.67[e]	0.46–0.92	0.91
	Average ± *SEM*	0.635 ± 0.040		
Sample 5, mol. wt. = 1375, 86% peptide	48.8 ± 8.5	0.88	0.72–1.08	0.90
	39.0 ± 4.6	0.79[e]	0.65–0.97	0.95
	33.0 ± 11.4	0.70[d]	0.55–0.89	0.93
	41.5 ± 9.4	0.83[e]	0.71–0.98	0.95
	44.5 ± 7.4	0.71[e]	0.59–0.87	0.97
	Average ± *SEM*	0.782 ± 0.035		
Sample 6, mol. wt. = 1338, 88% peptide	34.0 ± 6.0	0.86	0.69–1.07	0.99
	39.4 ± 13.2	0.89	0.72–1.10	0.99
	45.6 ± 6.1	0.95	0.83–1.09	0.99
	53.4 ± 10.9	1.04	0.86–1.26	0.99
	Average ± *SEM*	0.935 ± 0.039		

[a] Potency determined relative to Sample 7. [b] Confidence limits. [c] Relative bioassay precision. [d] $p < 0.01$. [e] $p < 0.05$. [f] Standard error of the mean.

to the other systems in elucidation of contaminants in luteinizing hormone releasing hormone preparations. Preparations were dissolved in 95% ethanol, and 30 μg of each sample was applied to thin-layer plates followed by one-dimensional chromatography and exposure to iodine vapor for visualization.

Anterior pituitary cells were isolated from diestrous female rats[12] (200–250 g) and incubated as described previously (4), except that Hanks balanced salt solution[13] (calcium and magnesium free) was substituted for *N*-(2-hydroxyethyl)piperazine-*N*-2-ethanesulfonic acid buffer and enzymatic cell dispersion was carried out in a humidified carbon dioxide incubator[14]. The sensitivity of the primary cell culture system was compared to the classical luteinizing hormone releasing hormone bioassay (5) employing ovariectomized estrogen–progesterone-blocked rats as described previously (6, 7).

Fresh luteinizing hormone releasing hormone solutions were prepared for each assay from the lyophilized powder stored over a desiccant. Samples, 1–2 mg, were weighed[15] on the day of assay, and solutions were prepared at three or four treatment levels to extend over the effective dose–response range of luteinizing hormone releasing hormone in the cell culture (0.06–0.60 ng/ml). Included in each assay was Sample 7; all curves within an assay were compared to the curve for the standard.

Luteinizing hormone concentrations of media removed from cell cultures were evaluated by double antibody radioimmunoassay (8) employing reagents for rat luteinizing hormone[16]. Anti-rat luteinizing hormone serum-2 (final dilution 1:250,000) and ^{125}I-rat luteinizing hormone-I-3[17] were added per test tube. A computer program (9) was employed for analysis of radioimmunoassay data[18].

Comparison of 10 luteinizing hormone assays, selected at random, indicated that 31.59 ± 1.98% (mean ± *SEM*) of labeled hormone was found in the absence of unlabeled hormone, the midrange of the luteinizing hormone dose–response curve was 1.31 ± 0.05 ng/ml, and the minimum detectable concentration was 77.51 ± 10.87 pg/ml. Within assay variability at the 80 and 20% binding points on the luteinizing hormone curve was 13.93 ± 2.54 and 7.00 ± 1.29%, respectively. Within each radioimmunoassay, analyses of two rat serum pools containing either high (71.69 ± 2.91 ng/ml) or low (6.87 ± 0.20 ng/ml) luteinizing hormone levels were employed for determining between assay variability. The coefficients of variation between assays for these two serum pools were 8.87 and 9.37%, respectively.

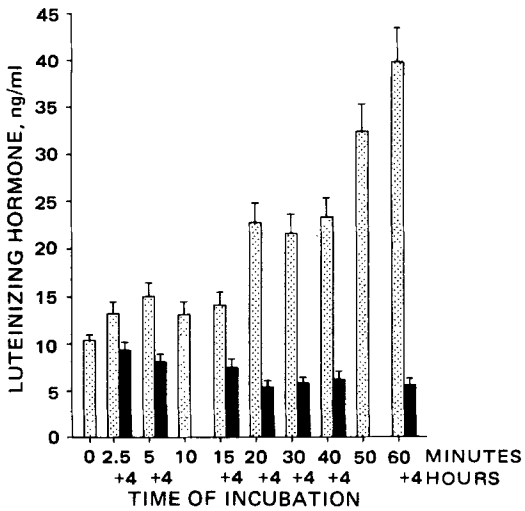

Figure 1—*Luteinizing hormone concentrations in the presence (dotted bars) and following removal (black bars) of luteinizing hormone releasing hormone. The 4-hr samples following luteinizing hormone releasing hormone for 10 and 50 min were lost. Values represent the mean* ± SEM *of triplicate observations.*

Potency estimates were determined within each cell culture experiment relative to Sample 7 (potency = 1.0). Each luteinizing hormone releasing hormone dose–response curve was first tested for linearity (*t* test) and then for parallelism (*F* test) to the Sample 7 curve prior to estimation of potency. Relative precision (λ) for symmetrical experimental designs was determined according to Finney (10).

RESULTS AND DISCUSSION

Some preliminary studies were necessary to validate and standardize the *in vitro* system. Cell culture experiments were performed to determine if luteinizing hormone releasing hormone (0.6 ng/ml) had to be in

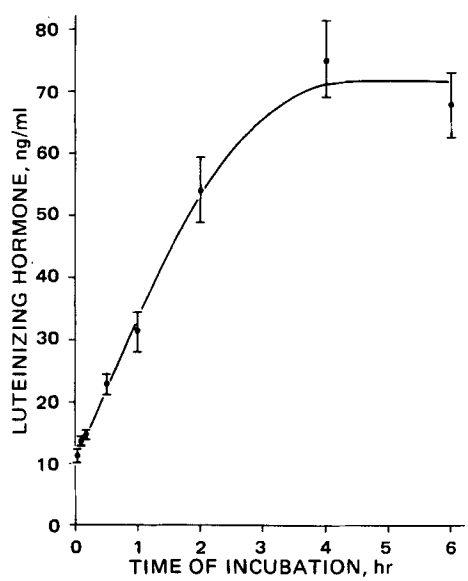

Figure 2—*Time course of luteinizing hormone releasing hormone-induced luteinizing hormone release. Values represent the mean* ± SEM *of triplicate observations.*

[12] Holtzman Laboratory Animals, Madison, Wis.
[13] Grand Island Biological Co., Grand Island, N.Y.
[14] Model 329, Forma Scientific Co., Marietta, Ohio.
[15] H 10 T, Mettler Instrument Co., Hightstown, N.J.
[16] Reagents supplied by the Rat Pituitary Hormone Distribution Program, National Institute of Arthritis, Metabolic and Digestive Diseases, Bethesda, Md.
[17] Counted in model 588 gamma counter, Micromedic Systems, Niles, Ill.
[18] IBM 370/158.

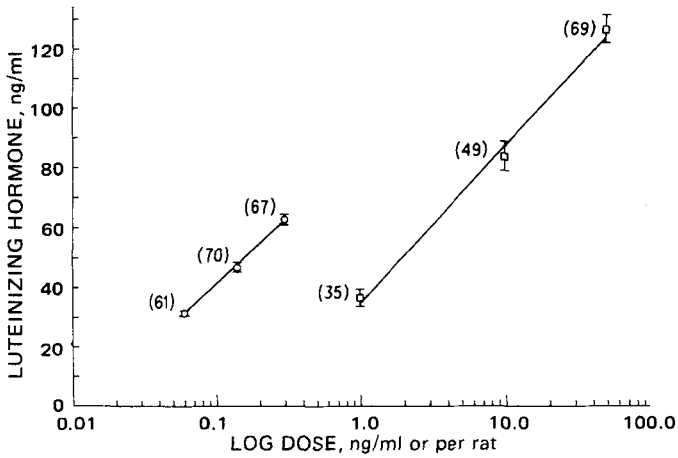

Figure 3—*Sample 7 dose–response curves* in vitro *(tissue culture, ○) and* in vivo *(chronically ovariectomized steroid-blocked rats, □). Figures in parentheses indicate the number of observations at each point. Vertical bars denote the standard error of the mean.*

constant contact with cells for continued luteinizing hormone secretion and at what time maximum luteinizing hormone concentrations were found in the medium. Media were removed at selected times and assayed for luteinizing hormone (Fig. 1). Cells were washed and fresh medium, without luteinizing hormone releasing hormone, was added; incubations were continued for an additional 4 hr. In the presence of luteinizing hormone releasing hormone, the increase in luteinizing hormone concentration in the medium was linearly related to time during the 60-min observation. Following removal of luteinizing hormone releasing hormone, there was a dramatic fall in the luteinizing hormone concentration observed at the end of 4 hr of additional incubation. Data indicate that luteinizing hormone secretion depends upon constant cell contact with luteinizing hormone releasing hormone. Maximum luteinizing hormone

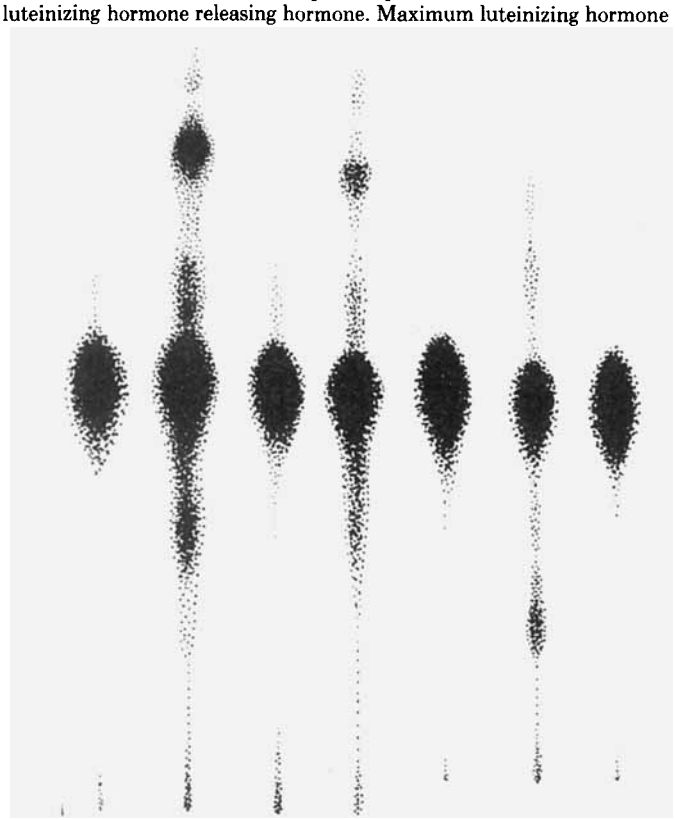

Figure 4—*Thin-layer chromatograms of luteinizing preparations. In Solvent System 2, the* R_f *of luteinizing hormone releasing hormone was 0.25 visualized by iodine vapor. From left to right, the preparations (30 μg each) were: Samples 7, 2, 5, 4, 7, 3, and 6.*

levels in the medium were observed after 4 hr of incubation with luteinizing hormone releasing hormone (Fig. 2); therefore, all subsequent experiments involved 4-hr incubation periods.

Various assays may be employed to determine the potency of luteinizing hormone releasing hormone preparations. Dose–response curves were compared (Fig. 3) for bioassays employing chronically ovariectomized, steroid-blocked rats (7–9) and primary pituitary cell culture. The slope of the dose–response curve obtained *in vivo* was 53.84 ± 5.15 (n = 5) over the dose range of 1–50 ng/rat. The average slope of Sample 7 dose–response curves in cell cultures was 44.32 ± 3.20 (n = 14). Similar luteinizing hormone responses of 30.90 ± 2.21 ng/ml in cell cultures and 39.64 ± 4.73 ng/ml *in vivo* were obtained in response to 0.06 ng/ml and 1.0 ng/rat, respectively. Primary cell cultures were selected for evaluation of synthetic luteinizing hormone releasing hormone preparations due to greater assay sensitivity and economy.

Of the five preparations compared to Sample 7, all but Sample 6[6] were less potent ($p < 0.05$) (Table I). The average potency of the preparations varied from 0.49 to 0.94. Differences in molecular weights were minor (8%) and could not account for the potency differences. Thin-layer chromatograms of 30-μg samples of the preparations (Fig. 4) showed the presence of materials that do not migrate with luteinizing hormone releasing hormone. These contaminants may account for the lower potencies of Samples 1–4. Identification of the impurities was not germane to the current investigation. However, the contaminants may create difficulties in radioimmunoassays (11), where the purity of the labeled antigen is critical.

The data indicate that a sensitive and precise assay for luteinizing hormone releasing hormone was obtained by utilizing primary cultures of enzymatically dispersed rat anterior pituitary cells. This assay procedure demonstrated differences in biological potency of synthetic luteinizing hormone releasing hormone preparations that might account for certain reported biological and immunological differences.

REFERENCES

(1) A. V. Schally, A. J. Kastin, and A. Arimura, *Am. J. Obstet. Gynecol.*, **114**, 423 (1972).

(2) A. V. Schally, T. W. Redding, J. Matsuo, and A. Arimura, *Endocrinology*, **90**, 1561 (1972).

(3) A. V. Schally, A. Arimura, W. H. Carter, T. W. Redding, R. Geiger, W. Konig, H. Wissman, G. Jaeger, J. Sandow, N. Yanaihara, C. Yanaihara, T. Hashimoto, and M. Sakagami, *Biochem. Biophys. Res. Commun.*, **48**, 366 (1972).

(4) W. Vale, G. Grant, M. Amoss, R. Blackwell, and R. Guillemin, *Endocrinology*, **91**, 562 (1972).

(5) V. D. Ramirez and S. M. McCann, *ibid.*, **72**, 193 (1963).

(6) R. R. Humphrey, W. C. Dermody, H. O. Brink, F. G. Bousley, N. H. Schottin, R. Sakowski, J. W. Vaitkus, H. T. Veloso, and J. R. Reel, *ibid.*, **92**, 1515 (1973).

(7) W. C. Dermody, E. A. Becvar, B. L. Windsor, A. L. Wong, J. W. Vaitkus, J. E. Caple, and R. Sakowski, in "Hypothalamic Hormones," E. S. E. Hafez and J. R. Reel, Eds., Ann Arbor Science Publishers, Ann Arbor, Mich., 1975, p. 71.

(8) G. D. Niswender, A. R. Midgley, Jr., S. E. Monroe, and L. E. Reichert, Jr., *Proc. Soc. Exp. Biol. Med.*, **128**, 807 (1968).

(9) W. G. Duddelson, A. R. Midgley, Jr., and G. D. Niswender, *Computers Biomed. Res.*, **5**, 205 (1972).

(10) D. J. Finney, "Statistical Methods in Biological Assay," 1st ed., Griffin, London, England, 1952, p. 179.

(11) A. W. Root, E. O. Reiter, G. E. Duckett, M. Sweetland, and R. O. Russ, Program of the 57th Meeting of the Endocrine Society, June 1975, Abstract 104.

ACKNOWLEDGMENTS AND ADDRESSES

Received February 25, 1976, from the *Department of Pharmacology, Research and Medical Affairs Division, Parke, Davis and Company, Ann Arbor, MI 48106.*

Accepted for publication May 21, 1976.

The authors are indebted to Dr. T. F. Mich and Mr. M. P. Hutt for preparation of Sample 7, to Mr. John L. Fu for development of the parallel-line bioassay statistical program, to Mrs. A. Wong for TLC, and to Dr. R. A. Edgren for editorial comments.

[x] To whom inquiries should be directed. Present address: Frederick Cancer Research Center, Frederick, MD 21701.

Quantitative Assay of Physostigmine in Human Whole Blood

WILLIAM A. GROFF ˣ, ROBERT I. ELLIN, and RICKIE L. SKALSKY

Abstract □ A quantitative assay for measuring physostigmine in human whole blood is described. Blood samples are maintained at 37°, and cholinesterase activity is measured periodically. The time required for enzyme reactivation is related to physostigmine concentration. The precision of the method is within ±4% over a physostigmine concentration range of 0.5–5.0 × 10^{-7} M.

Keyphrases □ Physostigmine—quantitative analysis by measurement of duration of cholinesterase inhibition, human blood □ Cholinesterase—duration of inhibition by physostigmine measured, related to physostigmine concentration, human blood □ Cholinergics, ophthalmic—physostigmine, quantitative analysis by measurement of duration of cholinesterase inhibition, human blood

Physostigmine has been used to treat various clinical conditions: to reduce intraocular pressure in glaucoma (1), to treat muscular weakness in myasthenia gravis (2), to counteract atropine coma (3) and scopolamine delirium (4), and as an antidote against certain hallucinogenic agents (5). The primary physiological effect of physostigmine results from the inhibition or inactivation of cholinesterase at sites of cholinergic transmission.

BACKGROUND

The inhibition of cholinesterase by carbamates occurs by a mechanism analogous to that of organophosphorus inhibition. With both, a reversible complex is formed first, followed by acylation of the enzyme and, finally, deacylation to yield the original enzyme. However, since the rate of decarbamylation is relatively fast as compared with dephosphorylation (6), progressive carbamate inhibition levels off before complete inhibition is attained.

The cyclic reaction of carbamate inhibition is shown in Scheme I. In the presence of excess inhibitor, an apparent steady-state condition ensues, since the free enzyme, E, resulting from decarbamylation is promptly recomplexed. Since k_1 is extremely fast with relation to k_{-1}, one can simplify the cyclic reaction as shown in Scheme II. Because the rate of carbamylation (k_2 = ~10 min^{-1}) is slower than the rate of complex formation ($K_a = k_{-1}/k_1 = 3.3 \times 10^{-6}$ mole/liter) and the rate of decarbamylation ($k_3 = 1.8 \times 10^{-2}$ min^{-1}) is much slower than the rate of carbamylation, there is a small accumulation of the complex, ECX. Almost all inhibited enzyme is the carbamylated enzyme, EC. The ECX complex is readily reversible (6–9) by high concentration of substrate, dilution, and dialysis. Due to this reversibility and the rate of decarbamylation, it is not possible to demonstrate complete enzyme inhibition even with high concentrations of carbamate (7).

The degree of inhibition of blood cholinesterase is generally accepted as a reflection of the intensity and duration of action of the drug in the body. The purpose of this work was to develop a method that would quantitatively relate the duration of enzyme inhibition to the concentration of physostigmine in blood. Since the drug is given to patients in low doses (2 mg) and its metabolism in the body is quite rapid, only nanogram levels of the drug are found in the blood. Existing colorimetric (10), spectrophotofluorometric (11), phosphorescent (12), and TLC (13) methods are not sufficiently sensitive to measure these low levels.

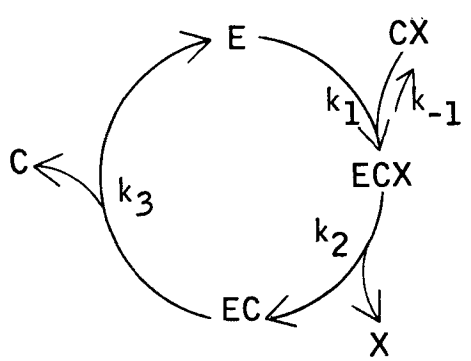

Scheme I

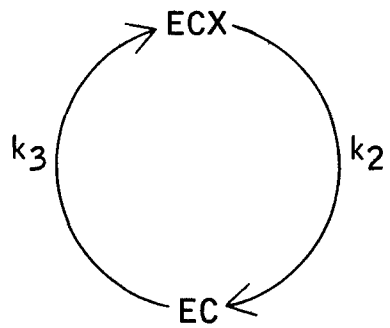

Scheme II

The problem is further complicated by the fact that inhibition of the enzyme by physostigmine is reversible. However, by taking these parameters into consideration, along with temperature and time control of a sample obtained under clinical conditions, an assay for physostigmine sensitive to 2.5 × 10^{-8} M or 7 ng of drug/ml of blood was developed.

EXPERIMENTAL

Materials—Physostigmine salicylate[1] USP was used as received. A stock solution (10^{-3} M) was prepared by dissolving 0.0413 g in 100 ml of distilled water. A working solution (10^{-5} M) was prepared fresh each week by diluting 1 ml of the stock solution to 100 ml with isotonic saline. These solutions were stored at 4°. An aliquot of the working solution was brought to room temperature each day before use. Human whole blood[2] was collected by vacuum tubes[3], with edetic acid as the anticoagulant.

Cholinesterase Measurement—Whole blood cholinesterase activity was determined by an automated procedure (14). Enzyme activity was expressed as micromoles of substrate hydrolyzed by 1 ml of sample per minute of incubation time. The substrate was acetylthiocholine iodide at 2 × 10^{-3} M. The reaction mixture, containing sample, substrate, and 5,5′-dithiobis(2-nitrobenzoic acid) (I), was buffered to pH 8.2 with 0.05 M tromethamine and incubated for approximately 6 min at 37°. Thiocholine, resulting from enzymatic hydrolysis of the substrate, reacts with I to form a colored anion. This colored anion is dialyzed into pH 8.2 buffer, and the absorbance was measured at 420 nm.

***In Vitro* Assay**—Microliter volumes of physostigmine solution were added, using micropipets[4], to 5-ml aliquots of whole blood. Concentrations of inhibitor were 0.25, 0.50, 1.00, 1.25, 2.50, and 5.00 × 10^{-7} M; 10 whole blood samples were prepared at each concentration. Each tube was immediately stoppered, shaken, and placed in a water bath at 37°. Zero time was recorded for each tube. At selected times, the blood samples were gently mixed; transfer pipets were used to remove aliquots to sample cups[5] for enzyme assay. Each aliquot was assayed within 1 min after removal from the incubation bath.

***In Vivo* Assay**—Physostigmine was administered intravenously to 10 subjects and intramuscularly to nine subjects. Blood samples for the physostigmine assay were collected from all subjects 30 min after dosing. These samples were placed immediately in a 37° incubation bath, and

[1] Control No. 932-LCA-11, S. B. Penick and Co., New York, N.Y.

[2] The volunteers in these tests were enlisted U.S. Army personnel. These tests were governed by the principles, policies, and rules for medical volunteers as established in AR 70-25 and the Declaration of Helsinki.

[3] Vacutainer, Scientific Products, Columbia, MD 21045.

[4] Eppendorf pipets, Arthur H. Thomas, Philadelphia, PA 19105.

[5] Technicon sample cups, Technicon Instruments Corp., Tarrytown, NY 10591.

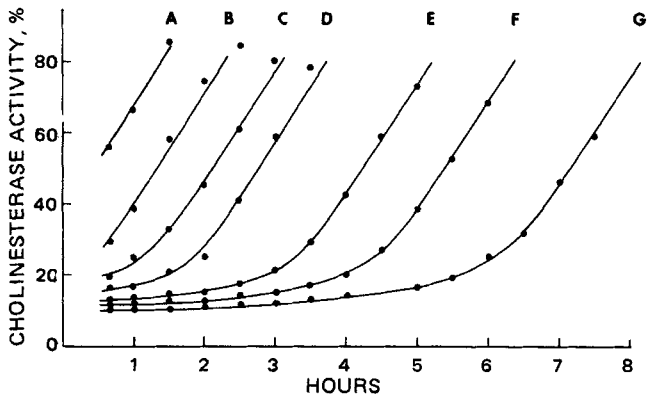

Figure 1—*Time course of whole blood cholinesterase activity after inhibition by physostigmine. Key: A, 0.5 × 10^{-7}; B, 1.0 × 10^{-7}; C, 1.5 × 10^{-7}; D, 2.0 × 10^{-7}; E, 3.0 × 10^{-7}; F, 4.0 × 10^{-7}; and G, 5.0 × 10^{-7}* M.

the time was recorded. Cholinesterase activity was measured periodically as described. The concentration obtained is a measure of the physostigmine present in the blood at the time the sample is withdrawn.

Precision—The precision of the method was determined by statistical analysis of the data obtained at the six concentrations of physostigmine that were added to blood *in vitro*.

Correlation—Concentration values measured in the precision study were correlated with concentrations added, and a regression curve was plotted.

RESULTS

The time course of human whole blood cholinesterase inhibition produced by physostigmine exhibits three phases: rapid inhibition; steady state, during which the cyclic reaction occurs; and reactivation (decarbamylation). A family of curves is shown in Fig. 1 for physostigmine concentrations ranging from 0.5 to 5.0 × 10^{-7} *M* at 37°. Percent cholinesterase activity is plotted *versus* time on Cartesian coordinate graph paper for each concentration of inhibitor until the enzyme activity has recovered to approximately 80% of the control level. The plot of activity *versus* time over the range of 30–70% activity is nearly linear, even though the decarbamylation rate is not zero order. This apparent linearity was used to determine the concentration of physostigmine present at the time of inhibition.

The time required for activity to reach a given percent activity level (between 30 and 70% on each curve) is proportional to the initial physostigmine concentration. For example, at the 50% cholinesterase activity level in Fig. 1, time values are 1.8 hr at 1.50 × 10^{-7} *M*, 2.4 hr at 2.00 × 10^{-7} *M*, 3.9 hr at 3.00 × 10^{-7} *M*, 5.0 hr at 4.00 × 10^{-7} *M*, and 6.8 hr at 5.00 × 10^{-7} *M* physostigmine. These values and values for other activity levels are plotted *versus* concentration on Cartesian coordinate graph paper in Fig. 2. This set of standard curves is used to convert time/percent activity values of an unknown blood sample to physostigmine concentration.

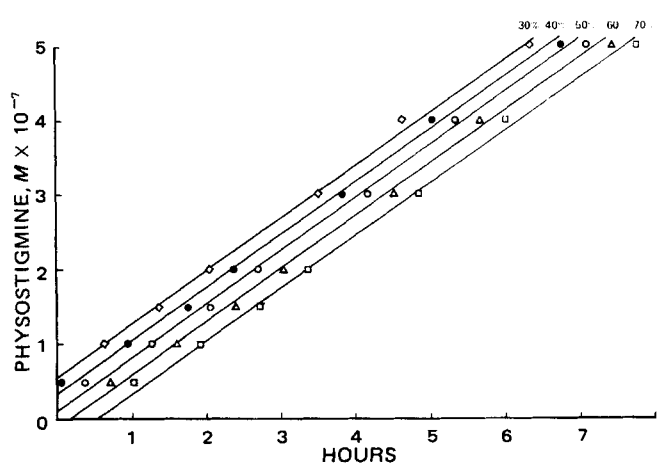

Figure 2—*Standard curves to convert time/percent activity values to physostigmine concentration.*

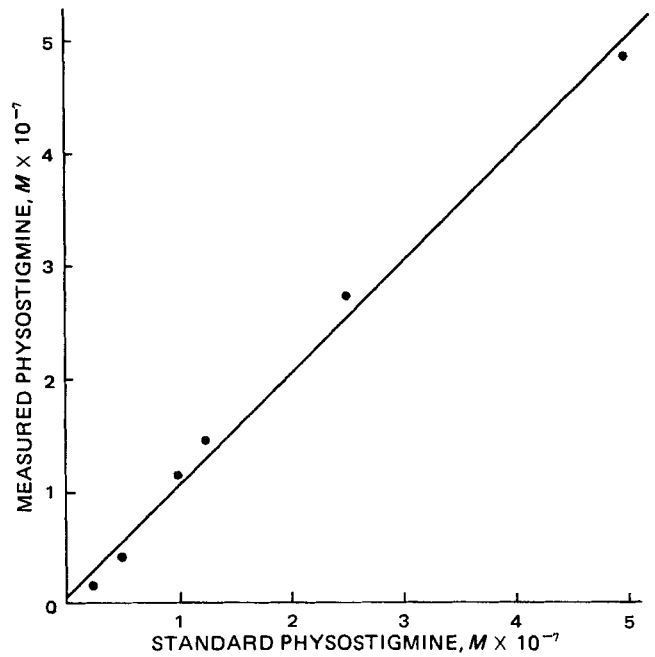

Figure 3—*Comparison of measured physostigmine concentrations with theoretical concentrations added to whole blood samples* (y = 0.975x + 0.079; r = 0.996_6).

A blood sample containing an unknown concentration of physostigmine is incubated at 37° and periodically assayed to determine cholinesterase activity until several data points are obtained that fall within the 30–70% activity range. These points are plotted on Cartesian coordinate graph paper, and a line is drawn through the points. A time value is taken from this line at any activity level for which a line is graphed in Fig. 2. The time value is then converted to concentration by means of this figure. The resulting concentration value must be corrected for any difference between the control (uninhibited) activity (in micromoles per milliliter per minute) of the unknown blood sample and the control activity of the standard blood sample. This correction is necessary because the time required for decarbamylation is proportional to the enzyme concentration in the blood.

The physostigmine concentration in the unknown can be calculated from:

$$\text{physostigmine concentration } [\times 10^{-7} \text{ mole/liter}] = \frac{\text{unknown control activity}}{\text{standard control activity}} \times \frac{\text{concentration}}{\text{(from Fig. 2)}} \quad \text{(Eq. 1)}$$

A micromole per milliliter per minute activity unit is a fixed unit for the conditions of assay expressed in this report. A percent activity unit is variable and is dependent upon the relative activity of each blood sample.

If the control activity level of the unknown blood sample cannot be determined in advance, it must be obtained by assaying the sample until no further increase in activity is obtained.

The precision of the method was determined by statistical evaluation

Table I—Precision of Physostigmine Assay

Concentration Added, × 10^{-7} *M*	Concentration Measured: Mean, × 10^{-7} *M*	*SD*, × 10^{-7} *M*	Coefficient of Variation, %
0.25	0.19	0.019	±10.0
0.50	0.42	0.016	±3.8
1.00	1.13	0.021	±1.9
1.25	1.43	0.029	±2.0
2.50	2.71	0.049	±1.8
5.00	4.83	0.159	±3.3

Table II—Blood Physostigmine Levels ($\times 10^{-7}$ *M*) in Humans 30 min after Administration

Route	Dose Administered, μg/kg				
	15	20	25	30	45
Intravenous	—[a]			0.40	0.90
	—[a]			0.29	0.59
	—[a]				0.90
	—[a]				0.78
Intramuscular	—[a]	0.35	0.25		
	—[a]	—[a]	0.31		
		—[a]	0.27		
			—[a]		

[a] $<0.25 \times 10^{-7}$ *M*.

of data obtained from a reproducibility study. Ten whole blood samples were prepared at each of six different concentrations of physostigmine, ranging from 0.25 to 5.00 $\times 10^{-7}$ *M*. Means, standard deviations, and coefficients of variation for each set of 10 assays are presented in Table I. Precision was within ±3.8% for physostigmine concentrations ranging from 0.50 to 5.00 $\times 10^{-7}$ *M*. At 0.25 $\times 10^{-7}$ *M*, precision was ±10.0%.

The mean physostigmine concentrations obtained in the precision study were correlated with the concentrations added to the blood samples. The plot of data points and the equation of the regression line are given in Fig. 3.

Blood levels at 30 min after intravenous and intramuscular injections of physostigmine are presented in Table II. The relationship of dose administered to blood levels was approximately the same for both routes of administration.

DISCUSSION

To relate physostigmine concentration to cholinesterase inhibition, it is necessary to measure enzyme activity after inhibition has progressed until none of the enzyme remains in the complexed form. At this time, when the enzyme activity is between 30 and 70% of the control level, only decarbamylation occurs. The time course at 37°, from inhibition until a near linear reactivation rate is attained, together with the enzyme activity level at this time, can be used to determine the concentration of physostigmine in the blood at the time the *in vitro* sample was inhibited. With an *in vivo* blood sample, the physostigmine concentration can be determined for the time the blood was withdrawn from the patient.

This assay method assumes that decarbamylation occurs over the entire period from the time of inhibition. The error in the assumption is quite small, since an initial time period of less than 2 min is required for formation of an appreciable concentration of carbamylated enzyme. The time required for enzyme reactivation should be, and has been shown to be, a function of the inhibitor concentration. The time required to complete an assay varies directly with the physostigmine concentration, from approximately 1 hr for 0.50 $\times 10^{-7}$ *M* to approximately 7.5 hr for 5.00 $\times 10^{-7}$ *M*. Considering the inherent errors, the precision of this method is excellent.

REFERENCES

(1) F. H. Rodin, *Am. J. Ophthalmol.*, **30**, 19 (1947).

(2) M. D. Walker, *Lancet*, **1**, 1200 (1934).

(3) G. R. Farrer and J. J. Miller, *Am. J. Psychiat.*, **115**, 455 (1958).

(4) E. B. Crowell, Jr., and J. S. Ketchum, *Clin. Pharm. Ther.*, **8**, 409 (1967).

(5) I. Christenson, *Acta Pharm. Suec.*, **6**, 287 (1969).

(6) R. D. O'Brien, B. D. Hilton, and L. Gilmour, *Mol. Pharm.*, **2**, 593 (1966).

(7) R. D. O'Brien, *ibid.*, **4**, 121 (1968).

(8) F. F. Foldes and J. C. Smith, *Ann. N.Y. Acad. Sci.*, **135**, 287 (1966).

(9) F. P. W. Winteringham and K. S. Fowler, *Biochem. J.*, **101**, 127 (1966).

(10) O. E. Schultz and R. Kratzer, *Arch. Pharm.*, **295**, 444 (1962).

(11) S. Udenfriend, D. E. Duggan, B. M. Vasta, and B. B. Brodie, *J. Pharmacol. Exp. Ther.*, **120**, 26 (1957).

(12) J. D. Winefordner, in "Fluorescence and Phosphorescence Analysis; Principles and Applications," D. M. Hercules, Ed., Wiley, New York, N.Y., 1966, p. 169.

(13) A. R. Rogers and G. Smith, *J. Chromatogr.*, **87**, 125 (1973).

(14) W. A. Groff, A. Kaminskis, and R. I. Ellin, *Clin. Toxicol.*, **9**, 353 (1976).

ACKNOWLEDGMENTS AND ADDRESSES

Received March 1, 1976, from the *Biomedical Laboratory, Edgewood Arsenal, Aberdeen Proving Ground, MD 21010.*

Accepted for publication May 18, 1976.

The views of the authors do not purport to reflect the position of the Department of Defense. The use of trade names does not constitute an official endorsement or approval of such commercial hardware or software. This report may not be cited for advertisement purposes.

[x] To whom inquiries should be directed.

Influence of Zinc–Ligand Mixtures on Serum Zinc Levels in Rats

EUGENE GIROUX [x] and N. J. PRAKASH

Abstract □ The influence of various salts, chelates, and other complexes of zinc given by gavage on serum zinc levels in rats was studied. Serum zinc concentrations were determined over 6 hr after administration of zinc sulfate at doses of 5, 10, 20, 50, and 100 mg of zinc/kg. Serum zinc levels following doses of zinc salts and complexes were compared with those after zinc sulfate. Phytic acid, aminopolycarboxylic acids (including edetate disodium), and penicillamine significantly suppressed increases in serum zinc concentration. Some natural amino acid–zinc sulfate mixtures (those with lysine, cysteine, glycine, and histidine) produced greater levels than the equivalent dose of zinc sulfate alone. Several thiocarboxylic acids, such as mercaptoacetic acid and thiosalicylic acid, also increased serum zinc concentrations. These observations form a basis for attempted modification of zinc absorption in other species.

Keyphrases □ Zinc—serum levels, effect of various salts, chelates, and other complexes, rats □ Salts, zinc—effect on serum zinc levels, rats □ Chelates, various—with zinc, effect on serum zinc levels, rats □ Complexes, various—with zinc, effect on serum zinc levels, rats □ Metals—zinc, various salts, chelates, and other complexes, effect on serum zinc levels, rats

Treatment of humans with zinc usually involves administration of zinc sulfate heptahydrate, taken with meals to avoid gastric irritation. However, Schelling *et al.* (1) reported that when it is given simultaneously with meals, the apparent absorption of zinc may be nil. Poor absorption may partly account for equivocal clinical results of zinc therapy (2–7).

GI absorption of zinc in several species has been studied

Table II—Blood Physostigmine Levels ($\times 10^{-7}$ *M*) in Humans 30 min after Administration

Route	Dose Administered, μg/kg				
	15	20	25	30	45
Intravenous	—[a]			0.40	0.90
	—[a]			0.29	0.59
	—[a]				0.90
	—[a]				0.78
Intramuscular	—[a]	0.35	0.25		
	—[a]	—[a]	0.31		
		—[a]	0.27		
			—[a]		

[a] $<0.25 \times 10^{-7}$ *M*.

of data obtained from a reproducibility study. Ten whole blood samples were prepared at each of six different concentrations of physostigmine, ranging from 0.25 to 5.00 $\times 10^{-7}$ *M*. Means, standard deviations, and coefficients of variation for each set of 10 assays are presented in Table I. Precision was within ±3.8% for physostigmine concentrations ranging from 0.50 to 5.00 $\times 10^{-7}$ *M*. At 0.25 $\times 10^{-7}$ *M*, precision was ±10.0%.

The mean physostigmine concentrations obtained in the precision study were correlated with the concentrations added to the blood samples. The plot of data points and the equation of the regression line are given in Fig. 3.

Blood levels at 30 min after intravenous and intramuscular injections of physostigmine are presented in Table II. The relationship of dose administered to blood levels was approximately the same for both routes of administration.

DISCUSSION

To relate physostigmine concentration to cholinesterase inhibition, it is necessary to measure enzyme activity after inhibition has progressed until none of the enzyme remains in the complexed form. At this time, when the enzyme activity is between 30 and 70% of the control level, only decarbamylation occurs. The time course at 37°, from inhibition until a near linear reactivation rate is attained, together with the enzyme activity level at this time, can be used to determine the concentration of physostigmine in the blood at the time the *in vitro* sample was inhibited. With an *in vivo* blood sample, the physostigmine concentration can be determined for the time the blood was withdrawn from the patient.

This assay method assumes that decarbamylation occurs over the entire period from the time of inhibition. The error in the assumption is quite small, since an initial time period of less than 2 min is required for formation of an appreciable concentration of carbamylated enzyme. The time required for enzyme reactivation should be, and has been shown to be, a function of the inhibitor concentration. The time required to complete an assay varies directly with the physostigmine concentration, from approximately 1 hr for 0.50 $\times 10^{-7}$ *M* to approximately 7.5 hr for 5.00 $\times 10^{-7}$ *M*. Considering the inherent errors, the precision of this method is excellent.

REFERENCES

(1) F. H. Rodin, *Am. J. Ophthalmol.*, **30**, 19 (1947).

(2) M. D. Walker, *Lancet*, **1**, 1200 (1934).

(3) G. R. Farrer and J. J. Miller, *Am. J. Psychiat.*, **115**, 455 (1958).

(4) E. B. Crowell, Jr., and J. S. Ketchum, *Clin. Pharm. Ther.*, **8**, 409 (1967).

(5) I. Christenson, *Acta Pharm. Suec.*, **6**, 287 (1969).

(6) R. D. O'Brien, B. D. Hilton, and L. Gilmour, *Mol. Pharm.*, **2**, 593 (1966).

(7) R. D. O'Brien, *ibid.*, **4**, 121 (1968).

(8) F. F. Foldes and J. C. Smith, *Ann. N.Y. Acad. Sci.*, **135**, 287 (1966).

(9) F. P. W. Winteringham and K. S. Fowler, *Biochem. J.*, **101**, 127 (1966).

(10) O. E. Schultz and R. Kratzer, *Arch. Pharm.*, **295**, 444 (1962).

(11) S. Udenfriend, D. E. Duggan, B. M. Vasta, and B. B. Brodie, *J. Pharmacol. Exp. Ther.*, **120**, 26 (1957).

(12) J. D. Winefordner, in "Fluorescence and Phosphorescence Analysis; Principles and Applications," D. M. Hercules, Ed., Wiley, New York, N.Y., 1966, p. 169.

(13) A. R. Rogers and G. Smith, *J. Chromatogr.*, **87**, 125 (1973).

(14) W. A. Groff, A. Kaminskis, and R. I. Ellin, *Clin. Toxicol.*, **9**, 353 (1976).

ACKNOWLEDGMENTS AND ADDRESSES

Received March 1, 1976, from the *Biomedical Laboratory, Edgewood Arsenal, Aberdeen Proving Ground, MD 21010.*

Accepted for publication May 18, 1976.

The views of the authors do not purport to reflect the position of the Department of Defense. The use of trade names does not constitute an official endorsement or approval of such commercial hardware or software. This report may not be cited for advertisement purposes.

[x] To whom inquiries should be directed.

Influence of Zinc–Ligand Mixtures on Serum Zinc Levels in Rats

EUGENE GIROUX [x] and N. J. PRAKASH

Abstract □ The influence of various salts, chelates, and other complexes of zinc given by gavage on serum zinc levels in rats was studied. Serum zinc concentrations were determined over 6 hr after administration of zinc sulfate at doses of 5, 10, 20, 50, and 100 mg of zinc/kg. Serum zinc levels following doses of zinc salts and complexes were compared with those after zinc sulfate. Phytic acid, aminopolycarboxylic acids (including edetate disodium), and penicillamine significantly suppressed increases in serum zinc concentration. Some natural amino acid–zinc sulfate mixtures (those with lysine, cysteine, glycine, and histidine) produced greater levels than the equivalent dose of zinc sulfate alone. Several thiocarboxylic acids, such as mercaptoacetic acid and thiosalicylic acid, also increased serum zinc concentrations. These observations form a basis for attempted modification of zinc absorption in other species.

Keyphrases □ Zinc—serum levels, effect of various salts, chelates, and other complexes, rats □ Salts, zinc—effect on serum zinc levels, rats □ Chelates, various—with zinc, effect on serum zinc levels, rats □ Complexes, various—with zinc, effect on serum zinc levels, rats □ Metals—zinc, various salts, chelates, and other complexes, effect on serum zinc levels, rats

Treatment of humans with zinc usually involves administration of zinc sulfate heptahydrate, taken with meals to avoid gastric irritation. However, Schelling *et al.* (1) reported that when it is given simultaneously with meals, the apparent absorption of zinc may be nil. Poor absorption may partly account for equivocal clinical results of zinc therapy (2–7).

GI absorption of zinc in several species has been studied

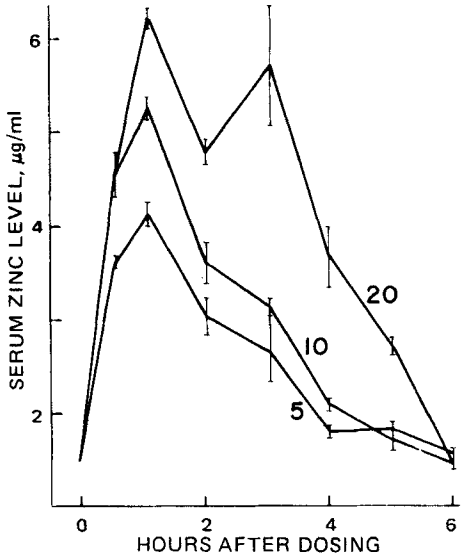

Figure 1—*Serum zinc levels following gavage of 5, 10, and 20 mg of zinc/kg, given as zinc sulfate heptahydrate dissolved in water. Points indicate mean values; vertical bars denote ± SEM. At least five rats were used for each point except for the 1- and 4-hr points at 5 mg of zinc/kg, where three and four rats were used, respectively.*

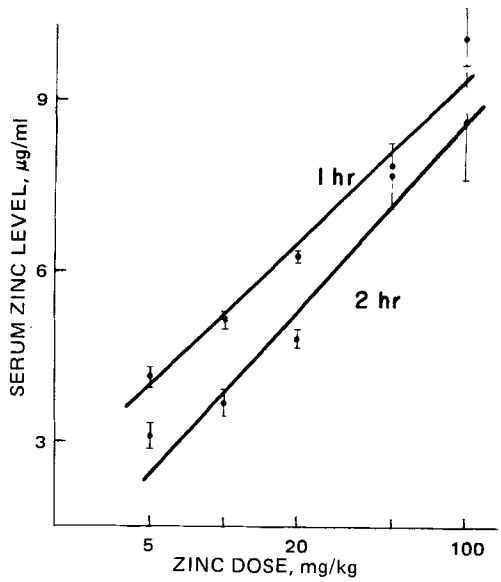

Figure 2—*Serum zinc levels 1 and 2 hr after gavaging of zinc sulfate heptahydrate dissolved in water. (See Fig. 1 for further explanation.)*

in vivo and *in vitro*. Various experimental designs have been employed including conventional balance studies, radioisotopic tracer studies, and studies of the bioavailability of zinc from foodstuffs as monitored by correction of zinc deficiency symptoms. Zinc absorption was discussed in several reviews (8–12). In one study, edetate and ascorbic acid depressed gut mucosal uptake of zinc but enhanced transmural transport during *in vitro* perfusion experiments on rats (13). Zinc–edetate complexes and zinc–histidine complexes were absorbed intact from the gut and appeared in the plasma of chickens further complexed with plasma proteins (14). Zinc–aspirin complexes were broken down and did not appear intact in serum (14).

Apparently, some compounds potentiate zinc absorption when given with an oral dose of zinc sulfate while other substances suppress it. Accordingly, serum zinc levels were measured in rats after gavage of mixtures of zinc sulfate with various complexing agents. Compounds with different zinc coordinating sites were studied including thiol, amino, and carboxylic acid groups. Phytic acid and various amino acids were chosen because of their relevance to trace metal metabolism.

EXPERIMENTAL

Materials[1]—Reagents and chemicals, including bis[*N*,*N*-di(carboxymethyl)aminoethoxy]ethane (I), the ammonium salt of pyrrolidine-*N*-carboxydithioic acid (II), and 3-mercaptopropionylglycine (III), were obtained commercially, except for *N*-acetylhydroxyproline, which was prepared in this laboratory.

Animals and *In Vivo* Procedure—Male Sprague–Dawley rats[2], 140–240 g, were maintained in open mesh, stainless steel cages for at least 1 week in the laboratory environment (12-hr dark cycle beginning at 7 pm and controlled temperature and humidity). They were fed laboratory ration[3] and tap water *ad libitum* until 20–24 hr before an experiment. From that time and throughout the experiment, animals were fasted and allowed access only to demineralized water.

Each experiment began at 9–10 am. Various zinc mixtures were introduced by gavage. After 0.5–6 hr, animals were lightly anesthetized with ether and blood was taken from the heart with plastic syringes and stainless steel needles. The blood was allowed to clot in acid-washed glass tubes, and serum was obtained by centrifugation. A second centrifugation removed from the serum traces of erythrocytes carried over from the initial centrifugation.

Aliquots of serum were treated with trichloroacetic acid to a final concentration of 5% (15), and protein-free supernates were analyzed for zinc by atomic absorption spectrophotometry[4]. Zinc contamination was reduced through use of plastic zinc-free labware, disposable plastic test tubes, acid-washed pipets, and demineralized, double-distilled water for preparation of all reagents. Statistical comparison of means was by the Student two-tailed *t*-test with the assumption that variances of the populations were not necessarily identical (16).

Preparation of Mixtures—With few exceptions, test mixtures were prepared by combining aqueous zinc sulfate with an aqueous solution (or suspension) of the other component. A few mixtures were adjusted to pH 5–6, but the pH of the test mixtures generally was not controlled. The concentration of zinc in the final mixture was always chosen so that the volume administered was 5 ml/kg. If the mixture contained insoluble components, it was homogenized[5] immediately prior to gavage.

Butanol Solubility Measurements—Solubility of zinc in an organic phase as modified by the presence of ligand was determined by partitioning zinc-65 between 1-butanol and an aqueous solution [0.1 *M* NaCl–0.1 *M* 2-(*N*-morpholino)ethanesulfonic acid] buffered at pH 6.5. Each mixture contained 2 ml of aqueous buffer, 2.5 ml of 1-butanol, 5 μmoles of complexing agent, and 2 μmoles of ^{65}Zn-labeled zinc sulfate. Butanol and aqueous phases were repeatedly mixed and then separated by centrifugation. An aliquot of the butanol phase was counted in a γ-spectrometer[6].

[1] Anthranilic acid and 1-butanol from J. T. Baker, Deventer, Holland; 8-hydroxyquinoline, 8-hydroxyquinoline-5-sulfonic acid, 2-mercapto-1-methylimidazole, 3-mercaptopropionic acid, III, penicillamine, and thiosalicylic acid from Fluka, Buchs, Switzerland; 2-(*N*-morpholino)ethanesulfonic acid from Hopkin and Williams, Essex, England; acetylacetone from K & K Laboratories, Plainsview, N.Y.; asparagine, citric acid, cysteine, galacturonic acid, glycine, histidine, β-hydroxybutyric acid, imidazole, lysine, oxalic acid, trichloroacetic acid, and zinc sulfate heptahydrate from E. Merck, Darmstadt, Germany; ^{65}Zn-labeled zinc chloride from NEN Chemicals, GmbH, Dreieichenhain, Germany; malonic acid and salicylic acid from Prolabo, Paris, France; edetate disodium and II from Karl Roth, Karlsruhe, Germany; *N*-acetylcysteine, β-alanine, and I from Serva, Heidelberg, Germany; 2,4-diaminobutyric acid, dithioerythritol, ethylenediaminediacetic acid, nitrilotriacetic acid, sodium phytate, and 1,2-transcyclohexyldiaminetetraacetic acid from Sigma Chemical Co., St. Louis, Mo.; all others from Aldrich-Europe, Beerse, Belgium.

[2] Charles River France, St.-Aubin-des-Elbeuf.

[3] Diet A 04 (containing 85 mg of zinc/kg), U.A.R., Villemoisson-sur-Orge, France.

[4] Perkin-Elmer model 403 atomic absorption spectrophotometer.

[5] Potter–Elvehjem apparatus.

[6] Auto-Gamma scintillation spectrometer, Packard Instrument Co.

Table I—Serum Zinc Levels after Gavage of Zinc Sulfate–Ligand Mixtures at a Dose of 10 mg of Zinc/kg

Ligand	Zinc–Ligand Molar Ratio	Serum Zinc, μg/ml (Mean ± *SEM*)[a] 1 hr	4 hr
Sodium phytate	1:1	1.50 ± 0.02 (6)[b]	1.69 ± 0.03 (5)[b]
I	1:1	1.94 ± 0.12 (6)[b]	1.84 ± 0.27 (4)
8-Thioquinoline	1:2	2.06 ± 0.10 (6)[b]	—[c]
Penicillamine	1:2	2.06 ± 0.15 (5)[b]	1.54 ± 0.13 (5)[b]
Oxalic acid	1:1	2.39 ± 0.19 (5)[b]	1.76 ± 0.08 (4)
Edetate disodium	1:1	2.60 ± 0.13 (5)[b]	1.75 ± 0.17 (5)
1,3-Dimercapto-2-propanol	1:1	2.65 ± 0.19 (6)[b]	3.85 ± 0.34 (5)[d]
Dithioerythritol	1:1	2.77 ± 0.08 (6)[b]	3.02 ± 0.48 (5)[d]
2,3-Dimercapto-1-propanol	1:1	3.43 ± 0.24 (6)[b]	2.46 ± 0.13 (5)
8-Hydroxyquinoline	1:2	3.60 ± 0.20 (6)[b]	2.48 ± 0.09 (4)
2,3-Diaminopyridine	1:2	3.70 ± 0.20 (6)[b]	4.45 ± 0.22 (10)[d]
II	1:2	3.79 ± 0.26 (6)[b]	4.51 ± 0.20 (5)[d]
III	1:1	3.99 ± 0.22 (6)[b]	2.10 ± 0.18 (5)
2-Pyridylacetic acid	1:2	4.22 ± 0.22 (5)[b]	2.79 ± 0.22 (5)[d]
Anthranilic acid	1:1	4.31 ± 0.13 (6)[b]	2.39 ± 0.19 (5)
N-Acetylcysteine	1:2	4.72 ± 0.33 (6)	2.09 ± 0.15 (5)
3-Mercaptopropionic acid	1:1	4.96 ± 0.41 (6)	3.08 ± 0.18 (5)[d]
Salicylic acid	1:1	5.02 ± 0.10 (6)	2.33 ± 0.16 (5)
2-Mercapto-1-methylimidazole	1:2	5.03 ± 0.37 (6)	3.20 ± 0.23 (5)[d]
N-Acetylhydroxyproline	1:1	5.07 ± 0.34 (5)	2.14 ± 0.22 (5)
Acetylacetone	1:2	5.15 ± 0.22 (5)	4.06 ± 0.32 (5)[d]
8-Hydroxyquinoline-5-sulfonic acid	1:2	5.27 ± 0.20 (6)	2.81 ± 0.28 (5)[d]
Zinc sulfate heptahydrate (control)		5.29 ± 0.12 (15)	2.12 ± 0.06 (16)
2,4-Diaminobutyric acid	1:1	5.41 ± 0.23 (6)	2.29 ± 0.10 (5)
Asparagine	1:2	5.42 ± 0.16 (6)	2.77 ± 0.24 (5)
β-Alanine	1:2	5.46 ± 0.25 (6)	2.06 ± 0.15 (5)
Histidine methyl ester	1:2	5.56 ± 0.24 (12)	2.24 ± 0.16 (10)
3,4-Diaminobenzoic acid	1:2	5.59 ± 0.33 (5)	3.37 ± 0.27 (5)[d]
1,3-Diamino-2-propanol	1:2	5.78 ± 0.22 (6)	2.28 ± 0.25 (5)
Imidazole	1:2	5.87 ± 0.17 (6)	2.46 ± 0.12 (5)
Lysine	1:2	5.91 ± 0.13 (6)[d]	2.38 ± 0.07 (5)
Cysteine	1:2	5.97 ± 0.15 (12)[d]	—[c]
Citric acid	1:1	6.02 ± 0.37 (6)	—[c]
Histidine	1:2	6.23 ± 0.58 (6)	—[c]
Glycine	1:2	6.61 ± 0.42 (6)[d]	—[c]
Malonic acid	1:1	6.66 ± 0.24 (11)[d]	2.63 ± 0.11 (14)[d]
Mercaptoacetic acid	1:2	6.68 ± 0.46 (5)[d]	3.71 ± 0.54 (4)[d]
2-Mercapto-3-pyridinol	1:2	6.76 ± 0.17 (5)[d]	3.19 ± 0.24 (5)[d]
β-Hydroxybutyric acid	1:2	6.77 ± 0.46 (10)[d]	2.95 ± 0.24 (5)
Mercaptosuccinic acid	1:1	6.83 ± 0.28 (6)[d]	2.31 ± 0.14 (5)
α-D-Galacturonic acid	1:2	7.22 ± 0.42 (6)[d]	2.18 ± 0.18 (5)
Thiosalicylic acid	1:1	9.93 ± 0.36 (22)[d]	4.28 ± 0.28 (15)[d]

[a] The numbers in parentheses are the number of animals. [b] Significantly below control value, $p < 0.005$. [c] Data obtained 3 hr following dosing were not significantly different from control values. [d] Significantly above control value, $p < 0.005$.

RESULTS

Serum Zinc Levels following Zinc Sulfate—The serum zinc concentration was determined 1, 2, 3, 4, and 6 hr after gavage of rats with demineralized water. The mean values at these points were not significantly different from one another; the overall mean (28 rats) was 1.50 ± 0.03 (*SEM*) μg of zinc/ml of serum. Serum zinc levels were determined at 0.5, 1, 2, 3, 4, 5, and 6 hr following doses of 5, 10, 20, 50, and 100 mg of zinc/kg, given as aqueous solutions of zinc sulfate heptahydrate.

Serum concentration–time curves after 5, 10, and 20 mg of zinc/kg are shown in Fig. 1. With these doses, maximum serum zinc concentrations were observed 1 hr after gavage, and the level returned to the baseline concentration within 6 hr. Semilogarithmic curves relating all doses administered to the resulting serum concentrations were approximately linear (Fig. 2). The data indicated that measurable increases in serum zinc concentrations would not be observed at doses less than 1–2 mg of zinc/kg. Peak serum levels of 20 μg of zinc/ml (approximately 15 times greater than normal) did not produce any lethality over 8 hr.

Serum Zinc Levels following Zinc–Ligand Mixtures—Serum zinc concentrations were measured 1 and 4 hr following gavage (Table I). Doses of test mixtures contained 10 mg of zinc/kg, and the molar ratio of zinc to ligand was either 1:1 or 1:2. Serum zinc levels following gavage of zinc–ligand mixtures ranged from little or no increase above serum zinc levels in untreated animals to highly significant increases beyond the increase caused by zinc sulfate alone. Aminopolycarboxylic acids of the edetate type suppressed increases in serum zinc concentrations. Other aminopolycarboxylic acids tested in addition to those listed in Table I were nitrilotriacetic acid, ethylenediaminediacetic acid, and 1,2-*trans*-cyclohexyldiaminetetraacetic acid. These chelators also significantly ($p < 0.005$) diminished the increase in the serum zinc level.

The dithiol compounds 1,3-dimercapto-2-propanol, 2,3-dimercapto-1-propanol, and dithioerythritol significantly inhibited the elevation of serum zinc levels at 1 hr, but the levels were greater than the control value after 4 hr. After gavage of several compounds listed in Table I, serum levels of zinc were greater than those following equivalent doses of zinc sulfate. Notable among these latter compounds were some natural amino acids (lysine, glycine, cysteine, and histidine) and compounds containing thiol and carboxylic acid groups such that five- and six-membered chelate complexes with zinc could be formed.

Time–concentration curves following gavage of mixtures of zinc sulfate with penicillamine and with thiosalicylic acid are shown in Fig. 3A. Maximum serum zinc levels were noted 1 hr after dosing, with return to baseline concentration within 6 hr. When given in a mixture with zinc sulfate, D,L-penicillamine significantly ($p < 0.005$) suppressed the increase in the serum zinc level while thiosalicylic acid significantly ($p < 0.005$) enhanced the increase. The levels following gavage of ligands in the absence of zinc sulfate also were determined. Penicillamine reduced and thiosalicylic acid increased the serum zinc levels (Fig. 3B).

Time–serum zinc concentration curves for sodium phytate and β-hydroxybutyric acid given with and without zinc sulfate were obtained similarly (Fig. 4). Areas between the curves (Figs. 3 and 4) in the presence and absence of zinc sulfate were calculated: zinc sulfate (control), 9.2; thiosalicylic acid, 21.1; β-hydroxybutyric acid, 11.5; penicillamine, 3.8; and sodium phytate, 0.1 μg hr/ml. These results are consistent with the hypothesis that thiosalicylic acid and β-hydroxybutyric acid increase zinc absorption while penicillamine and sodium phytate suppress zinc absorption from zinc sulfate heptahydrate.

Butanol Solubility of Zinc–Ligand Mixtures—Partitioning of zinc-65 between aqueous buffer and butanol was compared for poorly absorbed and well-absorbed zinc–ligand mixtures. Ligands that sup-

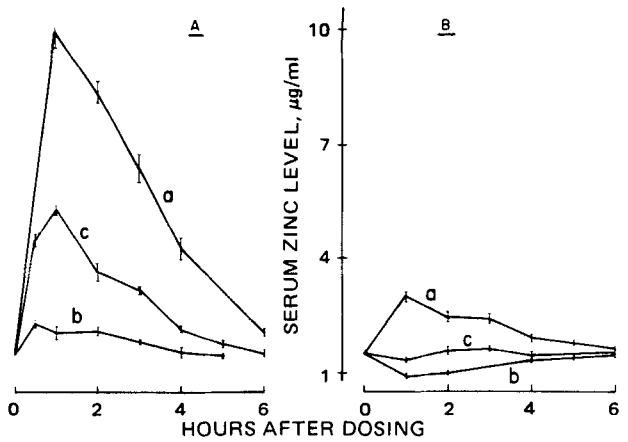

Figure 3—(*A*) *Serum zinc levels following gavage of zinc sulfate* (*c*) (*10 mg of zinc/kg*) *given alone or mixed with* D,L-*penicillamine* (*b*) (*1:2 molar ratio*) *or thiosalicylic acid* (*a*) (*1:1 molar ratio*). (*B*) *Serum zinc levels following gavage of thiosalicylic acid* (*a*) *or penicillamine* (*b*) *at the same concentrations as in A or of distilled water* (*c*). *Points* (*at least five rats per point*) *indicate mean values; vertical bars denote* ± SEM.

pressed zinc absorption also tended to suppress zinc solubility in the butanol phase (Table II), as did some ligands that augmented zinc absorption. In the absence of ligand, 0.9% of the ^{65}Zn-radioactivity was recovered in the butanol phase.

DISCUSSION

Ligands markedly influenced the serum zinc levels following their administration by gavage together with zinc sulfate. While these ligands might influence distribution or elimination of zinc after their absorption, it seems more likely that their major effect is on zinc absorption from the GI tract, particularly when the time course of serum zinc concentrations after dosing with ligands is similar to that seen after zinc sulfate. Thus, the form in which zinc is presented to the GI tract apparently influences zinc absorption. Phytic acid, considered responsible for dietary zinc deficiencies reported in Near Eastern adolescents (17), completely prevented increases in the serum zinc levels when coadministered with zinc sulfate. Most α-amino acids enhanced the increases. Penicillamine markedly suppressed such increases, but the structurally similar cysteine enhanced them. These two compounds form equally stable zinc complexes (18). For some mixtures of zinc sulfate and ligand, serum zinc levels at 4 hr were greater than at 1 hr after gavage; thus, the temporal pattern of zinc levels after these mixtures did not resemble that after zinc sulfate.

Constants for zinc complex formation are available (18) for several tested compounds. There was no obvious relationship between the effect on serum zinc levels and the complex formation constant, although some of the strongest complexes were among the most poorly absorbed mixtures. Furthermore, the solubility of the complexes in the test mixture did not seem to be the decisive factor. The water-soluble edetate–zinc mixture suppressed apparent zinc absorption, as did the insoluble 2,3-dimercapto-1-propanol–zinc mixture. The insoluble thiosalicylic acid–zinc mixture appeared significantly effective in enhancing zinc absorption. Lipid solubility of zinc species presented to GI absorption sites may play a role in absorption, but the data on the effect of ligands on butanol solubility of zinc are inconclusive in support of this hypothesis.

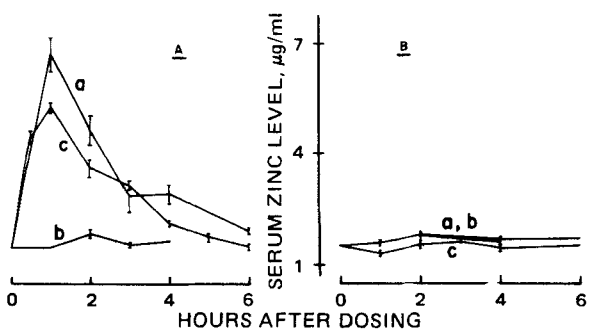

Figure 4—(*A*) *Serum zinc levels following gavage of zinc sulfate* (*c*) (*10 mg of zinc/kg*) *given alone or mixed with sodium phytate* (*b*) (*1:1 molar ratio*) *or β-hydroxybutyric acid* (*a*) (*1:2 molar ratio*). (*B*) *Serum zinc levels following gavage of β-hydroxybutyric acid* (*a*) *or sodium phytate* (*b*) *at the same concentrations as in A or of distilled water* (*c*). *Points* (*at least four rats per point*) *indicate mean values; vertical bars denote* ± SEM.

Table II—Stability and Butanol Solubility of Zinc Complexes

Ligand	Apparent Log K_1 pH 6.5[a]	Butanol-Soluble ^{65}Zn[b], %
Sodium phytate	—	<0.1
I	9.2	<0.1
8-Thioquinoline	8.3	55
Penicillamine	4.2	0.9
Oxalic acid	4.9	0.3
Edetate disodium	12.5	<0.1
1,3-Dimercapto-2-propanol	—	<0.1
Dithioerythritol	—	0.1
2,3-Dimercapto-1-propanol	7.3	0.5
8-Hydroxyquinoline	5.1	37
Cysteine	3.8	0.5
Histidine	3.8	1.3
Glycine	2.0	0.9
Malonic acid	2.8	0.9
Mercaptoacetic acid	4.2	1.4
2-Mercapto-3-pyridinol	—	85
β-Hydroxybutyric acid	1.1	1.0
Mercaptosuccinic acid	4.6	<0.1
α-D-Galacturonic acid	1.7[c]	0.8
Thiosalicylic acid	6.1	34

[a] Data were taken from Ref. 18; values at pH 6.5 were calculated as described in Ref. 22. [b] Distribution of isotope in presence of ligand between aqueous and 1-butanol phases as described in the text; each value is the average of two determinations. Butanol-soluble isotope in absence of ligand, 0.9%. [c] Ref. 19.

These observations apply only to the rat. However, in other species, oral intake of certain zinc–ligand mixtures may also increase serum levels of zinc more than oral zinc sulfate treatment. Alternatively, a smaller amount of zinc–ligand mixture may provide the equivalent effect of a greater amount of zinc sulfate, thereby reducing GI side effects of oral zinc sulfate therapy. Ligand effects may also partly account for diminished apparent zinc absorption when zinc sulfate is administered with meals (1, 20, 21).

REFERENCES

(1) J. L. Schelling, S. Muller-Hess, and F. Thonney, *Lancet*, **2**, 968 (1973).

(2) K. Haeger, E. Lanner, and P. O. Magnusson, *VASA, J. Vasc. Dis.*, **1**, 62 (1972).

(3) S. L. Husain, *Lancet*, **1**, 1069 (1969).

(4) G. R. Sergeant, R. E. Galloway, and M. C. Gueri, *ibid.*, **2**, 891 (1970).

(5) T. Hallböök and E. Lanner, *ibid.*, **2**, 891 (1970).

(6) B. M. Myers and G. Cherry, *Am. J. Surg.*, **120**, 77 (1970).

(7) M. W. Greaves and F. A. Ive, *Br. J. Dermatol.*, **87**, 632 (1972).

(8) B. L. O'Dell, *Am. J. Clin. Nutr.*, **22**, 1315 (1969).

(9) W. G. Hoekstra, in "Trace Element Metabolism in Animals," C. F. Mills, Ed., E. and S. Livingstone, Edinburgh, Scotland, 1970, pp. 347–353.

(10) E. J. Underwood, "Trace Elements in Human and Animal Nutrition," 3rd ed., Academic, New York, N.Y., 1971, pp. 208–252.

(11) W. M. Becker and W. G. Hoekstra, in "Intestinal Absorption of Metal Ions, Trace Elements and Radionuclides," S. C. Skoryna and D. W. Edwards, Eds., Pergamon, Oxford, England, 1971, pp. 229–256.

(12) B. L. O'Dell, *Ann. N.Y. Acad. Sci.*, **199**, 70 (1972).

(13) B. M. Sahagian, I. Harding-Barlow, and H. M. Perry, Jr., *J. Nutr.*, **93**, 291 (1967).

(14) F. A. Suso and H. M. Edwards, Jr., *Nature*, **236**, 230 (1972).
(15) I. J. T. Davies, M. Musa, and T. L. Dormandy, *J. Clin. Pathol.*, **21**, 359 (1968).
(16) R. D. Remington and M. A. Schork, "Statistics with Applications to the Biological and Health Sciences," Prentice-Hall, Englewood Cliffs, N.J., 1970, pp. 212, 213.
(17) J. G. Reinhold, K. Nasr, A. Lahimgarzadeh, and H. Hedayati, *Lancet*, **1**, 283 (1973).
(18) L. G. Sillén and A. E. Martell, "Stability Constants of Metal-Ion Complexes," The Chemical Society Special Publication No. 17, London, England, 1964. L. G. Sillén and A. E. Martell, "Stability Constants of Metal-Ion Complexes," Supplement No. 1, The Chemical Society Special Publication No. 25, London, England, 1971.
(19) G. K. R. Makar, M. L. D. Touche, and D. R. Williams, *J. Chem. Soc. Dalton Trans.*, **1976**, 1016.
(20) A. Pécoud, P. Donzel, and J. L. Schelling, *Clin. Pharmacol. Ther.*, **17**, 469 (1975).
(21) F. J. Oelshlegel, Jr., and G. J. Brewer, *Clin. Res.*, **23**, 2221 (1975).
(22) W. J. O'Sullivan, in "Data for Biochemical Research," 2nd ed., R. M. C. Dawson, D. C. Elliott, W. H. Elliott, and K. M. Jones, Eds., Clarendon, Oxford, England, 1969, pp. 423–434.

ACKNOWLEDGMENTS AND ADDRESSES

Received March 10, 1976, from *Centre de Recherche Merrell International, 16, rue d'Ankara, F 67000 Strasbourg, France.*
Accepted for publication May 19, 1976.
[x] To whom inquiries should be directed.

Pharmacokinetics of Δ^9-Tetrahydrocannabinol in Dogs

EDWARD R. GARRETT [x] and C. ANTHONY HUNT [x]

Abstract □ The pharmacokinetics of intravenously administered ^{14}C-Δ^9-tetrahydrocannabinol and derived radiolabeled metabolites were studied in three dogs at two doses each at 0.1 or 0.5 and 2.0 mg/kg. Two dogs were biliary cannulated; total bile was collected in one and sampled in the other. The time course for the fraction of the dose per milliliter of plasma was best fit by a sum of five exponentials, and there was no dose dependency. No drug was excreted unchanged. The mean apparent volume of distribution of the central compartment referenced to total drug concentration in the plasma was 1.31 ± 0.07 liters, approximately the plasma volume, due to the high protein binding of 97%. The mean metabolic clearance of drug in the plasma was 124 ± 3.8 ml/min, half of the hepatic plasma flow, but was 4131 ± 690 ml/min referenced to unbound drug concentration in the plasma, 16.5 times the hepatic plasma flow, indicating that net metabolism of both bound and unbound drug occurs. Apparent parallel production of several metabolites occurred, but the pharmacokinetics of their appearance were undoubtedly due to their sequential production during liver passage. The apparent half-life of the metabolic process was 6.9 ± 0.3 min. The terminal half-life of Δ^9-tetrahydrocannabinol in the pseudo-steady state after equilibration in an apparent overall volume of distribution of 2170 ± 555 liters referenced to total plasma concentration was 8.2 ± 0.23 days, based on the consistency of all pharmacokinetic data. The best estimate of the terminal half-life, based only on the 7000 min that plasma levels could be monitored with the existing analytical sensitivity, was 1.24 days. However, this value was inconsistent with the metabolite production and excretion of 40–45% of dose in feces, 14–16.5% in urine, and 55% in bile within 5 days when 24% of the dose was unmetabolized and in the tissue at that time. These data were consistent with an enterohepatic recirculation of 10–15% of the metabolites. Intravenously administered radiolabeled metabolites were totally and rapidly eliminated in both bile and urine: 88% of the dose in 300 min with an apparent overall volume of distribution of 6 liters. These facts supported the proposition that the return of Δ^9-tetrahydrocannabinol from tissue was the rate-determining process of drug elimination after initial fast distribution and metabolism and was inconsistent with the capability of enzyme induction to change the terminal half-life.

Keyphrases □ Δ^9-Tetrahydrocannabinol—intravenous, radiochemical study of pharmacokinetics, dogs □ Pharmacokinetics—intravenous, Δ^9-tetrahydrocannabinol, radiochemical study, dogs □ Radiochemistry—study of pharmacokinetics of intravenous Δ^9-tetrahydrocannabinol, dogs

(−)-Δ^9-Tetrahydrocannabinol is the major active component of marijuana. An essential prerequisite to understand its pharmacological action, presumably related to the plasma levels of the drug and its metabolites (1, 2), is the quantification of the time course of the drug and its metabolites in biological tissues to relate to the psychoactive effects.

Agurell *et al.* (3, 4) demonstrated that when tritium-labeled Δ^9-tetrahydrocannabinol was intravenously administered to the mouse and rabbit, the radioactivity was slowly excreted as metabolites in the feces and urine with no unchanged drug observed in the urine. The relative amounts excreted biliary and renally varied with the species (3–5), and enterohepatic recirculation of metabolites was indicated (5, 6). The major studies to date with pharmacokinetic significance are those of Agurell *et al.* (4, 5) in rabbits and humans and Lemberger *et al.* (5, 7, 8) in humans. The general pattern appears to be a rapid initial fall of Δ^9-tetrahydrocannabinol concentration in plasma with an apparent half-life of 12 min in rabbits (4) and 30 min in humans (8), with a slower decline to a terminal apparent half-life of 50–60 hr in humans (8). A similar pattern was observed in a preliminary experiment with dogs (9). Metabolite levels in human plasma increased rapidly to two to three times that of the drug (8). The slower terminal phase decline of the log metabolite level with time paralleled the similarly plotted decline of plasma Δ^9-tetrahydrocannabinol.

It has been proposed (7, 10) that these facts can be explained by concomitant rapid hepatic metabolism and distribution to binding sites and other tissues such as fat (11) with a subsequent slow release of sequestered Δ^9-tetrahydrocannabinol from these stores. The suggestion that induced metabolism significantly lessens the terminal half-life of Δ^9-tetrahydrocannabinol in chronic users over that of naive individuals (2, 12) is inconsistent with this premise. The release rate from the "deep" tissues should be rate determining, not the metabolic rate. Changes in the latter would merely affect the relative plasma Δ^9-tetrahydrocannabinol levels, not the terminal half-life.

The purposes of this paper are to present the results of studies designed to elucidate the rate-determining pro-

(14) F. A. Suso and H. M. Edwards, Jr., *Nature*, **236**, 230 (1972).
(15) I. J. T. Davies, M. Musa, and T. L. Dormandy, *J. Clin. Pathol.*, **21**, 359 (1968).
(16) R. D. Remington and M. A. Schork, "Statistics with Applications to the Biological and Health Sciences," Prentice-Hall, Englewood Cliffs, N.J., 1970, pp. 212, 213.
(17) J. G. Reinhold, K. Nasr, A. Lahimgarzadeh, and H. Hedayati, *Lancet*, **1**, 283 (1973).
(18) L. G. Sillén and A. E. Martell, "Stability Constants of Metal-Ion Complexes," The Chemical Society Special Publication No. 17, London, England, 1964. L. G. Sillén and A. E. Martell, "Stability Constants of Metal-Ion Complexes," Supplement No. 1, The Chemical Society Special Publication No. 25, London, England, 1971.
(19) G. K. R. Makar, M. L. D. Touche, and D. R. Williams, *J. Chem. Soc. Dalton Trans.*, **1976**, 1016.
(20) A. Pécoud, P. Donzel, and J. L. Schelling, *Clin. Pharmacol. Ther.*, **17**, 469 (1975).
(21) F. J. Oelshlegel, Jr., and G. J. Brewer, *Clin. Res.*, **23**, 2221 (1975).
(22) W. J. O'Sullivan, in "Data for Biochemical Research," 2nd ed., R. M. C. Dawson, D. C. Elliott, W. H. Elliott, and K. M. Jones, Eds., Clarendon, Oxford, England, 1969, pp. 423–434.

ACKNOWLEDGMENTS AND ADDRESSES

Received March 10, 1976, from *Centre de Recherche Merrell International, 16, rue d'Ankara, F 67000 Strasbourg, France.*
Accepted for publication May 19, 1976.
[x] To whom inquiries should be directed.

Pharmacokinetics of Δ^9-Tetrahydrocannabinol in Dogs

EDWARD R. GARRETT [x] and C. ANTHONY HUNT [x]

Abstract □ The pharmacokinetics of intravenously administered ^{14}C-Δ^9-tetrahydrocannabinol and derived radiolabeled metabolites were studied in three dogs at two doses each at 0.1 or 0.5 and 2.0 mg/kg. Two dogs were biliary cannulated; total bile was collected in one and sampled in the other. The time course for the fraction of the dose per milliliter of plasma was best fit by a sum of five exponentials, and there was no dose dependency. No drug was excreted unchanged. The mean apparent volume of distribution of the central compartment referenced to total drug concentration in the plasma was 1.31 ± 0.07 liters, approximately the plasma volume, due to the high protein binding of 97%. The mean metabolic clearance of drug in the plasma was 124 ± 3.8 ml/min, half of the hepatic plasma flow, but was 4131 ± 690 ml/min referenced to unbound drug concentration in the plasma, 16.5 times the hepatic plasma flow, indicating that net metabolism of both bound and unbound drug occurs. Apparent parallel production of several metabolites occurred, but the pharmacokinetics of their appearance were undoubtedly due to their sequential production during liver passage. The apparent half-life of the metabolic process was 6.9 ± 0.3 min. The terminal half-life of Δ^9-tetrahydrocannabinol in the pseudo-steady state after equilibration in an apparent overall volume of distribution of 2170 ± 555 liters referenced to total plasma concentration was 8.2 ± 0.23 days, based on the consistency of all pharmacokinetic data. The best estimate of the terminal half-life, based only on the 7000 min that plasma levels could be monitored with the existing analytical sensitivity, was 1.24 days. However, this value was inconsistent with the metabolite production and excretion of 40–45% of dose in feces, 14–16.5% in urine, and 55% in bile within 5 days when 24% of the dose was unmetabolized and in the tissue at that time. These data were consistent with an enterohepatic recirculation of 10–15% of the metabolites. Intravenously administered radiolabeled metabolites were totally and rapidly eliminated in both bile and urine: 88% of the dose in 300 min with an apparent overall volume of distribution of 6 liters. These facts supported the proposition that the return of Δ^9-tetrahydrocannabinol from tissue was the rate-determining process of drug elimination after initial fast distribution and metabolism and was inconsistent with the capability of enzyme induction to change the terminal half-life.

Keyphrases □ Δ^9-Tetrahydrocannabinol—intravenous, radiochemical study of pharmacokinetics, dogs □ Pharmacokinetics—intravenous, Δ^9-tetrahydrocannabinol, radiochemical study, dogs □ Radiochemistry—study of pharmacokinetics of intravenous Δ^9-tetrahydrocannabinol, dogs

(−)-Δ^9-Tetrahydrocannabinol is the major active component of marijuana. An essential prerequisite to understand its pharmacological action, presumably related to the plasma levels of the drug and its metabolites (1, 2), is the quantification of the time course of the drug and its metabolites in biological tissues to relate to the psychoactive effects.

Agurell *et al.* (3, 4) demonstrated that when tritium-labeled Δ^9-tetrahydrocannabinol was intravenously administered to the mouse and rabbit, the radioactivity was slowly excreted as metabolites in the feces and urine with no unchanged drug observed in the urine. The relative amounts excreted biliary and renally varied with the species (3–5), and enterohepatic recirculation of metabolites was indicated (5, 6). The major studies to date with pharmacokinetic significance are those of Agurell *et al.* (4, 5) in rabbits and humans and Lemberger *et al.* (5, 7, 8) in humans. The general pattern appears to be a rapid initial fall of Δ^9-tetrahydrocannabinol concentration in plasma with an apparent half-life of 12 min in rabbits (4) and 30 min in humans (8), with a slower decline to a terminal apparent half-life of 50–60 hr in humans (8). A similar pattern was observed in a preliminary experiment with dogs (9). Metabolite levels in human plasma increased rapidly to two to three times that of the drug (8). The slower terminal phase decline of the log metabolite level with time paralleled the similarly plotted decline of plasma Δ^9-tetrahydrocannabinol.

It has been proposed (7, 10) that these facts can be explained by concomitant rapid hepatic metabolism and distribution to binding sites and other tissues such as fat (11) with a subsequent slow release of sequestered Δ^9-tetrahydrocannabinol from these stores. The suggestion that induced metabolism significantly lessens the terminal half-life of Δ^9-tetrahydrocannabinol in chronic users over that of naive individuals (2, 12) is inconsistent with this premise. The release rate from the "deep" tissues should be rate determining, not the metabolic rate. Changes in the latter would merely affect the relative plasma Δ^9-tetrahydrocannabinol levels, not the terminal half-life.

The purposes of this paper are to present the results of studies designed to elucidate the rate-determining pro-

cesses for disposition of intravenously administered Δ^9-tetrahydrocannabinol in the dog and to give a detailed pharmacokinetic analysis and model to fit the data. The effects of dose and other variables on the metabolism of drug and biliary and renal excretion of metabolites are delineated. Sensitive analytical methods, previously developed (9, 13, 14) for Δ^9-tetrahydrocannabinol in biological tissues, were used. The metabolites were characterized by the partition properties of their radiolabels derived from ^{14}C-labeled drug and were monitored in all available biological fluids. In addition, radiolabeled metabolites were intravenously administered to challenge the pharmacokinetic model. The previously studied physicochemical properties and protein binding (13) were taken into account.

EXPERIMENTAL

Preparation of Δ^9-Tetrahydrocannabinol Intravenous Dosages—Labeled and unlabeled Δ^9-tetrahydrocannabinols were purified on the evening prior to a pharmacokinetic study by methods given previously (14). They were combined to give the desired specific activity, and amounts sufficient to dose at 0.1, 0.5, or 2.0 mg/kg were transferred to a 50-ml glass centrifuge tube and dried in a water bath (50°) under a nitrogen stream. The residue was dissolved in 1 ml of absolute ethanol. The solution and 3 × 1-ml ethanol rinsings were transferred to a 20-ml vial and reduced to dryness. The residue in the vial was dissolved in 0.5 ml of absolute ethanol, and the vial was capped and placed in a freezer. On the morning of the study, the vial containing a small stirring bar[1] was placed on a magnetic stirrer set at low speed and 1 ml of water was added dropwise over 2–3 min to form an emulsion.

Dog plasma, 10 ml taken 1 hr after the last meal, was added to ultrafiltration cones[2] and centrifuged (3000 rpm) until an ultrafiltrate (2–5 ml) was obtained. The concentrated plasma was delivered dropwise from a pipet to the aqueous ethanol emulsion of Δ^9-tetrahydrocannabinol. This method produced a true solution of drug in plasma protein which, within 10 min, was administered intravenously to the dog in a 10-ml silanized syringe. This method is the method of choice for intravenously administering highly protein-bound materials normally insoluble in water.

Treatment of Animals—Two weeks prior to the first pharmacokinetic study, each mongrel dog was transferred to a metabolic cage. The next day, the dog was weighed and anesthetized with pentobarbital (30 mg/kg iv). One external jugular vein of the neck was exposed and cannulated under sterile conditions with 51 cm of 0.32-cm (0.125-in.) o.d. tubing[3]; at least 20.3 cm was inserted into the vein. The incision was closed after verifying the patency of the cannula and filling with heparinized[4] saline.

On the following day, the dog was placed on a table in a standing position and restrained by two straps placed around the fore- and hindlegs and fixed to a horizontal bar above. After 8 hr, the dog was returned to the cage. This training procedure was repeated daily until the dog would remain on the table unattended and unrestrained. At the end of each day, the dog was walked briefly, the regularly deposited stool sample was collected uncontaminated on an aluminum foil sheet, and the patency of the jugular cannula was checked.

A laparatomy was performed on Dogs A and C at the same time as the jugular was cannulated. The gallbladder was tied off, and an incision was made in the common bile duct distal to the gallbladder. One end of a 1.22-m length of 0.32-cm (0.125-in.) o.d. tubing was inserted in the bile duct incision approximately 6 cm toward the liver, and the other end was inserted in the incision approximately 16 cm into the intestine. When bile flow was visibly observed through the tubing, an incision was made in the abdominal wall; the tube was then passed through the opening and subcutaneously to an exit incision on the back of the neck. All incisions were closed, and the exposed bile cannula was cut. Bile flow was checked, and unrestricted flow to the intestine was confirmed. The tube was reconnected with 14-gauge stainless steel tubing.

After a 1-day recovery period, the dogs were transferred to a table and conditioned as described. At the end of all surgical procedures, the dogs were given 8×10^6 units of penicillin G intravenously.

Table I—Doses and Biliary Modifications in the Pharmacokinetic Studies after Intravenous Administration of ^{14}C-Δ^9-Tetrahydrocannabinol

Dog	Weight, kg	Average Hematocrit	Dose, mg/kg	10^{-6} × Total, cpm	Bile Cannulation
A	12.4	0.30	0.1	145.2	Yes[a]
A	14.1	0.42	2.0	85.36	Yes[a,b]
B	12.7	0.31	0.5	76.22	No
B	14.4	0.38	2.0	116.3	No
C	13.3	0.39	0.5	229.4	Yes[c]
C	16.6	0.38	2.0	150.8	Yes[c,d]

[a] Bile was sampled, but all was returned to the intestine. [b] Bile flow was stopped at approximately 1300 min after dosing. [c] All bile was collected, and none was allowed to return to the intestine. [d] Metabolites were extracted from the bile of this dog, and 8.62×10^6 cpm was administered intravenously to this biliary-cannulated 14.1-kg dog.

The dogs were fasted for 24 hr before each experiment and then weighed. A water load of 10 ml/kg was administered through a stomach tube, and a continuous 0.9% NaCl iv drip (0.5 ml/min) was started 30 min prior to dosing.

Experiments on a given dog were spaced at least 28 days apart. All dogs required transfer of the jugular cannula to the remaining jugular vein between the first and second pharmacokinetic experiments.

The bile from Dog A was collected over a specified time, sampled, and then returned *via* the intestinal tube. The bile from Dog C was collected but not returned *via* the intestinal tube. Bile flow in Dog C was maintained by four daily oral doses (with food) of 150 mg of taurocholic acid[5] and by incorporating taurocholic acid into the 0.5-ml/min iv saline drip at 0.833 mg/ml.

The weights, hematocrits, and intravenous doses administered to the dogs are listed in Table I, and their treatments for bile study are summarized.

Collection and Treatment of Samples—Δ^9-Tetrahydrocannabinol was administered intravenously as a freshly prepared suspension solubilized in doubled plasma protein concentration, prepared by plasma filtration through filters[6]. The drug was injected into the jugular catheter over 0.05 min. The dosing syringe and catheter were flushed with 10 ml of normal saline.

Blood was withdrawn from the jugular catheter, after filling the dead space of the catheter with fresh undiluted blood, into a sterile, disposable syringe containing 0.01 ml of heparin (10,000 units/ml). The blood sample was transferred to a sterile 15-ml centrifuge tube and centrifuged at 1500 rpm for 10 min. Plasma, 1–2 ml, was transferred to a 50-ml centrifuge tube with a sterile pipet, and the tube was quickly stoppered and frozen. A known volume (0.05–0.2 ml) of the remaining plasma was analyzed for total carbon-14 as described previously (14). The small amount of blood remaining in the syringe was used to determine blood pH in selected instances.

The separated red blood cells were refrigerated at 5°. Blood, 5 ml, was sampled at 0.5, 1, 1.5, 2, 3, 5, 7, 10, 13, 16, 19, 22, 27, 32, 37, 45, 55, 65, 80, 100, 130, 180, 210, 260, 310, 400, 500, 600, 700, and 1000 min and at 500-min intervals up to 7000 min (4.86 days). Sterile red blood cells were collected over the first 1500 min. They were pooled, washed once with an equal volume of sterile normal saline, resuspended in 50 ml of normal saline, and returned to the animal in equal portions after the next three blood samplings. Hematocrits were obtained on selected blood samples prior to centrifugation.

Urine was collected from the catheterized animal at approximately 20, 40, 60, 85, and 100 min; then every 50 min up to 500 min; then every 200 min through Day 1; then every 6 hr of Day 2; and then twice daily thereafter for 5–25 days. The volumes of each collection were measured. Urine pH was determined in selected instances, and an aliquot was removed to determine total carbon-14. A 2-ml aliquot of freshly collected urine was transferred to a 50-ml centrifuge tube, which was stoppered and frozen. The remaining urine (up to 50 ml) was stored frozen.

Bile was collected in glass tubes (containing 0.2–0.5 ml of cyclohexane) and pooled between the following times: 0, 1, 2, 3, 4, 8, 11, 14, 18, 22, 26, 30, 35, 40, 45, 50, 60, 70, 80, 110, 140, 170, 200, 250, 300, 350, and 400 min

[1] Teflon (du Pont).
[2] Amicon Corp., Lexington, Mass.
[3] Silastic, Dow Corning Corp., Midland, Mich.
[4] The Upjohn Co., Kalamazoo, Mich.
[5] N.B.C., Cleveland, Ohio.
[6] Amicon.

and thereafter as plasma samples were taken. The volumes of the pooled bile samples were recorded, and aliquots were obtained for extraction and determination of total carbon-14.

The pooled bile samples from Dog A were returned through the intestinal side of the biliary cannula during the next collection period. Pooled bile samples from Dog C were stored frozen.

Biliary Elimination and Enterohepatic Recirculation of Δ^9-Tetrahydrocannabinol and Its Metabolites—The collected bile fractions from Dog A were sampled prior to their intestinal return and analyzed for tetrahydrocannabinol and metabolites. Bile flow rates were determined at the start of each interval of bile flow collection, and the averages of the flow rates at the start and end of each interval were multiplied by the concentration of metabolites as equivalents of ^{14}C-Δ^9-tetrahydrocannabinol in bile and by the time of collection to obtain the total biliary excretion of metabolites in that interval. No bile was collected from Dog B. No enterohepatic recirculation would be possible with Dog C. The feces of Dog C between 0 and 24 hr were collected and analyzed for total carbon-14 to confirm complete collection of all bile.

Pharmacokinetics of ^{14}C-Labeled Metabolites—The 0–300-min bile from the 0.5-mg/kg study in Dog C was pooled, the volume was measured, and the solution was adjusted to pH 10.0–10.5 with 0.5 *M* Na_2CO_3 and extracted twice with an equal volume of heptane (containing 1.5% isopentyl alcohol), which removed approximately 2% of the radioactivity. The remaining bile solution was adjusted to pH 2.0, saturated with sodium chloride, and extracted twice with three equivalent volumes of tetrahydrofuran, which removed over 90% of the original radioactivity.

An aliquot (30 ml) of the metabolites extracted into tetrahydrofuran at pH 2 was reduced to dryness, reconstituted in 1 ml of ethanol, and diluted with 9 ml of normal saline. Two 0.1-ml aliquots were counted for total carbon-14, and 9.5 ml of the solution was administered intravenously to Dog C. Blood, bile, and urine collections were the same as described for tetrahydrocannabinol.

Effect of Isotope Placement on Pharmacokinetics and Metabolism of Δ^9-Tetrahydrocannabinol—Two types of ^{14}C-labeled Δ^9-tetrahydrocannabinol were available: C-11 labeled[7] and aromatic ring labeled[8]. Metabolism at C-11 could result in loss of the ^{14}C-label. This hypothesis was tested by conducting the 0.5-ml/kg study in Dog C with the ring-labeled tetrahydrocannabinol and the 2.0-mg/kg study in Dog C with C-11 labeled agent. The null hypothesis was that no difference in metabolism or distribution would result.

Effect of Altered Bile Flow on Pharmacokinetics of Δ^9-Tetrahydrocannabinol—After the 2.0-mg/kg injection of Δ^9-tetrahydrocannabinol in Dog C, 150 mg of taurocholic acid was rapidly infused (30 mg/min and 6 mg/ml in normal saline) at 400 min over 5 min in lieu of the normally infused 0.417 mg/min. Additional blood samples (1 ml) were taken at 410, 420, 430, 460, 530, and 560 min; additional bile samples were collected between 400, 410, 420, 430, 460, 480, 510, and 550 min. These samples were analyzed for total carbon-14 only. Oral taurocholic acid (150 mg four times a day) was reinstituted after 24 hr.

The taurocholic acid infusion was designed to increase bile flow sharply, which presumably would decline after cessation of infusion.

Analysis of Δ^9-Tetrahydrocannabinol in Biological Fluids—A 2-ml plasma sample was adjusted between pH 9.5 and 11.0, extracted, treated, and analyzed as described by Garrett and Hunt (9, 14). It was shown (14) that the electron-capture GLC analysis of the high-pressure liquid chromatographic (HPLC) collected tetrahydrocannabinol gave the same assay results as the liquid scintillation analysis of the separated tetrahydrocannabinol when both methods of analysis were conducted in Dog A on administration of 0.1 and 0.5 mg of Δ^9-tetrahydrocannabinol/kg iv. However, the sensitivity of the GLC analysis was approximately 1 ng/ml of plasma and that of the radiochemical analysis was 0.16 ng/ml. Since the former method only permitted plasma assays no more than 1000 min and the latter no more than 7000 min after the stated doses were administered (Table I), all other assays of plasma tetrahydrocannabinol in the remaining pharmacokinetic studies were obtained by the liquid scintillation analysis of the radiolabel after collection and separation of ^{14}C-tetrahydrocannabinol from plasma on the normal phase HPLC.

A 2-ml urine sample suspected of containing Δ^9-tetrahydrocannabinol was adjusted to pH 9.5–11 by addition of 0.2 ml of 0.5 *M* Na_2CO_3. A bile sample was diluted with distilled water to yield a 5–25% (v/v) solution. A 2-ml aliquot of this solution was adjusted to pH 9.5–11 by addition of 0.2 ml of 0.5 *M* Na_2CO_3. Subsequent steps for urine and bile were the same as described for the liquid scintillation analysis of tetrahydrocannabinol (14) in plasma.

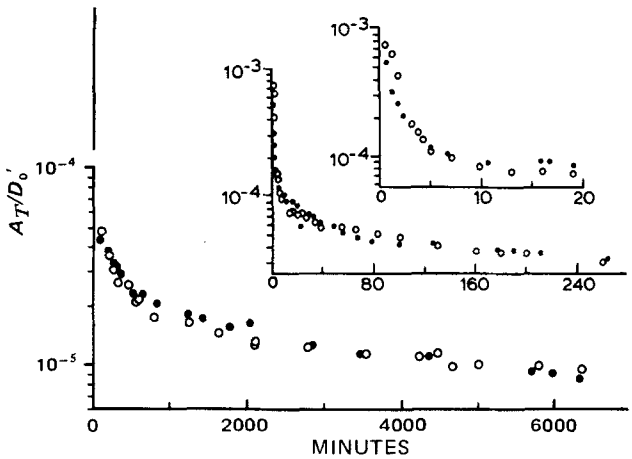

Figure 1—*Semilogarithmic plots of the fractions, A_T/D_0', of the total radioactive dose, D_0', per milliliter of plasma against time for the 2.0-mg/kg (●) (116.3 × 10^6 cpm) and 0.5-mg/kg (○) (76.22 × 10^6 cpm) doses of ^{14}C-Δ^9-tetrahydrocannabinol in Dog B. The activities per milliliter corresponding to $A_T/D_0' = 10^{-4}$ are 11,630 (●) and 7620 (○) cpm and correspond to 2880 and 635 ng/ml as Δ^9-tetrahydrocannabinol equivalents, respectively.*

Determination of Total Carbon-14 in Urine and Bile—An aliquot (0.2 or 0.4 ml) of freshly collected urine was transferred to a scintillation vial containing 0.1 ml of 0.1 *N* KOH. The sample was bleached to avoid quench by adding 0.2 ml of *tert*-butyl hydroperoxide[9]. The vial was tightly capped, placed in a water bath (50°), and reacted for 12–24 hr. Residual peroxide was hydrolyzed by the addition of 0.5 ml of water, and the capped vial was returned to the water bath for 1–3 hr. Six milliliters of scintillation solution was added to the vial, which was dark adapted for at least 6 hr before counting.

An aliquot of 0.05–0.2 ml of freshly collected bile was transferred to a vial containing 0.1 ml of 0.1 *N* KOH. Samples were bleached after addition of 0.1 ml of *tert*-butyl hydroperoxide/0.1 ml of bile. Subsequent manipulations were the same as for urine.

Samples with low counts (less than 400 cpm) were counted twice and averaged. This procedure resulted in negligible quench for 95% of all urine and bile samples.

Determination of Total Carbon-14 in Plasma—An aliquot of 0.05, 0.1, 0.2, or 0.5 ml of fresh plasma was transferred to a vial and 0.6, 0.5, 0.4, or 0.2 ml, respectively, of water was added. Six milliliters of scintillation solution was added to each, and the capped samples were dark adapted for at least 6 hr. Samples with low counts were counted twice and averaged. Selected plasma samples were checked for sedimentation error; if this error was observed, each sample was counted twice manually after vigorous shaking. Plasma samples showing evidence of hemolysis were treated as described for bile samples. This procedure resulted in negligible quench for all plasma samples.

Determination of Total Carbon-14 in Feces—The collected feces were transferred to a weighed sheet of aluminum foil, wrapped, weighed, and frozen. At the time of analysis, the frozen feces were transferred to a flask containing a measured volume of 15% ethanol in water. The volume of solvent was designed to give a 10–25% fecal suspension. The suspension was homogenized[10] for 15 min, and a 0.5-ml aliquot was transferred to a vial containing 0.2 ml of 0.5 *N* KOH and 0.5 ml of *tert*-butyl hydroperoxide. The vial was capped and placed in a water bath (50°) for 12–24 hr. One milliliter of water and 10 ml of scintillation solution were added, and the samples were dark adapted for at least 6 hr before counting. When an error due to sedimentation was suspected, each sample was manually counted twice after vigorous shaking. Quench corrections were required on all fecal samples.

Analysis of Metabolites in Plasma—The concentration of total metabolites in plasma, $[M_p]$, in terms of equivalents of Δ^9-tetrahydrocannabinol was calculated from:

$$[M_p] = (A_T/S) - C \qquad \text{(Eq. 1)}$$

[7] Sample DW-III-23, 68 μCi/mg, R.T.I., Research Triangle Park, N.C.
[8] Sample 3168-145-37, 38.7 μCi/mg, R.T.I., Research Triangle Park, N.C.
[9] Mallinckrodt Chemical Works, St. Louis, Mo.
[10] Polytron, Kinematica, Lucerne, Switzerland.

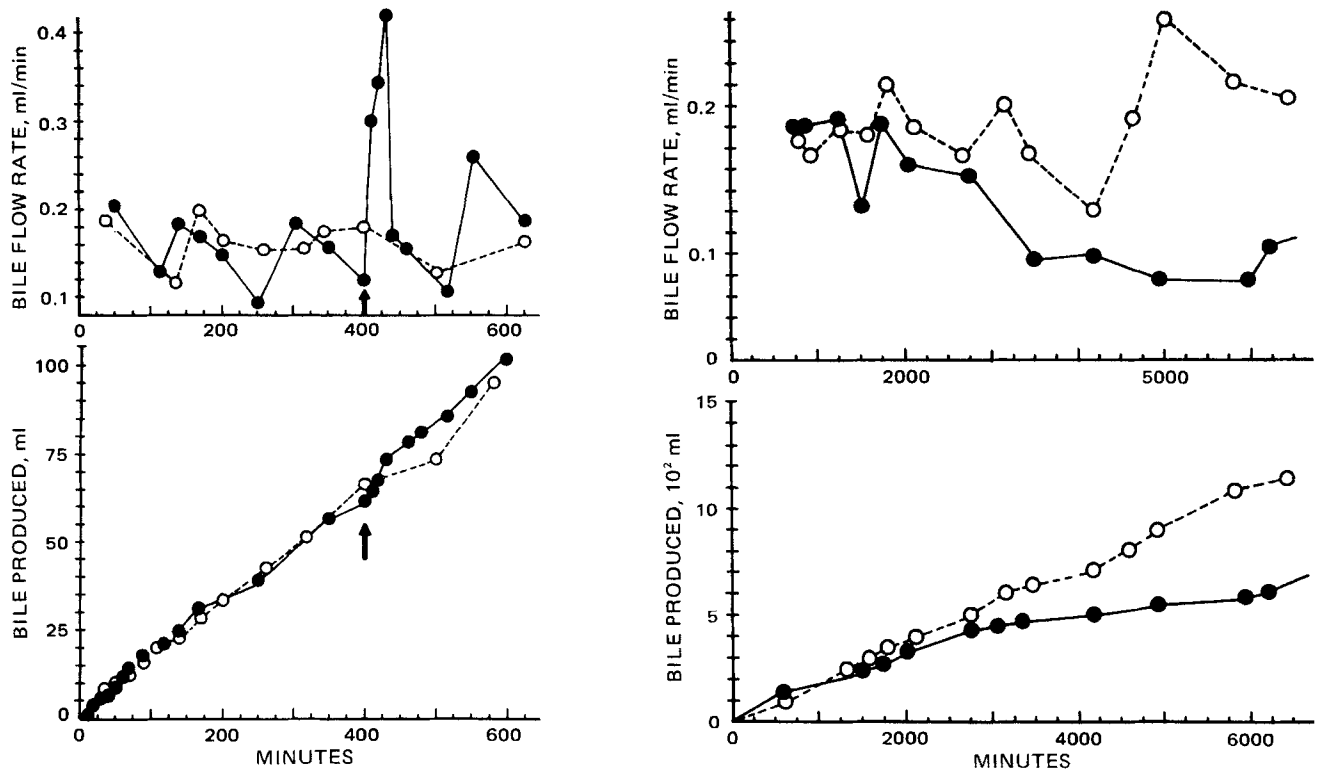

Figure 2—*Bile flow rates and cumulative volumes of bile produced with time after the 0.5- (○) and 2.0- (●) mg/kg iv doses of Δ^9-tetrahydrocannabinol in Dog C. The arrows indicate the time of increased infusion of taurocholic acid from 0.42 to 30 mg/min for 5 min.*

where A_T is the total radioactivity per milliliter of plasma, S is the activity of tetrahydrocannabinol in counts per minute per nanogram, and C is the experimentally observed plasma concentration of tetrahydrocannabinol. After extraction of plasma with heptane for determination of tetrahydrocannabinol and other heptane-extractable metabolites, the aqueous layer was adjusted to pH 2.0–2.3 by addition of 0.2–0.4 ml of a hydrochloric acid–acetic acid buffer [5.2 *N* HCl–1.0 *M* acetic acid–water (1:3:2)]. The final volume was either (*a*) adjusted to 3.0 ml by addition of 0.01 *M* acetic acid and then adding 15 ml of ethyl acetate or (*b*) prepared by adding 1 g of sodium chloride and 15 ml of tetrahydrofuran. The tube was stoppered, shaken for 15 min, and centrifuged.

In Case *a*, an aliquot (1–14 ml) of the organic layer was transferred to a scintillation vial and dried. The remaining organic layer was aspirated off, and 15 ml of tetrahydrofuran and 1 g of sodium chloride were added. This solution was shaken and centrifuged as before. An aliquot (1–14 ml) of the organic layer was transferred to a scintillation vial and dried. The contents of both vials were counted for total carbon-14 as described previously. In Case *b*, an aliquot (1–14 ml) of the organic layer was transferred to a scintillation vial, dried, and counted as described previously.

The concentration of metabolites in plasma in terms of tetrahydrocannabinol equivalents, extracted into heptane at pH 10.5, $[M_h]$, was calculated from:

$$[M_h] = (A_h/F_1S) - C \qquad \text{(Eq. 2)}$$

where A_h is the activity extracted per milliliter of plasma, F_1 is the extraction efficiency of tetrahydrocannabinol (14), S is the specific activity of the dose, and C is the concentration of tetrahydrocannabinol in plasma. The calculation assumed that the metabolites extractable into heptane had extraction efficiencies equivalent to tetrahydrocannabinol. The plasma concentration of metabolites extracted into ethyl acetate, $[M_{ea}]$, or tetrahydrofuran, $[M_{thf}]$, under acid conditions following a heptane extraction was calculated from:

$$[M_{ea}] = \frac{A_{ea} - A_h/(1 - F_1)}{S} \qquad \text{(Eq. 3)}$$

and:

$$[M_{thf}] = \frac{A_{thf} - A_h/(1 - F_1)}{S} \qquad \text{(Eq. 4)}$$

where A_{ea} and A_{thf} are the activities of the extracts per milliliter of plasma and are corrected for the unextracted heptane-extractable metabolites; *i.e.*, $A_h/(1 - F_1)$.

RESULTS AND DISCUSSION

Time Course of Total Radioactivity in Plasma—Semilogarithmic plots of the total radioactivity in plasma as A_T/D_0', where A_T is the total activity per milliliter of plasma and D_0' is the activity of the dose, are given in Fig. 1 for typical studies at two dose levels of ^{14}C-Δ^9-tetrahydrocannabinol for Dog B (Table I). The data plotted in this manner from the different doses were superimposable for the high and low doses in Dogs A and B, demonstrating no significant dose dependency. Differences in bile flow (Fig. 2) may have been responsible for the greater discrepancy between plasma levels for the two doses given to Dog C (Fig. 3).

An extended study of plasma levels of total carbon-14 was conducted in Dog C for 23 days at 2.0 mg/kg (Fig. 4). The data after 2000 min were

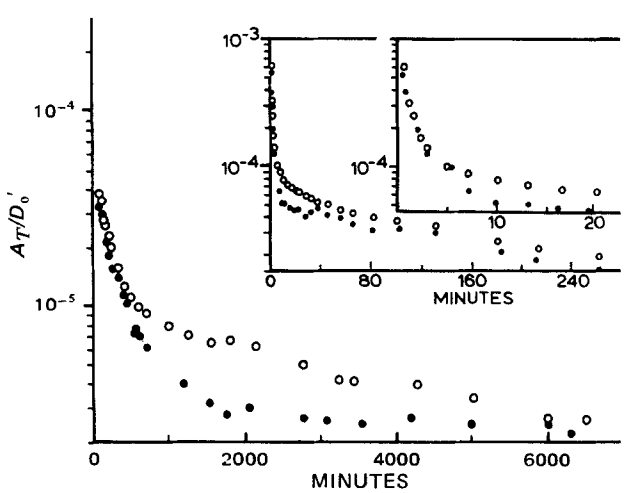

Figure 3—*Semilogarithmic plots of the fractions, A_T/D_0', of the total radioactive dose, D_0', per milliliter of plasma against time for the 2.0-mg/kg (●) (150.8 × 10^6 cpm) and 0.5-mg/kg (○) (229.4 × 10^6 cpm) doses of ^{14}C-Δ^9-tetrahydrocannabinol in Dog C. The activities per milliliter corresponding to $A_T/D_0' = 10^{-4}$ are 15,080 (●) and 22,940 (○) cpm and correspond to 3320 and 665 ng/ml as Δ^9-tetrahydrocannabinol equivalents, respectively.*

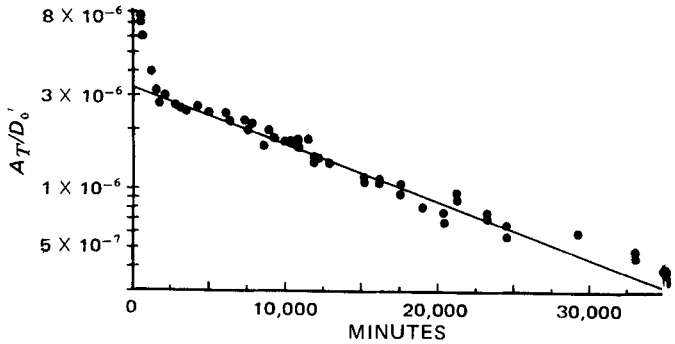

Figure 4—*Semilogarithmic plot of the fraction A_T/D_0' of the total radioactive dose, D_0', per milliliter of plasma against an extended time of study for the 2.0-mg/kg dose of Δ^9-tetrahydrocannabinol in Dog C. The apparent rate constant, k_5, obtained by least-squares regression was 6.74×10^{-5} min^{-1}.*

consistent with a single exponential of 171.4 hr half-life ($k_i = 6.7 \times 10^{-5}$ min). It was presumed that the terminal half-life for each study would be similar.

The variability of the data prior to 300 min was no different among dogs than within dogs. After 300 min, the total activity in plasma for both doses in Dog C (Fig. 3) dropped significantly below the levels in Dogs A and B (Fig. 1). The collection of total bile from Dog C (Table I), preventing any enterohepatic circulation of metabolites, could explain this difference.

Excretion of Total Radioactivity in Urine and Bile—No significant amount (<0.01%) of tetrahydrocannabinol was in the urine or bile on analysis of the HPLC collection (14). The total radioactivity as the percentage of dose recovered in urine was plotted against time (Fig. 5) and ranged from 14.7 to 16.6% at 7000 min for Dogs A and B.

The excretion rate of total radiolabeled metabolites in bile, dB_T/dt, in Dog C, where all bile was collected and bile flow was maintained by intravenous or oral solutions of taurocholic acid, was proportional to the radioactivity concentration in bile, $[B_T]$, and both values peaked between 25 and 45 min after drug administration. The concentrations of metabolites in bile were approximately 500 times the concentrations of total activity in plasma at this time and subsequently decreased to less than 50% of the plasma concentration at $t \geq 2500$ min.

Linear plots of the bile flow rates and the cumulative volume of bile produced as a function of time are given in Fig. 2 for the high and low dose studies in Dog C.

The percent of the dose recovered in bile for both doses in Dogs C (all bile collected) and A (bile sampled) was approximately 50% after 1 day or 1400 min (Fig. 5). Thereafter, only 5% of the dose was recovered.

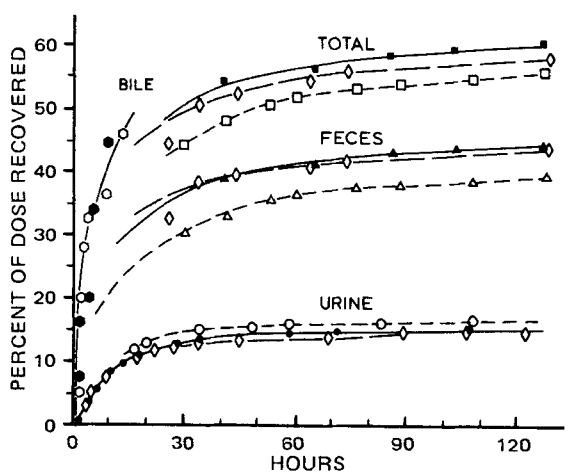

Figure 5—*Linear plots of the percent of dose recovered in urine and feces against time for the two intravenous doses in Dogs A and B. Key: Dog B urine, 0.5 (●) and 2.0 (○) mg/kg; Dog B feces, 0.5 (△) and 2.0 (▲) mg/kg; Dog B total (urine plus feces), 0.5 (□) and 2.0 (■) mg/kg; Dog A urine, feces, and total, 0.1-mg/kg dose (◇). The percent of dose excreted in the sampled bile of Dog A, corrected for the "dead" time of the cannula, is given as ○ for the 0.1-mg/kg dose and as ● for the 2.0-mg/kg dose. The percent of dose was calculated from [Δt × bile flow rate (mg/min) × 100]/dose, where Δt is the time of collection.*

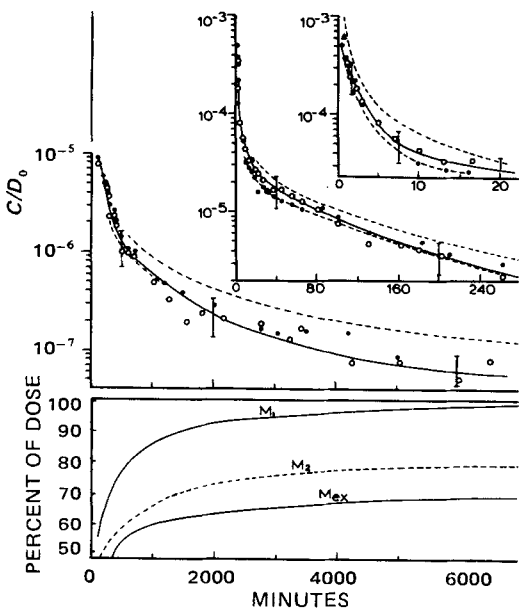

Figure 6—*Semilogarithmic plots of the plasma levels of Δ^9-tetrahydrocannabinol as C/D_0 against time for the 0.5- (○) and 2.0- (●) mg/kg iv doses to Dog C. The solid curve gives the calculated values for C/D_0, $\hat{Y}$, for the five-exponential fit of the 0.5-mg/kg data, and the vertical bars are the range for ±2 SD of the weighted residuals (Table II). The dashed lines represent the range for the maximum and minimum of all $\hat{Y}$ values calculated. The concentrations of Δ^9-tetrahydrocannabinol in plasma corresponding to the fraction $C/D_0 = 10^{-4}$ are 665 (○) and 3320 (●) ng/ml. Curves M_1 and M_2 were calculated from Eq. 14 using the $\hat{Y}$ expressions of Eqs. 5 and 6, respectively, and represent the total metabolite in percent of dose formed with time, where M_{ex} is the experimentally determined metabolite in percent of dose excreted in both urine and bile.*

During this time, the biliary excretion rate decreased asymptotically to approximately 0.72%/week.

The rates of excretion of total metabolites per unit dose and their concentrations in bile were similar for both Dogs A and C. The consistency in the percent of radiolabeled dose recovered in bile for both doses in Dogs A (Fig. 5) and C demonstrated no significant dose dependency. The percentage recovered in feces ranged from 39.5 to 44.5% over 130 hr for Dogs A and B, whereas the percentage recovered in bile (Dog A) was always consistently higher at any given time (Fig. 5). When all bile was collected, as for Dog C, approximately 55% of the radioactive dose was excreted therein for the same time period. No radioactivity was found in feces when all bile was collected.

Since the percent of the dose recovered in urine was essentially the same for $t > 1000$ min between doses and among dogs, the 10–15% excess recovered in bile compared to feces can be attributed to the enterohepatic circulation of 15% of the biliary excreted metabolites.

Pharmacokinetics of Intravenously Administered Δ^9-Tetrahydrocannabinol—There may not be a unique linear sum of time exponentials, $\hat{Y}$, that best fits the actual data, $Y = C/D_0$, where C is the concentration per milliliter of Δ^9-tetrahydrocannabinol in plasma, and D_0 is the dose; instead, there may be several. A unique solution could only be obtained if the drug transferred into other compartments or transformed into metabolites was analyzed with time in its respective compartments. For example, the plasma data for Dog C at the dose of 0.5 mg of Δ^9-tetrahydrocannabinol/kg where the fraction of the dose per milliliter of plasma is plotted against time (Fig. 6) could be fitted by the method of residuals (15) to:

$$\hat{Y}_1 = \hat{C}/D_0 = 6.80 \times 10^{-4}e^{-1.01t} + 1.25 \times 10^{-4}e^{-0.202t} + 2.30 \times 10^{-5}e^{-0.0206t} + 7.65 \times 10^{-6}e^{-4.36\times10^{-3}t} + 5.30 \times 10^{-7}e^{-3.87\times10^{-4}t} \quad \text{(Eq. 5)}$$

or to:

$$\hat{Y}_2 = \hat{C}/D_0 = 5.02 \times 10^{-4}e^{-0.587t} + 4.25 \times 10^{-5}e^{-0.0877t} + 2.15 \times 10^{-5}e^{-1.16\times10^{-2}t} + 1.88 \times 10^{-6}e^{-1.28\times10^{-3}t} + 9.50 \times 10^{-8}e^{-4.98\times10^{-5}t} \quad \text{(Eq. 6)}$$

Table II—Parameters of the Best Fit Sum-of-Exponentials, $\hat{Y} = \sum_{i=1}^{5} A_i e^{-k_i t}$, Describing the Fraction of the Dose of Δ^9-Tetrahydrocannabinol per Milliliter of Plasma against Time in Minutes

Parameter[a]	Dog A		Dog B		Dog C		Mean[b]	Apparent $t_{1/2}$, min
	0.1 mg/kg	2.0 mg/kg	0.5 mg/kg	2.0 mg/kg	0.5 mg/kg	2.0 mg/kg		
$10^4 A_1$	6.40	5.40	13.7	8.0	5.02	6.70	7.54 (1.31)	—
$10^5 A_2$	7.45	3.93	11.3	14.0	4.25	3.80	7.46 (1.77)	—
$10^5 A_3$	2.10	1.30	2.70	2.35	2.15	1.50	2.02 (0.21)	—
$10^6 A_4$	1.48	2.06	1.90	2.05	1.88	2.45	1.97 (0.13)	—
$10^7 A_5$	1.92	1.92	2.70	1.95	0.95	1.15	1.77 (0.26)	—
$10\ k_1$	9.21	4.35	9.82	10.42	5.87	7.03	7.78 (0.99)	0.90 min
$10\ k_2$	1.26	0.37	1.43	1.31	0.88	0.90	1.03 (0.16)	6.8 min
$10^2 k_3$	1.09	0.70	1.16	1.01	1.16	0.93	1.01 (0.07)	1.15 hr
$10^3 k_4$	1.18	1.54	1.17	1.26	1.28	1.27	1.28 (0.05)	9.0 hr
$10^5 k_5$	5.0	5.0	6.80	6.60	4.98	6.74	5.85 (0.39)	197 hr
$10^2 \bar{\epsilon}$, mean of residuals[c]	0.96	0.40	−1.3	0.17	−0.16	2.1	—	—
$2s$[d]	0.273	0.191	0.284	0.162	0.363	0.289	—	—

[a] The A_i values are in fraction of dose per milliliter of plasma; k_i are in minutes^{-1}. [b] The parenthetical values are standard errors of the mean. [c] The average values of the weighted residuals, $\epsilon = (Y - \hat{Y})/\hat{Y}$, where $\hat{Y}$ is the predicted value and Y is the experimental, none of which is significantly statistically different than zero. [d] Twice the standard deviation of the weighted residuals.

where time, t, is in minutes. The terminal data of the 7000-min span in Fig. 6 were approximated by the best straight line for estimation of the parameters of the last exponential in Eq. 5. The parameters for the last exponential in Eq. 6 were based on the assumption that the terminal slope was close to the rate constant characteristic of the rate of decline of the total radioactivity in the plasma up to 35,000 min (Fig. 5).

The validities of both Eqs. 5 and 6 were confirmed by the demonstration that a plot of the weighted residuals:

$$\epsilon = \frac{Y - \hat{Y}_i}{\hat{Y}_i} \qquad \text{(Eq. 7)}$$

for both $\hat{Y}_1$ and $\hat{Y}_2$ against log Y = log C/D_0 gave a calculated mean, $\bar{\epsilon}$, of zero and where the standard deviations of their ϵ values were practically the same, *i.e.*, 0.13 for Eq. 5 and 0.12 for Eq. 6 (16).

The decision that a linear sum of five exponentials was necessary to fit the plasma tetrahydrocannabinol data for all studies was based on the fact that, when a linear sum of four or less exponentials was used, the plot of the weighted residuals (Eq. 8) against log C/D_0 demonstrated biases above and below the line of the mean of the n weighted residuals:

$$\bar{\epsilon} = \sum_{i=1}^{n} \left[\frac{(Y - \hat{Y})_i}{\hat{Y}_i} \right] \Big/ n \qquad \text{(Eq. 8)}$$

which were not statistically significant from zero (Table II). In the particular case of the data of Fig. 6, the standard deviation for a best fit of a linear sum of four exponentials was higher, *i.e.*, 0.21, than for five. The best fitting to a linear sum of six exponentials was similar to the sum of five and did not show significant nonrandom scatter about $\bar{\epsilon} \sim 0$, but the standard deviation (0.15) was not significantly improved.

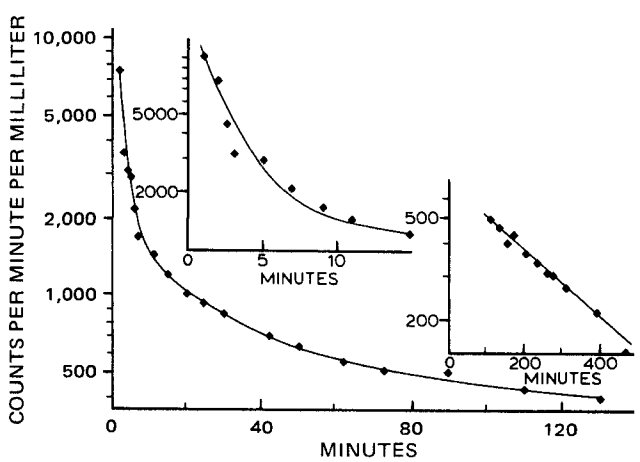

Figure 7—*Semilogarithmic plot of the activity (counts per minute) per milliliter of plasma against time for the intravenous administration of biliary Δ^9-tetrahydrocannabinol metabolites to Dog C. The inserts are for expanded and extended time scales. The curves through the data are given by* $\hat{Y}_m = \sum_{i=1}^{3} A_i e^{-k_i t}$, *where* $A_1 = 15{,}013$, $A_2 = 1330$, *and* $A_3 = 584$ *cpm/ml and* $k_1 = 0.542$, $k_2 = 0.0477$, *and* $k_3 = 3.005 \times 10^{-3}$ *min*$^{-1}$.

When the fraction of the dose per milliliter of plasma as tetrahydrocannabinol or its logarithm (Fig. 6) was plotted against time for widely variant doses, the curves were superimposable, indicative of no dose dependency.

Pharmacokinetics of Intravenously Administered Biliary Metabolites of Δ^9-Tetrahydrocannabinol—The plasma levels of the intravenously administered radiolabeled metabolites were adequately described in Dog C by a sum of three exponentials (Fig. 7). These metabolites were those collected in the bile for 300 min after ^{14}C-Δ^9-tetrahydrocannabinol administration, and 98% of the collected radioactivity was retained after heptane extraction at pH 10 to remove highly lipid-soluble components. The metabolites administered were those extracted from the aqueous bile by tetrahydrofuran. This extract contained over 90% of the original radioactivity. The calculated terminal half-life for these metabolites in plasma was 230 min. At 500 min, a total of 90.7% of the administered dose was eliminated in bile and urine (Fig. 8). Ninety-six percent of the administered dose was eliminated by 24 hr, with the majority (73%) eliminated in bile. The final ratio of metabolites eliminated in bile to that in urine, 2.4, was slightly lower than the ratio, 3.2, for *in vivo* produced metabolites.

Evidence that Rates of Terminal Decline of Total Plasma Radioactivity Estimates Rates of Terminal Decay of Plasma Tetrahydrocannabinol Concentration and that the Ultimate Rate-Determining Step for Elimination is Return from Deep Tissues—Since no dose-dependent pharmacokinetics for tetrahydrocannabinol or its metabolites were observed, it can be postulated that the metabolism was first order and dependent only on the estimated concentration, $\hat{C}$, of tetrahydrocannabinol in the central compartment or:

$$dM/dt = k_m V_c \hat{C} \qquad \text{(Eq. 9)}$$

where $k_m V_c$ is the metabolic clearance. Thus:

$$M = \int_0^M dM = k_m V_c \int_0^t \hat{C}\, dt \qquad \text{(Eq. 10)}$$

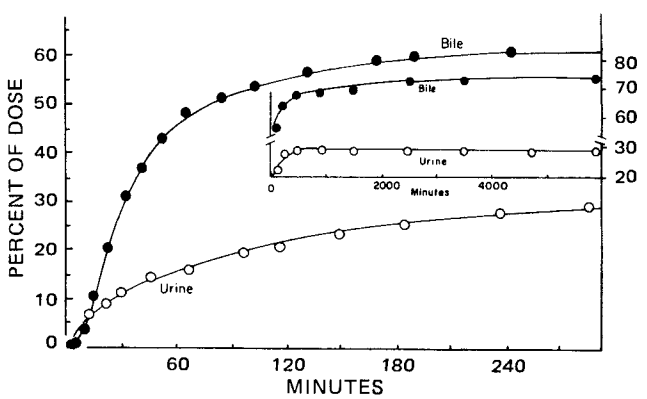

Figure 8—*Linear plots of the percent of the radioactivity recovered in bile (●) and urine (○) against time for the intravenous administration of biliary Δ^9-tetrahydrocannabinol metabolites to Dog C.*

Table III—Apparent Volumes of Distribution, Clearances, and First-Order Metabolic Rate Constants for Δ⁹-Tetrahydrocannabinol

Parameter	Dog A		Dog B		Dog C		
	0.1 mg/kg	2.0 mg/kg	0.5 mg/kg	2.0 mg/kg	0.5 mg/kg	2.0 mg/kg	Mean (*SEM*)
$10^4 C_0/D_0$[a]	7.37	5.95	15.1	9.66	5.68	7.26	8.50 (1.44)
V_c[b], liters	1.36	1.68	0.66	1.04	1.76	1.38	1.31 (0.17)
Cl_p[c], ml/min	120.4	106.9	98.9	114.3	152.2	151.0	124.0 (9.2)
$10^2 k_m$[d], min^{-1}	8.87	6.36	14.96	11.0	8.64	10.96	10.13 (1.19)
V_{ss}[e], liters	0.77	0.95	0.90	0.90	0.811	1.05	0.90 (0.04)
$Cl_p{}^{uf}$, ml/min	4013	3563	3297	3810	5073	5033	4131 (307)
$V_{p_{ss}}$[g], liters	2405	2136	1454	1732	3055	2239	2170 (227)

[a] The fractions of the dose of tetrahydrocannabinol per milliliter of plasma at time zero estimated from $\hat{Y} = \Sigma_{i=1}^{5} A_i e^{-k_i t}$ for $t = 0$, where the A_i and k_i parameters are given in Table II. [b] Apparent volume of distribution of the central compartment referenced to total drug concentration in plasma, $D_0/10^3\ C_0$. [c] Clearance referenced to total concentration in plasma, calculated from Eq. 14 where the parameters of Y are given in Table II. [d] The rate constant with respect to total concentration in plasma calculated from $Cl_p/10^3\ V_c$. [e] The volume of plasma in the dog calculated from $(1 - H)\ V_{B,\text{true}}$, where $V_{B,\text{true}}$ = dog weight in kilograms × 100 ml/kg (18), and H is the hematocrit (Table I). [f] Clearance referenced to unbound drug in plasma, calculated from $Cl^u = Cl_p/f_u$, where f_u is the fraction of the unbound drug in plasma and is 0.03 (13). [g] The apparent volume of distribution referenced to total plasma concentration in the ultimate pseudo-steady state of tetrahydrocannabinol elimination from the body calculated from $10^{-3}\ Cl_p/k_5$, where k_5 is given in Table II.

where M is the amount of metabolite(s) produced in the first metabolic step from tetrahydrocannabinol, k_m is the first-order metabolic rate constant, and $V_c = D_0/C_0$ (Table III) is the apparent volume of distribution of the central compartment for tetrahydrocannabinol of dose D_0. The $\hat{C}_0$ is the estimated concentration of tetrahydrocannabinol in plasma at $t = 0$ and can be calculated from Eq. 5 or 6 with $t = 0$.

Substitution of Eq. 5 or 6 into Eq. 10 gives:

$$M = k_m V_c D_0 \int_0^t \hat{Y}\, dt \qquad \text{(Eq. 11)}$$

At $t = \infty$, $M = M_\infty = D_0$, since tetrahydrocannabinol was not excreted unchanged but was transformed to metabolites. Thus, the apparent metabolic rate constant is:

$$k_m = 1/V_c \int_0^\infty \hat{Y}\, dt \qquad \text{(Eq. 12)}$$

Substitution of Eq. 12 into Eq. 11 yields:

$$M = D_0 \frac{\int_0^t \hat{Y}\, dt}{\int_0^\infty \hat{Y}\, dt} = D_0 A_t / A_\infty \qquad \text{(Eq. 13)}$$

and the total metabolites, both excreted and unexcreted, produced at time t can be calculated from the pertinent fit, $\hat{Y}$, of the plasma tetrahydrocannabinol data against time or from the ratio of the area under the *C versus t* plot at time t, A_t, to the total area, A_∞. The values calculated for total metabolites with time, M_1 and M_2, as the percent of dose from the $\hat{Y}_1$ and $\hat{Y}_2$ obtained with Eqs. 5 and 6, respectively, are plotted in Fig. 6 against time. For comparative purposes, the experimentally determined total amount of radiolabeled drug, M_{ex}, excreted into bile and urine as the percent of dose is also plotted against time for 0.5 mg/kg. At 7000 min, the total amounts of metabolites excreted by Dog C (Table IV), M_{ex}, comprised 68% of the dose, whereas the calculated amounts of metabolites formed, M_1 and M_2, were 98 and 79%, respectively (Fig. 8).

If the M_1 values, and thus the parameters of Eq. 5 with an apparent terminal half-life of 30 hr, were accepted as valid for tetrahydrocannabinol administration, it must be concluded that tetrahydrocannabinol metabolism was virtually concluded at 7000 min, that 98 − 68% = 30% of the formed metabolites was still in the body, and that this large amount of metabolites was very slowly eliminated well after 7000 min (Fig. 4) with an apparent half-life of 171 hr. The result implies that these metabolites are highly sequestered in, and/or bound to, body tissues so that they have extremely large apparent volumes of distribution. However, these hypotheses are inconsistent with the fact (Fig. 8) that 90.7% of intravenously administered biliary metabolites was eliminated in both bile and urine within 500 min of administration, with 96% eliminated by 1500 min. Also, the terminal plasma half-life of administered radiolabeled metabolites of 230 min (Fig. 7) supports the hypothesis that the rate-determining step for metabolite elimination on Δ⁹-tetrahydrocannabinol administration is not the elimination of such metabolites.

The estimate of M_2 from Eq. 13 as the amount of total metabolites formed at any time is greater than M_1, since M_2 was obtained from the $\hat{Y}_2$ of Eq. 6 where the terminal slope was smaller and the plotted area, A_∞, was greater than would be obtained in Eq. 13 from the M_1 calculated from the $\hat{Y}_1$ of Eq. 5. This M_2 is more consistent than M_1 with the fraction of the dose excreted as metabolites, M_{ex} (Fig. 6). It follows that the ob-

Table IV—Percent Disposition of Δ⁹-Tetrahydrocannabinol at 7000 min after Intravenous Administration

	Dog A		Dog B		Dog C[a]	
	0.1 mg/kg	2.0 mg/kg[b]	0.5 mg/kg	2.0 mg/kg	0.5 mg/kg	2.0 mg/kg
Δ⁹-Tetrahydrocannabinol in central compartment[c]	0.018	0.023	0.011	0.013	0.012	0.010
Δ⁹-Tetrahydrocannabinol in tissues[d]	29.2	29.0	24.4	21.3	20.4	16.1
Metabolized[e]	70.8	71.0	75.6	78.7	79.6	83.9
Excreted metabolites[f]	57.1	—	56.0	59.5	68.4	71.5
Metabolites in body[g]	13.7	—	19.6	19.2	11.2	12.4

[a] All bile was collected, and enterohepatic circulation was not possible. [b] Study terminated at 1300 min; all values given are extrapolated values, and no feces were collected. [c] $10^5 \times V_c \hat{Y}$, where $\hat{Y} = \Sigma_{i=1}^{5} A_i e^{-k_i t}$ in fraction of dose per milliliter of plasma, and the A_i and k_i parameters of Table II were used. The V_c values in liters are listed in Table III. [d] $10^2\ T/D_0$, where T is the amount of the dose, D_0, not in the central compartment, $V_c C$, or transformed to metabolite, M; *i.e.*, $D_0 - V_c C - M$, where $V_c C = 10^2\ V_c \hat{Y} D_0$. [e] The percent metabolized is $10^2\ M/D_0$, where M was obtained from Eq. 13, $M = D_0 \int_0^t \hat{Y}\, dt / \int_0^\infty Y\, dt$. [f] Percent of dose excreted in urine plus bile (Dog C) or feces (Dogs A and B). [g] Difference of above two values.

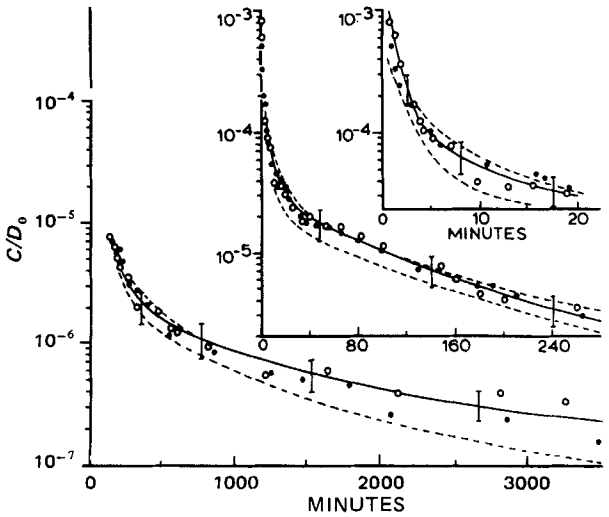

Figure 9—*Semilogarithmic plots of the plasma Δ^9-tetrahydrocannabinol levels as C/D_0 against time for the 0.5- (○) and 2.0- (●) mg/kg iv doses to Dog B. The solid curve gives the calculated values for C/D_0, $\hat{Y}$, for the five-exponential fit of the 0.5-mg/kg data, and the vertical bars are the range for ±2 SD of the weighted residuals (Table II). The dashed lines represent the range for the maximum and minimum of all $\hat{Y}$ values calculated. The concentrations of Δ^9-tetrahydrocannabinol in plasma corresponding to the fraction $C/D_0 = 10^{-4}$ are 635 (○) and 2880 (●) ng/ml.*

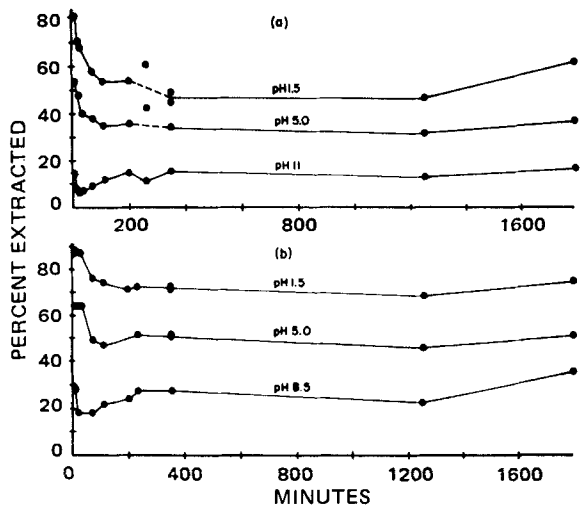

Figure 10—*Percent of biliary metabolites in a given sample that were extracted into benzene (a) or ethyl acetate (b) at selected pH values plotted against time after the administration of 0.5 mg of Δ^9-tetrahydrocannabinol/kg iv to Dog C.*

served rate of terminal loss of plasma total radioactivity from 2000 to 35,000 min (Fig. 4) is consistent with the terminal loss of Δ^9-tetrahydrocannabinol in the plasma as characterized by the last exponential in Eq. 6, which cannot normally be observed since the available analytical sensitivity did not permit assay of plasma tetrahydrocannabinol for more than 5000–6000 min after administration of the given doses.

This terminal rate of the 171.4-hr half-life (Fig. 4) for the loss of total radioactivity provided initial estimates of the terminal half-life and the derived k_5 values for the plasma Δ^9-tetrahydrocannabinol data in each dog. The determined parameters for the linear sum of five exponentials used to fit the assayed plasma levels of Δ^9-tetrahydrocannabinol with time (Figs. 6 and 9) are given in Table II and are considered as the most appropriate parameters. An expression for $\hat{Y}$ using the mean values of the parameters obtained for all studies reasonably fit all plasma–time data for tetrahydrocannabinol. The data from each study lay within ±2 *SD* of the resultant common equation (Figs. 6 and 9).

The consistency of these terminal rates of plasma total radioactivity and Δ^9-tetrahydrocannabinol decay indicates a typical "flip-flop" (17), where the rate-determining step in plasma decay of both tetrahydrocannabinol and its formed metabolites is the slow return of the tetrahydrocannabinol in the tissues to the central compartment where it can be metabolized (Eq. 9). A logical consequence of this assertion is that the composition of the metabolites would remain constant and in pseudo-steady-state equilibrium when the rate-determining step is return of tetrahydrocannabinol from the tissues since metabolism is a relatively fast process. This was confirmed (Fig. 10) by the reasonable constancy of the percent of biliary metabolites extracted into benzene and ethyl acetate after 100–200 min. The similarity of data for the low and high doses of Δ^9-tetrahydrocannabinol confirmed the lack of dose dependency. Similarly, the percent of urinary metabolites extracted into various solvents at selected pH values did not significantly vary with time (Fig. 11), and the pseudo-steady state exemplified by these studies was reached prior to the collection of the 50–73-min urine.

The plasma levels of metabolites, $[M_p]$, in terms of tetrahydrocannabinol equivalents were calculated from Eq. 1. The fact that the ratio of plasma levels of total metabolites, M_p, to Δ^9-tetrahydrocannabinol, C, were constant after 3000 min subsequent to drug administration provided further evidence that the return of tetrahydrocannabinol from tissues was the rate-determining step for metabolism and subsequent elimination of metabolites.

Clearance and Apparent Volume of Distribution of Δ^9-Tetrahydrocannabinol—Tetrahydrocannabinol was cleared from the body solely by metabolism. This clearance, Cl_p, referenced to total plasma concentration is a product of the metabolic microscopic rate constant, k_m, and the apparent volume of distribution of the central compartment, V_c, and can be obtained from a rearrangement of Eq. 12 to:

$$Cl_p = k_m V_c = 1 \Big/ \int_0^\infty \hat{Y}\, dt \qquad \text{(Eq. 14)}$$

where the values of $\hat{Y}$ can be obtained from the linear sum of five exponentials using the parameters of Table II.

The average metabolic clearance, Cl_p, for all six studies was 124 ± 22.6 ml/min (Table III). The calculated hepatic blood flow for these dogs ranged from 372 to 747 ml/min, 30–45 ml/min/kg (18). Multiplication of the hepatic blood flow by $(I - \overline{H})$, where $\overline{H} = 0.363$ was the mean hematocrit (Table I), gave a range for hepatic plasma flows of 237–476 ml/min and was approximately twice the metabolic clearance of both bound and unbound drug in plasma. Thus, Δ^9-tetrahydrocannabinol was not completely cleared in a single pass through the liver as previously reported (10). If only the unbound drug were cleared, then the mean clearance referenced to unbound drug, $Cl_p{}^u = Cl_p/f^u$ (Table III), would be 4132 ± 753 ml/min, an order of magnitude greater than hepatic plasma flow, where $f^u = 0.03$ (13), the fraction of unbound drug in plasma. Since the liver is the primary metabolizing organ (19), an apparent substantial fraction of the bound drug was cleared in a single pass through the liver.

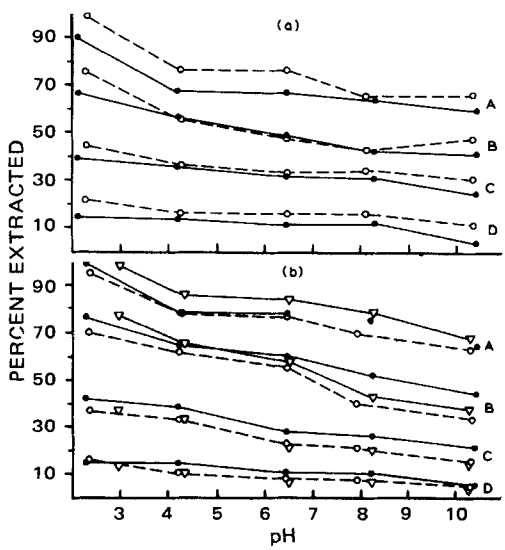

Figure 11—*Plots of the percent of urinary metabolites extracted into various solvents as a function of pH. Aliquots of the urine from the 2.0-mg Δ^9-tetrahydrocannabinol/kg study in Dog B were adjusted to the indicated pH and extracted with tetrahydrofuran (A), ethyl acetate (B), heptane containing 1% butanol (C), or heptane containing 1.5% isopentyl alcohol (D). Urine collection intervals in (a) were 50–73 (○) and 133–195 (●) min; in (b), they were 325–381 (●), 646–855 (○), and 1244–1474 (▽) min.*

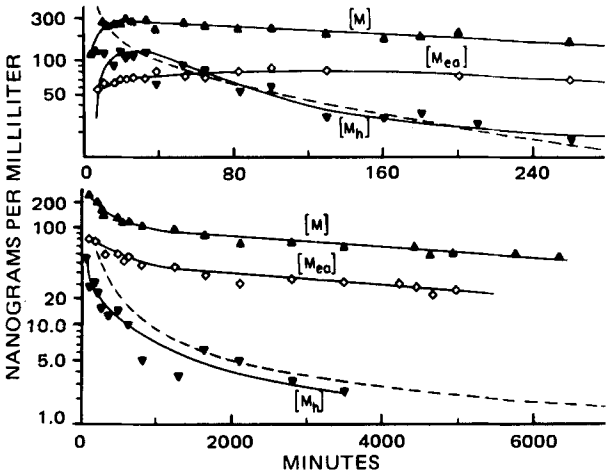

Figure 12—*Semilogarithmic plots of Δ^9-tetrahydrocannabinol metabolites in plasma against time for the 0.5-mg/kg iv dose of Δ^9-tetrahydrocannabinol in Dog B. The concentration of total metabolites in plasma [M] (▲), as nanograms per milliliter equivalents of Δ^9-tetrahydrocannabinol, was calculated from Eq. 1. The concentration of heptane-extractable metabolites (at pH 10.5) in plasma, [M_h] (▽), as nanograms per milliliter equivalents of Δ^9-tetrahydrocannabinol, is given by Eq. 2. The concentration of ethyl acetate-extractable metabolites (at pH 2.5; 5 ml of solvent/ml of plasma) in plasma, [M_{ea}] (◇), as nanograms per milliliter equivalents is given by Eq. 3. The best fit values for $C/D_0\hat{Y}$ (Table II), are given as concentration of Δ^9-tetrahydrocannabinol per milliliter of plasma in the dashed curve.*

The transit time of plasma in the liver may be sufficient for a series of reequilibrations between bound and unbound drug, with only the latter being actually metabolized.

The apparent first-order metabolic rate constants, k_m (Table III), calculated from the metabolic clearances (Eq. 14) ranged from 0.0636 to 0.1446 min^{-1} and were consistent with rapid metabolism ($t_{1/2}$ values from 4.8 to 10.9 min).

The high plasma protein binding (97%) and comparatively lower red blood cell partitioning (13) from plasma of Δ^9-tetrahydrocannabinol require that the expected apparent volume of distribution of the central compartment referenced to total plasma Δ^9-tetrahydrocannabinol concentration should be close to the plasma volume. Consistent with this premise, the apparent volumes of distribution, V_c, ranged from 0.66 to 1.76 liters, close to those of the calculated plasma volumes, V_p, which ranged from 0.77 to 1.05 liters (Table III).

Unfortunately, it is difficult to estimate accurately the apparent volume of distribution of the central compartment referenced to unbound drug in plasma when a drug such as Δ^9-tetrahydrocannabinol is highly bound, *i.e.*, 97%. The equation (20) for the estimation of this volume depends on the fraction unbound, the apparent volume of distribution, and the true volume, V_p, of the plasma. When the latter two are similar, as in the present case, and literature values of V_p are used, large errors in such estimates are inevitable.

The apparent volume of distribution ($V_{p_{ss}}$ in Table III) of the pseudo-equilibrated fluids in the final pseudo-steady state of drug elimination referenced to the total drug concentration in plasma can be obtained from the quotient of the metabolic clearance, Cl_p (Table III), and the terminal apparent first-order rate constant of metabolism, k_5 (Table II). The value of $V_{p_{ss}}$ ranged from 1500 to 3000 liters. This apparent volume of distribution would be much higher (20) if it could be referenced to the unbound concentration in plasma. The high degree of sequestration and distribution of Δ^9-tetrahydrocannabinol in body tissues is apparent from the fact that dog weights ranged only from 12 to 17 kg.

Time Course of Plasma Levels of Total and Extractable Metabolites—Typical plasma levels of total metabolites, [M_p], were calculated from Eq. 1 for the six studies (Table I) where Δ^9-tetrahydrocannabinol was administered intravenously and are given in Fig. 12 for the 0.5-mg/kg dose in Dog B. Peak concentrations, in terms of tetrahydrocannabinol equivalents, ranged from 1050 to 1450 ng/ml at 22–36 min in Dogs B and C for the 2.0-mg/kg doses and from 250 to 280 ng/ml at 22–28 min in Dogs B and C for the 0.5-mg/kg doses; a peak of 58 ng/ml occurred at 28 min for the 0.1-mg/kg dose given to Dog. A. The peak levels were proportional to dose and confirmed the lack of dose dependency.

The pH 10.5 heptane-extractable metabolites, [M_h], from plasma (Eq. 2), corrected for any possible tetrahydrocannabinol in plasma (Fig. 12), increased rapidly to a broad maximum between 12 and 40 min and then decreased, paralleling the loss of tetrahydrocannabinol (Fig. 12) from plasma to indicate a similar metabolic clearance of these relatively nonpolar metabolites. At the earliest times, [M_h] accounted for less than 50% of the concentration of [M_p] in plasma, whereas at later times ($t > 2000$ min) [M_h] accounted for less than 10% of [M_p]. The semilogarithmic plots of the pH 2.0 ethyl acetate-extractable metabolites, [M_{ea}] (Eq. 3), which were identical with the tetrahydrofuran-extractable metabolites (Eq. 4), against time (Fig. 11) paralleled the total metabolite concentration in plasma [M_p] after its maximum was achieved. This finding indicated that these more polar acidic metabolites maintained a constant ratio to the total metabolites in plasma subsequent to 70–100 min after tetrahydrocannabinol administration.

The simultaneous appearance in plasma of both nonpolar (heptane extractable, [M_h]) and acidic polar metabolites (ethyl acetate and tetrahydrofuran extractable, [M_{ea}] and [M_{thf}]) may be explained by either parallel metabolic processes or by sequential metabolic processes during each pass through the liver.

This extremely rapid appearance of metabolites in the plasma, which peaked at 25–30 min, demonstrated the extremely rapid metabolism of tetrahydrocannabinol consistent with the metabolic half-lives of 4.8–10.9 min estimated from the derived k_m values (Table III). Since the experimentally observed plasma tetrahydrocannabinol values persisted for 7000 min, it must be stated that the nonmetabolized drug rapidly distributed into tissues concomitantly with its rapid metabolic clearance from the central compartment. Estimates of the disposition at that time are given in Table IV.

These phenomena can be dramatically demonstrated by analog computer fitting of the data obtained for the first 60 min after intravenous administration of Δ^9-tetrahydrocannabinol; the computer need only be programmed to a three-compartment body model, rather than the five needed for 7000 min, since negligible amounts of drugs were returned from the deeper third and fourth tissues during the 60 min. Programs, techniques, and procedures for fitting pharmacokinetic data by the analog computer were described previously (20).

The most highly divergent data from the various studies, the 0.1- and 0.5-mg/kg studies in Dogs A and C, were used for the analog computer fitting of the scheme in Fig. 13. They included the experimentally obtained plasma levels of Δ^9-tetrahydrocannabinol with time and the total amount of metabolites, M, produced with time as calculated from Eq. 13. The sets of microscopic rate constants are listed in Table V. The simultaneous rapid distribution of large amounts of drug into the tissues—*viz.*, T_1 and T_2, and the transformation into metabolites, M, are apparent from the example of Fig. 13.

Pseudo-Clearances and Pseudo-Apparent Volumes of Distribu-

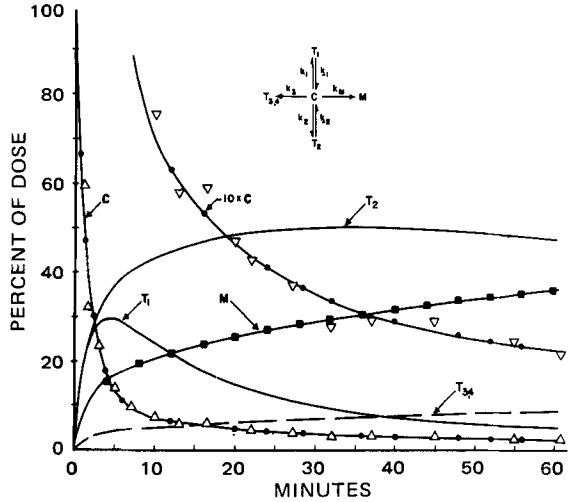

Figure 13—*Analog computer fitting of plasma Δ^9-tetrahydrocannabinol data (△) and metabolites (■) produced, M (as calculated from Eq. 13), for 60 min after the 0.1-mg/kg study in Dog A for the scheme given. The plasma values (●) were calculated with the pertinent constants of Table II. The plasma values of Δ^9-tetrahydrocannabinol (▽) were also fit on a 10-fold expanded ordinate. The generated tissue levels of Δ^9-tetrahydrocannabinol, T_1, T_2, and $T_{3,4} = T_3 + T_4$, are also given.*

Table V—Pharmacokinetic Parameters after Intravenous Administration of Δ^9-Tetrahydrocannabinol Obtained by Analog Computer Fitting to the Scheme in Fig. 13[a]

Parameter	Dog A 0.1 mg/kg	Dog C 0.5 mg/kg
V_c, liters	1.35	1.77
$10^2 k_M$, min^{-1}	9.11	8.68
$10^2 k_1$, min^{-1}	34.62	21.83
$10^2 k_{-1}$, min^{-1}	20.11	11.38
$10^2 k_2$, min^{-1}	29.74	19.73
$10^2 k_{-2}$, min^{-1}	1.81	1.27
$10^2 k_3$, min^{-1}	7.59	2.11

[a]The fit was considered adequate when the experimental values of $10^5 V_C C/D_0$ in terms of percent of dose in plasma (where V_C is apparent volume of distribution of the central compartment in liters from Table III) and the $10^2 M/D_0$ values (from M calculated by Eq. 13) were reasonably fit.

tion of Metabolites of Δ^9-Tetrahydrocannabinol—Pseudo-clearances, Cl_R and Cl_B, of total metabolites after tetrahydrocannabinol administration were estimated from the quotients of the rates of appearance of total radioactivity in the urine or bile, respectively, and the plasma concentrations of radiolabeled metabolites, $[M_p]$, where:

$$Cl_R = (\Delta U_T/\Delta t)/[M_p] \quad \text{(Eq. 15)}$$

and:

$$Cl_B = (\Delta B_T/\Delta t)/[M_p] \quad \text{(Eq. 16)}$$

where ΔU_T and ΔB_T are the amounts of radioactivity collected in an interval, Δt, and $[M_p]$ is the plasma concentration at the midpoint of the interval. These apparent clearances were plotted against the time at the midpoint of the collection interval, and typical examples are given for bile (Fig. 14) and urine (Fig. 15).

The maximum pseudo-renal clearances (Fig. 15) for Dogs A and B (5.5–8.4 ml/min at about 300 min) were similar, but those for Dog C were higher (17–21 ml/min). The pseudo-renal clearances did plateau after their decrease from the maximum during the 400–1200-min interval and then gradually decreased toward zero over the remaining 5000 min. The pseudo-biliary clearances (Fig. 14) for Dog C (80–100 ml/min) showed a maximum slightly earlier at 60 min but did plateau after their decrease during the 100–500-min interval and then gradually decreased to an apparent asymptote of 1–3 ml/min by 3000 min.

The initially low, but subsequently increasing, pseudo-renal and biliary clearances are consistent with an initial production of nonpolar metabolites that can be extensively reabsorbed back to plasma in the kidneys and liver. The fact that peak renal clearances are low (Fig. 15) implies high plasma protein binding of metabolites and/or their large tubular reabsorption. A glomerular filtration rate of 80 ml/min (18) and a 92% plasma protein binding of such metabolites, a fact substantiated in preliminary binding studies, could account for the observed low peak pseudo-renal clearances of 6.0–6.4 ml/min in Dog B (Fig. 15).

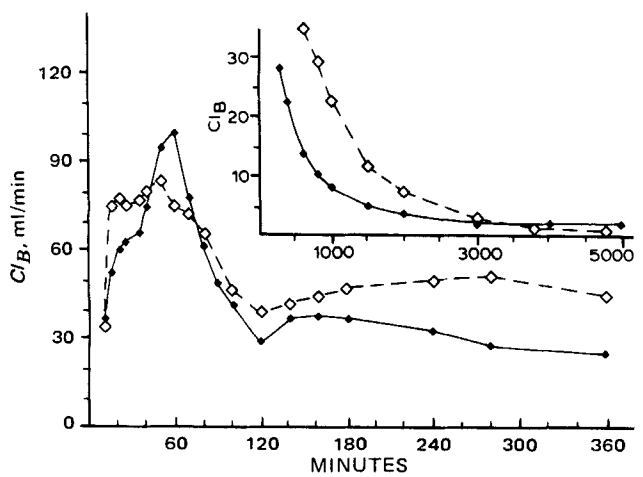

Figure 14—*Plots of the biliary clearance,* Cl_B, *against time for the 0.5- (♦) and 2.0- (◊) mg/kg iv doses in Dog C.* $Cl_B = (dB_T/dt)/[M_p]$, *where* dB_T/dt *and* $[M_p]$ *were estimated from data such as are given in Figs. 8 and 12, respectively.*

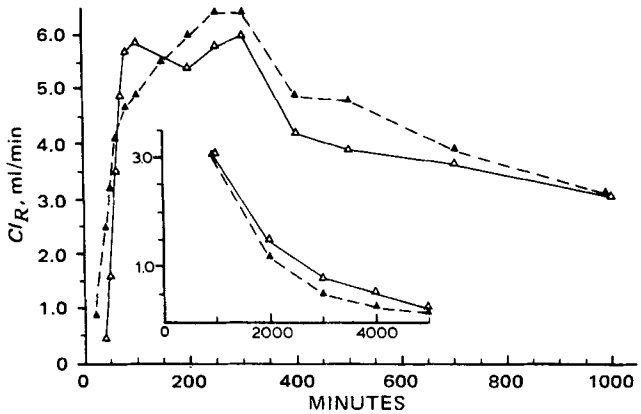

Figure 15—*Plots of the renal clearance,* Cl_R, *of total metabolites excreted in urine against time for the 0.5- (△) and 2.0- (▲) mg/kg doses in Dog B.* $Cl_R = (dU_T/dt)/[M_p]$, *where* dU_T/dt *and* $[M_p]$ *were estimated from data such as are given in Figs. 8 and 12, respectively.*

These observed differences in pseudo-clearances with time undoubtedly reflected changes in the metabolite composition of plasma where the approach to the maximum resulted from the transition from production of less polar, reabsorbable metabolites to those of higher polarity. The subsequent decrease resulted from the relatively rapid elimination of these more polar compounds, with a subsequently relatively higher retention and accumulation in the circulating fluids of less rapidly eliminated metabolites. The fact that over 88% of the biliary metabolites intravenously administered was eliminated by 300 min (Fig. 8) is confirmatory. It should be remembered that material, <10%, had been extracted by heptane before these metabolites had been administered. The general invariance of extraction characteristics for the metabolites in bile (Fig. 10) and urine (Fig. 11) in the 200–1000-min interval was consistent with the reasonable constancy of the pseudo-clearances (Fig. 14) in the same interval.

The subsequent slow decay to the lower asymptotic value achieved after 2000–3000 min can only be explained by the formation of a metabolite that is not further metabolized easily which is initially a small percent of the dose but is not readily biliary or renally excreted. Thus, at a later time, it accounts for an increasing percentage of the radiolabeled metabolites in the plasma until a new pseudo-steady state among metabolite components is reached at 3000 min. At this time, sufficient amounts of this metabolite have accumulated so that its formation rate is approximately equal to its elimination rate from the body. This is the achievement of the final pseudo-steady state when the rate-determining step for the overall elimination of Δ^9-tetrahydrocannabinol from the body is the slow return of the drug from the deepest tissues where it has been sequestered.

Pseudo-apparent volumes of distribution, V_m, of the metabolite formed on intravenous administration of Δ^9-tetrahydrocannabinol as a function of time (Fig. 16) can be calculated from the quotient of the amount of metabolites in the body, M_{in}, and the observed concentration of metabolites in the plasma, $[M_p]$ (Fig. 12). These M_{in} values were estimated from the differences between the predicted amount, M, of total metabolites produced (Eq. 13 and Fig. 6) and the total amounts of radiolabeled metabolites, M_{ex}, excreted in the bile and urine at a given time (Fig. 8) so that:

$$M_{in} = M - M_{ex} \quad \text{(Eq. 17)}$$

Thus:

$$V_m = M_{in}/[M_p] = (M - M_{ex})/[M_p] \quad \text{(Eq. 18)}$$

These pseudo-apparent volumes of distribution as a function of time depend on the calculated M values (Eq. 13) and, thus, the set of parameters chosen to describe the time course, $\hat{Y}$, of tetrahydrocannabinol in plasma. Curves A and B in Fig. 16 were calculated on the premises of the validity of Eqs. 6 and 5, respectively, where the former was based on presumption that the half-life of tetrahydrocannabinol elimination was reflected by the terminal half-life for total radioactivity in the body (Fig. 4). Support for this presumption was afforded by the fact that the estimated apparent volume of distribution, $(V_m)_{est}$, of the intravenously administered biliary metabolites (curve C) was the same 6 liters between

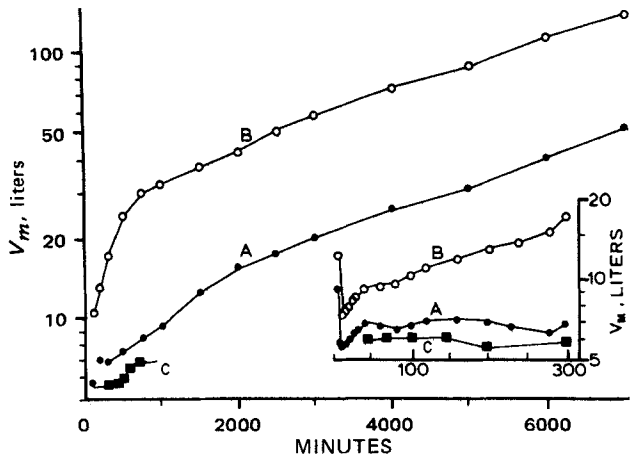

Figure 16—*Pseudo-apparent volumes of distribution of total metabolites for the intravenously administered biliary metabolites,* $V_{m_{est}}$ *(curve C), and those formed on intravenous administration of 0.5 mg of* Δ^9*-tetrahydrocannabinol/kg to Dog C,* V_m*. The calculations of* V_m *for curves A and B were based on the premise of the validity of Eqs. 6 and 5, respectively, for the* Δ^9*-tetrahydrocannabinol administration.*

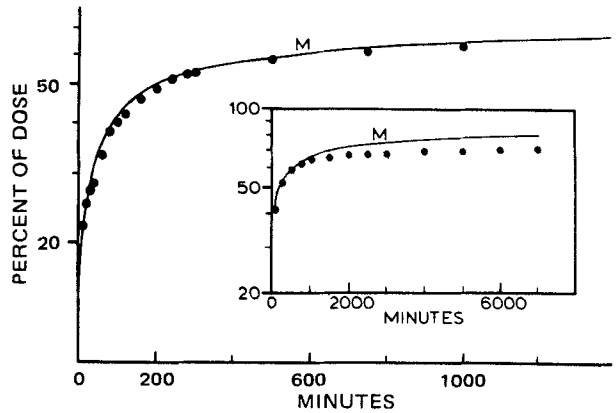

Figure 17—*Semilogarithmic plots of the total metabolites,* M, *produced as percent of dose against time for the 0.5-mg* Δ^9*-tetrahydrocannabinol/kg dose in Dog C. The values were calculated from Eq. 16 using an estimated pseudo-apparent volume of distribution,* $(V_m)_{est}$ *= 6.0 liters, and the drawn curve was calculated from Eq. 13.*

50 and 300 min as observed with curve A. These values were obtained from:

$$(V_m)_{est} = \frac{CPM_0 - CPM_{ex}}{[CPM]_p} \qquad \text{(Eq. 19)}$$

where CMP_0 is the total activity of the administered metabolites, CPM_{ex} is the total activity excreted in bile and urine at a given time, and $[CPM]_p$ is the concentration of activity per milliliter in plasma at that time.

The presumption of 6 liters as the apparent volume of distribution of metabolites should permit proper estimation of the cumulative total, M (Eq. 13), of metabolites produced:

$$M_{est} = (V_m)_{est}[M_p] + M_{ex} \qquad \text{(Eq. 20)}$$

if the composition of the metabolites comprising $[M_p]$ did not change significantly with time. The fact that M_{est} satisfactorily estimates M prior to 1000 min is clearly shown in Fig. 17. The deviations between them after 1000 min of approximately 10% at 7000 min are a consequence of the increase in the pseudo-apparent V_m (Fig. 16, curve A). This increase could have resulted from the accumulation in tissues of slowly eliminated nonpolar metabolites comprising less than 10% of the total metabolites formed, a fact consistent with: (*a*) the previous explanations of the observed declines in the apparent biliary and urinary clearances of total metabolites, (*b*) the fact that the biliary metabolites intravenously administered had 10% of the radiolabeled metabolites removed prior to administration and also had 88% of the administered dose eliminated by 300 min (Fig. 7), and (*c*) the fact that the fraction of the dose as metabolites in the body at 7000 min during the final pseudo-steady state was close to these 10% values (Table IV).

Significances and Implications of Observed Pharmacokinetics—The sequestration of administered Δ^9-tetrahydrocannabinol in deep tissues (Table IV) and its large retention over long periods produced a terminal half-life of approximately 8 days on acute dosing. Thus, there should be significant accumulation of drug on chronic administration. If daily chronic dosing is intravenously administered, a steady state of the amount of drug in the central compartment associated with the plasma results by approximately 7 days, oscillating between 0.03% of the daily dose at 3 hr after dosing and 2% at 24 hr after dosing. However, a steady-state oscillation of the amount of drug in the tissues is not achieved until after 30 days of chronic dosing and varies after each dose, from 450% of the single dose at 3 hr to 360% at 24 hr. The amounts in the tissues increase fivefold over that from a single dose at 7 days and 10-fold by 27 days. Thus, a pharmacodynamic response could increase with chronic dosing or be maintained for weeks after its cessation if tolerance did not develop.

The rate-determining step in drug elimination from the body, subsequent to the first several hundred minutes after administration, is not the rate of metabolism but the rate of return from deep tissues. Thus, it is unlikely that any claimed decrease (8, 12) in the apparent half-life for tetrahydrocannabinol in the plasma of chronic marijuana smokers relative to naive smokers could be a consequence of marijuana-induced enzymes. If this were the case, the relative plasma levels would change but not the terminal half-life of decay.

The calculated accumulation in tissues is consistent with the observations of Kreuz and Axelrod (11) that the drug accumulates in the body fat of rats after repetitive administration and implies that significant differences in the disposition and pharmacodynamics of tetrahydrocannabinol may be anticipated between lean and obese individuals. If the fat to lean ratio of the chronic marijuana smokers were higher than that of naive smokers, claimed apparent differences (12) in apparent plasma half-lives could be best explained as resulting from differences in the rates of return of plasma of the rate-determining release of drug from such lipophilic deep compartments.

11-Hydroxy-Δ^9-tetrahydrocannabinol, a metabolite of Δ^9-tetrahydrocannabinol (21–29), has similar pharmacological properties and could contribute to the total pharmacodynamic action. In fact, it was suggested (1, 30) that the action was primarily due to this metabolite, although other researchers did not reach the same conclusion (31–34).

Since the disposition and metabolism of the intravenously administered metabolite were claimed (32–34) to be similar to that of Δ^9-tetrahydrocannabinol, equivalent pharmacokinetic parameters may be assumed. It is on this premise that the scheme in Fig. 18 is based, where *PI* is considered to be the primary intermediate(s) in metabolism, including pharmacodynamically active metabolites such as 11-hydroxy-Δ^9-tetrahydrocannabinol that can be metabolized further. The analog computer-generated curves in Fig. 18 demonstrate the time course of the maximum amounts of *PI* as percent of dose in its central compartment

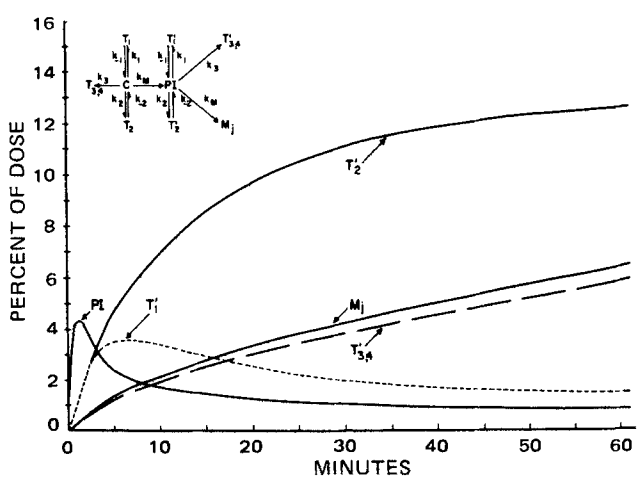

Figure 18—*Analog computer-generated curves of active metabolites,* PI, *which are primary intermediates in the metabolic sequence to* M_j *in the specified scheme for 60 min after intravenous administration of* Δ^9*-tetrahydrocannabinol in the 0.1-mg/kg study in Dog A. The generated* M_j *and tissue levels of* PI *in the tissues* T_1', T_2', *and* $T_{3,4}' = T_3' + T_4'$ *are also given.*

and in the various tissues, T_1', T_2', and $T_{3,4}'$, for 60 min after Δ^9-tetrahydrocannabinol administration. The time course of the amounts of the inactive metabolites, M_j, produced subsequently is also given. The ratios, R, of the amounts of PI to Δ^9-tetrahydrocannabinol in corresponding tissues approached asymptotes within these 60 min (compare Figs. 13 and 18). For example, T_1'/T_1 or PI/C approached one-half, whereas T_2'/T_1 or $T_{3,4}'/T_{3,4}$ approached lower values (one-fourth to one-third). Thus, PI would make the largest contribution to the observed activity if T_1 and T_1' were the biophases. Ryrfeldt *et al.* (6) observed R ratios in mice in blood and brain of this magnitude after intravenous administration of Δ^9-tetrahydrocannabinol.

Extant evidence from experimental animals (33) suggests that the relative potency, r, of 11-hydroxy-Δ^9-tetrahydrocannabinol to Δ^9-tetrahydrocannabinol ranges between 2 and 18; and if the central compartment and its rapidly equilibrating tissues, T_1 or T_1', are taken as the biophase, the contribution of PI to the observed pharmacological effect would be 50% at $r = 2$ and 90% at $r = 18$. If other tissues are the biophase, the contributions would be less.

However, these are maximum estimates since they are based on the premises that all PI produced in the liver is active and wholly returned to the plasma unchanged. This would not be so if PI were metabolized at the same rate as Δ^9-tetrahydrocannabinol. The fraction of the Δ^9-tetrahydrocannabinol entering the liver that left unmetabolized could be given by:

$$q = C_2/C_1 = e^{-\alpha T} \qquad \text{(Eq. 21)}$$

where α is the intrinsic first-order metabolic rate constant, and T is the time required for complete replacement of the liver blood volume, *i.e.*, the time of blood transit through the liver. The C_1 and C_2 are the concentrations in the plasma entering and leaving the liver, respectively. If the active metabolites are further metabolized to M_j with the same rate dependency, the rate of change in the amount of PI in the liver could be given by:

$$d(PI)_L/dt = \alpha V_L C_1 - \alpha(PI)_L \qquad \text{(Eq. 22)}$$

The fraction of the entering concentration, C_1, that retains its identity at the end of the interval, T, can be obtained by the integration (35) of Eq. 22 over the interval $t = T$ and is:

$$p = (PI)_L/V_L C_1 = \alpha T e^{-\alpha T} \qquad \text{(Eq. 23)}$$

where V_L is the apparent volume of distribution of the liver.

If the logarithms of both sides of Eq. 19 are taken:

$$\alpha T = \ln q \qquad \text{(Eq. 24)}$$

which may be substituted into Eq. 23. Equation 23 can be rearranged and divided by $1 - q$ to give the fraction of metabolites formed from Δ^9-tetrahydrocannabinol in the liver that remain as PI on exit from the liver:

$$p/(1 - q) = q \ln q/(q - 1) \qquad \text{(Eq. 25)}$$

Since the apparent metabolic efficiency of tetrahydrocannabinol, $q = C_2/C_1$, is 0.5, only 69.3% of the PI formed in the liver would exit from this organ. Thus, if the central compartment is taken as the biophase for a relative potency of 2, the estimated ratio of amounts therein at 60 min becomes 0.35 rather than 0.5, and the contribution of PI to the observed pharmacological effect would be 41% rather than the 50% estimated if PI is not metabolized further during its passage through the liver prior to its return to the plasma.

On the basis of this discussion, an appropriate model for the pharmacokinetics of Δ^9-tetrahydrocannabinol is given in Fig. 18 on the premise that PI has pharmacokinetic properties similar to its precursor, where PI and M_j appear to be produced in parallel rather than sequentially when Δ^9-tetrahydrocannabinol is supplied continuously to the liver. When the hepatic efficiency, $q = C_2/C_1$, is small, negligible PI would be formed by the route designated with the microscopic rate constant $k_m[1 - p/(1 - q)]$. Even if PI were 20 times more potent than tetrahydrocannabinol, it could account for a maximum of only 30% of the observed response for a central compartment biophase when $q = 0.01$. The contribution of PI-type active metabolites, such as 11-hydroxy-Δ^9-tetrahydrocannabinol, to the observed pharmacological response of its precursor cannot be resolved until the true biophase is ascertained, their unique metabolic efficiencies are known, and the true relative potencies are determined.

Effects of ^{14}C-Label Position on Pharmacokinetics of ^{14}C-Δ^9-Tetrahydrocannabinol—Although the differently labeled ^{14}C-Δ^9-tetrahydrocannabinol in plasma, when radioactivity of the separated compound was monitored with time, showed the same pharmacokinetics (Fig. 6), this was not so for total concentrations of radioactivity in plasma (Fig. 3) where the C-11-labeled drug showed significantly less plasma concentration per unit dose than the 1,3-ring-labeled drug at comparable times. A definite conclusion that metabolites tend to lose the C-11 group, as through decarboxylation of C-11 carboxylic acid metabolites, is clouded by the fact that the studies were conducted in biliary-cannulated Dog C where different bile flows had a pronounced effect on biliary excretions of the two studies (Fig. 2).

However, the total percents of dose excreted into bile for the differently labeled tetrahydrocannabinols were equivalent, although the metabolite derived from C-11-labeled drug showed less of a percentage excreted in the urine and totally excreted than the ring labeled. Nevertheless, the variation in total radioactivity as percent of dose excreted for the two differently labeled compounds in Dog C at the two different doses was not significantly different from the variation in total radioactivity as percent of dose excreted for the two studies at different doses of 1,3-^{14}C-Δ^9-tetrahydrocannabinol in Dog B (Fig. 5), where the relative amounts recovered in feces accounted for the latter's variability. Thus, the null hypothesis that there were no significant differences between the pharmacokinetics in the dog of the radiolabeled compounds derived from the two differently labeled Δ^9-tetrahydrocannabinols cannot yet be rejected.

REFERENCES

(1) L. Lemberger, *Drug Metab. Disp.*, **1**, 461 (1973).

(2) L. Lemberger, *Adv. Pharmacol. Chemother.*, **10**, 221 (1972).

(3) S. Agurell, I. M. Nilsson, A. Ohlsson, and F. Sandberg, *Biochem. Pharmacol.*, **18**, 1195 (1969).

(4) *Ibid.*, **19**, 1333 (1970).

(5) W. D. M. Paton and R. G. Pertwee, in "Marijuana," R. Mechoulam, Ed., Academic, New York, N.Y., 1973, chap. 5, pp. 243–248.

(6) A. Ryrfeldt, C. H. Ramsey, I. M. Nilsson, W. Widman, and S. Agurell, *Acta Pharm. Suec.*, **10**, 13 (1973).

(7) L. Lemberger, S. D. Silberstein, J. Axelrod, and I. J. Kopin, *Science*, **170**, 1320 (1970).

(8) L. Lemberger, J. Axelrod, and I. J. Kopin, *Ann. N.Y. Acad. Sci.*, **191**, 142 (1971).

(9) E. R. Garrett and C. A. Hunt, *J. Pharm. Sci.*, **62**, 1211 (1973).

(10) H. A. Klausner and J. V. Dingell, *Life Sci.*, **10**, 49 (1971).

(11) D. S. Kreuz and J. Axelrod, *Science*, **179**, 391 (1973).

(12) L. Lemberger, N. R. Tamarkin, J. Axelrod, and I. J. Kopin, *ibid.*, **173**, 72 (1971).

(13) E. R. Garrett and C. A. Hunt, *J. Pharm. Sci.*, **63**, 1056 (1974).

(14) *Ibid.*, **66**, 20 (1977).

(15) D. S. Riggs, "The Mathematical Approach to Physiological Problems," 2nd ed., M.I.T. Press, Cambridge, Mass., 1972, pp. 146–161.

(16) F. J. Anscombe and J. W. Tukey, *Technometrics*, **5**, 141 (1963).

(17) A. Rescigno and G. Segre, "Drug and Tracer Kinetics," Blaisdell, Waltham, Mass., 1966, p. 21.

(18) P. L. Altman and D. S. Dittmer, "Respiration and Circulation," Biological Handbooks, American Societies for Experimental Biology, Bethesda, Md., 1971, pp. 382, 429.

(19) "Marijuana," R. Mechoulam, Ed., Academic, New York, N.Y., 1973, pp. 167–189.

(20) E. R. Garrett and H. J. Lambert, *J. Pharm. Sci.*, **62**, 550 (1973).

(21) I. M. Nilsson, S. Agurell, J. L. G. Nilsson, A. Ohlsson, F. Sandberg, and M. Wahlquist, *Science*, **168**, 1228 (1970).

(22) S. H. Burstein and D. Kupfer, *Chem. Biol. Interact.*, **3**, 316 (1971).

(23) Z. Ben-Zvi and S. Burstein, *Res. Commun. Chem. Pathol. Pharmacol.*, **8**, 223 (1974).

(24) F. Mikes, A. Hofmann, and P. G. Waser, *Biochem. Pharmacol.*, **20**, 2469 (1971).

(25) Z. Ben-Zvi, R. Mechoulam, and S. H. Burstein, *Tetrahedron Lett.*, **1970**, 4495.

(26) M. E. Wall, D. R. Brine, G. A. Brine, C. G. Pitt, R. I. Freudenthal, and H. D. Christensen, *J. Am. Chem. Soc.*, **92**, 3466 (1970).

(27) Z. Ben-Zvi, R. Mechoulam, and S. Burstein, *ibid.*, **92**, 3468 (1970).

(28) R. Mechoulam, *Science*, **168**, 1159 (1970).

(29) Y. Grunfeld and H. Edery, *Psychopharmacologica*, **14**, 200 (1969).

(30) L. Lemberger, R. E. Crabtree, and H. M. Rowe, *Science*, **177**, 62 (1972).

(31) E. W. Gill, G. Jones, and D. K. Lawrence, *Biochem. Pharmacol.*, **22**, 175 (1973).
(32) R. Karler and W. Cely, *Fed. Proc.*, **33**, 540 (1974).
(33) E. W. Gill and D. K. Lawrence, *J. Pharm. Pharmacol.*, **25**, 988 (1973).
(34) B. T. Ho, V. S. Estevez, and L. F. Englert, *ibid.*, **25**, 488 (1973).
(35) F. H. Dost, "Grundlagen der Pharmakokinetik," Geog. Thieme Verlag, Stuttgart, Germany, 1968, pp. 41–43.

ACKNOWLEDGMENTS AND ADDRESSES

Received November 26, 1975, from *The Beehive, College of Pharmacy, University of Florida, Gainesville, FL 32610.*

Accepted for publication May 12, 1976.

Abstracted in part from a dissertation submitted by C. A. Hunt to the Graduate School, University of Florida, in partial fulfillment of the Doctor of Philosophy degree requirements.

Supported in part by Grant DA-00743 from the National Institute of Mental Health, Bethesda, MD 20014.

The technical assistance of Mrs. Kathleen Eberst and the contributions of Dr. Lester L. Rolf and Dr. Andre Jackson with dog surgery are gratefully acknowledged.

* Present address: School of Pharmacy, University of California, San Francisco, CA 94143.

x To whom inquiries should be directed.

Determination of Porosity and Pore-Size Distribution of Aspirin Tablets Relevant to Drug Stability

H. GUCLUYILDIZ *, G. S. BANKER, and G. E. PECK x

Abstract □ Total porosity and pore-size distribution of aspirin tablets prepared from aspirin, starch USP, and precipitated colloidal silicon dioxide were determined using mercury porosimetry. The model represented a hydrolyzable drug substance in combination with simple excipients. The role of starch and silicon dioxide on the microstructure of the tablets was investigated, as was the chemical stability of various systems. In general, the porosity of tablets containing a constant quantity of starch increased linearly with silicon dioxide concentration. Examination of the pore-size distribution, however, revealed that at low concentrations silicon dioxide functioned primarily to reduce the size and volume of coarse pores representing the spaces between the agglomerates of starch and aspirin particles. This effect was optimum at 3%. A further increase in silicon dioxide concentration produced tablets with relatively larger pore sizes. Studies of changes in the porosity characteristics of tablets as influenced by water vapor over time showed distinct differences in this complex parameter. A unique trend in the change of the pore-size distribution was noted with tablets containing 3% silicon dioxide. These observations are discussed relative to the stability of aspirin tablets in which this concentration of silicon dioxide produced a maximum stabilizing effect.

Keyphrases □ Aspirin—tablets, stability, porosity and pore-size distribution determined, effect of colloidal silicon dioxide □ Porosity and pore-size distribution—aspirin tablets, effect of colloidal silicon dioxide □ Stability—aspirin tablets, porosity and pore-size distribution determined, effect of colloidal silicon dioxide □ Silicon dioxide, colloidal—effect on stability of aspirin tablets, porosity and pore-size distribution determined □ Dosage forms—aspirin tablets, stability, porosity and pore-size distribution determined, effect of colloidal silicon dioxide

In any systematic and fundamental approach to the design of solid dosage forms, a comprehensive elucidation of the physical characteristics of the solid components is necessary and basic. Knowledge of the physical nature of solid pharmaceutical systems is often confined to determinations of such properties as particle size, particle-size distribution, and true and bulk density. To relate the disintegration, dissolution, and stability characteristics to meaningful physicochemical parameters, a direct examination of the porosity characteristics also may be essential.

The pharmaceutical and chemical literature clearly documents that the pore-size distribution of solids is frequently among the controlling variables in processes involving disintegration, dissolution, adsorption, and diffusion. In tablet disintegration and dissolution, the initial stage is probably typically the penetration of the solvent medium into the tablet through the tablet pore system. The solvent penetration rate, in turn, was shown to be intimately related to the volume and size of tablet pores (1–6). From the standpoint of tablet stability, especially when dealing with hydrolyzable drugs, a physical description of the porous state of tablets may be important, since porosity and pore-size distribution affect the diffusion of water vapor and the accessibility of condensed vapor to the labile drug.

Studies on the porous nature of tablets have been conducted with increasing frequency recently (7). Porosity characteristics of tablets are primarily influenced by compression as a result of fragmentation, deformation, and consolidation of particles. Additional factors include particle size, particle shape, and the compressibility of particles (5, 6, 8).

As evident from review articles, the stability of aspirin in the solid state was the subject of numerous studies (9, 10). Many adjuvants have been proposed to enhance aspirin stability. Studies in these laboratories showed that inclusion of precipitated colloidal silicon dioxide into tablets prepared from aspirin and starch significantly improved aspirin stability. The maximum stabilizing effect of silicon dioxide occurred at 3%. Above this level, a continuous decrease in the stability of aspirin was observed. Although the major mechanism of this effect may be the large adsorptive capacity of silicon dioxide which functions as an internal tablet desiccant, an evaluation of tablet porosity characteristics may add significant dimensions in the interpretation of the physicochemical phenomena involved in aspirin decomposition.

The present study was undertaken to determine the influence of colloidal silicon dioxide on the porosity and pore-size distribution of aspirin tablets using mercury

(31) E. W. Gill, G. Jones, and D. K. Lawrence, *Biochem. Pharmacol.*, **22**, 175 (1973).
(32) R. Karler and W. Cely, *Fed. Proc.*, **33**, 540 (1974).
(33) E. W. Gill and D. K. Lawrence, *J. Pharm. Pharmacol.*, **25**, 988 (1973).
(34) B. T. Ho, V. S. Estevez, and L. F. Englert, *ibid.*, **25**, 488 (1973).
(35) F. H. Dost, "Grundlagen der Pharmakokinetik," Geog. Thieme Verlag, Stuttgart, Germany, 1968, pp. 41–43.

ACKNOWLEDGMENTS AND ADDRESSES

Received November 26, 1975, from *The Beehive, College of Pharmacy, University of Florida, Gainesville, FL 32610.*

Accepted for publication May 12, 1976.

Abstracted in part from a dissertation submitted by C. A. Hunt to the Graduate School, University of Florida, in partial fulfillment of the Doctor of Philosophy degree requirements.

Supported in part by Grant DA-00743 from the National Institute of Mental Health, Bethesda, MD 20014.

The technical assistance of Mrs. Kathleen Eberst and the contributions of Dr. Lester L. Rolf and Dr. Andre Jackson with dog surgery are gratefully acknowledged.

* Present address: School of Pharmacy, University of California, San Francisco, CA 94143.

x To whom inquiries should be directed.

Determination of Porosity and Pore-Size Distribution of Aspirin Tablets Relevant to Drug Stability

H. GUCLUYILDIZ *, G. S. BANKER, and G. E. PECK x

Abstract □ Total porosity and pore-size distribution of aspirin tablets prepared from aspirin, starch USP, and precipitated colloidal silicon dioxide were determined using mercury porosimetry. The model represented a hydrolyzable drug substance in combination with simple excipients. The role of starch and silicon dioxide on the microstructure of the tablets was investigated, as was the chemical stability of various systems. In general, the porosity of tablets containing a constant quantity of starch increased linearly with silicon dioxide concentration. Examination of the pore-size distribution, however, revealed that at low concentrations silicon dioxide functioned primarily to reduce the size and volume of coarse pores representing the spaces between the agglomerates of starch and aspirin particles. This effect was optimum at 3%. A further increase in silicon dioxide concentration produced tablets with relatively larger pore sizes. Studies of changes in the porosity characteristics of tablets as influenced by water vapor over time showed distinct differences in this complex parameter. A unique trend in the change of the pore-size distribution was noted with tablets containing 3% silicon dioxide. These observations are discussed relative to the stability of aspirin tablets in which this concentration of silicon dioxide produced a maximum stabilizing effect.

Keyphrases □ Aspirin—tablets, stability, porosity and pore-size distribution determined, effect of colloidal silicon dioxide □ Porosity and pore-size distribution—aspirin tablets, effect of colloidal silicon dioxide □ Stability—aspirin tablets, porosity and pore-size distribution determined, effect of colloidal silicon dioxide □ Silicon dioxide, colloidal—effect on stability of aspirin tablets, porosity and pore-size distribution determined □ Dosage forms—aspirin tablets, stability, porosity and pore-size distribution determined, effect of colloidal silicon dioxide

In any systematic and fundamental approach to the design of solid dosage forms, a comprehensive elucidation of the physical characteristics of the solid components is necessary and basic. Knowledge of the physical nature of solid pharmaceutical systems is often confined to determinations of such properties as particle size, particle-size distribution, and true and bulk density. To relate the disintegration, dissolution, and stability characteristics to meaningful physicochemical parameters, a direct examination of the porosity characteristics also may be essential.

The pharmaceutical and chemical literature clearly documents that the pore-size distribution of solids is frequently among the controlling variables in processes involving disintegration, dissolution, adsorption, and diffusion. In tablet disintegration and dissolution, the initial stage is probably typically the penetration of the solvent medium into the tablet through the tablet pore system. The solvent penetration rate, in turn, was shown to be intimately related to the volume and size of tablet pores (1–6). From the standpoint of tablet stability, especially when dealing with hydrolyzable drugs, a physical description of the porous state of tablets may be important, since porosity and pore-size distribution affect the diffusion of water vapor and the accessibility of condensed vapor to the labile drug.

Studies on the porous nature of tablets have been conducted with increasing frequency recently (7). Porosity characteristics of tablets are primarily influenced by compression as a result of fragmentation, deformation, and consolidation of particles. Additional factors include particle size, particle shape, and the compressibility of particles (5, 6, 8).

As evident from review articles, the stability of aspirin in the solid state was the subject of numerous studies (9, 10). Many adjuvants have been proposed to enhance aspirin stability. Studies in these laboratories showed that inclusion of precipitated colloidal silicon dioxide into tablets prepared from aspirin and starch significantly improved aspirin stability. The maximum stabilizing effect of silicon dioxide occurred at 3%. Above this level, a continuous decrease in the stability of aspirin was observed. Although the major mechanism of this effect may be the large adsorptive capacity of silicon dioxide which functions as an internal tablet desiccant, an evaluation of tablet porosity characteristics may add significant dimensions in the interpretation of the physicochemical phenomena involved in aspirin decomposition.

The present study was undertaken to determine the influence of colloidal silicon dioxide on the porosity and pore-size distribution of aspirin tablets using mercury

Table I—Porosity and Related Characteristics of Aspirin Tablets

Silicon Dioxide Concentration, %	Apparent Volume, ml	True Volume, ml	Displacement Volume[a], ml	Total Porosity, %	Porosity in Pore Radius Range, %	
					$r > 0.006$ μm	$r < 0.006$ μm
Control	0.3508	0.3281	0.3504	6.46	5.54	0.92
0	0.3669	0.3426	0.3663	6.62	6.44	0.18
1	0.3684	0.3418	0.3682	7.21	6.85	0.36
3	0.3700	0.3392	0.3698	8.33	7.44	0.89
5	0.3732	0.3366	0.3730	9.81	9.14	0.67
10	0.3765	0.3302	0.3763	12.29	11.44	0.85
15	0.3830	0.3239	0.3825	15.43	15.24	0.19

[a] Determined by displacement of mercury at 1.6 psia.

porosimetry. Of major interest were the structural changes that occur in tablets under the influence of water vapor. On the basis of these observations, the role played by silicon dioxide was assessed and, inferentially, extended to the general utility and significance of pore-size distribution measurements in compressed pharmaceutical systems.

EXPERIMENTAL

Materials—Aspirin USP (200–250-mesh powder), starch USP (80 mesh), and an experimental precipitated colloidal silicon dioxide meeting NF specifications were used in the preparation of aspirin tablets. Before use, starch and silicon dioxide were pretreated for about 12 hr by evacuation in a vacuum oven at 60 and 150°, respectively. The nitrogen surface areas of these substances were determined by the Brunauer, Emmett, and Teller (BET) method (11) using a commercially available instrument[1]. The corresponding values were 0.6 m^2/g for starch and 556 m^2/g for silicon dioxide. The true density measurements were performed by a helium-displacement technique utilizing the instrument[1] employed in the BET surface area determinations. The following values were obtained: aspirin, 1.40 g/ml; starch, 1.59 g/ml; and silicon dioxide, 2.29 g/ml.

Tablet Preparation—Several tablet formulations with various silicon dioxide concentrations (0, 1, 3, 5, 10, and 15%) were prepared. Each tablet contained 23 mg of starch in addition to the total aspirin–silicon dioxide content of 460 mg. Silicon dioxide concentrations were expressed on the basis of a 460-mg tablet weight, excluding the weight of starch. Tablets also were made from aspirin powder alone to serve as control samples. The components for 10 tablets of each formulation were weighed and mixed for 15 min in a miniblender of approximately 20-g capacity. The miniblender consisted of a V-shaped shell fabricated from clear plastic prescription bottles and was operated at 14 rpm by a motor.

An accurately weighed quantity of the powder mixture was then placed in a 12.7-mm flat-faced punch and die set and compressed at a calculated punch face pressure of 15.3×10^3 psi between the plates of a hydraulic press[2]. The weight of the compressed sample was again determined, and the tablet dimensions were measured with a micrometer. These physical measurements assured compliance of each tablet to identical compression conditions for consecutive samples and allowed the calculation of the apparent volume of the tablet.

To evaluate the chemical stability of tablets and the changes in their porosity characteristics with time, a relative water vapor pressure of 0.82 and a temperature of 40° were selected as the storage conditions. Constant relative pressure was maintained in a desiccator by a saturated potassium chloride solution (12). Samples were placed in the desiccator and stored in an oven until testing.

Evaluation of Porosity and Pore-Size Distribution—The total porosity of a tablet was determined from its apparent volume, its weight, and the true density of the individual tablet components. Pore-size distribution determinations were performed by intrusion of mercury using a commercial porosimeter[3] with a pressuring capacity of 15,000 psi. Approximately 20 increments of pressure were recorded in a typical determination, allowing sufficient time at each pressure for mercury to reach equilibrium in the sample. Equilibrium was assumed to have been reached when the liquid ceased penetration into the sample or penetrated at a rate of not more than 0.0001 ml/min.

In the derivation of pore-size distribution from basic intrusion data, the equation derived by Washburn (13) was used. The surface tension of mercury was taken to be 484 dynes/cm at 24°, the temperature of the measurements, as the best available value (14, 15). In the absence of specific data for the contact angle between mercury and the samples studied, this value was assumed to be 130°, a value commonly used for most solids (16, 17). Appropriate corrections were applied for the compressibility of mercury and of the residual air entrapped in the penetrometer in the initial evacuation step. Any volume change due to the compressibility of the sample itself was considered negligible. A correction factor for effective compressibility of mercury was determined by measuring the effect of applied pressure on the penetrometer (sample cell) filled entirely with mercury, *i.e.*, without any sample being present. Under the experimental conditions, the required corrections did not exceed 0.0075 ml. A description of the pore-size distribution calculations is presented elsewhere (18).

Evaluation of Aspirin Stability—The residual aspirin content of the tablets was determined by a spectrophotometric method (19). Basically, this procedure was based on a simultaneous determination of aspirin with salicylic acid in a pH 7.0 buffer solution at 296.5 and 262 nm.

RESULTS AND DISCUSSION

Effect of Silicon Dioxide on Porosity Characteristics—The results of pore volume and porosity determinations of aspirin tablets prepared with varying concentrations of silicon dioxide are outlined in Table I. The data are based on calculations from tablet dimensions and on results of mercury intrusion studies. The pore volume determined by intrusion of mercury represents the volume of pores in the pore radius range of about 60–0.006 μm. These limits of measurable pore radius are imposed by the pressure used in the initial introduction of mercury to the sample and by the maximum pressuring capacity of the instrument.

The close agreement seen in Table I between the measurements of apparent and displacement volumes of tablets shows that pores with radii larger than 60 μm were absent. The pore-size range determined by mercury intrusion represents virtually all of the pore volume present. The pore volume calculated to be present but remaining unintruded by mercury, in fact, constitutes an overestimate of the volume of pores smaller than 0.006 μm in radii. This unintruded volume also includes:

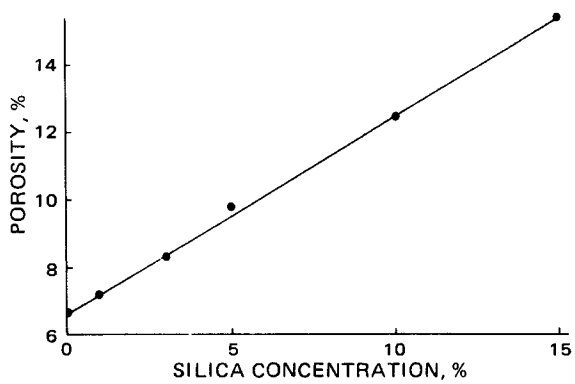

Figure 1—*Effect of colloidal silicon dioxide on total porosity of aspirin tablets.*

[1] Orr surface-area pore-volume analyzer, model 2100, Micromeritics Instrument Corp., Norcross, Ga.
[2] Carver laboratory press, model C, Fred S. Carver Inc., Summit, N.J.
[3] Aminco, Catalog No. 5-7121, American Instrument Co., Silver Spring, Md.

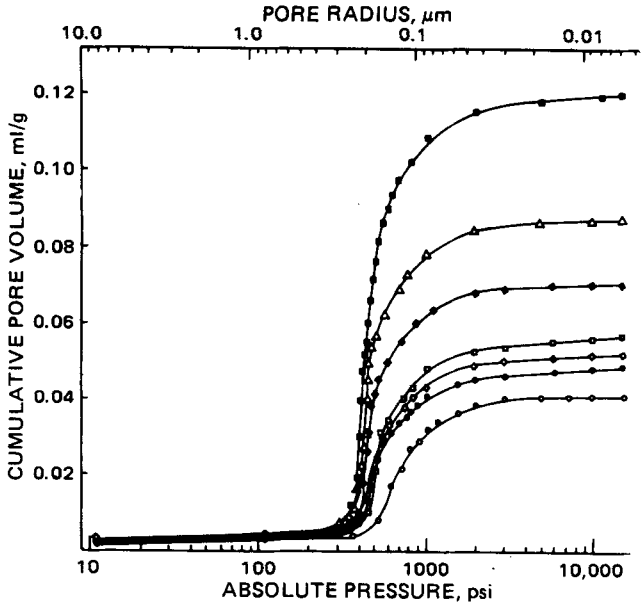

Figure 2—*Cumulative pore-size distribution of aspirin tablets containing various silicon dioxide concentrations. Key:* ○, *control;* ●, *0%;* ◇, *1%;* □, *3%;* ◆, *5%;* △, *10%; and* ■, *15%.*

(*a*) the volume of pores with radii larger than 0.006 μm but accessible to mercury only through smaller openings, and (*b*) the volume of pores that may be completely isolated from the pore network in the tablets. The total measured porosity (Table I) is in excellent agreement with the porosity calculated from the apparent volume and the true volume (Table I). However, the pore sizes determined by the mercury intrusion method represent the size of pore openings rather than the actual size of the pores.

A comparison of tablet porosity results given in Table I reveals that the total porosity of tablets prepared from aspirin only (control) was slightly lower than that prepared with 0% silicon dioxide. Since the latter formulation contained starch (5% of the total aspirin–silicon dioxide content), starch apparently did not alter significantly total tablet porosity under these compression conditions. On the other hand, the major effect of silicon dioxide on the porosity characteristics of aspirin tablets, containing a constant 5% level of starch, was immediately evident as a consistent increase in the total porosity with silicon dioxide concentration (Fig. 1). Despite its smaller specific volume, silicon dioxide contributed to the porosity of tablets to a greater extent than aspirin.

The manner by which silicon dioxide alters the porosity characteristics of aspirin tablets can best be inferred by examining the pore-size distribution of the samples shown in Fig. 2, where the cumulative pore volume intruded by mercury is plotted *versus* the pressure applied on the sample. The corresponding pore radius is also indicated on the upper abscissa. The data are presented in the form of a cumulative distribution function, which has the advantage that the fraction of pore volume between any arbitrary bounds of pore radii can be quickly assessed. The sigmoid shape of the cumulative distribution curves is characteristic of this determination. Although the pore-size measurements were originally made starting from a pore radius of about 60 μm, almost negligible intrusion was observed in the pore-size range of 60–10 μm. Therefore, these portions of the curves were omitted from the graph. The experimental points shown represent the average of at least two separate determinations. The reproducibility of the data was excellent.

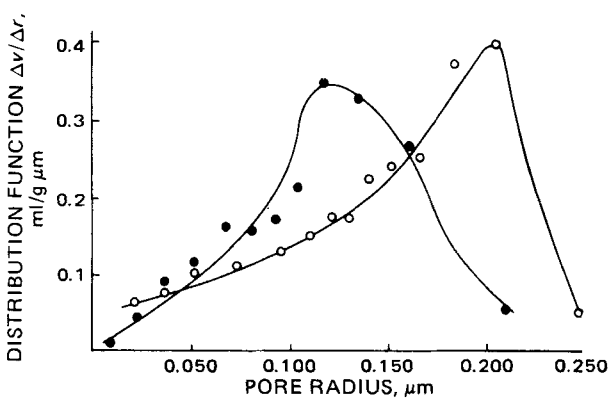

Figure 3—*Pore-size distribution of aspirin tablets. Key:* ●, *aspirin (control); and* ○, *aspirin with 5% starch (0% silicon dioxide).*

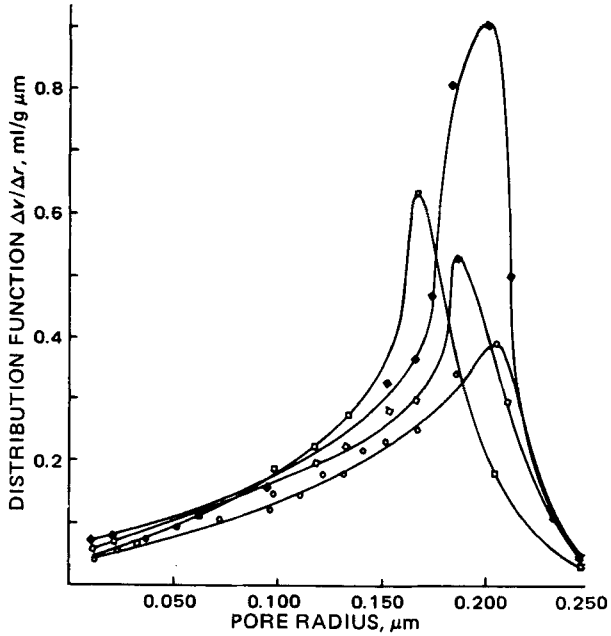

Figure 4—*Pore-size distribution of aspirin tablets containing various silicon dioxide concentrations. Key:* ○, *0%;* ◇, *1%;* □, *3%; and* ◆, *5%.*

Inspection of Fig. 2 shows the absence of significant pore volume for pores larger than about 0.2 μm followed by an abrupt upward trend, indicating that the distribution of pores was confined over a relatively narrow size range in all formulations. A greater portion of the pore volume was in the lower pore-size region as the silicon dioxide concentration increased. Judging from the slopes of the curves toward the lower pore-size limit of the instrumentation employed, essentially all of the pore volume present in tablets existed in accessible pores larger than 0.006 μm in radii.

The distribution curves display an apparent threshold radius characterized by a sudden, significant intrusion of mercury into the tablet pore system. The threshold radius may represent the minimum radius of pores that are essentially continuous throughout the tablet.

An alternative way of examining the results is to present the distribution curves as the derivative distribution function, *i.e.*, differential or derived pore-size distribution curves. Figures 3–5 represent typical distribution curves for the aspirin tablets investigated. The pore system developed in each formulation had a simple continuous distribution of pores. The pore-size distribution of tablets was drastically altered by the addition of 5% starch to the tablets, as judged from the shift in the maximum frequency toward a greater pore radius (Fig. 3). Apparently, starch promotes a tablet pore system characterized by a relatively larger size and volume of coarser pores. This observation seems to be rather significant in view of the fact that the influence of starch to total porosity is not quite so pronounced (Table I).

On the other hand, tablets containing 1% silicon dioxide in addition to starch showed a pore-size distribution with a maximum frequency at a smaller pore size (Fig. 4) than the tablets prepared from aspirin and starch only. This trend continued upon further addition of silicon dioxide, *i.e.*, up to 3%, but it was reversed at higher levels of silicon dioxide (Figs. 4 and 5). When the silicon dioxide concentration exceeded 3%, the general distribution moved consistently to relatively larger pore sizes with increasing silicon dioxide concentration. This concentration appeared to be rather characteristic, since the observed maximum frequency corresponded to the smallest pore size among tablets containing various silicon dioxide concentrations.

The major differential effect of incorporating silicon dioxide in the formulations was to decrease the size of coarser pores (Figs. 4 and 5). At a concentration level of 5%, the pore size corresponding to the maximum frequency of the distribution approached that of tablets containing no

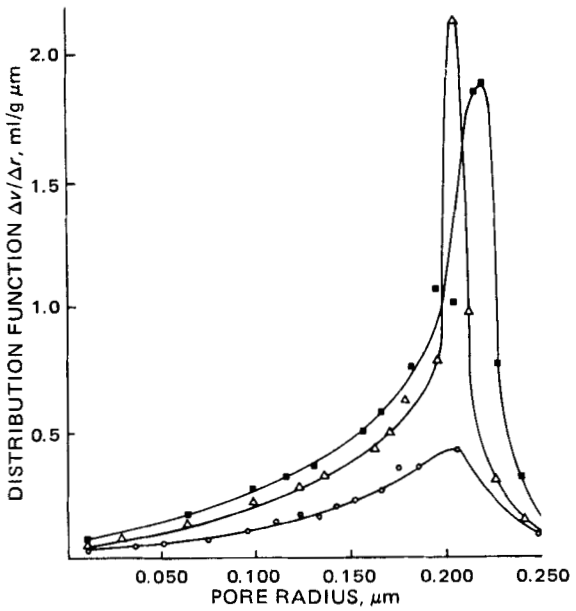

Figure 5—*Pore-size distribution of aspirin tablets containing various silicon dioxide concentrations. Key:* ○, *0%;* △, *10%; and* ■, *15%.*

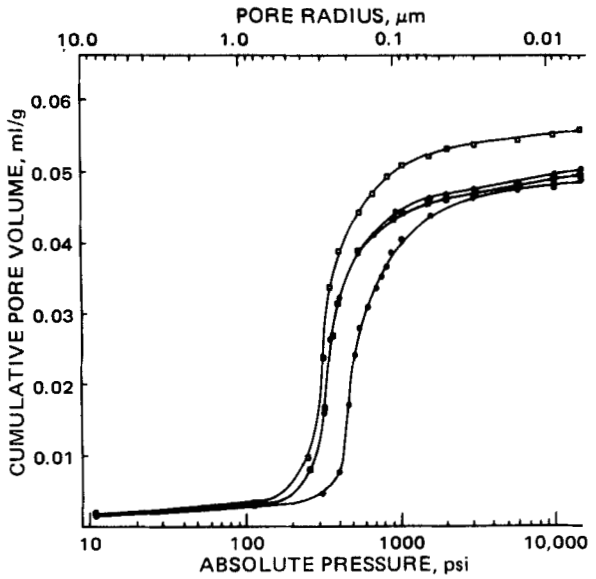

Figure 7—*Cumulative pore-size distribution of aspirin tablets containing 0% silicon dioxide after exposure to a relative water vapor pressure of 0.82 at 40° for various periods. Key:* ○, *0 month;* □, *1 month;* ●, *3 months; and* ■, *5 months.*

silicon dioxide (Fig. 4). This finding suggests that the process of reduction in pore size by the addition of silicon dioxide was essentially completed at 3% silicon dioxide.

The aforementioned observations may be explained by considering that the small silicon dioxide particles were capable of filling the coarse interparticle voids developed by starch. Although the net effect of the presence of silicon dioxide in the formulations was to increase the total pore volume of tablets, in fact, silicon dioxide reduced the size and volume of coarser pores at low concentrations. This phenomenon is not at all in contrast with what is expected. From the value of the BET nitrogen surface area (556 m^2/g) and knowledge of the density of silicon dioxide (2.29 g/ml), it can be shown that the volume–surface diameter of spherical silicon dioxide particles corresponds to 4.7 nm. As compared to the size of aspirin and starch particles, which lie in the micrometer range, it does not appear unusual that silicon dioxide particles can easily undergo such a packing arrangement at low concentrations so as to limit the size of coarser pores.

In discussing the pore-size distribution of aspirin tablets, attention also must be focused on the compression characteristics of the tablet components. The absence of coarse pores in tablets prepared from aspirin powder alone can be attributed to relatively superior compressibility as well as deformability of aspirin particles. On the other hand, the development of coarser pores with formulations containing starch reflects the poor ability of this material to bond and compress. Similarly, the trend toward larger pore sizes with increasing silicon dioxide concentration presumably results from the resistance of silicon dioxide particles to consolidation during the compaction process.

Changes in Porosity Characteristics of Aspirin Tablets with Time—The susceptibility of the porosity characteristics of aspirin tablets to various changes with time is presented in Figs. 6–12 in the order of increasing silicon dioxide content. These figures depict the cumulative pore-size distribution of the samples exposed to a relative water vapor pressure of 0.82 at 40° for various times. The volume parameter is expressed in milliliters of pore space intruded by mercury per gram of sample previously outgassed in a vacuum oven at room temperature.

The mercury intruded pore volume of aspirin tablets (control) decreased consistently with increasing exposure to water vapor (Fig. 6). On the other hand, comparison of the distribution curves of the tablet for-

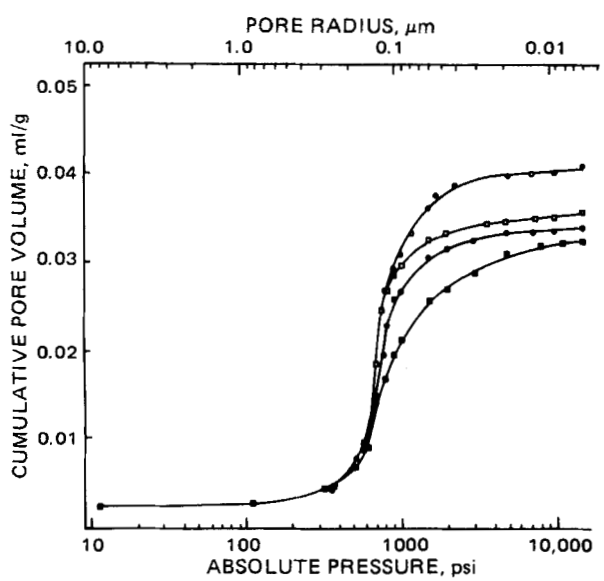

Figure 6—*Cumulative pore-size distribution of aspirin tablets (control) after exposure to a relative water vapor pressure of 0.82 at 40° for various periods. Key:* ○, *0 month;* □, *1 month;* ●, *3 months; and* ■, *5 months.*

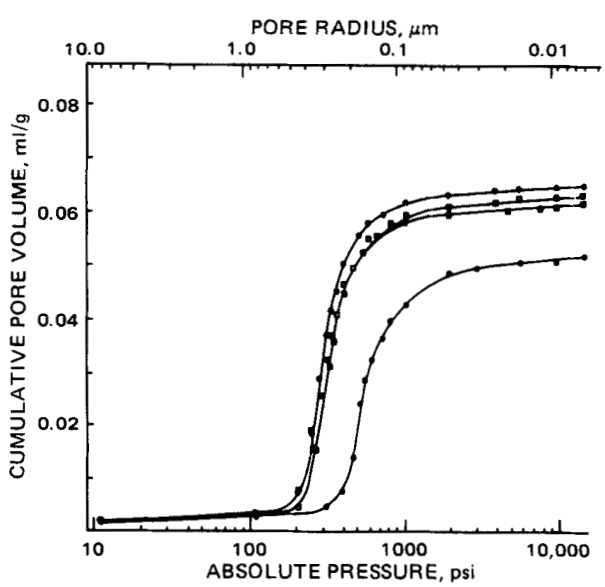

Figure 8—*Cumulative pore-size distribution of aspirin tablets containing 1% silicon dioxide after exposure to a relative water vapor pressure of 0.82 at 40° for various periods. Key:* ○, *0 month;* □, *1 month;* ●, *3 months; and* ■, *5 months.*

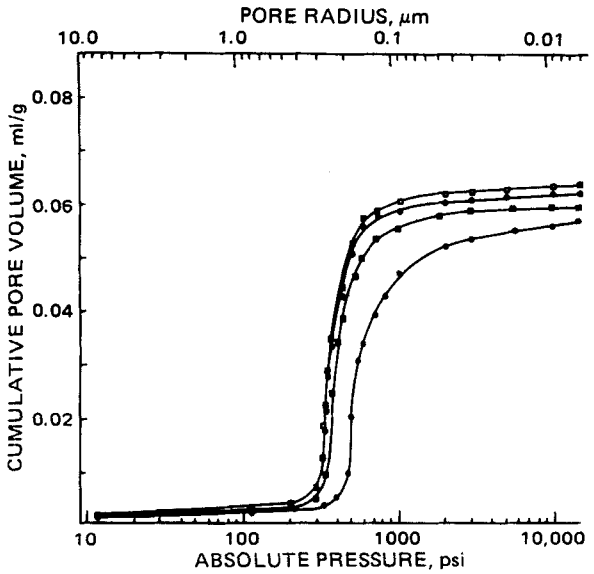

Figure 9—*Cumulative pore-size distribution of aspirin tablets containing 3% silicon dioxide after exposure to a relative water vapor pressure of 0.82 at 40° for various periods. Key: ○, 0 month; □, 1 month; ●, 3 months; and ■, 5 months.*

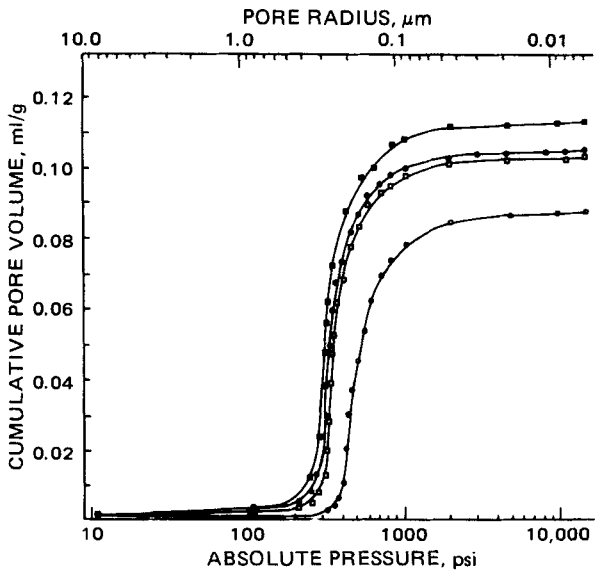

Figure 11—*Cumulative pore-size distribution of aspirin tablets containing 10% silicon dioxide after exposure to a relative water vapor pressure of 0.82 at 40° for various periods. Key: ○, 0 month; □, 1 month; ●, 3 months; and ■, 5 months.*

mulation containing 0% silicon dioxide (Fig. 7) shows that the pore volume first increased on 1 month of exposure to water vapor and then decreased. This initial increase in the pore volume on exposure of the samples to water vapor for 1 month can also be seen by inspection of Figs. 8–12, which represent the cumulative pore-size distribution of aspirin tablets containing 1, 3, 5, 10, and 15% silicon dioxide. Further changes that occurred with time in the measured pore volume and the pore-size distribution differed depending on the silicon dioxide content of the samples.

At the end of 3 months, samples containing 1, 5, 10, and 15% silicon dioxide (Figs. 8 and 10–12) displayed additional increases in the pore volumes intruded by mercury, whereas the measured pore volume of the tablets having 3% silicon dioxide (Fig. 9) actually decreased with respect to the volume determined at the end of 1 month. Examination of the samples exposed to water vapor over 5 months revealed that the pore volumes of the tablets containing 5, 10, and 15% silicon dioxide continued to increase (Figs. 10–12) and those of the tablets having 3% silicon dioxide showed a further decrease (Fig. 9). Interestingly, as opposed to the previously observed trend that the mercury-intruded volume of tablets with 1% silicon dioxide increased with time, these samples appeared to have smaller pore volumes at the end of 5 months (Fig. 8).

Attention can be focused more sharply on these results with reference to Table II, where the values for the total pore volumes intruded by mercury are expressed as the percent of those obtained with corresponding samples not subjected to water vapor. The data may be explained as follows. When aspirin tablets are subjected to water vapor, water vapor is adsorbed on the surfaces of the tablet components. Since the tablet matrix is porous, and the relative pressure of water vapor is high enough for capillary condensation to occur, it is reasonable to expect that adsorption is accompanied by condensation of vapor to liquid in the small pores of the tablet. The quantity of water vapor adsorbed and subsequently condensed invariably depends on the adsorptive capacity of the particular formulation, which, as was experimentally confirmed, increases consistently with silicon dioxide concentration. Once the water vapor enters the tablet, decomposition of aspirin results, giving acetic acid and salicylic acid as the decomposition products. Acetic acid is highly volatile, but salicylic acid is partly sublimed through the tablet, as evidenced by the appearance of the crystals of this material on the sample

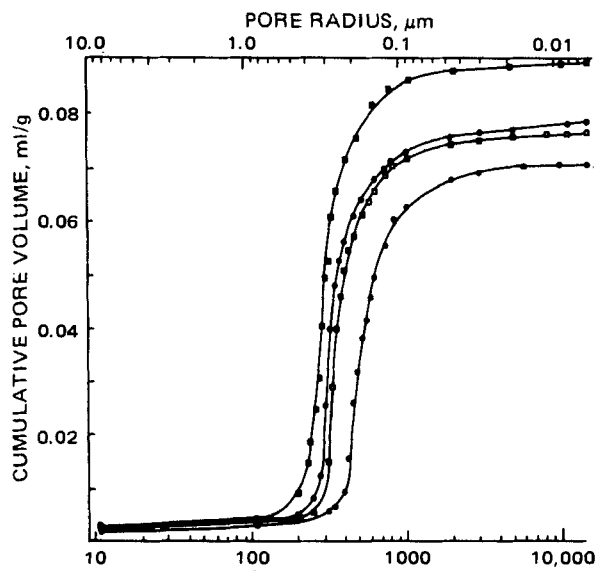

Figure 10—*Cumulative pore-size distribution of aspirin tablets containing 5% silicon dioxide after exposure to a relative water vapor pressure of 0.82 at 40° for various periods. Key: ○, 0 month; □, 1 month; ●, 3 months; and ■, 5 months.*

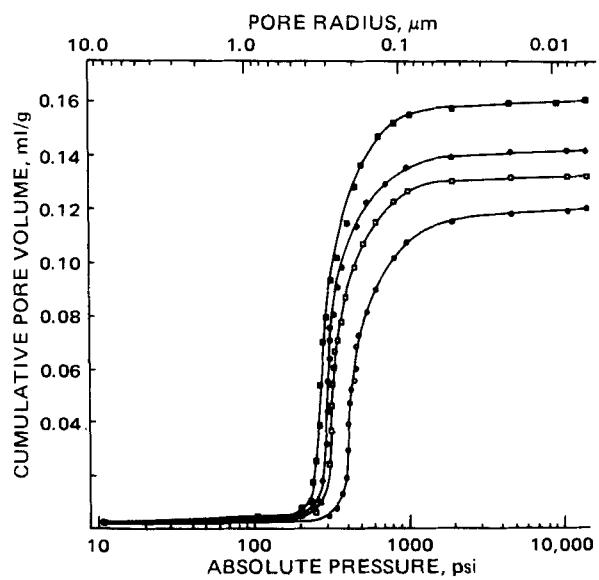

Figure 12—*Cumulative pore-size distribution of aspirin tablets containing 15% silicon dioxide after exposure to a relative water vapor pressure of 0.82 at 40° for various periods. Key: ○, 0 month; □, 1 month; ●, 3 months; and ■, 5 months.*

Table II—Percent Pore Volume Ratios of Aspirin Tablets Exposed to a Relative Water Vapor Pressure of 0.82 at 40° for Various Periods

Silicon Dioxide Concentration, %	Pore Volume Ratio after Indicated Period of Exposure, %		
	1 Month	3 Months	5 Months
Control	86.2	82.5	79.3
0	116.8	104.2	100.7
1	121.9	124.7	117.9
3	112.8	109.5	105.5
5	110.7	111.3	126.4
10	111.6	117.9	124.5
15	110.0	117.1	129.1

surface. A substantial portion of salicylic acid, however, is undoubtedly deposited in the pore system of the tablets. This result is evident from Table II, which shows a continual reduction with time in the pore volume ratios of control samples prepared from aspirin only.

Aside from influencing the porosity and pore-size distribution of the samples by causing chemical changes, water vapor also affects these parameters by physically altering the arrangement of pore spaces between the particles of the tablet components. The presence of starch in the formulations significantly increased their porosity, as reflected clearly by the increase in the pore volume ratios of the samples exposed to water vapor for 1 month (Table II). This result is naturally due to the swelling of starch grains upon penetration of water vapor into the tablet, which, in turn, distorts the arrangement and size distribution of pores. After exposure to water vapor for 1 month, tablets containing the lowest silicon dioxide concentration (1%) exhibited the maximum increase in pore volume. Further addition of silicon dioxide to the tablet formulations resulted in the reduction of the pore volume ratios with respect to this value. However, when the silicon dioxide concentration exceeded 3%, the pore volume ratios were essentially unaffected by silicon dioxide concentration. This trend presumably reflects the fact that the presence of silicon dioxide in tablets at concentration levels of 3% or above restricts the access of water vapor to starch in the tablet so that the swelling of this material is impeded.

Examination of the pore volume results obtained at the end of 3 months (Table II) shows that the samples containing starch but no silicon dioxide had a smaller pore volume ratio than that of corresponding samples analyzed after 1 month of exposure to water vapor. The deposition of salicylic acid in the tablet pores becomes the important factor in affecting the volume as well as the distribution of pores. Further reduction in the pore volume occurred when identical samples were exposed to water vapor for 5 months.

The situation, however, is quite different for tablets containing silicon dioxide, with the notable exception of tablets with 3% silicon dioxide. The data obtained at the end of 3 months show that the pore volume ratios of the samples with silicon dioxide were higher than their respective values determined after 1 month of exposure to water vapor. The divergence observed with samples containing 3% silicon dioxide indicates that in this particular formulation of the two opposing factors influencing porosity, *i.e.*, swelling of starch grains and deposition of salicylic acid in the pores, the latter predominates. Inspection of data resulting from the analysis of tablets at the end of 5 months showed that at the 3% silicon dioxide level the pore volume ratios continued to decrease. At this stage, a similar pattern is also evident with tablets containing 1% silicon dioxide.

Table IV—Stability of Aspirin Tablets under a Relative Vapor Pressure of 0.82 at 40°

Silicon Dioxide Concentration, %	Undegraded Aspirin after Indicated Period, %			
	1 Month	2 Months	3 Months	4 Months
Control	95.0	94.4	93.6	93.3
0	95.1	94.5	93.9	93.6
1	98.9	98.6	—	98.1
3	99.1	99.4	—	99.0
5	97.6	97.0	97.0	96.7
10	97.8	96.4	—	—
15	96.7	95.5	94.3	93.6

However, the increase in the pore volume ratios at higher silicon dioxide concentrations indicates that the effect of swelling of starch grains is more pronounced in these formulations. This suggests that the presence of a higher silicon dioxide content not only favors the adsorption of greater quantities of water vapor, but also as a result of this, the water vapor recedes from the silicon dioxide surface as it approaches the liquid state and becomes available for hydration of starch.

In discussing the changes in the pore characteristics of aspirin tablets with time, changes taking place in the pore sizes of the various formulations should also be considered. Therefore, the values of pore radii that may be used to characterize the pore-size distribution of aspirin tablets investigated are presented in Table III. With the exception of the control tablets, there was a general tendency for the pore sizes to attain greater values with increasing exposure of samples to water vapor. This observation is in accord with ordinary expectations based on the pore volume changes of the tablets. For a given formulation, the numerical change was the greatest between the untreated samples and samples exposed to water vapor for 1 month and diminished at longer periods of exposure. The trends evident in Table III are consistent with those obtained while considering the changes in the pore volume (Table II).

Table III also shows that the agreement between respective values of r_{med}, median pore radius, and r_{mode}, radius corresponding to the maximum frequency of pores in the sample, was reasonably close and that the pattern of change in their values was somewhat similar. Furthermore, after any period of exposure to water vapor, except for control tablets, samples containing 3% silicon dioxide exhibited the smallest values for r_{med} and r_{mode}. This finding reflects the apparent ability of this particular formulation to retain its unique feature irrespective of relative changes in the size and volumes of pores.

Interpretation of Stabilizing Properties of Colloidal Silicon Dioxide in Hydrolytic Decomposition of Aspirin—The pore-size distribution results discussed previously clearly indicate that this parameter is of significant value in following the microstructural changes that occur in aspirin tablets as a result of exposure to water vapor. Furthermore, the examination of such changes sheds considerable light on the stabilizing properties of silicon dioxide in the hydrolytic decomposition of aspirin in tablets (Table IV).

The results obtained from a direct examination of the changes in porosity characteristics indicate that the desiccant effect of silicon dioxide apparently was not the only factor favoring aspirin stability in these formulations. The pore volume data (Table II) indicate that the presence of silicon dioxide in the tablets did not preclude the access of water vapor to starch. Water vapor continued to be available for aspirin hydrolysis. The availability of water vapor to starch and, presumably, to aspirin was

Table III—Characteristic Pore Radii (Micrometers) of Aspirin Tablets

Silicon Dioxide Concentration, %	Untreated Samples		Samples Exposed to Water Vapor[a]					
			1 Month		3 Months		5 Months	
	r_{med}[b]	r_{mode}[c]	r_{med}	r_{mode}	r_{med}	r_{mode}	r_{med}	r_{mode}
Control	0.130	0.118	0.140	0.136	0.135	0.118	0.115	0.136
0	0.175	0.206	0.275	0.315	0.254	0.268	0.254	0.268
1	0.168	0.185	0.290	0.328	0.299	0.328	0.293	0.300
3	0.164	0.167	0.234	0.240	0.241	0.257	0.241	0.257
5	0.177	0.200	0.250	0.277	0.268	0.277	0.304	0.321
10	0.184	0.205	0.244	0.283	0.259	0.283	0.276	0.305
15	0.194	0.220	0.248	0.283	0.262	0.292	0.280	0.336

[a] At a relative pressure of 0.82 at 40°. [b] Median pore radius, the radius corresponding to 50% of the mercury intruded pore volume. [c] The radius corresponding to the maximum frequency of pores in the sample.

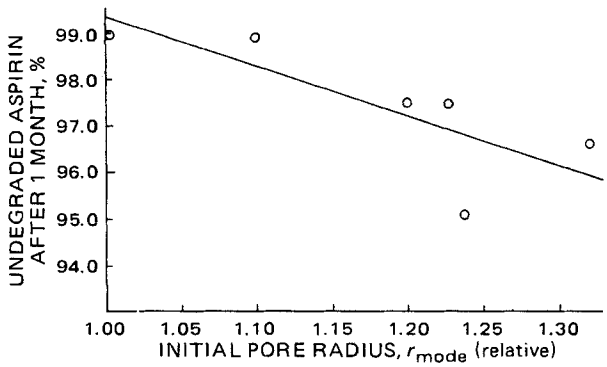

Figure 13—*Relationship between aspirin stability and pore size.*

not a simple function of silicon dioxide concentration in the tablets studied. Undoubtedly, the precise mechanism by which silicon dioxide affected the stabilization of aspirin did not involve the simple retention of water vapor by silicon dioxide to limit the availability of water vapor to aspirin *per se*. A complex combination of factors was possibly responsible for the optimum stability observed at the 3% silicon dioxide concentration.

Aspirin decomposition in tablets involves a heterogeneous reaction, the rate of which may be controlled both by diffusional processes and the hydrolytic reaction at the unreacted aspirin surface. The two general diffusional processes of importance include the diffusion of water vapor into the tablet and the transfer of salicylic acid in and out of the tablet pores. As the present experimental data verify, salicylic acid is deposited in the tablet pore system. In this process, salicylic acid may easily form a protective layer on the aspirin surface, which, in turn, results in slow diffusion of water vapor through this layer. It is also possible to conceive that the hydrolytic reaction may approach an equilibrium state. In either event, the aspirin degradation rate becomes diffusion controlled, and the complex internal pore structure and the nature of individual pores may become determining factors in the accessibility of water vapor to the aspirin surface. The characteristic pore-size distribution pattern observed with tablets containing 3% silicon dioxide may, therefore, be helpful in interpreting the relatively small extent of aspirin degradation in this formulation.

To determine whether a simple correlation existed between aspirin stability and the pore size attained in the formulations, the stability results shown in Table IV were plotted against the values of r_{mode}, the pore radius corresponding to the maximum frequency of pores in the tablet. The trend representing aspirin stability at the end of 1 month as a function of initial pore size is illustrated in Fig. 13, where r_{mode} is expressed in normalized form relative to that of the tablets having the smallest pore size (Table III). Figure 13 shows that aspirin stability is apparently related to the initial pore size.

An extension of the relationship seen in Fig. 13 to stability data over longer periods did not appear feasible, because of the complexity of the interactions of various variables involved in aspirin stability. When a similar plot was prepared for the 3-month data, for example, the trend remained the same, but the correlation was relatively poor. The deviation occurred primarily due to the formulation containing 1% silicon dioxide, which had relatively greater stability despite the larger pore size attained in this formulation with time (Table III).

This apparent lack of direct correlation between aspirin stability and pore size suggests that the water vapor accessible to starch is not equally available to the aspirin surface. Presumably, at low silicon dioxide concentration, starch itself retains the water vapor, resulting in its greater hydration and an increased pore volume and pore size in the tablets. With increased silicon dioxide concentration, however, starch grains are isolated from each other; silicon dioxide adsorbs the water vapor to a greater extent, since it has a much larger surface area and greater adsorption capacity than starch.

Another explanation that may be offered for the slower decomposition of aspirin in formulations containing low silicon dioxide concentrations may be related to the effect of salicylic acid on the system. As pointed out previously, a protective layer of salicylic acid is probably formed on the aspirin surface to control further the access of water vapor to the aspirin. Additionally, the deposition of salicylic acid in the tablet pore system at low silicon dioxide concentrations (Tables II and III) decreases the pore volumes and sizes with longer periods of exposure to water vapor. With formulations containing silicon dioxide levels higher than 3%, the accessibility of water vapor to aspirin is expected to be much greater. This is attributed to the fact that the increased silicon dioxide concentration favors the adsorption of greater quantities of water vapor which recede from the silicon dioxide surface with time as it approaches the liquid state and becomes available for aspirin degradation. The superior adsorptive capacity of these formulations and the favorable pore size may simultaneously operate to facilitate the access of water to unreacted aspirin surfaces. The transfer of salicylic acid also may be enhanced because of the greater pore sizes. This point is evidenced simply by the physical appearance of the tablets, which showed more localized salicylic acid crystals on the external surfaces consistent with increasing silicon dioxide content.

Finally, none of the aforementioned factors, *i.e.*, the superior water vapor adsorptive capacity of silicon dioxide, sublimation of salicylic acid, and the distinct pore size distribution of each formulation, can alone be directly related to the differences in the stability of aspirin at various silicon dioxide levels. However, the present observations along with the foregoing discussion promote additional insight into the stabilizing properties of silicon dioxide in aspirin degradation. It should also be evident that pore-size distribution can be a very useful parameter in interpreting aspirin stability in compressed pharmaceutical systems.

SUMMARY AND CONCLUSIONS

1. The influence of colloidal silicon dioxide on the porosity characteristics of aspirin tablets containing a constant quantity of starch was investigated. The porosity of the samples prepared under constant compression conditions increased linearly with silicon dioxide concentration.

2. Pore-size distribution determinations by mercury intrusion allowed a complete elucidation of the microstructural changes produced by the inclusion of silicon dioxide. At low concentrations, silicon dioxide functioned primarily to reduce the size and volume of coarser pores, presumably representing the spaces between the aggregations of starch and aspirin particles. This effect was optimum at 3%.

3. An assessment of the changes in the pore-size distribution patterns occurring under the influence of water vapor revealed distinct differences in this parameter as functions of the silicon dioxide concentration and the period of exposure to water vapor. These results were explained in terms of the accessibility of water vapor to tablet components.

4. A unique trend in the change of pore-size distribution was noted with tablets containing 3% silicon dioxide. Irrespective of relative changes in the size and volume of pores as a result of swelling of starch grains and the deposition of salicylic acid in the tablet pore system, this formulation consistently exhibited the smallest average pore size among the tablets containing several concentrations of silicon dioxide.

5. The present observations shed considerable light on the interpretation of the stabilizing properties of silicon dioxide in aspirin tablets. It was concluded that pore-size distribution measurements appear to be useful in elucidating aspirin stability in compressed pharmaceutical systems.

REFERENCES

(1) H. Nogami, J. Hasegawa, and M. Miyamoto, *Chem. Pharm. Bull.*, **15**, 279 (1967).

(2) P. Singh, S. J. Desai, A. P. Simonelli, and W. I. Higuchi, *J. Pharm. Sci.*, **57**, 217 (1968).

(3) D. Ganderton, *J. Pharm. Pharmacol.*, **21**, 9S (1969).

(4) D. Ganderton and A. B. Selkirk, *ibid.*, **22**, 345 (1970).

(5) D. Ganderton and D. R. Fraser, *ibid.*, **22**, 95S (1970).

(6) A. B. Selkirk and D. Ganderton, *ibid.*, **22**, 86S (1970).

(7) W. Lowenthal, *J. Pharm. Sci.*, **61**, 1695 (1972).

(8) A. B. Selkirk and D. Ganderton, *J. Pharm. Pharmacol.*, **22**, 79S (1970).

(9) C. A. Kelly, *J. Pharm. Sci.*, **59**, 1053 (1970).

(10) B. K. Martin, in "Advances in Pharmaceutical Sciences," vol. 3, H. S. Bean, A. H. Beckett, and J. E. Carless, Eds., Academic, London, England, 1971, p. 107.

(11) S. Brunauer, P. H. Emmett, and E. Teller, *J. Am. Chem. Soc.*, **60**, 309 (1938).

(12) D. S. Carr and B. L. Harris, *Ind. Eng. Chem.*, **41**, 2014 (1949).

(13) E. W. Washburn, *Proc. Nat. Acad. Sci. USA*, **7**, 115 (1921).

(14) M. E. Nicholas, P. A. Joyner, B. M. Tassem, and M. D. Olsen, *J. Phys. Chem.*, **65**, 1373 (1961).

(15) C. Kembell, *Trans. Faraday Soc.*, **42**, 526 (1946).

(16) H. M. Rootare, *Aminco Lab News*, **4**, 4A (1968).

(17) C. Orr, Jr., *Powder Technol.*, **3**, 117 (1969/70).
(18) H. Gucluyildiz, G. E. Peck, and G. S. Banker, *J. Chem. Ed.*, **49**, 440 (1972).
(19) A. Y. Gore, K. B. Naik, D. O. Kildsig, G. E. Peck, V. F. Smolen, and G. S. Banker, *J. Pharm. Sci.*, **57**, 1850 (1968).

ACKNOWLEDGMENTS AND ADDRESSES

Received November 6, 1975, from the *Department of Industrial and Physical Pharmacy, School of Pharmacy and Pharmacal Sciences, Purdue University, West Lafayette, IN 47907.*

Accepted for publication May 19, 1976.

Presented at the Industrial Pharmaceutical Technology Section, APhA Academy of Pharmaceutical Sciences, Atlanta meeting, November 1975.

Supported in part by a David Ross Fellowship, Purdue Research Foundation.

* Present address: Warner-Lambert Research Institute, Morris Plains, NJ 07950.

[x] To whom inquiries should be directed.

Analysis of Sulindac and Metabolites by Combined Isotope Dilution–Radioimmunoassay

L. E. HARE, C. A. DITZLER, M. HICHENS, A. ROSEGAY, and D. E. DUGGAN [x]

Abstract □ Sulindac, a new anti-inflammatory agent, and its sulfone and sulfide metabolites were conjugated to bovine serum albumin by the *N*-hydroxysuccinimide active ester procedure. Antiserum from rabbits immunized with each of these haptens exhibited extensive cross-reactivity, precluding differential analyses of the three species by displacement assay without prior separation. Therefore, an analytical method based on a combination of isotope dilution and radioimmunoassay was devised. A known mixture of the three chemical species, each labeled with tritium, was equilibrated with plasma or urine samples, reisolated chromatographically, and quantitated by binding to an appropriate immunoglobulin. The radiolabeled materials thus served as recovery standards as well as labeled antigens for each displacement assay. Sulindac and each of its metabolites in plasma or urine at concentrations as low as 500 ng/sample were differentially determined by this procedure. However, since an extraction is required, several milliliters of plasma can be used for each sample, thus increasing the actual sensitivity of the assay.

Keyphrases □ Sulindac—and metabolites, combined isotope dilution–radioimmunoassay, human plasma and urine □ Radioimmunoassay—combined with isotope dilution, analysis of sulindac and metabolites, human plasma and urine □ Isotope dilution–radioimmunoassay—analysis of sulindac and metabolites, human plasma and urine □ Anti-inflammatory agents—sulindac and metabolites, combined isotope dilution–radioimmunoassay, human plasma and urine

Sulindac, *cis*-5-fluoro-2-methyl-1-[*p*-(methylsulfinyl)benzylidenyl]indene-3-acetic acid (I), is a new anti-inflammatory agent (1, 2) currently in clinical trials. Its two principal metabolites, the sulfone (II) and sulfide (III), differ from the parent drug only with respect to the oxidation state of the sulfur moiety (3). Metabolic reduction of sulindac to the sulfide is reversible, but oxidation to the sulfone is irreversible; thus, disposition patterns of this drug are complex. Furthermore, the sulfide metabolite has been proposed as the pharmacologically active species[1]. Thus, any analytical procedure should ideally be capable of distinguishing among these closely related compounds.

GC analysis of sulindac and metabolites was attempted without success[2]. The principal difficulties encountered were the lack of sensitivity for sulfide and the insufficient separation of sulindac and its sulfone metabolite. Another potentially useful method is mass fragmentography, and such an assay for sulindac is in the final stages of development[3].

A third possible method is radioimmunoassay, provided that specific antiserums to each compound are available. Early results suggested that specific antibodies to sulindac and metabolites could not be obtained. One solution to the problem of poor selectivity is to separate the compounds chromatographically prior to radioimmunoassay. This approach has been applied to assays of steroids and prostaglandins (4–6). A slightly different technique utilizing isotope dilution in combination with radioimmunoassay has been devised for the differential determination of sulindac and its metabolites and is the subject of this report.

EXPERIMENTAL

Materials—Bovine serum albumin[4], *N*-hydroxysuccinimide[5], dicyclohexylcarbodiimide[5], neutral charcoal[6], and dextran[7] were used. Dextran-coated charcoal was prepared by suspending 6.25 g of prewashed charcoal and 0.625 g of dextran in 100 ml of 0.05 *M* phosphate buffer, pH 7.5.

Preparation of Labeled Antigens—*[^{3}H-Methylene]sulindac Sulfide*—A mixture of sulindac sulfide (0.5 g), potassium *tert*-butoxide (0.6 g), and tritiated water (2 ml, 25 Ci) was heated at 90° for 2 hr. Water was then added, and the mixture was acidified. The labeled sulfide that precipitated was collected and dissolved in methanol. The solution was evaporated (several times) to remove labile tritium. Several recrystallizations from benzene afforded pure tritiated sulfide (350 mg), mp 186–187°, specific activity 172 μCi/mg.

[^{3}H-Methylene]sulindac—Sodium metaperiodate (144 mg) in water (2 ml) was added to a solution of tritiated sulindac sulfide (102 mg) in methanol (8 ml) and acetone (2 ml), and the mixture was stirred at 25° for 16 hr. The mixture was concentrated, diluted with water, acidified, and extracted with ethyl acetate. The solid obtained by evaporating the ethyl acetate was recrystallized several times from ethyl acetate to yield 53 mg of pure sulindac, mp 181–183°, specific activity 167 μCi/mg.

[1] C. G. Van Arman, Merck Sharp & Dohme Research Laboratories, unpublished data.

[2] H. B. Hucker and G. O. Breault, Merck Sharp & Dohme Research Laboratories, personal communication.

[3] W. J. A. VandenHeuvel, Merck Sharp & Dohme Research Laboratories, personal communication.

[4] Nutritional Biochemical Co.

[5] Pierce Chemical Co.

[6] Norit A, Amend Drug and Chemical Co.

[7] T-70, Pharmacia Labs.

(17) C. Orr, Jr., *Powder Technol.*, **3**, 117 (1969/70).
(18) H. Gucluyildiz, G. E. Peck, and G. S. Banker, *J. Chem. Ed.*, **49**, 440 (1972).
(19) A. Y. Gore, K. B. Naik, D. O. Kildsig, G. E. Peck, V. F. Smolen, and G. S. Banker, *J. Pharm. Sci.*, **57**, 1850 (1968).

ACKNOWLEDGMENTS AND ADDRESSES

Received November 6, 1975, from the *Department of Industrial and Physical Pharmacy, School of Pharmacy and Pharmacal Sciences, Purdue University, West Lafayette, IN 47907.*

Accepted for publication May 19, 1976.

Presented at the Industrial Pharmaceutical Technology Section, APhA Academy of Pharmaceutical Sciences, Atlanta meeting, November 1975.

Supported in part by a David Ross Fellowship, Purdue Research Foundation.

* Present address: Warner-Lambert Research Institute, Morris Plains, NJ 07950.

[x] To whom inquiries should be directed.

Analysis of Sulindac and Metabolites by Combined Isotope Dilution–Radioimmunoassay

L. E. HARE, C. A. DITZLER, M. HICHENS, A. ROSEGAY, and D. E. DUGGAN [x]

Abstract □ Sulindac, a new anti-inflammatory agent, and its sulfone and sulfide metabolites were conjugated to bovine serum albumin by the *N*-hydroxysuccinimide active ester procedure. Antiserum from rabbits immunized with each of these haptens exhibited extensive cross-reactivity, precluding differential analyses of the three species by displacement assay without prior separation. Therefore, an analytical method based on a combination of isotope dilution and radioimmunoassay was devised. A known mixture of the three chemical species, each labeled with tritium, was equilibrated with plasma or urine samples, reisolated chromatographically, and quantitated by binding to an appropriate immunoglobulin. The radiolabeled materials thus served as recovery standards as well as labeled antigens for each displacement assay. Sulindac and each of its metabolites in plasma or urine at concentrations as low as 500 ng/sample were differentially determined by this procedure. However, since an extraction is required, several milliliters of plasma can be used for each sample, thus increasing the actual sensitivity of the assay.

Keyphrases □ Sulindac—and metabolites, combined isotope dilution–radioimmunoassay, human plasma and urine □ Radioimmunoassay—combined with isotope dilution, analysis of sulindac and metabolites, human plasma and urine □ Isotope dilution–radioimmunoassay—analysis of sulindac and metabolites, human plasma and urine □ Anti-inflammatory agents—sulindac and metabolites, combined isotope dilution–radioimmunoassay, human plasma and urine

Sulindac, *cis*-5-fluoro-2-methyl-1-[*p*-(methylsulfinyl)benzylidenyl]indene-3-acetic acid (I), is a new anti-inflammatory agent (1, 2) currently in clinical trials. Its two principal metabolites, the sulfone (II) and sulfide (III), differ from the parent drug only with respect to the oxidation state of the sulfur moiety (3). Metabolic reduction of sulindac to the sulfide is reversible, but oxidation to the sulfone is irreversible; thus, disposition patterns of this drug are complex. Furthermore, the sulfide metabolite has been proposed as the pharmacologically active species[1]. Thus, any analytical procedure should ideally be capable of distinguishing among these closely related compounds.

GC analysis of sulindac and metabolites was attempted without success[2]. The principal difficulties encountered were the lack of sensitivity for sulfide and the insufficient separation of sulindac and its sulfone metabolite. Another potentially useful method is mass fragmentography, and such an assay for sulindac is in the final stages of development[3].

A third possible method is radioimmunoassay, provided that specific antiserums to each compound are available. Early results suggested that specific antibodies to sulindac and metabolites could not be obtained. One solution to the problem of poor selectivity is to separate the compounds chromatographically prior to radioimmunoassay. This approach has been applied to assays of steroids and prostaglandins (4–6). A slightly different technique utilizing isotope dilution in combination with radioimmunoassay has been devised for the differential determination of sulindac and its metabolites and is the subject of this report.

EXPERIMENTAL

Materials—Bovine serum albumin[4], *N*-hydroxysuccinimide[5], dicyclohexylcarbodiimide[5], neutral charcoal[6], and dextran[7] were used. Dextran-coated charcoal was prepared by suspending 6.25 g of prewashed charcoal and 0.625 g of dextran in 100 ml of 0.05 *M* phosphate buffer, pH 7.5.

Preparation of Labeled Antigens—*[^{3}H-Methylene]sulindac Sulfide*—A mixture of sulindac sulfide (0.5 g), potassium *tert*-butoxide (0.6 g), and tritiated water (2 ml, 25 Ci) was heated at 90° for 2 hr. Water was then added, and the mixture was acidified. The labeled sulfide that precipitated was collected and dissolved in methanol. The solution was evaporated (several times) to remove labile tritium. Several recrystallizations from benzene afforded pure tritiated sulfide (350 mg), mp 186–187°, specific activity 172 μCi/mg.

[^{3}H-Methylene]sulindac—Sodium metaperiodate (144 mg) in water (2 ml) was added to a solution of tritiated sulindac sulfide (102 mg) in methanol (8 ml) and acetone (2 ml), and the mixture was stirred at 25° for 16 hr. The mixture was concentrated, diluted with water, acidified, and extracted with ethyl acetate. The solid obtained by evaporating the ethyl acetate was recrystallized several times from ethyl acetate to yield 53 mg of pure sulindac, mp 181–183°, specific activity 167 μCi/mg.

[1] C. G. Van Arman, Merck Sharp & Dohme Research Laboratories, unpublished data.

[2] H. B. Hucker and G. O. Breault, Merck Sharp & Dohme Research Laboratories, personal communication.

[3] W. J. A. VandenHeuvel, Merck Sharp & Dohme Research Laboratories, personal communication.

[4] Nutritional Biochemical Co.

[5] Pierce Chemical Co.

[6] Norit A, Amend Drug and Chemical Co.

[7] T-70, Pharmacia Labs.

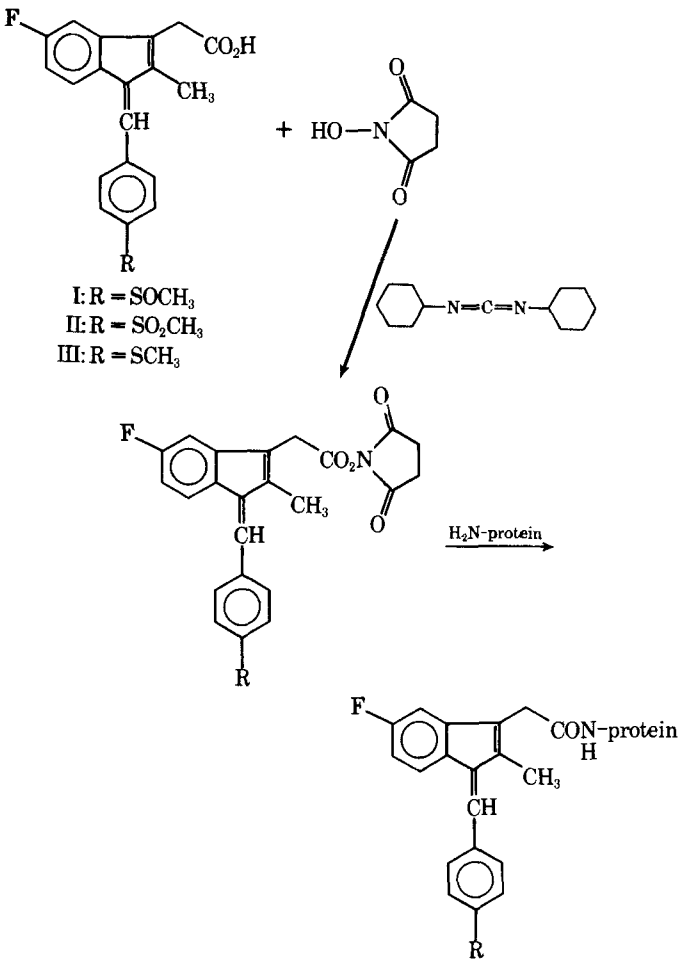

Scheme I

[^{3}*H-Methylene, vinyl*]*sulindac Sulfone*—Sulindac sulfone was labeled in the same manner as the sulfide. The crude product was redissolved in 1 *N* sodium hydroxide for 5 min and then precipitated with acid (several times) to remove labile tritium from the sulfonylmethyl and carboxyl groups. Two recrystallizations from acetic acid–water afforded pure tritiated sulfone, mp 200–201°, specific activity 337 μCi/mg. The NMR spectrum of the deuterated analog showed partial exchange of the vinyl proton as well as the methylene protons.

Preparation of Conjugates—Sulindac and metabolites were each conjugated through the carboxylic acid moiety to bovine serum albumin by the *N*-hydroxysuccinimide active ester procedure (7, 8) (Scheme I). Conversion of the acids to the succinimide esters was verified by the appearance of characteristic imide peaks at 1800, 1780, and 1720 cm^{-1} in the IR spectrum. Each active ester (0.15 mmole) in dioxane (4 ml) was added dropwise to a solution of albumin (340 mg, 0.3 mmole of lysine equivalents) in 0.1 *M* borate buffer, pH 9.0 (30 ml).

The solutions were allowed to stand at room temperature overnight and then were extensively dialyzed against distilled water. Insoluble material was removed by centrifugation, and the solution was lyophilized. The extent of conjugation was 10–30 molecules of sulindac or metabolites per molecule of protein, as estimated by UV absorption (sulindac, ϵ 325 nm = 1.31×10^4; sulindac sulfone, ϵ 327 nm = 1.17×10^4; and sulindac sulfide, ϵ 350 nm = 1.72×10^4).

Immunization of Animals—New Zealand White rabbits were given sulindac–albumin conjugates (2–5 mg im) dissolved in saline and emulsified with an equal volume of Freund's complete adjuvant. Booster injections of 1 mg of conjugate were given at monthly intervals in incomplete adjuvant. Bleedings were taken from central ear arteries about 2 weeks after booster injections.

To determine antibody titer, the quantity of tritiated sulindac and metabolites bound to the various antiserums was compared with the binding observed for normal serums. The high degree of sulindac sulfide binding to serum proteins necessitated the purification of the γ-globulin fraction of antiserum to this compound by precipitation from 18% sodium sulfate (9). Antiserums were used at dilutions that bound 30–50% of the added label in control tubes containing no unlabeled antigen.

Table I—Cross-Reactivity of Sulindac Antiserums

	Unlabeled Antigen, I_{50}[a], ng/ml		
Immunoglobulin	I	II	III
Anti-I or anti-II[b]	40	40	>1000
Anti-III[c]	29	23	33

[a] I_{50} = drug concentration resulting in 50% inhibition of binding of labeled antigen. [b] Labeled antigen = ^{3}H-I or ^{3}H-II (50 ng). [c] Labeled antigen = ^{3}H-III (20 ng).

Combined Isotope Dilution–Radioimmunoassay—A known mixture of I–III, each labeled with tritium (250 ng, ~1×10^5 dpm each), was equilibrated with 1-ml plasma or urine samples containing standard or unknown solutions of sulindac and metabolites in the 500–3000-ng/ml range. The aqueous solutions were adjusted to pH 5 by the addition of 0.2 ml of 1 *M* citrate buffer, pH 5, and were extracted with 3 ml of benzene–2-propanol (9:1). The aqueous phase was discarded.

The organic phase was removed and evaporated to dryness. The residue was dissolved in 0.03 ml of ethanol, and approximately one-third was chromatographed on paper[8] with toluene–xylene–2-propanol–dioxane–6% ammonium hydroxide (1:1:3:3:2) as the developing solvent. Areas containing the three chemical species (sulindac, R_f 0.45; sulindac sulfone, R_f 0.54; and sulindac sulfide, R_f 0.71) were excised and eluted with 15 m*M* sodium hydroxide (1 ml). The aqueous solutions were adjusted to pH 7.5 by the addition of 30 m*M* monobasic sodium phosphate (0.5 ml), and one 0.3-ml aliquot was used for determination of recovery.

For the binding assay, a solution consisting of 0.9 ml of the eluate and 0.1 ml of the appropriate immunoglobulin was mixed and allowed to equilibrate at 4° overnight. "Bound" and "free" antigens were separated by addition of 0.2 ml of dextran-coated charcoal. The charcoal suspension was kept at 4° for 10–12 min and then separated by centrifugation; the supernate was counted to determine the fraction of radioactivity bound to the antibody.

Standard curves were plotted as drug concentration (labeled plus unlabeled drug) in the assay tube *versus* percent of total radioactivity bound to antibody. Concentrations of unknowns (*C*, nanograms per milliliter) were calculated from the following equation: $C = (c/r) - 250$, where *c* and *r* represent drug concentration as extrapolated from the standard curve and recovery, respectively. The 250 value represents the mass of each radioactive species added to the original sample.

In urine, glucuronide conjugates were hydrolyzed before analysis, thereby providing a measure of the total amount of each species present in free and conjugated forms. Appropriately diluted urine samples (0.75 ml) and 0.25 ml of 1 *N* sodium hydroxide were incubated for 30 min at room temperature and adjusted to pH 5 by the addition of 2 *M* acetic acid (0.17 ml). The mixture of the labeled compounds was added, and the samples were chromatographed and assayed as described.

Cross-Reactivity—Conventional radioimmunoassay was used for the estimation of cross-reactivity. This procedure was similar to that already described, except that extraction was necessary only in the case of sulindac sulfide due to binding of this species to plasma proteins. In addition, all chromatography steps were eliminated.

Comparison of Methods—Plasma samples containing labeled sulindac and metabolites of low specific activity (8 μCi/mg) were prepared to mimic concentrations found in humans following sulindac administration. Each sample was analyzed by isotope dilution–radioimmunoassay as already described and by reverse isotope dilution. In the latter procedure, samples (1 ml) were equilibrated with a known mixture (0.25 μmole each) of the three compounds and were extracted with benzene–2-propanol (9:1). The organic phase was evaporated to dryness, and the mixture was chromatographed as described. Papers were eluted with ethanol, and drug concentrations were determined spectrophotometrically. The eluates were counted, and the concentration of each component was determined from the specific activities of each species and the known ratio of carrier to radioactivity initially present.

RESULTS

Antibodies to sulindac and metabolites were detected within 6 weeks after immunization of rabbits. Antibody titers reached plateau values after 6 months and began to fall off after 1 year despite continued boosting. The amount of drug attached to the protein did not appear to

[8] Whatman No. 1.

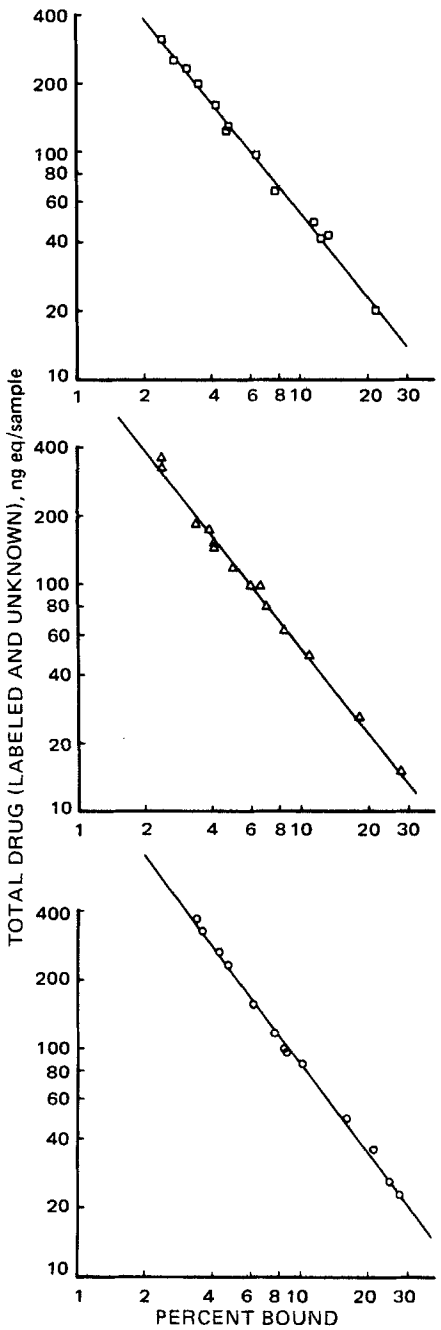

Figure 1—*Typical standard displacement curves for determination of sulindac* (○), *sulindac sulfone* (△), *and sulindac sulfide* (□).

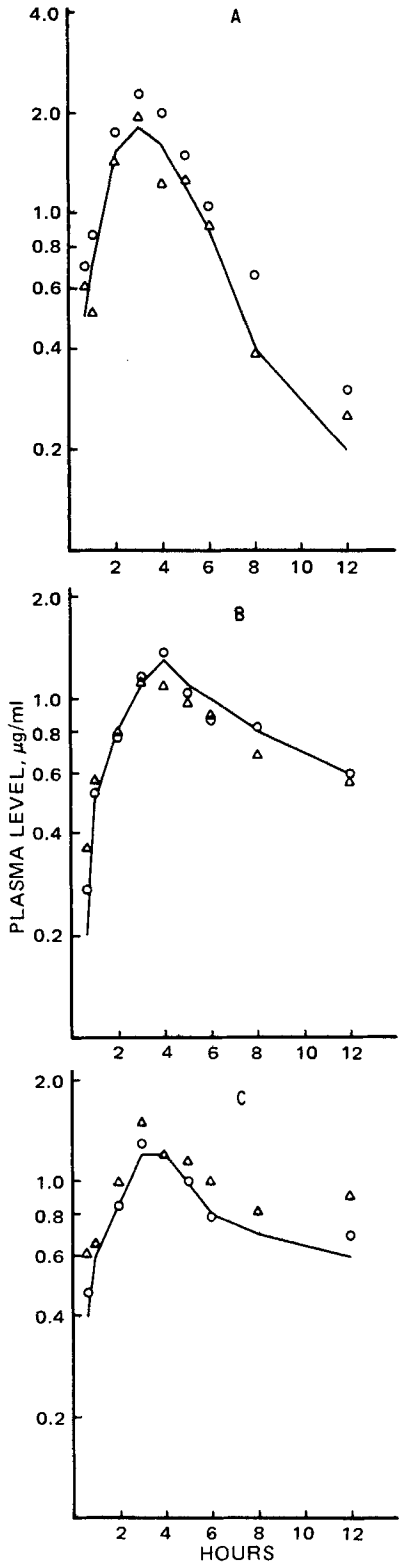

Figure 2—*Observed plasma concentrations of sulindac* (*A*), *sulindac sulfone* (*B*), *and sulindac sulfide* (*C*) *determined by isotope dilution–radioimmunoassay* (△) *and reverse isotope dilution* (○). *The line represents theoretical values.*

be critical, since conjugates in which 25–50% of the lysine residues were modified afforded equivalent antibody titers. Final antiserum dilutions of approximately 1:500 in the reaction tube bound 35% of labeled antigen and were used for routine assay.

All antiserums exhibited extensive cross-reactivity (Table I). Antiserums to I and II each possessed identical affinity for I and II. However, neither antibody bound III significantly. The anti-III immunoglobulin was less selective, exhibiting virtually 100% cross-reactivity to all three compounds. Thus, these serums possessed high affinity but low selectivity and were unsuitable for direct, differential determinations of sulindac and metabolites.

The combined isotope dilution–radioimmunoassay method produced the necessary specificity *via* the chromatography step while retaining the sensitivity of the antibody-binding assay. Radioactive recovery following sample extraction, aliquoting, and chromatography ranged from 20 to 70%, and good reproducibility of the assay was obtained within this range. This variability of recovery was probably due to the inability to locate with certainty the three redox species on the paper. Absolute recovery is not critical, since the recovery standard also serves as labeled antigen.

Standard displacement curves are illustrated in Fig. 1. These curves were linear when drawn on a log–log scale and possessed correlation coefficients greater than 0.997. Significant displacement was obtained with approximately 20 ng of unlabeled antigen/tube. Therefore, the effective sensitivity of the assay was 200 ng/sample, assuming a 50% re-

Table II—Assay of Sulindac and Metabolites Added to Normal Plasma

Standard Concentrations, μg/ml	Experimental Values[a]								
	Sulindac			Sulindac Sulfone			Sulindac Sulfide		
	μg/ml	CV	Recovery, %	μg/ml	CV	Recovery, %	μg/ml	CV	Recovery, %
0.1	0.07 ± 0.015	0.22	70 ± 15	0.089 ± 0.012	0.13	89 ± 12	0.046 ± 0.023	0.50	46 ± 23
0.5	0.5 ± 0.042	0.08	99 ± 8	0.55 ± 0.062	0.11	111 ± 12	0.44 ± 0.022	0.05	89 ± 4
1.0	1.2 ± 0.083	0.07	115 ± 8	1.1 ± 0.051	0.05	106 ± 5	0.89 ± 0.057	0.06	89 ± 6

[a] Means of 10 samples ± *SD*.

covery. However, since an extraction step is employed, sensitivity can be increased by using sample volumes larger than 1 ml with a concomitant increase in the volume of the first organic phase.

Precision and accuracy were demonstrated by analysis of replicate standards in pooled normal plasma (Table II). Coefficients of variance for sulindac and the sulfide at 0.1 μg/ml were unacceptable. However, at concentrations near the midpoint of the standard curves, *i.e.*, 0.5–1.0 μg/ml, coefficients of variance averaged 7% while mean accuracy was 102 ± 7% for all three compounds. Thus, samples should be adjusted to the 0.5–5.0-μg range by dilution or concentration prior to assay.

Results obtained by this method also were validated by comparison with results of the classical reverse isotope dilution assay. The two methods were employed to analyze levels of ^{3}H-sulindac and its sulfone and sulfide metabolites in plasma. The specific activity of these samples was much lower than that of the labeled antigen and did not interfere with the combined isotope dilution–radioimmunoassay procedure. Plasma concentrations are shown in Fig. 2. In general, good correlation was seen among values obtained by the two methods.

Since sulfoxides are enantiomeric, the binding of partially resolved biogenic sulindac to the antibody was examined. Biogenic material was purified from the urine of rabbits treated with sulindac sulfide and possessed an $[\alpha]_D$ of +11° compared to the value of +21° determined for chemically resolved compound[9]. Thus, biogenic sulindac was approximately 67% enriched with respect to the dextrorotatory isomer. Standard displacement curves for the biogenic sample and for racemic sulindac were identical.

DISCUSSION

A common disadvantage of many radioimmunoassay procedures is a lack of specificity. Thus, closely related compounds often cannot be distinguished. For this reason, separation procedures have been utilized in combination with radioimmunoassay in several cases. For example, prostaglandins E, A, and F were separated on silicic acid columns (4), estrogens were analyzed by dextran gel[10] chromatography (5), and dehydroepiandrosterone was purified by paper chromatography (6) prior to radioimmunoassay. In all of these procedures, tracer quantities of radiolabeled drug were added to samples to determine recovery. Then, larger amounts of radioactive drug, usually two to 10 times the tracer amount, were added as labeled antigen for radioimmunoassay. Relatively high specific activities are required to ensure that the recovery standard is indeed added in negligible amounts relative to the material being measured and, therefore, will not interfere with radioimmunoassay.

The described procedure (combined isotope dilution–radioimmunoassay) for sulindac differs from radioimmunoassay in that it is fundamentally an isotope dilution method employing a binding assay for detection. Added radioactive drug serves as both the recovery standard and labeled antigen, and standard curves represent total labeled and unlabeled drug (*i.e.*, specific activity of diluted material) present in the assay tube. Thus, whereas radioimmunoassay is an indirect measurement of unlabeled material causing a certain degree of displacement of labeled antigen from the antibody, combined isotope dilution–radioimmunoassay is a direct measure of the total material bound to the antibody. Therefore, the modified procedure offers the advantages that absolute recovery is not a limiting factor and that standards are treated in the same manner as unknowns, thus avoiding unaccountable procedural changes or losses. In addition, a lower specific activity of the labeled antigens is acceptable and a pipetting step is eliminated.

An apparent disadvantage of this method is that the critical antibody–labeled antigen ratio can vary with recovery, resulting in irreproducible data. This is true if recovery falls below a certain critical value of approximately 15%. However, as indicated by the precision of the assay, this is not generally a problem. Combined isotope dilution–radioimmunoassay requires that labeled antigens be chemically identical to each compound being determined and is not applicable to materials such as peptide hormones that utilize iodine-labeled antigens.

Incorporation of isotope dilution into radioimmunoassay procedures does result in a rather tedious method, but such a combination will, in most cases, provide specificity and sensitivity not otherwise obtainable. The disadvantages, in the case of sulindac, may be eliminated in some instances by determining the parent drug plus sulfone or all three compounds directly by radioimmunoassay using a nonselective antibody such as the anti-III immunoglobulin (Table I). Such an approach might be justified in certain bioavailability or drug interaction studies in which drug absorption is the principal consideration.

Examination of the sulindac metabolic pattern suggested that the sulfoxide might be resolved into one enantiomeric form *in vivo* by repeated reduction to sulfide followed by reoxidation, and this has been shown to be the case. The stereospecificity of antibodies was first demonstrated by Landsteiner and Scheer (10), who found that antibodies produced against one enantiomer of a pair were far less reactive to the second enantiomer. Since the sulindac antibody was produced against a recemic compound, the possibility exists of altered displacement kinetics involving an optically pure or even partially resolved enantiomer of the drug. However, the superimposability of standard curves for biogenic and racemic sulfoxide indicates that partial resolution does not compromise the validity of this assay.

[9] H. Jones, Merck Sharp & Dohme Research Laboratories, personal communication.

[10] Sephadex LH-20.

REFERENCES

(1) T. Y. Shen, B. E. Witzel, H. Jones, B. O. Linn, J. McPherson, R. Greenwald, M. Fordice, and A. Jacobs, *Fed. Proc.*, **31**, 577 (1972).

(2) C. G. Van Arman, E. A. Risley, and G. W. Nuss, *ibid.*, **31**, 577 (1972).

(3) H. B. Hucker, S. C. Stauffer, S. D. White, R. E. Rhodes, B. H. Arison, E. R. Umbenhauer, R. J. Bower, and F. G. McMahon, *J. Pharmacol. Exp. Ther.*, **1**, 721 (1973).

(4) B. M. Jaffe, H. R. Behrman, and C. W. Parker, *J. Clin. Invest.*, **52**, 398 (1973).

(5) C.-H. Wu and L. E. Lundy, *Steroids*, **18**, 91 (1971).

(6) H. Sekihara, T. Yamaji, N. Ohsawa, and H. Ibayashi, *Endocrinol. Jpn.*, **21**, 115 (1974).

(7) G. W. Anderson, J. E. Zimmerman, and F. M. Callahan, *J. Am. Chem. Soc.*, **86**, 1839 (1964).

(8) M. Hichens and A. F. Hogans, *Clin. Chem.*, **20**, 266 (1974).

(9) K. Heide and H. G. Schwick, in "Handbook of Experimental Immunology," 2nd ed., D. M. Weir, Ed., Blackwell Scientific Publications, Oxford, England, 1973, chap. 6.

(10) K. Landsteiner and J. van der Scheer, *J. Exp. Med.*, **48**, 315 (1928).

ACKNOWLEDGMENTS AND ADDRESSES

Received October 8, 1975, from the *Merck Institute for Therapeutic Research, West Point, PA 19486.*

Accepted for publication May 26, 1976.

Presented in part at the American Society for Pharmacology and Experimental Therapeutics, Montreal, Canada, fall meeting, 1974 [*Pharmacologist*, **16**, 221 (1974)].

The authors thank Dr. J. E. Baer for encouragement and comments and Ms. K. F. Hooke for assistance with animals.

[x] To whom inquiries should be directed.

Synthesis and *In Vivo* Antimalarial Evaluation of Isopropyl [(4-Chlorophenyl)amino]iminomethylcarbamimidate

VICTOR D. WARNER *x, **DONALD M. LYNCH** *, **CHARLES A. MESZOELY** ‡, and **WILLIAM G. DYKSTRA, Jr.** ‡

Abstract □ Isopropyl [(4-chlorophenyl)amino]iminomethylcarbamimidate was synthesized as a potential antimalarial agent. Biological activity was evaluated against *Plasmodium lophurae* in turkeys. The activity of this compound was compared to its nitrogen isostere, chloroguanide.

Keyphrases □ Carbamimidate ester, substituted—synthesized, screened for antimalarial activity, turkeys □ Antimalarial activity—screened in substituted carbamimidate ester, turkeys □ Structure–activity relationships—substituted carbamimidate ester screened for antimalarial activity, turkeys

During an *in vitro* study of the antiplaque activity of N^1-(4-chlorophenyl)-N^5-alkylbiguanides (I), it became necessary to prepare larger quantities of these compounds (1). To optimize yields, the ratio of alkylamine to N^1-(4-chlorophenyl)-N^3-cyanoguanidine (II) in ethanol was changed from 4:1 to 1:1. The product obtained from this reaction was the ethyl ester of [(4-chlorophenyl)amino]-iminomethylcarbamimidic acid (III) rather than the expected alkylbiguanide. The similarity between this compound and chloroguanide (IV) prompted the synthesis of the isopropyl derivative (V) as a potential antimalarial agent.

Reaction of II with isopropyl alcohol in the presence of triethylamine and copper acetate (Scheme I) yielded isopropyl [(4-chlorophenyl)amino]iminomethylcarbamimidate (V). This compound and chloroguanide were tested as their acetate salts against turkeys infected with *Plasmodium lophurae*.

EXPERIMENTAL

Chemistry[1]—N^1-*(4-Chlorophenyl)*-N^3-*cyanoguanidine (II)*—This compound was prepared from 4-chloroaniline hydrochloride and sodium dicyanamide, as previously reported (2), mp 202–203° [lit. (2) mp 204–205°].

Isopropyl [(4-Chlorophenyl)amino]iminomethylcarbamimidate (V)—Compound II (4.86 g, 0.025 mole), copper acetate monohydrate (2.5 g, 0.0125 mole), triethylamine (10 ml), and isopropyl alcohol (100 ml) were refluxed with stirring for 12 hr. The purple reaction mixture was evaporated *in vacuo* to yield a semisolid. Water (100 ml) was added, and the remaining alcohol was removed by azeotropic distillation. An additional 100 ml of water was then added, and the insoluble copper complex was destroyed with acetic acid (25 ml).

Gaseous hydrogen sulfide was bubbled through the mixture, and the resulting copper sulfide was removed by filtration. The filtrate was adjusted to pH 7 with concentrated ammonium hydroxide and allowed to stand at 4° for 12 hr, which resulted in the precipitation of the acetate salt. The acetate salt was then recrystallized using methanol to yield 2.88 g (36.2%) of a white solid, mp 181–182°.

Anal.—Calc. for $C_{13}H_{19}ClN_4O_3$: C, 49.60; H, 6.08; N, 17.80. Found: C, 49.65; H, 6.15; N, 17.85.

Antimalarial Activity—Turkey poults (3–4 weeks old) from the same brood were used. The turkeys were given food and water *ad libitum*. The strain[2] of *P. lophurae* used was maintained by weekly serial blood passage from an infected donor turkey to an uninfected poult. The turkeys used in both the Davey test (eight turkeys) and the Patency test (six turkeys) were infected intravenously *via* the wing vein with an inoculum (50 million parasitized red blood cells in 0.2 ml) taken from the same donor turkey.

Modified Davey Test—This test was modified as suggested by Peters (3). The day of infection was termed D 0, and the following day was designated D + 1. The drugs were given as aqueous solutions by oral intubation. The first dose of the drug (10 mg/kg) was given 4 hr prior to infection. Doses of 5 mg/kg were then administered twice daily for 3 days for a total of seven doses (40 mg/kg). Blood smears were taken daily, and the percent parasitemia was determined by counting the parasites in 500 red blood cells.

Patency Test[3]—This test involved the measurement of the schizonticidal activity of the test compounds. Percent parasitemia levels of the untreated, infected turkeys were determined daily. When the levels were above 10%, a large, single oral dose (100 mg/kg) was administered.

RESULTS AND DISCUSSION

The results of the modified Davey test are summarized in Table I. Chloroguanide displayed suppressive activity against the blood forms of *P. lophurae* 7 days after infection. The carbamimidate ester suppressed parasitemia for only 1 day. At D + 8, the controls and carbamimidate ester-treated turkeys died, but the chloroguanide-treated animals showed only a trace of parasitemia. According to the Davey test criterion (percent parasitemia on D + 4), the carbamimidate ester-treated turkeys did not show a significant difference of suppression from that of the controls.

From these results, it may be concluded that the carbamimidate ester has no suppressive activity at a total dose of 40 mg/kg. Conceivably, the carbamimidate ester may display suppressive activity at a higher dose,

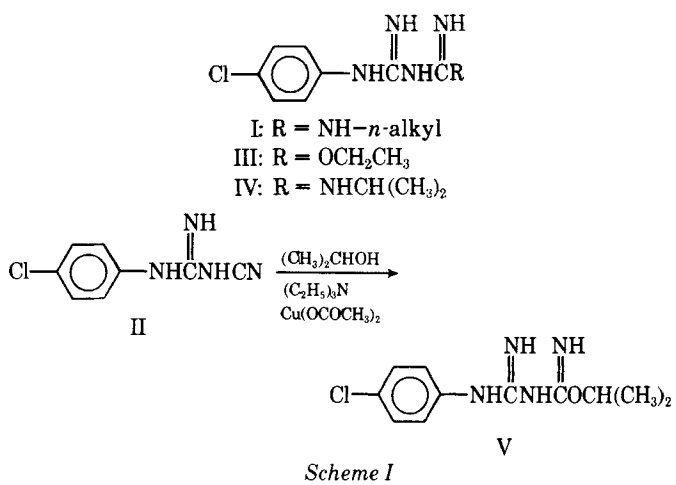

Scheme I

[1] Melting points were determined on a Thomas-Hoover capillary melting-point apparatus and are uncorrected. Microanalysis was performed by Midwest Microlab, Ltd., Indianapolis, Ind. A Varian Associates model T-60 NMR spectrometer and a Perkin-Elmer model 700 IR spectrometer were used. Spectral data were in accord with assigned structures.

[2] Donated by Dr. Richard Beaudoin, Malaria Division, Naval Medical Research Institute, Bethesda, Md.

[3] R. Beaudoin, Malaria Division, Naval Medical Research Institute, Bethesda, Md., personal communication.

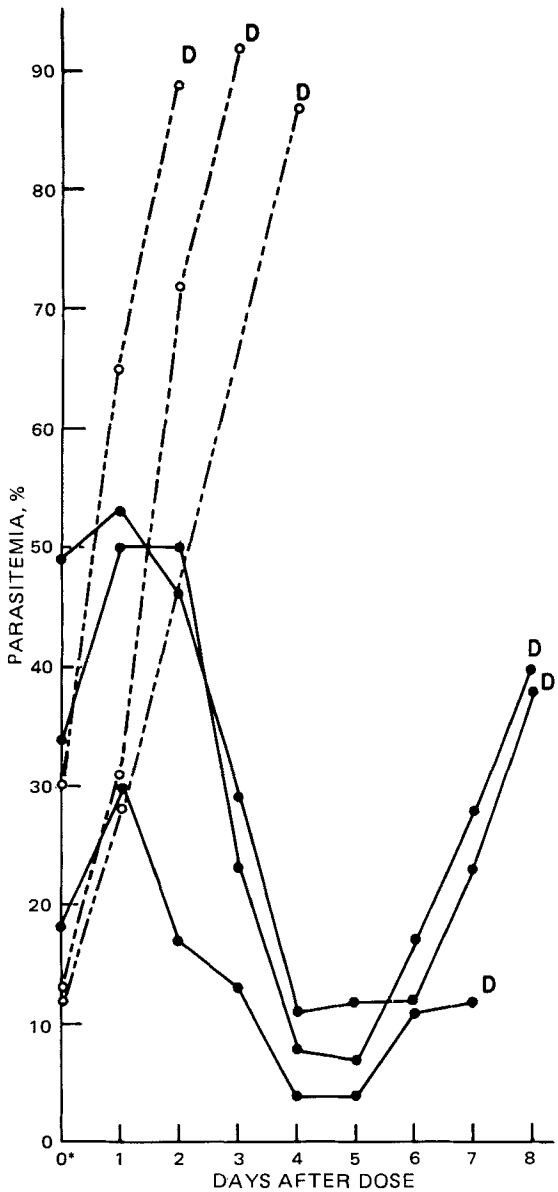

Figure 1—*Schizonticidal activity of single oral dose (100 mg/kg) of the test compounds. Key: *, birds given oral dose; O, carbamimidate ester; ●, chloroguanide; and D, bird died.*

Table I—Results of the Davey Test[a]

Time	Control	Chloroguanide[b]	Carbamimidate[b]
D + 1	1 ± 1	0	0
D + 2	1.1 ± 0.3	0	1
D + 3	3.5 ± 2.5	0	3.1 ± 2.1
D + 4	22.3 ± 13.3	0	15.5 ± 10.5
D + 5	65.3 ± 25.3	0	36.0 ± 17
D + 6	89.6 ± 9.4	0	58.0 ± 25
D + 7	97[c]	0	82[d]
D + 8	Death	1	Death
D + 9		6 ± 4	
D + 10		13.3 ± 5.3	
D + 11		54.3 ± 17.7	
D + 12		83.0 ± 3[d]	
D + 13		Death	

[a] Blood smears compared on D + 4 are used as Davey test criteria; there were three turkeys in each group. [b] Percent parasitemia is expressed as mean ± range. [c] Death of two birds. [d] Death of one bird.

but results from the Patency test (Fig. 1) indicate that this effect is not too likely. The blood smears taken at daily intervals show that chloroguanide possesses potent schizonticidal activity, whereas the carbamimidate ester displays no schizonticidal activity at the same dose (100 mg/kg).

The apparent lack of antimalarial activity for the carbamimidate ester may be due to: (*a*) an inability to form some biologically active metabolite [chloroguanide must cyclize prior to displaying antimalarial activity (4)] or (*b*) nonspecific esterase hydrolysis of the isopropyl group, yielding a product that could rearrange to a urea derivative.

REFERENCES

(1) V. D. Warner, D. M. Lynch, R. S. Ajemian, and S. S. Turesky, Medicinal Chemistry Section, APhA Academy of Pharmaceutical Sciences, San Francisco meeting, Apr. 1975, Abstract 2.

(2) F. H. S. Curd and F. F. Rose, *J. Chem. Soc.*, **1946**, 729.

(3) W. Peters, "Chemotherapy and Drug Resistance in Malaria," Academic, New York, N.Y., 1970, p. 85.

(4) E. A. Steck, "The Chemotherapy of Protozoan Diseases," Walter Reed Army Institute of Research, Washington, D.C., 1971, p. 23.

ACKNOWLEDGMENTS AND ADDRESSES

Received February 12, 1976, from the **Department of Medicinal Chemistry and Pharmacology, College of Pharmacy and Allied Health Professions, and the* [‡]*Department of Biology, College of Liberal Arts, Northeastern University, Boston, MA 02115.*

Accepted for publication April 23, 1976.

Supported in part by Department of Health, Education, and Welfare Grant RR 07143.

[x] To whom inquiries should be directed.

β-Lipoproteins: Possible Plasma Transport Proteins for Basic Drugs

J. J. VALLNER ˣ and L. CHEN

Abstract □ Various drugs were screened for possible interaction with β-lipoprotein. The results suggest that β-lipoproteins may act in conjunction with albumin in the plasma transport of basic or cationic drugs.

Keyphrases □ β-Lipoproteins—interactions with various acidic and basic drugs screened □ Drug–biomolecule interactions—various acidic and basic drugs with β-lipoproteins □ Interactions, drug–biomolecule—various acidic and basic drugs with β-lipoproteins □ Plasma transport proteins—β-lipoprotein interactions with various acidic and basic drugs screened

Numerous literature reports deal with the binding of drugs to human or bovine serum albumin, and it is generally agreed that albumin is the main transport protein for many anionic drug molecules. In contrast, there have been few reports of albumin binding of positively charged species.

When the binding of three sulfonylureas to serum proteins was examined (1), almost no binding to lipoproteins could be demonstrated. The largest portion of each hypoglycemic was bound to the albumin fraction. However, in an examination of the binding of the basic drugs chlorpromazine and imipramine (2), the interaction with lipoproteins was as avid as that with albumin or red cells. In this same study, the binding of an anionic agent, salicylic acid, to lipoprotein could not be shown. In another study, lipoproteins demonstrated an affinity for the basic drug quinidine almost equal to that of serum albumin (3). The high affinity quinidine site on lipoprotein (low and high density) was about 2×10^5.

This work was undertaken to test whether lipoproteins have a greater affinity for basic drugs than other agents. β-Lipoproteins may serve as plasma transporters of basic drugs as albumin does of primarily anionic species. To examine this possibility, numerous acidic and basic drugs were screened. The method of absorbance difference spectrophotometry was employed because of its capability for detecting small changes should binding occur between the drug and lipoprotein.

EXPERIMENTAL

The drugs were used as received from the manufacturers without further purification. All other materials were USP grade. The β-lipoprotein[1] was used as supplied, except that, in some experiments, it was dialyzed against 10 volumes of buffer for 5 hr prior to the drug binding examination. Sorenson phosphate buffer, adjusted to pH 7.4, was used throughout this study.

The drug–macromolecule interaction was assessed on a spectrophotometer[2] using the tandem cell technique (4). As in a previous study employing the difference spectrophotometric method, the concentrations of drug and protein had to be kept constant in both reference and sample beams throughout the titration of the macromolecule (5). All reported results are the averages of at least 3-μl aliquot titrations of the β-lipoprotein with the drug.

[1] Cohn fraction III-0, lot 4351, Nutritional Biochemical Corp., Cleveland, Ohio.

[2] Cary model 118C, Cary Instruments, Monrovia, Calif.

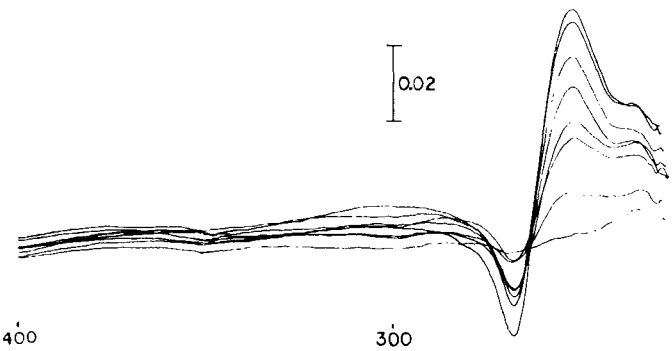

Figure 1—*Example of a difference spectrophotometric titration of β-lipoprotein (0.02%) with trifluoperazine dihydrochloride (0.104 mg/ml). The lower curve is the baseline, and each subsequent curve was generated by the addition of 50 μl of drug as described in the text.*

RESULTS AND DISCUSSION

Interactions between β-lipoprotein and various drugs were examined by difference spectrophotometry. Typical difference absorption spectra for the association of a drug with lipoprotein in phosphate buffer are shown in Fig. 1. A family of curves was generated by the incremental addition of a drug to a protein solution of constant concentration; the solutions ranged from 0.01 to 0.8% in lipoprotein. Drug solutions employed in the titrations ranged from 0.005 to 0.5 mg/ml.

Inspection of these difference absorbance spectra suggests that more than a single class of sites exists on the β-lipoprotein. A distinct isosbestic point was not maintained throughout the titration with any drug. However, the phenomenon of increased difference absorption spectra in the presence of increased amounts of β-lipoprotein was upheld throughout the range of lipoprotein employed.

Table I presents the results of the screening of drugs for binding to

Table I—Results of Drug Screening for Binding Interaction with β-Lipoprotein

Drug	Character	Absorbance Difference[a]	Drug–Protein Ratio
Trifluoperazine hydrochloride	Basic	0.089	0.08
Pyridostigmine bromide	Basic	0.103	1.25
Tolbutamide sodium	Acidic	0[b]	—
Tolazoline hydrochloride	Basic	0	—
Decamethonium bromide	Basic	0.010	5.00
Chlorpromazine hydrochloride	Basic	0.041	0.15
Phenylbutazone sodium	Acidic	0	—
Edrophonium chloride	Basic	0.051	3.07
Isopropamide iodide	Basic	0	—
Propranolol hydrochloride	Basic	0.027	1.67
Warfarin sodium	Acidic	0	—
Clofibrate sodium	Acidic	0.020	2.50
Prednisone	Neutral	0.068	1.10
Phenobarbital sodium	Acidic	0	—
Phenoxybenzamine hydrochloride	Basic	0.017	3.33
Hexamethonium chloride	Basic	0	—

[a] The absorbance difference is measured from a peak (or trough) to the adjacent trough (or peak). The drug to protein ratio at which this absorbance difference occurs is given in the succeeding column. [b] If the absorbance difference is zero, the drug–protein ratio is not given. However, with most drugs, a ratio greater than 8 was tried.

β-lipoproteins. A large number of the basic drugs examined resulted in a perturbation of the macromolecule baseline, reflecting that an interaction had taken place. Most of the cationic drugs showing a perturbation had a large hydrophobic portion in the molecule. Perhaps the β-lipoprotein, in order to bind these basic drugs, requires not only the center of deficient electron density but also a hydrophobic area. With the two aliphatic, yet basic, drugs tested, decamethonium and hexamethonium, only a very weak interaction resulted from the larger drug, decamethonium.

The description of the interaction was based on measuring a suitable absorbance difference from at least three titrations and also providing the drug–lipoprotein ratio of such absorbance diferences. In a number of aliquot titrations of the protein, saturation was not reached. In these instances, the results in Table I are the largest absorbance differences recorded at the ratio causing the perturbation.

Considering the results of Refs. 1–3 and those of this preliminary work, it is possible that cationic drugs may be preferentially transported by β-lipoproteins as well as other plasma proteins. If so, then research can be directed toward examining drug–β-lipoprotein interactions when new basic drugs are introduced. The β-lipoprotein can be assessed as to the strength of binding and the numbers of binding sites if some work is done on purification and exact molecular weight determination. Competitive displacement of drugs by concurrently administered agents may be an area in need of further examination if β-lipoproteins have a high affinity for specific basic drugs.

REFERENCES

(1) J. Judis, *J. Pharm. Sci.*, **61**, 89 (1972).

(2) M. H. Bickel, *J. Pharm. Pharmacol.*, **27**, 733 (1975).

(3) O. G. Nilsen and S. Jacobsen, *Biochem. Pharmacol.*, **24**, 995 (1975).

(4) A. S. Brill and H. E. Sandberg, *Biophys. J.*, **8**, 664 (1968).

(5) J. J. Vallner, L. A. Sternson, and D. L. Parsons, *J. Pharm. Sci.*, **65**, 873 (1976).

ACKNOWLEDGMENTS AND ADDRESSES

Received January 19, 1976, from the *Department of Pharmaceutics, School of Pharmacy, University of Georgia, Athens, GA 30602.*

Accepted for publication May 4, 1976.

[x] To whom inquiries should be directed.

GLC Determination of Opium Alkaloids in Papaveretum

G. FISHER [x] and R. GILLARD

Abstract □ A GLC method for the determination of the opium alkaloids in papaveretum, based on the formation of the acetyl derivatives of morphine and codeine, is described. The analytical results are compared with those obtained by the official method. The proposed method is fast and accurate and is particularly suited to the analysis of the raw material.

Keyphrases □ Opium alkaloids—GLC analysis in papaveretum, prepared samples □ Papaveretum—GLC analysis of opium alkaloids, prepared samples □ GLC—analysis, opium alkaloids in papaveretum, prepared samples □ Narcotics—GLC analysis of opium alkaloids in papaveretum, prepared samples

Papaveretum raw material (1) is a synthetic mixture of the hydrochlorides of the opium alkaloids, containing the equivalent of anhydrous morphine (47.5–52.5%), anhydrous codeine (2.5–5.0%), noscapine (16.0–22.0%), and papaverine (2.5–7.0%). It has the analgesic and narcotic properties of morphine but is claimed to produce fewer side effects and may be used in all cases where morphine or opium is indicated (2).

The official method of analysis (1, p. 346), involves a titrimetric method for morphine and gravimetric methods for the other alkaloids. Gravimetric analyses, due to their very nature (3), are prone to error, and the many operations required in the official procedure make it tedious and time consuming. For example, the method involves some 30 extractions, more than 40 washings (*i.e.*, of filter papers and solvent layers), and more than 20 actual transfers of the substances to be determined. A skilled and experienced analyst would require about 2 working days to complete an assay in duplicate.

The GLC determination of the opium alkaloids has been described (4–9). These methods involve initial extraction of the alkaloids, followed by GLC as either the free bases or derivatives. The direct injection of hydrochlorides of various other classes of drugs, which relies on subsequent quantitative breakdown to the free base, was reported (10, 11).

In the present study, a GLC method was investigated involving derivatization of the alkaloid hydrochlorides in papaveretum without prior extraction, followed by direct injection into the gas chromatograph. The acetate derivatives of the hydrochlorides of morphine and codeine are formed, while the hydrochlorides of noscapine and papaverine are not derivatized due to the absence of any free hydroxyl groups. Since no extractions are required, some error-prone steps are eliminated. This study apparently was the first application of this technique specifically to the hydrochlorides of the opium alkaloids in papaveretum.

EXPERIMENTAL

Materials—Standards of morphine, codeine, papaverine, and noscapine bases[1] were used, together with morphine hydrochloride[2]. These materials were dried at 120° for 2 hr immediately before use. Anhydrous analytical reagent grade pyridine was used, and all other solvents were also analytical reagent grade.

A solution of 100 mg of squalane in 100 ml of 95% ethyl acetate and 5% acetic acid was prepared as the internal standard solution.

Equipment and Operating Conditions—The analysis was performed on a gas chromatograph[3] equipped with dual flame-ionization detectors and a 5-mv recorder with a chart speed of 10 mm/min. The columns used were 1120-mm (4-ft) × 3-mm o.d. glass-lined metal tubing[4] packed with

[1] All alkaloid bases were BP grade material, recrystallized before use until they assayed at >99.5% by both GLC and nonaqueous titration.

[2] Customs Department, Sydney, Australia.

[3] Perkin-Elmer F30.

[4] Scientific Glass Engineering, Melbourne, Australia.

β-lipoproteins. A large number of the basic drugs examined resulted in a perturbation of the macromolecule baseline, reflecting that an interaction had taken place. Most of the cationic drugs showing a perturbation had a large hydrophobic portion in the molecule. Perhaps the β-lipoprotein, in order to bind these basic drugs, requires not only the center of deficient electron density but also a hydrophobic area. With the two aliphatic, yet basic, drugs tested, decamethonium and hexamethonium, only a very weak interaction resulted from the larger drug, decamethonium.

The description of the interaction was based on measuring a suitable absorbance difference from at least three titrations and also providing the drug–lipoprotein ratio of such absorbance diferences. In a number of aliquot titrations of the protein, saturation was not reached. In these instances, the results in Table I are the largest absorbance differences recorded at the ratio causing the perturbation.

Considering the results of Refs. 1–3 and those of this preliminary work, it is possible that cationic drugs may be preferentially transported by β-lipoproteins as well as other plasma proteins. If so, then research can be directed toward examining drug–β-lipoprotein interactions when new basic drugs are introduced. The β-lipoprotein can be assessed as to the strength of binding and the numbers of binding sites if some work is done on purification and exact molecular weight determination. Competitive displacement of drugs by concurrently administered agents may be an area in need of further examination if β-lipoproteins have a high affinity for specific basic drugs.

REFERENCES

(1) J. Judis, *J. Pharm. Sci.*, **61**, 89 (1972).

(2) M. H. Bickel, *J. Pharm. Pharmacol.*, **27**, 733 (1975).

(3) O. G. Nilsen and S. Jacobsen, *Biochem. Pharmacol.*, **24**, 995 (1975).

(4) A. S. Brill and H. E. Sandberg, *Biophys. J.*, **8**, 664 (1968).

(5) J. J. Vallner, L. A. Sternson, and D. L. Parsons, *J. Pharm. Sci.*, **65**, 873 (1976).

ACKNOWLEDGMENTS AND ADDRESSES

Received January 19, 1976, from the *Department of Pharmaceutics, School of Pharmacy, University of Georgia, Athens, GA 30602.*

Accepted for publication May 4, 1976.

[x] To whom inquiries should be directed.

GLC Determination of Opium Alkaloids in Papaveretum

G. FISHER [x] and R. GILLARD

Abstract □ A GLC method for the determination of the opium alkaloids in papaveretum, based on the formation of the acetyl derivatives of morphine and codeine, is described. The analytical results are compared with those obtained by the official method. The proposed method is fast and accurate and is particularly suited to the analysis of the raw material.

Keyphrases □ Opium alkaloids—GLC analysis in papaveretum, prepared samples □ Papaveretum—GLC analysis of opium alkaloids, prepared samples □ GLC—analysis, opium alkaloids in papaveretum, prepared samples □ Narcotics—GLC analysis of opium alkaloids in papaveretum, prepared samples

Papaveretum raw material (1) is a synthetic mixture of the hydrochlorides of the opium alkaloids, containing the equivalent of anhydrous morphine (47.5–52.5%), anhydrous codeine (2.5–5.0%), noscapine (16.0–22.0%), and papaverine (2.5–7.0%). It has the analgesic and narcotic properties of morphine but is claimed to produce fewer side effects and may be used in all cases where morphine or opium is indicated (2).

The official method of analysis (1, p. 346), involves a titrimetric method for morphine and gravimetric methods for the other alkaloids. Gravimetric analyses, due to their very nature (3), are prone to error, and the many operations required in the official procedure make it tedious and time consuming. For example, the method involves some 30 extractions, more than 40 washings (*i.e.*, of filter papers and solvent layers), and more than 20 actual transfers of the substances to be determined. A skilled and experienced analyst would require about 2 working days to complete an assay in duplicate.

The GLC determination of the opium alkaloids has been described (4–9). These methods involve initial extraction of the alkaloids, followed by GLC as either the free bases or derivatives. The direct injection of hydrochlorides of various other classes of drugs, which relies on subsequent quantitative breakdown to the free base, was reported (10, 11).

In the present study, a GLC method was investigated involving derivatization of the alkaloid hydrochlorides in papaveretum without prior extraction, followed by direct injection into the gas chromatograph. The acetate derivatives of the hydrochlorides of morphine and codeine are formed, while the hydrochlorides of noscapine and papaverine are not derivatized due to the absence of any free hydroxyl groups. Since no extractions are required, some error-prone steps are eliminated. This study apparently was the first application of this technique specifically to the hydrochlorides of the opium alkaloids in papaveretum.

EXPERIMENTAL

Materials—Standards of morphine, codeine, papaverine, and noscapine bases[1] were used, together with morphine hydrochloride[2]. These materials were dried at 120° for 2 hr immediately before use. Anhydrous analytical reagent grade pyridine was used, and all other solvents were also analytical reagent grade.

A solution of 100 mg of squalane in 100 ml of 95% ethyl acetate and 5% acetic acid was prepared as the internal standard solution.

Equipment and Operating Conditions—The analysis was performed on a gas chromatograph[3] equipped with dual flame-ionization detectors and a 5-mv recorder with a chart speed of 10 mm/min. The columns used were 1120-mm (4-ft) × 3-mm o.d. glass-lined metal tubing[4] packed with

[1] All alkaloid bases were BP grade material, recrystallized before use until they assayed at >99.5% by both GLC and nonaqueous titration.

[2] Customs Department, Sydney, Australia.

[3] Perkin-Elmer F30.

[4] Scientific Glass Engineering, Melbourne, Australia.

Table I—Recovery Results for Papaveretum Alkaloid Bases and Morphine Hydrochloride

Alkaloid	Amount Added, mg	Amount Recovered, mg	Recovery, %
Codeine	54.5	53.2	97.6
	119.1	119.6	100.4
	202.7	201.1	99.2
	216.9	216.7	99.9
			$\bar{x}$ = 99.4
			s = 1.2
Morphine	65.9	63.5	96.4
	128.5	127.9	99.2
	190.7	191.1	100.2
	251.8	251.5	99.9
			$\bar{x}$ = 98.9
			s = 1.7
Papaverine	66.9	65.2	97.5
	120.0	118.9	99.1
	196.9	194.0	98.6
	206.2	207.6	100.7
			$\bar{x}$ = 99.0
			s = 1.3
Noscapine	116.4	117.1	100.6
	191.8	191.5	99.8
	177.4	176.6	99.5
	406.3	401.2	98.9
			$\bar{x}$ = 99.7
			s = 1.3
Morphine hydrochloride	64.2	64.6	100.6
	121.8	120.6	98.9
	192.5	192.7	100.1
	256.5	256.2	99.9
			$\bar{x}$ = 99.9
			s = 0.7

2% OV-101 on 100–120-mesh Gas Chrom Q. The injector and detector were maintained at 300° and the sample was chromatographed under the following conditions: initially at 180° for 5 min, then programmed from 180 to 250° at the rate of 7°/min, and then held at 250° for 3 min. The nitrogen carrier gas flow rate was 30 ml/min, and the air and hydrogen flow rates were adjusted to give optimum detector response. The packed columns were conditioned overnight at 325° with low nitrogen flow (10 ml/min).

Preparation of Standard Solution—*Solution A*—Weigh accurately 200 mg of morphine base and 80 mg of noscapine into a 50-ml volumetric flask. Dilute to volume with anhydrous pyridine.

Solution B—Weigh accurately 80 mg of codeine base and 80 mg of papaverine into a 200-ml volumetric flask. Dilute to volume with anhydrous pyridine.

Table II—Comparison of Chemical (1973 BPC) and GLC Results[a]

Alkaloid	Chemical, % w/w		GLC, % w/w	
	Sample 1			
Codeine	3.83	3.87	3.45	3.25
Morphine	51.66	52.22	51.70	51.54
Papaverine	4.62	4.62	4.19	4.56
Noscapine	20.53	20.70	18.06	18.52
	Sample 2			
Codeine	3.89	3.98	4.05	3.89
Morphine	51.90	51.49	50.93	51.92
Papaverine	4.22	4.33	4.39	4.43
Noscapine	20.03	19.85	18.21	18.98
	Sample 3			
Codeine	2.94		2.53	
Morphine	50.45		50.09	
Papaverine	3.81		3.90	
Noscapine	19.83		19.61	

[a] Duplicate assays.

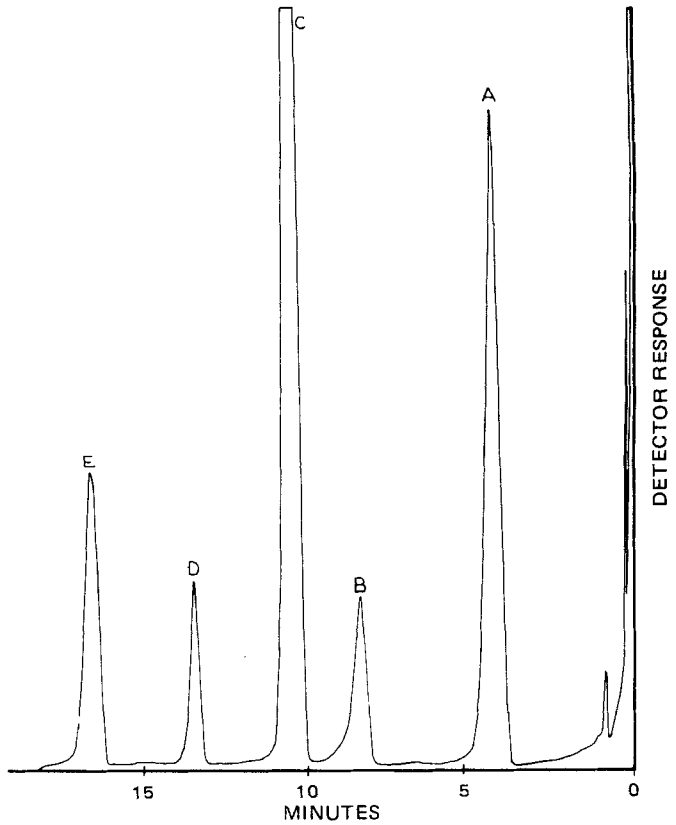

Figure 1—*Typical chromatogram of papaveretum standard preparation. Key: A, squalane; B, codeine; C, morphine; D, papaverine; and E, noscapine.*

Pipet 1.0 ml of Solution A and 1.0 ml of Solution B into a 10-ml conical flask[5] fitted with a septum[6]. Add 1.0 ml of acetic anhydride and allow to stand for 20 min. Evaporate to dryness with a stream of dry nitrogen and add 0.5 ml of internal standard solution. Inject 0.5 μl of this solution into the gas chromatograph, recording the areas of each component using an electronic digital integrator[7].

Preparation of Sample Solution—Accurately weigh approximately 170 mg of the papaveretum sample into a 50-ml volumetric flask, diluting to volume with anhydrous pyridine. Pipet a 2.0-ml aliquot of this solution into a 10-ml flask and then proceed as under *Preparation of Standard Solution* beginning with: "Add 1.0 ml of acetic anhydride . . . ."

The assay is normally performed in duplicate.

Quantitation—Calculate R_{st} and R_s for each component peak from the standard and sample chromatograms, respectively, as follows:

$$R_s = \frac{\text{peak area of particular component in sample chromatogram}}{\text{peak area of internal standard in sample chromatogram}} \quad \text{(Eq. 1)}$$

$$R_{st} = \frac{\text{peak area of particular component in standard chromatogram}}{\text{peak area of internal standard in standard chromatogram}} \quad \text{(Eq. 2)}$$

The amounts of the respective alkaloids in the papaveretum sample are then calculated from the following equation:

$$C_a = \frac{R_s \times C_{st}}{R_{st} \times C_s \times 2} \times 100 \quad \text{(Eq. 3)}$$

where C_a = percent (w/w) of the particular alkaloid base, C_{st} = concentration of that alkaloid in the standard solution in milligrams per milliliter, and C_s = concentration of papaveretum in the sample solution in milligrams per milliliter.

Linearity of Response—The linearity of response of the GLC procedure was checked for each alkaloid using a sample of papaveretum raw

[5] Reacti-Flask, Pierce Chemical Co.
[6] Lined with Teflon (du Pont).
[7] Infotronics CRS-208.

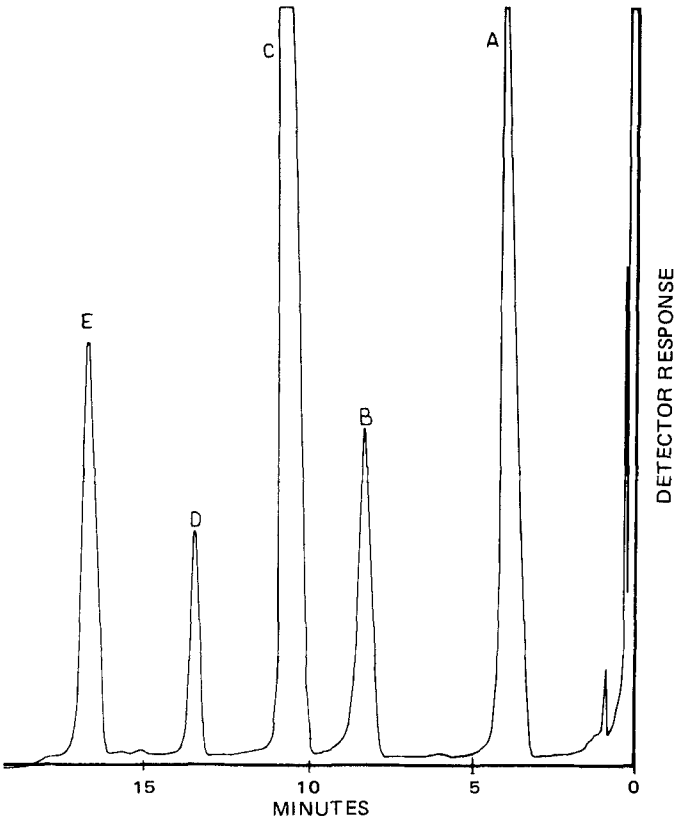

Figure 2—*Typical chromatogram of papaveretum sample preparation. Key: A, squalane; B, codeine; C, morphine; D, papaverine; and E, noscapine.*

material. The response was linear over the 2–20-mg/ml range of papaveretum in the sample solution under the assay conditions described.

RESULTS AND DISCUSSION

Figures 1 and 2 illustrate typical chromatograms of a standard and sample, respectively. The peak due to the acetyl derivative of codeine showed a tendency to tail slightly due to hydrolysis of the derivative to codeine base, brought about by the trace presence of moisture. Normally, the derivatives were stable for at least 4 hr if protected from moisture.

A mixed solvent (95% ethyl acetate and 5% acetic acid) was necessary to keep the derivatives in solution. Ethyl acetate is, by itself, an excellent recrystallizing solvent for diacetylmorphine; therefore, acetic acid was added to increase the solubility of this derivative. The original column has been in use for over 12 months, and no significant deterioration has been observed due to the injection of the acetic acid onto the column.

Recovery experiments were also carried out to check the validity of the method. Table I lists the results for the four alkaloid bases and morphine hydrochloride. Recoveries were quantitative, with an acceptable standard deviation for each alkaloid determination. With the morphine hydrochloride, the results were calculated as morphine base and then factored to the hydrochloride using the theoretical molecular weight ratio. The recovery results obtained in this way verify that the morphine hydrochloride does break down quantitatively to the free base on introduction to the chromatographic system under the conditions described.

Three different commercial lots of papaveretum raw material were assayed in duplicate by both the 1973 BPC method and the proposed GLC method (Table II). Agreement between the two methods was excellent, further validating the applicability of the GLC method.

REFERENCES

(1) "British Pharmaceutical Codex," Pharmaceutical Press, London, England, 1973.

(2) "Martindale: The Extra Pharmacopoeia," 26th ed., Pharmaceutical Press, London, England, 1972, p. 1129.

(3) D. A. Skoog and D. M. West, "Fundamentals of Analytical Chemistry," 2nd ed., Holt, Rinehart & Winston, London, England, 1971, p. 121.

(4) E. Brochmann-Hanssen and A. B. Svendsen, *J. Pharm. Sci.*, **51,** 1095 (1962).

(5) K. D. Parker, C. R. Fontan, and P. L. Kirk, *Anal. Chem.*, **35,** 346 (1963).

(6) S. J. Mule, *ibid.*, **36,** 1907 (1964).

(7) E. Brochmann-Hanssen and C. R. Fontan, *J. Chromatogr.*, **19,** 296 (1965).

(8) E. Brochmann-Hanssen and A. B. Svendsen, *J. Pharm. Sci.*, **52,** 1134 (1963).

(9) A. Bechtel, *Chromatographia*, **5,** 404 (1972).

(10) H. Kern, P. Schulling, and S. H. Müller, "Gas Chromatographic Analysis of Pharmaceuticals and Drugs," Varian Aerograph, Palo Alto, Calif., 1968.

(11) C. K. Wong, J. R. Urbigkit, N. Conca, D. M. Cohen, and K. P. Munnelly, *J. Pharm. Sci.*, **62,** 1340 (1973).

ACKNOWLEDGMENTS AND ADDRESSES

Received September 15, 1975, from *Abbott Laboratories Australia, Captain Cook Drive, Kurnell, N.S.W. 2231, Australia.*

Accepted for publication March 10, 1976.

[x] To whom inquiries should be directed. Present address: Merck Sharp & Dohme (Australia) Pty. Ltd., 54–68 Ferndell Street, South Granville, N.S.W. 2142, Australia.

Synthesis and Antiparasitic Activity of Certain 2-Imino-3-[(*N*-arylcarbamoyl)methyl]-2,3,4,5-tetrahydrothiazoles

H. H. FARAG [*], ADEL F. YOUSSEF [*x], and LAILA A. OMRAN [‡]

Abstract □ New derivatives of 2-imino-3-[(*N*-arylcarbamoyl)methyl]-2,3,4,5-tetrahydrothiazole were prepared. Six compounds were tested for their antiparasitic activities and were active in varying degrees against *Hymenolepis diminuta* without any clinical toxicity manifestations.

Keyphrases □ Thiazoles, substituted—synthesized, screened for antiparasitic activity, rats □ Antiparasitic activity—various substituted thiazoles screened □ Structure–activity relationships—substituted thiazoles screened for antiparasitic activity

During the past few years, significant progress has been made in the continuing struggle against parasitic diseases. However, better drugs are still needed for the treatment of many debilitating human and animal parasites. A number of reviews (1, 2) provide background information on the types of chemical structures that possess antipar-

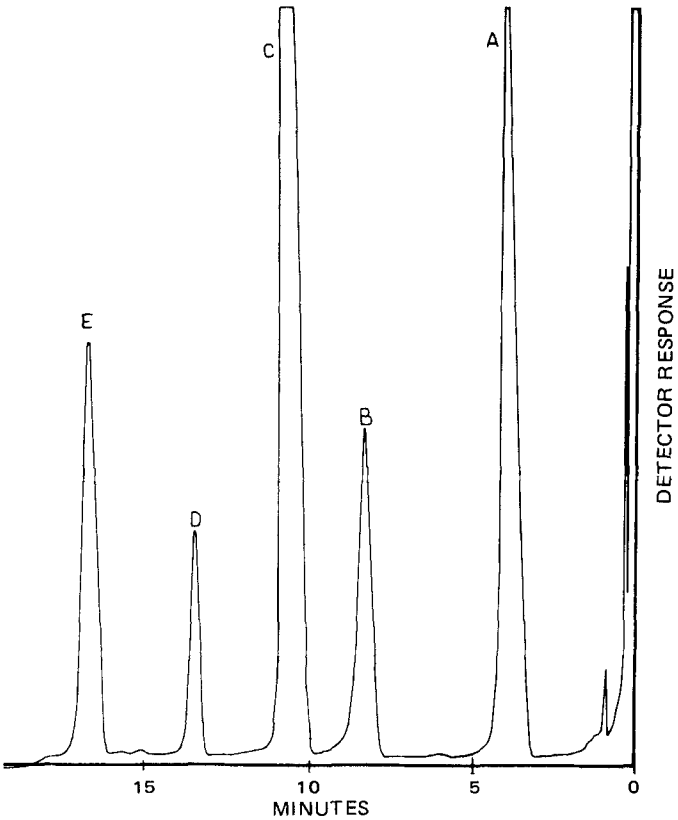

Figure 2—*Typical chromatogram of papaveretum sample preparation. Key: A, squalane; B, codeine; C, morphine; D, papaverine; and E, noscapine.*

material. The response was linear over the 2–20-mg/ml range of papaveretum in the sample solution under the assay conditions described.

RESULTS AND DISCUSSION

Figures 1 and 2 illustrate typical chromatograms of a standard and sample, respectively. The peak due to the acetyl derivative of codeine showed a tendency to tail slightly due to hydrolysis of the derivative to codeine base, brought about by the trace presence of moisture. Normally, the derivatives were stable for at least 4 hr if protected from moisture.

A mixed solvent (95% ethyl acetate and 5% acetic acid) was necessary to keep the derivatives in solution. Ethyl acetate is, by itself, an excellent recrystallizing solvent for diacetylmorphine; therefore, acetic acid was added to increase the solubility of this derivative. The original column has been in use for over 12 months, and no significant deterioration has been observed due to the injection of the acetic acid onto the column.

Recovery experiments were also carried out to check the validity of the method. Table I lists the results for the four alkaloid bases and morphine hydrochloride. Recoveries were quantitative, with an acceptable standard deviation for each alkaloid determination. With the morphine hydrochloride, the results were calculated as morphine base and then factored to the hydrochloride using the theoretical molecular weight ratio. The recovery results obtained in this way verify that the morphine hydrochloride does break down quantitatively to the free base on introduction to the chromatographic system under the conditions described.

Three different commercial lots of papaveretum raw material were assayed in duplicate by both the 1973 BPC method and the proposed GLC method (Table II). Agreement between the two methods was excellent, further validating the applicability of the GLC method.

REFERENCES

(1) "British Pharmaceutical Codex," Pharmaceutical Press, London, England, 1973.

(2) "Martindale: The Extra Pharmacopoeia," 26th ed., Pharmaceutical Press, London, England, 1972, p. 1129.

(3) D. A. Skoog and D. M. West, "Fundamentals of Analytical Chemistry," 2nd ed., Holt, Rinehart & Winston, London, England, 1971, p. 121.

(4) E. Brochmann-Hanssen and A. B. Svendsen, *J. Pharm. Sci.*, **51,** 1095 (1962).

(5) K. D. Parker, C. R. Fontan, and P. L. Kirk, *Anal. Chem.*, **35,** 346 (1963).

(6) S. J. Mule, *ibid.*, **36,** 1907 (1964).

(7) E. Brochmann-Hanssen and C. R. Fontan, *J. Chromatogr.*, **19,** 296 (1965).

(8) E. Brochmann-Hanssen and A. B. Svendsen, *J. Pharm. Sci.*, **52,** 1134 (1963).

(9) A. Bechtel, *Chromatographia*, **5,** 404 (1972).

(10) H. Kern, P. Schulling, and S. H. Müller, "Gas Chromatographic Analysis of Pharmaceuticals and Drugs," Varian Aerograph, Palo Alto, Calif., 1968.

(11) C. K. Wong, J. R. Urbigkit, N. Conca, D. M. Cohen, and K. P. Munnelly, *J. Pharm. Sci.*, **62,** 1340 (1973).

ACKNOWLEDGMENTS AND ADDRESSES

Received September 15, 1975, from *Abbott Laboratories Australia, Captain Cook Drive, Kurnell, N.S.W. 2231, Australia.*

Accepted for publication March 10, 1976.

[x] To whom inquiries should be directed. Present address: Merck Sharp & Dohme (Australia) Pty. Ltd., 54–68 Ferndell Street, South Granville, N.S.W. 2142, Australia.

Synthesis and Antiparasitic Activity of Certain 2-Imino-3-[(*N*-arylcarbamoyl)methyl]-2,3,4,5-tetrahydrothiazoles

H. H. FARAG [*], ADEL F. YOUSSEF [*x], and LAILA A. OMRAN [‡]

Abstract □ New derivatives of 2-imino-3-[(*N*-arylcarbamoyl)methyl]-2,3,4,5-tetrahydrothiazole were prepared. Six compounds were tested for their antiparasitic activities and were active in varying degrees against *Hymenolepis diminuta* without any clinical toxicity manifestations.

Keyphrases □ Thiazoles, substituted—synthesized, screened for antiparasitic activity, rats □ Antiparasitic activity—various substituted thiazoles screened □ Structure–activity relationships—substituted thiazoles screened for antiparasitic activity

During the past few years, significant progress has been made in the continuing struggle against parasitic diseases. However, better drugs are still needed for the treatment of many debilitating human and animal parasites. A number of reviews (1, 2) provide background information on the types of chemical structures that possess antipar-

Table I—2-Imino-3-[(*N*-arylcarbamoyl)methyl]-2,3,4,5-tetrahydrothiazoles

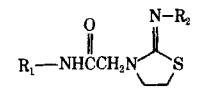

Compound	R_1	R_2	Yield, %	Crystallization Solvent	Melting Point	Molecular Formula	Analysis, %	Calc.	Found
I	C_6H_5	H	45	Ethanol–petroleum ether	218–219°	$C_{11}H_{13}N_3OS$ (hydrochloride)	C	48.61	49.21
							H	5.15	4.76
							N	15.46	15.29
II	C_6H_5	$COCH_3$	40	Water	186–187°	$C_{13}H_{15}N_3O_2S$	C	56.31	55.85
							H	5.41	5.42
							N	15.16	14.92
III	$2\text{-}CH_3C_6H_4$	H	43	Ethanol	218–219°	$C_{12}H_{15}N_3OS$ (hydrochloride)	C	50.43	50.31
							H	5.60	5.70
							N	14.71	14.27
IV	$4\text{-}OC_2H_5C_6H_4$	H	60	Hydrochloric acid–water (1:1)	212–213°	$C_{13}H_{17}N_3O_2S$ (hydrochloride)	C	49.44	48.95
							H	5.70	5.78
							N	13.31	12.95
V	$4\text{-}COOC_2H_5C_6H_4$	H	60	Ethanol	209–210° dec.	$C_{14}H_{17}N_3O_2S$ (hydrochloride)	C	48.90	48.77
							H	5.24	5.27
							N	12.22	11.69
VI	$4\text{-}BrC_6H_4$	H	61	Butanol	230–232°	$C_{11}H_{12}BrN_3OS$[a] (base)	C	42.04	43.39
							H	3.82	3.53
							N	—	—
VII	$3\text{-}ClC_6H_4$	H	33	Isopropyl ether	210–211° dec.	$C_{11}H_{12}ClN_3OS$ (hydrochloride)	C	43.13	42.99
							H	3.92	4.18
							N	13.72	13.63
VIII	$4\text{-}NO_2C_6H_4$	H	71	10% Hydrochloric acid	250° dec.	$C_{11}H_{12}N_4O_3S$ (hydrochloride)	C	41.64	41.72
							H	4.10	4.08
							N	17.69	17.29
IX	1-Naphthyl	H	54	Water	230° dec.	$C_{15}H_{15}N_3OS$ (hydrochloride)	C	55.98	56.56
							H	4.97	4.95
							N	—	—

[a] Could not be purified further.

asitic activity.

Recent research on the thiazoles resulted in the development of the leading antiparasitic compounds including nithiamide (3), niridazole (4), thiabendazole (5), and tetramisole (6). Most of these compounds are nitrated thiazole derivatives (3, 4, 7); however, some nonnitrated derivatives are active too (4–6). Certain totally or partially hydrogenated thiazoles (6, 8) are among the active compounds. Antiparasitic nonalkylated thiazoles (4) as well as ring-nitrogen alkylated derivatives (9) also were reported in the literature.

The present paper is concerned with the synthesis and preliminary parasitological testing of new 2-imino-3-[(*N*-arylcarbamoyl)methyl] -2,3,4,5-tetrahydrothiazoles (Table I).

EXPERIMENTAL[1]

2-Aminothiazole—This compound was prepared according to the reported method (10), yielding 39%, mp 76–78° [lit. (10) mp 84–85°].

***N*-Aryl-2-chloroacetamides (X–XVII, Table II)**—These compounds were prepared according to the reported methods.

2-Imino-3-[(*N*-arylcarbamoyl)methyl]-2,3,4,5-tetrahydrothiazoles (I and III–IX, Table I)—To a solution of 2-aminothiazole (0.01 mole) in 10 ml of 2-propanol, 0.01 mole of the appropriate *N*-aryl-2-chloroacetamide was added. The mixture was refluxed for 1.5 hr, and the separated compound was filtered off, washed with cold 2-propanol, and dried. In experiments where no solid separated after cooling, 2-propanol was distilled under reduced pressure and the residue was crystallized from the proper solvent.

2-Acetylimino-3-[(*N*-phenylcarbamoyl)methyl] -2,3,4,5-tetrahydrothiazole (II, Table I)—To a mixture of 2.7 g (0.01 mole) of I and 1.6 g (0.02 mole) of pyridine in 20 ml of chloroform was added 2.04 g (0.02 mole) of acetic anhydride. The mixture was stirred and refluxed for 1.5 hr. After cooling, the mixture was made alkaline with dilute ammonium hydroxide and the organic layer was separated. The aqueous layer was extracted twice with 20 ml of chloroform, and the combined chloroform extract was washed with water and dried (magnesium sulfate). The residue remaining after the distillation of chloroform was crystallized from water.

Materials and Methods of Anthelmintic Testing—The diagnosis of natural infection in laboratory rats was carried out by examination of their stools. Each positive rat was isolated in a separate cage. Positive controls were also isolated in separate cages. A dose of 100 mg/rat (mean weight 100 g) was given orally to a group of rats (two rats were given the same drug). A dose of 20 mg/rat was given in the same way. The stools of all rats were examined daily for *Hymenolepis* ova. Positive rats were redosed and followed up. Negative rats were autopsied to look for the adult worms or scolices. The rat was considered cured when neither ova nor cestodes were recovered.

RESULTS AND DISCUSSION

Chemistry—The new compounds (Table I) were prepared by the interaction of the proper *N*-aryl-α-chloroacetamide (Table II) with 2-aminothiazole (10). Alkylation of 2-aminothiazole by alkyl halides took place at the nuclear nitrogen (19). Compound I was acetylated with acetic anhydride to yield II. The IR spectrum of I showed multiple bands in the 3300–3200-cm^{-1} region (NH stretching), broad multiple bands at

Table II—*N*-Aryl-α-chloroacetamides

$RNHCOCH_2Cl$

Compound	R	Yield, %	Melting Point	Reference
X	C_6H_5	71	137–138°	11
XI	$2\text{-}CH_3C_6H_4$	80	112°	12
XII	$4\text{-}OC_2H_5C_6H_4$	84	142–144°	13
XIII	$4\text{-}COOC_2H_5C_6H_4$	75	116°	14
XIV	$4\text{-}BrC_6H_4$	70	180–181°	15
XV	$3\text{-}ClC_6H_4$	50	101°	16
XVI	$4\text{-}NO_2C_6H_4$	85	185°	17
XVII	1-Naphthyl	56	160°	18

[1] Melting points were determined in open capillary tubes and are uncorrected. IR spectra were determined in potassium bromide using a Beckman IR-20 spectrometer. Elemental microanalysis and IR spectra were performed by El-Nasr Co., A.R. Egypt.

3100–3000 cm^{-1} (secondary amine salt), and strong bands at 1700 and 1570 cm^{-1} (amide, I and II). Compound II revealed broad multiple bands at 3200–3100 cm^{-1} (NH stretching) and strong bands at 1700 (amide-I), 1620 (tertiary amide), and 1540 cm^{-1} (amide-II) (20).

Parasitological Screening—Compounds III, V, and VIII were tested for anthelmintic efficacy in mice naturally infected with *H. diminuta* and were active at the dose level (100 mg/rat, single dose) that showed no activity for VI and VII. Only VIII was active at 20 mg/rat (single dose); a further dose reduction abolished the activity.

Preliminary test revealed the activity of II against *Oxyuris* in naturally infected rats (100 mg/rat, single dose).

All of the drugs tested showed no clinical toxic manifestations even at the highest dose level.

CONCLUSION

The experimental results demonstrate that the replacement of the nitro group in 2-imino-3-[(*N*-4-nitrophenylcarbamoyl)methyl]-2,3,4,5-tetrahydrothiazole (VIII) by ethoxycarbonyl (V) or bromo (VI) substituents results in partial or complete loss of anthelmintic activity. Electronegativity alone cannot explain the crucial role played by the nitro group, and *in vivo* drug bioactivation may be involved.

REFERENCES

(1) "Annual Reports in Medicinal Chemistry 1965," C. K. Cain, Ed., Academic, New York, N.Y., 1966, pp. 136–163.

(2) "Annual Reports in Medicinal Chemistry 1966," C. K. Cain, Ed., Academic, New York, N.Y., 1967, pp. 131–156.

(3) A. C. Cuckler, A. B. Kupferberg, and N. Millman, *Antibiot. Chemother.*, **5**, 540 (1955).

(4) R. D. Westland, L. M. Werbel, J. R. Dice, J. L. Holmes, and B. G. Zahm, *J. Med. Chem.*, **14**, 916 (1971).

(5) H. D. Brown, A. R. Matzuk, I. R. Ilves, L. H. Peterson, S. A. Harris, L. A. Sarrett, J. R. Egerton, J. J. Yakstis, W. C. Campbell, and A. C. Cuckler, *J. Am. Chem. Soc.*, **83**, 1764 (1961).

(6) D. C. I. Thienpont, O. F. J. Vanparijs, A. H. M. Raeymaekers, J. Vandenberk, P. J. A. Demoen, F. T. N. Allewijn, R. P. H. Marsboom, C. J. E. Neimegeors, K. H. L. Schellekens, and P. A. J. Janssen, *Nature*, **209**, 1084 (1966).

(7) P. J. Islip, M. D. Closier, and J. E. Weale, *J. Med. Chem.*, **16**, 1027 (1973).

(8) P. J. Islip, M. D. Closier, M. C. Neville, L. M. Werbel, and D. B. Capps, *ibid.*, **15**, 951 (1972).

(9) A. H. M. Raeymaekers, F. T. N. Allewijn, J. Vandenberk, P. J. A. Demoen, T. T. T. Offenwert, and P. A. J. Janssen, *ibid.*, **9**, 545 (1966).

(10) S. Gabriel, *Chem. Ber.*, **22**, 1140 (1889).

(11) T. Zincke and O. Kegel, *ibid.*, **23**, 243 (1890).

(12) W. Abenium, *J. Prakt. Chem.*, **38**, 299 (1888).

(13) A. Bistrzycki and F. Ulffers, *Chem. Ber.*, **31**, 2790 (1898).

(14) G. Sanna and M. Granata, *Chem. Zentralbl.*, **1937**, 108.

(15) "Dictionary of Organic Compounds," vol. 1, I. M. Heilbron and H. M. Bunbury, Eds., Eyre and Spatteswoode, London, England, 1946, p. 271.

(16) H. Beckurts and G. Frerichs, *Arch. Pharm.*, **253**, 244 (1915).

(17) "Dictionary of Organic Compounds," vol. 3, I. M. Heilbron and H. M. Bunbury, Eds., Eyre and Spatteswoode, London, England, 1946, p. 87.

(18) *Ibid.*, p. 31.

(19) G. Yong and S. I. Crooks, *J. Chem. Soc.*, **89**, 59 (1906).

(20) R. M. Silverstein and G. C. Bassler, "Spectrometric Identification of Organic Compounds," 2nd ed., Wiley, New York, N.Y., 1967, pp. 94–96.

ACKNOWLEDGMENTS AND ADDRESSES

Received December 11, 1975, from the *Department of Pharmaceutical Chemistry, Faculty of Pharmacy, and the ‡Department of Parasitology, Faculty of Medicine, Assiut University, Assiut, A. R. Egypt.

Accepted for publication April 29, 1976.

Presented in part at the XIV Egyptian Conference of Pharmaceutical Sciences, Cairo, December 1975.

ˣ To whom inquiries should be directed.

Quantitative High-Pressure Liquid Chromatographic Determination of Epinephrine in Pharmaceutical Formulations

CHERNG-CHYI FU and MURRAY J. SIBLEY ˣ

Abstract □ A quantitative high-pressure liquid chromatographic method, using a cationic exchange resin column and an aqueous phosphate buffer as the mobile phase, was employed for the determination of epinephrine in liquid pharmaceutical preparations. The method is stability determining and can differentiate epinephrine in the presence of oxidative and other degradation products.

Keyphrases □ Epinephrine—high-pressure liquid chromatographic analysis, liquid pharmaceutical preparations □ High-pressure liquid chromatography—analysis, epinephrine, liquid pharmaceutical preparations □ Adrenergics—epinephrine, high-pressure liquid chromatographic analysis, liquid pharmaceutical preparations

Epinephrine solutions are widely used for the treatment of open angle glaucoma and are also used as cardiac stimulants and vasoconstrictors. Air oxidation is a major degradation process involved in epinephrine pharmaceutical preparations (1). Antioxidants such as bisulfite are used in many commercial liquid formulations. Bisulfite causes a degradation of epinephrine to form 1-(3,4-dihydroxyphenyl)-2-methylaminoethanesulfonic acid (2).

A stability-indicating method that differentiates epinephrine from its oxidation products as well as sulfonic acid derivatives is needed. The USP XIX assay method requires the formation of the triacetyl epinephrine derivative and is very lengthy (3). Several spectrofluorometric methods have the disadvantage of interference from the antioxidants (4). The addition of antioxidants is necessary to stabilize the final fluorescence in these assay methods.

This report describes a high-pressure liquid chromatographic (HPLC) assay method for epinephrine in liquid pharmaceutical preparations which will differentiate epinephrine from these major degradation products.

3100–3000 cm^{-1} (secondary amine salt), and strong bands at 1700 and 1570 cm^{-1} (amide, I and II). Compound II revealed broad multiple bands at 3200–3100 cm^{-1} (NH stretching) and strong bands at 1700 (amide-I), 1620 (tertiary amide), and 1540 cm^{-1} (amide-II) (20).

Parasitological Screening—Compounds III, V, and VIII were tested for anthelmintic efficacy in mice naturally infected with *H. diminuta* and were active at the dose level (100 mg/rat, single dose) that showed no activity for VI and VII. Only VIII was active at 20 mg/rat (single dose); a further dose reduction abolished the activity.

Preliminary test revealed the activity of II against *Oxyuris* in naturally infected rats (100 mg/rat, single dose).

All of the drugs tested showed no clinical toxic manifestations even at the highest dose level.

CONCLUSION

The experimental results demonstrate that the replacement of the nitro group in 2-imino-3-[(*N*-4-nitrophenylcarbamoyl)methyl]-2,3,4,5-tetrahydrothiazole (VIII) by ethoxycarbonyl (V) or bromo (VI) substituents results in partial or complete loss of anthelmintic activity. Electronegativity alone cannot explain the crucial role played by the nitro group, and *in vivo* drug bioactivation may be involved.

REFERENCES

(1) "Annual Reports in Medicinal Chemistry 1965," C. K. Cain, Ed., Academic, New York, N.Y., 1966, pp. 136–163.

(2) "Annual Reports in Medicinal Chemistry 1966," C. K. Cain, Ed., Academic, New York, N.Y., 1967, pp. 131–156.

(3) A. C. Cuckler, A. B. Kupferberg, and N. Millman, *Antibiot. Chemother.*, **5**, 540 (1955).

(4) R. D. Westland, L. M. Werbel, J. R. Dice, J. L. Holmes, and B. G. Zahm, *J. Med. Chem.*, **14**, 916 (1971).

(5) H. D. Brown, A. R. Matzuk, I. R. Ilves, L. H. Peterson, S. A. Harris, L. A. Sarrett, J. R. Egerton, J. J. Yakstis, W. C. Campbell, and A. C. Cuckler, *J. Am. Chem. Soc.*, **83**, 1764 (1961).

(6) D. C. I. Thienpont, O. F. J. Vanparijs, A. H. M. Raeymaekers, J. Vandenberk, P. J. A. Demoen, F. T. N. Allewijn, R. P. H. Marsboom, C. J. E. Neimegeors, K. H. L. Schellekens, and P. A. J. Janssen, *Nature*, **209**, 1084 (1966).

(7) P. J. Islip, M. D. Closier, and J. E. Weale, *J. Med. Chem.*, **16**, 1027 (1973).

(8) P. J. Islip, M. D. Closier, M. C. Neville, L. M. Werbel, and D. B. Capps, *ibid.*, **15**, 951 (1972).

(9) A. H. M. Raeymaekers, F. T. N. Allewijn, J. Vandenberk, P. J. A. Demoen, T. T. T. Offenwert, and P. A. J. Janssen, *ibid.*, **9**, 545 (1966).

(10) S. Gabriel, *Chem. Ber.*, **22**, 1140 (1889).

(11) T. Zincke and O. Kegel, *ibid.*, **23**, 243 (1890).

(12) W. Abenium, *J. Prakt. Chem.*, **38**, 299 (1888).

(13) A. Bistrzycki and F. Ulffers, *Chem. Ber.*, **31**, 2790 (1898).

(14) G. Sanna and M. Granata, *Chem. Zentralbl.*, **1937**, 108.

(15) "Dictionary of Organic Compounds," vol. 1, I. M. Heilbron and H. M. Bunbury, Eds., Eyre and Spatteswoode, London, England, 1946, p. 271.

(16) H. Beckurts and G. Frerichs, *Arch. Pharm.*, **253**, 244 (1915).

(17) "Dictionary of Organic Compounds," vol. 3, I. M. Heilbron and H. M. Bunbury, Eds., Eyre and Spatteswoode, London, England, 1946, p. 87.

(18) *Ibid.*, p. 31.

(19) G. Yong and S. I. Crooks, *J. Chem. Soc.*, **89**, 59 (1906).

(20) R. M. Silverstein and G. C. Bassler, "Spectrometric Identification of Organic Compounds," 2nd ed., Wiley, New York, N.Y., 1967, pp. 94–96.

ACKNOWLEDGMENTS AND ADDRESSES

Received December 11, 1975, from the *Department of Pharmaceutical Chemistry, Faculty of Pharmacy, and the ‡Department of Parasitology, Faculty of Medicine, Assiut University, Assiut, A. R. Egypt.

Accepted for publication April 29, 1976.

Presented in part at the XIV Egyptian Conference of Pharmaceutical Sciences, Cairo, December 1975.

ˣ To whom inquiries should be directed.

Quantitative High-Pressure Liquid Chromatographic Determination of Epinephrine in Pharmaceutical Formulations

CHERNG-CHYI FU and MURRAY J. SIBLEY ˣ

Abstract □ A quantitative high-pressure liquid chromatographic method, using a cationic exchange resin column and an aqueous phosphate buffer as the mobile phase, was employed for the determination of epinephrine in liquid pharmaceutical preparations. The method is stability determining and can differentiate epinephrine in the presence of oxidative and other degradation products.

Keyphrases □ Epinephrine—high-pressure liquid chromatographic analysis, liquid pharmaceutical preparations □ High-pressure liquid chromatography—analysis, epinephrine, liquid pharmaceutical preparations □ Adrenergics—epinephrine, high-pressure liquid chromatographic analysis, liquid pharmaceutical preparations

Epinephrine solutions are widely used for the treatment of open angle glaucoma and are also used as cardiac stimulants and vasoconstrictors. Air oxidation is a major degradation process involved in epinephrine pharmaceutical preparations (1). Antioxidants such as bisulfite are used in many commercial liquid formulations. Bisulfite causes a degradation of epinephrine to form 1-(3,4-dihydroxyphenyl)-2-methylaminoethanesulfonic acid (2).

A stability-indicating method that differentiates epinephrine from its oxidation products as well as sulfonic acid derivatives is needed. The USP XIX assay method requires the formation of the triacetyl epinephrine derivative and is very lengthy (3). Several spectrofluorometric methods have the disadvantage of interference from the antioxidants (4). The addition of antioxidants is necessary to stabilize the final fluorescence in these assay methods.

This report describes a high-pressure liquid chromatographic (HPLC) assay method for epinephrine in liquid pharmaceutical preparations which will differentiate epinephrine from these major degradation products.

Table I—Comparison of Spectrofluorometric and HPLC Methods for Epinephrine Determination

Assay Method	Epinephrine Found, Product A[a], %	Percentage of Label Claim	Epinephrine Found, Product B[a], %	Percentage of Label Claim
Spectrofluorometric[b]	0.262	105	2.14	107
HPLC	0.255	102	2.10	105

[a] Label claim of Product A was 0.25%; label claim of Product B was 2%. [b] See Footnote 4.

EXPERIMENTAL

Apparatus—A high-pressure liquid chromatograph[1], composed of a pump (7000 psig maximum) and equipped with dual-channel UV detectors at 254 and 280 nm, was used. A 3 × 500-mm stainless steel column was packed with cationic exchange resin[2]. The mobile phase consisted of 0.05 *M* KH_2PO_4 at pH 4.5, which was degassed by using vacuum suction.

Reagents—1-(3,4-Dihydroxyphenyl)-2-methylaminoethanesulfonic acid was prepared according to a literature method (5).

Preparation of Epinephrine Standard Solutions—Dissolve epinephrine bitartrate[3], 181.8, 272.7, and 363.6 mg, in water and dilute to 100 ml. These solutions represent concentrations of 0.1, 0.15, and 0.2% of epinephrine base, respectively.

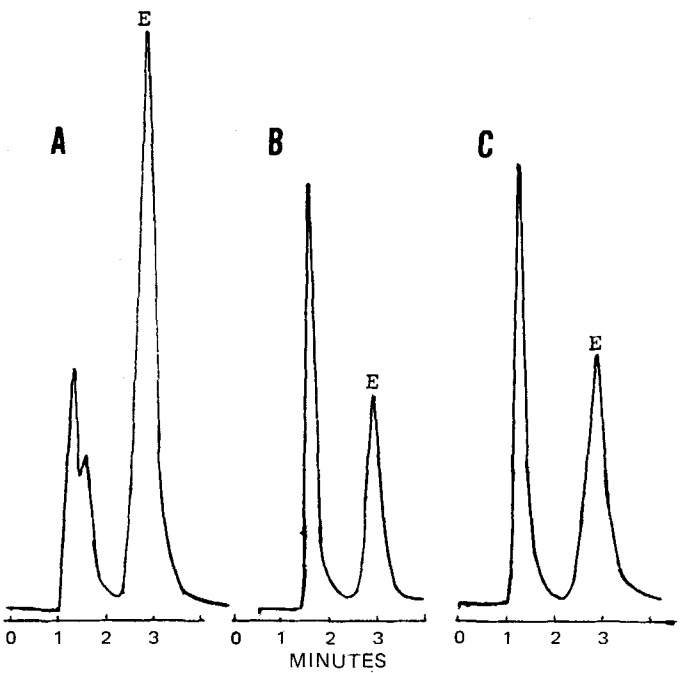

Figure 1—*Chromatographic separation of epinephrine (E) from degradation products. Key: A, air oxidation of 0.1% epinephrine at pH 7; B, hydrogen peroxide oxidation of epinephrine solution at pH 5; and C, mixture of epinephrine and its sulfonic acid derivative.*

[1] Spectra Physics Isocratic model 3500B.
[2] Vydac, Applied Science Laboratories, State College, Pa.
[3] 3M Laboratories, Loughborough, England.

Degradation of Epinephrine—*Method A*—Dissolve 181.8 mg of epinephrine bitartrate in water, adjust the pH to about 7 with 0.02 *N* NaOH, and dilute to 100 ml. Bubble air through this solution overnight.

Method B—Dissolve 181.8 mg of epinephrine bitartrate in water, adjust the pH to about 5 with 0.02 *N* NaOH, and dilute to 100 ml. To 50 ml of this solution, add 2 ml of 30% hydrogen peroxide and heat the mixture in an 80° water bath for 1 hr.

Preparation of Sample Solution—Dilute the liquid sample with water to obtain a concentration of 0.1% epinephrine.

Chromatographic Separation—The procedure was run at ambient temperature, and the solvent flow was 1.6 ml/min. The UV monitor was set at 280 nm with a sensitivity of 0.32 absorbance unit. The samples and standards were injected at 10 μl in duplicate. Peak heights were used for calculating epinephrine concentrations; the concentration of epinephrine samples was obtained from a standard curve.

RESULTS AND DISCUSSION

Excellent linearity of peak height response over the concentration range from 0 to 2 mg/ml was obtained. Figure 1 contains three individual chromatograms and shows the different retention times of epinephrine, the oxidation products, and the sulfonic acid derivative. The difference in chromatograms A and B is probably the result of the complexity of the epinephrine oxidation process. Epinephrine eluted at about 3 min; therefore, the degradation products did not interfere with the epinephrine assay.

The results of adding known amounts of epinephrine to a commercially available formulation[4] in two different concentrations were assayed by both HPLC and spectrofluorometric (4) methods. The results are given in Table I.

REFERENCES

(1) T. D. Sokoloski and T. Higuchi, *J. Pharm. Sci.*, **51**, 172 (1962).

(2) T. Higuchi and L. C. Schroeter, *J. Am. Pharm. Assoc., Sci. Ed.*, **48**, 535 (1959).

(3) "The United States Pharmacopeia," 19th rev., Mack Publishing Co., Easton, Pa., 1975, p. 170.

(4) V. K. Prasad, R. A. Ricci, B. C. Nunning, and A. P. Granatek, *J. Pharm. Sci.*, **62**, 1130 (1973).

(5) L. C. Schroeter and T. Higuchi, *J. Am. Pharm. Assoc., Sci. Ed.*, **49**, 331 (1960).

ACKNOWLEDGMENTS AND ADDRESSES

Received March 12, 1976, from the *Research Department, Barnes-Hind Pharmaceuticals, Inc., Sunnyvale, CA 94086.*

Accepted for publication May 4, 1976.

[x] To whom inquiries should be directed.

[4] EPPY/N, Barnes-Hind Pharmaceuticals, Sunnyvale, Calif.

Complement Fixing Site of Human IgG1

BRIAN J. JOHNSON ˣ and KENNETH E. THAMES

Abstract □ A number of chemical modifications were made to purified human IgG1. The effects of these modifications on the complement activity of the immunoglobulin were studied using aggregation on latex and measuring the consumption of the complement by CH_{50}-quantitation. Tryptophan and tyrosine are implicated in the complement fixing site of this human immunoglobulin, and an arginine moiety probably provides a binding site for the complement.

Keyphrases □ Complement fixing—human IgG1, effect of chemical modifications on active site □ Immunoglobulins—human IgG1, effect of chemical modifications on complement activity □ Amino acids—residues of human IgG1 involved in complement fixing defined

It has been shown that modification of a few tryptophan residues of rabbit immunoglobulin G with 2-hydroxy-5-nitrobenzyl bromide reduces the anticomplementary activity of this protein (1, 2). This observation prompted interest in defining some of the amino acid residues of human immunoglobulin G1 (IgG1[1]) involved in its complement fixing ability. For this purpose, studies were conducted on the change in anticomplementary activity by chemical modification of human IgG1.

EXPERIMENTAL

Preparation of Human IgG1—The plasma[2] containing IgG1 was isolated from a patient with multiple myeloma. Sufficient ϵ-aminocaproic acid was added to the plasma to make the final concentration of the amino acid 1×10^3 *M*. For every 100 ml of plasma, 1 ml of 25% $CaCl_2$ and 1 ml of 10% NaN_3 were added. The material was allowed to clot overnight at 4°, the clot was then removed, and ammonium sulfate (50%) precipitation of the serum was performed.

The precipitate was dissolved in distilled water and reprecipitated with ammonium sulfate (33%). This latter precipitation was repeated. Then the precipitate was dissolved in distilled water and dialyzed against tris(hydroxymethyl)aminomethane buffer, 0.005 *M*, pH 8.0. This solution was concentrated[3] and then chromatographed on a column (44 × 2.5 cm) of cellulose[4] in the same buffer. Elution of the column with 0.015 *M* tris(hydroxymethyl)aminomethane, pH 8.0, produced human IgG1.

The purity of the product was indicated by Ouchterlony double diffusion in agar gels using goat anti-human serum, from which only a single precipitin band was obtained. Similarly, only a single band was obtained upon polyacrylamide electrophoresis of the sample of human IgG1.

Modifications of Human IgG1—*2-Hydroxy-5-nitrobenzyl Bromide (I)*—The reaction with I was performed in a similar manner to that described by Allen and Isliker (1, 2). To 4 ml of a 2.7% solution of human IgG1 in 0.1 *M* sodium acetate buffer, pH 4.5, was added 0.2 ml of a 0.33 *M* dioxane solution of I. The mixture was stirred for 1 hr at room temperature, centrifuged, and then dialyzed for 24 hr against 4 × 250 ml of 0.1 *M* sodium acetate. The number of moles of I bound per mole of IgG1 was calculated by determining the absorbance at 410 nm (E_{410} = 18,000 M^{-1} cm^{-1}, pH >12.0) (6) for the modified IgG1 and at 280 nm ($E^{1\%}_{1cm}$ = 13.6, pH 7.0) for IgG1. A molecular weight of 150,000 was used for human IgG1.

5-(Dimethylamino)-1-naphthalenesulfonyl Chloride (II)—The reaction with II was performed in a similar manner to that previously reported (7, 8). Typically, 2.50 ml of a 7.4×10^{-3} *M* II solution in acetone was added to 8.75 ml of a 5.4% solution of human IgG1 dissolved in 0.1 *M* $NaHCO_3$, pH 8.0. The mixture was stirred for 2 hr at 4°. The ratio of II to protein was 6:1. The reaction mixture was dialyzed for 24 hr against 4 × 250 ml of 0.05 *M* tris(hydroxymethyl)aminomethane–0.15 *M* NaCl, pH 8.0. Then the solution was centrifuged, and the number of moles of the 5-(dimethylamino)-1-naphthalenesulfonyl moiety bound per mole of IgG1 was calculated by determining the absorbance at 280 nm ($E^{1\%}_{1cm}$ = 13.6, pH 7.0) for IgG1 and at 335 nm ($E_{335} = 4.4 \times 10^6\ M^{-1}\ cm^{-1}$) for bound IgG1. A molecular weight of 150,000 was assumed for human IgG1.

Tetranitromethane (III)—The method of Atassi and Habeeb (9) was used for the nitration of human IgG1. To a solution of 1.8 μmoles of human IgG1 in 5 ml of 0.05 *M* tris(hydroxymethyl)aminomethane–1 *M* NaCl, pH 8.0, was added 21.4 μmoles of III in 75 μl of ethanol. The mixture was stirred at room temperature for 2 hr and then dialyzed for 24 hr against 4 × 250 ml of barbital-buffered saline, pH 7.4, containing 0.15 m*M* calcium and 1.0 m*M* magnesium ions (10). The number of moles of nitrotyrosine associated with each mole of IgG1 was calculated by determining the absorbance at 280 nm ($E^{1\%}_{1cm}$ = 13.6, pH 7.0) for IgG1 and at 428 nm ($E = 3800\ M^{-1}\ cm^{-1}$) (11) for nitro IgG1. Amino acid analysis of the modified IgG1 confirmed this result.

2,3-Butanedione (IV)—This modification of human IgG1 was done using the method of Grossberg and Pressman (12). To 2 ml of a 5.4% solution of human IgG1 in 0.001 *M* phosphate buffer, pH 7.5, was added 2 ml of IV reagent (optical density = 0.5/ml), and the pH of the reaction mixture was adjusted to 8.6. After 6 hr at room temperature, the mixture was centrifuged and dialyzed for 24 hr against 4 × 250 ml of barbital-buffered saline, pH 7.4, containing 0.15 m*M* calcium and 1.0 m*M* magnesium ions (10). Comparison of the amino acid analysis of acid hydrolysates of IgG1 and modified IgG1 showed that half of the arginine residues of the immunoglobulin had been modified.

Protein Absorption on Latex Particles—To 0.25-ml aliquots of an aqueous 1.5% latex suspension (particle size 0.81 μm) was added 1 ml of barbital-buffered saline, pH 7.4, containing 0.15 m*M* calcium and 1.0 m*M* magnesium ions (8). To each sample was added 20 μg of the pertinent human IgG1 or its modifications, and the suspension was gently inverted through 180° every 5 sec to ensure complete mixing. Complete adsorption of the protein to the latex was accomplished by incubation for 16 hr at 4°.

Hemolytic Complement Fixation Assay—The method employed for the quantitative fixation test was based on one described previously (10). All operations were performed in barbital-buffered saline, pH 7.4, containing optimal concentrations of calcium and magnesium ions. The protein–latex suspensions were centrifuged, and to each pellet was added 1.2 ml of human complement containing 20 CH_{50} units/ml. Each pellet was suspended in the complement and incubated for 2 hr at 37°. The suspensions were inverted every 15 min to ensure reaction.

After this incubation, the suspensions were centrifuged and 1 ml of the supernate from each reaction mixture was removed. These supernates were assayed for residual complement activity. Each supernate was diluted in ratios of 1:7, 1:10, and 1:15 with barbital-buffered saline containing 0.15 m*M* calcium and 1.0 m*M* magnesium ions. To 1-ml aliquots of each dilution were added 5×10^8 sensitized sheep erythrocytes, and

Table I—Anticomplementary Activity of Modified Human IgG1

Protein[a]	Amount of Modification[a]	Number of CH_{50} Units Removed per Microgram of Protein	Decrease in Anticomplementary Activity, %
Human IgG1	None	1	0
II-Bound IgG1	4.5	0.65	35
I-Bound IgG1	6.6	0.41	59
Nitro IgG1	7.3	0.28	72
IV-Modified IgG1	16.0	0.23	77

[a] The amount of protein used was 20 μg adsorbed to 3.75 mg of latex. [b] Moles of chemical modifier per mole of immunoglobulin.

[1] Nomenclature recommended by International Union of Immunological Societies (3–5).

[2] Courtesy of Dr. W. T. Hammack, Veterans Administration Hospital, Birmingham, Ala.

[3] Diaflo-filtration using a PM-30 filter.

[4] DE-52.

Table II—Comparison of Amino Acid Sequences of Various Anticomplementary Immunoglobulins

Immunoglobulin C_H2 Domain	Amino Acid Residues	Sequence
Human IgG1 (Ref. 13)	271–282	Pro-Gln-Val-Lys-Phe-Asn-Trp-Tyr-Val-Asp-Val-Gln
Guinea pig IgG2 (Ref. 14)	271–282	Pro-Glu-Val-Gln-Phe-Thr-Trp-Phe-Val-Asp-Lys-Pro
Rabbit IgG (Ref. 15)	271–282	Pro-Glu-Val-Glx-Phe-Thr-Trp-Ile-Asx-Glu-Gln-Val
Murine IgG2a (Ref. 16)	271–282	Pro-Asp-Val-Gln-Ile-Ser-Trp-Phe-Val-Asp-Val-Glu

the volumes were made up to 7.5 ml with the barbital buffer. These suspensions were incubated for 1 hr at 37° and then centrifuged.

The optical density of each supernate was obtained at 541 nm. The following controls were run concurrently with the latex–protein samples: no latex–protein, latex only, sensitized sheep erythrocytes without complement, complement only, and total lysis of sensitized sheep erythrocytes.

RESULTS

The 2,3-butanedione reagent (12) modified 16 moles of arginine/mole of human IgG1. The amino acid analysis indicated no reaction with the lysine residues. Each mole of human IgG1 bound 4.5 moles of 5-(dimethylamino)-1-naphthalenesulfonyl moiety. Nitration, using tetranitromethane, of human IgG1 indicated 7.3 moles of nitrotyrosine bound/mole of immunoglobulin. Alkylation of the tryptophan residues with 2-hydroxy-5-nitrobenzyl bromide showed that 6.6 moles of this alkylating agent was bound per mole of IgG1.

To quantitate the complement fixing abilities of the human IgG1 and its various modifications, it was necessary to aggregate the various proteins on latex particles. The standard used was 20 μg of human IgG1 aggregated to 3.75 mg of latex particles. At this ratio, all immunoglobulin was adsorbed. This amount of IgG1 routinely removed all of the measurable complement from human serum. Of the controls run concurrently with the samples, the latex by itself removed 5–10% of the available complement. This reduction of complement for consumption by the immunoglobulins has been incorporated in the results shown in Table I.

By using these standard conditions, it was possible to compare the complement fixing abilities of human IgG1 with those of the various modifications of the immunoglobulin. Compared to the native immunoglobulin, the complement fixing activity of the alkylated material was reduced by 59%. Binding of human IgG1 to II was not as effective, causing a decrease of 35% in the complement fixing ability of the modified immunoglobulin. Nitration of human IgG1 lowered the anticomplementary activity by 72%. This finding suggests that a tyrosine residue may be implicated as a moiety in the complement fixing area of the immunoglobulin. The reaction of IgG1 with the 2,3-butanedione reagent (12) gave the greatest decrease, 77%, in the complement fixing activity of the immunoglobulin. However, amino acid analysis of this material indicated that only the arginine residues were affected by this reagent.

DISCUSSION

Allen and Isliker (1, 2) showed that modification of rabbit IgG with 2-hydroxy-5-nitrobenzyl bromide reduced the complement fixing ability of the immunoglobulin. It was suggested that the moiety modified by this alkylating agent was a tryptophan residue located in the Fc portion (3–5) of the immunoglobulin close to the hinge region (3–5). Furthermore, the tryptophan at position 277 within the first domain of the Fc portion of rabbit immunoglobulin appears to be involved in complement fixation (1).

With human IgG1, a similar change in anticomplementary activity was observed when tryptophan was alkylated. Nitration of the tyrosine residues also affected the anticomplementary activity of the modified immunoglobulin. Comparison of the sequences of immunoglobulins that possess anticomplementary activity is shown in Table II. There is a great similarity of amino acid residues around the tryptophan moiety at position 277. The close proximity of the aromatic residues, phenylalanine and tyrosine, is also evident. Possibly nitration of human IgG1 with tetranitromethane modified one of these residues.

The present results also implicate an arginine residue playing a role in complement consumption. However, the sequences shown in Table II do not include this amino acid residue. It has been suggested (2) that different parts of the Fc region (3–5) of the immunoglobulin may provide points of attachment for the Clq subcomponent of complements (17). Thus, a possible explanation for the reduction in anticomplementary activity of human IgG1 upon modification of the arginine residues is that such residues are necessary for the binding of the complement to the immunoglobulin.

The synthesis of peptides and polypeptides that mimic the sequences shown in Table II and their anticomplementary activities will be reported later.

REFERENCES

(1) R. Allen and H. Isliker, *Immunochemistry*, **11**, 175 (1974).

(2) *Ibid.*, **11**, 243 (1974).

(3) *Bull. WHO*, **30**, 447 (1964).

(4) *Ibid.*, **41**, 975 (1969).

(5) *Biochemistry*, **11**, 3311 (1972).

(6) T. E. Barman and D. E. Koshland, *J. Biol. Chem.*, **242**, 5771 (1967).

(7) G. Weber, *Biochem. J.*, **51**, 145 (1952).

(8) P. Wohl and G. Weber, *J. Mol. Biol.*, **30**, 371 (1967).

(9) M. Z. Atassi and A. F. S. A. Habeeb, *Biochemistry*, **8**, 1385 (1969).

(10) E. A. Kabat and M. M. Mayer, in "Experimental Immunochemistry," 2nd ed., Charles C Thomas, Springfield, Ill., 1969, p. 133.

(11) J. F. Riordan, M. Sokolovsky, and B. L. Vallee, *J. Am. Chem. Soc.*, **88**, 4104 (1966).

(12) A. L. Grossberg and D. Pressman, *Biochemistry*, **7**, 272 (1968).

(13) G. M. Edelman, *ibid.*, **9**, 3197 (1970).

(14) D. E. Tracey and J. J. Cebra, *ibid.*, **13**, 4796 (1974).

(15) E. Appella, A. Chersi, R. G. Mage, and S. Dubiski, *Proc. Nat. Acad. Sci. USA*, **68**, 1341 (1971).

(16) J. M. Kehoe, A. Bourgois, J. D. Capra, and M. Fougereau, *Biochemistry*, **13**, 2499 (1974).

(17) *Bull. WHO*, **39**, 935 (1968).

ACKNOWLEDGMENTS AND ADDRESSES

Received February 25, 1976, from the *Department of Microbiology, University of Alabama Medical School, Birmingham, AL 35294.*

Accepted for publication May 5, 1976.

Supported by Grant AI 11970 from the National Institutes of Health.

[x] To whom inquiries should be directed.

Determination of Oxamniquine in Serum

N. M. WOOLHOUSE [x] and P. R. WOOD

Abstract □ A method for the analysis of oxamniquine in serum (or plasma), sensitive to 10 ng/ml, was developed. Oxamniquine and a close structural analog as the internal standard were extracted from serum with ether. After derivatization with *N,O*-bis(trimethylsilyl)acetamide, oxamniquine was determined as its trimethylsilyl ether derivative by GLC using an electron-capture detector. The method was developed to study serum concentration profiles of different dosage forms of oxamniquine.

Keyphrases □ Oxamniquine—GLC analysis, human serum or plasma □ GLC—analysis, oxamniquine, human serum or plasma □ Antischistosomals—oxamniquine, GLC analysis, human serum or plasma

Oxamniquine[1], 6-hydroxymethyl-2-isopropylaminomethyl-7-nitro-1,2,3,4-tetrahydroquinoline (I), is a potent schistosomicide, active principally against *Schistosoma mansoni*. Extensive clinical trials with this drug in South America and in Africa have shown that oxamniquine is curative after a single intramuscular dose (1–6) and is also effective when given orally (7).

An assay was developed so that serum and plasma concentration profiles of the drug could be determined after both intramuscular and oral administrations of different dosage forms to humans and experimental animals.

EXPERIMENTAL

Reagents—The following were used: ether[2]; ethyl acetate[2], redistilled from molecular sieve 4A; pyridine[2], dried over potassium hydroxide; *N,O*-bis(trimethylsilyl)acetamide[3]; citrate–phosphate buffer, pH 5.0, prepared from stock solutions by mixing 51.5 ml of 0.2 *M* Na_2HPO_4 with 48.5 ml of 0.1 *M* citric acid; and 8-hydroxymethyl-3-isopropyl-9-nitro-2,3,4,4a,5,6-hexahydro-1*H*-pyrazine[1,2-*a*]quinoline (II), synthesized according to Baxter and Richards (8).

GLC—A gas-liquid chromatograph[4] fitted with a glass column, 1.85 m in length × 1.0 mm i.d., and a ^{63}Ni-electron-capture detector was used. The stationary phase was dimethyl silicone (OV-101), 5%, on Gas Chrom Q, 80–100 mesh. Operating temperatures were: injector, 250°; oven, 260°; and detector, 290°. The carrier gas was oxygen-free nitrogen with a flow rate of 40 ml/min. Retention times were: oxamniquine, 5 min; and internal standard (II), 7 min.

Standard Curve—Solutions of I and II were prepared daily at a concentration of 50 μg/ml by dissolving 2.5 mg of the compounds in methanol (5.0 ml) and adjusting the volume to 50 ml with distilled water.

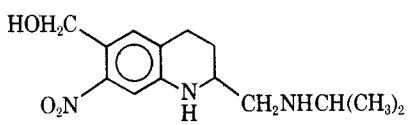

I

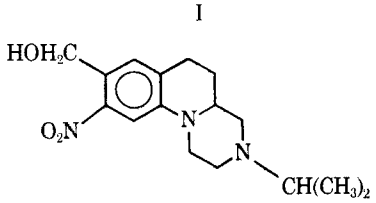

II

A standard calibration curve was prepared daily by spiking blank serum samples with varying amounts of oxamniquine together with a fixed amount of internal standard. To 1.0 ml of control samples of serum in 10-ml stoppered tubes, 50, 100, 200, 300, and 400 ng of oxamniquine were added (*i.e.*, 1, 2, 4, 6, and 8 μl of the stock solution) using a 10-μl syringe[5]. A constant amount of internal standard, 250 ng, was then added

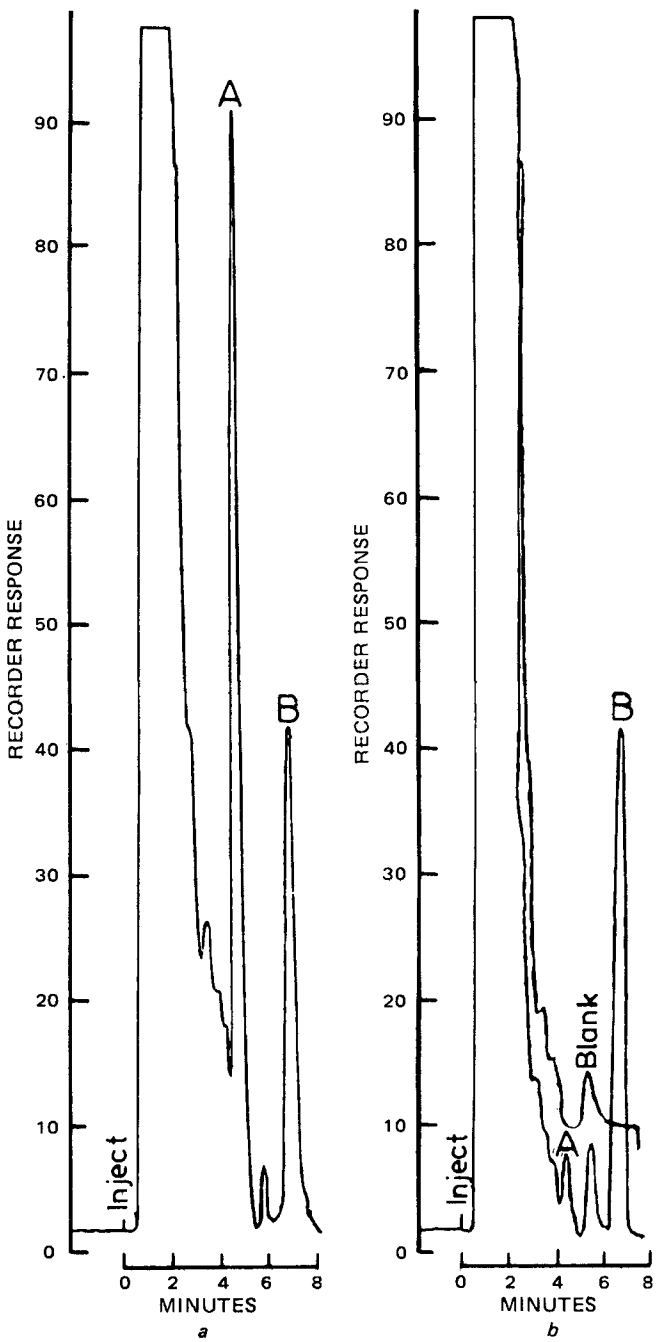

Figure 1—*Chromatograms of oxamniquine (A) and internal standard (B) showing* (a) *a high (440 ng/ml) and* (b) *a low (30 ng/ml) concentration of oxamniquine in human serum and a superimposed blank serum sample chromatogram.*

[1] Mansil, Pfizer.
[2] Analar.
[3] Phase Separations Ltd.
[4] Varian 1400.
[5] Hamilton.

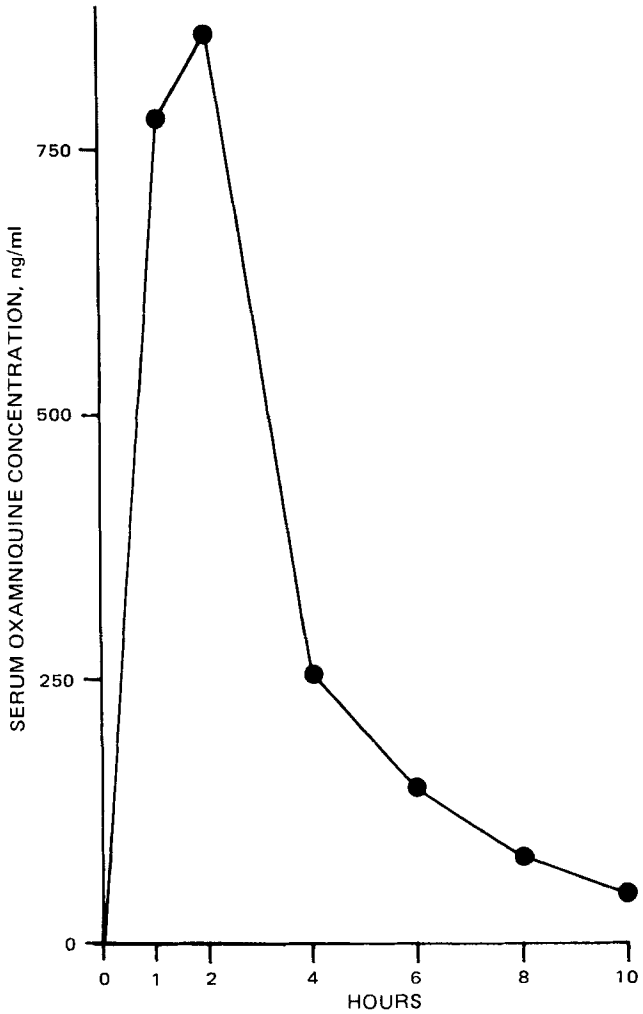

Figure 2—*Serum concentrations of oxamniquine in a human volunteer following administration of a single oral dose of oxamniquine (1000 mg).*

to each of the spiked serum samples containing different amounts of oxamniquine. Sodium hydroxide, 1 *M* (1.0 ml), and ether (4.0 ml) were added and the samples were extracted by mixing for 30 sec using a vortex mixer.

The phases were separated by centrifugation, and the organic layer was carefully removed to a second stoppered tube. A second ether extraction was carried out, and the second extract was added to the first. The combined organic extracts were extracted with citrate–phosphate buffer (5.0 ml) and, after separation of the phases by centrifugation, the organic layer was removed and discarded. Sodium hydroxide, 1 *M* (1.0 ml), was added, and the aqueous phase was then extracted twice with 4.0-ml portions of ether as described.

The extracts were combined in a clean centrifuge tube and placed in a water bath at ambient temperature, and the solvent was evaporated to dryness under a stream of nitrogen. Dry pyridine (50 μl) was added to redissolve the extract. *N,O*-Bis(trimethylsilyl)acetamide (10 μl) was then added, and the tube was stoppered and allowed to stand for 5 min at room temperature. The derivatized material was then diluted with ethyl acetate (0.5 ml) and, after mixing, an accurately measured aliquot (2 μl) was injected onto the column.

The peak heights due to oxamniquine and the internal standard were measured, and peak height ratios (oxamniquine–internal standard) were calculated. The relationship between peak height ratio and oxamniquine concentration was linear for serum concentrations up to 500 ng/ml. The actual mean recovery of oxamniquine in ether extracts of serum determined by comparison of peak height ratios using the described method with those obtained by direct injection of pure sample mixtures was 92 ± 4% (*SEM*).

Sample Analysis—Test serum samples or suitably diluted samples (1.0 ml) to be assayed were transferred to chemically clean stoppered tubes and spiked with 250 ng of the internal standard. These samples were analyzed as already described. The typical sample chromatograms obtained, showing high (440 ng/ml) and low (30 ng/ml) concentrations of oxamniquine in human serum, and a blank sample chromatogram are shown in Fig. 1. A typical serum concentration *versus* time curve in a healthy human volunteer following administration of a single oral dose of oxamniquine (1000 mg) is shown in Fig. 2.

Accuracy and Reproducibility—The accuracy of the assay over the 50–500-ng/ml concentration range was determined. Eight spiked serum samples of concentrations unknown to the operator were assayed. The spiked concentrations (nanograms per milliliter) together with the assayed values (in parentheses) were 49 (50), 98 (97), 123 (128), 148 (168), 197 (202), 246 (240), 395 (404), and 450 (470).

Six replicate assays were carried out on a serum sample spiked at a concentration of 115 ng/ml. The mean value found was 114.5 ± 4.0 ng/ml (*SEM*).

Identity of Oxamniquine Derivative—After derivatization of oxamniquine with *N,O*-bis(trimethylsilyl)acetamide under the described conditions, only one peak was seen on the gas–liquid chromatogram. Combined GLC–mass spectrometry indicated a mass of 351, showing that only a monotrimethylsilyl derivative is formed under the conditions employed. A prominent M − 89 fragment ion peak in the mass spectrum confirmed that the trimethylsilyl group is attached to oxygen (9).

DISCUSSION

A method for the assay of oxamniquine was first developed in these laboratories to determine serum concentrations in toxicity trial animals. The method employed was essentially the same as that described here but used a flame-ionization detector. With this method, drug concentrations down to 750 ng/ml could be determined. However, the method was not sufficiently sensitive to determine with precision the serum concentrations achieved at therapeutic dose levels in clinical trials.

The presence of the nitro group in the oxamniquine molecule suggested that an increase in sensitivity might be gained by employing an electron-capture detector. This change increased the sensitivity of detection some 75-fold, and concentrations of oxamniquine in serum or plasma can be readily determined down to 10 ng/ml. This sensitivity makes the method suitable for the determination of serum concentration profiles of oxamniquine in patients receiving therapeutic doses where maximum plasma concentrations of drug ranging up to approximately 1 μg/ml are found.

REFERENCES

(1) A. Coutinho, A. L. C. Domingues, and J. R. A. Bonfim, *Rev. Inst. Med. Trop. S. Paulo (Supplement 1)*, **15**, 10 (1973).

(2) N. Katz, J. Pellegrino, E. Grinbaum, A. Chaves, and F. Zicker, *ibid.*, **15**, 35 (1973).

(3) J. R. Coura, C. A. Argento, N. de Figueiredo, B. Wanke, and G. C. de Queiroz, *ibid.*, **15**, 41 (1973).

(4) A. Prata, J. F. M. Figueiredo, J. C. Brandt, and L. Lauria, *ibid.*, **15**, 47 (1973).

(5) V. M. Eyakuse, *ibid.*, **15**, 67 (1973).

(6) P. H. Rees, J. M. D. Roberts, B. A. Woodger, and H. O. Pamba, *ibid.*, **15**, 78 (1973).

(7) L. C. da Silva, H. Sette, Jr., D. A. F. Chamone, A. Saez Alquezar, J. A. Punskas, and S. Raia, *Rev. Inst. Med. Trop. S. Paulo*, **16**, 103 (1974).

(8) C. A. R. Baxter and H. C. Richards, *J. Med. Chem.*, **15**, 351 (1972).

(9) H. Budzikiewicz, C. Djerassi, and D. H. Williams, "Mass Spectrometry of Organic Compounds," Holden-Day, San Francisco, Calif., 1967, p. 473.

ACKNOWLEDGMENTS AND ADDRESSES

Received January 19, 1976, from *Pfizer Central Research, Pfizer Ltd., Sandwich, Kent, CT13 9NJ, England.*

Accepted for publication May 5, 1976.

[x] To whom inquiries should be directed.

Synthetic Acetylenic Antifungal Agents

D. Z. SIMON, S. BROOKMAN [x], J. BELIVEAU, and R. L. SALVADOR

Abstract □ Several monoamino bis(propynyloxy)benzenes were prepared by a Mannich reaction and tested for antifungal activity against *Trichophyton schoenleini, T. mentagrophytes, T. tonsurans, Candida albicans,* and *Epidermophyton flocossum.* In addition, the bis(propynyloxy)benzene intermediates were tested and comparisons were made with standard drugs. The intermediates were found to be the most active, although two Mannich bases possessed considerable activity.

Keyphrases □ Bis(propynyloxy)benzenes and monoamino derivatives—synthesized, screened for antifungal activity □ Antifungal activity—screened in various bis(propynyloxy)benzenes and monoamino derivatives □ Structure–activity relationships—various bis(propynyloxy)benzenes and monoamine derivatives screened for antifungal activity

The isolation of 1-oxo-1-phenylhexa-2,4-diyne from the essential oil of *Artemisia capillaris* Thunb. (Compositae) (1) and the subsequent isolation and synthesis of acetylenecarboxamide (2, 3) have led many investigators to synthesize related acetylenic compounds and to examine their antifungal properties (4). Some mercury acetylides (5), amino polyenes (6), and monoamino alkynes (7) were prepared that were effective antifungal agents. In addition, acetylenic amino esters and diamines with antifungal action were synthesized (8).

Among a large series of compounds (9–13), 3-iodopropargyl ethers exhibited considerable antifungal activity when they possessed an aryl group that was either phenyl or naphthyl substituted by at least one electronegative group. This finding led to the clinically successful agent haloprogin, 1,2,4-trichloro-5-[(3-iodo-2-propynyl)-oxy]benzene (14). A new series of phenyl ethers, which might prove interesting from this aspect, was synthesized (Scheme I).

RESULTS AND DISCUSSION

Bis(propynyloxy)benzenes (I) were prepared *via* a Williamson synthesis, as previously described (15). Under Mannich reaction conditions with formaldehyde solution and various dialkylamines, a series of monoamino bis(propynyloxy)benzenes (II) was obtained; confirmation was by elemental analysis and IR and NMR spectroscopy (Table I). Attempts at synthesizing the *o*-dimethylamino and *o*-diethylamino Mannich bases failed, probably due to steric hindrance.

The antifungal activity of all compounds, *i.e.*, types I and II, was determined *in vitro* [1] against *Trichophyton schoenleini, T. mentagrophytes, T. tonsurans, Candida albicans,* and *Epidermophyton flocossum.* All compounds were dissolved in dimethyl sulfoxide at a concentration of 5 μg/ml. The antifungal properties of the active substances are reported in Table II and were compared to haloprogin and griseofulvin.

Antifungal activity was observed with I*a*, I*b*, and I*c*. The Mannich bases II*a* and II*d* showed some activity, although the remaining bases did not. In addition, considerable growth inhibition was visible by II*a* against *E. flocossum.* Therefore, it appeared that the introduction of an alkylamino group onto one propargyl chain led to diminished antifungal properties.

[1] A cylinder plate method on a Sabouraud dextrose agar medium (Difco), pH 5.9, was used. The plates were subjected to preincubation (period of diffusion) at 4° for 1 hr and then incubated at 25° for 72 hr. The zones of inhibition were measured, each value representing the average of three trials. Control agar plates using dimethyl sulfoxide were included in each trial series. The microorganisms were obtained from the fungi collection of the Department of Microbiology, University of Montreal, Montreal 101, Canada.

EXPERIMENTAL [2]

1,2-Bis(2-propynyloxy)benzene (I*a*)—To 75 ml of acetone, 11 g (0.1 mole) of catechol, 27.6 g (0.2 mole) of anhydrous potassium carbonate, and 23.8 g (0.2 mole) of propargyl bromide were added, and the mixture was refluxed under nitrogen for 8 hr. The mixture was filtered, and the resulting filtrate was evaporated under reduced pressure. The residue was dissolved in ether, washed with 10% sodium hydroxide and water, and dried over anhydrous potassium carbonate. The solvent was evaporated under reduced pressure, and the resulting oil was heated in *n*-pentane. Decanting and evaporating the supernate yielded 13.1 g (70%) of I*a*, mp 30.5–31°; IR (ν_{max}): 3285 (acetylenic CH) and 2115 (monosubstituted C≡C) cm^{-1}; NMR: 2.4 (t, 2H, J = 2.6 Hz), 4.65 (d, 4H, J = 2.6 Hz), and 6.95 (s, 4H) ppm; TLC: R_f 0.50 (chloroform).

1,3-Bis(2-propynyloxy)benzene (I*b*)—Compound I*b* was prepared from resorcinol as described for I*a*, yielding 15.8 g (85%), mp 37.5–38°; NMR: 2.6 (t, 2H, J = 2.6 Hz), 4.7 (d, 4H, J = 2.6 Hz), 6.6 (m, 3H), and 7.2 (t, 1H, J = 8.0 Hz) ppm; TLC: R_f 0.8 (chloroform).

1,4-Bis(2-propynyloxy)benzene (I*c*)—Compound I*c* was prepared from hydroquinone as described for I*a*, yielding 16.8 g (87%), mp 49.5–50°; NMR: 2.6 (t, 2H, J = 2.6 Hz), 4.8 (d, 4H, J = 2.6 Hz), and 7.2 (s, 4H) ppm; TLC: R_f 0.55 [chloroform–carbon tetrachloride (7:3)].

1-(4-Dimethylamino-2-butynyloxy)-4-(2-propynyloxy)benzene (II*a*)—To 35 ml of dioxane, 16.2 ml (0.216 mole) of 40% formaldehyde and 10 g (0.054 mole) of I*c* were added, and the solution was placed in a 250-ml pressure flask. Dimethylamine, 19.4 g (0.432 mole), was added, and the flask was sealed and heated at 80° for 140 hr. The reaction flask was cooled prior to opening. The solvents were evaporated under reduced pressure; the residue was dissolved in ether and washed with several portions of 10% sodium bisulfite and then water until neutral washings resulted. The organic phase was extracted with 250 ml of 10% HCl, the aqueous fraction was made alkaline with a slurry of sodium bicarbonate, and the free base was extracted with ether and dried over anhydrous potassium carbonate. The solvent was removed to yield 4.02 g (31%) of II*a*, mp 34–35°; IR (ν_{max}): 3290 (acetylenic CH) and 2110 (monosubstituted C≡C) cm^{-1}; NMR: 2.15 (s, 6H), 2.4 (t, 1H, J = 2.6 Hz), 3.2 (d, 2H, J = 2.0 Hz), 4.6 (m, 4H), and 6.9 (s, 4H) ppm.

Mannich Bases—The following Mannich bases were prepared similarly.

1-(4-Diethylamino-2-butynyloxy)-4-(2-propynyloxy)benzene (II*b*)—NMR: 1.0 (t, 6H, J = 6.3 Hz), 2.4 (m, 5H), 3.35 (t, 2H, J = 2.0 Hz), 4.6 (m, 4H), and 6.85 (s, 4H) ppm.

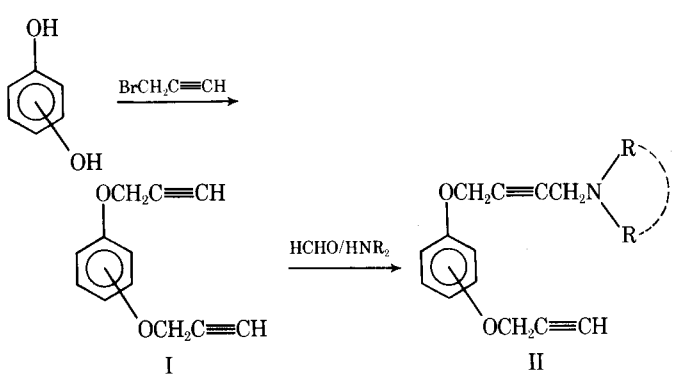

Scheme I

[2] Melting points were measured by the capillary method on a Buchi melting-point apparatus and are uncorrected. Carbon, hydrogen, and nitrogen were determined by Dr. C. Daessle, Montreal, Canada. Amine bases were analyzed in the form of their picrate salts, and the results obtained are within 0.4% of the theoretical values. IR spectra were recorded on a Beckman IR 18A spectrophotometer. NMR spectra were recorded on a Perkin-Elmer R 12B spectrometer in carbon tetrachloride. The tetramethylsilane signal was taken as the internal reference. The proton signals are designated by the following abbreviations: s, singlet; d, doublet; t, triplet; and m, multiplet. TLC plates, 0.5 mm thick, were prepared using silica gel G, and the compounds were detected with iodine vapors.

Table I—Physical Constants of Monoamino Bis(propynyloxy)benzenes

Compound	Yield, %	Melting Point	Boiling Point	Formula (Picrate)	Analysis, % Calc.	Found
II*a*	31	34–35°	—	$C_{21}H_{20}N_4O_9$	C 53.39	53.16
					H 4.24	4.47
					N 11.86	11.68
II*b*	38	20–21°	—	$C_{23}H_{24}N_4O_9$	C 55.20	54.92
					H 4.80	5.07
					N 11.20	10.96
II*c*	31	44–46°	—	$C_{23}H_{22}N_4O_{10}$	C 53.70	53.46
					H 4.28	4.14
					N 10.89	11.10
II*d*	22	49–51°	—	$C_{23}H_{22}N_4O_{10}$	C 53.70	53.48
					H 4.28	4.27
					N 10.89	11.14
II*e*	12	—	118°/ 0.005 mm	$C_{21}H_{20}N_4O_9$	C 53.39	53.43
					H 4.24	4.44
					N 11.86	12.13
II*f*	13	—	130–132°/ 0.005 mm	$C_{23}H_{24}N_4O_9$	C 55.20	55.13
					H 4.80	5.05
					N 11.20	11.31
II*g*	30	152–153° (picrate)	—	$C_{23}H_{22}N_4O_{10}$	C 53.70	53.96
					H 4.28	4.44
					N 10.89	11.05

Table II—Antifungal Activity of Bis(propynyloxy)benzenes and Their Mannich Bases[a]

Compound	*T. schoenleini*	*T. tonsurans*	*T. mentagrophytes*	*E. flocossum*	*C. albicans*
Control	–	–	–	–	–
I*a*	+	+	+	2+	+
I*b*	+	2+	2+	2+	2+
I*c*	+	2+	2+	2+	2+
II*a*	+	+	+	+	+
II*d*	+	+	+	2+	+
Griseofulvin	+	+	+	2+	–
Haloprogin	+	2+	3+	3+	2+

[a] Inhibition zones expressed as follows: –, inhibition; +, 10–25 mm; 2+, 26–40 mm; and 3+, 41–55 mm.

1-(4-Morpholino-2-butynyloxy)-4-(2-propynyloxy)benzene (II*c*) —NMR: 2.5 (m, 5H), 3.3 (t, 2H, J = 2.0 Hz), 3.7 (m, 4H), 4.7 (t, 4H, J = 5.3 Hz), and 6.9 (s, 4H) ppm.

1-(4-Morpholino-2-butynyloxy)-2-(2-propynyloxy)benzene (II*d*) —NMR: 2.5 (m, 5H), 3.35 (t, 2H, J = 2.0 Hz), 3.7 (t, 4H, J = 5.3 Hz), 4.8 (m, 4H), and 7.0 (s, 4H) ppm.

1-(4-Dimethylamino-2-butynyloxy)-3-(2-propynyloxy)benzene (II*e*)—NMR: 2.2 (s, 6H), 2.4 (t, 1H, J = 2.6 Hz), 3.25 (t, 2H, J = 2.0 Hz), 4.6 (m, 4H), and 6.5–7.2 (m, 4H) ppm.

1-(4-Diethylamino-2-butynyloxy)-3-(2-propynyloxy)benzene (II*f*)—NMR: 1.1 (t, 6H, J = 6.3 Hz), 2.5 (m, 5H), 3.45 (t, 2H, J = 2.0 Hz), 4.7 (m, 4H), and 6.6–7.3 (m, 4H) ppm.

1-(4-Morpholino-2-butynyloxy)-3-(2-propynyloxy)benzene (II*g*) —NMR: 2.5 (m, 5H), 3.4 (t, 2H, J = 2.0 Hz), 3.7 (t, 4H, J = 5.3 Hz), 4.8 (m, 4H), and 6.8–7.4 (m, 4H) ppm.

REFERENCES

(1) K. Imai, N. Ikeda, K. Tanaka, and S. Sugawa, U.S. pat. 2,868,839 (Jan. 13, 1959).

(2) S. Suzuki, G. Nakamura, K. Okuna, and Y. Tomiyama, *J. Antibiot. (Tokyo)*, **11**, 81 (1958).

(3) A. J. Saggiomo, *J. Org. Chem.*, **22**, 1171 (1957).

(4) K. Tanaka, I. Iwai, Y. Okajima, and T. Konotsune, *Antibiot. Chemother.*, **9**, 151 (1959).

(5) J. H. Wotiz (to Diamond Alkali Co.), U.S. pat. 3,219,677 (Nov. 23, 1965).

(6) J. H. Wotiz (to Diamond Alkali Co.), U.S. pat. 3,210,426 (Oct. 5, 1965).

(7) J. L. Neumeyer and J. G. Cannon, *J. Pharm. Sci.*, **51**, 804 (1962).

(8) J. Waters and G. A. Wiese, *J. Am. Pharm. Assoc., Sci. Ed.*, **49**, 112 (1960).

(9) C. S. L. Baker, P. D. Landor, and S. R. Landor, *J. Chem. Soc.*, **1965**, 4659.

(10) F. Hoffmann-La Roche & Co. A.-G., Netherlands pat. appl. 6,601,926; through *Chem. Abstr.*, **66**, 2362d (1967).

(11) F. Hoffmann-La Roche & Co. A.-G., Netherlands pat. appl. 6,612,646; through *Chem. Abstr.*, **67**, 73349p (1967).

(12) F. Hoffmann-La Roche & Co. A.-G., Netherlands pat. appl. 6,612,647; through *Chem. Abstr.*, **67**, 73350g (1967).

(13) Y. Seki, F. Kai, and H. Ogawa (to Meiji Confectionary Co.), Japanese pat. 11,734 (July 4, 1967).

(14) S. Seki, B. Nomiya, T. Koeda, K. Umemura, M. Oda, and H. Ogawa, *Antimicrob. Ag. Chemother.*, **1963**, 569.

(15) R. Bolduc, M.S. thesis, University of Montreal, Montreal, Canada (1965).

ACKNOWLEDGMENTS AND ADDRESSES

Received October 29, 1975, from the *Faculty of Pharmacy, University of Montreal, Montreal 101, Quebec, Canada.*

Accepted for publication April 19, 1976.

The authors thank Ayerst Laboratories, Montreal, Canada, and Mead Johnson Canada, Toronto, for furnishing reference samples. The authors are indebted to Miss C. Lepage and Mr. M. A. Fattah for technical assistance. They also thank the Medical Research Council of Canada for financial support and Dr. T. El-Kersh for helpful suggestions.

[x] To whom inquiries should be directed. Present address: Institut de médecine et de chirurgie expérimentales, Université de Montreal, Montreal 101, Quebec, Canada.

Fluorometric Determination of Naproxen in Serum

MARKKU ANTTILA

Abstract □ The fluorometric measurement of naproxen following its extraction from serum by a two-step procedure is described. Different parameters in the analysis were examined. The method was useful in biopharmaceutic and pharmacokinetic studies of naproxen.

Keyphrases □ Naproxen—fluorometric analysis, human serum □ Fluorometry—analysis, naproxen in human serum □ Anti-inflammatory agents—naproxen, fluorometric analysis, human serum

Naproxen, (+)-6-methoxy-α-methyl-2-naphthaleneacetic acid, is a potent nonsteroidal anti-inflammatory, analgesic, and antipyretic drug (1). The pharmacokinetics of naproxen in various animal species and in humans have been reported (2). These studies were based on an assay method, described briefly previously (2), which involves GLC with flame-ionization detection. In the present study, a fluorometric method was developed; it is more sensitive and, because of its simplicity, may be more widely applicable than the GLC method.

EXPERIMENTAL

Materials and Equipment—Naproxen was synthesized[1], and all other chemicals were analytical grade and used as supplied[2]. Standard solutions were prepared by dissolving naproxen in 0.1 *M* NaOH. Fluorescence spectra (uncorrected) and measurements were made with a fluorescence spectrophotometer[3].

Procedure—Serum or plasma, 0.10 ml, was added to 1 ml of 1 *M* hydrochloric acid and 5.00 ml of benzene containing 1.5% isoamyl alcohol in 10-ml screw-capped[4] tubes. These tubes were then shaken for 10 min on a reciprocating shaker. Following a brief centrifugation (5 min at 2000×*g*), 4.00 ml of the organic phase was transferred to a second tube containing 3.00 ml of 0.1 *M* sodium hydroxide.

After shaking and centrifuging again, the organic phase was aspirated and discarded. The fluorescence of the water phase was measured at excitation and emission maxima of 330 and 355 nm, respectively. The concentrations of naproxen in the samples were estimated by reference to standard solutions of naproxen in serum prepared simultaneously.

RESULTS AND DISCUSSION

Naproxen showed strong native fluorescence in aqueous solution with three distinct excitation maxima at wavelengths of 240, 275, and 330 nm and an emission maximum at 355 nm (Fig. 1). The fluorescence was insensitive to changes in pH (the fluorescence changed by less than 3% over the pH 0.1–14.0 range). For routine assay, the excitation maximum at 330 nm was used because fluorescence remained linearly related to naproxen concentration up to 10 μg/ml. At excitation maxima of 240 and 270 nm, linearity was preserved only up to 2.5 and 1 μg/ml, respectively.

The extraction of naproxen from serum into several organic solvents was tested. Quantitative recovery was obtained with heptane and benzene (both containing 1.5% isoamyl alcohol); 99 ± 2% (mean ± *SD*, *n* = 10) of the drug added at a concentration of 50 μg/ml to serum samples was found in the aqueous phase after two extractions. Benzene was selected for the assay because it produced a lower background fluorescence.

The optimum conditions for extraction of naproxen from aqueous solution into organic solvents were found by studying the distribution of the compound between various buffer solutions and benzene. For the transfer of naproxen from an aqueous into an organic phase, a pH lower than 7 was required; reextraction into water required a pH above 9.

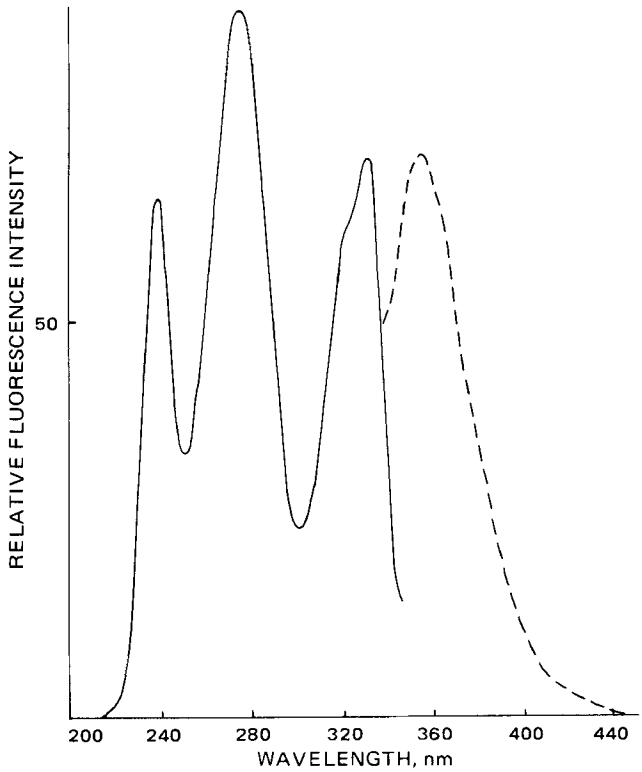

Figure 1—*Uncorrected excitation (—) and emission (- - -) spectra of the fluorescence of naproxen (1 μg/ml of 0.1 M NaOH).*

The detection limit of the present method is 0.5 μg/ml of serum. At this concentration, the fluorescence is twice that of the reagent blank. The sensitivity of the procedure is such that it will detect therapeutic plasma concentrations of naproxen. The sensitivity could be increased by using larger volumes (to 1 ml) of serum, since this change did not excessively increase background fluorescence and did not affect the recovery. Because

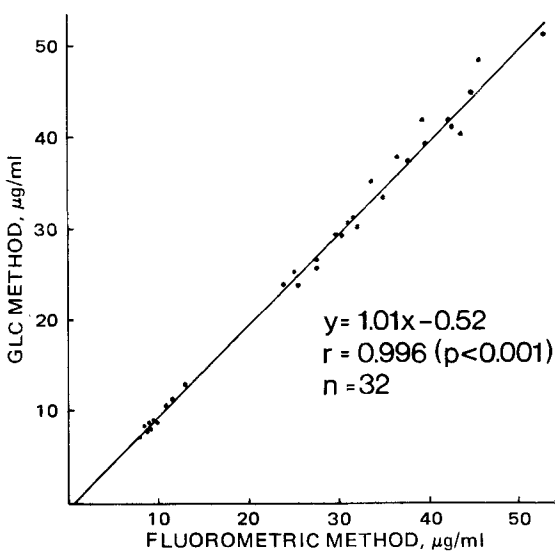

Figure 2—*Comparison of the serum levels of naproxen as determined by the fluorometric and GLC methods.*

[1] Synthetic laboratory of Farmos Group, Research Center, Turku, Finland.
[2] E. Merck, Darmstadt, Germany.
[3] Model MPF-2A, Perkin-Elmer Corp., Norwalk, Conn.
[4] Lined with Teflon (du Pont).

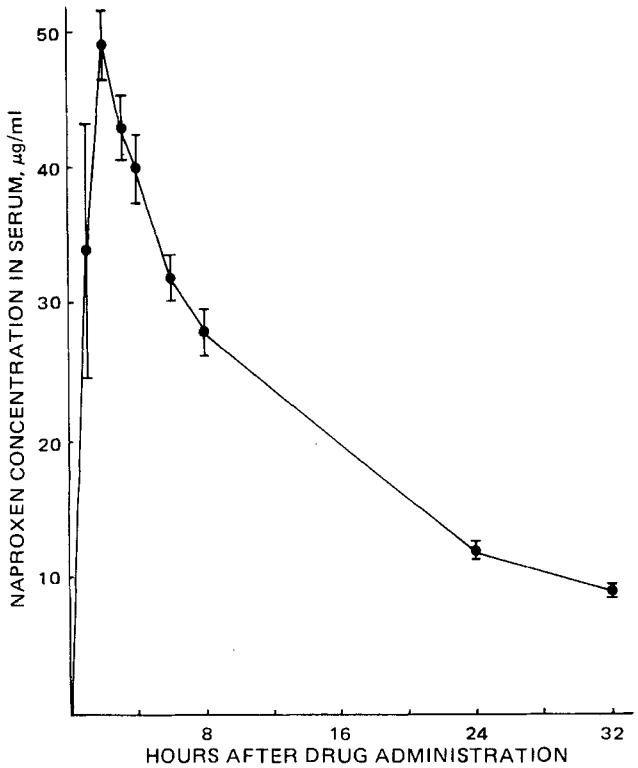

Figure 3—*Mean (±SEM) serum levels of naproxen in humans (n = 6) following single-dose oral administration of 250 mg of drug as a compressed tablet.*

of the linearity of the standard curve, serum concentrations up to 250 μg/ml can be measured using 0.1 ml of sample.

Several drugs at normal serum concentrations were examined for interference with this fluorometric assay of naproxen. Basic drugs were removed in the extraction procedure and caused no interference. The following acidic drugs also did not interfere: chlorpropamide, furosemide, ibuprofen, indomethacin, mefenamic acid, phenobarbital, phenylbutazone, phenytoin, sulfamethoxazole, and warfarin. Interference was observed with salicylic acid; 200 μg of salicylic acid/ml of serum gave a fluorescence value equivalent to about 10 μg of naproxen/ml. Therefore, this fluorometric assay method is not suitable for the determination of serum levels of naproxen in patients simultaneously receiving salicylates.

Interference by metabolites of naproxen was not studied, because the concentrations of metabolites in serum after naproxen administration are negligible (3).

The precision of the method was determined at three different concentrations. Naproxen solution was added to serum to give final concentrations of 5, 50, and 200 μg/ml. Ten 0.1-ml samples of each serum solution were analyzed by the proposed method at the same time. The relative standard deviations obtained were 2.6, 1.4, and 1.1%, respectively.

To test the accuracy of the method, 32 serum samples containing unknown concentrations of naproxen were assayed by both the present method and the GLC method (2). The results (Fig. 2) showed excellent correlation between the two methods.

To demonstrate the utility of this fluorometric method, serum concentrations of naproxen were measured in six normal human subjects after oral administration of a single dose of 250 mg of naproxen (one 250-mg tablet). The resulting serum levels (Fig. 3) agreed well with the serum levels of naproxen obtained by other workers using the GLC method (2).

The described fluorometric method is simple, rapid, and sensitive and can serve as a useful tool in the study of biopharmaceutics and pharmacokinetics of naproxen.

REFERENCES

(1) A. P. Roszkowski, W. H. Rooks, A. J. Tomolonis, and L. M. Miller, *J. Pharmacol. Exp. Ther.*, **179**, 114 (1971).

(2) R. Runkel, M. Chaplin, G. Boost, E. Segre, and E. Forchielli, *J. Pharm. Sci.*, **61**, 703 (1972).

(3) G. Boost, *Arzneim.-Forsch.*, **25**, 281 (1975).

ACKNOWLEDGMENTS AND ADDRESSES

Received March 9, 1976, from the *Farmos Group, Research Center, P.O. Box 425, 20101 Turku 10, Finland.*

Accepted for publication May 5, 1976.

Fluorescent Inhibitors of Thymidylate Synthetase

THOMAS L. DEITS, GEORGE R. GAPSKI, and JOHN M. WHITELEY ×

Abstract □ Two fluorescent derivatives of 2′-deoxy-5-fluorouridine 5′-*p*-aminophenyl phosphate were prepared by treatment of this compound with fluorescein isothiocyanate in dimethyl sulfoxide or 5-(dimethylamino)naphthalenesulfonyl chloride in pyridine. The products of the reactions were isolated by diethylaminoethylcellulose chromatography and were shown to be homogeneous by polyacrylamide electrophoresis and TLC. Confirmation of the structure was provided by elemental analysis, absorption and fluorescence spectra, PMR measurements, and liberation of nucleotide upon hydrolysis with snake venom phosphodiesterase. The fluorescent derivatives are good competitive inhibitors ($K_i \simeq 10^{-6}$ *M*) of thymidylate synthetase from a methotrexate-resistant strain of *Lactobacillus casei*.

Keyphrases □ Thymidylate synthetase—inhibition by fluorescent derivatives of 2′-deoxy-5-fluorouridylate ester evaluated □ 2′-Deoxy-5-fluorouridylate ester—fluorescent derivatives synthesized, inhibition of thymidylate synthetase evaluated □ Enzyme inhibitors—fluorescent derivatives of 2′-deoxy-5-fluorouridylate ester synthesized, effect on thymidylate synthetase

The *de novo* enzymatic synthesis of thymidylate (2′-deoxy-5-methyluridylate) is achieved by transfer of the methylene substituent of 5,10-methylenetetrahydrofolate to 2′-deoxyuridylate with the associated conversion of the hypothetical methylene intermediate (1) to methyl using the inherent reducing power of the folate cofactor (Scheme I). A metabolic cycle is completed when the ensuing dihydrofolate is reduced to the tetrahydro level in the presence of dihydrofolate reductase, and an additional one-carbon unit is reintroduced enzymatically (2). Because

5,10-methylenetetrahydrofolate + 2′-deoxyuridylate $\xrightarrow{\text{thymidylate synthetase}}$ dihydrofolate + thymidylate

Scheme I

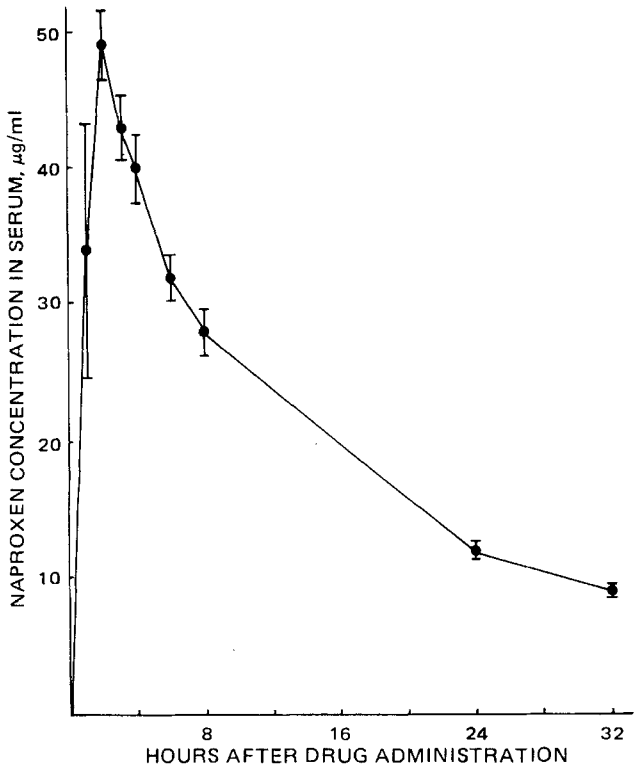

Figure 3—*Mean (±SEM) serum levels of naproxen in humans (n = 6) following single-dose oral administration of 250 mg of drug as a compressed tablet.*

of the linearity of the standard curve, serum concentrations up to 250 μg/ml can be measured using 0.1 ml of sample.

Several drugs at normal serum concentrations were examined for interference with this fluorometric assay of naproxen. Basic drugs were removed in the extraction procedure and caused no interference. The following acidic drugs also did not interfere: chlorpropamide, furosemide, ibuprofen, indomethacin, mefenamic acid, phenobarbital, phenylbutazone, phenytoin, sulfamethoxazole, and warfarin. Interference was observed with salicylic acid; 200 μg of salicylic acid/ml of serum gave a fluorescence value equivalent to about 10 μg of naproxen/ml. Therefore, this fluorometric assay method is not suitable for the determination of serum levels of naproxen in patients simultaneously receiving salicylates.

Interference by metabolites of naproxen was not studied, because the concentrations of metabolites in serum after naproxen administration are negligible (3).

The precision of the method was determined at three different concentrations. Naproxen solution was added to serum to give final concentrations of 5, 50, and 200 μg/ml. Ten 0.1-ml samples of each serum solution were analyzed by the proposed method at the same time. The relative standard deviations obtained were 2.6, 1.4, and 1.1%, respectively.

To test the accuracy of the method, 32 serum samples containing unknown concentrations of naproxen were assayed by both the present method and the GLC method (2). The results (Fig. 2) showed excellent correlation between the two methods.

To demonstrate the utility of this fluorometric method, serum concentrations of naproxen were measured in six normal human subjects after oral administration of a single dose of 250 mg of naproxen (one 250-mg tablet). The resulting serum levels (Fig. 3) agreed well with the serum levels of naproxen obtained by other workers using the GLC method (2).

The described fluorometric method is simple, rapid, and sensitive and can serve as a useful tool in the study of biopharmaceutics and pharmacokinetics of naproxen.

REFERENCES

(1) A. P. Roszkowski, W. H. Rooks, A. J. Tomolonis, and L. M. Miller, *J. Pharmacol. Exp. Ther.*, **179**, 114 (1971).

(2) R. Runkel, M. Chaplin, G. Boost, E. Segre, and E. Forchielli, *J. Pharm. Sci.*, **61**, 703 (1972).

(3) G. Boost, *Arzneim.-Forsch.*, **25**, 281 (1975).

ACKNOWLEDGMENTS AND ADDRESSES

Received March 9, 1976, from the *Farmos Group, Research Center, P.O. Box 425, 20101 Turku 10, Finland.*

Accepted for publication May 5, 1976.

Fluorescent Inhibitors of Thymidylate Synthetase

THOMAS L. DEITS, GEORGE R. GAPSKI, and JOHN M. WHITELEY ×

Abstract □ Two fluorescent derivatives of 2′-deoxy-5-fluorouridine 5′-*p*-aminophenyl phosphate were prepared by treatment of this compound with fluorescein isothiocyanate in dimethyl sulfoxide or 5-(dimethylamino)naphthalenesulfonyl chloride in pyridine. The products of the reactions were isolated by diethylaminoethylcellulose chromatography and were shown to be homogeneous by polyacrylamide electrophoresis and TLC. Confirmation of the structure was provided by elemental analysis, absorption and fluorescence spectra, PMR measurements, and liberation of nucleotide upon hydrolysis with snake venom phosphodiesterase. The fluorescent derivatives are good competitive inhibitors ($K_i \simeq 10^{-6}$ *M*) of thymidylate synthetase from a methotrexate-resistant strain of *Lactobacillus casei*.

Keyphrases □ Thymidylate synthetase—inhibition by fluorescent derivatives of 2′-deoxy-5-fluorouridylate ester evaluated □ 2′-Deoxy-5-fluorouridylate ester—fluorescent derivatives synthesized, inhibition of thymidylate synthetase evaluated □ Enzyme inhibitors—fluorescent derivatives of 2′-deoxy-5-fluorouridylate ester synthesized, effect on thymidylate synthetase

The *de novo* enzymatic synthesis of thymidylate (2′-deoxy-5-methyluridylate) is achieved by transfer of the methylene substituent of 5,10-methylenetetrahydrofolate to 2′-deoxyuridylate with the associated conversion of the hypothetical methylene intermediate (1) to methyl using the inherent reducing power of the folate cofactor (Scheme I). A metabolic cycle is completed when the ensuing dihydrofolate is reduced to the tetrahydro level in the presence of dihydrofolate reductase, and an additional one-carbon unit is reintroduced enzymatically (2). Because

5,10-methylenetetrahydrofolate + 2′-deoxyuridylate $\xrightarrow{\text{thymidylate synthetase}}$ dihydrofolate + thymidylate

Scheme I

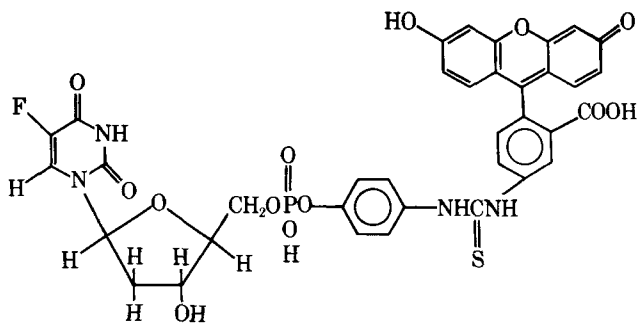

I

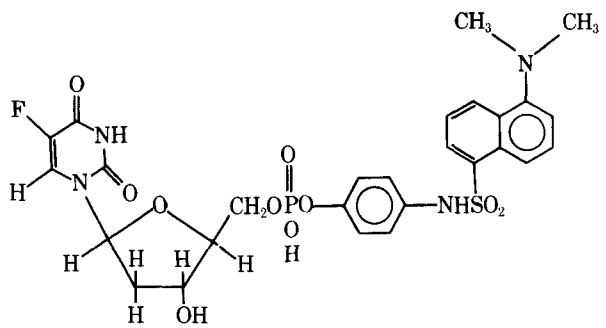

II

thymidylate is a required precursor of DNA, these two enzymes are essential for cellular replication; their interrelationship and mechanism of action have been of considerable interest during the past decade (3, 4).

Earlier experiments showed that fluorescein isothiocyanate coupled *via* a diaminopentyl group to methotrexate gives a compound that exhibits significant fluorescence changes in the presence of dihydrofolate reductase but retains its inhibitory properties and coelectrophoreses with this enzyme on polyacrylamide gels (5). As a result of this observation and earlier reports by Stryer (6) who demonstrated how variations in fluorescence intensity could be used as indicators of the nature of the heme-binding site in myoglobin, it appeared possible that similar fluorescent derivatives of the potent inhibitor of thymidylate synthetase, 2′-deoxy-5-fluorouridylate[1], might be useful as probes for the active site of this enzyme.

The syntheses and properties of the fluorescein and 5-(dimethylamino)naphthalenesulfonyl derivatives of 2′-deoxy-5-fluorouridylate are described in this paper. The two compounds (I and II) were obtained by condensing equimolar quantities of 2′-deoxy-5-fluorouridine 5′-*p*-aminophenyl phosphate (III), a compound previously synthesized in this laboratory (7), with fluorescein isothiocyanate[2] in dimethyl sulfoxide or 5-(dimethylamino)-naphthalenesulfonyl chloride[2] in pyridine. In each case, the desired fluorescent products were purified by chromatography on diethylaminoethylcellulose[3] and isolated by lyophilization. Further purification was achieved by fractional crystallization of the barium salts from ethanol–water. When I and II were irradiated at 492 and 360 nm, respectively, they showed strong fluorescence maxima at 523 and 543 nm, respectively, and the intensity varied markedly with the polarity of the solvent. Both compounds were good competitive inhibitors of thymidylate synthetase from a methotrexate-resistant strain of *Lactobacillus casei* (4).

EXPERIMENTAL[4]

Materials and Methods—Quantum yields were determined by comparison with quinine sulfate as a standard. Two systems were used for TLC: A, cellulose layers developed with 1-butanol–5 *N* acetic acid (2:1); and B, diethylaminoethylcellulose layers developed with 0.5 *M* ammonium acetate.

Thymidylate synthetase was isolated from a methotrexate-resistant strain of *L. casei* according to the procedure of Whiteley *et al.* (7) and was assayed spectrophotometrically (8). Inhibition constants were obtained from plots of $1/v$ against i at varying substrate concentrations, where v is the initial rate of reaction and i is the inhibitor concentration. Disc electrophoresis on 7.5% (w/v) polyacrylamide gels was carried out in 0.6 × 6-cm tubes. Enzymatic hydrolysis of the fluorescent derivatives was achieved by incubating an aliquot of the sample with snake venom phosphodiesterase[5] in 0.5 *M* tromethamine hydrochloride[2] buffer, pH 9, at ambient temperatures for 1 hr. The nucleotide product was identified by comparison with an authentic standard on TLC using System A.

Preparation of Fluorescent Derivatives of III—*Fluorescein Derivative (I)*—Fluorescein isothiocyanate (61.8 mg, 0.159 mmole) and the barium salt of III (89.7 mg, 0.159 mmole) were dissolved in dimethyl sulfoxide (1 ml). After standing for 4 hr at room temperature, the solution was applied to a 2 × 40-cm column of diethylaminoethylcellulose, which was then washed with 0.3 *M* ammonium acetate (2 liters). The product (I) was recovered by eluting with a 0.6 *M* solution of the same buffer, followed by lyophilization (126 mg, 99%). The product was either isolated as the free acid at this stage by trituration with 1-propanol and filtration or converted to the barium salt by dissolving in water and adjustment of the resulting solution to pH 8 with saturated barium hydroxide.

After lyophilization, the residue was taken up in the minimum quantity of water, precipitated with absolute ethanol, filtered, and dried; TLC: System A, R_f 0.69; System B, R_f 0.22; λ_{max} (0.1 *M* HCl) 251 and 438 nm (ϵ 41,200 and 40,000); λ_{max} (0.1 *M* potassium phosphate, pH 7) 236, 262, and 492 nm (ϵ 48,200, 35,300, and 53,900); λ_{max} (0.1 *M* NaOH) 237, 260, and 488 nm (ϵ 56,700, 34,600, and 67,700); fluorescence maximum (0.1 *M* potassium phosphate, pH 7): 492 nm (excitation) and 523 nm (emission) (quantum yield = 0.51); PMR (D_2O): δ 2.1 (2H, m) (2′-protons), 4.0 (3H, m) (4′- and 5′-protons), 4.3 (1H, m) (3′-proton), 6.0 (1H, m) (1′-proton), and 6.2–7.8 (broad multiplet containing the remaining 14 nonexchangeable proteins attached to unsaturated carbon).

Anal.—Calc. for $C_{36}H_{28}FN_4O_{13}PS \cdot 5.5\ H_2O$: C, 47.74; H, 4.34. Found: C, 47.48; H, 3.93.

5-(Dimethylamino)naphthalenesulfonyl Derivative (II)—A mixture of 5-(dimethylamino)naphthalenesulfonyl chloride (59.4 mg, 0.22 mmole) and the barium salt of III (113 mg, 0.2 mmole) dissolved in pyridine (5 ml) was allowed to react at ambient temperatures for 20 hr. The solution was then applied directly to a 2 × 40-cm column of diethylaminoethylcellulose. Application of water (300 ml) followed by 0.2 *M* ammonium bicarbonate (2 liters) eluted the gold fluorescent product (II). The principal fractions were combined and lyophilized (111 mg, 86%). The free acid was purified by dissolving the residue in a minimum quantity of methanol, followed by precipitation with ether. To obtain the barium salt, the material was taken up in water (15 ml), adjusted to pH 8 with barium hydroxide, filtered, and lyophilized.

The residue was dissolved in a minimum quantity of water, and the nucleotide was precipitated by the addition of acetone; TLC: System A, R_f 0.60; λ_{max} (0.1 *M* HCl) 275 and 320 nm (ϵ 13,300 and 2850); λ_{max} (0.1 *M* potassium phosphate, pH 7) 248 and 320 nm (ϵ 17,800 and 4040); λ_{max} (0.1 *M* NaOH) 244 and 318 nm (ϵ 22,400 and 5240); fluorescence maximum (0.1 *M* potassium phosphate, pH 7): 360 nm (excitation) and 543 nm (emission) (quantum yield = 0.02); PMR (D_2O): δ 2.0 (8H, m) (*N*-dimethyl and 2′-protons), 3.9 (3H, broad s) (4′- and 5′-protons), 4.2 (1H, m) (3′-proton), 6.0 (1H, m) (1′-proton), and 6.3–8.2 (broad multiplet containing the remaining 11 nonexchangeable protons attached to unsaturated carbon).

Anal.—Calc. for $C_{27}H_{28}FN_4O_{10}PS \cdot 2.5H_2O$: C, 46.62; H, 4.78. Found: C, 46.63; H, 5.03.

[1] Floxuridine is the USAN name for 2′-deoxy-5-fluorouridine.
[2] Sigma Chemical Co.
[3] Whatman Biochemicals, Ltd.

[4] Absorption, fluorescence, and PMR spectra were recorded with Cary model 14, Turner model 210, and Jeol model JNM-PS-100 (courtesy of Dr. J. Rivier, Salk Institute for Biological Studies) spectrometers, respectively.
[5] Worthington Biochemical Corp.

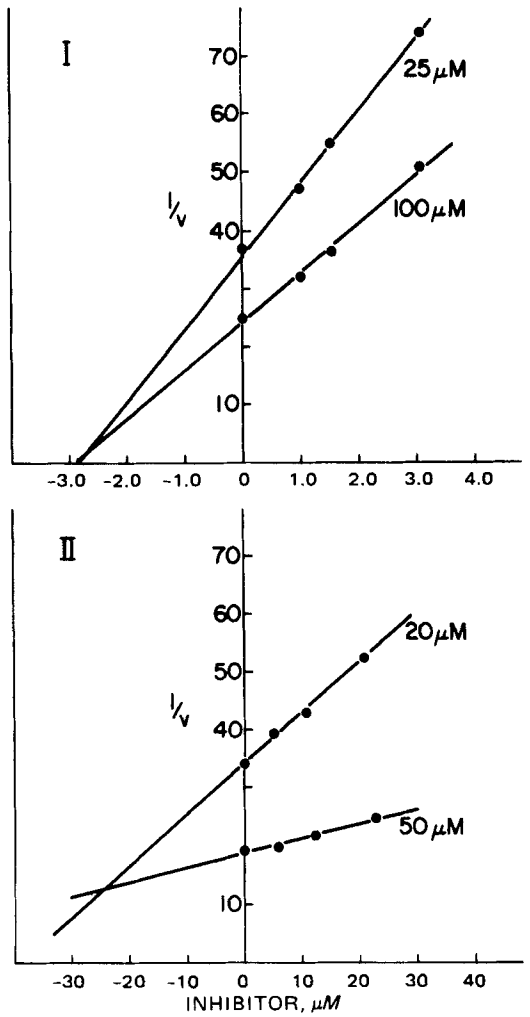

Figure 1—*Inhibition of thymidylate synthetase by I and II. The activity of the synthetase from a methotrexate-resistant strain of* L. casei *(specific activity = 3; 1.2 μg of protein) was measured as described under* Experimental. *Enzyme, 5,10-methylenetetrahydrofolate, and inhibitor were incubated together for 10 min prior to the addition of the indicated concentrations of 2′-deoxyuridylate to initiate the reaction.*

RESULTS AND DISCUSSION

The two fluorescent derivatives (I and II) were shown to be homogeneous by polyacrylamide electrophoresis and TLC. Structure confirmation was afforded by hydrolysis with snake venom phosphodiesterase to liberate free 2′-deoxy-5-fluorouridylate, elemental analysis, and PMR and absorption spectra. The absorption spectrum of each product contained the chromophore of the fluorescent moiety superimposed on that of the nucleotide ester; however, the absorptivity of the fluorescein derivative at 492 nm (pH 7) was only 54,000. This figure is 26% lower than the value recorded for free fluorescein under the same conditions (9), which suggests that there may be some interaction between the pyrimidine and fluorescein components.

This inference is supported (Table I) by the lower quantum yield (0.51) recorded for this compound when compared with the quantum yield (0.64) of free fluorescein at pH 7 (10). In the presence of ethanol, the quantum yield was depressed a further 40%, suggesting that the interaction of the two chromophores is increased in the less polar solvent. Derivative II showed a much smaller efficiency of fluorescence (quantum yield = 0.019, *cf.*, Table I); but in the presence of increasing amounts of ethanol, solutions of this compound showed a progressive increase in quantum yield. These disparate observations suggest that the two derivatives may complement each other when used as probes for the active site of the enzyme.

Table I—Quantum Yields for I and II

Derivative	Solvent	Quantum Yield
I	0.1 *M* PO_4, pH 7.0	0.51
	0.1 *M* PO_4–25% ethanol	0.31
	0.1 *M* PO_4–50% ethanol	0.32
II	0.1 *M* PO_4, pH 7.0	0.019
	0.1 *M* PO_4–25% ethanol	0.047
	0.1 *M* PO_4–50% ethanol	0.10

The inhibition constants (K_i) derived at pH 7 for the interaction of purified thymidylate synthetase with I, II, and III were 2.8, 24, and 8 μM, respectively. Clearly, introduction of the fluorescent groups made little change in the inhibitory properties. In fact, the large fluorescein moiety slightly enhanced the inhibitory capacity of the nucleotide ester, although a small decrease was observed for II. That the inhibition (for both I and II) was competitive with the normal substrate of the reaction is shown in Fig. 1, where the reciprocal velocity is plotted *versus* the inhibitor concentration at different concentrations of the substrate (2′-deoxyuridylate).

The strongly inhibitory properties demonstrated by I and II, coupled with their observed variation in fluorescence intensity with solvent polarity, suggest that these compounds may be useful aids for probing the active site of thymidylate synthetase. The compounds may provide information concerning the interaction of the nucleotide substrate or its fluorinated analog with the synthetase and may also have an additional function as visual protein markers during enzyme purification.

REFERENCES

(1) M. Friedkin and A. Kornberg, in "A Symposium on the Chemical Basis of Heredity," W. D. McElroy and B. Glass, Eds., Johns Hopkins University Press, Baltimore, Md., 1957, p. 609.

(2) R. L. Blakley, "The Biochemistry of Folic Acid and Related Pteridines," North Holland Press, Amsterdam, The Netherlands, 1969, p. 231.

(3) M. Friedkin, *Adv. Enzymol.*, **38**, 235 (1973).

(4) R. B. Dunlap, N. G. L. Harding, and F. M. Huennekens, *Biochemistry*, **10**, 88 (1971).

(5) G. R. Gapski, J. M. Whiteley, J. I. Rader, P. L. Cramer, G. B. Henderson, V. Neef, and F. M. Huennekens, *J. Med. Chem.*, **18**, 526 (1975).

(6) L. Stryer, *J. Mol. Biol.*, **13**, 482 (1965).

(7) J. M. Whiteley, I. Jerkunica, and T. Deits, *Biochemistry*, **13**, 2044 (1974).

(8) A. J. Wahba and M. Friedkin, *J. Biol. Chem.*, **236**, PC 11 (1961).

(9) W. B. Dandliker and R. Alonso, *Immunochemistry*, **4**, 191 (1967).

(10) J. M. Whiteley, G. R. Gapski, V. Neef, G. Henderson, P. DiGirolamo, P. Cramer, and J. I. Rader, *Fed. Proc.*, **33**, 508 (1974).

ACKNOWLEDGMENTS AND ADDRESSES

Received March 26, 1976, from the *Department of Biochemistry, Scripps Clinic and Research Foundation, La Jolla, CA 92037.*

Accepted for publication May 19, 1976.

Supported by U.S. Public Health Service Grant CA-11778 from the National Cancer Institute, National Institutes of Health.

The authors are indebted to Dr. S. A. Levison for advice on the determination of quantum yields, Ms. A. Russell for technical assistance, and Ms. K. Vitols for help in preparing this manuscript.

[x] To whom inquiries should be directed. Recipient of a U.S. Public Health Service Research Career Development Award (CA-00106) from the National Cancer Institute.

Survival of Pleomorphic Sarcoma-37 Transplanted Virgin Female DBA/2J Mice: Hyperthermia and Hyperglycemia, Alone and in Combination with Drugs

RONALD E. ORTH ˣ, HOWARD J. SWIDLER, and MILO S. ZARAKOV

Abstract □ Sarcoma-37 (S-37) transplanted DBA/2J mice were submitted to a controlled whole body hyperglycemic–hyperthermic ("double attack") treatment. A single exposure to the 3-hr 400–500-mg % blood glucose level coupled with 1 hr of whole body 40.0° warming was safe and extended longevity by 40% over the nontreated controls. This increase suggests that additive or potentiated effects follow the two-parameter procedure. The treatment safety and resultant increased longevity were not enhanced by single-dose chemotherapy with doxorubicin and/or dacarbazine.

Keyphrases □ Blood glucose—high levels, combined with hyperthermia and doxorubicin or dacarbazine, effect on survival of tumor-transplanted mice □ Dextrose infusion—combined with hyperthermia and doxorubicin or dacarbazine, effect on survival of tumor-transplanted mice □ Hyperthermia—combined with dextrose infusion and doxorubicin or dacarbazine, effect on survival of tumor-transplanted mice □ Doxorubicin—combined with hyperglycemia and hyperthermia, effect on survival of tumor-transplanted mice □ Dacarbazine—combined with hyperglycemia and hyperthermia, effect on survival of tumor-transplanted mice □ Antineoplastics—doxorubicin and dacarbazine, combined with hyperglycemia and hyperthermia, effect on survival of tumor-transplanted mice

Nearly a half century ago, investigators attempting to characterize functional differences between normal and cancerous tissue from the same organ found a higher rate of aerobic glucose metabolism for the latter (1). von Ardenne (2) attempted to capitalize on the resultant higher intracellular lactic acid levels in glucose-stressed cancerous tissue. The premise is that the more acidic neoplastic tissue offers a better substrate for support of intrinsic catabolic lysosomal enzyme activity. A single safe 3-hr 400–500-mg % blood glucose level was followed by a significant increase in the longevity for Sarcoma-37 (S-37) transplanted virgin female DBA/2J mice (3).

A review on the association of heat and cancer (4) and data on whole body hyperthermia in humans (5) and animals (6) are available. One hour of whole body 40.0° warming was found to be a safe, statistically significant factor in prolonging the longevity of S-37 transplanted DBA/2J mice[1].

Doxorubicin (I) and dacarbazine (II), drugs known to interfere with cell membrane protein synthesis, were effective alone and in combination against human (7) and mouse (8) sarcomas *in vivo*.

A dextrose infusion–whole body warming technique was evaluated *in vitro* and *in vivo* in seven different rodent tumor types (9), and tumor diameter decreases were noted.

The effects of a single incident of 3-hr 400–500-mg % whole blood glucose levels, 1 hr of warming at 40.0°, 5 mg/kg sc of I, and 200 mg/kg ip of II were individually evaluated for safety and resultant longevity under controlled conditions in S-37 transplanted mice (Table I, cages 2–5). Various combinations of these four treatments also were evaluated (Table I, cages 6–10 and 12). Virgin female DBA/2J mice were the treatment and control subjects in cages 2–10 and 1, respectively. Transplanted male DBA/2J mice were subjected to control and dextrose–warming ("double attack") procedures (cages 11 and 12, respectively) to determine differences in responses by sex.

[1] R. E. Orth, H. J. Swidler, and M. S. Zarakov, unpublished results.

EXPERIMENTAL

Transplantation—An S-37 bearing donor mouse[2] was sacrificed 7 days after serial subcutaneous transplantation. The tumor was removed, moistened with isotonic saline, and minced. One cubic millimeter of tissue was placed in a 15-gauge trocar and administered to 15–20-g DBA/2J mice subcutaneously into the thigh 6 days before treatment.

Drugs—Whenever drugs were administered to experimental animals, isotonic saline was given to the paired control animal in the same way, at the same site, and in the same chronological sequence. When used, I[3] and II[3] were given 15 min prior to the hypnotic agent. Pentobarbital sodium, 80 mg/kg po, was administered (3.2 mg/ml of 1:2150 diluted B complex elixir). Aqueous dextrose (40% w/v) and isotonic saline were the infusion solutions used.

Dextrose Intravenous Infusion Procedure —Unconscious mice were secured with their heads down (shock position), on their backs, with immobilized tails. An adapted infusion pump[4] syringe holder contained six 1-ml syringes[5]. Each syringe was connected by tubing[6] to a 26-gauge 12.7-mm needle[7] for insertion into the tail vein of each of six mice. The syringes, filled with the dextrose solution[8], were activated at pump speed setting No. 19. Postorbital venous blood samples of approximately 0.05 ml were periodically obtained using heparinized capillary tubes[9].

Blood glucose levels were determined by reading glucose oxidase–peroxidase reagent strips[10] in a reflectance colorimeter[11]. Once 400–500-mg % levels were obtained, the infusion was slowed to a replacement rate with a pump setting of No. 20 or 21, and these levels were maintained for 2 hr.

Water Bath Procedures—Conscious mice were immersed to the neck in a water bath[12] for 1 hr at 40.0 ± 0.3°[13] (Table I, cages 3, 7–10, and 12) or 37.0 ± 0.3° (Table I, cages 1, 2, 4–6, and 11) following oral administration of 0.01 ml of B complex elixir. A stream of 95% O_2 was directed to the head of each animal during this period. Following the immersion, the animals were gently toweled and placed in a 37.0° oxygenated compartment for 1 hr before being returned to their cages.

[2] Sarcoma-37 tumor-in-host and genetically standardized inbred DBA/2J mice, Jackson Laboratory, Bar Harbor, ME 04609.

[3] Doxorubicin (NSC 123,127) hydrochloride and dacarbazine (NSC 45,388), supplied by Division of Cancer Treatment, National Cancer Institute, National Institutes of Health, Bethesda, MD 20014.

[4] Model 975, Harvard Apparatus Co., Millis, MA 02254.

[5] Plastipak disposable syringe 5602, sterile-tuberculin, Becton-Dickinson, Rutherford, NJ 07064.

[6] PE 20 (7407) Intramedic, Animal Tested Medical Formulation, Clay Adams Co., Parsippany, NJ 07064.

[7] B-D Yale hypodermic needle, Luer-lok hub, sterile disposable, stainless steel cannula, Becton-Dickinson, Rutherford, NJ 07070.

[8] Diluted 50% dextrose injection USP obtained from McGaw Laboratories, Division of American Hospital Supply Corp., Glendale, CA 91201.

[9] Van-Lab, yellow band with heparin, Catalog No. 15401-683, VWR Scientific Co., Phoenix, AZ 85001.

[10] Dextrostix, Ames Co., Elkhart, IN 46514.

[11] Reflectance meter, Ames Co., Elkhart, IN 46514.

[12] NAPCO bath model 87251 with Cenco 19245 0–100° thermometer with 0.1° divisions.

[13] Tele-thermometer model 43TA with appropriate sensor probes, Yellow Springs Instrument Co.

Table I—Dextrose, Heat, and Drug Treatment of Sarcoma-37 Transplanted Mice

Cage	Treatment[a]	Fraction Surviving Treatment[b]	Longevity beyond Transplant Date[c]
1	Female controls[d]	32/32	26.5 ± 0.7
2	Dextrose intravenous infusion[e]	12/12	31.4 ± 0.9
3	Whole body 40.0° warming[f]	12/12	30.1 ± 0.9
4	I, 5 mg/kg sc[d]	8/8	28.2 ± 1.8
5	II, 200 mg/kg ip[d]	8/8	32.2 ± 1.1
6	I, 2.5 mg/kg sc, plus II, 100 mg/kg ip[d]	8/8	29.4 ± 1.5
7	Dextrose intravenous infusion plus whole body 40.0° warming (double attack)[g]	8/8	37.0 ± 1.1
8	I, 2.5 mg/kg sc, plus double attack[g]	7/8	36.3 ± 1.5
9	II, 100 mg/kg ip, plus double attack[g]	8/8	35.2 ± 1.1
10	I, 2.5 mg/kg sc, plus II, 100 mg/kg ip, plus double attack[g]	6/8	31.5 ± 1.6
11	Male controls[d]	16/16	30.8 ± 0.6
12	Male double attack[g]	24/24	33.2 ± 0.9

[a] All mice were anesthetized with pentobarbital sodium, 80 mg/kg po, prior to immobilization. [b] (Number surviving treatment + 24 hr)/(number of mice treated). [c] Days of life between transplant date and death date (mean ± *SEM*). [d] Isotonic saline tail vein 3-hr 0.5-ml iv infusion. Whole body 37.0° water bath immersion during the 3rd hr. [e] Forty percent (w/v) dextrose tail vein intravenous infusion at rate that maintains 3-hr 400–500-mg % blood glucose level. Whole body 37.0° water bath immersion during the 3rd hr. [f] Isotonic saline tail vein 3-hr 0.5-ml iv infusion. Whole body 40.0° water bath immersion during the 3rd hr. [g] Forty percent (w/v) dextrose tail vein infusion at rate that maintains 3-hr 400–500-mg % blood glucose level. Whole body 40.0° water bath immersion during the 3rd hr.

RESULTS AND DISCUSSION

All mice (cages 1–12) were subcutaneously transplanted with S-37, given B complex, anesthetized, secured, infused (dextrose or saline), subjected to blood sampling, immersed 1 hr in a water bath (40.0 or 37.0°), and dried. The use of I and/or II was the only variation.

Blood glucose levels of 450–500 mg % were obtained in 60 ± 15 min by infusing approximately 0.2 ml of the 40% dextrose solution. Blood glucose samples obtained after warming the mice remained at or above 400 mg %. Therefore, 1 hr after discontinuing the infusion or 3 hr after establishing the necessary blood glucose level, the desired concentration still existed. To obviate excessive dextrose or volume problems, no more than 0.5 ml was given to any subject.

Treatment of S-37 transplanted virgin female DBA/2J mice with dextrose (cage 2), 1 hr of warming at 40° (cage 3), or 200 mg/kg ip of II (cage 5) was safe (100% treatment survival) and significantly increased longevity. The dextrose–40.0°/1-hr therapy (cage 7) was safe and effectively increased longevity by 40% over the transplanted controls of cage 1. The adjunctive use of I and/or II (cages 8–10) did not enhance this combination. In this study, only mice treated with 5 mg/kg sc of I (cage 4) failed to show a significant increase in lifespan over the controls of cage 1 according to the Student two-tailed t test with 95% confidence limits.

Male mice transplanted with S-37 responded less dramatically to either the tumor (cage 11) or the dextrose–40.0°/1-hr treatment (cage 12) than did virgin females of the same DBA/2J strain (cages 1 and 7). The control males lived significantly longer than the control females; however, the dextrose–1-hr warmed males lived longer than the male controls but not as long as the treated females.

The results of this study are in good general agreement with those of von Ardenne (6). Under different conditions, 1 hr of warming at 40°[2] increased the length of life for S-37 transplanted mice, and 3-hr 400–500 mg % blood glucose levels (3) were even more effective at safely prolonging longevity. A single application of these two procedures together is safe and appears to effect an additive if not a potentiated longevity increase. The results are not improved upon by concurrently administering I and/or II, although II is effective alone. The tumor is less virulent and more susceptible to the "double attack" in males than in females of the DBA/2J strain.

REFERENCES

(1) O. Warburg, "The Metabolism of Tumors," 1st ed., Constable, London, England, 1930.

(2) M. von Ardenne, *Vortr. Heidelberger Krebsforschungszentrum*, **24,** 9 (1965).

(3) R. E. Orth, H. J. Swidler, and M. S. Zarakov, *J. Pharm. Sci.*, **66,** 279 (1977).

(4) R. Cavaliere, E. C. Ciocatto, B. C. Giovanella, C. Heidelberger, R. O. Johnson, M. Margottini, B. Mondovi, G. Moricca, and A. Rossi-Fanelli, *Cancer*, **20,** 1351 (1967).

(5) M. A. Henderson and R. T. Pettigrew, *Lancet*, **1,** 1275 (1971).

(6) M. von Ardenne, "Theoretische and Experimentelle Grundlagen der Krebs-Mehrschritt-Therapie," vols. 1 and 2, 2nd ed., VEB Verlag Volk und Gesundheit, Berlin, Germany, 1971.

(7) J. A. Gottlieb, L. H. Baker, J. M. Quagliana, J. K. Luce, J. P. Whitecar, J. G. Sinkovics, S. E. Rivkin, R. Brownlee, and E. Frei, III, *Cancer*, **30,** 1632.

(8) F. M. Schabel, Jr., "Pharmacological Basis of Cancer Chemotherapy," Williams & Wilkins, Baltimore, Md., 1975, pp. 595–623.

(9) S. Garattini, A. Goldin, F. Hawking, and I. J. Kopin, "Advances in Pharmacology and Chemotherapy," vol. 10, Academic, New York, N.Y., 1972, pp. 362–366.

ACKNOWLEDGMENTS AND ADDRESSES

Received November 26, 1975, from the *College of Pharmacy, University of Arizona, Tucson, AZ 85721.*

Accepted for publication May 19, 1976.

Supported by the University of Arizona Foundation, the University of Arizona Vice President for Research, and the Pharmacy College Overhead Allocation.

The authors thank Mr. Fred Smith for assistance.

[x] To whom inquiries should be directed.

IR Spectrophotometric Assay of Carbachol Solutions

JOHN FRANK and LESTER CHAFETZ ˣ

Abstract □ Carbachol ophthalmic solutions can be assayed by evaporating a measured volume, dissolving the residue in methanol, and scanning the carbonyl stretching frequency in an IR spectrophotometer using a cell with calcium fluoride windows. Methylcellulose and other formulation vehicle components do not interfere. The method is stability indicating with respect to hydrolysis. It affords a recovery of 99.5 ± 0.51% (*RSD*).

Keyphrases □ Carbachol—IR spectrophotometric analysis, commercial ophthalmic preparations □ IR spectrophotometry—analysis, carbachol, commercial ophthalmic preparations □ Cholinergics, ophthalmic—carbachol, IR spectrophotometric analysis, commercial preparations

Carbachol, the carbamoyl ester of choline, has been shown to be stable in aqueous solution at pH values lower than 7. A kinetic study of its hydrolysis was reported in which choline separated from carbachol by TLC was determined photometrically as its dipicrylamine complex (1). USP XVIII (2) used a reinecke salt colorimetric method for the assay of carbachol ophthalmic solution; however, the method does not discriminate between carbachol and choline. It was replaced in the First Supplement (3) by a stability-indicating method, apparently based on the work of Puckett and Poe (4). The procedure involves formation of the *N*-chloro derivative of carbachol by reaction with alkaline hypochlorite, destruction of excess hypochlorite with phenol, and oxidation of iodide by the *N*-chloro derivative to iodine, which is determined as its amylose complex. Erratic results with the method led to the development of the simple and highly selective IR spectrophotometric method described here.

EXPERIMENTAL

Pipet a volume of carbachol ophthalmic solution[1], equivalent to about 90 mg of carbachol, into a 250-ml round-bottom flask. Add about 10 ml of methanol and evaporate the solution to dryness in a rotary evaporation apparatus[2], using reduced pressure and a water bath temperature of 50°. Add exactly 10.0 ml of methanol to the flask, stopper, and swirl to dissolve the carbachol. (Methylcellulose, in the test preparations used in this work, forms a thin film which does not dissolve.)

Fill a 0.1-mm path length IR cell, equipped with calcium fluoride windows, with the solution. Record its spectrum in the carbonyl region (1970–1550 cm^{-1}) three times, using a suitable double-beam IR spectrophotometer[3] and a matched cell filled with methanol in the reference beam. Concomitantly scan the carbonyl region of a methanol solution of carbachol USP reference standard containing a known concentration of about 9 mg/ml. Draw a horizontal straight line from the shoulder at about 1980 cm^{-1} and draw a straight line from the absorption band maximum at 1720 cm^{-1} perpendicular to the first line and intercepting it. The length of this line, in the units of the recorder chart paper, is the percent transmittance from which absorbance is calculated from the relation $A = \log_{10}(1/T)$.

Calculate the concentration, in percent (w/v), of carbachol in the ophthalmic solution from the formula $C/V(A_U/A_S)$, where C is the concentration, in milligrams per milliliter, of carbachol in the standard solution; V is the volume, in milliliters, of carbachol ophthalmic solution taken for assay; and A_U and A_S are the average absorbances determined for the assay preparation and the standard solution, respectively.

[1] Carbacel 1.5 and 3%, Softcon Products Division, Warner-Lambert Co., Morris Plains, NJ 07950.

[2] Buchler flash evaporator.

[3] Perkin-Elmer model 621 ratio-recording double-beam IR spectrophotometer.

Table I—Recovery of Carbachol Added to 1.5 and 3.0% Formulation Vehicles

Vehicle	Amount Added, mg	Amount Found, mg	Percent Recovered
1.5%	39.1	39.0	99.7
	78.2	78.0	99.7
	156.4	155.0	99.1
3.0%	94.9	94.4	99.5
	189.9	189.0	99.5
	379.8	380.0	100.0

RESULTS AND DISCUSSION

The feasibility of the method was first investigated using ordinary sodium chloride cells; however, these cells are fogged by methanol and require polishing after only a few uses. Calcium fluoride windows are impervious to methanol. Methanol was chosen as the solvent because of its excellent solvent powers for carbachol and its transparency in the spectral area of interest.

Precision and Recovery—The vehicles for the 1.5 and 3.0% test preparations differ in that the latter contains a borate buffer and sodium chloride as well as methylcellulose and benzalkonium chloride. However, both vehicles gave IR spectra indistinguishable from a methanol blank when tested in the procedure. Carbachol was added in three concentrations to each vehicle. Average recovery (Table I) for the six trials was 99.6% with a relative standard deviation of ±0.51%.

Standard solutions containing 3.91, 7.82, and 15.64 mg of carbachol/ml in methanol provided absorbances of 0.140, 0.280, and 0.572, respectively. These data afford a straight-line graph that intercepts the origin.

Selectivity—None of the constituents of the ophthalmic solution vehicles used interfered in the assay. Other commercially available carbachol eye solutions list 1.4% polyvinyl alcohol and edetate disodium as vehicle components. Since polyvinyl alcohol contains acetate ester groups to some extent and edetate disodium has carboxyl functions, solutions of 1.4% polyvinyl alcohol and 0.1% edetate were assayed by the proposed method. Neither interfered in the assay; both gave spectra identical with the blank in the spectral region used for analysis.

The validity of the assay as a stability-indicating method was verified by heating 5 ml of water containing 100 mg of carbachol and 4 ml of 1 *N* sodium hydroxide in a sealed ampul at 105° overnight to saponify the carbamate. Assay of this solution by the proposed method showed no carbonyl band.

REFERENCES

(1) P. Lundgren, *Acta Pharm. Suec.*, **6**, 299 (1969).

(2) "The United States Pharmacopeia," 18th rev., Mack Publishing Co., Easton, Pa., 1970, p. 98.

(3) "First Supplement to USP XVIII," Mack Publishing Co., Easton, Pa., 1971, p. 3.

(4) R. Puckett and R. E. Poe, *J. Pharm. Sci.*, **58**, 602 (1969).

ACKNOWLEDGMENTS AND ADDRESSES

Received February 23, 1976, from the *Pharmaceutical Research and Development Laboratories, Warner-Lambert Research Institute, Morris Plains, NJ 07950.*

Accepted for publication May 20, 1976.

ˣ To whom inquiries should be directed.

Synthesis of Sulfonates of 4-Chloro-3,5-dimethylphenol and 5-Chloro-7-iodo-8-quinolinol

JITENDRA J. SHAH

Abstract □ Seven sulfonates of 4-chloro-3,5-dimethylphenol and seven sulfonates of 5-chloro-7-iodo-8-quinolinol were synthesized, characterized, and evaluated for antimalarial activity. None of the sulfonates was effective against *Plasmodium berghei*.

Keyphrases □ Sulfonates—of substituted phenols and quinolinols, synthesized and evaluated for antimalarial activity □ Phenols, substituted—sulfonates synthesized and evaluated for antimalarial activity □ Quinolinols, substituted—sulfonates synthesized and evaluated for antimalarial activity □ Antimalarial activity—sulfonates of substituted phenols and quinolinols evaluated □ Structure–activity relationships—sulfonates of substituted phenols and quinolinols evaluated for antimalarial activity

The sulfonation of quinoline occurs more readily than that of pyridine but less readily than that of naphthalene. Sulfonation with 30% sulfuric acid at approximately 80° yields 8-quinolinesulfonic acid (54% recovered after isolation) and possibly some 5- and 7-quinolinesulfonic acid as well (1). With mercury as a catalyst, however, 5-quinolinesulfonic acid is the sole reaction product (2). Sulfonation of quinoline with sulfur trioxide in the presence of mercury as a catalyst at 180° leads to a mixture of the 5- and 8-quinolinesulfonic acids (3). The velocity constant of sulfonation is influenced only by the temperature of the reaction and varies considerably.

The methyl group in either the 2- or 4-position to the hydroxyl group has the effect of retarding the speed of sulfonation at all temperatures from 20 to 80°. The methyl group in the 3-position both accelerates and retards the speed of sulfonation according to reaction temperature. Phenol is sulfonated at 2.11 times the rate of 4-methylphenol and 2.21 times the rate of 2,4-dimethylphenol at 40°. The esters, carbonates, and sulfonates of clopidol (3,5-dichloro-2,6 dimethyl-4-pyridinol) were prepared by treating the sodium salt of clopidol suspended in dimethylformamide with the corresponding alkyl or aryl chlorides (4, 5).

This study reports the synthesis of sulfonates of 4-chloro-3,5-dimethylphenol and 5-chloro-7-iodo-8-quinolinol. Sulfonation was carried out with different sulfonyl chlorides in the presence of sodium hydride and dimethylformamide at 3° (4). These sulfonates were evaluated for their antimalarial activity against *Plasmodium berghei* and toxicity in albino mice.

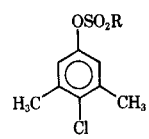

Table I—Sulfonates of 4-Chloro-3,5-dimethylphenol

Compound	R	Melting Point	Molecular Formula	Analysis, % Calc.	Analysis, % Found	IR[a], cm^{-1}	UV[b] λ_{max} ($CHCl_3$)	Toxicity[c] Test
I	p-$C_6H_4CH_3$	95°	$C_{15}H_{15}ClO_3S$	C 57.78 H 4.81 N 11.39	57.90 4.92 11.49	925 (s), 1017 (s), 1225 (b), 1424 (w)	241, 274	—
II	$C_6H_4NHCOCH_3$	148°	$C_{16}H_{16}ClNO_4S$	C 54.31 H 4.52 N 10.04	54.13 4.65 9.86	927 (s), 1018 (s), 1224 (b), 1418 (w)	261	—
III	α-$H_2CC_6H_4$	102°	$C_{15}H_{15}ClO_3S$	C 57.97 H 4.83 N 11.43	57.87 4.95 11.26	924 (s), 1022 (s), 1232 (b), 1430 (w)	236, 239	Nontoxic
IV	$C_6H_3(CH_3)_2$	78°	$C_{16}H_{17}ClO_3S$	C 59.16 H 5.23 N 10.93	59.21 5.34 10.87	922 (s), 1019 (s), 1227 (b), 1420 (w)	241, 278, 286	Nontoxic
V	C_6H_4Cl	110°	$C_{14}H_{12}Cl_2O_3S$	C 50.75 H 3.62 N 21.45	50.74 3.74 21.36	923 (s), 1019 (s), 1226 (b), 1428 (w)	240	Nontoxic
VI	C_6H_5	64°	$C_{14}H_{13}ClO_3S$	C 56.66 H 4.38 N 11.97	56.79 4.47 12.08	922 (s), 1016 (s), 1230 (b), 1415 (w)	241, 259, 266, 273	—
VII	o-$C_6H_4CH_3$	58°	$C_{15}H_{15}ClO_3S$	C 57.78 H 4.81 N 11.39	57.87 4.99 11.31	926 (s), 1025 (s), 1233 (b), 1418 (w)	241, 271, 280	—

[a] Baird atomic IR recording spectrophotometer; s = strong, b = broad, and w = weak. [b] Beckman Acta CIII spectrophotometer. [c] The mortality observed after administration of 5 g/kg of III, IV, and V was 10, 30, and 10%, respectively, during 14 days. Gross necropsies performed in mice after administration of III–V showed normal pathology.

EXPERIMENTAL[1]

Preparation of Sulfonates—To a slurry of 10.8 g of sodium hydride (0.22 mole, 50% mixture in oil) in 100 ml of dimethylformamide was added 0.20 mole of 4-chloro-3,5-dimethylphenol or 5-chloro-7-iodo-8-quinolinol.

[1] Melting points were taken in open capillary tubes and are uncorrected. All compounds were analyzed for carbon, hydrogen, and nitrogen content by M.H.W. Laboratories, Garden City, MI 48135.

Table II—Sulfonates of 5-Chloro-7-iodo-8-quinolinol

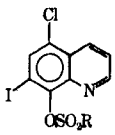

Compound	R	Melting Point	Molecular Formula	Analysis, % Calc.	Analysis, % Found	IR, cm^{-1}	UV λ_{max} ($CHCl_3$)	Toxicity[a] Test
VIII	C_6H_4Cl	116–117°	$C_{15}H_8Cl_2INO_3S$	C 37.57 H 1.67 N 2.92	37.65 1.56 2.87	920 (s), 1020 (s), 1232 (b), 1414 (w)	241	—[b]
IX	p-$C_6H_4CH_3$	139–140°	$C_{16}H_{11}ClINO_3S$	C 41.78 H 2.39 N 3.04	41.73 2.42 2.96	926 (s), 1022 (s), 1230 (b), 1416 (w)	242	Nontoxic
X	o-$C_6H_4CH_3$	110°	$C_{16}H_{11}ClINO_3S$	C 41.78 H 2.39 N 3.04	41.82 2.43 2.96	918 (s), 1026 (s), 1224 (b), 1410 (w)	242.5	—
XI	$C_6H_4NHCOCH_3$	160°	$C_{17}H_{12}ClIN_2O_4S$	C 40.59 H 2.38 N 5.57	40.49 2.45 5.63	922 (s), 1025 (s), 1234 (b), 1408 (w)	454.5	—[b]
XII	α-$CH_2CH_6H_4$	86–87°	$C_{16}H_{11}ClINO_3S$	C 41.78 H 2.39 N 3.04	41.68 2.47 3.10	920 (s), 1021 (s), 1228 (b), 1405 (w)	258	—[b]
XIII	$C_6H_3(CH_3)_2$	125–126°	$C_{17}H_{13}ClINO_3S$	C 43.08 H 2.74 N 2.95	43.17 2.84 3.03	930 (s), 1025 (s), 1232 (b), 1407 (w)	242	Nontoxic
XIV	C_6H_5	98–99°	$C_{15}H_9ClINO_3S$	C 40.04 H 2.00 N 3.11	39.96 2.09 3.16	923 (s), 1026 (s), 1224 (b), 1407 (w)	241	—

[a] The mortality observed after administration of 5 g/kg of VIII, IX, XI, XII, and XIII was 90, 40, 100, 100, and 30%, respectively, during 14 days. Gross necropsies performed in mice treated with VIII, IX, and XI–XIII showed congested lungs of varying degree; advanced autolysis was found in mice treated with VIII and XI–XIII. [b] Due to mortality, classification of toxicity cannot be made because the compound may be highly toxic.

The mixture was cooled to 3° and added to the desired sulfonyl chloride (0.22 mole) dissolved in 75 ml of dimethylformamide. The reaction mixture was stirred for 1.5 hr, filtered, and washed with chloroform. The filtrate was partially concentrated under reduced pressure and, on cooling, gave the desired product. The analytical product was purified by two recrystallizations from ethanol. The sulfonates of 4-chloro-3,5-dimethylphenol and 5-chloro-7-iodo-8-quinolinol are recorded in Tables I and II, respectively.

Antimalarial Activity—All sulfonates were evaluated[2] for antimalarial activity (6) against *P. berghei* in mice. They were inactive at dose levels of 40, 160, and 640 mg/kg.

Toxicity Studies[3]—The acute oral toxicity was determined by oral administration of sulfonates by stomach tube to 10 albino mice[4], 12–20 g, kept on an *ad libitum* diet. Each sulfonate was administered as a 50% (w/v) suspension in corn oil[5] at a dose of 5 g/kg. The mice were kept in two cages of five animals each and starved for 18 hr prior to the sulfonate administration. The animals were observed closely, and their mortality was recorded. Gross necropsies were performed on the mice that died during the 14-day period. The surviving mice were weighed and then sacrificed by cervical dislocation, and gross necropsies were performed.

[2] Evaluated by Dr. Leo Rane, University of Miami, Miami, Fla., and furnished by Dr. E. A. Stack, Walter Reed Army Institute of Research, Washington, D.C.
[3] Hill Top Research Laboratory, Miamiville, OH 45147 [by using Federal Hazardous Substances Act (Revised), Federal Register, Sept. 17, 1964].
[4] Laboratory Supply Company, Indianapolis, IN 46241.
[5] Mazola.

REFERENCES

(1) G. E. McCasland, *J. Org. Chem.*, **11**, 277 (1946).
(2) N. Grier, U.S. pat. 2,689,850 (1954); through *Chem. Abstr.*, **49**, 11725 (1955).
(3) H. Fuerst and W. Kretzschmann, East German pat. 23,315 (1962); through *Chem. Abstr.*, **58**, 9088 (1963).
(4) L. D. Markley, J. C. VanHeertum, and H. E. Doorenbus, *J. Med. Chem.*, **15**, 1188 (1972).
(5) H. K. Hall, *J. Am. Chem. Soc.*, **78**, 2717 (1956).
(6) T. S. Osdene, P. B. Russell, and L. Rane, *J. Med. Chem.*, **10**, 431 (1967).

ACKNOWLEDGMENTS AND ADDRESSES

Received September 2, 1975, from *Woodson-Tenent Laboratories, Inc., Memphis, TN 38102.*
Accepted for publication May 10, 1976.
Presented at the American Chemical Society Midwest Regional Meeting, Carbondale, Ill., October 1975.

Use of ^{99m}Tc-Labeled Triethylenetetramine–Polystyrene Resin for Measuring the Gastric Emptying Rate in Humans

Keyphrases □ Technetium Tc 99m—as radiolabel on triethylenetetramine–polystyrene resin, scintigraphic determination of gastric emptying rate, humans □ Scintigraphy, external—determination of gastric emptying rate using ^{99m}Tc-labeled triethylenetetramine–polystyrene resin □ Triethylenetetramine–polystyrene resin—^{99m}Tc-labeled, use in scintigraphic determination of gastric emptying rate, humans □ Gastric emptying rate—scintigraphic determination using ^{99m}Tc-labeled triethylenetetramine–polystyrene resin, humans □ Radiopharmaceuticals—^{99m}Tc-labeled triethylenetetramine–polystyrene resin, scintigraphic determination of gastric emptying rate, humans

To the Editor:

The introduction of γ-emitting short-lived radionuclides provides the opportunity for the determination of gastric emptying time using external scintigraphy. Quantitative dynamic data can be obtained with these radionuclides without physical or physiological influences on the GI tract (1). Futhermore, excellent scintigraphic images of the stomach, intestines, and colon can be obtained with a low target organ and total body radiation dose.

Several radiopharmaceutical preparations have been introduced for measuring gastric motility and emptying: ^{51}Cr-sodium chromate (2, 3), ^{113m}In- or ^{99m}Tc-labeled diethylenetriaminepentaacetic acid (3, 4), ^{113m}In-microcolloid (5), an insoluble colloid of ^{99m}Tc-antimony sulfide (6), ^{99m}Tc-labeled human albumin microspheres (7), and their combinations (3, 8).

After a meal, the liquid phase of gastric contents is discharged through the pylorus more rapidly than the solid phase. Therefore, radiopharmaceutical preparations dispensed as liquids give lower values for the half-time of gastric emptying (4), and minor deviations in time would provide opportunity for greater error. Comparison of emptying rates using ^{113m}In-diethylenetriaminepentaacetic acid and ^{51}Cr-sodium chromate showed that significantly slower rates were obtained with chromate. Subsequent *in vitro* studies demonstrated adsorption of chromate on the solid component of the meal (3). Thus, difficulties may be encountered with radiopharmaceuticals that appear to interact with the solid particles in a meal and the stomach wall. Colloidal preparations are difficult to prepare, and their physicochemical properties offer disadvantages such as the formation of micelles and coagulation.

Additional criteria in selecting a radiopharmaceutical preparation for gastric emptying are that it should: (*a*) not influence the osmolality of the stomach content (9), (*b*) be nonabsorbable and nonadsorbable (10), (*c*) bind the radionuclide tenaciously and provide no opportunity for physical or chemical interaction with food particles or the stomach wall, (*d*) possess ideal food mixing characteristics and have a particle size comparable to that of food, and (*e*) be nontoxic and inert and give reproducible and noninvasive estimates of the gastric emptying time without exposing the patient to a high radiation dose. The last prerequisite becomes exceedingly important in gastric emptying determinations involving pediatric patients (5).

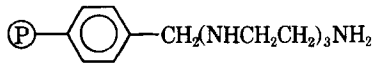

I

Polystyrene beads (40–100 mesh) bearing triethylenetetramine (I) functions (11) (2 mEq/g) efficiently and quantitatively chelated pertechnetate[1] ($^{99m}TcO_4^-$) from aqueous solutions (12). The ^{99m}Tc-labeled resin is stable in simulated gastric juice USP, releasing only 2.0% of the radioactivity in 25 hr at 37°. When the ^{99m}Tc-complex with I was administered to dogs and humans with a standardized meal, it satisfied all of the previously mentioned criteria for the determination of gastric emptying times. The release of radioactivity from the resin was monitored by collecting blood and urine samples from dogs and human volunteers. Less than 0.2% of the radioactivity was released during the passage of the resin throughout the entire GI tract.

In a typical experiment, 0.25 g of I in 20 ml of water was stirred with the $^{99m}TcO_4^-$ solution[1] (20 μCi) for 10 min. The resin was recovered by filtration, washed with water, and subsequently added to the test meal. This meal consisted of 33.3 g of cream of wheat and 2.4 g of sodium chloride in 235 ml of water. After the subject ingested the labeled test meal, the time was recorded and the subject was placed in a supine position under the collimated detector of a multicrystal scintillation γ-camera[2]. The positions of the γ-camera and of the patient were adjusted so that the entire stomach appeared in the center of the monitoring oscilloscope.

Several scintiphotos of the stomach were obtained at certain time intervals. In each time interval, a series of seven or eight points was collected. Each point represented the integrated relative radioactivity per minute of the desired flagged area of the stomach. The data were stored on a magnetic tape for future reference. The logarithm of the relative radioactivity of the stomach was plotted against time. The half-time of the gastric emptying of the test meal and the ^{99m}Tc-labeled I resin beads was determined from the slope of the line. A whole body survey at the end of each study failed to show any detectable activity outside of the GI tract.

By utilizing the described technique, gastric emptying times ranging from 45 to 60 min were obtained for 10 healthy volunteers (Fig. 1). These times agree with results obtained with other radiopharmaceuticals (6). In all normal subjects studied, monoexponential kinetics were obtained for gastric emptying. Similar kinetic profiles were obtained with patients with pyloric stenosis, although

[1] Technetium Tc 99m, obtained from a ^{99}Mo-generator (E. R. Squibb and Sons, Princeton, NJ 08540) in its pertechnetate form ($^{99m}TcO_4^-$), is a γ-emitting radionuclide with a half-life of 6 hr and an energy of 140 Kev.

[2] Baird Atomic System 77 (Baird Atomic Nuclear Division, Bedford, MA 01730) equipped with a computer and magnetic tape and possessing storage and replay capability.

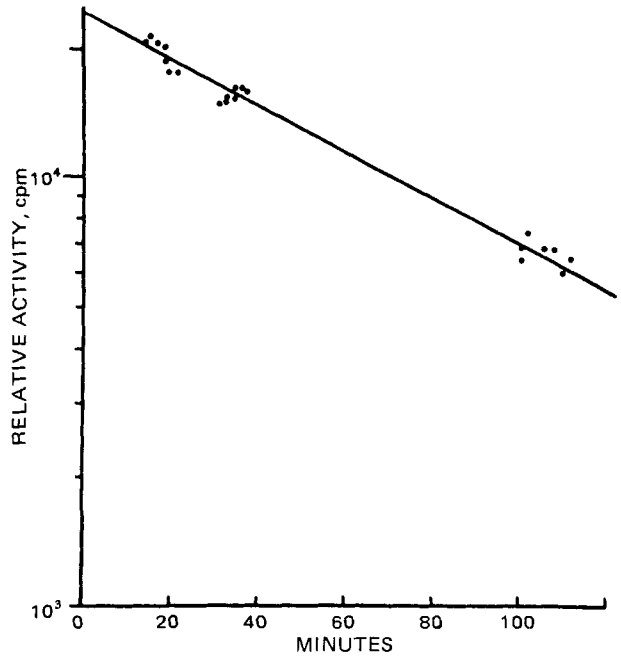

Figure 1—*Rate of clearance of ^{99m}Tc-labeled polystyrene beads bearing triethylenetetramine functions from the stomach of a normal human male subject (half-time of gastric emptying = 51 min).*

these subjects exhibited longer gastric emptying times (115 min) (Fig. 2).

Measurement of gastric emptying is an important aid to the clinician studying gastroduodenal disease, dumping syndrome, and postvagotomy disturbances. Gastric emptying is delayed in malignant disease of the stomach, gastric ulcers, and pyloric stenosis. On the other hand, hastened emptying has been associated with duodenal ulcers. Symptoms of dumping syndrome and diarrhea following gastrectomy and vagotomy are due to altered gastric emptying (10). A simple, accurate, and noninvasive technique for measuring gastric emptying is needed. ^{99m}Tc-Labeled I has a great potential for becoming a popular radiodiagnostic agent for routine clinical determinations of gastric emptying times.

Gastric emptying has been suggested to be a major determinant in the absorption rate of drugs. Individual variations in the rate of drug absorption from any one dosage form may be due largely to differences in the rate of gastric emptying (13, 14). Experiments are now in progress to assess ^{99m}Tc-labeled I in studying the effects of drugs on the gastric emptying rate as well as the gastric emptying influence on drug bioavailability.

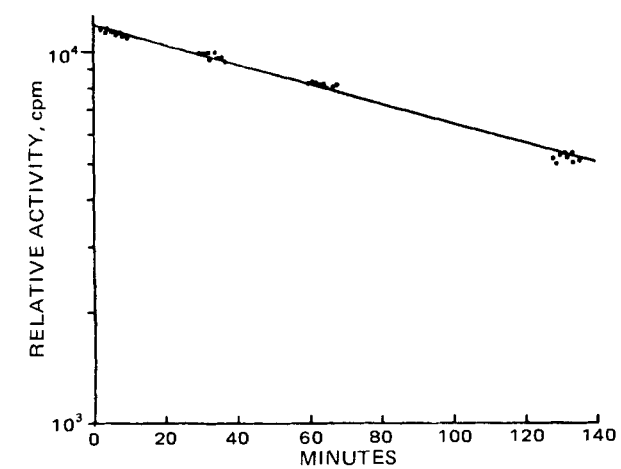

Figure 2—*Rate of clearance of ^{99m}Tc-labeled polystyrene beads bearing triethylenetetramine functions from the stomach of a female patient with pyloric stenosis (half-time of gastric emptying = 115 min).*

(1) R. F. Harvey, N. J. Brown, D. B. Mackie, D. H. Keeling, and W. T. Davies, *Lancet*, **1**, 16 (1970).

(2) G. H. Griffith, G. M. Owen, S. Kirkman, and R. Shields, *ibid.*, **1**, 1244 (1966).

(3) R. C. Heading, P. Tothill, A. J. Laidlaw, and D. J. C. Shearman, *Gut*, **12**, 611 (1971).

(4) T. K. Chaudhuri, *J. Nucl. Med.*, **15**, 391 (1974).

(5) E. Signer and R. Fridrich, *Acta Paediatr. Scand.*, **64**, 525 (1975).

(6) A. P. M. van Dam, *Radiology*, **110**, 155 (1974).

(7) M. Calderon, R. E. Sonnemaker, T. Hersh, and J. A. Burdine, *ibid.*, **101**, 371 (1974).

(8) R. C. Heading, P. Tothill, and G. P. McLoughlin, *Br. J. Radiol.*, **48**, 508 (1975).

(9) A. R. Cooke, *Gastroenterology*, **68**, 804 (1975).

(10) T. K. Chaudhuri, A. J. Greenwald, R. C. Heading, and T. K. Chaudhuri, *Dig. Dis.*, **20**, 1063 (1975).

(11) M. B. Shambhu, M. C. Theodorakis, and G. A. Digenis, *J. Polym. Sci.*, in press.

(12) M. C. Theodorakis, Ph.D. thesis, University of Kentucky, Lexington, Ky., 1975.

(13) R. C. Heading, J. Nimmo, L. F. Prescott, and P. Tothill, *Br. J. Pharmacol.*, **47**, 415 (1973).

(14) J. B. Houston and G. Levy, *J. Pharm. Sci.*, **64**, 1504 (1975).

George A. Digenis [x]
Robert M. Beihn
Michael C. Theodorakis
Manvendra B. Shambhu
Divisions of Medicinal Chemistry and Nuclear Medicine
Colleges of Pharmacy and Medicine
University of Kentucky
Lexington, KY 40506

Received March 16, 1976.
Accepted for publication December 9, 1976.
We thank Ms. S. Yonts for assistance and Dr. F. DeLand for guidance and encouragement.
[x] To whom inquiries should be directed.

Identification of an Impurity in Illicit Amphetamine Tablets

Keyphrases □ Amphetamine—illicit tablets, impurity identified as α-benzylphenethylamine ■ α-Benzylphenethylamine—identified as impurity in illicit amphetamine tablets ■ Contaminants—α-benzylphenethylamine identified in illicit amphetamine tablets

To the Editor:

An impurity detected in exhibits of illicit amphetamine tablets has been identified as α-benzylphenethylamine (I). The tablets, of a type known as "mini-bennies," were found to contain caffeine as well as *dl*-amphetamine (II), the latter as a sulfate salt. TLC examination on silica gel plates[1] revealed an additional spot, R_f 0.7, which, upon

[1] Mobile phase consisted of ammonia-saturated chloroform–methanol (18:1); visualization was by shortwave UV.

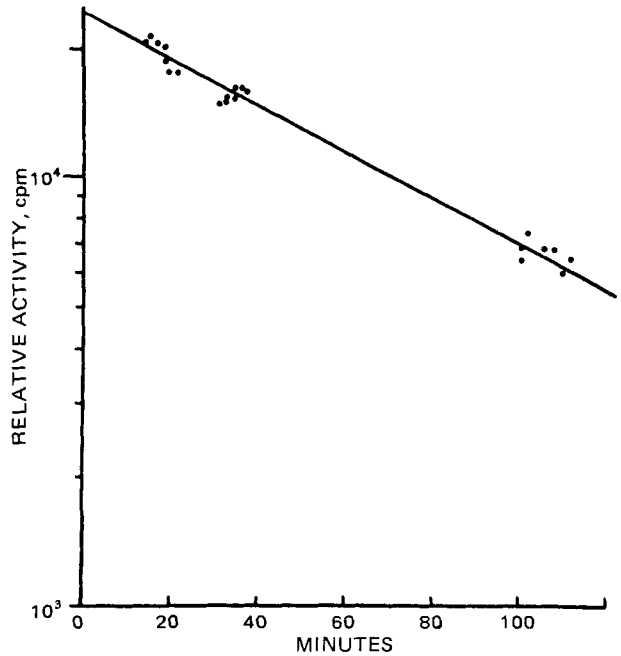

Figure 1—*Rate of clearance of ^{99m}Tc-labeled polystyrene beads bearing triethylenetetramine functions from the stomach of a normal human male subject (half-time of gastric emptying = 51 min).*

these subjects exhibited longer gastric emptying times (115 min) (Fig. 2).

Measurement of gastric emptying is an important aid to the clinician studying gastroduodenal disease, dumping syndrome, and postvagotomy disturbances. Gastric emptying is delayed in malignant disease of the stomach, gastric ulcers, and pyloric stenosis. On the other hand, hastened emptying has been associated with duodenal ulcers. Symptoms of dumping syndrome and diarrhea following gastrectomy and vagotomy are due to altered gastric emptying (10). A simple, accurate, and noninvasive technique for measuring gastric emptying is needed. ^{99m}Tc-Labeled I has a great potential for becoming a popular radiodiagnostic agent for routine clinical determinations of gastric emptying times.

Gastric emptying has been suggested to be a major determinant in the absorption rate of drugs. Individual variations in the rate of drug absorption from any one dosage form may be due largely to differences in the rate of gastric emptying (13, 14). Experiments are now in progress to assess ^{99m}Tc-labeled I in studying the effects of drugs on the gastric emptying rate as well as the gastric emptying influence on drug bioavailability.

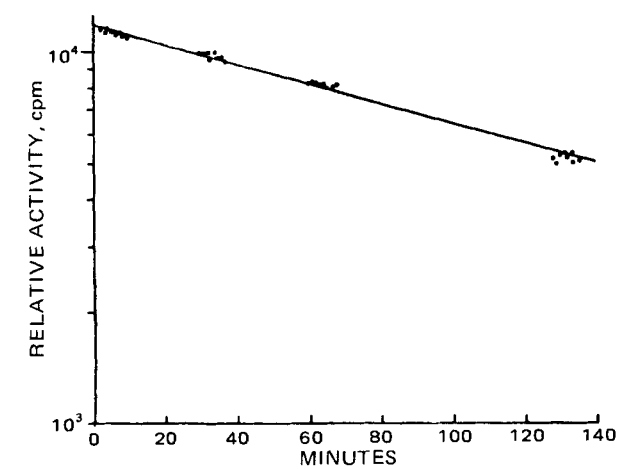

Figure 2—*Rate of clearance of ^{99m}Tc-labeled polystyrene beads bearing triethylenetetramine functions from the stomach of a female patient with pyloric stenosis (half-time of gastric emptying = 115 min).*

(1) R. F. Harvey, N. J. Brown, D. B. Mackie, D. H. Keeling, and W. T. Davies, *Lancet*, **1**, 16 (1970).

(2) G. H. Griffith, G. M. Owen, S. Kirkman, and R. Shields, *ibid.*, **1**, 1244 (1966).

(3) R. C. Heading, P. Tothill, A. J. Laidlaw, and D. J. C. Shearman, *Gut*, **12**, 611 (1971).

(4) T. K. Chaudhuri, *J. Nucl. Med.*, **15**, 391 (1974).

(5) E. Signer and R. Fridrich, *Acta Paediatr. Scand.*, **64**, 525 (1975).

(6) A. P. M. van Dam, *Radiology*, **110**, 155 (1974).

(7) M. Calderon, R. E. Sonnemaker, T. Hersh, and J. A. Burdine, *ibid.*, **101**, 371 (1974).

(8) R. C. Heading, P. Tothill, and G. P. McLoughlin, *Br. J. Radiol.*, **48**, 508 (1975).

(9) A. R. Cooke, *Gastroenterology*, **68**, 804 (1975).

(10) T. K. Chaudhuri, A. J. Greenwald, R. C. Heading, and T. K. Chaudhuri, *Dig. Dis.*, **20**, 1063 (1975).

(11) M. B. Shambhu, M. C. Theodorakis, and G. A. Digenis, *J. Polym. Sci.*, in press.

(12) M. C. Theodorakis, Ph.D. thesis, University of Kentucky, Lexington, Ky., 1975.

(13) R. C. Heading, J. Nimmo, L. F. Prescott, and P. Tothill, *Br. J. Pharmacol.*, **47**, 415 (1973).

(14) J. B. Houston and G. Levy, *J. Pharm. Sci.*, **64**, 1504 (1975).

George A. Digenis [x]
Robert M. Beihn
Michael C. Theodorakis
Manvendra B. Shambhu
Divisions of Medicinal Chemistry and Nuclear Medicine
Colleges of Pharmacy and Medicine
University of Kentucky
Lexington, KY 40506

Received March 16, 1976.
Accepted for publication December 9, 1976.
We thank Ms. S. Yonts for assistance and Dr. F. DeLand for guidance and encouragement.
[x] To whom inquiries should be directed.

Identification of an Impurity in Illicit Amphetamine Tablets

Keyphrases □ Amphetamine—illicit tablets, impurity identified as α-benzylphenethylamine ■ α-Benzylphenethylamine—identified as impurity in illicit amphetamine tablets ■ Contaminants—α-benzylphenethylamine identified in illicit amphetamine tablets

To the Editor:

An impurity detected in exhibits of illicit amphetamine tablets has been identified as α-benzylphenethylamine (I). The tablets, of a type known as "mini-bennies," were found to contain caffeine as well as *dl*-amphetamine (II), the latter as a sulfate salt. TLC examination on silica gel plates[1] revealed an additional spot, R_f 0.7, which, upon

[1] Mobile phase consisted of ammonia-saturated chloroform–methanol (18:1); visualization was by shortwave UV.

$C_6H_5CH_2COCH_3 \rightarrow C_6H_5CH_2CH(CH_3)NHCHO \rightarrow C_6H_5CH_2CH(CH_3)NH_2$

IV III II

Scheme I

extraction with chloroform and subsequent conversion to the hydrochloride salt, produced an IR spectrum somewhat similar to that of II hydrochloride. The pattern at 2300–2700 cm^{-1} was typical of primary amine salts; strong, sharp bands at 703 and 754 cm^{-1} were indicative of monosubstituted phenyl; intense bands appearing at 1452, 1491, and 1599 cm^{-1} were attributed to phenyl and methylene absorption.

The mass spectrum of I[2] exhibited a base peak at *m/e* 120 with further fragmentation indicative of benzyl (*m/e* 91, 77, 65, 51, and 39). Additional intense ions appeared at *m/e* 103 and 42. Considering that amines generally produce their most intense peaks by β-fission or α,β'-fission with hydrogen rearrangement (1), it was felt that the amino group was attached to a carbon atom with two substituents. The absence of any significant fragmentation above *m/e* 120 ruled out additional substitution. The possibility of a single α-substituent was eliminated by the absence of an intense *m/e* 30 fragment. From the foregoing considerations, the structure of I was deduced.

Support for the proposed structure was obtained from the NMR spectrum[3] of the salt (deuterium oxide), which displayed the following features: singlet at 7.37 ppm[4] (phenyl), multiplet at 3.0–4.0 ppm (methine), and a pair of doublets at 3.00 and 3.02 ppm (nonequivalent methylene hydrogens). Integration indicated a ratio of two phenyl and two methylene groups to one methine.

For verification of the assigned structure, a hydrochloride salt, mp 202–202.5° [lit. (2–5) mp 200–205°], was prepared from a known material[5]; IR and NMR spectra were identical to those prepared from extracts of the unknown substance.

The origin of I as a contaminant has been postulated as follows.

The presence of traces of *N*-formylamphetamine (III) in the tablet extracts, as determined by GLC–mass spectrometry (6), indicated that II was prepared by some form of the Leuckart synthesis, in which methyl benzyl ketone (IV) reacted with ammonium formate or formamide (7, 8), producing III as an intermediate. Subsequent hydrolysis converted it to II (Scheme I).

$(C_6H_5CH_2)_2CO \rightarrow (C_6H_5CH_2)_2CHNHCHO \rightarrow (C_6H_5CH_2)_2CHNH_2$

V VI I

Scheme II

Dibenzyl ketone (V), a by-product in the Aonuma *et al.* (9) synthesis of IV, was found as a contaminant accompanying IV in illicit preparations of amphetamine-type drugs (6). It has already been reported to produce I *via* Leuckart procedures (2, 10; Scheme II); hence, its presence as an impurity in IV is a likely cause for the accompaniment of II by I.

The appearance of I as an amphetamine contaminant poses serious implications due to its reported toxicity (11, 12).

(1) R. S. Gohlke and F. W. McLafferty, *Anal. Chem.*, **34**, 1281 (1962).

(2) S. Rajagopalan, *Proc. Ind. Acad. Sci.*, **14A**, 126 (1941); through *Chem. Abstr.*, **36**, 1604[2] (1942).

(3) A. Ogata and S. Niinobu, *J. Pharm. Soc. Jpn.*, **62**, 152 (1942); through *Chem. Abstr.*, **45**, 1728d (1951).

(4) M. Minchilli, *Atti Relaz. Acad. Pugliese Sci.*, **3**, 167 (1945); through *Chem. Abstr.*, **43**, 5027a (1949).

(5) T. Sasa, *J. Soc. Org. Synth. Chem. Jpn.*, **12**, 105 (1954); through *Chem. Abstr.*, **51**, 2780d (1957).

(6) T. C. Kram and A. V. Kruegel, *J. Forensic Sci.*, **22**, 40 (1977).

(7) A. W. Ingersoll, J. H. Brown, C. K. Kim, W. D. Beauchamp, and G. Jennings, *J. Am. Chem. Soc.*, **58**, 1808 (1936).

(8) F. S. Crossley and M. L. Moore, *J. Org. Chem.*, **9**, 529 (1944).

(9) S. Aonuma, T. Hama, and T. Kametami, *Jpn. J. Pharm. Chem.*, **27**, 607 (1955); through *Chem. Abstr.*, **50**, 13292g (1956).

(10) C. F. Koelsch, *J. Am. Chem. Soc.*, **67**, 1720 (1945).

(11) J. Hano and W. Wojewodkki, *Arch. Immunol. Ter. Dosw.*, **9**, 7 (1961); through *Chem. Abstr.*, **59**, 15769f (1963).

(12) E. M. DeEspanés and B. Weksler, *Rev. Soc. Arg. Biol.*, **29**, 195 (1953); through *Chem. Abstr.*, **48**, 7774h (1954).

T. C. Kram

Department of Justice
Drug Enforcement Administration
Special Testing and Research Laboratory
McLean, VA 22101

Received September 1, 1976.
Accepted for publication December 13, 1976.
The author thanks Dr. A. V. Kruegel for her comments.

[2] Finnigan model 3100D quadrupole EI-MS.
[3] Jeol C-60HL.
[4] From sodium 3-trimethylsilylpropionate-2,2,3,3-d_4.
[5] ICN Pharmaceuticals, Plainview, N.J.

REVIEWS

Ethical Safeguards in Research on Humans. Vol. 5. Philosophy and Technology of Drug Assessment. Edited by JOSEPH D. COOPER and HERBERT L. LEY. Interdisciplinary Communication Associates, 1717 Massachusetts Ave., N.W., Washington, DC 20036, 1976. 235 pp. 14.5 × 23 cm. Price $9.00.

This publication consists primarily of the transcripts of an April 1973 conference on "Ethical Problems in Drug Experimentation," which was the fifth in a series on the Philosophy and Technology of Drug Assessment. The 3-year time lag was due to the death of the coordinator, Dr. Joseph D. Cooper, following the seventh conference of the series in March 1975. Human research is a subject with many recent developments, and there are current publications that diminish the significance and timeliness of these proceedings.

The conference dialog was divided into several aspects of human research including surgical experimentation, patients and prisoners as subjects, state moratoriums on research, how to turn off an experiment, national and local review mechanisms, extrapolating results from animal to human, and payments and indemnification. Unfortunately, the majority of the book is merely transcripts of the dialog among the 22 nationally renown medical scientists who are listed as the conference participants. Other than the brief introductory summaries of each chapter, the dialog is sometimes difficult to follow. With the emphasis on dialog, the book suffers from a lack of references that might be useful in documenting the seemingly anecdotal comments of the participants.

The most valuable portion of the book is the introductory "Background Notes on Issues in Experimentation with Human Subjects." This 32-page segment of preconference material summarizes the issues prior to 1973 rather well. The background includes 63 references and a selected bibliography of eight publications. Readers who are following the human experimentation issue very closely may be interested in this publication.

Reviewed by William F. McGhan
College of Pharmacy
University of Minnesota
Minneapolis, MN 55414

Drug Metabolism Reviews. Vol. 4. Edited by FREDERICK J. DiCARLO. Dekker, 270 Madison Ave., New York, NY 10016, 1976. 340 pp. 16 × 24 cm. Price $32.50.

According to the press release for reviewers, "Volume 4 includes treatises on the disposition of used and abused drugs, the effects of liver disease upon drug disposition, the biotransformation of insecticides by insects, the clinical usefulness of organic nitrates and the logistics of drug metabolism studies." This is a factual and bald description of a fascinating volume.

The trend toward the complete integration of drug metabolism and pharmacokinetics continues and is very apparent in these reviews. We might as well stop referring to drug metabolism and pharmacokinetics and recognize that we are dealing with an integrated science of drug disposition. The term "drugs" does not just refer to human health products but also to animal health products, pesticides, industrial chemicals, and just about any other nonnutritive material that can enter any type of living organism.

There are three reviews on compounds that have been in use from centuries to millenia: morphine and heroin (Boerner, Abbot, and Roe), nitroglycerin (DiCarlo), and caffeine (Burg). It is always surprising to realize that, despite the length of their use, a great deal about each of them remains unknown. They present active and ongoing research problems of fundamental importance. The review on nitroglycerin is fun to read as well as informative. It got some "Gee whiz, I didn't know that" reactions from me. I'd recommend it as a model for authors.

A great deal of experimental work has been done, and clinical experience exists concerning renal dysfunction and its effects on drug disposition. Much less information exists on the effects of dysfunction of the liver, the other major organ of drug elimination. Wilkinson and Schenker's review on drug disposition and liver disease plays its part in redressing this balance.

The two most important reviews in this volume were written by Ruelius and Weiner on the logistics of drug disposition studies. The discipline of drug disposition is of fundamental importance in industry, where it constitutes an important part of the safety evaluation process, *de facto* or *de jure*. This is not simply to meet regulatory requirements; the regulatory agencies can only lag and react to what is found in the research laboratory and in the field when a drug is in use. Drug disposition studies can occupy a central place in the development process and interact with screening studies, pathology, toxicology, and "clinical" development and use. An academically engendered desire to know all that there is possible to know must give way to the imposition of priorities and the use of finite resources to find out what is of fundamental but practical importance. The primary question must be: "Within what limits is this agent safe and effective?" Each new drug represents a different problem. It would be impractical and impossible to impose rigid checklists or rules of procedure on drug disposition studies. The only valid approach, which both Ruelius and Weiner adapted, is to discuss general principles and then to illustrate the application of those principles by case studies of the problems presented by specific compounds. Many times they are saying the same things but what they are saying needs a lot of repetition.

This book costs almost 10¢ a page but it's well worth it. Buy a copy through your library or your own budget or even personally (it is tax deductible). Once you've got a copy, read it!

Reviewed by Morris Pfeffer
Bristol Laboratories
Syracuse, NY 13201

Calculations in Pharmacy. Third Edition. By SUE H. ROUSE and M. GEORGE WEBBER. Lippincott, East Washington Square, Philadelphia, PA 19105, 1976. 264 pp. 15.5 × 23.5 cm. Price $12.75.

The familiar strengths of this useful textbook in pharmaceutical calculations have for the most part remained intact in the second revision of the work. Substantially little has changed in format, content, or presentation of the third edition. Most helpful is its continued logical approach to the reasoned solution for pharmaceutical calculations in a way that deemphasizes rote methods and confusing proportionalities.

To accommodate newer concepts, nearly 800 revised practice problems with answers have been prepared, and "much of the emphasis on the 'art of compounding' has been reduced or neglected in favor of orientation toward patients." The art of the printer, however, is very much evident in the presentation of the book. The new table of contents is expanded in topical outline and detail. It visually organizes the material chapter by chapter, thereby eliminating any need for an index. Answers for sample problems in the text are always given and in many instances underlined for added clarity and emphasis. The use of unit labels is judiciously observed; and wherever factor reduction by cancellation occurs in the sample problems, smaller faced type indicates the results of the operation, thereby making this edition uniformly more readable and understandable for the student.

Chapter 6 contains useful additions contemplated for inclusion in the second edition (1968) but dropped because of a perceived overlap

REVIEWS

Ethical Safeguards in Research on Humans. Vol. 5. Philosophy and Technology of Drug Assessment. Edited by JOSEPH D. COOPER and HERBERT L. LEY. Interdisciplinary Communication Associates, 1717 Massachusetts Ave., N.W., Washington, DC 20036, 1976. 235 pp. 14.5 × 23 cm. Price $9.00.

This publication consists primarily of the transcripts of an April 1973 conference on "Ethical Problems in Drug Experimentation," which was the fifth in a series on the Philosophy and Technology of Drug Assessment. The 3-year time lag was due to the death of the coordinator, Dr. Joseph D. Cooper, following the seventh conference of the series in March 1975. Human research is a subject with many recent developments, and there are current publications that diminish the significance and timeliness of these proceedings.

The conference dialog was divided into several aspects of human research including surgical experimentation, patients and prisoners as subjects, state moratoriums on research, how to turn off an experiment, national and local review mechanisms, extrapolating results from animal to human, and payments and indemnification. Unfortunately, the majority of the book is merely transcripts of the dialog among the 22 nationally renown medical scientists who are listed as the conference participants. Other than the brief introductory summaries of each chapter, the dialog is sometimes difficult to follow. With the emphasis on dialog, the book suffers from a lack of references that might be useful in documenting the seemingly anecdotal comments of the participants.

The most valuable portion of the book is the introductory "Background Notes on Issues in Experimentation with Human Subjects." This 32-page segment of preconference material summarizes the issues prior to 1973 rather well. The background includes 63 references and a selected bibliography of eight publications. Readers who are following the human experimentation issue very closely may be interested in this publication.

Reviewed by William F. McGhan
College of Pharmacy
University of Minnesota
Minneapolis, MN 55414

Drug Metabolism Reviews. Vol. 4. Edited by FREDERICK J. DiCARLO. Dekker, 270 Madison Ave., New York, NY 10016, 1976. 340 pp. 16 × 24 cm. Price $32.50.

According to the press release for reviewers, "Volume 4 includes treatises on the disposition of used and abused drugs, the effects of liver disease upon drug disposition, the biotransformation of insecticides by insects, the clinical usefulness of organic nitrates and the logistics of drug metabolism studies." This is a factual and bald description of a fascinating volume.

The trend toward the complete integration of drug metabolism and pharmacokinetics continues and is very apparent in these reviews. We might as well stop referring to drug metabolism and pharmacokinetics and recognize that we are dealing with an integrated science of drug disposition. The term "drugs" does not just refer to human health products but also to animal health products, pesticides, industrial chemicals, and just about any other nonnutritive material that can enter any type of living organism.

There are three reviews on compounds that have been in use from centuries to millenia: morphine and heroin (Boerner, Abbot, and Roe), nitroglycerin (DiCarlo), and caffeine (Burg). It is always surprising to realize that, despite the length of their use, a great deal about each of them remains unknown. They present active and ongoing research problems of fundamental importance. The review on nitroglycerin is fun to read as well as informative. It got some "Gee whiz, I didn't know that" reactions from me. I'd recommend it as a model for authors.

A great deal of experimental work has been done, and clinical experience exists concerning renal dysfunction and its effects on drug disposition. Much less information exists on the effects of dysfunction of the liver, the other major organ of drug elimination. Wilkinson and Schenker's review on drug disposition and liver disease plays its part in redressing this balance.

The two most important reviews in this volume were written by Ruelius and Weiner on the logistics of drug disposition studies. The discipline of drug disposition is of fundamental importance in industry, where it constitutes an important part of the safety evaluation process, *de facto* or *de jure*. This is not simply to meet regulatory requirements; the regulatory agencies can only lag and react to what is found in the research laboratory and in the field when a drug is in use. Drug disposition studies can occupy a central place in the development process and interact with screening studies, pathology, toxicology, and "clinical" development and use. An academically engendered desire to know all that there is possible to know must give way to the imposition of priorities and the use of finite resources to find out what is of fundamental but practical importance. The primary question must be: "Within what limits is this agent safe and effective?" Each new drug represents a different problem. It would be impractical and impossible to impose rigid checklists or rules of procedure on drug disposition studies. The only valid approach, which both Ruelius and Weiner adapted, is to discuss general principles and then to illustrate the application of those principles by case studies of the problems presented by specific compounds. Many times they are saying the same things but what they are saying needs a lot of repetition.

This book costs almost 10¢ a page but it's well worth it. Buy a copy through your library or your own budget or even personally (it is tax deductible). Once you've got a copy, read it!

Reviewed by Morris Pfeffer
Bristol Laboratories
Syracuse, NY 13201

Calculations in Pharmacy. Third Edition. By SUE H. ROUSE and M. GEORGE WEBBER. Lippincott, East Washington Square, Philadelphia, PA 19105, 1976. 264 pp. 15.5 × 23.5 cm. Price $12.75.

The familiar strengths of this useful textbook in pharmaceutical calculations have for the most part remained intact in the second revision of the work. Substantially little has changed in format, content, or presentation of the third edition. Most helpful is its continued logical approach to the reasoned solution for pharmaceutical calculations in a way that deemphasizes rote methods and confusing proportionalities.

To accommodate newer concepts, nearly 800 revised practice problems with answers have been prepared, and "much of the emphasis on the 'art of compounding' has been reduced or neglected in favor of orientation toward patients." The art of the printer, however, is very much evident in the presentation of the book. The new table of contents is expanded in topical outline and detail. It visually organizes the material chapter by chapter, thereby eliminating any need for an index. Answers for sample problems in the text are always given and in many instances underlined for added clarity and emphasis. The use of unit labels is judiciously observed; and wherever factor reduction by cancellation occurs in the sample problems, smaller faced type indicates the results of the operation, thereby making this edition uniformly more readable and understandable for the student.

Chapter 6 contains useful additions contemplated for inclusion in the second edition (1968) but dropped because of a perceived overlap

REVIEWS

Ethical Safeguards in Research on Humans. Vol. 5. Philosophy and Technology of Drug Assessment. Edited by JOSEPH D. COOPER and HERBERT L. LEY. Interdisciplinary Communication Associates, 1717 Massachusetts Ave., N.W., Washington, DC 20036, 1976. 235 pp. 14.5 × 23 cm. Price $9.00.

This publication consists primarily of the transcripts of an April 1973 conference on "Ethical Problems in Drug Experimentation," which was the fifth in a series on the Philosophy and Technology of Drug Assessment. The 3-year time lag was due to the death of the coordinator, Dr. Joseph D. Cooper, following the seventh conference of the series in March 1975. Human research is a subject with many recent developments, and there are current publications that diminish the significance and timeliness of these proceedings.

The conference dialog was divided into several aspects of human research including surgical experimentation, patients and prisoners as subjects, state moratoriums on research, how to turn off an experiment, national and local review mechanisms, extrapolating results from animal to human, and payments and indemnification. Unfortunately, the majority of the book is merely transcripts of the dialog among the 22 nationally renown medical scientists who are listed as the conference participants. Other than the brief introductory summaries of each chapter, the dialog is sometimes difficult to follow. With the emphasis on dialog, the book suffers from a lack of references that might be useful in documenting the seemingly anecdotal comments of the participants.

The most valuable portion of the book is the introductory "Background Notes on Issues in Experimentation with Human Subjects." This 32-page segment of preconference material summarizes the issues prior to 1973 rather well. The background includes 63 references and a selected bibliography of eight publications. Readers who are following the human experimentation issue very closely may be interested in this publication.

Reviewed by William F. McGhan
College of Pharmacy
University of Minnesota
Minneapolis, MN 55414

Drug Metabolism Reviews. Vol. 4. Edited by FREDERICK J. DiCARLO. Dekker, 270 Madison Ave., New York, NY 10016, 1976. 340 pp. 16 × 24 cm. Price $32.50.

According to the press release for reviewers, "Volume 4 includes treatises on the disposition of used and abused drugs, the effects of liver disease upon drug disposition, the biotransformation of insecticides by insects, the clinical usefulness of organic nitrates and the logistics of drug metabolism studies." This is a factual and bald description of a fascinating volume.

The trend toward the complete integration of drug metabolism and pharmacokinetics continues and is very apparent in these reviews. We might as well stop referring to drug metabolism and pharmacokinetics and recognize that we are dealing with an integrated science of drug disposition. The term "drugs" does not just refer to human health products but also to animal health products, pesticides, industrial chemicals, and just about any other nonnutritive material that can enter any type of living organism.

There are three reviews on compounds that have been in use from centuries to millenia: morphine and heroin (Boerner, Abbot, and Roe), nitroglycerin (DiCarlo), and caffeine (Burg). It is always surprising to realize that, despite the length of their use, a great deal about each of them remains unknown. They present active and ongoing research problems of fundamental importance. The review on nitroglycerin is fun to read as well as informative. It got some "Gee whiz, I didn't know that" reactions from me. I'd recommend it as a model for authors.

A great deal of experimental work has been done, and clinical experience exists concerning renal dysfunction and its effects on drug disposition. Much less information exists on the effects of dysfunction of the liver, the other major organ of drug elimination. Wilkinson and Schenker's review on drug disposition and liver disease plays its part in redressing this balance.

The two most important reviews in this volume were written by Ruelius and Weiner on the logistics of drug disposition studies. The discipline of drug disposition is of fundamental importance in industry, where it constitutes an important part of the safety evaluation process, *de facto* or *de jure*. This is not simply to meet regulatory requirements; the regulatory agencies can only lag and react to what is found in the research laboratory and in the field when a drug is in use. Drug disposition studies can occupy a central place in the development process and interact with screening studies, pathology, toxicology, and "clinical" development and use. An academically engendered desire to know all that there is possible to know must give way to the imposition of priorities and the use of finite resources to find out what is of fundamental but practical importance. The primary question must be: "Within what limits is this agent safe and effective?" Each new drug represents a different problem. It would be impractical and impossible to impose rigid checklists or rules of procedure on drug disposition studies. The only valid approach, which both Ruelius and Weiner adapted, is to discuss general principles and then to illustrate the application of those principles by case studies of the problems presented by specific compounds. Many times they are saying the same things but what they are saying needs a lot of repetition.

This book costs almost 10¢ a page but it's well worth it. Buy a copy through your library or your own budget or even personally (it is tax deductible). Once you've got a copy, read it!

Reviewed by Morris Pfeffer
Bristol Laboratories
Syracuse, NY 13201

Calculations in Pharmacy. Third Edition. By SUE H. ROUSE and M. GEORGE WEBBER. Lippincott, East Washington Square, Philadelphia, PA 19105, 1976. 264 pp. 15.5 × 23.5 cm. Price $12.75.

The familiar strengths of this useful textbook in pharmaceutical calculations have for the most part remained intact in the second revision of the work. Substantially little has changed in format, content, or presentation of the third edition. Most helpful is its continued logical approach to the reasoned solution for pharmaceutical calculations in a way that deemphasizes rote methods and confusing proportionalities.

To accommodate newer concepts, nearly 800 revised practice problems with answers have been prepared, and "much of the emphasis on the 'art of compounding' has been reduced or neglected in favor of orientation toward patients." The art of the printer, however, is very much evident in the presentation of the book. The new table of contents is expanded in topical outline and detail. It visually organizes the material chapter by chapter, thereby eliminating any need for an index. Answers for sample problems in the text are always given and in many instances underlined for added clarity and emphasis. The use of unit labels is judiciously observed; and wherever factor reduction by cancellation occurs in the sample problems, smaller faced type indicates the results of the operation, thereby making this edition uniformly more readable and understandable for the student.

Chapter 6 contains useful additions contemplated for inclusion in the second edition (1968) but dropped because of a perceived overlap

with pharmacology. This edition more boldly and appropriately includes the material on dosage calculations based on body surface area and Fried's rule for the calculation of children's doses based upon age in months. Standard nomograms are included for the conversion of doses based on body weight to doses based on body surface.

Much less successful is the material added in the newly appended Chapter 14. The authors preface their book with an indication that the material contained in this last chapter results from acknowledgment of requests from many instructors. The appended chapter, prepared by two of the authors' colleagues, attempts to review important concepts from chemistry [milliequivalents, electrolyte replenishment, and operator p (pH and pK)], pharmaceutics (alligation involving the HLB system), and mathematics (logarithms, unit label analysis, and elementary statistics), all within 18 pages and 29 practice problems! The task is hopelessly more global than the space allotted, with the result that nothing in the chapter works well. A seven-page section (with nine practice problems on the elements of statistics, the operator p, and the unit analysis) is totally inadequate and will confuse even the proficient student who turns to it for review. It has no potential as a teaching chapter and the authors would have been wiser in reapplying their reasoning from the preface of the second edition: to reject the inclusion of these materials in the third edition because of duplication with much more authoritative and useful treatments in other standard pharmaceutical textbooks, rather than blemish the new edition with so inadequate a treatment.

Ignoring at least portions of the newly appended chapter as a misplaced and nonfunctioning appendage to the book, Rouse and Webber have provided a useful third edition that will undoubtedly continue to serve as a mainstay textbook for traditional courses in pharmaceutical calculations and as a wealthy storehouse of reference material and practice problems for the student engaged in competency based self-directed study.

Reviewed by Robert G. Mrtek
College of Pharmacy
University of Illinois at the Medical Center
Chicago, IL 60680

Amino-Acids, Peptides, and Proteins. Vol. 7. Edited by R. C. SHEPPARD. The Chemical Society, Burlington House, London, W1V OBN, England, 1976. 431 pp. 14.5 × 22.5 cm. Price $57.75.

This volume is the seventh in the series of literature reviews in the field of amino acids, peptides, and proteins. Under the leadership of Dr. Sheppard, a selected group of researchers summarize the developments during 1974 in six chapters. As with previous volumes, the reader can expect the high standards associated with publications of the Chemical Society.

The first four chapters are primarily concerned with an extensive review of the literature regarding amino acids, structural investigations of peptides and proteins, peptide synthesis, and peptides with structural features not typical of proteins. In addition to the usual format, the second chapter contains tables summarizing features of affinity chromatography separations, molecular weights and subunit composition of proteins, uses of chemical modifications of proteins, affinity labeling of proteins, and proteins whose partial or complete sequence was published in 1974. These tables are followed by a summary of references to authors and published articles in an orderly and useful fashion.

A most important feature of this seventh edition is Chapter 5, which covers enzymes for the first time in the series. Dr. Fersht, in a sophisticated yet enjoyable manner, reviews some of the more important papers published during 1974 that were concerned with chemical structure and biological activity of enzymes; very appropriately mentions earlier work done in the area; and presents all sides of current work and some current problems. Chapter 6 is the biennial review of metal derivatives of amino acids, peptides, and proteins. The format is that followed by previous volumes, and the reader is given a survey of the literature for 1973–1974.

This seventh volume presents the reader with some interesting developments, with further applications of known chemistry, and some presentations of old principles which have been given ingenious new applications. This volume is certainly a comprehensive source of information to researchers interested in amino acids, peptides, proteins, and enzymes. The information should, of course, be supplemented by reading the original literature, especially by students.

Reviewed by A. Kapoor
Department of Pharmaceutical Sciences
College of Pharmacy and Allied Health Professions
St. John's University
Jamaica, NY 11439

Advances in Mass Spectrometry In Biochemistry and Medicine. Vol. 1. Edited by ALBERTO FRIGERIO and NEAL CASTAGNOLI. Spectrum Publications, 86-19 Sancho St., Holliswood, NY 11423, 1976. 586 pp. 16 × 23.5 cm.

This volume is a compilation of 51 separate papers of varying quality, with titles ranging from "Biomedical Applications of Chemical Ionization" to "Gas Chromatography–Mass Fragmentography Pharmacokinetics of Antineoplastic Agents." The text was taken from the proceedings of the Second International Symposium of Mass Spectrometry in Biochemistry and Medicine at the Mario Negri Institute for Pharmocological Research, Milan, Italy, in June 1974. Each chapter was contributed by different authors, and each relates to a different potential application of mass spectrometry in biochemistry and medicine. The topics range in value from prime import to minimal interest. Most chapters contain illustrations such as normalized mass spectra, gas chromatographs, and fragmentation schemes. The illustrations are clearly presented and well labeled. Each chapter includes a thorough bibliography which would enable the reader to do further research on the given theme, if desired.

Topics such as mass fragmentography, gas chromatography–mass spectrometry, stable isotope measurements, field ionization, field desorption, chemical ionization, atmospheric pressure ionization, high-resolution studies, and data acquisition and processing are discussed. In particular, the major topics include detection and identification of drug metabolites and other biomedical applications including biosynthesis and toxicology studies. Applications of mass spectrometry to the study of such important groups of compounds as peptides, steroids, prostaglandins, nucleotides, carbohydrates, and many other natural products and medicinal agents are given. Although mass spectrometry is the principal means of identification of these compounds, various means of isolation and separation are discussed. Also described are derivatization techniques that not only enhance volatility but also generate more intense ions in their spectra.

The papers contained in this volume represent a large cross section of mass spectrometric techniques presently being developed over a broad range field of mass spectrometry. Owing to the scope of this book, it is impossible to evaluate all of the topics covered at one level of criticism. This book does, however, have definite merit, since various mass spectrometry systems represent one of the most powerful means of analysis now available for the study of samples of biologic origin.

This book should serve as a useful source of information to many chemists, biochemists, pharmacologists, and medical researchers. Mass spectrometrists, in particular, will find this book useful in keeping abreast of the many faceted advances in their technology.

Reviewed by Charles F. Kuhlman
Wyeth Laboratories, Inc.
Research Division
Radnor, PA 19087

with pharmacology. This edition more boldly and appropriately includes the material on dosage calculations based on body surface area and Fried's rule for the calculation of children's doses based upon age in months. Standard nomograms are included for the conversion of doses based on body weight to doses based on body surface.

Much less successful is the material added in the newly appended Chapter 14. The authors preface their book with an indication that the material contained in this last chapter results from acknowledgment of requests from many instructors. The appended chapter, prepared by two of the authors' colleagues, attempts to review important concepts from chemistry [milliequivalents, electrolyte replenishment, and operator p (pH and pK)], pharmaceutics (alligation involving the HLB system), and mathematics (logarithms, unit label analysis, and elementary statistics), all within 18 pages and 29 practice problems! The task is hopelessly more global than the space allotted, with the result that nothing in the chapter works well. A seven-page section (with nine practice problems on the elements of statistics, the operator p, and the unit analysis) is totally inadequate and will confuse even the proficient student who turns to it for review. It has no potential as a teaching chapter and the authors would have been wiser in reapplying their reasoning from the preface of the second edition: to reject the inclusion of these materials in the third edition because of duplication with much more authoritative and useful treatments in other standard pharmaceutical textbooks, rather than blemish the new edition with so inadequate a treatment.

Ignoring at least portions of the newly appended chapter as a misplaced and nonfunctioning appendage to the book, Rouse and Webber have provided a useful third edition that will undoubtedly continue to serve as a mainstay textbook for traditional courses in pharmaceutical calculations and as a wealthy storehouse of reference material and practice problems for the student engaged in competency based self-directed study.

Reviewed by Robert G. Mrtek
College of Pharmacy
University of Illinois at the Medical Center
Chicago, IL 60680

Amino-Acids, Peptides, and Proteins. Vol. 7. Edited by R. C. SHEPPARD. The Chemical Society, Burlington House, London, W1V OBN, England, 1976. 431 pp. 14.5 × 22.5 cm. Price $57.75.

This volume is the seventh in the series of literature reviews in the field of amino acids, peptides, and proteins. Under the leadership of Dr. Sheppard, a selected group of researchers summarize the developments during 1974 in six chapters. As with previous volumes, the reader can expect the high standards associated with publications of the Chemical Society.

The first four chapters are primarily concerned with an extensive review of the literature regarding amino acids, structural investigations of peptides and proteins, peptide synthesis, and peptides with structural features not typical of proteins. In addition to the usual format, the second chapter contains tables summarizing features of affinity chromatography separations, molecular weights and subunit composition of proteins, uses of chemical modifications of proteins, affinity labeling of proteins, and proteins whose partial or complete sequence was published in 1974. These tables are followed by a summary of references to authors and published articles in an orderly and useful fashion.

A most important feature of this seventh edition is Chapter 5, which covers enzymes for the first time in the series. Dr. Fersht, in a sophisticated yet enjoyable manner, reviews some of the more important papers published during 1974 that were concerned with chemical structure and biological activity of enzymes; very appropriately mentions earlier work done in the area; and presents all sides of current work and some current problems. Chapter 6 is the biennial review of metal derivatives of amino acids, peptides, and proteins. The format is that followed by previous volumes, and the reader is given a survey of the literature for 1973–1974.

This seventh volume presents the reader with some interesting developments, with further applications of known chemistry, and some presentations of old principles which have been given ingenious new applications. This volume is certainly a comprehensive source of information to researchers interested in amino acids, peptides, proteins, and enzymes. The information should, of course, be supplemented by reading the original literature, especially by students.

Reviewed by A. Kapoor
Department of Pharmaceutical Sciences
College of Pharmacy and Allied Health Professions
St. John's University
Jamaica, NY 11439

Advances in Mass Spectrometry In Biochemistry and Medicine. Vol. 1. Edited by ALBERTO FRIGERIO and NEAL CASTAGNOLI. Spectrum Publications, 86-19 Sancho St., Holliswood, NY 11423, 1976. 586 pp. 16 × 23.5 cm.

This volume is a compilation of 51 separate papers of varying quality, with titles ranging from "Biomedical Applications of Chemical Ionization" to "Gas Chromatography–Mass Fragmentography Pharmacokinetics of Antineoplastic Agents." The text was taken from the proceedings of the Second International Symposium of Mass Spectrometry in Biochemistry and Medicine at the Mario Negri Institute for Pharmocological Research, Milan, Italy, in June 1974. Each chapter was contributed by different authors, and each relates to a different potential application of mass spectrometry in biochemistry and medicine. The topics range in value from prime import to minimal interest. Most chapters contain illustrations such as normalized mass spectra, gas chromatographs, and fragmentation schemes. The illustrations are clearly presented and well labeled. Each chapter includes a thorough bibliography which would enable the reader to do further research on the given theme, if desired.

Topics such as mass fragmentography, gas chromatography–mass spectrometry, stable isotope measurements, field ionization, field desorption, chemical ionization, atmospheric pressure ionization, high-resolution studies, and data acquisition and processing are discussed. In particular, the major topics include detection and identification of drug metabolites and other biomedical applications including biosynthesis and toxicology studies. Applications of mass spectrometry to the study of such important groups of compounds as peptides, steroids, prostaglandins, nucleotides, carbohydrates, and many other natural products and medicinal agents are given. Although mass spectrometry is the principal means of identification of these compounds, various means of isolation and separation are discussed. Also described are derivatization techniques that not only enhance volatility but also generate more intense ions in their spectra.

The papers contained in this volume represent a large cross section of mass spectrometric techniques presently being developed over a broad range field of mass spectrometry. Owing to the scope of this book, it is impossible to evaluate all of the topics covered at one level of criticism. This book does, however, have definite merit, since various mass spectrometry systems represent one of the most powerful means of analysis now available for the study of samples of biologic origin.

This book should serve as a useful source of information to many chemists, biochemists, pharmacologists, and medical researchers. Mass spectrometrists, in particular, will find this book useful in keeping abreast of the many faceted advances in their technology.

Reviewed by Charles F. Kuhlman
Wyeth Laboratories, Inc.
Research Division
Radnor, PA 19087

with pharmacology. This edition more boldly and appropriately includes the material on dosage calculations based on body surface area and Fried's rule for the calculation of children's doses based upon age in months. Standard nomograms are included for the conversion of doses based on body weight to doses based on body surface.

Much less successful is the material added in the newly appended Chapter 14. The authors preface their book with an indication that the material contained in this last chapter results from acknowledgment of requests from many instructors. The appended chapter, prepared by two of the authors' colleagues, attempts to review important concepts from chemistry [milliequivalents, electrolyte replenishment, and operator p (pH and pK)], pharmaceutics (alligation involving the HLB system), and mathematics (logarithms, unit label analysis, and elementary statistics), all within 18 pages and 29 practice problems! The task is hopelessly more global than the space allotted, with the result that nothing in the chapter works well. A seven-page section (with nine practice problems on the elements of statistics, the operator p, and the unit analysis) is totally inadequate and will confuse even the proficient student who turns to it for review. It has no potential as a teaching chapter and the authors would have been wiser in reapplying their reasoning from the preface of the second edition: to reject the inclusion of these materials in the third edition because of duplication with much more authoritative and useful treatments in other standard pharmaceutical textbooks, rather than blemish the new edition with so inadequate a treatment.

Ignoring at least portions of the newly appended chapter as a misplaced and nonfunctioning appendage to the book, Rouse and Webber have provided a useful third edition that will undoubtedly continue to serve as a mainstay textbook for traditional courses in pharmaceutical calculations and as a wealthy storehouse of reference material and practice problems for the student engaged in competency based self-directed study.

Reviewed by Robert G. Mrtek
College of Pharmacy
University of Illinois at the Medical Center
Chicago, IL 60680

Amino-Acids, Peptides, and Proteins. Vol. 7. Edited by R. C. SHEPPARD. The Chemical Society, Burlington House, London, W1V OBN, England, 1976. 431 pp. 14.5 × 22.5 cm. Price $57.75.

This volume is the seventh in the series of literature reviews in the field of amino acids, peptides, and proteins. Under the leadership of Dr. Sheppard, a selected group of researchers summarize the developments during 1974 in six chapters. As with previous volumes, the reader can expect the high standards associated with publications of the Chemical Society.

The first four chapters are primarily concerned with an extensive review of the literature regarding amino acids, structural investigations of peptides and proteins, peptide synthesis, and peptides with structural features not typical of proteins. In addition to the usual format, the second chapter contains tables summarizing features of affinity chromatography separations, molecular weights and subunit composition of proteins, uses of chemical modifications of proteins, affinity labeling of proteins, and proteins whose partial or complete sequence was published in 1974. These tables are followed by a summary of references to authors and published articles in an orderly and useful fashion.

A most important feature of this seventh edition is Chapter 5, which covers enzymes for the first time in the series. Dr. Fersht, in a sophisticated yet enjoyable manner, reviews some of the more important papers published during 1974 that were concerned with chemical structure and biological activity of enzymes; very appropriately mentions earlier work done in the area; and presents all sides of current work and some current problems. Chapter 6 is the biennial review of metal derivatives of amino acids, peptides, and proteins. The format is that followed by previous volumes, and the reader is given a survey of the literature for 1973–1974.

This seventh volume presents the reader with some interesting developments, with further applications of known chemistry, and some presentations of old principles which have been given ingenious new applications. This volume is certainly a comprehensive source of information to researchers interested in amino acids, peptides, proteins, and enzymes. The information should, of course, be supplemented by reading the original literature, especially by students.

Reviewed by A. Kapoor
Department of Pharmaceutical Sciences
College of Pharmacy and Allied Health Professions
St. John's University
Jamaica, NY 11439

Advances in Mass Spectrometry In Biochemistry and Medicine. Vol. 1. Edited by ALBERTO FRIGERIO and NEAL CASTAGNOLI. Spectrum Publications, 86-19 Sancho St., Holliswood, NY 11423, 1976. 586 pp. 16 × 23.5 cm.

This volume is a compilation of 51 separate papers of varying quality, with titles ranging from "Biomedical Applications of Chemical Ionization" to "Gas Chromatography–Mass Fragmentography Pharmacokinetics of Antineoplastic Agents." The text was taken from the proceedings of the Second International Symposium of Mass Spectrometry in Biochemistry and Medicine at the Mario Negri Institute for Pharmocological Research, Milan, Italy, in June 1974. Each chapter was contributed by different authors, and each relates to a different potential application of mass spectrometry in biochemistry and medicine. The topics range in value from prime import to minimal interest. Most chapters contain illustrations such as normalized mass spectra, gas chromatographs, and fragmentation schemes. The illustrations are clearly presented and well labeled. Each chapter includes a thorough bibliography which would enable the reader to do further research on the given theme, if desired.

Topics such as mass fragmentography, gas chromatography–mass spectrometry, stable isotope measurements, field ionization, field desorption, chemical ionization, atmospheric pressure ionization, high-resolution studies, and data acquisition and processing are discussed. In particular, the major topics include detection and identification of drug metabolites and other biomedical applications including biosynthesis and toxicology studies. Applications of mass spectrometry to the study of such important groups of compounds as peptides, steroids, prostaglandins, nucleotides, carbohydrates, and many other natural products and medicinal agents are given. Although mass spectrometry is the principal means of identification of these compounds, various means of isolation and separation are discussed. Also described are derivatization techniques that not only enhance volatility but also generate more intense ions in their spectra.

The papers contained in this volume represent a large cross section of mass spectrometric techniques presently being developed over a broad range field of mass spectrometry. Owing to the scope of this book, it is impossible to evaluate all of the topics covered at one level of criticism. This book does, however, have definite merit, since various mass spectrometry systems represent one of the most powerful means of analysis now available for the study of samples of biologic origin.

This book should serve as a useful source of information to many chemists, biochemists, pharmacologists, and medical researchers. Mass spectrometrists, in particular, will find this book useful in keeping abreast of the many faceted advances in their technology.

Reviewed by Charles F. Kuhlman
Wyeth Laboratories, Inc.
Research Division
Radnor, PA 19087

Journal of Pharmaceutical Sciences

MARCH 1977

VOLUME 66 NUMBER 3

MARY H. FERGUSON
Editor

L. LUAN CORRIGAN
Assistant Editor

SHELLY ELLIOTT
Production Editor

JANET D. SHOFF
Copy Editor

EDWARD G. FELDMANN
Contributing Editor

SAMUEL W. GOLDSTEIN
Contributing Editor

LELAND J. ARNEY
Director of Publications

EDITORIAL ADVISORY BOARD

JOHN AUTIAN
HARRY B. KOSTENBAUDER
NORMAN R. FARNSWORTH
HERBERT A. LIEBERMAN
WILLIAM O. FOYE
DAVID E. MANN, JR.
WILLIAM J. JUSKO
GERALD J. PAPARIELLO

The *Journal of Pharmaceutical Sciences* is published monthly by the American Pharmaceutical Association at 2215 Constitution Ave., N.W., Washington, DC 20037. Second-class postage paid at Washington, D.C., and at additional mailing office.

All expressions of opinion and statements of supposed fact appearing in articles or editorials carried in this journal are published on the authority of the writer over whose name they appear and are not to be regarded as necessarily expressing the policies or views of the American Pharmaceutical Association.

Offices—Editorial, Advertising, and Subscription Offices: 2215 Constitution Ave., N.W., Washington, DC 20037. Printing Offices: 20th & Northampton Streets, Easton, PA 18042.

Annual Subscriptions—United States and foreign, industrial and government institutions $50, educational institutions $50, individuals *for personal use only* $30; single copies $5. All foreign subscriptions add $5 for postage. Subscription rates are subject to change without notice. Members of the American Pharmaceutical Association may elect to receive the *Journal of Pharmaceutical Sciences* as a part of their annual $60 (foreign $65) APhA membership dues.

Claims—Missing numbers will not be supplied if dues or subscriptions are in arrears for more than 60 days or if claims are received more than 60 days after the date of the issue, or if loss was due to failure to give notice of change of address. The Association cannot accept responsibility for foreign delivery when its records indicate shipment has been made.

Change of Address—Members and subscribers should notify at once both the Post Office and the American Pharmaceutical Association, 2215 Constitution Ave., N.W., Washington, DC 20037, of any change of address.

© Copyright 1977, American Pharmaceutical Association, 2215 Constitution Ave., N.W., Washington, DC 20037; all rights reserved.

HOW MUCH IS "ENOUGH"?

For the past year or two, articles, speeches, testimony, and assorted other means of communication have been rife with comment and opinion to the effect that either additional regulation is needed in the area of drug discovery and introduction or, conversely, that already drug discovery and introduction are subjected to excessive regulation.

On the one side, those who advocate additional legal controls present persuasive arguments based upon statistics showing significant toxicity, adverse reactions, and related harmful effects associated with a particular drug which often come to light only after its widespread or long-term use. On the other hand, opponents to further regulation present equally persuasive arguments that already drug innovation has been inhibited, a so-called "drug lag" has developed, and patients are presently being denied the benefit of important new drug discoveries, all due to what they regard as the excessively restrictive current regulations which delay or prevent new drug marketing approval.

It is, of course, just such differences of viewpoint which are said "to make a horse race." All of this reminds us of an anecdote which may or may not have basis in fact but certainly is pertinent. We were told that the river which ran through a small rural town was closed to swimming by the local health department on grounds that it was polluted and a menace to health. The town leaders went to extensive effort to correct the problem and to clean up their river. But when they then requested the health department to open the river to swimming, their request was again denied—this time with the explanation that the river constituted the source of the local drinking water supply and it would be unsanitary, therefore, to permit swimming!

Whether or not such an incident actually occurred, we do know for a fact that rather comparable incidents repeatedly have happened in the area of drug standards. For example, on many occasions, critics from the drug industry have alleged that official compendia specifications were insufficient to assure an aspect of drug quality whether it be potency, identity, bioavailability, stability, or some other related characteristic. Subsequently, the compendia proposed adoption of either a new or more stringent specification in order to remedy the alleged deficiency. Not uncommonly, such proposals then met with objection from the very same critics on grounds that such test requirements were excessive, or would contribute prohibitively to manufacturing costs, or even that the proposed requirements were too "severe" because their own products could not meet the new standard!

It is well to recognize that the genesis of any proposed new law or regulation generally can be traced back to some sort of abuse or problem. For example, the Good Laboratory Practice regulations which were discussed in our February editorial were the direct result of falsified test data submitted to FDA in support of certain New Drug Applications. Consequently, as a general observation, most disinterested parties would tend to feel that society and government must impose regulatory controls to avoid problems or to prevent repeated abuses.

Our view tends to concur but, at the same time, we also recognize that such regulations must be reasonable and properly tempered to avoid excessive restrictions which will unduly inhibit and discourage future research by destroying legitimate incentives. Drug regulation is particularly susceptible to "overkill," and care must be exercised to avoid a result which might be even more disastrous than the problem it is intended to control.

Edward G. Feldmann

Journal of Pharmaceutical Sciences

APRIL 1977

VOLUME 66 NUMBER 4

MARY H. FERGUSON
Editor

L. LUAN CORRIGAN
Assistant Editor

SHELLY ELLIOTT
Production Editor

JANET D. SHOFF
Copy Editor

EDWARD G. FELDMANN
Contributing Editor

SAMUEL W. GOLDSTEIN
Contributing Editor

LELAND J. ARNEY
Director of Publications

EDITORIAL ADVISORY BOARD

JOHN AUTIAN
NORMAN R. FARNSWORTH
WILLIAM O. FOYE
WILLIAM J. JUSKO
HARRY B. KOSTENBAUDER
HERBERT A. LIEBERMAN
DAVID E. MANN, JR.
GERALD J. PAPARIELLO

The *Journal of Pharmaceutical Sciences* is published monthly by the American Pharmaceutical Association at 2215 Constitution Ave., N.W., Washington, DC 20037. Second-class postage paid at Washington, D.C., and at additional mailing office.

All expressions of opinion and statements of supposed fact appearing in articles or editorials carried in this journal are published on the authority of the writer over whose name they appear and are not to be regarded as necessarily expressing the policies or views of the American Pharmaceutical Association.

Offices—Editorial, Advertising, and Subscription Offices: 2215 Constitution Ave., N.W., Washington, DC 20037. Printing Offices: 20th & Northampton Streets, Easton, PA 18042.

Annual Subscriptions—United States and foreign, industrial and government institutions $50, educational institutions $50, individuals *for personal use only* $30; single copies $5. All foreign subscriptions add $5 for postage. Subscription rates are subject to change without notice. Members of the American Pharmaceutical Association may elect to receive the *Journal of Pharmaceutical Sciences* as a part of their annual $60 (foreign $65) APhA membership dues.

Claims—Missing numbers will not be supplied if dues or subscriptions are in arrears for more than 60 days or if claims are received more than 60 days after the date of the issue, or if loss was due to failure to give notice of change of address. The Association cannot accept responsibility for foreign delivery when its records indicate shipment has been made.

Change of Address—Members and subscribers should notify at once both the Post Office and the American Pharmaceutical Association, 2215 Constitution Ave., N.W., Washington, DC 20037, of any change of address.

© Copyright 1977, American Pharmaceutical Association, 2215 Constitution Ave., N.W., Washington, DC 20037; all rights reserved.

"ZERO-BASED" DRUG STANDARDS

President Carter has introduced the management approach of "zero-based budgeting" in reviewing federal programs and their financing. Indeed, so much has been said and written about this concept in recent months that few of our readers are probably unfamiliar with the term and its meaning. However, a brief explanation may be useful.

Basically, in contrast to taking last year's projects and programs and simply adding to them by way of staff, budget, and so on, zero-based budget calls for a complete reassessment of each such project or program to determine if the activity itself, as well as all of its components, can be currently justified. The premise is that there is a natural tendency for activities to be initiated which in time come to outlive their usefulness, in part or in whole. In the absence of any positive step to reassess their function and value by today's perspective, they drone on indefinitely.

The thought has long been with us that some such comprehensive reassessment would be highly desirable with respect to drug standards and specifications—particularly those appearing in the official compendia. Frequently, additions or revisions are made to *United States Pharmacopeia* or *National Formulary* monographs which interrelate with other elements within the compendia.

Those responsible for the compendial revision programs generally have done a good job of making whatever modifications were necessary to avoid any outright discrepancies or contradictions. However, in the absence of a "start from scratch" review, any process that introduces changes or new material in a piecemeal fashion will result in a patchwork product to some degree.

An example or two might help to explain both what we have in mind as well as how it happens to come about.

Effective April 1 of this year, a new standard requires that certain drugs be packaged in containers meeting specified criteria of "tightness." This significant advance now provides the compendia with objective procedures to test the tightness of containers and to specify well-defined limits of performance that the containers must meet. The drugs involved are all those whose individual monographs specifically include provision for such packaging. And, a review of the USP and NF reveals that a substantial number of monographs do call for use of either "well-closed" or "tight" containers.

However, such provisions were placed in most, if not all, of these drug monographs at a time when there was no real method for evaluating container tightness. Hence, the standard was more qualitative than quantitative.

The question now arises as to whether all drugs, for which there is a tightness requirement in the pertinent monographs, actually need this degree of protection now that we have defined it and have established methodology for its determination.

Compendia officials are well aware of this situation, but there is only one way that it can be rectified. That would require a drug-by-drug, monograph-by-monograph review, complete with stability data and the like, in order to conclude that the requirement may safely be deleted from certain monographs. But this review would necessitate considerable time and effort just to "clean up" the subject; that is, there is no risk or hazard with the present situation—it simply is one that, on purely scientific grounds, probably could not be justified as necessary to the extent that it applies.

Drug identification tests are another illustration of this problem. For many years, simple qualitative tests were included in compendia monographs to confirm the identity of a specimen. For example, such a test might describe a certain color change in a solution of the sample upon addition of a certain reagent.

With the introduction and wide application of infrared spectrophotometry—especially in conjunction with a reference standard—these antiquated spot tests and color tests became superfluous in the extreme. Yet they often were not deleted because certain parties—due to limitations in available equipment or misguided nostalgia—argued for their retention.

Again, there is nothing wrong *per se* with their continued presence. However, they have outlived their usefulness and they add a lot of undesirable "clutter" to what should be a concise set of drug standards.

All of these defects could be remedied by a start from scratch review of the entire USP and NF content. In line with President Carter's approach to budget development, it appears timely to consider a zero-based review of the compendial standards, with a goal of streamlining the monographs, eliminating duplication, correcting inconsistencies, and achieving uniformity of treatment.

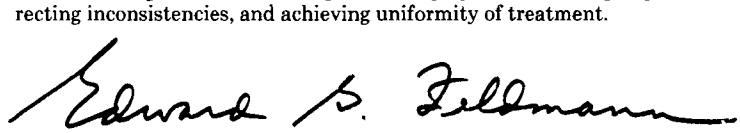

Journal of Pharmaceutical Sciences

APRIL 1977
VOLUME 66 NUMBER 4

REVIEW ARTICLE

Binding of Drugs by Albumin and Plasma Protein

JOSEPH J. VALLNER

Keyphrases □ Binding, protein—various drugs to albumin and plasma proteins, pharmacokinetics, drug displacement, and clinical significance, review □ Protein binding—various drugs to albumin and plasma proteins, pharmacokinetics, drug displacement, and clinical significance, review □ Pharmacokinetics—various drugs, binding to albumin and plasma proteins, review □ Displacement, drug—various drugs, binding to albumin and plasma proteins, review

Many drug–protein binding papers have been published since the often-cited review by Meyer and Guttman (1). This review is intended to be a sequel to that one; published research on drug–albumin binding since 1969 is covered. Only results with human or bovine serum albumin are discussed, and attention is focused on the physical and clinical significance of drug–protein binding and on results obtained with particular drug classes.

Various reviews and articles have appeared since 1969 concerning methods of investigating drug–protein binding phenomena. These methods can be summarized into two broad categories: (*a*) equilibrium methods based upon measuring changes in ligand concentration as a result of the establishment of a binding equilibrium, and (*b*) direct measurement methods in which a property of the drug, protein, or complex may be examined during the binding process. A short but complete coverage of the various specific methods in these two categories was pubished (2). Other articles dealing solely with one method may also be of interest (3–9).

Once binding data are accumulated, the binding parameters must be obtained by employing some data reduction technique. Various articles have appeared dealing with graphical and computer treatment of binding data. It is now well recognized that the Scatchard (10) and Klotz (11) methods of examining binding data are suitable when only one class of sites is displayed by the protein but are at best approximate when more than a single class exists on the protein. The subject of binding data reduction is not dealt with here; however, Refs. 12–22 are either applications of various methods or critical treatises of existing techniques.

Articles dealing with ways to estimate drug–albumin affinity constants rapidly (23) have extremely limited use, since most apply mathematics of the mass action law based upon a single protein site for the drug and require that the free concentration of the drug in the blood be known or determined. Presumably, if one is interested in the binding constant from the clinical standpoint, the affinity is high and measurement of the minute amount free from a therapeutic dose is at best hazardous.

Drug binding to various blood proteins and tissue proteins can influence the therapeutic, pharmacodynamic, and toxicologic actions of drugs. Protein binding may also exert profound effects on drug distribution. The protein–drug complex acts as a transport system to carry drug to the sites of action; this transport is extremely important for drugs that exhibit low solubility in the water portion of the plasma. Protein binding slows the disappearance of free drug from the plasma into tissues by decreasing the concentration gradient. It also provides a source of free drug to replace that removed by various distribution and elimination processes.

In a short overview of the consequences of drug–protein binding, Gillette (24) suggested some important questions to be answered from experiments examining binding phenomena. For example, he pointed out that not only are drugs bound to serum albumin but that other proteins in the blood and tissues may be important in the drug complexation interaction. In addition, the volumes of distribution of the bound forms of the drug usually differ from that of unbound drug. Also lacking in most articles is the consideration that the blood contains other substances that compete with drugs for binding sites. In addition,

correlation of *in vitro* binding results with *in vivo* drug–macromolecule interactions is sorely lacking.

Serum or plasma protein binding, principally to albumin, may have a profound effect on overall drug activity. The following effects have become evident from protein binding investigations: (*a*) only free drug (unbound) is available for activity or tissue distribution; (*b*) tightly bound drugs tend to be distributed in a smaller body space or volume; (*c*) marked decreases in protein binding occur in uremia, hypoalbuminemia, hyperbilirubinemia, and hepatic failure; and (*d*) the delayed elimination of highly bound drugs is a result of glomerular filtration and hepatic uptake being directly proportional to free drug in the serum.

PHYSICAL SIGNIFICANCE OF PROTEIN BINDING

Pharmacokinetics—Until the 1960's, protein binding as a basic principle in drug behavior was neglected in pharmacokinetic models. Drug–albumin interactions may profoundly influence the kinetics of drug elimination, *e.g.*, some sulfa drugs, or the relationship between renal clearance and the apparent biological half-life of the drug (25, 26).

In a short review article, Wagner (27) discussed plasma protein binding effects on nonlinear pharmacokinetic models. He pointed out that drugs showing a high affinity for serum albumin may have their plasma concentration–time profiles convex curvilinear in the terminal phase, and, indeed, this was the case in several reports (25–27). Wagner also pointed out, as did Gillette (24), that tissue binding may be much more important pharmacokinetically than albumin binding.

Gillette (24) added a useful criticism of some pharmacokinetic interpretations of bioavailability data by stating that estimations of volumes of distribution from area under the plasma concentration–time curves and the rate constant of the terminal phase of elimination assume that the drug is not highly bound to plasma proteins and that the ratio of the concentrations of bound and unbound drug in the plasma is constant. The researcher may make erroneous conclusions if it is not determined that the areas under the blood level–time curves are dose dependent.

The binding of chlorpromazine was examined pharmacokinetically (28) in an attempt to explain rapid drug decreases in the plasma. Through theoretical computer simulations, it was determined that a rapid redistribution is possible for such a highly protein-bound drug after small changes in tissue binding. As with many other studies, these results suggest that more experimental work on the actual degree of tissue binding may be important in determining a drug's time course in the plasma.

The pharmacokinetic consequences of plasma protein binding were examined for one- and two-compartment models (29). The computer-simulated data treatment suggested that, if an elimination process operates on bound drug in the plasma for either the one- or two-compartment case, considerable alterations in half-life and area under the free drug concentration–time curve would be seen. However, no *in vivo* data were presented to show the existence of such an elimination mechanism for the bound drug.

Drug Displacement—Concurrent administration of drugs with high albumin binding affinities may produce competition at the binding sites, producing a higher free drug concentration and greater biological activity of each drug than if either is administered alone. Competitive protein binding was studied by using sulfaethidole and bovine serum albumin (30). By using a circular dichroic technique, the drug was found to exhibit optical activity only at its primary binding site, resulting in the unique opportunity to examine the effects of added drugs on the optical activity of sulfaethidole. Drugs that underwent binding at the same site, but were not themselves optically active, reduced the signal due to the sulfa drug. The data for acidic drugs showed that the same primary binding site may be shared by a wide variety of these molecules; basic drugs did not compete for the sulfaethidole site on bovine albumin. However, these same investigators reported that a series of basic alkyldimethylbenzylammonium chlorides did displace sulfaethidole from bovine serum albumin (31). Tryptophan and tyrosine residues of the protein may be involved, and some conformational changes may take place when these surfactant molecules are added to the protein solutions.

In another study employing the circular dichroic technique (32), various drugs were examined with regard to their competition for the two binding sites of dicumarol on human serum albumin. Acidic drugs displaced dicumarol, whereas basic drugs displayed no competition at the binding sites.

The displacing effect of endogenous fatty acids on diazepam bound to human serum albumin was examined (33). At therapeutic levels of diazepam, about 14% of the drug was displaced by laurate anion. The investigators concluded that, if the albumin binding of a drug was extensive, displacement interactions with other endogenous substances should not be ignored. Also, fluctuations of diazepam in blood could result from such a free fatty acid competition phenomenon. Considerable support for such a hypothesis could have been warranted if an attempt had been made to support these *in vitro* results with *in vivo* findings.

Diazepam competed for binding sites on thyroxine binding globulin and thyroxine binding prealbumin in a study using electrophoresis of serum containing thyroid hormone isotopes (34). Since this steroid binding globulin and prealbumin are endogenous macromolecules, the *in vivo* displacement of diazepam may be quite complex. A series of equilibrium–displacement–redistribution may take place *in vivo*. In some individuals having either a diminished concentration or malfunctioning macromolecules, a clinical manifestation of fluctuating drug concentrations and perhaps related toxicities may ensue.

Wardell (35) and McQueen (36), working independently and together (37), examined displacement of protein-bound drug and found that the displacement of initially bound drug upon injection of a more highly protein-bound drug results mainly in redistribution of the initially administered agent. The redistribution is caused by a displacement of drug from plasma protein, not from changes in absorption, metabolism, and excretion.

Dayton *et al.* (38), in a brief discussion of possible clinical effects resulting from plasma binding displacement, noted that drug displacement had not been studied adequately *in vivo*. A clinically oriented study was published concerning the displacement of warfarin from human al-

bumin (39). Drugs used as competitors included diazoxide and ethacrynic, mefenamic, and nalidixic acids. Levy and Oie (40) suggested that displacement can be quantitated for bilirubin. They found a strong correlation between the free fraction of bilirubin in plasma containing no drugs and the free fraction of bilirubin when sulfisoxazole or salicylic acid was present.

The effects of sodium 2-(4-chlorophenoxy)-2-methylpropanoate, the active form of clofibrate, on the possible displacement of phenindione derivatives from human albumin were investigated (41). This work was undertaken because clofibrate presumably had the same binding site on albumin as phenylbutazone. Moreover, phenylbutazone was shown to induce hemorrhagic accidents if patients were concurrently receiving coumarin drugs but not if they were receiving phenindione derivatives. 2-(4-Chlorophenoxy)-2-methylpropanoate inhibited the binding of coumarin agents but did not alter the binding of phenindione derivatives.

The displacement of urate from plasma proteins by anti-inflammatory drugs was examined (42, 43). A relationship was shown between the ability of acidic uricosuric agents to displace albumin-bound urate and to interact at the primary albumin binding site of 5-dimethylaminonaphthalene-1-sulfonamide *in vitro*. Since some of the uricosuric action of these agents was thought to depend on displacement of urate, four of the seemingly best displacing agents were tested clinically. All four drugs tested *in vivo* lowered serum urate concentrations. These two papers demonstrated excellent *in vitro–in vivo* correlations of drug displacement data.

Effect of Fatty Acids—The effects of free fatty acids on the subsequent binding of drugs to human and bovine serum albumins were studied extensively (44). Albumin solutions were prepared with 7, 3.5, or <0.05 mole of palmitate or oleate per mole of protein. Palmitate and oleate are the major free fatty acids of mammalian plasma. By using the equilibrium dialysis technique, studies were conducted on the binding of eight drugs to these fatty acid–albumin solutions. The results indicated that inhibition of drug binding was greater with palmitate than oleate and that inhibition was manifested either as a reduction in the number of drug binding sites or in the association constant for that binding site. The experiments suggested that free fatty acids in serum in the 7–3.5-mole ratio range are inhibitors of serum albumin binding of many drugs. At ratios less than 3.5 (free fatty acid to albumin), the inhibition is essentially negligible.

Spector *et al.* (45) examined the effects of palmitate and oleate at free fatty acid to albumin ratios of 0 to 4 on the ability of previously defatted human serum albumin to bind the antihypertriglyceridemics 2-(4-chlorophenoxy)-2-methylpropanoate and halofenate. The added fatty acid greatly reduced the binding of the 2-(4-chlorophenoxy)-2-methylpropanoate while little effect on halofenate binding was seen. The affinity of halofenate to fatty acid free albumin is much greater than the affinity of the 2-methylpropanoate drug to free albumin. As a result of their data, the investigators suggested that the ability of free fatty acids to regulate drug binding depended upon the affinity with which the drug was bound to albumin. They also suggested a hypothetical mechanism to explain the variation in results for free fatty acid effects on drug binding: that at low mole ratios, allosterism predominates, while both allosterism and a competitive interaction ensue at high mole ratios.

Effect on Bilirubin—Albumin binds significant amounts of the endogenous substance bilirubin. Numerous clinical studies document displacement of bilirubin by sulfa drugs, particularly sulfisoxazole. Many drugs have the ability to displace bilirubin from albumin and thereby potentiate its cytotoxicity (46). Albumin was shown to have two classes of bilirubin binding sites from *in vitro* studies. Of highest affinity was a single site from which bilirubin was not displaced by drugs; however, the availability of this site to bilirubin may be related to free fatty acid concentrations in the serum. The second class of site was multiple in nature, and it was from this class of site that drugs may have displaced bilirubin.

A model was postulated for bilirubin–albumin binding and the propensity of drugs to compete with this highly bound endogenous material. A rapid methodology for detection of free bilirubin in plasma or serum, especially in the newborn, has become important from the standpoint of concurrent drug administration. Published methods attempt to quantitate bilirubin in the presence of various drugs, and some of these methods are quite complex (47–51).

Although drugs may increase the free concentration of bilirubin, as already pointed out, a recent study (52) suggested that phototherapy in the case of hyperbilirubinemia did not increase the unbound fraction of bilirubin in blood. In fact, the bound fractions of both bilirubin and salicylate to albumin remained unchanged after phototherapy compared to prephototherapy levels.

CLINICAL SIGNIFICANCE OF PROTEIN BINDING

Most clinicians and pharmaceutical scientists believe that a drug's action is dependent on its concentration in plasma water. However, most blood level measurement methods include the amount of drug bound to plasma proteins as well as the free amount. The concept of a plasma therapeutic level is now becoming more important (53). Information on the changes in free and bound levels in the presence of various disease states is in its initial stages.

In Renal Dysfunction—Recent studies indicated that, for many drugs, the percent of therapeutic amounts of drug bound to albumin in the plasma was significantly reduced in patients with uremia (54). Patients with renal dysfunction have a higher incidence of adverse drug reaction. Drug dosage modification to obtain plasma therapeutic levels appears most beneficial in patients with these abnormalities of drug excretion. The dosage modification in uremic patients was quantitated using a one-compartment model to predict changes in the elimination rate constant of drugs (55).

The protein binding of phenytoin (diphenylhydantoin) in the uremic patient has been well studied. Phenytoin binding was reduced in such patients, and this reduction was not strongly dependent on concentration of albumin or total protein (56). It was suggested that there had been a qualitative change in the drug binding proteins in uremic patients. The decrease in drug binding was not due to the presence of dialyzable substances in the plasma.

Blum *et al.* (57) concurred with these results and also showed that the principal metabolite of phenytoin was not responsible for a competition phenomenon and therefore could not be decreasing phenytoin binding. They postulated that the free plasma concentration of phenytoin may have been much lower in the uremic patient than in a normal individual, yet adequate seizure control was maintained. To the contrary, Andreasen (58) found phenytoin to have increased binding after dialysis of the plasma proteins from both normal and uremic individuals. He concluded that: (*a*) a competing substance of molecular weight greater than 700 may have been present (nondialyzable in his experiments), (*b*) some very strongly bound small molecules may have been present, or (*c*) alterations in the macromolecules may have been involved. Shoeman *et al.* (59) also suggested a qualitative difference in the albumins of normal and uremic patients.

Other studies showed decreased phenytoin binding in patients with renal abnormalities (60–62). In an excellent comparative study (62), it was pointed out that both normal and uremic patients should have about equal levels of unbound drug in plasma, provided tissue binding has not changed. The total plasma phenytoin concentration would, however, be decreased since there was a smaller amount of protein-bound drug and therefore a shift to a new equilibrium amount. The investigators stated that decreased plasma protein binding in uremic patients would potentiate pharmacological effects only if the drug was highly protein bound in normal subjects and, thus, minimal free drug levels were required for the principal pharmacological action. They further stated that monitoring of the plasma levels of drugs in uremic patients should be combined with the knowledge of the extent of the drug's binding to plasma protein. A more recent study (63) provided information on phenytoin binding to blood cells and showed that the distribution of drug in whole blood was different in the uremic *versus* the healthy subjects.

The binding of sulfamethazine to albumin was reduced in six nephrectomized patients (64). Dialysis of the patient blood did not increase the *in vivo* binding capacity over nondialyzed blood samples, supporting the belief that a defect in the binding properties of serum albumin existed in uremic patients. Also, a study of furosemide binding in patients with acute renal failure seemed to support the possibility of a defective drug binding mechanism (65, 66). The furosemide binding affinities determined in these two studies were in close agreement.

In the case of diazoxide in uremia (67), it appeared that the main determinant of decreased binding was the reduction in serum albumin concentration. Likewise, morphine binding was reduced in patients with renal failure and was shown to be dependent on the concentration of total serum proteins and albumin but not on the severity of renal dysfunction measured by creatinine clearance (68). Other studies were conducted with phenylbutazone (69) and cardiac glycosides (70, 71) in the plasma of uremic patients, and similar reductions in binding in uremic conditions were found.

The pharmacokinetics of trimethoprim, sulfamethoxazole, and cefazolin were studied in normal and uremic patients (72, 73). The distribution of free sulfamethoxazole in tissues increased during renal insufficiency, and this result was suggested to be due to reduced protein binding. However, no change in tissue distribution was seen for trimethoprim. With cefazolin, higher serum levels were observed in uremic subjects after identical doses to uremic and normal subjects, and serum half-lives increased with decreasing renal function. The apparent volume of distribution of cefazolin was elevated in the uremic state, probably due to decreased protein binding.

Campion (74) and Dromgoole (75) examined the reduction in binding of dyes during renal failure. Both found a decrease in binding; but while Campion determined that the decrease was unrelated to competition with metabolites, Dromgoole suggested either competition or conformational changes in albumin as the reason for the reduction. The binding of drugs, essential amino acids, and waste metabolites was investigated in normal and uremic subjects (76). Binding was reduced in the uremic subjects in all cases.

In Hypoalbuminemia—Generally, the concentration of albumin or total protein is decreased in various chronic diseases. Therefore, the unbound fraction of most drugs could be elevated; that is, the concentration of drug in plasma water could be increased. The intensity of drug effect may become greater than expected and may fall into the toxic range, as was documented in the case of phenytoin (77). Phenytoin was extensively bound to albumin and had increased adverse reactions when decreased serum albumin levels were present. A similar explanation was advanced for toxicity due to prednisolone, the major metabolite of prednisone (78).

Perhaps the best *in vivo* correlation of serum protein concentration and adverse drug reaction was reported by Greenblatt and Koch-Weser (79). In more than 1200 patients monitored while receiving diazepam, adverse reactions ranged from 2.9% in patients with normal serum albumin concentrations ($\geq$4.0 g %) to 9.3% in those with hypoalbuminemia (<3.0 g %). Similarly, methadone has a large variation in its binding fraction as a result of varying albumin levels in patients (80).

Another study (81) examined diluted serum from two subjects with regard to its binding of four drugs. In all cases, the amount of unbound drug increased as the albumin concentration was diminished. It was recommended that the albumin concentration be determined when examining plasma drug levels.

Wosilait (82) computed the theoretical amount of free drug in the plasma at various clinical concentrations of a number of drugs and at levels of albumin ranging from 2 to 5 g %. His results implied that the amount of free drug increased significantly in hypoalbuminemia and that care should be exercised when using highly protein-bound drugs in patients with decreased albumin levels.

In Liver Dysfunction—The influence of liver disease on the binding and kinetics of drugs in humans has received limited attention. Some reported results conflict as to the importance, if any, of drug–protein binding in hepatic dysfunction. The binding of five drugs to plasma proteins from patients with alcoholic liver disease was studied (83). The data for basic drugs indicated that liver disease decreased binding. With quinidine, the unbound fraction increased three times over normal amounts, an elevated level that may be clinically significant. For the organic bases studied, the decreased binding was most sensitive to decreased levels of serum albumin. Since cir-

rhotic patients have lower albumin concentrations, they consequently should have increased fractions of unbound drug. The data presented for acidic drugs lacked correlation with liver disease or albumin levels.

The percentage of unbound phenytoin increased by about 33% in five patients with acute viral hepatitis (84). In patients with hepatic dysfunction, monitoring plasma drug concentrations was the best means for adjusting dosages and schedules. The unbound phenytoin fraction in patients with hepatic disease increased by about 50% over that in normal healthy individuals (61). These changes in protein binding correlated better with changes in albumin and bilirubin levels in plasma than with any of 13 other biochemical parameters monitored. The binding of both morphine and phenytoin was decreased in liver failure (66). The binding depended on albumin concentration, but more data are needed to assess the effect of liver dysfunction on protein binding.

The degree of protein binding of amobarbital was reduced in five chronic liver disease patients who also had abnormally low serum albumin levels but was normal in five chronic liver diseased patients with normal serum albumin concentrations (85). Meperidine disposition and elimination were examined in patients with acute viral hepatitis (86). The significant increase in plasma half-life in patients with hepatitis was tested against protein binding of meperidine in normal *versus* hepatitis patients. The binding of meperidine was about equal in both groups; although elimination was significantly impaired in acute viral hepatitis, the effect seemed independent of protein binding.

Likewise, the effect of cirrhosis on the disposition and elimination of clindamycin was examined (87) and compared to normal individuals. Although the half-life was prolonged in the cirrhotic condition, the effect of clindamycin protein binding was about equal in both groups. The effect of liver disease in patients taking diazepam was studied (88). Plasma protein binding of diazepam in cirrhosis was decreased compared to that in normal subjects.

In Neonates—The neonate may respond quite differently than adults to drug substances (89). Drug binding to plasma proteins is of special interest in the neonate due to its regulatory effect on pharmacodynamic processes. Neonatal distribution, metabolism, and excretion processes differ from adults partly because infants have a greater total body water and lower fat content. This composition difference is larger and of extreme importance in premature infants.

The binding of phenytoin, salicylate, and nafcillin to plasma protein from newborn infants was investigated (90). The unbound fraction of phenytoin was significantly greater in neonates than adults, and the percentage of unbound drug correlated with the serum bilirubin level, suggestive of a possible competition phenomenon. Likewise, salicylate binding differed in the newborn as compared to adults. Nafcillin binding in the neonate exhibited large reductions from amounts bound to adult serum, and the levels of unbound drug were much higher. In a more recent paper (91), the low degree of nafcillin binding suggested that albumin was not the primary binding protein for this drug. Diazepam binding to neonatal and adult serum proteins also was discussed; in this case, the same binding affinity was observed with both the adult and newborn proteins.

Two studies (92, 93) compared the binding of some drugs to adult, fetal, and neonatal plasma. Both studies found reduced binding capacity in the newborn as compared with plasma from adults. Differences in the total protein concentration between these two age groups may have been responsible for the binding disparity. Hyperbilirubinemia further decreased the binding capacity. Data were given for phenytoin, imipramine, diazoxide, and cephalothin (92) at levels comparable to therapeutic concentrations; neonatal binding was reduced by 4–12% compared to adult plasma in all cases.

It was similarly reported (94) that drugs were less bound in newborn than in adult plasma, but this study also fractionated the plasma from each group into albumin and globulin fractions. With the six drugs studied, no difference was found in binding in the albumin fraction of newborn or adult plasma; however, binding to the globulin fraction was less in the newborn than in adults. Three possible mechanisms were suggested for the observed binding disparities: (*a*) a bilirubin competition phenomenon, (*b*) the decrease in globulin–drug interaction, and (*c*) the possibility for less drug binding due to albumin–globulin interaction in the plasma of the newborn.

A binding disparity between maternal and fetal plasma protein affinities for bupivacaine also was reported (95). Maternal protein bound approximately twice as much drug as did fetal protein on a per gram basis. The drug concentration was in the therapeutic range of 0.05–5.0 μg/ml, and the binding decreased from 92–78% to 35–31% in the maternal and fetal plasma, respectively. However, Gorodischer *et al.* (96), in an attempt to rationalize high digoxin doses in infants, reported that at therapeutic levels the affinity of digoxin for cord serum was low and about equal to that in adult serum. The higher therapeutic concentrations of digoxin in infants probably are a result of a higher dose (per unit body weight or surface area) than in adults. The pharmacological basis for the traditionally used high doses of digoxin in infants cannot be rationalized as due to binding differences, and more work is required.

In a study of hydrocortisone binding to plasma proteins from maternal, fetal, and infant plasma, a large difference was found in the binding capacity of maternal and fetal plasma (97). That this result might be due to a physicochemical difference in the respective proteins was deemed unlikely because the binding or affinity constants (K_a) were similar ($5–8 \times 10^8\ M^{-1}$) in all blood compartments examined. It was also reported (98) that the binding proteins in the maternal compartment may be highly active in the control of steroid metabolism. This report (98) found that, in comparison with nongravid women, fetal and neonatal steroid serum binding protein concentrations were one-thirtieth in the 5th month of gestation, one-twentieth immediately postpartum, and at normal adult nongravid levels 1 month postpartum.

In attempts to understand the binding disparity of phenytoin in neonatal and adult stages, it has been suggested (99) that there are large variations in circulating free fatty acids during the neonatal period and that the differences in both the acids present and their concentrations can influence the degree of drug binding during this period.

In plasma from newborn infants, phenytoin binding correlated with the albumin concentration and with the concentration ratios of bilirubin and free fatty acid to albumin. A reasonable correlation coefficient for phenytoin binding was obtained when compared to the ratio of total plasma bilirubin and albumin concentrations in infants (100).

RESULTS OBTAINED WITH PARTICULAR DRUG CLASSES

Antibacterial Chemotherapeutic Agents—*Penicillins and Cephalosporins*—A paper dealing with the pharmacological effects of the binding of various antibiotics (101) noted that, although most penicillins are bound by serum proteins, in only a few cases does this binding exceed 80%. (This percentage figure is misleading, because it is definitely related to some specific concentration or at least a concentration range.) Consequences of extensive binding of antibiotics by serum proteins may be interference with biological activity, delayed renal excretion, reduced urine concentration, restricted distribution volume, and decreased penetration of drug into intracellular spaces or inflammatory fluids. These effects were examined in relation to the binding of antibiotics by serum proteins and other endogenous substances. It was concluded that serum protein binding exerted an effect on these parameters and that this effect was particularly important for penicillinase-resistant penicillin and newer analogs of tetracyclines. Also included in this paper was a tabulation of binding percentages for various penicillin and tetracycline analogs.

In a study of six antibiotics, binding was well correlated with the ability of antibiotics to diffuse into interstitial fluid (102), as suggested previously. By using an *in vivo* skin chamber device, antibiotics with lower percentages of protein binding were found to diffuse into the interstitial fluid better than those with high binding percentages. Floxacillin (flucloxacillin), 95% of which is bound to protein, exhibited no detectable interstitial fluid levels. Also, increased protein binding influenced the renal clearance of four penicillins inversely (103).

Using a diafiltration technique to examine the association–dissociation rate of drug–protein interactions, a question about which information is still scarce, Barza *et al.* (104) presented data for oxacillin, nafcillin, and cephalothin. The binding of all three antibiotics was rapidly reversible and complete. The results of their experiments, in terms of percentages bound, are included in Table I, along with the results of some other papers having protein-binding data on penicillin and cephalosporin drugs.

In another study designed to demonstrate the reversible-ion binding between a series of penicillins and bovine serum albumin (105), the penicillin side chain had considerable influence over the binding process. According to the reactions of hydrated electrons produced by pulse radiolysis, the binding of the first molecule of penicillin G (benzylpenicillin) or penicillin V (phenoxymethylpenicillin) resulted in a greater decrease in protein reactivity towards e_{aq}^- than succeeding molecules. The results were interpreted in terms of the carboxyl group of penicillins interacting with cationic sites on the protein; however, other short-range weak forces may be significant.

In a study of the pharmacokinetics of various cephalosporins compared to cefazolin (106), extensive binding of a few congeners to serum protein took place. This degree of binding (Table I) apparently affected the serum half-life, the renal clearance, and the apparent volume of distribution of these drugs. Cefazolin, the most highly bound cephalosporin, had the lowest distribution volume, a result also obtained by other workers (110). In a study of the levels of ampicillin and cloxacillin in synovial fluid of arthritic patients, the non-highly-bound ampicillin reached about the same concentration in synovial fluid as in serum; the highly bound cloxacillin had synovial fluid levels much lower than serum levels (111). A rapid equilibrium apparently was established between the free concentration of cloxacillin in serum and synovial fluid. The primary effect of binding was to confine the drug to the vascular fluid. Distribution to other fluids was governed by levels of free drug in serum and not total levels. Along these same lines, a wide variation was found in the clearance of seven antibiotics by an artificial kidney (112). These differences were attributed to the variation in protein binding among the antibiotics.

Table I—Penicillin and Cephalosporin Antibiotic Binding to Human Serum

Antibiotic	Antibiotic Concentration, μg/ml[a]	Percent of Antibiotic Bound[b]	Reference
Oxacillin	20 (99)	85.2 (83.5)	103
Nafcillin	20 (100)	87.2 (80.5)	103
Cephalothin	10 (40)	57.0 (53.9)	103
Carbenicillin	80	50	107, 109
Ticarcillin	124	65	107
Penicillin V	30 (60)	52.7 (45.2)	108
Cefazolin	30	86	106
Cephanone	30	88	106
Cephaloridine	30	20	106
Cephalexin	30	15	106
Cephalothin	30	65	106
Cephradine	86.9	12.5	110
Ampicillin	—	13.5	111

[a] Number in parenthesis denotes second concentration of drug used in the literature report; results for this concentration are given in parenthesis in percent bound column. [b] Results are given in terms of percent of drug concentration bound. The serum consisted of 100% human serum or 100% pooled human serum.

Tetracyclines—A quantitative study of the interaction of therapeutic concentrations of tetracycline with human serum proteins was reported (113). In serum, 53% of tetracycline was complexed with various proteins and just over half of that amount was with albumin (most of the rest being associated with lipoprotein fractions). The results showed that tetracycline bound to two sites on albumin. The high affinity site had an association constant of $4.38 \times 10^4\ M^{-1}$ but very limited capacity (0.032 site/mole of albumin); the low affinity site exhibited a binding constant of $1.01 \times 10^2\ M^{-1}$ but had 39.50 sites associated with it. The physical meaning of having less than one-tenth of a binding site per mole of albumin was not discussed and was quite confusing to the reader. Such a minute number of sites on a large globular protein is difficult to envision.

The binding of tetracycline and various analogs to human serum albumin was examined using a probe displacement technique (114). Methacycline displaced the greatest amount of probe followed, in order, by doxycycline, chlortetracycline, oxytetracycline, and tetracycline. The association constants are included in Table II. As with

Table II—Literature Values for the Binding of Tetracycline Antibiotics to Serum Albumin

Tetracycline Analog	Primary Binding Constant or Percentage Bound	Number of Binding Sites or Concentration of Tetracycline	Reference
Tetracycline[a]	$4.38 \times 10^4\ M^{-1}$	0.032	113
Tetracycline[a]	$3.15 \times 10^4\ M^{-1}$	—	114
Oxytetracycline[a]	$3.53 \times 10^4\ M^{-1}$	—	114
Chlortetracycline[a]	$4.03 \times 10^4\ M^{-1}$	—	114
Doxycycline[a]	$5.32 \times 10^4\ M^{-1}$	—	114
Methacycline[a]	$6.28 \times 10^4\ M^{-1}$	—	114
Oxytetracycline[a,b]	$4.44 \times 10^3\ M^{-1}$	0.27	115
Demeclocycline	38%	10 μg/ml	116
Oxytetracycline	31%	10 μg/ml	116
Doxycycline	52%	10 μg/ml	116

[a] The tetracycline concentration was varied over a wide range, and more than one protein concentration was used in most cases. [b] Study used bovine serum albumin; 50% of the drug was bound at therapeutic concentrations.

other probe studies, the number of binding sites associated with these binding constants cannot be calculated. However, the technique was confined solely to the number of sites upon which the probe itself was bound. A drug binding at a site different than the probe may not have been detected. In addition, the possibility of probe-caused conformational changes in the protein structure was not, or cannot be, accounted for with such a technique.

Aminoglycosides—Conflicting reports concerning aminoglycoside antibiotic binding exist. The problem seemingly arose due to the ion content of the buffers used in various studies. For example, human serum binding of gentamicin, tobramycin, and kanamycin was about zero whereas streptomycin was about 35% bound (117). The system was not described except that a physiological pH was used with an ultrafiltration method.

In contrast, at gentamicin concentrations between 1.7 and 8.9 μg/ml (therapeutic levels of this antibiotic), 70% was bound to human serum albumin (118, 119). When the concentration was increased to 10–20 μg/ml, the binding of gentamicin was decreased to about 50% (118). Similar results were obtained for tobramycin, sisomicin, kanamycin, and amikacin; they were bound to the extent of 75, 85, 54, and 69%, respectively, at therapeutic levels. However, under *in vivo* conditions, these binding levels would not be expected to be reached; these values were obtained in 0.05 *M* tromethamine–hydrochloric acid buffer, which was void of any divalent cations. As levels of Ca^{2+} and Mg^{2+} increased, the binding of these agents decreased (118). The variations reported for *in vitro* experiments might carry over to the *in vivo* situation only under certain pathological conditions.

Another conflict arose from the results of a report comparing the pharmacokinetics of kanamycin and amikacin (120). Only 3.6% binding of amikacin could be detected when 15 μg of drug/ml was present in an *in vitro* system. This figure was about 200% less than the results reported previously (118).

Erythromycin, Lincomycin, and Clindamycin—Few papers have been published since 1969 concerning the binding of these drugs to human serum albumin. Prior to 1969, various reports stated that these molecules bound with high affinity while other papers indicated that only a low binding of these drugs occurred.

The binding of these three related antibiotics to serum albumin was studied using an ultrafiltration technique (121) (Table III). Also included in this work was a discussion of erroneous techniques and conclusions that resulted in some previously reported low levels of binding of these drugs. In a report examining the protein binding influence on the relative merits of the blood levels produced by erythromycin stearate and erythromycin estolate (erythromycin propionate lauryl sulfate) (122), doubts were raised as to the ability of blood levels to predict the effectiveness of these two forms of the same drug. Of utmost importance, in the author's opinion, was that the unbound levels of the estolate form were significantly lower than the unbound parent drug levels, even though total levels were higher. Thus, the difference in serum levels produced by the two forms of erythromycin reflected the difference in protein binding (Table III). It was suggested that unbound drug was a better measure of activity in the case of erythromycin congeners (122).

Table III—*In Vitro* Human Serum Binding of Erythromycin, Lincomycin, and Clindamycin[a]

Antibiotic	Percentage Bound	Antibiotic Concentration, μg/ml	Reference
Erythromycin base	73.4	5	121
	81.4	0.59–2.87	122
Erythromycin propionate	92.6	5	121
Erythromycin estolate	95.7	0.94–4.05	122
Lincomycin	71.9	5	121
	57	1	123
Clindamycin	93.6	5	121
	93	1	123

[a] Protein consisted of human serum (in a few cases pooled). The results reported are with 100% human serum, although some studies also used 25, 50, and 75% serum solutions.

Sulfas—In a series of articles dealing with drug–macromolecule complex formation, sulfa drug–albumin interactions were studied (124–127). For the many sulfas studied, the binding was considerably greater for the ionic form of the drugs than for the nonionized form. Also, two sets of binding sites apparently existed on albumin for most of these agents. Various drugs, such as phenobarbital and penicillin V (phenoxymethylpenicillin), were able to compete for these sulfa binding sites. Some of the binding data results are given in Table IV.

Table IV—Literature Parameters for Sulfa Drug Binding by Human Serum Albumin

Agent[a]	Primary Binding Affinity	Number of Binding Sites	Reference
Sulfadiazine	$3.6 \times 10^3\ M^{-1}$	1	125
Sulfamerazine	$2.9 \times 10^4\ M^{-1}$	1	125
Sulfamethazine	$4.4 \times 10^4\ M^{-1}$	1	125
Sulfameter	$5.9 \times 10^4\ M^{-1}$	1	125
Sulfadimethoxine	$1.8 \times 10^5\ M^{-1}$	1	125
Sulfisomidine	$5 \times 10^3\ M^{-1}$	1.1	128
Sulfamethomidine	$1 \times 10^4\ M^{-1}$	2.1	128
Sulfaortho-dimethoxine	$1.25 \times 10^4\ M^{-1}$	2.1	128
Sulfadimethoxy-pyrimidine	$4 \times 10^3\ M^{-1}$	2.2	128
Sulfadimethoxine	$1 \times 10^4\ M^{-1}$	1.9	128
Sulfaethidole[b]	1.2×10^5 liters/mole	1 primary (3 secondary)	129
Sulfathiazole[b]	2.96×10^3 liters/mole	1.98 primary (9.77 secondary)	130

[a] The concentration of drug used for these data varied over a wide range; the albumin concentration was also varied in most cases. [b] Study used bovine serum albumin.

The influence of sulfa drug binding on the excretion of two very long-acting, two long-acting, and one short-acting sulfa drugs was reported (128). The short-acting agent was bound to a lesser extent at clinical concentrations, and only a single binding site was evident for this drug in contrast to the two sites for the other sulfas. Small changes in sulfa drug structure may have altered plasma protein binding. At the plasma concentration of 0.4 mM, which is within the therapeutic range of these drugs, the short-acting agent was 67% bound whereas the longer acting drugs were 90–96% bound.

Perrin and Nelson (129), using the highly specific direct technique of induced optical activity, especially appropriate at low levels of added drug, found that with sulfaethidole only the single high affinity site was being examined by their method. Dialysis investigations had shown two classes of binding sites and thus made drug competition examination difficult. A primary binding affinity of 1.2×10^5 was obtained for sulfaethidole binding to bovine serum albumin. Binding constants of various drugs competing for the sulfaethidole binding site were reported.

Recently, the binding of sulfathiazole to bovine serum albumin and other blood constituents was examined (130). The results for serum albumin are included in Table IV. Also, some interesting possibilities were offered to explain unusual binding data. Data treatment of binding may be altered in whole blood systems, so normal methods to characterize the data may be inappropriate in these instances.

Rifampin—The binding of rifampin (rifampicin), a semisynthetic antibiotic with a broad antibacterial spectrum, often used as an antituberculous agent, has been examined (131–135). Rifampin concentrations ranging from 0.8 to 1000 μg/ml were used, and all studies except one (134) showed the drug to be 70–91% bound. This extent of binding resulted from using human and bovine serum as well as the albumin fractions of each. The report with percentage binding outside this range used human serum and a rifampin concentration of 10 μg/ml in an equilibrium dialysis investigation (134). The binding was 8–41%; however, these results are confusingly reported as rates of binding.

In one study (135), binding was examined in healthy volunteers (mean 88.9% bound) as well as in tuberculous patients (mean 86.1% bound). The difference between these two groups was significant, but the binding of rifampin to plasma proteins was of relatively minor importance clinically.

Anticoagulants—The interaction of warfarin and dicumarol with human albumin has been the subject of many investigations. This is to be expected since the relatively low therapeutic index of these agents and the propensity for other concurrently administered drugs to displace small amounts of the anticoagulants from their binding sites raise free drug levels and possibly increase prothrombin time.

O'Reilly (136–138) found that warfarin was bound to albumin with an affinity constant of $2.17 \times 10^5\ M^{-1}$ at 37° (137) and that the 6-, 7-, and 8-hydroxy metabolites showed a 7–23-fold reduction in binding (136). These data (136) suggested that the interaction was exothermic and had a positive entropy and that the albumin–drug interaction was probably the result of cooperative hydrogen bonding–hydrophobic forces. Recent studies (139, 140) discussed the effect of protein binding of warfarin in rats related to its pharmacological action, distribution, and elimination. A substantial variation was found in the free fraction of drug in the serum, and strong correlations were observed between the free serum fraction and the elimination rate constant, the volume of distribution, and the total plasma clearance of the drug. The amount of total warfarin required to elicit a specific anticoagulant response varied widely between animals, and this response was a function of free warfarin levels in plasma (140).

An investigation of warfarin and dicumarol interaction with human serum albumin was reported using a circular dichroic technique (141). Warfarin, in contrast to dicumarol, gave no induced Cotton effect, suggesting a different mode of binding for the two anticoagulants. On the other hand, another study (142) found that warfarin was capable of generating extrinsic Cotton effects and that the binding constant could be calculated from such data. Based on equilibrium dialysis data, Chignell (141) also reported that dicumarol (bishydroxycoumarin) was bound to human serum albumin at three primary homogeneous sites and exhibited a binding constant of $2 \times 10^5\ M^{-1}$. However, he also studied the interaction by monitoring the quenching of the single tryptophan residue of human serum albumin and concluded that one primary binding site existed with a binding affinity of $5.2 \times 10^5\ M^{-1}$. In addition, he showed that the dicumarol–albumin interaction gave rise to large negative extrinsic Cotton effects. Thus, it was proven that the interaction could be studied by the circular dichroic technique, but no quantitative attempt was made.

Recently, a report (32) appeared using this sensitive circular dichroic method for low dicumarol to protein ratios (*i.e.*, those of clinical significance), and a binding constant of $2.9 \pm 10\% \times 10^6\ M^{-1}$ at the single high affinity site was calculated. Results from dicumarol displacement studies using other acidic drug molecules are contained in the same report (32). A competition between warfarin and dicumarol for a human albumin binding site also was shown.

A computer program was used to determine the binding capacities, association constants, and amounts of unbound and bound dicumarol at different drug levels as well as at various levels of protein concentrations (143–145). An association constant of 2.2×10^6 liters/mole containing two homogeneous sites was reported. A second class of seven sites with a binding constant of 1.3×10^4 liters/mole also was determined (144), and for warfarin a primary binding affinity of 8.9×10^4 liters/mole at two equivalent binding sites was found.

Warfarin, dicumarol, sulfonamides, and other acidic drugs may share the same binding site on albumin (146). However, such acidic drug competition may not always be the case. A recent report dealt with the lack of interaction between warfarin and ibuprofen (147). Ibuprofen, an acidic drug bound to plasma protein when administered alone, failed to inhibit competitively or to interfere with warfarin binding, thus producing no alteration in the degree of hypoprothrombinemia.

Antiepileptics—Phenytoin has been well studied with respect to its protein binding and pharmacokinetic characteristics. In normal human plasma, 92.6% of the drug was bound at a therapeutic concentration of 16 μg/ml using an

ultrafiltration technique (148). No binding differences were found with respect to sex, and there was a 64% increase in the unbound fraction of drug at 37°. Thirteen drugs were also examined as to their propensity to affect phenytoin binding. Only salicylic acid, sulfisoxazole (sulfafurazole), and phenylbutazone were able to increase the unbound fraction of phenytoin. In another study (149), phenytoin was extensively bound to both human and rat albumin and the major metabolite (the 5-*p*-hydroxy species) was also strongly plasma protein bound. The binding levels of both the parent compound and the metabolite were suggested as possible explanations of the species selectivity in the drug-induced toxicity observed.

A study was designed to examine the protein binding of phenytoin in eight patients with epilepsy and in drug-free volunteers as well as to determine total drug in plasma and cerebrospinal fluid (150). Only minor variations were seen between individuals in each group. The mean unbound fraction of phenytoin in patient plasma was 6.3% at room temperature and 10.3% at body temperature at a mean drug level of 11.2 μg/ml. The ratio of total phenytoin in cerebrospinal fluid to that in plasma in the eight patients was unusually constant with a mean of 9.6%. A comparison between the unbound fraction of phenytoin in plasma and the same cerebrospinal fluid to plasma ratio exhibited a good correlation, a result not unexpected since only the unbound fraction of drug was available for equilibration.

Phenytoin binding was examined to determine if individual differences in the degree of protein binding might explain the variance between total serum levels and clinical intoxication (151). Adverse clinical symptoms were better correlated to free levels of the drug than to total serum concentration. When free phenytoin levels were above 5 μg/ml, signs of intoxication would probably be present no matter what the total serum level. These individual variations in ability to bind this drug may have been due to a qualitative change in the drug binding proteins (152). In a study of plasma from 11 different species of mammal, such a change in binding proteins was observed.

For highly bound phenytoin, the unbound plasma level can be readily obtained in the clinical laboratory by measuring the red blood cell to plasma concentration ratio of an unknown sample (153). The red blood cell binding to plasma binding ratio was constant throughout therapeutic plasma phenytoin levels. As a result of this finding, one could readily individualize drug dosage and minimize adverse effects. A recent paper (154) concerned with phenytoin effects and plasma protein binding reported that, in rats, prior treatment with phenylbutazone had no effect on the potency of unbound phenytoin. Thus, the action of this antiepileptic depends upon the unbound concentration in plasma and not upon dose or total plasma concentration. These results agree well with those previously described (151–153).

A recent abstract (155) further supported the idea of binding when more than one highly bound drug was present. Diazoxide lowered the phenytoin binding levels, requiring considerable dosage adjustment. Concurrent drug administration may also have changed the rate of drug metabolism, further necessitating dosage adjustment.

The protein binding of the antiepileptic carbamazepine was the topic of two recent investigations (156, 157). Carbamazepine had a low association constant for albumin (1.35×10^3 liters/mole) at approximately one site per mole (156). For therapeutic concentrations of drug (5–30 μg/ml), the unbound fraction was 24% following ultrafiltration of plasma samples from six volunteers. The results from an excellent study (157) confirmed this observation of the unbound fraction. A linear relationship was observed between unbound and total drug throughout the therapeutic region of 5–50 μg/ml. Carbamazepine binding in 54 plasma samples from treated patients was examined with the result that 26.9% of the drug was found to be unbound. Erythrocyte uptake, measured in 23 of these patients, was 38.3% of the plasma levels. Six other anticonvulsants were examined at high therapeutic concentrations for effects on carbamazepine binding and were shown not to alter carbamazepine free drug levels significantly. Also, no difference was seen when renal disease was present and only a slightly lower percentage of carbamazepine was bound if the patient had hepatic dysfunction.

Antihypertensives—The binding of diazoxide to human albumin was investigated, and the binding accounted for its long half-life. At 37°, the dissociation constant for the diazoxide–albumin interaction was $5.2 \times 10^5\ M^{-1}$, with 1.2 sites exhibiting this constant. At pH 7.4, the free energy change upon binding was −5.9 kcal/mole and was accounted for from hydrogen and ionic bonds (158). Protein binding may be implicated in the kinetics of the diazoxide effect (159). A rapid intravenous injection produced an effective hypotensive action, whereas injections lasting longer than 1 min greatly reduced the intensity. At therapeutic concentrations, 97.6% of the drug was in the protein-bound form, so free diazoxide reached effective levels at the arteriolar wall only during rapid injection. These results duplicated those of Andreasen (160).

Propranolol binding was studied and related to its disposition in humans (161–163). At therapeutic concentrations, 93.2% of the drug was bound to human plasma (163); the volume of distribution increased as the free propranolol fraction in the blood increased (162). However, the ratio of the volume of distribution to the free drug was relatively constant. After examination of propranolol binding in four species (humans, monkeys, dogs, and rats) as well as the clearance, half-life, and volume of distribution, it was concluded that increased drug binding was associated with a decrease in drug half-life when the influence of variable drug clearance was accounted for. Differences in binding were responsible for interindividual variations in the half-life of the drug in humans after intravenous administration. This was the result of an increase in the rate of drug delivery to the elimination sites (163). Human albumin (5%) alone accounted for only about 50–60% of the binding to plasma over the drug concentration of 1–10 μg/ml. Similarly, serum albumin alone accounted for only 42% of propranolol binding at drug concentrations less than $1 \times 10^{-4}\ M$ (164). From these data, an intrinsic binding constant of very low magnitude was calculated for propranolol (about 120 liters/mole). The binding of the β-adrenergic receptor antagonists alprenolol, its 4-hydroxy derivative, and a chemically related compound metoprolol[1]

[1] H 93/26.

Table V—Summary of Results Obtained from Investigations of Analgesic–Anti-Inflammatory Agent Binding to Plasma or Serum Albumin

Drug	Drug Concentration	Protein	Protein Concentration	Affinity Constant or Percent Bound	Number of Sites	Reference
Salicylate	50 μg/ml	Human plasma	5.3%	72%	—	166
Salicylate	50 μg/ml	Human albumin	3%	73%	—	166
Salicylate	Wide range	Bovine albumin	4%	5×10^4 liters/mole	1.04	130
Salicylate	Wide range	Human albumin	0.7%	$2.19 \times 10^5\ M^{-1}$	4	169
Salicylic acid	$0.002–5 \times 10^{-3}\ M$	Human albumin	0.3%	$7.07 \times 10^4\ M^{-1}$	1.28	168
Indomethacin	$0.002–2 \times 10^{-3}\ M$	Human albumin	$1 \times 10^{-4}\ M$	$8.4 \times 10^5\ M^{-1}$	4–5	169
Indomethacin	57–756 μg/ml	Human plasma	2.35%	$3 \times 10^5\ M^{-1}$	1	174
Phenylbutazone	Wide range	Human albumin	$1 \times 10^{-5}\ M$	$1 \times 10^5\ M^{-1}$	1	177
Fenoprofen	40 μg/ml	Human albumin	$7.1 \times 10^{-5}\ M$	$3 \times 10^4\ M^{-1}$ (>99% bound)	4–5	180
Fenoprofen	$0.075–37.9 \times 10^{-5}\ M$	Human albumin	$7.25 \times 10^{-5}\ M$	$1.86 \times 10^5\ M^{-1}$	1	181
Pentazocine	—	Human plasma	—	61.1%	—	182
Diftalone	Wide range	Human albumin	$2.5 \times 10^{-5}\ M$	3.85×10^4 liters/mole	1.38	183
Methadone	$0.006–2.87 \times 10^{-5}\ M$	Human plasma	—	83–87%	—	185
Morphine	$1.3–1.7 \times 10^{-7}\ M$	Human albumin	4%	31.4 ± 1.4%	—	187

also was studied. Alprenolol had about the same percentage binding and intrinsic constant for human serum albumin as propranolol; however, alprenolol was bound to a much higher extent in human serum *in vitro* (165).

Analgesic–Anti-Inflammatory Agents—Many of these agents have been examined for the intensity of their interaction with albumin or plasma. Some of these results are given in Table V.

Salicylic acid and its salts and aspirin have been the subject of many investigations, often with wide variations in results. Salicylate binding in the plasma obtained from six mammalian species was compared (166). After equalizing the protein concentration from each species, the binding was greatest in humans (72% at a drug concentration of 50 μg/ml). Salicylate bound to albumin was closely correlated with that bound to plasma in four species, including humans, but was not correlated in rats and dogs. Similar results were obtained for salicylate binding to adult plasma, but binding was progressively and perhaps significantly less in children (5–8 years) and newborns (to 5 days old) (167).

Cruze and Meyer (130), studying salicylate binding to bovine serum albumin and bovine plasma, found close agreement in the extent of binding for these two systems. Keresztes-Nagy *et al.* (168) examined the salicylate–albumin interaction by two methods and found results compatible with those of Cruze and Meyer (130). Another investigation of the salicylic acid–human albumin interaction found four strong primary binding sites exhibiting an affinity constant of about 2.19×10^5 (Table V) (169). The culmination of such *in vitro* binding experiments can be seen in a report by Levy and Yaffe (170), which pointed out the protein binding and dose-dependent change in the volume of distribution of salicylate. These data were used to explain the clinical severity of salicylate poisoning in cases of single-dose ingestion (171): once the binding capacity of available serum proteins was surpassed, the apparent volume of distribution increased and a given serum salicylate level reflected larger amounts of total salicylate in the body than at low doses. The larger volume of distribution possibly includes the central nervous system, which then may manifest toxicity.

Aspirin and salicylates also were examined from the standpoint of their effects on endogenous substances. The ingestion of aspirin caused a release of tryptophan from its serum albumin binding site (172). Subsequently, there was a decrease in bound and total serum amino acid levels, a rise in free levels of tryptophan, and an increased effect on tryptophan metabolism. Aspirin produced an increase in free 11-hydroxysteroids in an *in vitro* system employing human plasma (173). In summary, salicylate may not be highly protein bound, but the levels ingested may have some deleterious effects on the binding of concomitantly administered agents or on endogenous substances.

The interaction of indomethacin with human plasma protein was investigated at 37° using an ultrafiltration technique (174). A surprisingly high affinity constant was obtained for indomethacin (Table V), and plasma protein displayed one primary site and at least seven secondary sites for the drug. Displacement of albumin-bound indomethacin was also investigated. Hvidberg *et al.* (175) found about 90% indomethacin binding to human plasma over the therapeutic concentration range of 0.5–10 μg/ml. From these data, they calculated an association constant of $8.6 \times 10^2\ M^{-1}$ with about 15 sites present on the albumin; however, this binding constant may be somewhat suspect in relation to other indomethacin binding studies due to the fact that only 4 hr was used for the equilibrium dialysis procedure and more time to equilibrate may be required. The indomethacin–human plasma interaction also was studied using an equilibrium dialysis procedure (176). The results showed plasma binding to an extent of about 75% at a drug concentration of $2 \times 10^{-4}\ M$.

The binding of phenylbutazone, flufenamic acid, and some of their analogs to human serum albumin was investigated using a circular dichroic method (177, 178). Based upon the induced Cotton effects and solvent perturbation studies, it appears that hydrophobic interactions, along with polar binding, were important for the phenylbutazone–protein complex (177). Likewise, these forces may play a major role in the flufenamic acid–albumin interaction. The primary association constant for flufenamic acid bound to albumin appears to be very large; when less than 2 moles of drug were bound per mole of protein, no free drug apparently existed (178).

The binding of the nonsteroidal anti-inflammatory drug fenoprofen (I) and some of its analogs to human serum

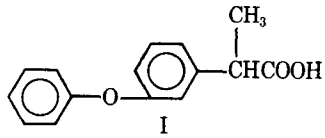

I

albumin was investigated using the circular dichroic technique (179). Fenoprofen was bound nonstereospecifically to albumin as a result of hydrophobic bonding of the aromatic rings and hydrogen bonding of the carbonyl and ether oxygen. Another study (180) found an association constant of about 3×10^4 for the fenoprofen–human albumin interaction. In an investigation of competition phenomena, only the highly bound phenylbutazone, in concentrations 10 times that of fenoprofen, was able to displace fenoprofen from human serum albumin. These data supported the binding constant data of Vallner (181) for the fenoprofen–human albumin interaction. He found a primary association constant of 1.86×10^5 liters/mole at a single site on albumin, indicating that displacement by added drugs would probably require a strongly bound agent.

In a study of the relationship of the nonsteroidal anti-inflammatory agent diftalone to its interaction with human serum proteins (183), the largest association took place with the albumin fraction, and an association constant of 3.85×10^4 liters/mole was calculated (Table V). The diftalone–albumin interaction was strongly temperature dependent. It was concluded that the binding was primarily due to either van der Waals or hydrophobic forces.

Recently, morphine, heroin, and methadone have been examined with regard to their plasma and albumin binding capacity. Initially, Olsen (184, 185) found that the percent of methadone bound to albumin was independent of drug concentration but dependent on albumin concentration. He obtained a range of 8.0–43.8% bound as the albumin increased from 0.4 to 5.0 g % (184). Subsequently, Olsen (185) examined the contribution of γ-globulin to the total amount of methadone binding and found a small addition of 13–17% bound to this macromolecule fraction. At therapeutic levels in human plasma, methadone was about 85% bound (185).

Morphine and heroin binding to human serum proteins and red blood cells was examined and found to be minimal (186). The morphine–plasma protein interaction also was investigated; morphine bound to albumin and γ-globulin (187). In the therapeutic range, 34.0–37.5% of morphine was bound to human plasma, with albumin accounting for the largest binding fraction. A recent report concerned the possible production of a morphine-binding globulin in subcutaneous pellet-implanted rabbits receiving narcotic drugs (188). Opiates could form specific protein conjugates, so binding to albumin may be minimal. The possibility that immunogenic drug–protein complexes were formed deserves further study.

Antitumor Agents—A paucity of information is available concerning the plasma protein binding of antineoplastic agents. Binding information coupled with pharmacokinetic data could be exploited advantageously in the clinical cancer chemotherapy setting. In a report (189) on protein binding and renal clearance data for methotrexate, the mean protein-bound methotrexate was 70% of the serum levels (in 15 patients) over the 90–200-ng/ml range. Alterations in renal clearance of the antimetabolite were affected by concomitant administration of organic acid drugs. These alterations may have been due to altered protein binding or renal mechanism and may be useful in the clinical situation. These results (189) were confirmed in a recent study (190) employing a different technique.

Camptothecin binding to various plasma proteins as well as to whole plasma has been investigated in various species including humans (191). This antitumor agent was extensively bound in human plasma: 98.3% at a drug concentration of 30 μg/ml. It also showed a high association constant, $7.9 \times 10^6\ M^{-1}$, for human plasma albumin at a single site on the macromolecule. Albumin, however, was not the only plasma protein with significant affinity for this agent. High binding levels in the human may be one reason that significant antineoplastic effects have not been seen, whereas this agent showed marked potential in the mouse but had a low binding affinity.

The binding of the antineoplastic agents vinblastine, vincristine, and colchicine to plasma and serum proteins was examined (192). These agents adsorbed to serum proteins, with the result that vinblastine and vincristine were about 75% bound while colchicine was 50% bound. Saturation of binding could not be shown with these drugs; however, it was evident that α- and β-globulins were the more important macromolecular serum species involved in the adsorption.

A subsequent study (193) showed that, although vinblastine binding in two patients was highest in their platelet fractions, red blood cells and white blood cells also accounted for significant binding. The extent of protein binding of this agent was not so great as to prevent rapid distribution into other body organs. A study (194) of the binding of a number of antineoplastic dinitrophenylaziridines found that the five congeners studied were weakly and reversibly bound to bovine serum albumin.

Barbiturates—Most protein binding work concerning these agents was done prior to 1969. However, the influence of pH on the bovine albumin binding of barbituric acid and amobarbital was evaluated (195). At pH 4, barbituric acid had an association constant of $1.6 \times 10^3\ M^{-1}$ for albumin; at pH 2, no binding occurred. According to the report, such behavior was consistent with an ionic mechanism of binding for this agent. Similarly, with amobarbital, no binding was evident at pH 5.8 but was detected at a higher pH.

In a subsequent study (196), the binding of amobarbital, pentobarbital, and phenobarbital to human albumin was examined over the pH range of 5.7–8.4; the ionized forms of these drugs were preferentially bound, with the primary binding constant ranging from 2.0 to 6.2×10^3. In a pharmacokinetic study of pentobarbital at therapeutic levels in seven human volunteers, little of this drug was associated with plasma protein whereas tissue binding was extensive (197). The large extent of tissue binding elevated the distribution volume such that it exceeded total body water. In another patient study (198), thiopental binding was better correlated with hemoglobin than with plasma protein levels. That such a conclusion was reached was not surprising since therapeutic levels of barbiturates do not seem to have a high affinity for albumin or other plasma proteins.

Cardiovascular Agents—An excellent study concerned the binding of digitoxin and digoxin and related cardiac glycosides and genins (199). Digitoxin in the plasma was bound almost exclusively by a single site on albumin and to the extent of 97% of concentrations ranging

Table VI—Literature Results of *In Vitro* Binding of Diuretics to Human Serum Albumin

Drug	Drug Concentration, μg/ml	Albumin Concentration, %	Binding Constant or Percent Bound	Number of Sites	Reference
Chlorothiazide	5–100	0.1–4	3–3.4 × 10^4 M^{-1}	1 or 2	208
Hydroflumethiazide	—	5	74%	—	209
Bendroflumethiazide	—	5	94%	—	209
Furosemide	3.4	5	97.2%	—	212

as high as 12 μg/ml. An association constant of 9.62 × 10^4 liters/mole at 37° was calculated. The digitoxin–albumin interaction was endothermic with a gain in enthalpy of 3.5 kcal/mole, a free energy change of −7.06 kcal/mole, and an entropy change of 33.8 cal/mole/°K. These results were suggestive of a hydrophobic mechanism between digitoxin and albumin. In contrast to digitoxin, only 23% of digoxin bound to albumin at concentrations up to 2 μg/ml. The binding differences for these two closely related drugs are reflected by higher plasma levels, lower urinary excretion rates, and a longer half-life of digitoxin compared to digoxin when these agents are administered to humans.

In other studies of digitoxin (200) and digoxin (201) binding to human serum proteins, digitoxin had a large association constant for albumin (K = 1–5 × 10^5 liters/mole), but the number of sites calculated was 0.5 in contrast to the 1.0 site seen previously. The binding was observed to be pH dependent; maximum binding occurred at pH 4.8. This finding might explain the somewhat lower binding constant observed by Lukas and DeMartino (199) who carried out their work at pH 7.4. For the digoxin–albumin interaction, Brock (201) found that increases in pH from 5 to 9 decreased the association constant from 8 × 10^2 to 1 × 10^2 liters/mole at 37°. The binding of these same two drugs was examined in a wide variety of mammalian species, and some substantial binding differences were noted, especially in the less tightly bound digoxin (202).

Two other studies (203, 204) on digoxin binding reported results contradictory to those given above. One study (203) found a total lack of protein binding of digoxin in human serum, and the other (204) showed that digoxin was about 30% bound in human serum using a wide range of digoxin concentrations. The calculated association constant was 6.8 × 10^4 liters/mole at an infinite number of digoxin sites on the albumin molecule (204). Seemingly, the binding constant calculated was larger than expected based on results of other studies and the low percentage binding in the plasma.

The antiarrhythmic drug quinidine was bound to albumin at two different classes of sites, and the primary binding affinity was 2.06 × 10^4 M^{-1} (205). Another study also examined the binding of quinidine to human plasma and human albumin (206). At a concentration of 1.6 × 10^{-5} M quinidine, 74% of the drug was bound to plasma and 71% to albumin. Like the previous study, two classes of sites on albumin were found, and the primary binding affinity was calculated to be 1.28 × 10^4. In the same study, binding of the new antiarrhythmic disopyramide had a lower binding affinity (4.6 × 10^3). A computer program was used to predict free and bound levels of quinidine, based on binding to albumin at two sets of sites (209). The analysis was limited to drug concentrations that may be obtained clinically (1–10 μg/ml). Over this concentration range, 74–88% of the drug would be predicted to be bound to serum albumin.

Diuretics—Relatively little work has been done concerning the binding of diuretic drugs to serum albumin since the Meyer and Guttman (1) review. A study of the binding of chlorothiazide to plasma proteins found that plasma binding was due almost entirely to the albumin fraction (208). At 37° with a 0.4% albumin solution and a drug concentration of 5–100 μg/ml, a maximum of 68% of chlorothiazide was bound; larger percentages of binding occurred at lower temperatures. Other binding data for diuretic agents are given in Table VI. In addition, it was found that the chlorothiazide–albumin interaction was accompanied by a negative entropy change and a relatively large change in enthalpy (208). It was suggested that the interactive force was due to nonionic bond formation.

Agren and Back (209), examining the binding of hydroflumethiazide and bendroflumethiazide to human serum albumin, found the primary binding affinity for hydroflumethiazide to be 1.8 × 10^3. For bendroflumethiazide, the affinity constant was 2.6 × 10^5 when the drug was ionized to 6.5% (at pH 7.35) and about 50 times less if 0.7% ionized. It was concluded that bendroflumethiazide was bound primarily by ionic bond formation. Another study (210) mentioned that bumetamide was 95–97% bound to human plasma protein *in vitro*.

Furosemide binding has been studied both *in vitro* and *in vivo* in cardiac patients and normal volunteers. In these individuals, the diuretic was bound exclusively to plasma albumin; at concentrations of furosemide from 10 to 400 μg/ml, 99.1–95.8% of the drug was bound (211). Similar results were observed using therapeutic concentrations of furosemide (212); phenytoin, phenobarbital, diazoxide, trifluoperazine, or chloramphenicol did not displace any furosemide.

Hypoglycemics—The natural hypoglycemic agent insulin has been studied in the serum of normal and diabetic patients. With a gel permeation method, addition of iodine-labeled insulin to normal human serum showed a binding of 4.3% if analyzed immediately and 5.4% if incubated for 24 hr (213). In contrast, these values were 37.7 and 66.9%, respectively, in insulin-treated diabetics. Another study (214) found that the binding of insulin to macromolecular serum proteins was about 10 times higher in the diabetic than the normal individual.

An investigation of the binding of acetohexamide, chlorpropamide, and tolbutamide to human serum proteins showed that the albumin fraction was responsible for the greatest binding (215). At pH 7.4, the primary binding affinities were 3.4 × 10^4, 1.1 × 10^4, and 4.1 × 10^4 for acetohexamide, chlorpropamide, and tolbutamide, respectively. The interaction of a number of drugs with the sulfonylurea–albumin complex was examined for each of these agents. Sulfaphenazole appeared to be a potent in-

Table VII—Reported Sulfonylurea–Albumin Binding Parameters

Drug	Drug Concentration, M	Albumin Source	Albumin Concentration	Primary Binding Constant	Number of Sites	Reference
Tolbutamide	$2–84 \times 10^{-5}$	Human serum	2.9×10^{-4} M	4.06×10^{4} M^{-1}	1.36	215
Tolbutamide	—	Human serum	1%	2.18×10^{5} liters/mole	2.27	216
Tolbutamide	$10^{-6}–10^{-3}$	Human serum	1×10^{-4} M	1.35×10^{5} M^{-1}	—	217
Tolbutamide	—	Human serum	$0.25–1.0 \times 10^{-4}$ M	1.65×10^{5} M^{-1}	—	221
Chlorpropamide	$6–84 \times 10^{-5}$	Human serum	2.9×10^{-4} M	1.09×10^{4} M^{-1}	1.64	215
Chlorpropamide	—	Human serum	1%	4.51×10^{4} liters/mole	2.19	216
Chlorpropamide	$10^{-6}–10^{-3}$	Human serum	1×10^{-4} M	6.80×10^{4} M^{-1}	—	217
Acetohexamide	$2–81 \times 10^{-5}$	Human serum	2.9×10^{-4} M	3.39×10^{4} M^{-1}	1.39	215
Acetohexamide	—	Bovine serum	$0.25–1.0 \times 10^{-4}$ M	1.60×10^{4} M^{-1}	—	221
Carbutamide	$10^{-6}–10^{-3}$	Human serum	1×10^{-4} M	3.75×10^{4} M^{-1}	—	217
Glipizide	—	Bovine serum	1.38×10^{-6} M	$2.45–6.88 \times 10^{4}$ M^{-1}	—	220
Glipizide	—	Bovine serum	$0.25–1.0 \times 10^{-4}$ M	4.90×10^{4} M^{-1}	—	221
Glipizide	—	—[a]	—	92–99% bound	—	219
Glyburide	—	Bovine serum	1.38×10^{-6} M	3.26×10^{5} M^{-1}	—	220
Glyburide	—	Bovine serum	$0.25–1.0 \times 10^{-4}$ M	6.13×10^{4} M^{-1}	—	221

[a] In this report, human plasma was used as the biomacromolecule.

hibitor of the sulfonylurea–albumin binding while aspirin had little displacing ability. In contrast to these data (215), substantial differences were reported in the binding of tolbutamide and chlorpropamide (216). This study demonstrated that an interaction between buffer contents and serum albumin may have had significant effects upon the binding parameters calculated by Judis (215).

In 1% human serum albumin using phosphate buffer and tromethamine buffer, the numbers of primary binding sites were 2.27 and 1.42 and the primary affinity constants were 21.86×10^4 and 0.97×10^4 liters/mole, respectively (216). It appears important to characterize binding at several buffer or protein concentrations and perhaps employ more than a single buffer system to calculate more meaningful constants. Various other studies using the same sulfonylureas, tolbutamide, chlorpropamide, and acetohexamide, and newer agents, such as glyburide and glipizide, have appeared (217–222). These results are given in Table VII.

Hsu *et al.* (220) reported that the binding of glipizide and glyburide to human and bovine serum albumin was fundamentally different than the other sulfonylureas. Using a fluorescent probe study, they found a difference in competition for the probe binding site between glipizide and glyburide, which interacted with one of their probes, and the other sulfonylureas, which interacted with a probe with which glipizide and glyburide did not. In their opinion, this probe-specific interaction differentiated the binding sites. Zia and Price (221), on the other hand, showed that acetohexamide, glipizide, glyburide, and tolbutamide bound at the same or closely located sites on the protein.

An evaluation was made recently of the nature of the molecular interaction between sulfonylureas and serum albumin using a circular dichroic technique (222). The sulfonylurea–albumin complex failed to generate a specific conformation among these various agents. This finding could be interpreted in terms of a dissimilar mode of binding for these agents. The binding of the biguanides metformin, buformin, and phenformin to human and dog whole blood and plasma was studied (223). Relatively small percentages (7.4–12%) of these agents were bound in human plasma at drug concentrations from 0 to 3×10^{-4} M.

Local Anesthetics—The binding of the anilide-type local anesthetic agents lidocaine, mepivacaine, and bupivacaine was reported (224). The binding of these agents was evaluated in two patients at plasma drug concentrations of 0.4–23.3 μg/ml. Binding of bupivacaine was greatest (96.5–61.5%), mepivacaine was less (84.3–31.5%), and lidocaine was least (75.0–28.2%). At levels greater than 5.0–10.0 μg/ml of any of these agents, there was a marked reduction in binding, presumably due to binding site saturation. Identification of the main plasma binding macromolecule for these basic drugs was not successful; however, albumin was probably not the protein of greatest importance. A subsequent paper reported that differences between the plasma binding of these three agents may partly explain observed differences between their umbilical–maternal concentrations (225).

The results of another study (226) examining the interaction of bupivacaine with human plasma proteins are in close agreement with those of Tucker *et al.* (224). It was found (226) that at bupivacaine levels of 1 μg/ml, the mean unbound fraction of drug in 10 healthy volunteers was 6.3%. In a study of lidocaine disposition kinetics (227), 60.8% of the drug was bound over the plasma concentration range of 0.8–4.1 μg/ml. A rapid bolus injection of lidocaine and its seemingly rapid saturation of binding sites may be important in determining the immediate toxicity of this drug (227). The suggestion of administering this drug over 1–2 min may be important in decreasing toxic symptoms.

Psychopharmacological Agents—Many reports concerning the binding of tricyclic and benzodiazepine derivatives to human plasma and albumin have been published since 1969. An ultrafiltration technique was used to examine the binding of various tricyclic antidepressants to human plasma proteins (228). At a total concentration of 0.29 μg/ml, the percentage of unbound desipramine (desmethylimipramine) was 9.5 ± 1.4 in 41 individuals; this degree of binding was relatively constant over a wide drug concentration range. Other tricyclics studied at 1.1 μM concentrations had the following percentages of unbound drug: nortriptyline, 5.5 ± 0.6; amitriptyline, 3.6 ± 0.8; and protriptyline, 8.0 ± 0.6. The *in vitro* percentage of unbound nortriptyline correlated well with *in vivo* measurements of free drug concentration in cerebrospinal fluid. The protein responsible for the greatest amount of binding in the plasma was not determined.

Imipramine interacted with bovine serum albumin at six equivalent binding sites, possibly involving tyrosyl

Table VIII—Reported Tricyclic Antidepressant–Protein Binding Parameters

Drug	Drug Concentration, M	Protein	Protein Concentration, M	Primary Binding Constant	Number of Sites	Reference
Chlorpromazine	—	Human albumin	1.8×10^{-5}	4.2×10^{4} liters/mole	4	7
Trifluopromazine	$0.365–14.6 \times 10^{-5}$	Human albumin	1.8×10^{5}	5.5×10^{4} liters/mole	4	7
Chlorpromazine	$40–1600 \times 10^{-6}$	Human plasma	—	$1.5 \times 10^{4}\ M^{-1}$	—	236
Chlorpromazine	$40–1600 \times 10^{-6}$	Human albumin	—	$1.3 \times 10^{3}\ M^{-1}$	—	236
Imipramine	$40–1600 \times 10^{-6}$	Human plasma	—	$1 \times 10^{4}\ M^{-1}$	—	236
Imipramine	$40–1600 \times 10^{-6}$	Human albumin	—	$4.9 \times 10^{2}\ M^{-1}$	—	236
Chlorpromazine	$1–20 \times 10^{-6}$	Human albumin	6.8×10^{6}	1.9×10^{5} liters/mole	1.94	237
Promazine	$1–20 \times 10^{-6}$	Human albumin	5.8×10^{-6}	8.5×10^{4} liters/mole	1.31	237
Promethazine	$1–20 \times 10^{-6}$	Human albumin	5.8×10^{-6}	7.9×10^{4} liters/mole	1.64	237
Trifluoperazine	$1–20 \times 10^{-6}$	Human albumin	5.8×10^{-6}	2.86×10^{5} liters/mole	1.18	237
Imipramine	$1–20 \times 10^{-6}$	Human albumin	5.8×10^{-6}	2.39×10^{4} liters/mole	1.31	237
Trimipramine	$1–20 \times 10^{-6}$	Human albumin	5.8×10^{-6}	2.38×10^{4} liters/mole	1.24	237
Clomipramine	$1–20 \times 10^{-6}$	Human albumin	5.8×10^{-6}	7.35×10^{4} liters/mole	1.03	237
Desipramine	$1–20 \times 10^{-6}$	Human albumin	5.8×10^{-6}	7.02×10^{4} liters/mole	1.53	237
Chlorpromazine	4.6×10^{-5}, 15×10^{-4}	Bovine albumin	6.9×10^{-5}	$2.57 \times 10^{4}\ M^{-1}$	—	221
Trifluoperazine	4.6×10^{-5}, 15×10^{-4}	Bovine albumin	6.9×10^{-5}	$2.32 \times 10^{4}\ M^{-1}$	—	221
Perphenazine	4.6×10^{-5}, 15×10^{-4}	Bovine albumin	6.9×10^{-5}	$1.96 \times 10^{4}\ M^{-1}$	—	221
Fluphenazine	4.6×10^{-5}, 15×10^{-4}	Bovine albumin	6.9×10^{-5}	$1.82 \times 10^{4}\ M^{-1}$	—	221
Promazine	4.6×10^{-5}, 15×10^{-4}	Bovine albumin	6.9×10^{-5}	$1.04 \times 10^{4}\ M^{-1}$	—	221

residues of the protein, with an intrinsic association constant of $5 \times 10^{3}\ M^{-1}$ (229). The related tricyclic desipramine exhibited a more complicated binding mechanism, perhaps involving a drug-induced conformational change. From a study of nortriptyline binding in seven identical and 10 fraternal sets of twins, Alexanderson and Borga (230) concluded that drug binding was influenced by environmental, that is, statistically significant differences in the binding ratio within monozygotic twin pairs, as well as genetic factors. They found no significant correlation between the bound to free nortriptyline ratio and the steady-state drug concentration.

Another study (231) showed that there was far less variation in plasma protein binding of imipramine among children (bound fraction 77–94.6%) (92) than among adults and that children bound substantially less of this drug. Adult-like binding values may be reached at about age 13, and the relatively high doses of imipramine administered at bedtime to children with behavior disorders may be unsound from a binding–pharmacokinetic standpoint.

In a study relating the plasma protein binding of chlorpromazine to the apparent volume of distribution and the rate constant of elimination, chlorpromazine plasma binding influenced tissue localization; a high degree of tissue localization occurred in the species in which plasma protein binding was low and vice versa (232). It was also shown that over 90% of chlorpromazine in human plasma was present in bound form (233). The binding was reversible, and very large amounts of chlorpromazine, 15 μg/ml of plasma or more, were required to saturate the plasma binding sites.

One study (234) found that the apparent binding constant for chlorpromazine was 1355 with human albumin and 1545 with a human α-globulin fraction; although each of these proteins demonstrated a large number of binding sites for the drug, the results indicated that a different plasma protein fraction may display a larger affinity. Mao and Noval (235) suggested that the serum protein binding of the phenothiazines might explain the low *in vivo* hemolytic activity found for these agents. Administration of large amounts of tricyclics over extended times showed that erythrocytes were protected from hemolysis due to the plasma protein binding of these agents.

Another study determined the groups or positions on the phenothiazines responsible for drug–albumin complexation (7). The whole phenothiazine nucleus takes part in the binding process; predominantly hydrophobic forces are involved, but ionic interactions must not be completely ignored. The binding parameters are included in Table VIII.

Chlorpromazine and imipramine were bound to three major blood components: erythrocyte membranes, albumin, and lipoproteins (236). The affinity displayed by lipoprotein for these drugs was as high as that of albumin. The binding of various tranquilizer–antidepressant drugs to human albumin was examined (237) (Table VIII). A drug displacement study of these drugs found that phenothiazines displace iminodibenzyl compounds but not vice versa, since the affinities of the phenothiazines for the albumin are greater than the affinities of the iminodibenzyl agents.

In a subsequent study (238), the binding of tricyclic compounds to human albumin was correlated with linear free energy models. The major force in the binding of these molecules was electronic, and only a minor contribution of hydrophobic forces was involved. To the contrary, a previous report (221) stated that the interaction of phenothiazine drugs with bovine serum albumin was of a predominantly hydrophobic nature. Another study (239) also showed that the binding of phenothiazines to bovine serum albumin was of a hydrophobic nature. Recently, excellent evidence was presented that hydrophobic forces are more responsible for the phenothiazine–albumin interaction than are charge transfer or electronic forces (240).

Dialysis of plasma from 14 patients receiving diazepam (0.1 mg/kg) showed that plasma bound 97.7% of this benzodiazepine (241). Similarly, in seven patients the plasma proteins bound 98% of the diazepam in the serum from a 10-mg im dose (242). Diazepam was among 11 benzodiazepine derivatives quantitatively studied for binding to bovine serum albumin (243). Diazepam had a binding constant of 8.23×10^{3} liters/mole with 5.56 binding sites on bovine albumin. Binding constants calculated for the 11 benzodiazepines demonstrated that their binding affinities for bovine albumin were smaller than for human

albumin. Furthermore, these agents have more than the characteristic one or two binding sites on bovine albumin than would be expected on human albumin.

Some benzodiazepines were shown to be competitors for the binding of L-tryptophan to human serum albumin (244). There was a single highly stereospecific site on human albumin which bound L-tryptophan and with which the benzodiazepines competed. Lucek and Coutinho (245) presented results showing that the protein binding of benzodiazepines increased with increases in the lipophilic character of substituents in the 1-, 2-, 3-, 4-, 7-, and 4′-positions. The electronic character of 1-, 3-, and 7-substituents also correlated with protein binding but to a lesser degree than the lipophilic parameter.

Amphetamine binding was studied *in vitro* in different species, including humans (246), and was less than 45% in all species in the drug concentration range of 2.5×10^{-7}–4×10^{-6} *M*. Drug diffusion to cerebrospinal and ocular fluids was not retarded by the binding. An *in vitro* investigation of bovine serum albumin and amphetamine and one of its derivatives (247) arrived at similar results (246). Amphetamines appeared to be bound primarily to the albumin fraction of plasma. However, Δ^1-tetrahydrocannabinol was 80–95% bound to lipoprotein fractions *in vitro,* and no binding to albumin could be demonstrated (248).

Steroids and Catecholamines—Most steroid hormones are bound to hormone-specific macromolecules such as various binding globulins. However, some literature reports have concerned steroid–albumin binding. The protein binding of 10 steroids was studied in women with benign breast disease, early breast cancer, and advanced breast cancer and was compared to the binding in normal women (249). The data showed that the percentage binding in the plasma varied considerably between steroids. However, for a given steroid, there was no significant difference in the mean amount of steroid bound among these groups of women.

An investigation of progesterone binding to different polymeric fractions of human serum albumin found similar parameters in the mono- and dimeric species; two independent sets of binding sites were determined (250). In the first class, there was one site with an affinity of 3.6×10^5 M^{-1}; in the second class, there were eight sites with an affinity of 6×10^3 M^{-1}. The trimeric and higher forms had significantly lower binding affinities. Clark and Bird (251) examined the binding of 5α-androstane-3α,17β-diol, an important biologically active metabolite of testosterone, to human plasma proteins. They found that 96.6% of the drug was bound in male plasma and that the albumin fraction contained the greatest amount of the steroid. Albumin bound more of this steroid than the parent testosterone, and the authors concluded that this result was due to a higher association constant for the metabolic dihydroxysteroid.

Estriol and some of its conjugates were studied for their binding to plasma proteins during pregnancy (252). These compounds were bound principally in the albumin fraction, and such binding was stated to play an important role in the transport, metabolism, and excretion of these steroidal agents. Although albumin has been reported to be the main binding protein for some steroid hormones and related molecules, other results suggest that the globulin fraction may be principally responsible (253, 254). Ryan and Gibbs (255) found that Ca^{2+} was bound to human serum albumin in direct competition with testosterone and that such ion binding was associated with inhibition of testosterone binding to hydrophobic albumin sites but not with inhibition to sites involving hydrogen bonding.

Recently, several studies were published concerning the binding of catecholamine hormones to plasma proteins. Two distinct plasma binding sites were found for epinephrine; the binding was highly specific, similar to that reported for steroids (256). The first site was present in small numbers and had a large binding constant (6.9×10^5 liters/mole). The second site was more plentiful and had a smaller binding affinity. The enthalpy associated with the epinephrine–plasma protein interaction was small, because the activation energies for association and dissociation were essentially equal.

Both epinephrine and norepinephrine binding to human serum albumin was studied, and a similar binding affinity of approximately 10^7 was observed (257). Other catechols were studied, and neither the nature of the alkyl side chain nor it presence affected the binding affinity. It was also determined that 50% of a physiologic concentration of norepinephrine circulates bound to plasma protein. In apparent contrast to these results, Zia *et al.* (258) reported that the most probable binding site on epinephrine, when bound to bovine albumin, was the alkyl side chain. A possible reason for such a conclusion was that the concentrations of epinephrine used were high. Therefore, Zia *et al.* (258) were examining nonspecific binding in contrast to Danon and Sapira (257). Another report (259) implicated the phenolic hydroxyl groups as well as the alkyl side chain of catecholamines as being responsible for the binding interaction. In a recent study (260), an excellent discussion of the binding observed (257–259) in human serum was given. Several serum macromolecules were implicated as being responsible for catecholamine binding, and such binding may be responsible for the stability of these agents in blood.

Miscellaneous—The interaction of the antimalarial agent pamaquine with bovine albumin was examined (261), and three pamaquine molecules were bound per molecule of protein; the primary binding affinity was very strong, 6.4×10^7. Because the drug was positively charged and the binding constant was large, the binding site on the protein probably involved negatively charged groups. The binding of dapsone, a drug important in the treatment of leprosy, and its principal metabolite, monoacetyldapsone, was studied *in vitro* and *in vivo* in patients known to be rapid acetylators of the drug and in patients metabolizing the agent normally (262). At therapeutic concentrations of dapsone, 70–80% was bound to plasma protein while 90–100% of the monoacetyldapsone was bound. No difference in binding was seen in the plasma of rapid and normal acetylators. The results suggested that protein binding of monoacetyldapsone may account for limited excretion of this compound in the urine and the long plasma half-lives of these agents.

The binding of the antiprotozoal agent metronidazole and four derivatives to plasma proteins was assessed (263). The nature of the alkyl side chain had a significant effect on binding; however, the lipophilicity of these agents was not correlated with plasma protein binding. The parent compound showed good lipophilic character, as did one of

the metabolites, yet these compounds were bound to very small extents (less than 5% over a wide concentration range). A metabolite with poor ability to partition exhibited extensive binding (65–70%), and the binding was principally related to the frontier electron density on the terminal portion of the alkyl side chain. Recently, a good correlation was observed between lipophilicity in a series of related drugs, measured by a reversed-phase thin-layer technique, and the drug binding constants (264). Seemingly, if hydrophobic forces are responsible for the binding interaction, good correlation between partition coefficient and protein binding should be observed. The binding of therapeutic levels of ornidazole and metronidazole to human plasma proteins was less than 15% (265), and this binding was not correlated with the lipophilicity of these agents.

The binding of dantrolene sodium to human serum albumin recently was reported (266). The binding constant, calculated over a wide range of drug concentrations by two different techniques, was 4×10^4–$4 \times 10^5\ M^{-1}$. Ionic as well as hydrophobic forces were responsible for the interaction. Dantrolene added to a cationic surfactant produced perturbations similar to the drug added to human albumin solutions. Albumin also was shown to be the plasma protein most responsible for the binding of prostaglandins (267, 268). The binding of prostaglandins A_2, E_2 (dinoprostone), and F_2 to human plasma was reported to be 88, 73, and 58%, respectively, over the 10–120-ng/ml concentration range (267). The apparent association constants were $1–4 \times 10^4$ liters/mole. Another report (268) also indicated that albumin was the plasma protein principally responsible for binding prostaglandin E_1 and that no E_1 interaction with blood cells or γ-globulin occurred.

Conclusions—The binding of drugs by plasma proteins in general and isolated specific proteins, such as serum albumin and various lipoproteins and globulins, has continued to interest many researchers. Binding parameters (n's and K's), percentages bound, and possible displacement effects may be the clinically important contributions of this research and may be beneficial to dosage adjustment and prediction of the duration of drug action. From a physical standpoint, drug–protein interactions are studied to gain information about denaturation or unfolding of the protein, to determine cooperative interactions and mechanisms, to examine saturation and the total number of binding sites on the protein, and to examine molecular phenomena such as the active site, molecular conformation, or molecular distance involved in the drug–protein complex.

The vast majority of articles reviewed here were *in vitro* investigations and provided quantitative binding data. However, much of the work was of a more qualitative nature, since data were presented in terms of percent binding without specification of the drug concentration to which the binding data pertain; at times, drug concentrations were higher than therapeutic or toxic concentrations expected in the *in vivo* situation. Often plasma was considered by itself as the binding biomacromolecule without an attempt to define the primary protein component responsible for the binding interaction. Seldom were *in vitro–in vivo* correlations of binding attempted. Many results failed to furnish the reader with the temperature of the binding study, and it is well known that less binding is found at 37° than at ambient temperatures. Much of the binding literature could serve as a useful source of information to the clinician, pharmacokineticist, and other interested pharmaceutical researchers if the data presentation, data reduction, and use of multiple methods to support conclusions could be uniformly imposed on new articles pertaining to drug binding results.

Considerable research attention in the area of drug–protein binding could be directed at one or more of the following points, as well as inclusion of the calculated binding parameters: tissue binding, complexation of drugs by red cells and blood vessels, binding effects on pharmacokinetic models and parameters, protein active sites, and other molecular events associated with binding phenomena, displacement interactions, especially in the *in vivo* situation, and binding changes that may alter the course or effects of therapy associated with specific disease states. It is quite evident that strongly bound drugs influence drug effects and drug dynamics, and new drugs ought to be assessed as to whether or not they fit in the category of strongly bound agents.

REFERENCES

(1) M. C. Meyer and D. E. Guttman, *J. Pharm. Sci.*, **57**, 895 (1968).

(2) J. Steinhardt and J. A. Reynolds, "Multiple Equilibria in Proteins," Academic, New York, N.Y., 1969, pp. 34–70.

(3) C. J. Halfman and J. Steinhardt, *Biochemistry*, **10**, 3564 (1971).

(4) C. J. Halfman and T. Nishida, *ibid.*, **11**, 3493 (1972).

(5) J. K. Ma, H. W. Jun, and L. A. Luzzi, *J. Pharm. Sci.*, **62**, 2038 (1973).

(6) J. Blanchard, T. N. Tozer, D. L. Sorby, and L. D. Tuck, *Mol. Pharmacol.*, **11**, 133 (1975).

(7) P. C. Huang and S. Gabay, *Biochem. Pharmacol.*, **23**, 957 (1974).

(8) J. H. Perrin and P. A. Hart, *J. Pharm. Sci.*, **59**, 431 (1970).

(9) H. J. Weder and M. H. Bickel, *ibid.*, **59**, 1563 (1970).

(10) G. F. Scatchard, *Ann. N.Y. Acad. Sci.*, **51**, 660 (1949).

(11) I. M. Klotz, *Arch. Biochem.*, **9**, 109 (1946).

(12) B. W. Madsen and J. S. Robertson, *J. Pharm. Pharmacol.*, **28**, 807 (1974).

(13) H. G. Weder, J. Schildknecht, R. A. Lutz, and P. Kesselring, *Eur. J. Biochem.*, **42**, 475 (1974).

(14) J. H. Perrin, J. J. Vallner, and S. Wold, *Biochim. Biophys. Acta*, **371**, 482 (1974).

(15) C. J. Thompson and I. M. Klotz, *Arch. Biochem. Biophys.*, **147**, 178 (1974).

(16) H. A. Feldman, *Anal. Biochem.*, **48**, 317 (1972).

(17) J. E. Fletcher, J. D. Ashbrook, and A. A. Spector, *Ann. N.Y. Acad. Sci.*, **226**, 69 (1973).

(18) J. P. Raynaud, *Comput. Programs Biomed.*, **3**, 63 (1973).

(19) J. P. Tillement, R. Zini, P. d'Athis, and G. Vassent, *Eur. J. Clin. Pharmacol.*, **7**, 307 (1974).

(20) D. L. Hunston, *Anal. Biochem.*, **63**, 99 (1975).

(21) I. M. Klotz and D. L. Hunston, *J. Biol. Chem.*, **250**, 3001 (1975).

(22) J. J. Vallner, J. H. Perrin, and S. Wold, *J. Pharm. Sci.*, **65**, 1182 (1976).

(23) H. M. Solomon and G. B. Thomas, *Clin. Pharmacol. Ther.*, **12**, 445 (1971).

(24) J. R. Gillette, *Ann. N.Y. Acad. Sci.*, **226**, 15 (1973).

(25) G. Evans and D. Shand, *Clin. Pharmacol. Ther.*, **14**, 494 (1973).

(26) W. A. Craig and C. M. Kunin, *Ann. Intern. Med.*, **78**, 491 (1973).

(27) J. G. Wagner, *J. Pharmacokinet. Biopharm.*, **1**, 384 (1973).

(28) S. H. Curry, *J. Pharm. Pharmacol.*, **22**, 753 (1970).

(29) P. T. Schoenemann, D. W. Yesair, J. J. Coffey, and F. J. Bullock, *Ann. N.Y. Acad. Sci.*, **226**, 162 (1973).

(30) J. H. Perrin and D. A. Nelson, *J. Pharm. Pharmacol.*, **25,** 125 (1973).
(31) J. H. Perrin and D. A. Nelson, *Biochem. Pharmacol.*, **23,** 3139 (1974).
(32) J. H. Perrin, J. J. Vallner, and D. A. Nelson, *ibid.*, **24,** 769 (1975).
(33) E. Tsutsumi, T. Inaba, W. A. Maon, and W. Kalow, *ibid.*, **24,** 1361 (1975).
(34) G. C. Schussler, *J. Pharmacol. Exp. Ther.*, **178,** 204 (1971).
(35) W. M. Wardell, *Br. J. Pharmacol.*, **43,** 325 (1971).
(36) E. G. McQueen, *Progr. Biochem. Pharmacol.*, **9,** 122 (1974).
(37) E. G. McQueen and W. M. Wardell, *Br. J. Pharmacol.*, **43,** 312 (1971).
(38) P. G. Dayton, Z. H. Israili, and J. M. Perel, *Ann. N.Y. Acad. Sci.*, **226,** 188 (1973).
(39) E. M. Sellers and J. Koch-Weser, *Clin. Pharmacol. Ther.*, **11,** 514 (1970).
(40) G. Levy and S. Oie, *Pediatr. Res.*, **9,** 284 (1975).
(41) J. P. Tillement, C. Mattei, and R. Zini, *Experientia*, **30,** 460 (1974).
(42) M. W. Whitehouse, I. Kippen, and J. R. Klinenberg, *Biochem. Pharmacol.*, **20,** 3309 (1971).
(43) L. H. Schlosstein, I. Kippen, M. W. Whitehouse, R. Bluestone, H. E. Paulus, and J. R. Klinenberg, *J. Lab. Clin. Med.*, **82,** 412 (1973).
(44) D. Rudman, T. J. Bixler, and A. E. DelRio, *J. Pharmacol. Exp. Ther.*, **176,** 261 (1971).
(45) A. A. Spector, E. C. Santos, J. D. Ashbrook, and J. E. Fletcher, *Ann. N.Y. Acad. Sci.*, **226,** 247 (1973).
(46) G. B. Odell, *ibid.*, **226,** 225 (1973).
(47) C. B. Coutinho, R. W. Lucek, J. A. Cheripko, and R. Kuntzman, *ibid.*, **226,** 238 (1973).
(48) R. Brodersen, *J. Clin. Invest.*, **54,** 1353 (1974).
(49) S. Athanassiadis, D. R. Chopra, M. Fisher, and J. McKenna, *Pediatr. Res.*, **7,** 399/177 (1973).
(50) D. Schiff, G. Chan, and L. Stern, *Rev. Can. Biol.*, **32,** 135 (1973).
(51) L. Stern, *Pediatrics*, **49,** 916 (1972).
(52) A. Windorfer, Jr., G. Faxelius, and L. O. Boreus, *Acta Paediatr. Scand.*, **64,** 293 (1975).
(53) M. M. Reidenberg, *Med. Clin. N. Am.*, **58,** 1103 (1974).
(54) M. Black and I. M. Arias, in "Handbook of Experimental Pharmacology," vol. 28, J. R. Gillette and J. R. Mitchell, Eds., 1975, p. 258.
(55) P. G. Welling, W. A. Craig, and C. M. Kunin, *Clin. Pharmacol. Ther.*, **18,** 45 (1975).
(56) M. M. Reidenberg, I. Odar-Cederlof, C. von Bahr, O. Borga, and F. Sjoqvist, *N. Engl. J. Med.*, **285,** 264 (1971).
(57) M. R. Blum, S. Riegelman, and C. E. Becker, *ibid.*, **286,** 109 (1972).
(58) F. Andreasen, *Acta Pharmacol. Toxicol.*, **34,** 284 (1974).
(59) D. W. Shoeman, D. M. Benjamin, and D. L. Azarnoff, *Ann. N.Y. Acad. Sci.*, **226,** 127 (1973).
(60) L. Zathurecky, A. Szelepcsenyiova, E. Brunckova, V. Masarykova, and F. Hajnovic, *Acta Pharm. Suec.*, **11,** 653 (1974).
(61) W. D. Hooper, F. Bochner, M. J. Eadie, and J. H. Tyrer, *Clin. Pharmacol. Ther.*, **15,** 276 (1974).
(62) I. Odar-Cederlof and O. Borga, *Eur. J. Clin. Pharmacol.*, **8,** 445 (1975).
(63) M. Ehrnebo and I. Odar-Cederlof, *ibid.*, **8,** 445 (1975).
(64) A. H. Anton and W. T. Corey, *Fed. Proc.*, **30,** 629 (1971).
(65) F. Andreasen and P. Jacobsen, *Acta Pharmacol. Toxicol.*, **35,** 49 (1974).
(66) J. Prandota and A. W. Pruitt, *Clin. Pharmacol. Ther.*, **17,** 159 (1975).
(67) K. O'Malley, M. Velasco, A. Pruitt, and J. L. McNay, *ibid.*, **18,** 53 (1975).
(68) G. D. Olsen, W. M. Bennett, and G. A. Porter, *ibid.*, **17,** 677 (1975).
(69) M. M. Mussche, F. M. Belpaire, and M. G. Bogaert, *Eur. J. Clin. Pharmacol.*, **9,** 69 (1975).
(70) P. Kramer, E. Kothe, J. Saul, and F. Scheler, *Eur. J. Clin. Invest.*, **4,** 53 (1974).
(71) D. W. Shoeman and D. L. Azarnoff, *Fed. Proc.*, **31,** 517 (1972).
(72) P. G. Welling, W. A. Craig, G. L. Amidon, and C. M. Kunin, *J. Infect. Dis.*, **128,** S556 (1973).
(73) P. G. Welling, W. A. Craig, G. L. Amidon, and C. M. Kunin, *Clin. Pharmacol. Ther.*, **15,** 344 (1974).
(74) D. S. Campion, *Toxicol. Appl. Pharmacol.*, **25,** 391 (1973).
(75) S. H. Dromgoole, *J. Pharmacol. Exp. Ther.*, **191,** 318 (1974).
(76) P. C. Farrell, N. L. Grib, D. L. Fry, R. P. Popovich, J. W. Broyiac, and A. L. Babb, *Trans. Am. Soc. Artif. Int. Organs*, **18,** 268 (1972).
(77) Boston Collaborative Drug Surveillance Program, *Clin. Pharmacol. Ther.*, **14,** 529 (1973).
(78) G. P. Lewis, W. J. Jusko, C. W. Burke, and L. Graves, *Lancet*, **2,** 778 (1971).
(79) D. J. Greenblatt and J. Koch-Weser, *Eur. J. Clin. Pharmacol.*, **7,** 259 (1974).
(80) G. D. Olsen, *Science*, **176,** 525 (1972).
(81) M. M. Reidenberg and M. Affrime, *Ann. N.Y. Acad. Sci.*, **226,** 115 (1973).
(82) W. D. Wosilait, *Res. Commun. Chem. Pathol. Pharmacol.*, **9,** 681 (1974).
(83) M. Affrime and M. M. Reidenberg, *Eur. J. Clin. Pharmacol.*, **8,** 267 (1975).
(84) T. F. Blaschke, P. J. Meffin, K. L. Melmon, and M. Rowland, *Clin. Pharmacol. Ther.*, **17,** 685 (1975).
(85) G. E. Mawer, N. E. Miller, and L. A. Turnberg, *Br. J. Pharmacol.*, **44,** 549 (1972).
(86) T. S. McHorse, G. R. Wilkinson, R. F. Johnson, and S. Schenker, *Gastroenterology*, **68,** 775 (1975).
(87) G. R. Avant, S. Schenker, and R. H. Alford, *Digest. Dis.*, **20,** 223 (1975).
(88) C. R. Avant, U. Klotz, G. R. Wilkinson, A. Hoyumpa, and S. Schenker, *J. Clin. Invest.*, **53,** 2a (1974).
(89) S. J. Yaffe and M. R. Juchau, *Ann. Rev. Pharmacol.*, **14,** 308 (1974).
(90) J. Krasner, G. P. Giacoia, and S. J. Yaffe, *Ann. N.Y. Acad. Sci.*, **226,** 101 (1973).
(91) J. Krasner and S. J. Yaffe, in "Basic and Therapeutic Aspects of Perinatal Pharmacology," P. L. Morselli, S. Garattini, and F. Sereni, Eds., Raven, New York, N.Y., 1975, p. 357.
(92) A. W. Pruitt and P. G. Dayton, *Eur. J. Clin. Pharmacol.*, **4,** 59 (1971).
(93) M. Ehrnebo, S. Agurell, B. Jalling, and L. O. Boreus, *ibid.*, **3,** 189 (1971).
(94) H. Stickel, H. Kurz, and H. Michels, *Naunyn-Schmiedeberg's Arch. Pharmacol.*, **287,** R 67 (1975).
(95) L. E. Mather, G. J. Long, and J. Thomas, *J. Pharm. Pharmacol.*, **23,** 359 (1971).
(96) R. Gorodischer, J. Krasner, and S. J. Yaffe, *Res. Commun. Chem. Pathol. Pharmacol.*, **9,** 387 (1974).
(97) A. J. Hadjian, M. Chedin, C. Cochet, and E. M. Chambaz, *Pediatr. Res.*, **9,** 40 (1975).
(98) H. Sakata, *Acta Obstet. Gynacol., Jpn.*, **19,** 210 (1973).
(99) B. B. Fredholm, A. Rane, and B. Persson, *Pediatr. Res.*, **9,** 26 (1975).
(100) A. Rane, P. K. M. Lunde, B. Jalling, S. J. Yaffe, and F. Sjoqvist, *Pediatr. Pharmacol. Ther.*, **78,** 877 (1971).
(101) C. M. Kunin, W. A. Craig, M. Kornguth, and R. Monson, *Ann. N.Y. Acad. Sci.*, **226,** 214 (1973).
(102) J. S. Tan, A. Trott, J. P. Phair, and C. Watanakunakorn, *J. Infect. Dis.*, **126,** 492 (1972).
(103) K. A. Desante, *Diss. Abstr.*, **1973,** 4364-B.
(104) M. Barza, H. Vine, and L. Weinstein, *Antimicrob. Ag. Chemother.*, **1,** 427 (1972).
(105) G. O. Phillips, D. M. Power, C. Robinson, and J. V. Davies, *Biochim. Biophys. Acta*, **215,** 491 (1970).
(106) W. M. M. Kirby and C. Regamey, *J. Infect. Dis.*, **128,** 5341 (1973).
(107) R. D. Libke, J. T. Clarke, E. D. Ralph, R. P. Luthy, and W. M. M. Kirby, *Clin. Pharmacol. Ther.*, **17,** 441 (1975).
(108) W. Chojnowski, *Acta Pol. Pharm.*, **28,** 545 (1971).
(109) H. C. Standiford, M. C. Jordan, and W. M. M. Kirby, *J. Infect. Dis.*, **122,** 59 (1970).
(110) H. Lode, S. Gebert, and A. Hendrisck, *Chemotherapy*, **21,** 19 (1975).
(111) A. Howell, R. Sutherland, and G. N. Rolinson, *Clin. Pharmacol. Ther.*, **13,** 724 (1972).
(112) J. Verhoef, P. L. Oe, and S. Simonian, *Chemotherapy*, **19,** 272 (1973).
(113) G. Powis, *J. Pharm. Pharmacol.*, **26,** 113 (1974).
(114) H. Zia and J. C. Price, *J. Pharm. Sci.*, **65,** 226 (1976).
(115) M. Pilloud, *Res. Vet. Sci.*, **15,** 224 (1973).

(116) V. P. Yakovlev, *Antibiotiki*, **16**, 354 (1971).
(117) R. C. Gordon, C. Regamey, and W. M. M. Kirby, *Antimicrob. Ag. Chemother.*, **2**, 214 (1972).
(118) C. H. Ramirez-Ronda, R. K. Holmes, and J. P. Sanford, *J. Clin. Invest.*, **53**, 63A (1974).
(119) C. H. Ramirez-Ronda, R. K. Homes, and J. P. Sanford, *Antimicrob. Ag. Chemother.*, **7**, 239 (1975).
(120) J. T. Clarke, R. D. Libke, C. Regamey, and W. M. Kirby, *Clin. Pharmacol. Ther.*, **15**, 610 (1974).
(121) R. C. Gordon, C. Regamey, and W. M. M. Kirby, *J. Pharm. Sci.*, **62**, 1074 (1973).
(122) R. G. Wiegand and A. H. C. Chun, *ibid.*, **61**, 425 (1972).
(123) W. T. Sokolski, *Ann. Soc. Microbiol.*, **75**, 10 (1975).
(124) R. Elofsson, S. O. Nilsson, and A. Agren, *Acta Pharm. Suec.*, **7**, 473 (1970).
(125) R. Elofsson, S. O. Nilsson, and B. Kluczykowska, *ibid.*, **8**, 465 (1971).
(126) A. Agren, R. Elofsson, and S. O. Nilsson, *ibid.*, **8**, 475 (1971).
(127) S. O. Nilsson, A. Agren, J. O. Branstad, and U. Meresaar, *ibid.*, **10**, 455 (1973).
(128) S. R. Walker, *J. Pharm. Pharmacol.*, **22**, 574 (1970).
(129) J. H. Perrin and D. A. Nelson, *ibid.*, **25**, 125 (1973).
(130) C. A. Cruze and M. C. Meyer, *J. Pharm. Sci.*, **65**, 33 (1976).
(131) W. Riess, K. Schmid, H. Keberle, L. Dettli, and P. Spring, *Progr. Antimicrob. Anticancer Chemother.*, **2**, 905 (1970).
(132) K. Mashimo, *ibid.*, **2**, 1198 (1970).
(133) J. K. Seydel, *Antibiot. Chemother.*, **16**, 380 (1970).
(134) T. Aoyagi, *Scand. J. Resp. Dis., Suppl.*, **84**, 44 (1973).
(135) G. Boman and V. A. Ringberger, *Eur. J. Clin. Pharmacol.*, **7**, 369 (1974).
(136) R. A. O'Reilly, *J. Clin. Invest.*, **48**, 193 (1969).
(137) R. A. O'Reilly, *Ann. N.Y. Acad. Sci.*, **226**, 293 (1973).
(138) R. A. O'Reilly, *Mol. Pharmacol.*, **7**, 209 (1971).
(139) A. Yacobi and G. Levy, *J. Pharm. Sci.*, **64**, 1660 (1975).
(140) A. Yacobi and G. Levy, *Res. Commun. Chem. Pathol. Pharmacol.*, **12**, 405 (1975).
(141) C. F. Chignell, *Mol. Pharmacol.*, **6**, 1 (1970).
(142) J. H. Perrin and D. A. Nelson, *Life Sci.*, **11**, 277 (1972).
(143) S. Garten and W. D. Wosilait, *Comput. Programs Biomed.*, **2**, 61 (1971).
(144) S. Garten and W. D. Wosilait, *Comp. Gen. Pharmacol.*, **3**, 83 (1972).
(145) W. D. Wosilait and S. Garten, *Res. Commun. Chem. Pathol. Pharmacol.*, **3**, 535 (1972).
(146) Basic Pharmaceutics Symposium, APhA Academy of Pharmaceutical Sciences, New Orleans meeting, Apr. 1976.
(147) J. A. Penner and P. H. Abbrecht, *Curr. Ther. Res.*, **18**, 862 (1975).
(148) P. K. M. Lunde, A. Rane, S. J. Yaffe, L. Lund, and F. Sjoqvist, *Clin. Pharmacol. Ther.*, **11**, 846 (1970).
(149) G. J. Gordon, C. O. Haavik, and K. F. Finger, *J. Pharm. Sci.*, **60**, 1642 (1971).
(150) L. Lund, A. Berlin, and P. K. M. Lunde, *Clin. Pharmacol. Ther.*, **13**, 196 (1972).
(151) H. E. Booker and B. Darcey, *Epilepsia*, **14**, 177 (1973).
(152) J. D. Baggot and L. E. Davis, *Comp. Gen. Pharmacol.*, **4**, 399 (1973).
(153) D. Kurata and G. Wilkinson, *Clin. Pharmacol. Ther.*, **16**, 355 (1974).
(154) D. W. Shoeman and D. L. Azarnoff, *J. Pharmacol. Exp. Ther.*, **195**, 84 (1975).
(155) T. F. Roe, R. L. Podosin, and M. E. Blaskovics, *Pediatr. Res.*, **9**, 285 (1975).
(156) E. DiSalle, G. M. Pacifici, and P. L. Morselli, *Pharmacol. Res. Commun.*, **6**, 193 (1974).
(157) W. D. Hooper, D. K. Dubetz, F. Bochner, L. M. Cotter, G. A. Smith, M. J. Eadie, and J. H. Tyrer, *Clin. Pharmacol. Ther.*, **17**, 433 (1975).
(158) E. M. Sellers and J. Koch-Weser, *Pharmacologist*, **11**, 293 (1969).
(159) E. M. Sellers and J. Koch-Weser, *Fed. Proc.*, **28**, 613 (1969).
(160) F. V. V. Andreasen, *ibid.*, **28**, 614 (1969).
(161) D. G. Shand, A. S. Nies, and G. H. Evans, *ibid.*, **32**, 715 (1973).
(162) G. H. Evans and D. G. Shand, *Clin. Pharmacol. Ther.*, **14**, 494 (1973).
(163) G. H. Evans, A. S. Nies, and D. G. Shand, *J. Pharmacol. Exp. Ther.*, **186**, 114 (1973).
(164) C. Appelgren, K. O. Borg, R. Elofsson, and K. A. Johansson, *Acta Pharm. Suec.*, **11**, 325 (1974).
(165) K. A. Johansson, C. Appelgren, K. O. Borg, and R. Elofsson, *ibid.*, **11**, 333 (1974).
(166) J. L. Kucera and F. J. Bullock, *J. Pharm. Pharmacol.*, **21**, 293 (1969).
(167) A. Windorfer, Jr., W. Kuenzer, and R. Urbanek, *Eur. J. Clin. Pharmacol.*, **7**, 227 (1974).
(168) S. Keresztes-Nagy, R. F. Mais, Y. T. Oester, and J. F. Zaroslinski, *Anal. Biochem.*, **48**, 80 (1972).
(169) D. Hultmark, K. O. Borg, R. Elofsson, and L. Palmer, *Acta Pharm. Suec.*, **12**, 259 (1975).
(170) G. Levy and S. J. Yaffe, *Pediatrics*, **54**, 713 (1974).
(171) A. K. Done, *ibid.*, **54**, 670 (1974).
(172) H. G. Smith and C. Lakatos, *J. Pharm. Pharmacol.*, **23**, 180 (1971).
(173) J. B. Stenlake, W. D. Williams, A. G. Davidson, W. Downie, and K. Whaley, *ibid.*, **21**, 451 (1969).
(174) R. W. Mason and E. G. McQueen, *Pharmacology*, **12**, 12 (1974).
(175) E. Hvidberg, H. H. Lausen, and J. A. Jansen, *Eur. J. Clin. Pharmacol.*, **4**, 119 (1972).
(176) J. N. McArthur, P. D. Dawkins, and M. J. H. Smith, *J. Pharm. Pharmacol.*, **23**, 32 (1971).
(177) C. F. Chignell, *Mol. Pharmacol.*, **5**, 244 (1969).
(178) *Ibid.*, **5**, 455 (1969).
(179) J. H. Perrin, *J. Pharm. Pharmacol.*, **25**, 208 (1973).
(180) A. Rubin, P. Warrick, R. L. Wolen, S. M. Chernish, A. S. Ridolfo, and C. M. Gruber, *J. Pharmacol. Exp. Ther.*, **183**, 449 (1972).
(181) J. J. Vallner, Ph.D. thesis, University of Wisconsin, Madison, Wis., 1974, p. 108.
(182) M. Ehrnebo, S. Agurell, L. O. Boreus, E. Gordon, and U. Lonroth, *Clin. Pharmacol. Ther.*, **16**, 424 (1974).
(183) A. Assandri, A. Zerial, M. Strolin-Benedetti, and A. Perazzi, *Biochem. Pharmacol.*, **24**, 1767 (1975).
(184) G. D. Olsen, *Science*, **176**, 525 (1972).
(185) G. D. Olsen, *Clin. Pharmacol. Ther.*, **14**, 338 (1973).
(186) G. L. Cohn, J. A. Cramer, W. McBride, R. C. Brown, and H. D. Kleber, *Proc. Soc. Exp. Biol. Med.*, **147**, 664 (1974).
(187) G. D. Olsen, *Clin. Pharmacol. Ther.*, **17**, 31 (1975).
(188) B. L. Herndon, D. H. Baeder, and D. A. Ringle, *Clin. Exp. Immunol.*, **23**, 367 (1976).
(189) D. G. Liegler, E. S. Henderson, M. A. Hahn, and V. T. Oliverio, *Clin. Pharmacol. Ther.*, **10**, 849 (1969).
(190) M. Esposito, R. Rosso, and L. Santi, *Res. Basic Pharmacol.*, **3**, 1180 (1974).
(191) A. M. Guarino, J. B. Anderson, D. K. Starkweather, and C. F. Chignell, *Cancer Chemother. Rep.*, **57**, 125 (1973).
(192) D. W. Donigian and R. J. Owellen, *Biochem. Pharmacol.*, **22**, 2113 (1973).
(193) R. J. Owellen and C. A. Hartke, *Cancer Res.*, **35**, 975 (1975).
(194) J. A. Hickman, *Biochem. Pharmacol.*, **23**, 2833 (1974).
(195) W. Mikikits, A. Skinner, R. G. Spector, and D. C. Watts, *Br. J. Pharmacol.*, **41**, 76 (1971).
(196) J. O. Branstad, U. Meresaar, and A. Agren, *Acta Pharm. Suec.*, **9**, 129 (1972).
(197) M. Ehrnebo, *ibid.*, **11**, 655 (1974).
(198) R. Edwards and F. R. Ellis, *Br. J. Anaesth.*, **45**, 891 (1973).
(199) D. S. Lukas and A. G. DeMartino, *J. Clin. Invest.*, **48**, 1041 (1969).
(200) A. Brock, *Acta Pharmacol. Toxicol.*, **36**, 13 (1975).
(201) *Ibid.*, **34**, 260 (1974).
(202) J. D. Baggot and L. E. Davis, *Res. Vet. Sci.*, **15**, 81 (1973).
(203) J. E. Doherty and W. H. Hall, *Am. J. Cardiol.*, **28**, 326 (1971).
(204) E. E. Ohnhaus, P. Spring, and L. Dettli, *Eur. J. Clin. Pharmacol.*, **5**, 34 (1972).
(205) R. F. Mais, S. Keresztes-Nagy, J. F. Zaroslinski, and Y. T. Oester, *J. Pharm. Sci.*, **63**, 1423 (1974).
(206) Y. W. Chien, H. J. Lambert, and A. Karim, *ibid.*, **63**, 1877 (1974).
(207) W. Wosilait, *Res. Commun. Chem. Pathol. Pharmacol.*, **12**, 147 (1975).
(208) A. Breckenridge and A. Rosen, *Biochim. Biophys. Acta*, **229**, 610 (1971).
(209) A. Agren and T. Back, *Acta Pharm. Suec.*, **10**, 223 (1973).
(210) D. L. Davies, A. F. Lant, N. R. Millard, A. J. Smith, J. W. Ward,

and G. M. Wilson, *Clin. Pharmacol. Ther.*, **15,** 153 (1974).
(211) F. Andreasen and E. Mikkelsen, *Acta Pharmacol. Toxicol., Suppl.*, **35,** 18 (1974).
(212) J. Prandota and A. W. Pruitt, *Pediatr. Res.*, **8,** 365 (1974).
(213) A. Lev-Ran, L. Ratt, and A. Bar-Ayal, "Kupat-Holim Year Book," Tel Aviv, **2,** 215 (1972).
(214) A. H. Christiansen and A. Volund, *Diabetologia*, **7,** 475 (1971).
(215) J. Judis, *J. Pharm. Sci.*, **61,** 89 (1972).
(216) M. J. Crooks and K. F. Brown, *ibid.*, **62,** 1904 (1973).
(217) B. Nilsson and A. Agren, *Acta Pharm. Suec.*, **11,** 391 (1974).
(218) K. F. Brown and M. J. Crooks, *Can. J. Pharm. Sci.*, **9,** 75 (1974).
(219) H. A. E. Schmidt, M. Schoog, K. H. Schveer, and E. Winkler, *Diabetologia*, **9,** 320 (1973).
(220) P. L. Hsu, J. K. H. Ma, and L. A. Luzzi, *J. Pharm. Sci.*, **63,** 570 (1974).
(221) H. Zia and J. C. Price, *ibid.*, **64,** 1177 (1975).
(222) W. E. Muller and U. Wollert, *Res. Commun. Chem. Pathol. Pharmacol.*, **13,** 551 (1976).
(223) E. R. Garrett, J. Tsau, and P. H. Hinderling, *J. Pharm. Sci.*, **61,** 1411 (1972).
(224) G. T. Tucker, R. N. Boyes, P. O. Bridenbaugh, and D. C. Moore, *Anesthesiology*, **33,** 287 (1970).
(225) *Ibid.*, **33,** 304 (1970).
(226) M. M. Ghoneim and H. Pandya, *Br. J. Anaesth.*, **46,** 435 (1974).
(227) N. Benowitz, R. P. Forsyth, K. L. Melmon, and M. Rowland, *Clin. Pharmacol. Ther.*, **16,** 87 (1974).
(228) O. Borga, D. L. Azarnoff, G. P. Forshell, and F. Sjoqvist, *Biochem. Pharmacol.*, **18,** 2135 (1969).
(229) H. J. Weder and M. H. Bickel, *J. Pharm. Sci.*, **59,** 1563 (1970).
(230) B. Alexanderson and O. Borga, *Eur. J. Clin. Pharmacol.*, **4,** 196 (1972).
(231) B. G. Winsberg, J. M. Perel, M. J. Hurwic, and A. Klutch, in "The Phenothiazines and Structurally Related Drugs," I. S. Forrest, C. J. Can, and E. Usdin, Eds., Raven, New York, N.Y., 1974, p. 425.
(232) S. H. Curry, *J. Pharm. Pharmacol.*, **24,** 818 (1972).
(233) *Ibid.*, **22,** 193 (1970).
(234) J. J. Noval and V. Champion, *Res. Commun. Chem. Pathol. Pharmacol.*, **6,** 123 (1973).
(235) T. S. S. Mao and J. J. Noval, *Biochem. Pharmacol.*, **22,** 2497 (1973).
(236) M. H. Bickel, *J. Pharm. Pharmacol.*, **27,** 733 (1975).
(237) D. Sharples, *ibid.*, **27,** 379 (1975).
(238) *Ibid.*, **28,** 100 (1976).
(239) J. Krieglstein, F. Lier, and J. Michaelis, *Naunyn-Schmiedebergs Arch. Pharmacol.*, **272,** 121 (1972).
(240) A. Hulshoff, Ph.D. thesis, University of Utrecht, Utrecht, The Netherlands, 1976, p. 111.
(241) U. Klotz, K. H. Antonin, and P. Bieck, *Naunyn-Schmiedebergs Arch. Pharmacol.*, **287,** 121 (1972).
(242) L. Kangas, J. Kanto, and T. Siirtola, *Acta Pharmacol. Toxicol. Suppl.*, **35,** 35 (1975).
(243) W. E. Muller and U. Wollert, *Biochem. Pharmacol.*, **25,** 141 (1976).
(244) W. E. Muller and U. Wollert, *Naunyn-Schmiedebergs Arch. Pharmacol.*, **287,** R66 (1975).
(245) R. W. Lucek and C. B. Coutinho, *Fed. Proc.*, **35,** 487 (1976).
(246) J. D. Baggot, L. E. Davis, and C. A. Neff, *Biochem. Pharmacol.*, **21,** 1813 (1972).
(247) S. P. Baker and B. A. Hemsworth, *J. Pharm. Pharmacol.*, **24,** 164P (1972).
(248) M. Wahlqvist, I. M. Nilsson, F. Sandberg, and S. Agurell, *Biochem. Pharmacol.*, **19,** 2579 (1970).
(249) D. Y. Wang and F. D. Bulbrook, *Eur. J. Cancer*, **5,** 247 (1969).
(250) U. Westphal and G. B. Harding, *Biochim. Biophys. Acta*, **310,** 518 (1973).
(251) A. F. Clark and C. E. Bird, *J. Endocrinol.*, **57,** 289 (1973).
(252) U. Goebelsmann, L. C. Chen, M. Saga, R. M. Nakamura, and R. B. Jaffe, *Acta Endrocrinol.*, **74,** 592 (1973).
(253) J. A. Blaquier and M. S. deCameo, *Steroids*, **15,** 219 (1970).
(254) E. Nunez, G. Vallette, C. Benassayag, and M. F. Jayle, *Biochem. Biophys. Res. Commun.*, **57,** 126 (1974).
(255) M. T. Ryan and G. Gibbs, *Biochim. Biophys. Acta*, **222,** 206 (1970).
(256) J. C. Russell and D. M. Doty, *Physiol. Chem. Phys.*, **5,** 75 (1973).
(257) A. Danon and J. D. Sapira, *J. Pharmacol. Exp. Ther.*, **182,** 295 (1972).
(258) H. Zia, R. H. Cox, and L. A. Luzzi, *J. Pharm. Sci.*, **60,** 89 (1971).
(259) P. May, F. J. Sanders, and R. K. Donabedian, *Experientia*, **30,** 304 (1974).
(260) G. Powis, *Biochem. Pharmacol.*, **24,** 707 (1975).
(261) D. V. Naik, W. L. Paul, and S. G. Schulman, *J. Pharm. Sci.*, **64,** 1677 (1975).
(262) J. T. Biggs and L. Levy, *Proc. Soc. Exp. Biol. Med.*, **137,** 692 (1971).
(263) D. R. Sanvordeker, Y. W. Chien, T. K. Lin, and H. J. Lambert, *J. Pharm. Sci.*, **64,** 1797 (1975).
(264) A. Hulshoff and J. H. Perrin, *J. Chromatogr.*, in press.
(265) D. E. Schwartz and F. Jeunet, *Chemotherapy*, **22,** 19 (1976).
(266) J. J. Vallner, L. A. Sternson, and D. L. Parsons, *J. Pharm. Sci.*, **65,** 873 (1976).
(267) A. Raz, *Biochem. J.*, **130,** 631 (1972).
(268) W. G. Unger, *J. Pharm. Pharmacol.*, **24,** 470 (1972).

ACKNOWLEDGMENTS AND ADDRESSES

Received from the *Department of Pharmaceutics, School of Pharmacy, University of Georgia, Athens, GA 30602.*

The author expresses appreciation to Dr. L. C. Schramm for discussions during the preparation of this review and to Ms. K. Minter and Ms. J. Lemmon for help with manuscript preparation.

Fenbufen, a New Anti-Inflammatory Analgesic: Synthesis and Structure–Activity Relationships of Analogs

RALPH G. CHILD ˣ, ARNOLD C. OSTERBERG, ADOLPH E. SLOBODA, and ANDREW S. TOMCUFCIK

Abstract □ One hundred analogs of fenbufen were prepared and tested using the carrageenan, polyarthritis, and UV erythema anti-inflammatory tests and the 2-phenyl-1,4-benzoquinone writhing and inflamed paw pressure analgesic tests. Only three retained the same full spectrum of activity as fenbufen: *dl*-4-(4-biphenylyl)-4-hydroxybutyric acid, *dl*-4-(4-biphenylyl)-1,4-butanediol, and 4-biphenylacetic acid. Fenbufen had the same spectrum of activity as aspirin, phenylbutazone, and indomethacin in the five tests. In addition, dose–response derived potencies show fenbufen more potent than aspirin and at least as potent as phenylbutazone in all five tests. Two related compounds were generally similar.

Keyphrases □ Fenbufen—and various analogs, synthesized and evaluated for anti-inflammatory and analgesic activity □ Anti-inflammatory activity—evaluated in fenbufen and various analogs □ Analgesic activity—evaluated in fenbufen and various analogs □ Structure–activity relationships—fenbufen and various analogs, evaluated for anti-inflammatory and analgesic activity

While designing and synthesizing compounds for an immunosuppressive program, fenbufen (I) (1) was prepared as an intermediate potentially capable of imparting anti-inflammatory activity. Although fenbufen was uninteresting as an immunosuppressive, its activity in the ancillary anti-inflammatory tests (2) and its recognition as belonging to the well-known arylaliphatic carboxylic ("arylalkanoic") acid class of anti-inflammatory analgesics (3–5) prompted its full testing in this area. The biological testing program supporting this effort included the carrageenan-induced edema of the rat paw (6) and the guinea pig erythema (7) as anti-inflammatory tests, the polyarthritis test in rats as a model of chronic inflammation (8, 9), and the 2-phenyl-1,4-benzoquinone writhing (10) and paw pressure threshold (11) tests for analgesic action. When the preliminary screening data on I indicated activity in all five tests, a program was initiated to explore the structure–activity relationships of a series of analogs.

DISCUSSION

Chemistry—Most of the synthesized compounds were prepared by the Friedel–Crafts condensation of succinic anhydride with various aromatic compounds catalyzed by aluminum chloride. The reaction was described previously (12), and no unexpected difficulties were encountered. Twelve compounds were prepared by modification of preformed aryl keto acids. Thus, the benzylphenyl analog (VIII) was oxidized with chromic acid to the benzoylphenyl analog (XVI); similarly, the fluorene ring (III) gave the oxofluorene analog (XXV). Oxidation of the thioether (XIX) with peroxide gave the sulfoxide (XXI), whereas chromic oxide gave the sulfone (XX). Diazotization of the *p*-aminophenyl analog (13) followed by coupling to 2,6-diaminopyridine gave the azo compound (XXVII), which was oxidatively cyclized to the triazolo analog (XXVIII). The same *p*-aminophenyl analog reacted with *p*-chlorobenzoyl chloride to give the benzamido derivative (X). Table I summarizes the physical and pharmacological properties of the 3-(4-arylcarbonyl)propionic acids synthesized.

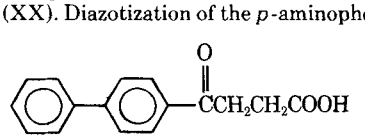

I

In the miscellaneous group (Table II) of compounds not previously described, sodium borohydride reduction of 4-phenoxybenzoylpropionic acid (V) gave the 4-hydroxybutyric acid analog (XXXIII) and bromination of 4-benzylbenzoylpropionic acid (VIII) gave the 3-bromopropionic acid analog (XXXIV).

The compounds listed in Table III consist of variations in the alkyl chain with the biphenyl moiety kept constant. The procedures used to modify the acid function of I or to replace it with various terminal substituents included esterification of I with ethanol and sulfuric acid to give the ester (XXXVIII) (Scheme I, R_1 = biphenylyl). The 4-hydroxy acid hydrazide (LXXII) came from the lactone (LX) (Scheme I) and hydrazine; the three polyols (XCI, C, and CI) were produced by reduction of the keto ester (XXXVIII), the diketone (XCVII), and the diketo ester (XCVI), respectively, with sodium bis(2-methoxyethoxy)aluminum hydride[1]. The chloro derivative (XLIV), obtained by Friedel–Crafts reaction of 3-chloropropionyl chloride and biphenyl, served as the intermediate for a number of products: the sodium sulfonate (L) *via* the acrylophenone (XLIII), the thioimidazoline (LI) from the corresponding imidazoline-2-thione, the nitrile (LII), and the *p*-tolylsulfinate (LIV).

The three amides (LXV, LXVI, and LXVII) were readily prepared directly from I and the corresponding amine at room temperature with the aid of the peptide-forming reagent, 1-ethoxycarbonyl-2-ethoxy-1,2-dihydroquinoline[1] (CIII), in tetrahydrofuran (Scheme I, R_1 = biphenylyl). The procedure is simple, the by-products are volatile, and the yields are good.

Modifications to the carbonyl included the enol lactone (XXXIX) from I in boiling acetic anhydride (Scheme I, R_1 = biphenylyl). Reduction of I with excess sodium borohydride gave the *dl*-4-hydroxy analog (LV) (Scheme I). Resolution into the *d*- and *l*-isomers (LVI and LVII) was accomplished using the *d*- and *l*-isomers, respectively, of 2-aminobutanol. The *dl*-4-hydroxy acid (LV) cyclized readily in acid media to the lactone (LX) (Scheme I).

The keto group of I reacted with aminoguanidine to give the corresponding guanylhydrazone (XLI) and with hydroxylamine to give the oxime (LXI) (Scheme I, R_1 = biphenylyl). Reduction of the oxime with zinc and ammonium hydroxide afforded the 4-amino derivative (LXXXII). Methyl magnesium iodide added to the 4-carbonyl of the ester (XXXVIII), which subsequently lactonized by loss of ethanol to the lactone (LXII) (Scheme I). Dilute alkali opened the lactone to the corresponding 4-hydroxyvaleric acid analog (LXIII).

The Wittig reaction was employed in two instances to prepare biphenylbutenoic acids with the unsaturation conjugated to the biphenyl group. Thus, 4-acetylbiphenyl and the Wittig reagent, 2-carboxyethyltriphenylphosphonium chloride, yielded 4-(4-biphenylyl)-3-pentenoic acid (LXX). Similarly, 4-biphenylcarboxaldehyde yielded the 3-butenoic acid (XCIV).

The preparation of the sulfonyl (in place of carbonyl) analog of I required the preparation of 4-phenylthiophenol from diazotized 4-aminobiphenyl followed by condensation with 3-bromopropionic acid to give the thioether. This thioether was then oxidized *in situ* with peroxide to give the desired 3-(4-biphenylsulfonyl)propionic acid (LXXV).

The α,β-unsaturated chain analog of I was prepared directly from bi-

[1] Aldrich Chemical Co.

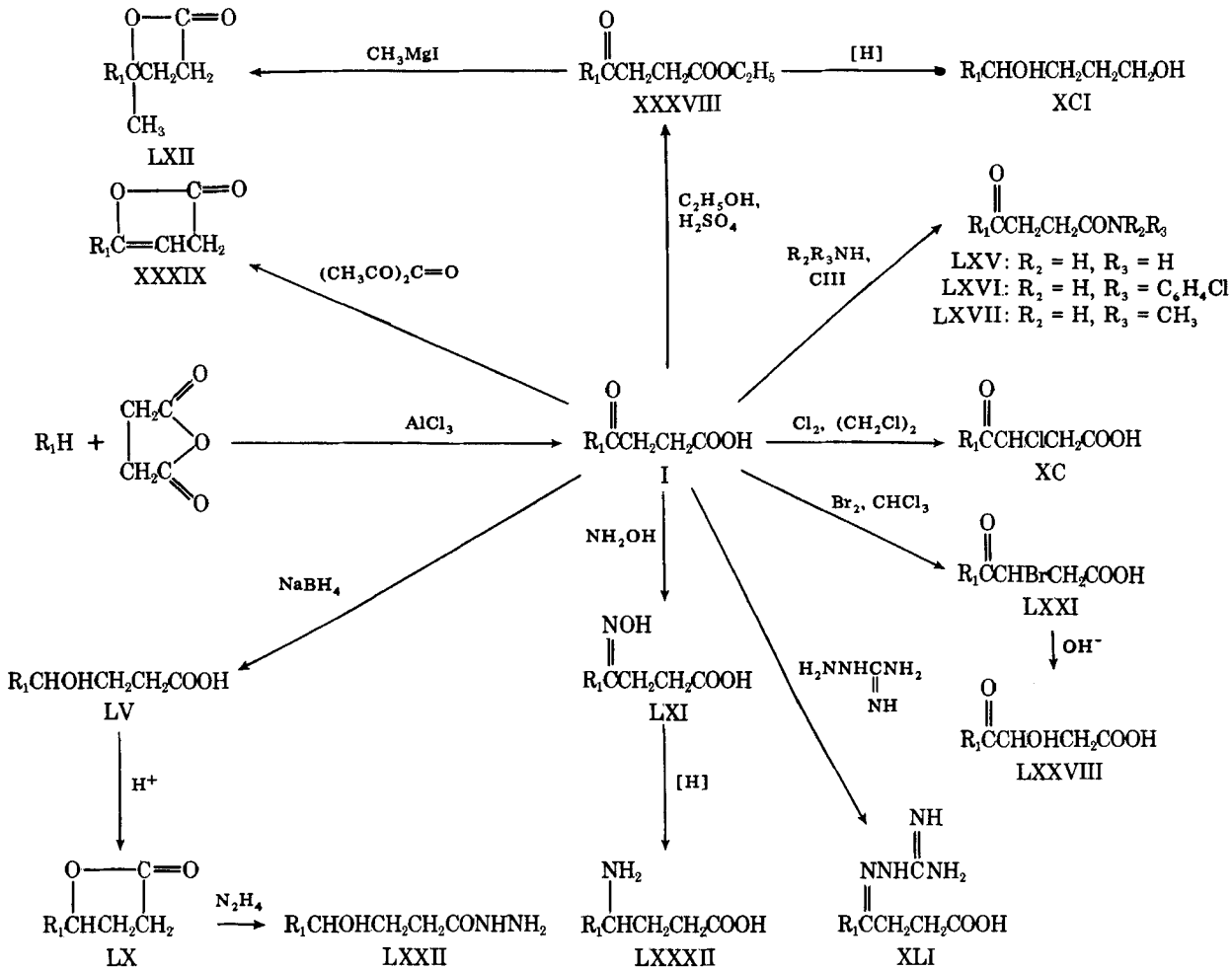

Scheme I

phenyl and maleic anhydride *via* the Friedel–Crafts reaction, giving 3-(4-biphenylylcarbonyl)acrylic acid (XL). On reduction with sodium borohydride, XL gave the unsaturated alcohol derivative (XCIII) (Scheme II, R_1 = biphenylyl).

The α,β-unsaturated analog (XL) was used to prepare a series of products by addition to the double bond. Thus, bromination in acetic acid gave one racemate isomer of the 2,3-dibromo analog (LXXX); bromination in chloroform gave the other 2,3-dibromo racemate (LXXXI) (Scheme II, R_1 = biphenylyl). Chlorination in acetic acid gave a 2,3-dichloro derivative (LXXXIX). Refluxing XL in dilute hydrochloric acid gave the 2-hydroxy analog (LXXIX) (Scheme II).

Bromination of I in ethanol-free chloroform gave the 3-bromo analog (LXXI) (Scheme I, R_1 = biphenylyl), which when stirred in dilute sodium carbonate solution, hydrolyzed to the 3-hydroxy derivative (LXXVIII). Similarly, chlorination of I in dichloroethane gave the 3-chloro analog (XC) (Scheme I).

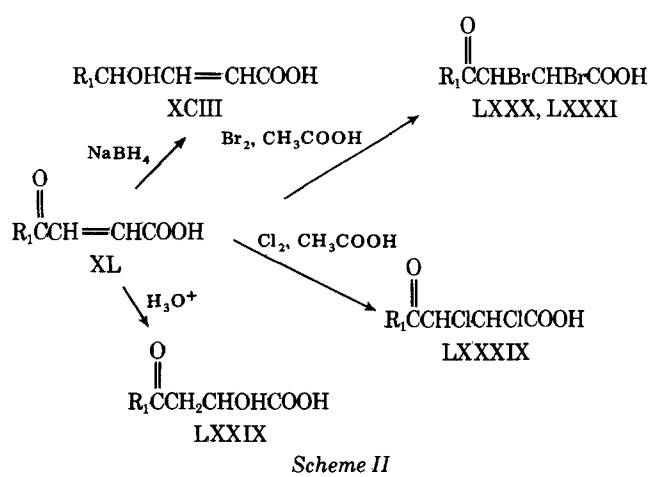

Scheme II

Only the 2-methyl analog (XLVIII) was isolated from the Friedel–Crafts reaction of biphenyl and methylsuccinic anhydride. The 2-phenyl congener (XLIX) was prepared by hydrochloric acid hydrolysis in acetic acid of the corresponding nitrile (XLVII) which, in turn, was obtained by addition of hydrocyanic acid to 4′-phenylchalcone.

The Friedel–Crafts reaction of biphenyl and glutaric anhydride gave far lower yields than with succinic anhydride. Nevertheless, 4-(4-phenylbenzoyl)butyric acid (LXIX) was obtained in sufficient quantity and also brominated to the 4-bromo derivative (LXXVI). Finally, 4-biphenylcarboxaldehyde condensed smoothly with cyanoacetic acid in base to give good yields of 3-(4-biphenylyl)-2-cyanoacrylic acid (LXXXVIII).

Biological Activity—All compounds were tested in the carrageenan anti-inflammatory and 2-phenyl-1,4-benzoquinone writhing analgesic tests. The decision to use the remaining three tests was dictated by the activity in the two basic tests and the availability of sufficient quantities of the compounds. These initial screening data were not designed to provide a comparison between compounds in any one test. The spectrum of activity over the range of all five tests using a standard large dose (250 mg/kg) provided a rapid initial evalution of a fairly large series of compounds, enabling selection of compounds for further study.

Table I lists the modifications to the biphenyl moiety or its replacement by other bulky groups and shows that all changes generally resulted in a reduced spectrum of activity. For example, substitution in the 4-position of the terminal phenyl group by chloro (II), methoxy (XI), phenyl (XVII), or fluoro (XXIX) groups decreased the carrageenan anti-inflammatory activity overall, and, where tested, there was a similar decrease in polyarthritis, UV erythema, and analgesic activity. In the single instance of a substituent on the ring adjacent to the alkyl chain, the 2-methoxy-5-phenyl analog (XII), there was complete loss of activity.

Separation of the two phenyl groups by oxygen, as in V, depressed

Table I—3-(4-Arylcarbonyl)propionic Acids

$RCOCH_2CH_2CO_2H$

Compound	R	Method	Reaction Solvent	Yield, %	Recrystallization Solvent	Melting Point	Formula	Analyses, % Calc.	Analyses, % Found	Carrageenan Edema, C/T, Paw Volume	Adjuvant Arthritis, % Inhibition	UV Erythema % Inhibition	2-Phenyl-1,4-benzoquinone, Number of Writhes	Paw Pressure Threshold, T/C
I	4-$C_6H_5C_6H_4$—[a]	A	$C_6H_5NO_2$	70	C_2H_5OH	185–187°	$C_{16}H_{14}O_3$	—	—	1.9	71	100	3	2.3
II	4-(4-ClC_6H_4)C_6H_4—[b]	A	CS_2	38	$CHCl_3$	185.5–186.5°	$C_{16}H_{13}ClO_3$	—	—	NA[c]	61	NA	16	1.8
III	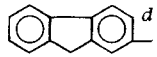 [d]	A	C_6H_6	80	—[e]	212–215°	$C_{17}H_{15}O_3$	—	—	NA	—	NA	NA	—
IV	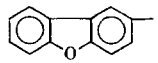 [f]	A	$(CHCl_2)_2$, $C_6H_5NO_2$	28	$CH_3COOC_2H_5$	185–187°	$C_{16}H_{12}O_4$	—	—	1.8	3.7	NA	NA	—
V	4-(C_6H_5O)C_6H_4—[g]	A	C_6H_6	67	—[e]	117–119°	$C_{16}H_{14}O_4$	—	—	1.9	NA	94	8	NA
VI	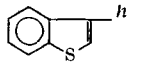 [h]	A	$C_6H_5NO_2$	8	C_6H_6	133°	$C_{12}H_{10}O_3S$	—	—	NA	—	—	—	—
VII	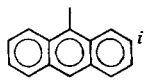 [i]	A	$C_6H_5NO_2$	43	C_2H_5OH	158–160°	$C_{18}H_{14}O_3$	—	—	NA	—	—	NA	—
VIII	4-($C_6H_5CH_2$)C_6H_4—[j]	A	$C_6H_5NO_2$	37	C_6H_6	125–127°	$C_{17}H_{17}O_3$	—	—	1.7	—	—	NA	—
IX	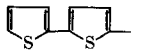	A	$C_6H_5NO_2$	10	C_6H_6	175–177°	$C_{12}H_{10}O_3S_2$	C 54.11 H 3.79 S 24.08	54.54 3.84 23.78	NA	NA	NA	NA	—
X	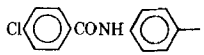	—	Aqueous NaOH	20	$CH_3OCH_2CH_2OH$	270–271°	$C_{17}H_{14}ClNO_4$	C 61.55 H 4.25 H 4.22 Cl 10.69	61.32 4.34 3.92 10.70	NA	NA	—	9	—
XI	4-($CH_3OC_6H_4$)C_6H_4—	A	$(CH_2Cl)_2$	9	—	201–202°	$C_{17}H_{16}O_4$	—	—	NA	—	—	8	NA
XII	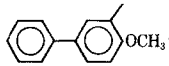 [j]	A	$(CHCl_2)_2$, $C_6H_5NO_2$	43	—	147–149°	$C_{17}H_{16}O_4$	—	—	NA	—	—	NA	—
XIII	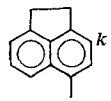 [k]	A	$C_6H_5NO_2$	90	—[l]	205–208°	$C_{16}H_{14}O_3$	—	—	NA	—	—	13	NA
XIV	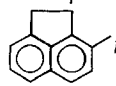 [k]	A	$C_6H_5NO_2$	1.4	—[m]	125–126°	$C_{16}H_{14}O_3$	—	—	NA	—	—	NA	—
XV	4-(*n*-C_4H_9O)C_6H_4—[n]	A	$C_6H_5NO_2$	82	—[d]	108–110°	$C_{14}H_{18}O_4$	—	—	NA	—	—	NA	—
XVI	4-(C_6H_5CO)C_6H_4—[o]	—	CH_3COOH	43	$(CH_2Cl)_2$, C_6H_{14}	125–127°	$C_{17}H_{14}O_4$	C 72.33 H 5.00	72.23 5.02	2.2	NA	NA	—	NA

XVII	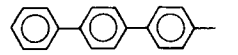	A	$C_6H_5NO_2$	24	CH_3COOH	255–258°	$C_{22}H_{18}O_3$	C 79.98 80.63 H 5.49 5.54	NA	—	—	NA	—
XVIII	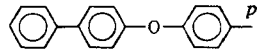 [p]	A	C_6H_6	63	C_2H_5OH	185–187°	$C_{22}H_{18}O_4$	C 76.28 75.84 H 5.24 5.14	NA	—	—	NA	—
XIX	4-(C_6H_5S)C_6H_4—	A	C_6H_6	75	C_6H_6	143–145°	$C_{16}H_{14}O_3S$	C 67.12 67.30 H 4.93 4.87 S 11.18 11.21	1.7	40	NA	8	NA
XX	4-($C_6H_5SO_2$)C_6H_4—	—	CH_3COOH	65	Aqueous C_2H_5OH	157–159°	$C_{16}H_{14}O_5S$	C 60.08 59.79 H 4.42 4.33 S 10.05 10.31	NA	—	—	NA	—
XXI	4-(C_6H_5SO)C_6H_4—	—	$(CH_3)_2CO$	95	Aqueous C_2H_5OH	162–163°	$C_6H_{14}O_4S$	C 63.57 63.96 H 4.67 4.56 S 10.59 10.56	NA	—	—	NA	—
XXII	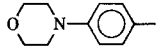	A	$(CHCl_2)_2$	6	H_2O	163–164°	$C_{14}H_{17}NO_4$	C 63.86 63.97 H 6.41 6.45 N 5.32 5.18	NA	—	—	NA	—
XXIII	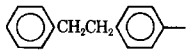	A	$C_6H_5NO_2$	80	Aqueous C_2H_5OH	125–127°	$C_{18}H_{18}O_3$	C 76.57 76.48 H 6.43 6.28	NA	NA	—	NA	—
XXIV	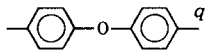 [q]	A	$(CHCl_2)_2$	22	—[r]	226–228°	$C_{20}H_{18}O_7$	— —	NA	—	—	NA	—
XXV	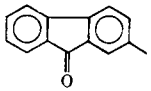	—	CH_3COOH	10	—[d]	—	$C_{17}H_{12}O_4$	C 72.85 72.09 H 4.32 4.43	NA	—	—	NA	—
XXVI	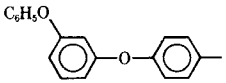	A	C_6H_6	16	C_6H_6	134–135°	$C_{22}H_{18}O_5$	C 72.92 73.18 H 5.01 5.11	NA	—	—	NA	—
XXVII	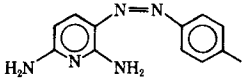	—	H_2O	54	—[r]	265–270°	$C_{15}H_{15}N_5O_3$	C 57.50 56.42 H 4.83 5.01 N 22.35 22.71	NA	NA	—	NA	—
XXVIII	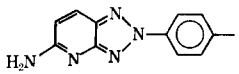	—	C_5H_5N	17	—[s]	>300°	$C_{15}H_{13}N_6O_3$	N 22.50 22.66	NA	NA	—	11	—
XXIX	4-(4-FC_6H_4)C_6H_4—	A	CS_2	23	CH_3COOH	169–171°	$C_{16}H_{13}FO_3$	C 70.57 70.72 H 4.81 4.70 F 6.98 6.35	1.7	NA	NA	10	NA
XXX	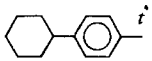 [t]	A	$C_6H_5NO_2$	66	C_6H_6	135–137°	$C_{16}H_{19}O_3$	— —	NA	—	—	NA	—

[a] Reference 1. [b] Reference 14. [c] NA = not active. [d] Reference 15. [e] Precipitates from sodium carbonate solution with hydrochloric acid. [f] References 16 and 17. [g] Reference 18. [h] Reference 19. [i] Reference 20. [j] Reference 21. [k] Reference 22. [l] Purified as the sodium salt and liberated with acid. [m] Purified *via* the methyl ester. [n] Reference 23. [o] Mass spectrum showed a mass ion of 282 and a strong 209 of $C_6H_5COC_6H_4CO$. [p] UV λ_{max} (methanol): 273 nm. Compound V λ_{max} (methanol): 268 nm; XI λ_{max} (methanol): 302 nm. [q] Reference 24. [r] Aqueous dimethylformamide. [s] Precipitated from ammonia solution with acetic acid. [t] Reference 25.

Table II—Miscellaneous Compounds

Compound	R	Method	Reaction Solvent	Yield, %	Recrystallization Solvent	Melting Point	Formula	Analyses, %		Carrageenan Edema, C/T, Paw Volume	Adjuvant Arthritis, % Inhibition	UV Erythema, % Inhibition	2-Phenyl-1,4-benzoquinone, Number of Writhes	Paw Pressure Threshold, T/C
								Calc.	Found					
XXXI	[a]	A	$(CH_2Cl)_2$	36	C_2H_5OH	87–90°	$C_{11}H_{10}OS_2$	—	—	NA[b]	—	—	14	NA
XXXII	[a]	A	$(CH_2Cl)_2$	32	C_2H_5OH	117–180°	$C_{14}H_{14}O_2S_2$	—	—	NA	NA	NA	—	—
XXXIII	4-$(C_6H_5O)C_6H_4CH(OH)CH_2CH_2CO_2H$	—	H_2O	88	—[c]	102–103°	$C_{16}H_{16}O_4$	C 70.57 H 5.92	70.22 5.82	2.2	NA	NA	12	1.8
XXXIV	4-$(C_6H_5CH_2)C_6H_4CO$-$CHBrCH_2CO_2H$[d]	—	$(CH_2Cl)_2$	43	C_6H_6	137–138°	$C_{17}H_{15}BrO_3$	C 58.81 H 4.26 Br 23.02	59.23 4.49 23.13	1.7	—	—	NA	—
XXXV	4-$(C_6H_5S)C_6H_4$-$(CH_2)_3CO_2H$[e]	—	—[f]	95	—[g]	66–67°	$C_{16}H_{16}O_2S$	—	—	2.3	NA	NA	NA	—

[a] Reference 26. [b] NA = not active. [c] See *Experimental*. [d] Mass spectrum showed a mass ion of 346 and a 195, 4-$(C_6H_5CH_2)C_6H_4CO$, indicative of bromination in the propionic acid chain. [e] Reference 27. [f] Triethylene glycol. [g] Precipitated from alkaline solution by addition of hydrochloric acid.

activity in all five tests; the addition of a dibenzofuran group (IV) reduced activity further.

Separation by sulfur (XIX) showed about the same order of reduction of activity as the oxygen analog (V). Oxidation of the sulfur in XIX to sulfoxide (XXI) and sulfone (XX) destroyed activity completely. In contrast, where the phenyl groups were separated by a methylene (VIII), oxidation to a carbonyl (XVI) caused a slight increase in the low order of activity. Again, addition of a fluorene (III) or 9-oxofluorene (XXV) reduced activity further.

Separation of the two phenyl groups by an ethylene (XXIII) resulted in total loss of activity. Similarly, separation by a carboxamide group (X) gave much lower activity when compared to the analogous II. With phenyl as a separating group in the terphenyl analog (XVII), activity was totally eliminated.

Replacement of the terminal phenyl group by various substituents such as butoxy (XV), morpholino (XXII), 3-phenoxyphenoxy (XXVI), diaminopyridylazo (XXVII), its cyclized triazolopyridyl (XXVIII), and cyclohexyl (XXX) likewise eliminated all activity.

None of the other various bulky aromatic groups such as VI, VII, IX, XIII, XIV, and XVIII showed any activity. The one case of a bis(carboxypropionic acid)-substituted diphenyl ether (XXIV) similarly was inactive.

With the miscellaneous compounds of Table II, reduction of the carbonyl of V to a carbinol (XXXIII) made no significant change, nor did the complete reduction of the carbonyl of XIX to a methylene (XXXV). Similarly, bromination of the chain in the 3-position of VIII giving XXXIV made no change in the activity spectrum.

Among the numerous changes to the alkyl chain moiety of I listed in Table III, only three retained the full spectrum of activity: the racemic 4-hydroxy analog (LV), the racemic 1,4-diol (XCI), and the acetic acid analog (CII). Although the full spectrum of tests was not carried out on the *d*-LVI and *l*-LVII isomers of LV, it appears that they were comparable.

Halogenation in the 3-position of I, *e.g.*, the 3-bromo product (LXXI), or its ester (LXIV) and the 3-chloro product (XC), retained the anti-inflammatory activity but reduced the analgesic activity. The 2,3-dichloro derivative (LXXXIX), as well as both racemates of the 2,3-dibromo analog (LXXX and LXXXI), showed minimal activity in both the anti-inflammatory and analgesic tests.

The effect of modifying the carboxylic acid group of I was dramatic and surprising in that only the 4-hydroxy acid hydrazide (LXXII) and the 1,4-diol (XCI) of 13 congeners retained anti-inflammatory activity. Unexpectedly, the ethyl ester (XXXVIII) and the three amides (LXV, LXVI, and LXVII) were devoid of carrageenan activity. Other substitutions for the carboxylic acid function that were inactive were the chloro (XLIV), the sodium sulfonate (L), the thioimidazole (LI), the nitrile (LII), the *p*-toluenesulfonate (LIV), the acetyl (XCVII), and the hydroxyethyl (C).

Modifications of the 4-carbonyl function of I, other than its reduction to a carbinol (LV), produced less active compounds. Thus, complete reduction to the methylene (XXXVI) eliminated the polyarthritis and paw pressure activity. The lactone (LX) of the 4-hydroxy acid (LV) showed only UV erythema and writhing activity, whereas the enol lactone (XXXIX) showed no activity. The oxime (LXI) and the 4-amino derivative (LXXXII) were completely inactive, yet the guanyl hydrazone ester (XLI) showed carrageenan activity. Reductive alkylation of the carbonyl to the 4-methyl-4-hydroxy analog (LXIII) and its lactone (LXII) also reduced overall activity. Replacement of the carbonyl by sulfonyl (LXXV) or oxygen (LXXIV) likewise reduced activity.

Unsaturation along the butyric acid chain at the 2,3-position as in XL or its ester (LXVIII) and XCIII eliminated anti-inflammatory activity, leaving minimal analgesic activity. However, unsaturation at the 3,4-position (XCIV) retained, except for the paw pain, a full spectrum of activity. Similarly, the 4-methyl 3,4-unsaturated analog (LXX) retained carrageenan activity but lost analgesic activity.

Aryl substitution as in the 2-phenyl (XLIX) and 3-phenyl (LXXVII) derivatives destroyed all activity. Alkyl substitution as in the 2-methyl (XLVIII) derivative retained only writhing activity.

Lengthening the alkyl chain as in the valeric acid 5-oxo analog (LXIX) reduced anti-inflammatory activity and eliminated analgesic activity. The 4-bromo derivative (LXXVI) was completely inactive.

Both the 2- and 3-hydroxy-substituted analogs of I (LXXIX and LXXVIII, respectively) showed only carrageenan activity. The remaining miscellaneous substituted biphenyls of Table III were inactive.

Summary—The only modifications or analogs of I that, at best, did not reduce the spectrum of activity over the five tests were the reduction of the 4-carbonyl to a carbinol, giving *dl*-4-(4-biphenylyl)-4-hydroxy-

Table III—Substituted Biphenyls

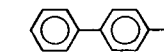

Compound	R	Yield, %	Recrystallization Solvent	Melting Point	Formula	Analyses, % Calc.	Analyses, % Found	Carrageenan Edema, C/T, Paw Volume	Adjuvant Arthritis, % Inhibition	UV Erythema, % Inhibition	2-Phenyl-1,4-benzoquinone, Number of Writhes	Paw Pressure Threshold, T/C
XXXVI	$-(CH_2)_3CO_2H$[a]	—	—	—	—	—	—	1.8	NA[b]	94	2	NA
XXXVII	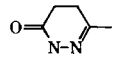	33	—[c]	241–242°	$C_{16}H_{14}N_2O$	C 76.77 H 5.64 N 11.19	C 76.48 H 5.69 N 10.92	1.2	—	—	38	—
XXXVIII	$-CO(CH_2)_2CO_2C_2H_5$	31	C_2H_5OH	48–49°	$C_{18}H_{18}O_3$	C 76.57 H 6.43	C 76.65 H 6.32	NA	—	NA	10	NA
XXXIX	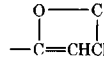	40	$(CH_3CO)_2O$	182–184°	$C_{16}H_{12}O_2$	C 81.33 H 5.12	C 80.91 H 5.03	NA	—	NA	NA	—
XL	$-COCH{=}CHCO_2H$[d]	35	CH_3COOH	172–175°	$C_{16}H_{12}O_2$	—	—	NA	—	NA	4	NA
XLI	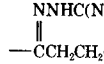	44	C_2H_5OH	193–194°	$C_{17}H_{18}N_4O_2$	C 60.87 H 6.18 N 14.95	C 60.64 H 6.04 N 14.98	2.2[e]	—	NA	NA[f]	—
XLII	$-SO_2NH_2$[g]	55	—[h]	227–228°	$C_{12}H_{11}NSO_2$	—	—	NA	—	—	NA	—
XLIII	$-COCH{=}CH_2$[i]	23	C_2H_5OH	82–84°	$C_{15}H_{12}O$	—	—	NA	—	—	10	NA
XLIV	$-COCH_2CH_2Cl$[i]	70	C_6H_6	119–120°	$C_{15}H_{13}ClO$	—	—	NA	—	—	NA	—
XLV	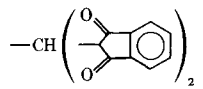	50		188–190°	$C_{31}H_{20}O_4$	C 81.56 H 4.42	C 81.21 H 4.36	NA	—	—	NA	—
XLVI	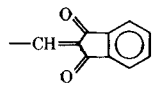	54	CH_3COOH	167–169°	$C_{22}H_{14}O$	C 85.14 H 4.55	C 85.05 H 4.36	NA	—	—	NA	—
XLVII	$-COCH_2CH(C_6H_5)CN$	77	—[c]	175–176°	$C_{22}H_{17}NO$	C 84.86 H 5.50 N 4.50	C 85.68 H 5.45 N 4.30	NA	—	—	13	NA
XLVIII	$-COCH_2CH(CH_3)CO_2H$[j]	55	CH_3OH	212–215°	$C_{17}H_{16}O_3$	—	—	NA	NA	NA	4	NA
XLIX	$-COCH_2CH(C_6H_5)CO_2H$	63	—[k]	180–181°	$C_{22}H_{18}O_3$	C 79.78 H 5.49	C 79.78 H 5.45	NA	NA	NA	NA	—
L	$-COCH_2CH_2SO_3Na$	56	H_2O	278–280°	$C_{15}H_{13}NaO_4S$	C 56.18 H 4.37 S 10.00	C 56.72 H 4.36 S 9.44	NA	—	NA	NA	—
LI	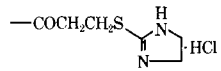	27	C_2H_5OH	163–165°	$C_{18}H_{18}NOS{\cdot}HCl$	C 63.13 H 4.99 N 9.25 S 10.57	C 62.87 H 4.84 N 9.11 S 10.58	NA	—	—	NA	—
LII	$-COCH_2CH_2CN$[l]	75	C_2H_5OH	171–173°	$C_{16}H_{13}NO$	—	—	NA	—	—	NA	—
LIII	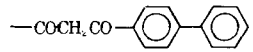	3	C_6H_6	132–133°	$C_{29}H_{24}O$	C 86.11 H 5.98	C 86.45 H 6.00	NA	—	—	NA	—
LIV	$-COCH_2CH_2SO_2C_6H_4$-4-CH_3	49	—[m]	179–180°	$C_{22}H_{20}O_3S$	C 72.50 H 5.53 S 8.80	C 72.39 H 5.41 S 8.83	NA	NA	NA	NA	—
LV	$-CH(OH)CH_2CH_2CO_2H$	97	—[n]	135–136°	$C_{16}H_{16}O_3$	C 74.98 H 6.29	C 74.67 H 6.32	1.8	52	100	3	1.4
LVI	d-$CH(OH)CH_2CH_2CO_2H$	10	C_2H_5OH	153–155°	$C_{16}H_{16}O_3$	C 74.98 H 6.29	C 74.70 H 6.45	2.1	61	92	—	—
LVII	l-$CH(OH)CH_2CH_2CO_2H$	10	C_2H_5OH	153–155°	$C_{16}H_{16}O_3$	C 74.98 H 6.29	C 74.73 H 6.42	2.2	—	82	12	NA

(continued)

Table III—*Continued*

Compound	R	Yield, %	Recrystallization Solvent	Melting Point	Formula	Analyses, % Calc.	Analyses, % Found	Carrageenan Edema, C/T, Paw Volume	Adjuvant Arthritis, % Inhibition	UV Erythema, % Inhibition	2-Phenyl-1,4-benzoquinone, Number of Writhes	Paw Pressure Threshold, T/C
LVIII	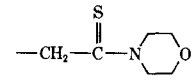	39	C_2H_5OH	138–140°	$C_{18}H_{19}NOS$	C 72.69 H 6.44 N 4.71 S 10.78	72.34 6.56 4.63 11.27	NA	NA	—	NA	—
LIX	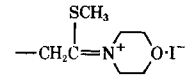	97	$(CH_3)_2CO$	163–167°	$C_{19}H_{22}NOS$	C 51.94 H 5.05 N 3.19 S 7.30	52.02 5.12 3.12 7.56	NA	—	—	NA	—
LX	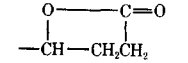	75	—[o]	105°	$C_{16}H_{14}O_2$	C 80.44 H 5.92	80.15 5.77	NA	NA	100	0	NA
LXI	—C(=NOH)$CH_2CH_2CO_2H$	60	C_2H_5OH	188–190°	$C_{16}H_{15}NO_3$	C 71.36 H 5.61 N 5.20	71.79 5.76 5.10	NA	—	—	NA	—
LXII	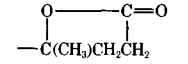	66	C_2H_5OH	107–110°	$C_{17}H_{16}O_2$	C 80.92 H 6.39	80.68 6.50	NA	34	—	NA	—
LXIII	—C(OH)$(CH_3)CH_2CH_2CO_2H$	61	—[n]	133–135°	$C_{17}H_{18}O_3$	C 75.03 H 6.71	74.85 6.67	NA	NA	—	NA	—
LXIV	—$COCHBrCH_2CO_2C_2H_5$	65	CH_3OH	77–78°	$C_{18}H_{17}BrO_3$	C 59.84 H 4.75 Br 22.12	59.96 4.87 21.97	2.3	58	91	NA	NA
LXV	—$COCH_2CH_2CONH_2$	47	C_2H_5OH	191–192°	$C_{16}H_{15}NO_2$	C 75.87 H 5.97 N 5.53	75.61 5.84 4.84	NA	—	—	6	NA
LXVI	—$COCH_2CH_2CONHC_6H_4$-4-Cl	55	C_2H_5OH	200°	$C_{22}H_{18}ClNO$	C 72.61 H 4.98 N 3.85	72.90 4.89 3.74	NA	—	—	NA	—
LXVII	—$COCH_2CH_2CONHCH_3$	40	C_2H_5OH	172–173°	$C_{17}H_{17}NO_2$	C 76.83 H 6.41 N 5.24	76.62 6.49 4.93	NA	—	—	NA	—
LXVIII	—$COCH{=}CHCO_2C_2H_5$	57	CH_3OH	87–88°	$C_{18}H_{16}O_3$	C 77.12 H 5.75	76.91 5.63	NA	—	—	NA	—
LXIX	—$COCH_2CH_2CH_2CO_2H$	3	CH_3COOH	160–161°	$C_{17}H_{16}O_3$	C 76.10 H 6.01	74.90 5.89	1.6	37	NA	NA	—
LXX	—C(CH_3)=$CHCH_2CO_2H$	5	C_6H_6, C_6H_{14}	175–176°	$C_{17}H_{16}O_2$	C 80.92 H 6.39	79.86 6.29	2.0	—	—	NA	—
LXXI	—$COCHBrCH_2CO_2H$	60	C_6H_{14}	161–162°	$C_{16}H_{13}BrO_3$	C 57.67 H 3.94 Br 23.99	57.77 4.11 23.12	2.6	64	70	16	NA
LXXII	—C(OH)$HCH_2CH_2CONHNH_2$	36	C_2H_5OH	186–187°	$C_{16}H_{18}N_2O_2$	C 71.09 H 6.71 N 10.36	70.86 6.60 10.28	1.8	—	—	15	NA
LXXIII	—OCH_2CH_2CN[p]	30	$CH_2{=}CH_2CN$	130–131°	$C_{15}H_{13}NO$	—	—	NA	—	—	16	NA
LXXIV	—$OCH_2CH_2CO_2H$[p]	65	C_2H_5OH	174–175°	$C_{15}H_{14}O_3$	—	—	2.3	—	—	NA	—
LXXV	—$SO_2CH_2CH_2CO_2H$	25	C_2H_5OH, H_2O	174–176°	$C_{15}H_{14}O_4S$	S 11.04	11.25	NA	—	—	—	—
LXXVI	—$COCHBrCH_2CH_2CO_2H$	58	C_6H_6	163–164°	$C_{17}H_{15}BrO_3$	C 58.81 H 4.35 Br 23.03	58.85 4.25 23.32	NA	—	—	NA	—
LXXVII	—$COC(C_6H_5)HCH_2CO_2H$	6	CH_3COOH	175–177°	$C_{22}H_{18}O_3$	C 79.98 H 5.49	79.92 5.25	NA	—	—	NA	—
LXXVIII	—$COC(OH)HCH_2CO_2H$	78	—[q]	170–172°	$C_{16}H_{14}O_4$	C 71.10 H 5.22	71.25 5.02	1.8	NA	NA	NA	—
LXXIX	—$COCH_2C(OH)HCO_2H$	70	H_2O	174–175°	$C_{16}H_{14}O_4$	C 71.10 H 5.22	70.94 5.18	1.6	NA	NA	NA	—

LXXX	—COCHBrCHBrCO$_2$H(A)	30	C_6H_6	190–192°	$C_{16}H_{12}Br_2O_3$	C 46.63 46.81 H 2.94 2.87 Br 38.78 38.43	5.6	NA	NA	6	NA
LXXXI	—COCHBrCHBrCO$_2$H(B)	60	C_6H_6	181–182°	$C_{16}H_{12}Br_2O_3$	C 46.63 47.38 H 2.94 2.96 Br 38.78 38.43	4.2	NA	—	4	NA
LXXXII	—C(NH$_2$)HCH$_2$CH$_2$CO$_2$H	13	—[r]	182–184°	$C_{16}H_{19}NO_2$	C 75.27 75.48 H 6.71 6.80 N 5.48 5.31	NA	—	—	NA	—
LXXXIII	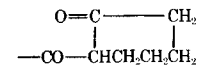	13	C_6H_6, C_7H_{16}	130–132°	$C_{19}H_{18}O_2$	C 81.99 81.70 H 6.52 6.31	NA	NA	—	NA	—
LXXXIV	—OCOCH=CHCO$_2$H	20	C_6H_6	218–219°	$C_{16}H_{12}O_4$	C 71.63 71.71 H 4.51 4.37	NA	—	—	9	NA
LXXXV	—COCH$_2$SCH$_2$CO$_2$C$_2$H$_5$	80	Aqueous C$_2$H$_5$OH	60–62°	$C_{18}H_{18}O_3S$	C 68.76 68.90 H 5.77 5.74 S 10.20 10.01	NA	—	—	NA	—
LXXXVI	—C(NNH$_2$)CH$_2$SCH$_2$CO$_2$C$_2$H$_5$	27	C$_2$H$_5$OH	78–79°	$C_{18}H_{20}N_2O_2S$	C 65.82 66.03 H 6.14 6.11 N 8.53 8.32 S 9.76 9.33	NA	—	—	NA	—
LXXXVII	—COCH$_2$SCH$_2$CO$_2$H	41	Aqueous C$_2$H$_5$OH	118–120°	$C_{16}H_{14}O_3S$	C 67.13 67.55 H 4.93 4.98 S 11.20 10.81	NA	NA	—	8	1.7
LXXXVIII	—CH=C(CN)CO$_2$H	77	—	243–245°	$C_{16}H_{11}NO_2$	C 77.09 77.15 H 4.45 4.40 N 5.62 5.78	1.8	NA	—	NA	—
LXXXIX	—COCHClCHClCO$_2$H	28	C_6H_6	180–184°	$C_{16}H_{12}Cl_2O_3$	C 59.46 59.52 H 3.74 3.66 Cl 21.94 22.05	4.8	NA	NA	15	NA
XC	—COCHClCH$_2$CO$_2$H	85	C_6H_6	158–159°	$C_{16}H_{13}ClO_3$	C 66.54 66.68 H 4.53 4.46 Cl 12.28 12.40	2.3	61	85	12	NA
XCI	—C(OH)HCH$_2$CH$_2$CH$_2$OH	50	Aqueous C$_2$H$_5$OH	79–80°	$C_{16}H_{18}O_2$	C 79.31 79.06 H 7.49 7.36	1.9	59	88	5	1.8
XCII	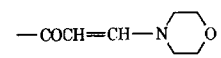	62	(CH$_3$)$_2$CO	191–193°	$C_{19}H_{19}NO_2$	C 77.79 77.71 H 6.53 6.68 N 4.77 4.66	NA	NA	—	NA	—
XCIII	—C(OH)HCH=CHCO$_2$H	43	Aqueous CH$_3$OH	155–157°	$C_{16}H_{14}O_3$	C 75.57 75.20 H 5.55 5.51	NA	NA	—	8	1.6
XCIV	—CH=CHCH$_2$CO$_2$H	25	C_6H_6	183–185°	$C_{16}H_{14}O_2$	C 80.64 81.01 H 5.92 5.92	1.8	50	85	9	NA
XCV	—COCH=CHNHC$_6$H$_5$	33	C_6H_6	220–222°	$C_{21}H_{17}NO$	C 84.25 83.95 H 5.72 5.37 N 4.68 4.50	NA	NA	—	NA	—
XCVI	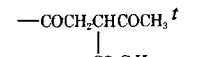	65	C$_2$H$_5$OH	87–89°	$C_{20}H_{20}O_4$	— —	NA	NA	—	NA	—
XCVII	—COCH$_2$CH$_2$COCH$_3$[t]	41	C$_2$H$_5$OH	111–112°	$C_{17}H_{16}O_2$	— —	NA	NA	—	14	NA
XCVIII	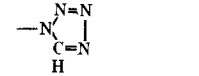	54	C_6H_6, C_6H_{14}	161–162°	$C_{13}H_{10}N_4$	C 70.25 69.95 H 4.54 4.89 N 25.21 25.58	NA	NA	—	16	NA
XCIX	—COCHBrCH$_2$Br[i]	7	—[u]	84–86°	$C_{15}H_{12}Br_2O$	— —	NA	NA	NA	8	NA
C	—C(OH)HCH$_2$CH$_2$C(OH)-HCH$_3$	43	C_6H_6	106–107°	$C_{17}H_{20}O_2$	C 79.65 79.33 H 7.86 7.60	NA	NA	—	NA	—
CI	—C(OH)HCH$_2$C(CH$_2$OH)-HC(OH)HCH$_3$	80	—	Oil	$C_{18}H_{22}O$	C 75.49 76.26 H 7.74 7.50	NA	—	—	4	—
CII	—CH$_2$COOH[v]	—	—	—	—	— —	1.7	55	97	4	2.8

[a] Alfred Bader Chemicals, AB 3391. [b] NA = not active. [c] Ethanol–dimethylformamide (2:1). [d] Reference 28. [e] Toxic. [f] Dose was 5 mg/kg po. [g] Reference 29. [h] Dioxane–water (1:1). [i] Reference 30. [j] Reference 31. [k] Dimethylformamide–water (1:1). [l] Reference 32. [m] Ethanol–dimethylformamide (10:1). [n] Precipitated from solution with acetic acid. [o] Precipitated from acetic acid solution by dilution with water. [p] Reference 33. [q] Precipitated from sodium carbonate solution with acetic acid. [r] Dimethylformamide–2-methoxyethanol. [s] Reference 34. [t] Reference 35. [u] Cyclohexane–hexane. [v] Safron Laboratories.

Table IV—Potency Relative to Aspirin

Compound	Anti-Inflammatory			Analgesic	
	Carrageenan Edema	Adjuvant Arthritis	UV Erythema	2-Phenyl-1,4-benzoquinone-Induced Writhing	Paw Pain Pressure Threshold
Aspirin	1	1	1	1	1
Phenylbutazone	4.1	4.5	5.5	0.8	10.0
Indomethacin	25.0	118.0	9.2	119.0	20.0
Fenbufen (I)	4.2	6.3	6.3	3.7	10.0
4-Biphenylacetic acid (CII)	4.2	11.9	22.0	2.9	—
dl-4-(4-Biphenylyl)-4-hydroxybutyric acid (LV)	10.0	4.8	4.9	—	—

butyric acid (LV); the reduction of the carboxylic acid function to a carbinol, giving *dl*-4-(4-biphenylyl)-1,4-butanediol (XCI); and the acetic acid analog (CII).

From these data, I, CII, and LV were selected for dose–response studies. Table IV gives their relative potencies compared to aspirin, as the standard, along with phenylbutazone and indomethacin for comparison. The detailed pharmacological examination of fenbufen is the subject of a recent paper[2]; however, the long duration of action of this compound was noteworthy. It can be seen that all three compounds were considerably more potent than aspirin and at least as potent as phenylbutazone in the five test systems. Moreover, CII was more potent than indomethacin in the UV erythema test.

EXPERIMENTAL

Biological Tests—The carrageenan edema test was a modification of the test of Winter *et al.* (6). Drugs were administered by gavage at a dose of 250 mg/kg, except when resultant mortality required lower doses. Foot volume measurements were made 5 hr after drug administration (4 hr after carrageenan challenge). Results were expressed as a control (C)/treated (T) efficacy ratio (the ratio of mean edema volume of eight control rats over the mean edema volume of two treated rats). Compounds found to have activity were retested, and the final decision concerning such drugs was based on 32 control rats and eight treated rats.

The adjuvant-induced arthritis test was based on the procedures of Newbould (8) as well as Ward and Cloud (9). Test compound was administered orally at a dose of 50 mg/kg (occasionally lower because of toxicity) once daily on Days 0–13 postchallenge. On the 14th day postchallenge, the diameter of the injected paw (primary lesion) was measured with a micrometer caliper. From these measurements of inflamed paws, a determination was made of the rat paw volume. Results are expressed as the percent inhibition of inflamed control paw volume (mean volume of three treated rats compared with paw volume of 12 controls). Decisions of interesting activity were based on a minimum of 36 controls and nine treated rats.

The UV-induced erythema test followed that of Winder *et al.* (7). Groups of four albino guinea pigs received by gavage a 250-mg/kg dose (occasionally lower because of toxicity) 1 hr prior to UV exposure (−1 hr). At +1 and +4 hr after UV exposure, the degree of erythema for each of the three sites was assessed according to the following scoring system: 0, no erythema; 0.5, incomplete circle or faint erythema; and 1.0, complete circle of distinct erythema. In general, only compounds showing greater than 70% inhibition of erythema were considered of interest. The activity of compounds was confirmed with a second independent run; thus, the decision concerning activity was based on a minimum of 16 control guinea pigs and eight treated guinea pigs.

The 2-phenyl-1,4-benzoquinone test for analgesic activity was a modification of that described by Hindershot and Forsaith (10). The test compounds were administered orally at a dosage of 200 mg/kg to groups of two mice each 30 min before injection of 2-phenyl-1,4-benzoquinone. A compound was considered active if it reduced the total number of writhes in two test mice from a control value of approximately 30 per pair to 18 or less during a 3-min observation.

The inflamed paw pressure analgesic test was based on a modification of the method of Randall and Selitto (11). Pressure-pain thresholds were recorded 2 hr after the brewer's yeast injection. The agents being tested were given at the same time as the yeast at a dosage of 200 mg/kg. The ratios of treated (T)/control (C) reaction threshold were calculated as estimates of analgesic efficacy. A compound was considered an active analgesic if its T/C ratio was >1.5.

All results indicating activity were statistically significant ($p < 0.05$) by the t test.

Chemistry—Each analytical sample had an IR (potassium bromide) spectrum compatible with its assigned structure. Where deemed necessary, IR, mass, UV, and NMR spectral data are given. The melting points[3] of known compounds agreed with reported values within narrow limits.

General Method A: Friedel–Crafts Condensation of Succinic Anhydride and Aromatic Compounds—With the solvent listed in Table I in sufficient quantity to dissolve or suspend 0.2 mole of the aromatic compound and 0.21 mole of succinic anhydride at 0°, 0.42 mole of aluminum chloride was added portionwise with stirring. The reaction was allowed to warm to room temperature. It was stirred a few hours and then poured into 1 liter of ice water containing 125 ml of 12.2 *N* HCl. The solvents were removed by vacuum or steam distillation, and the residue was recrystallized from the solvent listed in Table I.

3-(4-Benzoylbenzoyl)propionic Acid (XVI)—A solution of 5.36 g (0.02 mole) of VIII in 150 ml of acetic acid and 1.9 ml of concentrated sulfuric acid was heated with 10.14 g (0.34 mole) of sodium dichromate and stirred at 40–60° for 4 hr. After standing at 20° for 2.5 days, the mixture was filtered. The filtrate was diluted with 1 liter of water, giving a crude product. This product was filtered, washed with water, and dried. Recrystallization gave 2.6 g of faintly green crystals. The mass spectrum showed *m/e* 282 and a strong 209 for 4-$(C_6H_5CO)C_6H_4CO$.

3-[4-(5-Amino-2H-triazolo[4,5-b]pyridin-2-yl)benzoyl]propionic Acid (XXVIII)—Eleven grams (0.035 mole) of XXVII was dissolved in 750 ml of refluxing pyridine. A solution of 32 g (0.2 mole) of copper sulfate in 250 ml of water was then added carefully (exotherm!). After the addition, refluxing was continued for a further 3 hr. Spot tests indicated complete conversion of the azo dye in about 30 min. The hot solution was added to 6 liters of water, and the suspension was treated with 12.2 *N* HCl until a clear solution was obtained. Solid sodium acetate was then added until the pH reached 4–5.

After cooling at 4° overnight, the precipitate was collected and extracted with 200 ml of boiling 12.2 *N* HCl. The insoluble portion was filtered off hot, washed with ethanol and ether, and dried. It was dissolved in 25 ml of hot water and 15 ml of concentrated ammonia, clarified with charcoal, and precipitated with 15 ml of acetic acid, giving 1.8 g of a bright-yellow product.

3-(4-Biphenylyl)-4,5-dihydro-6(1H)-pyridazinone (XXXVII)—A solution of 12.6 g (0.05 mole) of I in 300 ml of water containing 3.2 g (0.05 mole) of 85% KOH was treated with 2.5 ml of hydrazine hydrate (0.05 mole), and the mixture was stirred and heated on the steam bath for 4 hr. Acidification with 10 ml of acetic acid gave a precipitate, which was collected, washed with water, and dried. Recrystallization gave 4.1 g of pure product.

2,2′-[4-Biphenylylmethylene]bis(1,3-indandione) (XLV)—A mixture of 7.3 g (0.05 mole) of 1,3-indandione and 9.1 g (0.05 mole) of *p*-biphenylcarboxaldehyde in 125 ml of ethanol was refluxed for 3 hr and cooled. The formed solid was filtered off, washed well with ethanol, and dried, leaving 11 g of a pale-yellow solid. Recrystallization gave colorless crystals.

2-(4-Phenylbenzylidene)-1,3-indandione (XLVI)—A mixture of 4.4 g (0.03 mole) of 1,3-indandione and 5.5 g (0.03 mole) of *p*-biphenylcarboxaldehyde in 100 ml of acetic acid and 3 drops of concentrated sulfuric acid was heated on a steam bath for 2.5 hr and cooled. The formed bright-yellow plates were filtered and washed with acetic acid, water, and ethanol, yielding 5.0 g.

γ-Oxo-α-phenyl-4-biphenylbutyronitrile (XLVII)—A solution of 14.2 g (0.05 mole) of 4′-phenylchalcone, 700 ml of ethanol, 150 ml of di-

[2] See A. Sloboda and A. Osterberg, *Inflammation*, 1, 415 (1976).

[3] Melting points were taken on a Fisher-Johns block and are uncorrected.

methylformamide, and 3 ml of acetic acid at 55–60° was treated with 6.5 g (0.1 mole) of potassium cyanide in 25 ml of water during 15 min. The solution was stirred at 55–60° for an additional 5 hr and then at 20° for 2 days. The precipitate was collected, washed with water, dried, and recrystallized, giving 9.5 g of product. Concentration of the mother liquor to half-volume and cooling gave an additional 2.6 g with the same melting point. The total yield was 12.1 g.

1,4-Bis(4-biphenylyl)butane-1,4-dione (LIII)—An intimate mixture of 15.4 g (0.1 mole) of biphenyl and 11.4 g (0.1 mole) of glutaric anhydride was added portionwise to a cold (5°) solution of 28 g (0.21 mole) of aluminum chloride in 175 ml of nitrobenzene. The mixture was allowed to warm to 20° and was stirred for 4 days. After working up in the usual way, the crude product was precipitated from sodium carbonate solution with hydrochloric acid. After recrystallizing from acetic acid and benzene, 1.2 g of straw-yellow rods was obtained.

d-*4-(4-Biphenylyl)-4-hydroxybutyric Acid (LVI)*—A solution of 2.56 g (0.1 mole) of LV in 50 ml of warm ethanol was filtered, treated with 0.9 g (0.01 mole) of *d*-2-aminobutanol[1], and cooled. After 2 days at 5°, 1 g of colorless crystals was filtered off, mp 144–146°. Concentration of the mother liquor to half-volume gave a second crop (0.2 g, mp 144–148°). Two recrystallizations of the combined crops from ethanol gave 0.5 g (mp 152–153°) of the salt. Acidification of the salt in 50 ml of water with 5 *N* HCl to pH 2 gave a white precipitate. This precipitate was filtered, washed well with water, and dried, yielding the optically pure hydroxy acid, 0.2 g, $[\alpha]_D^{25}$ + 14.1 ± 0.18° (ethanol). The IR curve was identical to that of the racemic acid (LV).

l-*4-(4-Biphenylyl)-4-hydroxybutyric Acid (LVII)*—In the same manner as described for the previous resolution, *l*-2-aminobutanol[1] was used to separate the stereoisomeric salt (mp 150–152°) and yielded the optically pure hydroxy acid, $[\alpha]_D^{25}$ −14.1 ± 0.2° (ethanol). The IR curve was identical to that of the racemic acid (LV).

4-(4-Biphenylylthioacetyl)morpholine (LVIII)—A mixture of 29.4 g (0.15 mole) of 4′-phenylacetophenone, 8 g (0.25 mole) of sulfur, and 50 ml of morpholine was refluxed on steam for 8 hr and cooled. The reaction mass was triturated with 100 ml of ether; the insolubles were collected, washed with 100 ml of petroleum ether (bp 30–60°), and dried. Recrystallization gave 16.4 g.

4-[1-(4-Biphenylyl)-2-(methylthio)ethylidene]morpholinium Iodide (LIX)—A solution of 25.5 g (0.09 mole) of LVIII in 600 ml of acetone and 15 ml of methyl iodide was allowed to stand at 20° for 3 days. The crystalline precipitate was collected, washed with ether, and dried, giving 34.0 g.

4-(4-Biphenylyl)-4-valerolactone (LXII)—Grignard reagent, made in the usual way from 10 g (0.07 mole) of methyl iodide and 1.71 g (0.07 mole) of magnesium in ether, was added dropwise to a cold (5°) suspension of 14.1 g (0.05 mole) of the ester (XXXVIII) in 500 ml of ether (Scheme I, R_1 = biphenylyl). After stirring at 5° for 1.5 hr, the complex was decomposed with 15 ml of saturated ammonium chloride solution, allowed to warm to 20°, filtered, dried over calcium chloride, and concentrated to dryness. The residue was crystallized, yielding 10 g of lactone; IR (KBr): 5.65 μm.

Ethyl 3-Bromo-3-(4-phenylbenzoyl)propionate (LXIV)—A solution of 2.54 g (0.01 mole) of I in 300 ml of commercial grade chloroform containing ethanol was treated dropwise with 1.6 g (0.01 mole) of bromine in 25 ml of chloroform over 0.5 hr. The mixture was then refluxed for 4 hr and stripped to dryness. The residual oil was crystallized once from ether–hexane and finally from methanol, yielding 2.3 g; mass spectrum: *m/e* 360.

3-(4-Phenylbenzoyl)propionamide (LXV)—A saturated solution of ammonia in 75 ml of tetrahydrofuran was treated with 2.54 g (0.01 mole) of I (Scheme I). The resulting suspension of ammonium salt was treated with 2.96 g (0.012 mole) of CIII and stirred overnight at 20°. The mixture was stripped to dryness, and the residue was recrystallized, giving 1.2 g of colorless flakes.

Ethyl 3-(4-Phenylbenzoyl)acrylate (LXVIII)—A warm mixture of 2.7 g (0.045 mole) of acetic acid and 2.77 g (0.028 mole) of triethylamine in 100 ml of acetone was treated all at once with 1.805 g (0.005 mole) of LXIV and stirred for 2 hr. After cooling and filtering, the acetone solution was poured into two volumes of water. The formed solid was filtered, washed with water, dried, and recrystallized, yielding 0.8 g.

4-(4-Phenylbenzoyl)butyric Acid (LXIX)—Glutaric anhydride (12 g, 0.11 mole) was condensed with biphenyl (15.4 g, 0.1 mole) in tetrachloroethane by addition of aluminum chloride according to Carter *et al.* (36); 0.8 g of a yellow material was obtained.

4-(4-Biphenylyl)-3-pentenoic Acid (LXX)—By using the general procedure described by Corey *et al.* (37), 4-acetylbiphenyl (14.72 g, 0.075 mole) was condensed with the Wittig reagent, (2-carboxyethyl)triphenylphosphonium chloride, in the presence of sodium hydride. A pale-yellow solid (1 g) was obtained; UV λ_{max} (ethanol): 276 nm, consistent with an unsaturated alkyl conjugated with biphenyl.

3-(4-Biphenylylsulfonyl)propionic Acid (LXXV)—A solution of 7.2 g (0.04 mole) of crude 4-phenylthiophenol (38) in a mixture of 100 ml of water, 50 ml of ethanol, and 4.5 ml of 10 *N* NaOH was treated with a mixture of 6.3 g (0.04 mole) of 3-bromopropionic acid, 100 ml of water, and 4.5 g (0.04 mole) of sodium bicarbonate. The mixture was heated and stirred on the steam bath for 4 hr and then clarified. The filtrate was successively acidified (concentrated hydrochloric acid) and basified (concentrated ammonium hydroxide).

The insolubles in ammonia solution were removed by filtration, and the filtrate was reacidified with concentrated hydrochloric acid. The acid mixture was extracted with 250 ml of chloroform. Removal of the chloroform left 1.0 g of oily residue, which was taken up in acetic acid. Addition of 4 ml of 30% H_2O_2 and heating on steam for 5 hr, followed by dilution with 450 ml of cold water, produced a precipitate. This precipitate was collected, dried, and recrystallized, yielding 200 mg.

3-(4-Phenylbenzoyl)-3-phenylpropionic Acid (LXXVII)—A suspension of 13.6 g (0.05 mole) of benzyl biphenyl ketone (39) in 500 ml of absolute ethanol was treated with 1.2 g (0.05 mole) of sodium hydride followed by 8.35 g (0.05 mole) of ethyl bromoacetate. After refluxing for 20 min, the mixture was treated with 5 g of potassium hydroxide in 25 ml of water, refluxed for 2 hr more, and then poured into 1 liter of water. After filtering, acidification of the filtrate with concentrated hydrochloric acid gave a crude product. This product, when crystallized from acetic acid once and finally from benzene–hexane, gave 1 g of a colorless product.

3-Hydroxy-3-(4-phenylbenzoyl)propionic Acid (LXXVIII)—A mixture of 5 g (0.015 mole) of LXXI in 500 ml of 10% Na_2CO_3 was stirred at room temperature for 16 hr (33) (Scheme I). The formed peach-colored sodium salt was removed, suspended in water, and acidified with acetic acid, giving 3.2 g of colorless product; mass spectrum: *m/e* 270; $C_6H_5C_6H_4C{\equiv}O^+$, 181; and $C_6H_5C_6H_4^+$, 153.

2-Hydroxy-3-(4-phenylbenzoyl)propionic Acid (LXXIX)—A mixture of 5.7 g (0.023 mole) of XL and 100 ml of concentrated hydrochloric acid in 400 ml of water was refluxed for 20 hr and filtered hot, yielding 5.6 g of unreacted XL (Scheme II). On cooling, the filtrate yielded 0.2 g of a product whose IR curve indicated it to be a hydroxy keto acid. Boiling the unreacted material three times with large volumes of 1:4 diluted hydrochloric acid gave an accumulation of 5 g of crude product, mp 160–165°. Recrystallization gave 4.3 g of colorless product. A mixed melting point of this product with the 3-hydroxy analog (LXXVIII) was 150–155°; mass spectrum: *m/e* 270; $C_6H_5C_6H_4C{\equiv}O^+$, 181; $C_6H_5C_6H_4^+$, 153; and a 196 which results from a McLafferty rearrangement (40) of a β-hydroxy ketone (Scheme III). The α-hydroxy ketone (LXXVIII) described previously cannot undergo this fragmentation and does not show an *m/e* 196.

2,3-Dibromo-3-(4-phenylbenzoyl)propionic Acid (LXXX): Racemic Mixture A—In a manner similar to that described by Rice (41), 7.5 g (0.03 mole) of XL in 400 ml of acetic acid at 15° was treated dropwise with 4.8 g (0.03 mole) of bromine (Scheme II). The solution was then concentrated to dryness, and the residue was washed with water and dried. Recrystallization yielded 4.1 g of colorless grains.

4-Amino-4-biphenylbutyric Acid (LXXXII)—By using the general method of Tochims (42), 9.5 g (0.035 mole) of LXI was stirred into 500 ml of concentrated ammonium hydroxide, warmed, and held at 60–65° while 50 g of zinc dust was carefully added in small portions (Scheme I). After the addition, stirring at 60–65° was continued for 18 hr. The reaction mixture was clarified by filtration, and the filtrate was taken to dryness *in vacuo*. The residue was shaken with 500 ml of 0.1 *N* NaOH solution and clarified, and the filtrate was acidified with 10 ml of acetic acid. The semigelatinous precipitate was collected, washed with water, and dried. It was then extracted with 500 ml of boiling ethanol. The insoluble portion was recrystallized, giving 0.8 g of the amino acid. Con-

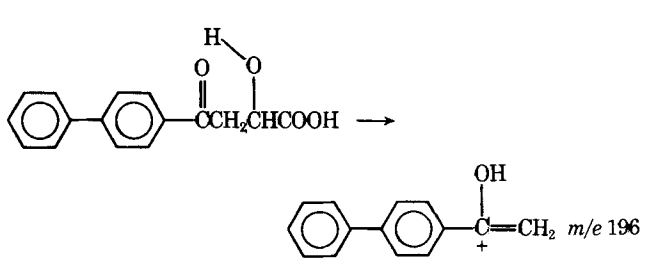

Scheme III

centration of the ethanol extract to 250 ml and cooling gave an additional 0.4 g; the total yield was 1.2 g.

2-(4-Phenylbenzoyl)cyclohexanone (*LXXXIII*)—4-Phenylbenzoyl chloride [formed from 19.8 g (0.1 mole) of 4-phenylbenzoic acid, benzene, and thionyl chloride under reflux for 1 hr] was dissolved in 250 ml of chloroform and added during 2 hr to a stirred mixture of 18.5 g (0.11 mole) of 1-morpholinocyclohexene, 18 ml (0.13 mole) of triethylamine, and 250 ml of chloroform at 30–35°. After stirring at 20° for 16 hr, 50 ml of water and 25 ml of concentrated hydrochloric acid were added; the mixture was then refluxed for 2 hr. The chloroform layer was separated, washed with water, dried over magnesium sulfate, and concentrated to dryness. The residual oil was dissolved in a hot mixture of 150 ml of benzene and 300 ml of *n*-heptane, decolorized with carbon, and cooled, yielding 3.6 g.

Maleic Acid Mono-4-biphenylyl Ester (*LXXXIV*)—A solution of 5.04 g (0.02 mole) of XL in 200 ml of acetic acid was treated with 12 ml of 30% H_2O_2 and heated at 60° for 24 hr. An additional 10 ml of hydrogen peroxide was added, and the reaction was stirred on steam overnight. Dilution of the clear yellow solution with 1.5 volumes of water gave a crude product. When this product was recrystallized, 1.0 g of colorless product was obtained. Hydrolysis of a sample of the product yielded 4-phenylphenol, mp 164–165°; mass spectrum: *m/e* 268; and $C_6H_5C_6H_4OH$, 170.

Ethyl 4-Phenylbenzoylmethylthioacetate (*LXXXV*)—A solution of 7.2 g (0.06 mole) of ethyl mercaptoacetate and 3.4 g (0.06 mole) of sodium methoxide in 500 ml of ethanol was treated with 13.8 g (0.05 mole) of 2-bromo-4′-phenylacetophenone. The mixture was stirred at 20° for 5 hr, refluxed for 4 hr, and then concentrated to a thick oil. Trituration with 250 ml of cold water left a solid, which was filtered, washed with water, and dried, yielding 19 g. Recrystallization gave 15 g of colorless crystals.

Ethyl 4-Phenylbenzoylmethylthioacetate Hydrazone (*LXXXVI*)—A solution of 7.0 g (0.022 mole) of LXXXV in 200 ml of boiling ethanol was treated with 1.1 ml (0.022 mole) of 100% $N_2H_4 \cdot H_2O$ and refluxed for 6 hr, clarified with carbon, filtered, and cooled, yielding 2 g of hydrazone.

3-(4-Phenylbenzoyl)-2,3-dichloropropionic Acid (*LXXXIX*)—A solution of 5 g (0.02 mole) of XL in 300 ml of acetic acid at 20° was treated with a steady stream of chlorine for 3 hr (Scheme II). The yellow solution was concentrated to dryness, and the residue was washed with water and dried. Two recrystallizations gave 1.8 g of colorless crystals.

3-Morpholino-4′-phenylacrylophenone (*XCII*)—A solution of 4.1 g (0.01 mole) of LXXX in 500 ml of boiling benzene was treated with 6 ml (0.07 mole) of morpholine. Extensive carbon dioxide evolution was detected by bubbling the evolved gas through barium hydroxide solution. After 8 hr of refluxing, the precipitate of morpholine salt was filtered off (3.2 g, 95%). The benzene filtrate was concentrated to 100 ml, diluted with 200 ml of petroleum ether (bp 30–60°), and cooled. The precipitate was collected and recrystallized, giving 1.5 g of product; IR (KBr): C=O, 6.08 (vinylogous amide); C=C, 6.5; *trans*-CH=CH, 10.1 μm; no COOH; mass spectrum: *m/e* 293.

3-Anilino-4′-phenylacrylophenone (*XCV*)—A mixture of 8.3 g (0.02 mole) of LXXX, 15 ml (0.16 mole) of aniline, and 500 ml of benzene was stirred under reflux for 16 hr. The precipitate of aniline salt was filtered from the hot suspension and washed with 100 ml of benzene. Concentration of the filtrate and wash to 150 ml and cooling to 20° gave a precipitate, which was washed with 100 ml of warm water and dried, giving 2.0 g.

1-(4-Biphenylyl)tetrazole (*XCVIII*)—A solution of 4.23 g (0.025 mole) of 4-aminobiphenyl in 180 ml of ethyl orthoformate was distilled slowly until the temperature reached 143° (3 hr). The remainder was evaporated to dryness, dissolved in 40 ml of acetic acid, treated with 6.5 g (0.1 mole) of sodium azide, and stirred at 20° for 24 hr. After addition of 100 ml of water, the solid was filtered off, washed with water, dried, and recrystallized (two times), giving pale-yellow crystals, 3.0 g.

REFERENCES

(1) D. H. Hey and R. Wilkinson, *J. Chem. Soc.*, **1940**, 1030.

(2) A. S. Tomcufcik, R. G. Child, and A. E. Sloboda, U.S. pat. 3,784,701 (Jan. 1974).

(3) D. I. Barron, P. T. Bysouth, R. W. Clarke, A. R. Copley, O. Stephenson, D. K. Vallance, and A. W. Wild, *J. Med. Chem.*, **11**, 1139 (1968).

(4) F. Krausz, H. Demarne, J. Vaillant, B. Brunaud, and J. Navarro, *Arzneim.-Forsch.*, **24**, 1360 (1974).

(5) S. Wong, in "Annual Reports in Medicinal Chemistry," vol. 10, R. V. Heinzelman, Ed., Academic, New York, N.Y., 1975.

(6) C. A. Winter, E. A. Risley, and G. W. Nuss, *Proc. Soc. Exp. Biol. Med.*, **111**, 544 (1962).

(7) C. V. Winder, J. Wax, V. Burr, M. Been, and C. E. Rosiere, *Arch. Int. Pharmacodyn. Ther.*, **116**, 261 (1958).

(8) B. B. Newbould, *Br. J. Pharmacol. Chemother.*, **21**, 127 (1963).

(9) J. R. Ward and R. S. Cloud, *J. Pharmacol. Exp. Ther.*, **152**, 116 (1966).

(10) L. C. Hendershot and J. Forsaith, *ibid.*, **125**, 237 (1958).

(11) L. O. Randall and J. J. Selitto, *Arch. Int. Pharmacodyn. Ther.*, **111**, 409 (1957).

(12) E. Berliner, in "Organic Reactions," vol. 5, R. Adams, Ed., Wiley, New York, N.Y., 1949, p. 229.

(13) J. P. English, R. C. Clapp, Q. P. Cole, and J. Krapcho, *J. Am. Chem. Soc.*, **67**, 2263 (1945).

(14) W. V. Curran and A. Ross, *J. Med. Chem.*, **17**, 273 (1974).

(15) C. F. Koelsch, *J. Am. Chem. Soc.*, **55**, 3885 (1933).

(16) H. Gilman, P. T. Parker, J. C. Bailie, and G. E. Brown, *ibid.*, **61**, 2836 (1939).

(17) R. R. Martel, J. G. Rockefort, J. Klicins, and T. A. Dobson, *Can. J. Phys. Pharmacol.*, **52**, 669 (1974).

(18) Huang-Minlon, *J. Am. Chem. Soc.*, **68**, 2487 (1946).

(19) N. P. Buu-Hoi and P. Cagniant, *Chem. Ber.*, **76**, 1269 (1943).

(20) J. W. Cook, A. M. Robinson, and E. M. F. Roe, *J. Chem. Soc.*, **1939**, 266.

(21) L. F. Fieser and C. K. Bradsher, *J. Am. Chem. Soc.*, **58**, 1738 (1936).

(22) L. F. Fieser, *Org. Syn.*, Collect. Vol. **III**, 6 (1955).

(23) J. Travedi and K. S. Nargsenel, *J. Univ. Bombay*, **11**, 127 (1942).

(24) E. Ochiai and Y. Tamai, *Itsuu Kenkyusho Newpo*, **12**, 39 (1962); through *Chem. Abstr.*, **59**, 7414b (1963).

(25) N. P. Buu-Hoi, P. Caignant, and C. Mentzer, *Bull. Soc. Chem. Fr.*, **11**, 127 (1944).

(26) J. H. Uhlenbroek and J. D. Bijloo, *Rec. Trav. Chem.*, **79**, 1181 (1960).

(27) Belgian pat. 667,498; through *Chem. Abstr.*, **65**, 3802d (1966).

(28) H. G. Oddy, *J. Am. Chem. Soc.*, **45**, 2158 (1923).

(29) W. D. Kumler and I. F. Halverstadt, *ibid.*, **63**, 2182 (1941).

(30) R. J. Mohrbacher and N. H. Cromwell, *ibid.*, **79**, 401 (1957).

(31) F. G. Badder, H. A. Fahim, and A. M. Fleifel, *J. Chem. Soc.*, **1955**, 2199.

(32) J. H. Burckhalter and J. H. Short, *J. Org. Chem.*, **23**, 1281 (1958).

(33) J. D. Loudon and R. K. Razden, *J. Chem. Soc.*, **1954**, 4299.

(34) R. D. Obolentsev, V. G. Bukharov, T. E. Pozdnyakova, L. A. Alalykina, L. A. Bakalo, and A. E. Pototskaya, *Khim. Sera Azotorg. Soedin.* **3**, 9 (1960); through *Chem. Abstr.*, **58**, 4496f (1962).

(35) S. Fatutta, *Gazz. Chim. Ital.*, **90**, 1645 (1960); through *Chem. Abstr.*, **56**, 14208i.

(36) F. D. Carter, J. L. Simonsen, and H. O. Williams, *J. Chem. Soc.*, **1940**, 451.

(37) H. S. Corey, J. R. D. McCormick, and W. E. Swenson, *J. Am. Chem. Soc.*, **86**, 1884 (1964).

(38) H. Niwa, *Tohoku Yakka Daigaku Kiyo*, **4**, 19 (1957); through *Chem. Abstr.*, **52**, 7234d (1958).

(39) V. Papcke, *Chem. Ber.*, **21**, 1331 (1888).

(40) F. McLafferty, "Interpretations of Mass Spectra," W. A. Benjamin, New York, N.Y., 1966, p. 123.

(41) G. P. Rice, *J. Am. Chem. Soc.*, **48**, 269 (1926).

(42) J. C. Tochims, *Monatsh. Chem.*, **94**, 677 (1963).

ACKNOWLEDGMENTS AND ADDRESSES

Received February 26, 1976, from *Lederle Laboratories, A Division of American Cyanamid Company, Pearl River, NY 10965.*

Accepted for publication May 20, 1976.

The authors thank Mr. F. M. Brancone and staff for microanalyses and Mr. W. Fulmor, Mr. G. O. Morton, and Dr. G. Van Lear for the spectroanalytical results and their assistance with interpretation.

[x] To whom inquiries should be directed.

Determination of Pentobarbital in Serum by Electron-Capture GLC

SY-RONG SUN [x] **and A. H. C. CHUN**

Abstract □ A GLC method was developed for pentobarbital in serum. After extraction from serum, a pentafluorobenzyl derivative was prepared and quantitated by electron-capture detection. The method has a sensitivity of 0.1 μg/ml of serum, and the amount detectable is less than 0.2 ng/injection. Hexethal was used as the internal standard. Derivatives of other barbiturates were also made. NMR and mass spectrometric analyses confirmed the proposed structure of the 1,3-bis(pentafluorobenzyl) derivative of pentobarbital. The procedure was successfully applied to measurement of serum pentobarbital levels in humans.

Keyphrases □ Pentobarbital—electron-capture GLC analysis, human serum □ GLC, electron capture—analysis, pentobarbital in human serum, retention times, various barbiturates □ Barbiturates, various—electron-capture GLC retention times □ Sedatives—pentobarbital, electron-capture GLC analysis in human serum, retention times, various barbiturates

The GLC determination of barbiturates was reported by numerous authors in the past several years. Some investigators (1, 2) methylated the barbiturate with dimethyl sulfate prior to GLC analysis. A direct "on-column" flash-heater methylation of barbiturates with trimethylanilinium hydroxide was also reported. Ehrnebo *et al.* (4) used similar methodology to assay amobarbital and pentobarbital in serum after ether extraction at pH 5.5. Other investigators (5–12) also described the determination of barbiturates in biological fluids. These methods primarily utilized GLC with flame-ionization detection.

This report describes a new GLC method for the determination of pentobarbital (I). It is sensitive to 0.2 ng/injection, using electron-capture detection of the 1,3-bis(pentafluorobenzyl) derivative of pentobarbital (III, Scheme I) in serum.

EXPERIMENTAL

Reagents and Materials—Pentobarbital[1] (I), hexethal[2] (II), the internal standard, and pentafluorobenzyl bromide[3] were used as supplied. Ether[4] and benzene[4] were nanograde, absolute alcohol[5] was USP grade, and the other chemicals were analytical reagent grade. Aqueous solutions of sodium tungstate (10%), sodium bicarbonate (3%), sodium carbonate (250 μg/ml), and sulfuric acid (1 *N*) were stored in glass containers.

Apparatus—A two-speed reciprocating shaker[6] and a refrigerated centrifuge[7] were used. Sample solutions in the test tubes were mixed by a mixer[8]. Pentafluorobenzyl derivative formation at high temperature was carried out on a heating block[9].

GLC—A gas chromatograph[10] equipped with a ^{63}Ni-electron-capture detector containing a 2-mCi ^{63}Ni-β-ionization source and an electronic integrator were used for the GLC assay. The glass column was 1.82 m (6 ft) × 2 mm (i.d.), packed with 3% OV-17[11] on Gas Chrom Q[11] (80–100 mesh). The column was conditioned at 280° for 1 hr without carrier gas flow and for 16 hr with a carrier gas [argon–methane[12] (95:5)] at a flow rate of 50 ml/min. Before connecting the column to the detector, three to five 5-μl injections of *N,O*-bis(trimethylsilyl)acetamide[13] were made into the column every 10 min.

The cylinder of the carrier gas was fitted with an oxygen trap filter[14]. The operating conditions were: column oven temperature, 225°; electron-capture detector temperature, 325°; injection port temperature,

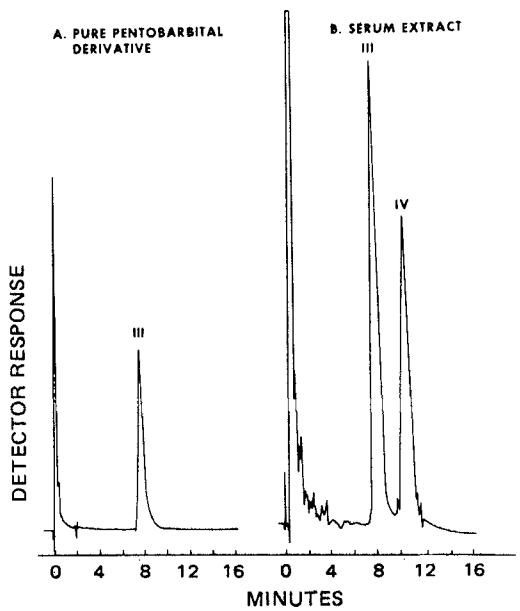

Figure 1—*Gas-liquid chromatogram (electron-capture detection) of pentafluorobenzyl derivatives. Key: A, 0.2 ng of pure III injected; B, serum extract from human subject at 24 hr after single-dose oral administration of 100 mg of pentobarbital sodium (capsule form); and IV, pentafluorobenzyl derivative of the internal standard (hexethal).*

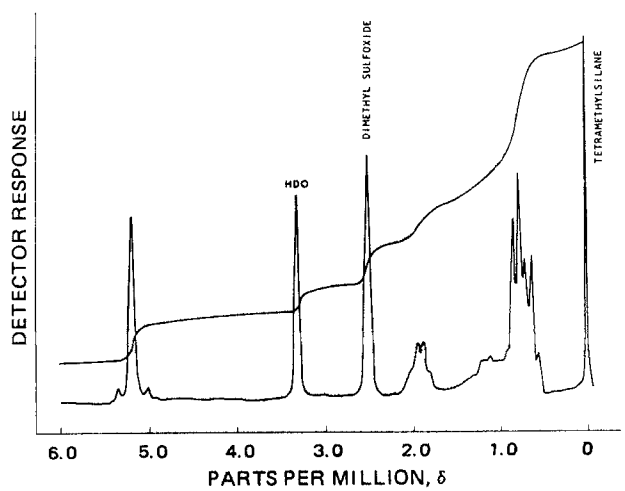

Figure 2—*NMR spectrum of III.*

[1] Internal reference standard, Nembutal acid, lot 3330-113, Abbott Laboratories, North Chicago, Ill.
[2] Internal reference standard, lot A-13271, Abbott Laboratories, North Chicago, Ill.
[3] Bendix Corp., Ronceverte, W. Va.
[4] Mallinckrodt Chemicals, St. Louis, Mo.
[5] Reagent, Abbott Laboratories, North Chicago, Ill.
[6] Eberbach Corp., Ann Arbor, Mich.
[7] Model RC-3, Sorvall, Newtown, Conn.
[8] Vortex Genie model K-550-GT, Scientific Industries, Springfield, Mass.
[9] Dri-block DB-3, Techne, Inc., Princeton, N.J.
[10] Hewlett-Packard model 7620.
[11] Applied Science Laboratories, State College, Pa.
[12] Matheson Gas Products, Elk Grove Village, Ill.
[13] Pierce Chemicals Co., Rockford, Ill.
[14] Altech Associates, Arlington Heights, Ill.

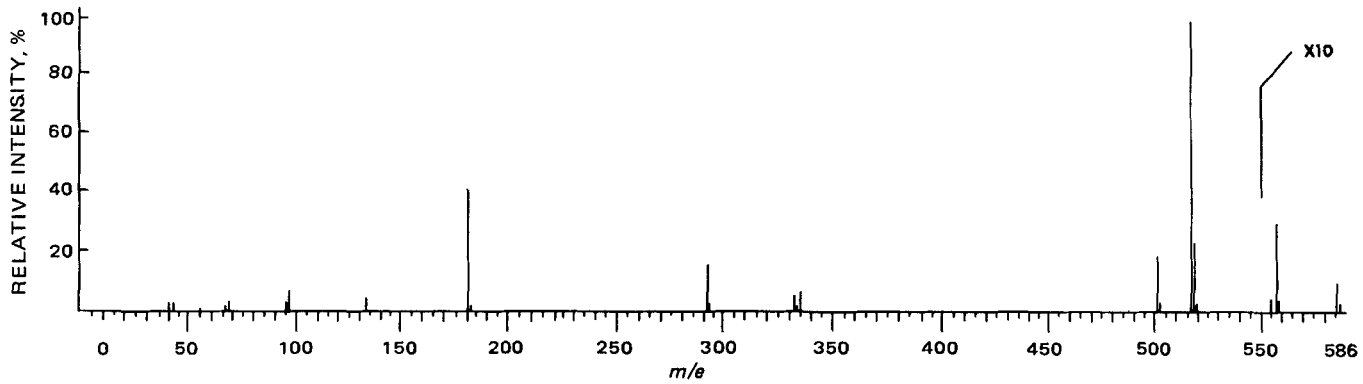

Figure 3—*Mass spectrum of III.*

250°; carrier gas flow rate, 50 ml/min; detector pulse interval, 150 μsec; electrometer range, 10^3; recorder presentation, 2 mv; and slope sensitivity, 0.3 mv/min.

Spectrometry—A mass spectrometer[15] was used under the following conditions: energy of the ionization beam, 70 ev; ion source temperature,

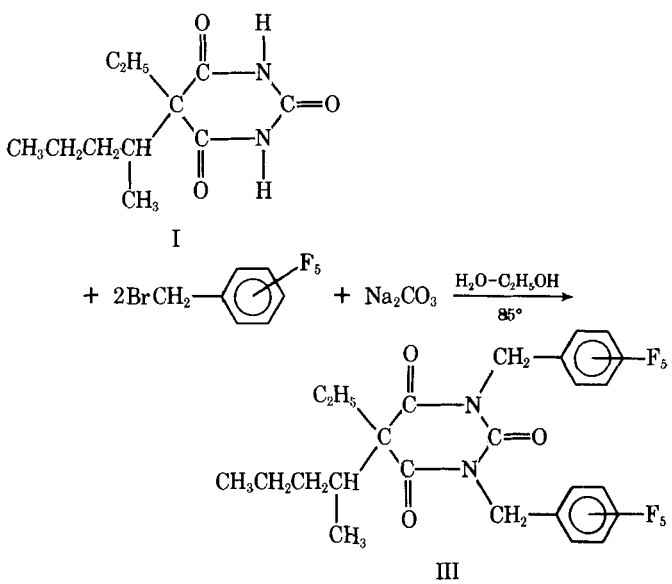

Scheme I

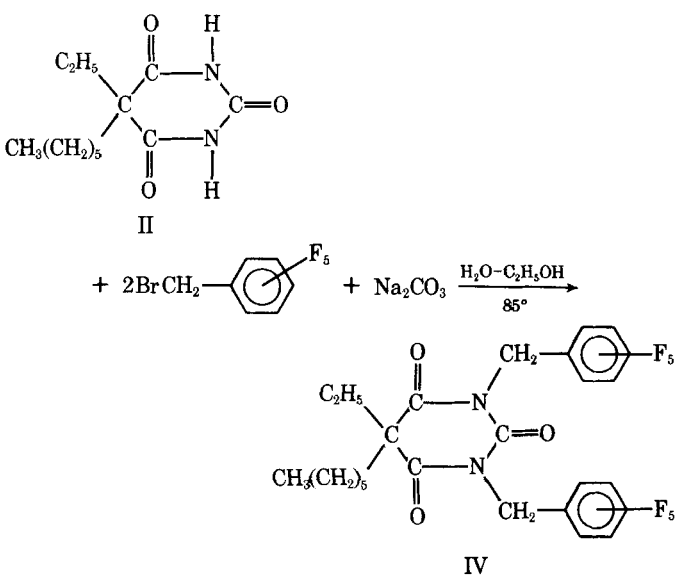

Scheme II

[15] MS-902, Associate Electronic Industry, Manchester, England.

160°; accelerating voltage, 8 kv; and trap current, 100 μamp. The NMR spectrum was recorded at ambient temperatures on a spectrometer[16] using a solution in dimethyl sulfoxide containing tetramethylsilane as the internal standard. The IR spectrum[17] was measured using a potassium bromide pellet.

Preparation of Serum Standards—For human studies, serum standards spiked with I at 0.5, 1.0, 1.5, 2.0, and 2.5 μg/ml were used. This range covered the human serum pentobarbital levels expected after oral administration of a 100-mg dose of pentobarbital sodium capsules[18].

Extraction Procedure—To 1.0 ml of serum in a 20-ml screw-capped test tube were added 3.0 ml of hexethal internal standard solution in water (1 μg/ml) and 1.0 ml of 1 *N* H_2SO_4. The tube was vortexed, 1.0 ml of 10% sodium tungstate solution in water was added, and the tube was then shaken mechanically for 10 min. After centrifugation at 3000 rpm for 15 min at 20°, all of the aqueous phase (supernate) was separated and transferred to a 15-ml conical test tube and recentrifuged at 3000 rpm for 10 min at 20°. Four milliliters of aqueous phase was then pipetted into a 20-ml screw-capped test tube and extracted with 11.5 ml of ether by shaking for 10 min and centrifuging at 3000 rpm for 10 min at 10°.

Ten milliliters of the organic phase was transferred to a 20-ml screw-capped test tube and washed with 2 ml of 3% $NaHCO_3$ aqueous solution by shaking and centrifuging as previously described. The ether layer (9 ml) was transferred into the 15-ml screw-capped conical test tube and evaporated to dryness at 40° with filtered air. The residue was reconstituted with 1 ml of ether and dried again at 40° with filtered air.

1,3-Bis(pentafluorobenzyl) Derivative (III) Formation—To the dry residue were added 0.1 ml of sodium carbonate solution (250 μg/ml of water), 0.1 ml of alcohol, and 50 μl of pentafluorobenzyl bromide in alcohol (2 μg/μl) (Schemes I and II). The mixture was capped and vortexed twice for 15 sec and reacted at 85° for 4 hr on the heating block. Then the mixture was cooled to room temperature; 0.5 ml of water and 4.5 ml of benzene were added, followed by shaking and centrifugation for 10 min. Four milliliters of the benzene extract was separated and evaporated to dryness at 40° with filtered air. The clear residue was reconstituted with 1.0 ml of benzene by vortexing for about 30 sec, and 2 μl of the solution was injected into the GLC column by the automatic sampler[19].

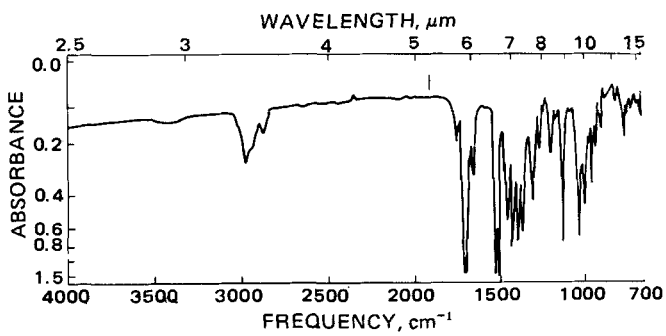

Figure 4—*IR spectrum of III in potassium bromide pellet.*

[16] Varian XL-100.
[17] Perkin-Elmer model 521 IR spectrometer.
[18] Nembutal sodium capsules, 100 mg, lot 38-465-AR, Abbott Laboratories.
[19] Hewlett-Packard model 7670A.

Table I—Peak Area Ratio of III to IV at Various Pentobarbital Serum Concentrations

Pentobarbital Serum Concentration, μg/ml	Peak Area Ratio	Mean ± *SD*	*RSD*
0.1	0.35 0.32 0.38	0.35 ± 0.03	8.6
0.2	0.83 0.70 0.73	0.75 ± 0.07	9.3
0.3	1.03 1.39 1.40	1.27 ± 0.21	16.5
0.4	1.70 1.82 2.14	1.89 ± 0.23	12.2
0.5	2.25 2.39 2.21	2.28 ± 0.10	4.4
0.6	2.54 2.73 2.70	2.66 ± 0.10	3.8
0.8	3.64 3.69	Average 3.67	—
1.0	4.92 5.17 5.13	5.07 ± 0.13	2.6

Under these conditions, derivatization of pentobarbital with pentafluorobenzyl bromide gave one peak on GLC analysis with a retention time of 7.7 min. Hexethal also gave a single peak with a retention time of 10.6 min. Spiked standards of pentobarbital in serum were extracted and reacted with pentafluorobenzyl bromide as previously described.

Calculations—The peak area ratios of III to IV were plotted against known standards of pentobarbital expressed as micrograms per milliliter of serum. Values for unknown concentrations of pentobarbital in serum were calculated by the least-squares regression method from the calibration curve.

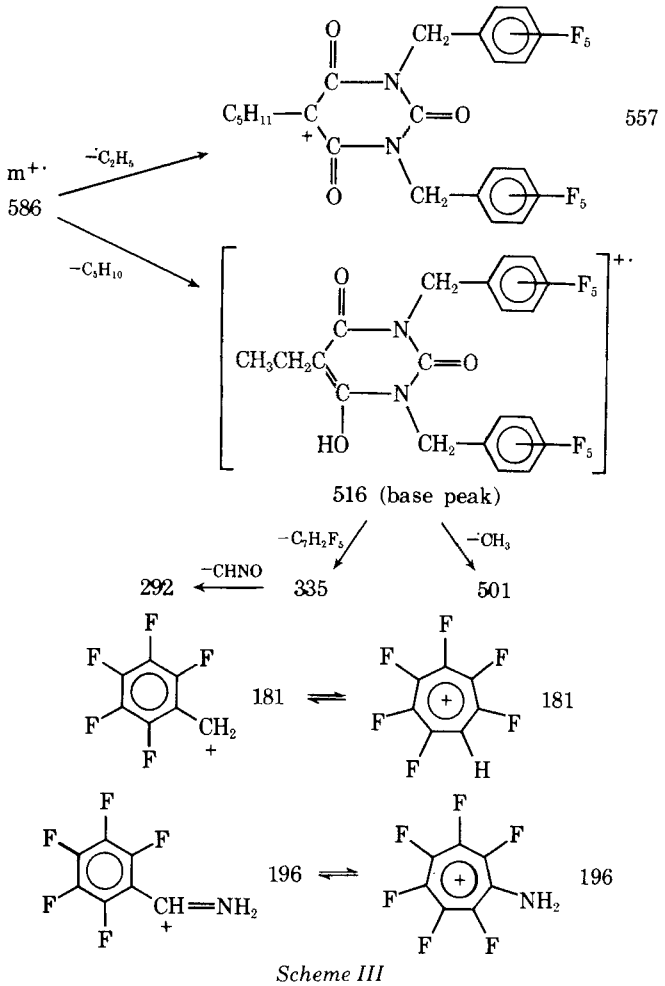

Scheme III

RESULTS AND DISCUSSION

Synthesis and Identification of 1,3-Bis(pentafluorobenzyl) Derivative of Pentobarbital (III)—Structural confirmation of III was accomplished by synthesizing sufficient pure drug under similar conditions. The derivative collected was white crystalline material, mp 106–107°. The gas chromatogram (Fig. 1A) of pure III thus formed was identical to that prepared with the serum extract under the same conditions (Fig. 1B).

The NMR spectrum (Fig. 2) showed the presence of benzyl protons at a chemical shift 5.20 ppm downfield from tetramethylsilane. High-resolution mass spectral measurement (Fig. 3) confirmed a small, but distinct, molecular ion at *m/e* 586, consistent with the proposed structure (III). From the empirical formulas calculated, Scheme III was proposed, indicating two pentafluorobenzyl groups attached to the two nitrogen atoms. The IR spectrum (Fig. 4) showed bands at 1700 and 1760 cm^{-1}, assigned to carbonyl stretching. This spectrum also indicates that derivatization occurs on the ring nitrogens and not on the oxygen.

Assay Sensitivity, Reproducibility, and Specificity—The amount of III detectable by the electron-capture detector was less than 0.2 ng/

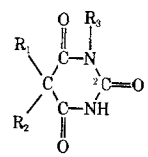

Table II—Retention Times of the Pentafluorobenzyl Derivatives of 15-Barbiturates by the Electron-Capture Detector

Barbiturate	R_1	R_2	R_3	R_f, min
Metharbital[a]	C_2H_5	C_2H_5	CH_3	1.34
Phenobarbital	C_2H_5	C_6H_5	H	1.83 dec.
Barbital	C_2H_5	C_2H_5	H	4.73
Hexobarbital	CH_3	C_6H_9	CH_3	5.15
Allobarbital	CH_2=$CHCH_2$	CH_2=$CHCH_2$	H	5.66
Mephobarbital	C_2H_5	C_6H_5	CH_3	5.66
Butalbital	CH_2=$CHCH_2$	$(CH_3)_2CHCH_2$	H	5.76
Aprobarbital	CH_2=$CHCH_2$	$(CH_3)_2CH$	H	6.08 dec.
Butethal	C_2H_5	C_4H_9	H	6.35
Butabarbital	C_2H_5	$CH_3CH_2CH(CH_3)$	H	6.59 dec.
Amobarbital	C_2H_5	$(CH_3)_2CHCH_2CH_2$	H	6.85 dec.
Pentobarbital	C_2H_5	$CH_3CH_2CH_2CH(CH_3)$	H	7.71
Thiopental (S replaces O on C-2)	C_2H_5	$CH_3CH_2CH_2CH(CH_3)$	H	7.86
Secobarbital	CH_2=$CHCH_2$	$CH_3CH_2CH_2CH(CH_3)$	H	8.39
Hexethal	C_2H_5	$CH_3(CH_2)_5$	H	10.58

[a] Gemonil, Abbott.

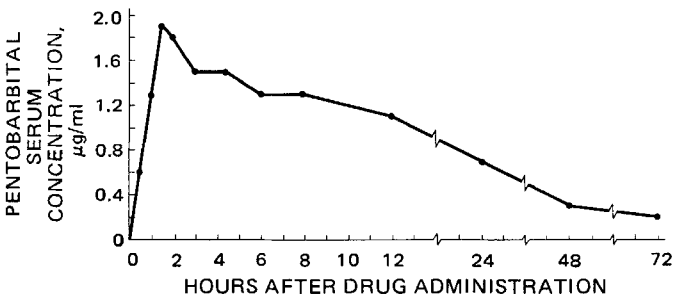

Figure 5—*Serum concentration of pentobarbital* versus *time in one human subject after single-dose oral administration of 100 mg of drug/capsule.*

injection (Fig. 1A). However, under the assay conditions, the lower limit of quantitation for I in extracts of human serum was 0.1 μg/ml, using 1 ml of serum sample (Table I). A linear relationship between peak area ratios and concentrations was obtained for I up to 1.0 μg/ml. Analyses of triplicate serum samples at 0.1–1.0 μg/ml gave a relative standard deviation of 2.6–16.5% with 1 μg of internal standard (Table I).

The method is specific for pentobarbital. Except for thiopental, it was resolved from 13 other barbiturates. The retention times for the pentafluorobenzyl derivatives of 15 barbiturates synthesized individually under similar conditions and detected by the electron-capture detector are shown in Table II. However, the derivatives did not resolve well when all 15 barbiturates were reacted simultaneously with pentafluorobenzyl bromide.

Serum Pentobarbital Levels in Humans—This analytical methodology was used for the measurement of serum pentobarbital (I) concentrations in normal human subjects after a single oral dose of 100 mg of pentobarbital sodium (capsule form). The subjects were fasted for a minimum of 12 hr prior to dosing and for 2 hr after dosing. The drug was administered with 120 ml (4 oz) of water.

Peak levels of pentobarbital ranged from 1.2 and 3.1 μg/ml and were observed at 0.5–2.0 hr after drug administration. Substantial amounts of drug (0.30 ± 0.08 μg/ml) were found in the 48-hr serum samples. A typical serum concentration *versus* time curve for one subject is shown in Fig. 5.

REFERENCES

(1) H. F. Martin and J. L. Driscoll, *Anal. Chem.*, **38**, 345 (1966).

(2) E. A. Fiereck and N. W. Tietz, *Clin. Chem.*, **17**, 1024 (1971).

(3) E. Brochmann-Hanssen and T. O. Oke, *J. Pharm. Sci.*, **58**, 370 (1969).

(4) M. Ehrnebo, S. Agurell, and L. O. Boreus, *Eur. J. Clin. Pharmacol.*, **4**, 191 (1972).

(5) J. MacGee, *Clin. Chem.*, **17**, 587 (1971).

(6) R. C. Driscoll, F. S. Barr, B. J. Gragg, and G. W. Moore, *J. Pharm. Sci.*, **60**, 1492 (1971).

(7) R. G. Cooper, M. S. Greaves, and G. Oaen, *Clin. Chem.*, **18**, 1343 (1972).

(8) R. J. Flanagan and G. Withers, *J. Clin. Pathol.*, **25**, 899 (1972).

(9) R. B. Smith, L. W. Dittert, W. O. Griffen, Jr., and J. T. Doluisio, *J. Pharmacokinet. Biopharm.*, **1**, 5 (1973).

(10) D. J. Berry, *J. Chromatogr.*, **86**, 89 (1973).

(11) L. T. Sennello and F. E. Kohn, *Anal. Chem.*, **46**, 752 (1974).

(12) D. D. Breimer and J. M. Van Rossum, *J. Chromatogr.*, **88**, 235 (1974).

ACKNOWLEDGMENTS AND ADDRESSES

Received December 29, 1975, from the *Pharmaceutical Products Division, Abbott Laboratories, North Chicago, IL 60064.*

Accepted for publication April 29, 1976.

The authors thank S. L. Mueller and members of the Structural Chemistry Section, Abbott Laboratories, for the spectrometric measurements and helpful discussions. Technical assistance from L. R. Hardy and discussions with Dr. D. Hoffman are also gratefully acknowledged.

[x] To whom inquiries should be directed.

In Vitro Adsorption of Acetaminophen onto Activated Charcoal

CAROL A. BAINBRIDGE [*], ERNEST L. KELLY [‡], and W. DOUGLAS WALKLING [x]

Abstract □ *In vitro* experiments supported *in vivo* evidence that activated charcoal is effective in adsorbing acetaminophen. In the physiologic pH range, adsorption was rapid and pH independent. Adsorption, however, was dependent upon the quantity of activated charcoal employed, becoming more complete as the quantity of activated charcoal was increased.

Keyphrases □ Acetaminophen—*in vitro* adsorption onto activated charcoal, effect of pH □ Adsorption, *in vitro*—acetaminophen onto activated charcoal, effect of pH □ Charcoal, activated—*in vitro* adsorption of acetaminophen, effect of pH □ Analgesics—acetaminophen, *in vitro* adsorption onto activated charcoal, effect of pH

The use of activated charcoal has been overlooked as an emergency procedure in acute acetaminophen overdose. Activated charcoal, given in powdered form, effectively decreased absorption of acetaminophen *in vivo* (1–3). When 2 g of acetaminophen was administered simultaneously with 10 g of activated charcoal suspended in a

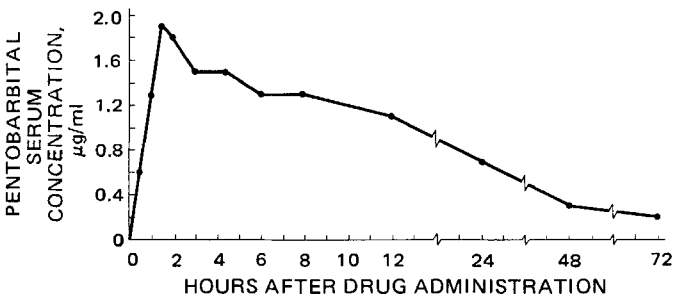

Figure 5—*Serum concentration of pentobarbital* versus *time in one human subject after single-dose oral administration of 100 mg of drug/capsule.*

injection (Fig. 1A). However, under the assay conditions, the lower limit of quantitation for I in extracts of human serum was 0.1 μg/ml, using 1 ml of serum sample (Table I). A linear relationship between peak area ratios and concentrations was obtained for I up to 1.0 μg/ml. Analyses of triplicate serum samples at 0.1–1.0 μg/ml gave a relative standard deviation of 2.6–16.5% with 1 μg of internal standard (Table I).

The method is specific for pentobarbital. Except for thiopental, it was resolved from 13 other barbiturates. The retention times for the pentafluorobenzyl derivatives of 15 barbiturates synthesized individually under similar conditions and detected by the electron-capture detector are shown in Table II. However, the derivatives did not resolve well when all 15 barbiturates were reacted simultaneously with pentafluorobenzyl bromide.

Serum Pentobarbital Levels in Humans—This analytical methodology was used for the measurement of serum pentobarbital (I) concentrations in normal human subjects after a single oral dose of 100 mg of pentobarbital sodium (capsule form). The subjects were fasted for a minimum of 12 hr prior to dosing and for 2 hr after dosing. The drug was administered with 120 ml (4 oz) of water.

Peak levels of pentobarbital ranged from 1.2 and 3.1 μg/ml and were observed at 0.5–2.0 hr after drug administration. Substantial amounts of drug (0.30 ± 0.08 μg/ml) were found in the 48-hr serum samples. A typical serum concentration *versus* time curve for one subject is shown in Fig. 5.

REFERENCES

(1) H. F. Martin and J. L. Driscoll, *Anal. Chem.*, **38**, 345 (1966).

(2) E. A. Fiereck and N. W. Tietz, *Clin. Chem.*, **17**, 1024 (1971).

(3) E. Brochmann-Hanssen and T. O. Oke, *J. Pharm. Sci.*, **58**, 370 (1969).

(4) M. Ehrnebo, S. Agurell, and L. O. Boreus, *Eur. J. Clin. Pharmacol.*, **4**, 191 (1972).

(5) J. MacGee, *Clin. Chem.*, **17**, 587 (1971).

(6) R. C. Driscoll, F. S. Barr, B. J. Gragg, and G. W. Moore, *J. Pharm. Sci.*, **60**, 1492 (1971).

(7) R. G. Cooper, M. S. Greaves, and G. Oaen, *Clin. Chem.*, **18**, 1343 (1972).

(8) R. J. Flanagan and G. Withers, *J. Clin. Pathol.*, **25**, 899 (1972).

(9) R. B. Smith, L. W. Dittert, W. O. Griffen, Jr., and J. T. Doluisio, *J. Pharmacokinet. Biopharm.*, **1**, 5 (1973).

(10) D. J. Berry, *J. Chromatogr.*, **86**, 89 (1973).

(11) L. T. Sennello and F. E. Kohn, *Anal. Chem.*, **46**, 752 (1974).

(12) D. D. Breimer and J. M. Van Rossum, *J. Chromatogr.*, **88**, 235 (1974).

ACKNOWLEDGMENTS AND ADDRESSES

Received December 29, 1975, from the *Pharmaceutical Products Division, Abbott Laboratories, North Chicago, IL 60064.*

Accepted for publication April 29, 1976.

The authors thank S. L. Mueller and members of the Structural Chemistry Section, Abbott Laboratories, for the spectrometric measurements and helpful discussions. Technical assistance from L. R. Hardy and discussions with Dr. D. Hoffman are also gratefully acknowledged.

[x] To whom inquiries should be directed.

In Vitro Adsorption of Acetaminophen onto Activated Charcoal

CAROL A. BAINBRIDGE [*], ERNEST L. KELLY [‡], and W. DOUGLAS WALKLING [x]

Abstract □ *In vitro* experiments supported *in vivo* evidence that activated charcoal is effective in adsorbing acetaminophen. In the physiologic pH range, adsorption was rapid and pH independent. Adsorption, however, was dependent upon the quantity of activated charcoal employed, becoming more complete as the quantity of activated charcoal was increased.

Keyphrases □ Acetaminophen—*in vitro* adsorption onto activated charcoal, effect of pH □ Adsorption, *in vitro*—acetaminophen onto activated charcoal, effect of pH □ Charcoal, activated—*in vitro* adsorption of acetaminophen, effect of pH □ Analgesics—acetaminophen, *in vitro* adsorption onto activated charcoal, effect of pH

The use of activated charcoal has been overlooked as an emergency procedure in acute acetaminophen overdose. Activated charcoal, given in powdered form, effectively decreased absorption of acetaminophen *in vivo* (1–3). When 2 g of acetaminophen was administered simultaneously with 10 g of activated charcoal suspended in a

Table I—Percent Acetaminophen Adsorbed onto Activated Charcoal from Two Sources[a] at pH 6.0 and 37.5°

Activated Charcoal, g[b]	Percent Adsorbed	
	Powder 1	Powder 2
0.3	53.7	65.2
0.4	68.0	86.1
0.5	81.2	93.8
0.6	90.0	97.1
0.7	95.9	98.9
1.0	99.0	99.8

[a] Powder 1 was Norit A, Matheson, Coleman and Bell, Norwood, Ohio. Powder 2 was from Amend Drug and Chemical Co., New York, N.Y. [b] Quantities per 50 ml of acetaminophen solution, 2.5 mg/ml.

methylcellulose solution, absorption in humans was reduced by 63% (1). When activated charcoal was given 60 min after acetaminophen ingestion, a 23% reduction in absorption was noted. When 10 g of activated charcoal was administered immediately after a 1-g dose of acetaminophen, a reduction of 69–77% was observed (2). Activated charcoal can be administered alone or following ipecac or apomorphine-induced emesis. A 10:1 ratio of activated charcoal to acetaminophen reduced absorption by 51% within 30 min (3).

Large quantities of activated charcoal can be administered safely, are well tolerated, and can be used in an emergency for various poisonings (4). To understand the effects of time of administration, pH of the medium, and amount of activated charcoal on the adsorption of acetaminophen, the following study was performed.

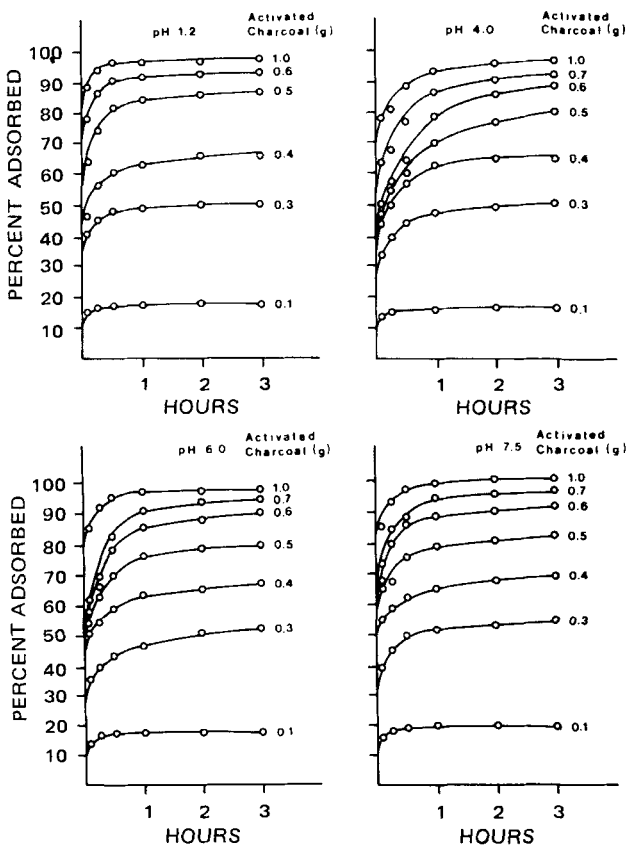

Figure 1—*Percent acetaminophen adsorbed onto activated charcoal at 37.5°.*

Table II—Parameters for the Langmuir Adsorption Isotherm at 37.5°

pH	*n*	*b*	Correlation Coefficient (*r*)
1.2	4.39	0.268	0.996
4.0	4.63	0.223	0.999
6.0	4.16	0.269	0.997
7.5	3.84	0.288	0.998
Composite	4.28	0.282	0.991

EXPERIMENTAL

Materials—Acetaminophen solutions, 2.5 mg/ml, were prepared with the following vehicles: simulated gastric fluid USP without pepsin (pH 1.2), McIlvaine citrate-phosphate buffers (pH 4.0, 4.5, and 6.0), and simulated intestinal fluid USP without pancreatin (pH 7.5).

Analytical—Concentrations of acetaminophen were determined by diluting the samples with acidified methanol and analyzing on a spectrophotometer[1] at 247 nm.

Particle Size—Particle diameters were determined on an automated counter[2].

Adsorption—Various amounts of activated charcoal powder[3] (0.1–1.0 g) were shaken with 50 ml of standard acetaminophen solution at various hydrogen-ion concentrations. The suspensions were shaken at 37.5°, and samples were priodically removed, filtered, and assayed. Samples for equilibrium studies were shaken for 24 hr and centrifuged, and the supernates were assayed.

Desorption—Three variations in desorption experiments were performed.

1. To determine the rate of desorption, various amounts of activated charcoal (0.1–1.0 g) were equilibrated (shaken) overnight with acetaminophen solutions (pH 1.2, 4.5, and 7.5) at 37.5°. The suspensions were centrifuged, the supernates were assayed, and the excess supernates were aspirated. Fifty milliliters of fresh buffer (without acetaminophen) of the same pH as the equilibrating solution was added to the bottles, and the suspensions were shaken again. Samples were removed periodically, filtered, and assayed.

Once it was established that desorption equilibrium could be achieved within 1 hr, the effects of activated charcoal concentration and pH were studied by using only the results from 1-hr samples.

2. Various amounts of activated charcoal (0.2–1.0 g) were equilibrated for 1 hr with pH 1.2 acetaminophen solution. The desorption procedure was the same as Variation 1, but the eluting solutions were of a different pH (4.0 and 7.5).

3. Various amounts of activated charcoal (0.05–1.00 g) were equilibrated for 1 hr with pH 1.2 acetaminophen solution. The desorption procedure was the same as Variation 1 with pH 1.2 eluting solutions. However, each elution was performed four times to determine how repeated elution would affect the accumulative amount of acetaminophen desorbed.

RESULTS AND DISCUSSION

Activated charcoal was demonstrated to be an effective adsorbant for acetaminophen. Within 30 min, most acetaminophen was adsorbed onto the activated charcoal (Fig. 1). Within 1 hr, adsorption was complete at all activated charcoal quantities and over the pH range tested. The percent of acetaminophen adsorbed depended upon the quantity of activated charcoal present. The addition of each 0.1 g of activated charcoal above 0.5 g did not appreciably improve the effectiveness of the activated charcoal for adsorbing 125 mg of acetaminophen. With the reduction of each 0.1 g of activated charcoal below 0.5 g, a large difference in the effectiveness of adsorbing 125 mg of acetaminophen was seen. Consequently, at least four times as much activated charcoal as acetaminophen was required for effective adsorption.

This observation agreed well with suggested doses derived from *in vivo* experiences. Picchioni (5) suggested that a dose of activated charcoal five times the estimated overdose of acetaminophen be employed in acute situations. Levy and Gwilt (3) suggested a 10:1 ratio of activated charcoal to acetaminophen.

[1] Acta III, Beckman Instruments, Fullerton, Calif.
[2] Coulter counter model T, Coulter Electronics Inc., Hialiah, Fla.
[3] Norit A, Matheson, Coleman and Bell, Norwood, Ohio.

Table III—Percent Acetaminophen Adsorbed on Activated Charcoal as a Function of pH at 37.5°

Activated Charcoal, g[a]	Percent Adsorbed			
	pH 1.2	pH 4.0	pH 6.0	pH 7.5
0.05	10.3	8.4	11.2	8.7
0.1	16.8	17.2	19.4	16.4
0.2	29.0	34.1	36.8	36.7
0.3	58.2	50.2	53.7	59.1
0.4	64.9	65.3	68.0	71.0
0.5	77.7	77.7	81.2	85.3
0.6	87.2	87.0	90.0	93.9
0.7	94.5	89.9	95.9	97.2
1.0	98.3	98.8	99.0	99.7

[a] Quantities per 50 ml of acetaminophen solution, 2.5 mg/ml.

Activated charcoal powder from another source[4] was compared to the activated charcoal[3] employed throughout the rest of the study. The mean particle diameters of the activated charcoal powder from the two sources were similar (one source[4] had a mean of 8.3 μm and a 70% range of 3.6–16.5 μm; the other[3] had a mean of 9.1 μm and a 70% range of 3.7–18.5 μm). Only slight differences in their equilibrium concentrations were found. Table I shows the differences in the percent adsorbed at equilibrium onto the two brands of activated charcoal. These differences should not have a bearing on the effectiveness of activated charcoal in overdose situations.

Langmuir adsorption isotherms were determined for the adsorption of acetaminophen onto activated charcoal powder at various hydrogen-ion concentrations. The Langmuir isotherm is defined as follows:

$$c/(x/m) = nc + b \qquad \text{(Eq. 1)}$$

where c = concentration of acetaminophen in milligrams per milliliter at equilibrium, x/m = amount of adsorbed drug in milligrams (x) per milligram of activated charcoal (m), and n and b are constants for the isotherms. The constants (n and b) were determined by linear regression analysis at each pH (Table II). Since the differences between the isotherms at various pH values were not significant, the data from all four pH values were pooled and a composite isotherm was obtained. The parameters for this isotherm are listed in Table II as "composite."

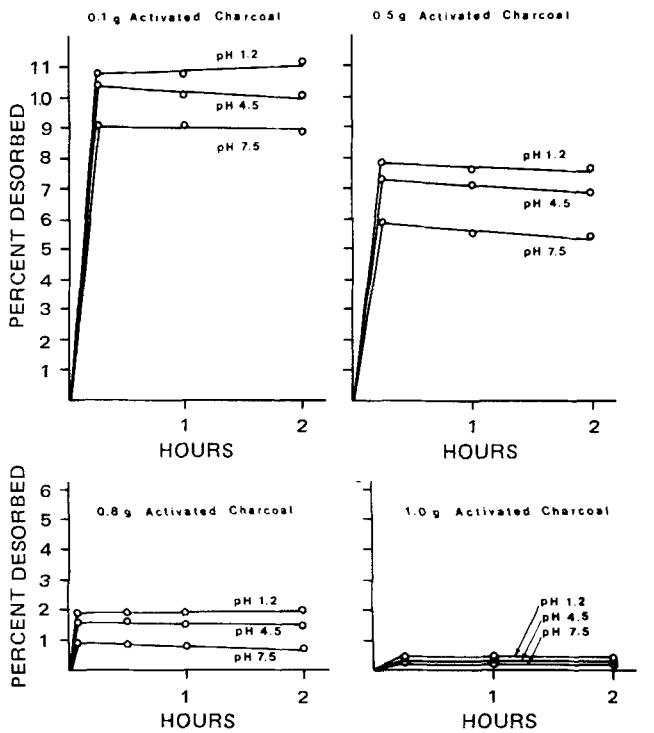

Figure 2—*Percent acetaminophen desorbed from activated charcoal at 37.5°.*

[4] Amend Drug and Chemical Co., New York, N.Y.

Table IV—Percent Acetaminophen Desorbed from Activated Charcoal at 37.5°

Activated Charcoal, g[a]	Percent Desorbed	
	pH 4.0	pH 7.5
0.2	25.7	17.8
0.3	19.9	13.7
0.4	15.9	10.2
0.5	12.0	7.2
0.6	8.3	4.4
0.7	5.8	2.3
1.0	1.4	0.3

[a] Equilibrium was attained with 50 ml of pH 1.2 acetaminophen solution, 2.5 mg/ml, and elution was performed with 50 ml of pH 4.0 and 7.5 buffers.

Table V—Desorption by Four Successive Elutions at 37.5°[a]

Activated Charcoal, g	Accumulative Percent Desorbed			
	Elution 1	Elution 2	Elution 3	Elution 4
0.05	30.8	40.3	45.8	48.8
0.1	26.5	36.1	41.4	45.1
0.2	18.9	27.5	32.5	36.0
0.3	13.7	21.0	25.7	29.0
0.4	10.4	16.5	20.6	23.6
0.5	7.4	12.2	15.7	18.8
0.6	4.2	7.3	9.9	12.0
0.7	2.0	3.7	5.1	6.5
1.0	0.4	0.7	0.9	1.2

[a] Equilibrium was attained with 50 ml of pH 1.2 acetaminophen solution, 2.5 mg/ml, and elution was performed with 50 ml of pH 1.2 solution.

Adsorption onto activated charcoal is greater for unionized compounds. Since acetaminophen has a pKa of 9.9 (6), it is unionized in the pH 1.2–7.5 range. Therefore, the compound is well adsorbed at all physiological pH values. Under *in vivo* conditions, small differences such as were seen in the Langmuir isotherms would probably be negated by ions, enzymes, *etc.*, which would also be adsorbed onto the charcoal.

The maximum adsorption capacity (1/n) was 234 mg of acetaminophen/g of activated charcoal. This value is in agreement with the 279 mg of acetaminophen/g of activated charcoal found by Levy and Gwilt (3).

The effect of pH on the percent of acetaminophen adsorbed at equilibrium onto activated charcoal is more evident from the data in Table III. For each activated charcoal quantity, only a slight difference was seen. For example, 0.5 g of activated charcoal adsorbed 77.7% of acetaminophen at pH 1.2 and 85.3% at pH 7.5. Normal deviations in data and the use of different buffer systems might account for the differences seen.

Desorption studies were performed to determine if acetaminophen, once adsorbed, could be desorbed from activated charcoal as a result of a change in pH or in the acetaminophen concentration in the solution. Figure 2 illustrates the effect of variations in the quantity of activated charcoal employed and in the pH of the desorption medium. Desorption was essentially complete within 15 min. Desorption decreased with decreasing pH and with increasing quantities of activated charcoal.

Table IV describes desorption when the eluting solution was at a pH (4.0 and 7.0) higher than the pH (1.2) of the adsorbing solution. Desorption was greater in the pH 4.0 solution than in the pH 7.0 solution. The exact reason for this result is not known, but it is probably related to the buffer compositions. Also, as in the previous case, the greater the amount of activated charcoal employed, the smaller was the percent desorption of acetaminophen.

Data in Table V indicate that the most desorption occurred with the first elution. Subsequent elutions had a much smaller effect on desorption, especially when large amounts of activated charcoal were employed.

REFERENCES

(1) B. Dordoni, R. Willson, R. P. H. Thompson, and R. Williams, *Br. Med. J.*, **3**, 86 (July 14, 1973).

(2) G. Levy and P. R. Gwilt, *J. Am. Med. Assoc.*, **219**, 621 (1972).

(3) G. Levy and P. R. Gwilt, *Pharmacologist*, **16**, 208 (1974).

(4) D. Corby and W. Decker, *Pediatrics*, **54**, 324 (1974).

(5) A. Picchioni, *Pediat. Clin. N. Am.*, **17**, 535 (1970).
(6) G. B. Berlin and D. D. Perrin, *Q. Rev.*, **20**, 75 (1966).

ACKNOWLEDGMENTS AND ADDRESSES

Received February 9, 1976, from the *Pharmacy Research Department, McNeil Laboratories, Inc., Fort Washington, PA 19034.*

Accepted for publication June 7, 1976.

* Present address: Medical College of Pennsylvania, Philadelphia, PA 19129.

‡ Present address: Villanova University, Villanova, PA 19085.

x To whom inquiries should be directed.

Conformational Studies of Antiradiation Agents by NMR: Cysteamine and Its Derivatives

VITHAL M. KULKARNI and GIRJESH GOVIL x

Abstract □ The conformations of cysteamine, thiazolidine, and thiazolidine-4-carboxylic acid were determined in aqueous solutions using NMR spectroscopy. At physiological pH, the population ratio of *gauche*- and *trans*-conformers was 3:1. The *gauche*-rotamer is probably responsible for the antiradiation activity and acts through metal chelation involving sulfur and nitrogen atoms. The puckering of the thiazolidine ring was calculated using NMR coupling constants. The observed results were compared with those obtained in the solid state using X-ray diffraction.

Keyphrases □ Cysteamine—and derivatives, NMR conformational study in aqueous solutions □ Thiazolidine—and derivatives, NMR conformational study in aqueous solutions □ NMR—conformational study of cysteamine, thiazolidine, and derivatives in aqueous solutions □ Conformations—cysteamine, thiazolidine, and derivatives, NMR study in aqueous solutions □ Antiradiation agents—cysteamine, thiazolidine, and derivatives, NMR conformational study in aqueous solutions

Cysteamine (2-aminoethanethiol, I) is a well-established antiradiation agent (1). The sulfur-substituted derivative of this molecule (2), 2-aminoethanethiosulfuric acid (II), is as active as I. Some 2-substituted thiazolidines (III and IV), prepared by condensing I with carbonyls, are also good antiradiation agents (3). To explain the mechanism of radioprotection offered by these compounds, several postulations (4, 5) have been suggested such as mixed disulfide formation (6) with protein constituents, chelation of vital metal ions (7), and binding to DNA (8).

The conformations in the solid state by X-ray diffraction for these molecules were reported (9–12). Recently, quantum chemical calculations using extended Hückel theory (EHT) and complete neglect of differential overlap (CNDO) methods were made in this laboratory. The results showed that I has both *gauche*- and *trans*-conformations, with a preference toward the *trans*-structure.

In this paper, the application of NMR spectroscopy for the determination of the preferred conformation in solution of cysteamine and some thiazolidine derivatives is reported. Attempts were made to correlate these findings with their biological action.

$HSCH_2CH_2NH_2$ I

$HO_3SSCH_2CH_2NH_2$ II

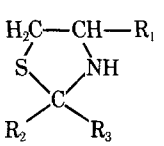

III: $R_1 = COOH$, $R_2 = R_3 = H$
IV: $R_1 = H$, $R_2 = R_3 = CH_3$

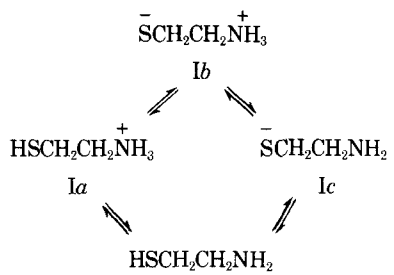

Scheme I

In physiological solution, cysteamine undergoes multiple ionization (9) (Scheme I). The ionization constants governing these equilibria have been reported, so it is possible to calculate the fraction of each species as a function of pH. The concentration of I is low at all pH values. Form I*a* predominates in acidic media, while I*c* predominates at pH values greater than 12. Form I*b* is present at intermediate pH's and reaches its maximum concentration of 84.6% around pH 9.5. Therefore, NMR studies of cysteamine were made at three different pH values. Other compounds were studied in neutral solution and in deuterochloroform.

EXPERIMENTAL

Materials—Cysteamine hydrochloride[1] was recrystallized from 95% ethyl alcohol until it was free from disulfide traces. 2-Aminoethanethiosulfuric acid and thiazolidine derivatives were prepared using reported procedures (3, 13).

NMR Measurements—Samples were dissolved in deuterium oxide to a known concentration, and spectra[2] were recorded using the sodium salt of 2,2-dimethyl-2-silapentane-5-sulfonic acid as the internal reference. The pH values were adjusted using trifluoroacetic acid.

RESULTS AND DISCUSSION

Spectral Analysis—The studied molecules are of the 1,2-disubstituted ethane type and show the usual rotational isomerism around the carbon–carbon bond. In the case of thiazolidines, this rotation is hindered, but a small degree of conformational freedom is still present due to the puckering modes of the ring. The spectrum of cysteamine recorded in

[1] Fluka grade.
[2] Varian Associates HA-100 and A-60 spectrometers.

(5) A. Picchioni, *Pediat. Clin. N. Am.*, **17**, 535 (1970).
(6) G. B. Berlin and D. D. Perrin, *Q. Rev.*, **20**, 75 (1966).

ACKNOWLEDGMENTS AND ADDRESSES

Received February 9, 1976, from the *Pharmacy Research Department, McNeil Laboratories, Inc., Fort Washington, PA 19034.*

Accepted for publication June 7, 1976.

* Present address: Medical College of Pennsylvania, Philadelphia, PA 19129.

‡ Present address: Villanova University, Villanova, PA 19085.

x To whom inquiries should be directed.

Conformational Studies of Antiradiation Agents by NMR: Cysteamine and Its Derivatives

VITHAL M. KULKARNI and GIRJESH GOVIL x

Abstract □ The conformations of cysteamine, thiazolidine, and thiazolidine-4-carboxylic acid were determined in aqueous solutions using NMR spectroscopy. At physiological pH, the population ratio of *gauche*- and *trans*-conformers was 3:1. The *gauche*-rotamer is probably responsible for the antiradiation activity and acts through metal chelation involving sulfur and nitrogen atoms. The puckering of the thiazolidine ring was calculated using NMR coupling constants. The observed results were compared with those obtained in the solid state using X-ray diffraction.

Keyphrases □ Cysteamine—and derivatives, NMR conformational study in aqueous solutions □ Thiazolidine—and derivatives, NMR conformational study in aqueous solutions □ NMR—conformational study of cysteamine, thiazolidine, and derivatives in aqueous solutions □ Conformations—cysteamine, thiazolidine, and derivatives, NMR study in aqueous solutions □ Antiradiation agents—cysteamine, thiazolidine, and derivatives, NMR conformational study in aqueous solutions

Cysteamine (2-aminoethanethiol, I) is a well-established antiradiation agent (1). The sulfur-substituted derivative of this molecule (2), 2-aminoethanethiosulfuric acid (II), is as active as I. Some 2-substituted thiazolidines (III and IV), prepared by condensing I with carbonyls, are also good antiradiation agents (3). To explain the mechanism of radioprotection offered by these compounds, several postulations (4, 5) have been suggested such as mixed disulfide formation (6) with protein constituents, chelation of vital metal ions (7), and binding to DNA (8).

The conformations in the solid state by X-ray diffraction for these molecules were reported (9–12). Recently, quantum chemical calculations using extended Hückel theory (EHT) and complete neglect of differential overlap (CNDO) methods were made in this laboratory. The results showed that I has both *gauche*- and *trans*-conformations, with a preference toward the *trans*-structure.

In this paper, the application of NMR spectroscopy for the determination of the preferred conformation in solution of cysteamine and some thiazolidine derivatives is reported. Attempts were made to correlate these findings with their biological action.

$HSCH_2CH_2NH_2$ I

$HO_3SSCH_2CH_2NH_2$ II

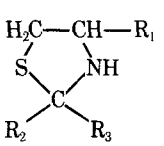

III: $R_1 = COOH$, $R_2 = R_3 = H$
IV: $R_1 = H$, $R_2 = R_3 = CH_3$

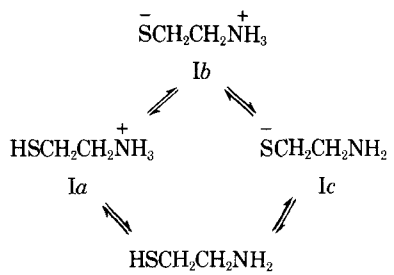

Scheme I

In physiological solution, cysteamine undergoes multiple ionization (9) (Scheme I). The ionization constants governing these equilibria have been reported, so it is possible to calculate the fraction of each species as a function of pH. The concentration of I is low at all pH values. Form I*a* predominates in acidic media, while I*c* predominates at pH values greater than 12. Form I*b* is present at intermediate pH's and reaches its maximum concentration of 84.6% around pH 9.5. Therefore, NMR studies of cysteamine were made at three different pH values. Other compounds were studied in neutral solution and in deuterochloroform.

EXPERIMENTAL

Materials—Cysteamine hydrochloride[1] was recrystallized from 95% ethyl alcohol until it was free from disulfide traces. 2-Aminoethanethiosulfuric acid and thiazolidine derivatives were prepared using reported procedures (3, 13).

NMR Measurements—Samples were dissolved in deuterium oxide to a known concentration, and spectra[2] were recorded using the sodium salt of 2,2-dimethyl-2-silapentane-5-sulfonic acid as the internal reference. The pH values were adjusted using trifluoroacetic acid.

RESULTS AND DISCUSSION

Spectral Analysis—The studied molecules are of the 1,2-disubstituted ethane type and show the usual rotational isomerism around the carbon–carbon bond. In the case of thiazolidines, this rotation is hindered, but a small degree of conformational freedom is still present due to the puckering modes of the ring. The spectrum of cysteamine recorded in

[1] Fluka grade.
[2] Varian Associates HA-100 and A-60 spectrometers.

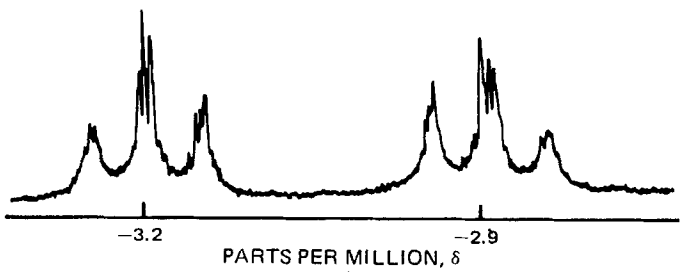

Figure 1—*The 100-MHz spectrum of cysteamine in deuterium oxide (pH 7).*

a neutral medium (pH 7.0) is shown in Fig. 1. Figures 2 and 3 show the spectra of thiazolidine-4-carboxylic acid hydrochloride and 2,2′-dimethylthiazolidine hydrochloride, respectively.

The chemical shift and coupling constant data for all these molecules are given in Table I. The spectra of I and IV show two methylene proton absorptions due to the CH_2CH_2 fragment. The chemical shift difference in acidic solution is greater than in neutral and basic solutions, indicating the effect of pH on the acid–base equilibrium. The spectrum is of the *AA′BB′* type and was analyzed by an iterative LAOCOON program (14). As usual with such spectra, only the sum of the coupling constants ($J_{AB} + J_{AB'}$) was estimated accurately. The spectrum of thiazolidinecarboxylic acid, on the other hand, is of the *ABC* type and all coupling constants were evaluated accurately. 2-Aminoethanethiosulfuric acid shows a single methylene proton at −3.00 ppm (δ), indicating a very small chemical shift difference (spectrum not shown).

Conformational Analysis of Cysteamine—Due to rotation about the carbon–carbon bond, the spectrum is an average of the individual rotamers, each of which belongs to the *AA′BB′* class (15). In the system of three equilibrating staggered rotamers, G, T, and G′ (Fig. 4), the weighted mean of the couplings between protons *A* and *B* are observed.

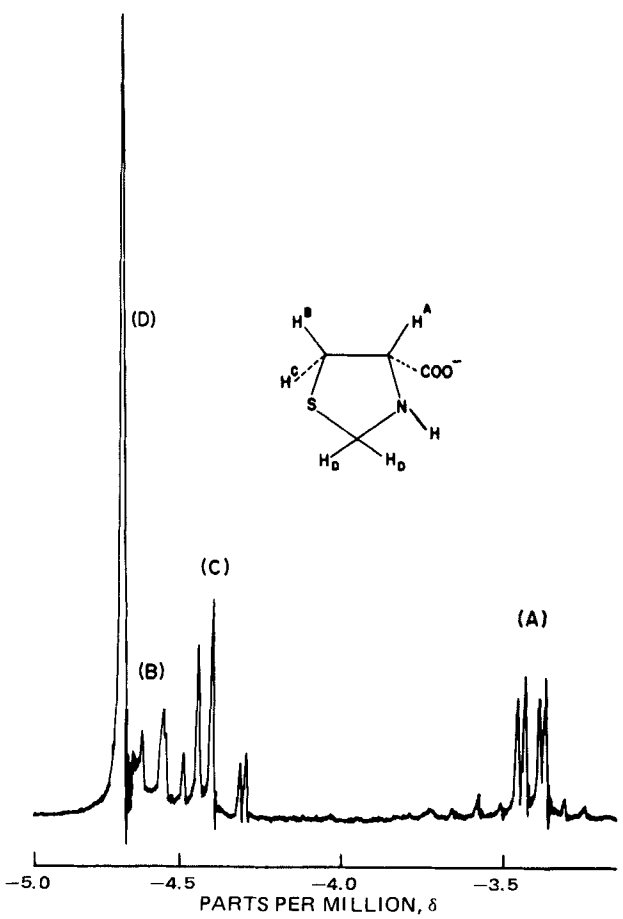

Figure 2—*The 100-MHz spectrum of thiazolidine-4-carboxylic acid in deuterium oxide.*

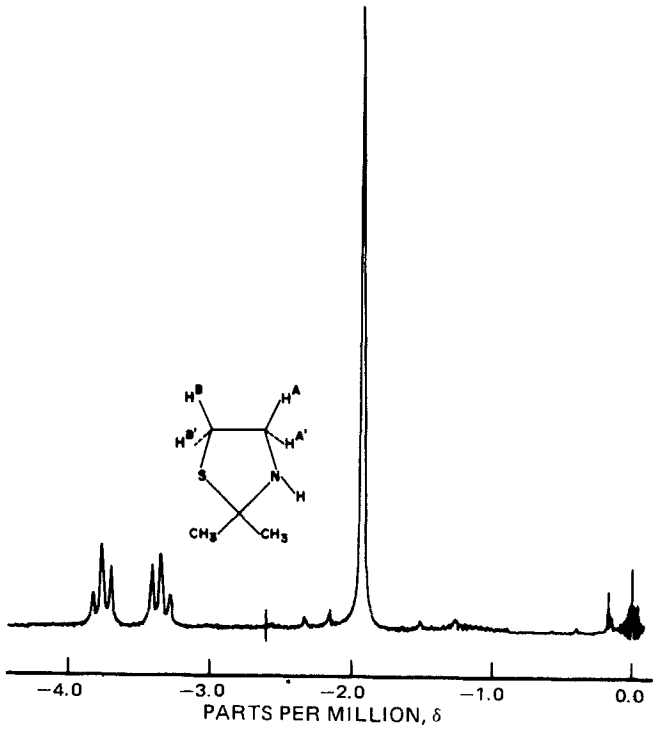

Figure 3—*The 100-MHz spectrum of 2,2-dimethylthiazolidine in deuterochloroform.*

In the present case, rotamers G and G′ are identical. The observed coupling constants (J_{AB} and $J_{AB'}$) contain information about the relative populations of the three rotamers.

In an $X\text{-}CH_2CH_2\text{-}Y$ fragment, the *vicinal* coupling constants depend on the electronegativity of the substituents and the dihedral angles. Abraham and Gatti (16) made a detailed analysis of the two effects. For staggered conformations of 1,2-disubstituted ethanes, the individual *gauche-* and *trans-vicinal* proton–proton couplings (J_g and J_t) are related to the electronegativities of the substituent atoms X and Y as follows.

For *trans*-rotamer T:

$$J_g{}^T = 1.35 + 0.63(E_X + E_Y) \quad \text{(Eq. 1)}$$

$$J_t{}^T = 18.07 - 0.88(E_X + E_Y) \quad \text{(Eq. 2)}$$

For *gauche*-rotamers G and G′:

$$J_g{}^G = 8.94 - 0.94(E_X + E_Y) \quad \text{(Eq. 3)}$$

$$J_{g'}{}^G + J_t{}^G = 26.92 - 2.03(E_X + E_Y) \quad \text{(Eq. 4)}$$

where E_X and E_Y are Huggins electronegativities (17) for atoms S and N, which are 2.60 and 3.05, respectively. From Eqs. 1–4, $J_g{}^T = 4.91$, $J_t{}^T = 13.04$, $J_g{}^G = 3.63$, and $J_t{}^G = 11.83$. From these values, one estimates $(J_{AB} + J_{AB'})^T = J_g{}^T + J_t{}^T = 17.95$ and $(J_{AB} + J_{AB'})^{G,G'} = \frac{1}{2}[(J_{AB} + J_{AB'})^G + (J_{AB} + J_{AB'})^{G'}] = \frac{1}{2}[3J_g{}^G + J_t{}^G] = 11.36$. The population of the *trans*-isomer, p_T, can now be evaluated using the observed values of $(J_{AB} + J_{AB'})$:

$$(J_{AB} + J_{AB'})_{obs} = 17.95p_T + 11.36(1 - p_T) \quad \text{(Eq. 5)}$$

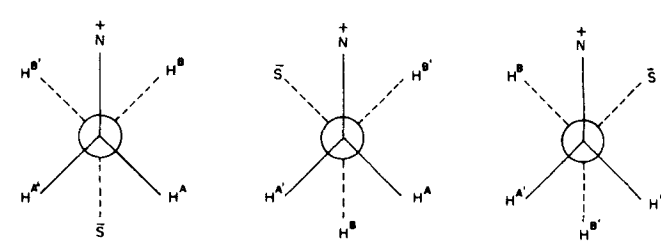

Figure 4—*Conformational rotamers of cysteamine.*

Table I—Proton Chemical Shifts and Coupling Constants in Cysteamine and Thiazolidines

Compound	Chemical Shift (Downfield) A	B	C	Coupling Constant, Hz	p_T
Cysteamine[a]					
pH 3	−3.11	−3.54	—	$J_{A,B} \sim 6.5$, $J_{A,B'} \sim 7.8$ $\lvert J_{A,B} + J_{A,B'} \rvert = 14.3$	0.44
pH 7	−3.04	−3.35	—	$J_{A,B} \sim 7.2$, $J_{A,B'} \sim 5.8$ $\lvert J_{A,B} + J_{A,B'} \rvert = 13.0$	0.25
pH 11	−3.05	−3.37	—	$J_{A,B} \sim 6.8$, $J_{A,B'} \sim 6.8$ $\lvert J_{A,B} + J_{A,B'} \rvert = 13.6$	0.34
Thiazolidinecarboxylic acid[a]	−3.43	−4.58	−4.46	$J_{A,B} \sim 6.6$, $J_{A,C} \sim 2.1$, $J_{B,C} \sim -11.7$	—
Dimethylthiazolidine[b]	−3.35	−3.78	—	$J_{A,B} \sim 6.6$, $J_{A,B'} \sim 6.6$ $\lvert J_{A,B} + J_{A,B'} \rvert = 13.2$	—

[a] In deuterium oxide relative to sodium 2,2-dimethyl-2-silapentane-5-sulfonate. [b] In deuterochloroform relative to tetramethylsilane.

or:

$$p_T = \frac{(J_{AB} + J_{AB'})_{obs} - 11.36}{6.59} \quad \text{(Eq. 6)}$$

The population analysis of the rotamer isomers is given in Table I.

Two factors can contribute to errors in the estimates of the population distributions reported in Table I. Basic values of component coupling constants, estimated using empirical generalizations made on the basis of experimental measurements on a large number of compounds (16), may be in error. Recently, Feeney (18) made an accurate determination of component coupling constants for carbon–carbon bonds in peptides using data from methyl-substituted piperidine and cyclohexylamine. The electronegativities of the substituents in this case are similar to those in cysteamine, as are the component coupling constants for the G and T isomers. Nevertheless, errors of ~0.5 Hz in the estimation of $J_{AB} + J_{AB'}$ for either the G or T isomer are possible and will be reflected as a maximum error of 6 in the estimated population of the *trans*-conformer.

Errors also may occur in the observed values of $J_{AB} + J_{AB'}$. In neutral and acidic media, the NMR lines are fairly sharp and the sum of the coupling constants can be estimated to an accuracy of ±0.1 Hz. This value corresponds to an accuracy of ±2 in estimated percentage values of p_T. However, in basic solutions, the linewidths are about 1 Hz and the sum of the estimated coupling constants can be in error by ±0.5 Hz, leading to an error of ±10 in the percentage values of p_T.

Clearly, a significant population of both *gauche*- and *trans*-conformers is present at all three pH values. The population distribution of p_G to p_T is close to the value of 2:1 expected from purely statistical considerations. If it is assumed that the component coupling constants are not sensitive to the ionization state of the molecule, then the population distribution does show a detectable change with pH. At physiological pH, the ratio of p_G to p_T is around 3:1. A slightly higher population of the *gauche*-conformer around pH 7 may be associated with a preferential stabilization of such a conformer by electrostatic charge–charge interaction or the nitrogen–hydrogen–sulfur–hydrogen bond.

Puckering Angle in Thiazolidine and Thiazolidinecarboxylic Acid—Thiazolidine and its derivatives cannot acquire fully staggered conformations about their various single bonds because of the restrictions imposed by ring closure. In general, a saturated five-member ring system may lie in a twisted conformation, with two of its atoms lying out of the plane defined by the other three.

It is possible to estimate the dihedral angle (δ) along the nitrogen–carbon–carbon–sulfur bond (Fig. 5) using *vicinal* NMR coupling constants between protons on the two carbon atoms[3]. In general, a Karplus-type relationship between the *vicinal* hydrogen–carbon–carbon–hydrogen coupling constant and the relevant dihedral angle (ϕ) is used in such studies:

$$J(\phi) = A\cos^2\phi + B\cos\phi + C \quad \text{(Eq. 7)}$$

The first term in the Karplus relationship generally dominates, since the value of A is almost 10 times larger than that of B or C.

The available coupling constants, $J_g^G(\phi = 60°)$ and $J_t^G(\phi = 180°)$, for cysteamine can be used to calibrate the Karplus relationship for thiazolidine. However, these data are insufficient for estimating all three parameters. Fortunately, as will be seen later, results are not sensitive to values of B and C. Accordingly, attempts are made on the following combinations of A, B, and C values to estimate δ in thiazolidine and thiazolidinecarboxylic acid: (*a*) $A = 10.93$, $B = 0$, and $C = 0.90$ (analogous to the relationship suggested by Feeney (18) for amino acids); (*b*) $A = 12.7$, $B = 0.9$, and $C = 0$; (*c*) $A = 11.8$, $B = 0$, and $C = 0$; and (*d*) $A = 14.5$, $B = 0$, and $C = 0$. The estimated value of δ does not differ by more than ±5° from the mean values reported in the subsequent discussion.

For thiazolidine itself, two identical conformations correspond to positive or negative values of δ. The NMR spectrum of the NCH_2CH_2S fragment is a weighted average of the two identical conformers. As is evident from Fig. 5*b*, the sum of coupling constants $J_{AB'} + J_{A'B}$ is related to δ by the following equation:

$$(J_{AB'} + J_{A'B})_{obs} = \tfrac{1}{2}[2J(\delta) + J(120 - \delta) + J(120 + \delta)] \quad \text{(Eq. 8)}$$

Using a value of 13.2 Hz for $J_{AB'} + J_{A'B}$, one obtains $\delta = 42 \pm 3°$.

With thiazolidinecarboxylic acid, the two conformers become nonequivalent, but the NMR spectrum (*ABC* type) enables one to determine which of the two conformers is preferred because both J_{AB} and J_{AC} are measurable. The observed values of 2.1 Hz for J_{AC} and 6.6 Hz for J_{AB} indicate that the preferred conformer in solution is as shown in Fig. 5c with $\delta = 45 \pm 5°$. The result is not significantly affected when the parameters of the Karplus relationship are calibrated using $J_g^G = 3.2$ and $J_t^G = 11.4$, which are the values obtained when allowing for the electronegativity of the substituent on thiazolidine.

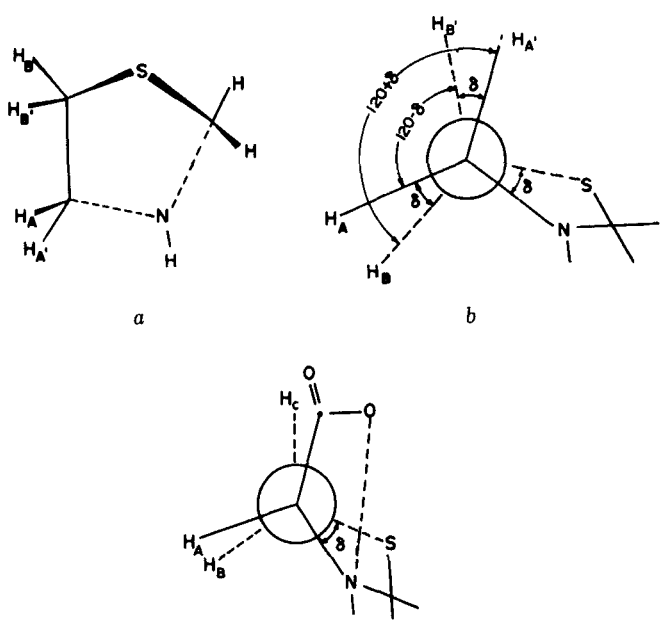

Figure 5—*Conformations of thiazolidine. Key:* a, *ring puckering of thiazolidine showing both nitrogen and sulfur atoms puckered with respect to the plane passing through the three carbon atoms (twisted conformation);* b, *dihedral angles around the carbon–carbon bond in thiazolidine; and* c, *ring puckering in thiazolidinecarboxylic acid.*

[3] In principle, it is also possible to estimate dihedral angles along the carbon–carbon–nitrogen–carbon and carbon–nitrogen–carbon–sulfur bonds through hydrogen–carbon–nitrogen–hydrogen coupling constants. Unfortunately, such coupling constants were not detected in the molecules under study.

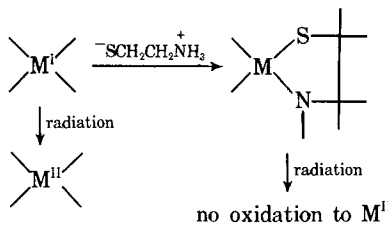

Scheme II

Comparison with Conformational Studies by Other Methods—While the solid-state and solution data on the preferred conformations of the compounds are not identical, they do show a high degree of similarity. For cysteamine in deuterium oxide at physiological pH, the relative population of the *gauche*-conformer is greater (75%) than the *trans*-conformer. X-ray diffraction studies (9), on the other hand, showed that in the solid state the molecule crystallizes only in the *gauche*-form. In crystals, the observed structure is stabilized by intramolecular nitrogen–hydrogen–sulfur bonds.

For thiazolidinecarboxylic acid, X-ray crystallography indicates that the ring has a one-atom pucker (envelope) conformation, with the sulfur atom lying about 0.8 Å ($\delta = 27°$) out of the plane described by the other four atoms. The solution data indicate a slightly higher pucker ($\delta = 45°$) for both thiazolidine and thiazolidinecarboxylic acid. If the bond length and bond angles observed in the solid state are preserved in solution, then the NMR data indicate that both sulfur and nitrogen atoms are puckered relative to the plane described by the three ring carbon atoms. The structure of thiazolidinecarboxylic acid is held in the crystal by several intra- and intermolecular NH···O=C hydrogen bonds. When such hydrogen bonds are replaced by solute–solvent hydrogen bonds in aqueous solutions, the molecular conformation apparently switches to a more relaxed two-atom twisted conformation.

The solution results are in better agreement with those predicted by EHT and CNDO theory. Theoretical results correspond more closely to conformations for isolated molecules and indicate a slight preference for the intramolecularly hydrogen-bonded form of I*b* while almost equal energies are predicted for the G, T, and G′ conformers of I*a* and I*c*. For thiazolidine systems, such calculations indicate that a two-atom twisted conformation (with $\delta = 38°$) is most stable.

Biological Action—Based on the conformer population of cysteamine in solution, it can be argued that the radioprotective action of this molecule arises from a structure in which the essential atoms, sulfur and nitrogen, are placed in a *gauche*-arrangement. In this conformation, the sulfur and nitrogen atoms come in close proximity and their steric repulsion may be offset by intramolecular hydrogen bond NH···S and charge interactions. This type of molecular arrangement allows the possibility of chelation of metal ions involving sulfur and nitrogen atoms (Scheme II) and prevents their oxidation by free radicals formed in the biophase by the radiolysis of water (19). With thiazolidines, the antiradiation action may be due to their *in vivo* hydrolysis (20) to a protective compound, cysteamine, which then undergoes molecular arrangement as shown in Scheme II.

REFERENCES

(1) Z. M. Bacq, A. Herre, J. Leomte, P. Fischer, J. Blavier, G. Dechamps, M. LeBihan, and P. Rayet, *Arch. Int. Physiol.*, **59**, 442 (1951).

(2) B. Sorbo, *Acta Chem. Scand.*, **12**, 1990 (1952).

(3) V. M. Kulkarni and H. P. Tipnis, *Curr. Sci.*, **41**, 637 (1972).

(4) W. O. Foye, *J. Pharm. Sci.*, **58**, 283 (1969).

(5) Z. M. Bacq, "Chemical Protection Against Ionizing Radiation," Charles C Thomas, Springfield, Ill., 1965.

(6) A. Pihl and L. Eldjarn, *Pharmacol. Rev.*, **10**, 437 (1958).

(7) E. C. Knoblock and W. C. Purdy, *Radiat. Res.*, **15**, 94 (1961).

(8) E. Jellum, *Int. J. Radiat. Biol.*, **9**, 185 (1965).

(9) R. J. Jandacek and H. M. Swartz, *Radiat. Res.*, **44**, 523 (1970).

(10) W. E. Keefe and J. M. Stewart, *Acta Crystallogr.*, **28(B)**, 2459 (1972).

(11) J. Loscalzo, R. G. Kallen, and D. Voet, *Arch. Biochem. Biophys.*, **157**, 426 (1973).

(12) M. Goodman, V. Chen, E. Benedetti, C. Pedone, and P. Corradini, *Biopolymers*, **11**, 1779 (1972).

(13) D. L. Klayman, M. M. Grenan, and D. P. Jacobus, *J. Med. Chem.*, **12**, 510 (1969).

(14) S. Castellano and A. A. B. By, *J. Chem. Phys.*, **41**, 3863 (1964).

(15) L. M. Jackman and S. Sternhell, "Applications of Nuclear Magnetic Resonance Spectroscopy in Organic Chemistry," 2nd ed., Pergamon Press, Oxford, England, 1969, p. 368.

(16) R. J. Abraham and G. Gatti, *J. Chem. Soc. B*, **1969**, 961.

(17) M. L. Huggins, *J. Am. Chem. Soc.*, **75**, 4123 (1953).

(18) J. Feeney, *J. Mag. Res.*, **21**, 473 (1976).

(19) N. Haugaard, *Physiol. Rev.*, **48**, 339 (1968).

(20) H. P. Tipnis and L. D. Small, *Diss. Abstr.*, **25**, 2773 (1964).

ACKNOWLEDGMENTS AND ADDRESSES

Received March 10, 1975, from the *Tata Institute of Fundamental Research, Homi Bhabha Road, Bombay 400005, India.*

Accepted for publication May 12, 1976.

The authors are grateful to Prof. M. V. Bhatt, Indian Institute of Science, Bangalore, for use of the 100-MHz NMR spectrometer and to Dr. M. M. Dhingra of this Institute for discussions and help.

[x] To whom inquiries should be directed.

Radioimmunoassay of Indomethacin in Biological Fluids

L. E. HARE, C. A. DITZLER, and D. E. DUGGAN [x]

Abstract □ A radioimmunoassay was developed for the determination of indomethacin in biological fluids at concentrations as low as 50 ng/ml. Antibodies were produced in rabbits immunized with a conjugate of bovine serum albumin and indomethacin. This conjugate was prepared by an *N*-hydroxysuccinimide active ester procedure. Antiserums exhibited minimal cross-reactivity with the *O*-desmethyl and deschlorobenzoyl metabolites. However, the glucuronide conjugate was about three times as reactive as indomethacin, thus invalidating direct determinations of indomethacin in urine. This difficulty was circumvented by analyzing urine aliquots before and after conjugate hydrolysis. Concentrations of free and conjugated indomethacin were calculated by difference.

Keyphrases □ Indomethacin—radioimmunoassay, human plasma and urine □ Radioimmunoassay—indomethacin, human plasma and urine □ Anti-inflammatory agents—indomethacin, radioimmunoassay, human plasma and urine

Analyses of the widely used anti-inflammatory agent indomethacin[1] have previously been accomplished by spectrofluorometric (1) or radioisotopic (2) methods. These procedures are useful in certain situations but are subject to limitations. The spectrofluorometric method lacks sensitivity, and the presence of other fluorescent materials,

[1] Indocin, Merck Sharp & Dohme.

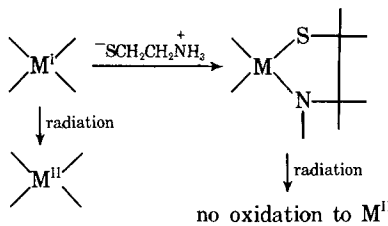

Scheme II

Comparison with Conformational Studies by Other Methods—While the solid-state and solution data on the preferred conformations of the compounds are not identical, they do show a high degree of similarity. For cysteamine in deuterium oxide at physiological pH, the relative population of the *gauche*-conformer is greater (75%) than the *trans*-conformer. X-ray diffraction studies (9), on the other hand, showed that in the solid state the molecule crystallizes only in the *gauche*-form. In crystals, the observed structure is stabilized by intramolecular nitrogen–hydrogen–sulfur bonds.

For thiazolidinecarboxylic acid, X-ray crystallography indicates that the ring has a one-atom pucker (envelope) conformation, with the sulfur atom lying about 0.8 Å ($\delta = 27°$) out of the plane described by the other four atoms. The solution data indicate a slightly higher pucker ($\delta = 45°$) for both thiazolidine and thiazolidinecarboxylic acid. If the bond length and bond angles observed in the solid state are preserved in solution, then the NMR data indicate that both sulfur and nitrogen atoms are puckered relative to the plane described by the three ring carbon atoms. The structure of thiazolidinecarboxylic acid is held in the crystal by several intra- and intermolecular NH···O=C hydrogen bonds. When such hydrogen bonds are replaced by solute–solvent hydrogen bonds in aqueous solutions, the molecular conformation apparently switches to a more relaxed two-atom twisted conformation.

The solution results are in better agreement with those predicted by EHT and CNDO theory. Theoretical results correspond more closely to conformations for isolated molecules and indicate a slight preference for the intramolecularly hydrogen-bonded form of I*b* while almost equal energies are predicted for the G, T, and G′ conformers of I*a* and I*c*. For thiazolidine systems, such calculations indicate that a two-atom twisted conformation (with $\delta = 38°$) is most stable.

Biological Action—Based on the conformer population of cysteamine in solution, it can be argued that the radioprotective action of this molecule arises from a structure in which the essential atoms, sulfur and nitrogen, are placed in a *gauche*-arrangement. In this conformation, the sulfur and nitrogen atoms come in close proximity and their steric repulsion may be offset by intramolecular hydrogen bond NH···S and charge interactions. This type of molecular arrangement allows the possibility of chelation of metal ions involving sulfur and nitrogen atoms (Scheme II) and prevents their oxidation by free radicals formed in the biophase by the radiolysis of water (19). With thiazolidines, the antiradiation action may be due to their *in vivo* hydrolysis (20) to a protective compound, cysteamine, which then undergoes molecular arrangement as shown in Scheme II.

REFERENCES

(1) Z. M. Bacq, A. Herre, J. Leomte, P. Fischer, J. Blavier, G. Dechamps, M. LeBihan, and P. Rayet, *Arch. Int. Physiol.*, **59**, 442 (1951).

(2) B. Sorbo, *Acta Chem. Scand.*, **12**, 1990 (1952).

(3) V. M. Kulkarni and H. P. Tipnis, *Curr. Sci.*, **41**, 637 (1972).

(4) W. O. Foye, *J. Pharm. Sci.*, **58**, 283 (1969).

(5) Z. M. Bacq, "Chemical Protection Against Ionizing Radiation," Charles C Thomas, Springfield, Ill., 1965.

(6) A. Pihl and L. Eldjarn, *Pharmacol. Rev.*, **10**, 437 (1958).

(7) E. C. Knoblock and W. C. Purdy, *Radiat. Res.*, **15**, 94 (1961).

(8) E. Jellum, *Int. J. Radiat. Biol.*, **9**, 185 (1965).

(9) R. J. Jandacek and H. M. Swartz, *Radiat. Res.*, **44**, 523 (1970).

(10) W. E. Keefe and J. M. Stewart, *Acta Crystallogr.*, **28(B)**, 2459 (1972).

(11) J. Loscalzo, R. G. Kallen, and D. Voet, *Arch. Biochem. Biophys.*, **157**, 426 (1973).

(12) M. Goodman, V. Chen, E. Benedetti, C. Pedone, and P. Corradini, *Biopolymers*, **11**, 1779 (1972).

(13) D. L. Klayman, M. M. Grenan, and D. P. Jacobus, *J. Med. Chem.*, **12**, 510 (1969).

(14) S. Castellano and A. A. B. By, *J. Chem. Phys.*, **41**, 3863 (1964).

(15) L. M. Jackman and S. Sternhell, "Applications of Nuclear Magnetic Resonance Spectroscopy in Organic Chemistry," 2nd ed., Pergamon Press, Oxford, England, 1969, p. 368.

(16) R. J. Abraham and G. Gatti, *J. Chem. Soc. B*, **1969**, 961.

(17) M. L. Huggins, *J. Am. Chem. Soc.*, **75**, 4123 (1953).

(18) J. Feeney, *J. Mag. Res.*, **21**, 473 (1976).

(19) N. Haugaard, *Physiol. Rev.*, **48**, 339 (1968).

(20) H. P. Tipnis and L. D. Small, *Diss. Abstr.*, **25**, 2773 (1964).

ACKNOWLEDGMENTS AND ADDRESSES

Received March 10, 1975, from the *Tata Institute of Fundamental Research, Homi Bhabha Road, Bombay 400005, India.*

Accepted for publication May 12, 1976.

The authors are grateful to Prof. M. V. Bhatt, Indian Institute of Science, Bangalore, for use of the 100-MHz NMR spectrometer and to Dr. M. M. Dhingra of this Institute for discussions and help.

[x] To whom inquiries should be directed.

Radioimmunoassay of Indomethacin in Biological Fluids

L. E. HARE, C. A. DITZLER, and D. E. DUGGAN [x]

Abstract □ A radioimmunoassay was developed for the determination of indomethacin in biological fluids at concentrations as low as 50 ng/ml. Antibodies were produced in rabbits immunized with a conjugate of bovine serum albumin and indomethacin. This conjugate was prepared by an *N*-hydroxysuccinimide active ester procedure. Antiserums exhibited minimal cross-reactivity with the *O*-desmethyl and deschlorobenzoyl metabolites. However, the glucuronide conjugate was about three times as reactive as indomethacin, thus invalidating direct determinations of indomethacin in urine. This difficulty was circumvented by analyzing urine aliquots before and after conjugate hydrolysis. Concentrations of free and conjugated indomethacin were calculated by difference.

Keyphrases □ Indomethacin—radioimmunoassay, human plasma and urine □ Radioimmunoassay—indomethacin, human plasma and urine □ Anti-inflammatory agents—indomethacin, radioimmunoassay, human plasma and urine

Analyses of the widely used anti-inflammatory agent indomethacin[1] have previously been accomplished by spectrofluorometric (1) or radioisotopic (2) methods. These procedures are useful in certain situations but are subject to limitations. The spectrofluorometric method lacks sensitivity, and the presence of other fluorescent materials,

[1] Indocin, Merck Sharp & Dohme.

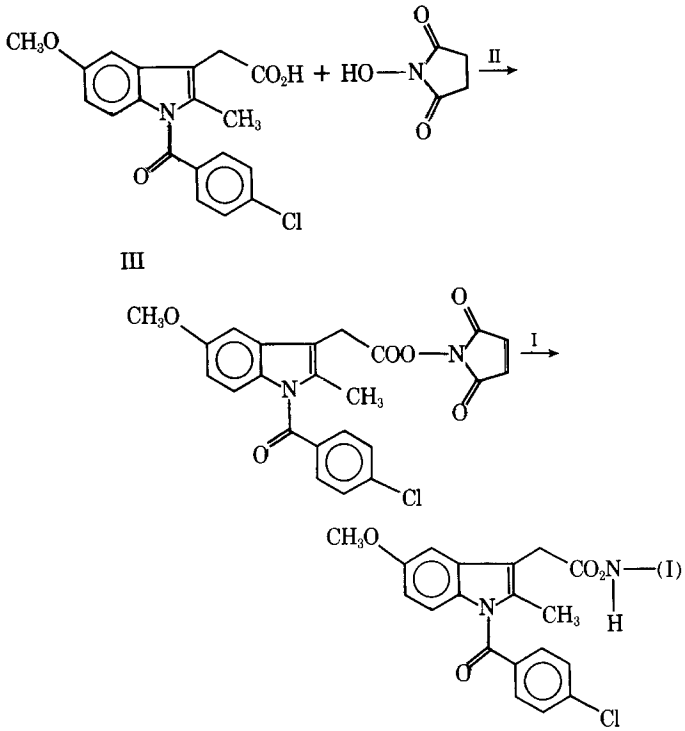

Scheme I

such as salicylic acid, causes interference. Reverse isotope dilution offers the advantage of quantitating all metabolites but necessitates administration of radioactive drug.

GC (3), mass fragmentographic (4), and liquid chromatographic (5) techniques recently were developed. Their primary disadvantages are the necessity of careful sample preparation and the relatively slow rate of analysis. This paper reports a radioimmunoassay procedure for the direct analysis of indomethacin in biological fluids requiring no prior isolation.

EXPERIMENTAL

2-^{14}C-Indomethacin[2] (52 μCi/mg), bovine serum albumin[3] (I), *N*-hydroxysuccinimide[4], dicyclohexylcarbodiimide[4] (II), β-glucuronidase[5], neutral charcoal[6], and dextran[7] were used as received. Dextran-coated charcoal was prepared by suspending 6.25 g of previously washed charcoal and 0.625 g of dextran in 100 ml of 0.05 *M* phosphate buffer (pH 7.5).

Preparation of Conjugates—Indomethacin (III) was conjugated through the carboxylic acid moiety to I by an *N*-hydroxysuccinimide active ester procedure (6, 7) (Scheme I). Conversion of indomethacin to the succinimide ester was verified by the appearance of characteristic imide peaks at 1800, 1780, and 1720 cm^{-1} in the IR spectrum. Indomethacin active ester (125 mg, 0.35 mmole) in dioxane (3 ml) was added dropwise to a solution of I (200 mg, 0.18 mmole lysine equivalents) in 0.05 *M* phosphate buffer (pH 7.8) (20 ml).

The solution was allowed to stand at room temperature overnight and was then extensively dialyzed against distilled water. The small amount of insoluble material present was removed by centrifugation, and the solution was lyophilized. The extent of conjugation was 17 molecules of indomethacin/molecule of I as estimated by UV absorption (indomethacin $\epsilon_{320} = 6.3 \times 10^3$). Protein concentration was determined by a microbiuret method (8).

Immunization of Animals—New Zealand White rabbits were injected intramuscularly with indomethacin–I conjugates (5 mg), which had been dissolved in 0.5 ml of saline and emulsified with an equal volume of Freund's complete adjuvant. Booster injections of 1 mg of conjugate were given at monthly intervals in incomplete adjuvant. Bleedings were taken from central ear arteries about 2 weeks after booster injections. The antibody titer was determined from the binding of 2-^{14}C-indomethacin by the antiserums, corrected for binding to normal serum.

Radioimmunoassay of Plasma—Antiserum was used at a dilution that bound 35–50% of the added label in control tubes containing no unlabeled antigen. The assay solution consisted of 0.1 ml of pooled human plasma containing unlabeled indomethacin standards (50–3000 ng/ml) or 0.1 ml of plasma from indomethacin-treated subjects, 0.1 ml of a 1:12 dilution of the antiserum, 20 ng of 2-^{14}C-indomethacin (2.3×10^3 dpm) in 0.1 ml of 0.05 *M* phosphate buffer (pH 7.4), and sufficient buffer to achieve a final volume of 1.0 ml. The solutions were allowed to equilibrate at 4° overnight, and then 0.2 ml of dextran-coated charcoal suspension was added with thorough mixing. The tubes were allowed to stand at 4° for 10–12 min, and the charcoal was separated by centrifugation. Antibody-bound radioactivity contained in the supernate was determined by scintillation counting.

Standard curves were plotted on log-probit paper as unlabeled indomethacin added *versus* percent of control binding ($100 \times B/B_0$, where B = bound antigen in the presence of unknown sample, and B_0 = bound antigen in the absence of unlabeled drug).

Radioimmunoassay of Urine—*Unconjugated Indomethacin*—One aliquot (1 ml) of each appropriately diluted urine sample (5–300 ng/ml) was treated with 0.2 ml of 1 *M* citrate buffer (pH 5.0) and extracted with 3 ml of benzene–2-propanol (9:1). The organic phase was allowed to evaporate, and the residue was dissolved in 0.1 ml of 0.05 *M* phosphate buffer (pH 7.4). Radioimmunoassay was performed as described for plasma.

Total Indomethacin—A second 1-ml aliquot (5–300 ng/ml) was treated with 1 ml (5000 units) of β-glucuronidase in the same buffer as was used for unconjugated indomethacin for 3 hr at 37° to hydrolyze the glucuronide conjugate. Thereafter, this aliquot was treated in an identical manner as the first.

Indomethacin Glucuronide—The numerical difference between results of total and unconjugated procedures represents conjugated indomethacin.

RESULTS

Antibodies to indomethacin could be detected in two of five rabbits 8 weeks after immunization. With continued boosting, antibody titers increased slowly up to about 4 months, at which time a final antiserum dilution of 1:120 bound 35% of added 2-^{14}C-indomethacin in the absence of unlabeled drug. Antiserum was used at this dilution for routine assay.

Standard curves for detecting indomethacin in human plasma were prepared as described under *Experimental*. Significant displacement was seen with 5 ng of added indomethacin, and the curves were linear (r = 0.98) up to about 300 ng. Thus, the useful range of the method is 50–3000 ng/ml plasma. Nonspecific binding to antiserum was less than 5%, indicating that there were no interfering substances in normal plasma. Assay of standards prepared in urine resulted in standard curves that were slightly displaced from plasma curves but had identical slopes. Thus, separate standard curves are required for urine and plasma.

Recovery and reproducibility of the assay were determined by 10 replicate assays of known indomethacin samples in pooled normal plasma:

standard concentration, ng	7	25	100
mean ± *SD* of 10 assays, ng	9.5 ± 0.9	29 ± 1.5	98 ± 7.0
CV, %	9.5	5.2	7.1
recovery, %	135 ± 13	115 ± 6	98 ± 7

Recovery was rather poor at lower indomethacin levels due, in part at least, to errors in sample preparation as well as variations in the assay itself.

Potential interference of metabolites and other substances with the assay was evaluated by determining the concentrations of these compounds necessary to displace 50% of the bound 2-^{14}C-indomethacin from the antibody (Table I). The *O*-desmethyl metabolite (IV) was 12% as reactive as indomethacin, whereas the deschlorobenzoyl metabolite (V) was nonreactive. Salicylate, which is sometimes present in indomethacin plasma samples (following simultaneous aspirin administration), also did not interfere with the assay. However, several ester and amide derivatives of indomethacin were highly cross-reactive. The glycoside de-

[2] Prepared by Dr. R. L. Ellsworth, Merck Sharp & Dohme Research Laboratories.
[3] Nutritional Biochemical Co.
[4] Pierce Chemical Co.
[5] Ketodase, Warner-Chilcott.
[6] Norit A, Amend Drug and Chemical Co.
[7] T-70, Pharmacia Labs.

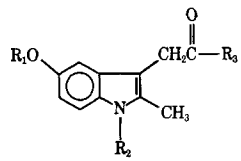

Table I—Cross-Reactivity of Indomethacin–I Antiserum

Compound	R_1	R_2	R_3	Mass Required to Displace 50% of Bound 2-^{14}C-Indomethacin, ng	Relative Cross-Reactivity, %
III	CH_3	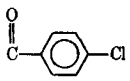	OH	35	100
IV	H	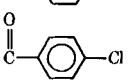	OH	296	12
V	CH_3	H	OH	>20,000	<0.2
VI	CH_3	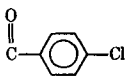	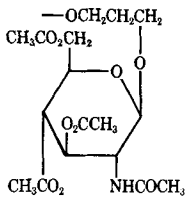	9	390
VII	CH_3	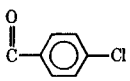	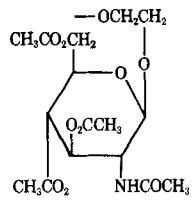	3	1170

rivatives (VI and VII) were several times more reactive than indomethacin. Thus, the glucuronide conjugate of indomethacin, which accounts for at least 50% of the drug-derived material excreted in urine, might be expected to interfere with the determination of urine indomethacin levels.

To explore this possibility, indomethacin and indomethacin glucuronide concentrations were determined in human urine by both radioimmunoassay and reverse isotope dilution (2) (Table II). In this study, 2-^{14}C-indomethacin (25 mg, 1 μCi/mg) was administered intravenously; urine was collected over the 0–2-hr period. The specific activity of the injected indomethacin was <2% of that used in radioimmunoassay and, therefore, did not interfere.

Both methods afforded comparable total indomethacin concentrations following glucuronidase treatment of the samples. Unconjugated indomethacin was determined by extraction of the urine samples with benzene–2-propanol (9:1) prior to analysis. Similar results were obtained by both methods. The slightly high radioimmunoassay value may have been due to 10% interference by IV (2.6 μg equivalent/ml as determined by reverse isotope dilution).

Direct radioimmunoassay or reverse isotope dilution of untreated urine samples should also afford unconjugated indomethacin concentrations if the glucuronide conjugate does not interfere with either method. Values obtained by reverse isotope dilution (3.7 μg/ml) were as expected, but results of the radioimmunoassay analysis were much too high (17.3 μg/ml). Thus, the assay is highly cross-reactive to indomethacin glucuronide. Whether this effect involves perturbation(s) of the indomethacin–antibody or indomethacin–charcoal equilibria or both is not apparent.

The difference between free indomethacin measured by radioimmunoassay after extraction (4.63 μg/ml) and total indomethacin in unextracted samples (17.3 μg/ml) represents the apparent glucuronide level. This value (12.7 μg equivalent/ml) is 3.25 times higher than the true conjugate concentration (3.91 μg equivalent/ml). Radioimmunoassay of indomethacin in unextracted urine samples, therefore, will result in high estimates of indomethacin concentrations. Furthermore, the small but significant cross-reactivity to the desmethyl metabolite (Table I), which is a major constituent of later urine samples (2), precludes the use of direct radioimmunoassay for specific measurement of indomethacin in urine. However, urine concentrations can be determined by analyzing aliquots before and after conjugate hydrolysis as described later.

The utility of the assay for determination of plasma indomethacin concentrations was also demonstrated by a comparison of results obtained by radioimmunoassay and reverse isotope dilution following administration of labeled drug (Fig. 1). Results from the two procedures were in excellent agreement (r = 0.995).

DISCUSSION

The production of antiserums to indomethacin has permitted development of a simple and sensitive method for the determination of this drug in biological fluids. The present sensitivity (50 ng/ml) is adequate for pharmacological levels commonly encountered but could be improved by the use of radiolabeled indomethacin of greater specific activity.

The indomethacin radioimmunoassay is not a totally specific method. The described antiserum is not reactive with V but is about threefold more reactive with indomethacin glucuronide than with indomethacin

Table II—Indomethacin and Indomethacin Glucuronide Concentrations in Urine[a]

Method	Total Indomethacin[b] and Indomethacin Glucuronide	Unconjugated[c] Indomethacin	Indomethacin[d] Glucuronide	Indomethacin[e] and Indomethacin Glucuronide	Indomethacin[f] Glucuronide
Reverse isotope dilution	9.20 ± 0.42	3.70 ± 0.45	5.50	—	—
Radioimmunoassay	8.54 ± 0.47	4.63 ± 0.55	3.91	17.3 ± 1.35	12.0 ± 0.76

[a] Mean ± *SD* of 10 determinations. Values are in micrograms per milliliter. [b] β-Glucuronidase treatment. [c] Reverse isotope dilution data were obtained by direct analysis; radioimmunoassay data were obtained after extraction of free indomethacin. [d] Determined by difference. [e] Direct determination by radioimmunoassay. [f] Radioimmunoassay of aqueous phase from reverse isotope dilution method.

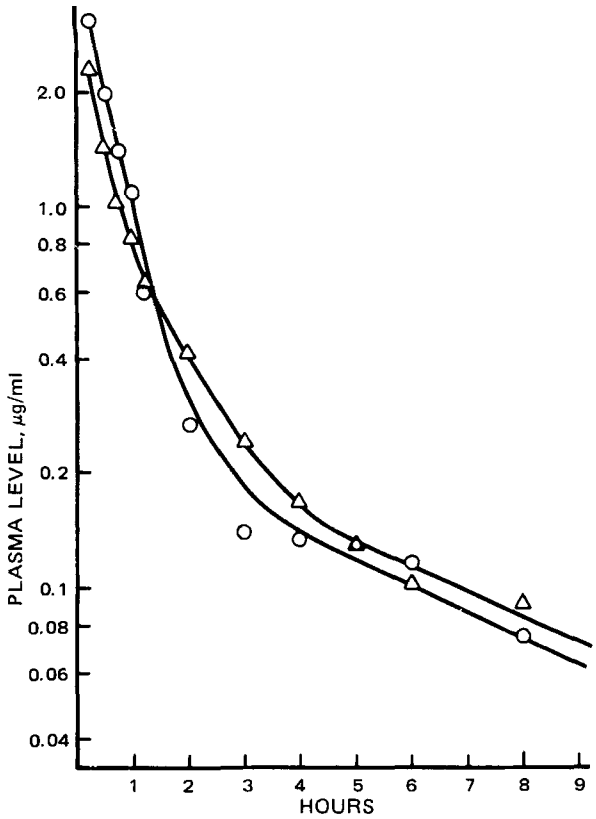

Figure 1—*Human plasma indomethacin concentrations determined by radioimmunoassay (○) and reverse isotope dilution (△). Subjects received 25 mg of 2-^{14}C-indomethacin (1 μCi/mg) intravenously.*

itself. Furthermore, IV exhibits 12% cross-reactivity to the antibody used, and some animals produce serums with 100% cross-reactivity to IV. Even animals with serums of good selectivity produce less selective antibodies over time. Therefore, care must be taken to select appropriate antiserums. Several animals should be immunized, and bleedings should be taken very early.

The cross-reactivity of the antiserum with indomethacin glucuronide is not surprising, since the material used for immunization of rabbits was an acyl conjugate of indomethacin and I. Thus, antibodies were expected to be more reactive to amide and ester derivatives than to the free acid of indomethacin. This supposition was verified by cross-reactivity studies in which glycosyl esters were bound more tightly to the antibody than was free indomethacin and by experiments with human urine samples.

Indomethacin and its conjugate in urine can be estimated accurately by analyzing two sample aliquots as described under *Experimental*. One aliquot is extracted with benzene–2-propanol, thus providing a measure of unconjugated indomethacin. The second aliquot is treated with β-glucuronidase to hydrolyze the conjugate before assay. The value obtained by the latter procedure represents total indomethacin, and the difference between the two values is an estimate of indomethacin glucuronide concentration.

Plasma samples can be analyzed directly without extraction. The small amount of interference (12%) caused by IV would not generally be a problem, since plasma levels of this metabolite only begin to approach indomethacin concentrations about 6 hr after administration of the parent drug, whose plasma half-life is about 2 hr (2). Urinary concentrations of indomethacin are also much greater than concentrations of IV for the first 4 hr. However, IV equals or exceeds indomethacin levels for the 4–48-hr period; IV will, therefore, interfere with the radioimmunoassay procedure outlined for urine.

If differentiation is necessary, a combined isotope dilution–radioimmunoassay method analogous to that described for sulindac (9) could be used. In this case, metabolites are separated chromatographically prior to radioimmunoassay, thus allowing the determination of each compound if suitable antiserums and labeled antigens are available.

REFERENCES

(1) H. B. Hucker, A. G. Zacchei, S. V. Cox, D. A. Brodie, and N. H. R. Cantwell, *J. Pharmacol. Exp. Ther.*, **153**, 237 (1966).

(2) D. E. Duggan, A. F. Hogans, K. C. Kwan, and F. G. McMahon, *ibid.*, **181**, 563 (1972).

(3) D. G. Ferry, D. M. Ferry, P. W. Moller, and E. G. McQueen, *J. Chromatogr.*, **89**, 110 (1974).

(4) G. Alvan, M. Orme, L. Bertilsson, R. Ekstrand, and L. Palmer, *Clin. Pharmacol. Ther.*, **18**, 364 (1975).

(5) J. Skellern and E. Salole, *J. Chromatogr.*, **114**, 483 (1975).

(6) G. W. Anderson, J. E. Zimmerman, and F. M. Callahan, *J. Am. Chem. Soc.*, **86**, 1839 (1964).

(7) M. Hichens and A. F. Hogans, *Clin. Chem.*, **20**, 266 (1974).

(8) R. F. Itzhaki and D. M. Gill, *Anal. Biochem.*, **9**, 401 (1964).

(9) L. E. Hare, C. A. Ditzler, M. Hichens, A. Rosegay, and D. E. Duggan, *J. Pharm. Sci.*, **66**, 414 (1977).

ACKNOWLEDGMENTS AND ADDRESSES

Received March 22, 1976, from the *Merck Institute for Therapeutic Research, West Point, PA 19486.*

Accepted for publication June 7, 1976.

The authors thank Dr. F. G. McMahon of Tulane University and Dr. A. W. Czerwinski of Oklahoma University for the biological samples. The known metabolites of indomethacin (IV and V) and the acyl esters (VI and VII) were supplied by Dr. T.-Y. Shen of the Merck Sharp & Dohme Research Laboratories, Rahway, N.J. The authors also acknowledge the interest and support of Dr. J. E. Baer.

[x] To whom inquiries should be directed.

Sustained-Release Hormonal Preparations XV: Release of Progesterone from Cholesterol Pellets *In Vivo*

A. A. JOSEPH *, J. L. HILL ‡, J. PATEL §, S. PATEL ¶, and FRED A. KINCL ˣ

Abstract □ Progesterone–sterol pellets were made that provided a zero-order release of progesterone for 80 days. 4-^{14}C-Progesterone was used to measure the release *in vitro* and *in vivo*. The dissolution rate *in vitro* (distilled water as the desorbing medium) for progesterone–cholesterol (59:41 w/w) and progesterone–β-sitosterol (47:53 w/w) pellets was 72 μg/100 mm^2/24 hr. The average *in vivo* absorption from subcutaneously implanted pellets in rabbits was 2 ± 0.1 μg/ml of plasma/cm^2 of surface area. Of this amount, 20–25% was progesterone; the remainder was progesterone metabolites and conjugates. Zero-order release (plasma levels) was obtained for approximately 80 days or until about 70% of the available progesterone was exhausted. During this time, the level of excreted radioactivity in urine continuously decreased, indicating that monitoring only this parameter would lead to erroneous conclusions. A long-term effect and increased effectiveness were obtained with a 5–20-mg progesterone equivalent dose, using gel prepared from 2% methylcellulose as the suspending medium.

Keyphrases □ Progesterone—in sustained-release cholesterol implant pellets, *in vivo* and *in vitro* release, biological effectiveness, rabbits and rats □ Cholesterol—implant pellets containing progesterone, *in vivo* and *in vitro* release and biological effectiveness, rabbits and rats □ Dosage forms—sustained-release progesterone–cholesterol implant pellets, *in vivo* and *in vitro* release and biological effectiveness of progesterone, rabbits and rats □ Sustained-release implant pellets—progesterone–cholesterol, *in vivo* and *in vitro* release and biological effectiveness of progesterone, rabbits and rats □ Hormones—progesterone in sustained-release cholesterol implant pellets, *in vivo* and *in vitro* release, biological effectiveness, rabbits and rats

Over the past several years, the biological effectiveness of drugs as a function of dosage form has been evaluated. In most studies, subcutaneously implanted sustained-release poly(dimethylsiloxane) capsules were used as the drug carrier (1). Animal studies demonstrated a significant increase in the potency of steroid hormones given in a sustained-release form; when released continuously from silicone rubber implants, considerably less hormone was needed to produce a given biological effect than when the same compound was given by injection or orally (2). The lower dose resulted in lower plasma levels and less accumulation of the steroid and of its metabolites in various organs (3).

Steroid–lipid implants as drug carriers have also been used (4–8). Mixing of steroids and lipids in arbitrary proportions resulted in steroid release in sufficient amounts to provide a pharmacological effect, but "the reproducibility of pellets of the same composition but made at different times varied . . . ." (4).

The present experiments were designed to test the release and biological effectiveness of steroid–sterol pellets combined in the region of eutectic mixtures.

EXPERIMENTAL

Pellet Preparation—Weighed amounts of progesterone and the respective sterol were dissolved in minimal amounts of chloroform. The solvent was removed by evaporation in a rotary evaporator, and the resulting crystalline mass was dried at 37°. The dry powder was transferred into a hand press preheated to about 100°. The temperature of the brass block was then slowly raised until the mass began to soften (115–120°). The soft mass was extruded through a perforated disk; the emerging rods (3 and 1 mm thick), which cooled and hardened rapidly, were cut into 1–3-mm long, cylindrical sections and marumerized to spherical pellets.

Marumerizer—The marumerizer was made from a Plexiglas block containing a circular chamber 6.4 cm in diameter. The wall was inlaid with aluminum oxide-coated abrasive[1]. For operation, the chamber was loaded with about 2–5 g of material; a current of air led in through tangential air inlets imparted a rapid rotation to the pellets. The average time for a 3-g load was 15 min with an air flow of about 200 liters/hr.

To minimize the loss of material, the outlets of the marumerizer were connected to a small Plexiglas cyclone separator. Five different pellet sizes between 177 and 1705 μm were obtained by screening marumerized material through a set of analytical sieves.

Preparation of Radioactive Progesterone—A known amount of 4-^{14}C-progesterone was added to cold progesterone dissolved in chloroform. The solvent was removed by distillation in a rotary evaporator, and the crystalline material was dried *in vacuo*. Specific activity of the resulting material was determined by weighing two or three samples on an analytical microbalance. Weighed samples were dissolved in toluene, and the radioactivity was determined.

Determination of Radioactivity—Toluene-based scintillation medium containing 1% of a fluor was used; plasma samples (1 ml) were solubilized with 1 ml of a tissue solubilizer[2] by digesting at 45–50° for about 1.5 hr. When a clear solution was obtained, 10 ml of a medium[3] was added. Prior to counting, the samples were kept at 0° for approximately 24 hr to eliminate photoluminescence. Urine and feces samples (*vide infra*) were decolorized with 30% aqueous hydrogen peroxide solution (0.5 ml) by incubating at 37° for 48–64 hr. A solubilizing solution (10 ml) prepared from two parts of toluene and one part of a surfactant[4] and containing 1% of a fluor was added. Counting efficiency (liquid spectrophotometer[5]) was determined by using external (and where appropriate, internal) standards. The efficiency in toluene scintillation medium was 80–85%; the efficiency in aqueous scintillation medium was 20–45%.

Studies *In Vitro*—A known weight (and number) of pellets was gently shaken[6] in 100 ml of distilled water at room temperature. To determine the amount of progesterone in the desorbing medium, 2-ml aliquots were taken periodically. Water was evaporated (IR lamps), and the radioactivity present was counted upon addition of toluene scintillation medium. Fresh desorbing medium was used every 24–72 hr. Other conditions were as stated previously (4).

Metabolic Studies in Rabbits—With the use of a local anesthetic[7], ethylene oxide-sterilized pellets (suspended in a sterile medium prepared from 2% aqueous gel of methylcellulose; 0.75 ml of the medium to suspend 100 mg of pellets) were implanted in the left hindleg of rabbits[8] by means of a thin walled No. 9 trocar. One-milliliter graduated pipets were used to deliver the desired amount. The wound was closed by clips[9].

Two rabbits were implanted with 23 and 27 tablets (compressed in a small press, hardness >5 kg) having a surface area of 456 and 535 mm^2, respectively. Two rabbits were implanted with 67 and 70 pellets with an average diameter of 1705 μm (surface area of 612 and 639 mm^2, respectively), and two rabbits were implanted with 78 and 94 pellets with an average diameter of 1205 μm (surface area of 356 and 429 mm^2, respectively). The average hardness of the pellets was <1 kg.

The animals were kept in metabolic cages, and water and food were given *ad libitum*. Peripheral blood (by ear puncture), urine, and feces were collected as stated. For blood collection, the ear and the collection

[1] Norton 120-J, Behr-Manning Division, Troy, N.Y.
[2] NCS solubilizer, Amersham/Searle, Arlington Heights, Ill.
[3] PCS, Amersham/Searle.
[4] Triton X, Rohm and Haas Co., Philadelphia, Pa.
[5] Model 720, Nuclear Chicago.
[6] Burrel wrist-action shaker, Burrel Corp., Pittsburgh, Pa.
[7] Xylocaine.
[8] Rockland, Inc., Gilbertsville, Pa.
[9] Justerite wound clips, 11 mm, Clay Adams, Parsippany, N.J.

Table I—Dissolution of Progesterone from Lipid Pellets into Water (Based on Unit Weight)

Lipid Used (% w/w)	Micrograms of Progesterone/24 hr/100-mg Pellets ± *SE*				
	1705[a]	1205	750	375	177
Cholesterol (41%)	560 ± 22	905 ± 33	1320 ± 96	3620 ± 289	5015 ± 409
β-Sitosterol (53%)	640 ± 25	1115 ± 72	1210 ± 93	4090 ± 435	3960 ± 278
	Based on Unit Area, μg of Progesterone/24 hr/100-mm² Area				
Cholesterol (41%)	252	224	239	245	Not calculated
β-Sitosterol (53%)	288	276	219	278	Not calculated

[a] Average pellet size, micrometers (obtained by sieving).

Table II—Observed Plasma Progesterone[a] Levels in Rabbits following Subcutaneous Implantation of Progesterone–Cholesterol Pellets

Animal	Progesterone, μg/100 ml of Plasma											
	1[b]	3	8	18	25	32	39	57	64	71	81	89
1	NS[c]	98	97	75	99	94	84	121	NS	94	56	76
2	226	NS	83	86	109	102	118	116	102	102	103	74
3	211	NS	97	134	121	120	117	132	127	131	NS	68
4	180	NS	98	125	112	112	101	129	128	127	NS	73
5	165	NS	80	135	110	121	109	(Died)				
6	226	NS	79	110	114	91	NS	93	88			

[a] Based on the amount of detected radioactivity. [b] Days after implantation. [c] NS = no sample.

vessel were siliconized to minimize hemolysis. Citrate solution, 1 ml/10 ml of blood, was added, and plasma was separated by centrifugation. At autopsy, body weights were recorded and blood was collected by heart puncture. Liver and kidneys were excised, weighed, and frozen. The implantation site was examined for capsule formation, and the pellets were collected.

Sample Preparation—*Urine*—Weekly collections were combined, and the volume was reduced about fourfold by evaporation in a rotary evaporator under reduced pressure. The resulting volume was recorded, and a 30-ml aliquot was diluted with 70 ml of absolute ethanol. The solution was kept for 48 hr at −20° to precipitate the proteins and was then centrifuged, and the clear supernate was separated. Radioactivity was determined in 2-ml aliquots.

Feces—Feces collected separately two or three times a week were combined and weighed. A 30-g sample was ground in a blender[10] with 100 ml of 70% aqueous methanol, and the resulting slurry was centrifuged. An aliquot of the clear supernate diluted with an equal volume of absolute methanol was kept at −20° for 48 hr. Radioactivity was determined in 1-ml aliquots.

Implantation Site—Surrounding tissue, including the pellets, was excised; the tissue was exhaustively extracted at room temperature with acetone–dichloromethane (1:3), the extracts were combined, and the solvent was removed by evaporation. Then the residue was redissolved in methanol, the volume was brought to 10 ml, and the residual radioactivity was determined by counting 1-ml aliquots in a toluene scintillation medium.

Calculations—Data were usually expressed in micrograms of progesterone per milliliter of plasma per surface area of the implant in square centimeters. *In vivo* data were analyzed with a two-factor repeated-measures design analysis of variance (9). Factors found to be significant were further analyzed with Duncan's new multiple range tests (10). All data met the assumptions of variance homogeneity and independence of means and variance (11, 12).

Two separate analyses were performed because data for some individuals were not collected for the entire experimental period. Data for all six animals were available for the first 5 weeks, and these data were utilized in one analysis. Data for four animals, the two given hard tablets and the two given large (1705-μm diameter) pellets, were available for Weeks 6 and 8–10. These data were analyzed independently.

The amount of radioactivity excreted in urine was submitted to regression analysis to determine if there was a significant change in the amount of progesterone excreted as a function of time. Data were expressed as $\log_{10}$ micrograms of progesterone equivalent per day per 100-mm² surface area of implanted pellets. Only the data from four animals, the two given hard tablets and the two given large pellets, were available for the entire period, and only these data were analyzed.

Biological Experiments—Pellets having an average particle size of 750 μm suspended in 2% aqueous methylcellulose gel were used in all experiments. Subcutaneous insertion was used in both tests.

Antiovulatory Tests—Following subcutaneous insertion, ovulation was induced in rabbits (different periods of therapy) by intravenous injection of 0.3 ml of 1% copper acetate–sodium chloride solution (13). Laparotomy was performed 18–24 hr after the injection, and the ovaries were examined for ovulation points.

Maintenance of Pregnancy—Rats[11] were bilaterally ovariectomized (ether anesthesia) on Day 5 following insemination, and progesterone pellets were inserted in the neck region. At autopsy, on Day 18 of the test, the number of viable (and resorbing) fetuses was counted and recorded. On the day of the ovariectomy and 1 week later, some animals received (in addition to progesterone) 1 μg of estradiol benzoate dissolved in 0.2 ml of sesame oil. A small group of ovariectomized animals with no treatment was included for comparison.

RESULTS

The present studies confirmed previous observations (4) that the amount of progesterone found in the desorbing medium is dependent upon the frequency of sample collection and the total pellet surface area exposed to the desorbing medium. As noted (4), dissolution rates were high during the first few days of the test, most likely due to the liberation of small particles loosely attached to the surface of the pellets; after a few days, the values became more uniform and variations between different samples of the same pellet size from day to day were small. In addition to the sampling frequency, the *in vitro* release rate was also influenced by the volume and temperature of the desorbing medium and the frequency (or speed) of agitation.

Table I shows average dissolution of progesterone from cholesterol (41% w/w) and β-sitosterol (53% w/w) pellets of various sizes based on 4- and 6-hr sampling (observation period of 6–28 days) calculated as micrograms of progesterone released per 24-hr interval from 100-mg pellets. The relative dissolution rate of progesterone per unit weight increased with the decrease in pellet size. This finding is in accord with the observation that the dissolution rate is dependent upon the surface area of the pellets; smaller pellets have a large surface area per unit weight. When calculated on the basis of unit area (100 mm²), good correlation between the various sizes was obtained.

Progesterone absorption (as total radioactivity) from pellets of three different sizes, monitored by measuring plasma levels, is shown in Table

[10] Warington Products, New Hartford, Conn.

[11] Holtzman Co., Madison, Wis.

Table III—Material Balance of Progesterone Used in Implantation Studies

Animal	Progesterone Available, mg	Progesterone Equivalent[a] Found, mg			
		Urine, %	Feces, %[b]	Implant Site, %	Total Recovered, %
1	43.04	24.05 (55.4)	0.94 (2.2)	13.46 (31.0)	88.6
2	63.09	28.22 (44.7)	0.97 (1.5)	27.00 (42.8)	89.0
3	92.09	72.97 (78.7)	5.30 (5.7)	3.60 (3.9)	88.3
4	93.82	55.68 (59.3)	5.05 (5.4)	17.39 (18.5)	93.3
5	37.39	19.14 (51.2)	3.39 (9.1)	—[c]	—[c]
6	45.43	38.15 (84.0)	3.92 (8.6)	2.97 (6.5)	99.1

[a] Based on the amount of detected radioactive material. [b] Collected 54 days of the experiment. [c] Not autopsied.

II. The release of radioactive material was high the 1st day after implantation; there was then a decrease in circulating levels, which remained stable until about Day 80. On Day 90, the amount of radioactivity in peripheral blood was found to be declining. Statistical evaluation (calculated in terms of unit surface area) revealed no differences in values between the three types of pellets used. The high levels noted immediately after implantation were significantly higher ($F = 6.79$, $df = 41$, $p < 0.005$) as compared to Weeks 1–4. This difference resulted because the plasma level for Week 0 was significantly greater ($\bar{x} \pm SE = 3.8 \pm 0.6$ μg/ml/cm^2) than that of the other 4 weeks, which did not differ from each other (overall $\bar{x} \pm SE = 2.1 \pm 0.2$ μg/ml/cm^2).

For Weeks 6 and 8–10, there was no significant difference between individual animals and there was no significant difference due to the time factor. The mean overall plasma level of 2.0 ± 0.1 μg/ml/cm^2 for this period did not differ significantly from that for Weeks 1–4 ($t = 0.75$, $df = 38$, $p > 0.40$). These data indicate that high plasma progesterone levels are reached shortly after implantation. Within less than 1 week, the plasma progesterone level decreased to a stable level, which was maintained for at least 10 weeks.

Of the total radioactivity in plasma, about 40% was ether extractable. The remaining 60% was in the aqueous phase, presumably associated with polar progesterone metabolites and conjugates. Partial purification of the ether extract by TLC in silica separated 40–60% of material with the same mobility as progesterone. This result indicates that the 100-mm^2 surface area of pellets provided 0.3–0.5 μg of progesterone/ml of plasma; the balance was presumably free and conjugated progesterone metabolites.

Elimination of radioactive progesterone metabolites was significantly lower in feces than in urine (Table III). The average values were below 5% for Animals 1–4 and less than 10% for Animals 5 and 6. Since excretion of progesterone metabolites in feces represented usually less than 5% of the total metabolic products (occasional higher values being due most likely to contamination from urine), the metabolic cages were modified to minimize this possibility; feces were not collected during the last 2 weeks of the experiment.

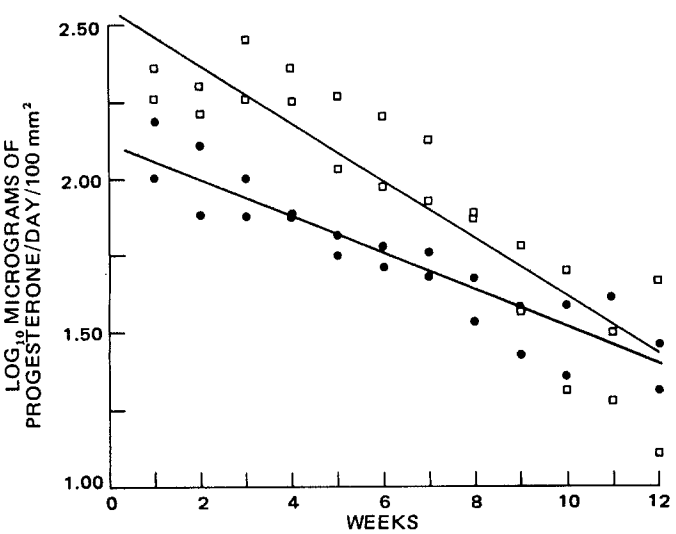

Figure 1—*Excretion of radioactivity in rabbits implanted with progesterone–cholesterol acetate pellets. Key: ●, Animals 1 and 2 (hard tablet); and □, Animals 3 and 4 (large pellet).*

The patterns of excreted radioactivity, expressed as $\log_{10}$ micrograms of progesterone per day per 100-mm^2 surface area implanted pellets, are shown in Fig. 1. There was a significant difference between the slopes of the two regression lines shown ($t = 4.06$, $df = 44$, $p < 0.001$); the amount of progesterone excreted by the animals implanted with the large pellets was initially at a higher level and declined more rapidly than in those animals implanted with the hard tablets. For both treatments there was no significant deviation from linearity; the r^2 values (the proportion of the variation in progesterone excreted explained by a linear relationship with time) were 0.81 for Animals 1 and 2 and 0.86 for Animals 3 and 4.

There was a significant increase in body weight during the 10-week experiment. The average initial body weight was 1430 g (1110–1680 g), and the final body weight was 2100 (1860–2445 g); this difference represents an average increase of 47%. Because the animals implanted with the large pellets had a higher average proportional weight increase than did those implanted with the hard tablets (60 *versus* 50%), the data were submitted to the following transformation to adjust for any differential effects of weight gain. For each individual for each week, the amount of progesterone excreted ($\log_{10}$ micrograms progesterone equivalent per day per 100-mm^2 surface area of implanted pellets) was multiplied by the estimated weight of that individual for that week and divided by that individual's initial weight.

Only initial and final body weights were recorded, so estimation of an individual's weight for each week was made by linear interpolation. For the data so treated, the regression equations are: for the hard tablet, $y = 2.10 - 0.005x$; and for the large pellets, $y = 2.59 - 0.029x$. The difference between the slopes is not significant ($t = 1.46$, $df = 44$, $p > 0.10$), which suggests that the difference in the slopes of the excretion rates in Fig. 1 is probably a function of the difference in weight gain.

Pellets were routinely recovered from the deposits under the skin; some migrated into the proximal muscle. In a few animals, the implant site was covered with a thin membrane, forming a pouch. No macroscopic manifestation of an inflammatory reaction at the implantation site was observed in any animal. The amount of radioactivity left in the remaining pellets varied from 4 to 27%. The overall recovery of ^{14}C-radioactive material in urine (and feces) and from the subcutaneous tissue at implant site varied from 70 to 99%; the average value was about 85%.

The results of antiovulation tests in rabbits are summarized in Table IV. The weights of pellets used in the experiment were 25, 75, and 225 mg, representing a dose of progesterone from 13.5 to 121.5 mg. Ovulation was inhibited for at least 45 days (duration of experiment) at the highest dose used. Based on the *in vivo* release data, it can be assumed that this dose released about 145 μg of progesterone/day.

Gravid rats deprived of progesterone by ovariectomy lost the ability to maintain pregnancy, and fetuses were rapidly resorbed; none was viable after 2 weeks (Table V). A single dose of 25 mg of progesterone pellets (13.5 mg progesterone equivalent) provided an incomplete fetal support;

Table IV—Duration of Antiovulatory Activity with Progesterone–Cholesterol Pellets

Progesterone Dose, mg	Rabbits Used	Average Ovulation ± *SE*	
		15 Days	45 Days
0	6	4.5 ± 0.4	6.5 ± 0.7
13.5	4	2.5 ± 0.4	4.0 ± 1.0
40.5[a]	5	0.5 ± 0.1	2.0 ± 0.3
121.5	5	0.0	0.0

[a] Estimated daily release, 450 μg.

Table V—Pregnancy Maintenance in Ovariectomized Rats with Progesterone–Cholesterol Pellets

Progesterone Dose, mg	Number of Rats			Mean Number (Range)	
	Total	with Fetuses	with Resorbed Fetuses	Fetuses	Resorbed Fetuses
4	6	0	0	0	0
13.5	6	0	3	0	7.2 (0–14)
13.5[a]	5	4	4	3.8 (3–13)	4.2 (0–6)
27.0[b]	4	2	4	4.5 (4–5)	4.8 (2–9)
27.0[a]	5	5	4	11.6 (10–14)	1.2 (0–2)
54	8	3	5	3.8 (0–8)	6.9 (3–12)
54[a]	3	3	0	12.0 (11–13)	0

[a] Indicates groups injected twice with 1 μg of estradiol benzoate. [b] Estimated daily release, 300 μg.

only resorption sites were found at autopsy. Addition of 1 μg of estradiol at weekly intervals was sufficient to increase significantly fetal salvage. In animals given 50-mg pellets (27 mg progesterone equivalent), there was an average of 11.6 live fetuses (a value usually seen in our colony) and only a few resorbing sites. Based on the same assumption as already given, the dose used was about 32 μg of progesterone/day.

DISCUSSION

Properties that influence absorption rates of drug implants, such as area, dissociation constant, solubility, and the diffusion coefficient, have been recorded (14). Most investigators considered absorption of materials released from pure crystalline implants of spherical shape. Mathematical relationships have been derived to predict the rates, but such relationships are not valid for drug systems combining two substances of unequal dissolutions.

Progesterone dissolution from steroid–sterol pellets was more rapid than sterol dissolution. When a "diffusion" constant was calculated using the slope of the regression line of cumulative release rate ($b^2\pi/16/3600$), similar values were obtained for progesterone regardless of pellet diameter. The values varied from 1.90×10^{-11} to 2.22×10^{-11} cm^2/sec for 750-, 1205-, and 1705-μm diameter pellets independent of period. The calculated value for 375-μm diameter pellets was 1.05×10^{-11} cm^2/sec, while the value for a "powder" (particle size <177-μm diameter) was 3.48×10^{-12} cm^2/sec. Corresponding values for β-sitosterol pellets (1205 and 1705 μm) were 1.87×10^{-11} and 1.99×10^{-11}, respectively.

Measurement of radioactivity in peripheral plasma showed a steady dissolution of progesterone, indicative of zero-order release rates in the presence of continuously declining excretion of radioactive material in urine and feces. The overall decline in the amount of progesterone excreted with time was most likely associated with the increase in body weight of the individuals. The difference in the origins in the regression equations (Fig. 1) suggests that animals implanted with the large pellets had a higher rate of progesterone excretion than did animals implanted with the hard tablets. However, this possible difference was not a function of any difference in circulating levels of progesterone in plasma, because these levels did not differ significantly as a function of treatment difference. Also, circulating plasma progesterone levels did not change as a function of time, as did the levels of excreted progesterone, which further indicates that plasma and excretory levels may vary independently.

Weight gain could have been the result of progesterone therapy; overeating and weight gain induced by progesterone have been observed in several species (15). Since there was no control group in these experiments and food consumption was not measured, additional experiments would be needed to confirm this conclusion. However, it is well documented that many steroid hormones, including progesterone, are deposited selectively in lipid tissues. In the present study, the concentration of radioactivity in intestinal fat (five observations) was 0.4 μg progesterone equivalent/g of fat. This observation supports the data showing that, in part, released progesterone was stored in the continuously formed lipid tissue.

These observations lead to the conclusion that, in studying absorption dynamics from implanted material, measurement of plasma levels provides more reliable information than measurements of excretion rates.

Progesterone was released from the pellets in a sufficient amount to exert biological effects. The effectiveness of sustained-release progesterone in maintaining pregnancy in ovariectomized rats was potentiated by injecting small amounts of estradiol as reported by others (16). Based on previously published data, it is possible to estimate that progesterone in a lipid delivery system is about 20 times more active than a daily injection of progesterone dissolved in oil. This value is in good agreement with previous findings (2).

REFERENCES

(1) F. A. Kincl and H. W. Rudel, *Acta Endocrinol.*, **66**, Suppl. 151 (1971).

(2) C. C. Chang and F. A. Kincl, *Fertil. Steril.*, **21**, 134 (1970).

(3) F. A. Kincl, I. Angee, C. C. Chang, and H. W. Rudel, *Acta Endocrinol.*, **64**, 508 (1970).

(4) F. A. Kincl, K. Sundaram, C. C. Chang, and H. W. Rudel, *ibid.*, **64**, 253 (1970).

(5) M. B. Shimkin and J. White, *Endocrinology*, **29**, 1020 (1941).

(6) C. D. Kochakian, *Am. J. Physiol.*, **145**, 549 (1945).

(7) A. Lipschutz and R. Iglesias, *Nature (London)*, **190**, 174 (1961).

(8) A. F. Pi, A. Oriol, L. H. Lasso, M. Maqueo, R. I. Dorfman, and F. A. Kincl, *Acta Endocrinol.*, **48**, 602 (1965).

(9) J. L. Bruning and B. L. Kintz, "Computational Handbook of Statistics," Scott, Foresman & Co., Glenview, Ill., 1968.

(10) J. C. R. Li, "Statistical Inference," vol. 1, Edwards Brothers, Ann Arbor, Mich., 1964.

(11) C. I. Bliss, "Statistics in Biology," vol. 1, McGraw-Hill, New York, N.Y., 1967.

(12) R. R. Sokal and F. J. Rohlf, "Biometry," Freeman, San Francisco, Calif., 1969.

(13) F. A. Kincl, *Endokrinologie*, **44**, 67 (1963).

(14) B. E. Ballard, *Ph.D. thesis, University of California, San Francisco, Calif., 1961.*

(15) S. Roberts, W. S. Kenney, and D. G. Mook, *Horm. Behav.*, **3**, 267 (1972).

(16) W. R. Lyons, *Proc. Soc. Exp. Biol. Med.*, **54**, 65 (1943).

ACKNOWLEDGMENTS AND ADDRESSES

Received March 5, 1976, from the *Department of Pure and Applied Sciences, Richmond College of the City University of New York, Staten Island, NY 10301.*

Accepted for publication May 27, 1976.

Supported in part by Contract NIH-71-2235.

* Present address: Department of Clinical Laboratories, Brookdale Hospital Centers, Brooklyn, NY 11212.

‡ Present address: Department of Zoology, Michigan State University, East Lansing, Mich.

§ Present address: Phoenix, Ariz.

¶ Present address: Schering Corp., Bloomfield, N.J.

x To whom inquiries should be directed.

Dissolution Rates of Corticosteroids Utilizing Sugar Glass Dispersions

LOYD V. ALLEN, Jr. ˣ, VICTOR A. YANCHICK *, and DALE D. MANESS *

Abstract □ A method of increasing the dissolution rates of some orally administered corticosteroids was investigated. This method involved glass dispersions using dextrose, galactose, and sucrose as the carriers. These dispersions were prepared by the fusion process and were subjected to a modified NF XIII dissolution rate determination. The results revealed a marked increase in the dissolution rate of the corticosteroids contained in the solid dispersions when compared to the dissolution rate of the plain corticosteroid powder. The increase in dissolution rates was attributed to the presence of the corticosteroid in a very fine state of subdivision and to the increased wettability of the corticosteroid powder.

Keyphrases □ Corticosteroids, various—glass dispersions using sugar carriers, dissolution rates compared to plain powder □ Glass dispersions—various corticosteroids, sugar carriers, dissolution rates compared to plain powder □ Dissolution rates—various corticosteroids, glass dispersions using sugar carriers compared to plain powder □ Sugars—dextrose, galactose, and sucrose as carriers in glass dispersions of various corticosteroids, dissolution rates compared to plain powder □ Solid-state dispersions—various corticosteroids, sugar carriers, dissolution rates compared to plain powder

In 1961, Sekiguchi and Obi (1) introduced a unique approach of utilizing solid dispersions to reduce the particle size of drugs and to increase their dissolution and absorption rates. They proposed the formation of a eutectic mixture of a poorly soluble drug, such as sulfathiazole, with a physiologically inert, easily soluble carrier, such as urea.

The possibility of using a solid solution approach in which a drug is molecularly dispersed in a soluble carrier was subsequently introduced (2, 3). A series of reports (4–7) presented a detailed discussion of the advantages of the solid solution over the eutectic mixture.

A method was reported for preparing aqueous colloidal dispersions of β-carotene by using water-soluble polymers, *e.g.*, povidone (8). The dissolution rate of griseofulvin was enhanced markedly when dispersed in povidone by the same solvent method (9). The term "solid-state dispersions" was used to refer to these solid dispersions. The mechanisms of increased dissolution rates of drugs solid dispersed in povidone carriers were reviewed (10). Additional studies supported the significance of the solid dispersion technique (11–19).

The concept of glass solutions was introduced recently to increase dissolution rates (14). This concept also was discussed in an extensive review of the pharmaceutical applications of solid dispersions (20). In this investigation, when a melt of a griseofulvin–citric acid mixture, which was highly viscous, was solidified, it was transformed into a glassy state. This glassy state, or glass solution, exhibited a very rapid dissolution rate with griseofulvin. The glass dispersion technique was used successfully with sulfabenzamide (21).

The corticosteroids are considered to be generally poorly water soluble and have demonstrated unpredictable dissolution rates (22–27). Polyethylene glycol solid dispersions were used to increase the dissolution rates of prednisolone acetate and hydrocortisone acetate (15). The purpose of this investigation was to apply the glass dispersion technique to alter the dissolution rates of several orally administered corticosteroids, *e.g.*, betamethasone acetate, cortisone acetate, hydrocortisone acetate, methylprednisolone acetate, prednisolone, and prednisone. Conceptually, this method could result in increased and more predictable dissolution rates, benefiting the therapeutic response.

EXPERIMENTAL

It was desired to use nontoxic, physiologically acceptable carriers that possessed no significant therapeutic effects and had melting points less than or close to the melting points of the corticosteroids used. The latter was considered a requirement since the corticosteroids melt with some decomposition. The use of sucrose and dextrose as glass-forming substances was discussed (14) and, upon investigation, galactose also was found to form a glass upon rapid cooling from a melt. These three sugars also met the other listed criteria.

Preparation of Dispersion Systems—All dispersion systems were prepared by the fusion method as follows. A suitable amount of the drug–carrier mixture [in a ratio containing 6 mg of betamethasone acetate or methylprednisolone acetate added to 200 mg of the carriers (sugars), or 5 mg of each of the other corticosteroids added to 200 mg of the carriers] was weighed and placed in a preformed aluminum foil boat, 7 cm in diameter and 2 cm in depth. The materials were mixed thoroughly and placed on a wire screen positioned on a preheated electric heating plate. Heat was applied with constant stirring until a melt was obtained.

This melt was heated further to the following temperatures: dextrose carriers, 185°; galactose carriers, 169°; and sucrose carriers, 200°. This melt was rapidly solidified by placing the boat containing the melt on a hollowed out portion of a block of dry ice. After solidification, the dispersion system was quickly removed from the dry ice to prevent water condensation and placed in a glass desiccator containing a drying agent where it was stored for 24 hr at 37°.

The solid was pulverized to the desired particle size, and the 60–100-mesh fraction (250–150-μm particle size) was collected by standard sieves[1] placed on a sieve shaker[2] and shaken for 5 min. The powder was then placed in an amber, screw-capped glass vial and stored in a desiccator at 25°. The plain corticosteroids used as the controls possessed a particle size of 250–150 μm (60–100-mesh fraction).

Dissolution Rate Determinations—The dissolution rate determinations were carried out using a modified NF XIII dissolution rate apparatus (23).

An appropriate amount of the dispersion system, containing 6 mg of betamethasone acetate or methylprednisolone acetate or 5 mg of the other corticosteroids, was weighed and placed in the basket of the dissolution apparatus. This amount was used because it allowed absorption within the 0.2–0.8 range on a spectrophotometer[3] (all corticosteroids followed Beer's law throughout the concentration ranges used). A thin circular piece of clear plastic was fitted at the bottom of the dissolution basket to prevent the powder from falling out. The temperature and sample flow rate were established, and the basket was lowered into 1000 ml of the dissolution medium (deionized water) to a point 2 cm from the bottom of the kettle and rotated at a constant speed of 100 rpm. There was a lag time of about 4 sec for the sample to reach the flowcell, and a complete circuit required about 10 sec.

As the dispersion system dissolved, the concentration of the corticosteroid in solution was monitored and recorded with a chart recorder[4].

[1] Sargent-Welch Scientific Co., Skokie, Ill.
[2] W. S. Tyler, Inc., Mentor, Ohio.
[3] Beckman DB, Beckman Instruments, Fullerton, Calif.
[4] Beckman Instruments, Fullerton, Calif.

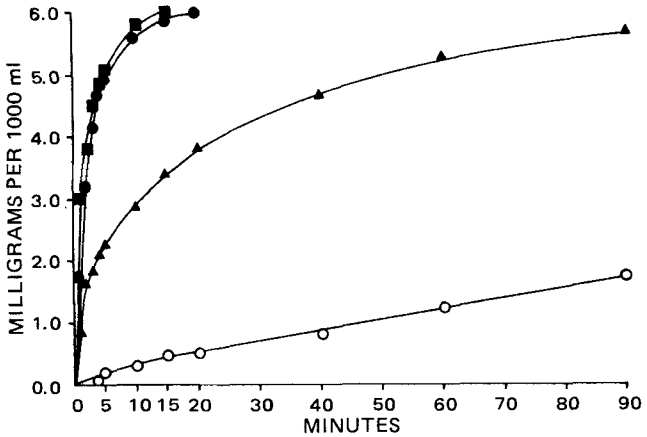

Figure 1—*Dissolution rates of betamethasone acetate. Key:* ○, *plain;* ▲, *dextrose carrier;* ●, *galactose carrier; and* ■, *sucrose carrier.*

The determinations were made for 90 min and were done at least in duplicate. The wavelengths of maximum absorption used were determined experimentally in aqueous solutions and were: betamethasone acetate, 239 nm; cortisone acetate, 238 nm; hydrocortisone acetate, 243 nm; methylprednisolone acetate, 243 nm; prednisolone, 242 nm; and prednisone, 239 nm. These substances followed Beer's law in the concentration range used.

Short-Term Stability Study—A short-term stability study was performed by storing the powdered dispersion systems at 25° for 30 days and repeating the dissolution rate determinations described.

Corticosteroid Stability Studies—The chemical stability of the corticosteroids during the preparation of the dispersion systems was studied using TLC. Chromatogram sheets[5] were spotted with an aqueous solution of the respective dispersion systems and a methanol solution of the reference corticosteroids. The sheets were allowed to dry at room temperature and placed in a chamber containing chloroform–ether–methanol (6:3:1). The plates were removed, air dried, and visualized under UV light. UV scans of the dispersion systems in deionized water also were obtained before and after preparation of the dispersion systems.

RESULTS

Glass Formation—Dextrose, galactose, and sucrose formed glasses quite readily. Dry ice was used to hasten solidification of all melts so that the systems would not be exposed to atmospheric moisture and contamination longer than necessary. The corticosteroids were not necessarily completely miscible with the carriers in the glass systems because of the generally lower temperatures used in their preparation. Complete melting was not attempted in these cases because of decomposition of the sugars and the corticosteroids at the high temperatures that would be required. All systems were relatively easy to prepare. The glass dispersion systems were hygroscopic and, as such, required storage in a desiccator.

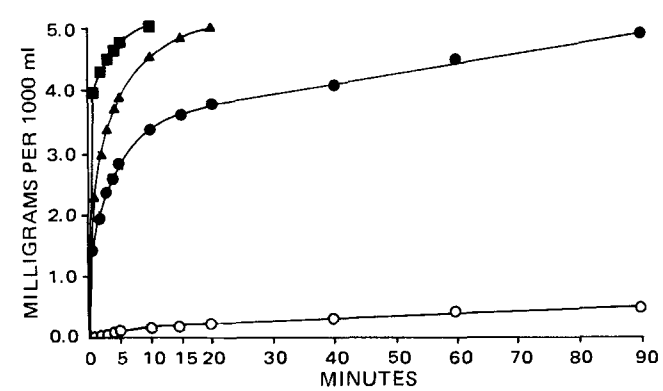

Figure 2—*Dissolution rates of cortisone acetate. Key:* ○, *plain;* ▲, *dextrose carrier;* ●, *galactose carrier; and* ■, *sucrose carrier.*

[5] Eastman Chromagram Sheets, Eastman Kodak Co., Rochester, N.Y.

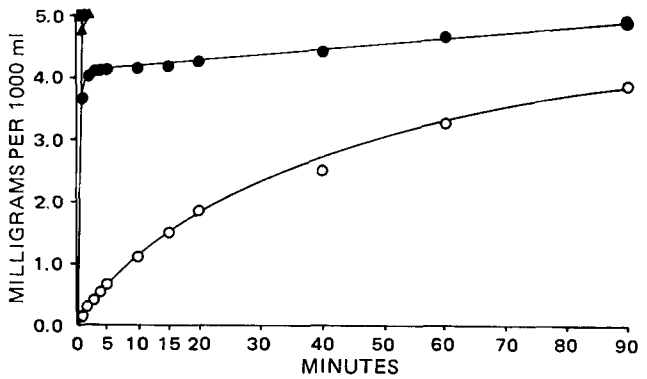

Figure 3—*Dissolution rates of hydrocortisone acetate. Key:* ○, *plain;* ▲, *dextrose carrier;* ●, *galactose carrier; and* ■, *sucrose carrier.*

Dissolution Rate Determinations—As shown in Figs. 1–6, the dissolution rate determinations revealed marked increases in the dissolution rates of all corticosteroids utilizing all three sugar carriers. The dextrose and sucrose glass dispersions possessed the fastest release characteristics for 50 and 100% dissolution (Table I).

Samples of the glass dispersions prepared at different times reproduced these results. The glass dispersion samples assayed after storage for 30 days showed no decrease in the dissolution rates. These amorphous systems may recrystallize upon aging for a longer time. One would expect that a return to the crystalline state would result in a decrease in the dissolution rate of the system. The time required for these systems to return to the crystalline state has not been determined.

Stability of Components—None of the corticosteroids demonstrated any decomposition products after being subjected to the preparation of the dispersion systems according to the analytical methods used. TLC revealed no additional spots, and there was good correspondence with the reference samples. UV spectra of the dispersion systems in deionized water revealed no decomposition products, and the absorbance values were unchanged.

A light-amber discoloration of the melt and of the cooled glass was observed during the dextrose and sucrose glass formation process, possibly indicating slight decomposition of these sugars. This color change did not appear to interfere with the fast release characteristics of the carrier.

DISCUSSION

The dissolution of these powders occurred in two phases: a very rapid initial phase followed by a slower, more prolonged, second phase. The rapid initial rate was attributed to the release of the corticosteroid present in a state of very fine subdivision. With the glass dispersion, a portion of the corticosteroid probably is solubilized during preparation by the molten carrier. Since this melt quickly solidifies, crystallization would be retarded because of the high viscosity of the melt and the very short time interval required for solidification. When this portion of the dis-

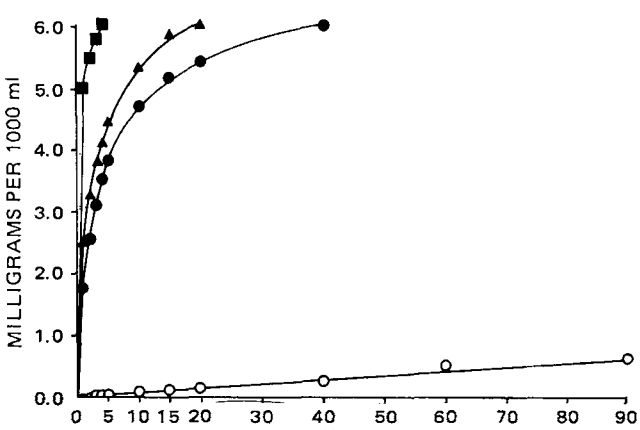

Figure 4—*Dissolution rates of methylprednisolone acetate. Key:* ○, *plain;* ▲, *dextrose carrier;* ●, *galactose carrier; and* ■, *sucrose carrier.*

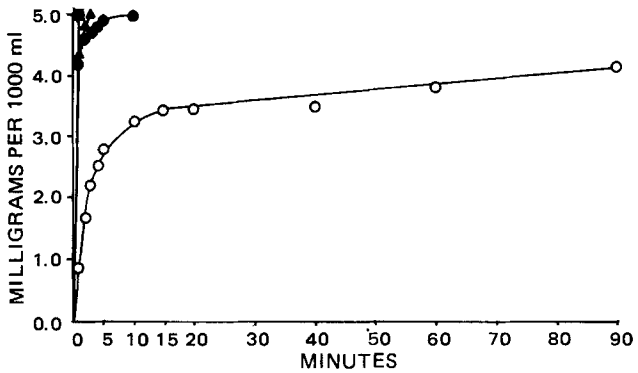

Figure 5—*Dissolution rates of prednisolone. Key:* O, *plain;* ▲, *dextrose carrier;* ●, *galactose carrier; and* ■, *sucrose carrier.*

persion system is exposed to the aqueous medium, the corticosteroid would immediately be released in its molecular state.

The second phase of dissolution, exhibited by most systems, was the more prolonged phase. The dissolution rates of the second phase of the glass dispersions were somewhat more rapid than that of the plain powder. This difference can be attributed to the increased wettability of the corticosteroid powders. Glass carriers may act similarly to wetting agents, as follows.

It is frequently difficult to disperse a finely divided powder in a liquid because of entrapped or adsorbed air or some other contaminant. When a strong affinity exists between a liquid and a solid, the liquid easily forms a film over the surface of the solid. However, when this affinity is nonexistent or weak, the liquid has difficulty displacing the air or other substances surrounding the solid. The sugars used in this investigation are readily soluble in an aqueous medium. During the preparation of the dispersion system, intimate contact was achieved between the sugar and the corticosteroid particles. The high temperatures involved in the preparation process aided in removing adsorbed and entrapped air. Upon exposure of this system to an aqueous medium, the sugar rapidly dissolved and a complete wetting of the corticosteroid occurred at the same time.

The temperatures reached during the preparation of the melts were greater than the melting points of the sugars but less than the melting points of the corticosteroids. There were two main reasons for reaching this temperature before quenching the melt. First, since this temperature was somewhat less than the melting point of the corticosteroids, decomposition of the corticosteroid did not occur or was negligible. This factor was desirable since the corticosteroids decompose to some degree at their melting points (22). Second, the sugars could not be heated much higher than the preparation temperatures because of decomposition, manifested by an amber discoloration. The temperatures used were a compromise between the melting points of the corticosteroids and the decomposition ranges of the sugars.

These solutions were not glass solutions, since complete melting of both components did not occur and a molecular dispersion of the corticosteroid in the glassy carrier did not result. The portion of the corticosteroid molecularly dispersed in the glass carriers could account in part for the extremely rapid initial release rate. This phase was followed by a slower rate of release of the dispersed particles.

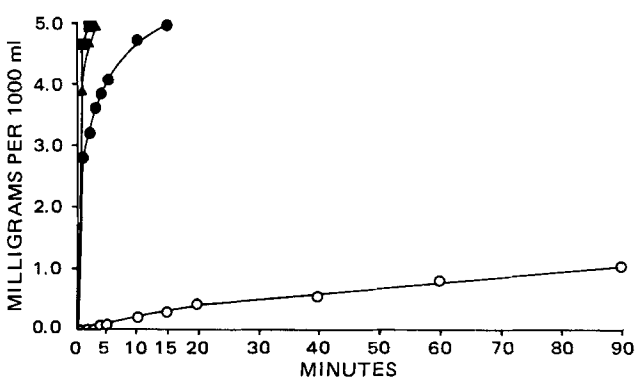

Figure 6—*Dissolution rates of prednisone. Key:* O, *plain;* ▲, *dextrose carrier;* ●, *galactose carrier; and* ■, *sucrose carrier.*

Table I—50 and 100% Dissolution Times (Minutes) for Corticosteroids in Glass Dispersions

Corticosteroid	$t_{50\%}$	$t_{100\%}$
Dextrose carrier		
Betamethasone acetate	<15	>90
Cortisone acetate	<2	20
Hydrocortisone acetate	<1	2
Methylprednisolone acetate	<2	20
Prednisolone	<1	3
Prednisone	<1	3
Galactose carrier		
Betamethasone acetate	<2	20
Cortisone acetate	<4	>90
Hydrocortisone acetate	<1	>90
Methylprednisolone acetate	<3	40
Prednisolone	<1	10
Prednisone	<1	15
Sucrose carrier		
Betamethasone acetate	1	15
Cortisone acetate	<1	10
Hydrocortisone acetate	<1	<1
Methylprednisolone acetate	<1	4
Prednisolone	<1	1
Prednisone	<1	2

In view of present-day considerations of the effect of dissolution rates on drug bioavailability, these glass dispersions offer a unique opportunity of making available an extremely fine state of subdivision of active ingredients and a unique method of increasing the wettability of the active ingredients. The sugars enjoy many advantages over other forms of solid dispersion carriers in addition to their being relatively nontoxic, inexpensive, and physiologically acceptable. They have long been utilized in the preparation of pharmaceutical dosage forms, and the only difference in their past use and the newly proposed use is in the physical state. In the past, they have been used in physical mixtures; now it is suggested that they be used as solid dispersion carriers in a glassy state. These solid dispersions should be considered as potential dosage form modifications for the corticosteroids and for other poorly soluble or insoluble drugs with fairly high melting points where an increase in the dissolution rate is desirable.

REFERENCES

(1) K. Sekiguchi and N. Obi, *Chem. Pharm. Bull.*, **9**, 866 (1961).
(2) G. Levy, *Am. J. Pharm.*, **135**, 78 (1963).
(3) J. L. Kanig, *J. Pharm. Sci.*, **53**, 188 (1964).
(4) A. H. Goldberg, M. Gibaldi, and J. L. Kanig, *ibid.*, **54**, 1145 (1965).
(5) *Ibid.*, **55**, 484 (1966).
(6) *Ibid.*, **55**, 487 (1966).
(7) *Ibid.*, **55**, 581 (1966).
(8) T. Tachibana and A. Nakamura, *Kolloid-Z. Polym.*, **203**, 103 (1965).
(9) M. Mayersohn and M. Gibaldi, *J. Pharm. Sci.*, **55**, 1323 (1966).
(10) A. P. Simonelli, S. C. Mehta, and W. I. Higuchi, *ibid.*, **58**, 538 (1969).
(11) W. L. Chiou, *ibid.*, **60**, 1406 (1971).
(12) W. L. Chiou and S. Riegelman, *ibid.*, **59**, 937 (1970).
(13) *Ibid.*, **60**, 1376 (1971).
(14) *Ibid.*, **58**, 1505 (1969).
(15) *Ibid.*, **60**, 1569 (1971).
(16) W. L. Chiou and S. Niazi, *J. Pharm. Sci.*, **60**, 1333 (1971).
(17) W. L. Chiou and L. D. Smith, *ibid.*, **60**, 125 (1971).
(18) A. P. Simonelli, S. C. Mehta, and W. I. Higuchi, *ibid.*, **59**, 633 (1970).
(19) E. I. Stupak and T. R. Bates, *ibid.*, **61**, 401 (1972).
(20) W. L. Chiou and S. Riegelman, *ibid.*, **60**, 1281 (1971).
(21) J. W. McGinty, D. D. Maness, and G. J. Yakatan, *Drug. Dev. Commun.*, **1**, 369 (1974–75).
(22) "The United States Pharmacopeia," 18th rev., Mack Publishing Co., Easton, Pa., 1970, pp. 8, 148, 308, 529, 535, 936.
(23) "The National Formulary," 13th ed., Mack Publishing Co., Easton, Pa., 1970, pp. 88, 451, 802.
(24) G. Levy, *Am. J. Hosp. Pharm.*, **17**, 757 (1960).
(25) G. Levy, N. A. Hall, and E. Nelson, *ibid.*, **21**, 402 (1964).
(26) G. H. Schneller, *Drug Inf. Bull.*, **3**, 100 (1969).
(27) H. C. Shirkey, *J. Pediatr.*, **76**, 774 (1970).

ACKNOWLEDGMENTS AND ADDRESSES

Received March 27, 1973, from the *College of Pharmacy, University of Oklahoma, Norman, OK 73069.*

Accepted for publication May 28, 1976.

Abstracted from a dissertation submitted by Loyd V. Allen, Jr., to the graduate school, University of Texas, in partial fulfillment of the Doctor of Philosophy degree requirements.

The authors thank The Upjohn Co. and Schering Co. for the corticosteroids.

* Present address: College of Pharmacy, University of Texas, Austin, TX 78712.

ˣ To whom inquiries should be directed.

Distribution, Dilution, and Elimination of Polychlorinated Biphenyl Analogs in Growing Swine

L. G. HANSEN ˣ and M. E. WELBORN

Abstract □ Growing swine were given 15 mg/kg po of purified polychlorinated biphenyl analogs and a commercial mixture. Backfat biopsies for 16–18 weeks exhibited two-compartment elimination kinetics when based on concentration. Total body fat was estimated from potassium-40 abundance, and the calculated total fat load indicated that most of the decline in residue concentrations was due to dilution by growth and expansion of the fat compartment. Redistribution in the fat was apparent for various analogs at different times, and tissue distribution varied significantly among analogs.

Keyphrases □ Biphenyls, polychlorinated—tissue distribution, dilution by growth, and elimination, swine □ Polychlorinated biphenyls—tissue distribution, dilution by growth, and elimination, swine □ Distribution, tissue—various polychlorinated biphenyls, swine □ Elimination—various polychlorinated biphenyls, swine

Stable compounds of low water solubility and high lipid affinity such as chlorinated pesticides and polychlorinated biphenyls comprise a special class of pharmacokinetically distinct xenobiotics. Recent studies involving intravenous and oral administrations of a polychlorinated biphenyl mixture containing 54% chlorine to swine and sheep showed that component peaks were distributed at different rates (1, 2). The smaller isomers of low chlorine content generally distributed at a faster rate than those of higher chlorination and were metabolized to a greater extent (1–4).

The high fat–blood concentration ratios of polychlorinated biphenyls (PCB) make sampling of the fat more meaningful for pharmacokinetic modeling. Because the apparent $t_{1/2}$ for elimination is on the order of weeks when fat concentration alone is presented (5), dilution due to growth is a required parameter for studies of rapidly growing animals such as young swine. In addition, the fat compartment is neither static nor a constant proportion of body weight.

This paper presents methods for evaluating the total amount of three pure polychlorinated biphenyl analogs and a commercial mixture[1] in the fat of growing swine. The "total fat load," L_t, is defined as the weight of chlorinated biphenyl present in the fat compartment. The pharmacokinetic parameters defined from these calculations demonstrate that traditional models must be reconstructed for persistent chemicals in food-producing animals.

EXPERIMENTAL

Fifteen matched weanling pigs of mixed Yorkshire/Hampshire breeding were divided into four experimental and one control group of three animals each. The pigs were fed a wet mash containing 100 ppm of 2,5,2′,5′-tetrachlorobiphenyl (I), 2,4,5,3′,4′-pentachlorobiphenyl (II), 2,4,5,2′,4′,5′-hexachlorobiphenyl (III), and a commercial mixture[1] (IV) for 1 week. The mash was offered every morning and left until totally consumed in quantities sufficient to produce a 2.14-mg/kg/day or 15-mg/kg/week dosing regimen.

Total body fat was estimated by a variation of the potassium-40

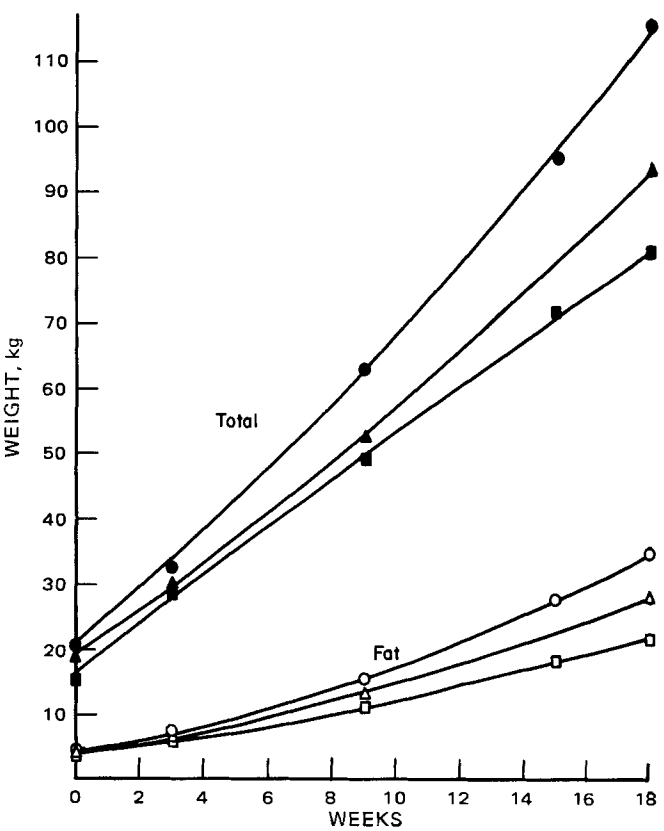

Figure 1—*Comparison of body weight (solid symbols) and body fat (open symbols) in single pigs receiving control (circles), hexachlorobiphenyl (triangles), and 54% chlorine mixture (squares) feed.*

[1] Aroclor 1254, Monsanto electrical grade, lot KB-05-612.

ACKNOWLEDGMENTS AND ADDRESSES

Received March 27, 1973, from the *College of Pharmacy, University of Oklahoma, Norman, OK 73069.*

Accepted for publication May 28, 1976.

Abstracted from a dissertation submitted by Loyd V. Allen, Jr., to the graduate school, University of Texas, in partial fulfillment of the Doctor of Philosophy degree requirements.

The authors thank The Upjohn Co. and Schering Co. for the corticosteroids.

* Present address: College of Pharmacy, University of Texas, Austin, TX 78712.

ˣ To whom inquiries should be directed.

Distribution, Dilution, and Elimination of Polychlorinated Biphenyl Analogs in Growing Swine

L. G. HANSEN ˣ and M. E. WELBORN

Abstract □ Growing swine were given 15 mg/kg po of purified polychlorinated biphenyl analogs and a commercial mixture. Backfat biopsies for 16–18 weeks exhibited two-compartment elimination kinetics when based on concentration. Total body fat was estimated from potassium-40 abundance, and the calculated total fat load indicated that most of the decline in residue concentrations was due to dilution by growth and expansion of the fat compartment. Redistribution in the fat was apparent for various analogs at different times, and tissue distribution varied significantly among analogs.

Keyphrases □ Biphenyls, polychlorinated—tissue distribution, dilution by growth, and elimination, swine □ Polychlorinated biphenyls—tissue distribution, dilution by growth, and elimination, swine □ Distribution, tissue—various polychlorinated biphenyls, swine □ Elimination—various polychlorinated biphenyls, swine

Stable compounds of low water solubility and high lipid affinity such as chlorinated pesticides and polychlorinated biphenyls comprise a special class of pharmacokinetically distinct xenobiotics. Recent studies involving intravenous and oral administrations of a polychlorinated biphenyl mixture containing 54% chlorine to swine and sheep showed that component peaks were distributed at different rates (1, 2). The smaller isomers of low chlorine content generally distributed at a faster rate than those of higher chlorination and were metabolized to a greater extent (1–4).

The high fat–blood concentration ratios of polychlorinated biphenyls (PCB) make sampling of the fat more meaningful for pharmacokinetic modeling. Because the apparent $t_{1/2}$ for elimination is on the order of weeks when fat concentration alone is presented (5), dilution due to growth is a required parameter for studies of rapidly growing animals such as young swine. In addition, the fat compartment is neither static nor a constant proportion of body weight.

This paper presents methods for evaluating the total amount of three pure polychlorinated biphenyl analogs and a commercial mixture[1] in the fat of growing swine. The "total fat load," L_t, is defined as the weight of chlorinated biphenyl present in the fat compartment. The pharmacokinetic parameters defined from these calculations demonstrate that traditional models must be reconstructed for persistent chemicals in food-producing animals.

EXPERIMENTAL

Fifteen matched weanling pigs of mixed Yorkshire/Hampshire breeding were divided into four experimental and one control group of three animals each. The pigs were fed a wet mash containing 100 ppm of 2,5,2′,5′-tetrachlorobiphenyl (I), 2,4,5,3′,4′-pentachlorobiphenyl (II), 2,4,5,2′,4′,5′-hexachlorobiphenyl (III), and a commercial mixture[1] (IV) for 1 week. The mash was offered every morning and left until totally consumed in quantities sufficient to produce a 2.14-mg/kg/day or 15-mg/kg/week dosing regimen.

Total body fat was estimated by a variation of the potassium-40

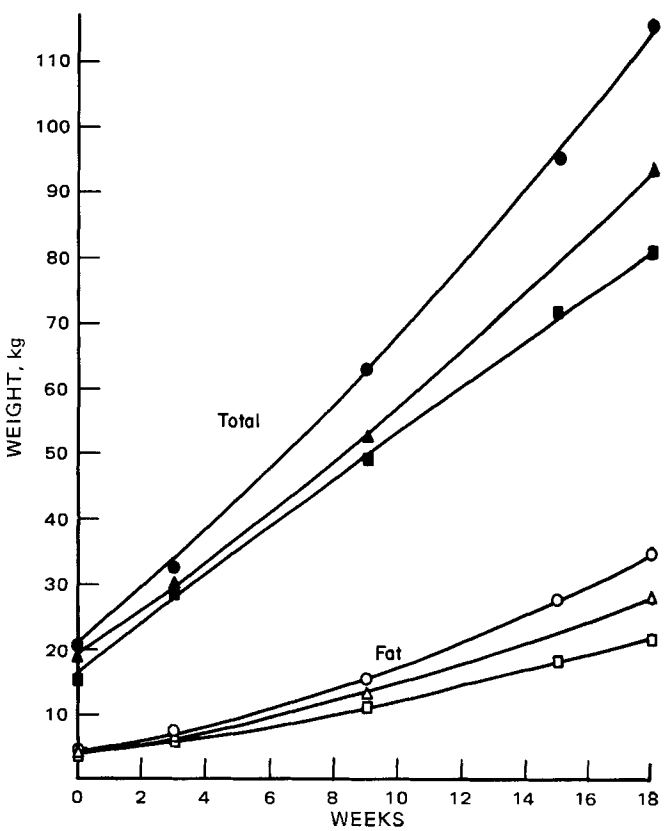

Figure 1—*Comparison of body weight (solid symbols) and body fat (open symbols) in single pigs receiving control (circles), hexachlorobiphenyl (triangles), and 54% chlorine mixture (squares) feed.*

[1] Aroclor 1254, Monsanto electrical grade, lot KB-05-612.

Table I—Polynomial Coefficients for Total Pig Weight *versus* Time[a]

Pig	A_0	A_1	A_2 (× 10^3)	D_{max}, kg
1	17.04	4.91	0.62	0.76
2	22.40	2.74	109.57	0.90
3	11.44	4.11	−24.70	1.56
4	17.76	2.74	39.81	2.16
5	18.65	3.07	53.70	0.65
6	17.85	3.26	57.41	1.85
7	18.38	3.93	28.70	0.58
8	21.21	4.07	63.33	1.01
9	17.58	3.04	82.41	1.08
10	18.95	3.41	40.74	0.45
11	14.60	3.79	48.15	0.40
12	15.92	2.58	101.85	0.42
13	18.97	3.89	43.21	0.03
14	18.73	3.66	−4.32	0.33
15	16.43	3.82	−12.96	1.23

[a] $Y_{(kg)} = A_0 + A_1X_{weeks} + A_2X^2_{weeks}$.

Table II—Polynomial Coefficients for Potassium-40 *versus* Time[a]

Pig	B_0	B_1	B_2	D_{max}, kg
1	3.283	1.250	0.03148	0.317
2	4.731	0.481	0.06636	0.431
3	2.128	0.994	0.00679	0.472
4	3.603	0.636	0.02068	0.503
5	5.535	0.843	0.02241	0.065
6	4.225	0.631	0.03981	0.225
7	3.580	1.020	0.02000	0.020
8	4.199	0.882	0.04522	0.199
9	3.995	0.333	0.06800	0.695
10	3.951	0.732	0.03344	0.251
11	3.040	0.804	0.03407	0.040
12	3.436	0.319	0.06327	0.336
13	3.844	0.794	0.04753	0.044
14	3.928	0.744	0.02346	0.228
15	3.317	0.783	0.01296	0.317

[a] $Y_{(fat\ weight)} = B_0 + B_1X_{weeks} + B_2X^2_{weeks\ kg}$.

method of Lohman *et al.* (6). The equation describing the conversion of potassium-40 to total potassium and finally to body fat is:

$$\text{potassium (g)} = \frac{[(A_1 - A_2) + (0.0583B) - (A_3)][C]}{(0.2028 - 0.000174B)(\gamma)} \quad \text{(Eq. 1)}$$

where:

A_1 = total potassium-40 counts per second
A_2 = background potassium-40 counts per second
A_3 = net counting capsule counts per second
B = weight of subject (pounds); $0.0583B$ is background depression factor, correcting for background absorbed by mass of subject

$$C = \frac{\text{net cps of standard on date of calibration}}{\text{net cps of standard on date of subject count}} = \frac{10^5 \text{ cps}}{\text{std cps}}$$

γ = gamma ray disintegrations/sec/g, $K = 3.0$

The $(0.2028 - 0.000174B)$ function was determined experimentally by Lohman *et al.* (6).

Blood samples and bilateral backfat biopsies were taken on Days 3, 7 (last day of treatment), 14, 28, and every 28 days thereafter for 16 or 18 weeks. A pilot study showed that backfat concentrations accurately reflected concentrations of polychlorinated biphenyl in other dissectible fat stores of swine (e.g., mesenteric and perirenal); concentrations within the same pig did not vary anteriorly-posteriorly, but each side varied consistently from the other. Bilateral biopsies were analyzed independently, and the results are reported as an average of the two. Blood and tissues were analyzed by electron-capture GLC as described previously (1, 7).

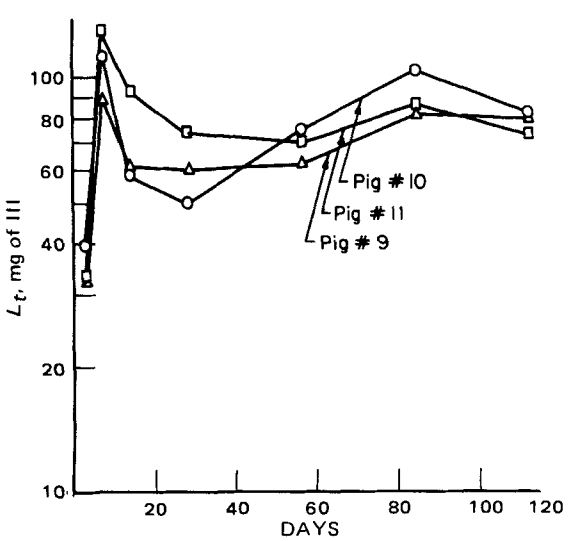

Figure 2—*Total fat content of III in three pigs receiving 2.14 mg/kg/day for 7 days.*

The animals were weighed and counted in a whole body counter for potassium-40 at 0, 3, 9, and 15 or 18 weeks. Fat content was calculated, and both the gross weight and fat compartment weight were plotted against time. The data were fit to a second-degree polynomial using the Chebyshev method where $\max|P(X_i - Y_i)|$ is a minimum for all A_i.

The program was run on a computer[2] and produced the polynomial parameters A_0, A_1, A_2, and D_{max} (maximum deviation from fit) so that:

$$Y \text{ (total weight)} = A_0 + A_1t + A_2t^2 \quad \text{(Eq. 2)}$$

where t is weeks after dosing, and:

$$Y \text{ (fat weight)} = B_0 + B_1t + B_2t^2 \quad \text{(Eq. 3)}$$

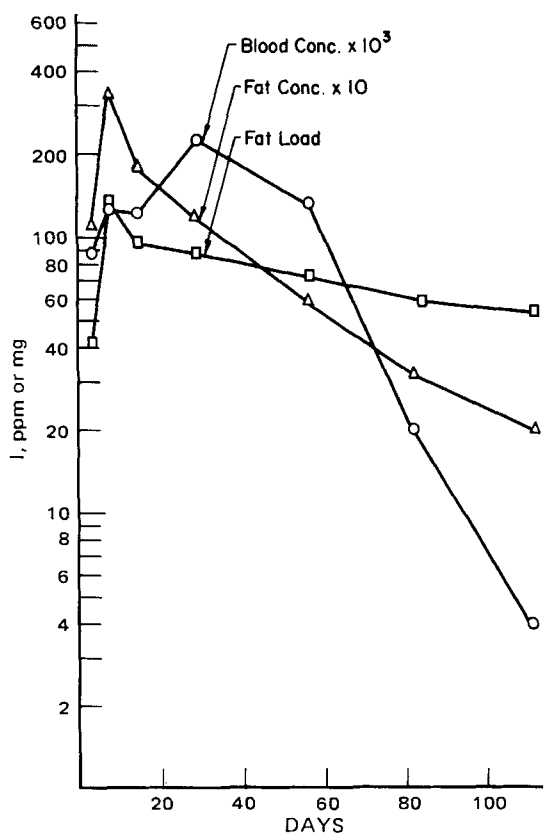

Figure 3—*Mean blood and fat concentrations (parts per million) and total fat content (milligrams) in pigs receiving 2.14 mg/kg/day of I for 7 days* (n = 3).

[2] IBM 360/65.

Table III—Apparent Pharmacokinetic Parameters for Fat Elimination

Treatment	Concentration Basis		Total Load Basis	
	$t_{1/2}$ Elimination, weeks	K_{el}, week^{-1}	$t_{1/2}$ Elimination, weeks	K_{el}, week^{-1}
I[a]	3.43	0.202	15.4	0.045
II[a]	3.57	0.194	38.3	0.018
III[b]	9.00	0.077	DI[c]	DI[c]
IV[b]	6.00	0.116	40.5	0.017
Peak 127[d]	5.36	0.129	24.2	0.028
Peak 149[e]	6.00	0.116	23.3	0.030

[a] Start of elimination phase at 2 weeks. [b] Start of elimination phase at 4 weeks. [c] Data were inadequate for estimate; a longer sample time was required. [d] 16.7% of polychlorinated biphenyl mixture; predominantly II. [e] 13.7% of polychlorinated biphenyl mixture; III is a significant, but not predominant, component.

The total fat load, L_t, is calculated by:

$$L_t \text{ (mg PCB)} = \text{(concentration PCB)}(t)(B_0 + B_1t + B_2t^2) \quad \text{(Eq. 4)}$$

RESULTS AND DISCUSSION

Computer Design—The computer-generated coefficients and D_{max} values for total weight and fat weight are presented in Tables I and II. Three sample curves are given in Fig. 1: for a control animal, for one treated with III, and for one treated with IV. The computer-fitted curves were drawn with the raw data points to permit visual comparison of fit to the polynomial. The trends in growth shown are consistent with the means and indicative of possible effects of polychlorinated biphenyls on swine performance. Percent weight gains (n = 3) were: control, 555 ± 105; III, 482 ± 62; II, 471 ± 52; I, 410 ± 67; and IV, 372 ± 42.

Pharmacokinetics—Figure 2 shows the total fat load data for pigs given the hexachlorobiphenyl ration[3]. In each case, a rise in total load occurred at 60–84 days after dosing due to the possible redistribution of residues (8). If the means of each group are examined for total fat load, fat concentration, and blood levels (Figs. 3–6), it becomes apparent that a redistributive phase existed in the pigs receiving II and III between 56 and 84 days after dosing. Although redistribution also may have occurred with I, its lower molecular weight and size made it easier to mobilize in the animal and the redistribution phase may have been missed in the sampling.

Generally, the amplitude and time shift of this redistribution are directly proportional to lipid solubility and degree of chlorination and inversely proportional to mobility and water solubility. The large time lag before redistribution discounts the more common factors responsible for nonlinearity such as enterohepatic recirculation and saturated tubular secretion. Changes in plasma protein binding characteristics might be suspect, but the volume of the blood compartment is less than fat and the concentration in blood is 10^{-3} that of fat so that the amounts in blood are inadequate.

Induction of microsomal oxidases by polychlorinated biphenyls (4) may account for the more rapid elimination rate at early times, followed

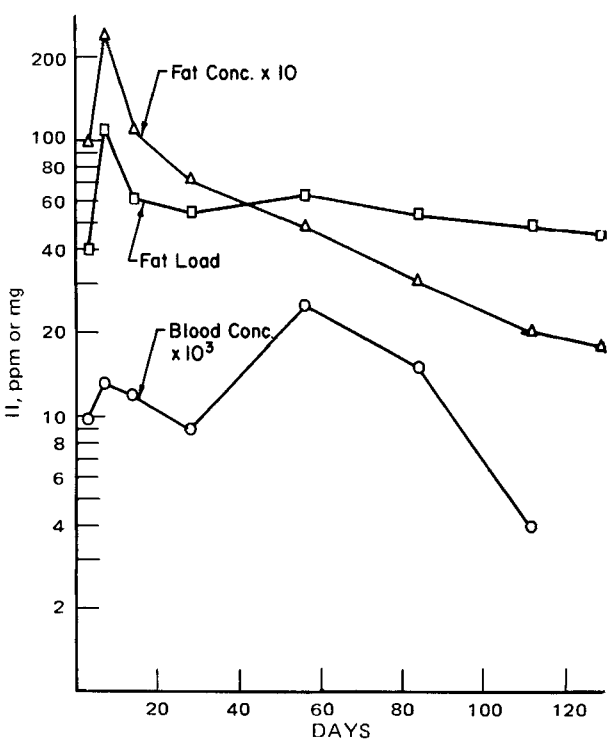

Figure 4—*Mean blood and fat concentrations and total fat content in pigs receiving II.*

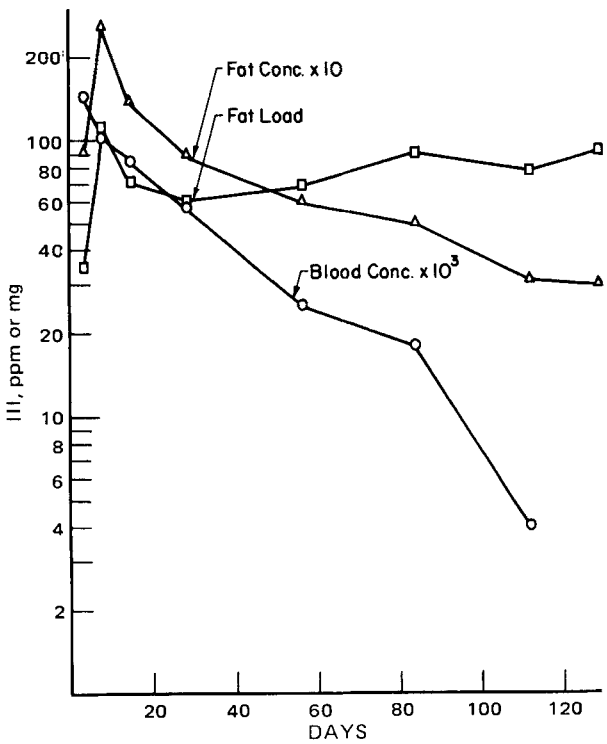

Figure 5—*Mean blood and fat concentrations and total fat content in pigs receiving III.*

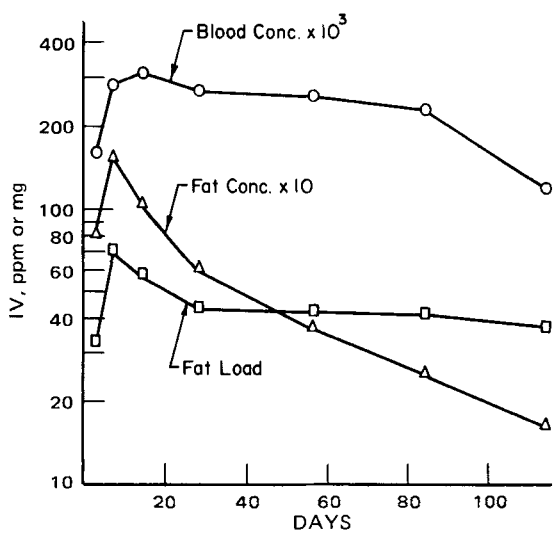

Figure 6—*Mean blood and fat concentrations and total fat content in pigs receiving a commercial mixture containing 54% chlorine.*

[3] Lines connected to raw data points were drawn by hand.

Table IV—Mean Terminal Tissue Residues 16 or 18 Weeks after 2.14 mg/kg/day of Polychlorinated Biphenyl for 7 Days

Treatment	Concentration, ppb					
	Fat	Blood	Liver	Kidney	Muscle	Spleen
I[a]	1987 ± 732	4 ± 3	330 ± 51	535 ± 71	689 ± 55	321 ± 14
II[b]	1807 ± 631	4 ± 1	140 ± 14	31 ± 2	71 ± 1	59 ± 22
III[b]	3117 ± 445	4 ± 2	358 ± 49	59 ± 10	81 ± 11	64 ± 16
IV[a]	1660 ± 360	120 ± 10	1593 ± 208	340 ± 76	780 ± 280	577 ± 217
Peak 127	354 ± 65	3.3 ± 0	127 ± 28	12 ± 7	27 ± 10	20 ± 10
Peak 149	283 ± 42	2.7 ± 0	ND[c]	11 ± 7	23 ± 5	26 ± 16

[a] Sixteen weeks. [b] Eighteen weeks. [c] Not determined due to interference.

by reduced activity as the blood concentration drops and microsomal parameters return to near normal; however, this should result in a flattening in the decline of the fat load rather than a rise. The redistribution must result from, or be partially dependent on, changes in concentration throughout the sampled fat subcompartment due to nonparallel changes in this and other fat subcompartments. Further delineation of the redistribution requires more extensive (destructive or more traumatically invasive) sampling of several subcompartments.

Fat concentration alone provides pharmacokinetic curves indicative of the fast distribution and slow elimination phases of a two-compartment model (9). The elimination from a single compartment and the β-elimination phase are calculated exactly the same as long as both processes exhibit a first-order decline.

Elimination constants (K_{el} in Table III) were calculated on the basis of first-order elimination from the fat compartment using:

$$K_{el} = 0.693/t_{1/2} \qquad \text{(Eq. 5)}$$

The values based on concentration half-lives are not indicative of elimination only but rather a combination of elimination and dilution due to compartment growth. Elimination constants based on total fat load, however, can be used as a precise measure of true elimination from fat. Compared to fat concentrations, blood concentrations indicate a faster elimination rate for all compounds (Figs. 3–6); however, the actual elimination phase for blood is delayed beyond that for fat. In addition, blood concentrations tend to increase (Fig. 4) or deviate from linearity (Fig. 5) at the times the total fat load indicates a redistribution of residues. The smaller, more mobile tetrachlorobiphenyl (I) maintains relatively higher blood concentrations than the heavier analogs and implicates a redistribution at about 28 days (Fig. 3).

Total fat load curves show that the true elimination half-lives based on total content are much longer than indicated by concentration (Figs. 2–6). In no case did the total fat load curve ever reach a half-life due to true elimination (starting at 2–4 weeks, depending on the isomer). In Table III, elimination half-lives based on total fat load are compared to those computed from more familiar concentration methods. It is necessary to use the apex of the redistributive phase as the initial start of elimination, since growth at this time is linear and a decrease in total load seems due to metabolism and elimination. It is possible that the total body load of polychlorinated biphenyls does not decrease at all in swine (10); however, the declines seen after redistribution is complete (Figs. 3 and 4) indicate that, although slow, some elimination does occur.

The commercial mixture (IV) used in this study contained 54% chlorine by weight and was composed of several components identified by GLC retention times (11, 12). Two predominant peaks produced by GLC separation occurred at retention times of 127 and 149 with respect to 1,1-dichloro-2,2-bis(*p*-chlorophenyl)ethane = 100. Peak compositions were confirmed by mass spectrometry, and studies of individual components were conducted previously (4, 11, 12).

When components 127 and 149 of IV are compared to their respective analogs (Figs. 7 and 8), the pentachlorobiphenyl analog (II) more closely matches the course of absorption and redistribution than the hexachlorobiphenyl analog (III). This result must be considered primarily due to the fact that II is a major component of peak 127 while III is only a minor component of peak 149 (11, 12). Therefore, conclusions concerning the behavior of the purified analogs compared with their behavior in a mixture cannot be drawn from these data alone.

Tissue Residues—According to the data in Table IV, II is the least persistent in all tissues analyzed, including blood. The fat load curves in Figs. 3–6 show, however, that fat content remains high. This finding indicates an increased vulnerability to metabolism rather than low lipophilicity. Compound II is the only isomer present that can assume two adjacent *ortho*-positions which are open to attack. This singularity would also produce a more planar molecule, which would be susceptible to dibenzofuran formation or hydroxylation.

The tetrachlorobiphenyl (I) maintained its presence in the blood and in the highly vascularized liver and kidney to a greater degree than did II and III, indicating a low level of biotransformation. It was the only analog significantly eliminated from the fat compartment, but this elimination was probably due to mobility rather than biotransformation.

The components of the mixture were generally distributed in the tissues according to degree of chlorination (Table V). Peaks 85 and 105, tetra- and pentachlorobiphenyl(s) (12), were eliminated from most tissues after 16 weeks. Peak 85 was apparently highly mobile and present in high levels in blood and liver only. Peaks 83 and 99 were concentrated in all

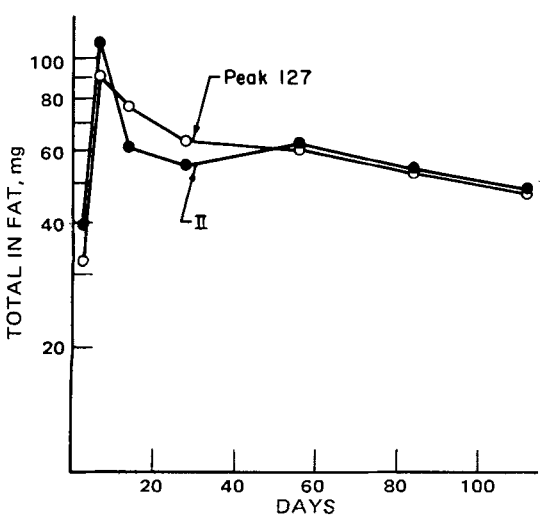

Figure 7—*Comparative fat dynamics of II and peak 127 of the commercial mixture.*

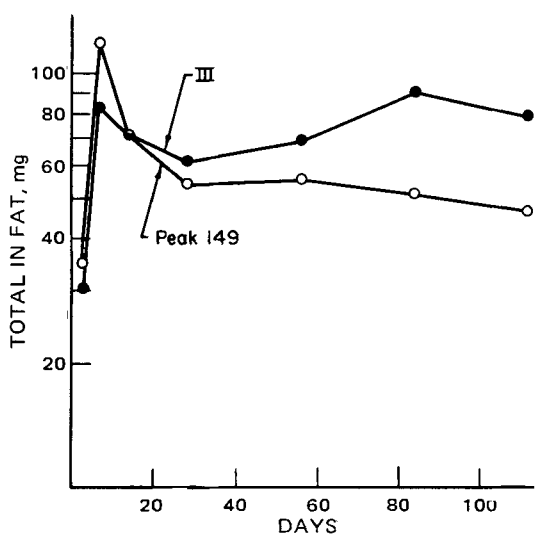

Figure 8—*Comparative fat dynamics of III and peak 149 of the commercial mixture.*

Table V—Distribution of Polychlorinated Biphenyl Mixture Components in Swine Tissues

Component	Mean Concentration, ppm Relative to Standard						Percent Total Polychlorinated Biphenyl						
	Fat	Liver	Kidney	Muscle	Spleen	Blood	Fat	Liver	Kidney	Muscle	Spleen	Blood	Standard
70	0.96	2.57	0.26	0.99	0.34	0.04	7.9	24.8	11.5	20.3	8.2	5.05	16.1
83	3.81	8.08	2.26	4.93	4.27	0.73	15.9	39.6	51.0	51.6	52.2	47.0	8.2
85	0.00	2.63	0.00	0.00	0.00	0.31	0.0	12.9	0.0	0.0	0.0	20.0	8.2
99	3.11	1.27	0.82	0.98	1.49	0.20	16.0	7.7	22.8	12.6	22.4	15.9	10.1
105	0.00	0.00	0.00	0.00	0.00	0.00	0.0	0.0	0.0	0.0	0.0	0.0	10.1
127	2.12	0.76	0.07	0.16	0.12	0.02	18.0	7.6	3.2	3.4	3.0	2.6	16.7
149	2.06	ND	0.08	0.17	0.19	0.02	14.4	ND[a]	3.0	3.0	3.9	2.2	13.7
176	3.61	0.35	0.11	0.19	0.15	0.04	15.1	1.7	2.5	2.0	1.8	2.6	8.2
208	3.56	0.23	0.13	0.27	0.30	0.02	3.8	0.3	0.8	0.7	0.9	0.3	2.1
253	3.47	0.16	0.09	0.23	0.32	0.02	3.4	0.2	0.5	0.6	0.9	0.3	1.9
286	4.79	1.44	0.43	2.43	1.63	0.04	1.5	0.5	0.7	1.9	1.5	0.2	0.6
332	5.36	12.93	ND	ND	8.04	0.03	0.3	0.8	ND	ND	1.2	Trace	0.1
Total	1.66	1.59	0.34	0.78	0.58	0.12							

[a] Not determined due to interference.

tissues above the relative levels present in the mixture administered. Otherwise, the peaks of longer relative retention time (more highly chlorinated) accumulated in fat while blood carried the peaks of shorter relative retention time. Other tissues were intermediate, except that the liver maintained high levels of component 70, which is rapidly distributed or eliminated from swine and sheep fat and blood (1, 2, 4, 5); the level of peak 253, which is rapidly eliminated by fish (13), was lower in the liver than in any other tissue.

REFERENCES

(1) R. E. Borchard, L. G. Hansen, W. G. Huber, R. L. Metcalf, and M. E. Welborn, *Arch. Environ. Contam. Toxicol.*, **2**, 179 (1974).

(2) R. E. Borchard, M. E. Welborn, W. B. Wiekhorst, D. W. Wilson, and L. G. Hansen, *J. Pharm. Sci.*, **64**, 1294 (1975).

(3) R. L. Metcalf, J. R. Sanborn, P.-Y. Lu, and D. Nye, *Arch. Environ. Contam. Toxicol.*, **3**, 151 (1975).

(4) L. G. Hansen, M. E. Welborn, R. E. Borchard, R. H. Teske, and R. L. Metcalf, *ibid.*, **5**, 257 (1977).

(5) R. E. Borchard, M. E. Welborn, L. G. Hansen, R. P. Link, and R. H. Teske, *ibid.*, **4**, 226 (1976).

(6) T. G. Lohman, B. C. Breidenstein, A. R. Twardock, G. S. Smith, and H. W. Norton, *J. Anim. Sci.*, **25**, 1218 (1966).

(7) M. E. Welborn, R. E. Borchard, L. G. Hansen, and R. L. Metcalf, *J. Assoc. Offic. Anal. Chem.*, **57**, 1248 (1974).

(8) L. G. Hansen, D. W. Wilson, R. L. Metcalf, and M. E. Welborn, *J. Agr. Food Chem.*, **24**, 256 (1976).

(9) J. T. Doluisio and L. W. Dittert, *Am. J. Pharm. Educ.*, **32** (1968).

(10) N. S. Platonow and H. D. Geissinger, *Vet. Rec.*, **93**, 287 (1973).

(11) S. N. Hirwe, R. E. Borchard, L. G. Hansen, and R. L. Metcalf, *Bull. Environ. Contam. Toxicol.*, **12**, 138 (1974).

(12) R. G. Webb and A. C. McCall, *J. Assoc. Offic. Anal., Chem.*, **55**, 746 (1972).

(13) S. F. Sundlof, M.S. thesis, University of Illinois, Urbana, Ill., 1975.

ACKNOWLEDGMENTS AND ADDRESSES

Received December 16, 1975, from the *Comparative Environmental Pharmacology and Toxicology Program, College of Veterinary Medicine, University of Illinois, Urbana, IL 61801.*

Accepted for publication June 11, 1976.

Supported by Research Contract FDA 72-116 from the Bureau of Veterinary Medicine, Food and Drug Administration.

The authors thank Monsanto Chemical Co. for supplying Aroclor 1254, S. B. Dorn and S. N. Hirwe for the synthesis and purification of the analogs, and R. E. Borchard, T. G. Lohman, R. H. Teske, and D. W. Wilson for their advice and assistance.

[x] To whom inquiries should be directed.

Renal Function Testing: Differentiation between a Nephrotoxic Agent and Diuretic Drugs

E. E. VOGIN

Abstract □ Preliminary studies indicate that it may be possible to differentiate the effects of a nephrotoxic substance from those of diuretic agents by the measurement of both urine and plasma osmolality. The nephrotoxic substance, mercuric chloride, decreases urinary osmolality and increases plasma or serum osmolality. The diuretic agents, at exceedingly high dosages, may show a dose-related decrease in urine osmolality. However, serum osmolality either remains unchanged or is only slightly lowered. This difference in the serum response of animals treated with a nephrotoxin or diuretic agents may allow for the differentiation in toxicological studies.

Keyphrases □ Osmolality, urine and plasma—effects of nephrotoxic and diuretic agents compared, dogs □ Renal function testing—differentiation between nephrotoxic and diuretic agents by urine and plasma osmolality measurements, dogs □ Nephrotoxic agents—mercuric chloride, effect on urine and plasma osmolality compared to various diuretic agents, dogs □ Diuretics, various—effects on urine and plasma osmolality compared to nephrotoxic agent, dogs □ Mercuric chloride—effect on urine and plasma osmolality compared to various diuretic agents, dogs

The evaluation of nephrotoxicity in safety evaluation studies has always posed a problem to the toxicologist. The need to determine histopathological changes in the urinary bladder prohibits catheterization because of possible irritant effects. The clinical evaluation of nephrotoxicity evolves about the determination of blood (serum) urea

Table V—Distribution of Polychlorinated Biphenyl Mixture Components in Swine Tissues

Component	Mean Concentration, ppm Relative to Standard						Percent Total Polychlorinated Biphenyl						
	Fat	Liver	Kidney	Muscle	Spleen	Blood	Fat	Liver	Kidney	Muscle	Spleen	Blood	Standard
70	0.96	2.57	0.26	0.99	0.34	0.04	7.9	24.8	11.5	20.3	8.2	5.05	16.1
83	3.81	8.08	2.26	4.93	4.27	0.73	15.9	39.6	51.0	51.6	52.2	47.0	8.2
85	0.00	2.63	0.00	0.00	0.00	0.31	0.0	12.9	0.0	0.0	0.0	20.0	8.2
99	3.11	1.27	0.82	0.98	1.49	0.20	16.0	7.7	22.8	12.6	22.4	15.9	10.1
105	0.00	0.00	0.00	0.00	0.00	0.00	0.0	0.0	0.0	0.0	0.0	0.0	10.1
127	2.12	0.76	0.07	0.16	0.12	0.02	18.0	7.6	3.2	3.4	3.0	2.6	16.7
149	2.06	ND	0.08	0.17	0.19	0.02	14.4	ND[a]	3.0	3.0	3.9	2.2	13.7
176	3.61	0.35	0.11	0.19	0.15	0.04	15.1	1.7	2.5	2.0	1.8	2.6	8.2
208	3.56	0.23	0.13	0.27	0.30	0.02	3.8	0.3	0.8	0.7	0.9	0.3	2.1
253	3.47	0.16	0.09	0.23	0.32	0.02	3.4	0.2	0.5	0.6	0.9	0.3	1.9
286	4.79	1.44	0.43	2.43	1.63	0.04	1.5	0.5	0.7	1.9	1.5	0.2	0.6
332	5.36	12.93	ND	ND	8.04	0.03	0.3	0.8	ND	ND	1.2	Trace	0.1
Total	1.66	1.59	0.34	0.78	0.58	0.12							

[a] Not determined due to interference.

tissues above the relative levels present in the mixture administered. Otherwise, the peaks of longer relative retention time (more highly chlorinated) accumulated in fat while blood carried the peaks of shorter relative retention time. Other tissues were intermediate, except that the liver maintained high levels of component 70, which is rapidly distributed or eliminated from swine and sheep fat and blood (1, 2, 4, 5); the level of peak 253, which is rapidly eliminated by fish (13), was lower in the liver than in any other tissue.

REFERENCES

(1) R. E. Borchard, L. G. Hansen, W. G. Huber, R. L. Metcalf, and M. E. Welborn, *Arch. Environ. Contam. Toxicol.*, **2**, 179 (1974).

(2) R. E. Borchard, M. E. Welborn, W. B. Wiekhorst, D. W. Wilson, and L. G. Hansen, *J. Pharm. Sci.*, **64**, 1294 (1975).

(3) R. L. Metcalf, J. R. Sanborn, P.-Y. Lu, and D. Nye, *Arch. Environ. Contam. Toxicol.*, **3**, 151 (1975).

(4) L. G. Hansen, M. E. Welborn, R. E. Borchard, R. H. Teske, and R. L. Metcalf, *ibid.*, **5**, 257 (1977).

(5) R. E. Borchard, M. E. Welborn, L. G. Hansen, R. P. Link, and R. H. Teske, *ibid.*, **4**, 226 (1976).

(6) T. G. Lohman, B. C. Breidenstein, A. R. Twardock, G. S. Smith, and H. W. Norton, *J. Anim. Sci.*, **25**, 1218 (1966).

(7) M. E. Welborn, R. E. Borchard, L. G. Hansen, and R. L. Metcalf, *J. Assoc. Offic. Anal. Chem.*, **57**, 1248 (1974).

(8) L. G. Hansen, D. W. Wilson, R. L. Metcalf, and M. E. Welborn, *J. Agr. Food Chem.*, **24**, 256 (1976).

(9) J. T. Doluisio and L. W. Dittert, *Am. J. Pharm. Educ.*, **32** (1968).

(10) N. S. Platonow and H. D. Geissinger, *Vet. Rec.*, **93**, 287 (1973).

(11) S. N. Hirwe, R. E. Borchard, L. G. Hansen, and R. L. Metcalf, *Bull. Environ. Contam. Toxicol.*, **12**, 138 (1974).

(12) R. G. Webb and A. C. McCall, *J. Assoc. Offic. Anal., Chem.*, **55**, 746 (1972).

(13) S. F. Sundlof, M.S. thesis, University of Illinois, Urbana, Ill., 1975.

ACKNOWLEDGMENTS AND ADDRESSES

Received December 16, 1975, from the *Comparative Environmental Pharmacology and Toxicology Program, College of Veterinary Medicine, University of Illinois, Urbana, IL 61801.*

Accepted for publication June 11, 1976.

Supported by Research Contract FDA 72-116 from the Bureau of Veterinary Medicine, Food and Drug Administration.

The authors thank Monsanto Chemical Co. for supplying Aroclor 1254, S. B. Dorn and S. N. Hirwe for the synthesis and purification of the analogs, and R. E. Borchard, T. G. Lohman, R. H. Teske, and D. W. Wilson for their advice and assistance.

[x] To whom inquiries should be directed.

Renal Function Testing: Differentiation between a Nephrotoxic Agent and Diuretic Drugs

E. E. VOGIN

Abstract □ Preliminary studies indicate that it may be possible to differentiate the effects of a nephrotoxic substance from those of diuretic agents by the measurement of both urine and plasma osmolality. The nephrotoxic substance, mercuric chloride, decreases urinary osmolality and increases plasma or serum osmolality. The diuretic agents, at exceedingly high dosages, may show a dose-related decrease in urine osmolality. However, serum osmolality either remains unchanged or is only slightly lowered. This difference in the serum response of animals treated with a nephrotoxin or diuretic agents may allow for the differentiation in toxicological studies.

Keyphrases □ Osmolality, urine and plasma—effects of nephrotoxic and diuretic agents compared, dogs □ Renal function testing—differentiation between nephrotoxic and diuretic agents by urine and plasma osmolality measurements, dogs □ Nephrotoxic agents—mercuric chloride, effect on urine and plasma osmolality compared to various diuretic agents, dogs □ Diuretics, various—effects on urine and plasma osmolality compared to nephrotoxic agent, dogs □ Mercuric chloride—effect on urine and plasma osmolality compared to various diuretic agents, dogs

The evaluation of nephrotoxicity in safety evaluation studies has always posed a problem to the toxicologist. The need to determine histopathological changes in the urinary bladder prohibits catheterization because of possible irritant effects. The clinical evaluation of nephrotoxicity evolves about the determination of blood (serum) urea

Table I—Drug Dosage for 3 Days

Compound	Milligrams per Kilogram per Day
Hydrochlorothiazide	12.5, 25, 50
Chlorothiazide	125, 250, 500
Acetazolamide	10, 20, 40
Ethacrynic acid	2.5, 5.0, 10.0[a]

[a] Administered as two 5-mg/kg successive doses.

nitrogen and urine analytical studies. Osmolality measurements have been used extensively in clinical situations to assess renal function. The concept, physiology, and clinical application of this procedure were described previously (1).

One of the most easily studied functions of the kidney is its capacity to conserve water under dehydration conditions. In these circumstances, water is reabsorbed from the tubular fluid against an osmotic gradient through the influence of endogenous antidiuretic hormones, and the maximum concentration of the solutes is used as an indication of the kidney's capacity to perform osmotic work (2).

Low protein diets and habitual consumption of large quantities of fluid may result in the excretion of urine of low specific gravity or inhibit the concentrating ability of the kidneys. Since diuretics also can reduce the renal concentrating capacity, preliminary studies were undertaken to determine if osmolality measurements of urine and serum can differentiate between pharmacodynamic and nephrotoxic effects of chemical agents. This report presents the initial findings.

EXPERIMENTAL

Eighteen purebred male and female beagle dogs were individually housed in metabolism cages in air-conditioned and humidity-controlled quarters and were maintained on a standard laboratory chow. Osmolality measurements were made according to the following procedures. At approximately 1 pm on the test day, all food and water were withdrawn from the cages. At 4:30 pm, a clean urine-collecting vessel was placed beneath the cage. A filter was positioned above the vessel to prevent contamination of the urine with feces, hair, *etc.*

Urine was collected from each animal until 8:30 am the following morning, at which time aliquots were taken for the determination of osmolality. Blood, with or without anticoagulant, was obtained from representative dogs by venipuncture. Following centrifugation, 2 ml of plasma or serum was used for the determination of osmolality. Osmolality measurements[1] were performed by the freezing-point method.

Physiological measurements included the volume, sodium, potassium, chloride, and specific gravity of urine and the sodium, potassium, chloride, urea nitrogen, alkaline phosphatase, and glutamic oxaloacetic transaminase of plasma or serum.

Six dogs were divided into three groups (one male and one female in each) and dosed with the diuretic agents according to the schedule shown in Table I; a table of random numbers was used for assignments to drug and dosage level. Seven days were allowed to elapse between each drug or dosage change to obviate measurable drug interactions. Twelve dogs were given two intravenous doses of mercuric chloride for 2 consecutive days. Dosage levels were 0.5, 1.0, 2.0, and 3.0 mg/kg. Following collection of urine and plasma for the various physiological measurement, these animals were sacrificed and examined in detail at necropsy, and histomorphological studies of renal tissues were made.

RESULTS

Urine osmolality measurements made on 88 colony dogs revealed values ranging from 975 to 2904 mOsm/kg. The results also indicated a linear correlation with specific gravity. Plasma osmolality measurements were made on 46 dogs and resulted in a mean value of 325 ± 3.7 (*SD*) mOsm/kg. Serum values were somewhat less, about 307 mOsm/kg. The ratio of urine osmolality to plasma osmolality (for 24 dogs on which both measurements were performed) was 7.51 ± 1.49 (*SD*).

[1] Advance Instrument osmometer with direct readouts.

Table II—Effect of Intravenous Mercuric Chloride on Blood Chemistry

Dog Number (Sex)	Dose, mg/kg	Urea[a] Nitrogen, mg %	Alkaline[a] Phosphatase Units	Transaminase[a] Units
313 (F)	0.5	16/21	15/11	23/17
267 (F)	0.5	12/18	20/20	16/19
315 (F)	1.0	10/16	24/14	20/21
265 (F)	1.0	12/15	12/12	15/17
266 (M)	2.0	15/17	18/16	16/13
393 (M)	2.0	9/247	10/72	16/1070
392 (M)	3.0	13/131	16/12	14/183
280 (M)	3.0	16/139	14/14	18/147
630 (F)	3.0	17/129	18/13	15/108
493 (F)	3.0	11/133	13/24	14/111
494 (M)	3.0	10/156	13/39	11/129
495 (F)	3.0	14/174	11/12	17/75

[a] The numerator is the predrug value; the denominator is the postdrug value.

The effects of mercuric chloride administration on blood chemistry and osmolality measurements are shown in Tables II and III. At doses of 0.5 and 1.0 mg/kg for 2 consecutive days, no overt renal toxicity was evident. Values for urea nitrogen, transaminase, and urine and serum osmolality were within the normal ranges. The urine–plasma (U/P) ratio was reduced but also remained within normal limits.

One of two dogs at 2.0 mg/kg and all dogs at 3.0 mg/kg showed clinical evidence of nephrotoxicity as manifested by elevated urea nitrogen and serum osmolality values, marked inhibition in renal concentrating ability with marked reduction in urine osmolality, and reduction of U/P ratios to unity. Alkaline phosphate values were not altered; transaminase was markedly elevated. Histopathological examinations showed evidence of renal tubular pathology consistent with the clinical findings.

The results of administration of the diuretic agents resulted in slight to marked reductions in urine osmolality. These data are shown in Tables IV, V, VI, and VII for hydrochlorothiazide, chlorothiazide, acetazolamide, and ethacrynic acid, respectively. Acetazolamide and ethacrynic acid were most potent in decreasing urine osmolality. Dogs given hydrochlorothiazide or chlorothiazide generally had urine osmolality levels within the normal range. If the measurements had been obtained under circumstances whereby treatment was not known, the values would have been considered as normal.

Serum osmolality was slightly decreased following administration of hydrochlorothiazide or chlorothiazide, whereas variable responses were seen in dogs administered ethacrynic acid or acetazolamide. The U/P ratio of the dogs treated with hydrochlorothiazide, although reduced, was still greater than 3, which clinically has served as an indication of normality of the renal concentrating ability. Only one dog, Dog 4, in the group treated with chlorothiazide showed a U/P ratio of less than 3. Ethacrynic acid and acetazolamide resulted in marked decreases in U/P ratios in most instances. In general, the posttreatment values were less than 3.

Table III—Effect of Intravenous Mercuric Chloride on Osmolality of Urine and Plasma

Dog Number (Sex)	Dose, mg/kg	Specific[a] Gravity (1.0 +)	Urine[a], mOsm/kg	Serum[a], mOsm/kg	U/P[a]
313 (F)	0.5	60/50	2470/2199	298/304	8.3/7.2
267 (F)	0.5	35/40	1624/1591	297/303	5.5/5.3
315 (F)	1.0	55/48	2413/1914	300/296	8.0/6.5
265 (F)	1.0	52/36	2304/1449	284/299	7.8/4.8
266 (M)	2.0	37/30	1605/1316	292/295	5.5/4.5
393 (M)	2.0	35/06	1563/294	294/397	5.3/0.7
392 (M)	3.0	50/00	2223/252	297/342	7.5/0.7
280 (M)	3.0	40/10	1605/356	300/335	5.4/1.1
630 (F)	3.0	35/10	1596/285	297/332	5.4/0.9
493 (F)	3.0	60/15	2399/261	310/321	7.7/0.8
494 (M)	3.0	45/03	2275/417	316/387	7.2/1.1
494 (F)	3.0	35/05	2098/401	320/387	6.6/1.0

[a] The numerator is the predrug value; the denominator is the postdrug value.

Table IV—Effect of Hydrochlorothiazide on Serum Urea Nitrogen, Electrolytes, and Urine and Serum Osmolality

Dog Number	Dose, mg/kg	Sodium, mEq/liter	Potassium, mEq/liter	Chloride, mEq/liter	Blood Urea Nitrogen, mg %	Urine[a], mOsm/kg	Serum[a], mOsm/kg	U/P[a]
1	12.5	147/144	4.8/4.5	105/99	15/17	2118/1760	305/299	6.95/5.90
2	12.5	147/146	5.1/4.8	105/98	15/17	2940/2475	307/298	9.55/8.28
3	25	150/145	5.0/4.1	105/96	13/16	1225/975	308/293	4.07/3.34
4	25	148/146	5.0/4.4	105/95	15/16	1675/1045	308/296	5.45/3.57
5	50	148/146	4.6/3.7	109/99	15/15	2025/1460	298/298	6.80/4.89
6	50	147/146	4.7/4.8	104/99	19/19	1000/1055	302/294	3.33/3.60

[a] The numerator is the predrug value; the denominator is the postdrug value.

In an attempt to analyze the data with regard to pharmacological effects, urinary excretion of sodium, potassium, and chloride ions was determined after treatment with the respective diuretic agents. While some pre- and postdrug values differed markedly, considerable overlap was seen and no definite increase in the excretion of electrolytes was observed. These findings are shown in Table IV for hydrochlorothiazide, which served as the prototype agent. Similar patterns were seen in chronic toxicity studies with diuretics when urine was collected on the 3rd day of dosing. This response is not unusual and appears to reflect the homeostatic mechanisms of the animal to maintain normal electrolyte balance.

No significant changes were found in sodium levels subsequent to the administration of the diuretic agent. Administration of chlorothiazide and acetazolamide tended to reduce blood potassium-ion levels, while animals given hydrochlorothiazide and chlorothiazide generally showed a slight reduction in the blood chloride-ion levels. However, the values recorded are within the normal limits for the species. In general, only dogs given ethacrynic acid demonstrated slight elevations in blood urea nitrogen values.

Microscopic examination of renal tissue from these animals revealed no pathological changes attributable to the administration of diuretic agents.

DISCUSSION

These studies indicate that the use of plasma or serum and urine osmolality tests may be useful in evaluating renal function during subacute or chronic toxicity studies with diuretic agents.

Mercuric chloride administration resulted in an apparent dose–response in renal pathology. At doses less than 2.0 mg/kg, no clinical evidence of nephrotoxicity was evident; however, U/P osmolality ratios were reduced in a manner consistent with diuretic activity. This finding appears to reflect the mercuric-ion effect on sulfhydryl enzymes at these subtoxic levels (3). At higher dosages (2 and 3 mg/kg), the dogs showed renal toxicity that could be correlated with marked elevations of urea nitrogen, serum osmolality, and histopathology affecting the proximal renal tubule.

Table V—Effect of Chlorothiazide on Osmolality

Dog Number	Dose, mg/kg	Urine[a], mOsm/kg	Serum[a], mOsm/kg	U/P[a]
1	125	1675/1475	288/276	5.85/5.32
2	125	2075/2475	280/287	7.40/8.61
3	250	1300/875	290/279	4.50/3.19
4	250	1300/650	296/275	4.46/2.36
5	500	1475/1225	281/268	5.25/3.58
6	500	1650/1125	279/276	5.92/4.09

[a] The numerator is the predrug value; the denominator is the postdrug value.

Table VI—Effect of Acetazolamide on Osmolality

Dog Number	Dose, mg/kg	Urine[a], mOsm/kg	Serum[a], mOsm/kg	U/P[a]
1	40	2427/575	289/293	8.35/1.97
2	40	NS/475	298/307	— /1.52
3	20	2025/275	315/298	6.45/0.92
4	20	1400/600	298/291	4.72/2.06
5	10	1475/1575	293/314	5.05/5.01
6	10	1725/550	298/282	5.80/1.95

[a] The numerator is the predrug value; the denominator is the postdrug value.

Table VII—Effect of Ethacrynic Acid on Osmolality

Dog Number	Dose, mg/kg	Urine[a], mOsm/kg	Serum[a], mOsm/kg	U/P[a]
1	2.5	2125/800	309/316	6.89/2.54
2	2.5	2825/2750	307/308	9.17/8.95
3	5.0	1775/925	328/314	5.40/2.95
4	5.0	1625/1175	318/308	5.13/3.83
5	10.0	1825/750	293/304	6.22/2.47
6	10.0	1350/600	304/312	4.45/1.92

[a] The numerator is the predrug value; the denominator is the postdrug value.

Mercuric chloride toxicity causes severe tubular necrosis with acute oliguric renal failure (4) but sparing of the glomeruli (5). Renal blood flow and glomerular filtration continue at rates which, in chronic renal failure, should provide adequate volumes of urine. However, it is postulated that oliguria results from filtrate disappearance by nonselective back-diffusion through damaged tubules (5).

Since serum osmolality is primarily dependent upon electrolyte concentration and concentrations of urea and glucose, the high levels seen in these nephrotoxic dogs may be attributed to the oliguric state and consequent uremia resulting from mercuric chloride toxicity.

Although diuretics can reduce the renal concentrating ability of the kidney and likewise alter the U/P ratio in a manner similar to that caused by the nephrotoxin mercuric chloride, the determination of plasma or serum osmolality may serve as the basis for the differentiation of effects. In cases of renal disease, serum or plasma osmolality is generally elevated; however, in the present program, serum osmolality remained unchanged or was slightly decreased subsequent to the administration of diuretic agents. Serum sodium concentrations and urea nitrogen levels were not elevated.

The data indicate that this method appears to be of value in assessing and differentiating renal function subsequent to diuretic agents and a nephrotoxic agent. While these results are preliminary, they can serve as a basis for extending the scope of testing by evaluating a series of less potent nephrotoxins during subacute oral toxicity studies and comparing these data to those obtained subsequent to more prolonged administration of a diuretic agent.

REFERENCES

(1) R. M. Warhol, A. Eichenholz, and R. O. Mulhausen, *Arch. Intern. Med.*, **116**, 743 (1965).

(2) B. E. Miles, A. Paton, and H. E. deWardener, *Br. Med. J.*, **2**, 901 (1954).

(3) A. Osol, R. Pratt, and M. D. Altschule, "The United States Dispensatory," 26th ed., Lippincott, Philadelphia, Pa., 1967, pp. 1005, 1006.

(4) M. D. Milne, in "Diseases of the Kidney," 2nd ed., M. B. Strauss and L. G. Welt, Eds., Little, Brown, Boston, Mass., 1971, pp. 1071–1138.

(5) J. P. Merrill, in *ibid.*, pp. 637–666.

ACKNOWLEDGMENTS AND ADDRESSES

Received August 28, 1972, from *Food and Drug Research Laboratories, Inc., Maspeth, NY 11378.*

Accepted for publication June 9, 1976.

Present address: Vogin Associates, 9768 Susan Road, Philadelphia, PA 19115.

Instrumentation of an Automatic Capsule-Filling Machine

L. E. SMALL and L. L. AUGSBURGER [x]

Abstract □ Techniques similar to those used in instrumenting tablet presses were applied to an automatic capsule-filling machine. The dosing unit was modified to allow the bonding of strain gauges to the compression piston. The gauges formed the arms of a Wheatstone bridge circuit. Thus, compression and ejection events were monitored by measuring the bridge unbalance voltage using a suitable amplifier–recording system. The instrumented piston was calibrated in a physical testing machine. Dosing unit rotation required the interposing of a mercury contact swivel between the amplifier and instrumented piston. The instrumentation system required only one minor, permanent modification to the machine, a cut in the dosator tube. Since the same dosator piston sensed both compression and ejection, only one of the two dosing units was instrumented and the other was removed from the machine. A solenoid switching system was devised which only permitted the feeding of empty gelatin shells into the filling cycle for the instrumented piston. Representative fillers were run at constant powder bed and piston heights. Oscilloscope tracings showed two stages in slug formation: (*a*) "precompression," representing the force sensed during dipping of the dosator into the powder before actual compression, and (*b*) actual piston compression. Generally, the maximum slug compression force fell to zero rapidly on retraction of the piston, but in some cases a retention force was noted, possibly due to elastic rebound of the slug against the retracted piston. A negative deflection due to binding of the piston also was observed in tracings of one material. Lubricated batches exhibited ejection forces of less than 1 kg.

Keyphrases □ Capsule-filling machine, automatic—instrumentation for monitoring compression and ejection forces described □ Instrumentation—described for monitoring compression and ejection forces in automatic capsule-filling machine □ Compression forces—in automatic capsule-filling machine, instrumentation described □ Ejection forces—in automatic capsule-filling machine, instrumentation described □ Technology, pharmaceutical—instrumentation described for monitoring compression and ejection forces in automatic capsule-filling machine

One significant advance in pharmaceutical technology in recent decades was the application of instrumentation techniques to monitor the forces developed in the formation and ejection of tablets. Applied first to single-punch presses and later to high-speed rotary presses, this instrumentation has brought about great insights into the fundamentals of tablet compaction, facilitated product formulation, and permitted continuous in-process monitoring and control of tablet weight (1–4). In light of the successful application of instrumentation to tablet formulation and production, the application of this technology to modern capsule-filling equipment should be of equal value.

Modern, fully automatic, capsule-filling equipment, employing filling principles similar to tablet compression, appeared uniquely suited to the application of instrumentation techniques. Although both the traditional semiautomatic and the newer fully automatic capsule-filling machines generally require that formulations have good flow properties and be lubricious, the machine used in this study[1] required that formulations also be compressible enough to form slugs sufficiently cohesive to be transported within the machine and ejected into open capsules.

The similarity of this filling mechanism to tablet compression suggested that slug compression force and ejection force would be meaningful parameters that could be monitored in a manner similar to that presently used in tableting. Therefore, the specific aim of this research was the development of an instrumentation system capable of monitoring the compression and ejection forces developed during the filling cycle of this capsule filling machine.

A literature review revealed only two references related to the instrumentation of capsule filling machines. Cole and May (5), in a short article, noted the instrumentation of the same model automatic capsule filling machine[1] using strain gauges but gave no details regarding the method of instrumentation. They did, however, report forces ranging from 5 to 350 N (0.5–35 kg) required for compression and ejection of the powder slugs.

Coinciding with the completion of the present work, Cole and May (6) reported in detail their method of instrumentation. A size No. 00 piston was fitted with strain gauges. The rotating dosator head was modified by incorporating a planetary gear system, which prevented the continuous twisting of the cable connecting the gauges with the monitoring equipment. Compression, retention, and ejection forces of representative capsule fillers were reported. However, as will be pointed out, several important differences exist between the methodology and results of Cole and May and those reported here.

EXPERIMENTAL

A primary concern throughout the design process was to keep the modification of the machine to a minimum. The attachment of mounting brackets or guides should be by existing hardware. The system should not alter the normal functioning of the filling process nor reduce normal operating speeds. Finally, the machine should retain the capability of operating uninstrumented, and restoration to this mode should be easily accomplished.

Modification of Dosator Piston—The dosator piston of this capsule filling machine is analogous to the upper punch of a single-punch tableting machine and also to the lower punch in both single-punch and rotary machines because the piston is responsible for both compression of the powder slug and ejection of the slug from the filling head. Since the piston must, therefore, sense the forces generated during compression and ejection, it provided the logical site for bonding of the strain gauges used to detect these forces.

The piston (Fig. 1A) can be conveniently divided into four areas: (1) an upper graduated shank, (2) a collar supporting a metal rod used to adjust the height of the piston in the dosator, and (3) a middle shank tapering to (4) a lower shank with a slightly flared, flattened end. To facilitate bonding of strain gauges and to increase sensitivity, a new piston was machined from No. 304 machinable stainless steel (Fig. 1B). The new piston is identical in all respects to the original, except that the normally cylindrical middle shank was altered to a rectangular cross-section 1.12 cm wide and 0.234 cm thick. In addition, part of this area was reduced to a 0.742-cm width, affecting a portion of the middle shank 1.89 cm in length.

This reduced area (1.89 × 0.742 × 0.234 cm) is the bonding site of the strain gauges. This reduction further increases sensitivity and provides clearance for connecting wires to pass to the reverse side of the piston

[1] Zanasi LZ-64 automatic capsule filling machine, USM Corp., Machinery Division, Beverly, MA 01915.

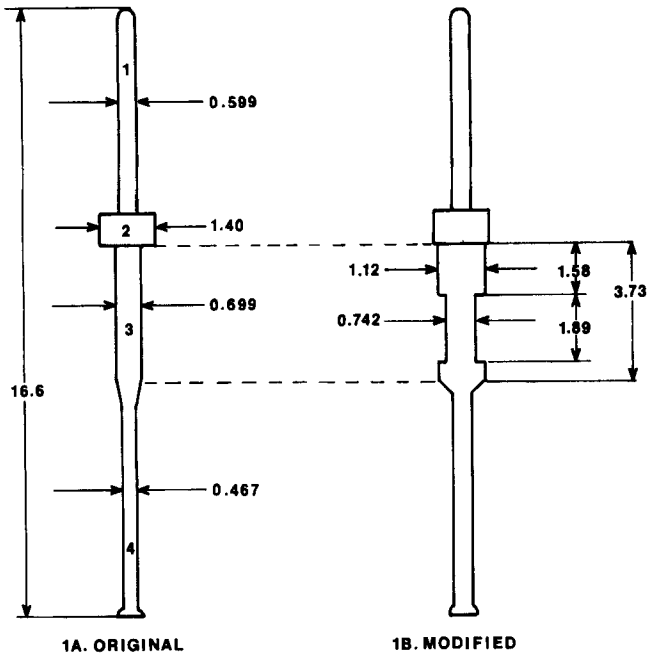

Figure 1—*Sketch of original and modified pistons (all dimensions in centimeters).*

when in the dosator unit. A groove was also cut into the collar on one side of the piston, 3.18 mm wide, to allow passage of connecting wires. The plane of the modified rectangular cross section is parallel to the axis of the hole drilled in the collar. The piston, thus modified, is fitted in the dosator unit in the same fashion as the original piston.

Axial strain produced in the bonding area originates only from stress generated at the flared end of the lower shank. The piston is pushed downward, externally, at the tip of the upper shank. The flared, lower end presses on the powder sectioned by the filling head during compression and ejection. The piston is retracted to its original position by a spring acting on the base of the collar.

Installation of Strain Gauges—Two sets of strain gauges[2] were bonded to the reduced area of the modified piston, one set on each side. The strain-gauge configuration chosen for this project consisted of two grid elements, perpendicular to each other, mounted along the length of the gauge backing. The gauges were oriented so that the grid elements closest to the flared end of the piston were parallel to the axis of the piston.

Bonding of the gauges was carried out according to a standard procedure provided by the strain-gauge manufacturer (7). The gauges were mounted such that the center alignment mark of one gauge was perfectly matched with the center alignment mark of the gauge on the opposite side of the piston. A four-post terminal strip was bonded to the grooved collar side of the piston, midway between the collar and gauges (Fig. 2).

Circuitry and Connections—The gauge elements parallel to the axis of the piston serve as the active arms of a Wheatstone bridge. The gauge elements perpendicular to the piston axis serve as temperature-compensating gauges and complete the Wheatstone bridge circuit. The active gauges are connected in opposite arms of the Wheatstone bridge to double the sensitivity of the instrumented piston (Fig. 3).

To protect the bridge and eliminate strain on the gauges induced by the connecting wiring, the terminal strip was interposed between the bridge circuitry and connecting wiring. The connecting wiring was fed from the terminal strip through the groove in the collar and loosely wrapped once counterclockwise behind the upper shank of the piston. Narrow strips of plastic electrical tape secured the connecting wires on each side of the collar. The completed bridge was coated with a polyurethan preparation[3].

Assembly of Dosator with Instrumented Piston—The dosator was assembled in the same manner as an original piston. The retracting spring was fitted over the lower and middle shanks of the piston, coming to rest

[2] Type EA-06-125TF-120, MicroMeasurements, Romulus, MI 48174.
[3] M-Coat A, MicroMeasurements, Romulus, MI 48174.

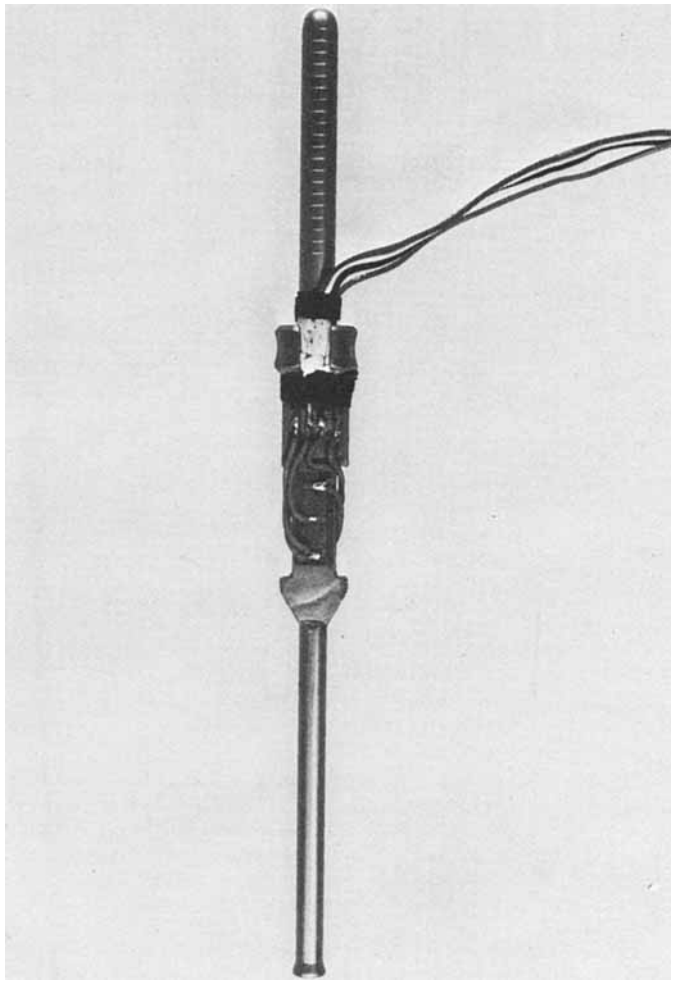

Figure 2—*Overall view of instrumented piston.*

against the lower edge of the collar. The spring and piston were then inserted into the dosator tube. The piston was then manually pushed below the adjusting rings, the cross bar was inserted through the collar, and the set screw was tightened.

The adjusting rings thread onto the outside of the dosing tube. The ends of the cross bar in the collar of the piston protrude from the dosing tube through slots, cut on a quarter-turn, extending most of the threaded length of the dosing tube. Since the rings function as a stop for the cross bar, the position of the adjusting rings determines the piston height. Thus, as the piston is pushed downward, it is caused to rotate a quarter-turn (or less, depending on the initial piston height) counterclockwise and then clockwise to its original position upon retraction. Since the connecting wire from the terminal strip through the groove in the collar was also wrapped counterclockwise, the piston unwraps the wire slightly as it descends and recoils the wire as it is retracted. In this manner, the required length of wire inside the dosing tube is held as compactly as possible to avoid damage.

To facilitate the installation and removal of the instrumented piston, one of the quarter-turn slots was continued vertically by making a cut in the dosing tube. This modification enabled the connecting wires to pass freely through the side of the dosing tube. This modification was the *only* permanent one made in the capsule filling machine.

The connecting wire was then supported at the upper end of the dosing tube by an auxiliary set of adjusting rings and a wire brace. The wire brace around the dosing tube was held securely by tightening the rings, one on either side of the brace. A cap, which centers the upper shank of the piston, was then screwed in the top of the dosing tube. The assembled dosator was then mounted, with the filling head, to the dosator arm.

The completed assembly is depicted in Fig. 4. The graduated shank of the piston (A) can be seen projecting from the dosator (B) mounted to the dosator arm (C). As the cable passes through the quarter-turn slot in the dosator, it is supported by the wire brace (D).

Mercury Contact Swivel—One problem inherent in the instru-

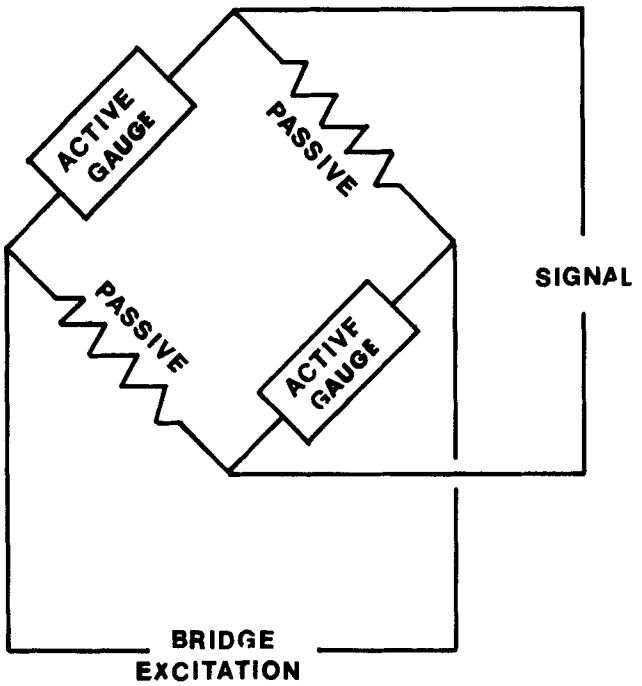

Figure 3—*Diagram of Wheatstone bridge circuit for the instrumented piston.*

mentation of this capsule filling machine was that the dosator arm, carrying the instrumented dosator, continuously rotated through 360°. To prevent the continuous twisting of the connecting cable, it was necessary to interpose a slip ring or swivel between the instrumented dosator and monitoring equipment. A mercury contact swivel[4] was selected in lieu of the usual mechanical type to minimize the possibility of noise in the output.

Figure 4 shows the swivel (E) mounted on the bracket (F) fashioned from 0.48-mm thick, 3003-H14 aluminum. The bracket is bolted to the machine by the existing mounting bolts of the capsule hopper. The swivel is supported by the bracket level with the top of the capsule hopper and directly over the dosator arm.

The swivel consists of a stationary plate and a rotating wheel. The upper cable connects the stationary plate to the monitoring equipment. The lower cable connects the piston with the wheel, which moves freely with the rotation of the dosator. Electrical continuity is maintained through the swivel by means of platinum-tipped electrodes, mounted on the stationary plate, which dip into mercury-filled annular canals cut into the rotating wheel. Additional electrodes passing through the bottom of each canal are connected to a standard connector by wires passing through the hollow axle of the swivel. Figure 4 shows the lower cable extending from the dosator to the standard connector.

Since the dosator arm not only rotates but also moves up and down to position the dosator, slack must be provided in the cable between the dosator and the swivel. To prevent the slackened cable from being snagged by the compression and/or ejection knobs, a wire guide was fashioned and mounted, using existing bolts, to the compression–ejection arm (Fig. 4G).

The compression and ejection events, detected by the instrumented piston, are monitored by measuring the bridge unbalance voltage using a carrier preamplifier[5], which also serves to activate the bridge. The compression and ejection events are recorded continuously on an oscillographic recorder[6] or displayed on an oscilloscope[7].

Calibration of Piston—Calibration was necessary to convert microstrains to kilograms of force. The associated monitoring equipment was capable of directly measuring the strain on the gauges during compression and ejection. The instrumented piston was calibrated statically by applying known loads to the piston in a physical testing machine[8].

Two trials were run, and the observed microstrain readings, resulting from the applied loads, were noted (Table I). Linear regression analysis, using data from both trials, revealed excellent linearity over the range of forces tested (correlation coefficient = 0.999). The slope was 3.96 microstrains/kg. The internal calibration of the recording system, determined by the gauge factor and the gain set on the galvanometer pen, set each millimeter of deflection equal to 1.60 microstrains. Dividing the internal calibration factor by the slope of the regression line resulted in the calibration factor of 0.404 kg/mm for this system.

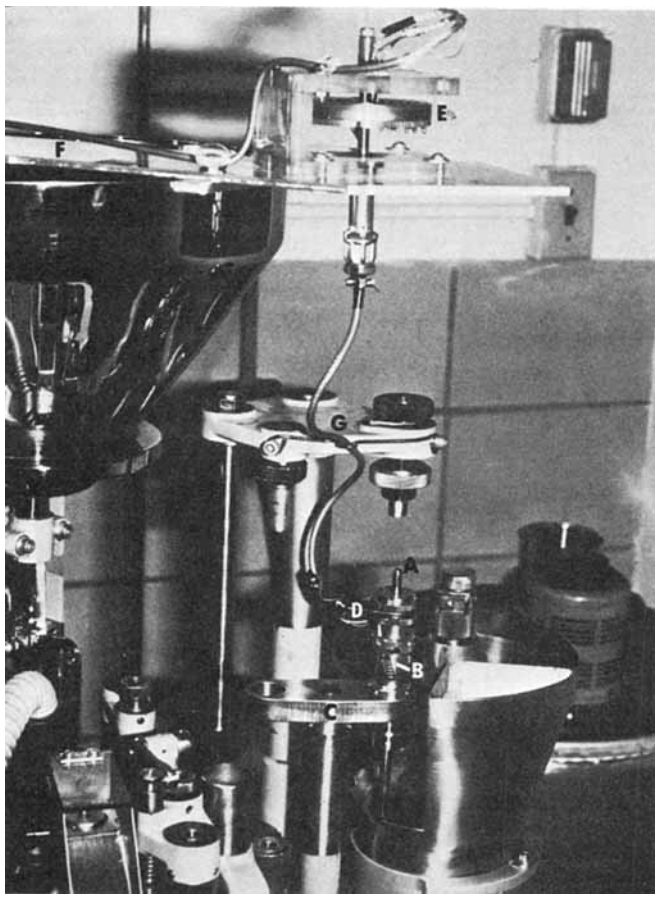

Figure 4—*Perspective view of instrumented dosator, cable, and swivel. Key: A, piston; B, dosator; C, dosator arm; D, wire brace; E, mercury contact swivel; F, swivel bracket; and G, compression–ejection arm.*

Alternate Feeding of Capsule Shells—Since the same dosator was used to monitor both compression and ejection, only one dosator was instrumented. This procedure also eliminated errors that could occur because of possible differences in piston height adjustment. This filling machine was designed to operate with two dosators in place. Thus, for every capsule that was filled, the machine ejected one empty capsule that had gone through the filling cycle but had not been filled because of the missing dosator.

This procedure presented a number of problems. The empty capsules had to be manually separated from the filled capsules for economic reasons and simply for ease of handling the filled capsules for further study. However, even when the capsules were separated, they risked being contaminated by the formulation used. Furthermore, damage to the capsule may have occurred during a previous run, which could cause the machine to stop during a subsequent run.

To eliminate these problems, a means to feed the capsules alternately into the filling cycle was devised. A standard 120-v solenoid[9] (Fig. 5A) was mounted and connected to the rod (Fig. 5B) controlling the position of the metal shoulder (Fig. 5C), which lifts the rocker arm assembly to allow one capsule to feed into the turntable bushings. Again, mounting was accomplished using existing hardware. The solenoid, energized by house current, was connected in series with a microswitch mounted on the support rod of the orientating block so that the lever of the microswitch rode on the edge of the turntable.

When the lever was tripped, the solenoid was activated to retract the

[4] Technical Concepts, Bronx, NY 14063.
[5] Model 8805A, Hewlett-Packard, Palo Alto, CA 94306.
[6] Model 7702B, Hewlett-Packard, Palo Alto, CA 94306.
[7] Oscilloscope system 5103N, Tektronix, Beaverton, OR 97005.
[8] Instron model TM-M, load cell CCTM, Instron Corp., Canton, Mass.
[9] Trible's and Associates, Baltimore, Md.

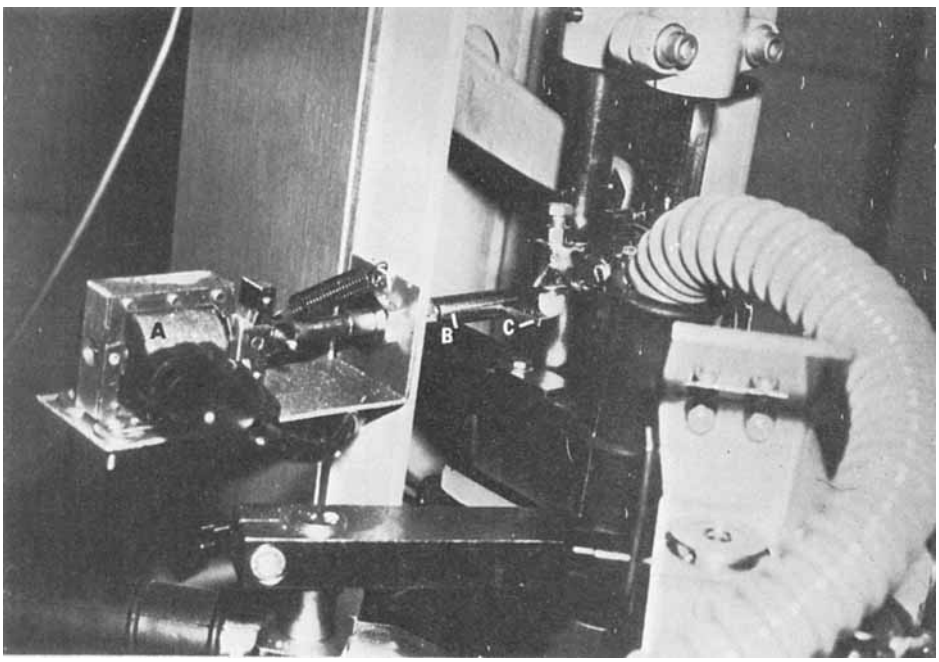

Figure 5—*Solenoid mechanism for alternate capsule feed. Key: A, solenoid; B, rod; and C, metal shoulder.*

metal shoulder, thereby preventing capsule feed. The tripping of the microswitch was timed so that omission of a capsule feed coincided with the missing dosator cycle by causing the lever to ride over hex nuts strategically fixed to the turntable edge. A return spring caused the metal shoulder to return to its original position, which permitted capsule feed for the instrumented dosator.

Preliminary Experience with Instrumentation System—To evaluate the system and to obtain force–time traces, No. 1 capsules were filled with representative fillers. The fillers were microcrystalline cellulose[10] NF, lactose[11] USP, pregelatinized starch[12] USP (compressible starch), and dibasic calcium phosphate[13] NF (unmilled). Fifteen hundred-gram batches of these materials were lubricated with 0.5% magnesium stearate[14], 80 mesh, by mixing in a twin-shell blender[15] for 15 min. The intensifier bar was run during the final 2 min to ensure efficient distribution of the lubricant. Abbreviated runs with unlubricated materials were also made.

The two piece star-wheel, which rotates at the bottom of the hopper, was adjusted to yield the maximum powder bed height of 49.4 mm. This was the height of the bed into which the dosators dipped. Then, with the star-wheel rotating and the dosators removed, powder was gradually added and allowed to come to an equilibrium bulk density at a hopper reservoir powder height of 25 mm. To prevent any possible change in powder bulk density due to changes in reservoir powder weight, care was taken to maintain this reservoir bed height to within approximately ±12 mm during all runs.

The dosator was then fitted to the dosator arm, and the instrumented piston was set to a height of 18.7 mm. This piston height, representing a setting of 9.5 graduated divisions on the upper shank of the piston, was the highest setting that would allow the apparent complete fill of the capsule at zero compaction at the maximum powder bed height regardless of the material being filled. The powder bed height and piston height were then kept constant throughout the evaluation.

The Zanasi filling principle includes compression of the dosed powder prior to ejection into the capsule. The degree of compression or the compaction level is controlled by the extent of displacement of the piston. This, in turn, is regulated by the length of the compression knob located on the compression–ejection arm. The length of the compression knob was adjusted such that it just touched the tip of the upper shank of the piston when the compression–ejection arm was at the lowest point of its downward stroke. At this setting, no displacement of the piston would occur for this piston height. This setting was taken to be the zero reference for compaction. Batches were run first at this setting and then, starting from this point, at knob length increments of 1.27 mm until the final free displacement of the piston was 6.35 mm.

Free displacement is, however, a theoretical displacement because, under filling conditions, the piston may or may not actually be displaced the full adjusted distance due to an overload relief mechanism. Much like the overload mechanism in a rotary tablet press, the compression knob is equipped with a spring in its support to prevent damage to the machine. Care was taken not to exceed the limits of this system.

DISCUSSION

Analysis of Force–Time Trace—Study of the force–time trace yields information about the forces generated during the filling cycle and the

Table I—Calibration of Instrumented Piston

Trial 1		Trial 2	
Applied Load, kg	Resulting Strain, microstrains	Applied Load, kg	Resulting Strain, microstrains
0	0	0	0
1.0	4.0	1.0	4.0
2.0	8.0	2.0	8.0
4.0	16.0	3.0	11.0
5.0	20.0	4.0	15.0
8.0	32.0	5.0	20.0
10.	40.0	6.0	24.0
15	60.0	7.0	27.0
20.	80.0	8.0	32.0
25	99.0	9.0	36.0
30.	119	10.	40.0
35	136	12	48.0
40.	158	15	60.0
45	179	18	72.0
50.	199	20.	80.0
		25	99.0
		30.	118
		35	135
		40.	156
		45	178
		50.	197
		60.	235
		70.	279
		75	299

Correlation coefficient = 0.999
Intercept = −0.0352 microstrain
Slope = 3.96 microstrains/kg

[10] Avicel PH101, FMC Corp., American Viscose Division, Marcus Hook, PA 19061.
[11] Fast Flo, Foremost Dairies, San Francisco, CA 94104.
[12] StaRx 1500, A. E. Staley Manufacturing Co., Decatur, Ill.
[13] Stauffer Chemical Co., Industrial Chemical Division, Westport, CT 06880.
[14] Ruger Chemical Co., Irvington-on-Hudson, NY.
[15] Liquid solids blender P-K LB5695, Patterson-Kelly Co., East Stroudsburg, Pa.

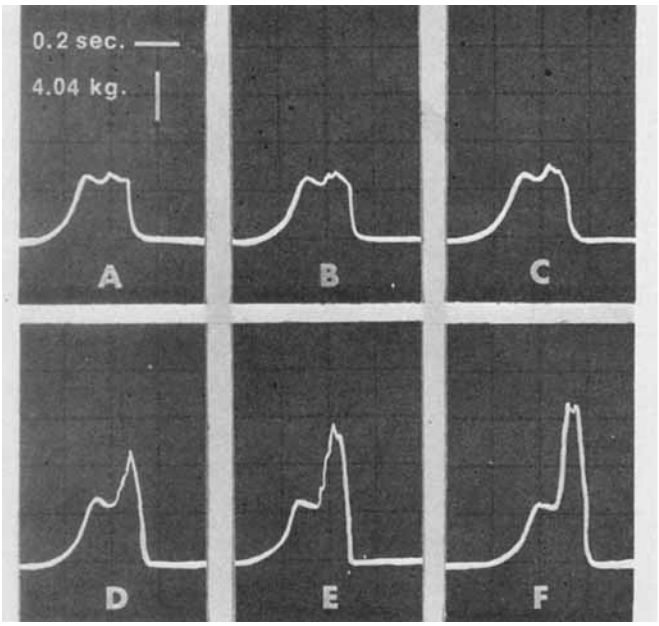

Figure 6—*Progressive changes in the force–time trace of lubricated microcrystalline cellulose.*

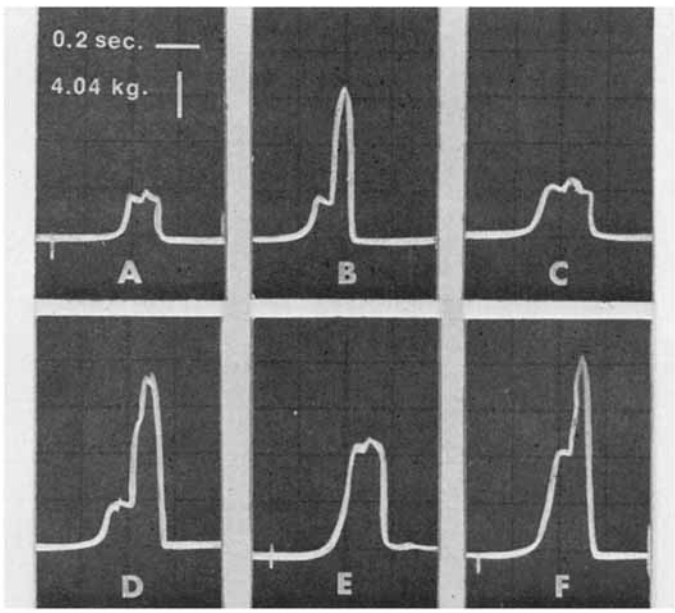

Figure 7—*Contrast of force–time traces of three materials (lactose, A and B; compressible starch, C and D; and dibasic calcium phosphate, E and F) at 0- (A, C, and E) and 6.35- (B, D, and F) mm compaction levels.*

sequence in which these forces occur. Figure 6 is a composite of single-compression force tracings of microcrystalline cellulose containing 0.5% magnesium stearate. Tracing A represents no compaction due to piston displacement (zero compaction level); tracings B–F represent the force trace changes as a result of continually increasing the compaction level with all other factors being held constant.

As the dosator dips into the powder bed, no force is recorded until the dosator penetrates the powder bed to a depth equal to the piston height. However, as the dosator continues its downward stroke, a force begins to be recorded and builds to a maximum at the maximum penetration of the filling head into the powder bed. At zero compaction level, this "precompression" force remains until the dosator is withdrawn from the powder bed (Fig. 6A). Since the powder bed height is greater than the piston height, it follows that the volume of powder sectioned by the filling head during the downward stroke of the dosing unit be either displaced or compressed into the adjusted volume of the filling head, resulting in the precompression force.

The pulse that appears to separate the wave form in Fig. 6A is not attributable to actual compression by the piston. This pulse coincides with the downward stroke of the compression–ejection arm which, when the compression knob is so adjusted, would ordinarily cause the piston to compress the sectioned powder. Because of the mechanical linkage between the compression–ejection arm and the dosator arm, some slight downward motion takes place in the dosator arm as the compression–ejection arm is in its lowest downward travel. Thus, the complete dosator unit essentially acts to compress the powder slightly at an adjusted zero compaction level.

As the compaction level increases, the second half of the trace begins to rise. This increase in compression force reflects the actual compression of the powder in the filling head. The rise in compression, to a maximum of 12.9 kg of force, is shown in Figs. 6B–6F.

The precompression force decays slightly in every case. After the dosator penetrates the powder bed and the precompression force is generated, there is a lag time (about 0.1 sec) that represents the travel time of the compression knob to the piston. During this period, the compressed powder probably undergoes some rearrangement or slight displacement of powder between the lower end of the filling head and the floor of the powder hopper.

Some slight decay also occurs in the compression part of the trace (Figs. 6D and 6E) during the short, but finite, dwell time of the maximum compressive force. As the compression knob lifts, the spring retracts the piston and the force trace drops rapidly to the zero baseline.

Figure 6F, for microcrystalline cellulose, and Figs. 7B, 7D, and 7F, for lactose, compressible starch, and dibasic calcium phosphate, respectively, depict the force responses generated by a constant piston displacement or compression of 6.35 mm. An evaluation of these tracings reveals the following decreasing order of compression forces developed under these circumstances: dibasic calcium phosphate, 16.2 kg; compressible starch, 14.8 kg; lactose, 13.3 kg; and microcrystalline cellulose, 12.9 kg.

These differences are, no doubt, due to differences in initial packing densities as well as to differences in the relative ability of these substances to undergo further consolidation and voids reduction under the present experimental conditions. As previously noted, all samples were allowed to reach their own characteristic equilibrium packing density (due to the agitation induced by the star-wheel) at the same powder bed height prior to capsule filling. Under these relatively low compressive forces, such consolidation is likely mainly due to particle rearrangement with only slight elastic and/or permanent deformation.

Regardless of the material, all force tracings resemble one another in these runs. Also, all lubricated batches exhibit barely measurable ejection forces of less than 1 kg. This finding is surprising in view of the fact that these batches employ only 0.5% magnesium stearate. Stoyle (8), for instance, empirically determined lubricant requirements of up to 3% magnesium stearate for running lactose in a larger model of the same type of machine. Although there were no indications of poor lubrication in the small batches run here, lubrication requirements possibly would be greater under the stress conditions of a full-scale production run. For a given compression force, longer slug lengths may also increase lubrication requirements due to the increased area of contact with the filling tube.

Cole and May (5) made no mention of the compaction adjustment in their report, although the Zanasi filling principle clearly is based on the compaction of the slug prior to positioning over the capsule body. Also, the tracings published by Cole and May did not reflect the two stages, precompression and compression, as presented in this work.

Unlubricated Materials—The effect of varying levels of lubricant on the ejection force was not an objective of this work. However, the force–time traces of unlubricated materials were considered important, particularly since two fillers, microcrystalline cellulose and compressible starch, are self-lubricating when used alone as tablet fillers (9, 10). The force–time traces of these two materials are shown in Fig. 8. The compression event precedes ejection. The occasional small spikes appearing between the compression and ejection events are due to the cycling solenoid.

Figure 8A shows the usual compression trace (compression force = 9.7 kg) and the ejection event (ejection force = 5.5 kg) of microcrystalline cellulose. This trace contrasts markedly with the trace for the compressible starch (Fig. 8B), which exhibits a retention force (positive deflection of trace above baseline between compression and ejection) and a negative deflection just after ejection. Similar findings were reported by Cole and May (6).

The retention force noted in the unlubricated starch run (Fig. 8B) indicates a residual pressure on the end of the piston as the slug is trans-

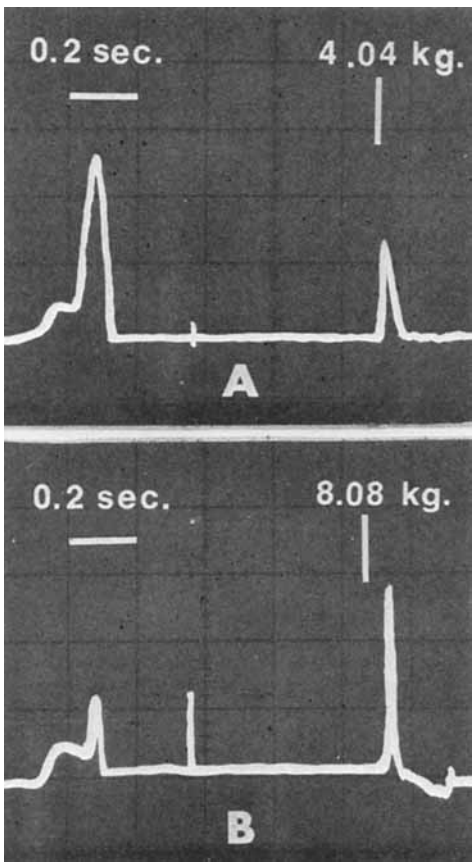

Figure 8—*Force–time traces of unlubricated materials. Key: A, microcrystalline cellulose; and B, compressible starch.*

ported to be ejected, possibly due to elastic rebound of the slug against the piston. This phenomenon occurs not only with compressible starch but also with unlubricated microcrystalline cellulose and lactose when run under conditions of relatively low compression force (*i.e.*, low powder bed heights and zero or low compaction levels). Apparently, under these conditions, bonding within the slug is insufficient to prevent expansion against the piston. However, unlubricated starch also produces a retention force when compressed at the maximum powder bed height and/or with a high compression force. This result is possibly due to a high modulus of elasticity in the case of starch. Lubricants presumably allow the slug to slip to relieve the residual pressure; this phenomenon was not observed in any lubricated run.

The negative deflection following ejection in Fig. 8B indicates tension on the piston as it is being retracted. A similar observation was reported by Cole and May (6), who suggested that this tension is likely to be caused by the adherence of material between the wall of the filling head and the piston. Under such circumstances, binding of the piston would be expected to occur, thereby leading to tension on the piston as it is being retracted by the spring. In the present study, particle adherence was observed in such cases, particularly on the piston. A similar phenomenon in tableting gives rise to a lower punch pulldown force (11).

Extreme care was taken when running unlubricated lactose and basic dicalcium phosphate. Very high ejection forces (up to 30 kg) developed after only 20–30 capsules had been filled, and the runs were terminated to prevent possible damage to the machine.

REFERENCES

(1) P. E. Wray, J. G. Vincent, F. W. Moller, and G. J. Jackson, presented at the Industrial Pharmacy Section, APhA Academy of Pharmaceutical Sciences, Dallas meeting, Apr. 1966.

(2) K. Marshall, presented at the Industrial Pharmaceutical Technology Section, APhA Academy of Pharmaceutical Sciences, Cherry Hill, N.J., meeting, 1972.

(3) E. L. Knoechel, C. C. Sperry, and C. J. Lintner, *J. Pharm. Sci.*, **56,** 116 (1967).

(4) A. M. Salpekar, Ph.D. thesis, University of Maryland, Baltimore, Md., 1975.

(5) G. C. Cole and G. May, *J. Pharm. Pharmacol., Suppl.*, **24,** 122P (1972).

(6) G. C. Cole and G. May, *J. Pharm. Pharmacol.*, **27,** 353 (1975).

(7) "Strain Gage Installations with M-Bond 200 Adhesive," Micro-Measurements, Instruction Bulletin B-127-4, Romulus, Mich., June 1974.

(8) L. E. Stoyle, Jr., presented at the Industrial Pharmacy Section, APhA Academy of Pharmaceutical Sciences, Dallas meeting, Apr. 1966.

(9) C. D. Fox, M. D. Richman, G. E. Reier, and R. F. Shangraw, *Drug Cosmet. Ind.*, **92,** 161 (1963).

(10) K. W. Manudhane, A. M. Contractor, H. Y. Kim, and R. F. Shangraw, *J. Pharm. Sci.*, **58,** 616 (1969).

(11) F. W. Goodhart, M. Gustavo, and F. C. Ninger, *ibid.*, **58,** 248 (1969).

ACKNOWLEDGMENTS AND ADDRESSES

Received February 9, 1976, from the *Department of Pharmacy (Pharmaceutics), School of Pharmacy, University of Maryland, Baltimore, MD 21201.*

Accepted for publication June 11, 1976.

Presented at the Industrial Pharmaceutical Technology Section, APhA Academy of Pharmaceutical Sciences, Atlanta meeting, November 1975.

Abstracted in part from a thesis submitted by L. E. Small to the Graduate School, University of Maryland, in partial fulfillment of the Master of Science degree requirements.

Supported in part by General Research Support Grant 1-SO1-RR05770-01.

The authors express their appreciation to Mr. Leslie Jakab, Senior Scientist, Johnson & Johnson Research Center, for his assistance in the calibration of the instrumented piston and to Johnson & Johnson for the use of their Instron testing machine. They also thank Mr. David Beach for assistance in the design and construction of the solenoid switching mechanism.

The authors gratefully acknowledge the assistance of Mrs. Vicki Leone in the preparation of this manuscript.

ˣ To whom inquiries should be directed.

Physical Processes of Tableting

E. N. HIESTAND ˣ, J. E. WELLS, C. B. PEOT, and J. F. OCHS

Abstract □ Shear deformation was shown to occur during the decompression of large compacts made by nonisostatic compression. Some materials undergo fracture when these shear stresses are developed. Other materials withstand these stresses but fracture upon ejection when the stress concentrations at the edge of the die are large. Failure to fracture seems to be related to the ability to relieve stresses by plastic deformation. A test was devised to measure this property, called the brittle fracture propensity.

Keyphrases □ Tablet formation—fracture caused by shear stresses during decompression, effect of plastic deformation □ Dosage forms—tablets, fracture caused by shear stresses during decompression, effect of plastic deformation □ Plastic deformation—effect on tablet fracture caused by shear stresses during decompression

It is generally accepted that compact formation by pressure occurs because of forces acting at the areas of true interparticle contact. However, the failure to obtain an intact compact from the compression–decompression cycle is a bit more mysterious. A series of arguments and some supporting evidence indicate that the stresses induced by elastic rebound and the associated deformation processes during decompression are principally responsible for the success or failure of compact formation. This report presents experimental results obtained by using several, sometimes complementary procedures. These data support the shift of emphasis to the decompression process.

To present a coherent, conceptual thesis, the discussion of each individual experimental procedure is not comprehensive. Instead, the emphasis is on the contribution of the results to the total concept. Bits are taken from various on-going research investigations. Cumulatively, these studies, even though incomplete, contribute much to the evidence.

Under high compression pressures, the powder particles in a compact are forced into intimate contact, and extensive areas of true contact between particles are formed. Because the magnitude of van der Waals forces across these interfaces is adequate to provide strong bonds, one might expect all materials to form strong, intact compacts after being subjected to compression. However, if too much energy is stored elastically when under compression, the elastic recovery during decompression may break most of these bonds and a soft, crumbly compact will be formed. Excipients are added to most pharmaceutical formulations to compensate for inherent, undesirable properties of the medicament. For example, it is possible to eliminate the storage of excess elastic energy during compression by mixing a plastic excipient with the harder "elastic" material. The plastic material will permanently deform and establish large, true contact areas with the harder material and will do so at relatively low pressures. Thus, during recovery, the stored elastic energy will be inadequate to separate extensive areas of contact, and strong bonding will result.

Even though these statements are reasonable explanations of many observations, every tablet formulator knows that they are inadequate. Often a laminated compact is produced. The individual pieces are dense, strongly bonded fragments. Therefore, sufficient areas of true contact must form during compression; in general, these areas are not destroyed during the elastic recovery, even though those in the fracture plane are destroyed. Thus, the mechanism of fracture is different from that of the formation of a crumbly tablet. Both are believed to result from inadequate plastic flow. A much more detailed look at compression and decompression is necessary to explain the compaction properties of materials and the fracture phenomenon.

EXPERIMENTAL

Tablet Compression—Many of the tablets used were made in a hand press. A square die was used. The cross section of the faces of the punches was 38.1 mm on a side. The tablet compression force was applied by placing the assembly, with punches in place, into an 18-metric ton hydraulic press[1]. The hand press could be pumped manually or by a motor-driven external cylinder to obtain the desired compression force. Both the punch and die had inserts containing diaphram-type strain gauges on the end of a screw[2]. One gauge was flush with the face of the die, and the other gauge was flush with the face of the punch and centered in it.

In one mode of operation, the output from the gauges was coupled at the y-input of an x–y recorder through a switching circuit that converts the recorder into a two-channel input on the y-axis. Calibration was made by placing a square rubber plug into the die and compressing it with known force. At low pressures, a rubber bag filled with water was used in a similar manner.

The known total force on the punches was obtained from a load cell[3] mounted on the press. The load cell was calibrated by applying a dead weight to check the supplier's calibration. Its output could be coupled to the x-input of the x–y recorder. Thus, it was possible to record simultaneously the total applied force, a local punch face pressure, and a local die wall pressure throughout the entire compression–decompression cycle.

An alternative mode of operation was to monitor the output of the load cell on a voltmeter[4] and to couple the die wall gauge to the y-axis and the punch gauge to the x-axis of the recorder.

In addition to the plain punch and an instrumented one, a special punch was made which contained at its center a spring-loaded, retractable pin 1.09 mm in diameter. This punch was used to form the tablet with a center hole to be used in the brittle fracture propensity determination.

The rotary tableting machine used in the lamination study was an instrumented (1) 16-station press[5]. A direct compaction formulation[6], selected to produce desired levels of lamination, was used. Dies and punches (extra deep cup 12.7 mm diameter) were used in the major study. Flat punches were used only to demonstrate the effect of punch shape. To obtain the data on fracture conditions, the precompression force and speeds were selected arbitrarily, with the final compression increased stepwise until lamination or capping occurred.

Tensile Strength—The tensile strength measurements were made by the transverse compression of square compacts. The procedure and apparatus were described previously (2). Since the hydraulic pressure

[1] Model 341-20, Loomis Engineering and Manufacturing Co., Caldwell, N.J.
[2] Model EPS-1228S (die wall) and model EPS-2528-1800 (punch), Entran Devices Inc., Little Falls, N.J.
[3] Model 1221-AF load cell, Interface Inc., Scottsdale, Ariz.
[4] Model 160B digital multimeter, Keithley Instruments, Cleveland, Ohio.
[5] Manesty Betapress, Manesty Machines, Ltd., Liverpool L24 9LQ, England.
[6] With the cupped punches, each tablet contained 150 mg of phenacetin (bolted), 325 mg of microcrystalline cellulose (Avicel 102), 2 mg of colloidal silicon dioxide (Cab-O-Sil), 167 mg of lactose (bolted), and 6 mg of magnesium stearate. With the flat punches, each tablet contained 150 mg of phenacetin (bolted), 221 mg of spray-dried lactose, and 39 mg of magnesium stearate.

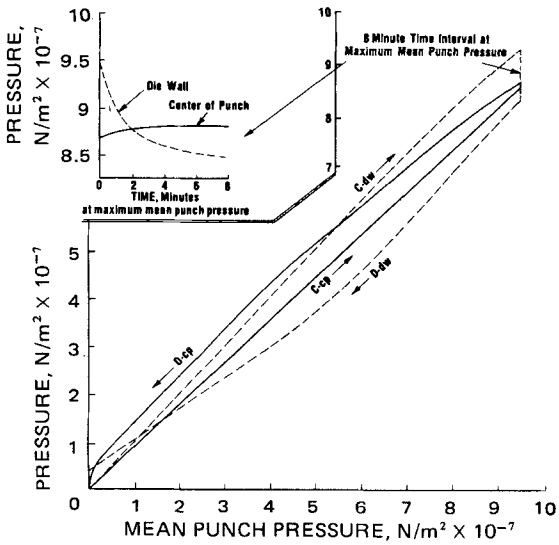

Figure 1—*Sitosterols: change of pressures at die wall and center of punch with average punch pressure during a compression–decompression cycle with a time delay at maximum pressure. Key (dashed lines): C-dw, die wall during compression; and D-dw, die wall during decompression. Key (solid lines): C-cp, center of punch during compression; and D-cp, center of punch during decompression. Insert graph shows changes with time while at maximum compression force.*

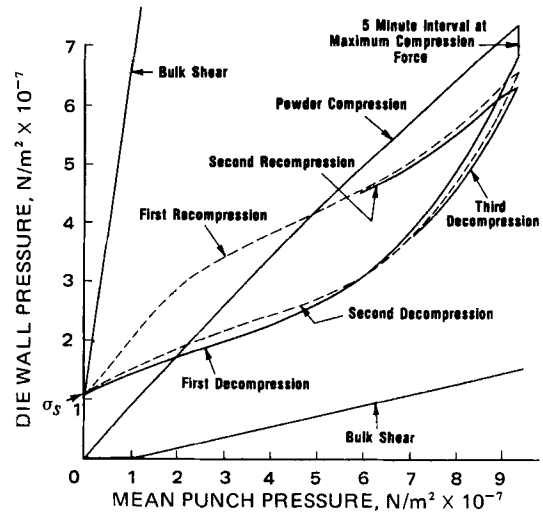

Figure 2—*Die wall* versus *average punch pressure for some compression–recompression cycles of the same sucrose compact. Constant maximum pressure was held on the punch for 5 min before the first decompression. Note that each successive recompression led to a lower maximum die wall pressure. Bulk shear lines were estimated from the uniaxial compression test, which gave* $\alpha = 67°$; σ_s *is failure stress under uniaxial compression.*

in the jack was developed by compression from an external motor-driven cylinder whose speed could be selected, the rate of stress application was controlled. This rate was not critical in experiments exploring this factor. Nevertheless, it is desirable to use a standard rate so that any time-dependent effects are reproduced, should they become important. Even though the external cylinder was driven at a constant rate, the rate of increase of force approximates an exponential curve. In the work reported herein, the rate was selected so that the time between $1/e$ of maximum force to the maximum force was 15 sec.

This apparatus also was used to determine the uniaxial compressive force required to cause a compact to shear. A 38.1-mm square compact was cut into two pieces. One-half was placed in the press with the long axis vertical. The platens covered the entire end of the compact. Blotter material was used on the platen as a pad.

A ring strain-gauge system was used to supply input to a chart recorder to observe the force at fracture. The area of the compact under the platen was calculated from measured dimensions obtained with a micrometer.

Stress Relaxation—The apparatus used by Milosovich was used in the form described by Shlanta and Milosovich (3). One addition was made—*viz.*, an oscilloscope[7] to the output. This oscilloscope permitted one to record photographically the transducer output for the first few seconds of the experiment. The output for the remaining time was recorded on a strip-chart recorder. A 12.7-mm diameter die was used in the studies done in air. The vacuum die was 13 mm in diameter. Powder weights were adjusted to give the same tablet thickness in the two dies.

Another procedure for observing stress relaxation was performed with the hand press, using the instrumented die and punch described previously. This apparatus is flexible, and various procedures may be used. In the work reported in Fig. 1, while the total force on the punch was held constant, the x–y recorder monitored the output of the strain gauges in the punch and die wall. Local pressure changes were observed at the center of the punch face while the mean pressure remained constant. With sucrose (Fig. 2), the punch gauge was not used (due to gauge failure), but the relaxation of the die wall pressure was followed. The load cell on the press indicated the total force on the punch.

Indentation Hardness—The indentation hardness values were measured using the dynamic impact method described previously (4). The chordal radius of the dent was measured with a low powered microscope. The initial and rebound heights were calculated from the arc of the pendulum movement. The indenter was a 25.4-mm diameter steel ball suspended on a 1-m long steel wire (to form the pendulum).

[7] Model B, type 202-1, Tektronix Inc., Portland, Ore.

RESULTS AND DISCUSSION

Compression—The nonisostatic compression of a powdered or granular material to produce a compact is not a simple process. The complexity arises from the numerous simultaneous internal processes that lead to consolidation and bonding. These events include particle rearrangement (consolidation), fracture, and plastic deformation. At the start of the compression, the first dominates; at the end of the compression, the third dominates. In some cases, a fourth phenomenon occurs (5, 6)—*viz.*, localized melting at the interparticle contact points. This phenomenon is believed to be important only with relatively low melting materials. Even very hard asperities are pushed into a more plastic substrate. Thus, the stresses that could produce melting of an asperity are limited by particle hardness. Particle fracture occurs when the stresses within the particles become large enough for a crack to propagate. With some materials, the particles need not fracture because the stresses are relieved by plastic deformation of the particle before their magnitude is sufficient to initiate fracture.

Except in the case of localized asperity melting, the effective area of true contact in a cross-sectional area normal to the direction of pressure application is determined by the product of the force across the plane divided by the permanent deformation pressure of the solid. For simplicity, assume that only one material is present. If the deformation pressure is a constant, then:

$$F = PA \qquad \text{(Eq. 1)}$$

where F is the applied force, P is the permanent deformation pressure of the solid, and A is the effective true contact area in the normal plane.

Therefore, under pressure, a desired maximum true contact area can be established simply by applying adequate pressure. Equation 1 gives no information about the true contact area after elastic recovery; therefore, it is not adequate to predict final compact strength.

By making some general assumptions about the maximum interatomic separation distances that permit significant contributions to bond strength and then applying the Hertz elastic contact relationships (7), it can be deduced that smaller particles should yield larger true contact areas and, thereby, stronger bond strengths. However, the results are not independent of the particle permanent deformation pressures, *i.e.*, their hardness, and hardness may vary with particle size. Furthermore, plastic deformation tends to increase the number of dislocations in a crystal; a hard crystal may first become softer and, if sufficiently "worked," may then become hard again. Thus, the magnitude of P in Eq. 1 usually is unknown. Also, particle size and shape changes may influence the packing density. Thus, speculations on the effect of particle size on tablet bond strength are at best precarious.

Theoretical approaches that use models for the summation of contact areas and forces over a cross-sectional area to obtain true contact areas

are interesting (8, 9) but have not found significant application for solving real problems. Usually, the results deviate only slightly from a linear relationship between true area and force. Unfortunately, the proportionality constant is not known; it is known that the extent of the plastic deformation influences the magnitude of the proportionality constant. Thus, P is an important parameter influencing bond strength.

A more complete description of compaction must include the effects of interparticle friction and friction with the die wall and punches. These contribute to variations of the degree of packing in the die and, therefore, cause a nonuniform density compact to be formed. The variations of density within a compact were reported by Train (10). Furthermore, the effect of die wall friction on pressure at various levels in a compact was studied and described by (11):

$$P_b = P_a \exp\left(-\frac{4L\mu\eta}{D}\right) \qquad \text{(Eq. 2)}$$

where P_a is the applied pressure (punch), P_b is the transmitted pressure at L distance from the punch, D is the diameter, μ is the coefficient of friction, and η is the ratio of radial to axial stress in the compact.

Compression involving movement of both upper and lower punches significantly reduces the density variation within a compact; however, this fact does not eliminate the problem completely. Also, the use of a lubricant and glidant to reduce both interparticle friction and friction with the surfaces of the punch and die contribute significantly to the formation of a more homogeneous compact. Usually, these agents cause an increase in the die wall pressure for a given punch pressure (12), probably because the particles compact more tightly before plastic deformation becomes the dominant consolidation process. Possibly, interparticle "wedging" occurs more easily when friction is reduced and, thereby, increases the die wall pressure.

Thus, several factors may influence the structure of a compact and the magnitude of the die wall pressure at the maximum compression force. It is not easy to establish the relative importance of each. However, a valid qualitative generalization is that when either powders or granules are compressed into a compact, regions of different relative density are produced and the die wall pressure is of higher magnitude than would result from the elastic deformation of a single piece of an isotropic solid. During decompression, this extra die wall pressure may lead to excessively large shear stresses in the compact.

It is instructive to think of plastic deformation both as a change in particle shape and as the sliding of groups of particles within the compact. This approach provides a more macroscopic perspective and is used to explain the redistribution of stresses when under compression. For example, when sitosterols were held under constant compressional force (the total punch force held constant), a localized die wall pressure decreased as a function of time and the pressure at the center of the punch increased simultaneously (Fig. 1, insert graph, which was obtained with the instrumented 38.1-mm square punch and die set). Apparently, at maximum compression, some points in the compact were stressed to the limit of their strength. Since their instantaneous or dynamic shear strength exceeded their static shear strength, internal plastic flow occurred over time to relieve some stress[8]. The center of the punch always is a lower pressure region (10), so the flow was toward the center. Thus, regional density changes occurred and the compact density became slightly less heterogeneous as a result of this macroscopic plastic flow. The rate of the process decreased sharply; thus, a totally uniform density compact did not result.

In Fig. 1, the pressures reported were local pressures known at only two small regions because the strain gauges were less than 6.35 mm in diameter; the compact was a 38.1-mm square. In the absence of better data, it is expedient to use these pressures as very rough estimates of the principal stresses for an assumed isotropic homogeneous compact. In this case, the shear stress is given by:

$$\tau = \frac{\sigma_a - \sigma_r}{2} \sin 2\alpha \qquad \text{(Eq. 3)}$$

where τ is the shear stress at angle α from the direction of the minor principal stress, σ_a is the axial or punch pressure, and σ_r is the radial or die wall pressure.

Whenever τ just exceeds the shear strength of the material, shear failure occurs. If the failure does not cause a fracture plane to develop, the failure is by plastic flow. Obviously, τ has its largest value when $\alpha = 45°$. The shear strength also is a function of the angle α; therefore, the shear strength may be exceeded at some angle greater than 45° before

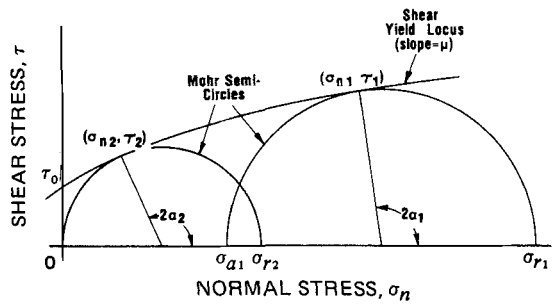

Figure 3—*Shear yield conditions based on the use of a geometric representation of stress analysis equations, a Mohr diagram. Semicircle on right (subscript 1) represents the higher pressure case when the radial pressure is less than the axial pressure. Semicircle on left (subscript 2) represents case when the axial pressure is zero and the residual die wall pressure is* σ_{r2} *(*σ_{r0} *in Eq. 6); it also could describe the uniaxial compression case. In Eq. 5, the yield locus is assumed to be a straight line and* μ *is a constant.*

it is exceeded at $\alpha = 45°$. For a Mohr body, the shear strength is assumed to be a nearly linear function of the compressive stress normal to the shear plane. The normal stress, σ_n, is given by:

$$\sigma_n = \frac{\sigma_a + \sigma_r}{2} + \frac{\sigma_a - \sigma_r}{2} \cos 2\alpha \qquad \text{(Eq. 4)}$$

For the Mohr body, the internal friction coefficient, μ, becomes the proportionality constant for calculating the shear strength, τ_f, and for the linear case:

$$\tau_f = \mu\sigma_{nf} + \tau_0 \qquad \text{(Eq. 5)}$$

where σ_{nf} is the magnitude of the normal stress, σ_n, at failure; τ_0 is the shear strength when $\sigma_n = 0$; and μ is the internal friction coefficient and is related to α by $\mu = -\cot 2\alpha$.

Equations 3–5 are useful in providing some insight into shear failure conditions. A standard geometric representation of Eqs. 3–5 is called a Mohr diagram. Because of symmetry, only half of a Mohr diagram is shown in Fig. 3. It should be useful to use Eqs. 3–5 and the Mohr diagram to discuss shear failure in both the compression and decompression of compacts. The graphical representation of shear failure is correct only when the Mohr circle of stress is tangent to the shear failure yield locus.

Decompression—In this discussion, it is assumed that adequate compressional force was applied to produce densification and bonding; *i.e.*, crumbling from lack of adequate compression with plastic deformation will not be considered further. Even though adequate pressure is applied, the compression–decompression cycle may or may not produce an intact compact without fracture lines in it. Success is determined primarily by the internal processes that occur as the compression stresses are removed. These processes include both removal of punch pressure and ejection from the die.

Powder under compression in a cylindrical die is confined in a radial direction until ejected from the die. Therefore, the major dimensional change during decompression is in the axial direction. Of course, the same is true for recompression of the compact if it is recompressed without removal from the die. Equation 6 describes the stresses associated with elastic deformation of an isotropic solid when the strain in the radial direction is zero:

$$\sigma_r - \sigma_{r0} = \frac{\nu}{1 - \nu} \sigma_a \qquad \text{(Eq. 6)}$$

where ν is the Poisson ratio[9], and σ_{r0} is the die wall pressure intercept value.

The residual die wall pressure, σ_{r0}, would be zero if the compression of an isotropic solid is started with a confined, but unstressed, solid body. If only elastic deformation occurred during compression and decompression, σ_{r0} would remain zero. When one starts with a powder, a finite residual die wall pressure is always observed after completion of the compression–decompression cycle. Obviously, if the compact undergoes shear deformation in both recompression and decompression, gross deviations from the elastic case would be expected and Eq. 6 would not be applicable. (Later, it will become obvious that Eq. 6 is not applicable

[8] This viscoelastic flow is believed to result from random thermal fluctuations breaking prestressed bonds.

[9] The Poisson ratio is defined as the transverse expansion per unit dimension of a solid of uniform cross section to its contraction per unit length when subjected to a uniaxial compressive stress (during elastic deformation).

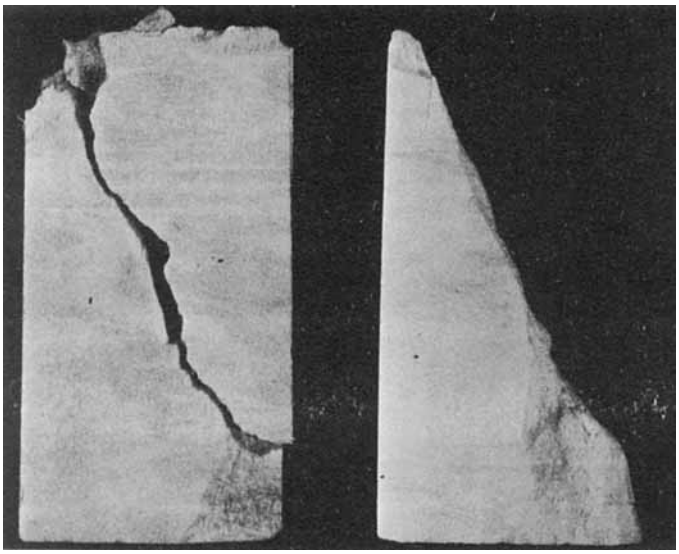

Figure 4—*Sucrose compact fractured in shear under uniaxial compressive stress of 1.1 × 10⁷ N/m². Compact was compressed at 9.2 × 10⁷ N/m². Fracture plane was irregular so value of α was not precise. With various compacts, values ranged from 64 to 67°.*

during the decompression process.) Others (13, 14) considered the possibility of plastic deformation during decompression but approached the subject differently than will be done in the following discussion.

To describe the magnitudes of the die wall and punch pressures that would cause the compact to fail in shear, the following equations are developed. Taking derivatives of Eqs. 3 and 4 with respect to σ_r and combining to obtain $d\tau_f/d\sigma_{rf}$ yield:

$$\frac{d\tau_f}{d\sigma_{nf}} = \frac{\left(\frac{d\sigma_{af}}{d\sigma_{rf}} - 1\right)\sin^2 2\alpha_f + 2(\sigma_{af} - \sigma_{rf})\frac{d\alpha_f}{d\sigma_{rf}}}{\left(\frac{d\sigma_{af}}{d\sigma_{rf}} + 1\right)\cos 2\alpha_f + \left(\frac{d\sigma_{af}}{d\sigma_{rf}} - 1\right)\cos^2 2\alpha_f - 2(\sigma_{af} - \sigma_{rf})\frac{d\alpha_f}{d\sigma_{rf}}} \cot 2\alpha_f \qquad \text{(Eq. 7)}$$

The subscript f was added to indicate a condition of failure.

By definition:

$$\frac{d\tau_f}{d\sigma_{nf}} = \mu = -\cot 2\alpha \qquad \text{(Eq. 8)}$$

Combining Eqs. 7 and 8 gives:

$$\frac{d\sigma_{af}}{d\sigma_{rf}} = \frac{1 - \cos 2\alpha}{1 + \cos 2\alpha} = \frac{\sqrt{1+\mu^2} + 1}{\sqrt{1+\mu^2} - 1} \qquad \text{(Eq. 9)}$$

Equation 9 permits the estimation of the limiting stresses beyond which shear occurs once μ or an equivalent value has been determined. While μ may not be a constant, large variations are not expected as long as only compressive stresses are used.

At least in theory, the uniaxial compression of a compact should provide the necessary data for use of Eq. 9. For this experiment, a large square compact was cut into two equal pieces and a compressive stress was applied along its long axis until it fractured. If both the fracture angle, α, and the compressive stress at fracture can be measured, Eqs. 8 and 9 can be evaluated. Figure 4 shows a sucrose compact fractured under uniaxial stress; the magnitude of the observed fracture stress is plotted on Fig. 2 (point σ_s). The irregular fracture line shown in Fig. 4 makes an accurate evaluation difficult. Compacts of most materials are even less satisfactory because of laminations and other aberrant fracture planes.

The two bulk shear lines in Fig. 2 have slopes calculated by Eq. 9 using the uniaxial compression data. Both α and μ were taken as constants; hence, straight lines are shown. These lines cross the axis at the uniaxial compression stress for fracture. The slopes of the two lines are reciprocals of each other; the distinction between σ_{af} and σ_{rf} in Eq. 9 is artificial; *i.e.*, it does not matter which is larger, only the difference is important. As is obvious in Fig. 2, these lines do not correspond to the experimental range of σ_{rf} *versus* σ_{af}. While this finding suggests that the experimental compression–decompression stresses are within the elastic limits of the material, further examination, such as of the data in Fig. 5, indicates that shear is occurring in the regions between these lines.

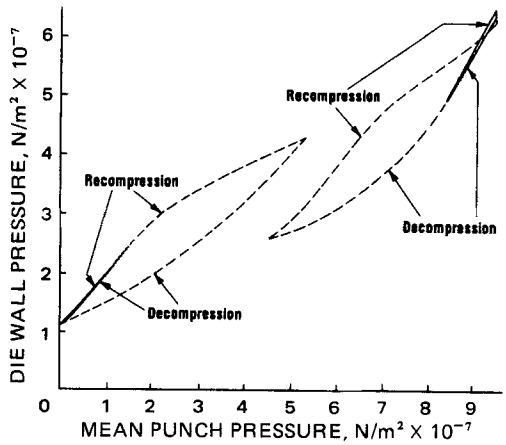

Figure 5—*Sucrose compact compressed as in Fig. 2 but recompression–decompression cycles were partials. Key: solid lines on left, recompression–decompression over very limited range of pressure; dashed lines on left, recompression–decompression cycle extended into decreasing slope region; solid lines on right, decompression–recompression cycle over limited range of pressures but starting from maximum values; and dashed lines on right, decompression–recompression cycle extended into decreasing slope region. Loops are believed to indicate that plastic deformation occurred at local points. Very small loops with solid lines may be due to friction resisting punch movement.*

The uniaxial fracture stress is an estimate of the magnitude of the die wall pressure at failure when the punch pressure is zero and vice versa. Figure 2 shows data for die wall *versus* punch pressures obtained for compression–decompression cycles using sucrose. The die wall pressure is that measured at the center of one side of a square compact. The punch pressure is the mean value based on the total force applied to the punch. When the punch pressure went to zero, the die wall pressure became identical to the uniaxial compressive strength, σ_s. Obviously, the shear strength limited the residual die wall pressure. This value remained essentially constant even after repeated recompression cycles.

The shapes of the decompression plot reported here are very different from those reported by Leigh *et al.* (13) and Carless and Leigh (14). Possibly, the differences arise from differences in the procedure and instrumentation. Those investigators measured total die wall force and not local pressures. Furthermore, the present apparatus is very rigid; *i.e.*, the entire die expands very little under pressure. Other differences are size and shape of compacts and the rate of compression and decompression. When Poisson ratios are calculated from the data reported here, unrealistically large values are obtained. Thus, the data measured at separated regions of the compact surface do not seem to be representative of a single, small volume element. However, the theoretical arguments developed from these data do not depend on the exact shape of the die wall *versus* punch pressure plot.

Upon recompression followed by decompression, as was done to obtain the data in Fig. 2, a "hysteresis" type of loop is formed. If the compression–decompression involves only elastic deformation, the compression–decompression pathway should be identical. Therefore, plastic deformation must be occurring during each recompression–decompression cycle. Partial recompression–decompression cycles are even more revealing (Fig. 5). If the recompression pressure is limited to a value below the first bend, the decompression line from that point superimposes onto the compression line (solid lines on the left of Fig. 5). However, when the recompression pressure is increased to a point beyond the first bend, a loop is formed upon decompression. Apparently, the first portion of the recompression curve represents elastic deformation while larger compression forces introduce plastic deformation.

Results of a similar experiment at the start of the decompression is shown on the right side of Fig. 5. If the decompression from maximum applied force is stopped short of the first bend, recompression from that point retraces essentially the same line. (A slight deviation occurs, possibly due to friction.) Therefore, the first part of the decompression is an elastic deformation. However, if the decompression is stopped at a pressure beyond the first bend, the recompression from that point forms a loop. Therefore, shear or plastic deformation is occurring during much of the decompression.

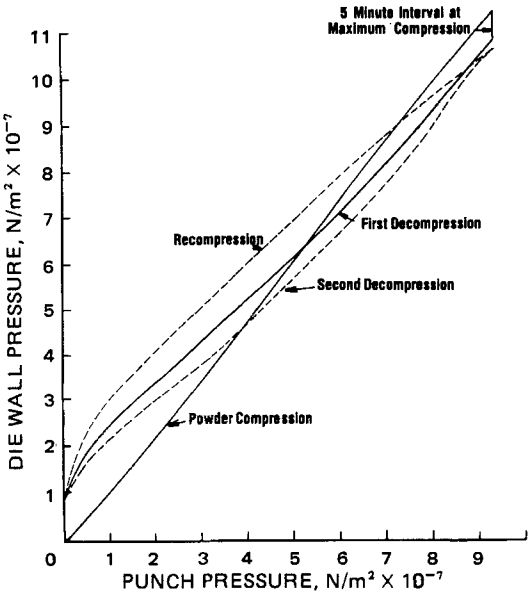

Figure 6—*Sitosterols: local die wall pressure* versus *mean punch pressure for compression–decompression cycles.*

The authors hope to equip the apparatus with a distance-measuring sensor so that the work of recompression and decompression may be determined. Certainly, the loop in Fig. 2 suggests that the work of recompression is much greater than the work done on the punch during decompression. Without a distance or volume measurement, the calculations cannot be made.

Figures 6–13 show similar results for sitosterols, spray-dried lactose, erythromycin, and sodium chloride. While differences in the detailed shapes of the curves are apparent, the general characteristics remain the same. Apparently, the previous discussion for sucrose applies equally to these materials.

Localized plastic deformation may occur at lower stresses than would be required to produce gross shear across the compact. The local shear stresses exceed the shear strength because of stress concentrations that occur around imperfections such as pores and density gradients. These internal local regions of shear may account for the apparently anelastic behavior in the recompression–decompression cycle. If localized shear occurs, the recompression–decompression cycle might not be completely reproducible, since there is no reason to expect the shapes of the stress concentrator regions that flow plastically during compression to be reconstructed in the decompression stage. Thus, it is not surprising that the observed maximum die wall pressure is less after each recompression (Fig. 2). This direction of change would be expected, since the die wall

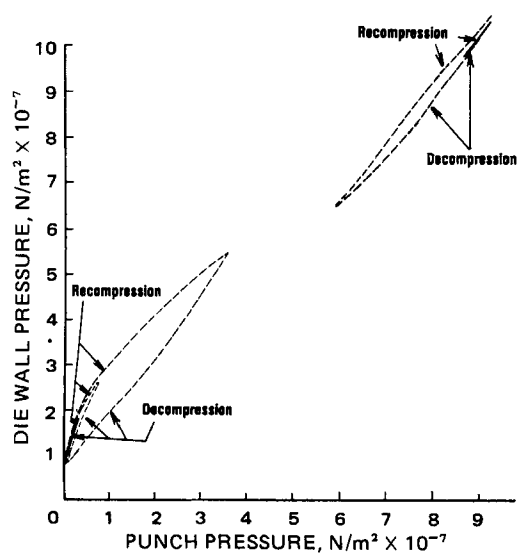

Figure 7—*Sitosterols: partial recompression–decompression cycles of a compact.*

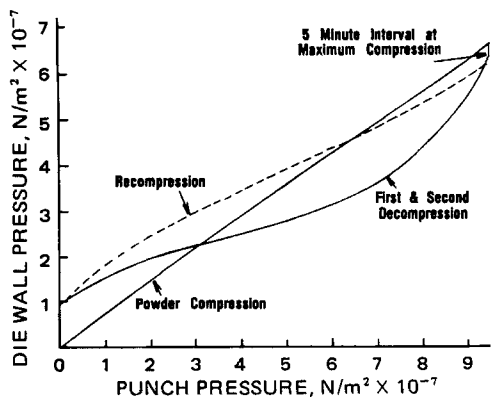

Figure 8—*Spray-dried lactose USP (hydrous): local die wall pressure* versus *mean punch pressure for compression–decompression cycles.*

pressure decreased during stress relaxation under constant punch pressure. The combined evidence of these observations and the time-dependent stress redistribution reported in Figs. 1, 2, and 14[10] strongly indicates the conclusion that local plastic deformation occurs in compacts.

Table I shows tensile strength values for compacts subjected to recompression–decompression cycling. The increase in strength that occurred with these materials is interpreted as an increase in true contact area between particles. Shear under a compressive load could produce an increased contact area. However, shear also may induce fracture, especially during decompression. Since the two processes produce opposite effects on the strength, not all materials will show the same trend. Most plastic materials, such as those used for the data in Table I, show increased strength. Figure 15 illustrates the case where the stresses during decompression led to fracture on the first decompression. Obviously, tensile strengths could not be determined. Phenacetin, methenamine, and acetaminophen, materials known to induce capping, show this kind of fracture. Apparently, these materials do not adequately relieve local stresses by plastic deformation; hence, fracture in shear occurs across the entire compact. For these materials, recompression curves are meaningless.

Brittle Fracture—The Griffith crack theory teaches that, for crack growth to occur, the energy stored at the tip of a crack must just exceed the energy required to form the two new surfaces resulting from the propagation of the crack. Also, the amount of energy stored at the tip of a crack is a function of the dimensions of the crack. An elementary description of the critical condition for crack growth is given by:

$$\sigma_c = K\sqrt{\frac{\gamma E}{L}} \qquad \text{(Eq. 10)}$$

where σ_c is the critical tensile stress for crack growth, γ is the surface energy, E is Young's modulus of elasticity, L is one-half the crack length, and K is a constant. In deriving this equation, the radius of curvature at the tip of the crack was assumed to be of molecular dimensions. The radius does not appear in Eq. 10 because it cancels against the same radius term, which occurs in the expression for the applicable stress concentration factor.

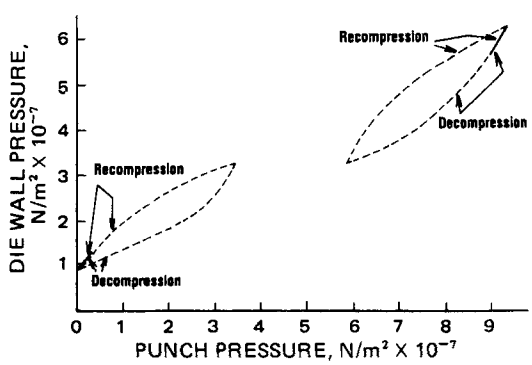

Figure 9—*Spray-dried lactose USP (hydrous): partial recompression–decompression cycles of a compact.*

[10] Figure 14 is basically a stress relaxation determination using the Milosovich apparatus (3) to obtain the data.

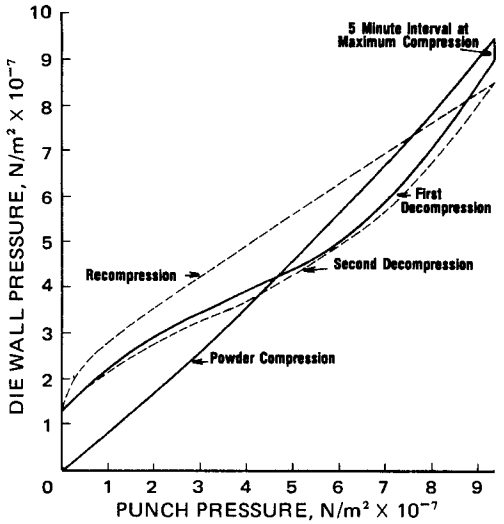

Figure 10—*Erythromycin USP: local die wall pressure* versus *mean punch pressure for compression–recompression cycles.*

The extent of the stress concentration, the stress concentration factor f, is a multiplier applied to the magnitude of the uniform stress calculated as if no flaw were present. A simple case may be used to illustrate stress concentration. If a slab is subjected to only a uniform tensile stress and the slab contains an elliptical hole with the long axis normal to the direction of the tensile stress, the tensile stress at the edge of the hole, as long as the hole is much smaller than the width of the slab, is given by:

$$f = 1 + 2\sqrt{\frac{L}{R}} \qquad \text{(Eq. 11)}$$

where L is one-half the length of the hole, and R is the radius of curvature of the tip of the hole.

Note that Eq. 11 reduces to a stress concentration factor of 3 for a round hole, regardless of its radius (its size still must be very much less than the slab size). When a second uniform stress is applied to the slab normal to the direction of the tensile stress, the stress concentration factor around a hole is not exactly 3. Figure 16 shows the stress concentration factor at a hole for various stress conditions (15).

The stress concentration concept is useful in understanding why ejection from a die can cause a compact to laminate. Theoretically, the radius of curvature at the edge of the die could be of molecular dimensions. Therefore, the stress concentration factor to be applied to the die wall pressure when a compact is partially ejected could be a very large number. Figure 17 is a photograph of an erythromycin compact that split off many layers as it was slowly ejected. The assumed mechanism is that a crack initiated at the edge and propagated across the compact. Materials that exhibit a high shear strength and, therefore, a high residual die wall pressure and also have a high propensity for brittle fracture may undergo

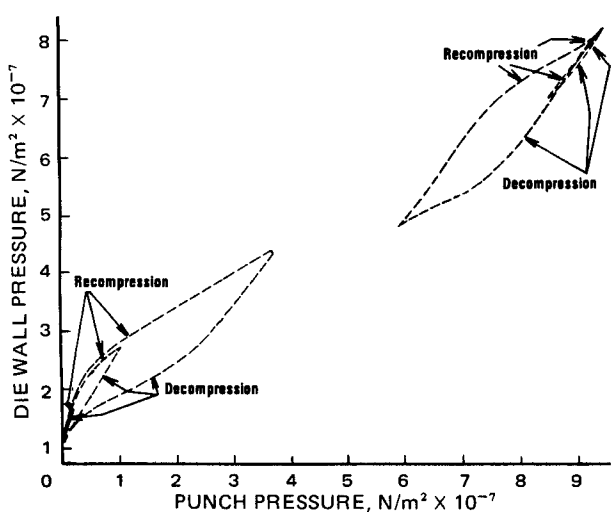

Figure 11—*Erythromycin USP: partial recompression–decompression cycles of a compact.*

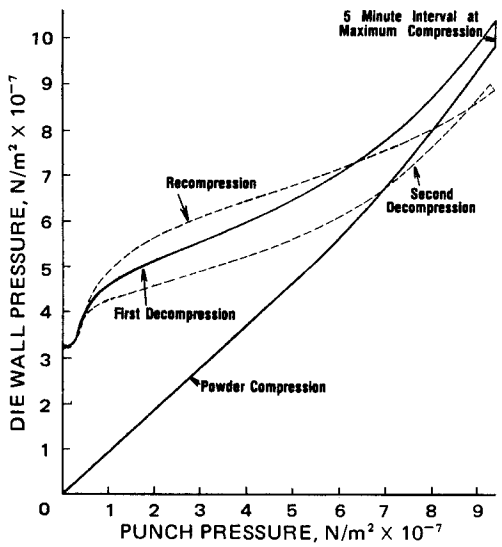

Figure 12—*Sodium chloride: local die wall pressure* versus *mean punch pressure for compression–decompression cycles different from other materials. The die wall pressure increased during the 5-min interval the maximum punch pressure was held constant.*

brittle fracture from points of very high stress concentration such as the die edge.

It should be possible to use the knowledge of stress relief at sites of stress concentration to characterize the tendency of compacts to propagate cracks. Suppose that a round hole is placed in the center of a compact and that it is subjected to a tensile stress. Tensile fracture might be expected to occur at exactly one-third of the tentile stress required to produce tensile fracture when no hole is present. However, this would be true only if the compact did not relieve the locally concentrated stresses at the edge of the hole by plastic deformation. If all excess stresses at the hole's edge were relieved, no observable differences in the tensile fracture force would be observed. Real materials should fracture at some intermediate value, the magnitude depending on their ability to relieve localized stresses. Since fracture by crack propagation from a flaw that concentrates stress is called brittle fracture, comparison of the strength with and without a hole has been used to define a parameter called the brittle fracture propensity (BFP). The BFP is calculated by:

$$\text{BFP} = 1/2\left[\frac{\sigma_T}{\sigma_{TO}} - 1\right] \qquad \text{(Eq. 12)}$$

where σ_T is the tensile strength without a hole, and σ_{TO} is the apparent tensile strength with a hole present.

The subtraction of one and division by two normalize the values of BFP so that the theoretical value range is 0–1 when the stress concentration factor is 3. Since the BFP value is an inverse measure of localized stress relief, it should indicate the tendency of a compact to laminate or cap.

A technique for measuring the BFP of compacts is based on the transverse compression of squares (2). Earlier work showed that if a

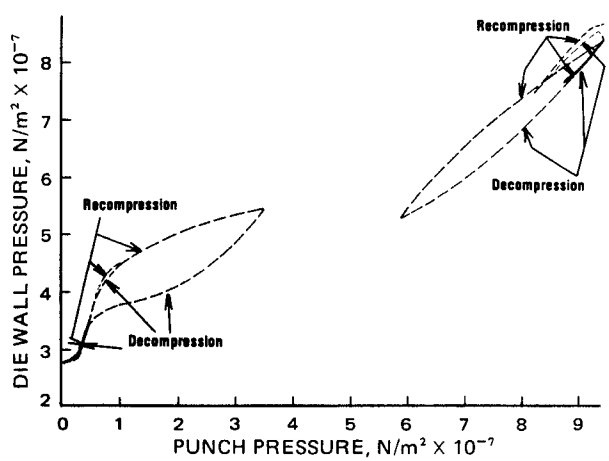

Figure 13—*Sodium chloride: partial recompression–decompression cycles of a compact.*

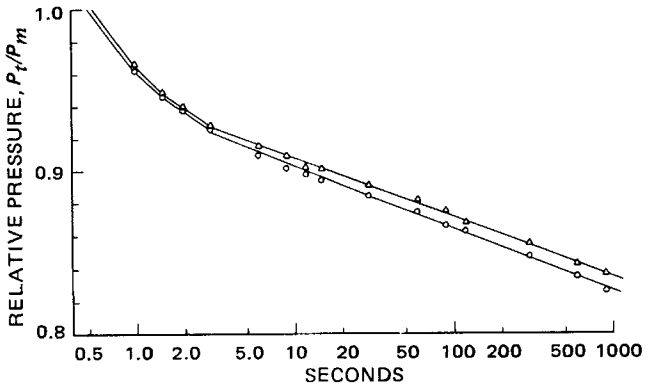

Figure 14—*Microcrystalline cellulose: relative punch pressure* versus *log time;* P_t *is pressure at time* t, P_m *is the maximum pressure applied, zero time corresponds to the start of the stress application, circles are data for an in air measurement, and triangles are data for an* in vacuo *measurement. Escape of air following compression did not alter the general shape of the curve. Maximum pressures applied were* 7.24×10^7 N/m^2 *in air and* 6.89×10^7 N/m^2 in vacuo; *slope values varied slightly with the maximum applied compression pressure and were usually steeper with an increase in the maximum pressure.*

square compact is centered on edge between two platens whose width is four-tenths of the width of the compact, the central region of the compact is under a nearly uniform shear stress (16). Figure 18 shows the fringe patterns obtained with polarized light through a transparent model substance, poly(methyl methacrylate). (Photoelastic methods of determining stress distributions use more sophisticated techniques to obtain and evaluate fringe patterns.) Comparison of the two fringe patterns clearly shows that when the hole is present, the magnitude of the stresses is changed markedly. Although isochromatic fringe lines are isoshear stress lines, one cannot determine the principal stresses without additional information. The techniques of photoelasticity are outside the scope of this discussion but do indeed permit the determination of stress concentration factors such as those shown in Fig. 16.

The stress condition at the center of a square compact in transverse compression is not simple tension. A compression stress is present in the direction normal to the tensile stress. Therefore, from the data displayed in Fig. 16 and from the analysis of Berenbaum and Brodie (16), which show that the ratio of tension to compression is approximately 0.28, it is evident that the stress concentration factor is approximately 3.25. The use of Eq. 12 with this method of tensile strength measurement will not limit the BFP values to less than unity, at least in theory, since the equation was normalized for a stress concentration factor of 3. In practice, one probably cannot make an intact compact of a material with a BFP of 1. Therefore, the observed range of values may not exceed the 0–1 range.

While it might be preferable to base the BFP on an exact theoretical analysis, one must recognize that the heterogeneous relative densities of a compact make a high level of precision most difficult to attain. Furthermore, difficulties not yet understood arise with this test. Therefore, the authors elected to use Eq. 12 to estimate the BFP, even when the evaluation of tensile strengths was made by the transverse compression of squares[11]. Added specifications should include the relative density of the compact because very soft compacts do not yield useful data. Nevertheless, sufficient accuracy exists for useful relative values to be obtained simply by adopting a standard procedure. Of course, compacts containing other flaws such as laminations will yield false values. When one observes a stepped fracture plane, one should suspect lamination and reject the data. If various laboratories were to attempt to obtain identical values for the BFP, very detailed specifications would be needed for high levels of precision.

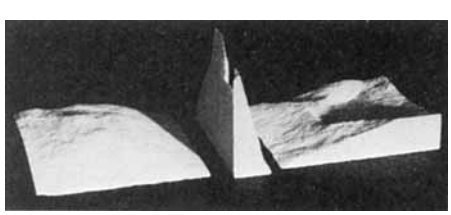

Figure 15—*Phenacetin compact that fractured in the die without ejection. Similar fracture occurs with acetaminophen and with some mixtures of these materials with excipients.*

[11] In the authors' studies, the platen width was 0.4 the tablet width, pads were used on the platens, and the hole diameter was 1.09 mm in a 38.1-mm square compact.

Table I—Tensile Strength of Compacts Subject to Various Compression Procedures

Material	Number of Compressions	Tensile[a] Strength, $N/m^2 \times 10^{-6}$	Significant[b] Difference, p
Aspirin	1	1.10	] <0.001
	4	1.26	
Sucrose	1	1.32	] 0.18
	4	1.37	
Lactose (spray dried)	1	1.45	] 0.08
	4	1.50	

[a] Average of five compacts. Maximum compression of 9.50×10^7 N/m^2. [b] Strengths are significantly different at listed p values. Brackets indicate the pair of values compared to obtain p value.

Experimental values for a few materials are listed in Table II. Materials known to induce capping have relatively large BFP values, as expected. The punch used to form compacts with a hole in the center is shown in Fig. 19.

Stress Relaxation—So far, the discussion has ignored an important variable—*viz.*, time. Plastic deformation is a time-dependent phenomenon. Shlanta and Milosovich (3) showed that compression stresses are relieved with time. Their experiments were similar to a relaxation study, since the size of the compact was fixed and the change in punch pressure with time was recorded. The authors used the Milosovich apparatus and confirmed the basic observation. Furthermore, every material examined by the authors with this apparatus underwent relaxation of the punch pressure (Figs. 14, 20, and 21). Because the compact is not under uniaxial compression during the stress relaxation, the quantitative interpretation of the experimental results is complicated. Furthermore, the slope is a function of the porosity of the compact. However, for the examples shown, the rank order is obvious. Materials that are known to cap exhibit slower stress relaxation.

The change of slope at the short time intervals observed in these stress *versus* log time plots suggests that some initially prominent mechanism soon becomes negligible. Because air entrapment has been propounded as the cause of lamination and capping, it was of interest to establish whether the diffusion of air from the compact was an initially prominent mechanism. Therefore, the stress relaxation experiments were repeated but with the powders in an evacuated die[12]. In no case were the general characteristics of the stress relaxation curves altered. Apparently, the air must escape in less than 0.4–0.7 sec from these materials (Figs. 14, 20, and 21). An apparatus that reduces the compression time to very small values is needed to explore this point further.

The relaxation of die wall pressure was discussed previously. Obviously, pressures at all points in a compact may not be undergoing stress relaxation identically. As indicated previously, the pressure at the center of the punch was increasing while the die wall pressure decreased (Fig. 1).

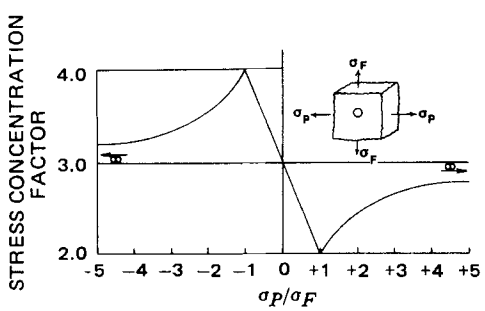

Figure 16—*Tensile stress concentration factor at the edge of a hole for biaxial stress conditions;* σ_P *and* σ_F *are stresses acting at right angles to each other. A negative value arises for* σ_P/σ_F *when one stress is compression and the other is tension. Hole diameter is much much smaller than dimensions in direction of stress. (Data from Ref. 12.)*

[12] Evacuable die 186-0002, Perkin-Elmer Corp., Norwalk, Conn.

Table II—Deformation and Fracture Properties of Pure Materials

Material	BFP[a]	P/σ_t[b]	E_e/E_p[c]
Methenamine	0.83	58	0.134
Erythromycin base	0.65	25	3.56
Ibuprofen	0.40	87	0.145
Sucrose	0.35	102	0.590
Starch, modified[d]	0.27	78	1.07
Lactose (spray dried)	0.18	193	0.844
Microcrystalline cellulose	0.04	25	1.45

[a] Brittle fracture propensity. All compacts were compressed at 9.5×10^7 N/m². [b] Mean deformation pressure divided by the tensile strength. All compacts had a relative density of 0.85. [c] Relative deformation energies (elastic/plastic) for deformation beneath a steel sphere; $E_e + E_p$ was the same for all materials. The relative density of all compacts was 0.85. [d] StaRx.

However, mean pressures may be decreasing if the compact increases its relative density as a result of stress relaxation, *i.e.*, as a function of time. Therefore, there is no reason to conclude that the two apparatuses yield conflicting results.

The evidence clearly indicates the existence in compacts of time-dependent properties of plastic deformation and stress relief. Therefore, the incidence of fracture also should be time dependent. Intact compacts of some pure medicaments, *e.g.*, acetaminophen, methenamine, and erythromycin, were made when the decompression was extended over several hours, even though rapid decompression produced fractured compacts.

Differences in the slopes of the initial segments of these plots should reflect the ability of the material to relieve stresses in a tableting machine. As expected, the stresses in methenamine decayed very slowly while those in sitosterols decayed much more rapidly. Stresses in erythromycin decayed much more rapidly than might be expected since they produced laminated compacts. This finding may account for the ability of erythromycin to withstand (not fracture) decompression but to fracture upon ejection where the time interval for decay of stress is very short.

Indentation Hardness—If a sphere is pressed against a compact surface hard enough to produce plastic flow beneath it, the mean pressure over the sphere–compact interface is essentially a constant when the chordal radius of the dent is much less than the radius of the sphere. This mean deformation pressure[13], P, is a measure of the hardness of the compact. The yield value for plastic flow is approximately 0.36 P.

The role of plastic flow in determining residual die wall pressure and in relieving concentrated stresses was emphasized in the preceding discussion. Therefore, the determination of P should be of direct interest. A method based on the rebound of a steel sphere from a compact was used (4). For comparison, the values of P for compacts with a relative density, ρ_r, of 0.85 were used for all materials. Plots of log P *versus* ρ_r are nearly straight lines and were used in interpolation to obtain the 0.85 relative density value.

Perhaps the ratio of the deformation pressure, P, divided by the tensile strength is of more interest than the deformation pressure alone. If both shear strength and tensile strength arise from the same bonded areas in a given compact, then the ratio P/σ_T for materials should have similar values unless the mechanical structure of the compact influences disproportionally the magnitude of these terms. The magnitude of P should not be influenced by crack propagation, but that of σ_T should be. Thus, if the ratio of P to σ_T varies over a large range, the pore structure may be affecting the tensile strength values. Crack propagation occurs

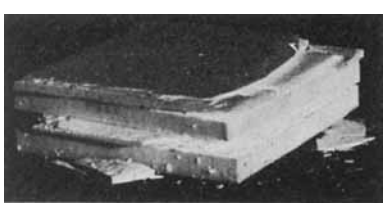

Figure 17—*Erythromycin base compact that fractured when ejected from the die. Starch and methenamine compacts fractured in a similar manner.*

[13] Analogous to P in Eq. 1, except that Eq. 1 was measured at contact points between particles. Here, the mean pressure is over a macroscopic area that may contain pores. Nevertheless, the equations for nonporous materials may be used (4).

Table III—Influence of Machine Speed and Precompression Force on the Final Compression Force that Produced Fractured Tablets[a]

Machine Speed, rpm	Precompression Force, Metric Tons	Final Compression Force, Metric Tons	
		No Lamination	Lamination
	Cupped Punches[b]		
44	0	0.907	1.134
	0.225	1.361	1.814
	0.454	1.814	1.905
32	0	1.270	1.361
	0.225	1.814	1.905
	0.454	1.905	2.041
24	0	1.588	1.814
	0.225	2.268	2.495
	0.454	2.268	2.495
	Flat Punches[c]		
37	0	1.361	2.268

[a] See footnote 6 in text for the composition of the formulas. [b] When 11.9-mm flat punches and die were used with the same formulation, no lamination was observed. [c] Very little work was done with the flat punches because a formula that produced a good bond at lower pressures and laminated at the highest pressures was not developed.

when the tensile stresses at a flaw exceed the tensile strength without the shear stresses exceeding the shear strength, *i.e.*, without stress relief occurring by plastic flow. Thus, the ratio of P/σ_T might correlate with the BFP. If true, a relatively large value of P/σ_T should indicate an increased propensity for brittle fracture. Factors that could affect this comparison are differences in the surface energy of the solid, the modulus of elasticity of the compact, and the internal flaw structure that concentrates stresses. Table II shows the results of these measurements.

It is obvious from Table II that the P/σ_T values do not correlate with the BFP values. Nor do the P/σ_T values correlate with the tendency to form fractured tablets. It seems more reasonable to conclude that both σ_T and P are measuring different manifestations of the strength of the true contact areas without gross effects from stress concentration at pores controlling the values.

The impact–rebound method of determining P provides measurements of both the energy used in the permanent deformation and the energy of the elastic recovery from the impact. A high energy of elastic deformation per unit of plastic deformation energy, E_e/E_p, could indicate that large elastic stresses develop within the compact. Thus, it is of interest to compare the magnitude of E_e/E_p for the various materials. The last column of Table II lists the experimental values for several materials. Obviously, the magnitudes of the ratios of E_e/E_p do not correlate with the brittle fracture properties of the compact.

Tablet Making—Stress relaxation is believed to explain some practical problems encountered in tableting. When lamination is a problem and the production volume of a rotary machine is needed, a machine that provides precompression should be selected. The precompressed compact has time to undergo some stress relaxation before the final compression is applied. To maximize the stress relaxation, the precompression pressure should be near the maximum that will not by itself introduce lamination. This will maximize the stress relaxation that can occur before the final compression. A long dwell time under compression also will increase the time for stress relaxation. Thus, a slow operating speed also increases the time available for stress relaxation. The final compression should use as small a force as possible to obtain an acceptable tablet, since there is less stress acting at a smaller compression force to cause the compact to fracture. If the BFP of the formulation is not too high, one should be able to make a satisfactory product under the conditions described.

The use of deep oval punches is known to engender capping. Obviously, a large quantity of material in the "dome" is expanding radially as the punch is removed. Since the main body of the tablet cannot expand radially into the die wall, large shear stresses develop. Flat punches avoid this contribution to the shear stress. Therefore, when possible, tablet shape selection should be made to reduce stress gradients during tableting.

Other studies have demonstrated the effects of precompression[14]. They were repeated in the present study to observe the effects of precom-

[14] A. C. Shah, The Upjohn Co., unpublished data.

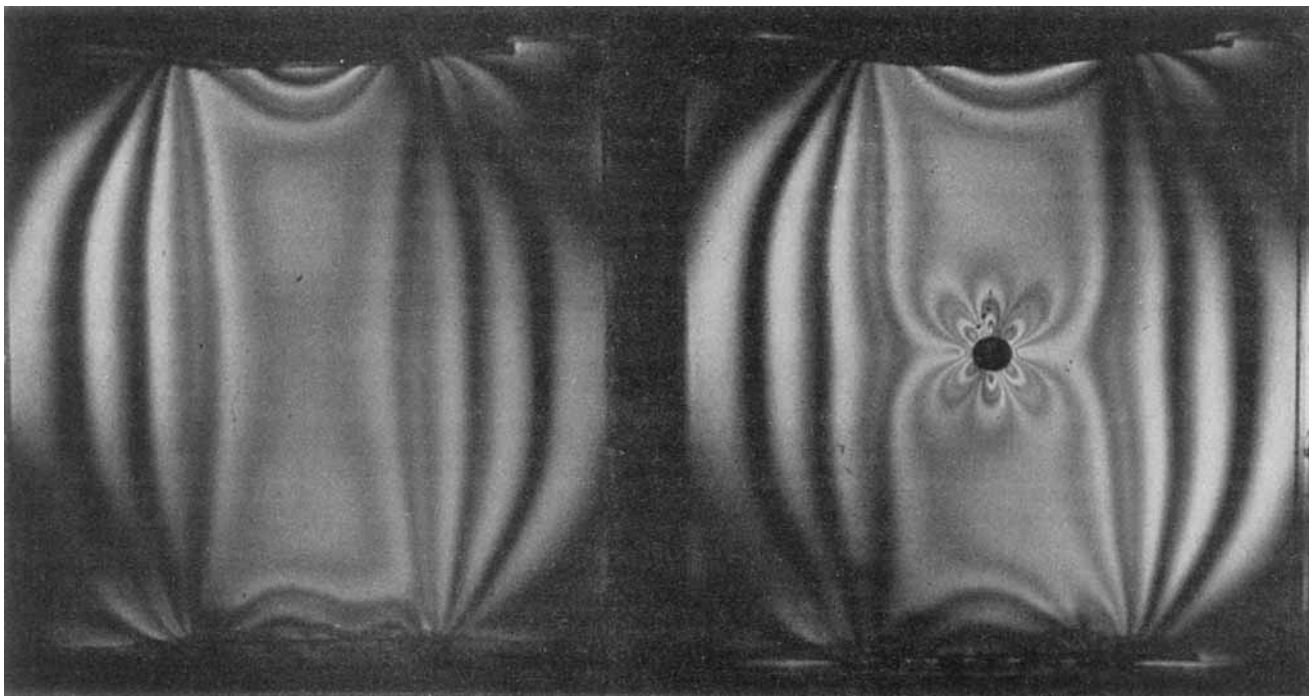

Figure 18—*Examples of simple fringe patterns obtained with and without a hole in a compact subjected to transverse compression. These photographs were made with white light and simple polarizers and are not suitable for stress analysis use. However, they identify high stress gradient areas.*

pression on final compression, the influence of machine speed, and the influence of punch shape (Table III). The theory predicts the pattern of the experimental results. Of course, quantitative predictions are not possible with the present knowledge. The minimum precompression force for intact compacts was a function of machine speed, final compression force, and punch shape. Conversely, the maximum final compression force that produced intact compacts was a function of the precompression force, the machine speed, and the punch shape. Conditions that increased the amount of stress relaxation permitted increased compression force and vice versa.

If even the best conditions of tableting still produce laminated tablets, reformulation is necessary. One should then seek an excipient material that has a very low BFP value to add to the high BFP medicament. Of course, in practice, one must also consider effects on disintegration, *etc.* Nevertheless, an understanding of the discussed principles provides much guidance in the formulation of the compressed tablet dosage form.

SUMMARY

Under the nonisostatic compression force of tableting, the powder particles undergo sufficient plastic deformation to produce a die wall pressure in excess of that that can be relieved by the elastic recovery accompanying the removal of the punch pressure. This die wall pressure produces internal stress sufficiently high to cause internal shear in the compact during the decompression. Plastic deformation occurs in repeated recompression and decompression cycles. In some materials, the internal shear stresses cause a crack to propagate and fragmentation occurs. If the stresses during decompression are not sufficient to produce crack propagation within the die during decompression, the stress concentrations developed at the edge of the die may produce crack propagation (lamination) as the tablet is ejected.

Since shear stresses develop during decompression and/or ejection, the failure to fracture appears to be due to the ability of a material to relieve shear stresses by localized shear flow, *i.e.*, plastic deformation. This property can be measured by comparing the tensile strength of a compact that contains a built-in stress concentrator "defect" with one that does not. By using this knowledge, a test was designed that indicates a property of a material called the "brittle fracture propensity." The brittle fracture propensity value indicates whether or not capping or lamination may be a problem in tableting the material.

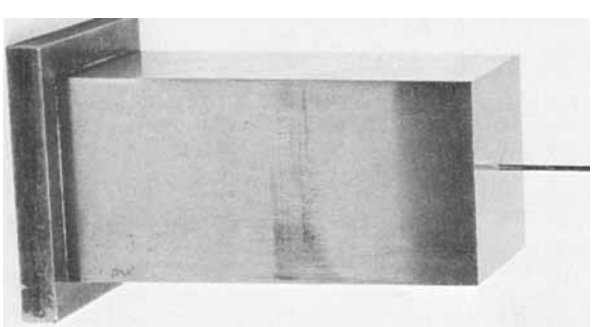

Figure 19—*Special punch used to make compacts with small hole in center. Pin is spring loaded and retractable so that any reasonable compact thickness can be used.*

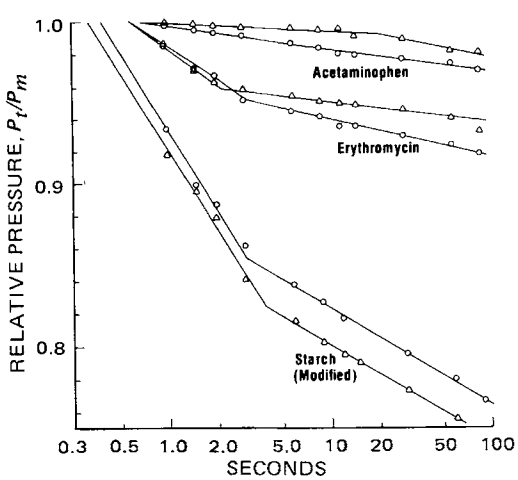

Figure 20—*Relative punch pressure* versus *log time. Zero time corresponds to the start of the stress application. Circles are data from an in air measurement; triangles are data from an* in vacuo *measurement. Material with the slowest rate of relaxation fractured upon decompression in the die; erythromycin laminated upon ejection. Maximum pressures (in* $N/m^2 \times 10^{-7}$*) were: acetaminophen, air 7.31 and* in vacuo *7.03; erythromycin, air 7.86 and* in vacuo *8.89; and modified starch, air 6.62 and* in vacuo *5.31.*

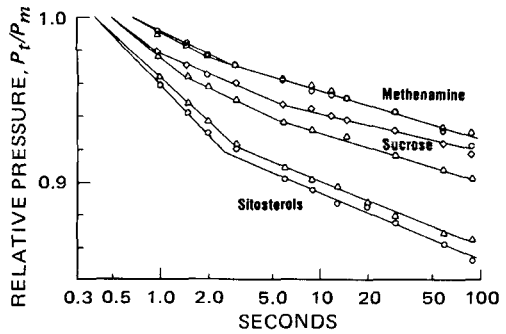

Figure 21—*Relative punch pressure* versus *log time. Zero time corresponds to the start of stress application. Circles and diamonds are data from an in air measurement; triangles are data from an* in vacuo *measurement. Only material with the slowest rate of relaxation fractured upon rapid decompression in the die. Maximum pressures (in* $N/m^2 \times 10^{-7}$*) were: methenamine, air 8.34 and* in vacuo *8.41; sucrose, air 6.96 and* in vacuo *6.52; and sitosterols, air 4.62 and* in vacuo *4.07.*

The time-dependent nature of plastic flow or stress relaxation also must be considered and may account for differences in the properties of tablets produced on various machines or at various machine settings.

REFERENCES

(1) E. L. Knoechel, C. C. Sperry, H. E. Ross, and C. J. Linter, *J. Pharm. Sci.*, **56**, 109 (1967).

(2) E. N. Hiestand and C. B. Peot, *ibid.*, **63**, 605 (1974).

(3) S. Shlanta and G. Milosovich, *ibid.*, **53**, 562 (1964).

(4) E. N. Hiestand, J. M. Bane, Jr., and E. P. Strzelinski, *ibid.*, **60**, 758 (1971).

(5) A. S. Rankell and T. Higuchi, *ibid.*, **57**, 574 (1968).

(6) P. York and N. Pilpel, *J. Pharm. Pharmacol.*, **25**, S-1P (1973).

(7) E. N. Hiestand, *Pharm. Ind.*, **34**, 262 (1972).

(8) P. Dyachenko, N. Tolkacheva, G. Andrew, and T. Karpova, "The Actual Contact Area Between Touching Surfaces," Consultants Bureau, New York, N.Y., 1964.

(9) F. C. Yip and J. E. S. Venart, *J. Phys. D., Appl. Phys.*, **4**, 1470 (1971).

(10) D. Train, *J. Pharm. Pharmacol.*, **8**, 745 (1956).

(11) E. Shotton and J. A. Hersey, in "Theory and Practice of Industrial Pharmacy," L. Lachman, H. Lieberman, and J. Kanig, Eds., Lea & Febiger, Philadelphia, Pa., 1970, chap. 9.

(12) E. Nelson, *J. Am. Pharm. Assoc., Sci. Ed.*, **44**, 494 (1955).

(13) S. Leigh, J. E. Carless, and B. W. Burt, *J. Pharm. Sci.*, **56**, 888 (1967).

(14) J. E. Carless and S. Leigh, *J. Pharm. Pharmacol.*, **26**, 289 (1973).

(15) C. Lipson and R. C. Juvinall, "Handbook of Stress and Strength," Macmillan, New York, N.Y., 1963.

(16) R. Berenbaum and I. Brodie, *Br. J. Appl. Phys.*, **10**, 281 (1959).

ACKNOWLEDGMENTS AND ADDRESSES

Received December 4, 1975, from *Pharmacy Research, The Upjohn Company, Kalamazoo, MI 49001.*

Accepted for publication June 8, 1976.

The authors thank the many people that assisted in various ways with this research. Mr. H. Ballen and Mr. C. C. Sperry designed the special apparatuses used. Dr. G. Milosovich and the University of Michigan School of Pharmacy loaned the stress relaxation apparatus. Mr. L. H. Macdonald and Mr. J. F. Glasscock worked with the phenacetin formulations.

[x] To whom inquiries should be directed.

Solubility Studies of Silver Sulfadiazine

R. U. NESBITT, Jr. *, and B. J. SANDMANN [x]

Abstract □ The solubility of silver sulfadiazine as a function of pH was determined in nitric acid–potassium nitrate buffer for pH 2–3 and in 2-(*N*-morpholino)ethanesulfonic acid buffer for pH 6–7. As the salt of a weak organic acid, silver sulfadiazine exhibits the anticipated increase in solubility with an increasing hydrogen-ion concentration. Measurement of the silver-ion concentration was carried out using a silver-ion selective electrode. The methods of known subtraction and known addition were utilized to measure the total concentration of the silver ion in solution. Evidence was obtained to indicate that the salt is completely ionized in aqueous solution.

Keyphrases □ Silver sulfadiazine—solubility as a function of pH, potentiometric study □ Solubility—silver sulfadiazine as a function of pH, potentiometric study □ pH—effect on solubility of silver sulfadiazine, potentiometric study □ Potentiometry—study of solubility of silver sulfadiazine as a function of pH □ Anti-infectives, topical—silver sulfadiazine, solubility as a function of pH, potentiometric study

Silver sulfadiazine, a substance with extremely low water solubility, was reported to be particularly efficacious as a topical antibacterial agent for the control of *Pseudomonas* infection in burns (1). When applied locally to burned skin, silver sulfadiazine is claimed to offer definite therapeutic advantages over other similar chemotherapeutic agents used to treat infection. Unlike other drugs that diffuse rapidly or deplete chloride ions from body fluids, silver sulfadiazine remains in the wound exudate for a prolonged effect and appears to enhance conditions favorable for epithelial regeneration.

BACKGROUND

The mode of antibacterial action is different than that of sulfonamides, because the drug is not antagonized *in vitro* by aminobenzoic acid. In binding studies using radioactive silver sulfadiazine prepared from radioactive ^{110}Ag- and ^{35}S-tracers, the silver ion was found to bind with the *Pseudomonas* cells. No cellular binding of sulfadiazine was detected (2, 3).

The binding of silver to bacterial DNA was proposed as important for inhibiting microbial growth. Silver displaces the hydrogen bonds between adjacent nitrogens of the purines (adenine or guanine) and pyrimidines (thymine and cytosine) in the DNA molecule. The nitrogen–silver bonds, once formed, appear to be stronger than the nitrogen–hydrogen bonds; therefore, bacteria having this silver–nucleic acid complex presumably

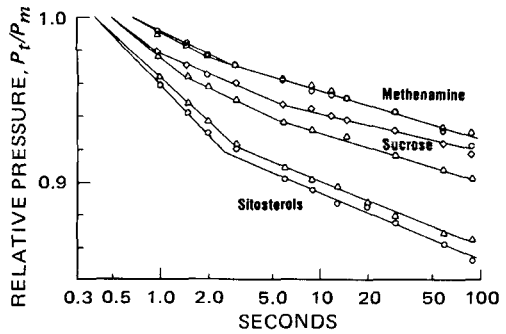

Figure 21—*Relative punch pressure* versus *log time. Zero time corresponds to the start of stress application. Circles and diamonds are data from an in air measurement; triangles are data from an* in vacuo *measurement. Only material with the slowest rate of relaxation fractured upon rapid decompression in the die. Maximum pressures (in* $N/m^2 \times 10^{-7}$*) were: methenamine, air 8.34 and* in vacuo *8.41; sucrose, air 6.96 and* in vacuo *6.52; and sitosterols, air 4.62 and* in vacuo *4.07.*

The time-dependent nature of plastic flow or stress relaxation also must be considered and may account for differences in the properties of tablets produced on various machines or at various machine settings.

REFERENCES

(1) E. L. Knoechel, C. C. Sperry, H. E. Ross, and C. J. Linter, *J. Pharm. Sci.*, **56**, 109 (1967).

(2) E. N. Hiestand and C. B. Peot, *ibid.*, **63**, 605 (1974).

(3) S. Shlanta and G. Milosovich, *ibid.*, **53**, 562 (1964).

(4) E. N. Hiestand, J. M. Bane, Jr., and E. P. Strzelinski, *ibid.*, **60**, 758 (1971).

(5) A. S. Rankell and T. Higuchi, *ibid.*, **57**, 574 (1968).

(6) P. York and N. Pilpel, *J. Pharm. Pharmacol.*, **25**, S-1P (1973).

(7) E. N. Hiestand, *Pharm. Ind.*, **34**, 262 (1972).

(8) P. Dyachenko, N. Tolkacheva, G. Andrew, and T. Karpova, "The Actual Contact Area Between Touching Surfaces," Consultants Bureau, New York, N.Y., 1964.

(9) F. C. Yip and J. E. S. Venart, *J. Phys. D., Appl. Phys.*, **4**, 1470 (1971).

(10) D. Train, *J. Pharm. Pharmacol.*, **8**, 745 (1956).

(11) E. Shotton and J. A. Hersey, in "Theory and Practice of Industrial Pharmacy," L. Lachman, H. Lieberman, and J. Kanig, Eds., Lea & Febiger, Philadelphia, Pa., 1970, chap. 9.

(12) E. Nelson, *J. Am. Pharm. Assoc., Sci. Ed.*, **44**, 494 (1955).

(13) S. Leigh, J. E. Carless, and B. W. Burt, *J. Pharm. Sci.*, **56**, 888 (1967).

(14) J. E. Carless and S. Leigh, *J. Pharm. Pharmacol.*, **26**, 289 (1973).

(15) C. Lipson and R. C. Juvinall, "Handbook of Stress and Strength," Macmillan, New York, N.Y., 1963.

(16) R. Berenbaum and I. Brodie, *Br. J. Appl. Phys.*, **10**, 281 (1959).

ACKNOWLEDGMENTS AND ADDRESSES

Received December 4, 1975, from *Pharmacy Research, The Upjohn Company, Kalamazoo, MI 49001.*

Accepted for publication June 8, 1976.

The authors thank the many people that assisted in various ways with this research. Mr. H. Ballen and Mr. C. C. Sperry designed the special apparatuses used. Dr. G. Milosovich and the University of Michigan School of Pharmacy loaned the stress relaxation apparatus. Mr. L. H. Macdonald and Mr. J. F. Glasscock worked with the phenacetin formulations.

[x] To whom inquiries should be directed.

Solubility Studies of Silver Sulfadiazine

R. U. NESBITT, Jr. *, and B. J. SANDMANN [x]

Abstract □ The solubility of silver sulfadiazine as a function of pH was determined in nitric acid–potassium nitrate buffer for pH 2–3 and in 2-(*N*-morpholino)ethanesulfonic acid buffer for pH 6–7. As the salt of a weak organic acid, silver sulfadiazine exhibits the anticipated increase in solubility with an increasing hydrogen-ion concentration. Measurement of the silver-ion concentration was carried out using a silver-ion selective electrode. The methods of known subtraction and known addition were utilized to measure the total concentration of the silver ion in solution. Evidence was obtained to indicate that the salt is completely ionized in aqueous solution.

Keyphrases □ Silver sulfadiazine—solubility as a function of pH, potentiometric study □ Solubility—silver sulfadiazine as a function of pH, potentiometric study □ pH—effect on solubility of silver sulfadiazine, potentiometric study □ Potentiometry—study of solubility of silver sulfadiazine as a function of pH □ Anti-infectives, topical—silver sulfadiazine, solubility as a function of pH, potentiometric study

Silver sulfadiazine, a substance with extremely low water solubility, was reported to be particularly efficacious as a topical antibacterial agent for the control of *Pseudomonas* infection in burns (1). When applied locally to burned skin, silver sulfadiazine is claimed to offer definite therapeutic advantages over other similar chemotherapeutic agents used to treat infection. Unlike other drugs that diffuse rapidly or deplete chloride ions from body fluids, silver sulfadiazine remains in the wound exudate for a prolonged effect and appears to enhance conditions favorable for epithelial regeneration.

BACKGROUND

The mode of antibacterial action is different than that of sulfonamides, because the drug is not antagonized *in vitro* by aminobenzoic acid. In binding studies using radioactive silver sulfadiazine prepared from radioactive ^{110}Ag- and ^{35}S-tracers, the silver ion was found to bind with the *Pseudomonas* cells. No cellular binding of sulfadiazine was detected (2, 3).

The binding of silver to bacterial DNA was proposed as important for inhibiting microbial growth. Silver displaces the hydrogen bonds between adjacent nitrogens of the purines (adenine or guanine) and pyrimidines (thymine and cytosine) in the DNA molecule. The nitrogen–silver bonds, once formed, appear to be stronger than the nitrogen–hydrogen bonds; therefore, bacteria having this silver–nucleic acid complex presumably

do not replicate (4). In another report, silver sulfadiazine was said to bind to cell membranes rather than to interact with cellular DNA (5).

The mechanism of action of silver sulfadiazine is incompletely defined, and the exact role of the sulfadiazine moiety remains unclear. One proposal suggests that sulfadiazine localizes the action of the drug to the microbial cells (2). The very slow reaction of silver sulfadiazine with endogenous chloride ions is interesting when enough silver ions are apparently present to produce a strong antibacterial effect, but silver chloride reportedly does not precipitate in tissue fluids. The dissociation of silver sulfadiazine during inhibition of bacterial growth was described (3) in contrast to an earlier report that silver sulfadiazine does not ionize (6). Additional studies to determine the solubility and ionization properties of silver sulfadiazine are necessary for a complete understanding of its mechanism of action.

The crystallization and structure of silver sulfadiazine were recently reported, and the drug was characterized as a salt of a weak acid (7). A study using X-ray diffraction confirmed the assigned structure (8). The current report is concerned with the behavior of silver sulfadiazine in aqueous solutions in the presence of electrolytes and buffers. The objectives of this study were to investigate the ionization and solubility of silver sulfadiazine using recently developed potentiometric methods and to relate these properties with those of the silver salts of other N^1-substituted sulfonamides.

EXPERIMENTAL

Equipment—Potentiometric measurements were made using a pH meter[1], accurate to ±0.1 mv or ±0.001 pH unit, in a thermostated bath regulated at 25 ± 0.1°. The silver-ion concentration was measured with a silver-ion selective electrode[2]. The hydronium-ion concentration was measured with a triple-purpose pH electrode[3]. A double-junction silver chloride reference electrode[4] with a filling solution of 10% KNO_3 was used to eliminate the possible precipitation of silver chloride in the sample solutions.

Reagents—All reagents were of analytical grade, unless otherwise stated. Water with a specific conductivity of $1–10 \times 10^{-7}$ ohm^{-1} cm^{-1} was employed. Silver nitrate[5] and sodium sulfadiazine[5] were obtained commercially. Silver sulfadiazine was prepared by the method of Braun and Towle (9) and recrystallized as previously described (7). The 2-(*N*-morpholino)ethanesulfonic acid buffer[6] was prepared by titration of the acid with a standard sodium hydroxide solution.

Preparation of Equilibrium Mixtures—Silver sulfadiazine was screened through a size 80 standard screen[7]. Paraffin-coated vials with film-covered[8] rubber closures held in place by aluminum bands were utilized. Mixtures of 100 mg of silver sulfadiazine, 25 ml of nitric acid buffer, or 25 ml of 0.05 *M* 2-(*N*-morpholino)ethanesulfonic acid buffer were prepared, adjusted to an ionic strength of 0.1 *M* with potassium nitrate, and placed in the coated vials. For the measurement of total silver, 27 ml of buffer solution was used. The vials were rotated end-over-end in the thermostated bath until equilibrium solubility was obtained.

Measurement of Silver—After filtration of the equilibrated mixtures, the solutions were analyzed at 25 ± 0.1° in paraffin-coated beakers for the silver-ion concentration using a silver-ion selective electrode[2] standardized at 25 ± 0.1° and an ionic strength of 0.1 *M*. The electrode displayed a Nerstian response throughout the concentration range of 1×10^{-2}–1.5×10^{-6} *M* for the silver ion. The pH was measured with a pH electrode[3] standardized using standard buffers meeting National Bureau of Standards requirements (10). The total silver concentration was determined by the method of known subtraction (11, 12) in the nitric acid-buffered solution, to which a sufficient amount of a standard solution of potassium iodide was added to precipitate approximately one-half of the free silver ion. In the 2-(*N*-morpholino)ethanesulfonic acid-buffered solutions, the total silver concentration was determined by the method of known addition (12); the added reagent was a standard solution of silver nitrate representing a 100-fold increase in the free silver ion present in the sample solutions.

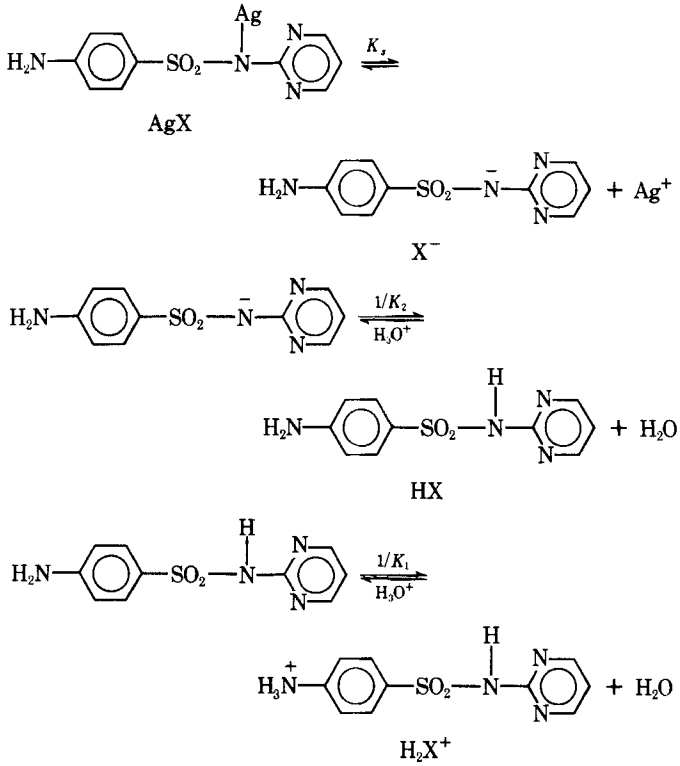

Scheme I

RESULTS AND DISCUSSION

In aqueous solutions, silver sulfadiazine would be expected to exhibit the general properties of the salt of a weak acid. The measurement of these properties, however, presents an analytical problem due to its extremely low water solubility. The recent development of ion selective electrode technology along with two new techniques for measuring total ion concentrations suggested the application of a potentiometric method for the analysis of silver sulfadiazine. In distilled water, the solubility of silver sulfadiazine is below the limits of analysis by any potentiometric method. However, in dilute acid, enough silver ions are ionized to give a concentration well within the sensitivity of a silver-ion specific electrode. Hydrolysis of the silver ion at near neutral or alkaline pH limits the study of silver sulfadiazine solubility to pH values less than 7.

The tendency of the silver ion to complex with various molecules and other ions reduced the number of possible buffering agents. Of the common inorganic salts of strong electrolytes, only nitrate and perchlorate ions remain in solution in the presence of silver ions. Nitric acid–potassium nitrate buffers were employed over a limited pH range. A suitable buffer for silver ions in the pH 6–7 range has not been identified. The sulfonic acid buffer system chosen exhibits minimal complexation with the silver ion (13). The use of conditional solubility product constants permits limited conclusions on solubility at this pH range.

Saturated solutions of silver sulfadiazine were analyzed for free and total silver concentrations by the analytical techniques of known addition (12) and known subtraction (11, 12). These methods were necessary due to the high probability of complexation of the silver with the sulfonic acid buffer as well as the uncertainty of the ionization properties of silver sulfadiazine. With nitrate buffers, the known subtraction method was utilized to determine the extent of ionization of the silver ion from the sulfadiazine. With this method, a complexing agent that will completely precipitate about one-half of the ion measured is added to the sample and the observed change in potential is used to calculate the original total ion concentration. By measuring the activity of free ion by a direct measurement using a calibration curve, it is possible to calculate the amount undissociated.

Due to the complexation of silver with the sulfonic acid buffer, the known addition method was used wherein a known solution of the ion being measured is added to the sample of interest. The original ion concentration is then calculated from the observed increase in potential. The usefulness of these methods depends on how well the system obeys the inherent assumptions.

The equilibria of the saturated solutions depicted by Scheme I may

[1] Corning digital 112 research pH meter, Corning Scientific Instruments, Medfield, Mass.
[2] No. 94-16, Orion Research, Cambridge, Mass.
[3] Corning Scientific Instruments, Medfield, Mass.
[4] No. 90-02, Orion Research, Cambridge, Mass.
[5] Marion Laboratories, Kansas City, Mo.
[6] United States Biochemical Corp., Cleveland, Ohio.
[7] W. S. Tyler Co., Minton, Ohio.
[8] Parafilm, American Can Co., Neenah, Wis.

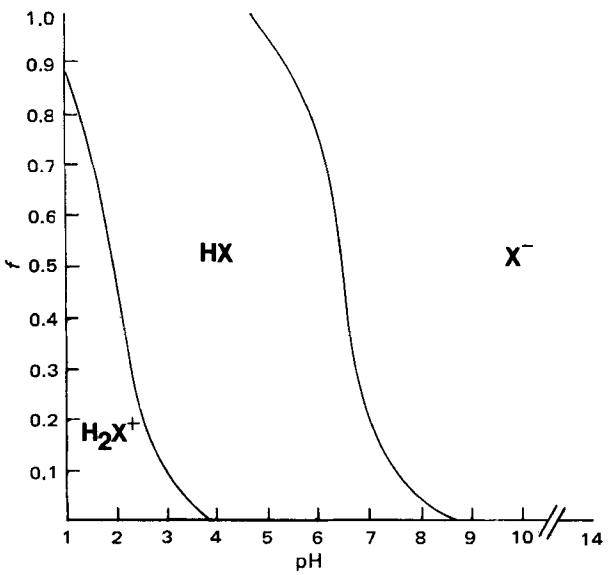

Figure 1—*Distribution diagram: fraction of sulfadiazine present as some particular form, f, as a function of pH; $pK_1 = 2.09$, and $pK_2 = 6.45$ (14).*

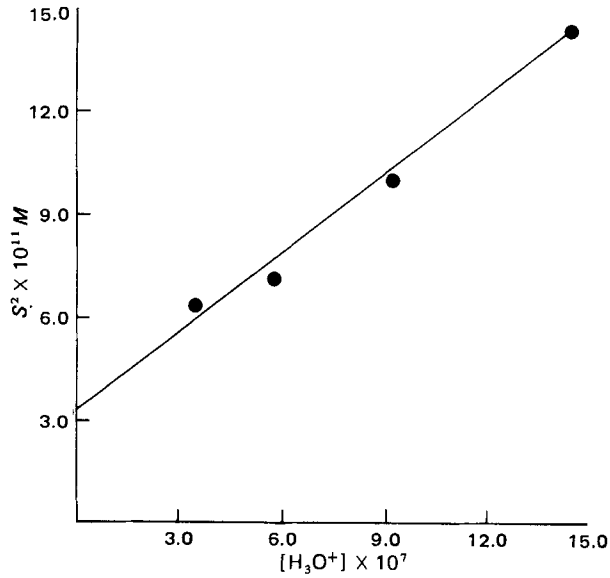

Figure 3—*Equilibrium values of* S^2 versus $[H_3O^+]$ *in 0.05* M *2-(N-morpholino)ethanesulfonic acid buffer at 0.1* M *ionic strength and 25 ± 0.1°.*

be described by:

$$K_s = [Ag^+][X^-] \quad \text{(Eq. 1)}$$

$$\frac{1}{K_2} = \frac{[HX]}{[H_3O^+][X^-]} \quad \text{(Eq. 2)}$$

$$\frac{1}{K_1} = \frac{[H_2X^+]}{[HX][H_3O^+]} \quad \text{(Eq. 3)}$$

$$S = [Ag^+] \quad \text{(Eq. 4)}$$

$$S = [H_2X^+] + [HX] + [X^-] \quad \text{(Eq. 5)}$$

where S is the total molar solubility of silver sulfadiazine. Substituting Eqs. 1–4 into Eq. 5 gives an equation that describes the solubility of silver sulfadiazine in terms of only the silver- and hydronium-ion concentrations of the saturated solution:

$$S^2 = [Ag^+]^2 = \frac{[H_3O^+]^2K_s}{K_1K_2} + \frac{[H_3O^+]K_s}{K_2} + K_s \quad \text{(Eq. 6)}$$

where K_s is the solubility product constant, and K_1 and K_2 are the ionization constants of the N^4- and N^1-hydrogens, respectively.

Equation 6 may be simplified by using the limiting conditions of low pH (2–3) and high pH (6–7). These approximations were derived by using the theoretical distribution diagram for sulfadiazine (Fig. 1), noting which species of sulfadiazine were not present in the pH range of interest, and neglecting this term in the mass balance (Eq. 5).

At the low pH range, Eq. 6 may be approximated to give:

$$S^2 = [Ag^+]^2 = \frac{[H_3O^+]^2K_s}{K_1K_2} + \frac{[H_3O^+]K_s}{K_2} \quad \text{(Eq. 7)}$$

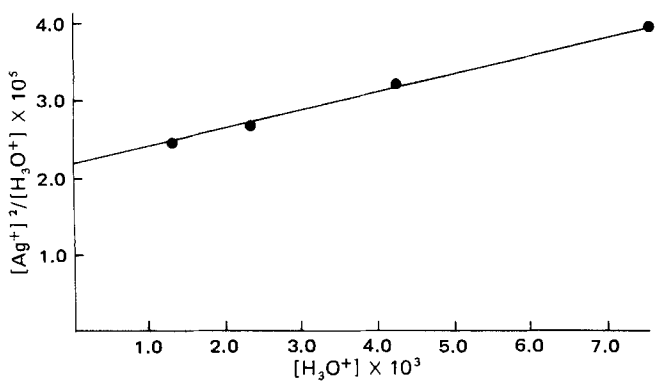

Figure 2—*Equilibrium values of* $[Ag^+]^2/[H_3O^+]$ versus $[H_3O^+]$ *at 0.1* M *ionic strength and 25 ± 0.1°.*

by neglecting the X^- species in Eq. 5. This equation may be linearized by dividing both sides by the hydronium-ion concentration, giving Eq. 8:

$$\frac{[Ag^+]^2}{[H_3O^+]} = \frac{[H_3O^+]K_s}{K_1K_2} + \frac{K_s}{K_2} \quad \text{(Eq. 8)}$$

When $[Ag^+]^2/[H_3O^+]$ is plotted against $[H_3O^+]$, a linear relationship should exist with an intercept of K_s/K_2 and a slope of K_s/K_2 $(1/K_1)$. From the slope and intercept, K_1 may be experimentally determined under the given conditions.

In the pH range of 6–7, Eq. 6 may be approximated to give:

$$S^2 = [Ag^+]^2 = \frac{[H_3O^+]K_s}{K_2} + K_s \quad \text{(Eq. 9)}$$

where the H_2X^+ species in Eq. 5 has been neglected. The application of Eq. 9 to the experimental data in the presence of the 2-(*N*-morpholino)-ethanesulfonic acid buffer does not completely represent the system due to apparent complexation of the free silver ion with the buffer, giving an increased value of the solubility, S, and subsequently a higher value for K_s, the solubility product constant.

A suitable modification of Eq. 9 to include this complexation may be made by using a conditional solubility product constant, K_s', defined by:

$$K_s' = [Ag^+]'[X^-] \quad \text{(Eq. 10)}$$

where $[Ag^+]'$ represents the concentration of all silver in solution irrespective of the form in which the silver ion may be present. Equation 9 may now be rewritten as:

$$S^2 = \frac{[H_3O^+]K_s'}{K_2} + K_s' \quad \text{(Eq. 11)}$$

Table I—Comparison of Total Molar Solubility, *S*, of Silver Sulfadiazine Determined by the Method of Known Subtraction with the Molar Concentration of the Silver Ion Determined by Direct Potentiometry on Identical Samples at 25 ± 0.1°, Ionic Strength 0.1 *M*, in Nitric Acid Buffers

	pH 2.128		pH 3.851	
	$S \times 10^5$	$[Ag^+] \times 10^5$	$S \times 10^5$	$[Ag^+] \times 10^5$
	59.18	59.11	6.690	6.455
	58.06	57.97	6.690	6.517
	59.35	59.34	6.434	6.517
	58.53	58.42	6.768	6.475
	59.19	60.00	6.586	6.375
	57.30	57.97	6.612	6.455
Mean	58.60	58.80	6.466	6.629

Table II—Calculation of Solubility Product of Silver Sulfadiazine Using Eq. 13 at 25 ± 0.1° and Ionic Strength 0.1 *M*

pH	f_0[a]	$[Ag^+]^2$	K_s
2.122	2.688×10^{-5}	2.980×10^{-7}	8.04×10^{-12}
2.373	6.024×10^{-5}	1.352×10^{-7}	8.16×10^{-12}
2.630	1.279×10^{-4}	6.165×10^{-8}	7.90×10^{-12}
2.891	2.583×10^{-4}	3.139×10^{-8}	8.14×10^{-12}
Mean	$8.06 \times 10^{-12} \pm 0.12$		

[a] $K_1 = 8.59 \times 10^{-3}$, and $K_2 = 3.82 \times 10^{-7}$.

where S is the total molar solubility, and K_2 is defined by Eq. 2. A plot of S^2 *versus* $[H_3O^+]$ would be expected to be linear with an intercept of K_s' and a slope of K_s'/K_2, from which K_2 may be experimentally determined.

Figure 2 is a linear plot of the equilibrium values of $[Ag^+]^2/[H_3O^+]$ against the equilibrium $[H_3O^+]$ value, having a slope of 2.459×10^{-3} and an intercept of 2.112×10^{-5}. From the slope and intercept, pK_1 was found to be 2.07 ± 0.06 at an ionic strength of 0.1 *M*. This value is in agreement with a literature value of 2.09 (14). As shown in Fig. 3, a plot of S^2 *versus* $[H_3O^+]$ at equilibrium is linear with an intercept of 3.05×10^{-11} and a slope of 7.98×10^{-5}. From the slope and intercept, pK_2 was evaluated experimentally to be 6.42 ± 0.04, in agreement with a previously reported value of 6.45 (14).

The possibility of intact silver sulfadiazine in solution in a pH range of 2.1–3.8 was investigated by comparison of the total molar solubility, S, as determined by the method of known subtraction, with the molar concentration of free silver ion, $[Ag^+]$, by direct potentiometric analysis on identical samples under the given experimental conditions. By the use of one-way analysis of variance, the means displayed in Table I are not statistically different at the 5% level. Therefore, in the pH 2–3 range,

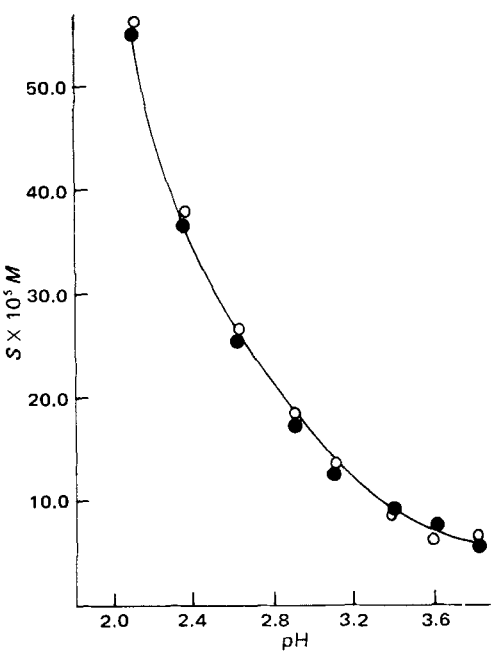

Figure 4—*Molar solubility (S) of silver sulfadiazine* versus *pH at 0.1 M ionic strength and 25 ± 0.1°. Key: ●, experimental values; and ○, calculated from Eq. 7 and the equilibrium constants determined in this study.*

the solubility, S, of silver sulfadiazine is given by Eqs. 4 and 5. The solubility product of silver sulfadiazine is given by Eq. 1. By substituting Eqs. 2 and 3 into Eq. 5, an expression may be derived giving the ratio, f_0, of the sulfadiazine anion to the total solubility, where:

$$f_0 = \frac{[X^-]}{S} = \left(1 + \frac{[H_3O^+]}{K_2} + \frac{[H_3O^+]^2}{K_1K_2}\right)^{-1} \quad \text{(Eq. 12)}$$

Combining this expression with Eq. 1 gives:

$$K_s = f_0S^2 \quad \text{(Eq. 13)}$$

Application of this equation to the experimental data at the low pH range is given in Table II, where the mean solubility product constant for silver sulfadiazine was $8.06 \pm 0.12 \times 10^{-12}$.

A plot of the molar solubility, S, of silver sulfadiazine against pH over the pH range studied is displayed in Fig. 4. This plot at pH 2–3 compares very closely with the distribution of the sulfadiazine cation over the same pH range. Thus, the solubility of silver sulfadiazine is directly a function of sulfadiazine ionization.

The solubility would be expected to be nearly pH independent in the pH 4–5 range where the predominant sulfadiazine species is the neutral molecule. For pH 6–7, the solubility is estimated by Eq. 9. At pH 6, the calculated solubility, S, was 5.40×10^{-6} *M*; at pH 7, it was 3.19×10^{-6} *M*. Where the predominant sulfadiazine species is the sulfadiazine anion, the limiting value of the solubility would be expected to be the square root of the solubility product constant, $\sqrt{K_s} = 2.83 \times 10^{-6}$ *M*.

REFERENCES

(1) C. L. Fox, Jr., B. W. Rappole, and W. Stanford, *Surg. Gynecol. Obstet.*, **128**, 1021 (1968).

(2) S. M. Modak and C. L. Fox, Jr., *Biochem. Pharmacol.*, **22**, 2391 (1973).

(3) C. L. Fox, Jr., and S. M. Modak, *Antimicrob. Ag. Chemother.*, **6**, 582 (1974).

(4) R. H. Jensen and N. Davidson, *Biopolymers*, **4**, 17 (1966).

(5) J. C. Ballin, *J. Am. Med. Assoc.*, **230**, 1184 (1974).

(6) H. S. Rosenkranz and S. Rosenkranz, *Antimicrob. Ag. Chemother.*, **11**, 373 (1972).

(7) B. J. Sandmann, R. U. Nesbitt, Jr., and R. A. Sandmann, *J. Pharm. Sci.*, **63**, 948 (1974).

(8) A. W. Struss, *Diss. Abstr. Int. B*, **35** (12, Part 1), 580 (1975).

(9) C. E. Braun and J. L. Towle, *J. Am. Chem. Soc.*, **63**, 3223 (1941).

(10) R. G. Bates, "Determination of pH Theory and Practice," 2nd ed., Wiley, New York, N.Y., 1973, p. 96.

(11) R. A. Durst, in "Ion Selective Electrodes," R. A. Durst, Ed., National Bureau of Standards Special Publication No. 314, U.S. Government Printing Office, Washington, D.C., 1969, pp. 381–385.

(12) *Orion Research Inc. Newsletter*, **1**, 25 (1969).

(13) R. K. Murmann, "Inorganic Complex Compounds," Reinhold, New York, N.Y., 1964, p. 41.

(14) H. A. Krebs and J. C. Speakman, *J. Chem. Soc.*, **1945**, 593.

ACKNOWLEDGMENTS AND ADDRESSES

Received December 9, 1975, from the *School of Pharmacy, University of Missouri–Kansas City, Kansas City, MO 64110.*

Accepted for publication May 19, 1976.

Presented at the Basic Pharmaceutics Section, APhA Academy of Pharmaceutical Sciences, Atlanta meeting, November 1975.

Partial support from Marion Laboratories is gratefully acknowledged.

* Fellow, Robert Lincoln McNeil Memorial, American Foundation for Pharmaceutical Education.

[x] To whom inquiries should be directed.

GLC Assay of Conjugated Estrogen Formulations

K. M. McERLANE ˣ and N. M. CURRAN

Abstract □ A procedure is described for the enzyme hydrolysis and GLC assay of conjugated estrogens in commercial formulations. Resolution of up to nine of the components is achieved on a methyl phenyl cyanopropyl silicone-coated column using a dual-derivatization and dual-injection technique. Replicate results from analyses of a commercial tablet formulation yielded coefficients of variation between 1.0 and 17.2%, depending mainly on the quantity present; a coefficient of variation of 0.4% was obtained for the assay for total conjugated estrogens. Similar results were obtained with other commercial formulations.

Keyphrases □ Estrogens, conjugated—enzyme hydrolysis and GLC analysis, commercial formulations □ GLC—analysis, conjugated estrogens, commercial formulations □ Enzyme hydrolysis—for GLC analysis of conjugated estrogens, commercial formulations □ Hormones—conjugated estrogens, enzyme hydrolysis and GLC analysis, commercial formulations

According to the USP (1), conjugated estrogens contain "a mixture of the sodium salts of the sulfate esters of the estrogenic substances, principally estrone and equilin, that are of the type excreted by pregnant mares." The USP also requires that conjugated estrogens contain dihydroequilin-17α, dihydroequilin-17β, estradiol-17α, estradiol-17β, 8-dehydroestrone, and equilenin. In addition, other sulfate esters of dihydroequilenin-17α and dihydroequilenin-17β have been identified in the urine of pregnant mares (2).

The USP XIX assay for conjugated estrogens is a long and difficult procedure, in which only estrone (I) and equilin (II) are quantified after acid hydrolysis of the sulfates. Dihydroequilin-17α and 17β (III), estradiol-17α and 17β (IV), 8-dehydroestrone (V), and equilenin (VI) are separately identified only by GLC following enzyme hydrolysis. The assay for total conjugated estrogens is performed separately using a color-producing reagent.

Experience in these laboratories indicated that the acid hydrolysis of the sulfate may lead to decomposition of some estrogens, notably dihydroequilin.

Because of the complex nature of the product, many methods have been suggested to resolve the components including column (3–6), thin-layer (7, 8), paper (9–13), high-speed liquid (14), and gas–liquid (15–17) chromatographic techniques. Earlier studies (18) showed the feasibility of resolving the estrogen steroids by GLC using a dual-derivatization and dual-injection procedure on a methyl phenyl cyanopropyl silicone (OV-225) column.

In the present procedure, the sulfate esters of equine estrogens are hydrolyzed by enzyme incubation and subsequently quantified by GLC.

EXPERIMENTAL

Enzyme Hydrolysis—*Tablet Samples*—Twenty tablets were weighed and finely powdered, and an aliquot equivalent to 1.5 mg of conjugated estrogens was weighed directly into a 50-ml round-bottom, polytetrafluoroethylene[1]-lined, screw-capped centrifuge tube. Fifteen milliliters of acetate buffer (pH 5.2, 0.02 *M*) was added, and the tubes were shaken on a horizontal shaker for 30 min.

Injectable Samples —The contents of a multiple injection vial (25 mg) were transferred quantitatively to a 50-ml volumetric flask, using the acetate buffer, and brought to volume. A 3-ml aliquot (1.5 mg) of this solution was then placed in a 50-ml round-bottom, polytetrafluoroethylene-lined, screw-capped centrifuge tube containing 12 ml of acetate buffer.

Redistilled benzene (10 ml) was added to all tubes, and they were gently shaken on a horizontal shaker for 20 min. The tubes were centrifuged, and the top benzene layer was removed as completely as possible with a 10-ml pipet. An additional 10 ml of benzene was added, and the process was repeated. The tubes were then shaken to resuspend the solid material, and the contents were transferred to a 250-ml round-bottom flask; the tubes were rinsed with 2 × 2 ml of acetate buffer, which was added to the flask. By using a rotary evaporator and taking care to avoid frothing, the residual benzene was removed until its odor was no longer apparent. Traces of benzene remaining in the centrifuge tube were removed with a gentle stream of air.

The contents of the flask were then transferred back to the original centrifuge tube with 3 × 2 ml of acetate buffer, 7500 units of sulfatase enzyme was added, and the tubes were incubated for 30 min at 45° with occasional shaking. The tubes were then cooled to room temperature, 15 ml of pure redistilled chloroform was added, and the tubes were shaken for 30 min on a horizontal shaker.

After centrifuging, the chloroform layer was removed as completely as possible by driving the tip of a pipet down through the aqueous layer and gently blowing out any water that may have entered the pipet before drawing up the chloroform. The chloroform was transferred to a stoppered tube through a funnel containing a pledget of glass wool covered with a bed of anhydrous sodium sulfate. The free phenolic estrogens were stored in the refrigerator until required for derivatization. (Storage times did not exceed 2 days.)

Sample Preparation—Two 5-ml polytetrafluoroethylene-lined, screw-capped, conical vials[2] were used for each sample. One milliliter of an ethanolic solution of the internal standard, ethinyl estradiol[3] (VII), was added to one vial, and then 3 ml of the estrogen hydrolysate in chloroform was added to each vial. To the vial containing the estrogens and the internal standard, 0.1 ml of pyridine and 0.05 ml of a silylating reagent[4] were added; the sample was capped and heated for 10 min at 60°. To the other sample (no internal standard), 0.1 ml of a 2% solution of methoxamine in pyridine was added; this sample was heated at 60° for 3 hr. After this time, 0.05 ml of silylating reagent was added and the solution was further heated at 60° for 10 min.

At the completion of the silylation reaction, 2–4-μl aliquots of the samples were injected in the 3% OV-225 column.

Column Packing—Experience has shown that the method of column preparation is important in achieving good resolution. Therefore, the procedure is described in detail.

The coated support, 3% OV-225 on Chromosorb W (HP), 100–120 mesh[5], was prepared by uniformly depositing a chloroform solution (50 ml) of the stationary phase (0.75 g), using a Pasteur pipet, over the surface of a bed of the support phase (25 g) uniformly dispersed in a 13.97-cm (5.5-in.) petri dish. The vessel in which the stationary phase was prepared was rinsed with 2–3 ml of chloroform onto the support in the same manner.

The barely moist cake of coated support was then transferred to a fluidizer sitting on a hot plate. With a gentle stream of clean dry nitrogen flowing through the fluidizer, the temperature of the hot plate was raised until a thermometer inserted in the base of the fluidizer registered about 175°. Heating was continued for 0.5 hr or until the coated support tumbled freely and no odor of chloroform was detectable.

A 1.8-m × 0.63-cm (6-ft × 0.25-in.) o.d., glass, U-shaped column was filled with chromic acid and allowed to sit for 0.5 hr. The column was emptied, rinsed with water and methanol, and then dried by drawing air through it. It was then filled with 5% dimethylchlorosilane in dry toluene

[1] Teflon (du Pont).

[2] ReactiVials, Pierce Chemical Co., Rockford, Ill.
[3] USP reference standard.
[4] TRISIL TBT, Pierce Chemical Co., Rockford, Ill.
[5] Chromatographic Specialties, Brockville, Ontario, Canada.

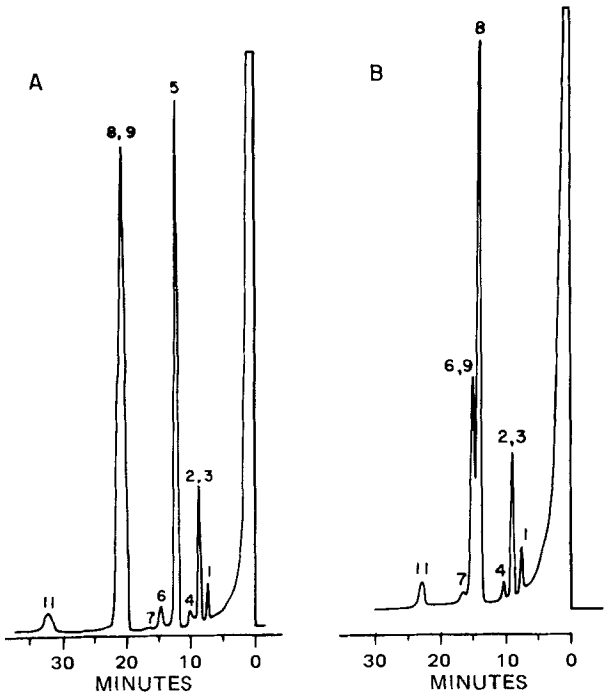

Figure 1—*Trimethylsilyl (A) and methoxamine–trimethylsilyl (B) derivatives of a synthetic composite of equine estrogens. Key: 1, estradiol-17α; 2, estradiol-17β; 3, dihydroequilin-17α; 4, dihydroequilin-17β; 5, ethinyl estradiol; 6, dihydroequilenin-17α; 7, dihydroequilenin-17β; 8, estrone; 9, equilin; and 11, equilenin.*

and allowed to stand for 1 hr. Then it was emptied, rinsed with methanol and acetone, and thoroughly dried as before.

The column was packed by applying vacuum on one end while adding about 15.2-cm (6-in.) sections of coated support to the other and gently vibrating each section.

The column was conditioned in the gas chromatograph oven at 175° with a nitrogen flow of 45 ml/min for 8 hr. The oven temperature was then raised to 235° at 3°/min and held for an additional 16 hr or until a stable baseline was achieved. An occasional injection of a mixture of *N,O*-bis-(trimethylsilyl)acetamide, trimethylsilyldiethylamine, and hexamethyldisilazane[6] shortened conditioning times.

RESULTS AND DISCUSSION

The resolution achieved using a 3% methyl phenyl cyanopropyl silicone (OV-225) column for the trimethylsilyl derivatives of a synthetic composite of sulfates of equine estrogens (I–VIII) is shown in Fig. 1A. In this chromatogram, baseline separation of all steroids is apparent except for the pairs estradiol-17β–dihydroequilin-17α and estrone–equilin within a total chromatographic analysis time of less than 55 min.

Separation of the two major steroids, estrone and equilin, was achieved by forming the methoxamine–trimethylsilyl derivatives of the keto steroids present in the mixture with the resulting resolution (R = 0.8) of the keto steroids as shown in Fig. 1B. The pair estradiol-17β–dihydroequilin-17α could not be resolved under any conditions employed. However, since the former is known to contribute little to the normal natural balance of the components of equine estrogens (2), little interference would be observed in the determination of dihydroequilin-17α. (The steroid 8-dehydroestrone was not included in the synthetic mixture due to a short supply.)

Quantitative Aspects—To utilize this resolution of estrogens as the basis of a quantitative method for the individual determination of most, if not all, of the components of conjugated estrogens, area response factors for the trimethylsilyl derivatives of the estrogens were determined in relation to an internal standard, ethinyl estradiol (Table I).

With the addition of a known amount of internal standard, the absolute amounts of each steroid in a mixture could then be determined from:

$$A = \frac{B \times C \times D}{E} \qquad \text{(Eq. 1)}$$

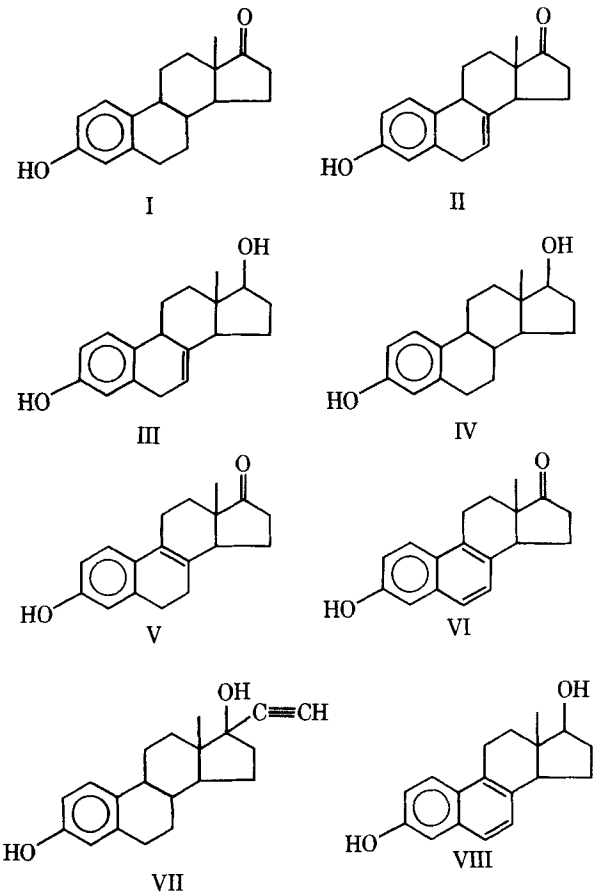

where A = weight of steroid, B = response factor, C = weight of internal standard, D = area of steroid, and E = area of internal standard.

The determination of the amounts of the equine estrogens observed in a sample from the foregoing calculation will yield a total for estrone and equilin. However, the proportions of these two steroids can be determined from the chromatogram of the methoxamine–trimethylsilyl derivatives (which does not contain any internal standard) by their relative peak heights. Peak height responses for estrone and equilin were identical. The peak observed for equilin as its methoxamine–trimethylsilyl derivative overlaps with that for the trimethylsilyl derivative of dihydroequilenin-17α (VIII). The contribution of the latter is most easily determined by the peak height ratio between the chromatogram of the trimethylsilyl derivatives and that for the methoxamine–trimethylsilyl derivatives by:

$$F = \frac{G \times H}{I} \qquad \text{(Eq. 2)}$$

where F = height of dihydroequilenin-17α in the methoxamine–trimethylsilyl chromatogram, G = height of dihydroequilenin-17α in the trimethylsilyl chromatogram, H = height of dihydroequilenin in the methoxamine–trimethylsilyl chromatogram, and I = height of dihydroequilin in the trimethylsilyl chromatogram.

Subtraction of the contribution of dihydroequilenin-17α from equilin

Table I—Response Factors for Equine Estrogens

Trimethylsilyl Steroid Ethers	Response[a]
Estradiol-17α	0.91
Estradiol-17β	1.04
Dihydroequilin-17α	1.04
Dihydroequilin-17β	1.03
Dihydroequilenin-17α	0.95
Dihydroequilenin-17β	1.04
Estrone	1.20
Equilin	1.20
8-Dehydroestrone	1.00
Equilenin	1.12

[a] Relative to ethinyl estradiol.

[6] Silyl-8, Pierce Chemical Co.

Table II—Assay of Synthetic Composite of Equine Estrogens

Steroid	Percent Added	Range Found, %	Average Found, %	CV, %
Estradiol-17α	1.9	1.7–1.8	1.8	3.2
Estradiol-17β–dihydro-equilin-17α	7.8	6.4–8.6	7.1	4.9
Dihydroequilin-17β	1.6	0.8–1.3	1.1	14.4
Dihydroequilenin-17α	2.0	2.2–2.4	2.2	6.8
Dihydroequilenin-17β	0.8	0.8–0.9	0.9	6.7
Estrone	58.4	59.1–59.5	59.3	0.3
Equilin	22.5	21.4–22.6	21.9	2.4
Equilenin	5.1	4.6–6.3	5.8	6.6
Assay[a]		(96.9–99.0)	(98.1)	0.9

[a] $n = 6$.

Table III—Assay of 2.5-mg Tablet

Steroid	Range, %	Average, %	CV, %
Estradiol-17α	4.5–4.8	4.7	3.1
Estradiol-17β–dihydro-equilin-17α	14.7–15.4	15.2	1.7
Dihydroequilin-17β	1.1–1.2	1.2	4.0
Dihydroequilenin-17α	1.9–2.3	2.0	5.8
Dihydroequilenin-17β	0.3–0.4	0.3	17.2
Estrone	50.7–52.0	51.4	1.0
Equilin	19.5–21.2	20.2	3.3
8-Dehydroestrone	1.6–1.9	1.8	5.2
Equilenin	2.8–3.7	3.4	9.6
Assay[a]	2.49–2.51 mg	2.5 mg	0.4

[a] $n = 6$.

yields the true height of the equilin peak. This value can then be used, along with the height of the peak observed for estrone, to determine the relative amounts of estrone and equilin from the total of these two estrogens obtained as their combined trimethylsilyl derivatives. The quantitation of the individual estrogens is then complete, and these values can simply be added to give the total assay amount of the free phenolic estrogens. The equivalent weight of the conjugates can then be calculated by:

$$\text{total assay} = \text{weight of free steroids} \times 1.38 \times \text{dilution factor} \quad \text{(Eq. 3)}$$

where 1.38 represents the weighted molecular weight ratio between free phenol and the sulfate ester.

To test the robustness of the 3% OV-225 column to varying conditions of the gas chromatograph, the column oven temperature was adjusted ±15° around the normal 225° used for the assay. The nitrogen flow was also adjusted ±15 ml/min around the 40 ml/min employed. None of these conditions, either singly or in combination, markedly affected the assay results of the individual steroids or the total assay. Under the extreme conditions of the column temperature and gas flow, the total chromatogram time for the trimethylsilyl derivatives varied between 20 and 45 min with no apparent lack of resolution.

To evaluate the variability of the GLC assay of a synthetic mixture of equine estrogens, a sample of the free phenolic steroids was prepared and then assayed according to the described method (Table II).

Enzyme Hydrolysis—Before the assay method could be applied to commercial conjugated estrogen formulations, the hydrolytic cleavage

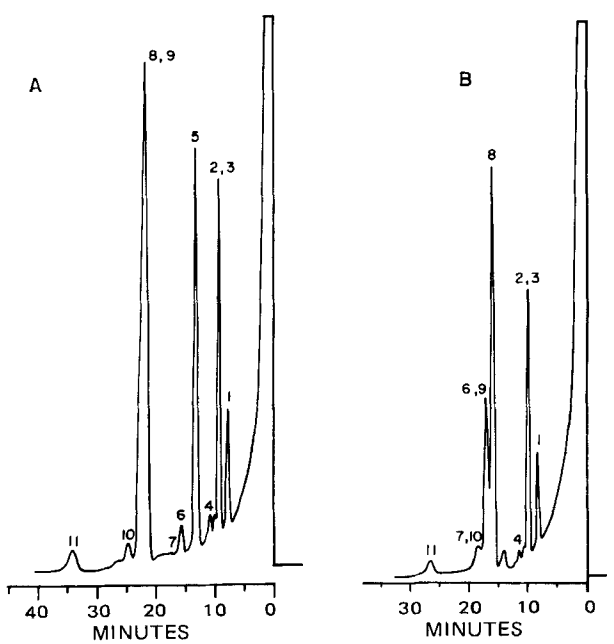

Figure 2—*Trimethylsilyl (A) and methoxamine–trimethylsilyl (B) derivatives of equine estrogens obtained from a 2.5-mg commercial tablet. Key: 1, estradiol-17α; 2, estradiol-17β; 3, dihydroequilin-17α; 4, dihydroequilin-17β; 5, ethinyl estradiol; 6, dihydroequilenin-17α; 7, dihydroequilenin-17β; 8, estrone; 9, equilin; 10, 8-dehydroestrone; and 11, equilenin.*

of the sodium sulfate esters of the phenolic steroids was investigated. The sulfatase enzyme derived from *Helix pomatia*[7] was subjected to varying time, temperature, buffer concentration, and pH conditions. Many methods (19, 20) showed the effectiveness of sulfatase enzyme in pH 5.2 acetate buffer at 37° toward the hydrolysis of estrone sulfate. However, the time interval quoted was frequently about 18 hr, and this time was deemed inappropriate for this study. Therefore, the variables of temperature (40, 45, 50, and 55°), pH (4.5, 5.2, 5.5, and 6.0), hydrolysis time (20, 30, and 40 min), and acetate buffer molarity (0.02, 0.1, and 0.2) were studied. The results indicated that quantitative recovery of the free steroid could be expected under all conditions and combinations of these conditions when potassium estrone sulfate was used as a substrate. As a laboratory convenience, commercial sulfate conjugates of equine estrogens were routinely hydrolyzed at 45° for 30 min in 0.02 *M* acetate buffer at pH 5.2.

When conjugated estrogen samples were initially hydrolyzed under these conditions and then extracted into chloroform (a single extraction was quantitative), the samples revealed, after evaporation and silylation, an extraneous peak in the chromatogram interfering with the less retentive diols. A benzene prewash of the formulation samples, after they had been extracted into the acetate buffer, removed the interference. This peak, appearing between the trimethylsilyl derivatives of estradiol-17α and dihydroequilin-17α, was purified by preparative GLC of the silylated prewash residue. Mass spectral analysis of the compound giving rise to the impurity showed an apparent molecular ion at *m/e* 396 with other prominent ions at *m/e* 381, 323, 277, 217, 216, 203, 189, 188, 187, and 159. Comparisons of the mass spectra with other similarly prepared estrogen samples failed to provide any similarities between the samples.

To ascertain that sufficient enzyme was being used to obtain complete hydrolysis of estrogen conjugates in formulations (phosphate inhibits the action of sulfatase enzyme and is used in tablet formulas), a series of tablet samples was prepared using 1000, 2000, 4000, 8000, and 10,000 units of sulfatase. In some cases, 1000 units of enzyme was sufficient to yield theoretical quantitative recovery of the estrogens, but other samples required at least 4000 units. Consequently, for new tablet formulations, each analysis was performed in triplicate using 1000, 5000, and 7500 units of enzyme to expose enzyme inhibition.

Formulation Quantitation—A commercial 2.5-mg tablet was assayed by obtaining the trimethylsilyl derivative of the steroid hydrolysate (Fig. 2A). The peak due to dihydroequilenin-17β is not noticeable in the chromatogram but was detected by the integrator. A peak following the estrone–equilin peak was identified as 8-dehydroestrone from chromatographic comparison with authentic material. The chromatogram of the methoxamine–trimethylsilyl derivative (Fig. 2B) displays the partial resolution of estrone and equilin, sufficient to allow their quantitation (Table III).

The chromatograms of the trimethylsilyl and methoxamine–trimethylsilyl derivatives of a 1.25-mg tablet obtained from the same manufacturer are shown in Figs. 3A and 3B, and the quantitative assay is given in Table IV. The similarity of relative estrogen amounts is quite obvious and would likely be related to the manufacturer's source of pregnant mare's urine. The label claim of 1.25 mg was exceeded in this instance by 16%, the USP maximum.

Similar results (Table V) were obtained for the analysis of an injectable preparation from the same manufacturer; again the similarity of the relative proportions of steroids points to a uniform source.

The method has been applied with equal facility to various tablet

[7] Type H-2, Sigma Chemical Co., St. Louis, Mo.

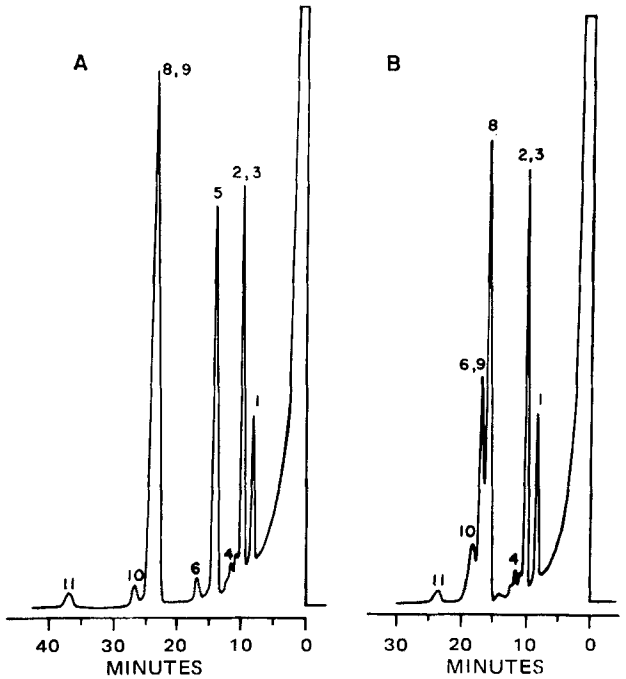

Figure 3—*Trimethylsilyl (A) and methoxamine–trimethylsilyl (B) derivatives of equine estrogens obtained from a 1.25-mg commercial tablet. Key: 1, estradiol-17α; 2, estradiol-17β; 3, dihydroequilin-17α; 4, dihydroequilin-17β; 5, ethinyl estradiol; 6, dihydroequilenin-17α; 8, estrone; 9, equilin; 10, 8-dehydroestrone; and 11, equilenin.*

formulations and has provided the basis of a GLC identification and quantitation of the main estrogenic components of conjugated estrogen preparations.

Comparison with Literature Methods—Other GLC methods for the quantitative analysis of esterified (16) and conjugated (17) estrogens have been reported. They are based on the resolution of the trimethylsilyl ether derivatives of the free equine estrogens on a diethylene glycol succinate-coated column. The steroids are resolved, except that the peak due to estradiol-17β appears as a shoulder on the dihydroequilin-17α peak. On an OV-225 column as used in the present study, the peak due to the minor constituent, estradiol-17β, is not resolved from dihydroequilin-17α.

The proposed OV-225 column is apparently indefinitely stable under conditions of normal usage. Diethylene glycol succinate columns, however, are limited to a useful lifetime to 2–3 weeks in equine estrogen analysis (2), probably due to column breakdown from oxidative processes and to bleed at the temperature of the analysis (21). In addition, there are reportedly batch-to-batch variations in the properties of diethylene glycol succinate (22), and these variations may affect the chromatographic behavior of the steroids.

The time and cost of the OV-225 and diethylene glycol succinate procedures are comparable. The time required for preparation of the additional samples for the OV-225 procedure is compensated for by the chromatographic time of 55 min as compared to 75 min for the diethylene glycol method. The peaks observed on the OV-225 column are sharp, whereas those seen on the diethylene glycol succinate are broadened due to the longer retention times; the peak due to equilenin, therefore, may be difficult to quantify. Calculations associated with the OV-225 method are marginally longer due to the double-injection technique, but this factor is not significant in practice[8].

Both the OV-225 and diethylene glycol succinate methods have advantages. For the analysis of a single sample, the preference may be for the diethylene glycol succinate method because of the slightly better resolution. For the long-term analysis of many samples, the stability and robustness of the OV-225 method appear to be highly advantageous.

Table IV—Assay of 1.25-mg Tablet

Steroid	Weight, mg	Percent
Estradiol-17α	0.08	5.5
Estradiol-17β–dihydro-equilin-17α	0.21	14.5
Dihydroequilin-17β	0.01	0.7
Dihydroequilenin-17α	0.03	1.7
Dihydroequilenin-17β	0.01	0.3
Estrone	0.74	50.6
Equilin	0.32	21.9
8-Dehydroestrone	0.03	2.0
Equilenin	0.04	2.7
Total	1.46 mg	(116% of label claim)

Table V—Assay of 25-mg Multiple Injection Vial

Steroid	Weight, mg	Percent
Estradiol-17α	0.81	3.0
Estradiol-17β–dihydro-equilin-17α	4.14	15.4
Dihydroequilin-17β	0.97	3.6
Dihydroequilenin-17α	0.36	1.3
Dihydroequilenin-17β	0.06	0.2
Estrone	12.66	47.2
Equilin	6.64	24.7
8-Dehydroestrone	0.56	2.1
Equilenin	0.68	2.5
Total	26.9 mg/vial	(107% of label claim)

REFERENCES

(1) "The United States Pharmacopeia," 18th rev., Mack Publishing Co., Easton, Pa., 1970.

(2) R. Roman, C. H. Yates, J. F. Millar, and W. J. A. VandenHeuvel, *Can. J. Pharm. Sci.*, **10**, 8 (1975).

(3) G. A. Grant and D. Beall, *Rec. Progr. Hormone Res.*, **5**, 307 (1950).

(4) K. Savard and B. Bierdules, *Endocrinology*, **68**, 411 (1961).

(5) B. R. Bhavani, R. V. Short, and S. Solomen, *ibid.*, **85**, 1172 (1969).

(6) G. J. Krol, R. P. Masserano, J. F. Carney, and B. T. Kho, *J. Pharm. Sci.*, **59**, 1483 (1970).

(7) L. E. Crocker and B. A. Lodge, *J. Chromatogr.*, **62**, 158 (1971).

(8) *Ibid.*, **67**, 419 (1972).

(9) J. E. Cox, *J. Chromatogr.*, **61**, 193 (1971).

(10) G. J. Krol, G. R. Bayden, R. H. Moady, J. C. Comeau, and B. T. Kho, *ibid.*, **61**, 187 (1971).

(11) E. Heltman, *Science*, **111**, 571 (1950).

(12) E. Heltman, *J. Am. Chem. Soc.*, **73**, 851 (1951).

(13) R. E. Oakey, *J. Chromatogr.*, **8**, 2 (1962).

(14) A. G Butterfield, B. A. Lodge, and N. J. Pound, *J. Chromatogr. Sci.*, **11**, 401 (1973).

(15) I. Schroeder, J. C. Medina-Scivedo, and G. Lopez-Sanches, *ibid.*, **10**, 183 (1972).

(16) R. Roman, C. H. Yates, J. F. Millar, and W. J. A. VandenHeuvel, *Can. J. Pharm. Sci.*, **10**, 12 (1975).

(17) R. Johnson, R. Masserano, R. Haring, B. Kho, and G. Schilling, *J. Pharm. Sci.*, **64**, 1007 (1975).

(18) K. M. McErlane, *J. Chromatogr. Sci.*, **12**, 97 (1975).

(19) M. F. Jayle, R. Scholler, P. Jarrige, and S. Metay, *Bull. Soc. Chim. Biol.*, **41**, 1593 (1959).

(20) J. Jarrige and M. F. Boyle, *ibid.*, **45**, 783 (1963).

(21) R. F. Kruppa, and R. S. Henly, Paper 144 presented at the Pittsburgh Conference, Cleveland, Ohio, Mar. 1974.

(22) J. R. Mann and S. T. Preston, *J. Chromatogr. Sci.*, **11**, 216 (1973).

ACKNOWLEDGMENTS AND ADDRESSES

Received June 20, 1975, from the *Pharmaceutical Chemistry Division, Health Protection Branch, Health and Welfare Canada, Tunney's Pasture, Ottawa, Ontario, Canada K1A 0L2.*

Accepted for publication May 27, 1976.

Presented in part at the APhA Academy of Pharmaceutical Sciences, Chicago meeting, August 1974.

The authors thank Dr. B. A. Lodge for helpful discussions and Ayerst Laboratories, St-Laurent, Québec, Canada, for supplying the pure individual steroids.

ˣ To whom inquiries should be directed.

[8] A program for the Hewlett-Packard 9810 calculator is available on request.

GLC Analysis of Acetazolamide in Blood, Plasma, and Saliva following Oral Administration to Normal Subjects

SYLVIA M. WALLACE *, VINOD P. SHAH ‡, and SIDNEY RIEGELMAN ˣ

Abstract □ An electron-capture GLC assay for acetazolamide in biological fluids was developed. Extraction efficiency was 96–104%. The minimum detectable amount of acetazolamide was 10 ng/sample. Concentrations of acetazolamide were determined by GLC in blood, plasma, plasma water, and saliva after oral administration of a single 250-mg dose to five volunteers. Erythrocyte levels were calculated from whole blood and plasma data. Concentration of free drug in the plasma was measured in samples of plasma water obtained by microultrafiltration. Peak plasma levels of 10–18 μg/ml were reached 1–3 hr after the dose. At least 1 hr later, erythrocyte levels reached peak concentrations of 13–29 μg/ml. Over 31 hr, plasma levels declined more rapidly than erythrocyte levels. Saliva concentrations averaged 1% of those in plasma and decreased at a rate equal to that of plasma. Saliva levels were proportional to, but not equal to, plasma water concentration. Saliva to plasma ratios were consistent for any given individual and, therefore, offer a means of monitoring drug dosage without resorting to frequent blood sampling.

Keyphrases □ Acetazolamide—GLC analysis, human blood, plasma, and saliva □ GLC—analysis, acetazolamide, human blood, plasma, and saliva □ Carbonic anhydrase inhibitors—acetazolamide, GLC analysis, human blood, plasma, and saliva

Acetazolamide is used primarily to control intraocular pressure in the treatment of glaucoma. Side effects of the drug, although not life threatening, are often severe enough to warrant discontinuing therapy. At present, dosage regimens are adjusted empirically to balance therapeutic and toxic effects. However, by using as a guideline the minimum effective plasma concentration for lowering intraocular pressure (10 μg/ml) established by Lehmann *et al.* (1), a more efficient, individualized control of therapy should be possible.

The present study was designed to:

1. Develop a rapid, sensitive method for quantitating acetazolamide in biological fluids. Until recently (2), techniques for analyzing acetazolamide have been limited to the carbonic anhydrase inhibition method (3). However, the lower limit of the enzyme assay is 0.2 μg/ml of plasma.

2. Determine the feasibility of monitoring acetazolamide dosage in glaucoma patients by measurement of saliva concentrations. Saliva has been suggested (4–6) as a satisfactory alternative to plasma for routine monitoring of pharmacokinetic parameters. Use of saliva as the sampling fluid precludes the discomfort and inconvenience of multiple venipunctures but still yields the requisite information for dosage regimen adjustment.

3. Establish the relationship between plasma, saliva, and erythrocyte (red blood cell) concentrations of acetazolamide after oral administration of a single 250-mg dose to humans. Acetazolamide has a high affinity for binding sites, purportedly carbonic anhydrase enzymes, within the red blood cells (7). To define the kinetics of multiple dosing, the pool of drug within the red blood cells must be examined.

EXPERIMENTAL

Materials—Acetazolamide[1], fluoranthene[2], analytical grade solvents[3] (ether, dichloromethane, and 2-propanol), and trimethylphenylammonium hydroxide[4] (0.1 *M* in methanol) were used as obtained from standard sources without further purification. Tetramethylammonium hydroxide[5] (20% in methanol) diluted with methanol to 0.2% was used as an alternative derivatizing reagent, since many lots of trimethylphenylammonium hydroxide produce interfering peaks on electron-capture GLC.

Sample Preparation—Aliquots of blood, plasma (50–100 μl), and saliva (1–2 ml), adjusted to approximately pH 5 by the addition of 0.5 ml of 0.1 *M* acetate buffer, were extracted with 10 ml of organic solvent (six volumes of ether, four volumes of dichloromethane, and two volumes of 2-propanol). Tubes were centrifuged[6] for 15 min at 1500 rpm. The lower aqueous layer was frozen in a dry ice–acetone bath, and the upper organic layer was decanted quantitatively. Alternatively, if the concentration of acetazolamide in plasma or saliva exceeded the linear range of the standard curve, an aliquot of the organic layer was removed. The organic extract was evaporated to dryness under a slow stream of nitrogen.

Chromatographic Analysis—The internal standard, fluoranthene (2.5 μg in an ether solution), was added to the dried organic extract of plasma and saliva samples. The solvent was evaporated to dryness under nitrogen. After addition of 50 μl of methylating reagent (0.1 *M* trimethylphenylammonium hydroxide or 0.2% tetramethylammonium hydroxide in methanol), 2-μl aliquots were chromatographed. Chromatograms obtained with the two methylating reagents were identical.

The gas chromatograph[7] equipped with a ^{63}Ni-electron-capture detector was operated at 280, 215, and 340° for the injector, column, and detector, respectively. Solutions were chromatographed on a 1.8-m, 0.3-cm (6-ft, 0.124-in.) o.d. glass column packed with 3% OV-17 on Gas Chrom Q[8] (100–120 mesh). Carrier gas (95% argon, 5% methane) flow was 30 ml/min.

Sample Collection—Five healthy volunteers (two females and three males) between the ages of 24 and 31 years were each given a 250-mg tablet of acetazolamide[9] on an empty stomach. Blood samples were collected in heparinized tubes[10] at 0, 0.25, 0.5, 1, 2, 3, 5, 7, 9, 24, 27, and 31 hr after drug administration. At the same time, saliva (stimulated by chewing an elastic band) was collected in wide mouth vials. Saliva and plasma (separated from whole blood by centrifugation) were stored at 0° prior to analysis. Aliquots (100 μl) of plasma water were obtained from the 1-, 2-, 3-, 5-, 7-, and 9-hr plasma samples using a microultrafiltration procedure (8).

Calculation of Red Blood Cell Levels—Concentrations of acetazolamide in plasma, plasma water, blood, and saliva were measured directly by electron-capture GLC. Concentrations of the drug in the red blood cell fraction were calculated using the hematocrit:

$$C_B = C_{RBC}(H) + C_P(1 - H) \quad \text{(Eq. 1)}$$

$$C_{RBC} = \frac{C_B - C_P(1 - H)}{H} \quad \text{(Eq. 2)}$$

where C_B is the concentration in the blood, C_P is the concentration in the plasma, C_{RBC} is the concentration in the red blood cells, and H is the hematocrit.

[1] Sigma Chemical Co., St. Louis, Mo.
[2] Chem Service, Inc., West Chester, Pa.
[3] Mallinckrodt Chemical Works, St. Louis, Mo.
[4] Eastman Organic Chemicals, Rochester, N.Y.
[5] Aldrich Chemical Co., San Leandro, Calif.
[6] Centrifuge model UV, International Equipment Co., Needham, Mass.
[7] Model 1200, Varian Aerograph, Walnut Creek, Calif.
[8] Applied Science Laboratories, State College, Pa.
[9] Diamox, Lederle Laboratories, Pearl River, N.Y.
[10] Becton-Dickinson Co., Rutherford, N.J.

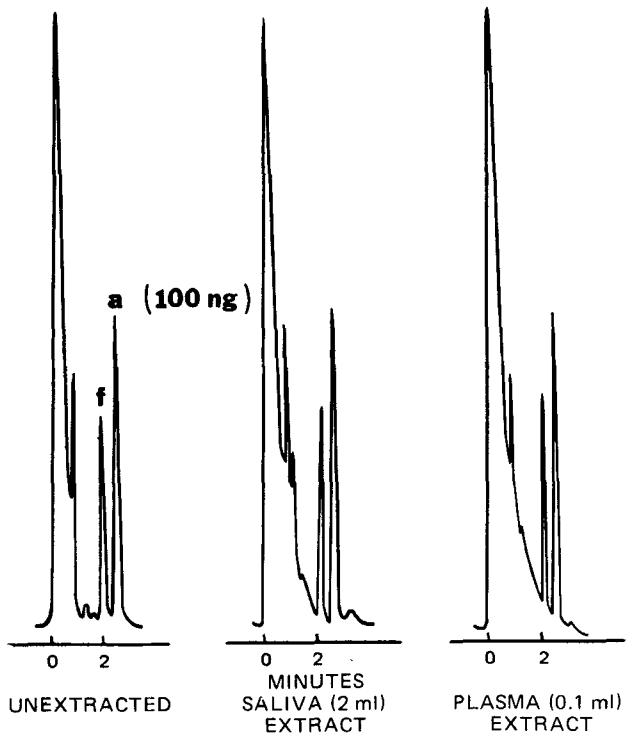

Figure 1—*Gas chromatogram of 2.5 μg of fluoranthene (f) internal standard and 100 ng of acetazolamide (a) unextracted, extracted from 2 ml of saliva, and extracted from 100 μl of plasma.*

RESULTS AND DISCUSSION

With a single extraction into the organic solvent mixture, recovery of acetazolamide from blood, plasma, and saliva was 96–104%. Two milliliters of saliva and up to 100 μl of plasma did not produce any significant interfering peaks. With a column temperature of 215° and a carrier gas flow of 30 ml/min, retention times for fluoranthene and acetazolamide were 2 and 2.5 min, respectively (Fig. 1). Peak height ratios of acetazolamide relative to fluoranthene were calculated, and standard curves were plotted as peak height ratio *versus* acetazolamide concentration.

Standard curves, prepared daily using at least four concentrations of acetazolamide, were linear ($r^2 = 0.98$) to a maximum concentration of 100 ng of acetazolamide/50 μl of methylating reagent. Concentrations of 10 ng/50 μl were easily visualized. Thus, for a 2-ml sample of saliva and a 100-μl sample of plasma or blood, the GLC method could quantitate saliva levels of 5 ng/ml and plasma or blood levels of 100 ng/ml.

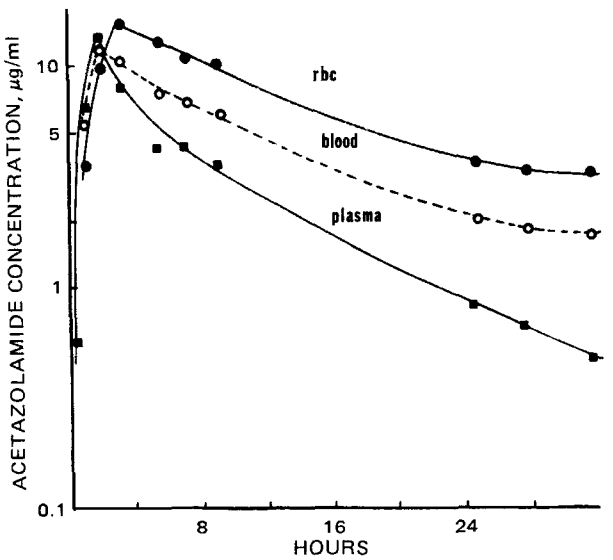

Figure 3—*Semilogarithmic plot of plasma, blood, and red blood cell levels of acetazolamide in Subject TS after a 250-mg oral dose.*

In the five subjects studied, peak plasma levels of 10–18 μg/ml were reached 1–3 hr after oral administration of the 250-mg dose (Figs. 2 and 3). These levels were approximately half those reported (1) after oral administration of a 500-mg dose. At least 1 hr later, whole blood and red blood cell levels reached peak concentrations of 10–19 and 13–29 μg/ml, respectively (Table I). This lag between the time for plasma and red blood cell levels to reach peak concentrations was apparent in all subjects.

Previous studies of elimination kinetics of acetazolamide in humans rarely analyzed plasma beyond 12 hr. These levels, if determined, were usually single-point measurements at 24 hr. Subsequent plasma concentrations were frequently too low to be measured accurately by the carbonic anhydrase inhibition method. Thus, data have heretofore not permitted evaluation of more than one exponential decay phase. With the more sensitive GLC assay, elimination from the plasma no longer appears to be a simple monoexponential process.

Over the 31 hr studied, plasma levels decayed more rapidly than red blood cell or blood levels. The area under the blood level–time curve from 0 to 31 hr was 1.5 times that under the plasma curve. If sufficient data are available, *i.e.*, for times greater than 31 hr after the dose, plasma levels should eventually decline parallel to red blood cell levels. This conjecture is suggested by the data for Subject PJ (Fig. 2). The plasma decay curve appeared biexponential with a half-life of just over 2 hr for the initial phase and 13 hr for the terminal phase. The half-life for the decay curve in the red blood cells was also 13 hr.

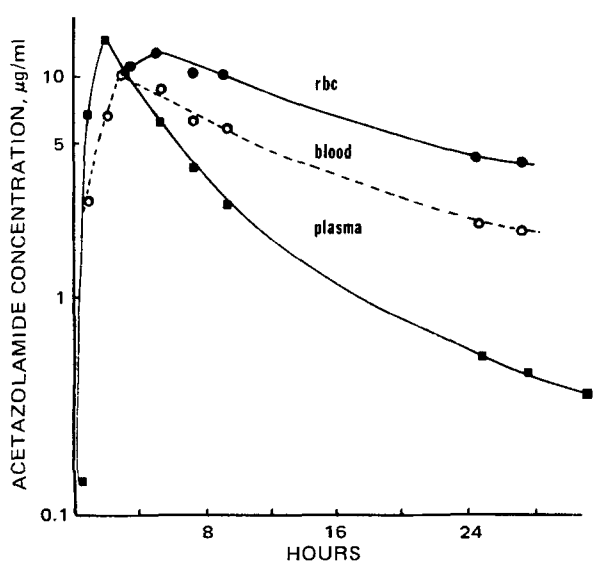

Figure 2—*Semilogarithmic plot of plasma, blood, and red blood cell levels of acetazolamide in Subject PJ after a 250-mg oral dose.*

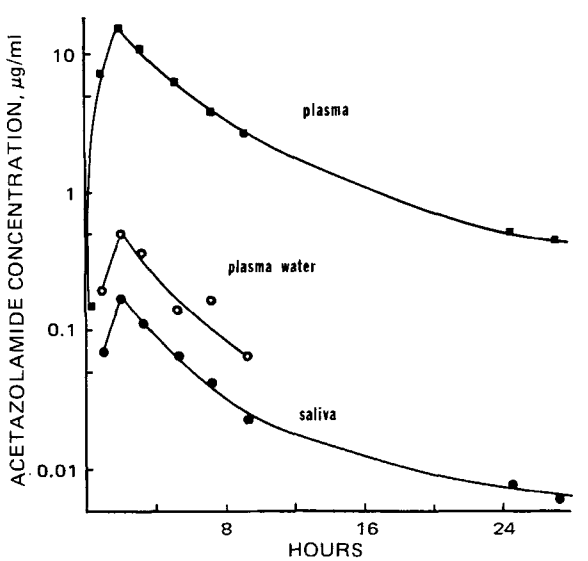

Figure 4—*Semilogarithmic plot of plasma, plasma water, and saliva levels of acetazolamide in Subject PJ.*

Table I—Blood, Plasma, and Red Blood Cell Levels (Micrograms per Milliliter) of Acetazolamide in Five Normal Subjects following Oral Administration of a 250-mg Tablet

	Hours										
	0.25	0.5	1	2	3	5	7	9	24	27	31
Subject PJ											
Blood	0	—	2.77	6.96	10.50	9.21	6.56	5.92	2.06	2.00	—
Plasma	0	0.15	7.23	14.54	10.33	6.30	3.87	2.69	0.52	0.45	0.35
Red blood cell	0	—	0	0	10.72	13.07	10.14	10.21	4.11	4.06	—
Subject CA											
Blood	0	0	0	4.79	8.42	10.54	10.65	9.61	2.91	2.68	—
Plasma	0	0	0	8.74	10.61	8.92	8.04	6.26	1.06	0.76	0.63
Red blood cell	0	0	0	0.16	5.85	12.44	13.71	13.54	5.09	4.93	—
Subject SG											
Blood	1.40	9.16	14.53	19.37	—	12.92	11.26	8.26	2.47	2.05	—
Plasma	1.20	7.91	13.77	12.95	9.12	8.97	5.97	5.24	0.84	0.78	0.35
Red blood cell	1.69	11.04	15.66	29.00	—	14.70	19.20	12.79	4.92	3.95	—
Subject AS											
Plasma	0	7.90	12.95	18.12	10.43	7.01	6.61	4.60	0.74	0.64	0.45
Subject TS											
Blood	0	0.29	5.34	11.71	11.12	7.89	7.12	6.41	1.87	1.73	1.61
Plasma	0	0.60	6.66	13.31	7.95	4.41	4.41	3.58	0.80	0.67	0.45
Red blood cell	0	0	3.51	9.49	15.47	12.71	10.86	10.12	3.40	3.19	3.21

Red blood cell levels obtained up to 27 hr could be fit adequately to a one-compartment pharmacokinetic model with an elimination half-life of 10–12 hr. However, when more samples were obtained beyond 24 hr, a second elimination phase was apparent. In Subject TS (Fig. 3), where data at 24, 28, and 31 hr were available, the down slope of the red blood cell *versus* time curve was biphasic with half-lives of 6 and 33 hr. For Subjects PJ (Fig. 2), CA, and SG, data were only available at 24 and 28 hr. Obviously, although a straight line with a half-life of 40–50 hr can be drawn through these last two data points, such estimates of a terminal slope are highly questionable. Maren *et al.* (7) reported similar biphasic decay curves for red blood cell binding of acetazolamide in dogs with half-lives of 12 hr for the initial phase and 2–3 days for the terminal phase.

Saliva levels were approximately 1% of plasma levels and decreased at a rate equal to that of the plasma rather than the blood (Fig. 4). The proportionality factors relating plasma to saliva concentration calculated by least-squares linear regression analysis (Figs. 5 and 6) and by an arithmetic average were similar (Table II). The saliva–plasma ratio did not change with time or plasma concentration of acetazolamide. However, saliva samples obtained within the 1st hr after oral administration frequently gave unpredictable results (Fig. 5). In the population tested, saliva levels were 0.7–1.1% of plasma levels. Maren and Robinson (9) reported that in hydrocephalic children treated with acetazolamide, cerebrospinal fluid levels were also 1% of plasma levels. Although there was no significant difference (analysis of variance, $p < 0.05$) between the saliva–plasma ratio of the five subjects, it is still advisable to obtain individual estimates of the ratio rather than rely on a population average.

The fraction of drug bound to plasma protein did not change significantly for the first 9 hr after oral administration. Thereafter, free drug concentration in the 100 μl of ultrafiltrate [using the microultrafiltration apparatus (8)] was too low to measure accurately. Plasma water, or free drug, concentrations averaged 6% of plasma concentrations (Table II). Thus, saliva levels were proportional to, but not equal to, levels of unbound drug in plasma (Fig. 4). In addition to protein binding, other parameters such as the oil-in-water partition coefficient and the degree of ionization obviously affect membrane transport and secretion into the saliva and cerebrospinal fluid.

CONCLUSIONS

In this single-dose study, although saliva–plasma ratios varied in the normal population, they were consistent for a given individual. Thus, saliva measurements offer a convenient means of monitoring plasma acetazolamide levels in glaucoma patients. The biexponential decay of saliva levels mirrors that of plasma.

Blood and plasma levels of acetazolamide were not equivalent. From

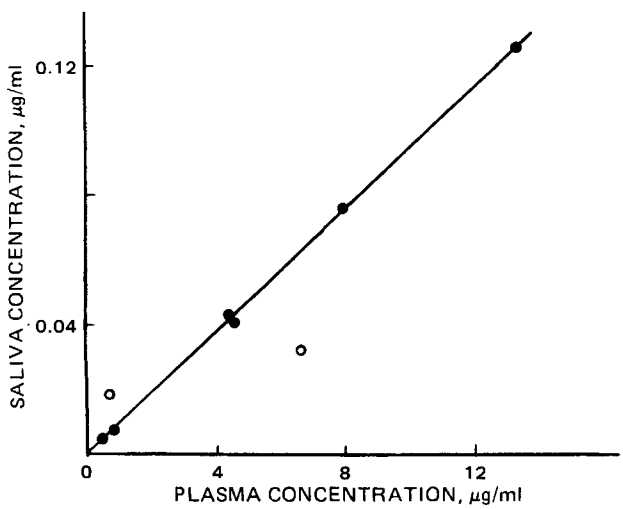

Figure 5—*Correlation of saliva and plasma concentrations of acetazolamide in Subject TS. Open circles represent samples taken within the 1st hr after oral administration. The line was calculated by least-squares linear regression analysis.*

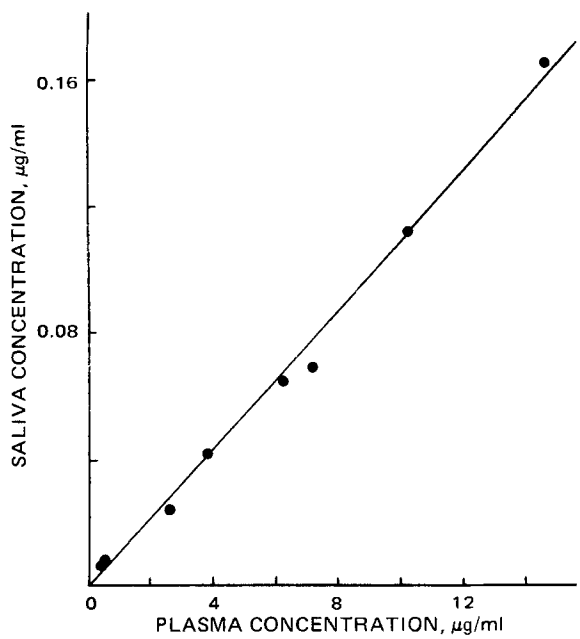

Figure 6—*Correlation of saliva and plasma concentrations of acetazolamide in Subject PJ. The line was calculated by least-squares linear regression analysis.*

Table II—Relationship of Saliva, Plasma, and Plasma Water Concentrations of Acetazolamide in Five Subjects after Oral Administration of a 250-mg Dose

Subject	Saliva Concentration / Plasma Concentration × 100			Plasma Water Concentration / Plasma Concentration × 100	
	Mean	(± *SEM*)	Linear Regression Slope	Mean	(± *SEM*)
PJ	1.11	(±0.07)	1.12	3.02	(±0.32)
CA	0.70	(±0.10)	0.51	4.22	(±0.41)
SG	0.85	(±0.09)	0.77	10.74	(±0.73)
AS	0.94	(±0.14)	0.93	5.17	(±0.52)
TS	0.84	(±0.06)	0.92	5.35	(±0.40)
Pooled data	0.90	(±0.04)	0.88	5.66	(±0.58)

24 to 31 hr after administration of a single oral dose, the ratio of red blood cells to plasma levels was greater than 4:1. Therefore, to ensure accurate determination of plasma levels, plasma should be separated from blood immediately, before hemolysis occurs. An appreciable degree of hemolysis may lead to overestimation of plasma concentrations.

The significance of the slowly declining red blood cell levels during chronic therapy with the drug remains to be determined.

REFERENCES

(1) B. Lehmann, E. Linner, and P. J. Wistrand, *Adv. Biosci.*, **5**, 197 (1969).

(2) W. F. Bayne, G. Rogers, and N. Crisologo, *J. Pharm. Sci.*, **64**, 402 (1975).

(3) T. H. Maren, V. I. Ash, and E. M. Bailey, *Bull. Johns Hopkins Hosp.*, **95**, 244 (1954).

(4) G. Graham and M. Rowland, *J. Pharm. Sci.*, **61**, 1219 (1972).

(5) U. Groth, W. Prellwitz, and E. Jahnchen, *Clin. Pharmacol. Ther.*, **16**, 490 (1974).

(6) R. Koysooko, E. F. Ellis, and G. Levy, *Clin. Pharmacol. Ther.*, **15**, 454 (1974).

(7) T. H. Maren, B. Robinson, R. F. Palmer, and M. E. Griffith, *Biochem. Pharmacol.*, **6**, 21 (1961).

(8) V. P. Shah, S. M. Wallace, and S. Riegelman, *J. Pharm. Sci.*, **63**, 1364 (1974).

(9) T. H. Maren and B. Robinson, *Bull. Johns Hopkins Hosp.*, **106**, 1 (1960).

ACKNOWLEDGMENTS AND ADDRESSES

Received November 26, 1975, from the *Department of Pharmacy, School of Pharmacy, University of California, San Francisco, CA 94143.*

Accepted for publication May 26, 1976.

Presented at the Basic Pharmaceutics Section, APhA Academy of Pharmaceutical Sciences, San Francisco meeting, April 1975.

Supported in part by U.S. Public Health Service Grant NIGMS 16496-05 and Lederle Laboratories.

The authors thank Dr. Dunbar Hoskins, Dr. Ernst Martin, and Ms. Lucy Roman for the screening and supervision of subjects.

* Postdoctoral fellow, Killam Foundation Fellowship, University of British Columbia, Canada. Present address: College of Pharmacy, University of Saskatchewan, Saskatoon, Canada S7N-OWO.

‡ Present address: Division of Biopharmaceutics, Bureau of Drugs, Food and Drug Administration (HFD-529), Washington, DC 20204.

ˣ To whom inquiries should be directed.

Pharmacokinetic Analysis of Drug Concentration Data Obtained during Repetitive Drug Administration

WAYNE A. COLBURN and MILO GIBALDI ˣ

Abstract □ A digital computer curve-fitting method, designed to estimate pharmacokinetic model constants by utilizing all drug concentration–time data collected during repetitive dosing studies, was applied to data manifesting systematic dose-to-dose variability in one or another of the pharmacokinetic parameters. The method accurately determined dose-to-dose changes in absorption or elimination rate constants or in the apparent volume of distribution, and it would be useful for detecting phenomena such as self-induction and self-inhibition that may occur during multiple-dose administration. The method can also be used to analyze multiple-dose data of drugs exhibiting capacity-limited elimination and to obtain estimates of the Michaelis–Menten parameters.

Keyphrases □ Pharmacokinetics—model constants estimated by computer curve-fitting method, drug concentration data obtained during repetitive drug administration □ Computer curve-fitting method—pharmacokinetic model constants estimated, drug concentration data obtained during repetitive drug administration □ Repetitive drug administration—drug concentration data obtained, model constants estimated by computer curve-fitting method

A previous report (1) described the development of a digital computer method which utilized all plasma or blood concentration data collected during repetitive dosing studies to estimate pharmacokinetic model constants and, simultaneously, to fit the entire time course of drug concentration in plasma or blood. The method readily accommodates changes in dose or dosing interval during a multiple-dose regimen.

Several investigations found that pharmacokinetic parameters of certain drugs change in a systematic way

Table II—Relationship of Saliva, Plasma, and Plasma Water Concentrations of Acetazolamide in Five Subjects after Oral Administration of a 250-mg Dose

Subject	Saliva Concentration / Plasma Concentration × 100			Plasma Water Concentration / Plasma Concentration × 100	
	Mean	(± *SEM*)	Linear Regression Slope	Mean	(± *SEM*)
PJ	1.11	(±0.07)	1.12	3.02	(±0.32)
CA	0.70	(±0.10)	0.51	4.22	(±0.41)
SG	0.85	(±0.09)	0.77	10.74	(±0.73)
AS	0.94	(±0.14)	0.93	5.17	(±0.52)
TS	0.84	(±0.06)	0.92	5.35	(±0.40)
Pooled data	0.90	(±0.04)	0.88	5.66	(±0.58)

24 to 31 hr after administration of a single oral dose, the ratio of red blood cells to plasma levels was greater than 4:1. Therefore, to ensure accurate determination of plasma levels, plasma should be separated from blood immediately, before hemolysis occurs. An appreciable degree of hemolysis may lead to overestimation of plasma concentrations.

The significance of the slowly declining red blood cell levels during chronic therapy with the drug remains to be determined.

REFERENCES

(1) B. Lehmann, E. Linner, and P. J. Wistrand, *Adv. Biosci.*, **5**, 197 (1969).

(2) W. F. Bayne, G. Rogers, and N. Crisologo, *J. Pharm. Sci.*, **64**, 402 (1975).

(3) T. H. Maren, V. I. Ash, and E. M. Bailey, *Bull. Johns Hopkins Hosp.*, **95**, 244 (1954).

(4) G. Graham and M. Rowland, *J. Pharm. Sci.*, **61**, 1219 (1972).

(5) U. Groth, W. Prellwitz, and E. Jahnchen, *Clin. Pharmacol. Ther.*, **16**, 490 (1974).

(6) R. Koysooko, E. F. Ellis, and G. Levy, *Clin. Pharmacol. Ther.*, **15**, 454 (1974).

(7) T. H. Maren, B. Robinson, R. F. Palmer, and M. E. Griffith, *Biochem. Pharmacol.*, **6**, 21 (1961).

(8) V. P. Shah, S. M. Wallace, and S. Riegelman, *J. Pharm. Sci.*, **63**, 1364 (1974).

(9) T. H. Maren and B. Robinson, *Bull. Johns Hopkins Hosp.*, **106**, 1 (1960).

ACKNOWLEDGMENTS AND ADDRESSES

Received November 26, 1975, from the *Department of Pharmacy, School of Pharmacy, University of California, San Francisco, CA 94143.*

Accepted for publication May 26, 1976.

Presented at the Basic Pharmaceutics Section, APhA Academy of Pharmaceutical Sciences, San Francisco meeting, April 1975.

Supported in part by U.S. Public Health Service Grant NIGMS 16496-05 and Lederle Laboratories.

The authors thank Dr. Dunbar Hoskins, Dr. Ernst Martin, and Ms. Lucy Roman for the screening and supervision of subjects.

* Postdoctoral fellow, Killam Foundation Fellowship, University of British Columbia, Canada. Present address: College of Pharmacy, University of Saskatchewan, Saskatoon, Canada S7N-OWO.

‡ Present address: Division of Biopharmaceutics, Bureau of Drugs, Food and Drug Administration (HFD-529), Washington, DC 20204.

ˣ To whom inquiries should be directed.

Pharmacokinetic Analysis of Drug Concentration Data Obtained during Repetitive Drug Administration

WAYNE A. COLBURN and MILO GIBALDI ˣ

Abstract □ A digital computer curve-fitting method, designed to estimate pharmacokinetic model constants by utilizing all drug concentration–time data collected during repetitive dosing studies, was applied to data manifesting systematic dose-to-dose variability in one or another of the pharmacokinetic parameters. The method accurately determined dose-to-dose changes in absorption or elimination rate constants or in the apparent volume of distribution, and it would be useful for detecting phenomena such as self-induction and self-inhibition that may occur during multiple-dose administration. The method can also be used to analyze multiple-dose data of drugs exhibiting capacity-limited elimination and to obtain estimates of the Michaelis–Menten parameters.

Keyphrases □ Pharmacokinetics—model constants estimated by computer curve-fitting method, drug concentration data obtained during repetitive drug administration □ Computer curve-fitting method—pharmacokinetic model constants estimated, drug concentration data obtained during repetitive drug administration □ Repetitive drug administration—drug concentration data obtained, model constants estimated by computer curve-fitting method

A previous report (1) described the development of a digital computer method which utilized all plasma or blood concentration data collected during repetitive dosing studies to estimate pharmacokinetic model constants and, simultaneously, to fit the entire time course of drug concentration in plasma or blood. The method readily accommodates changes in dose or dosing interval during a multiple-dose regimen.

Several investigations found that pharmacokinetic parameters of certain drugs change in a systematic way

Table I—Average Parameter Estimates for 10 Sets of Errant Multiple-Dose Data that Can Be Described by First-Order Absorption and Simultaneous Michaelis–Menten and First-Order Elimination

	K_m[a], mg/liter	V_m[b], mg/hr	Vc[c], liters	Cl[d], liters/hr	k_a[e], hr^{-1}
Parameter value	0.961	0.388	101	0.405×10^{-3}	1.02
Computer estimate	1.08	0.407	103	0.413×10^{-3}	1.06
SD	0.281	0.053	6.0	0.009×10^{-3}	0.109
CV, %	26.0	13.0	5.8	2.1	10.3
Bias, %	12.4	4.9	2.0	2.0	3.9

[a]Michaelis constant. [b]Maximum elimination rate. [c]Apparent volume of distribution. [d]First-order clearance. [e]First-order absorption rate constant.

during repetitive drug administration (2–8). Self-induction, self-inhibition, and product inhibition of metabolism are possible causes of variation in elimination rate constants. Variability in absorption rate constants and/or the amount absorbed as well as changes in the apparent volume of distribution from dose to dose may also occur during a repetitive dose regimen.

Changes in elimination rate constants are usually detected by comparing the half-life of a drug after a single dose with that determined during the washout period following the last dose of a multiple-dose regimen. The interpretation of such results may be obscure if an inappropriate pharmacokinetic model is assigned to the data (9). In situations where self-induced changes in metabolism appear to be operative, little is known about the time course of these changes. No studies have been directed to detecting systematic variations in bioavailability or in the apparent volume of distribution from dose to dose during repetitive administration.

Under certain conditions, a drug subject to capacity-limited metabolism will demonstrate pharmacokinetic characteristics similar to those of a drug subject to self-inhibition or product inhibition; *i.e.*, the half-life will appear to increase during multiple dosing. The characterization of Michaelis–Menten kinetics is usually attempted by analyzing data after administration of a large single dose, administration of different single doses, or administration of the last dose of a repetitive dose regimen. Although the most dramatic consequences of capacity-limited elimination are the unusual rate and extent of drug accumulation, little effort has been directed to the characterization of such kinetics by analyzing data obtained during repetitive drug administration.

Table II—Parameter Estimates for 10 Sets of Errant Data that Can Be Described by First-Order Absorption and Elimination (the Absorption Rate Constant Fluctuates during Repetitive Dosing)

Parameter	Parameter Value	Computer Estimate	*SD*	*CV*, %	Bias, %
$k_{a(1)}$[a]	1.98	1.95	0.15	7.7	−1.5
$k_{a(2)}$	2.92	2.84	0.65	22.9	−2.7
$k_{a(3)}$	1.98	1.96	0.31	15.8	−1.0
$k_{a(4)}$	2.92	2.99	0.79	26.4	+2.4
$k_{a(5)}$	1.98	1.93	0.26	13.5	−2.5
$k_{a(6)}$	2.92	2.78	0.50	18.0	−4.8
$k_{a(7)}$	1.98	2.07	0.21	10.1	+4.5
$k_{a(8)}$	2.92	3.01	0.78	25.9	+3.1
Kb[b]	0.346	0.351	0.005	1.4	+1.4
Vc[c]	99.7	98.7	1.78	1.8	−1.0

[a]The term $k_{a(n)}$ denotes the first-order absorption rate constant after the nth dose (hours^{-1}). [b]First-order elimination rate constant (hours^{-1}). [c]Apparent volume of distribution (liters).

Table III—Parameter Estimates for 10 Sets of Errant Data that Can Be Described by First-Order Absorption and Elimination (the Absorption Rate Constant Decreases during Repetitive Dosing)

Parameter	Parameter Value	Computer Estimate	*SD*	*CV*, %	Bias, %
$k_{a(1)}$[a]	3.14	3.29	0.658	20.0	+4.8
$k_{a(2)}$	2.71	2.91	0.783	26.9	+7.4
$k_{a(3)}$	2.10	2.13	0.372	17.5	+1.4
$k_{a(4)}$	1.53	1.52	0.136	8.9	−0.7
$k_{a(5)}$	1.02	1.00	0.069	6.9	−2.0
$k_{a(6)}$	0.509	0.500	0.020	4.0	−1.8
$k_{a(7)}$	0.507	0.519	0.029	5.6	+2.4
$k_{a(8)}$	0.505	0.495	0.029	5.9	−2.0
Kb	0.344	0.346	0.010	2.9	+0.6
Vc	100.7	100.2	3.1	3.1	−0.5

[a]The term $k_{a(n)}$ denotes the first-order absorption rate constant after the nth dose (hours^{-1}). [b]First-order elimination rate constant (hours^{-1}). [c]Apparent volume of distribution (liters).

The present report concerns the use of the previously described digital computer method (1) for detecting changes in pharmacokinetic model constants and for characterizing Michaelis–Menten kinetics during repetitive drug administration.

COMPUTER METHOD

The development of the computer method was detailed previously (1). The main element of the method is NONLIN (10), a nonlinear least-squares regression computer program specifically developed for pharmacokinetic applications, used in conjunction with DASCRU[1] (11), a subprogram that provides numerical solutions to differential equations.

To detect changes in pharmacokinetic constants during repetitive dosing, it is necessary to estimate independently model parameters for drug concentration data after each dose. While this approach is possible in principle, it requires considerably more data than are obtained in the usual metabolic or clinical study. Hence, it was decided that only one parameter would be estimated independently for each dose while all other parameters would be estimated by assuming that they were invariant from dose to dose. This procedure can be repeated for each parameter, and it becomes possible to detect systematic variability in absorption rate constants, amounts absorbed or volumes of distribution, and elimination rate constants.

To estimate a parameter for individual doses independently, the DFUNC section of NONLIN requires that each dose uses a separate in-

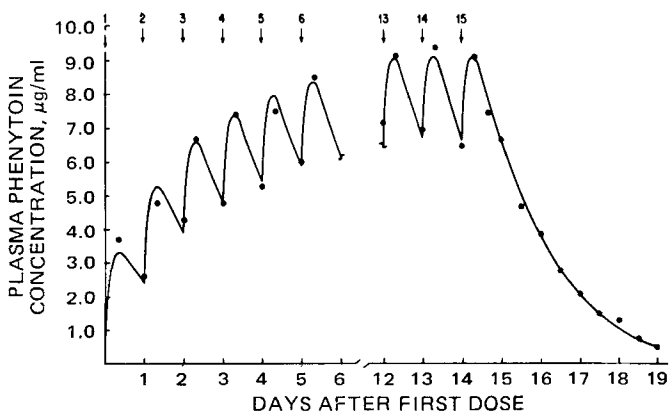

Figure 1—*Curve fit to plasma phenytoin concentrations during repetitive oral dosing, 300 mg/day for 14 consecutive days. Each point is the mean of determinations in 12 subjects. Data were fit using Program I.*

[1] Available from IMSL, 6200 Hillcroft, Houston, TX 77036.

Table IV—Parameter Estimates for 10 Sets of Errant Data that Can Be Described by First-Order Absorption and Elimination (the Elimination Rate Constant Increases during Repetitive Dosing)

Parameter	Parameter Value	Computer Estimate	SD	CV, %	Bias, %
k_a[a]	1.00	1.03	0.129	12.5	+3.0
V[b]	100.0	101.4	7.5	7.4	+1.4
$K_{(1)}$[c]	0.043	0.042	0.018	42.9	−2.3
$K_{(2)}$	0.087	0.086	0.009	10.5	−1.1
$K_{(3)}$	0.130	0.129	0.007	5.4	−0.8
$K_{(4)}$	0.173	0.172	0.013	7.6	−0.6
$K_{(5)}$	0.260	0.260	0.016	6.2	0.0
$K_{(6)}$	0.346	0.338	0.021	6.2	−2.3
$K_{(7)}$	0.346	0.348	0.026	7.5	+0.6
$K_{(8)}$	0.346	0.346	0.026	7.5	0.0

[a] First-order absorption rate constant (hours^{-1}). [b] Apparent volume of distribution (liters). [c] The term $K_{(n)}$ denotes the first-order elimination rate constant after the nth dose (hours^{-1}).

Table V—Parameter Estimates for 10 Sets of Errant Data that Can Be Described by First-Order Absorption and Elimination (the Elimination Rate Constant Decreases during Repetitive Dosing)

Parameter	Parameter Value	Computer Estimate	SD	CV, %	Bias, %
k_a[a]	1.00	1.02	0.149	14.6	+2.0
V[b]	100.0	100.9	8.8	8.7	+0.9
$K_{(1)}$[c]	0.779	0.777	0.063	8.1	−0.3
$K_{(2)}$	0.693	0.700	0.065	9.3	+1.0
$K_{(3)}$	0.606	0.610	0.038	6.2	+0.7
$K_{(4)}$	0.519	0.528	0.043	8.1	+1.7
$K_{(5)}$	0.433	0.446	0.039	8.7	+3.0
$K_{(6)}$	0.346	0.347	0.027	7.8	+0.3
$K_{(7)}$	0.346	0.350	0.029	8.3	+1.2
$K_{(8)}$	0.346	0.349	0.026	7.4	+0.9

[a] First-order absorption rate constant (hours^{-1}). [b] Apparent volume of distribution (liters). [c] The term $K_{(n)}$ denotes the first-order elimination rate constant after the nth dose (hours^{-1}).

tegration routine. Therefore, an F subroutine was included for each dose. The integration subprogram DASCRU was called using the F subroutine corresponding to the number of the dose.

Specific programs[2] were developed to fit data described by the following one-compartment pharmacokinetic models: I, constant first-order absorption and constant simultaneous Michaelis–Menten and first-order elimination; II, variable first-order absorption and constant first-order elimination; III, constant first-order absorption and variable first-order elimination; and IV, constant first-order absorption and elimination but variable apparent volume of distribution.

APPLICATIONS

Ideal drug concentration–time data after repetitive dosing were generated by means of appropriate equations satisfying the conditions of each program. Each data set consisted of five values during the first dosing interval, four values during the last interval, and two values for each of the six interceding intervals. A normally distributed random absolute error of 10% was introduced into each data set as previously described (1). Ten errant data sets were generated for each ideal data set. The errant data and the appropriate differential equations served as input for Programs I–IV.

Table I shows the average computer-estimated pharmacokinetic parameters for data described by first-order absorption and simultaneous Michaelis–Menten and first-order elimination. Good agreement between the pharmacokinetic parameters used to generate the ideal data and the means of the parameter estimates that best describe the errant data was obtained.

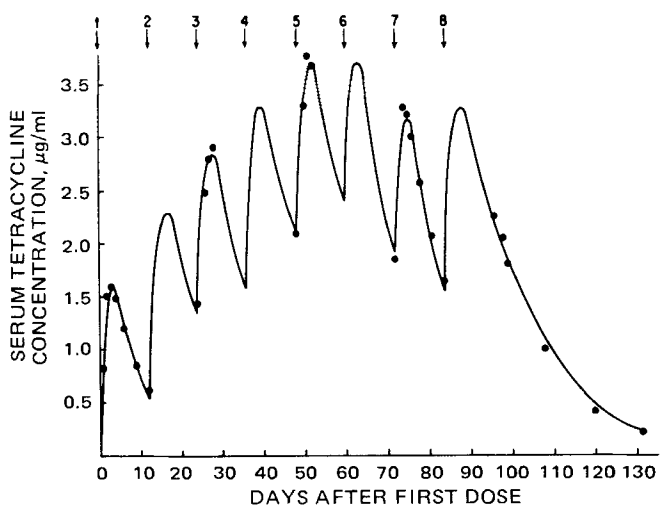

Figure 2—*Curve fit to mean serum tetracycline concentrations during repetitive oral dosing of 500 mg twice a day for eight consecutive doses to 12 healthy subjects. Data were fit using Program III.*

[2] Information concerning these programs may be obtained by writing the authors.

Programs II, III, and IV, which were intended to characterize dose-to-dose variation in the absorption rate constant (Tables II and III), in the elimination rate constant (Tables IV and V), and in the amount absorbed or the apparent volume of distribution (Table VI), respectively, also provided highly acceptable results.

The computer programs were evaluated further by determining their applicability to previously published experimental data. In a multiple-dose trial, subjects were given 300-mg oral doses of phenytoin once daily for 14 days (12). Blood samples were obtained during the first 6 days and the last 3 days of dosing as well as for 3 days following the last dose. These data were evaluated using Program I, which assumes first-order absorption and simultaneous Michaelis–Menten and first-order elimination. The computer fit to the average drug concentration data is shown in Fig. 1. The correlation coefficient was 0.996. The parameter estimates are listed in Table VII.

Several investigations indicated that the elimination of phenytoin in humans is capacity limited and can be described by Michaelis–Menten kinetics or simultaneous first-order and Michaelis–Menten kinetics (13–15). The values of the pharmacokinetic parameters determined in the present study differ considerably from previous estimates. For example, the K_m value of 20.7 mg/liter is three to five times larger than those values previously reported from single-dose data. The V_m value is about 100% larger than previously reported average values but comparable to values observed in certain individuals (14). The ratio of V_m/K_m is comparable to that reported by Gerber and Wagner (13) but much smaller than the ratios found by others (14, 15). In view of the narrow therapeutically effective range of plasma concentrations found with phenytoin, additional studies are needed to determine which set of parameter estimates is more realistic in predicting the relation between the dose and steady-state concentration of the drug.

Doluisio and Dittert (8) found that the average apparent half-life of

Table VI—Parameter Estimates for 10 Sets of Errant Data that Can Be Described by First-Order Absorption and Elimination (the Apparent Volume of Distribution Increases during Repetitive Dosing)

Parameter	Parameter Value	Computer Estimate	SD	CV, %	Bias, %
k_a[a]	0.782	0.778	0.019	2.4	−0.5
K[b]	0.360	0.362	0.004	1.1	+0.6
$V_{(1)}$[c]	68.0	68.0	1.29	1.9	0.0
$V_{(2)}$	73.4	73.1	2.27	3.1	−0.4
$V_{(3)}$	82.7	82.8	3.16	3.8	+0.1
$V_{(4)}$	94.9	94.2	3.88	4.1	−0.7
$V_{(5)}$	108	108	4.31	4.0	0.0
$V_{(6)}$	123	122	4.06	3.3	−0.8
$V_{(7)}$	143	141	3.16	2.2	−1.4
$V_{(8)}$	165	167	3.77	2.3	+1.2

[a] First-order absorption rate constant (hours^{-1}). [b] First-order elimination rate constant (hours^{-1}). [c] The term $V_{(n)}$ denotes the apparent volume of distribution after the nth dose (liters).

Table VII—Pharmacokinetic Model Parameters Derived from Fitting Multiple-Dose Phenytoin Data Assuming First-Order Absorption and Simultaneous Michaelis–Menten and First-Order Elimination

	K_m[a], mg/liter	V_m[b], mg/hr	V[c], liters	Cl[d], liters/hr	k_a[e], hr^{-1}
Computer estimate	20.7	0.605	72.7	7×10^{-4}	0.320
SD of estimate	5.6	0.119	2.5	4×10^{-4}	0.072

[a] Michaelis constant. [b] Maximum elimination rate. [c] Apparent volume of distribution. [d] First-order clearance. [e] First-order absorption rate constant.

tetracycline in 10 subjects increased from 6.3 hr (after the first dose) to 10 hr (after the eighth dose) during 4 days of repetitive oral dosing (every 12 hr). Although at least one blood sample was taken during each dosing interval, pharmacokinetic analysis was limited to the data obtained from the first and last doses.

The average serum concentration–time data from this study were fit using Program III, which accommodates dose-to-dose variation in the first-order elimination rate constant. The computer fit of the data is shown in Fig. 2. The correlation coefficient was 0.997. The parameter estimates are listed in Table VIII.

A substantial change in the elimination rate constant is evident when the first dose is compared with each subsequent dose. The elimination rate constants for Doses 2–8 tend to fluctuate about a mean value of 0.078 hr^{-1} ($t_{1/2} \simeq 9$ hr), which is much smaller than the value estimated after the first dose.

Table VIII—Pharmacokinetic Model Parameters Derived from Fitting Multiple-Dose Tetracycline Data Assuming Constant First-Order Absorption and Variable First-Order Elimination

Parameter	Computer Estimate	*SD* of Estimate
k_a[a]	0.563	0.046
V/F[b]	191.1	4.6
$K_{(1)}$[c]	0.164	0.010
$K_{(2)}$	0.083	0.007
$K_{(3)}$	0.086	0.014
$K_{(4)}$	0.066	0.007
$K_{(5)}$	0.061	0.010
$K_{(6)}$	0.089	0.006
$K_{(7)}$	0.099	0.005
$K_{(8)}$	0.061	0.003

[a] First-order absorption rate constant ($hours^{-1}$). [b] Ratio of the apparent volume of distribution, V, to the fraction, F, of the dose absorbed (liters). [c] The term $K_{(n)}$ denotes the first-order elimination rate constant after the nth dose ($hours^{-1}$).

The reason for this apparent change in half-life remains obscure. Whether it is due to a real change in the pharmacokinetics of the drug upon repetitive dosing or to a mathematical artifact that arises from selecting the wrong pharmacokinetic model (9) is not known. The present analysis suggests that if an inhibitory mechanism is operative, it is fully induced after the first dose.

The described analyses of hypothetical and experimental multiple-dose data further support the utility and flexibility of the recently reported digital computer-fitting method (1).

REFERENCES

(1) W. A. Colburn, D. Shen, and M. Gibaldi, *J. Pharmacokinet. Biopharm.*, **4**, 469 (1976).

(2) P. L. Morselli and A. Frigerio, *Drug Metab. Rev.*, **4**, 97 (1975).

(3) R. M. Welch, Y. E. Harrison, and J. J. Burns, *Toxicol. Appl. Pharmacol.*, **10**, 340 (1967).

(4) P. S. Misra, A. Lefevre, H. Ishii, E. Rubin, and C. S. Lieber, *Am. J. Med.*, **51**, 346 (1971).

(5) B. Solymoss, S. Toth, S. Varga, and M. Krajny, *Steroids*, **16**, 263 (1970).

(6) V. Nitti, F. Delli Veneri, A. Ninni, and G. Meola, *Chemotherapy*, **17**, 121 (1972).

(7) R. Sellman, J. Kanto, E. Raijola, and A. Pekkarinen, *Acta Pharmacol. Toxicol.*, **37**, 345 (1975).

(8) J. T. Doluisio and L. W. Dittert, *Clin. Pharmacol. Ther.*, **10**, 690 (1969).

(9) M. Gibaldi and H. Weintraub, *J. Pharm. Sci.*, **60**, 624 (1971).

(10) C. M. Metzler, Technical Report 7292/69/7292/005, The Upjohn Co., Kalamazoo, Mich.

(11) J. Christiansen, *Numer. Math.*, **14**, 317 (1970).

(12) A. J. Glazko, in "Bioavailability of Drugs," B. B. Brodie and W. M. Heller, Eds., S. Karger, New York, N.Y., 1972, p. 170.

(13) N. Gerber and J. G. Wagner, *Res. Commun. Chem. Pathol. Pharmacol.*, **3**, 455 (1972).

(14) G. E. Mawer, P. W. Mullen, M. Rodgers, A. J. Robins, and S. B. Lucas, *Br. J. Clin. Pharmacol.*, **1**, 163 (1974).

(15) L. K. Garrettson and W. J. Jusko, *Clin. Pharmacol. Ther.*, **17**, 481 (1975).

ACKNOWLEDGMENTS AND ADDRESSES

Received March 25, 1976, from the *Department of Pharmaceutics, School of Pharmacy, State University of New York at Buffalo, Buffalo, NY 14214.*

Accepted for publication May 27, 1976.

Supported in part by Grant GM-20852 from the National Institute of General Medical Sciences, National Institutes of Health.

[x] To whom inquiries should be directed.

Metal-Ion Interaction with Penicillins: Kinetics of Complexation of Nickel(II)

G. V. FAZAKERLEY [x] and G. E. JACKSON

Abstract □ The kinetics of complexation of nickel(II) with some penicillins and related compounds show that the zwitterionic form of the ligand has very low reactivity compared to the anionic form. The resolved rate constants are interpreted in terms of binding to the ring nitrogen and carboxyl group and not to the side chain.

Keyphrases □ Penicillin G—and related compounds, complexation with nickel(II) ions, reaction kinetics □ Nickel(II)—complexation with penicillin G and related compounds, reaction kinetics □ Complex formation—penicillin G and related compounds with nickel(II) ions, reaction kinetics □ Kinetics, reaction—complexation of nickel(II) with penicillin G and related compounds □ Metal ions—nickel(II), complexation with penicillin G and related compounds, reaction kinetics □ Antibacterials—penicillin G and related compounds, complexation with nickel(II) ions, reaction kinetics

Penicillin antibiotics interact with metal ions in a complex manner. Copper(II) has a very pronounced effect on the hydrolysis rate of the β-lactam ring (1, 2), which is not shown by other first-row transition metal ions (3, 4).

Table VII—Pharmacokinetic Model Parameters Derived from Fitting Multiple-Dose Phenytoin Data Assuming First-Order Absorption and Simultaneous Michaelis–Menten and First-Order Elimination

	K_m[a], mg/liter	V_m[b], mg/hr	V[c], liters	Cl[d], liters/hr	k_a[e], hr^{-1}
Computer estimate	20.7	0.605	72.7	7×10^{-4}	0.320
SD of estimate	5.6	0.119	2.5	4×10^{-4}	0.072

[a] Michaelis constant. [b] Maximum elimination rate. [c] Apparent volume of distribution. [d] First-order clearance. [e] First-order absorption rate constant.

tetracycline in 10 subjects increased from 6.3 hr (after the first dose) to 10 hr (after the eighth dose) during 4 days of repetitive oral dosing (every 12 hr). Although at least one blood sample was taken during each dosing interval, pharmacokinetic analysis was limited to the data obtained from the first and last doses.

The average serum concentration–time data from this study were fit using Program III, which accommodates dose-to-dose variation in the first-order elimination rate constant. The computer fit of the data is shown in Fig. 2. The correlation coefficient was 0.997. The parameter estimates are listed in Table VIII.

A substantial change in the elimination rate constant is evident when the first dose is compared with each subsequent dose. The elimination rate constants for Doses 2–8 tend to fluctuate about a mean value of 0.078 hr^{-1} ($t_{1/2} \simeq 9$ hr), which is much smaller than the value estimated after the first dose.

Table VIII—Pharmacokinetic Model Parameters Derived from Fitting Multiple-Dose Tetracycline Data Assuming Constant First-Order Absorption and Variable First-Order Elimination

Parameter	Computer Estimate	*SD* of Estimate
k_a[a]	0.563	0.046
V/F[b]	191.1	4.6
$K_{(1)}$[c]	0.164	0.010
$K_{(2)}$	0.083	0.007
$K_{(3)}$	0.086	0.014
$K_{(4)}$	0.066	0.007
$K_{(5)}$	0.061	0.010
$K_{(6)}$	0.089	0.006
$K_{(7)}$	0.099	0.005
$K_{(8)}$	0.061	0.003

[a] First-order absorption rate constant ($hours^{-1}$). [b] Ratio of the apparent volume of distribution, V, to the fraction, F, of the dose absorbed (liters). [c] The term $K_{(n)}$ denotes the first-order elimination rate constant after the nth dose ($hours^{-1}$).

The reason for this apparent change in half-life remains obscure. Whether it is due to a real change in the pharmacokinetics of the drug upon repetitive dosing or to a mathematical artifact that arises from selecting the wrong pharmacokinetic model (9) is not known. The present analysis suggests that if an inhibitory mechanism is operative, it is fully induced after the first dose.

The described analyses of hypothetical and experimental multiple-dose data further support the utility and flexibility of the recently reported digital computer-fitting method (1).

REFERENCES

(1) W. A. Colburn, D. Shen, and M. Gibaldi, *J. Pharmacokinet. Biopharm.*, **4**, 469 (1976).

(2) P. L. Morselli and A. Frigerio, *Drug Metab. Rev.*, **4**, 97 (1975).

(3) R. M. Welch, Y. E. Harrison, and J. J. Burns, *Toxicol. Appl. Pharmacol.*, **10**, 340 (1967).

(4) P. S. Misra, A. Lefevre, H. Ishii, E. Rubin, and C. S. Lieber, *Am. J. Med.*, **51**, 346 (1971).

(5) B. Solymoss, S. Toth, S. Varga, and M. Krajny, *Steroids*, **16**, 263 (1970).

(6) V. Nitti, F. Delli Veneri, A. Ninni, and G. Meola, *Chemotherapy*, **17**, 121 (1972).

(7) R. Sellman, J. Kanto, E. Raijola, and A. Pekkarinen, *Acta Pharmacol. Toxicol.*, **37**, 345 (1975).

(8) J. T. Doluisio and L. W. Dittert, *Clin. Pharmacol. Ther.*, **10**, 690 (1969).

(9) M. Gibaldi and H. Weintraub, *J. Pharm. Sci.*, **60**, 624 (1971).

(10) C. M. Metzler, Technical Report 7292/69/7292/005, The Upjohn Co., Kalamazoo, Mich.

(11) J. Christiansen, *Numer. Math.*, **14**, 317 (1970).

(12) A. J. Glazko, in "Bioavailability of Drugs," B. B. Brodie and W. M. Heller, Eds., S. Karger, New York, N.Y., 1972, p. 170.

(13) N. Gerber and J. G. Wagner, *Res. Commun. Chem. Pathol. Pharmacol.*, **3**, 455 (1972).

(14) G. E. Mawer, P. W. Mullen, M. Rodgers, A. J. Robins, and S. B. Lucas, *Br. J. Clin. Pharmacol.*, **1**, 163 (1974).

(15) L. K. Garrettson and W. J. Jusko, *Clin. Pharmacol. Ther.*, **17**, 481 (1975).

ACKNOWLEDGMENTS AND ADDRESSES

Received March 25, 1976, from the *Department of Pharmaceutics, School of Pharmacy, State University of New York at Buffalo, Buffalo, NY 14214.*

Accepted for publication May 27, 1976.

Supported in part by Grant GM-20852 from the National Institute of General Medical Sciences, National Institutes of Health.

[x] To whom inquiries should be directed.

Metal-Ion Interaction with Penicillins: Kinetics of Complexation of Nickel(II)

G. V. FAZAKERLEY [x] and G. E. JACKSON

Abstract □ The kinetics of complexation of nickel(II) with some penicillins and related compounds show that the zwitterionic form of the ligand has very low reactivity compared to the anionic form. The resolved rate constants are interpreted in terms of binding to the ring nitrogen and carboxyl group and not to the side chain.

Keyphrases □ Penicillin G—and related compounds, complexation with nickel(II) ions, reaction kinetics □ Nickel(II)—complexation with penicillin G and related compounds, reaction kinetics □ Complex formation—penicillin G and related compounds with nickel(II) ions, reaction kinetics □ Kinetics, reaction—complexation of nickel(II) with penicillin G and related compounds □ Metal ions—nickel(II), complexation with penicillin G and related compounds, reaction kinetics □ Antibacterials—penicillin G and related compounds, complexation with nickel(II) ions, reaction kinetics

Penicillin antibiotics interact with metal ions in a complex manner. Copper(II) has a very pronounced effect on the hydrolysis rate of the β-lactam ring (1, 2), which is not shown by other first-row transition metal ions (3, 4).

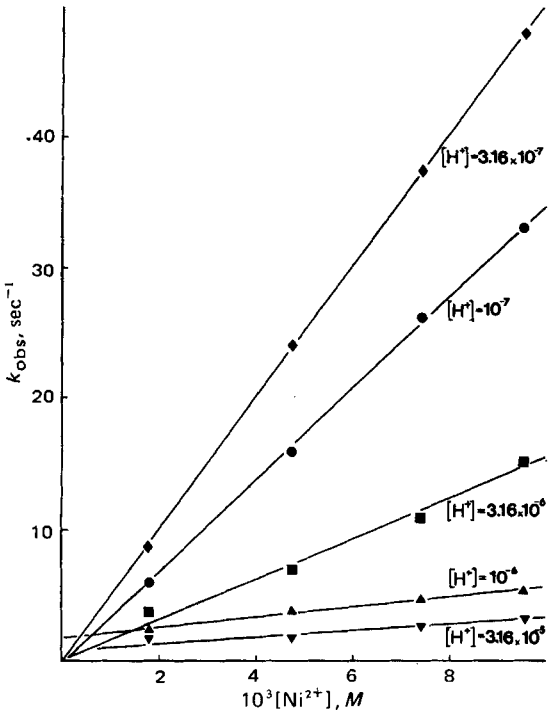

Figure 1—*Plot of* k_{obs} versus $[Ni^{2+}]$ *at constant* $[H^+]$ *for penicilloic acid.*

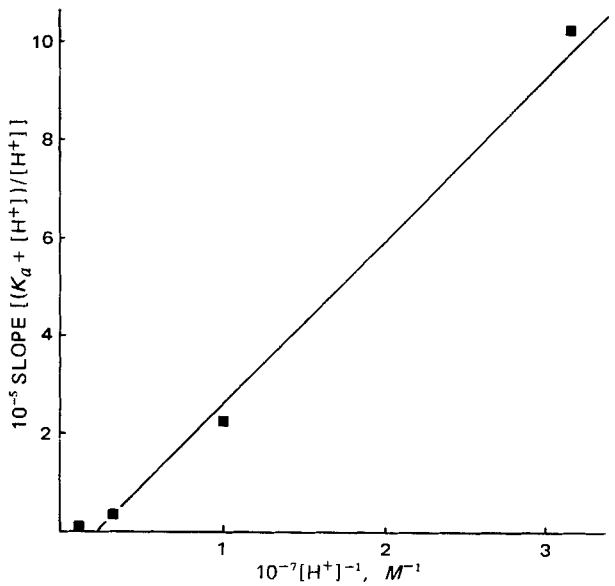

Figure 2—*Plot of slope* $(K_a + [H^+])/[H^+]$ versus $1/[H^+]$ *for penicilloic acid.*

Previous kinetic studies dealt exclusively with the hydrolysis rate in the presence of metal ions rather than with the complexation reaction itself. The differing effects of metal ions have been explained in terms of two possible binding sites (1). This paper describes the complexation reaction kinetics of nickel(II) with penicillin G and some related compounds.

EXPERIMENTAL

Penicillin G sodium, ampicillin, and thiaproline were commercial products used without further purification. Penicilloic acid was prepared by the method of Rapson and Bird (5). Nickel(II) perchlorate was prepared from nickel(II) sulfate and sodium bicarbonate by treating the nickel bicarbonate produced with perchloric acid. Excess nickel bicarbonate was filtered off, and nickel perchlorate was crystallized. Solutions of nickel perchlorate were standardized by adding a known concentration of edetate and back titrating[1] with standard magnesium sulfate.

Reactions were followed at 220 nm for thiaproline and penicillin G, 225 nm for ampicillin, and 250 nm for penicilloic acid on a stopped-flow spectrophotometer at 298 ± 0.5° K. The ionic strength was adjusted to 0.15 *M* with sodium perchlorate, and a 0.02 *M* sodium borate–mannitol buffer was used to maintain the pH.

The pH measurements were made using a glass–calomel electrode in which the potassium chloride had been replaced by sodium chloride. The meter was calibrated at pH 4 and 7. Reactions were carried out in the following pH regions: penicillin G, pH 6.1–7.8; thiaproline, pH 4.5–6.0; ampicillin, pH 6.7–7.4; and penicilloic acid, pH 4.5–6.5.

Ligand concentrations were 10^{-4} *M*. Reactions were run under pseudo-first-order conditions with nickel(II) concentrations in 10–100-fold excess to ensure that only 1:1 species were formed. Oscilloscope traces yielded excellent first-order rate constants, linear for at least 90% completion of the reaction. Value of k_{obs} used in evaluating further parameters were an average of three to five individual determinations.

RESULTS AND DISCUSSION

Penicilloic Acid, Ampicillin, and Thiaproline—All three ligands showed the same behavior in that the observed rate of reaction, k_{obs}, increased markedly with increasing pH at constant nickel(II) concentration. Figure 1 shows the effect of pH upon the reaction rate with penicilloic acid. The reactions showed the same characteristics as those of nickel(II) with amino acids (6) and were accounted for by the increasing concentration of the deprotonated zwitterion at high pH.

The reactions are shown in Scheme I, where L is the singly charged anion for thiaproline and ampicillin and the doubly charged anion for penicilloic acid. The pKa's for thiaproline, penicilloic acid, and ampicillin are 6.1 (7), 5.19 (7), and 7.25 (5), respectively.

$$Ni^{2+} + L \xrightarrow{k_1} [NiL]^{2+}$$

$$Ni^{2+} + LH^+ \xrightarrow{k_2} [NiL]^{2+} + H^+$$

$$LH^+ \overset{K_a}{\rightleftharpoons} L + H^+$$

Scheme I

The usual rate equation (6) is:

$$k_{obs} = \frac{k_1K_a + k_2[H^+]}{K_a + [H^+]}[Ni^{2+}] \qquad \text{(Eq. 1)}$$

Thus, the slopes in Fig. 1 are equal to $(k_2[H^+] + k_1K_a)/(K_a + [H^+])$. Since the intercepts are not experimentally different from zero, the dissociation reactions can be ignored.

Rearranging Eq. 1 gives:

$$\text{slope}\frac{(K_a + [H^+])}{[H^+]} = \frac{k_2 + k_1K_a}{[H^+]} \qquad \text{(Eq. 2)}$$

Figure 2 shows a graph of the left-hand side of Eq. 2 against $1/[H^+]$ for penicilloic acid. The slope is k_1K_a, and the intercept is k_2. However, the intercepts are not experimentally different from zero, so only the overall forward rate constant, k_f, is determined (Table I).

The unreactivity of the protonated species has been explained (6) in

Table I—Rate Constants for the Formation (k_f) and Dissociation (k_d) of Nickel(II) Complexes at 25° and Ionic Strength 0.15 *M*

Ligand	Reacting Form of Ligand	k_f, M^{-1} sec^{-1}	k_d, sec^{-1}
Thiaproline	L^-	7.5×10^2	0.15[a]
Penicilloic acid	L^{2-}	5.2×10^3	4.3[a]
Ampicillin	L^-	6.9×10^2	—
Penicillin G	L^-	2.3×10^3	19.3

[a] Calculated using $k_d = k_f/K$ (9).

[1] Using Erichrome Black T as indicator.

terms of an extreme sterically controlled substitution (SCS) mechanism, since, upon protonation, first-bond formation must switch from the amino group to the carboxylic group. The rate of ring closure is comparable with, or smaller than, the rate at which the first bond is broken.

Penicillin G—The reaction was again found to be first order with respect to ligand concentration, the metal being in at least 10-fold excess. It was also first order with respect to the metal-ion concentration observed in the linearity of the k_{obs} *versus* $[Ni^{2+}]$ graph. In the region of study, pH 6.1–7.8, k_{obs} was independent of $[H^+]$. This finding was expected because the reactions were carried out well above the pKa (2.73) and, thus, in the absence of the protonated species.

The reaction shown in Scheme II:

$$[Ni^{2+}] + L^- \underset{k_{-1}}{\overset{k_1}{\rightleftharpoons}} [NiL]^+$$

Scheme II

gives the rate equation (8):

$$k_{obs} = k_1[Ni^{2+}] + k_{-1} \qquad \text{(Eq. 3)}$$

The forward and dissociation rate constants are shown in Table I.

At lower pH values, there was no observable reaction.

The rate constant for thiaproline was much lower than that expected for "normal" substitution (9). There are two possible explanations for this finding: a shift to another rate-determining step (an SCS mechanism) occurs or hydrogen bonding between a water molecule in the metal-ion coordination sphere and the sulfur atom disorients the ligand for attack on the metal. The value of k_f was an order of magnitude less than for proline and hydroxyproline (9). Some reduction in k_f was observed with hydroxyproline relative to proline and was attributed to a hydrogen bonding mechanism. However, the large drop with thiaproline cannot be explained in this way because hydrogen bonding through sulfur is weaker than that through oxygen. Thus, a shift to another rate-determining step is postulated.

The inductive effect of sulfur is known (10) to reduce the basicity of nitrogen. This effect increases the rate at which the first bond formed is broken. This result is shown by the dissociative rate constant (0.15), which was higher than that for proline (0.024) and hydroxyproline (0.014).

The forward rate constant for penicillin G was also lower than that for normal substitution mechanisms but higher than that for thiaproline. If reaction occurs at the ring nitrogen and carboxyl group, then, by analogy with thiaproline, an SCS mechanism will lower the rate. The increase in rate over thiaproline can be explained by hydrogen bonding of the β-lactam carbonyl to water around the metal ion, which promotes the correct orientation of the ligand for attack in an internal conjugate base type of mechanism (11).

The alternative site, β-lactam carbonyl and side-chain amide nitrogen, would react as a neutral species for which the normal substitution rate is about 3×10^3, in good agreement with the observed rate. However, this normal value was obtained for strong nitrogen chelates. If comparison is made with acetylacetonate in the enol form, a value of 5.0 is found (12) because an SCS mechanism is operative. From this discussion, a similar mechanism seems to be operative, suggesting a forward rate constant much lower than 10^3 for coordination at the side chain. For this reason, and by comparison with penicilloic acid, the former postulate is favored.

The reaction rate with penicilloic acid was 5.2×10^3. A potentiometric study (7) indicated that penicilloic acid acts as a bidentate ligand, with one carboxyl group not being involved in coordination. The lower than normal rate is attributed to the nitrogen basicity.

The reactions with ampicillin are known (13) to involve coordination only at the side chain through the amino and carbonyl groups. As an effectively neutral donor involving no ring strain, a forward rate constant of $3–4 \times 10^3$ is expected. Since the pKa of the amino group is 7.25, an SCS mechanism is not likely. The decreased reactivity must be due to hydrogen bonding.

The two most likely coordination metal sites on penicillin are: A, the β-lactam carbonyl and the side-chain amide nitrogen; and B, the carboxyl group and the ring nitrogen. Structure A has been used to explain the rapid hydrolysis rate in the presence of certain metal ions of penicillin G compared to penicillanic acid (2). This interpretation is suspect because the hydrolysis rate of acylamino-substituted β-lactams is known to be several orders of magnitude faster than that of unsubstituted β-lactams in the absence of metal ions (14). Structure B is supported by potentiometric studies of nickel(II) with *N*-benzylpipecolic acid and *N*-hippurylpipecolic acid (15). The two complexes have similar stability constants, although one has the penicillin G side chain and the other does not.

Amide nitrogens are poor donors because binding results in a loss of the amide resonance stabilization energy through change in hybridization from sp^2 to sp^3. The ring nitrogen of penicillin G is already much distorted from an sp^2 planar structure. The nitrogen lies 0.4 Å out of the plane and close to the position (0.56 Å) expected for sp^3 (16). Consequently, the amide resonance is already largely lost even before coordination, making this nitrogen a better donor.

Furthermore, molecular models show that whereas it is possible to accommodate a metal ion in Structure B with normal metal ion–ligand bond lengths, a very long (~3.4 Å) and consequently weak metal nitrogen bond would result from Structure A.

From these results and those from potentiometry (7) and NMR (13) studies, it is clear that the dominant binding site for penicillin G is at the ring nitrogen and carboxyl group. In itself, this finding does not explain the different hydrolysis rates in the presence of different metal ions. This result must arise from the nature of the binding rather than a shift in the site of binding. Copper(II) will form a stronger bond to the ring nitrogen than nickel(II). The stronger tendency of copper(II) to remove electrons from the nitrogen will weaken the β-lactam ring and promote hydrolysis.

REFERENCES

(1) W. A. Cressman, E. T. Sugita, J. T. Doluisio, and P. J. Niebergall, *J. Pharm. Pharmacol.*, **18**, 801 (1966).

(2) W. A. Cressman, E. T. Sugita, J. T. Doluisio, and P. J. Niebergall, *J. Pharm. Sci.*, **58**, 1471 (1969).

(3) G. Gunther, *Pharmazie*, **5**, 577 (1950).

(4) J. Johnson, H. Clarke, and R. Robinson, "The Chemistry of Penicillin," Princeton University Press, Princeton, N.J., p. 14.

(5) H. Rapson and A. Bird, *J. Pharm. Pharmacol., Suppl.*, **15**, 222T (1963).

(6) J. C. Cassatt and R. G. Wilkens, *J. Am. Chem. Soc.*, **90**, 6045 (1968).

(7) G. V. Fazakerley, G. E. Jackson, and P. W. Linder, *J. Inorg. Nucl. Chem.*, **38**, 1397 (1976).

(8) F. Basolo and R. G. Pearson, "Mechanics of Inorganic Reactions," 2nd ed., Wiley, New York, N.Y., 1967.

(9) K. Kustin and S. Liu, *J. Chem. Soc. Dalton*, **1973**, 278.

(10) J. Johnson, H. Clarke, and R. Robinson, "The Chemistry of Penicillin," Princeton University Press, Princeton, N.J., p. 417.

(11) D. B. Rarabacher, *Inorg. Chem.*, **5**, 1891 (1966).

(12) R. Pearson and D. Anderson, *ibid.*, **9**, 39 (1970).

(13) G. V. Fazakerley and G. E. Jackson, *J. Inorg. Nucl. Chem.*, **37**, 2371 (1975).

(14) J. Johnson, H. Clarke, and R. Robinson, "The Chemistry of Penicillin," Princeton University Press, Princeton, N.J., p. 978.

(15) A. Weiss and S. Fallab, *Helv. Chim. Acta*, **40**, 611 (1962).

(16) R. Sweet and L. Dahl, *J. Am. Chem. Soc.*, **92**, 5489 (1970).

ACKNOWLEDGMENTS AND ADDRESSES

Received November 24, 1975, from the *Department of Inorganic Chemistry, University of Cape Town, Rondebosch, 7700, South Africa.*

Accepted for publication May 26, 1976.

The authors thank the University of Cape Town and the Council for Scientific and Industrial Research for financial support and for an AE&CI fellowship (to G. E. Jackson).

[x] To whom inquiries should be directed.

Synthesis of ^{14}C-Meglumine Salicylate and Its Disposition in Humans after Oral Administration

NAGY A. FARID *, GORDON S. BORN ×, WAYNE V. KESSLER, HENRY T. RUSSELL ‡, STANLEY M. SHAW, and WINTHROP E. LANGE §

Abstract □ The synthesis of ^{14}C-meglumine salicylate was accomplished by heating ^{14}C-meglumine with salicylic acid, in equimolar ratios, in 2-propanol. The average radiochemical yield was 97.5%. Ten healthy adult male volunteers were given 1.2 g of the compound orally. Five took 1.2 g of 1-deoxy-1-[^{14}C]-methylamino-D-glucitol salicylate (containing about 47 μCi), and five others took 1.2 g of 1-deoxy-1-methylamino-D-[U-^{14}C]-glucitol salicylate (containing about 45 μCi). Urine and feces were collected for 5 days, and blood was sampled for 24 hr. The peak urinary excretion of meglumine and/or its metabolites occurred between 4 and 8 hr after administration (about 7.2% of the administered dose). Meglumine was excreted primarily in the feces (72.4% over 5 days) and, to a smaller extent, in urine (21.3% over 5 days). No activity was detected in blood. The excretion rate and percentage excreted were the same for both groups of subjects, suggesting that meglumine was not metabolized by *N*-demethylation or conversion to carbon dioxide. The highest blood salicylate level, 44.4 ± 1.9 μg/ml, was observed 1 hr after administration. Urinary levels of salicylic acid and its metabolites were observed to be at a maximum at 8 hr. Total salicylate recovery was 94.7 ± 1.5% in 48 hr. Salicyluric acid was the major metabolite, accounting for 69.5 ± 3.6% of the dose. Salicylic acid accounted for 6.8 ± 1.2%.

Keyphrases □ ^{14}C-Meglumine salicylate—synthesized, administered orally, biological distribution and excretion measured, humans □ Distribution, biological—^{14}C-meglumine salicylate, oral administration, humans □ Excretion—^{14}C-meglumine salicylate, oral administration, humans □ Radiochemistry—^{14}C-meglumine salicylate synthesized, administered orally, biological distribution and excretion measured, humans

Meglumine[1] (I) was first synthesized in 1935 (1). The use of I in pharmaceuticals began with the preparation of I antimonate for the treatment of leishmaniasis. Presently, several pharmaceutical preparations contain I. Some X-ray contrast media, for example, contain I as a solubilizing agent, and I was found to decrease the toxicity of such contrast media (2–4). Also, it was reported that I–coumermycin mixtures (4:1) elevated the blood antibiotic levels five- to 15-fold over those for the antibiotic alone (5, 6). The disposition of I in rats and dogs was reported recently (7).

Meglumine salicylate (II) is a promising new water-soluble salicylate under investigation. The suggested indications for the use of II include all conditions requiring systemic salicylate therapy. Since the compound is relatively new, its blood and urinary salicylate levels have not been reported. The literature also does not contain information about the disposition of I in humans.

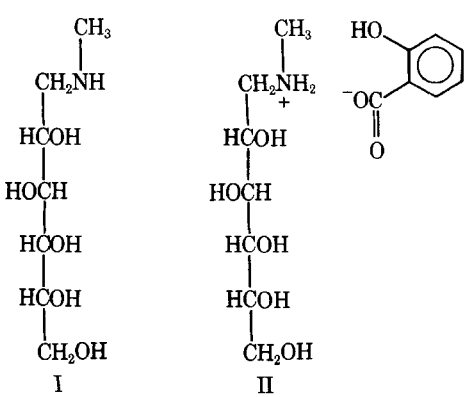

The purpose of this study was to gain such information and to show the effect, if any, I had on the absorption and urinary excretion of the salicylate moiety. To this end, 1-deoxy-1-[^{14}C]-methylamino-D-glucitol salicylate (II-M) and 1-deoxy-1-methylamino-D-[U-^{14}C]-glucitol salicylate (II-G) were synthesized and administered orally to humans. Two different positions of ^{14}C-labeling were used to gain preliminary information on the metabolism of I in humans.

EXPERIMENTAL

Radiosyntheses—The syntheses of I-M and I-G were described previously (8). Several preliminary reactions for the synthesis of II were conducted with ethanol or 2-propanol as a reaction medium. When ethanol was used, as previously suggested (9), a syrup of II was formed. By using a small volume of 2-propanol and conducting the synthesis in low humidity (50%), II could be synthesized in high yields.

Compound II-M—A solution of 2.91 g of I-M (14.9 mmoles, 0.067 mCi/mmole) and 2.06 g of salicylic acid in 35 ml of 2-propanol was warmed in a water bath at 50° to allow complete dissolution of I-M. After the solution was allowed to cool to room temperature, it was placed in a refrigerator overnight. The resulting compound was filtered in a low humidity (50%) atmosphere, since it was slightly hygroscopic, and dried under vacuum. The yield was 4.90 g (first crop, 98.6% of theoretical) of II-M, mp 98–101°. The specific activity was 0.19 ± 0.002 μCi/mg or 0.063 mCi/mmole.

Anal.[2]—Calc. for $C_{14}H_{23}NO_8$: C, 50.45; H, 6.90; N, 4.20. Found: C, 50.52; H, 7.08; N, 4.09.

Compound II-G—A solution of 849 mg of I-G (4.35 mmoles, 0.204 mCi/mmole) and 601 mg of salicylic acid in 10 ml of 2-propanol was treated as described for II-M. The yield was 1.4 g (first crop, 96.5% of theoretical) of II-G, mp 98–100°. The specific activity was 0.56 ± 0.005 μCi/mg or 0.19 mCi/mmole.

Anal.—Found: C, 50.23; H, 7.30; N, 4.00.

A mixed melting point of each labeled compound gave no melting-point depression. The IR spectrum of II (Fig. 1) was compared with spectra of the labeled compounds. From these analyses, the two ^{14}C-labeled compounds were determined to be chemically pure.

TLC analysis of II for radiochemical purity determination was not successful. Solvent systems of varying polarities and compositions failed to give a single spot for II. Two spots, one corresponding to I and the other to salicylic acid, were obtained, apparently due to the dissociation of II when dissolved in water or methanol. The two labeled compounds were assumed to be radiochemically pure, since it was predetermined that the ^{14}C-labeled I compounds had a radiochemical purity of 98.4%.

Procedure—Two volunteer groups of five healthy male subjects were used. Their weight range was 66–90 kg (average 77.6 kg), and their age range was 21–29 years. Blood and urine samples were collected from each volunteer at 7:30 am to serve as controls. At 8 am following an overnight fast, each subject received orally a capsule (assigned by random number drawing) containing an exactly weighed amount of either II-M (referred to as the M group) or II-G (referred to as the G group). The range of

[1] 1-Deoxy-1-methylamino-D-glucitol or *N*-methylglucamine.

[2] Midwest Microlab, Ltd., Indianapolis, Ind.

Table I—Excretion of ^{14}C-Meglumine and/or Its Metabolites in Urine and Feces[a]

	Time Interval, hr												
	Urine								Feces				
Subject[b]	0–4	4–8	8–12	12–24	24–48	48–72	72–96	96–120	0–24	24–48	48–72	72–96	96–120
M-1	2.6	1.8	0.75	0.87	1.4	5.1	0.62	0.25	41.4	31.1	NS[c]	6.0	0.05
M-2	5.4	2.5	1.7	1.8	6.7	2.6	3.2	2.1	NS	37.0	8.0	7.7	NS
M-3	3.8	2.1	0.87	1.9	2.7	2.0	0.87	0.15	11.4	62.1	NS	12.9	0.07
M-4	9.8	19.8	6.5	2.9	2.6	2.0	0.55	0.11	29.7	7.4	11.3	2.8	0.67
M-5	5.9	8.9	2.4	1.9	4.0	5.2	1.6	0.28	NS	1.0	57.3	10.6	0.89
$\bar{X}_M$	5.5	7.0	2.4	1.9	3.5	3.4	1.3	0.58	16.5	27.7	15.3	8.0	0.34
SEM	1.2	3.4	1.0	0.32	0.90	0.73	0.49	0.38	8.2	10.9	10.7	1.7	0.18
G-1	8.2	18.3	4.1	1.8	0.98	0.25	0.10	0.12	0.04	59.3	6.0	NS	1.0
G-2	2.4	2.3	0.85	0.75	0.56	0.20	0.12	0.05	4.0	64.4	1.5	0.33	0.71
G-3	6.4	2.2	0.66	0.96	1.0	1.4	1.9	1.2	0.04	39.6	28.7	0.25	8.5
G-4	1.6	0.96	0.38	0.50	0.58	0.15	0.00	0.00	15.9	72.3	2.5	0.11	0.14
G-5	5.5	13.4	2.9	0.46	1.2	0.39	0.14	0.07	0.09	29.1	44.0	5.9	0.35
$\bar{X}_G$	4.8	7.4	1.8	0.89	0.86	0.48	0.45	0.29	4.0	52.9	16.5	1.3	2.1
SEM	1.2	3.5	0.73	0.24	0.28	0.23	0.36	0.23	3.0	8.0	8.4	1.1	1.6
$\bar{X}_{M+G}$	5.2	7.2	2.1	1.4	2.2	1.9	0.91	0.43	10.3	40.3	15.9	4.7	1.2
SEM	0.83	2.3	0.62	0.25	0.61	0.60	0.33	0.22	4.6	7.6	6.4	1.5	0.82

[a] Expressed as percentage of administered dose. [b] Prefixes M and G refer to the position of the ^{14}C-label. See text. [c] No sample was supplied; subject was constipated. Result was entered as zero in average calculations.

^{14}C-activity ingested was 42.2–49.3 μCi, based on the determined specific activities. Each subject also received two more capsules containing II to make the total ingested amount of II equal to 1200 mg. Food, but not water, was withheld until noon, when the same lunch was served to all subjects.

Urine and feces were collected for 5 days. Urine was collected at the intervals shown in Table I. Feces were collected during each 24-hr period and were pooled for each subject before analysis when there were more than one. All urine and feces samples were frozen until analyzed. Blood was collected at 1, 2, 4, 8, 12, and 24 hr after drug administration in tubes containing edetic acid. All blood samples were refrigerated until analyzed.

Salicylate Analysis—The levels of salicylic acid, salicyluric acid, and total salicylate in urine were determined (at least in duplicate) using the method of Farid *et al.* (10). Blood salicylate was determined using the method of Trinder (11), with at least three determinations per sample. Blood and urine salicylate data from the 10 volunteers were pooled for the determination of the mean and standard error of the mean at each time interval.

Sample Preparation and Radioanalysis—The volume of urine of each subject for a given time interval was measured. Aliquots of 0.5 ml, or 1 ml when the activity was expected to be low, of urine in triplicate were placed in low potassium vials, and 0.1 ml of acetic acid was added. Fifteen milliliters of scintillator[3] was added, and the radioactivity was determined.

A preliminary study compared three agents for digesting feces: a quaternary ammonium hydroxide[4], perchloric acid–hydrogen peroxide (12), and a tissue digestant[5]. The use of perchloric acid–hydrogen peroxide led to a loss of about 15% of the activity in the case of I-G. The quaternary ammonium hydroxide caused a loss of about 12%. These losses were attributed to the long digestion times required for feces. The use of the tissue digestant did not cause a loss of activity and, moreover, gave the highest counting efficiency (77.9%).

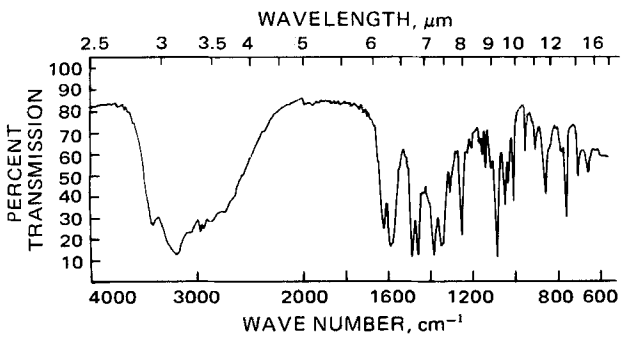

Figure 1—*IR spectrum of meglumine salicylate.*

The tissue digestant procedure was as follows. Feces were weighed and placed in a blender. Water, two to three times the sample weight, was added, and the mix was blended for 5–7 min. Quadruplicate samples of the resulting slurry, weighing 150–250 mg, were accurately weighed in tared counting vials. Two milliliters of tissue digestant and 0.3 ml of hydrogen peroxide were added, and the samples were left at room temperature. Six hours later, 0.3 ml of hydrogen peroxide was added, and the samples were left at room temperature for 24–36 hr. Then 0.1 ml of acetic acid was added followed by 15 ml of scintillator, and the radioactivity in the sample was determined.

Triplicate blood samples were prepared for counting by heating, in a counting vial, 0.1 ml of blood and 2 ml of tissue digestant at 50° for 4 hr. The vial was cooled to room temperature, and 0.3 ml of hydrogen peroxide was added dropwise. Four hours later, 0.3 ml of hydrogen peroxide was added. The samples were counted 3–4 hr later after the addition of 15 ml of scintillator.

All counting data were converted to disintegrations per minute with corrections for background and counter efficiency by internal standardization. Disintegrations per minute for the total volume or weight were calculated, and the result was reported as the percentage of the administered dose for each subject.

RESULTS AND DISCUSSION

Blood analysis showed no detectable activity above background. With the method used, the detection limit was 10 μg/ml of blood. Table I shows the concentration of ^{14}C-I and/or its radioactive metabolites in the urine and feces, expressed as the percentage of the administered dose. As can

Table II—Blood Salicylate Levels

	Salicylate Level, μg/ml	
Hours	Mean[a] ± *SEM*	Range
Control	16.6 ± 0.6	13.2[b]–19.5
1	44.4 ± 1.9	35.6–53.9
2	43.0 ± 1.6	37.5–53.2
4	35.6 ± 1.2	31.1–40.9
8	26.7 ± 1.4	20.0–32.2
12	20.6 ± 1.0	15.6–25.3
24	16.9 ± 0.7	13.2–20.3

[a] All values are the average of at least three determinations. [b] Ten subjects. See text for details.

[3] Phase combining system, Amersham-Searle, Arlington Heights, Ill.
[4] Hydroxide of Hyamine 10-X, a 1 *M* solution in methanol, Packard Instrument Co., Downers Grove, Ill.
[5] Soluene 100, Packard Instrument Co., Downers Grove, Ill.

Table III—Recovery of Salicylic Acid, Salicyluric Acid, and Total Salicylate in Urine

	Amount, mg						Cumulative Amount as Percentage of Administered Dose of Salicylic Acid				
	Control	0–4 hr	4–8 hr	8–12 hr	12–24 hr	24–48 hr	0–4 hr	0–8 hr	0–12 hr	0–24 hr	0–48 hr
Salicylic acid											
Mean ± *SEM*	0.12 ± 0.03	9.1 ± 3.1	9.8 ± 2.5	6.5 ± 1.2	2.3 ± 0.5	5.9 ± 1.7	1.8 ± 0.63	3.8 ± 0.88	5.1 ± 0.92	5.6 ± 0.94	6.8 ± 1.2
Range	0.00–0.30[a]	1.7–34.4	3.0–26.9	2.7–15.6	0.48–6.2	0.0–17.7	0.35–6.9	1.4–8.8	2.1–9.7	2.3–10.4	2.3–13.6
Salicyluric acid											
Mean ± *SEM*	1.8 ± 0.8	165.3 ± 11.1	177.9 ± 13.5	97.0 ± 6.8	40.5 ± 4.8	7.4 ± 1.4	23.6 ± 1.6	48.9 ± 3.0	62.7 ± 3.6	68.5 ± 3.5	69.5 ± 3.6
Range	0.23–8.4[b]	127.8–227.0	111.4–237.2	70.3–147.4	14.5–65.2	2.6–17.8	18.2–32.3	34.4–64.3	44.6–85.3	50.1–87.3	50.5–89.9
Total salicylate											
Mean ± *SEM*	2.0 ± 0.7	152.1 ± 8.2	167.5 ± 5.4	90.8 ± 4.9	47.2 ± 5.1	13.2 ± 1.3	30.6 ± 1.7	64.3 ± 1.9	82.6 ± 2.1	92.1 ± 1.6	94.7 ± 1.5
Range	0.27–6.7	119.4–209.2	143.6–190.2	66.0–114.8	13.3–79.8	4.9–19.8	24.0–42.1	55.5–71.6	73.8–93.4	84.3–101.5	87.5–102.5

[a] All values are the average of at least two determinations per sample. Values listed were not corrected for background salicylic acid levels because of the daily variability of the background levels. [b] For salicyluric acid, the amount in milligrams is listed as salicyluric acid; percentage of dose, however, is based on salicylic acid equivalent.

be seen, the excretion of I and/or its metabolites in the urine peaked 4–8 hr after drug administration. The average of the excreted I-M and/or its metabolites in urine over 5 days was 25.6 ± 5.7% of the administered dose. For the G group, the average was 17.0 ± 5.5% over the same period. This difference was attributed to biological variations between subjects. A t-test indicated that there was no significant difference in the excretion rate and the percentage excreted of I and/or its metabolites in urine over time between the M and G groups ($p > 0.1$).

About 68% of I-M and 77% of I-G and/or their metabolites were excreted in the feces (Table I) over 5 days. Again, a t-test indicated there was no significant difference between the excretion rate and the percentage of the administered activity excreted in the feces between the two groups ($p > 0.1$).

The 10 data points for each time interval were averaged (Table I), and the cumulative percentage of activity excreted in both the urine and feces was calculated. The resulting data showed that 21.3 ± 4.0% of the administered activity was excreted in the urine and 72.4 ± 4.1% was excreted in the feces over 5 days. Thus, 93.7 ± 2.8% of the administered dose was excreted in 5 days. Further examination of the data indicated that 50% of the administered dose was excreted during the first 35 hr.

After a single oral dose of 1.2 g of II, equivalent to 0.65 g of aspirin, blood salicylate levels (Table II) were 44.4 ± 1.9 and 43.0 ± 1.6 μg/ml in the 1st and 2nd hr, respectively. These values are comparable to the published blood salicylate levels after equivalent single doses of aspirin (13, 14), buffered aspirin (15), and sodium salicylate (16).

Table III shows the recovery of salicylic acid, salicyluric acid, and total salicylate in urine over 48 hr. Total salicylate concentration in urine samples collected beyond the 48-hr postdrug period were within the same concentration range as in the control samples and, therefore, were not included in Table III.

A semilogarithmic plot of the percentage of salicylate remaining in the body *versus* time showed that the half-life of the salicylate moiety in II was 6 hr. This value is in agreement with the previously reported half-life of a single 1-g dose of aspirin of 6 hr (17).

As with other salicylates (18), the major metabolite excreted in the urine was salicyluric acid, which accounted for 69.5 ± 3.6% of the administered dose. Salicylic acid excretion accounted for 6.8 ± 1.2% of the administered dose. Total salicylate excretion was 92.1 ± 1.6 and 94.7 ± 1.5% of the administered dose 24 and 48 hr after dosing, respectively.

These results show that the blood salicylate levels and the excretion of salicylic acid and its metabolites in urine followed the well-documented pattern of other salicylates. Thus, the salicylate moiety in II is absorbed and metabolized in humans like other salicylates.

The fact that, regardless of the position of the ^{14}C-label on I, the same percentage of the administered dose was excreted indicates that I is not metabolized through N-demethylation or through the formation of carbon dioxide. Whether I is excreted unchanged in the urine or metabolized needs further investigation.

REFERENCES

(1) R. B. Flint and P. L. Salzberg, U.S. pat. 2,016,962 (1935); through *Chem. Abstr.*, **29**, 8007[8] (1935).

(2) T. Greitz, R. Teleinus, and G. Tornell, *Acta Radiol. Suppl.*, **270**, 208 (1967).

(3) H. W. Fischer, S. R. Reuter, and N. P. Moscow, *Invest. Radiol.*, **3**, 324 (1968).

(4) S. H. Cornell and H. W. Fischer, *ibid.*, **2**, 41 (1967).

(5) H. L. Newmark and J. Berger, *J. Pharm. Sci.*, **59**, 1246 (1970).

(6) H. L. Newmark, J. Berger, and J. T. Carstensen, *ibid.*, **59**, 1249 (1970).

(7) J. F. Heeg, G. S. Born, W. V. Kessler, S. M. Shaw, and W. E. Lange, *ibid.*, **66**, 96 (1977).

(8) J. F. Heeg, G. S. Born, W. V. Kessler, S. M. Shaw, J. E. Christian, and W. E. Lange, *Can. J. Pharm. Sci.*, **10**, 75 (1975).

(9) H. Suter, Belgian pat. 626,944 (1964); through *Chem. Abstr.*, **61**, 10769d (1964).

(10) N. A. Farid, G. S. Born, W. V. Kessler, S. M. Shaw, and W. E. Lange, *Clin. Chem.*, **21**, 1167 (1975).

(11) P. Trinder, *Biochem. J.*, **57**, 301 (1954).

(12) R. H. Bishara, G. S. Born, and J. E. Christian, *J. Pharm. Sci.*, **61**, 1912 (1972).

(13) A. J. Cummings, in "Salicylates, An International Symposium," A. St. J. Dixon, B. K. Martin, M. J. H. Smith, and P. H. N. Wood, Eds., Little, Brown, Boston, Mass., 1963, pp. 28–31.

(14) S. Riegelman, in "Aspirin, Platelets and Stroke," W. S. Fields and W. K. Hass, Eds., W. H. Green, St. Louis, Mo., 1971, pp. 105–114.

(15) J. R. Leonards, *Clin. Pharmacol. Ther.*, **4**, 476 (1963).

(16) J. R. Leonards and G. Levy, *ibid.*, **14**, 62 (1973).

(17) B. B. Brodie, J. J. Burns, and M. Weiner, *Med. Exp.*, **1**, 290 (1959).

(18) C. Davidson, in "Drug Metabolism in Man," E. S. Vesell, Ed., *Ann. N.Y. Acad. Sci.*, **179**, 249 (1971).

ACKNOWLEDGMENTS AND ADDRESSES

Received June 19, 1975, from the *Bionucleonics Department, School of Pharmacy and Pharmacal Sciences, Purdue University, West Lafayette, IN 47907.*

Accepted for publication May 28, 1976.

Presented in part at the APhA Academy of Pharmaceutical Sciences, Atlanta meeting, November 1975.

Supported in part by the Purdue Frederick Co., Norwalk, CT 06856.

* Present address: Methodist Hospital, Indianapolis, IN 46202.

‡ Present address: Saint Elizabeth Hospital, Covington, KY 41014.

§ Purdue Frederick Co., Norwalk, CT 06856.

ˣ To whom inquiries should be directed.

Comparative Bioavailability of Four Commercial Quinidine Sulfate Tablets

JEFFREY D. STRUM, JOHN L. COLAIZZI ×, JAMES M. JAFFE, PERRY C. MARTINEAU *, and ROLLAND I. POUST

Abstract □ A comparative bioavailability study was performed using four commercially available, chemically equivalent brands of quinidine sulfate tablets. Two 200-mg tablets were administered to 11 different subjects following a completely randomized crossover design. Serum levels, urinary excretion data, and derived pharmacokinetic parameters were compared statistically. There were no statistical differences in the extent of quinidine absorption from the four brands of tablets as evidenced by the cumulative urinary excretion values and the areas under the serum level–time curves. Significant differences in the mean serum levels at 0.5 and 1 hr and differences in the peak times and absorption rate constants indicate that there was a difference in the absorption rate between Treatments A and D and C and D. A significant difference in the peak times also was noted for Treatments B and C. When mean disintegration times for the four tablet formulations were compared with their values for k_a, t_{max}, and mean serum levels at 0.5 and 1 hr, rank-order correlations were observed. A considerable degree of variability in quinidine elimination was noted, with half-life values ranging from 2.71 to 8.12 hr (mean half-life of 5.36 hr).

Keyphrases □ Quinidine sulfate—bioavailability of four commercial tablets compared, humans □ Bioavailability—quinidine sulfate, four commercial tablets compared, humans □ Cardiac depressants—quinidine sulfate, bioavailability of four commercial tablets compared, humans

Emphasis has been placed recently on the importance of establishing the biological equivalence of quinidine sulfate tablets. The APhA Academy of Pharmaceutical Sciences classified quinidine sulfate as one of the "commonly prescribed multiple source drugs whose solid dosage forms exhibit the most serious bioavailability and/or quality assurance problems" (1). However, since no published articles report the comparative bioavailability of chemically equivalent quinidine sulfate tablets, the classification of the Academy of Pharmaceutical Sciences must be taken to mean that there is a potential for bioavailability differences with this drug dosage form.

The Food and Drug Administration (FDA) also indicated that quinidine sulfate is one drug for which a bioequivalence requirement is currently anticipated and specified that *in vivo* testing would be necessary to compare different commercial products (2). A list of approved manufacturers and distributors of bioequivalent problem drugs recently published by the FDA included four manufacturers[1] and one distributor[2] of quinidine sulfate tablets (3).

BACKGROUND

Quinidine is a frequently prescribed antiarrhythmic drug. In 1975, it ranked 14th among the most frequently prescribed generic drugs in the United States (4). Currently, at least 60 different generic brands of 200-mg quinidine sulfate tablets are on the market (5). Studies established the blood level profiles of several salt and sustained-release dosage forms of quinidine to define an optimal dosage regimen (6–11). Other reports compared the blood levels produced by administering quinidine by different routes (12). The bioavailability of the drug is variable, especially when taken with food, since it is known to interact with bile anions to form an insoluble complex (13).

A specific range of serum quinidine levels (3–6 μg/ml) must be maintained to achieve the desired pharmacological effect (14). This therapeutic range varies, however, depending upon the assay methodology employed and may be as low as 2–4 μg/ml (11). Several studies indicated that there is a definite correlation between serum levels and clinical effect (15–17). However, a recent report (18) stressed cautious interpretation of serum level when predicting therapeutic or toxic response since individual patient sensitivity to the drug may be more important. Toxic reactions may occur at any serum level due to allergy or idiosyncrasy but are more likely to appear at levels above 8 μg/ml (19, 20).

Studies employing intravenous infusions of quinidine gluconate defined the kinetic disposition of the drug and showed that there is considerable interpatient variability in quinidine elimination (21). A recent study[3] employing capsule, tablet, and solution forms of quinidine sulfate and an intramuscular injection of the gluconate confirmed that there is a high degree of intersubject and intrasubject variability in the biological half-life of the drug as well as a difference in the bioavailability of the tablet and intramuscular dosage forms.

Based on the low therapeutic index of this drug, the critical purpose for which it is indicated, its reported potential for bioequivalency problems, its wide generic availability, and the lack of published comparative bioequivalency data, the objective of this study was to compare the bioavailability of four commonly available, chemically equivalent brands of quinidine sulfate tablets.

EXPERIMENTAL

***In Vivo* Study Protocol**—Eleven healthy, normal adult male volunteers, 20–37 years of age, were the subjects. The treatments consisted of four different brands of quinidine sulfate tablets acquired by the normal channels of drug distribution. A dose of 400 mg of quinidine sulfate (as two 200-mg tablets) was administered to each subject with approximately 180 ml of water. The subjects received each of the four treatments, A[4], B[5], C[6], and D[7], in a completely randomized crossover design. A 2-week period was employed between each dosage interval to allow for complete drug elimination. All subjects fasted for 8 hr before and 3 hr following drug administration.

Blood samples (6 ml) were drawn using evacuated glass containers[8] just prior to dosing and at 0.5, 1, 2, 3, 4, 6, 8, 12, 24, and 32 hr following drug administration. The samples were immediately centrifuged[9] at 3000 rpm, and the serum was separated and analyzed for quinidine. Complete urine voids were collected at intervals of 2, 4, 6, 8, 12, 16, 24, 28, 32, 40, 48, 58, and 72 hr following drug administration and analyzed for quinidine.

***In Vitro* Assessment of Dosage Forms**—Weight variation tests were performed on 20 tablets of each of the four brands following the method outlined in USP XIX (22) for determining permissible limits of weight variation.

Disintegration times were determined using an apparatus conforming

[1] Merrell-National, Parke-Davis, Phillips Roxane, and Rexall.
[2] Alliance.

[3] W. D. Mason, J. O. Covinsky, J. C. Valentine, K. C. Kelly, G. H. Weddle, and B. C. Martz, School of Medicine, University of Missouri, Kansas City, Mo., personal communication.
[4] Quinidine sulfate tablets USP, Lot 76F83A, Eli Lilly & Co., Indianapolis, Ind.
[5] Quinidine sulfate tablets USP, Lot 7088A, Phillips Roxane Laboratories, Columbus, Ohio.
[6] Quinora, Lot 72755, Lakeside Laboratories, Milwaukee, Wis.
[7] Quinidine sulfate tablets USP, Lot 15840, Stanlabs, Portland, Ore.
[8] Vacutainers, silicone-coated interior, Becton-Dickinson and Co., Rutherford, N.J.
[9] Clinical centrifuge model CL, International Equipment Co., Needham Heights, Mass.

Table I—Parameters Derived from Serum Levels and Urinary Excretion of Unchanged Drug

Parameter	Treatment[a] A	B	C	D	Statistical Method	Statistical Evaluation
Mean value of peaks of individual serum concentration–time curves, μg/ml	1.42	1.45	1.43	1.33	ANOVA	NS[b]
Mean time of peak value of individual serum concentration–time curves, hr	1.84	2.27	1.63	2.54	Wilcoxon's matched-pairs signed ranks test	$p < 0.05$
Mean corrected area under individual serum concentration–time curves, (μg/ml) × hr	14.41	15.80	15.11	14.63	ANOVA	NS
Mean k_a value of individual serum concentration–time curves, hr^{-1}	2.88	2.08	2.91	1.12	Wilcoxon's matched-pairs signed ranks test	$p < 0.05$
Mean K_E value of individual serum concentration–time curves, hr^{-1}	0.142	0.130	0.125	0.138	Wilcoxon's matched-pairs signed ranks test	NS

[a] See text for explanation of treatment conditions. [b] NS = not statistically significant.

to USP specifications[10] and employing six tablets of each of the four products. Tablets were tested according to the official specifications with purified water maintained at 37 ± 2° as the immersion fluid.

Although a content uniformity test is not specified for quinidine sulfate tablets, the relative potency of the tablets was determined by performing individual assays on each of 10 randomly chosen tablets of the four different brands. An additional 10 tablets of each brand were chosen and collectively assayed for mean quinidine content. The assay was conducted by following the nonaqueous titration procedure outlined in USP XIX (23) for quinidine sulfate tablets.

Fluorometric Determination of Quinidine in Biological Fluids—The analytical method used for the determination of quinidine in serum and urine was a modified form of the fluorometric assay developed by Cramer and Isaksson (24). This method utilizes a double-extraction procedure, which limits the extraction of water-soluble metabolites of quinidine and dihydroquinidine. Fluorescence was determined on a spectrofluorometer[11] at 450-nm emission and 340-nm excitation. Stock solutions for the calibration plots were prepared such that results are reported in terms of quinidine base.

Statistical Evaluation of Results—The following parameters were analyzed for variance for a crossover design using a computerized statistical program (BMD08V) (25): (*a*) serum concentrations at each time period, (*b*) peak serum concentrations, (*c*) corrected area under the serum concentration–time curve, and (*d*) total urinary excretion of the unchanged drug. Any variance established among treatments was further analyzed for differences between all possible treatment pairs using Tukey's allowable difference test (26).

Wagner (27) and Westlake (28) pointed out that univariate parameters, such as absorption rate constants and elimination rate constants estimated from serum level–time data, should not be analyzed by methods assuming uniform error variance. Therefore, values for the absorption rate constant, k_a, elimination rate constant, K_E, and calculated peak time, t_{max}, were analyzed nonparametrically using Wilcoxon's matched-pairs signed ranks test (29).

RESULTS

Based on the shapes of semilogarithmic plots of individual serum concentration–time data for the 11 subjects, the data were fitted to the classical one-compartment model, both with and without a lag time (30, 31), using a nonlinear least-squares regression computer program (32) on a digital computer[12]. Comparison of the values of the individual sums of squares of the deviations between experimental data and calculated values showed the one-compartment model with a lag time to have the better fit. The individual areas under the serum concentration–time curves (*AUC*) were calculated using the trapezoidal rule, including a correction for the *AUC* beyond the last data point. The peak time is the sum of the calculated peak time and the calculated lag time, t_{lag}. The calculated peak time was determined using (33):

$$t_{max} = \frac{2.303}{k_a - K_E} \log \frac{k_a}{K_E} \quad \text{(Eq. 1)}$$

The lag time was calculated from (34):

$$t_{lag} = \frac{2.303(\log A_2 - \log A_1)}{k_a - K_E} \quad \text{(Eq. 2)}$$

where A_2 and A_1 represent the coefficients for the exponential terms describing absorption and elimination, respectively.

Table I summarizes the pharmacokinetic data obtained from the individual serum and urinary excretion data. An analysis of variance and Wilcoxon's matched-pairs signed ranks test were performed on the appropriate parameters. A statistical difference was evidenced for the time of the peak concentration of the individual serum concentration–time curves between Treatments A and D, B and C, and C and D at the 95% level of confidence. Statistical differences ($p < 0.05$) were also found between Treatments A and D and C and D for the k_a values derived from the individual serum concentration–time curves.

Figure 1 illustrates the mean cumulative urinary excretion of the unchanged drug for the four brands of tablets. Statistical analyses (ANOVA)

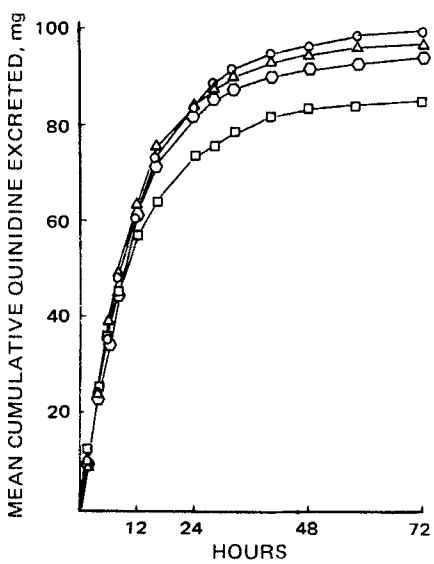

Figure 1—*Mean cumulative milligrams of unchanged quinidine excreted in urine (0–72 hr). Key: ○, Treatment A; △, Treatment B; □, Treatment C; and ○, Treatment D.*

[10] Van Kel Industries, Livingston, N.J.
[11] Turner model 430, G. K. Turner Associates, Palo Alto, Calif.
[12] PDP-10, Digital Equipment Corp., Maynard, Mass.

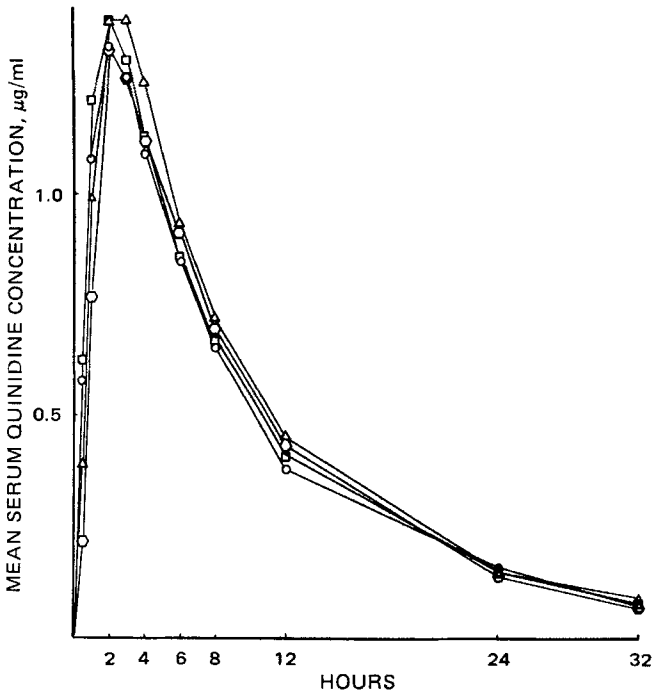

Figure 2—*Mean serum concentrations for 11 subjects for four different brands of quinidine sulfate tablets (0–32 hr). Key: ○, Treatment A; △, Treatment B; □, Treatment C; and ◇, Treatment D.*

revealed no differences between the four tablet brands based on the urinary excretion data. Figure 2 represents the mean serum level values for each treatment at each of the 10 sampling times following drug administration. An analysis of variance revealed a statistical difference ($p < 0.05$) among the treatment values for the mean serum values obtained at 0.5 and 1.0 hr following drug administration.

Differences among treatments were analyzed to determine the difference between treatment pairs using Tukey's test. A statistical difference was evidenced between Treatments A and D and C and D at 0.5 hr. There was also a statistical difference between Treatments C and D at 1.0 hr. The mean elimination half-life was calculated using (35):

$$t_{1/2} = \frac{0.693}{K_E} \qquad \text{(Eq. 3)}$$

and the individual K_E values were obtained from the computer program. The mean $t_{1/2}$ for all subjects and all treatments was 5.36 ± 1.07 hr, with all values falling into a range of 2.71–8.12 hr.

All four brands passed the weight variation and disintegration tests for quinidine sulfate tablets as specified in USP XIX. Mean disintegration times were 4.08 ± 0.20 min for Treatment A, 7.16 ± 1.94 min for Treatment B, 1.00 ± 0.0 min for Treatment C, and 17.83 ± 2.22 min for Treatment D. The relative potency of the individual tablets was also confirmed, with all individual tablet assays for all four brands resulting in 86.7–104.9% of the average of the monograph potency definition for the drug (36). The data confirmed the assumption that the various brands were chemical equivalents.

DISCUSSION

The bioavailability of a drug from tablet dosage forms depends on both the rate and extent of drug absorption into the general circulation. These factors can be evaluated by examining the pharmacokinetic parameters derived from blood level–time profiles and urinary excretion patterns for the unchanged drug. Bioequivalence is assured when the serum level–time curves for different brands of tablets are superimposable. Bioequivalence can also be established by comparing the peak serum concentrations of the drug, the times of the peak concentration, and the extent of absorption as reflected by the areas under the serum level–time curves.

Comparison of the area under the curve values revealed no significant differences in the extent of absorption of quinidine sulfate among the four different brands of tablets tested. The amount of drug excreted unchanged in the urine was also employed as an indicator of drug absorption. The urinary excretion of quinidine sulfate is pH dependent (37). Although no attempts were made to control urine pH in this study, comparison of the amounts excreted unchanged in the urine for 72 hr following administration showed no significant differences among the four brands tested. No apparent differences in urine pH values for the different treatments were noted.

The peak concentration and time of the peak concentration serve as indicators of the drug absorption rate. The peak concentration is generally achieved 2–3 hr following oral administration of a single dose of quinidine sulfate (38). Analyses of the data in Table I revealed a significant difference in the times of peak concentration between Treatments A and D, C and D, and B and C. A statistical difference also was evidenced for the mean serum levels between Treatments A and D and C and D at 0.5 hr and between Treatments C and D at 1.0 hr. Examination of the k_a values also revealed significant differences between Treatments A and D and C and D. The treatment pairs that exhibited significant differences in mean serum levels (A and D and C and D) and k_a values (A and D and C and D) also showed a statistical difference in the peak times (A and D and C and D), indicating that there was a difference in the absorption rate between these two formulation pairs. Treatment pair B and C also demonstrated a statistical difference in the peak time but not in serum levels or k_a values.

When mean disintegration times for the tablet brands were compared with the values for k_a, t_{max}, and mean serum levels at 0.5 and 1.0 hr, rank-order correlations were observed. Treatment C, with the shortest mean disintegration time, had the largest k_a value, highest serum levels at the first two sampling times, and the shortest t_{max}. Treatments A, B, and D followed in numerical ranking of mean disintegration times. There is currently no dissolution requirement in the compendial monograph of quinidine sulfate tablets, but dissolution studies are now underway in these laboratories to determine if a correlation between dissolution rates and *in vivo* parameters exist.

Although there was no significant difference among treatments for the mean biological half-life of the drug, there was considerable intersubject variability, in agreement with previously reported variability in the biological elimination of quinidine (39). The mean half-life for all subjects using all formulations was 5.36 ± 1.07 hr with a range of 2.71–8.12 hr. This range is less than that reported by Mason *et al.*[3] of 1.16–15.75 hr but corresponds more closely to the results of Ueda *et al.* (21), who reported a half-life of 6.33 hr with a range of 3.61–9.00 hr.

REFERENCES

(1) *J. Am. Pharm. Assoc.*, **NS14,** 557 (1974).
(2) *Fed. Reg.*, **40,** 26168 (1975).
(3) *FDC Rep.*, **38,** B16 (1976).
(4) *Pharm. Times*, **42,** 37 (1976).
(5) "Drug Topics Red Book," Medical Economics Co., Oradell, N.J., 1976, pp. 356–357.
(6) W. M. Goldberg and S. G. Charkrabarti, *Can. Med. Assoc. J.*, **91,** 991 (1964).
(7) E. M. Ditlefson and H. E. Loken, *Acta Med. Scand.*, **179,** 333 (1966).
(8) G. Cramer, E. Varnauskas, and L. Werko, *ibid.*, **173,** 511 (1963).
(9) S. Bellet, D. Finkelstein, and H. Gilmore, *Arch. Intern. Med.*, **100,** 750 (1957).
(10) J. J. Sampson, H. Foreman, and B. Solomon, *Circulation*, **5,** 534 (1952).
(11) R. Henning and G. Nyberg, *Eur. J. Clin. Pharm.*, **6,** 239 (1973).
(12) R. W. Kalmansohn and J. J. Sampson, *Circulation*, **1,** 569 (1950).
(13) S. Riegelman, *Pharmacology*, **8,** 127 (1972).
(14) "The Pharmacological Basis of Therapeutics," L. S. Goodman and A. Gilman, Eds., Macmillan, New York, N.Y., 1971, p. 17.
(15) A. J. Lisenthal, S. Ulich, and L. A. Patterson, *J. Clin. Invest.*, **26,** 1188 (1947).
(16) A. B. Houston and W. F. Perry, *Can. Med. Assoc. J.*, **63,** 59 (1950).
(17) A. F. Delevett and C. A. Poindexter, *Am. Heart J.*, **32,** 697 (1946).
(18) J. P. Van Dueme and M. G. Bogaert, *Circulation*, **50,** 1284 (1974).
(19) H. L. Conn and R. J. Luchi, *Am. J. Med.*, **37,** 685 (1964).
(20) A. F. Lyon and A. C. DeGraff, *Am. Heart J.*, **70,** 140 (1965).
(21) C. T. Ueda, D. S. Hirschfeld, M. M. Scheinman, M. Rowland, B.

J. Williamson, and B. S. Dzindzio, *Clin. Pharmacol. Ther.*, **19**, 30 (1976).
(22) "The United States Pharmacopeia," 19th rev., Mack Publishing Co., Easton, Pa., 1974, pp. 670, 671.
(23) *Ibid.*, p. 435.
(24) G. Cramer and B. Isaksson, *Scand. J. Clin. Lab. Invest.*, **15**, 553 (1963).
(25) P. Sampson, in "BMD, Biomedical Computer Programs," W. J. Dixon, Ed., University of California Press, Berkeley, Calif., 1974, pp. 693–704.
(26) D. U. Huntsberger and P. E. Leaverston, "Statistical Inference in the Biomedical Sciences," Allyn and Bacon, Boston, Mass., 1970, p. 213.
(27) J. G. Wagner, "Fundamentals of Clinical Pharmacokinetics," 1st ed., Drug Intelligence Publications, Hamilton, Ill., 1975, p. 351.
(28) W. J. Westlake, *J. Pharm. Sci.*, **62**, 1585 (1973).
(29) N. M. Downie and R. W. Heath, "Basic Statistical Methods," 2nd ed., Harper and Row, New York, N.Y., 1965, pp. 237–239.
(30) G. A. Portmann, in "Biopharmaceutics," J. Swarbrick, Ed., Lea & Febiger, Philadelphia, Pa., 1970, pp. 4–6.
(31) J. G. Wagner, "Fundamentals of Clinical Pharmacokinetics," 1st ed., Drug Intelligence Publications, Hamilton, Ill., 1975, p. 81.
(32) NLIN, Share Library No. 360 D-13.6.007, Research Triangle Park, NC 27709.
(33) G. A. Portman, in "Biopharmaceutics," J. Swarbrick, Ed., Lea & Febiger, Philadelphia, Pa., 1976, p. 17.
(34) J. G. Wagner, "Fundamentals of Clinical Pharmacokinetics," 1st ed., Drug Intelligence Publications, Hamilton Ill., 1975, pp. 81, 82.
(35) J. G. Wagner, "Biopharmaceutics and Relevant Pharmacokinetics," 1st ed., Drug Intelligence Publications, Hamilton, Ill., 1971, p. 252.
(36) "The United States Pharmacopeia," 19th rev., Mack Publishing Co., Easton, Pa., 1974, p. 648.
(37) R. E. Gerhardt, R. F. Knouss, P. T. Thyum, R. J. Luchi, and J. J. Morris, *Ann. Intern. Med.*, **5**, 927 (1969).
(38) A. F. Lyon and A. C. DeGraff, *Am. Heart J.*, **69**, 834 (1965).
(39) K. M. Kessler, D. T. Lowenthal, H. Warner, T. Gibson, W. Briggs, and Reidenberg, *N. Engl. J. Med.*, **290**, 706 (1974).

ACKNOWLEDGMENTS AND ADDRESSES

Received March 26, 1976, from the *Department of Pharmaceutics, University of Pittsburgh, Pittsburgh, PA 15261.*

Accepted for publication June 11, 1976.

Abstracted from a thesis submitted by Jeffrey D. Strum to the University of Pittsburgh in partial fulfillment of the Master of Science degree requirements.

* Medical Laboratories, McKeesport Hospital, McKeesport, Pa.

[x] To whom inquiries should be directed.

Mechanism of Histamine Binding II: Effect of Alkali Metal and Alkaline Earth Cations on Histamine Binding to Peptide H

PAUL A. KRAMER, JOHN R. HAZLETT, and DANE O. KILDSIG [x]

Abstract □ The association constants of histamine with Mg^{2+}, Ca^{2+}, Sr^{2+}, and Ba^{2+} were determined in buffer solutions at constant pH using an ion selective electrode. These cations enabled histamine to bind to peptide H. A minimum cation binding concentration was required for histamine binding. A linear relationship existed between the minimum cation binding concentration and the log of the equilibrium constant for the histamine–cation complexes, indicating that the specificity of the alkaline earth cations in promoting histamine binding was due to the difference in their ability to complex with histamine. The monovalent cations, Na^+, K^+, and Cs^+, inhibited histamine binding to peptide H, with the extent of inhibition dependent on cation concentration. An ion-exchange mechanism or a conformation change in the peptide may account for the inhibition.

Keyphrases □ Histamine—binding to peptide H, effect of alkali metal and alkaline earth cations, association constants determined □ Peptide H—binding to histamine, effect of alkali metal and alkaline earth cations, association constants determined □ Alkali metal and alkaline earth cations—effect on binding of histamine to peptide H, association constants determined □ Binding—histamine to peptide H, effect of alkali metal and alkaline earth cations, association constants determined □ Association constants—determined for binding of histamine to peptide H, effect of alkali metal and alkaline earth cations □ Metals—alkali metal and alkaline earth cations, effect on binding of histamine to peptide H

Previous reports indicated that Ca^{2+} is involved in the binding of histamine to serum protein (1, 2). Cations other than Ca^{2+} also appear to affect histaminopexy. Serum Mg^{2+} levels in asthmatics are low during attacks but normal while patients are free of symptoms (3); magnesium sulfate given intravenously to severe asthmatics gives relief for 18–20 hr (3). Injections of magnesium chloride restore histaminopexy in adrenalectomized and ovariectomized rats for up to 3 months, an effect similar to that of Ca^{2+} but longer lasting (4). In contrast to the divalent alkaline earth cations, the monovalent cation K^+ appears to inhibit histaminopexy (2, 5–7).

Previously (8), histamine was found to bind to a plasma peptide, termed peptide H, through the formation of a Ca^{2+}–histamine complex. Apparently, only one extensive investigation of histamine–alkaline earth complexes has been reported. Chawla (9) measured association and other thermodynamic constants for Be^{2+}, Ca^{2+}, and Mg^{2+} complexes with histamine, antistine, and similar molecules at several temperatures. Several studies determined association constants for histamine complexes with various other metals (10–12), and the method of pH titration generally has been used. For accurate results, this technique requires extensive experimental precautions such as those used by Chawla (9).

This report describes the determination of histamine–cation constants at constant pH, using a cation selective electrode. The purpose of this investigation was to deter-

J. Williamson, and B. S. Dzindzio, *Clin. Pharmacol. Ther.*, **19**, 30 (1976).
(22) "The United States Pharmacopeia," 19th rev., Mack Publishing Co., Easton, Pa., 1974, pp. 670, 671.
(23) *Ibid.*, p. 435.
(24) G. Cramer and B. Isaksson, *Scand. J. Clin. Lab. Invest.*, **15**, 553 (1963).
(25) P. Sampson, in "BMD, Biomedical Computer Programs," W. J. Dixon, Ed., University of California Press, Berkeley, Calif., 1974, pp. 693–704.
(26) D. U. Huntsberger and P. E. Leaverston, "Statistical Inference in the Biomedical Sciences," Allyn and Bacon, Boston, Mass., 1970, p. 213.
(27) J. G. Wagner, "Fundamentals of Clinical Pharmacokinetics," 1st ed., Drug Intelligence Publications, Hamilton, Ill., 1975, p. 351.
(28) W. J. Westlake, *J. Pharm. Sci.*, **62**, 1585 (1973).
(29) N. M. Downie and R. W. Heath, "Basic Statistical Methods," 2nd ed., Harper and Row, New York, N.Y., 1965, pp. 237–239.
(30) G. A. Portmann, in "Biopharmaceutics," J. Swarbrick, Ed., Lea & Febiger, Philadelphia, Pa., 1970, pp. 4–6.
(31) J. G. Wagner, "Fundamentals of Clinical Pharmacokinetics," 1st ed., Drug Intelligence Publications, Hamilton, Ill., 1975, p. 81.
(32) NLIN, Share Library No. 360 D-13.6.007, Research Triangle Park, NC 27709.
(33) G. A. Portman, in "Biopharmaceutics," J. Swarbrick, Ed., Lea & Febiger, Philadelphia, Pa., 1976, p. 17.
(34) J. G. Wagner, "Fundamentals of Clinical Pharmacokinetics," 1st ed., Drug Intelligence Publications, Hamilton Ill., 1975, pp. 81, 82.
(35) J. G. Wagner, "Biopharmaceutics and Relevant Pharmacokinetics," 1st ed., Drug Intelligence Publications, Hamilton, Ill., 1971, p. 252.
(36) "The United States Pharmacopeia," 19th rev., Mack Publishing Co., Easton, Pa., 1974, p. 648.
(37) R. E. Gerhardt, R. F. Knouss, P. T. Thyum, R. J. Luchi, and J. J. Morris, *Ann. Intern. Med.*, **5**, 927 (1969).
(38) A. F. Lyon and A. C. DeGraff, *Am. Heart J.*, **69**, 834 (1965).
(39) K. M. Kessler, D. T. Lowenthal, H. Warner, T. Gibson, W. Briggs, and Reidenberg, *N. Engl. J. Med.*, **290**, 706 (1974).

ACKNOWLEDGMENTS AND ADDRESSES

Received March 26, 1976, from the *Department of Pharmaceutics, University of Pittsburgh, Pittsburgh, PA 15261.*

Accepted for publication June 11, 1976.

Abstracted from a thesis submitted by Jeffrey D. Strum to the University of Pittsburgh in partial fulfillment of the Master of Science degree requirements.

* Medical Laboratories, McKeesport Hospital, McKeesport, Pa.

[x] To whom inquiries should be directed.

Mechanism of Histamine Binding II: Effect of Alkali Metal and Alkaline Earth Cations on Histamine Binding to Peptide H

PAUL A. KRAMER, JOHN R. HAZLETT, and DANE O. KILDSIG [x]

Abstract □ The association constants of histamine with Mg^{2+}, Ca^{2+}, Sr^{2+}, and Ba^{2+} were determined in buffer solutions at constant pH using an ion selective electrode. These cations enabled histamine to bind to peptide H. A minimum cation binding concentration was required for histamine binding. A linear relationship existed between the minimum cation binding concentration and the log of the equilibrium constant for the histamine–cation complexes, indicating that the specificity of the alkaline earth cations in promoting histamine binding was due to the difference in their ability to complex with histamine. The monovalent cations, Na^+, K^+, and Cs^+, inhibited histamine binding to peptide H, with the extent of inhibition dependent on cation concentration. An ion-exchange mechanism or a conformation change in the peptide may account for the inhibition.

Keyphrases □ Histamine—binding to peptide H, effect of alkali metal and alkaline earth cations, association constants determined □ Peptide H—binding to histamine, effect of alkali metal and alkaline earth cations, association constants determined □ Alkali metal and alkaline earth cations—effect on binding of histamine to peptide H, association constants determined □ Binding—histamine to peptide H, effect of alkali metal and alkaline earth cations, association constants determined □ Association constants—determined for binding of histamine to peptide H, effect of alkali metal and alkaline earth cations □ Metals—alkali metal and alkaline earth cations, effect on binding of histamine to peptide H

Previous reports indicated that Ca^{2+} is involved in the binding of histamine to serum protein (1, 2). Cations other than Ca^{2+} also appear to affect histaminopexy. Serum Mg^{2+} levels in asthmatics are low during attacks but normal while patients are free of symptoms (3); magnesium sulfate given intravenously to severe asthmatics gives relief for 18–20 hr (3). Injections of magnesium chloride restore histaminopexy in adrenalectomized and ovariectomized rats for up to 3 months, an effect similar to that of Ca^{2+} but longer lasting (4). In contrast to the divalent alkaline earth cations, the monovalent cation K^+ appears to inhibit histaminopexy (2, 5–7).

Previously (8), histamine was found to bind to a plasma peptide, termed peptide H, through the formation of a Ca^{2+}–histamine complex. Apparently, only one extensive investigation of histamine–alkaline earth complexes has been reported. Chawla (9) measured association and other thermodynamic constants for Be^{2+}, Ca^{2+}, and Mg^{2+} complexes with histamine, antistine, and similar molecules at several temperatures. Several studies determined association constants for histamine complexes with various other metals (10–12), and the method of pH titration generally has been used. For accurate results, this technique requires extensive experimental precautions such as those used by Chawla (9).

This report describes the determination of histamine–cation constants at constant pH, using a cation selective electrode. The purpose of this investigation was to deter-

Table I—Values for the Stoichiometry and Association Constants for Alkaline Earth Cation–Histamine Complexes at 37° and pH 7.4

Cation	n	log K	K, M^{-1}
Mg^{2+}	1.00	2.50	3.2×10^2
Ca^{2+}	1.02	3.07	11.8×10^2
Sr^{2+}	0.88	2.96	9.2×10^2
Ba^{2+}	0.80	2.87	7.4×10^2

mine the effect of the alkaline earth and alkali metal cations on the binding of histamine to peptide H.

EXPERIMENTAL

Materials—Histamine dihydrochloride[1] and tromethamine hydrochloride, ultrapure[1], were used. All other chemicals were reagent grade. The isolation of peptide H and the preparation of the tromethamine buffer were described previously (8).

Minimum Detectable Binding Concentration—To determine the minimum concentration of the alkaline earth cation necessary for detectable histamine–peptide binding, a series of dynamic dialysis runs was carried out with increasing concentrations of the alkaline earth cation added to internal and external solutions. The apparatus and experimental procedure for dynamic dialysis were described previously (8). Plots of log total histamine remaining in the internal cell *versus* time were made. When no binding occurred, the slopes of these linear plots were the same as the slope with no peptide present. When binding occurred, the slope decreased, indicating less free histamine present.

Association Constants for Histamine and Alkaline Earth Cations—Calcium-ion and calomel electrodes were used with a pH meter[2]. Solutions were maintained at 37 ± 0.1° in a jacketed beaker and agitated with a magnetic stirrer. A titrant, alkaline earth chloride solution in isotonic tromethamine buffer (pH 7.4), was added in 0.1-ml increments to either 50 ml of 1.81×10^{-3} M histamine in the same tromethamine buffer or 50 ml of a buffer blank containing no histamine. Each 0.1-ml increment of titrant produced a 0.0005 M increment of cation.

Plots of cation concentration *versus* millivolt reading, both in the presence and absence of histamine, were made. From these plots, the concentration of free cation and, by subtraction, the concentration of bound cation were determined.

Millivolt Titrations with Histamine, Peptide, and Calcium: Effect of Alkali Metal Cation—Alkali metal chloride was added to 25 ml of peptide H, 7.8 mg/ml, in 0.9% NaCl. Sodium, potassium, and cesium chlorides were used. Since 0.9% NaCl was used in the buffer system throughout all investigations, 0.154 M, corresponding to 0.9% NaCl, was the lowest concentration of potassium and cesium chlorides used. The peptide H solution was also made 0.770 and 1.1540 M in sodium chloride; 0.308, 0.616, and 1.232 M in potassium chloride; and 0.308 and 0.770 M in cesium chloride. To these solutions, histamine dihydrochloride solution was added in 0.1-ml increments such that each addition produced a 0.001 M increment in histamine.

A pH meter[3] was used with combination electrode to determine the millivolt readings. Identical runs were conducted with calcium chloride added to the peptide H–alkali metal chloride solutions.

RESULTS AND DISCUSSION

Cation–Histamine Association Constants—Total valence electron calculations show that histamine, in both its neutral and monoprotonated forms, exists in a configuration theoretically favorable to metal and intramolecular hydrogen binding (13). The equilibria involved are shown in Schemes I and II:

$$n_1M^{2+} + Hi^+ \overset{K}{\rightleftharpoons} M_{n_1}Hi^+$$

Scheme I

$$n_2M^{2+} + Hi \overset{K'}{\rightleftharpoons} M_{n_2}Hi$$

Scheme II

[1] Schwarz/Mann, Orangeburg, NY 10962.
[2] Orion model 801, Orion Research, Cambridge, MA 02139.
[3] Sargent model NX, Sargent-Welch Co., Skokie, IL 60076.

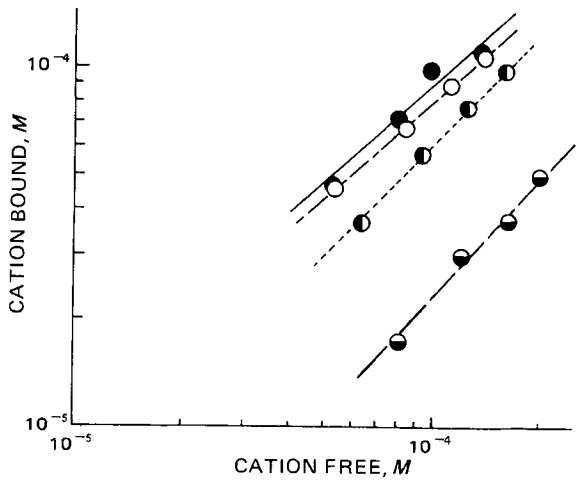

Figure 1—*Log–log plot of the bound alkaline earth cation* versus *the free alkaline earth cation for various histamine–alkaline earth cation complexes. The slope is equal to the number of cations bound per histamine molecule. Key:* ◒, *Mg;* ◐, *Ba;* ○, *Sr; and* ●, *Ca.*

where Hi and Hi^+ are the unionized and monoprotonated forms of histamine, M^{2+} is the alkaline earth divalent cation concentration, n is the number of moles of cation bound per mole of histamine, and $M_{n_1}Hi^+$ and $M_{n_2}Hi$ are the concentrations of the complexes formed.

If $n_1 = n_2 = n$, then:

$$K'/K = [M_nHi]/[M_nHi^+]\{[Hi^+]/[Hi]\} \qquad \text{(Eq. 1)}$$

Since the side-chain pKa of histamine is about 9.4, the ratio Hi^+/Hi is between 30 and 100 at a physiologic pH of 7.4. Therefore, the species M_nHi makes only a minor contribution to the total bound alkaline earth cation at pH 7.4 unless the affinity constant, K', for the unionized histamine–metal complex is an order of magnitude higher than that for ionized histamine, K. Assuming Scheme I represents the primary association, one can calculate the cation–histamine$^+$ association constant, K, for Mg^{2+}, Ca^{2+}, Sr^{2+}, and Ba^{2+} from determinations of free and bound alkaline earth cation concentrations at pH's where Hi^+ predominates. The equilibrium expression for Scheme I is:

$$K = \frac{[M_nHi^+]}{[M^{2+}]^n[Hi^+]} \qquad \text{(Eq. 2)}$$

which may be written as:

$$\log K = \log [M_nHi^+] - \log [Hi^+] - n \log [M^{2+}] \qquad \text{(Eq. 3)}$$

or:

$$\log [M^{2+}_{\text{bound}}] = \log K + \log [Hi^+] + n \log [M^{2+}_{\text{free}}] \qquad \text{(Eq. 4)}$$

where $\log [M^{2+}_{\text{bound}}] = \log [M_nHi^+]$. A plot of log cation bound *versus* log cation free was linear (Fig. 1), and the slope, n, was approximately one for all four cations, indicating a 1:1 complex (Table I). The association constants may then be calculated using Eq. 2, since the concentrations of bound and free cation, and thus of complex and free histamine, are known (Table I). The complexes of histamine with Ca^{2+}, Sr^{2+}, Ba^{2+}, and Mg^{2+} were found to be 1:1 with association constants for Ca^{2+}, Sr^{2+}, and Ba^{2+} with histamine being fairly close at about 10^3 M^{-1} and for the histamine–Mg^{2+} complex being considerably lower.

The association constants determined for the histamine–alkaline earth complexes by the ion selective electrode at constant pH are in good agreement with Chawla's (9) results (for Mg^{2+}, a log K of 2.26; for Ca^{2+}, a log K of 2.91) determined at 25° using the pH titration method. The

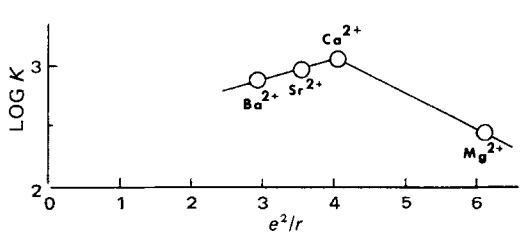

Figure 2—*Log* K versus e^2/r *for histamine–alkaline earth cation complexes.*

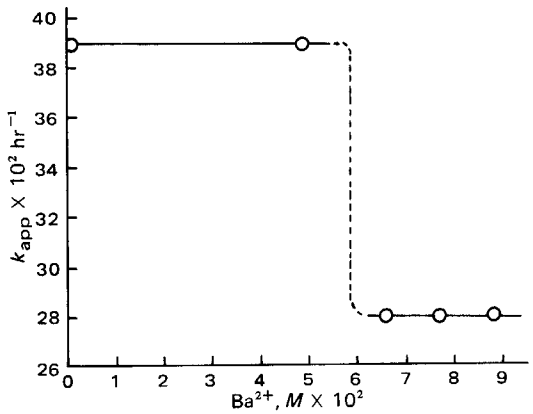

Figure 3—*Relationship between apparent first-order dialysis rate constant, k_{app}, and concentration of Ba^{2+} indicating the minimum detectable binding concentration of Ba^{2+}.*

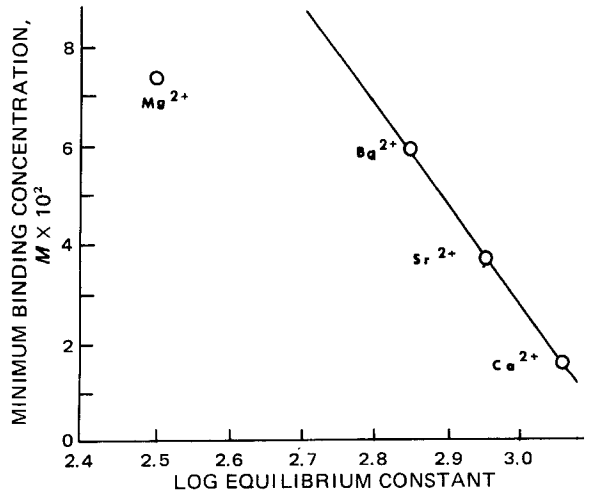

Figure 4—*Relationship between the minimum detectable binding concentration and log of the histamine–alkaline earth cation association constants.*

pH titration method, however, approaches its limit of application for association constants under 10^3, limiting the accuracy of Chawla's values for Ca^{2+}–histamine and, particularly, for Mg^{2+}–histamine (9). While it is difficult to draw conclusions based on only these two systems, the larger deviation of Chawla's log K for Mg^{2+}–histamine from the log K determined by the ion selective electrode was most likely due to the pH titration limitation, with the ion selective electrode measurement of log K being the more accurate.

A plot of the data according to the Born equation, as described by Martell and Calvin (14), provides some insight into the influence of the charge and radius of the alkaline earth ion on the binding constant:

$$E = \frac{e^2}{2r}\left(1 - \frac{1}{D}\right) \qquad \text{(Eq. 5)}$$

where E = energy of solvation for gaseous ions, r = ionic radius, e = charge, and D = dielectric constant of solvent. If the energy of solvation is assumed to be directly related to log K, then a linear relationship should exist between log K and e^2/r. When the log of the association constants for histamine–alkaline earth cations are plotted *versus* e^2/r, it is seen (Fig. 2) that while Ba^{2+}, Sr^{2+}, and Ca^{2+} follow the expected order, Mg^{2+} is low. It is not unusual, however, for Ca^{2+} complexes to have higher log K's than Mg^{2+}, particularly with ligands forming a highly chelated structure.

One might also expect a relationship between the proton affinity (pK) of the chelating agent and the free energy of the binding process as represented by log K. Martell and Calvin (14) showed a plot of log K *versus* pK for the alkaline earth complexes of a series of structurally similar weak acid chelating agents. A linear relationship was observed for each alkaline earth cation studied. For chelating agents with pK's above 9, the affinity constants were in the order $Mg^{2+} > Ca^{2+} > Sr^{2+} > Ba^{2+}$. At pK's below 7.5, the order seemed to be altered; this same order, $Ca^{2+} > Sr^{2+} > Ba^{2+} > Mg^{2+}$, was observed for histamine affinities. The present system seems to exhibit the expected metal specificity for a species with a conjugate acid dissociation constant below 7.5, *i.e.*, the monoprotonated form of histamine, the conjugate acid of which has a pK of 5.8, and for a species that predominates at pH 7.4. The binding affinities of the alkaline earth cations for vitamin D-induced calcium binding protein also follow the order $Ca^{2+} > Sr^{2+} > Ba^{2+} > Mg^{2+}$ (15). This effect may be due to ionizable groups of pK less than 7.5 on the binding protein.

Effect of Alkaline Earth Divalent Cations—When Sr^{2+}, Ba^{2+}, or Mg^{2+} was substituted for Ca^{2+} in the dynamic dialysis runs, it also enabled the peptide to bind histamine. The difference was only in the concentration of cation necessary to promote binding.

When the apparent first-order rate constants were determined from the slopes of plots of log total histamine remaining in the dialysis cell *versus* time and plotted against the concentration of cation at which they were obtained, the apparent first-order rate constants were the same whether the cation was present or not until a minimum cation concentration was reached. At this point, the rate constants decreased, indicating that binding, perhaps mediated by a conformational change, had occurred (Fig. 3). The minimum concentrations of the alkaline earth cation required for binding are shown in Table II. As the divalent cation concentration was increased beyond the minimum for binding, a rate of dialysis independent of cation concentration was reached (Fig. 3). Since the concentration of peptide H was much smaller than the histamine or divalent cation concentrations and was constant, the peptide H concentration probably became a limiting factor, resulting in the apparent constancy of the binding.

When association constants for histamine–alkaline earth cations were logarithmically plotted *versus* their respective minimum detectable binding concentrations (Fig. 4), a linear relationship was observed between the threshold concentration and the free energy of the binding process. Thus, the specificity of the alkaline earth cations in promoting binding of histamine to peptide H is due to the difference in their ability to complex with histamine as indicated by their association constants.

Botre *et al.* (16) studied the binding of histamine to bovine serum albumin at various ionic strengths and reported that, for a given ionic strength, the protein required a threshold concentration of histamine for binding and that this threshold varied with the nature of the inorganic cations present in the system. The explanation given is that the albumin undergoes a "conformational perturbation that is induced by histamine and dependent on ionic strength." Apparently, a similar phenomenon occurs for peptide H, where the conformational change is induced by the alkaline earth cation–histamine complex.

Effect of Monovalent Cations on Histamine–Ca^{2+}–Peptide H Binding—Peptide H in distilled water, with varying concentrations of alkali metal chloride added, was titrated with histamine dihydrochloride, and the millivolt readings were recorded using a pH electrode. A plot of the millivolt readings *versus* the log of the concentration of histamine added was linear (Fig. 5). Since histamine does not bind to peptide H in the absence of Ca^{2+} (8) (or other divalent cations), the pH electrode was responding to free histamine hydrochloride. The addition of calcium chloride resulted, as expected, in a decrease in free histamine due to binding to peptide H, as evidenced by a decreased slope of the millivolt titration curve. This Ca^{2+} effect was most noticeable at the lower concentrations of the alkali metal chlorides, 0.154 M, with the effect of the alkali metal chloride increasing as its concentration increased.

Table II—Minimum Detectable Binding Concentrations for the Alkaline Earth Cations

Cation	Minimum Binding Concentrations, M
Mg^{2+}	7.4×10^{-2}
Ca^{2+}	1.6×10^{-2}
Sr^{2+}	3.7×10^{-2}
Ba^{2+}	5.9×10^{-2}

Table III—Minimum Alkali Metal Chloride Concentrations for Complete Inhibition of Histamine Binding

Cation	Inhibitory Concentration, M
Cs^+	0.52
Na^+	0.86
K^+	1.43

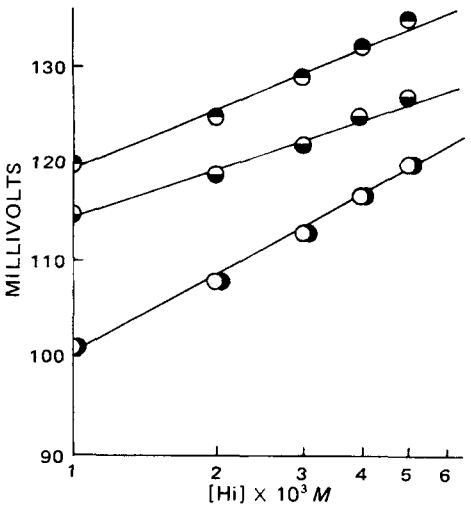

Figure 5—*Relative millivolt readings* versus *concentration of histamine for determining the effect of Na^+ on peptide–histamine–Ca^{2+} binding. Key: ◓, peptide, low Na^+; ◒, peptide, Ca^{2+}, low Na; ○, peptide, high Na^+; and ●, peptide, Ca^{2+}, high Na^+. The concentrations were: peptide, 1.7 × 10^{-4} M; Ca^{2+}, 1.8 × 10^{-2} M; low Na^+, 0.154 M; and high Na^+, 0.770 M.*

As seen in Fig. 5, the curves for both the peptide H and peptide H–calcium chloride solutions containing the higher alkali metal concentration approach one another. Apparently, an alkali metal chloride concentration can be reached that completely inhibits histamine binding to peptide H. That this is indeed the case is shown in Fig. 6, where the millivolt difference between the peptide H and peptide H–calcium chloride solutions was plotted *versus* the concentration of alkali metal chloride present in the solution. An extrapolation to the abscissa gives the concentration of alkali metal chloride necessary to inhibit histamine binding completely. This finding is verified by the complete inhibition of binding by Na^+ and Cs^+ at concentrations over the predicted inhibitory concentration.

The alkali metal cations may inhibit the histamine–peptide H binding

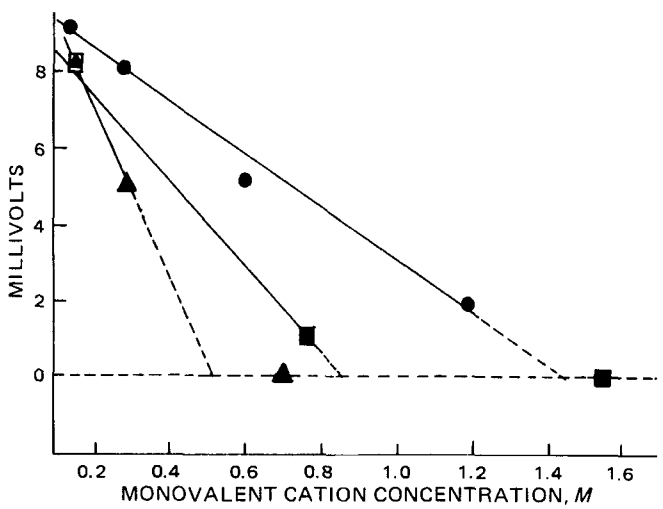

Figure 6—*Relationship between the change in millivolt reading produced by added Ca^{2+} and the concentration of the monovalent cation present in solution. The intercept at 0 mv is predictive of the minimum inhibitory concentration of the monovalent cation. Key: ▲, Cs^+; ■, Na^+; and ●, K^+.*

by affecting either the Ca^{2+}–histamine complex formation or the binding of the complex to peptide H. To determine if Na^+ affected the complexation between histamine and Ca^{2+}, histamine was titrated with Ca^{2+} solution using a Ca^{2+} ion selective electrode in the same manner as was used to determine the histamine–Ca^{2+} association constant, except that more sodium chloride was added to increase the Na^+ concentration from 0.154 to 0.770 *M*. There was no difference in the concentration of bound Ca^{2+} in the presence of increased Na^+. However, the increase of Na^+ to 0.770 *M* did interfere with the Ca^{2+}-mediated binding of histamine to peptide H (Fig. 5); therefore, the Na^+ effect must occur in the interaction between the histamine–Ca^{2+} complex and peptide H.

Two possible mechanisms for the alkali metal cation inhibition of histamine binding may be considered. One possibility is an ion exchange between the alkali metal cation and the bound calcium–histamine complex, similar to that reported by Aborg and Uvnas (17) for Na^+ inhibition of histamine binding to a heparin–clupeine complex. The inhibition by Na^+ was due to a competition with histamine for carboxyl groups on the clupeine. Peptide H provides nine weak acid groups per peptide molecule, and a similar competitive displacement from these anionic sites is a possible explanation of the present observations. Alternatively, conformational changes in peptide H favorable to binding may be induced by the Ca^{2+}–histamine complex and, above a critical alkali metal salt concentration, these conformational changes cannot be effected. It was reported that alkali metal cations prevent a conformational change in bovine serum albumin that is essential for albumin–histamine binding (16). The order of specificity of this inhibitory effect was $K^+ > Rb^+ > Na^+ > Li^+ = Cs^+$, which is the reverse of the order observed for the inhibition of Ca^{2+}–histamine binding to peptide H (Table III).

REFERENCES

(1) J. L. Parrot and M. Mordelet-Dambrine, *J. Physiol.*, **53,** 439 (1961).

(2) J. L. Parrot, M. Mordelet-Dambrine, and G. Trinquet, *Bull. Acad. Nat. Med. (Paris)*, **146,** 335 (1962).

(3) V. G. Haury, *J. Lab. Clin. Med.*, **26,** 340 (1940).

(4) M. Mordelet-Dambrine and J. L. Parrot, *J. Physiol.*, **58,** 303 (1966).

(5) J. L. Parrot, M. Laborde, and M. Mordelet-Dambrine, *C. R. Soc. Biol.*, **149,** 2094 (1955).

(6) J. L. Parrot and M. Mordelet-Dambrine, *ibid.*, **153,** 750 (1959).

(7) J. L. Parrot and M. Mordelet-Dambrine, *J. Physiol.*, **53,** 439 (1961).

(8) J. R. Hazlett and D. O. Kildsig, *J. Pharm. Sci.*, **63,** 701 (1974).

(9) I. D. Chawla, Ph.D. thesis, Kansas State University, Manhattan, Kans., 1962.

(10) M. Karapetyants and E. Slenskaya, *Zh. Fiz. Khim.*, **38,** 1312 (1964).

(11) P. Kiralo and R. V. Schalien, *Suom. Kemistil.*, **35B,** 7 (1962).

(12) J. Zarembowitch, *J. Chim. Phys.*, **63,** 438 (1966).

(13) J. P. Green, S. Kang, and S. Margolis, *Mem. Soc. Endocrinol.*, **19,** 727 (1971).

(14) A. E. Martell and M. Calvin, "Chemistry of the Metal Chelate Compounds," Prentice-Hall, New York, N.Y., 1952, p. 191.

(15) R. J. Ingersoll and R. H. Wasserman, *J. Biol. Chem.*, **246,** 2808 (1971).

(16) C. Botre, M. Marchetti, and S. Borghi, *Biochim. Biophys. Acta*, **154,** 360 (1968).

(17) C. H. Aborg and B. Uvnas, *Acta Physiol. Scand.*, **74,** 552 (1968).

ACKNOWLEDGMENTS AND ADDRESSES

Received April 5, 1976, from the *Department of Industrial and Physical Pharmacy, School of Pharmacy and Pharmacal Sciences, Purdue University, West Lafayette, IN 47907.*

Accepted for publication May 28, 1976.

* To whom inquiries should be directed.

Synthesis and PMR and Mass Spectra of Potential Metabolites and Other Derivatives of Bis(2-ethylhexyl) Phthalate

JAMES E. CARTER, ROBERT V. PETERSEN, and DAVID B. ROLL ˣ

Abstract □ The 3- and 4-hydroxylated derivatives of the plasticizer bis(2-ethylhexyl) phthalate and the monoesters derived from these hydroxylated derivatives were synthesized. The structures of the two 4-hydroxy monoesters were confirmed by lithium borohydride reduction to their corresponding hydroxymethylbenzoic acids, followed by cyclization of the reduced compounds to known phthalides. All compounds were characterized by PMR and mass spectra. The PMR data reiterate the difficulty in predicting chemical shifts in multisubstituted benzene rings.

Keyphrases □ Phthalate esters, mono- and bis(2-ethylhexyl)—3- and 4-hydroxy derivatives synthesized and characterized by PMR and mass spectra □ Hydroxyphthalate esters, mono- and bis(2-ethylhexyl)—synthesized and characterized by PMR and mass spectra □ PMR—characterization of mono- and bis(2-ethylhexyl) esters of 3- and 4-hydroxyphthalic acid □ Mass spectrometry—characterization of mono- and bis(2-ethylhexyl) esters of 3- and 4-hydroxyphthalic acid

It has been shown that bis(2-ethylhexyl) phthalate (I) is converted into the corresponding monoester, mono(2-ethylhexyl) phthalate (II), both *in vivo* (1) and *in vitro* (2) followed by ω and ω-1 oxidation of II (3). Since II is 50–100 times more toxic than I (4), as determined by acute LD_{50} studies in mice and rats, other toxic metabolites, such as those formed by aromatic hydroxylation of I, might be formed in the body. In conjunction with studies aimed at the identification of such metabolites, the 3-hydroxy (III*a* and III*b*) and 4-hydroxy (IV*a*–IV*c*) derivatives of I and II and related compounds necessary for their unequivocal structural elucidation were synthesized and characterized by PMR and mass spectra.

EXPERIMENTAL

Instrumentation—PMR spectra[1] were obtained using dimethyl sulfoxide-d_6[2] as the solvent and sodium 2,2-dimethyl-2-silapentane-5-sulfonate as the internal standard and are reported in δ, parts per million (ppm), relative to the internal standard. Mass spectra[3] were obtained by direct probe operating at 70 ev with an accelerating voltage of 3.5 kv and an ion source temperature of 250°.

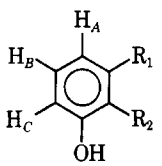

III*a*: $R_1 = R_2 = COOCH_2CH(C_2H_5)(CH_2)_3CH_3$
III*b*: $R_1 = COOCH_2CH(C_2H_5)(CH_2)_3CH_3$, $R_2 = COOH$

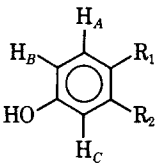

IV*a*: $R_1 = R_2 = COOCH_2CH(C_2H_5)(CH_2)_3CH_3$
IV*b*: $R_1 = COOH$, $R_2 = COOCH_2CH(C_2H_5)(CH_2)_3CH_3$
IV*c*: $R_1 = COOCH_2CH(C_2H_5)(CH_2)_3CH_3$, $R_2 = COOH$

Melting points were determined using a micro hot stage or, where specified, a capillary melting-point apparatus[4] and are uncorrected. The TLC solvent system employed was chloroform–methanol–acetic acid (250:10:1).

For the PMR spectra, the aromatic protons in both the 3-hydroxy (III*a* and III*b*) and 4-hydroxy (IV*a*–IV*c*) derivatives were designated H_A, H_B, and H_C. The PMR data for the relevant protons of the 4-hydroxy derivatives are shown in Table I.

Mono(2-ethylhexyl) Phthalate (II)—This compound was synthesized from phthalic anhydride[5] and 2-ethylhexanol[5] according to the procedure of Kenyon and Platt (5); PMR: δ 7.65 (m, 4), 4.17 (d, 2), and 0.77–1.58 (m, 15) ppm; mass spectrum[6]: *m/e* 278 (M^+, 0.5%), 279 (M + 1, 7.5), 167 (30), 149 ($C_8H_5O_3$, 100), 113 (6), 112 (13), 104 (14), 57 (29), and 43 (55).

Bis(2-ethylhexyl) 4-Hydroxyphthalate (IV*a*)—To 3 g (16.4 mmoles) of 4-hydroxyphthalic acid[5] (V*a*) were added 33.4 g (256 mmoles) of 2-ethylhexanol and 3 drops of concentrated sulfuric acid dissolved in 75 ml of toluene (Scheme I, R = 2-ethylhexyl). The mixture was refluxed for 16 hr, the sulfuric acid was removed by shaking with 5% $NaHCO_3$, and the organic phase was washed with water. Toluene was removed with a flash evaporator, and 2-ethylhexanol was removed by vacuum distillation, leaving 5 g (75%) of crude liquid. The product was purified by silica gel[7] dry column chromatography (3.0 × 15 cm) (6) employing chloroform as the eluent; IV*a* eluted mainly in the first 100 ml, which then was concentrated and placed over a second silica gel dry column (1.2 × 20 cm). Elution with chloroform and solvent removal resulted in a clear viscous liquid of analytical quality; mass spectra: *m/e* 406 (M^+, 0.8%), 295 (21), 183 (43) m* 113.5, 165 (100) m* 148.8, 113 (9.5), 112 (20), 71 (25), 70 (30), 59 (29), and 43 (25).

Anal.[8]—Calc. for $C_{24}H_{38}O_5$: C, 70.90; H, 9.42. Found: C, 70.71; H, 9.18.

2-(2-Ethylhexyl) 4-Hydroxyphthalate (IV*b*)—Two grams (10.9 mmoles) of V*a* was sublimed under vacuum to 4-hydroxyphthalic anhydride (V*b*) (1.69 g, 94%) and refluxed for 6 hr with 1.2 equivalents (1.6 g, 13 mmoles) of 2-ethylhexanol in 20 ml of toluene (Scheme I, R = 2-ethylhexyl). The reaction mixture contained only one product, as shown by TLC. The solution was filtered while hot. On cooling, the product crystallized in 70% (2.1 g) yield, mp 142–144°, when recrystallized from acetone–hexane; mass spectra: *m/e* 294 (M^+, 0.3%), 295 (M + 1, 0.9), 183 (10), 165 (50), 164 (82.5), 120 (100), 112 (19), 98 (28), 92 (25), 84 (30), 70 (40), 69 (35), and 57 (90).

Anal.—Calc. for $C_{16}H_{22}O_5$: C, 65.29, H, 7.53. Found: C, 65.51; H, 7.62.

1-(2-Ethylhexyl) 4-Hydroxyphthalate (IV*c*)—Two grams (10.9 mmoles) of V*a*, 8.2 g (62.9 mmoles) of 2-ethylhexanol, and 2 drops of concentrated sulfuric acid were refluxed in 20 ml of toluene for 16 hr and yielded IV*a*, which was hydrolyzed by refluxing for 4 hr after the addition of 2 g of sodium hydroxide (Scheme I). In addition to the desired product (IV*c*), small amounts of IV*b* and V*a* were shown to be present by silica gel[9] TLC. The reaction mixture was acidified with 4 *N* sulfuric acid and extracted with ether, and the product was purified by passage through a silica gel dry column (1.5 × 16 cm). The column was eluted with 100 ml of chloroform followed by increasing concentrations of methanol in chloroform, resulting in elution of the product (1.1 g, 34%) with 25% methanol, mp 124–126° from acetone–hexane; mass spectra: *m/e* 294

[1] JNM-C-60 spectrometer.
[2] Stohler Isotope Chemicals.
[3] LKB 9000S.
[4] A. H. Thomas.
[5] Eastman Chemical Co.
[6] The m* designates metastable ions.
[7] Brinkmann, 0.05–0.20 mm.
[8] Heterocyclic Chemical Corp.
[9] Mallinckrodt Chemical Works.

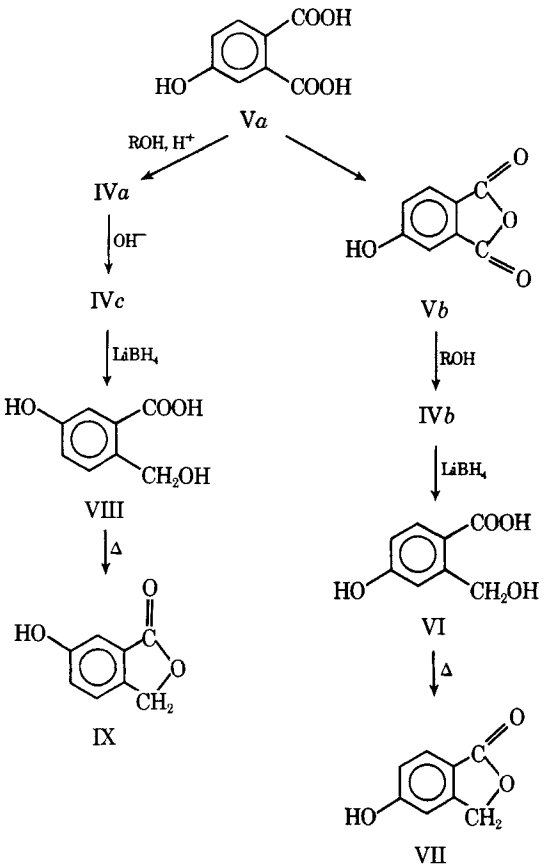

Scheme I

(M+, 0.3%), 295 (M + 1, 1.0), 183 (19.5), 165 (95), 164 (20.0), 120 (40), 92 (28), 83 (26), 70 (45), 57 (100), 43 (35), and 41 (33).

2-Hydroxymethyl-4-hydroxybenzoic Acid (VI)—To confirm the structure of IV*b*, VI was prepared by refluxing IV*b* (0.81 g, 2.77 mmoles) for 24 hr with a 10-fold excess of lithium borohydride[10] (0.60 g, 28 mmoles) in 30 ml of dioxane (Scheme I). The reaction mixture was acidified with 2 *N* hydrochloric acid and extracted with ether, and the ether was removed under vacuum. The product (0.27 g, 58%), recrystallized from methanol–water, slowly sublimed between 140 and 170°, probably forming the corresponding lactone but never giving a sharp melting point; mass spectra: *m/e* 168 (M+, 4%), 150 (70), 121 (100) m* 97.6, 93 (19) m* 71.5, and 65 (21) m* 45.4.

2-Hydroxymethyl-4-hydroxybenzolactone (VII)—To aid in the identification of IV*b*, VI was converted quantitatively to its corresponding lactone (VII) by heating at 100° for 72 hr (Scheme I), mp 219° with softening at 210° (capillary) [lit. (7) mp 223° with softening at 210°]; mass spectra: *m/e* 150 (M+, 74%), 121 (100) m* 97.6, 93 (21) m* 71.5, and 65 (25) m* 45.4.

2-Hydroxymethyl-5-hydroxybenzoic Acid (VIII)—This compound was prepared by refluxing 2.5 g of IV*c* (8.5 mmoles) with 1.85 g (85 mmoles) of lithium borohydride in dioxane for 36 hr (Scheme I). Excess borohydride was destroyed by the addition of 2 *N* hydrochloric acid, the solution was extracted with ether and dried with sodium sulfate, and the ether was removed, giving the desired product (0.52 g, 36%). This product was recrystallized from methanol–water, mp 129–130° (capillary); mass spectra: *m/e* 168 (M+, 1.1%), 150 (46), 121 (100) m* 97.6, 93 (28) m* 71.5, and 65 (26) m* 45.4.

2-Hydroxymethyl-5-hydroxybenzolactone (IX)—Compound VIII was quantitatively converted to IX by heating at 100° for 6 hr (Scheme I), mp 199–200° (capillary) [lit. (7) mp 201–202°]; mass spectra: *m/e* 150 (M+, 57%), 121 (100) m* 97.6, 93 (35) m* 71.5, and 65 (25) m* 45.4.

3-Hydroxyphthalic Anhydride (X*c*)—3-Aminophthalic acid[5] (X*a*) (2.0 g, 11.0 mmoles) was diazotized with 0.76 g (11.0 mmoles) of sodium nitrite in 20 ml of 15 *N* sulfuric acid (Scheme II, R = 2-ethylhexyl) following the procedure of Eliel *et al.* (8). The resultant 3-hydroxyphthalic acid (X*b*) was sublimed *in vacuo* to the anhydride (X*c*) (0.71 g, 40%), mp 195–196° [lit. (9) mp 199–200°], and was used without further purification in the following syntheses.

Table I—Chemical Shift Values (δ) for Derivatives of 4-Hydroxyphthalic Acid (V*a*)

Compound	H_A	H_B	H_C	$-CH_2-$
V*a*	7.65 (d, $J \simeq 9$)	6.90	6.90	—
↓ IV*a*	7.66 (d, $J \simeq 9$)	6.95	6.90	4.10
↓ IV*c*	7.35 (d, $J \simeq 8$)	6.72 (dd, $J \simeq 2,8$)	7.00 (d, $J \simeq 2$)	4.05
↓ VIII	7.47 (d, $J \simeq 8$)	6.94 (dd, $J \simeq 2,8$)	7.28 (d, $J \simeq 2$)	4.73
↓ IX	7.53 (d, $J \simeq 9$)	7.23	7.15	5.30
IV*b*	7.72 (d, $J \simeq 8$)	6.92	6.83	4.13
↓ VI	7.77 (d, $J \simeq 8$)	6.67 (dd, $J \simeq 2,8$)	7.12 (d, $J \simeq 2$)	4.82
↓ VII	7.67 (d, $J \simeq 9$)	6.97	6.97	5.27

Bis(2-ethylhexyl) 3-Hydroxyphthalate (III*a*)—Compound X*c* (1.0 g, 6.1 mmoles) was added to 20 ml of 2-ethylhexanol (16.7 g, 128.5 mmoles) in 30 ml of toluene plus 3 drops of concentrated sulfuric acid and refluxed for 16 hr (Scheme II, R = 2-ethylhexyl). The reaction mixture was treated similarly to that in the synthesis of IV*a*. The crude product (1.5 g, 60%) was purified for analysis by silica gel dry column chromatography (1.4 × 15 cm) by elution with hexane followed by increasing concentrations of chloroform in hexane. Fractions containing III*a* were concentrated and placed over a neutral alumina[11] dry column (1.2 × 20 cm), which was eluted with benzene followed by 25% chloroform in benzene. Removal of the solvent yielded a clear, viscous liquid; PMR: δ 7.68 (dd, H_A), 6.98 (m, H_B and H_C), 4.15 (d, 4), and 0.77–1.58 (m, 30) ppm; mass spectra: *m/e* 406 (M+, 7.5%), 295 (9), 294 (10.5), 183 (31.5), 182 (28.5), 165 (100), 164 (29), 149 (24), 113 (30), 112 (56), and 71 (47.5).

Anal.—Calc. for $C_{24}H_{38}O_5$: C, 70.90; H, 9.42. Found: C, 71.02; H, 9.86.

1-(2-Ethylhexyl) 3-Hydroxyphthalate (III*b*)—This compound was synthesized from X*c* (0.71 g, 4.3 mmoles) and 2-ethylhexanol (1.1 g, 8.6 mmoles) by refluxing in 20 ml of pyridine for 8 hr (Scheme II, R = 2-ethylhexyl). The reaction mixture was acidified to pH 3 with 4 *N* sulfuric acid, extracted with ether, and then shaken with 50 ml of 5% Na_2CO_3. The basic solution was carefully acidified, resulting in the precipitation of III*b* (0.85 g, 72%), mp 191–192° when recrystallized from acetone–hexane. TLC indicated that only one isomer was formed (R_f 0.51). Attempts to synthesize the other isomer of III*b* by hydrolysis of III*a* (analogous to hydrolysis of IV*a* to IV*c*) were unsuccessful. Compound III*b* is probably the 1-(2-ethylhexyl) ester; PMR: δ 7.20 (dd, H_A), 6.88 (m, H_B and H_C), 4.08 (d, 2), and 0.77–1.58 (m, 15) ppm; mass spectra: *m/e* 294 (M+, 1.3%), 221 (32), 183 (2.5), 182 (3.5), 165 (20), 164 (100), 120 (95), 112 (36), 92 (90), 83 (86), and 70 (60).

RESULTS AND DISCUSSION

Chemistry—Scheme I shows the reactions involved in the synthesis of the various derivatives of 4-hydroxyphthalic acid (V*a*). The reaction

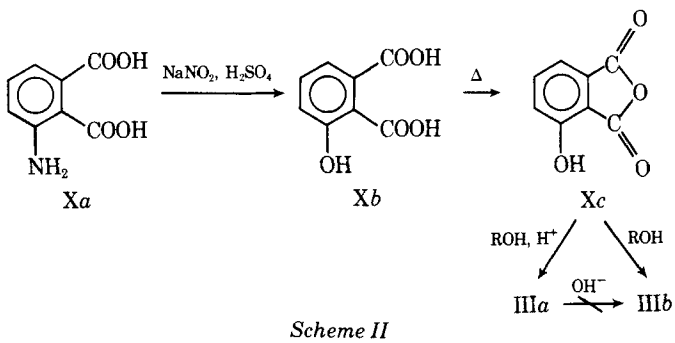

Scheme II

[10] ICN, Inc.

[11] Woelm, Waters Associates.

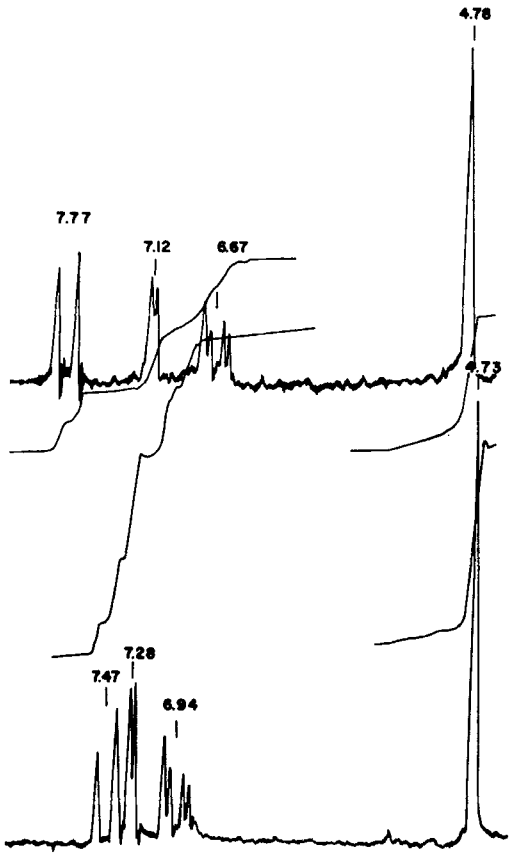

Figure 1—*PMR spectra of the hydroxymethylbenzoic acids VI (upper) and VIII (lower).*

of 4-hydroxyphthalic anhydride (V*b*) and 2-ethylhexanol yielded only one isomer, subsequently shown to be IV*b*. Alkaline hydrolysis of IV*a*, however, resulted mainly in the formation of the geometric isomer, IV*c*; small amounts of phthalic acid and IV*b* also were obtained. The results in both cases are explicable when one considers that the 2-ethylhexanol or the hydroxide ion in the two reactions, respectively, would be most likely to attack the more electropositive carbonyl group, which is the one *meta* to the phenolic hydroxyl in both cases.

Scheme II shows the reaction pathway for the synthesis of the derivatives of 3-hydroxyphthalic acid (X*b*). Although the position of the ester group in the 3-hydroxy monoester (III*b*) was not unequivocally established, the electron-donating effect of the hydroxyl group to the *ortho*-position suggests that the 1-(2-ethylhexyl) ester is the compound formed under the reaction conditions employed. There was no evidence by TLC of formation of the isomer of III*b*, even when III*a* was subjected to hydrolysis in base, a procedure successful in the conversion of IV*a* to IV*c*. Regardless of the preparation method of III*b*, the products isolated had identical PMR and mass spectra. Compound III*b* was the only hydroxylated metabolite subsequently found on incubation of liver homogenates[12].

Lithium borohydride was chosen as the reducing agent for IV*b* and IV*c*, since this reagent selectively reduces esters in the presence of carboxylic acids (10). A large excess of lithium borohydride was required for quantitative reduction because of the ionization of the carboxylic acid and consequent insolubility of the complex. The hydroxymethylbenzoic acids formed (VI and VIII) were then cyclized to their known lactones. This conversion was quite facile, particularly in the case of IX, since it was formed when the reaction mixture for the synthesis of VIII from IV*c* was made too acidic when destroying the excess borohydride.

Attempted reduction of III*b* with lithium borohydride to distinguish unequivocally the position of the 2-ethylhexyl group was unsuccessful.

PMR Spectra—The relevant PMR data for the various derivatives of 4-hydroxyphthalic acid are shown in Table I. The assignment of the signals of H_A, H_B, and H_C were made by their coupling constants and chemical shifts. Whereas the signal for H_A in V*a* (δ 7.65) and IV*a* (δ 7.66) had nearly identical chemical shifts, the same signal in two monoesters, IV*b* (δ 7.72) and IV*c* (δ 7.35), showed a significant difference. From these data, it became obvious that the unequivocal structural assignment of IV*b* and IV*c* could not be made on the basis that H_A was adjacent to the acid in one isomer and the ester in the other. Although it is difficult to predict the chemical shift of a given proton on multiple-substituted benzene rings (11), it was felt that selective reduction of the ester carbonyl of IV*c* to the corresponding hydroxymethyl compound (VIII) would result in a significant upfield shift of H_A and that a similar reduction of the ester group of IV*b* would result in little change in the chemical shift of H_A.

Similarly, the signal of H_C in VIII would be expected to remain relatively unchanged compared to that of H_C in IV*c*, and the signal of H_C in VI might be expected to move upfield compared to that of IV*b*; in the latter case, H_C would be *ortho* to the hydroxymethyl group instead of the deshielding carbonyl moiety. From an examination of Table I, it is apparent that, upon reduction of IV*b* and IV*c*, there was an unexpected small downfield shift in the signal of H_A in both cases whereas there was a more significant downfield shift of 0.29 and 0.28 ppm in the signal of H_C of the reduced products, VI and VIII, respectively.

The PMR spectra of VI and VIII are shown in Fig. 1. The assignments of H_A in VI (upper spectrum, δ 7.77) and VIII (δ 7.47) were made on the basis of their being furthest downfield and their coupling constants of 8 Hz. The signal of H_C was assigned at δ 7.12 and 7.28 in VI and VIII, respectively, by the small *meta*-coupling of 2 Hz; the signal of H_B was the furthest upfield in both cases, appearing as a doublet of doublets with coupling constants of about 8 and 2 Hz, respectively.

Although the PMR data for the reduction of IV*b* and IV*c* were not entirely expected, as expected the signals of H_A and H_C were at lower fields when adjacent to a carbonyl group than when adjacent to a hydroxymethyl group; *i.e.*, the signal of H_A was downfield in VI compared to VIII and, similarly, the signal of H_C was downfield in VIII compared to VI (Table I). Unequivocal proof of structure of the monoesters IV*b* and IV*c* was obtained by conversion of VI and VIII to their corresponding known lactones, VII and IX, respectively, which were characterized by their melting points and PMR and mass spectra. The most noteworthy feature of the PMR spectra of these compounds was that the signal for the methylene protons was downfield approximately 0.5 ppm from the analogous signals in VI and VIII. This downfield shift was consistent with that observed for the methylene protons of alcohols and their corresponding esters (12).

The PMR spectra of the 3-hydroxyphthalates, III*a* and III*b*, were unremarkable but consistent with the structures assigned.

Mass Spectrometry—The mass spectral data for II and IV*a*–IV*c* were consistent with the assigned structures. One of the most characteristic fragments for phthalate esters occurred at *m/e* 149 (13), and this fragment was the base peak for II. Since IV*a*–IV*c*, III*a*, and III*b* are hydroxyphthalates (with 16 additional amu), the main fragment for these compounds appeared at *m/e* 165. For diesters such as IV*a*, the most characteristic fragmentation was the loss of the alkyl fragment with transfer of one or two hydrogen atoms to produce the carboxylic acid ion or the protonated carboxylic acid ion, respectively (14). In the case of IV*a*, the protonated carboxylic acid ion (*m/e* 295) was formed, which then lost a second 2-ethylhexyl fragment in a typical McClafferty reaction (15) to form the protonated diacid (*m/e* 183). This transition, although uncomplicated, was also supported by the metastable ion[13] at *m/e* 113.5. Loss of water gave a peak at *m/e* 165 (again consistent with a metastable ion at *m/e* 148.8) and was followed by loss of CO_2 (*m/e* 121). Fragments between 41 and 113 amu mostly arose from fragmentation of the 2-ethylhexyl side chain.

The mass spectra of IV*b* and IV*c* were similar and explicable, except that an artifact appeared for both compounds at *m/e* 295, 1 amu higher than the expected molecular ion *m/e* 294. Such an artifact also appeared in the mass spectrum of II. This unexpected peak was shown to be the result of a bimolecular collision, with a fragment ion donating a proton to the molecular ion. The abundance of the M + 1 species was dependent upon the sample pressure in the ion source. The proper identification of the molecular ion and of M + 1 as an artifact was accomplished by scanning the total ion current peak and noting the disappearance of M + 1 as the sample pressure decreased.

The mass spectra of the 3-hydroxyphthalates were consistent with the structures assigned. In the case of the monoester III*b*, the formation of both the carboxylic acid ion (*m/e* 182) and the protonated carboxylic acid ion (*m/e* 183) was apparent, but the formation of the base peak at *m/e*

[12] Unpublished data.

[13] Metastable peaks (m*) are formed when an ion, m, decomposes during flight through the instrument and is analyzed with a mass m_2. The masses are related by the expression $m^* = (m_2^2/m_1)$ (16).

164 (182 − H_2O) indicated that the former fragmentation path predominated.

The mass spectral data for the reduced products VI and VIII and their corresponding lactones, although unremarkable, were compatible with the assigned structures. As might be expected for the hydroxymethylbenzoic acids, a major fragment at *m/e* 150 indicated the loss of water with cyclization to the corresponding lactones.

REFERENCES

(1) P. W. Albro, R. Thomas, and L. Fishbein, *J. Chromatogr.*, **76**, 321 (1973).

(2) J. E. Carter, D. B. Roll, and R. V. Petersen, *Drug Metab. Disp.*, **2**, 341 (1974).

(3) J. W. Daniel and H. Bratt, *Toxicology*, **2**, 51 (1974).

(4) R. V. Petersen, D. J. Lyman, D. B. Roll, and E. A. Swinyard, "Toxicology of Plastic Devices Having Contact with Blood," Final Report (Contract NIH-NHLI-73-2908-B, distributed by Clearinghouse for Federal, Scientific and Technical Information), 1975, pp. 35–41.

(5) J. Kenyon and B. D. Platt, *J. Chem. Soc.*, **1939**, 633.

(6) B. Loev and M. M. Goodman, *Chem. Ind.*, **1967**, 2026.

(7) J. Tirouflet, *Bull. Soc. Sci. Bretagne*, **26**, 7 (1951); through *Chem. Abstr.*, **47**, 8692g (1953).

(8) E. L. Eliel, A. W. Burgstahler, D. E. Rivard, and L. Haefele, *J. Am. Chem. Soc.*, **77**, 5092 (1955).

(9) O. Gisvold, *J. Am. Pharm. Assoc., Sci. Ed.*, **31**, 302 (1942).

(10) L. F. Fieser and M. Fieser, "Reagents for Organic Synthesis," Wiley, New York, N.Y., 1967 p. 603.

(11) L. M. Jackman and S. Sternhell, "Applications of Nuclear Magnetic Resonance Spectroscopy in Organic Chemistry," 2nd ed., Pergamon, New York, N.Y., 1969, pp. 202, 203.

(12) L. M. Jackman, "Applications of Nuclear Magnetic Spectroscopy in Organic Chemistry," Pergamon, New York, N.Y., 1964, p. 55.

(13) H. Budzikiewicz, C. Djerassi, and D. H. Williams, "Mass Spectroscopy of Organic Compounds," Holden-Day, San Francisco, Calif., 1967, p. 203.

(14) *Ibid.*, p. 184.

(15) P. Laszlo and P. J. Stang, "Organic Spectroscopy," Harper and Row, New York, N.Y., 1971, p. 139.

(16) *Ibid.*, p. 137.

ACKNOWLEDGMENTS AND ADDRESSES

Received February 17, 1976, from the *College of Pharmacy, University of Utah, Salt Lake City, UT 84112.*

Accepted for publication June 7, 1976.

Supported in part by Contract NIH-NHLI-73-2908-B, National Heart and Lung Institute, National Institutes of Health, Bethesda, MD 20014.

The authors gratefully acknowledge the technical assistance of G. Anderson, D. Gerdes, L. Ingersoll, and H. Law. The mass spectra and aid in their interpretation were provided by Dr. K. Schram, Dr. G. Puzo, P. Crane, and U. Cramer.

[x] To whom inquiries should be directed.

Bioavailability of Ampicillin and Amoxicillin in Fasted and Nonfasted Subjects

P. G. WELLING [*x], H. HUANG [*], P. A. KOCH [*], W. A. CRAIG [‡], and P. O. MADSEN [‡]

Abstract □ The influence of various test meals and fluid volume on the relative bioavailability of ampicillin and amoxicillin was studied in healthy human subjects. Serum amoxicillin levels were somewhat, but not always, significantly higher than those of ampicillin from equivalent oral doses. Food ingested immediately before dosing reduced serum levels and urinary excretion of both antibiotics to a similar extent. Reduction of dosed water volume caused a marked decrease in serum amoxicillin levels in fasted subjects.

Keyphrases □ Ampicillin—bioavailability, oral administration, effect of fasting and fluid volume, humans □ Amoxicillin—bioavailability, oral administration, effect of fasting and fluid volume, humans □ Bioavailability—ampicillin and amoxicillin, oral administration, effect of fasting and fluid volume, humans □ Antibacterial agents—ampicillin and amoxicillin, bioavailability, oral administration, effect of fasting and fluid volume, humans

Ampicillin and amoxicillin have similar antibacterial activity against various organisms (1). Amoxicillin has twice the activity of ampicillin against enterococci and *Salmonella* species but is somewhat less active than ampicillin against *Haemophilus* and *Shigella* species (2, 3).

Various reports indicated that, despite the similar antibacterial spectrum of the two compounds, amoxicillin has superior bioavailability properties from oral dosage forms and may, therefore, be the compound of choice when this route of administration is used (4–6). Amoxicillin absorption may be less influenced by food than ampicillin absorption, so less variation in circulating antibiotic levels might be expected during repeated oral doses of amoxicillin (7, 8).

In this study, the bioavailability of ampicillin and amoxicillin was compared in fasted and nonfasted subjects under carefully controlled conditions.

EXPERIMENTAL

The subjects were three male and three female healthy volunteers. Male subjects were 24–30 years old (mean 27) and weighed 64–81 kg (mean 74). Female subjects were 21–27 years old (mean 23) and weighed 50–68 kg (mean 60). All subjects were shown by medical examination to be in good physical condition with normal blood and urine laboratory values. The subjects had no histories of allergic reaction to penicillins.

Protocol—Verbal assurance was obtained from all subjects that they had taken no known enzyme-inducing agents for 1 month and no other drugs for 1 week preceding the study. Subjects were instructed to take no drugs other than the required doses of antibiotic during the study.

The subjects were fasted overnight before each treatment and were permitted to eat no food, apart from test meals, until 4 hr after dosing. On the morning of a treatment, each subject drank 250 ml of water on arising, at least 1 hr before dosing. Medication was administered at 8 am; blood samples (4–5 ml) were collected from a forearm vein into vacuum tubes[1] containing no anticoagulant immediately before dosing and at 20 and 40 min and 1, 1.5, 2, 3, 4, 6, and 8 hr after dosing. Serum was separated and deep frozen at −18° until assayed. Urine was collected through 8 hr

[1] Vacutainers.

164 (182 − H_2O) indicated that the former fragmentation path predominated.

The mass spectral data for the reduced products VI and VIII and their corresponding lactones, although unremarkable, were compatible with the assigned structures. As might be expected for the hydroxymethylbenzoic acids, a major fragment at *m/e* 150 indicated the loss of water with cyclization to the corresponding lactones.

REFERENCES

(1) P. W. Albro, R. Thomas, and L. Fishbein, *J. Chromatogr.*, **76**, 321 (1973).

(2) J. E. Carter, D. B. Roll, and R. V. Petersen, *Drug Metab. Disp.*, **2**, 341 (1974).

(3) J. W. Daniel and H. Bratt, *Toxicology*, **2**, 51 (1974).

(4) R. V. Petersen, D. J. Lyman, D. B. Roll, and E. A. Swinyard, "Toxicology of Plastic Devices Having Contact with Blood," Final Report (Contract NIH-NHLI-73-2908-B, distributed by Clearinghouse for Federal, Scientific and Technical Information), 1975, pp. 35–41.

(5) J. Kenyon and B. D. Platt, *J. Chem. Soc.*, **1939**, 633.

(6) B. Loev and M. M. Goodman, *Chem. Ind.*, **1967**, 2026.

(7) J. Tirouflet, *Bull. Soc. Sci. Bretagne*, **26**, 7 (1951); through *Chem. Abstr.*, **47**, 8692g (1953).

(8) E. L. Eliel, A. W. Burgstahler, D. E. Rivard, and L. Haefele, *J. Am. Chem. Soc.*, **77**, 5092 (1955).

(9) O. Gisvold, *J. Am. Pharm. Assoc., Sci. Ed.*, **31**, 302 (1942).

(10) L. F. Fieser and M. Fieser, "Reagents for Organic Synthesis," Wiley, New York, N.Y., 1967 p. 603.

(11) L. M. Jackman and S. Sternhell, "Applications of Nuclear Magnetic Resonance Spectroscopy in Organic Chemistry," 2nd ed., Pergamon, New York, N.Y., 1969, pp. 202, 203.

(12) L. M. Jackman, "Applications of Nuclear Magnetic Spectroscopy in Organic Chemistry," Pergamon, New York, N.Y., 1964, p. 55.

(13) H. Budzikiewicz, C. Djerassi, and D. H. Williams, "Mass Spectroscopy of Organic Compounds," Holden-Day, San Francisco, Calif., 1967, p. 203.

(14) *Ibid.*, p. 184.

(15) P. Laszlo and P. J. Stang, "Organic Spectroscopy," Harper and Row, New York, N.Y., 1971, p. 139.

(16) *Ibid.*, p. 137.

ACKNOWLEDGMENTS AND ADDRESSES

Received February 17, 1976, from the *College of Pharmacy, University of Utah, Salt Lake City, UT 84112.*

Accepted for publication June 7, 1976.

Supported in part by Contract NIH-NHLI-73-2908-B, National Heart and Lung Institute, National Institutes of Health, Bethesda, MD 20014.

The authors gratefully acknowledge the technical assistance of G. Anderson, D. Gerdes, L. Ingersoll, and H. Law. The mass spectra and aid in their interpretation were provided by Dr. K. Schram, Dr. G. Puzo, P. Crane, and U. Cramer.

[x] To whom inquiries should be directed.

Bioavailability of Ampicillin and Amoxicillin in Fasted and Nonfasted Subjects

P. G. WELLING [*x], H. HUANG [*], P. A. KOCH [*], W. A. CRAIG [‡], and P. O. MADSEN [‡]

Abstract □ The influence of various test meals and fluid volume on the relative bioavailability of ampicillin and amoxicillin was studied in healthy human subjects. Serum amoxicillin levels were somewhat, but not always, significantly higher than those of ampicillin from equivalent oral doses. Food ingested immediately before dosing reduced serum levels and urinary excretion of both antibiotics to a similar extent. Reduction of dosed water volume caused a marked decrease in serum amoxicillin levels in fasted subjects.

Keyphrases □ Ampicillin—bioavailability, oral administration, effect of fasting and fluid volume, humans □ Amoxicillin—bioavailability, oral administration, effect of fasting and fluid volume, humans □ Bioavailability—ampicillin and amoxicillin, oral administration, effect of fasting and fluid volume, humans □ Antibacterial agents—ampicillin and amoxicillin, bioavailability, oral administration, effect of fasting and fluid volume, humans

Ampicillin and amoxicillin have similar antibacterial activity against various organisms (1). Amoxicillin has twice the activity of ampicillin against enterococci and *Salmonella* species but is somewhat less active than ampicillin against *Haemophilus* and *Shigella* species (2, 3).

Various reports indicated that, despite the similar antibacterial spectrum of the two compounds, amoxicillin has superior bioavailability properties from oral dosage forms and may, therefore, be the compound of choice when this route of administration is used (4–6). Amoxicillin absorption may be less influenced by food than ampicillin absorption, so less variation in circulating antibiotic levels might be expected during repeated oral doses of amoxicillin (7, 8).

In this study, the bioavailability of ampicillin and amoxicillin was compared in fasted and nonfasted subjects under carefully controlled conditions.

EXPERIMENTAL

The subjects were three male and three female healthy volunteers. Male subjects were 24–30 years old (mean 27) and weighed 64–81 kg (mean 74). Female subjects were 21–27 years old (mean 23) and weighed 50–68 kg (mean 60). All subjects were shown by medical examination to be in good physical condition with normal blood and urine laboratory values. The subjects had no histories of allergic reaction to penicillins.

Protocol—Verbal assurance was obtained from all subjects that they had taken no known enzyme-inducing agents for 1 month and no other drugs for 1 week preceding the study. Subjects were instructed to take no drugs other than the required doses of antibiotic during the study.

The subjects were fasted overnight before each treatment and were permitted to eat no food, apart from test meals, until 4 hr after dosing. On the morning of a treatment, each subject drank 250 ml of water on arising, at least 1 hr before dosing. Medication was administered at 8 am; blood samples (4–5 ml) were collected from a forearm vein into vacuum tubes[1] containing no anticoagulant immediately before dosing and at 20 and 40 min and 1, 1.5, 2, 3, 4, 6, and 8 hr after dosing. Serum was separated and deep frozen at −18° until assayed. Urine was collected through 8 hr

[1] Vacutainers.

Table I—Average Serum Concentrations of Ampicillin and Amoxicillin from All Treatments (±1 *SD*)

Treatment	0.0	20 min	40 min	1.0 hr	1.5 hr	2 hr	3 hr	4 hr	6 hr	8 hr
Serum Ampicillin Concentration, μg/ml										
1	0.0	0.0	0.1 ± 0.1	0.4 ± 0.1	1.5 ± 1.1	2.6 ± 1.7	3.4 ± 1.3	3.1 ± 1.3	0.8 ± 0.2	0.4 ± 0.1
2	0.0	0.0	0.2 ± 0.2	0.5 ± 0.2	1.8 ± 0.7	2.7 ± 0.4	2.7 ± 0.4[a]	2.3 ± 0.6	1.3 ± 0.6	0.6 ± 0.3
3	0.0	0.0	0.2 ± 0.1	0.7 ± 0.7	2.1 ± 1.1	2.8 ± 1.1	2.4 ± 0.6[a]	1.8 ± 0.3[a]	0.7 ± 0.2[a]	0.3 ± 0.1[a]
4	0.0	0.6 ± 0.5	2.8 ± 1.4	3.5 ± 1.8	4.0 ± 2.0	4.7 ± 2.1	6.1 ± 2.5	4.2 ± 2.6	2.3 ± 2.1	0.7 ± 0.6
5	0.0	0.2 ± 0.3	3.3 ± 1.6	4.3 ± 1.7	5.4 ± 1.7	6.1 ± 1.7	4.8 ± 1.3	3.3 ± 1.3[a]	1.4 ± 1.5	0.1 ± 0.1
Paired[b] *t*-test		4 > 2,3,5	4,5 > 1–3	4,5 > 1–3	4 > 1,2; 5 > 1–3	4 > 1,2; 5 > 1–3	4 > 2,3; 5 > 1–3	4,5 > 3	NSD[c]	1,2 > 5
Serum Amoxicillin Concentration, μg/ml										
1	0.0	0.0	0.3 ± 0.3	0.9 ± 0.8	2.2 ± 0.7	3.1 ± 2.1	5.0 ± 1.9	4.4 ± 0.7	1.4 ± 0.8	0.6 ± 0.4
2	0.0	0.0	0.3 ± 0.2	1.3 ± 1.1	3.6 ± 2.1	5.0 ± 3.1	5.5 ± 2.3	4.7 ± 1.9	2.2 ± 1.1	0.7 ± 0.4
3	0.0	0.0	0.5 ± 0.6	1.2 ± 0.8	3.0 ± 1.9	4.1 ± 2.3	5.0 ± 1.6	4.3 ± 1.0	2.2 ± 0.8	0.7 ± 0.4
4	0.0	0.5 ± 0.4	2.8 ± 1.3	4.1 ± 1.3	6.6 ± 1.2	6.6 ± 1.7	4.1 ± 1.5	1.9 ± 0.6	0.6 ± 0.2	0.2 ± 0.1
5	0.0	0.1 ± 0.2	3.6 ± 2.7	7.3 ± 5.3	9.6 ± 5.8	10.0 ± 3.3	8.7 ± 2.7	7.0 ± 2.6	3.2 ± 3.2	0.9 ± 0.7
Paired *t*-test		4 > 1–3	4,5 > 1–3	4,5 > 1–3	4,5 > 1–3	4 > 1; 5 > 1–3	5 > 1,2,4	1–3 > 4; 5 > 2,4	1–3 > 4; 2,3 > 1	1–3,5 > 4

[a] Amoxicillin levels significantly higher ($p < 0.05$) than ampicillin levels for this sampling time and treatment. [b] Significant at $p < 0.05$ among treatments. [c] No significant differences.

Figure 1—*Average serum ampicillin levels.*

after dosing, and aliquots were deep frozen until assayed. All assays were carried out within 72 hr of sampling.

Treatments—It is recognized that bioavailability comparisons between compounds are best studied in a crossover fashion. However, the primary aim of the overall study was to compare bioavailability among treatments for each compound. Therefore, the amoxicillin study was done immediately following the ampicillin study. All subjects participated in both studies.

Subjects received single 500-mg doses of ampicillin[2] or amoxicillin[3] as two 250-mg capsules. High carbohydrate, high fat, and high protein test meals were prepared and standardized as described previously (9). Each drug was administered as the following treatments:

Treatment 1—Two capsules with 250 ml of water immediately following a standard high carbohydrate meal.

Treatment 2—Two capsules with 250 ml of water immediately following a standard high fat meal.

Treatment 3—Two capsules with 250 ml of water immediately following a standard high protein meal.

Treatment 4—Two capsules with 25 ml of water on an empty stomach.

Treatment 5—Two capsules with 250 ml of water on an empty stomach.

All subjects received the same treatment at the same time. Treatments were administered 2 weeks apart, and all subjects received all treatments. Capsules were swallowed whole.

Assay—Serum and urine ampicillin and amoxicillin were assayed using a microbiological disk diffusion method with *Sarcina lutea* (ATCC 9341) as the test organism as described elsewhere (10).

Interpretation of Results—Individual serum antibiotic levels were fitted graphically to the standard one-compartment open model with first-order absorption and elimination. With this model, serum concentrations, C, at any time, t, after dosing are described by:

$$C = \frac{FD}{V}\frac{k}{k-K}(e^{-Kt} - e^{-kt}) \qquad \text{(Eq. 1)}$$

where F is the fraction of the dose, D, absorbed, V is the drug distribution volume in the body, and k and K are first-order rate constants for absorption and elimination, respectively. Improved estimates of parameters, together with coefficients of determination, r^2, were obtained by iterative least-squares methods using the program NREG on a digital computer[4] (11). Data fitting was improved in some cases by incorporating a lag time, t_0, representing the time period between dosing and the appearance of the antibiotic in the circulation.

Serum levels at each sampling time, urine data, and pharmacokinetic parameters were examined by analysis of variance. If significant differences due to treatments were obtained ($p < 0.05$), results from individual treatments were compared by a paired t-test.

RESULTS

Serum Levels—Mean serum antibiotic concentrations, together with statistical analysis, are given in Table I; the data are summarized

[2] Ampicillin trihydrate, Polycillin, Bristol Laboratories.
[3] Amoxicillin trihydrate, Polymox, Bristol Laboratories.
[4] Univac model 1110.

Table II—Concentrations and Percentage Recoveries of Ampicillin and Amoxicillin in 8-hr Urine (±1 *SD*)

Compound	Treatment 1	2	3	4	5	Paired *t*-Test
Ampicillin						
Concentration, μg/ml	313 ± 131	781[a]	207 ± 89	1105 ± 411	970[a]	4 > 1,3
Recovery, %	27.2 ± 17.5	42.8[a]	21.8 ± 5.7[b]	66.4 ± 24.9	82.8[a]	4 > 1,3
Amoxicillin						
Concentration, μg/ml	540 ± 278	478 ± 143	341 ± 247	827 ± 289	1491 ± 382	5 > 1–4
Recovery, %	41.3 ± 20.1	55.7 ± 21.4	36.6 ± 25.0	49.1 ± 9.2	85.3 ± 29.7	5 > 1–4

[a] Complete recoveries were obtained from two subjects only. [b] Amoxicillin recoveries significantly higher than ampicillin recoveries.

graphically in Figs. 1 and 2. Urine antibiotic concentrations and recoveries are summarized in Table II, and averaged results from the pharmacokinetic analyses are given in Tables III and IV.

It is clear from Table I and Figs. 1 and 2 that circulating levels of both ampicillin and amoxicillin were significantly reduced by the test meals under conditions used in this study. Treatments 4 and 5 yielded high serum levels of ampicillin compared to the food treatments for the first 3 hr after dosing. After this time, similar serum levels were obtained from all treatments. Serum amoxicillin levels were reduced similarly by the food treatments. These levels also were reduced following the 2-hr postdosing period when amoxicillin was given with 25 ml of water (Treatment 4).

Despite the higher serum levels generally observed with amoxicillin, differences between ampicillin and amoxicillin levels for the same treatment were significant in only a few cases. No significant differences were obtained during the first 2 hr after dosing, due, in part at least, to the scatter between individual serum levels. No significant differences were observed in serum levels among food treatments for either compound.

Urine Recovery—Failure by some subjects to provide complete 8-hr urine samples prevented the statistical comparison of urine concentration and recovery data in some instances (Table II). However, both fasting treatments resulted in higher urine concentrations and recoveries of ampicillin than the food treatments. Whereas Treatment 5 also resulted in increased amoxicillin concentrations and recoveries than the food treatments, values from Treatment 4 did not differ significantly from food treatment values.

Pharmacokinetic Analysis—Analysis of individual serum ampicillin and amoxicillin levels in terms of the simple one-compartment model was complicated by the similar numerical values obtained in many cases for the absorption and elimination rate constants. Almost identical values for these rate constants were reported before for ampicillin and amoxicillin (12). In this type of situation, it is difficult to determine which of the two rate constants, obtained by graphical analysis, represents absorption and elimination. This type of "flip-flop" model was discussed previously (13). Where this problem arose in the present study, the rate constant equivalent to an elimination half-life closest to 1 hr was designated as the elimination rate constant. This arbitrary designation was based on considerable evidence from the literature that both ampicillin and amoxicillin half-lives are close to 1 hr in normal subjects (4–6, 12).

The degree of fit of individual serum levels to the one-compartment model is reflected in the coefficient of determination values in Tables III and IV. Although less than perfect fits were obtained in some cases, this result appeared to be a function of data noise rather than the model. Analysis of the data in terms of the two-compartment model resulted in a greater variance in pharmacokinetic parameter values and no improvement in the coefficients of determination.

From Tables III and IV, it is apparent that the various treatments had little influence on absorption and elimination rates. Ampicillin appeared to be eliminated somewhat faster after Treatment 5 than after all other treatments, although this finding may have been due to the continued absorption of small amounts of antibiotic during the postabsorptive phase in the food treatments resulting in a prolonged apparent elimination half-life.

The influence of food on the overall absorption efficiency of both compounds was reflected in reduced peak heights and FD/V values, reduced areas under serum level–time curves to 2 and 8 hr after dosing, and reduced calculated areas from time zero to infinity. Both fasting treatments yielded significantly greater values for these parameters than the food treatments for ampicillin. In the case of amoxicillin, however, Treatment 5 tended to give higher values than all other treatments. The serum levels, urinary excretion, and pharmacokinetic parameter values from Treatment 5 were similar to reported values in fasted subjects (1–6).

DISCUSSION

Although the superior bioavailability of amoxicillin over ampicillin in fasted subjects is well documented (4–6), there is less comparative information to support the popular notion that amoxicillin absorption is not significantly influenced by food. Neu and Winshell (14) obtained similar serum amoxicillin levels in four fasted and nonfasted subjects. However, the nature of the meal and the actual time relationship between eating and dosing were not described. No comparison was made with ampicillin.

In a subsequent study (2), the times of average peak ampicillin levels were delayed by 2 hr and amoxicillin levels by 1 hr in nonfasting subjects. Peak serum amoxicillin levels were unchanged by food, while peak serum ampicillin levels were reduced by approximately 20%. A third study reported similar serum amoxicillin levels when the drug was administered as repeated doses either before or 0.5 hr after lunch (7). The actual time

Table III—Values of Pharmacokinetic Parameters (±1 *SD*) for Ampicillin

Parameter	Treatment 1	2	3	4	5	Paired *t*-Test
k, hr^{-1}	0.36 ± 0.15	0.34 ± 0.13	0.64 ± 0.25	0.45 ± 0.23	0.57 ± 0.22	NSD
$t_{1/2(abs)}$, hr	2.2 ± 0.8	2.4 ± 1.2	1.2 ± 0.4	0.3 ± 2.0	1.4 ± 0.5	NSD
K, hr^{-1}	0.52 ± 0.13	0.66 ± 0.32	0.46 ± 0.10	0.53 ± 0.18	0.76 ± 0.15[a]	5 > 1–3
$t_{1/2(elim)}$, hr	1.4 ± 0.4	1.2 ± 0.5	1.6 ± 0.4	1.4 ± 0.5	0.9 ± 0.2[a]	1–3 > 5
FD/V[b], μg/ml	9.4 ± 4.9[a]	5.3 ± 1.7[a]	5.7 ± 1.9[a]	18.3 ± 10.0	18.6 ± 3.9	4 > 2,3; 5 > 1–3
Area 0 → 2[c], μg × hr/ml	1.6 ± 1.0	1.8 ± 0.4	2.1 ± 1.0	6.0 ± 2.5	7.1 ± 2.2	4,5 > 1–3
Area 0 → 8[c], μg × hr/ml	13.1 ± 4.6	12.4 ± 2.1[a]	10.1 ± 3.1	26.1 ± 9.3	22.7 ± 6.9[a]	4,5 > 1–3
Area 0 → ∞[d], μg × hr/ml	9.6 ± 4.0[a]	13.2 ± 6.3	10.7 ± 5.7[a]	25.8 ± 8.1	19.4 ± 5.0[a]	4,5 > 1–3
t_0, hr	0.4 ± 0.1	0.5 ± 0.2	0.4 ± 0.2	0.0	0.2 ± 0.2	1–3 > 4
r^{2e}	0.85	0.94	0.93	0.90	0.96	—
Peak height, μg/ml	4.0 ± 1.8	2.9 ± 0.4[a]	2.9 ± 1.0[a]	6.9 ± 2.0[a]	6.5 ± 1.6[a]	4,5 > 2,3
Time of peak height, hr	3.2 ± 0.8	2.5 ± 0.8	2.3 ± 0.5	2.7 ± 0.5	1.9 ± 0.8	1 > 5

[a] Values in this table significantly different from those for amoxicillin (Table IV). [b] Fraction of dose absorbed expressed as concentration in its distribution volume in the body. [c] Obtained by trapezoidal rule. [d] Obtained from FD/VK. [e] $(\Sigma obs^2 - \Sigma dev^2)/\Sigma obs^2$.

Table IV—Values of Pharmacokinetic Parameters (±1 *SD*) for Amoxicillin[a]

Parameter	Treatment 1	2	3	4	5	Paired *t*-Test
k, hr^{-1}	0.29 ± 0.10	0.32 ± 0.18	0.40 ± 0.11	0.69 ± 0.20	0.65 ± 0.35	4 > 1–3
$t_{1/2(abs)}$, hr	2.6 ± 0.7	3.2 ± 2.7	1.9 ± 0.5	1.1 ± 0.3	1.6 ± 1.1	NSD
K, hr^{-1}	0.56 ± 0.16	0.53 ± 0.13	0.41 ± 0.14	0.62 ± 0.10	0.50 ± 0.12	NSD
$t_{1/2(elim)}$, hr	1.3 ± 0.4	1.4 ± 0.3	1.8 ± 0.6	1.2 ± 0.2	1.5 ± 0.4	NSD
FD/V, μg/ml	14.6 ± 4.3	18.4 ± 6.0	12.0 ± 4.7	14.2 ± 4.6	26.4 ± 6.9	5 > 1–4
Area 0 → 2, μg × hr/ml	2.3 ± 1.8	3.7 ± 2.2	3.2 ± 1.8	7.7 ± 1.5	11.5 ± 6.5	4,5 > 1–3
Area 0 → 8, μg × hr/ml	18.8 ± 3.0	23.9 ± 5.8	21.9 ± 5.6	19.2 ± 3.8	42.9 ± 6.4	5 > 1–4
Area 0 → ∞, μg × hr/ml	21.8 ± 8.2	21.7 ± 6.4	19.6 ± 8.0	18.1 ± 5.8	39.4 ± 8.4	5 > 1–4
t_0, hr	0.4 ± 0.2	0.3 ± 0.0	0.4 ± 0.3	0.1 ± 0.1	0.2 ± 0.2	1,2 > 4,5
r^2	0.84	0.90	0.90	0.91	0.92	—
Peak height, μg/ml	5.4 ± 1.3	6.5 ± 2.5	5.4 ± 1.6	7.0 ± 1.3	12.6 ± 3.0	4 > 1; 5 > 1–4
Time of peak height, hr	3.5 ± 0.6	3.7 ± 1.4	3.0 ± 0.6	1.8 ± 0.3	2.5 ± 1.8	1–3 > 4

[a] Symbols are as defined in Table III.

elapsed between the prelunch dose and eating was not indicated, and no comparison was made with ampicillin.

When 500 mg of ampicillin and amoxicillin were given immediately following a standard breakfast, peak serum levels of 2.1 and 5.9 μg/ml were obtained, respectively (8). These values were similar to those obtained from the food treatments in the present study.

During this study, in which nonfasted subjects received the drugs immediately following a standard meal, all food treatments reduced peak serum antibiotic levels by about 50%. However, serum amoxicillin levels in nonfasted subjects were almost identical to ampicillin levels in fasted subjects. Thus, although serum levels of both antibiotics appeared to be reduced to the same extent by food, the reduction was probably of less clinical significance for amoxicillin.

Reducing the dosed water volume from 250 to 25 ml in fasted subjects caused a significant reduction in serum amoxicillin levels, but ampicillin levels were affected to only a small extent. This difference may be explained by comparing the water solubilities of the antibiotics. One gram of ampicillin trihydrate dissolves in about 90 ml of water whereas 1 g of amoxicillin trihydrate dissolves in about 370 ml (15). Thus, any reduction in dosed water volume is likely to reduce the dissolution and subsequent absorption of amoxicillin to a greater extent than ampicillin.

The results of this study indicate that oral absorption of both ampicillin and amoxicillin is reduced to a similar extent when administered immediately following a meal, although the reduction in ampicillin levels may be of greater clinical significance. The bioavailability of amoxicillin is reduced when given with small water volumes in fasted subjects.

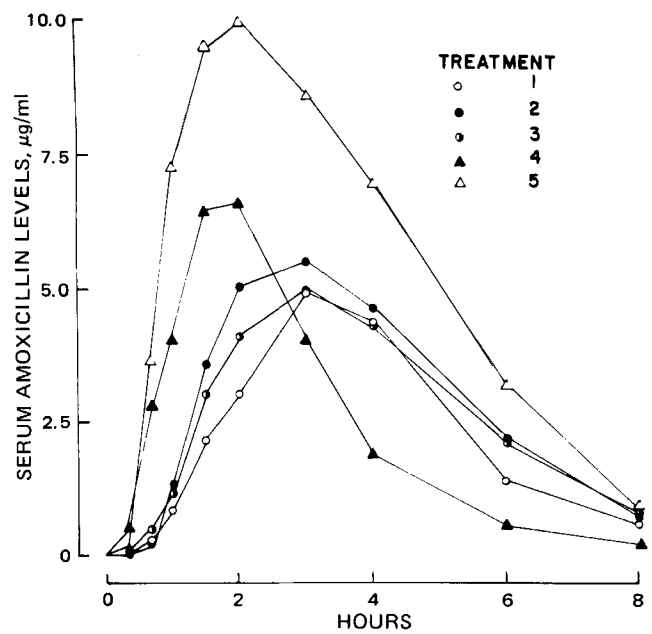

Figure 2—*Average serum amoxicillin levels.*

REFERENCES

(1) G. P. Bodey and J. Nance, *Antimicrob. Ag. Chemother.*, **1**, 358 (1972).

(2) H. C. Neu, *J. Infect. Dis., Suppl.*, **129**, S123 (1974).

(3) G. N. Rolinson, *ibid.*, **129**, S139 (1974).

(4) R. C. Gordon, C. Regamey, and W. M. M. Kirby, *Antimicrob. Ag. Chemother.*, **1**, 504 (1972).

(5) W. M. M. Kirby, R. C. Gordon, and C. Regamey, *J. Infect. Dis., Suppl.*, **129**, S154 (1974).

(6) L. Verbist, *Antimicrob. Ag. Chemother.*, **6**, 588 (1974).

(7) P. J. Little and B. A. Peddie, *Med. J. Aust.*, **2**, 598 (1974).

(8) T. G. Vitti, M. J. Gurwith, and A. R. Ronald, *J. Infect. Dis., Suppl.*, **129**, S149 (1974).

(9) P. G. Welling, L. L. Lyons, W. A. Craig, and G. A. Trochta, *Clin. Pharmacol. Ther.*, **17**, 475 (1975).

(10) T. B. Kjaer and P. O. Madsen, *Invest. Urol.*, in press.

(11) P. G. Welling, W. A. Craig, G. L. Amidon, and C. M. Kunin, *J. Infect. Dis., Suppl.*, **128**, S556 (1973).

(12) H. Lode, P. Janisch, G. Küpper, and H. Weuta, *ibid.*, **129**, S156 (1974).

(13) M. Gibaldi and D. Perrier, "Pharmacokinetics," Dekker, New York, N.Y., 1975, p. 35.

(14) H. C. Neu and E. B. Winshell, *Antimicrob. Ag. Chemother.*, **1970**, 423 (1971).

(15) "Remington's Pharmaceutical Sciences," 15th ed., Mack Publishing Co., Easton, Pa., 1975, pp. 1128, 1133.

ACKNOWLEDGMENTS AND ADDRESSES

Received April 8, 1976, from the *Center for Health Sciences, School of Pharmacy, and the ‡Veterans Administration Hospital, University of Wisconsin, Madison, WI 53706.

Accepted for publication June 8, 1976.

Supported by NIH Grant GM 20327.

ˣ To whom inquiries should be directed.

Dissolution Profile for Multisized Drug Particles: New Approximate Expression

JOHN W. MAUGER *, DANA BROOKE ‡x, and EARL Z. DAMEWOOD §

Abstract □ New approximate expressions for the weight fraction undissolved were obtained using the Taylor series expansion. These approximations were tested using simulated data for multisized drug particle populations. The resulting calculations show that: (*a*) the approximations are not dependent on a knowledge of the analytical form of the particle-size density function, (*b*) the distribution effects are accounted for, but only a knowledge of the sample mean and standard deviation is required, and (*c*) the approximations (especially on a weight basis) lead to values within the limits of error in dissolution studies, thus posing the question of whether published exact expressions have practical value.

Keyphrases □ Dissolution—multisized drug particles, approximate expressions for weight fraction undissolved □ Particles, multisized—dissolution profile, approximate expressions for weight fraction undissolved □ Weight fraction undissolved—multisized drug particles, approximate expressions

The effects of multisized particle distributions on dissolution kinetics were studied using either experimental or simulated data (1–7). One area of particular concern has been the acceptability of treating the kinetics of dissolution for a multisized particle population with an approximate mathematical treatment for the kinetic model of interest.

The importance of including the distribution effects was recognized in the mathematical treatment of a diffusional model proposed for the dissolution of micronized methylprednisolone (1, 2). The complexity of these equations led to simplified forms *via* an approximation for the particle-size density function.

Approximate expressions were discussed in connection with the cube root kinetic model (3–5). For example, an approximation to the cube root model was described for a log-normal particle-size population that relaxes to the exact cube root law when the standard deviation of the particle population approaches zero. However, such an approximation, requiring a knowledge of the mean and variance of the log normal population, has limited practical value (5). Certainly, the approximation could not be used intelligently unless the powder of interest was *confirmed* to obey the log-normal distribution and the parameters of the distribution could be estimated.

An interest in an approximation illustrating the effects of different particle sizes derives, in part, from difficulties in obtaining monosized powder cuts for dissolution studies. The mathematical treatment of dissolution data from actual drug powders, which may contain a range of sizes, has often been based on the assumption of monosized particles. Recent papers (8, 9) proposed treatments of dissolution data on powders without a calculation of the effect of a distribution of particle sizes. Because of such difficulties, the relationship between dissolution theory and its experimental justification remains fragile. The approximations reported here enable one to estimate the effect of varying particle sizes on dissolution data and may strengthen the relationship between theory and data.

Interest in an approximation can also be appreciated if one considers the complex and cumbersome calculations involved. The use of a distribution function in connection with the dissolution model of interest, *i.e.*, cube root, Dankwert's, *etc.*, requires integration over the random variable of particle size as well as a consideration of time. Therefore, any reasonable approximation is inviting.

To date, no convenient treatment can be justified for any particular kinetic model with a particular distribution function. This report describes a simplified procedure that can be justified by a standard mathematical (and statistical) derivation. The procedure utilizes estimators of the dispersion of sizes in a powder, which are readily accessible from particle-size data (*e.g.*, automated counter and microscopic data). The limitations and uses of the procedure are tested using simulated data.

THEORETICAL

Let there be a population of spherical particles of initial diameters A_0 that are randomly distributed on a numbers basis according to the continuous density function $f_n(A_0)$ or on a weight basis according to the density function $f_w(A_0)$. The dissolution profile of such a population of particles exposed to a dissolution medium is often analytically expressed in terms of the weight fraction undissolved. Let there be a function $g(A_0, t)$ of the random variable A_0 and the dissolution time t that reflects a suitable dissolution model. For example, let A_τ be the diameter of a particle exposed to a dissolution medium for some function τ of time so that:

$$g(A_0, t) = A_\tau{}^3 \qquad \text{(Eq. 1)}$$

If the dissolution is diffusion rate limited and takes place under sink conditions, then $g(A_0, t)$ describes the well-known cube root law kinetic model:

$$g(A_0, t) = A_\tau{}^3 = (A_0 - \tau)^3 \qquad \text{(Eq. 2)}$$

For a numbers distribution, the weight fraction undissolved, W_{fn}, will be seen to be a ratio of expected values as follows:

$$W_{fn} = \frac{\int_{\text{all } A_0 \text{ undissolved}} g(A_0, t) f_n(A_0) d(A_0)}{\int_{\text{all } A_0} g(A_0, 0) f_n(A_0) d(A_0)} = \frac{E(A_\tau{}^3)}{E(A_0{}^3)} \qquad \text{(Eq. 3)}$$

If the initial population of particles is described on a weight basis, the weight fraction undissolved, W_{fw}, is the expected value of a ratio as follows:

$$W_{fw} = \int_{\text{all } A_0 \text{ undissolved}} \frac{g(A_0, t)}{g(A_0, 0)} f_w(A_0) dA_0 = \int_{\text{all } A_0 \text{ undissolved}} h(A_0, t) f_w(A_0) dA_0 = E\left(\frac{A_\tau{}^3}{A_0{}^3}\right) \qquad \text{(Eq. 4)}$$

where $h(A_0, t)$ is $g(A_0, t)$ divided by $g(A_0, 0)$.

If the mean $E(A_0) = \mu$ and variance $V(A_0) = \sigma^2$ of the population of particles are known, the important expected value terms in Eqs. 3 and 4 can be approximated, provided that $f(A_0)$ takes significant values in an interval near $A_0 = \mu$ of the order of σ and that $g(A_0, t)$ is "smooth" in this interval. The approximation given in Eqs. 5 and 6 in the terminology of this derivation is found in standard texts on probability and statistics (10, 11) and can be proved using a Taylor series expansion[1]. The ap-

[1] See *Appendix* for additional information on this technique.

Table I—Dissolution Profiles for Simulated Log-Normal Powders with Narrow Distribution Using the Cube Root Law

Summary of Population Parameters	
Numbers Basis	Weight Basis
$E(\ln A_0) = 3.68888$	$E(\ln A_0) = 3.71888$
$V(\ln A_0) = 0.01$	$V(\ln A_0) = 0.01$
$E(A_0) = 40.20$	$E(A_0) = 41.43$
$V(A_0) = 16.24$	$V(A_0) = 17.25$

τ	W_f(exact)	W_{fn}(approx)	W_{fw}(approx)	$\left(\frac{\bar{A}_0 - \tau}{\bar{A}_0}\right)^3_w$
10	0.4337	0.4336	0.4337	0.4366
20	0.1381	0.1379	0.1381	0.1384
29.63	0.0255	0.02534	0.02575	0.0231
30	0.0234	0.02328	0.02370	0.0210
35	0.0063	0.00589	0.00646	0.0037

proximations of interest are:

$$E(A_\tau{}^3) = g(\mu, t) + \frac{\sigma^2}{2} g''(\mu, t) \quad \text{(Eq. 5)}$$

and:

$$E\left(\frac{A_\tau{}^3}{A_0{}^3}\right) = h(\mu, t) + \frac{\sigma^2}{2} h''(\mu, t) \quad \text{(Eq. 6)}$$

Thus, approximations for the weight fraction undissolved on a numbers basis or a weight basis are:

$$W_{fn}(\text{approx}) = \frac{g(\mu, t) + \frac{\sigma^2}{2} g''(\mu, t)}{g(\mu, 0) + \frac{\sigma^2}{2} g''(\mu, 0)} \quad \text{(Eq. 7)}$$

and:

$$W_{fw}(\text{approx}) = h(\mu, t) + \frac{\sigma^2}{2} h''(\mu, t) \quad \text{(Eq. 8)}$$

Generally, the sample mean, μ, of a population will be understood to be the numbers or weight average, $\bar{A}_0$, and the variances, σ^2, will be the square of the sample standard deviations[2]. Thus, for the cube root dissolution model, the weight fraction undissolved of a multisized particle distribution will be:

$$W_{fn}(\text{approx}) = \frac{(\bar{A}_0 - \tau)^3 + 3\sigma^2(\bar{A}_0 - \tau)}{\bar{A}_0{}^3 + 3\sigma^2\bar{A}_0} \quad \text{(Eq. 9)}$$

or:

$$W_{fw}(\text{approx}) = \left(\frac{\bar{A}_0 - \tau}{\bar{A}_0}\right)^3 - \frac{\sigma^2}{2}\left(\frac{6\tau}{\bar{A}_0{}^3} - \frac{18\tau^2}{\bar{A}_0{}^4} + \frac{12\tau^3}{\bar{A}_0{}^5}\right) \quad \text{(Eq. 10)}$$

For another popular dissolution model, the Higuchi–Hiestand model (1):

$$g(A_0, t) = A_\tau{}^3 = (A_0{}^2 - \tau)^{3/2} \quad \text{(Eq. 11)}$$

and the weight fractions become:

$$W_{fn}(\text{approx}) = \frac{(\bar{A}_0{}^2 - \tau)^{3/2} + \frac{3\sigma^2}{2}\left[\frac{\bar{A}_0{}^2}{(\bar{A}_0{}^2 - \tau)^{1/2}} + (\bar{A}_0{}^2 - \tau)^{1/2}\right]}{\bar{A}_0{}^3 + 3\sigma^2\bar{A}_0} \quad \text{(Eq. 12)}$$

or:

$$W_{fw}(\text{approx}) = \left(\frac{\bar{A}_0{}^2 - \tau}{\bar{A}_0{}^2}\right)^{3/2} + \frac{\sigma^2}{2}\left[\frac{3\tau}{\bar{A}_0{}^5}\right]\left[\frac{\tau}{(\bar{A}_0{}^2 - \tau)^{1/2}} - 3(\bar{A}_0{}^2 - \tau)^{1/2}\right] \quad \text{(Eq. 13)}$$

RESULTS AND DISCUSSION

An examination of the adequacy of the approximations derived for the cube root model (Eqs. 9 and 10) or for the Higuchi–Hiestand model (Eqs. 12 and 13) is limited to cases where drug particle sizes follow the log-normal distribution as given by:

$$f(\ln A_0) = \frac{1}{s\sqrt{2\pi}} e^{-(\ln A_0 - m)^2/2s^2} \quad \text{(Eq. 14)}$$

where m and s^2 refer to the (numbers basis) population mean $E(\ln A_0)$ and variance $V(\ln A_0)$, respectively. The approximations, however, require a knowledge of the arithmetic mean $E(A_0)$ and the corresponding variance $V(A_0)$. These may be calculated from:

$$E(A_0) = e^{m + s^2/2} \quad \text{(Eq. 15)}$$

and:

$$V(A_0) = E(A_0{}^2) - [E(A_0)]^2 = (e^{s^2} - 1)e^{2m + s^2} \quad \text{(Eq. 16)}$$

These transformations arise from the appropriate use of Eq. 9 of Ref. 4. Since approximations are given for populations where particle-size parameters are evaluated on a numbers basis or a weight basis, it is also necessary to use the Hatch and Choate relationships for log-normal distributions (12), which state:

$$m_{\text{weight}} = m_{\text{numbers}} + 3s^2_{\text{numbers}} \quad \text{(Eq. 17)}$$

$$s^2_{\text{weight}} = s^2_{\text{numbers}} \quad \text{(Eq. 18)}$$

Cube Root Model—The exact and approximate weight fraction undissolved quantities for the cube root kinetic model are presented in Tables I–III. The exact weight fraction undissolved is taken from published data (4). The data in Table I are for a log-normal population with a relatively narrow distribution, as evidenced by the near quality between $E[A_0]_{\text{numbers}}$ and $E[A_0]_{\text{weight}}$. The approximate W_f values are reasonably close to W_f(exact) throughout the dissolution profile, although W_{fw}(approx) from Eq. 10 appears to give slightly better results.

The populations shown in Tables II and III stress the approximations by increasing the magnitude of the standard deviation. The approximation values given in Table II are adequate throughout most of the dissolution time frame. Only at $\tau = 40$ do the approximate values for W_{fw}(approx) begin to diverge from the exact values. The W_{fn}(approx) values begin to diverge from the exact values at $\tau = 25$, but this approx-

Table II—Dissolution Profiles for Simulated Log-Normal Powders with Moderate Distribution Using the Cube Root Law

Summary of Population Parameters	
Numbers Basis	Weight Basis
$E(\ln A_0) = 3.68888$	$E(\ln A_0) = 3.95888$
$V(\ln A_0) = 0.09$	$V(\ln A_0) = 0.09$
$E(A_0) = 41.84$	$E(A_0) = 54.81$
$V(A_0) = 164.87$	$V(A_0) = 282.92$

τ	W_f(exact)	W_{fn}(approx)	W_{fw}(approx)	$\left(\frac{\bar{A}_0 - \tau}{\bar{A}_0}\right)^3_w$
5	0.7320	0.7262	0.7314	0.7505
10	0.5215	0.5113	0.5197	0.5464
16.26	0.3273	0.3129	0.3240	0.3479
25	0.1575	0.1395	0.1547	0.1609
40	0.0372	0.00975	0.04533	0.0197

Table III—Dissolution Profiles for Simulated Log-Normal Powders with Wide Distribution Using the Cube Root Law

Summary of Population Parameters	
Numbers Basis	Weight Basis
$E(\ln A_0) = 3.68888$	$E(\ln A_0) = 4.43888$
$V(\ln A_0) = 0.25$	$V(\ln A_0) = 0.25$
$E(A_0) = 45.33$	$E(A_0) = 95.96$
$V(A_0) = 583.51$	$V(A_0) = 2615$

τ	W_f(exact)	W_{fn}(approx)	W_{fw}(approx)	$\left(\frac{\bar{A}_0 - \tau}{\bar{A}_0}\right)^3_w$
8.93	0.6929	0.6469	0.6875	0.7460
10	0.6625	0.6142	0.6559	0.7188
20	0.4326	0.3513	0.4140	0.4960
40	0.1831	0.0549	0.1639	0.1983

[2] The authors use $\bar{A}_0$ to represent the numbers average diameter in those approximations derived for distributions evaluated on a numbers basis. The same character, $\bar{A}_0$, represents a weight mean diameter in those approximations offered for distributions stated on a weight basis.

Table IV—Dissolution Profiles for Simulated Log-Normal Powders with Narrow Distribution Using the Higuchi–Hiestand Model

Summary of Population Parameters	
Numbers Basis	Weight Basis
$E(\ln A_0) = 2.99573$	$E(\ln A_0) = 3.02573$
$V(\ln A_0) = 0.01$	$V(\ln A_0) = 0.01$
$E(A_0) = 20.10$	$E(A_0) = 20.712$
$V(A_0) = 4.061$	$V(A_0) = 4.3116$

τ	W_f(numerical integration)	W_{fn}(approx)	W_{fw}(approx)	$\left(\frac{\bar{A}_0^2-\tau}{\bar{A}_0^2}\right)^{1.5}_w$
30.77	0.8911	0.8913	0.8913	0.8944
92.31	0.6873	0.6874	0.6874	0.6953
153.85	0.5032	0.5031	0.5031	0.5136
246.15	0.2702	0.2697	0.2689	0.2783
307.69	0.1519	0.1501	0.1477	0.1504
369.23	0.07189	0.07870	0.06739	0.0520
400.00	0.04596	—	0.05706	0.0176

imation is satisfactory over at least 80% of the total dissolution profile.

A log-normal population, where $E[\ln A_0]_{\text{numbers}} = 3.68888$ and $V[\ln A_0]_{\text{numbers}} = 0.25$, represents a rigorous test for the approximate expressions for the weight fraction undissolved. This population stresses the approximations by virtue of the large standard deviation and the skewed shape of the density function. The approximate and exact W_f values for this population are presented in Table III. Both the W_{fn} and W_{fw} values are consistently lower than the exact values. Again, the weight fractions undissolved calculated using Eq. 10 are more satisfactory than those calculated using Eq. 9.

Also presented in Tables I–III are $(\bar{A}_0 - \tau)^3/\bar{A}_0^3$ values, which reflect the dissolution profile for a monosized powder that obeys the cube root law. This term obtains from either approximation in Eq. 9 or 10 when σ^2 becomes zero. For a monosized population, the average diameter on a numbers basis is equal to the average diameter on a weight basis so that $(\bar{A}_0 - \tau)^3/\bar{A}_0^3$ calculated on either basis leads to the same estimate of weight fraction undissolved. However, for powders where particles have a wide range of sizes, the calculation on a *weight basis* generally provides a better estimate of the undissolved weight fraction. The calculation provided in Tables I–III employs the average diameters on a weight basis as signified by a subscript w.

The first term of Eq. 10 is actually $[(\bar{A}_0 - \tau)^3/\bar{A}_0^3]_w$. The remaining term in Eq. 10 indicates the effect of the particle-size distribution on the dissolution profile. Thus, this approximation provides a means of quantitating the errors that may occur when data on a polydisperse powder are treated as having come from a monosized powder. Although the simple $[(\bar{A}_0 - \tau)^3/\bar{A}_0^3]_w$ is useful for narrow distributions, the data of Tables I–III indicate that the weight basis approximation, which includes consideration of size distribution, provides better estimates of the weight fraction undissolved.

Table V—Dissolution Profiles for Simulated Log-Normal Powders with Moderate Distribution Using the Higuchi–Hiestand Model

Summary of Population Parameters	
Numbers Basis	Weight Basis
$E(\ln A_0) = 2.99573$	$E(\ln A_0) = 3.11573$
$V(\ln A_0) = 0.04$	$V(\ln A_0) = 0.04$
$E(A_0) = 20.40$	$E(A_0) = 23.01$
$V(A_0) = 16.99$	$V(A_0) = 21.60$

τ	W_f(numerical integration)	W_{fn}(approx)	W_{fw}(approx)	$\left(\frac{\bar{A}_0^2-\tau}{\bar{A}_0^2}\right)^{1.5}_w$
30.77	0.9036	0.9031	0.9040	0.9141
92.31	0.7229	0.7215	0.7232	0.7502
153.85	0.5603	0.5579	0.5587	0.5975
246.15	0.3580	0.3529	0.3471	0.3914
307.69	0.2554	0.2533	0.2340	0.2711
369.23	0.1774	0.2145	0.1502	0.1665
461.54	0.09972	—	0.1185	0.0046

Table VI—Dissolution Profiles for Simulated Log-Normal Powders with Moderately Wide Distribution Using the Higuchi–Hiestand Model

Summary of Population Parameters	
Numbers Basis	Weight Basis
$E(\ln A_0) = 2.99573$	$E(\ln A_0) = 3.26573$
$V(\ln A_0) = 0.09$	$V(\ln A_0) = 0.09$
$E(A_0) = 20.92$	$E(A_0) = 27.41$
$V(A_0) = 41.22$	$V(A_0) = 70.73$

τ	W_f(numerical integration)	W_{fn}(approx)	W_{fw}(approx)	$\left(\frac{\bar{A}_0^2-\tau}{\bar{A}_0^2}\right)^{1.5}_w$
30.77	0.9203	0.9194	0.9225	0.9392
92.31	0.7710	0.7684	0.7750	0.8215
153.85	0.6373	0.6326	0.6384	0.7091
246.15	0.4710	0.4651	0.4560	0.5513
307.69	0.3819	0.3883	0.3512	0.4537
369.23	0.3112	—	0.2620	0.3627
461.54	0.2279	—	0.1637	0.2395
500.00	0.2007	—	0.1385	0.1935

Equation 10 can be written in expanded form and expressed as:

$$W_{fw}(\text{approx}) = 1 - 3\left(\frac{\tau}{\bar{A}_0}\right)\left(1 + \frac{\sigma^2}{\bar{A}_0^2}\right) + 3\left(\frac{\tau}{\bar{A}_0}\right)^2\left(1 + 3\frac{\sigma^2}{\bar{A}_0^2}\right) - \left(\frac{\tau}{\bar{A}_0}\right)^3\left(1 + 6\frac{\sigma^2}{\bar{A}_0^2}\right) \quad \text{(Eq. 19)}$$

If $\bar{A}_0$ and σ^2 are known, Eq. 19 can be solved by using a one-parameter model. Furthermore, as $\sigma^2 \to 0$, Eq. 19 assumes a perfect cube form:

$$W_f = 1 - 3\frac{\tau}{\bar{A}_0} + 3\left(\frac{\tau}{\bar{A}_0}\right)^2 - \left(\frac{\tau}{\bar{A}_0}\right)^3 \quad \text{(Eq. 20)}$$

Recently, dissolution data for 20–40-mesh salicylic acid particles were reported (9). These data were treated using the cubic form of the expression to fit the experimental weight fraction undissolved values. For a sieve cut of this width, a considerable bias can be introduced if the terms accounting for the distribution effects are neglected. In fact, the curve fitting of data to a cubic form without regard for particle-size effects would lead to a parameter that would be in error by a factor having a value between $[1 + (\sigma^2/\bar{A}_0^2)]$ and $[1 + 6(\sigma^2/\bar{A}_0^2)]^{1/3}$. For a powder uniformly distributed over a size range of 20–40 mesh, the factor would be between 1.037 and 1.069[3]. This point is significant in cases where critical model testing is the objective.

Higuchi–Hiestand Model—The approximate expressions for the Higuchi–Hiestand kinetic model (Eqs. 12 and 13) were tested (Tables IV–VI). The exact weight fraction undissolved was calculated from Eq. 4 using standard numerical integration techniques.

The weight fraction undissolved values shown in Table IV are for a log-normal population where $E[\ln A_0]_{\text{numbers}} = 2.99573$ and $V[\ln A_0]_{\text{numbers}} = 0.01$. The approximate expressions yield values that are less than 3% in error when compared with those calculated using numerical integration over almost the total dissolution profile. At $\tau = 369.23$, the approximate expressions give values that are more than 5% in error when compared with the "exact" values. However, at this point, more than 90% of the initial population weight has dissolved.

The data in Table V are for a log-normal population where $E[\ln A_0]_{\text{numbers}} = 2.99573$ and $V[\ln A_0]_{\text{numbers}} = 0.04$. This population was designed to provide a more exacting test of the approximations by virtue of a large population variance. In this case, the coefficient of variation, *i.e.*, $(V[A_0])^{1/2}/E[A_0]$, is about 20%; the coefficient of variation for the data in Table IV is about 10%. The W_{fw}(approx) values for this example follow the exact values closely over about 75% of the total dissolution profile. At $\tau = 369.23$ and 461.54, the approximations begin to drift away from the exact values; at $\tau = 470$, the approximation fails. The failure at the latter end of the dissolution profile is closely related to the magnitude of the variance and the form of the approximate expression. It can be seen from Eq. 13 that as $(\bar{A}_0^2 - \tau) \to 0$, $\tau/(\bar{A}_0^2 - \tau)^{1/2}$ approaches infinity and becomes the dominating term.

Analysis of the W_{fn}(approx) values shown in Table II shows that the approximation is useful over about 75% of the total dissolution profile.

[3] The terms $E(A_0)$ and $V(A_0)$ for a uniform distribution are calculable from Eq. 3 of Ref. 13 where $R = 1$.

Again, however, the magnitude of the variance and the form of the approximation contribute to the failure. According to Eq. 12, the term $\overline{A}_0^2/(\overline{A}_0^2 - \tau)^{1/2}$ approaches infinity as $\overline{A}_0^2 - \tau$ approaches zero. This is even more critical for a population based on numbers because $E[A_0]_{\text{numbers}} < E[A_0]_{\text{weight}}$ for the log-normal populations under study.

The data in Table VI are for a log-normal drug population where $E[\ln A_0]_{\text{numbers}} = 2.99573$ and $V[\ln A_0]_{\text{numbers}} = 0.09$. The coefficient of variation for this population is about 30%. Therefore, this population represents a severe test of the approximation. The data in Table VI show that the approximations are useful over about 60% of the total dissolution even for this population. Again, the failure of the approximations is related to the magnitude of the standard deviation and the form of the approximate expression.

The first term in Eq. 13, $[(\overline{A}_0^2 - \tau)/\overline{A}_0^2]^{1.5}$, was also tested as an approximation for the weight fraction undissolved. The data presented in Tables IV–VI show that this approximation is only useful for narrow distributions. Therefore, experimental dissolution data for many multisized drug populations will be incorrectly interpreted if the term for the distribution effects is not included.

When testing the approximate expressions for different kinetic models, some consideration must be given to the mathematical form of the kinetic equation. For the cube root model, each particle, independent of size, dissolves at the same rate with regard to diameter. On the other hand, small particles dissolving according to the Higuchi–Hiestand model dissolve much more rapidly than larger particles. The approximate expressions for the cube root model are only concerned with a population of particles all dissolving at a uniform rate. Approximate expressions for the Higuchi–Hiestand kinetic model, however, must deal with a population where the temporal characteristics of the sample mean and variance at time τ are more complex. With this in mind, it is interesting to compare the data in Table II with the data in Table VI. The approximate weight fraction undissolved values in Table II are for the cube root model, and those in Table VI are for the Higuchi–Hiestand model. The coefficient of variation in both cases is about 30%. Comparison of the data in Tables II and VI shows that the approximations for the cube root model are better than those for the Higuchi–Hiestand model.

SUMMARY

Approximate expressions for the weight fraction undissolved were tested using multisized (log-normal) distributions in connection with the cube root and Higuchi–Hiestand kinetic models. These simulated data show several important features:

1. The approximations are based on a recognized mathematical treatment and *not* on empirical relationships.
2. The distribution effects are accounted for, but only a knowledge of the arithmetic mean and standard deviation of the sample is required.
3. The approximations are not dependent upon a knowledge of the exact analytical form of the particle-size density function, *i.e.*, whether gamma, normal, log normal, *etc.*
4. The approximations lend themselves to usefulness with real laboratory data such as might be acquired by an automated counter (number or weight data), microscopic examination (numbers data), or sieve fractions (weight data).
5. The approximations are general and are potentially useful with any kinetic model that is at least twice differentiable at $A_0 = \mu$.
6. The approximations may find usefulness in a modeling technique to determine dissolution rate constants from dissolution data.

APPENDIX

The approximation of an expected value of a function of a random variable, as set forth in various texts on statistics (10, 11), first requires approximating that function through a Taylor series expansion and then taking the expected value of the approximation to the function. In this case, the function of the random variable A_0 (the initial particle diameter) is the dissolution model, *e.g.*, $g(A_0, t)$. It must be appreciated that the expected value of this function:

$$E[g(A_0, t)] = \int_{\text{all } A_0 \text{ remaining}} g(A_0, t) f(A_0) dA_0 \qquad \text{(Eq. A1)}$$

must be evaluated considering t as a constant whose value can be supplied after the integration. This consideration is important in derivations of dissolution equations by Brooke (4, 5, 13) and Pedersen and Brown (7). Therefore, it is imperative that all operations prior to the actual calculation of W_f consider t a constant.

The Taylor series approximation to a function of the random variable A_0, *e.g.*, $g(A_0, t)$, is most accurate in a region where values of A_0 are within 1 *SD*, σ, of the initial population mean, μ. Both μ and σ are parameters of the initial (time zero) particle-size distribution. The expansion about μ is written:

$$g(A_0, t) \simeq g(\mu, t) + (A_0 - \mu)g'(\mu, t) + \tfrac{1}{2}(A_0 - \mu)^2 g''(\mu, t) + \ldots \qquad \text{(Eq. A2)}$$

For t as a constant, $g(\mu, t)$, $g'(\mu, t)$, *etc.*, are constants and the expected value $E[g(A_0, t)]$ is approximated by:

$$g(\mu, t) + g'(\mu, t)E(A_0 - \mu) + \tfrac{1}{2} g''(\mu, t)E(A_0 - \mu)^2 + \ldots \qquad \text{(Eq. A3)}$$

By neglecting higher order terms in the expansion and by recognizing that $E(A_0 - \mu)$ is zero and $E(A_0 - \mu)^2$ is σ^2, the approximation for $E[g(A_0, t)]$ is written:

$$E[g(A_0, t)] \simeq g(\mu, t) + \tfrac{1}{2} g''(\mu, t)\sigma^2 \qquad \text{(Eq. A4)}$$

The use of Eq. A4 is illustrated by deriving the approximate weight fraction undissolved when the particle distribution is expressed on a numbers basis and the particles dissolve according to the Higuchi–Hiestand model. Here:

$$g(A_0, t) = (A_0^2 - \tau)^{3/2} = A_\tau^3 \qquad \text{(Eq. A5)}$$

which is twice differentiated in respect to the initial particle size, A_0, while t is considered a constant. That is:

$$g'(A_0, t) = 3(A_0^2 - \tau)^{1/2} A_0 \qquad \text{(Eq. A6)}$$

and:

$$g''(A_0, t) = 3(A_0^2 - \tau)^{1/2} + 3A_0^2/(A_0^2 - \tau)^{1/2} \qquad \text{(Eq. A7)}$$

In using Eq. A4, it is necessary to evaluate $g(A_0, t)$ and $g''(A_0, t)$ at the population mean μ. For this purpose, the arithmetic mean of the initial diameters, $\overline{A}_0$, is considered an appropriate estimator. Furthermore, it is experimentally available. Therefore:

$$E[g(A_0, t)] = E(A_\tau^3) \simeq (\overline{A}_0^2 - \tau)^{3/2} + \frac{3\sigma^2}{2}\left[\frac{\overline{A}_0^2}{(\overline{A}_0^2 - \tau)^{1/2}} + (\overline{A}_0^2 - \tau)^{1/2}\right] \qquad \text{(Eq. A8)}$$

and:

$$E[g(A_0, t)_{t=0}] = E(A_0^3) \simeq \overline{A}_0^3 + 3\sigma^2\overline{A}_0 \qquad \text{(Eq. A9)}$$

and W_{fn}(approx) for the Higuchi–Hiestand model becomes Eq. 12 of the text by dividing Eq. A8 by Eq. A9.

The use of the approximate equations for weight undissolved is illustrated by considering W_{fn}(approx) for the Higuchi–Hiestand model. Here, data are taken from Table V where the average particle size, $\overline{A}_0$, for the numbers distribution is 20.40 μm and the squared standard deviation, $V(A_0)$, is 16.99 μm^2. By using Eq. 12 of the text, W_{fn}(approx) for $\tau = 153.85$ μm is:

$$W_{fn}(\text{approx}) = \frac{[(20.40)^2 - 153.85]^{3/2} + \tfrac{3}{2}(16.99)\left[\dfrac{(20.40)^2}{[(20.40)^2 - 153.85]^{1/2}} - [(20.40)^2 - 153.85]^{1/2}\right]}{(20.40)^3 + 3(16.99)(20.40)} = 0.5587 \qquad \text{(Eq. A10)}$$

REFERENCES

(1) W. Higuchi and E. Hiestand, *J. Pharm. Sci.*, **52**, 67 (1963).
(2) W. Higuchi, E. Rowe, and E. Hiestand, *ibid.*, **52**, 162 (1963).
(3) J. Carstensen and M. Musa, *ibid.*, **61**, 223 (1972).
(4) D. Brooke, *ibid.*, **62**, 795 (1973).
(5) *Ibid.*, **63**, 344 (1974).
(6) J. Mauger and S. Howard, *J. Pharm. Sci.*, **65**, 1042 (1976).
(7) P. V. Pedersen and K. F. Brown, *ibid.*, **64**, 1192 (1975).
(8) M. P. Short, P. Sharkey, and C. T. Rhodes, *ibid.*, **61**, 1732 (1972).

(9) J. Cobby, M. Mayersohn, and B. Farlinger, *Can. J. Pharm. Sci.*, **9**, 91 (1974).
(10) A. Papoulis, "Probability, Random Variables, and Stochastic Processes," McGraw-Hill, New York, N.Y., 1965, p. 151.
(11) P. L. Meyer, "Introductory Probability and Statistical Applications," Addison-Wesley, Reading, Mass., 1965, p. 126.
(12) R. R. Irani and C. F. Callis, "Particle Size: Measurement, Interpretation, and Application," Wiley, New York, N.Y., 1963, p. 45.
(13) D. Brooke, *J. Pharm. Sci.*, **64**, 1409 (1975).

ACKNOWLEDGMENTS AND ADDRESSES

Received November 17, 1975, from the *School of Pharmacy, West Virginia University, Morgantown, WV 26506, the ‡Mead Johnson Research Center, Mead Johnson and Company, Evansville, IN 47712, and the §Department of Industrial Engineering, West Virginia University, Morgantown, WV 26506.

Accepted for publication June 7, 1976.

ˣ To whom inquiries should be directed.

Dissolution Profiles for Multisized Prednisolone Acetate Suspensions

STEPHEN A. HOWARD ˣ, JOHN W. MAUGER, and LAWAN PHUSANTI

Abstract □ Particle-size measurements and *in vitro* dissolution characteristics of commercial and formulated suspensions of prednisolone acetate were determined using a resistance particle counter and a spinning filter apparatus, respectively. Significant differences in dissolution rates were noted for the commercial suspensions. Particle size affected dissolution but did not account for all observed variations in the dissolution rate. Formulation differences, specifically the presence of hydroxypropyl methylcellulose, in suspensions seemed to be important in dissolution.

Keyphrases □ Prednisolone acetate—multisized suspensions, dissolution profiles and particle-size measurements □ Suspensions, multisized—prednisolone acetate, dissolution profiles and particle-size measurements □ Dissolution—multisized suspensions of prednisolone acetate, effect of particle size □ Particle size—effect on dissolution of prednisolone acetate suspensions □ Glucocorticoids—prednisolone acetate, multisized suspensions, dissolution profiles and particle-size measurements

The dissolution rate and *in vivo* physiological availability of drugs are important research areas (1–5). The dissolution rate of a solid dosage form such as a tablet or a capsule can be the rate-limiting step in availability for the *in vivo* absorption of the active ingredient (6–8), particularly for poorly soluble or poorly wetted drugs (9).

At present, almost all dissolution rate research efforts are directed toward tablets and capsules. Although suspensions share many physical–chemical characteristics of tablets and capsules with respect to the dissolution process, they are almost completely ignored. Since tablets and capsules disintegrate into powder suspensions, pharmaceutical suspensions share the dissolution process as a rate-limiting step for absorption and bioavailability.

Bates *et al.* (10) studied the dissolution rates of nitrofurantoin tablets and suspensions and commented that it was inconsistent to provide a USP dissolution test for nitrofurantoin tablets without including a dissolution rate test for the suspension. They concluded that: "the rationale underlying the official dissolution rate specification for nitrofurantoin tablets appears quite arbitrary and inconsistent with the dissolution profile and potential toxicity of the official suspension dosage form."

These comments substantiate a need to pursue dissolution rate testing of suspension dosage forms. In the current study, the dissolution and particle-size profiles of several commercially available suspensions were determined to obtain information about brand-to-brand variation and formulation characteristics directly related to dissolution.

Commercially available steroid ophthalmic/otic suspensions were studied. They represent a dosage form that requires dissolution as a prerequisite to therapeutic availability. These products contain a poorly soluble micronized steroid in a suitable vehicle. The solubility and particle-size characteristics of these products make them desirable prototype suspensions to study.

EXPERIMENTAL

Dissolution Testing—All reported dissolution data were obtained using a device[1] described by Shah *et al.* (11). The basic features of the apparatus are a large volume fluid container, a rotating filter assembly, and an external variable-speed magnetic stirrer. The sample basket was removed.

The rotating filter assembly provides variable intensity of mild laminar liquid agitation and also functions as an *in situ* nonclogging filter to permit efficient intermittent or continuous filtration of dissolution fluid samples during the dissolution process. The assembly is suspended and freely rotates in the center of the flask on the flared end of a glass capillary pilot tube. The assembly rotates by means of a controlled, variable-speed, external magnetic stirrer coupled with a magnetic bar embedded in the bottom part of the assembly. A 0.5-μm porosity sintered stainless steel filter also was employed.

One liter of distilled water was transferred into the flask, and the fluid was allowed to equilibrate at 25°. The stirring speed of the filter assembly was 960 rpm. A strobe lamp[2] was used to standardize the stirring speed.

Filtered fluid samples were continuously withdrawn through the capillary pilot tube at the rate of 100 ml/min and were circulated through the spectrophotometer and back to the flask. Air bubbles were periodically released from an air trap. The system was allowed to run for at least 15 min to ensure the consistency of the flow and stirring rate. The spectrophotometer[3] was then calibrated for zero absorbance at 246 nm with the dissolution medium in the reference cell. The baseline on the stripchart[4] paper also was adjusted corresponding to zero absorbance.

[1] The dissolution apparatus was made available through the courtesy of The Upjohn Co., Kalamazoo, Mich.
[2] Glass Instrument Co., Quincy, Mass.
[3] Perkin-Elmer double-beam spectrophotometer, Coleman 124, Hitachi, Ltd., Tokyo, Japan.
[4] Chart recorder model SRG, Sargent-Welch Scientific Co., Cleveland, Ohio.

(9) J. Cobby, M. Mayersohn, and B. Farlinger, *Can. J. Pharm. Sci.*, **9**, 91 (1974).
(10) A. Papoulis, "Probability, Random Variables, and Stochastic Processes," McGraw-Hill, New York, N.Y., 1965, p. 151.
(11) P. L. Meyer, "Introductory Probability and Statistical Applications," Addison-Wesley, Reading, Mass., 1965, p. 126.
(12) R. R. Irani and C. F. Callis, "Particle Size: Measurement, Interpretation, and Application," Wiley, New York, N.Y., 1963, p. 45.
(13) D. Brooke, *J. Pharm. Sci.*, **64**, 1409 (1975).

ACKNOWLEDGMENTS AND ADDRESSES

Received November 17, 1975, from the *School of Pharmacy, West Virginia University, Morgantown, WV 26506, the ‡Mead Johnson Research Center, Mead Johnson and Company, Evansville, IN 47712, and the §Department of Industrial Engineering, West Virginia University, Morgantown, WV 26506.

Accepted for publication June 7, 1976.

ˣ To whom inquiries should be directed.

Dissolution Profiles for Multisized Prednisolone Acetate Suspensions

STEPHEN A. HOWARD ˣ, JOHN W. MAUGER, and LAWAN PHUSANTI

Abstract □ Particle-size measurements and *in vitro* dissolution characteristics of commercial and formulated suspensions of prednisolone acetate were determined using a resistance particle counter and a spinning filter apparatus, respectively. Significant differences in dissolution rates were noted for the commercial suspensions. Particle size affected dissolution but did not account for all observed variations in the dissolution rate. Formulation differences, specifically the presence of hydroxypropyl methylcellulose, in suspensions seemed to be important in dissolution.

Keyphrases □ Prednisolone acetate—multisized suspensions, dissolution profiles and particle-size measurements □ Suspensions, multisized—prednisolone acetate, dissolution profiles and particle-size measurements □ Dissolution—multisized suspensions of prednisolone acetate, effect of particle size □ Particle size—effect on dissolution of prednisolone acetate suspensions □ Glucocorticoids—prednisolone acetate, multisized suspensions, dissolution profiles and particle-size measurements

The dissolution rate and *in vivo* physiological availability of drugs are important research areas (1–5). The dissolution rate of a solid dosage form such as a tablet or a capsule can be the rate-limiting step in availability for the *in vivo* absorption of the active ingredient (6–8), particularly for poorly soluble or poorly wetted drugs (9).

At present, almost all dissolution rate research efforts are directed toward tablets and capsules. Although suspensions share many physical–chemical characteristics of tablets and capsules with respect to the dissolution process, they are almost completely ignored. Since tablets and capsules disintegrate into powder suspensions, pharmaceutical suspensions share the dissolution process as a rate-limiting step for absorption and bioavailability.

Bates *et al.* (10) studied the dissolution rates of nitrofurantoin tablets and suspensions and commented that it was inconsistent to provide a USP dissolution test for nitrofurantoin tablets without including a dissolution rate test for the suspension. They concluded that: "the rationale underlying the official dissolution rate specification for nitrofurantoin tablets appears quite arbitrary and inconsistent with the dissolution profile and potential toxicity of the official suspension dosage form."

These comments substantiate a need to pursue dissolution rate testing of suspension dosage forms. In the current study, the dissolution and particle-size profiles of several commercially available suspensions were determined to obtain information about brand-to-brand variation and formulation characteristics directly related to dissolution.

Commercially available steroid ophthalmic/otic suspensions were studied. They represent a dosage form that requires dissolution as a prerequisite to therapeutic availability. These products contain a poorly soluble micronized steroid in a suitable vehicle. The solubility and particle-size characteristics of these products make them desirable prototype suspensions to study.

EXPERIMENTAL

Dissolution Testing—All reported dissolution data were obtained using a device[1] described by Shah *et al.* (11). The basic features of the apparatus are a large volume fluid container, a rotating filter assembly, and an external variable-speed magnetic stirrer. The sample basket was removed.

The rotating filter assembly provides variable intensity of mild laminar liquid agitation and also functions as an *in situ* nonclogging filter to permit efficient intermittent or continuous filtration of dissolution fluid samples during the dissolution process. The assembly is suspended and freely rotates in the center of the flask on the flared end of a glass capillary pilot tube. The assembly rotates by means of a controlled, variable-speed, external magnetic stirrer coupled with a magnetic bar embedded in the bottom part of the assembly. A 0.5-μm porosity sintered stainless steel filter also was employed.

One liter of distilled water was transferred into the flask, and the fluid was allowed to equilibrate at 25°. The stirring speed of the filter assembly was 960 rpm. A strobe lamp[2] was used to standardize the stirring speed.

Filtered fluid samples were continuously withdrawn through the capillary pilot tube at the rate of 100 ml/min and were circulated through the spectrophotometer and back to the flask. Air bubbles were periodically released from an air trap. The system was allowed to run for at least 15 min to ensure the consistency of the flow and stirring rate. The spectrophotometer[3] was then calibrated for zero absorbance at 246 nm with the dissolution medium in the reference cell. The baseline on the stripchart[4] paper also was adjusted corresponding to zero absorbance.

[1] The dissolution apparatus was made available through the courtesy of The Upjohn Co., Kalamazoo, Mich.
[2] Glass Instrument Co., Quincy, Mass.
[3] Perkin-Elmer double-beam spectrophotometer, Coleman 124, Hitachi, Ltd., Tokyo, Japan.
[4] Chart recorder model SRG, Sargent-Welch Scientific Co., Cleveland, Ohio.

All test conditions (*i.e.*, fluid temperature, stirring rate, cycling through the flowcell, and calibration of the spectrophotometer) were adjusted properly. The dissolution experiment was started by injecting a measured amount of suspension (0.5 ml except for Product A which was 1 ml) at a fixed position in the beaker using a syringe fitted with an extra long needle. The strip-chart paper was marked at the exact same time that the suspension was introduced into the flask. The recorder was switched to "stand by" until the drug readings, which were taken periodically, reached a plateau. The plateau of the curve was recorded and represented the equilibrium value. Generally, 2 hr was needed to reach equilibrium in this study.

The absorbance of dissolution profiles was then edited from the chart recording. For this report, the absorbance was edited at 5-sec intervals until 200 sec and then at every 100-sec interval until 1500 sec. The edited value was then used to calculate the weight fraction undissolved at any time t by simply dividing each absorption value by the equilibrium value and subtracting the resulting fraction from one.

Particle-Size Analysis—All particle-size data were obtained with a resistance particle counter[5] that employs the basic automated principle of sizing particles for a 16-channel (size) distribution analysis.

One convenient aspect provided by this instrument is that the volumetric size of the particle is automatically converted to the equivalent spherical diameter without any calculations by the operator. The calibration materials for the 50- and 200-μm aperture tubes were 2.02-μm diameter latex[6] beads and 27–28-μm diameter Lycopodium[7], respectively.

To avoid coincidence errors, size distribution must be measured within the limits given in the instrument manual. A meter on the instrument facilitates this process. A reading of approximately 0.05 on the concentration meter essentially eliminates coincidence problems.

The particle-size distribution data obtained from the resistance particle counter were provided by a numeric display of the cumulative and differential distributions. An oscilloscope display and the histograms were also available. Readout of total particle counts accumulated in the active channels was available during accumulation and held until the counter was reset. Also available were elapsed time data. Accumulations were continued for approximately 60 sec.

Electrolyte Preparation—Particle-size determinations of the suspensions were made using a balanced electrolyte[8] saturated with prednisolone acetate. Particulate contamination of the electrolyte was avoided by filtering the saturated solutions twice through a 0.22-μm filter[9].

Sample Preparation and Assay—The handmade suspensions were prepared in a glass mortar. Air-micronized prednisolone acetate[10] was triturated with presaturated water with or without hydroxypropyl methylcellulose[11], depending on the experiment.

The dissolution of prednisolone acetate from a suspension was measured by a spectrophotometric assay. A Beer's law plot was obtained at 246 nm. The linearity throughout the full range of concentrations was evidenced by a correlation coefficient of 0.9998.

An analytical methodology was developed to determine if components in the formulations, other than prednisolone acetate, interfered with the assay. A sample of the commercial suspension was filtered through a 0.22-μm filter, and the filtrate was diluted to the same concentration as that used for the actual dissolution study. These solutions showed little or no absorbance.

RESULTS AND DISCUSSION

Prednisolone acetate suspensions were chosen as the first product to be tested. This drug product was chosen for the following reasons: (*a*) multiple brands were marketed, (*b*) formulations were available from the labels, (*c*) dissolution of the active ingredient could be followed spectrophotometrically, (*d*) only the active ingredient was suspended, and (*e*) the dissolution rate was presumed to be the rate-limiting step for therapeutic availability.

Commercially available products were purchased from a pharmaceutical source other than directly from the manufacturer. Product A (ophthalmic suspension) contained prednisolone acetate, 0.12%; phenylephrine hydrochloride, 0.12%; antipyrine, 0.1%; benzalkonium chloride; polysorbate 80; boric acid; sodium citrate–sodium bisulfite; edetate disodium–sodium chloride; hydroxypropyl methylcellulose; and purified water.

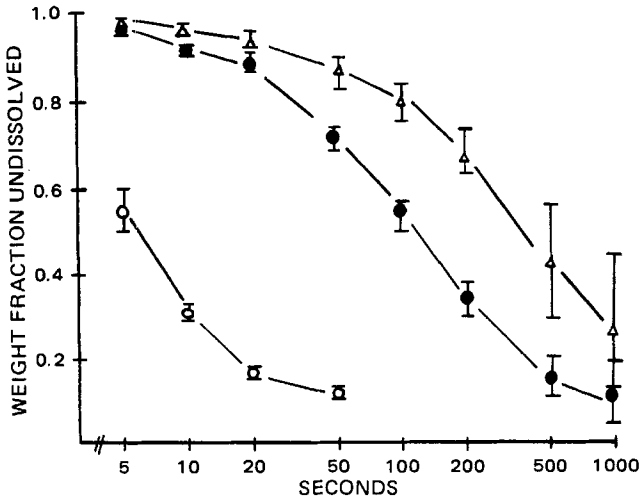

Figure 1—*Dissolution profiles for three commercial prednisolone acetate suspension products. Key: ○, Product A; ●, Product B; and △, Product C. Each point is the average of three experiments, and the bars show the extremes of the experiments.*

Product B (otic–ophthalmic suspension) contained prednisolone acetate, 2.5 mg/ml; neomycin sulfate, 5.0 mg/ml; sodium citrate; polyethylene glycol 4000; povidone; myristyl γ-picolinium chloride; sodium hydroxide and/or hydrochloric acid when necessary to adjust the pH; and water for injection.

Product C (ophthalmic suspension) contained prednisolone acetate, 0.25%; phenylephrine hydrochloride, 0.125%; benzalkonium chloride, 0.01%; hydroxypropyl methylcellulose, 0.2%; sodium bisulfite, 0.2%; edetate disodium; monobasic and dibasic sodium phosphates; sodium chloride; and water.

The results of the dissolution studies for the three commercial prednisolone suspensions are shown in Fig. 1. The dissolution of Product A was the most rapid; 80% dissolved in about 20 sec.

The initial release rate of Product B was much more rapid than that of Product C; the half-life of B occurred at approximately 110 sec, and the half-life of C occurred at approximately 550 sec. Moreover, 65% of Product B dissolved in about 200 sec, while only about 30% of Product C dissolved in the same period.

Since dissolution characteristics are closely related to particle size, a

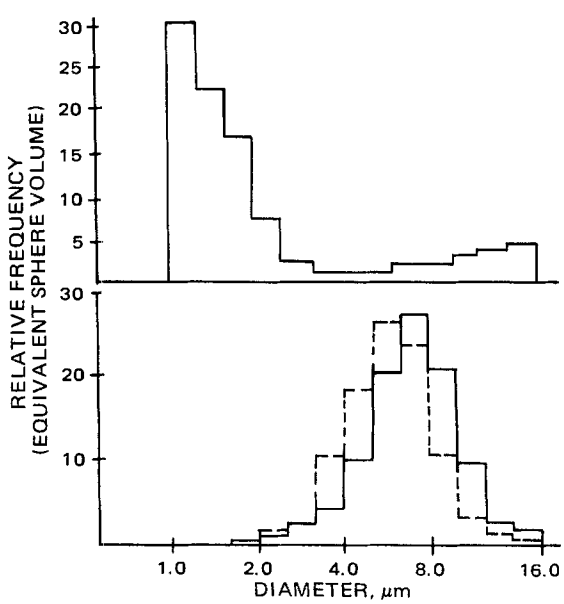

Figure 2—*Particle-size distributions of Products A (—, top), B (- - -, bottom) and C (—, bottom) measured by an automated counter using a 50-μm aperture tube.*

[5] Coulter counter model TA, Coulter Electronics, Hialeah, Fla.
[6] Lot 11001, Coulter Electronics, Hialeah, Fla.
[7] Coulter Diagnostics, Miami Springs, Fla.
[8] Isoton, distributed by Coulter Electronics, Hialeah, Fla.
[9] Millipore Corp., Bedford, Mass.
[10] Prednisolone acetate USP, code 6610, MI19636, Schering Corp., Kenilworth, N.J.
[11] Methocel 60 HG, 4000 cps, lot QP-291021-A, Dow, Midland, Mich.

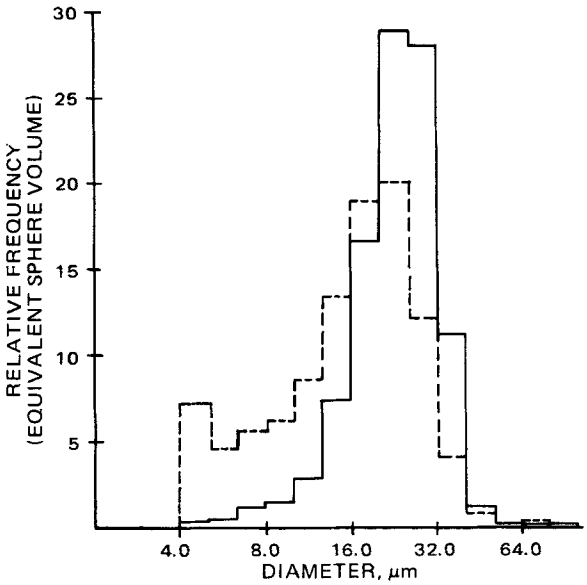

Figure 3—*Particle-size distributions of suspensions of prednisolone acetate (- - -) and prednisolone acetate with hydroxypropyl methylcellulose (——) measured by an automated counter using a 200-μm aperture tube.*

comparison of the particle-size distributions for Products A, B, and C is shown in Fig. 2. Product A was characterized by a population of small particles; about 70% of the particles, by volume, were less than 2 μm in diameter. The cutoff on the left side of Fig. 2 is the limitation of the 50-μm aperture tubes. The very rapid dissolution profile for Product A correlates with the particle-size analysis, because a particle-size reduction is generally regarded as a means of increasing the dissolution rate. According to label information, Product A utilizes a patented micronization process; at one time the package insert specifically mentioned the relationship between particle size and dissolution rate.

The bottom section of Fig. 2 shows the size distribution of Products B and C using the same scale as for Product A. These two products yielded essentially log-normal distributions with an approximate mean diameter of 6–7 μm. The similar particle-size distributions did not predict the significantly different dissolution profiles that were experimentally determined for these products. Since particle size did not provide an explanation, formulation differences between the two suspensions might have been responsible.

A comparison of the formulas for Products B and C shows that C contains hydroxypropyl methylcellulose whereas B does not. To test the effect of this ingredient, aqueous suspensions containing 0.25% prednisolone acetate and 0.2% hydroxypropyl methylcellulose were prepared. Aqueous suspensions containing just 0.25% prednisolone acetate and prepared in exactly the same manner served as a control. A mortar and pestle were used; this method yielded the finest and most reproducible suspensions compared to any other small-scale method of preparation attempted. No dispersing agent was used because it might have altered the dissolution of the suspensions.

Figure 3 shows the size distribution for these two handmade suspensions. The particle-size analysis for each suspension yielded similar distributions. The suspension containing hydroxypropyl methylcellulose yielded a slightly higher percentage of large particles. The mean particle diameter for the hydroxypropyl methylcellulose-containing formula was approximately 26 μm, whereas the mean particle diameter for the control formula was approximately 22 μm.

The dissolution data (Fig. 4) showed a striking difference between the two handmade prednisolone acetate suspensions that would not be predicted on the basis of particle-size analysis. Hydroxypropyl methylcellulose increased the dissolution time of prednisolone acetate compared to the control suspension. Twenty percent of the hydroxypropyl methylcellulose-containing suspension dissolved in about 750 sec, whereas only 100 sec was required for the control suspension. These data were similar

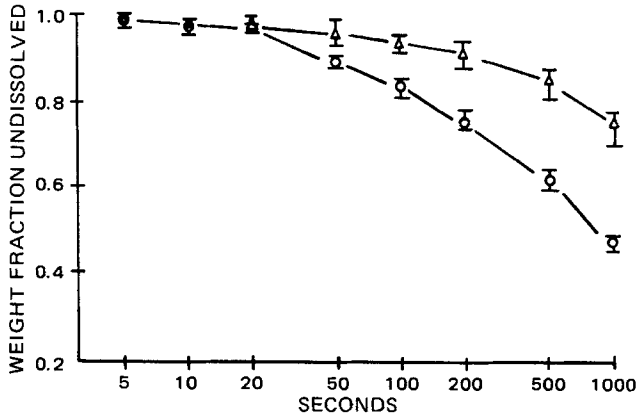

Figure 4—*Dissolution profiles for suspensions of prednisolone acetate (○) and prednisolone acetate containing hydroxypropyl methylcellulose (△) prepared by using a mortar and pestle.*

to those for Products C and B, where C is the hydroxypropyl methylcellulose-containing product. Although Product A also contains hydroxypropyl methylcellulose, the extremely small particle size seemed to dominate to yield a more rapid dissolution rate.

These data suggested that the hydroxypropyl methylcellulose in Product C may be related to its slower dissolution characteristics when compared to Product B, a suspension with similar particle size but without the polymer. It was also evident from a dissolution profile and particle-size analysis for Product A that the particle size can be the dominating factor.

In view of the results, it is believed that dissolution equivalency testing of pharmaceutical suspensions and the factors that cause the dissolution inequivalency, other than particle size, should be the subject of further study.

Although the therapeutic importance of these findings is only speculative, one would argue that the dissolution rate is usually interpreted as being the rate-limiting step for bioavailability. However, the dissolution profiles (Fig. 1) showed that there was inequivalency between the products. Establishment of routine dissolution tests can, therefore, considerably affect the control of lot-to-lot uniformity of the suspension dissolution rate.

REFERENCES

(1) G. Levy and B. A. Hayes, *N. Engl. J. Med.*, **262**, 1053 (1960).

(2) G. Levy and R. H. Gumtow, *J. Pharm. Sci.*, **52**, 1139 (1963).

(3) R. A. Castello, G. Jellinek, J. M. Konieczny, K. C. Kwan, and R. O. Toberman, *ibid.*, **57**, 485 (1968).

(4) R. J. Glazko, A. W. Kinkel, W. C. Alegnani, and E. L. Holmes, *Clin. Pharmacol. Ther.*, **9**, 472 (1968).

(5) P. J. Tannenbaum, E. Rosen, T. Flanagan, and A. P. Crosley, Jr., *ibid.*, **9**, 598 (1968).

(6) J. G. Wagner, *J. Pharm. Sci.*, **50**, 359 (1961).

(7) K. A. Lee, *J. Pharm. Pharmacol., Suppl.*, **15**, 43T (1963).

(8) L. J. Edwards, *Trans. Faraday Soc.*, **47**, 1191 (1951).

(9) E. Nelson, *J. Am. Pharm. Assoc., Sci. Ed.*, **48**, 96 (1959).

(10) T. Bates, H. Rosenberg, and A. Tembo, *J. Pharm. Sci.*, **62**, 2057 (1973).

(11) A. C. Shah, C. B. Peot, and J. F. Ochs, *ibid.*, **62**, 671 (1973).

ACKNOWLEDGMENTS AND ADDRESSES

Received February 20, 1976, from the *School of Pharmacy, West Virginia University, Morgantown, WV 26506.*

Accepted for publication June 14, 1976.

Acknowledgment is made to Schering Corp. and Allergan Pharmaceuticals for their donation of chemicals and to The Upjohn Co. for the loan of the dissolution apparatus.

[x] To whom inquiries should be directed.

Selective GLC Determination of Epinephrine, Isoproterenol, and Phenylephrine in Pharmaceutical Dosage Forms

J. R. WATSON ˣ and R. C. LAWRENCE

Abstract □ A simple, specific GLC analytical procedure for the quantitation of epinephrine, isoproterenol, and phenylephrine in commercial tablets, powders, inhalation solutions, ophthalmic and nasal drops, and injectable preparations is presented. Samples are taken to dryness where required, the dried residue is reacted with an appropriate trimethylsilylating reagent, and the derivatives are eluted from a methyl silicone column using temperature programming. Quantitation of the flame-ionization detector signal is achieved relative to the dibenzyl succinate internal standard by an electronic integrator. The results obtained by applying the method to the analysis of each of the three drugs in several simulated decomposed mixtures were in good agreement with theoretical values, even at impurity levels of up to 80% by weight. When applied to commercial formulations, the procedure was feasible for tablets, powders, and solutions at drug concentrations of 0.2% or greater. The commonly incorporated buffering and antioxidant excipients did not interfere.

Keyphrases □ Epinephrine—GLC analysis, pharmaceutical dosage forms □ Isoproterenol—GLC analysis, pharmaceutical dosage forms □ Phenylephrine—GLC analysis, pharmaceutical dosage forms □ GLC—analyses, epinephrine, isoproterenol, and phenylephrine, pharmaceutical dosage forms □ Adrenergics—epinephrine, isoproterenol, and phenylephrine, GLC analysis, pharmaceutical dosage forms

The sympathomimetic drugs epinephrine (I), isoproterenol (II), and phenylephrine (III) comprise some of the most extensively studied pharmacological agents employed in chemotherapeutics. Their wide acceptance is reflected by the many marketed formulations and the variety of pharmaceutical dosage forms.

BACKGROUND

Because of their amphoteric properties and attendant highly unfavorable extraction characteristics into organic solvents, the analysis of epinephrine, isoproterenol, and phenylephrine in pharmaceutical dosage forms is difficult. Moreover, in an alkaline medium, the water-soluble salts formed by the catecholamines epinephrine and isoproterenol are very unstable and undergo a rapid but complex oxidative decomposition to reddish aminochromes and, subsequently, to brown melanin-type compounds (1, 2). Degradation of phenylephrine occurs less readily, but, above pH 7, cleavage of the side chain of the parent molecule results in the formation of formaldehyde, which immediately reacts with a second molecule of phenylephrine in a Pictet–Spengler-type reaction to produce a mixture of isomeric dihydroxytetrahydroisoquinoline derivatives (2).

In view of the intrinsic susceptibility of these drugs to oxidative degradation, most of their preparations are stabilized with antioxidants such as chlorobutanol, ascorbic acid, or sodium bisulfite. Several reports showed that the stability of many important epinephrine and isoproterenol pharmaceutical products may be seriously impaired by anaerobic interaction of these drugs with sodium bisulfite to give zwitterionic sulfonate derivatives. These derivatives are both optically and physiologically inactive and exhibit UV spectra identical in absorption characteristics to the parent compounds (3–8). Phenylephrine differs in this respect apparently because it lacks the 4-hydroxyl group and the required resonating quinoid structure (4).

The current USP (9) and BP (10) procedures for the assay of epinephrine in commercial formulations are based on the measurement of the specific optical rotation after conversion to the triacetyl derivative. This method is self-limiting in scope and specificity and involves tedious and time-consuming manipulations. Although limit tests for the presence of adrenalone and levarterenol (norepinephrine) are described in the monographs for the drug substance, none is specified for pharmaceutical dosage forms.

In the USP (9), both isoproterenol and phenylephrine hydrochlorides are extracted quantitatively from pharmaceutical solutions or tablet matrixes by ion-pair formation with bis(2-ethylhexyl)phosphoric acid in ether, followed by partition chromatography of the solution through a suitably buffered siliceous earth column. Isoproterenol sulfonic acid, if present, reportedly remains adsorbed on the stationary phase (8). The USP monographs include a limit test for congeneric ketone compounds in the drug substances and in the commercial isoproterenol formulations. The assay procedure may lack precision because many important variables, such as tightness of the column packing and rate of elution, are not described.

Both BP 1973 (10) and NF XIV (11) employ a nonspecific colorimetric method for the analysis of isoproterenol sulfate in tablets and aerosol spray preparations. In the former pharmacopeia, phenylephrine hydrochloride injection is determined by simple absorbance measurement at 273 nm after appropriate dilution with aqueous sulfuric acid. This procedure would be inadequate where the product has undergone oxidative decomposition or is contaminated with other UV-absorbing phenylalcoholamine substances.

As a consequence of the limitations, most notably in specificity, of the compendial assay procedures for epinephrine, isoproterenol, and phenylephrine in dosage forms, alternative methods that encompass various analytical techniques have appeared (12–30).

Evidence was given previously that the highly polar functional groups of levodopa (31), α-methyldopa (32), and their respective congeners can be suitably altered by trimethylsilylation to give less polar and more thermally stable derivatives. These derivatives can be easily eluted as single sharp peaks from a methyl silicone column under relatively moderate temperature conditions. Since the catecholamines and other related sympathomimetic amines readily undergo similar well-documented transformations, it seemed reasonable to apply essentially the same quantitative GLC method to the analysis of epinephrine, isoproterenol, and phenylephrine.

The present investigation was conducted to integrate the available information and to develop a rapid, accurate, and selective GLC procedure for the analysis of epinephrine, isoproterenol, and phenylephrine in both liquid and solid pharmaceutical dosage forms in the presence of excipients and high levels of decomposition products and/or contaminating congeners. The method obviates the need for extraction or prior on-column cleanup manipulations inherent in most published procedures.

EXPERIMENTAL

Materials and Solutions—The following were used: *dl*-epinephrine hydrochloride[1], *dl*-norepinephrine hydrochloride[2], adrenalone hydrochloride[1], *l*-adrenochrome free base[1], epinephrine bitartrate[3], isoproterenol hydrochloride[3], isoproterenol sulfate[4], *N*-isopropylnoradrenalone sulfate[1], phenylephrine hydrochloride[3], norphenylephrine hydrochloride[2], *N,O*-bis(trimethylsilyl)acetamide[5], and *N*-trimethylsilylimidazole[5].

Epinephrine sulfonic acid and isoproterenol sulfonic acid were synthesized by applying the general method of Schroeter and Higuchi (5). The structures of the synthesized compounds were confirmed by elemental analysis and by their IR and NMR spectral characteristics.

The following examined excipients were all analytical grade standards: glycerin, lactic acid, ascorbic acid, citric acid, lactose, chlorobutanol,

[1] ICN Laboratories Inc., Montreal, Canada.
[2] Aldrich Chemical Co., Montreal, Canada
[3] United States Pharmacopeial Convention, Rockville, Md.
[4] Abbott Laboratories, Montreal, Canada.
[5] Pierce Chemical Co., Rockford, Ill.

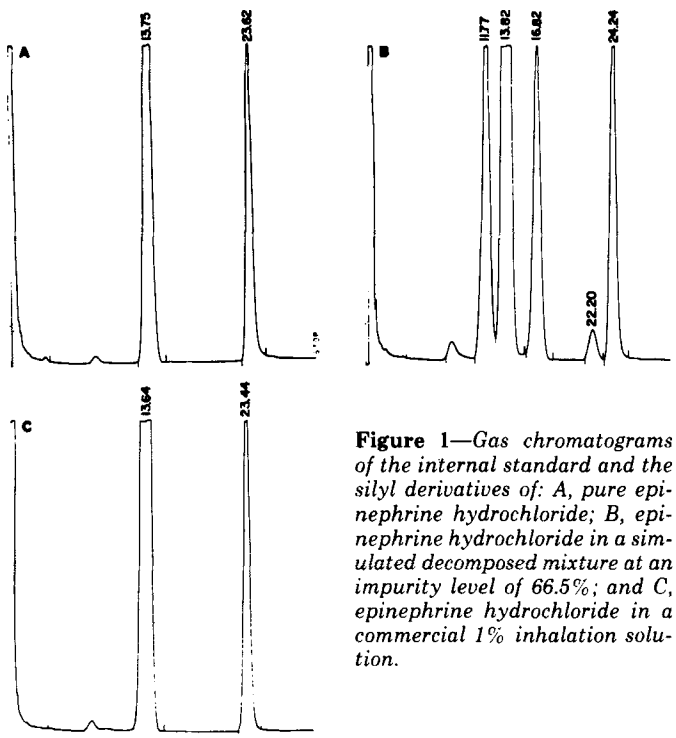

Figure 1—*Gas chromatograms of the internal standard and the silyl derivatives of: A, pure epinephrine hydrochloride; B, epinephrine hydrochloride in a simulated decomposed mixture at an impurity level of 66.5%; and C, epinephrine hydrochloride in a commercial 1% inhalation solution.*

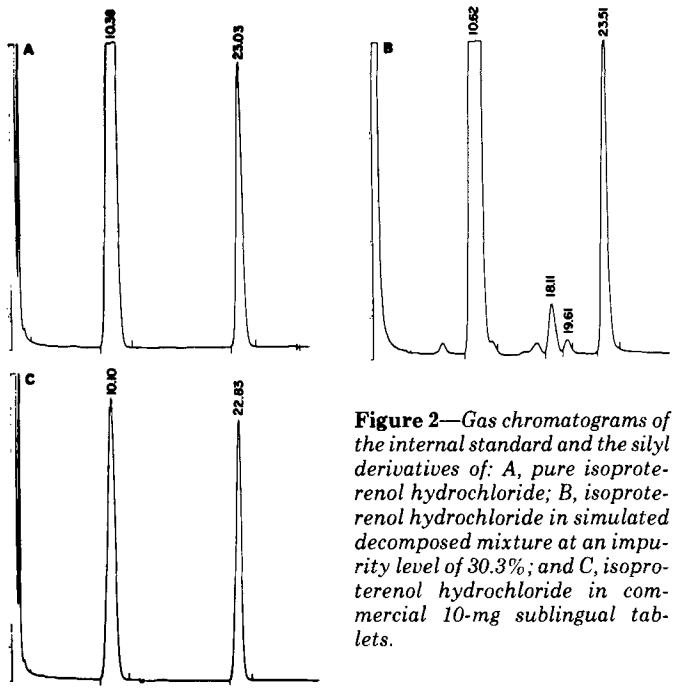

Figure 2—*Gas chromatograms of the internal standard and the silyl derivatives of: A, pure isoproterenol hydrochloride; B, isoproterenol hydrochloride in simulated decomposed mixture at an impurity level of 30.3%; and C, isoproterenol hydrochloride in commercial 10-mg sublingual tablets.*

saccharin sodium, sodium bisulfite, sodium citrate, edetate sodium, phenol, and benzalkonium chloride.

The internal standard solution was dibenzyl succinate[6] in spectrograde dimethylformamide[6], accurately weighed to contain about 2.5 mg/ml.

Sample Preparation—*Response Factor Calibration Mixtures*—For I, II, or III, varying quantities of the pure substance (as the salt), ranging from about 2 to 18 mg, were accurately weighed into five separate 5-ml septum-sealed vials. Then 2.00 ml of the internal standard solution was dispensed into each vial from a 5-ml microburet graduated in 0.01 ml.

Simulated Decomposed Mixtures—For each drug, five separate simulated decomposed mixtures of widely differing impurity levels were prepared by accurately weighing known quantities of the following compounds into 5-ml septum-sealed vials to obtain about 20–30 mg of material in each mixture.

For epinephrine mixtures (Series 1), epinephrine hydrochloride, epinephrine sulfonic acid, norepinephrine hydrochloride, adrenalone hydrochloride, and adrenochrome free base were used. The impurity range varied from about 20 to 80%.

For isoproterenol mixtures (Series 2), isoproterenol hydrochloride, isoproterenol sulfonic acid, norepinephrine hydrochloride, and *N*-isopropylnoradrenalone sulfate were used. The impurity range was from about 16 to 77%.

For phenylephrine mixtures (Series 3), phenylephrine hydrochloride and norphenylephrine hydrochloride were used. The impurity range was from about 7 to 26%.

To simulate the analysis of aqueous commercial formulations, each of the 15 mixtures was dissolved in water (1 ml) and the water was then removed at 60° under a stream of pure dry nitrogen on a heating block module[5]. To ensure complete desiccation, the vial was placed in a drying pistol assembly under vacuum over phosphorus pentoxide at 80° for 30 min under subdued light conditions. The dried residues were then treated with 2.00 ml of the internal standard solution.

Commercial Products—Ten tablets were selected at random, weighed, and finely powdered. An amount of powdered tablet (or powder) equivalent to about 10–15 mg of isoproterenol hydrochloride (or sulfate) was weighed into a 5-ml vial, and 2.00 ml of the internal standard solution was dispensed into the vial.

Aqueous formulations included inhalation solutions, ophthalmic and nasal drops, and injectable preparations. A volume of solution theoretically equivalent to about 5–15 mg of active drug was pipetted into a 5-ml vial, and the water was removed as indicated previously. Then 2.00 ml of the internal standard solution was added to the dried residue in the vial.

[6] J. T. Baker Chemical Co., Phillipsburg, N.J.

Derivatization Procedure—Each isoproterenol sample solution containing the internal standard was treated with *N*-trimethylsilylimidazole (1.0 ml) and allowed to stand for 30 min in the dark at ambient temperature with occasional shaking.

Each epinephrine and phenylephrine sample solution containing the internal standard was treated with *N,O*-bis(trimethylsilyl)acetamide (1.0 ml) and allowed to stand for 30 min in the dark at ambient temperature with occasional shaking.

GLC—Two microliters of silylated solution was injected into a gas chromatograph[7] (flame-ionization detector) fitted with a 5% OV-101[5] on Chromosorb 750[8] (100–120-mesh) U-shaped glass column [1.82 m (6 ft) × 6 mm o.d.] preconditioned at 265° for 18 hr. The support was coated using a fluidizer[9] maintained at 150° for 2 hr with a suitable nitrogen flow to ensure gentle, yet thorough, drying of the packing material.

Temperature conditions were: column, 170° (10 min) and then programmed to 245° at 2°/min; injection port, 225°; and detector, 225°. Gas flows were: nitrogen, 70 ml/min; hydrogen, 40 ml/min; and air, 380 ml/min.

The detector signal was fed to an electronic integrator[10] with an input signal range capacity of 0–1 v.

RESULTS AND DISCUSSION

Although the catecholamine acids are readily silylated in acetonitrile, the catecholamine salts are not, probably because of poor solubility in this solvent. For these drugs, dimethylformamide is a superior medium because it possesses enhanced solubilizing properties and accelerates the trimethylsilylation 10–20 times by comparison with pyridine and other solvents (23).

The criteria adopted for choosing the appropriate silylating reagent for each of the three drugs were based on the following considerations: (*a*) the derivatization of the drug should take place quantitatively in a minimum amount of time and at ambient temperature if possible, (*b*) the silyl derivative of the pure drug should elute as a single sharp peak, and (*c*) this peak should be clearly resolved from that of the internal standard and from the peak or peaks generated by potential contaminating by-products or decomposition products. In the present study, *N,O*-bis(trimethylsilyl)acetamide was employed for the silylation of epinephrine hydrochloride (and bitartrate) and phenylephrine hydrochloride but was less suitable for isoproterenol sulfate, yielding two peaks in the approximate area ratio of 4:1. Consequently, *N*-trimethylsilylimidazole was selected as the preferred silyl donor for the analysis of isoproterenol hydrochloride and isoproterenol sulfate formulations.

[7] Bendix series 2500.
[8] Applied Science Laboratories Inc., State College, Pa.
[9] Hi-Eff, Applied Science Laboratories.
[10] Hewlett-Packard series 3380A reporting integrator.

Table I—GLC Data on Epinephrine, Isoproterenol, Phenylephrine, and Associated Compounds

Compound	Silylation Method[a]	Number of Peaks	Retention Time, min	Relative[b] Response Factor, %
Epinephrine hydrochloride	A	1	13.7	0.528 ± 2.52
Epinephrine bitartrate	A	2	3.1 (tartaric acid)	—
			13.7	0.849 ± 1.52
Norepinephrine hydrochloride	A	1	11.5	—
Adrenalone hydrochloride	A	1	16.3	—
Epinephrine sulfonic acid	A	—	—	—
Adrenochrome	A	1	22.6 (broad and small)	—
Isoproterenol hydrochloride	B	1	10.4	0.608 ± 2.67
Isoproterenol sulfate	B	1	10.4	0.686 ± 1.84
Norepinephrine hydrochloride	B	2	18.1 (91%)	—
			19.5 (9%)	—
N-Isopropylnoradrenalone sulfate	B	3	9.2 (12%)	—
			14.7 (11%)	—
			16.1 (77%)	—
Isoproterenol sulfonic acid	B	—	—	—
Phenylephrine hydrochloride	A	1	6.3	0.604 ± 2.38
Norphenylephrine hydrochloride	A	1	5.2	—
Dibenzyl succinate	—	1	23.4	1.0000

[a] A = *N,O*-bis(trimethylsilyl)acetamide in dimethylformamide, and B = *N*-trimethylsilylimidazole in dimethylformamide. [b] Relative to dibenzyl succinate, expressed as weight/area, and representing the average of five determinations.

Table II—GLC Analysis of Simulated Mixtures[a]

Mixture Series	Components	1		2		3		4		5	
		Added	Rec[b]	Added	Rec[b]	Added	Rec[b]	Added	Rec[b]	Added	Rec[b]
1	Epinephrine hydrochloride	17.99	17.78	14.15	14.32	11.84	11.93	8.47	8.23	5.44	5.28
	Norepinephrine hydrochloride	1.03	—	3.60	—	2.15	—	4.12	—	5.31	—
	Adrenalone hydrochloride	1.33	—	3.09	—	2.87	—	4.37	—	5.36	—
	Epinephrine sulfonic acid	1.04	—	2.82	—	2.02	—	4.18	—	7.65	—
	Adrenochrome	1.01	—	2.86	—	2.02	—	4.17	—	5.51	—
	Percent impurity in mixture	19.7		46.6		43.4		66.5		81.4	
2	Isoproterenol hydrochloride	17.30	17.89	14.38	14.76	11.44	11.54	8.62	8.48	5.22	4.95
	Norepinephrine hydrochloride	1.02	—	1.77	—	3.27	—	4.10	—	5.33	—
	Isoproterenone sulfate	1.10	—	1.73	—	3.10	—	4.17	—	6.24	—
	Isoproterenol sulfonic acid	1.07	—	2.76	—	3.06	—	4.23	—	5.50	—
	Percent impurity in mixture	15.6		30.3		45.2		59.3		76.6	
3	Phenylephrine hydrochloride	19.57	19.28	18.54	18.62	17.45	17.58	16.50	16.49	15.48	15.31
	Norphenylephrine hydrochloride	1.35	—	2.13	—	3.17	—	4.20	—	5.50	—
	Percent impurity in mixture	6.5		10.3		15.4		20.3		26.2	

[a] All values are in milligrams. [b] The recovery values listed represent the average of duplicate injections of the mixture.

Table III—GLC Analysis of Commercial Formulations

Drug	Dosage Form	Manufacturer	Label Claim[a]	Percent Recovery of Label Claim
Epinephrine hydrochloride	Inhalation solution	M	3.5%	97.9
	Inhalation solution	D	2.25%	102.9
	Ophthalmic solution	C	2.0%	106.8
	Inhalation solution	H	2.25%	87.8
	Inhalation solution	H	2.25%	94.0
	Ophthalmic solution	B	2.0%	102.5
	Inhalation solution	K	2.25%	114.5
	Inhalation solution	I	1.0%	114.3
Epinephrine bitartrate	Ophthalmic solution	F	2.0%	95.9
Isoproterenol hydrochloride	Tablets	O	10 mg/tablet	104.8
	Tablets	O	10 mg/tablet	102.5
	Inhalation solution	O	0.5%	107.9
	Inhalation solution	L	0.5%	112.9
Isoproterenol sulfate	Powder mix	A	25%	106.0
Phenylephrine hydrochloride	Nasal drops	O	1.0%	94.0
	Nasal drops	E	0.25%	91.7
	Ophthalmic solution	G	0.2%	90.1
	Ophthalmic solution	O	10%	99.5
	Ophthalmic solution	J	10%	100.6
	Ophthalmic solution	N	10%	106.4
	Injection	O	1%	91.7

[a] The percent values are defined in grams per 100 ml of solution.

Relevant information on the average retention times of epinephrine, isoproterenol, and phenylephrine salts and their respective congeners and/or interaction and degradation products are presented in Table I. In the epinephrine series, the bitartrate salt of the drug afforded two peaks. The first (at 3.1 min) was due to the tartaric acid moiety while the adrenochrome gave only one small broad noninterfering peak at around 22 min. For the two compounds in the isoproterenol series for which more than one peak was generated, the individual peak values, expressed as percentages of total area, have been included in parentheses. *N*-Isopropylnoradrenalone sulfate appears to be particularly prone to multiple peak formation, due perhaps to *in situ* enolization, but none of the peaks would interfere with the quantitation of isoproterenol even in the presence of unusually large amounts of *N*-isopropylnoradrenalone.

No data are given with respect to the aminochrome analog of isoproterenol since it was not commercially available and is not readily prepared in the laboratory. However, it appears safe to assume a flame-ionization detector response for this compound quite similar to that of adrenochrome. The sulfonic acids of epinephrine and isoproterenol were not converted to silyl derivatives of sufficient volatility or thermal stability to be detectable under the GLC conditions. However, attempts to investigate further the nonelutive properties of these two compounds were not made.

In Table I, the listed response factors of the pure drugs were computed automatically by the digital processor and are expressed in weight/area relative to dibenzyl succinate. Their respective coefficients of variation were well within acceptable limits of precision. The chromatograms of the silyl derivatives of pure epinephrine hydrochloride, isoproterenol hydrochloride, and phenylephrine hydrochloride are reproduced in Figs. 1A, 2A, and 3A, respectively.

The results obtained by applying the GLC method to the analysis of several simulated decomposed mixtures of each drug are given in Table II and support the conclusion that the procedure is feasible and selective even at unrealistically high levels of contamination. The term "decomposed" is employed here in the broader sense to embrace other chemical entities that would not arise from the normal degradation but rather are artifacts incompletely removed during drug synthesis. The mixtures were dissolved in water prior to sample treatment and analysis to duplicate as closely as possible the conditions existing in the assay of commercial aqueous formulations and to demonstrate that the correct amount of chemically intact parent drug could be recovered.

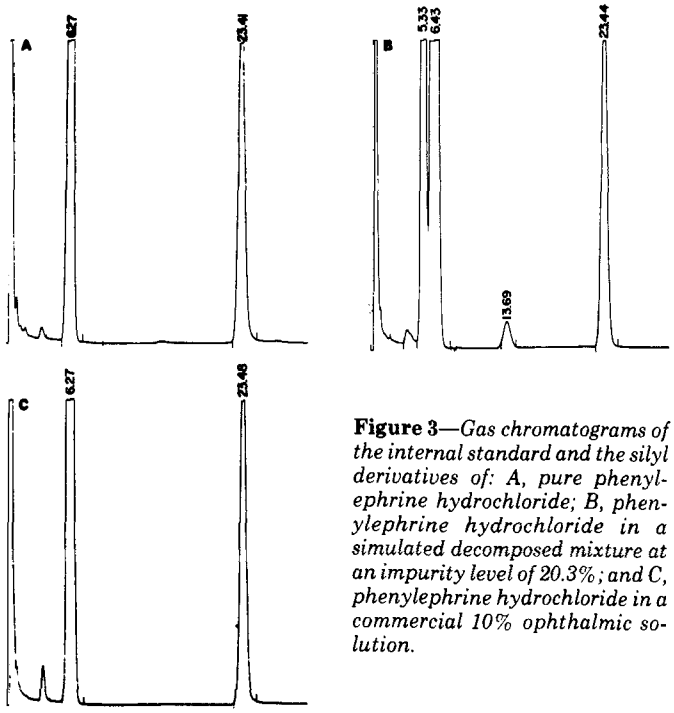

Figure 3—*Gas chromatograms of the internal standard and the silyl derivatives of: A, pure phenylephrine hydrochloride; B, phenylephrine hydrochloride in a simulated decomposed mixture at an impurity level of 20.3%; and C, phenylephrine hydrochloride in a commercial 10% ophthalmic solution.*

The percent recovery values varied from 97.2 to 101.2% for epinephrine, from 94.9 to 103.4% for isoproterenol, and from 98.5 to 100.7% for phenylephrine. The value of 94.9% for isoproterenol Mixture 5 is admittedly somewhat of an outlier, but the high level of impurity in this case (76.6%) is really not one that would normally be encountered in the day-to-day analysis of commercial formulations. Sample chromatograms of each of the three drugs in simulated decomposed mixtures are presented in Figs. 1B, 2B, and 3B.

To document further the validity of the present GLC method for the analysis of commercial formulations, 12 commonly incorporated buffering and antioxidant excipient compounds were chromatographed after dissolution or suspension in the silylation medium at ambient temperature for 30 min. No potentially interfering signals were observed for any substance examined. Most adjuvants listed under *Experimental* either gave peaks that were eluted close to or under the solvent or produced no peak that could be detected under the temperature conditions used. Single sharp peaks, well resolved from those of the particular drug with which they were formulated, were observed for citric acid (7.6 min) and ascorbic acid (12.6 min). Benzalkonium chloride gave four small noninterfering peaks at about 17, 26, 36, and 44 min.

The results of the analysis of commercial tablets, powder mixes, nasal drops, inhalation and ophthalmic solutions, and an injectable preparation are delineated in Table III. Chromatograms for epinephrine, isoproterenol, and phenylephrine in commercial formulations are given in Figs. 1C, 2C, and 3C.

REFERENCES

(1) T. D. Sokoloski and T. Higuchi, *J. Pharm. Sci.*, **51**, 172 (1962).

(2) B. J. Millard, D. J. Priaulx, and E. Shotton, *J. Pharm. Pharmacol., Suppl.*, **25**, 24P (1973).

(3) L. C. Schroeter, T. Higuchi, and E. E. Schuler, *J. Am. Pharm. Assoc., Sci. Ed.*, **47**, 723 (1958).

(4) T. Higuchi and L. C. Schroeter, *ibid.*, **48**, 535 (1959).

(5) L. C. Schroeter and T. Higuchi, *ibid.*, **49**, 331 (1960).

(6) T. Higuchi and L. C. Schroeter, *J. Am. Chem. Soc.*, **82**, 1904 (1960).
(7) B. R. Hajratwala, *J. Pharm. Sci.*, **64**, 45 (1975).
(8) L. H. Welsh and O. R. Sammul, *J. Assoc. Offic. Anal. Chem.*, **51**, 176 (1968).
(9) "The United States Pharmacopeia," 19th rev., Mack Publishing Co., Easton, Pa., 1975 pp. 169–172, 274–276, 377–379.
(10) "The British Pharmacopoeia 1973," Her Majesty's Stationery Office, London, England, 1973, pp. 14, 15, 257, 365, 366.
(11) "The National Formulary," 14th ed., Mack Publishing Co., Easton, Pa., 1975, pp. 253, 368–371.
(12) V. K. Prasad, R. A. Ricci, B. C. Nunning, and A. P. Granatek, *J. Pharm. Sci.*, **62**, 1130 (1973).
(13) *Ibid.*, **62**, 1135 (1973).
(14) T. James, *J. Pharm. Sci.*, **62**, 669 (1973).
(15) K. K. Kaistha, *ibid.*, **59**, 241 (1970).
(16) J. Levine and T. D. Doyle, *ibid.*, **56**, 619 (1967).
(17) E. Shotton and D. J. Priaulx, *J. Pharm. Pharmacol.*, **26**, 197 (1974).
(18) J. Doulakas, *Pharm. Acta Helv.*, **50**, 66 (1975).
(19) R. B. Salama and S. K. W. Khalil, *J. Pharm. Sci.*, **63**, 1301 (1974).
(20) N. H. Choulis, *ibid.*, **56**, 196 (1967).
(21) D. Cantin, J. Alary, and A. Coeur, *Analusis*, **2**, 654 (1974).
(22) *Ibid.*, **3**, 5 (1975).
(23) S. Kawai and Z. Tamura, *J. Chromatogr.*, **25**, 471 (1966).
(24) G. M. Anthony, C. J. W. Brooks, I. Maclean, and I. Sangster, *J. Chromatogr. Sci.*, **7**, 623 (1969).
(25) P. F. G. Boon and A. W. Mace, *J. Pharm. Pharmacol., Suppl.*, **21**, 49S (1969).
(26) L. J. Dombrowski, P. M. Comi, and E. L. Pratt, *J. Pharm. Sci.*, **62**, 1761 (1973).
(27) H. G. Lovelady and L. L. Foster, *J. Chromatogr.*, **108**, 43 (1975).
(28) E. Gelpi, E. Peralta, and J. Segura, *J. Chromatogr. Sci.*, **12**, 701 (1974).
(29) K. P. Wong, C. R. J. Ruthven, and M. Sandler, *Clin. Chim. Acta*, **47**, 215 (1973).
(30) L. Bertilsson, *J. Chromatogr.*, **87**, 147 (1973).
(31) J. R. Watson, *J. Pharm. Sci.*, **63**, 96 (1974).
(32) J. R. Watson and R. C. Lawrence, *J. Chromatogr.*, **103**, 63 (1975).

ACKNOWLEDGMENTS AND ADDRESSES

Received April 5, 1976, from the *Drug Research Laboratories, Health Protection Branch, Health and Welfare Canada, Ottawa, Canada.*
Accepted for publication June 11, 1976.
[x] To whom inquiries should be directed.

High-Performance Liquid Chromatographic Analysis of Isoniazid and Its Dosage Forms

LEONARD C. BAILEY [x] and HAMED ABDOU

Abstract □ A high-performance liquid chromatographic analysis is described for isoniazid as a drug entity and in its tablet and injectable dosage forms. After incorporation of the drug or dosage form in a solvent mixture and addition of an internal standard, tribenzylamine, an aliquot is chromatographed using a pellicular silica gel medium followed by UV spectrophotometric detection at 254 nm. The response of the chromatographic system was linear over a concentration range corresponding to 20–200% of the labeled amount of isoniazid. Comparison of the results with those obtained by the official USP XIX method indicates similar accuracy and precision. The advantages of the proposed method are its simplicity and rapidity, its potential for automation, and its specificity. The specificity was demonstrated in the presence of potential degradation products of isoniazid, other drugs used with isoniazid in combination dosage forms, and an adduct formed by the reaction of isoniazid with lactose in the tablet.

Keyphrases □ Isoniazid—high-performance liquid chromatographic analysis, tablets and injectables □ High-performance liquid chromatography—analysis, isoniazid, tablets and injectables □ Tuberculostatic antibacterials—isoniazid, high-performance liquid chromatographic analysis, tablets and injectables

Because isoniazid (isonicotinic acid hydrazide) is the drug of choice for the treatment of tuberculosis, many attempts have been made to develop methods for its quantitation in dosage formulations. The procedures rely primarily on the redox reactivity of the hydrazide group or upon color formation with an appropriate chromogen.

One analysis is based on the addition of excess standard iodine followed by back-titration with standard thiosulfate (1). This procedure was official in four USP revisions but was supplanted in the current USP XIX (2) by a nitrous acid titration similar to that used for the determination of sulfa drugs. The method official in the BP (3) is similar to the earlier USP method, except that excess bromine is used instead of iodine. These oxidimetric methods and a nonaqueous titration procedure were reviewed and compared previously (4).

Another method (5) involves the determination of isoniazid and other hydrazine-derived drugs by potentiometric titration in an acid solution, using chloramine-T as the titrant. However, its applicability to dosage forms was not explored. A colorimetric method was proposed based on the reaction of isoniazid with 7-chloro-4-nitrobenzo-2-oxa-1,3-diazole (6). A colorimetric procedure uses 9-chloracridine as the chromogenic reagent (7).

The purpose of this study was to investigate the utility of high-performance liquid chromatography (HPLC) in the determination of isoniazid in its dosage forms. The speed and accuracy of this technique and the availability of relatively inexpensive modular instrumentation should make such analysis particularly applicable in quality assurance situations.

The proposed method is simple, involving only the dissolution of the sample, addition of the internal standard, and introduction of an aliquot of the resulting mixture onto a liquid chromatograph with an adsorption column and a

(6) T. Higuchi and L. C. Schroeter, *J. Am. Chem. Soc.*, **82**, 1904 (1960).
(7) B. R. Hajratwala, *J. Pharm. Sci.*, **64**, 45 (1975).
(8) L. H. Welsh and O. R. Sammul, *J. Assoc. Offic. Anal. Chem.*, **51**, 176 (1968).
(9) "The United States Pharmacopeia," 19th rev., Mack Publishing Co., Easton, Pa., 1975 pp. 169–172, 274–276, 377–379.
(10) "The British Pharmacopoeia 1973," Her Majesty's Stationery Office, London, England, 1973, pp. 14, 15, 257, 365, 366.
(11) "The National Formulary," 14th ed., Mack Publishing Co., Easton, Pa., 1975, pp. 253, 368–371.
(12) V. K. Prasad, R. A. Ricci, B. C. Nunning, and A. P. Granatek, *J. Pharm. Sci.*, **62**, 1130 (1973).
(13) *Ibid.*, **62**, 1135 (1973).
(14) T. James, *J. Pharm. Sci.*, **62**, 669 (1973).
(15) K. K. Kaistha, *ibid.*, **59**, 241 (1970).
(16) J. Levine and T. D. Doyle, *ibid.*, **56**, 619 (1967).
(17) E. Shotton and D. J. Priaulx, *J. Pharm. Pharmacol.*, **26**, 197 (1974).
(18) J. Doulakas, *Pharm. Acta Helv.*, **50**, 66 (1975).
(19) R. B. Salama and S. K. W. Khalil, *J. Pharm. Sci.*, **63**, 1301 (1974).
(20) N. H. Choulis, *ibid.*, **56**, 196 (1967).
(21) D. Cantin, J. Alary, and A. Coeur, *Analusis*, **2**, 654 (1974).
(22) *Ibid.*, **3**, 5 (1975).
(23) S. Kawai and Z. Tamura, *J. Chromatogr.*, **25**, 471 (1966).
(24) G. M. Anthony, C. J. W. Brooks, I. Maclean, and I. Sangster, *J. Chromatogr. Sci.*, **7**, 623 (1969).
(25) P. F. G. Boon and A. W. Mace, *J. Pharm. Pharmacol., Suppl.*, **21**, 49S (1969).
(26) L. J. Dombrowski, P. M. Comi, and E. L. Pratt, *J. Pharm. Sci.*, **62**, 1761 (1973).
(27) H. G. Lovelady and L. L. Foster, *J. Chromatogr.*, **108**, 43 (1975).
(28) E. Gelpi, E. Peralta, and J. Segura, *J. Chromatogr. Sci.*, **12**, 701 (1974).
(29) K. P. Wong, C. R. J. Ruthven, and M. Sandler, *Clin. Chim. Acta*, **47**, 215 (1973).
(30) L. Bertilsson, *J. Chromatogr.*, **87**, 147 (1973).
(31) J. R. Watson, *J. Pharm. Sci.*, **63**, 96 (1974).
(32) J. R. Watson and R. C. Lawrence, *J. Chromatogr.*, **103**, 63 (1975).

ACKNOWLEDGMENTS AND ADDRESSES

Received April 5, 1976, from the *Drug Research Laboratories, Health Protection Branch, Health and Welfare Canada, Ottawa, Canada.*
Accepted for publication June 11, 1976.
[x] To whom inquiries should be directed.

High-Performance Liquid Chromatographic Analysis of Isoniazid and Its Dosage Forms

LEONARD C. BAILEY [x] and HAMED ABDOU

Abstract □ A high-performance liquid chromatographic analysis is described for isoniazid as a drug entity and in its tablet and injectable dosage forms. After incorporation of the drug or dosage form in a solvent mixture and addition of an internal standard, tribenzylamine, an aliquot is chromatographed using a pellicular silica gel medium followed by UV spectrophotometric detection at 254 nm. The response of the chromatographic system was linear over a concentration range corresponding to 20–200% of the labeled amount of isoniazid. Comparison of the results with those obtained by the official USP XIX method indicates similar accuracy and precision. The advantages of the proposed method are its simplicity and rapidity, its potential for automation, and its specificity. The specificity was demonstrated in the presence of potential degradation products of isoniazid, other drugs used with isoniazid in combination dosage forms, and an adduct formed by the reaction of isoniazid with lactose in the tablet.

Keyphrases □ Isoniazid—high-performance liquid chromatographic analysis, tablets and injectables □ High-performance liquid chromatography—analysis, isoniazid, tablets and injectables □ Tuberculostatic antibacterials—isoniazid, high-performance liquid chromatographic analysis, tablets and injectables

Because isoniazid (isonicotinic acid hydrazide) is the drug of choice for the treatment of tuberculosis, many attempts have been made to develop methods for its quantitation in dosage formulations. The procedures rely primarily on the redox reactivity of the hydrazide group or upon color formation with an appropriate chromogen.

One analysis is based on the addition of excess standard iodine followed by back-titration with standard thiosulfate (1). This procedure was official in four USP revisions but was supplanted in the current USP XIX (2) by a nitrous acid titration similar to that used for the determination of sulfa drugs. The method official in the BP (3) is similar to the earlier USP method, except that excess bromine is used instead of iodine. These oxidimetric methods and a nonaqueous titration procedure were reviewed and compared previously (4).

Another method (5) involves the determination of isoniazid and other hydrazine-derived drugs by potentiometric titration in an acid solution, using chloramine-T as the titrant. However, its applicability to dosage forms was not explored. A colorimetric method was proposed based on the reaction of isoniazid with 7-chloro-4-nitrobenzo-2-oxa-1,3-diazole (6). A colorimetric procedure uses 9-chloracridine as the chromogenic reagent (7).

The purpose of this study was to investigate the utility of high-performance liquid chromatography (HPLC) in the determination of isoniazid in its dosage forms. The speed and accuracy of this technique and the availability of relatively inexpensive modular instrumentation should make such analysis particularly applicable in quality assurance situations.

The proposed method is simple, involving only the dissolution of the sample, addition of the internal standard, and introduction of an aliquot of the resulting mixture onto a liquid chromatograph with an adsorption column and a

UV detector operated at 254 nm. The accuracy and precision of the method are comparable to those of the current USP XIX analysis, but the time required for a determination is significantly less. In addition, the HPLC method is more specific in that it is insensitive to isonicotinic acid, a possible hydrolysis product of isoniazid, and 1-isonicotinoyl-2-lactosylhydrazine, the hydrazone formed by the reaction of isoniazid with lactose, which may be present as a diluent in the formulation.

EXPERIMENTAL

Reagents and Chemicals—High purity isoniazid[1] was recrystallized twice from 95% ethanol, dried at 105° for 4 hr, and stored in a vacuum desiccator, mp 171°. Isonicotinic acid[1] was recrystallized twice from distilled water. Tribenzylamine[2] was recrystallized twice from 95% ethanol and dried *in vacuo*, mp 93–93.5°.

The lactose hydrazone of isoniazid, 1-isonicotinoyl-2-lactosylhydrazine, was prepared as follows. Isoniazid, 6.85 g (0.05 mole), was mixed with 300 ml of 95% ethanol in a 500-ml round-bottom flask and warmed on a steam bath until solution was complete. In a 100-ml beaker, 17.1 g (0.05 mole) of lactose was mixed with 40 ml of distilled water and warmed on a hot plate until the lactose was dissolved. The aqueous lactose solution was added slowly, with continuous stirring, to the isoniazid solution and refluxed for 8 hr. The mixture was concentrated under vacuum until a pasty mass was obtained.

After mixing the crude product with 20 ml of methanol and refrigerating overnight, the resulting slurry was filtered and the residue was dried in a desiccator under vacuum. Recrystallization from the minimum amount of 95% ethanol–water (3:1) yielded white needles, mp 199° (uncorr.) [lit. (8) mp 202°]; λ_{max} (ethanol, 95%): 261.5 nm.

Anal.—Calc. for $C_{18}H_{27}N_3O_{12}$: C, 46.85; H, 5.90; N, 9.10; O, 38.14. Found: C, 46.24; H, 6.04; N, 9.14; O, 35.58.

TLC of the hydrazone, using silica gel G plates[3] and a mobile phase of methanol–chloroform (60:65) (9), showed a single spot with an R_f of 0.17 (R_f of isoniazid under these conditions is 0.60). Analysis of the product using the USP XIX procedure specified for isoniazid (2) indicated an apparent purity of 97%.

Solvents—Reagent grade methanol[4] was redistilled from an all-glass apparatus. Reagent grade methylene chloride[4] and spectranalyzed chloroform[4] and 2-propanol[4] were used as received.

Apparatus—HPLC was performed with an apparatus consisting of a pump[5] with a pulse dampener[6] and a UV monitor[6] operated at 254 nm. Samples were introduced through a septum injector[6] using a 10-μl syringe[7]. The output of the detector was displayed on a recorder[8] having a full-scale range of 10 mv. The output signal was integrated, and results were calculated using an electronic integrator[9]. A 1-m × 2.1-mm i.d. stainless steel column was packed with a pellicular silica gel adsorbent[10] according to the manufacturer's instructions. The mobile phase was pumped at a pressure of 300 psig, which resulted in a flow rate of 1.20 ml/min.

USP analyses for isoniazid were performed using standard 10.00- and 50.00-ml burets[11] and an expanded scale pH meter[12].

Mobile Phase—The mobile phase was a mixture of either methylene chloride or chloroform with methanol, 2-propanol, and water in the following proportions: 85:5:10:0.5.

Standard Solutions—*Solvent Mixture* —The solvent mixture used was methylene chloride (or chloroform, if the mobile phase was chloroform based)–methanol–2-propanol (85:5:10).

Isoniazid Standard Solution—Accurately weigh 0.2000 g of isoniazid, transfer to a 100-ml volumetric flask, and dilute to the mark with the solvent mixture.

Internal Standard Solution—Accurately weigh 3.0000 g of tribenzylamine, transfer to a 100-ml volumetric flask, and dilute to the mark with the solvent mixture.

Standard Preparation—Into a 50-ml volumetric flask, pipet 25.0 ml of isoniazid standard solution, 5.0 ml of internal standard solution, and 0.5 ml of water. Mix well to ensure incorporation of the water into the solution. Dilute to volume with the solvent mixture and shake until a homogeneous mixture is obtained. Introduce 5 μl into the liquid chromatograph. Measure the areas under the two peaks and calculate the ratio, R_s, by dividing the area of the isoniazid peak by the area of the internal standard peak.

Isoniazid—*Assay Preparation*—Dissolve 100 mg of isoniazid, accurately weighed, in 50 ml of the solvent mixture in a 100-ml volumetric flask. Then add 1.0 ml of water and 10.0 ml of internal standard solution and shake until the water is incorporated. Dilute to the mark with the solvent mixture and mix until homogeneous.

Assay Procedure—Introduce a 5-μl portion into the liquid chromatograph. Measure the areas under the two peaks and calculate the ratio, R_u, by dividing the area of the isoniazid peak by the area of the internal standard peak. Calculate the quantity, in milligrams, of isoniazid present in the sample taken by the formula:

$$\text{isoniazid} = W_s(R_u/R_s) \qquad \text{(Eq. 1)}$$

where R_u and R_s are as defined previously, and W_s is the weight, in milligrams, of isoniazid in 100.0 ml of the standard preparation.

Isoniazid Tablets—*Assay Preparation*—Weigh and finely powder not less than 20 isoniazid tablets. Weigh accurately a portion of the powder, equivalent to 100 mg of isoniazid, and transfer it to a 100-ml volumetric flask using about 50 ml of the solvent mixture. Add 1.0 ml of water and 10.0 ml of internal standard solution. Mix well for 1 min to ensure extraction of the isoniazid from the powder. Dilute to volume with the solvent mixture and mix until homogeneous.

Assay Procedure—Proceed as directed in the assay procedure for isoniazid.

Isoniazid Injection—*Assay Preparation*—Transfer 1.0 ml of isoniazid injection to a 100-ml volumetric flask and add about 75 ml of the solvent mixture. Mix well to ensure incorporation of the aqueous injection vehicle with the solvent mixture and add 10.0 ml of internal standard. Dilute to volume with the solvent mixture and mix until homogeneous.

Assay Procedure—Proceed as directed in the assay procedure for isoniazid.

RESULTS AND DISCUSSION

Mobile Phase—The mobile phase may contain either methylene chloride or chloroform as its main constituent. The initial separations were accomplished using methylene chloride, but lot-to-lot variations with this solvent were more pronounced than with chloroform.

Some batches of methylene chloride contained impurities which deactivated the surface of the column packing after 2–3 liters of mobile

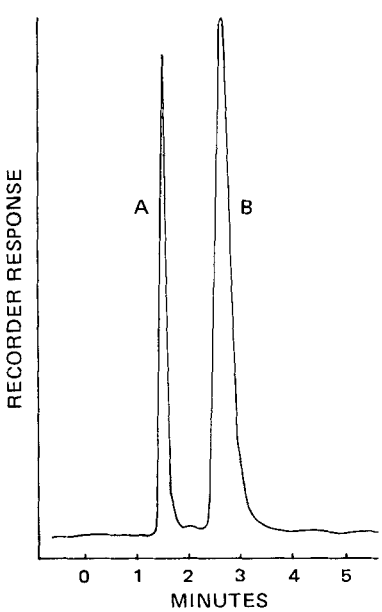

Figure 1—*Typical chromatogram obtained from the analysis of powdered tablet material. Key: A, internal standard (3.0 μg/liter); and B, isoniazid (1.0 μg/liter).*

[1] Eastman Kodak Co., Rochester, N.Y.
[2] Matheson, Coleman and Bell, Norwood, Ohio.
[3] Eastman No. 6061.
[4] Fisher Scientific Co., Fairlawn, N.J.
[5] LDC Minipump, Milton Roy Co., Riviera Beach, Fla.
[6] Laboratory Data Control, Riviera Beach, Fla.
[7] Hamilton model No. 701.
[8] Omniscribe model 5211-151, Houston Instruments, Austin, Tex.
[9] Model 3380A, Hewlett-Packard, Avondale, Pa.
[10] HC Pellosil, Whatman, Inc., Clifton, N.J.
[11] Scientific Glass Apparatus, Bloomfield, N.J.
[12] Model 7413, Leeds and Northrop, North Wales, Pa.

Table I—Determination of Isoniazid by the HPLC and USP XIX Methods

Drug Entity	Manufacturer	Label Claim	Method of Analysis			
			HPLC	n^a	USP XIX	n
Powder	C	—	99.24 ± 0.41[b] 98.75 ± 0.42	4 12	98.14 ± 0.18	6
Tablet	B	100 mg/tablet	98.45 ± 0.44 98.36 ± 0.69	5 20	97.68 ± 0.28	8
Tablet	A (Lot 1)	100 mg/tablet	85.96 ± 0.63[c]	8	95.53 ± 0.24	6
Tablet	A (Lot 2)	100 mg/tablet	93.23 ± 0.96[c]	3	98.41 ± 0.23	6
Injection	A	100 mg/ml	104.31 ± 0.41 104.23 ± 0.43	6 19	103.13 ± 0.48	5

[a] Number of samples analyzed. [b] Percent of label claim ± *SD*. [c] Tablets were shown to contain isoniazid as the lactose hydrazone (see text).

phase passed over it. Moreover, the compound(s) responsible for this effect could not be removed by distillation or by passing the solvent through a column packed with 6–16-mesh silica gel. For batches of solvent containing these deactivating impurities, a suitable level of purity may be attained by passing the solvent twice through 2.8 × 25-cm columns of small particle (76–230 mesh) silica gel 60.

Because the solvent properties of chloroform and methylene chloride are very similar, there were only slight differences in the separations achieved when either of them was in the mobile phase. As a measure of the efficiency of the separation of tribenzylamine and isoniazid, the resolution factor, R, was calculated as described in USP XIX (10). For the methylene chloride-based mobile phase, R was 4.12; for the chloroform-based system, it was 3.14. Either of these results is indicative of a separation greater than 99%.

The overlap between the isoniazid and internal standard peaks was, therefore, slightly greater when chloroform was used, but no effect on the quantitative results was noted whether peak heights or areas were used. No significant difference (t-test) was found between samples of the same dosage forms when analyzed using chloroform or methylene chloride.

Chromatographic Response—The typical response of the internal standard and isoniazid to the chromatographic system is shown in Fig. 1. This chromatogram was obtained from the analysis of a quantity of powdered tablet material containing 100 mg of isoniazid. A methylene chloride-based mobile phase was used.

To determine the linearity of the chromatographic response, a calibration curve was run in which the concentration of the internal standard was maintained constant while that of isoniazid was varied. The curve was linear (r = 0.999) over a 10-fold range, corresponding to quantities of isoniazid that would be obtained in the analysis of dosage forms containing 20–200% of the label claim. The intercept was essentially zero.

The integration method used to measure the response of each component was not critical, since both peaks were nearly symmetrical and almost completely resolved. Peak heights, peak areas obtained by manual methods (height times width at half-height), and electronic integration were used, and similar results were obtained.

Analysis of Dosage Forms—Table I gives the results obtained from the analysis of a number of commercially available dosage forms containing isoniazid. To verify the reliability of the method, portions of the same material taken for analysis by HPLC were also assayed using the method official in USP XIX. The results obtained by the HPLC method were comparable in accuracy and precision to those given by the USP method, with the exception of the two different lots of tablets from Manufacturer A (Table I). These lots gave results consistently 5–10% lower in isoniazid content than indicated by the USP method. Since it was assumed initially that the cause of the lower results was incomplete extraction of the isoniazid from the powdered tablet mass, various techniques, including heating, longer extraction times, and the use of an ultrasonic generator, were employed to improve recoveries. However, none of these procedures resulted in an increase in the quantity of isoniazid found.

To determine the cause of the anomalously low results, a study was initiated based on the observations (9) that isoniazid was capable of interacting with dosage form ingredients, particularly reducing sugars, to form hydrazones. These derivatizations were reported to occur even in the solid state. A portion of powdered material from the tablets that assayed at 85.90% isoniazid by HPLC was extracted by shaking with methanol. The same was done to the powdered mass of a tablet that had been shown to contain 99.24% isoniazid by HPLC.

Aliquots of the filtered extracts were applied to a TLC sheet along with methanol solutions of isoniazid and its lactose hydrazone. After development in methanol–chloroform (60:65), the lane containing the extract of the anomalous tablet showed two spots under UV light. The R_f of one spot corresponded to that of isoniazid; the other was the same as that of its lactose hydrazone. The lane containing the extract of the normal tablet had only one spot, that of pure isoniazid.

It was apparent, therefore, that the low results were due to the derivatization of a portion of the isoniazid by the lactose used as a diluent in the tablet formulation. Blake *et al.* (4) reported, and this work has verified, that the USP analysis does not distinguish between free isoniazid and the hydrazone it forms with a reducing sugar. The fact that HPLC is stability indicating in this regard is considered advantageous in view of the observations of Rao *et al.* (11), which indicated that the absorption of isoniazid from syrups containing reducing sugars was seriously impaired. Attempts to elute the lactose hydrazone of isoniazid using the conditions specified for the analysis of isoniazid were unsuccessful, with no peaks being observed even after 1 hr. Since the hydrazones formed by isoniazid with other reducing sugars would have similar structures and polarities, it is assumed that they too will not interfere with the HPLC method.

Potential Interfering Substances—Retention times were determined, using a chloroform-based mobile phase, for a number of compounds that might potentially interfere with the HPLC analysis. The results (Table II) indicate that the method retains its specificity despite the presence of degradation products of isoniazid or of other drugs frequently administered in combination dosage forms with isoniazid.

Two possible degradation products, isonicotinic acid and *N,N'*-bis-(isonicotinoyl)hydrazine, were completely separated. Aminosalicylic acid, an antitubercular drug available in combination with isoniazid, was also completely resolved by HPLC. Pyridoxine hydrochloride, which is administered concurrently with isoniazid to counteract the latter's antagonistic effect on vitamin B_6 activity, also did not interfere.

Table II—Retention Times of Isoniazid, Tribenzylamine, and Potential Interferences

Compound	Retention Time, min
Isoniazid	2.3
Tribenzylamine (internal standard)	1.5
Isonicotinic acid	44.0
Niacin	57.0
N,N'-Bis(isonicotinoyl)hydrazine	8.6
1-Isonicotinoyl-2-lactosylhydrazine	>60.0
Aminosalicylic acid	34.5
Pyridoxine hydrochloride	4.1

REFERENCES

(1) T. Canback, *J. Pharm. Pharmacol.*, **4**, 407 (1952).

(2) "The United States Pharmacopeia," 19th rev., Mack Publishing Co., Easton, Pa., 1975, pp. 272–274, 626, 772.

(3) "The British Pharmacopoeia," Pharmaceutical Press, London, England, 1968, p. 535.

(4) M. I. Blake, D. Bode, and H. J. Rhodes, *J. Pharm. Sci.*, **63**, 1303 (1974).

(5) S. Pinzauti, V. Dal Piaz, and E. La Porta, *ibid.*, **63**, 1446 (1974).

(6) H. S. I. Tan, *ibid.*, **62**, 993 (1973).
(7) J. T. Stewart and D. A. Settle, *ibid.*, **64**, 1403 (1975).
(8) R. Yamamoto and H. Tanaka, *Yakuzaigaku*, **17**, 219 (1957).
(9) W. H. Wu, T. F. Chin, and J. L. Lach, *J. Pharm. Sci.*, **59**, 1234 (1970).
(10) "The United States Pharmacopeia," 19th rev., Mack Publishing Co., Easton, Pa., 1975, p. 640.
(11) K. V. N. Rao, S. Kallasam, V. K. Menon, and L. Radhakrishna, *Indian J. Med. Res.*, **59**, 1343 (1971).

ACKNOWLEDGMENTS AND ADDRESSES

Received March 29, 1976, from the *Department of Pharmaceutical Chemistry, College of Pharmacy, Rutgers—the State University, New Brunswick, NJ 08903.*

Accepted for publication June 9, 1976.

The authors express their appreciation to Carole A. Bailey for technical assistance and to Dr. Thomas Medwick for helpful discussions.

[x] To whom inquiries should be directed.

Comparative Pharmacokinetics of Coumarin Anticoagulants XXI: Effect of Plasma Protein Binding on Distribution Kinetics of Warfarin in Rats

AVRAHAM YACOBI and GERHARD LEVY [x]

Abstract □ The purpose of this investigation was to determine the effect of plasma protein binding on the pharmacokinetic parameters for warfarin that are used conventionally to describe its distribution kinetics on the basis of the time course of plasma warfarin concentrations. Following rapid intravenous injection, warfarin concentrations in the plasma of 14 selected adult male rats declined triexponentially, with the terminal exponential phase starting at about 5 hr. The free fraction, f, of warfarin in the serum of individual animals ranged from 0.303×10^{-2} to 2.89×10^{-2}. The parameters of the equation $C_t = Pe^{-\pi t} + Ae^{-\alpha t} + Be^{-\beta t}$ for plasma concentration C_t at time t were obtained from the experimental data by nonlinear least-squares computer fitting and varied markedly between animals. Strong and highly statistically significant positive correlations with f were obtained for P, B, and β, but no significant correlation was found for A, π, and α. Rate constants and apparent volumes for a three-compartment open mammillary model with elimination from the central compartment were calculated. No apparent correlation was found between f and the intercompartment distribution rate constants. However, strong positive correlations between f and the elimination rate constant, the volume of the central compartment, and the volume of distribution, V_{area}, were observed. There also was a strong linear correlation between f and total clearance. Excellent replication of the experimental data was obtained when the experiments were repeated in some animals after 2 weeks. A detailed analysis of practical pharmacokinetic problems associated with and revealed by such repeated experiments is presented.

Keyphrases □ Warfarin—distribution kinetics, effect of plasma protein binding, rats □ Distribution—pharmacokinetic parameters, effect of plasma protein binding, rats □ Pharmacokinetics—warfarin distribution, effect of plasma protein binding, rats □ Binding, plasma protein—effect on warfarin distribution kinetics, rats □ Protein binding, plasma—effect on warfarin distribution kinetics □ Anticoagulants—warfarin, distribution kinetics, effect of plasma protein binding, rats

Plasma protein binding is a major determinant of the elimination kinetics of warfarin in rats (1) and humans (2). Consistent with theoretical considerations (3), the total clearance, TC, of warfarin by the body was found to be proportional to the free fraction, f, of warfarin in plasma or serum. Wide intersubject differences in f and, consequently, in the TC of warfarin have been observed.

The purpose of this investigation was to determine the relationship between f and the pharmacokinetic constants conventionally used to describe the kinetics of warfarin distribution on the basis of the time course of drug concentrations in plasma after rapid intravenous injection. A detailed analysis of certain practical problems of pharmacokinetic data interpretation was also undertaken.

EXPERIMENTAL

Single 3-ml blood samples were obtained from 63 adult male Sprague–Dawley rats[1] for determination of f, and 14 animals with widely differing f values were selected for further study. Three weeks later, with

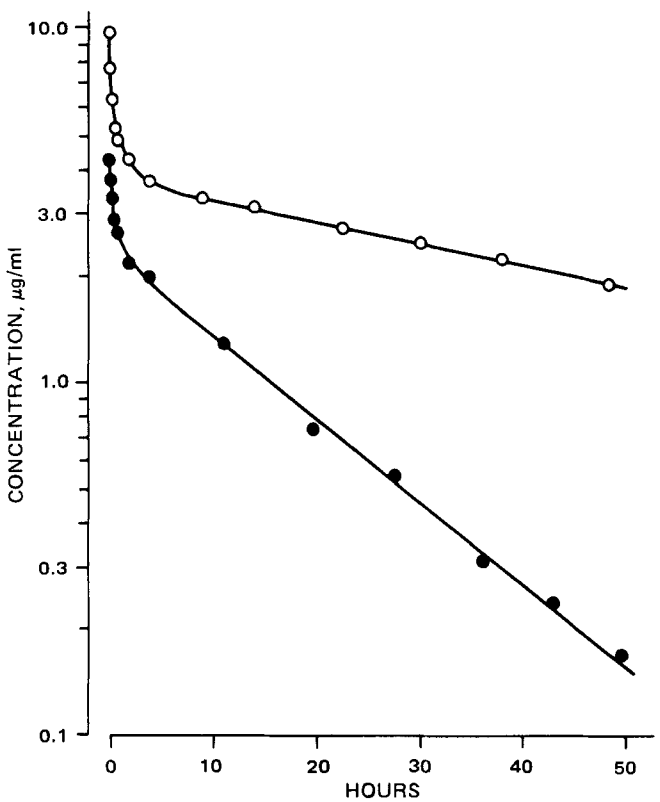

Figure 1—*Warfarin concentration in the plasma of two rats as a function of time after intravenous injection of* ^{14}*C-warfarin, 0.51 mg/kg. Key:* ●, *Rat 1; and* ○, *Rat 14. The curves were fitted to the data by a nonlinear least-squares computer program.*

[1] Blue Spruce Farms, Altamont, N.Y.

(6) H. S. I. Tan, *ibid.*, **62**, 993 (1973).
(7) J. T. Stewart and D. A. Settle, *ibid.*, **64**, 1403 (1975).
(8) R. Yamamoto and H. Tanaka, *Yakuzaigaku*, **17**, 219 (1957).
(9) W. H. Wu, T. F. Chin, and J. L. Lach, *J. Pharm. Sci.*, **59**, 1234 (1970).
(10) "The United States Pharmacopeia," 19th rev., Mack Publishing Co., Easton, Pa., 1975, p. 640.
(11) K. V. N. Rao, S. Kallasam, V. K. Menon, and L. Radhakrishna, *Indian J. Med. Res.*, **59**, 1343 (1971).

ACKNOWLEDGMENTS AND ADDRESSES

Received March 29, 1976, from the *Department of Pharmaceutical Chemistry, College of Pharmacy, Rutgers—the State University, New Brunswick, NJ 08903.*

Accepted for publication June 9, 1976.

The authors express their appreciation to Carole A. Bailey for technical assistance and to Dr. Thomas Medwick for helpful discussions.

[x] To whom inquiries should be directed.

Comparative Pharmacokinetics of Coumarin Anticoagulants XXI: Effect of Plasma Protein Binding on Distribution Kinetics of Warfarin in Rats

AVRAHAM YACOBI and GERHARD LEVY [x]

Abstract □ The purpose of this investigation was to determine the effect of plasma protein binding on the pharmacokinetic parameters for warfarin that are used conventionally to describe its distribution kinetics on the basis of the time course of plasma warfarin concentrations. Following rapid intravenous injection, warfarin concentrations in the plasma of 14 selected adult male rats declined triexponentially, with the terminal exponential phase starting at about 5 hr. The free fraction, f, of warfarin in the serum of individual animals ranged from 0.303×10^{-2} to 2.89×10^{-2}. The parameters of the equation $C_t = Pe^{-\pi t} + Ae^{-\alpha t} + Be^{-\beta t}$ for plasma concentration C_t at time t were obtained from the experimental data by nonlinear least-squares computer fitting and varied markedly between animals. Strong and highly statistically significant positive correlations with f were obtained for P, B, and β, but no significant correlation was found for A, π, and α. Rate constants and apparent volumes for a three-compartment open mammillary model with elimination from the central compartment were calculated. No apparent correlation was found between f and the intercompartment distribution rate constants. However, strong positive correlations between f and the elimination rate constant, the volume of the central compartment, and the volume of distribution, V_{area}, were observed. There also was a strong linear correlation between f and total clearance. Excellent replication of the experimental data was obtained when the experiments were repeated in some animals after 2 weeks. A detailed analysis of practical pharmacokinetic problems associated with and revealed by such repeated experiments is presented.

Keyphrases □ Warfarin—distribution kinetics, effect of plasma protein binding, rats □ Distribution—pharmacokinetic parameters, effect of plasma protein binding, rats □ Pharmacokinetics—warfarin distribution, effect of plasma protein binding, rats □ Binding, plasma protein—effect on warfarin distribution kinetics, rats □ Protein binding, plasma—effect on warfarin distribution kinetics □ Anticoagulants—warfarin, distribution kinetics, effect of plasma protein binding, rats

Plasma protein binding is a major determinant of the elimination kinetics of warfarin in rats (1) and humans (2). Consistent with theoretical considerations (3), the total clearance, TC, of warfarin by the body was found to be proportional to the free fraction, f, of warfarin in plasma or serum. Wide intersubject differences in f and, consequently, in the TC of warfarin have been observed.

The purpose of this investigation was to determine the relationship between f and the pharmacokinetic constants conventionally used to describe the kinetics of warfarin distribution on the basis of the time course of drug concentrations in plasma after rapid intravenous injection. A detailed analysis of certain practical problems of pharmacokinetic data interpretation was also undertaken.

EXPERIMENTAL

Single 3-ml blood samples were obtained from 63 adult male Sprague–Dawley rats[1] for determination of f, and 14 animals with widely differing f values were selected for further study. Three weeks later, with

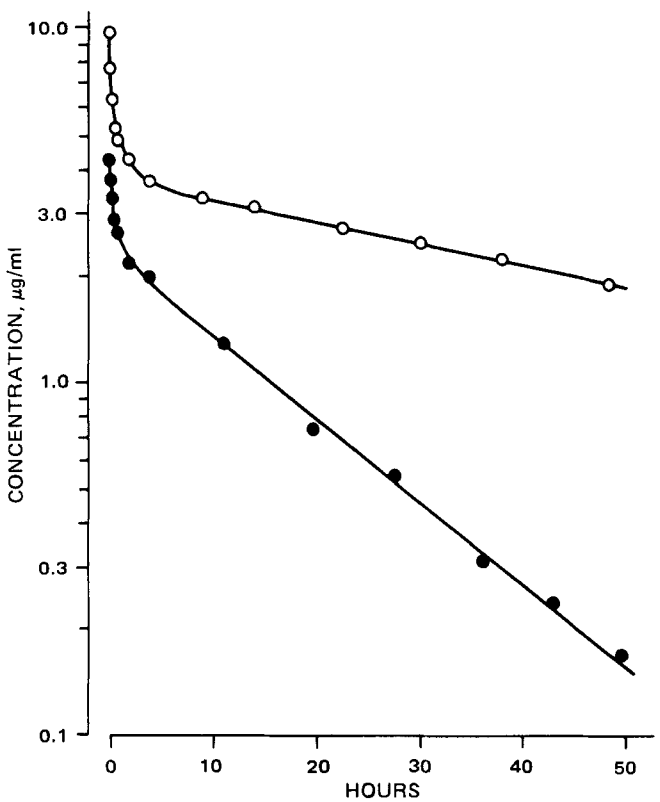

Figure 1—*Warfarin concentration in the plasma of two rats as a function of time after intravenous injection of* ^{14}*C-warfarin, 0.51 mg/kg. Key:* ●, *Rat 1; and* ○, *Rat 14. The curves were fitted to the data by a nonlinear least-squares computer program.*

[1] Blue Spruce Farms, Altamont, N.Y.

Table I—Warfarin Kinetics in Rats

Parameter	Mean	Range
P, μg/ml[a]	4.67	1.28–8.78
A, μg/ml[a]	1.76	0.359–3.59
B, μg/ml[a]	3.08	2.36–4.10
π, hr^{-1}	6.98	2.34–19.0
α, hr^{-1}	1.03	0.348–1.83
β, hr^{-1}	0.0310	0.0117–0.0580

[a]For a 0.51-mg/kg dose.

Table II—Warfarin Kinetics in Rats

Constant	Mean	Range
k_{10}, hr^{-1}	0.0851	0.0422–0.141
k_{12}, hr^{-1}	3.11	0.134–8.73
k_{21}, hr^{-1}	4.21	1.73–9.18
k_{13}, hr^{-1}	0.640	0.0897–1.97
k_{31}, hr^{-1}	0.552	0.248–1.13
V_c, ml/kg	59.6	31.7–96.9
V_{area}, ml/kg	165	123–209
$V_{intercept}$, ml/kg	170	124–220
TC, ml/(hr × kg)	5.59	1.74–11.4

the animals then weighing 380–490 g, a two-piece cannula of silicone rubber–polyethylene was implanted in the right jugular vein under light ether anesthesia (4, 5). One or 2 days after cannulation, the rats were placed in individual metabolism cages with food[2] and water freely available.

Racemic warfarin, 0.51 mg/kg including about 5 μCi of ^{14}C-warfarin[3]/kg, was injected rapidly through the cannula; 0.25-ml blood samples were obtained at 5, 10, 20, 40, 60, and 120 min and then at less frequent intervals for about 50 hr by a technique described previously (5). Plasma was separated, and warfarin was extracted, purified by TLC, and assayed as previously described (6). At the end of the experiment, a large volume of blood was obtained for the determination of the free fraction of warfarin in serum by equilibrium dialysis (1, 7).

The warfarin concentrations in plasma as a function of time after injection were fitted to a multiexponential equation by nonlinear least-squares regression (8). Convergence was defined as a relative change in the residual sum of squares $<10^{-4}$. Data in all functions were weighted numerically equal. The parameter estimates of the multiexponential equation were used to calculate rate constants for a multicompartment open model (9). Simulations were carried out with a digital analog simulator program (10).

RESULTS

Figure 1 shows the time course of plasma warfarin concentrations in two rats, one a relatively rapid eliminator and the other a relatively slow

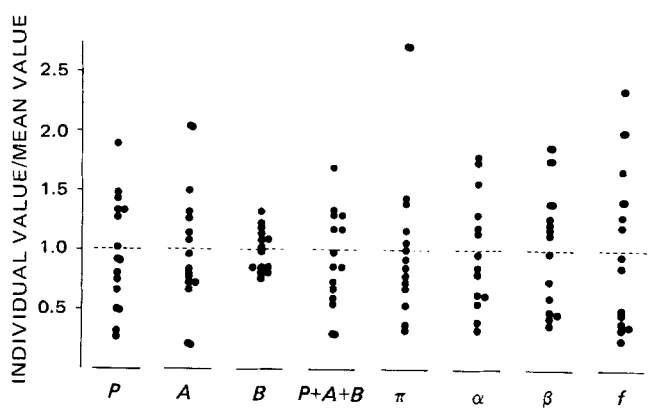

Figure 2—*Intersubject distribution of values for the parameters of the triexponential equation that describes the time course of plasma warfarin concentrations and of values for the free fraction of warfarin in the serum of 14 rats.*

[2] Charles River formula 4RF.
[3] Amersham/Searle Corp., Arlington Heights, Ill.

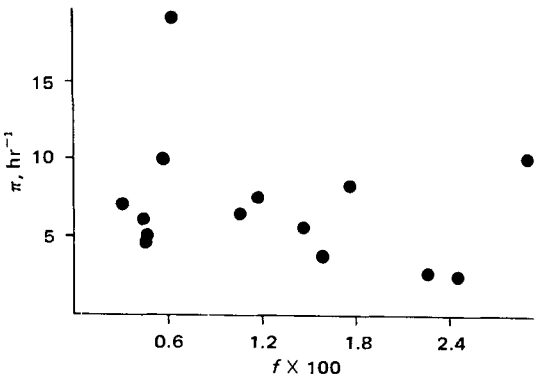

Figure 3—*Relationship between the serum free fraction, f, of warfarin and the parameter π, which characterizes the slope of the first exponential phase of the triexponential decline of warfarin concentrations in the plasma of 14 rats after intravenous injection.*

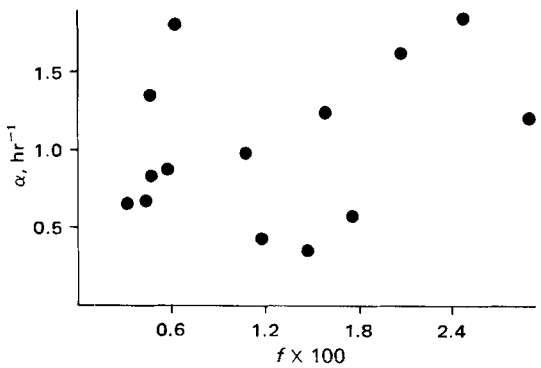

Figure 4—*Relationship between the serum free fraction, f, of warfarin and the parameter α, which characterizes the slope of the second exponential phase of the triexponential decline of warfarin concentrations in the plasma of 14 rats after intravenous injection.*

eliminator of the drug. Experimental data of similar quality were obtained for the other 12 animals. A triexponential equation of the type $C_t = Pe^{-\pi t} + Ae^{-\alpha t} + Be^{-\beta t}$ was required to describe the plasma warfarin concentrations, C_t, as a function of time, t. Substantially fewer than 20 iterations were required in all cases to obtain convergence; the correlation coefficient was ≥0.997 for each set of data.

The mean values and ranges for the parameters of the triexponential equation fitted to the individual data from 14 animals are listed in Table I. As is evident from the values of these constants and from Fig. 1, the terminal exponential phase of plasma concentrations began about 5 hr after injection. Rate constants for a linear three-compartment mam-

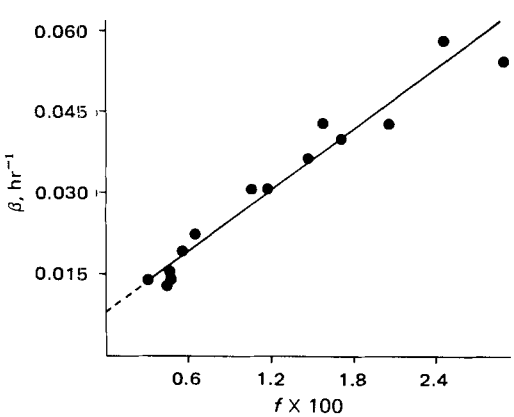

Figure 5—*Relationship between the serum free fraction, f, of warfarin and the parameter β, which characterizes the slope of the terminal exponential phase of the triexponential decline of warfarin concentrations in the plasma of 14 rats after intravenous injection. Correlation coefficient = 0.962, p < 0.001.*

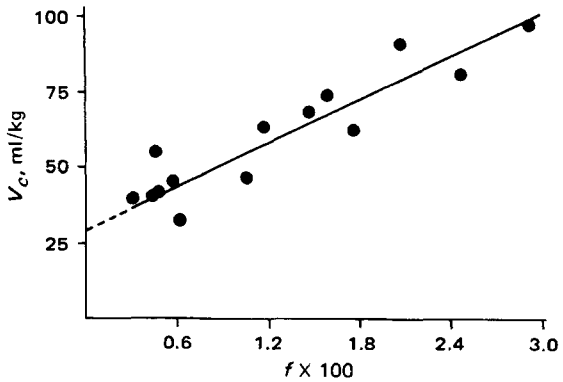

Figure 6—*Relationship between the serum free fraction, f, of warfarin and the volume of the hypothetical central compartment,* V_c *[which is dose* $(P + A + B)^{-1}$*] for warfarin in 14 rats. Correlation coefficient = 0.921,* $p < 0.001$.

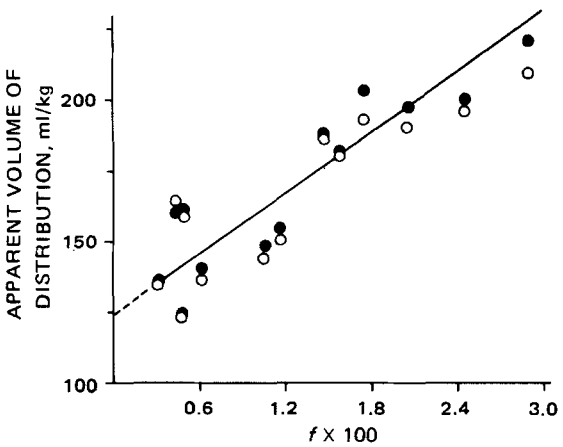

Figure 7—*Relationship between the serum free fraction, f, of warfarin and the apparent volume of distribution of the drug in 14 rats. Key: ●, based on the terminal exponential curve [one-compartment model, (dose)* B^{-1}*]; and ○, based on the triexponential curve [three-compartment model,* V_{area} *= (dose)* $(P/\pi + A/\alpha + B/\beta)^{-1}\beta^{-1}$*]. Regression line fitted to ●, correlation coefficient = 0.911,* $p < 0.001$.

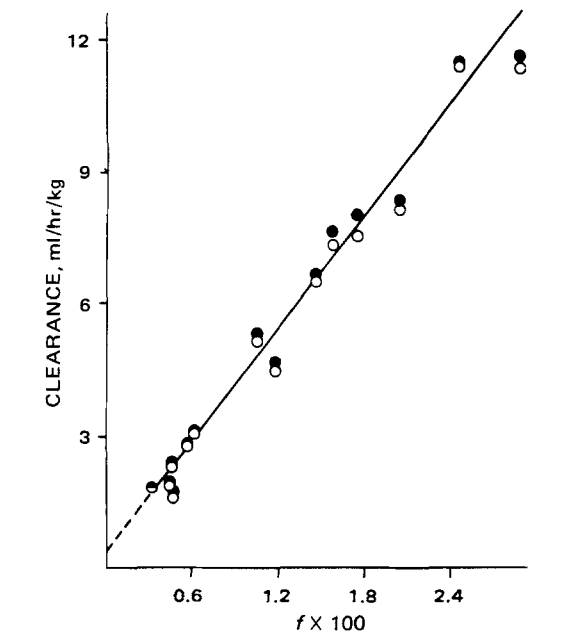

Figure 8—*Relationship between the serum free fraction, f, of warfarin and the total body clearance of warfarin in 14 rats. Key: ●, based on one-compartment model [(dose)* $B^{-1}\beta$*]; and ○, based on three-compartment model (*$V_{area}\beta$*). Regression line fitted to ●, correlation coefficient = 0.988,* $p < 0.001$.

Table III—Correlation between Pharmacokinetic Parameters for Warfarin in Rats and the Free Fraction of Warfarin in Serum

Parameter	Correlation Coefficient	Statistical Significance[a]
P	0.873	+
A	0.384	–
B	0.816	+
π	0.234	–
α	0.310	–
β	0.962	+
k_{10}	0.810	+
k_{12}	0.287	–
k_{21}	0.350	–
k_{13}	0.066	–
k_{31}	0.453	–
V_c	0.921	+
V_{area}	0.871	+
$V_{intercept}$	0.911	+
TC	0.988	+

[a] + = statistically significant ($p < 0.001$), and – = not statistically significant ($p > 0.1$).

millary open model, with elimination arbitrarily defined as occurring from the central compartment (Compartment 1), were obtained for each set of experimental data and are listed in Table II.

Table II also contains the values for the apparent volume of the central compartment, V_c, the apparent volume of distribution based on the area under the triexponential curve, V_{area}, the apparent volume of distribution estimated from the dose divided by B, $V_{intercept}$, and the total body clearance, $TC = V_{area}\beta$ or $\simeq V_{intercept}\beta$. The average ± SD of the individual ratios of $V_{intercept}/V_{area}$ was 1.03 ± 0.051, indicating only a very small contribution of the initial distribution phase to the total area under the concentration–time curve.

Figure 2 shows the distribution of values for the triexponential equation (to be referred to as the direct pharmacokinetic parameters) and for f, the serum free fraction, which ranged from 0.303×10^{-2} to 2.89×10^{-2}. Since the 14 rats were selected from 63 animals to obtain a wide range of f values, the distribution patterns in Fig. 2 are not characteristic of a normal population.

The direct pharmacokinetic parameters π and α were apparently not affected by changes in f (Figs. 3 and 4), but the β values showed a strong positive correlation with f (Fig. 5). The volumes V_c, V_{area}, and $V_{intercept}$ were also strongly and positively correlated with f (Figs. 6 and 7). Linear

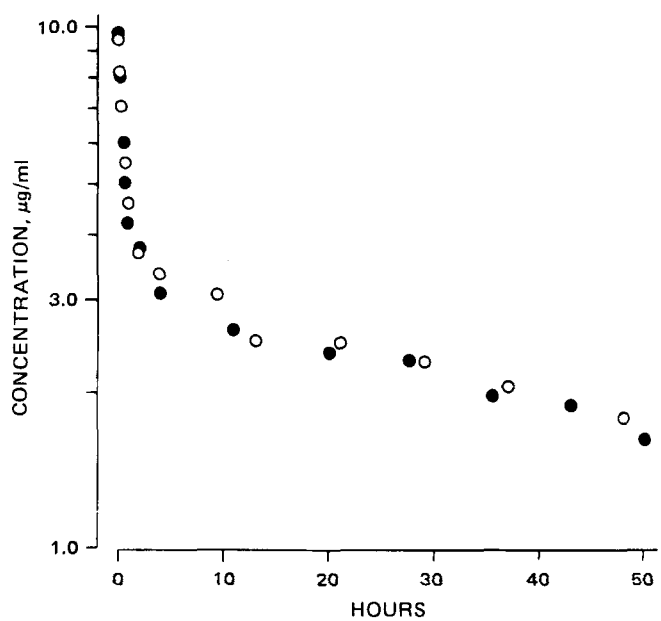

Figure 9—*Warfarin concentrations in the plasma of Rat 13 as a function of time after intravenous injection of* ^{14}C*-warfarin, 0.51 mg/kg, on two separate occasions. Key: ●, first experiment; and ○, 2 weeks later.*

Table IV—Warfarin Kinetics in Rat 3 in Two Separate Experiments

Direct Parameter	First Experiment	Second Experiment[a]	Derived Constant	First Experiment	Second Experiment[a]
P, μg/ml[b]	1.38 ± 13.5[c]	5.17 ± 0.65	k_{10}, hr^{-1}	0.0894	0.160
A, μg/ml[b]	1.60 ± 13.7	0.766 ± 0.131	k_{12}, hr^{-1}	0.320	6.23
B, μg/ml[b]	2.60 ± 0.19	2.40 ± 0.12	k_{21}, hr^{-1}	2.36	4.09
π, hr^{-1}	2.87 ± 12.2	10.5 ± 1.50	k_{13}, hr^{-1}	0.711	0.208
α, hr^{-1}	1.36 ± 4.63	0.407 ± 0.153	k_{31}, hr^{-1}	0.790	0.316
$\beta \times 100$ hr^{-1}	4.28 ± 0.32	4.84 ± 0.20	V_c, ml/kg	91.4	61.2
			V_{area}, ml/kg	191	203
			TC, ml/(hr × kg)	8.17	9.82

[a] Two weeks after first experiment. [b] For a 0.51-mg/kg dose. [c] Standard deviation.

Table V—Warfarin Kinetics in Rat 8 in Two Separate Experiments

Direct Parameter	First Experiment	Second Experiment[a]	Derived Constant	First Experiment	Second Experiment[a]
P, μg/ml[b]	6.27 ± 0.45[c]	3.56 ± 0.37	k_{10}, hr^{-1}	0.113	0.0924
A, μg/ml[b]	1.27 ± 0.48	2.27 ± 0.32	k_{12}, hr^{-1}	2.95	2.12
B, μg/ml[b]	3.49 ± 0.09	3.23 ± 0.081	k_{21}, hr^{-1}	3.00	3.97
π, hr^{-1}	6.43 ± 0.97	6.32 ± 0.63	k_{13}, hr^{-1}	0.717	0.476
α, hr^{-1}	1.00 ± 0.46	0.752 ± 0.154	k_{31}, hr^{-1}	0.697	0.444
$\beta \times 100$ hr^{-1}	3.68 ± 0.10	3.42 ± 0.11	V_c, ml/kg	46.2	56.4
			V_{area}, ml/kg	142	152
			TC, ml/(hr × kg)	5.24	5.21

[a] Two weeks after first experiment. [b] For a 0.51-mg/kg dose. [c] Standard deviation.

regression lines in Figs. 5–7 do not necessarily imply an exactly linear relationship between the variables. There was a strong ($r = -0.913$) and highly statistically significant ($p < 0.001$) negative correlation between the plasma warfarin concentration at 5 min and f. This finding constitutes an independent and direct verification of the positive correlation between f and the computer-derived values of V_c. As demonstrated previously (1–3), there was a direct linear relationship between f and the total clearance of warfarin by the body (Fig. 8).

A summary of the relationship between f and the various direct and derived pharmacokinetic parameters for warfarin is presented in Table III. Of the derived constants, the elimination constant k_{10} was strongly correlated with f while the intercompartment distribution rate constants k_{12}, k_{21}, k_{13}, and k_{31} were not.

The warfarin experiment was repeated in three animals 2 weeks after the first experiment. Excellent replication of experimental data was obtained, as shown in Figs. 9 and 10 for one of the best and the "worst" case. Nevertheless, nonlinear least-squares regression analyses yielded substantial numerical intrasubject differences in P, A, π, and α (Tables IV–VI). On the other hand, there was very little intrasubject variation in B and β, and these values had small standard deviations. The same pattern obtained with respect to the derived pharmacokinetic constants and the volume terms; there was good replication of k_{10}, V_c, and V_{area} but not of the other constants (Tables IV–VI).

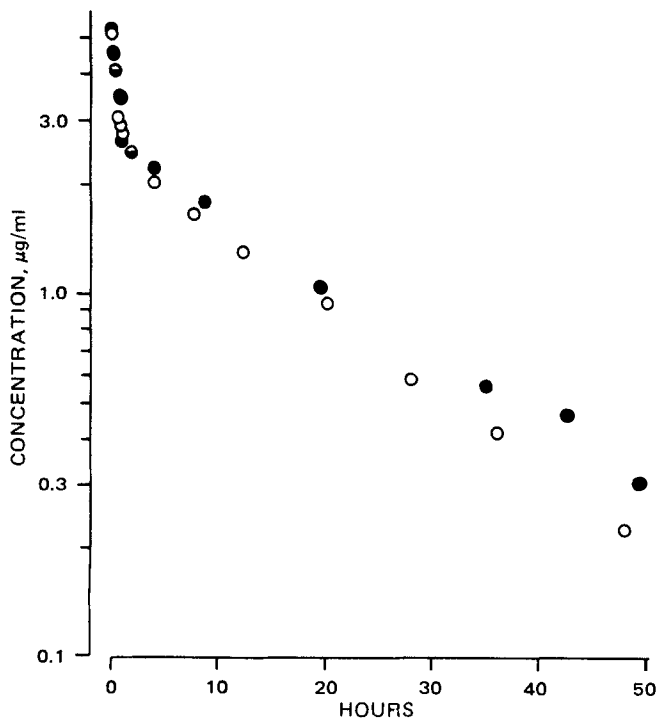

Figure 10—*Warfarin concentrations in the plasma of Rat 3 as a function of time after intravenous injection of ^{14}C-warfarin, 0.51 mg/kg, on two separate occasions. Key: ●, first experiment; and ○, 2 weeks later.*

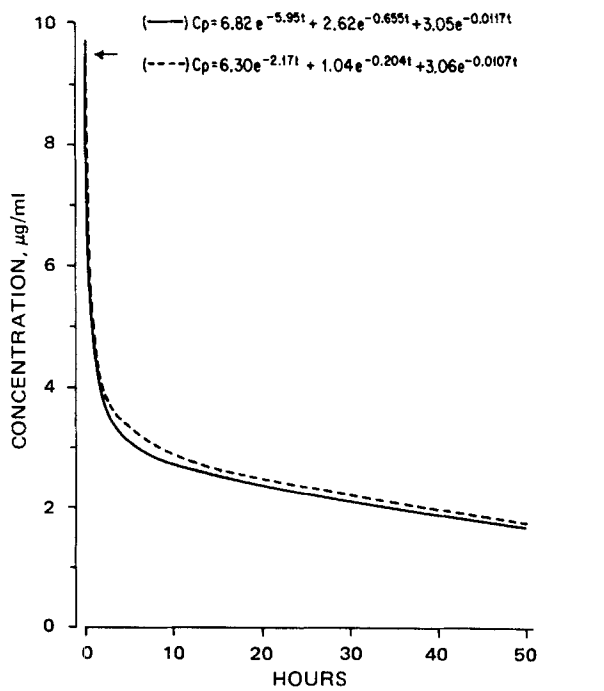

Figure 11—*Curves fitted to the data in Fig. 9 by nonlinear least-squares computer program. Key: ——, first experiment; and - - - -, second experiment.*

Table VI—Warfarin Kinetics in Rat 13 in Two Separate Experiments

Direct Parameter	First Experiment	Second Experiment[a]	Derived Constant	First Experiment	Second Experiment[a]
P, μg/ml[b]	6.82 ± 0.61[c]	6.30 ± 0.44	k_{10}, hr^{-1}	0.0472	0.0352
A, μg/ml[b]	2.62 ± 0.46	1.04 ± 0.38	k_{12}, hr^{-1}	2.67	1.16
B, μg/ml[b]	3.05 ± 0.13	3.06 ± 0.34	k_{21}, hr^{-1}	2.88	0.897
π, hr^{-1}	5.95 ± 1.09	2.17 ± 0.33	k_{13}, hr^{-1}	0.679	0.137
α, hr^{-1}	0.655 ± 0.178	0.204 ± 0.193	k_{31}, hr^{-1}	0.336	0.149
$\beta \times 100$ hr^{-1}	1.17 ± 0.13	1.07 ± 0.31	V_C, ml/kg	40.6	49.0
			V_{area}, ml/kg	164	162
			TC, ml/(hr × kg)	1.92	1.73

[a] Two weeks after first experiment. [b] For a 0.51-mg/kg dose. [c] Standard deviation.

Table VII—Effect of Initial Estimates on Computer-Derived Parameters for Triexponential Equation, Rat 14

Parameter	Initial Estimate	Computer Output[a]				
		N.C.	−30%*	+30%*	−30%* +30%+	+30%* −30%+
P	5.00	6.74	6.74*	6.74*	6.74*	6.74*
A	3.00	2.32	2.33*	2.32*	2.32+	2.32+
B	3.80	3.77	3.77	3.77	3.77	3.77
π	5.00	7.08	7.08*	7.06*	7.07*	7.07*
α	0.693	0.652	0.652*	0.650*	0.651+	0.651+
$\beta \times 100$	1.40	1.38	1.38	1.38	1.38	1.38

[a] The computer outputs when the initial estimates were not changed (N.C.) and when P, A, π, and α were increased or decreased by 30% as specified by the superscripts in the column headings.

To examine the effect of the initial estimates on the computer-calculated direct pharmacokinetic parameters, the initial estimates for P, A, π, and α were increased or decreased in different combinations by 30%[4]. For 12 of the 14 rats, this change had no effect (<5%) on the calculated values. Tables VII and VIII show the results of this exercise for one of the best and for the worst case, respectively.

Despite the numerically pronounced intrasubject differences in several direct pharmacokinetic parameters for warfarin (Tables IV–VI), the plasma concentration–time curves generated by the triexponential equations for replicate experiments in any one animal were very similar (Figs. 11 and 12). However, the curves obtained from the derived constants for the time course of warfarin in the two hypothetical peripheral compartments of the three-compartment model differed greatly between experiments in any one animal (Figs. 13 and 14).

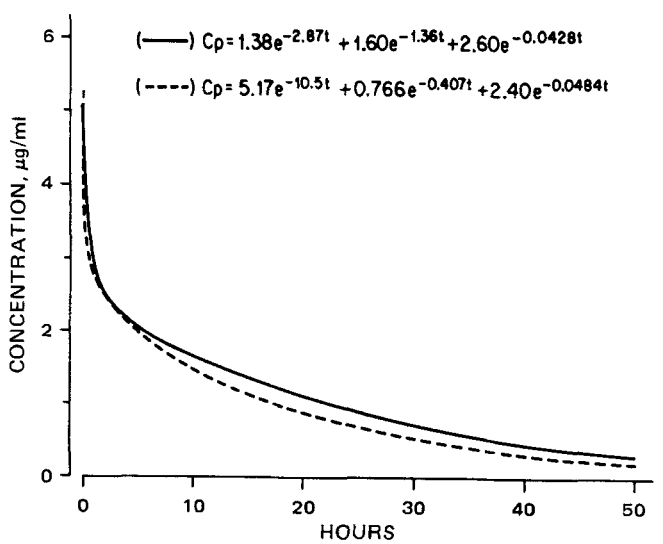

Figure 12—*Curve fitted to the data in Fig. 10 by nonlinear least-squares computer program. Key: ——, first experiment; and - - - -, second experiment.*

[4] The initial estimates for B and β were so close to the computer outputs in all cases that there was no need to vary these estimates.

DISCUSSION

The experiments were carried out under relatively ideal conditions for pharmacokinetic analysis: a large number of blood samples were obtained through an indwelling cannula; a sensitive, specific, and precise assay method was used; the experiments were done twice in some animals; and the concentration data were sufficiently "clean" so that computer calculations were not affected by substantial variations in the initial estimates of the parameters.

As expected on the basis of earlier investigations (1–3), plasma protein

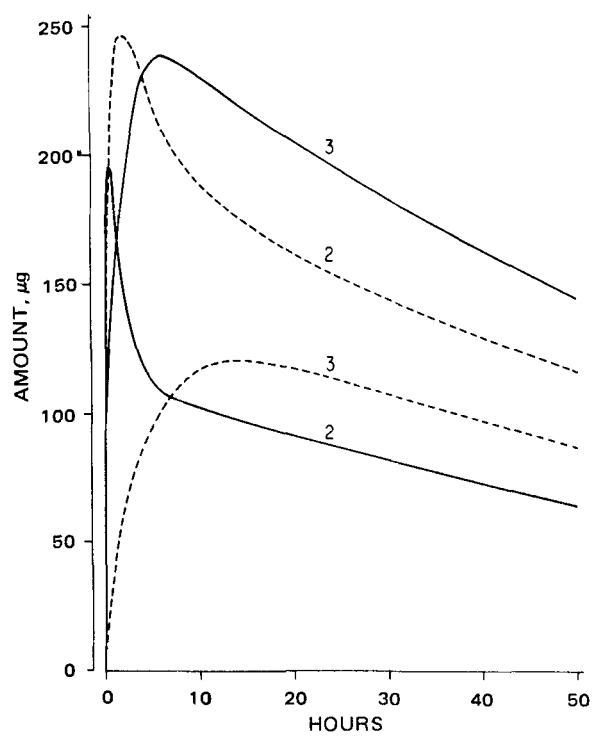

Figure 13—*Inferred time course of warfarin in the hypothetical shallow and deep peripheral compartments, based on the triexponential curves shown in Fig. 11. Key: ——, first experiment; - - - -, second experiment; 2, Compartment 2; and 3, Compartment 3.*

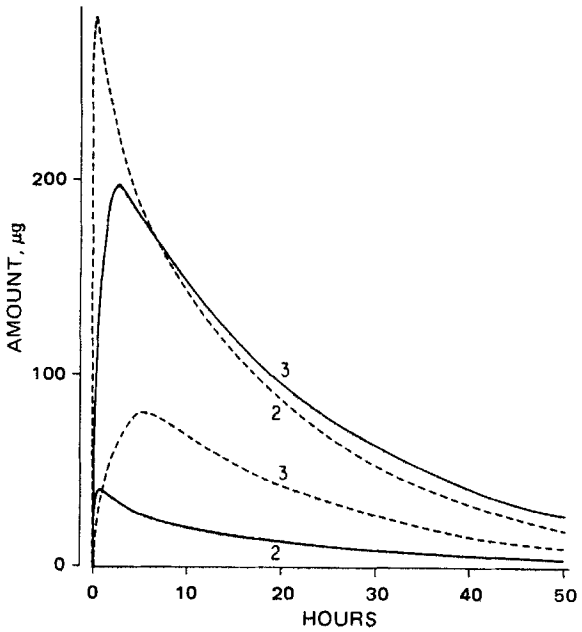

Figure 14—*Inferred time course of warfarin in the hypothetical shallow and deep peripheral compartments, based on the triexponential curves shown in Fig. 12. Key: ——, first experiment; - - - -, second experiment; 2, Compartment 2; and 3, Compartment 3.*

binding had a pronounced effect on the total clearance of warfarin. Our previous practice of using $V_{intercept}$ rather than V_{area} values to estimate TC[5] was entirely acceptable for warfarin, since the differences were on the order of 3 ± 5%.

Protein binding of warfarin in plasma had no apparent effect on the directly determined pharmacokinetic parameters π and α and on the derived rate constants k_{12}, k_{21}, k_{13}, and k_{31}, which are conventionally used to describe the distribution kinetics of a drug on the basis of plasma concentration data. This conclusion must be viewed in the context that these parameters are also the ones with the greatest uncertainty in their calculated values (as reflected by their relative coefficients of variation and by the results of replicate experiments).

Of interest are the strong correlations of P and V_c [*i.e.*, $D/(P + A + B)$] with f (Table III). If V_c is the volume of a "real" initial homogeneous compartment, then differences in plasma protein binding should not affect its value. The increase of V_c with f suggests that V_c is a hybrid affected by some aspects of drug distribution and that it does not reflect the volume of a distinct, homogeneous, well-defined, and instantaneously accessible (by intravenous injection) physiological space under the experimental conditions. However, V_c is essentially equal to the plasma volume of 35 ml/kg in Sprague–Dawley rats (11) when f is very small (Fig. 6).

From a theoretical assessment of problems associated with the analysis of pharmacokinetic models, Westlake (12) concluded that: "When a pharmacokinetic model is fitted to blood levels of a drug, the estimates of the pharmacokinetic parameters are likely to be subject to considerable error. These errors are probably unimportant as long as the model is used only to predict blood levels. However, when the parameters are used to predict other features of the system (*e.g.*, tissue drug levels), considerable errors in prediction may result." The results of our replicate studies, carried out under ideal conditions for good replication, afford the best opportunity to examine this problem experimentally.

[5] This practice is necessitated by the requirement of nonheparinized blood for most of these studies, since it is usually desired to determine not only drug concentrations but also the intensity of the anticoagulant effect. Blood samples must then be collected by serial arterial punctures (rather than by cannula) and at more frequent time intervals at later times, thereby limiting the number and frequency of early samples.

Table VIII—Effect of Initial Estimates on Computer-Derived Parameters for Triexponential Equation, Rat 3

Parameter	Initial Estimate	Computer Output[a] N.C.	−30%*	+30%*	−30%* +30+	+30%* −30%+
P	1.20	1.38	1.36*	1.78*	1.50*	0.888*
A	2.00	1.60	1.39*	1.19*	1.51+	2.35+
B	2.59	2.60	2.59	2.57	2.61	2.67
π	3.50	2.87	2.42*	2.37*	2.15*	5.14*
α	1.40	1.36	1.01*	1.32*	1.93+	1.97+
$\beta \times 100$	4.26	4.28	4.27	4.23	4.29	4.40

[a] The computer outputs when the initial estimates were not changed (N.C.) and when P, A, π, and α were increased or decreased by 30% as specified by the superscripts in the column headings.

Pharmacokinetic analysis of the data demonstrated that Westlake's conclusions are fully justified. The tool of pharmacokinetics is powerful and effective when focused on directly measurable concentrations or effects but becomes a potentially misleading and meaningless mathematical manipulation when used to infer the events or conditions that are thought (often mistakenly) to occur in the "black box" portion of the body and that cannot be measured directly.

REFERENCES

(1) A. Yacobi and G. Levy, *J. Pharm. Sci.*, **64**, 1660 (1975).

(2) A. Yacobi, J. A. Udall, and G. Levy, *Clin. Pharmacol. Ther.*, **19**, 552 (1976).

(3) G. Levy and A. Yacobi, *J. Pharm. Sci.*, **63**, 805 (1974).

(4) J. R. Weeks and J. D. Davis, *J. Appl. Physiol.*, **19**, 540 (1964).

(5) J. J. Ashley and G. Levy, *Res. Commun. Chem. Pathol. Pharmacol.*, **4**, 297 (1972).

(6) A. Yacobi, L. B. Wingard, Jr., and G. Levy, *J. Pharm. Sci.*, **63**, 868 (1974).

(7) A. Yacobi and G. Levy, *J. Pharmacokinet. Biopharm.*, **3**, 439 (1975).

(8) C. M. Metzler, "NONLIN, a Computer Program for Parameter Estimation in Nonlinear Situations," The Upjohn Co., Kalamazoo, Mich., 1969.

(9) M. Gibaldi and D. Perrier, "Pharmacokinetics," Dekker, New York, N.Y., 1975.

(10) "MIMED, State University of New York at Buffalo Computer Center Adaptation of MIMIC," Publication 44610400, Control Data Corp., Special Systems Publications, St. Paul, Minn., 1968.

(11) R. J. K. Julkunen, M. Kekki, J.-J. Himberg, and B. Wahlström, *Acta Pharmacol. Toxicol.*, **38**, 90 (1976).

(12) W. J. Westlake, *J. Pharm. Sci.*, **60**, 882 (1971).

ACKNOWLEDGMENTS AND ADDRESSES

Received March 10, 1976, from the *Department of Pharmaceutics, School of Pharmacy, State University of New York at Buffalo, Buffalo, NY 14214.*

Accepted for publication June 14, 1976.

Supported in part by Grant GM 20852 from the National Institute of General Medical Sciences, National Institutes of Health.

Previous paper in this series: A. Yacobi, J. A. Udall, and G. Levy, *Clin. Pharmacol. Ther.*, **20**, 300 (1976).

[x] To whom inquiries should be directed.

Kinetics and Mechanisms of Hydrolysis of 1,4-Benzodiazepines II: Oxazepam and Diazepam

WESLEY W. HAN ˣ, GERALD J. YAKATAN, and DALE D. MANESS

Abstract □ The hydrolysis kinetics of oxazepam and diazepam leading to a benzophenone product and a glycine derivative were quantified from pH 1 to 11. For oxazepam, two intermediates were isolated and identified, indicating a parallel consecutive reaction mechanism. The hydrolysis occurred uncatalyzed and demonstrated acid–base catalysis for both reaction steps. One intermediate was observed by TLC for diazepam hydrolysis. This intermediate, resulting from breakage of the azomethine linkage, was different than the major intermediate isolated for oxazepam hydrolytic degradation (amide hydrolysis preferred). Stability parameters involving rate constant–temperature dependence are reported.

Keyphrases □ Oxazepam—kinetics and mechanism of hydrolysis, effect of pH □ Diazepam—kinetics and mechanism of hydrolysis, effect of pH □ Hydrolysis—oxazepam and diazepam, kinetics and mechanism, effect of pH □ 1,4-Benzodiazepines—oxazepam and diazepam, kinetics and mechanism of hydrolysis, effect of pH

In a previous report (1), the kinetics and mechanisms of hydrolysis of chlordiazepoxide and demoxepam, 1,4-benzodiazepines of therapeutic interest, were quantitatively described. Chlordiazepoxide undergoes facile transformation to demoxepam by hydrolysis of the methylamino substituent in the 2-position. Subsequently, the 1,4-benzodiazepine nucleus is lost by hydrolysis of the 1,2- and 4,5-bonds, leading to the final products: 2-amino-5-chlorobenzophenone and a glycine derivative.

Although the kinetic and TLC data indicated a parallel consecutive reaction mechanism (*i.e.*, either 1,2- or 4,5-bond hydrolysis may initially occur), complete data analysis showed that initial azomethine hydrolysis was relatively unimportant to the overall hydrolysis kinetics. An investigation of kinetics and mechanisms of hydrolysis of oxazepam (I*a*) and diazepam (I*b*) was initiated to delineate structural effects on the relative importance of the two mechanistic paths leading to the final products.

EXPERIMENTAL

Materials—TLC was used to verify the purity of oxazepam[1], 2-amino-5-chlorobenzophenone[1], and diazepam[2]. These compounds were chromatographically pure and were used as received. All other chemicals were reagent grade quality. Aqueous solutions were prepared using distilled deionized water. All aqueous solutions were buffered using the following systems: hydrochloric acid, acetate, phosphate, borate, and sodium hydroxide.

Kinetic Measurements and Compound Identification—Hydrolysis kinetics were followed spectrophotometrically. Detailed procedures describing the kinetic measurements and methods used in isolation and identification were reported previously (1). TLC analysis of hydrolytic reaction solutions of diazepam was identical to that used for chlordiazepoxide (1).

For oxazepam, samples of about 10^{-3} *M* solution were withdrawn at appropriate times. These samples were extracted three times with an equal volume of chloroform. A UV scan of the aqueous phase indicated that extraction was complete. The chloroform extract was concentrated and subjected to TLC analysis, using 250-μm silica gel GF plates and chloroform–toluene–methanol (52:48:7) as the developing solvent.

[1] Wyeth Laboratories, Philadelphia, Pa.
[2] Hoffmann-La Roche Inc., Nutley, N.J.

RESULTS AND DISCUSSION

Scheme I gives the general expected mechanism if concomitant 1,2-amide and 4,5-azomethine hydrolyses occur. Compound II would result from 1,2-amide hydrolysis; III is the intermediate derived from hydrolysis of the 4,5-azomethine bond; and IV represents the final products, the substituted benzophenone and the glycine derivative. The initial parallel reaction steps may be reversible under appropriate conditions (1, 2) and are shown. A mathematical treatment of this scheme according to differential absorbance measurements may be found in a prior report (1).

Spectral Changes and Rate Constant Determinations—Two pKa's, 1.7 and 11.6, have been reported for oxazepam at 25° (3). The lower value is attributable to protonation of the azomethine nitrogen, and the larger one is due to deprotonation of the amide nitrogen. Since the proposed intermediates and products are also subject to prototropic reactions, it is not surprising that the kinetic spectra are influenced by pH changes. Throughout the entire pH region, two apparent reaction steps were spectrally observed for oxazepam. Typical spectral changes, demonstrating a two-step reaction, are shown in Fig. 1. The final spectrum is identical to that of 2-amino-5-chlorobenzophenone.

For oxazepam, time plots of the logarithm of differential absorbance measurements at any time and time infinity ($A_t - A_\infty$) consisted of two linear segments according to the biexponential equation:

$$A_t - A_\infty = M \exp(-b_1 t) + N \exp(-b_2 t) \qquad \text{(Eq. 1)}$$

where M and N are preexponential constants and b_1 and b_2 are exponential factors related to the observed rate constants of the first-order reactions in Scheme I. Typical apparent first-order plots are given in Figs. 2 and 3. Feathering was employed to differentiate the two linear seg-

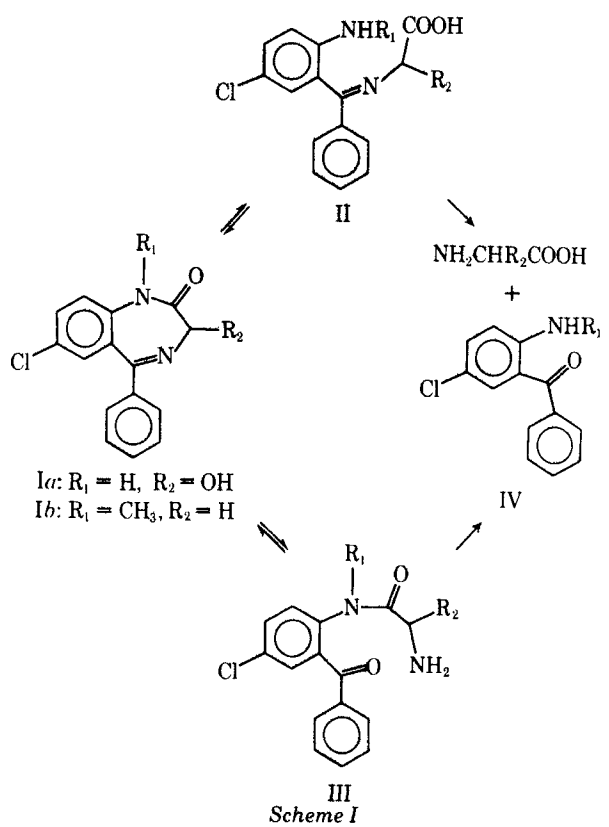

Scheme I

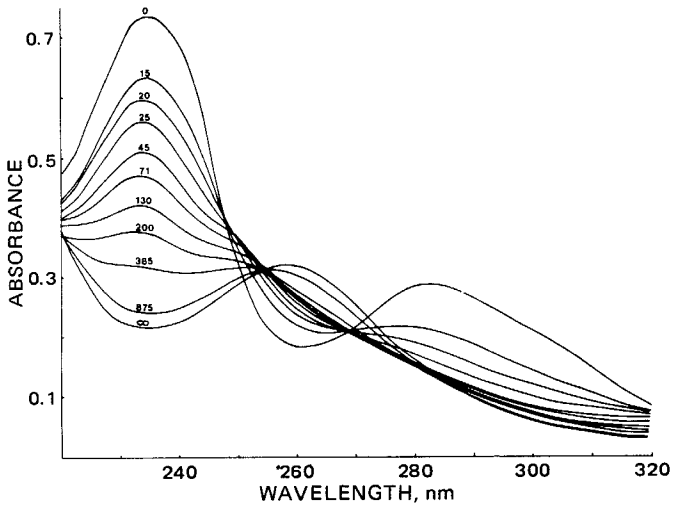

Figure 1—*Typical spectral changes for the hydrolysis of 10^{-5} M oxazepam in 0.1 N HCL, μ = 1.0, at 80°. Curves are labeled as to minutes after initiation of the reaction.*

ments. The apparent first-order rate constants, calculated by least-squares fitting, are reported in Table I.

Diazepam differs from oxazepam in that only one pKa has been observed in the normal pH region (3). The pKa of 3.3 is reportedly due to protonation at the azomethine nitrogen in the 4-position. Due to the methyl substitution on the amide nitrogen, the higher pKa observed with oxazepam, attributable to deprotonation of the amide proton, is absent. At pH values below the pKa of diazepam, observed spectral changes indicated an apparent two-step reaction, both being first order. Above this pKa, spectra of sequential samples demonstrated clear isosbestic points, implicating a single reaction step in a one-to-one kinetic transformation of diazepam to 2-methylamino-5-chlorobenzophenone. Throughout the pH region, the final spectrum was superimposable on that of an equimolar solution of this product.

Below the pKa of diazepam, the apparent rate constants were calculated by the same procedure as used for oxazepam. In the pH region showing a single reaction step, the observed rate constants were determined according to the integrated first-order expression:

$$\ln(A_t - A_\infty) = \ln(A_0 - A_\infty) - kt \qquad \text{(Eq. 2)}$$

Linear segments for both the biexponential and monoexponential plots were clearly first order, as indicated by the correlation coefficients, r, in Tables I and II. The least-squares estimates of the rate constants for diazepam are given in Table II.

Rate–pH Profiles—The log k–pH profile for oxazepam hydrolysis (Fig. 4) was generated from the rate constants given in Table I. The two reaction steps are shown on the same log k–pH profile: the initial step, hydrolysis of oxazepam to an intermediate(s), and the second, slower reaction representing hydrolysis of the intermediate(s) to the final products. For the initial hydrolytic step, the equation that defines the

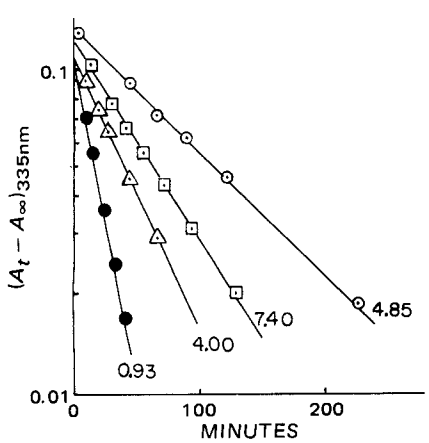

Figure 2—*Typical apparent first-order plots for the first hydrolytic reaction step of oxazepam at 85°, μ = 1.0. Feathered lines are labeled as to pH values.*

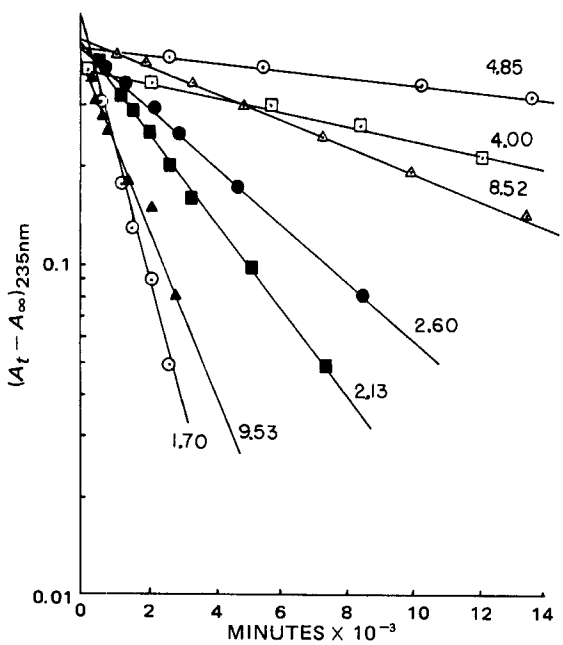

Figure 3—*Typical apparent first-order plots for the second hydrolytic reaction step of oxazepam at 85°, μ = 1.0. Lines are labeled as to pH values.*

theoretical curve drawn through the experimental points is:

$$k_{obs} = k_H[H^+]f_{H_2S} + k_{H'}[H^+]f_{HS} + k'_{H_2O}f_{HS} + k_{OH'}[OH^-]f_{HS} + k_{OH''}[OH^-]f_S \qquad \text{(Eq. 3)}$$

where the observed rate constant (k_{obs}) is defined as a function of the specific bimolecular rate constants (k_H, k_{H_2O}, and k_{OH}), the specific catalyzing species (H^+ and OH^-), and the fractions of diprotic (f_{H_2S}), monoprotic or uncharged (f_{HS}), and deprotonated oxazepam (f_S), respectively. This general equation may be substituted with the following

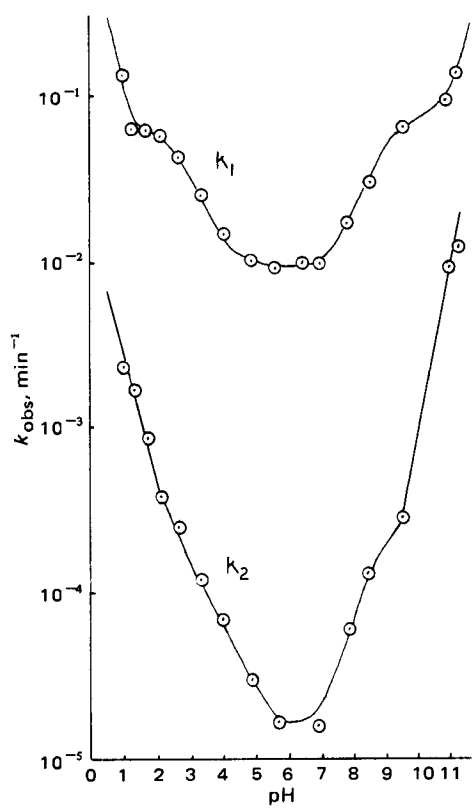

Figure 4—*Log k–pH profile for the hydrolysis of oxazepam at 85°, μ = 1.0.*

Table I—Apparent First-Order Rate Constants, 10^4 k (in Minutes^{-1}) for Oxazepam at 85°, μ = 1.0

pH	Buffer, M		k_1[a]	k_2[a]	r_1	r_2
		[HCl]				
0.93		0.1000	1324.9 ± 280.2	24.42 ± 4.01	0.93	0.93
1.24		0.0398	669.0 ± 128.5	16.95 ± 0.08	0.96	0.99
1.70		0.0158	633.9 ± 62.98	8.66 ± 0.20	0.99	0.99
2.13		0.0063	589.6 ± 79.6	3.84 ± 0.11	0.97	0.99
2.60		0.0025	436.5 ± 49.8	2.50 ± 0.08	0.97	0.99
	[CH_3COOH]	[CH_3COO^-]				
3.24	0.0957	0.0043	254.2 ± 9.2	1.18 ± 0.11	0.99	0.98
4.00	0.0761	0.0239	151.0 ± 6.2	0.68 ± 0.03	0.99	0.99
4.85	0.0322	0.0678	102.1 ± 1.1	0.28 ± 0.01	0.99	0.99
	[$H_2PO_4^-$]	[HPO_4^{2-}]				
5.58	0.0553	0.0011	92.9 ± 1.7	0.16 ± 0.008	0.99	0.99
6.47	0.0275	0.0391	103.1 ± 2.1	0.29 ± 0.008	0.99	0.99
	[H_3BO_3]	[$H_2BO_3^-$]				
6.96	0.103	0.003	100.8 ± 10.3	0.15 ± 0.02	0.97	0.98
7.93	0.103	0.029	177.9 ± 1.8	0.59 ± 0.05	0.99	0.98
8.52	0.061	0.112	331.1 ± 4.8	1.33 ± 0.11	0.99	0.99
9.53	0.003	0.100	628.8 ± 160.0	2.87 ± 1.33	0.94	0.77
		[NaOH]				
10.90		0.05	980.8 ± 18.3	95.54 ± 27.83	0.99	0.77
11.23		0.10	1421.9 ± 55.7	126.75 ± 1.15	0.99	0.99

[a] Standard deviations were calculated from a linear regression analysis of the data.

kinetic equivalents:

$$k_{H_2O}f_{H_2S} = k_{H'}[H^+]f_{HS} \quad \text{(Eq. 4)}$$

$$k_{OH}[OH^-]f_{H_2S} = k'_{H_2O}f_{HS} \quad \text{(Eq. 5)}$$

$$k_{OH'}[OH^-]f_{HS} = k''_{H_2O}f_S \quad \text{(Eq. 6)}$$

The respective fractions may also be written in terms of proton concentration and the acidity constants of oxazepam, K_1 and K_2, as, for example:

$$f_{H_2S} = \frac{[H^+]^2}{[H^+]^2 + K_1[H^+] + K_1K_2} \quad \text{(Eq. 7)}$$

The bimolecular rate constants and kinetic pKa's that provided the optimal fit to the experimental data points are listed in Table III. The calculated pKa's, 3.0 and 8.8, deviated substantially from those previously given as 1.7 and 11.6 at 25°. This deviation is reconcilable with the temperature difference between 85° (kinetic determination) and 25° (literature value). The directions of the shifts would be expected from thermodynamic consideration of the charged species in the protropic reactions.

The log k–pH profile for the second reaction step mirrors that of the initial step, and Eq. 3 may be used to generate the theoretical curve through the experimental data points. However, the fractions present (f_{H_2S}, f_{HS}, and f_S) would in this case refer to the intermediate(s), as would the kinetic pKa's. The theoretical curve was constructed from the values of the bimolecular rate constants and pKa values given in Table III.

The log k–pH profile for diazepam is given in Fig. 5. For pH values below the pKa of diazepam, two reaction steps were observed. The first reaction step is quantitatively described by the expression:

$$k_{obs} = k_{H_2O}f_{HS} \quad \text{(Eq. 8)}$$

or by its kinetic equivalent:

$$k_{obs} = k_H[H^+]f_S \quad \text{(Eq. 9)}$$

The kinetic pKa was determined to be 2.9, compared to the value of 3.3 at 25°. The magnitude and direction of the change in the pKa do not agree with those observed for the lower pKa value of oxazepam, both involving deprotonation of the azomethine nitrogen. The reason for this difference is not apparent. The second reaction step, as well as the single reaction step at higher pH values, is attributable to hydrolysis of a reaction intermediate according to the expression:

$$k_{obs} = k_H[H^+]f_{HS} + k_{H'}[H^+]f_S + k_{OH}[OH^-]f_S \quad \text{(Eq. 10)}$$

The second term, involving acid catalysis of the deprotonated intermediate, is kinetically equivalent to uncatalyzed hydrolysis of the protonated form. Table III lists the bimolecular rate constants and pKa values used to generate the theoretical curve shown in Fig. 5.

Isolation and Identification—Oxazepam samples withdrawn at appropriate times were subjected to TLC analysis as previously described. Throughout the entire pH region, the oxazepam spot (R_f 0.23) showed a gradual decrease in intensity with a concomitant relative intensity increase for that of the product 2-amino-5-chlorobenzophenone (R_f 0.75). The glycine derivative was observed at the origin upon spraying with

Table II—Apparent First-Order Rate Constants, 10^4 k (in Minutes^{-1}) for Diazepam at 80°, μ = 1.0

pH	Buffer, M		k_1[a]	k_2[a]	r_1	r_2
		[HCl]				
0.93		0.1000	940 ± 188	5.30 ± 0.11	0.97	0.99
1.70		0.0158	562 ± 104	1.71 ± 0.04	0.98	0.99
2.60		0.0025	640 ± 100	0.56 ± 0.07	0.90	0.97
	[CH_3COOH]	[CH_3COO^-]				
3.24	0.0957	0.0043	279 ± 6.15	0.26 ± 0.03	0.99	0.97
4.00	0.0761	0.0239	—	<0.10	—	—
4.85	0.0322	0.0678	—	<0.10	—	—
5.64	0.0081	0.0919	—	<0.10	—	—
	[$H_2PO_4^-$]	[HPO_4^{2-}]				
5.58	0.0553	0.0011	—	<0.10	—	—
6.47	0.0275	0.0391	—	<0.10	—	—
	[H_3BO_3]	[$H_2BO_3^-$]				
6.96	0.103	0.003	—	<0.10	—	—
7.93	0.103	0.029	—	<0.10	—	—
8.52	0.061	0.112	0.18 ± 0.01	—	0.99	—
9.63	0.003	0.100	0.57 ± 0.01	—	0.99	—
		[NaOH]				
10.18		0.01	1.75 ± 0.77	—	0.99	—
10.90		0.05	26.10 ± 0.77	—	0.99	—

[a] Standard deviations were calculated from a linear regression analysis of the data.

Table III—Bimolecular Rate Constants[a] for Hydrolysis of Oxazepam and Diazepam, μ = 1.0

k_H	k_H'	k_{H_2O}	k'_{H_2O}	k''_{H_2O}	k_{OH}	k_{OH}'	k_{OH}''	pKa[b]
				Oxazepam, k_1, 85°				
1.0	65	0.065	0.0098	0.072	4.18×10^7	487	2.0	3.0, 8.8
				Oxazepam, k_2, 85°				
0.023	1.44	0.000115	0.000014	0.00012	4070	4.07	0.4	4.1, 8.1
				Diazepam, k_1, 80°				
—	—	—	0.09	—	0.08	—	—	2.9
				Diazepam, k_2, 80°				
0.0045	0.11	—	—	—	—	—	—	3.4

[a] Except that 55.5 M water is incorporated into the k_{H_2O}, the rate constants are in units of minutes^{-1} M^{-1}. [b] The calculated kinetic pKa for the hydrolysis.

ninhydrin aerosol (0.5%). Two additional spots appeared transiently (R_f 0.48 and 0.68) and were ascribed to reaction intermediates. At pH values below pKa, the relative intensities of the intermediate spots appeared similar. However, at higher pH values, the spot at R_f 0.68 was much more intense than that at R_f 0.48.

The intermediates were isolated by preparative TLC and characterized spectroscopically. Structure IIa of Scheme I was assigned to the intermediate (R_f 0.68) predominating at the higher pH values by these measurements. The IR spectrum of a potassium bromide disk showed a typical carbonyl absorption peak at 1725 cm^{-1} for the carboxylic acid functional group. The NMR spectrum taken in dimethyl sulfoxide-d_6 demonstrated an acid proton (τ = −0.2). The expected molecular ion at m/e 304 was not observed in the mass spectrum analysis. The ion of greatest mass was observed at m/e 284. Sadee and Kleijn (4) demonstrated that the thermolysis of oxazepam leads to 6-chloro-4-phenylquinazoline-2-carboxaldehyde in GLC. It is possible that a comparable rearrangement of intermediate IIa, leading to the formation of 6-chloro-4-phenylquinazoline-2-carboxylic acid (mol. wt. 284), occurred in the ionization chamber of the mass spectrometer.

The IR and NMR spectra of the second intermediate were compatible with Structure IIIa of Scheme I but not definitive. The mass spectrum showed a parent peak of m/e 287 instead of the molecular ion of IIIa (m/e 304). Oxazepam, mol. wt. 286, gives a parent peak at m/e 269, indicating that dehydroxylation is a favored fragmentation. A similar preference for IIIa would account for the absence of the 304 peak and the appearance of the 287 peak. Thus, Structure IIIa was tentatively assigned to the intermediate (R_f 0.48).

TLC analysis of the hydrolysis of diazepam indicated formation of one intermediate (R_f 0.58) at pH values below the pKa. Diazepam and the product 2-methylamino-5-chlorobenzophenone were observed at R_f 0.43 and 0.69, respectively. At pH values above the pKa, no spots attributable to reaction intermediates were observed. The product glycine was identified at the origin by spraying with 0.5% ninhydrin aerosol reagent throughout the entire pH region. Attempts to isolate sufficient quantities of the intermediate for identification were unsuccessful due to the small amount present.

If the assumption is made that the intermediate is either IIb or IIIb, then the log k–pH profile may be used to suggest which is the most likely candidate. The discontinuity observed for the first reaction step at pH values above the pKa may be attributable to a recyclization reaction, adding a reversible reaction to the consecutive kinetic scheme. Structure IIb would exist as a protonated amine at pH values below its pKa and in the neutral form above the pKa. No recyclization would be expected with the protonated form due to the expected decreased nucleophilicity. However, the free base form could be expected to undergo facile recyclization. Thus, Structure IIIb was tentatively assigned to the intermediate resulting from diazepam hydrolysis.

Hydrolytic Mechanisms—The mechanisms of hydrolysis for oxazepam and diazepam may be interpreted according to Scheme I. For each, the pKa in the acidic pH region provides a pivotal point. At pH values above this point, II should exist as the carboxylate anion. This charge character would decrease the likelihood of nucleophilic attack of the aromatic amine necessary for reversibility. At lower pH values, the conjugate acid form should be susceptible to recyclization analogous to that observed with chlordiazepoxide (1) and demoxepam (2).

Intermediate III should demonstrate the opposite charge character as a function of pH. At pH values below its pKa, the amine function should be predominately protonated and thus have a resident positive charge. In this form, the nitrogen should be ineffective as a nucleophile, and recyclization would not occur. As the conjugate base above the pKa, reversibility would be much more favorable.

The observation that two intermediates are present during oxazepam hydrolysis implies that the parallel consecutive reaction mechanism shown in Scheme I is operable throughout the entire pH region. At pH values below the pKa, biphasic kinetic behavior was observed. These kinetics would be consistent with the parallel consecutive scheme if the transformation of the intermediates to final products is of approximately equal magnitude. The appearance and loss of the intermediates were qualitatively observed by TLC to be occurring at equal rates. At pH values above the pKa, TLC indicated that IIa formation was preferred. This phenomenon, coupled with the biphasic character of the kinetics, implies that the kinetically relevant mechanism is that shown in Scheme II.

$$Ia \rightarrow IIa \rightarrow IVa$$

Scheme II

Recyclization of intermediate IIIa and the absence of reversible reaction for Ia → IIa kinetically favor this pathway. Models show that sterically amide hydrolysis should be preferential to breakage of the azomethine bond. The competitiveness observed in the lower pH region appears to be attributable to the reversibility differences of the initial,

Table IV—Apparent First-Order Rate Constants, 10^4 k (in Minutes^{-1}) and Thermodynamic Parameters for Hydrolysis of Diazepam and Oxazepam

pH	k_i	85°	80°	75°	70°	E_a[a], kcal/mole	ln P[a]
				Diazepam			
0.93	k_1	157.0	94.0	67.0	49.6	18.4 ± 1.9	24.0 ± 2.8
	k_2	8.46	5.22	3.43	2.06	22.7 ± 0.6	24.7 ± 0.8
10.18	k_1	2.3	1.7	1.2	0.8	17.2 ± 0.6	15.9 ± 0.9
				Oxazepam			
0.93	k_1	1325	806	466	288	24.2 ± 0.5	33.0 ± 0.8
	k_2	24.4	18.6	12.9	10.9	13.5 ± 1.3	13.0 ± 1.9
3.24	k_1	254	208	118	78.1	20.0 ± 2.3	24.6 ± 3.3
	k_2	1.18	0.92	0.63	0.51	12.9 ± 1.1	9.1 ± 1.6
8.52	k_1	331	247	100	74.9	26.1 ± 4.2	33.4 ± 6.0
10.90	k_1	981	757	479	243	22.5 ± 3.0	29.5 ± 4.3
	k_2	95.5	67.1	42.2	21.7	24.0 ± 2.2	29.2 ± 3.1

[a] Standard deviations were calculated from a linear regression analysis of the data.

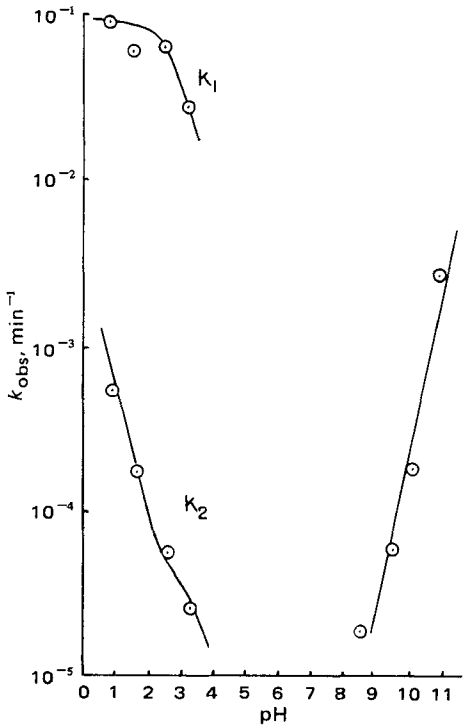

Figure 5—*Log* k–*pH profile for the hydrolysis of diazepam at 80°, μ = 1.0.*

parallel steps. Additionally, the charge character of the intact benzodiazepine, brought about by protonation of the azomethine nitrogen at lower pH values, electronically favors nucleophilic attack on the 5-position.

Diazepam hydrolysis proceeds through one intermediate (Scheme III).

$$Ib \rightarrow IIIb \rightarrow IVb$$

Scheme III

Apparently, methyl substitution on the amide nitrogen makes initial azomethine hydrolysis the preferred pathway. At pH values below the pKa, III*b* is not subject to recyclization; clear biphasic kinetics result. In the higher pH region, facile recyclization of III*b* causes the kinetics to be monophasic in character (Scheme IV).

$$Ib \rightleftharpoons IIIb \rightarrow IVb$$

Scheme IV

The Arrhenius parameters for hydrolysis were obtained from the slope and intercept of a plot of the logarithm of the apparent first-order rate constant, k, *versus* the reciprocal of the absolute temperature, T, shown by the expression:

$$\ln k = \ln P - E_a/RT \qquad \text{(Eq. 11)}$$

where R is the gas constant equal to 1.987 cal deg^{-1} mole^{-1}; $\ln P$ is related to the entropy of activation, ΔS_a, by:

$$\Delta S_a = R[\ln P - \ln(kT/h) - 1] \qquad \text{(Eq. 12)}$$

where h and k are the Planck and Boltzman constants, respectively; and E_a is related to the enthalpy of activation of the hydrolysis, ΔH_a, by:

$$\Delta H_a = E_a - RT \qquad \text{(Eq. 13)}$$

The Arrhenius parameters for oxazepam and diazepam hydrolyses at various pH values are given in Table IV. These values allow stability prediction in the pH regions showing rapid degradation. For oxazepam, buffer catalysis was studied according to the relationship:

$$k_{obs} = k_0 + \left(\frac{k_{HA}[H^+]}{K_a} + k_A\right)[A^-] \qquad \text{(Eq. 14)}$$

where K_a is the dissociation constant for the buffer species; k_0 is the hydrolysis rate constant in the absence of buffer catalysis; and k_{HA} and k_A are the rate constants for buffer catalysis of the acid buffer species, HA, and its conjugate base, A^-, respectively. Buffer effects were investigated by changing the original buffer concentration fourfold in a gradient manner. Buffer effects were not significant, and thus the specific rate constants were not delineated.

REFERENCES

(1) W. W. Han, G. J. Yakatan, and D. D. Maness, *J. Pharm. Sci.*, **65,** 1198 (1976).

(2) L. H. Sternback and E. Reeder, *J. Org. Chem.*, **26,** 4936 (1961).

(3) J. Barrett, W. F. Smyth, and I. E. Davidson, *J. Pharm. Pharmacol.*, **25,** 387 (1973).

(4) W. Sadee and V. D. Kleijn, *J. Pharm. Sci.*, **60,** 135 (1971).

ACKNOWLEDGMENTS AND ADDRESSES

Received November 28, 1975, from the *College of Pharmacy, University of Texas at Austin, Austin, TX 78712.*

Accepted for publication June 15, 1976.

Presented in part at the Basic Pharmaceutics Section, APhA Academy of Pharmaceutical Sciences, San Francisco meeting, April 1975.

Abstracted in part from a dissertation submitted by W. W. Han to the University of Texas at Austin in partial fulfillment of the Doctor of Philosophy degree requirements.

Supported in part by a grant from the University Research Institute, University of Texas at Austin.

The authors express their gratitude to Dr. W. E. Scott, Hoffmann–La Roche Inc., and to Dr. G. Schneller, Wyeth Laboratories, for samples supplied and to Dr. Jay Nematollahi for helpful discussions.

[x] To whom inquiries should be directed. Present address: Searle Laboratories, Chicago, IL 60680.

Thermal Decomposition of 1,3-Dimethyl Derivative of Phenobarbital in Trimethylanilinium Hydroxide

PATRICK S. CALLERY and JAMES LESLIE ˣ

Abstract □ Extensive degradation of the 1,3-dimethyl derivative of phenobarbital occurs when it is injected with trimethylanilinium hydroxide in methanol into a gas chromatograph. The application of mass spectrometry demonstrated that the major products are *N*-methyl-2-phenylbutyramide, *N,N*-dimethyl-2-phenylbutyramide, methyl 2-phenylbutyrate, *N,N,N'*-trimethylethylphenylmalondiamide, and *N,N,N',N'*-tetramethylethylphenylmalondiamide. The methyl group of the ester arises from the methanol solvent, whereas the methyl groups of the substituted amides arise from the parent compound or the methylating reagent. Tetramethylammonium hydroxide causes much more degradation than trimethylanilinium hydroxide under comparable conditions.

Keyphrases □ 1,3-Dimethyl derivative of phenobarbital—thermal decomposition in gas chromatograph, major products identified by mass spectrometry □ Phenobarbital 1,3-dimethyl derivative—thermal decomposition in gas chromatograph, major products identified by mass spectrometry □ Decomposition, thermal—1,3-dimethyl derivative of phenobarbital, in gas chromatograph, major products identified by mass spectrometry □ GLC–mass spectrometry—thermal decomposition of 1,3-dimethyl derivative of phenobarbital, major products identified

Phenobarbital is frequently analyzed by a GC technique in which the drug is injected simultaneously with trimethylanilinium hydroxide (I) (1). The peak quantified was shown to be the 1,3-dimethyl derivative of phenobarbital (II) (2), but the presence of an additional peak with a much shorter retention time was consistently reported (3–7). This "early peak" was identified as *N*-methyl-2-phenylbutyramide (V) (5), although the presence of *N,N*-dimethyl-2-phenylbutyramide (VI) also was demonstrated (7).

In preliminary studies, a mixture of I and II was injected into a gas chromatograph under the conditions of phenobarbital analysis, and it was observed that II degraded to several products (8). In view of the extensive use of the on-column GC methylation procedure for phenobarbital determination and the interest in the structure of the early peak, the products of the reaction of I and II were examined by mass spectrometry; the results are reported in this paper.

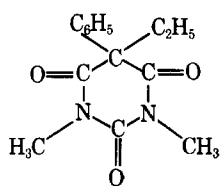

II

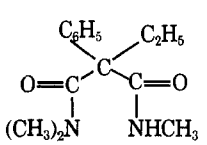

III

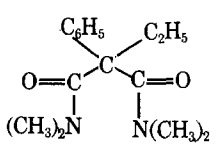

IV

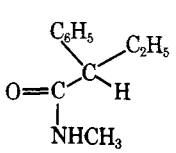

V

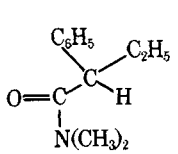

VI

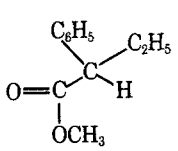

VII

RESULTS

Injection of II in methanol into a gas chromatograph[1] yielded a single peak, whereas injection of this compound in I (0.1–1.8 *M*) at temperatures usually used in the analysis of phenobarbital yielded several peaks (Fig. 1). Peaks A and B had the same retention times as the early peak and major peak, respectively, observed when phenobarbital is injected with I under the same conditions. Peaks C and D were not reported previously.

Furthermore, analysis of the mixture of I and II at a programmed temperature starting at 90° revealed the presence of two additional components, E and F, and resolved peak A into two peaks, A_1 and A_2 (Fig. 2*a*). The relative areas of the peaks were dependent on a number of factors, including the absolute and relative concentrations of I and II, the water content of the mixture injected, and the pH of the solution of I used. By comparison of their mass spectra to those obtained for authentic compounds, the identities of peaks A_1, A_2, B, E, and F were established as VI, V, II, dimethylaniline, and methyl 2-phenylbutyrate (VII), respectively.

The mass spectra of peaks C and D (Figs. 3 and 4) indicated that these compounds were *N,N,N'*-trimethylphenylethylmalondiamide (III) and *N,N,N',N'*-tetramethylphenylethylmalondiamide (IV), respectively. The fragmentation pattern of peak D corresponded closely to the literature values for IV (9). Peak C was assigned Structure III on the basis of

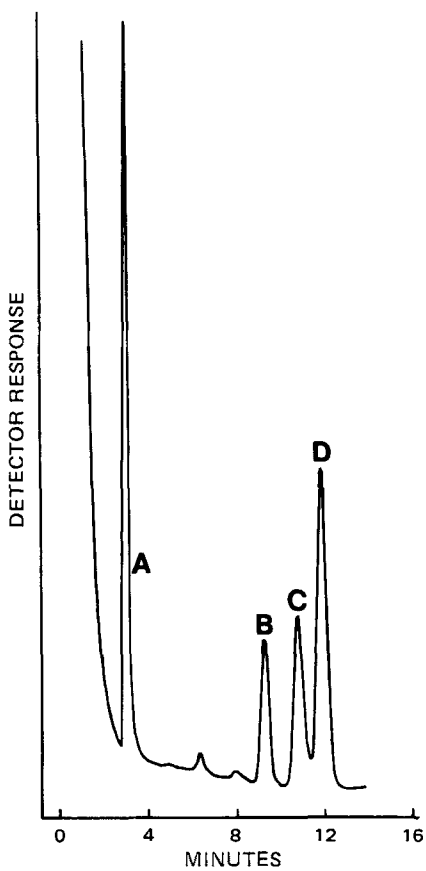

Figure 1—*Gas chromatogram of a mixture of I and II isothermally at 220°.*

[1] Varian series 1400.

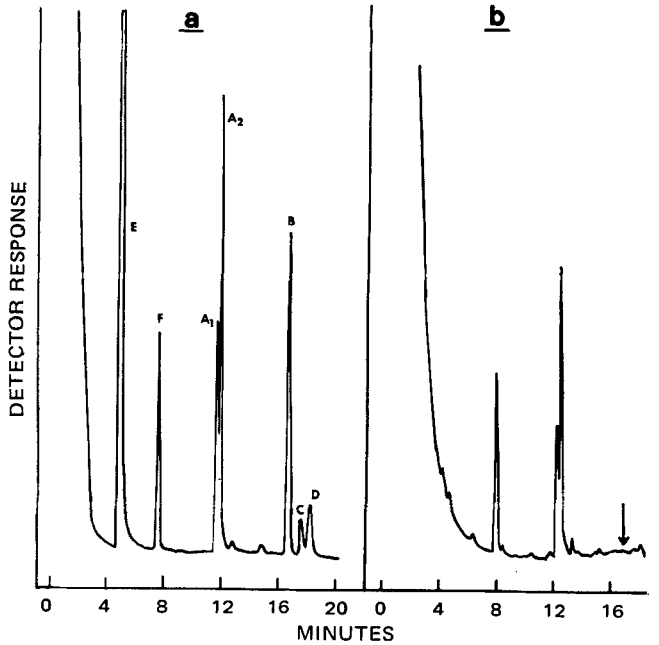

Figure 2—(a) *Gas chromatogram of a mixture of I and II programmed from 90 to 260° at 10°/min.* (b) *Gas chromatogram of a mixture of II and tetramethylammonium hydroxide programmed from 90 to 260° at 10°/min. The arrow indicates where unchanged II would have appeared.*

an analysis of its fragmentation pattern. Peak C exhibited significant ions also found for IV at *m/e* 120, 117, 103, 91, and 72, which suggested that C and D were derived from a similar skeleton structure.

The molecular ion of peak C (*m/e* 248), which was 14 mass units less than the tetramethyl Compound IV, was consistent with the trimethyldiamide III. Ions at *m/e* 176 $[M-(CH_3)_2NCO]^+$ and 72 $[(CH_3)_2NCO]^+$ indicated that peak C contained a dimethylamide moiety; the ion at *m/e* 58 $(CH_3NHCO)^+$ suggested that the parent molecule also contained a monomethylamide group. Further support for the presence of a monomethylamide function was derived from an intense ion at *m/e* 191, which can be accounted for by the loss of methylisocyanate by a McLafferty-type rearrangement of the molecular ion.

On-column methylation performed with deuterated I coupled with mass spectrometric analysis demonstrated that deuterium was incorporated into one methyl group in VI and into one and two methyl groups in III and IV, respectively. No deuterium was observed in VII under these conditions. However, deuterium was incorporated into the ester when the methylation was carried out in the presence of deuterated methanol[2], indicating that the source of the methyl group in this compound was the methanol solvent. When a mixture of I and II was allowed to stand for several days at room temperature and then neutralized with dilute hydrochloric acid, only the peaks corresponding to dimethylaniline and II were observed upon GLC analysis. This result indicates that the decomposition of the barbiturate in alkaline solution occurs after injection and not at ambient temperatures and that the decomposition is base catalyzed. Injection of the amides V and VI into the gas chromatograph with I in methanol did not result in the formation of the ester VII.

When II was injected into the gas chromatograph with 0.13 *M* tetramethylammonium hydroxide[3] in methanol, the results were more striking. As illustrated in Fig. 2*b*, II was almost completely degraded under these conditions to V–VII. Acidification of the reaction mixture prior to injection resulted in little or no decomposition of II upon injection.

DISCUSSION

A GLC–mass spectrometric study of the reaction of I and II shows that extensive degradation of the barbiturate occurs at high temperatures to form a number of products. This degradation is of interest, since phenobarbital is frequently determined by quantification of the area of its

[2] Stohler Isotope Chemicals.
[3] Supplied as 24% solution, Matheson, Coleman and Bell.

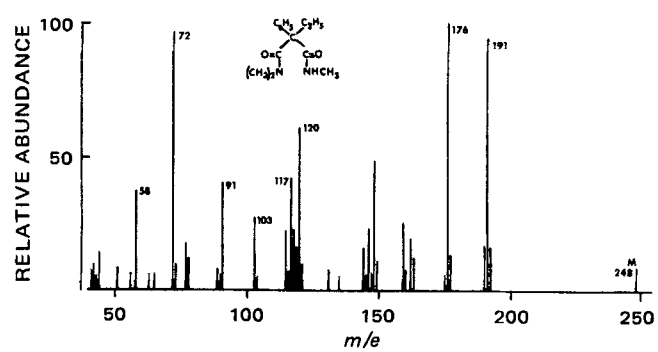

Figure 3—*Mass spectrum of peak C of Fig. 2.*

1,3-dimethyl derivative obtained after on-column methylation with I (1) and in at least one laboratory by quantification of the area of the early peak (7).

The degradation of II occurs in the injector port at high temperatures in the presence of base, since it does not occur in alkaline solutions at ambient temperatures or in neutral solutions at high temperatures. The first step in the degradation is likely to be the loss of a carbonyl group from II with the formation of *N,N*-dimethylphenylethylmalondiamide, which is then subsequently methylated to the tri- and tetramethyl derivatives. The formation of IV was observed previously in the reaction of phenobarbital with methylsulfinylmethide carbanion and methyl iodide (9) but not with phenobarbital and diazomethane (10). The methylated phenylbutyramides probably arise from III and IV, since it was shown that phenylethylmalondiamide forms V and VI when injected into a gas chromatograph with I (7), although this result was interpreted as either V and phenylethylmalondiamide having similar retention times (5) or the early peak being phenylethylmalondiamide (4).

The reaction pathway leading to the formation of VII has not been elucidated at this time, but it apparently is not formed from the methylated 2-phenylbutyramides. A possibility is that a 1,6-cleavage of II occurs, leading to a product that could form the ester with methanol. It was demonstrated that 1,6-cleavage in addition to 3,4-cleavage can occur in the degradation of barbiturates (11).

In view of the instability of II in solutions of I at high temperatures, the on-column methylation of phenobarbital might be expected to result in the formation of degradation products. The lack of the formation of significant amounts of products other than V indicates that reactions involving methylation and decomposition of I are completed before extensive degradation of II can occur. However, it does suggest that any analytical method for phenobarbital determination involving quantification of a decomposition product should be applied with caution, since the amounts of degradation products depend on experimental parameters such as injection port temperatures and the concentration of the methylating reagent.

EXPERIMENTAL

Materials—Compound II was prepared by reacting 2.3 g of phenobarbital[4] with 11.4 g of methyl iodide and 0.5 g of sodium hydroxide in 10 ml of methanol for 4 hr at ambient temperature. The product, which separated from the mixture upon dilution with water, was recrystallized from ethanol–water. The purified product, mp 88° [lit. (12) mp 84°],

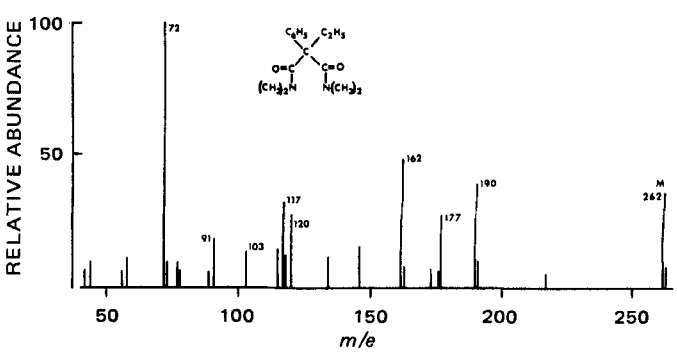

Figure 4—*Mass spectrum of peak D of Fig. 2.*

[4] Merck and Co.

chromatographed as a single peak with the same retention time as that observed by on-column methylation of phenobarbital; its mass spectrum was consistent with that previously reported (13). Compound I was prepared by the method of Brochmann-Hanssen and Oke (2), and deuterated I was prepared in a similar manner using methyl iodide-d_3[5]. A 1.8 *M* solution of I was obtained from a commercial source[6].

2-Phenylbutyryl chloride was prepared by refluxing 10 g of 2-phenylbutyric acid[7] and 15 g of thionyl chloride for 30 min and then distilling off the excess thionyl chloride. The acid chloride was divided into three portions. Compounds V and VI were prepared by reacting portions of the 2-phenylbutyryl chloride with 20 g of methylamide hydrochloride and 25 g of dimethylamine hydrochloride, respectively, which had been previously adjusted to about pH 12. The reaction mixture was allowed to stand overnight, during which time the crude products separated. The mixture was again made alkaline and extracted with ether. The extract was dried with anhydrous sodium sulfate, and the ether was evaporated. Compound V was obtained as a solid, which was purified by treatment with charcoal[8] in ethanol. Then the ethanol was evaporated, and the compound was recrystallized from hexane, mp 97° [lit. (14) mp 95–96°]. Compound VI was obtained as a viscous liquid, which was purified by repeated treatment with charcoal in ethanol.

Compound VII was prepared by refluxing 5 g of 2-phenylbutyric acid, 10 ml of methanol, and 0.2 ml of concentrated sulfuric acid for 4 hr. Then the cooled reaction mixture was poured into 25 ml of water and saturated with sodium bicarbonate. The alkaline solution was extracted with ether and dried overnight with anhydrous sodium sulfate, the ether was evaporated, and the ester was distilled, bp 225° [lit. (15) bp 228°].

Methods—GLC was performed on a 1.82-m × 3.2-mm o.d. glass column packed with 3% OV-17 on Chromosorb WHP[9]. The carrier gas was helium at a flow rate of 30 ml/min, the injector temperature was 250°, and the oven temperature was either maintained at 220° or programmed from 90 to 260° at 10°/min during the chromatography. A flame-ionization detector was used.

In the appropriate experiments, a portion of the effluent was passed through a heated glass jet separator into a mass spectrometer[10] operating in the electron-impact mode with an ionizing voltage of 70 ev. A mass range of 41–500 was automatically scanned at 2 sec/decade approximately every 5 sec during the elution of peaks. Normalized mass spectra of compounds included all ions within the mass range scanned with intensity greater than 5% of the base peak.

[5] Merck Sharp and Dohme Isotope Division.
[6] Supelco.
[7] Aldrich Chemical Co.
[8] Norit-A, Fisher Scientific Co.
[9] Applied Science Laboratories.
[10] DuPont 21-490 interfaced with a DuPont 21-094 data system.

REFERENCES

(1) H. J. Kupferberg, *Clin. Chim. Acta*, **29**, 283 (1970).

(2) E. Brochmann-Hanssen and T. O. Oke, *J. Pharm. Sci.*, **58**, 370 (1969).

(3) G. W. Stevenson, *Anal. Chem.*, **38**, 1948 (1966).

(4) J. C. Van Meter and H. W. Gillen, *Clin. Chem.*, **19**, 359 (1973).

(5) A. Wu, *ibid.*, **20**, 630 (1974).

(6) R. J. Perchalski, K. N. Scott, B. J. Wilder, and R. H. Hammer, *J. Pharm. Sci.*, **62**, 1735 (1973).

(7) R. Osiewicz, V. Aggarwal, R. M. Young, and I. Sunshine, *J. Chromatogr.*, **88**, 157 (1974).

(8) P. S. Callery and J. Leslie, *Clin. Chem.*, **22**, 926 (1976).

(9) R. M. Thompson and D. M. Desiderio, *Org. Mass Spectrom.*, **7**, 989 (1973).

(10) D. J. Harvey, J. Nowlin, P. Hickert, C. Butler, O. Gansow, and M. G. Horning, *Biomed. Mass Spectrom.*, **1**, 340 (1974).

(11) H. V. Maulding, J. Nazareno, J. Polesuk, and A. Michaelis, *J. Pharm. Sci.*, **61**, 1389 (1972).

(12) S. Dilli and D. N. Pillai, *Aust. J. Chem.*, **28**, 2265 (1975).

(13) J. N. T. Gilbert, B. J. Millard, and J. W. Powell, *J. Pharm. Pharmacol.*, **22**, 897 (1970).

(14) J. Bojarski, W. Kahl, and M. Melzacka, *Rocz. Chem.*, **39**, 875 (1965); through *Chem. Abstr.*, **64**, 5088f (1966).

(15) "Dictionary of Organic Compounds," vol. 4, Oxford University Press, New York, N.Y., 1965, p. 2677.

ACKNOWLEDGMENTS AND ADDRESSES

Received April 30, 1976, from the *School of Pharmacy, University of Maryland, Baltimore, MD 21201.*

Accepted for publication June 17, 1976.

[x] To whom inquiries should be directed.

Use of Pharmacological Data for Bioavailability and Pharmacokinetic Analyses

PAUL A. KRAMER

Abstract □ The use of pharmacological responses such as pupil diameter for dosage individualization, bioavailability, and pharmacokinetic analyses is becoming more widespread. Attempts to use pupil diameter to assess morphine bioavailability illuminate the fact that multiple responses, nonlinearities, and the condition of the subject can produce misleading results unless the applicability of the method is confirmed.

Keyphrases □ Pharmacological response data—use in bioavailability and pharmacokinetic analyses, situations producing misleading results determined □ Bioavailability—analyses based on pharmacological response data, situations producing misleading results determined □ Pharmacokinetics—analyses based on pharmacological response data, situations producing misleading results determined □ Pupil diameter—measurements used to assess morphine bioavailability □ Morphine—bioavailability analyzed using pupil diameter measurements

Several recent publications underscored the utility of pharmacological response data for performing drug bioavailability and pharmacokinetic analyses (1–3). The theoretical foundation and limits of applicability of the approach were described in detail (2, 4), and this approach was applied successfully to several systems that would have been difficult or impossible to analyze by conventional means (5, 6). An obvious necessity for using pharmacological data is the existence of a clearly defined, measurable, graded response to the administered drug, but the availability and quantitation of such responses are often cited (7) as limiting factors in applying the method.

The objective of this study is to determine the usefulness of pharmacological methods for analyzing the bioavail-

chromatographed as a single peak with the same retention time as that observed by on-column methylation of phenobarbital; its mass spectrum was consistent with that previously reported (13). Compound I was prepared by the method of Brochmann-Hanssen and Oke (2), and deuterated I was prepared in a similar manner using methyl iodide-d_3[5]. A 1.8 *M* solution of I was obtained from a commercial source[6].

2-Phenylbutyryl chloride was prepared by refluxing 10 g of 2-phenylbutyric acid[7] and 15 g of thionyl chloride for 30 min and then distilling off the excess thionyl chloride. The acid chloride was divided into three portions. Compounds V and VI were prepared by reacting portions of the 2-phenylbutyryl chloride with 20 g of methylamide hydrochloride and 25 g of dimethylamine hydrochloride, respectively, which had been previously adjusted to about pH 12. The reaction mixture was allowed to stand overnight, during which time the crude products separated. The mixture was again made alkaline and extracted with ether. The extract was dried with anhydrous sodium sulfate, and the ether was evaporated. Compound V was obtained as a solid, which was purified by treatment with charcoal[8] in ethanol. Then the ethanol was evaporated, and the compound was recrystallized from hexane, mp 97° [lit. (14) mp 95–96°]. Compound VI was obtained as a viscous liquid, which was purified by repeated treatment with charcoal in ethanol.

Compound VII was prepared by refluxing 5 g of 2-phenylbutyric acid, 10 ml of methanol, and 0.2 ml of concentrated sulfuric acid for 4 hr. Then the cooled reaction mixture was poured into 25 ml of water and saturated with sodium bicarbonate. The alkaline solution was extracted with ether and dried overnight with anhydrous sodium sulfate, the ether was evaporated, and the ester was distilled, bp 225° [lit. (15) bp 228°].

Methods—GLC was performed on a 1.82-m × 3.2-mm o.d. glass column packed with 3% OV-17 on Chromosorb WHP[9]. The carrier gas was helium at a flow rate of 30 ml/min, the injector temperature was 250°, and the oven temperature was either maintained at 220° or programmed from 90 to 260° at 10°/min during the chromatography. A flame-ionization detector was used.

In the appropriate experiments, a portion of the effluent was passed through a heated glass jet separator into a mass spectrometer[10] operating in the electron-impact mode with an ionizing voltage of 70 ev. A mass range of 41–500 was automatically scanned at 2 sec/decade approximately every 5 sec during the elution of peaks. Normalized mass spectra of compounds included all ions within the mass range scanned with intensity greater than 5% of the base peak.

[5] Merck Sharp and Dohme Isotope Division.
[6] Supelco.
[7] Aldrich Chemical Co.
[8] Norit-A, Fisher Scientific Co.
[9] Applied Science Laboratories.
[10] DuPont 21-490 interfaced with a DuPont 21-094 data system.

REFERENCES

(1) H. J. Kupferberg, *Clin. Chim. Acta*, **29**, 283 (1970).

(2) E. Brochmann-Hanssen and T. O. Oke, *J. Pharm. Sci.*, **58**, 370 (1969).

(3) G. W. Stevenson, *Anal. Chem.*, **38**, 1948 (1966).

(4) J. C. Van Meter and H. W. Gillen, *Clin. Chem.*, **19**, 359 (1973).

(5) A. Wu, *ibid.*, **20**, 630 (1974).

(6) R. J. Perchalski, K. N. Scott, B. J. Wilder, and R. H. Hammer, *J. Pharm. Sci.*, **62**, 1735 (1973).

(7) R. Osiewicz, V. Aggarwal, R. M. Young, and I. Sunshine, *J. Chromatogr.*, **88**, 157 (1974).

(8) P. S. Callery and J. Leslie, *Clin. Chem.*, **22**, 926 (1976).

(9) R. M. Thompson and D. M. Desiderio, *Org. Mass Spectrom.*, **7**, 989 (1973).

(10) D. J. Harvey, J. Nowlin, P. Hickert, C. Butler, O. Gansow, and M. G. Horning, *Biomed. Mass Spectrom.*, **1**, 340 (1974).

(11) H. V. Maulding, J. Nazareno, J. Polesuk, and A. Michaelis, *J. Pharm. Sci.*, **61**, 1389 (1972).

(12) S. Dilli and D. N. Pillai, *Aust. J. Chem.*, **28**, 2265 (1975).

(13) J. N. T. Gilbert, B. J. Millard, and J. W. Powell, *J. Pharm. Pharmacol.*, **22**, 897 (1970).

(14) J. Bojarski, W. Kahl, and M. Melzacka, *Rocz. Chem.*, **39**, 875 (1965); through *Chem. Abstr.*, **64**, 5088f (1966).

(15) "Dictionary of Organic Compounds," vol. 4, Oxford University Press, New York, N.Y., 1965, p. 2677.

ACKNOWLEDGMENTS AND ADDRESSES

Received April 30, 1976, from the *School of Pharmacy, University of Maryland, Baltimore, MD 21201.*

Accepted for publication June 17, 1976.

[x] To whom inquiries should be directed.

Use of Pharmacological Data for Bioavailability and Pharmacokinetic Analyses

PAUL A. KRAMER

Abstract □ The use of pharmacological responses such as pupil diameter for dosage individualization, bioavailability, and pharmacokinetic analyses is becoming more widespread. Attempts to use pupil diameter to assess morphine bioavailability illuminate the fact that multiple responses, nonlinearities, and the condition of the subject can produce misleading results unless the applicability of the method is confirmed.

Keyphrases □ Pharmacological response data—use in bioavailability and pharmacokinetic analyses, situations producing misleading results determined □ Bioavailability—analyses based on pharmacological response data, situations producing misleading results determined □ Pharmacokinetics—analyses based on pharmacological response data, situations producing misleading results determined □ Pupil diameter—measurements used to assess morphine bioavailability □ Morphine—bioavailability analyzed using pupil diameter measurements

Several recent publications underscored the utility of pharmacological response data for performing drug bioavailability and pharmacokinetic analyses (1–3). The theoretical foundation and limits of applicability of the approach were described in detail (2, 4), and this approach was applied successfully to several systems that would have been difficult or impossible to analyze by conventional means (5, 6). An obvious necessity for using pharmacological data is the existence of a clearly defined, measurable, graded response to the administered drug, but the availability and quantitation of such responses are often cited (7) as limiting factors in applying the method.

The objective of this study is to determine the usefulness of pharmacological methods for analyzing the bioavail-

Table I—Miotic Response of Rabbits to Intravenous Doses of Morphine Sulfate[a]

Rabbit Number	Dose, mg/kg	I_{max}[b]	t_{max}[c], min	Duration of Action $I > 0.1$, min	Total Morphine Plasma Level at End of Effect ($I = 0.1$), μg/ml
1	5	0.58	3	180	2.0
2	5	0.59	1	240	0.35
3	7.5	0.52	1	17	6.5
4	4	0	—	—	6.0[d]
5	6	0	—	—	13.2[d]
6	6	0	—	—	20.0[d]
7	5	0.32	1	120	3.0
8	5	0	—	—	8.0[d]
9	5	0.40	1.5	120	3.6

[a] Using 50 mg/ml in normal saline. [b] Maximum miotic response intensity defined by $(D_0 - D_{t_{max}})/D_0$, where D_0 = baseline pupillary diameter and $D_{t_{max}}$ = diameter at time of maximum miosis. [c] Time of occurrence of maximum miotic response intensity. [d] Measured 30 min after dosing by radioimmunoassay.

ability and pharmacokinetics of narcotics or narcotic antagonists. Narcotics such as morphine and heroin produce pupillary diameter changes that can be quantitated accurately, and the abolition of these changes by narcotic antagonists might also be interpreted as a pharmacological effect and used to assess the bioavailability and absorption characteristics of these agents. The steady-state miotic response to morphine could, for example, be utilized to determine the rate and extent of bioavailability of naloxone from a sustained-release device by analysis of the antagonist's ability to abolish these miotic effects.

Besides a graded pharmacological response, another criterion for using the method is that the rate-limiting process in the production of that response be the drug's ability to gain access to the biophase. All processes must also be entirely reversible, *i.e.*, nonhysteretic and the instantaneous result of a continuous equilibrium between free and receptor-bound drug, and the biokinetic behavior of the drug must be linear. As pointed out previously: "It is not generally sufficient to assume arbitrarily that these conditions are met for any given drug and biological system" (4).

Preliminary results with morphine in rabbits are reported here to underscore the importance of testing these assumptions before using a dose–effect curve to perform pharmacokinetic analyses.

EXPERIMENTAL

Pupillometry—Male New Zealand White rabbits, 3.0–4.0 kg, were fasted overnight and placed in a rabbit restrainer consisting of a rectangular metal box with a neck ring through which the rabbit's head could extend. An IR illuminator provided a constant low level of background light for accentuating the miotic effects of morphine and facilitated drug administration and plasma sampling. All rabbits were acclimated to the experimental setup by putting them through mock experiments for several weeks.

A closed circuit TV camera[1], equipped with an IR light source and a telephoto lens[2], was positioned about 17 cm from the rabbit's right eye and connected to a 22.9-cm television monitor[3]. The near IR light used did not affect pupillary diameter. The camera was set at a fixed focal length and was not altered during the measurements of pupillary diameter. Head movements, which were infrequent, were corrected for by repositioning the camera so that the pupil was returned to perfect focus.

Pupillary diameters were calibrated to the TV screen image by measuring with calipers the TV image size of a series of dots of known diameter located at the position of the rabbit's eye. Pupil diameters were then measured with the calipers on the TV screen and converted to actual diameters using the calibration curve. When a rabbit pupil was not a perfect circle, all measurements were made vertically through the center point of the pupil. Pupil diameters at any given time were measured four times, and the average value was recorded.

Drug Administration—A 23-gauge butterfly infusion set was placed in the marginal vein of one ear. After a brief acclimation, pupillary diameters were measured in the absence of drug to obtain baseline miotic data. Morphine sulfate was then administered in 0.9% NaCl either as a bolus dose or with an infusion pump[4]. Saline solutions buffered to the pH (4.8) of morphine sulfate did not produce a miotic effect when injected into the ear vein as a control.

Plasma Sampling and Radioimmunoassay—Blood samples (100 μl) were collected in heparinized capillary tubes through a small cut in the marginal vein of the opposite ear. The cut was made prior to the experiment and reopened by gentle rubbing to minimize discomfort. Plasma was obtained by centrifugation and was assayed using a commercially available tritiated morphine radioimmunoassay kit[5]. Dialysis studies showed that the procedure measured both free and plasma protein-bound morphine. However, at the high plasma concentrations found in this study during miosis (1–20 μg/ml), a negligible fraction (less than 3%) of the total morphine present was protein bound.

RESULTS

Table I lists the miotic responses of nine rabbits to intravenous doses of morphine sulfate. The intensity of response, I, was taken to be the fractional reduction in pupil diameter at any given time after dosing. Large intrasubject variability was observed, with four rabbits showing substantial responses, four not responding, and one exhibiting a transient response. Plasma morphine levels in nonresponders verified that high plasma levels often did not produce miosis.

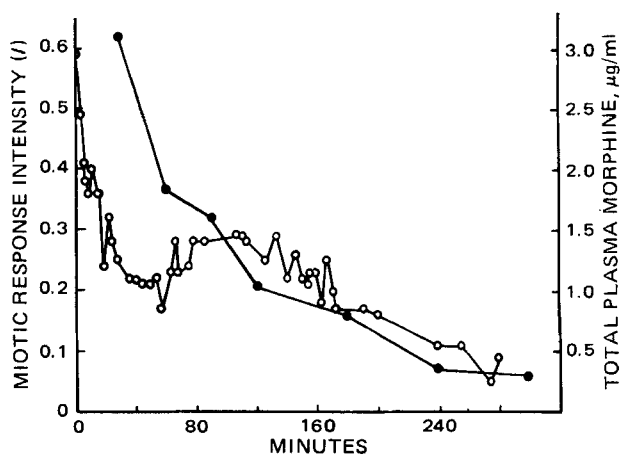

Figure 1—*Typical plot of miotic response intensity (I) as a function of time in a responding rabbit (Rabbit 2) after intravenous administration of a 5-mg/kg dose of morphine sulfate. Each response is the average of four determinations.*

[1] Shibaden model HV40SU, Nucleus Video Co., Indianapolis, Ind.
[2] Wollensack Reptar 7.62 cm f/2.5.
[3] Sony.
[4] Harvard dual syringe, model 2681, Millis, Mass.
[5] Roche Diagnostics, Nutley, N.J.

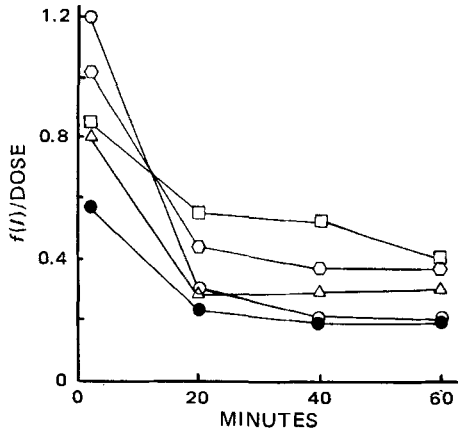

Figure 2—*Congruency test on dose-normalized relative quantities of drug in the biophase, f(I). Each value is the average of four replications on the rabbit that provided the dose–effect data (Fig. 3) used to determine f(I). Doses were 2.0 (□), 3.0 (○), 4.0 (△), 5.0 (○), and 6.0 (●) mg/kg. Curves would be superimposable if system were linear.*

Plots of the time course of I in responding rabbits (Fig. 1) consisted of three phases: an initial rapid decline, a plateau where response was independent of time, and a final slow decline. The relative quantities of drug in the biophase, $f(I)$, at various times were computed from these data (4) and normalized for dose. Plots of dose-normalized values of $f(I)$ *versus* time (Fig. 2) for various intravenous doses are not superimposable as they would be if the system were linear. Therefore, this "congruency test" (4) indicates that the use of a linear compartment model to describe the data is inappropriate. Failure to recognize this nonlinearity can lead to erroneous predictions of expected responses in multiple dose or infusion therapy (see *Discussion*).

When the maximum response intensities (occurring 1–3 min after administration) were plotted as a function of dose, a hyperbolic dose–effect curve was obtained (Fig. 3). The fact that a parallel curve was not obtained when intensities were chosen at times other than t_{max} (such as 30 min) indicated that the response to the drug was hysteretic and not solely the instantaneous result of a continuous equilibrium between free and receptor-bound drug at the site of action ["function of I ratio test" (4)]. Identical challenge doses of morphine were administered to a responding rabbit 1 week after each experiment that contributed to the dose–effect curve (Fig. 3) over several months. No alteration in the miotic response to the challenge dose was observed, indicating that the development of tolerance to morphine did not affect the dose–response relationship.

DISCUSSION

While the rabbit may not be the ideal species for studying the miotic effects of morphine because of the large number of nonresponders, researchers are not totally free to select an appropriate species for many applications; the effective utilization of pharmacological response data ultimately depends on measurements made in a single species, humans.

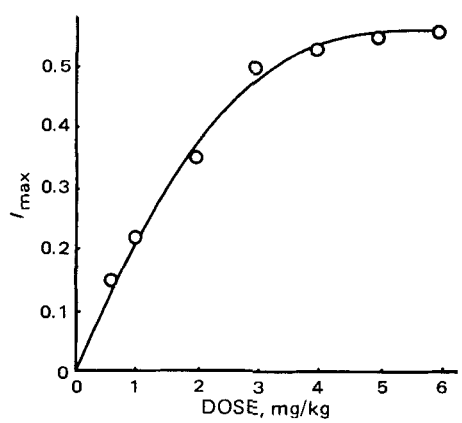

Figure 3—*Intravenous dose–response curve for morphine sulfate in a responding rabbit (Rabbit 2). Response was taken at time of maximum miotic effect (1–3 min), and each response is the average of four determinations. Parallel curves are not obtained using I values obtained at longer times (such as 30 min) after dosing.*

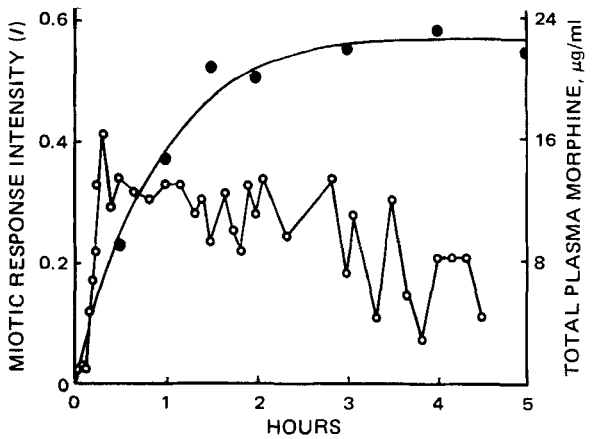

Figure 4—*Miotic response intensity (I) and plasma total morphine levels during an intravenous infusion of morphine sulfate (48 mg/hr) into a responding rabbit (Rabbit 2). Each response is the average of four determinations.*

The presented results are indicative of the potential pitfall one may encounter when a substantial number of nonresponding subjects are encountered for a given drug in a given species. While careful selection of responding subjects or averaging of results over a large number of subjects might prove adequate for some applications such as the determination of bioavailability, dosage individualization using pharmacological responses and attendant calculations specific to a particular subject may not be possible in a substantial fraction of a given subject population.

Even when graded responses are observed in an individual subject, one could easily obtain a dose–effect curve like that shown in Fig. 3, fail to check if the required conditions were met before applying the pharmacological method, and proceed to predict erroneously the outcome of subsequent drug administrations. Figure 4 shows measured plasma total morphine levels during intravenous drug infusion and the miotic response that resulted in a single responding rabbit. This analysis could serve as a model for dosage individualization in a single human or as a check on the validity of using miotic response data to determine the bioavailability from a zero-order sustained-release dosage form.

The responses to the intravenous bolus doses were nonlinear, and one would not expect the miotic response data to be useful in calculating the cumulative amount of drug entering the bloodstream for comparison with what was actually administered. The data confirm that this was indeed the case. The peak miotic responses (Fig. 4) occurred much earlier than peak plasma total morphine levels, and the miotic response to the zero-order infusion never really plateaued but rather continuously diminished with time. Kinukawa (8) also was unable to observe plateau miotic responses during infusions in rabbits.

One must also be aware of factors that may confound the pharmacological response of interest. These factors can render certain pharmacological response baselines so "noisy" that the use of the technique for dosage individualization may be jeopardized. Factors of potential concern include the effects of coadministered drugs in the patient's overall therapy, physiological effects associated with the patient's disease state, and multiple pharmacological responses that are not independent but rather interact. The last factor is illustrated by these data in rabbits. Previous investigators observed a parallelism between morphine miosis and respiratory rate in the rabbit and showed that miosis increased as the carbon dioxide content of plasma rose (9). Thus, observation of the primary pharmacological effect (miosis) appears to be confounded by the depressant effects of the drug. Patients often take several drugs simultaneously, so similar effects in human subjects can be expected to complicate the practical application of pharmacological response methods.

Pharmacological methods of analysis are extremely powerful and hold great potential in systems where they can be quantitated accurately and applied properly. This preliminary study points out that investigators must proceed cautiously in selecting responses to be monitored.

REFERENCES

(1) V. F. Smolen, R. D. Barile, and T. G. Theophanous, *J. Pharm. Sci.*, **61**, 467 (1972).

(2) V. F. Smolen and W. A. Weigand, *J. Pharmacokinet. Biopharm.*, **1**, 329 (1973).

(3) V. F. Smolen, *Can. J. Pharm. Sci.*, **1**, 1 (1972).
(4) V. F. Smolen and R. D. Schoenwald, *J. Pharm. Sci.*, **60**, 96 (1971).
(5) V. F. Smolen, E. J. Williams, and P. B. Kuehn, *Can. J. Pharm. Sci.*, **10**, 95 (1975).
(6) V. F. Smolen, H. R. Murdock, W. P. Stoltman, J. W. Cleavenger, L. W. Combs, and E. J. Williams, *J. Clin. Pharmacol.*, **15**, 734 (1975).
(7) J. G. Wagner, "Fundamentals of Clinical Pharmacokinetics," Drug Intelligence Publications, Hamilton, Ill., 1975, p. 3.
(8) C. Kinukawa, *Tohoku J. Exp. Med.*, **22**, 174 (1933).
(9) V. E. Henderson and R. W. Graham, *J. Pharmacol. Exp. Ther.*, **26**, 469 (1925).

ACKNOWLEDGMENTS AND ADDRESSES

Received April 5, 1976, from the *Department of Industrial and Physical Pharmacy, School of Pharmacy and Pharmacal Sciences, Purdue University, West Lafayette, IN 47907.*

Accepted for publication June 17, 1976.

Supported by Grant R03 DA 00725 from the National Institute of Mental Health.

The author is indebted to Mrs. Sandra Diskin for technical assistance.

Present address: Pharmacy Department, University of Connecticut, Farmington, CT 06032.

High-Pressure Liquid Chromatographic Analysis of Drugs in Biological Fluids II: Determination of an Antiarrhythmic Drug, Tocainide, as Its Dansyl Derivative Using a Fluorescence Detector

PETER J. MEFFIN ˣ, SANDRA R. HARAPAT, and DONALD C. HARRISON

Abstract □ A sensitive and specific method is described for the determination of a new primary aliphatic amine antiarrhythmic drug, tocainide. Tocainide, together with an internal standard, is selectively extracted from plasma or blood and reacted with dansyl chloride. The highly fluorescent dansyl derivatives are separated using high-pressure liquid chromatography and measured using a fluorescence detector. The method can measure therapeutic and subtherapeutic concentrations of the drug (0.1–5.0 μg/ml of plasma) with a standard deviation of less than 2%.

Keyphrases □ Tocainide—high-pressure liquid chromatographic analysis, plasma or blood □ High-pressure liquid chromatography—analysis, tocainide, plasma or blood □ Dansyl chloride—derivatizing reagent in high-pressure liquid chromatographic analysis of tocainide □ Antiarrhythmics—tocainide, high-pressure liquid chromatographic analysis, plasma or blood

Within the last 5 years, advances in high-pressure liquid chromatography (HPLC), the commercial availability of reliable HPLC equipment, and the development of efficient columns have resulted in the application of HPLC to many analytical problems. However, the application of HPLC to drug analysis has lagged behind the increase in its general use (1, 2). Many papers reported the chromatographic conditions required to separate drugs (3–7), but only a few described the quantitative application of HPLC to the analysis of drugs in dosage forms (8–11).

A major cause of the failure to apply HPLC to the analysis of drugs in biological fluids has been the lack of suitable detectors. UV absorption detectors have been commonly used in HPLC. The microgram or nanogram per milliliter concentrations of many drugs found in plasma after therapeutic doses have confined the use of HPLC analysis to drugs having high molar absorptivities at 254 or 280 nm, the wavelengths most frequently used in these detectors (12–18).

The derivatization of pesticides with reagents yielding fluorescent derivatives and their subsequent HPLC analysis have been reported (19–22). Many drugs unsuited for analysis with UV absorption or fluorescence detectors have primary or secondary amino, phenolic or alcoholic hydroxyl, or aldehyde and keto functions suitable for the formation of fluorescent derivatives. The ability of HPLC to resolve compounds with small differences in molecular structure permits derivatization prior to injection onto the column while still achieving adequate separation of the drug of interest from other molecules reacting with the reagent.

This paper reports the use of HPLC with a commercially available fluorescence detector to determine blood and plasma concentrations of a new primary aliphatic amine antiarrhythmic drug, tocainide [2-amino-*N*-(2,6-dimethylphenyl)propanamide], after derivatization with dansyl chloride [5-(dimethylamino)-1-naphthalenesulfonyl chloride]. The described techniques should be generally applicable to drugs containing derivatizable functional groups. The use of reagents such as dansyl chloride may result in the increased utilization of HPLC for drug analysis in biological fluids, in a manner similar to that which occurred with electron-capture detection in GLC when halogenated acylating and alkylating reagents became available.

EXPERIMENTAL

Reagents—Ethyl acetate[1], hexane[1], acetone[1], and carbon tetrachloride[1] were used as received. Hexane[2], dichloromethane[2], and methanol[2] were used as chromatographic solvents. Stock solutions of tocainide[3] were prepared in 0.05 *N* HCl over the range of 0.1–10 μg/100 μl. The internal standard [2-amino-*N*-(2,6-dimethylphenyl)butanamide hydrochloride[3] (I)] was prepared in 0.05 *N* HCl at a concentration of 0.675 μg/50 μl.

A solution of dansyl chloride (1 mg/ml) was prepared in acetone and

[1] Nanograde quality, Mallinckrodt, St. Louis, Mo.
[2] SpectrAR quality, Mallinckrodt.
[3] Astra Pharmaceutical Products, Worcester, Mass.

(3) V. F. Smolen, *Can. J. Pharm. Sci.*, **1**, 1 (1972).
(4) V. F. Smolen and R. D. Schoenwald, *J. Pharm. Sci.*, **60**, 96 (1971).
(5) V. F. Smolen, E. J. Williams, and P. B. Kuehn, *Can. J. Pharm. Sci.*, **10**, 95 (1975).
(6) V. F. Smolen, H. R. Murdock, W. P. Stoltman, J. W. Cleavenger, L. W. Combs, and E. J. Williams, *J. Clin. Pharmacol.*, **15**, 734 (1975).
(7) J. G. Wagner, "Fundamentals of Clinical Pharmacokinetics," Drug Intelligence Publications, Hamilton, Ill., 1975, p. 3.
(8) C. Kinukawa, *Tohoku J. Exp. Med.*, **22**, 174 (1933).
(9) V. E. Henderson and R. W. Graham, *J. Pharmacol. Exp. Ther.*, **26**, 469 (1925).

ACKNOWLEDGMENTS AND ADDRESSES

Received April 5, 1976, from the *Department of Industrial and Physical Pharmacy, School of Pharmacy and Pharmacal Sciences, Purdue University, West Lafayette, IN 47907.*

Accepted for publication June 17, 1976.

Supported by Grant R03 DA 00725 from the National Institute of Mental Health.

The author is indebted to Mrs. Sandra Diskin for technical assistance.

Present address: Pharmacy Department, University of Connecticut, Farmington, CT 06032.

High-Pressure Liquid Chromatographic Analysis of Drugs in Biological Fluids II: Determination of an Antiarrhythmic Drug, Tocainide, as Its Dansyl Derivative Using a Fluorescence Detector

PETER J. MEFFIN ˣ, SANDRA R. HARAPAT, and DONALD C. HARRISON

Abstract □ A sensitive and specific method is described for the determination of a new primary aliphatic amine antiarrhythmic drug, tocainide. Tocainide, together with an internal standard, is selectively extracted from plasma or blood and reacted with dansyl chloride. The highly fluorescent dansyl derivatives are separated using high-pressure liquid chromatography and measured using a fluorescence detector. The method can measure therapeutic and subtherapeutic concentrations of the drug (0.1–5.0 μg/ml of plasma) with a standard deviation of less than 2%.

Keyphrases □ Tocainide—high-pressure liquid chromatographic analysis, plasma or blood □ High-pressure liquid chromatography—analysis, tocainide, plasma or blood □ Dansyl chloride—derivatizing reagent in high-pressure liquid chromatographic analysis of tocainide □ Antiarrhythmics—tocainide, high-pressure liquid chromatographic analysis, plasma or blood

Within the last 5 years, advances in high-pressure liquid chromatography (HPLC), the commercial availability of reliable HPLC equipment, and the development of efficient columns have resulted in the application of HPLC to many analytical problems. However, the application of HPLC to drug analysis has lagged behind the increase in its general use (1, 2). Many papers reported the chromatographic conditions required to separate drugs (3–7), but only a few described the quantitative application of HPLC to the analysis of drugs in dosage forms (8–11).

A major cause of the failure to apply HPLC to the analysis of drugs in biological fluids has been the lack of suitable detectors. UV absorption detectors have been commonly used in HPLC. The microgram or nanogram per milliliter concentrations of many drugs found in plasma after therapeutic doses have confined the use of HPLC analysis to drugs having high molar absorptivities at 254 or 280 nm, the wavelengths most frequently used in these detectors (12–18).

The derivatization of pesticides with reagents yielding fluorescent derivatives and their subsequent HPLC analysis have been reported (19–22). Many drugs unsuited for analysis with UV absorption or fluorescence detectors have primary or secondary amino, phenolic or alcoholic hydroxyl, or aldehyde and keto functions suitable for the formation of fluorescent derivatives. The ability of HPLC to resolve compounds with small differences in molecular structure permits derivatization prior to injection onto the column while still achieving adequate separation of the drug of interest from other molecules reacting with the reagent.

This paper reports the use of HPLC with a commercially available fluorescence detector to determine blood and plasma concentrations of a new primary aliphatic amine antiarrhythmic drug, tocainide [2-amino-*N*-(2,6-dimethylphenyl)propanamide], after derivatization with dansyl chloride [5-(dimethylamino)-1-naphthalenesulfonyl chloride]. The described techniques should be generally applicable to drugs containing derivatizable functional groups. The use of reagents such as dansyl chloride may result in the increased utilization of HPLC for drug analysis in biological fluids, in a manner similar to that which occurred with electron-capture detection in GLC when halogenated acylating and alkylating reagents became available.

EXPERIMENTAL

Reagents—Ethyl acetate[1], hexane[1], acetone[1], and carbon tetrachloride[1] were used as received. Hexane[2], dichloromethane[2], and methanol[2] were used as chromatographic solvents. Stock solutions of tocainide[3] were prepared in 0.05 *N* HCl over the range of 0.1–10 μg/100 μl. The internal standard [2-amino-*N*-(2,6-dimethylphenyl)butanamide hydrochloride[3] (I)] was prepared in 0.05 *N* HCl at a concentration of 0.675 μg/50 μl.

A solution of dansyl chloride (1 mg/ml) was prepared in acetone and

[1] Nanograde quality, Mallinckrodt, St. Louis, Mo.
[2] SpectrAR quality, Mallinckrodt.
[3] Astra Pharmaceutical Products, Worcester, Mass.

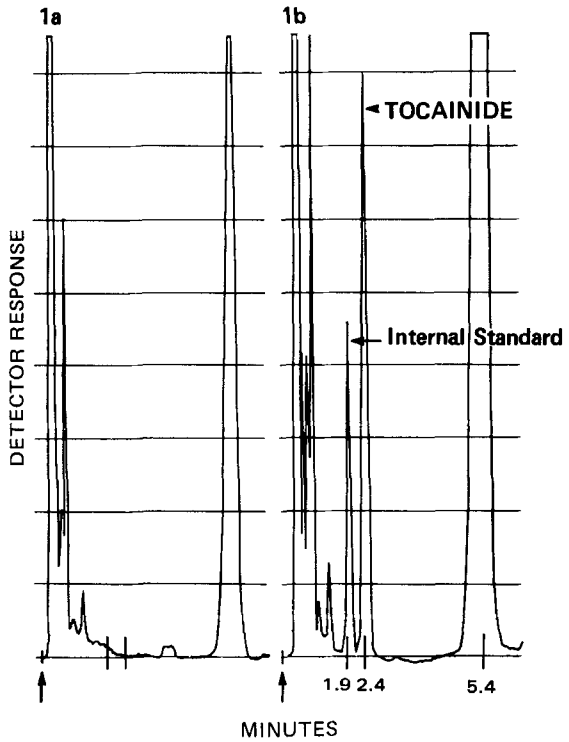

Figure 1—*Chromatograms obtained with plasma from a patient prior to receiving tocainide* (a) *and with a plasma concentration of tocainide of 1.10 μg/ml* (b). *The vertical lines in Fig. 1a correspond to the retention times of tocainide and the internal standard.*

stored in the dark under refrigeration. A fresh solution was prepared each week. Buffer (pH 6.0) was prepared by making a half-saturated solution of disodium citrate in water and adjusting the pH to 6.0 with 85% H_3PO_4. Solutions of 2 and 0.5 *N* NaOH, 0.1 *N* H_2SO_4, and 1 *M* $NaHCO_3$ were also employed.

General Procedure: Extraction and Derivatization of Tocainide—Between 0.05 and 2.0 ml of plasma or whole blood containing an estimated 0.1–5.0 μg of tocainide was transferred with a pipet[4] to a screw-capped[5] centrifuge tube (15 ml) together with 50 μl of internal standard solution containing 0.675 μg of 1, 200 μl of 2 *N* NaOH, and 3 ml of ethyl acetate. The samples were extracted by mixing, using gentle hand-tilting of the tubes for 5 min, followed by centrifugation at 2500 rpm for 10 min to separate the organic and aqueous phases.

The aqueous phase was discarded. Approximately 2 ml of the ethyl acetate phase was transferred to a second tube, which had an elongated cone at its base of nominal 0.1-ml capacity, containing 50 μl of 0.1 *N* H_2SO_4. The tube was mixed[6] for 1 min and centrifuged for 5 min to separate the phases. The ethyl acetate phase was then discarded, and hexane (1 ml) was added to the acidic extract in the tube. The mixing and centrifugation steps were then repeated. The tube was then immersed in a dry ice–acetone bath to freeze the aqueous phase; the hexane, together with the remaining ethyl acetate, was decanted and discarded.

After thawing, 50 μl of 1 *M* $NaHCO_3$ and 200 μl of dansyl chloride solution were added to the tube, which was heated[6] for 30 min at 40°. Sodium hydroxide solution (100 μl of 0.5 *N*) was then added to the tube to convert the remaining dansyl chloride to the sodium salt of 5-(dimethylamino)-1-naphthalenesulfonic acid. Most of the acetone was then removed by heating[6] the tube to 40°, at reduced pressure, for 3 min. Buffer (pH 6.0, 1 ml) was added, together with 200 μl of carbon tetrachloride. The tube was mixed for 2 min and centrifuged for 5 min to separate the aqueous and organic phases. Between 2 and 5 μl of the carbon tetrachloride phase, sampled through the aqueous phase with a 10-μl syringe, was injected into the chromatograph.

Chromatography—A high-pressure liquid chromatograph[7] fitted with a 30-cm × 4-mm i.d. column[8] was used. A fluorometer[9] having both excitation[10] and emission[11] filters was used as a detector. Pressure was maintained in the detector to prevent the formation of bubbles by a 0.5-μm porosity stainless steel frit[12], placed on the efferent side of the detector. One pump of the dual-pump gradient elution chromatograph contained hexane, and the other contained 2% methanol in dichloromethane. An isocratic 1:1 mixture of the two solvents was used in the analysis[13].

Calibration and Accuracy—Calibration curves were constructed by adding known amounts of tocainide and the internal standard to blood and plasma, which were then taken through the analytical procedure. The peak height ratio of tocainide to the internal standard was plotted *versus* the amount of tocainide added to construct the calibration curve. Replicates (10 samples) at tocainide concentrations of 0.3 and 3.0 μg were carried through the procedure to determine the reproducibility of the method.

To calibrate the method and obtain an estimate of accuracy for each particular batch of unknown samples, standards of 0.1, 1.0, and 5.0 μg of tocainide were added to 1-ml samples of blank plasma, which were assayed for tocainide at the same time as the unknown samples. The peak height ratio of each standard was divided by the amount of tocainide added to give a normalized peak height ratio. The average normalized peak height ratio was used to calculate the amount of tocainide in the unknown samples and to estimate accuracy. The effect of sample size on the method was investigated by adding 1.0 μg of tocainide to tubes containing 0.05–2.0 ml of plasma and then assaying for tocainide.

Mass Spectra—Solvent corresponding to the peaks resulting from tocainide and internal standard was collected and reduced to a small volume with a stream of air at room temperature. The mass spectra of these materials were determined by direct probe insertion into the mass spectrometer[14], which had undergone minor modifications to permit use in the chemical ionization mode (23). The reactant gas was isobutane, and the instrument was operated at 200°.

Plasma Level Study—Tocainide tablets were administered to a patient (60 years old, 67 kg) on two separate occasions after approximately 12 hr of fasting. Either 400 or 800 mg of tocainide was administered on each occasion, and food was allowed after 3 hr. Samples of venous blood (10 ml) were withdrawn by means of heparinized containers[15] at appropriate intervals for 60 hr after dosing. The blood samples were centrifuged, and the plasma was transferred to glass containers and stored at −15° until analyzed.

RESULTS AND DISCUSSION

Preliminary work showed that tocainide was satisfactorily and conveniently extracted from plasma by ethyl acetate under strongly alkaline conditions. The conditions for the reaction of tocainide with dansyl chloride were optimized for pH, reagent concentration, solvent composition, temperature, and time using published data on the reaction of the reagent with primary aliphatic amines as a guide (24). The excitation and emission maxima of the peaks corresponding to both tocainide and internal standard in the mixture of solvents used for the chromatography were at 360 and 490 nm, respectively. The excitation and emission filters used in the detector (see *Experimental*) were chosen to minimize the radiation from sources other than the fluorescence of the dansyl derivatives reaching the photomultiplier tube, consistent with a high input in the region of the excitation maxima.

With the solvents used in this analysis, the column[8] required a pressure of 120 atm to produce a flow rate of 300 ml/hr. Under these conditions, the peaks corresponding to tocainide and the internal standard had retention times of 2.4 and 1.9 min, respectively. A large peak at 5.4 min, present also in reagent blanks, prevented injection of samples into the chromatograph at intervals more frequent than 6 min. A typical chromatogram of a patient sample having 1.10 μg of tocainide/ml of plasma is shown in Fig. 1*b*. A chromatogram of blank plasma from this patient is also shown in Fig. 1*a*. In general, no peaks that interfered with the tocainide or internal standard peak, other than the partially resolved small peaks shown in Fig. 1*a*, were encountered in analysis of plasma from some 20 patients. To date, only one column[8] has been used and has shown no deterioration in performance after 6 months of use on a daily basis under the conditions described.

[4] Eppendorf, V.W.R. Scientific, San Francisco, Calif.
[5] Lined with Teflon (du Pont).
[6] Vortex-evaporator, Buchler Instruments, Fort Lee, N.J.
[7] Model 8500, Varian, Palo Alto, Calif.
[8] μBondapack NH_2, Waters, Milford, Mass.
[9] Fluoromonitor, American Instrument Co., Silver Spring, Md.
[10] Corning 7–51, Scientific Products.
[11] Wratten 8, Eastman Kodak, Rochester, N.Y.
[12] Varian, Palo Alto, Calif.
[13] Minor adjustments in the ratio of the two solvents were made each day to give the retention times reported.
[14] AEI MS 902.
[15] Vacutainers, V.W.R. Scientific, San Francisco, Calif.

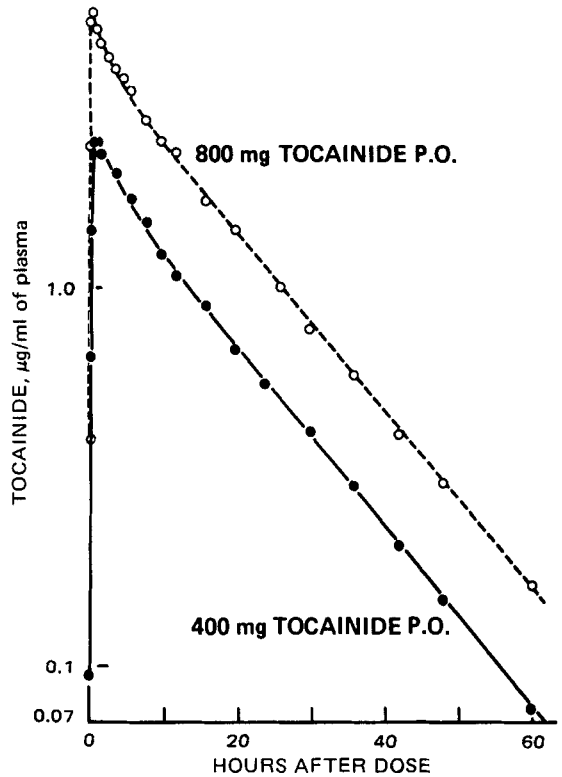

Figure 2—*Plasma concentrations of tocainide at various times in a patient receiving 400 and 800 mg po of tocainide on two separate occasions.*

Calibration curves from water, plasma, and whole blood were superimposable within the error of the method. However, the increased background observed in the chromatograms of blood extracts made the application of the method unreliable at tocainide concentrations below approximately 0.5 μg/ml of blood. The calibration curve from plasma was linear in the 0.1–5.0-μg range and passed through the origin. The average normalized peak height ratio (see *Experimental*) obtained from the daily three-point calibration curves had a mean coefficient of variation of 3.4% for 32 separate calibration curves obtained over approximately 6 months.

This estimate of accuracy probably gives a higher estimate of error than normally would be encountered during the routine application of the method to pharmacokinetic studies, since two of the three calibration points (at 0.1 and 5.0 μg of tocainide/ml of plasma) are at the maximum and minimum of the calibration curve. At the time of analysis of unknown samples, sample volumes were chosen to yield peak height ratios as close to 1.0 as possible to minimize error. Replicates of 10 samples of 3.0 and 0.3 μg of tocainide/ml of plasma had coefficients of variation of 1.1 and 1.8%, respectively.

Since it was convenient to take variable volumes of plasma to determine the tocainide concentration in unknown samples, the effect of plasma volume on the peak height ratio of tocainide to the internal standard was examined. The results of this investigation indicated that the peak height ratios were independent of the volume of plasma added between 0.05 and 2.0 ml of plasma, having a coefficient of variation of 3.7% with no systematic trend apparent in the data.

The sensitivity of the method is more than adequate to measure antiarrhythmic concentrations of tocainide, which preliminary data indicate to be in the range of 4–10 μg/ml of plasma. The sensitivity of the presently described method could be increased by extracting the final reaction mixture into a volume of carbon tetrachloride less than the 0.2 ml used or by sampling a larger portion of solvent than the 1–2% injected into the chromatograph. The lower limit of sensitivity is imposed by the competition of solvent with the drug during the derivatization step. It is impractical to scale down the derivatization conditions described (total volume of 300 μl) by more than an order of magnitude. The addition of excess dansyl chloride to compensate for the low concentrations of drug gives rise to an increased solvent signal and produces no net beneficial result.

The described method was applied during the initial clinical evaluation of tocainide in some 20 patients and yielded consistent data after both single and multiple oral doses. The use of the vortex-evaporator[6] in conjunction with the rapid chromatographic analysis allowed the extraction and analysis of 30–35 samples in 8 hr. Typical data are shown in Fig. 2 for a patient who received 400 and 800 mg of tocainide on two separate occasions. Computation of the area under the plasma concentration–time curve from zero to infinite time for the low dose divided by the high dose yields a value of 0.497. This ratio is very close to 0.5, which would be expected if the product of the fraction of the dose absorbed and the clearance of the drug remained constant in this subject.

The use of dansyl chloride as a reagent for the determination of drugs and their metabolites in the biological fluids has been restricted by the lack of suitable methods for the routine separation of the compounds of interest from the many other products of the reaction. Dansyl chloride undergoes many side reactions and, as a result, the compound being assayed may be a minor constituent of the reaction mixture (24). The utility of HPLC in achieving difficult separations is evidenced in the separation of the dansyl derivative of tocainide from its internal standard. The structures of these two compounds, differing by only one methylene unit, are supported by their mass spectra.

The protonated molecular ion, *m/e* 426, was the base peak of the chemical ionization mass spectrum of the dansyl derivative to tocainide (mol. wt. 425). Peaks were also observed at *m/e* 277 (relative abundance 36%) and 191 (55), corresponding to the fragments shown in Structure II (tocainide, R = CH_3; internal standard, R = CH_2CH_3).

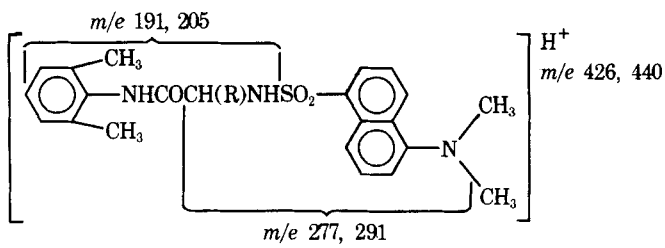

II

A similar series of peaks at *m/e* 440 (relative abundance 100%), 291 (30), and 205 (25), 14 amu higher than those obtained for the dansyl derivative of tocainide, was observed for the derivative of the internal standard (mol. wt. 439). All of these data are consistent with the proposed structures of the derivatives.

The ability of HPLC to separate the dansyl derivatives of two such similar compounds may be indicative of the usefulness of the combination of HPLC and fluorescence detectors. The use of similar reagents with this combination might increase significantly the number of drugs that can be measured in biological fluids and the sensitivity with which they can be measured.

REFERENCES

(1) A. F. Michaelis, D. W. Cornish, and R. Vivilecchia, *J. Pharm. Sci.*, **62**, 1399 (1973).

(2) R. E. Heuttemann, M. L. Cotter, C. J. Shaw, C. A. Janicki, H. R. Almond, E. S. Moyer, A. P. Schroff, and F. Vestano, *Anal. Chem.*, **47**, 233R (1975).

(3) E. Murgia, P. Richards, and H. F. Walton, *J. Chromatogr.*, **87**, 523 (1973).

(4) R. G. Muusze and J. F. K. Huber, *ibid.*, **83**, 405 (1973).

(5) J. H. Knox and J. Jurand, *ibid.*, **82**, 398 (1973).

(6) *Ibid.*, **87**, 95 (1973).

(7) F. J. Evans, *J. Chromatogr.*, **88**, 411 (1973).

(8) F. Bailey and P. N. Brittain, *ibid.*, **83**, 431 (1973).

(9) M. Vecchi, J. Vesely, and G. Oesterhelt, *ibid.*, **83**, 477 (1973).

(10) R. H. King, L. T. Grady, and J. T. Reamer, *J. Pharm. Sci.*, **63**, 1591 (1974).

(11) I. L. Honigberg, J. T. Stewart, A. P. Smith, R. D. Plunkett, and D. W. Hester, *ibid.*, **63**, 1762 (1974).

(12) C. V. Manion, D. W. Shoeman, and D. L. Azarnoff, *J. Chromatogr.*, **101**, 169 (1974).

(13) R. D. Thompson, H. T. Nagasawa, and J. W. Jenne, *J. Lab. Clin. Med.*, **84**, 584 (1974).

(14) J. E. Evans, *Anal. Chem.*, **45**, 2428 (1973).

(15) K. S. Albert, M. R. Hallmark, M. E. Carroll, and J. G. Wagner, *Res. Commun. Chem. Pathol. Pharmacol.*, **3**, 845 (1973).

(16) E. W. Vesell and C. A. Shively, *Science*, **184**, 466 (1974).

(17) N. J. Pound and R. W. Sears, *J. Pharm. Sci.*, **64**, 284 (1975).
(18) W. F. Bayne, G. Rodgers, and N. Crisologo, *ibid.*, **64**, 402 (1975).
(19) J. F. Lawrence and R. W. Frei, *Anal. Chem.*, **44**, 2047 (1972).
(20) R. W. Frei and J. F. Lawrence, *J. Chromatogr.*, **83**, 321 (1973).
(21) J. F. Lawrence and R. W. Frei, *Chromatogr. Rev.*, **17**, 253 (1974).
(22) R. W. Frei, J. F. Lawrence, J. Hope, and R. M. Cassidy, *J. Chromatogr. Sci.*, **12**, 40 (1974).
(23) W. A. Garland, R. J. Weinkam, and W. F. Trager, *Chem. Inst.*, 271 (1973).
(24) N. Seiler and M. Weichman, in "Progress in Thin-Layer Chromatography and Related Methods," vol. 1, A. Nieder-Wieser and G. Pataki, Eds., Ann Arbor Science Publishers, Ann Arbor, Mich., 1970, chap. 4.

ACKNOWLEDGMENTS AND ADDRESSES

Received October 8, 1975, from the *Cardiology Division, Stanford University School of Medicine, Stanford, CA 94305.*

Accepted for publication June 22, 1976.

Supported by NIH Grant HL-5866 and Program Project Grant 1-P01-15833.

The assistance of Mr. Joseph B. Keenaghan in supplying a number of compounds for investigation as internal standards is appreciated. The authors also thank Mrs. Dorothy McCain for her editorial assistance.

[x] To whom inquiries should be directed.

NOTES

Cytotoxic and Tumor Inhibitory Agent from *Polygala macradenia* Gray (Polygalaceae): 4′-Demethyldeoxypodophyllotoxin

JOSEPH J. HOFFMANN, RICHARD M. WIEDHOPF, and JACK R. COLE [x]

Abstract □ The chloroform fraction of *Polygala macradenia* exhibited activity against the P-388 lymphocytic leukemia and human epidermoid carcinoma of the nasopharynx test systems. The constituent responsible for this activity was a lignan, 4′-demethyldeoxypodophyllotoxin ($C_{21}H_{20}O_7$). The identity was proven by elemental analysis; PMR, IR, mass spectrometric, and melting-point determinations; and preparation of a derivative.

Keyphrases □ *Polygala macradenia*—chloroform fraction of extract of aerial parts, lignan isolated, evaluated for cytotoxic and tumor inhibitory activity □ 4′-Demethyldeoxypodophyllotoxin—isolated from chloroform fraction of extract of aerial parts of *Polygala macradenia*, evaluated for cytotoxic and tumor inhibitory activity □ Cytotoxic activity—lignan isolated from chloroform fraction of extract of aerial parts of *Polygala macradenia* evaluated □ Tumor inhibitory activity—lignan isolated from chloroform fraction of extract of aerial parts of *Polygala macradenia* evaluated

In the continuing search for plants having tumor inhibitory constituents, it was found that the chloroform fraction of *Polygala macradenia* Gray (Polygalaceae)[1], obtained by partitioning the ethanol extract of the stems, leaves, flowers, and fruit between chloroform and water, showed inhibitory activity against the P-388 lymphocytic leukemia (PS) test system and the human epidermoid carcinoma of the nasopharynx (KB) test system[2].

DISCUSSION

The lignan 4′-demethyldeoxypodophyllotoxin (I), previously isolated from *Polygala paenea* L. (Polygalaceae) (1), was isolated from the chloroform fraction by column chromatography, treatment with activated charcoal, preparative TLC, and recrystallization. The structure of the lignan was confirmed by elemental analysis; PMR, IR, mass spectrometric, and melting-point determinations; and conversion to the known lignan, deoxypodophyllotoxin (II).

Compound I demonstrated an ED_{50} of 0.0012 μg/ml in the KB test system. Activity in the KB system is defined as $ED_{50} \leq 20$ μg/ml (2). In the PS test system, the lignan demonstrated activity of 132% test/control (T/C) at 2.1 mg/kg. Activity in the PS system is defined as an increase in the survival of treated animals over that of control animals resulting in a T/C ≥ 125% (3).

EXPERIMENTAL[3]

Isolation Procedure—The stems, leaves, flowers, and fruit of *P. macradenia* (16 kg) were ground and extracted exhaustively in a Lloyd-type extractor with ethanol. The air-dried residue was partitioned between chloroform (10 liters) and water (10 liters). A 200-g sample of the air-dried chloroform phase was then subjected to alumina III (2 kg) column (7 × 65 cm) chromatography. The solvents used, in increasing order of polarity, were hexane, hexane–benzene (1:1), benzene, chloroform, and methanol; elution was continued with each solvent until the eluent was colorless. The benzene fraction (1.2 g) was subjected to silica gel 60 (75 g) column (3.5 × 24 cm) chromatography, eluting with benzene–ether (4:1). Fractions 16–38 (25 ml each), consisting of one major component according to TLC, exhibited activity.

Isolation of I—The combined active fractions were treated with activated charcoal and purified by preparative TLC with a chloroform–

[1] The plant was collected in Texas in August 1974. Identification was confirmed by Dr. Robert E. Perdue, Jr., Medicinal Plant Resources Laboratory, U.S. Department of Agriculture, Bethesda, Md. A reference specimen is maintained by the U.S. Department of Agriculture.

[2] Of the Drug Evaluation Branch, Drug Research and Development, Division of Cancer Treatment, National Cancer Institute, National Institutes of Health, Department of Health, Education, and Welfare, Bethesda, Md.

[3] Carbon and hydrogen analyses were performed by Chemalytics, Inc., Tempe, Ariz. PMR, IR, and mass spectra were determined using a Varian T-60 spectrophotometer, a Beckman IR-33, and a Hitachi Perkin-Elmer double-focusing spectrometer (model RMU-6E), respectively. The melting points were determined on a Kofler hot-stage apparatus and are uncorrected.

(17) N. J. Pound and R. W. Sears, *J. Pharm. Sci.*, **64**, 284 (1975).
(18) W. F. Bayne, G. Rodgers, and N. Crisologo, *ibid.*, **64**, 402 (1975).
(19) J. F. Lawrence and R. W. Frei, *Anal. Chem.*, **44**, 2047 (1972).
(20) R. W. Frei and J. F. Lawrence, *J. Chromatogr.*, **83**, 321 (1973).
(21) J. F. Lawrence and R. W. Frei, *Chromatogr. Rev.*, **17**, 253 (1974).
(22) R. W. Frei, J. F. Lawrence, J. Hope, and R. M. Cassidy, *J. Chromatogr. Sci.*, **12**, 40 (1974).
(23) W. A. Garland, R. J. Weinkam, and W. F. Trager, *Chem. Inst.*, 271 (1973).
(24) N. Seiler and M. Weichman, in "Progress in Thin-Layer Chromatography and Related Methods," vol. 1, A. Nieder-Wieser and G. Pataki, Eds., Ann Arbor Science Publishers, Ann Arbor, Mich., 1970, chap. 4.

ACKNOWLEDGMENTS AND ADDRESSES

Received October 8, 1975, from the *Cardiology Division, Stanford University School of Medicine, Stanford, CA 94305.*

Accepted for publication June 22, 1976.

Supported by NIH Grant HL-5866 and Program Project Grant 1-P01-15833.

The assistance of Mr. Joseph B. Keenaghan in supplying a number of compounds for investigation as internal standards is appreciated. The authors also thank Mrs. Dorothy McCain for her editorial assistance.

[x] To whom inquiries should be directed.

NOTES

Cytotoxic and Tumor Inhibitory Agent from *Polygala macradenia* Gray (Polygalaceae): 4′-Demethyldeoxypodophyllotoxin

JOSEPH J. HOFFMANN, RICHARD M. WIEDHOPF, and JACK R. COLE [x]

Abstract □ The chloroform fraction of *Polygala macradenia* exhibited activity against the P-388 lymphocytic leukemia and human epidermoid carcinoma of the nasopharynx test systems. The constituent responsible for this activity was a lignan, 4′-demethyldeoxypodophyllotoxin ($C_{21}H_{20}O_7$). The identity was proven by elemental analysis; PMR, IR, mass spectrometric, and melting-point determinations; and preparation of a derivative.

Keyphrases □ *Polygala macradenia*—chloroform fraction of extract of aerial parts, lignan isolated, evaluated for cytotoxic and tumor inhibitory activity □ 4′-Demethyldeoxypodophyllotoxin—isolated from chloroform fraction of extract of aerial parts of *Polygala macradenia*, evaluated for cytotoxic and tumor inhibitory activity □ Cytotoxic activity—lignan isolated from chloroform fraction of extract of aerial parts of *Polygala macradenia* evaluated □ Tumor inhibitory activity—lignan isolated from chloroform fraction of extract of aerial parts of *Polygala macradenia* evaluated

In the continuing search for plants having tumor inhibitory constituents, it was found that the chloroform fraction of *Polygala macradenia* Gray (Polygalaceae)[1], obtained by partitioning the ethanol extract of the stems, leaves, flowers, and fruit between chloroform and water, showed inhibitory activity against the P-388 lymphocytic leukemia (PS) test system and the human epidermoid carcinoma of the nasopharynx (KB) test system[2].

DISCUSSION

The lignan 4′-demethyldeoxypodophyllotoxin (I), previously isolated from *Polygala paenea* L. (Polygalaceae) (1), was isolated from the chloroform fraction by column chromatography, treatment with activated charcoal, preparative TLC, and recrystallization. The structure of the lignan was confirmed by elemental analysis; PMR, IR, mass spectrometric, and melting-point determinations; and conversion to the known lignan, deoxypodophyllotoxin (II).

Compound I demonstrated an ED_{50} of 0.0012 μg/ml in the KB test system. Activity in the KB system is defined as $ED_{50} \leq 20$ μg/ml (2). In the PS test system, the lignan demonstrated activity of 132% test/control (T/C) at 2.1 mg/kg. Activity in the PS system is defined as an increase in the survival of treated animals over that of control animals resulting in a T/C ≥ 125% (3).

EXPERIMENTAL[3]

Isolation Procedure—The stems, leaves, flowers, and fruit of *P. macradenia* (16 kg) were ground and extracted exhaustively in a Lloyd-type extractor with ethanol. The air-dried residue was partitioned between chloroform (10 liters) and water (10 liters). A 200-g sample of the air-dried chloroform phase was then subjected to alumina III (2 kg) column (7 × 65 cm) chromatography. The solvents used, in increasing order of polarity, were hexane, hexane–benzene (1:1), benzene, chloroform, and methanol; elution was continued with each solvent until the eluent was colorless. The benzene fraction (1.2 g) was subjected to silica gel 60 (75 g) column (3.5 × 24 cm) chromatography, eluting with benzene–ether (4:1). Fractions 16–38 (25 ml each), consisting of one major component according to TLC, exhibited activity.

Isolation of I—The combined active fractions were treated with activated charcoal and purified by preparative TLC with a chloroform–

[1] The plant was collected in Texas in August 1974. Identification was confirmed by Dr. Robert E. Perdue, Jr., Medicinal Plant Resources Laboratory, U.S. Department of Agriculture, Bethesda, Md. A reference specimen is maintained by the U.S. Department of Agriculture.

[2] Of the Drug Evaluation Branch, Drug Research and Development, Division of Cancer Treatment, National Cancer Institute, National Institutes of Health, Department of Health, Education, and Welfare, Bethesda, Md.

[3] Carbon and hydrogen analyses were performed by Chemalytics, Inc., Tempe, Ariz. PMR, IR, and mass spectra were determined using a Varian T-60 spectrophotometer, a Beckman IR-33, and a Hitachi Perkin-Elmer double-focusing spectrometer (model RMU-6E), respectively. The melting points were determined on a Kofler hot-stage apparatus and are uncorrected.

ethyl acetate (9:1) solvent system, and the residue was crystallized from methanol to yield colorless plates, mp 246–248° [lit. (1) mp 244–248°]. The IR and PMR spectra were identical to the previously reported spectra (1). Mass spectrometry indicated a parent peak at *m/e* 384.

Anal.—Calc. for $C_{21}H_{20}O_7$: C, 65.61; H, 5.24; mol. wt., 384. Found: C, 65.52; H, 5.08; *m/e* 384.

Compound II—Methylation of I (25 mg) with ethereal diazomethane in dry dichloromethane for 48 hr at room temperature yielded II, which crystallized from methanol as colorless prisms, mp 168° [lit. (1) mp 167–169°]. The IR spectrum was identical to the previously reported spectrum (1).

REFERENCES

(1) J. Polonsky, J. Moron, and H. Pourrat, *Mem. Present. Soc. Chim.*, **1962**, 1722.

(2) R. I. Geran, N. H. Greenberg, M. N. MacDonald, A. M. Schumacher, and B. J. Abbott, *Cancer Chemother. Rep.*, **3**, 17 (1972).

(3) *Ibid.*, **3**, 9 (1972).

ACKNOWLEDGMENTS AND ADDRESSES

Received March 29, 1976, from the *Division of Pharmaceutical Chemistry, College of Pharmacy, University of Arizona, Tucson, AZ 85721.*

Accepted for publication May 19, 1976.

Supported by Contract NOI-CM-33750 from the Division of Cancer Treatment, National Cancer Institute, National Institutes of Health, Department of Health, Education, and Welfare, Bethesda, Md., and the Elsa U. Pardee Foundation, Midland, Mich.

[x] To whom inquiries should be directed.

Topical Mosquito Repellents X: 2-Oxazolidones

W. A. SKINNER [x], H. T. CRAWFORD, D. SKIDMORE, and H. I. MAIBACH *

Abstract □ A number of 2-oxazolidones were evaluated for their effectiveness as topical mosquito repellents. Although some compounds approached diethyltoluamide in potency, none was superior.

Keyphrases □ 2-Oxazolidones, various—synthesized, evaluated as topical mosquito repellents □ Repellents, mosquito—various 2-oxazolidones synthesized and evaluated □ Structure–activity relationships—various 2-oxazolidones evaluated as topical mosquito repellents

Several derivatives of 2-oxazolidone have been prepared and evaluated for effectiveness as topical mosquito repellents. The repellency of all of the compounds against female *Aedes aegypti* (yellow fever) mosquitoes was determined by topical application on human subjects as previously described (1).

Since the majority of effective repellents are either amides or esters, it is surprising that carbamates have not been more extensively investigated. The two literature reports (2, 3) of repellent carbamates indicate that simple alkyl derivatives of the type $R_1OC(=O)N(R_2)R_3$ have provided some degree of protection against *A. aegypti* mosquitoes.

The fact that little data were available in a structural area of reported repellent activity, combined with the intriguing similarity between the two most common classes of repellents (esters and amides) and carbamates, encouraged further studies. 2-Oxazolidones were chosen because of practical considerations. Physical properties for a number of 2-oxazolidones were available (proper volatility is an important consideration for a topically applied insect repellent), as were some well-documented synthetic methods for their preparation.

With few exceptions, all compounds tested were prepared *via* published procedures. Table I gives their structures, boiling points, and topical repellency data. Diethyltoluamide was used as the standard repellent in all tests.

EXPERIMENTAL[1]

Preparation of 3-Methoxymethyl-2-oxazolidone (XIX)—Thionyl chloride (9.5 g, 0.08 mole) was placed in a 20-ml flask and stirred at room temperature. 3-Hydroxymethyl-2-oxazolidone (3.2 g, 0.03 mole) was added dropwise over 30 min, and the resulting solution was stirred overnight.

Excess thionyl chloride was removed *in vacuo*, and the residue was distilled. The desired product (bp 100–103°/0.25 mm) was obtained as a colorless oil, 2.9 g; IR (film): 2970, 1740, 1480, 1260, 1031, and 766 cm^{-1}; NMR ($CDCl_3$): δ 5.31 (s, 2H), 4.45 (t, 2H), and 3.74 (t, 2H).

The 3-chloromethyl-2-oxazolidone was not stable at room temperature (loss of hydrogen chloride), but it could be stored for short periods at −20°.

A solution of sodium methoxide in methanol was prepared by the addition of sodium (0.345 g, 0.015 mole) to a stirred solution of dry methanol under nitrogen. 3-Chloromethyl-2-oxazolidone (2.0 g, 0.015 mole) was then added dropwise over 30 min. After stirring for 1 hr at room temperature, TLC indicated no remaining starting material.

The crude reaction mixture was filtered, and methanol was removed under reduced pressure. Distillation (bp 76°/0.20 mm) afforded XIX as a colorless oil, 1.2 g; IR (film): 2930, 1740, 1421, 1259, and 1080 cm^{-1}; NMR ($CDCl_3$): δ 4.70 (s, 2H), 4.45 (t, 2H), 3.71 (t, 2H), and 3.38 (s, 3H).

Anal.—Calc. for $C_5H_9NO_3$: C, 45.79; H, 6.92; N, 10.68. Found: C, 45.82; H, 6.81; N, 10.95.

Preparation of 3-Acetoxymethyl-2-oxazolidone (XX)—Acetic anhydride (2.04 g, 0.02 mole) was added dropwise to a stirred solution of 3-hydroxymethyl-2-oxazolidone (2.0 g, 0.017 mole) in dry pyridine (5 ml). The colorless solution was then stirred overnight at room temperature.

The crude reaction mixture was concentrated *in vacuo;* the residue was dissolved in methylene chloride, washed with saturated sodium chloride, dried, and reconcentrated *in vacuo*. Distillation (100–104°/0.1 mm) afforded XX as a colorless oil, 1.9 g; IR (film): 2950, 1760, 1740, 1420, 1210, 1020, and 940 cm^{-1}; NMR ($CDCl_3$): δ 5.37 (s, 2H), 4.40 (t, 2H), 3.76 (t, 2H), and 2.07 (s, 3H).

[1] Melting points were determined on a capillary melting-point apparatus and are uncorrected. Boiling points were determined using a short path distillation apparatus and also are uncorrected. IR and NMR spectra were taken of all compounds and were consistent with the assigned structures. Elemental analyses were performed by the Microanalytical Laboratory, Department of Chemistry, Stanford University, Stanford, Calif.

ethyl acetate (9:1) solvent system, and the residue was crystallized from methanol to yield colorless plates, mp 246–248° [lit. (1) mp 244–248°]. The IR and PMR spectra were identical to the previously reported spectra (1). Mass spectrometry indicated a parent peak at *m/e* 384.

Anal.—Calc. for $C_{21}H_{20}O_7$: C, 65.61; H, 5.24; mol. wt., 384. Found: C, 65.52; H, 5.08; *m/e* 384.

Compound II—Methylation of I (25 mg) with ethereal diazomethane in dry dichloromethane for 48 hr at room temperature yielded II, which crystallized from methanol as colorless prisms, mp 168° [lit. (1) mp 167–169°]. The IR spectrum was identical to the previously reported spectrum (1).

REFERENCES

(1) J. Polonsky, J. Moron, and H. Pourrat, *Mem. Present. Soc. Chim.*, **1962**, 1722.

(2) R. I. Geran, N. H. Greenberg, M. N. MacDonald, A. M. Schumacher, and B. J. Abbott, *Cancer Chemother. Rep.*, **3**, 17 (1972).

(3) *Ibid.*, **3**, 9 (1972).

ACKNOWLEDGMENTS AND ADDRESSES

Received March 29, 1976, from the *Division of Pharmaceutical Chemistry, College of Pharmacy, University of Arizona, Tucson, AZ 85721.*

Accepted for publication May 19, 1976.

Supported by Contract NOI-CM-33750 from the Division of Cancer Treatment, National Cancer Institute, National Institutes of Health, Department of Health, Education, and Welfare, Bethesda, Md., and the Elsa U. Pardee Foundation, Midland, Mich.

[x] To whom inquiries should be directed.

Topical Mosquito Repellents X: 2-Oxazolidones

W. A. SKINNER [x], H. T. CRAWFORD, D. SKIDMORE, and H. I. MAIBACH *

Abstract □ A number of 2-oxazolidones were evaluated for their effectiveness as topical mosquito repellents. Although some compounds approached diethyltoluamide in potency, none was superior.

Keyphrases □ 2-Oxazolidones, various—synthesized, evaluated as topical mosquito repellents □ Repellents, mosquito—various 2-oxazolidones synthesized and evaluated □ Structure–activity relationships—various 2-oxazolidones evaluated as topical mosquito repellents

Several derivatives of 2-oxazolidone have been prepared and evaluated for effectiveness as topical mosquito repellents. The repellency of all of the compounds against female *Aedes aegypti* (yellow fever) mosquitoes was determined by topical application on human subjects as previously described (1).

Since the majority of effective repellents are either amides or esters, it is surprising that carbamates have not been more extensively investigated. The two literature reports (2, 3) of repellent carbamates indicate that simple alkyl derivatives of the type $R_1OC(=O)N(R_2)R_3$ have provided some degree of protection against *A. aegypti* mosquitoes.

The fact that little data were available in a structural area of reported repellent activity, combined with the intriguing similarity between the two most common classes of repellents (esters and amides) and carbamates, encouraged further studies. 2-Oxazolidones were chosen because of practical considerations. Physical properties for a number of 2-oxazolidones were available (proper volatility is an important consideration for a topically applied insect repellent), as were some well-documented synthetic methods for their preparation.

With few exceptions, all compounds tested were prepared *via* published procedures. Table I gives their structures, boiling points, and topical repellency data. Diethyltoluamide was used as the standard repellent in all tests.

EXPERIMENTAL[1]

Preparation of 3-Methoxymethyl-2-oxazolidone (XIX)—Thionyl chloride (9.5 g, 0.08 mole) was placed in a 20-ml flask and stirred at room temperature. 3-Hydroxymethyl-2-oxazolidone (3.2 g, 0.03 mole) was added dropwise over 30 min, and the resulting solution was stirred overnight.

Excess thionyl chloride was removed *in vacuo*, and the residue was distilled. The desired product (bp 100–103°/0.25 mm) was obtained as a colorless oil, 2.9 g; IR (film): 2970, 1740, 1480, 1260, 1031, and 766 cm^{-1}; NMR ($CDCl_3$): δ 5.31 (s, 2H), 4.45 (t, 2H), and 3.74 (t, 2H).

The 3-chloromethyl-2-oxazolidone was not stable at room temperature (loss of hydrogen chloride), but it could be stored for short periods at −20°.

A solution of sodium methoxide in methanol was prepared by the addition of sodium (0.345 g, 0.015 mole) to a stirred solution of dry methanol under nitrogen. 3-Chloromethyl-2-oxazolidone (2.0 g, 0.015 mole) was then added dropwise over 30 min. After stirring for 1 hr at room temperature, TLC indicated no remaining starting material.

The crude reaction mixture was filtered, and methanol was removed under reduced pressure. Distillation (bp 76°/0.20 mm) afforded XIX as a colorless oil, 1.2 g; IR (film): 2930, 1740, 1421, 1259, and 1080 cm^{-1}; NMR ($CDCl_3$): δ 4.70 (s, 2H), 4.45 (t, 2H), 3.71 (t, 2H), and 3.38 (s, 3H).

Anal.—Calc. for $C_5H_9NO_3$: C, 45.79; H, 6.92; N, 10.68. Found: C, 45.82; H, 6.81; N, 10.95.

Preparation of 3-Acetoxymethyl-2-oxazolidone (XX)—Acetic anhydride (2.04 g, 0.02 mole) was added dropwise to a stirred solution of 3-hydroxymethyl-2-oxazolidone (2.0 g, 0.017 mole) in dry pyridine (5 ml). The colorless solution was then stirred overnight at room temperature.

The crude reaction mixture was concentrated *in vacuo;* the residue was dissolved in methylene chloride, washed with saturated sodium chloride, dried, and reconcentrated *in vacuo*. Distillation (100–104°/0.1 mm) afforded XX as a colorless oil, 1.9 g; IR (film): 2950, 1760, 1740, 1420, 1210, 1020, and 940 cm^{-1}; NMR ($CDCl_3$): δ 5.37 (s, 2H), 4.40 (t, 2H), 3.76 (t, 2H), and 2.07 (s, 3H).

[1] Melting points were determined on a capillary melting-point apparatus and are uncorrected. Boiling points were determined using a short path distillation apparatus and also are uncorrected. IR and NMR spectra were taken of all compounds and were consistent with the assigned structures. Elemental analyses were performed by the Microanalytical Laboratory, Department of Chemistry, Stanford University, Stanford, Calif.

Table I—Physical Properties of 2-Oxazolidones

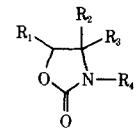

Compound	R_1	R_2	R_3	R_4	Boiling Point (mm) or Melting Point	Repellency, hr[a] (0.35 mg/cm²)	Reference
I	H	CH_3	CH_3	H	55°	1.0 (2)	4
II	CH_3	H	H	H	111° (0.5)	0.3 (2)	5
III	H	H	C_2H_5	H	141° (0.5)	1.0 (2)	4
IV	H	H	H	CH_3	82° (0.5)	1.3 (2)	4
V	H	H	H	C_2H_5	88° (0.5)	1.0 (2)	4
VI	H	H	H	$C(CH_3)_3$	78° (0.5)	1.3 (2)	6
VII	H	H	H	$CH_2CH(CH_3)_2$	112° (0.5)	1.8 (2)	—[b]
VIII	H	H	H	C_5H_{11}	120° (0.5)	5.5 (5)	7
IX	H	H	H	C_6H_{13}	131° (0.5)	5.3 (7)	—[c]
X	H	H	H	C_7H_{15}	138° (0.5)	4.8 (4)	—[d]
XI	H	H	H	C_8H_{17}	143° (0.5)	3.8 (2)	—[e]
XII	H	H	H	Cyclohexyl	134° (0.5)	4.8 (4)	—[f]
XIII	H	H	H	o-Tolyl	131° (0.5)	1.0 (2)	6
XIV	H	H	H	Furfuryl	142° (0.5)	1.0 (2)	—[g]
XV	H	H	H	$CH_2N(C_2H_5)_2$	140° (0.5)	1.3 (2)	8
XVI	H	H	H	*N*-Methylene-pyrrolidino	137° (0.5)	1.0 (2)	8
XVII	H	H	H	$CH_2N(C_4H_9)_2$	145° (0.5)	2.0 (2)	8
XVIII	H	H	H	CH_2OH	58°	1.0 (2)	9
XIX	H	H	H	CH_2OCH_3	91° (0.5)	1.0 (2)	—[h]
XX	H	H	H	CH_2OCOCH_3	124° (0.5)	1.5 (2)	—[h]
XXI	H	H	H	$(CH_2)_3Cl$	124° (0.5)	1.0 (2)	10
Diethyltoluamide					100° (0.5)	6.5	

[a] Number of determinations is given in parentheses; for more than one determination, reproducibility was ±0.5 hr. [b] *Anal.*—Calc. for $C_7H_{13}NO_2$: C, 58.72; H, 9.15; N, 9.78. Found: C, 58.31; H, 9.21; N, 9.32. [c] *Anal.*—Calc. for $C_9H_{17}NO_2$: C, 63.12; H, 10.01; N, 8.18. Found: C, 62.95; H, 10.25; N, 7.91. [d] *Anal.*—Calc. for $C_{10}H_{19}NO_2$: C, 64.83; H, 10.34; N, 7.56. Found: C, 65.07; H, 10.50; N, 7.60. [e] *Anal.*—Calc. for $C_{11}H_{21}NO_2$: C, 66.29; H, 10.62; N, 7.03. Found: C, 65.88; H, 10.69; N, 7.04. [f] *Anal.*—Calc. for $C_9H_{15}NO_2$: C, 63.88; H, 8.94; N, 8.28. Found: C, 63.74; H, 9.15; N, 8.14. [g] *Anal.*—Calc. for $C_8H_9NO_3$: C, 57.49; H, 5.43; N, 8.39. Found: C, 57.43; H, 5.49; N, 8.31. [h] See *Experimental*.

Anal.—Calc. for $C_6H_9NO_4$: C, 45.28; H, 5.70; N, 8.80. Found: C, 45.22; H, 5.83; N, 8.59.

Tests on Skin—Compounds were uniformly applied in ethanol to an exposed area of the forearm of a human subject as described previously (1). Repellency was evaluated utilizing female *A. aegypti*.

RESULTS AND DISCUSSION

As discussed previously (11), the utility of a particular compound as a topical insect repellent is determined by its volatility and its inherent intrinsic repellency. Analysis of the data presented in Table I allows structural characteristics resulting in maximum intrinsic repellency as well as a range of volatilities appropriate to the 2-oxazolidones (resulting in maximum duration of repellency) to be elucidated.

Of the 2-oxazolidones examined (Table I), the 3-alkyl derivatives were the best repellents. Compounds containing an unsubstituted nitrogen or those having electronegative atoms or an aromatic substituent in the side chain attached at position 3 all afforded less protection. Since some compounds have boiling points similar to the more repellent 3-alkyl derivatives, the differences in protection time probably reflect differences in intrinsic repellencies or skin absorption differences. The apparent decrease in intrinsic repellency with the introduction of an aromatic substituent (XIII and XIV) was surprising and contradictory to results obtained earlier in the isoquinoline system (11).

Another interesting observation concerns the relationship between steric bulk and repellency. Wright (12) recently suggested that repellents function by blocking moisture-sensitive pores in the cuticle of the mosquito's sensory hairs, thus preventing the sensors from responding normally to the raised humidity levels of a host. The argument is that steric bulkiness is a desirable characteristic of an effective repellent (pore blocker).

The bulky, somewhat spherically shaped, repellents dimethyl phthalate and 2-ethyl-1,3-hexanediol were compared with their essentially long and flat isomers, dimethyl terephthalate and 1,6-hexanediol, both poor repellents. The facts that dimethyl phthalate has a boiling point of 250° while dimethyl terephthalate melts at 142° and that 2-ethyl-1,3-hexanediol and 1,6-hexanediol are not isomers at all were overlooked. In addition, just how the lipophilic repellent dimethyl phthalate is to be attracted to, and held in, the presumably hydrophilic environment of a pore designed to be a water receptor was not discussed.

Data obtained with the 3-alkyl-2-oxazolidones indicate that proper volatility (not steric bulkiness) is the major factor in determining duration of repellency and that there are no great differences in intrinsic repellency among the various 3-alkyl-2-oxazolidones. The sterically bulky 3-*tert*-butyl-2-oxazolidone (VI) had a repellency nearly identical to the much less bulky 3-methyl (IV) and 3-ethyl (V) derivatives. All have similar boiling points. The same is true of the 3-hexyl (IX) and 3-cyclohexyl (XII) compounds. In the alkyl-substituted 2-oxazolidone series, steric bulk and molecular shape did not appear to be major factors determining repellency.

Of interest, however, in this series is the lower protection time attained by the electronegatively substituted compounds (XV–XVII, XX, and XXI) when compared with saturated alkyl derivatives having comparable boiling points.

None of the compounds evaluated here offers a significant advantage in terms of increased protection times over topical repellents currently available. However, interesting synthetic possibilities in the area of the 3-alkyl-2-oxazolidones remain to be explored and will be the subject of future work wherein a membrane *in vitro* system will be used for initial screening rather than human subjects.

REFERENCES

(1) H. L. Johnson, W. A. Skinner, D. Skidmore, and H. I. Maibach, *J. Med. Chem.*, **11**, 1256 (1968).

(2) Y. Naumov, A. Mentus, V. Kazhadan, and I. Dunaeva, *Khim. Sredstva Zashch. Rast.*, **2**, 269 (1972); through *Chem. Abstr.*, **81**, 135422g (1974).

(3) Section of Insect Repellent Research (Institute of Zoology, Academy of Science, Peoples Republic of China), *K'un Ch'ung Hseueh Pao*, **16**, 39 (1973); through *Chem. Abstr.*, **82**, 150466p (1975).

(4) P. G. Sears and H. L. Huffman, *J. Solution Chem.*, **1**, 187 (1972).

(5) J. B. Bell and J. D. Malkemus (to Jefferson Chemical Co.), U.S. pat. 2,755,286, July 17, 1956; through *Chem. Abstr.*, **51**, P2871i (1957).

(6) R. Oda, M. Miyanoki, and M. Okano, *Bull. Chem. Soc. Jpn.*, **35**, 1309 (1962).

(7) A. Boucherle, G. Carraz, and J. Bonnin, *Bull. Soc. Chim. Fr.*, **1958**, 231.

(8) Badische Anilin and Soda Fabrik Akt. Ges., British pat. 728,699, Apr. 27, 1955; through *Chem. Abstr.*, **50**, P6521b (1956).

(9) S. Okamara and T. Endo (to Seitesy Chem. Ind. Co.), Japanese pat. 69 32,048 (C1. 16E 341), Dec. 20, 1969; through *Chem. Abstr.*, **72**, P79016c (1970).

(10) R. Delaby, R. Damiens, and G. d'Huyteza, *Ann. Pharm. Fr.*, **13**, 565 (1955).

(11) W. A. Skinner, H. T. Crawford, H. Tong, D. Skidmore, and H. I. Maibach, *J. Pharm. Sci.*, **65**, 1404 (1976).

(12) R. H. Wright, *Sci. Am.*, **233**, 104 (1975).

ACKNOWLEDGMENTS AND ADDRESSES

Received January 16, 1976, from the *Life Sciences Division, Stanford Research Institute, Menlo Park, CA 94025.*

Accepted for publication May 28, 1976.

Supported by U.S. Army Medical Research and Development Command Contract DADA 17-70-C-0112 (W. A. Skinner) and DADA 70-C-0190 (H. I. Maibach).

* Present address: Division of Dermatology, School of Medicine, University of California, San Francisco Medical Center, San Francisco, Calif.

[x] To whom inquiries should be directed.

GLC Determination of Methenamine in Tablets

J. G. STROM, Jr., and H. W. JUN [x]

Abstract □ A rapid and sensitive GLC method was developed for the quantitative determination of methenamine in tablets. The method was shown to possess several advantages over the official NF assay. After dissolution of the whole tablet in absolute ethanol and addition of an internal standard (pentylenetetrazol), an aliquot was injected into the gas chromatograph for analysis. The sample was chromatographed using a stainless steel column packed with 10% OV-17 on Chromosorb W-HP. Quantitation was achieved by measuring peak heights. The simplicity, directness, extreme rapidity, and accuracy of the method represent an improvement over the official method and the other proposed assays.

Keyphrases □ Methenamine—GLC analysis, commercial tablets □ GLC—analysis, methenamine, commercial tablets □ Antibacterials, urinary—methenamine, GLC analysis, commercial tablets

Methenamine is a urinary antibacterial useful in the long-term therapy of chronic urinary tract infections. The method most often used for the determination of methenamine is based on the hydrolysis of methenamine to formaldehyde and ammonia in a strong acid solution. The formaldehyde may be volatilized by continued heating and the excess acid may be back-titrated, or the liberated formaldehyde may be determined by colorimetry. However, these assays do not differentiate between decomposed and unhydrolyzed methenamine. The NF XIII (1) method involves the back-titration procedure and may be subject to errors due to the uncertainty of complete hydrolysis.

The official NF XIV (2) method and other commonly used techniques (3–5) for the determination of methenamine are based on reaction of formaldehyde with chromotropic acid. Since the decomposition product, formaldehyde, and not the intact methenamine is the analytically available moiety, any formaldehyde released by decomposition and trapped in the tablet is determined with the drug.

Other proposed methods include complexation (6), fluorometry (7), NMR spectroscopy (8), and a 2-hydrazinobenzothiazole reaction (9). This report presents a direct method of analysis of the intact methenamine by GLC. The procedure is rapid, simple, and accurate.

EXPERIMENTAL

Apparatus—A gas chromatograph[1] equipped with a dual flame-ionization detector was used. The chromatographic column was a 3-mm (i.d.) stainless steel coiled column, 1.83 m in length, packed with 10% OV-17 on 80–100-mesh Chromosorb W-HP. The operating temperatures were 250° for the injection port, 190° (isothermal) for the column oven, and 250° for the detector. Nitrogen, with a flow rate of 60 ml/min, was the carrier gas. The flow rates of hydrogen and compressed air were adjusted to optimum sensitivity. The electrometer range was 10^{-10} amp/mv.

Materials and Reagents—Methenamine[2] and pentylenetetrazol[3] were used as received. Methenamine tablets[4,5] from two different companies were purchased in a local pharmacy. Absolute alcohol[6] USP was also used.

Analytical Calibration Curve—Six samples of methenamine[2], 105.0, 210.0, 420.0, 634.0, 845.0, and 1680.0 mg, were weighed. Each sample was placed into a 100-ml volumetric flask, and 10.0 ml of pentylenetetrazol internal standard alcoholic solution (50 mg/ml) was added and diluted to volume with absolute alcohol. Three microliters of each solution was injected into the chromatograph. The calibration curve was then obtained by plotting the known concentrations of methenamine against the corresponding peak height ratios (methenamine–pentylenetetrazol).

Tablet Analysis—Randomly selected tablets were individually wrapped inside glassine weighing paper and crushed. The powder was transferred to a 25-ml volumetric flask containing about 10 ml of absolute alcohol, shaken until dissolved, and diluted to 25 ml with absolute alcohol. Methenamine tablets contain no insoluble excipients and are totally soluble in the alcohol. Aliquots of 4.0 ml each were removed, placed into 10-ml volumetric flasks containing 1.0 ml of pentylenetetrazol internal standard solution (50 mg/ml), and diluted to 10 ml with absolute alcohol. Three-microliter samples of each tablet solution were injected into the chromatograph.

Calculations—The ratio of the peak height of the sample to the internal standard for each tablet solution was determined. The amount of methenamine per tablet was calculated from:

$$\text{mg/tablet} = \frac{R_{sa}}{R_{st}} \times \text{standard weight} \times \text{dilution factor} \quad \text{(Eq. 1)}$$

where R_{sa} is the ratio of the methenamine peak height to the internal standard peak height for the sample solution, and R_{st} is the methenamine–pentylenetetrazol peak height ratio for the known standard solution (5 mg/ml in absolute alcohol).

[1] Varian Aerograph model 1830.
[2] Riker Laboratories, Northridge, CA 91324.
[3] Metrazol, Knoll Pharmaceutical Co., Whippany, NJ 07981.
[4] Eli Lilly and Co., Indianapolis, IN 46206.
[5] Uritone, Parke-Davis and Co., Detroit, MI 48232.
[6] U.S. Industrial Chemicals Co., New York, N.Y.

(7) A. Boucherle, G. Carraz, and J. Bonnin, *Bull. Soc. Chim. Fr.*, **1958**, 231.

(8) Badische Anilin and Soda Fabrik Akt. Ges., British pat. 728,699, Apr. 27, 1955; through *Chem. Abstr.*, **50**, P6521b (1956).

(9) S. Okamara and T. Endo (to Seitesy Chem. Ind. Co.), Japanese pat. 69 32,048 (C1. 16E 341), Dec. 20, 1969; through *Chem. Abstr.*, **72**, P79016c (1970).

(10) R. Delaby, R. Damiens, and G. d'Huyteza, *Ann. Pharm. Fr.*, **13**, 565 (1955).

(11) W. A. Skinner, H. T. Crawford, H. Tong, D. Skidmore, and H. I. Maibach, *J. Pharm. Sci.*, **65**, 1404 (1976).

(12) R. H. Wright, *Sci. Am.*, **233**, 104 (1975).

ACKNOWLEDGMENTS AND ADDRESSES

Received January 16, 1976, from the *Life Sciences Division, Stanford Research Institute, Menlo Park, CA 94025.*

Accepted for publication May 28, 1976.

Supported by U.S. Army Medical Research and Development Command Contract DADA 17-70-C-0112 (W. A. Skinner) and DADA 70-C-0190 (H. I. Maibach).

* Present address: Division of Dermatology, School of Medicine, University of California, San Francisco Medical Center, San Francisco, Calif.

[x] To whom inquiries should be directed.

GLC Determination of Methenamine in Tablets

J. G. STROM, Jr., and H. W. JUN [x]

Abstract □ A rapid and sensitive GLC method was developed for the quantitative determination of methenamine in tablets. The method was shown to possess several advantages over the official NF assay. After dissolution of the whole tablet in absolute ethanol and addition of an internal standard (pentylenetetrazol), an aliquot was injected into the gas chromatograph for analysis. The sample was chromatographed using a stainless steel column packed with 10% OV-17 on Chromosorb W-HP. Quantitation was achieved by measuring peak heights. The simplicity, directness, extreme rapidity, and accuracy of the method represent an improvement over the official method and the other proposed assays.

Keyphrases □ Methenamine—GLC analysis, commercial tablets □ GLC—analysis, methenamine, commercial tablets □ Antibacterials, urinary—methenamine, GLC analysis, commercial tablets

Methenamine is a urinary antibacterial useful in the long-term therapy of chronic urinary tract infections. The method most often used for the determination of methenamine is based on the hydrolysis of methenamine to formaldehyde and ammonia in a strong acid solution. The formaldehyde may be volatilized by continued heating and the excess acid may be back-titrated, or the liberated formaldehyde may be determined by colorimetry. However, these assays do not differentiate between decomposed and unhydrolyzed methenamine. The NF XIII (1) method involves the back-titration procedure and may be subject to errors due to the uncertainty of complete hydrolysis.

The official NF XIV (2) method and other commonly used techniques (3–5) for the determination of methenamine are based on reaction of formaldehyde with chromotropic acid. Since the decomposition product, formaldehyde, and not the intact methenamine is the analytically available moiety, any formaldehyde released by decomposition and trapped in the tablet is determined with the drug.

Other proposed methods include complexation (6), fluorometry (7), NMR spectroscopy (8), and a 2-hydrazinobenzothiazole reaction (9). This report presents a direct method of analysis of the intact methenamine by GLC. The procedure is rapid, simple, and accurate.

EXPERIMENTAL

Apparatus—A gas chromatograph[1] equipped with a dual flame-ionization detector was used. The chromatographic column was a 3-mm (i.d.) stainless steel coiled column, 1.83 m in length, packed with 10% OV-17 on 80–100-mesh Chromosorb W-HP. The operating temperatures were 250° for the injection port, 190° (isothermal) for the column oven, and 250° for the detector. Nitrogen, with a flow rate of 60 ml/min, was the carrier gas. The flow rates of hydrogen and compressed air were adjusted to optimum sensitivity. The electrometer range was 10^{-10} amp/mv.

Materials and Reagents—Methenamine[2] and pentylenetetrazol[3] were used as received. Methenamine tablets[4,5] from two different companies were purchased in a local pharmacy. Absolute alcohol[6] USP was also used.

Analytical Calibration Curve—Six samples of methenamine[2], 105.0, 210.0, 420.0, 634.0, 845.0, and 1680.0 mg, were weighed. Each sample was placed into a 100-ml volumetric flask, and 10.0 ml of pentylenetetrazol internal standard alcoholic solution (50 mg/ml) was added and diluted to volume with absolute alcohol. Three microliters of each solution was injected into the chromatograph. The calibration curve was then obtained by plotting the known concentrations of methenamine against the corresponding peak height ratios (methenamine–pentylenetetrazol).

Tablet Analysis—Randomly selected tablets were individually wrapped inside glassine weighing paper and crushed. The powder was transferred to a 25-ml volumetric flask containing about 10 ml of absolute alcohol, shaken until dissolved, and diluted to 25 ml with absolute alcohol. Methenamine tablets contain no insoluble excipients and are totally soluble in the alcohol. Aliquots of 4.0 ml each were removed, placed into 10-ml volumetric flasks containing 1.0 ml of pentylenetetrazol internal standard solution (50 mg/ml), and diluted to 10 ml with absolute alcohol. Three-microliter samples of each tablet solution were injected into the chromatograph.

Calculations—The ratio of the peak height of the sample to the internal standard for each tablet solution was determined. The amount of methenamine per tablet was calculated from:

$$\text{mg/tablet} = \frac{R_{sa}}{R_{st}} \times \text{standard weight} \times \text{dilution factor} \quad \text{(Eq. 1)}$$

where R_{sa} is the ratio of the methenamine peak height to the internal standard peak height for the sample solution, and R_{st} is the methenamine–pentylenetetrazol peak height ratio for the known standard solution (5 mg/ml in absolute alcohol).

[1] Varian Aerograph model 1830.
[2] Riker Laboratories, Northridge, CA 91324.
[3] Metrazol, Knoll Pharmaceutical Co., Whippany, NJ 07981.
[4] Eli Lilly and Co., Indianapolis, IN 46206.
[5] Uritone, Parke-Davis and Co., Detroit, MI 48232.
[6] U.S. Industrial Chemicals Co., New York, N.Y.

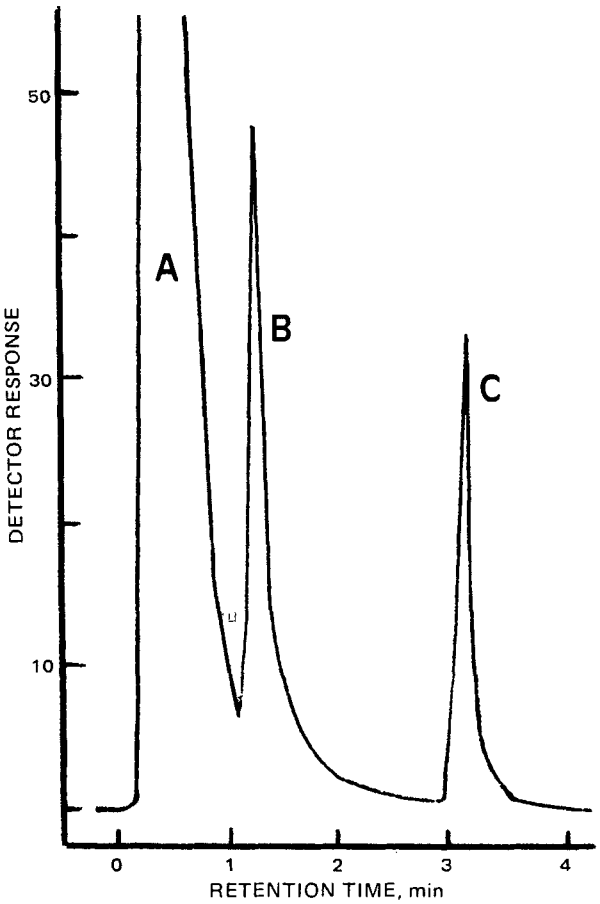

Figure 1—*GLC peaks. Key: A, solvent; B, methenamine; and C, pentylenetetrazol.*

RESULTS AND DISCUSSION

Figure 1 shows a typical gas chromatogram obtained for a tablet solution. Both the methenamine and the calibration marker, pentylenetetrazol, gave sharp, narrow, well-resolved peaks with no tailing. The retention time for each compound was relatively short, 1.2 min for methenamine and 3.0 min for pentylenetetrazol.

This analytical method was specific for intact methenamine. The retention time for formaldehyde, one of the decomposition products, was about 0.8 min. The flame-ionization detector did not respond to ammonia, the other decomposition product.

The linearity of the system was shown by analyzing various amounts of methenamine over the concentration range of 1.05–16.80 mg/ml with a constant amount of pentylenetetrazol (5 mg/ml). The correlation coefficient of the linear regression line was 0.998.

Results obtained by applying the proposed GLC method to known weights of methenamine are presented in Table I. The overall recovery for the five samples was 101.0 ± 1.85% (*SD*).

Six individual tablets from each commercial product were analyzed,

Table I—Assay Data for Known Amounts of Methenamine[a]

Amount Weighed, mg/ml	Amount Found, mg/ml	Recovery, %
3.10	3.12	100.6
3.75	3.85	102.6
4.80	4.92	102.5
5.30	5.20	98.1
5.60	5.68	101.4
	Mean recovery, %	101.1
	SD	1.85

[a] Crystalline powder, Merck & Co., Rahway, N.J.

Table II—Results of Analysis of Commercially Available Methenamine Tablets (325 mg/Tablet)

Tablet Number	Amount Found, mg/Tablet[a]	Percent of Claim
A 1	312.8	96.2
A 2	316.4	97.4
A 3	314.7	96.8
A 4	321.9	99.0
A 5	313.3	96.4
A 6	315.5	97.1
	Mean recovery, %	97.2
	SD	1.01
B 1	315.0	96.9
B 2	314.8	96.9
B 3	311.3	95.8
B 4	308.0	94.8
B 5	316.5	97.4
B 6	313.2	96.4
	Mean recovery, %	96.3
	SD	0.95

[a] Average of duplicate assays.

Table III—ANOVA Table for the Assayed Weight of Methenamine Tablets

Source	*df*	*SS*	*MS*	F_0
Companies	1	20.803	20.803	2.051
Error	10	101.427	10.143	—
Total	11	122.230	—	—

and the data are summarized in Table II. The ANOVA values for the assay of the tablets, based on a one-factor analysis of variance, are given in Table III. From the *F* table (10), $F_{1,10(0.05)}$ is 4.96. The statistical analysis of the data shows that there was no detectable difference in the means of the two different commercial tablets at the 5% level of significance.

The method presented represents an improvement over the official method and over other assays for methenamine. The GLC procedure is applicable to methenamine dosage form analysis and is simple, direct, and rapid.

REFERENCES

(1) "The National Formulary," 13th ed., Mack Publishing Co., Easton, Pa., 1970, p. 433.

(2) "The National Formulary," 14th ed., Mack Publishing Co., Easton, Pa., 1975, p. 444.

(3) V. Knight, J. W. Drapper, E. A. Brady, and C. A. Attmore, *Antibiot. Chemother.*, **2**, 615 (1952).

(4) D. A. MacFadyen, H. D. Watkins, and P. R. Anderson, *J. Biol. Chem.*, **158**, 107 (1945).

(5) C. E. Bricker and H. R. Johnson, *Anal. Chem.*, **17**, 400 (1945).

(6) C. A. Gaglia, Jr., L. A. Gossei, and L. Chafetz, *ibid.*, **44**, 1690 (1972).

(7) S. Belman, *Anal. Chim. Acta*, **29**, 120 (1963).

(8) J. W. Turczan and B. A. Goldwitz, *J. Assoc. Off. Anal. Chem.*, **56**, 669 (1973).

(9) J. K. Lim and C. C. C. Chen, *J. Pharm. Sci.*, **62**, 1503 (1973).

(10) B. Ostle, "Statistics in Research," 2nd ed., Iowa State University Press, Ames, Iowa, 1973, p. 529.

ACKNOWLEDGMENTS AND ADDRESSES

Received February 11, 1976, from the *Department of Pharmacy, School of Pharmacy, University of Georgia, Athens, GA 30602.*

Accepted for publication June 7, 1976.

Presented at the Pharmaceutical Analysis and Control Section, APhA Academy of Pharmaceutical Sciences, Atlanta meeting, November 1975.

[x] To whom inquiries should be directed.

Comparison of Two Spectrofluorometric Procedures for Quinidine Determination in Biological Fluids

THO HUYNH-NGOC * and GERARD SIROIS ˣ

Abstract □ Different methods for the spectrofluorometric determination of quinidine in plasma and urine were studied. The alkaline washings of plasma and urine extracts remove fluorescent metabolites, as shown by TLC analysis of urine extracts, and do not lead to a significant loss of alkaloids. The spectrofluorometric assays without alkaline washings of the benzene extract averaged 18% higher than the assays with alkaline washings. Since unchanged quinidine and hydroquinidine are responsible for antiarrhythmic activity, the method with alkaline washing is more appropriate for the control of quinidinemia than are other methods. The therapeutic plasma concentration range becomes 0.8–2.5 μg/ml with this method.

Keyphrases □ Quinidine—spectrofluorometric analysis, human plasma and urine, effect of alkaline washings □ Spectrofluorometry—analysis, quinidine, human plasma and urine, effect of alkaline washings □ Antiarrhythmics—quinidine, spectrofluorometric analysis, human plasma and urine, effect of alkaline washings

Quinidine, in spite of its well-known potential toxicity, remains a useful antiarrhythmic agent. The incidence of toxic reactions gets higher with increasing plasma drug concentration. Several spectrofluorometric methods were reported (1) for the estimation of quinidine in plasma, not only to prevent toxic levels but also to ensure adequate plasma concentrations of unchanged quinidine, which is responsible for activity.

The methods currently used involve either a protein precipitation with metaphosphoric acid and a direct spectrofluorometric determination on the filtrate (2–4) or an extraction with benzene followed by a transfer of the drug to sulfuric acid for spectrofluorometric determination (5). Although benzene is the most specific extraction solvent for unchanged quinidine, Armand and Badinand (6) found that alkaline washings of benzene extracts of dog urine removed an additional amount of metabolites without reducing significantly the amount of quinidine.

The purposes of this investigation were to study the effect of alkaline washings of the benzene extract of human plasma and urine samples containing known amounts of quinidine and to compare the data obtained with and without alkaline washing of the benzene extract of plasma and urine samples of patients treated with quinidine.

EXPERIMENTAL

Materials—Commercial quinidine base[1] was used without further purification. Benzene was spectrophotometric grade. All other chemicals were analytical grade.

Spectrofluorometric Determinations of Quinidine—Heparinized blood samples[2] from patients treated with quinidine were centrifuged. The plasma samples were kept at −20° until assayed by the method of Armand and Badinand (6) with and without alkaline washing of the benzene extract. In this procedure, 1 ml of plasma is alkalinized with 1 ml of 0.1 *N* NaOH. Then 30 ml of benzene is added. The resulting mixture is vigorously shaken (30 min), and the clear benzene extract is removed and washed twice by shaking for 5 min with 10 ml of 0.1 *N* NaOH. Twenty milliliters of this washed extract is mixed with 3 ml of 0.1 *N* H_2SO_4. The mixture is shaken for 10 min, and the sulfuric acid extract is analyzed by spectrofluorometry[3].

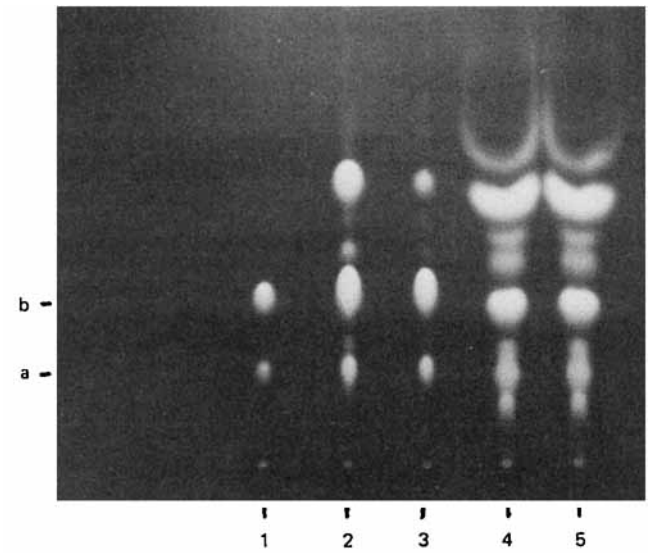

Figure 1—*Separation of hydroquinidine, quinidine, and their metabolites from urine by TLC. Key: 1, commercial quinidine containing hydroquinidine; 2, benzene extract; 3, benzene extract with alkaline washings; 4, pentanol–benzene (1:1) extract; and 5, pentanol–benzene extract with alkaline washings. Fluorescence bands for hydroquinidine and quinidine are designated by a and b, respectively (6).*

The precision and reproducibility of the alkaline washing procedure were evaluated by adding known amounts of quinidine to human plasma[2] and urine and by comparing the results obtained in the plasma with those of the protein precipitation method of Brodie and Udenfriend (2) in the same drug concentration range. The urine of one patient was also extracted with a pentanol–benzene (1:1) solvent mixture, which has been found optimal for the simultaneous extraction of quinidine, hydroquinidine, and their metabolites (7).

TLC—One urine sample from a patient receiving only quinidine was analyzed by TLC. Two 1-ml aliquots of this urine were alkalinized with 1 ml of 0.1 *N* NaOH; one was extracted with 25 ml of benzene and the other was extracted with 25 ml of pentanol–benzene (1:1). Ten milliliters of each organic extract was then washed twice with 5 ml of 0.1 *N* NaOH. Ten milliliters of the four washed and unwashed organic extracts was evaporated, and the residue was dissolved in 0.5 ml of the corresponding organic solvent.

Two hundred microliters of each resulting solution was applied on a silica gel plate[4]. Two hundred microliters of a benzene solution, containing 50 mg of commercial quinidine/liter, was also run for comparison. The chromatoplates were developed by the ascending technique with methanol (6) as the developing solvent. Fluorescent spots representing quinidine, hydroquinidine, and their metabolites were observed under UV light.

RESULTS AND DISCUSSION

The precision and reproducibility of the analytical procedure were verified by adding known amounts of commercial quinidine to human plasma and urine samples.

[1] K & K Laboratories, Plainview, N.Y.

[2] Supplied by M. Pierre Lemieux, Centre Hospitalier Notre-Dame of Montréal, and/or Dr. Michel Chabot, Institute of Cardiology of Montréal.

[3] Aminco-Bowman spectrofluorometer, American Instrument Co., Silver Spring, Md.

[4] Precoated TLC plates, Catalog No. 5765, Brinkmann Instruments, Rendale, Ontario, Canada.

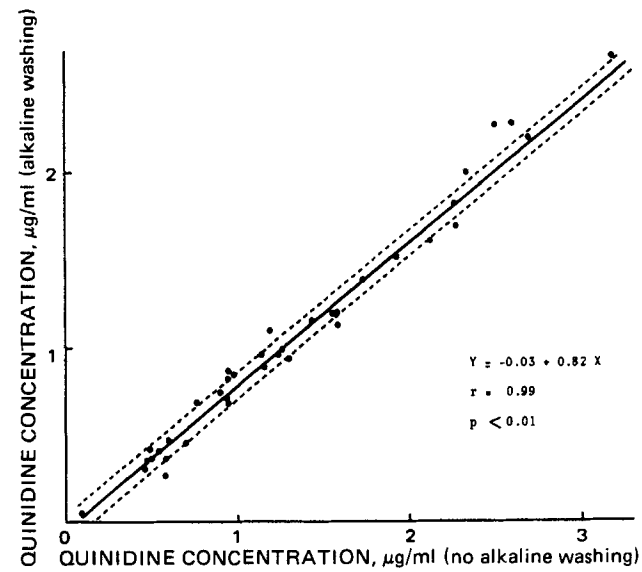

Figure 2—*Correlation of plasma quinidine concentration as measured by the method of Armand and Badinand (6) with (abscissa) and without (ordinate) alkaline washing of the benzene extract. The two dashed lines (- - -) parallel to the regression line (—) have a vertical distance from it that is equal to the standard error of estimate.*

When quinidine was added to eight plasma samples to obtain 0.1–5-µg/ml concentrations, the mean values of the percent found were 98.5 (*SD* = 4.1 and *CI*[5] = 3.4) and 100.9 (*SD* = 3.2 and *CI* = 2.6) for the protein precipitation method and benzene extraction procedure with alkaline washing, respectively. These results demonstrate that there is a good recovery of quinidine and hydroquinidine (8) with no significant loss of the alkaloids resulting from the alkaline washings of the benzene extract.

The addition of 0.1–150 µg/ml of quinidine to 14 urine samples led to a mean percent of 98.1 (*SD* = 2.5 and *CI* = 1.5) when the benzene extract was washed with an alkaline solution. The reproducibility of the extraction procedures was also checked by five measurements on the patient urine sample used for TLC analysis. The mean values of urine concentrations found in the benzene extract without and with alkaline washing were 109.75 (*SD* = 3.75 and *CI* = 4.66) and 66.43 (*SD* = 3.08 and *CI* = 3.83) µg/ml, respectively. On the other hand, mean concentration values of 182.08 (*SD* = 3.53 and *CI* = 439) and 182.92 (*SD* = 4.80 and *CI* = 5.97) µg/ml were found in the unwashed and washed pentanol–benzene (1:1) extract, respectively, of the same urine sample. In this last extraction method, the concentration of fluorescent quinidine molecules (quinidine, hydroquinidine, and their metabolites) is not reduced by the alkaline washings because of their high solubility in the pentanol–benzene solvent system.

The importance of alkaline washings of the benzene extract is illustrated in Fig. 1 where quinidine, hydroquinidine, and their metabolites were separated by TLC. In this figure, the metabolite spots have nearly completely disappeared with this treatment. This figure demonstrates also that the high quinidine concentration values obtained with the pentanol–benzene extraction solvent mixture result from fluorescent metabolites which are not removed by alkaline washing of the extract.

Thirty-seven plasma samples obtained from patients treated with quinidine were examined to test the importance of the alkaline washing. The plasma quinidine concentrations found spectrofluorometrically from washed and unwashed benzene extracts are shown in Fig. 2. As indicated by the regression line, the unwashed benzene extract assay averaged 18% higher than the washed benzene extract assay. With this additional removal of fluorescent metabolites, the quinidine therapeutic plasma concentration range would then become 0.8–2.5 µg/ml instead of 1–3 (9) or 3–7 (10) µg/ml. Since unchanged quinidine and hydroquinidine are responsible for antiarrhythmic activity (1), the procedure of Armand and Badinand (6) should be considered more appropriate than other methods for the control of quinidinemia. Furthermore, there is always the possibility in clinical practice that the rate of quinidine metabolism can be different in some patients because of physiopathological conditions or drug interactions.

[5] Confidence interval of the mean at the 0.05 level of significance.

REFERENCES

(1) T. Huynh-Ngoc and G. Sirois, *J. Pharm. Belg.*, **29**, 152 (1974).

(2) B. B. Brodie and S. Udenfriend, *J. Pharmacol. Exp. Ther.*, **78**, 154 (1943).

(3) A. L. Edgar and M. Sokolow, *J. Lab. Clin. Med.*, **36**, 478 (1950).

(4) H. C. Archer, D. Weitzman, and H. L. Kay, *Br. Heart J.*, **17**, 534 (1955).

(5) G. Cramer and B. Isaksson, *Scand. J. Clin. Lab. Invest.*, **15**, 553 (1963).

(6) J. Armand and A. Badinand, *Ann. Biol. Clin.*, **30**, 599 (1972).

(7) G. Hartel and A. Korhonen, *J. Chromatogr.*, **49**, 70 (1968).

(8) T. Huynh-Ngoc and G. Sirois, *Pharm. Acta Helv.*, **49**, 37 (1974).

(9) G. Hartel, A. Louhija, A. Konttinen, and P. I. Halonen, *Br. Heart J.*, **32**, 57 (1970).

(10) L. Resnekov, D. Gibson, S. Waich, J. Muir, and L. McDonald, *ibid.*, **33**, 220 (1971).

ACKNOWLEDGMENTS AND ADDRESSES

Received May 3, 1976, from the *Faculté de Pharmacie, Université de Montréal, C.P. 6128, Succ. A, Montréal, Québec, H3C 3J7, Canada.*

Accepted for publication June 7, 1976.

Supported by the Medical Research Council of Canada, MA-5337.

* Studentship of the Ministère de l'Education du Québec.

x To whom inquiries should be directed.

Alkaloids of *Glaucium oxylobum* Boiss and Buhse, Population Ab-Ali

A. SHAFIEE ˣ, I. LALEZARI, and M. MAHJOUR

Abstract □ *Glaucium oxylobum* Boiss and Buhse, population Ab-Ali, was demonstrated to contain one major alkaloid, glaucine (0.7%), and two minor alkaloids, *O*-methylatheroline and predicentrine, in the aerial parts. The root also contains protopine. Glaucine and *O*-methylatheroline were detected for the first time in this species, and predicentrine was detected for the first time in the *Glaucium* genus.

Keyphrases □ *Glaucium oxylobum*—aerial parts and roots, alkaloids isolated and identified □ Alkaloids—isolated and identified in *Glaucium oxylobum* aerial parts and roots

As part of chemotaxonomic studies of Iranian wild *Papaveraceae* (1–4), the alkaloids of *Glaucium oxylobum* Boiss and Buhse[1], population Ab-Ali (a perennial wild plant scattered in Ab-Ali, located on the southern slopes of the Alborz mountains north of Tehran at about 2200 m above sea level), were isolated and identified. The height of the plant is 50–100 cm. The plant blooms from April to September. The four petals are yellow at the edge and orange at the bottom with a brown spot at the base of each petal.

EXPERIMENTAL

Plant Material—The whole aerial parts or roots were collected during May, air dried in the shade, then dried at 60° to a constant weight, and powdered so that all material possesses a mesh size not greater than 0.5 mm. The aerial parts and roots were extracted separately.

Extraction—Powdered plant material, 200 g, was moistened with 200 ml of 15% NH_4OH, stirred with 600 ml of chloroform at room temperature for 1 hr, and filtered. The extraction was repeated four times. After evaporation of the solvent, the residue was extracted with 100 ml of 5% sulfuric acid. The solution was filtered and extracted with petroleum ether (3 × 20 ml) to remove the colored material. The aqueous layer was made alkaline with 15% NH_4OH and extracted with chloroform (4 × 50 ml). Evaporation of the solvent gave 1.8 g of the crude alkaloids.

RESULTS AND DISCUSSION[2]

Chromatography of the crude alkaloids from the aerial parts [TLC, silica gel, ethyl acetate–methanol–ammonia (85:10:5)] gave glaucine (I, 1.4 g, 0.7%), mp 118–119° [lit. (5) mp 117–118°], mixed melting point with an authentic sample 117–119°. For the hydrobromide, the melting point was 239–241° (ethanol) [lit. (6) mp 241°]. The UV, IR, and NMR data of the separated alkaloid were identical with those reported previously (7, 8).

Glaucine was isolated by Bubeva-Ivanova *et al.* (9) from *Glaucium flavum* and claimed to have antitussive, spasmolytic, antiedematous, and tranquilizer effects but no depressing activity.

O-Methylatheroline (II) was obtained as a minor alkaloid, mp 224° [lit. mp 225–227° (10), 227–229° (11), and 235–236° (12)]. The IR spectrum was identical to the published spectrum for II (12), and the UV and

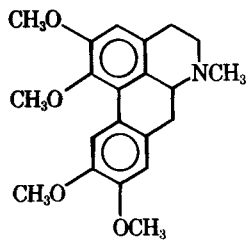

I

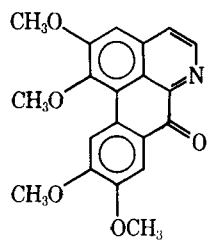

II

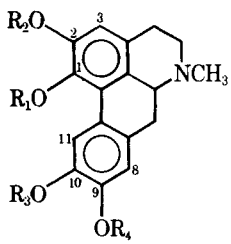

III: R_2 = H, R_1 = R_3 = R_4 = CH_3
IV: R_1 = H, R_2 = R_3 = R_4 = CH_3 (thaliporphine)
V: R_3 = H, R_1 = R_2 = R_4 = CH_3
VI: R_4 = H, R_1 = R_2 = R_3 = CH_3 (*N*-methyllaurotetanine)

NMR spectral data were in accord with published data (11, 13). The mass spectrum had major peaks at *m/e* 351, 336, 320, 308, and 234.

Anal.—Calc. for $C_{20}H_{17}NO_5$: C, 68.38; H, 4.84; N, 3.99. Found: C, 68.21; H, 4.93; N, 4.05.

A second minor alkaloid was an oil which could not be crystallized in various solvents. Its hydrochloride salt was a solid, mp 214–217° (methanol–ethyl acetate). As the free base, the UV spectrum showed λ_{max} (ethanol) 301 (log ϵ 4.11) and 280 (4.15) nm and λ_{min} 252 (3.73) nm; UV λ_{max} (ethanol, 2 drops of 10% NaOH): 301 and 280 nm; NMR ($CDCl_3$): δ 2.50 (s, 3H, NCH_3), 3.56 (3H, s, OCH_3), 3.88 (s, 3H, OCH_3), 3.90 (s, 3H, OCH_3), 6.56 (s, 1H, aromatic), 6.73 (s, 1H, aromatic), and 7.88 (s, 1H, aromatic) ppm. The mass spectrum had peaks at *m/e* 341 (M^+), 340 (M − 1), 326 (M − CH_3), 310 (M − OCH_3), 298 (M − CH_2=NCH_3), 165, 152, and 149.

Anal.—Calc. for $C_{20}H_{23}NO_4$: C, 70.38; H, 6.74; N, 4.11. Found: C, 70.42; H, 6.68; N, 4.02.

The UV spectrum was similar to that of dicentrine and glaucine (7); in addition, its mass spectrum fragmentation pattern was characteristic of aporphine alkaloids (14). The three singlet aromatic protons in the NMR spectrum showed that adjacent aromatic protons did not exist; in addition, the most deshielded aromatic proton must be at C_{11}. The NMR spectrum was in agreement with the four possible structures (III–VI) for this compound.

The UV spectrum in a basic solution did not show a hypsochromic shift given above, indicating that the hydroxyl was not at C-9. In addition, the spectral data for this alkaloid were different from the data for IV–VI (8, 15, 16). The UV, NMR, and IR (chloroform) spectra were identical with the spectra of predicentrine[3], which was synthesized by Charubala *et al.* (17). This alkaloid is, therefore, predicentrine. It was reported to exist also in *Ocotea macropoda*[4].

From the root of the plant, protopine was also isolated, mp 205–207° [lit. (18) mp 207°], mixed melting point with an authentic sample 205–207°. The NMR spectrum was identical with the one reported previously (19).

[1] The plant was identified by Dr. C. R. Gunn, Plant Taxonomy Laboratory, Plant Genetics and Germplasm Institute, Agricultural Research Service, Beltsville, MD 20705. A herbarium sample was deposited in the Herbarium of the College of Pharmacy, Tehran University.

[2] Melting points were taken with a Koffler hot-stage microscope and are uncorrected. UV spectra were recorded on a Varian Techtron 635 instrument. NMR spectra were taken with a Varian T-60A instrument, using tetramethylsilane as the internal standard. Mass spectra were recorded on a CH5 spectrometer at Arya-Mehr Technical University. IR spectra were obtained with a Leitz model III spectrograph.

[3] The spectra of predicentrine was provided by Professor B. R. Pai, Presidency College, Madras, India.

[4] M. P. Cava, Y. Watanabe, J. Kumitomo, K. Bessho, M. J. Mitchell, A. I. Da-Rocha, B. Hwang, J. A. Weisbach, and B. Douglas, Abstracts of Papers at the Second Natural Products Symposium, 1968, p. 3.

A literature survey (20, 21) revealed that glaucine and *O*-methylatheroline had not been found previously in *G. oxylobum* and predicentrine had not been detected in the genus *Glaucium*.

REFERENCES

(1) N. Sharghi and I. Lalerzai, *Nature*, **213**, 1244 (1967).

(2) I. Lalezari, A. Shafiee, and P. Nasseri-Nouri, *J. Pharm. Sci.*, **62**, 1718 (1973).

(3) I. Lalezari, P. Nasseri-Nouri, and R. Asgharian, *ibid.*, **63**, 1331 (1974).

(4) A. Shafiee I. Lalezari, P. Nasseri-Nouri, and R. Asgharian, *ibid.*, **64**, 1570 (1975).

(5) K. Warnt, *Chem. Ber.*, **59**, 85 (1926).

(6) J. Go, *J. Pharm. Soc. Jpn.*, **50**, 933 (1930); through *Chem. Abstr.*, **25**, 518 (1931).

(7) L. Slavikova, *Collect. Czech. Chem. Commun.*, **33**, 635 (1968).

(8) W. H. Baarschers, R. R. Arndt, K. Pachler, J. A. Weisbach, and B. Douglas, *J. Chem. Soc.*, **1964**, 4778.

(9) L. Bubeva-Ivanova, N. Donev, E. Mermerska, B. Avramova, P. Ioncheva, and S. Stefanov, *Postep Dziedzinie Leku Rosl., Pr. Ref. Dosw. Wygloszone Symp.*, **1970**, 104; through *Chem. Abstr.*, **78**, 88550y (1973). N. T. Donev, *Farmatsiya (Sofia)*, **14**, 49 (1964); through *Chem. Abstr.*, **61**, 9928g (1964).

(10) M. Tomita, T. H. Yang, H. Furukawa, and H. M. Yang, *Yakugaku Zasshi*, **82**, 1574 (1962); through *Chem. Abstr.*, **58**, 14012 (1963).

(11) J. Cohen, W. von Langenthal, and W. I. Taylor, *J. Org. Chem.*, **26**, 4143 (1961).

(12) M. A. Buchanan and E. E. Dickey, *ibid.*, **25**, 1389 (1960).

(13) I. R. C. Bick and G. K. Douglas, *Tetrahedron Lett.*, **1965**, 2399. *Ibid.*, **1965**, 4655.

(14) M. Ohashi, J. M. Wilson, H. Budzikiewicz, M. Shamma, W. A. Slusarchyk, and C. Djerassi, *J. Am. Chem. Soc.*, **85**, 2807 (1963).

(15) M. Shamma and W. A. Slusarchyk, *Tetrahedron Lett.*, **1965**, 1509.

(16) H. Guinaudeau, M. Leboeuf, and A. Cave, *Lloydia*, **38**, 286 (1975).

(17) R. Charubala, B. R. Pai, T. R. Govindachari, and N. Viswanathan, *Chem. Ber.*, **101**, 2665 (1968).

(18) W. H. Perkin, *J. Chem. Soc.*, **109**, 1023 (1916).

(19) F. A. L. Anet and M. A. Brown, *Tetrahedron Lett.*, **1967**, 4881.

(20) J. Slavik and L. Slavikova, *Collect. Czech. Chem. Commun.*, **28**, 253 (1963).

(21) F. Santavy, in "The Alkaloids," vol. 12, R. H. Manske and H. L. Holmes, Eds., Academic, New York, N.Y., 1970, p. 337.

ACKNOWLEDGMENTS AND ADDRESSES

Received December 29, 1975, from the *Institute of Medicinal Plants, College of Pharmacy, Tehran University, Tehran, Iran.*

Accepted for publication April 20, 1976.

Supported by Grant 13 of the International Foundation for Science and by a grant from the Ministry of Science and Higher Education Research Development Council.

[x] To whom inquiries should be directed.

Synthesis of 5,6-Benzo-2-azabicyclo[2.2.2]octane Derivatives as Potential Benzomorphan-Type Analgesic Agents

RONALD F. BORNE [x], SAY-JONG LAW, PHILIP W. WIRTH, and JAMES C. MURPHY

Abstract □ The synthesis of two *N*-substituted 5,6-benzo-2-azabicyclo[2.2.2]octane analogs of benzomorphan-type analgesics *via* benzyne addition to appropriate *N*-substituted *N*-alkyl-2-pyridones is described. Neither derivative possessed observable analgesic activity at the doses tested.

Keyphrases □ 5,6-Benzo-2-azabicyclo[2.2.2]octanes, *N*-substituted—synthesized, analgesic activity evaluated, mice □ Structure–activity relationships—*N*-substituted 5,6-benzo-2-azabicyclo[2.2.2]octanes synthesized, analgesic activity evaluated, mice □ Analgesic activity—*N*-substituted 5,6-benzo-2-azabicyclo[2.2.2]octanes evaluated, mice

The structural features of narcotic analgesics related to morphine have been well documented (1, 2). Studies of structure–analgesic activity requirements within the benzomorphan-type analgesics have also received considerable attention. While the structural features of benzomorphans are generally incorporated in structures such as I, many analogous structures have been demonstrated to possess significant analgesic activity. For example, 2-methyl-6,7-benzomorphan (II) (3), 7-methoxy-2-methyl-B-norbenzomorphan (III) (4), and 5-methano-3-methyl-6-phenyl-1,2,3,4,5,6-hexahydro-3-benzazocine (IV) (5)

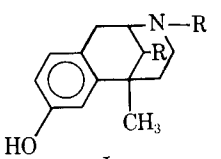

I

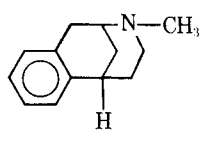

II

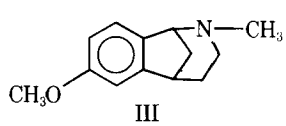

III

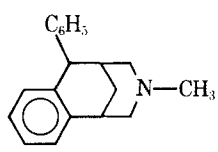

IV

possessed analgesic potencies comparable to that of codeine.

Compounds II–IV all lack "quaternary central carbon atoms," a structural feature once thought to be essential for activity (1, 2). Additionally, II and IV lack phenolic functions, and IV contains only a one-carbon separation from the basic nitrogen and the central carbon atom. While the active benzomorphans are characterized by the presence of a basic nitrogen atom 4.1 Å from the center of an

A literature survey (20, 21) revealed that glaucine and *O*-methylatheroline had not been found previously in *G. oxylobum* and predicentrine had not been detected in the genus *Glaucium*.

REFERENCES

(1) N. Sharghi and I. Lalerzai, *Nature*, **213**, 1244 (1967).

(2) I. Lalezari, A. Shafiee, and P. Nasseri-Nouri, *J. Pharm. Sci.*, **62**, 1718 (1973).

(3) I. Lalezari, P. Nasseri-Nouri, and R. Asgharian, *ibid.*, **63**, 1331 (1974).

(4) A. Shafiee I. Lalezari, P. Nasseri-Nouri, and R. Asgharian, *ibid.*, **64**, 1570 (1975).

(5) K. Warnt, *Chem. Ber.*, **59**, 85 (1926).

(6) J. Go, *J. Pharm. Soc. Jpn.*, **50**, 933 (1930); through *Chem. Abstr.*, **25**, 518 (1931).

(7) L. Slavikova, *Collect. Czech. Chem. Commun.*, **33**, 635 (1968).

(8) W. H. Baarschers, R. R. Arndt, K. Pachler, J. A. Weisbach, and B. Douglas, *J. Chem. Soc.*, **1964**, 4778.

(9) L. Bubeva-Ivanova, N. Donev, E. Mermerska, B. Avramova, P. Ioncheva, and S. Stefanov, *Postep Dziedzinie Leku Rosl., Pr. Ref. Dosw. Wygloszone Symp.*, **1970**, 104; through *Chem. Abstr.*, **78**, 88550y (1973). N. T. Donev, *Farmatsiya (Sofia)*, **14**, 49 (1964); through *Chem. Abstr.*, **61**, 9928g (1964).

(10) M. Tomita, T. H. Yang, H. Furukawa, and H. M. Yang, *Yakugaku Zasshi*, **82**, 1574 (1962); through *Chem. Abstr.*, **58**, 14012 (1963).

(11) J. Cohen, W. von Langenthal, and W. I. Taylor, *J. Org. Chem.*, **26**, 4143 (1961).

(12) M. A. Buchanan and E. E. Dickey, *ibid.*, **25**, 1389 (1960).

(13) I. R. C. Bick and G. K. Douglas, *Tetrahedron Lett.*, **1965**, 2399. *Ibid.*, **1965**, 4655.

(14) M. Ohashi, J. M. Wilson, H. Budzikiewicz, M. Shamma, W. A. Slusarchyk, and C. Djerassi, *J. Am. Chem. Soc.*, **85**, 2807 (1963).

(15) M. Shamma and W. A. Slusarchyk, *Tetrahedron Lett.*, **1965**, 1509.

(16) H. Guinaudeau, M. Leboeuf, and A. Cave, *Lloydia*, **38**, 286 (1975).

(17) R. Charubala, B. R. Pai, T. R. Govindachari, and N. Viswanathan, *Chem. Ber.*, **101**, 2665 (1968).

(18) W. H. Perkin, *J. Chem. Soc.*, **109**, 1023 (1916).

(19) F. A. L. Anet and M. A. Brown, *Tetrahedron Lett.*, **1967**, 4881.

(20) J. Slavik and L. Slavikova, *Collect. Czech. Chem. Commun.*, **28**, 253 (1963).

(21) F. Santavy, in "The Alkaloids," vol. 12, R. H. Manske and H. L. Holmes, Eds., Academic, New York, N.Y., 1970, p. 337.

ACKNOWLEDGMENTS AND ADDRESSES

Received December 29, 1975, from the *Institute of Medicinal Plants, College of Pharmacy, Tehran University, Tehran, Iran.*

Accepted for publication April 20, 1976.

Supported by Grant 13 of the International Foundation for Science and by a grant from the Ministry of Science and Higher Education Research Development Council.

[x] To whom inquiries should be directed.

Synthesis of 5,6-Benzo-2-azabicyclo[2.2.2]octane Derivatives as Potential Benzomorphan-Type Analgesic Agents

RONALD F. BORNE [x], SAY-JONG LAW, PHILIP W. WIRTH, and JAMES C. MURPHY

Abstract □ The synthesis of two *N*-substituted 5,6-benzo-2-azabicyclo[2.2.2]octane analogs of benzomorphan-type analgesics *via* benzyne addition to appropriate *N*-substituted *N*-alkyl-2-pyridones is described. Neither derivative possessed observable analgesic activity at the doses tested.

Keyphrases □ 5,6-Benzo-2-azabicyclo[2.2.2]octanes, *N*-substituted—synthesized, analgesic activity evaluated, mice □ Structure–activity relationships—*N*-substituted 5,6-benzo-2-azabicyclo[2.2.2]octanes synthesized, analgesic activity evaluated, mice □ Analgesic activity—*N*-substituted 5,6-benzo-2-azabicyclo[2.2.2]octanes evaluated, mice

The structural features of narcotic analgesics related to morphine have been well documented (1, 2). Studies of structure–analgesic activity requirements within the benzomorphan-type analgesics have also received considerable attention. While the structural features of benzomorphans are generally incorporated in structures such as I, many analogous structures have been demonstrated to possess significant analgesic activity. For example, 2-methyl-6,7-benzomorphan (II) (3), 7-methoxy-2-methyl-B-norbenzomorphan (III) (4), and 5-methano-3-methyl-6-phenyl-1,2,3,4,5,6-hexahydro-3-benzazocine (IV) (5)

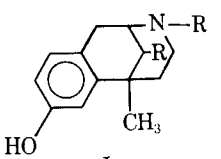

I

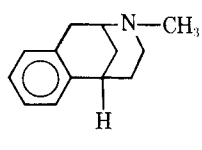

II

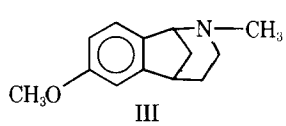

III

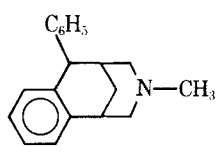

IV

possessed analgesic potencies comparable to that of codeine.

Compounds II–IV all lack "quaternary central carbon atoms," a structural feature once thought to be essential for activity (1, 2). Additionally, II and IV lack phenolic functions, and IV contains only a one-carbon separation from the basic nitrogen and the central carbon atom. While the active benzomorphans are characterized by the presence of a basic nitrogen atom 4.1 Å from the center of an

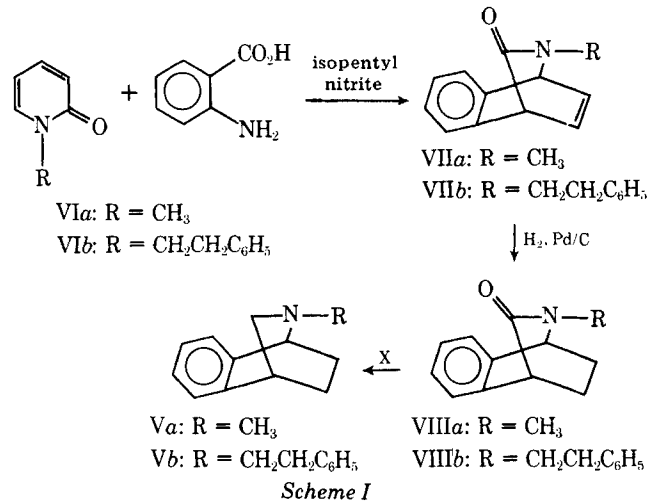

Scheme I

aromatic ring and 1.5 Å above the plane of that ring, derivatives possessing these characteristics alone proved to be inactive as analgesics (6). This discussion illustrates the flexibility of structural features for analgesic activity within the benzomorphan series.

These factors, along with interest in 2-azabicyclo[2.2.2]-octane analogs of analgesics (7), prompted the preparation and evaluation of V*a* and V*b* for analgesic and central nervous system (CNS) activity. These analogs lack a quaternary carbon atom, a phenolic function, and a two-carbon separation between the basic nitrogen and the central carbon atom but do orient the basic nitrogen 3.6 Å from the center of the aromatic ring and 1.3 Å above the plane of this ring. Additionally, these analogs may be considered as semirigid analogs of phenethylamine derivatives.

DISCUSSION

Chemistry—The synthetic approach to V*a* was essentially that previously reported (8) with some modifications (Scheme I). Benzyne was generated by the action of isopentyl nitrite on anthranilic acid in the presence of *N*-methyl-2-pyridone (VI*a*). The adduct, VII*a*, was obtained in only 10% yield. Subsequent catalytic hydrogenation gave VIII*a*, which was further reduced with sodium bis(2-methoxyethoxy)aluminum hydride (X) to give V*a*.

The synthesis of V*b* was somewhat more difficult. The synthesis of IX (Scheme II) was attempted with the anticipation that reduction, carbamate hydrolysis, and subsequent reductive alkylation with phenylacetaldehyde would give V*b*. However, condensation of benzyne with *N*-carbethoxy-1,2-dihydropyridine yielded no isolatable adduct. Thus, VI*b* was prepared by the oxidation of the quaternary salt obtained from pyridine and 2-bromoethylbenzene with potassium hydroxide and potassium ferricyanide. Condensation of this pyridone and benzyne gave only a 7% yield of VII*b*. Isolation of the diazonium salt prior to benzyne generation did not improve the yield of the adduct. Catalytic hydrogenation of VII*b* gave VIII*b* in a 92% yield. Subsequent lactam reduction gave V*b* in an overall 6% yield from VI*b*.

Pharmacology—Compounds V*a* and V*b* were evaluated for analgesic activity in mice using the D'Amour–Smith (9) tail-flick method. The toxicity of both compounds limited the maximum doses at which they could be evaluated. Both compounds failed to display analgesic activity, V*a* at 25 mg/kg and V*b* at 50 mg/kg, but produced some CNS effects.

Compound V*a* was tested at 50, 25, and 10 mg/kg. The 50-mg/kg dose was lethal to all subjects within 12 min of injection. Death was preceded by profuse salivation, Straub tail, and tremors. The 25-mg/kg dose produced tremors which lasted for about 20 min following injection. Consistent failure in tests involving muscular coordination was seen at 25 mg/kg, but spontaneous activity and reactivity were not affected. The 10-mg/kg dose produced no effects within the scope of this screen.

Compound V*b* was tested at 100, 50, and 25 mg/kg. All mice injected with 100 mg/kg died within 10 min of injection following clonic convulsions. The mice injected with 50 mg/kg showed a loss of spontaneous activity as evidenced by observer ratings and failures on the dish, pedestal, and chimney tests. Both the finger touch and tail pull tests showed a loss of reactivity. No ptosis or loss of skeletal muscle tone was observed. The pinna reflex was abolished, indicating that the effect of V*b* at 50 mg/kg may not be purely depressant. One death occurred within 24 hr at 50 mg/kg, while only marginal effects and no lethality were observed at 25 mg/kg.

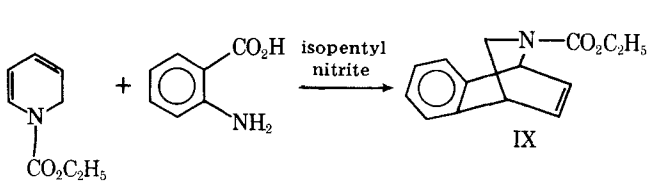

Scheme II

EXPERIMENTAL[1]

2-Methyl-5,6-benzo-2-azabicyclo[2.2.2]oct-7-en-3-one (VII*a*)—A solution of anthranilic acid (20.0 g, 0.145 mole) in 125 ml of acetone was added dropwise over 1.0 hr to a refluxing solution of 15.0 g (0.137 mole) of VI*a* and 20.0 g (0.17 mole) of isopentyl nitrite in 400 ml of dichloromethane. The reaction mixture was refluxed an additional 1.0 hr and the resulting solution was washed with 2 × 200 ml of 10% hydrochloric acid and 2 × 200 ml of water. The organic phase was dried over sodium sulfate and evaporated to give a dark oil.

The oil was taken up in benzene, placed on a basic alumina column[2] (80–200 mesh, 520 g), and eluted with ether–benzene (1:1). Isopentyl alcohol eluted first, followed by the adduct, VII*a* (2.5 g, 10%); NMR: δ 3.0 (s, 3H, NCH_3), 4.8 (doublet of doublets, 1H, J = 2.5 Hz), 5.2 (doublet of doublets, 1H, J = 2.5 Hz), and 7.1–7.7 (m, 6H, olefinic and aromatic); IR (liquid film): 1680 cm^{-1} (NC=O).

2-Methyl-5,6-benzo-2-azabicyclo[2.2.2]octan-3-one (VIII*a*)—To a solution of VII*a* (4.8 g, 0.026 mole) in 100 ml of ethanol was added 10% palladium-on-charcoal (0.48 g), and the resulting mixture was hydrogenated at 3.1 kg/cm^2. The mixture was filtered through diatomaceous earth[3], and the filtrate was evaporated to give a clear oil (3.9 g, 81%); NMR: δ 2.95 (s, 3H, NCH_3), 4.0 (s, 1H, NCH), and 7.25 (s, 4H, aromatic); IR (liquid film): 1680 cm^{-1} (NC=O).

2-Methyl-5,6-benzo-2-azabicyclo[2.2.2]octane (V*a*)—A solution of VIII*a* (2.3 g, 0.012 mole) in benzene (40 ml) was added dropwise to X (14 ml of a 70% benzene solution, 0.048 mole), and the resulting solution was refluxed for 3 hr. Ethanol was added to the cooled, stirring solution until bubbling ceased. Water was added until precipitation ceased. The precipitate was removed by filtration, and the filtrate was separated into organic and aqueous phases. The aqueous phase was extracted with chloroform (2 × 30 ml); the organic extracts were combined, dried over sodium sulfate, and evaporated to give a residue.

Distillation of the residue gave an oil (1.0 g, 47%), bp 70°/0.45 mm; NMR: δ 1.27–2.5 (m, 5H, H at C-7, C-8, and C-3), 2.03 (NCH_3), 2.97 (broad, 1H, H at C-4), 3.2–3.4 (doublet of doublets, 1H, H at C-3), 3.6 (broad, 1H, H at C-1), and 7.2–7.4 (broad, 4H, aromatic); *m/e* 173 (M+) and 144 (base). The hydrochloride salt was prepared in the normal manner, mp 236.5–238.5°.

Anal.—Calc. for $C_{12}H_{16}ClN$: C, 68.72; H, 7.69; N, 6.68. Found: C, 68.63; H, 7.73; N, 6.53.

1-(2-Phenylethyl)-2-pyridone (VI*b*)—To a solution of 13.0 g (0.049 mole) of 1-(2-phenylethyl)pyridinium bromide (prepared from pyridine and 2-bromoethylbenzene, mp 123–125°) in 60 ml of water was added a solution of 65.0 g (0.2 mole) of potassium ferricyanide in 400 ml of water. After addition was complete, a yellow suspension was obtained. Benzene (125 ml) was added, and the reaction mixture was warmed to 40°. A so-

[1] All melting points were taken on a Mel-Temp apparatus and are corrected. IR spectra were obtained with a Beckman IR-33 spectrophotometer. NMR spectra were taken in deuterochloroform on a Jeolco C-60-HL spectrometer, and values are reported in parts per million (δ) from tetramethylsilane as the internal standard. Mass spectral data were obtained on a Dupont model 21-492 spectrometer. Elemental analyses were performed by Galbraith Laboratories, Knoxville, Tenn. Sodium bis(2-methoxyethoxy)aluminum hydride (Red Al) was purchased from Aldrich Chemical Co.

[2] Fisher.

[3] Celite.

lution of potassium hydroxide (27.0 g, 0.5 mole) in 75 ml of water was added dropwise, and the resulting mixture was stirred for 2 hr.

The organic layer was separated, and the aqueous layer was extracted with benzene (2 × 75 ml). The organic phases were combined, dried over sodium sulfate, and evaporated to give a tan solid (6.5 g, 66%). Recrystallization from benzene–petroleum ether yielded colorless crystals, mp 104–106°; IR (mineral oil): 1660 cm^{-1} (C=O).

2-(2-Phenylethyl)-5,6-benzo-2-azabicyclo[2.2.2]oct-7-en-3-one (VII*b*)—A solution of anthranilic acid (61.6 g, 0.45 mole) in 500 ml of ethanol was cooled to 5°. Concentrated hydrochloric acid (35 ml) was added followed by isopentyl nitrite (85 ml). The temperature was maintained below 10° throughout addition. Ether (500 ml) was added; the resulting diazonium salt was collected by filtration, washed with anhydrous ether, and suspended in 650 ml of dichloromethane. To the suspension were added 18.3 g (0.092 mole) of VI*b* and 35.0 g (0.6 mole) of propylene oxide in 50 ml of dichloroethane. The mixture was stirred at room temperature for 1.5 hr, and the solvents were evaporated.

The residual oil was taken up in benzene, placed on a silica gel column[4] (0.05–0.20 mm, 800 g), and eluted with ether–hexane (1:1) to give 1.75 g (7%) of VII*b*, mp 124–125°; NMR: δ 2.73 (t, 2H, $CH_2C_6H_5$), 3.4–3.7 (m, 2H, NCH_2), 4.5–4.7 (doublet of doublets, 1H, H at C-4), 4.8–4.9 (doublet of doublets, 1H, H at C-1), and 6.5–7.3 (broad, 11H, olefinic and aromatic); IR (mineral oil): 1675 cm^{-1} (C=O); *m/e* 275 (M+) and 128 (base).

Anal.—Calc. for $C_{19}H_{17}NO$: C, 82.85; H, 6.23; N, 5.09. Found: C, 82.81; H, 6.26; N, 5.38.

2-(2-Phenylethyl)-5,6-benzo-2-azabicyclo[2.2.2]octan-3-one (VIII*b*)—A solution of 3.56 g (0.0129 mole) of VI*b* in 175 ml of ethanol was hydrogenated in the presence of 0.4 g of palladium-on-charcoal at 3.1 kg/cm^2 until hydrogen uptake ceased. The catalyst was removed by filtration, and the filtrate was evaporated to give a solid. The solid was recrystallized from benzene–petroleum ether to yield 3.3 g (92%) of VIII*b*, mp 127–129°; IR (KBr): 1665 cm^{-1} (C=O); *m/e* 277 (M+) and 130 (base).

Anal.—Calc. for $C_{19}H_{19}NO$: C, 82.27; H, 6.90; N, 5.05. Found: C, 82.33; H, 7.00; N, 5.01.

2-(2-Phenylethyl)-5,6-benzo-2-azabicyclo[2.2.2]octane (V*b*)—A solution of 2.18 g of VIII*b* (0.0079 mole) in 40 ml of benzene was added dropwise to X (8 ml, 0.0277 mole), and the resulting mixture was refluxed for 4 hr. The mixture was cooled, ethanol and water were added to destroy excess hydride, and the mixture was filtered. The organic phase of the filtrate was separated, and the aqueous layer was extracted with chloroform (2 × 30 ml).

The organic phases were combined, dried over sodium sulfate, and evaporated to give a residue which was chromatographed on a silica gel column[4] (0.05–0.20 mm, 45 g). Elution with ether–hexane (1:1) gave 1.85 g (89%) of V*b*; NMR: δ 1.27–2.9 (m, 9H, $NCH_2CH_2C_6H_5$ and H at C-7, C-8, and C-3), 2.9–3.1 (broad, 1H, H at C-4), 3.32–3.5 (doublet of doublets, 1H, H at C-3), 3.7–3.9 (broad, 1H, H at C-1), and 7.0–7.4 (broad, 9H, aromatic); *m/e* 263 (M+) and 172 (base). The hydrochloride salt was prepared in the normal manner, mp 142–144°.

Anal.—Calc. for $C_{19}H_{22}ClN$: C, 76.11; H, 7.40; Cl, 11.83; N, 4.67. Found: C, 76.30; H, 7.42; Cl, 11.76; N, 4.77.

Pharmacological Methods—Both V*a* and V*b* were tested for biological activity with blind screening techniques standard to this laboratory. All tests were conducted in groups of four to six male Swiss mice, 18–23 g, and were conducted according to published protocols (10, 11). This mouse assay consists of: (*a*) rating of spontaneous activity, (*b*) rating of skeletal muscle tone, (*c*) the tail pull and finger touch tests of reactivity, (*d*) the righting time test, (*e*) measurement of pinna reflex, (*f*) the test for catalepsy, (*g*) the dish test, (*h*) the pedestal test, (*i*) the traction test, (*j*) the chimney test, and (*k*) a modification of the D'Amour–Smith tail flick test for analgesia (9).

The tail-flick test was performed 30 min after intraperitoneal injection. All other tests were performed at 15 and 60 min postinjection. Sixteen standard observations of autonomic activity and abnormal behavior were made in addition to the tests listed. Appropriate vehicle and positive controls were included in the test protocols.

[4] Woelm.

REFERENCES

(1) N. B. Eddy and E. L. May, in "Synthetic Analgesics," J. Rolfe, Ed., Pergamon, London, England, 1965, part IIB.

(2) E. L. May and L. J. Sargent, in "Analgetics," G. deStevens, Ed., Academic, New York, N.Y., 1965, pp. 123–177.

(3) K. Kanematsu, M. Takeda, A. E. Jacobson, and E. L. May, *J. Med. Chem.*, **12**, 405 (1969).

(4) A. E. Jacobson and M. Molotoff, *ibid.*, **13**, 7 (1970).

(5) W. K. Chang, L. A. Walter, and R. I. Taber, *ibid.*, **14**, 1011 (1971).

(6) R. L. Clarke, A. J. Gambino, and S. J. Daun, *ibid.*, **17**, 1040 (1974).

(7) C. R. Clark, R. F. Borne, and J. M. Holbrook, *ibid.*, **19**, 852 (1976).

(8) E. B. Sheinin, G. E. Wright, C. L. Bell, and L. Bauer, *J. Heterocycl. Chem.*, **5**, 859 (1968).

(9) F. E. D'Amour and D. L. Smith, *J. Pharmacol. Exp. Ther.*, **72**, 74 (1941).

(10) R. A. Turner, "Screening Methods in Pharmacology," Academic, New York, N.Y., 1965.

(11) F. R. Domer, "Animal Experiments in Pharmacological Analysis," Charles C Thomas, Springfield, Ill., 1971.

ACKNOWLEDGMENTS AND ADDRESSES

Received March 22, 1976, from the *School of Pharmacy, University of Mississippi, University, MS 38677.*

Accepted for publication June 7, 1976.

Supported in part by Grant I R01 NS 09188 from the National Institute of Neurological Diseases and Stroke and in part by the Research Institute of Pharmaceutical Sciences, School of Pharmacy, University of Mississippi.

[x] To whom inquiries should be directed.

Polarographic Study of New Antibacterial Isoxazolium Salts: 2,3-Dialkyl-5-arylisoxazolium Perchlorates

NABIL M. OMAR ˣ and NAWAL A. EL-RABBAT

Abstract □ The polarographic reduction of new antibacterial 2,3-dialkyl-5-arylisoxazolium salts is described. The electrode process involves an irreversible two-electron transfer and is pH independent within the 6.0–10.0 range. In more acidic media, hydrogen waves are observed; at higher pH values, a chemical degradation of the isoxazolium salt proceeds. Values of the half-wave potential of the salts are dependent on the polar contribution of the 5-aryl substituents in terms of the Hammett equation. The *in vitro* minimum inhibitory concentrations of these compounds are best correlated with Hansch π-values.

Keyphrases □ Isoxazolium salts, substituted—polarographic reduction, effect of pH, polar contribution of 5-aryl substituents correlated with antibacterial activity □ Polarography—reduction, substituted isoxazolium salts, effect of pH, polar contribution of 5-aryl substituents correlated with antibacterial activity □ Antibacterial activity—substituted isoxazolium salts, correlated with polar contribution of 5-aryl substituents, polarographic reduction □ Structure–activity relationships—substituted isoxazolium salts, polar contribution of 5-aryl substituents correlated with antibacterial activity, polarographic reduction

In a search for new antimicrobial cationic agents, the synthesis and antibacterial evaluation of a series of 2,3-dialkyl-5-arylisoxazolium perchlorates (I–XIII) were undertaken (1). Since differences in the antibacterial effectiveness of these salts were roughly assigned to substituent effects, it was of interest to evaluate such effects by tracing the possible electronic contributions of the isoxazolium 2- and 5-substituents and to correlate the corresponding microbiological data with these effects.

This report describes the polarographic reduction of I–XIII and its suitability as a measure of the polar substituent effect. Correlation of the antibacterial effectiveness to the polar substituent effect and the substituent solubility effect also was attempted.

EXPERIMENTAL

Materials—Analytically pure 2,3-dimethyl- and 2-ethyl-3-methyl-5-arylisoxazolium perchlorates (I–XIII) were prepared by quaternizing the appropriate isoxazoles as reported previously (2). Double-distilled water was used for all solutions.

Reagents—A Britton–Robinson phosphate–acetate–borate buffer was used. Adjustment to the required pH value was effected by addition of 0.2 *N* carbonate-free sodium hydroxide solution (3). Potassium chloride and tetraethylammonium perchlorate were utilized as the supporting electrolytes in 0.1–1.0 *M* solutions. Octoxynol[1] (0.1% v/v) and freshly prepared gelatin (0.2% w/v) solutions were the maximum suppressors. For deoxygenation, oxygen-free nitrogen was prepared by passing commercial nitrogen through 5% (w/v) aqueous vanadous sulfate solution (4).

Instrumentation—Current–voltage curves were recorded on a suitable polarograph[2] using 25-ml H-type polarographic cells, a dropping mercury electrode, and a saturated calomel electrode. Temperature control was achieved with an ultrathermostat[3], switched at 25° (±0.1).

Capillary characteristics were: drop time, 3.0 sec; and rate of mercury flow, 3.5 mg/sec, measured at a 30.0-cm mercury column height without applied potential. Recording conditions were: full scale deflection, 0.1 μamp; applied potential, 0.0–2.0 at a rate of 200 mv/min; and shunt, $\frac{1}{200}$. A pH meter[4] fitted with a sealed calomel electrode and a shielded glass electrode was used. For the spectrophotometric monitoring, a manual spectrophotometer[5] and 1-cm thick quartz cells were employed.

Procedure—The corresponding weight of the isoxazolium salt was dissolved in an appropriate volume of 0.5 *M* potassium chloride solution (or in a selected buffer solution), 0.5–1.0 ml of the maximum suppressor solution was added, and the solution was diluted with the supporting electrolyte solution to a final concentration of 5×10^{-4} *M* depolarizer/liter. Electrolysis was conducted at 25° after deoxygenation with pure nitrogen for 10 min.

RESULTS AND DISCUSSION

A literature review revealed that data pertaining to the polarographic reduction of the isoxazolium cation are not available, although the electroactivity of other 6π-isoelectronic analogs has been established (5–7). When tested for such activity in 0.5 *M* potassium chloride solution (pH 6.60–6.75), 2,3-dimethyl-5-phenylisoxazolium perchlorate (I) afforded a single well-defined cathodic wave with a half-wave value of −1.05 v (Fig. 1). This value was not significantly affected by variations in the ionic strength of the potassium chloride solution (0.10–2.0 *M*).

The use of 0.1 *M* aqueous tetraethylammonium perchlorate solution as the supporting electrolyte brought about a negative shift in the wave ($E_{1/2}$ = −1.12 v), reflecting the relatively high electrophilicity of the isoxazolium cation relative to its isosteric pyrazolium analog. The $E_{1/2}$ of 1,2,3-trimethyl-5-phenylpyrazolium perchlorate is −1.69 v (5).

As revealed from the dependence of the limiting current values of I, both on concentration (1×10^{-3}–5×10^{-4} *M*) and on the square root of the mercury column height (20–45 cm), its reduction wave is diffusion controlled. Comparison of the wave height and slope with relevant data of the similarly investigated pyrazolium analog gives the electron transfer of I a value of $n \sim 2$ (5). Theoretical logarithmic analysis of the observed wave gave rise to a straight line; however, the slope corresponded to a nonintegral value for n ($\alpha = 0.134$, $\alpha n \neq 0.059$), thus suggesting the irreversibility of the electrode reaction (8). Based on reported electrophilic interactions of the isoxazolium cation (9), the polarographic reduction of I might be similarly expected to afford the corresponding isoxazoline (Scheme I).

With the Britton–Robinson buffer as the supporting electrolyte, no apparent change in the wave characteristics of I could be traced within pH 6.0–10.0. At lower pH values (2.0–5.5), gradual reduction of the hydrogen ion seriously precluded the observation of the isoxazolium wave, while an increase of alkalinity (10.5–11.9) brought about a remarkable fall in the wave height. The $E_{1/2}$ value was little affected by such pH variations. At pH values higher than 11.9, a continous prominent drop of the limiting current was observed.

Estimations of the actual concentration of I at such pH values by UV spectrophotometric[6] and polarographic monitoring were similar. This finding denotes a considerable instability of the isoxazolium cation at elevated pH values, probably because of a base-induced cleavage of the cation (10). Since the antibacterial effectiveness of most cationic agents

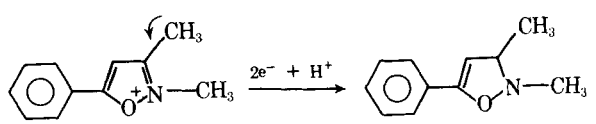

Scheme I

[1] Triton-X 100.
[2] LP-60 A, Prague, Czechoslovakia.
[3] T-606 MTA, Budapest, Hungary.
[4] *Radelkis OP-401/2, Budapest, Hungary.*
[5] Spektromom-203, Budapest, Hungary.
[6] The 282-nm absorption maximum of I was not affected by variations in the buffer pH.

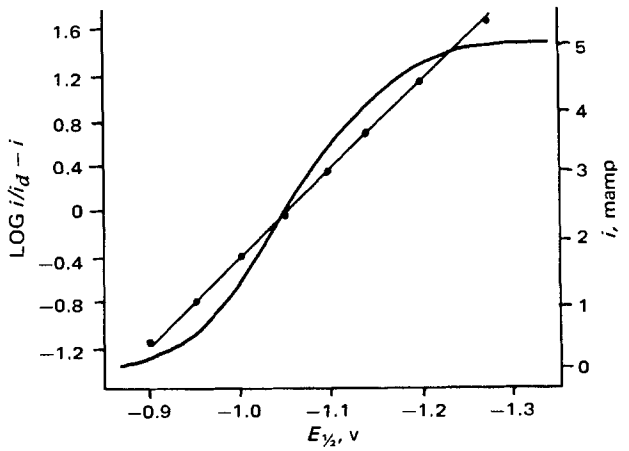

Figure 1—*Wave equation of I, 5 × 10⁻⁴ M in 0.5 M potassium chloride solution.*

is enhanced with increased pH values, further antimicrobial investigations of this series of isoxazolium salts will be carried out at pH values up to 10.0.

Polarographic reduction of II–XIII was carried out under the same conditions (Table I). Except for the two nitro derivatives, VII and XIII, comparison of the wave characteristics of the investigated salts (in 0.5 *M* potassium chloride) indicated that their electrode processes were identical to those of I. Compounds VII and XIII were reduced with the production of two waves; the first ($E_{1/2} \sim -0.68$ v) corresponded, however, to a four-electron transfer for the reduction of the nitro group (5). The second wave ($E_{1/2} \sim -1.28$ v) involved a two-electron reduction of the nitro-reduced isoxazolium cation.

The polar contribution of the 5-aryl substituents of I–XIII can be determined with the modified Hammett equation (11):

$$\Delta E_{1/2} = E_{1/2}^{x} - E_{1/2}^{0} = \sigma\rho \qquad \text{(Eq. 1)}$$

where $E_{1/2}^{x}$ and $E_{1/2}^{0}$ are the polarographic half-wave potentials of the benzene-substituted and unsubstituted derivatives of a particular series, respectively; ρ represents the reaction constant; and σ is the Hammett substituent constant. For I–VI and VIII–XII, correlation of their $E_{1/2}$ values to the corresponding 5-aryl σ-constants was fairly significant (r = 0.90 and 0.96, ρ = 0.26 and 0.28, and s = ±68 and ±46 mv for the *N*-methyl and *N*-ethyl sets, respectively).

The weak sensitivity of the polarographic reaction center of the investigated salts to the polar substituent effect was readily reflected by the relatively low values of the electrode reaction constant. Since such values are usually encountered when substituents are far away from reaction centers (12), this result would favor the representation of the isoxazolium 3-carbon for the polarographic reaction center (Scheme I).

The fact that substitution of the *N*-methyl radical for an *N*-ethyl analog did not affect the electrophilic tendency of the carrier isoxazolium cation (Table I) is explained by the electronic leveling effect of polar contributions of the *N*-methyl and *N*-ethyl moieties; σ-constants are −0.15 and −0.17, respectively (13). In contradiction to the reported polarographic data for related nitrophenyl heterocycles (5, 6), the $E_{1/2}$ values of the nitrophenylisoxazolium salts were not linearly correlated to their NHOH-substituent constant, probably due to a difference between their electrode reaction and other 5-arylisoxazolium derivatives.

Moreover, no correlations could be set up between the $E_{1/2}$ values of the investigated salts and their corresponding minimum inhibitory concentration (MIC) values. Added to the fact that VIII–XIII are more microbiologically effective than their *N*-methyl congeners (I–VII), these data suggest a weak operation of the polar contributions of both of the 2- and 5-isoxazolium substituents. In fact, the correlation of logarithmic MIC values of I–VII to the corresponding Hansch partition values of the

Table I—Antibacterial Activity and Substituent Constants of 2,3-Dialkyl-5-arylisoxazolium Perchlorates

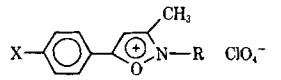

Compound	R	X	$E_{1/2}$, v	σX^- Constant[a]	πX^- Value[a]	MIC, μg/ml[b]
I	CH_3	H	−1.050	0.00	0.00	800
II	CH_3	CH_3	−1.070	−0.17	+0.56	300
III	CH_3	OCH_3	−1.085	−0.27	−0.02	400
IV	CH_3	OC_2H_5	−1.075	−0.24	+0.38	300
V	CH_3	Cl	−0.960	+0.23	+0.71	200
VI	CH_3	Br	−0.940	+0.27	+0.86	150
VII	CH_3	NO_2	−1.275[c]	+0.78	−0.28	1000
VIII	C_2H_5	H	−1.045	0.00	0.00	500
IX	C_2H_5	CH_3	−1.050	−0.17	+0.56	200
X	C_2H_5	OCH_3	−1.075	−0.27	−0.02	250
XI	C_2H_5	OC_2H_5	−1.070	−0.24	+0.38	120
XII	C_2H_5	Br	−0.960	+0.27	+0.86	100
XIII	C_2H_5	NO_2	−1.280[c]	+0.78	−0.28	600

[a] From Ref. 13. [b] Minimum inhibitory concentration against *Staphylococcus aureus*. [c] Another wave existed at $E_{1/2}$ = −0.675 v.

5-phenyl substituents (π-values, Table I) was fairly significant (r = 0.97 and r^2 = 0.94 for n = 7). Such data also favor interpretation of the increased effectiveness of the *N*-ethylisoxazolium congeners in terms of their enhanced lipophilicity, π-CH_3 and C_2H_5 = +0.56 and +1.02, respectively (13).

REFERENCES

(1) N. M. Omar and A. A. El-Kader, *Can. J. Pharm. Sci.*, **8**, 128 (1973).

(2) C. Munsante, *Gazz. Chim. Ital.*, **72**, 448, 537 (1942).

(3) U. U. Lyrie, "Handbook of Analytical Chemistry," Khimia, Moscow, Russia, 1967, p. 230.

(4) L. Meites and T. Meites, *Anal. Chem.*, **20**, 984 (1948).

(5) N. M. Omar and N. A. El-Rabbat, *J. Pharm. Sci.*, **63**, 937 (1974).

(6) Z. N. Timoofeeva, N. M. Omar, L. S. Tikhonova, and A. V. Eltsov, *Zh. Obshch. Khim.*, **40**, 2072 (1970).

(7) Z. N. Timoofeeva and A. V. Eltsov, *ibid.*, **37**, 2599 (1967).

(8) I. K. Kolthoff and J. J. Lingane, "Polarography," vol. I, Interscience, New York, N.Y., 1965, p. 120.

(9) A. Ikou, H. Kaoru, and K. Heido, *Tetrahedron Lett.*, **55**, 4875 (1969).

(10) R. B. Woodward and R. Olofson, *J. Am. Chem. Soc.*, **83**, 1007 (1961).

(11) P. Zuman, *Collect. Czech. Chem. Commun.*, **19**, 599 (1954).

(12) U. A. Jdanov and V. I. Minkin, "Correlation Analysis in Organic Chemistry," Khimia, Moscow, Russia, 1968, p. 134.

(13) C. Hansch, A. Leo, S. H. Unger, K. H. Kim, D. Nikaitani, and E. J. Lien, *J. Med. Chem.*, **16**, 1207 (1973).

ACKNOWLEDGMENTS AND ADDRESSES

Received March 11, 1976, from the *Department of Pharmaceutical Chemistry, Faculty of Pharmacy, University of Assiut, Assiut, Egypt.*

Accepted for publication June 15, 1976.

The authors are indebted to M. A. El-Soukarry, Department of Microbiology, University of Assiut, for supplying the microbiological data.

[x] To whom inquiries should be directed. Present address: Institut für Pharm. Chem. der Universität, Hittorfstr. 58/62, 4400 Münster/Westf., Bundesrepublik Deutschland.

Micromethod for Determination of Meperidine in Plasma

M. A. EVANS [x] **and R. D. HARBISON**

Abstract □ A GLC method utilizing a flame-ionization detector is described for the analysis of meperidine in blood plasma. Meperidine is extracted with ether from plasma that has been made basic with sodium hydroxide. The ether extract is evaporated to dryness, and the residue is dissolved in carbon disulfide for GLC analysis. An internal standard, *N',N'*-diethylaminoacetyl-2,6-xylidine, is used to quantitate meperidine. The extraction efficiency from plasma is 85%, and as little as 0.05 μg of meperidine can be quantitatively determined in 1 ml of plasma.

Keyphrases □ Meperidine—GLC analysis, human plasma □ GLC—analysis, meperidine, human plasma □ Analgesics, narcotic—meperidine, GLC analysis, human plasma

Since the development (1) of a spectrophotometric analysis of meperidine[1] (I), several investigators reported procedures with greater sensitivity and specificity for plasma meperidine (2). However, some of these newer methods require several extractions (3), lack internal standard techniques (4), and demonstrate long retention times, which limit the number of samples that can be processed (5).

During prolonged administration of meperidine to pediatric patients, a micromethod of analysis is needed for the determination of peak plasma concentrations and the half-life of the drug. Therefore, a GLC method was developed for the rapid analysis of small amounts of meperidine in plasma using an internal standard for quantitation. The sensitivity of this method was greater than 0.05 μg/ml of plasma, and no interference was observed with peak identification. To evaluate this method, meperidine disappearance in plasma was studied in two infants following therapeutic drug administration.

EXPERIMENTAL

Apparatus—A gas chromatograph[2] equipped with a flame-ionization detector was maintained with gas flows of 20, 30, and 300 ml/min for nitrogen, hydrogen, and air, respectively. A column oven temperature of 215° was used; the injection port and detector temperatures were maintained at 240°.

Column—A glass column, 2 m × 2 mm, was packed with 3% SP 2250 on Chromosorb W, AW/DMCS[3] (80–100 mesh). The column was rinsed before packing with methanol and acetone; it was then dried and conditioned for 6 hr with a 10% solution of dimethyldichlorosilane[4] in toluene to silylate reactive sites. Following silylation, the column was again rinsed with acetone and dried.

Analytical Procedures—One milliliter of blood plasma was transferred to a 25-ml glass-stoppered centrifuge tube, mixed with the internal standard *N',N'*-diethylaminoacetyl-2,6-xylidine[5] (II) (1.0 μg/0.5 ml), made basic with 1 *N* NaOH (0.2 ml), and extracted with reagent grade ether (10 ml) by stirring on a vortex mixer (30 sec). The ether was then transferred by disposable pipet to a dry, clean, 12-ml centrifuge tube and evaporated to dryness in a water bath (45°) using nitrogen flow. The residue was redissolved in 20 μl of spectrophotometric grade carbon disulfide[6], and 1 μl was injected into the gas chromatograph.

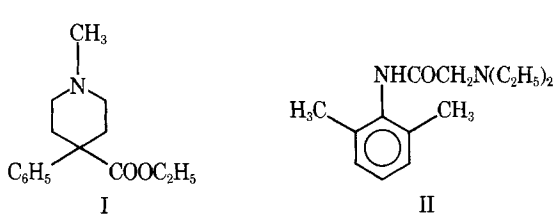

I

II

A standard calibration curve was prepared by adding aliquots of an aqueous solution of meperidine hydrochloride to 1 ml of plasma to give a final concentration ranging from 0.05 to 0.20 μg/ml of meperidine in plasma. The internal standard (1 μg) was then added to the sample, and the analyses were made. Sixteen samples, four per concentration of meperidine, were analyzed for the determination of the standard curve. Each sample was injected in triplicate, and the determination for the entire standard was replicated once.

[^{14}C-*N*-Methyl]-meperidine hydrochloride[7] was used to estimate the extraction efficiency of meperidine from plasma by measurement of the total radioactivity in the extract[8].

RESULTS AND DISCUSSION

The GLC retention times for I and II were 1.4 and 2.5 min, respectively. A gas chromatogram from a control human plasma and plasma containing 0.1 μg of meperidine/ml with the internal standard (0.5 μg/ml) is shown in Fig. 1. Since peaks for both agents were symmetrical, quantitation was made by comparison of peak heights. Detector responses and calibration curves were linear for both compounds over the 0.05–0.20-μg/ml range. Blanks were prepared from plasma of drug-free subjects, and no peaks were observed that would interfere with the measurement of meperidine or the internal standard.

Linear regression analysis of the individual data points from the standards, plotted as the ratio of peak height of meperidine–peak height of the internal standard *versus* concentration of meperidine in plasma gave a computed slope of 1.37/μg of meperidine with a 0.01 *SE* of the

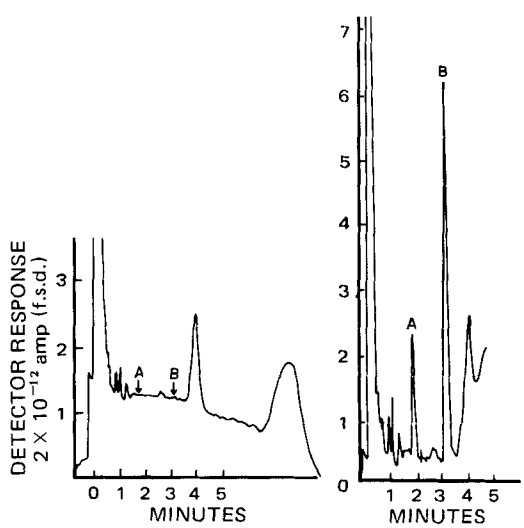

Figure 1—*Gas chromatogram of human plasma. Left: control plasma. Right: plasma containing 0.1 μg of meperidine/ml (A) and 0.5 μg of the internal standard/ml (B).*

[1] Demerol, Sterling-Winthrop Research Institute.
[2] Packard model 419.
[3] Supelco, Inc. Bellefonte, Pa.
[4] Applied Science Laboratories, State College, Pa.
[5] Astra Pharmaceutical Inc., Worcester, Mass.
[6] Mallinckrodt Chemicals, St. Louis, Mo.
[7] California Bionuclear, Sun Valley, Calif.
[8] Packard Tri-Carb model 3320.

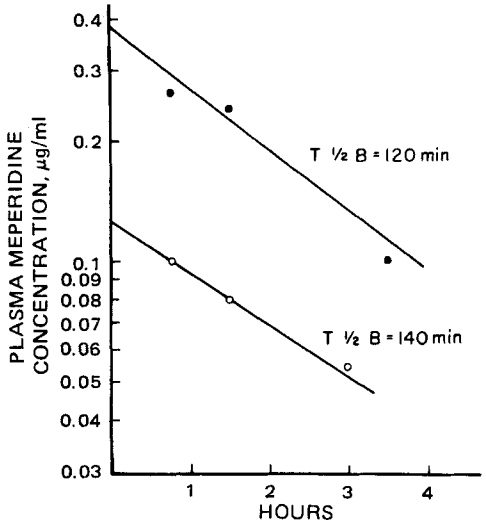

Figure 2—*Plasma concentration–time profile for meperidine in two infants following therapeutic drug administration. Sample size ranged from 0.5 to 1.5 ml of plasma.*

estimate and an intercept of zero. Extraction efficiency based on results from 10 samples using ^{14}C-meperidine hydrochloride was estimated at 85%.

Results of meperidine analysis in two infants following therapeutic intravenous administration of the drug are shown in Fig. 2. Although the calculated half-life was 1.5 hr for both infants, no clear definition of biological half-life in infants can be made since only two subjects were available for complete analysis. Burns *et al.* (1) demonstrated a biological half-life of 3–4 hr in adult humans with variations up to 100%.

This rapid method of analysis may prove useful for meperidine determinations when sample size is limited and many samples must be analyzed.

REFERENCES

(1) J. J. Burns, B. L. Berger, P. A. Lief, A. Wollack, E. M. Papper, and B. B. Brodie, *J. Pharmacol. Exp. Ther.*, **114**, 289 (1955).

(2) T. J. Goehl and C. Davison, *J. Pharm. Sci.*, **62**, 907 (1973).

(3) S. L. Tompsett, *Acta Pharmacol. Toxicol.*, **17**, 295 (1960).

(4) A. H. Beckett and J. F. Taylor, *J. Pharm. Pharmacol. Suppl.*, **19**, 505 (1967).

(5) V. R. Jenkins, II, P. V. Dilts, Jr., and W. M. Tolbert, *Obstet. Gynecol.*, **39**, 254 (1972).

ACKNOWLEDGMENTS AND ADDRESSES

Received November 6, 1975, from the *Department of Pharmacology, Vanderbilt Medical Center, Nashville, TN 37232.*

Accepted for publication June 8, 1976.

Supported in part by U.S. Public Health Service Grants ES00267 and DA00141. M. A. Evans was supported by Research Development Award NS00346.

[x] To whom inquiries should be directed.

Flavonoid Constituents from *Eupatorium altissimum* L. (Compositae)

R. H. DOBBERSTEIN, M. TIN-WA, H. H. S. FONG, F. A. CRANE, and N. R. FARNSWORTH [x]

Abstract □ An aqueous ethanol extract of *Eupatorium altissimum* L. (Compositae) showed confirmed activity in the P-388 lymphocytic leukemia assay in mice, and the chloroform solubles showed both cytotoxic activity in the 9KB carcinoma of the nasopharynx cell culture assay and antitumor activity in the P-388 lymphocytic leukemia assay. Two flavones, eupatorin and 5-hydroxy-3′,4′,6,7-tetramethoxyflavone, were isolated and identified. Both were devoid of cytotoxic and antitumor activity.

Keyphrases □ *Eupatorium altissimum*—aqueous ethanol whole plant extract, two flavones isolated, cytotoxic and antitumor activity evaluated □ Flavones—isolated from *Eupatorium altissimum* aqueous ethanol whole plant extract, cytotoxic and antitumor activity evaluated □ Cytotoxic activity—evaluated in *Eupatorium altissimum* aqueous ethanol whole plant extract and isolated flavones □ Antitumor activity—evaluated in *Eupatorium altissimum* aqueous ethanol whole plant extract and isolated flavones

As part of a continuing search for antitumor compounds from plant sources, it was found that an aqueous ethanol extract of *Eupatorium altissimum* L. (Compositae) showed confirmed activity against the P-388 leukemia assay in mice and that the chloroform solubles showed both antitumor activity in the P-388 leukemia and marginal activity against the 9KB cell culture (cytotoxicity). In the only previous investigation of *E. altissimum*, a defatted ethanol extract was reported to exhibit antimicrobial activity against *Leuconostoc citrovorum* (1).

Extracts of various *Eupatorium* species have been reported to possess cytotoxic and/or antitumor activity. Cytotoxic flavonoids have been isolated from *E. semiserratum* (2–4) and *E. cuneifolium* (4); cytotoxic and antitumor sesquiterpene lactones have been isolated from *E. semiserratum* (5), *E. cuneifolium* (6, 7), *E. formosanum* (8), and *E. rotundifolium* (9–11).

In this investigation, two flavonoids were isolated from a fraction possessing cytotoxic activity. One was identified as eupatorin (I), a flavone previously isolated from *E. semiserratum* (2). The other flavonoid was verified as 5-hydroxy-3′,4′,6,7-tetramethoxyflavone (II). Although II

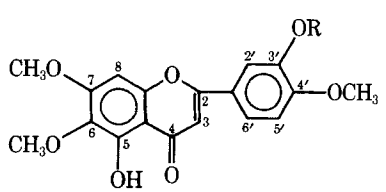

I: R = H

II: R = CH_3

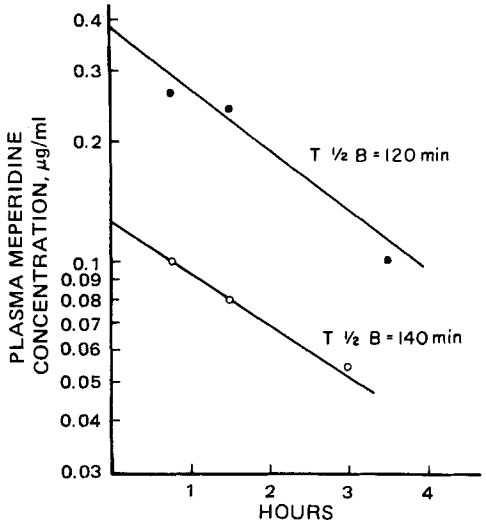

Figure 2—*Plasma concentration–time profile for meperidine in two infants following therapeutic drug administration. Sample size ranged from 0.5 to 1.5 ml of plasma.*

estimate and an intercept of zero. Extraction efficiency based on results from 10 samples using ^{14}C-meperidine hydrochloride was estimated at 85%.

Results of meperidine analysis in two infants following therapeutic intravenous administration of the drug are shown in Fig. 2. Although the calculated half-life was 1.5 hr for both infants, no clear definition of biological half-life in infants can be made since only two subjects were available for complete analysis. Burns *et al.* (1) demonstrated a biological half-life of 3–4 hr in adult humans with variations up to 100%.

This rapid method of analysis may prove useful for meperidine determinations when sample size is limited and many samples must be analyzed.

REFERENCES

(1) J. J. Burns, B. L. Berger, P. A. Lief, A. Wollack, E. M. Papper, and B. B. Brodie, *J. Pharmacol. Exp. Ther.*, **114**, 289 (1955).

(2) T. J. Goehl and C. Davison, *J. Pharm. Sci.*, **62**, 907 (1973).

(3) S. L. Tompsett, *Acta Pharmacol. Toxicol.*, **17**, 295 (1960).

(4) A. H. Beckett and J. F. Taylor, *J. Pharm. Pharmacol. Suppl.*, **19**, 505 (1967).

(5) V. R. Jenkins, II, P. V. Dilts, Jr., and W. M. Tolbert, *Obstet. Gynecol.*, **39**, 254 (1972).

ACKNOWLEDGMENTS AND ADDRESSES

Received November 6, 1975, from the *Department of Pharmacology, Vanderbilt Medical Center, Nashville, TN 37232.*

Accepted for publication June 8, 1976.

Supported in part by U.S. Public Health Service Grants ES00267 and DA00141. M. A. Evans was supported by Research Development Award NS00346.

[x] To whom inquiries should be directed.

Flavonoid Constituents from *Eupatorium altissimum* L. (Compositae)

R. H. DOBBERSTEIN, M. TIN-WA, H. H. S. FONG, F. A. CRANE, and N. R. FARNSWORTH [x]

Abstract □ An aqueous ethanol extract of *Eupatorium altissimum* L. (Compositae) showed confirmed activity in the P-388 lymphocytic leukemia assay in mice, and the chloroform solubles showed both cytotoxic activity in the 9KB carcinoma of the nasopharynx cell culture assay and antitumor activity in the P-388 lymphocytic leukemia assay. Two flavones, eupatorin and 5-hydroxy-3′,4′,6,7-tetramethoxyflavone, were isolated and identified. Both were devoid of cytotoxic and antitumor activity.

Keyphrases □ *Eupatorium altissimum*—aqueous ethanol whole plant extract, two flavones isolated, cytotoxic and antitumor activity evaluated □ Flavones—isolated from *Eupatorium altissimum* aqueous ethanol whole plant extract, cytotoxic and antitumor activity evaluated □ Cytotoxic activity—evaluated in *Eupatorium altissimum* aqueous ethanol whole plant extract and isolated flavones □ Antitumor activity—evaluated in *Eupatorium altissimum* aqueous ethanol whole plant extract and isolated flavones

As part of a continuing search for antitumor compounds from plant sources, it was found that an aqueous ethanol extract of *Eupatorium altissimum* L. (Compositae) showed confirmed activity against the P-388 leukemia assay in mice and that the chloroform solubles showed both antitumor activity in the P-388 leukemia and marginal activity against the 9KB cell culture (cytotoxicity). In the only previous investigation of *E. altissimum*, a defatted ethanol extract was reported to exhibit antimicrobial activity against *Leuconostoc citrovorum* (1).

Extracts of various *Eupatorium* species have been reported to possess cytotoxic and/or antitumor activity. Cytotoxic flavonoids have been isolated from *E. semiserratum* (2–4) and *E. cuneifolium* (4); cytotoxic and antitumor sesquiterpene lactones have been isolated from *E. semiserratum* (5), *E. cuneifolium* (6, 7), *E. formosanum* (8), and *E. rotundifolium* (9–11).

In this investigation, two flavonoids were isolated from a fraction possessing cytotoxic activity. One was identified as eupatorin (I), a flavone previously isolated from *E. semiserratum* (2). The other flavonoid was verified as 5-hydroxy-3′,4′,6,7-tetramethoxyflavone (II). Although II

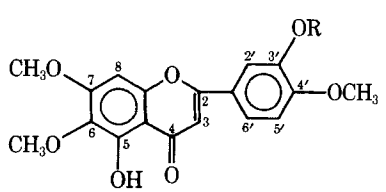

I: R = H

II: R = CH_3

was synthesized previously (12), it was only recently isolated from a natural source, *Salvia lavanduloides* (13). This paper reports the first isolation of these two flavones from *E. altissimum*.

EXPERIMENTAL[1]

Biological Activity—A 50% aqueous ethanol extract of *E. altissimum* was evaluated for cytotoxicity and antitumor activity[2]; it was active against the P-388 lymphocytic leukemia in mice[3] (T/C 144, 133, and 144 at 150, 100, and 66 mg/kg, respectively). The chloroform solubles, obtained by partitioning the concentrated aqueous ethanol extract between chloroform and water, possessed both cytotoxic[4] (ED_{50} = 20 μg/ml) and antitumor activity (T/C 150 and 159 at 200 and 100 mg/kg, respectively).

Extraction and Fractionation—A sample of whole plant material (5.5 kg) was continuously extracted[5] with petroleum ether (bp 30–60°) until the extract was colorless. The extract was then concentrated *in vacuo* to a viscous syrup weighing 296 g (Fraction A). The defatted plant material was air dried and then continuously extracted with methanol until the extract was nearly colorless. The methanol extract was concentrated *in vacuo* to yield 599 g of a thick dark-green syrup (Fraction B).

Fraction B was partitioned between chloroform (2 liters) and distilled water (2 liters). After two additional extractions of the aqueous layer with chloroform (2 liters), the combined chloroform fraction (Fraction C) was dried over anhydrous sodium sulfate and concentrated to dryness *in vacuo* to give a residue weighing 172 g. The aqueous phase was lyophilized to yield a residue weighing 387 g (Fraction D). A precipitate, which formed between the chloroform and water phases, was redissolved in methanol and concentrated *in vacuo* to a viscous brown syrup weighing 35 g (Fraction E).

Fraction C was partitioned between petroleum ether (bp 30–60°; 2 liters) and 20% aqueous methanol (2 liters). The petroleum ether fraction (Fraction F) was separated and concentrated *in vacuo* to a viscous green syrup weighing 32 g. The aqueous methanol phase was filtered, and a dark-green waxy material weighing 19 g (Fraction G) was collected. The filtrate was concentrated *in vacuo* to remove the methanol, diluted with distilled water (500 ml), and lyophilized to yield Fraction H (118 g).

Chromatography of Fraction H—A portion (25 g) of Fraction H was dissolved in chloroform and carefully added to the top of a chloroform slurry-packed column containing 500 g of silica gel PF_{254}[6] (Column 1). Elution was initiated with chloroform, and 20-ml fractions were collected.

The eluent was changed by the addition of increasing amounts of methanol as the fractions were monitored by TLC[7]. The fractions were combined into 24 groups on the basis of their TLC patterns.

Isolation and Characterization of Eupatorin (I)—Fraction 8 (690 mg), which was eluted from the column with chloroform–methanol (99:1), was dissolved in benzene–ethyl acetate (6:1) and rechromatographed over a column of silica gel PF_{254}. Elution was initiated with benzene–ethyl acetate (6:1), and 20-ml fractions were collected. The polarity of the eluent was increased by the addition of ethyl acetate. Finally, the column was washed with methanol. Fractions were combined into 18 groups according to their similarity following TLC[8]. Yellow crystals (I, 460 mg) spontaneously crystallized from fractions 13–15. Recrystallization from benzene–chloroform gave 245 mg of yellow needles, mp 189–190°. Additionally, a small sample (20 mg) was recrystallized from dioxane–water, mp 191–192°.

A UV spectrum of I in methanol exhibited absorptions with λ_{max} at 342 (log ε 4.50), 274 (4.35), 254 (4.32), and 243 (4.34) nm. Bands were observed in the IR spectrum (KBr) at ν_{max} 3430 (OH) and 1658 (chelated CO) cm^{-1}. These data are typical of flavones having a hydroxyl substituent at C-5 and hydroxyl or methoxyl substituents at both C-3′ and C-4′ positions (15–17). The mass spectrum showed a molecular ion at *m/e* 344 (100%), in agreement with an empirical formula of $C_{18}H_{16}O_7$. The NMR spectrum of I in dimethyl sulfoxide-d_6 was in good agreement with that reported for eupatorin (4).

The TLC, UV, IR, and mass spectral properties of I were identical with those of authentic eupatorin[9], and there was no depression of the melting point following a mixed melting-point determination. This evidence establishes the identity of I as eupatorin.

Isolation and Characterization of II—Fraction 5 (860 mg), which had been eluted from Column 1 with chloroform, was dissolved in benzene–ethyl acetate (4:1) and rechromatographed over a column of silica gel PF_{254} using benzene–ethyl acetate (4:1) as the eluent. Fractions (20 ml) were collected and combined into 13 groups on the basis of their TLC[8] similarities. Fractions 6–9 were combined and evaporated to dryness *in vacuo* (210 mg). Crystallization and recrystallization of this material from 95% ethanol yielded pale-yellow microcrystals (II, 142 mg), mp 188–189°.

The UV spectrum of II in methanol showed absorption maxima at 339 (log ε 4.49), 275 (4.32), and 242 (4.34) nm; the IR spectrum (KBr) showed bands at ν_{max} 3410 (OH) and 1660 (chelated CO) cm^{-1}. Again these data suggested a flavone nucleus having a hydroxyl substituent at C-5 and hydroxyl or methoxyl substituents at both C-3′ and C-4′ positions. The mass spectrum of II showed a molecular ion at *m/e* 358 (100%, $C_{19}H_{18}O_7$) with significant ions at *m/e* 343 (94%), 329 (22), 315 (23), 312 (25), 181 (17), and 153 (40). The NMR spectrum of II in deuterochloroform showed a 3H singlet at δ 3.92 (OCH_3), a 9H singlet at δ 4.00 (3-OCH_3), a 1H singlet at δ 6.58 (olefinic H), a 1H singlet at δ 6.61 (ArH), a 1H doublet at δ 7.01 [J = 9 Hz (ArH)], a 1H doublet at δ 7.37 [J = 2 Hz (ArH)], a 1H doublet of doublets at δ 7.64 [J = 9 Hz, J = 2 Hz (ArH)], and a 1H singlet at δ 12.76 (ArOH).

These data suggested that II was eupatorin 3′-methyl ether. Therefore, a sample of eupatorin was methylated. Eupatorin (52 mg) in methanol (100 ml) was treated with excess diazomethane (18) in ether at room temperature for 24 hr. The solvent was removed *in vacuo*, and the product, dissolved in benzene–ethyl acetate (6:1), was chromatographed over a column of silica gel PF_{254} (5 g) using benzene–ethyl acetate (6:1) as the developing solvent. The second fraction eluted (25 mg) was crystallized from 95% ethanol to give pale-yellow microcrystals (20 mg), mp 188–189°. Comparison of the TLC, UV, IR, NMR, and mass spectral properties of methylated I with those of II showed that they were identical.

Finally, an authentic sample of II[9] was shown to be identical with the isolated product in all respects. There was no depression of the melting point following a mixed melting-point determination.

DISCUSSION

As part of a program of screening plants for antitumor activity, it was observed that an aqueous ethanol extract of *E. altissimum* (Compositae) showed confirmed *in vivo* activity against the P-388 lymphocytic leukemia assay in mice. The chloroform-soluble fraction was marginally active against Eagle's 9KB carcinoma of the nasopharnyx in cell culture (cytotoxic) and active against the P-388 lymphocytic leukemia assay in mice. Compounds I and II were isolated from Fraction C. Both compounds, however, were inactive in the two test systems.

Eupatorin (I) was previously isolated from *E. semiserratum* and was reported to show cytotoxic activity (2, 4). However, the cytotoxicity of I, isolated from *E. altissimum*, could not be confirmed even after repeated testing.

Flavone II was recently isolated from *S. lavanduloides* (Labiatae) (13), representing its first reported natural occurrence. The present investigation establishes the first occurrence of this compound in the genus *Eupatorium* of the unrelated Compositae family.

Work is currently in progress to isolate and identify the compound(s) present in *E. altissimum* responsible for the antitumor activity.

[1] The plant material consisted of the whole plant of *E. altissimum* L. (Compositae), collected in Lisle, Ill., during October 1972. Identification was made by Floyd A. Swink of the Morton Arboretum, Lisle, Ill. Voucher specimens are deposited in the Herbarium of the Department of Pharmacognosy and Pharmacology, University of Illinois at the Medical Center, Chicago, IL 60612.

Melting points were determined using a Kofler hot-stage instrument and are uncorrected. Mixed melting points were determined on a Thomas-Hoover Uni-Melt apparatus. UV spectra were recorded using a Beckman model DB-G grating spectrophotometer. IR spectra were run using a Beckman model IR-18A spectrophotometer. NMR spectra were recorded on a Varian T-60A instrument at 60 MHz. Mass spectral data were obtained on a Hitachi Perkin-Elmer model RMU-6D spectrophotometer.

[2] The test methods employed were those of the Drug Research and Development Branch of the National Cancer Institute (14).

[3] An active fraction is one that exhibits a T/C of ≧125%.

[4] An active fraction is one that exhibits an ED_{50} ≦20 μg/ml.

[5] Lloyd extractor.

[6] Silica gel PF_{254} for preparative layer chromatography, E. Merck, Darmstadt, Germany.

[7] TLC analyses were carried out on silica gel G precoated plates (E. Merck, Darmstadt, Germany) using chloroform–methanol (19:1) as the solvent. The developed plates were sprayed with 70% methanolic sulfuric acid and were heated at 100° for 5 min.

[8] TLC analyses were conducted on silica gel G precoated plates using benzene–ethyl acetate (2:1) as the developing solvent.

[9] Supplied by Professor L. Farkas, Hungarian Academy of Sciences, Budapest, Hungary, and/or by Professor N. Morita, University of Toyama, Japan.

REFERENCES

(1) N. R. Farnsworth, L. K. Henry, G. H. Svoboda, R. N. Blomster, M. J. Yates, and K. L. Euler, *Lloydia*, **29**, 101 (1966).

(2) S. M. Kupchan, J. R. Knox, and M. S. Udayamurthy, *J. Pharm. Sci.*, **54**, 929 (1965).

(3) S. M. Kupchan, C. W. Sigel, J. R. Knox, and M. S. Udayamurthy, *J. Org. Chem.*, **34**, 1460 (1969).

(4) S. M. Kupchan, C. W. Sigel, R. J. Hemingway, J. R. Knox, and M. S. Udayamurthy, *Tetrahedron*, **25**, 1603 (1969).

(5) S. M. Kupchan, T. Fujita, M. Maruyama, and R. W. Britton, *J. Org. Chem.*, **38**, 1260 (1973).

(6) S. M. Kupchan, M. Maruyama, R. J. Hemingway, J. C. Hemingway, S. Shibuya, T. Fujita, P. D. Cradwick, A. D. U. Hardy, and G. A. Sim, *J. Am. Chem. Soc.*, **93**, 4914 (1971).

(7) S. M. Kupchan, M. Maruyama, R. J. Hemingway, J. C. Hemingway, S. Shibuya, and T. Fujita, *J. Org. Chem.*, **38**, 2189 (1973).

(8) K.-H. Lee, H.-C. Huang, E.-S. Huang, and H. J. Furukawa, *J. Pharm. Sci.*, **61**, 629 (1972).

(9) S. M. Kupchan, J. C. Hemingway, J. M. Cassady, J. R. Knox, A. T. McPhail, and G. A. Sim, *J. Am. Chem. Soc.*, **89**, 465 (1967).

(10) S. M. Kupchan, J. E. Kelsey, M. Maruyama, and J. M. Cassady, *Tetrahedron Lett.*, **1968**, 3517.

(11) S. M. Kupchan, J. E. Kelsey, M. Maruyama, J. M. Cassady, J. C. Hemingway, and J. R. Knox, *J. Org. Chem.*, **34**, 3876 (1969).

(12) N. Morita, *Chem. Pharm. Bull.*, **8**, 59 (1960).

(13) J. Rodríguez, H. Tello, L. Quijano, J. Calderón, F. Gómez, J. Romo, and T. Ríos, *Rev. Latinoam. Quim.*, **5**, 41 (1974).

(14) R. I. Geran, N. H. Greenberg, M. M. Macdonald, A. M. Shumacher, and B. J. Abbott, *Cancer Chemother. Rep.*, **3**(2), 1 (1972).

(15) T. J. Mabry, K. R. Markham, and M. B. Thomas, "The Systematic Identification of Flavonoids," Springer Verlag, New York, N.Y., 1970, p. 44.

(16) L. Jurd, in "The Chemistry of Flavonoid Compounds," T. A. Geissman, Ed., Macmillan, New York, N.Y., 1962, pp. 108–118.

(17) K. Yamaguchi, "Spectral Data of Natural Products," vol. 1, Elsevier, New York, N.Y., 1970, p. 89.

(18) J. A. Moore and D. E. Reed, *Org. Synth.*, **41**, 16 (1961).

ACKNOWLEDGMENTS AND ADDRESSES

Received November 22, 1975, from the *Department of Pharmacognosy and Pharmacology, College of Pharmacy, University of Illinois at the Medical Center, Chicago, IL 60612.*

Accepted for publication June 8, 1976.

Presented at the joint meeting of the American Society of Pharmacognosy and the Pharmacognosy and Natural Products Section, APhA Academy of Pharmaceutical Sciences, Chicago meeting, August 1974.

[x] To whom inquiries should be directed.

Thiocardenolides II: Synthesis and Pharmacological Evaluation of 3β-Thioacetyl-14β-hydroxy-5β-card-20(22)-enolide

HANLEY N. ABRAMSON [x], CHIAN L. HUANG, CHIU-CHUNG HO, LAWRENCE L. WALNY, and YOU-MEEI HSU

Abstract □ The synthesis of a 3β-thioacetylcardenolide is described. The thioacetate exhibited effects similar to those seen with digitoxigenin acetate on the isolated frog and guinea pig hearts at 1×10^{-7} dilution. In the intact rat heart, the lethal dose was 5 mg/kg for the thioacetate and 2.5 mg/kg for digitoxigenin acetate. The thioacetate inhibited sodium- and potassium-activated adenosine triphosphatase to the same extent as digitoxigenin, but it was somewhat less inhibitory than digitoxigenin acetate.

Keyphrases □ Thiocardenolides—3β-thioacetyl - 14β - hydroxy - 5β - card-20(22)-enolide synthesized, screened for cardiotonic activity and effect on sodium- and potassium-activated adenosine triphosphatase □ Cardiotonic activity—screened in 3β-thioacetyl-14β-hydroxy-5β-card-20(22)-enolide □ Adenosine triphosphatase, sodium and potassium activated—effect of 3β-thioacetyl-14β-hydroxy-5β-card-20(22)-enolide

The naturally occurring cardioactive steroids are widely used in the therapy of congestive heart failure and atrial arrhythmias and have low therapeutic indexes. There have been numerous efforts to synthesize and evaluate cardenolide derivatives with improved margins of safety, and the literature in this area was reviewed (1). As part of a program to replace oxygens of various cardenolides by sulfur atoms with the aim of separating the therapeutic and toxic actions of the digitalis glycosides, the synthesis and pharmacological actions of the 3β-thioacetyl analog (I) of digitoxigenin (II) are herein reported. A previous paper (2) described the preparation and biological actions of a 3β-thiocyanato analog.

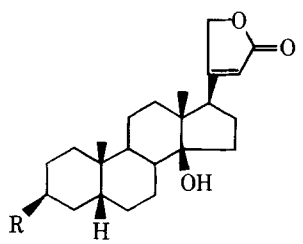

I: R = $SCOCH_3$
II: R = OH
III: R = $OCOCH_3$

EXPERIMENTAL[1]

Chemistry—A solution of 584 mg (1.29 mmoles) of 3-epidigitoxigenin 3-methanesulfonate (2) and 577 mg (5.0 mmoles) of freshly recrystallized (ethanol–water) potassium thioacetate in 10 ml of dimethylformamide (freshly distilled over potassium hydroxide) was heated at 70–90° for 3 hr under dry nitrogen. The reaction mixture was poured onto ice, and the solid product was collected by filtration, dried, dissolved in chloroform,

[1] Melting points were taken on a Fisher-Johns melting-point stage and are uncorrected. UV absorption spectra were determined in 95% ethanol on a Beckman model DK2A recording spectrophotometer. IR absorption spectra were recorded in chloroform on a Beckman model 8 recording spectrophotometer. NMR spectra were determined on a Varian EM 360 spectrometer, using tetramethylsilane as the internal standard and deuterochloroform as the solvent. Microanalyses were conducted by Spang Microanalytical Laboratory, Ann Arbor, Mich. TLC was carried out using Merck silica gel G 254 (0.25-mm thick, analytical plates) or Merck silica gel PF 254 + 366 (0.75-mm thick, preparative plates). Analytical plates were visualized by charring with 5% $Ce(SO_4)_2$ in 6 *N* H_2SO_4; preparative plates were visualized under UV light.

REFERENCES

(1) N. R. Farnsworth, L. K. Henry, G. H. Svoboda, R. N. Blomster, M. J. Yates, and K. L. Euler, *Lloydia*, **29**, 101 (1966).

(2) S. M. Kupchan, J. R. Knox, and M. S. Udayamurthy, *J. Pharm. Sci.*, **54**, 929 (1965).

(3) S. M. Kupchan, C. W. Sigel, J. R. Knox, and M. S. Udayamurthy, *J. Org. Chem.*, **34**, 1460 (1969).

(4) S. M. Kupchan, C. W. Sigel, R. J. Hemingway, J. R. Knox, and M. S. Udayamurthy, *Tetrahedron*, **25**, 1603 (1969).

(5) S. M. Kupchan, T. Fujita, M. Maruyama, and R. W. Britton, *J. Org. Chem.*, **38**, 1260 (1973).

(6) S. M. Kupchan, M. Maruyama, R. J. Hemingway, J. C. Hemingway, S. Shibuya, T. Fujita, P. D. Cradwick, A. D. U. Hardy, and G. A. Sim, *J. Am. Chem. Soc.*, **93**, 4914 (1971).

(7) S. M. Kupchan, M. Maruyama, R. J. Hemingway, J. C. Hemingway, S. Shibuya, and T. Fujita, *J. Org. Chem.*, **38**, 2189 (1973).

(8) K.-H. Lee, H.-C. Huang, E.-S. Huang, and H. J. Furukawa, *J. Pharm. Sci.*, **61**, 629 (1972).

(9) S. M. Kupchan, J. C. Hemingway, J. M. Cassady, J. R. Knox, A. T. McPhail, and G. A. Sim, *J. Am. Chem. Soc.*, **89**, 465 (1967).

(10) S. M. Kupchan, J. E. Kelsey, M. Maruyama, and J. M. Cassady, *Tetrahedron Lett.*, **1968**, 3517.

(11) S. M. Kupchan, J. E. Kelsey, M. Maruyama, J. M. Cassady, J. C. Hemingway, and J. R. Knox, *J. Org. Chem.*, **34**, 3876 (1969).

(12) N. Morita, *Chem. Pharm. Bull.*, **8**, 59 (1960).

(13) J. Rodríguez, H. Tello, L. Quijano, J. Calderón, F. Gómez, J. Romo, and T. Ríos, *Rev. Latinoam. Quim.*, **5**, 41 (1974).

(14) R. I. Geran, N. H. Greenberg, M. M. Macdonald, A. M. Shumacher, and B. J. Abbott, *Cancer Chemother. Rep.*, **3**(2), 1 (1972).

(15) T. J. Mabry, K. R. Markham, and M. B. Thomas, "The Systematic Identification of Flavonoids," Springer Verlag, New York, N.Y., 1970, p. 44.

(16) L. Jurd, in "The Chemistry of Flavonoid Compounds," T. A. Geissman, Ed., Macmillan, New York, N.Y., 1962, pp. 108–118.

(17) K. Yamaguchi, "Spectral Data of Natural Products," vol. 1, Elsevier, New York, N.Y., 1970, p. 89.

(18) J. A. Moore and D. E. Reed, *Org. Synth.*, **41**, 16 (1961).

ACKNOWLEDGMENTS AND ADDRESSES

Received November 22, 1975, from the *Department of Pharmacognosy and Pharmacology, College of Pharmacy, University of Illinois at the Medical Center, Chicago, IL 60612.*

Accepted for publication June 8, 1976.

Presented at the joint meeting of the American Society of Pharmacognosy and the Pharmacognosy and Natural Products Section, APhA Academy of Pharmaceutical Sciences, Chicago meeting, August 1974.

[x] To whom inquiries should be directed.

Thiocardenolides II: Synthesis and Pharmacological Evaluation of 3β-Thioacetyl-14β-hydroxy-5β-card-20(22)-enolide

HANLEY N. ABRAMSON [x], CHIAN L. HUANG, CHIU-CHUNG HO, LAWRENCE L. WALNY, and YOU-MEEI HSU

Abstract □ The synthesis of a 3β-thioacetylcardenolide is described. The thioacetate exhibited effects similar to those seen with digitoxigenin acetate on the isolated frog and guinea pig hearts at 1×10^{-7} dilution. In the intact rat heart, the lethal dose was 5 mg/kg for the thioacetate and 2.5 mg/kg for digitoxigenin acetate. The thioacetate inhibited sodium- and potassium-activated adenosine triphosphatase to the same extent as digitoxigenin, but it was somewhat less inhibitory than digitoxigenin acetate.

Keyphrases □ Thiocardenolides—3β-thioacetyl - 14β - hydroxy - 5β - card-20(22)-enolide synthesized, screened for cardiotonic activity and effect on sodium- and potassium-activated adenosine triphosphatase □ Cardiotonic activity—screened in 3β-thioacetyl-14β-hydroxy-5β-card-20(22)-enolide □ Adenosine triphosphatase, sodium and potassium activated—effect of 3β-thioacetyl-14β-hydroxy-5β-card-20(22)-enolide

The naturally occurring cardioactive steroids are widely used in the therapy of congestive heart failure and atrial arrhythmias and have low therapeutic indexes. There have been numerous efforts to synthesize and evaluate cardenolide derivatives with improved margins of safety, and the literature in this area was reviewed (1). As part of a program to replace oxygens of various cardenolides by sulfur atoms with the aim of separating the therapeutic and toxic actions of the digitalis glycosides, the synthesis and pharmacological actions of the 3β-thioacetyl analog (I) of digitoxigenin (II) are herein reported. A previous paper (2) described the preparation and biological actions of a 3β-thiocyanato analog.

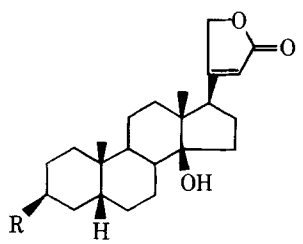

I: R = $SCOCH_3$
II: R = OH
III: R = $OCOCH_3$

EXPERIMENTAL[1]

Chemistry—A solution of 584 mg (1.29 mmoles) of 3-epidigitoxigenin 3-methanesulfonate (2) and 577 mg (5.0 mmoles) of freshly recrystallized (ethanol–water) potassium thioacetate in 10 ml of dimethylformamide (freshly distilled over potassium hydroxide) was heated at 70–90° for 3 hr under dry nitrogen. The reaction mixture was poured onto ice, and the solid product was collected by filtration, dried, dissolved in chloroform,

[1] Melting points were taken on a Fisher-Johns melting-point stage and are uncorrected. UV absorption spectra were determined in 95% ethanol on a Beckman model DK2A recording spectrophotometer. IR absorption spectra were recorded in chloroform on a Beckman model 8 recording spectrophotometer. NMR spectra were determined on a Varian EM 360 spectrometer, using tetramethylsilane as the internal standard and deuterochloroform as the solvent. Microanalyses were conducted by Spang Microanalytical Laboratory, Ann Arbor, Mich. TLC was carried out using Merck silica gel G 254 (0.25-mm thick, analytical plates) or Merck silica gel PF 254 + 366 (0.75-mm thick, preparative plates). Analytical plates were visualized by charring with 5% $Ce(SO_4)_2$ in 6 *N* H_2SO_4; preparative plates were visualized under UV light.

Table I—Adenosine Triphosphatase Inhibition

Compound	Adenosine Triphosphatase Activity, μmoles of Inorganic Phosphate Released/mg of Protein/hr
Control	11.45[a]
I	6.17[b]
II	6.15[b]
III	5.28[b]

[a] Average of four determinations. [b] Average of two determinations.

and filtered. After concentration to dryness, the filtrate was washed with absolute ethanol and filtered to give 378 mg of 3β-thioacetyl-14β-hydroxy-5β-card-20(22)-enolide (I), mp 198–204°.

TLC (1% methanol in chloroform) showed one major spot (R_f 0.3) with two minor products of lower R_f values. Preparative TLC (1% methanol in chloroform) gave 225 mg of a crystalline solid, mp 211–214°. Recrystallization from ethyl acetate–chloroform gave an analytical sample, mp 213–217°; IR: ν_{max} 3600 (OH), 1795 and 1750 (butenolide doublet), 1690 (SC=O), 1610 (C=C), and 730 (CS) cm^{-1}; UV: ν_{max} 219 nm (ϵ = 22,600); NMR: δ 0.88 (3H, s, 18-CH_3), 0.95 (3H, s, 19-CH_3), 2.33 [3H, s, $CH_3C(=O)S$], 4.06 (1H, broad s, 3-H), 4.95 (2H, broad s, 22-CH_2), and 5.90 (1H, s, 21-CH).

Anal.—Calc. for $C_{25}H_{36}O_4S$: C, 69.41; H, 8.39; S, 7.41. Found: C, 69.44; H, 8.45; S, 7.48.

The IR and NMR spectra indicated that the attack by thioacetate anion on the 3α-methanesulfonate occurred from the β-face of the molecule. The medium absorption band at 730 cm^{-1} (CS) stretch was consistent with the stereochemical assignment of a 3β-thioacetyl *A/B cis*-steroid (3). The epimeric 3β-thioacetyl compound would be expected to absorb at a higher frequency (755–762 cm^{-1}) (3). The broad singlet at δ 4.06 was attributed to the equatorial (α) proton at position 3, indicating that the thioacetyl substituent was axially (β) oriented (4). An axial proton at position 3 should show a peak centered considerably upfield in the δ 3.4 region (4).

Biological Evaluation—Isolated frog hearts (six preparations) were used to evaluate the cardiotonic effect of I according to Straub's method (5). Saline was used as the control, and digitoxigenin acetate (III) was used as the reference standard. The frog hearts were perfused with Frog–Ringer solutions of both compounds, and the changes in chronotropic and inotropic responses were recorded on a smoked-drum kymograph. Analytically pure samples of I were used in this and succeeding experiments.

The action of I on the isolated guinea pig heart was studied using the Langendorff preparation (6). The hearts (six preparations) were perfused with Krebs–Henseleit solutions of I, II, and III, and the inotropic changes were measured on a polygraph recorder[2].

The effect of I on the intact rat heart was studied using three animals anesthetized with pentobarbital (45 mg/kg ip). The cardiac actions were recorded on a polygraph recorder[2]. Saline was used as the control, and digitoxigenin acetate was used as the standard.

Studies of sodium- and potassium-activated adenosine triphosphatase inhibition were carried out using the enzyme obtained from guinea pig brain. The brain of a freshly decapitated guinea pig was homogenized in five volumes of an ice-cold solution (pH 6.8) containing 0.25 *M* sucrose, 5 m*M* histidine, 5 m*M* edetic acid, and 0.2% deoxycholate. The homogenate was centrifuged at 12,000×*g* for 30 min. The supernate was centrifuged at 35,000×*g* for 30 min, and the pellet was suspended in a solution (pH 7.0) containing 0.25 *M* sucrose, 5 m*M* histidine, and 1 m*M* edetic acid. This suspension was centrifuged again at 35,000×*g* for 30 min, and the pellet was resuspended in 20 ml of the same suspending solution. These procedures were carried out at 2°. The quantity of protein in the preparation was assayed by the method of Lowry *et al.* (7).

The enzyme solution (1.0 ml) was diluted to 10.0 ml with the ice-cold suspending solution. To 0.9 ml of the final solution was added 0.1 ml of a 10^{-3} *M* solution of I, II, or III in dimethylformamide and 1.0 ml of a solution containing 50 m*M* tromethamine hydrochloride buffer (pH 7.5), 5 m*M* magnesium chloride, 5 m*M* adenosine triphosphate, 100 m*M* sodium chloride, and 15 m*M* potassium chloride. The control contained the equivalent amount of dimethylformamide. After an 8-min preincubation period, the mixture was incubated at 37° for 20 min. Then 1.0 ml of 15% aqueous ice-cold trichloroacetic acid was added to terminate the reaction.

This mixture was centrifuged for 10 min. The supernate was decanted and mixed with 1.0 ml of a solution prepared by dissolving 400 mg of ferrous sulfate in 10 ml of a 1% ammonium molybdate solution in 1.15 *N* sulfuric acid. The resulting absorbance was read at 700 nm 30 min after the addition of the reagent. Reagent blanks and unincubated tests were also included. The resulting absorbance was converted into micromoles of inorganic phosphate released by comparison with a standard curve (Table I).

RESULTS AND DISCUSSION

In the isolated frog heart, I elicited a positive inotropic action at 1×10^{-8} dilution as well as at 1×10^{-7} dilution. A negative inotropic effect was seen at dilutions of 5×10^{-6} and lower. On the other hand, digitoxigenin acetate (III) demonstrated a positive inotropic response at 1×10^{-7} dilution and a negative inotropic effect at 5×10^{-5} dilution and lower.

Both I and III had similar actions on the guinea pig heart, causing a prominent inotropic response at 1×10^{-7} dilution and a negative inotropic effect at 5×10^{-5} dilution and lower. Digitoxigenin (II) exhibited a positive inotropic action at dilutions of 1×10^{-7} and 1×10^{-6} and a negative inotropic effect at 1×10^{-5} dilution and lower. At doses of 1 mg/kg, both I and III had a noticeable effect on the lead II ECG of the intact rat heart, as evidenced by decreases in the amplitudes of the T wave and the QRS complex, a prolongation of the PR interval, and a shortened QT segment. A dose of 2.5 mg/kg of III was lethal to the three rats tested; each of those receiving the same dosage of I survived. At a dosage level of 5 mg/kg of I, none of the animals survived.

The results of the interaction of I with sodium- and potassium-activated adenosine triphosphatase indicate that the inhibitory effect is approximately the same as that of digitoxigenin but less than that of digitoxigenin acetate.

It appears that the presence of a 3β-thioacetate moiety on the cardiotonic steroid nucleus does not reduce the cardioactivity associated with digitalis compounds. The results of the lethal dose study on the intact rat heart are encouraging, since they demonstrated that the thioacetyl grouping leads to decreased toxicity. This work is currently being expanded to a study of other thiocardenolides containing thiol and thioacetyl groupings at position 3β to ascertain whether such compounds may have improved margins of safety compared to those currently used in therapeutics.

REFERENCES

(1) R. Thomas, J. Boutagy, and A. Gelbart, *J. Pharm. Sci.*, **63**, 1649 (1974).

(2) H. N. Abramson, C. L. Huang, T. F. Wu, and T. Tobin, *ibid.*, **65**, 765 (1976).

(3) D. A. Swann and J. H. Turnbull, *Tetrahedron*, **22**, 231 (1966).

(4) *Ibid.*, **20**, 1265 (1964).

(5) W. Straub, *Biochem. Z.*, **75**, 132 (1916).

(6) E. Langendorff, *Pfluger's Arch. Ges. Physiol.*, **61**, 291 (1895).

(7) O. H. Lowry, N. J. Rosenbrough, A. L. Farr, and R. J. Randall, *J. Biol. Chem.*, **193**, 265 (1951).

ACKNOWLEDGMENTS AND ADDRESSES

Received April 2, 1976, from the *College of Pharmacy and Allied Health Professions, Wayne State University, Detroit, MI 48202.*

Accepted for publication June 14, 1976.

Supported by a grant from the Michigan Heart Association.

The authors thank Dr. Bernard Marks and Dr. Saradindu Dutta, Department of Pharmacology, School of Medicine, Wayne State University, for helpful discussions.

[x] To whom inquiries should be directed.

[2] Sanborn model 964.

Simultaneous GLC Determination of Acetaminophen, Dichloralantipyrine, and Isometheptene Mucate

FOTIOS M. PLAKOGIANNIS ˣ and AHMED M. SAAD

Abstract □ A rapid GLC assay for acetaminophen, dichloralantipyrine, and isometheptene mucate in capsules was developed. These substances are chromatographed directly, using phenyl methyl silicone gum as the stationary phase. The standard calibration curves are linear up to 14 mg/ml, with a lower limit of sensitivity of 2 mg/ml. This method is simple and rapid and does not require derivative formation.

Keyphrases □ Acetaminophen—GLC analysis in capsules with dichloralantipyrine and isometheptene mucate □ Dichloralantipyrine—GLC analysis in capsules with acetaminophen and isometheptene mucate □ Isometheptene mucate—GLC analysis in capsules with acetaminophen and dichloralantipyrine □ GLC—analyses, acetaminophen, dichloralantipyrine, and isometheptene mucate in combination capsules □ Analgesics—acetaminophen and dichloralantipyrine, GLC analysis in capsules with isometheptene mucate □ Adrenergics—isometheptene mucate, GLC analysis in capsules with acetaminophen and dichloralantipyrine

Among the reasons for the pharmaceutical popularity of acetaminophen is that it is a nonsalicylate analgesic and antipyretic. Dichloralantipyrine is also used as a hypnotic analgesic, while isometheptene is a sympathomimetic agent effective as adjunctive therapy in the treatment of peptic ulcer. A mixture of the three agents is formulated in a pharmaceutical dosage form that is effective in the relief of vascular, tension, and migraine headaches.

Acetaminophen has been assayed by spectrophotometric (1–4) and chromatographic (5–9) methods. One spectrophotometric method has been reported for the assay of dichloralantipyrine (10), but there is none for the determination of isometheptene mucate. The lack of information regarding the simultaneous determination of acetaminophen, dichloralantipyrine, and isometheptene mucate in capsules, together with the tedious extraction requirements and derivative formation required in other assays, led to this investigation.

EXPERIMENTAL

Materials—Acetaminophen[1], dichloralantipyrine[2], isometheptene mucate[3], and pure ethanol[4] (all analytical grade) were used.

Apparatus—GLC analyses were performed on a gas chromatograph[5] equipped with a dual flame-ionization detector. The column was coiled stainless steel tubing (240 cm × 3 mm i.d.) packed with 1% phenyl methyl silicone gum (OV-17) on high-performance Chromosorb WHP[6] (80–100 mesh).

Helium was used as a carrier gas at a flow rate of 25 ml/min. The flow rates of hydrogen and air were 25 and 30 ml/min, respectively. The temperature of both the injection port and the flame-ionization detector was 190°. The columns were conditioned at 200° for 24 hr before use. During analysis, the temperature was programmed as follows: 3 min of 70°, increased to 185° at 5°/min, and finally held for 5 min at 185°.

Assay Procedures—Into each of three glass-stoppered centrifuge tubes, weigh accurately 20 mg of the capsule formulation containing 325 mg of acetaminophen, 100 mg of dichloralantipyrine, and 65 mg of isometheptene mucate. Add to each tube 10 ml of a 50 μg % ethanol solution of tuaminoheptane sulfate[7]. Mix the contents of each tube for 2 min using a vortex mixer and then centrifuge for 5 min at 5000 rpm.

Transfer the ethanol solution quantitatively to another glass-stoppered tube and evaporate it in a water bath at 50° under a nitrogen stream. Redissolve the residue in 0.20 ml of pure ethanol and transfer it to a 0.2-ml injection vial[8]. Evaporate the ethanol again under nitrogen and redissolve the residue in 40 μl of pure ethanol; then cap the injection vial.

Samples of 1 μl were injected into the gas chromatograph with a 1-μl syringe[9]. Standard calibration curves were established with ethanol solutions of known concentrations (2, 4, 6, 8, 10, 12, and 14 μg/ml) of the individual drugs to be assayed. Computation was done with both peak area and peak height measurements. Reproducibility was better with the peak area than the peak height technique.

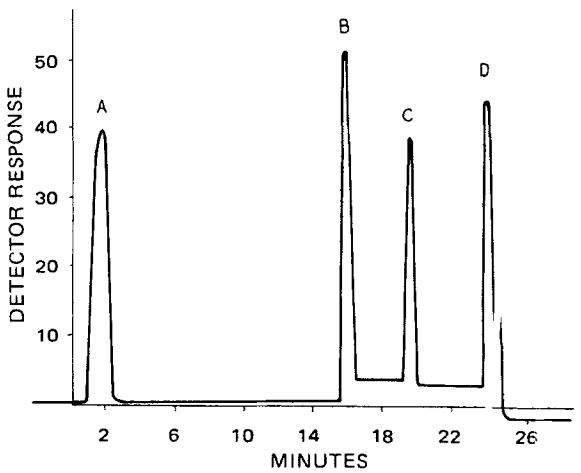

Figure 1—*Gas-liquid chromatogram. Key: A, dichloralantipyrine; B, acetaminophen; C, isometheptene; and D, tuaminoheptane sulfate (internal standard).*

RESULTS AND DISCUSSION

The standard calibration curves obtained by plotting the peak area ratio of acetaminophen, dichloralantipyrine, and isometheptene mucate *versus* their concentrations gave a straight line ($y = mx$) over the 2–14-μg/ml range with mean slope values of 0.66, 0.40, and 0.75, respectively.

Figure 1 shows a typical gas chromatogram of an acetaminophen, dichloralantipyrine, and isometheptene mucate mixture analyzed according to the described procedure. The retention times for dichloralantipyrine, acetaminophen, and isometheptene mucate were 3, 16, and 19 min, respectively; the retention time for the internal standard, tuaminoheptane sulfate, was 24 min. The overall recovery was constant from one test run to another. The results obtained with the procedure are illustrated by the examples in Table I.

The GLC determination of acetaminophen was accomplished either by measuring the unmodified drug directly (5, 6) or by converting acetaminophen to its trimethylsilyl ether or acetyl derivatives (7, 8, 11). McMartin and Street (11) reported that the reason for preparing a derivative of acetaminophen is that the unchanged drug is a highly polar compound that shows marked "tailing" during chromatography. However, there are two important disadvantages with acetaminophen de-

[1] McNeil Laboratories.
[2] Delmar Chemicals Co.
[3] Graham Laboratories.
[4] J. T. Baker Chemical Co.
[5] Hewlett-Packard model 7620A.
[6] Alltech Assoc. Inc., Arlington Heights, Ill.
[7] K and K Laboratories, Plainview, N.Y.
[8] Hewlett-Packard.
[9] Hamilton.

Table I—Arithmetic Mean of Determination of an Accurately Weighed Capsule Formulation

Compound	Labeled Amount, mg/ Capsule	Recovered Amount, mg/Capsule		Mean Percent
Acetaminophen	325	323.5		99.5
		322.8		99.3
		322.5		99.2
		Mean 322.9	Mean	99.3
Dichloralantipyrine	100	98.3		98.3
		97.6		97.6
		98.1		98.1
		Mean 98.0	Mean	98.0
Isometheptene mucate	65	63.20		97.2
		63.90		98.3
		Mean 63.5	Mean	97.7

rivatives. They are time consuming and are readily hydrolyzed by moisture even in the presence of excess reagents.

A comparison showed that the described method is more rapid than previously described GLC methods that required preparation of a derivative (7, 8, 11). It is not more rapid than other reported methods (5, 6), but the use of the 1% OV-17 on high-performance Chromosorb WHP eliminates the tailing and, therefore, increases the efficiency and accuracy.

REFERENCES

(1) J. B. Vaughn, *J. Pharm. Sci.*, **58**, 469 (1969).

(2) L. Chafetz, R. E. Daly, H. Schriftman, and J. J. Lomnev, *ibid.*, **60**, 463 (1971).

(3) F. M. Plakogiannis and A. M. Saad, *ibid.*, **64**, 1547 (1975).

(4) A. A. D'Souza and K. C. Slenoy, *Can. J. Pharm. Sci.*, **3**, 90 (1968).

(5) J. Grove, *J. Chromatogr.*, **59**, 289 (1971).

(6) M. J. Stewart and R. G. Willis, *Ann. Clin. Biochem.*, **12**, 4 (1975).

(7) H. V. Street, *J. Chromatogr.*, **109**, 29 (1975).

(8) L. F. Prescott, *J. Pharm. Pharmacol.*, **23**, 111 (1971).

(9) R. M. Riggin, A. L. Schmidt, and R. T. Kissinger, *J. Pharm. Sci.*, **64**, 680 (1975).

(10) A. W. Archer and E. A. Hougas, *J. Pharm. Pharmacol.*, **12**, 751 (1960).

(11) C. McMartin and H. V. Street, *J. Chromatogr.*, **22**, 274 (1966).

ACKNOWLEDGMENTS AND ADDRESSES

Received March 22, 1976, from the *Department of Pharmaceutics, Arnold & Marie Schwartz College of Pharmacy & Health Sciences of Long Island University, Brooklyn, NY 11201.*

Accepted for publication June 9, 1976.

Presented in part at the APhA Academy of Pharmaceutical Sciences, Atlanta meeting, November 1975.

[x] To whom inquiries should be directed.

New Compounds: Synthesis of 2-Amino-5*H*-1,3,4-benzotriazepin-5-ones

ROBERT W. LEIBY and NED D. HEINDEL [x]

Abstract □ *N*-Methyl-2-aminobenzohydrazides, when treated with cyanogen bromide, were found to yield 2-amino-5*H*-1,3,4-benzotriazepin-5-ones.

Keyphrases □ 2-Amino-5*H*-1,3,4-benzotriazepin-5-ones—various derivatives synthesized □ Benzotriazepinones, substituted—various derivatives synthesized

Benzotriazepines as bioisosteric homologs of the well-established benzodiazepine psychotherapeutics have received considerable attention recently. Several synthetic methods and claims of sedative activity have been published (1–8) for the 1,3,4-benzotriazepine subclass, but a few earlier structural assignments (as benzotriazepines) were revised recently (9).

DISCUSSION

As a continuation of investigations on 1,4-benzodiazepin-3,5-diones derived from anthranilamides (10–12), this study reports the preparation of 2-amino-1,4-dihydro-5*H*-1,3,4-benzotriazepin-5-ones (II), a new type of 1,3,4-benzotriazepine obtained from the cyclization of anthranilohydrazides (I). By use of cyanogen bromide and a suitably methylated anthranilohydrazide, cyclization can be directed in an unambiguous fashion to the hydrobromide salts of the benzotriazepines, thus avoiding the classic pitfalls and uncertainties of structure that occur when alternative closure pathways are possible (9).

Anthranilohydrazides bearing a methyl on the amide-like nitrogen (*i.e.*, *N*-methyl-2-aminobenzohydrazides, I) were obtained by the opening of isatoic anhydride with methylhydrazine (13, 14). These hydrazides condensed instantaneously in chilled ethanol with cyanogen bromide (Scheme I) to give IIa–IIg in 36–85% yield. When the *ortho*-amino group was deactivated by conjugation to a nitro moiety, *i.e.*, If and Ig, condensation in refluxing dioxane was necessary to obtain a satisfactory yield.

The monomethylated benzotriazepines displayed four NH absorptions in the IR spectra between 3440 and 3080 cm^{-1}, while the dimethylated benzotriazepines (II, $R_2 = CH_3$) displayed only three absorptions between 3360 and 3080 cm^{-1}. Since tautomerism is possible in monomethylated compounds but not in IId, IIe, or IIg, these results may indicate a tautomeric equilibrium in the monomethyl isomers. No present structural evidence can eliminate their alternative formulation as 2-amino-3,4-dihydro-5*H*-1,3,4-benzotriazepin-5-ones.

In the PMR spectra, the N_4 methyl resonances appeared between 3.75 and 3.85 ppm; the N_1 methyl singlets were observed at 2.75–2.90 ppm. The NH resonances were variable in position, with the C_2 amino protons

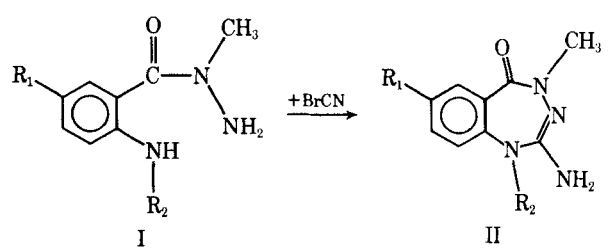

Scheme I

Table I—Arithmetic Mean of Determination of an Accurately Weighed Capsule Formulation

Compound	Labeled Amount, mg/ Capsule	Recovered Amount, mg/Capsule		Mean Percent
Acetaminophen	325	323.5		99.5
		322.8		99.3
		322.5		99.2
		Mean 322.9	Mean	99.3
Dichloralantipyrine	100	98.3		98.3
		97.6		97.6
		98.1		98.1
		Mean 98.0	Mean	98.0
Isometheptene mucate	65	63.20		97.2
		63.90		98.3
		Mean 63.5	Mean	97.7

rivatives. They are time consuming and are readily hydrolyzed by moisture even in the presence of excess reagents.

A comparison showed that the described method is more rapid than previously described GLC methods that required preparation of a derivative (7, 8, 11). It is not more rapid than other reported methods (5, 6), but the use of the 1% OV-17 on high-performance Chromosorb WHP eliminates the tailing and, therefore, increases the efficiency and accuracy.

REFERENCES

(1) J. B. Vaughn, *J. Pharm. Sci.*, **58**, 469 (1969).

(2) L. Chafetz, R. E. Daly, H. Schriftman, and J. J. Lomnev, *ibid.*, **60**, 463 (1971).

(3) F. M. Plakogiannis and A. M. Saad, *ibid.*, **64**, 1547 (1975).

(4) A. A. D'Souza and K. C. Slenoy, *Can. J. Pharm. Sci.*, **3**, 90 (1968).

(5) J. Grove, *J. Chromatogr.*, **59**, 289 (1971).

(6) M. J. Stewart and R. G. Willis, *Ann. Clin. Biochem.*, **12**, 4 (1975).

(7) H. V. Street, *J. Chromatogr.*, **109**, 29 (1975).

(8) L. F. Prescott, *J. Pharm. Pharmacol.*, **23**, 111 (1971).

(9) R. M. Riggin, A. L. Schmidt, and R. T. Kissinger, *J. Pharm. Sci.*, **64**, 680 (1975).

(10) A. W. Archer and E. A. Hougas, *J. Pharm. Pharmacol.*, **12**, 751 (1960).

(11) C. McMartin and H. V. Street, *J. Chromatogr.*, **22**, 274 (1966).

ACKNOWLEDGMENTS AND ADDRESSES

Received March 22, 1976, from the *Department of Pharmaceutics, Arnold & Marie Schwartz College of Pharmacy & Health Sciences of Long Island University, Brooklyn, NY 11201.*

Accepted for publication June 9, 1976.

Presented in part at the APhA Academy of Pharmaceutical Sciences, Atlanta meeting, November 1975.

[x] To whom inquiries should be directed.

New Compounds: Synthesis of 2-Amino-5*H*-1,3,4-benzotriazepin-5-ones

ROBERT W. LEIBY and NED D. HEINDEL [x]

Abstract □ *N*-Methyl-2-aminobenzohydrazides, when treated with cyanogen bromide, were found to yield 2-amino-5*H*-1,3,4-benzotriazepin-5-ones.

Keyphrases □ 2-Amino-5*H*-1,3,4-benzotriazepin-5-ones—various derivatives synthesized □ Benzotriazepinones, substituted—various derivatives synthesized

Benzotriazepines as bioisosteric homologs of the well-established benzodiazepine psychotherapeutics have received considerable attention recently. Several synthetic methods and claims of sedative activity have been published (1–8) for the 1,3,4-benzotriazepine subclass, but a few earlier structural assignments (as benzotriazepines) were revised recently (9).

DISCUSSION

As a continuation of investigations on 1,4-benzodiazepin-3,5-diones derived from anthranilamides (10–12), this study reports the preparation of 2-amino-1,4-dihydro-5*H*-1,3,4-benzotriazepin-5-ones (II), a new type of 1,3,4-benzotriazepine obtained from the cyclization of anthranilohydrazides (I). By use of cyanogen bromide and a suitably methylated anthranilohydrazide, cyclization can be directed in an unambiguous fashion to the hydrobromide salts of the benzotriazepines, thus avoiding the classic pitfalls and uncertainties of structure that occur when alternative closure pathways are possible (9).

Anthranilohydrazides bearing a methyl on the amide-like nitrogen (*i.e.*, *N*-methyl-2-aminobenzohydrazides, I) were obtained by the opening of isatoic anhydride with methylhydrazine (13, 14). These hydrazides condensed instantaneously in chilled ethanol with cyanogen bromide (Scheme I) to give IIa–IIg in 36–85% yield. When the *ortho*-amino group was deactivated by conjugation to a nitro moiety, *i.e.*, If and Ig, condensation in refluxing dioxane was necessary to obtain a satisfactory yield.

The monomethylated benzotriazepines displayed four NH absorptions in the IR spectra between 3440 and 3080 cm^{-1}, while the dimethylated benzotriazepines (II, $R_2 = CH_3$) displayed only three absorptions between 3360 and 3080 cm^{-1}. Since tautomerism is possible in monomethylated compounds but not in IId, IIe, or IIg, these results may indicate a tautomeric equilibrium in the monomethyl isomers. No present structural evidence can eliminate their alternative formulation as 2-amino-3,4-dihydro-5*H*-1,3,4-benzotriazepin-5-ones.

In the PMR spectra, the N_4 methyl resonances appeared between 3.75 and 3.85 ppm; the N_1 methyl singlets were observed at 2.75–2.90 ppm. The NH resonances were variable in position, with the C_2 amino protons

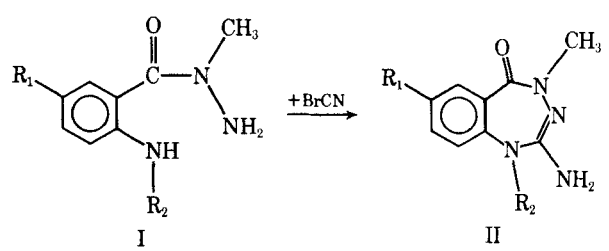

Scheme I

Table I—2-Amino-1,4-dihydro-5*H*-1,3,4-benzotriazepin-5-ones[a]

Compound	R_1	R_2	Yield, %	Melting Point	Formula	Analysis, % Calc.	Found
II*a*	H	H	80	226.0–226.5°	$C_9H_{11}BrN_4O$	C 39.87	39.75
						H 4.09	4.31
II*b*	Cl	H	72	218–219°	$C_9H_{10}BrClN_4O$	C 35.37	35.54
						H 3.30	3.51
II*c*	Br	H	36	177–179°[b]	$C_9H_{10}Br_2N_4O \cdot 1/2H_2O$	C 30.10	30.19
						H 3.08	3.05
II*d*	H	CH_3	76	212.0–212.5°	$C_{10}H_{13}BrN_4O$	C 42.12	42.07
						H 4.60	4.79
II*e*	Cl	CH_3	85	240.0–240.5°	$C_{10}H_{12}BrClN_4O$	C 37.58	37.57
						H 3.77	3.96
II*f*	NO_2	H	69	212.0–212.5°	$C_9H_{10}BrN_5O_3$	C 34.19	33.96
						H 3.19	3.43
II*g*	NO_2	CH_3	79	246–247°	$C_{10}H_{12}BrN_5O_3$	C 36.38	36.33
						H 3.65	3.73

[a] The title compounds were isolated as hydrobromide salts. [b] Compound forms hemihydrate; presence of water can also be demonstrated by PMR spectroscopy.

evident between 5.40 and 7.70 ppm and the N_1 (or N_3) protons detected at 8.55–8.80 ppm.

EXPERIMENTAL[1]

Preparation of Anthranilohydrazides—The synthesis of hydrazides I*a*–I*g* was described previously (13, 14).

General Procedure for 2-Amino-1,4-dihydro-5*H*-1,3,4-benzotriazepin-5-one Hydrobromide Salts (II*a*–II*e*)—A solution of 0.10 mole of the requisite anthranilohydrazide (I*a*–I*e*) in 100 ml of absolute ethanol was chilled in an ice bath, and 0.10 mole of cyanogen bromide in 20 ml of ethanol was added rapidly. The solution was stirred vigorously, and almost immediately the yellow crystalline hydrobromide salt began to precipitate. The solid was collected on a filter, washed with 100 ml of cold ether, and recrystallized from ethanol (Table I).

2-Amino-4-methyl-7-nitro-1,4-dihydro-5*H* -1,3,4- benzotriazepin-5-one Hydrobromide (II*f*)—To a solution of 5.25 g (25.0 mmoles) of *N*-methyl-2-amino-5-nitrobenzohydrazide (I*f*) dissolved in refluxing dioxane was added a solution of 2.65 g (25.0 mmoles) of cyanogen bromide in dioxane. Immediately upon addition, the solution became cloudy and precipitated a yellow semisolid mass. This semisolid crystallized on cooling in an ice bath. The solid was recrystallized from acetic acid and washed with absolute ethanol and ether. The analytical product (II*f*) was obtained in 68.5% (5.40 g) yield as fine yellow needles, mp 212.0–212.5°.

2-Amino- 1,4- dimethyl-7-nitro-1,4-dihydro-5*H*-1,3,4-benzotriazepin-5-one Hydrobromide (II*g*)—A dioxane–cyanogen bromide solution was prepared from 15 ml of dioxane and 2.65 g (25.0 mmoles) of cyanogen bromide. This solution was then added to 5.61 g (25.0 mmoles) of *N*-methyl-2-methylamino-5-nitrobenzohydrazide (I*g*) dissolved in refluxing dioxane. Upon addition, the solution became blood red with concomitant precipitation of a tan solid. The crude II*g* was recrystallized from absolute ethanol (sparingly soluble), giving 6.48 g (79%), mp 246–247°.

[1] IR spectra were obtained in potassium bromide disks on a Beckman IR-33 spectrometer. A Hitachi Perkin-Elmer R20A magnetic resonance spectrometer was employed to obtain the PMR spectra. Melting points were obtained in capillaries on a Thomas Hoover apparatus and are uncorrected. Combustion analyses were obtained from Robertson Microanalytical Laboratory, Florham Park, N.J.

REFERENCES

(1) M. Nair, *Indian J. Chem.*, **11**, 109 (1973).

(2) Ferlux-Chimie S.A., Fr. Demande 2,191,893 (1974); through *Chem. Abstr.*, **81**, 25703s (1974).

(3) D. Bailey, U.S. pat. 3,607,866 (1971); through *Chem. Abstr.*, **75**, 140910v (1971).

(4) A. Langis and M. Charest, *Chim. Ther.*, **2**, 349 (1967).

(5) A. Langis, U.S. pat. 3,542,767 (1970); through *Chem. Abstr.*, **74**, 88089 (1971).

(6) O. Hromatka, F. Krenmueller, and Knollmueller, *Monatsh. Chem.*, **100**, 934 (1969).

(7) T. Sulkowski and S. Childress, *J. Med. Chem.*, **7**, 386 (1964).

(8) T. Sulkowski and S. Childress, U.S. pat. 3,176,008 (1965); through *Chem. Abstr.*, **62**, 16284 (1965).

(9) N. P. Peet and S. Sunder, *J. Org. Chem.*, **40**, 1909 (1975).

(10) N. D. Heindel, *Psychopharm. Bull.*, **5** (2), 23 (1969).

(11) N. D. Heindel, W. P. Fives, T. F. Lemke, J. E. Rowe, H. W. Snady, and R. A. Carrano, *J. Med. Chem.*, **14**, 1233 (1971).

(12) N. D. Heindel, V. B. Fish, and T. F. Lemke, *J. Org. Chem.*, **32**, 3997 (1968).

(13) R. W. Leiby and N. D. Heindel, *Syn. Comm.*, **6**, 295 (1976).

(14) R. W. Leiby and N. D. Heindel, *J. Org. Chem.*, **41**, 2736 (1976).

ACKNOWLEDGMENTS AND ADDRESSES

Received April 22, 1976, from the *Department of Chemistry, Lehigh University, Bethlehem, PA 18015.*

Accepted for publication June 8, 1976.

Abstracted in part from a thesis submitted by R. W. Leiby to Lehigh University in partial fulfillment of the Doctor of Philosophy degree requirements.

The authors thank Stuart Pharmaceuticals, Division of ICI United States Inc., for their generous support of this research.

[x] To whom inquiries should be directed.

USP Dissolution Test I: Adequacy of Mixing

Keyphrases □ Dissolution apparatus—effect of sampling depth, temperature, and time on results □ Apparatus, dissolution—effect of sampling depth, temperature, and time on results

To the Editor:

This laboratory is presently engaged in a study aimed at characterizing the hydrodynamics (1, 2) of the USP dissolution apparatus. Phenomena have been observed akin to those reported by Withey (3) and Withey and Bowker (4), who found that "spurious results could be obtained if its sampling depth is varied." This communication assesses the seriousness of this problem and suggests a means of minimizing it.

Three pellets of pure oxalic acid dihydrate, 1.113 cm in diameter and 0.38 cm in thickness, were subjected to dissolution in a USP dissolution apparatus operated at 50 rpm in 900 ml of 0.1 *N* HCl at 25°. It was visually apparent that there was a schlieren effect; one can actually observe the discrete schlierens of oxalic acid solution move out into the liquid, sink somewhat, and then disperse. The results are shown in the lower curve in Fig. 1.

Four experiments were run in which the dissolution was carried out for 150 sec, the basket was removed, and the entire 900 ml of liquid in the dissolution vessel was assayed. This procedure was repeated at other time points, and the results are shown in the top curve in Fig. 1. Point-to-point *t*-comparisons and rank tests showed that the two sets of data differed significantly at the 99.9% confidence level.

The described tests were performed at 25°, and the sampling was carried out close to (1 cm below) the surface. The problems encountered at 25° probably would occur at 37° as well and be even more pronounced. The chosen point of sampling, of course, emphasized differences due to improper mixing. To establish the effect of temperature and sampling points, the experiments were repeated at 37° at various sampling points (Table I).

The USP description (5) states that "one of the outer ports *may* be used for insertion of a thermometer. Samples *may* be removed . . . through the other two ports." No actual dimensions or positioning details are given other than the drawing in the cited reference. Therefore, experiments were carried out (at 37°) with a setup that dimensionally matched the drawing in the USP.

Two experiments were performed (Table I). In one, a syringe was attached to the sampling tube and the dissolution was carried out with air in the dip tube (the air was there because the syringe was attached prior to the addition of liquid). This method is denoted USP-2 in Table I. In the other experiment (USP-1 in Table I), the syringe was added after the liquid was added to the vessel, so the liquid level in the dip tube matched that of the liquid in the vessel during dissolution. In this latter setup, a stagnant column of liquid will be sampled. In most sampling situations, the concentration at the sampling point will not equal the average concentration of the liquid in the vessel. If the volume of liquid is multiplied by the concentration, the amount obtained from the sampling will differ from the amount actually dissolved.

Table I—Concentrations Multiplied by Volume for Sampling at Various Points at 37° Compared with Amounts Actually Dissolved

Seconds	Position	Volume × Concentration, mg: At Sampling Point[a]	Volume × Concentration, mg: Entire Content Assayed[a]
120	0.5 cm below surface	57[a]	455
120	1 cm below surface	284[a]	455
120	2 cm above bottom	611[a]	455
120	At bottom	597	455
120	USP-1	270[a]	470
120	USP-2	398[a]	470
240	0.5 cm below surface	583[a]	796
240	1 cm below surface	753	796
240	2 cm above bottom	867[a]	796
240	At bottom	870[a]	796
240	USP-1	754[a]	839
240	USP-2	810	839

[a] Assays shown are averages of duplicate experiments. The sample standard deviation is 20 mg; on a two-way comparison, differences over 63 are significant on the 95% level.

This fact does not *per se* invalidate the test, although it places several restrictions on it, some rather severe. If the position and dimensions of the thermometer and sampling tube are defined carefully, curves can be obtained that will be reproducible. If such curves can be shown to correlate with *in vivo* data, then the test conceivably may be used as a control tool (6). However, dimensional specificity would be a necessity in such a case, as would duplication validation between apparatuses to be used.

The method denoted USP-2 in Table I gives the results closest to the actual content. It is felt that continuous monitoring by pumping liquid continuously through a flowcell comes close to this condition, since it eliminates the stagnant column of liquid in the sampling tube.

The use of a highly soluble substance (oxalic acid dihy-

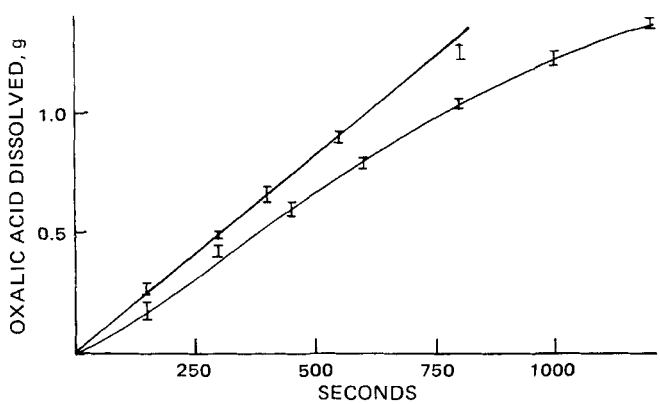

Figure 1—*Results from dissolution of oxalic acid dihydrate pellets in USP dissolution apparatus operated at 25° and 50 rpm. Key: upper curve, entire liquid mass assayed at each time point; and lower curve, samples taken 1 cm below surface.*

drate) accentuates the positional difference in concentration. The differences, furthermore, will be most pronounced in the beginning of the curve. Eventually, of course, all material will dissolve (provided the amount of liquid suffices) and molecular diffusion will provide a state of complete mixedness at very high time values.

The described phenomena were found with dissolution at higher revolutions per minute as well, although not to the same extent. They offer an added explanation of why dissolution curves are often sigmoid shaped[1], although a sigmoid shape *per se* should not be taken as a criterion for poor mixing since other factors affect curve shape.

(1) J. T. Carstensen and K. Dhupar, *J. Pharm. Sci.*, **65**, 1634 (1976).
(2) K. Dhupar, M.S. thesis, University of Wisconsin, Madison, Wis., 1976.
(3) R. J. Withey, *J. Pharm. Pharmacol.*, **23**, 573 (1971).
(4) R. J. Withey and A. J. Bowker, *ibid.*, **24**, 345 (1972).
(5) "The United States Pharmacopeia," 19th ed., Mack Publishing Co., Easton, Pa., 1975, p. 651.
(6) L. J. Leeson, *J. Pharm. Sci.*, **62** (4), iv (1973).

J. T. Carstensen [x]
Tom Lai
School of Pharmacy
University of Wisconsin
Madison, WI 53706

V. K. Prasad
Biopharmaceutics Laboratory
Food and Drug Administration
Washington, DC 20204

Received October 28, 1976.
Accepted for publication January 1, 1977.
[x] To whom inquiries should be directed.

[1] Unpublished results.

Polymorphic and Dissolution Properties of Mercaptopurine

Keyphrases □ Mercaptopurine—polymorphic form, dissolution rate, differential thermographic and X-ray diffraction analyses □ Polymorphic form—of mercaptopurine, dissolution rate, differential thermographic and X-ray diffraction analyses □ Dissolution rate—polymorphic form of mercaptopurine, differential thermographic and X-ray diffraction analyses □ Antineoplastics—mercaptopurine, polymorphic form, dissolution rate, differential thermographic and X-ray diffraction analyses

To the Editor:

Mercaptopurine is an effective purine antagonist (1) that has significant activity against human leukemia and other neoplastic disorders. It distributes throughout the body tissues rapidly and is extensively metabolized (2). Upon oral administration, it shows erratic and incomplete absorption (3). Although the structural similarity of mercaptopurine with natural purines makes the mechanism of its absorption complicated, its dissolution rate probably affects its bioavailability in view of its low water solubility.

The purpose of this communication is to report a fast dissolving polymorphic form of mercaptopurine which can be useful in increasing the bioavailability of this compound.

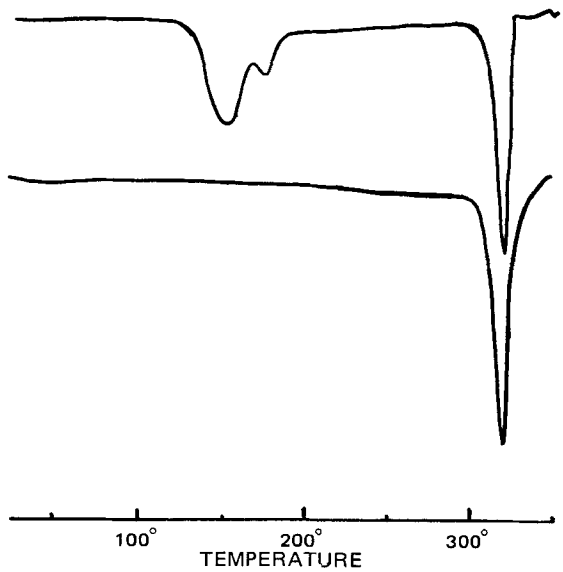

Figure 1—*Differential thermogram of original (top) and heat-treated or rerun (bottom) samples of mercaptopurine.*

The sample of mercaptopurine supplied by the manufacturer[1] yielded a differential thermogram[2] with two endothermic peaks (Fig. 1). The second peak is attributed to the melting of the compound as confirmed by a visual method[3]. The first endothermic peak can be attributed to, among other possibilities, a mercaptopurine polymorph (4). A rerun (Fig. 1) on the same sample showed only one peak corresponding to the final melting point. A similar thermogram with one peak was obtained when the sample was incubated at 225° for 20 min (4), strengthening the possibility of the polymorphic transition observed as the first endothermic peak in the original thermogram.

A sample of the high energy polymorph was prepared by incubating the original drug at 225° for 20 min; then it was subjected to X-ray diffraction analysis[4] (Fig. 2). The

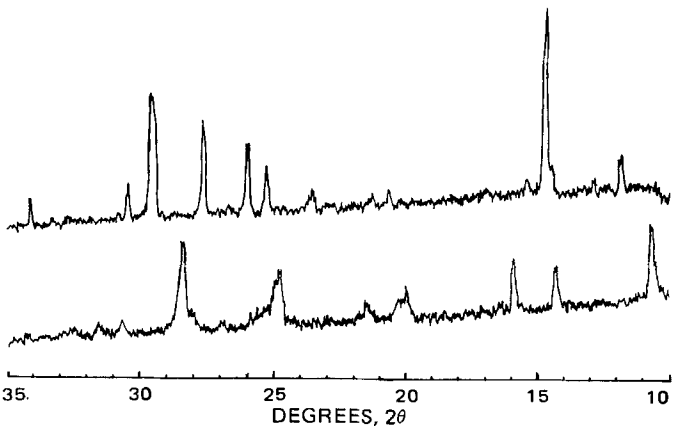

Figure 2—*X-ray diffraction spectra of original (top) and heat-treated (bottom) samples of mercaptopurine.*

[1] Supplied by Burroughs Wellcome Co., Research Triangle Park, N.C.
[2] DuPont 990 thermal analyzer, E. I. du Pont de Nemours & Co., Wilmington, Del.
[3] Arthur H. Thomas Co., Philadelphia, Pa.
[4] Picker X-ray diffractometer.

drate) accentuates the positional difference in concentration. The differences, furthermore, will be most pronounced in the beginning of the curve. Eventually, of course, all material will dissolve (provided the amount of liquid suffices) and molecular diffusion will provide a state of complete mixedness at very high time values.

The described phenomena were found with dissolution at higher revolutions per minute as well, although not to the same extent. They offer an added explanation of why dissolution curves are often sigmoid shaped[1], although a sigmoid shape *per se* should not be taken as a criterion for poor mixing since other factors affect curve shape.

(1) J. T. Carstensen and K. Dhupar, *J. Pharm. Sci.*, **65**, 1634 (1976).
(2) K. Dhupar, M.S. thesis, University of Wisconsin, Madison, Wis., 1976.
(3) R. J. Withey, *J. Pharm. Pharmacol.*, **23**, 573 (1971).
(4) R. J. Withey and A. J. Bowker, *ibid.*, **24**, 345 (1972).
(5) "The United States Pharmacopeia," 19th ed., Mack Publishing Co., Easton, Pa., 1975, p. 651.
(6) L. J. Leeson, *J. Pharm. Sci.*, **62** (4), iv (1973).

J. T. Carstensen [x]
Tom Lai
School of Pharmacy
University of Wisconsin
Madison, WI 53706

V. K. Prasad
Biopharmaceutics Laboratory
Food and Drug Administration
Washington, DC 20204

Received October 28, 1976.
Accepted for publication January 1, 1977.
[x] To whom inquiries should be directed.

[1] Unpublished results.

Polymorphic and Dissolution Properties of Mercaptopurine

Keyphrases □ Mercaptopurine—polymorphic form, dissolution rate, differential thermographic and X-ray diffraction analyses □ Polymorphic form—of mercaptopurine, dissolution rate, differential thermographic and X-ray diffraction analyses □ Dissolution rate—polymorphic form of mercaptopurine, differential thermographic and X-ray diffraction analyses □ Antineoplastics—mercaptopurine, polymorphic form, dissolution rate, differential thermographic and X-ray diffraction analyses

To the Editor:

Mercaptopurine is an effective purine antagonist (1) that has significant activity against human leukemia and other neoplastic disorders. It distributes throughout the body tissues rapidly and is extensively metabolized (2). Upon oral administration, it shows erratic and incomplete absorption (3). Although the structural similarity of mercaptopurine with natural purines makes the mechanism of its absorption complicated, its dissolution rate probably affects its bioavailability in view of its low water solubility.

The purpose of this communication is to report a fast dissolving polymorphic form of mercaptopurine which can be useful in increasing the bioavailability of this compound.

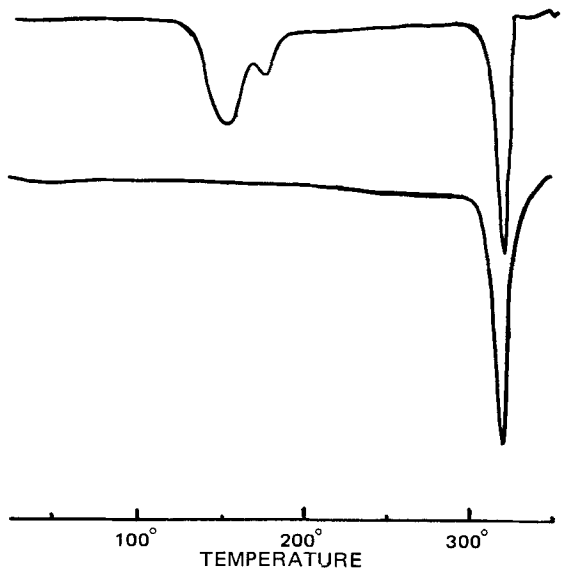

Figure 1—*Differential thermogram of original (top) and heat-treated or rerun (bottom) samples of mercaptopurine.*

The sample of mercaptopurine supplied by the manufacturer[1] yielded a differential thermogram[2] with two endothermic peaks (Fig. 1). The second peak is attributed to the melting of the compound as confirmed by a visual method[3]. The first endothermic peak can be attributed to, among other possibilities, a mercaptopurine polymorph (4). A rerun (Fig. 1) on the same sample showed only one peak corresponding to the final melting point. A similar thermogram with one peak was obtained when the sample was incubated at 225° for 20 min (4), strengthening the possibility of the polymorphic transition observed as the first endothermic peak in the original thermogram.

A sample of the high energy polymorph was prepared by incubating the original drug at 225° for 20 min; then it was subjected to X-ray diffraction analysis[4] (Fig. 2). The

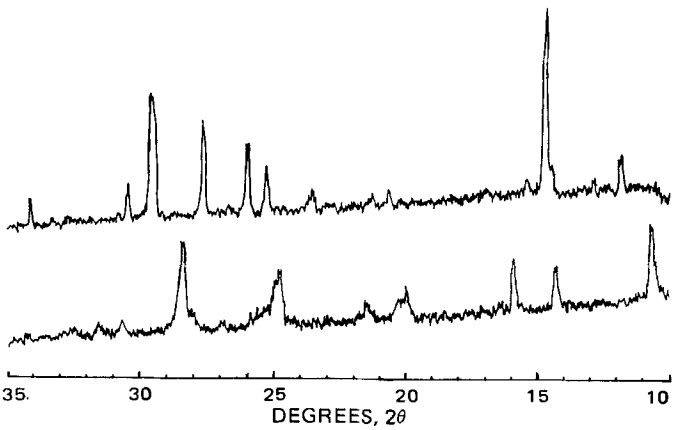

Figure 2—*X-ray diffraction spectra of original (top) and heat-treated (bottom) samples of mercaptopurine.*

[1] Supplied by Burroughs Wellcome Co., Research Triangle Park, N.C.
[2] DuPont 990 thermal analyzer, E. I. du Pont de Nemours & Co., Wilmington, Del.
[3] Arthur H. Thomas Co., Philadelphia, Pa.
[4] Picker X-ray diffractometer.

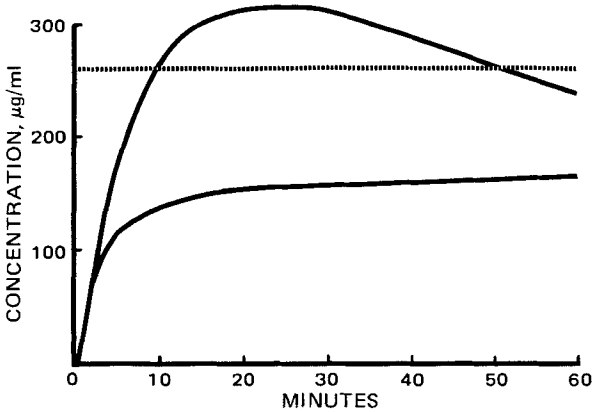

Figure 3—*Dissolution of high energy (top) and low energy (bottom) polymorphs of mercaptopurine. Broken line indicates equilibrium solubility at 37° in water.*

powder X-ray diffraction spectrum of the heat-treated sample was entirely different from that of the original compound, confirming the existence of at least two polymorphic forms. The IR spectra[5] were also different, with increased CH stretching and bending and additional CN and CC stretching and CH rocking in the heat-treated, high energy polymorphic form.

The purpose of this study was to show that a higher energy, relatively stable form of mercaptopurine can exist compared to the form of the drug used in commercial dosage forms. It is possible that the original compound may itself be composed of several polymorphic forms, especially in view of the peak splitting observed in the thermogram (Fig. 1). This aspect is currently being investigated in our laboratory.

The equilibrium solubilities of the two polymorphic forms were determined by placing excess drug in dialysis tubing[3], which was sealed, placed in an erlenmeyer flask containing 100 ml of distilled water, and equilibrated at 37° for up to 5 days. Prior studies excluded any interactions in the analysis due to leaching from the tubing.

This method allows direct sampling of the solution without filtration, which can result in significant loss due to adsorption. The solutions were analyzed spectrophotometrically[6] and gave the identical solubility value of 259.2 ± 4.3 μg/ml (mean ± *SEM*) for the two polymorphic forms. This observation, in spite of the differences in energy of the two polymorphic forms, can be attributed to the possible conversion of the high energy form to the low energy form when placed in water, a phenomenon reported for other drugs (5). However, the differences between the dissolution rates can still be observed, depending on dissolution conditions (4).

The dissolution rates of the two polymorphic forms were determined in water at 37° using a membrane filtration[7] method, which has often been shown to correlate better with *in vivo* dissolution rates and absorption (6, 7). Initial dissolution rate studies showed (Fig. 3) that the release from the high energy polymorph was twice that obtained from the low energy polymorph, resulting in supersaturation of the solution. These initial dissolution rate data (up to 20 min) showed an excellent log-linear relationship ($r > 0.98$) with corresponding rate constants of 0.25 and 0.16 min^{-1} for the high and low energy polymorphs, respectively. However, if the dissolution was continued for up to 1 hr, the high energy polymorphic form decreased in concentration, indicating precipitation and conversion to the low energy polymorph.

The effect of the nature of the medium on the dissolution rate and *in vivo* bioavailability aspects are currently being investigated in our laboratories.

[5] Perkin-Elmer IR spectrophotometer.

[6] Beckman DBGT spectrophotometer, Beckman Instrument Co., Fullerton, Calif.

[7] Sartorius membrane filter solubility simulator, Sartorius Filters, Inc., San Francisco, Calif.

(1) G. B. Elion, E. Burgi, and G. Hitchings, *J. Am. Chem. Soc.*, **74**, 411 (1952).

(2) G. B. Elion, S. Bieber, and G. Hitching, *Ann. N.Y. Acad. Sci.*, **60**, 297 (1954).

(3) T. L. Loo, J. K. Luce, M. P. Sullivan, and E. Frei, *Clin. Pharmacol. Ther.*, **9**, 180 (1968).

(4) S. Niazi, *J. Pharm. Sci.*, **65**, 302 (1976).

(5) W. I. Higuchi, P. O. Bernardo, and S. C. Mehta, *ibid.*, **56**, 200 (1967).

(6) H. Stricker, *Pharm. Ind.*, **31**, 794 (1969).

(7) *Ibid.*, **33**, 446 (1971).

M. L. Huang
Sarfaraz Niazi ˣ
Department of Pharmacy
College of Pharmacy
University of Illinois at the Medical Center
Chicago, IL 60612

Received November 8, 1976.
Accepted for publication January 18, 1977.
ˣ To whom inquiries should be directed.

Absolute Availability of Lithium

Keyphrases □ Lithium carbonate—bioavailability, calculations based on perturbation of renal clearance, commercial dosage form □ Bioavailability—lithium carbonate, calculations based on perturbation of renal clearance, commercial dosage form □ Renal clearance perturbation—calculations used to determine bioavailability of lithium carbonate, commercial dosage form □ Antidepressants—lithium carbonate, bioavailability, calculations based on perturbation of renal clearance, commercial dosage form

To the Editor:

It is generally accepted that lithium carbonate is completely absorbed when given orally to humans (1–3). This absorption, however, has not been demonstrated pharmacokinetically by comparison of oral plasma level–time curves with those obtained following intravenous dose administration, due largely to the legal and ethical considerations involved in giving this drug parenterally. It has been shown (4) that the lithium absorption rate can be influenced significantly by formulation differences between different brands. Thus, poorly formulated solid dosage forms may present a potential bioavailability problem for lithium carbonate.

Lalka and Feldman (5) recently reported an indirect method for calculating absolute bioavailability based on perturbation of renal clearance that does not require parenteral data. The purpose of this communication is to report the absolute bioavailability of one commercially

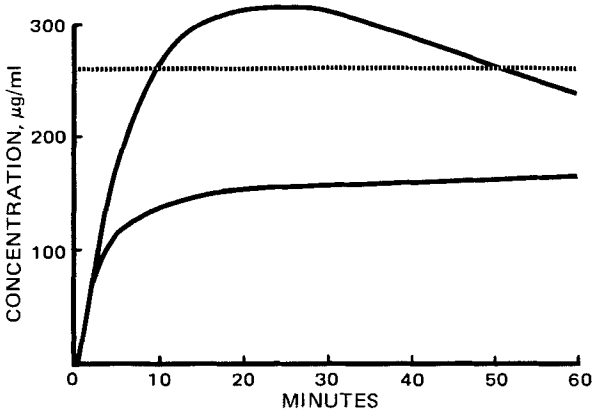

Figure 3—*Dissolution of high energy (top) and low energy (bottom) polymorphs of mercaptopurine. Broken line indicates equilibrium solubility at 37° in water.*

powder X-ray diffraction spectrum of the heat-treated sample was entirely different from that of the original compound, confirming the existence of at least two polymorphic forms. The IR spectra[5] were also different, with increased CH stretching and bending and additional CN and CC stretching and CH rocking in the heat-treated, high energy polymorphic form.

The purpose of this study was to show that a higher energy, relatively stable form of mercaptopurine can exist compared to the form of the drug used in commercial dosage forms. It is possible that the original compound may itself be composed of several polymorphic forms, especially in view of the peak splitting observed in the thermogram (Fig. 1). This aspect is currently being investigated in our laboratory.

The equilibrium solubilities of the two polymorphic forms were determined by placing excess drug in dialysis tubing[3], which was sealed, placed in an erlenmeyer flask containing 100 ml of distilled water, and equilibrated at 37° for up to 5 days. Prior studies excluded any interactions in the analysis due to leaching from the tubing.

This method allows direct sampling of the solution without filtration, which can result in significant loss due to adsorption. The solutions were analyzed spectrophotometrically[6] and gave the identical solubility value of 259.2 ± 4.3 μg/ml (mean ± *SEM*) for the two polymorphic forms. This observation, in spite of the differences in energy of the two polymorphic forms, can be attributed to the possible conversion of the high energy form to the low energy form when placed in water, a phenomenon reported for other drugs (5). However, the differences between the dissolution rates can still be observed, depending on dissolution conditions (4).

The dissolution rates of the two polymorphic forms were determined in water at 37° using a membrane filtration[7] method, which has often been shown to correlate better with *in vivo* dissolution rates and absorption (6, 7). Initial dissolution rate studies showed (Fig. 3) that the release from the high energy polymorph was twice that obtained from the low energy polymorph, resulting in supersaturation of the solution. These initial dissolution rate data (up to 20 min) showed an excellent log-linear relationship ($r > 0.98$) with corresponding rate constants of 0.25 and 0.16 min^{-1} for the high and low energy polymorphs, respectively. However, if the dissolution was continued for up to 1 hr, the high energy polymorphic form decreased in concentration, indicating precipitation and conversion to the low energy polymorph.

The effect of the nature of the medium on the dissolution rate and *in vivo* bioavailability aspects are currently being investigated in our laboratories.

[5] Perkin-Elmer IR spectrophotometer.

[6] Beckman DBGT spectrophotometer, Beckman Instrument Co., Fullerton, Calif.

[7] Sartorius membrane filter solubility simulator, Sartorius Filters, Inc., San Francisco, Calif.

(1) G. B. Elion, E. Burgi, and G. Hitchings, *J. Am. Chem. Soc.*, **74**, 411 (1952).

(2) G. B. Elion, S. Bieber, and G. Hitching, *Ann. N.Y. Acad. Sci.*, **60**, 297 (1954).

(3) T. L. Loo, J. K. Luce, M. P. Sullivan, and E. Frei, *Clin. Pharmacol. Ther.*, **9**, 180 (1968).

(4) S. Niazi, *J. Pharm. Sci.*, **65**, 302 (1976).

(5) W. I. Higuchi, P. O. Bernardo, and S. C. Mehta, *ibid.*, **56**, 200 (1967).

(6) H. Stricker, *Pharm. Ind.*, **31**, 794 (1969).

(7) *Ibid.*, **33**, 446 (1971).

M. L. Huang
Sarfaraz Niazi ˣ
Department of Pharmacy
College of Pharmacy
University of Illinois at the Medical Center
Chicago, IL 60612

Received November 8, 1976.
Accepted for publication January 18, 1977.
ˣ To whom inquiries should be directed.

Absolute Availability of Lithium

Keyphrases □ Lithium carbonate—bioavailability, calculations based on perturbation of renal clearance, commercial dosage form □ Bioavailability—lithium carbonate, calculations based on perturbation of renal clearance, commercial dosage form □ Renal clearance perturbation—calculations used to determine bioavailability of lithium carbonate, commercial dosage form □ Antidepressants—lithium carbonate, bioavailability, calculations based on perturbation of renal clearance, commercial dosage form

To the Editor:

It is generally accepted that lithium carbonate is completely absorbed when given orally to humans (1–3). This absorption, however, has not been demonstrated pharmacokinetically by comparison of oral plasma level–time curves with those obtained following intravenous dose administration, due largely to the legal and ethical considerations involved in giving this drug parenterally. It has been shown (4) that the lithium absorption rate can be influenced significantly by formulation differences between different brands. Thus, poorly formulated solid dosage forms may present a potential bioavailability problem for lithium carbonate.

Lalka and Feldman (5) recently reported an indirect method for calculating absolute bioavailability based on perturbation of renal clearance that does not require parenteral data. The purpose of this communication is to report the absolute bioavailability of one commercially

Table I—Parameters Used for Calculation of Lithium Availability in Each of Four Subjects

Subject	ΔCl_R, liters/hr	AUC, mEq/liter × hr	AUC', mEq/liter × hr	F
I	0.644	3.337	4.448	1.043
II	0.516	4.823	6.805	1.037
III	0.779	3.740	5.810	0.991
IV	0.191	5.206	5.816	1.152

available dosage form of lithium carbonate using this method.

Four healthy male subjects were given one 300-mg capsule of lithium carbonate[1] under fasting conditions. Plasma concentrations were measured periodically for 30 hr. Three weeks later, the same four subjects ingested 500 mg of chlorothiazide[2] daily for 8 days. On the 8th day, they again were given a single 300-mg dose of lithium carbonate. Details of these experiments were reported elsewhere (6, 7). The coadministration of chlorothiazide and lithium led to an average reduction in renal lithium clearance of 26.5%, thus fulfilling the requirement of renal clearance perturbation (7).

The equation presented by Lalka and Feldman (5) for calculating absolute availability is:

$$F = \frac{\Delta Cl_R}{D}\left[\frac{(AUC)(AUC')}{AUC' - AUC}\right] \qquad \text{(Eq. 1)}$$

where F is the fraction of dose absorbed, ΔCl_R is the change in renal clearance that occurs as a result of changes in the experimental conditions, D is the dose administered (8.25 mEq in this case), and AUC and AUC' are the resulting areas under the plasma concentration–time curves for the two experimental conditions.

Values employed in calculating F for each subject are given in Table I along with the calculated F values. As shown, the F value for each subject is very close to unity, indicating that lithium carbonate is completely absorbed under the conditions of these experiments. Thus, we have demonstrated the applicability of this method for determining absolute availability and have shown that this particular brand of lithium carbonate is completely absorbed.

(1) U. Groth, W. Prellwitz, and E. Jahnchen, *Clin. Pharmacol. Ther.*, **16**, 490 (1974).

(2) E. M. Trautner, R. Morris, C. H. Noack, and S. Gershon, *Med. J. Aust.*, **2**, 280 (1955).

(3) M. Schou and D. M. Shaw, *Practitioner*, **210**, 105 (1973).

(4) E. T. Sugita, J. W. Stokes, A. Frazer, P. Grof, J. Mendels, F. J. Goldstein, and P. J. Niebergall, *J. Clin. Pharmacol.*, **13**, 264 (1973).

(5) D. Lalka and H. Feldman, *J. Pharm. Sci.*, **63**, 1812 (1974).

(6) R. I. Poust, A. G. Mallinger, J. Mallinger, J. M. Himmelhoch, and I. Hanin, *Psychopharmacol. Commun.*, **2**, 91 (1976).

(7) R. I. Poust, A. G. Mallinger, J. Mallinger, J. M. Himmelhoch, J. F. Neil, and I. Hanin, *ibid.*, **2**, 273 (1976).

R. I. Poust [x]
Department of Pharmaceutics
School of Pharmacy
University of Pittsburgh
Pittsburgh, PA 15261

A. G. Mallinger
J. Mallinger
J. M. Himmelhoch
J. F. Neil
I. Hanin
Department of Psychiatry
Western Psychiatric Institute and Clinic
School of Medicine
University of Pittsburgh
Pittsburgh, PA 15261

Received December 15, 1976.
Accepted for publication January 18, 1977.
[x] To whom inquiries should be directed.

[1] Eskalith capsules, Smith Kline and French Laboratories, Philadelphia, PA 19101.

[2] Diuril tablets, Merck Sharp and Dohme, West Point, PA 19486.

BOOKS

REVIEWS

Clinical Pharmacy Sourcebook. Key Articles from the American Journal of Hospital Pharmacy. Publishing Sciences Group, 162 Great Road, Acton, MA 01720, 1976. xvi + 396 pp. 22 × 28 cm. Price $20.00.

"Clinical Pharmacy Sourcebook" is, as its title indicates, a collection of carefully selected articles relating to clinical aspects of pharmacy service which have been published previously in the *American Journal of Hospital Pharmacy*. Thus, although not reflecting the entire universe of the clinically oriented pharmacy literature, the "Sourcebook" has tapped one of the most fertile sources of material on this important facet of pharmacy practice.

Stressing clinically oriented pharmacy practice rather than education, the "Sourcebook" is an excellent source of background information for pharmacy students, practicing pharmacists interested, but as yet not fully involved, in clinical practice, industrial representatives, and other health care professionals who desire to learn more about the contributions to direct patient care which can be offered by the clinically oriented pharmacist.

Readers of the "Sourcebook" will benefit also from its convenient organization. The book is divided into seven sections: Introduction; Clinical Pharmacy Services: Implementation and Administration; Clinical Pharmacy Services: The Hospitalized Patient; Clinical Pharmacy Services: The Ambulatory Patient; Clinical Pharmacy Services: Therapeutic Considerations; Clinical Pharmacy Services: Biopharmaceutics and Pharmacokinetics; and Clinical Pharmacy Services: Evaluation. This format does more than compartmentalize the material; it enables readers to select a specific area of interest such as therapeutics, develop the appropriate "mind set," and review easily a series of related articles in the area of interest selected.

In addition to the extensive number of references cited in each individual article, the "Sourcebook" contains a useful bibliography of approximately 160 selected references dealing with the clinical aspects of pharmacy practice and education. The book's index, which was computer generated from the International Pharmaceutical Abstracts Information

Table I—Parameters Used for Calculation of Lithium Availability in Each of Four Subjects

Subject	ΔCl_R, liters/hr	AUC, mEq/liter × hr	AUC', mEq/liter × hr	F
I	0.644	3.337	4.448	1.043
II	0.516	4.823	6.805	1.037
III	0.779	3.740	5.810	0.991
IV	0.191	5.206	5.816	1.152

available dosage form of lithium carbonate using this method.

Four healthy male subjects were given one 300-mg capsule of lithium carbonate[1] under fasting conditions. Plasma concentrations were measured periodically for 30 hr. Three weeks later, the same four subjects ingested 500 mg of chlorothiazide[2] daily for 8 days. On the 8th day, they again were given a single 300-mg dose of lithium carbonate. Details of these experiments were reported elsewhere (6, 7). The coadministration of chlorothiazide and lithium led to an average reduction in renal lithium clearance of 26.5%, thus fulfilling the requirement of renal clearance perturbation (7).

The equation presented by Lalka and Feldman (5) for calculating absolute availability is:

$$F = \frac{\Delta Cl_R}{D}\left[\frac{(AUC)(AUC')}{AUC' - AUC}\right] \qquad \text{(Eq. 1)}$$

where F is the fraction of dose absorbed, ΔCl_R is the change in renal clearance that occurs as a result of changes in the experimental conditions, D is the dose administered (8.25 mEq in this case), and AUC and AUC' are the resulting areas under the plasma concentration–time curves for the two experimental conditions.

Values employed in calculating F for each subject are given in Table I along with the calculated F values. As shown, the F value for each subject is very close to unity, indicating that lithium carbonate is completely absorbed under the conditions of these experiments. Thus, we have demonstrated the applicability of this method for determining absolute availability and have shown that this particular brand of lithium carbonate is completely absorbed.

(1) U. Groth, W. Prellwitz, and E. Jahnchen, *Clin. Pharmacol. Ther.*, **16**, 490 (1974).

(2) E. M. Trautner, R. Morris, C. H. Noack, and S. Gershon, *Med. J. Aust.*, **2**, 280 (1955).

(3) M. Schou and D. M. Shaw, *Practitioner*, **210**, 105 (1973).

(4) E. T. Sugita, J. W. Stokes, A. Frazer, P. Grof, J. Mendels, F. J. Goldstein, and P. J. Niebergall, *J. Clin. Pharmacol.*, **13**, 264 (1973).

(5) D. Lalka and H. Feldman, *J. Pharm. Sci.*, **63**, 1812 (1974).

(6) R. I. Poust, A. G. Mallinger, J. Mallinger, J. M. Himmelhoch, and I. Hanin, *Psychopharmacol. Commun.*, **2**, 91 (1976).

(7) R. I. Poust, A. G. Mallinger, J. Mallinger, J. M. Himmelhoch, J. F. Neil, and I. Hanin, *ibid.*, **2**, 273 (1976).

R. I. Poust [x]
Department of Pharmaceutics
School of Pharmacy
University of Pittsburgh
Pittsburgh, PA 15261

A. G. Mallinger
J. Mallinger
J. M. Himmelhoch
J. F. Neil
I. Hanin
Department of Psychiatry
Western Psychiatric Institute and Clinic
School of Medicine
University of Pittsburgh
Pittsburgh, PA 15261

Received December 15, 1976.
Accepted for publication January 18, 1977.
[x] To whom inquiries should be directed.

[1] Eskalith capsules, Smith Kline and French Laboratories, Philadelphia, PA 19101.

[2] Diuril tablets, Merck Sharp and Dohme, West Point, PA 19486.

BOOKS

REVIEWS

Clinical Pharmacy Sourcebook. Key Articles from the American Journal of Hospital Pharmacy. Publishing Sciences Group, 162 Great Road, Acton, MA 01720, 1976. xvi + 396 pp. 22 × 28 cm. Price $20.00.

"Clinical Pharmacy Sourcebook" is, as its title indicates, a collection of carefully selected articles relating to clinical aspects of pharmacy service which have been published previously in the *American Journal of Hospital Pharmacy*. Thus, although not reflecting the entire universe of the clinically oriented pharmacy literature, the "Sourcebook" has tapped one of the most fertile sources of material on this important facet of pharmacy practice.

Stressing clinically oriented pharmacy practice rather than education, the "Sourcebook" is an excellent source of background information for pharmacy students, practicing pharmacists interested, but as yet not fully involved, in clinical practice, industrial representatives, and other health care professionals who desire to learn more about the contributions to direct patient care which can be offered by the clinically oriented pharmacist.

Readers of the "Sourcebook" will benefit also from its convenient organization. The book is divided into seven sections: Introduction; Clinical Pharmacy Services: Implementation and Administration; Clinical Pharmacy Services: The Hospitalized Patient; Clinical Pharmacy Services: The Ambulatory Patient; Clinical Pharmacy Services: Therapeutic Considerations; Clinical Pharmacy Services: Biopharmaceutics and Pharmacokinetics; and Clinical Pharmacy Services: Evaluation. This format does more than compartmentalize the material; it enables readers to select a specific area of interest such as therapeutics, develop the appropriate "mind set," and review easily a series of related articles in the area of interest selected.

In addition to the extensive number of references cited in each individual article, the "Sourcebook" contains a useful bibliography of approximately 160 selected references dealing with the clinical aspects of pharmacy practice and education. The book's index, which was computer generated from the International Pharmaceutical Abstracts Information

System's data base, is easy to use and provides the reader with fast access to the text's subject matter.

Finally, it will be apparent to readers of "Clinical Pharmacy Sourcebook" who are familiar with the literature of pharmacy that the articles included in this reference were published between 1971 and 1975. It is unfortunate, however, that the dates of original publication for each article are not included in the text—if only to provide a perspective to the chronology of the development of different programs, concepts, and philosophies. Nevertheless, "Clinical Pharmacy Sourcebook" represents a convenient compilation of the literature of clinically oriented pharmacy and would be a valuable addition to the libraries of all health care professionals interested in providing improved service(s) to their patients.

Staff Review

Liquid Scintillation Counting. By K. D. NEAME and C. A. HOMEWOOD. Halsted, 605 Third Ave., New York, NY 10016, 1974. 180 pp. 16 × 24 cm. Price $13.75.

"Liquid Scintillation Counting" could be considered as a "McGuffey Reader" for this radiation detection technique. The book describes the elementary principles of liquid scintillation counter operation and presents information helpful in resolving fundamental practical considerations of proper operation. The authors have written a book that should be required reading for the beginning user of liquid scintillation counters.

After presenting information on radioactivity in general, the authors discuss the liquid scintillation counter, counting efficiency and quenching, and the selection and quantity of tracers to use in experimentation. With the basics covered, they then take up topics of a more applied nature. They discuss preparation of samples for counting, determination of counting efficiency for making quench correction, and double-isotope analysis. Such subjects as errors from various sources and what the user should be concerned about in correcting or evaluating them are considered. The authors omit discussion of errors that are common to all methods of analysis but cover in detail several errors peculiar to the nature of radioactivity and to its measurement by liquid counting.

The book could be considered by educators as a text in courses that teach principles of nuclear detection and the liquid scintillation method.

Reviewed by Gordon S. Born
Bionucleonics Department
Purdue University
West Lafayette, IN 47907

A Flexible Design for Health Professions Education. Edited by RICHARD M. JACOBS. Wiley, 605 Third Ave., New York, NY 10016, 1976. 260 pp. 16 × 23.5 cm.

"Flexible Design" is essential reading for anyone involved in the field of health education, particularly for those who are involved in, or are getting ready to embark on, "experiments" in new instructional techniques and/or curriculum design.

The chapters, which represent the thinking of 23 outstanding educators from the disciplines of medicine, dentistry, pharmacy, nursing, and allied health, are based on material originally presented at an invitational conference (by the same title) held in Iowa City in April 1975.

The editor's introduction succinctly states the book's purpose: "Recent trends in education, health care, and society in general have stimulated serious efforts to find alternatives to the traditional approaches to the health professions education." The volume examines how societal expectations and individual aspirations might be more effectively fulfilled outside the context of the "traditional, highly regimented and stereotyped health professions education programs"—through educational flexibility.

The 20 chapters are grouped into five parts: Basic Educational Considerations and Instructional Strategies; An Overview of Individualized Instructional Practices in the Major Health Professions, (included is the paper on "Flexible Approaches to Pharmacy Education" by L. C. Weaver and H. R. Manassee, Jr.); Planning, Implementation, and Evaluation: Case Studies; Cost of Flexibility; and Broader Dimensions of Flexibility.

The flexibility to which the work is addressed involves a personalized approach to education: individualized curricular content, individualized modes of instruction, flexible scheduling of instruction, and flexible admissions.

Several notable experiments in health professions education are elaborated upon. The authors provide excellent insights into such areas as outreach programs, individual and elective study, hospital programs, different modes of instruction, multitrack systems, independent study programs, computer-aided instruction, use of simulation, social costs, and flexible tuition.

Douglas R. Whitney's chapter on the Placement, Monitoring, and Evaluation System (PME) is important for the distinction it makes between flexible and traditional instruction in view of the demands that the flexible approach places on the system. PME is a decision-making network that collects data; a management system to hold and control data; and an output system to produce reports, documents, and summaries for use in decision making.

Alvin L. Morris, in his chapter on "Implementation," raises important questions and presents a broader perspective on the subject. He argues that: "While flexible education introduces varieties of time and methods to bring all students to the same end point, traditional education does just the opposite.

There is something disturbing about the idea of all students being the same at the end of an educational experience. Conversely, it can be argued that the identification of a wide range of achievements and achievers through traditional education has served both the students and their professions well." Dr. Morris cautions that: "Educators must be willing to reconcile their views and aspirations with those of the 'real world' where the products of the educational process must ultimately function."

"A Flexible Design for Health Professions Education" presents a balanced and timely discussion about the traditional and experimental approaches being used to educate health professionals.

Staff Review

Radiopharmacy. Edited by MANUEL TUBIS and WALTER WOLF. Wiley, 605 Third Ave., New York, NY 10016, 1976. 911 pp. 16 × 24 cm. Price $44.50.

This book is very pertinent and timely considering the current expansion of radiopharmacy in the curricula of schools of pharmacy both at the undergraduate and graduate levels. The editors themselves have been key figures in the development of radiopharmacy and its establishment in pharmacy education. They are eminent researchers in their own right and have assembled a highly knowledgeable group of contributors to aid them in their presentation of the subject matter. The problems of multiple-author books and variability in style and presentation occur to some extent in this text. For example, the author of Chapter 1 decided that *in vitro* tests would not be considered in the scope of the book from his vantage point, while the editors considered it pertinent and devoted Chapter 26 to a discussion of competitive binding assay procedures. This reviewer considers that the radiopharmacist does need to have an appreciation of such procedures since they will clearly become more important both clinically and industrially.

The structure of the text is orderly in the presentation of material. It is composed of six basic sections dealing with history, physics and instrumentation, biology, chemistry, radiopharmaceutics, and nuclear medicine. The organization is certainly desirable, providing the student with the background material in these various scientific areas that impinge directly on the practice of radiopharmacy. Additionally, there is an important section on regulations and legal aspects in the handling and dispensing of radiopharmaceuticals. Obviously, such information is of importance to the potential practitioner.

There is also a chapter on radionuclides in space biology and medicine by two very knowledgeable individuals. Such material will certainly gain importance with time, but presently its general application is limited and of a highly specialized nature.

In conclusion, this is a most worthwhile and highly informative text and one that will undoubtedly be widely used by those in academia for teaching purposes and by those who wish to familiarize themselves with the exciting opportunities presented by radiopharmacy. Clearly,

System's data base, is easy to use and provides the reader with fast access to the text's subject matter.

Finally, it will be apparent to readers of "Clinical Pharmacy Sourcebook" who are familiar with the literature of pharmacy that the articles included in this reference were published between 1971 and 1975. It is unfortunate, however, that the dates of original publication for each article are not included in the text—if only to provide a perspective to the chronology of the development of different programs, concepts, and philosophies. Nevertheless, "Clinical Pharmacy Sourcebook" represents a convenient compilation of the literature of clinically oriented pharmacy and would be a valuable addition to the libraries of all health care professionals interested in providing improved service(s) to their patients.

Staff Review

Liquid Scintillation Counting. By K. D. NEAME and C. A. HOMEWOOD. Halsted, 605 Third Ave., New York, NY 10016, 1974. 180 pp. 16 × 24 cm. Price $13.75.

"Liquid Scintillation Counting" could be considered as a "McGuffey Reader" for this radiation detection technique. The book describes the elementary principles of liquid scintillation counter operation and presents information helpful in resolving fundamental practical considerations of proper operation. The authors have written a book that should be required reading for the beginning user of liquid scintillation counters.

After presenting information on radioactivity in general, the authors discuss the liquid scintillation counter, counting efficiency and quenching, and the selection and quantity of tracers to use in experimentation. With the basics covered, they then take up topics of a more applied nature. They discuss preparation of samples for counting, determination of counting efficiency for making quench correction, and double-isotope analysis. Such subjects as errors from various sources and what the user should be concerned about in correcting or evaluating them are considered. The authors omit discussion of errors that are common to all methods of analysis but cover in detail several errors peculiar to the nature of radioactivity and to its measurement by liquid counting.

The book could be considered by educators as a text in courses that teach principles of nuclear detection and the liquid scintillation method.

Reviewed by Gordon S. Born
Bionucleonics Department
Purdue University
West Lafayette, IN 47907

A Flexible Design for Health Professions Education. Edited by RICHARD M. JACOBS. Wiley, 605 Third Ave., New York, NY 10016, 1976. 260 pp. 16 × 23.5 cm.

"Flexible Design" is essential reading for anyone involved in the field of health education, particularly for those who are involved in, or are getting ready to embark on, "experiments" in new instructional techniques and/or curriculum design.

The chapters, which represent the thinking of 23 outstanding educators from the disciplines of medicine, dentistry, pharmacy, nursing, and allied health, are based on material originally presented at an invitational conference (by the same title) held in Iowa City in April 1975.

The editor's introduction succinctly states the book's purpose: "Recent trends in education, health care, and society in general have stimulated serious efforts to find alternatives to the traditional approaches to the health professions education." The volume examines how societal expectations and individual aspirations might be more effectively fulfilled outside the context of the "traditional, highly regimented and stereotyped health professions education programs"—through educational flexibility.

The 20 chapters are grouped into five parts: Basic Educational Considerations and Instructional Strategies; An Overview of Individualized Instructional Practices in the Major Health Professions, (included is the paper on "Flexible Approaches to Pharmacy Education" by L. C. Weaver and H. R. Manassee, Jr.); Planning, Implementation, and Evaluation: Case Studies; Cost of Flexibility; and Broader Dimensions of Flexibility.

The flexibility to which the work is addressed involves a personalized approach to education: individualized curricular content, individualized modes of instruction, flexible scheduling of instruction, and flexible admissions.

Several notable experiments in health professions education are elaborated upon. The authors provide excellent insights into such areas as outreach programs, individual and elective study, hospital programs, different modes of instruction, multitrack systems, independent study programs, computer-aided instruction, use of simulation, social costs, and flexible tuition.

Douglas R. Whitney's chapter on the Placement, Monitoring, and Evaluation System (PME) is important for the distinction it makes between flexible and traditional instruction in view of the demands that the flexible approach places on the system. PME is a decision-making network that collects data; a management system to hold and control data; and an output system to produce reports, documents, and summaries for use in decision making.

Alvin L. Morris, in his chapter on "Implementation," raises important questions and presents a broader perspective on the subject. He argues that: "While flexible education introduces varieties of time and methods to bring all students to the same end point, traditional education does just the opposite.

There is something disturbing about the idea of all students being the same at the end of an educational experience. Conversely, it can be argued that the identification of a wide range of achievements and achievers through traditional education has served both the students and their professions well." Dr. Morris cautions that: "Educators must be willing to reconcile their views and aspirations with those of the 'real world' where the products of the educational process must ultimately function."

"A Flexible Design for Health Professions Education" presents a balanced and timely discussion about the traditional and experimental approaches being used to educate health professionals.

Staff Review

Radiopharmacy. Edited by MANUEL TUBIS and WALTER WOLF. Wiley, 605 Third Ave., New York, NY 10016, 1976. 911 pp. 16 × 24 cm. Price $44.50.

This book is very pertinent and timely considering the current expansion of radiopharmacy in the curricula of schools of pharmacy both at the undergraduate and graduate levels. The editors themselves have been key figures in the development of radiopharmacy and its establishment in pharmacy education. They are eminent researchers in their own right and have assembled a highly knowledgeable group of contributors to aid them in their presentation of the subject matter. The problems of multiple-author books and variability in style and presentation occur to some extent in this text. For example, the author of Chapter 1 decided that *in vitro* tests would not be considered in the scope of the book from his vantage point, while the editors considered it pertinent and devoted Chapter 26 to a discussion of competitive binding assay procedures. This reviewer considers that the radiopharmacist does need to have an appreciation of such procedures since they will clearly become more important both clinically and industrially.

The structure of the text is orderly in the presentation of material. It is composed of six basic sections dealing with history, physics and instrumentation, biology, chemistry, radiopharmaceutics, and nuclear medicine. The organization is certainly desirable, providing the student with the background material in these various scientific areas that impinge directly on the practice of radiopharmacy. Additionally, there is an important section on regulations and legal aspects in the handling and dispensing of radiopharmaceuticals. Obviously, such information is of importance to the potential practitioner.

There is also a chapter on radionuclides in space biology and medicine by two very knowledgeable individuals. Such material will certainly gain importance with time, but presently its general application is limited and of a highly specialized nature.

In conclusion, this is a most worthwhile and highly informative text and one that will undoubtedly be widely used by those in academia for teaching purposes and by those who wish to familiarize themselves with the exciting opportunities presented by radiopharmacy. Clearly,

System's data base, is easy to use and provides the reader with fast access to the text's subject matter.

Finally, it will be apparent to readers of "Clinical Pharmacy Sourcebook" who are familiar with the literature of pharmacy that the articles included in this reference were published between 1971 and 1975. It is unfortunate, however, that the dates of original publication for each article are not included in the text—if only to provide a perspective to the chronology of the development of different programs, concepts, and philosophies. Nevertheless, "Clinical Pharmacy Sourcebook" represents a convenient compilation of the literature of clinically oriented pharmacy and would be a valuable addition to the libraries of all health care professionals interested in providing improved service(s) to their patients.

Staff Review

Liquid Scintillation Counting. By K. D. NEAME and C. A. HOMEWOOD. Halsted, 605 Third Ave., New York, NY 10016, 1974. 180 pp. 16 × 24 cm. Price $13.75.

"Liquid Scintillation Counting" could be considered as a "McGuffey Reader" for this radiation detection technique. The book describes the elementary principles of liquid scintillation counter operation and presents information helpful in resolving fundamental practical considerations of proper operation. The authors have written a book that should be required reading for the beginning user of liquid scintillation counters.

After presenting information on radioactivity in general, the authors discuss the liquid scintillation counter, counting efficiency and quenching, and the selection and quantity of tracers to use in experimentation. With the basics covered, they then take up topics of a more applied nature. They discuss preparation of samples for counting, determination of counting efficiency for making quench correction, and double-isotope analysis. Such subjects as errors from various sources and what the user should be concerned about in correcting or evaluating them are considered. The authors omit discussion of errors that are common to all methods of analysis but cover in detail several errors peculiar to the nature of radioactivity and to its measurement by liquid counting.

The book could be considered by educators as a text in courses that teach principles of nuclear detection and the liquid scintillation method.

Reviewed by Gordon S. Born
Bionucleonics Department
Purdue University
West Lafayette, IN 47907

A Flexible Design for Health Professions Education. Edited by RICHARD M. JACOBS. Wiley, 605 Third Ave., New York, NY 10016, 1976. 260 pp. 16 × 23.5 cm.

"Flexible Design" is essential reading for anyone involved in the field of health education, particularly for those who are involved in, or are getting ready to embark on, "experiments" in new instructional techniques and/or curriculum design.

The chapters, which represent the thinking of 23 outstanding educators from the disciplines of medicine, dentistry, pharmacy, nursing, and allied health, are based on material originally presented at an invitational conference (by the same title) held in Iowa City in April 1975.

The editor's introduction succinctly states the book's purpose: "Recent trends in education, health care, and society in general have stimulated serious efforts to find alternatives to the traditional approaches to the health professions education." The volume examines how societal expectations and individual aspirations might be more effectively fulfilled outside the context of the "traditional, highly regimented and stereotyped health professions education programs"—through educational flexibility.

The 20 chapters are grouped into five parts: Basic Educational Considerations and Instructional Strategies; An Overview of Individualized Instructional Practices in the Major Health Professions, (included is the paper on "Flexible Approaches to Pharmacy Education" by L. C. Weaver and H. R. Manassee, Jr.); Planning, Implementation, and Evaluation: Case Studies; Cost of Flexibility; and Broader Dimensions of Flexibility.

The flexibility to which the work is addressed involves a personalized approach to education: individualized curricular content, individualized modes of instruction, flexible scheduling of instruction, and flexible admissions.

Several notable experiments in health professions education are elaborated upon. The authors provide excellent insights into such areas as outreach programs, individual and elective study, hospital programs, different modes of instruction, multitrack systems, independent study programs, computer-aided instruction, use of simulation, social costs, and flexible tuition.

Douglas R. Whitney's chapter on the Placement, Monitoring, and Evaluation System (PME) is important for the distinction it makes between flexible and traditional instruction in view of the demands that the flexible approach places on the system. PME is a decision-making network that collects data; a management system to hold and control data; and an output system to produce reports, documents, and summaries for use in decision making.

Alvin L. Morris, in his chapter on "Implementation," raises important questions and presents a broader perspective on the subject. He argues that: "While flexible education introduces varieties of time and methods to bring all students to the same end point, traditional education does just the opposite.

There is something disturbing about the idea of all students being the same at the end of an educational experience. Conversely, it can be argued that the identification of a wide range of achievements and achievers through traditional education has served both the students and their professions well." Dr. Morris cautions that: "Educators must be willing to reconcile their views and aspirations with those of the 'real world' where the products of the educational process must ultimately function."

"A Flexible Design for Health Professions Education" presents a balanced and timely discussion about the traditional and experimental approaches being used to educate health professionals.

Staff Review

Radiopharmacy. Edited by MANUEL TUBIS and WALTER WOLF. Wiley, 605 Third Ave., New York, NY 10016, 1976. 911 pp. 16 × 24 cm. Price $44.50.

This book is very pertinent and timely considering the current expansion of radiopharmacy in the curricula of schools of pharmacy both at the undergraduate and graduate levels. The editors themselves have been key figures in the development of radiopharmacy and its establishment in pharmacy education. They are eminent researchers in their own right and have assembled a highly knowledgeable group of contributors to aid them in their presentation of the subject matter. The problems of multiple-author books and variability in style and presentation occur to some extent in this text. For example, the author of Chapter 1 decided that *in vitro* tests would not be considered in the scope of the book from his vantage point, while the editors considered it pertinent and devoted Chapter 26 to a discussion of competitive binding assay procedures. This reviewer considers that the radiopharmacist does need to have an appreciation of such procedures since they will clearly become more important both clinically and industrially.

The structure of the text is orderly in the presentation of material. It is composed of six basic sections dealing with history, physics and instrumentation, biology, chemistry, radiopharmaceutics, and nuclear medicine. The organization is certainly desirable, providing the student with the background material in these various scientific areas that impinge directly on the practice of radiopharmacy. Additionally, there is an important section on regulations and legal aspects in the handling and dispensing of radiopharmaceuticals. Obviously, such information is of importance to the potential practitioner.

There is also a chapter on radionuclides in space biology and medicine by two very knowledgeable individuals. Such material will certainly gain importance with time, but presently its general application is limited and of a highly specialized nature.

In conclusion, this is a most worthwhile and highly informative text and one that will undoubtedly be widely used by those in academia for teaching purposes and by those who wish to familiarize themselves with the exciting opportunities presented by radiopharmacy. Clearly,

System's data base, is easy to use and provides the reader with fast access to the text's subject matter.

Finally, it will be apparent to readers of "Clinical Pharmacy Sourcebook" who are familiar with the literature of pharmacy that the articles included in this reference were published between 1971 and 1975. It is unfortunate, however, that the dates of original publication for each article are not included in the text—if only to provide a perspective to the chronology of the development of different programs, concepts, and philosophies. Nevertheless, "Clinical Pharmacy Sourcebook" represents a convenient compilation of the literature of clinically oriented pharmacy and would be a valuable addition to the libraries of all health care professionals interested in providing improved service(s) to their patients.

Staff Review

Liquid Scintillation Counting. By K. D. NEAME and C. A. HOMEWOOD. Halsted, 605 Third Ave., New York, NY 10016, 1974. 180 pp. 16 × 24 cm. Price $13.75.

"Liquid Scintillation Counting" could be considered as a "McGuffey Reader" for this radiation detection technique. The book describes the elementary principles of liquid scintillation counter operation and presents information helpful in resolving fundamental practical considerations of proper operation. The authors have written a book that should be required reading for the beginning user of liquid scintillation counters.

After presenting information on radioactivity in general, the authors discuss the liquid scintillation counter, counting efficiency and quenching, and the selection and quantity of tracers to use in experimentation. With the basics covered, they then take up topics of a more applied nature. They discuss preparation of samples for counting, determination of counting efficiency for making quench correction, and double-isotope analysis. Such subjects as errors from various sources and what the user should be concerned about in correcting or evaluating them are considered. The authors omit discussion of errors that are common to all methods of analysis but cover in detail several errors peculiar to the nature of radioactivity and to its measurement by liquid counting.

The book could be considered by educators as a text in courses that teach principles of nuclear detection and the liquid scintillation method.

Reviewed by Gordon S. Born
Bionucleonics Department
Purdue University
West Lafayette, IN 47907

A Flexible Design for Health Professions Education. Edited by RICHARD M. JACOBS. Wiley, 605 Third Ave., New York, NY 10016, 1976. 260 pp. 16 × 23.5 cm.

"Flexible Design" is essential reading for anyone involved in the field of health education, particularly for those who are involved in, or are getting ready to embark on, "experiments" in new instructional techniques and/or curriculum design.

The chapters, which represent the thinking of 23 outstanding educators from the disciplines of medicine, dentistry, pharmacy, nursing, and allied health, are based on material originally presented at an invitational conference (by the same title) held in Iowa City in April 1975.

The editor's introduction succinctly states the book's purpose: "Recent trends in education, health care, and society in general have stimulated serious efforts to find alternatives to the traditional approaches to the health professions education." The volume examines how societal expectations and individual aspirations might be more effectively fulfilled outside the context of the "traditional, highly regimented and stereotyped health professions education programs"—through educational flexibility.

The 20 chapters are grouped into five parts: Basic Educational Considerations and Instructional Strategies; An Overview of Individualized Instructional Practices in the Major Health Professions, (included is the paper on "Flexible Approaches to Pharmacy Education" by L. C. Weaver and H. R. Manassee, Jr.); Planning, Implementation, and Evaluation: Case Studies; Cost of Flexibility; and Broader Dimensions of Flexibility.

The flexibility to which the work is addressed involves a personalized approach to education: individualized curricular content, individualized modes of instruction, flexible scheduling of instruction, and flexible admissions.

Several notable experiments in health professions education are elaborated upon. The authors provide excellent insights into such areas as outreach programs, individual and elective study, hospital programs, different modes of instruction, multitrack systems, independent study programs, computer-aided instruction, use of simulation, social costs, and flexible tuition.

Douglas R. Whitney's chapter on the Placement, Monitoring, and Evaluation System (PME) is important for the distinction it makes between flexible and traditional instruction in view of the demands that the flexible approach places on the system. PME is a decision-making network that collects data; a management system to hold and control data; and an output system to produce reports, documents, and summaries for use in decision making.

Alvin L. Morris, in his chapter on "Implementation," raises important questions and presents a broader perspective on the subject. He argues that: "While flexible education introduces varieties of time and methods to bring all students to the same end point, traditional education does just the opposite.

There is something disturbing about the idea of all students being the same at the end of an educational experience. Conversely, it can be argued that the identification of a wide range of achievements and achievers through traditional education has served both the students and their professions well." Dr. Morris cautions that: "Educators must be willing to reconcile their views and aspirations with those of the 'real world' where the products of the educational process must ultimately function."

"A Flexible Design for Health Professions Education" presents a balanced and timely discussion about the traditional and experimental approaches being used to educate health professionals.

Staff Review

Radiopharmacy. Edited by MANUEL TUBIS and WALTER WOLF. Wiley, 605 Third Ave., New York, NY 10016, 1976. 911 pp. 16 × 24 cm. Price $44.50.

This book is very pertinent and timely considering the current expansion of radiopharmacy in the curricula of schools of pharmacy both at the undergraduate and graduate levels. The editors themselves have been key figures in the development of radiopharmacy and its establishment in pharmacy education. They are eminent researchers in their own right and have assembled a highly knowledgeable group of contributors to aid them in their presentation of the subject matter. The problems of multiple-author books and variability in style and presentation occur to some extent in this text. For example, the author of Chapter 1 decided that *in vitro* tests would not be considered in the scope of the book from his vantage point, while the editors considered it pertinent and devoted Chapter 26 to a discussion of competitive binding assay procedures. This reviewer considers that the radiopharmacist does need to have an appreciation of such procedures since they will clearly become more important both clinically and industrially.

The structure of the text is orderly in the presentation of material. It is composed of six basic sections dealing with history, physics and instrumentation, biology, chemistry, radiopharmaceutics, and nuclear medicine. The organization is certainly desirable, providing the student with the background material in these various scientific areas that impinge directly on the practice of radiopharmacy. Additionally, there is an important section on regulations and legal aspects in the handling and dispensing of radiopharmaceuticals. Obviously, such information is of importance to the potential practitioner.

There is also a chapter on radionuclides in space biology and medicine by two very knowledgeable individuals. Such material will certainly gain importance with time, but presently its general application is limited and of a highly specialized nature.

In conclusion, this is a most worthwhile and highly informative text and one that will undoubtedly be widely used by those in academia for teaching purposes and by those who wish to familiarize themselves with the exciting opportunities presented by radiopharmacy. Clearly,

this book also will be well used by those engaged in research in which radionuclides are a very important factor.

Reviewed by Albert H. Soloway
College of Pharmacy and Allied Health Professions
Northeastern University
Boston, MA 02115

The Alkaloids. Vol. 6. Edited by M. F. GRUNDON *et al.* The Chemical Society, Burlington House, London W1V 0BN, England, 1976. x + 310 pp. 13.5 × 21.5 cm. Price £19.50.

M. F. Grundon has succeeded J. E. Saxton as senior reporter for the sixth volume of this excellent series on alkaloids. This comprehensive review of the literature published between July 1974 and June 1975 follows the format established by the previous volumes.

Chapter 1 deals with biosynthesis, which continues to be an area of considerable interest. In addition to the work on various alkaloids, many biosynthetic studies are reported on secondary microbial metabolites, including gliotoxin, mycelianamide, demethyltomaymycin, actinomycin, the cytochalasins, mitomycin, rifamycin, penicillins, and prodigiosins.

The ensuing 13 chapters cover the major types of alkaloids grouped by chemical structure: pyrrolidine, piperidine, and pyridine; tropane; pyrrolizidine; indolizidine; quinolizidine; quinoline, quinazoline, and acridone; β-phenethylamine and isoquinoline; aporphinoids; indole; *Lycopodium;* diterpenoid; steroidal alkaloids of the *Apocynaceae, Buxaceae, Asclepidaceae,* and *Salamandra-Phyllobates* groups; and *Solanum* and *Veratrum* steroidal alkaloids. Included in these chapters are discussions on the isolation of new alkaloids, structure determinations, chemical synthesis, miscellaneous general chemical studies, analytical methods, and pharmacological studies, depending on the literature available concerning a particular group of alkaloids during the period reviewed.

The centers of greatest activity remain the indole and isoquinoline alkaloids. Miscellaneous alkaloids, such as the imidazole, peptide, and purine alkaloids, have not been included, with the explanation that they will be covered in Volume 7.

Like its predecessors, Volume 6 is well organized. Each chapter is thorough, yet with the conciseness necessary for such a review. That such a review is available so promptly after the time period covered is a tribute to its contributors. While it is somewhat expensive, this volume is recommended very highly for those who wish to keep up-to-date in the field of alkaloid chemistry.

Reviewed by Susan Tafur
Lilly Research Laboratories
Eli Lilly and Company
Indianapolis, IN 46206

Microbiology–1975. Edited by DAVID SCHLESSINGER. American Society for Microbiology, 1913 I St., N.W., Washington, DC 20006, 1975. vii + 521 pp. 17 × 25 cm. Price $16.00.

This book is a compilation of contributed articles of ASM-sponsored meetings in 1975. The title is misleading, since the book does not deal with topics that follow classical treatment of taxonomic, cultural, and biochemical aspects of microorganisms. The book addresses itself to subject matter areas of methodological and conceptual importance, intended to assist the investigator in the diagnosis and treatment of human diseases. These are provided in the form of "extensive exposures rather than an intensive high-level research." On this premise, a title such as "Recent Advances in Clinical Microbiology" or "Modern Approaches to Clinical Microbiology" or "Selected Topics of Current Interest in Clinical Microbiology" would have been more appropriate.

The book is divided into five sections, each of which is preceded by a short introductory note. Section I, Rapid Diagnostic Techniques in Clinical Microbiology, defines the extent to which new microbiological techniques that give rapid and/or automated results can be applied to clinical microbiology. It provides 14 contributed articles in 97 pages.

Section II, Pathogenic Mechanisms in Bacterial Diseases, discusses current concepts in pathogenesis of microorganisms that cause diseases in humans. It provides 43 contributed articles in 325 pages (about half of the book).

Section III, Mycotoxins, reveals basic interactions and biochemical aspects of mycotoxins in disease processes. It provides five contributed articles in 53 pages.

Section IV, New Vaccines, deals with most recent development and application of specific vaccines and immune serum globulins to the treatment of infections caused by "troublesome" organisms including *Haemophilus influenzae, Neisseria meningitidis,* and *Pseudomonas aeruginosa.* It provides four contributed articles in 17 pages.

Section V, Cell Differentiation and Communication, provides perspectives of morphogenesis in very simple organisms as they pertain to basic problems in developmental biology. It provides 11 contributed articles in 95 pages.

The contributed articles are well written and organized. Many of them show strong interactions between basic and applied concepts of microbiology. With few exceptions, *e.g.,* Considerations in Computer Data Entry by Paul D. Ellner (p. 73) and Polyvalent Vaccine and Human Globulin for Controlling *Pseudomonas aeruginosa* Infections by Mike W. Fisher (p. 416), leading references to original research articles are provided. Each article, however, includes a review, summary, and projections for future work in the specific area.

The book should find an interested audience among graduate students and microbiologists as well as health professionals in related disciplines at universities, hospital laboratories, and industry who may want to follow up on specific subjects.

Reviewed by Sammuel M. Heman-Ackah
Department of Pharmacy
College of Pharmacy and Pharmacal Sciences
Howard University
Washington, DC 20059

Marihuana. Chemistry, Biochemistry and Cellular Effects. Edited by GABRIEL G. NAHAS, WILLIAM D. M. PATON, and JUHANA E. IDÄNPÄÄN-HEIKKILÄ. Springer-Verlag, 175 Fifth Ave., New York, NY 10010, 1976. 556 pp. 16 × 24.5 cm. Price $19.80.

This volume contains the proceedings of a Satellite Symposium on Marihuana held at Matinkylä, Finland, before the Sixth International Congress of Pharmacology in Helsinki, Finland, in the summer of 1975. The conference was held primarily to pursue scientifically the areas of marihuana toxicology developed in 1974 spring hearings before the Senate Internal Security Subcommittee of the Committee on the Judiciary (Eastland Subcommittee). Many of the original government witnesses appeared again (Nahas, Morishima, Stenchever, Heath, and Leuchtenberger), but the meeting really was much broader, attracting 43 papers and more than 126 participants and contributors.

The areas covered include marihuana chemistry, the detection and identification of cannabinoids and their metabolites, kinetics and biotransformation, biochemical and cellular effects in isolated cell systems, neurotransmitter effects, and biochemical effects on organ development. The two largest groups of papers were devoted to the chemistry of detection and metabolism and inhibitory effects in isolated cell systems. Many new hydroxylated side-chain metabolites were reported for the first time (Agurell). Parts of the Greek chronic marihuana smoking study in humans were presented, but the majority of papers dealt with animals as subjects. Unfortunately, the discussion that is much needed to help evaluate these research publications is missing. A subject index is included to aid in rapid location of items of interest. Color plates are used in two hematology papers but not for all pathology.

Dr. W. D. M. Paton's concluding state-of-the-cannabis-art summary is recommended. He successfully perceives the limitations of the neurochemical basis for explaining marihuana action, the need for *in vivo* corroboration of isolated cell system work, and the elegant chemical and biochemical studies that undergird the field.

Reviewed by Edward B. Truitt, Jr.
Northeastern Ohio Universities College of Medicine
Kent, OH 44240

this book also will be well used by those engaged in research in which radionuclides are a very important factor.

Reviewed by Albert H. Soloway
College of Pharmacy and Allied Health Professions
Northeastern University
Boston, MA 02115

The Alkaloids. Vol. 6. Edited by M. F. GRUNDON *et al.* The Chemical Society, Burlington House, London W1V 0BN, England, 1976. x + 310 pp. 13.5 × 21.5 cm. Price £19.50.

M. F. Grundon has succeeded J. E. Saxton as senior reporter for the sixth volume of this excellent series on alkaloids. This comprehensive review of the literature published between July 1974 and June 1975 follows the format established by the previous volumes.

Chapter 1 deals with biosynthesis, which continues to be an area of considerable interest. In addition to the work on various alkaloids, many biosynthetic studies are reported on secondary microbial metabolites, including gliotoxin, mycelianamide, demethyltomaymycin, actinomycin, the cytochalasins, mitomycin, rifamycin, penicillins, and prodigiosins.

The ensuing 13 chapters cover the major types of alkaloids grouped by chemical structure: pyrrolidine, piperidine, and pyridine; tropane; pyrrolizidine; indolizidine; quinolizidine; quinoline, quinazoline, and acridone; β-phenethylamine and isoquinoline; aporphinoids; indole; *Lycopodium;* diterpenoid; steroidal alkaloids of the *Apocynaceae, Buxaceae, Asclepidaceae,* and *Salamandra-Phyllobates* groups; and *Solanum* and *Veratrum* steroidal alkaloids. Included in these chapters are discussions on the isolation of new alkaloids, structure determinations, chemical synthesis, miscellaneous general chemical studies, analytical methods, and pharmacological studies, depending on the literature available concerning a particular group of alkaloids during the period reviewed.

The centers of greatest activity remain the indole and isoquinoline alkaloids. Miscellaneous alkaloids, such as the imidazole, peptide, and purine alkaloids, have not been included, with the explanation that they will be covered in Volume 7.

Like its predecessors, Volume 6 is well organized. Each chapter is thorough, yet with the conciseness necessary for such a review. That such a review is available so promptly after the time period covered is a tribute to its contributors. While it is somewhat expensive, this volume is recommended very highly for those who wish to keep up-to-date in the field of alkaloid chemistry.

Reviewed by Susan Tafur
Lilly Research Laboratories
Eli Lilly and Company
Indianapolis, IN 46206

Microbiology–1975. Edited by DAVID SCHLESSINGER. American Society for Microbiology, 1913 I St., N.W., Washington, DC 20006, 1975. vii + 521 pp. 17 × 25 cm. Price $16.00.

This book is a compilation of contributed articles of ASM-sponsored meetings in 1975. The title is misleading, since the book does not deal with topics that follow classical treatment of taxonomic, cultural, and biochemical aspects of microorganisms. The book addresses itself to subject matter areas of methodological and conceptual importance, intended to assist the investigator in the diagnosis and treatment of human diseases. These are provided in the form of "extensive exposures rather than an intensive high-level research." On this premise, a title such as "Recent Advances in Clinical Microbiology" or "Modern Approaches to Clinical Microbiology" or "Selected Topics of Current Interest in Clinical Microbiology" would have been more appropriate.

The book is divided into five sections, each of which is preceded by a short introductory note. Section I, Rapid Diagnostic Techniques in Clinical Microbiology, defines the extent to which new microbiological techniques that give rapid and/or automated results can be applied to clinical microbiology. It provides 14 contributed articles in 97 pages.

Section II, Pathogenic Mechanisms in Bacterial Diseases, discusses current concepts in pathogenesis of microorganisms that cause diseases in humans. It provides 43 contributed articles in 325 pages (about half of the book).

Section III, Mycotoxins, reveals basic interactions and biochemical aspects of mycotoxins in disease processes. It provides five contributed articles in 53 pages.

Section IV, New Vaccines, deals with most recent development and application of specific vaccines and immune serum globulins to the treatment of infections caused by "troublesome" organisms including *Haemophilus influenzae, Neisseria meningitidis,* and *Pseudomonas aeruginosa.* It provides four contributed articles in 17 pages.

Section V, Cell Differentiation and Communication, provides perspectives of morphogenesis in very simple organisms as they pertain to basic problems in developmental biology. It provides 11 contributed articles in 95 pages.

The contributed articles are well written and organized. Many of them show strong interactions between basic and applied concepts of microbiology. With few exceptions, *e.g.,* Considerations in Computer Data Entry by Paul D. Ellner (p. 73) and Polyvalent Vaccine and Human Globulin for Controlling *Pseudomonas aeruginosa* Infections by Mike W. Fisher (p. 416), leading references to original research articles are provided. Each article, however, includes a review, summary, and projections for future work in the specific area.

The book should find an interested audience among graduate students and microbiologists as well as health professionals in related disciplines at universities, hospital laboratories, and industry who may want to follow up on specific subjects.

Reviewed by Sammuel M. Heman-Ackah
Department of Pharmacy
College of Pharmacy and Pharmacal Sciences
Howard University
Washington, DC 20059

Marihuana. Chemistry, Biochemistry and Cellular Effects. Edited by GABRIEL G. NAHAS, WILLIAM D. M. PATON, and JUHANA E. IDÄNPÄÄN-HEIKKILÄ. Springer-Verlag, 175 Fifth Ave., New York, NY 10010, 1976. 556 pp. 16 × 24.5 cm. Price $19.80.

This volume contains the proceedings of a Satellite Symposium on Marihuana held at Matinkylä, Finland, before the Sixth International Congress of Pharmacology in Helsinki, Finland, in the summer of 1975. The conference was held primarily to pursue scientifically the areas of marihuana toxicology developed in 1974 spring hearings before the Senate Internal Security Subcommittee of the Committee on the Judiciary (Eastland Subcommittee). Many of the original government witnesses appeared again (Nahas, Morishima, Stenchever, Heath, and Leuchtenberger), but the meeting really was much broader, attracting 43 papers and more than 126 participants and contributors.

The areas covered include marihuana chemistry, the detection and identification of cannabinoids and their metabolites, kinetics and biotransformation, biochemical and cellular effects in isolated cell systems, neurotransmitter effects, and biochemical effects on organ development. The two largest groups of papers were devoted to the chemistry of detection and metabolism and inhibitory effects in isolated cell systems. Many new hydroxylated side-chain metabolites were reported for the first time (Agurell). Parts of the Greek chronic marihuana smoking study in humans were presented, but the majority of papers dealt with animals as subjects. Unfortunately, the discussion that is much needed to help evaluate these research publications is missing. A subject index is included to aid in rapid location of items of interest. Color plates are used in two hematology papers but not for all pathology.

Dr. W. D. M. Paton's concluding state-of-the-cannabis-art summary is recommended. He successfully perceives the limitations of the neurochemical basis for explaining marihuana action, the need for *in vivo* corroboration of isolated cell system work, and the elegant chemical and biochemical studies that undergird the field.

Reviewed by Edward B. Truitt, Jr.
Northeastern Ohio Universities College of Medicine
Kent, OH 44240

this book also will be well used by those engaged in research in which radionuclides are a very important factor.

Reviewed by Albert H. Soloway
College of Pharmacy and Allied Health Professions
Northeastern University
Boston, MA 02115

The Alkaloids. Vol. 6. Edited by M. F. GRUNDON *et al.* The Chemical Society, Burlington House, London W1V 0BN, England, 1976. x + 310 pp. 13.5 × 21.5 cm. Price £19.50.

M. F. Grundon has succeeded J. E. Saxton as senior reporter for the sixth volume of this excellent series on alkaloids. This comprehensive review of the literature published between July 1974 and June 1975 follows the format established by the previous volumes.

Chapter 1 deals with biosynthesis, which continues to be an area of considerable interest. In addition to the work on various alkaloids, many biosynthetic studies are reported on secondary microbial metabolites, including gliotoxin, mycelianamide, demethyltomaymycin, actinomycin, the cytochalasins, mitomycin, rifamycin, penicillins, and prodigiosins.

The ensuing 13 chapters cover the major types of alkaloids grouped by chemical structure: pyrrolidine, piperidine, and pyridine; tropane; pyrrolizidine; indolizidine; quinolizidine; quinoline, quinazoline, and acridone; β-phenethylamine and isoquinoline; aporphinoids; indole; *Lycopodium;* diterpenoid; steroidal alkaloids of the *Apocynaceae, Buxaceae, Asclepidaceae,* and *Salamandra-Phyllobates* groups; and *Solanum* and *Veratrum* steroidal alkaloids. Included in these chapters are discussions on the isolation of new alkaloids, structure determinations, chemical synthesis, miscellaneous general chemical studies, analytical methods, and pharmacological studies, depending on the literature available concerning a particular group of alkaloids during the period reviewed.

The centers of greatest activity remain the indole and isoquinoline alkaloids. Miscellaneous alkaloids, such as the imidazole, peptide, and purine alkaloids, have not been included, with the explanation that they will be covered in Volume 7.

Like its predecessors, Volume 6 is well organized. Each chapter is thorough, yet with the conciseness necessary for such a review. That such a review is available so promptly after the time period covered is a tribute to its contributors. While it is somewhat expensive, this volume is recommended very highly for those who wish to keep up-to-date in the field of alkaloid chemistry.

Reviewed by Susan Tafur
Lilly Research Laboratories
Eli Lilly and Company
Indianapolis, IN 46206

Microbiology–1975. Edited by DAVID SCHLESSINGER. American Society for Microbiology, 1913 I St., N.W., Washington, DC 20006, 1975. vii + 521 pp. 17 × 25 cm. Price $16.00.

This book is a compilation of contributed articles of ASM-sponsored meetings in 1975. The title is misleading, since the book does not deal with topics that follow classical treatment of taxonomic, cultural, and biochemical aspects of microorganisms. The book addresses itself to subject matter areas of methodological and conceptual importance, intended to assist the investigator in the diagnosis and treatment of human diseases. These are provided in the form of "extensive exposures rather than an intensive high-level research." On this premise, a title such as "Recent Advances in Clinical Microbiology" or "Modern Approaches to Clinical Microbiology" or "Selected Topics of Current Interest in Clinical Microbiology" would have been more appropriate.

The book is divided into five sections, each of which is preceded by a short introductory note. Section I, Rapid Diagnostic Techniques in Clinical Microbiology, defines the extent to which new microbiological techniques that give rapid and/or automated results can be applied to clinical microbiology. It provides 14 contributed articles in 97 pages.

Section II, Pathogenic Mechanisms in Bacterial Diseases, discusses current concepts in pathogenesis of microorganisms that cause diseases in humans. It provides 43 contributed articles in 325 pages (about half of the book).

Section III, Mycotoxins, reveals basic interactions and biochemical aspects of mycotoxins in disease processes. It provides five contributed articles in 53 pages.

Section IV, New Vaccines, deals with most recent development and application of specific vaccines and immune serum globulins to the treatment of infections caused by "troublesome" organisms including *Haemophilus influenzae, Neisseria meningitidis,* and *Pseudomonas aeruginosa.* It provides four contributed articles in 17 pages.

Section V, Cell Differentiation and Communication, provides perspectives of morphogenesis in very simple organisms as they pertain to basic problems in developmental biology. It provides 11 contributed articles in 95 pages.

The contributed articles are well written and organized. Many of them show strong interactions between basic and applied concepts of microbiology. With few exceptions, *e.g.,* Considerations in Computer Data Entry by Paul D. Ellner (p. 73) and Polyvalent Vaccine and Human Globulin for Controlling *Pseudomonas aeruginosa* Infections by Mike W. Fisher (p. 416), leading references to original research articles are provided. Each article, however, includes a review, summary, and projections for future work in the specific area.

The book should find an interested audience among graduate students and microbiologists as well as health professionals in related disciplines at universities, hospital laboratories, and industry who may want to follow up on specific subjects.

Reviewed by Sammuel M. Heman-Ackah
Department of Pharmacy
College of Pharmacy and Pharmacal Sciences
Howard University
Washington, DC 20059

Marihuana. Chemistry, Biochemistry and Cellular Effects. Edited by GABRIEL G. NAHAS, WILLIAM D. M. PATON, and JUHANA E. IDÄNPÄÄN-HEIKKILÄ. Springer-Verlag, 175 Fifth Ave., New York, NY 10010, 1976. 556 pp. 16 × 24.5 cm. Price $19.80.

This volume contains the proceedings of a Satellite Symposium on Marihuana held at Matinkylä, Finland, before the Sixth International Congress of Pharmacology in Helsinki, Finland, in the summer of 1975. The conference was held primarily to pursue scientifically the areas of marihuana toxicology developed in 1974 spring hearings before the Senate Internal Security Subcommittee of the Committee on the Judiciary (Eastland Subcommittee). Many of the original government witnesses appeared again (Nahas, Morishima, Stenchever, Heath, and Leuchtenberger), but the meeting really was much broader, attracting 43 papers and more than 126 participants and contributors.

The areas covered include marihuana chemistry, the detection and identification of cannabinoids and their metabolites, kinetics and biotransformation, biochemical and cellular effects in isolated cell systems, neurotransmitter effects, and biochemical effects on organ development. The two largest groups of papers were devoted to the chemistry of detection and metabolism and inhibitory effects in isolated cell systems. Many new hydroxylated side-chain metabolites were reported for the first time (Agurell). Parts of the Greek chronic marihuana smoking study in humans were presented, but the majority of papers dealt with animals as subjects. Unfortunately, the discussion that is much needed to help evaluate these research publications is missing. A subject index is included to aid in rapid location of items of interest. Color plates are used in two hematology papers but not for all pathology.

Dr. W. D. M. Paton's concluding state-of-the-cannabis-art summary is recommended. He successfully perceives the limitations of the neurochemical basis for explaining marihuana action, the need for *in vivo* corroboration of isolated cell system work, and the elegant chemical and biochemical studies that undergird the field.

Reviewed by Edward B. Truitt, Jr.
Northeastern Ohio Universities College of Medicine
Kent, OH 44240

this book also will be well used by those engaged in research in which radionuclides are a very important factor.

Reviewed by Albert H. Soloway
College of Pharmacy and Allied Health Professions
Northeastern University
Boston, MA 02115

The Alkaloids. Vol. 6. Edited by M. F. GRUNDON *et al.* The Chemical Society, Burlington House, London W1V 0BN, England, 1976. x + 310 pp. 13.5 × 21.5 cm. Price £19.50.

M. F. Grundon has succeeded J. E. Saxton as senior reporter for the sixth volume of this excellent series on alkaloids. This comprehensive review of the literature published between July 1974 and June 1975 follows the format established by the previous volumes.

Chapter 1 deals with biosynthesis, which continues to be an area of considerable interest. In addition to the work on various alkaloids, many biosynthetic studies are reported on secondary microbial metabolites, including gliotoxin, mycelianamide, demethyltomaymycin, actinomycin, the cytochalasins, mitomycin, rifamycin, penicillins, and prodigiosins.

The ensuing 13 chapters cover the major types of alkaloids grouped by chemical structure: pyrrolidine, piperidine, and pyridine; tropane; pyrrolizidine; indolizidine; quinolizidine; quinoline, quinazoline, and acridone; β-phenethylamine and isoquinoline; aporphinoids; indole; *Lycopodium;* diterpenoid; steroidal alkaloids of the *Apocynaceae, Buxaceae, Asclepidaceae,* and *Salamandra-Phyllobates* groups; and *Solanum* and *Veratrum* steroidal alkaloids. Included in these chapters are discussions on the isolation of new alkaloids, structure determinations, chemical synthesis, miscellaneous general chemical studies, analytical methods, and pharmacological studies, depending on the literature available concerning a particular group of alkaloids during the period reviewed.

The centers of greatest activity remain the indole and isoquinoline alkaloids. Miscellaneous alkaloids, such as the imidazole, peptide, and purine alkaloids, have not been included, with the explanation that they will be covered in Volume 7.

Like its predecessors, Volume 6 is well organized. Each chapter is thorough, yet with the conciseness necessary for such a review. That such a review is available so promptly after the time period covered is a tribute to its contributors. While it is somewhat expensive, this volume is recommended very highly for those who wish to keep up-to-date in the field of alkaloid chemistry.

Reviewed by Susan Tafur
Lilly Research Laboratories
Eli Lilly and Company
Indianapolis, IN 46206

Microbiology–1975. Edited by DAVID SCHLESSINGER. American Society for Microbiology, 1913 I St., N.W., Washington, DC 20006, 1975. vii + 521 pp. 17 × 25 cm. Price $16.00.

This book is a compilation of contributed articles of ASM-sponsored meetings in 1975. The title is misleading, since the book does not deal with topics that follow classical treatment of taxonomic, cultural, and biochemical aspects of microorganisms. The book addresses itself to subject matter areas of methodological and conceptual importance, intended to assist the investigator in the diagnosis and treatment of human diseases. These are provided in the form of "extensive exposures rather than an intensive high-level research." On this premise, a title such as "Recent Advances in Clinical Microbiology" or "Modern Approaches to Clinical Microbiology" or "Selected Topics of Current Interest in Clinical Microbiology" would have been more appropriate.

The book is divided into five sections, each of which is preceded by a short introductory note. Section I, Rapid Diagnostic Techniques in Clinical Microbiology, defines the extent to which new microbiological techniques that give rapid and/or automated results can be applied to clinical microbiology. It provides 14 contributed articles in 97 pages.

Section II, Pathogenic Mechanisms in Bacterial Diseases, discusses current concepts in pathogenesis of microorganisms that cause diseases in humans. It provides 43 contributed articles in 325 pages (about half of the book).

Section III, Mycotoxins, reveals basic interactions and biochemical aspects of mycotoxins in disease processes. It provides five contributed articles in 53 pages.

Section IV, New Vaccines, deals with most recent development and application of specific vaccines and immune serum globulins to the treatment of infections caused by "troublesome" organisms including *Haemophilus influenzae, Neisseria meningitidis,* and *Pseudomonas aeruginosa.* It provides four contributed articles in 17 pages.

Section V, Cell Differentiation and Communication, provides perspectives of morphogenesis in very simple organisms as they pertain to basic problems in developmental biology. It provides 11 contributed articles in 95 pages.

The contributed articles are well written and organized. Many of them show strong interactions between basic and applied concepts of microbiology. With few exceptions, *e.g.,* Considerations in Computer Data Entry by Paul D. Ellner (p. 73) and Polyvalent Vaccine and Human Globulin for Controlling *Pseudomonas aeruginosa* Infections by Mike W. Fisher (p. 416), leading references to original research articles are provided. Each article, however, includes a review, summary, and projections for future work in the specific area.

The book should find an interested audience among graduate students and microbiologists as well as health professionals in related disciplines at universities, hospital laboratories, and industry who may want to follow up on specific subjects.

Reviewed by Sammuel M. Heman-Ackah
Department of Pharmacy
College of Pharmacy and Pharmacal Sciences
Howard University
Washington, DC 20059

Marihuana. Chemistry, Biochemistry and Cellular Effects. Edited by GABRIEL G. NAHAS, WILLIAM D. M. PATON, and JUHANA E. IDÄNPÄÄN-HEIKKILÄ. Springer-Verlag, 175 Fifth Ave., New York, NY 10010, 1976. 556 pp. 16 × 24.5 cm. Price $19.80.

This volume contains the proceedings of a Satellite Symposium on Marihuana held at Matinkylä, Finland, before the Sixth International Congress of Pharmacology in Helsinki, Finland, in the summer of 1975. The conference was held primarily to pursue scientifically the areas of marihuana toxicology developed in 1974 spring hearings before the Senate Internal Security Subcommittee of the Committee on the Judiciary (Eastland Subcommittee). Many of the original government witnesses appeared again (Nahas, Morishima, Stenchever, Heath, and Leuchtenberger), but the meeting really was much broader, attracting 43 papers and more than 126 participants and contributors.

The areas covered include marihuana chemistry, the detection and identification of cannabinoids and their metabolites, kinetics and biotransformation, biochemical and cellular effects in isolated cell systems, neurotransmitter effects, and biochemical effects on organ development. The two largest groups of papers were devoted to the chemistry of detection and metabolism and inhibitory effects in isolated cell systems. Many new hydroxylated side-chain metabolites were reported for the first time (Agurell). Parts of the Greek chronic marihuana smoking study in humans were presented, but the majority of papers dealt with animals as subjects. Unfortunately, the discussion that is much needed to help evaluate these research publications is missing. A subject index is included to aid in rapid location of items of interest. Color plates are used in two hematology papers but not for all pathology.

Dr. W. D. M. Paton's concluding state-of-the-cannabis-art summary is recommended. He successfully perceives the limitations of the neurochemical basis for explaining marihuana action, the need for *in vivo* corroboration of isolated cell system work, and the elegant chemical and biochemical studies that undergird the field.

Reviewed by Edward B. Truitt, Jr.
Northeastern Ohio Universities College of Medicine
Kent, OH 44240

Journal of Pharmaceutical Sciences

APRIL 1977

VOLUME 66 NUMBER 4

MARY H. FERGUSON
Editor

L. LUAN CORRIGAN
Assistant Editor

SHELLY ELLIOTT
Production Editor

JANET D. SHOFF
Copy Editor

EDWARD G. FELDMANN
Contributing Editor

SAMUEL W. GOLDSTEIN
Contributing Editor

LELAND J. ARNEY
Director of Publications

EDITORIAL ADVISORY BOARD

JOHN AUTIAN
NORMAN R. FARNSWORTH
WILLIAM O. FOYE
WILLIAM J. JUSKO
HARRY B. KOSTENBAUDER
HERBERT A. LIEBERMAN
DAVID E. MANN, JR.
GERALD J. PAPARIELLO

The *Journal of Pharmaceutical Sciences* is published monthly by the American Pharmaceutical Association at 2215 Constitution Ave., N.W., Washington, DC 20037. Second-class postage paid at Washington, D.C., and at additional mailing office.

All expressions of opinion and statements of supposed fact appearing in articles or editorials carried in this journal are published on the authority of the writer over whose name they appear and are not to be regarded as necessarily expressing the policies or views of the American Pharmaceutical Association.

Offices—Editorial, Advertising, and Subscription Offices: 2215 Constitution Ave., N.W., Washington, DC 20037. Printing Offices: 20th & Northampton Streets, Easton, PA 18042.

Annual Subscriptions—United States and foreign, industrial and government institutions $50, educational institutions $50, individuals *for personal use only* $30; single copies $5. All foreign subscriptions add $5 for postage. Subscription rates are subject to change without notice. Members of the American Pharmaceutical Association may elect to receive the *Journal of Pharmaceutical Sciences* as a part of their annual $60 (foreign $65) APhA membership dues.

Claims—Missing numbers will not be supplied if dues or subscriptions are in arrears for more than 60 days or if claims are received more than 60 days after the date of the issue, or if loss was due to failure to give notice of change of address. The Association cannot accept responsibility for foreign delivery when its records indicate shipment has been made.

Change of Address—Members and subscribers should notify at once both the Post Office and the American Pharmaceutical Association, 2215 Constitution Ave., N.W., Washington, DC 20037, of any change of address.

© Copyright 1977, American Pharmaceutical Association, 2215 Constitution Ave., N.W., Washington, DC 20037; all rights reserved.

"ZERO-BASED" DRUG STANDARDS

President Carter has introduced the management approach of "zero-based budgeting" in reviewing federal programs and their financing. Indeed, so much has been said and written about this concept in recent months that few of our readers are probably unfamiliar with the term and its meaning. However, a brief explanation may be useful.

Basically, in contrast to taking last year's projects and programs and simply adding to them by way of staff, budget, and so on, zero-based budget calls for a complete reassessment of each such project or program to determine if the activity itself, as well as all of its components, can be currently justified. The premise is that there is a natural tendency for activities to be initiated which in time come to outlive their usefulness, in part or in whole. In the absence of any positive step to reassess their function and value by today's perspective, they drone on indefinitely.

The thought has long been with us that some such comprehensive reassessment would be highly desirable with respect to drug standards and specifications—particularly those appearing in the official compendia. Frequently, additions or revisions are made to *United States Pharmacopeia* or *National Formulary* monographs which interrelate with other elements within the compendia.

Those responsible for the compendial revision programs generally have done a good job of making whatever modifications were necessary to avoid any outright discrepancies or contradictions. However, in the absence of a "start from scratch" review, any process that introduces changes or new material in a piecemeal fashion will result in a patchwork product to some degree.

An example or two might help to explain both what we have in mind as well as how it happens to come about.

Effective April 1 of this year, a new standard requires that certain drugs be packaged in containers meeting specified criteria of "tightness." This significant advance now provides the compendia with objective procedures to test the tightness of containers and to specify well-defined limits of performance that the containers must meet. The drugs involved are all those whose individual monographs specifically include provision for such packaging. And, a review of the USP and NF reveals that a substantial number of monographs do call for use of either "well-closed" or "tight" containers.

However, such provisions were placed in most, if not all, of these drug monographs at a time when there was no real method for evaluating container tightness. Hence, the standard was more qualitative than quantitative.

The question now arises as to whether all drugs, for which there is a tightness requirement in the pertinent monographs, actually need this degree of protection now that we have defined it and have established methodology for its determination.

Compendia officials are well aware of this situation, but there is only one way that it can be rectified. That would require a drug-by-drug, monograph-by-monograph review, complete with stability data and the like, in order to conclude that the requirement may safely be deleted from certain monographs. But this review would necessitate considerable time and effort just to "clean up" the subject; that is, there is no risk or hazard with the present situation—it simply is one that, on purely scientific grounds, probably could not be justified as necessary to the extent that it applies.

Drug identification tests are another illustration of this problem. For many years, simple qualitative tests were included in compendia monographs to confirm the identity of a specimen. For example, such a test might describe a certain color change in a solution of the sample upon addition of a certain reagent.

With the introduction and wide application of infrared spectrophotometry—especially in conjunction with a reference standard—these antiquated spot tests and color tests became superfluous in the extreme. Yet they often were not deleted because certain parties—due to limitations in available equipment or misguided nostalgia—argued for their retention.

Again, there is nothing wrong *per se* with their continued presence. However, they have outlived their usefulness and they add a lot of undesirable "clutter" to what should be a concise set of drug standards.

All of these defects could be remedied by a start from scratch review of the entire USP and NF content. In line with President Carter's approach to budget development, it appears timely to consider a zero-based review of the compendial standards, with a goal of streamlining the monographs, eliminating duplication, correcting inconsistencies, and achieving uniformity of treatment.

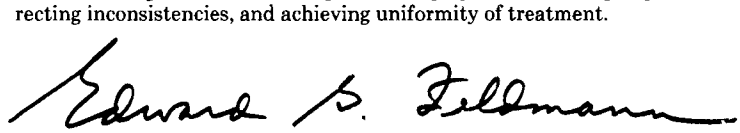

Journal of Pharmaceutical Sciences

MAY 1977

VOLUME 66 NUMBER 5

MARY H. FERGUSON
Editor

L. LUAN CORRIGAN
Assistant Editor

SHELLY ELLIOTT
Production Editor

JANET D. SHOFF
Copy Editor

EDWARD G. FELDMANN
Contributing Editor

SAMUEL W. GOLDSTEIN
Contributing Editor

EDITORIAL ADVISORY BOARD

JOHN AUTIAN	HARRY B. KOSTENBAUDER
NORMAN R. FARNSWORTH	HERBERT A. LIEBERMAN
WILLIAM O. FOYE	DAVID E. MANN, JR.
WILLIAM J. JUSKO	GERALD J. PAPARIELLO

The *Journal of Pharmaceutical Sciences* is published monthly by the American Pharmaceutical Association at 2215 Constitution Ave., N.W., Washington, DC 20037. Second-class postage paid at Washington, D.C., and at additional mailing office.

All expressions of opinion and statements of supposed fact appearing in articles or editorials carried in this journal are published on the authority of the writer over whose name they appear and are not to be regarded as necessarily expressing the policies or views of the American Pharmaceutical Association.

Offices—Editorial, Advertising, and Subscription Offices: 2215 Constitution Ave., N.W., Washington, DC 20037. Printing Offices: 20th & Northampton Streets, Easton, PA 18042.

Annual Subscriptions—United States and foreign, industrial and government institutions $50, educational institutions $50, individuals *for personal use only* $30; single copies $5. All foreign subscriptions add $5 for postage. Subscription rates are subject to change without notice. Members of the American Pharmaceutical Association may elect to receive the *Journal of Pharmaceutical Sciences* as a part of their annual $60 (foreign $65) APhA membership dues.

Claims—Missing numbers will not be supplied if dues or subscriptions are in arrears for more than 60 days or if claims are received more than 60 days after the date of the issue, or if loss was due to failure to give notice of change of address. The Association cannot accept responsibility for foreign delivery when its records indicate shipment has been made.

Change of Address—Members and subscribers should notify at once both the Post Office and the American Pharmaceutical Association, 2215 Constitution Ave., N.W., Washington, DC 20037, of any change of address.

© Copyright 1977, American Pharmaceutical Association, 2215 Constitution Ave., N.W., Washington, DC 20037; all rights reserved.

IMPEDING METRIC CONVERSION

For many years, this writer had served as a self-styled good will ambassador for the metric system. Whenever the subject happened to be discussed with family, friends, or professional acquaintances, we always talked up the merits of the system and the desirability of the United States converting *in toto* to its use.

Moreover, we felt very comfortable in doing so. The metric system is "the system" of the physical and biological sciences; it is "the system" of pharmacy; it is officially endorsed as "the system" by the American Pharmaceutical Association. Hence, by training, background, career, and affiliation, we were in concert with the metric theme. Indeed, we even had several occasions to participate as a witness in presenting testimony before U.S. Congressional committees which were hearing bills dealing with national conversion to the metric system.

On all these occasions, we have repeated what so many others have said in arguing the merits of such conversion; namely, we would be adopting a pure, uniform, and simple system which can be easily learned and, once learned, will remain unchanged forever.

But then some unsettling things began to happen. The first hint that all may not be quite as rosy as we thought was when the controversy arose over whether the preferred unit of volume was a "cubic centimeter" (cc) or a "milliliter" (ml). After what seemed to be a good deal of haggling, this was eventually settled with the result that much revising was necessary in style books, in texts, in calibrations on laboratory equipment, and in the labeling on numerous containers, particularly those of chemicals and drugs.

Then one day the local weather report began to give temperatures in terms of degrees celsius rather than the familiar degrees centigrade. And when we could not immediately explain the difference to our children, we suffered both embarrassment as well as a blow to our personal credibility.

We hardly had time to track this one down when we learned that the presses must be halted for our publications in order that the typesetters could scurry about changing all the "microns" to "micrometers" and the "millimicrons" to "nanometers"—along with corresponding changes in the symbols and abbreviations used in their stead.

What was happening? Why were these and other changes like them being made? Was no one else distressed and disturbed by what to us appeared to be a series of confusing, pointless, and disturbing disruptions?

Well, in the letters column of a recent issue of the American Chemical Society's publication, *Chemical and Engineering News*, we learned that there is at least one fellow sufferer. Dean W. Gibbons of Detroit wrote about his experience trying to keep up with such changes as those mentioned above, as well as a number of others including "torr" to honor Torricelli, the inventor of the barometer, and "kilopascals," presumably in honor of Pascal and his law of the pressure-volume relationship.

"There are better ways to honor our scientific forefathers than to rename familiar metric units," writes Gibbons. And he goes on to add: *"Public acceptance of the metric system will depend on whether the system is perceived as simple and logical, or regarded as a jumble of confusion. The use of long-established, descriptive units, instead of the latest fads, will aid the transition from the English to the metric system."*

His point is both well taken and well stated. Hopefully, the scientific community is more stable and sedate than the local town officials who will rename Main Street at the drop of a hat to honor—for political reasons—some celebrity or other public figure who is currently in the news.

Those of us who deal with measurement terms and their symbols on a daily basis have difficulty enough remembering which is what, and which is correct. For the general public to cope with such changes is simply asking too much. We hope that the scientists responsible for initiating such changes will recognize that they are doing a real disservice by needlessly impeding the process of metric conversion.

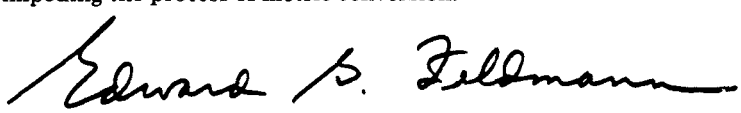

Journal of Pharmaceutical Sciences

MAY 1977
VOLUME 66 NUMBER 5

RESEARCH ARTICLES

GI Motor Inhibition Associated with Acute Exposure to Methyl Methacrylate Vapor

MARTIN F. TANSY ˣ, JOHN S. MARTIN, SEROUYA BENHAIM, WENDELL E. LANDIN, and FRANK M. KENDALL

Abstract □ A mixture of monomeric methyl methacrylate vapor in air was delivered into the breathing air of chloralose–urethan anesthetized dogs. Fixed length exposures to 2000-ppm doses of the vapor resulted in a transient drop in arterial blood pressure and a marked inhibition of ongoing GI motor activities. Motor inhibition always continued for a variable time (~10–15 min) subsequent to the cessation of methyl methacrylate vapor administration. This inhibitory response was not blocked by bilateral vagotomy, spinal transection, splanchnectomy, or the intravenous administration of tetraethylammonium chloride. Another series of experiments determined that the administration of blood from a dog receiving methyl methacrylate vapor produced GI motor inhibition in another dog not connected to the experimental gas mixture. Therefore, it is concluded that, aside from any reflex effects produced, methyl methacrylate vapor in sufficient concentration probably exerts a direct inhibitory effect upon GI smooth muscle that is mediated by the cardiopulmonary systems.

Keyphrases □ Methyl methacrylate monomeric vapor—pulmonary exposure, effects on GI motor activities, dogs □ GI motor activities—effect of pulmonary exposure to monomeric methyl methacrylate vapor, dogs □ Toxicity—monomeric methyl methacrylate vapor, pulmonary exposure, effects on GI motor activities, dogs

Published experiments (1) from this laboratory previously demonstrated that short exposures of conscious rats to relatively high concentrations of methyl methacrylate vapor in air were associated with rapid declines in the amplitudes of gastric pressure events. These pressure events gradually reestablished normal patterns within 4 min of cessation of methyl methacrylate vapor exposures for 5–10 min. A similar observation was made with a single human subject during an exposure comparable to that received occupationally (1).

The second objective of these acute motility experiments (1) was to determine a possible reflex mechanism that could reasonably be inferred to mediate the inhibition of gastric motor activity associated with the acute exposure of the rat to methyl methacrylate vapor. However, the results were equivocal because cervical vagotomy does not define a reflex originating in the pulmonary apparatus having its afferent and efferent limbs in the vagus and subdiaphragmatic vagotomy cannot be performed as surely in the rat. For this surgical reason, the chloralose–urethan anesthetized dog was employed as the experimental animal after satisfying the requirement that a similar inhibitory response can be produced. Therefore, the experimental observations were extended to another species.

EXPERIMENTAL

Animals and General Procedure—Twelve adult mongrel dogs of both sexes were equilibrated for at least 3 days in the local animal facility prior to use. All experiments were undertaken after the animals had been fasted overnight but with water allowed *ad libitum*. All dogs were individually titrated to a surgical plane of anesthesia by the intravenous administration of a mixture of α-chloralose (5%, dissolved in polyethylene glycol 200) and urethan (50% in 0.9% saline). Further injections of the chloralose–urethan mixture were given when necessary.

Surgical and Recording Procedures—The femoral artery was cannulated to permit the continuous measurement of systemic blood pressure, and the ipsilateral vein was cannulated to permit administration of tetraethylammonium chloride[1] and fluids. Each animal was tracheostomized to permit monitoring of respiration, artificial respiration, and administration of methyl methacrylate vapor. On occasion, a pneumograph was used to record respiratory movements.

A midline laparotomy was then performed. Recording balloons were inserted *via* the oral route for gastric recording and retrograde *via* a stab wound in the ileum for small intestinal recording. Polygraphic control tracings were obtained before and at stated intervals after the physical and chemical stimulatory procedures in each group of dogs. In all in-

[1] Etamon, Parke, Davis.

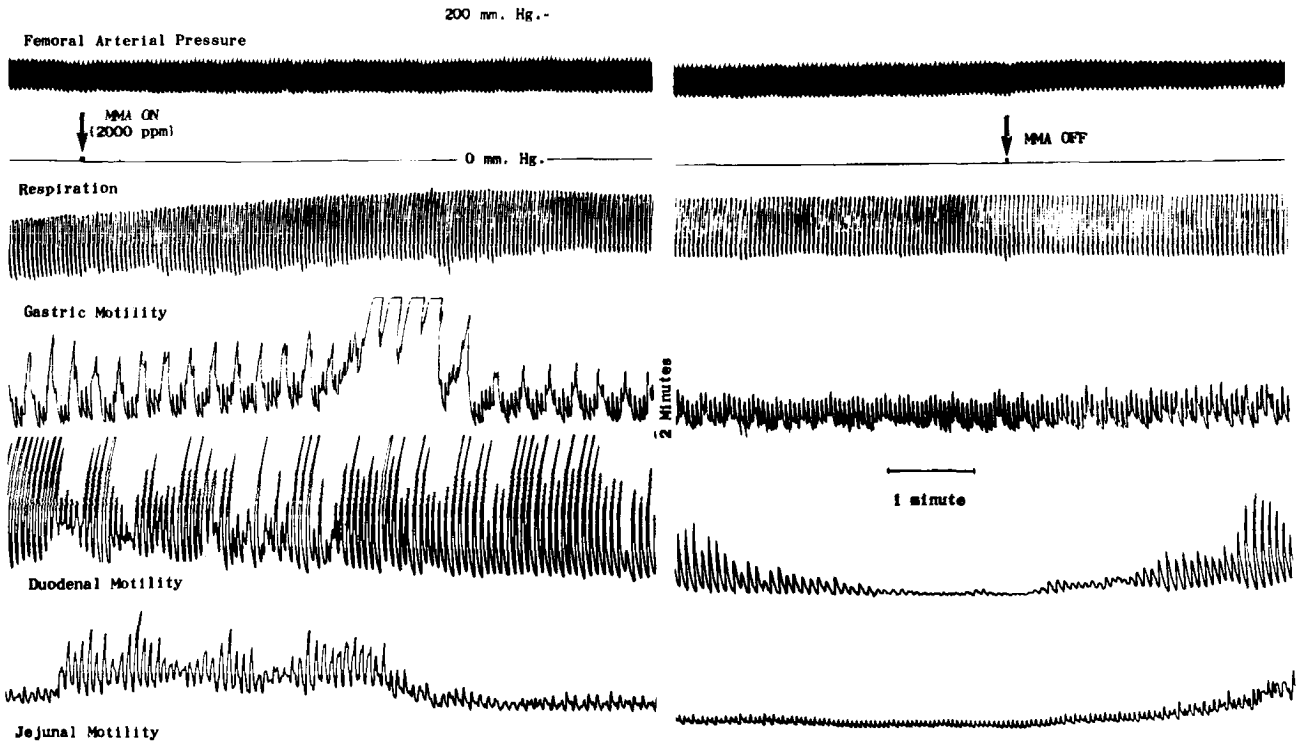

Figure 1—*Polygram of physiological parameters observed during the acute exposure of a chloralose–urethan anesthetized dog to methyl methacrylate (MMA) vapor at 2000 ppm in air. A slight, transient decline in arterial blood pressure was observed. Respiratory rate and relative tidal volume (as measured by a pneumograph) were substantially unchanged. Gastric pressure indications suggest an initial augmentation of active contractile activity followed by a decline in the active component with little effect upon tonus. Duodenal motor activity suggests a drastic decline in active contractile activity as well as a reduction in tonus. The jejunum fortuitously began a bout of contractile activity just before the exposure commenced. Both the active and tonus components of this activity were inhibited during exposure.*

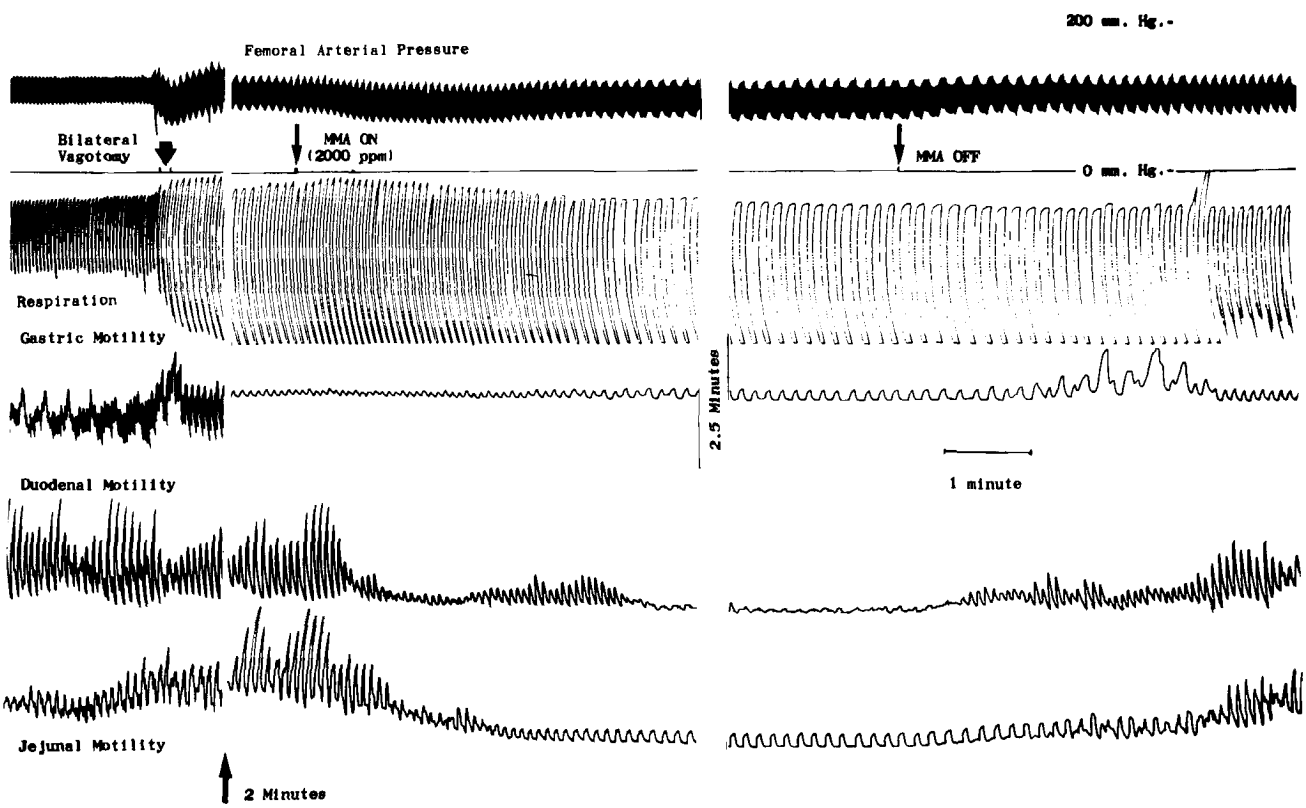

Figure 2—*Continuation of the experiment depicted in Fig. 1. Both vagi were severed, and the gas exposure was repeated. Gastric, duodenal, and jejunal motor activities continued to be inhibited during exposure. The transient depression in arterial blood pressure was more evident in magnitude and duration during the exposure to 2000 ppm of methyl methacrylate (MMA) vapor in air.*

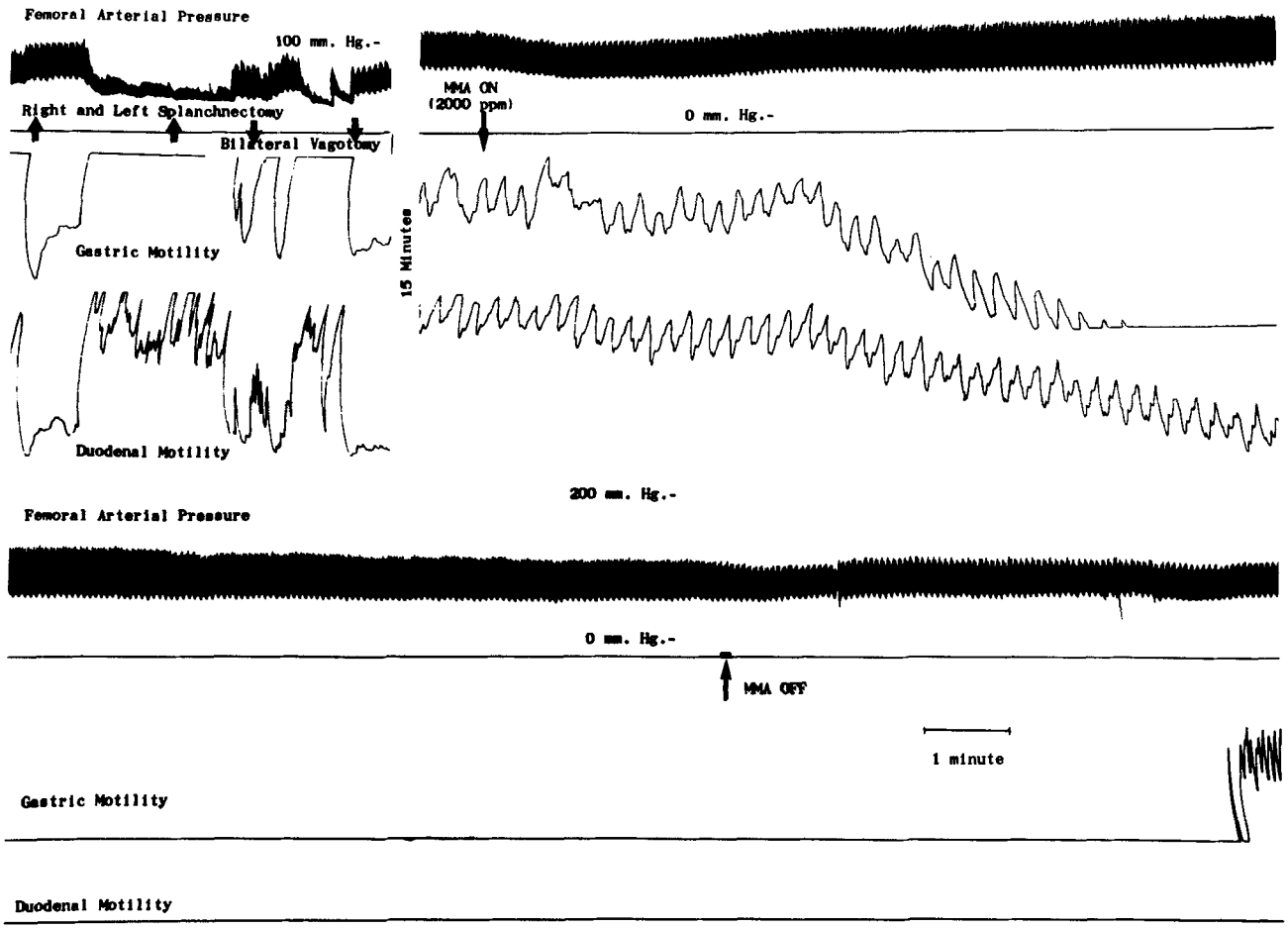

Figure 3—*Effects of acute exposure to 2000 ppm of methyl methacrylate (MMA) vapor in air following bilateral vagotomy and splanchnectomy (top panel) in a chloralose–urethan anesthetized dog. The active and tonus components of gastric and duodenal motor activities were severely inhibited (top of lower panels). Arterial blood pressure was transiently affected.*

stances, the designation of intestinal pressure records as signifying a particular type of motility response is justified on the basis of a visual observation that such a response occurred concurrently with the recorded pressure events.

Vapor Administration and Analyses—The methyl methacrylate monomer[2] used contained 10 ppm of the monoethyl ether of hydroquinone as an inhibitor. During all methyl methacrylate vapor administrations, the dogs were ventilated at a fixed minute volume of 4–6 liters. Pilot experiments were performed to determine empirically a rate of methyl methacrylate vapor introduction that would consistently produce the motor effects desired. Once this rate was determined, samples of the resulting gas mixture were analyzed by GLC[3] and the average measured concentration was assumed to be constant throughout the balance of the experiments. In view of the minute volume, it was assumed that the methyl methacrylate vapor rapidly disappeared from the respirator system when the supply of methyl methacrylate vapor was turned off.

RESULTS AND DISCUSSION

For all practical purposes, each animal was used for at least one control run prior to the performance of any procedure not already outlined. Figure 1 represents a typical polygram produced by such a run. Gastric antral pressure amplitudes became depressed during exposure. In all cases, a transient but vigorous bout of gastric contraction appeared shortly after the first introduction of methyl methacrylate vapor. This effect never occurred more than once. Gastric antral pressure activity became depressed during exposure and gradually approached control values after cessation of exposure. Small intestinal pressure amplitudes also were depressed.

The rate of onset of inhibition was not apparently a necessary function of the observed organs. In this polygram, it can be seen that the duodenum exhibited a higher degree of contractile activity during the control period. In this case, degradation of duodenal activity followed a longer time course than that of jejunum activity, which became quiescent much sooner. The latency of the inhibitory response was generally proportional to the degree of pressure activity produced by the organ prior to administration of methyl methacrylate vapor.

Figure 2 shows the responses of the previous animal to methyl methacrylate vapor following subdiaphragmatic vagotomy. A short administration of methyl methacrylate vapor quickly reduced intestinal pressure activity, which remained depressed for the duration of the exposure. In this particular experiment, the motor activity of the gastric antrum had not recovered from the transient effects of vagotomy by the time that this exposure was performed. In this record, only the onset of the return of antral motor activity is apparent. Subsequently, this activity returned and was inhibited by further methyl methacrylate exposures. There appeared to be a transient fall in arterial blood pressure in the vagotomized animal following the start of methyl methacrylate vapor administration.

Figure 3 depicts polygrams obtained from a mechanically ventilated, splanchnectomized, vagectomized dog anesthetized with chloralose–urethan. These recordings depict the time course of arterial blood pressure and gastric and duodenal motor activities. The left portion of the top panel shows the artifacts produced by sectioning of the splanchnic nerves and vagi. Methyl methacrylate vapor was introduced into the air supply, and motor activities were abruptly reduced, primarily in terms of loss of tonus. Contractile events were not seen because the pens bottomed in the channel stops. Within 7–8 min after cessation of exposure, gastric tone abruptly reappeared.

The polygrams shown in Fig. 4 were obtained as a continuation of the

[2] Rohm and Haas.

[3] The column was 1.5-m × 0.3-cm (5-ft × 0.125-in.) o.d. stainless steel, packed with 20% Carbowax 20M, coated onto 80–100-mesh Chromosorb W. The chromatographic conditions were: column oven (starting) temperature, 100°; injection port temperature, 200°; detector temperature, 200°; helium pressure, 68 psi; helium flow, 30 ml/min; hydrogen pressure, 20 psi; air pressure, 20 psi; attenuation, 32×10^{-11}; recorder sensitivity, 1 mv; and sample size, 1 ml.

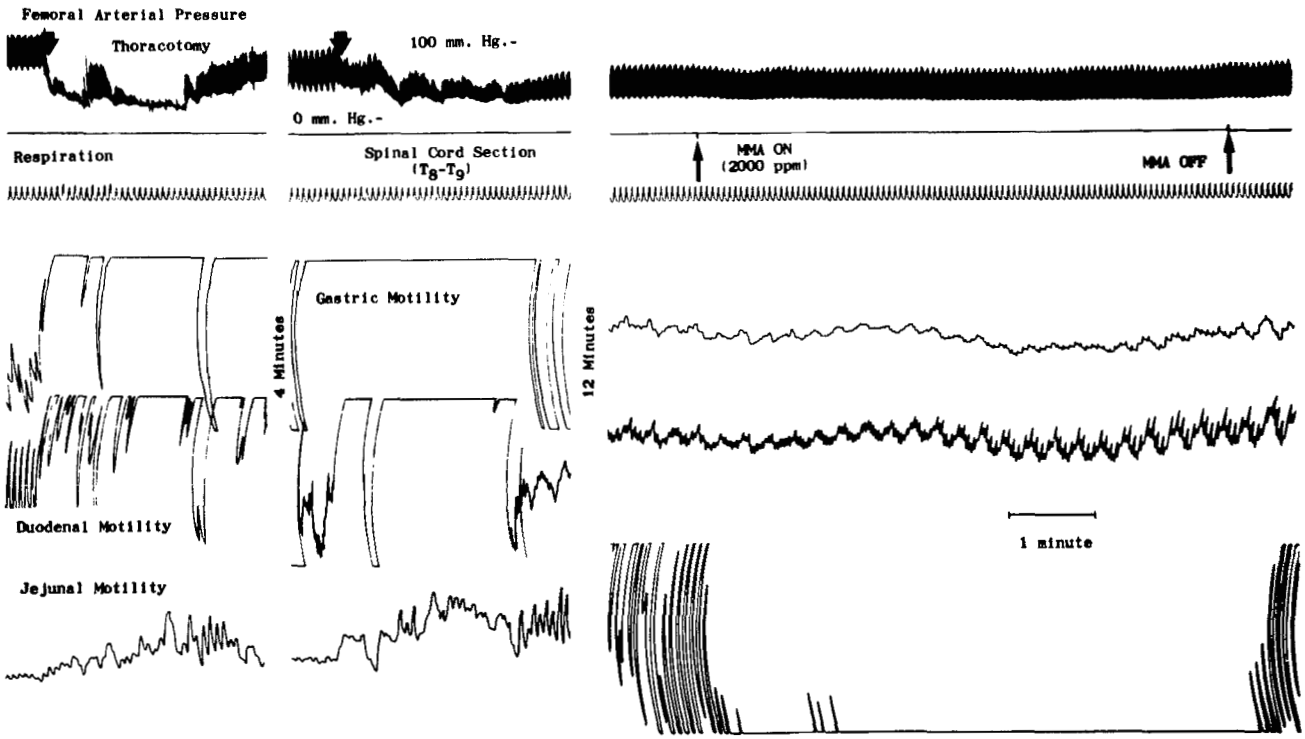

Figure 4—*Continuation of the experiment depicted in Fig. 3. Following recovery from the previous exposure, the dog was ventilated mechanically, a thoracotomy was performed, and the spinal cord was severed at the T_8–T_9 level. Tonus components of gastric and duodenal motor activities were slightly depressed. No remarkable changes in active contractile activity were apparent, because there was very little in evidence at the start of exposure. In contrast, the high amplitude jejunal activity present was abruptly abolished and spontaneously restored at the cessation of vapor exposure. A slight depressor effect on arterial blood pressure was seen.*

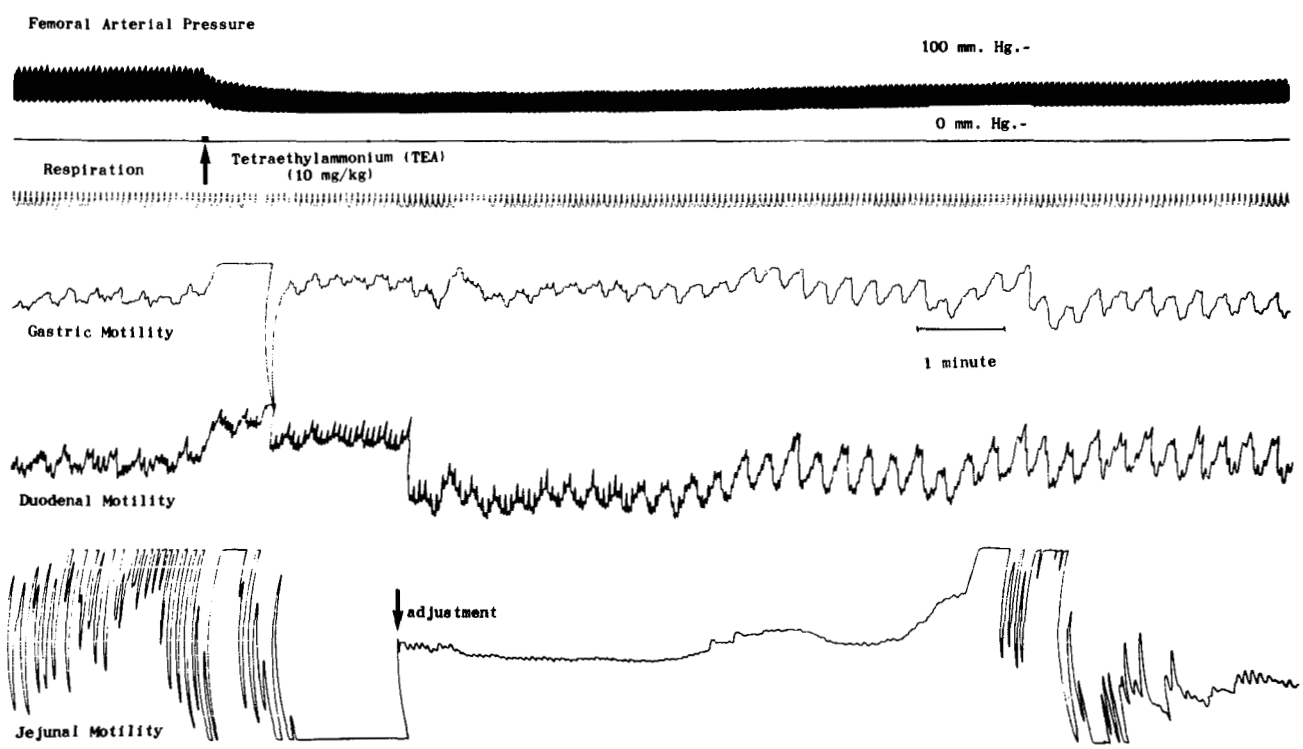

Figure 5—*Continuation of the experiment depicted in Figs. 3 and 4 following recovery from the previous exposure with a dog that has been bilaterally vagotomized, splanchnectomized, and spinally transected. Administration of the ganglionic blocking agent tetraethylammonium chloride (10 mg/kg) was associated with a decline in arterial mean and pulse pressures, a transient decline in duodenal active and tonus contractile components, and little effect upon gastric pressure activity. Jejunal contractile activity was inhibited. The baseline for jejunal pressure activity was reset to determine the effects of tetraethylammonium chloride on the active component.*

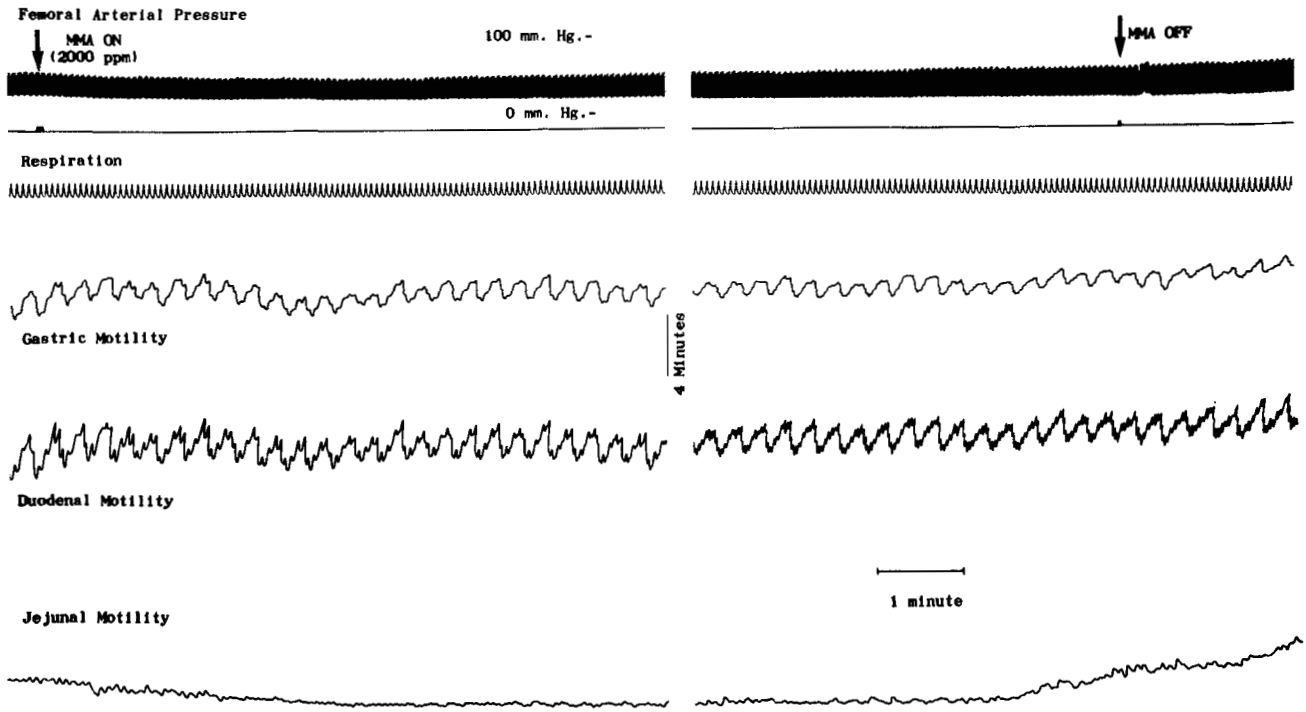

Figure 6—*Continuation of the experiment depicted in Figs. 3–5 following a recovery period from the previous procedures. At this point, reexposure to 2000 ppm of methyl methacrylate (MMA) vapor in air resulted in a slight decline in mean arterial blood pressure and a definite reduction in jejunal tonus.*

observations made during the experiment depicted in Fig. 3. In this record, relative respiratory motion and jejunal motor activities are included. The left and center panels depict the artifacts produced by retraction of the open chest and transection of the spinal cord between T_8 and T_9. During methyl methacrylate administration, gastric antral and duodenal motor activities were only slightly affected but jejunal tonus was drastically reduced.

Further observations were then conducted utilizing the by now surgically denervated viscera. The polygram in Fig. 5 shows the observed effects of tetraethylammonium chloride administration, which produced

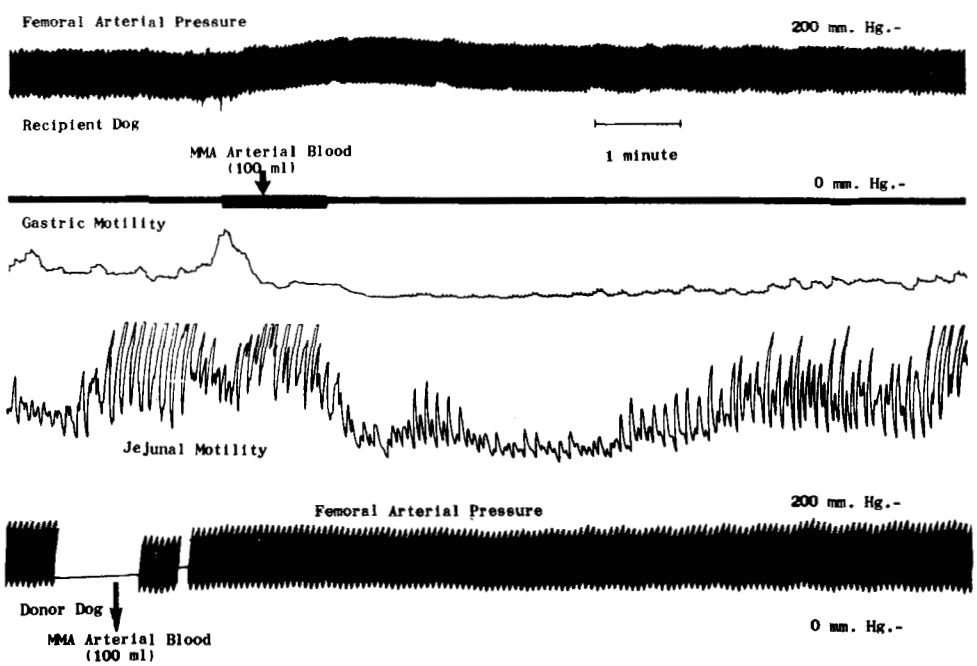

Figure 7—*Parallel polygrams obtained from chloralose–urethan anesthetized dogs. The donor dog (lower trace) was continuously exposed to 2000 ppm of methyl methacrylate (MMA) vapor in air for about 1 hr before these records were made. Arterial blood (100 ml) was obtained from the arterial pressure cannula of the exposed dog and rapidly infused into the femoral vein of the unexposed recipient dog (top traces). Gastric tonus of the recipient was depressed, but no inference can be drawn concerning an effect upon the active component of gastric activity which was not present at this time. The active and tonic components of jejunal activity were both depressed transiently in the recipient. The increase in mean arterial blood pressure of the recipient was most likely due to the hypervolemia produced by the infusion of 100 ml of whole blood, which would tend to obscure any transient decline due to the methyl methacrylate content of the donor blood.*

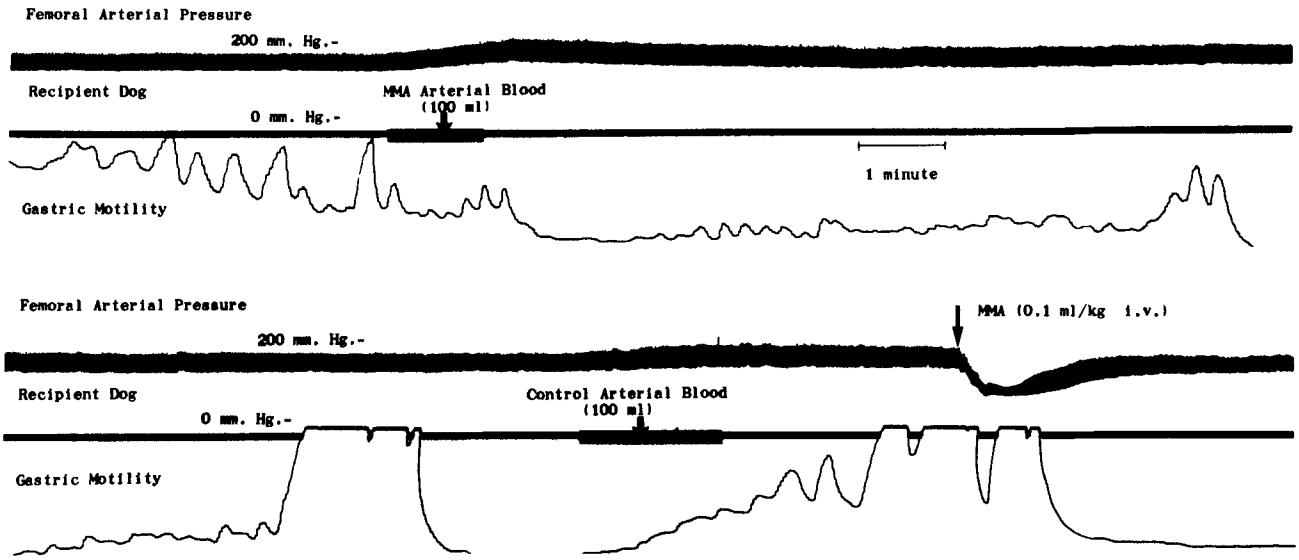

Figure 8—*Gastric contractile activity and arterial blood pressure events produced in a chloralose–urethan anesthetized dog following the infusion of 100 ml of whole blood from a donor dog (continuation of the experiment depicted in Fig. 7). In the top traces, the active and tonic gastric contractile activity of the recipient dog were depressed when 100 ml of whole blood, obtained during the exposure to 2000 ppm of methyl methacrylate (MMA) vapor in air, was infused via a femoral vein. The same experiment was repeated in the lower traces, where 100 ml of donor blood, obtained prior to methyl methacrylate exposure, was infused into the venous system of the recipient. Gastric contractile activity appeared to be normal following the infusion of blood from the donor prior to methyl methacrylate exposure, but recipient gastric motor activity was depressed following infusion from the methyl methacrylate exposed donor. At the end of the lower trace, the reactivity of the recipient was verified by the results of an intravenous administration of 0.1 mg/kg of the methyl methacrylate monomer. Gastric contractile activity was abolished and femoral arterial blood pressure was sharply, but transiently, affected.*

a transient fall in duodenal tonus and jejunal tonus and contractile activity. In this recording, the baseline of the jejunal pressure channel was reset to permit observation of the resulting motor activity, which was minimal.

Figure 6, a continuation of the record of Fig. 5, shows that the administration of methyl methacrylate vapor following ganglionic blockade with tetraethylammonium chloride was principally associated with a further depression of jejunal tonus and the by now minimal jejunal contractile activity. Jejunal tonus began to appear prior to the cessation of methyl methacrylate vapor administration.

A series of observations were then conducted simultaneously in real time utilizing four chloralose–urethan anesthetized dogs. These dogs had been subjected to identical surgical procedures: tracheostomies, arterial and venous cannulation, gastric antral recording balloons (oral route), and duodenal recording balloons (retrograde from the ileum). The purpose of these observations was to test the hypothesis that the motor effects associated with methyl methacrylate vapor administration could not be mediated in part by the circulation. Accordingly, methyl methacrylate vapor was only administered to one of each pair of dogs, and an arterial blood sample from the exposed (donor) dog was infused into the femoral vein of the nonexposed (recipient) dog. During these procedures, the monitored parameters were recorded graphically upon the same strip chart.

Figure 7 shows the time course of events in the recipient (top traces) and the donor (lower trace only) during these experiments. During the span of this record, the donor dog was continuously exposed to 2000 ppm of methyl methacrylate vapor *via* the breathing system. The top traces show that the slow infusion of 100 ml of donor blood resulted in a decrease in gastric and duodenal tonus and contractile activity. These activities gradually returned to control levels.

Figure 8 shows a continuation of the observations of the gastric antral activity of the recipient dog. Antral activity and tonus were reduced following intravenous administration of another sample of exposed donor blood (top traces). The lower traces show that recipient gastric activity was unchanged when an equal volume of donor blood, drawn during the control period prior to methyl methacrylate exposure, was infused.

Cardiovascular activity was monitored on a routine basis to indicate the general viability of the preparation and the responsiveness following certain procedures and as a general indication of cardiovascular toxicity. The time rate of the GI motor phenomena is unfortunately too low to permit adequate recording of faster cardiovascular phenomena without producing records of unusable length. As a result, the cardiovascular data are unsuitable for acquiring data for dynamic analysis. However, the records do show that direct administration of methyl methacrylate produced a decreased pulse pressure and probably a reflex tachycardia. These effects could be accounted for by two possible mechanisms: a direct toxic increase in arterial compliance and a direct toxic decrease in myocardial contractility. If, indeed, the general toxic effect of this agent resides in an inhibition of active contractile force, a further examination of the cardiovascular effects appears to be warranted.

The remainder of the foregoing data may be interpreted as follows. The acute studies indicated that the administration of methyl methacrylate is associated with a depression of tonus and contractile activity of the canine gastric antrum and proximal small bowel. Regardless of the presence or absence of visceral innervation, this effect had a latency on the order of 10 min when the agent was administered in vapor form. This latency was very short when either blood from an exposed dog or liquid methyl methacrylate was introduced intravenously. Although it was not included previously, a short latency was observed when the agent was administered intravenously to a surgically and chemically denervated preparation. Thus, the short latency might be indicative of a reflex response. However, the manifestation of the same effect in the denervated preparation, while not excluding the possibility that some reflex effects are produced, makes a reflex explanation for the observed response unlikely.

Inasmuch as this laboratory (2) and others (3) have observed that the monomer vapor depresses the spontaneous motor activity of intestinal strips *in vitro*, it may be concluded that methyl methacrylate vapor probably exerts a direct inhibitory effect upon GI smooth muscle and that the cardiopulmonary system is capable of mediating this effect when exposure is by inhalation.

REFERENCES

(1) M. F. Tansy, S. Benhaim, S. Probst, and J. S. Jordan, *J. Am. Dent. Assoc.*, **89**, 372 (1974).

(2) M. F. Tansy, J. S. Martin, W. Landin, and S. Benhaim, *Clin. Res.*, **23**, 258 (1975).

(3) G. N. Mir, W. H. Lawrence, and J. Autian, *J. Pharm. Sci.*, **62**, 1258 (1973).

ACKNOWLEDGMENTS AND ADDRESSES

Received November 28, 1975, from the *Department of Physiology and Biophysics, Health Sciences Center, Temple University, Philadelphia,*

PA 19140.
Accepted for publication June 22, 1976.
Presented at the Pharmacology and Biochemistry Section, APhA Academy of Pharmaceutical Sciences, Atlanta meeting, November 1975.
Supported by Public Health Service Research Grant OH-00518 from the National Institute of Occupational Safety and Health.
[x] To whom inquiries should be directed.

Disposition of Sulfonamides in Food-Producing Animals IV: Pharmacokinetics of Sulfamethazine in Cattle following Administration of an Intravenous Dose and Three Oral Dosage Forms

RICHARD F. BEVILL [*x], LEWIS W. DITTERT [‡], and DAVID W. A. BOURNE [‡]

Abstract □ The plasma and urine data obtained following intravenous administration of sulfamethazine to cattle were fit to a one-compartment pharmacokinetic model with a half-life of elimination of 9 hr and a volume of distribution of 0.35 liter/kg. Sulfamethazine was eliminated by excretion of unchanged sulfamethazine (18%) into urine and by formation of three metabolites subsequently excreted into urine. Sulfamethazine also was administered as a solution, a rapid-release bolus, and a sustained-release bolus. The change in the urinary metabolic pattern with different routes of administration suggested that first-pass metabolism was occurring during the absorption process. The absorption half-life was 6 hr. The absorption process for the two solid boluses kinetically appeared to include a dissolution step.

Keyphrases □ Sulfamethazine—absorption, metabolism, and excretion, various dosage forms compared, cattle □ Sulfonamides—sulfamethazine, absorption, metabolism, and excretion, various dosage forms compared, cattle □ Absorption—sulfamethazine, various dosage forms compared, cattle □ Metabolism—sulfamethazine, various dosage forms compared, cattle □ Excretion—sulfamethazine, various dosage forms compared, cattle □ Pharmacokinetics—sulfamethazine, various dosage forms compared, cattle □ Antibacterials—sulfamethazine, absorption, metabolism, and excretion, various dosage forms compared, cattle

Sulfamethazine is used extensively in veterinary medicine for the treatment of various infections in food-producing animals. Commercially available oral dosage forms for large animals include a solution, a bolus of the sodium salt, and a sustained-release bolus of the free acid. The comparative bioavailabilities and plasma concentration–time profiles of these dosage forms in large animals have not been reported.

The present study investigated the rate and extent of sulfamethazine absorption from three oral dosage forms compared with an intravenous solution of sulfamethazine sodium in 1-year-old cross-bred heifer feeder calves.

EXPERIMENTAL

Intravenous Administration—Three Hereford × Angus heifers, 1 year old, were weighed, fitted with urinary retention catheters[1] attached to 4-liter plastic collection bottles, and assigned to individual slot-floored metabolism cages 3 days prior to dosing. The weights of Animals 1, 2, and 3 were 235, 226, and 245 kg, respectively. Good quality grass hay and water were provided *ad libitum* during acclimatization and postdosing periods. A concentrate mixture, formulated from shelled corn and linseed meal and containing 12% protein, was limit fed to each animal during the study.

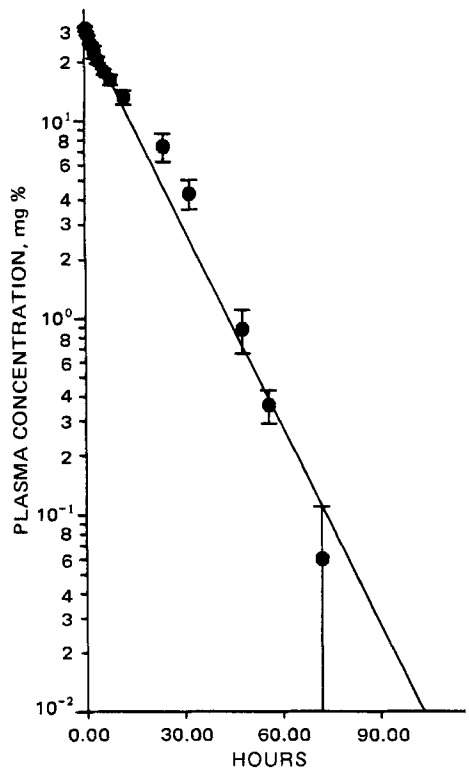

Figure 1—*Semilog plot of average plasma sulfamethazine concentration* (±SD) versus *time following intravenous administration of sulfamethazine sodium (107 mg/kg) to three calves. Points were experimentally observed, and the line was calculated by iterative least-squares fitting to a one-compartment model* ($t_{1/2}$ = *9 hr*, V_D = *0.35 liter/kg*).

A dose of 107 mg/kg (¾ gr/lb) of sulfamethazine as a 12.5% solution of sulfamethazine sodium[2] was rapidly injected *via* the right jugular vein in each animal. All blood specimens were collected from the left jugular vein by serial venipuncture using disposable plastic syringes prerinsed with a 1% solution of heparin sodium in normal saline.

Blood and urine specimens were collected at 0, 0.5, 1, 2, 3, 4, 6, 8, 12, 24, 32, 48, 56, and 72 hr following drug administration. The volume of urine collected over each interval was recorded, and a clean collection

[1] Bardex, 24 Fr, C. R. Bard Inc., Murray Hill, N.J.

[2] Prepared by diluting sulfamethazine sodium, 25% (American Cyanamid Co.), with an equal volume of sterile distilled water.

PA 19140.
Accepted for publication June 22, 1976.
Presented at the Pharmacology and Biochemistry Section, APhA Academy of Pharmaceutical Sciences, Atlanta meeting, November 1975.
Supported by Public Health Service Research Grant OH-00518 from the National Institute of Occupational Safety and Health.
[x] To whom inquiries should be directed.

Disposition of Sulfonamides in Food-Producing Animals IV: Pharmacokinetics of Sulfamethazine in Cattle following Administration of an Intravenous Dose and Three Oral Dosage Forms

RICHARD F. BEVILL [*x], LEWIS W. DITTERT [‡], and DAVID W. A. BOURNE [‡]

Abstract □ The plasma and urine data obtained following intravenous administration of sulfamethazine to cattle were fit to a one-compartment pharmacokinetic model with a half-life of elimination of 9 hr and a volume of distribution of 0.35 liter/kg. Sulfamethazine was eliminated by excretion of unchanged sulfamethazine (18%) into urine and by formation of three metabolites subsequently excreted into urine. Sulfamethazine also was administered as a solution, a rapid-release bolus, and a sustained-release bolus. The change in the urinary metabolic pattern with different routes of administration suggested that first-pass metabolism was occurring during the absorption process. The absorption half-life was 6 hr. The absorption process for the two solid boluses kinetically appeared to include a dissolution step.

Keyphrases □ Sulfamethazine—absorption, metabolism, and excretion, various dosage forms compared, cattle □ Sulfonamides—sulfamethazine, absorption, metabolism, and excretion, various dosage forms compared, cattle □ Absorption—sulfamethazine, various dosage forms compared, cattle □ Metabolism—sulfamethazine, various dosage forms compared, cattle □ Excretion—sulfamethazine, various dosage forms compared, cattle □ Pharmacokinetics—sulfamethazine, various dosage forms compared, cattle □ Antibacterials—sulfamethazine, absorption, metabolism, and excretion, various dosage forms compared, cattle

Sulfamethazine is used extensively in veterinary medicine for the treatment of various infections in food-producing animals. Commercially available oral dosage forms for large animals include a solution, a bolus of the sodium salt, and a sustained-release bolus of the free acid. The comparative bioavailabilities and plasma concentration–time profiles of these dosage forms in large animals have not been reported.

The present study investigated the rate and extent of sulfamethazine absorption from three oral dosage forms compared with an intravenous solution of sulfamethazine sodium in 1-year-old cross-bred heifer feeder calves.

EXPERIMENTAL

Intravenous Administration—Three Hereford × Angus heifers, 1 year old, were weighed, fitted with urinary retention catheters[1] attached to 4-liter plastic collection bottles, and assigned to individual slot-floored metabolism cages 3 days prior to dosing. The weights of Animals 1, 2, and 3 were 235, 226, and 245 kg, respectively. Good quality grass hay and water were provided *ad libitum* during acclimatization and postdosing periods. A concentrate mixture, formulated from shelled corn and linseed meal and containing 12% protein, was limit fed to each animal during the study.

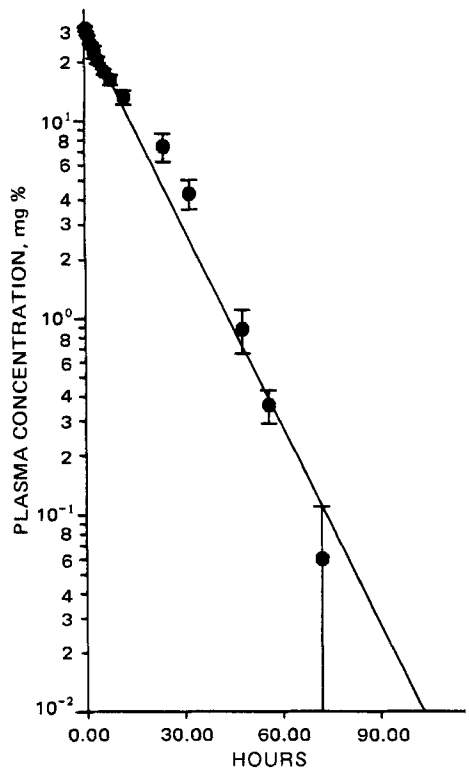

Figure 1—*Semilog plot of average plasma sulfamethazine concentration* (±SD) versus *time following intravenous administration of sulfamethazine sodium (107 mg/kg) to three calves. Points were experimentally observed, and the line was calculated by iterative least-squares fitting to a one-compartment model* ($t_{1/2}$ = *9 hr*, V_D = *0.35 liter/kg*).

A dose of 107 mg/kg (¾ gr/lb) of sulfamethazine as a 12.5% solution of sulfamethazine sodium[2] was rapidly injected *via* the right jugular vein in each animal. All blood specimens were collected from the left jugular vein by serial venipuncture using disposable plastic syringes prerinsed with a 1% solution of heparin sodium in normal saline.

Blood and urine specimens were collected at 0, 0.5, 1, 2, 3, 4, 6, 8, 12, 24, 32, 48, 56, and 72 hr following drug administration. The volume of urine collected over each interval was recorded, and a clean collection

[1] Bardex, 24 Fr, C. R. Bard Inc., Murray Hill, N.J.

[2] Prepared by diluting sulfamethazine sodium, 25% (American Cyanamid Co.), with an equal volume of sterile distilled water.

Table I—Average Plasma Sulfamethazine Concentration in Three Calves following Intravenous Administration of 107 mg/kg (3/4 gr/lb) of Sulfamethazine Sodium

Hours	Concentration, mg %
0.5	29.66
1.0	27.35
2.0	24.64
3.0	22.53
4.0	20.46
6.0	17.80
8.0	16.20
12.0	13.20
24.0	7.40
32.0	4.30
48.0	0.88
56.0	0.36
72.0	0.06

bottle was substituted at each collection time. Urine specimens were stored in plastic bottles at −10° until assayed. Within 1 hr of collection, the blood specimens were centrifuged at 3000 rpm for 10 min; plasma was harvested and stored in screw-capped glass tubes at −10° until assayed. All assays were completed within 1 week of specimen collection.

Oral Solution Administration—The three calves were allowed to rest for 21 days between the intravenous and oral solution administrations. Three days prior to dosing, they were reweighed (1 = 232 kg, 2 = 232 kg, and 3 = 250 kg), refitted with urinary retention catheters, and reassigned to individual metabolism cages. The animals were fed and watered as previously described, except that hay and grain were withheld for 24 hr prior to drug administration to avoid regurgitation of the rumen contents and drug during the dosing procedure.

A dose of 107 mg/kg (¾ gr/lb) of sulfamethazine as a 12.5% solution of sulfamethazine sodium was administered to each animal *via* a stomach tube.

Plasma and urine specimens were collected, stored, and assayed as previously described at 0, 1, 4, 5, 7, 9, 12, 24, 32, 48, 56, 72, 96, 120, and 140 hr following drug administration.

Oral Rapid-Release Bolus Administration—The three calves were allowed to rest for 30 days between oral solution and oral bolus administrations. Three days prior to dosing, they were reweighed (1 = 255 kg, 2 = 264 kg, and 3 = 273 kg), refitted with urinary retention catheters, and reassigned to individual metabolism cages. The animals were fed and watered as described for the oral solution administration.

Two boluses[3] containing a total of 30 g of sulfamethazine sodium (27.8 g of sulfamethazine) were administered to each animal using a balling gun. The dose was similar on a milligram per kilogram basis to the dose used in the intravenous and oral solution studies. Slight variations in the milligram per kilogram doses for each animal were tolerated so that intact boluses could be administered.

Plasma and urine specimens were collected, stored, and assayed as previously described at 0, 1, 2, 3, 4, 6, 8, 12, 24, 32, 48, 56, 72, 80, 96, 104, 120, and 144 hr following drug administration.

Oral Sustained-Release Bolus Administration—The three calves were allowed to rest for 30 days between oral rapid-release bolus and oral sustained-release bolus administrations. Three days prior to dosing, they were reweighed (1 = 255 kg, 2 = 268 kg, and 3 = 289 kg), refitted with urinary retention catheters, and reassigned to individual metabolism cages. The animals were fed and watered as described for the oral solution administration.

Three sustained-release boluses[4] containing a total of 67.5 g of sulfamethazine were administered to each animal using a balling gun. The 67.5-g dose was higher than the doses used in the other studies so as to produce comparable plasma sulfamethazine levels. Slight variations in the milligram per kilogram doses for each animal were tolerated so that intact boluses could be administered.

Plasma and urine specimens were collected, stored, and assayed as previously described at 0, 1, 3, 5, 7, 9, 12, 15, 24, 30, 36, 48, 60, 72, 84, 96, 108, 120, 144, and 168 hr following drug administration.

Analytical Methods—All assays were carried out using the methods described previously (1).

Table II—Average Plasma Sulfamethazine Concentration in Three Calves following Oral Administration of 107 mg/kg (3/4 gr/lb) of Sulfamethazine as a Solution of the Sodium Salt

Hours	Concentration, mg %
1.0	4.82
4.0	11.31
5.0	12.38
7.0	12.92
9.0	13.04
12.0	12.80
24.0	9.69
32.0	6.82
48.0	2.53
56.0	1.25

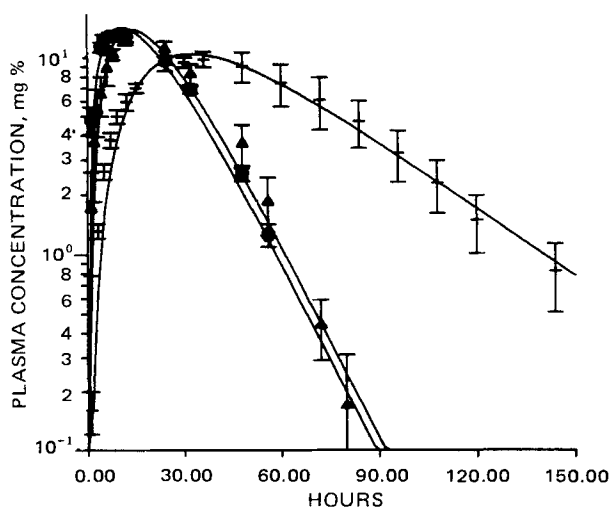

Figure 2—*Semilog plot of average plasma sulfamethazine concentration* (±SD) versus *time following oral administration of sulfamethazine in solution (107 mg/kg)* (●), *in a rapid-release bolus (27.8 g)* (▲), *and in a sustained-release bolus (67.5 g)* (+) *to three calves. Points were experimentally observed, and lines were calculated according to Schemes I and III.*

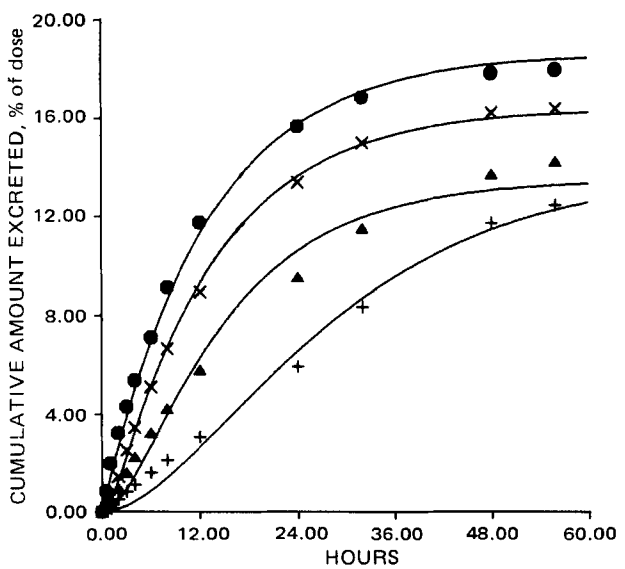

Figure 3—*Plot of average cumulative amount of unchanged sulfamethazine* (●) *and its polar* (▲), *hydroxy* (+), *and acetyl* (×) *metabolites excreted in urine* versus *time following intravenous administration of sulfamethazine sodium (107 mg/kg) to three calves. Points were experimentally observed, and lines were calculated according to Scheme I.*

[3] American Cyanamid Co.

[4] Spanbolets, Norden Laboratories.

Table III—Average Plasma Sulfamethazine Concentration in Three Calves following Oral Administration of 27.8 g of Sulfamethazine as a Rapid-Release Bolus of the Sodium Salt

Hours	Concentration, mg %
1.0	1.69
2.0	3.67
3.0	5.40
4.0	6.50
6.0	8.80
8.0	10.40
12.0	12.40
24.0	11.10
32.0	8.20
48.0	3.63
56.0	1.83
72.0	0.44
80.0	0.17

RESULTS AND DISCUSSION

Average plasma sulfamethazine concentrations following intravenous administration of 107-mg/kg doses of sulfamethazine to calves are presented in Table I and plotted in Fig. 1. Average plasma sulfamethazine concentrations following oral administration of a solution of sulfamethazine sodium, a rapid-release bolus of sulfamethazine sodium, and a sustained-release bolus of sulfamethazine are presented in Tables II, III, and IV, respectively, and plotted in Fig. 2. The cumulative amounts of sulfamethazine and its metabolites excreted in urine following the intravenous and oral administrations of sulfamethazine are presented in Tables V–VIII and plotted in Figs. 3 and 4.

The plasma sulfamethazine *versus* time curve obtained following intravenous administration (Fig. 1) appears to be monoexponential, suggesting that a one-compartment pharmacokinetic model is sufficient to describe the time course of sulfamethazine in cattle. Analysis of urine following sulfamethazine administration indicated the presence of unchanged sulfamethazine and three metabolites: the acetyl and hydroxy derivatives and a polar metabolite[5]. If the formations of all three metabolites in plasma are assumed to follow first-order kinetics and the eliminations of sulfamethazine and the three metabolites from plasma are assumed to follow first-order kinetics, Scheme I describes the time course of sulfamethazine and its metabolites in the plasma and urine of cattle.

The value of the overall elimination rate constant, $k_{el} = k_{12} + k_{13} + k_{14} + k_{15} + k_{16} = 0.0774\ hr^{-1}$, was calculated by weighted iterative least-squares fitting (2) to the plasma concentration–time data obtained following intravenous administration. This calculation also estimated a volume of distribution of 0.35 liter/kg. Values of the individual rate constants, k_{12}, k_{13}, k_{14}, k_{15}, and k_{16}, were estimated from the value of k_{el} and the ratios of the total amounts of unchanged sulfamethazine and the three metabolites excreted in urine over the 0–72-hr period after drug administration. Values of the rate constants for the elimination of the metabolites, acetyl (k_{69}), hydroxy (k_{58}), and polar (k_{47}), were estimated from the urinary excretion data for these metabolites.

With all of these values as initial estimates, a least-squares fit of the model shown in Scheme I to the urine–time data for unchanged sulfamethazine and the metabolites (Table V) was obtained using the SAAM 23 program (2) and a digital computer[6]. The final calculated values ($\pm SD$) for the parameters of Scheme I are shown in Table IX. These values were used to generate the calculated lines in Figs. 1 and 3. The good fits of the calculated lines to the experimental data points suggest that the one-compartment pharmacokinetic model is sufficient to describe the disposition and elimination of sulfamethazine in cattle and that the formations and eliminations of the metabolites are first-order processes at the dosage levels studied. The one-compartment model shown in Scheme I and the final calculated parameter values shown in Table IX were subsequently used in analyzing the results obtained following oral administrations.

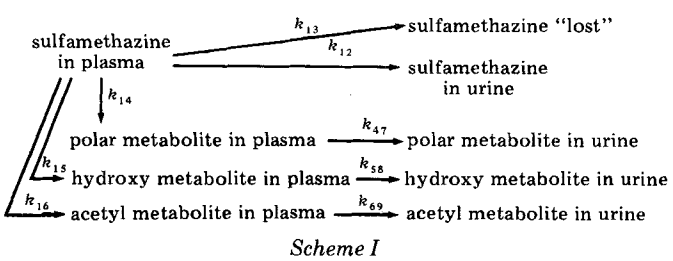

Scheme I

[5] Determination of the exact structures of the hydroxy and polar metabolites will be the subject of a future publication.

[6] IBM 360/60.

Table IV—Average Plasma Sulfamethazine Concentration in Three Calves following Oral Administration of 67.5 g of Sulfamethazine as a Sustained-Release Bolus

Hours	Concentration, mg %
1.0	0.16
3.0	1.31
5.0	2.63
7.0	3.80
9.0	5.02
12.0	5.95
15.0	7.01
24.0	9.33
30.0	9.43
36.0	9.80
48.0	9.00
60.0	7.41
72.0	6.06
84.0	4.70
96.0	3.26
108.0	2.29
120.0	1.49
144.0	0.82

The relative absorptions of the oral dosage forms of sulfamethazine (Table X) were calculated by comparing the total amount of drug (unchanged drug plus metabolites) excreted in urine following oral administration with the total amount excreted following intravenous administration. The results suggest that the oral solution and the oral rapid-release bolus are relatively efficiently absorbed but that the oral sustained-release bolus is not. This calculation does not take into account that there may be relatively more metabolism following oral administration of any dosage form compared with intravenous administration as a result of greater exposure of the drug to the enzymes of the gut and liver.

A more accurate estimate of the therapeutic potential of the various oral dosage forms is given by their systemic availabilities (3), which were calculated by comparing the total amount of unchanged drug excreted in urine following oral administration with that following intravenous administration (Table X). This calculation measures delivery of active drug to the blood and reflects the different metabolic patterns observed following oral and intravenous administrations. The results suggest that the oral solution and oral rapid-release bolus are relatively efficient at delivering active drug to the blood whereas the oral sustained-release bolus is not. Although the sustained-release bolus does not appear to be an efficient dosage form from the standpoint of relative absorption or systemic availability, inspection of its plasma concentration–time curve (Fig. 2) shows that it maintains plasma concentrations above the mini-

Table V—Average Cumulative Percent of Dose Excreted as Sulfamethazine and Its Metabolites in the Urine of Three Calves following Intravenous Administration of 107 mg/kg (3/4 gr/lb) of Sulfamethazine as the Sodium Salt

Hours	Sulfamethazine	Metabolites		
		Polar	Hydroxy	Acetyl
0.0	0.0	0.0	0.0	0.0
0.5	0.84	0.05	0.06	0.12
1.0	1.98	0.30	0.19	0.56
2.0	3.24	0.88	0.50	1.44
3.0	4.32	1.54	0.82	2.51
4.0	5.39	2.19	1.11	3.46
6.0	7.13	3.19	1.61	5.11
8.0	9.14	4.17	2.12	6.66
12.0	11.77	5.75	3.07	8.95
24.0	15.68	9.49	5.94	13.39
32.0	16.86	11.44	8.35	14.97
48.0	17.84	13.65	11.73	16.22
56.0	17.99	14.16	12.47	16.37

Table VI—Average Cumulative Percent of Dose Excreted as Sulfamethazine and Its Metabolites in the Urine of Three Calves following Oral Administration of 107 mg/kg (3/4 gr/lb) of Sulfamethazine as a Solution of the Sodium Salt

Hours	Sulfamethazine	Metabolites		
		Polar	Hydroxy	Acetyl
0.0	0.0	0.0	0.0	0.0
1.0	0.07	0.02	0.05	0.08
4.0	0.31	0.31	0.32	0.53
5.0	0.72	0.77	0.62	1.32
7.0	1.35	1.33	0.96	2.45
9.0	2.29	1.89	1.36	3.87
12.0	3.65	2.71	1.95	6.00
24.0	8.08	5.80	4.77	15.13
32.0	10.23	7.59	6.89	18.54
48.0	12.61	9.93	10.69	23.09
56.0	13.19	10.66	12.17	24.31
72.0	14.07	11.21	14.24	25.16
96.0	14.45	11.52	15.20	25.44
120.0	14.54	11.71	15.76	25.63

mum therapeutic level (5 mg %) (4) for at least 70 hr. This time is more than twice as long as that with the rapid-release bolus and the solution and probably represents a therapeutic advantage.

The different metabolic patterns of sulfamethazine following intravenous and oral administrations may be seen by comparing Figs. 3 and 4 and Tables V and VI. Figure 3 and Table V show that the major excretion product following intravenous administration was unchanged sulfamethazine, which amounted to 18% of the dose. On the other hand, the major excretion product following administration of the oral solution (Fig. 4 and Table VI) was the acetyl metabolite of sulfamethazine, amounting to more than 25% of the dose. The fraction of the dose excreted as the hydroxy metabolite also increased from 12.5% following intravenous administration to 15.8% following oral administration. Thus, a significant part of the reduction in systemic availability observed with the oral dosage forms of sulfamethazine apparently can be attributed to increased metabolism during movement from the rumen to peripheral plasma.

The kinetics of sulfamethazine absorption following oral administration of sulfamethazine sodium in solution were investigated using the method of Wagner and Nelson (5). The percentage of the dose remaining to be absorbed at each time was calculated from the plasma level data using the value of k_{el} obtained in the intravenous study. A semilog plot of the percent of the dose remaining to be absorbed *versus* time appeared to be linear, indicating that sulfamethazine absorption from solution in cattle is a first-order process with a half-life of about 6 hr (k_a = 0.115 hr^{-1}).

This value of k_a was used as an initial estimate for calculating the final value of the absorption rate constant by least-squares fitting to the plasma concentration *versus* time data using the SAAM 23 program (2).

Table VII—Average Cumulative Percent of Dose Excreted as Sulfamethazine and Its Metabolites in the Urine of Three Calves following Oral Administration of 27.8 g of Sulfamethazine as a Rapid-Release Bolus of the Sodium Salt

Hours	Sulfamethazine	Metabolites		
		Polar	Hydroxy	Acetyl
0.0	0.0	0.0	0.0	0.0
1.0	0.01	0.01	0.01	0.01
2.0	0.08	0.05	0.09	0.08
3.0	0.18	0.22	0.25	0.22
4.0	0.30	0.39	0.40	0.37
6.0	0.52	0.74	0.70	0.75
8.0	0.82	1.24	1.11	1.46
12.0	1.55	2.06	1.76	3.06
24.0	4.80	4.93	4.19	9.26
32.0	6.65	6.65	5.95	12.64
48.0	9.32	9.43	9.36	16.54
56.0	10.00	10.24	10.65	17.53
72.0	10.92	11.61	12.97	18.97
80.0	11.13	11.81	13.39	19.42
96.0	11.32	12.00	13.99	19.95
104.0	11.37	12.05	14.10	20.02

Table VIII—Average Cumulative Percent of Dose Excreted as Sulfamethazine and Its Metabolites in the Urine of Three Calves following Oral Administration of 67.5 g of Sulfamethazine as a Sustained-Release Bolus

Hours	Sulfamethazine	Metabolites		
		Polar	Hydroxy	Acetyl
0.0	0.0	0.0	0.0	0.0
1.0	0.0	0.0	0.0	0.0
3.0	0.02	0.04	0.03	0.02
5.0	0.04	0.12	0.11	0.05
7.0	0.08	0.23	0.22	0.12
9.0	0.13	0.34	0.32	0.22
12.0	0.24	0.55	0.46	0.45
15.0	0.34	0.70	0.58	0.76
24.0	0.98	1.35	1.13	1.89
30.0	1.46	1.76	1.47	2.65
36.0	2.05	2.30	1.94	3.55
48.0	2.97	3.30	2.87	5.25
60.0	3.89	4.29	3.92	6.82
72.0	4.49	5.15	4.84	8.14
84.0	4.97	5.97	5.68	9.19
96.0	5.27	6.54	6.37	9.95
108.0	5.45	7.03	7.04	10.41
120.0	5.58	7.43	7.68	10.75
144.0	5.71	7.85	8.54	11.15
168.0	5.75	8.00	8.88	11.27

The value of the overall elimination rate constant was set equal to the value obtained in the intravenous study. This calculation yielded an absorption rate constant of 0.113 hr^{-1}.

To account for the different metabolic patterns of sulfamethazine following intravenous and oral administrations, a kinetic model was tested where the absorption process consisted of simultaneous transfer of sulfamethazine from solution in the rumen to sulfamethazine in plasma and to the three metabolites in plasma (Scheme II). The remainder of the model, *i.e.*, that describing disposition and elimination of sulfamethazine and its metabolites in plasma, was identical to Scheme I. The values of the rate constants of Scheme I obtained by fitting the plasma and urine data from the intravenous study were used as initial estimates in the least-squares fitting of the oral data.

Initial estimates of $k_{10,1}$, $k_{10,4}$, $k_{10,5}$, and $k_{10,6}$ were calculated by mass balance from the urinary excretion–time data. In fitting the oral data, the following constraints were employed: the value of k_{el} was fixed at the value obtained from the intravenous study, and the value of $k_a = (k_{10,1}$

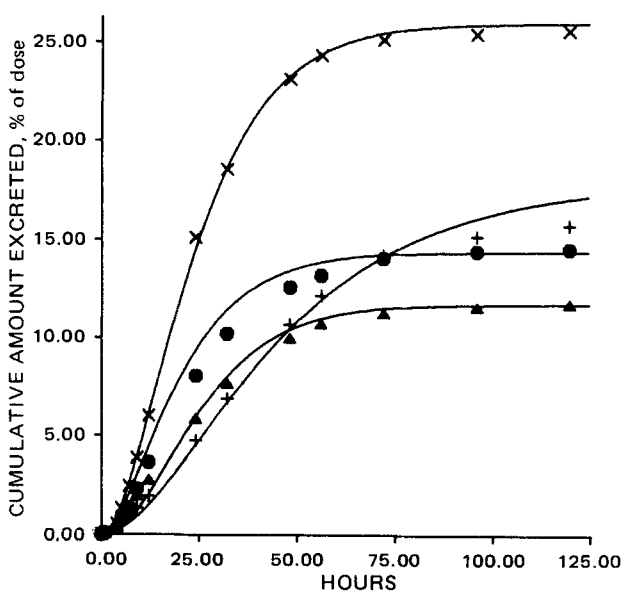

Figure 4—*Plot of average cumulative amount of unchanged sulfamethazine* (●) *and its polar* (▲), *hydroxy* (+), *and acetyl* (×) *metabolites excreted in urine* versus *time following oral administration of sulfamethazine sodium in solution (107 mg/kg) to three calves. Points were experimentally observed, and lines were calculated according to Schemes I and II.*

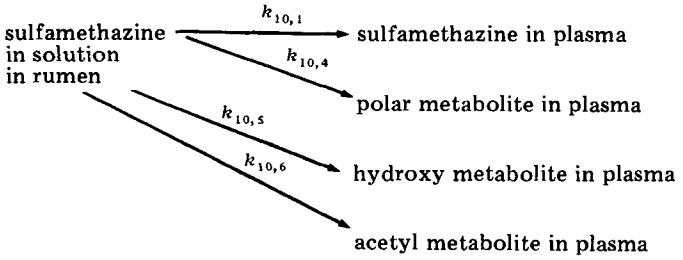

Scheme II

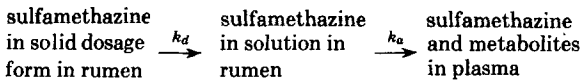

Scheme III

$+ k_{10,4} + k_{10,5} + k_{10,6}$) was fixed at the value obtained by iterative fitting of the plasma concentration–time data. The values of $k_{10,1}$, $k_{10,4}$, $k_{10,5}$, $k_{10,6}$, k_{47}, k_{58}, and k_{69} were then calculated by least-squares fitting to the data for unchanged sulfamethazine and metabolites in urine (Table VI). The results of this calculation are shown in Table XI. The calculated lines of Fig. 4 were generated using the parameter values in Table XI and appear to fit the experimental points well.

The kinetics of sulfamethazine absorption following administration of the oral rapid-release bolus of sulfamethazine sodium and the oral sustained-release bolus of sulfamethazine were investigated by the method of Wagner and Nelson (5) using the value of k_{el} obtained in the intravenous study. In both cases, the semilog plot of the percent of dose remaining to be absorbed *versus* time appeared to be biexponential. This finding suggested that the absorption process consisted of two successive first-order processes, the initial process being dissolution of the drug and the second process being absorption of the dissolved drug from the rumen (Scheme III).

An estimate of the *in vivo* dissolution rate constant, k_d, was obtained from the semilog plot of percent of dose remaining to be absorbed *versus* time. The value of k_{el} obtained in the intravenous study and the value of k_a obtained in the oral solution study were then used to calculate values for the *in vivo* dissolution rate constants for the rapid-release bolus and the sustained-release bolus by iterative least-squares fitting to the plasma concentration–time data using the SAAM 23 program (2). The values of k_{el}, k_d, and k_a calculated from the plasma data were then fixed; values for $k_{10,1}$, $k_{10,4}$, $k_{10,5}$, $k_{10,6}$, k_{47}, k_{58}, and k_{69} were calculated by least-squares iterative fitting to urine data for unchanged sulfamethazine and its metabolites (Tables VII and VIII). The results of these calculations are shown in Table XI.

The calculated dissolution rate for the sustained-release bolus is much slower than that for the rapid-release bolus. This reduced dissolution rate appears to be effective in reducing the rate of appearance of sulfamethazine in plasma and also in maintaining effective plasma sulfamethazine levels for longer times. Peak plasma levels following administration of the sustained-release bolus were about 75% of those following oral administration of the solution or the rapid-release bolus. The sustained-release bolus, although less efficient (less bioavailable) than the other oral dosage forms (Table X), maintained plasma concentrations of active drug above the minimum effective concentration (5 mg %) (4) for above twice as long as the other dosage forms.

Apparently, a compromise must be considered in designing a "best" oral dosage form of sulfamethazine for cattle. If longer dosing intervals and smoother plasma levels are important factors in sulfamethazine therapy, then the lower bioavailability of the sustained-release dosage form becomes less important than its prolonged release, and this dosage form is preferable. However, if the dosing interval can be shorter and the higher peak plasma levels do not cause increased toxicity, the more completely absorbed rapid-release bolus dosage form (82% relative absorption) may be preferred to either the incompletely absorbed sustained-release dosage form (46%) or the less convenient solution dosage form (99%).

Table IX—Values of the Parameters[a] of the Pharmacokinetic Model (Scheme I) Describing the Metabolism and Excretion of Sulfamethazine in Cattle following Intravenous Administration of 107 mg/kg

Parameter	Value ± *SD*
k_{12}	0.0144 ± 0.0002 hr^{-1}
k_{13}	0.0290 ± 0.0007 hr^{-1}
k_{14}	0.0104 ± 0.0002 hr^{-1}
k_{15}	0.0108 ± 0.0006 hr^{-1}
k_{16}	0.0127 ± 0.0002 hr^{-1}
k_{47}	0.28 ± 0.05 hr^{-1}
k_{58}	0.057 ± 0.009 hr^{-1}
k_{69}	0.9 ± 0.2 hr^{-1}
V_D	0.346 ± 0.002 liter/kg
k_{el}	0.077 ± 0.002 hr^{-1}

[a] Values from SAAM 23.

Table X—Bioavailabilities of Three Oral Dosage Forms of Sulfamethazine Compared with Intravenous Administration

Dosage Form	Relative Absorption	Systemic Availability
Solution	99.2	80.8
Rapid-release bolus	82.2	63.2
Sustained-release bolus	46.4	32.0

Table XI—Values of the Parameters[a] of the Pharmacokinetic Models (Schemes I–III) Describing the Absorption, Metabolism, and Excretion of Sulfamethazine in Cattle following Oral Administration

Parameter	Unit	Solution	Rapid-Release Bolus	Sustained-Release Bolus
k_d	$Hours^{-1}$	—	0.405	0.0261
k_a	$Hours^{-1}$	0.113	0.113[b]	0.113[b]
k_{el}	$Hours^{-1}$	0.077[c]	0.077[c]	0.077[c]
$k_{10,1}$	$Hours^{-1}$	0.0884	0.0808	0.0780
$k_{10,4}$	$Hours^{-1}$	0.00149	0.00619	0.00893
$k_{10,5}$	$Hours^{-1}$	0.00830	0.0119	0.0108
$k_{10,6}$	$Hours^{-1}$	0.0152	0.0145	0.0157
k_{47}	$Hours^{-1}$	0.145	0.0673	0.110
k_{58}	$Hours^{-1}$	0.0298	0.0274	0.0486
k_{69}	$Hours^{-1}$	0.0979	0.0763	0.127
V_D	Liters per kilogram	0.25	0.20	0.13

[a] Values from SAAM 23. [b] Value from oral solution study. [c] Value from intravenous study.

REFERENCES

(1) R. F. Bevill, S. H. Meachum, D. W. A. Bourne, L. W. Dittert, and R. M. Sharma, *Am. J. Vet. Res.*, in press.

(2) M. Berman and M. F. Weiss, "Users Manual for SAAM," National Institute of Arthritis and Metabolic Diseases, National Institutes of Health, Bethesda, Md., 1968.

(3) M. Gibaldi and D. Perrier, "Pharmacokinetics," Dekker, New York, N.Y., 1975, p. 237.

(4) S. M. Finegold and I. Ziment, in "Antimicrobial Therapy," B. M. Kagan, Ed., Saunders, Philadelphia, Pa., 1970, p. 102.

(5) J. G. Wagner and E. Nelson, *J. Pharm. Sci.*, **53**, 1392 (1964).

ACKNOWLEDGMENTS AND ADDRESSES

Received March 16, 1976, from the *Department of Veterinary Physiology and Pharmacology, College of Veterinary Medicine, University of Illinois, Urbana, IL 61801, and the ‡College of Pharmacy, University of Kentucky, Lexington, KY 40506.

Accepted for publication June 17, 1976.

Presented in part at the Basic Pharmaceutics Section, APhA Academy of Pharmaceutical Sciences, New Orleans meeting, April 1976.

Supported by Food and Drug Administration Grant 71-69.

* To whom inquiries should be directed.

Determination of Aqueous Solubility and pKa Values of Estrogens

A. R. HURWITZ ˣ and S. T. LIU

Abstract □ Reported estrone pKa and solubility data show wide variation. Improved experimental procedures were designed and used to obtain reproducible results. The pKa values for several estrogens and related compounds also were determined to assess the effects of structural differences on ionization. No evidence was obtained for long-range D to A ring electronic transmission affecting pKa. Significant differences in pKa values resulted only when conjugated unsaturation was added into the B ring of estrone or estradiol. The aqueous solubilities of estrone and 17α-estradiol were 0.8 and 3.9 μg/ml, respectively, at 25°.

Keyphrases □ Estrogens, various—aqueous solubilities, pKa values, effects of structural differences on ionization □ Solubility, aqueous—various estrogens, effects of structural differences on ionization □ pKa values—various estrogens, effects of structural differences on ionization □ Ionization—various estrogens, effects of structural differences □ Structure-activity relationships—various estrogens, aqueous solubilities and pKa values

Estrogen steroids undergo ionization in alkaline solution. Differences in the UV spectra of the ionized and neutral species of these compounds provide a suitable method for determining ionization constants (1). Previously, the spectrophotometric method was used to study the ionization constants of five estrogens (2). The same technique was also used in determining the pKa value differences between 17β-estradiol and six other estrogens (3). Considerable differences were claimed to exist between the ionization constants of the estrogens studied (2, 3). The results were explained in terms of long-range interaction and conjugation effects. Recent investigations (4, 5) of the ionization constants of 10 phenolic steroids also claimed that the character of the substitutions in the D ring would greatly affect the ionization constant of the C-3 hydroxyl group.

Reported observed ionization constant values for estrone ranged from 9.36 to 11.0 (2–7). This discrepancy may be due to differences in experimental conditions. In the present work, the thermodynamic ionization constants of nine phenolic steroids were studied spectrophotometrically. The ionization of 5,6,7,8-tetrahydro-2-naphthol also was investigated for comparison. A solubility method was employed to determine the ionization constant of equilenin. Aqueous solubility values of estrone, estradiol, equilin, and equilenin also were determined by either UV or GLC methods.

EXPERIMENTAL

Reagents—Estrone[1], 17α-estradiol[1], equilin[1], equilenin[1], 17α-dihydroequilin[1], 17β-dihydroequilenin[1], ethinyl estradiol[1], estriol[2], 1,3,5(10),6-estratetraen-3-ol-17-one (6-dehydroestrone)[2], and 5,6,7,8-tetrahydro-2-naphthol[3] were used with no prior treatment. Standard buffer solutions[4] of pH 9 and 10 were used for calibration of the glass electrode.

Apparatus—UV spectra were obtained with a recording spectrophotometer[5], and the pH was measured with a digital pH meter[6]. GLC analyses were performed on a gas chromatograph with flame-ionization detection[7], and the data were recorded with a recorder with a disk integrator[8].

Solubility Determination—Excess solid material was introduced into 200 ml of distilled water in a 250-ml jacketed beaker. The experiments were carried out at 25 ± 0.02° under nitrogen. Suspensions were magnetically stirred for at least 4 hr to allow the solution to reach equilibrium. Although 4 hr of such vigorous stirring was adequate to achieve equilibrium, several samples were stirred up to 24 hr. An aliquot of the suspension was filtered through a 0.2-μm filter membrane[9]. To prevent error due to possible filtration adsorption losses[10], at least 25 ml of suspension was first passed through the membrane. Additional suspension was collected for GLC analysis.

For GLC analysis, 5 ml of filtrate and a known amount of testosterone standard were mixed and evaporated to dryness under nitrogen. To the residue were added 15 ml of pyridine and 65 ml of *N,O*-bis(trimethylsilyl)trifluoroacetamide plus 1% trimethylchlorosilane[11]. The tube was immediately capped and mixed thoroughly on a vortex mixer[12]. The derivatized sample was injected onto a column packed with 2% DEGS on 100–120-mesh Gas Chrom Q. Analyses were performed under conditions described previously (8).

Equilenin was analyzed also by a UV method. Equilenin solubility was determined as a function of pH. The solution pH was adjusted with 0.1 *N* sodium hydroxide or 0.1 *N* hydrochloric acid, and the final pH was measured at the time of filtration. The filtrate pH was adjusted to 11.5 with 0.1 *N* sodium hydroxide. The solution concentration was determined from the absorbance at 245 nm with the molar absorptivity ($\epsilon = 5.22 \times 10^4$) for the ionized form.

Solutions for Spectrophotometric Determinations—While solution concentrations were higher than 2.0×10^{-5} *M* in previous investigations (2, 4, 5), relatively low concentrations, ranging from 2.4×10^{-6} to 1.5×10^{-5} *M* depending on the compound solubility, were used in this study. These concentrations gave either stable unsaturated or slightly oversaturated metastable solutions. The slightly oversaturated solutions were checked by UV to determine their turbidity. All solutions were stable without precipitation during the time of measurement.

Stock solutions of estrogens, 3.0×10^{-3} *M*, were prepared by dissolving weighed amounts in 100 ml of pure ethanol. Aliquots of 0.12–0.5 ml were then diluted to 100 ml with distilled water. During the dilution process, the stock solution was added dropwise with stirring to prevent localized precipitation. The solution pH was adjusted with 0.1 *N* hydrochloric acid or 0.1 *N* sodium hydroxide. The UV spectrum of the solution was recorded immediately after a stable pH reading was obtained. Spectrophotometric determinations were carried out at room temperature, 23 ± 2°.

Experimental pKa—Three distinct absorption spectra were observed for the compounds. Figure 1 shows the UV spectra of 17α-estradiol at different pH conditions. In acid solution, the molar absorptivity at the 278-nm absorption peak was 1.81×10^3 cm^{-1} *M*$^{-1}$. Two absorption peaks at 238 ($\epsilon = 9.07 \times 10^3$ cm^{-1} *M*$^{-1}$) and 296 (2.67×10^3) nm were found in alkaline solution. Other compounds with similar absorption spectra included estrone, estriol, equilin, 17α-dihydroequilin, ethinyl estradiol, and 5,6,7,8-tetrahydro-2-naphthol; they had corresponding molar absorptivities in acid solution at 278 nm of 1.85×10^3, 1.84×10^3, 1.81×10^3, 1.93×10^3, 1.89×10^3, and 2.00×10^3 cm^{-1} *M*$^{-1}$, respectively.

In alkaline solution, the molar absorptivities at the two absorption peaks were 9.26×10^3 and 2.76×10^3 cm^{-1} *M*$^{-1}$ for estrone, 9.20×10^3

[1] Ayerst Research Laboratories, Montreal, Quebec, Canada.
[2] Searle Chemical Inc.
[3] Aldrich Chemical Co.
[4] Anachemia Chemicals.
[5] Cary model 14.
[6] Corning model 110.
[7] Bendix model 2500.
[8] Honeywell model 19.
[9] Nuclepore.
[10] A. Hurwitz and S. Liu, to be published.
[11] Regisil, RC2, Regis Chemical Co.
[12] Lab-line, Melrose Park, Ill.

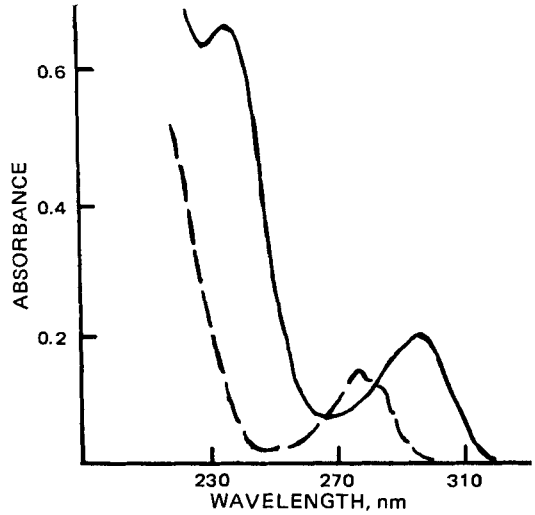

Figure 1—*UV spectrum of 17α-estradiol at a concentration of 1.50 × 10^{-5} M and a cell length of 5 cm. Key: ——, pH 12.3; and - - -, pH 3.6.*

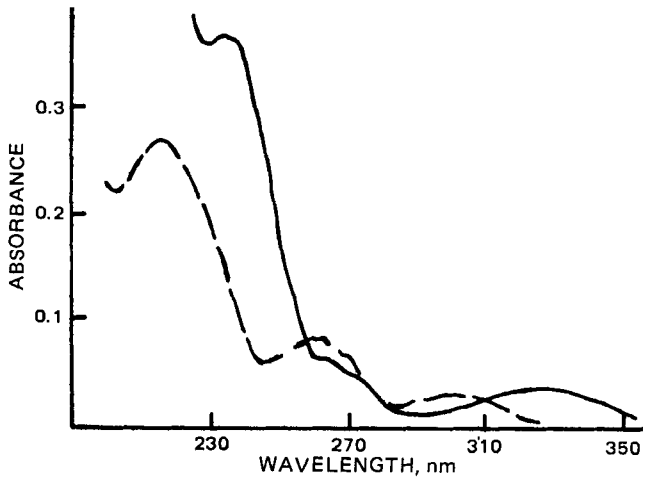

Figure 2—*UV spectrum of 6-dehydroestrone at a concentration of 2.40 × 10^{-6} M and a cell length of 5 cm. Key: ——, pH 12.0; and - - -, pH 3.0.*

and 2.73 × 10^3 cm^{-1} M^{-1} for estriol, 8.93 × 10^3 and 2.56 × 10^3 cm^{-1} M^{-1} for equilin, 8.80 × 10^3 and 2.65 × 10^3 cm^{-1} M^{-1} for 17α-dihydroequilin, 9.00 × 10^3 and 2.72 × 10^3 cm^{-1} M^{-1} for ethinyl estradiol, and 7.33 × 10^3 and 2.75 × 10^3 cm^{-1} M^{-1} for 5,6,7,8-tetrahydro-2-naphthol. Figures 2 and 3 show the UV spectrum of 1,3,5(10),6-estratetraen-3-ol-17-one and equilenin, respectively. From these figures, the influence on the UV spectra of the addition of one or two conjugated double bonds in the B ring can be seen. In contrast, equilin, having a nonconjugated double bond in the B ring, gave the same absorption spectrum as estrone.

The absorption maxima for 1,3,5(10),6-estratetraen-3-ol-17-one was at 235 (ε = 3.08 × 10^4 cm^{-1} M^{-1}) and 325 (2.58 × 10^3) nm in alkaline solution and at 215 (ε = 2.29 × 10^4 cm^{-1} M^{-1}), 261 (7.17 × 10^3), 271 (5.83 × 10^3), and 331 (2.50 × 10^3) nm in acid solution. Equilenin had maxima at 242 (ε = 5.22 × 10^4 cm^{-1} M^{-1}), 274 (6.80 × 10^3), 285 (7.47 × 10^3), 295 (4.53 × 10^3), and 355 (3.13 × 10^3) nm for the ionized form and at 228 (ε = 5.47 × 10^4 cm^{-1} M^{-1}), 269 (4.53 × 10^3), 280 (5.33 × 10^3), 292 (4.00 × 10^3), and 338 (2.47 × 10^3) nm for the neutral species.

Wavelengths selected for the pKa determinations were 240, 248, 295, and 300 nm for estrone, 17α-estradiol, estriol, ethinyl estradiol, 5,6,7,8-tetrahydro-2-naphthol, equilin, and 17α-dihydroequilin; 235 and 248 nm for 1,3,5(10),6-estratetraen-3-ol-17-one; 230, 240, and 250 nm for equilenin; and 355 and 370 nm for 17β-dihydroequilenin. All experiments were carried out using 5-cm cells, except for equilenin and 5,6,7,8-tetrahydro-2-naphthol where 2-cm cells were used.

RESULTS AND DISCUSSION

Solubility Determinations—Several studies reported the solubilities of estrone and estradiol in organic solvents (9) and aqueous solutions containing amino acids (10) or surfactants (11). However, few solubility values for estrogens in pure water are available. It was important to determine estrogen aqueous solubilities first in order to choose suitable concentration ranges for the spectrophotometric pKa determination. The improper choice of concentration may result in serious interference due to precipitation. A solubility value of 1.17 × 10^{-4} *M* was reported (12) for estrone in pure water. However, precipitation resulted when a concentrated estrone–ethanol solution was diluted in pure water to 1.5 × 10^{-5} *M*. This finding clearly indicated that the solubility of estrone in pure water is much less than 1.17 × 10^{-4} *M*.

Solubility determinations were made for estrone, 17α-estradiol, equilin, equilenin, 17α-dihydroequilin, 17α-dihydroequilenin, estriol, and ethinyl estradiol. No detectable difference in solubility values was observed for samples stirred for 4 or 24 hr. Satisfactory agreement between the UV and GLC results was found for equilenin. The experimental variation was within ±5%. Solubility values for estrone and 17α-estradiol determined by UV were about 20% to more than 50% higher than values obtained by GLC. This result indicated that these two compounds contained trace impurities of either high absorbance or relatively high solubility. Results of the GLC determinations of solubilities are shown in Table I.

The aqueous solubility observed for 17α-estradiol, 1.43 × 10^{-5} *M*, was in agreement with a literature value (1.40 × 10^{-5} *M*) obtained in 0.02 *M*

Table I—Solubility Values of Some Estrogens

Compound	Solvent	Solubility μg/ml	Solubility *M*
Estrone	Water	0.8	2.96 × 10^{-6}
17α-Estradiol	Water	3.9	1.43 × 10^{-5}
Ethinyl estradiol	Water	9.7	3.28 × 10^{-5}
Estriol	Water	3.2	1.11 × 10^{-5}
Equilin	Water	1.4	5.22 × 10^{-6}
Equilenin	pH 7.20 buffer	1.5	5.64 × 10^{-6}
	pH 8.30 buffer	1.6	6.10 × 10^{-6}
	pH 9.63 buffer	2.9	1.11 × 10^{-5}
	pH 9.85 buffer	3.6	1.37 × 10^{-5}
	pH 9.98 buffer	4.6	1.72 × 10^{-5}
	pH 10.2 buffer	6.5	2.46 × 10^{-5}
17α-Dihydroequilin	Water	10.7	3.96 × 10^{-5}
17α-Dihydroequilenin	Water	6.1	2.28 × 10^{-5}

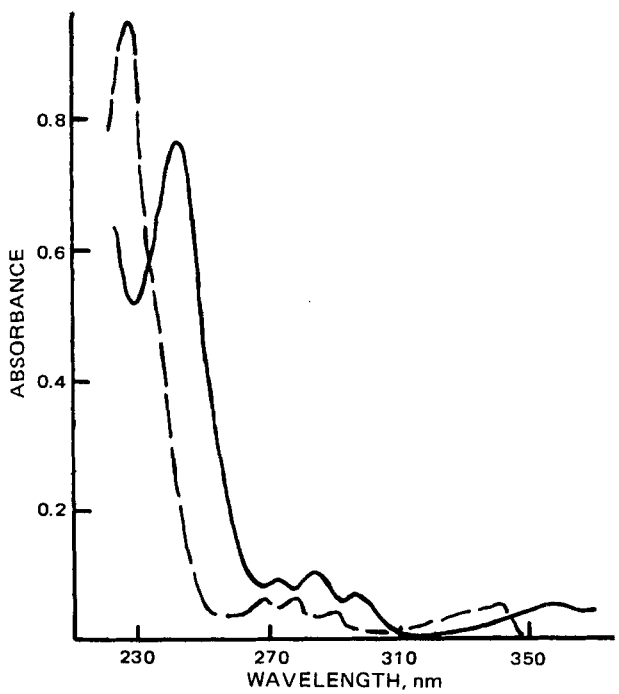

Figure 3—*UV spectrum of equilenin at a concentration of 7.5 × 10^{-6} M and a cell length of 2 cm. Key: ——, pH 12.0; and - - -, pH 3.0.*

Table II—Spectrophotometric Determination of pKa of 17α-Estradiol[a]

pH	240 nm Absorbance	240 nm pKa	248 nm Absorbance	248 nm pKa	295 nm Absorbance	295 nm pKa	300 nm Absorbance	300 nm pKa
12.3	0.670	—	0.423	—	0.200	—	0.192	—
3.6	0.047	—	0.015	—	0.007	—	0.0	—
10.37	0.342	10.42	0.218	10.38	0.096	10.44	0.089	10.43
10.51	0.360	10.51	0.227	10.48	0.102	10.52	0.098	10.49
10.38	0.326	10.47	0.200	10.46	0.095	10.46	0.090	10.44
10.65	0.421	10.47	0.265	10.45	0.120	10.50	0.115	10.47
10.30	0.298	10.47	0.180	10.47	0.086	10.46	0.080	10.45
				pKa = 10.46 ± 0.03				

[a] Cell length = 5 cm; concentration = 1.50×10^{-5} *M*.

sodium chloride solution (10). Experimental results show that estradiol is more soluble than estrone in pure water. Other investigations also revealed that estradiol has higher solubility in aqueous solutions containing surfactant materials (11). From the estrogen compounds examined, it would be expected that corresponding compounds would show a similar range of solubilities.

Spectrophotometric Determination of pKa Values—The thermodynamic ionization constant is expressed by $HA \rightleftharpoons H^+ + A^-$ and:

$$K_a = \frac{A_{H^+}[A^-]f_1}{[HA]} \quad \text{(Eq. 1)}$$

where A_{H^+} is the activity of hydrogen ion, f_1 is the activity coefficient of univalent ion, and $[A^-]$ and $[HA]$ represent the concentration of ionic and neutral species of the estrogen, respectively. At the low concentrations used, the activity coefficient, f_1, should approach 1. The following equation was employed to determine the ionization constant:

$$pKa = pH - \log\frac{[A^-]}{[HA]} = pH - \log\frac{A - A_a}{A_b - A} \quad \text{(Eq. 2)}$$

where A is the absorbance of a solution at a specific pH. The corresponding absorbances of the same concentration solution in alkaline and acid solution are A_b and A_a. The advantage of calculation with Eq. 2 and comparison of solutions at the same concentration was that the possible error due to the dilution process could be reduced. The present study was carried out in very dilute solution without salt or buffer reagents to eliminate f_1 in Eq. 1.

In previous studies, usually only one wavelength was used experimentally. However, more than one wavelength was used in the present study. Typical results for the pKa determination of 17α-estradiol are shown in Table II. Absorbance at 240 nm was about three times higher than that at 295 nm. Excellent agreement was obtained between the pKa values determined at different wavelengths. The reproducibility of these results illustrated the reliability of the present procedure. The pKa of 17α-estradiol obtained was 10.46 ± 0.03 *SD*.

A summary of the pKa values of the compounds studied is given in Table III. 17α-Estradiol, estriol, and ethinyl estradiol showed pKa values of 10.38–10.46, which were slightly higher than 10.34 observed for estrone. The difference in the pKa value between estradiol and estrone was 0.12, in good agreement with the value of 0.10 reported previously (3). The thermodynamic pKa values of estrone and 17α-estradiol observed in the present study were quite close to the apparent pKa of 10.26 for estrone and of 10.30 for estradiol reported by Egorova *et al.* (4, 5). Since these latter studies were done in buffered solutions, the slightly lower apparent pKa value reported may be due to neglected correction of the activity coefficient.

Kirdani and Burgett (2) used a spectral technique to study the ionization of five estrogens and reported a pKa value 10.91 for estrone. However, this high value resulted from certain errors in their calculations. Recalculation of their data gave a value of 10.10, close to their reported values of 10.08 for 17β-estradiol and 10.10 for 17α-estradiol.

Other reported pKa values include 11.0 for estrone determined by a back-titration technique (6) and 9.36 for estrone and 9.11 for estriol in methanol solution (7) determined by a conductiometric titration method. The great discrepancy in reported values may result from different experimental conditions. Since the present experiments were made at relatively low concentrations, possible interference due to precipitation can be eliminated. In contrast, most of the previous studies were made at quite high supersaturated conditions. For example, Egorova *et al.* (4, 5) and Kirdani and Burgett (2) employed concentrations from 3.0×10^{-5} to 8.8×10^{-5} *M*. As mentioned before, the metastable supersaturation limit of estrone in pure water is less than 1.5×10^{-5} *M*. Therefore, it would be quite difficult to prepare clear solutions, free from precipitation, at such a high concentration. The unavoidable colloidal precipitation that would result would cause serious error in the pKa determination. Furthermore, only one wavelength, 300 nm, was used (2) in the determination of the pKa values of estrone and estradiol. Due to the low absorbance at this wavelength, any interference would cause a large error in the measurements. The advantages of using stable, low concentration solutions and different wavelengths were illustrated by the good agreement obtained for pKa value determinations.

Table III—pKa Values of Several Estrogens and Related Compounds

Compound	Number of Determinations	Concentration, *M*	pKa	Literature pKa
Estrone	5	7.5×10^{-6}	10.34 ± 0.05	10.91 (2), 10.26 (4, 5)
	2	5.4×10^{-6}	—	—
17α-Estradiol	5	1.5×10^{-5}	10.46 ± 0.03	10.10 (2), 10.30 (4, 5)
Estriol	3	1.5×10^{-5}	10.38 ± 0.02	—
	2	9.0×10^{-6}	—	—
Ethinyl estradiol	6	1.5×10^{-5}	10.40 ± 0.01	—
Equilin	3	1.5×10^{-5}	10.26 ± 0.04	—
	4	9.0×10^{-6}	—	—
17α-Dihydroequilin	2	1.5×10^{-5}	10.29 ± 0.02	—
	3	9.0×10^{-6}	—	—
6-Dehydroestrone	4	2.4×10^{-6}	10.17 ± 0.04	—
Equilenin	4	7.5×10^{-6}	9.75 ± 0.06	—
17β-Dihydroequilenin[a]	5	—	9.77 ± 0.04	—
Phenol	—	—	—	10.00 (1)
m-Cresol	—	—	—	10.09 (1)
p-Cresol	—	—	—	10.26 (1)
5,6,7,8-Tetrahydro-2-naphthol	6	1.5×10^{-5}	10.51 ± 0.02	10.32 (1) (20°)
1-Naphthol	—	—	—	9.30 (1) (20°)
2-Naphthol	—	—	—	9.63 (1) (20°)

[a] The material used also contained 17β-dihydroequilin. Determinations were made at 370 nm to prevent interference.

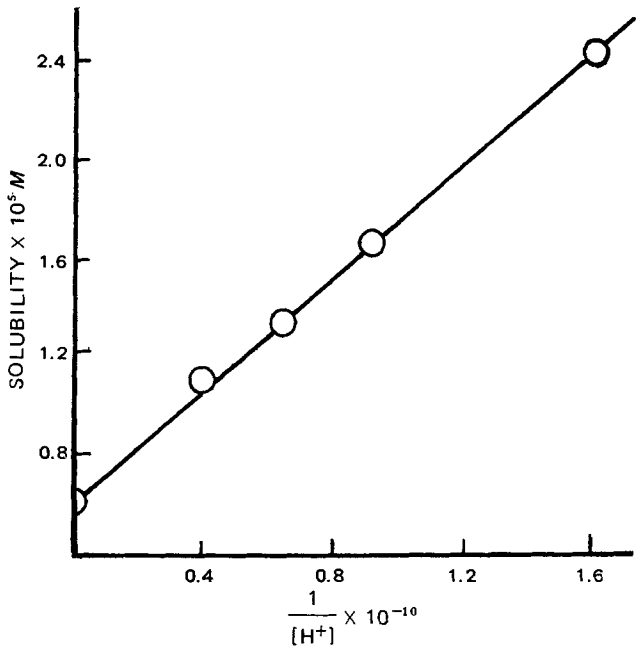

Figure 4—*Plot of solubility* versus *the reciprocal of the hydrogen-ion concentration for equilenin.*

In previous studies (2–5), small pKa value differences between estrone and estradiol were explained in terms of long-range D to A ring transmission effects. While conformational or steric transmission effects have important consequences in some reaction systems, it is not likely that electronic transmission affecting pKa occurs for estrone and estradiol. The experimental data obtained show small differences in pKa values. However, these differences apparently fall within anticipated experimental reproducibility ranges. No significant effect on pKa values occurred when the C-17 substituent was varied between carbonyl and hydroxyl for three pairs of compounds. Values for estrone, 17α-estradiol, ethinyl estradiol, and estriol ranged from 10.34 to 10.46. Where an unconjugated double bond was present in the B ring, as in equilin and 17α-dihydroequilin, pKa values were 10.26 and 10.29, respectively. When a single double bond in the B ring was in conjugation with the A ring, as in 1,3,5(10),6-estratetraen-3-ol-17-one, the pKa value observed was 10.17. For fully unsaturated B ring compounds such as equilenin and 17β-dihydroequilenin, pKa values were 9.75 and 9.77, respectively.

The acidity of the estrogens was increased by introduction of one or more double bonds in the B ring. The pKa values of estrone and related derivatives followed the order estrone > equilin > 1,3,5(10),6-estratetraen-3-ol-17-one > equilenin. The conjugated double bond in 1,3,5(10),6-estratetraen-3-ol-17-one had a greater effect in increasing acidity than the nonconjugated double bond in the B ring of equilin. Among the compounds examined, the fully conjugated B ring of equilenin produced the most profound effect in reduced pKa value. The pKa of equilenin was 0.59 unit lower than that of estrone. Similar inductive effects were found among estradiol, 17α-dihydroequilin, and 17β-dihydroequilenin.

Literature pKa values of phenol and some simple derivatives are listed in Table III for comparison. Comparison of the pKa values of 5,6,7,8-tetrahydro-2-naphthol and phenol shows that the attachment of a saturated B ring at the *meta*- and *para*-positions caused an increase in pKa of 0.5 unit. By contrast, a fully unsaturated naphthol such as 1-naphthol or 2-naphthol showed an increased acidity greater than that of phenol. The results with the more complicated estrogens were consistent with these general observations.

Solubility Method Determination of Equilenin pKa—The phenolic steroids studied are quite insoluble weak acids. Solubility changes as a function of pH provide a useful method for determining the ionization constants of these compounds. Equilenin was chosen for the comparison of pKa determination methods. Solubility values of equilenin at different pH values are listed in Table I. It was expected that a sharp increase in solubility would occur at pH values near or greater than the pKa value. Solubility values, S, can be expressed for the present experimental conditions by:

$$S = [HA] + [A^-] = [HA] + \frac{K_a[HA]}{[H^+]} \qquad \text{(Eq. 3)}$$

where [HA] is the intrinsic solubility of the neutral or undissociated species of equilenin. A linear relationship was found between S and $1/[H^+]$, as shown in Fig. 4. A value of [HA] can be obtained either from the intercept of this plot or by direct measurement in acid solution. The value for [HA] obtained from direct measurement was 5.71×10^{-6} M, which was close to that obtained from the intercept, 6.10×10^{-6} M. Linear regression was employed to determine the slope of the plot. The association constant was calculated from the equation: slope = $K_a \times [HA] = 1.13 \times 10^{-15}$. The pKa thus obtained was 9.72, in excellent agreement with the value obtained by spectrophotometric determination.

This solubility technique could also be applied in the determination of the ionization constants of other phenolic steroids. However, if a spectrophotometric method is employed for analysis, special precautions must be taken to avoid possible interference by impurities.

REFERENCES

(1) A. Albert and E. P. Serjeant, "Ionization Constant of Acids and Bases," T. and A. Constable Ltd., Edinburgh, Scotland, 1971.

(2) R. Kirdani and M. Burgett, *Arch. Biochem. Biophys.*, **118**, 33 (1967).

(3) M. Legrand, V. Delaroff, and J. Mathieu, *Bull. Soc. Chim. Fr.*, **1961**, 1346.

(4) V. Egorova, A. Zakharychev, and S. Ananchenko, *Izv. Akad. Nauk SSSR Ser. Khim.*, **3**, 726 (1972).

(5) V. Egorova, A. Zakharychev, and S. Ananchenko, *Tetrahedron*, **29**, 301 (1973).

(6) G. F. Marrian, *Biochem. J.*, **24**, 1019 (1930).

(7) A. Butenandt and U. Z. Westphal, *Physiol. Chem.*, **223**, 147 (1934).

(8) R. Johnson, R. Masserano, R. Haring, B. Kho, and G. Schilling, *J. Pharm. Sci.*, **64**, 1007 (1975).

(9) M. W. Ruchelman and P. Haines, *J. Gas Chromatogr.*, **5**, 290 (1967).

(10) R. Hahnel, *J. Steroid Biochem.*, **2**, 61 (1971).

(11) C. Blomquist and L. Sjoblom, *Acta Chem. Scand.*, **18**, 2404 (1964).

(12) "The Merck Index," 8th ed., Merck and Co., Rahway, N.J., 1968, p. 924.

ACKNOWLEDGMENTS AND ADDRESSES

Received March 15, 1976, from the *Pharmaceutical Research and Development Division, Ayerst Laboratories, Inc., Rouses Point, NY 12979.*

Accepted for publication June 17, 1976.

The authors thank Dr. R. Johnson for cooperation and assistance in obtaining the estrogen samples and are grateful for the technical assistance of Mr. R. Haring in performing GLC analysis.

[x] To whom inquiries should be directed.

Acetylacroninium Salts as Soluble Prodrugs of the Antineoplastic Agent Acronine

D. W. A. BOURNE *§, T. HIGUCHI ‡, and A. J. REPTA ‡x

Abstract □ The low aqueous solubility of acronine (~2 mg/liter) has been overcome by identification of quaternary prodrug salts exhibiting apparent molar solubilities two to five orders of magnitude greater than acronine. The synthesis and kinetics of hydrolysis of the various prodrug acetylacroninium salts were studied, and the half-life for hydrolysis under conditions approximating the *in vivo* situation was estimated to be about 5 min. Such rapid reversion, together with the greatly increased solubility, appears to qualify the prodrug for intravenous use.

Keyphrases □ Acronine—quaternary salts of acetyl derivative synthesized as prodrugs for intravenous use, solubilities and kinetics of hydrolysis studied □ Acetylacroninium salts—synthesized as prodrugs for intravenous use, solubilities and kinetics of hydrolysis studied □ Prodrugs, potential—quaternary salts of acetyl derivative of acronine synthesized for intravenous use, solubilities and kinetics of hydrolysis studied □ Antineoplastic agents—acronine, quaternary salts of acetyl derivative synthesized as prodrugs for intravenous use, solubilities and kinetics of hydrolysis studied

Acronine (I), a derivative of 1,3-dihydroxy-9-acridanone[1], was first isolated in 1948 (2, 3). Later, the compound was found to exhibit activity (4) against various rodent tumor system cultures when administered as an aqueous suspension by different routes. However, the extremely low solubility of acronine (2–3 mg/liter[2]) has presented problems in the clinical evaluation of the drug administered orally as a capsule[3].

A suitable intravenous formulation of acronine would obviate problems associated with the GI absorption of the nearly insoluble drug. However, the problem of low solubility, together with the estimated adult human dose of 100 mg[3], presented a significant barrier to intravenous use.

BACKGROUND

A coprecipitate of acronine with povidone (5) was about 15 times as water soluble as acronine alone, and the cytotoxic activity of acronine in the coprecipitate was about twice that of acronine itself. This study (5) demonstrated that increased solubility yielded improved drug activity, but the coprecipitate approach did not appear capable of producing the concentration increases necessary for a suitable intravenous dosage form.

The objective of the present study was to identify physical and/or chemical approaches for the solubilization of acronine in vehicle systems suitable for intravenous administration. Various approaches were considered including complexation, simple salt formation, and mixed solvent systems. Most approaches were ruled out due to the physicochemical properties of acronine (*e.g.*, its weakly basic nature) and/or the insufficient increase in solubility expected.

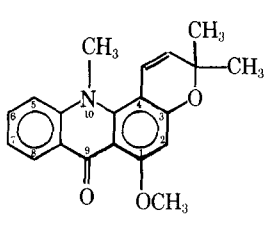

I

It was concluded that the required solubility increase would best be accomplished through the identification of a chemically derived prodrug of acronine. This report deals with the identification, synthesis, and properties of a derivative of acronine. It presumably satisfies the increased solubility requirement and yet lies within those constraints (6, 7) inherent in a satisfactory prodrug.

Acronine, mol. wt. 321.3, pKa (protonated form) 1.6, mp 176–178°, has solubilities at 25° of 3.2, 27.5, and 3×10^{-4} g/100 ml in acetone, chloroform, and water, respectively. The low aqueous solubility of acronine is probably due to its very hydrophobic nature rather than to strong interactions among molecules in the crystalline state. Therefore, a prodrug with greatly increased hydrophilic character (8, 9) might afford the greatest probability for attaining the desired solubility increase (~1 mg/ml).

Compound I contains no functional groups that could be derivatized to yield a soluble prodrug that would rapidly revert to I following intravenous administration. However, the apparent solubility of I in aqueous hydrochloric acid was >1 mg/ml at pH ~0. Although the pharmaceutical use of such a highly acidic solution is impractical, this observed solubility of acroninium chloride suggested that the presence of a formal charge on the acronine molecule might yield an increased solubility of the magnitude desired.

Evaluation of the reported acid–base behavior of 9-acridanone (II, Scheme I) indicates that protonation of that weak base occurs at the carbonyl oxygen (10), resulting in a fully aromatic 9-acridanonium ion (II*a*) where the positive charge resides on the nitrogen. Since acronine is structurally similar to 9-acridanone, an equilibrium similar to that shown in Scheme I may be found for acronine under strongly acid conditions. The existence of such an equilibrium suggests that the carbonyl oxygen of acronine might react under suitable conditions to form an ether or ester derivative at the 9-position.

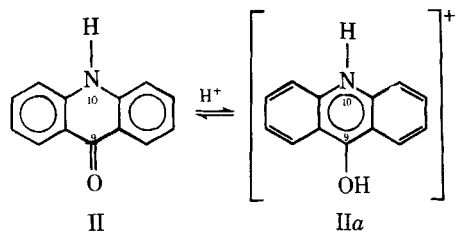

II IIa

Scheme I

A derivative such as I*a* is a quaternary salt analogous to the protonated form of acronine and would be worthy of evaluation as a soluble prodrug of acronine, since its ester linkage might be more rapidly cleaved (6) to yield the parent drug than would the corresponding ethers. Various acetylacroninium salts (I*a*, R = methyl) were chosen as the desired candidates for initial evaluation. The anions expected to influence solubility were chosen from the more common strong inorganic acids.

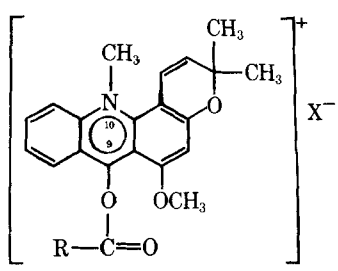

I*a*

[1] All species discussed that contain the acridine skeleton are treated as derivatives of acridine. Therefore, the numbering system employed is that most widely used for acridine (1) and not acronine (3,12-dihydro-6-methoxy-3,3,12-trimethyl-7*H*-pyrano[2,3-c]acridin-7-one).

[2] See C. A. Hewitt, Stanford Research Institute Report (SRI 758 and 770) to the National Cancer Institute, Aug. 20, 1968.

[3] J. P. Davignon, National Cancer Institute, personal communication.

RESULTS AND DISCUSSION

Preparation and Characterization of Prodrug Salts—Acetylacroninium perchlorate was synthesized by heating a suspension of acroninium perchlorate in acetic anhydride[4] at ~100° for a short period and then cooling to room temperature. The acetylacroninium perchlorate formed was isolated as a burgundy-colored crystalline solid after the reaction filtrate was diluted with cold ether.

The solid material contained ~80% of acetylacroninium perchlorate; the remaining ~20% of the sample consisted of I and the perchlorate salt of I. Attempts to purify the samples (relative to acetylacroninium perchlorate content) were unsuccessful due to the instability of the compound. Since the impurities did not present a major problem in the evaluation of approximate solubilities and stability properties, extensive efforts to obtain high purity samples of acetylacroninium perchlorate did not appear justified.

The assignment of the structure of the acetylacroninium species was based on NMR and IR spectra and the fact that the compound hydrolyzed rapidly to yield acronine.

Solubility of Salts—Following the characterization of acetylacroninium perchlorate, the chloride, sulfate, phosphate, and bromide salts were prepared. These salts were appreciably less stable and less pure than the perchlorate salt. Because of the rather rapid hydrolysis of the acetylacroninium ion, it was not possible to obtain equilibrium data on the solubility of the various salts. However, approximate values were obtained by shaking excess quantities of the solid samples with 0.05 *M* phosphate buffer (pH 7.0) for several minutes, filtering, and allowing the filtrates to stand at 22° until hydrolysis of the acetylacroninium ion was complete. The acronine content of each filtrate was then determined spectrophotometrically. The salt solubilities, expressed as acronine content in grams per 100 ml, were: perchlorate, 0.025–0.030; sulfate, 0.15–0.2; bromide, 0.6–0.8; chloride, 1.2–1.5; and phosphate, 1.2–2.0. Since the aqueous equilibrium solubility of acronine was less than 1% of that observed for the various acetylacroninium salts, the acronine content of the filtrate was essentially completely attributable to the salt itself. Although considerable error was inherent in such determinations, the results appeared meaningful.

The solubility of the chloride salt was about the same as that of the phosphate salt, possibly because of the *in situ* formation of the phosphate salt under these conditions.

A comparison of the solubility values of the salts with those of acronine (about 2–3 mg/liter) demonstrated that even the perchlorate salt, which was the least soluble, exhibited about a 100-fold greater solubility than acronine; the more soluble chloride and phosphate salts were about 10,000 times more soluble than free acronine. Therefore, the use of any acetylacroninium salt would yield at least the minimum required increase in solubility necessary to formulate a parenteral solution of reasonable volume. However, it was yet to be determined whether these salts would be otherwise suitable for use in such solutions. Therefore, the hydrolysis of the acetylacroninium salts was studied.

Hydrolysis of Prodrug—When near-saturated aqueous solutions of the acetylacroninium salts were prepared and allowed to stand, a precipitate of acronine formed. Additionally, when aqueous solutions of the salts were prepared and examined by TLC [benzene–acetone (1:1) on silica gel] at various times, two spots were observed initially: a yellow spot (R_f 0.76) and a purple or wine-colored spot (R_f 0.17) corresponding to acronine and the prodrug, respectively. In several hours, the wine-colored spot disappeared completely and the acronine spot was enlarged, indicating a rapid and complete reversion of the acetylacroninium perchlorate (wine-colored spot) to acronine.

The rate at which the acetylacroninium perchlorate was hydrolyzed to yield acronine was studied quantitatively in pH 0–11 aqueous solutions. A plot (Fig. 1) of the logarithm of the observed half-life *versus* pH data indicated that the hydrolytic rate was pH independent at pH <8. The data for pH ≥2.6 were obtained in various buffers at 3×10^{-3} to 5×10^{-2} *M*. From these and other data[5], it appeared that the hydrolytic rate was relatively unaffected by various buffer components at low concentrations and that the spontaneous rate of hydrolysis under such conditions occurred with a half-life of about 20–25 min. At pH >8, however, there appeared to be hydroxide-ion catalysis, as evidenced by a negative slope of approximately unity at pH >9.

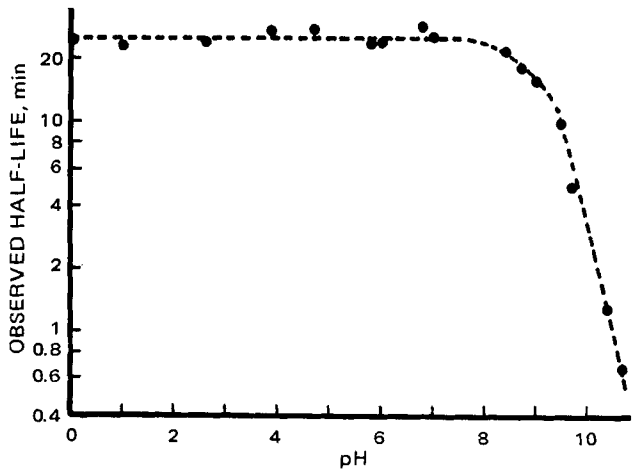

Figure 1—*Plot of observed half-life for the hydrolysis of acetylacroninium perchlorate at 25.4° in various buffers.*

The hydrolysis rate of the prodrug in pH 6.9 phosphate buffer (0.1 *M*) was also studied at 15, 25, and 30°; these data were used to construct an Eyring plot. From the slope and intercept of that plot were determined the enthalpy of activation (19.5 kcal/mole) and the entropy of activation (−16 cal/mole degree), respectively. On the basis of the temperature study data, it was estimated that the half-life for hydrolysis at body temperature of 37° would be about 5 min or even less if enzymatic enhancement (6) occurred *in vivo*.

Some studies of the influence of both the ionic strength of aqueous buffers and the dielectric constant of a mixed aqueous–organic solvent on the hydrolysis rate of acetylacroninium perchlorate were also carried out. When the ionic strength of an aqueous phosphate buffer (0.1 *M*, pH 7) was varied fivefold from 0.02 to 0.1 *M*, no significant difference was observed for the hydrolysis rate of the prodrug at 25°. However, when the hydrolytic rate of the acetylacroninium salt was followed in solutions prepared by mixing given volumes of acetone with a phosphate buffer (pH 7.0, 0.05 *M*, I = 0.1 *M*), the rate increased nearly linearly with the percent (v/v) acetone from 0 to 60%. The observed half-life of the reactions over that range of acetone concentration decreased from about 23 to 10 min.

These data suggested that the decrease in the dielectric constant when going from simply aqueous media to increasing concentrations of acetone enhanced the reaction rate. Since the reaction was hydrolytic, the rate was also a function of the water concentration. Therefore, the decrease in the water concentration at increased acetone concentrations perhaps accounted for the fact that little or no difference in the hydrolytic rate was observed in solutions containing 60 and 80% acetone in water.

When the hydrolytic rates of the other prepared salts were studied in phosphate buffer (pH 7, 0.05 *M*, I = 0.1), none differed significantly from that of the perchlorate. These latter results were not unexpected, since all prepared salts probably were completely dissociated in dilute aqueous solution and, therefore, the hydrolysis of the acetylacroninium ion should have been independent of the anion.

Applications—On the basis of these studies, it appears that the acylacroninium salts may be suitable for use as prodrugs of acronine. The major feature of the quaternary salts is the greatly enhanced solubility coupled with their rapid reversion to the parent alkaloid under conditions approximately like those encountered *in vivo*.

The information presented here together with data on the acetylacroninium perchlorate salt served as the basis for the formulation of an experimental intravenous prodrug formulation of acronine (11).

EXPERIMENTAL

Materials—Acronine[6] was used as obtained, mp 175–177° [lit. (3) mp 174–176°] and homogeneous by TLC [benzene–acetone (2:1) on silica gel[7]], R_f 0.45. All other chemicals were reagent grade. Water was distilled from acid permanganate solution in an all-glass still.

Procedures—*Acroninium Salts*—The simple acroninium salts were prepared by dissolving acronine (5 g) in acetone (175 ml) and adding 4

[4] When reactions were attempted using acetyl chloride as the acetylating agent under conditions similar to these described here, insignificant quantities of the prodrug salt were obtained.

[5] Changes in the acetate buffer concentration (pH 4.6) from 0.1 to 0.5 *M* decreased the half-life for hydrolysis by only approximately 5 min.

[6] Batch 1, Sample MH, CSIRO, obtained from the National Cancer Institute.

[7] Polygram Sil G/uv, Brinkmann Instruments.

ml of the appropriate aqueous acid. The acid solutions used were 37% (w/w) hydrochloric, 71% (w/w) perchloric, 53% (w/w) phosphoric, and 50% (w/w) hydrobromic acids. Upon mixing, the respective salts precipitated as bright red-orange solids. All but the phosphate were isolated at room temperature. The phosphate salt required cooling (~0°) to obtain good yields. The yield of all salts was 95% or better. All acroninium salts melted with decomposition as follows: perchlorate, 245–255°; chloride, 158–160°; bromide, 188–190°; sulfate, 158–160°; and phosphate, 182–184°.

Acetylacroninium Salts—Each acetylacroninium salt was prepared by heating the corresponding acroninium salt (~1 g) with acetic anhydride (~20 ml) at 100° for 10–15 min in a suitable flask fitted with a water-cooled condenser and calcium chloride-filled drying tube. The reaction mixture was then cooled to room temperature. Undissolved acroninium salt was removed by filtration, and the filtrate was quickly added to cold (~0°) ether (~200 ml). The acetylacroninium salt readily separated as a fluffy purple solid. This solid was immediately separated by filtration, rinsed with cold ether (50 ml), dried, and stored in a desiccator.

Solid acetylacroninium perchlorate was quite stable and could be stored at room temperature in a desiccator over calcium chloride for months with little or no change. However, the other salts were extremely hygroscopic and thus unstable due to hydrolysis. Therefore, these salts were stored in a desiccator cooled with solid carbon dioxide. The chloride salt was so hygroscopic that all handling procedures were carried out in a dry box under a nitrogen atmosphere.

Characterization of Acetylacroninium Salts—The characterization of acetylacroninium perchlorate was based primarily on spectral data and chemical behavior. The IR[8] spectra of acetylacroninium perchlorate and acroninium perchlorate (as potassium bromide pellets) were qualitatively quite similar, except for strong carbonyl absorption at 1790 cm^{-1} for the acetylacroninium salt. Absorption at that wave number was completely absent in the simple acroninium salt. The absorption at 1790 cm^{-1} was attributed to the carbonyl absorption (12) of the acetyl group.

The NMR[9] spectrum of the acetylacroninium perchlorate (in formamide and in dimethyl sulfoxide-d_6) exhibited a sharp singlet at δ 2.65, which integrated for about three protons and was consistent (13) with an acetate ester of the type Ia. Upon standing in such solutions, the absorption at δ 2.65 decreased and a new singlet appeared at δ 2.08. Since acetic acid also produced a sharp singlet at δ 2.08 when added to either of the solvents, it was concluded that acetic acid was being produced in the NMR tube as a result of the hydrolysis of the ester linkage. While ester hydrolysis was fairly rapid initially in the NMR studies, the rate decreased with time, apparently due to consumption of the limited amounts of water present in such solvents.

Another observation was that the *gem*-dimethyl protons of acetylacroninium perchlorate absorbed at δ 1.70 while those of acronine absorbed at δ 1.47. The hydrolysis of the ester (as already described) resulted in a decrease in the δ 1.70 peak and the corresponding appearance of a peak at δ 1.47.

When an aqueous solution of acetylacroninium perchlorate was freshly prepared, it was deep burgundy in color. Upon standing, the color became yellow and a yellow precipitate formed. This precipitate was identified as acronine. The hydrolysis was also followed by TLC as described under *Results and Discussion*.

In view of the impurity of the samples obtained, elemental analysis data were not considered meaningful, although agreement with theory was good. On the basis of all of these data, the characterization of acetylacroninium perchlorate as having Structure Ia (R = methyl) seemed conclusive.

The other acetylacroninium salts were characterized mainly on the basis that color, spectral characteristics, and chemical behavior were essentially identical to those of the perchlorate salt.

Composition of Acetylacroninium Salt Samples—Acetylacroninium perchlorate samples were dissolved in acetone and subjected to TLC [benzene–acetone (2:1) on silica gel]. Three spots were observed directly: an orange spot at the origin corresponding to authentic acroninium perchlorate, a yellow spot at R_f 0.45 corresponding to authentic acronine, and a purple spot at R_f 0.05 due to the acetylacroninium salt. No other spots were observed using iodine or UV light.

When a TLC sample of acetic acid–acetone (1:5) on silica gel was used, only two spots were observed at R_f 0.77 and 0.25. The yellow spot at 0.77 arose when both acronine and acroninium perchlorate were used[10]. The spot at R_f 0.25 was purple, corresponding to the acetylacroninium salt. When the other acetylacroninium salts were studied using the acetic acid–acetone TLC system, they behaved almost identically. On the basis of these data, the sample appeared to consist of only the prodrug salts, the corresponding acroninium salt, and acronine.

An estimate of the acetylacroninium salt present in the prepared sample was made from the NMR spectra in formamide. The ratio of the peak height at δ 1.70 to that at δ 1.47, corresponding to the *gem*-dimethyl proton in the acetylacroninium salt and acronine, respectively, was used as a simple indication of the composition. Since decomposition occurred in these solutions, it was necessary to follow the ratio as a function of time and extrapolate back to the time at which the solution was prepared. The prodrug appeared to comprise about 80% of the acetylacroninium perchlorate-containing samples. The content of the acetylacroninium salt in the other samples, such as the chloride and phosphate, was only 50–60%.

Kinetic Measurements—The hydrolysis of the acetylacroninium salts was studied spectrophotometrically[11] (520 nm) by following the disappearance of the absorption peak due to the acetylacroninium ion. The reaction mixtures were prepared by shaking a sample of the salt ($\simeq$2 mg) for about 1 min with the buffer solution[12] (10 ml). This reaction mixture was then rapidly filtered through a sintered-glass funnel of a medium or coarse pore size and diluted to 40 ml with additional buffer solution.

A portion of this solution was transferred to a quartz spectrophotometer cell. The buffer solution was used as the reference solution. Cells with 10-cm pathlengths were selected so that dilute reaction mixtures could be used and, therefore, followed spectrophotometrically for longer times. The use of larger cells was necessary because, as the reaction proceeded, the reaction solutions became supersaturated with acronine and precipitation often occurred before an absorbance value could be obtained at the completion of the reaction.

Since acronine does not absorb energy at 520 nm, the spectrophotometer was balanced carefully against air prior to initiation of the reaction; a final absorbance value (at the end of the reaction) of zero was used in the calculation of the reaction rate constant. Some sufficiently dilute solutions that did not show precipitation were found to be first order in ester concentration over three to four half-lives.

Solubility Determination of Acronine and Acroninium Salts—Acronine solubility in various solvent systems was determined by shaking excess acronine with the solvent at room temperature ($\simeq$22°) until equilibration was reached ($\simeq$24 hr). The filtered solutions, after suitable dilution with water and adjustment to pH 7, were then assayed spectrophotometrically for acronine at 277 nm ($\log \epsilon = 4.60$).

Since the acroninium salts were hydrolyzed quickly in water, determination of equilibrium solubility values for these substances was not practical. The "estimated solubility" of the salts was taken as the amount of ester dissolved (expressed as acronine content) after 2 min of constant agitation of excess sample in buffer at 22°. The resulting solution was quickly filtered through a sintered-glass funnel or filter[13]. The filtrate was allowed to stand overnight to ensure the complete hydrolysis of the ester and then was diluted with methanol to dissolve the precipitated acronine. The resulting solution was assayed spectrophotometrically for acronine (277 nm, $\log \epsilon = 4.60$).

REFERENCES

(1) R. M. Acheson, "The Chemistry of Heterocyclic Compounds. Acridines," 2nd ed., R. M. Acheson, Ed., Interscience, New York, N.Y., 1973, pp. 1–7.

(2) G. K. Hughes, F. N. Lahey, J. R. Price, and L. J. Webb, *Nature*, **162**, 223 (1948).

(3) F. L. Lahey and W. C. Thomas, *Aust. J. Sci. Res.*, **A2**, 423 (1949).

(4) G. H. Svoboda, G. A. Poore, P. J. Simpson, and G. B. Bodor, *J. Pharm. Sci.*, **55**, 758 (1966).

(5) G. H. Svoboda, M. J. Sweeney, and W. D. Walkling, *ibid.*, **60**, 333 (1971).

(6) A. J. Repta, B. J. Rawson, R. D. Shaffer, K. B. Sloan, N. Bodor, and T. Higuchi, *ibid.*, **64**, 392 (1975).

[8] Beckman model IR-33.

[9] Varian model T60.

[10] Apparently, the acroninium perchlorate salt underwent hydrolysis in the presence of the developing solvent.

[11] Cary model 14, 15, or 16 spectrophotometer.

[12] Buffer systems used in the various pH ranges were: pH $\leq$ 1, hydrochloric acid; pH 2.6, chloroacetate; pH 3.5–5.80, acetate; pH 6–7, phosphate; pH 7–10, borate; and pH > 10.7, sodium hydroxide.

[13] Millipore.

(7) A. J. Repta, *ACS Symposium Series, 14*, **1975**, 197.
(8) I. Kovatch, I. H. Pitman, and T. Higuchi, *J. Pharm. Sci.*, **64**, 1070 (1975).
(9) V. Stella and T. Higuchi, *ibid.*, **62**, 962 (1973).
(10) A. Albert, "The Acridines," 2nd ed., St. Martins Press, New York, N.Y., 1966, pp. 371–373.
(11) C.-H. Huang, B. Kreilgård, and A. J. Repta, *Bull. Parenteral Drug Assoc.*, **30**, 1 (1976).
(12) R. M. Silverstein and G. C. Bassler, "Spectrometric Identification of Organic Compounds," 2nd ed., Wiley, New York, N.Y., 1967, pp. 87, 92.
(13) *Ibid.*, p. 137.

ACKNOWLEDGMENTS AND ADDRESSES

Received July 28, 1975, from the *Victorian College of Pharmacy, Melbourne, Australia 3052 and the ‡Department of Pharmaceutical Chemistry, School of Pharmacy, University of Kansas, Lawrence, KS 66045.

Accepted for publication June 21, 1976.

Presented in part at the Basic Pharmaceutics Section, APhA Academy of Pharmaceutical Sciences, San Diego meeting, November 1973.

Abstracted in part from a dissertation submitted by D. W. A. Bourne to the University of Kansas and the Victorian College of Pharmacy in partial fulfillment of the Intersearch Doctor of Philosophy degree requirements.

Supported in part by Contract NO1-CM-23217 from the Division of Cancer Treatment, National Cancer Institute, National Institutes of Health, Department of Health, Education, and Welfare. Additional support was provided (to D. W. A. Bourne) by the Intersearch Fund.

The authors thank Wanda Waugh for technical assistance.

§ Present address: College of Pharmacy, University of Kentucky, Lexington, KY 40506.

ˣ To whom inquiries should be directed.

Microencapsulation of Phenobarbital by Spray Polycondensation

C. VOELLMY, P. SPEISER ˣ, and M. SOLIVA

Abstract □ A new method for the microencapsulation of solids is described. It is based on the polycondensation of amphiphilic and, thus, tensioactive precondensates on a melamine–formaldehyde base on the surface of suspended particles during spray drying. A film-forming agent, preferably one that reacts chemically with the resin, is indispensable for spray drying and also for the formation of an efficient membrane around the drug particles. The resulting microcapsules are essentially spherical and have, after appropriate curing, a sustained-release effect *in vitro*. The factors that most influence the formation and properties of the microcapsules are the composition (qualitative and quantitative), pH, and viscosity of the suspension.

Keyphrases □ Phenobarbital—microencapsulation by spray polycondensation, effect of composition, pH, and viscosity □ Microencapsulation—of solids by spray polycondensation, effect of composition, pH, and viscosity □ Spray polycondensation—microencapsulation of solids, effect of composition, pH, and viscosity □ Technology, pharmaceutical—microencapsulation of solids by spray polycondensation, effect of composition, pH, and viscosity

Microencapsulation can be defined as a method to provide solid particles or liquid droplets with an individual coat, thereby modifying their physical, chemical, and physiological characteristics. This effect is useful for separating reactive or incompatible components, covering disagreeable odors and tastes of substances, and converting liquids into solids.

In pharmacy, microencapsulation is used to improve the stability and handling properties of drugs and to prepare controlled-release products. Release may be accomplished by rupture (mechanical or after swelling) or diffusion through the intact or swollen wall. The size of microcapsules generally ranges from several microns to about 200 μm (1).

Various specific technological aspects and limitations of microencapsulation have been studied (2, 3), as have the different variables that influence microcapsule formation. In most cases, the microcapsules were prepared by simple coacervation (4–9). The aim of this work was to gain insight into the possibilities and limitations of a new microencapsulation method; the influence of some important technological variables on the properties of the microcapsules was studied.

THEORETICAL

Spray drying is used to separate the microcapsules from the vehicle (8, 10) or to prepare microcapsules in a single operation (11, 12). The procedure is, in principle, as follows. After dissolving the coating material in a preferably aqueous medium and dispersing the core material in it, the dispersion is spray dried. The core material is thereby microencapsulated in its original state.

Clearly, different products are obtained when a true solution of coating material and drug is spray dried. The active substance is in an X-ray amorphous state and shows crystallinity only when the drug–polymer ratio is increased (13, 14).

The fundamentals of spray polycondensation were presented previously (15, 16). One processes a dispersion of core material that contains in the continuous phase aminoplast monomers or aminoplast precondensates of relatively low molecular weight in addition to other coating material (film-forming agents) and the catalyst. The resin-forming monomers and precondensates play an essential role. In contrast to the monomers, the reactive tensides (17–19) exhibit pronounced tensioactive properties. They are derived from hexamethylolmelamine whose hydroxymethyl groups are substituted partly with hydrophilic polyglycol ethers and partly with lipophilic alcohols (usually C_4–C_{18}), forming low molecular weight precondensates. Due to their physicochemical properties, they are adsorbed selectively at the surface of the inner phase of the dispersion.

The insoluble polymer microcapsule is formed upon spray drying at 150–200° by vaporization of water and simultaneous polycondensation of the monomers and the precondensates by acid catalysis. Details of the basic chemical reactions can be found in textbooks (20). The quality of the shell can be improved by the use of a film-forming agent that reacts chemically with the monomers and also by curing.

EXPERIMENTAL

Materials—Phenobarbital[1], with a mean particle size of 30–35 μm, was chosen as the model drug. As a film-forming agent, polyvinyl alcohol[2]

[1] Phenobarbital Ph. Helv. VI pulvis alcoholisatus, Siegfried Ltd., Zofingen, Switzerland.
[2] Mowiol 4-88, Hoechst, Plüss-Stauffer, Oftringen, Switzerland.

(7) A. J. Repta, *ACS Symposium Series, 14*, **1975**, 197.
(8) I. Kovatch, I. H. Pitman, and T. Higuchi, *J. Pharm. Sci.*, **64**, 1070 (1975).
(9) V. Stella and T. Higuchi, *ibid.*, **62**, 962 (1973).
(10) A. Albert, "The Acridines," 2nd ed., St. Martins Press, New York, N.Y., 1966, pp. 371–373.
(11) C.-H. Huang, B. Kreilgård, and A. J. Repta, *Bull. Parenteral Drug Assoc.*, **30**, 1 (1976).
(12) R. M. Silverstein and G. C. Bassler, "Spectrometric Identification of Organic Compounds," 2nd ed., Wiley, New York, N.Y., 1967, pp. 87, 92.
(13) *Ibid.*, p. 137.

ACKNOWLEDGMENTS AND ADDRESSES

Received July 28, 1975, from the *Victorian College of Pharmacy, Melbourne, Australia 3052 and the ‡Department of Pharmaceutical Chemistry, School of Pharmacy, University of Kansas, Lawrence, KS 66045.

Accepted for publication June 21, 1976.

Presented in part at the Basic Pharmaceutics Section, APhA Academy of Pharmaceutical Sciences, San Diego meeting, November 1973.

Abstracted in part from a dissertation submitted by D. W. A. Bourne to the University of Kansas and the Victorian College of Pharmacy in partial fulfillment of the Intersearch Doctor of Philosophy degree requirements.

Supported in part by Contract NO1-CM-23217 from the Division of Cancer Treatment, National Cancer Institute, National Institutes of Health, Department of Health, Education, and Welfare. Additional support was provided (to D. W. A. Bourne) by the Intersearch Fund.

The authors thank Wanda Waugh for technical assistance.

§ Present address: College of Pharmacy, University of Kentucky, Lexington, KY 40506.

ˣ To whom inquiries should be directed.

Microencapsulation of Phenobarbital by Spray Polycondensation

C. VOELLMY, P. SPEISER ˣ, and M. SOLIVA

Abstract □ A new method for the microencapsulation of solids is described. It is based on the polycondensation of amphiphilic and, thus, tensioactive precondensates on a melamine–formaldehyde base on the surface of suspended particles during spray drying. A film-forming agent, preferably one that reacts chemically with the resin, is indispensable for spray drying and also for the formation of an efficient membrane around the drug particles. The resulting microcapsules are essentially spherical and have, after appropriate curing, a sustained-release effect *in vitro*. The factors that most influence the formation and properties of the microcapsules are the composition (qualitative and quantitative), pH, and viscosity of the suspension.

Keyphrases □ Phenobarbital—microencapsulation by spray polycondensation, effect of composition, pH, and viscosity □ Microencapsulation—of solids by spray polycondensation, effect of composition, pH, and viscosity □ Spray polycondensation—microencapsulation of solids, effect of composition, pH, and viscosity □ Technology, pharmaceutical—microencapsulation of solids by spray polycondensation, effect of composition, pH, and viscosity

Microencapsulation can be defined as a method to provide solid particles or liquid droplets with an individual coat, thereby modifying their physical, chemical, and physiological characteristics. This effect is useful for separating reactive or incompatible components, covering disagreeable odors and tastes of substances, and converting liquids into solids.

In pharmacy, microencapsulation is used to improve the stability and handling properties of drugs and to prepare controlled-release products. Release may be accomplished by rupture (mechanical or after swelling) or diffusion through the intact or swollen wall. The size of microcapsules generally ranges from several microns to about 200 μm (1).

Various specific technological aspects and limitations of microencapsulation have been studied (2, 3), as have the different variables that influence microcapsule formation. In most cases, the microcapsules were prepared by simple coacervation (4–9). The aim of this work was to gain insight into the possibilities and limitations of a new microencapsulation method; the influence of some important technological variables on the properties of the microcapsules was studied.

THEORETICAL

Spray drying is used to separate the microcapsules from the vehicle (8, 10) or to prepare microcapsules in a single operation (11, 12). The procedure is, in principle, as follows. After dissolving the coating material in a preferably aqueous medium and dispersing the core material in it, the dispersion is spray dried. The core material is thereby microencapsulated in its original state.

Clearly, different products are obtained when a true solution of coating material and drug is spray dried. The active substance is in an X-ray amorphous state and shows crystallinity only when the drug–polymer ratio is increased (13, 14).

The fundamentals of spray polycondensation were presented previously (15, 16). One processes a dispersion of core material that contains in the continuous phase aminoplast monomers or aminoplast precondensates of relatively low molecular weight in addition to other coating material (film-forming agents) and the catalyst. The resin-forming monomers and precondensates play an essential role. In contrast to the monomers, the reactive tensides (17–19) exhibit pronounced tensioactive properties. They are derived from hexamethylolmelamine whose hydroxymethyl groups are substituted partly with hydrophilic polyglycol ethers and partly with lipophilic alcohols (usually C_4–C_{18}), forming low molecular weight precondensates. Due to their physicochemical properties, they are adsorbed selectively at the surface of the inner phase of the dispersion.

The insoluble polymer microcapsule is formed upon spray drying at 150–200° by vaporization of water and simultaneous polycondensation of the monomers and the precondensates by acid catalysis. Details of the basic chemical reactions can be found in textbooks (20). The quality of the shell can be improved by the use of a film-forming agent that reacts chemically with the monomers and also by curing.

EXPERIMENTAL

Materials—Phenobarbital[1], with a mean particle size of 30–35 μm, was chosen as the model drug. As a film-forming agent, polyvinyl alcohol[2]

[1] Phenobarbital Ph. Helv. VI pulvis alcoholisatus, Siegfried Ltd., Zofingen, Switzerland.
[2] Mowiol 4-88, Hoechst, Plüss-Stauffer, Oftringen, Switzerland.

Table I—Effect of Ratio of Reactive Tenside to Monomer: Composition of Suspensions and Release Rate Constants K of the Respective Products

	Batch						
	800	801	802	805	806	807	808
Polyvinyl alcohol	4.0	4.0	4.0	4.0	4.0	4.0	4.0
Water	46.0	46.0	46.0	46.0	46.0	46.0	46.0
Phenobarbital	10.0	10.0	10.0	10.0	10.0	10.0	10.0
Reactive tenside IV	12.0	10.5	9.0	6.0	3.0	1.5	0
Monomer I	0	0.75	1.5	3.0	4.5	5.25	6.0
Approximate mole-percent of reactive tenside[a]	100.0	25.9	13.0	4.8	1.6	0.7	—
K[b]	35.9	41.3	42.1	41.3	32.6	25.4	25.5
$t_{75\%}$, min	4.4	3.3	3.2	3.3	5.3	8.7	8.6
K[c]	27.6	18.9	12.2	12.0	12.5	13.1	15.3
$t_{75\%}$, min	7.4	15.8	37.9	39.3	35.8	33.0	24.0

[a] Refers to total quantity of moles of reactive tenside and monomer. [b] No curing. [c] Curing for 1 hr at 100°.

(mol. wt. ~34,000) was used. As monomers, hexamethylolmelamine hexamethyl ether[3] (I), trimethylolmelamine trimethyl ether[3] (II), and dimethylolurea dimethyl ether[3] (III) were used as well as a cationic reactive tenside on a melamine–formaldehyde base[4] (IV). Hydrochloric acid (1 N) was added as a catalyst.

Microcapsule Preparation—After dissolving the polyvinyl alcohol, the monomers, and the precondensate in distilled water, the pH was adjusted[5] with hydrochloric acid. Unless specified otherwise, a pH of 2.5 was used. The phenobarbital was homogeneously dispersed with a high-speed stirrer[6] and immediately spray dried[7]. The following conditions were used: inlet temperature, 220°; outlet temperature, 90°; spray-disk speed, about 30,000 rpm; and feed rate, 1 liter/hr[8].

After spray drying, the product that adhered to the wall was brushed off and collected. The yield of microcapsules in the cyclone was low due to the small dimensions of the spray drier. Unless otherwise indicated, curing was performed in a drying oven under standard conditions (1 hr at 100°).

Microcapsule Evaluation—*Phenobarbital Content*—A 60–100-mg sample was accurately weighed into a 100.0-ml volumetric flask. Then about 50 ml of 0.1 N NaOH solution was added, and the suspension was treated with ultrasound[9] for about 90 sec. The microcapsules were thereby ruptured, and the drug dissolved. Then 0.1 N NaOH solution was again added to give 100.0 ml, and a 1.0-ml sample was withdrawn through a G 3 sintered-glass plate. After appropriate dilution, phenobarbital was assayed spectrophotometrically[10] at 256 nm. All samples were analyzed in duplicate.

Release Studies—Phosphate buffer solution (200 ml, pH 7.2, μ = 0.2, 0.1% polysorbate 80) in a 400-ml beaker was maintained at 37° and stirred at a constant rate of 133 rpm[11]. The length of the stirring rod[12] was approximately 6 cm and its diameter was 1.1 cm. The sample containing 50.0 mg of phenobarbital was placed on a small sieve (mesh size approximately 0.75 mm) laid on the beaker. Scratching the sieve caused the powder to fall into the liquid without forming clumps (time t = 0). Filtered[13] 1-ml samples were removed after 1, 2, 4, 8, 16, *etc.*, min until about 90% of the core material was released. The samples were assayed as specified. The release rate studies were carried out in duplicate.

RESULTS AND DISCUSSION

Evaluation of Release Data—For the characterization and comparison of microcapsules prepared under different conditions, it is useful to express the release results by a representative constant.

In some cases, the release pattern follows a first-order mechanism (21). Other investigators suggested a linearization of release curves of different dosage forms by using the Weibull function (22). It was found that the calculation of the linear regression of:

$$y = K^* t^n \quad \text{(Eq. 1)}$$

where y is the percent drug released at time t and K^* is a constant, yielded an exponent, n, in the range of about 0.5. The release rate constant K was calculated by linear regression of:

$$y = Kt^{1/2} \quad \text{(Eq. 2)}$$

The fit of the experimental results with the calculated points was satisfactory, and the statistical linearity was significant for most cases.

Effect of Resin-Forming Agent on Microcapsules—No satisfactory microcapsules resulted with the exclusive use of either I or reactive tenside IV. In the former case, agglomerates of irregular shape and size, which can hardly be regarded as microcapsules, were produced (Fig. 1). In the latter case, the core material was completely coated by spherical microcapsules (Fig. 2) in which no defective coats could be discerned. However, these products were highly hydrophilic (but insoluble in water, acetone, alcohols, dimethylformamide, *etc.*) without any noteworthy sustained-release effect even after curing.

Spray polycondensation with mixtures of I and IV in different ratios was performed; the compositions and dissolution rate constants are given in Table I. The shape of the microcapsules of Batches 800–805 was spherical. Due to the low amount of reactive tenside, Batches 806 and

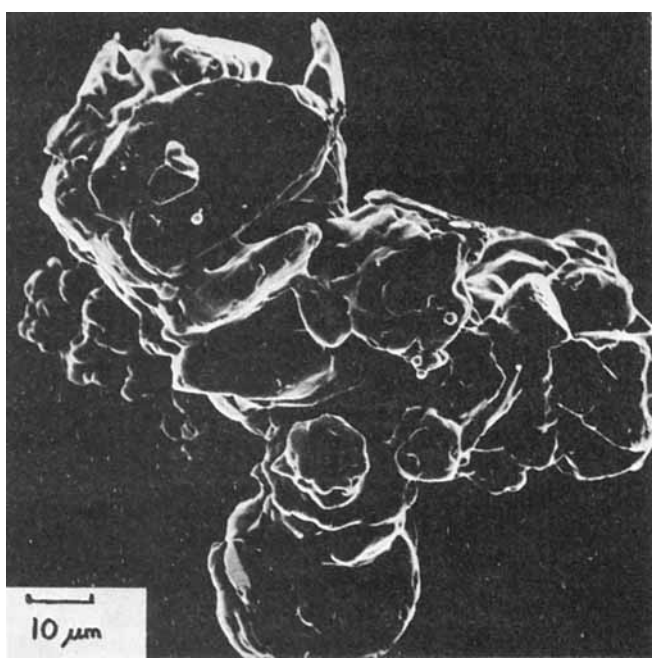

Figure 1—*Typical structure of product manufactured by spray polycondensation with monomer I (Batch 808). Coating is irregular and defective.*

[3] Ciba-Geigy Ltd., Basel, Switzerland.
[4] Reactive tenside 709 LS 50% aqueous solution, Ciba-Geigy Ltd., Basel, Switzerland.
[5] pH Meter E 520, Metrohm, Herisau, Switzerland.
[6] Polytron PT 20 OD, Kinematica, Lucerne, Switzerland.
[7] Niro Minor, Niro A/S, Copenhagen, Denmark.
[8] Peristaltic pump LP-A Standard, W. Bachofen, Basel, Switzerland.
[9] Ultrasonic bath, Elgasonic TS-100 (50 kHz), Biel, Switzerland.
[10] Model 635, Varian, Basel, Switzerland.
[11] Magnetic stirrers were constructed using a Philips motor 9904 111 04131, transmission BA/UR, Philips, Zürich, Switzerland.
[12] Covered with Teflon (du Pont).
[13] Sartorius SM 113 03 1.2-µm membrane filters and Sartorius SM 165 14 filter-support, diameter 13 mm, Instrumentengesellschaft, Zürich, Switzerland.

Table II—Effect of Monomers: Composition of Suspensions and Release Rate Constants of the Respective Products[a]

	Batch		
	816	866	870
Polyvinyl alcohol	6.0	6.0	6.0
Water	44.0	44.0	44.0
Phenobarbital	10.0	10.0	10.0
Reactive tenside IV	6.0	6.0	6.0
Monomer			
Type	I	II	III
Amount	3.0	3.0	3.0
K	8.1	9.3	23.2
$t_{75\%}$, min	85.1	64.7	10.5

[a] Curing for 1 hr at 100°.

807 tended toward the structures shown in Fig. 1. In all cases, the release rate was high ($t_{75\%} < 10$ min) for the original products. This property differed distinctly after curing, depending on the ratio between I and IV. It was lowest when the fraction of IV was 0.25–0.75 based on the total amount of I and IV, as in Batches 802, 805, and 806.

To obtain products that best met the expectations (*i.e.*, spherical microcapsules with slow release effect and relatively low amount of reactive tenside used), a IV to I ratio of 1:1 was chosen for the subsequent experiments.

The excessive permeability of the original product could be explained by the relatively low molecular weight of the resin. The results demonstrate that curing distinctly reduced the permeability only of products containing I. The comparatively small molecular size of I probably formed a more intimate network than when using reactive tenside alone. A mechanism similar to steric hindrance can be assumed. Methanol evaporates when the ether groups of I are broken up; with reactive tenside, large and much less volatile molecules that could impede cross-linking are separated.

Effect of Curing Conditions on Release Properties—As already stated, curing is necessary to attain slow release microcapsules. It was found by microscopical examination that the morphology of the products was not affected by this process. The influence of the curing conditions on the release rate constant is shown in Fig. 3. The permeability of the products can only be reduced to a certain degree, characteristic for the respective formulation. The chemical reactions occurring during this process are, among others, the formation of methylene bridges by liberation of formaldehyde (organoleptic identification; see also Ref. 20) and the dehydration of resin and polyvinyl alcohol. The latter is characterized

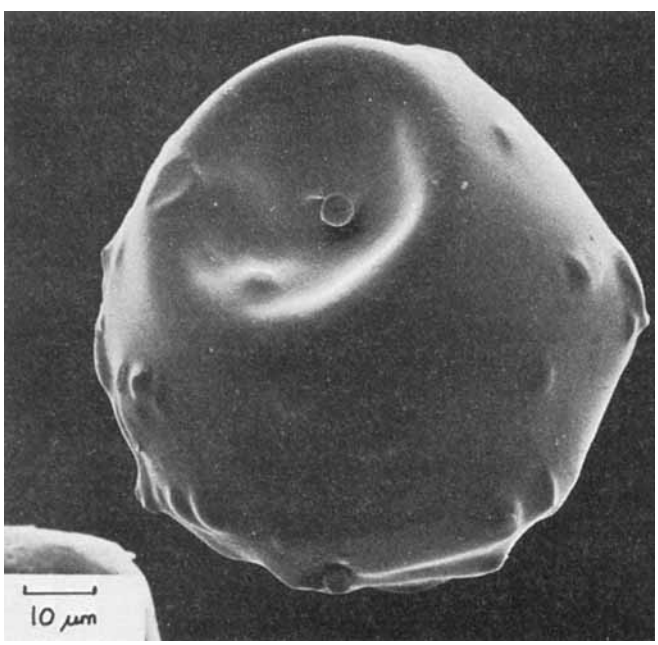

Figure 2—*Typical microcapsule manufactured using reactive tenside IV. Active substance is entirely coated.*

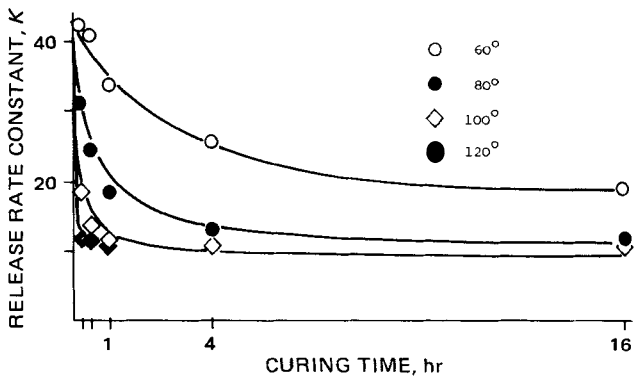

Figure 3—*Effect of curing conditions on release rate constant of Batch 805 (composition given in Table I).*

by a discoloration to yellow of the originally white product at 120° and after more than 4 hr at 100° (23).

Effect of Monomers of Low Tensioactivity on Release Properties—The composition and release rate constants are shown in Table II. The distinct differences in the release rate of the products depending on the chemical nature of the monomer used can be explained by the fact that I has more potential cross-linking sites than II and the latter has more than III. The consequence is a wall structure with a more or less intimate network which is primarily responsible for the different permeabilities. Microscopically (scanning electron microscope), no differences in the surface structure could be discerned.

Effect of pH on Release Properties—Polycondensation is catalyzed by acid pH. Consequently, pH influences the quality of the coat. The suspensions adjusted to different pH values were immediately spray dried and cured. The batches showed no morphological differences. The results of the release studies (Fig. 4) reflect the basic importance of this factor. The effect of pH on the release of phenobarbital was distinct and was not suppressed by the obligatory curing process.

A suspension with pH 1.5 could not be processed because it gelled in a few minutes; at higher pH values, gelling was observed only after several hours or days.

Effect of Viscosity on Microcapsules—Suspensions with identical compositions diluted with water to polyvinyl alcohol concentrations of 2, 4, 8, and 12% exhibited Newtonian flow[14]. The microcapsules resulting from the two high viscosity suspensions were spherical. The low viscosity suspensions, however, yielded products with irregular shapes similar to those shown in Fig. 1. The respective release patterns are shown in Fig. 5.

Viscosity is known to be an important factor in spray drying technology (24). Its influence on the formation and properties of the microcapsules is also demonstrated by the following experiment. A suspension with 16% polyvinyl alcohol does not yield discrete microcapsules but rather long and fine insoluble threads. It is obvious that in this case the water vaporizes before discrete droplets are formed by spraying; *i.e.*, the atomization of the dispersion is impeded by the high viscosity.

Effect of Resin to Polyvinyl Alcohol Ratio on Microcapsules—

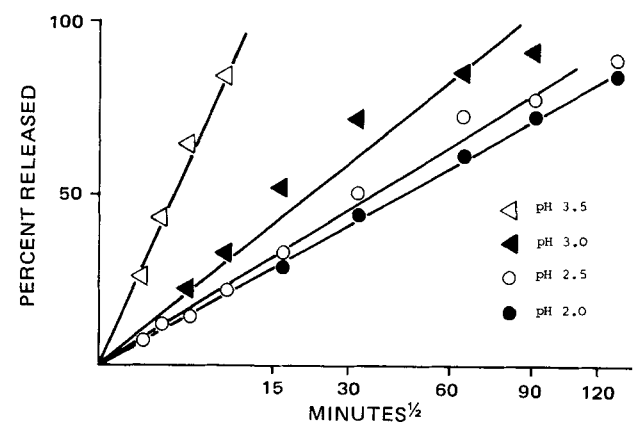

Figure 4—*Effect of pH on release rate.*

[14] Measured with a Epprecht Rheomat, Contraves, Zürich, Switzerland.

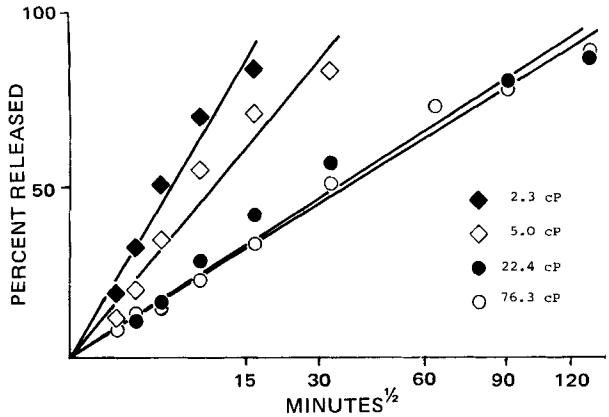

Figure 5—*Effect of viscosity on release rate.*

The composition of the batches, their respective release rate constants, and the evaluation of the results are shown in Fig. 6. In the evaluation of the results, the composition of the formulation with the maximum sustained release as well as its expected value for K was calculated. The following polynomial equation was computed after having found by analysis of variance that the regression of second order was adequate:

$$y = 33.084 - 6.133x_1 - 63.380x_2 + 25.251x_1^2 + 64.400x_2^2 - 43.796x_1x_2 \quad \text{(Eq. 3)}$$

where y is the dissolution rate constant, x_1 is the level of factor Compounds I and IV, and x_2 is the level of factor polyvinyl alcohol.

The coordinates x_{1s} and x_{2s} (Fig. 6) for the stationary point were computed by partial differentiation and setting the results equal to zero. By setting these values into the polynomial equation, the expected value for K, a true minimum, was calculated. The comparison of the computed and experimentally found values demonstrated a good fit when it was considered that the confidence limits were relatively large due to the not unimportant residual term in the analysis of variance.

The coordinates of the stationary point were within the experimental field. Thus, no significant improvement of the sustained-release effect could be expected by investigating further levels of these factors. The quality of the coat was largely determined by an interaction of the factors investigated. The slope of the ellipse in Fig. 6 and the results of the statistical analysis, however, indicated that the variable polyvinyl alcohol was somewhat more critical in its influence on the release rate constant.

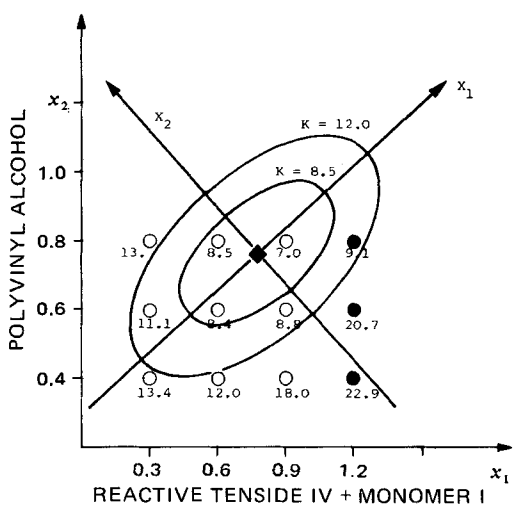

Figure 6—*Contour plot for release rate constants* K = *12.0 and 8.5. The numbers inserted give the experimental* K; x_1 *and* x_2 *are relative amounts of reactive tenside IV + monomer I and polyvinylalcohol, respectively. The relative amount of phenobarbital is unity. The polyvinyl alcohol concentration is 8%. Key:* ○, *experimental range evaluated;* ●, *residual experimental range; and* ♦, *stationary point,* K = *6.39.*

REFERENCES

(1) L. A. Luzzi, *J. Pharm. Sci.*, **59**, 1367 (1970).

(2) J. A. Herbig, in "Encyclopedia of Chemical Technology," vol. 13, Wiley, New York, N.Y., 1967, p. 436.

(3) C. E. Anderson, "Microencapsulation," Management Reports, Boston, Mass., 1963.

(4) L. A. Luzzi and R. J. Gerraughty, *J. Pharm. Sci.*, **56**, 634 (1967).

(5) *Ibid.*, **56**, 1174 (1967).

(6) *Ibid.*, **53**, 429 (1964).

(7) H. P. Merkle, Ph.D. thesis, Swiss Federal Institute of Technology, Zürich, Switzerland, 1972.

(8) J. R. Nixon, S. A. H. Khalil, and J. E. Carless, *J. Pharm. Pharmacol.*, **20**, 528 (1968).

(9) N. N. Salib, *Pharm. Ind.*, **34**, 671 (1972).

(10) L. A. Luzzi, M. A. Zoglio, and H. V. Maulding, *J. Pharm. Sci.*, **59**, 338 (1970).

(11) H. J. Robinson and E. V. Svedres, U.S. pat. 2,805,977 (1957).

(12) N. Macaulay, U.S. pat. 3,016,308 (1962).

(13) H. Junginger, *Pharm. Ind.*, **36**, 100 (1974).

(14) *Ibid.*, **36**, 333 (1974).

(15) DT (OS) 2,233,428 (1973, unexamined).

(16) H. P. Merkle and P. Speiser, *Pharm. Ind.*, **37**, 555 (1975).

(17) C. Voellmy, Ph.D. thesis, Swiss Federal Institute of Technology, Zürich, Switzerland, 1975.

(18) L. Schibler, French pat. 1,381,811 (1964).

(19) L. Schibler, French pat. 1,470,103 (1967).

(20) R. Wegler, in "Methoden der Organischen Chemie" (Houben-Weyl), vol XIV/2, E. Müller, Ed., Thieme Verlag, Stuttgart, Germany, 1963, pp. 319, 357, 361.

(21) "Theory and Practice of Industrial Pharmacy," L. Lachman, H. Lieberman, and J. Kanig, Eds., Lea & Febiger, Philadelphia, Pa., 1970, p. 384.

(22) F. Langenbucher, *J. Pharm. Pharmacol.*, **24**, 979 (1972).

(23) J. G. Pritchard, "PVA, Basic Properties and Uses," Gordon & Breach Science Publishers, London, England, 1970.

(24) W. Beuttner, Ph.D. thesis, Swiss Federal Institute of Technology, Zürich, Switzerland, 1959.

ACKNOWLEDGMENTS AND ADDRESSES

Received April 15, 1976, from the *Department of Pharmacy, Swiss Federal Institute of Technology, CH 8006 Zürich, Switzerland.*

Accepted for publication June 23, 1976.

Abstracted in part from a thesis submitted by C. Voellmy to the Swiss Federal Institute of Technology in partial fulfillment of the Doctor of Philosophy degree requirements.

The authors thank Dr. H. P. Merkle, University of Heidelberg, Germany, for valuable suggestions and Dr. L. Schibler, Ciba-Geigy Ltd., Basel, Switzerland, for the synthesis of the monomers and the reactive tensides.

[x] To whom inquiries should be directed.

GLC Determination of Acetohexamide and Hydroxyhexamide in Biological Fluids

J. W. KLEBER [x], J. A. GALLOWAY, and B. E. RODDA

Abstract □ A sensitive and specific GLC assay was developed for acetohexamide and hydroxyhexamide, its major metabolite, in plasma and urine. The assay uses tolbutamide as a mass internal standard. Compounds are extracted from acidified plasma or urine with toluene, converted to methylated derivatives with dimethyl sulfate, and measured by GLC using a flame-ionization detector. With GLC–mass spectrometry, the compounds measured are the *N*-methylsulfonamides resulting from GLC pyrolysis. Plasma and urine data are presented from a bioavailability study to demonstrate the utility of this method.

Keyphrases □ Acetohexamide—GLC analysis, human plasma and urine □ Hydroxyhexamide—GLC analysis, human plasma and urine □ GLC—analyses, acetohexamide and hydroxyhexamide, human plasma and urine □ Antidiabetic agents—acetohexamide, GLC analysis, human plasma and urine

Earlier methods for the determination of plasma concentrations of acetohexamide utilized isotope dilution analysis (1–3), the Spingler (4) method, or the Toolan–Wagner (5) procedure. None of these methods is sufficiently sensitive or suitable for the assay of the multiple samples needed in a bioavailability study, nor do they permit the assay of acetohexamide and hydroxyhexamide in urine.

The earliest GLC method for the determination of hypoglycemic sulfonylureas (6) involved conversion of tolbutamide and chlorpropamide to their *N*-methylated derivatives by treatment with dimethyl sulfate. Difficulty in consistently reproducing this work was reported (7, 8), and similar difficulties were experienced in this laboratory. Prescott and Redman (9) later described a method for the GLC estimation of tolbutamide and chlorpropamide, which served as the basis for the present determination of acetohexamide and hydroxyhexamide in plasma and urine.

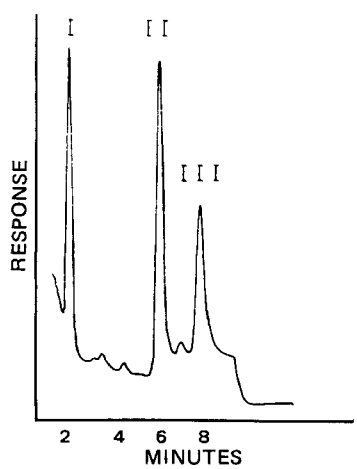

Figure 1—*Gas–liquid chromatograph of extract of plasma spiked with 10 μg of tolbutamide (I)/ml and 20 μg of acetohexamide (II) and hydroxyhexamide (III)/ml.*

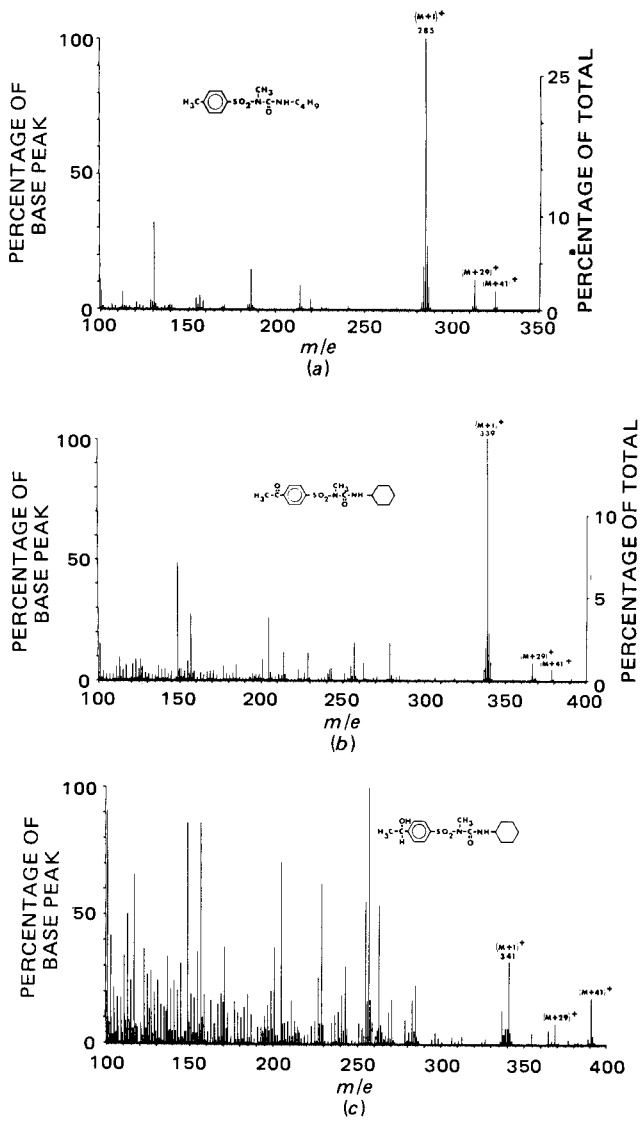

Figure 2—*Chemical ionization mass spectra of* N*-methyl derivatives of tolbutamide* (a), *acetohexamide* (b), *and hydroxyhexamide* (c).

EXPERIMENTAL

Reagents—Acetohexamide, hydroxyhexamide, and tolbutamide were synthesized[1]; tolbutamide was used as the mass internal standard for GLC analysis. All solvents were analytical reagent quality except hexane[2], which was distilled in glass. Commercially available GLC packing material, 0.5% PEG 20M on Gas Chrom Q[3] (80–100 mesh), and the methylating reagent dimethyl sulfate[4] were used.

Apparatus—The basic instrument was a gas–liquid chromatograph[5] with dual-column capability, equipped with a flame-ionization detector

[1] At the Lilly Research Laboratories, Eli Lilly and Co., Indianapolis, Ind.
[2] Burdick and Jackson Laboratories, Muskegon, Mich.
[3] Ohio Valley Specialty Chemicals Inc., Marietta, Ohio.
[4] Mallinckrodt Chemical Works, St. Louis, Mo.
[5] Model 402, Hewlett-Packard, Avondale, Pa.

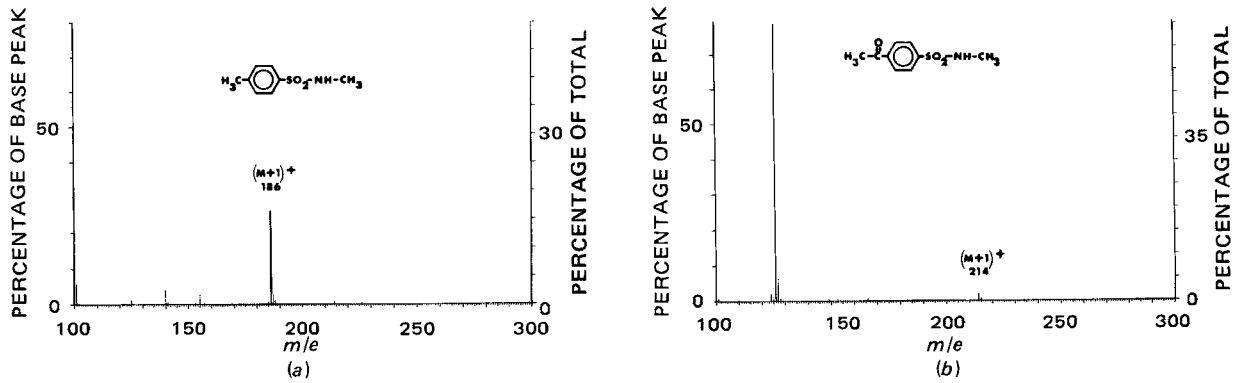

Figure 3—*Chemical ionization mass spectra of* N-*methyltoluenesulfonamide* (a) *and* N-*methyl*-p-*acetylbenzenesulfonamide* (b) *obtained after GLC.*

and 1-mv recorder[6]. Disposable 15-ml centrifuge tubes[7] were used for the extraction procedure; previously siliconized, tapered 15-ml glass centrifuge tubes[8] were used for the methylation step and hexane evaporation[9].

Chromatographic Conditions—The gas chromatograph was operated in the dual-column mode. The two glass columns, 0.61 m × 3 mm i.d., were operated initially at 190° with a programmed 5°/min increase to 240° during analyses. The recorder was operated at a chart speed of 0.63 cm/min, the detector temperature was 260°, and the oxygen and hydrogen flow rates were 90 ml/min. Helium carrier gas (flow rate of 90 ml/min) was filtered through a molecular sieve preconditioned overnight at 240° with dry nitrogen.

Under these conditions, the following retention times were observed: *N*-methyl-*p*-toluenesulfonamide, 90 sec; *N*-methyl-*p*-acetylbenzenesulfonamide, 300 sec; and *p*-(1-hydroxyethyl)-*N*-methylbenzenesulfonamide, 480 sec. When using the instrument in the dual-column mode, a satisfactory baseline was obtained as the oven was heated.

Procedure—The 15-ml tapered centrifuge tubes were washed with chromic acid cleaning solution, rinsed with water, dried, and siliconized with a 1% solution of dimethyldichlorosilane in toluene[10]. Standard solutions of acetohexamide and hydroxyhexamide were added to 1 ml of blank plasma or urine to give calibration concentrations of 0, 5, 10, 20, and 40 μg of each drug/ml. To each tube were added 20 μl (10 μg) of the mass internal standard solution and 1 ml of 1.0 *N* HCl. The mixture was vortexed to ensure uniform distribution, and 5 ml of toluene was then added[11] to each tube.

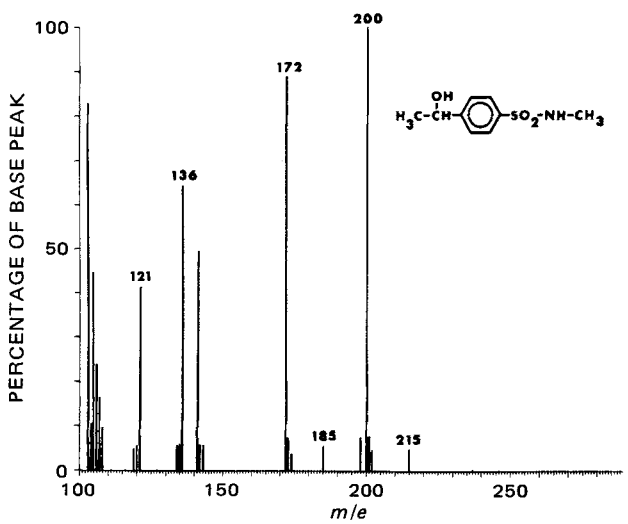

Figure 4—*Electron-impact mass spectrum of* p-(*1-hydroxyethyl*)-N-*methylbenzenesulfonamide obtained after GLC.*

The samples were shaken for 2 min and then centrifuged at 2000 rpm for 4 min. The upper organic phase was transferred to a conical screw-capped centrifuge tube containing 1 ml of 7.5% aqueous potassium carbonate solution, and the samples were again shaken and centrifuged. The toluene was aspirated and discarded. To the aqueous phase were added 1 ml of methanol and 0.1 ml of dimethyl sulfate. Then the tubes were loosely capped and placed in a water bath at 60° for 10 min.

After cooling, 1 ml of 1 *M* acetate buffer (pH 5.2) was added. The methylated sulfonylureas were extracted with 5 ml of *n*-hexane, which was transferred to a 15-ml siliconized, tapered centrifuge tube. The hexane was evaporated to dryness at 50° under a gentle stream of dry nitrogen. Dissolution of the residue in 25 μl of carbon disulfide–chloroform (1:1) was aided by vortex mixing, and 2 μl of each sample solution was then injected onto the GLC column (Fig. 1).

Following chromatography of the calibration standards, peak height ratios[12] of the *N*-methylsulfonamides to the *N*-methyl-*p*-toluenesulfonamide mass internal standard were calculated. These ratios, plotted against concentrations of acetohexamide and hydroxyhexamide in the 5.0–40.0-μg/ml range, gave straight lines passing through the origin (r = 1.0). Mean slope values of 0.080 ± 0.005 and 0.043 ± 0.004 were obtained for acetohexamide and hydroxyhexamide, respectively.

Chemical ionization mass spectra[13] of the *N*-methylated derivatives of tolbutamide, acetohexamide, and hydroxyhexamide were obtained before GLC; those of the respective *N*-methylated sulfonamides were determined after chromatography.

A bioavailability study was conducted to compare acetohexamide tablets[14] and to demonstrate the utility of this method. Tablets from three different lots[15], plus a placebo tablet to estimate basal response, were administered to eight subjects in a four-way crossover study. Each subject fasted for 8 hr before receiving a therapeutic dose of 1.5 tablets, 750 mg, of acetohexamide. Blood samples were drawn at −1, 0, 1, 2, 3, 4, 6, and 8 hr after administration, and urine was collected for the 0–8-hr period. In addition to the determination of acetohexamide and hydrox-

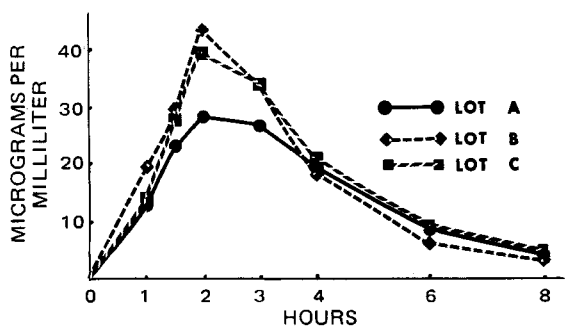

Figure 5—*Mean plasma concentrations of acetohexamide after administration of 750 mg of acetohexamide to eight subjects.*

[6] Model 7128A, Hewlett-Packard, Avondale, Pa.
[7] Corning Glass Co., Corning, N.Y.
[8] Matheson Scientific Co., Chicago, Ill.
[9] Model 106 N-Evap, Organomation Associates, Shrewsbury, Mass.
[10] This treatment appears to prevent adsorption of the *N*-methylsulfonylureas to the glassware.
[11] Repipet, Labindustries, Berkeley, Calif.

[12] Results were virtually unaffected when relative peak areas were used instead of relative peak heights.
[13] Using a Finnigan model 3100 Quadrupole M/S. Column was 45 cm long, contained 3% Dexsil, and was operated at 210°.
[14] Dymelor, Lilly, tablets 1843.
[15] Lot A was formulated with starch hydrolyzed powder and was 30 months old; Lots B and C were formulated with starch gelatinized powder and were 2 months old.

Table I—Precision and Accuracy in Measurement of Acetohexamide and Hydroxyhexamide Added to Plasma

Amount Added, μg/ml	Acetohexamide Measured[a]			Hydroxyhexamide Measured[a]		
	μg/ml	*RSD*, %	*RE*, %	μg/ml	*RSD*, %	*RE*, %
10.0	9.9 (8.1–11.5)	11.5	−1.0	14.1 (12.5–15.5)	7.2	41
20.0	19.8 (18.9–20.7)	3.2	−1.0	18.2 (14.9–21.6)	15.9	9
40.0	39.4 (37.7–41.5)	3.0	−1.5	40.0 (36.8–44.0)	7.4	1

[a] Mean of eight replicate samples (range).

Table II—Dissolution Studies[a] of Acetohexamide Tablets at 1 hr

Formulation	Mean, %	Range, %	*RSD*, %
Lot A	59.5	16.6	10.8
	58.5	17.7	11.3
Lot B	67.7	11.0	6.2
	72.7	25.5	12.4
	68.1	8.7	4.4
Lot C	51.2	—	11.5
	58.4	11.5	10.2
	68.0	14.6	7.7

[a] Using pH 7.6, 100 rpm, and 900 ml (USP XIX, 1975, p. 15).

Table III—Recovery of Acetohexamide and Hydroxyhexamide in 8-hr Urines

	Acetohexamide, mg		Hydroxyhexamide, mg		Total	Recovery, %	
Lot	Mean	*SD*	Mean	*SD*	Mean	Mean	*SD*
A	31	16	189	93	220	29.2	13.7
B	30	12	223	28	253	33.7	4.1
C	35	8	247	67	282	37.5	9.7

yhexamide concentrations in blood and urine, blood glucose (10) and serum insulin (11) concentrations were measured.

Dissolution of the acetohexamide tablets was determined by the method in USP XIX.

RESULTS AND DISCUSSION

To estimate the precision and accuracy of the procedure, plasma samples with known amounts of acetohexamide and hydroxyhexamide were assayed; the results are presented in Table I.

The chemical ionization mass spectra by which the structures of the *N*-methylated sulfonylureas were identified are shown in Fig. 2. When these compounds were chromatographed using the described conditions, they were quantitatively pyrolyzed to the respective *N*-methylsulfonamides. The GLC–mass spectra for *N*-methyl-*p*-toluenesulfonamide and *N*-methyl-*p*-acetylbenzenesulfonamide are shown in Fig. 3. *p*-(1-Hydroxyethyl)-*N*-methylbenzenesulfonamide did not elute from the column under the conditions used and was investigated by GLC–electron-impact mass spectrometry[16]. The fragmentation pattern shown in Fig. 4 is consistent with that expected for the *N*-methyl-substituted pyrolysis product of *N*-methylhydroxyhexamide.

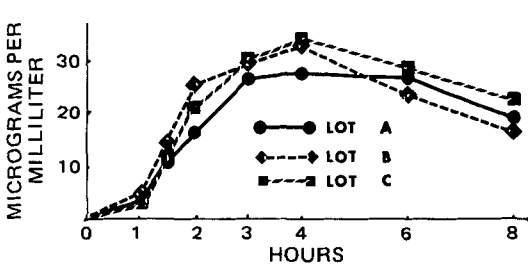

Figure 6—*Mean plasma concentrations of hydroxyhexamide after administration of 750 mg of acetohexamide to eight subjects.*

[16] Using an LKB 9000S GC–mass spectrometer with column and conditions used in this procedure.

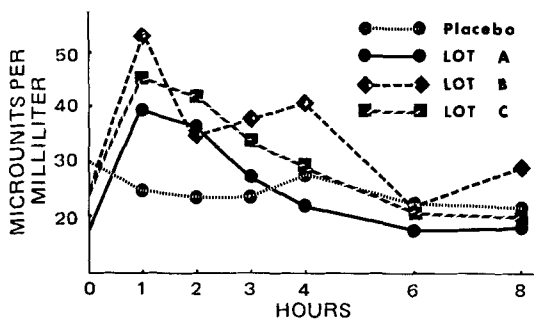

Figure 7—*Mean insulin levels in serum after administration of 750 mg of acetohexamide to eight subjects.*

Dissolution profiles are shown in Table II; all lots met the USP XIX dissolution requirement. Although Lot B appeared to have more rapid dissolution, the variability was such that all lots were judged to have relatively similar dissolution patterns.

The average plasma concentration–time curves observed for acetohexamide and hydroxyhexamide are given in Figs. 5 and 6, respectively. Recovery of drug and metabolite in the 0–8-hr urines is shown in Table III, and mean serum insulin and blood glucose responses associated with these three tablet formulations are shown in Figs. 7 and 8. The three lots were compared with respect to the area under the plasma concentration–time curves (*AUC*) and the peak plasma concentration responses for both acetohexamide and hydroxyhexamide. Analysis of variance suggested a lower bioavailability of acetohexamide for Lot A than for B or C. While it is difficult to be certain why Lot A appeared poorer than the other lots, the formulation used in preparing Lot A tablets was different from that used for Lots B and C, and Lot A tablets were approximately 30 months old at the time of this study while the other lots were only 2 months old.

The physiological responses (elevation of serum insulin and lowering of blood glucose) may more truly reflect the bioavailability of acetohexamide from the three tablet formulations, because the metabolite, hydroxyhexamide, is not only physiologically active but also has a more prolonged effect than the parent drug. Since no substantial differences were found in the plasma concentrations of hydroxyhexamide from these tablet lots, the physiological responses may more closely reflect the plasma metabolite concentrations or a combination of the plasma concentrations of drug and metabolite.

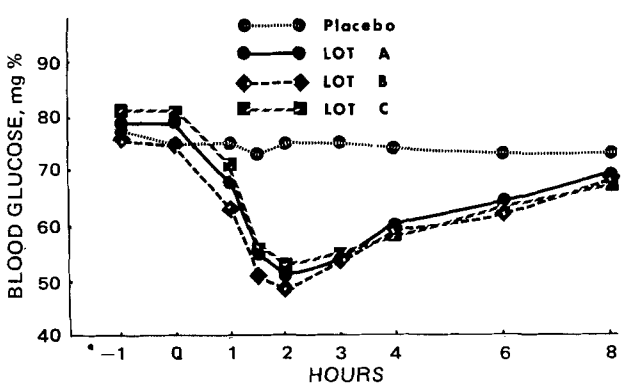

Figure 8—*Mean blood glucose responses after administration of 750 mg of acetohexamide to eight subjects.*

REFERENCES

(1) D. L. Smith, T. J. Vecchio, and A. A. Forist, *Metabolism*, **14**, 229 (1965).

(2) B. D. Cohen, J. A. Galloway, R. E. McMahon, H. W. Culp, M. A. Root, and K. J. Henriques, *Am. J. Med. Sci.*, **254**, 608 (1967).

(3) R. E. McMahon, F. J. Marshall, and H. W. Culp, *J. Pharmacol. Exp. Ther.*, **149**, 272 (1965).

(4) H. Spingler, *Klin. Wochenschr.*, **35**, 533 (1957).

(5) T. J. Toolan and R. L. Wagner, *Ann. N.Y. Acad. Sci.*, **74**, 449 (1959).

(6) K. Sabih and K. Sabih, *J. Pharm. Sci.*, **59**, 782 (1970).

(7) S. B. Matin and M. Rowland, *J. Pharm. Pharmacol.*, **25**, 186 (1973).

(8) D. L. Simmons, R. J. Ranz, and P. Picotte, *J. Chromatogr.*, **71**, 421 (1972).

(9) L. F. Prescott and D. R. Redman, *J. Pharm. Pharmacol.*, **24**, 713 (1972).

(10) W. S. Hoffman, *J. Biol. Chem.*, **120**, 51 (1937).

(11) L. Heding, *Diabetologia*, **8**, 260 (1972).

ACKNOWLEDGMENTS AND ADDRESSES

Received October 17, 1975, from the *Lilly Research Laboratories, Indianapolis, IN 46206.*

Accepted for publication June 22, 1976.

Presented in part at the Pharmaceutical Analysis and Control Section, APhA Academy of Pharmaceutical Sciences, New Orleans meeting, November 1974.

The authors thank Mr. T. Collins for collecting the blood and urine samples, Mrs. N. Werner for blood glucose determinations, Mr. J. Ferguson for insulin determinations, Dr. R. Wolen for GLC–chemical ionization mass spectrometry, Mr. C. Novotny for GLC–electron-impact mass spectrometry, and Dr. A. Kossoy for interpretation of the data. The authors also thank Mr. P. Page for analysis of the plasma and urine samples.

[x] To whom inquiries should be directed.

Quantitative Analysis of Degradation Products in Pilocarpine Hydrochloride Ophthalmic Formulations

GEORGE A. NEVILLE [*x], FARIZA B. HASAN [‡], and IAN C. P. SMITH [‡]

Abstract □ The presence of isopilocarpine, an epimer of pilocarpine, and of pilocarpinic acid, a hydrolytic degradation product of pilocarpine, was established and all three substances were assayed in various commercial ophthalmic formulations of pilocarpine hydrochloride by ^{13}C-Fourier transform spectroscopy. Assay was based upon integrated intensities of selected resonances from any formulation calibrated against the intensity of tetramethylammonium bromide, used as a common external reference. The normalized intensities were then related to those of a reference solution of pilocarpine hydrochloride, thereby eliminating any factor arising from variability of ^{13}C-relaxation times. The ^{13}C-resonance for the *N*-methyl group, being common to all products, provides a convenient basis for the assay of the total alkaloid content whereas the C-8 resonances are best suited for assaying residual pilocarpine and its degradation products. This procedure, estimated as accurate to ±5%, constitutes the first comprehensive analytical method to differentiate between pilocarpine and its degradation products.

Keyphrases □ Pilocarpine hydrochloride—and degradation products, ^{13}C-NMR analysis, commercial ophthalmic formulations □ Isopilocarpine—^{13}C-NMR analysis in commercial ophthalmic formulations of pilocarpine hydrochloride □ Pilocarpinic acid—^{13}C-NMR analysis in commercial ophthalmic formulations of pilocarpine hydrochloride □ ^{13}C-NMR spectroscopy—analysis, pilocarpine hydrochloride and degradation products, commercial ophthalmic formulations □ Ophthalmic formulations, commercial—^{13}C-NMR analysis of pilocarpine hydrochloride and degradation products

No satisfactory methodology[1] is available for the analysis of the degradation products, isopilocarpine (II) and pilocarpinic acid[2] (III), in aqueous formulations of pilocarpine (I). The analysis of such impurities has received little attention because of: (*a*) their apparent relatively low concentrations in pilocarpine formulations, (*b*) the great difficulty in effecting any separation, and (*c*) the difficulty in realizing unequivocal characterization. However, numerous procedures for the determination of pilocarpine, including colorimetric, volumetric, polarimetric, and polarographic (3, 4), have been developed.

All commonly used procedures for the assay of pilocarpine have drawbacks (5). A common deficiency is the inability to distinguish between the parent alkaloid and its degradation products. For example, various colorimetric methods use the ferric hydroxamate reaction in aqueous (4, 6) or alcoholic (7) media, the sodium nitroprusside reaction (8), the hydrogen peroxide dichromate reaction (9), and the phosphomolybdic acid reaction (10). Although none of these colorimetric procedures excludes the contribution from degradation products from the total assay,

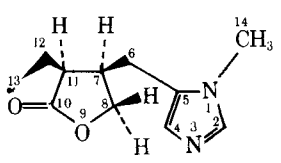

I

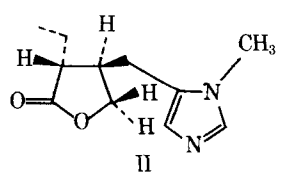

II

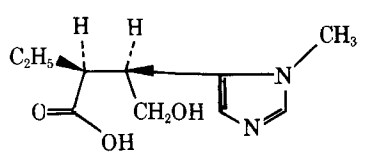

III

[1] The simultaneous determination of pilocarpine and isopilocarpine in pharmaceutical preparations (1) was published after this paper was submitted. The same method had been used to analyze isopilocarpine and pilocarpine in the synthesis of *d*-pilocarpine-*N*-$^{14}CH_3$ (2).

[2] Pilocarpinic acid has also been called pilocarpic acid (T. A. Henry, in "The Plant Alkaloids," 4th ed., Blakiston, Philadelphia, Pa., 1949) and pilocarpoic acid (R. H. F. Manske, in "The Alkaloids," vols. 3 and 5, Academic, New York, N.Y., 1953 and 1955).

REFERENCES

(1) D. L. Smith, T. J. Vecchio, and A. A. Forist, *Metabolism*, **14**, 229 (1965).

(2) B. D. Cohen, J. A. Galloway, R. E. McMahon, H. W. Culp, M. A. Root, and K. J. Henriques, *Am. J. Med. Sci.*, **254**, 608 (1967).

(3) R. E. McMahon, F. J. Marshall, and H. W. Culp, *J. Pharmacol. Exp. Ther.*, **149**, 272 (1965).

(4) H. Spingler, *Klin. Wochenschr.*, **35**, 533 (1957).

(5) T. J. Toolan and R. L. Wagner, *Ann. N.Y. Acad. Sci.*, **74**, 449 (1959).

(6) K. Sabih and K. Sabih, *J. Pharm. Sci.*, **59**, 782 (1970).

(7) S. B. Matin and M. Rowland, *J. Pharm. Pharmacol.*, **25**, 186 (1973).

(8) D. L. Simmons, R. J. Ranz, and P. Picotte, *J. Chromatogr.*, **71**, 421 (1972).

(9) L. F. Prescott and D. R. Redman, *J. Pharm. Pharmacol.*, **24**, 713 (1972).

(10) W. S. Hoffman, *J. Biol. Chem.*, **120**, 51 (1937).

(11) L. Heding, *Diabetologia*, **8**, 260 (1972).

ACKNOWLEDGMENTS AND ADDRESSES

Received October 17, 1975, from the *Lilly Research Laboratories, Indianapolis, IN 46206.*

Accepted for publication June 22, 1976.

Presented in part at the Pharmaceutical Analysis and Control Section, APhA Academy of Pharmaceutical Sciences, New Orleans meeting, November 1974.

The authors thank Mr. T. Collins for collecting the blood and urine samples, Mrs. N. Werner for blood glucose determinations, Mr. J. Ferguson for insulin determinations, Dr. R. Wolen for GLC–chemical ionization mass spectrometry, Mr. C. Novotny for GLC–electron-impact mass spectrometry, and Dr. A. Kossoy for interpretation of the data. The authors also thank Mr. P. Page for analysis of the plasma and urine samples.

[x] To whom inquiries should be directed.

Quantitative Analysis of Degradation Products in Pilocarpine Hydrochloride Ophthalmic Formulations

GEORGE A. NEVILLE [*x], FARIZA B. HASAN [‡], and IAN C. P. SMITH [‡]

Abstract □ The presence of isopilocarpine, an epimer of pilocarpine, and of pilocarpinic acid, a hydrolytic degradation product of pilocarpine, was established and all three substances were assayed in various commercial ophthalmic formulations of pilocarpine hydrochloride by ^{13}C-Fourier transform spectroscopy. Assay was based upon integrated intensities of selected resonances from any formulation calibrated against the intensity of tetramethylammonium bromide, used as a common external reference. The normalized intensities were then related to those of a reference solution of pilocarpine hydrochloride, thereby eliminating any factor arising from variability of ^{13}C-relaxation times. The ^{13}C-resonance for the *N*-methyl group, being common to all products, provides a convenient basis for the assay of the total alkaloid content whereas the C-8 resonances are best suited for assaying residual pilocarpine and its degradation products. This procedure, estimated as accurate to ±5%, constitutes the first comprehensive analytical method to differentiate between pilocarpine and its degradation products.

Keyphrases □ Pilocarpine hydrochloride—and degradation products, ^{13}C-NMR analysis, commercial ophthalmic formulations □ Isopilocarpine—^{13}C-NMR analysis in commercial ophthalmic formulations of pilocarpine hydrochloride □ Pilocarpinic acid—^{13}C-NMR analysis in commercial ophthalmic formulations of pilocarpine hydrochloride □ ^{13}C-NMR spectroscopy—analysis, pilocarpine hydrochloride and degradation products, commercial ophthalmic formulations □ Ophthalmic formulations, commercial—^{13}C-NMR analysis of pilocarpine hydrochloride and degradation products

No satisfactory methodology[1] is available for the analysis of the degradation products, isopilocarpine (II) and pilocarpinic acid[2] (III), in aqueous formulations of pilocarpine (I). The analysis of such impurities has received little attention because of: (*a*) their apparent relatively low concentrations in pilocarpine formulations, (*b*) the great difficulty in effecting any separation, and (*c*) the difficulty in realizing unequivocal characterization. However, numerous procedures for the determination of pilocarpine, including colorimetric, volumetric, polarimetric, and polarographic (3, 4), have been developed.

All commonly used procedures for the assay of pilocarpine have drawbacks (5). A common deficiency is the inability to distinguish between the parent alkaloid and its degradation products. For example, various colorimetric methods use the ferric hydroxamate reaction in aqueous (4, 6) or alcoholic (7) media, the sodium nitroprusside reaction (8), the hydrogen peroxide dichromate reaction (9), and the phosphomolybdic acid reaction (10). Although none of these colorimetric procedures excludes the contribution from degradation products from the total assay,

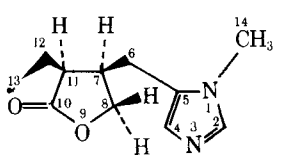

I

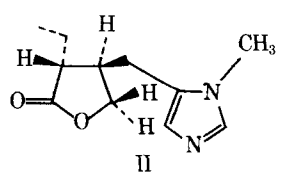

II

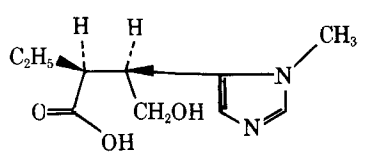

III

[1] The simultaneous determination of pilocarpine and isopilocarpine in pharmaceutical preparations (1) was published after this paper was submitted. The same method had been used to analyze isopilocarpine and pilocarpine in the synthesis of *d*-pilocarpine-*N*-$^{14}CH_3$ (2).

[2] Pilocarpinic acid has also been called pilocarpic acid (T. A. Henry, in "The Plant Alkaloids," 4th ed., Blakiston, Philadelphia, Pa., 1949) and pilocarpoic acid (R. H. F. Manske, in "The Alkaloids," vols. 3 and 5, Academic, New York, N.Y., 1953 and 1955).

Table I—Measurements and Calculated Parameters

Pilocarpine Hydrochloride Formulation (%)[a]	Density of Concentrated Formulation[b]	Relative Peak Intensities[c]					Calculated Parameters		
		IV	C-14	C-8			C_t	F	C_0
				Pilocarpine	Isopilocarpine	Pilocarpinic Acid			
A (4)	1.12	55	55	94	—	—	25.5	7.5	3.4
A (3)	1.12	60	42	84	5	5	18.1	6.7	2.7
A (2)	1.15	65	51	95	—	—	19.0	10	1.9
A (1)	1.13	84	75	41	—	—	22.0	20	1.1
B (6)	1.03	97	72	85	6	6	20.5	3.3	6.2
B (4)	1.18	121	59	81	—	5	12.0	4.0	3.0
C (4)	0.92	82	40	80	—	4	15.0	3.75	4.0
D (2)	1.12	73	43	81	4	4	15.0	7.5	2.0
E (4)	1.11	114	24	23	—	—	5.4	1.7	3.2

[a] Percent concentration as read from labeled formulation. [b] Density of concentrated (freeze-dried) sample of formulation in deuterium oxide. [c] To measure the intensities of the small peaks due to isopilocarpine and pilocarpinic acid, the C-8 peak intensities were integrated separately on one intensity scale; integration of the C-14 and IV peak intensities was performed on a different, common scale.

new, similar colorimetric procedures with the same limitations continue to appear.

A recently reported procedure based on the oxidative cleavage of pilocarpine by benzoyl peroxide and colorimetric estimations of the formaldehyde formed after additions of chromotropic acid (11) is alleged to hold some advantage in obviating interferences present in the USP hydroxylamine hydrochloride method for pilocarpine formulations. However, this new procedure probably will account for every substance having the *N*-methyl group (degradation products included) in a pilocarpine solution.

Dissatisfaction with traditional methods prompted the development of rather sophisticated chemical procedures for the indirect assay of pilocarpine and associated impurities. One such procedure employs phase solubility analysis of slightly soluble picrate salts in aqueous buffered solutions (12), but it is assumed that the reference pilocarpine samples are pure and that no chemical alteration occurs upon dissolution. A kinetic method for analyzing microgram quantities of pilocarpine in aqueous solution is based on the catalytic activity of the imidazole portion of the alkaloids on the hydrolysis of 2,4-dinitrophenyl acetate (12). The catalytic constants obtained for pilocarpine, pilocarpinic acid, isopilocarpinic acid, *etc.*, like the rate constants for the same substances obtained in related kinetic studies of the hydrolysis of pilocarpine (13, 14), may be based upon false assumptions regarding the constitution of pilocarpine reference solutions.

From a detailed study of the hydrolysis and epimerization of pilocarpine in aqueous solutions with changing pH using ^{13}C-NMR spectroscopy (15), an unequivocal basis for the characterization of aqueous solutions of pilocarpine and isopilocarpine was reported. The purpose of this paper is to discuss the application of ^{13}C-NMR spectroscopy to the assay of pilocarpine formulations for the content of pilocarpine and its degradation products.

EXPERIMENTAL

Procedure—^{13}C-Fourier transform NMR spectra were obtained[3] from various concentrated formulations of pilocarpine using 10-mm o.d. tubes and operating at 30°. The samples were scanned over 4000 Hz, and chemical shifts were measured in parts per million downfield from a tetramethylsilane external reference. The noise–signal ratio was kept at a constant minimum for each sample. Comparisons of the spectra obtained from commercial formulations with those of reference solutions of pilocarpine and isopilocarpine with varying pH (15) allowed the determination of the ratio of pilocarpine, isopilocarpine, and the corresponding hydroxy acids in the samples.

The spectra used for the calculations were obtained by using 4K data points, an acquisition time of 0.5 sec, a pulse angle of 30°, and no pulse delay. To check the accuracy of the observed intensities, spectra of two samples, 4% A and 4% E, were obtained using 8K data points within a 2000-Hz spectral width, an acquisition time of 2 sec, and a pulse delay of 1 sec. These conditions eliminated any error due to insufficient data points and to differences in relaxation times in the spectra. The results from these spectra were in good agreement (±5% of the measured values) with the results obtained by the more rapid method.

A known pipetted volume of each formulation was reduced to dryness by freeze drying. The residue was dissolved in deuterium oxide and carefully transferred, together with washings, to a volumetric flask (3.0 or 5.0 ml). The final concentration of pilocarpine was usually kept close to 20%; however, more dilution was sometimes necessary to dissolve the residue completely due to the presence of buffering agents and other preservatives. Table I lists the original and prepared pilocarpine concentrations for the various formulations.

For the quantitation of components in the pilocarpine formulations, a solution (2.04 *M*) of tetramethylammonium bromide in deuterium oxide was used for calibration. First, ^{13}C-NMR spectra of a solution (reference standard) of pilocarpine hydrochloride (0.159 *M*) in deuterium oxide were obtained in an NMR tube in which a coaxial inner tube containing the calibration solution of tetramethylammonium bromide had been inserted (Fig. 1). From the resulting proton-decoupled spectra, correlations were made between the peak intensities of the tetramethylammonium carbon resonances and the peak intensities for selected carbon resonances of pilocarpine and their respective solution concentrations. The same coaxial tube of tetramethylammonium bromide solution was then inserted in each formulation analyzed to calibrate them in terms of a common standard. A typical spectrum is shown in Fig. 2.

The following ophthalmic formulations of pilocarpine hydrochloride were examined: 4% A (expiration date December 1972), 3% A (expiration date February 1973), 2% A (expiration date September 1973), 1% A (expiration date December 1972), 6% B (expiration date February 1974), 4% B (expiration date June 1974), 4% C (no expiration date), 2% D (no expiration date), and 4% E (expiration date December 1975). Pilocarpine hydrochloride[4] (mp 204–205°) and tetramethylammonium bromide[5] were used for calibration.

Formulations and Calculations—The integrated intensity of any ^{13}C-NMR resonance from the reference solution of pilocarpine hydrochloride = P_n (where n refers to the carbon numbering position); the intensity of the ^{13}C-peak for tetramethylammonium bromide (IV) calibration solution (2.04 *M*) observed in the reference solution = S; the ratio of any pilocarpine peak intensity to peak IV intensity = P_n/S; the concentration of reference pilocarpine solution, P_R, per unit concentration

[3] Varian CFT-20 spectrometer.

[4] BDH.

[5] Eastman, White Label.

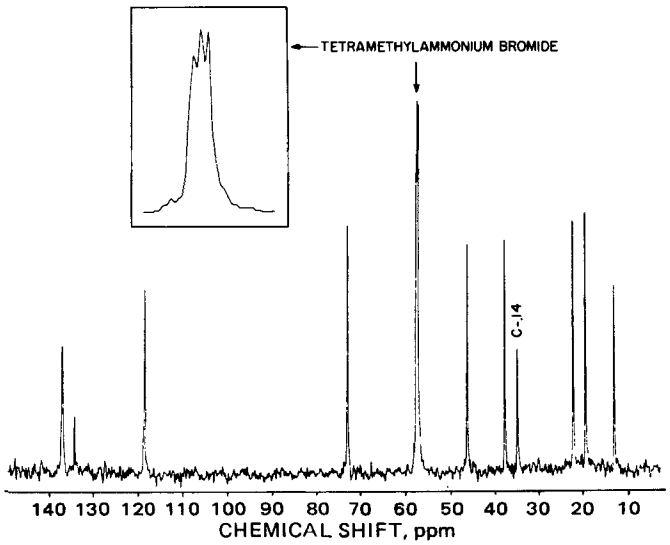

Figure 1—^{13}C-*NMR spectrum of pilocarpine hydrochloride (0.159* M*) in deuterium oxide with tetramethylammonium bromide (2.04* M*) in deuterium oxide as the external standard.*

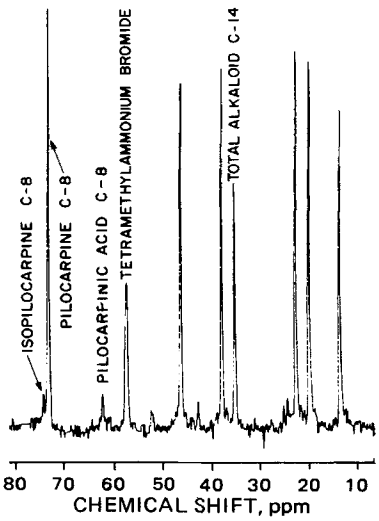

Figure 2—^{13}C-*NMR spectrum of freeze-dried sample from 6% B with tetramethylammonium bromide (2.04* M*) in deuterium oxide as the external standard.*

of IV calibration solution = $[P_R]/[IV] = 0.159/2.04 = 0.078$; and the normalized concentration of reference pilocarpine solution per normalized unit intensity, N, of any pilocarpine resonance peak = $[P_R]/[IV] \times S/P_n$. Thus, for any pilocarpine formulation, the total molar concentration, M_t, of all components having the N-methyl group may be expressed as follows:

$$M_t = \frac{\text{intensity of C-14 peak}}{\text{intensity of internal peak IV}} \times [IV] \times N \text{ (moles/liter)} \quad \text{(Eq. 1)}$$

The percent concentration (% total alkaloid) is:

$$C_t = \frac{M_t \times \text{mol. wt. of pilocarpine hydrochloride}}{1000 \text{ (ml)} \times \text{solution density (g/ml)}} \times 100 \quad \text{(Eq. 2)}$$

The calculated original concentration C_0, of pilocarpine hydrochloride in any formulation is C_t/F, where the concentration factor is:

$$F = \frac{\text{volume of labeled formulation pipetted}}{\text{final volume of concentrated formulation}} \quad \text{(Eq. 3)}$$

For a particular sample, 3% A, the total concentration of the species that contains the imidazole ring was calculated using Eqs. 1–3. From the known concentrations of the standard solutions of pilocarpine hydrochloride (0.159 *M*) and IV (2.04 *M*) and their peak intensities [16 and 117, respectively (Table I)], $N = 0.57$, $M_t = 0.81$ mole/liter, $C_t = 17.8$ moles/liter, $F = 6.7$, and $C_0 = 2.7\%$.

From the intensities of the C-8 peaks for pilocarpine, isopilocarpine, and the corresponding hydroxy acids in any particular sample, the relative quantities of the different species were calculated as follows:

$$\text{total intensity of C-8 resonances} = I_t = I_1 + I_2 + I_3 \ldots + I_n \quad \text{(Eq. 4)}$$

where $I_n = I_1$, I_2, *etc.*, C-8 intensities for pilocarpine, isopilocarpine, *etc.*

The ratio of any C-8 resonance to total C-8 intensity = I_n/I_t, and the percent species n in solution = $I_n/I_t \times C_0$. Therefore, for 3% A (Table I), pilocarpine = 2.4%, isopilocarpine = 0.1%, and pilocarpinic acid = 0.1%. Similar calculations were performed for each formulation (Table I).

RESULTS AND DISCUSSION

The results of ^{13}C-NMR analysis of pilocarpine formulations are summarized in Table II. Little change in pH resulted from the concentration of any formulation, and the small changes are ascribed to effects arising from the concentration of other formulating agents such as hydroxypropyl methylcellulose (0.33%), benzalkonium chloride (0.01%), edetate disodium (0.01%), potassium chloride (0.25%), boric acid (0.413%), and sodium carbonate (0.006%) present in a 2% pilocarpine hydrochloride formulation. The estimated amount of pilocarpine hydrochloride (percent) after concentration (Table I) was calculated from known changes in volume; usually, 20 ml reduced to 3.0 ml. However, in some instances the final volume had to be increased to keep all components of a formulation in solution. Formulations D and E were particularly troublesome for reconstitution of their components in deuterium oxide; consequently, their analyses were restricted to less concentrated solutions.

Baeschlin *et al.* (16) first utilized proton NMR spectroscopy to differentiate between pilocarpine hydrochloride in deuterium oxide and the lactone-cleaved sodium pilocarpinate in 2 *N* NaOD. Knowledge of these spectral features was then used to interpret the spectral changes observed when a formulation of pilocarpine hydrochloride (0.14 g) in deuterium oxide (2 ml) at pH 6.1, containing monobasic potassium phosphate (0.056 g) and dibasic sodium phosphate dihydrate (0.04 g), was heated at 70° for 240 hr. The gradual diminution of a multiplet at 0.4 ppm, attributed to the γ-methylene protons of the lactone ring, with the simultaneous development of a more complex multiplet at 1.1 ppm (not assigned) during prolonged heating of the formulations was attributed to hydrolysis (lactone ring cleavage) of pilocarpine. From comparison of the integrals from these multiplets, it was reported that 70% pilocarpine remained intact and that 28% of an "open form" was generated after 240 hr at 70°.

From inspection of the published spectra (16), most of the spectral change can be accounted for by isomerization to isopilocarpine, because obvious development of an additional methyl triplet can be seen on the high field side of the 3.7-ppm triplet for the methyl group of the ethyl substituent of pilocarpine. The recognition that the spectra reveal evidence for appreciable isomerization of pilocarpine also discounts the value of the colorimetric method designed by Brochmann-Hanssen *et al.* (17), with which the proton NMR method was compared because it also cannot distinguish between isopilocarpine and lactone-cleaved products.

Nunes and Brochmann-Hanssen (14) were the first to report that when pilocarpine and isopilocarpine are hydrolyzed in alkaline solution, the NMR triplets of the terminal methyl group of the ethyl substituents are shifted upfield to 1.31 ppm for both epimers and that the chemical shifts differ by 0.1 ppm for the two epimers. Nunes and Brochmann-Hanssen considered that integration of the methyl triplets due to pilocarpinate and isopilocarpinate, recorded with a 10-fold scale expansion and a 1.0-ppm offset, provided the best means of quantitating epimerization. For the best utilization of this method at 100 MHz, it is necessary to use a curve resolver for the expanded spectra (14). In addition, the assay-based integration of methyl triplets is limited to alkaline solutions and cannot be utilized under acidic or nearly neutral conditions where the chemical shifts for the methyl triplets of isopilocarpine and pilocarpine coincide.

Recently, a liquid chromatographic procedure was published for the simultaneous determination of pilocarpine and isopilocarpine in pharmaceutical preparations (1). This procedure involves separation of the isomers on an ion-exchange column followed by detection by UV absorption in the 217-nm region. The conditions used (1), *i.e.*, the buffered mobile phase was adjusted to pH 9, might lead to isomerization and hydrolysis of pilocarpine, as indicated by ^{13}C-NMR spectroscopic studies of the behavior of pilocarpine with varying pH (15). This concern for possible analytical modification of the sample by the chromatographic

Table II—Analysis of Pilocarpine Formulations[a]

Formulation	Pilocarpine Hydrochloride (from Label), %	pH	Estimated Concentration of Pilocarpine Hydrochloride (after Freeze Drying), %	pD after Freeze Drying	Total[b] Alkaloid	Calculated Concentration, %[c]		
						Pilocarpine	Isopilocarpine	Pilocarpinic Acid
A	4	3.85	30	4.60	3.4	3.4	n.d.[d]	n.d.
A	3	4.00	20	4.50	2.7	2.4	0.1	0.1
A	2	3.75	20	4.15	1.9	1.9	n.d.	n.d.
A	1	4.10	20	4.95	1.1	1.1	n.d.	n.d.
B	6	4.20	20	4.65	6.2	5.4	0.4	0.4
B	4	4.20	16	4.50	3.0	2.8	n.d.	0.2
C	4	4.10	15	4.55	4.0	3.8	n.d.	0.2
D	2	4.25	15	4.60	2.0	1.8	0.1	0.1
E	4	3.90	6.8	4.35	3.2	3.2	n.d.	n.d.

[a] Estimated accuracy of intensity measurement = ±5%; precision = ±3%. [b] Calculated on the basis of the C-14 ^{13}C-NMR resonance and expressed as if total intensity arose from pilocarpine hydrochloride. [c] Contents less than 0.1% could not be detected by the method of analysis employed. [d] Not detected.

procedure is especially pertinent when long retention times are involved.

While Urbànyi *et al.* (1) did not describe the determination of pilocarpinic acid, Weber[6] chromatographically determined this acid by treating a second aliquot of the ophthalmic solution with acid (pH <1) to convert pilocarpinic acid to pilocarpine. In contrast, the NMR spectroscopic technique permits pilocarpine, isopilocarpine, and pilocarpinic acid to be characterized and assayed simultaneously in the presence of one another and in the presence of excipients commonly found in commercial pilocarpine solutions.

In a detailed ^{13}C-NMR study of the hydrolysis and epimerization of pilocarpine in aqueous solution of varying pH (15), it was shown that the C-8 resonances[7] afford a particularly good spectral basis for distinguishing among pilocarpine, isopilocarpine, and pilocarpinic acid. In this study, this understanding was applied in the development of an assay procedure based on the relative intensities of the C-8 resonances for these compounds calibrated against the intensity of the ^{13}C-resonance from a known concentration of tetramethylammonium bromide.

Tetramethylammonium bromide (IV) was selected because its ^{13}C-resonance is well removed from any resonance of pilocarpine and the other compounds (Fig. 1). The insert in Fig. 1 reveals the triplet character for the resonance of IV due to quadrupole coupling by nitrogen; thus, the intensity of the resonance of IV was taken as the sum of the three integrated component intensities. Figure 2 illustrates the spectral features of a pilocarpine formulation, showing the C-8 resonances for pilocarpine, isopilocarpine, pilocarpinic acid, and IV.

Because the C-14 resonance for the *N*-methyl moiety has a common frequency for all components of a pilocarpine solution at any pH, its intensity can be used as a measure of the total alkaloid content of any pilocarpine formulation. The intensities of the C-8 resonances, however, cannot be compared directly with the C-14 resonances, because the ^{13}C-relaxation time for the C-14 is markedly different from that for C-8, as may be seen from inspection of the relative intensities in Fig. 2.

To calculate either the percentage composition or the total alkaloid content of any formulation, it is necessary to circumvent the difference in relaxation characteristics by relating any particular resonance intensity to the intensity of the common calibration resonance, IV. The ratio of intensities so obtained is then multiplied by a normalizing factor, *N*, calculated to relate the intensity of reference IV in terms of the intensity of any resonance of a reference solution of pilocarpine hydrochloride of known concentration. The details of these formulations together with sample calculations are outlined under *Experimental.*

The results of the analysis of a range of pilocarpine formulations having various labeled concentrations of drug and expiration dates are summarized in Table II. The samples were procured from various pharmacies in 1972 and were then stored at room temperature and protected from light. In most instances, no isopilocarpine was detected; where it was detected, it generally did not exceed 5% of the labeled pilocarpine content. In one instance, B (6%) showed degradation to 7% isopilocarpine and 7% pilocarpinic acid which was surprising in view of its more recent expiration date compared to most samples. However, this formulation apparently was the only one containing phenylmercuric nitrate as well as benzalkonium chloride as preservatives. One formulation, 4% E, showed a new resonance at 70.25 ppm, attributed to a ring carbon of povidone, an ingredient not found in the other formulations.

The calculated total alkaloid content agreed well with the labeled content of pilocarpine hydrochloride in each instance. Low results obtained by a colorimetric method for the determination of pilocarpine in ophthalmic solutions were attributed (18) to pilocarpine–methylcellulose interaction. In no case was there any evidence of interference with the ^{13}C-NMR method by methylcellulose, hydroxypropyl methylcellulose, or hydroxyethylcellulose.

In summary, this ^{13}C-NMR spectroscopic assay constitutes the first reported unequivocal and comprehensive method for analyzing degradation products of pilocarpine, isopilocarpine, and pilocarpinic acid, as well as unchanged pilocarpine, in pilocarpine formulations. This method provides for the differentiation and characterization *in situ* of products as well as their convenient assay utilizing resonance intensities treated in such a way as to avoid the limitation imposed upon ^{13}C-NMR spectroscopy for quantitation due to marked variability in relaxation times. The assay, as described, provides the percentage composition within ±5%.

[6] J. D. Weber, Food and Drug Administration, Washington, D.C., personal communication.

[7] By definition, the C-8 resonances arise from the γ-methylene carbon atom of the γ-lactone ring of pilocarpine, isopilocarpine, *etc.*

REFERENCES

(1) T. Urbànyi, A. Piedmont, E. Willis, and G. Manning, *J. Pharm. Sci.*, **65**, 257 (1976).

(2) J. I. DeGraw, J. S. Engstrom, and E. Willis, *ibid.*, **64**, 1700 (1975).

(3) T. Higuchi and E. Brochmann-Hanssen, "Pharmaceutical Analysis," Interscience, New York, N.Y., 1961, chap. 8.

(4) "The United States Pharmacopeia," 19th rev., Mack Publishing Co., Easton, Pa., 1975, pp. 385, 386.

(5) A. Repta and T. Higuchi, *J. Pharm. Sci.*, **60**, 1465 (1971).

(6) H. Wachsmuth and L. Vankaeckhoven, *J. Pharm. Belg.*, **14**, 456 (1959).

(7) E. Tomach and J. Major, *Acta Pol. Pharm.*, **17**, 139 (1960).

(8) V. G. Belikov and V. N. Berstein, USSR pat. 141,871 (1961); through *Chem. Abstr.*, **56**, 13020 (1962).

(9) F. Biederbach, *Apoth. Ztg.*, **48**, 736 (1933).

(10) J. Celechovesky and D. Sovobodava, *Cesk. Farm.*, **8**, 380 (1959).

(11) M. S. Karawya and M. G. Ghourab, *J. Assoc. Offic. Anal. Chem.*, **55**, 1180 (1972).

(12) A. J. Repta and P. Bansal, *J. Pharm. Sci.*, **61**, 1069 (1972).

(13) P.-H. Chung, T.-F. Chin, and J. L. Lach, *ibid.*, **59**, 1300 (1970).

(14) M. A. Nunes and E. Brochmann-Hanssen, *ibid.*, **63**, 716 (1974).

(15) G. A. Neville, F. B. Hasan, and I. C. P. Smith, *Can. J. Chem.*, **54**, 2094 (1976).

(16) K. Baeschlin, J. C. Etter, and H. Moll, *Pharm. Acta Helv.*, **44**, 301 (1969).

(17) E. Brochmann-Hanssen, P. Schmid, and J. D. Benmaman, *J. Pharm. Sci.*, **54**, 783 (1965).

(18) J. W. Steele and J. Thiessen, *J. Pharm. Pharmacol.*, **18**, 179 (1966).

ACKNOWLEDGMENTS AND ADDRESSES

Received March 15, 1976, from the **Drug Research Laboratories, Health Protection Branch, Health and Welfare Canada, Ottawa, Canada K1A OL2,* and the ‡ *Division of Biological Sciences, National Research Council of Canada, Ottawa, Canada K1A OR6.*

Accepted for publication June 17, 1976.

ˣ To whom inquiries should be directed.

Structure–Activity Studies Using Valence Molecular Connectivity

LOWELL H. HALL *ˣ and LEMONT B. KIER ‡

Abstract □ The extension of the molecular connectivity concept to the treatment of heteroatom molecules affords an opportunity to examine structure–activity relationships in a wide variety of molecule series that possess biological activity. Four series are described in this report. The correlations found indicate that molecular connectivity is an extremely useful descriptor of structure in studying drug molecule structure–activity relationships.

Keyphrases □ Molecular connectivity index—related to structure–activity relationships, various types of molecules □ Structure–activity relationships—various types of molecules, related to molecular connectivity index □ Topological indexes—molecular connectivity index, related to structure–activity relationships, various types of molecules

Recently (1, 2), the extension of molecular connectivity to the treatment of heteroatom molecules was described. By considering the valence electrons, whether bonded or nonbonded, an atom connectivity term, δ^v, for multiply bonded carbon atoms or heteroatoms was assigned.

The work presented in this paper tests the ability of δ^v to describe the atomic connectivity in heteroatoms so that the molecular connectivity indexes bear some relationship to structure influencing biological properties.

DISCUSSION

The simple prescription for assigning δ^v is $Z^v - h_i$, where Z^v is the number of valence electrons and h_i is the number of attached hydrogens. For alcohols, ethers, primary amines, and pyridine, the δ^v values for the heteroatoms are 5, 6, 3, and 5, respectively. The δ^v values for heteroatoms are shown in Table I.

Since halogen atoms have an identical number of valence electrons, this prescription yields identical values of δ^v. It is necessary to derive empirical values of δ^v for the halogens by calibrating them to a physical property. The molar refraction was chosen for this assignment (1, 2) (Table I).

Table I—Valence Delta, δ^v, Values for Heteroatoms

Atom	δ^v	Atom	δ^v
—NH_2	3	—OH	5
—NH—	4	—O—	6
	5	—C=O	6
—C≡N	5	Furan O	6
—C=NH	4	O=N—O	6
Pyridine N	5	H_2O	4
Nitro N	6	H_3O+	3
NH_3	2	F	(−)20
NH_4^+	1	Cl	0.690
	6	Br	0.254
=NH_2^+	3	I	0.085

The use of δ^v thus permits the calculation of a valence chi term of the first order, $^1\chi^v$, by the expression:

$$^1\chi^v = \sum (\delta_i^v \delta_j^v)^{-1/2} \qquad \text{(Eq. 1)}$$

The $^1\chi^v$ terms provide a further structural description of heteroatom molecules, eliminating the redundancies found when simple connectivity values are used. The refinement permits the close correlation of chi terms with physical properties such as boiling point, solubility, and molar refraction (1, 2).

Cytochrome Conversion by Phenols—The conversion of cytochrome P-450 to P-420 in the rabbit liver by a series of phenols was reported (3). An analysis of these molecules using $^1\chi^v$ reveals the following relationship to the minimum active concentration (−log *c*), p*C*:

$$pC = 0.816\ (\pm 0.105)\,^1\chi^v - 0.789\ (\pm 0.329) \qquad \text{(Eq. 2)}$$

$$r = 0.914 \quad s = 0.291 \quad n = 14$$

The calculated and observed values are listed in Table II.

The inclusion of the Hammett sigma value for each substituent in a multiple regression with $^1\chi^v$ does not improve the relationship. The re-

REFERENCES

(1) T. Urbànyi, A. Piedmont, E. Willis, and G. Manning, *J. Pharm. Sci.*, **65**, 257 (1976).

(2) J. I. DeGraw, J. S. Engstrom, and E. Willis, *ibid.*, **64**, 1700 (1975).

(3) T. Higuchi and E. Brochmann-Hanssen, "Pharmaceutical Analysis," Interscience, New York, N.Y., 1961, chap. 8.

(4) "The United States Pharmacopeia," 19th rev., Mack Publishing Co., Easton, Pa., 1975, pp. 385, 386.

(5) A. Repta and T. Higuchi, *J. Pharm. Sci.*, **60**, 1465 (1971).

(6) H. Wachsmuth and L. Vankaeckhoven, *J. Pharm. Belg.*, **14**, 456 (1959).

(7) E. Tomach and J. Major, *Acta Pol. Pharm.*, **17**, 139 (1960).

(8) V. G. Belikov and V. N. Berstein, USSR pat. 141,871 (1961); through *Chem. Abstr.*, **56**, 13020 (1962).

(9) F. Biederbach, *Apoth. Ztg.*, **48**, 736 (1933).

(10) J. Celechovesky and D. Sovobodava, *Cesk. Farm.*, **8**, 380 (1959).

(11) M. S. Karawya and M. G. Ghourab, *J. Assoc. Offic. Anal. Chem.*, **55**, 1180 (1972).

(12) A. J. Repta and P. Bansal, *J. Pharm. Sci.*, **61**, 1069 (1972).

(13) P.-H. Chung, T.-F. Chin, and J. L. Lach, *ibid.*, **59**, 1300 (1970).

(14) M. A. Nunes and E. Brochmann-Hanssen, *ibid.*, **63**, 716 (1974).

(15) G. A. Neville, F. B. Hasan, and I. C. P. Smith, *Can. J. Chem.*, **54**, 2094 (1976).

(16) K. Baeschlin, J. C. Etter, and H. Moll, *Pharm. Acta Helv.*, **44**, 301 (1969).

(17) E. Brochmann-Hanssen, P. Schmid, and J. D. Benmaman, *J. Pharm. Sci.*, **54**, 783 (1965).

(18) J. W. Steele and J. Thiessen, *J. Pharm. Pharmacol.*, **18**, 179 (1966).

ACKNOWLEDGMENTS AND ADDRESSES

Received March 15, 1976, from the **Drug Research Laboratories, Health Protection Branch, Health and Welfare Canada, Ottawa, Canada K1A OL2,* and the ‡ *Division of Biological Sciences, National Research Council of Canada, Ottawa, Canada K1A OR6.*

Accepted for publication June 17, 1976.

ˣ To whom inquiries should be directed.

Structure–Activity Studies Using Valence Molecular Connectivity

LOWELL H. HALL *ˣ and LEMONT B. KIER ‡

Abstract □ The extension of the molecular connectivity concept to the treatment of heteroatom molecules affords an opportunity to examine structure–activity relationships in a wide variety of molecule series that possess biological activity. Four series are described in this report. The correlations found indicate that molecular connectivity is an extremely useful descriptor of structure in studying drug molecule structure–activity relationships.

Keyphrases □ Molecular connectivity index—related to structure–activity relationships, various types of molecules □ Structure–activity relationships—various types of molecules, related to molecular connectivity index □ Topological indexes—molecular connectivity index, related to structure–activity relationships, various types of molecules

Recently (1, 2), the extension of molecular connectivity to the treatment of heteroatom molecules was described. By considering the valence electrons, whether bonded or nonbonded, an atom connectivity term, δ^v, for multiply bonded carbon atoms or heteroatoms was assigned.

The work presented in this paper tests the ability of δ^v to describe the atomic connectivity in heteroatoms so that the molecular connectivity indexes bear some relationship to structure influencing biological properties.

DISCUSSION

The simple prescription for assigning δ^v is $Z^v - h_i$, where Z^v is the number of valence electrons and h_i is the number of attached hydrogens. For alcohols, ethers, primary amines, and pyridine, the δ^v values for the heteroatoms are 5, 6, 3, and 5, respectively. The δ^v values for heteroatoms are shown in Table I.

Since halogen atoms have an identical number of valence electrons, this prescription yields identical values of δ^v. It is necessary to derive empirical values of δ^v for the halogens by calibrating them to a physical property. The molar refraction was chosen for this assignment (1, 2) (Table I).

Table I—Valence Delta, δ^v, Values for Heteroatoms

Atom	δ^v	Atom	δ^v
—NH_2	3	—OH	5
—NH—	4	—O—	6
	5	—C=O	6
—C≡N	5	Furan O	6
—C=NH	4	O=N—O	6
Pyridine N	5	H_2O	4
Nitro N	6	H_3O+	3
NH_3	2	F	(−)20
NH_4^+	1	Cl	0.690
	6	Br	0.254
=NH_2^+	3	I	0.085

The use of δ^v thus permits the calculation of a valence chi term of the first order, $^1\chi^v$, by the expression:

$$^1\chi^v = \sum (\delta_i^v \delta_j^v)^{-1/2} \qquad \text{(Eq. 1)}$$

The $^1\chi^v$ terms provide a further structural description of heteroatom molecules, eliminating the redundancies found when simple connectivity values are used. The refinement permits the close correlation of chi terms with physical properties such as boiling point, solubility, and molar refraction (1, 2).

Cytochrome Conversion by Phenols—The conversion of cytochrome P-450 to P-420 in the rabbit liver by a series of phenols was reported (3). An analysis of these molecules using $^1\chi^v$ reveals the following relationship to the minimum active concentration (−log *c*), p*C*:

$$pC = 0.816\ (\pm 0.105)\,^1\chi^v - 0.789\ (\pm 0.329) \qquad \text{(Eq. 2)}$$

$$r = 0.914 \quad s = 0.291 \quad n = 14$$

The calculated and observed values are listed in Table II.

The inclusion of the Hammett sigma value for each substituent in a multiple regression with $^1\chi^v$ does not improve the relationship. The re-

Table II—Cytochrome P-450 Conversions by Substituted Phenols

Phenol Substituent	$^1\chi^v$	Obs. pC^a	Calc. pC
H	2.134	1.07	0.95
3-Hydroxy	2.268	0.81	1.06
3-Amino	2.333	0.46	1.11
4-Methyl	2.545	1.48	1.29
4-Carboxy	2.722	1.15	1.43
3-Methyl	2.545	1.50	1.29
2-Chloro	2.653	1.60	1.38
3-Ethyl	3.105	1.82	1.74
4-Bromo	3.037	2.04	1.69
2-Iodo	3.766	2.09	2.28
2,4-Dichloro	3.165	2.11	1.79
2,4,6-Trichloro	3.604	2.21	2.15
2,3,4,6-Tetrachloro	4.208	2.65	2.64
Pentachloro	4.734	2.90	3.07

[a] Reference 3.

sults are interesting in that a single term, $^1\chi^v$, is capable of producing a fairly good correlation with biological potency. This is accomplished in a group of molecules containing oxygen, nitrogen, chlorine, bromine, and iodine in three different ring positions and singly as well as multiply substituted. The $^1\chi^v$ term thus encodes within it sufficient structural information to describe the salient features influencing biological activity.

From a mechanistic point of view, it might be concluded that the electronic influence of the substituent on the ring or on the phenolic hydroxyl group is not the critical process. The substituent itself must be participating in a characteristic way in some critical event leading to the activity.

Sweet-Tasting Nitroanilines—A series of substituted nitroanilines was reported to possess sweet taste potency of up to 4000 times the level of sucrose (4). Kier studied these and other sweet-tasting molecules and predicted that the substituent is a third member of the pharmacophore that may participate in a dispersion interaction (5).

The connectivity indexes $^1\chi$ and $^1\chi^v$ were calculated for these molecules and compared with the log of the relative (molar) sweetness to sucrose (Table III). The relationship is:

$$\log RS = 0.350\ (\pm 0.160)^1\chi + 0.694\ (\pm 0.153)^1\chi^v - 3.856\ (\pm 0.689) \quad \text{(Eq. 3)}$$

$$r = 0.953 \quad s = 0.222 \quad n = 9$$

In this case, the structural characteristics influencing the receptor role of the substituent are best quantified by the combination of the simple connectivity, $^1\chi$, and the valence connectivity, $^1\chi^v$, terms. The correlation is quite good and is of potential value in drug design.

Inhibition of *Aspergillus niger*—A group of substituted benzyl alcohols exhibited an inhibitory influence on the mold *A. niger* (6). The potency of these molecules is expressed as log $1/c$ for the minimum inhibitory concentration (Table IV).

Calculation of the $^1\chi^v$ values for each molecule reveals a fair correlation with log $1/c$ (0.890). The electronic influence of the substituents on the ring might be an additional structural factor influencing the activity. Accordingly, the use of the Hammett sigma term is suggested as a second term in a multiple regression analysis. The correlation improves in this case:

$$\log 1/c = 0.990\ (\pm 0.106)^1\chi^v + 0.656\ (\pm 0.197)\sigma - 1.268\ (\pm 0.361) \quad \text{(Eq. 4)}$$

$$r = 0.937 \quad s = 0.286 \quad n = 19$$

An inspection of other chi terms reveals that the fourth-order term, $^4\chi_P{}^v$, described previously (7), gives a significantly improved correlation along with σ:

$$\log 1/c = 1.987^4\chi_P{}^v + 0.507\sigma + 0.365 \quad \text{(Eq. 5)}$$

$$r = 0.962 \quad s = 0.217 \quad n = 19$$

These results indicate that both a connectivity structural characteristic and an electronic influence contribute to the activity within the series. Furthermore, the superiority of the $^4\chi_P{}^v$ term over the first-order term, $^1\chi^v$, is of interest. The $^4\chi_P{}^v$ term describes the important connectivity feature in a superior manner, resulting in a fine correlation.

Toxicity of Diethyl Phenyl Phosphates—A series of ring-substituted diethyl phenyl phosphates was toxic to the housefly (8) (Table V). An analysis using molecular connectivity and the Hammett sigma term reveals a very good correlation with the toxic concentration, pC, according to:

$$pC = 2.512\ (\pm 0.184)\sigma + 0.382\ (\pm 0.154)^1\chi^v - 1.350\ (\pm 0.420) \quad \text{(Eq. 6)}$$

$$r = 0.975 \quad s = 0.295 \quad n = 13$$

The predicted results are shown in Table V.

Equation 6 reveals that both a connectivity feature and an electronic influence play important roles in the activity of these molecules. The wide

Table III—Relative Sweet Taste of Nitroanilines

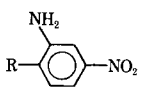

R	$^1\chi$	$^1\chi^v$	Obs. Log RS^a	Calc. Log RS
Propoxy	6.647	4.264	1.406	1.426
Iodo	5.109	4.279	0.675	0.899
Ethoxy	6.147	3.764	0.885	0.904
Bromo	5.109	3.556	0.566	0.398
Chloro	5.109	3.166	0.365	0.127
Methoxy	5.647	3.176	0.293	0.321
Methyl	5.109	3.064	0.337	0.561
Fluoro	5.109	2.452	−0.591	−0.368
Hydrogen	4.716	2.653	−0.538	−0.366

[a] Reference 4. Data converted to molar basis.

Table IV—Inhibition of *Aspergillus niger* by Substituted Benzyl Alcohols *versus* Chi and Hammett Sigma Terms

R	σ	$^4\chi_P{}^v$	Obs. Log $1/C^a$	Calc. Log $1/C$
Hydrogen	0	0.574	1.51	1.51
4-Chloro	0.23	0.718	2.07	1.91
2,4-Dichloro	0.45	1.153	3.07	2.88
3,4-Dichloro	0.60	0.980	3.07	2.61
2,4,5-Trichloro	0.82	1.365	3.32	3.49
3,4,5-Trichloro	0.97	1.400	3.63	3.64
2-Bromo	0.20	1.024	2.15	2.50
4-Bromo	0.23	0.851	2.27	2.17
4-Iodo	0.28	1.107	2.75	2.70
4-Methyl	−0.17	0.684	1.79	1.64
2,4-Dimethyl	−0.31	1.008	2.14	2.21
3,5-Dimethyl, 4-chloro	0.09	1.238	3.05	2.87
3,5-Dimethyl, 4-iodo	0.14	1.575	3.42	3.56
2-Nitro	0.76	0.786	2.49	2.31
4-Nitro	0.78	0.697	2.00	2.14
4-Cyano	0.63	0.676	1.67	2.03
2-Hydroxy	0.17	0.623	1.39	1.42
3-Hydroxy	0.17	0.635	1.39	1.63
4-Hydroxy	0.17	0.586	1.39	1.35

[a] Reference 6.

Table V—Toxicity of Substituted Diethyl Phenyl Phosphates *versus* Sigma and Chi Terms

Phenyl Substituent	σ	$^1\chi^v$	Obs. pC^a	Calc. pC
4-Nitro	1.24	2.358	2.40	2.66
4-Sulfoxymethyl	0.92	3.059	2.10	2.12
4-Cyano	0.88	2.295	1.85	1.74
3-Nitro	0.71	2.358	1.48	1.33
3-Sulfopentafluoro	0.68	1.530	1.38	0.94
4-Chloro	0.23	2.423	0.04	0.15
3-*tert*-Butyl	−0.10	3.571	−0.24	−0.24
Hydrogen	0	1.911	−0.82	−0.62
4-Carboxy	0.35	2.499	0.25	0.48
4-*tert*-Butyl	−0.20	3.571	−0.24	−0.49
3-Methoxy	0.12	2.433	−0.25	−0.12
4-Methoxy	−0.11	2.433	−0.25	−0.69
4-Methyl	−0.17	2.321	−1.32	−0.89

[a] Reference 8.

diversity of groups is a severe challenge for the connectivity concept, and the good correlation is testimony to the ability of the method to describe structural characteristics important in this case.

SUMMARY

These studies reveal the contribution that molecular connectivity may make in structure–activity studies. Recent advances made in this method, namely the treatment of heteroatoms (1) and the development of extended connectivity terms (7), make possible the consideration of a wide variety of molecules typically found in drug studies. Most importantly, molecular connectivity, as developed to this point, is capable of revealing good relationships with biological activities (9–13). It is expected that this method of structural analysis will find wide application in structure–activity studies.

Furthermore, the method of molecular connectivity relates molecular structure directly to biological activity. No intermediate physical properties are required for satisfactory correlation. The medicinal chemist's intuition concerning structure and activity can be applied directly and quantitatively to drug studies. The demonstrated ability to handle a variety of heteroatoms greatly strengthens the method of molecular connectivity.

REFERENCES

(1) L. B. Kier and L. H. Hall, *J. Pharm. Sci.*, **65**, 1806 (1976).

(2) L. B. Kier and L. H. Hall, "Molecular Connectivity in Chemistry and Drug Research," Academic, New York, N.Y., 1976.

(3) Y. Ichikawa and T. Yamano, *Biochim. Biophys. Acta*, **147**, 518 (1967).

(4) J. Blanksma and D. Hoegen, *Rec. Trav. Chim.*, **65**, 333 (1946).

(5) L. B. Kier, *J. Pharm. Sci.*, **61**, 1394 (1972).

(6) D. V. Carter, P. T. Charlton, A. H. Fenton, J. R. Housey, and B. Lessel, *J. Pharm. Pharmacol., Suppl.*, **10**, 149T (1958).

(7) L. B. Kier, W. J. Murray, M. Randić, and L. H. Hall, *J. Pharm. Sci.*, **65**, 1226 (1976).

(8) R. L. Metcalf and T. R. Fukuto, *J. Econ. Entomol.*, **55**, 340 (1962).

(9) L. B. Kier, L. H. Hall, W. J. Murray, and M. Randić, *J. Pharm. Sci.*, **64**, 1971 (1975).

(10) L. H. Hall, L. B. Kier, and W. J. Murray, *ibid.*, **64**, 1974 (1975).

(11) W. J. Murray, L. H. Hall, and L. B. Kier, *ibid.*, **64**, 1978 (1975).

(12) L. B. Kier, W. J. Murray, and L. H. Hall, *J. Med. Chem.*, **18**, 1272 (1975).

(13) T. DiPaolo, L. B. Kier, and L. H. Hall, *Mol. Pharmacol.*, **13**, 31 (1977).

ACKNOWLEDGMENTS AND ADDRESSES

Received March 10, 1976, from **Eastern Nazarene College, Quincy, MA 02170,* and the *‡Massachusetts College of Pharmacy, Boston, MA 02115.*

Accepted for publication June 23, 1976.

[x] To whom inquiries should be directed.

Bioavailability of Digoxin–Hydroquinone Complex: A New Oral Digoxin Formulation

FELIX BOCHNER *§, DAVID H. HUFFMAN ‡, DANNY D. SHEN *, and DANIEL L. AZARNOFF *x

Abstract □ A new oral digoxin formulation, a digoxin–hydroquinone complex (99% dissolution at 5 min), was evaluated in 12 healthy human volunteers with reference to bioavailability and extent and time of peak serum digoxin levels. This preparation was compared with a commercial digoxin tablet (26% dissolution at 5 min), digoxin elixir, and a parenteral digoxin solution. Bioavailability was assessed by the 24-hr area under the serum digoxin–time curve and 48-hr digoxin excretion in urine. The bioavailability of the complex was similar to that of the elixir but not statistically different from that of the tablet. The tablet was less bioavailable than the elixir. There was less interindividual variation in bioavailability with the complex than with the elixir. Peak serum digoxin levels were higher with the complex than the tablet and were achieved more quickly.

Keyphrases □ Digoxin—bioavailability of complex with hydroquinone compared to other digoxin dosage forms, humans □ Bioavailability—digoxin–hydroquinone complex compared to other digoxin dosage forms, humans □ Complexes—digoxin–hydroquinone, bioavailability compared to other digoxin dosage forms, humans □ Dosage forms, various—digoxin and digoxin–hydroquinone complex, bioavailability compared, humans □ Cardiotonic agents—digoxin–hydroquinone complex, bioavailability compared to other digoxin dosage forms, humans

The bioavailability of oral digoxin preparations has been studied recently (1–11), and several studies (4–10) showed that the bioavailability of solid digoxin dosage forms correlated with the dissolution rate but not the disintegration rate (11). This finding led to the assertion that existing *in vitro* dissolution tests are adequate for predicting commercial digoxin tablet bioavailability. Other investigations (12–16), however, demonstrated that the *in vitro* dissolution rate of commercial digoxin tablets need not correlate with bioavailability, since tablets that did not meet USP XVIII dissolution specifications showed *in vivo* bioavailability characteristics comparable to tablets that did. Thus, the relationship between bioavailability and dissolution rate appears to be unresolved.

The main cause of the unsatisfactory dissolution of digoxin tablets is related primarily to digoxin's low water solubility. Although improved formulation technology has resulted in significant improvement, an intrinsically more soluble form of digoxin should enhance dissolution. Higuchi and Ikeda (17) recently developed such a form by complexing digoxin and hydroquinone. This approach utilizes the concept of free energy of dissolution of molecular complexes (18). The digoxin–hydroquinone[1] complex is more readily soluble than digoxin itself, and total dissolution of digoxin occurs within 5 min (17).

This paper reports a comparison of the bioavailability in humans of the complex with that of a digoxin tablet[2] of

[1] Lot 828-264, supplied by Pennwalt Corp., Pharmaceutical Division, Rochester, N.Y.

[2] Lanoxin, lot 022-1, supplied by the Food and Drug Administration.

diversity of groups is a severe challenge for the connectivity concept, and the good correlation is testimony to the ability of the method to describe structural characteristics important in this case.

SUMMARY

These studies reveal the contribution that molecular connectivity may make in structure–activity studies. Recent advances made in this method, namely the treatment of heteroatoms (1) and the development of extended connectivity terms (7), make possible the consideration of a wide variety of molecules typically found in drug studies. Most importantly, molecular connectivity, as developed to this point, is capable of revealing good relationships with biological activities (9–13). It is expected that this method of structural analysis will find wide application in structure–activity studies.

Furthermore, the method of molecular connectivity relates molecular structure directly to biological activity. No intermediate physical properties are required for satisfactory correlation. The medicinal chemist's intuition concerning structure and activity can be applied directly and quantitatively to drug studies. The demonstrated ability to handle a variety of heteroatoms greatly strengthens the method of molecular connectivity.

REFERENCES

(1) L. B. Kier and L. H. Hall, *J. Pharm. Sci.*, **65**, 1806 (1976).

(2) L. B. Kier and L. H. Hall, "Molecular Connectivity in Chemistry and Drug Research," Academic, New York, N.Y., 1976.

(3) Y. Ichikawa and T. Yamano, *Biochim. Biophys. Acta*, **147**, 518 (1967).

(4) J. Blanksma and D. Hoegen, *Rec. Trav. Chim.*, **65**, 333 (1946).

(5) L. B. Kier, *J. Pharm. Sci.*, **61**, 1394 (1972).

(6) D. V. Carter, P. T. Charlton, A. H. Fenton, J. R. Housey, and B. Lessel, *J. Pharm. Pharmacol., Suppl.*, **10**, 149T (1958).

(7) L. B. Kier, W. J. Murray, M. Randić, and L. H. Hall, *J. Pharm. Sci.*, **65**, 1226 (1976).

(8) R. L. Metcalf and T. R. Fukuto, *J. Econ. Entomol.*, **55**, 340 (1962).

(9) L. B. Kier, L. H. Hall, W. J. Murray, and M. Randić, *J. Pharm. Sci.*, **64**, 1971 (1975).

(10) L. H. Hall, L. B. Kier, and W. J. Murray, *ibid.*, **64**, 1974 (1975).

(11) W. J. Murray, L. H. Hall, and L. B. Kier, *ibid.*, **64**, 1978 (1975).

(12) L. B. Kier, W. J. Murray, and L. H. Hall, *J. Med. Chem.*, **18**, 1272 (1975).

(13) T. DiPaolo, L. B. Kier, and L. H. Hall, *Mol. Pharmacol.*, **13**, 31 (1977).

ACKNOWLEDGMENTS AND ADDRESSES

Received March 10, 1976, from **Eastern Nazarene College, Quincy, MA 02170,* and the *‡Massachusetts College of Pharmacy, Boston, MA 02115.*

Accepted for publication June 23, 1976.

[x] To whom inquiries should be directed.

Bioavailability of Digoxin–Hydroquinone Complex: A New Oral Digoxin Formulation

FELIX BOCHNER *§, DAVID H. HUFFMAN ‡, DANNY D. SHEN *, and DANIEL L. AZARNOFF *x

Abstract □ A new oral digoxin formulation, a digoxin–hydroquinone complex (99% dissolution at 5 min), was evaluated in 12 healthy human volunteers with reference to bioavailability and extent and time of peak serum digoxin levels. This preparation was compared with a commercial digoxin tablet (26% dissolution at 5 min), digoxin elixir, and a parenteral digoxin solution. Bioavailability was assessed by the 24-hr area under the serum digoxin–time curve and 48-hr digoxin excretion in urine. The bioavailability of the complex was similar to that of the elixir but not statistically different from that of the tablet. The tablet was less bioavailable than the elixir. There was less interindividual variation in bioavailability with the complex than with the elixir. Peak serum digoxin levels were higher with the complex than the tablet and were achieved more quickly.

Keyphrases □ Digoxin—bioavailability of complex with hydroquinone compared to other digoxin dosage forms, humans □ Bioavailability—digoxin–hydroquinone complex compared to other digoxin dosage forms, humans □ Complexes—digoxin–hydroquinone, bioavailability compared to other digoxin dosage forms, humans □ Dosage forms, various—digoxin and digoxin–hydroquinone complex, bioavailability compared, humans □ Cardiotonic agents—digoxin–hydroquinone complex, bioavailability compared to other digoxin dosage forms, humans

The bioavailability of oral digoxin preparations has been studied recently (1–11), and several studies (4–10) showed that the bioavailability of solid digoxin dosage forms correlated with the dissolution rate but not the disintegration rate (11). This finding led to the assertion that existing *in vitro* dissolution tests are adequate for predicting commercial digoxin tablet bioavailability. Other investigations (12–16), however, demonstrated that the *in vitro* dissolution rate of commercial digoxin tablets need not correlate with bioavailability, since tablets that did not meet USP XVIII dissolution specifications showed *in vivo* bioavailability characteristics comparable to tablets that did. Thus, the relationship between bioavailability and dissolution rate appears to be unresolved.

The main cause of the unsatisfactory dissolution of digoxin tablets is related primarily to digoxin's low water solubility. Although improved formulation technology has resulted in significant improvement, an intrinsically more soluble form of digoxin should enhance dissolution. Higuchi and Ikeda (17) recently developed such a form by complexing digoxin and hydroquinone. This approach utilizes the concept of free energy of dissolution of molecular complexes (18). The digoxin–hydroquinone[1] complex is more readily soluble than digoxin itself, and total dissolution of digoxin occurs within 5 min (17).

This paper reports a comparison of the bioavailability in humans of the complex with that of a digoxin tablet[2] of

[1] Lot 828-264, supplied by Pennwalt Corp., Pharmaceutical Division, Rochester, N.Y.

[2] Lanoxin, lot 022-1, supplied by the Food and Drug Administration.

Table I—24-hr Area under Concentration–Time Curves (Nanograms × Hours per Milliliter)

Subject	Digoxin–Hydroquinone Complex	Digoxin Tablets	Digoxin Elixir	Digoxin Intravenous Injection
1	19.48	9.63	18.68	31.68
2	15.23	9.49	16.51	31.24
3	10.52	8.24	15.11	23.79
4	13.88	17.48	15.68	31.11
5	17.82	17.12	20.47	15.61
6	14.61	11.82	17.20	20.10
7	10.42	9.66	10.28	26.07
8	15.17	12.05	14.91	28.11
9	14.27	12.96	14.83	28.93
10	14.35	13.32	14.46	17.24
11	21.08	21.26	19.85	28.82
12	11.15	12.48	16.09	18.44
Mean	14.83	12.96	16.17	25.10
CV, %	22.52	29.90	16.90	23.40
Bioavailability, %	59.10	51.60	64.50	—

Analysis of Variance

Source	*df*	Sum of Squares	Mean of Squares	*F* Ratio	*p*
Between subjects	11	306.09	27.83	2.19	<0.05
Between periods	3	61.52	20.51	1.61	>0.1
Between treatments	3	1043.44	347.81	27.38	<0.0005
Error	30	381.16	12.71	—	—
Total	47	1792.21	—	—	—

Multiple Range Analysis

Complex *versus* tablets	$p < 0.08$
Complex *versus* intravenous injection	$p < 0.005$
Complex *versus* elixir	$p > 0.05$
Tablet *versus* intravenous injection	$p < 0.001$
Tablet *versus* elixir	$p < 0.01$
Intravenous injection *versus* elixir	$p < 0.001$

satisfactory dissolution and bioavailability, a digoxin elixir[3], and an intravenous injection[4].

EXPERIMENTAL

Subjects—Twelve healthy volunteers[5], seven female and five male, ages 22–41 years (median 31), were studied. There was no evidence of cardiac, hepatic, renal, GI, or hematopoietic disease from the history, physical examination, ECG, complete blood count, creatinine clearance, urinalysis, and bilirubin, alkaline phosphatase, glutamic-pyruvic transaminase, and thyroxine levels.

Drug Administration—The volunteers abstained from drugs, including alcohol, for at least 48 hr prior to each dosing period. The dosage form was administered between 7 and 8 am after an overnight fast of at least 10 hr. During the first 4 hr after drug administration, the subjects were not allowed to eat or to lie down. They were allowed to drink water at a maximum rate of 100 ml/hr.

In a random sequence with at least 2-week intervals, the individuals received each of the following dosage forms: (*a*) two 0.329-mg tablets of digoxin–hydroquinone complex[1] (equivalent to 0.5 mg of digoxin), (*b*) two 0.25-mg digoxin tablets[2], (*c*) 0.5 mg of digoxin elixir[3], and (*d*) 0.5 mg of digoxin intravenous injection[4]. The oral dosage forms were given with 200 ml of water. The parenteral digoxin was injected intravenously over 2–3 min, followed by 200 ml of water orally.

Specimen Collection and Assay—Blood (10 ml) for digoxin estimation was obtained from an antecubital vein with an indwelling catheter[6] at 0, 0.25, 0.50, 0.75, 1.0, 1.5, 2, 3, 4, 6, 8, 10, and 24 hr following an oral dose. Additional early samples were collected at 0.05, 0.1, 0.17, and 0.33 hr following the intravenous dose. Serum was separated from blood and frozen until assayed for digoxin by radioimmunoassay (19). The coefficients of variation of high and low internal standards analyzed daily were 5.3 and 6.4%, respectively.

Complete daily urine collections were obtained for 48 hr following dosing. Each 24-hr urine collection was thoroughly mixed, the volume was determined, and an aliquot was frozen until assayed by a modification of a reported method (20). Each sample also was assayed for creatinine content to aid in the assessment of the completeness of the urine collections.

Analysis—Bioavailability of the various preparations was determined by comparing the 24-hr area under the serum digoxin–time curve ($AUC_{0\rightarrow24}$) following intravenous administration to that following the oral dosage forms, *i.e.*:

$$\frac{(AUC_{0\rightarrow24})_{oral}}{(AUC_{0\rightarrow24})_{iv}} \times 100\%$$

The *AUC* was computed[7] by the trapezoidal rule. Furthermore, the 48-hr excretion of digoxin in urine following intravenous administration was compared to that following the oral dosage forms (20).

The time taken to achieve peak serum digoxin concentrations and the peak concentrations were obtained from the serum concentration profiles. Statistical significance was determined by a two-way analysis of variance (ANOVA). Differences between the individual groups were determined by Duncan's multiple range test (21, 22).

Table II—Time to Achieve Peak Plasma Digoxin Concentration (Hours)

	Digoxin–Hydroquinone Complex	Digoxin Tablets	Digoxin Elixir
Mean	0.83	1.31	0.68
SD	0.29	0.69	0.22

Analysis of Variance

Source of Variation	*df*	Sum of Squares	Mean of Squares	*F* Ratio	*p*
Between subjects	11	2.22	0.20	1.25	>0.05
Between periods	2	1.36	0.68	4.25	<0.05
Between treatments	2	3.27	1.64	10.25	<0.001
Error	20	3.11	0.16	—	—
Total	35	9.96	—	—	—

Multiple Range Analysis

Complex *versus* tablet	$p < 0.005$
Complex *versus* elixir	$p < 0.2$
Tablet *versus* elixir	$p < 0.005$

RESULTS

Dissolution Rate Tests—The dissolution of the complex was 99% complete within 5 min whereas that of the tablets was 26% at 5 min, 61% at 15 min, 74% at 30 min, and 88% at 60 min. All commercial dosage forms met USP specifications.

Bioavailability—The $AUC_{0\rightarrow24}$, time to achieve peak plasma digoxin levels, and peak digoxin levels are presented in Tables I–III. Based on the *AUC* values, the bioavailabilities of the complex, tablet, and elixir were 59.1 (40–83.2), 51.6 (30.4–77.3), and 64.5% (39.4–87.3%), respectively, compared to the intravenous dosage form. The bioavailability of the complex and the tablets was not significantly different ($p < 0.08$), but all oral preparations differed significantly from intravenous digoxin. The elixir was more available than the tablets ($p < 0.005$), but the tablet and the elixir did not differ significantly ($p < 0.2$).

The 48-hr excretion of digoxin in urine following the various dosage forms is given in Table IV. The intravenous form differed significantly from all oral formulations. The complex did not differ significantly from the tablet ($p > 0.3$) or the elixir ($p > 0.1$), although the elixir was different

[3] Lanoxin, lot 456-N, supplied by Burroughs Wellcome, Research Triangle Park, N.C.

[4] Lanoxin, lot 691-O, supplied by Burroughs Wellcome, Research Triangle Park, N.C.

[5] Written informed consent was obtained after discussing with each subject the inconveniences and hazards to be expected.

[6] Teflon (du Pont).

[7] Olivetti Programma 101.

Table III—Peak Plasma Digoxin Concentration (Nanograms per Milliliter)

	Digoxin—Hydroquinone Complex	Digoxin Tablets	Digoxin Elixir
Mean	2.79	1.73	3.27
SD	1.13	0.73	0.91

Analysis of Variance

Source of Variation	*df*	Sum of Squares	Mean of Squares	*F* Ratio	*p*
Between subjects	11	14.73	1.34	2.35	<0.05
Between periods	2	1.65	0.82	1.44	>0.05
Between treatments	2	15.75	7.88	13.82	<0.005
Error	20	11.48	0.57	—	—
Total	35	43.61	—	—	—

Multiple Range Analysis

Complex *versus* tablet	$p < 0.005$
Complex *versus* elixir	$p > 0.05$
Tablet *versus* elixir	$p < 0.005$

Table IV—Urine Digoxin Excretion (Micrograms per 48 hr)

Subject	Digoxin—Hydroquinone Complex	Digoxin Tablets	Digoxin Elixir	Digoxin Intravenous Injection
1	187.2	49.6	182.0	139.4
2	129.4	96.8	108.6	178.3
3	123.6	113.8	146.3	231.7
4	116.2	114.8	136.3	129.3
5	130.2	115.6	85.7	107.2
6	85.3	111.8	143.6	192.7
7	87.2	141.4	127.6	179.2
8	148.8	81.2	141.4	149.0
9	86.3	97.5	136.3	233.0
10	108.3	111.1	116.0	129.3
11	136.3	196.1	226.7	173.5
12	116.5	106.4	147.2	196.7
Mean	121.3	112.7	137.1	174.4
CV, %	24.1	32.05	19.1	24.92
Bioavailability, %	69.6	64.6	78.6	—

Analysis of Variance

Source	*df*	Sum of Squares	Mean of Squares	*F* Ratio	*p*
Between subjects	11	15,668.50	1424.41	1.27	>0.05
Between periods	3	1,732.56	577.52	0.52	>0.05
Between treatments	3	27,586.75	9195.58	8.22	<0.01
Error	30	33,570.13	1119.00	—	—
Total	47	78,557.94	—	—	—

Multiple Range Analysis

Complex *versus* tablet	$p > 0.3$
Complex *versus* intravenous injection	$p < 0.005$
Complex *versus* elixir	$p > 0.1$
Tablet *versus* intravenous injection	$p < 0.005$
Tablet *versus* elixir	$p < 0.01$
Intravenous injection *versus* elixir	$p < 0.005$

from the tablet ($p < 0.01$). If a 10% difference is assumed to be significant, the complex had greater bioavailability than the tablet in six subjects, the two preparations behaved equally in five subjects, and the tablet was more available than the complex in one individual.

Peak Time and Peak Concentration—The peak concentration and the time required to achieve it are presented in Tables II and III. A mean peak value of 2.79 ± 1.13 ng/ml was achieved in 0.83 ± 0.29 hr with the complex; 1.73 ± 0.73 ng/ml was achieved in 1.31 ± 0.69 hr with the tablet, and 3.27 ± 0.91 ng/ml was achieved in 0.68 ± 0.22 hr with the elixir. Compared to the tablet, both the complex ($p < 0.005$) and the elixir ($p < 0.05$) achieved significantly higher peak digoxin levels and in a shorter time (complex, $p < 0.005$; elixir, $p < 0.005$).

DISCUSSION

The bioavailability of oral liquid dosage forms has, in general, been shown to be greater than that of tablet forms (3, 20, 23). Although the bioavailability (based on comparison of *AUC*'s) of the complex, a digoxin preparation of very rapid dissolution, was not statistically different from that of the elixir, it also was not statistically different from that of a solid dosage form. This discrepancy may be related to the fact that the volunteers showed large intersubject variations in the bioavailability of various preparations (Table I).

A considerable variance from the mean $AUC_{0\rightarrow 24}$ and urine digoxin excretion was observed in subjects receiving the complex, but an even greater variance occurred with the tablet. Thus, the complex appeared to be less erratically absorbed than the tablet, which may be advantageous when administered on a chronic basis. The bioavailability of the oral preparations was lower in this study than in a previous one (20), where the elixir was 84.5% absorbed (*cf.*, 64.5% in this study) and a rapid dissolution tablet was 77.8% absorbed (*cf.*, 59.6% in this study). However, the $AUC_{0\rightarrow 24}$ (25.1) following intravenous digoxin agreed closely with values obtained in two other studies, one following single-dose digoxin (25.9) (20) and the other in a steady-state study (22.9) (23). In three subjects (Subjects 1, 4, and 5), the 48-hr excretion of digoxin in urine following intravenous administration was less than that following one of the oral preparations. There is no ready explanation for this finding, except inadequate urine collections by these volunteers; low creatinine excretion in urine confirmed this suspicion.

The complex produced a higher peak serum digoxin level earlier than the tablet. This characteristic may not be desirable, although there is no evidence (24, 25) to suggest that the peak digoxin concentration during absorption and distribution is related to toxicity. The rapid achievement of the higher peak level is similar to that attained with the elixir, which also has not been reported to be associated with more toxicity than a solid dosage form. On the other hand, steady-state serum digoxin concentrations do correlate with therapeutic and toxic responses in patients (26).

The absorption of incompletely absorbed drugs has more inter- and intraindividual variability than that of completely absorbed drugs (23, 27, 28). This variation may have harmful effects in humans if the drug has a narrow therapeutic index, such as digoxin. Considerable data (4–10) demonstrate a direct correlation between the dissolution rate of digoxin tablets and their bioavailability. This relationship is further supported by the observation that various digoxin solutions are more bioavailable than solid dosage forms (3, 20, 23).

The particle size of digoxin in relation to bioavailability was examined (29), and particles below 3.7 μm in size produced better availability than did particles above 12 μm. However, another study (9) found that the bioavailability of a digoxin elixir was not greater than that of digoxin tablets whose dissolution rate exceeded 85% in 1 hr. A recent study (30) compared the availability of a digoxin solution in capsules with tablets that were 97 and 78% dissolved in 1 hr. However, the tablet dissolution rate was not given. The solution in capsules performed better than the tablets, whose availability did not differ despite different *in vitro* dissolution rates. This latter finding is in accord with information obtained in other studies (13–16) and supports the finding of this study that dissolution rates above a certain point may not be associated with increased digoxin absorption. However, in these and other studies (4–10), oral preparations were compared only to each other, whereas in this study the bioavailability of oral digoxin was compared to other oral forms as well as to the intravenous form. Thus, absolute bioavailability cannot be ascertained in most other studies.

It appears, therefore, that the dissolution rate of digoxin tablets may not be the only limiting factor in their incomplete absorption and that the current method of dissolution testing does not discriminate satisfactorily. Digoxin is prescribed for chronic therapy. Single-dose studies may not assess the bioavailability of the dosage forms accurately during chronic use. The results in this single-dose study warrant the further evaluation of the chronic administration of the complex. Steady-state bioavailability studies of digoxin have been reported (23).

The principle of complexing a drug with substances such as hydroquinone to enhance dissolution might be applied to other medications whose absorption is erratic following poor *in vivo* dissolution.

REFERENCES

(1) J. Lindenbaum, M. H. Mellow, M. O. Blackstone, and V. P. Butler, *N. Engl. J. Med.*, **285**, 1344 (1971).

(2) V. Manninen, J. Melin, and G. Hartel, *Lancet*, **2**, 934 (1971).

(3) D. H. Huffman and D. L. Azarnoff, *J. Am. Med. Assoc.*, **222**, 957 (1972).

(4) B. F. Johnson, H. Greer, J. McCrerie, C. Bye, and A. Fowle, *Lancet*, **1**, 1473 (1973).

(5) J. Lindenbaum, V. P. Butler, J. E. Murphy, and R. M. Cresswell, *ibid.*, **1**, 1215 (1973).

(6) E. J. Fraser, R. H. Leach, J. W. Poston, A. M. Bold, L. S. Culank, and A. B. Lipede, *J. Pharm. Pharmacol.*, **25**, 968 (1973).

(7) B. F. Johnson, *Postgrad. Med. J., Suppl. 6*, **50**, 48 (1974).

(8) J. G. Wagner, M. Christensen, E. Sakmar, D. Blair, J. D. Yates, P. W. Willis, III, A. J. Sedman, and R. G. Stoll, *J. Am. Med. Assoc.*, **224**, 199 (1973).

(9) D. J. Greenblatt, D. W. Duhme, J. Koch-Weser, and T. W. Smith, *ibid.*, **229**, 1774 (1974).

(10) E. Steiness, V. Christensen, and H. Johansen, *Clin. Pharmacol. Ther.*, **14**, 949 (1973).

(11) P. F. Binnion, *ibid.*, **16**, 807 (1974).

(12) P. R. Klink, R. I. Poust, J. L. Colaizzi, and R. H. McDonald, *J. Pharm. Sci.*, **63**, 1231 (1974).

(13) P. Ylitalo, G. Wilen, and S. Lundell, *ibid.*, **64**, 1264 (1975).

(14) P. Ylitalo, G. Wilen, and S. Lundell, *Lancet*, **1**, 343 (1975).

(15) *Ibid.*, **1**, 744 (1975).

(16) P. T. Hairsnape, *Br. Med. J.*, **2**, 55 (1974).

(17) T. Higuchi and M. Ikeda, *J. Pharm. Sci.*, **63**, 809 (1974).

(18) E. Shefter and T. Higuchi, *ibid.*, **52**, 781 (1963).

(19) T. W. Smith, V. P. Butler, and E. Haber, *N. Engl. J. Med.*, **281**, 1212 (1969).

(20) D. H. Huffman, C. V. Manion, and D. L. Azarnoff, *J. Pharm. Sci.*, **64**, 433 (1975).

(21) D. B. Duncan, *Biometrics*, **11**, 1 (1955).

(22) H. L. Harter, *ibid.*, **16**, 671 (1960).

(23) D. H. Huffman, C. V. Manion, and D. L. Azarnoff, *Clin. Pharmacol. Ther.*, **16**, 310 (1974).

(24) D. A. Chamberlain, *Postgrad. Med. J., Suppl. 6*, **50**, 29 (1974).

(25) T. R. D. Shaw, K. Raymond, and H. Greenwood, *ibid.*, **50**, 55 (1974).

(26) D. H. Huffman, J. W. Crow, P. Pentikäinen, and D. L. Azarnoff, *Am. Heart J.*, **91**, 28 (1976).

(27) J. Koch-Weser, *N. Engl. J. Med.*, **291**, 233 (1974).

(28) J. G. Wagner, *Pharmacology*, **8**, 102 (1972).

(29) T. R. D. Shaw, J. E. Carless, M. R. Howard, and K. Raymond, *Lancet*, **2**, 209 (1973).

(30) G. J. Mallis, D. H. Schmidt, and J. Lindenbaum, *Clin. Pharmacol. Ther.*, **18**, 761 (1975).

ACKNOWLEDGMENTS AND ADDRESSES

Received April 26, 1976, from the **Clinical Pharmacology and Toxicology Center, Departments of Medicine and Pharmacology, University of Kansas Medical Center, Kansas City, KS 66103,* and the ‡*Medicine and Research Service (Project No. 3704-02), Veterans Administration Hospital, Kansas City, MO 64128.*

Accepted for publication July 1, 1976.

Supported by the Pharmaceutical Division, Pennwalt Corp., and U.S. Public Health Service Grant GM 15956.

The authors thank Jessie Fink for assistance, Dr. K. Hassanein for statistical analyses, and Billie Jean Milanez for technical help. Dissolution rate studies were performed by Dr. Lewis Amsel and Mr. Thomas Matochik, Pharmaceutical Development, Pharmaceutical Division, Pennwalt Corp.

§ Fellow in Clinical Sciences in Clinical Pharmacology of the National Health and Medical Research Council of Australia.

ˣ To whom inquiries should be directed.

Time-Dependent Kinetics I: Exponential Autoinduction of Carbamazepine in Monkeys

WILLIAM H. PITLICK * and RENÉ H. LEVY ˣ

Abstract □ The pharmacokinetics of carbamazepine were studied during a week-long infusion of the drug in 60% polyethylene glycol 400 solution in three rhesus monkeys. Serum concentrations approached steady state within 8–16 hr and then rapidly declined, within 72 hr, to a new asymptotic level approximately 46% of the maximum steady-state concentration. Serum concentrations remained at that level during the rest of the experimental period. The decline from the maximum value to the asymptotic steady state was exponential. It is postulated that the decline in the steady-state concentration is due to autoinduction by carbamazepine of its own metabolism.

Keyphrases □ Time-dependent pharmacokinetics—carbamazepine, 1-week infusion, monkeys □ Carbamazepine—time-dependent pharmacokinetics, 1-week infusion, monkeys □ Pharmacokinetics, time dependent—carbamazepine, 1-week infusion, monkeys □ Analgesics—carbamazepine, time-dependent pharmacokinetics, 1-week infusion, monkeys

Over the past 15 years, awareness of the various facets of dose dependency in drug disposition has increased. As a result, experimental designs of pharmacokinetic investigations often include studies at several dose levels. Examples of dose dependency in absorption, distribution, and elimination have been reported. However, the concept of *time dependency* in pharmacokinetics is still undefined.

BACKGROUND

Studies in this laboratory involving animals and humans clearly indicated that time dependency is a multifaceted phenomenon, at least as complex as dose dependency. Several types of time dependency exist, and this series of papers will provide examples. Carbamazepine is the drug of choice for the treatment of trigeminal neuralgia (1) and was recently approved for use as an anticonvulsant in adults (2). Single-dose intravenous and oral studies in monkeys indicated that the drug has a short biological half-life (1–2 hr) and that chronic oral administration during its efficacy testing in epileptic monkeys would be impractical (3, 4). Consequently, a continuous mode of administration such as constant-rate intravenous infusion in chronically catherized monkeys was considered.

Short-term infusion studies indicated that carbamazepine exhibits dose-dependent kinetics (5, 6). Infusion rates between 8.5 and 40 mg/hr yielded steady-state concentrations of carbamazepine between 2.0 and 5.8 μg/ml (6). However, the increase in steady-state concentration was more than proportional to the increase in infusion rate, and the time required to reach one-half of the steady-state level was not constant. A model with zero-order input and one capacity-limited elimination pathway was adequate to describe the pharmacokinetic behavior of the drug (6).

REFERENCES

(1) J. Lindenbaum, M. H. Mellow, M. O. Blackstone, and V. P. Butler, *N. Engl. J. Med.*, **285**, 1344 (1971).

(2) V. Manninen, J. Melin, and G. Hartel, *Lancet*, **2**, 934 (1971).

(3) D. H. Huffman and D. L. Azarnoff, *J. Am. Med. Assoc.*, **222**, 957 (1972).

(4) B. F. Johnson, H. Greer, J. McCrerie, C. Bye, and A. Fowle, *Lancet*, **1**, 1473 (1973).

(5) J. Lindenbaum, V. P. Butler, J. E. Murphy, and R. M. Cresswell, *ibid.*, **1**, 1215 (1973).

(6) E. J. Fraser, R. H. Leach, J. W. Poston, A. M. Bold, L. S. Culank, and A. B. Lipede, *J. Pharm. Pharmacol.*, **25**, 968 (1973).

(7) B. F. Johnson, *Postgrad. Med. J., Suppl. 6*, **50**, 48 (1974).

(8) J. G. Wagner, M. Christensen, E. Sakmar, D. Blair, J. D. Yates, P. W. Willis, III, A. J. Sedman, and R. G. Stoll, *J. Am. Med. Assoc.*, **224**, 199 (1973).

(9) D. J. Greenblatt, D. W. Duhme, J. Koch-Weser, and T. W. Smith, *ibid.*, **229**, 1774 (1974).

(10) E. Steiness, V. Christensen, and H. Johansen, *Clin. Pharmacol. Ther.*, **14**, 949 (1973).

(11) P. F. Binnion, *ibid.*, **16**, 807 (1974).

(12) P. R. Klink, R. I. Poust, J. L. Colaizzi, and R. H. McDonald, *J. Pharm. Sci.*, **63**, 1231 (1974).

(13) P. Ylitalo, G. Wilen, and S. Lundell, *ibid.*, **64**, 1264 (1975).

(14) P. Ylitalo, G. Wilen, and S. Lundell, *Lancet*, **1**, 343 (1975).

(15) *Ibid.*, **1**, 744 (1975).

(16) P. T. Hairsnape, *Br. Med. J.*, **2**, 55 (1974).

(17) T. Higuchi and M. Ikeda, *J. Pharm. Sci.*, **63**, 809 (1974).

(18) E. Shefter and T. Higuchi, *ibid.*, **52**, 781 (1963).

(19) T. W. Smith, V. P. Butler, and E. Haber, *N. Engl. J. Med.*, **281**, 1212 (1969).

(20) D. H. Huffman, C. V. Manion, and D. L. Azarnoff, *J. Pharm. Sci.*, **64**, 433 (1975).

(21) D. B. Duncan, *Biometrics*, **11**, 1 (1955).

(22) H. L. Harter, *ibid.*, **16**, 671 (1960).

(23) D. H. Huffman, C. V. Manion, and D. L. Azarnoff, *Clin. Pharmacol. Ther.*, **16**, 310 (1974).

(24) D. A. Chamberlain, *Postgrad. Med. J., Suppl. 6*, **50**, 29 (1974).

(25) T. R. D. Shaw, K. Raymond, and H. Greenwood, *ibid.*, **50**, 55 (1974).

(26) D. H. Huffman, J. W. Crow, P. Pentikäinen, and D. L. Azarnoff, *Am. Heart J.*, **91**, 28 (1976).

(27) J. Koch-Weser, *N. Engl. J. Med.*, **291**, 233 (1974).

(28) J. G. Wagner, *Pharmacology*, **8**, 102 (1972).

(29) T. R. D. Shaw, J. E. Carless, M. R. Howard, and K. Raymond, *Lancet*, **2**, 209 (1973).

(30) G. J. Mallis, D. H. Schmidt, and J. Lindenbaum, *Clin. Pharmacol. Ther.*, **18**, 761 (1975).

ACKNOWLEDGMENTS AND ADDRESSES

Received April 26, 1976, from the **Clinical Pharmacology and Toxicology Center, Departments of Medicine and Pharmacology, University of Kansas Medical Center, Kansas City, KS 66103,* and the ‡*Medicine and Research Service (Project No. 3704-02), Veterans Administration Hospital, Kansas City, MO 64128.*

Accepted for publication July 1, 1976.

Supported by the Pharmaceutical Division, Pennwalt Corp., and U.S. Public Health Service Grant GM 15956.

The authors thank Jessie Fink for assistance, Dr. K. Hassanein for statistical analyses, and Billie Jean Milanez for technical help. Dissolution rate studies were performed by Dr. Lewis Amsel and Mr. Thomas Matochik, Pharmaceutical Development, Pharmaceutical Division, Pennwalt Corp.

§ Fellow in Clinical Sciences in Clinical Pharmacology of the National Health and Medical Research Council of Australia.

ˣ To whom inquiries should be directed.

Time-Dependent Kinetics I: Exponential Autoinduction of Carbamazepine in Monkeys

WILLIAM H. PITLICK * and RENÉ H. LEVY ˣ

Abstract □ The pharmacokinetics of carbamazepine were studied during a week-long infusion of the drug in 60% polyethylene glycol 400 solution in three rhesus monkeys. Serum concentrations approached steady state within 8–16 hr and then rapidly declined, within 72 hr, to a new asymptotic level approximately 46% of the maximum steady-state concentration. Serum concentrations remained at that level during the rest of the experimental period. The decline from the maximum value to the asymptotic steady state was exponential. It is postulated that the decline in the steady-state concentration is due to autoinduction by carbamazepine of its own metabolism.

Keyphrases □ Time-dependent pharmacokinetics—carbamazepine, 1-week infusion, monkeys □ Carbamazepine—time-dependent pharmacokinetics, 1-week infusion, monkeys □ Pharmacokinetics, time dependent—carbamazepine, 1-week infusion, monkeys □ Analgesics—carbamazepine, time-dependent pharmacokinetics, 1-week infusion, monkeys

Over the past 15 years, awareness of the various facets of dose dependency in drug disposition has increased. As a result, experimental designs of pharmacokinetic investigations often include studies at several dose levels. Examples of dose dependency in absorption, distribution, and elimination have been reported. However, the concept of *time dependency* in pharmacokinetics is still undefined.

BACKGROUND

Studies in this laboratory involving animals and humans clearly indicated that time dependency is a multifaceted phenomenon, at least as complex as dose dependency. Several types of time dependency exist, and this series of papers will provide examples. Carbamazepine is the drug of choice for the treatment of trigeminal neuralgia (1) and was recently approved for use as an anticonvulsant in adults (2). Single-dose intravenous and oral studies in monkeys indicated that the drug has a short biological half-life (1–2 hr) and that chronic oral administration during its efficacy testing in epileptic monkeys would be impractical (3, 4). Consequently, a continuous mode of administration such as constant-rate intravenous infusion in chronically catherized monkeys was considered.

Short-term infusion studies indicated that carbamazepine exhibits dose-dependent kinetics (5, 6). Infusion rates between 8.5 and 40 mg/hr yielded steady-state concentrations of carbamazepine between 2.0 and 5.8 μg/ml (6). However, the increase in steady-state concentration was more than proportional to the increase in infusion rate, and the time required to reach one-half of the steady-state level was not constant. A model with zero-order input and one capacity-limited elimination pathway was adequate to describe the pharmacokinetic behavior of the drug (6).

Table I—Data Obtained from Three Monkeys following Infusion of Carbamazepine at a Constant Rate during 1 Week

Monkey	R_0, mg/hr	Initial Steady-State Concentration, C_0*, μg/ml	Lag Time, θ, hr	Final Steady-State Concentration, C_∞*, μg/ml	Apparent Total Body Clearance		Induction Half-Life, hr
					Initial, liters/hr	Final, liters/hr	
1	17.3	4.10	16	2.04	4.2	8.5	5.8
2	16.0	4.32	12	1.84	3.7	8.6	11.6
3	9.0	2.86	16	1.29	3.1	6.9	7.6

The present investigation was undertaken to define infusion schedules and involved continuous infusion of the drug during 7 days. The steady-state levels of carbamazepine decreased during long-term constant rate infusion. Thus, carbamazepine appears to be the first example of a drug exhibiting simultaneously two types of nonlinearities, dose and time dependency. Furthermore, the long-term constant rate infusion approach used allowed a characterization of the kinetics of autoinduction. These findings provide an experimental basis for the development of nonlinear pharmacokinetic models involving time dependency.

EXPERIMENTAL

Materials—Carbamazepine[1] in polyethylene glycol 400–water (60:40) at 8 mg/ml was used for intravenous infusions.

Animals—Three healthy, male, chaired rhesus (*Macaca mulatta*) monkeys, 3.5–4.5 kg, with chronic jugular and femoral catheters were used. The patency of the catheters was assured by a slow continuous saline infusion into each catheter. The animals were maintained on monkey chow and fresh fruit.

Procedures—Carbamazepine was infused at a constant rate for 1 week. The intravenous infusion was accomplished by pumping the drug solution from a 100-ml calibrated reservoir[2] into the femoral vein catheter through an appropriate chamber attached to a calibrated peristaltic pump[3]. Infusion rates ranged between 9.0 and 17.3 mg/hr (Table I).

Samples of 1.5 ml of blood were drawn from the jugular catheter into a 5-ml plastic disposable syringe through a three-way stopcock attached to the catheter. Each sample was transferred to a nonheparinized tube, allowed to clot, and centrifuged at 2000 rpm for extraction immediately or frozen until assayed. Following the collection of each sample, the catheter was flushed with 1.5 ml of saline.

Twenty to 22 samples were collected over 1 week, the majority of the samples being taken in the first 48 hr. Twenty-four-hour urine collections were taken during the infusion studies. Serum and urine samples of carbamazepine were assayed using a GLC method presented previously (7).

RESULTS AND DISCUSSION

Serum concentration–time plots for Monkeys 1 and 2 are shown in Figs. 1 and 2, respectively. Serum concentrations approached an initial steady state, C_0*, within 8–16 hr and then fell off to a new asymptotic level, C_∞*, which was reached within 72 hr after the start of the infusion. There was no further decline from this final steady state during the rest of the experimental period. The serum concentrations observed within the first 12 hr were within 10% of the levels predicted from short-term infusion studies (6), as shown by the dotted lines in Figs. 1 and 2.

On the average, the final steady-state concentrations represented 46% (42–50%) of the maximum levels seen within the first 8–16 hr (Table I). This decrease corresponded to a twofold increase in apparent total body clearance (Table I). In all animals, the decline in steady-state concentrations from 12 hr onward was remarkable from two aspects: (*a*) the decline began somewhat abruptly, after a lag time (θ) of 12–16 hr, and (*b*) the decline in levels during a continuous infusion at a constant rate appeared to be an exponential process (Figs. 1 and 2). Semilogarithmic plots of the serum concentration data after the lag time, log ($C - C_\infty$*) *versus* ($t - \theta$), appeared linear (Fig. 3). An induction rate constant, K_I, and a corresponding half-life of induction, $T_{I\,1/2}$, can be measured to characterize the decreases in concentration at times larger than θ. The values of $T_{I\,1/2}$ obtained for these monkeys ranged between 5.8 and 11.6 hr. Serum concentrations at times larger than θ could then be fitted to the equation:

$$C = C_\infty^* + (C_0^* - C_\infty^*)\, e^{-K_I(t-\theta)} \qquad \text{(Eq. 1)}$$

A good agreement was observed between experimental data points and the fitted lines (continuous lines in Figs. 1 and 2).

No unchanged carbamazepine could be measured in the 24-hr urine samples. This finding was consistent with an earlier report that less than 1% of single intravenous and oral doses could be recovered as unchanged carbamazepine in urine (3).

Many drugs and chemicals affect the activity of drug-metabolizing enzymes in the liver microsomes. A large amount of evidence indicates that an increase in activity could be due to the increased synthesis of microsomal protein (8). In addition, a period of time follows treatment before the effect is apparent, and this time delay corresponds to known rates of protein synthesis (8). Carbamazepine has affected the half-lives of other drugs (9–12). A reduction in the half-life of doxycycline from 15 to 8 hr was reported in patients receiving carbamazepine (10). Carbamazepine also caused a decrease in the elimination half-life of phenytoin in patients (11). Likewise, a reduction in the half-lives of phenytoin and carbamazepine in monkeys pretreated with carbamazepine was reported (12). The effect of carbamazepine on the metabolism of several drugs is considered to be due to an induction of the drug-metabolizing enzyme systems in the liver. Other studies in this laboratory (excretion of *d*-

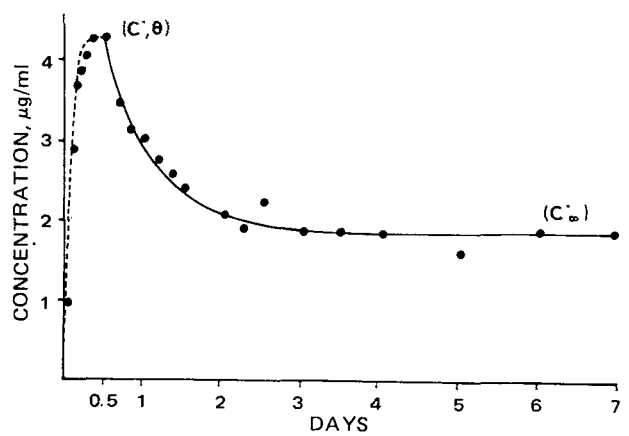

Figure 1—*Plot of serum carbamazepine concentrations* versus *time for Monkey 1 during 1 week on long-term infusion at a constant rate of* $R_0 = 17.3$ *mg/hr. The continuous line represents a fit to* $C = 2.04 + 2.06\, e^{-0.693/5.8(t-\theta)}$.

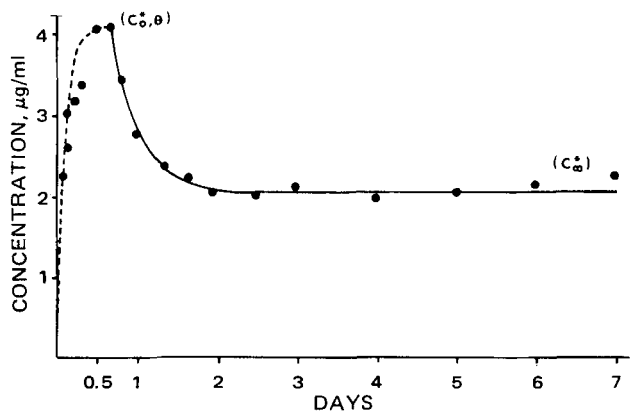

Figure 2—*Plot of serum carbamazepine concentration* versus *time for Monkey 2 during infusion for 1 week at a constant rate of* $R_0 = 16.0$ *mg/hr. The continuous line represents a fit to* $C = 1.84 + 2.48\, e^{-0.693/11.6(t-\theta)}$.

[1] Supplied by Ciba-Geigy Corp., Ardsley, N.Y.
[2] Soluset, Abbott Laboratories, North Chicago, Ill.
[3] Holter infusion pump, Extracorporeal Medical Specialties, King of Prussia, Pa.

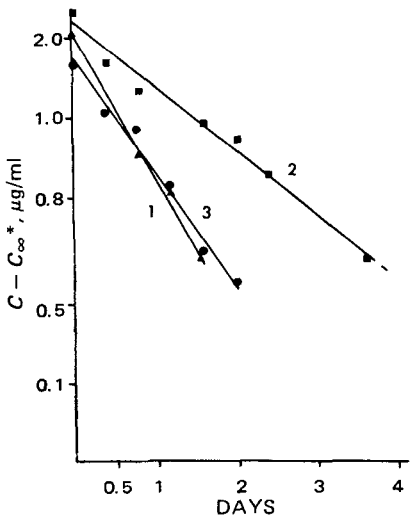

Figure 3—*Semilogarithmic plot of* (C − C_∞*) versus *time* (t − θ) *for Monkeys 1* (▲), *2* (■), *and 3* (●) *during 1 week of constant-rate infusion.*

glucaric acid) indicated that the observed autoinduction in steady-state plasma levels was probably due to enzyme induction.

Carbamazepine, in and of itself, is capable of stimulating its own metabolism in rhesus monkeys. Drug interaction studies with carbamazepine in other monkeys showed that the autoinduction phenomenon was consistently reproducible[4]. The possible role played by the solvent (polyethylene glycol 400) in the observed phenomenon was considered. Other anticonvulsants (ethosuximide, clonazepam, and dipropylacetic acid) were infused intravenously in rhesus monkeys with the same solvent for 1–2 weeks, and no index of autoinduction was observed[4]. In addition, Ronfeld and Benet (12) showed that the intravenous kinetics of phenytoin in rhesus monkeys were not altered after prolonged intravenous infusion of polyethylene glycol 400.

Several questions remain to be evaluated, particularly the relationship between the induction effect and the dosing regimen (dose or infusion rate and duration of infusion) of the inducing agent. It is not known whether the levels of carbamazepine achieved prior to induction (2.9–4.3 μg/ml) represent minimum or maximum inducing levels. However, it appears that the duration of infusion used in this study was long enough to permit an analysis of the time course of induction.

A significant feature of the present results is that the decrease in the steady-state concentration during autoinduction was exponential. In view of this relatively simple kinetic pattern, the phenomenon of autoinduction becomes quantifiable and, as such, predictable. Thus, it should be possible to design a pharmacokinetic model that will allow the calculation of dosage regimens that can maintain steady-state plasma concentrations of carbamazepine and overcome the phenomenon of autoinduction.

A one-compartment pharmacokinetic model with an exponentially increasing first-order elimination rate "constant" was proposed to explain the decreases in maximum and minimum serum levels of carbamazepine in human volunteers during a 3-week treatment (13). However, such a model would not be appropriate in the present study since short-term infusion studies (5, 6) indicated that the kinetics of carbamazepine in monkeys were dose dependent. A pharmacokinetic model involving simultaneous dose and time dependency is currently being investigated to account for the present results as well as additional chronic infusion data.

[4] Unpublished data.

REFERENCES

(1) S. Blom, *Lancet*, **1**, 839 (1962).

(2) J. J. Cereghino, in "Advances in Neurology," vol. II, J. K. Penry and D. D. Daly, Eds., Raven, New York, N.Y., 1975, p. 309.

(3) R. H. Levy, J. S. Lockard, J. R. Green, P. Friel, and L. Martis, *J. Pharm. Sci.*, **64**, 302 (1975).

(4) J. S. Lockard, R. H. Levy, V. Uhlir, and J. A. Farquhar, *Epilepsia*, **15**, 351 (1974).

(5) R. Ronfeld and L. Z. Benet, *Res. Commun. Chem. Pathol. Pharmacol.*, **10**, 303 (1975).

(6) W. H. Pitlick and R. H. Levy, "Abstracts," APhA Academy of Pharmaceutical Sciences, Atlanta meeting, 1975.

(7) R. H. Levy, W. H. Pitlick, A. S. Troupin, J. R. Green, and J. M. Neal, *Clin. Pharmacol. Ther.*, **17**, 657 (1975).

(8) A. Goldstein, L. Aronow, and S. M. Kalman, "Principles of Drug Action," 2nd ed., Wiley, New York, N.Y., 1974, p. 275.

(9) H. Meinardi, in "Antiepileptic Drugs," D. M. Woodbury, J. K. Penry, and R. P. Schmidt, Eds., Raven, New York, N.Y., 1972.

(10) O. Pentila, P. J. Neuvonen, K. Aho, and R. Lehtovaara, *Br. Med. J.*, **2**, 470 (1974).

(11) J. M. Hansen, K. Siersbaek-Nielsen, and L. Skovsted, *Clin. Pharmacol. Ther.*, **12**, 539 (1973).

(12) R. Ronfeld and L. Z. Benet, "Abstracts," APhA Academy of Pharmaceutical Sciences, Chicago meeting, 1974.

(13) W. H. Pitlick, R. H. Levy, A. S. Troupin, and J. R. Green, *J. Pharm. Sci.*, **65**, 462 (1976).

ACKNOWLEDGMENTS AND ADDRESSES

Received April 5, 1976, from the *Department of Pharmaceutical Sciences, School of Pharmacy, and the Department of Neurological Surgery, School of Medicine, University of Washington, Seattle, WA 98195.*

Accepted for publication June 28, 1976.

Presented at the Basic Pharmaceutics Section, APhA Academy of Pharmaceutical Sciences, Atlanta meeting, November 1975.

Abstracted in part from a thesis submitted by W. H. Pitlick to the Graduate School, University of Washington, in partial fulfillment of the Doctor of Philosophy degree requirements.

Supported by National Institutes of Health Research Contract NO1-NS-1-2282 and Research Grant NS-04053, National Institute of Neurological and Communicative Disorders and Stroke, U.S. Public Health Service.

* Present address: Department of Pharmaceutics, School of Pharmacy, University of Pittsburgh, Pittsburgh, PA 15261.

[x] To whom inquiries should be directed.

Time-Dependent Kinetics II: Diurnal Oscillations in Steady-State Plasma Ethosuximide Levels in Rhesus Monkeys

INDRAVADAN H. PATEL, RENÉ H. LEVY ˣ, and JOAN S. LOCKARD

Abstract □ Morning steady-state (9 am) plasma levels were significantly higher than the corresponding evening (5 pm) plasma levels during a 3-week zero-order infusion of ethosuximide to six monkeys. These differences could not be explained by experimental variables such as GLC assay and infusion pump. Circadian periodicity in steady-state plasma levels was investigated in three monkeys over 4 months under controlled experimental conditions: blood sampling at 2-hr intervals for 26 hr, 1 day/week; fixed lighting, feeding, and noise schedules; and electroencephalogram monitoring. The plasma concentration–time curves showed two minima in the 12 noon–2 pm and 8 pm–12 midnight periods, and the later involved the largest percent change in plasma levels (4–8%). The plasma concentration–time data were subjected to cross-correlation analysis, which indicated a circadian rhythm in steady-state plasma levels with a period of 24–26 hr.

Keyphrases □ Time-dependent kinetics—ethosuximide, circadian rhythm in steady-state plasma levels, monkeys □ Ethosuximide—circadian rhythm in steady-state plasma levels, monkeys □ Pharmacokinetics—ethosuximide, circadian rhythm in steady-state plasma levels, monkeys □ Circadian rhythm—in steady-state plasma levels of ethosuximide, monkeys □ Anticonvulsants—ethosuximide, circadian rhythm in steady-state plasma levels, monkeys

Time dependency in pharmacokinetics involves several types of phenomena. Previous studies dealt with the self-induced decreases in steady-state concentrations of carbamazepine during chronic administration of the drug to humans (1) and monkeys (2). More recently, the terms "cronodisponibilita" (3) (equivalent to chronoavailability) and "chronopharmacokinetics" (4) have been coined to stress the importance of temporal changes in bioavailability and pharmacokinetics, respectively.

Diurnal variations in excretion rates of several acidic and basic drugs (*e.g.*, salicylate, sulfasymazine, and amphetamine) were reported (5–7). In several instances, these variations could be explained on the basis of circadian rhythms in kidney functions (8–11). Diurnal fluctuations in plasma levels of dipyridamole could be related to circadian changes in GI absorption (12).

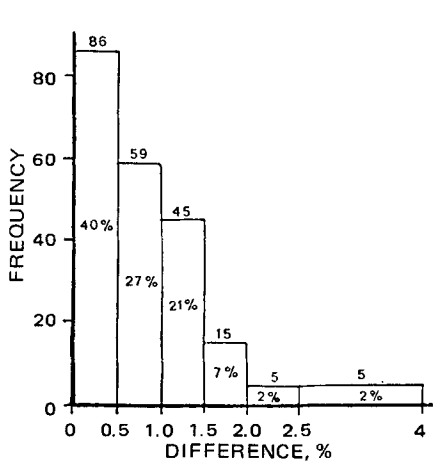

Figure 1—*Plot of frequency* versus *difference (percent) between duplicate assay determinations.*

In a previous study (13) designed to test for time dependency in elimination kinetics of ethosuximide in monkeys, the drug was chronically infused for 22 days to six animals. Morning (9 am) plasma concentrations were consistently higher than evening (5 pm) concentrations, and the presence of circadian rhythm in steady-state plasma levels was suspected. The present study was undertaken to elucidate this phenomenon under more rigorously controlled experimental and, particularly, environmental conditions. These conditions included frequent blood sampling (2-hr intervals); duplicate GLC assays; infusion pump monitoring; fixed lighting, feeding, and noise schedules; and electroencephalogram (EEG) monitoring (sleep staging).

EXPERIMENTAL

Experimental Subjects—Three chronically catheterized male rhesus monkeys (Animals 903, 923, and 983) were used. These monkeys were previously used to determine the pharmacokinetics of ethosuximide under single-dose and chronic dosing conditions (13, 14).

EEG Monitoring—Screw electrodes[1], 3 mm, were bilaterally implanted in the mastoid, occipital, central, and inferior lateral orbital regions of the skull. The left mastoid electrode served as a reference electrode. Electroculograms were recorded for each eye with respect to the reference electrode. Electromyograms were recorded from the temporal muscles. Electroencephalograms (EEG) were monitored from the right central electrode to the left mastoid electrode.

All leads were crimped to a miniature 16-pin socket, and the assembly was fixed to the skull with 3-mm screws[1] and cranioplastic fluid[2]. A chronic, shielded, flexible cable connected the leads of the socket assembly to the four-channel EEG machine[3].

The sleep stages were determined from the EEG data using a previously described procedure (15).

Environmental Conditions—The animals were housed in a room with glass windows and diurnal lighting (light during "day" period, 6 am–6 pm; dark during "night" period, 6 pm–6 am). They were fed twice a day, at 6 am (monkey chow) and 5:30 pm (monkey chow and fresh fruit). The glass windows were covered to prevent penetration of external light. The jugular and femoral catheters, as well as the EEG cable of each animal, were carried to an adjacent room through holes drilled in the glass window.

Infusion of drug solutions, blood sampling, and EEG monitoring were performed in the adjacent room. Continuous 24-hr music (moderately high volume, 6 am–6 pm; low volume, 6 pm–6 am) aided in the masking of external noise during the study. Activities in the monkey room and the adjacent room were kept to a minimum.

Experimental Protocol—The animals received a continuous zero-order infusion[4] of ethosuximide in normal saline over 4 months (infusion rate, 3.72–4.74 mg/hr; steady-state plasma concentration, 30–55 μg/ml). Plasma samples of 0.4 ml were collected 1 day/week at 2-hr intervals for 26 hr for 5 weeks. Fractions of 0.1 ml of the plasma samples were assayed for ethosuximide in duplicate using the GLC assay of Dill *et al.* (16). Only

[1] Vitallium, Howmedica Inc., Rutherford, N.J.
[2] Codman and Shartleff, Inc., Randolph, Mass.
[3] Grass model III-D, Grass Instruments Co., Quincy, Mass.
[4] Holter infusion pump, Extracorporeal Medical Specialties, King of Prussia, Pa.

Table I—Statistical Comparison[a] of Morning (9 am) and Evening (5 pm) Plasma Concentrations[b] (Micrograms per Milliliter) of Ethosuximide in Monkeys

	Stage 1			Stage 2			Stage 3		
Animal	Morning	Evening	p	Morning	Evening	p	Morning	Evening	p
733	23.24	22.20	0.05	—	—	—	—	—	—
743	26.30	24.85	0.01	53.84	51.40	0.01	86.00	79.29	0.05
753	27.21	26.00	0.05	50.12	49.93	NS	78.67	78.54	NS
903	25.10	23.17	0.01	50.08	46.01	0.01	76.97	72.05	0.01
923	29.90	28.75	NS[c]	56.10	54.12	0.01	89.40	86.45	0.01
983	28.99	27.51	NS	—	—	—	—	—	—
Mean	26.79	25.41	0.01	52.54	50.37	0.01	82.76	79.09	0.01

[a] Paired t-test. [b] Each concentration value represents a mean of six to eight determinations, excluding the concentrations obtained during the first 24 hr of each stage. [c] Not significant at $p = 0.05$.

3 weeks of data for Animal 983 could be obtained because of technical difficulties with the catheters.

Continuous EEG monitoring was performed from 10 am to 10 am or from 10 pm to 6 am with and without blood sampling.

RESULTS

Preliminary Observations—Previously (13), it was pointed out that morning steady-state plasma concentrations of ethosuximide were consistently higher than the corresponding evening concentrations during a three-stage zero-order infusion of the drug to six monkeys. A statistical evaluation of the differences between morning and evening concentrations was performed (Table I). The differences between morning and evening plasma concentrations ranged from 3.8 to 7.7% in Stage 1, from 0.4 to 8.1% in Stage 2, and from 0.2 to 7.8% in Stage 3. These differences were significant in the majority of animals in each stage. However, these differences were of a small magnitude and could be explained by fluctuations in several experimental variables (*e.g.*, drug assay and infusion pump). Thus, it became necessary to evaluate the potential contribution of these experimental factors to the observed differences in plasma concentrations.

The precision of the GLC assay was calculated from duplicate determinations of approximately 200 plasma samples (concentration range of 30–55 μg/ml), and a frequency plot was constructed from these data (Fig. 1). The percent difference was less than 1% in 67% of the cases, 1–2% in 28% of the cases, and 2–4% in the remaining instances. These results indicated that the GLC procedure can establish differences in plasma concentrations of 4–7%. Furthermore, morning and evening plasma samples were always assayed simultaneously (within the same run). Since assay error would tend to be random, it could not explain the observed systematic differences between morning and evening plasma concentrations.

Fluctuations in the voltage of the electrical line could influence the operational pump voltage, rotational speed, and, consequently, delivery rate. The delivery rates of two infusion pumps were determined by recording the volume delivered between 9 am and 5 pm and between 5 pm and 9 am for 5–10 consecutive days. These measurements utilized six different pump chambers. In three instances, delivery rates increased during the 5 pm–9 am period (0.3–0.7%); in the other three, they decreased (0.5–2.4%). There were no significant differences between the delivery rates of the 9 am–5 pm and 5 pm–9 am periods in five of six cases.

These experiments suggested that experimental variables such as infusion pump and drug assay did not contribute to the observed fluctuations in steady-state plasma levels. However, the sampling schedule employed in the previous study (13) was limited. Therefore, additional studies were undertaken where steady-state plasma levels were obtained at 2-hr intervals over 26 hr under rigorously controlled experimental conditions.

EEG–Time and Plasma Concentration–Time Data—EEG data were collected to determine the sleeping behavior of monkeys during day and night periods. The data indicated that the animals were awake during most of the day periods and slept an appreciable portion of the night periods (Fig. 2 and Table II).

Typical diurnal variations in steady-state plasma levels for Animals 903, 923, and 983 during a single sampling period are represented in Figs. 3A–5A. The observed oscillations were reproducible within a given animal over 3–5 weeks. Consequently, plasma concentrations were averaged, and plots of mean percent change in plasma level (using the 8 am concentration as a reference value) as a function of time were constructed (Figs. 3B–5B). Certain features were present in the profiles of all animals: a decline from 8 am to 2–4 pm, a small rise or plateau between 4 and 6 pm, and a steady decline until 8 pm–12 midnight followed by a steady rise until 8–10 am (next day). Thus, in each plot, there appeared to be two minima, in the 12 noon–2 pm and 8 pm–12 midnight time periods. However, the minimum occurring during the night period involved the largest percent change in plasma levels (4–8%).

The evidence suggesting a circadian rhythm in steady-state plasma levels can be summarized as follows:

1. The earlier multistage infusion studies (13) indicated that the pattern of oscillations in plasma levels was similar on several consecutive days (up to 3 weeks).
2. The percent change in plasma concentration–time profiles obtained in the present study defined the actual time course of steady-state plasma levels within a 26-hr period.
3. The concentrations observed in the 8–10 am period on 2 consecutive days were quite close.
4. The time course of steady-state plasma levels within a 26-hr period was reproducible on successive weeks (on the same day of the week).

Several techniques (moving variate analysis, Fourier analysis, auto- and cross-correlation, and cosinor analysis) are available to estimate the

Table II—Sleeping Behavior of Rhesus Monkeys during Night Period[a], 10 pm–6 am

	Percent of Night Period Spent in Stage					
Animal	0	1	2	3	4	REM
903[b]	31	27	15	10	9	8
923[b]	28	27	20	10	7	9
983[c]	38	22	2	14	17	7

[a] Calculated from continuous EEG data obtained from 10 pm to 6 am. [b] The values shown for Animals 903 and 923 represent the mean values of five night periods. [c] The values obtained for Animal 983 are from a single night period.

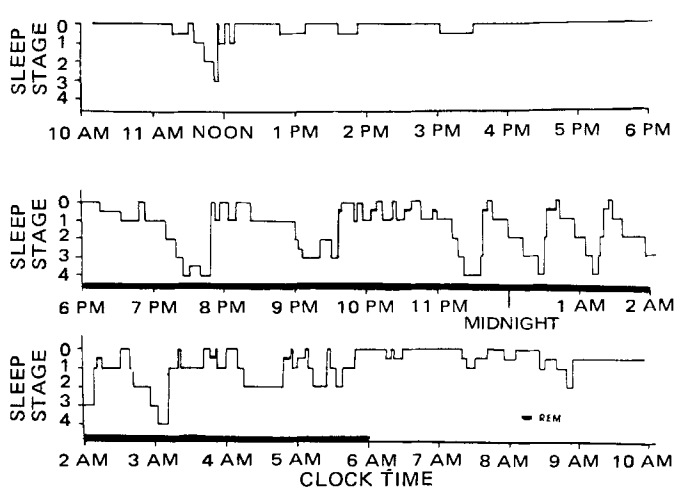

Figure 2—*The 24-hr sleep pattern of Animal 903.*

Table III—Cross-Correlation Analysis of Experimental Data

Animal	Week	Estimated Value of Period, hr	Estimated Value of Amplitude, %
903	1[a]	34.5	0.92
	2	26.0	2.62
	3	29.5	1.77
	4	25.5	1.13
	5	24.5	1.55
	Mean	28.0	1.60
923	1[a]	27.0	3.86
	2	24.0	4.50
	3	25.5	2.28
	4	26.0	2.75
	5	21.5	2.80
	Mean	24.8	3.24
983	1[a]	21.0	2.09
	2	39.5	2.65
	3	25.0	3.99
	Mean	28.5	2.91
903	Mean profile	25.5	1.24
923	Mean profile	25.5	3.05
983	Mean profile	24.5	2.49

[a] Plasma samples were collected over 22 hr. Mean values obtained at 24 and 26 hr were substituted for the missing values.

parameters of a periodic function, namely, period and amplitude (17–24). However, a literature review failed to demonstrate applications of these analyses to blood level data of exogenous compounds such as drugs. In the present study, an attempt was made to analyze the observed data by cross-correlation analysis (22).

In view of the relatively small oscillations in plasma levels found in this study, the cross-correlation method was first evaluated with generated data using the equation $y = a + b\cos(cX)$. The following input values were used: period = 24 hr, amplitude = 5%, sampling interval = 2 hr, and observation timespan = 26 hr. The method yielded values of the period within 2% and values of the amplitude within 14% of the input values even with 1–4% random error in the data. These results indicated that the cross-correlation method could be applied to the experimental observations.

Sets of plasma concentration–time data of individual animals, as well as the mean set of data of each animal, were subjected to the cross-correlation analysis (Table III). The mean periods obtained from individual sets of data were 28.0, 24.8, and 28.5 hr for Animals 903, 923, and 983, respectively. The corresponding periods obtained from mean plasma concentration–time data were 25.5, 25.5, and 24.5 hr. These values are close to the circadian period (24 hr) and provide further support for the hypothesis of a circadian rhythm in steady-state plasma levels.

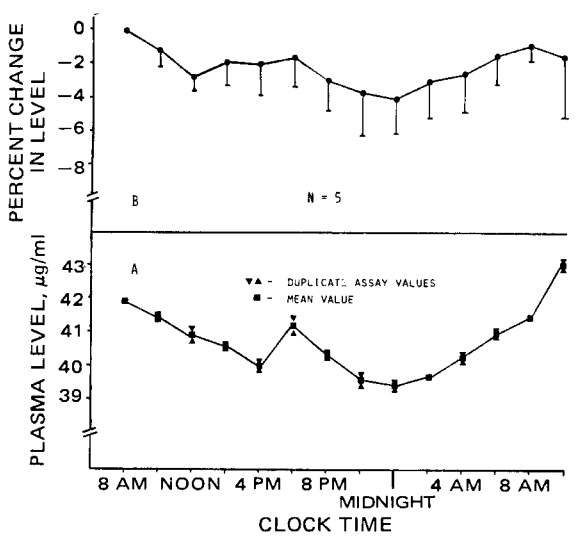

Figure 3—*Plots of typical diurnal changes in steady-state plasma levels observed during a given sampling period (A) and mean (±SD) percent changes in plasma levels* versus *time (B) for Animal 903.*

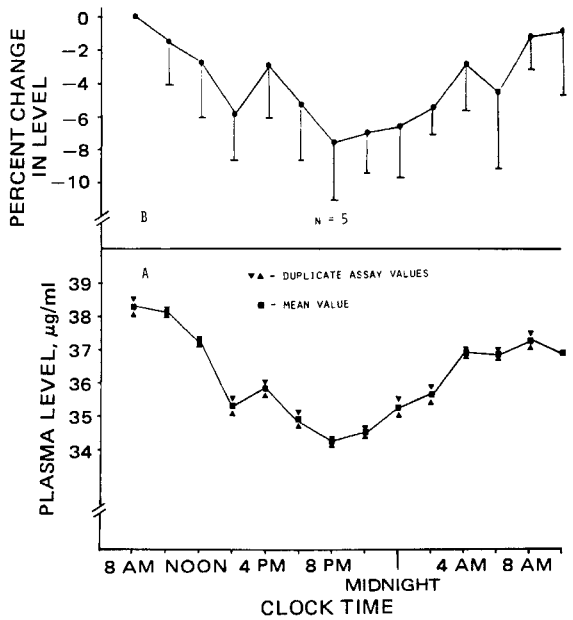

Figure 4—*Plots of typical diurnal changes in steady-state plasma levels observed during a given sampling period (A) and mean (±SD) percent changes in plasma levels* versus *time (B) for Animal 923.*

DISCUSSION

The present study revealed diurnal fluctuations (circadian periodicity) in steady-state plasma levels of ethosuximide in monkeys. An analysis of the possible causes for fluctuations in plasma levels during zero-order infusion suggested a circadian rhythm in total body clearance. Diurnal variations in the volume of distribution, renal excretion, and/or metabolism could explain the observed periodicity in plasma levels.

Circadian variations in the excretion rates of several drugs (*e.g.*, salicylate, sulfasymazine, and amphetamine) have been reported in humans and were believed to be associated with the diurnal urinary pH rhythm (5–7). It is not known whether such a circadian rhythm in urine pH exists in monkeys. However, even if such a cycle exists, it should include urine pH values close to 9 to influence the urinary excretion of ethosuximide (pKa = 9.4). In the present study, it was not possible to determine the existence of a circadian rhythm in the excretion rate of ethosuximide,

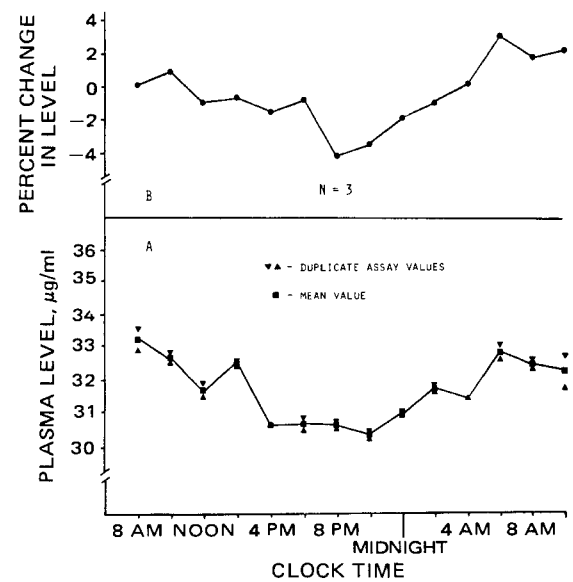

Figure 5—*Plots of typical diurnal changes in steady-state plasma levels observed during a given sampling period (A) and mean (±SD) percent changes in plasma levels* versus *time (B) for Animal 983.*

primarily because of the additional technical problems (trauma and infection) posed by chronic urethral catheters.

Circadian variations in the rates of *in vitro* metabolism of drugs (hexobarbital, aminopyrine, *p*-nitroanisole, and 4-dimethylaminoazobenzene) have been documented (25–32). However, whenever a circadian rhythm in metabolism has been reported, it has usually been associated with an oxidative metabolic process (33). Ethosuximide is metabolized to a significant extent (60–65%) in monkeys (13, 14, 34), and all known metabolic pathways (in rats, monkeys, and humans) involve oxidative processes (35–38). Thus, the possibility of circadian variations in the activities of hepatic drug-metabolizing enzymes in monkeys is not unrealistic.

This study shows that the phenomenon of circadian rhythm in steady-state levels is real. Although the extent of oscillations reported here is limited, ongoing studies show that other anticonvulsants (valproic acid and clonazepam) exhibit diurnal oscillations in plasma levels likely to have therapeutic consequences.

REFERENCES

(1) W. H. Pitlick, R. H. Levy, A. S. Troupin, and J. R. Green, *J. Pharm. Sci.*, **65,** 462 (1976).

(2) W. H. Pitlick and R. H. Levy, presented at the Basic Pharmaceutics Section, APhA Academy of Pharmaceutical Sciences, Atlanta meeting, Nov. 1975, Abstract 32.

(3) A. Carandente, *Chronobiologia, Suppl. 1,* **1,** 15 (1974).

(4) F. Halberg, *ibid.*, **1,** 27 (1974).

(5) A. Reinberg, Z. W. Zagula-Mally, J. Ghata, and F. Halberg, *Proc. Soc. Exp. Biol. Med.*, **124,** 826 (1967).

(6) L. Dettli and P. Spring, *Helv. Med. Acta,* **33,** 291 (1967).

(7) A. H. Beckett and M. Rowland, *Nature (London),* **204,** 1203 (1964).

(8) J. L. Hastings and B. Eisele, *Proc. Soc. Exp. Biol. Med.*, **43,** 308 (1940).

(9) S. W. Stanbury and A. E. Thomson, *Clin. Sci.*, **10,** 267 (1951).

(10) J. N. Mills and S. W. Stanbury, *J. Physiol.*, **117,** 22 (1952).

(11) J. S. Elliot, R. F. Sharp, and L. Lewis, *J. Urol.*, **81,** 339 (1959).

(12) T. J. Mellinger and J. G. Bohorfoush, *Arch. Int. Pharmacodyn. Ther.*, **163,** 471 (1966).

(13) I. H. Patel and R. H. Levy, *Epilepsia,* **16,** 717 (1975).

(14) I. H. Patel, R. H. Levy, and T. G. Bauer, *ibid.*, **16,** 705 (1975).

(15) A. Rechtschaffen and A. Kales, "A Manual of Standardized Terminology, Technique, and Scoring System for Sleep Stages of Human Subjects," U.S. Department of Health, Education and Welfare, Public Health Service, National Institutes of Health, National Institute of Neurological Diseases and Blindness, Neurological Information Network, Bethesda, Md., 1968.

(16) W. A. Dill, L. Peterson, T. Chang, and A. J. Glazko, presented at the American Chemical Society, 149th National Meeting, Detroit, Mich., Apr. 1965, Abstract 30N.

(17) J. T. Enright, in "Circadian Clocks," Proceedings of the Feldafing Summer School, J. Aschoff, Ed., North Holland Publishing Co., Amsterdam, the Netherlands, 1964, pp. 31–42.

(18) J. T. Enright, *J. Theoret. Biol.*, **8,** 426 (1965).

(19) A. Sollberger, "Supplement to the Reports from the Fifth Conference of the Society for Biological Rhythm," Stockholm, Sweden, 1960, pp. 30–34.

(20) W. P. Colquhoun, "Biological Rhythms and Human Performance," Academic, New York, N.Y., 1971, pp. 1–38.

(21) Y. W. Lee, "Statistical Theory of Communication," Wiley, New York, N.Y., 1963, pp. 4–104.

(22) F. Koehler, F. K. Okano, L. R. Elveback, F. Halberg, and J. Bittner, *Exp. Med. Surg.*, **14,** 5 (1956).

(23) D. M. A. Mercer, *Cold Spring Harbor Symp. Quant. Biol.*, **25,** 73 (1960).

(24) F. Halberg, Y. L. Tong, and E. A. Johnson, in "The Cellular Aspects of Biorhythms," H. Von Mayersback, Ed., Springer-Verlag, New York, N.Y., 1967, pp. 20–48.

(25) V. Nair and R. Casper, *Life Sci.*, **8,** 1291 (1969).

(26) F. M. Radzialowski and W. F. Bousquet, *ibid.*, **6,** 2545 (1967).

(27) F. M. Radzialowski and W. F. Bousquet, *J. Pharmacol. Exp. Ther.*, **163,** 229 (1968).

(28) E. S. Vesell, *Ann. N.Y. Acad. Sci.*, **151,** 900 (1968).

(29) P. Roberts, M. J. Turnbull, and A. Winterburn, *Eur. J. Pharmacol.*, **12,** 375 (1970).

(30) M. Civen, R. Uhrich, B. M. Trimmer, and C. B. Brown, *Science,* **157,** 1563 (1967).

(31) A. Jori, E. DiSalle, and V. Santini, *Biochem. Pharmacol.*, **20,** 2965 (1971).

(32) A. Jori, S. Caccia, and E. DiSalle, *Eur. J. Pharmacol.*, **21,** 37 (1973).

(33) A. R. DiSanto and J. G. Wagner, *J. Pharm. Sci.*, **61,** 1086 (1972).

(34) T. Chang, W. A. Dill, and A. J. Glazko, in "Antiepileptic Drugs," D. M. Woodbury, J. K. Penry, and R. P. Schmidt, Eds., Raven, New York, N.Y., 1972, pp. 417–423.

(35) T. Chang, A. R. Burkett, and A. J. Glazko, in *ibid.*, pp. 425–429.

(36) A. R. Burkett, T. Chang, and A. J. Glazko, *Fed. Proc.*, **30,** 391 (1971).

(37) M. G. Horning, C. Stratton, J. Nowlin, D. J. Harvey, and R. M. Hill, *Drug Metab. Disp.*, **1,** 569 (1973).

(38) P. G. Preste, C. E. Westerman, N. P. Das, B. J. Wilder, and J. H. Duncan, *J. Pharm. Sci.*, **63,** 467 (1974).

ACKNOWLEDGMENTS AND ADDRESSES

Received April 19, 1976, from the *Department of Pharmaceutical Sciences, School of Pharmacy, and the Department of Neurological Surgery, School of Medicine, University of Washington, Seattle, WA 98195.*

Accepted for publication June 15, 1976.

Presented at the Basic Pharmaceutics Section, APhA Academy of Pharmaceutical Sciences, New Orleans meeting, April 1976.

Supported by National Institutes of Health Research Contract NO1-NS-1-2282 and Research Grant NS-04053, National Institute of Neurological and Communicative Disorders and Stroke, U.S. Public Health Service.

The authors thank Parke-Davis & Co. for the generous supply of ethosuximide powder. They also thank Mr. L. L. Ducharme, Mr. W. C. Congdon, Mr. L. Lombard, and Ms. R. Nepenphe (deceased) for technical assistance.

[x] To whom inquiries should be directed.

Diffusion Model for Drug Release from Suspensions I: Theoretical Considerations

JAMES W. AYRES * and F. TOM LINDSTROM ‡x

Abstract □ A new mathematical model based on physicochemical principles is presented; it does not require a "diffusion layer" for the release of a suspended drug from a semisolid vehicle. This general model has wide range application to systems where release is controlled by the diffusion rate or dissolution rate of a drug. The appropriate mathematical relationships are derived and evaluated. Theoretical drug concentration distributions in the vehicle and a membrane and the predicted cumulative drug mass uptake by blood under specified conditions are presented. The dissolution rate of solid drug in the vehicle markedly influences predicted drug release using the model presented. It is anticipated that the model will stimulate further research to confirm or reject the assumption that the dissolution rate may be slow enough to be important in the systems studied.

Keyphrases □ Diffusion—suspended drug in semisolid vehicle, mathematical model based on physicochemical principles □ Dissolution—suspended drug in semisolid vehicle, mathematical model based on physicochemical principles □ Pharmacokinetic models—diffusion and dissolution of suspended drug in semisolid vehicle □ Drug release—from suspensions, diffusion model based on physicochemical principles □ Suspensions—drug release, diffusion model based on physicochemical principles

Many physical models for diffusion from solutions were defined and the appropriate mathematical equations were presented in standard texts (1–3). The release of drug from a topically applied ointment was considered (4) when the drug was initially uniformly dissolved in a homogeneous base and the rate-controlling step was in either the applied phase or the skin. The theoretical analysis of drug diffusion through emulsion systems was extensively studied and reported (5–8).

Physical models for diffusion of drug from suspension systems were also reported (4, 5, 9). In one case, the suspension was considered as a potential barrier to drug diffusion (5); in others (4, 9), the suspended drug was considered a source of drug supply.

The most widely accepted theory for dissolution rates was proposed by Noyes and Whitney in 1897 and subsequently modified to include the stagnant or unstirred diffusion layer concept of Nernst and Brunner. These and other theories for dissolution models were reviewed previously (10–12).

The purposes of this study were to describe dissolution and diffusion for a suspended drug in a semisolid vehicle in terms of the molecular rates of escape from, and the return to, a particle surface; to present a mathematical model (a set of nonlinear diffusion equations) for the mass transport of the drug through the suspension and a permeable barrier system to a perfect sink; and to solve the appropriate linearized equations for a general least upper bound case as well as for several specific cases.

Consideration is given to the condition where dissolution is either very slow or very fast with respect to diffusion in the continuous phase of the suspension as well as where dissolution and diffusion occur at about the same rate. Special emphasis is placed on the condition of slow dissolution and fast diffusion, because this case is not treated in the literature and the need for such equations has been stated (13).

MODEL DEVELOPMENT

Suppose that the ointment–skin–blood system can be approximated by the system shown in Fig. 1. The barrier enclosing the ointment on three sides penetrates the skin only as a means of illustrating that the drug is required to move perpendicular to the membrane in this model. Assume that there is a uniformly distributed source (at time $t = 0$) in the region $-L_1 \leq x < 0$ and that this source operates in the following way. In any plane sheet of thickness Δx and cross-section area A (cm^2) in Medium I ($-L_1 \leq x < 0$), the time rate of change of the source mass is equal to the difference between the mass dissolution rate and the crystallization rate. Or:

$$\frac{\partial[\rho_s A\, \Delta x \epsilon(x,t)]}{\partial t} = -K_{dis} A_s(x,t) C_{sol} + K_{cry} A_s(x,t) C_1(x,t) \quad \text{(Eq. 1)}$$

where:

C_{sol} = solvent concentration (grams per milliliter)
ρ_s = crystal or powder density (grams per milliliter)
K_{dis} = dissolution rate constant (centimeters per second)
K_{cry} = crystallization rate constant (centimeters per second)
$A_s(x,t)$ = effective source (crystal) surface area at (x, t) (square centimeters)
$\epsilon(x,t)$ = volume fraction measure of source (milliliters per milliliter)

These relationships between dissolution and crystallization provide a general model and are developed from standard theories of velocity of adsorption and desorption (14) as well as crystallization and dissolution (15). In addition, the coefficients K_{dis} and K_{cry} are assumed to be temperature and activation energy dependent in the sense of their definitions as stated by Szinai and Hunt (16). The volume fraction measure of the source ϵ simply measures how much of the source is left at point (x, t).

Again using the ideas of Rowler (15), let $A_s(x,t) = \kappa A\, \Delta x[\epsilon(x,t)]^{2/3}$, where κ is a surface area to volume constant.

Putting all these hypotheses together yields for the time rate of change of the source mass in the incremental volume $A\, \Delta x$:

$$\frac{\partial \epsilon}{\partial t} = -\frac{K_{dis}\kappa}{\rho_s}\epsilon^{2/3} C_{sol} + \frac{K_{cry}\kappa}{\rho_s}\epsilon^{2/3} C_1 \quad \text{(Eq. 2)}$$

Suppose that at time $t = 0$, $C_1(x,0) = C_s$, the saturation concentration for the free ointment phase drug distribution. Also, let $\epsilon(x,0) = \epsilon_0$, a prescribed positive constant volume fraction. Then, assuming uniform equilibrium conditions between the dissolution and crystallization pro-

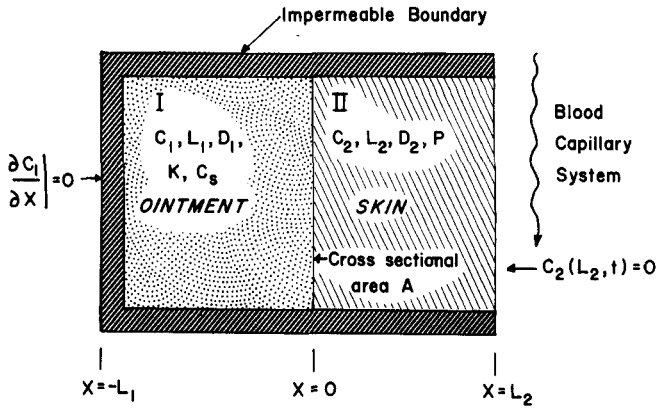

Figure 1—*Model geometry approximating the transport system.*

cesses at time $t = 0$, *i.e.*, $(\partial\epsilon/\partial t)|_{t=0} = 0$, results in:

$$K_{dis}C_{sol} = K_{cry}C_s \qquad \text{(Eq. 3)}$$

and:

$$\frac{\partial \epsilon}{\partial t} = -\frac{\kappa}{\rho_s}\epsilon^{2/3}K_{cry}(C_s - C_1) \qquad \text{(Eq. 4)}$$

This expression may be rewritten as:

$$\frac{\partial(\epsilon^{1/3} - \epsilon_0{}^{1/3})}{\partial t} = -\frac{\kappa}{3\rho_s}K_{cry}(C_s - C_1) \qquad \text{(Eq. 5)}$$

which can be integrated to yield:

$$\epsilon(x, t) = \left\{\epsilon_0{}^{1/3} - \frac{\kappa}{3\rho_s}K_{cry}\int_0^t [C_s - C_1(x, \tau)]d\tau\right\}^3 \qquad \text{(Eq. 6)}$$

The free or solution phase mass balance in the plane sheet then admits the equation[1]:

$$A\,\Delta x\frac{\partial C_1}{\partial t} = -D_1 A\frac{\partial C_1}{\partial x}\bigg|_{x-\Delta x/2} + D_1 A\frac{\partial C_1}{\partial x}\bigg|_{x+\Delta x/2} - \frac{\partial[\rho_s A\,\Delta x\epsilon(x, t)]}{\partial t} \qquad \text{(Eq. 7)}$$

or, in words, the net instantaneous free drug mass gain in the sheet is equal to the mass flux in minus the mass flux out plus the source mass flux into the solution phase from the suspended phase. Substitution for $\rho_s A\,\Delta x[\partial\epsilon(x, t)/\partial t]$ from Eq. 4 into Eq. 7, with subsequent passage to the limit as $\Delta x \to 0$, yields the solution phase concentration distribution rule in Medium I:

$$\frac{\partial C_1}{\partial t} = D_1\frac{\partial^2 C_1}{\partial x^2} + K(C_s - C_1)\left\{1 - \frac{K}{3\rho_s\epsilon_0}\int_0^t [C_s - C_1(x, \tau)]d\tau\right\}^2 \qquad \text{(Eq. 8)}$$

for $t > 0$ and $-L_1 < x < 0$ with K defined as:

$$K = \kappa K_{cry}\epsilon_0{}^{2/3} \qquad \text{(Eq. 9)}$$

Based upon mass balance considerations at time $t = 0$, it is not too difficult to show that:

$$\epsilon_0 = \frac{\frac{M_{DT}}{AL_1} - C_s}{\rho_s - C_s} \qquad \text{(Eq. 10)}$$

for $C_s \leq (M_{DT}/AL_1) \leq \rho_s$, where M_{DT} is equal to the total drug mass in the solution plus suspended phases at time $t = 0$, and AL_1 is the total volume of the ointment slab.

While Eq. 8 incorporates the realistic ideas of source area changes with time and a decreasing local solvent concentration with an increasing local free phase drug concentration, it is nonlinear and thus out of the realm of classical linear problem solution methods such as integral transforms and eigenfunction expansion.

The analysis presented later in this paper concerns a linear approximation to Eq. 8 valid for small values of time[2].

Since all physical parameters of the dissolution process are positive and $C_s - C_1(x, t) \geq 0$ for all (x, t) such that $-L_1 < x < 0$ and $t > 0$, the source function defined in Eq. 8 is a strictly monotone decreasing function of increasing time t, making the local source term less important; *i.e.*, locally, the source contributes less and less to the overall drug distribution process as time goes on. Hence, setting the source function term equal to 1.0 for all $t > 0$ and $-L_1 < x < 0$, as is done in the remainder of this paper, generates an upper bound on the actual physical process. That is, the assumption is made that the free phase drug concentration distribution in the ointment slab obeys the linearized distribution rule:

$$\frac{\partial C_1}{\partial t} = D_1\frac{\partial^2 C_1}{\partial x^2} + K(C_s - C_1) \qquad -L_1 < x < 0 \qquad t > 0 \qquad \text{(Eq. 11)}$$

By proceeding formally in an analogous manner in Medium II, the solution phase concentration distribution rule can be shown to be:

$$\frac{\partial C_2}{\partial t} = D_2\frac{\partial^2 C_2}{\partial x^2} \qquad t > 0 \qquad 0 < x < L_2 \qquad \text{(Eq. 12)}$$

The following initial conditions are assumed:

$$C_1(x, 0+) = C_s \qquad -L_1 \leq x < 0 \qquad \text{(Eq. 13)}$$

and:

$$C_2(x, 0+) = 0 \qquad 0 < x < L_2 \qquad \text{(Eq. 14)}$$

and the following boundary conditions are assumed:

$$C_1(0, t) = PC_2(0, t) \qquad t > 0 \qquad \text{(Eq. 15)}$$

$$D_1\frac{\partial C_1(0, t)}{\partial x} = D_2\frac{\partial C_2(0, t)}{\partial x} \qquad t > 0 \qquad \text{(Eq. 16)}$$

$$\frac{\partial C_1}{\partial x}\bigg|_{x=-L_1} = 0 \qquad t \geq 0 \qquad \text{(Eq. 17)}$$

and:

$$C_2(L_2, t) = 0 \qquad t \geq 0 \qquad \text{(Eq. 18)}$$

The coefficients D_1 and D_2 are assumed to be constant in this model and are, respectively, the solution phase diffusion coefficients in Media I and II (square centimeters per second), while P is the equilibrium coefficient of partition between solution concentrations in Media I and II. The authors were unable to find this particular mass transport system or its heat conduction analog listed in the literature or in standard references (1, 2, 17, 18). Churchill (19) considered a similar problem and used Laplace transform techniques, which led to a solution of the system by operational methods[3].

A paper (20) important to this discussion reported the conduction of heat in a semi-infinite solid of two different materials.

Laplace transform techniques lead to the following forms for the solution phase drug concentration distributions. In Medium I (ointment):

$$C_1(x, t) = C_s - C_s\frac{\cosh\left[(L_1 + x)\sqrt{\frac{K}{D_1}}\right]}{\cosh\left(L_1\sqrt{\frac{K}{D_1}}\right) + P\sqrt{\frac{KD_1L_2{}^2}{D_2{}^2}}\sinh\left(L_1\sqrt{\frac{K}{D_1}}\right)} + C_s\sum_{n=1}^{\infty}\frac{\sin(2\beta_n)\cosh\left(\frac{L_1 + x}{L_2}\sqrt{\frac{D_2}{D_1}}\sqrt{\frac{K}{D_2}L_2{}^2 - \beta_n{}^2}\right)\exp[-(\beta_n{}^2D_2t/L_2{}^2)]}{\beta_n\Delta_n\cosh\left(\frac{L_1}{L_2}\sqrt{\frac{D_2}{D_1}}\sqrt{\frac{K}{D_2}L_2{}^2 - \beta_n{}^2}\right)} \qquad \text{(Eq. 19)}$$

for $-L_1 \leq x < 0$ and $t > 0$. In Medium II:

$$C_2(x, t) = C_s\frac{\sqrt{\frac{KD_1L_2{}^2}{D_2{}^2}}\left(1 - \frac{x}{L_2}\right)\sinh\left(L_1\sqrt{\frac{K}{D_1}}\right)}{\cosh\left(L_1\sqrt{\frac{K}{D_1}}\right) + P\sqrt{\frac{KD_1L_2{}^2}{D_2{}^2}}\sinh\left(L_1\sqrt{\frac{K}{D_1}}\right)} + \frac{2C_s}{P}\sum_{n=1}^{\infty}\frac{\cos\beta_n\sin\left[\beta_n\left(1 - \frac{x}{L_2}\right)\right]\exp[-(\beta_n{}^2D_2t/L_2{}^2)]}{\beta_n\Delta_n} \qquad \text{(Eq. 20)}$$

where β_n is the nth zero of the transcendental equations:

$$\cot\beta + \frac{P\sqrt{\frac{D_1}{D_2}}\sqrt{\frac{K}{D_2}L_2{}^2 - \beta^2}}{\beta}\tanh\left(\frac{L_1}{L_2}\sqrt{\frac{D_2}{D_1}}\sqrt{\frac{K}{D_2}L_2{}^2 - \beta^2}\right) = 0 \qquad \text{(Eq. 21)}$$

for $0 < \beta \leq L_2\sqrt{K/D_2}$, and:

$$\cot\beta - \frac{P\sqrt{\frac{D_1}{D_2}}\sqrt{\beta^2 - \frac{K}{D_2}L_2{}^2}}{\beta}\tan\left(\frac{L_1}{L_2}\sqrt{\frac{D_2}{D_1}}\sqrt{\beta^2 - \frac{K}{D_2}L_2{}^2}\right) = 0 \qquad \text{(Eq. 22)}$$

[1] The reviewer correctly pointed out that, as $\epsilon \to 0$, D_1 will be a variable of position and time and Medium I will probably undergo contraction. While these assumptions will be dealt with in future work, they are not included in this first approximation model.

[2] The full numerical analysis will be the subject of a later paper in this series.

[3] The solution procedure is to be published elsewhere.

for $\beta \geqq L_2\sqrt{K/D_2}$, and where:

$$\Delta_n = 1 + P\frac{L_1}{L_2}\sin^2\beta_n\left[1 - \sqrt{\frac{D_1}{D_2}}\tanh^2\left(\frac{L_1}{L_2}\sqrt{\frac{D_2}{D_1}}\sqrt{\frac{K}{D_2}L_2^2 - \beta_n^2}\right)\right] + P\sqrt{\frac{D_1}{D_2}}\frac{KL_2^2}{\beta_n^2 D_2}\frac{\sin^2\beta_n \tanh\left(\frac{L_1}{L_2}\sqrt{\frac{D_2}{D_1}}\sqrt{\frac{K}{D_2}L_2^2 - \beta_n^2}\right)}{\sqrt{\frac{K}{D_2}L_2^2 - \beta_n^2}} \quad \text{(Eq. 23)}$$

While the concentration distributions (formal solutions) are important for some work, two other important formulas to obtain are the cumulative drug mass taken up by the receptor phase (blood in some cases), $M_{but}(t)$, and the cumulative mass loss from the ointment, $M_1(t)$. These two drug mass distribution functions are defined as:

$$M_{but}(t) = \int_0^t \left(-D_2 A \left.\frac{\partial C_2}{\partial x}\right|_{x=L_2}\right) d\tau \quad \text{(Eq. 24)}$$

and:

$$M_1(t) = \int_0^t \left(-D_1 A \left.\frac{\partial C_1}{\partial x}\right|_{x=0}\right) d\tau \quad \text{(Eq. 25)}$$

Performing the indicated partial differentiations with subsequent evaluations of these results at $x = L_2$ and $x = 0$, respectively, obtains (after some algebra and use of Eqs. 19–22):

$$M_{but}(t) = AC_s\sqrt{KD_1}t\frac{\sinh\left(L_1\sqrt{\frac{K}{D_1}}\right)}{\cosh\left(L_1\sqrt{\frac{K}{D_1}}\right) + P\sqrt{\frac{KD_1L_2^2}{D_2^2}}\sinh\left(L_1\sqrt{\frac{K}{D_1}}\right)} + \frac{2AL_2C_s}{P}\sum_{n=1}^{\infty}\frac{\cos\beta_n\{1 - \exp[-(\beta_n^2 D_2 t/L_2^2)]\}}{\beta_n^2\Delta_n} \quad \text{(Eq. 26)}$$

and:

$$M_1(t) = AC_s\sqrt{KD_1}t\frac{\sinh\left(L_1\sqrt{\frac{K}{D_1}}\right)}{\cosh\left(L_1\sqrt{\frac{K}{D_1}}\right) + P\frac{L_2}{L_1}\sqrt{KD_1}\sinh\left(L_1\sqrt{\frac{K}{D_1}}\right)} + \frac{2AL_2C_s}{P}\sum_{n=1}^{\infty}\frac{\cos^2\beta_n}{\beta_n^2\Delta_n}[1 - \exp(-\beta_n^2 D_2 t/L_2^2)] \quad \text{(Eq. 27)}$$

Uniform convergence of the resulting series is confirmed by an analysis similar to that mentioned by Churchill (19).

Before pursuing an in-depth study of these least upper bounding distributions for published literature values of the transport parameters, a brief discussion is included for the following asymptotic forms to which the relative cumulative receptor phase uptake, $\mu_{but}(t) = M_{but}(t)/M_0$, and/or the cumulative drug mass loss from the ointment, μ_1, converge in the limit of small and large K values.

For finite D_1 and D_2 values, $0 \leq K \leq 0.25\,(D_1/L_1^2)$, $t \geqq (4L_2^2/\beta_1^2 D_2)$, and $M_0 = AL_1C_s$:

$$\mu_{but}(t) \sim \frac{Kt}{1 + KP\frac{L_1L_2}{D_2}} + 2\left(\frac{L_2}{L_1}\right)\frac{\cos\beta_1}{P\beta_1^2\Delta_1} \quad \text{(Eq. 28)}$$

and:

$$\mu_1(t) \sim \frac{Kt}{1 + KP\frac{L_1L_2}{D_2}} + 2\left(\frac{L_2}{L_1}\right)\frac{\cos^2\beta_1}{P\beta_1^2\Delta_1} \quad \text{(Eq. 29)}$$

Again for finite D_1 and D_2 values, $K \geqq 25\,(D_1/L_1^2)$, $t \geqq (4L_2^2/\beta_1^2 D_2)$, and $M_0 = AL_1C_s$:

$$\mu_{but}(t) \sim \frac{\sqrt{KD_1}}{L_1}\frac{t}{1 + P\frac{L_2}{D_2}\sqrt{KD_1}} + 2\frac{L_2}{L_1}\frac{\cos\beta_1}{P\beta_1^2\Delta_1} \quad \text{(Eq. 30)}$$

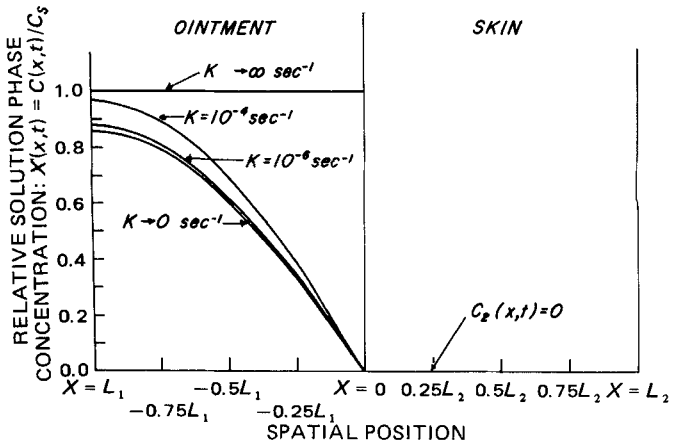

Figure 2—*Plots of relative solution phase drug concentration distribution in the ointment and the skin when* $D_2 \to \infty$ *and time* t = 600 *sec* ($D_1 = 10^{-9}$ *cm²/sec).*

and:

$$\mu_1(t) \sim \frac{\sqrt{KD_1}}{L_1}\frac{t}{1 + P\frac{L_2}{D_2}\sqrt{KD_1}} + 2\frac{L_2}{L_1}\frac{\cos^2\beta_1}{P\beta_1^2\Delta_1} \quad \text{(Eq. 31)}$$

An ointment–drug–stirred water system represents the extreme case of large D_2. Mathematically, if $D_2 \to \infty$, the perfect sink at $x = L_2$ becomes operable throughout the entire skin region; *i.e.*, there is no barrier to overcome. The practical situation might be the topical application of a product containing drug suspended in a vehicle directly to the capillary system exposed due to skin abrasion. Thus, in the limit as $D_2 \to \infty$, $K \geqq 25\,(D_1/L_1^2)$, and $t \geqq 5/[(9\pi^2 D_1/4L_1^2) + K]$, the relative receptor phase uptake of drug mass, μ_{but}, is:

$$\mu_{but} \sim \frac{\sqrt{D_1K}}{L_1}t + \frac{1}{2L_1}\sqrt{\frac{D_1}{K}} \quad \text{(Eq. 32)}$$

RESULTS AND DISCUSSION

Since the main purpose of formulating this mathematical model is to aid in understanding the passive diffusion process (one type of mass transport process) of a drug from a suspension dosage form through the dermal layer to the blood capillary bed, attention is now turned to an evaluation of the equations of the model itself.

The drug cortisone was chosen as an example of a commonly used drug in an ointment form, and a literature search revealed the following estimates for the model parameters. For the partition coefficient and average skin diffusion coefficient:

$$P = \frac{K_{hex}}{K_{skin}} = \frac{0.28}{8.5} = \frac{1}{30} \quad \text{(Eq. 33)}$$

and:

$$D_2 = 10^{-12}\ \text{cm}^2/\text{sec} \quad \text{(Eq. 34)}$$

respectively (21). From a diffusion path length viewpoint, the effective composite layer through which substances must diffuse to enter the bloodstream was estimated to be about 200 μm (21). However, the main skin barrier in most cases of percutaneous absorption is the stratum corneum, reported to be about 10 μm in depth. Since the thickness of the stratum corneum varies with its location on the body, a thickness of 20 μm for L_2 is used in Fig. 2 as a first approximation of the main skin barrier. Variable pathways of diffusion and differing diffusion rates through appendages in the skin (21) are not considered, since Medium II in Fig. 2 is assumed to be homogeneous in the model, although skin is, in reality, a heterogeneous system. This "artificial" membrane, although not an exact equivalent of skin, is used as an approximation in solving the model.

Let it be assumed that a thinly applied ointment or salve is also around 20 μm in thickness. Thus, $L_1 = 2 \times 10^{-3}$ cm. The authors were unable to find any specific diffusion coefficient data on cortisone in different lipophilic bases. However, the value of $D_1 = 10^{-9}$ cm²/sec was finally chosen, since it is less than the average value for diffusion of steroids in aqueous solution and greater than diffusion through the skin barrier. The knowledge that the vehicle composition can influence the release (22)

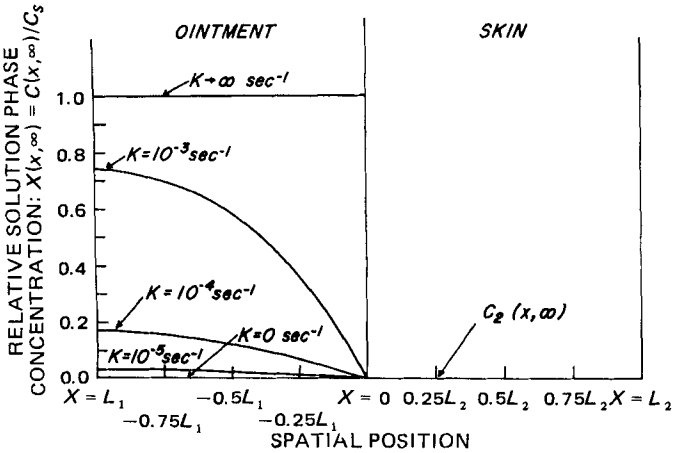

Figure 3—*Plots of relative solution phase drug concentration distribution in the ointment and the skin when* $D_2 \to \infty$ *and time* $t \to \infty$, i.e., *"steady state"* ($D_1 = 10^{-9}$ *cm*^{2}*/sec).*

and physiological response (23) for some steroids makes this value a reasonable estimate.

Finally, the dissolution rate constant K, for which the authors were unable to find any specific values for cortisone in semisolid vehicles, is used as an active parameter. For the remainder of this paper, K is simply assigned order of magnitude values.

Substitution of these parameter values into the appropriate equations, *e.g.*, Eqs. 19, 20, and 26, allows the drug concentration distributions in the solution phases of both media to be estimated at any time after drug application. In addition, the drug mass uptake as a function of time also can be calculated. The discussion of these distributions is carried out starting with the extreme cases ($D_1 \to \infty$, $D_2 \to \infty$, or any subcase thereof) and progressing toward the most general situation, namely, an evaluation of Eqs. 19, 20, and 26.

Extreme Case $D_2 \to \infty$—It is assumed that mass transport through the skin is carried out infinitely fast, as would approximately be the case for some *in vitro* studies or if there is no skin covering the capillary bed and the dosage form is applied directly to the capillary bed. Evaluation of the limiting forms of Eqs. 19, 20, and 26 gives the concentration distributions shown in Figs. 3 and 4 and the relative cumulative drug mass uptake by the blood shown in Fig. 5, respectively. This type of mass transport system may be an example of ointment or salve applied directly to an open wound or abrasion.

Mathematically, the perfect sink boundary condition $C_2(L_2, t) = 0$ is moved left to $C_1(0, t) = 0$ (Fig. 2). Also, as $K \to \infty$, the solution phase concentration phase distribution in Medium I (the ointment) tends to stay at saturation concentrations, C_s, as expected. The distribution curves shown in Fig. 3 are all for one fixed time, $t = 600$ sec, after ointment application. The long time or steady-state concentration distributions to which $C_1(x, t)$ converges for the various K values chosen in this work are shown in Fig. 3.

The cumulative mass of drug taken up by the blood for this special case is shown in Fig. 4. If $K = 0$, then only the finite amount of original solution phase drug in the ointment can be taken up by the blood, because this quantity is the only drug mass available to be taken up. However, if $K > 0$, then the blood uptake of drug distribution over time is seen. The abscissa in all time plots is the square root of time.

This time scale was chosen because it compresses the abscissa, allowing a greater time period to be shown on the graph, and because some models of diffusion[4] have resulted in equations where the total amount of drug transferred from the donor phase is linearly dependent on time$^{1/2}$.

While still operating under the assumption that $D_2 \to \infty$, the asymptotic form (Eq. 32) can be used for the relative cumulative blood uptake of drug mass, μ_{but}. Suppose that $K \geq 25\ (D_1/L_1^2)$ ($= 6.25 \times 10^{-3}$ sec^{-1} based on D_1 and L_1 used for Figs. 2–4) and time t is such that:

$$t \geq t_{min} = 5 \Big/ \left(\frac{9\pi^2 D_1}{4L_1^2} + K\right) \qquad \text{(Eq. 35)}$$

This time would be variable for Figs. 2–4, depending on the value of K. The t_{min} would be 42.3 sec for $K = 10^{-2}$ sec^{-1}. Then the asymptotic form

[4] A comparison among different diffusion models for the predicted release of drug is included in Part II of this series (24).

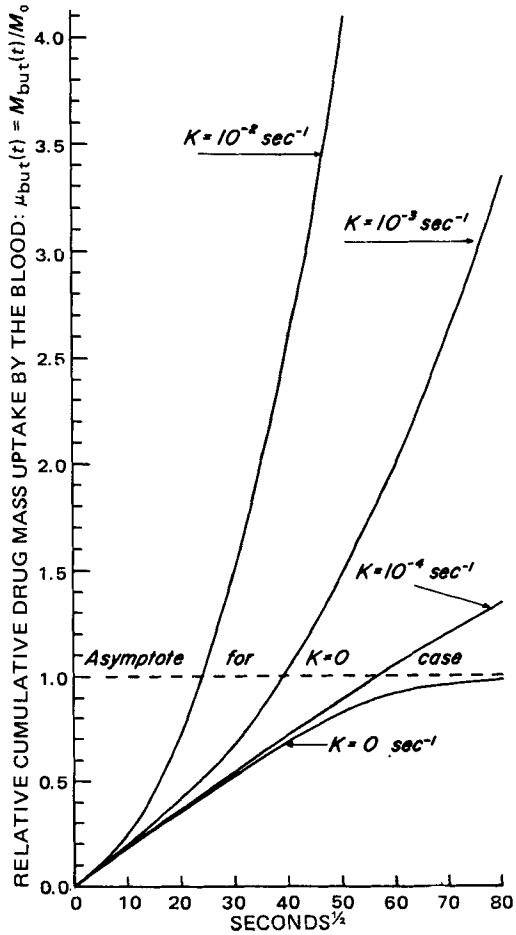

Figure 4—*Plots of relative cumulative drug mass uptake by the blood,* $\mu_{but}(t) = M_{but}(t)/M_0$, $M_0 = AL_1C_s$, *for* $D_2 \to \infty$. *The ordinate is linear while the abscissa is the square root of time with each curve carrying its respective* K *value* ($D_1 = 10^{-9}$ *cm*^{2}*/sec).*

for μ_{but} (Eq. 32) demonstrates directly that under these conditions μ_{but} is proportional to the total drug mass, M_{DT}, to the one-third power, close to agreement with the classical model for drug release from ointments (9). Since:

$$K = \kappa K_{cry} \epsilon_0^{2/3} \qquad \text{(Eq. 36)}$$

and:

$$\epsilon_0 = \left(\frac{M_{DT}}{AL_1} - C_s\right) \Big/ (\rho_s - C_s) \qquad \text{(Eq. 37)}$$

K is directly proportional to $M_{DT}^{2/3}$ and, hence, $\mu_{but} \propto M_{DT}^{1/3}$. Note, however, that the amount of drug taken up by the receptor phase is only predicted to be proportional to the cube root of the total drug mass when the restrictions on K and t are satisfied.

Recasting the classical equation into the notation of the proposed model gives:

$$\mu_H = \frac{\sqrt{D_1 t \left(2\frac{M_{DT}}{M_0} - 1\right)}}{L_1} \qquad \text{(Eq. 38)}$$

where the subscript H stands for the classical model (9).

The major difference between μ_{but} and μ_H is that μ_{but} is proportional to t for large values of time while μ_H is proportional to $t^{1/2}$ for all time values. Furthermore, in the case of small values of time, μ_H is proportional to $t^{1/2}$ while the asymptotic form for μ_{but} for small time can easily be shown to be root t like in this linearized model; that is:

$$\mu_{but} \sim \frac{2\sqrt{D_1 t}}{L_1}\left[1 + \frac{Kt}{3} - O(Kt)^2\right] \qquad \text{(Eq. 39)}$$

where the O notation of Heaviside has been used to collect all higher order terms.

No matter which of these equations is assumed to describe the drug release phenomenon, they are all invalid for values of time $t > t_{C_s}$, the

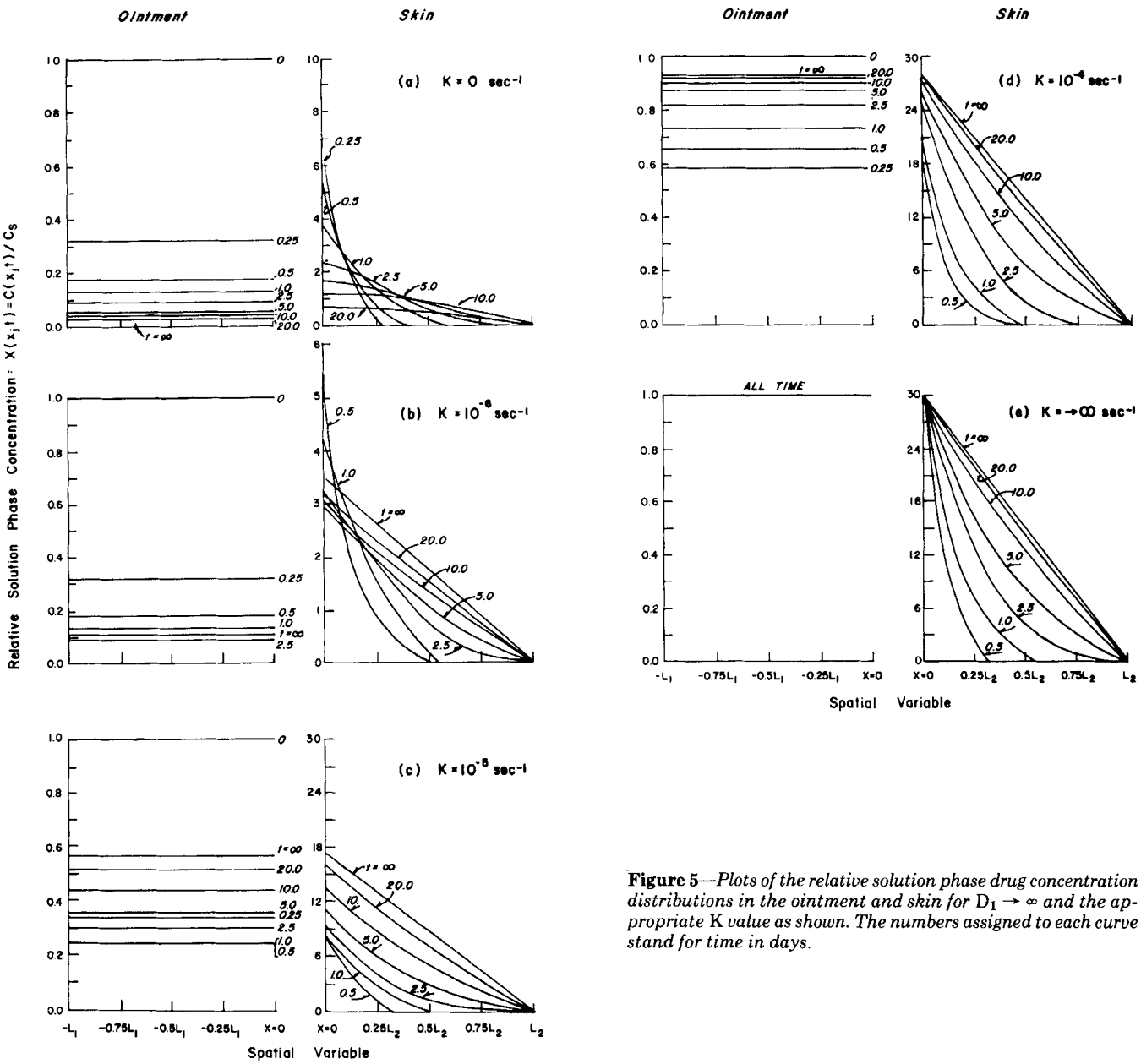

Figure 5—*Plots of the relative solution phase drug concentration distributions in the ointment and skin for* $D_1 \to \infty$ *and the appropriate* K *value as shown. The numbers assigned to each curve stand for time in days.*

exhaustion of source time. The analytical expressions derived here for the cumulative drug mass uptake by the blood are only useful for estimation purposes, since they are actually upper bounding distributions for realistic release situations.

A cursory look at preliminary numerical analysis data for the more realistic model (Eq. 8), *i.e.*, if the source function is *not* constrained at 1.0 but is free to vary in the natural way, shows that, depending upon the magnitude of K, the cumulative relative drug mass uptake by the blood distribution begins to flatten out considerably before t_{C_s} is reached. The preliminary data also show that, for any fixed value of time $t > 0$, μ_{but}, when looked upon as a function of M_{DT}, increases monotonically but nonlinearly toward an asymptotic bounding curve. That is, the release does not continue to be proportional to $(M_{DT})^{1/3}$ at all times, as predicted by Eq. 32, but a maximum release rate is predicted by Eq. 8 with increasing M_{DT}, as reported experimentally (13).

Finally, it should be seen that even in the upper bounding case (Eq. 32), when the crystal or powder density increases, as would be the case in using a finer grind of powder, *i.e.*, a larger surface area to volume ratio, κ increases. Moreover, since μ_{but} is proportional to $\kappa^{1/2}$ (for time t sufficiently large), μ_{but} increases with the increasing surface area of the suspended drug. This increase in the drug release rate with an increasing surface area to volume ratio (smaller suspended particles) has been observed experimentally (13, 24, 25).

For this special case ($D_2 \to \infty$), it can be seen that the relative cumulative blood uptake of drug mass, μ_{but}, is: (*a*) rather linearly dependent upon total drug mass for small time t, (*b*) almost proportional to $t^{1/2}$ for small t, (*c*) linearly dependent upon t for t large, (*d*) proportional to $(M_{DT})^{1/3}$ for large M_{DT} and moderate to large values of time t, and (*e*) increasing accordingly as the surface area to volume ratio of the suspended drug increases for both small and large time values. Another physical factor affecting the release rate is the Arrhenius-type temperature dependence of K_{dis} and K_{cry}; *i.e.*, as T (absolute temperature) goes up, the release rate increases.

Extreme Case $D_1 \to \infty$—This case corresponds to having the transport rate-limiting step occurring in the skin, which is a diffusion barrier-type process. The solution phase concentration distributions are given by limiting forms of Eqs. 19 and 20. The large D_1 limiting form of Eq. 26 is evaluated to demonstrate the cumulative drug mass uptake by the blood. Other special subcases ($K = 0$ and $K \to \infty$) are included here for reference purposes.

Before any actual evaluation of the limiting forms of Eqs. 19, 20, and 26 can be made, the first several zeros, β_n, of the associated transcendental equation (limiting form of Eqs. 21 and 22) must be found for the parameter values of interest. The first 12 zeros for the various values of K and the other designated parameters are listed in Table I.

When using the β values in Table I, the solution phase concentration phase distributions are obtained by evaluating the appropriate distribution equations. Figure 5 was prepared as an aid in understanding the

Table I—Set of First 12 Zeros of the Transcendental Expression: $\beta \cot \beta - P(L_1/L_2)(\beta^2 - K/D_2 L_2^2) = 0, 0 < \beta < \infty$

Zero (β_i) i	K, sec^{-1}					
	0[a]	10^{-7}	10^{-6}	10^{-5}	10^{-4}	∞
1	1.5202	1.5286	1.6007	2.0880	2.9214	3.1416
2	4.5615	4.5643	4.5891	4.8272	5.8368	6.2832
3	7.6057	7.6073	7.6217	7.7670	8.7435	9.4248
4	10.6544	10.6554	10.6652	10.7648	11.6435	12.5664
5	13.7086	13.7094	13.7164	13.7890	14.5448	15.7080
6	16.7691	16.7697	16.7750	16.8298	17.4585	18.8850
7	19.8362	19.8366	19.8408	19.8831	20.3943	21.9911
8	22.9098	22.9102	22.9134	22.9467	23.3572	25.1327
9	25.9897	25.9900	25.9926	26.0191	26.3473	28.2743
10	29.0754	29.0757	29.0778	29.0992	29.3620	31.4159
11	32.1665	32.1667	32.1684	32.1859	32.3976	34.5575
12	35.2625	35.2627	35.2641	35.2784	35.4502	37.6991

[a]This set of zeros follows from setting $K = 0$, yielding the well-known form $\beta \tan \beta - (L_2/PL_1) = 0$.

effect of varying the dissolution rate coefficient K upon the overall system. The distribution curves in Fig. 5 clearly show that as K sequences in value from $K = 0$ to $K \to \infty$, the solution phase concentration in the skin builds up in time toward the well-known constant negative gradient situation. The magnitude of the slope of the "steady-state" distribution clearly depends upon the value of K. Linear ordinates and abscissa axes are used throughout Fig. 5. The much larger ordinate numbers for Medium II (the skin) are simply a reflection of P being a 30:1 ratio of skin to ointment; *i.e.*, the drug cortisone likes to be in the solution phase in the skin much better than in the ointment vehicle for the conditions described.

Initially (small times, $t < \frac{1}{4}$ day), drug is lost rapidly from the ointment to the surface layers of the skin. Indeed, if $K = 0$ (Fig. 5*a*), then about 87% of the total "available" drug has been lost from the ointment by the end of Day 1 and resides in the outermost region of the skin. Since there is no dissolution from the suspension when $K = 0$, the only available drug is that in the solution phase initially. With the blood capillary system supposedly forming a perfect sink for the drug, both C_1 and $C_2 \to 0$ as time $t \to \infty$.

In cases where $K > 0$, a finite steady state in the skin is easily observable as time $t \to \infty$. At small times, the same apparent rapid loss of drug from the ointment to the skin is seen. However, as time progresses, some drug released by the ointment at previous times is being replaced by the finite dissolution rate process occurring in the suspension (Medium I).

Another interesting phenomenon that occurs as K increases is the generation of a "deficit" zone in the solution phase of the ointment. The drug in the ointment appears to be lost to the skin too rapidly to be replaced by the dissolution from the suspension until a certain solution phase concentration balance between the drug concentration in the solution phase of the ointment and the solution phase in the skin is reached (Figs. 5*b*–5*d*). The time at which this turning point occurs is dependent on K, as expected. The magnitude of the initial drop and the subsequent return to a long time or steady-state level are also dependent on K.

With the cumulative drug mass uptake by the blood distributions (Fig. 6), it is much easier to see why there is little drug mass transmitted to the blood until after time $t = 4$ days. In fact, it is easy to show that if the drug solution phase concentration at the boundary $x = 0$ remains constant at the relative concentration of 1.0 in the ointment (30.0 on the surface of the skin), it takes at least 3.5 days for the concentration at a point 20 μm from this barrier to reach 1% of the surface concentration. A clear indication of the barrier or rate-limiting action of the skin for this particular drug is seen by a careful study of Figs. 5 and 6. The buildup of drug in Medium II (the skin), which is predicted by this model and shown in Fig. 5, is in agreement with the recognized fact that the stratum corneum is a reservoir for drugs (26).

The cumulative drug mass uptake by the blood (Fig. 6) is bounded above for the case $K = 0$ by the asymptote $M_0 = C_s A L_1$. The same reason for this asymptote holds as in the previously discussed limiting case, $D_2 \to \infty$ and D_1 remaining finite. For values of $K > 0$, the drug mass delivered to the blood increases rapidly for values of time t greater than 9 days (77.76×10^4 sec).

Figure 7 demonstrates the relative cumulative drug mass loss from the ointment, $\mu_1(t) = [M_1(t)/M_0]$ (based upon the limiting form of Eq. 27).

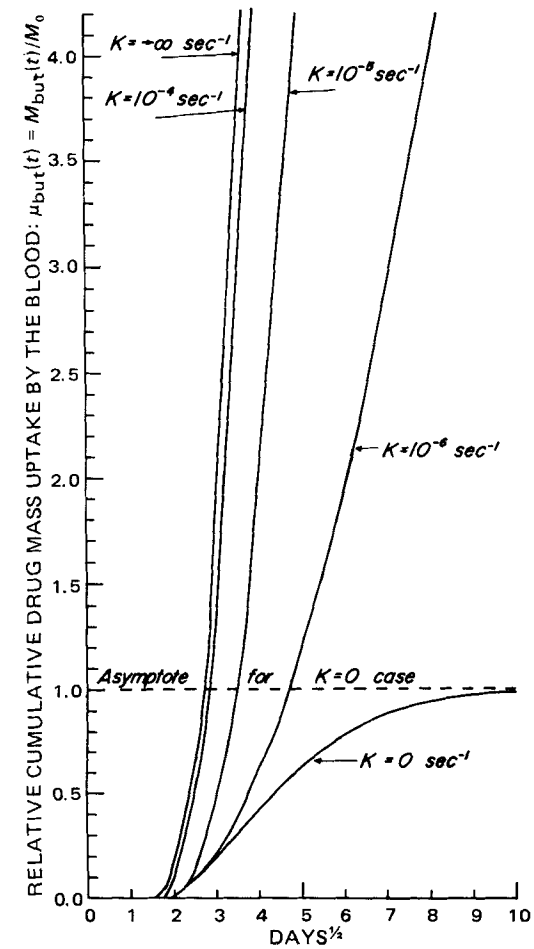

Figure 6—*Plots of the relative cumulative drug mass uptake by the blood, $\mu_{but}(t)$ (see Fig. 4), for $D_1 \to \infty$ and the appropriate K value as shown. The ordinate is linear in drug mass units, M_0, while the abscissa is the square root of time.*

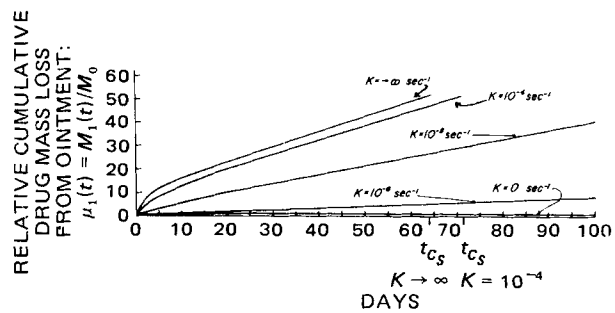

Figure 7—*Plots of the relative cumulative drug mass loss from the ointment under the assumption $D_1 \to \infty$. Both ordinate and abscissa are linear scales. The curves carry their appropriate K values.*

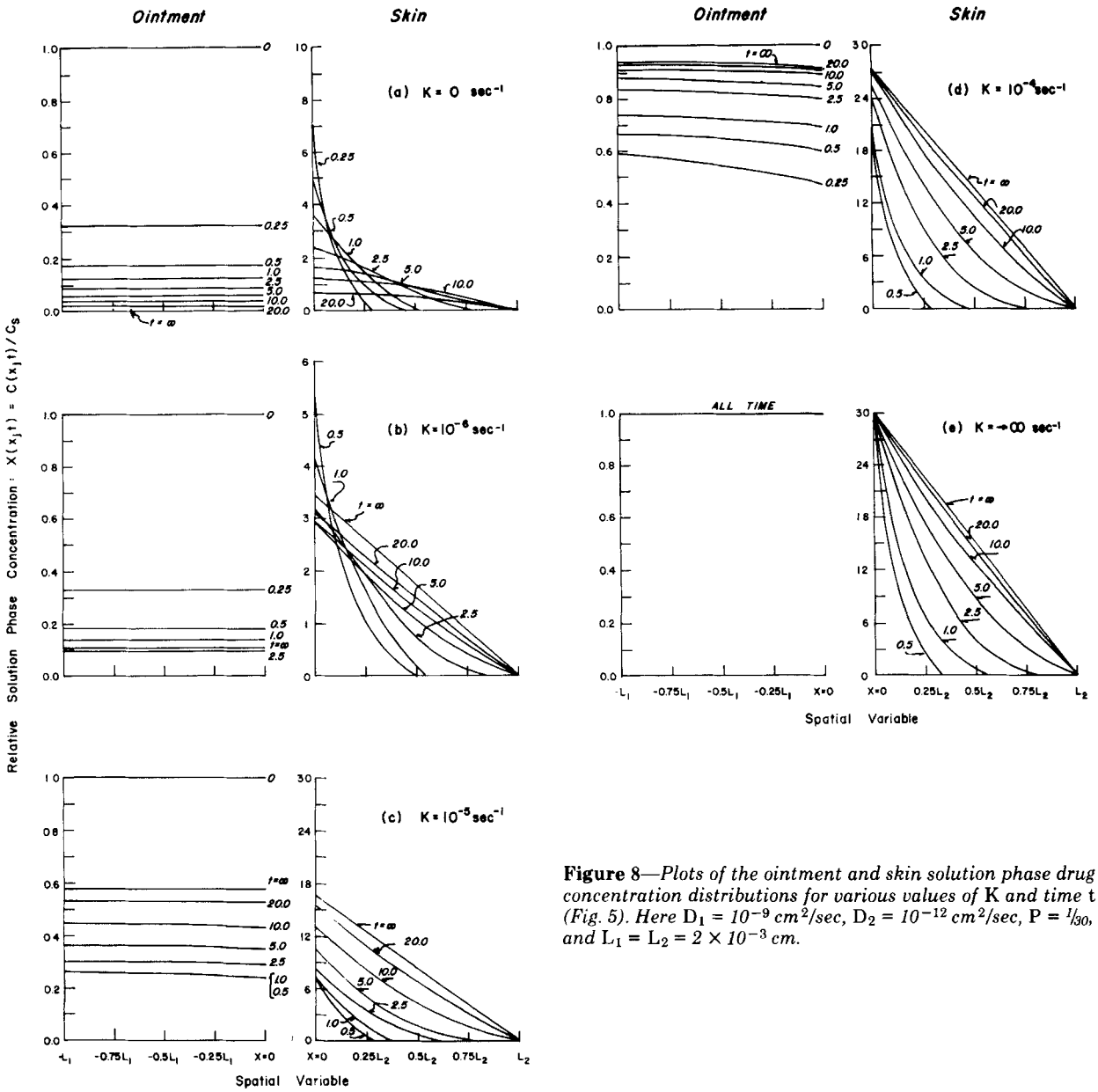

Figure 8—*Plots of the ointment and skin solution phase drug concentration distributions for various values of* K *and time* t *(Fig. 5). Here* $D_1 = 10^{-9}$ *cm²/sec,* $D_2 = 10^{-12}$ *cm²/sec,* P = 1/30, *and* $L_1 = L_2 = 2 \times 10^{-3}$ *cm.*

The scales on this plot are both linear. Suppose, for example, that at time $t = 0$ there exist 50 initial M_0 units of drug in the suspended phase of the ointment and one M_0 unit of drug in the solution phase of the ointment for a total of 51 M_0 units of drug mass. Under the hypothesis of $D_1 \to \infty$, with all other parameters as previously stated, the time t_{C_s} (the time at which 50 M_0 units of drug mass have been lost from the ointment) is easily seen to be 65 days for $K \to \infty$ sec^{-1}, 69 days for $K = 10^{-4}$ sec^{-1}, and > 100 days for $0 < K < 10^{-5}$ sec^{-1}.

If a smaller value of the total initial drug mass is used, then the appropriate values of t_{C_s} can be read off the graphs shown in Fig. 7. The curves in Fig. 7 are peculiar to $D_2 = 10^{-12}$ cm^2/sec. If some other value of D_2 is used, then the relative cumulative mass loss distributions also would be different from those shown in Fig. 7.

General Case D_1 and D_2 Both Finite—As in the special cases, a set of zeros, β_n, associated with the particular transcendental Eqs. 21 and 22 must be obtained. The first 12 zeros of the general case for these transcendental equation(s) for the parameter values $D_1 = 10^{-9}$ cm^2/sec, $D_2 = 10^{-12}$ cm^2/sec, $L_1 = L_2 = 2 \times 10^{-3}$ cm, $P = 1/30$, and several orders of magnitude values of K are listed in Table II.

A careful comparison of the β_n values in Table II with those (for a corresponding K value) in Table I reveals that one should not expect any major differences in the solution phase concentration distributions in either the ointment or the skin (Fig. 2). In fact, an order of magnitude sequence of D_1 values with D_2 fixed at $D_2 = 10^{-12}$ cm^2/sec, *e.g.*, ($D_1 =$: $10^{-9}, 10^{-8}, 10^{-7}, \ldots$), gives essentially no differences between the solution phase concentration distributions for these D_1 values and those obtained under the special case $D_1 \to \infty$. This fact follows from the physical reasoning that, as $D_1 \to \gg D_2$, diffusion across the skin barrier becomes the rate-limiting process. However, if D_2 is about the same order of magnitude as the D_1 value ($D_1 = 10^{-9}$ cm^2/sec), then considerable differences would arise between the general case $D_2 \cong D_1 = 10^{-9}$ cm^2/sec and the special case $D_2 = 10^{-9}$ cm^2/sec and $D_1 \to \infty$.

Figures 8 and 9 summarize the solution phase concentration distributions in the ointment and the skin and the cumulative drug mass blood uptake, respectively. The close similarity of the distributions shown in Figs. 8 and 9 with those in Figs. 5 and 6 is expected as explained. Table III shows some selected values of $\chi_1(x, t)$ and $\chi_1(x, t) = C_1(x, t)/C_s$ and the relative solution phase concentration distribution for several values of (x, t) and K. Note that the slope

$$\left.\frac{\partial \chi_1}{\partial x}\right|_{\substack{-L_1<x<0 \\ t>0}}$$

is almost zero. Only in the case considered, $K = 10^{-4}$ sec^{-1}, does even a shallow gradient exist at small negative x values and small values of time. Somewhere between $K = 10^{-5}$ sec^{-1} and $K \to \infty$ sec^{-1} for small time values, the gradient has a finite maximum value. The spatial position of this maximum gradient lies on the boundary $x = 0$; the exact time at which this maximum occurs is primarily of academic interest and is beyond the scope of this paper.

Table II—Set of First 12 Zeros of the Transcendental Expressions:

$$\beta \cot \beta + P\sqrt{\frac{D_1}{D_2}}\sqrt{\frac{K}{D_2}L_2^2-\beta^2}\tanh\left(\frac{L_1}{L_2}\sqrt{\frac{D_2}{D_1}}\sqrt{\frac{K}{D_2}L_2^2-\beta^2}\right)=0,\ 0<\beta\leqq L_2\sqrt{\frac{K}{D_2}}$$

$$\beta \cot \beta - P\sqrt{\frac{D_1}{D_2}}\sqrt{\beta^2-\frac{K}{D_2}L_2^2}\tan\left(\frac{L_1}{L_2}\sqrt{\frac{D_2}{D_1}}\sqrt{\beta^2-\frac{K}{D_2}L_2^2}\right)=0,\ \beta>L_2\sqrt{\frac{K}{D_2}}$$

	K, sec^{-1}					
Zero (β_i)	0[a]	10^{-7}	10^{-6}	10^{-5}	10^{-4}	∞
1	1.5201	1.5286	1.6007	2.0840	2.8965	3.1416
2	4.5605	4.5633	4.5884	4.8266	5.7950	6.2832
3	7.6012	7.6028	7.6177	7.7664	8.6977	9.4248
4	10.6423	10.6435	10.6539	10.7593	11.6069	12.5664
5	13.6841	13.6850	13.6928	13.7727	14.5249	15.7080
6	16.7266	16.7273	16.7335	16.7966	17.4535	18.8850
7	19.7700	19.7706	19.7756	19.8266	20.3942	21.9911
8	22.8143	22.8148	22.8189	22.8609	23.3475	25.1327
9	25.8596	25.8600	25.8634	25.8989	26.3134	28.2743
10	28.9058	28.9061	28.9090	28.9385	29.2912	31.4159
11	31.9529	31.9532	31.9556	31.9805	32.2799	31.9529
12	35.0008	35.0010	35.0031	35.0243	35.2785	37.6991

[a] This set of zeros follows from setting $K = 0$, yielding the transcendental equation:

$$\cot \beta - P\sqrt{\frac{D_1}{D_2}}\tan\left(\frac{L_1}{L_2}\sqrt{\frac{D_2}{D_1}}\beta\right)=0$$

The model developed in this report is based on parameters known or anticipated to affect drug release. Therefore, for semisolids containing suspensions for topical application, the following are predicted to affect drug release and uptake: (*a*) powder density or particle size, (*b*) partition coefficient between the vehicle and the receptor phase, (*c*) solubility of the drug in the vehicle, (*d*) area of application, (*e*) viscosity of the vehicle (affects the diffusion coefficient), (*f*) temperature (affects release and would be different for semisolids applied rectally compared to semisolids applied to the forearm), and, (*g*) total time the material remains in contact with the receptor phase.

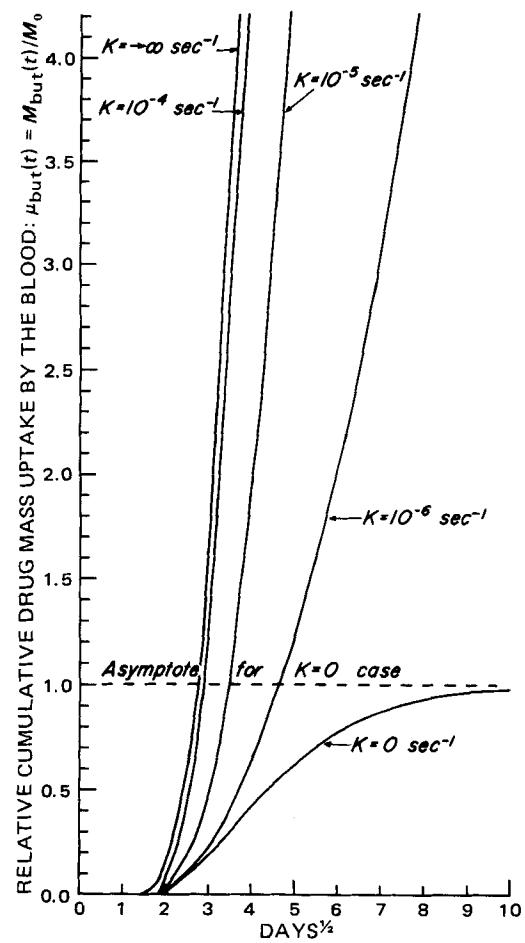

Figure 9—*Plots of the relative drug mass uptake by the blood, $\mu_{but}(t)$, versus the square root of time for the general case (Fig. 8).*

CONCLUSIONS

A general model system for the mass transport of drug in a suspension through the suspension and a permeable barrier to a perfect sink was presented. The appropriate equations for a general case and several specific cases were solved and evaluated. Drug distribution in a vehicle and a membrane and the cumulative drug mass uptake by a receptor phase were all related to the dissolution rate of the drug in the vehicle and diffusion through the vehicle and membrane for specified model conditions. If dissolution is essentially nonexistent during the time considered, then a suspension system behaves as a solution with respect to drug release. Where dissolution of the suspended drug into a semisolid vehicle is slower than diffusion, the rate of dissolution markedly influences the rate of drug release from the vehicle.

The classical model (9) for drug release from suspensions is simple to apply and describes drug release in many systems. It should certainly be used where the model requirements are satisfied. The system presented

Table III—Typical Example Values for the First Few Values of the Relative Solution Phase Concentration Distribution for Finite D_1; $D_1 = 10^{-9}$ cm^2/sec

	$\chi_1(x, t) = C_1(x, t)/C_S$			
Days	$x = -0.75L_1$	$x = -0.5L_1$	$x = -0.25L_1$	$x = 0L_1$
		$K = 0$ sec^{-1}		
0.5	0.1717	0.1711	0.1699	0.1684
1.0	0.1245	0.1242	0.1238	0.1232
2.5	0.0800	0.0800	0.798	0.0797
5.0	0.0569	0.0569	0.0568	0.0568
10.0	0.0398	0.0398	0.0397	0.0397
		$K = 10^{-6}$ sec^{-1}		
0.5	0.1823	0.1814	0.1799	0.1777
1.0	0.1408	0.1402	0.1393	0.1381
2.5	0.1081	0.1077	0.1071	0.1062
5.0	0.0984	0.0981	0.0975	0.0967
10.0	0.0999	0.0996	0.0994	0.0987
		$K = 10^{-4}$ sec^{-1}		
0.5	0.6649	0.6534	0.6339	0.6059
1.0	0.7446	0.7356	0.7202	0.6981
2.5	0.8316	0.8254	0.8149	0.8000
5.0	0.8794	0.8749	0.8673	0.8565
10.0	0.9134	0.9102	0.9047	0.8969

here is more complex and results in equations that are not simple and do not predict a simple relationship between drug release and time, particle size, or drug concentration. This model should be considered if its assumptions appear to be met and if experimental data are not described by the classical model.

The model presented here probably will provide some insight into the formulation of suspensions for application to the skin or mucous membranes. The equations presented are only valid for systems that satisfy the requirements of the model. Parameters other than dissolution rate that can affect drug release and parameter interrelationships will be investigated and discussed in a subsequent publication based on the model presented here.

REFERENCES

(1) R. M. Barrer, "Diffusion in and Through Solids," Cambridge University Press, London, England, 1941.

(2) J. Crank, "The Mathematics of Diffusion," Oxford University Press, London, England, 1956.

(3) M. H. Jacobs, "Diffusion Processes," Springer-Verlag, New York, N.Y., 1967.

(4) T. Higuchi, *J. Soc. Cosmet. Chem.*, **11**, 85 (1960).

(5) W. I. Higuchi and T. Higuchi, *J. Am. Pharm. Assoc., Sci. Ed.*, **49**, 598 (1960).

(6) T. Koizumi and W. I. Higuchi, *J. Pharm. Sci.*, **57**, 87 (1968).

(7) *Ibid.*, **57**, 93 (1968).

(8) T. Yotsuyanagi, W. I. Higuchi, and A.-H. Ghanem, *J. Pharm. Sci.*, **62**, 40 (1973).

(9) T. Higuchi, *ibid.*, **50**, 874 (1961).

(10) W. I. Higuchi, *ibid.*, **56**, 315 (1967).

(11) D. E. Wurster and P. W. Taylor, *ibid.*, **54**, 169 (1965).

(12) J. Swarbrick, "Current Concepts in the Pharmaceutical Sciences, Biopharmaceutics," Lea & Febiger, Philadelphia, Pa., 1970, pp. 265–296.

(13) J. Haleblian, R. Runkel, N. Mueller, J. Christopherson, and K. Ng, *J. Pharm. Sci.*, **60**, 541 (1971).

(14) D. O. Hayward and B. M. W. Trapnell, "Chemisorption," Butterworths, London, England, 1964.

(15) P. S. Rowler, *J. Phys. Chem.*, **39**, 221 (1935).

(16) S. S. Szinai and C. A. Hunt, *Can. J. Pharm. Sci.*, **7**, 78 (1972).

(17) H. S. Carslaw and J. C. Jaeger, "Conduction of Heat in Solids," Oxford University Press, London, England, 1959.

(18) W. Jost, "Diffusion in Solids, Liquids and Gases," Academic, New York, N.Y., 1952.

(19) R. V. Churchill, *Duke Math. J.*, **2**, 405 (1936).

(20) A. N. Lowan, *ibid.*, **1**, 94 (1935).

(21) R. J. Scheuplein, in "Pharmacology and the Skin," W. Montague, R. B. Stoughton, and E. J. Van Scott, Eds., in "Advances in Biology of Skin," vol. 12, Appleton-Century-Crofts, New York, N.Y., 1972, pp. 125–151.

(22) B. J. Poulson, E. Young, V. Coquilla, and M. Katz, *J. Pharm. Sci.*, **57**, 928 (1968).

(23) J. Ostrenga, C. Steinmetz, and B. J. Poulson, *ibid.*, **60**, 1175 (1971).

(24) F. T. Lindstrom and J. W. Ayres, *ibid.*, **66**, 662 (1977).

(25) C. W. Barrett, J. W. Jadgraft, G. A. Caron, and I. Sarkany, *Br. J. Dermatol.*, **77**, 576 (1965).

(26) C. F. H. Vickers, in "Pharmacology and the Skin," W. Montague, R. B. Stoughton, and E. J. Van Scott, Eds., in "Advances in Biology of Skin," vol. 12, Appleton-Century-Crofts, New York, N.Y., 1972, pp. 177–205.

ACKNOWLEDGMENTS AND ADDRESSES

Received September 15, 1975, from the *Department of Pharmaceutical Science, School of Pharmacy, and the ‡Department of Statistics, College of Science, Oregon State University, Corvallis, OR 97331.

Accepted for publication June 14, 1976.

Supported in part by Grant ES00040 from the National Institute of Environmental Health Sciences and issued as Technical Paper 3940 from the Oregon Agricultural Experiment Station, Corvallis, OR 97331.

* To whom inquiries should be directed.

Diffusion Model for Drug Release from Suspensions II: Release to a Perfect Sink

F. TOM LINDSTROM *x and JAMES W. AYRES ‡

Abstract □ Numerical mathematical methods are applied to a diffusion model based on physicochemical principles to predict drug release from suspensions of drug in semisolid vehicles. The predicted mass of drug released *versus* time curves using this model are in agreement with some reported experimental data but differ from predictions using the classical model for semisolid suspensions. The differences are discussed in relation to the drug dissolution rate and diffusion rate in the vehicle.

Keyphrases □ Diffusion—suspended drug in semisolid vehicle, mathematical model based on physicochemical principles □ Dissolution—suspended drug in semisolid vehicle, mathematical model based on physicochemical principles □ Pharmacokinetic models—diffusion and dissolution of suspended drug in semisolid vehicle □ Drug release—from suspensions, diffusion model based on physicochemical principles □ Suspensions—drug release, diffusion model based on physicochemical principles

Previously (1), the complete theoretical development of a general nonlinear mass transport model was presented. Thus, this paper simply gives the nonlinear mass transport equations that incorporate local drug dissolution mechanics as already reported. The case under consideration is the mass transfer of drug out of an ointment vehicle containing dissolved and suspended drug when the semisolid is in immediate contact with a perfect sink (Fig. 1). A typical "real world" case where these conditions can exist

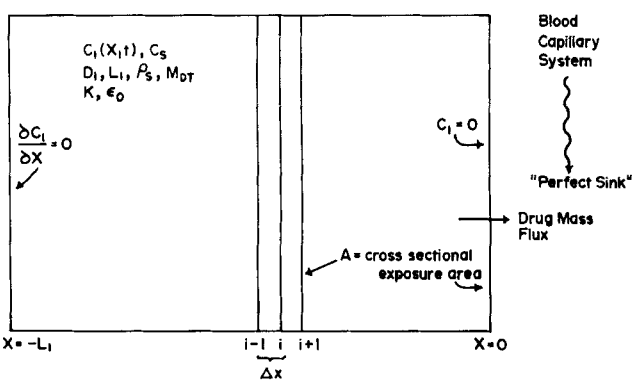

Figure 1—*Schematic of the model system for drug release directly to a perfect sink.*

here is more complex and results in equations that are not simple and do not predict a simple relationship between drug release and time, particle size, or drug concentration. This model should be considered if its assumptions appear to be met and if experimental data are not described by the classical model.

The model presented here probably will provide some insight into the formulation of suspensions for application to the skin or mucous membranes. The equations presented are only valid for systems that satisfy the requirements of the model. Parameters other than dissolution rate that can affect drug release and parameter interrelationships will be investigated and discussed in a subsequent publication based on the model presented here.

REFERENCES

(1) R. M. Barrer, "Diffusion in and Through Solids," Cambridge University Press, London, England, 1941.

(2) J. Crank, "The Mathematics of Diffusion," Oxford University Press, London, England, 1956.

(3) M. H. Jacobs, "Diffusion Processes," Springer-Verlag, New York, N.Y., 1967.

(4) T. Higuchi, *J. Soc. Cosmet. Chem.*, **11**, 85 (1960).

(5) W. I. Higuchi and T. Higuchi, *J. Am. Pharm. Assoc., Sci. Ed.*, **49**, 598 (1960).

(6) T. Koizumi and W. I. Higuchi, *J. Pharm. Sci.*, **57**, 87 (1968).

(7) *Ibid.*, **57**, 93 (1968).

(8) T. Yotsuyanagi, W. I. Higuchi, and A.-H. Ghanem, *J. Pharm. Sci.*, **62**, 40 (1973).

(9) T. Higuchi, *ibid.*, **50**, 874 (1961).

(10) W. I. Higuchi, *ibid.*, **56**, 315 (1967).

(11) D. E. Wurster and P. W. Taylor, *ibid.*, **54**, 169 (1965).

(12) J. Swarbrick, "Current Concepts in the Pharmaceutical Sciences, Biopharmaceutics," Lea & Febiger, Philadelphia, Pa., 1970, pp. 265–296.

(13) J. Haleblian, R. Runkel, N. Mueller, J. Christopherson, and K. Ng, *J. Pharm. Sci.*, **60**, 541 (1971).

(14) D. O. Hayward and B. M. W. Trapnell, "Chemisorption," Butterworths, London, England, 1964.

(15) P. S. Rowler, *J. Phys. Chem.*, **39**, 221 (1935).

(16) S. S. Szinai and C. A. Hunt, *Can. J. Pharm. Sci.*, **7**, 78 (1972).

(17) H. S. Carslaw and J. C. Jaeger, "Conduction of Heat in Solids," Oxford University Press, London, England, 1959.

(18) W. Jost, "Diffusion in Solids, Liquids and Gases," Academic, New York, N.Y., 1952.

(19) R. V. Churchill, *Duke Math. J.*, **2**, 405 (1936).

(20) A. N. Lowan, *ibid.*, **1**, 94 (1935).

(21) R. J. Scheuplein, in "Pharmacology and the Skin," W. Montague, R. B. Stoughton, and E. J. Van Scott, Eds., in "Advances in Biology of Skin," vol. 12, Appleton-Century-Crofts, New York, N.Y., 1972, pp. 125–151.

(22) B. J. Poulson, E. Young, V. Coquilla, and M. Katz, *J. Pharm. Sci.*, **57**, 928 (1968).

(23) J. Ostrenga, C. Steinmetz, and B. J. Poulson, *ibid.*, **60**, 1175 (1971).

(24) F. T. Lindstrom and J. W. Ayres, *ibid.*, **66**, 662 (1977).

(25) C. W. Barrett, J. W. Jadgraft, G. A. Caron, and I. Sarkany, *Br. J. Dermatol.*, **77**, 576 (1965).

(26) C. F. H. Vickers, in "Pharmacology and the Skin," W. Montague, R. B. Stoughton, and E. J. Van Scott, Eds., in "Advances in Biology of Skin," vol. 12, Appleton-Century-Crofts, New York, N.Y., 1972, pp. 177–205.

ACKNOWLEDGMENTS AND ADDRESSES

Received September 15, 1975, from the *Department of Pharmaceutical Science, School of Pharmacy, and the ‡Department of Statistics, College of Science, Oregon State University, Corvallis, OR 97331.

Accepted for publication June 14, 1976.

Supported in part by Grant ES00040 from the National Institute of Environmental Health Sciences and issued as Technical Paper 3940 from the Oregon Agricultural Experiment Station, Corvallis, OR 97331.

* To whom inquiries should be directed.

Diffusion Model for Drug Release from Suspensions II: Release to a Perfect Sink

F. TOM LINDSTROM *x and JAMES W. AYRES ‡

Abstract □ Numerical mathematical methods are applied to a diffusion model based on physicochemical principles to predict drug release from suspensions of drug in semisolid vehicles. The predicted mass of drug released *versus* time curves using this model are in agreement with some reported experimental data but differ from predictions using the classical model for semisolid suspensions. The differences are discussed in relation to the drug dissolution rate and diffusion rate in the vehicle.

Keyphrases □ Diffusion—suspended drug in semisolid vehicle, mathematical model based on physicochemical principles □ Dissolution—suspended drug in semisolid vehicle, mathematical model based on physicochemical principles □ Pharmacokinetic models—diffusion and dissolution of suspended drug in semisolid vehicle □ Drug release—from suspensions, diffusion model based on physicochemical principles □ Suspensions—drug release, diffusion model based on physicochemical principles

Previously (1), the complete theoretical development of a general nonlinear mass transport model was presented. Thus, this paper simply gives the nonlinear mass transport equations that incorporate local drug dissolution mechanics as already reported. The case under consideration is the mass transfer of drug out of an ointment vehicle containing dissolved and suspended drug when the semisolid is in immediate contact with a perfect sink (Fig. 1). A typical "real world" case where these conditions can exist

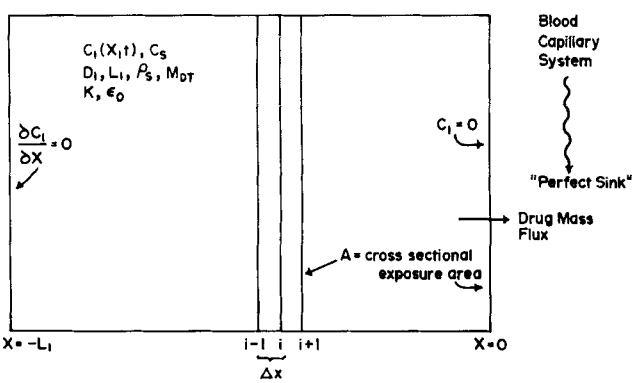

Figure 1—*Schematic of the model system for drug release directly to a perfect sink.*

Table I—Relative Cumulative Mass Release Values for the Distribution $\mu(t)$ as a Function of Time t in Minutes ($\epsilon_0 = 0.025$)[a]

	K, min^{-1}							
Minutes	0.0	0.01	0.1	1.0	10	100	1000	10,000
0	0.00	0.00	0.00	0.00	0.00	0.00	0.00	0.00
30	0.78	0.79	0.85	1.29	3.02	5.57	6.59	6.73
60	0.96	0.99	1.17	2.33	5.93	11.04	13.16	13.46
120	1.05	1.11	1.63	4.39	11.64	21.63	26.17	26.91
180	1.05	1.17	2.07	6.44	17.20	31.52	38.46	38.94
240	1.05	1.22	2.50	8.49	22.61	40.25	43.29	43.44
300	1.05	1.27	2.93	10.52	27.86	46.76	47.74	47.94
360	1.05	1.32	3.36	12.55	32.95	51.02	52.18	52.43
420	1.05	1.37	3.79	14.56	37.87	55.06	56.61	56.92
480	1.05	1.42	4.22	16.57	42.62	59.03	60.99	61.41
960	1.05	1.82	7.64	32.29	74.34	84.32	85.75	86.09
1440	1.05	2.23	11.04	47.42	96.14	103.63	104.48	104.74

[a] $D = 6 \times 10^{-8}$ cm^2/min, $L = 2 \times 10^{-3}$ cm, $C_s = 100$ μg/cm^3, $\rho_s = 1.0$ g/cm^3, and $\Delta t = 0.5$ min.

would be the application of ointment directly to an exposed capillary bed when the skin has been abraded.

This model also simulates certain laboratory experiments where a drug suspended in a semisolid is in direct contact with a large, well-stirred, uniform temperature receptor phase for a period of time. Drug release from suspension experiments have been carried out in this manner (2–4). This case was solved previously (1) using classical nonnumerical mathematical methods. This paper explores the predicted drug release from such systems obtained by numerical analysis of the system simulated in Fig. 1.

MASS TRANSPORT MODEL

The heart of the mass transport model for drug movement in the solution phase in an ointment base (1) is:

$$\frac{\partial C_1}{\partial t} = D_1 \frac{\partial^2 C_1}{\partial x^2} + K(C_s - C_1)\left(\epsilon_0^{1/3} - \frac{K}{3\rho_s}\int_0^t [C_s - C_1(x,\tau)]\,d\tau\right)^2 \quad \text{(Eq. 1)}$$

where:

C_1 = solution phase drug concentration distribution (grams per cubic centimeter)
D_1 = solution phase drug diffusion coefficient (square centimeters per minute)
C_s = solution phase drug saturation concentration (grams per cubic centimeter)
ρ_s = suspended phase drug density (powder density) (grams per cubic centimeter)
ϵ_0 = initial volume fraction of ointment that is suspended drug (cubic centimeter per cubic centimeter) and equals:

$$\left(\frac{M_{DT}}{AL_1} - C_s\right) \Big/ (\rho_s - C_s) \qquad C_s \leqq \frac{M_{DT}}{AL_1} \leqq \rho_s$$

M_{DT} = total drug mass in ointment sample (free and suspended) (grams)
A = exposure surface area of ointment (square centimeters) (Fig. 1)
L_1 = ointment slab thickness
$K = \kappa K_{cry}$, where K is the overall dissolution rate constant (min^{-1}), the product of the crystal surface area to volume constant and the energy-dependent reverse dissolution rate or crystallization rate constant K_{cry}. A more complete explanation of these terms is found in Ref. 1.

The subscripts (suppressed for the remainder of this paper) simply denote that a particular parameter or dependent variable belongs to the ointment portion of the model (Fig. 1).

The concentration distributions $C(x, t)$ can be obtained by solving the numerical analog of Eq. 1 subject to a no flux–perfect sink set of boundary conditions. The simulated system (Fig. 1) can be described mathematically as:

$$\frac{\partial C}{\partial t} = D\frac{\partial^2 C}{\partial x^2} + K(C_s - C)\left(\epsilon_0^{1/3} - \frac{K}{3\rho_s}\int_0^t [C_s - C(x,\tau)]\,d\tau\right)^2 \quad \text{(Eq. 2)}$$

The initial conditions are:

$$C(x, +0) = C_s \qquad -L \leqq x < 0 \quad \text{(Eq. 3)}$$

The boundary conditions are:

$$\left.\frac{\partial C}{\partial x}\right|_{x=-L} = 0 \qquad \text{no flux boundary, } t > 0 \quad \text{(Eq. 4)}$$

$$C(0, t) = 0 \qquad \text{perfect sink, } t > 0 \quad \text{(Eq. 5)}$$

Since the system of mass transport (Eqs. 2–5) is nonlinear and the parameter values (especially K) may be large, the more classical math-

Table II—Relative Cumulative Mass Release Values for the Distribution $\mu(t)$ as a Function of Time t in Minutes ($\epsilon_0 = 0.05$)[a]

	K, min^{-1}							
Minutes	0.0	0.01	0.1	1.0	10	100	1000	10,000
0	0.00	0.00	0.00	0.00	0.00	0.00	0.00	0.00
30	0.78	0.79	0.88	1.51	3.56	5.94	6.65	6.74
60	0.96	1.00	1.27	2.82	7.04	11.83	13.29	13.48
120	1.05	1.15	1.93	5.43	13.92	23.50	26.56	26.95
180	1.05	1.23	2.56	8.02	20.69	34.96	39.78	40.43
240	1.05	1.31	3.19	10.62	27.34	46.15	52.92	53.89
300	1.05	1.39	3.82	13.20	33.88	56.97	65.89	67.33
360	1.05	1.47	4.45	15.77	40.30	67.26	77.36	77.48
420	1.05	1.55	5.08	18.34	46.60	76.68	81.83	81.98
480	1.05	1.63	5.71	20.89	52.77	84.56	86.31	86.48
960	1.05	2.26	10.72	41.05	97.22	119.08	121.91	122.44
1440	1.05	2.89	15.71	60.67	132.03	146.51	147.42	147.66

[a] $D = 6 \times 10^{-8}$ cm^2/min, $L = 2 \times 10^{-3}$ cm, $C_s = 100$ μg/cm^3, $\rho_s = 1.0$ g/cm^3, and $\Delta t = 0.5$ min.

Table III—Relative Cumulative Mass Release Values for the Distribution $\mu(t)$ as a Function of Time t in Minutes ($\epsilon_0 = 0.1$)[a]

	K, min^{-1}							
Minutes	0.0	0.01	0.1	1.0	10	100	1000	10,000
0	0.00	0.00	0.00	0.00	0.00	0.00	0.00	0.00
30	0.78	0.80	0.94	1.79	4.13	6.21	6.69	6.74
60	0.96	1.02	1.43	3.42	8.19	12.39	13.37	13.49
120	1.05	1.21	2.33	6.68	16.23	24.72	26.74	26.97
180	1.05	1.34	3.23	9.92	24.29	36.99	40.09	40.46
240	1.05	1.46	4.12	13.16	32.26	49.18	53.44	53.94
300	1.05	1.58	5.01	16.39	40.09	61.29	66.76	67.42
360	1.05	1.71	5.91	19.62	47.87	73.29	80.07	80.91
420	1.05	1.83	6.80	22.83	55.58	85.18	93.36	94.38
480	1.05	1.95	7.69	26.04	63.20	96.92	106.61	107.86
960	1.05	2.94	14.80	51.44	120.96	171.51	172.32	172.51
1440	1.05	3.92	21.89	76.35	172.05	206.02	208.15	208.49

[a] $D = 6 \times 10^{-8}$ cm^2/min, $L = 2 \times 10^{-3}$ cm, $C_S = 100$ μg/cm^3, $\rho_S = 1.0$ g/cm^3, and $\Delta t = 0.5$ min.

ematical methods such as perturbations (regular in this case) are not applicable. Thus, it is necessary to consider numerical methods for obtaining the close approximation concentration distributions. The exact numerical method used is that of backward finite differences, where the global error involved at any point in time and space always remains bounded and goes as $O(\Delta x^2 + \Delta t)$. The details of sectioning the ointment slab up into N discrete, but adjoining, compartments (analogous to N discrete, but intimately connected, well-mixed chemical reactors) are contained in the *Appendix*.

RESULTS AND DISCUSSION

The model drug–vehicle system chosen was cortisone powder suspended in a semisolid vehicle that is not soluble in the receptor sink. Thus, the following parameter data estimates are available (1): $N = 10$ compartments, $\Delta x = L/N$, $D = 6 \times 10^{-8}$ cm^2/min, $L = 2 \times 10^{-3}$ cm, $C_s = 100$ μg/cm^3, $\rho_s = 1.0$ g/cm^3, K is variable, $0 \leqq \kappa < \infty$ min^{-1}, and ϵ_0 is variable ($0 \leqq \epsilon_0 < 1$).

Since the relative cumulative drug mass release (grams) at any time t after the release process has begun is defined as (1):

$$\mu(t) = \frac{\int_0^t \left\{ -AD \left. \frac{\partial C}{\partial x} \right|_{x=0} \right\} d\tau}{M_0} \qquad \text{(Eq. 6)}$$

and $M_0 = ALC_s$, the actual formula used in calculating the relative cumulative drug mass release from the ointment is:

$$\mu(t) = -\frac{D}{L} \int_0^t \left\{ \left. \frac{\partial \eta}{\partial x} \right|_{x=0} \right\} d\tau \qquad \text{(Eq. 7)}$$

where $\eta(x, t) = C(x, t)/C_s$, and the partial derivative in Eq. 7 is replaced by a sufficiently high order (2 or higher) numerical approximation so that $O(\Delta x^2)$ is always retained (see *Appendix* for details).

For the finite sequence $\epsilon_0 = 0.025$, 0.05, 0.1, 0.2, and 0.4, the relative cumulative drug mass release, $\mu(t)$, as a function of time (minutes) over the interval 0–24 hr is summarized in Tables I–V. Note that $\epsilon_0 = 0.025$ is equivalent to a concentration of 2.5% drug in the semisolid and would give a maximum $\mu(t)$ value of 250. In like manner, the other ϵ_0 values follow suit and the maximum $\mu(t)$ for $\epsilon_0 = 0.4$ would be 4000.

Several important effects on the cumulative relative drug mass loss distribution can be observed by study of the distributions in Tables I–V. In the true case of no dissolution of drug in the vehicle ($K = 0$), there is no release of drug since none dissolves. This model assumes a C_s of 100 μg/cm^3; therefore, this total amount is predicted to be released when $K = 0$, since no more drug can dissolve to replace the released drug. Each 100 μg/cm^3 gives a relative release of 1.0; if the numerical approximation is exact, $\mu(t) = 1.00$ for the case $K = 0$ as $t \rightarrow$ large.

However, since the numerical simulation is actually formed from a truncated Taylor series, it is not exact but does remain close to the exact value as time $\rightarrow$ large (*i.e.*, the error remains bounded in time). For low overall dissolution rate constants, $0 \leqq K \leqq 0.1$ min^{-1} (the choice of 0.1 is, of course, dependent on D and L), the cumulative drug mass loss is quite slow and becomes linear with time after about 120 min (Tables I–IV, bottom three curves in Fig. 2). The exact value of time where this more or less zero-order type of drug release commences can be seen from the tables to be close to 120 min regardless of the initial total drug mass (ϵ_0). This type of phenomenon is expected for such low values of K, because the rate-limiting step in this region of K values is clearly dissolution. The drug simply cannot go into solution fast enough to replace what has been transported toward the boundary ($x = 0$) by diffusion when $D = 6 \times 10^{-8}$ cm^2/min.

In the highest case of $\epsilon_0 = 0.4$ (40% of the ointment slab consists of suspended drug initially), it can be calculated that as $t \rightarrow \infty$, $\mu(t) \rightarrow 4000$ for the example presented here. At the end of 24 hr, less than 1.0% of the total drug has been released due to the slow dissolution.

For values of K in the range $0.1 \leqq K \leqq 100.0$ min^{-1}, a substantial increase in the cumulative relative drug mass release distribution is seen compared to $K \leqq 0.1$ min^{-1}. This region (again dependent upon D and L) contains those values of K where the dissolution and diffusion processes are somewhat comparable and neither one is clearly the rate-limiting step. In this region of K values (over the first 24 hr anyway), the distributions are somewhat linear (Fig. 2) in time after a similar initial curvilinear buildup, as was observed for K in $0 \leqq K \leqq 0.1$ min^{-1}. The maximum cumulative drug release at 24 hr ($\epsilon_0 = 0.4$) is about 6%.

Table IV—Relative Cumulative Mass Release Values for the Distribution $\mu(t)$ as a Function of Time t in Minutes ($\epsilon_0 = 0.2$)[a]

	K, min^{-1}							
Minutes	0.0	0.01	0.1	1.0	10	100	1000	10,000
0	0.00	0.00	0.00	0.00	0.00	0.00	0.00	0.00
30	0.78	0.81	1.02	2.14	4.68	6.39	6.71	6.75
60	0.96	1.05	1.65	4.15	9.32	12.77	13.42	13.49
120	1.05	1.30	2.88	8.18	18.57	25.53	26.84	26.98
180	1.05	1.49	4.10	12.19	27.78	38.26	40.25	40.46
240	1.05	1.68	5.32	16.20	36.95	50.97	53.67	53.97
300	1.05	1.87	6.54	20.20	46.08	63.65	67.08	67.46
360	1.05	2.06	7.76	24.19	55.16	76.31	80.48	80.95
420	1.05	2.26	8.99	28.18	64.19	88.94	93.88	94.44
480	1.05	2.45	10.21	32.16	73.18	101.54	107.28	107.93
960	1.05	3.97	19.95	63.77	143.27	200.81	214.22	215.82
1440	1.05	5.50	29.68	94.94	209.69	293.54	308.42	308.55

[a] $D = 6 \times 10^{-3}$ cm^2/min, $L = 2 \times 10^{-3}$ cm, $C_S = 100$ μg/cm^3, $\rho_S = 1.0$ g/cm^3, and $\Delta t = 0.5$ min.

Table V—Relative Cumulative Mass Release Values for the Distribution $\mu(t)$ as a Function of Time t in Minutes ($\epsilon_0 = 0.4$)[a]

	K, min^{-1}							
Minutes	0.0	0.01	0.1	1.0	10	100	1000	10,000
0	0.00	0.00	0.00	0.00	0.00	0.00	0.00	0.00
30	0.78	0.82	1.13	2.56	5.19	6.52	6.73	6.75
60	0.96	1.10	1.95	5.02	10.35	13.03	13.45	13.50
120	1.05	1.43	3.57	9.94	20.66	26.05	26.90	27.00
180	1.05	1.73	5.19	14.85	30.95	39.07	40.35	40.48
240	1.05	2.02	6.80	19.76	41.21	52.08	53.80	53.98
300	1.05	2.31	8.42	24.66	51.46	65.08	67.24	67.47
360	1.05	2.60	10.04	29.55	61.68	78.07	80.69	80.97
420	1.05	2.89	11.65	34.44	71.87	91.05	94.13	94.46
480	1.05	3.18	13.27	39.32	82.05	104.03	107.58	107.96
960	1.05	5.51	26.18	78.19	162.56	207.51	215.09	215.91
1440	1.05	7.84	39.07	116.68	241.33	310.21	322.50	323.85

[a] $D = 6 \times 10^{-8}$ cm^2/min, $L = 2 \times 10^{-3}$ cm, $C_s = 100$ μg/cm^3, $\rho_s = 1.0$ g/cm^3, and $\Delta t = 0.5$ min.

In the region $100 \leqq K < \infty$ min^{-1} (∞ = 10,000 for Tables I–V), diffusion is the rate-limiting step. When diffusion is the rate-limiting process, the model predicts the following very interesting "moving source" phenomenon, which is in good agreement with literature data for release of medroxyprogesterone acetate from a cylindrical silicone polymer (5). Notice that under the columns labeled K = 10,000 min^{-1}, the relative cumulative drug mass distribution initially has a zero-order (Fig. 3) type of buildup ($0 < t < 60$ min). Then (especially at low ϵ_0 values), the release becomes non-zero order as the suspended drug in the surface layer [first compartment adjacent to the boundary ($x = 0$) in the numerical scheme] becomes exhausted and a type of diffusion layer or ointment boundary is created by the portion of the semisolid vehicle that is now drug free.

Initially, under high K values, a large burst of drug is obtained from the surface layer of ointment only. The other deeper regions in the ointment slab have essentially not yet begun to feel any concentration gradient in the local regions and are thus, for all practical purposes, just sitting still in time. However, as time goes on and the surface layer (first compartment) is exhausted of its suspended drug, the second layer (second compartment) begins to contribute drug by diffusion of dissolved drug and by sending suspended drug into solution. But this newly dissolved drug must diffuse through a thin permeable slab of ointment, the empty first compartment which is now devoid of any suspended drug, to the boundary $x = 0$.

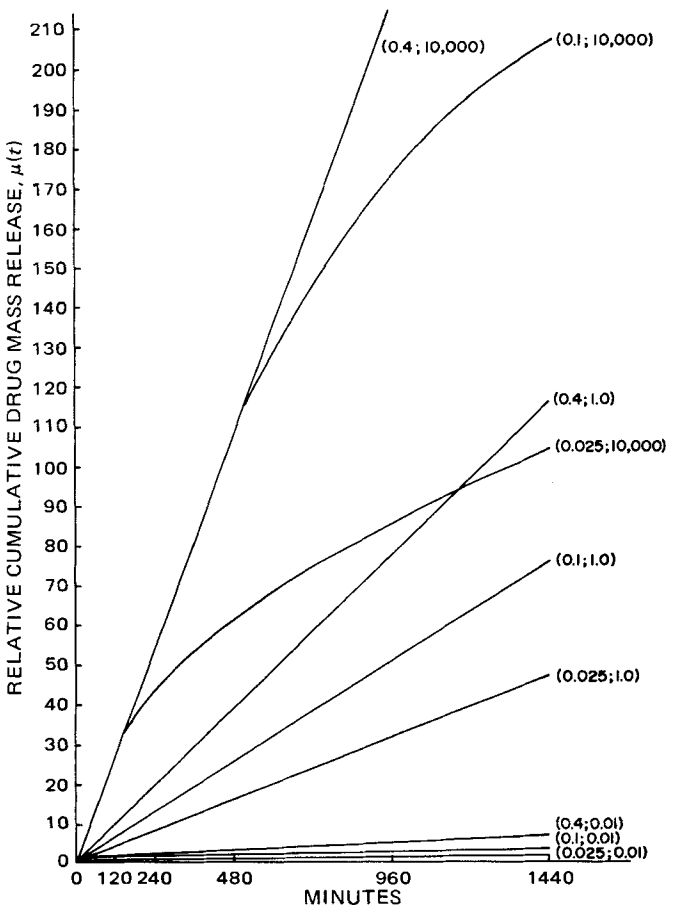

Figure 2—*Relationship between relative cumulative mass loss* μ(t) versus *time* t *in minutes for three different* ϵ_0 *values and three* K *values for each* ϵ_0 *value. The combinations are characterized via the order pair designation* (ϵ_0 = —; K = —).

As time goes on, the second layer is also depleted of its suspended drug and the third compartment begins to contribute. Now drug coming from the third compartment must diffuse through the first two compartments. This sequence is repeated in time until the entire ointment slab is devoid of all suspended and free drug under the hypothesis of this model. The net effect of these large values of K is to produce a moving source of suspended drug, very much like an earlier model (6) in which diffusion is the rate-limiting step.

From Table VI, it can be seen that after 24 hr the first four compartments are nearly exhausted of their initially suspended drug mass (K large) in the case of ϵ_0 being a 2.5% suspension, whereas only the first compartment is extensively depleted when ϵ_0 = 40%. This moving source phenomenon is the reason for the extreme curvilinearity in the case of ϵ_0 small and almost complete linearity for 24 hr for ϵ_0 large (Fig. 3).

Although the current model is in agreement with an earlier model (6) with respect to a moving source when dissolution is very rapid, the models predict different cumulative drug mass release *versus* time curves. The classical model (6) results in Eq. 8 to relate the amount and rate of release of drug suspended in an ointment vehicle to time and variables of the system (when $C_s \ll A$):

$$Q = S\sqrt{2ADC_s t} \qquad \text{(Eq. 8)}$$

where Q = amount of drug released at time t, S = surface area of exposure, A = concentration of drug (units per cubic centimeter), C_s = solubility of drug (units per cubic centimeter) in the vehicle, D = diffusion constant of the drug in the vehicle, and t = time.

Equation 8 predicts that the amount of drug released would be proportional to the square root of the total drug present. The model presented here predicts a limiting or upper bounding distribution (for large K values) as ϵ_0 increases (Fig. 3). Obviously, ϵ_0 cannot be increased beyond 1.0. However, it appears from the tables that ϵ_0 = 40% is probably close to the upper bounding distribution. This upper limit distribution is important and was observed experimentally (7).

Other experimental data indicate that the release of drug from a sus-

Table VI—Relative Cumulative Mass Loss Data and Relative Initial Mass Data (K = 10,000 min^{-1})

ϵ_0	Initial Relative Mass in Boundary Compartment	1440-min μ Reading
0.025	25	105
0.05	50	148
0.1	100	208
0.2	200	308
0.4	400	324

Table VII—Comparison of Relative Amounts of Predicted Drug Release Using Two Different Diffusion Models Assuming Rapid Dissolution[a]

	$\epsilon_0 = 0.025$		$\epsilon_0 = 0.10$		$\epsilon_0 = 0.20$		$\epsilon_0 = 0.40$	
Minutes	μ	μ_H	μ	μ_H	μ	μ_H	μ	μ_H
120	26.9	29.98	26.9	59.96	26.9	84.57	26.9	119.22
960	86	84.85	173	169.71	216	239.28	216	338.43
1440	105	103.94	209	207.89	309	337.43	324	413.37

[a] Relative amounts obtained for μ and μ_H using Eq. 7 and converting Eq. 8 to a form (1) that also predicts relative cumulative drug mass release at time t, namely, $\mu_H = \sqrt{2Dt}/L\ \sqrt{\rho\epsilon_0/C_S}$ or $\mu_H = Q/LC_S$.

pension in a semisolid is not always proportional to the square root of drug concentration and the ratio changes with time. Examples are sulfacetamide in hydrogenated cottonseed oil with surfactant and sulfathiazole in hydrogenated cottonseed oil (8). Salicylic acid suspended in several different vehicles was not released as predicted by Eq. 8, possibly due to an inadequate dissolution rate of the suspended particles (9). Release of suspended benzocaine from white petrolatum was not proportional to the square root of concentration for each sample obtained over the time period investigated (10).

Introduction of a membrane between the vehicle and the receptor phase, when the membrane is not rate limiting for release (as occurred in some experiments), would not change the relationship predicted by the model for Eq. 8 between concentration and amount released, although a lag time may be evident. A matrix–boundary diffusion layer model (5, 11, 12) was proposed to explain some cases where the release is not proportional to the square root of concentration. Such models incorporate the realistic assumption of a desorptive phenomenon occurring at the semisolid–receptor phase interface. This assumption is compatible with the model presented here and will be considered in a future publication.

The differences in predicted relative cumulative drug mass release using Eqs. 7 and 8 are shown in Table VII and Fig. 4. In the range of rapid dissolution for increasing drug concentrations, the model presented predicts little effect on the amount of drug released at short times and a limiting upper bound for drug release at longer times. In contrast, the classical model predicts a large effect at short times for increasing drug concentrations. The predicted effect at short times is highly dependent on the parameter constants being used and will vary for each drug–vehicle system. An upper bound, however, is predicted for all systems by the current model and not by the classical model.

The apparent linearity of μ *versus* $\sqrt{t}$ in Fig. 4 is due to computer time limitations. If this numerical simulation were plotted for 10 or 20 days consecutively, a pronounced negative curvature, especially at smaller ϵ_0 values, would clearly be seen at longer times. This negative curvature has no place in the theory of heat and mass transfer when simple $\sqrt{t}$ behavior is assumed. However, the negative curvature is a well-known phenomenon in heat and mass transfer theory when the complete Fourier series representation is given to the drug concentration distribution $C(x, t)$ across the ointment slab, $-L \leqq x < 0$.

The previous discussion was obtained from a rather good (as evidenced by the column labeled $K = 0$) numerical simulation of the transport model under the hypothesis that $D = 6 \times 10^{-8}$ cm^2/min and $L = 20$ μm. When these parameter values are changed for systems other than the one presented here, a new set of drug mass release distribution tables over the same range of K values can be easily obtained[1].

Since this scheme is numerical, it is instructive to consider the effects of changes in the mesh size, Δx, and time step size, Δt, on the distributions, $\mu(t)$. Since it is difficult to generate a large set of tables for the

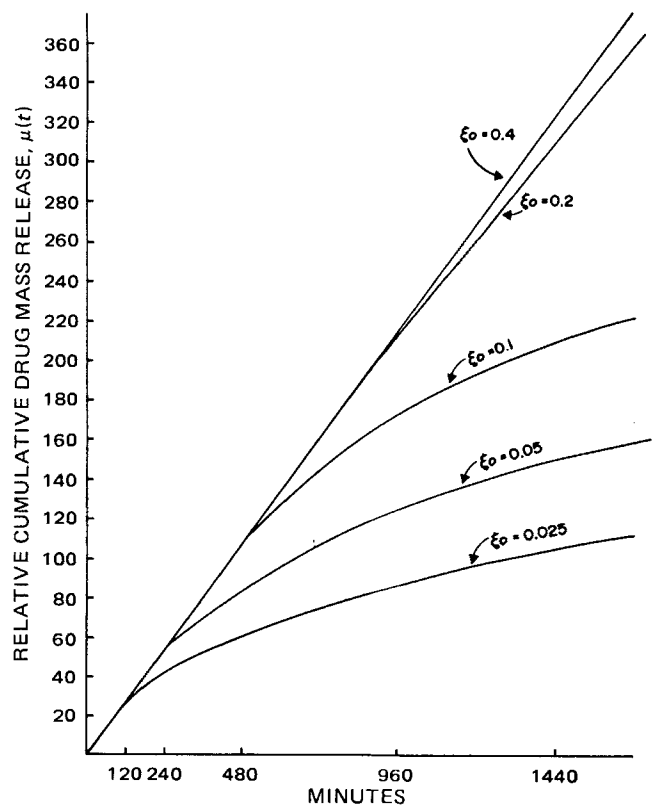

Figure 3—*Relationship of* μ(t) versus t *for* K = *10,000 min*$^{-1}$ *and* ϵ_0 *varying from* ϵ_0 = *0.025 to 0.4. Other parameters used in generating the curves are listed in the text.*

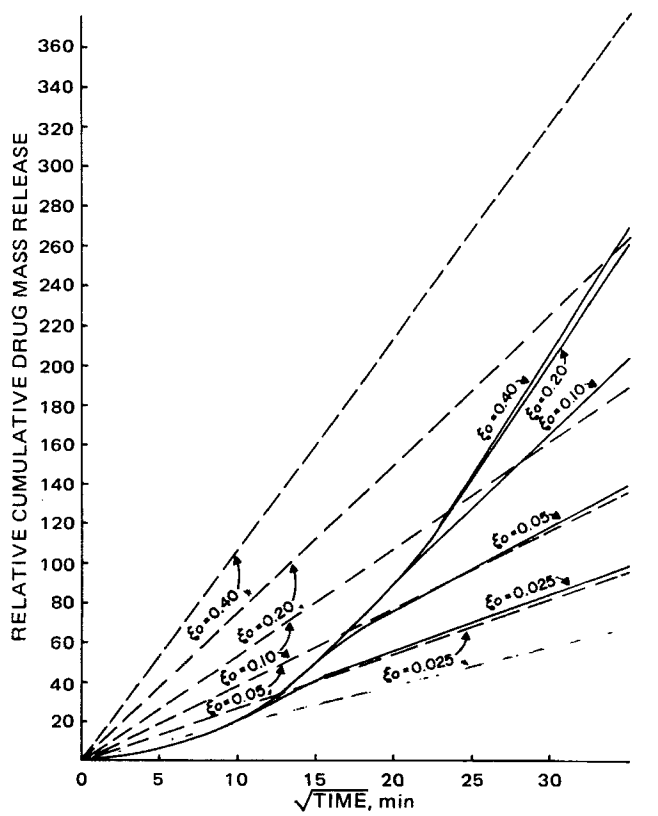

Figure 4—*Relationship of* μ(t) *or* μ_Ht versus $\sqrt{t}$ *for* K = *10,000 min*$^{-1}$ *and* ϵ_0 *varying from* ϵ_0 = *0.025 to 0.4. Other parameters used in generating the curves are listed in the text. Key:* μ(t), ——; *and* μ_H(t), - - -.

[1] This will be discussed in Part III of this series.

Table VIII—Relative Cumulative Mass Release Values for the Distribution $\mu(t)$ as a Function of Time t in Minutes ($\epsilon_0 = 0.1$ and $\Delta t = 0.25$ min)[a]

	K, min^{-1}							
Minutes	0.0	0.01	0.1	1.0	10	100	1000	10,000
0	0.00	0.00	0.00	0.00	0.00	0.00	0.00	0.00
30	0.76	0.77	0.91	1.77	4.12	6.20	6.69	6.74
60	0.94	0.99	1.41	3.40	8.18	12.39	13.37	13.49
120	1.02	1.18	2.31	6.66	16.27	24.72	26.74	26.97
180	1.03	1.31	3.20	9.90	24.28	36.99	40.09	40.46
240	1.03	1.43	4.10	13.14	32.21	49.18	53.43	53.94
300	1.03	1.56	4.99	16.37	40.07	61.28	66.76	67.42
360	1.03	1.68	5.88	19.60	47.86	73.29	80.07	80.91
420	1.03	1.80	6.77	22.81	55.56	85.17	93.36	94.38
480	1.03	1.93	7.66	26.02	63.18	96.91	106.60	107.86
960	1.03	2.91	14.78	51.42	120.94	171.41	172.15	172.28
1440	1.03	3.90	21.87	76.32	172.03	205.91	207.97	208.26

[a] $D = 6 \times 10^{-6}$ cm^2/min, $L = 2 \times 10^{-3}$ cm, $C_S = 100$ μg/cm^3, and $\rho_S = 1.0$ g/cm^3.

Table IX—Relative Cumulative Mass Release Values for the Distribution $\mu(t)$ as a Function of Time t in Minutes ($\epsilon_0 = 0.1$ and $\Delta t = 1.0$ min)[a]

	K, min^{-1}							
Minutes	0.0	0.01	0.1	1.0	10	100	1000	10,000
0	0.00	0.00	0.00	0.00	0.00	0.00	0.00	0.00
30	0.83	0.85	0.99	1.83	4.15	6.21	6.69	6.74
60	1.02	1.07	1.48	3.46	8.22	12.40	13.37	13.49
120	1.10	1.26	2.39	6.72	16.30	24.73	26.74	26.97
180	1.11	1.39	3.28	9.97	24.31	37.00	40.09	40.46
240	1.11	1.52	4.17	13.21	32.25	49.19	53.44	53.94
300	1.11	1.64	5.07	16.44	40.11	61.30	66.76	67.43
360	1.11	1.76	5.96	19.66	47.90	73.3	80.07	80.91
420	1.11	1.89	6.85	22.88	55.61	85.19	93.36	94.38
480	1.11	2.01	7.74	26.09	63.23	96.94	106.61	107.86
960	1.11	2.99	14.86	51.48	121.00	171.71	172.67	172.93
1440	1.11	3.98	21.95	76.39	172.11	206.22	208.49	208.91

[a] $D = 6 \times 10^{-6}$ cm^2/min, $L = 2 \times 10^{-3}$ cm, $C_S = 100$ μg/cm^3, and $\rho_S = 1.0$ g/cm^3.

various ϵ_0 *versus* K combinations for selected values of Δx and Δt while still retaining the total ointment thickness, L, and run time $t = 1440$ min, the cases of $\Delta t = 1$ min and $\Delta t = 0.25$ min for $\epsilon_0 = 0.1$ and $N = 10$ were chosen for evaluation. In accordance with theory (13), when N increases and Δx and Δt decrease, the order of the error goes down rapidly. Hence, the approximation becomes better and better.

Although this paper does not attempt to give an exact error analysis for the model presented, Tables III, VIII, and IX illustrate the accuracy and error stability of the numerical simulator used to approximate the solution to the complete nonlinear mass transport system. Tables VIII, III, and IX reflect the values $\Delta t = 0.25$, 0.5, and 1.0 min, respectively. All have the common parameter values used earlier. Examination of the tables shows that not only does the error remain bounded in all cases, as theory says it should (13), but also that the percentage difference between values for corresponding K values decreases with increasing time when Tables III and VIII are compared and when Tables VIII and IX are compared. The worst error occurs at early times and small K values ($0 \leqq K \leqq 0.1$). This finding is justified, however, by the error analysis (13) for parabolic-type partial differentio-integral equations of the type adapted for the transport model.

The value of Δt throughout this paper is 0.5 min. This value is the geometric mean of the two values 1.0 and 0.25, although the main reason for choosing 0.5 min is simply that it gives reasonably accurate μ values coupled with ease of computation.

SUMMARY

A numerical method was used to solve the equations associated with a new model for the release of suspended drug from a semisolid vehicle to an infinite sink. Evaluation of the method through the consideration of increasing t values shows the mathematics to be stable and bounded in the scheme presented. The model predicts a curvilinear relationship between the amount of drug released and the amount of drug present and the time elapsed other than time$^{1/2}$.

The release pattern may or may not appear linear with time or time$^{1/2}$ if release is evaluated over short time intervals. Use of such linear relationships to project drug release at earlier or later times than those actually evaluated may introduce considerable error with respect to the actual amount released.

APPENDIX

Consider the following nonlinear parabolic integro-differential problem for mass transport of drug in an ointment–perfect sink system:

$$\frac{\partial \eta}{\partial t} = D\frac{\partial^2 \eta}{\partial x^2} + K(1-\eta)\left(\epsilon_0^{1/3} - \frac{KC_s}{3\rho_s}\int_0^t [1-\eta(x,\tau)]\,d\tau\right)^2 \quad \text{(Eq. A1)}$$

for all (x, t) in $\{(-L_1 < x < 0) \times (t > 0)\}$ subject to the initial conditions:

$$\eta(x, +0) = 1.0 \qquad -L_1 \leqslant x > 0 \quad \text{(Eq. A2)}$$

and boundary conditions:

$$\left.\frac{\partial \eta}{\partial x}\right|_{x=-L_1} = 0 \qquad t > 0 \quad \text{(Eq. A3}a\text{)}$$

and:

$$\eta(0, t) = 0 \qquad t > 0 \quad \text{(Eq. A3}b\text{)}$$

and $\eta(x, t) = C(x, t)/C_s$. Note that D, K, ϵ_0, ρ_s, C_s, and L_1 are all positive parameters.

By using a reported scheme (13), the time derivative $\partial\eta/\partial t$ can be replaced by a backward in time difference quotient:

$$\left.\frac{\partial \eta}{\partial t}\right|_{t_{n+1}} \doteq \frac{\eta^{(n+1)} - \eta^{(n)}}{\Delta t} \quad \text{(Eq. A4)}$$

while the space derivative is approximated by a space-centered difference quotient:

$$\frac{\partial^2 \eta}{\partial x^2} \doteq \frac{1}{\Delta x^2}(\eta_{i-1} - 2\eta_i + \eta_{i+1}) \quad \text{(Eq. A5)}$$

and the integral term is evaluated backward in time by the trapezoidal rule. Note that $\Delta x = L_1/N$ and Δt is chosen arbitrarily small but positive. The $\eta_i^{(n)}$ notation used for the remainder of the paper means simply this:

$$\eta_i^{(n)} = \eta(x_i, t_n) = \eta(i\Delta x, n\Delta t)$$
$$i = 0, 1, 2, \ldots, N \qquad n = 0, 1, 2, \ldots \qquad \text{(Eq. A6)}$$

The space, time, and integral operators have been approximated in such a way that an implicit, irreducible, diagonal dominant linear system must be solved at each time step. The resulting iterative scheme is not only unconditionally stable but has been shown (13) to produce an approximating solution which converges uniformly to the true solution as Δx and $\Delta t \to 0$.

Define:

$$I_i^{(n)} = \left(\epsilon_0^{1/3} - \frac{KC_s}{3\rho_s}\int_0^{t_n}[1 - \eta_i(\tau)]\,d\tau\right)^2 \qquad \text{(Eq. A7)}$$

For computer computation, define:

$$J_i^{(n)} = \int_0^{t_n}[1 - \eta_i(\tau)]\,d\tau \qquad \text{(Eq. A8)}$$

By using the trapezoid rule, which retains $O(\Delta t)^2$ globally:

$$J_i^{(n)} = J_i^{(n-1)} + \frac{\Delta t}{2}\{2 - [\eta_i^{(n)} + \eta_i^{(n-1)}]\} \qquad \text{(Eq. A9)}$$

with $J_i^{(0)} = 0$ and $i = 0, 1, 2, \ldots, N$. Hence:

$$I_i^{(n)} = \left[\epsilon_0^{1/3} - \frac{KC_s}{3\rho_s}J_i^{(n)}\right]^2 \qquad \text{(Eq. A10)}$$

Putting all parts together gives the numerical scheme (tridiagonal system):

$$\frac{\eta_i^{(n+1)} - \eta_i^{(n)}}{\Delta t} = \frac{D}{\Delta x^2}\left[\eta_{i-1}^{(n+1)} - 2\eta_i^{(n+1)} + \eta_{i+1}^{(n+1)}\right] + K[1 - \eta_i^{(n+1)}]I_i^{(n)} \qquad \text{(Eq. A11)}$$

where $i = 1, 2, 3, \ldots, N-1$. The boundary conditions (no flux boundary) at $x = -L_1$, which corresponds to $i = 0$ in the "bookkeeping" of this numerical scheme, is approximated as:

$$\left.\frac{\partial\eta^{(n+1)}}{\partial x}\right|_{x=-L_1} \doteq \frac{1}{2\Delta x}[-3\eta_0^{(n+1)} + 4\eta_1^{(n+1)} - \eta_2^{(n+1)}] \qquad \text{(Eq. A12)}$$

where the $O(\Delta x^2)$ accuracy is preserved *via* this approximation. Since the boundary condition requires $(\partial\eta/\partial x)|_{x=-L_1} = 0$ for all $t \geq 0$, then:

$$\eta_0^{(n+1)} = \frac{4}{3}\eta_1^{(n+1)} - \frac{1}{3}\eta_2^{(n+1)} \qquad \text{(Eq. A13)}$$

This equation, together with the boundary condition at $i = N$ ($x = 0$), $\eta_N^{(n+1)} = 0$, and $n = 0, 1, 2, \ldots$, and Eq. A11 give, after some algebra, the tridiagonal system (interative):

$$\begin{aligned}
a_{11}\eta_1^{(n+1)} + a_{12}\eta_2^{(n+1)} + 0\eta_3^{(n+1)} + \ldots + 0\eta_{N-1}^{(n+1)} &= \eta_1^{(n)} + K\Delta t I_i^{(n)} \\
a_{21}\eta_1^{(n+1)} + a_{22}\eta_2^{(n+1)} + a_{21}\eta_3^{(n+1)} + 0\eta_4^{(n+1)} + \ldots + 0\eta_{N-1}^{(n+1)} &= \eta_2^{(n)} + K\Delta t I_2^{(n)} \\
&\vdots \quad \vdots \quad \vdots \\
0\eta_1^{(n+1)} + \ldots + a_{21}\eta_{N-2}^{(n+1)} + a_{N-1,N-1}\eta_{N-1}^{(n+1)} &= \eta_{N-1}^{(n)} + K\Delta t I_{N-1}^{(n)}
\end{aligned} \qquad \text{(Eq. A14)}$$

where:

$$a_{11} = 1 + \frac{2}{3}\frac{D\Delta t}{\Delta x^2} + K\Delta t I_1^{(n)}$$
$$a_{12} = -\frac{2}{3}\frac{D\Delta t}{\Delta x^2}$$
$$a_{21} = -\frac{D\Delta t}{\Delta x^2}$$
$$a_{ii} = 1 + \frac{D\Delta t}{\Delta x^2} + K\Delta t I_i^{(n)},\ i = 2, 3, 4, \ldots, N-1$$

Hence, by iteration with the matrix system:

$$A^{(n)}\eta^{(n+1)} = \eta^{(n)} + K\Delta t\,\mathbf{I}^{(n)} \qquad \text{(Eq. A15)}$$

the relative concentration distribution $\eta^{(n+1)} = [\eta_0^{(n+1)}, \eta_1^{(n+1)}, \eta_2^{(n+1)} \ldots \eta_N^{(n+1)}]^1$, is obtained in terms of the previous time level relative concentration distribution and any new drug which has come into solution in the intervening time.

It remains now to calculate $\mu_1(t)$, the relative cumulative drug mass loss from the ointment system. Since $\mu_1(t)$ is defined as:

$$\mu_1(t) = \frac{\int_0^t\left\{-DA\left.\frac{\partial C}{\partial x}\right|_{x=0}\right\}}{AL_1C_s}d\tau = -\frac{D}{L_1}\int_0^t\left.\frac{\partial\eta}{\partial x}\right|_{x=0}d\tau \qquad \text{(Eq. A16)}$$

the space derivative at the right-hand boundary $x = 0$ is replaced by the numerical approximation which preserves the $O(\Delta x^2)$ accuracy locally and globally in time:

$$\left.\frac{\partial\eta}{\partial x}\right|_{x=0} \doteq \frac{1}{2\Delta x}[\eta_{N-2} - 4\eta_{N-1} + 3\eta_N] \qquad \text{(Eq. A17)}$$

Under the assumption that there is a perfect sink condition operating at all times at the ointment–sink boundary, $x = 0$, $\eta_N^{(n)} = 0$, and $n = 1, 2, \ldots$. Hence, substituting for this space derivative approximation and again using the trapezoid rule for numerical quadrature in time yield:

$$\mu^{(n+1)} = \frac{D}{2\Delta x L_1}I_2^{(n+1)} \qquad \text{(Eq. A18)}$$

where:

$$I_2^{(n+1)} = I_2^{(n)} + \frac{\Delta t}{2}\{4[\eta_{N-1}^{(n+1)} + \eta_{N-1}^{(n)}] - [\eta_{N-2}^{(n+1)} + \eta_{N-2}^{(n)}]\} \qquad \text{(Eq. A19)}$$

with $I_2^{(0)} = 0$.

Equations A9, A10, A13, and A14 constitute the numerical simulation for the relative solution phase drug concentration at any point in time, while Eqs. A18 and A19 are used to obtain the relative cumulative drug mass release from the ointment slab at time $t \geq 0$.

REFERENCES

(1) J. W. Ayres and F. T. Lindstrom, *J. Pharm. Sci.*, **66,** 654 (1977).

(2) B. J. Poulsen, E. Young, U. Coquilla, and M. Katz, *ibid.*, **57,** 928 (1968).

(3) R. E. Dempski, J. B. Portnoff, and A. W. Wase, *ibid.*, **58,** 579 (1969).

(4) J. Ostrenga, C. Steinmetz, and B. Poulsen, *ibid.*, **60,** 1175 (1971).

(5) T. J. Roseman and W. I. Higuchi, *ibid.*, **59,** 353 (1970).

(6) T. Higuchi, *ibid.*, **50,** 874 (1961).

(7) J. Haleblian, R. Runkel, N. Mueller, J. Christopherson, and K. Ng, *ibid.*, **60,** 541 (1971).

(8) C. W. Whitworth and C. H. Becker, *ibid.*, **54,** 569 (1965).

(9) F. Bottari, G. Di Colo, E. Nannipieri, M. F. Saettone, and M. F. Serafini, *ibid.*, **63,** 1779 (1974).

(10) J. W. Ayres and P. A. Laskar, *ibid.*, **63,** 1402 (1974).

(11) Y. W. Chien, H. J. Lambert, and O. E. Grant, *ibid.*, **63,** 364 (1974).

(12) Y. W. Chien and H. J. Lambert, *ibid.*, **63,** 515 (1974).

(13) L. Douglas and B. F. Jones, *Numerische Mathematik,* **4,** 96 (1962).

ACKNOWLEDGMENTS AND ADDRESSES

Received September 15, 1975, from the *Department of Statistics, College of Science, and the ‡Department of Pharmaceutical Science, School of Pharmacy, Oregon State University, Corvallis, OR 97331.

Accepted for publication June 14, 1976.

Supported in part by Grant ES00040 from the National Institute of Environmental Health Sciences and issued as Technical Paper 4097 from the Oregon Agricultural Experiment Station, Corvallis, OR 97331.

The authors express their appreciation to Mr. William E. McCoy, III, for assistance in writing and running the Fortran 4 algorithms on the Oregon State University CDC 3300 computer.

ˣ To whom inquiries should be directed.

Polymorphism of Phenylbutazone: Properties and Compressional Behavior of Crystals

H. G. IBRAHIM ˣ, F. PISANO, and A. BRUNO

Abstract □ Data from X-ray diffraction, thermal analysis, IR spectroscopy, and solubility studies were used for the identification and characterization of four crystalline modifications of phenylbutazone. The thermal behavior of the polymorphs under different treatment conditions also was investigated. Compression of the thermodynamically unstable forms, at a compression force of 1590–2040 kg, induced polymorphic changes in the crystals. Similar changes also were produced through grinding. The apparent equilibrium solubilities of polymorphs were determined, as was the dissolution of the polymorphs as compressed disks in an aqueous medium. The small effective surface area possessed by one polymorph resulted in slow dissolution.

Keyphrases □ Phenylbutazone—four polymorphic forms identified, thermal and compressional behavior and solubilities compared □ Polymorphism—phenylbutazone, four crystalline forms identified, thermal and compressional behavior and solubilities compared □ Thermal behavior—four polymorphic forms of phenylbutazone compared □ Compressional behavior—four polymorphic forms of phenylbutazone compared □ Solubility—four polymorphic forms of phenylbutazone compared □ Antirheumatic agents—phenylbutazone, four polymorphic forms identified, thermal and compressional behavior and solubilities compared

Different polymorphs are known to possess different physical properties. From a practical point of view, solubility, surface tension, density, crystal shape, and hardness are the most significant differences. The bioavailability of a drug as well as the chemical and physical stability of a solid compound in a particular dosage form can be modified by presenting the drug in the appropriate crystal form (1, 2). This approach, of course, requires a thorough knowledge of the properties and behavior of the different crystalline modifications.

While several reports discussed the bioavailability of drugs that can exist in more than one crystalline modification (3, 4), little information is available on the role of polymorphism and crystal habit in solid dosage form and powder technology. The orientation of crystals during a packing or compression process is influenced by the dominant faces in the crystal and, therefore, by crystal habit. Using data from X-ray powder diffraction, Shell (5) described crystal habit as it relates to a good or poor tableting performance.

Polymorphous transformations at high pressures occur in some inorganic and organic substances (6, 7). The possibility of phase transitions with pressure during tableting and their effects on dissolution rates and availability of drugs have not been adequately investigated, probably because of the general contention that tableting pressures will not induce phase transformations. Nevertheless, such phase changes during compression are conceivable and would occur at individual points of contact between particles where local pressures are extremely large (pressure being force per unit area). These pressures probably would promote transitions toward structures of higher coordination and higher density.

The present work reports on polymorphism in phenylbutazone and provides information regarding the feasibility of crystalline structural changes under tableting conditions.

EXPERIMENTAL

Crystal Forms—Cyclohexane (Form II), *n*-heptane (III), 2-propanol (IV), and isobutyl alcohol (I) were used as crystallization solvents for the polymorphs. All solvents were analytical grade. A single batch of commercial phenylbutazone[1] was used. The techniques of crystallization of the different polymorphs from the different solvents were essentially the same. An adequate amount of the drug was added to the warm solvent, and the resultant saturated solution was allowed to cool.

For the preparation of Form IV, water was added to the 2-propanol solution until the cloud point. Then the solution was warmed again and allowed to cool. The separated crystals were filtered off using a sintered-glass funnel and then dried under vacuum.

Polymorph Characterization—*Differential Scanning Calorimetry*—The thermograms of the different crystalline modifications were recorded on a thermal analyzer[2] equipped with a differential scanning calorimetry cell. Indium (99.99% purity) was used to check instrument calibration. The thermal behavior of the four polymorphs was studied at different heating rates and under different conditions of sample treatment; *i.e.*, crystals were heated in an open pan, covered pan, or as a crimped sample.

Heating rates of 2 and 5°/min and, to a much lesser extent, 10°/min promoted solid–solid transformation. To minimize such transformation, the samples routinely were heated throughout the investigation at 20°/min. Phase transition temperatures obtained from the thermograms were corrected for the nonlinear response of the chromel–alumel thermocouple.

IR Spectroscopy—A double-beam IR spectrophotometer[3] was used for recording the spectra of the polymorphs. Grinding, as will be shown later, induced polymorphic changes in the samples. Since the sample must be sufficiently ground to obtain a good mineral oil[4] mull, this technique and the potassium bromide disk technique were considered unsuitable for handling such grinding-sensitive material. For this reason, attenuated total reflectance, using a TR-9 ATR unit with a 45° KRS-5 (thallous bromide–iodide) crystal, was employed to record the IR spectra. An adhesive tape technique similar to that used by Kang *et al.* (8) was utilized in preparing the samples for IR analysis.

X-Ray Analysis—X-ray diffraction patterns were recorded using an X-ray diffractometer with K_α radiation[5]. The settings used with the instrument were: 1° beam slit, 0.2° detector slit, copper tube-K_α radiation, and nickel filter.

Dissolution and Solubility Studies—All dissolution studies were conducted in a 0.067 *M* aqueous phosphate buffer of pH 6.95. The apparatus used in the dissolution rate determinations was similar to that described by Wood *et al.* (9). Approximately 100 mg of the crystals was compressed[6] into a disk in an 8-mm stainless steel tablet die at approximately 1590 kg. The tablet die, with one face of the compressed disk exposed and in plane with the die surface, was placed in a plastic holder. The tablet assembly was rotated in 500 ml of dissolution medium at 50 rpm. The drug concentration in solution was continuously monitored by circulating the solution into a spectrophotometer[7] and continuously measuring the absorbance at 264 nm.

For the determination of the equilibrium solubility, an excess quantity of the crystals was shaken with 100 ml of the buffer solution in an erlen-

[1] Ciba-Geigy, Suffern, N.Y.
[2] Du Pont 990.
[3] Beckman model IR-33.
[4] Nujol.
[5] General Electric XRD-5.
[6] Carver press.
[7] Beckman DU.

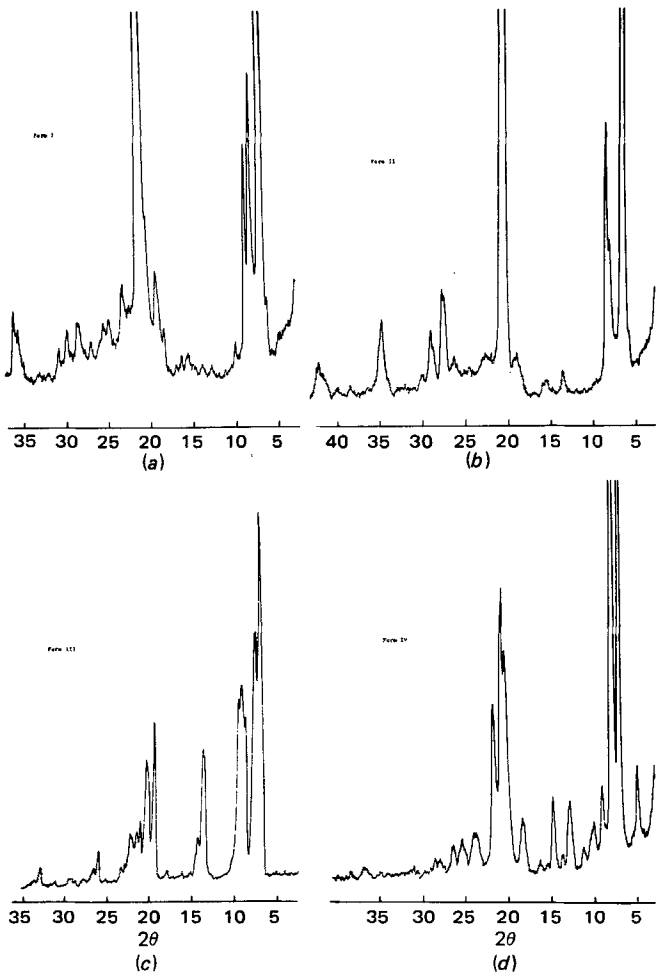

Figure 1—*X-ray diffraction patterns of phenylbutazone polymorphs. Forms I (a), II (b), and IV (d) were recorded at 1000-cps range, and Form III (c) was recorded at 2000-cps range.*

meyer flask immersed in a water bath thermostated to ±0.02°. No attempt was made to control the particle size of the crystals. At specific time intervals, 5 ml of the solution was withdrawn with a pipet fitted with a glass wool plug. Aliquots of 1 ml were withdrawn from the filtered solution and appropriately diluted, and the absorbance was measured spectrophotometrically at 264 nm.

Scanning Electron Microscopy—Compressed disks prepared in the same manner as those used for dissolution rate determinations were used for the scanning electron microscopy investigation[8]. The disks were flushed with air, and the photomicrographs were taken at magnifications ranging from 200 to 10,000×.

RESULTS AND DISCUSSION

Four crystalline modifications of phenylbutazone were obtained by the crystallization technique described and identified using data from X-ray diffraction, thermal analysis, and IR spectroscopy. Figure 1 shows the X-ray diffraction patterns of Forms I, II, III, and IV prepared from isobutyl alcohol, cyclohexane, *n*-heptane, and 2-propanol–water, respectively. Distinct differences are apparent and are attributed to differences in the arrangements of the molecules in the crystal lattices of the polymorphs.

The IR absorption spectra of the various forms showed recognizable differences in the detailed structure and intensities of some major absorption bands. Differences in the carbonyl stretching vibration region, specifically from 1760 to 1700 cm^{-1}, and in the 750–650-cm^{-1} region were peculiar for each form and could be used for the characterization and identification of the different crystalline phases. Differences in the ketone

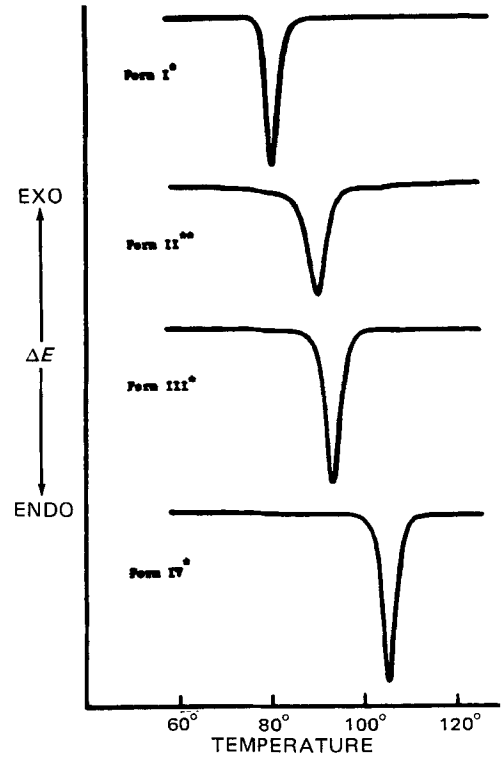

Figure 2—*Thermograms of the different crystal modifications at a heating rate of 20°/min. Key: *, crimped sample; and **, crystals heated in a covered pan with no pressure applied.*

skeletal vibration region (1350–1000 cm^{-1}) could also be attributed to differences in crystal structures. No attempt was made, however, to associate these differences with the modes of association of the molecules in the crystal lattice. The possibility of a solvate formation was excluded

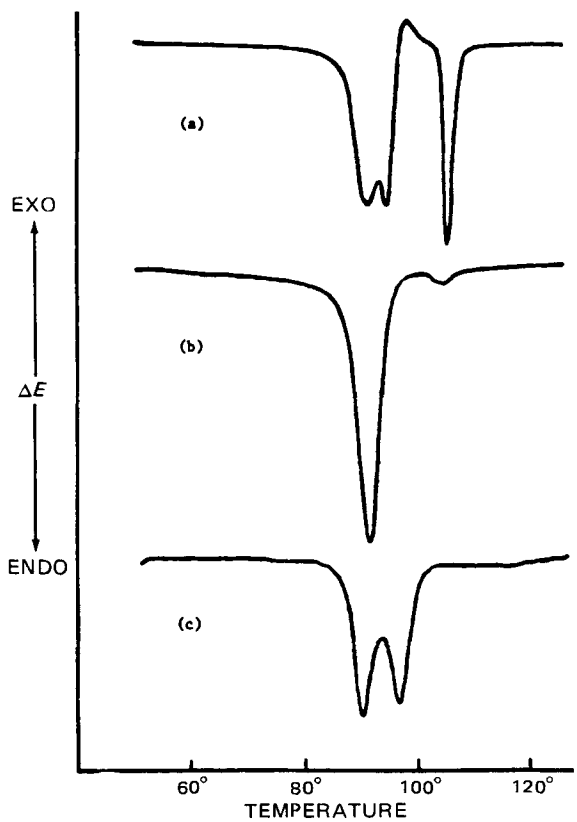

Figure 3—*Thermograms of polymorph II under different conditions of sample treatment. Key: (a), open pan; (b), covered pan; and (c), crimped sample.*

[8] Performed by Microne, Inc., Analytical & Consulting Services, Wilmington, DE 19807.

on the basis that both IR spectra and thermal analysis did not show any trace of the solvents used in the crystallization processes.

Differential scanning thermograms of I–IV are depicted in Fig. 2. In all instances, a lowering of 0.5–1° was noted in the recorded transition temperatures if the sample was crimped as compared to determinations in an open or covered pan. This decrease probably resulted from better thermal contact between the sample and the aluminum pan. Thermograms obtained for Forms III and IV were independent of the conditions of sample packing, whereas those of Forms I and II showed various phase changes depending on whether the heating was conducted in an open pan or a covered pan or whether the sample was crimped before heating.

The thermal behavior of Form II under different conditions of sample treatment is illustrated in Fig. 3. Samples heated in an open pan showed a noticeable solid–solid transformation and crystallization from melt. These effects are evident from the two endothermic peaks at 94 and 105° and the exotherm at 98° in the upper thermogram. The covered and crimped samples did not show any apparent crystallization from melt, probably because of the reduced thermal gradient within the sample.

The thermogram of the crimped sample in Fig. 3 is qualitatively in agreement with the middle thermogram in Fig. 4, where a small portion of a compressed disk of Form II was heated in a covered pan. Correlation between the two thermograms indicates that the appearance of an endotherm at 97–98° (which could possibly correspond to another form that has not been isolated as individual crystals yet) was caused by the compression pressure used in preparing the disk or even in crimping the sample.

Form IV, when heated up to 120°, cooled either naturally or with liquid nitrogen, and then subjected to thermal analysis, showed an endothermic peak at 97–98° instead of the original melting peak at 105°. On the other hand, slow controlled cooling of the melt resulted in the regeneration of the original crystals, *i.e.*, Form IV. Grinding of the rapidly cooled mass, as judged from the thermal behavior of the ground material, induced transformation to the most stable form, IV. Also, water caused such polymorphic changes when the rapidly cooled mass was kept in contact with aqueous buffer solutions. Despite the recorded differences in the X-ray diffraction patterns of the solidified mass and Forms III and IV, judgment on the authenticity of these differences should be made with great care because of the influence of the preferred orientations of the crystals in the solidified mass.

In a recent report concerning a nonclassical dissolution behavior of

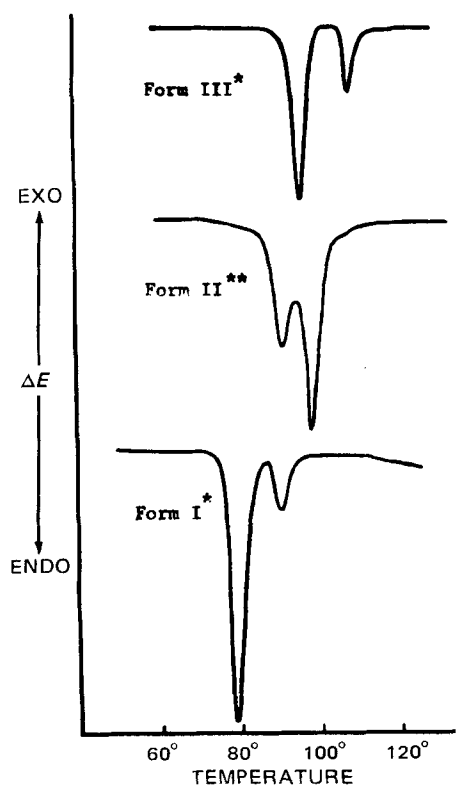

Figure 4—*Differential scanning thermograms of portions of compressed disks of Forms I–III. Key: *, crimped sample; and **, crystals heated in a covered pan with no pressure applied.*

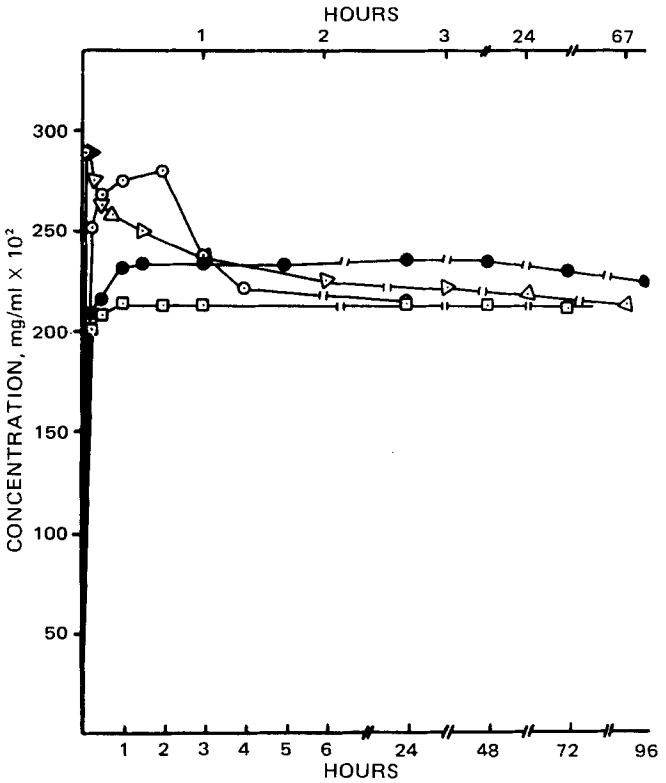

Figure 5—*Solubility profile of phenylbutazone polymorphs in phosphate buffer at 36°. Key: △, Form I (upper time scale); ⊙, Form II (lower time scale); ●, Form III (lower time scale); and □, Form IV (lower time scale).*

phenylbutazone, Stella (10) noted the existence of three crystalline phases of the compound. Melting points of 86, 96, and 106° were the only information provided about the polymorphs. The reported melting point of 96° is close to the melting point of 97–98° obtained for the rapidly cooled mass. So far, attempts to obtain phenylbutazone as individual

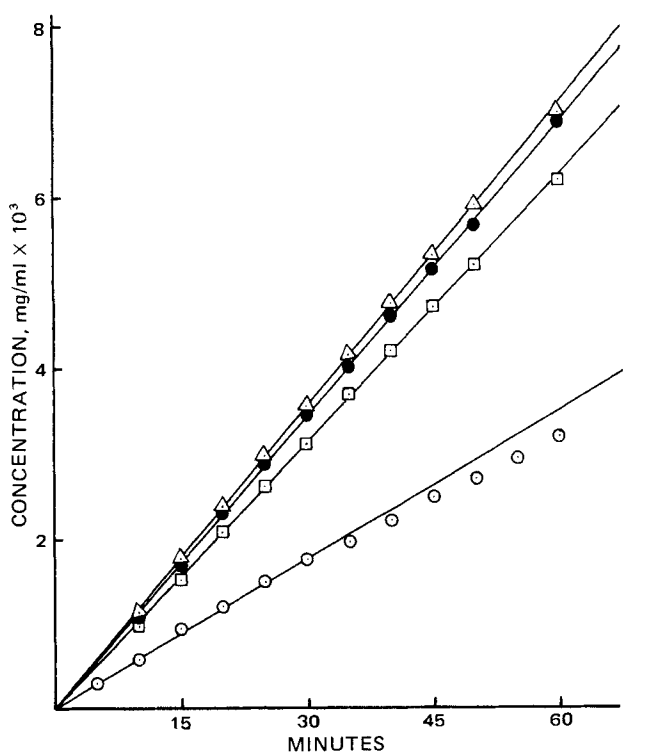

Figure 6—*Comparison of dissolution rates of phenylbutazone Forms I (△), II (⊙), III (●), and IV (□) in phosphate buffer at 36°.*

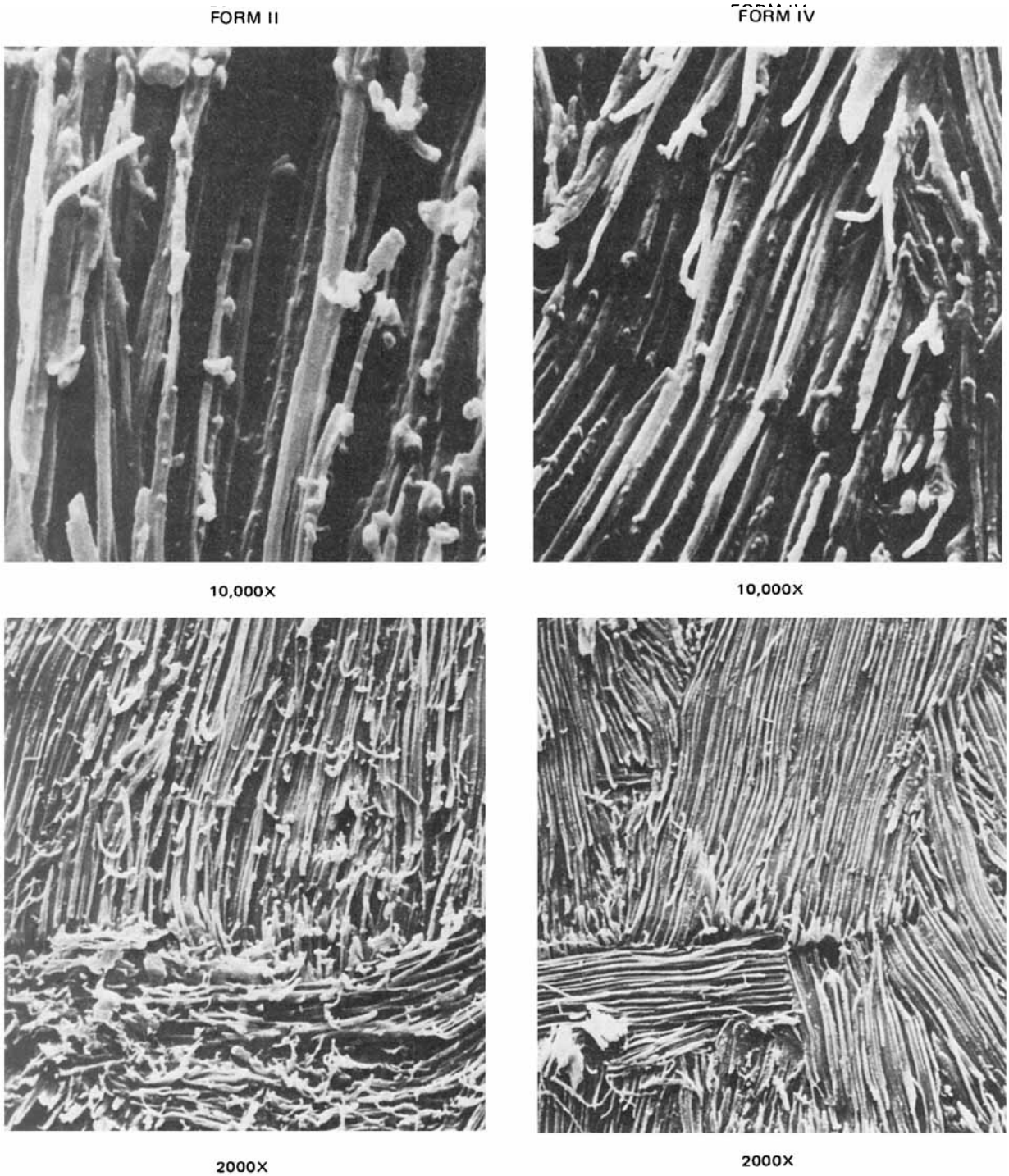

Figure 7—*Scanning electron photomicrographs of compressed disks of Forms II and IV.*

crystals with melting and spectral characteristics similar to those of the rapidly cooled mass, *e.g.*, by crystallization, have failed.

Similarly, Form I exhibited various transitions when heated under different conditions of sample treatment (Table I). Apparently, Form I is not as sensitive to crimping pressure as is Form II; however, heating of Form I in a covered pan induced solid–solid transformation to Form II.

Figure 4 shows thermograms obtained by heating a small portion of disks of Forms I–III, previously prepared by compacting approximately 100 mg of the crystals in an 8-mm die at 1590–2040 kg. Form III, during compression, was transformed to the most stable modification, Form IV. Forms I and II gave thermodynamically unstable phases, *i.e.*, Form II and a polymorphic species melting at 97–98°, respectively. Grinding of Forms I–III in a mortar induced polymorphic changes analogous to those observed when the respective crystal forms were compressed into disks. While compression of Form II into a disk consistently produced a polymorphic species melting at 97–98°, mortar grinding sometimes resulted in Form IV instead.

In view of the observed results, it is likely that similar effects on the crystals were produced by the shear stresses dominating in the mortar assembly and the shear stresses operative during compression and decompression of the disks. The notion of an active ingredient undergoing polymorphic changes during compression was discussed previously (11, 12). The variation and apparent increase in the dissolution rate of unlubricated sulfathiazole disks with pressure, as reported by Milosovich (13), were interpreted by Nogami *et al.* (14) to be caused by a change in the crystalline form. The effects of such polymorphic transformations on the dissolution rates as determined from compressed disks as well as from tablets containing transformation-labile ingredients are important to recognize. In fact, the determined dissolution rates vary depending

Table I—Phase Transitions in Form I when Heated under Different Conditions of Sample Treatment

Condition	Endothermic Transition	Exothermic Transition
Open pan	80°, 105°	92–94°
Covered pan	80°, 90°	—
Crimped sample	80°	—

on the type and proportions of the polymorphic species produced during compact preparation. This variation might affect drug bioavailability in an unpredictable and undesirable manner.

The dissolution profiles of the four crystal modifications (Fig. 5) show differences in solubilities and physical stabilities of the various forms in the aqueous medium. The apparent equilibrium solubilities (Table II) correspond in value to the peak solubilities as determined from the dissolution profiles. Form I gave the highest solubility in the aqueous buffer solution and was the fastest to achieve the degree of supersaturation necessary for the nucleation process. Apparent slower nucleation and crystal growth processes were associated with Form III compared to Forms I and II (Fig. 5). Since the degree of supersaturation achieved in a system containing Form III was much less than that in a system containing Form I or II, a much smaller driving force for the crystal growth process existed. Transformation of Forms I–III to the most stable modification, Form IV, at the end of the dissolution experiment was confirmed by IR and thermal analysis.

Solubility measurements at different temperatures were used to obtain information concerning enthalpy and entropy of transition from Form I to Form IV. The thermodynamic background of the relationship between polymorphism and solubility was extensively reviewed (15). A straight-line relationship between the logarithm of the solubility ratio of the two forms and the reciprocal of the absolute temperature was obtained, and the extrapolation of the line to a solubility ratio of unity corresponded to a transition temperature of 74.1°. The calculated enthalpy and entropy of transition were −1613 cal/mole and −4.6 eu, respectively. The observed entropy difference between phenylbutazone Forms I and IV suggests differences in the molecular association in the crystalline lattice of the two forms.

A comparison between the dissolution rates of the different crystal modifications is shown in Fig. 6. Because of the crystal changes that took place during the compression of Forms I–III into disks, the respective dissolution rates of the three forms are apparent rather than intrinsic dissolution rates. Unexpectedly, the dissolution rate of Form II was consistently lower than that of the most stable modification, IV. This low dissolution behavior persisted even for compressed disks prepared from 50% mixtures of II and IV and of II and I. The slopes of the concentration–time curves for the dissolution of such disks were of intermediate values between those of II and IV.

If a transport-controlled dissolution from the disk surface is assumed, the dissolution curves in Fig. 6 should adhere to the Noyes–Whitney equation and, in the initial stages of dissolution, the relationship between concentration in solution and time could be given by:

$$\frac{dC}{dt} = \frac{D}{Vh} AC_s \qquad \text{(Eq. 1)}$$

where D is the diffusion coefficient, h is the thickness of the diffusion layer, A is the surface area, and C_s is the saturated solubility of the crystalline solid in the medium. The volume of the dissolution medium, V, was kept constant by using 500 ml of the medium in each experiment. The four polymorphs should have the same values of D and h irrespective of the crystal form, and the increase in the slopes of the straight lines in Fig. 6 should follow the order reflected in their saturated solubilities. The latter holds true only when the area exposed to dissolution is the same for the four polymorphs. In view of the obtained results, it is likely that the physical characteristics of phenylbutazone Form II crystals are such that, upon compression, they produce disks with a smaller effective surface area compared to those of Form IV, even though the same conditions are maintained carefully during compression.

Table II—Differential Scanning Transition Temperatures and Peak Solubilities of the Different Polymorphs

Form	Solvent of Crystallization	Transition Temperature	Peak Solubility[a], mg/100 ml
I	Isobutyl alcohol	80°	288.7
II	Cyclohexane	90°	279.9
III	*n*-Heptane	93°	233.6
IV	2-Propanol–water	105°	213.0

[a] Solubility in phosphate buffer, pH 6.95, at 36°.

A qualitative assessment of the surfaces of compressed disks of Forms II and IV was sought through the use of the scanning electron microscope. Photomicrographs (Fig. 7) indicate differences in the surface characteristics of the disks. Also, it can be inferred from the pictures that the extent of corrugation per unit area of the surfaces differed. Although it is too difficult to describe differences in surface area in a quantitative manner, these differences reflect that crystals of different forms behave differently under compression. This fact could, at least in part, account for the observed anomaly in the dissolution rates of compressed disks of Form II compared to Form IV.

REFERENCES

(1) J. K. Haleblian, *J. Pharm. Sci.*, **64**, 1269 (1975).

(2) J. K. Haleblian and W. McCrone, *ibid.*, **58**, 911 (1969).

(3) D. L. Simmons, R. L. Ranz, and N. D. Gyanchandani, *Can. J. Pharm. Sci.*, **8**, 125 (1973).

(4) S. Khalil, M. Moustafa, A. Ebian, and M. Motawi, *J. Pharm. Sci.*, **61**, 1615 (1972).

(5) J. W. Shell, *ibid.*, **52**, 100 (1963).

(6) P. W. Bridgeman, *J. Appl. Phys.*, **27**, 659 (1956).

(7) H. G. Drickamer, *Science*, **156**, 1183 (1967).

(8) I. P. S. Kang, C. E. Kendall, and R. W. Lee, *J. Pharm. Pharmacol.*, **26**, 201 (1973).

(9) J. H. Wood, J. E. Syatto, and H. Letterman, *J. Pharm. Sci.*, **54**, 1068 (1965).

(10) V. J. Stella, *ibid.*, **64**, 706 (1975).

(11) J. E. Rees, *Bull. Chim. Farm.*, **112**, 216 (1973).

(12) J. K. Haleblian, R. T. Koda, and J. A. Biles, *J. Pharm. Sci.*, **60**, 1485 (1971).

(13) G. Milosovich, *ibid.*, **53**, 484 (1964).

(14) H. Nogami, T. Nagai, and A. Suzuki, *Chem. Pharm. Bull.*, **14**, 329 (1966).

(15) W. I. Higuchi, P. K. Lau, T. Higuchi, and J. W. Shell, *J. Pharm. Sci.*, **52**, 150 (1963).

ACKNOWLEDGMENTS AND ADDRESSES

Received April 23, 1976, from *Pharmacy Research & Development, Pharmaceuticals Division, Ciba-Geigy Corporation, Suffern, NY 10901.*

Accepted for publication July 1, 1976.

The authors thank Dr. H. Stober of Analytical Research & Development for assistance in the X-ray diffraction work.

[x] To whom inquiries should be directed.

Antipyretic Testing of Commercial Aspirin Formulations in Rats

J. J. LOUX *x, P. D. DePALMA *, R. Z. EBY ‡, and S. L. YANKELL *§

Abstract □ Four commercial aspirin formulations and aspirin powder USP were assayed in yeast-fevered rats for antipyretic activity. Tablets allowed to disintegrate spontaneously prior to dosing yielded aggregates of various sizes which failed to produce uniform patterns of antipyresis. When tested at smaller, more uniform particle sizes of total product, consistent, statistically significant antipyresis was observed with no significant variation among formulations. The ED_{50} values and parallel line assays were homogeneous.

Keyphrases □ Aspirin—four commercial formulations evaluated for antipyretic activity, compared to powder, effect of particle size, rats □ Antipyretic activity—aspirin, four commercial formulations evaluated and compared to powder, effect of particle size, rats □ Particle size—effect on antipyretic activity of aspirin, four commercial formulations evaluated and compared to powder, rats

Previously, this laboratory reported a method for obtaining statistically significant antipyresis in yeast-fevered rats utilizing low doses of aspirin (1). Since the aspirin tested was the pure chemical (white, crystalline powder, USP), those results provided little information on the pharmacological effects of commercial formulations. Thus, experiments were conducted, utilizing the same basic methodology, in which several commercially available products were assayed for their comparative antipyretic activity. Since it was anticipated that differences in activity might be realized with the various products, an attempt also was made to determine what factor(s) might be responsible for such variances.

EXPERIMENTAL

Male albino Charles River rats, 200–250 g, were used. Fever was induced by 20 ml/kg of a 20% aqueous suspension of brewer's yeast[1], which was injected subcutaneously in the back below the nape of the neck. The animals were then fasted for the duration of the experiment (approximately 24 hr). Water was available *ad libitum*.

Temperatures[2] were taken with a lubricated[3] thermistor probe[4] inserted approximately 4 cm into the rectum for 45 sec. Rectal temperatures were taken 24 hr after the yeast injection to determine the pyretic response to yeast. This response ranged between 1.25 and 2.0° above the normal nonfevered control value of 36.40°. No marked variability was encountered. These temperatures, taken 24 hr after yeast administration and 30 min prior to drug administration on fevered animals, served as the predrug controls.

Study 1—Eight animals were used per dose for each compound studied, with eight animals serving as controls. The following were tested: Formulation 1, an aspirin tablet[5]; Formulation 2, a generic aspirin tablet[6]; Formulation 3, a buffered aspirin tablet[7]; Formulation 4, an effervescent aspirin tablet[8]; and Formulation 5, aspirin powder USP[9] as the positive control.

All preparations were tested at equal doses in terms of aspirin content, determined from the "Handbook of Non-Prescription Drugs" (2), label statements, and multiple weighings of groups of 10 tablets.

All preparations except the effervescent one were allowed to disintegrate spontaneously in 0.5% tragacanth; water was employed for the effervescent preparation. Disintegration was considered complete when the respective test preparations had fallen apart into small particles, usually in 5 min or less. After the stock bottles were manually shaken, a stirring bar[10] was added to each. The bottles remained on magnetic stirring plates throughout the animal dosing. Doses employed were 18.75, 37.50, 75, and 150 mg/kg po at a dose volume of 10 ml/kg. Control animals received 0.5% tragacanth at 10 ml/kg. Antipyretic activity was measured at 15, 30, 60, 120, 180, and 240 min after administration.

Study 2—The data from Study 1 indicated variable antipyretic activity among the test formulations. Thus, in this study the following variables were controlled carefully.

Differences in Aspirin Content, Tablet to Tablet—Groups of 10 tablets were ground, and an aliquot was taken of the resulting powder.

Particle Size—All preparations were further extensively ground to a uniform fine particle size in a mortar prior to suspension in the vehicle. With standard USP XVIII sieves (3), it was determined that all products assayed in Study 2, prior to suspension in a vehicle, had a particle-size composition of which 60% passed a 60-mesh, 20% passed an 80-mesh, and 20% passed a 100-mesh sieve.

Dilutions—All doses of a given formulation were prepared by serial dilutions of the respective formulation.

Pyretic Response—The pyretic response to yeast injections was controlled by not using any animal that did not demonstrate a minimum 1.5° elevation in rectal temperature.

Experimenters—The entire study was performed by the same experimenter to eliminate any variability between technical personnel.

The time action study in Study 1 showed that the peak antipyretic activity of aspirin occurred between 1 and 2 hr. The tight, within-group variability in Study 2 along with the steep slope seen in a preliminary dose range study suggested that only four animals per dose were needed. This modification was introduced based on complete statistical analysis of the data. Previous unreported work in this laboratory has repeatedly demonstrated that control yeast responding animals maintain a long pyretic response (up to 4 or 5 hr).

Each of the five preparations was tested at the following doses in terms of aspirin content: 18.75, 37.50, 75, and 150 mg/kg po. Two animals were tested at each dose of each preparation on 2 consecutive days. Thus, any day-to-day variability effect was balanced over all preparations to yield unbiased comparisons. The antipyretic activity assay was measured at 60 and 120 min.

The data were analyzed for the presence of statistically significant antipyretic activity, and ED_{50} values with 95% confidence limits were calculated by paired analysis (4). The ED_{50} refers to the dose of test compound (milligrams per kilogram) that reduced the rectal temperature in treated fevered rats to 50% of the response observed in the fevered nontreated control groups. "Significant antipyretic activity" indicates statistical significance at p values of <0.05. Parallel-line bioassay was performed to test deviation from linearity and parallelism (5).

RESULTS

Study 1—The data from Study 1 indicated that all compounds tested produced effective antipyresis for the duration of the study (4 hr). The time to peak effect was between 2 and 3 hr. Controls did not vary significantly over the 4-hr test period.

Since all preparations were tested at equivalent doses of aspirin, an attempt was made statistically to prepare comparative dose–response

[1] Mead Johnson, Evansville, Ind.
[2] Tele-Thermometer, model 44DT, Yellow Springs Instrument Co., Yellow Springs, Ohio.
[3] K-Y Jelly, Johnson & Johnson, New Brunswick, N.J.
[4] Series 400, Yellow Springs Instrument Co., Yellow Springs, Ohio.
[5] Bayer aspirin, Bayer Co., Glenbrook Laboratories, Division of Sterling Drug, New York, NY 10016.
[6] Rite Aid aspirin, Rite Aid Corp., Shiremanstown, PA 17091.
[7] Bufferin, Bristol-Myers Co., New York, NY 10022.
[8] Alka-Seltzer, Miles Laboratories, Elkhart, IN 46514.
[9] Pure aspirin crystalline powder from bulk lot used in Ecotrin, Smith Kline and French Laboratories, Philadelphia, PA 19101.
[10] Coated with Teflon (du Pont).

Table I—Mean Antipyretic Responses of Test Formulations in Yeast-Fevered Rats Given Spontaneously Disintegrated Tablets

Formulation	Dose, mg/kg	Predrug Rectal Temperature	Time after Administration, min: 15	30	60	120	180	240
			Mean Decrease in Temperature					
1	150	37.94°	0.32°	0.96°	2.02°	2.46°	2.73°	2.42°
	75	37.88°	0.61°	0.86°	1.34°	1.92°	1.94°	1.77°
	37.5	37.80°	0.32°	0.82°	0.94°	1.01°	1.04°	0.95°
	18.75	37.52°	0.01°	0.28°	0.27°	0.51°	0.60°	0.42°
2	150	37.82°	0.33°	0.98°	1.56°	2.12°	2.03°	1.92°
	75	37.74°	0.50°	0.91°	1.53°	2.01°	2.11°	1.79°
	37.5	37.69°	0.05°	0.36°	0.37°	0.67°	0.88°	0.69°
	18.75	37.85°	0.15°	0.20°	0.51°	0.51°	0.46°	0.47°
3	150	37.94°	0.17°	0.73°	1.47°	1.93°	1.99°	2.13°
	75	37.72°	0.02°	0.44°	0.88°	1.68°	1.63°	1.46°
	37.5	37.75°	0.13°	0.49°	0.98°	0.72°	0.78°	0.75°
	18.75	37.92°	0.16°	0.36°	0.49°	0.68°	0.38°	0.46°
4	150	37.78°	0.25°	0.73°	1.08°	1.74°	1.69°	1.33°
	75	37.95°	0.51°	1.02°	1.32°	1.81°	1.81°	1.62°
	37.5	37.79°	0.37°	0.23°	0.48°	0.55°	0.52°	0.32°
	18.75	37.71°	0.10°	0.10°	0.48°	0.59°	0.80°	0.52°
5	150	37.92°	0.38°	1.29°	2.27°	2.78°	3.08°	2.82°
	75	37.62°	0.18°	0.51°	0.96°	1.59°	1.63°	1.47°
	37.5	37.74°	0.22°	0.51°	0.78°	1.16°	0.78°	0.86°
	18.75	37.80°	0.48°	0.37°	0.64°	0.73°	0.59°	0.68°
Controls	—	37.85°	0.13°	0.05°	0.04°	0.06°	0.16°	0.15°

curves. However, significant variations were present that precluded fitting linear and parallel lines to the data. As an alternative, the 1- and 2-hr postdrug responses to the highest dose tested were compared and ranked according to effectiveness. This approach showed that Formulation 5 was the most effective, closely followed by Formulation 1. These agents did not differ from each other. The remaining formulations were statistically less effective, with Formulation 2 better than Formulation 3. Formulation 4 was the least effective. Table I presents the mean antipyretic responses for each dose of the five test formulations at each time period.

Study 2—The mean antipyretic responses for each dose of the five test formulations at each time period are presented in Table II. The ED_{50} values with 95% confidence limits are presented in Table III for both the 2- and 3-hr data. Statistically significant antipyresis was observed for all formulations. The ED_{50} values ranged between 17.2 and 22.7 mg/kg. All responses were linear and parallel. No significant variation was observed between any two formulations. The statistical evaluation of the 2-hr data is presented in Table IV.

The test of validity showed that deviations from parallelism and from linearity were not significant. Thus, relative potencies and 95% confidence limits were calculated. The relative potencies were very near 1.0 (*i.e.*, equality) with 95% confidence limits that bracket 1.0. There was no significant difference in potency between any of these preparations.

Table II—Mean Antipyretic Responses of Test Formulations in Yeast-Fevered Rats Given Finely Ground Tablets

Formulation	Dose, mg/kg	Predrug Rectal Temperature	Time after Administration, min: 120	180
			Mean Decrease in Temperature	
1	150	37.88°	2.10°	2.00°
	75	37.95°	1.80°	1.78°
	37.5	37.55°	1.35°	1.78°
	18.75	37.88°	0.95°	1.25°
2	150	37.85°	2.40°	2.08°
	75	37.78°	1.78°	1.95°
	37.5	37.95°	1.60°	1.40°
	18.75	38.00°	0.88°	0.77°
3	150	37.78°	1.95°	1.98°
	75	37.78°	1.72°	1.52°
	37.5	37.78°	1.60°	1.52°
	18.75	37.80°	0.80°	1.10°
4	150	37.92°	2.52°	2.20°
	75	37.82°	1.78°	1.58°
	37.5	37.92°	1.17°	1.35°
	18.75	37.80°	0.65°	0.50°
5	150	37.85°	2.10°	2.05°
	75	37.98°	2.08°	1.80°
	37.5	37.88°	1.60°	1.65°
	18.75	37.72°	0.85°	0.75°
Controls	—	37.95°	0.20°	0.25°

DISCUSSION

The initial study (1) described the criteria for significant antipyresis; *i.e.*, the test substance must reduce the pyretic response induced by yeast to 50% of the value obtained for the controls. The pyretic control value in this study was 1.86° above the value before yeast administration, which indicated a satisfactory response to the pyretic agent. All test formulations allowed to disintegrate spontaneously prior to testing exhibited effective antipyretic responses (Table I). However, the study indicated wide variability; some preparations exhibited poor activity at doses as high as 75 mg/kg while another demonstrated good activity at half that dose.

Examination of these data for the time course of activity also demonstrated variability in that one preparation effected favorable activity at 30 min with 75 mg/kg whereas another preparation required 120 min to exhibit similar activity at the same dose. Since it had previously been determined that the ED_{50} for aspirin was 10.3 (1.8–23) mg/kg, the lack of significant antipyresis at doses up to 75 mg/kg in this portion of the study was questioned. However, these results were not entirely unexpected. Apparently, one may not assume that equal doses of the same compounds (in terms of active ingredient) will produce the same degree of pharmacological effect. The results clearly indicate that the behavior of several commercial preparations of aspirin was variable when tested under similar experimental conditions.

Some factors contributing to the variability in drug response include nonuniformity of dose among the test preparations (6), disintegration

Table III—ED_{50} and Relative Potency of Test Formulations

Formulation	ED_{50} (95% Confidence Limits), mg/kg	Relative Potency (95% Confidence Limits)
	120-min Data	
1	20.6 (14.4–28.0)	0.85 (0.57–1.27)
2	17.4 (11.9–23.8)	1.01 (0.68–1.51)
3	21.6 (15.2–29.3)	0.81 (0.54–1.21)
4	21.2 (14.9–28.7)	0.83 (0.55–1.23)
5	17.5 (12.0–24.0)	Standard
	180-min Data	
1	17.9 (11.1–26.4)	0.96 (0.57–1.59)
2	17.5 (10.8–25.9)	0.98 (0.59–1.63)
3	18.1 (11.2–26.7)	0.95 (0.57–1.57)
4	22.7 (14.5–32.9)	0.76 (0.45–1.25)
5	17.2 (10.5–25.3)	Standard

Table IV—Analysis of Variance for 2-hr Data, Study II, Antipyresis in Rats

Source	*df*	*MS*	*F*
Treatments	20	1.310	9.51
Control *versus* preparations	1	3.197	23.2
Among preparations	4	0.078	0.57
Regression	1	20.566	149.3
Deviation from parallelism	4	0.216	1.57 N.S.
Deviation from linearity	10	0.126	0.92 N.S.
Error	143	0.138	
Total	163		

and dissolution characteristics of the various preparations (7), additives that alter the absorptive processes in the GI tract (8), particle size (9, 10), fasted *versus* nonfasted subjects (7), and normal *versus* febrile (disease) states (11). In these studies, nonuniformity of dose was controlled by testing all preparations at equivalent aspirin doses. The disintegration parameter was controlled by allowing complete disintegration of tablets prior to dosing the animal. Since it has been pointed out that the amounts of buffering agents contained in analgesic products are probably insufficient in quantity to affect drug action or gastric pH (8, 12), this parameter was considered insignificant. Finally, all animals were fasted and febrile. However, one parameter was not controlled: particle size.

The particle size of a drug influences dissolution or disintegration rates of tablets (9) and absorption from the GI tract (10, 13). Study 2 attempted, in part, to control particle size more closely. In this second study, in which testing parameters were more tightly controlled, the data obtained indicated statistically significant antipyresis for all test preparations, and no statistical or pharmacological differences could be determined among the various test preparations.

Relatively few reports have been published wherein an attempt was made to ascertain the variability of pharmacological response relative to controlled particle sizes. One report (11) detailed the variability of responses not only due to different particle sizes but also due to differences in dissolution rates and absorption rates, all of which are interdependent. An interesting factor was noted, *i.e.*, that the plasma concentration and time course activity of aspirin not only differs with the particle size of aspirin crystals but also differs between febrile and normal rabbits; febrile rabbits obtain faster, higher, and longer blood levels than the nonfevered controls.

Additionally, data reported (11) for the antipyretic activity of various aspirin preparations of different particle sizes in fevered rabbits correlate with the present data for fevered rats dosed with random particle-size aspirin. Itami *et al.* (11) concluded that the data supported the theory that as the particle size of aspirin decreases, antipyretic activity is more pronounced and more rapid in onset. Study 2 results also supported this theory, particularly at low dose levels where the antipyretic activity (Table II) was markedly different than the activity of the larger sized aggregates (Table I).

On the other hand, the favorable improvement in the physical properties of aspirin crystals may be reversed when subjected to the tableting process (9), a factor that also could compromise much of the pharmacological benefits derived from smaller crystal size. Thus, the recent suggestion (14) that aspirin tablets be crushed or chewed to a fine powder prior to being swallowed merits some attention.

REFERENCES

(1) J. J. Loux, P. D. DePalma, and S. L. Yankell, *Toxicol. Appl. Pharmacol.*, **22**, 672 (1972).

(2) W. H. Barr and R. P. Penna, in "Handbook of Non-Prescription Drugs," G. B. Griffenhagen and L. L. Hawkins, Eds., American Pharmaceutical Association, Washington, D.C., 1973, p. 36 *ff.*

(3) "The United States Pharmacopeia," 18th rev., Mack Publishing Co., Easton, Pa., 1970, p. 940.

(4) K. A. Brownlee, in "Statistical Theory and Methodology in Science and Engineering," Wiley, New York, N.Y., 1965, p. 346.

(5) D. J. Finney, in "Statistical Methods in Biological Assay," Hafner, New York, N.Y., 1952, chap. 4.

(6) W. L. Chiou, *J. Clin. Pharmacol.*, **14**, 277 (1974).

(7) G. Levy, *J. Pharm. Sci.*, **50**, 388 (1961).

(8) G. Levy and B. A. Hayes, *N. Engl. J. Med.*, **262**, 1053 (1960).

(9) E. Cid and F. Jaminet, *Farmaco, Ed. Prat.*, **27**, 298 (1972).

(10) G. Levy, *Am. J. Pharm.*, **135**, 78 (1963).

(11) T. Itami, M. Yoshida, and S. Kahoh, *Eisei Shikenjo Hokohu*, **91**, 27 (1973).

(12) R. Rubin, E. W. Pelikan, and C. J. Kensler, *N. Engl. J. Med.*, **261**, 1208 (1959).

(13) S. Ljungberg and G. Otto, *Acta Pharm. Suec.*, **7**, 449 (1970).

(14) M. I. Blake, *J. Am. Med. Assoc.*, **230**, 1385 (1974).

ACKNOWLEDGMENTS AND ADDRESSES

Received September 8, 1975, from the *Department of Biological Sciences, Research and Development Division, Menley & James Laboratories, Ltd., Philadelphia, PA 19101, and the ‡Department of Biostatistics, Smith Kline and French Laboratories, Philadelphia, PA 19101.

Accepted for publication July 6, 1976.

§ Present address: University of Pennsylvania School of Dental Medicine, Philadelphia, PA 19174.

ˣ To whom inquiries should be directed. Present address: Department of Pharmacology, Cooper Laboratories, Cedar Knolls, NJ 07927.

Effect of Temperature and Relative Humidity on Nitrazepam Stability in Solid State

D. GENTON and U. W. KESSELRING ˣ

Abstract □ The decomposition of a 1% dilution of nitrazepam in microcrystalline cellulose was established by quantitative determination of the two main breakdown products, 2-amino-5-nitrobenzophenone and 3-amino-6-nitro-4-phenyl-2(1*H*)-quinolone, using *in situ* diffuse reflectance measurements on thin-layer chromatograms. The decomposition and formation rate constants of nitrazepam and of the breakdown products, respectively, were determined at four temperatures and six relative humidities. By means of a three-parameter regression equation, it was possible to correlate quantitatively the decomposition constant of nitrazepam to both temperature and relative humidity.

Keyphrases □ Nitrazepam, solid—decomposition in microcrystalline cellulose, effect of temperature and humidity □ Decomposition—nitrazepam in solid state in microcrystalline cellulose, effect of temperature and humidity □ Stability—nitrazepam in solid state in microcrystalline cellulose, effect of temperature and humidity □ Anticonvulsants—nitrazepam in solid state in microcrystalline cellulose, decomposition, effect of temperature and humidity □ Solid state—decomposition, nitrazepam in microcrystalline cellulose, effect of temperature and humidity

Stability studies of drugs in pure form and in solid dosage forms were reviewed and summarized previously (1, 2). Apparently, no workers have attempted to combine the influences of both temperature and humidity (or water content) in a unique mathematical expression.

The purpose of this work was to assess quantitatively

Table IV—Analysis of Variance for 2-hr Data, Study II, Antipyresis in Rats

Source	*df*	*MS*	*F*
Treatments	20	1.310	9.51
Control *versus* preparations	1	3.197	23.2
Among preparations	4	0.078	0.57
Regression	1	20.566	149.3
Deviation from parallelism	4	0.216	1.57 N.S.
Deviation from linearity	10	0.126	0.92 N.S.
Error	143	0.138	
Total	163		

and dissolution characteristics of the various preparations (7), additives that alter the absorptive processes in the GI tract (8), particle size (9, 10), fasted *versus* nonfasted subjects (7), and normal *versus* febrile (disease) states (11). In these studies, nonuniformity of dose was controlled by testing all preparations at equivalent aspirin doses. The disintegration parameter was controlled by allowing complete disintegration of tablets prior to dosing the animal. Since it has been pointed out that the amounts of buffering agents contained in analgesic products are probably insufficient in quantity to affect drug action or gastric pH (8, 12), this parameter was considered insignificant. Finally, all animals were fasted and febrile. However, one parameter was not controlled: particle size.

The particle size of a drug influences dissolution or disintegration rates of tablets (9) and absorption from the GI tract (10, 13). Study 2 attempted, in part, to control particle size more closely. In this second study, in which testing parameters were more tightly controlled, the data obtained indicated statistically significant antipyresis for all test preparations, and no statistical or pharmacological differences could be determined among the various test preparations.

Relatively few reports have been published wherein an attempt was made to ascertain the variability of pharmacological response relative to controlled particle sizes. One report (11) detailed the variability of responses not only due to different particle sizes but also due to differences in dissolution rates and absorption rates, all of which are interdependent. An interesting factor was noted, *i.e.*, that the plasma concentration and time course activity of aspirin not only differs with the particle size of aspirin crystals but also differs between febrile and normal rabbits; febrile rabbits obtain faster, higher, and longer blood levels than the nonfevered controls.

Additionally, data reported (11) for the antipyretic activity of various aspirin preparations of different particle sizes in fevered rabbits correlate with the present data for fevered rats dosed with random particle-size aspirin. Itami *et al.* (11) concluded that the data supported the theory that as the particle size of aspirin decreases, antipyretic activity is more pronounced and more rapid in onset. Study 2 results also supported this theory, particularly at low dose levels where the antipyretic activity (Table II) was markedly different than the activity of the larger sized aggregates (Table I).

On the other hand, the favorable improvement in the physical properties of aspirin crystals may be reversed when subjected to the tableting process (9), a factor that also could compromise much of the pharmacological benefits derived from smaller crystal size. Thus, the recent suggestion (14) that aspirin tablets be crushed or chewed to a fine powder prior to being swallowed merits some attention.

REFERENCES

(1) J. J. Loux, P. D. DePalma, and S. L. Yankell, *Toxicol. Appl. Pharmacol.*, **22**, 672 (1972).

(2) W. H. Barr and R. P. Penna, in "Handbook of Non-Prescription Drugs," G. B. Griffenhagen and L. L. Hawkins, Eds., American Pharmaceutical Association, Washington, D.C., 1973, p. 36 *ff.*

(3) "The United States Pharmacopeia," 18th rev., Mack Publishing Co., Easton, Pa., 1970, p. 940.

(4) K. A. Brownlee, in "Statistical Theory and Methodology in Science and Engineering," Wiley, New York, N.Y., 1965, p. 346.

(5) D. J. Finney, in "Statistical Methods in Biological Assay," Hafner, New York, N.Y., 1952, chap. 4.

(6) W. L. Chiou, *J. Clin. Pharmacol.*, **14**, 277 (1974).

(7) G. Levy, *J. Pharm. Sci.*, **50**, 388 (1961).

(8) G. Levy and B. A. Hayes, *N. Engl. J. Med.*, **262**, 1053 (1960).

(9) E. Cid and F. Jaminet, *Farmaco, Ed. Prat.*, **27**, 298 (1972).

(10) G. Levy, *Am. J. Pharm.*, **135**, 78 (1963).

(11) T. Itami, M. Yoshida, and S. Kahoh, *Eisei Shikenjo Hokohu*, **91**, 27 (1973).

(12) R. Rubin, E. W. Pelikan, and C. J. Kensler, *N. Engl. J. Med.*, **261**, 1208 (1959).

(13) S. Ljungberg and G. Otto, *Acta Pharm. Suec.*, **7**, 449 (1970).

(14) M. I. Blake, *J. Am. Med. Assoc.*, **230**, 1385 (1974).

ACKNOWLEDGMENTS AND ADDRESSES

Received September 8, 1975, from the *Department of Biological Sciences, Research and Development Division, Menley & James Laboratories, Ltd., Philadelphia, PA 19101, and the ‡Department of Biostatistics, Smith Kline and French Laboratories, Philadelphia, PA 19101.

Accepted for publication July 6, 1976.

§ Present address: University of Pennsylvania School of Dental Medicine, Philadelphia, PA 19174.

ˣ To whom inquiries should be directed. Present address: Department of Pharmacology, Cooper Laboratories, Cedar Knolls, NJ 07927.

Effect of Temperature and Relative Humidity on Nitrazepam Stability in Solid State

D. GENTON and U. W. KESSELRING ˣ

Abstract □ The decomposition of a 1% dilution of nitrazepam in microcrystalline cellulose was established by quantitative determination of the two main breakdown products, 2-amino-5-nitrobenzophenone and 3-amino-6-nitro-4-phenyl-2(1*H*)-quinolone, using *in situ* diffuse reflectance measurements on thin-layer chromatograms. The decomposition and formation rate constants of nitrazepam and of the breakdown products, respectively, were determined at four temperatures and six relative humidities. By means of a three-parameter regression equation, it was possible to correlate quantitatively the decomposition constant of nitrazepam to both temperature and relative humidity.

Keyphrases □ Nitrazepam, solid—decomposition in microcrystalline cellulose, effect of temperature and humidity □ Decomposition—nitrazepam in solid state in microcrystalline cellulose, effect of temperature and humidity □ Stability—nitrazepam in solid state in microcrystalline cellulose, effect of temperature and humidity □ Anticonvulsants—nitrazepam in solid state in microcrystalline cellulose, decomposition, effect of temperature and humidity □ Solid state—decomposition, nitrazepam in microcrystalline cellulose, effect of temperature and humidity

Stability studies of drugs in pure form and in solid dosage forms were reviewed and summarized previously (1, 2). Apparently, no workers have attempted to combine the influences of both temperature and humidity (or water content) in a unique mathematical expression.

The purpose of this work was to assess quantitatively

Table I—Sample Storage Conditions

Temperature[a]			
42.5°	55.0°	73.8°	83.4°
Relative Humidity[b], %			
29.9	30.6	32.1	29.3
38.6	55.3	40.9	38.1
47.9	49.2	51.7	53.1
60.6	60.3	59.3	60.2
66.3	67.5	69.0	70.0
82.2	82.7	83.8	83.8

[a] Mean values of 30 control measurements taken with a precision thermometer in 40 days. The corresponding standard deviations are ±0.6, ±0.1, ±1.4, and ±1.3° for 42.5, 55.0, 73.8, and 83.4°, respectively. [b] Precision was better than ±2% using a SINAequiHygroscope type eZFBA-PP, Sina AG, Zurich, Switzerland.

the separate and combined influences of temperature and humidity on the decomposition of a 1% dilution of nitrazepam in microcrystalline cellulose.

EXPERIMENTAL

Compounds—Nitrazepam[1] (1,3-dihydro-7-nitro-5-phenyl-2*H*-1,4-benzodiazepin-2-one) (I), 2-amino-5-nitrobenzophenone[1] (II), 3-amino-6-nitro-4-phenyl-2(1*H*)-quinolone[1] (III), and microcrystalline cellulose[2] were used as received. All reagents were of analytical grade or Pharm. Helv. VI quality.

Sample Storage Conditions—Individual samples of about 300 mg of microcrystalline cellulose containing 1.00% nitrazepam were stored as described previously (3) at relative humidities of about 30, 40, 50, 60, 70, and 80% (4) and at around 40, 55, 70, and 85° (Table I).

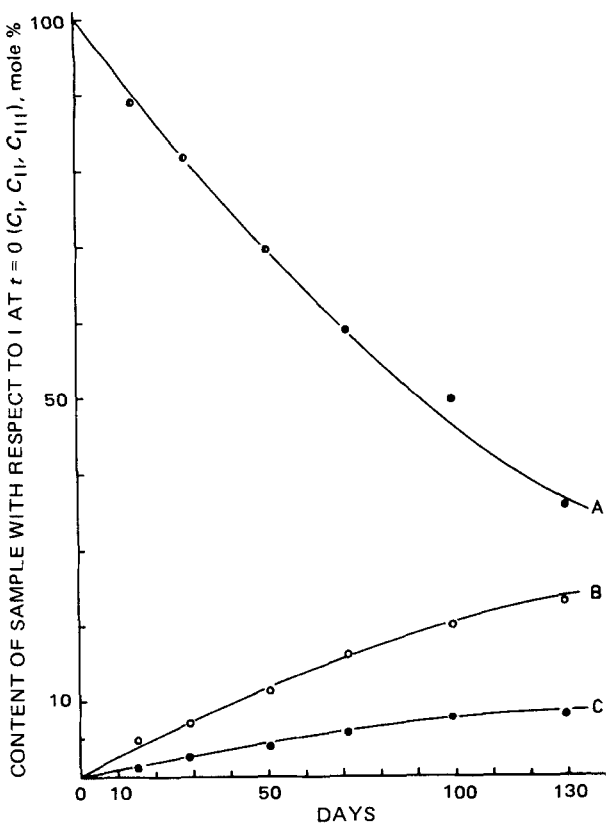

Figure 1—*Nitrazepam stability at 38.1% relative humidity and 83.4°. Key: A, decomposition of I; B, formation of II; and C, formation of III.*

[1] F. Hoffmann–La Roche & Co. SA., Basel, Switzerland.
[2] Avicel PH-101, Interchemie, Zurich, Switzerland.

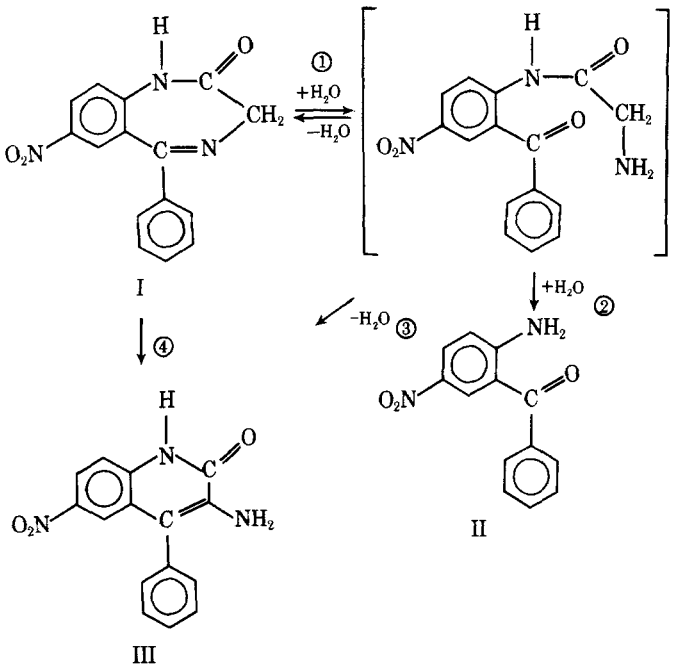

Scheme I

Quantitative Analysis—The quantitative analysis consisted essentially of extraction of I–III with methanol, their separation by TLC, and their quantitative determination by *in situ* diffuse reflectance measurements.

Extraction—Methanol, 3.00 ml, was added to the sample and vigorously shaken for 10 min. After the microcrystalline cellulose formed a deposit, the liquid layer was collected and centrifuged for 5 min. The clear solution, transferred to a hermetically sealable test tube, constituted the sample solution and eventually was diluted for quantitative determination, depending on the degree of decomposition.

Separation by TLC—The stationary phase was 0.40-mm kieselgel GF_{254}[3]-coated plates, dried for 12 hr at room temperature and activated just before use at 105° for 10 min. The mobile phase was benzene–ethyl acetate–acetic acid (60:36:4). The chamber saturation time was 1 hr, and the development time was 1 hr for the whole plate (about 18 cm).

Standard solutions, which were stable for about 6 months if stored away from light and at 4°, were at concentrations of 0.04–0.26, 0.02–0.10, and 0.02–0.10 mg/ml in methanol for I, II, and III, respectively.

One plate was used for the assay of each substance. With a precision syringe, seven spots (five standards and two samples) of 5 μl, one every 2.5 cm, were applied in increasing order of standard concentration with the samples placed third and fifth. The developed chromatograms were dried for 40 min in a cold air stream. The spots were located by visualizing with UV light at 254 nm.

Quantitative Evaluation—The spots were quantitatively evaluated by diffuse reflectance measurements[4] at 265, 365, and 295 nm for I, II, and III, respectively. The instrument conditions were: diaphragm opening, 12 mm; amplification, 10/10/I/A; scanning speed of the chromatogram, 3 cm/min; and chart flow (log scale), 10 cm/min. The peak surfaces, determined by direct integration[5], were linearly related to concentration in the ranges of 0–1.3 μg for I and 0–0.5 μg for II and III.

Kinetics (5)—The following decomposition scheme, reported previously (6–8) and confirmed by this work, shows the main decomposition routes of nitrazepam in the solid state under the influence of temperature and humidity (Scheme I). The bimolecular reactions 1 and 2 are acid–base catalyzed and depend on the amount of water available. The main decomposition product is II in aqueous solution and III in the solid state, with the II–III ratio depending on the availability of water (6). For low water concentrations, reactions 2 and 3 are competitive with preferential formation, especially in the solid state, of the quinolone derivative. The isomerization reaction 4 occurs only around and above the fusion temperature.

[3] E. Merck, Darmstadt, Germany.
[4] Zeiss PMQ II densitometer, Carl Zeiss, Oberkochen, Germany.
[5] W + W model 3212 recorder, Electronic Inc., Basel, Switzerland.

Table II—Experimental Values of k_1 and k_2

Temperature	Relative Humidity, %	k_1, day^{-1} × 10^5	y_0[a], %	r^2[b]	k_2, day^{-1} × 10^5	y_0[c], %	r^2[b]
42.5°	38.6	—	—	—	2.83	0.07	0.946
	47.9	2.69	0.01	0.998	2.97	0.08	0.900
	60.6	6.77	−0.25	0.887	11.67	−0.13	0.968
	66.3	6.09	−0.10	0.960	26.81	0.01	0.992
	82.2	5.30	−0.19	0.654	21.43	0.48	0.952
55.0°	30.6	—	—	—	4.42	0.03	0.981
	49.2	6.28	−0.06	0.867	12.48	−0.05	0.960
	55.3	11.03	−0.31	0.976	17.28	0.07	0.978
	60.3	14.73	−0.20	0.955	29.01	0.41	0.985
	67.5	32.26	−0.25	0.895	86.14	−0.27	0.993
	82.7	26.92	−0.47	0.810	101.11	0.18	0.966
73.8°	32.1	7.55	0.02	0.850	14.89	0.45	0.858
	41.0	19.10	−0.08	0.927	37.51	0.25	0.982
	51.7	29.05	0.02	0.950	84.99	0.48	0.988
	59.3	90.43	0.46	0.965	282.32	0.27	0.994
	69.0	246.89	0.47	0.979	482.52	0.25	0.996
	83.8	130.84	0.03	0.971	487.64	−0.17	0.989

[a] y_0 = y-intercept (*cf.*, Eq. 4); theoretically zero. [b] r^2 = coefficient of determination. [c] y_0 = y-intercept (*cf.*, Eq. 5); theoretically zero.

Nitrazepam (I) decomposes in two pseudo-first-order parallel reactions to II and III according to Scheme II:

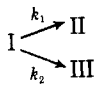

Scheme II

and:

$$C_I = C_{I_0}e^{-Kt} \quad \text{(Eq. 1)}$$

$$\log C_I = 0.4343Kt + \log C_{I_0} \quad \text{(Eq. 2)}$$

$$K = k_1 + k_2 \quad \text{(Eq. 3)}$$

$$C_{II} = \frac{k_1}{K} C_{I_0}(1 - e^{-Kt}) \quad \text{(Eq. 4)}$$

$$C_{III} = \frac{k_2}{K} C_{I_0}(1 - e^{-Kt}) \quad \text{(Eq. 5)}$$

where k_1 = formation constant of II, k_2 = formation constant of III, K = decomposition constant of I, C = mole percent content of the sample with respect to I at time t, and C_{I_0} = mole content of I at time t = 0 (=100%).

The value of K is obtained from the slope of the regression line calculated through Eq. 2. The obtained K values are used in Eqs. 4 and 5, whose corresponding regression lines reveal k_1 and k_2.

Table III—Experimental Values of K

Temperature	Relative Humidity, %	K, day^{-1} × 10^5	Confidence Interval, p = 0.05, day^{-1} × 10^5	n[a]	r^2[b]
42.5°	38.6	2.83	0.94	7	0.946
	47.9	5.98	1.72	5	0.976
	60.6	18.74	2.67	11	0.965
	66.3	32.68	3.08	7	0.993
	82.2	26.73	1.83	13	0.987
55.0°	30.6	4.42	1.30	5	0.975
	49.2	19.57	5.85	6	0.956
	55.3	28.72	2.18	10	0.990
	60.3	43.95	3.27	12	0.988
	67.5	120.64	27.55	4	0.984
	82.7	127.47	10.19	11	0.988
73.8°	32.1	24.82	4.27	7	0.979
	41.0	57.46	6.62	11	0.980
	51.7	125.29	21.83	7	0.978
	59.3	371.29	50.14	11	0.977
	69.0	729.96	55.91	5	0.990
	83.8	618.65	65.92	10	0.985
83.4°	29.3	567.83	89.54	7	0.981
	38.1	777.17	76.50	7	0.992
	53.1	1990.92	260.56	9	0.978
	60.2	3037.61	497.55	6	0.986
	70.0	5580.19	1253.77	3	0.999
	83.8	4612.95	1295.45	5	0.977

[a] n = number of experimental points. [b] r^2 = coefficient of determination.

RESULTS

Substances II and III are the only important decomposition products of I; both have to be followed to establish the decomposition kinetics of I (Figs. 1 and 2). Substances II and III were considered stable, although a few unidentified compounds (seemingly breakdown products of II and III) were observed in samples stored at 73.8 and 83.4° and high humidities. The appearance of these unidentified products was automatically detected on the chromatograms and helped establish the time limits for the system for the calculation of rate constants.

At 83.4°, the instability of II and III was such that only the disappearance constant K could be calculated (Tables II and III). For temperatures up to 83.4° and relative humidities up to 70%, the rate constants

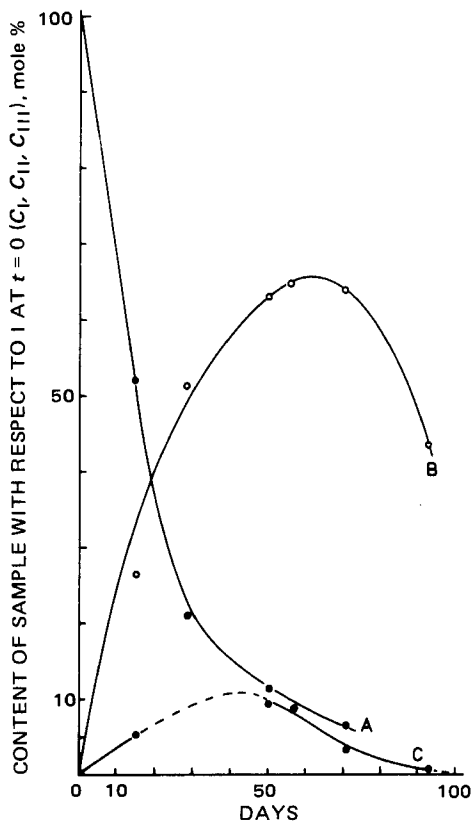

Figure 2—*Nitrazepam stability at 83.8% relative humidity and 83.4°. Key: A, decomposition of I; B, formation and decomposition of II; and C, formation and decomposition of III.*

Table IV—Regression Line Parameters for Logarithm $K \times 10^5$ as a Function of Relative Humidity

Temperature	42.5°	55.0°	73.8°	83.4°
Slope	0.03838	0.03718	0.04052	0.02492
Confidence interval, $p = 0.05$	0.00393	0.00960	0.00749	0.00348
y-Intercept	−1.0437	−0.5316	0.08549	1.9849
Confidence interval, $p = 0.05$	0.2141	0.5193	0.3917	0.1819
Coefficient of determination	0.988	0.980	0.990	0.994

followed an exponential pattern proportional to relative humidity. At 80% relative humidity, they diminished significantly. At about 75% relative humidity, an instability maximum was apparent at all temperatures (Fig. 3).

The parameters defining the regression equations relating log K, for a given temperature, to relative humidities are summarized in Table IV.

The slope values, discarding the result for 83.4°, were all within the confidence interval of each other. Therefore, if the straight lines are considered to be parallel with a slope equal to the mean value of the observed slopes at the three temperatures, then:

$$\log K \times 10^5 = 0.03869\% \text{ relative humidity} + A \qquad \text{(Eq. 6)}$$

where A represents a constant depending on temperature. Its values are obtained by putting the mean $\bar{x}, \bar{y}$ values of the regression lines for 42.5, 55.0, and 73.8° in Eq. 6. This approach yields $A = -1.0602$, -0.6105, and 0.1785 for the three temperatures, respectively. Treating the variation of A as a linear function of the reciprocal temperature, one obtains an Arrhenius-like relationship:

$$A = -4.3576 \times 10^3 \frac{1}{T} + 12.7207 \qquad \text{(Eq. 7)}$$

If Eqs. 6 and 7 represent truly straight lines, the decomposition constants of nitrazepam must be linearly related to both relative humidity and the reciprocal absolute temperature, in which case one might as well calculate directly the equation of the corresponding regression plane:

$$X_1 = a + bX_2 + cX_3 \qquad \text{(Eq. 8)}$$

where $X_1 = \log K \times 10^5$, $X_2 = 10^3\ T^{-1}$ (K), X_3 = relative humidity (percent), a = constant depending on the system, b = partial regression coefficient of log K on T^{-1} (relative humidity = constant), and c = partial regression coefficient of log K on relative humidity (T = constant).

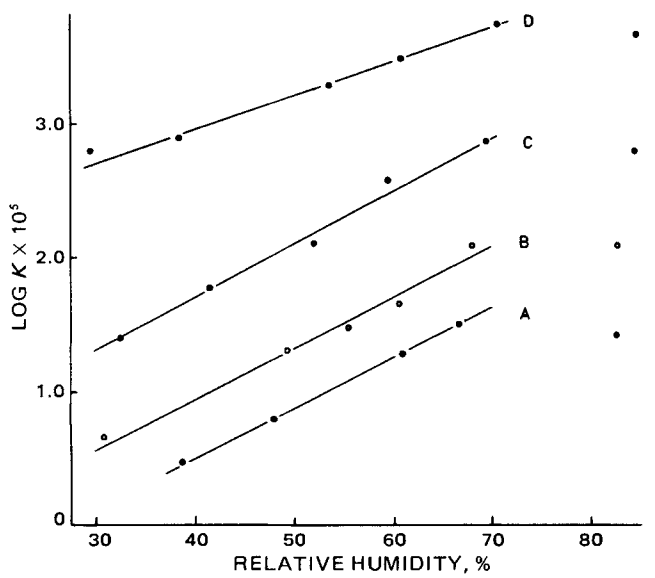

Figure 3—*Logarithm of the nitrazepam decomposition constant,* K, *as a function of relative humidity at various temperatures. Key: A, 42.5°; B, 55.0°; C, 73.8°; and D, 83.4°.*

Table V—Values of $t_{0.9}$ for Various Climatic Conditions

Climatic Condition	log $K \times 10^5$	$K \times 10^5$	$t_{0.9}$, years
North of Europe 18°; 50% relative humidity	−0.331	0.46	62.8
Central Europe 20°; 65% relative humidity	0.353	2.25	12.9
Tropical climate 30°; 70% relative humidity	1.040	11.0	2.7

The coefficients a, b, and c are found by solving the following system of equations (9):

$$\sum X_1 = aN + b\sum X_2 + c\sum X_3 \qquad \text{(Eq. 9)}$$

$$\sum X_1X_2 = a\sum X_2 + b\sum X_2^2 + c\sum X_2X_3 \qquad \text{(Eq. 10)}$$

$$\sum X_1X_3 = a\sum X_3 + b\sum X_2X_3 + c\sum X_3^2 \qquad \text{(Eq. 11)}$$

where N represents the number of storage conditions defined by temperature and relative humidity. Thus, the final result is obtained for all storage conditions where $T < 75°$ and relative humidity <80% (N = 14):

$$X_1 = 12.783 - 4.3804X_2 + 0.03877X_3 \qquad \text{(Eq. 12)}$$

or:

$$\log K \times 10^5 = 12.783 - 4.3804 \times 10^3T^{-1} + 0.03877\ (\%\text{ relative humidity}) \qquad \text{(Eq. 13)}$$

with a regression coefficient of $R_{1.23} = 0.995$. Figure 4 represents the plane corresponding to Eq. 13. Extrapolation with respect to T and interpolation with respect to relative humidity of the plane regression equation yields K for any other desired climatic condition. Therefore, the time interval $t_{0.9}$, after which only 90% of the initial nitrazepam concentration is left, may be calculated (Table V).

DISCUSSION

The presented results do not suggest adherence to any published model. In particular, the rate of disappearance of nitrazepam in a 1% dilution in microcrystalline cellulose apparently does not follow a sigmoid decomposition pattern like aspirin (10), and it does not reach an equilibrium level like thiamine hydrochloride in microcrystalline cellulose (11). Although this latter compound displays an instability maximum at a water content of about 5%, no comparison can be made with the instability maximum shown for the nitrazepam system at 75% relative humidity; no relationship between water content and relative humidity has yet been established, and thiamine hydrochloride is water soluble

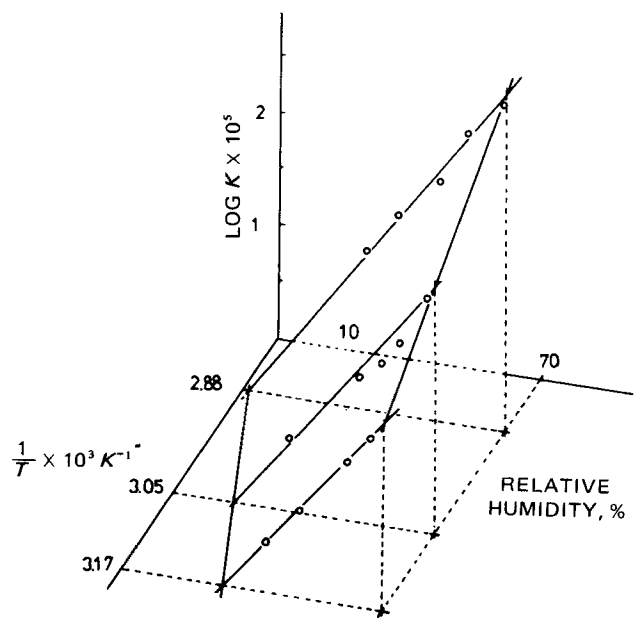

Figure 4—*Variation of log* K *as a function of relative humidity and reciprocal temperature.*

but nitrazepam is not. Kinetically limiting factors could be different in the two systems.

Nevertheless, there is now enough evidence to conclude that the rate of decomposition of pure and compound drugs in the solid state may be influenced as much by water as by temperature and that it is possible to relate the decomposition constants simply and simultaneously to temperature and to a term reflecting the influence of water. Relative humidity seems to be a good way to deal with this problem; combined with temperature, it can characterize climatic conditions and allows establishment of the corresponding $t_{0.9}$ values directly from experimental results.

REFERENCES

(1) J. T. Carstensen, *J. Pharm. Sci.*, **63**, 1 (1974).

(2) J. T. Carstensen, "Theory of Pharmaceutical Systems," vol. II, Academic, New York, N.Y., 1973, p. 294.

(3) F. Tripet and U. W. Kesselring, *Pharm. Acta Helv.*, **50**, 318 (1975).

(4) H. Landolt and R. Börnstein, "Physikalisch-Chemische Tabellen," Springer, Berlin, Germany, 1912, pp. 361, 419, 427.

(5) Z. G. Szabo in "Chemical Kinetics," vol. 2, C. H. Bamford and C. F. H. Tipper, Eds., Elsevier, New York, N.Y., 1969, p. 14.

(6) W. Mayer, S. Erbe, and R. Voigt, *Pharmazie*, **27**, 32 (1972).

(7) W. Mayer, S. Erbe, G. Wolf, and R. Voigt, *ibid.*, **29**, 700 (1974).

(8) J. T. Carstensen, K. S. E. Su, P. Maddrell, J. B. Johnson, and H. N. Newmark, *Bull. Parenteral Drug Assoc.*, **25**, 193 (1971).

(9) M. R. Spiegel, "Théorie et applications de la statistique," Ediscience SA., Paris, France, 1972, p. 222.

(10) L. J. Leeson and A. M. Mattocks, *J. Am. Pharm. Assoc., Sci. Ed.*, **47**, 329 (1958).

(11) J. T. Carstensen, M. Osadca, and S. H. Rubin, *J. Pharm. Sci.*, **58**, 549 (1969).

ACKNOWLEDGMENTS AND ADDRESSES

Received December 8, 1975, from the *Ecole de Pharmacie, 3, Place du Château, CH-1005 Lausanne, Switzerland.*

Accepted for publication June 28, 1976.

The authors thank M. Soliva for helpful discussions. They are indebted to Hoffmann–La Roche & Co. SA., Basel, Switzerland, and to the Swiss National Foundation for Scientific Research (Grant 3.730.72) who in part supported this work.

[x] To whom inquiries should be directed.

GI Drug Absorption in Rats Exposed to Cobalt-60 γ-Radiation III: *In Situ* Intestinal Absorption

MICHAEL E. BRADY [*] and WILLIAM L. HAYTON [x]

Abstract □ The absorption rate of sulfanilamide, bretylium tosylate, sulfisoxazole acetyl, and riboflavin from the *in situ* small intestine was studied in rats exposed to 850 rad of cobalt-60 γ-radiation. Compared to absorption from the intestine of sham-irradiated animals, the absorption rate of sulfanilamide declined following irradiation. It declined to a minimum that was 65% of the control value at 4 days postirradiation before it began to return toward the control value. The reduced absorption rate of sulfanilamide in irradiated animals was accompanied by, and appeared to result from, a reduction in the absorption rate of water from the intestinal drug solution. The sulfisoxazole acetyl absorption rate was reduced compared to the control rate at both 1 and 5 days postirradiation. While this reduced absorption rate at 5 days postirradiation may have resulted from a reduced absorption rate of water, postirradiation water absorption rates at 1 day were similar in irradiated and control animals. The absorption rates of bretylium and riboflavin were not affected by exposure of animals to radiation 1 or 5 days previously. The permeability of the small intestinal epithelium to the drugs studied appeared to be reduced slightly following its exposure to ionizing radiation. The reduced permeability is apparently an indirect effect of the reduced absorption rate of water.

Keyphrases □ Absorption, GI—sulfanilamide, bretylium tosylate, sulfisoxazole acetyl, and riboflavin, effect of γ-radiation on rate, rats □ Radiation, gamma—effect on rate of GI absorption of sulfanilamide, bretylium tosylate, sulfisoxazole acetyl, and riboflavin, rats □ Sulfanilamide—GI absorption, effect of γ-radiation on rate, rats □ Bretylium tosylate—GI absorption, effect of γ-radiation on rate, rats □ Sulfisoxazole acetyl—GI absorption, effect of γ-radiation on rate, rats □ Riboflavin—GI absorption, effect of γ-radiation on rate, rats

The bioavailability of drugs administered orally was altered in rats exposed to 850 rad of γ-radiation (1, 2). The alterations in bioavailability in irradiated animals compared to controls appeared to result primarily from a pronounced reduction in the gastric emptying rate. The effects of irradiation on bioavailability depended upon the physicochemical properties of the drug, the dosage form, and the time postirradiation at which the drug was administered.

While reduced gastric emptying appeared to be the principal mechanism by which irradiation of the gut altered bioavailability, damage resulting from irradiation of the intestine (3, 4) can also affect the absorption of orally administered drugs by alteration of the permeability of the intestinal epithelium. In irradiated rats, the apparent decrease in the absorption rate of sulfanilamide from the *in situ* intestine (5) and the altered permeability of the *in vitro* intestine to several drugs (6, 7) indicate that the permeability of the intestinal epithelium may be altered directly by its exposure to ionizing radiation. The purpose of this study was to explore further the effects of prior whole body exposure to 850 rad of γ-radiation on the apparent permeability of the *in situ* rat intestine to drugs.

EXPERIMENTAL

Materials—The chemicals and reagents used were described previously (1).

Intestinal Absorption Rate—Male Sprague–Dawley rats, 170–250 g, were either irradiated or sham-irradiated by a procedure described previously (1). At various times following irradiation, equal numbers of irradiated and sham-irradiated animals were fasted overnight, anesthetized with 1.3 g of ethyl carbamate/kg, and prepared surgically for the determination of the drug absorption rate from 7.0 ml of a solution instilled into the cannulated small intestine (8, 9). The drugs[1], at initial

[1] The following drugs were used: sulfisoxazole acetyl, Hoffmann–La Roche, Nutley, N.J.; bretylium tosylate, Burroughs Wellcome Co., Research Triangle Park, N.C.; 2-^{14}C-*d*-riboflavin, Amersham/Searle, Arlington Heights, Ill.; and sulfanilamide, Sigma Chemical Co., Irvington, N.Y.

but nitrazepam is not. Kinetically limiting factors could be different in the two systems.

Nevertheless, there is now enough evidence to conclude that the rate of decomposition of pure and compound drugs in the solid state may be influenced as much by water as by temperature and that it is possible to relate the decomposition constants simply and simultaneously to temperature and to a term reflecting the influence of water. Relative humidity seems to be a good way to deal with this problem; combined with temperature, it can characterize climatic conditions and allows establishment of the corresponding $t_{0.9}$ values directly from experimental results.

REFERENCES

(1) J. T. Carstensen, *J. Pharm. Sci.*, **63**, 1 (1974).

(2) J. T. Carstensen, "Theory of Pharmaceutical Systems," vol. II, Academic, New York, N.Y., 1973, p. 294.

(3) F. Tripet and U. W. Kesselring, *Pharm. Acta Helv.*, **50**, 318 (1975).

(4) H. Landolt and R. Börnstein, "Physikalisch-Chemische Tabellen," Springer, Berlin, Germany, 1912, pp. 361, 419, 427.

(5) Z. G. Szabo in "Chemical Kinetics," vol. 2, C. H. Bamford and C. F. H. Tipper, Eds., Elsevier, New York, N.Y., 1969, p. 14.

(6) W. Mayer, S. Erbe, and R. Voigt, *Pharmazie*, **27**, 32 (1972).

(7) W. Mayer, S. Erbe, G. Wolf, and R. Voigt, *ibid.*, **29**, 700 (1974).

(8) J. T. Carstensen, K. S. E. Su, P. Maddrell, J. B. Johnson, and H. N. Newmark, *Bull. Parenteral Drug Assoc.*, **25**, 193 (1971).

(9) M. R. Spiegel, "Théorie et applications de la statistique," Ediscience SA., Paris, France, 1972, p. 222.

(10) L. J. Leeson and A. M. Mattocks, *J. Am. Pharm. Assoc., Sci. Ed.*, **47**, 329 (1958).

(11) J. T. Carstensen, M. Osadca, and S. H. Rubin, *J. Pharm. Sci.*, **58**, 549 (1969).

ACKNOWLEDGMENTS AND ADDRESSES

Received December 8, 1975, from the *Ecole de Pharmacie, 3, Place du Château, CH-1005 Lausanne, Switzerland.*

Accepted for publication June 28, 1976.

The authors thank M. Soliva for helpful discussions. They are indebted to Hoffmann–La Roche & Co. SA., Basel, Switzerland, and to the Swiss National Foundation for Scientific Research (Grant 3.730.72) who in part supported this work.

[x] To whom inquiries should be directed.

GI Drug Absorption in Rats Exposed to Cobalt-60 γ-Radiation III: *In Situ* Intestinal Absorption

MICHAEL E. BRADY [*] and WILLIAM L. HAYTON [x]

Abstract □ The absorption rate of sulfanilamide, bretylium tosylate, sulfisoxazole acetyl, and riboflavin from the *in situ* small intestine was studied in rats exposed to 850 rad of cobalt-60 γ-radiation. Compared to absorption from the intestine of sham-irradiated animals, the absorption rate of sulfanilamide declined following irradiation. It declined to a minimum that was 65% of the control value at 4 days postirradiation before it began to return toward the control value. The reduced absorption rate of sulfanilamide in irradiated animals was accompanied by, and appeared to result from, a reduction in the absorption rate of water from the intestinal drug solution. The sulfisoxazole acetyl absorption rate was reduced compared to the control rate at both 1 and 5 days postirradiation. While this reduced absorption rate at 5 days postirradiation may have resulted from a reduced absorption rate of water, postirradiation water absorption rates at 1 day were similar in irradiated and control animals. The absorption rates of bretylium and riboflavin were not affected by exposure of animals to radiation 1 or 5 days previously. The permeability of the small intestinal epithelium to the drugs studied appeared to be reduced slightly following its exposure to ionizing radiation. The reduced permeability is apparently an indirect effect of the reduced absorption rate of water.

Keyphrases □ Absorption, GI—sulfanilamide, bretylium tosylate, sulfisoxazole acetyl, and riboflavin, effect of γ-radiation on rate, rats □ Radiation, gamma—effect on rate of GI absorption of sulfanilamide, bretylium tosylate, sulfisoxazole acetyl, and riboflavin, rats □ Sulfanilamide—GI absorption, effect of γ-radiation on rate, rats □ Bretylium tosylate—GI absorption, effect of γ-radiation on rate, rats □ Sulfisoxazole acetyl—GI absorption, effect of γ-radiation on rate, rats □ Riboflavin—GI absorption, effect of γ-radiation on rate, rats

The bioavailability of drugs administered orally was altered in rats exposed to 850 rad of γ-radiation (1, 2). The alterations in bioavailability in irradiated animals compared to controls appeared to result primarily from a pronounced reduction in the gastric emptying rate. The effects of irradiation on bioavailability depended upon the physicochemical properties of the drug, the dosage form, and the time postirradiation at which the drug was administered.

While reduced gastric emptying appeared to be the principal mechanism by which irradiation of the gut altered bioavailability, damage resulting from irradiation of the intestine (3, 4) can also affect the absorption of orally administered drugs by alteration of the permeability of the intestinal epithelium. In irradiated rats, the apparent decrease in the absorption rate of sulfanilamide from the *in situ* intestine (5) and the altered permeability of the *in vitro* intestine to several drugs (6, 7) indicate that the permeability of the intestinal epithelium may be altered directly by its exposure to ionizing radiation. The purpose of this study was to explore further the effects of prior whole body exposure to 850 rad of γ-radiation on the apparent permeability of the *in situ* rat intestine to drugs.

EXPERIMENTAL

Materials—The chemicals and reagents used were described previously (1).

Intestinal Absorption Rate—Male Sprague–Dawley rats, 170–250 g, were either irradiated or sham-irradiated by a procedure described previously (1). At various times following irradiation, equal numbers of irradiated and sham-irradiated animals were fasted overnight, anesthetized with 1.3 g of ethyl carbamate/kg, and prepared surgically for the determination of the drug absorption rate from 7.0 ml of a solution instilled into the cannulated small intestine (8, 9). The drugs[1], at initial

[1] The following drugs were used: sulfisoxazole acetyl, Hoffmann–La Roche, Nutley, N.J.; bretylium tosylate, Burroughs Wellcome Co., Research Triangle Park, N.C.; 2-^{14}C-*d*-riboflavin, Amersham/Searle, Arlington Heights, Ill.; and sulfanilamide, Sigma Chemical Co., Irvington, N.Y.

Table I—Drug Absorption from the *In Situ* Rat Intestine following Exposure to 850 rad of Cobalt-60 γ-Radiation or Sham Irradiation

Drug (Initial Concentration)	Day Post-irradiation	Absorption Rate Constant[a,b], min^{-1}		Volume of Water Absorbed[b,c], ml/hr		Gut Length[b], cm		Final pH of Drug Solution[b,d]	
		Sham	850 rad	Sham	850 rad	Sham	850 rad	Sham	850 rad
Sulfanilamide (60 μg/ml)	1	0.0395 ± 0.00755	0.0445 ± 0.00412	3.9 ± 1.0	4.2 ± 0.7	85.6 ± 2.88	84.8 ± 3.63	6.6 ± 0.03	6.6 ± 0.07
	4	0.0410 ± 0.00518	0.0268[e] ± 0.00566	3.2 ± 1.4	−0.4[e] ± 1.3	90.0 ± 6.30	87.0 ± 4.90	6.3 ± 0.12	6.4 ± 0.15
Bretylium (0.70 mg/ml)	1	0.00[f]	0.00[f]	—[g]	—[g]	84.3 ± 2.63	84.0 ± 3.37	6.6 ± 0.05	6.6 ± 0.04
	5	0.00[f]	0.00[f]	—[g]	—[g]	86.0 ± 1.41	87.5 ± 2.08	6.6 ± 0.05	6.7 ± 0.08
Sulfisoxazole acetyl (60 μg/ml)	1	0.156 ± 0.0111	0.138[e] ± 0.0150	4.5 ± 1.8	4.0 ± 1.5	87.9 ± 3.13	87.1 ± 2.04	6.7 ± 0.06	6.6 ± 0.08
	5	0.133 ± 0.0067	0.120[e] ± 0.0097	4.0 ± 0.6	1.7[e] ± 0.9	89.3 ± 3.98	89.4 ± 4.67	6.5 ± 0.09	6.5 ± 0.06
Riboflavin (20 μg/ml)	1	0.00155 ± 0.00081	0.00151 ± 0.00048	4.3 ± 0.5	3.2[e] ± 0.7	86.2 ± 4.32	85.8 ± 4.30	7.2 ± 0.11	7.1 ± 0.17
	5	0.00121 ± 0.00046	0.00167 ± 0.00085	4.1 ± 0.9	2.5[e] ± 1.3	85.3 ± 3.61	88.2 ± 3.19	7.0 ± 0.18	6.9 ± 0.08

[a] Corrected for loss of drug due to sampling. [b] Mean of five or more animals (four with bretylium) ± *SD*. [c] This volume is the difference between the volume of 0.9% NaCl solution added to maintain the volume of the drug solution constant and the volume of drug solution removed as samples. [d] Initial pH was 6.8, except for sulfanilamide at 4 days postirradiation where the pH was 6.5. [e] Significantly different ($p < 0.05$) from corresponding sham-irradiated animals. [f] Value was negative but not significantly different from zero. [g] Not recorded.

concentrations determined by assay sensitivity and drug solubility, were dissolved in 67 m*M* sodium phosphate buffer made isotonic with sodium chloride. The volume of the drug solution in the intestine was maintained at 7.0 ml by addition of 0.9% NaCl solution immediately prior to removal of each sample.

The rectal temperature of each animal was monitored[2] throughout the experiment and maintained at 37° by a rheostatically controlled heating pad. At the conclusion of each experiment, the following data were recorded: the volume of water absorbed[3], the pH of the intestinal drug solution, and the length of intestine perfused.

Absorption rate constants were estimated from the slopes of lines fitted by least squares to plots of the logarithm of drug concentration in the intestinal drug solution *versus* time. Each rate constant was corrected for the loss of drug due to sampling[4], and absorption half-lives were calculated from the corrected value of the rate constant.

Analytical Methods—To separate sulfisoxazole acetyl from sulfisoxazole present due to hydrolysis, samples of intestinal perfusate were made alkaline by addition of 0.6 *M* pH 8.0 sodium phosphate solution and extracted with chloroform. Sulfisoxazole acetyl in the chloroform layer was determined by spectrophotometry[5] at 278 nm. Methods for the determination of the other drugs and radioactivity were described previously (1). Tonicity (osmolality) was measured by dew point depression using an osmometer[6].

RESULTS AND DISCUSSION

A preliminary study showed that the absorption rate of sulfanilamide from the *in situ* rat intestine decreased to a minimum at 4–5 days following exposure of the animals to 850 rad of γ-radiation (Fig. 1). Therefore, additional experiments were performed at 4 days postirradiation (5), and the results showed a statistically significant decrease in the rate of sulfanilamide absorption in irradiated animals compared to controls (Table I). The reduced absorption rate could not be attributed to differences in the length of the intestine perfused nor to differences in the intestinal perfusate pH (Table I). The decrease in the apparent permeability of the intestinal mucosa to sulfanilamide at 4 days postirradiation did not affect significantly the overall *in vivo* rate or extent of absorption of sulfanilamide, since the slow step in its absorption tended to be gastric emptying (2).

The decreased rate of sulfanilamide absorption from the intestine of irradiated animals was accompanied by a similar decrease in the absorption rate of water from the intestine (Fig. 1 and Table I). The water absorption rate affects the rate of intestinal drug absorption directly due to a solvent drag effect (10–12). To examine the role of water absorption in the reduced rate of sulfanilamide absorption, the rate of water absorption from the *in situ* intestine was varied by altering the sodium chloride concentration in the intestinal perfusate (Table II). The ab-

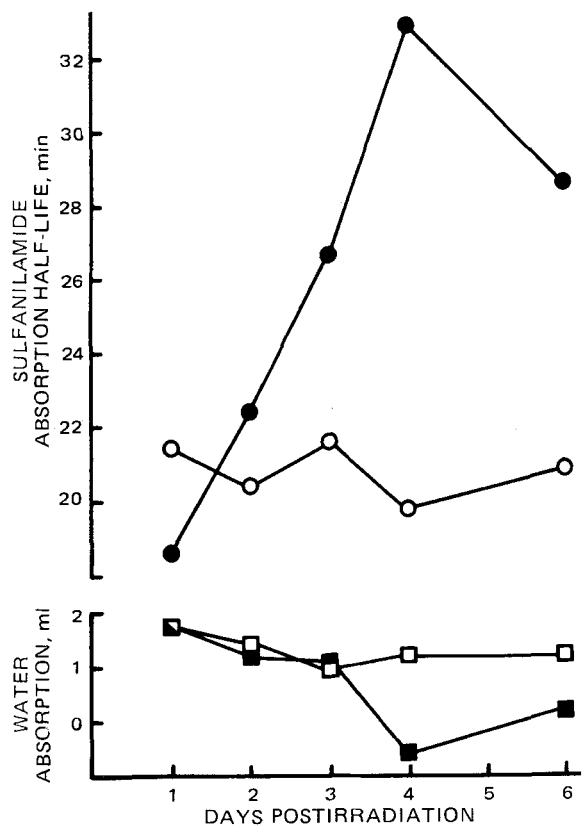

Figure 1—*Sulfanilamide (initial concentration of 60 μg/ml) absorption half-life from the* in situ *rat intestine at various times following irradiation. Key: ●, irradiated (850 rad); and ○, sham irradiated. Also shown is the volume of water absorbed over the 30-min absorption experiment. Key: ■, irradiated (850 rad); and □, sham irradiated. Each point represents the mean of two animals.*

[2] Tele-Thermometer model 44TD, Yellow Springs Instrument Co., Yellow Springs, Ohio.

[3] This volume is the difference between the volume of 0.9% NaCl solution added to maintain the volume of the drug solution constant and the volume of drug solution removed as samples.

[4] Rate constants were corrected by subtracting the quantity: sample size in milliliters/(sampling interval in minutes × 7 ml).

[5] Beckman DU (Beckman Instruments, Fullerton, Calif.), with a Gilford model 2000 multiple-sample recorder (Gilford Instrument Laboratories, Oberlin, Ohio).

[6] Vapor pressure osmometer, model 1500, Wescor, Logan, Utah.

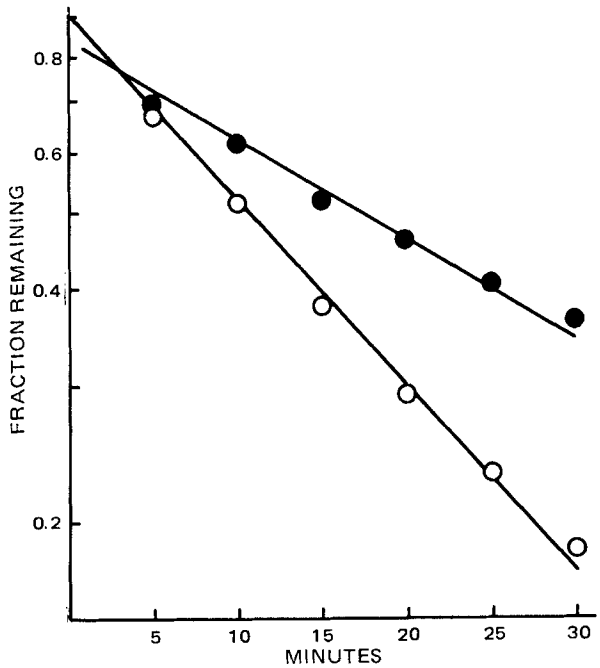

Figure 2—*Absorption of sulfanilamide (initial concentration of 60 μg/ml) from the* in situ *rat intestine under conditions of net water flux. Key: ●, hypertonic (548 mOsm/kg) perfusate; and ○, hypotonic (232 mOsm/kg) perfusate. Each point represents the mean of four animals.*

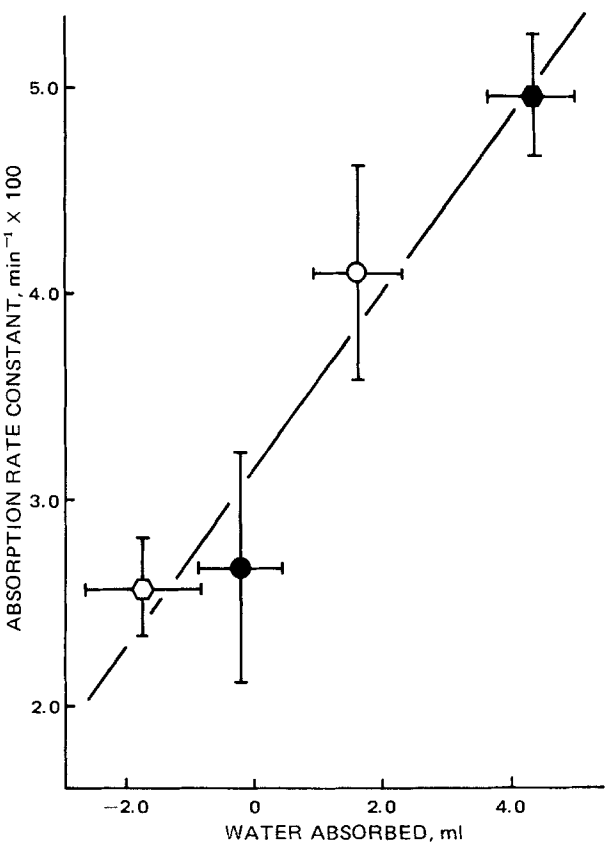

Figure 3—*Relationship between water flux and the rate constant for absorption of sulfanilamide (initial concentration of 60 μg/ml) over 30 min from the* in situ *rat intestine. Key: ○, sham-irradiated animals perfused with isotonic solution; ●, nonirradiated animals perfused with hypotonic solution (232 mOsm/kg); ○, nonirradiated animals perfused with hypertonic solution (548 mOsm/kg); and ●, irradiated animals perfused with isotonic solution at 4 days postirradiation.*

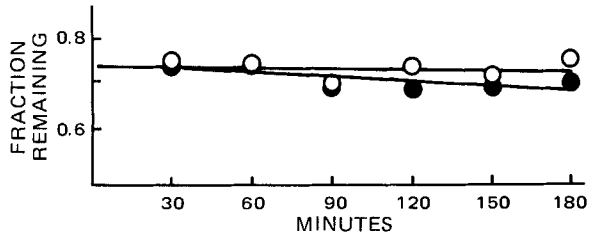

Figure 4—*Effect of 850 rad of γ-radiation on the absorption of bretylium (initial concentration of 0.70 mg/ml) from the* in situ *rat intestine at 5 days postirradiation. Key: ●, irradiated; and ○, sham irradiated. Each point represents the mean of four animals.*

sorption rate of sulfanilamide was significantly greater from a hypotonic than from a hypertonic perfusate (Fig. 2).

In nonirradiated animals, there was a linear relationship between the sulfanilamide absorption rate constant and the water absorption rate (Fig. 3). This relationship was similar to that reported for several other drugs (10–12). When the mean absorption rate constant of sulfanilamide in irradiated animals was plotted at the corresponding rate of water absorption, it was nearly on the line (Fig. 3). Thus, the reduction in the absorption rate constant of sulfanilamide in irradiated animals at 4 days postirradiation apparently resulted indirectly from a reduction in the water absorption rate and not from a direct alteration in the permeability of the intestinal mucosa to the drug. The possibility remains, however, that the rates of absorption of both water and sulfanilamide depend on a third factor affected by radiation.

Irradiation did not appear to alter the permeability of the intestinal epithelium to bretylium (Table I). No measurable absorption of bretylium occurred at 1 or 5 days postirradiation (Fig. 4). The initial relatively rapid decline in the fraction of bretylium remaining in the drug solution (Fig. 4) was possibly due to binding of the drug to the surface of the epithelial mucosa (13).

In a previous study (1), poor absorption of orally administered bretylium was demonstrated by low recovery of the drug in the urine of irradiated and sham-irradiated rats. The data reported here indicate that epithelial permeability is the rate-controlling step that limits both the rate and extent of drug absorption. In addition, this study indicates that the barrier properties of the intestinal epithelium to the transfer of positively charged compounds are not altered by prior exposure of the intestine to radiation.

Sulfisoxazole acetyl, a highly lipid-soluble drug, disappeared rapidly

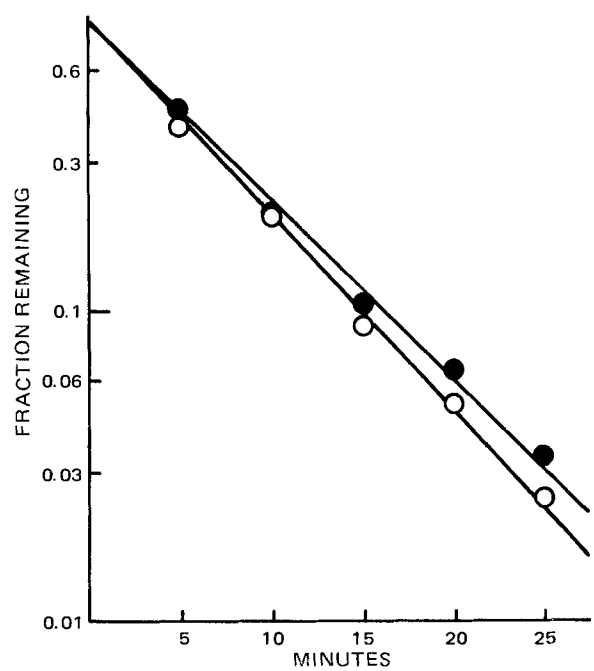

Figure 5—*Effect of 850 rad of γ-radiation on the absorption of sulfisoxazole acetyl (initial concentration of 60 μg/ml) from the* in situ *rat intestine at 5 days postirradiation. Key: ●, irradiated; and ○, sham irradiated. Each point represents the mean of at least five animals.*

Table II—Effect of Tonicity on the Absorption Rate Constant of Sulfanilamide[a] from the *In Situ* Rat Intestine

Tonicity, mOsm/kg	Absorption Rate Constant[b,c], min^{-1}	Volume of Water Absorbed[c,d], ml/hr	Gut Length[c], cm	Final pH of Drug Solution[c,e]
232	0.0497 ± 0.00299[f]	8.7 ± 1.4[f]	88.5 ± 4.80	6.6 ± 0.10
314 (Isotonic)	0.0410 ± 0.00518	3.2 ± 1.4	90.0 ± 6.30	6.3 ± 0.12
548	0.0258 ± 0.00236[f]	−3.5 ± 2.7[f]	88.5 ± 2.65	6.7 ± 0.08

[a] Initial concentration 60 μg/ml. [b] Corrected for loss of drug due to sampling. [c] Mean of four or more animals ± *SD*. [d] This volume is the difference between the volume of 0.9% NaCl solution added to maintain the volume of the drug solution constant and the volume of drug solution removed as samples. [e] Initial pH was 6.8, except for isotonic solutions where the pH was 6.5. [f] Significantly different ($p < 0.02$) from the isotonic value.

from the intestinal drug solution (Fig. 5). While the analytical method was specific for sulfisoxazole acetyl, deacetylation may have occurred simultaneously with absorption. When sulfisoxazole acetyl was incubated with intestinal epithelium, hydrolysis was accelerated compared to control studies in which the incubation medium did not contain intestinal epithelium (14). Thus, the rapid rate of disappearance of sulfisoxazole acetyl from the intestinal drug solution may reflect both rapid absorption and hydrolysis (15, 16).

Prior exposure of animals to 850 rad of γ-radiation reduced slightly, but significantly, the apparent absorption rate constant for sulfisoxazole acetyl at both 1 and 5 days (Table I). The reduction in the absorption rate of sulfisoxazole acetyl in irradiated animals was not due to a reduction in the length of intestine perfused nor to differences in the drug solution pH (Table I). Nor did a reduced rate of water absorption account entirely for the reduced rate of sulfisoxazole acetyl absorption in irradiated animals, since the water absorption rate at 1 day postirradiation was similar in irradiated and control animals (Table I).

Sulfisoxazole acetyl may penetrate the intestinal epithelium from solution so rapidly that blood flow to the intestine is the rate-controlling step in its absorption. Exposure to radiation reduced the rate of blood flow to the intestine of rats (17) and dogs (18) exposed 2–3 days previously. Absorption limited by blood flow was demonstrated for other rapidly absorbed drugs from the perfused *in situ* rat intestine (12, 19). The reduction in the sulfisoxazole acetyl absorption rate observed here was not clinically significant, since the intestinal absorption rate of the drug was still very high in irradiated animals.

Riboflavin disappeared slowly from the intestinal drug solution (Fig. 6). The absorption rate of the vitamin was not significantly different from that of the control at 1 or 5 days postirradiation (Table I). The initial rapid decline in the riboflavin concentration in the intestinal solution was similar to that observed for bretylium (Fig. 4) and may be attributed to binding of riboflavin to the intestinal mucosa rather than to absorption. In irradiated animals, the volume of water absorbed was lower than in sham-irradiated animals at 1 and 5 days postirradiation. The reduced rate of water absorption was not accompanied by a corresponding decrease in the rate of riboflavin absorption (Table I).

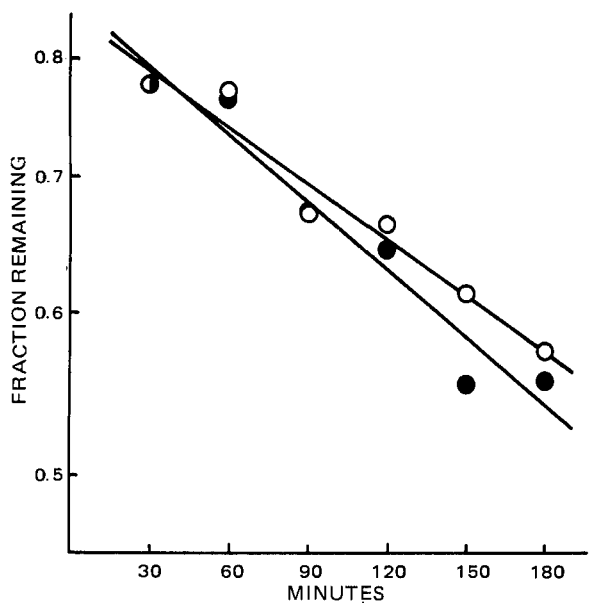

Figure 6—*Effect of 850 rad of γ-radiation on the absorption of riboflavin (initial concentration of 20 μg/ml) from the* in situ *rat intestine at 5 days postirradiation. Key: ●, irradiated; and ○, sham irradiated. Each point represents the mean of at least five animals.*

In general, prior irradiation of the small intestine tends to reduce its apparent permeability to drugs in an indirect manner by reducing the rate of water absorption by the intestine. In addition, the drug absorption rate may be reduced following irradiation due to a reduction in mesenteric blood flow, particularly for rapidly absorbed drugs. The magnitude of the observed radiation-induced reduction in the intestinal absorption rate was relatively small. If such a reduction in absorptive capacity occurred in humans following radiation therapy, it would not be clinically significant, although higher doses of radiation might have a more pronounced effect on intestinal drug absorption.

REFERENCES

(1) M. E. Brady and W. L. Hayton, *J. Pharm. Sci.*, **66**, 361 (1977).

(2) *Ibid.*, **66**, 366 (1977).

(3) H. R. Withers, *Cancer*, **28**, 75 (1971).

(4) K. E. Carr and P. G. Toner, *Virchows Arch. B*, **11**, 201 (1972).

(5) W. L. Hayton, *J. Pharm. Sci.*, **63**, 645 (1974).

(6) M. J. Mattila, S. Takki, and L. R. Holsti, *Arzneim.-Forsch.*, **18**, 889 (1968).

(7) M. J. Mattila, L. R. Holsti, V. M. K. Venho, and S. Takki, *ibid.*, **20**, 533 (1970).

(8) J. T. Doluisio, N. F. Billups, L. W. Dittert, E. T. Sugita, and J. V. Swintosky, *J. Pharm. Sci.*, **58**, 1196 (1969).

(9) W. L. Hayton and G. Levy, *ibid.*, **61**, 362 (1972).

(10) H. Ochsenfahrt and D. Winne, *Naunyn-Schmiedeberg's Arch. Pharmacol.*, **281**, 175 (1974).

(11) *Ibid.*, **281**, 197 (1974).

(12) S. Kojima and J. Miyake, *Chem. Pharm. Bull.*, **23**, 1247 (1975).

(13) R. M. Levine, M. R. Blair, and B. B. Clark, *J. Pharmacol. Exp. Ther.*, **114**, 78 (1955).

(14) S. Mizukami and K. Nagata, *Ann. Rep. Shionogi Res. Lab.*, **6**, 58 (1956); through *Chem. Abstr.*, **51**, 4560b (1957).

(15) R. E. Notari, J. L. DeYoung, and R. H. Reuning, *J. Pharm. Sci.*, **61**, 135 (1972).

(16) D. Perrier and M. Gibaldi, *ibid.*, **62**, 225 (1973).

(17) G. Janossy, *Acta Med. Acad. Sci. Hung.*, **26**, 13 (1969).

(18) J. Kabal, S. J. Baum, and L. J. Parkhurst, *Radiat. Res.*, **50**, 528 (1972).

(19) H. Ochsenfahrt and D. Winne, *Naunyn-Schmiedeberg's Arch. Pharmacol.*, **279**, 133 (1973).

ACKNOWLEDGMENTS AND ADDRESSES

Received March 29, 1976, from the *College of Pharmacy, Washington State University, Pullman, WA 99164.*

Accepted for publication July 1, 1976.

Presented in part at the Basic Pharmaceutics Section, APhA Academy of Pharmaceutical Sciences, San Francisco meeting, April 1975.

Abstracted from a dissertation submitted by M. E. Brady to Washington State University in partial fulfillment of the Doctor of Philosophy degree requirements.

Supported in part by funds provided for biological and medical research by Washington State University Initiative Measure No. 171.

The authors appreciate the gifts of sulfisoxazole acetyl provided by Dr. W. E. Scott, Research Division, Hoffmann-La Roche Inc., and bretylium tosylate provided by Dr. R. A. Maxwell, Burroughs Wellcome Co.

* AFPE Paul M. Scott Memorial Fellow. Present address: College of Pharmacy, University of Cincinnati, Cincinnati, OH 45221.

ˣ To whom inquiries should be directed.

High-Performance Liquid Chromatographic Determination of Chlordiazepoxide and Major Related Impurities in Pharmaceuticals

A. G. BUTTERFIELD ˣ, F. F. MATSUI, S. J. SMITH, and R. W. SEARS

Abstract □ A rapid, precise, forward-phase (adsorption) high-performance liquid chromatographic procedure is presented for the determination of chlordiazepoxide and two common impurities, 7-chloro-1,3-dihydro-5-phenyl-2*H*-1,4-benzodiazepin-2-one 4-oxide and 2-amino-5-chlorobenzophenone, in commercial formulations and for the determination of the benzophenone in the chlordiazepoxide drug substance. The method involves simultaneous quantitation of chlordiazepoxide and the 1,3-dihydro impurity, followed by quantitation of the benzophenone from a separate sample extract using a second mobile phase. A single microparticulate silica gel column is used throughout. Nitrazepam and *o*-dinitrobenzene are the internal standards. Quantitation is by peak area using a computing integrator, except that the peak due to the benzophenone is quantitated by peak height. The described procedure is of equivalent precision, but superior accuracy, to the BP 1973 spectrophotometric procedure for the analysis of chlordiazepoxide in chlordiazepoxide formulations. Quantitation of the 1,3-dihydro and the benzophenone impurities at levels as low as 6.3 and 0.9 ng, respectively, is demonstrated.

Keyphrases □ Chlordiazepoxide—and related impurities, high-performance liquid chromatographic analysis, commercial formulations □ High-performance liquid chromatographic analysis—chlordiazepoxide and related impurities, commercial formulations □ Tranquilizers—chlordiazepoxide and related impurities, high-performance liquid chromatographic analysis, commercial formulations

Pharmacopeial specifications for the tranquilizer chlordiazepoxide [7-chloro-2-(methylamino)-5-phenyl-3*H*-1,4-benzodiazepine 4-oxide] and its hydrochloride salt (I) include limit tests for the impurities 7-chloro-1,3-dihydro-5-phenyl-2*H*-1,4-benzodiazepin-2-one 4-oxide (II) and 2-amino-5-chlorobenzophenone (III) (1–3). These specifications allow a maximum of 0.1% of II and 0.01% (1, 2) or 0.05% (3) of III in the chlordiazepoxide drug substance. Specifications for capsules containing the hydrochloride salt permit a maximum of 3.0 and 0.1% for II and III, respectively (1, 3); tablets prepared with chlordiazepoxide base may contain up to 4.0% of II and 0.1% of III (2).

Numerous procedures have been reported for the quantitation of chlordiazepoxide in pharmaceuticals and biological fluids (1–9). However, none of these methods describes the quantitation of all three compounds. Spectrophotometric methods, such as those described in the pharmacopeias (1–3), are not specific for I since II exhibits a similar absorption spectrum. GLC has been used to quantitate I (8), but attempts in this laboratory to develop a GLC analysis for I–III were unsuccessful because of poor peak shape, lack of separation of I and II, long analysis times, sample decomposition, and/or poor precision.

High-performance liquid chromatography (HPLC) has been used extensively for the analysis of drugs in pharmaceuticals (10–14), including the qualitative (15) and quantitative (16) analysis of benzodiazepines. Chlordiazepoxide, but not II or III, has been quantitatively analyzed by HPLC (17).

This report describes a rapid, two-part HPLC method for the analysis of I–III in chlordiazepoxide formulations and for the analysis of III in I drug substance.

EXPERIMENTAL

Materials—Chlordiazepoxide hydrochloride[1] [tested to conform to USP (1) specifications], nitrazepam[1], and *o*-dinitrobenzene[2] were used as received. Compound II was prepared by controlled alkaline hydrolysis of I, recrystallized from ethanol–hexane, and dried at 56° *in vacuo* (mp 231–234°). Purity was established chromatographically (TLC and HPLC) by comparison to USP reference standard material[3]. Compound III[2] was recrystallized twice from ethanol and dried *in vacuo* at 61° (mp 97–98°). Reagent grade tetrahydrofuran[4] was distilled from ferrous sulfate[4] and stored over molecular sieves[5] under nitrogen. All other solvents and reagents were analytical reagent grade, except *n*-hexane[6] which was UV grade.

Apparatus—A liquid chromatograph[7], fitted with a septumless injection port[7], a fixed wavelength UV detector[7] (254 nm), and a computing integrator[8], was used. The detector was attenuated to 0.04 absorbance unit full scale (aufs) throughout. The column (25 × 0.216 cm i.d.), packed with 5-μm diameter silica gel[9] using a balanced density slurry technique similar to that described by Majors (18), was operated at ambient temperature and a flow rate of 60 ml/hr.

Mobile Phases—For the quantitation of I and II, System A, 5% ammoniacal ethanol and 30% tetrahydrofuran in *n*-hexane, was used. Ammoniacal ethanol (10% v/v) was prepared from concentrated ammonium hydroxide and absolute ethanol.

For the quantitation of III, System B, 25% tetrahydrofuran in *n*-hexane, was used.

Mobile phases were prepared as required, degassed (reflux, 5 min), and stored in the solvent reservoirs of the instrument.

Stock Solutions—*Nitrazepam (IV) Internal Standard Solution*—Approximately 15 mg of IV, accurately weighed, was transferred to a 500-ml volumetric flask, dissolved, and brought to volume with ethyl acetate (final concentration of 30 μg/ml).

o-Dinitrobenzene (V) Internal Standard Solution—Approximately 25 mg of V, accurately weighed, was transferred to a 500-ml volumetric flask, dissolved in a minimum of ethanol, and brought to volume with *n*-hexane (final concentration of 50 μg/ml).

Standard Solution of I—Approximately 25 mg of I, accurately weighed, was transferred to a 100-ml volumetric flask, dissolved, and brought to volume with 0.1 *N* aqueous hydrochloric acid (final concentration of 250 μg/ml).

Standard Solution of II—Approximately 20 mg of II, accurately weighed, was transferred to a 200-ml volumetric flask, dissolved, and brought to volume with ethyl acetate (final concentration of 100 μg/ml).

Standard Solution of III—Approximately 20 mg of III, accurately weighed, was transferred to a 200-ml volumetric flask, dissolved, and brought to volume with *n*-hexane. Then 10.0 ml of this solution was transferred to a 50-ml volumetric flask and brought to volume with *n*-hexane (final concentration of 20 μg/ml).

[1] Hoffmann-La Roche, Montreal, Quebec, Canada.
[2] Aldrich Chemical Co., Montreal, Quebec, Canada.
[3] The United States Pharmacopeial Convention, Inc., Rockville, Md.
[4] British Drug Houses, Toronto, Ontario, Canada.
[5] Fisher Scientific Co., Ottawa, Ontario, Canada.
[6] Burdick and Jackson Laboratories, Muskegon, Mich.
[7] Model 4100, Varian Aerograph, Palo Alto, Calif.
[8] Autolab System I, Spectra-Physics, Santa Clara, Calif.
[9] LiChrosorb SI 60, Brinkmann Instruments (Canada) Ltd., Rexdale, Ontario, Canada.

All stock solutions and sample preparations were protected from light by wrapping the tubes or flasks with aluminum foil.

Standard Curves for I and II—Five standard solutions were prepared to contain between 200 and 400 μg of I/ml in 0.1 *N* aqueous hydrochloric acid. Similarly, five solutions were prepared to contain between 1.7 and 300 μg of II/ml in ethyl acetate. Ten milliliters of the highest concentration solution of I and 1.0 ml of the highest concentration solution of II were pipetted into a 30-ml screw-capped tube[10] along with 1.0 ml of concentrated ammonium hydroxide and 12.5 ml of IV internal standard solution. The other standard solutions were prepared in the corresponding manner. The five tubes were tumbled on a rotator[11] at 30 rpm for 30 min and then centrifuged[12] at 2000 rpm for 10 min. Duplicate 5-μl aliquots of the supernatant ethyl acetate layer were chromatographed using mobile phase System A.

Linearity Curve for III—Six solutions were prepared to contain between 1.0 and 35 μg of III/ml in *n*-hexane. Aliquots of 1.0 ml of each solution were pipetted into individual 5-ml volumetric flasks along with 3.0 ml of V internal standard solution. The solutions were diluted to volume with *n*-hexane, and duplicate 5-μl aliquots of each solution were chromatographed using mobile phase System B.

Daily Calibration Standards—For the determination of I and II, 10.0 ml of I standard solution, 1.0 ml of II standard solution, 1.0 ml of concentrated ammonium hydroxide, and 12.5 ml of IV internal standard solution were pipetted into a 30-ml screw-capped tube. The tube was tumbled at 30 rpm for 30 min and then centrifuged at 2000 rpm for 10 min. Duplicate 5-μl aliquots of the ethyl acetate layer were chromatographed using mobile phase System A.

For the determination of III, 15.0 ml of 0.1 *N* hydrochloric acid, 1.0 ml of III standard solution, and 3.0 ml of V internal standard solution were pipetted into a 30-ml screw-capped tube. The tube was tumbled at 30 rpm for 1 hr and then centrifuged at 2000 rpm for 10 min. Duplicate 5-μl aliquots of the *n*-hexane layer were chromatographed using mobile phase System B.

Analysis of Pharmaceuticals—*Determination of I and II*—Powdered tablet or capsule contents equivalent to 25 mg of chlordiazepoxide hydrochloride or to 20 mg of chlordiazepoxide base, accurately weighed, were transferred to a 100-ml volumetric flask along with 60 ml of 0.1 *N* hydrochloric acid. The stoppered flask was shaken[13] vigorously for 1 hr, brought to volume with 0.1 *N* hydrochloric acid, mixed well, and filtered[14] with the aid of suction.

Ten milliliters of the filtrate, 1.0 ml of ammonium hydroxide, 1.0 ml of ethyl acetate, and 12.5 ml of IV internal standard solution were transferred to a 30-ml screw-capped tube. The tube was tumbled on a rotator for 30 min at 30 rpm and centrifuged at 2000 rpm for 10 min. Duplicate 5-μl aliquots of the supernatant ethyl acetate layer were chromatographed using mobile phase System A.

Determination of III—Powdered tablets or capsule contents equivalent to 25 mg of chlordiazepoxide hydrochloride or to 20 mg of chlordiazepoxide base, accurately weighed, were transferred to a 30-ml screw-capped tube. Then 15.0 ml of 0.1 *N* hydrochloric acid, 1.0 ml of *n*-hexane, and 3.0 ml of V internal standard solution were added. The tubes were tumbled on a rotator for 1 hr at 30 rpm and centrifuged at 2000 rpm for 10 min. Duplicate 5-μl aliquots of the *n*-hexane layer were chromatographed using mobile phase System B.

Calculations—The slopes of the calibration curves, S_C, determined each time the mobile phase was replenished, were calculated from:

$$S_C = N_S C_I / N_I C_S \qquad \text{(Eq. 1)}$$

where N_S is the number of integrator counts for I or II or the peak height for III, N_I is the number of integrator counts for the internal standard, C_I is the concentration of the internal standard, and C_S is the concentration of the test compound I, II, or III.

The amount of each component found, expressed as a percentage of the label claim of chlordiazepoxide hydrochloride, was calculated from:

$$\% \text{ label claim} = \frac{N_S C_I F}{N_I S_C M_I} \qquad \text{(Eq. 2)}$$

where M_I is the theoretical weight of I injected (based on label claim), and F is a scaling factor (13,500 for I and II, 400 for III).

[10] Canadian Laboratory Supplies, Montreal, Quebec, Canada.
[11] Scientific Industries Ltd., Springfield, Mass.
[12] Model K, International Equipment Co., Needham Heights, Mass.
[13] Model 00, Burrell Corp., Pittsburgh, Pa.
[14] Whatman No. 3, Canadian Laboratory Supplies, Ottawa, Ontario, Canada.

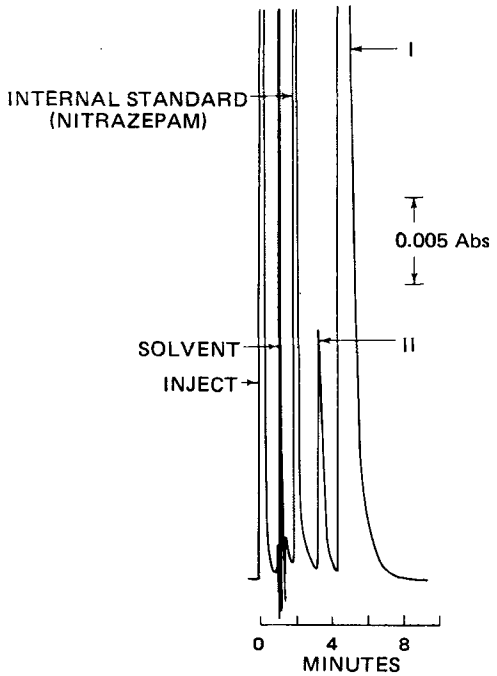

Figure 1—*High-performance liquid chromatogram of a standard solution containing 0.223 mg of chlordiazepoxide hydrochloride/ml, 7.06 μg of II/ml, and 33.0 μg of nitrazepam/ml (internal standard) using mobile phase System A.*

RESULTS AND DISCUSSION

Evaluation of Chromatographic Systems—Liquid–solid (adsorption) and bonded-phase chromatography are the modes of HPLC most applicable to the analysis of chlordiazepoxide and related impurities. Due to availability, cost, simplicity, stability, and column efficiency, liquid–solid chromatography, using a column packed with microparticulate silica gel, was chosen.

Various isocratic and gradient mobile phase systems were tried before the systems described were chosen. Attempts to find an isocratic mobile phase that eluted III behind the solvent front while eluting I and II within a reasonable time were unsuccessful because of the large relative differences in polarity among the three compounds. The inclusion of tetrahydrofuran in mobile phase System A was necessary to elute II before I. Also, III could not be detected at the low levels required (<0.01% in I) while maintaining the amount of I within the linear range of the system. The first problem was overcome by using a gradient system, but this approach had several disadvantages: lower precision, major baseline shifts during the gradient run, and longer total time due to a long column re-equilibration time. The sensitivity problem could possibly have been overcome by using a two-injection technique (overload the column with I to quantitate III and proceed normally to quantitate I and II). However, it was decided that this approach, combined with a gradient mobile phase system, would be less precise and offer little, if any, timesaving over the use of two separate isocratic systems for the analysis of III and for I and II. This latter approach allows optimum partition and chromatographic conditions to provide maximum peak size and minimum chromatograph time for all compounds.

Figure 1 shows a chromatogram obtained when the contents of a chlordiazepoxide hydrochloride capsule were analyzed for I and II using the described procedure. The internal standard, nitrazepam, and I and II were well resolved in less than 8 min. The peaks tailed somewhat, despite the basic mobile phase, but this tailing did not affect quantitation.

Figure 2 shows a chromatogram obtained when a 5-μl aliquot of a calibration standard, containing 4 μg/ml of III, was analyzed using mobile phase System B. The peaks for III and the internal standard, *o*-dinitrobenzene, were well resolved and eluted in less than 6 min.

Linearity and Standard Curves—A plot of peak area *versus* the amount of I injected was linear over the concentration range of 40–300 μg/ml[15] (0.2–1.5 μg/injection).

[15] Compound I was dissolved in 0.3% ammonium hydroxide in absolute ethanol (v/v).

Table I—Analysis of Synthetic Solutions of I and II

Sample	I			II		
	Calculated, μg/ml	Found, μg/ml	Recovery, %	Calculated, μg/ml	Found, μg/ml	Recovery, %
1	300	296	98.8	12.8	12.6	98.4
2	192	193	100.4	5.9	6.0	101.7
3	180	183	101.5	2.9	2.9	100.0
4	244	245	100.4	7.3	7.1	97.3
5	211	211	100.2	20.3	20.6	101.5
Mean recovery, %			100.3			99.8
RSD, %			±1.0			±2.6

A standard curve for I, covering the concentration range of 150–300 μg/ml (0.75–1.50 μg/injection) was linear with a slope of 1.37 ± 0.02 and a negligible intercept (0.005). By using the sample preparation procedure described, this standard curve is applicable to samples containing 80–160% of the theoretical weight of I (25 mg).

Duplicate calibration standards were prepared daily and injected periodically to determine the slope of the standard curve. The slope varied by less than 1% on any given day and by less than 3% over the study. Since the current value of the slope was experimentally determined and used in the calculations, small variations in the slope did not affect the accuracy of the procedure.

An identical procedure was followed for the determination of II. A plot of peak area *versus* the amount injected was linear to 140 μg/ml (0.7 μg/injection). A standard curve over the range of 1.2–20 μg/ml (0.006–0.1 μg/injection), the equivalent of 0.7–11% of the theoretical weight of I (25 mg), was linear with a slope of 1.10 ± 0.01 and a negligible intercept (0.0003). Duplicate calibration standards were used to check the slope of the standard curve, as for I.

A standard curve was not used for the analysis of III. Instead, linearity, partition, and calibration standard data were combined to show that the slope obtained from subsequent calibration standard data alone allowed III to be determined directly.

A plot of the ratio of peak height to internal standard counts *versus* the amount of III injected was linear between 1 and 35 ng/injection and passed through the origin. This range represented, using the sample preparation scheme described under *Experimental*, levels of III between 0.003 and 0.11% of the theoretical amount of I (25 mg).

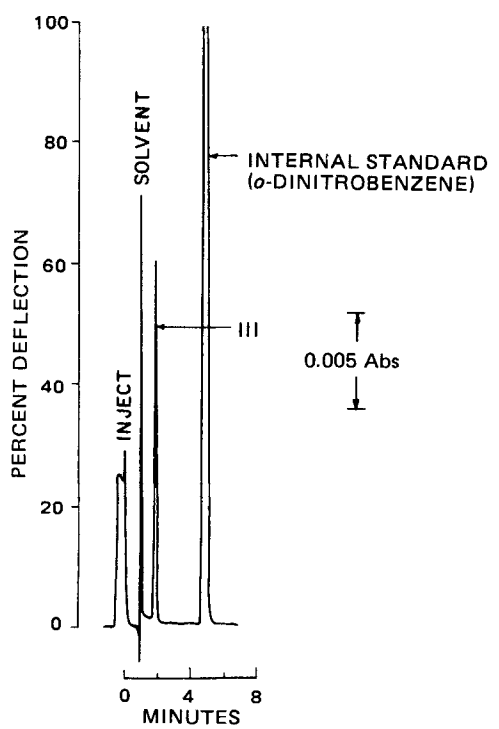

Figure 2—*High-performance liquid chromatogram of a standard solution containing 4.0 μg of III/ml and 56.0 μg of o-dinitrobenzene/ml (internal standard) using mobile phase System B.*

Sample Preparation—The times necessary for constant and complete extraction and partition of I and II from formulations were determined in two stages. Time for extraction into 0.1 *N* hydrochloric acid was determined by shaking capsule composite samples for 30, 60, and 90 min. The samples were then made alkaline and partitioned into ethyl acetate, as described, for 60 min. When the ethyl acetate layer was analyzed for I and II, levels in the samples extracted for 60 and 90 min were identical but somewhat higher than in the sample extracted for 30 min. With a 60-min extraction, the time for constant partition was determined by tumbling capsule composite samples, as described, for various times up to 60 min. No change in the peak heights for I or II were noted after 20 min.

Quantitative partition of I and II from hydrochloric acid (made basic) into ethyl acetate was demonstrated by chromatographing both layers of a capsule composite sample tumbled for 30 min. Also, when the described procedure was applied to capsule composite samples equivalent to 10, 20, and 30 mg of I, the ratio of concentrations for I and for II in the three samples was 1:2:3 in both cases.

To determine the time required to attain equilibrium in the partition of II, capsule composite samples in 0.1 *N* hydrochloric acid were tumbled with *n*-hexane, as described, for various times up to 90 min. No change in the size of the peak for III, obtained by chromatographing 5-μl aliquots of the *n*-hexane layer using mobile phase System B, was observed after 40 min.

When both layers of a calibration standard were analyzed for the internal standard (*o*-dinitrobenzene) and III, both compounds were partitioned quantitatively into the *n*-hexane layer (<99:1 concentration ratio). In addition, when the described extraction procedure was applied to capsule composite samples equivalent to 10, 20, and 30 mg of I, the concentrations of III were in the ratio 1:2:3. These data indicated complete and constant partition of III under the described conditions.

Compounds I and II did not interfere with the analysis of III since no peaks were observed for I or II when 5-μl aliquots of the *n*-hexane layer of a capsule composite sample, prepared using the procedure described for the determination of III, were chromatographed using mobile phase System A.

Quantitation—Compounds I and II were quantitated using peak area; however, quantitation of III was more precise using peak height. Since the internal standard peak was integrated in both cases, the assay for III was based on the peak height to peak area ratio and the assay for I and II was based on peak area ratios.

Reproducibility of the chromatographic system was shown by chromatographing six 5-μl aliquots of a calibration standard containing 0.19 mg of I/ml and 0.006 mg of II/ml (0.95 and 0.02 μg/injection, respectively)

Table II—Analysis of Synthetic Solutions of III

Sample	Calculated, μg/ml	Found, μg/ml	Recovery, %
1	0.179	0.178	99.6
2	0.358	0.356	99.5
3	1.79	1.83	102.1
4	4.00	3.90	97.5
5	8.10	7.90	97.5
6	16.1	16.1	100.0
7	24.9	24.8	99.6
8	32.3	31.8	98.4
Mean recovery, %			99.3
RSD, %			±1.5

Table III—Analysis of Chlordiazepoxide Formulations for I and II by HPLC and Spectrophotometric[a] Methods

Sample	Type	HPLC			Spectrophotometric, "I"[b], %
		I[b], %	II[b], %	Total[b], %	
A	Tablet, base	98.0	0.73	98.7	98.8
B	Capsule, hydrochloride	97.3	0.81	98.1	98.1
C	Capsule, hydrochloride	96.6	4.12	100.7	101.2
D	Capsule, hydrochloride	91.5	5.62	97.4	96.4
E	Tablet, hydrochloride	87.1	8.54	95.7	95.7

[a] Reference 3. [b] Percent of label claim amount of chlordiazepoxide *or* chlordiazepoxide hydrochloride.

along with the 0.03-mg/ml nitrazepam internal standard. The relative standard deviations of the peak area ratios were 0.32% for I and 2.7% for II. The analogous figure for III at a level of 0.0036 mg/ml (0.018 μg/injection) was 2.3%.

Calibration standards, stored in the dark at 4° between analyses, were analyzed for I, II, and III on each of 5 consecutive days; the relative standard deviations were 1.1, 2.7, and 2.5%, respectively. While the standards appeared to be stable for at least 1 week at 4°, fresh calibration standards were prepared daily to check the slopes of the calibration curves.

The minimum detectable amounts of II and III under the conditions described were 1 and 0.2 ng/injection, respectively. The lowest levels actually quantitated were 6.3 and 0.9 ng/injection, respectively. Under the extraction conditions described, these amounts of II and III represented 0.7 and 0.0003%, respectively, of the label claim of I.

Analysis of Solutions of Known Concentration—Five solutions of I and II, prepared in the same manner as the calibration standard solutions, were analyzed using the described procedure. Table I shows that the mean recoveries for I and II were 100.2 and 99.8% with relative standard deviations of 1.0 and 2.6%, respectively.

Similarly, eight solutions were prepared to contain known concentrations of III (0.18–32 μg/ml) in the same way as solutions used for the determination of linearity. Table II shows that the mean recovery was 99.3% with a relative standard deviation of 1.5%. For this assay, only the calibration standard used to determine the slope of the standard curve was prepared in the same way as for linearity samples. For the analysis of pharmaceuticals, the procedure described in *Experimental* was used.

Analysis of Pharmaceuticals—Five formulations of chlordiazepoxide or chlordiazepoxide hydrochloride, capsules or tablets, were analyzed by the BP spectrophotometric procedure (3) and by the described HPLC procedure for I and II. Aliquots of the same tablet or capsule composite were analyzed in each case. The spectrophotometric method is nonspecific, since both I and II exhibit absorbance maxima at 308 nm, the wavelength used in the assay. It was not surprising, therefore, that the sum of the levels of I and II determined by the HPLC procedure agreed closely with the level of I determined by the spectrophotometric method (Table III). The level of II exceeded the allowed limit in three cases; however, the samples assayed were several years old and were not representative of current formulations.

The precision of the procedure for the determination of I and II in formulations was determined by analyzing Sample B (Table III) five times. Percent relative standard deviations of 0.2 and 1.8% were measured for I and II, respectively.

Five formulations of chlordiazepoxide or chlordiazepoxide hydrochloride were analyzed for III using the described procedure (Table IV). Very low levels of III were encountered; in all cases, these levels were well within the allowable limits. Results for Formulation E (Tables III and IV) showed that a high level of II did not necessarily imply a high level of III. The other four samples listed in Table IV were selected to contain the highest levels of III from over 30 screened by the appropriate TLC limit test (1–3). The precision of the procedure for the determination of III in formulations was shown by analyzing Sample F five times. A percent relative standard deviation of 1.4% was measured.

Table IV—Analysis of Chlordiazepoxide Formulations for III by HPLC[a]

Sample	Type	III[b], %
E	Tablet, hydrochloride	0.030
F	Capsule, hydrochloride	0.015
G	Capsule, hydrochloride	0.009
H	Capsule, hydrochloride	0.006
I	Capsule, hydrochloride	0.015

[a] Using mobile phase System B. [b] Percent of label claim amount of chlordiazepoxide hydrochloride.

Five samples of chlordiazepoxide or chlordiazepoxide hydrochloride drug substance also were analyzed for III. In all cases, levels below the quantifiable limit of 0.003% were found, well below the allowable limits of 0.01%.

The described method is applicable to both tablets and capsules and both the free base and hydrochloride salt forms of chlordiazepoxide. Interference from excipients was not experienced. The method could be adapted to the analysis of single 5- or 10-mg tablets or capsules by reducing the volumes used for extraction and may be used as described for single 25-mg tablets or capsules.

REFERENCES

(1) "The United States Pharmacopeia," 19th rev., Mack Publishing Co., Easton, Pa., 1975, pp. 79, 80.

(2) "The National Formulary," 14th ed., Mack Publishing Co., Easton, Pa., 1975, pp. 131, 132.

(3) "British Pharmacopoeia," Her Majesty's Stationery Office, London, England, 1973, pp. 96, 97.

(4) B. A. Koechlin and L. D'Arconte, *Anal. Biochem.*, **5**, 195 (1963).

(5) C. S. Frings and P. S. Cohen, *Am. J. Clin. Pathol.*, **56**, 216 (1971).

(6) M. A. Schwartz and E. Postma, *J. Pharm. Sci.*, **55**, 1358 (1966).

(7) M. R. Hackman, M. A. Brooks, J. A. F. de Silva, and T. S. Ma, *Anal. Chem.*, **46**, 1075 (1974).

(8) I. A. Zingales, *J. Chromatogr.*, **61**, 237 (1971).

(9) G. Caille, J. Braun, and J. A. Mockle, *Can. J. Pharm. Sci.*, **5**, 78 (1970).

(10) J. S. Wragg and G. W. Johnson, *Pharm. J.*, **601**, 28 (1974).

(11) A. G. Butterfield, D. W. Hughes, W. L. Wilson, and N. J. Pound, *J. Pharm. Sci.*, **64**, 316 (1975).

(12) A. G. Butterfield, B. A. Lodge, N. J. Pound, and R. W. Sears, *ibid.*, **64**, 441 (1975).

(13) L. D. Bighley and J. P. McDonnell, *ibid.*, **64**, 1549 (1975).

(14) R. K. Gilpin, J. A. Korpi, and C. A. Janicki, *J. Chromatogr.*, **107**, 115 (1975).

(15) C. G. Scott and P. Bommer, *J. Chromatogr. Sci.*, **8**, 446 (1970).

(16) D. J. Webber, *J. Pharm. Sci.*, **61**, 1797 (1972).

(17) D. H. Rodgers, *J. Chromatogr. Sci.*, **12**, 742 (1974).

(18) R. E. Majors, *Anal. Chem.*, **44**, 1722 (1972).

ACKNOWLEDGMENTS AND ADDRESSES

Received March 15, 1976, from the *Drug Research Laboratories, Health Protection Branch, Ottawa, Ontario, Canada, K1A 0L2.*

Accepted for publication June 28, 1976.

[x] To whom inquiries should be directed.

Pharmacokinetics of Methsuximide and a Major Metabolite in Dogs

MICHAEL R. DOBRINSKA * and PETER G. WELLING ˣ

Abstract □ The pharmacokinetics of methsuximide and its major metabolite 2-methyl-2-phenylsuccinimide were studied in dogs after single intravenous doses. Plasma methsuximide levels were described by a two-compartment open model, and those of the metabolite were described by a one-compartment open model. An expression was derived that describes both methsuximide and metabolite plasma levels after methsuximide administration. Excellent fits were obtained between observed data and those predicted from the model. The metabolite accounted for 40% of the overall elimination of methsuximide, and the half-life of the metabolite (15 hr) was much greater than that of the parent drug (1–3.5 hr). The results suggest that pharmacological effects after methsuximide administration may be due primarily to the metabolite, which may accumulate in the body during repeated doses.

Keyphrases □ Methsuximide and metabolite—pharmacokinetics in dogs after single intravenous doses, GLC analysis in plasma □ Pharmacokinetics—methsuximide and metabolite, after single intravenous doses in dogs □ GLC—analysis, methsuximide and metabolite, dog plasma □ Anticonvulsants—methsuximide and metabolite, pharmacokinetics in dogs after single intravenous doses, GLC analysis in plasma

Methsuximide is a succinimide derivative useful in the treatment of petit mal epilepsy (1–4). In rats, it is distributed rapidly into most major tissues and organs (5). Metabolism studies in rats, guinea pigs, dogs, and humans (6–8) indicate not only that methsuximide is metabolized extensively but also that a prime biotransformation route is *N*-demethylation, leading to 2-methyl-2-phenylsuccinimide, which is pharmacologically active (2, 5, 9). There is evidence that this metabolite is cleared slowly from the body relative to the parent drug (10–12). This phenomenon is not uncommon; several other antiepileptic drugs undergo *N*-demethylation to yield slowly cleared, active metabolites (13).

The *N*-demethylated metabolite may be responsible for the therapeutic activity of methsuximide. Plasma levels of methsuximide and the metabolite were measured by mass fragmentography in 17 patients receiving chronic methsuximide therapy (11). Plasma metabolite levels exceeded those of the parent drug by 700-fold. However, this number reflects the extremely low methsuximide concentrations that the assay was capable of detecting. Metabolite levels of less than 10 μg/ml were judged ineffective, while levels in excess of 40 μg/ml were toxic.

As exemplified in a recent case report (12), special caution must be exercised in the management of a methsuximide overdose. After ingestion of 10 g of methsuximide, the time course of toxicity was biphasic. The initial phase of toxicity was attributed to the high circulating level of the parent drug. After a period of improvement, the patient regressed into an extended, profound coma. This second phase of toxicity was attributed to the sustained, high concentrations of the metabolite in plasma, which were about 20 times those of the parent drug.

A primary objective of this study was to obtain the pharmacokinetic profiles in the dog of both methsuximide and the metabolite after single intravenous doses. By combining the individual models, it was then possible to quantitate the rate and extent to which methsuximide was biotransformed into the metabolite after single doses of the parent drug. This report also describes an improved, sensitive, and fast GLC assay for the simultaneous measurement of methsuximide and its metabolite in plasma.

EXPERIMENTAL

Pure samples of methsuximide[1], phensuximide[1], and 2-methyl-2-phenylsuccinimide[2] were the racemic forms. Two male beagle dogs were used; Dog A weighed 14 kg and Dog B weighed 17.5 kg. The dogs had free access to water at all times, but food was withheld 12 hr prior to an experiment.

Due to the limited water solubility of methsuximide (10), the intravenous dosage form, used in all experiments, consisted of 250 mg of methsuximide dissolved in 5 ml of an aqueous solution of 75% propylene glycol. For consistency, the metabolite was also administered in this dosage form.

Procedure—Each dog was placed in a restraining apparatus with its limbs held secure by pediatric limb restraints. A vein infusion set[3] was positioned in each of the two front limbs. One set was used to administer 5 ml iv (250 mg) of the drug solution by rapid injection (120 sec or less) and was then immediately flushed with 10 ml of normal saline solution to ensure quantitative delivery of the dose. This set was then removed. The other infusion set was used to collect multiple samples at short intervals during the 1st hr of the experiment. The set was kept open by filling with heparin sodium solution, 10 units/ml, between samples.

Blood samples (5 ml) were collected in vacuum tubes[4] at 0, 2–5, 10, 15, 30, 45, 60, and 120 min and then at longer time intervals up to 48 hr. After 3 hr, the infusion set was removed and the dog was freed from the restraints. Blood samples after this time were obtained by direct venipuncture. When the set was used, the blood collection procedure was to withdraw 5 ml of the heparin-diluted blood, draw the 5-ml blood sample, inject 5 ml of saline, reinject the diluted blood, and refill the set with about 1 ml of the dilute heparin solution. The blood samples were centrifuged, and the plasma was deep frozen until analyzed, usually within 1 week.

To eliminate the possibility of drug-related changes in the pharmacokinetic parameters, the minimum time between experiments on the same dog was 1 month.

Assay—The assay was a modification of that of Kinkel *et al.* (10). One milliliter of plasma, or blank plasma containing known quantities of methsuximide and metabolite, was pipetted into a 13-ml glass-stoppered centrifuge tube and acidified with 0.5 ml of 0.5 *N* hydrochloric acid. Five milliliters of chloroform[5] was added, and the tubes were shaken horizontally on a flat-bed shaker for 15 min and then centrifuged[6]. A 4-ml aliquot of the chloroform layer was transferred to clean tubes, and 1 ml of phensuximide solution (6 μg/ml in chloroform) was added as an external standard. The chloroform was evaporated to dryness carefully in a 40° water bath under a gentle stream of nitrogen. The residue was immediately redissolved in about 100 μl of carbon disulfide[7], and the samples were analyzed by GLC.

The gas chromatograph[8], equipped with flame-ionization detectors, was run isothermally using a U-shaped glass column (1.8 m × 2 mm i.d.) packed with 3% OV-17 on 100–120-mesh Gas Chrom Q[9]. The temperatures employed were: column, 175°; flame-ionization detector, 200°; and

[1] Donated by Parke-Davis and Co., Detroit, Mich.
[2] Aldrich Chemical Co., Milwaukee, Wis.
[3] Miniset vein infusion set, Travenol, Deerfield, Ill.
[4] Ten milliliter green stoppered with 143 units of heparin sodium, Becton-Dickinson, Rutherford, N.J.
[5] Analytical reagent, Mallinckrodt, as supplied.
[6] Dynac centrifuge, Clay Adams, Parsippany, N.J.
[7] Analytical reagent, Fisher Scientific Co.
[8] Nuclear Chicago 5000 dual-column, programmable gas chromatograph.
[9] Applied Science Laboratories, State College, Pa.

Table I—Summary of Experiments

Experiment	Dog	Compound Administered, Dose and Route
A	A[a]	Methsuximide, 250 mg iv
B	B	Methsuximide, 250 mg iv
C	B	Methsuximide, 250 mg iv
D	B	2-Methyl-2-phenylsuccinimide, 250 mg iv
E	B	2-Methyl-2-phenylsuccinimide, 250 mg iv

[a] Dog A had some difficulty adapting to the restraining apparatus and was replaced by Dog B.

injection block, 210°. The electrometer settings varied between 8 and 64 $\times 10^{-11}$ amp. Sample volume, introduced by the on-column injection technique, was 3 μl; the recorder chart speed was 38 cm/hr.

The flame gases were hydrogen and compressed air, and their flow rates were systematically adjusted until maximum flame-ionization detector response to the compounds was obtained at 20 and 200 ml/min, respectively. The carrier gas was nitrogen, and its optimal flow rate of 20 ml/min was obtained from an experimentally determined Van Deemter plot (14). Under the conditions used, the column had 321 and 435 theoretical plates/30.5 cm for methsuximide and the metabolite, respectively.

Compounds were quantitated using peak height ratios. This method was faster than, and as accurate as, peak area determination by disk integration or planimetry. The assay method was sensitive to plasma compound concentrations of 0.5 μg/ml.

Standard curves, run in triplicate on separate days, were constructed from the assay results of blank dog plasma containing known quantities of methsuximide and the metabolite at 10 concentrations over the range of 0.5–25.0 μg/ml. The standard curves were checked at the time of assay of unknowns by including in each run a blank plasma sample containing 10 μg of methsuximide and the metabolite; recoveries were 93 ± 3 (*SD*) and 88 ± 5%, respectively.

The experiments conducted are summarized in Table I.

Pharmacokinetic Analysis—Plasma level data were fitted to the appropriate pharmacokinetic equations by graphical methods (15). Improved estimates of pharmacokinetic parameters, including confidence limits and coefficients of determination, were obtained using the iterative nonlinear least-squares program NREG on a digital computer[10] as described previously (16).

RESULTS AND DISCUSSION

Assay—Carbon disulfide was substituted for chloroform as the final solvent for injection into the gas chromatograph, because flame-ionization detectors respond poorly to carbon disulfide and compound peaks are obtained from a flat baseline. Chromatograms obtained by the two methods are compared in Fig. 1. Although evaporation of chloroform solutions was reported to result in drug losses (10), no loss of methsuximide or metabolite was observed. The entire chromatogram was obtained within 6 min of injection.

Pharmacokinetic Model for Methsuximide—The decline in plasma methsuximide levels in Experiments A, B, and C was biphasic. A typical plasma profile from Experiment B is shown in Fig. 2. Therefore, these data were analyzed in terms of the two-compartment open model (17) as depicted in Scheme I. This model describes the instantaneous introduction of an intravenous dose, D, of drug into a rapidly accessible central or plasma compartment having an apparent distribution volume, V_1, and equilibration of this compartment with a less readily accessible tissue compartment. The quantities A_1 and A_2 refer to the amounts of unchanged drug in the central and tissue compartments, respectively. The disposition first-order rate constants k_1 and k_{-1} govern the transfer of drug between the compartments, while k_2 is the first-order rate constant representing loss of drug from the central compartment by all routes except k_1.

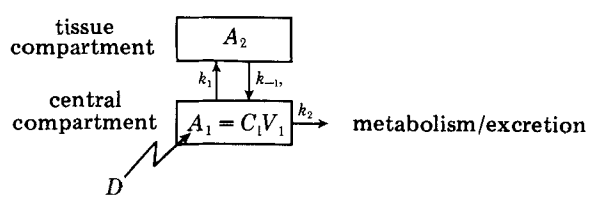

Scheme I

[10] Univac 1118.

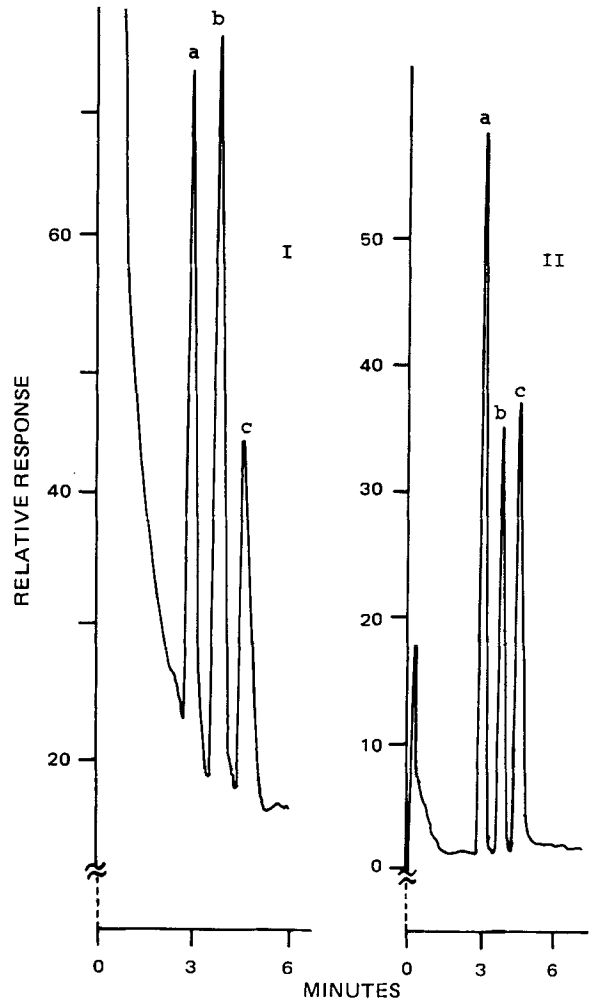

Figure 1—*Representative GLC chromatograms using chloroform (I) and carbon disulfide (II) as solvents. The lettered peaks and their retention times are:* (a) *methsuximide, 191 sec;* (b) *phensuximide external standard, 239 sec; and* (c) *2-methyl-2-phenylsuccinimide, 281 sec. Curves I and II are different plasma samples run at different chart speeds.*

Equation 1 describes the plasma drug concentration *versus* time profile appropriate to this model (17):

$$C_1 = \frac{D}{V_1(\alpha - \beta)}\left[(\alpha - k_{-1})\,e^{-\alpha t} + (k_{-1} - \beta)e^{-\beta t}\right] \qquad \text{(Eq. 1)}$$

where:

$$\begin{matrix}\alpha \\ \beta\end{matrix} = \tfrac{1}{2}\{(k_1 + k_{-1} + k_2) \pm [(k_1 + k_{-1} + k_2)^2 - 4k_{-1}k_2]^{1/2}\} \qquad \text{(Eq. 2)}$$

The composite rate constant β is the slope of the postdistributive log-linear phase of loss of drug from the body multiplied by −2.303, and α is the log-linear slope multiplied by −2.303 obtained by the method of curve stripping (17).

The broken line in Fig. 2 represents the computer fit to unweighted data. Low concentrations were consistently underestimated by the computer. Since NREG is a least-squares fitting routine, a small relative error in the higher concentrations contributes more to the sums of squares than an equivalent error in the lower concentration range. Thus, to make all concentrations contribute equally, data points were weighted by the reciprocal of their concentrations. This weighting scheme improved the curve fitting in all cases (solid line in Fig. 2) and was used in all nonlinear regression procedures.

Table II gives the computer-estimated parameters for Experiments A, B, and C. The distribution characteristics of methsuximide (k_1, k_{-1}, α, V_1, and T/P) differed between the two dogs, although they were of similar order of magnitude. There was more rapid equilibration of drug between compartments in Dog B (α, k_1, and k_{-1}), while Dog A had a

Table II—Pharmacokinetic Parameters after Intravenous Administration of Methsuximide to the Dog

Parameter[a]	Experiment A	Experiment B	Experiment C
k_1, hr^{-1}	2.80 (0.32–5.29)[b]	3.61 (1.02–6.32)	1.86 (0.074–3.65)
k_{-1}, hr^{-1}	1.47 (0.69–2.26)	3.40 (1.89–4.91)	3.28 (0.73–5.82)
k_2, hr^{-1}	0.63 (0.35–0.91)	1.67 (1.21–2.13)	0.84 (0.70–0.97)
D/V_1, mg/liter	23.3 (12.9–33.7)	18.5 (13.4–23.6)	11.1 (9.6–12.6)
D, mg	250	250	250
V_1, liters	10.7	13.5	22.5
α, hr^{-1}	4.71	8.03	5.48
β, hr^{-1}	0.20	0.71	0.50
$t_{1/2}$, hr	3.47	0.98	1.39
T/P[c]	2.20	1.36	0.67
R^2[d]	0.9930	0.9977	0.9972

[a] First four parameters are primary while the balance are derived. [b] The 95% confidence limits. [c] Amount of drug in the tissue compartment to that in the plasma compartment at equilibrium (17). [d] Coefficient of determination, $(\Sigma obs^2 - \Sigma dev^2)/\Sigma obs^2$.

greater amount of drug in the tissue compartment at equilibrium (T/P). The elimination characteristics (k_2, β, and $t_{1/2}$) also differed between the dogs, with Dog A eliminating and/or metabolizing methsuximide more slowly than Dog B.

The rate constant k_2 reflects excretion and metabolism of methsuximide. Since the metabolite was determined in all methsuximide experiments, it was possible to separate k_2 into components representing (*a*) formation of 2-methyl-2-phenylsuccinimide and (*b*) excretion of unchanged methsuximide and/or formation of any other metabolites. Before the metabolite data could be incorporated into Scheme I, its apparent distribution volume and individual pharmacokinetic model had to be obtained by intravenous administration of the pure metabolite.

Pharmacokinetic Model for Metabolite—Figures 3 and 4 are semilogarithmic plots of the data from Experiments D and E after intravenous metabolite administration (250 mg). Since the initial data points did not show sufficient curvilinearity to justify two-compartment model kinetics, the one-compartment open model (Scheme II) was used. The symbolism used in this model for the metabolite is equivalent to that used in Scheme I for unchanged drug.

The plasma metabolite level *versus* time profiles are described by:

$$C_m = \frac{D}{V_3} e^{-k_3 t} \qquad \text{(Eq. 3)}$$

so that, when plotted semilogarithmically, the concentration axis intercept is D/V_3 while the slope is $-k_3/2.303$. The solid lines in Figs. 3 and 4 are the lines of best fit as determined by linear regression analysis[11].

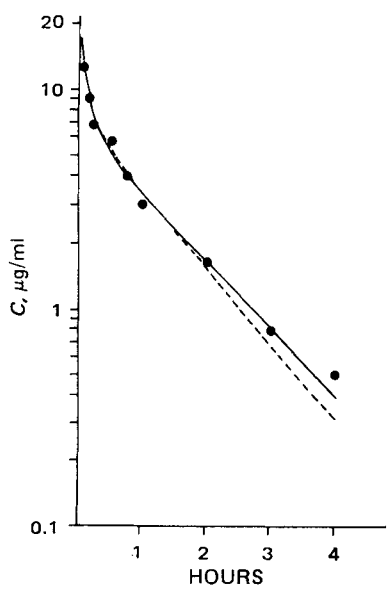

Figure 2—*Semilogarithmic plot of methsuximide concentration* versus *time data from Experiment B. The computer-determined equations of best fit using unweighted data* (- - -) *and data weighted by 1/C* (—) *are* $C_1 = 12.1e^{-9.95t} + 7.7e^{-0.81t}$ *and* $C_1 = 11.7e^{-8.03t} + 6.8e^{-0.71t}$, *respectively. See text for explanation.*

[11] Performed on a Compucorp 344 statistician microcomputer, Computer Design Corp., Los Angles, Calif.

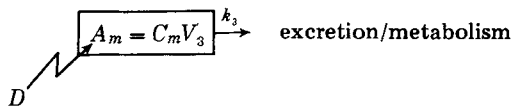

Scheme II

Table III summarizes the regression-determined parameters of Scheme II.

The elimination rate constant k_3, representing excretion or further metabolism, was identical in both experiments and the biological half-life, $t_{1/2}$, was about seven times greater than that of the parent drug (*cf.*, Table II). The apparent distribution volumes of the two compounds were similar.

Since the models and pharmacokinetic parameters for methsuximide and its major metabolite in plasma were obtained independently, it was possible to develop a model to quantitate the rate and extent of formation of the metabolite after an intravenous dose of methsuximide.

Pharmacokinetics of Methsuximide Including Metabolite Formation—Scheme III depicts the model describing intravenous administration of methsuximide with subsequent formation of the metabolite. In Scheme III, D is the amount of methsuximide administered intravenously, k_1 and k_{-1} are as previously defined, k_{el} is the first-order rate constant describing excretion and metabolism of methsuximide to compounds other than 2-methyl-2-phenylsuccinimide, k_f is the first-order rate constant describing formation of the metabolite, and k_3 is the first-order rate constant representing excretion and/or further metabolism of 2-methyl-2-phenylsuccinimide. The remaining symbols are as in Schemes I and II.

The differential equations for the rate of change of C_1 and C_m, with time, can be solved to yield Eqs. 1 and 4:

$$C_m = \frac{WDk_f}{V_3}\left\{\left[\frac{k_{-1}-\alpha}{(k_3-\alpha)(\beta-\alpha)}\right]e^{-\alpha t} + \left[\frac{k_{-1}-\beta}{(k_3-\beta)(\alpha-\beta)}\right]e^{-\beta t} + \left[\frac{k_{-1}-k_3}{(\beta-k_3)(\alpha-k_3)}\right]e^{-k_3 t}\right\} \qquad \text{(Eq. 4)}$$

Since all concentrations are expressed on a mass per volume basis, the factor W, the molecular weight ratio of the metabolite to the parent drug (189/203), is required in Eq. 4.

The composite rate constants α and β are now defined by Eq. 5. The significance of these constants is the same as that in Eq. 2. However, in Eq. 5, k_2 from Eq. 2 is separated into $k_{el} + k_f$:

$$\begin{matrix}\alpha \\ \beta\end{matrix} = \tfrac{1}{2}\{(k_1 + k_{-1} + k_{el} + k_f) \pm [(k_1 + k_{-1} + k_{el} + k_f)^2 - 4(k_{-1}k_f + k_{el}k_{-1})]^{1/2}\} \qquad \text{(Eq. 5)}$$

Table III—Metabolite Pharmacokinetic Parameters after Intravenous Administration to the Dog

Parameter	Experiment D	Experiment E
D, mg	250	250
V_3, liters	14.6	11.8
D/V_3, mg/liter	17.1	21.1
k_3, hr^{-1}	0.047	0.047
$t_{1/2}$, hr	14.7	14.7

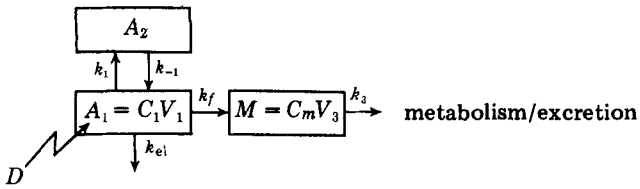

Scheme III

Figures 5 and 6 give the experimental data for methsuximide and the metabolite in Experiments B and C. Experiment A had to be terminated early, and the metabolite was followed over a time period less than its half-life (14.7 hr). Thus, this experiment could not be used to test the validity of the model in Scheme III.

Initial estimates of the parameters are needed for the computer analysis of the data in terms of Scheme III, but stripping of triexponential curves (Eq. 4) is an inaccurate procedure (18). However, initial estimates of α, β, k_1, and k_{-1} can be obtained from the computer values obtained from methsuximide alone (Table II). The estimate of k_3 can be obtained in two ways; it can be estimated from the independent metabolite experiments or from Eq. 4. Since it is already established that $\alpha > \beta > k_3$, after a certain time Eq. 4 will become essentially monoexponential and the resulting log-linear slope will equal $-k_3/2.303$. The volume V_3 can be estimated as the average volume obtained in Experiments D and E, and an estimate of k_f can be obtained by area analysis. Equations 1 and 4 can be integrated between the limits of zero and infinite time to yield Eqs. 6 and 7, respectively:

$$\text{area } C_1 = \frac{Dk_{-1}}{V_1\alpha\beta} \qquad \text{(Eq. 6)}$$

$$\text{area } C_m = \frac{Wk_fk_{-1}D}{V_3k_3\alpha\beta} \qquad \text{(Eq. 7)}$$

Combining Eqs. 6 and 7 and solving for k_f yield:

$$k_f = \frac{V_3k_3}{WV_1}\frac{\text{area } C_m}{\text{area } C_1} \qquad \text{(Eq. 8)}$$

The areas under the methsuximide and metabolite curves, area C_1 and area C_m, respectively, were determined using the trapezoidal rule; the areas from the time of the terminal data points to time infinity were calculated (17). The remaining parameter, k_{el}, was determined from:

$$k_{el} = \frac{\alpha\beta - k_{-1}k_f}{k_{-1}} \qquad \text{(Eq. 9)}$$

obtained directly from Eq. 5.

Table IV—Pharmacokinetic Parameters for Methsuximide and Metabolite after Intravenous Doses of Methsuximide

Parameter[a]	Experiment B	Experiment C
k_1, hr^{-1}	3.84 (0.52–7.17)[b]	0.71 (0.20–1.23)
k_{-1}, hr^{-1}	3.80 (1.92–5.68)	1.14 (0.26–2.02)
k_{el}, hr^{-1}	1.01 (0.69–1.33)	0.50 (0.42–0.58)
k_f, hr^{-1}	0.77 (0.54–1.00)	0.28 (0.24–0.31)
k_3, hr^{-1} (F)[c]	0.047	0.047
D/V_1, mg/liter	18.9 (12.8–25.0)	10.4 (9.3–11.5)
D/V_3, mg/liter (F)	18.9	18.9
V_1, liters	13.2	24.0
V_3, liters	13.2	13.2
α, hr^{-1}	8.64	2.24
β, hr^{-1}	0.78	0.40
$t_{1/2}$, hr (methsuximide)	0.9	1.7
$t_{1/2}$, hr (metabolite)	14.7	14.7
R^2 (methsuximide)	0.9979	0.9937
R^2 (metabolite)	0.9919	0.9914
R^2 (overall)	0.9950	0.9928

[a] First seven parameters are primary while the balance are derived. [b] The 95% confidence limits. [c] Indicates parameter was fixed in the regression analysis.

The methsuximide and metabolite data from Experiments B and C were simultaneously fitted to Eqs. 1 and 4. Since high correlations existed between some parameters, it was necessary to fix two of the seven primary parameters so that they would not contribute to the nonlinear regression analysis. Since V_3 was determined accurately in Experiments D and E and since identical values of k_3 were obtained by both initial estimate methods, these parameters were fixed. This procedure significantly reduced not only the correlations but also the 95% confidence limits of the parameters.

The computer parameter values are given in Table IV. The solid curves in Figs. 5 and 6 are the computer fits to the data. These figures and the R^2 values in Table IV indicate that Scheme III excellently describes the experimental data.

The simultaneous fitting only slightly changed the methsuximide parameters obtained in the absence of metabolite data (*cf.*, Table II).

Of particular interest is the relative importance of the rate of biotransformation of methsuximide to the metabolite, k_f, compared to the overall methsuximide elimination rate constant, $k_{el} + k_f$. This metabolic step accounted for 43 and 36% of the overall elimination of methsuximide in Experiments B and C, respectively. The large value of k_f together with the small k_3 led to sustained, high metabolite concentrations. This fact

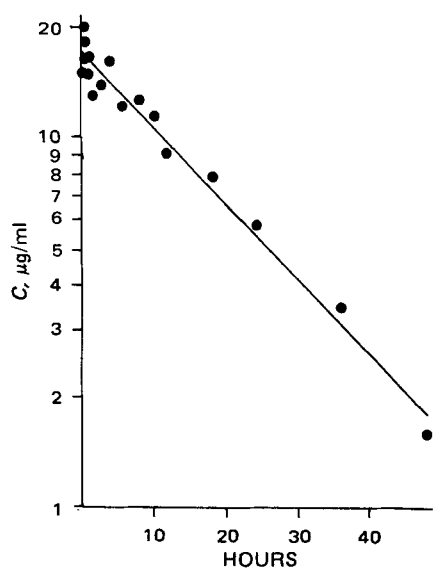

Figure 3—*Semilogarithmic plot of 2-methyl-2-phenylsuccinimide concentration* versus *time data from Experiment D after intravenous injection of this metabolite in the dog. The solid line was determined by linear regression analysis, the equation of which, including the 95% confidence limits, was log* $C_m = -0.0205(\pm 0.0015)t + 1.2326(\pm 0.0261)$.

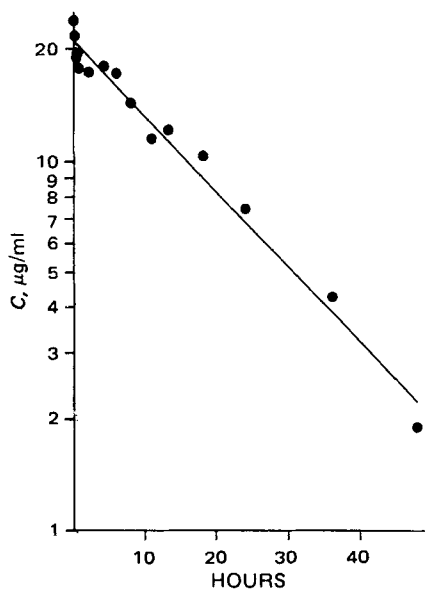

Figure 4—*Semilogarithmic plot of 2-methyl-2-phenylsuccinimide concentration* versus *time data from Experiment E after intravenous injection of this metabolite in the dog. The solid line was determined by linear regression analysis, the equation of which, including the 95% confidence limits, was log* $C_m = -0.0203(\pm 0.0017)t + 1.3245(\pm 0.0314)$.

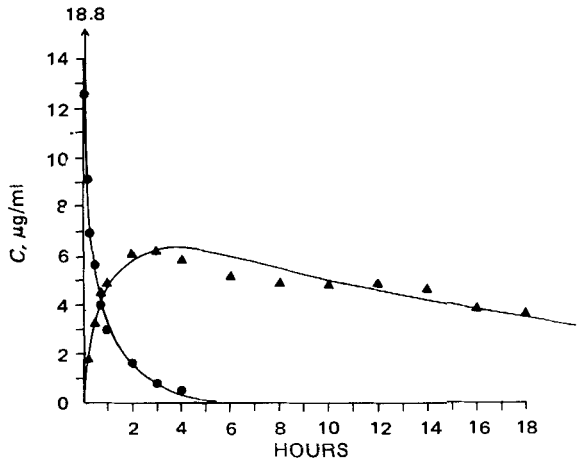

Figure 5—*Methsuximide and 2-methyl-2-phenylsuccinimide plasma level* versus *time profiles after a 250-mg intravenous injection of methsuximide (Experiment B). The computer-determined equations were: methsuximide* (●), $C_1 = 11.6e^{-8.64t} + 7.2e^{-0.78t}$; *and the metabolite* (▲), $C_m = -1.0e^{-8.64t} - 7.1e^{-0.78t} + 8.1e^{-0.047t}$.

lends support to the underlying assumption in this study that the dog is a suitable model for the pharmacokinetics of methsuximide in humans, since it has been shown that metabolite levels are also high and sustained in an overdose patient (12).

Multiple dosing of methsuximide results in induction of drug-metabolizing enzymes (10, 19). Thus, after multiple dosing, it might be expected that the metabolic step studied here would be increasingly important, both from a therapeutic and toxicological point of view. It cannot be discounted, however, that the metabolite may itself be responsible for some or all of the hepatic enzyme induction seen after repeated methsuximide doses.

Methsuximide is available for human use only as an oral dosage form. Since this drug is cleared from the body primarily by metabolism (7), the "first-pass effect," reported by Gibaldi *et al.* (20), may be an important phenomenon in methsuximide therapy. In light of the discussed enzyme induction and a possible first-pass effect, the pharmacological activity of methsuximide in humans may be due primarily to 2-methyl-2-phenylsuccinimide.

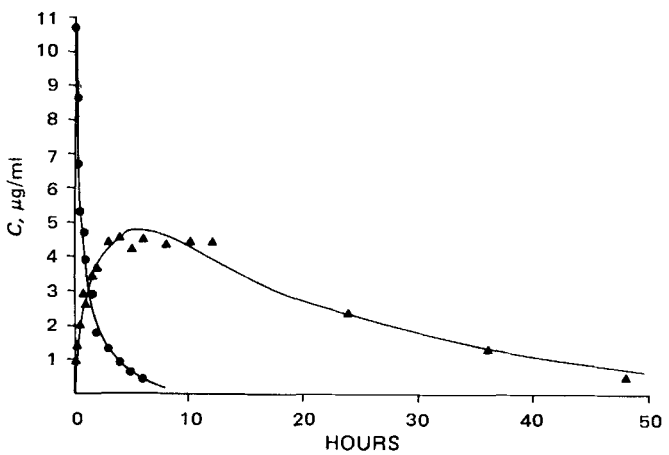

Figure 6—*Methsuximide and 2-methyl-2-phenylsuccinimide plasma level* versus *time profiles after a 250-mg intravenous injection of methsuximide (Experiment C). The computer-determined equations were: methsuximide* (●), $C_1 = 6.2e^{-2.24t} + 4.2e^{-0.40t}$; *and the metabolite* (▲), $C_m = -1.4e^{-2.24t} - 5.6e^{-0.40t} + 7.0e^{-0.047t}$.

REFERENCES

(1) C. A. Miller and L. M. Long, *J. Am. Chem. Soc.*, **73**, 4895 (1951).

(2) G. Chen, R. Portman, C. R. Ensor, and A. C. Bratton, Jr., *J. Pharmacol. Exp. Ther.*, **103**, 54 (1951).

(3) F. T. Zimmerman and B. B. Burgemeister, *Neurology (Suppl.)*, **8**, 769 (1958).

(4) V. R. Vossen, *Dtsch. Med. Wochenschr.*, **83**, 1227 (1958).

(5) P. J. Nicholls and T. C. Orton, *Br. J. Pharmacol.*, **43**, 459P (1971).

(6) M. G. Horning, C. Butler, D. J. Harvey, R. M. Hill, and T. E. Zion, *Res. Commun. Chem. Pathol. Pharmacol.*, **6**, 565 (1973).

(7) K. H. Dudley, D. L. Bius, and C. D. Waldrop, *Drug Metab. Dispos.*, **2**, 113 (1974).

(8) A. L. German, C. D. Pfaffenberger, J.-P. Thenot, M. G. Horning, and E. C. Horning, *Anal. Chem.*, **45**, 930 (1973).

(9) P. J. Nicholls and T. C. Orton, *Br. J. Pharmacol.*, **45**, 48 (1972).

(10) A. J. Glazko and W. A. Dill, in "Antiepileptic Drugs," D. M. Woodbury, J. K. Penry, and R. P. Schmidt, Eds., Raven, New York, N.Y., 1972, pp. 455–459.

(11) J. M. Strong, T. Abe, E. L. Gibbs, and A. J. Atkinson, Jr., *Neurology*, **24**, 250 (1974).

(12) S. B. Karch, *J. Am. Med. Assoc.*, **223** (13), 1463 (1973).

(13) T. C. Butler and W. J. Waddell, *Neurology, Suppl. 1*, **8**, 106 (1958).

(14) K. A. Connors, "A Textbook of Pharmaceutical Analysis," 1st ed., Wiley, New York, N.Y., 1967.

(15) P. G. Welling, A. Mosegaard, M. R. Dobrinska, and P. O. Madsen, *J. Clin. Pharmacol.*, **16**, 142 (1976).

(16) P. G. Welling, W. A. Craig, G. L. Amidon, and C. M. Kunin, *J. Infect. Dis., Suppl.*, **128**, S556 (1973).

(17) J. G. Wagner, "Pharmacokinetic Notes," J. M. Richards Laboratory, Grosse Pointe Park, Mich., 1969.

(18) J. G. Wagner, "Biopharmaceutics and Relevant Pharmacokinetics," Drug Intelligence Publications, Hamilton, Ill., 1971, p. 267.

(19) T. C. Orton and P. J. Nicholls, *Biochem. Pharmacol.*, **21**, 2253 (1972).

(20) M. Gibaldi, R. N. Boyes, and S. Feldman, *J. Pharm. Sci.*, **60**, 1338 (1971).

ACKNOWLEDGMENTS AND ADDRESSES

Received March 29, 1976, from the *Center for Health Sciences, School of Pharmacy, University of Wisconsin, Madison, WI 53706.*

Accepted for publication July 9, 1976.

Presented at the APhA Academy of Pharmaceutical Sciences, New Orleans meeting, April 1976.

Abstracted from a thesis submitted by M. R. Dobrinska to the University of Wisconsin in partial fulfillment of the Master of Science degree requirements.

The authors thank Dr. H. E. Booker of the Neurological and Rehabilitation Hospital, University of Wisconsin, Madison, for helpful discussions.

* AFPE fellow at the University of Wisconsin.

ˣ To whom inquiries should be directed.

Stable Nonaqueous Pentobarbital Sodium Solutions for Use in Laboratory Animals

SAUL BORODKIN ˣ, LOWELL MACY, GEORGE THOMPSON, and RONALD SCHMITS

Abstract □ The degradation kinetics of pentobarbital sodium in propylene glycol-based solutions were studied along with the *in vivo* effects in laboratory animals. The degradation rate constant was directly proportional to the water concentration in propylene glycol–water solvent systems. An activation energy of 23.4 kcal/mole was obtained in propylene glycol–water (1:1). Pentobarbital sodium solutions in anhydrous propylene glycol and 9:1 mixtures of propylene glycol with ethanol, glycerin, or dimethylacetamide gave relatively slow degradation rates at 100°, with all projected 25° $t_{99\%}$ values greater than 4.5 years. Intravenous administration of pentobarbital sodium in various anhydrous propylene glycol-based vehicles to rats produced no hemolysis or gross organ damage that would interfere with pathological evaluations. Results of an intraperitoneal sleeptime study indicated that pentobarbital sodium produced consistent hypnotic effects when administered as an aqueous solution or in anhydrous propylene glycol-based vehicles.

Keyphrases □ Pentobarbital sodium—degradation kinetics in propylene glycol-based solutions, *in vivo* effects in laboratory animals □ Degradation kinetics—pentobarbital sodium in propylene glycol-based solutions, *in vivo* effects in laboratory animals □ Stability—pentobarbital sodium in propylene glycol-based solutions, *in vivo* effects in laboratory animals □ Hypnotics—pentobarbital sodium, degradation kinetics in propylene glycol-based solutions, *in vivo* effects in laboratory animals

Pentobarbital has been recommended frequently as a drug of choice for producing euthanasia in laboratory animals whenever its use will not interfere with experimental results (1). In the dog, the maximum lethal dose is generally considered to be about 50 mg/kg. It is also widely used intraperitoneally to induce anesthesia in small laboratory animals.

A major concern in the use of injectable pentobarbital sodium products is the chemical instability in aqueous solutions (2, 3). At the high pH level necessary to maintain pentobarbital sodium in solution, the degradation rate is fast enough to cause crystallization of the water-insoluble degradation product within several months at room temperature. The use of vehicles containing 20–60% propylene glycol in water to overcome the stability problem was reported (4, 5), but detailed kinetic and toxicological data were not included. However, the utility of propylene glycol in parenteral products is well established (6).

This paper describes studies on propylene glycol-based solutions of pentobarbital sodium intended for parenteral use in producing euthanasia or anesthesia in laboratory animals. High temperature kinetic studies established the degradation rate reduction in the propylene glycol-based vehicles. The effects of water concentration and other solvents on the degradation rate also were evaluated. Additionally, acute intravenous toxicity and intraperitoneal sleeptime studies were conducted in rats to evaluate the drug availability and pathological changes associated with propylene glycol-based formulations.

EXPERIMENTAL

Kinetic Procedure—Solutions were prepared by dissolving sufficient pentobarbital sodium in the desired solvent to give a concentration of 50 mg/ml. The solution was then divided into several 10-ml ampuls, which were sealed and placed in a mechanical convection oven[1] maintained at a constant temperature ±0.2°. Periodically, ampuls were removed and assayed for the remaining pentobarbital sodium concentration.

Approximately 15 assays were obtained in each kinetic study, with each assay obtained from a separate ampul. All data were treated statistically, using linear regression analyses to establish rate constants and confidence intervals (7).

Assay—A differential UV method, similar to that reported by Tishler *et al.* (8) for phenobarbital degradation, was used to assay the remaining pentobarbital sodium. The sample was diluted in 1.0 *N* NH_4OH to a concentration of 4–20 μg/ml of pentobarbital sodium, and a UV spectrum from 220 to 300 nm was obtained[2]. An additional sample was diluted similarly in 0.1 *N* HCl, and a UV spectrum was obtained.

The difference in acidic and basic absorbances at 240 nm was used to determine the drug concentration. A standard curve obtained with this method, using concentrations of 4, 8, 12, 16, and 20 μg/ml, showed a slope of 0.03598 with an intercept of 0.0089 and a correlation coefficient of 0.9999.

Acute Intravenous Toxicity Studies—Forty-four male Sprague–Dawley rats[3], 160–180 g (7–8 weeks old), were divided into 11 treatment groups of four each. All animals were housed individually in stainless steel hanging cages with ambient temperature maintained at 22–24°. Food[4] and water were supplied *ad libitum*.

Single 100-mg/kg doses of five pentobarbital sodium formulations (200

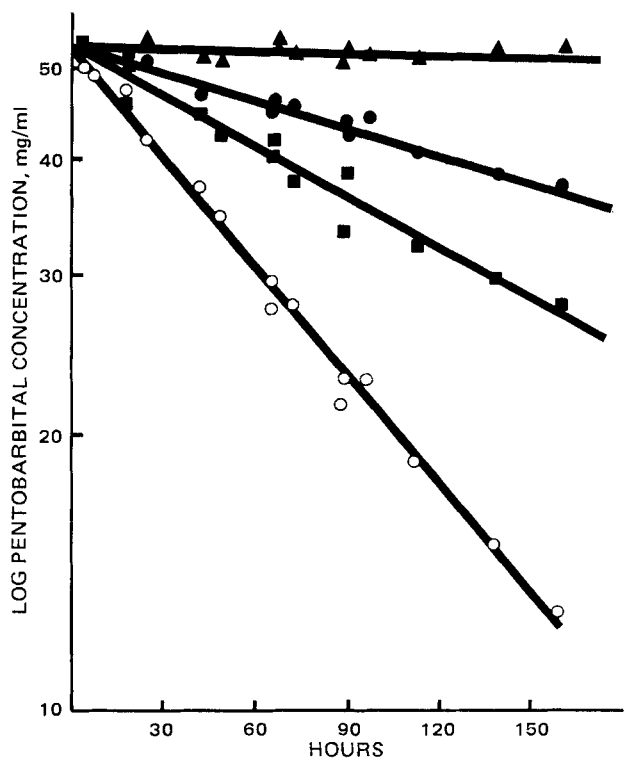

Figure 1—*Hydrolysis of pentobarbital sodium at 100° in solvents composed of varying propylene glycol–water ratios and an initial concentration of 50 mg/ml. Key: ○, 0:4; ■, 2:2; ●, 3:1; and ▲, 4:0.*

[1] Stabil-Therm, Blue M Electric Co., Blue Island, Ill.
[2] Coleman model 124, Perkin-Elmer Co., Norwalk, Conn.
[3] Sprague-Dawley Co., Madison, Wis.
[4] Purina rat chow, Ralston-Purina Co., St. Louis, Mo.

Table I—Effect of Propylene Glycol–Water Ratio on Hydrolysis Rate of Pentobarbital Sodium at 100°

Propylene Glycol–Water Ratio[a]	$k_1 \times 10^3$, hr^{-1} ± 95% Confidence Interval	$t_{1/2}$, hr
0:4	8.92 ± 0.45	78
2:2	4.07 ± 0.63	170
3:1	2.10 ± 0.54	330
4:0	0.04 ± 0.33	16,100

[a] Relationship between k_1 and percent water yields a correlation coefficient of 0.999 by linear regression analysis.

Table II—Effect of Temperature on Rate Constants Obtained from a Pentobarbital Sodium Solution in Propylene Glycol–Water (1:1)

Temperature	$k_1 \times 10^3$, hr^{-1} ± 95% Confidence Interval	$t_{1/2}$, hr
100°	4.07 ± 0.63	170
90°	1.61 ± 0.16	430
80°	0.683 ± 0.064	1016
70°	0.252 ± 0.049	2750

mg/ml), the five corresponding vehicles (0.5 ml/kg), or 100 mg/kg of a pentobarbital sodium aqueous solution (positive control) were administered to each group intravenously by the tail vein. In the drug-treated animals, euthanasia was produced by the intravenous administration of the pentobarbital sodium; these rats were evaluated for gross anatomical changes. Vehicle-treated rats were placed in a carbon dioxide chamber immediately after injection as a means of inducing euthanasia for evaluation of pathological changes associated with vehicle treatment. Immediately after death, all animals were necropsied; observations were made for gross pathological changes in the heart, liver, lungs, kidneys, spleen, and brain.

Intraperitoneal Sleeptime Studies—Eighty-five male Sprague–Dawley rats[3], 160–180 g (7–8 weeks old), were divided into six groups of 10 rats and five groups of five rats each. Pentobarbital sodium doses of 25 mg/kg in five different formulations and an aqueous solution (200 mg/ml) were administered to each group of 10 rats by the intraperitoneal route. The corresponding formulation vehicles without drug were administered to the five remaining groups of five rats using volumes equivalent to those used for the drug-treated rats (0.125 ml/kg). Sleeptime was defined as the time interval from loss to restoration of the righting reflex. The righting reflex was considered recovered when the animal erected itself three times within 30 sec.

RESULTS AND DISCUSSION

Degradation Kinetics—In all cases, the degradation of pentobarbital sodium followed first-order kinetics with the logarithm of drug concentration remaining linear with time. Garrett *et al.* (3) demonstrated first-order kinetics in hydrolysis studies with barbiturates, including pentobarbital, under neutral and alkaline conditions. Since the rate constant is independent of the initial concentration in first-order kinetics, the values obtained using 50 mg/ml (in most experiments) would be applicable to any other pentobarbital sodium concentration.

Table III—Degradation Rate Constants for Pentobarbital Sodium at 100° in Nonaqueous Solvent Systems

Solvent[a]	$k_1 \times 10^4$, hr^{-1} ± 95% Confidence Interval	Maximum $k_1 \times 10^4$ hr^{-1}	Minimum Projected $t_{99\%}$ at 25°, years[b]
100% Propylene glycol	0.43 ± 3.29	3.72	8.84
10% Ethanol in propylene glycol	3.69 ± 1.14	4.83	6.81
10% Glycerin in propylene glycol	5.67 ± 1.36	7.03	4.68
10% Dimethylacetamide in propylene glycol	3.40 ± 0.55	3.95	8.32

[a] Percentage refers to grams per 100 ml of solution. [b] Time for 1% degradation calculated from maximum rate constant at 100° and energy of activation of 23.4 kcal/mole.

Table IV—Stability of Nonaqueous Pentobarbital Sodium Solutions in 100-ml Injectable Vials[a] Maintained at 40°

Solvent System	Pentobarbital Sodium Concentration[b], mg/ml at Initial	3 Months	6 Months	9 Months	19 Months
Propylene glycol	206.1	205.1	203.9	204.7	201.4
10% Dimethylacetamide in propylene glycol	207.4	205.9	210.5	205.3	205.2
20% Dimethylacetamide in propylene glycol	207.0	199.8	200.6	201.1	209.0
10% Ethanol in propylene glycol	211.2	208.2	210.1	204.9	205.1
10% Glycerin in propylene glycol	205.0	206.9	207.0	202.4	201.4

[a] Type 2 glass and butyl rubber closures. [b] All assay values for stability samples are means from two vials, one maintained in an upright position and the other inverted. Initial values are from a single assay.

Propylene Glycol–Water Ratio—Kinetic experiments were run at 100° using various ratios of propylene glycol–water as the solvent to assess the magnitude of the degradation rate reduction with increasing proportions of propylene glycol (Fig. 1 and Table I). The data clearly show the decrease in the hydrolysis rate constant with an increased percentage of propylene glycol in the solvent. In fact, the rate constant appeared to be approximately proportional to the water concentration in the solvent, a condition consistent with a consideration of water as a first-order reactant in the hydrolysis. In anhydrous propylene glycol, the calculated rate constant was extremely low, with the statistical maximum still less than one-fifth of the rate constant in 75% propylene glycol.

Temperature Effect—Table II summarizes the kinetic results obtained at four temperatures with a 50-mg/ml pentobarbital sodium solution in propylene glycol–water (1:1). When the data were fitted to the Arrhenius relationship by plotting the logarithm of the rate constant *versus* the reciprocal of absolute temperature, excellent linearity was obtained, with a calculated activation energy of 23.4 kcal/mole (Fig. 2).

Table V—Acute Intravenous Toxicity[a] and Intraperitoneal Sleeptime in Rats

Pentobarbital Sodium Concentration, mg/ml	Solvent System[b]	Sleeptime Duration, min[c]
200	Water	45.7 ± 4.5
200	Propylene glycol	49.5 ± 6.1
0	Propylene glycol	0
200	10% Dimethylacetamide in propylene glycol	51.6 ± 8.9
0	10% Dimethylacetamide in propylene glycol	0
200	20% Dimethylacetamide in propylene glycol	51.2 ± 8.6
0	20% Dimethylacetamide in propylene glycol	0
200	10% Glycerin in propylene glycol	46.6 ± 7.2
0	10% Glycerin in propylene glycol	0
200	10% Ethanol in propylene glycol	44.0 ± 6.2
0	10% Ethanol in propylene glycol	0

[a] No gross pathology was found based on observations of four rats using 0.5 ml/kg of solution, equivalent to a pentobarbital sodium dose of 100 mg/kg. [b] Percentage refers to grams per 100 ml of solution. [c] Values represent mean ± 1 *SD* from 10 rats treated with drug-containing solutions and five rats treated with vehicles. All doses were 0.125 ml/kg, equivalent to 25 mg/kg of pentobarbital sodium, except with propylene glycol vehicle where 0.5 ml/kg was used.

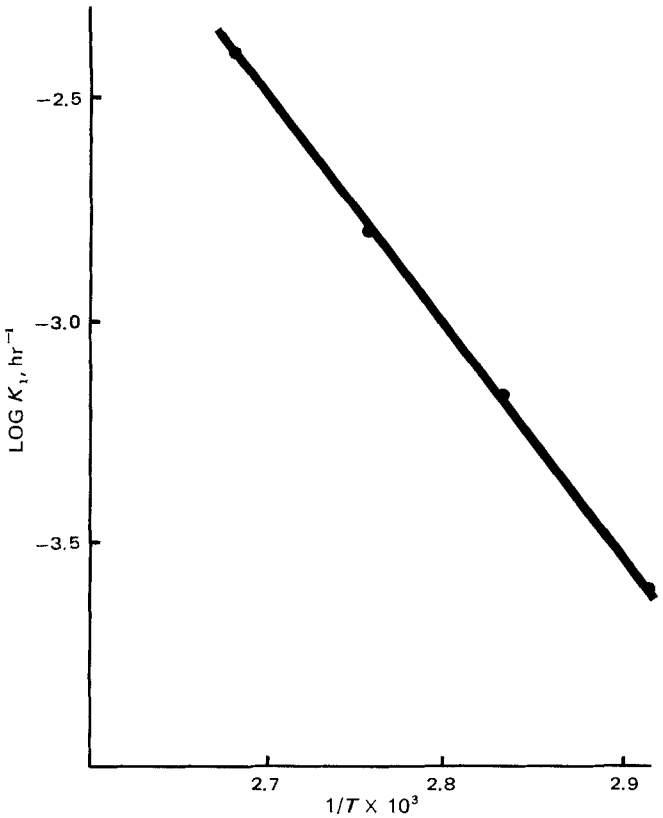

Figure 2—*Linear relationship between log* k_1 *and the reciprocal of absolute temperature in the hydrolysis of pentobarbital sodium in propylene glycol–water (1:1) using initial concentrations of 50 mg/ml. Energy of activation = 23,400 ± 1700 (p = 0.05) cal/mole; correlation coefficient = 0.9997.*

Extrapolation of this relationship to 25° yielded a rate constant of 1.42×10^{-6} hr^{-1}, a value 3.49×10^{-4} times the magnitude of the rate constant at 100°. When using this extrapolated constant, the calculated time for 1% pentobarbital sodium degradation in propylene glycol–water (1:1) at 25° would be 295 days; the time for 10% degradation would be 8.49 years.

Other Solvents—Degradation rates were determined at 100° for solutions containing 50 mg/ml of pentobarbital sodium and 10% ethanol, glycerin, or dimethylacetamide in propylene glycol (Table III). The glycerin-containing solvent gave the fastest degradation rate, while the pure propylene glycol system appeared to be the most stable. However, all anhydrous formulations showed substantially more stability than the propylene glycol–water solvent systems studied.

Based on the energy of activation determined with propylene glycol–water (1:1), the listed anhydrous solvents have projected minimum $t_{99\%}$ values (time for 1% degradation) at 25° of at least 4.68 years. As a comparison, the projected 25° $t_{99\%}$ values in water and propylene glycol–water (1:1) are 0.37 and 0.81 year, respectively. Actual stability assays on formulations based on the anhydrous systems showed no significant degradation, even after 19 months at 40° (Table IV).

Acute Intravenous Toxicity—Five anhydrous propylene glycol-based formulations containing 200 mg/ml of pentobarbital sodium were tested for acute intravenous toxicity in rats along with the corresponding vehicles (Table V). The pentobarbital sodium dose was 100 mg/kg, equivalent to 0.5 ml of formulation/kg. No drug-related pathological changes occurred in the organs of rats treated intravenously with the various pentobarbital sodium solutions or their corresponding vehicles. In all cases, organs were grossly normal. Thus, it may be concluded that the use of these solutions to produce euthanasia should not interfere with pathological evaluations or interpretations in rats.

Intraperitoneal Sleeptime—Sleeptimes induced by the various pentobarbital sodium solutions varied from 44.0 to 51.6 min (Table V). The values were not statistically different. The lack of statistically significant differences in the mean sleeptime durations indicated that the use of anhydrous propylene glycol-based vehicles did *not* affect pentobarbital sodium bioavailability. None of the vehicles (without drug) produced hypnotic effects in rats.

REFERENCES

(1) J. E. Breazile and R. L. Kitchell, *Fed. Proc.*, **28**, 1577 (1969).

(2) J. I. Bodin and A. Taub, *J. Am. Pharm. Assoc., Sci. Ed.*, **44**, 296 (1955).

(3) E. R. Garrett, J. T. Bojarski, and G. J. Yakatan, *J. Pharm. Sci.*, **60**, 1145 (1971).

(4) K. Ilver and B. Jochumsen, *Dan. Tidsskr. Farm.*, **39**, 307 (1965).

(5) D. L. Heine, P. F. Parker, and D. E. Frank, *Am. J. Soc. Hosp. Pharm.*, **7**, 8 (1950).

(6) A. J. Spiegel and M. M. Noseworthy, *J. Pharm. Sci.*, **52**, 917 (1963).

(7) A. Goldstein, "Biostatistics," Macmillan, New York, N.Y., 1964, p. 129.

(8) F. Tishler, L. F. Worrell, and J. E. Sinsheimer, *J. Pharm. Sci.*, **51**, 645 (1962).

ACKNOWLEDGMENTS AND ADDRESSES

Received March 18, 1976, from the *Agricultural and Veterinary Products Division, Abbott Laboratories, North Chicago, IL 60064.*

Accepted for publication July 9, 1976.

The authors thank Ms. Florence Tucker, Ms. Claire Crimmins, and Ms. Christine Yang for technical assistance.

[x] To whom inquiries should be directed. Present address: Pharmaceutical Products Division, Abbott Laboratories, North Chicago, IL 60064.

Bactericidal Properties of Quaternary Ammonium Compounds in Dispersed Systems

G. J. BALEY *, G. E. PECK x, and G. S. BANKER

Abstract □ Alkyltrimethylammonium bromides of selected chain length were synthesized and characterized with respect to their bactericidal properties. A partitioning method was developed, and the aqueous phases of the partitioned systems were evaluated for their antibacterial activity against *Staphylococcus aureus*. The relationships between the quaternary ammonium compound chain length and the aliphatic alcohol chain length were determined. The effect of selected hydrocarbons on the bactericidal effectiveness of the systems was studied. Cream systems corresponding to the partitioned systems were prepared and evaluated against *S. aureus*. The relationship between the aqueous phase concentration of the bactericidal agent was studied, and a correlation was shown between the bactericidal activity of the partitioned systems and cream systems.

Keyphrases □ Quaternary ammonium bromides, various—synthesized, bactericidal activity determined in simple partition systems, compared to cream systems □ Alkyltrimethylammonium bromides, various—synthesized, bactericidal activity determined in simple partition systems, compared to cream systems □ Bactericidal agents—various alkyltrimethylammonium bromides synthesized, activity determined in simple partition systems, compared to cream systems

In earlier studies (1), the partition coefficient of a series of quaternary ammonium compounds in selected aliphatic alcohols and hydrocarbons was evaluated and correlated to the physical stability of cream systems corresponding to the partitioned systems. In this study, the relationship between partitioning properties of selected quaternary ammonium compounds and their bactericidal properties in dispersed systems was evaluated.

The bactericidal effectiveness of a topical cream depends primarily on the inherent bactericidal properties of the bactericidal agent and its concentration in the aqueous phase of the system. The concentration in the aqueous phase depends upon the partition coefficient of the compound between the aqueous phase and the oil phase of the emulsion.

The partition coefficient of a solute is the ratio of the concentration of the agent in the oil phase divided by the concentration of the agent in the aqueous phase. The antimicrobial activities of antibacterials in oil-in-water systems were dependent on their aqueous phase concentration (2, 3), and another study (4) showed that the activity of solubilized iodine preparations was controlled by the concentration of iodine in the aqueous phase. In other reports, partition coefficients were used in the design of pharmaceutical dosage forms (5) and partitioning was related to preservative activity in emulsions (6).

Partitioning data were investigated relative to the preservation of multidose parenterals (7). An attempt was made to correlate partition coefficients, chemical structure, and solvent nature in dosage form design (8). Recent studies considered the availability of antimicrobial agents from emulsion systems and high petrolatum-based ointments (9, 10). Recently, the interaction of quaternary ammonium bactericides with biological materials was studied to understand their use (11, 12).

The purpose of this study was to correlate the partition characteristics of quaternary ammonium compounds with their bactericidal properties in simple partition and cream systems.

Table I—Critical Kill Dilutions of Aqueous Solutions of the Alkyltrimethylammonium Bromide Quaternary Ammonium Compounds

Alkyl Group	Experimental CKD	Literature[a] CKD
Lauryl	1:7,000	1:4,000
Myristyl	1:50,000	1:38,000
Cetyl	1:90,000	1:80,000
Stearyl	1:60,000	1:64,000

[a] Reference 15.

EXPERIMENTAL

The apparatus, materials, partitioned systems, and cream systems, including their method of manufacture, were described previously (1).

Test Culture—The Gram-positive bacteria, *Staphylococcus aureus*[1] (FDA 209, ATCC 6538), was maintained on nutrient agar, grown in nutrient broth, and tested in "Letheen" broth (13).

Preparation of Dilution—A 1% stock solution of the synthesized quaternary ammonium compounds was prepared in sterile distilled water. The final dilutions were made from the stock solution, directly into the medication tubes.

A 1:15 dilution of the aqueous phase from each partition study was prepared, and final dilutions were made directly into the medication tubes.

A 1:30 or greater dilution of each cream was prepared in sterile distilled water. The tube containing the cream dilution was shaken on a vortex mixer[2] until the contents appeared to be dispersed evenly. The phases were allowed to separate for 1 hr, after which a sample of the lower phase was removed with a 15.2-cm (6-in.), 18-gauge needle attached to a 10-ml syringe[3]. Final dilutions were made directly into the medication tubes.

Antibacterial Test Conditions—The critical kill dilution of each system was determined using the AOAC phenol coefficient method (14). The critical kill dilution is the highest dilution killing the test organism in 10 min but not in 5 min. Tests were conducted at 37° in a water bath, and results were read after 48 hr.

RESULTS AND DISCUSSION

Bactericidal Testing—The critical kill dilution (CKD) of each of the four synthesized quaternary ammonium compounds in distilled water was determined; the results are shown in Table I along with a comparison of reported data (15). In aqueous solution, the cetyl derivative was the most effective bactericidally, followed by stearyl-, myristyl-, and lauryltrimethylammonium bromides, respectively.

Ferguson (16) suggested that the toxicities of substances should be compared on the basis of their chemical potentials in the aqueous phase. Ecanow and Siegel (17) suggested that an extension of this concept may be applied to surfactants using the critical micelle concentration (CMC) as a standard state rather than a saturated solution as suggested by Ferguson. The thermodynamic activity and, therefore, the biological activity should be equal to a constant percent of the CMC of the drug.

The activities shown in Table II were calculated by obtaining the ratio of the test critical kill dilution divided by the CMC for each quaternary ammonium compound. The difference between the activities of the various compounds is relatively small, except for the stearyl derivative

[1] Also known as *Micrococcus pyogenes* var. *aureus*.
[2] Scientific Products, Evanston, Ill.
[3] Multifit (Luer-Lok), Becton Dickinson and Co., Rutherford, N.J.

Table II—Activity of Synthesized Quaternary Ammonium Compounds

Alkyl Group	CKD, *M*	CMC, *M*	Activity, CKD/CMC, *M*
Lauryl	4.63×10^{-7}	1.8×10^{-2}	2.57×10^{-5}
Myristyl	5.96×10^{-8}	3.6×10^{-3}	1.65×10^{-5}
Cetyl	3.03×10^{-8}	1.0×10^{-3}	3.03×10^{-5}
Stearyl	5.95×10^{-8}	3.3×10^{-4}	2.58×10^{-4}

which has an activity approximately 10-fold larger than the other three compounds.

On the other hand, a comparison indicated a 60-fold difference between the largest and smallest CMC values of the four quaternary ammonium compounds. Thus, Ferguson's principle appears to apply to the compounds studied, since the activities are in the same order of magnitude and substantiate the hypothesis that the bactericidal activity is the result of some nonspecific physical activity in contrast to the involvement of a specific chemical mechanism.

The equilibrated aqueous phases from the partitioning systems were evaluated for their critical kill dilutions. In the following experimental data, two critical kill dilutions are listed: an experimental and a corrected value. The experimental value is based on the actual dilution of the aqueous phase that was prepared to meet the critical kill dilution requirement. The corrected critical kill dilution takes into account the weight of the partitioned alcohol phase, which was not removed and evaluated; consequently, this value represents the total initial oil-in-water system. If the total nonaqueous phase was completely inert and acted only to dilute the aqueous phase, the corrected critical kill dilution would correspond to the experimental critical kill dilution for the whole cream formula.

The corrected critical kill dilution was calculated by substituting into the following equation:

$$\text{corrected CKD} = \frac{(\text{experimental CKD}) \times (\text{total weight of system})}{\text{weight of aqueous phase}} \quad \text{(Eq. 1)}$$

The relationships between quaternary ammonium compound chain length and aliphatic alcohol chain length were studied for the selected systems. Various systems were evaluated in which a hydrocarbon was included, and the change in bactericidal effectiveness was noted.

The lauryl-, myristyl-, cetyl-, and stearyltrimethylammonium bromides, at initial concentrations of 0.418, 0.452, 0.492, and 0.535%, respectively (corresponding to about 1.0 mEq/75.0 g), were each evaluated after equilibration with lauryl, myristyl, cetyl, and stearyl alcohols (15% each) against *S. aureus*. The relationships among the concentration of the quaternary ammonium compound in the aqueous phase, the quaternary ammonium compound chain length, the chain length of the aliphatic alcohol, and their effect on the critical kill dilution of the system are given in Table III.

The cetyl and stearyl quaternary ammonium compounds were ineffective as bactericidal agents, showing a corrected critical kill dilution of less than 1–13 with each alcohol. The poor killing properties may be related to the low concentration of quaternary ammonium compound present in the aqueous phase. The myristyl derivative was the most effective quaternary ammonium compound in the homologous series, even

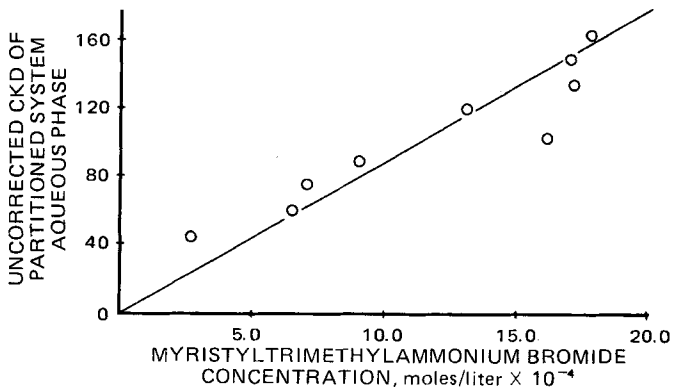

Figure 1—*Relationship between myristyltrimethylammonium bromide aqueous phase concentration and the uncorrected critical kill dilution of the aqueous phase.*

though the lauryl derivative was present in a greater concentration in each system. In the partitioning studies, the bactericidal properties of the quaternary ammonium compounds were a function of both their inherent bactericidal properties and their concentration in the aqueous phase. The myristyl quaternary ammonium compound, as a result of its intrinsic critical kill dilution, possessed the greatest bactericidal effectiveness for the concentration present in the aqueous phase.

Effect of Hydrocarbons—The critical kill dilutions for the lauryl, myristyl, and cetyl quaternary ammonium compounds in cetyl and stearyl alcohols were evaluated (Table IV) in systems that contained no hydrocarbon, 15% mineral oil, or 15% white petrolatum. The critical kill dilutions obtained appeared to be related to the inherent activity and the concentration of quaternary ammonium compound remaining in the aqueous phase of the partitioned systems.

The stearyl alcohol base systems were bactericidally more effective than the corresponding cetyl alcohol systems, due probably to the higher concentration of quaternary ammonium compound present in the aqueous phase. Both mineral oil and white petrolatum enhanced the critical kill dilution by decreasing the equilibrium partition distribution coefficient (1), thus making more quaternary ammonium compound available for bactericidal action.

The myristyltrimethylammonium bromide systems, without exception, were bactericidally more effective than either the lauryl or cetyl systems when combined with the same aliphatic alcohol and hydrocarbon. The greater activity of the myristyl compound was related to both its concentration in the aqueous phase and to its inherent bactericidal properties.

Effect of Percent Hydrocarbon—The effects of the percent hydrocarbon on the critical kill dilution of the myristyl quaternary ammonium compound in 15% cetyl or stearyl alcohol were evaluated (Table V). As the concentration of the hydrocarbon increased, the critical kill dilution of the system against *S. aureus* also increased. The addition of white petrolatum appeared to have a greater influence on increasing the critical kill dilution of a system than the corresponding percent mineral oil. The superiority of white petrolatum at increasing the critical kill dilution appeared to be related to the increase in the concentration of the myristyl compound remaining in the aqueous phase.

Relationship between Quaternary Ammonium Compound Concentration and Critical Kill Dilution—A relationship between the

Table III—Critical Kill Dilutions of Equilibrated Quaternary Ammonium Compounds in 15% Aliphatic Alcohol–Water Systems against *S. aureus*

	Lauryl Form			Myristyl Form			Cetyl Form			Stearyl Form		
Aliphatic Alcohol (15%)	Experimental CKD	Corrected CKD	Concentration of Active Compound in Aqueous Phase, moles/liter $\times 10^{-3}$	Experimental CKD	Corrected CKD	Concentration of Active Compound in Aqueous Phase, moles/liter $\times 10^{-3}$	Experimental CKD	Corrected CKD	Concentration of Active Compound in Aqueous Phase, moles/liter $\times 10^{-3}$	Experimental CKD	Corrected CKD	Concentration of Active Compound in Aqueous Phase, moles/liter $\times 10^{-3}$
Lauryl	30	25	7.05	45	40	2.19	<15	<13	0.95	<15	<13	0.77
Myristyl	30	25	7.51	45	40	2.35	<15	<13	1.17	<15	<13	1.14
Cetyl	30	25	9.02	45	40	3.05	<15	<13	1.53	<15	<13	1.42
Stearyl	30	25	10.05	75	65	4.58	<15	<13	2.68	<15	<13	1.58

Table IV—Critical Kill Dilutions of Equilibrated Quaternary Ammonium Compounds in Aliphatic Alcohol Combinations with and without 15% Hydrocarbon against *S. aureus*

Aliphatic Alcohol (15%)	Alkyl Group	No Hydrocarbon			15% Mineral Oil			15% White Petrolatum		
		Experimental CKD	Corrected CKD	Concentration of Active Compound in Aqueous Phase, moles/liter $\times 10^{-3}$	Experimental CKD	Corrected CKD	Concentration of Active Compound in Aqueous Phase, moles/liter $\times 10^{-3}$	Experimental CKD	Corrected CKD	Concentration of Active Compound in Aqueous Phase, moles/liter $\times 10^{-3}$
Cetyl	Lauryl	20	15	9.40	30	20	14.56	30	20	16.52
	Myristyl	45	40	3.11	90	65	11.45	105	75	16.19
	Cetyl	<15	<13	1.40	30	20	8.52	45	30	14.25
Stearyl	Lauryl	30	25	10.29	30	20	15.81	45	30	17.42
	Myristyl	75	60	4.45	120	85	13.08	135	95	17.17
	Cetyl	<15	<13	2.84	30	20	9.80	45	30	15.25

Table V—Critical Kill Dilutions of Equilibrated Myristyltrimethylammonium Bromide in 15% Aliphatic Alcohol with Increasing Concentrations of Hydrocarbon against *S. aureus*

Aliphatic Alcohol (15%)	Hydrocarbon, %	Mineral Oil			White Petrolatum		
		Experimental CKD	Corrected CKD	Concentration of Active Compound in Aqueous Phase, moles/liter $\times 10^{-3}$	Experimental CKD	Corrected CKD	Concentration of Active Compound in Aqueous Phase, moles/liter $\times 10^{-3}$
Cetyl	0	45	40	3.11	45	40	3.11
	5	60	45	4.45	60	45	8.15
	10	60	45	7.23	75	55	12.24
	15	90	65	11.45	105	75	16.19
	20	150	95	17.07	—	—	—
Stearyl	0	75	65	4.45	75	65	4.45
	5	90	70	6.59	90	70	6.57
	10	90	70	9.45	120	90	13.08
	15	120	85	13.08	135	95	17.17
	20	165	105	17.82	—	—	—

antibacterial agent concentration in the aqueous phase of an emulsion and the critical kill dilution of the emulsion has been suggested (2–8). It was observed throughout the study that the critical kill dilution of the aqueous phase was related to the aqueous phase concentration of quaternary ammonium compound determined in the partitioning studies. The concentration of the myristyl quaternary ammonium compound derivative in each partition study for which critical kill dilution data were available was averaged for each experimental critical kill dilution value, irrespective of the alcohol or additive present (Fig. 1). The average aqueous phase myristyl quaternary ammonium concentration was plotted against the uncorrected critical kill dilution of the systems. The uncorrected critical kill dilutions were employed because only the relationship between the critical kill dilution and concentration was being observed. This plot substantiates the hypothesis that the critical kill dilution is related to the concentration of quaternary ammonium compound in the aqueous phase.

Critical Kill Dilution Evaluation of Creams—The critical kill dilutions of creams prepared with the lauryl, myristyl, and cetyl quaternary ammonium compounds in cetyl and stearyl alcohols with 15% hydrocarbon were evaluated (Table VI). In general, the same critical kill dilution pattern was observed for the creams as for the corresponding partitioned systems (Table IV). The stearyl alcohol base creams with each quaternary ammonium compound were more effective than creams prepared with cetyl alcohol, except for the cetyl quaternary ammonium compound containing cream with 15% mineral oil. The increased effectiveness of the stearyl alcohol base creams may again be related to larger concentrations of quaternary ammonium compound in the aqueous phase, as was suggested in the partitioning studies.

The myristyl quaternary ammonium compound was the most effective compound in the series, while the lauryl compound showed one-fifth to two-thirds the effectiveness of myristyltrimethylammonium bromide. The reason the cetyl derivative was slightly less effective than the myristyl compound was probably related again to the lower concentration in the aqueous phase of the cream system—not to inherent bactericidal properties.

The inclusion of either 15% mineral oil or 15% white petrolatum increased the critical kill dilution of the cream, which again appeared to correlate with the increased aqueous phase concentration observed in the partitioning studies. Even more significant was the fact that the addition of white petrolatum to the formula permitted the preparation of systems exhibiting *both* acceptable bactericidal effectiveness and satis-

Table VI—Critical Kill Dilution Evaluation of Creams Prepared with and without 15% Hydrocarbon against *S. aureus*

Aliphatic Alcohol (15%)	Alkyl Group	No Hydrocarbon	15% Mineral Oil	15% White Petrolatum
Cetyl	Lauryl	45	30	60
	Myristyl	60	90	150
	Cetyl	<30	60	30
Stearyl	Lauryl	60	30	60
	Myristyl	120	150	180
	Cetyl	30	30	60

Table VII—Critical Kill Dilution Evaluation of Creams Prepared with and without Various Percent Hydrocarbons against *S. aureus*

Aliphatic Alcohol (15%)	Hydrocarbon, %	Mineral Oil	White Petrolatum
Cetyl	0	60	60
	5	75	120
	10	75	135
	15	90	150
	20	105	—
Stearyl	0	120	120
	5	135	150
	10	135	180
	15	150	180
	20	165	—

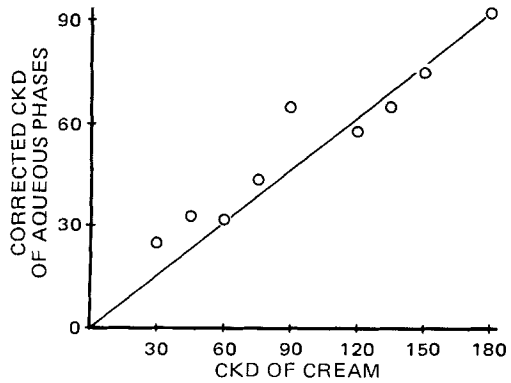

Figure 2—*Relationship between the critical kill dilutions of cream systems and the corrected critical kill dilutions of the partitioned aqueous phases.*

factory emulsion stability. A satisfactory combination of these two properties was not possible in the cream systems containing no hydrocarbon or 15% mineral oil.

Effect of Percent Hydrocarbon—The effect of the concentration of hydrocarbon on the critical kill dilution of creams emulsified with the myristyl quaternary ammonium compound and containing either cetyl or stearyl alcohol was evaluated (Table VII). The critical kill dilutions of the creams were similar in rank order to those observed in the critical kill dilution evaluation of the partitioned systems. The critical kill dilutions increased with increasing hydrocarbon concentration, with the stearyl alcohol creams being more effective than the corresponding cetyl alcohol base creams.

The white petrolatum creams showed a larger increase in critical kill dilution compared to the creams containing mineral oil of the same concentration. The increase may again be attributed to the greater concentration of quaternary ammonium compound present in the aqueous phase of the white petrolatum creams.

The relationship between the critical kill dilution of a cream and its corresponding aqueous phase was observed throughout the previous study. Figure 2 compares the relationship by pairing the corrected critical kill dilutions for the partitioned aqueous phases with the corresponding cream formula. The critical kill dilutions of the creams were ranked, and the corresponding corrected critical kill dilutions of the corresponding aqueous phases were averaged. From the data obtained, it appeared that on the average a cream was about twice as effective as the corresponding partitioned aqueous phase. The correlation technique appears to offer a method of correlating the bactericidal effectiveness of a cream and *in vitro* conditions, such as in the partitioning studies. The result also indicates that the nonaqueous phase also possesses antibacterial activity; otherwise, the slope of the plot would equal unity.

REFERENCES

(1) G. Baley, Ph.D. dissertation, Purdue University, West Lafayette, Ind., 1968.

(2) H. S. Bean, J. P. Richards, and J. Thomas, Proceedings of the 21st International Congress of Pharmaceutical Sciences, Pisa, Italy, 1961, p. 174.

(3) H. S. Bean and S. H. Heman-Ackah, *J. Pharm. Pharmacol.*, **16**, 58T (1964).

(4) N. A. Allawala and S. Riegelman, *J. Am. Pharm. Assoc., Sci. Ed.*, **42**, 267 (1953).

(5) E. R. Garrett and O. R. Woods, *ibid.*, **42**, 736 (1953).

(6) H. W. Hibbott and J. Monks, *J. Soc. Cosmet. Chem.*, **12**, 2 (1961).

(7) L. Lachman, T. Urbanyi, and S. Weinstein, *J. Pharm. Sci.*, **52**, 244 (1963).

(8) R. Collander, *Acta Chem. Scand.*, **4**, 1085 (1950).

(9) S. Tannenbaum, *TGA Cosmet. J.*, **2** (1), 24 (1970).

(10) K. Tsuji, E. Stapert, J. Robertson, and P. Waiyaki, *Appl. Microbiol.*, **20**, 798 (1970).

(11) D. Blois and J. Swarbrick, *J. Pharm. Sci.*, **61**, 390 (1972).

(12) *Ibid.*, **61**, 393 (1972).

(13) G. F. Reddish, "Antiseptics, Disinfectants, Fungicides, and Sterilization," Lea & Febiger, Philadelphia, Pa., 1954, p. 112.

(14) "Official and Tentative Methods of Analysis," 7th ed., Association of Official Agricultural Chemists, Washington, D.C., 1950, p. 88

(15) R. S. Shelton, M. G. VanCampen, C. H. Tilford, H. C. Lang, L. Nisonger, F. J. Bandelin, and H. L. Rubenkoenig, *J. Am. Chem. Soc.*, **68**, 753 (1946).

(16) J. Ferguson, *Proc. Roy. Soc.*, **B127**, 387 (1939).

(17) B. Ecanow and F. P. Siegel, *J. Pharm. Sci.*, **52**, 812 (1963).

ACKNOWLEDGMENTS AND ADDRESSES

Received November 28, 1973, from the *Department of Industrial and Physical Pharmacy, School of Pharmacy and Pharmacal Sciences, Purdue University, West Lafayette, IN 47907.*

Accepted for publication July 7, 1976.

Presented at the Industrial Pharmaceutical Technology Section, APhA Academy of Pharmaceutical Sciences, San Diego meeting, November 1973.

Supported by Miles Laboratories, Elkhart, IN 46514.

* Present address: Pharmaceutical Manufacturing Development, The Upjohn Co., Kalamazoo, MI 49001.

[x] To whom inquiries should be directed.

Determination of Solasodine in Fruits of *Solanum* Species

LEHEL TELEK

Abstract □ A potentiometric nonaqueous titration procedure was developed for the quantitative determination of solasodine in fruits of the *Solanum* species. The steroid glycoalkaloids were extracted from freshly harvested fruits with 2% acetic acid and methanol. After hydrolysis, the common aglycone solasodine was extracted with benzene. An aliquot was mixed with an equal volume of acetone and titrated potentiometrically with 0.005 *N* perchloric acid in dioxane, using glass and silver electrodes for the determination.

Keyphrases □ Solasodine—potentiometric analysis in fruits of *Solanum* species □ *Solanum* species—potentiometric analysis of solasodine in fruits □ Potentiometry—analysis, solasodine in fruits of *Solanum* species □ Steroids—solasodine, potentiometric analysis in fruits of *Solanum* species

The consumption of pharmacologically active steroids is increasing significantly (1). The use of steroidal contraceptives will spread with the pressing need for birth control. In the growing demand for raw materials, solasodine is the most competitive in supplementing diosgenin in the partial synthesis of steroid hormones (2). The special

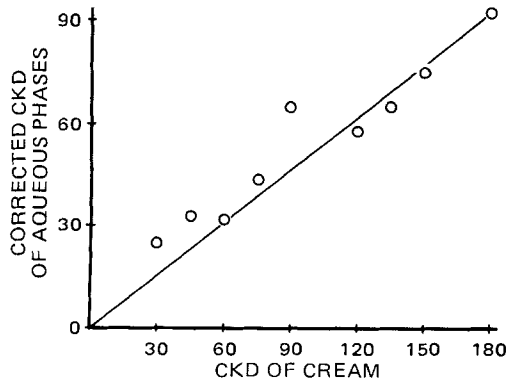

Figure 2—*Relationship between the critical kill dilutions of cream systems and the corrected critical kill dilutions of the partitioned aqueous phases.*

factory emulsion stability. A satisfactory combination of these two properties was not possible in the cream systems containing no hydrocarbon or 15% mineral oil.

Effect of Percent Hydrocarbon—The effect of the concentration of hydrocarbon on the critical kill dilution of creams emulsified with the myristyl quaternary ammonium compound and containing either cetyl or stearyl alcohol was evaluated (Table VII). The critical kill dilutions of the creams were similar in rank order to those observed in the critical kill dilution evaluation of the partitioned systems. The critical kill dilutions increased with increasing hydrocarbon concentration, with the stearyl alcohol creams being more effective than the corresponding cetyl alcohol base creams.

The white petrolatum creams showed a larger increase in critical kill dilution compared to the creams containing mineral oil of the same concentration. The increase may again be attributed to the greater concentration of quaternary ammonium compound present in the aqueous phase of the white petrolatum creams.

The relationship between the critical kill dilution of a cream and its corresponding aqueous phase was observed throughout the previous study. Figure 2 compares the relationship by pairing the corrected critical kill dilutions for the partitioned aqueous phases with the corresponding cream formula. The critical kill dilutions of the creams were ranked, and the corresponding corrected critical kill dilutions of the corresponding aqueous phases were averaged. From the data obtained, it appeared that on the average a cream was about twice as effective as the corresponding partitioned aqueous phase. The correlation technique appears to offer a method of correlating the bactericidal effectiveness of a cream and *in vitro* conditions, such as in the partitioning studies. The result also indicates that the nonaqueous phase also possesses antibacterial activity; otherwise, the slope of the plot would equal unity.

REFERENCES

(1) G. Baley, Ph.D. dissertation, Purdue University, West Lafayette, Ind., 1968.

(2) H. S. Bean, J. P. Richards, and J. Thomas, Proceedings of the 21st International Congress of Pharmaceutical Sciences, Pisa, Italy, 1961, p. 174.

(3) H. S. Bean and S. H. Heman-Ackah, *J. Pharm. Pharmacol.*, **16**, 58T (1964).

(4) N. A. Allawala and S. Riegelman, *J. Am. Pharm. Assoc., Sci. Ed.*, **42**, 267 (1953).

(5) E. R. Garrett and O. R. Woods, *ibid.*, **42**, 736 (1953).

(6) H. W. Hibbott and J. Monks, *J. Soc. Cosmet. Chem.*, **12**, 2 (1961).

(7) L. Lachman, T. Urbanyi, and S. Weinstein, *J. Pharm. Sci.*, **52**, 244 (1963).

(8) R. Collander, *Acta Chem. Scand.*, **4**, 1085 (1950).

(9) S. Tannenbaum, *TGA Cosmet. J.*, **2** (1), 24 (1970).

(10) K. Tsuji, E. Stapert, J. Robertson, and P. Waiyaki, *Appl. Microbiol.*, **20**, 798 (1970).

(11) D. Blois and J. Swarbrick, *J. Pharm. Sci.*, **61**, 390 (1972).

(12) *Ibid.*, **61**, 393 (1972).

(13) G. F. Reddish, "Antiseptics, Disinfectants, Fungicides, and Sterilization," Lea & Febiger, Philadelphia, Pa., 1954, p. 112.

(14) "Official and Tentative Methods of Analysis," 7th ed., Association of Official Agricultural Chemists, Washington, D.C., 1950, p. 88

(15) R. S. Shelton, M. G. VanCampen, C. H. Tilford, H. C. Lang, L. Nisonger, F. J. Bandelin, and H. L. Rubenkoenig, *J. Am. Chem. Soc.*, **68**, 753 (1946).

(16) J. Ferguson, *Proc. Roy. Soc.*, **B127**, 387 (1939).

(17) B. Ecanow and F. P. Siegel, *J. Pharm. Sci.*, **52**, 812 (1963).

ACKNOWLEDGMENTS AND ADDRESSES

Received November 28, 1973, from the *Department of Industrial and Physical Pharmacy, School of Pharmacy and Pharmacal Sciences, Purdue University, West Lafayette, IN 47907.*

Accepted for publication July 7, 1976.

Presented at the Industrial Pharmaceutical Technology Section, APhA Academy of Pharmaceutical Sciences, San Diego meeting, November 1973.

Supported by Miles Laboratories, Elkhart, IN 46514.

* Present address: Pharmaceutical Manufacturing Development, The Upjohn Co., Kalamazoo, MI 49001.

[x] To whom inquiries should be directed.

Determination of Solasodine in Fruits of *Solanum* Species

LEHEL TELEK

Abstract □ A potentiometric nonaqueous titration procedure was developed for the quantitative determination of solasodine in fruits of the *Solanum* species. The steroid glycoalkaloids were extracted from freshly harvested fruits with 2% acetic acid and methanol. After hydrolysis, the common aglycone solasodine was extracted with benzene. An aliquot was mixed with an equal volume of acetone and titrated potentiometrically with 0.005 *N* perchloric acid in dioxane, using glass and silver electrodes for the determination.

Keyphrases □ Solasodine—potentiometric analysis in fruits of *Solanum* species □ *Solanum* species—potentiometric analysis of solasodine in fruits □ Potentiometry—analysis, solasodine in fruits of *Solanum* species □ Steroids—solasodine, potentiometric analysis in fruits of *Solanum* species

The consumption of pharmacologically active steroids is increasing significantly (1). The use of steroidal contraceptives will spread with the pressing need for birth control. In the growing demand for raw materials, solasodine is the most competitive in supplementing diosgenin in the partial synthesis of steroid hormones (2). The special

advantages of solasodine are that all manufacturing processes based on diosgenin apply to it without any changes (3) and that its plant sources, some *Solanum* species, are easy to cultivate in the temperate zone.

Schreiber (4) reviewed the *Solanum* species that contain steroid glycoalkaloids in various plant parts. *S. laciniatum* Ait. is utilized industrially, and it is extensively cultivated in the Soviet Union (5) and New Zealand (6). In numerous *Solanum* species, the active ingredient is concentrated in their fruits. In Puerto Rico, *S. mammosum* L. and *S. khasianum* C. B. Clarke were studied as potential plant sources of steroid hormones[1].

In agronomic and plant biochemical research, a fast, reliable method was required for quantitative determination of solasodine in fruits of the *Solanum* species. Published procedures for the determination of solasodine in dried leaves of *S. laciniatum* include preparative gravimetry (7), colorimetry (8–11), titration in nonaqueous media (12, 13), and potentiometric titration in aqueous media (14). However, none of these methods is suitable for analyzing *Solanum* fruits.

The present report describes the direct quantitative determination of solasodine in fresh fruits, without drying, from the *Solanum* species grown in Puerto Rico in 1970 and 1971.

EXPERIMENTAL

Apparatus—An automatic system was used for the titrations[2]. A glass electrode[3] and a laboratory-made silver electrode, consisting of a folded silver strip 6.4 mm wide, 10 cm long, and 0.16 mm thick[4], were used. The sample was mixed using a magnetic stirrer and a 12.5-mm polytef[5]-coated stirring bar.

Reagents—Reagent grade acetic acid, benzene, methanol, and acetone were used without purification. Reagent grade dioxane was purified by the method of Chatten *et al.* (15) to eliminate browning with perchloric acid.

The 0.005 *N* perchloric acid titrant was prepared by dissolving 5 ml of 72% perchloric acid (reagent grade) in 100 ml of dioxane. From this 0.5 *N* $HClO_4$ stock solution, 5 ml was made up to 500 ml with purified dioxane. The perchloric acid titrant was standardized with atropine base[6] as a reference standard, which was purified by recrystallization from acetone and dried at 103°; its purity was checked by TLC (16).

Procedures—The fruits of *S. mammosum* and *S. khasianum* were harvested as soon as they reached a transition green-to-yellow color and were immediately extracted.

Extraction—Each of four or five fruits of *S. mammosum* or 20–25 fruits of *S. khasianum* of the same degree of maturity, collected from a single plant, was cut into four pieces with a sharp knife in a petri dish. The pieces were homogenized in a blender until they formed a thick, uniform slurry. The knife and dish were wiped with a small filter paper, which was added to the blender. From the homogenate, about a 10-g sample was weighed into a tared dish for determining the moisture content by drying to constant weight at 103°.

The glycoalkaloids were extracted by weighing 50 g of the homogenate in a beaker, transferring it quantitatively into a homogenizer[7] with 100 ml of 2% aqueous acetic acid, and mixing for 5 min. The slurry was centrifuged for 10 min, the supernate was decanted into an erlenmeyer flask, and the centrifuged solids were reblended and reextracted with 100 ml of methanol. After centrifugation, the methanol extract was combined with the acetic acid extract and again centrifuged. The clear solution was transferred into a 250-ml volumetric flask and diluted to volume with methanol.

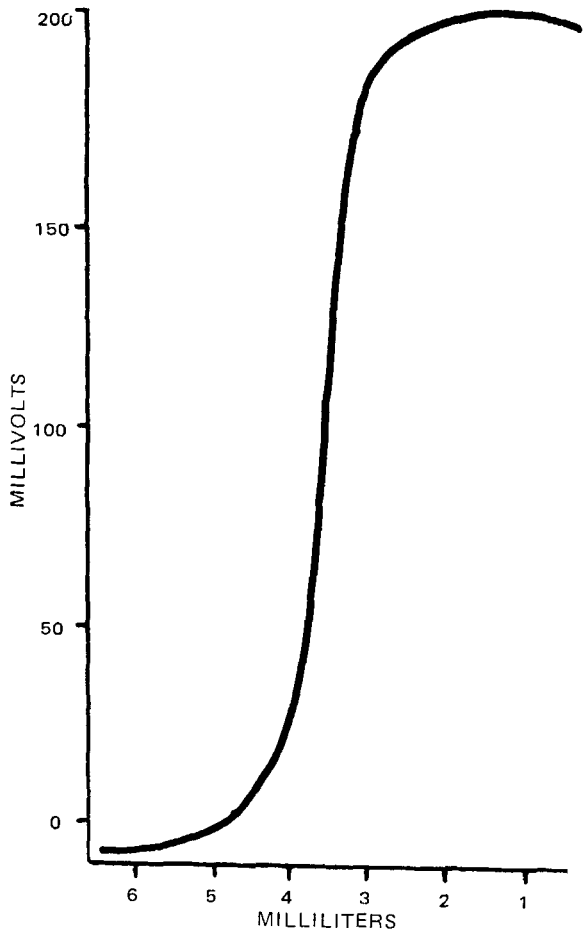

Figure 1—*Titration curve of solasodine.*

Hydrolysis—Duplicate 50-ml aliquots of the extracts were measured into 125-ml erlenmeyer flasks equipped with glass-tube condensers. Concentrated hydrochloric acid (5 ml) was added, and the mixture was heated in a boiling water bath for 2 hr. After cooling, 20 ml of 25% aqueous sodium hydroxide was added, and the mixture was heated in a water bath for 1 hr. After cooling, the content of the flask was transferred quantitatively into a separator and extracted with 25, 15, and 10 ml of benzene, consecutively. The pooled benzene extracts were dried with anhydrous sodium sulfate, transferred into a 50-ml volumetric flask, and brought to volume with benzene.

Twenty-five milliliters of the benzene extract was pipetted into the titration vessel, and 25 ml of reagent grade acetone was added. The extract was stirred at medium speed with a polytef stirring bar. The titration was monitored with a recorder by setting the electrode potential amplifier to the 100-mv scale and the recorder speed to 12.7 cm/min. Initially, the titrant was added rapidly; but as the first derivative curve began to appear, the rate of addition of titrant was decreased.

The percent of solasodine was calculated from:

$$\text{solasodine (\%)} = \frac{VF2.069 \times 100}{W_d} \qquad \text{(Eq. 1)}$$

where V = milliliters of titrant, F = normality factor of titrant, 2.069 = milliequivalents of solasodine, and W_d = weight of sample calculated as dry weight:

$$W_d = W_f - (W_f \times \%M) \qquad \text{(Eq. 2)}$$

where W_f = weight of fresh sample and $\%M$ = moisture content of fresh sample.

RESULTS AND DISCUSSION

Previously published analytical methods were developed for the evaluation of the solasodine content of dried and milled leaves of *S. la-*

[1] The plant materials used in this investigation were obtained by the Mayaguez Institute of Tropical Agriculture and identified by taxonomists of the Agricultural Research Service, U.S. Department of Agriculture, Plant Research Center, Beltsville, Md. Voucher specimens have been sent to the Herbarium, U.S. National Arboretum, Washington, D.C.

[2] Mettler DV 101 buret, DK 10 electrode potential amplifier, DV 103 command module, and Kentron 1110 pulse drive recorder.

[3] Beckman 1190-80.

[4] A. Thomas catalog No. C695-Q55.

[5] Teflon (du Pont).

[6] ICN Life Science Group, K and K Laboratories, Plainview, NY 11803.

[7] Omni mixer, Sorvall, Inc., Newtown, Conn.

Table I—Analysis of Isolated Solasodine

Sample[a]	Origin	End-Point Indication	Solasodine, %	Number of Analyses
Crude	*S. mammosum*	Potentiometric	86.5 ± 0.8	10
Crude	*S. khasianum*	Potentiometric	91.2 ± 0.6	10
Recrystallized	*S. mammosum*	Potentiometric	99.8 ± 0.4	10
Recrystallized	*S. khasianum*	Potentiometric	99.8 ± 0.4	10
Purified (preparative TLC)	*S. mammosum*	Potentiometric	100 ± 0.3	3
Purified (preparative TLC)	*S. mammosum*	Color indicator[b]	100 ± 0.4	2

[a] Every sample was heated to 105° for 2 hr before analysis. [b] From Ref. 13.

ciniatum. To achieve homogeneity of the sample, 250 g of dried leaves had to be milled through a fine mesh screen. The efficiency of extraction was inversely proportional to the particle size (17). To obtain a homogeneous sample using previous methods, serious problems would have been encountered. The steroid glycoalkaloids are not uniformly distributed in the fruit. The sap around the seed is very rich in the active principle, whereas the skin and seeds contain little or none.

It is difficult to dry a whole fruit quickly, and slow drying may cause decomposition. Moreover, the dried fruit cannot be minced because the high glycoalkaloid-containing sap tends to burn on the blades of the mill. Homogenization of fresh fruits yielded the best results. Extraction of freshly harvested fruits with weak acids and the subsequent precipitation of pectinous substances by methanol resulted in transparent yellow-colored solutions, free of suspended solids. The *Solanum* glycoalkaloids were removed quantitatively from the fruits.

In previously reported methods, the glycoalkaloids were isolated prior to hydrolysis. This step was unnecessary in the present procedure. After acid hydrolysis of the fruit extract, the solasodine was extracted with benzene from the hydrolysate.

Other methods suggested colorimetric techniques for determining solasodine based on its reaction with amphi-indicators such as methyl orange and tropaeoline 000 (8). However, these procedures are feasible only with purified compounds or colorless sample solutions.

The widely used gravimetric method, based on the weighing of a dried precipitate of solasodine hydrochloride, is not specific for solasodine and is subject to interference by inorganic coprecipitates.

The nonaqueous titration of secondary amines of alkaloids with 0.001 *N* *p*-toluenesulfonic acid, using dimethyl yellow as an indicator, is well established (18). It was applied (12, 13) to determine solasodine in leaves of *S. laciniatum*. When this method was applied to the colored fruit extracts, it was practically impossible to detect the transition color of the dimethyl yellow indicator. The chloroform solution of solasodine was also unstable, and the normality of *p*-toluenesulfonic acid in chloroform changed on standing.

Potentiometric determination of the end-point of the chloroform solutions of extracts of *Solanum* fruit titrated with *p*-toluenesulfonic acid also gave erratic results. Fritz and Burgett (19) titrated amines in acetone, using perchloric acid in dioxane as the titrant. When solasodine was titrated by this method, using calomel and glass electrodes, the resulting curves changed after each titration. By replacing the calomel electrode with a small strip of silver foil, titration of benzene extracts mixed with equal volumes of acetone gave good results. The titration curve and its first derivative curve are shown in Figs. 1 and 2.

The curves of purified solasodine and plant extracts were reproducible after repeated titrations. As a check of the procedure, the peak of the first derivative curve correlated well with the transition color of the added dimethyl yellow indicator when titrating colorless solutions of solasodine samples.

Fritz (20) recommended potassium acid phthalate in glacial acetic acid solution as a reference for standardization of perchloric acid in dioxane solution, using methyl violet as the indicator. The observation of the transition color of this indicator is very subjective, and potentiometric end-point determination of this system with glass and silver electrodes was unsuccessful.

Therefore, atropine was chosen for a reference standard. The purity of atropine was checked by TLC and by titration using the method of Gyenes (18). The titration of atropine base in benzene and acetone solution with perchloric acid in dioxane gave a curve similar to that of solasodine, and the first derivative curve showed a sharp end-point. The transition color of the dimethyl yellow indicator appeared exactly when the recorder reached the maximum of the first derivative curve.

The variable speed command module of the titration apparatus permitted the rapid addition of the bulk of the titrant; as the end-point was approached, the addition could be suitably slowed down. In this way, error due to temperature fluctuations could be minimized (21).

Titrations of crude, recrystallized, and chromatographically purified solasodine samples gave precise results. Titration of crystalline solasodine by the method of Bite (13) yielded the same result as that with the potentiometric determination (Table I).

The merits of this described method are illustrated in Table II. For the method development experiments, a composite sample was prepared of randomly picked yellow-green fruits of *S. mammosum* of different shapes. With the described extraction procedure of fresh samples, the average deviation in six assays was only 1.89% when the end-point was determined potentiometrically. However, when the methyl yellow indicator was used for the end-point determination, the average deviation of the results of four measurements was 18.4%. This deviation was further increased when the analytical samples were prepared by soxhlet extraction of dried and milled fruit (22). The titration of dark-colored samples was difficult using the methyl yellow indicator, and the average

Figure 2—*First derivative curve of solasodine.*

Table II—Analysis of a Composite Sample of Yellow-Green Fruits of *S. mammosum* for Method Development

Moisture Content[a], %	Extraction Method[b]	End-Point Indication	Solasodine Content, %	Number of Determinations
80.8	I	Potentiometric	1.06 ± 0.02	6
80.8	I	Color indicator[c]	0.98 ± 0.18	4
Dried	II	Potentiometric	0.94 ± 0.06	4
Dried	II	Color indicator[c]	0.92 ± 0.32	4
Previously extracted[d]	I	Potentiometric	2.04 ± 0.04	4

[a] Determined by drying to constant weight at 105°. [b] Extraction Method I is as outlined in this paper; Method II uses dried fruit and methanol extraction (22). [c] From Ref. 13. [d] Crystalline solasodine, 0.2 g, was added to 10 g of extracted sample.

Table III—Analyses of Fruits of *S. khasianum* and *S. mammosum*[a]

Fruit	Color	Shape	Moisture Content[b], %	Solasodine Content, %
S. khasianum	Green	Round	76.8	0.82 ± 0.04
S. khasianum	Yellow	Round	80.4	1.12 ± 0.06
S. mammosum	Yellow-green	Pear	79.1	1.05 ± 0.04
S. mammosum	Yellow-green	Round	81.9	0.99 ± 0.02
S. mammosum	Yellow-green	Pear with nipples	80.2	0.91 ± 0.03

[a] In all cases, the extraction method used was the one described in this report, and the end-point was determined potentiometrically (n = 3). [b] Determined by drying to constant weight at 105°

error of four titrations was 34.8%. Titrating the same sample with potentiometric end-point detection gave an average deviation of 6.4% in four measurements.

The recovery of added crystalline solasodine to an exhaustively extracted *S. mammosum* sample was quantitative within the experimental error of 2%, demonstrating the reliability of the extraction procedure outlined in this report.

Table III summarizes the results of solasodine determinations performed according to this procedure. Freshly harvested fruits of *S. khasianum* at different ripening stages and fruits of *S. mammosum* of different shapes were analyzed. Experimental errors were at the level previously experienced in the method development assays.

These analyses of *S. mammosum* and *S. khasianum* samples yielded more realistic values than those reported in the literature. Perez-Medina *et al.* (22) found 3.5–4% glycoalkaloids in *S. mammosum*. Maiti and Mathew (23) found 5% solasodine in *S. khasianum*. These investigators used the gravimetric method, and their results showed large variations and unusually high values when compared to solasodine levels found in other *Solanum* species. The present analyses showed alkaloid contents of 0.82–1.12% for these plants (Table III).

The easy operation of the titrating apparatus and the recorded end-point determination method should permit technicians to analyze single samples with sufficient accuracy for field evaluations.

REFERENCES

(1) N. Applezweig, *Chem. Week*, **May 17,** 58 (1969).
(2) R. Hardman, *Trop. Sci.*, **11,** 210 (1969).
(3) Y. Sato, *J. Am. Chem. Soc.*, **73,** 5009 (1951).
(4) K. Schreiber, in "The Alkaloids," vol. 10, R. H. F. Manske, Ed., Academic, New York, N.Y., 1968.
(5) N. N. Suvarov, *Med. Prom. SSSR*, **14,** 31 (1960).
(6) *N. Z. J. Agr.*, **123,** 15 (1960).
(7) P. Tuzson and F. Kiss, *Acta Chim. Acad. Sci. Hung.*, **12,** 31 (1957).
(8) K. Szasz, L. Gracza, and C. Lorincz, *Acta Pharm. Hung.*, **31,** 211 (1961).
(9) E. Balcar and M. Zalecka, *Biul. Inst. Rosl. Lecz.*, **8,** 90 (1962).
(10) J. Birner, *J. Pharm. Sci.*, **58,** 258 (1969).
(11) S. M. Khafagy and S. W. A. Amin, *Planta Med.*, **21,** 139 (1972).
(12) N. A. Valovics, *Herba Hung.*, **3,** 435 (1964).
(13) P. Bite, *Acta Chim. Acad. Sci. Hung.*, **64,** 199 (1970).
(14) A. K. Ruzhentsova and R. Tubina, *Med. Prom. SSSR*, **13,** 40 (1959).
(15) L. G. Chatten, M. Pernarowski, and L. Levi, *J. Am. Pharm. Assoc., Sci. Ed.*, **44,** 332 (1955).
(16) J. Buechi and A. Zimmerman, *Pharm. Acta Helv.*, **40,** 345 (1965).
(17) N. A. Valovics, *Med. Prom. SSSR*, **19,** 45 (1965).
(18) I. Gyenes, *Magy. Kem. Foly.*, **56,** 383 (1950).
(19) J. S. Fritz and C. A. Burgett, *Anal. Chem.*, **44,** 1673 (1972).
(20) J. S. Fritz, "Acid-Base Titrations in Nonaqueous Solvents," G. Frederick Smith Chemical Co., Columbus, Ohio, 1952.
(21) N. Adler, *Anal. Chem.*, **34,** 1668 (1962).
(22) L. A. Perez-Medina, E. Travecedo, and J. E. Devia, *Planta Med.*, **12,** 478 (1964).
(23) P. C. Maiti and R. Mathew, *Curr. Sci.*, **36,** 126 (1967).

ACKNOWLEDGMENTS AND ADDRESSES

Received April 16, 1975, from the *Agricultural Research Service, U.S. Department of Agriculture, Mayaguez Institute of Tropical Agriculture, Mayaguez, Puerto Rico 00708.*

Accepted for publication July 21, 1976.

Mention of a trademark or proprietary product does not constitute a guarantee or warranty of the product by the U.S. Department of Agriculture and does not imply its approval to the exclusion of other products.

Antimicrobial Action of Compound 48/80 against Protozoa, Bacteria, and Fungi

J. F. LENNEY *x, W. A. SIDDIQUI ‡, J. V. SCHNELL ‡, E. FURUSAWA *, and G. W. READ *

Abstract □ Compound 48/80 inhibited the growth of protozoa, bacteria, and fungi but had no effect on the multiplication of viruses. All susceptible organisms were inhibited by 10 μg/ml of crude compound 48/80, and some were inhibited by as little as 0.1 μg/ml. Against *Tetrahymena pyriformis*, this drug was seven times more potent than quinine. Separation of compound 48/80 into different fractions indicated that some antimicrobial activity could be separated from the histamine-liberating activity. It was found that compound 48/80 is not surface active at 500 μg/ml.

Keyphrases □ Compound 48/80—antimicrobial activity evaluated in protozoa, bacteria, fungi, and viruses □ Antimicrobial activity—compound 48/80 evaluated in protozoa, bacteria, fungi, and viruses □ Phenethylamine polymers—compound 48/80, antimicrobial activity evaluated in protozoa, bacteria, fungi, and viruses □ Polymers of phenethylamine—compound 48/80, antimicrobial activity evaluated in protozoa, bacteria, fungi, and viruses

In 1949, a family of polymers that lowered blood pressure was synthesized from *p*-methoxyphenethylmethylamine and formaldehyde (1). It was proposed that the products were various polymers of phenethylamine and that the most potent oligomer in the mixture was possibly the trimer. A widely distributed batch of this product was

Table III—Analyses of Fruits of *S. khasianum* and *S. mammosum*[a]

Fruit	Color	Shape	Moisture Content[b], %	Solasodine Content, %
S. khasianum	Green	Round	76.8	0.82 ± 0.04
S. khasianum	Yellow	Round	80.4	1.12 ± 0.06
S. mammosum	Yellow-green	Pear	79.1	1.05 ± 0.04
S. mammosum	Yellow-green	Round	81.9	0.99 ± 0.02
S. mammosum	Yellow-green	Pear with nipples	80.2	0.91 ± 0.03

[a] In all cases, the extraction method used was the one described in this report, and the end-point was determined potentiometrically (n = 3). [b] Determined by drying to constant weight at 105°

error of four titrations was 34.8%. Titrating the same sample with potentiometric end-point detection gave an average deviation of 6.4% in four measurements.

The recovery of added crystalline solasodine to an exhaustively extracted *S. mammosum* sample was quantitative within the experimental error of 2%, demonstrating the reliability of the extraction procedure outlined in this report.

Table III summarizes the results of solasodine determinations performed according to this procedure. Freshly harvested fruits of *S. khasianum* at different ripening stages and fruits of *S. mammosum* of different shapes were analyzed. Experimental errors were at the level previously experienced in the method development assays.

These analyses of *S. mammosum* and *S. khasianum* samples yielded more realistic values than those reported in the literature. Perez-Medina *et al.* (22) found 3.5–4% glycoalkaloids in *S. mammosum*. Maiti and Mathew (23) found 5% solasodine in *S. khasianum*. These investigators used the gravimetric method, and their results showed large variations and unusually high values when compared to solasodine levels found in other *Solanum* species. The present analyses showed alkaloid contents of 0.82–1.12% for these plants (Table III).

The easy operation of the titrating apparatus and the recorded end-point determination method should permit technicians to analyze single samples with sufficient accuracy for field evaluations.

REFERENCES

(1) N. Applezweig, *Chem. Week*, **May 17,** 58 (1969).
(2) R. Hardman, *Trop. Sci.*, **11,** 210 (1969).
(3) Y. Sato, *J. Am. Chem. Soc.*, **73,** 5009 (1951).
(4) K. Schreiber, in "The Alkaloids," vol. 10, R. H. F. Manske, Ed., Academic, New York, N.Y., 1968.
(5) N. N. Suvarov, *Med. Prom. SSSR*, **14,** 31 (1960).
(6) *N. Z. J. Agr.*, **123,** 15 (1960).
(7) P. Tuzson and F. Kiss, *Acta Chim. Acad. Sci. Hung.*, **12,** 31 (1957).
(8) K. Szasz, L. Gracza, and C. Lorincz, *Acta Pharm. Hung.*, **31,** 211 (1961).
(9) E. Balcar and M. Zalecka, *Biul. Inst. Rosl. Lecz.*, **8,** 90 (1962).
(10) J. Birner, *J. Pharm. Sci.*, **58,** 258 (1969).
(11) S. M. Khafagy and S. W. A. Amin, *Planta Med.*, **21,** 139 (1972).
(12) N. A. Valovics, *Herba Hung.*, **3,** 435 (1964).
(13) P. Bite, *Acta Chim. Acad. Sci. Hung.*, **64,** 199 (1970).
(14) A. K. Ruzhentsova and R. Tubina, *Med. Prom. SSSR*, **13,** 40 (1959).
(15) L. G. Chatten, M. Pernarowski, and L. Levi, *J. Am. Pharm. Assoc., Sci. Ed.*, **44,** 332 (1955).
(16) J. Buechi and A. Zimmerman, *Pharm. Acta Helv.*, **40,** 345 (1965).
(17) N. A. Valovics, *Med. Prom. SSSR*, **19,** 45 (1965).
(18) I. Gyenes, *Magy. Kem. Foly.*, **56,** 383 (1950).
(19) J. S. Fritz and C. A. Burgett, *Anal. Chem.*, **44,** 1673 (1972).
(20) J. S. Fritz, "Acid-Base Titrations in Nonaqueous Solvents," G. Frederick Smith Chemical Co., Columbus, Ohio, 1952.
(21) N. Adler, *Anal. Chem.*, **34,** 1668 (1962).
(22) L. A. Perez-Medina, E. Travecedo, and J. E. Devia, *Planta Med.*, **12,** 478 (1964).
(23) P. C. Maiti and R. Mathew, *Curr. Sci.*, **36,** 126 (1967).

ACKNOWLEDGMENTS AND ADDRESSES

Received April 16, 1975, from the *Agricultural Research Service, U.S. Department of Agriculture, Mayaguez Institute of Tropical Agriculture, Mayaguez, Puerto Rico 00708.*

Accepted for publication July 21, 1976.

Mention of a trademark or proprietary product does not constitute a guarantee or warranty of the product by the U.S. Department of Agriculture and does not imply its approval to the exclusion of other products.

Antimicrobial Action of Compound 48/80 against Protozoa, Bacteria, and Fungi

J. F. LENNEY *x, W. A. SIDDIQUI ‡, J. V. SCHNELL ‡, E. FURUSAWA *, and G. W. READ *

Abstract □ Compound 48/80 inhibited the growth of protozoa, bacteria, and fungi but had no effect on the multiplication of viruses. All susceptible organisms were inhibited by 10 μg/ml of crude compound 48/80, and some were inhibited by as little as 0.1 μg/ml. Against *Tetrahymena pyriformis*, this drug was seven times more potent than quinine. Separation of compound 48/80 into different fractions indicated that some antimicrobial activity could be separated from the histamine-liberating activity. It was found that compound 48/80 is not surface active at 500 μg/ml.

Keyphrases □ Compound 48/80—antimicrobial activity evaluated in protozoa, bacteria, fungi, and viruses □ Antimicrobial activity—compound 48/80 evaluated in protozoa, bacteria, fungi, and viruses □ Phenethylamine polymers—compound 48/80, antimicrobial activity evaluated in protozoa, bacteria, fungi, and viruses □ Polymers of phenethylamine—compound 48/80, antimicrobial activity evaluated in protozoa, bacteria, fungi, and viruses

In 1949, a family of polymers that lowered blood pressure was synthesized from *p*-methoxyphenethylmethylamine and formaldehyde (1). It was proposed that the products were various polymers of phenethylamine and that the most potent oligomer in the mixture was possibly the trimer. A widely distributed batch of this product was

identified by its code name "BW 48-80," which subsequently led to the adoption of the name "compound 48/80." Later, the dimeric and trimeric oligomers were synthesized by an alternative route and found to be inactive (2, 3). In 1972, dialysis and gel filtration were used to obtain evidence that the molecular size of the hypotensive constituents ranged from the tetramer to the octamer (4).

One study (5) reported that compound 48/80 caused the release of histamine and that this was the mechanism by which it lowered blood pressure. Since then, compound 48/80 has often been used as a tool to study the mechanism of mast cell degranulation and the pharmacological effects of the potent agents released from these cells. It is difficult to separate the direct effects of compound 48/80 from its indirect effects caused by the release of these agents, but several reports described actions for compound 48/80 that may not be related to mast cell degranulation: inhibition of the action of acetylcholine (6), central nervous system effects (7), ganglionic blockade (8), competitive inhibition of agonists that produce smooth muscle contraction (9), inhibition of skeletal muscle contraction (10), release of creatine phosphokinase from muscle (11), inhibition of viral-induced giant cell formation (12), and stimulation of tumor growth (13, 14). However, apparently no one has reported an antimicrobial action for compound 48/80.

The effects of compound 48/80 on the growth of protozoa, bacteria, fungi, and viruses were measured, and it was found that compound 48/80 is a moderately potent antimicrobial agent against all of these groups except the viruses. The relation between the antimicrobial activity and the histamine-liberating activity of this drug was also studied. A preliminary account of this work has been presented (15).

EXPERIMENTAL

Protozoa—*Tetrahymena pyriformis* GL (ATCC 30006) was grown in flasks containing Hogg's medium (1% proteose peptone, 0.1% K_2HPO_4, 0.1% dextrose, and 0.1% sodium acetate) on a rotary shaker at 27°. Growth was measured at intervals by counting cells that were freshly killed by dilution with 2.5% formaldehyde in 0.5% saline. In addition to compound 48/80 and its monomer, histamine diphosphate[1], diphenhydramine hydrochloride[2], and quinine hydrochloride[3] were tested for their effects on the growth of *Tetrahymena*.

Two strains of *Plasmodium falciparum* were employed: chloroquine resistant (FVO, Vietnam-Oak Knoll) and chloroquine sensitive (FUP, Uganda-Palo Alto). *P. falciparum*-infected blood was taken from Aotus monkeys and diluted with normal blood to obtain approximately 2% parasitemia. These diluted cultures were then incubated *in vitro* using a rocker dilution technique with a modified Harvard medium (16). The infections were synchronous, and experiments were begun with a majority of asexual parasites in the "ring" stage. At intervals, 100 or more parasites from each blood sample were examined microscopically and classified according to their maturation to trophozoite, schizont, or segmenter stages.

Fungi—Cultures of *Saccharomyces cerevisiae* (ATCC 7754) were grown at 30° in shake flasks containing 2% AC broth[4] on a rotary shaker. At intervals, aliquots of the cultures were diluted with water, and the transmittance of the yeast suspension was read at 755 nm. *Aspergillus niger* (ATCC 1004) was grown by the same procedure; however, growth was measured by weighing the dried mycelium, which was harvested by filtration through preweighed filter paper disks.

Bacteria—*Klebsiella pneumoniae* (ATCC 13883) and *Staphylococcus albus* (ATCC 3004) were grown in SMA broth, *Pediococcus cerevisiae* (ATCC 8081) and *Streptococcus faecalis* (ATCC 8042) were grown in Citrovorum factor assay medium[4] supplemented with 0.1 μg of calcium leucovorin/ml, and *Lactobacillus casei* (ATCC 7469) was grown in folic acid medium[4] supplemented with 0.1 μg of folic acid/ml. Cultures were incubated at 37°, and growth was followed by measuring the transmittance of the culture at 660 nm.

Viruses—Encephalomyocarditis (ATCC VR-129), vesicular stomatitis (ATCC VR-158), and vaccinia (ATCC VR-156) viruses were grown in KB cells at 37° in medium 199 supplemented with 2% calf serum (17). The concentration of the viruses in each inoculum was 100 times that necessary to infect 50% of the cells (100 $TCID_{50}$). The inoculum and compound 48/80 were added to the medium at the same time. Viral growth was followed microscopically by noting the degree of cytopathic effect caused by virus multiplication.

Gel Filtration—Compound 48/80 was fractionated in a 111 × 1.5-cm column of Sephadex G-25 medium[5]. A solution of 0.03 *N* acetic acid adjusted to pH 3.0 with hydrochloric acid was passed through the column at a flow rate of 12 ml/hr. Ten-milligram samples dissolved in 1 ml of acetic acid solution were placed on the column. The effluent was continuously monitored at 280 nm, and 8.5-ml fractions were collected.

Blood Pressure—Wistar male rats (300–600 g) were anesthetized with pentobarbital sodium[6] (50 mg/kg) and monitored on a polygraph[7]. Arterial pressure was measured with a liquid-pressure transducer[8] connected by a cannula to the right femoral artery. Heparin sodium[9] (10 mg/kg) and the fractions to be assayed were given through a cannula inserted into the right femoral vein. In each animal, the blood pressure was noted just before the infusion and again 5 min later. A dose–response curve was prepared for compound 48/80. The column fractions were analyzed in quadruplicate, and their potencies were expressed in terms of equivalent micrograms of compound 48/80 by reference to the dose–response curve.

Surface Activity—Test solutions were passed through a drop counter at a rate of approximately 15 drops/min. The volume obtained from 4000 drops provided a measure of drop size and, therefore, of surface tension. Benzalkonium chloride (0.01%) and other surfactants produced a volume that was 40–60% of the volume obtained with pure water.

RESULTS

The effects of compound 48/80 on the growth of microorganisms are presented in Table I. The growth of each protozoan, fungal, and bacterial species tested was inhibited, but there was no effect on the viruses used. The most sensitive species was *Staph. albus*, which did not grow at all in medium containing 2.5 μg of compound 48/80/ml. *L. casei* was also very sensitive, with 0.1 μg/ml causing a 37% inhibition of growth. The least sensitive of the affected organisms were *K. pneumoniae* and *A. niger*. In every case where the main reactant (*p*-methoxyphenethylmethylamine) for the synthesis of compound 48/80 was tested, it had no effect or was far less effective than an equal amount of compound 48/80.

Also shown in Table I are the effects of quinine, histamine, and diphenhydramine on the growth of *T. pyriformis*. Quinine and the antihistamine inhibited growth, whereas histamine had no significant effect. Quinine was about one-seventh as active as compound 48/80. Low levels of compound 48/80 had a static effect on *T. pyriformis* rather than a killing effect. After 24 hr of growth inhibition, dilution of the medium allowed growth to resume.

In separate experiments, compound 48/80 was about as active as pyrimethamine in inhibiting the maturation of *P. falciparum*, but it was only 10% as active as chloroquine. Compound 48/80 was more active against the chloroquine-sensitive strain of *Plasmodium* than it was against the chloroquine-resistant strain.

The activities of the fractions of compound 48/80 prepared by chromatography on Sephadex G-25 are shown in Fig. 1. The fractions that were the most potent histamine liberators also contained most of the antimicrobial activity. However, some fractions possessed antimicrobial activity but no hypotensive activity. When these fractions were tested against *P. falciparum*, all were active, including peaks 1, 2, and 3. Each fraction was more active against the chloroquine-sensitive strain of this protozoan than against the chloroquine-resistant strain.

In a preliminary experiment, peak 5 from the Sephadex G-25 column effluent was further purified by rechromatography on G-25 and then was

[1] City Chemical Corp.
[2] Tiffany Chemical Co.
[3] Merck and Co.
[4] Difco.
[5] Pharmacia.
[6] Abbott.
[7] Grass model 7.
[8] Statham P23Dc.
[9] Nutritional Biochemicals.

Table I—Effect of Compound 48/80 on the Growth of Microorganisms[a]

Group	Organism	Drug	Dose, μg/ml	Growth, % of Control
Protozoa	*T. pyriformis*	Compound 48/80	1	85[b]
		Compound 48/80	5	57
		Compound 48/80	25	19
		Monomer	100	95[c]
		Quinine	5	97[b]
		Quinine	25	81
		Quinine	100	21
		Histamine	10	101
		Histamine	100	106
		Diphenhydramine	1	89
		Diphenhydramine	10	73
		Diphenhydramine	100	17
	P. falciparum	Compound 48/80	2.5	75[d]
		Compound 48/80	25	0
		Monomer	10	100
Fungi	*S. cerevisiae*	Compound 48/80	5	100[e]
		Compound 48/80	10	15
		Compound 48/80	20	1
		Monomer	100	100
	A. niger	Compound 48/80	5	89[f]
		Compound 48/80	25	72
		Compound 48/80	100	1
		Monomer	100	47
Bacteria	*K. pneumoniae*	Compound 48/80	2.5	77[g]
		Compound 48/80	10	64
		Compound 48/80	25	37
		Compound 48/80	100	25
	L. casei	Compound 48/80	0.1	63
		Compound 48/80	0.25	40
		Compound 48/80	2.5	7
		Compound 48/80	25	0
		Monomer	200	93
	Ped. cerevisiae	Compound 48/80	2.5	68
		Compound 48/80	10	1
		Monomer	200	93
	Staph. albus	Compound 48/80	2.5	0
		Compound 48/80	10	0
		Monomer	100	71
	Strep. faecalis	Compound 48/80	2.5	87
		Compound 48/80	25	4
		Monomer	200	99
Viruses	Vesicular stomatitis	Compound 48/80	20	100[h]
	Encephalomyocarditis	Compound 48/80	40	100[i]
	Vaccinia	Compound 48/80	10	100[j]

[a] The assay at each concentration was performed two to five times. Only representative experiments at selected concentrations are shown. Monomer = *p*-methoxyphenethylmethylamine. [b] Cells per cubic millimeter after 24 hr. [c] Cells per cubic millimeter after 8 hr. [d] Number of parasitized red cells in which parasites grew to schizont stage in 35 hr. [e] Optical density of culture at 755 nm after 24 hr. [f] Mycelial dry weight after 24 hr. [g] Optical density of culture at 660 nm after 24 hr. [h] Cytopathic effect of the viruses in KB cells after 48 hr at the maximum nontoxic dose for 48 hr. [i] Cytopathic effect of the viruses in KB cells after 24 hr at the maximum nontoxic dose for 24 hr. [j] Cytopathic effect of the viruses in KB cells after 120 hr at the maximum nontoxic dose for 120 hr.

chromatographed on paper as previously described (4). The four resulting components were eluted from the paper and then analyzed for hypotensive activity and for activity against *L. casei*. One component displayed hypotensive activity only, another showed antibacterial activity only, and the other two components were inactive.

In another preliminary experiment, repurified peak 5 was chromatographed on a Bio Gel P-4[10] column. Four peaks were obtained in the effluent, representing compounds that were evidently separated by adsorption effects. As in the case of the paper chromatography, one peak showed hypotensive activity only, another had antibacterial activity only, and the other two were inactive.

Since compound 48/80 contains ionized nitrogen atoms, its antimicrobial and histamine-liberating activities were compared with those of a typical quaternary ammonium detergent. Benzalkonium chloride[11] was 100 times more potent than compound 48/80 as a hemolytic agent and 10 times more potent as an antimicrobial agent against yeast. However, benzalkonium chloride was one-third as potent as compound 48/80 as a histamine-releasing agent when tested *versus* mast cells *in vitro* and was only 1% as potent as a hypotensive agent. Detergents liberate histamine from mast cells by disrupting the plasma membrane, whereas compound 48/80 liberates histamine by a selective, noncytolytic action (18). The drop size procedure showed that compound 48/80 has no surface activity at 500 μg/ml; therefore, its antimicrobial activity is not attributable to surface activity or detergency.

DISCUSSION

The data show that compound 48/80 has a broad spectrum of activity in inhibiting the growth of microorganisms. In this respect, it resembles cationic detergents; however, the results indicate that compound 48/80 does not display the hemolytic and surface activities of a detergent. Although compound 48/80 is only moderately potent as an antimicrobial agent, it is not a pure substance; Fig. 1 shows that some components are inactive or are only weakly active. Thus, it is possible that the mixture may contain some very potent compounds.

In addition, since the assays were performed in the presence of growth media, complex formation with medium components may have reduced the concentration of free antimicrobial agent. (Each nitrogen atom of the polymer bears a positive charge.) Since different media were used for the growth of different organisms, the percentage of compound 48/80 complexed (if any) may have varied from one organism to another. Therefore, the relative sensitivities observed may be approximate. However, the salient point is that compound 48/80 inhibited the growth of all bacterial, fungal, and protozoal cultures tested.

Compound 48/80 (at 2–10 μg/ml) blocks the division of fertilized sea urchin (*Tripneustes gratilla*) eggs[12]. In KB cells and in sea urchin eggs, compound 48/80 alters the appearance of the cytoplasm and the shape of the nucleus. Evidently, compound 48/80 inhibits the division of a wide variety of cells, possibly by a similar mechanism.

[10] Bio-Rad.
[11] Zephiran, Calbiochem.
[12] R. Hino, School of Medicine, University of Hawaii personal communication.

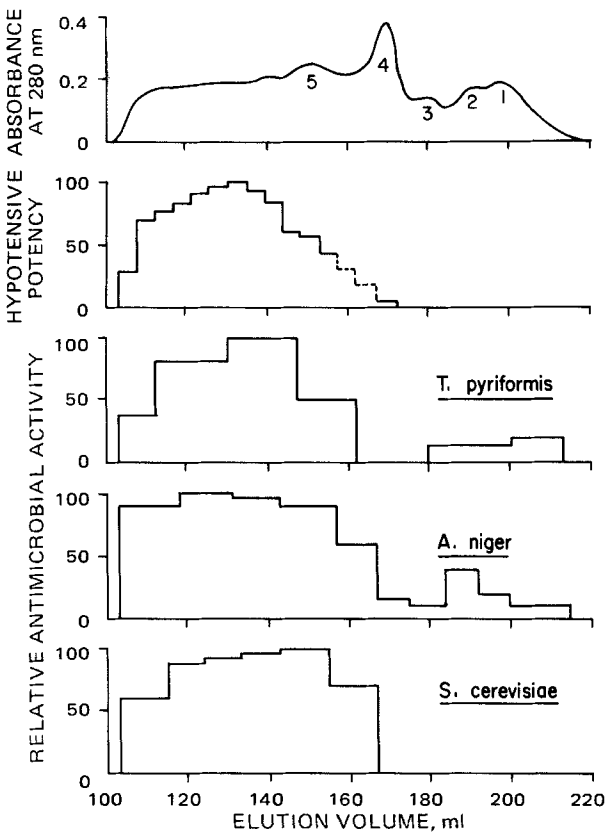

Figure 1—*Histamine-liberating and antimicrobial activities of fractions of compound 48/80. Compound 48/80 was fractionated by chromatography on Sephadex G-25 as previously described (4). The top curve is the tracing produced by a UV monitor. In the other four charts, the most potent fraction was assigned an activity of 100%.*

There are several indications that the histamine-liberating and antimicrobial activities of compound 48/80 may reside in different constituents of this mixture. Figure 1 shows that some antimicrobial activity was separated from the hypotensive fractions by chromatography on Sephadex G-25. A similar partial separation was achieved as measured by activity against *P. falciparum*. When peak 5 (Fig. 1) was separated into four components by chromatography on paper or on Bio Gel P-4, preliminary data indicated that a separation of the two activities had been effected. The fact that peak 5 contained at least four different compounds, all of approximately the same molecular size, suggests that the reaction for the synthesis of compound 48/80 may be more complex than previously assumed.

REFERENCES

(1) R. Baltzly, J. S. Buck, E. J. De Beer, and F. S. Webb, *J. Am. Chem. Soc.*, **71**, 1301 (1949).

(2) J. I. De Graw, V. H. Brown, S. A. Ferguson, N. E. Kontaxis, and W. A. Skinner, *J. Med. Chem.*, **9**, 292 (1965).

(3) *Ibid.*, **9**, 838 (1966).

(4) G. W. Read and J. F. Lenney, *J. Med. Chem.*, **15**, 320 (1972).

(5) W. D. M. Paton, *Br. J. Pharmacol.*, **6**, 499 (1951).

(6) P. B. Dews, A. L. Wnuck, R. V. Fanelli, A. E. Light, J. A. Tornaben, S. Norton, C. H. Ellis, and E. J. De Beer, *J. Pharmacol. Exp. Ther.*, **107**, 1 (1953).

(7) M. Rocha e Silva, *Br. J. Pharmacol.*, **14**, 243 (1959).

(8) S. B. Gertner, *ibid.*, **10**, 103 (1955).

(9) T. B. Paiva and A. C. M. Paiva, *Biochem. Pharmacol.*, **15**, 1303 (1966).

(10) G. Somjen and I. F. Uyldert, *Br. J. Pharmacol.*, **10**, 413 (1955).

(11) H. Y. Meltzer and P. Margulies, *Biochem. Pharmacol.*, **20**, 3501 (1971).

(12) D. Falke and G. F. Kahl, *J. Gen. Virol.*, **10**, 273 (1971).

(13) P. O. Montgomery, T. Dillon, and A. Goth, *Tex. Rep. Biol. Med.*, **14**, 432 (1956).

(14) G. Jasmin, *Proc. Soc. Exp. Biol. Med.*, **96**, 570 (1957).

(15) G. W. Read, J. F. Lenney, W. A. Siddiqui, J. V. Schnell, and E. Furusawa, *Fifth Int. Cong. Pharm.*, Abstract 1133 (1972).

(16) W. A. Siddiqui, J. V. Schnell, and Q. M. Geiman, *Am. J. Trop. Med. Hyg.*, **19**, 586 (1970).

(17) E. Furusawa and W. Cutting, *Ann. N.Y. Acad. Sci.*, **173**, 668 (1970).

(18) A. R. Johnson and N. C. Moran, *Fed. Proc.*, **28**, 1716 (1969).

ACKNOWLEDGMENTS AND ADDRESSES

Received March 8, 1976, from the *Department of Pharmacology and the ‡Department of Tropical Medicine and Medical Microbiology, School of Medicine, University of Hawaii, Honolulu, HI 96822.

Accepted for publication July 13, 1976.

Supported by grants from the University of Hawaii Research Council, the National Institutes of Health (GM 15198, GM 18740, and AIO-9558-01), and the Research and Development Command of the U.S. Army (DADA 17-70-C-0120).

The authors thank S. C. Chou and K. G. Conklin for the culture of *T. pyriformis* and instructions on its growth and assay. A sample of compound 48/80 was obtained from Burroughs Wellcome Co. through the generosity of David C. Daw. A sample of *p*-methoxyphenethylmethylamine was prepared by Edgar F. Kiefer of the Chemistry Department, University of Hawaii. The authors also acknowledge the technical assistance of Charlotte S. Oda, Clifford K. H. Lau, Edward Glenn, and Suzanne M. Richmond-Crum.

ˣ To whom inquiries should be directed.

Utilization of Cyclodextrin Complexation for Separation of E, A, and B Prostaglandins by Ion-Exchange Liquid Chromatography

K. UEKAMA [x], F. HIRAYAMA, K. IKEDA *, and K. INABA [‡]

Abstract □ Application of cyclodextrin complexation to the separation of E-, A-, and B-type prostaglandins by ion-exchange liquid chromatography is demonstrated. The addition of α- or β-cyclodextrin into the mobile phase on an anion-exchange support decreased the retention times of the prostaglandins significantly because of soluble complex formation. Chromatographic separation behavior is discussed on the basis of the stability of the inclusion complex. A rapid and sensitive method for the separation and quantification of the prostaglandins, using β-cyclodextrin in the mobile phase, is described.

Keyphrases □ Prostaglandins—ion-exchange liquid chromatographic analysis after cyclodextrin complexation, prepared samples □ Cyclodextrin complexation—with various prostaglandins, ion-exchange liquid chromatographic analysis, prepared samples □ Ion-exchange liquid chromatography—analysis, various prostaglandins after cyclodextrin complexation, prepared samples □ Complexes—various prostaglandins with cyclodextrins, ion-exchange liquid chromatographic analysis, prepared samples

The prostaglandins are essentially long chain unsaturated fatty acids containing a substituted cyclopentane ring system. The β-hydroxyketo moiety of E-type prostaglandins (I and II[1]) is susceptible to dehydration in acidic or alkaline conditions to form A-type prostaglandins (III and IV[2]), which are isomerized consecutively to form the corresponding B-type prostaglandins (V and VI[3]) in alkaline conditions (1, 2). The A- and B-type prostaglandins are isomeric compounds, differing only in the position of the double bond in the cyclopentanone ring.

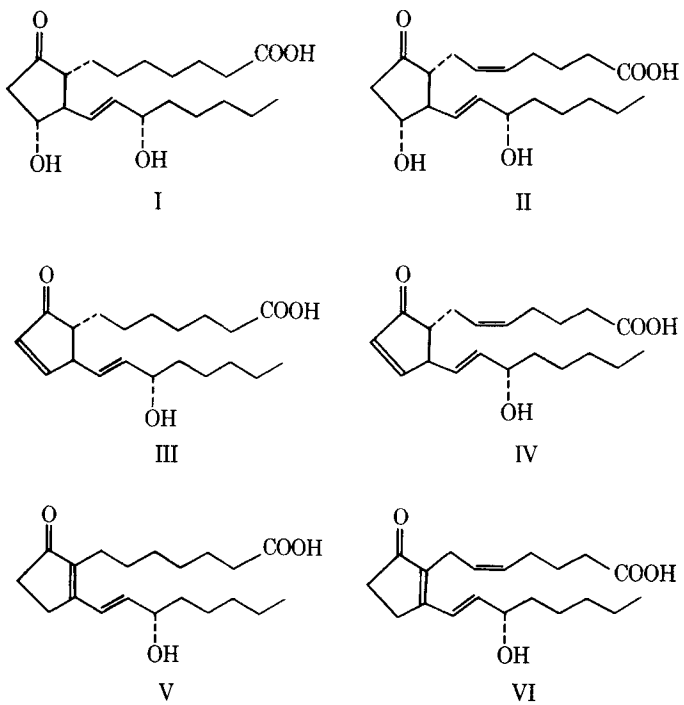

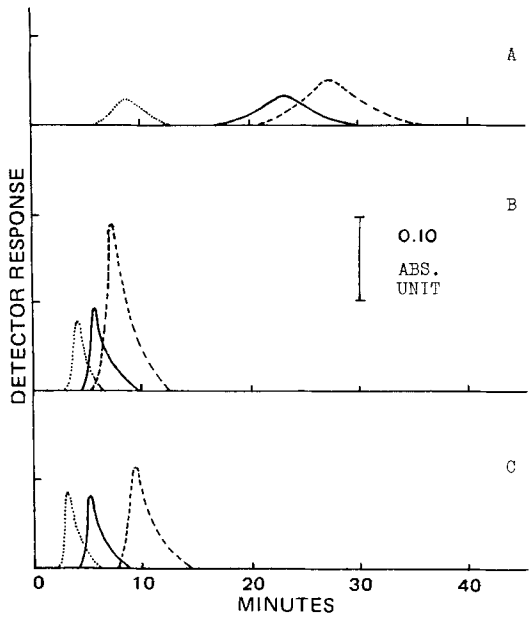

Figure 1—*Liquid chromatograms of I (20 μg), III (2.67 μg), and V (3.32 μg) on an anion-exchange column in the absence and presence of cyclodextrin in the mobile phase. Chromatographic conditions were: mobile phase, 0.1 M sodium phosphate buffer (pH 6.0, ionic strength 0.2); flow rate, 0.5 ml/min; and detection, 210, 221, and 282 nm for I, III, and V, respectively. Key: A, without cyclodextrin; B, with 0.5% α-cyclodextrin; C, with 0.5% β-cyclodextrin; ·····, I; —, III; and - - - -, V.*

High-performance liquid chromatography (HPLC) allows the direct analysis of closely related prostaglandins without protective derivatization (3). However, because the prostaglandins are hydrophobic, they generally exhibit long retention times with undesirable separation behavior on anion-exchange supports using an aqueous mobile phase. Therefore, a more rapid and sensitive HPLC method is required for the separation and detection of the prostaglandin isomers.

α- and β-Cyclodextrins form inclusion complexes with various drug molecules in water (4–9). The relatively hydrophobic environment of the cyclodextrin cavity is expected to attract the prostaglandins. A preliminary study indicated that I, III, and V formed soluble complexes with α- and β-cyclodextrins in water, which were stable in the neutral pH region (10).

The present paper deals with the application of cyclo-

[1] I is prostaglandin E_1 [(11α,13*E*,15*S*)-11,15-dihydroxy-9-oxoprost-13-en-1-oic acid], and II is dinoprostone [(5*Z*,11α,13*E*,15*S*)-11,15-dihydroxy-9-oxoprosta-5,13-dien-1-oic acid].

[2] III is prostaglandin A_1 [(13*E*,15*S*)-15-hydroxy-9-oxoprosta-10,13-dien-1-oic acid], and IV is prostaglandin A_2 [(5*Z*,13*E*,15*S*)-15-hydroxy-9-oxoprosta-5,10,13-trien-1-oic acid].

[3] V is prostaglandin B_1 [(13*E*,15*S*)-15-hydroxy-9-oxoprosta-8(12),13-dien-1-oic acid], and VI is prostaglandin B_2 [(5*Z*,13*E*,15*S*)-15-hydroxy-9-oxoprosta-5,8(12),13-trien-1-oic acid].

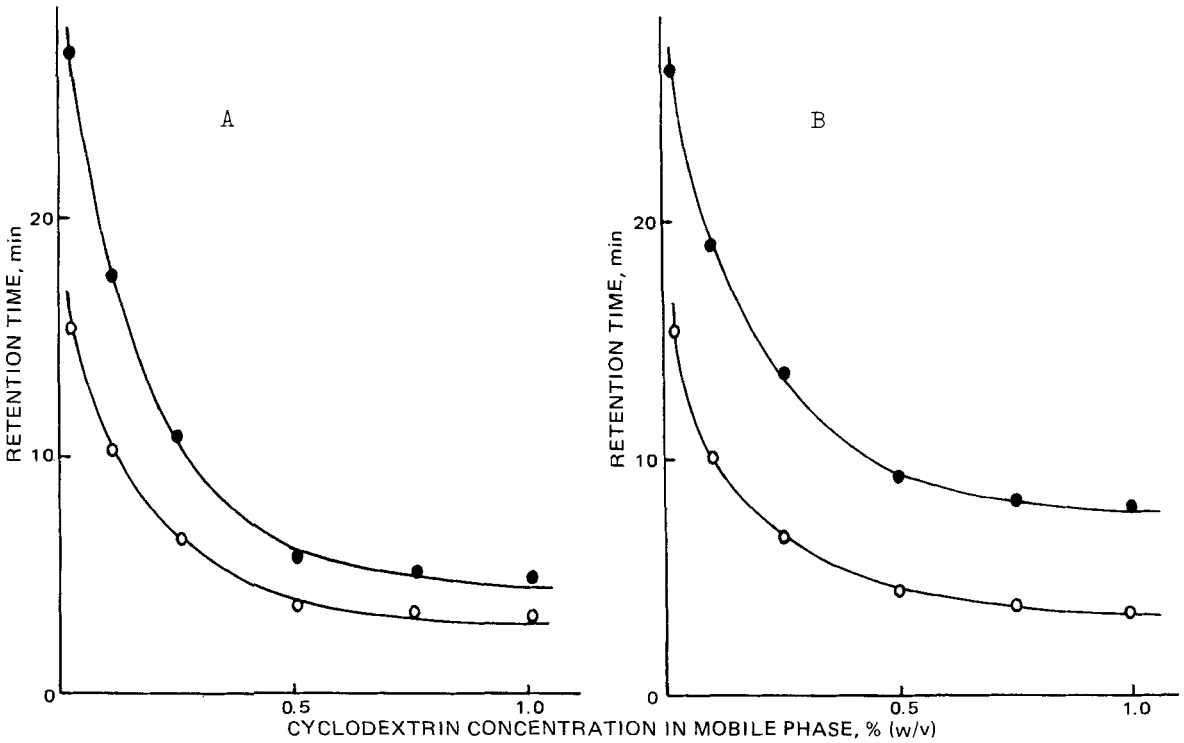

Figure 2—*Effects of cyclodextrin concentration on the retention times of III and V. Chromatographic conditions were the same as in Fig. 1. Key: A, α-cyclodextrin system; B, β-cyclodextrin system;* ○, *III; and* ●, *V.*

dextrin complexation to the separation of these prostaglandins by ion-exchange HPLC. α- or β-Cyclodextrin was added to the mobile phase on a strong anion-exchange support. To increase the detection sensitivity, A and B prostaglandins were monitored at their UV maximum wavelengths by a spectrophotometer equipped with a multiwavelength scanner. Furthermore, the concentration of cyclodextrin, pH, ionic strength, and solvent composition in the mobile phase were investigated to optimize resolution. The developed method is rapid, sensitive, and precise for the separation and quantification of the prostaglandins.

EXPERIMENTAL

Apparatus—The liquid chromatograph was equipped with a pump[4] (700 kg/cm^2 maximum), a double-beam spectrophotometric detector with a programmable multiwavelength scanner[5], an injection port[6], a microflowcell unit[7], and a strip-chart four-pen recorder[8].

Chromatographic Conditions—A 500 × 2.3-mm i.d. stainless steel column, packed with a strong anion-exchange pellicular support[9], was operated at a flow rate of 0.5 ml/min (about 1100 psi), unless otherwise stated. The pH and ionic strength of the mobile phase, phosphate buffer, were adjusted with 0.1 *M* phosphoric acid, 0.1 *M* sodium hydroxide, and sodium chloride.

Quantitative Analysis—Stock solutions of E, A, and B prostaglandins were prepared at concentrations of 6.63, 2.13, and 1.53 mg/ml in ethanol, respectively. A 2-μl aliquot of the sample was injected quantitatively with a 10-μl syringe[10]. The column temperature was ambient, and the chart speed of the recorder was 10 mm/min at a range of 0.2 absorbance unit full scale (aufs). Quantification was accomplished by the measurement of peak height. The retention time was measured as the elapsed time between injection and attainment of the chromatographic peak maximum.

Materials—α- and β-Cyclodextrins[11] and prostaglandins I–VI[12] were used as supplied. All other materials and solvents were reagent grade, and deionized, double-distilled water was used.

Solubility Studies—Solubility studies were carried out according to Higuchi and Lach (11). Excess amounts of the prostaglandins were added to aqueous α- or β-cyclodextrin solutions and were shaken at 25 ± 0.1°. After equilibration was attained, an aliquot was centrifuged and pipetted through a cotton filter. A 0.5-ml aliquot of the sample solution was extracted with 5 ml of ether from acidified media, and 2 ml of the ether phase was evaporated to dryness.

With I and III, the residues were converted to V by the treatment of 0.1 *M* sodium hydroxide solution at 80° for 1 hr (12). After cooling to room temperature, the resultant V was diluted suitably with 0.1 *M* sodium phosphate buffer (pH 7.0) and then subjected to UV spectrophotometry at 282 nm. With V, the residue was dissolved directly in a suitable amount of 0.1 *M* sodium phosphate buffer (pH 7.0) and subjected to UV spectrophotometry at 282 nm.

No appreciable degradations of I and III were confirmed during equilibration. The presence of cyclodextrin did not interfere in the spectrophotometric assay.

The stability constants for complexes were calculated from the phase diagrams obtained according to Higuchi and Lach (11).

Apparent Partition Coefficients—Solutions of E, A, and B prostaglandins (6.0×10^{-5} *M*) were prepared in chloroform, previously saturated with 0.1 *M* phosphate buffer (pH 6.0). These solutions were added to buffer solutions in suitable volume ratios and shaken at 25 ± 0.1° for 1 hr. After separation by centrifugation, an aliquot of the aqueous phase was assayed by the procedure described under *Solubility Studies*. The partition coefficient was defined as the ratio of the equilibrium concentration in the organic phase to that in the aqueous phase.

RESULTS AND DISCUSSION

Effects of Cyclodextrins on Retention Times of Prostaglandins—Figure 1 shows typical liquid chromatograms of I, III, and V on an anion-exchange support in the absence and presence of α- or β-cyclodextrin. The aqueous mobile phase was sodium phosphate buffer, since phosphate anions do not interfere with the inclusion complexation of cyclodextrins (13). A simple phosphate buffer gave long retention times

[4] Model FLC-A700, Jasco, Tokyo, Japan.
[5] Model UVIDEC-1M, Jasco, Tokyo, Japan.
[6] Model JP-350, Jasco, Tokyo, Japan.
[7] Jasco, Tokyo, Japan.
[8] Model D4R-1M, Ohkura Electric Co. Ltd., Tokyo, Japan.
[9] AV-02-500 (Vidac Anion), Jasco, Tokyo, Japan.
[10] Type MS-G10, Termo Co., Tokyo, Japan.
[11] Teijin Ltd., Tokyo, Japan.
[12] Ono Pharmaceutical Co. Ltd., Osaka, Japan.

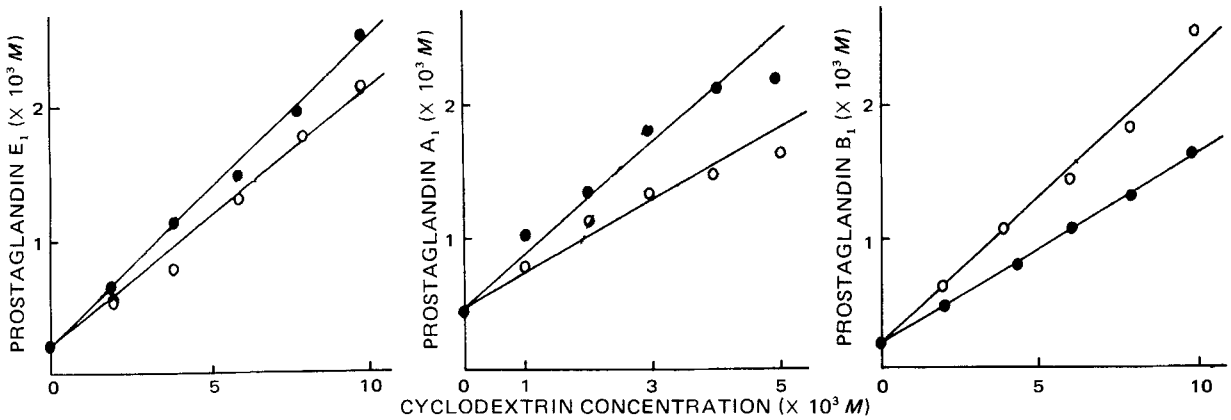

Figure 3—*Solubilities of prostaglandins as a function of α- or β-cyclodextrin concentration in water at 25°. Key: ○, α-cyclodextrin system; and ●, β-cyclodextrin system.*

with marked tailing, particularly for A and B prostaglandins. This result may have been due to the highly hydrophobic nature of the prostaglandins, as expected from their partition coefficients (Table I). When α- or β-cyclodextrin was added to the phosphate buffer, the retention times of the prostaglandins decreased significantly. The resolution of II, IV, and VI was somewhat better than that of I, III, and V (Table I).

Figure 2 shows that an increase in α- or β-cyclodextrin concentrations shortened the retention times of III and V. This result may be ascribed to the increase in the solubility of prostaglandins by complexation with cyclodextrins.

Solubility studies clearly indicated that prostaglandins form soluble complexes with α- and β-cyclodextrins in water (Fig. 3). Stability constants were calculated on the basis of 1:1 complexation from the straight-line portion of solubility diagrams (Table II).

Complexation of the prostaglandins with cyclodextrins was also studied by UV, circular dichroism, and ^{13}C-NMR spectrometry (10), where the importance of the spatial relationship between the guest and host molecules was suggested. For example, the small spectral changes observed for the β-cyclodextrin–V system may indicate that the inclusion of V in β-cyclodextrin of a larger cavity is loose compared to that of α-cyclodextrin and this is responsible for the magnitude of the stability constant in Table II.

The magnitude of the stability constants corresponds to the change in the retention times of the prostaglandins due to the presence of cyclodextrins. β-Cyclodextrin gave better resolution of the prostaglandin peaks compared to α-cyclodextrin, particularly for A and B prostaglandins. The insufficient separation of the peaks observed for α-cyclodextrin systems may reflect the smaller difference in the stability constants of A and B prostaglandins as compared to β-cyclodextrin systems. Use of β-cyclodextrin in the mobile phase (concentration of more than 0.5% w/v) yielded rapid separation of the A and B prostaglandins in anion-exchange HPLC (Fig. 2B).

Separation and Detection of A and B Prostaglandins—Morozowich (3) employed ion-exchange HPLC for the separation of IV and VI, followed by UV (254 nm) detection. The detector response of these

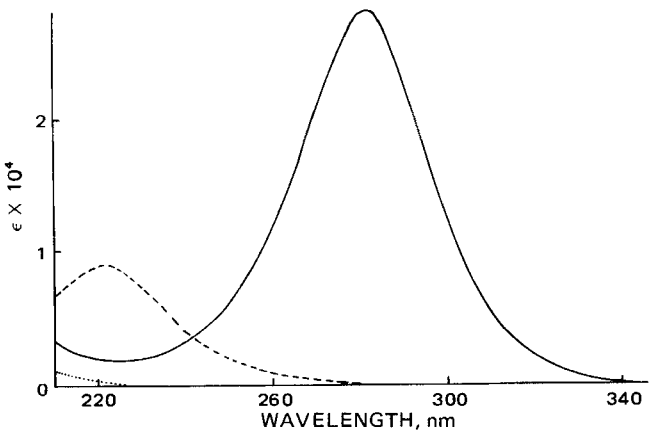

Figure 4—*UV absorption spectra of prostaglandins in 0.1 M sodium phosphate buffer at pH 6.0. Key: ·····, I; - - - -, III; and —, V.*

Table I—Retention Times[a] and Partition Coefficients[b] of Prostaglandins

Prostaglandin	Retention Time, min: Without Cyclodextrin	Retention Time, min: α-Cyclodextrin	Retention Time, min: β-Cyclodextrin	Partition Coefficient
I	8.63	4.15	3.81	1.14
II	7.42	3.93	3.51	0.638
III	23.0	5.63	5.39	80.8
IV	16.3	6.03	4.28	69.4
V	27.3	6.69	9.53	220
VI	22.5	7.67	8.49	192

[a] Chromatographic conditions were the same as in Fig. 1. [b] See text.

Table II—Stability Constants of Prostaglandin–Cyclodextrin Complexes in Water at 25°

Prostaglandin	Stability Constant, M^{-1}: α-Cyclodextrin	Stability Constant, M^{-1}: β-Cyclodextrin
I	1430	1700
III	1300	1400
V	1200	780

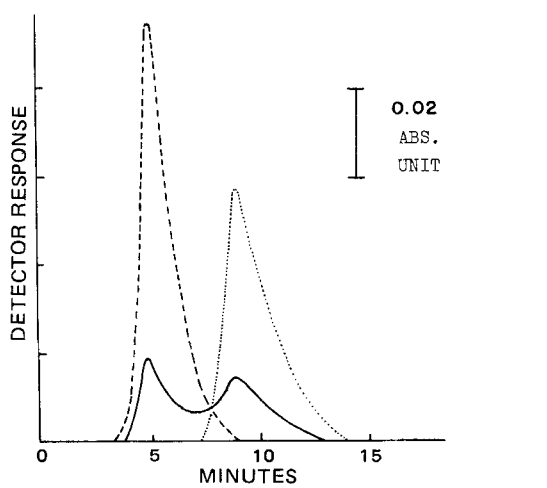

Figure 5—*Separation and detection of III (2.67 μg) and V (1.10 μg) by anion-exchange liquid chromatography using a multiwavelength scanner as the UV detector. Chromatographic conditions were: mobile phase, 0.1 M sodium phosphate buffer with 0.5% β-cyclodextrin (pH 6.0, ionic strength 0.2); and flow rate, 0.5 ml/min. The broken (- - - -), solid (—), and dotted (····) lines were monitored at 221, 254, and 282 nm, respectively.*

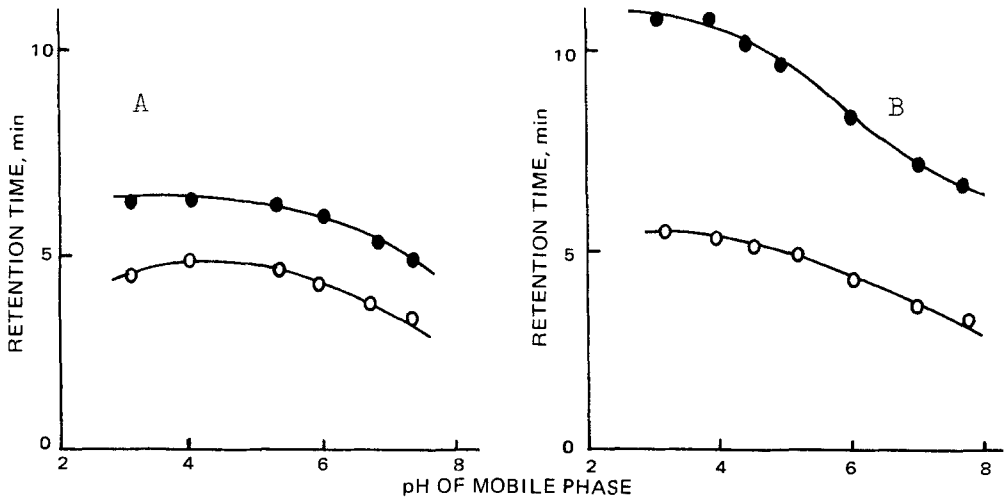

Figure 6—*Effects of pH on the retention times of III and V. Chromatographic conditions were: mobile phase, 0.1* M *sodium phosphate buffer with 0.5% cyclodextrin (ionic strength 0.2); flow rate, 0.5 ml/min; and detection, 221 and 282 nm for III and V, respectively. Key: A, α-cyclodextrin system; B, β-cyclodextrin system;* ○, *III; and* ●, *V.*

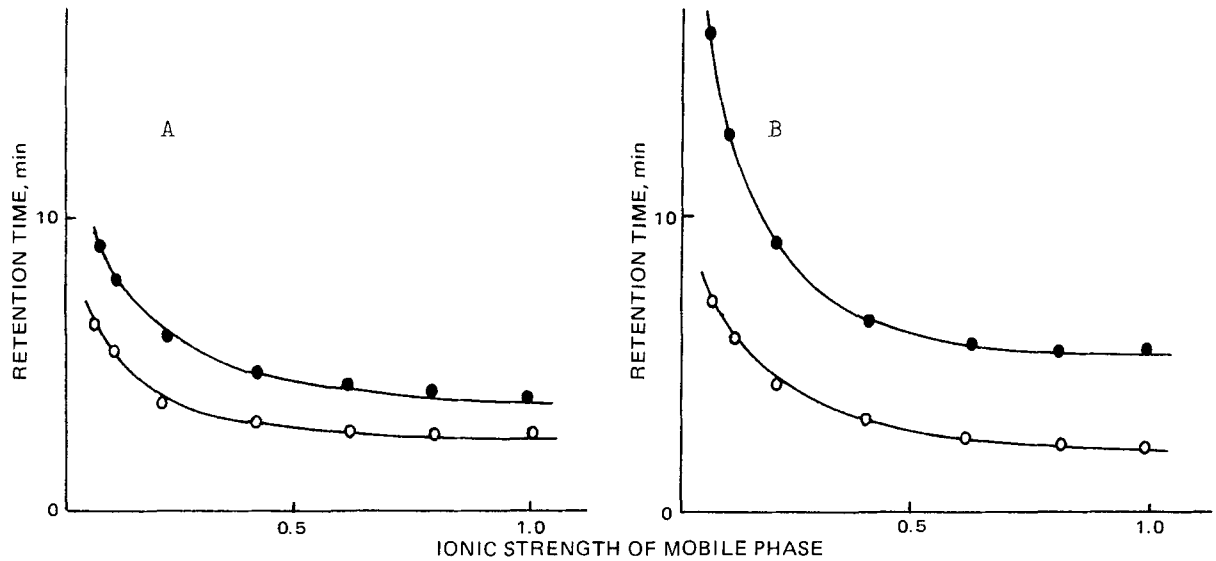

Figure 7—*Effect of ionic strength on the retention times of III and V. Chromatographic conditions were: mobile phase, 0.1* M *sodium phosphate buffer with 0.5% cyclodextrin (pH 6.0); flow rate, 0.5 ml/min; and detection, 221 and 282 nm for III and V, respectively. Key: A, α-cyclodextrin system; B, β-cyclodextrin system;* ○, *III; and* ●, *V.*

compounds, however, is expected to be quite low at 254 nm, as predicted from their molar absorption coefficients (Fig. 4).

The suitable selection of the detection wavelength would provide optimum resolution with higher sensitivity. In this study, A and B prostaglandins were monitored at their UV maximum wavelengths, using a programmable multiwavelength scanner connected to a double-beam spectrophotometer and multipen recorder. The multiwavelength scanner[13] was mapped continuously through a given set of detection wavelengths, and UV absorption data were taken at the desired wavelengths throughout the entire chromatogram.

Figure 5 shows liquid chromatograms of the mixtures of III and V, where their absorbances were monitored at 221, 254, and 282 nm. This method was also applicable to the separation and detection of IV and VI, using the β-cyclodextrin solution as the mobile phase; the resolution was somewhat better than that of III and V. These results indicate that use of the multiwavelength scanner as the detection system is a significant improvement in the separation and quantification of lower levels of prostaglandins compared to ordinary 254 nm detection.

Variations in pH, ionic strength, and solvent composition in the mobile phase were investigated to determine the best operating conditions. Figure 6 shows the effect of pH on the retention times of III and V, where the concentration of cyclodextrin (0.5%) and ionic strength (0.2) were fixed. No attempts were made at pH > 8, since III is susceptible to isomerization at room temperature. The pH–retention time profile showed the general chromatographic behavior of weak acids: the higher the pH, the faster the elution because of ionization of the acids. A lower pH of the eluent gave somewhat better resolution, but this advantage was offset by the longer retention time.

Figure 7 shows the effects of the variations of ionic strength on the retention times of III and V, where the pH and concentration of cyclodextrin were fixed. The mobility of the prostaglandins was increased significantly with an increasing sodium chloride concentration owing to a salting-out effect (14). These results indicate that use of higher pH and greater electrolyte concentration is preferable for the faster elution of prostaglandins.

Retention time also decreased with increasing concentrations of organic solvents such as methanol, ethanol, and acetonitrile in the mobile phase. The presence of higher organic solvent concentrations (about 10% v/v), however, led to undesirable separation behavior, particularly for the α-cyclodextrin systems. This result may be due to the fact that the effective concentration of cyclodextrin decreases with increasing organic solvent because of the interference of inclusion complexation with prostaglandins. The smaller size of the α-cyclodextrin cavity may be particularly susceptible to competitive complexation by solvent as compared with β-cyclodextrin. Combination of β-cyclodextrin with a small amount of organic solvent (less than 5%) as the mobile phase is suggested for the elution of the prostaglandins.

Quantification of Prostaglandins—Linearity of the chromatographic conditions was evaluated by running standard mixtures of various concentrations against their corresponding peak heights. The mobile phase was 0.1 *M* sodium phosphate buffer (pH 6.0 and ionic strength 0.2) containing 0.5% β-cyclodextrin. A linear response was obtained for E, A,

[13] The scanning rate and time interval between data points were 100 nm/sec and 2 sec, respectively.

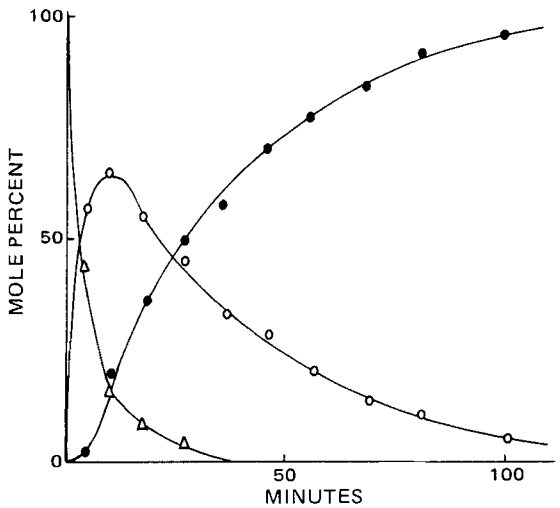

Figure 8—*Reaction profile of base-catalyzed conversion of I to III and V. A solution of I (0.863 mg/ml) in 0.05* M *sodium hydroxide at 30° under a nitrogen stream was periodically subjected to HPLC by direct injection of the alkaline mixture (pH 12.7) sample (4 μl) onto the column. Chromatographic conditions were the same as in Fig. 5. Key: △, I; ○, III; and ●, V.*

and B prostaglandins over concentration ranges of 0–30, 0–5, and 0–3 μg, respectively. In all cases, the correlation coefficient for the linear regression lines was 0.999. The minimum detection quantities of E, A, and B prostaglandins (followed at 210, 221, and 282 nm, respectively) were 150, 30, and 25 ng, respectively, when injected at a recorder range setting of 0.05 aufs.

The developed HPLC system is expected to have great utility in kinetic studies of the degradation of E and A prostaglandins. For example, Fig. 8 shows the reaction profile of base-catalyzed conversion of I to III and V. The rate constants of dehydration (0.267 min^{-1}) and isomerization (0.027 min^{-1}) were obtained by the direct analysis of the reaction species.

The described results were more rapid and sensitive than literature methods.

REFERENCES

(1) N. H. Andersen, *J. Lipid Res.*, **10**, 320 (1969).

(2) D. C. Monkhouse, L. Van Campen, and A. J. Aguiar, *J. Pharm. Sci.*, **62**, 576 (1973).

(3) W. Morozowich, *ibid.*, **63**, 800 (1974).

(4) J. Cohen and J. L. Lach, *ibid.*, **52**, 132 (1963).

(5) J. L. Lach and W. A. Pauli, *ibid.*, **55**, 32 (1966).

(6) A. L. Thakkar, P. B. Kuehn, J. H. Perrin, and W. L. Wilham, *ibid.*, **61**, 1841 (1972).

(7) K. Ikeda, K. Uekama, M. Otagiri, and M. Hatano, *ibid.*, **63**, 1186 (1974).

(8) K. Ikeda, K. Uekama, and M. Otagiri, *Chem. Pharm. Bull.*, **23**, 188, 201 (1975).

(9) Y. Yamada, N. Nambu, and T. Nagai, *ibid.*, **23**, 1205 (1975).

(10) K. Uekama, F. Hirayama, M. Otagiri, K. Ikeda, and K. Inaba, presented at the Pharmaceutics Section, Pharmaceutical Society of Japan, Nishinomiya, Japan, 1975.

(11) T. Higuchi and J. L. Lach, *J. Am. Pharm. Assoc., Sci. Ed.*, **43**, 349 (1954).

(12) S. Bergström, R. Ryhag, B. Samuelsson, and J. Sjorvall, *J. Biol.*, **238**, 3555 (1963).

(13) E. A. Lewis and L. D. Hansen, *J. Chem. Soc. Perkin II*, **1973**, 2081.

(14) K. S. Lee and D. W. Lee, *Anal. Chem.*, **46**, 1903 (1974).

ACKNOWLEDGMENTS AND ADDRESSES

Received January 14, 1976, from the *Faculty of Pharmaceutical Sciences, Kumamoto University, Kumamoto, Japan.*

Accepted for publication July 6, 1976.

The authors are grateful to Ono Pharmaceutical Co. Ltd. and Teijin Ltd. for supplying the materials. They also thank Miss Y. Mitsuda for assistance.

* Present address: Faculty of Pharmaceutical Sciences, Nagoya City University, Nagoya, Japan.

‡ Present address: Ono Pharmaceutical Co. Ltd., Osaka, Japan.

ˣ To whom inquiries should be directed.

Determination of Meclizine Hydrochloride by Ion-Pair Extraction with Methyl Orange

F. S. HOM ˣ and W. R. EBERT

Abstract □ A method, based on ion-pair extraction, is described for the quantification of meclizine hydrochloride in various pharmaceutical dosage forms, for content uniformity determination, and for concentration monitoring in dissolution and bioavailability studies. Methyl orange, dissolved in pH 2.8 MacIlvaine buffer, gave excellent recovery of meclizine after its isolation from aqueous solutions of gelatin, urine, and blood serum. The chloroform-extracted molecular species appeared to be a 1:1 ion-pair. Beer's law was obeyed for a wide concentration range. Because the extracted species seemed well defined and stable and since a surface or an interphase adsorption phenomenon was not a problem, the reported method is considered sensitive, accurate, precise, rapid, and simple.

Keyphrases □ Meclizine hydrochloride—spectrophotometric analysis using ion-pair extraction with methyl orange, pharmaceutical dosage forms and biological fluids □ Ion-pairs—meclizine hydrochloride–methyl orange, spectrophotometric analysis, pharmaceutical dosage forms and biological fluids □ Spectrophotometry—analysis, meclizine hydrochloride using ion-pair extraction with methyl orange, pharmaceutical dosage forms and biological fluids □ Antiemetics—meclizine hydrochloride, spectrophotometric analysis using ion-pair extraction with methyl orange, pharmaceutical dosage forms and biological fluids

Meclizine hydrochloride USP (1), an antiemetic, has been used in the management of motion sickness for many years. All available methods cited by Wong *et al.* (2), including the official ones (1), that are used for the determination of meclizine are not suitable or convenient for the rapid assay of numerous small quantities of the drug

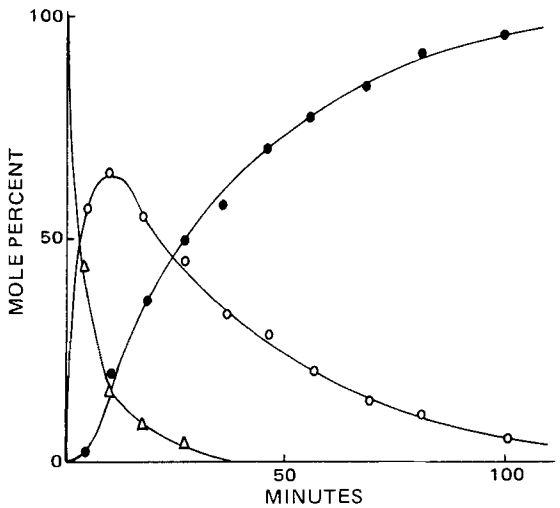

Figure 8—*Reaction profile of base-catalyzed conversion of I to III and V. A solution of I (0.863 mg/ml) in 0.05* M *sodium hydroxide at 30° under a nitrogen stream was periodically subjected to HPLC by direct injection of the alkaline mixture (pH 12.7) sample (4 μl) onto the column. Chromatographic conditions were the same as in Fig. 5. Key: △, I; ○, III; and ●, V.*

and B prostaglandins over concentration ranges of 0–30, 0–5, and 0–3 μg, respectively. In all cases, the correlation coefficient for the linear regression lines was 0.999. The minimum detection quantities of E, A, and B prostaglandins (followed at 210, 221, and 282 nm, respectively) were 150, 30, and 25 ng, respectively, when injected at a recorder range setting of 0.05 aufs.

The developed HPLC system is expected to have great utility in kinetic studies of the degradation of E and A prostaglandins. For example, Fig. 8 shows the reaction profile of base-catalyzed conversion of I to III and V. The rate constants of dehydration (0.267 min^{-1}) and isomerization (0.027 min^{-1}) were obtained by the direct analysis of the reaction species.

The described results were more rapid and sensitive than literature methods.

REFERENCES

(1) N. H. Andersen, *J. Lipid Res.*, **10**, 320 (1969).

(2) D. C. Monkhouse, L. Van Campen, and A. J. Aguiar, *J. Pharm. Sci.*, **62**, 576 (1973).

(3) W. Morozowich, *ibid.*, **63**, 800 (1974).

(4) J. Cohen and J. L. Lach, *ibid.*, **52**, 132 (1963).

(5) J. L. Lach and W. A. Pauli, *ibid.*, **55**, 32 (1966).

(6) A. L. Thakkar, P. B. Kuehn, J. H. Perrin, and W. L. Wilham, *ibid.*, **61**, 1841 (1972).

(7) K. Ikeda, K. Uekama, M. Otagiri, and M. Hatano, *ibid.*, **63**, 1186 (1974).

(8) K. Ikeda, K. Uekama, and M. Otagiri, *Chem. Pharm. Bull.*, **23**, 188, 201 (1975).

(9) Y. Yamada, N. Nambu, and T. Nagai, *ibid.*, **23**, 1205 (1975).

(10) K. Uekama, F. Hirayama, M. Otagiri, K. Ikeda, and K. Inaba, presented at the Pharmaceutics Section, Pharmaceutical Society of Japan, Nishinomiya, Japan, 1975.

(11) T. Higuchi and J. L. Lach, *J. Am. Pharm. Assoc., Sci. Ed.*, **43**, 349 (1954).

(12) S. Bergström, R. Ryhag, B. Samuelsson, and J. Sjorvall, *J. Biol.*, **238**, 3555 (1963).

(13) E. A. Lewis and L. D. Hansen, *J. Chem. Soc. Perkin II*, **1973**, 2081.

(14) K. S. Lee and D. W. Lee, *Anal. Chem.*, **46**, 1903 (1974).

ACKNOWLEDGMENTS AND ADDRESSES

Received January 14, 1976, from the *Faculty of Pharmaceutical Sciences, Kumamoto University, Kumamoto, Japan.*

Accepted for publication July 6, 1976.

The authors are grateful to Ono Pharmaceutical Co. Ltd. and Teijin Ltd. for supplying the materials. They also thank Miss Y. Mitsuda for assistance.

* Present address: Faculty of Pharmaceutical Sciences, Nagoya City University, Nagoya, Japan.

‡ Present address: Ono Pharmaceutical Co. Ltd., Osaka, Japan.

ˣ To whom inquiries should be directed.

Determination of Meclizine Hydrochloride by Ion-Pair Extraction with Methyl Orange

F. S. HOM ˣ and W. R. EBERT

Abstract □ A method, based on ion-pair extraction, is described for the quantification of meclizine hydrochloride in various pharmaceutical dosage forms, for content uniformity determination, and for concentration monitoring in dissolution and bioavailability studies. Methyl orange, dissolved in pH 2.8 MacIlvaine buffer, gave excellent recovery of meclizine after its isolation from aqueous solutions of gelatin, urine, and blood serum. The chloroform-extracted molecular species appeared to be a 1:1 ion-pair. Beer's law was obeyed for a wide concentration range. Because the extracted species seemed well defined and stable and since a surface or an interphase adsorption phenomenon was not a problem, the reported method is considered sensitive, accurate, precise, rapid, and simple.

Keyphrases □ Meclizine hydrochloride—spectrophotometric analysis using ion-pair extraction with methyl orange, pharmaceutical dosage forms and biological fluids □ Ion-pairs—meclizine hydrochloride–methyl orange, spectrophotometric analysis, pharmaceutical dosage forms and biological fluids □ Spectrophotometry—analysis, meclizine hydrochloride using ion-pair extraction with methyl orange, pharmaceutical dosage forms and biological fluids □ Antiemetics—meclizine hydrochloride, spectrophotometric analysis using ion-pair extraction with methyl orange, pharmaceutical dosage forms and biological fluids

Meclizine hydrochloride USP (1), an antiemetic, has been used in the management of motion sickness for many years. All available methods cited by Wong *et al.* (2), including the official ones (1), that are used for the determination of meclizine are not suitable or convenient for the rapid assay of numerous small quantities of the drug

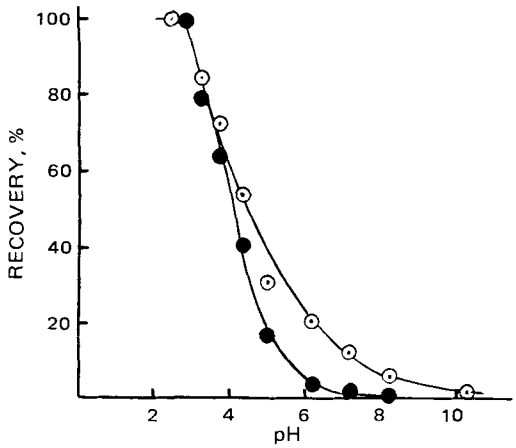

Figure 1—*Meclizine recovery pH profile after 150-ml chloroform extraction of 150-ml aqueous solution containing 2.0 × 10^{-5} M meclizine citrate, 7.6 × 10^{-5} M methyl orange, and 0.1 M dibasic sodium phosphate, which was made alkaline with sodium hydroxide and the pH was adjusted with citric acid. Key: ⊙, total meclizine extracted; and ●, meclizine extracted as methyl orange ion-pair.*

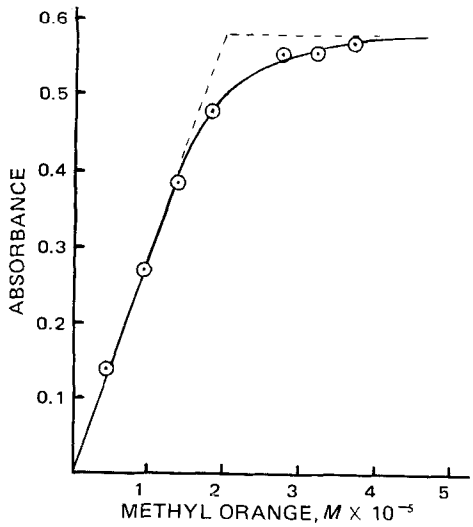

Figure 2—*Absorbance of the chloroform extract at 422 nm as a function of the methyl orange concentration with a constant 2 × 10^{-5} M meclizine in the aqueous layer.*

samples. For the Wong *et al.* (2) GLC method to be applicable to the present case, the small amounts of the isolated drug must be concentrated to a small volume, which is inconvenient.

Narrod *et al.* (3) used a modification of a literature method (4) in their study of the metabolism of meclizine in the rat. Their modified technique apparently worked well, but they experienced extraction and recovery problems. Similar analytical problems prompted the study of the chloroform extraction of meclizine from aqueous solutions (5) and the development of the present method.

EXPERIMENTAL

Apparatus—A spectrophotometer[1], matched 1-cm cells, a pH meter[2], and a rotating bottle (6) or the NF *in vitro* test apparatus (7) were used.

Reagents—USP meclizine hydrochloride reference standard, meclizine hydrochloride[3], type B gelatin[4], 25-mg meclizine hydrochloride tablets[5] and capsules[6], and analytical reagent grades of methyl orange[7], chloroform, citric acid monohydrate, dibasic sodium phosphate dodecahydrate, potassium chloride, anhydrous sodium sulfate, hydrochloric acid, and sodium hydroxide were used as received.

Methyl Orange Solution—Dissolve 250 mg of methyl orange and dilute to 1 liter with distilled water.

McIlvaine Buffer (8)—For Stock Solution A (0.2 *M*), dissolve 71.63 g of dibasic sodium phosphate dodecahydrate and dilute to 1 liter with distilled water. For Stock Solution B (0.1 *M*), dissolve 21.01 g of citric acid monohydrate and dilute to 1 liter with distilled water. To prepare pH 2.8 buffer, transfer 158 ml of Stock Solution A into a 1-liter volumetric flask and dilute to volume with Stock Solution B. Mix well and check and adjust pH, if necessary, with more Stock Solution A or B. Do not contaminate the pH 2.8 buffer solution with chloride ions from the electrode.

Reagent Solution—Dilute 100 ml of methyl orange solution to 1 liter with pH 2.8 buffer solution and mix well.

Standard Preparation—Dissolve 25 mg of USP meclizine hydrochloride reference standard, accurately weighed, by warming on a steam bath, if necessary, and dilute with 0.1 *N* HCl to volume in a 200-ml volumetric flask. Further dilute 10.0 ml with 0.1 *N* HCl to volume in a 200-ml volumetric flask.

Sample Preparation—Dissolve a sufficient sample equivalent to 25 mg of meclizine hydrochloride in 0.1 *N* HCl by warming on a steam bath, if necessary, so that the final solution contains a concentration of about 6.25 μg/ml. Adjust the pH of the solution with hydrochloric acid to a value of 1 or less.

Procedure—Concomitantly pipet 25.0-ml aliquots of standard and sample solutions into respective separators. Extract with 25 ml of chloroform by shaking for about 1 min. Allow the phases to separate and discard the aqueous layer. Wash the chloroform phase with 25 ml of 1 *N* NaOH by shaking for about 1 min and collect the chloroform layer into a 25-ml volumetric flask. Add more chloroform through the separator, if necessary, to bring to volume and mix well. Pipet 10.0-ml aliquots of the chloroform solutions into clean dry separators and use 10.0 ml of chloroform for the reagent blank. Add 20 ml of reagent solution to each. Shake each separator for about 1 min and allow the phases to separate.

Determine the absorbance of the chloroform extract at 422 nm *versus* the reagent blank in a suitable spectrophotometer after drying the extract with 1 g of anhydrous sodium sulfate. Calculate the amount of meclizine hydrochloride, in milligrams, in the sample by using:

$$\text{mg/sample} = \frac{4CA_u}{A_s} \qquad \text{(Eq. 1)}$$

where A_u and A_s are the absorbance values of the sample and standard, respectively; and C is the concentration of the standard solution in micrograms per milliliter.

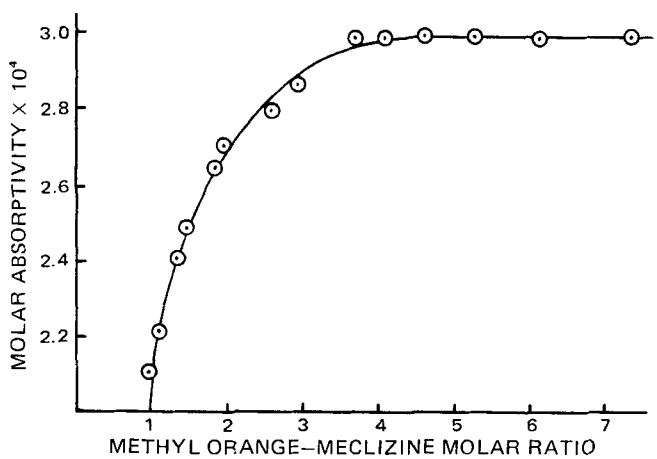

Figure 3—*Molar absorptivity of the chloroform extract at 422 nm as a function of the methyl orange to meclizine molar ratio in the aqueous layer.*

[1] Beckman model DU.
[2] Beckman Zeromatic.
[3] Napp Chemicals, Inc.
[4] Rousselot Corp.
[5] Bonine chewable tablets, 25 mg, Pfizer No. 24419.
[6] Meclizine hydrochloride gelatin capsules, 25 mg, R. P. Scherer, E-9736.
[7] Baker Chemical Co.

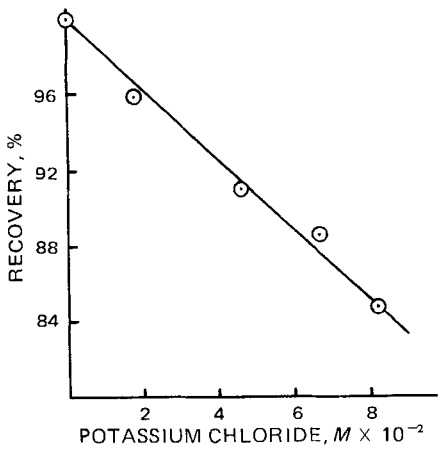

Figure 4—*Effect of chloride concentration on the percent recovery of meclizine.*

RESULTS AND DISCUSSION

It was necessary to study the effects of pH, various ions, and buffer systems to find an optimum condition for the chloroform extraction of meclizine with methyl orange (5). Figure 1 shows the percent meclizine extracted into chloroform from a citric acid–sodium phosphate–sodium hydroxide system as a function of pH (from basic to acidic). The open circles represent the total amounts of meclizine extracted into the chloroform layer, and the closed circles represent that portion extracted as the methyl orange ion-pair.

Absorbance reading at the 422-nm wavelength of the original chloroform extract from a given pH value only showed the amount of meclizine extracted as the methyl orange ion-pair (closed circles). The amount of meclizine extracted other than as the methyl orange ion-pair was visualized by a subsequent treatment of the original chloroform extract with an excess of reagent solution. The absorbance reading of the resulting chloroform layer represents the total meclizine extracted (open circles). The difference in the two curves between pH values of 4 and 10 is meclizine extracted possibly as the free base or as other ion-pairs. The shapes of the two curves indicate an apparent anomalous behavior because meclizine, an amine, should be extracted into chloroform rapidly and completely at the higher pH values but is not, probably because of the insolubility of meclizine in water (9).

This observed behavior is not reversible: if the system is made basic again, the meclizine remains in the chloroform layer. Apparently the rapid addition of alkali causes the meclizine in solution to form a colloidal suspension in water, making the complete chloroform extraction difficult and slow. Therefore, the observed difficulty may be a physical interphase phenomenon rather than a chemical one. To circumvent this difficulty, a method based on the chloroform extraction at pH 2.8, where all of the meclizine is extracted in the form of methyl orange ion-pairs, was developed.

Figure 2 is a plot of absorbance of the chloroform extract at 422 nm as a function of the methyl orange concentration with a constant 2×10^{-5} *M* meclizine in the aqueous layer. The extrapolation of the linear portions of the curve gives an intersect at about the 2×10^{-5} *M* methyl orange point, indicating an apparent 1:1 ion-pair of methyl orange to meclizine. However, a molar ratio greater than 1 must be used for the complete meclizine extraction, as indicated by the curve leveling off slowly after the intersect.

Figure 3 shows the molar absorptivity at 422 nm as a function of the methyl orange to meclizine molar ratio. As can be seen, a value of about 4 or greater is required before a constant molar absorptivity of about 2.91×10^4 is obtained. Unfortunately, Narrod *et al.* (3) did not give a value for this comparison. However, Chatten and Okamura (10) listed molar absorptivities for eight methyl orange ion-pairs ranging from 2.36 to 3.24×10^4. Their mean was 2.81 with a standard deviation of 0.33×10^4, which is close to the present value of about 2.91×10^4.

A typical Beer's law plot of absorbance at 422 nm *versus* meclizine concentration is linear if the methyl orange to meclizine molar ratio is 4 or greater and the system is freed of ions or molecules that can also form ion-pairs with meclizine or methyl orange. Figure 4 shows the effect of the chloride ion on the percent recovery of meclizine as the methyl orange ion-pair. The chloride ion competes with methyl orange to form an ion-pair with meclizine. For this reason, meclizine is converted to the free base to eliminate interfering ions before it is allowed to form the ion-pair with methyl orange.

Since this is an acid–dye method, color change could be a problem; however, the methyl orange–meclizine ion-pair in chloroform at these concentration levels was stable for 6 hr or longer, provided the chloroform was kept from evaporating. Methyl orange in the range from 2.95 to 29.5 mg/liter when dissolved in pH 2.8 McIlvaine buffer was stable for 2 weeks or longer, as shown by the constancy of the absorbance at 505 nm *versus* time in days. One fault with this reagent solution is that it supports mold growth. However, the reagent solution may be filtered and washed with chloroform before use. The absorbance of the reagent blank is zero or near zero and is unique for a colorimetric method of this type. Another property worth pointing out is surface or interphase adsorption. This phenomenon is a common source of difficulty in this type of analytical technique but is not a problem in the present method.

The extraction interphase is clean to the naked eye, perhaps the result of the use of rather dilute solutions. Glassware shows no sign of surface adsorption; consequently, special cleaning and handling are not necessary. Since methyl orange in solution exists in several forms, one has the choice of which form to use for the final absorbance reading. The cationic form has about a 30% advantage in sensitivity over the anionic form. However, use of the cationic form for the final absorbance reading requires an extra step in the procedure. For most purposes, this additional sensitivity is not necessary or worth the added effort. All recovery results reported were made on the anionic form of methyl orange.

Precision and Accuracy—Table I lists the replicate recovery results of 100 μg of meclizine hydrochloride from 20-ml solutions of water, 0.125% type B gelatin, and 50% urine. The mean recovery was from 97.0 to 100.2% of theory with a less than 1% *RSD*. Table II shows the replicate recovery results of 20 μg of meclizine hydrochloride from 20-ml solutions of water, 0.125% type B gelatin, 50% urine, and 10% blood serum. The mean recovery was from 98.5 to 99.5% of theory with a relative standard deviation of 2.5% or less. Gelatin binding of meclizine may have been the reason for the lower recovery in both cases. Table III summarizes the results on content uniformity determination of meclizine hydrochloride from 25-mg

Table I—Recovery Results of 100 μg of Meclizine Hydrochloride from 20-ml Solutions

	Wafer	0.125% Gelatin	50% Urine
	99.7	97.0	100.0
	99.7	96.0	99.4
	101.0	98.0	100.3
	99.7	97.4	99.4
	100.7	96.4	101.3
Mean ± *SD*	100.2 ± 0.6	97.0 ± 0.8	100.1 ± 0.8

Table II—Recovery Results of 20 μg of Meclizine Hydrochloride from 20-ml Solutions

	Water	0.125% Gelatin	50% Urine	10% Blood Serum
	20.0	19.5	19.7	19.2
	19.0	19.7	20.0	20.2
	20.2	20.0	19.8	20.3
	20.2	20.3	20.3	20.0
	19.8	19.2	19.4	19.7
Mean ± *SD*	19.8 ± 0.5	19.7 ± 0.5	19.8 ± 0 5	19.9 ± 0.4

Table III—Results from Content Uniformity Determinations of Meclizine Hydrochloride in Tablets and Solid Gelatin Capsules

	Milligrams per Tablet	Milligrams per Capsule
	26.0	24.4
	26.7	25.3
	25.9	25.2
	27.0	25.3
	27.3	25.5
Mean ± *SD*	26.5 ± 1.0	25.1 ± 0.4

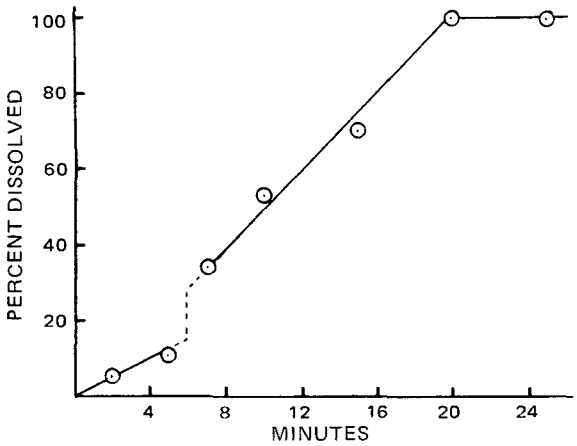

Figure 5—*Dissolution of meclizine hydrochloride from a 25-mg solid gelatin capsule in simulated gastric fluid (without pepsin) at 37° using the rotating-bottle method.*

solid gelatin capsules and 25-mg tablets. The mean recovery was 100.4 and 106.0% of labeled claim with relative standard deviations of 1.6 and 4.0%, respectively.

Figure 5 shows the dissolution of meclizine hydrochloride from a 25-mg solid gelatin capsule in simulated gastric fluid (without pepsin) at 37° using the rotating-bottle method (6,7). The initial portion of the curve represents the dissolution of the drug from the shell. When the shell dissolved, the slope of the curve changed from the dissolution of meclizine hydrochloride in the lesser concentrated shell to the more concentrated core. The core completely dissolved after about 20 min and the curve leveled off.

REFERENCES

(1) "The United States Pharmacopeia," 19th rev., Mack Publishing Co., Easton, Pa., 1975, p. 298.

(2) C. K. Wong, J. R. Urbigkit, N. Conca, D. M. Cohen, and K. P. Munnelly, *J. Pharm. Sci.*, **62**, 1340 (1973).

(3) S. A. Narrod, A. L. Wilk, and C. T. G. King, *J. Pharmacol. Exp. Ther.*, **147**, 380 (1965).

(4) B. B. Brodie and S. Udenfriend, *J. Biol. Chem.*, **158**, 705 (1945).

(5) F. S. Hom, "A Study of the Chloroform Extraction of Meclizine from Aqueous Solutions," presented at the First Detroit Anachem Symposium, Dearborn, Mich., Oct. 12, 1973.

(6) F. S. Hom and J. J. Miskel, *J. Pharm. Sci.*, **59**, 827 (1970).

(7) "The National Formulary," 14th ed., Mack Publishing Co., Easton, Pa., 1975, p. 985.

(8) "Lange's Handbook of Chemistry," rev. 10th ed., N. A. Lange, Ed., McGraw-Hill, New York, N. Y., 1967, p. 972.

(9) B. H. Berg, *Med. Norsk. Farm. Selskap.*, **30**, 155 (1968); through *Int. Pharm. Abstr.*, **6** (8), Abst. 1361, Apr. 30 (1969).

(10) L. G. Chatten and K. O. Okamura, *J. Pharm. Sci.*, **62**, 1328 (1973).

ACKNOWLEDGMENTS AND ADDRESSES

Received September 8, 1975, from the *Research and Development Department, R. P. Scherer Corp., Detroit, MI 48213.*

Accepted for publication July 16, 1976.

Presented at the First Detroit Anachem Symposium, Dearborn, Mich., October 12, 1973.

[x] To whom inquiries should be directed.

Recording pH Method of Characterizing Composition and Monitoring Dissolution Profile of an Anhydride–Acid Copolymer and Its Salt Derivatives

YEHCHUN MO, GARNET E. PECK, ALLEN HEYD, and GILBERT S. BANKER [x]

Abstract □ A sensitive potentiometric monitoring method was developed that permits the continuous measurement of the dissolution profiles of methyl vinyl ether–maleic anhydride–acid copolymers and salt derivatives. Three distinct rate periods were observed in the dissolution of the anhydride copolymer. The relative dissolution rate of the anhydride copolymer, expressed as percent anhydride dissolved, was independent of sample weight over the weight range studied. The acid form of the copolymer showed only one dissolution rate period, with dissolution being very rapid. The rapid initial pH decrease observed during the first stage of dissolution for a series of anhydride–acid copolymer powder samples correlated closely with the anhydride–acid ratio, permitting chemical characterization of the copolymer functionality simultaneously with the analysis of dissolution profiles. Similarly, the extent of copolymer alkaline salt conversion was inversely proportional to the initial maximum pH increase observed during the first stage of dissolution of these salts. Mechanisms of dissolution of copolymer powder materials are discussed and compared to the dissolution of compressed disks and films reported previously.

Keyphrases □ Maleic anhydride–acid copolymers—with methyl vinyl ether, potentiometric characterization of composition and measurement of dissolution profiles □ Methyl vinyl ether–maleic anhydride–acid copolymers—potentiometric characterization of composition and measurement of dissolution profiles □ Copolymers—methyl vinyl ether–maleic anhydride–acid, potentiometric characterization of composition and measurement of dissolution profiles □ Potentiometry—characterization of composition and measurement of dissolution profiles of methyl vinyl ether–maleic anhydride–acid copolymers □ Dissolution—methyl vinyl ether–maleic anhydride–acid copolymers, potentiometric measurement of profiles

Alkyl, aryl, and alkyl vinyl ether–maleic anhydride copolymers, their hydrolyzed acids, and various ester derivatives have been recommended for various pharmaceutical applications, including use as thickeners, suspension and emulsion stabilizers, topical product and cosmetic vehicles, complexing agents of iodine and other antiseptics, controlled-release matrixes, and protective, delayed-, or controlled-release coatings (1–4). Styrene,

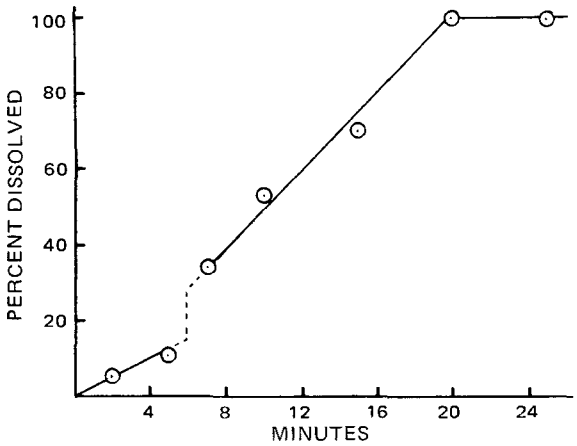

Figure 5—*Dissolution of meclizine hydrochloride from a 25-mg solid gelatin capsule in simulated gastric fluid (without pepsin) at 37° using the rotating-bottle method.*

solid gelatin capsules and 25-mg tablets. The mean recovery was 100.4 and 106.0% of labeled claim with relative standard deviations of 1.6 and 4.0%, respectively.

Figure 5 shows the dissolution of meclizine hydrochloride from a 25-mg solid gelatin capsule in simulated gastric fluid (without pepsin) at 37° using the rotating-bottle method (6,7). The initial portion of the curve represents the dissolution of the drug from the shell. When the shell dissolved, the slope of the curve changed from the dissolution of meclizine hydrochloride in the lesser concentrated shell to the more concentrated core. The core completely dissolved after about 20 min and the curve leveled off.

REFERENCES

(1) "The United States Pharmacopeia," 19th rev., Mack Publishing Co., Easton, Pa., 1975, p. 298.

(2) C. K. Wong, J. R. Urbigkit, N. Conca, D. M. Cohen, and K. P. Munnelly, *J. Pharm. Sci.*, **62**, 1340 (1973).

(3) S. A. Narrod, A. L. Wilk, and C. T. G. King, *J. Pharmacol. Exp. Ther.*, **147**, 380 (1965).

(4) B. B. Brodie and S. Udenfriend, *J. Biol. Chem.*, **158**, 705 (1945).

(5) F. S. Hom, "A Study of the Chloroform Extraction of Meclizine from Aqueous Solutions," presented at the First Detroit Anachem Symposium, Dearborn, Mich., Oct. 12, 1973.

(6) F. S. Hom and J. J. Miskel, *J. Pharm. Sci.*, **59**, 827 (1970).

(7) "The National Formulary," 14th ed., Mack Publishing Co., Easton, Pa., 1975, p. 985.

(8) "Lange's Handbook of Chemistry," rev. 10th ed., N. A. Lange, Ed., McGraw-Hill, New York, N. Y., 1967, p. 972.

(9) B. H. Berg, *Med. Norsk. Farm. Selskap.*, **30**, 155 (1968); through *Int. Pharm. Abstr.*, **6** (8), Abst. 1361, Apr. 30 (1969).

(10) L. G. Chatten and K. O. Okamura, *J. Pharm. Sci.*, **62**, 1328 (1973).

ACKNOWLEDGMENTS AND ADDRESSES

Received September 8, 1975, from the *Research and Development Department, R. P. Scherer Corp., Detroit, MI 48213.*

Accepted for publication July 16, 1976.

Presented at the First Detroit Anachem Symposium, Dearborn, Mich., October 12, 1973.

[x] To whom inquiries should be directed.

Recording pH Method of Characterizing Composition and Monitoring Dissolution Profile of an Anhydride–Acid Copolymer and Its Salt Derivatives

YEHCHUN MO, GARNET E. PECK, ALLEN HEYD, and GILBERT S. BANKER [x]

Abstract □ A sensitive potentiometric monitoring method was developed that permits the continuous measurement of the dissolution profiles of methyl vinyl ether–maleic anhydride–acid copolymers and salt derivatives. Three distinct rate periods were observed in the dissolution of the anhydride copolymer. The relative dissolution rate of the anhydride copolymer, expressed as percent anhydride dissolved, was independent of sample weight over the weight range studied. The acid form of the copolymer showed only one dissolution rate period, with dissolution being very rapid. The rapid initial pH decrease observed during the first stage of dissolution for a series of anhydride–acid copolymer powder samples correlated closely with the anhydride–acid ratio, permitting chemical characterization of the copolymer functionality simultaneously with the analysis of dissolution profiles. Similarly, the extent of copolymer alkaline salt conversion was inversely proportional to the initial maximum pH increase observed during the first stage of dissolution of these salts. Mechanisms of dissolution of copolymer powder materials are discussed and compared to the dissolution of compressed disks and films reported previously.

Keyphrases □ Maleic anhydride–acid copolymers—with methyl vinyl ether, potentiometric characterization of composition and measurement of dissolution profiles □ Methyl vinyl ether–maleic anhydride–acid copolymers—potentiometric characterization of composition and measurement of dissolution profiles □ Copolymers—methyl vinyl ether–maleic anhydride–acid, potentiometric characterization of composition and measurement of dissolution profiles □ Potentiometry—characterization of composition and measurement of dissolution profiles of methyl vinyl ether–maleic anhydride–acid copolymers □ Dissolution—methyl vinyl ether–maleic anhydride–acid copolymers, potentiometric measurement of profiles

Alkyl, aryl, and alkyl vinyl ether–maleic anhydride copolymers, their hydrolyzed acids, and various ester derivatives have been recommended for various pharmaceutical applications, including use as thickeners, suspension and emulsion stabilizers, topical product and cosmetic vehicles, complexing agents of iodine and other antiseptics, controlled-release matrixes, and protective, delayed-, or controlled-release coatings (1–4). Styrene,

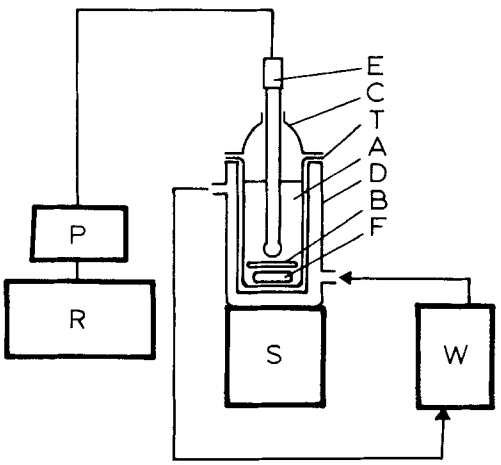

Figure 1—*Continuous pH-monitoring apparatus designed to record the dissolution processes of copolymer samples. Key: A, test solution; B, baffle plate; C, plastic cover; D, double-walled chamber; E, combination electrode; F, floating stirring bar; P, pH meter; R, recorder; S, magnetic stirrer; T, thin-walled beaker; and W, thermostat.*

ethylene, and various alkyl vinyl ether–maleic anhydride copolymers were studied extensively as delayed and enteric coatings (5–11), and some are now used commercially. Due to the reported low toxicity of this polymer class and its increasing acceptance in cosmetic and food applications, the importance and use of these materials in drug products probably will expand.

The dissolution of alkyl vinyl ether–maleic anhydride copolymers and ester derivatives from compressed disk and film structures, using an immersion refractometry method, was reported (12). Previously, Heyd *et al.* (13, 14) discussed the immersion refractometry method, studied the dissolution of a series of ethylene maleic anhydride and acid copolymers, and examined the surface phenomena associated with polymer dissolution. The dissolution of the anhydride copolymer as a compressed disk went through an induction period comprised of a lag time (no solute in solution), a stabilization period (rate of dissolution was nonlinear), and then a linear dissolution rate period (14). These periods were subsequently related to solvent penetration into the compressed disk and initial polymer swelling (the lag time), the formation of a hydrated layer on the disk surface and the attainment of a maximum hydrated layer thickness (the stabilization period), and a constant dissolution rate (polymer chain diffusion out of the hydrated layer probably being the rate-limiting step). Woodruff *et al.* (12) examined the effect of the degree of alkyl esterification of the alkyl vinyl ether–maleic acid copolymer and the effect of alkyl chain length of the ether substituent on dissolution properties of compressed disks. The dissolution of film structures was also characterized, and the effect of formulation factors such as the presence and concentration of plasticizers was examined.

While immersion refractometry provides a simple method of following polymer dissolution, it does not readily lend itself to continuous monitoring procedures. The method is also most applicable to polymer structures (compressed disks, matrixes, and films), but it lacks sensitivity at low polymer concentrations and has been of limited use in evaluating the dissolution characteristics of powdered polymer samples. This investigation was undertaken to develop a continuous dissolution monitoring method for anhydride–acid copolymers utilizing standard laboratory equipment. Additional objectives were to study powdered polymer materials, to examine the effect of the anhydride–acid ratio and the extent of alkaline salt formation on copolymer dissolution characteristics, and to find additional methods of characterizing these copolymers as to the anhydride–acid ratio or the extent of salt formation.

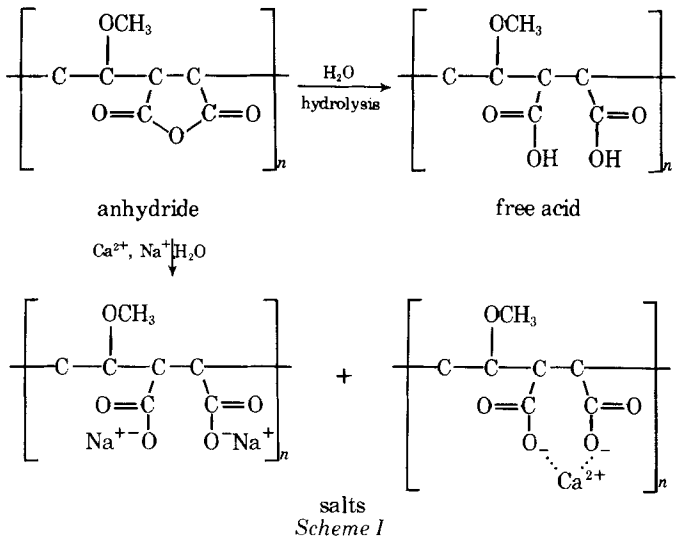

Scheme I

EXPERIMENTAL

Materials—The free acid of the copolymer[1] (mol. wt. 1,125,000) of methyl vinyl ether and maleic anhydride (Scheme I) was prepared by completely dissolving the anhydride copolymer [assayed purity = 99.9% using potentiometric method (12)] in water to produce the totally hydrolyzed free acid, which was then lyophilized to a white dry powder. The alkaline salt of this copolymer was produced in an aqueous solution, and the resultant copolymer salt was dried utilizing lyophilization. All copolymer samples were subjected to a sieve treatment, and the fraction of each sample in the 60–100-mesh cut (150–250 μm) was used.

Continuous Potentiometric Monitoring Apparatus—Figure 1 outlines the setup for the continuous potentiometric monitoring apparatus. The changing pH of the test solution (A) was monitored continuously using a calomel–glass combination electrode[2] (E) connected to a pH meter[3] (P) equipped with a 25.4-cm chart recorder[4]. Double-deionized water (50 ml) was pipetted into the thin-walled beaker (T), which was then fitted into the double-walled chamber (D). Water, at a constant temperature (37 ± 1°) controlled by a thermostat[5] (W), was circulated through the double-walled chamber to maintain the test solution at a constant temperature. For each test, the electrode (E) was introduced into the test solution to a fixed depth of 2 cm below the surface of solution.

A 2 × 1-cm "floating" stirring bar[6] (F), equipped with baffles (B), was placed in the bottom of the beaker and operated at a constant stirring rate (455 ± 10 rpm), which was verified with a strobe light. The floating stirring bar was used to avoid the grinding or the milling of the undissolved copolymer particles by the normal stirring operation; the baffles served to furnish a more smooth and homogeneous agitation as well as a more stable reading on the pH meter. A plastic cover (C) was placed on the top of the beaker to reduce evaporation and to avoid contamination during a prolonged dissolution monitoring process.

The pH meter was calibrated with standard pH buffer solutions. The recording chart of the recorder was adjusted to give a full scale of 5 (pH 2.0–7.0) or 10 (pH 2.0–12.0) pH units for the dissolution study of the anhydride or the alkaline salt copolymer sample, respectively.

[1] General Aniline & Film Co., New York, N.Y.
[2] Sargent-Welch, McGaw Hill, Ill.
[3] LSX, Sargent-Welch, McGaw Hill, Ill.
[4] SRG, Sargent-Welch, McGaw Hill, Ill.
[5] Heto Co. (Denmark), London Co., Westlake, Ohio.
[6] Spectroderm International, Inc., Fairfax, Va.

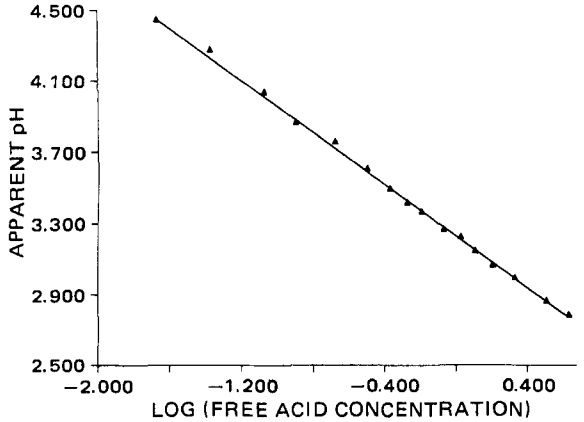

Figure 2—*Correlation of apparent pH values and logarithm values of the corresponding free acid concentrations of the copolymer standard solutions. Linear regression analysis produced a correlation coefficient of 0.998 over a concentration range of the free acid between 0.02 and 4.5 mg/ml.*

Quantitative Standardization of Copolymer Free Acid Solution—A copolymer free acid solution with an approximate concentration of 4.5 mg/ml was accurately prepared and potentiometrically titrated with a 0.1 *N* NaOH standard solution to determine its concentration quantitatively. An automatic titration system was used[7]. The free acid concentration was calculated as:

$$C_2\,(\text{mg/ml}) = \frac{174 \times N_1 \times V_1\,(\text{ml})}{V_2\,(\text{ml})} \qquad \text{(Eq. 1)}$$

where N_1 and V_1 are the normality and the amount of the sodium hydroxide standard solution consumed, respectively, and V_2 is the volume of the free acid sample solution.

RESULTS AND DISCUSSION

Correlation of Apparent pH Values with Copolymer Free Acid Concentrations in Aqueous Solutions—A series of standard copolymer free acid solutions (0.02–4.5 mg/ml) was prepared by diluting the standardized free acid solution with double-deionized water. The apparent pH value of 50 ml of each free acid solution was measured using the continuous pH-monitoring apparatus (Fig. 1) as described under *Experimental.* A linear calibration curve (r = 0.998) was observed when the measured apparent pH values of the free acid solutions were plotted against the logarithm of the corresponding concentrations (Fig. 2). The pH–concentration relationship may be expressed as:

$$\text{pH} = 3.2393 - 0.7382 \times \log\,(\text{free acid concentration}) \qquad \text{(Eq. 2)}$$

This finding coincides with the assumption (15) that the pH value of a dilute solution of a weak acid linearly correlates with the logarithm of its respective concentration:

$$\text{pH} = 0.5 \times \text{pKa} - 0.5 \times \log\,(\text{concentration}) \qquad \text{(Eq. 3)}$$

where the concentration is expressed in moles per liter. The value of the slope, 0.7382, obtained from Eq. 2 is different from the value of 0.5 of Eq. 3, because Eq. 2 expresses the concentration–pH relationship for a polyprotonic solution while Eq. 3 describes this relationship for a simple monomeric solution. For the polyacid aqueous solution, a modified form of the Henderson–Hasselbalch equation (16) was used:

$$\text{pH} = \text{pKa} - n \log \frac{(1-d)}{d} \qquad \text{(Eq. 4)}$$

where d is the degree of dissociation, pKa is the apparent dissociation constant, and n is a constant for a given set of conditions.

pH Dissolution Profile for Anhydride Copolymer—A carefully weighed sample of 100 mg of the anhydride copolymer, with a particle-size distribution ranging from 60 to 100 mesh, was added to a dissolution medium of 50 ml of double-deionized water in the sample beaker of the continuous pH-monitoring apparatus, maintained as described under *Experimental.* The pH value of the dissolution medium was continuously recorded on the recording chart (1 pH unit = 5.08-cm scale) over 10 hr (Fig. 3).

The observed decreasing pH value was due to the increased concentration of the free acid produced in the dissolution medium as the dissolution process proceeded. An initial abrupt decrease in the apparent pH value was followed by a slow and general decrease in pH until a plateau was reached, indicating that the dissolution process was complete.

Characterization of Dissolution Process of Anhydride Copolymer—The pH profile (Fig. 3) obtained by continuously monitoring the formation of the free acid in the dissolution medium was then trans-

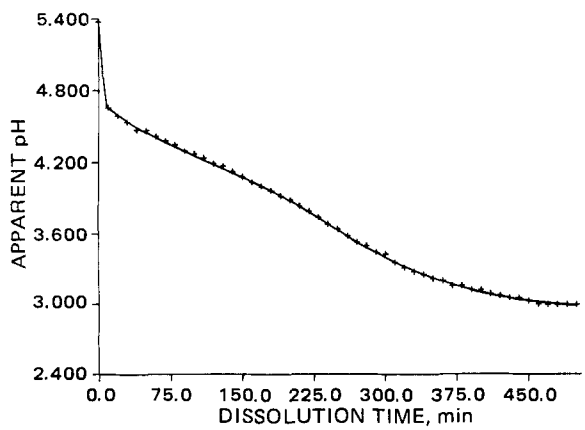

Figure 3—*The pH profile recorded during the dissolution process of the anhydride copolymer.*

[7] Radiometer, Coppenhagen, Denmark.

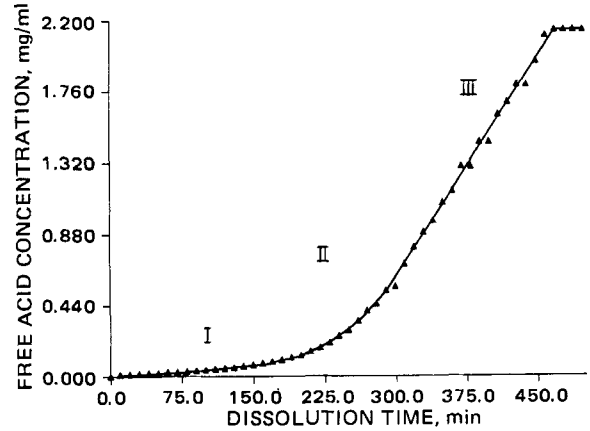

Figure 4—*Dissolution profile monitoring the formation of the free acid during the dissolution process of the anhydride copolymer. Key: I, initial lag period; II, intermediate accelerating rate period; and III, final zero-order rate period.*

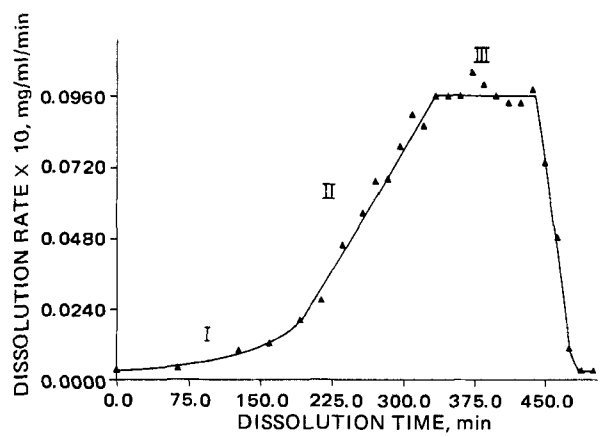

Figure 5—*Characterization of the anhydride copolymer dissolution rate process. These different periods are attributed to their different dissolution mechanisms. Key: I, wetting and penetration period; II, hydration and swelling period; and III, zero-order process period.*

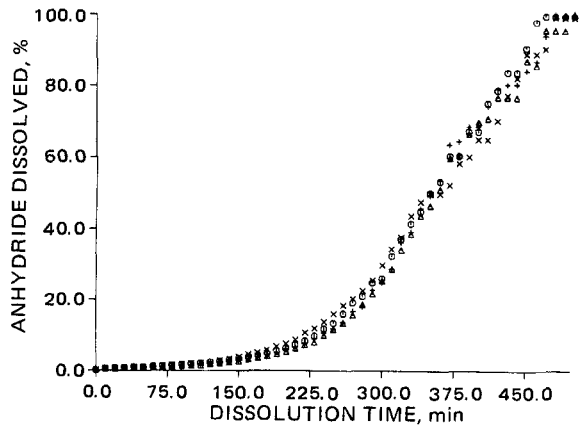

Figure 6—*Similarity of relative dissolution profiles observed for different weights of the anhydride copolymer sample. Key: ○, 100 mg; △, 75 mg; +, 50 mg; and ×, 30 mg.*

formed into a dissolution profile (Fig. 4). This profile correlated the formation of the free acid with the dissolution time by substituting the recorded pH values into the calibration equation (Eq. 2). The resultant dissolution profile was used to investigate the dissolution process of the anhydride copolymer powder.

Two possible mechanisms for the anhydride copolymer dissolution process are proposed, Schemes II and III. Scheme III is a more likely route for the copolymer dissolution process, where the hydrolysis reaction is the rate-limiting step.

anhydride copolymer (solid) —slow dissolution→ anhydride copolymer (in solution) —fast hydrolysis→ copolymer free acid (in solution)

Scheme II

anhydride copolymer (solid) —slow hydrolysis→ copolymer free acid (solid) —fast dissolution→ copolymer free acid (in solution)

Scheme III

Essentially, three different periods are observed for the dissolution process of the anhydride copolymer with respect to the formation of the free acid (Fig. 4). Period I, the initial lag period (0–180 min), is attributed to the slow process of wetting and penetration by the water molecules. Period II, an accelerating rate period, may be reflecting the hydration and swelling of the particles as well as the autocatalytic nature of the hydrolysis reaction in which the increased hydrogen-ion concentration accelerates the hydrolysis process (17). Period III is an apparent zero-order dissolution process.

The dissolution profile of the anhydride copolymer powder material correlated with reported dissolution studies of the polymer free acid film (14) and the compressed copolymer disk (12). In these studies, a similar lag time or induction period followed by an apparent zero-order dissolution process was observed.

The three different rate periods were further characterized by relating

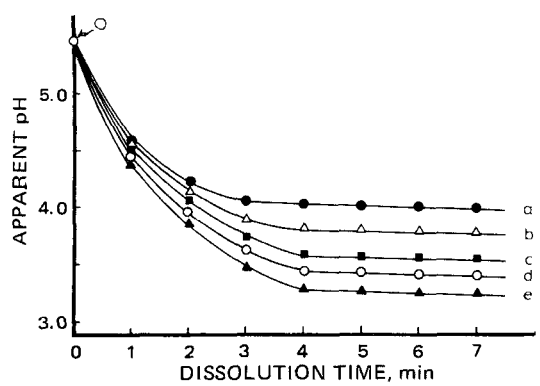

Figure 7—*Comparisons of initial dissolution profiles of copolymer anhydride–free acid mixtures. Key (anhydride–free acid ratio): a, 90:10; b, 80:20; c, 60:40; d, 40:60; and e, 0:100.*

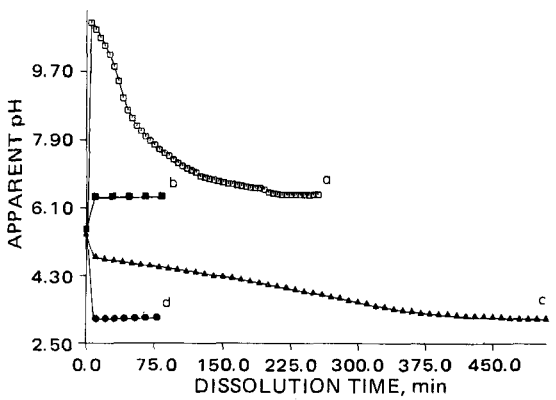

Figure 8—*Overall dissolution profiles observed for the copolymer anhydride, free acid, and salt. Key: a, mixture of the copolymer and the free alkaline salts; b, pure reacted copolymer salt; c, pure anhydride copolymer; and d, pure copolymer free acid.*

the calculated value of the initial rate of free acid formation with the dissolution time (Fig. 5). Initially, a slow dissolution rate was observed for Period I, followed by a rapidly increasing rate for Period II. The dissolution rate then reached a plateau and exhibited a constant and maximum value.

When 100-, 75-, 50-, and 30-mg powder samples of the anhydride copolymer were subjected to the dissolution test, nearly identical relative dissolution profiles were observed (Fig. 6). This result indicates that the dissolution process is essentially independent of the concentration of polymer already in solution over the concentration range studied. Figure 6 also indicates a high order of reproducibility for these recorded profiles.

Dissolution as Function of Anhydride–Free Acid Ratio—Fifty milligrams of each of a series of copolymer sample mixtures, composed of different anhydride–free acid compositions, was evaluated for dissolution characteristics as described under *Experimental.* As indicated in Fig. 7, samples containing different anhydride–free acid ratios exhibited different initial pH profiles. These profiles showed abruptly decreasing pH readings at the very beginning of the dissolution processes, followed by a much more gradual decrease in the pH values after the first 5 min (Figs. 3 and 7). In a separate experiment, the copolymer free acid completely dissolved within 5 min to give a concentration of 1.0 mg/ml.

The more abrupt drop in initial pH readings is attributed to the presence of the free acid (Fig. 8). Therefore, it is possible to determine the composition of the free acid in this mixed acid–anhydride polymer system by substituting the apparent pH reading of the dissolution medium recorded at the end of the first 5 min of the dissolution process into the calibration equation (Eq. 2) and solving for the free acid concentration. Thus, this method can be applied to the analysis of the acid–anhydride functionality of this type of polymer system. Only a very small amount of the copolymer anhydride was converted into the free acid during the first 5 min (Fig. 4). The amount of the copolymer anhydride

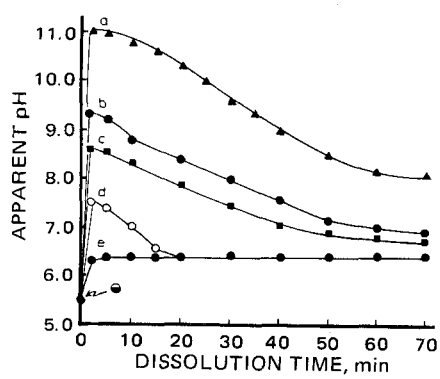

Figure 9—*Comparisons of dissolution profiles of copolymer mixtures of different anhydride–salt compositions. The half-open circle (◒) shows pH reading (5.50) prior to addition of samples. Key (anhydride–salt ratio): a, 80:20; b, 35:65; c, 25:75; d, 10:90; and e, 0:100. All samples contained identical content (29%) of alkaline salts, including both free (unreacted) and reacted salts. All profiles reached a similar plateau pH reading of 6.45 ± 0.05 toward the end of the dissolution processes.*

Table I—Correlation of the Anhydride–Salt Derivatives Ratio with the Maximum Dissolution pH Value and the Total Dissolution Time

Anhydride–Salt Derivatives Ratio[a]	Maximum pH	Total Dissolution Time, min
100/0	11.2 ± 0.1	210 ± 10
80/20	11.0 ± 0.1	180 ± 10
70/30	10.6 ± 0.1	165 ± 10
55/45	10.20 ± 0.05	140 ± 10
45/55	9.75 ± 0.05	115 ± 10
35/65	9.25 ± 0.05	95 ± 5
25/75	8.60 ± 0.05	85 ± 5
15/85	8.00 ± 0.05	55 ± 5
10/90	7.55 ± 0.05	17 ± 2
0/100	6.45 ± 0.05	1.5 ± 0.5

[a] Sample weight = 50 mg; dissolution medium = 50 ml; all samples were prepared in physical mixtures.

in a mixed anhydride–acid system is given by:

$$\text{copolymer anhydride (mg)} = 50\text{ mg} - \text{free acid concentration (mg/ml)} \times 50\text{ ml} \quad \text{(Eq. 5)}$$

Sample mixtures with higher free acid contents showed the greater initial pH drop.

Dissolution as a Function of Anhydride–Salt Ratio—When 50 mg of each anhydride–salt mixture was used for the dissolution study as discussed under *Experimental*, different characteristic dissolution profiles were recorded (Fig. 9). Free alkaline salts of calcium hydroxide and sodium carbonate were added to each sample mixture to maintain fixed salt concentrations. The profile of each sample abruptly rose from an initial reading of pH 5.5 to a maximum, after which the pH gradually decreased. The samples with a higher copolymer salt content exhibited a shorter dissolution process. In other words, the dissolution process of the anhydride copolymer was dramatically facilitated in the presence of alkaline salts (Fig. 8). One could, therefore, construct two working curves, correlating both the maximum pH readings and the total dissolution time values with the anhydride–acid salt ratios (Table I), to determine the anhydride–acid salt composition of an unknown sample mixture.

Four different dissolution profiles, representing the dissolution processes of the salt-catalyzed anhydride (a), the 100% totally reacted copolymer salt (b), the pure anhydride copolymer (c), and the pure copolymer free acid (d), are compared in Fig. 8. The copolymer sample that exhibited more polar functional groups as indicated by higher calculated hydrophilic–lipophilic balance (HLB) numbers (18) exhibited a faster dissolution process in aqueous solutions (Table II).

Table II—Correlation of the Total Dissolution Time and the Calculated HLB Number

Sample[a]	Total Dissolution Time, min[b]	HLB Number[c]
Copolymer salt	2	38.6
Pure copolymer free acid	5	9.8
Mixture of anhydride copolymer and free alkaline salts	210	—
Pure anhydride	540	7.3

[a] A 50-mg sample dissolved in 50 ml aqueous solution. [b] Determined as the time required to reach the plateau of the dissolution profile, which was recorded by the continuous pH-monitoring apparatus as described in the text. [c] Values were calculated for each repeating unit (Scheme I) of the copolymers using the reported HLB group numbers (7); (COO^-Na^+) or (COO^-Ca^+) = 20; (COOH) = 2.1; (—O—) = 1.3; (OCH_3) = 0.5; (C=O) = 0.2; and (CH) or (HCH) = 0.475. The HLB number (summation of group numbers) = +7.

REFERENCES

(1) "Poly(methyl vinyl ether/maleic anhydride) Resins," Tech. Bull. 7543-017, GAF Corp., New York, N.Y., 1965, p. 35.

(2) "Ethylene Maleic Anhydride Resins," Tech. Bull. I-261, Monsanto Co., St. Louis, Mo., p. 16.

(3) W. D. Niederhauser, U.S. pat. 2,752,281 (1956).

(4) W. A. Hosmer and A. C. Starke, U.S. pat. 3,087,853 (1963).

(5) L. C. Lappas and W. McKeehan, *J. Pharm. Sci.*, **51**, 808 (1962).

(6) *Ibid.*, **54**, 176 (1965).

(7) R. J. Nessel, H. G. DeKay, and G. S. Banker, *J. Pharm. Sci.*, **53**, 790 (1964).

(8) *Ibid.*, **53**, 882 (1964).

(9) J. W. Kleber, J. F. Nash, and C. Lee, *J. Pharm. Sci.*, **53**, 1519 (1964).

(10) J. G. Wagner, G. W. Ryan, E. Kabiak, and S. Lung, *J. Am. Pharm. Assoc., Sci. Ed.*, **49**, 133 (1960).

(11) C. R. Willis, G. S. Banker, and H. G. DeKay, *J. Pharm. Sci.*, **54**, 366 (1965).

(12) C. W. Woodruff, G. E. Peck, and G. S. Banker, *ibid.*, **61**, 1916 (1972).

(13) A. Heyd, D. O. Kildsig, and G. S. Banker, *ibid.*, **58**, 586 (1969).

(14) *Ibid.*, **59**, 947 (1970).

(15) J. G. Morris, "A Biologist's Physical Chemistry," Edward Arnold Ltd., London, England, 1968, p. 92.

(16) A. Katchalsky and P. Spitnik, *J. Polym. Sci.*, **2**, 432 (1947).

(17) T. Higuchi, T. Miki, A. C. Shah, and A. K. Herd, *J. Am. Chem. Soc.*, **85**, 3655 (1963).

(18) J. T. Davis, in "Proceedings of the Second International Congress of Surface Activity," vol. 1, Butterworths, London, England, 1957, p. 426.

ACKNOWLEDGMENTS AND ADDRESSES

Received May 3, 1976, from the *Industrial and Physical Pharmacy Department, School of Pharmacy and Pharmacal Sciences, Purdue University, West Lafayette, IN 47907.*

Accepted for publication July 1, 1976.

Presented in part at the Industrial Pharmaceutical Technology Section, APhA Academy of Pharmaceutical Sciences, New Orleans meeting, April 1976.

Supported by Vick Divisions Research and Development (Richardson Merrell, Inc.), Mount Vernon, N.Y.

[x] To whom inquiries should be directed.

Benzoyl Peroxide Stability in Pharmaceutical Gel Preparations

JAMES N. BOLLINGER ˣ, DELMA LEWIS, and VICTOR M. MENDEZ

Abstract □ The storage stability of benzoyl peroxide in the presence of both individual and combined pharmaceutical gel ingredients was investigated. Benzoyl peroxide was quite unstable in the presence of nucleophilic agents and certain acidic substances. At both 30 and 40° storage temperatures, benzoyl peroxide was destroyed rapidly (within 1 month) in the presence of ethanol and acidic chelating agents. The substitution of acetone for ethanol, the elimination of chelating agents, and the addition of sodium hydroxide to gel preparations markedly reduced degradation.

Keyphrases □ Benzoyl peroxide—stability in pharmaceutical gels, effect of temperature, pH, and various gel ingredients □ Stability—benzoyl peroxide in pharmaceutical gels, effect of temperature, pH, and various gel ingredients □ Gels—stability of benzoyl peroxide, effect of temperature, pH, and various gel ingredients □ Keratolytics—benzoyl peroxide, stability in pharmaceutical gels, effect of temperature, pH, and various gel ingredients

Benzoyl peroxide pharmaceutical preparations are widely used in the treatment of acne. However, due to the inherent chemical nature of benzoyl peroxide, degradation of these preparations is often encountered in storage. The purpose of this investigation, therefore, was to evaluate various parameters regarding the storage stability of benzoyl peroxide in pharmaceutical gel formulations.

BACKGROUND

A survey of existing products showed that most formulations contain either 5 or 10% benzoyl peroxide. The thickening agents commonly employed in the formation of the gels are carboxypolymethylene and hydroxypropyl methylcellulose. The stability of the gels formed with carboxypolymethylene is regulated by the addition of alkaline neutralizers such as sodium hydroxide, bis(2-propanol)amine, and triethanolamine. The stability of gels formulated with hydroxypropyl methylcellulose is usually enhanced by the addition of silicates.

Other gel components include the polyoxyethylene lauryl ether surfactants, which aid in the solubility of components in the gels themselves and enhance the contact of benzoyl peroxide with the skin. The latter effect probably is also enhanced by the presence of organic solvents.

Gels often contain various glycols such as glycerol, ethylene glycol, and propylene glycol. They serve several purposes including solvent action and humectant properties. The final major substance present is water, which may have a chelating agent added such as edetate disodium or citric acid.

Gels also may contain sodium lauryl sulfate, fragrances, and color, but these were not evaluated in this study.

Preliminary studies in this laboratory[1] indicated that certain ingredients in gels may influence the chemical stability of benzoyl peroxide—namely, that the benzoyl peroxide concentration is, with time, lowered due to its reactivity with the other ingredients. Original studies (1) on stability showed that, when heated, benzoyl peroxide, either in pure form or in nonpolar solvents, decomposed to yield carbon dioxide, biphenyl, phenyl benzoate, and benzene.

In the presence of alcohols, benzoyl peroxide decomposed to carbon dioxide, benzoic acid, and alcohol esters of benzoic acid (2). In the presence of acetic acid, it decomposed to form carbon dioxide, benzoic acid, phenylbenzoic acid, benzene, biphenyl, and phthalic acids (3). Since benzoyl peroxide is both a UV and a thermal free radical precursor, the resultant free radicals can interact with most molecules that, through electron shifts, are easily induced to possess reactive unshared electrons, such as certain alcohols, sulfhydryl compounds, alkanes, alkenes, and aromatic compounds.

The purpose of this study was not to identify reaction products but to evaluate the decomposition of benzoyl peroxide with respect to whether any ingredient used in the gel preparations enhances its degradation.

EXPERIMENTAL

Formulations—As shown in Table I, experimental test formulations were made to evaluate the stability of benzoyl peroxides as influenced by thickening agents, alkaline neutralizers, surfactants, solvents, chelating agents, and temperature. Except for the alkaline neutralizers, all ingredients were added on a gram-weight basis. The ingredients were added together and thoroughly mixed to a uniform gel using a high speed, high shear mixer. The benzoyl peroxide suspension was prepared by adding water and micropulverizing the mixture into a milky, stable suspension.

The final concentration of the ingredients, including benzoyl peroxide, was adjusted prior to the final mixing through the addition of weighed amounts of water; neutralization and pH adjustments were made during the final mixing using approximately 5–10 ml of a 10% solution of the amines and 5–7 ml of a 10% NaOH solution. A zero-time analysis of benzoyl peroxide was performed in triplicate by titrimetric means (4) on each final test sample batch.

Experimental Protocol—The 22 gel formulations (Table I) were individually evaluated in triplicate at zero time and after storage for 30, 60, and 90 days at both 30 and 40°. Approximately 2.5 g of the test gel was placed in tared glass vials and sealed with polyethylene- or polycarbonate–polyethylene-lined screw caps. Each vial was then reweighed and stored in the dark in either the 30 or 40° oven. Therefore, 18 samples were prepared for each test of the 22 gel formulations; an additional vial containing 20 g of the gel was used to evaluate pH changes.

The concentration of benzoyl peroxide was determined as indicated by employing the recently developed titrimetric procedure (4, 5), using acetone extractions with potassium iodide–thiosulfate titrations in the presence of phenyl sulfide.

Sample weight losses due to storage were determined gravimetrically for each sample. Hydrogen-ion concentrations were determined using glass electrodes and a digital readout pH meter.

GLC[2] and GLC–mass spectrometry[3] were employed to identify any unusual reaction products.

RESULTS AND DISCUSSION

Figures 1–7 graphically depict the mean percentage loss of benzoyl peroxide as influenced by the various ingredients and combination of ingredients used in the gels.

The first six test samples were stored in glass vials with polyethylene caps; at the 40° test temperature, several samples stored with these caps lost substantial weight (10–20%) due to heat softening of the caps and subsequent solvent leakage. Subsequent analysis indicated, however, that this loss had no influence on the stability of benzoyl peroxide. Loss in sample weight usually ranged from 1 to 3% of the original weight.

Influence of Alkaline Neutralizers in Carboxypolymethylene Gel—These gel systems contained 1.75% carboxypolymethylene, 10% benzoyl peroxide, and enough triethanolamine, bis(2-propanol)amine, or sodium hydroxide solution to bring the pH to approximately 5. As shown in Fig. 1*a*, at 30° there was practically no breakdown of benzoyl peroxide over 90 days in any of these test samples. At 40° (Fig. 1*b*) and after 60 days, a 5–10% loss in benzoyl peroxide occurred. After 90 days at this temperature, the breakdown or loss was 20% in the presence of bis(2-propanol)amine, 10% with triethanolamine, and 5% with sodium hydroxide. The pH of the 40° samples over 90 days dropped approximately from 5 to 4.5.

[1] J. N. Bollinger, unpublished investigations, 1969 and 1974.

[2] Hewlett-Packard.

[3] Varian.

Table I—Experimental Test Formulations (All Included Water)

Formulation	Thickening Agents	pH Regulator	pH	Organic Solvent	Surfactant	Humectant	Chelating Agent	Benzoyl Peroxide[a], %
1	Carboxypolymethylene[b] (1.75%)	Triethanolamine	5.02	—	—	—	—	10.88 ± 0.02
2	Carboxypolymethylene (1.75%)	Sodium hydroxide	4.85	—	—	—	—	11.02 ± 0.03
3	Carboxypolymethylene (1.75%)	Bis(2-propanol)amine	5.00	—	—	—	—	10.73 ± 0.05
4	Carboxypolymethylene (1.75%)	Triethanolamine	5.00	Ethanol (40%)	—	—	—	10.97 ± 0.26
5	Carboxypolymethylene (1.75%)	Sodium hydroxide	5.00	Ethanol (40%)	—	—	—	11.24 ± 0.05
6	Carboxypolymethylene (1.75%)	Triethanolamine	5.00	Acetone (10%)	—	—	—	11.25 ± 0.04
7	Carboxypolymethylene (1.75%)	Sodium hydroxide	4.85	Acetone (10%)	—	—	—	11.37 ± 0.02
8	Carboxypolymethylene (1.75%)	Triethanolamine	5.00	—	Polyoxyethylene 23 lauryl ether[c] (6%)	—	—	10.79 ± 0.03
9	Carboxypolymethylene (1.75%)	Triethanolamine	5.00	—	Polyoxyethylene 4 lauryl ether[d] (6%)	—	—	10.83 ± 0.14
10	Carboxypolymethylene (1.75%)	Triethanolamine	4.90	—	—	Propylene glycol (5%)	—	11.08 ± 0.04
11	Carboxypolymethylene (1.75%)	Triethanolamine	5.05	Ethanol (40%)	Polyoxyethylene 23 lauryl ether (6%)	Propylene glycol (5%)	Edetate disodium (0.1%)	11.34 ± 0.06
12	Carboxypolymethylene (1.75%)	Triethanolamine	5.00	Ethanol (40%)	Polyoxyethylene 23 lauryl ether (6%)	Propylene glycol (5%)	Citric acid (0.1%)	11.46 ± 0.04
13	Carboxypolymethylene (1.75%)	Sodium hydroxide	4.90	Ethanol (40%)	Polyoxyethylene 23 lauryl ether (6%)	Propylene glycol (5%)	Edetate disodium (0.1%)	11.43 ± 0.06
14	Carboxypolymethylene (1.75%)	Triethanolamine	4.95	Acetone (10%)	Polyoxyethylene 23 lauryl ether (6%)	Propylene glycol (5%)	Edetate disodium (0.1%)	11.26 ± 0.05
15	Carboxypolymethylene (1.75%)	Triethanolamine	4.90	Acetone (10%)	Polyoxyethylene 23 lauryl ether (6%)	Propylene glycol (5%)	Citric acid (0.1%)	11.21 ± 0.07
16	Carboxypolymethylene (1.75%)	Sodium hydroxide	4.92	Acetone (10%)	Polyoxyethylene 23 lauryl ether (6%)	Propylene glycol (5%)	Edetate disodium (0.1%)	11.40 ± 0.04
17	Hydroxypropyl methylcellulose (1%) and silicate[e] (1%)	Sodium hydroxide	6.15	—	—	—	—	11.56 ± 0.10
18	Hydroxypropyl methylcellulose (1%) and silicate (1%)	Sodium hydroxide	8.25	—	—	—	—	11.49 ± 0.05
19	Hydroxypropyl methylcellulose (1%) and silicate (1%)	Sodium hydroxide	5.95	Ethanol (40%)	Polyoxyethylene 23 lauryl ether (6%)	Propylene glycol (5%)	Edetate disodium (0.1%)	11.39 ± 0.03
20	Hydroxypropyl methylcellulose (1%) and silicate (1%)	Sodium hydroxide	6.10	Acetone (10%)	Polyoxyethylene 23 lauryl ether (6%)	Propylene glycol (5%)	Edetate disodium (0.1%)	11.53 ± 0.04
21	Hydroxypropyl methylcellulose (1%) and silicate (1%)	Sodium hydroxide	7.85	Ethanol (40%)	Polyoxyethylene 23 lauryl ether (6%)	Propylene glycol (5%)	Edetate disodium (0.1%)	11.45 ± 0.07
22	Hydroxypropyl methylcellulose (1%) and silicate (1%)	Sodium hydroxide	7.95	Acetone (10%)	Polyoxyethylene 23 lauryl ether (6%)	Propylene glycol (5%)	Edetate disodium (0.1%)	11.39 ± 0.19

[a] Lucidol-70, Pennwalt. [b] Carbopol 940, B. F. Goodrich. [c] Brij 35, ICI America. [d] Brij 30, ICI America. [e] Colloidal magnesium silicate, Veegum, Vanderbilt.

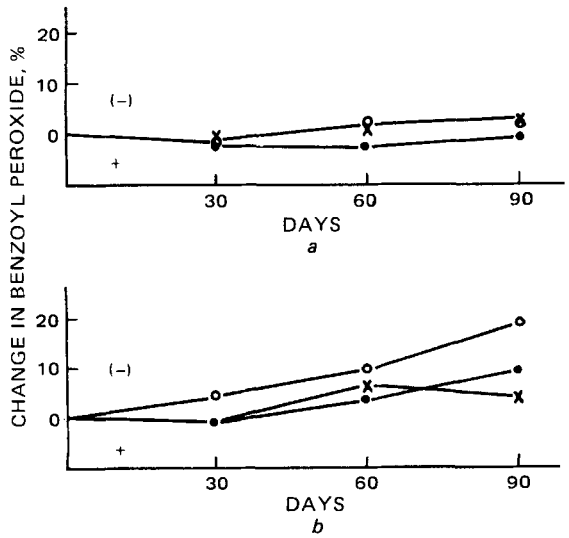

Figure 1—*Influence of alkaline neutralizers in carboxypolymethylene gel on the stability of benzoyl peroxide. Each gel consisted of carboxypolymethylene, benzoyl peroxide, and water. Alkaline neutralizers included triethanolamine (●), sodium hydroxide (×), and bis(2-propanol)amine (○). Key:* a, *storage at 30°; and* b, *storage at 40°.*

Influence of Organic Solvents—As shown in Fig. 2, two solvents, ethanol and acetone, were evaluated regarding their effect on benzoyl peroxide stability. The remainder of the preparation consisted of 10% benzoyl peroxide, 1.75% carboxypolymethylene, and both triethanolamine and sodium hydroxide as the polymer neutralizing-thickening agents.

At 30° (Fig. 2*a*), samples containing ethanol displayed 2–5% losses in benzoyl peroxide after 60 days. By 90 days, the samples containing ethanol and triethanolamine showed benzoyl peroxide losses of about 12%; those containing ethanol and sodium hydroxide had a 4% mean loss. None of the samples containing acetone showed measurable losses in benzoyl peroxide.

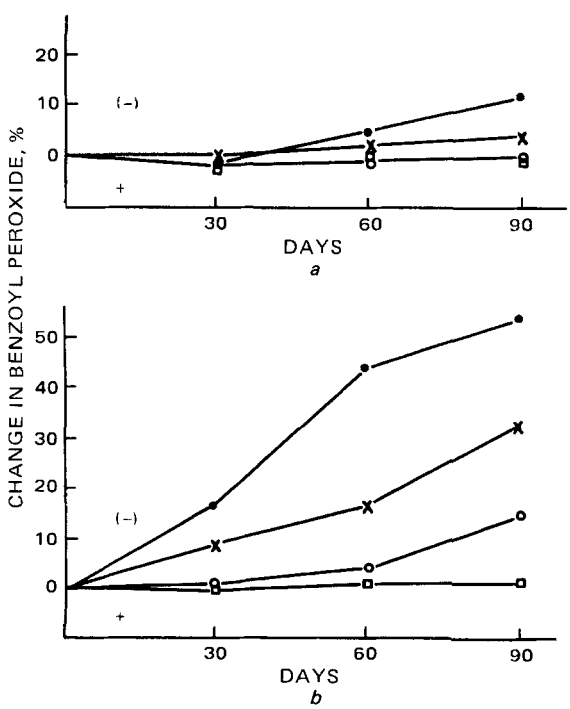

Figure 2—*Influence of organic solvents on benzoyl peroxide stability. Each gel mixture consisted of carboxypolymethylene, benzoyl peroxide, and water. Variants to the system included ethanol and triethanolamine (●), ethanol and sodium hydroxide (×), acetone and triethanolamine (○), and acetone and sodium hydroxide (□). Key:* a, *storage at 30°; and* b, *storage at 40°.*

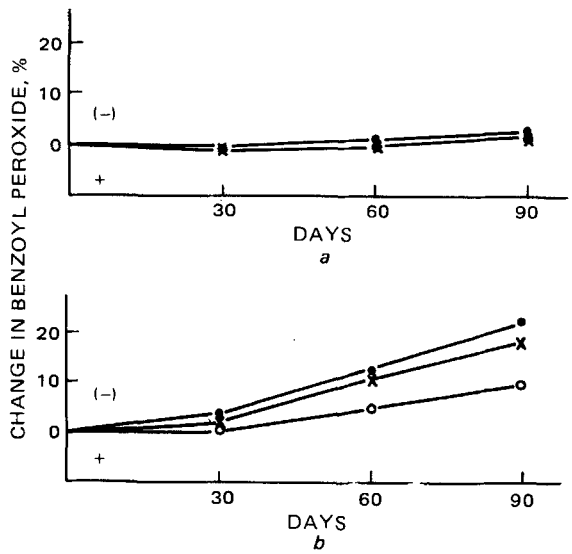

Figure 3—*Influence of surfactant and humectant on the stability of benzoyl peroxide. Each gel mixture consisted of carboxypolymethylene, benzoyl peroxide, and water. Variants to the system included polyoxyethylene 23 lauryl ether (●), polyoxyethylene 4 lauryl ether (×), and propylene glycol (○). Key:* a, *storage at 30°; and* b, *storage at 40°.*

These same effects were accentuated at the 40° storage temperature. By 90 days, the ethanol–triethanolamine samples sustained a 50% loss in benzoyl peroxide, the ethanol–sodium hydroxide samples had a 33% loss, and the acetone–triethanolamine-containing samples had a 15% loss. Samples containing acetone–sodium hydroxide showed no loss in benzoyl peroxide (Fig. 2*b*).

Indicative of the breakdown of the benzoyl peroxide was a marked pH change (*e.g.*, from a pH of 5 to ~3.5 in the ethanol–triethanolamine samples). After 90 days at 40°, samples containing ethanol–sodium hydroxide showed a decomposition of about 33% and the pH did not drop (from pH 5.0 to 4.2) as markedly.

Influence of Surfactant and Humectant—As shown in Fig. 3, neither the polyoxyethylene lauryl ethers nor propylene glycol appeared to influence the decomposition of benzoyl peroxide appreciably. After 90 days at 30°, there was no decomposition whatsoever; after 90 days at 40°, the decomposition of benzoyl peroxide was 20% in the presence of polyoxyethylene lauryl ethers as compared to 10% with propylene glycol.

Influence of Chelating Agents—These test systems contained all of the gel ingredients (Table I, Samples 11–16). The components held constant included carboxypolymethylene, polyoxyethylene lauryl ether, and propylene glycol. The ingredients that were varied included the solvents (ethanol and acetone), the neutralizers (sodium hydroxide and triethanolamine), and the chelating agents (edetate disodium and citric acid). It was not anticipated that any effect would be seen due to the chelating agents; however, as shown in Figs. 4 and 5, this assumption was erroneous.

Figure 4 graphically shows the influence of ethanol, triethanolamine, citric acid, and edetate disodium on the stability of benzoyl peroxide. The large decomposition of benzoyl peroxide (50–60%) at 30° after 90 days of storage (Fig. 4*a*) indicates that the chelating agents, citric acid and edetate disodium, somehow influenced the breakdown of benzoyl peroxide. The use of sodium hydroxide in this test system reduced the decomposition of benzoyl peroxide by more than 75% when compared to triethanolamine. The 15% level of decomposition noted in the sodium hydroxide-containing system was only slightly higher than that in the ethanol–sodium hydroxide system (5%) without chelating agents.

Figure 4*b* (40° test of the same mixtures) shows 90–100% destruction of benzoyl peroxide by 60 days, further indicating some form of catalytic activity due to the presence of chelating agents. The results were similar to the 30° test system discussed previously in that sodium hydroxide markedly delayed the decomposition of benzoyl peroxide during the initial 30 days.

Additional information on the effects of the solvent *versus* chelating agents can be seen in Fig. 5*a*. In these test systems, acetone was substituted for ethanol as the solvent. After 90 days at 30°, there was only a 10% decomposition in the acetone–triethanolamine–citric acid samples as

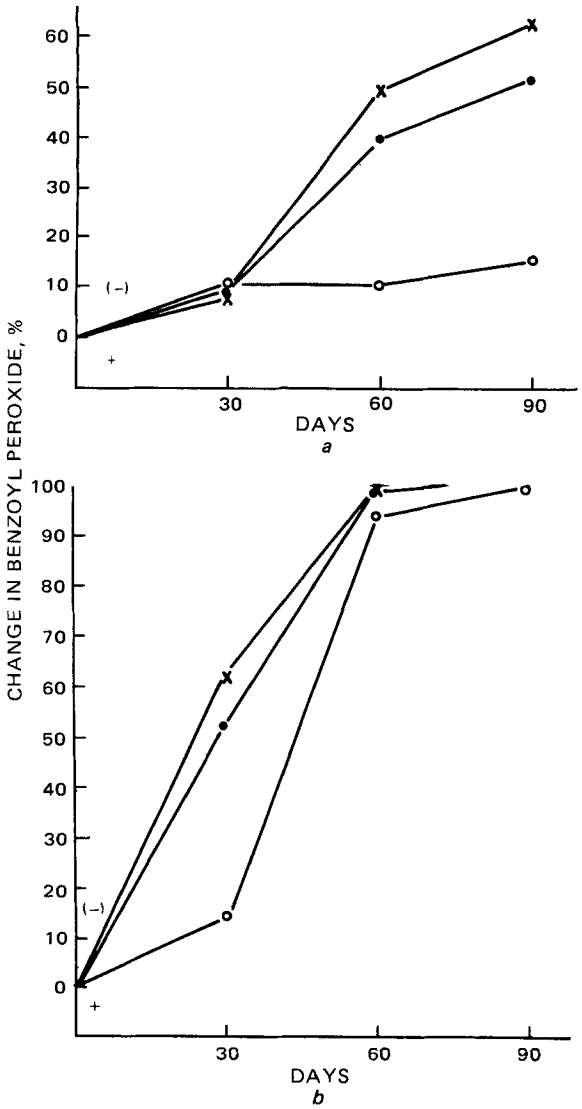

Figure 4—*Influence of ethanol in the presence of chelating agents on the stability of benzoyl peroxide. Each gel system contained carboxypolymethylene, benzoyl peroxide, ethanol, polyoxyethylene 23 lauryl ether, propylene glycol, and water. Variants in the system included triethanolamine and edetate disodium (●), triethanolamine and citric acid (×), and sodium hydroxide and edetate disodium (○). Key:* a, *storage at 30°; and* b, *storage at 40°.*

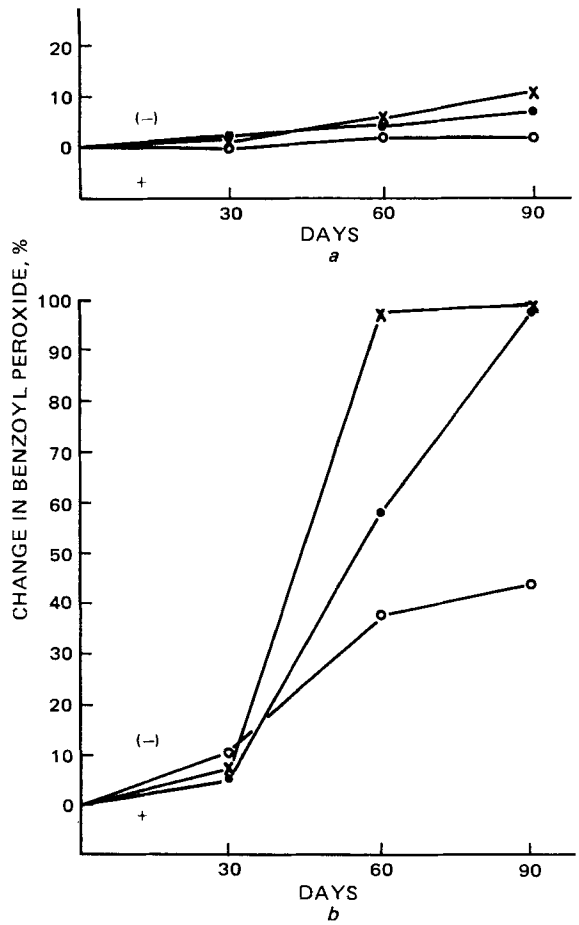

Figure 5—*Influence of acetone in the presence of chelating agents on the stability of benzoyl peroxide. Each test system consisted of the same ingredients as in Fig. 4, except that ethanol was replaced with acetone. Variants to the system included triethanolamine and edetate disodium (●), triethanolamine and citric acid (×), and sodium hydroxide and edetate disodium (○). Key:* a, *storage at 30°; and* b, *storage at 40°.*

compared to a 60% decomposition when ethanol was used in the same system. With the acetone–triethanolamine–edetate disodium system, there was a 7% decomposition of benzoyl peroxide but virtually no (<2%) decomposition in the acetone–sodium hydroxide–edetate disodium system.

Increasing the test storage temperature to 40° (Fig. 5*b*), however, induced the decomposition of benzoyl peroxide. During the initial 30 days of storage at this temperature, little decomposition occurred in any acetone sample; however, in the triethanolamine–citric acid–acetone system, there was 100% destruction of benzoyl peroxide by 60 days. It took 90 days to destroy benzoyl peroxide completely in the triethanolamine–edetate disodium–acetone system; with the sodium hydroxide–edetate disodium–acetone samples, only 45% destruction occurred after storage at 40° for 90 days.

These data indicate that the presence of chelating agents greatly enhanced the breakdown of benzoyl peroxide in the presence of ethanol. The partial decomposition noted in the presence of acetone and chelating agents at the higher temperatures was probably related to alcohol groups and other free-radical potentiating groups and not to acetone itself.

A GLC analysis of these samples indicated that the ethanol-containing preparations contained an additional reaction by-product. Both comparative GLC and GLC–mass spectrometry analysis showed this product to be ethyl benzoate.

Influence of Hydroxypropyl Methylcellulose and Silicate—Samples 16–22 (Table I) contained hydroxypropyl methylcellulose and magnesium aluminum silicate as the thickening agents instead of carboxypolymethylene. As opposed to gel thickened with carboxypolymethylene (pH 5), these samples were stored at pH 6 and 8. The results of these tests are shown in Figs. 6 and 7. The exception to the use of complete formulations was that one group of samples, prepared and stored at pH 6 and 8, contained only benzoyl peroxide, hydroxypropyl methylcellulose, silicate, and sodium hydroxide.

The ethanol-containing samples were the only ones to show appreciable (30%) decomposition of benzoyl peroxide after storage for 90 days at 40° (Figs. 6 and 7). Whether the test samples were initially stored at pH 8 or 6 had no influence on the degree of breakdown. The pH of the samples stored at pH 6 dropped approximately 1.7 units and that of the samples stored at pH 8 dropped approximately 3.7 units, to yield an average pH for all samples of 4.3 regardless of whether the samples contained acetone, ethanol, or no solvents. The effects of the catalytic activity of the chelating agents was not as evident in this gel system. However, since sodium hydroxide was used to adjust the pH, the breakdown of benzoyl peroxide would not be expected to be as great as if triethanolamine had been employed.

Influence of Temperature *versus* Gel Ingredients—An evaluation of the data showed that the storage temperature had only an indirect influence on the stability of benzoyl peroxide. Even at storage temperatures of 40° (104°F), little degradation (1–3%) occurred if no free-radical propagating-type molecules were present in the mixture. Molecules that enhanced the free-radical propagation-type reactions included hydroxyl-containing molecules, primarily ethanol, and, indirectly, the chelating agents.

The fact that neutralization of the gel with sodium hydroxide markedly reduced degradation of benzoyl peroxide in the presence of ethanol and

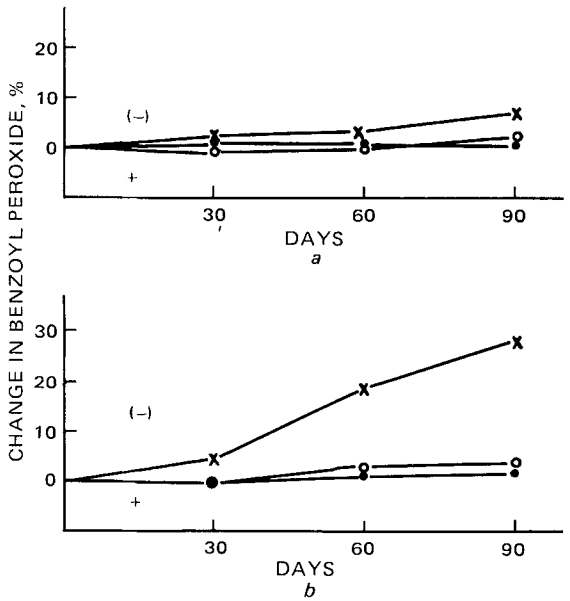

Figure 6—*Influence of hydroxypropyl methylcellulose and magnesium aluminum silicate gel system on the stability of benzoyl peroxide. The formulation contained benzoyl peroxide, sodium hydroxide, polyoxyethylene 23 lauryl ether, propylene glycol, edetate disodium, hydroxypropyl methylcellulose, magnesium aluminum silicates, and water. Variants to the system were: no solvent or chelating agent (●), ethanol as the solvent (×), and acetone as the solvent (○). Initial storage pH was 6.0. Key:* a, *storage at 30°; and* b, *storage at 40°.*

the chelating agents indicated that it interfered with the formation and entrance of ethanol radicals into the reaction. However, once the neutralization effect on the solvents is lost or lowered through either reaction with existing carboxyl groups or the thermal formation of benzoic acid (6), the entrance of free-radical propagating solvents such as ethanol into the reaction becomes increasingly unhindered. Acetone cannot readily, if at all, enter into free-radical reactions due to its electrochemical makeup. One might predict, based on data obtained in this study, that the polyoxyethylene lauryl ethers, glycols, carboxypolymethylene, and hydroxypropyl methylcellulose, in that order, can enter (on a limited basis) into a free-radical propagation-type reaction.

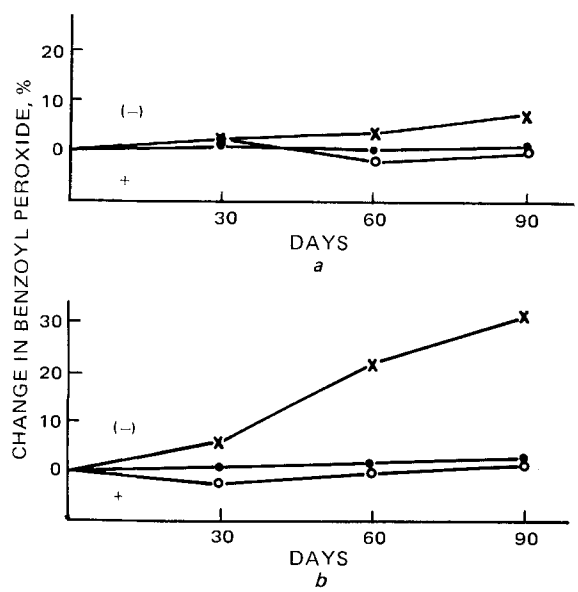

Figure 7—*Influence of pH on the storage stability of benzoyl peroxide in the hydroxypropyl methylcellulose–magnesium aluminum silicate gel. Basic gel system was the same as in Fig. 6, except that the samples were initially stored at a pH of 8. Variants were: no solvent or chelating agent (●), ethanol solvent (×), and acetone solvent (○). Key:* a, *storage at 30°; and* b, *storage at 40°.*

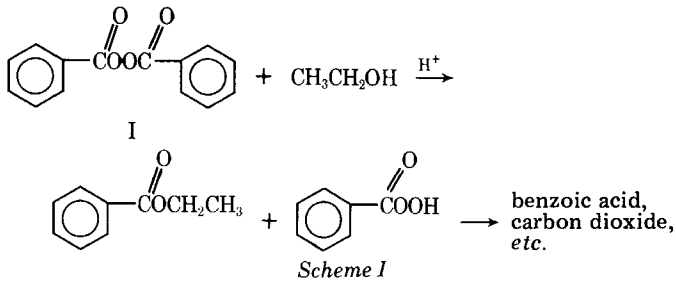

Scheme I

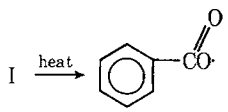

Scheme II

SUMMARY

The results of this investigation showed that triethanolamine, bis(2-propanol)amine, sodium hydroxide, carboxypolymethylene, hydroxypropyl methylcellulose, magnesium aluminum silicate, propylene glycol, the polyoxyethylene lauryl ethers, and acetone, individually, do not appreciably influence the storage stability of benzoyl peroxide (I). However, ethanol alone and, to a larger extent, in the presence of chelating agents and the carboxypolymethylene gel and, to a lesser degree, hydroxypropyl methylcellulose–silicate gel markedly enhanced the breakdown of benzoyl peroxide. The most pronounced degradation (100% within 30 days of storage at 30°) occurred in the presence of carboxypolymethylene, ethanol, and either edetate disodium or citric acid.

This latter phenomenon is thought to be due to the reaction shown in Scheme I. Classically, in the presence of heat, for example, benzoyl peroxide is thought to react as shown in Scheme II. However, the results of this investigation indicate that the Scheme II reaction did not occur to an appreciable extent even at the 40° storage temperature. Therefore, the partial degradation that occurred in the acetone samples containing the acidic chelating agents probably was due to some other alcohol or free-radical propagating groups, since acetone itself cannot be expected to react readily with benzoyl peroxide. In the absence of the chelating agents, for example, samples containing acetone were quite stable. In addition, the gel preparations containing sodium hydroxide as the neutralizing agent were far more stable than those containing triethanolamine, and the latter samples were slightly more stable than those containing bis(2-propanol)amine. These data indicate that sodium hydroxide hinders the formation of "solvent" radicals (*i.e.*, $CH_3CH_2O\cdot + \cdot H$), thus slowing the propagation of benzoyl peroxide decomposition.

In general, the results of this investigation demonstrated that the stability of benzoyl peroxide in pharmaceutical gel preparations is strongly influenced by the chemical makeup of the formulations and, secondarily, by the storage temperature due to increased reactivity.

REFERENCES

(1) H. Erlenmeyer and W. Schoenauer, *Helv. Chim. Acta*, **19**, 338 (1936).

(2) H. Gelissen and P. H. Hermans, *Ber. Dtsch. Chem. Ges.*, **58**, 765 (1925).

(3) M. T. Gladstone, *J. Am. Chem. Soc.*, **76**, 1581 (1954).

(4) "First Supplement to the United States Pharmacopeia," 19th rev., Mack Publishing Co., Easton, Pa., 1975.

(5) R. E. Daly, J. J. Lomner, and L. Chafetz, *J. Pharm. Sci.*, **64**, 1999 (1975).

(6) M. Gruber, R. Klein, and M. Foxx, *ibid.*, **58**, 566 (1969).

ACKNOWLEDGMENTS AND ADDRESSES

Received November 10, 1975, from the *Department of Environmental Sciences, Southwest Foundation for Research and Education, San Antonio, TX 78284.*

Accepted for publication July 14, 1976.

Supported by Texas Pharmacal Co., San Antonio, Tex.

ˣ To whom inquiries should be directed.

Spectrophotometry as a Tool for Assaying Endotoxins

NARBIK A. KARAMIAN *x and PAUL F. WATERS ‡

Abstract □ A spectrophotometric method is reported for assaying endotoxins over a wide concentration range, including low parts per billion levels. Five solutions of endotoxins, *Escherichia coli* 0127:B8, *Escherichia coli* 055:B5, *Salmonella abortus-equi*, *Salmonella enteritidis*, and *Shigella flexneri*, were examined. Each exhibited an absorption maximum at 259 nm, but the absorptivities differed in each case. Thus, rigorous quantification requires that the identity of the endotoxin be known. The UV absorbance and the statistical data for the standard curves for three groups of standard solutions are presented. The absorbance for each group was linear with concentration within acceptable limits.

Keyphrases □ Endotoxins, various—UV spectrophotometric analysis, prepared solutions, wide concentration range □ UV spectrophotometry—analysis, various endotoxins, prepared solutions, wide concentration range □ Pyrogens, various—UV spectrophotometric analysis, prepared solutions, wide concentration range □ Bacterial endotoxins, various—UV spectrophotometric analysis, prepared solutions, wide concentration range

Pyrogens are generally endotoxins produced by microorganisms growing in water or aqueous solutions. They cause inflammation and general fever when injected intravenously. They are colloidal in nature and persist even after the organisms that produced them are destroyed by sterilization.

Neither the mode(s) of their activity nor their structures are known (1). However, in Gram-negative bacteria, the glycopeptide basal layer usually is covered with a lipopolysaccharide constituting 20–30% of the cell wall. Lipopolysaccharides, components of the whole somatic antigen, with molecular weights of 10^6–10^7, exhibit endotoxin activity. It is difficult to construct a molecular model for a lipopolysaccharide that would adequately explain the shapes revealed by electron microscopy (2).

BACKGROUND

Endotoxins of high antigenic activity have been extracted from bacteria by using one of the recognized published procedures. The modified (3) Boivin trichloroacetic acid procedure (4) and the trypsin digestion method (5) produce bacterial endotoxins possessing properties adequate for most immunological and pathological studies. If more highly purified material is needed, the endotoxins are prepared by the phenol extraction procedure (6). The purified endotoxins are comparatively stable in the solid form but may become inactivated in solution by hydrolysis (7, 8).

Parenteral solutions are examined for pyrogens by using rabbits as test animals according to the USP procedure (9). This procedure was adopted in the early 1940's when the need for an official pyrogen test was first recognized.

Many attempts have been made to quantify the pyrogen test. One such procedure related solutions having less than 10,000 bacteria/liter to nonpyrogenicity (10). However, this procedure did not detect pyrogens at all unless viable bacteria were present in the sample. In 1971, a specific *in vitro* assay method, the "*Limulus* amebocyte lysate test," was developed. This test has a sensitivity level of 0.001–0.005 mg of pyrogen/ml of human plasma (11).

Although the test will normally detect a low level of endotoxins, it has not been used widely with sufficient confidence to replace the present rabbit test, primarily because there is a borderline region in the gelation process where the analyst must rely heavily on visual judgment. Furthermore, the gel-forming reaction is quite delicate and is irreversibly terminated with improper care.

Another disadvantage of the test lies in the production of the lysate itself. The lysate has been prepared by several different methods (11–15), and each study used different endotoxin references. At present, there is no universally adopted procedure or reference substance for this test.

A spectrophotometric approach was used in this research project, and an analytical method was developed that allows the detection of pyrogens from known sources below the 10-ppb level.

EXPERIMENTAL

Reagents and Equipment—A spectrophotometer[1] was used for measuring the absorbance of endotoxin solutions over a concentration range of 10–10,000 ppb. The endotoxins[2] used were: lipopolysaccharide *Escherichia coli* 0127:B8, lipopolysaccharide *Escherichia coli* 055:B5, lipopolysaccharide *Salmonella abortus-equi*, lipopolysaccharide *Salmonella enteritidis*, and lipopolysaccharide *Shigella flexneri*. All endotoxins were commercially prepared by a reported extraction method (6) and were shipped in powder form in vials that had to be kept refrigerated.

Endotoxin-free sterile double-distilled water was prepared in a still designed and constructed for that purpose (16).

Procedure—Stock solutions containing 50 ppm of endotoxin were prepared by dissolving 50 mg of each endotoxin in 1 liter of endotoxin-free sterile double-distilled water. The stock solutions were diluted to 7.5 ppm with endotoxin-free sterile double-distilled water, and the absorption curve of each was determined in a 10-cm cell.

To examine the linearity of the absorption *versus* concentration curve, a 1-liter solution of the five endotoxins containing a total of 50 ppm was prepared by mixing 200 ml of each 50-ppm endotoxin solution in a 1-liter volumetric flask. This solution was kept refrigerated at 10°. It was diluted to prepare a series of solutions for making the standard curve.

The solutions covered concentrations from 10 to 10,000 ppb. They were divided into three groups: (1) concentrations of 10, 25, and 50 ppb; (2) concentrations of 50–1000 ppb; and (3) concentrations of 500–10,000 ppb.

The measurements were made as follows. Aliquots of the stock solution, containing 50 ppm of the five mixed endotoxins, were diluted with endotoxin-free sterile double-distilled water to produce the desired concentrations. Each data point represents 49 readings of the absorbance

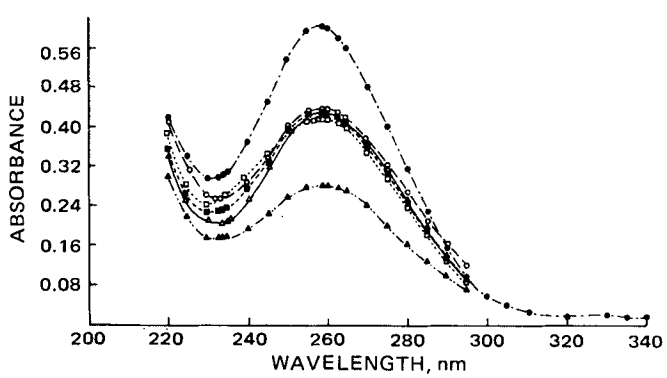

Figure 1—*UV absorption spectra of bacto-lipopolysaccharides. Key:* ●, E. coli *0127:B8;* □, Sh. flexneri; ■, S. enteritidis; △, S. abortus-equi; ▲, E. coli *055:B5; and* ○, *mixture of the five endotoxins.*

[1] ACTA MVI spectrophotometer, Beckman Instruments, Fullerton, CA 92634.

[2] Difco Laboratories, Detroit, MI 48201.

Table I—UV Absorbance and Statistical Data for Solutions of the Endotoxin Mixture Used for Preparing Standard Curves[a]

Concentration, ppb	Absorbance		
	$\bar{A}'$[b]	$\hat{A}$[c]	s[d]
	Group 1		
10	0.0024	0.002525	0.000371
25	0.0046	0.004398	0.000191
50	0.0074	0.007519	0.000353
	Group 2		
50	0.0074	0.008149	0.000353
100	0.0109	0.010908	0.000346
150	0.0138	0.013667	0.000325
200	0.0171	0.016426	0.000257
250	0.0192	0.019185	0.000186
350	0.0246	0.024704	0.000190
400	0.0281	0.027463	0.000397
500	0.0327	0.032981	0.000346
750	0.0463	0.046777	0.000324
1000	0.0607	0.060573	0.000247
	Group 3		
500	0.0327	0.031087	0.000346
750	0.0463	0.045093	0.000324
1000	0.0607	0.059099	0.000247
1500	0.0881	0.087111	0.001414
2500	0.1409	0.143136	0.000349
5000	0.2789	0.283196	0.000404
7500	0.4185	0.423256	0.000521
10000	0.5690	0.563317	0.000406

[a] Two independent groups of investigators at the National Institutes of Health tested the endotoxin mixture by both the rabbit and the *Limulus* amebocyte lysate methods, and each reported positive biological responses above 1.5 ppb. [b] Mean of 49 individual instrument readings expressed to the limit of the readability of the instrument. [c] $\hat{A} = A_0 + bC$, where $\hat{A}$ is the absorbance predicted from the fitted line, A_0 is the intercept of the fitted line, b is the slope, and C is the concentration of endotoxin mixture in parts per billion. [d] Standard deviation of each concentration.

for the solution of a given concentration. These readings were obtained in the following manner. For each concentration, the cell was filled seven separate times from a given prepared solution, and seven different readings were recorded for each filling by successively removing and then replacing the cell in the instrument. Each recorded reading was corrected by the absorbance of the blank, 0.0019 unit, measured with endotoxin-free sterile double-distilled water in each cell. The absorbance of the blank is ascribed to imperfect matching of the two 10-cm cells used.

RESULTS

The absorption curves for *E. coli* 0127:B8, *E. coli* 055:B5, *S. abortus-equi*, *S. enteritidis*, and *Sh. flexneri*, each at a concentration of 7.5 ppm, along with a mixture of the five endotoxins containing equal weights of each for a final total concentration of 7.5 ppm, are shown in Fig. 1. Each point represents the mean of two measurements made on a single solution without refilling the cell. Fresh solutions of each endotoxin were prepared, and the absorbance measurements were repeated. Essentially the same results as those reported here were observed. The absorption maxima for all endotoxins were practically the same—259 nm. The maximum for the mixture was at 258 nm.

The data for the determination of the standard curves are presented in Table I along with statistical information resulting from a regression analysis performed on the data from each of the three groups.

The regression equations for Groups 1, 2, and 3, respectively, are:

$$\hat{A} = 1.277 \times 10^{-3} + 1.248 \times 10^{-4} C \qquad r = 0.986 \qquad s = 3.5 \times 10^{-4} \quad \text{(Eq. 1)}$$

$$\hat{A} = 5.389 \times 10^{-3} + 5.518 \times 10^{-5} C \qquad r = 0.999 \qquad s = 5.1 \times 10^{-4} \quad \text{(Eq. 2)}$$

$$\hat{A} = 3.075 \times 10^{-3} + 5.602 \times 10^{-5} C \qquad r = 0.9998 \qquad s = 3.3 \times 10^{-3} \quad \text{(Eq. 3)}$$

where C is concentration, $\hat{A}$ is absorbance, r is the associated correlation coefficient, and s is the standard deviation about the regression.

The high concentrations show that within each group the absorbance is well approximated by a straight line, thereby indicating that Beer's law is approximately obeyed within each region. However, the high correlations are somewhat misleading. There were 49 observations at each concentration, and a lack of fit sum of squares is significant for each group. For practical purposes, the small, but significant, lack of fit does not seem important (17).

If all data from 10 to 10,000 ppb are represented by a single continuous curve, the linearity relationship between the absorbance and the concentration does not hold and Beer's law is not obeyed strictly, nor does it have to so long as the measurement regimen is reproducible. The reason(s) for this departure and the positive absorbance reading at 0 ppb are not known. It can be emphasized that endotoxins are macromolecules with molecular weights of 10^6–10^7. If portions of the molecular structure are polyelectrolytic, configurational changes can accompany dilution; these changes are accentuated at extremely low concentrations where unfolding might uncover more absorptive moieties. Disaggregation accompanying dilution could also be a possible cause of the increased slope in the low concentration region. Neither of these possibilities was proved in this work.

Scrupulous care must be exercised in handling glassware, cells, and solutions to achieve the precision reported. The data accumulated thus far are limited and, in the strictest sense, the method must be said to apply only to those bacterial endotoxins actually studied here. However, the endotoxins used were from an assortment of bacteria, and the results obtained hopefully presage wide applicability for the method[3].

REFERENCES

(1) A. I. Braude, *Sci. Am.*, **210**, 36 (1964).

(2) "Proceedings of a Symposium Held at the Institute of Microbiology at Rutgers—The State University," M. Landy and W. Braun, Eds., Quinn and Boden Co., Rahway, N.J., 1964.

(3) M. E. Webster, J. F. Sagin, M. Landy, and A. Johnson, *J. Immunol.*, **74**, 455 (1955).

(4) A. Boivin and L. Mesrobeanie, *C. R. Soc. Biol.*, **113**, 490 (1933). *Ibid.*, **128**, 5 (1938).

(5) J. L. Hartwell and M. J. Shear, *J. Nat. Cancer Inst.*, **4**, 107 (1943).

(6) V. O. Westphal, O. Luderitz, and F. Bister, *Z. Naturforsch.*, **7B**, 148 (1952).

(7) M. Dawson and J. P. Todd, *J. Pharm. Pharmacol.*, **4**, 97 (1952).

(8) J. Dorche and M. Castaing, *Ann. Pharm. Fr.*, **8**, 36 (1950).

(9) "The United States Pharmacopeia," 18th rev., Mack Publishing Co., Easton, Pa., 1970, p. 886.

(10) S. Marcus, C. Anselmo, and J. Luck, *J. Am. Pharm. Assoc., Sci. Ed.*, **49**, 616 (1960).

(11) R. B. Reinhold and J. Fine, *Proc. Soc. Exp. Biol. Med.*, **137**, 334 (1971).

(12) J. Levin and F. B. Bang, *Bull. Johns Hopkins Hosp.*, **115**, 265 (1964).

(13) J. F. Cooper, H. D. Hochstein, and E. B. Seligman, Jr., *Bull. Parenteral Drug Assoc.*, **26**, 153 (1972).

(14) E. T. Yin, C. Galanos, S. Kinsky, R. A. Bradshaw, S. Wessler, O. Luderitz, and M. E. Sarmiento, *Biochim. Biophys. Acta*, **261**, 284 (1972).

(15) H. D. Hochstein, R. J. Elin, J. F. Cooper, E. B. Seligman, Jr., and S. M. Wolff, *Bull. Parenteral Drug Assoc.*, **27**, 139 (1973).

(16) N. A. Karamian, *Am. Lab.*, 8 (3), 24 (1976).

(17) N. R. Draper and H. Smith, "Applied Regression Analysis," Wiley, New York, N.Y., 1966, p. 26.

ACKNOWLEDGMENTS AND ADDRESSES

Received August 1, 1975 from the *National Institutes of Health, Division of Research Services, Environmental Safety Branch, Bethesda, MD 20014, and the ‡Department of Chemistry, American University, Washington, DC 20016.

Accepted for publication June 17, 1976.

Adapted in part from a thesis submitted by N. A. Karamian to American University in partial fulfillment of the Doctor of Philosophy degree requirements.

ˣ To whom inquiries should be directed.

[3] U.S. patent applied for.

GLC Determination of Free Triclocarban in Blood

D. R. HOAR [x] and M. H. BOWEN *

Abstract □ A method is presented for the quantitative determination of free triclocarban in rat or human blood. The procedure involves the extraction from blood with acetone, a TLC cleanup, derivatization with *N,O*-bis(trimethylsilyl)acetamide, and GLC using an electron-capture detector. GLC–mass spectral analysis confirmed that the structure of the derivative was a bis(trimethylsilyl) molecule with one group on a nitrogen and the second group attached to the enol tautomer. The method is sensitive to 25 ng (12.5 μg/liter of blood). Recoveries of added triclocarban in the 12.5–50-μg/liter range were between 80 and 90%.

Keyphrases □ Triclocarban—GLC analysis, rat and human blood □ GLC—analysis, triclocarban, rat and human blood □ Disinfectants—triclocarban, GLC analysis, rat and human blood

The bacteriostatic agent triclocarban[1] is used exclusively in bar soaps. It is effective against both Gram-positive bacteria (*e.g.*, staphylococci) and fungi (1, 2). Its chemistry and antimicrobial properties were described previously (3). At the present time, the only methods for the determination of triclocarban are based on UV absorption (4) or HPLC[2]. Neither of these methods approaches the 10-μg/liter sensitivity of the GLC methods developed for the study of hexachlorophene (5) and triclosan[3] absorption.

A direct GLC measurement of triclocarban (4) was unsuccessful because of its low volatility. A method is now presented for the quantitative determination of free triclocarban in human and rat blood following derivatization. The procedure involves extraction from blood with acetone, a cleanup procedure by TLC, conversion to a trimethylsilyl derivative, and analysis by GLC using an electron-capture detector.

EXPERIMENTAL

Reagents—The following were used: triclocarban (>99% purity), acetone (analar grade), toluene (analar), ether (analar), acetonitrile (analar), and *N,O*-bis(trimethylsilyl)acetamide[4] (vacuum distilled).

Apparatus—GLC[5] was conducted on a glass column (1.5 m × 4 mm i.d.) containing 1.5% phenyl methyl silicone[6] and 1.95% trifluoropropyl methyl silicone[7] on 100–120-mesh Supelcon AW-DMCS[8].

All newly prepared columns were conditioned at 240° for 16 hr and then deactivated with 5 μl of hexamethyldisilazane. During analysis, the column and the detector were maintained at 210 and 300°, respectively. Nitrogen was used both as the carrier gas at 75 ml/min and as the purge gas to the ^{63}Ni-electron-capture detector at 25 ml/min.

GLC–Mass Spectrometry[9]—Combined GLC–mass spectrometry of the triclocarban derivative was conducted on a glass column (1.5 m × 4 mm i.d.) containing 3% methyl silicone[10] (OV-1) on 100–120-mesh Diatomite CLQ.

TLC—TLC was conducted on 250-μm silica gel GF plates[11] which had been prewashed overnight in a developing solvent [ether–toluene (1:4)]. After development, the separated bands were visualized by irradiation with a short wavelength (254 nm) UV lamp.

Calculation—The peak height for the trimethylsilyl derivative was measured and compared to a calibration curve prepared each day from known concentrations of triclocarban.

Assay Procedure—A 2.0-ml aliquot of whole blood (stored with edetate dipotassium dihydrate as an anticoagulant) was extracted twice by shaking with 10 ml of acetone. The mixture was centrifuged for 5 min at 1200×*g* after each extraction, and the solvent layers were removed. The combined extracts were placed in a warm water bath and concentrated to approximately 0.2 ml by a nitrogen stream. The concentrated extract was then applied to a silica gel GF plate as a narrow band. At least three aliquots of a standard solution containing 1 μg of triclocarban were spotted onto the plate, and the plate was developed for 10 cm and then allowed to dry at ambient temperature.

A 2-cm wide band of silica gel between the standards, located by irradiation with UV light, was scraped into a 10-ml tube and twice extracted with 10 ml of acetonitrile. The solvent was separated by centrifugation for 5 min at 1200×*g*, and the extracts were combined. The solution was placed on the water bath and concentrated to approximately 5 ml with nitrogen. This solution was transferred to a 10-ml tapered tube and blown to dryness. A 50-μl aliquot of *N,O*-bis(trimethylsilyl)acetamide was added to the residue, the tube was stoppered and placed in a water bath at 60° for 10 min, and a 5-μl aliquot was injected into the chromatograph.

RESULTS AND DISCUSSION

The structure of triclocarban suggests that the germicide might not be particularly well suited to direct GLC analysis. This compound was not eluted from nonpolar stationary phases even at high temperatures. Silylation gave a derivative that could be chromatographed at 210° on a mixed silicone column. Under these conditions, the derivative had a retention time of 7.8 min (Fig. 1).

Elucidation of Derivative Structure—The structure of the derivative was characterized by combined GLC–mass spectrometry. The mass spectrum (Fig. 2) corresponding to the peak from the flame-ionization detector gave significant fragments at *m/e* 458/460/462 (M, molecular ion), 386/388/390 (M − 72, loss of C_3H_8Si), 296/298/300 (further loss of C_3H_9Si + OH), and 73 (C_3H_9Si ion). This pattern confirms that the

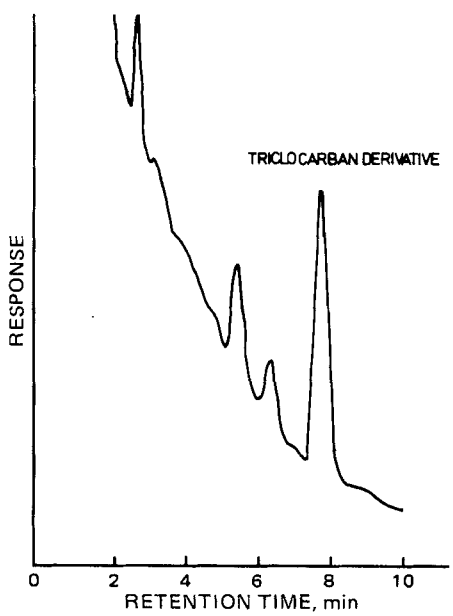

Figure 1—*Chromatogram of extract of whole blood containing 25 μg of triclocarban/liter.*

[1] TCC, 3,4,4′-trichlorocarbanilide, Monsanto.
[2] Paper presented by M. B. Graber and M. M. Goldstein, American Oil Chemists Society, Annual Spring Meeting, Mexico City, Mexico, 1974.
[3] Paper presented by D. R. Hoar and D. J. Sissons, Symposium at the University of Surrey, Surrey, England, September 1975. Triclosan is the generic name for 2′,4,4′-trichloro-2-hydroxydiphenyl ether (Irgasan DP300), Ciba-Geigy.
[4] Pierce Chemical Co.
[5] Pye series 104 chromatograph.
[6] SP 2250.
[7] SP 2401.
[8] Supelco Inc., Bellefonte, Pa.
[9] MS 902 mass spectrometer, AEI.
[10] Perkin-Elmer.
[11] Anachem.

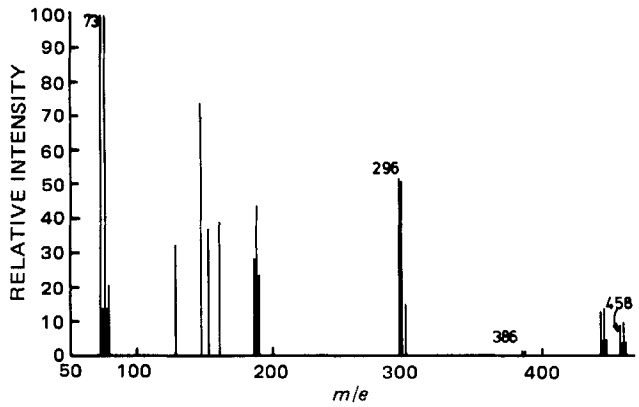

Figure 2—*Mass spectrum* (m/e *50–500*) *of the bis(trimethylsilyl) derivative of triclocarban.*

compound was a bis(trimethylsilyl) derivative. The relevant ions each displayed the characteristic trichloro isotope cluster. These particular ions show that only one nitrogen has a trimethylsilyl group while the second trimethylsilyl group is on the enol tautomer.

Examination of the spectra taken at intervals as the peak eluted showed that the ratio of *m/e* 458 to 386 decreased. This finding suggested that the derivative was capable of breaking down to the mono(trimethylsilyl) compound.

It was reported (6) that the drug rafoxanide[12] forms a similar bis(trimethylsilyl) derivative on a phenolic group and a secondary amide group. This derivative was shown to react with active sites on a chromatographic packing, exchanging one of its trimethylsilyl groups for a hydrogen atom to form a mono derivative. This effect was very small when carefully deactivated columns were used. Since electron-capture GLC of standard solutions gave only one peak, the column used for the GLC–mass spectral analysis may not have been completely deactivated.

This phenomenon of silyl donation was not completely unexpected since the amide structure of the derivative is similar to that of the silylating reagent. Therefore, it is important to maintain excess reagent to obtain a quantitative conversion to the bis(trimethylsilyl) derivative and to ensure that the column is completely deactivated. The optimum conditions of derivatization were determined to be 10 min and 60° with *N,O*-bis(trimethylsilyl)acetamide acting as the solvent as well as the derivatizing agent. A linear response was obtained over the range of 5–100 ng of triclocarban.

TLC of Blood Extracts—Ether–toluene (1:4), in which the R_f of triclocarban was 0.4, was by far the most effective solvent system. It separated triclocarban from interfering bands in the blood extract which were concentrated at the origin or solvent front.

Various solvents were evaluated for their ability to extract triclocarban from silica gel TLC plates. It was reported previously (7) that it is frequently necessary to use a solvent with a much greater polarity than the developing solvent. This suggestion was only partly relevant since, although acetonitrile gave 90% recovery, the more polar methanol gave only 41% recovery.

Recovery Experiments—A duplicate series of aliquots containing 25, 50, and 100 ng of triclocarban was blown to dryness in 10-ml tubes. Aliquots (2.0 ml) of whole blood were added to one series of tubes, and the samples were shaken and then analyzed by the described procedure. The second series of standards was taken up in 0.2 ml of acetone and put through the TLC cleanup procedure and the derivatization. The recoveries of these samples relative to a series of standard solutions that had only been concentrated and derivatized are given in Table I.

[12] Rafoxanide is generic name for 3′-chloro-4′-(*p*-chlorophenoxy)-2-hydroxy-3,5-diiodobenzanilide.

Table I—Recovery of Free Triclocarban Added to Whole Blood

Amount Added to Blood, ng	Amount through Cleanup, ng	Mean Recovery, %	*SD*
100	—	82	±4
—	100	80	±4
50	—	82	±6
—	50	86	±5
25	—	89	±15
—	25	90	±0

The results in Table I show that the recoveries of free triclocarban from whole blood in the 12.5–50-μg/liter range were between 80 and 90%. The results from the standard solutions that had been through only the cleanup procedure and derivatization were in good agreement with the recoveries from the blood samples. These results showed that the losses were occurring during the elution from the TLC plate rather than during the extraction from blood. This finding was confirmed by spotting aliquots containing 50 ng of triclocarban onto a TLC plate, allowing the spots to dry, scraping off the silica gel, and eluting with acetonitrile without developing the plate. The mean recovery was 90%.

Since the sensitivity of this method is comparable to methods used for other germicides, it should be applicable to studies on the absorption and metabolism of triclocarban. The metabolic pathway may be hydroxylation followed by conjugation with glucuronic acid or sulfate (8). Therefore, it is possible that this derivatization method may be applicable to the determination both of the amount and nature of the metabolite(s).

REFERENCES

(1) W. A. Hamilton, *J. Gen. Microbiol.*, **50**, 441 (1968).

(2) T. F. McNamara and M. Steinbach, *J. Am. Oil. Chem. Soc.*, **44**, 478 (1967).

(3) D. P. Roman, E. H. Barnett, and R. J. Balske, *Proc. Sci. Sect. Toilet Goods Assoc.*, **28**, 1213 (1957).

(4) H. S. C. Hong, R. J. Steltenkamp, and N. L. Smith, *J. Pharm. Sci.*, **64**, 860 (1975).

(5) D. G. Ferry and E. G. McQueen, *J. Chromatogr.*, **76**, 233 (1973).

(6) C. P. Talley, N. R. Trenner, G. V. Downing, and W. J. A. VandenHeuvel, *Anal. Chem.*, **43**, 1379 (1971).

(7) E. Stahl, "Thin Layer Chromatography," 2nd ed., George Allen and Unwin Ltd., London, England, 1969, p. 149.

(8) L. G. Scharpf, Jr., I. D. Hill, and H. I. Maibach, *Arch. Environ. Health*, **30**, 7 (1975).

ACKNOWLEDGMENTS AND ADDRESSES

Received January 12, 1976, from *Unilever Research, Colworth House, Sharnbrook, Bedford, England.*

Accepted for publication May 19, 1976.

The authors thank Mr. D. Welti for the GLC–mass spectral analysis.

* Present address: Edwin Cooper & Co. Ltd., Bracknell, Berkshire, England.

[x] To whom inquiries should be directed.

Effect of Surfactants on Absorption through Membranes V: Concentration-Dependent Effect of a Bile Salt (Sodium Deoxycholate) on Absorption of a Poorly Absorbable Drug, Phenolsulfonphthalein, in Humans

M. WAFIK GOUDA *x, NAWAL KHALAFALAH ‡, and SAID A. KHALIL ‡

Abstract □ The effect of administration of 600- and 300-mg doses of sodium deoxycholate 1 hr before phenolsulfonphthalein solution is reported. The 600-mg dose caused a decrease in drug bioavailability as measured by the total amount excreted in 24 hr. The 300-mg dose caused an increase in the initial phenolsulfonphthalein absorption rate, suggesting a direct action of the bile salt on membrane permeability. The decrease in absorption upon administration of 600 mg was attributed to micellar entrapment of the drug molecule.

Keyphrases □ Sodium deoxycholate—effect of preadministration on absorption and excretion of phenolsulfonphthalein, humans □ Phenolsulfonphthalein—absorption and excretion, effect of preadministration of sodium deoxycholate, humans □ Absorption—phenolsulfonphthalein, effect of preadministration of sodium deoxycholate, humans □ Excretion—phenolsulfonphthalein, effect of preadministration of sodium deoxycholate, humans □ Bile salts—sodium deoxycholate, effect of preadministration on absorption and excretion of phenolsulfonphthalein, humans

Bile salts, an important class of surface-active agents, play a significant role in the intestinal absorption of lipids (1, 2) and lipid-soluble vitamins. Several reports (3–6) indicated that bile salts influence drug absorption. Most accumulated data were derived from animal studies. Data obtained from human studies are limited. An increase in the urinary recovery of riboflavin in humans was reported when a 600-mg dose of sodium deoxycholate was administered 0.5 hr prior to the oral ingestion of the vitamin (7).

Sodium deoxycholate enhanced the absorption of phenolsulfonphthalein, a poorly absorbable drug, in the rat (4). The aim of the present study was to determine if a similar effect occurs in humans.

EXPERIMENTAL

The study was designed in a crossover fashion. The urinary excretion of phenolsulfonphthalein was determined following the administration of Treatments A, B, and C (Table I). Ten healthy volunteers (capable of informed consent) participated in Treatments A and B, and seven of these volunteers participated in Treatment C. Doses were administered at weekly intervals to fasting subjects. Fluid and food intake, as well as the analysis of the urine samples, was carried out as previously described (8).

RESULTS AND DISCUSSION

Administration of 600 mg of sodium deoxycholate 1 hr before phenolsulfonphthalein solution did not result in a significant change in the amount of the dye excreted in 1 hr. However, the total amount excreted in 24 hr was significantly less than the control (Table II). Administration of 300 mg of the bile salt increased significantly the amount of phenolsulfonphthalein excreted in 1 hr, while the total amount of the dye excreted in 24 hr was not significantly different from the control. The time course of phenolsulfonphthalein excretion following the various treatments is shown in Fig. 1. The average data in the figure are a good reflection of the individual results.

The increase in the initial rate of absorption (1-hr urinary excretion data, Table II) following the administration of 300 mg of sodium deoxycholate suggests a direct action of the bile salt on the membrane permeability, in agreement with other studies in animals (4, 5) and humans (7). Data in Table II and Fig. 1 indicate that 600 mg of sodium deoxycholate did not significantly affect the initial phenolsulfonphthalein absorption rate. Previous studies with bile salts indicated that the change in membrane permeability did not increase with an increase in the surfactant concentration (9). A minimum concentration of bile salt was usually sufficient to produce a maximum effect on membrane permeability. Hence, the higher dose of sodium deoxycholate was expected to produce a similar, but not necessarily greater, effect on the initial phenolsulfonphthalein absorption rate as that of the lower dose.

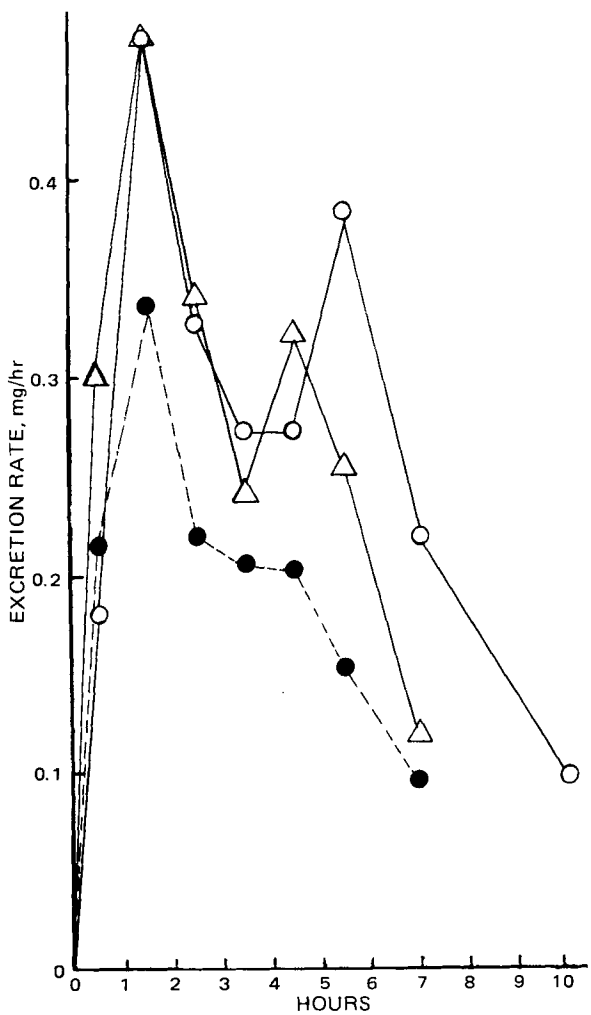

Figure 1—*Mean urinary excretion rates of phenolsulfonphthalein after oral administration of 20 mg in solution. Key: ○, control (average of 10 subjects); ●, pretreatment with 600 mg of sodium deoxycholate (average of 10 subjects); and △, pretreatment with 300 mg of sodium deoxycholate (average of seven subjects).*

Table I—Regimen of Treatments Administered to Human Volunteers

Hours	Treatment A	Treatment B	Treatment C
−1	100 ml of water	600 mg of sodium deoxycholate[a] with 100 ml of water	300 mg of sodium deoxycholate[a] with 100 ml of water
−0.5	100 ml of water in all treatments		
0	20 mg of phenolsulfonphthalein[b] dissolved in 50 ml of water[c] in all treatments		
1, 2, 3, 4, 5, 6, 8, 12, 24	Collection of urine in all treatments		

[a] Sodium deoxycholate (Mann Research Lab., New York, N.Y.) was administered in hard gelatin capsules, each containing 300 mg. [b] Nutritional Biochemical Corp., Cleveland, Ohio. [c] Contains 20 mg of sodium bicarbonate to aid the solubility of phenolsulfonphthalein.

The results obtained with Treatment B are not in agreement with this expectation and suggest that the direct effect of the bile salt on the membrane must have been masked by an opposing effect tending to decrease phenolsulfonphthalein absorption. The 24-hr urinary excretion data (Table II) give the same picture of two opposing effects of the bile salt on phenolsulfonphthalein absorption and provide evidence that the decrease in drug absorption becomes significant with the increase in the sodium deoxycholate concentration.

The decrease in the total excretion of phenolsulfonphthalein upon administration of 600 mg of the bile salt is believed to be the result of micellar solubilization. Entrapment of the dye in the micelles of sodium deoxycholate, with the resultant loss in thermodynamic activity, is expected to result in decreased absorption. Phenolsulfonphthalein was previously shown (5) to be a candidate for entrapment in the micelles of other bile salts. The concentration of bile salts in human intestinal content was reported (10) to be slightly above their critical micellar concentration. Therefore, it is expected that administration of both 300 and 600 mg of sodium deoxycholate will result in a micellar solution in the intestinal tract.

It seems that a direct membrane effect, resulting in potentiation of the initial rate of absorption, predominates at the lower dose, while more micelles entrap more drug at the higher dose, resulting in decreased absorption. The excretion pattern (Fig. 1) suggests this possibility. Higher concentrations of surfactants (3) including bile salts (11) decreased drug absorption. Although none of the volunteers reported experiencing a laxative effect, the possibility that the 600-mg dose of the bile salt resulted in an increased GI motility, and hence decreased absorption, cannot be ruled out. The delay in gastric emptying, suggested (7) as one possible explanation of the increased bioavailability of riboflavin after administration of a similar dose of the same bile salt, was not evident in the present study (Fig. 1).

The data of the present study and of Mayersohn *et al.* (7) suggest that, depending on the drug and its absorption mechanism, bile salts could decrease as well as increase drug absorption.

Table II—Effect of Sodium Deoxycholate on Phenolsulfonphthalein Absorption in Humans

Subject (Age, years; Weight, kg)	Amount of Phenolsulfonphthalein Excreted, mg: 1 hr A[a]	1 hr B	1 hr C	24 hr A	24 hr B	24 hr C
SK (41, 94)	0.122	0.148	0.378	3.430	1.210	2.280
OA (27, 90)	0.103	0.212	0.224	2.030	1.350	1.730
AH (50, 75)	0.218	0.179	0.231	2.150	1.480	1.940
SA (24, 71)	0.262	0.251	0.486	2.530	1.450	2.380
AR (31, 72)	0.181	0.254	0.196	1.750	1.630	1.840
MS (30, 61)	0.215	0.259	0.222	2.280	1.470	2.340
GM (29, 66)	0.167	0.120	0.349	1.860	1.490	2.660
WG (36, 72)	0.182	0.167		4.050	1.660	
ME (29, 63)	0.245	0.399		3.020	2.070	
AA (29, 69)	0.108	0.172		1.340	1.470	
Mean	0.180	0.216	0.298	2.444	1.528	2.167
RSD	31	37	36	34	15	16
Significance level[b]		N.S.	95.0%		99.0%	N.S.

[a] Treatment. [b] Paired *t* test *versus* Treatment A (same subjects).

REFERENCES

(1) A. M. Dawson, *Br. Med. Bull.*, **23**, 247 (1967).

(2) M. Gagnon and A. M. Dawson, *Proc. Soc. Exp. Biol. Med.*, **127**, 99 (1968).

(3) M. Gibaldi and S. Feldman, *J. Pharm. Sci.*, **59**, 579 (1970).

(4) S. Feldman, M. Salvino, and M. Gibaldi, *ibid.*, **59**, 705 (1970).

(5) K. Kakemi, H. Sezaki, R. Konishi, T. Kirmura, and M. Murakami, *Chem. Pharm. Bull.*, **18**, 275 (1970).

(6) K. Kakemi, H. Sezaki, R. Konishi, T. Kimura, and A. Okida, *ibid.*, **18**, 1034 (1970).

(7) M. Mayersohn, S. Feldman, and M. Gibaldi, *J. Nutr.*, **98**, 288 (1969).

(8) N. Khalafallah, M. W. Gouda, and S. A. Khalil, *J. Pharm. Sci.*, **64**, 991 (1975).

(9) S. Feldman and M. Gibaldi, *ibid.*, **58**, 425 (1969).

(10) A. F. Hofmann, *Gastroenterology*, **48**, 484 (1965).

(11) T. S. Gaginella, P. Bass, J. H. Perrin, and J. J. Vallner, *J. Pharm. Sci.*, **62**, 1121 (1973).

ACKNOWLEDGMENTS AND ADDRESSES

Received January 20, 1976, from the *School of Pharmacy, University of Montana, Missoula, MN 59801, and the ‡Faculty of Pharmacy, University of Alexandria, Alexandria, Egypt.

Accepted for publication June 17, 1976.

Supported by the National Science Foundation under SFC Program Grants GF 39207 and GF 38851.

ˣ To whom inquiries should be directed.

Uptake of Acetazolamide by Human Erythrocytes *In Vitro*

SYLVIA M. WALLACE [x] and SIDNEY RIEGELMAN

Abstract □ The binding of acetazolamide to human erythrocytes was studied *in vitro*. Blood and plasma samples were analyzed by electron-capture GLC. At 37°, drug equilibrated between plasma and erythrocytes in approximately 40 min. The effect of plasma concentration on the steady-state level of drug within the erythrocytes was examined. Erythrocyte accumulation of acetazolamide appeared to be a composite of two processes: a nonlinear, saturable process and a linear, diffusion-controlled process. By appropriate linear transformation of the data, estimates of the erythrocyte binding capacity and the dissociation constant for the drug were obtained.

Keyphrases □ Acetazolamide—*in vitro* binding to human erythrocytes, effect of plasma drug concentration on steady-state level within erythrocytes □ Binding—acetazolamide to human erythrocytes *in vitro*, effect of plasma drug concentration on steady-state level within erythrocytes □ Erythrocytes, human—binding of acetazolamide *in vitro*, effect of plasma drug concentration on steady-state level within erythrocytes □ Plasma drug concentration—effect on steady-state level of acetazolamide within human erythrocytes □ Carbonic anhydrase inhibitors—*in vitro* binding to human erythrocytes, effect of plasma drug concentration on steady-state level within erythrocytes

The erythrocyte compartment of the blood is often dismissed as an insignificant consideration in pharmacokinetics. Blood and plasma levels are often merely *assumed* to be equivalent terms. However, many drugs accumulate significantly in erythrocytes. Concentrations of salicylate (1), phenobarbital (1), phenytoin (2), chlorpromazine (3), and chlorthalidone (4) within the erythrocyte are all in excess of the free drug concentration in the plasma. The nature of the interaction and accumulation is unknown and probably varies, and the significance of these interactions in the overall pharmacokinetics of the drugs has not been determined.

After a single oral dose of acetazolamide to humans, concentration–time profiles of the drug in erythrocytes and plasma were significantly different[1]. Twenty-four hours after the dose, erythrocyte levels were four times greater than plasma levels. This accumulation was previously attributed to binding to erythrocyte carbonic anhydrase (5). Although Maren *et al.* (6) reported that erythrocyte uptake appears to have two components—one diffusible, *i.e.*, lost by washing, and the other bound—the extent and strength of binding have not been determined.

In vivo, in a dynamic situation, a single event such as erythrocyte uptake is difficult to isolate from the multiplicity of kinetic events occurring. Therefore, to determine the strength and capacity of acetazolamide binding, erythrocyte uptake of the drug was studied *in vitro* in a closed system.

EXPERIMENTAL

Time Course to Equilibration—Acetazolamide was added to whole human blood[2] and warmed to 37°, and the mixture was swirled gently on a water bath[3]. Aliquots were withdrawn at 10, 20, 40, 60, and 120 min and centrifuged[4] for 1 min to separate the plasma.

Equilibrium Studies—Whole blood containing varying concentrations of acetazolamide was incubated for 1 hr at 37° with gentle swirling. Aliquots (50 μl) of blood were withdrawn for analysis, and the remainder was centrifuged[5] for 15 min at 1500 rpm. Plasma and blood were analyzed, and the erythrocyte concentration was calculated from the difference using the hematocrit. The free drug concentration in the plasma was determined in plasma water samples obtained by microultrafiltration (7). Results of individual representative experiments are illustrated in Figs. 1–4.

Similar experiments were conducted using a synthetic blood medium consisting of erythrocytes washed three times with isotonic Sorenson's phosphate buffer (pH 7.4) and reconstituted to a hematocrit of approximately 0.5 with the buffer. To determine if washing erythrocytes altered acetazolamide uptake, erythrocytes washed three times with buffer were reconstituted with plasma and the results were compared to those obtained with whole blood.

GLC Analysis—Acetazolamide was determined in plasma and blood by GLC using a ^{63}Ni-electron-capture detector[6]. Samples were processed and chromatographed on a glass column packed with 3% OV-17 coated on Gas Chrom Q[7] (100–120 mesh).

RESULTS AND DISCUSSION

After addition of acetazolamide to whole blood *in vitro*, equilibration of acetazolamide between plasma and erythrocytes did not occur instantaneously. Steady state was established 40 min later (Fig. 1). *In vivo*, in subjects administered a single oral dose of acetazolamide, erythrocyte levels reached peak concentrations 1–2 hr after plasma levels. Presumably, this lag time *in vivo* reflects the equilibration time noted *in vitro*.

Uptake of acetazolamide by the erythrocytes is concentration dependent. Although a distinct plateau is not reached if the erythrocyte concentration of acetazolamide at equilibrium is plotted against the plasma concentration, the graph is curvilinear (Fig. 2). The ratio of the erythrocyte–plasma concentration decreases as the plasma concentration increases.

For example, at a hematocrit of 0.5 and plasma concentration of 1.6 μg/ml (blood concentration of 5 μg/ml), the erythrocyte–plasma ratio was 5.2:1. However, at a plasma concentration of 23.2 μg/ml (blood concentration of 30 μg/ml), the ratio was 1.6:1. Thus, over a wide range of plasma concentrations, the erythrocyte–plasma ratio cannot be characterized by a single value. As in the case of plasma protein binding of drugs, for a given percentage bound to have any significance, the total plasma concentration must be known.

Since erythrocyte uptake of acetazolamide is concentration dependent, it is assumed to be partially composed of a saturable process. The total erythrocyte concentration can be expressed as:

$$RBC_{total} = RBC_b + RBC_f \qquad \text{(Eq. 1)}$$

At equilibrium, the diffusible free drug concentration, RBC_f, within the erythrocytes is assumed to be equal to the concentration of free drug in the plasma, C_f; therefore:

$$RBC_b = RBC_{total} - C_f \qquad \text{(Eq. 2)}$$

The total uptake curve is a sum of two processes: a linear, presumably diffusion-controlled process such that RBC_f is equal to C_f and a nonlinear, saturable binding process such that the relationship of RBC_b to

[1] Presented at the Basic Pharmaceutics Section, APhA Academy of Pharmaceutical Sciences, San Francisco meeting, April 1975.

[2] Irwin Memorial Blood Bank, San Francisco, Calif.

[3] Metabolyte water bath shaker, New Brunswick Scientific Co., New Brunswick, N.J.

[4] Beckman/Spinco 152 microfuge.

[5] IEC model UV centrifuge, International Equipment Co.

[6] Varian series 1200 aerograph, Walnut Creek, Calif.

[7] Applied Science Laboratories, State College, Pa.

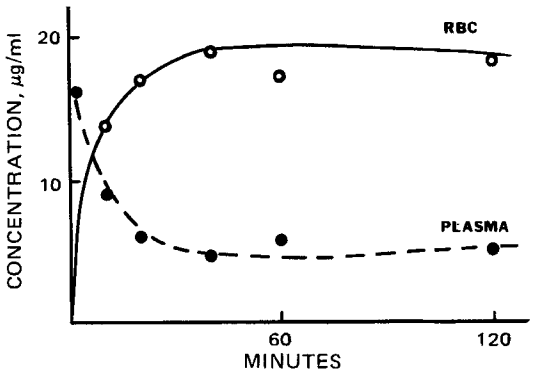

Figure 1—*Time course of erythrocyte (RBC) uptake of acetazolamide at a total blood concentration of 10 μg/ml. (All drug was assumed to be present initially in plasma.)*

C_f changes with the free concentration (Fig. 3). The curve for RBC_b is obtained by subtracting the values for RBC_f from the experimental curve, RBC_{total}.

The bound concentration, RBC_b, as calculated from Eq. 2, can also be expressed in terms of the law of mass action for the reversible macromolecule–ligand interaction:

$$RBC_b = \frac{nMk_aC_f}{1 + k_aC_f} \qquad \text{(Eq. 3)}$$

Since the macromolecule concentration is unknown, only the product of the number of binding sites, n, and the macromolecule concentration, M, can be calculated. However, the product nM is a useful parameter, because it represents the maximum binding capacity of the protein.

Linear transformation (8) of Eq. 3 yields:

$$\frac{RBC_b}{C_f} = nMk_a - k_aRBC_b \qquad \text{(Eq. 4)}$$

Thus, for a plot of RBC_b/C_f *versus* RBC_b, the absolute value of the slope is the association constant, k_a, and the intercept on the abscissa, the maximum binding capacity, nM (Fig. 4). The dissociation constant, k_d, is the reciprocal of the association constant.

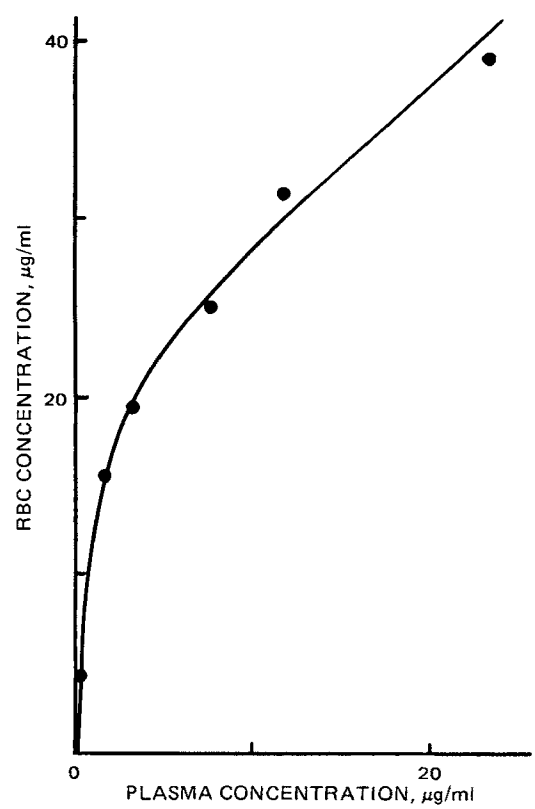

Figure 2—*Erythrocyte concentration of acetazolamide at equilibrium as a function of the total plasma concentration.*

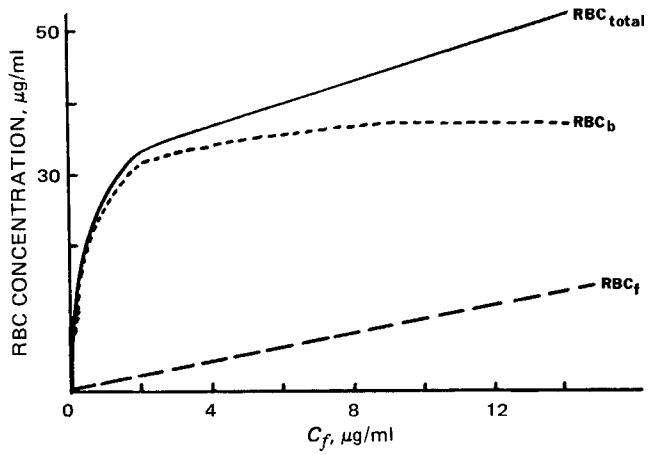

Figure 3—*Total (RBC_{total}, obtained experimentally), bound (RBC_b), and free (RBC_f) erythrocyte concentrations of acetazolamide as a function of the free drug concentration in plasma (C_f).*

Thus, to determine binding parameters for acetazolamide and erythrocytes, blood, total plasma, and free plasma concentrations were determined at equilibrium. Since greater than 90% of acetazolamide in plasma is bound to plasma protein (7), plasma ultrafiltrates were obtained to measure the freely diffusible drug in whole blood. By using a synthetic blood medium of erythrocytes suspended in isotonic buffer, the free drug concentration can be measured directly in the protein-free supernate. Washing the erythrocytes with isotonic buffer in the process of preparing the suspension does not alter the uptake of the drug. Uptake of acetazolamide from the plasma by untreated erythrocytes and by those washed with buffer is essentially the same (Fig. 4).

The concentration bound by erythrocytes was calculated by subtracting the unbound plasma concentration from the total erythrocyte concentration. Data were linearized according to Eq. 4, and the binding parameters were calculated by least-squares linear regression analysis (Fig. 4).

Blood samples varied in their maximum binding capacity and dissociation constant for acetazolamide (Table I). However, the values were in the same range as those reported (9) for human erythrocyte carbonic anhydrase B, *i.e.*, a molar concentration of 136 μM (30 μg/ml) and an inhibitory constant (K_i for acetazolamide) of 1 μM (0.22 μg/ml). These data strengthen the hypothesis (5) that the accumulation of the drug within the erythrocytes is due to binding to intracellular carbonic anhydrase.

Because blood samples varied not only in their erythrocyte binding but also in their plasma protein binding of acetazolamide, the plasma concentration at which erythrocyte binding sites become saturated cannot be closely defined. Lehmann *et al.* (9) suggested that inhibition of erythrocyte carbonic anhydrase may induce some of the side effects of acetazolamide therapy. However, attempts to delineate a maximum tolerable plasma level of drug sufficient to saturate erythrocyte enzyme may be thwarted by the large individual variation in binding parameters. Determination of the erythrocyte binding capacity for acetazolamide may

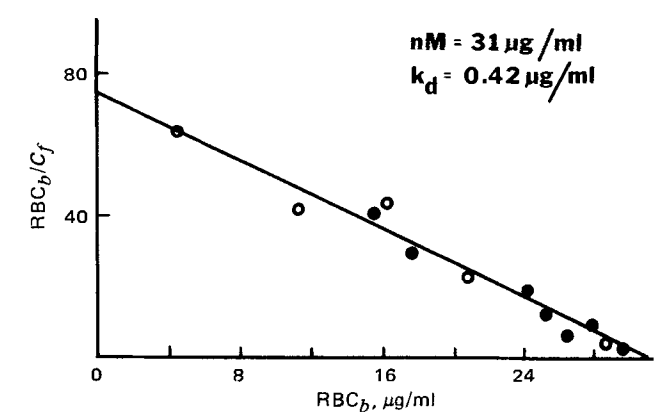

Figure 4—*Rosenthal plot of the binding of acetazolamide to human erythrocytes* in vitro, *Experiment 4. Key:* ○, *washed blood cells reconstituted with pH 7.4 phosphate buffer; and* ●, *whole blood.*

Table I—Binding of Acetazolamide to Human Erythrocytes *In Vitro*

		k_d, μg/ml	nM, μg/ml
1[a]	Erythrocytes in buffer, pH 7.4	0.50	21
2	Whole blood	0.23	27
	Erythrocytes in buffer, pH 7.4	0.23	28
3	Whole blood	0.41	29
	Erythrocytes in buffer, pH 7.4	0.24	27
4	Whole blood	0.43	32
	Erythrocytes in buffer, pH 7.4	0.40	31
	Mean	0.35	28
	SD	0.11	3.6

[a] Numbers indicate experiments performed with different units of whole blood.

still provide an estimate of the safe therapeutic limit for the plasma concentration of the drug.

REFERENCES

(1) J. N. McArthur, P. D. Dawkins, and J. H. Smith, *J. Pharm. Pharmacol.*, **23**, 32 (1971).

(2) D. Kurata and G. R. Wilkinson, *Clin. Pharmacol. Ther.*, **16**, 355 (1974).

(3) P. N. Kaul, M. K. Ticku, and M. L. Clark, *J. Pharm. Sci.*, **61**, 1753 (1972).

(4) B. Beerman, K. Hellstrom, B. Lindstrom, and A. Rosen, *Clin. Pharmacol. Ther.*, **17**, 424 (1975).

(5) T. H. Maren, *Physiol. Rev.*, **47**, 595 (1967).

(6) T. H. Maren, B. Robinson, R. F. Palmer, and M. C. Griffith, *Biochem. Pharmacol.*, **6**, 21 (1961).

(7) V. P. Shah, S. M. Wallace, and S. Riegelman, *J. Pharm. Sci.*, **63**, 1364 (1974).

(8) H. E. Rosenthal, *Anal. Biochem.*, **20**, 525 (1967).

(9) B. Lehmann, E. Linner, and P. J. Wistrand, *Adv. Biosci.*, **5**, 197 (1969).

ACKNOWLEDGMENTS AND ADDRESSES

Received February 26, 1976, from the *Department of Pharmacy, School of Pharmacy, University of California, San Francisco, CA 94143.*

Accepted for publication June 21, 1976.

Presented at the Basic Pharmaceutics Section, APhA Academy of Pharmaceutical Sciences, Atlanta meeting, November 1975.

Supported in part by U.S. Public Health Service Grant NIGMS 16496 and Lederle Laboratories.

[x] To whom inquiries should be directed. Postdoctoral Fellow, Killam Foundation, University of British Columbia, Vancouver, Canada. Present address: College of Pharmacy, University of Saskatchewan, Saskatoon, Canada S7N-0W0.

Direct Analysis of Salicylic Acid in Keratolytic Plaster by Gas–Solid Chromatography

PAK H. KO

Abstract □ A rapid gas–solid chromatographic method is reported for the direct analysis of salicylic acid in keratolytic plaster. The method requires no preseparation or derivatization and takes about 14 min. Since it requires only 2–7 mg of sample, it can determine the salicylic acid concentration in a particular area of plaster. The analyzing column is packed with porous polymer beads of 2,6-diphenyl-1,4-phenylene oxide. An automatic solid sampling system is used in connection with the gas chromatograph employing dual flame-ionization detectors. The average recovery of salicylic acid in synthetic samples containing 400–2700 μg was 100.6 ± 1.6%. The average correlation coefficient of the peak area against the standard was +0.9995 ± 0.0003 for samples in the 300–3000-μg range.

Keyphrases □ Salicylic acid—gas–solid chromatographic analysis, commercial plaster pads □ Gas–solid chromatography—analysis, salicylic acid in commercial plaster pads □ Keratolytics—salicylic acid, gas–solid chromatographic analysis in commercial plaster pads

The 40% salicylic acid (I) keratolytic plaster is a uniform mixture of I in a suitable base spread on a backing material such as paper or cloth. The USP (1) requires the plaster mass to contain not less than 90.0% and not more than 110.0% of the labeled amount of I.

To check for uniform distribution of I and for specification compliance, a specific method that does not require a fairly large sample is needed. Since the USP method (1) requires more than 1 g of the plaster base, excluding the backing material, it lacks the sensitivity desired for the type of product[1] with considerably less than 10 mg of the plaster base in a small disk. Furthermore, the USP method is very lengthy.

BACKGROUND

Literature methods for the determination of I that are based on measurement of UV absorption (2–4), color intensity of its ferric chelate (5, 6), fluorescence (7, 8), and alkalimetric titration (9) either required extensive separation manipulations or gave unsatisfactory results due to interference by the excipients in the plaster base.

Several investigators reported the use of GLC for the determination of I in pharmaceuticals and biological media (10–14). However, the methyl ester and methyl ether derivatives (11, 12) or the trimethylsilyl derivative (13, 14) of I had to be prepared before GLC analysis for sufficient volatility; otherwise, severe tailing occurred (10).

Because of the low solubility of the plaster base in most common solvents, methods requiring additional steps to extract I prior to GLC determination or other functional group analyses are less desirable than a direct method by which I in a plaster base can be analyzed without preseparation.

A direct method by gas–solid chromatography (GSC) for determining underivatized I with three other ingredients in a mixture was reported previously (15). This paper reports a rapid and specific GSC method using the same column (15) for the direct determination of I in the plaster base of callus pads without preliminary separation or derivatization.

[1] Zino Corn Pads, Scholl, Inc., Chicago, IL 60610.

Table I—Binding of Acetazolamide to Human Erythrocytes *In Vitro*

		k_d, μg/ml	nM, μg/ml
1[a]	Erythrocytes in buffer, pH 7.4	0.50	21
2	Whole blood	0.23	27
	Erythrocytes in buffer, pH 7.4	0.23	28
3	Whole blood	0.41	29
	Erythrocytes in buffer, pH 7.4	0.24	27
4	Whole blood	0.43	32
	Erythrocytes in buffer, pH 7.4	0.40	31
	Mean	0.35	28
	SD	0.11	3.6

[a] Numbers indicate experiments performed with different units of whole blood.

still provide an estimate of the safe therapeutic limit for the plasma concentration of the drug.

REFERENCES

(1) J. N. McArthur, P. D. Dawkins, and J. H. Smith, *J. Pharm. Pharmacol.*, **23**, 32 (1971).

(2) D. Kurata and G. R. Wilkinson, *Clin. Pharmacol. Ther.*, **16**, 355 (1974).

(3) P. N. Kaul, M. K. Ticku, and M. L. Clark, *J. Pharm. Sci.*, **61**, 1753 (1972).

(4) B. Beerman, K. Hellstrom, B. Lindstrom, and A. Rosen, *Clin. Pharmacol. Ther.*, **17**, 424 (1975).

(5) T. H. Maren, *Physiol. Rev.*, **47**, 595 (1967).

(6) T. H. Maren, B. Robinson, R. F. Palmer, and M. C. Griffith, *Biochem. Pharmacol.*, **6**, 21 (1961).

(7) V. P. Shah, S. M. Wallace, and S. Riegelman, *J. Pharm. Sci.*, **63**, 1364 (1974).

(8) H. E. Rosenthal, *Anal. Biochem.*, **20**, 525 (1967).

(9) B. Lehmann, E. Linner, and P. J. Wistrand, *Adv. Biosci.*, **5**, 197 (1969).

ACKNOWLEDGMENTS AND ADDRESSES

Received February 26, 1976, from the *Department of Pharmacy, School of Pharmacy, University of California, San Francisco, CA 94143.*

Accepted for publication June 21, 1976.

Presented at the Basic Pharmaceutics Section, APhA Academy of Pharmaceutical Sciences, Atlanta meeting, November 1975.

Supported in part by U.S. Public Health Service Grant NIGMS 16496 and Lederle Laboratories.

[x] To whom inquiries should be directed. Postdoctoral Fellow, Killam Foundation, University of British Columbia, Vancouver, Canada. Present address: College of Pharmacy, University of Saskatchewan, Saskatoon, Canada S7N-0W0.

Direct Analysis of Salicylic Acid in Keratolytic Plaster by Gas–Solid Chromatography

PAK H. KO

Abstract □ A rapid gas–solid chromatographic method is reported for the direct analysis of salicylic acid in keratolytic plaster. The method requires no preseparation or derivatization and takes about 14 min. Since it requires only 2–7 mg of sample, it can determine the salicylic acid concentration in a particular area of plaster. The analyzing column is packed with porous polymer beads of 2,6-diphenyl-1,4-phenylene oxide. An automatic solid sampling system is used in connection with the gas chromatograph employing dual flame-ionization detectors. The average recovery of salicylic acid in synthetic samples containing 400–2700 μg was 100.6 ± 1.6%. The average correlation coefficient of the peak area against the standard was +0.9995 ± 0.0003 for samples in the 300–3000-μg range.

Keyphrases □ Salicylic acid—gas–solid chromatographic analysis, commercial plaster pads □ Gas–solid chromatography—analysis, salicylic acid in commercial plaster pads □ Keratolytics—salicylic acid, gas–solid chromatographic analysis in commercial plaster pads

The 40% salicylic acid (I) keratolytic plaster is a uniform mixture of I in a suitable base spread on a backing material such as paper or cloth. The USP (1) requires the plaster mass to contain not less than 90.0% and not more than 110.0% of the labeled amount of I.

To check for uniform distribution of I and for specification compliance, a specific method that does not require a fairly large sample is needed. Since the USP method (1) requires more than 1 g of the plaster base, excluding the backing material, it lacks the sensitivity desired for the type of product[1] with considerably less than 10 mg of the plaster base in a small disk. Furthermore, the USP method is very lengthy.

BACKGROUND

Literature methods for the determination of I that are based on measurement of UV absorption (2–4), color intensity of its ferric chelate (5, 6), fluorescence (7, 8), and alkalimetric titration (9) either required extensive separation manipulations or gave unsatisfactory results due to interference by the excipients in the plaster base.

Several investigators reported the use of GLC for the determination of I in pharmaceuticals and biological media (10–14). However, the methyl ester and methyl ether derivatives (11, 12) or the trimethylsilyl derivative (13, 14) of I had to be prepared before GLC analysis for sufficient volatility; otherwise, severe tailing occurred (10).

Because of the low solubility of the plaster base in most common solvents, methods requiring additional steps to extract I prior to GLC determination or other functional group analyses are less desirable than a direct method by which I in a plaster base can be analyzed without preseparation.

A direct method by gas–solid chromatography (GSC) for determining underivatized I with three other ingredients in a mixture was reported previously (15). This paper reports a rapid and specific GSC method using the same column (15) for the direct determination of I in the plaster base of callus pads without preliminary separation or derivatization.

[1] Zino Corn Pads, Scholl, Inc., Chicago, IL 60610.

Table I—Recovery of Salicylic Acid Added to Placebo Plaster Base

Ratio of Salicylic Acid–Placebo Plaster Base	Salicylic Acid Added, μg	Salicylic Acid Found, μg	Recovery, %
0.31	408	400	98.0
0.24	517	517	100.0
0.26	598	605	101.2
0.31	651	660	101.4
0.27	739	750	101.5
0.26	785	797	101.5
0.64	854	850	99.5
0.37	969	946	97.6
0.45	1011	1035	102.4
0.37	1050	1040	99.0
0.50	1197	1176	98.2
0.80	1237	1256	101.5
0.85	1494	1533	102.6
0.39	1514	1506	99.5
0.61	1605	1621	101.0
0.43	2089	2136	102.2
0.41	2713	2783	102.6
			100.6 ± 1.6

EXPERIMENTAL

Standard—USP grade salicylic acid[2] was used.

GSC Column—A pair of 1.8-m × 0.32-cm o.d. stainless steel columns were packed with 60–80-mesh porous polymer beads of 2,6-diphenyl-1,4-phenylene oxide[3]. Newly packed columns were conditioned at 260° with helium carrier gas flow for 1 hr before use.

Apparatus—The GSC analyses were performed on a gas chromatograph[4] equipped with dual flame-ionization detectors. An automatic capsule sampling system[5] was fitted over the head of the analyzing column. A digital integrator[6] was used to analyze the signals from the flame-ionization detector. The interfacing mechanism was modified to link the integrator, the chromatograph, and the programmer of the automatic capsule sampling system, which were made by different manufacturers. An electronic microbalance[7] for weighing standards and samples, special aluminum capsules[8] for holding standards and samples, and a capsule cold-welding accessory[9] for sealing aluminum capsules containing standards and samples were used.

The chromatography conditions were: injection port, 280°; interface, 290°; column, initially 180° and (after the capsule is punctured) immediately programmed at 16°/min to the upper limit of 245° and maintained at the upper limit for 8 min; helium gas flow, 30 ml/min; detector hydrogen, 40 ml/min; and detector air, 500 ml/min.

Calibration Curve—Standard I samples were weighed into tared aluminum capsules to prepare a calibration curve with the range of 300–3000 μg. The capsules were sealed immediately. The samples were analyzed according to the suggested experimental condition using the gas chromatograph and the automatic sampling system. Specific information pertaining to the use of the automatic sampling system was given elsewhere[10].

The area of the I peak by each standard, as printed out by the digital integrator, was used to establish the calibration curve of area *versus* mass of I for the day's work. The least-squares linear regression method was perferred for showing the calibration.

Analysis of Samples—Samples of plaster base containing I were scraped from the backing cloth with a thin spatula and weighed in tared capsules. The size of the sample was chosen depending on the concentration of the I in the product in order to conform to the range of the calibration curve. The samples were analyzed in the same manner as the standards. The sample's peak area counts were used directly to calculate the I content in the samples according to the slope and intercept obtained by the least-squares linear regression analysis of the calibration runs.

[2] Tenneco Chemicals, Heydon Division, New York, NY 10017.
[3] Tenax GC, Applied Science Labs., State College, PA 16801.
[4] Perkin-Elmer model 3920, Norwalk, CT 06856.
[5] Perkin-Elmer model AS41.
[6] Hewlett-Packard model 3380A.
[7] Perkin-Elmer model AD-1.
[8] Perkin-Elmer part No. 009-0709.
[9] Perkin-Elmer identification No. 043680.
[10] See the Perkin-Elmer Manual for Autosampler AS-41.

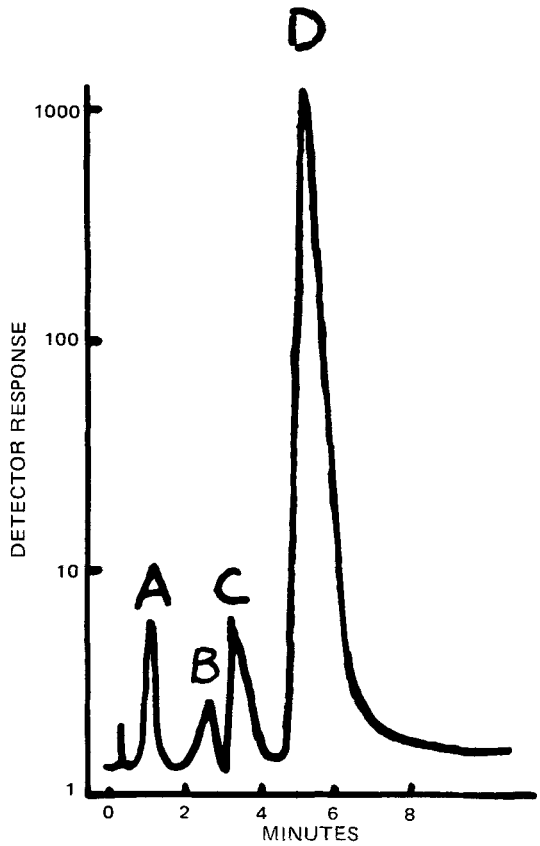

Figure 1—*Gas–solid chromatogram of keratolytic plaster. Key: A, B, and C, unidentified volatile ingredients; and D, salicylic acid.*

RESULTS AND DISCUSSION

Experimental results showed that underivatized solid I can be determined by this new method.

GSC Analysis Time Requirement—Complete elution of I was within 7 min from the time of injection, the time when the sample capsule was conveyed to the vaporizer port behind the trap door. A hollow thorn pierced the capsule, and the helium gas swept the sample vapors through the hollow thorn into the analyzing column. The complete cycle of temperature programming and cooling for the next sample required 14 min.

Calibration Curve Linearity and Sample Size Limitation—The correlation coefficients from various days were determined, and a mean value of +0.9995 was obtained with a standard deviation of 0.0003. Calibration routinely consisted of 15–29 individually weighed standards covering the range of 300–3000 μg of I, and the calibration curves obtained were linear.

When the I mass was less than 300 μg, the chromatographic response (peak area per unit weight of I) became slightly smaller. The cause for deviation has not been determined at this time. Therefore, sample sizes were adjusted to avoid having less than 300 μg of I. Samples with I content much higher than 3000 μg also were avoided because the volume in the aluminum capsule was limited. When the plaster base sample was too big and not enough empty space was available in the capsule, the gummy base material clogged the capillary of the thorn and blocked the carrier gas and the sample vapors from entering the column. Besides avoiding excessively large samples, a way to alleviate the clogging problem is to wrap the plaster base samples in small pieces of porous tissue paper before inserting samples into the capsules.

Continuous Calibration—Although experience showed no significant fluctuation of flame-ionization detector response during runs, slight changes of response were occasionally observed after shutdowns and startups of the instruments.

Since this method uses the I peak area for quantitation and the flame-ionization detector response is affected by the ratio of air and hydrogen, this laboratory routinely monitors the flame-ionization detector response during the span of analyses, usually for several days and nights, by intermittently analyzing known I standards along with unknown samples to ascertain the calibration validity.

Method Accuracy—Table I shows the amounts of I added and those recovered in the synthetic samples containing different ratios of placebo plaster base. The average recovery of I, covering the range of 400–2700 μg of I/sample, was 100.6 ± 1.6%. The accuracy of the method was maintained even when the I concentration was below the formula's theoretical level.

Advantages of Direct Solid Analysis—Because the plaster base samples were directly analyzed without preseparation such as extractions and filtrations, mechanical loss of I was avoided. The proposed method is superior to the methyl ester–methyl ether and trimethylsilyl GLC methods because multiple derivatives of I may be formed upon derivatization (11–14), which may lead to errors. With this method, interferences from solvents and derivatizing agents were totally eliminated.

Since all nonvolatile components in the plaster base were retained in the aluminum capsule and kept from contacting the column, there was essentially no contamination of the packing material. This undoubtedly contributed to the reproducible performance of the column, which has been used to analyze more than 1000 samples but shows no sign of deterioration.

No significant interference is caused by the other volatile ingredients for analysis of I using this method. Figure 1 shows a typical chromatogram (recorded in log scale of the digital integrator) for the analysis of I in a keratolytic plaster, illustrating the separation of I from the other impurities and the general elution characteristics of I.

REFERENCES

(1) "The United States Pharmacopeia," 19th rev., Mack Publishing Co., Easton, Pa., 1975.

(2) G. Ungar, E. Damgaard, and W. K. Wong, *Proc. Soc. Exp. Biol. Med.*, **80**, 45 (1952).

(3) G. W. Stevenson, *Anal. Chem.*, **32**, 1522 (1960).

(4) R. G. Reed and W. W. Davis, *J. Pharm. Sci.*, **54**, 1533 (1965).

(5) C. W. Strode, Jr., F. N. Stewart, H. O. Schott, and O. J. Coleman, *Anal. Chem.*, **29**, 1184 (1957).

(6) V. Cotty, F. Zurzola, T. Beezley, and A. Rogers, *J. Pharm. Sci.*, **54**, 868 (1965).

(7) S. Udenfriend, D. E. Duggan, B. M. Vasta, and B. B. Brodie, *J. Pharmacol. Exp. Ther.*, **120**, 26 (1957).

(8) W. E. Lange and S. A. Bell, *J. Pharm. Sci.*, **55**, 386 (1966).

(9) "Standard Methods of Chemical Analysis," 6th ed., vol. IIA, F. J. Welcher, Ed., Van Nostrand Reinhold, New York, N.Y., 1963, p. 597.

(10) J. G. Nikelly, *Anal. Chem.*, **36**, 2248 (1964).

(11) C. H. Morris, J. E. Christian, R. R. Landolt, and W. G. Hansen, *J. Pharm. Sci.*, **59**, 270 (1970).

(12) J. R. Watson, P. Crescuolo, and F. Matsui, *ibid.*, **60**, 454 (1971).

(13) L. J. Walter, D. F. Biggs, and R. T. Coutts, *ibid.*, **63**, 1754 (1974).

(14) M. J. Rance, B. J. Jordon, and J. D. Nichols, *J. Pharm. Pharmacol.*, **27**, 425 (1975).

(15) P. H. Ko, "Abstracts of Papers, No. 38," Analytical Chemistry Session, First Chemical Congress of the North American Continent, Mexico City, Mexico, Dec. 1975.

ACKNOWLEDGMENTS AND ADDRESSES

Received March 18, 1976, from the *Corporate Research and Development Department, Scholl, Inc., Chicago, IL 60610.*

Accepted for publication June 21, 1976.

The author thanks Ms. Patricia Liepins for laboratory assistance.

Present address: Johnson Products Co., Inc., Chicago, IL 60620.

Stability of Phenylbutazone in Presence of Pharmaceutical Colors

ROSALIND BAUGH, R. T. CALVERT, and J. T. FELL ˣ

Abstract □ The degradation of phenylbutazone was studied in the presence of lakes suitable for coloring the sugar coats of phenylbutazone tablets. The drug was degraded, in light, in the presence of erythrosine sodium. The degradation probably proceeds *via* singlet oxygen generated by the light-excited dye. The degradation may be important in some quality control procedures and can lead, for example, to unusual results in dissolution rate testing.

Keyphrases □ Phenylbutazone—stability in presence of various pharmaceutical colors, effect of light □ Stability—phenylbutazone in presence of various pharmaceutical colors, effect of light □ Colors, various pharmaceutical—effect on stability of phenylbutazone, effect of light □ Antirheumatic agents—phenylbutazone, stability in presence of various pharmaceutical colors, effect of light

Colors are used in pharmaceutical dosage forms for their aesthetic appeal and as an aid to identification. Coated tablets are frequently colored, and lakes are becoming increasingly popular for this purpose because they offer advantages in the speed of application and cover uniformity. The stability of pharmaceutical dyes and lakes was assessed (1, 2), but little attention has been paid to the possible interactions between colors and drugs.

Amaranth (FD&C Red No. 2 lake), erythrosine sodium (FD&C Red No. 3 lake), tartrazine (FD&C Yellow No. 5 lake), and FD&C Yellow No. 6 lake may be used in combination to give a color suitable for incorporation in the sugar coats of phenylbutazone tablets. This report is concerned with the interaction between these lakes and phenylbutazone.

EXPERIMENTAL

Materials—Amaranth lake[1], erythrosine sodium lake[1], tartrazine lake[1], and FD&C Yellow No. 6 lake[1] (sunset yellow) were obtained as separate powders and as a mixture in syrup[1]. Phenylbutazone[2] was of BP quality, and soluble erythrosine sodium[3] and methylene blue[3] were of reagent grade.

Irradiation of Samples—Suspensions or solutions of the materials in phosphate buffer (pH 7.4) were prepared and stored in subdued light. The test mixtures were exposed, in 1-cm quartz cells, to unfiltered light from a 300-w projector bulb situated 50 cm from the cell. Measurements of the liquid temperature during runs indicated no heating effect by the light beam. Due to the fine particle size of the lakes, sedimentation problems did not arise during the experiment.

[1] Colorcon Ltd., Orpington, England.
[2] Thomas Kerfoot Ltd., Ashton under Lyne, England.
[3] B.D.H. Ltd., Poole, England.

Method Accuracy—Table I shows the amounts of I added and those recovered in the synthetic samples containing different ratios of placebo plaster base. The average recovery of I, covering the range of 400–2700 μg of I/sample, was 100.6 ± 1.6%. The accuracy of the method was maintained even when the I concentration was below the formula's theoretical level.

Advantages of Direct Solid Analysis—Because the plaster base samples were directly analyzed without preseparation such as extractions and filtrations, mechanical loss of I was avoided. The proposed method is superior to the methyl ester–methyl ether and trimethylsilyl GLC methods because multiple derivatives of I may be formed upon derivatization (11–14), which may lead to errors. With this method, interferences from solvents and derivatizing agents were totally eliminated.

Since all nonvolatile components in the plaster base were retained in the aluminum capsule and kept from contacting the column, there was essentially no contamination of the packing material. This undoubtedly contributed to the reproducible performance of the column, which has been used to analyze more than 1000 samples but shows no sign of deterioration.

No significant interference is caused by the other volatile ingredients for analysis of I using this method. Figure 1 shows a typical chromatogram (recorded in log scale of the digital integrator) for the analysis of I in a keratolytic plaster, illustrating the separation of I from the other impurities and the general elution characteristics of I.

REFERENCES

(1) "The United States Pharmacopeia," 19th rev., Mack Publishing Co., Easton, Pa., 1975.

(2) G. Ungar, E. Damgaard, and W. K. Wong, *Proc. Soc. Exp. Biol. Med.*, **80**, 45 (1952).

(3) G. W. Stevenson, *Anal. Chem.*, **32**, 1522 (1960).

(4) R. G. Reed and W. W. Davis, *J. Pharm. Sci.*, **54**, 1533 (1965).

(5) C. W. Strode, Jr., F. N. Stewart, H. O. Schott, and O. J. Coleman, *Anal. Chem.*, **29**, 1184 (1957).

(6) V. Cotty, F. Zurzola, T. Beezley, and A. Rogers, *J. Pharm. Sci.*, **54**, 868 (1965).

(7) S. Udenfriend, D. E. Duggan, B. M. Vasta, and B. B. Brodie, *J. Pharmacol. Exp. Ther.*, **120**, 26 (1957).

(8) W. E. Lange and S. A. Bell, *J. Pharm. Sci.*, **55**, 386 (1966).

(9) "Standard Methods of Chemical Analysis," 6th ed., vol. IIA, F. J. Welcher, Ed., Van Nostrand Reinhold, New York, N.Y., 1963, p. 597.

(10) J. G. Nikelly, *Anal. Chem.*, **36**, 2248 (1964).

(11) C. H. Morris, J. E. Christian, R. R. Landolt, and W. G. Hansen, *J. Pharm. Sci.*, **59**, 270 (1970).

(12) J. R. Watson, P. Crescuolo, and F. Matsui, *ibid.*, **60**, 454 (1971).

(13) L. J. Walter, D. F. Biggs, and R. T. Coutts, *ibid.*, **63**, 1754 (1974).

(14) M. J. Rance, B. J. Jordon, and J. D. Nichols, *J. Pharm. Pharmacol.*, **27**, 425 (1975).

(15) P. H. Ko, "Abstracts of Papers, No. 38," Analytical Chemistry Session, First Chemical Congress of the North American Continent, Mexico City, Mexico, Dec. 1975.

ACKNOWLEDGMENTS AND ADDRESSES

Received March 18, 1976, from the *Corporate Research and Development Department, Scholl, Inc., Chicago, IL 60610.*

Accepted for publication June 21, 1976.

The author thanks Ms. Patricia Liepins for laboratory assistance.

Present address: Johnson Products Co., Inc., Chicago, IL 60620.

Stability of Phenylbutazone in Presence of Pharmaceutical Colors

ROSALIND BAUGH, R. T. CALVERT, and J. T. FELL ˣ

Abstract □ The degradation of phenylbutazone was studied in the presence of lakes suitable for coloring the sugar coats of phenylbutazone tablets. The drug was degraded, in light, in the presence of erythrosine sodium. The degradation probably proceeds *via* singlet oxygen generated by the light-excited dye. The degradation may be important in some quality control procedures and can lead, for example, to unusual results in dissolution rate testing.

Keyphrases □ Phenylbutazone—stability in presence of various pharmaceutical colors, effect of light □ Stability—phenylbutazone in presence of various pharmaceutical colors, effect of light □ Colors, various pharmaceutical—effect on stability of phenylbutazone, effect of light □ Antirheumatic agents—phenylbutazone, stability in presence of various pharmaceutical colors, effect of light

Colors are used in pharmaceutical dosage forms for their aesthetic appeal and as an aid to identification. Coated tablets are frequently colored, and lakes are becoming increasingly popular for this purpose because they offer advantages in the speed of application and cover uniformity. The stability of pharmaceutical dyes and lakes was assessed (1, 2), but little attention has been paid to the possible interactions between colors and drugs.

Amaranth (FD&C Red No. 2 lake), erythrosine sodium (FD&C Red No. 3 lake), tartrazine (FD&C Yellow No. 5 lake), and FD&C Yellow No. 6 lake may be used in combination to give a color suitable for incorporation in the sugar coats of phenylbutazone tablets. This report is concerned with the interaction between these lakes and phenylbutazone.

EXPERIMENTAL

Materials—Amaranth lake[1], erythrosine sodium lake[1], tartrazine lake[1], and FD&C Yellow No. 6 lake[1] (sunset yellow) were obtained as separate powders and as a mixture in syrup[1]. Phenylbutazone[2] was of BP quality, and soluble erythrosine sodium[3] and methylene blue[3] were of reagent grade.

Irradiation of Samples—Suspensions or solutions of the materials in phosphate buffer (pH 7.4) were prepared and stored in subdued light. The test mixtures were exposed, in 1-cm quartz cells, to unfiltered light from a 300-w projector bulb situated 50 cm from the cell. Measurements of the liquid temperature during runs indicated no heating effect by the light beam. Due to the fine particle size of the lakes, sedimentation problems did not arise during the experiment.

[1] Colorcon Ltd., Orpington, England.
[2] Thomas Kerfoot Ltd., Ashton under Lyne, England.
[3] B.D.H. Ltd., Poole, England.

Table I—Rate Constants for Degradation of 0.001% Phenylbutazone under Various Conditions

	Concentration, mg/liter													
	None	None	Lake Mixture, 9.00	Lake Mixture, 9.00	Erythrosine Sodium Lake, 1.23[a]	Erythrosine Sodium Lake, 2.45[a]	Erythrosine Sodium Lake, 4.90[a]	Erythrosine Sodium Lake, 9.80[a]	Erythrosine Sodium Lake, 19.60[a]	Soluble Erythrosine Sodium, 7.84	Amaranth Lake, 2.48	Tartrazine Lake, 2.45	FD&C Yellow No. 6 Lake, 2.51
Conditions	Light	Dark	Light	Dark	Light	Light	Light	Light	Light	Light	Light	Light	Light
Rate constant, min^{-1}	~0	~0	0.016	~0	0.017	0.019	0.091	0.155	0.195	0.062	~0	~0	~0

[a] Dye content = 40%.

At various intervals, the cell was removed from the beam, and the phenylbutazone concentration was measured spectrophotometrically at 264 nm. Corrections were applied for absorbance due to the lake. Interference from the degradation products of phenylbutazone was accounted for by measuring absorbance at the absorption peak of the degradation product (235 nm) and applying the simultaneous equations suggested by Beckstead *et al.* (3).

Identity of Degradation Products—Identification of the degradation products was accomplished by TLC using the method of Awang *et al.* (4). The use of silica gel–kieselguhr plates buffered at pH 6 prevented on-plate oxidation. As a further precaution, the plates were dried under nitrogen.

Dissolution Rates—Dissolution rates were measured by the method of Barrett and Fell (5). Coated phenylbutazone tablets were allowed to dissolve in 1 liter of phosphate buffer (pH 7.4) maintained at 37° and stirred at 70 rpm with a three-blade stirrer. Samples were removed at suitable intervals and filtered through membrane filters[4] (0.45 μm) mounted in special adaptors[4], and the phenylbutazone concentration was determined spectrophotometrically. The filtration procedure removed the majority of the lake.

RESULTS AND DISCUSSION

The concentration of phenylbutazone in solution (0.001% w/v) was monitored on exposure to light and to light in the presence of the lake mixture (0.0009% w/v). Rate constants for the degradation of phenylbutazone under these conditions were calculated from semilogarithmic plots derived from the original data shown in Fig. 1 (Table I). Comparative data for the changes of phenylbutazone concentration in the dark and in the dark in the presence of the lake mixture also are shown in Table I.

The rate constants indicate that phenylbutazone was stable in solution on illumination and in the dark and in the dark when mixed with the lakes. However, illumination of the phenylbutazone plus the lake mixture led to rapid phenylbutazone decomposition.

The effect of the individual lakes in approximately the same concentration as in the lake mixture on the degradation of phenybutazone was examined, and the resulting rate constants are given in Table I. Only erythrosine sodium lake caused measurable degradation of the phenylbutazone, the rate increasing with increasing lake concentration (Fig. 2 and Table I). This effect was also found with a solution of erythrosine sodium (0.00078% w/v), but a slower rate of degradation was noted than with an equivalent lake concentration (Table I), possibly due to a surface catalytic effect.

Only one degradation product could be isolated on TLC (4) from the phenylbutazone–erythrosine sodium mixture after illumination. It was identified as 1,2-diphenyl-4-*n*-butyl-4-hydroxypyrazolidine-3,5-dione

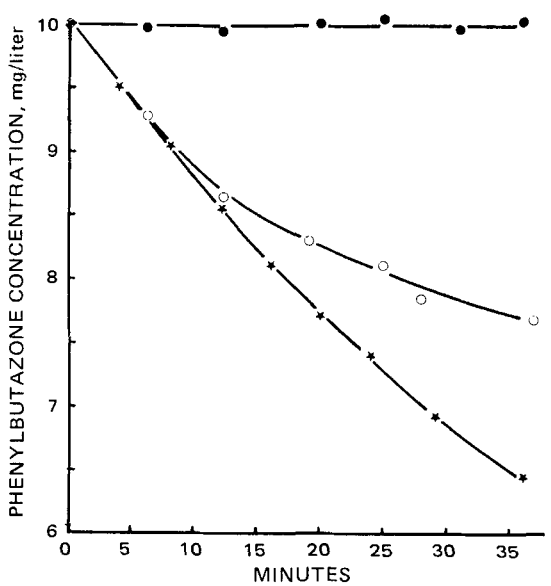

Figure 1—*Effect of the lake mixture on the degradation of 0.001% phenylbutazone solution under various conditions. Key: ★, phenylbutazone plus lake mixture in the light; ○, phenylbutazone plus lake mixture in the light after bubbling with nitrogen prior to irradiation; and ●, phenylbutazone plus lake mixture in the dark. Similar plots were obtained for phenylbutazone alone in the light and phenylbutazone plus other lake mixture components in the light.*

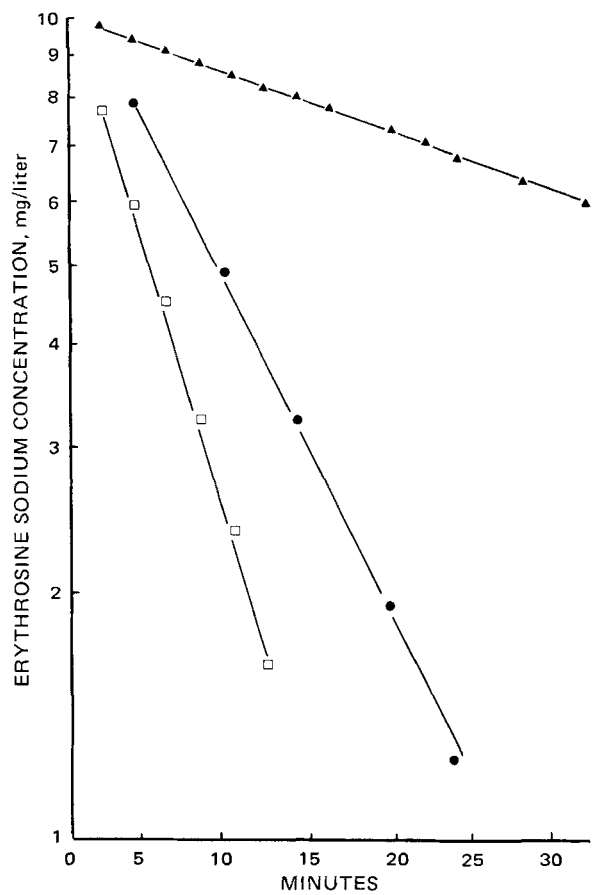

Figure 2—*Effect of erythrosine sodium lake concentration on the degradation of 0.001% phenylbutazone solution exposed to unfiltered light. Key: ▲, 1.23 mg/liter; ●, 4.90 mg/liter; and □, 9.80 mg/liter.*

[4] Millipore filters in Swinnex adaptors, Millipore Ltd., London, England.

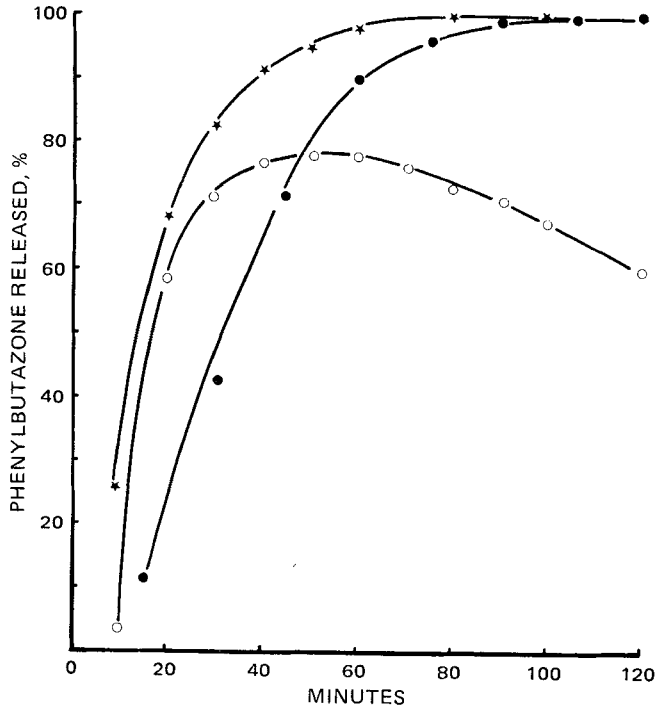

Figure 3—*Release rate of phenylbutazone from coated tablets containing erythrosine sodium in the light (○) and dark (★) or ponceau 4R in the light and dark (●).*

by comparison of R_f values on TLC with an authentic sample. This product is a known degradation product of phenylbutazone and is formed by oxidation (4). Illumination of phenylbutazone solution in the presence of the lake mixture after flushing the liquid with nitrogen markedly decreased the degradation rate of phenylbutazone (Fig. 1). This finding suggests that a mechanism involving oxygen is involved in the dye-catalyzed degradation of phenylbutazone on illumination.

Reactions involving dyes as photosensitizers are often mediated by singlet oxygen (6). A possible mechanism is suggested in Scheme I, where D = dye and R = oxidizable material. This mechanism involves the excitation of the dye into its triplet state by the light. The dye in the triplet state may return to the ground state with release of energy or may transfer the energy to ground-state triplet oxygen, generating singlet oxygen. The singlet oxygen may return to the ground state or attack oxidizable material present, in this case, phenylbutazone.

$$D + h\nu \rightarrow {}^3D^*$$
$$^3D^* \rightarrow D + h\nu'$$
$$^3D^* + {}^3O_2 \rightarrow D + {}^1O_2^*$$
$$^1O_2^* \rightarrow {}^3O_2$$
$$R + {}^1O_2^* \rightarrow RO_2$$

Scheme I

Further support for the suggestion that this scheme operates during the degradation of phenylbutazone by erythrosine sodium came from experiments in which methylene blue (10^{-7} *M*), a known generator of singlet oxygen, was substituted for erythrosine sodium and exposed to identical conditions. The phenylbutazone was degraded to the same degradation product as was produced with erythrosine sodium (first-order rate constant = 0.0282 min^{-1}).

The importance of this reaction lies in procedures where the drug, in solution, is brought into contact with erythrosine sodium in the presence of light, as in quality control procedures such as assays or dissolution rate testing. Figure 3 shows the results from the dissolution rate testing of coated phenylbutazone tablets. In one case, the color in the sugar coating contained erythrosine sodium; in the other, the erythrosine sodium had been replaced by ponceau 4R and the proportions of the other lakes had been altered to obtain an identical color. The tablets were not prepared from the same batch of cores, but comparison can be made between the types of dissolution profiles rather than absolute values.

The testing was carried out under normal laboratory lighting conditions, consisting of natural light from windows and artificial light from fluorescent fittings, and in the dark. When the tablet coat contained erythrosine sodium, the concentration of phenylbutazone in the beaker fell after a certain time due to degradation in the light in the manner described. Equivalent tests run in the dark showed no degradation, and the concentration of phenylbutazone rose to 100%. For tablets with the reformulated color, the drug dissolved and reached 100% in solution both in the dark and in the light, indicating that no degradation had occurred.

If tests are carried out in the light on tablets containing erythrosine sodium in the sugar coat and samples are taken only before the phenylbutazone concentration starts to fall, a falsely low dissolution rate will be indicated due to the competing reactions of dissolution and degradation.

REFERENCES

(1) F. W. Goodhart, H. A. Lieberman, D. S. Mody, and F. C. Ninger, *J. Pharm. Sci.*, **56**, 63 (1967).

(2) P. Turi, D. Brusco, H. V. Maulding, R. A. Tausendfreund, and A. F. Michaelis, *ibid.*, **61**, 1811 (1972).

(3) H. D. Beckstead, K. K. Kaistha, and S. J. Smith, *ibid.*, **57**, 1952 (1968).

(4) D. V. C. Awang, A. Vincent, and F. Matsui, *ibid.*, **62**, 1673 (1973).

(5) D. Barrett and J. T. Fell, *ibid.*, **64**, 335 (1975).

(6) R. Chapelon, G. Perichet, and B. Pouyet, *Mol. Photochem.*, **5**, 77 (1973).

ACKNOWLEDGMENTS AND ADDRESSES

Received April 9, 1976, from the *Pharmacy Department, University of Manchester, Manchester, M13 9PL, England.*

Accepted for publication June 22, 1976.

The authors thank Colorcon Ltd. for the lakes, Geigy Pharmaceuticals Ltd. for the phenylbutazone degradation products, and Thomas Kerfoot Ltd. for phenylbutazone.

[x] To whom inquiries should be directed.

High-Pressure Liquid Chromatographic Analysis of Polythiazide in Pharmaceutical Tablet Formulations

C. K. WONG, D. Y. J. TSAU, D. M. COHEN ˣ, and K. P. MUNNELLY

Abstract □ A high-pressure liquid chromatographic method was developed for the quantitative determination of polythiazide in pharmaceutical tablet formulations after extraction of the powdered tablets with a water–acetonitrile solvent. Analysis is accomplished by comparison of peak areas after chromatography.

Keyphrases □ Polythiazide—high-pressure liquid chromatographic analysis, pharmaceutical formulations □ High-pressure liquid chromatography—analysis, polythiazide in pharmaceutical formulations □ Diuretics—polythiazide, high-pressure liquid chromatographic analysis in pharmaceutical formulations □ Antihypertensives—polythiazide, high-pressure liquid chromatographic analysis in pharmaceutical formulations

Polythiazide {6-chloro-3,4-dihydro-2-methyl - 3 - [[(2,2,2-trifluoroethyl)thio]methyl] -2*H*- 1,2,4- benzothiadiazine-7-sulfonamide 1,1-dioxide}, an orally effective, nonmercurial diuretic and antihypertensive agent, is supplied as a tablet, alone and in combination with reserpine (1). Methods for the determination of polythiazide include TLC (2), spectrophotometry (3–5), column chromatography (6), and polarography (7, 8). However, these methods do not have the rapidity, simplicity, sensitivity, and accuracy of the high-pressure liquid chromatographic (HPLC) methodology.

Recently, a quantitative HPLC method for polythiazide involving reversed-phase partition chromatography was published (9). This method utilized a Bondapak phenyl/Corasil column[1], methanol–water (35:65 v/v) as the mobile phase, and peak height quantitation. The system, however, does not appear optimum since the absolute recovery of added polythiazide was reported as 106%, and baseline separation was not achieved between vanillin, a formulation excipient, and polythiazide, and polythiazide and the reported internal standard, quinoline. The subject of this report is the development of a simple, direct, extremely rapid, and precise HPLC procedure for the quantitation of polythiazide in several pharmaceutical tablet formulations.

EXPERIMENTAL

Apparatus—A high-pressure liquid chromatograph[2], operated at ambient temperature, was equipped with a UV detector for monitoring the column effluent at 254 nm. The column[3] was 25-cm × 4.6-mm (i.d.) stainless steel packed with Partisil 10-ODS. An electronic computing integrator[4] was used to obtain peak areas. A 10-μl loop injection valve[5] was used to introduce samples into the chromatographic system.

Reagents—Polythiazide NF reference standard was dried in vacuum at 60° for 2 hr. Reagent ACS grade acetonitrile[6] and distilled water were used in preparing the mobile phase.

Mobile Phase—Add 20 ml of distilled water to 980 ml of acetonitrile and shake vigorously. Degas prior to use.

Standard Solution—Accurately weigh approximately 50 mg of polythiazide reference standard, transfer quantitatively to a 250-ml volumetric flask, and dissolve in and dilute to volume with the mobile phase.

Sample Solution—Accurately weigh and finely powder 20 polythiazide tablets. Transfer an accurately weighed portion of the powder, equivalent to about 2 mg of polythiazide, to a glass-stoppered 30-ml centrifuge tube. Add 10 ml of the mobile phase, shake for 30 min, centrifuge, and filter the supernate through a 1-μm membrane filter[7]. Use the filtered supernate for analysis.

Chromatography—Condition the column for 24 hr with the mobile phase at a flow rate of 0.5 ml/min. This procedure is necessary for new columns; conditioning is not required for previously used columns. Inject 10 μl of the standard solution and adjust either the pressure or flow rate so that the polythiazide exhibits a retention time of about 3 min.

The approximate chromatographic conditions are a flow rate of 1 ml/min (at an inlet pressure of 300 psig), a chart speed of 1.3 cm (0.5 in.)/min, and a detector sensitivity of 0.32 absorbance unit full-scale (aufs). Data acquisition parameters for the electronic computing integrator were optimized according to the manufacturer's instructions.

For the analysis of a sample, two 10-μl aliquots of the standard solution are injected followed by two 10-μl injections of the sample solution. The peak areas obtained or peak heights may be used for the calculations.

RESULTS AND DISCUSSION

Initial studies concerned the selection of an appropriate column for the separation and quantitation of polythiazide. The adsorption mode of chromatography was investigated using a silica gel-type column[8]. With methanol as the mobile phase, a sharp and symmetrical peak was observed for polythiazide. As additional injections of polythiazide were made onto the column, peak broadening and finally peak splitting were observed. This phenomenon may be attributed either to a nonuniform adsorption of polythiazide on the column or to elution of residual polythiazide retained on the column from previous injections.

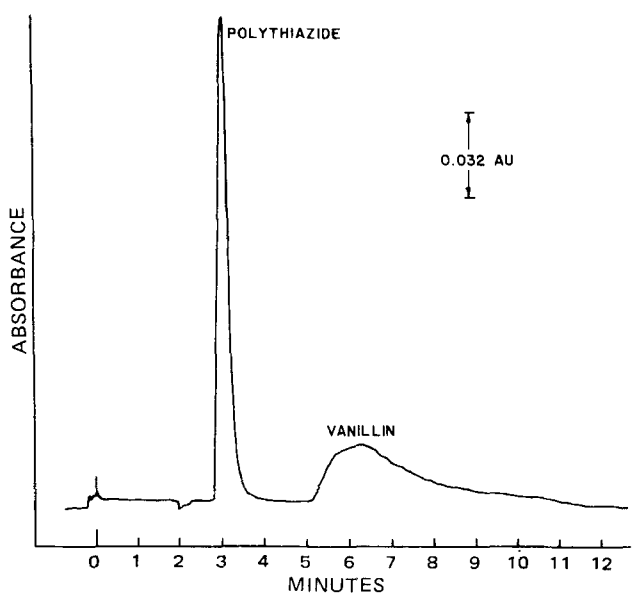

Figure 1—*Representative chromatogram of a polythiazide tablet formulation.*

[1] Catalog No. 27283, Waters Associates.
[2] DuPont model 840.
[3] Catalog No. PXS-1025-ODS, Whatman Inc.
[4] Autolab System I, Spectra-Physics Corp.
[5] Catalog No. 204590, DuPont.
[6] Eastman Kodak.
[7] Catalog No. FALP 02500, Millipore Corp.
[8] Pellosil-HS, catalog No. A011, Whatman Inc.

Table I—Percent Recovery of Polythiazide from Spiked Placeboes by HPLC

Formulation	Day	Weight	Injection Number 1	2
2 mg	1	1	102.3	102.3
		2	100.9	100.6
		3	101.0	103.6
	2	1	101.6	101.6
		2	99.7	99.7
		3	102.0	102.5
	3	1	100.4	99.0
		2	101.2	98.0
		3	99.2	99.7
Average = 100.8% (95% confidence limits of 99.8–101.8%)				
4 mg	1	1	101.0	100.9
		2	100.2	100.3
		3	99.8	100.6
	2	1	98.0	98.3
		2	98.7	100.3
		3	98.7	98.0
	3	1	102.1	101.6
		2	99.9	99.9
		3	100.1	99.9
Average = 99.9% (95% confidence limits of 99.0–100.8%)				
Combination[a]	1	1	99.5	100.0
		2	98.7	99.1
		3	101.2	101.7
	2	1	99.4	100.0
		2	100.9	100.6
		3	100.2	99.9
	3	1	101.8	102.2
		2	101.8	102.1
		3	101.1	102.1
Average = 100.6% (95% confidence limits of 99.8–101.4%)				

[a] Contained 2 mg of polythiazide and 0.25 mg of reserpine.

The addition of water to the methanolic mobile phase (50% v/v) produced a sharp and reproducible peak for polythiazide. However, the detector response was not linear and an interference was observed from some tablet excipients. Due to the problems encountered, adsorption chromatography was not investigated further.

Reversed-phase partition chromatography with a Partisil 10-ODS column was then investigated. With methanol as the mobile phase, the observed peak for polythiazide was sharp and the response was linear. However, vanillin, a tablet excipient, was not resolved from polythiazide. The addition of water to the methanolic mobile phase up to 50% (v/v) resulted in no observed improvement in resolution.

Because of vanillin's known solubility in methanol, acetonitrile was substituted for methanol in the mobile phase. A sharp peak was observed for polythiazide while no peak was observed for vanillin; it appeared to be retained by the column. However, continued injections of a polythiazide–vanillin solution resulted in tailing of the polythiazide peak, which may be attributed to the retained vanillin acting as a partition substrate. The addition of methanol (2:98 v/v) to the acetonitrile mobile phase resulted in elution of the vanillin while maintaining adequate resolution for polythiazide. However, continued injections of solutions prepared from spiked tablet placeboes resulted in peak broadening for polythiazide and decreased resolution between polythiazide and vanillin.

Table II—Estimates of Precision for Determination of Polythiazide in Pharmaceutical Tablet Formulations by HPLC

Weights per Day	Injections per Weight	Estimates of Precision[a], % 2 mg	4 mg	Combination[b]
1	1	±3.0	±2.6	±2.3
1	2	±2.6	±2.5	±2.2
2	2	±2.3	±2.2	±1.8
3	2	±2.2	±2.2	±1.6
Injection to injection within a weight		±2.0	±1.0	±0.7

[a] Ninety-five percent of the individual results or averages of two, four, or six results will not vary from each other by more than the percentages quoted. These estimates include variability due to days, weights, and injections. The estimates of precision for injection to injection within a weight exclude variability due to days and weights. [b] Contained 2 mg of polythiazide and 0.25 mg of reserpine.

Table III—Comparison of HPLC and Compendial Methods for Determination of Polythiazide in Pharmaceutical Tablet Formulations

Formulation	Day	Sample	Analysis, mg/Tablet HPLC	Spectrophotometric	TLC
2 mg	1	1	2.07	2.07	1.97
		2	2.07	2.09	1.96
		3	2.05	2.10	1.95
	2	1	2.09	2.05	2.00
		2	2.09	2.09	2.00
		3	2.08	2.05	1.97
	Average		2.08	2.08	1.98
4 mg	1	1	4.18	3.96	4.06
		2	4.18	4.03	3.99
		3	4.22	3.87	4.03
	2	1	4.18	4.12	3.99
		2	4.18	4.12	3.96
		3	4.22	4.18	4.03
	Average		4.18	4.06	4.03
Combination[a]	1	1	2.07	2.12	2.05
		2	2.07	2.12	1.99
		3	2.09	2.11	2.01
	2	1	2.06	2.07	1.97
		2	2.06	2.10	1.95
		3	2.06	2.10	1.97
	Average		2.07	2.10	1.99

[a] Contained 2 mg of polythiazide and 0.25 mg of reserpine.

The addition of water to the mobile phase was investigated and, after evaluating various combinations of acetonitrile, methanol, and water, optimum separation and column stability were obtained with a water–acetonitrile (2:98 v/v) system. With this system, baseline separation was obtained between polythiazide and vanillin and tablet placeboes did not interfere. Reserpine was retained on the column, and peak broadening or changing of retention time was not observed, indicating long-term column stability. The detector response for polythiazide was linear up to a concentration of 300 μg/ml when dissolved in the mobile phase. In addition, the column could be regenerated with water, the retained reserpine being washed off under this condition. A typical chromatogram of polythiazide is shown in Fig. 1.

The accuracy and precision of the HPLC method were determined by the following experiments. Three weights of the placeboes for the 2- and 4-mg tablets and 2-mg combination with 0.25 mg of reserpine, in which known quantities of polythiazide were added, were assayed each day for 3 consecutive days. The average percent recoveries of polythiazide were 100.8, 99.9, and 100.6, respectively (Table I).

Estimates of precision (Table II) were obtained using the analysis of variance statistical technique. Ninety-five percent of the individual results will not vary from each other (*i.e.*, from the mean) by more than ±3.0, ±2.6, and ±2.3% for the 2- and 4-mg tablets and 2-mg combination with reserpine, respectively. The standard errors for the average of two injections per sample were ±1.3, ±1.3, and ±1.1% for the 2- and 4-mg tablets and 2-mg combination with reserpine, respectively.

The proposed HPLC method was compared to the compendial TLC and colorimetric assays (2), and the results (Table III) were in agreement. All samples were within the requirements of NF XIV for polythiazide tablet formulations by HPLC methodology (2). Because of the speed, accuracy, and precision of the proposed procedure, it represents an alternative to present compendial and published methodologies.

REFERENCES

(1) "Physicians' Desk Reference," 30th ed., Medical Economics Co., Oradell, N.J., 1976, p. 1169.

(2) "The National Formulary," 14th ed., Mack Publishing Co., Easton, Pa., 1975, p. 590.

(3) J. F. Magalhaes and M. G. Piros, *Rev. Farm. Bioquim. Univ. Sao Paulo*, **8**, 273 (1970).

(4) J. B. Perez, A. C. Danhier, and J. A. Brieva, *An. Real. Acad. Farm.*, **33**, 233 (1967).

(5) R. Pinson, Jr., E. C. Schreiber, E. H. Wiseman, J. Chiaini, and D. Baumgarter, *J. Med. Pharm. Chem.*, **5**, 491 (1962).

(6) F. R. Fazzari, *J. Assoc. Offic. Anal. Chem.*, **56**, 677 (1973).
(7) P. Gantes and J. Barat, *Ann. Pharm. Fr.*, **25**, 447 (1967).
(8) E. Kkolos and J. Walker, *Anal. Chim. Acta*, **80**, 17 (1975).
(9) R. E. Moskalyk, R. A. Locock, L. G. Chatten, A. M. Veltman, and M. F. Bielech, *J. Pharm. Sci.*, **64**, 1406 (1975).

ACKNOWLEDGMENTS AND ADDRESSES

Received March 19, 1976, from *Quality Control, Pfizer Inc., Brooklyn, NY 11206.*

Accepted for publication July 1, 1976.

[x] To whom inquiries should be directed.

Quantitative High-Pressure Liquid Chromatographic Determination of Thimerosal in Pharmaceutical Formulations

CHERNG-CHYI FU and MURRAY J. SIBLEY [x]

Abstract □ A quantitative high-pressure liquid chromatographic method using an anion-exchange resin column and an aqueous perchlorate solution as the mobile phase is employed for the determination of thimerosal in pharmaceutical formulations. With a liquid formulation containing large amounts of edetate disodium, calcium chloride is used for complexation to eliminate the interference from edetate disodium.

Keyphrases □ Thimerosal—high-pressure liquid chromatographic analysis, pharmaceutical formulations □ High-pressure liquid chromatography—analysis, thimerosal in pharmaceutical formulations

Thimerosal is an organomercurial chemical with antibacterial activity. It is used as an antiseptic for applications such as skin disinfection, urethral irrigation, and preservation of ophthalmic formulations (1). Compendial analytical methods using atomic absorption spectroscopy lack specificity (2). Another analytical method employing colorimetry of a dithizone complex (3) is tedious, and the presence of metal ions in the reagents causes interference.

Described here is a high-pressure liquid chromatographic (HPLC) analysis of thimerosal using an anion-exchange resin column with buffered sodium perchlorate as the mobile phase. The method is specific and simple.

EXPERIMENTAL

Apparatus—A high-pressure liquid chromatograph[1] equipped with a pump (7000 psig maximum), dual-channel UV detectors at 254 and 280 nm, and a 3 × 500-mm stainless steel column packed with anion-exchange resin[2] was used.

Reagents—The mobile phase was 0.35% perchloric acid[3] in 0.001 *M* dibasic sodium phosphate with pH adjusted to 7.0 with 1 *N* sodium hydroxide.

Standard Solution—Dissolve 8, 10, and 12 mg of thimerosal, separately, in purified water and dilute to 1 liter. These solutions represent thimerosal concentrations of 0.0008, 0.001, and 0.0012%, respectively.

Sample Solution—Dilute the sample solutions with purified water to make a final thimerosal concentration of 0.001%.

Chromatographic Separation—The procedure is run at ambient temperature, and the solvent flow is 1.6 ml/min. The UV monitor is set at 254 nm with a sensitivity of 0.02 absorbance unit. The samples and standards are injected with a 30-μl loop. The concentration of thimerosal is calculated from a standard curve using peak area (*i.e.*, height times width at half-height) for quantitation.

[1] Spectra Physics isocratic model 3500B, Santa Clara, Calif.
[2] Vydac, Applied Science Laboratories, State College, Pa.
[3] J. T. Baker Chemical Co., Phillipsburg, N.J.

RESULTS AND DISCUSSION

A typical chromatogram of thimerosal is shown in Fig. 1*a*. The chromatogram of one sample was complete in less than 5 min. Areas were used for the calculation of thimerosal concentration. Linear response over the concentration range from 0 to 15 μg/ml was obtained.

Table I shows the results using both the HPLC and the dithizone complex colorimetric methods. A solution containing edetate disodium, a common ingredient in ophthalmic formulations, and thimerosal in the ratio of less than 10:1 was separated and analyzed by this method without further sample treatment. However, an overlap of peaks was observed if a formulation contained edetate disodium and thimerosal in a ratio of more than 10:1. In such cases, calcium chloride was added to the sample solution to suppress the edetate disodium peak. With this step, complete separation and analysis of thimerosal were obtained.

Figure 1*b* illustrates a typical chromatogram of a sample solution containing 0.02% edetate disodium and 0.001% thimerosal. Figure 1*c* shows the chromatogram of the sample solution after treating with calcium chloride (to each 5 ml of sample solution was added 0.1 ml of 2%

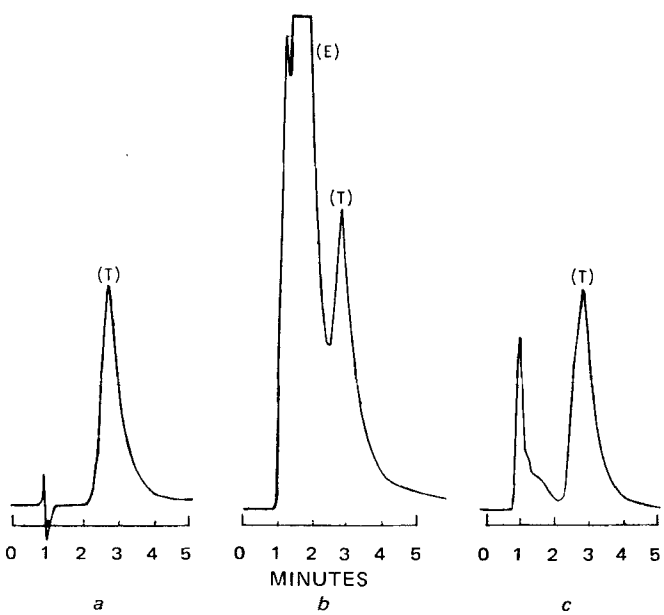

Figure 1—*Typical chromatograms of* (a) *thimerosal standard solution at 0.001%,* (b) *sample solution containing 0.02% edetate disodium and 0.001% thimerosal, and* (c) *0.1 ml of 2% $CaCl_2$ solution with 5 ml of sample solution* (b). *Key: T, thimerosal; and E, edetate disodium.*

(6) F. R. Fazzari, *J. Assoc. Offic. Anal. Chem.*, **56**, 677 (1973).
(7) P. Gantes and J. Barat, *Ann. Pharm. Fr.*, **25**, 447 (1967).
(8) E. Kkolos and J. Walker, *Anal. Chim. Acta*, **80**, 17 (1975).
(9) R. E. Moskalyk, R. A. Locock, L. G. Chatten, A. M. Veltman, and M. F. Bielech, *J. Pharm. Sci.*, **64**, 1406 (1975).

ACKNOWLEDGMENTS AND ADDRESSES

Received March 19, 1976, from *Quality Control, Pfizer Inc., Brooklyn, NY 11206.*

Accepted for publication July 1, 1976.

[x] To whom inquiries should be directed.

Quantitative High-Pressure Liquid Chromatographic Determination of Thimerosal in Pharmaceutical Formulations

CHERNG-CHYI FU and MURRAY J. SIBLEY [x]

Abstract □ A quantitative high-pressure liquid chromatographic method using an anion-exchange resin column and an aqueous perchlorate solution as the mobile phase is employed for the determination of thimerosal in pharmaceutical formulations. With a liquid formulation containing large amounts of edetate disodium, calcium chloride is used for complexation to eliminate the interference from edetate disodium.

Keyphrases □ Thimerosal—high-pressure liquid chromatographic analysis, pharmaceutical formulations □ High-pressure liquid chromatography—analysis, thimerosal in pharmaceutical formulations

Thimerosal is an organomercurial chemical with antibacterial activity. It is used as an antiseptic for applications such as skin disinfection, urethral irrigation, and preservation of ophthalmic formulations (1). Compendial analytical methods using atomic absorption spectroscopy lack specificity (2). Another analytical method employing colorimetry of a dithizone complex (3) is tedious, and the presence of metal ions in the reagents causes interference.

Described here is a high-pressure liquid chromatographic (HPLC) analysis of thimerosal using an anion-exchange resin column with buffered sodium perchlorate as the mobile phase. The method is specific and simple.

EXPERIMENTAL

Apparatus—A high-pressure liquid chromatograph[1] equipped with a pump (7000 psig maximum), dual-channel UV detectors at 254 and 280 nm, and a 3 × 500-mm stainless steel column packed with anion-exchange resin[2] was used.

Reagents—The mobile phase was 0.35% perchloric acid[3] in 0.001 *M* dibasic sodium phosphate with pH adjusted to 7.0 with 1 *N* sodium hydroxide.

Standard Solution—Dissolve 8, 10, and 12 mg of thimerosal, separately, in purified water and dilute to 1 liter. These solutions represent thimerosal concentrations of 0.0008, 0.001, and 0.0012%, respectively.

Sample Solution—Dilute the sample solutions with purified water to make a final thimerosal concentration of 0.001%.

Chromatographic Separation—The procedure is run at ambient temperature, and the solvent flow is 1.6 ml/min. The UV monitor is set at 254 nm with a sensitivity of 0.02 absorbance unit. The samples and standards are injected with a 30-μl loop. The concentration of thimerosal is calculated from a standard curve using peak area (*i.e.*, height times width at half-height) for quantitation.

[1] Spectra Physics isocratic model 3500B, Santa Clara, Calif.
[2] Vydac, Applied Science Laboratories, State College, Pa.
[3] J. T. Baker Chemical Co., Phillipsburg, N.J.

RESULTS AND DISCUSSION

A typical chromatogram of thimerosal is shown in Fig. 1*a*. The chromatogram of one sample was complete in less than 5 min. Areas were used for the calculation of thimerosal concentration. Linear response over the concentration range from 0 to 15 μg/ml was obtained.

Table I shows the results using both the HPLC and the dithizone complex colorimetric methods. A solution containing edetate disodium, a common ingredient in ophthalmic formulations, and thimerosal in the ratio of less than 10:1 was separated and analyzed by this method without further sample treatment. However, an overlap of peaks was observed if a formulation contained edetate disodium and thimerosal in a ratio of more than 10:1. In such cases, calcium chloride was added to the sample solution to suppress the edetate disodium peak. With this step, complete separation and analysis of thimerosal were obtained.

Figure 1*b* illustrates a typical chromatogram of a sample solution containing 0.02% edetate disodium and 0.001% thimerosal. Figure 1*c* shows the chromatogram of the sample solution after treating with calcium chloride (to each 5 ml of sample solution was added 0.1 ml of 2%

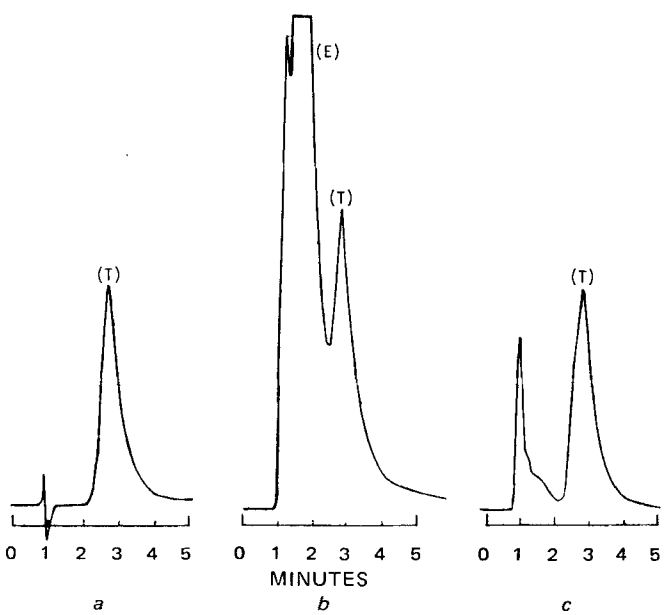

Figure 1—*Typical chromatograms of* (a) *thimerosal standard solution at 0.001%,* (b) *sample solution containing 0.02% edetate disodium and 0.001% thimerosal, and* (c) *0.1 ml of 2% $CaCl_2$ solution with 5 ml of sample solution* (b). *Key: T, thimerosal; and E, edetate disodium.*

Table I—Comparison of Dithizone Colorimetric and HPLC Methods for Thimerosal Determination

Sample	Thimerosal, μg/ml	
	Colorimetric	HPLC
1	11.5	11.9
2	11.5	11.7
3	11.8	12.3

calcium chloride solution). The amount of calcium chloride added to the sample solution depended on the actual amount of edetate disodium present. Since the complexation of edetate disodium with metal ions is pH dependent, one must adjust the sample solution pH to between 6.8 and 7.4 to obtain the best results.

REFERENCES

(1) "Textbook of Organic, Medicinal, and Pharmaceutical Chemistry," 4th ed., C. O. Wilson and O. Gisvold, Eds., Lippincott, Philadelphia, Pa., 1962, p. 188.

(2) "The National Formulary," 13th ed., Mack Publishing Co., Easton, Pa., 1970, pp. 703–706.

(3) V. L. Miller, D. Polley, and C. J. Gould, *Anal. Chem.*, **23**, 1286 (1951).

ACKNOWLEDGMENTS AND ADDRESSES

Received April 12, 1976, from the *Research Department, Barnes-Hind Pharmaceuticals, Inc., Sunnyvale, CA 94086.*

Accepted for publication June 30, 1976.

[x] To whom inquiries should be directed.

Sex Differences in Drug Evaluations

NANCY J. HORROM [x] and CLINTON C. BROWN

Abstract □ Twenty normal, nonobese subjects (10 male and 10 female) were administered a battery of seven psychomotor tests as well as affect checklists and physiological measurements on 6 alternate days. Subjects performed the entire battery predrug and at 45, 90, and 135 min postdrug. Fenfluramine, dextroamphetamine, two combined doses of the drugs, and a placebo were given in a double-blind, repeated measures design. Findings revealed significant sex-based differences in initial performance on five of the seven psychomotor tasks and in two physiological measures, with males performing at higher levels than females. Additionally, sex differences in postdrug changes were found in three psychomotor and two physiological measures, with females evidencing greater change scores than males.

Keyphrases □ Fenfluramine—alone and combined with dextroamphetamine, sex-based differences in psychomotor and physiological effects, humans □ Dextroamphetamine—alone and combined with fenfluramine, sex-based differences in psychomotor and physiological effects, humans □ Psychomotor effects—fenfluramine and dextroamphetamine, alone and in combination, sex-based differences, humans □ Physiological effects—fenfluramine and dextroamphetamine, alone and in combination, sex-based differences, humans □ Sex-based differences—fenfluramine and dextroamphetamine, alone and in combination, psychomotor and physiological effects, humans

Fenfluramine is an anorexic agent structurally similar to dextroamphetamine; however, it does not produce central nervous system (CNS) activation with respect to measures of sleep (1) or psychomotor performance (2). The mood elevation, euphoria, and lift produced by dextroamphetamine are well documented (3–5); fenfluramine, however, appears to have sedative properties (2, 4, 6). There is some evidence that fenfluramine may block the CNS stimulant effects of dextroamphetamine (7).

As with most psychopharmacological investigations, sex-based differences in drug reactivity were not explored in the studies cited (8). A chance assignment of subjects in a study to be reported elsewhere provided a comparison of pre- and postdrug performance and mood differences between the sexes given identical treatments. Based upon a preliminary analysis, it was hypothesized that males would have higher levels of performance on psychomotor tests than would females and that sex differences would occur in the pattern of drug reactivity.

EXPERIMENTAL

Twenty subjects (10 male and 10 female, age range of 21–30, $\bar{X}$ = 23.7) were recruited by newspaper advertisements and screened by psychiatric interview and psychological test (16 PF) (9). Informed consent was obtained and subjects were paid for their participation. Subjects were asked to abstain from all medication and alcohol and to maintain normal diet and sleeping habits during the 2-week testing period.

Subjects were tested at the same time of day (11:30 am–5:00 pm) on 6 alternate days. The 1st day was primarily for practice and familiarization with the tests, and this day's data were subsequently discarded. On each of the remaining 5 test days, the subject performed the entire test battery of psychomotor, perceptual, physiological, and affect evaluations prior to receiving medication and at 45, 90, and 135 min postmedication (exceptions noted in test descriptions).

Five treatments were used: (*a*) placebo (lactose), (*b*) fenfluramine alone (60 mg), (*c*) dextroamphetamine alone (10 mg), (*d*) a low combination (60 mg of fenfluramine plus 10 mg of dextroamphetamine), and (*e*) a high combination (90 mg of fenfluramine plus 10 mg of dextroamphetamine).

Each of the five conditions appeared equally on each test day, and subjects were randomly assigned to a treatment sequence upon acceptance. Postdrug measures were compared against the predrug baseline for each subject on each test day to minimize practice and potential day-of-week effects. Both the subject and experimenter were unaware of the contents of the identically appearing capsules. In the five treatment groups representing orders of administration of placebo and four drug conditions, males and females appeared in the ratios of 1:1, 0:1, 3:1, and 1:3. This approach provided the opportunity for an evaluation of study results with sex as a main factor.

The test battery included various psychomotor tasks, several physiological measures, and self-report mood evaluative forms. Psychomotor tests have been shown to be sensitive to various drug effects (8, 10) and were used previously in this laboratory (2).

Physiological Measures—Pulse rate, oral temperature, blood pressure, and salivary output were taken daily prior to drug administration and at 200 min postdrug; pupil size was measured predrug and at 45, 90, and 135 min postdrug. Additionally, the Lorr outpatient mood scale

Table I—Comparison of Dithizone Colorimetric and HPLC Methods for Thimerosal Determination

Sample	Thimerosal, μg/ml	
	Colorimetric	HPLC
1	11.5	11.9
2	11.5	11.7
3	11.8	12.3

calcium chloride solution). The amount of calcium chloride added to the sample solution depended on the actual amount of edetate disodium present. Since the complexation of edetate disodium with metal ions is pH dependent, one must adjust the sample solution pH to between 6.8 and 7.4 to obtain the best results.

REFERENCES

(1) "Textbook of Organic, Medicinal, and Pharmaceutical Chemistry," 4th ed., C. O. Wilson and O. Gisvold, Eds., Lippincott, Philadelphia, Pa., 1962, p. 188.

(2) "The National Formulary," 13th ed., Mack Publishing Co., Easton, Pa., 1970, pp. 703–706.

(3) V. L. Miller, D. Polley, and C. J. Gould, *Anal. Chem.*, **23**, 1286 (1951).

ACKNOWLEDGMENTS AND ADDRESSES

Received April 12, 1976, from the *Research Department, Barnes-Hind Pharmaceuticals, Inc., Sunnyvale, CA 94086.*

Accepted for publication June 30, 1976.

[x] To whom inquiries should be directed.

Sex Differences in Drug Evaluations

NANCY J. HORROM [x] and CLINTON C. BROWN

Abstract □ Twenty normal, nonobese subjects (10 male and 10 female) were administered a battery of seven psychomotor tests as well as affect checklists and physiological measurements on 6 alternate days. Subjects performed the entire battery predrug and at 45, 90, and 135 min postdrug. Fenfluramine, dextroamphetamine, two combined doses of the drugs, and a placebo were given in a double-blind, repeated measures design. Findings revealed significant sex-based differences in initial performance on five of the seven psychomotor tasks and in two physiological measures, with males performing at higher levels than females. Additionally, sex differences in postdrug changes were found in three psychomotor and two physiological measures, with females evidencing greater change scores than males.

Keyphrases □ Fenfluramine—alone and combined with dextroamphetamine, sex-based differences in psychomotor and physiological effects, humans □ Dextroamphetamine—alone and combined with fenfluramine, sex-based differences in psychomotor and physiological effects, humans □ Psychomotor effects—fenfluramine and dextroamphetamine, alone and in combination, sex-based differences, humans □ Physiological effects—fenfluramine and dextroamphetamine, alone and in combination, sex-based differences, humans □ Sex-based differences—fenfluramine and dextroamphetamine, alone and in combination, psychomotor and physiological effects, humans

Fenfluramine is an anorexic agent structurally similar to dextroamphetamine; however, it does not produce central nervous system (CNS) activation with respect to measures of sleep (1) or psychomotor performance (2). The mood elevation, euphoria, and lift produced by dextroamphetamine are well documented (3–5); fenfluramine, however, appears to have sedative properties (2, 4, 6). There is some evidence that fenfluramine may block the CNS stimulant effects of dextroamphetamine (7).

As with most psychopharmacological investigations, sex-based differences in drug reactivity were not explored in the studies cited (8). A chance assignment of subjects in a study to be reported elsewhere provided a comparison of pre- and postdrug performance and mood differences between the sexes given identical treatments. Based upon a preliminary analysis, it was hypothesized that males would have higher levels of performance on psychomotor tests than would females and that sex differences would occur in the pattern of drug reactivity.

EXPERIMENTAL

Twenty subjects (10 male and 10 female, age range of 21–30, $\bar{X}$ = 23.7) were recruited by newspaper advertisements and screened by psychiatric interview and psychological test (16 PF) (9). Informed consent was obtained and subjects were paid for their participation. Subjects were asked to abstain from all medication and alcohol and to maintain normal diet and sleeping habits during the 2-week testing period.

Subjects were tested at the same time of day (11:30 am–5:00 pm) on 6 alternate days. The 1st day was primarily for practice and familiarization with the tests, and this day's data were subsequently discarded. On each of the remaining 5 test days, the subject performed the entire test battery of psychomotor, perceptual, physiological, and affect evaluations prior to receiving medication and at 45, 90, and 135 min postmedication (exceptions noted in test descriptions).

Five treatments were used: (*a*) placebo (lactose), (*b*) fenfluramine alone (60 mg), (*c*) dextroamphetamine alone (10 mg), (*d*) a low combination (60 mg of fenfluramine plus 10 mg of dextroamphetamine), and (*e*) a high combination (90 mg of fenfluramine plus 10 mg of dextroamphetamine).

Each of the five conditions appeared equally on each test day, and subjects were randomly assigned to a treatment sequence upon acceptance. Postdrug measures were compared against the predrug baseline for each subject on each test day to minimize practice and potential day-of-week effects. Both the subject and experimenter were unaware of the contents of the identically appearing capsules. In the five treatment groups representing orders of administration of placebo and four drug conditions, males and females appeared in the ratios of 1:1, 0:1, 3:1, and 1:3. This approach provided the opportunity for an evaluation of study results with sex as a main factor.

The test battery included various psychomotor tasks, several physiological measures, and self-report mood evaluative forms. Psychomotor tests have been shown to be sensitive to various drug effects (8, 10) and were used previously in this laboratory (2).

Physiological Measures—Pulse rate, oral temperature, blood pressure, and salivary output were taken daily prior to drug administration and at 200 min postdrug; pupil size was measured predrug and at 45, 90, and 135 min postdrug. Additionally, the Lorr outpatient mood scale

Table I—Means, Standard Deviations, and t and p Data for Males and Females in Predrug Performance Level

Test		Female	Male	1 t 1	p
Tapping rate	Mean	305.06	400.42	3.60	0.005
	SD	22.01	14.73		
Card sorting	Mean	98.62	108.28	2.05	0.05
	SD	3.69	2.94		
Reaction time	Mean	0.81	0.57	4.59	0.0005
	SD	0.05	0.02		
Steadiness	Mean	11.28	5.23	2.93	0.005
	SD	1.96	0.64		
Handwriting	Mean	71.41	97.85	1.84	0.05
	SD	11.17	8.57		
Systolic blood pressure	Mean	104	111	4.47	0.0005
	SD	1.47	0.83		
Temperature	Mean	98.08	97.72	1.91	0.05
	SD	0.14	0.13		

(LOMS) and an adjective checklist were completed 160 min postmedication.

Psychomotor Performance Measures—*Tapping Rate*—The subject was instructed to tap as rapidly as possible with the forefinger of the preferred hand on a standard telegraph key for 1 min. The score was the number of taps.

Cross-Out Rate—The subject was required to make a slash through each X on a 21.6 × 28-cm sheet of paper with X's and O's in random order typed in continuous double-spaced rows. The score was the number of X's crossed out.

Reaction Time—The subject was instructed to react as quickly as possible to a signal light mounted on the response key 30.5 cm from the subject's hand by pressing the key at the appearance of the light. Twenty-five trials with randomized intertrial intervals were presented during 2 min. The score was the average reaction time in milliseconds.

Steadiness—The subject was given a pistol handle connected to a light metal rod 0.63 cm in diameter and 91.4 cm long, the end of which was placed in the center of a hole 1.2 cm in diameter. Contact between the rod and the hole produced an audible tone and activated a timer. The task was to hold the rod, with the elbow locked, in the center of the hole without touching the side for 60 sec. The score was time in milliseconds that the rod touched the side.

Number Path—The subject was instructed to connect the numbers one through 30 interspersed over a paper. The score was the number reached after 30 sec (11).

Card Sorting—The subject was required to sort four decks of playing cards into suits by placing them face down into the four divisions of a sorting bin. The score was the number of cards sorted.

Handwriting—The subject was asked to copy a standard paragraph on a piece of paper 21.6 × 28 cm. The score was the area in centimeters squared covered by the handwriting (12).

RESULTS

Male and female groups did not differ significantly on height–weight ratio, age, or 16 PF profiles.

Data were gathered across subjects and days with each subject serving as his or her own control. An analysis was undertaken to determine differences between sexes with regard to the baseline level of performance of the tests and differences in drug-modified performance.

Five of seven psychomotor tests, three physiological measures, and four LOMS factors revealed one or the other type of sex-based difference.

Predrug Sex Differences—Differences in the initial level of daily task performance between men and women were assessed by a t for correlated means (Table I). Significant pretreatment sex differences were found for five of the seven psychomotor tasks. In each case, the magnitude of male performance exceeded that of females. Males tapped more times in a minute, sorted more cards, reacted more quickly to a stimulus, were steadier, and covered a larger area with their handwriting than did females. Men also displayed a lower temperature and a higher systolic blood pressure.

Since the Lorr outpatient mood scale (LOMS) was given only once, 160 min postmedication, those ratings reflect a combination of drug-induced and predrug mood states. Males rated themselves significantly higher in total affect, energy level, "anger," and "cheerfulness" than did females.

Sex Differences in Drug Reactivity—Difference scores were obtained by subtracting each subject's predrug score from the scores obtained at 45, 90, and 135 min postdrug. A three-way analysis of variance (repeated measures) was employed on these difference scores, followed by t tests where significance was found. Sex appeared as a significant main factor in three psychomotor tasks and two physiological measures. In each case, females had greater change scores than did males (Table II).

Table II—Postdrug Change Scores for Males and Females

Test		Female	Male	F
Tapping rate	Mean	13.73	5.99	5.36[a]
	SD	3.23	1.89	
Card sorting	Mean	4.48	1.73	8.87[b]
	SD	1.04	1.18	
Steadiness	Mean	−1.91	−0.78	13.68[b]
	SD	0.39	0.29	
Systolic blood pressure	Mean	4	0	5.06[a]
	SD	1.92	1.15	
Pulse	Mean	0.28	−4.96	7.60[b]
	SD	1.32	1.94	

[a] Significant at 0.05. [b] Significant at 0.01.

Females had a significantly greater increase in card sorting, tapping rate, and steadiness after drugs than males had. Additionally, females showed greater changes in the physiological measures of systolic blood pressure and pulse rate. Although the systolic blood pressure of *both* males and females increased from pre- to postdrug, females increased significantly more than males. The differences in pulse rate change between the two sexes also achieved significance; while the pulse rate of women subjects increased after drugs, that of male subjects decreased.

DISCUSSION

These results suggest that there are significant sex-based differences in the initial performance of certain psychomotor tasks. Five of the seven psychomotor tasks used revealed significantly higher initial levels of test performance for males than for females. The rate of change in performance, *i.e.*, drug reactivity, following drugs may be partially determined by the sex of the subject. In this study, females had a greater change after drugs than did males.

The observed differences in certain physiological measures (pulse, blood pressure, and temperature) both pre- and postdrug may point to metabolic differences between males and females. Although there was no significant difference between the ratio of height to weight between males and females, the females were on the average 9.07 kg lighter than the males. This factor, along with probable differences in the proportion of fat and muscle, may contribute both to predrug differences as well as differences in reactivity. Further study of male–female reactivity to drugs and situational changes is definitely indicated.

The data from the Lorr outpatient mood scale, which showed that males rated themselves higher in affect, also need to be explored further. Since the design of the study had subjects completing the scale only after medication, it could not be determined if this sex difference was due to drug reactions, procedural factors, or basic difference between male and female awareness of and/or reporting of different feelings.

In the performance of the simple psychomotor tasks, the males excelled initially while the females showed greater postdrug changes. The effect of learning on the postdrug performance must be considered. Women have been shown to excel in performance of simple overlearned tasks (13). Postdrug increases in performance may be partially attributed to relearning occurring during the predrug testing.

The factor of sex of the experimenter may account for some differences between male and female subject performance. Studies have shown that subjects perform at a higher rate when the experimenter is of the opposite sex (14, 15). All subjects in this study were tested by the same female experimenter.

Sex-based differences in the performance of psychomotor tasks both initially and following drug treatment point out the need to consider the sex of the subject as an important factor in evaluating drug effects. Averaging the performance of an equal number of male and female subjects does not ensure results that can be generalized to both or, possibly, either sex. It may be inappropriate to generalize psychopharmacological research findings to the general population if only one sex has been used in the testing. Further study is indicated to determine if measurements other than psychomotor performance also show strong sex-based differences.

REFERENCES

(1) S. Lewis, in "International Symposium on Amphetamines and Related Compounds," E. Costa and S. Garattini, Eds., Raven, New York, N.Y., 1970, pp. 873–888.

(2) C. C. Brown, D. R. McAllister, and I. Turek, *J. Clin. Pharmacol.*, **14**, 369 (1974).

(3) J. H. Biel, in "International Symposium on Amphetamines and Related Compounds," E. Costa and S. Garattini, Eds., Raven, New York, N.Y., 1970, pp. 3–19.

(4) P. H. Connell, *Practitioner*, **200**, 234 (1968).

(5) J. P. Duncan and J. F. Munro, *ibid.*, **200**, 167 (1968).

(6) B. W. Elliott, *Curr. Ther. Res.*, **12**, 502 (1970).

(7) H. J. Berger, C. C. Brown, and J. C. Krantz, *J. Pharm. Sci.*, **62**, 788 (1973).

(8) F. M. Berger and J. Potterfield, in "The Psychopharmacology of the Normal Human," W. O. Evans and N. S. Kline, Eds., Charles C Thomas, Springfield, Ill., 1969, pp. 38–113.

(9) R. B. Cattell, "Personality and Motivation on Structure and Measurement," World Book, Yonkers-on-Hudson, N.Y., 1957.

(10) J. H. Stephens, J. W. Shaffer, and C. C. Brown, *J. Clin. Pharmacol.*, **14**, 543 (1974).

(11) G. P. Carl and W. D. Turner, *J. Psychol.*, **8**, 165 (1939).

(12) R. Fischer, T. Kappeler, P. Wisecup, and K. Thatcher, *Dis. Nerv. Syst.*, **31**, 181 (1970).

(13) D. M. Broverman and E. L. Klaiber, *Psychol. Rev.*, **75**, 23 (1968).

(14) M. Vonkerejarto, in "Non-Specific Factors in Drug Therapy," K. Rickels, Ed., Charles C Thomas, Springfield, Ill., 1968, pp. 128–131.

(15) H. W. Stevenson and S. Allen, *J. Abnormal Soc. Psychol.*, **68**, 214 (1964).

ACKNOWLEDGMENTS AND ADDRESSES

Received April 12, 1976, from the *Biomedical Sciences Division, Maryland Psychiatric Research Center, Baltimore, MD 21228.*

Accepted for publication June 23, 1976.

The clinical study was supported in part by Grant 3801 from the A. H. Robins Co., Richmond, Va., and administered by Friends Medical Science Research Center, Inc., Baltimore, Md.

[x] To whom inquiries should be directed.

Mathematical Description of Solute Velocities during Dissolution from a Horizontal Surface

ALLEN CHAO [*], CHONG-KOOK KIM, DANE O. KILDSIG [x], and PAUL A. KRAMER

Abstract □ A mathematical analysis of solute flow in a descending column following dissolution is presented. The acceleration of a solute particle from zero velocity, when it is in the solid phase, to its final equilibrium descending velocity was analyzed. The maximum velocity for *N*-(3-methylphenyl)acetamide developed essentially at the solid–liquid interface, contradicting the postulate of a microsize diffusional layer. The possibility of a diffusional layer existing for solids of lower solubility than *N*-(3-methylphenyl)acetamide is discussed.

Keyphrases □ Solute velocities—in descending column during dissolution from a horizontal surface, mathematical analysis □ Velocities, solute—in descending column during dissolution from a horizontal surface, mathematical analysis □ Dissolution—from a horizontal surface, mathematical analysis of solute velocities in descending column

Studies utilizing a descending column model to investigate the dissolution of a solid showed that convective transport of solute rather than molecular diffusion is the primary means of mass transfer for such a model (1, 2). Interfacial effects such as solvent penetration, wetting, and solvation of the solid seem to control the rate of mass transfer when dissolution from the solid surface occurs in the descending direction. Under such conditions, one would not anticipate the presence of a finite "diffusion layer." Calculations based on measurements of the rate of movement of a solute front in a descending dissolution column (1) are presented here to show that steady-state velocities are established within microseconds and essentially begin at the interface, thus eliminating the possibility of a microsize diffusion layer.

THEORY AND DISCUSSION

The velocity of solute flow in a vertical dissolution column was determined from observations of the movement of the solute front down the column (1). Since a linear relationship was observed between the solvent front location and time, the velocity appears to be independent of time. There must, however, be a time-variant laminar flow velocity profile, on a molecular basis, for molecules in the bulk fluid stream at times close to zero. A molecule in the solid phase obviously has a zero-velocity component contributing to its flow down the column.

Following the solvation step in a dissolution process, the solvated solute molecule descends from rest in a stationary fluid under the action of gravity. The molecule first accelerates as it would in a vacuum; but unlike the situation in a vacuum, its acceleration is retarded due to friction with the surrounding solvent medium. As the frictional force increases with an increase in velocity, this force eventually reaches a value equal to that of the gravitational force. From that point on, the two forces are balanced and the molecule continues to fall at a constant velocity. The exponentially increasing velocity of such a molecule descending from rest under the influence of gravity represents an interesting first-order system, because the dynamics are defined completely by the steady-state velocity and the time constant for the approach to steady state can be predicted from this velocity.

Consider the fall of a solvated solute molecule through an aqueous medium when the solvated solute and solvent differ in density and viscosity. Under the action of gravity, the downward force, F, acting on the molecule depends on the relative magnitudes of the forces of gravity and buoyancy. The gravitational force, F_w, acts on the molecule even when it is at rest and remains constant during the entire period of descent. The buoyancy, F_b, is dependent on the solvent medium. From Newton's second law of motion:

$$F = F_w - F_b \qquad \text{(Eq. 1a)}$$

$$F = (\rho - \rho_0)gV \qquad \text{(Eq. 1b)}$$

REFERENCES

(1) S. Lewis, in "International Symposium on Amphetamines and Related Compounds," E. Costa and S. Garattini, Eds., Raven, New York, N.Y., 1970, pp. 873–888.

(2) C. C. Brown, D. R. McAllister, and I. Turek, *J. Clin. Pharmacol.*, **14**, 369 (1974).

(3) J. H. Biel, in "International Symposium on Amphetamines and Related Compounds," E. Costa and S. Garattini, Eds., Raven, New York, N.Y., 1970, pp. 3–19.

(4) P. H. Connell, *Practitioner*, **200**, 234 (1968).

(5) J. P. Duncan and J. F. Munro, *ibid.*, **200**, 167 (1968).

(6) B. W. Elliott, *Curr. Ther. Res.*, **12**, 502 (1970).

(7) H. J. Berger, C. C. Brown, and J. C. Krantz, *J. Pharm. Sci.*, **62**, 788 (1973).

(8) F. M. Berger and J. Potterfield, in "The Psychopharmacology of the Normal Human," W. O. Evans and N. S. Kline, Eds., Charles C Thomas, Springfield, Ill., 1969, pp. 38–113.

(9) R. B. Cattell, "Personality and Motivation on Structure and Measurement," World Book, Yonkers-on-Hudson, N.Y., 1957.

(10) J. H. Stephens, J. W. Shaffer, and C. C. Brown, *J. Clin. Pharmacol.*, **14**, 543 (1974).

(11) G. P. Carl and W. D. Turner, *J. Psychol.*, **8**, 165 (1939).

(12) R. Fischer, T. Kappeler, P. Wisecup, and K. Thatcher, *Dis. Nerv. Syst.*, **31**, 181 (1970).

(13) D. M. Broverman and E. L. Klaiber, *Psychol. Rev.*, **75**, 23 (1968).

(14) M. Vonkerejarto, in "Non-Specific Factors in Drug Therapy," K. Rickels, Ed., Charles C Thomas, Springfield, Ill., 1968, pp. 128–131.

(15) H. W. Stevenson and S. Allen, *J. Abnormal Soc. Psychol.*, **68**, 214 (1964).

ACKNOWLEDGMENTS AND ADDRESSES

Received April 12, 1976, from the *Biomedical Sciences Division, Maryland Psychiatric Research Center, Baltimore, MD 21228.*

Accepted for publication June 23, 1976.

The clinical study was supported in part by Grant 3801 from the A. H. Robins Co., Richmond, Va., and administered by Friends Medical Science Research Center, Inc., Baltimore, Md.

[x] To whom inquiries should be directed.

Mathematical Description of Solute Velocities during Dissolution from a Horizontal Surface

ALLEN CHAO [*], CHONG-KOOK KIM, DANE O. KILDSIG [x], and PAUL A. KRAMER

Abstract □ A mathematical analysis of solute flow in a descending column following dissolution is presented. The acceleration of a solute particle from zero velocity, when it is in the solid phase, to its final equilibrium descending velocity was analyzed. The maximum velocity for *N*-(3-methylphenyl)acetamide developed essentially at the solid–liquid interface, contradicting the postulate of a microsize diffusional layer. The possibility of a diffusional layer existing for solids of lower solubility than *N*-(3-methylphenyl)acetamide is discussed.

Keyphrases □ Solute velocities—in descending column during dissolution from a horizontal surface, mathematical analysis □ Velocities, solute—in descending column during dissolution from a horizontal surface, mathematical analysis □ Dissolution—from a horizontal surface, mathematical analysis of solute velocities in descending column

Studies utilizing a descending column model to investigate the dissolution of a solid showed that convective transport of solute rather than molecular diffusion is the primary means of mass transfer for such a model (1, 2). Interfacial effects such as solvent penetration, wetting, and solvation of the solid seem to control the rate of mass transfer when dissolution from the solid surface occurs in the descending direction. Under such conditions, one would not anticipate the presence of a finite "diffusion layer." Calculations based on measurements of the rate of movement of a solute front in a descending dissolution column (1) are presented here to show that steady-state velocities are established within microseconds and essentially begin at the interface, thus eliminating the possibility of a microsize diffusion layer.

THEORY AND DISCUSSION

The velocity of solute flow in a vertical dissolution column was determined from observations of the movement of the solute front down the column (1). Since a linear relationship was observed between the solvent front location and time, the velocity appears to be independent of time. There must, however, be a time-variant laminar flow velocity profile, on a molecular basis, for molecules in the bulk fluid stream at times close to zero. A molecule in the solid phase obviously has a zero-velocity component contributing to its flow down the column.

Following the solvation step in a dissolution process, the solvated solute molecule descends from rest in a stationary fluid under the action of gravity. The molecule first accelerates as it would in a vacuum; but unlike the situation in a vacuum, its acceleration is retarded due to friction with the surrounding solvent medium. As the frictional force increases with an increase in velocity, this force eventually reaches a value equal to that of the gravitational force. From that point on, the two forces are balanced and the molecule continues to fall at a constant velocity. The exponentially increasing velocity of such a molecule descending from rest under the influence of gravity represents an interesting first-order system, because the dynamics are defined completely by the steady-state velocity and the time constant for the approach to steady state can be predicted from this velocity.

Consider the fall of a solvated solute molecule through an aqueous medium when the solvated solute and solvent differ in density and viscosity. Under the action of gravity, the downward force, F, acting on the molecule depends on the relative magnitudes of the forces of gravity and buoyancy. The gravitational force, F_w, acts on the molecule even when it is at rest and remains constant during the entire period of descent. The buoyancy, F_b, is dependent on the solvent medium. From Newton's second law of motion:

$$F = F_w - F_b \qquad \text{(Eq. 1a)}$$

$$F = (\rho - \rho_0)gV \qquad \text{(Eq. 1b)}$$

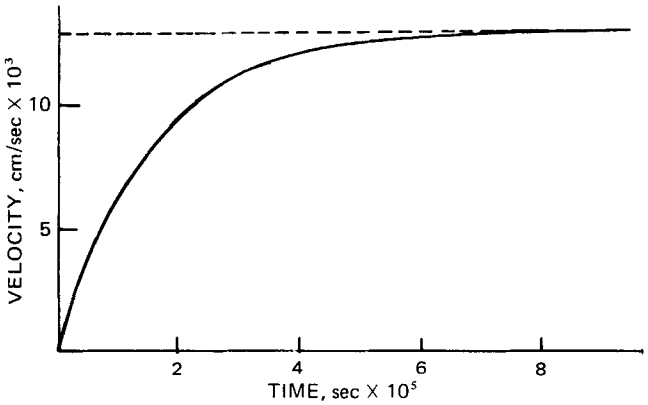

Figure 1—*Plot of velocity* versus *time for I using Eq. 9. The dashed line is the limiting maximum velocity:* v_{max} = *0.013 cm/sec.*

where g is the gravitational acceleration; ρ and ρ_0 are the densities of solvated solute and solvent, respectively; and V is the volume of the solvated solute molecule. The force F_w in Eq. 1*a* is the downward force of gravity acting on the solute molecule in the stationary medium. The term $\rho_0 gV$ represents the buoyancy effect. Although it is difficult to determine the volume of a molecule with an irregular shape, shape is an important factor contributing to the forces acting on a falling molecule. For the sake of simplicity, the solvated molecules are assumed to be spherical. If D is the diameter of a molecule, then:

$$V = \frac{\pi D^3}{6} \qquad \text{(Eq. 2)}$$

Substituting Eq. 2 into Eq. 1*b* yields:

$$F = \frac{\pi D^3 g}{6}(\rho - \rho_0) \qquad \text{(Eq. 3)}$$

The force resisting motion is generally referred to as the drag, R. It is assumed that its magnitude is a function of the diameter of the molecule, its velocity, v, and the viscosity of the surrounding fluid. On the basis of these assumptions, Stokes derived an equation for flow resistance in laminar flow systems (3):

$$R = KD\eta v \qquad \text{(Eq. 4)}$$

where η is the dynamic viscosity of the solvent medium, K is a shape factor for the solute and has been determined experimentally for a number of shapes, and v is velocity. For a spherical object, K has a value of 3π, so Eq. 4 takes the form:

$$R = 3\pi D\eta v \qquad \text{(Eq. 5)}$$

The net driving force, DF, acting on a molecule is:

$$DF = F - R \qquad \text{(Eq. 6)}$$

From Newton's law (3):

$$DF = \frac{F}{g}(dv/dt) \qquad \text{(Eq. 7}a\text{)}$$

$$DF = \frac{\pi D^3}{6}(\rho - \rho_0)dv/dt \qquad \text{(Eq. 7}b\text{)}$$

Substituting Eqs. 3, 5, and 7*b* into Eq. 6 yields:

$$\frac{\pi D^3}{6}(\rho - \rho_0)dv/dt = \frac{\pi D^3 g}{6}(\rho - \rho_0) - 3\pi D\eta v \qquad \text{(Eq. 8)}$$

Table I—Solubilities, Effective Interfacial Concentrations, and Velocities[a]

Solid	Saturation Solubility, C_s, $M \times 10^2$	Interfacial Concentration, C_i, $M \times 10^3$	Steady-State Velocity, V_{max}, cm/sec $\times 10^2$
Phenacetin	0.53	0.32	0.48
Salicylamide	2.0	1.1	1.6
I	4.1	2.8	1.3
Benzamide	12.5	4.0	4.2

[a] From Ref. 4.

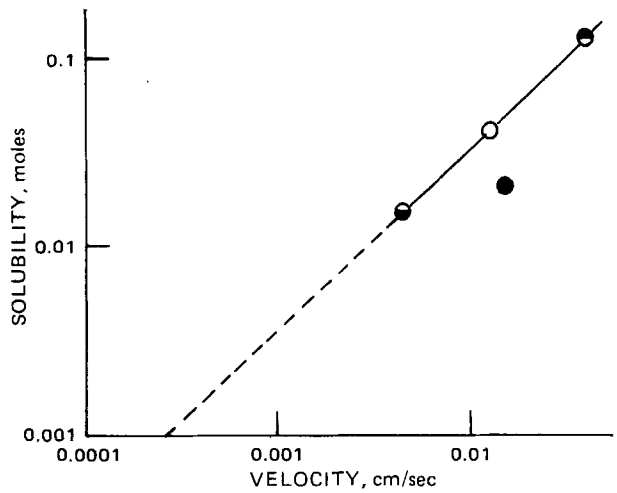

Figure 2—*Logarithmic plot of solubility* versus *velocity of flow. Key:* ○, *I;* ◓, *benzamide;* ◒, *phenacetin; and* ●, *salicylamide.*

By letting $v = 0$ at $t = 0$ since the molecules are initially at rest, the solution of Eq. 8 becomes:

$$v = \frac{D^2 g(\rho - \rho_0)}{18\eta}\left[1 - e^{-(18\eta/D^2)(\rho-\rho_0)t}\right] \qquad \text{(Eq. 9)}$$

As time increases, v approaches a constant limiting velocity, v_{max}, where:

$$v_{max} = \frac{D^2 g(\rho - \rho_0)}{18\eta} \qquad \text{(Eq. 10)}$$

In the descending dissolution of *N*-(3-methylphenyl)acetamide (I) in water, a v_{max} of 0.013 cm/sec was observed (1). A graph of the velocity of flow, v, as a function of time can be constructed according to Eq. 9 (Fig. 1). The descending molecules start at rest, exponentially gain velocity due to the effects of gravity, and reach their limiting velocity in an extremely short period (about 80 μsec).

The distance from the solid surface at which the maximum velocity is first attained is of particular interest. Since the solute velocity increases from 0 to 0.013 cm/sec, it is conceivable that diffusional velocities exist in the approximately 50-μm region usually described by diffusion layer theory. Equation 9 may be written as:

$$dx/dt = v_{max}\left[1 - e^{-(g/V_{max})t}\right] \qquad \text{(Eq. 11)}$$

where $v = dx/dt$ = the change in distance x with time for a solute front moving in the x direction. The solution of this equation for x with the initial condition $x = 0$ at $t = 0$ is:

$$x = v_{max}\left\{t + \frac{V_{max}}{g}\left[e^{-(g/V_{max})t}\right] - \frac{V_{max}}{g}\right\} \qquad \text{(Eq. 12)}$$

The solution of Eq. 12 at $t = 80$ μsec is 9.26×10^{-7} cm. As might be expected from the short time required, the maximum velocity for I is established essentially at the interface, contradicting any postulate of a microsize diffusional layer.

Since the steady-state velocity in the descending column is related to the solubility of the solid (Table I), the question arises as to the possibility of a diffusional layer existing for solids of a lower solubility than I. By using the solubility and descending solute front velocity values reported (2–4) for the solids I, benzamide, phenacetin, and salicylamide, a logarithmic plot of solubility *versus* velocity was constructed (Fig. 2) and an extrapolation was made to lower velocities. Since the velocity of solute flow down the column is related to the density difference between the solution at the interface and the bulk solution and since this density difference should, in general, decrease with the decreasing solubility of the solid, the extrapolation in Fig. 2 should reasonably reflect solute velocities at low solubilities.

The diffusional velocity of I can be estimated from reported ascending dissolution experiments (examining a true diffusion process) (1). When using the I diffusion coefficient of 1.25×10^{-5} cm^2/sec as representative of most solutes and a 60-min time period, a diffusion velocity of 2×10^{-4} cm/sec was obtained. The extrapolation in Fig. 2 indicated that velocities in the diffusional range are reached when the solubility falls below 0.001

M. Variations from Fig. 2 occur due to the fact that not all solids and their resulting solutions have the same density and convective velocity. For example, salicylamide has a lower solubility than I but a higher solution mass transfer velocity.

Finally, it must be stressed that a diffusional mass transfer step does not mean a diffusion-controlled mechanism for dissolution. While the dissolution of solids having solubilities below 0.001 M appears to be diffusion controlled, this does not mean that the interfacial rate is now fast compared to the diffusion rate. Certainly, the rate of interaction at the solid–liquid interface decreases as the solubility decreases, as indicated by the data in Table I showing that the effective interfacial concentration decreases with decreasing solubility. This phenomenon is not likely to change at even lower solubilities. Consequently, regardless of solubility or the approach to diffusional mass transfer, the interfacial rate will remain slower than the diffusion rate and dissolution must be considered as an interfacially controlled process.

REFERENCES

(1) R. L. Nedich and D. O. Kildsig, *J. Pharm. Sci.*, **61**, 214 (1972).

(2) C. D. Shively and D. O. Kildsig, *ibid.*, **61**, 1589 (1972).

(3) S. J. Michell, "Fluid and Particle Mechanics," Pergamon Press, London, England, 1970, pp. 289–292.

(4) C. D. Shively, Ph.D. thesis, Purdue University, West Lafayette, Ind., 1972.

ACKNOWLEDGMENTS AND ADDRESSES

Received April 5, 1976, from the *Department of Industrial and Physical Pharmacy, School of Pharmacy and Pharmacal Sciences, Purdue University, West Lafayette, IN 47907.*

Accepted for publication June 23, 1976.

* Present address: G. D. Searle & Co., Chicago, Ill.

ˣ To whom inquiries should be directed.

GLC–Mass Spectral Analysis of Psilocin and Psilocybin

DAVID B. REPKE ˣ, DALE THOMAS LESLIE *, DANIEL M. MANDELL ‡, and NICHOLAS G. KISH §

Abstract □ With the combined technique of GLC–mass spectrometry, psilocin and psilocybin, two hallucinogenic indoles, were analyzed as their trimethylsilyl derivatives. The method was applied to these two components in an extract of *Psilocybe cubensis* (Earle) Sing.

Keyphrases □ Psilocin—GLC–mass spectral analysis in extract of mushroom *Psilocybe cubensis* □ Psilocybin—GLC–mass spectral analysis in extract of mushroom *Psilocybe cubensis* □ GLC–mass spectrometry—analysis, psilocin and psilocybin in extract of mushroom *Psilocybe cubensis* □ Hallucinogenics—psilocin and psilocybin, GLC–mass spectral analysis in extract of mushroom *Psilocybe cubensis*

Psilocin and psilocybin, two hallucinogenic principles found in certain agarics (1), have aroused considerable interest since their isolation and characterization in the late 1950's (2, 3). The mushrooms in which they occur have been known and revered in southern Mexico for centuries. Their rediscovery in 1939 (4) and their subsequent study (5, 6) and popularization ultimately led to legislation to control their use (7).

BACKGROUND

Psilocin (3-[2-(dimethylamino)ethyl]indol-4-ol) and psilocybin, its dihydrogen phosphate ester, are unique in nature as indoles having a 4-substituent and a phosphate group. Both qualitative and quantitative methods have been utilized for their analysis. Paper chromatography (2) and TLC (8) have been used in conjunction with colorimetric reagents as well as UV spectroscopy. When pure samples are available, IR spectrometry can be used (9). Mass spectrometry (10) has been relied upon for identification of these compounds in various pharmaceutical preparations. Various fluorescence and phosphorescence techniques (11) as well as other emission spectral techniques (12) have also been used.

In an investigation of the genus *Psilocybe* and related genera, the need for a sensitive and accurate quantitative method for the analysis of psilocin and psilocybin became apparent. This method would have to be applicable to extracts of minute amounts of scarce herbarium material and vegetative mycelium obtained from liquid culture.

Previously, GLC was applied to the analysis of psilocin (13) and psilocybin (14), both as the free bases and their trimethylsilyl derivatives. GLC–mass spectrometry has been successfully applied to the bis(trimethylsilyl) derivative of bufotenine, the 5-hydroxy positional isomer of psilocin (15).

The possibility of utilizing GLC for the separation of organic molecules containing a phosphate group was suggested by work with trimethylsilyl derivatives of ribonucleotides (16).

EXPERIMENTAL[1]

Fifty milligrams of freeze-dried pileus tissue of *P. cubensis*[2] was ground to a fine powder with sand and transferred to a screw-capped vial. Methanol (5 ml) was added, and the tube was shaken at room temperature for 24 hr. The mixture was filtered, and the solid was washed with 5 ml of methanol. The filtrate was concentrated *in vacuo* to 0.5 ml, transferred to a 1.0-ml vial[3], and concentrated to dryness in a nitrogen stream. All traces of solvent were removed by evacuation on the oil pump. In an anhydrous nitrogen atmosphere, 100 μl of bis(trimethylsilyl)trifluoroacetamide[4] was added to the vial, which was then closed with a septum-lined aluminum seal[5].

The vial was heated at 140° for 15 min. Prolonged reaction periods (up to 2.5 hr) showed that this length of time was sufficient for quantitative

[1] GLC was carried out using a Hewlett-Packard model 402 gas chromatograph equipped with hydrogen flame-ionization detectors. The column used was a 1.6-m × 2.8-mm i.d. glass U-tube with 1.5% SE-30 on 100–120-mesh Chromosorb W. Chromatography conditions were: injection block, 220°; detector, 280°; oven, temperature programmed from 150 to 250° at 7.5°/min; chart speed, 0.64 cm/min; and helium carrier gas, 50 ml/min. TLC utilized glass plates with 0.25-mm layers of silica gel GF using 1-propanol–5% ammonium hydroxide (5:2) (17).

GLC–mass spectrometry was carried out with a Finnigan model 9500 gas chromatograph coupled to a Finnigan model 3100 D quadrupole mass spectrometer through a single-stage glass jet separator. A System/250 data system (Systems Industries) was used to control the mass spectrometer and acquire data. The mass spectrometer parameters were: interface temperature, 200–225°; transfer line, 150–175°; manifold temperature, 100°; and ion source potential, 70 ev. Two sets of chromatography conditions were employed: (*a*) essentially the same as those listed for GLC, and (*b*) a 0.75-m × 2-mm i.d. glass U-tube with 3% OV-101 on 100–120-mesh Gas Chrom Q temperature programmed from 200 to 275° at 10°/min with a helium flow rate of 20 ml/min.

[2] Carpophores of *Psilocybe cubensis* (Earle) Singer (= *Stropharia cubensis* Earle) (Strophariaceae) were obtained by aseptic cultivation of a strain of this fungus on sterile horse manure. The strain was isolated from pileus tissue of a fresh carpophore of *P. cubensis* collected Aug. 31, 1974, in Huautla de Jimenez, Oaxaca, Mexico, and was maintained on malt extract agar. The origin and maintenance of the culture and the production of fruiting bodies were similar to those reported previously (5, 6, 18). Carpophores were authoritatively identified by Dr. Gastón Guzmán, Escuela Nacional de Ciencias Biológicas (ENCB), I.P.N., Mexico, D.F., Mexico. Herbarium material is on deposit at the ENCB herbarium and the University of Michigan herbarium as LESLIE 1902 and at the Institute for Fermentation herbarium, Osaka, Japan, as IFO-H 11703. Subcultures are on deposit at the Institute for Fermentation (IFO 30176) and the Centraalbureau vorr Schimmelcultures, Baarn, The Netherlands (CBS 134.76).

[3] Hewlett-Packard 5080-8712.

[4] Regisil, Regis Chemical Co.

[5] Hewlett-Packard 5080-8713.

M. Variations from Fig. 2 occur due to the fact that not all solids and their resulting solutions have the same density and convective velocity. For example, salicylamide has a lower solubility than I but a higher solution mass transfer velocity.

Finally, it must be stressed that a diffusional mass transfer step does not mean a diffusion-controlled mechanism for dissolution. While the dissolution of solids having solubilities below 0.001 M appears to be diffusion controlled, this does not mean that the interfacial rate is now fast compared to the diffusion rate. Certainly, the rate of interaction at the solid–liquid interface decreases as the solubility decreases, as indicated by the data in Table I showing that the effective interfacial concentration decreases with decreasing solubility. This phenomenon is not likely to change at even lower solubilities. Consequently, regardless of solubility or the approach to diffusional mass transfer, the interfacial rate will remain slower than the diffusion rate and dissolution must be considered as an interfacially controlled process.

REFERENCES

(1) R. L. Nedich and D. O. Kildsig, *J. Pharm. Sci.*, **61**, 214 (1972).

(2) C. D. Shively and D. O. Kildsig, *ibid.*, **61**, 1589 (1972).

(3) S. J. Michell, "Fluid and Particle Mechanics," Pergamon Press, London, England, 1970, pp. 289–292.

(4) C. D. Shively, Ph.D. thesis, Purdue University, West Lafayette, Ind., 1972.

ACKNOWLEDGMENTS AND ADDRESSES

Received April 5, 1976, from the *Department of Industrial and Physical Pharmacy, School of Pharmacy and Pharmacal Sciences, Purdue University, West Lafayette, IN 47907.*

Accepted for publication June 23, 1976.

* Present address: G. D. Searle & Co., Chicago, Ill.

ˣ To whom inquiries should be directed.

GLC–Mass Spectral Analysis of Psilocin and Psilocybin

DAVID B. REPKE ˣ, DALE THOMAS LESLIE *, DANIEL M. MANDELL ‡, and NICHOLAS G. KISH §

Abstract □ With the combined technique of GLC–mass spectrometry, psilocin and psilocybin, two hallucinogenic indoles, were analyzed as their trimethylsilyl derivatives. The method was applied to these two components in an extract of *Psilocybe cubensis* (Earle) Sing.

Keyphrases □ Psilocin—GLC–mass spectral analysis in extract of mushroom *Psilocybe cubensis* □ Psilocybin—GLC–mass spectral analysis in extract of mushroom *Psilocybe cubensis* □ GLC–mass spectrometry—analysis, psilocin and psilocybin in extract of mushroom *Psilocybe cubensis* □ Hallucinogenics—psilocin and psilocybin, GLC–mass spectral analysis in extract of mushroom *Psilocybe cubensis*

Psilocin and psilocybin, two hallucinogenic principles found in certain agarics (1), have aroused considerable interest since their isolation and characterization in the late 1950's (2, 3). The mushrooms in which they occur have been known and revered in southern Mexico for centuries. Their rediscovery in 1939 (4) and their subsequent study (5, 6) and popularization ultimately led to legislation to control their use (7).

BACKGROUND

Psilocin (3-[2-(dimethylamino)ethyl]indol-4-ol) and psilocybin, its dihydrogen phosphate ester, are unique in nature as indoles having a 4-substituent and a phosphate group. Both qualitative and quantitative methods have been utilized for their analysis. Paper chromatography (2) and TLC (8) have been used in conjunction with colorimetric reagents as well as UV spectroscopy. When pure samples are available, IR spectrometry can be used (9). Mass spectrometry (10) has been relied upon for identification of these compounds in various pharmaceutical preparations. Various fluorescence and phosphorescence techniques (11) as well as other emission spectral techniques (12) have also been used.

In an investigation of the genus *Psilocybe* and related genera, the need for a sensitive and accurate quantitative method for the analysis of psilocin and psilocybin became apparent. This method would have to be applicable to extracts of minute amounts of scarce herbarium material and vegetative mycelium obtained from liquid culture.

Previously, GLC was applied to the analysis of psilocin (13) and psilocybin (14), both as the free bases and their trimethylsilyl derivatives. GLC–mass spectrometry has been successfully applied to the bis(trimethylsilyl) derivative of bufotenine, the 5-hydroxy positional isomer of psilocin (15).

The possibility of utilizing GLC for the separation of organic molecules containing a phosphate group was suggested by work with trimethylsilyl derivatives of ribonucleotides (16).

EXPERIMENTAL[1]

Fifty milligrams of freeze-dried pileus tissue of *P. cubensis*[2] was ground to a fine powder with sand and transferred to a screw-capped vial. Methanol (5 ml) was added, and the tube was shaken at room temperature for 24 hr. The mixture was filtered, and the solid was washed with 5 ml of methanol. The filtrate was concentrated *in vacuo* to 0.5 ml, transferred to a 1.0-ml vial[3], and concentrated to dryness in a nitrogen stream. All traces of solvent were removed by evacuation on the oil pump. In an anhydrous nitrogen atmosphere, 100 μl of bis(trimethylsilyl)trifluoroacetamide[4] was added to the vial, which was then closed with a septum-lined aluminum seal[5].

The vial was heated at 140° for 15 min. Prolonged reaction periods (up to 2.5 hr) showed that this length of time was sufficient for quantitative

[1] GLC was carried out using a Hewlett-Packard model 402 gas chromatograph equipped with hydrogen flame-ionization detectors. The column used was a 1.6-m × 2.8-mm i.d. glass U-tube with 1.5% SE-30 on 100–120-mesh Chromosorb W. Chromatography conditions were: injection block, 220°; detector, 280°; oven, temperature programmed from 150 to 250° at 7.5°/min; chart speed, 0.64 cm/min; and helium carrier gas, 50 ml/min. TLC utilized glass plates with 0.25-mm layers of silica gel GF using 1-propanol–5% ammonium hydroxide (5:2) (17).

GLC–mass spectrometry was carried out with a Finnigan model 9500 gas chromatograph coupled to a Finnigan model 3100 D quadrupole mass spectrometer through a single-stage glass jet separator. A System/250 data system (Systems Industries) was used to control the mass spectrometer and acquire data. The mass spectrometer parameters were: interface temperature, 200–225°; transfer line, 150–175°; manifold temperature, 100°; and ion source potential, 70 ev. Two sets of chromatography conditions were employed: (*a*) essentially the same as those listed for GLC, and (*b*) a 0.75-m × 2-mm i.d. glass U-tube with 3% OV-101 on 100–120-mesh Gas Chrom Q temperature programmed from 200 to 275° at 10°/min with a helium flow rate of 20 ml/min.

[2] Carpophores of *Psilocybe cubensis* (Earle) Singer (= *Stropharia cubensis* Earle) (Strophariaceae) were obtained by aseptic cultivation of a strain of this fungus on sterile horse manure. The strain was isolated from pileus tissue of a fresh carpophore of *P. cubensis* collected Aug. 31, 1974, in Huautla de Jimenez, Oaxaca, Mexico, and was maintained on malt extract agar. The origin and maintenance of the culture and the production of fruiting bodies were similar to those reported previously (5, 6, 18). Carpophores were authoritatively identified by Dr. Gastón Guzmán, Escuela Nacional de Ciencias Biológicas (ENCB), I.P.N., Mexico, D.F., Mexico. Herbarium material is on deposit at the ENCB herbarium and the University of Michigan herbarium as LESLIE 1902 and at the Institute for Fermentation herbarium, Osaka, Japan, as IFO-H 11703. Subcultures are on deposit at the Institute for Fermentation (IFO 30176) and the Centraalbureau vorr Schimmelcultures, Baarn, The Netherlands (CBS 134.76).

[3] Hewlett-Packard 5080-8712.

[4] Regisil, Regis Chemical Co.

[5] Hewlett-Packard 5080-8713.

derivatization. The resulting solution was cooled to room temperature, and 1.0-μl aliquots were used for subsequent analyses. Reference standards of psilocin and psilocybin were derivatized in the same manner, and quantitation was performed using an external standard of bis(trimethylsilyl)psilocin following the general method described by Gudzinowicz (19). The silanized solutions were stable for several weeks when stored at 4° under anhydrous conditions.

RESULTS AND DISCUSSION

Under the temperature-programmed chromatography conditions described (SE-30), the retention times for bis(trimethylsilyl)psilocin (I) and tris(trimethylsilyl)psilocybin (II) were 8.45 and 13.10 min, respectively. These two compounds were clearly separated from other components in the natural extract. Comparison with the external standard showed the concentrations to be 0.420% psilocin and 0.168% psilocybin. These values are not inconsistent with the total yields obtained by Heim and Hofmann (20) from various cultivated strains of *P. cubensis*. However, in the present analysis, the ratio of psilocin to psilocybin consistently exceeded 1, in contrast to the isolated yields of each compound reported by Heim and Hofmann (20). The present results were confirmed by TLC. The difference in these results might be attributed to the decomposition of psilocin during isolation procedures.

While the mass spectrum of I both as the standard and from the natural extract could be recorded easily, the mass spectrum of II could not be obtained with the longer SE-30 column. However, the conditions utilized with the OV-101 column proved rewarding, and a satisfactory spectrum was recorded. Under these conditions, II was eluted in 3.6 min.

The mass spectrum of I exhibited peaks at *m/e* 348 (M^+) (relative intensity 4%), 333 (1), 291 (6), 290 (21), 75 (3), 73 (39), and 58 (100). The mass spectrum of II showed peaks at *m/e* 500 (M^+) (1%), 485 (1), 442 (6), 77 (9), 75 (15), 73 (47), and 58 (100). While these two spectra are relatively simple in appearance, they are consistent with known fragmentation patterns of this type of compound. The parent peak at *m/e* 348 in I indicates the presence of two trimethylsilyl groups. As expected for 3-indolylethylamines, the significant fragments at *m/e* 290 and *m/e* 58 arise by fission of the bond beta to the nitrogen in the dimethylaminoethyl side chain (21). The M − 15 peak at *m/e* 333 and the peaks at *m/e* 75 and 73 are consistent with known fragmentations of trimethylsilyl ethers (22). The parent peak in the spectrum of II at *m/e* 500, the β-bond fission fragment at *m/e* 442 (M − 58), and the M − 15 peak at *m/e* 485 are evidence for the presence of three trimethylsilyl groups. Again, the peak at *m/e* 58 due to β-bond fission is the most prominent. The mass spectrum of the eluted psilocybin derivative confirms the stability of the silanized molecule under the instrumental conditions used.

Analyses by this method are routinely performed using 5–20 mg of dried fungal tissue.

REFERENCES

(1) R. E. Schultes and A. Hofmann, "The Botany and Chemistry of Hallucinogens," Charles C Thomas, Springfield, Ill., 1973, pp. 36–52.

(2) A. Hofmann, R. Heim, A. Brack, H. Kobel, A. Frey, H. Ott, T. Petrzilka, and F. Troxler, *Helv. Chim. Acta*, **42**, 1557 (1959).

(3) A. Hofmann, *Bull. Narc.*, **23**, 3 (1971).

(4) R. E. Schultes, *Bot. Mus. Leaft., Harv. Univ.*, **7**, 37 (1939).

(5) R. Heim and R. G. Wasson, "Les Champignons Hallucinogènes du Mexique," Museum National D'Histoire Naturelle, Paris, France, 1959, pp. 224–243.

(6) R. Singer, *Mycologia*, **50**, 239 (1958).

(7) 91st Congress of the United States, "Comprehensive Drug Abuse and Control Act of 1970," Public Law 91-513, Oct. 27, 1970.

(8) R. Heim, K. Genest, D. W. Hughes, and G. Belec, *J. Forensic Sci. Soc.*, **6**, 192 (1966).

(9) R. J. Mesley and W. H. Evans, *J. Pharm. Pharmacol.*, **22**, 321 (1970).

(10) S. W. Bellman, *J. Assoc. Offic. Anal. Chem.*, **51**, 164 (1968).

(11) J. J. Aaron, L. B. Sanders, and J. D. Winefordner, *Clin. Chim. Acta*, **45**, 375 (1973).

(12) N. Fiussello, *Mycopathol. Mycol. Appl.*, **39**, 329 (1969).

(13) B. Holmstedt, W. J. A. VandenHeuvel, W. L. Gardiner, and E. C. Horning, *Anal. Biochem.*, **8**, 151 (1964).

(14) M. Lerner and M. D. Katsiaficas, *Bull. Narc.*, **21**, 47 (1969).

(15) N. Narasimhachari, J. Spaide, and B. Heller, *J. Chromatogr. Sci.*, **9**, 502 (1971).

(16) T. Hashizume and Y. Sasaki, *Anal. Biochem.*, **15**, 199 (1966).

(17) A. Y. Leung, A. H. Smith, and A. G. Paul, *J. Pharm. Sci.*, **54**, 1576 (1965).

(18) L. R. Kneebone, in "Developments in Industrial Microbiology," vol. 1, Plenum, New York, N.Y., 1960, p. 109.

(19) B. J. Gudzinowicz, "Gas Chromatographic Analysis of Drugs and Pesticides," Dekker, New York, N.Y., 1967, pp. 164–174.

(20) R. Heim and A. Hofmann, *Rev. Mycol.*, **23**, 347 (1958).

(21) H. Budzikiewicz, C. Djerassi, and D. H. Williams, "Structural Elucidation of Natural Products by Mass Spectrometry," vol. 1, Holden-Day, San Francisco, Calif., 1964, pp. 42–45.

(22) A. E. Pierce, "Silylation of Organic Compounds," Pierce Chemical Co., Rockford, Ill., 1968, pp. 33–39.

ACKNOWLEDGMENTS AND ADDRESSES

Received May 14, 1976, from *148-B West Dana St., Mountain View, CA 94041.*

Accepted for publication July 7, 1976.

The authors thank Dr. Gastón Guzmán for identification and Jonathan Ott for deposition of the specimens at ENCB. They also thank Dr. R. E. Willette, National Institute on Drug Abuse, for supplying standards of psilocin and psilocybin.

* Present address: 104 Whitney Ave., Los Gatos, CA 95030.

‡ Present address: 1846 North Avenue 56, Los Angeles, CA 90042.

§ Present address: Ultrachem Corp., Walnut Creek, CA 94596.

ˣ To whom inquiries should be directed.

High-Pressure Liquid Chromatographic Separation of 5,6-*cis*- and *trans*-Prostaglandin A_2

DENNIS J. WEBER

Abstract □ A high-pressure liquid chromatographic procedure capable of separating the *cis*- and *trans*-isomers of prostaglandin A_2 is described.

Keyphrases □ Prostaglandin A_2—high-pressure liquid chromatographic analysis, *cis*- and *trans*-isomers □ High-pressure liquid chromatography—analysis, *cis*- and *trans*-prostaglandin A_2

Prostaglandin A_2 (I) normally has the *cis*-configuration at the 5,6-double bond. However, extracts from the gorgonian *Plexaura homomalla*, a soft coral found in the Caribbean area, contained significant amounts of 5,6-*trans*-prostaglandin A_2 (II) (1). Therefore, a procedure capable of separating the *cis*- and *trans*-isomers in prostaglandin samples is needed.

A recent paper (2) described the high-pressure liquid

derivatization. The resulting solution was cooled to room temperature, and 1.0-μl aliquots were used for subsequent analyses. Reference standards of psilocin and psilocybin were derivatized in the same manner, and quantitation was performed using an external standard of bis(trimethylsilyl)psilocin following the general method described by Gudzinowicz (19). The silanized solutions were stable for several weeks when stored at 4° under anhydrous conditions.

RESULTS AND DISCUSSION

Under the temperature-programmed chromatography conditions described (SE-30), the retention times for bis(trimethylsilyl)psilocin (I) and tris(trimethylsilyl)psilocybin (II) were 8.45 and 13.10 min, respectively. These two compounds were clearly separated from other components in the natural extract. Comparison with the external standard showed the concentrations to be 0.420% psilocin and 0.168% psilocybin. These values are not inconsistent with the total yields obtained by Heim and Hofmann (20) from various cultivated strains of *P. cubensis*. However, in the present analysis, the ratio of psilocin to psilocybin consistently exceeded 1, in contrast to the isolated yields of each compound reported by Heim and Hofmann (20). The present results were confirmed by TLC. The difference in these results might be attributed to the decomposition of psilocin during isolation procedures.

While the mass spectrum of I both as the standard and from the natural extract could be recorded easily, the mass spectrum of II could not be obtained with the longer SE-30 column. However, the conditions utilized with the OV-101 column proved rewarding, and a satisfactory spectrum was recorded. Under these conditions, II was eluted in 3.6 min.

The mass spectrum of I exhibited peaks at *m/e* 348 (M^+) (relative intensity 4%), 333 (1), 291 (6), 290 (21), 75 (3), 73 (39), and 58 (100). The mass spectrum of II showed peaks at *m/e* 500 (M^+) (1%), 485 (1), 442 (6), 77 (9), 75 (15), 73 (47), and 58 (100). While these two spectra are relatively simple in appearance, they are consistent with known fragmentation patterns of this type of compound. The parent peak at *m/e* 348 in I indicates the presence of two trimethylsilyl groups. As expected for 3-indolylethylamines, the significant fragments at *m/e* 290 and *m/e* 58 arise by fission of the bond beta to the nitrogen in the dimethylaminoethyl side chain (21). The M − 15 peak at *m/e* 333 and the peaks at *m/e* 75 and 73 are consistent with known fragmentations of trimethylsilyl ethers (22). The parent peak in the spectrum of II at *m/e* 500, the β-bond fission fragment at *m/e* 442 (M − 58), and the M − 15 peak at *m/e* 485 are evidence for the presence of three trimethylsilyl groups. Again, the peak at *m/e* 58 due to β-bond fission is the most prominent. The mass spectrum of the eluted psilocybin derivative confirms the stability of the silanized molecule under the instrumental conditions used.

Analyses by this method are routinely performed using 5–20 mg of dried fungal tissue.

REFERENCES

(1) R. E. Schultes and A. Hofmann, "The Botany and Chemistry of Hallucinogens," Charles C Thomas, Springfield, Ill., 1973, pp. 36–52.

(2) A. Hofmann, R. Heim, A. Brack, H. Kobel, A. Frey, H. Ott, T. Petrzilka, and F. Troxler, *Helv. Chim. Acta*, **42**, 1557 (1959).

(3) A. Hofmann, *Bull. Narc.*, **23**, 3 (1971).

(4) R. E. Schultes, *Bot. Mus. Leaft., Harv. Univ.*, **7**, 37 (1939).

(5) R. Heim and R. G. Wasson, "Les Champignons Hallucinogènes du Mexique," Museum National D'Histoire Naturelle, Paris, France, 1959, pp. 224–243.

(6) R. Singer, *Mycologia*, **50**, 239 (1958).

(7) 91st Congress of the United States, "Comprehensive Drug Abuse and Control Act of 1970," Public Law 91-513, Oct. 27, 1970.

(8) R. Heim, K. Genest, D. W. Hughes, and G. Belec, *J. Forensic Sci. Soc.*, **6**, 192 (1966).

(9) R. J. Mesley and W. H. Evans, *J. Pharm. Pharmacol.*, **22**, 321 (1970).

(10) S. W. Bellman, *J. Assoc. Offic. Anal. Chem.*, **51**, 164 (1968).

(11) J. J. Aaron, L. B. Sanders, and J. D. Winefordner, *Clin. Chim. Acta*, **45**, 375 (1973).

(12) N. Fiussello, *Mycopathol. Mycol. Appl.*, **39**, 329 (1969).

(13) B. Holmstedt, W. J. A. VandenHeuvel, W. L. Gardiner, and E. C. Horning, *Anal. Biochem.*, **8**, 151 (1964).

(14) M. Lerner and M. D. Katsiaficas, *Bull. Narc.*, **21**, 47 (1969).

(15) N. Narasimhachari, J. Spaide, and B. Heller, *J. Chromatogr. Sci.*, **9**, 502 (1971).

(16) T. Hashizume and Y. Sasaki, *Anal. Biochem.*, **15**, 199 (1966).

(17) A. Y. Leung, A. H. Smith, and A. G. Paul, *J. Pharm. Sci.*, **54**, 1576 (1965).

(18) L. R. Kneebone, in "Developments in Industrial Microbiology," vol. 1, Plenum, New York, N.Y., 1960, p. 109.

(19) B. J. Gudzinowicz, "Gas Chromatographic Analysis of Drugs and Pesticides," Dekker, New York, N.Y., 1967, pp. 164–174.

(20) R. Heim and A. Hofmann, *Rev. Mycol.*, **23**, 347 (1958).

(21) H. Budzikiewicz, C. Djerassi, and D. H. Williams, "Structural Elucidation of Natural Products by Mass Spectrometry," vol. 1, Holden-Day, San Francisco, Calif., 1964, pp. 42–45.

(22) A. E. Pierce, "Silylation of Organic Compounds," Pierce Chemical Co., Rockford, Ill., 1968, pp. 33–39.

ACKNOWLEDGMENTS AND ADDRESSES

Received May 14, 1976, from *148-B West Dana St., Mountain View, CA 94041.*

Accepted for publication July 7, 1976.

The authors thank Dr. Gastón Guzmán for identification and Jonathan Ott for deposition of the specimens at ENCB. They also thank Dr. R. E. Willette, National Institute on Drug Abuse, for supplying standards of psilocin and psilocybin.

* Present address: 104 Whitney Ave., Los Gatos, CA 95030.

‡ Present address: 1846 North Avenue 56, Los Angeles, CA 90042.

§ Present address: Ultrachem Corp., Walnut Creek, CA 94596.

ˣ To whom inquiries should be directed.

High-Pressure Liquid Chromatographic Separation of 5,6-*cis*- and *trans*-Prostaglandin A_2

DENNIS J. WEBER

Abstract □ A high-pressure liquid chromatographic procedure capable of separating the *cis*- and *trans*-isomers of prostaglandin A_2 is described.

Keyphrases □ Prostaglandin A_2—high-pressure liquid chromatographic analysis, *cis*- and *trans*-isomers □ High-pressure liquid chromatography—analysis, *cis*- and *trans*-prostaglandin A_2

Prostaglandin A_2 (I) normally has the *cis*-configuration at the 5,6-double bond. However, extracts from the gorgonian *Plexaura homomalla*, a soft coral found in the Caribbean area, contained significant amounts of 5,6-*trans*-prostaglandin A_2 (II) (1). Therefore, a procedure capable of separating the *cis*- and *trans*-isomers in prostaglandin samples is needed.

A recent paper (2) described the high-pressure liquid

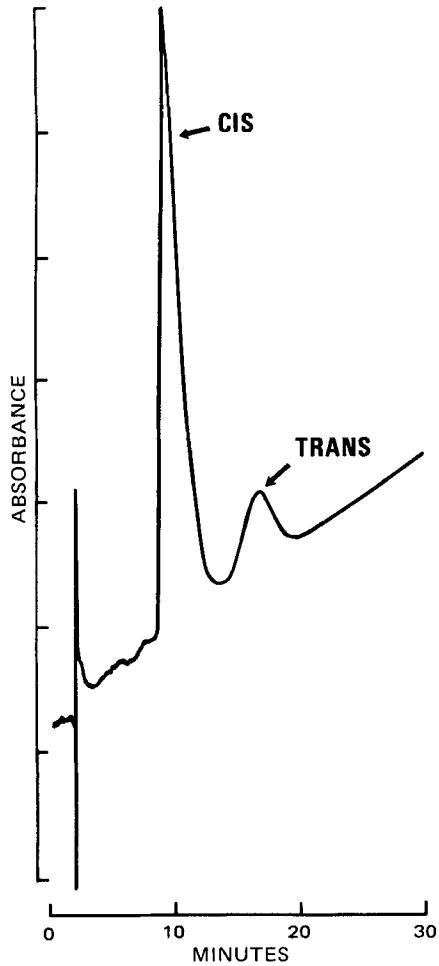

Figure 1—*Chromatogram of I and II methyl esters.*

chromatographic (HPLC) separation of a large number of prostaglandin *p*-nitrophenacyl esters using a microparticulate silica column. The partial separation of 5,6-*cis*- and *trans*-isomers of dinoprostone (III) and dinoprost (IV) was described, but no mention was made of the separation of prostaglandin A_2 or prostaglandin B_2 *cis*- and *trans*-isomers.

The separation of alkenes from saturated hydrocarbons (3, 4) and the resolution of *cis–trans*-isomers using silver-ion complexes are well-known procedures (5). The thermodynamics of alkene–silver-ion complexes in water show (6) that, although the enthalpy change favors formation, the entropy change is large and negative and causes the complex to be quite weak. Thus, temperatures near 25° are required for appreciable complexation. This low temperature requirement is easily satisfied by HPLC.

EXPERIMENTAL

Reagents and Samples—All solvents were distilled-in-glass quality[1], except water which was deionized. The anhydrous silver perchlorate[2] was used as received. The prostaglandin methyl esters[3] were used as received and stored as the methanol solutions.

Apparatus—The liquid chromatograph[4] was equipped with a 1-m column packed with 37-μm superficially porous beads with a bonded stationary phase of octadecylsilyl groups. Detection was by UV absorption at 254 nm. The mobile phase was 0.5 *M* $AgClO_4$ dissolved in methanol–water (20:80). The instrument was operated at 900 psi and room temperature. The sample concentrations were between 0.5 and 4 mg/ml, and 1–3-μl injections were used.

Because of the corrosive effect of the aqueous silver perchlorate on the copper drain tubing and on the brass pressure backup plate in the main pump, extensive plumbing changes were necessary. All copper drain tubing and brass fittings were replaced by perfluoropolyethylene tubing or stainless steel. The brass pressure backup plate was replaced by one made from ceramic-filled plastic.

The UV spectra were recorded on a recording spectrophotometer[5].

Mass spectra were taken on a high-resolution mass spectrometer[6] using an ionization potential of 70 v and direct probe sampling. Samples were prepared by evaporating an aliquot to dryness and reacting with reagent[7] to form the 15-trimethylsilyl derivative. Mass spectral samples from chromatographic cuts were obtained by running the aqueous chromatographic effluent into a flask containing about 10 ml of methylene chloride overlaid with about 3 ml of water. After each collection, the flask was immediately shaken to extract the prostaglandin into the organic phase. The phases were separated, and the methylene chloride fraction was washed with about 3 ml of water. The organic layer was taken to dryness and treated with derivatizing reagent as before.

Table I—Principal Ions in Mass Spectra of the 15-Trimethylsilyl Derivatives of I, II, and V Methyl Esters

Ion	*m/e* 15-Trimethylsilyl I and II Methyl Esters	*m/e* 15-Trimethylsilyl V Methyl Ester
$M^+\cdot$	420	420
$M^+\cdot - \cdot CH_3$	405	405
$M^+\cdot - \cdot C_2H_5$	391	391
$M^+\cdot - \cdot OCH_3$	389	389
$M^+\cdot - \cdot C_5H_{11}$	349	349
$M^+\cdot - (CH_3)_3SiOH$	330	330
$M^+\cdot - (\cdot C_5H_{11} + CO)$	321	321
$M^+\cdot - (\cdot C_5H_{11} + CH_3OH)$	317	317
—	199	247
—	190	

Table II—Comparison of Retention Times of 5,6-*cis*- and *trans*-Prostaglandin B_2 and Prostaglandin A_2 Methyl Esters

Compound	Retention Time, min
I Methyl ester	8.9
II Methyl ester	17.0
5,6-*cis*-V Methyl ester	16.4
5,6-*trans*-V Methyl ester	15.8

RESULTS AND DISCUSSION

Separation of I and II—Separation of I methyl ester from II methyl ester was achieved using a reversed-phase column[8] and a mobile phase of 0.5 *M* $AgClO_4$ in methanol–water (20:80). An example of the separation is shown in Fig. 1.

The retention times of the *cis*- and *trans*-isomers were 8.9 and 17.0 min, respectively. The *cis*-isomer eluted before the *trans*-isomer, because the complexation took place in the mobile phase and the stability constant of the silver–*cis*-isomer complex was greater (5). The relative sizes of the peaks were correct, since samples of I usually contained less than 15% of the *trans*-isomer.

An authentic sample of II methyl ester gave a single peak with a retention time of 17 min, which agreed very well with the peak assigned to the *trans*-isomer in Fig. 1.

[1] Burdick and Jackson Labs, Muskegon, Mich.
[2] G. F. Smith Chemical Co., Columbus, Ohio.
[3] Prepared by the Research Laboratory, The Upjohn Co., Kalamazoo, Mich.
[4] Model 820, DuPont Instrument Co., Wilmington, Del.
[5] Cary 15, Varian Inc., Palo Alto, Calif.
[6] Consolidated Electrodynamics Corp., Pasadena, Calif.
[7] Regisil, Regis Chemical Co., Morton Grove, Ill.
[8] ODS Permaphase, DuPont Instrument Co., Wilmington, Del.

Table III—Molar Absorptivities of Prostaglandin B_2 and Prostaglandin A_2 Methyl Esters

	Solvent 1[a]			Solvent 2[b]		
	λ_{max}	$\epsilon\lambda_{max}$	ϵ_{254}	λ_{max}	$\epsilon\lambda_{max}$	ϵ_{254}
Prostaglandin B_2	278	23,700	10,500	282	23,700	7560
Prostaglandin A_2	217	9,970	1,040	—[c]	—[c]	1520

[a] Solvent is methanol. [b] Solvent is 0.5 *M* $AgClO_4$ in methanol–water (20:80). [c] Data were not collectable due to solvent absorbance below 238 nm.

The possibility that the second, smaller peak of Fig. 1 was not the *trans*-isomer but an on-column degradation product of I methyl ester was checked by injecting a large amount, about 50 μg of the *cis–trans*-mixture, collecting the peak representing the *cis*-isomer, and reinjecting it. The reinjected material gave only one peak, and its retention time was the same as that for the *cis*-peak of the original mixture. Therefore, the chromatographic conditions had no apparent effect on the chemical stability of the samples and the peaks seen were not artifacts of the separation process.

A further check on the validity of the separation was carried out by injection of a biosynthetically produced I methyl ester. The material contains only the *cis*-isomer. Chromatographic analysis gave only one peak with a retention time of 9.2 min, in good agreement with the retention time of the *cis*-isomer in the mixture.

Mass Spectra of I and II Methyl Esters—The mass spectra of the pure biosynthetic I and pure II methyl esters were identical to each other and to the spectra of samples obtained by chromatographic cuts of elution curves. This finding is good evidence that the 8.9- and 17-min peaks differ only by a 5,6-*cis–trans*-relationship, since other prostaglandin A_2 methyl ester isomers or derivatives would be expected to give different mass spectra. The principal mass ions of the 15-trimethylsilyl derivative of I and II methyl esters are shown in Table I.

Chromatography of 5,6-*cis*- and *trans*-Prostaglandin B_2 Methyl Esters—Since I is often contaminated with prostaglandin B_2 (V), it was necessary to determine if the retention times of 5,6-*cis*- and *trans*-V methyl esters would interfere with the I or II methyl ester peak. Samples of the V methyl ester isomers[3] were chromatographed, and their retention times were close to each other and to the retention time of the II methyl ester (Table II).

Mass Spectra of V Methyl Esters—A chromatographic cut of 5,6-*cis*-V methyl ester was collected and submitted for mass spectral analysis as the trimethylsilyl derivative. Comparison with the mass spectra of the silylated unchromatographed 5,6-*cis*- and *trans*-V methyl esters showed no difference, indicating that the chromatographic process had no deleterious effect and that the samples of *cis*- and *trans*-V esters had the expected identical mass spectra. The principal mass ions of the 5,6-*cis–trans*-V methyl ester trimethylsilyl derivative are given in Table I. The 190 and 199 peaks in the prostaglandin A_2 series and the 247 peak in the prostaglandin B_2 series may be diagnostic of the differences among I, II, and V methyl esters.

UV Spectra of 5,6-*cis*- and *trans*-V, I, and II Methyl Esters—Additional evidence for the identity of the 5,6-*cis*- and *trans*-V, I, and II methyl esters was obtained from the UV spectra in methanol. The two samples of 5,6-*cis*- and *trans*-V methyl esters showed a peak at 278 nm and no evidence of a peak at 217 nm, indicating that neither sample contained any appreciable amount of I or II methyl ester. Conversely, the UV spectrum of II methyl ester, which had the same chromatographic retention time as the V isomers, indicated that the sample contained less than 5% of the V isomer. Approximately the same amount of V isomer was found in the biosynthetic I methyl ester.

The mass spectra and UV absorption data indicate that the assumed structures of the samples are correct. Therefore, the coincidence of the retention times of the *cis*- and *trans*-V methyl esters with the II methyl ester was real and not an artifact.

The UV spectra of V methyl ester in methanol–water (20:80), which was 0.5 *M* in silver perchlorate, showed a slight shift to a longer wavelength at the λ_{max} and no change in the molar absorptivity at the absorption maximum when compared to the spectrum in methanol. This finding indicates that the complexation of Ag^+ with I, II, and V methyl esters does not drastically change the chromophores. The molar absorptivities at the λ_{max} and at 254 nm are given in Table III.

Quantification of 5,6-*trans*-V Methyl Ester—An assay for the fraction of prostaglandin A_2 with the 5,6-*trans*-configuration is possible using the described procedure, but a reliable source of I methyl ester uncontaminated with the *trans*-isomer is needed to construct a calibration curve using a particular instrument and set of conditions. The 5,6-*cis*-isomer content can be found from HPLC data, and the sum of 5,6-*cis*- and 5,6-*trans*-isomers can be obtained from UV data. Therefore, the desired result can be calculated.

Possible Relationship of Structure to Lack of Separation of 5,6-*cis*- and *trans*-V Methyl Esters—A possible explanation as to why I and II methyl esters, but not the esters of 5,6-*cis*- and *trans*-V, can be separated in this system can be found in the differences in structure of prostaglandins B_2 and A_2. In prostaglandin A_2, the two side chains are *trans* to each other about the 8,12-bond. Thus, there is little or no interference of the lower side chain (C-13–C-20) with the approach of a silver ion to the 5,6-double bond. However, in prostaglandin B_2, the 8,12-double bond forces the side chains to be coplanar at the points of ring attachment. This orientation could result in a serious interference by the C-13–C-20 side chain with the approach of a silver ion to the 5,6-unsaturation. If no complexation occurs, there can be no separation of 5,6-*cis*- and *trans*-V esters, as is observed.

REFERENCES

(1) G. L. Bundy, E. G. Daniels, F. H. Lincoln, and J. E. Pike, *J. Am. Chem. Soc.*, **94**, 2124 (1972).

(2) W. Morozowich and S. L. Douglas, *Prostaglandins*, **10**, 19 (1975).

(3) B. W. Bradford, D. Harvey, and D. E. Chalkley, *J. Inst. Pet.*, **41**, 80 (1955).

(4) J. Janek, Z. Jagaric, and M. Dressler, *J. Chromatogr.*, **53**, 525 (1970).

(5) F. Armitage, *ibid.*, **2**, 655 (1959).

(6) D. S. Barnes, G. J. Ford, L. D. Pettit, and C. Sherrington, *J. Chem. Soc. D*, **1971**, 690.

ACKNOWLEDGMENTS AND ADDRESSES

Received March 25, 1976, from the *Research Laboratories, The Upjohn Company, Kalamazoo, MI 49001.*

Accepted for publication July 6, 1976.

Novel Method for Determination of Partition Coefficients of Penicillins and Cephalosporins by High-Pressure Liquid Chromatography

TSUKINAKA YAMANA ˣ, AKIRA TSUJI, ETSUKO MIYAMOTO, and OSAMU KUBO

Abstract □ Newly defined lipophilic indexes, log k', of a series of penicillins and cephalosporins were rapidly and reliably determined by reversed-phase high-pressure liquid chromatography (HPLC) on bonded octadecylsilane supports. The log k' values obtained from their retention times exhibited a linear relationship with methanol concentration (v/v %) in the mobile phase. The extrapolated log k' values to zero and those at 30% correlated well with the partition coefficients, log P, in 1-octanol–water and with R_m values from TLC. This HPLC technique provided some new log P and R_m values for highly ionizable β-lactam antibiotics. The HPLC method for the determination of partition coefficients of drugs has some advantages and is a useful alternative for the determination of log P and R_m.

Keyphrases □ Penicillins, various—high-pressure liquid chromatographic determination of lipophilic indexes, correlated to partition coefficients □ Cephalosporins, various—high-pressure liquid chromatographic determination of lipophilic indexes, correlated to partition coefficients □ High-pressure liquid chromatography—determination of lipophilic indexes of various penicillins and cephalosporins, correlated to partition coefficients □ Lipophilic indexes—log k' of various penicillins and cephalosporins determined by high-pressure liquid chromatography, correlated to partition coefficients □ Partition coefficients—various penicillins and cephalosporins, correlated to lipophilic indexes determined by high-pressure liquid chromatography □ Antibacterials—various penicillins and cephalosporins, high-pressure liquid chromatographic determination of lipophilic indexes, correlated to partition coefficients

Considerable effort has been expended to correlate biological properties of penicillins (1–7) and cephalosporins (5) with their partition coefficients. While the most useful and widely accepted lipophilic index is the logarithm of the partition coefficient, log P, determined in a 1-octanol–water system (8), such a measurement for penicillin molecules often presents practical difficulties because of their high instability in the acidic pH region near the pKa (~2.7). The log P values determined with a rapid pH-stat technique (9) seem to be the most accurate and reliable. Unfortunately, in spite of this technique, it is difficult to determine or compare the true log P values for β-lactam antibiotics because of two or more ionizable substituents in their side chains (*e.g.*, carbenicillin and sulbenicillin) and because of the zwitterion itself (*e.g.*, cyclacillin, ampicillin, amoxicillin, cephaloridine, cephaloglycin, cephalexin, and cephradine).

The R_m values, which are alternative lipophilic indexes, were determined from reversed-phase TLC for some penicillins (10) and cephalosporins (11). Recently, R_m values of penicillins were determined in another TLC system (9), but a difference between the actual pH on the plate and that of the mobile phase was observed (9). This pH difference is undesirable for acids such as β-lactam antibiotics, because the R_m values, in order to be an expression of the true partition coefficients, have to be corrected according to their degree of ionization at the mobile phase pH.

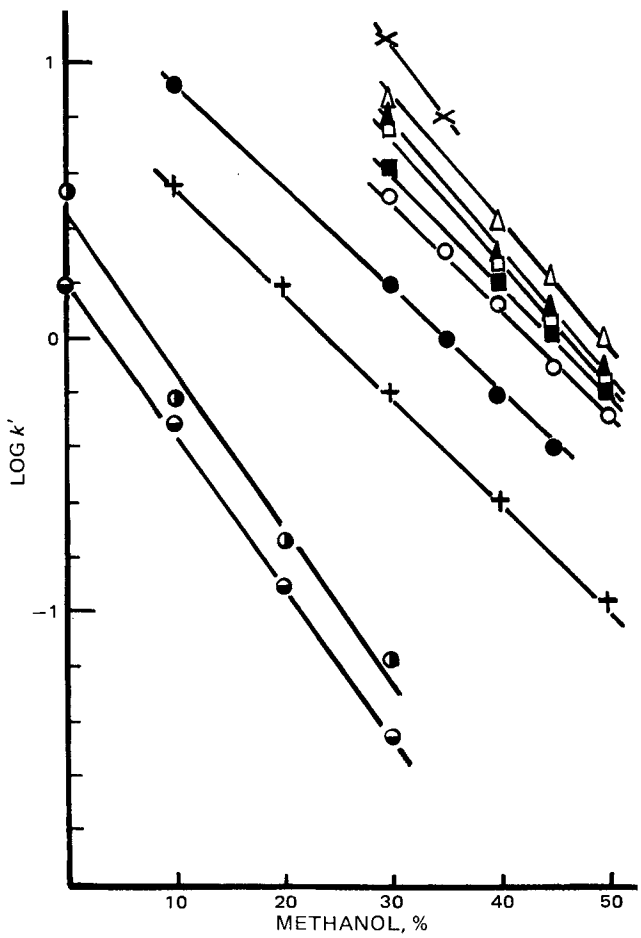

Figure 1—*Relationship between log* k' *values of penicillins and methanol concentration (v/v %) in the mobile phase. The compounds are numbered as in Table I. Key:* ×, *1;* △, *2;* ▲, *3;* □, *4;* ■, *7;* ○, *8;* ●, *9;* +, *11;* ◑, *12; and* ◒, *13.*

This paper reports a novel and useful method for the determination of partition coefficients of these β-lactam antibiotics by high-pressure liquid chromatography (HPLC). With the reversed-phase HPLC method developed recently (12), the lipophilic index, log k', can be defined as follows:

$$\log k' = \log [(t_R - t_0)/t_0] \quad \text{(Eq. 1)}$$

where t_R is the retention time of a retained peak, and t_0 is the retention time of an unretained peak. The term log k' is considered to be analogous to R_m.

EXPERIMENTAL

Materials—Carbenicillin phenyl sodium[1] (979 μg/mg), dicloxacillin

[1] Carfecillin (BRL 3475), Beecham Yakuhin Co., Tokyo, Japan.

Table I—Log k', Log P, and R_m Values of Penicillins and Cephalosporins

Number	Compound	Log k'[a] 30% Methanol	Log k'[a] Extrapolated[b]	Log $P_{octanol}$ Obs.[c]	Log $P_{octanol}$ Calc.[d]	$R_{m\,octanol}$ Obs.[e]	$R_{m\,octanol}$ Calc.[d]	$R_{m\,silicone}$ Obs.[f]	$R_{m\,silicone}$ Calc.[g]
1	Carbenicillin phenyl	1.09	2.68	3.10	3.14	—	0.77	—	2.05
2	Dicloxacillin	0.86	2.30	2.83	2.75	0.44	0.36	1.63	1.63
3	Floxacillin	0.79	2.14	2.67	2.58	—	0.19	—	1.45
4	Cloxacillin	0.77	2.04	2.44	2.48	0.01	0.08	1.34	1.33
5	Oxacillin	0.65	—	2.34	2.34	−0.15	−0.08	1.05	1.19
6	Propicillin	0.83	—	2.58	2.65	0.21	0.18	—	1.41
7	Phenethicillin	0.62	1.80	2.19	2.23	−0.23	−0.17	1.03	1.07
8	Penicillin V	0.51	1.62	2.01	2.05	−0.37	−0.37	0.89	0.86
9	Penicillin G	0.17	1.30	1.76	1.72	−0.66	−0.71	0.55	0.51
10	Cyclacillin	0.06	—	—	1.31	—	−0.93	—	0.46
11	Ampicillin	−0.19	0.94	—	1.35	—	−1.09	0.08	0.10
12	Amoxicillin	−1.14	0.48	—	0.87	—	−1.59	—	−0.41
13	Sulbenicillin	−1.50	0.20	—	0.59	—	−1.89	—	−0.73
14	Cephaloridine	0.37	—	—	1.85	—	—	0.98	0.85
15	Cephalothin	−0.08	—	0.94	1.07	—	—	0.40	0.29
16	Cephaloglyin	−0.10	—	—	1.04	—	—	0.29	0.27
17	Cephalexin	−0.32	—	—	0.65	—	—	—	0.00
18	Cephradine	−0.07	—	—	1.09	—	—	—	0.30
19	Cefazolin	−0.47	—	—	0.39	—	—	—	−0.19

[a] Log k' was defined in the text. A 2.1-mm × 25-cm stainless steel column was packed with Zorbax-ODS and eluted with 0.035 M NH_4Cl aqueous methanol solution of pH 7.4 at 150 kg/cm² and ambient temperature. [b] Extrapolated log k' value to 0% methanol from Fig. 1. [c] Data from Ref. 9, except those for Compounds 1, 3, and 15, which are averages of the values determined by employing the pKa values of 2.72 for Compounds 1 and 3 and of 2.22 for Compound 15 at four or more different pH's at 37° in this laboratory. [d] Calculated from corresponding Eqs. 2–4, except those for Compounds 5, 6, 10, and 14–19, which were calculated from Eqs. 5–7. [e] The R_m value determined at pH 4.0 (9); cellulose was the solid support, and 1-octanol was the stationary phase. [f] The R_m value determined at pH 7.4 (10, 11); silica gel was the solid support, and silicone oil was the stationary phase. [g] Calculated from Eq. 4 for the penicillins except Compounds 5, 6, and 10. Calculated from Eq. 7 for Compounds 5, 6, 10, and cephalosporins.

sodium[2] (900 μg/mg), floxacillin sodium[3] (893 μg/mg), cloxacillin sodium[2] (907 μg/mg), oxacillin sodium[4] (840 μg/mg), propicillin potassium[5] (993 μg/mg), phenethicillin potassium[2] (1444 units/mg), penicillin V potassium[2] (1490 units/mg), penicillin G potassium[2] (1600 units/mg), cyclacillin[5] (999 μg/mg), ampicillin sodium[5] (955 μg/mg), amoxicillin[3] (844 μg/mg), sulbenicillin disodium[5] (878 μg/mg), cephaloridine[6] (971 μg/mg), cephalothin sodium[6] (930 μg/mg), cephaloglycin[6] (864 μg/mg), cephalexin[6] (925 μg/mg), cephradine[7] (962 μg/mg), and cefazolin sodium[3] were used as supplied. Other chemicals[8] were of reagent grade and were used without further purification.

Procedures—A liquid chromatograph[9] equipped with a UV detector operating at 254 nm was used for HPLC. The stationary phase was totally porous silica gel bonded chemically with octadecyl chains prepacked into a 25-cm stainless steel column, 2.1 mm i.d.[10]. The mobile phase was a 0.035 M ammonium chloride–aqueous methanol solution adjusted to pH 7.4; ammonium salt was added to block the active silanol sites and to maintain the ionic strength. The instrument was operated at ambient temperature and 150 kg/cm². Solutions of penicillins and cephalosporins were prepared in the concentration range between 5×10^{-3} and 1×10^{-2} M. A 5-μl quantity of sample was injected into the column.

RESULTS AND DISCUSSION

Log k' values of the sample compounds were calculated from their t_R values by the application of Eq. 1, where the retention time of formamide was used for the t_0 value. The methanol concentration of the mobile phase was varied to obtain peaks with a reasonable retention time.

For the tested penicillins, plots of log k' *versus* methanol concentration (v/v %) showed a reasonable linear relationship (Fig. 1). Table I lists the log $k'_{(0\%)}$ values extrapolated to 0% methanol. The relationship between log $k'_{(0\%)}$ and the other reported lipophilic indexes (log P or R_m) (9, 10) is expressed by Eqs. 2–4 for penicillins and cephalosporins:

$$\log P_{octanol} = 1.03 \log k'_{(0\%)} + 0.38$$
$$n = 7 \quad r = 0.992 \quad s = 0.061 \qquad \text{(Eq. 2)}$$

$$R_{m\,octanol} = 1.07 \log k'_{(0\%)} - 2.10$$
$$n = 5 \quad r = 0.988 \quad s = 0.066 \qquad \text{(Eq. 3)}$$

$$R_{m\,silicone} = 1.12 \log k'_{(0\%)} - 0.95$$
$$n = 6 \quad r = 0.999 \quad s = 0.030 \qquad \text{(Eq. 4)}$$

where n, r, and s are number of experiments, correlation coefficient, and standard deviation, respectively. These equations show that log P and R_m in 1-octanol–water and silicone oil–water systems are satisfactorily correlated with log $k'_{(0\%)}$ values.

The slopes of Eqs. 2–4 are close to unity, which indicates that log $k'_{(0\%)}$ values should be regarded as those for the standard system in partition between a stationary phase and a mobile phase. However, such an extrapolation technique appears to be tedious and unreliable for highly lipophilic compounds, since one must extrapolate from a higher methanol concentration range. From the practical point of view, therefore, it would be desirable if log k' values at a suitable composition of the mobile phase could be used as an expression of the lipophilic character of the test compounds. For the present reference system, the log k' values at 30% methanol were selected because the 30% methanol concentration in the mobile phase provided a log $k'_{(30\%)}$ value in the range of maximum accuracy for most β-lactam antibiotics. The log $k'_{(30\%)}$ values (Table I) are considerably sensitive to the lipophilic balance of the substituents on the nucleus of penicillins and cephalosporins. Good correlations between log $k'_{(30\%)}$ values and log P or R_m are shown in Eqs. 5–7:

$$\log P_{octanol} = 1.74 \log k'_{(30\%)} + 1.21$$
$$n = 10 \quad r = 0.979 \quad s = 0.123 \qquad \text{(Eq. 5)}$$

$$R_{m\,octanol} = 1.45 \log k'_{(30\%)} - 1.02$$
$$n = 7 \quad r = 0.941 \quad s = 0.123 \qquad \text{(Eq. 6)}$$

$$R_{m\,silicone} = 1.23 \log k'_{(30\%)} + 0.39$$
$$n = 10 \quad r = 0.971 \quad s = 0.116 \qquad \text{(Eq. 7)}$$

The log P and R_m values calculated from Eqs. 2–7 with the corresponding log $k'_{(0\%)}$ or log $k'_{(30\%)}$ values are recorded in Table I. The results apparently confirm the usefulness of the log k' values as another expression of the lipophilic character and/or the conversion parameter for estimating unknown partition coefficients such as log P or Hansch π values (13) of β-lactam antibiotics.

For the determination of partition coefficients, Huber *et al.* (14) established a liquid–liquid chromatographic method; the HPLC method was recently proposed (12) as a useful alternative to the often tedious 1-octanol–water partition measurements. The HPLC method (12) is recommended for partition study of any compound because: (*a*) it is fast (*e.g.*, typical compounds can be eluted in less than 10 min) and repro-

[2] Meiji Seika Kaisha, Tokyo, Japan.
[3] Fujisawa Pharmaceutical Co., Osaka, Japan.
[4] Banyu Pharmaceutical Co., Tokyo, Japan.
[5] Takeda Chemical Industries, Osaka, Japan.
[6] Shionogi & Co., Osaka, Japan.
[7] Sankyo Co., Tokyo, Japan.
[8] Wako Pure Chemical Industries, Osaka, Japan.
[9] Shimadzu-DuPont 830.
[10] Zorbax-ODS, DuPont.

ducible, (*b*) the pH can be controlled, (*c*) it is applicable to compounds unstable in solution, (*d*) samples need not be pure, and (*e*) quantitative analytical methods need not be considered since any compound can be detected by a UV or refractive index detector.

However, an important unsolved problem remains. What system would produce the universal lipophilic index such as log *P*? A study is now in progress to develop a normalized method for correcting the differences in log *k'* determined with different columns from different sources, solvent compositions, pH's, and temperatures and to establish a general method for all kinds of chemical compounds.

REFERENCES

(1) C. Hansch and A. R. Steward, *J. Med. Chem.*, **7**, 691 (1964).

(2) C. Hansch and S. M. Anderson, *J. Org. Chem.*, **32**, 2583 (1967).

(3) A. E. Bird and A. C. Marshall, *Biochem. Pharmacol.*, **16**, 2275 (1967).

(4) W. Scholtan, *Arzneim.-Forsch.*, **18**, 505 (1968).

(5) G. L. Biagi, M. C. Barbaro, and M. F. Gamba, *J. Med. Chem.*, **13**, 511 (1970).

(6) A. E. Bird and J. H. C. Nayler, in "Drug Design," vol. II, E. J. Ariens, Ed., Academic, New York, N.Y., 1971, chap. 8.

(7) A. E. Bird, *J. Pharm. Sci.*, **64**, 1671 (1975).

(8) R. N. Smith, C. Hansch, and M. M. Ames, *ibid.*, **64**, 599 (1975).

(9) A. E. Bird and A. C. Marshall, *J. Chromatogr.*, **63**, 313 (1971).

(10) G. L. Biagi, A. M. Barbaro, M. C. Guerra, and M. F. Gamba, *ibid.*, **41**, 371 (1969).

(11) *Ibid.*, **44**, 195 (1969).

(12) J. M. McCall, *J. Med. Chem.*, **18**, 549 (1975).

(13) C. Hansch and T. Fujita, *J. Am. Chem. Soc.*, **86**, 1616 (1964).

(14) J. F. K. Huber, C. A. M. Meijers, and J. A. R. Hulsman, *Anal. Chem.*, **44**, 111 (1972).

ACKNOWLEDGMENTS AND ADDRESSES

Received February 5, 1976, from the *Faculty of Pharmaceutical Sciences, Kanazawa University, Takara-machi, Kanazawa 920, Japan.*

Accepted for publication July 9, 1976.

The authors acknowledge the gifts of penicillins and cephalosporins from Beecham Yakuhin Co., Meiji Seika Kaisha, Fujisawa Pharmaceutical Co., Takeda Chemical Industries, Banyu Pharmaceutical Co., Shionogi & Co., and Sankyo Co. The authors are grateful to Mr. I. Kagami for technical assistance.

[x] To whom inquiries should be directed.

Rapid GLC Determination of Ibuprofen in Serum

D. J. HOFFMAN

Abstract □ A rapid procedure for the determination of ibuprofen in human serum was developed using a single extraction with carbon tetrachloride after deproteinization with perchloric acid. The internal standard, 3-methyl-3-phenylbutyric acid, was added directly to the serum. Gas chromatograms were free of interfering peaks. Calibration curves (0–40 μg/ml) were linear with a sensitivity of 0.5 μg of ibuprofen/ml of serum. Relative standard deviations ranged from 1.1 to 25%.

Keyphrases □ Ibuprofen—GLC analysis, human serum □ GLC—analysis, ibuprofen in human serum □ Anti-inflammatory agents—ibuprofen, GLC analysis in human serum

Ibuprofen is a 2-phenylalkylcarboxylic acid derivative possessing potent anti-inflammatory, antipyretic, and analgesic properties (1–3). Recently, a GLC method for determining ibuprofen in human plasma was reported (4). The assay involved an extraction into benzene, followed by evaporation of the extract to dryness and subsequent derivatization of ibuprofen to the methyl ester. A rapid GLC method for the anticonvulsant valproic acid in serum utilized the underivatized acid and a 5% FFAP column (5). By using similar conditions, a GLC method was developed for the assay of serum ibuprofen levels. This method is rapid and precise and does not require derivative formation.

EXPERIMENTAL

Reagents—Reagent grade perchloric acid[1] and carbon tetrachloride[2] were used without further purification. Ibuprofen and 3-methyl-3-phenylbutyric acid were used as supplied[3].

Instrumentation—The GLC analyses were performed on a gas chromatograph[4] equipped with an automatic sampler[5], computing integrator[6], and flame-ionization detector. The chromatograph was fitted with a 1.83-m (6-ft) U-shaped glass column (2 mm i.d.) packed with 5% FFAP[7] on Gas Chrom W (HP), 80–100 mesh[8]. The column was conditioned before use at 255° for 15 hr with a carrier gas (nitrogen[9]) at a flow rate of 30 ml/min.

The chromatographic conditions were: carrier gas, 35 ml/min; air, 260 ml/min; hydrogen, 37 ml/min; injection port and detector temperatures, 250°; and oven temperature, 220°. The attenuation of the computing integrator was ×8, and the electrometer[10] range was 10^2. Under these conditions, the internal standard and ibuprofen had retention times of 2.9 and 4.3 min, respectively (Fig. 1).

Assay—*Preparation of Standards*—A 2-mg/ml stock solution of ibuprofen was prepared by dissolving 100 mg of ibuprofen in a 50-ml volumetric flask with 2 ml of 0.5 *N* NaOH and adjusting to 50 ml with distilled water. A working serum ibuprofen standard at 40 μg/ml was prepared by adding 1.0 ml of the stock solution to a 50-ml volumetric flask and adjusting to volume with commercial human serum[11]. Other serum standards were prepared from serial dilutions (with serum) of the 40-μg/ml serum standard.

The internal standard stock solution (2 mg/ml) was prepared by dissolving 100 mg of 3-methyl-3-phenylbutyric acid in a 50-ml volumetric flask with 2 ml of 0.5 *N* NaOH and adjusting to 50 ml with distilled water. A working internal standard solution (100 μg/ml) was prepared by diluting 5 ml of the internal standard stock solution to 100 ml with distilled water.

Extraction Procedure—To a 15-ml conical glass centrifuge tube were added 0.5 ml of the internal standard solution, 1.0 ml of serum, and 0.5 ml of 10% perchloric acid. After vigorous mixing[12], 0.4 ml of carbon tetrachloride was added, followed again by vigorous mixing for 15 sec. The

[1] Mallinckrodt reagent grade, 60%.
[2] Mallinckrodt (low sulfur) reagent grade.
[3] Supplied by A. Geisler, Abbott Laboratories.
[4] Hewlett-Packard model 7610A.
[5] Hewlett-Packard model 7671A.
[6] Hewlett-Packard model 3380A.
[7] Varian Aerograph.
[8] Applied Science Laboratories.
[9] Linde Division, Union Carbide Corp.
[10] Hewlett-Packard model 7650A.
[11] K-N Enterprises.
[12] Maxi Mix model M-16715, Thermolyne, Sybron Corp.

ducible, (*b*) the pH can be controlled, (*c*) it is applicable to compounds unstable in solution, (*d*) samples need not be pure, and (*e*) quantitative analytical methods need not be considered since any compound can be detected by a UV or refractive index detector.

However, an important unsolved problem remains. What system would produce the universal lipophilic index such as log *P*? A study is now in progress to develop a normalized method for correcting the differences in log *k'* determined with different columns from different sources, solvent compositions, pH's, and temperatures and to establish a general method for all kinds of chemical compounds.

REFERENCES

(1) C. Hansch and A. R. Steward, *J. Med. Chem.*, **7**, 691 (1964).

(2) C. Hansch and S. M. Anderson, *J. Org. Chem.*, **32**, 2583 (1967).

(3) A. E. Bird and A. C. Marshall, *Biochem. Pharmacol.*, **16**, 2275 (1967).

(4) W. Scholtan, *Arzneim.-Forsch.*, **18**, 505 (1968).

(5) G. L. Biagi, M. C. Barbaro, and M. F. Gamba, *J. Med. Chem.*, **13**, 511 (1970).

(6) A. E. Bird and J. H. C. Nayler, in "Drug Design," vol. II, E. J. Ariens, Ed., Academic, New York, N.Y., 1971, chap. 8.

(7) A. E. Bird, *J. Pharm. Sci.*, **64**, 1671 (1975).

(8) R. N. Smith, C. Hansch, and M. M. Ames, *ibid.*, **64**, 599 (1975).

(9) A. E. Bird and A. C. Marshall, *J. Chromatogr.*, **63**, 313 (1971).

(10) G. L. Biagi, A. M. Barbaro, M. C. Guerra, and M. F. Gamba, *ibid.*, **41**, 371 (1969).

(11) *Ibid.*, **44**, 195 (1969).

(12) J. M. McCall, *J. Med. Chem.*, **18**, 549 (1975).

(13) C. Hansch and T. Fujita, *J. Am. Chem. Soc.*, **86**, 1616 (1964).

(14) J. F. K. Huber, C. A. M. Meijers, and J. A. R. Hulsman, *Anal. Chem.*, **44**, 111 (1972).

ACKNOWLEDGMENTS AND ADDRESSES

Received February 5, 1976, from the *Faculty of Pharmaceutical Sciences, Kanazawa University, Takara-machi, Kanazawa 920, Japan.*

Accepted for publication July 9, 1976.

The authors acknowledge the gifts of penicillins and cephalosporins from Beecham Yakuhin Co., Meiji Seika Kaisha, Fujisawa Pharmaceutical Co., Takeda Chemical Industries, Banyu Pharmaceutical Co., Shionogi & Co., and Sankyo Co. The authors are grateful to Mr. I. Kagami for technical assistance.

[x] To whom inquiries should be directed.

Rapid GLC Determination of Ibuprofen in Serum

D. J. HOFFMAN

Abstract □ A rapid procedure for the determination of ibuprofen in human serum was developed using a single extraction with carbon tetrachloride after deproteinization with perchloric acid. The internal standard, 3-methyl-3-phenylbutyric acid, was added directly to the serum. Gas chromatograms were free of interfering peaks. Calibration curves (0–40 μg/ml) were linear with a sensitivity of 0.5 μg of ibuprofen/ml of serum. Relative standard deviations ranged from 1.1 to 25%.

Keyphrases □ Ibuprofen—GLC analysis, human serum □ GLC—analysis, ibuprofen in human serum □ Anti-inflammatory agents—ibuprofen, GLC analysis in human serum

Ibuprofen is a 2-phenylalkylcarboxylic acid derivative possessing potent anti-inflammatory, antipyretic, and analgesic properties (1–3). Recently, a GLC method for determining ibuprofen in human plasma was reported (4). The assay involved an extraction into benzene, followed by evaporation of the extract to dryness and subsequent derivatization of ibuprofen to the methyl ester. A rapid GLC method for the anticonvulsant valproic acid in serum utilized the underivatized acid and a 5% FFAP column (5). By using similar conditions, a GLC method was developed for the assay of serum ibuprofen levels. This method is rapid and precise and does not require derivative formation.

EXPERIMENTAL

Reagents—Reagent grade perchloric acid[1] and carbon tetrachloride[2] were used without further purification. Ibuprofen and 3-methyl-3-phenylbutyric acid were used as supplied[3].

Instrumentation—The GLC analyses were performed on a gas chromatograph[4] equipped with an automatic sampler[5], computing integrator[6], and flame-ionization detector. The chromatograph was fitted with a 1.83-m (6-ft) U-shaped glass column (2 mm i.d.) packed with 5% FFAP[7] on Gas Chrom W (HP), 80–100 mesh[8]. The column was conditioned before use at 255° for 15 hr with a carrier gas (nitrogen[9]) at a flow rate of 30 ml/min.

The chromatographic conditions were: carrier gas, 35 ml/min; air, 260 ml/min; hydrogen, 37 ml/min; injection port and detector temperatures, 250°; and oven temperature, 220°. The attenuation of the computing integrator was ×8, and the electrometer[10] range was 10^2. Under these conditions, the internal standard and ibuprofen had retention times of 2.9 and 4.3 min, respectively (Fig. 1).

Assay—*Preparation of Standards*—A 2-mg/ml stock solution of ibuprofen was prepared by dissolving 100 mg of ibuprofen in a 50-ml volumetric flask with 2 ml of 0.5 *N* NaOH and adjusting to 50 ml with distilled water. A working serum ibuprofen standard at 40 μg/ml was prepared by adding 1.0 ml of the stock solution to a 50-ml volumetric flask and adjusting to volume with commercial human serum[11]. Other serum standards were prepared from serial dilutions (with serum) of the 40-μg/ml serum standard.

The internal standard stock solution (2 mg/ml) was prepared by dissolving 100 mg of 3-methyl-3-phenylbutyric acid in a 50-ml volumetric flask with 2 ml of 0.5 *N* NaOH and adjusting to 50 ml with distilled water. A working internal standard solution (100 μg/ml) was prepared by diluting 5 ml of the internal standard stock solution to 100 ml with distilled water.

Extraction Procedure—To a 15-ml conical glass centrifuge tube were added 0.5 ml of the internal standard solution, 1.0 ml of serum, and 0.5 ml of 10% perchloric acid. After vigorous mixing[12], 0.4 ml of carbon tetrachloride was added, followed again by vigorous mixing for 15 sec. The

[1] Mallinckrodt reagent grade, 60%.
[2] Mallinckrodt (low sulfur) reagent grade.
[3] Supplied by A. Geisler, Abbott Laboratories.
[4] Hewlett-Packard model 7610A.
[5] Hewlett-Packard model 7671A.
[6] Hewlett-Packard model 3380A.
[7] Varian Aerograph.
[8] Applied Science Laboratories.
[9] Linde Division, Union Carbide Corp.
[10] Hewlett-Packard model 7650A.
[11] K-N Enterprises.
[12] Maxi Mix model M-16715, Thermolyne, Sybron Corp.

Table I—Precision and Sensitivity of Ibuprofen Assay in Serum

Ibuprofen Concentration, μg/ml	Peak Area Ratio[a] (Ibuprofen/Internal Standard)	*RSD*, %
0	0	—
0.5	0.016 ± 0.004	25.0
2.5	0.068 ± 0.005	7.4
5.0	0.135 ± 0.005	3.7
10.0	0.273 ± 0.003	1.1
20.0	0.563 ± 0.015	2.7
30.0	0.858 ± 0.031	3.6
40.0	1.18 ± 0.024	2.0

[a] Mean ± *SD* of four determinations at each concentration.

sample was centrifuged for 10 min at 2500 rpm, and the clear upper aqueous layer was discarded by aspiration. The lower carbon tetrachloride layer was transferred to a microvial[13] using a disposable pipet[14]. After the microvial was capped, a 5-μl aliquot was injected into the GLC using an automatic sampler.

Calculations—A calibration curve was constructed by plotting peak area ratios (ibuprofen/internal standard) against the serum ibuprofen concentration. All calibration curves were linear and passed through the origin. Unknowns were automatically calculated by a computing integrator, programmed with the slope of a least-squares calibration curve. A least-squares regression line from the values in Table I yielded parameters of 0.0293, −0.0085, and 0.999 for the slope, *y*-intercept, and correlation coefficient, respectively.

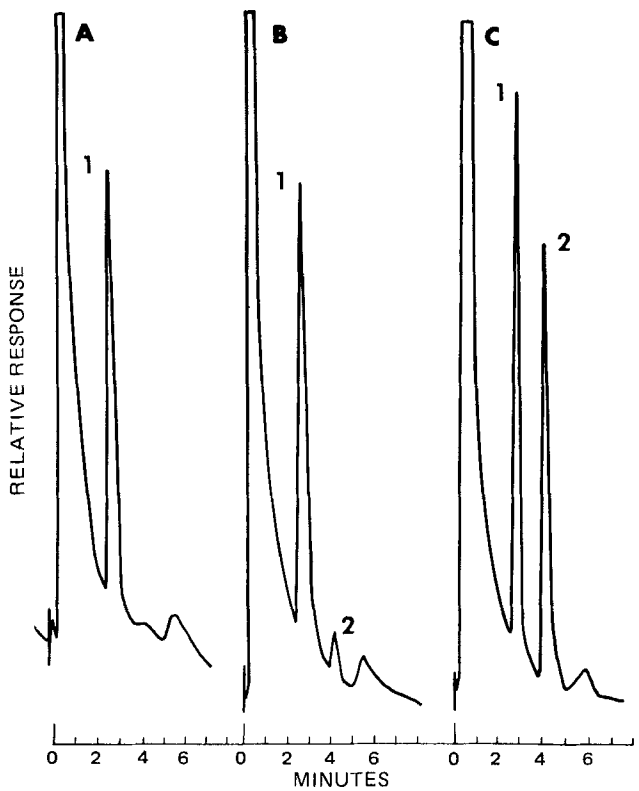

Figure 1—*GLC tracings of extracted serum samples. Key: A, serum blank with internal standard; B, serum containing ibuprofen at 5 μg/ml; C, serum containing ibuprofen at 40 μg/ml; 1, internal standard; and 2, ibuprofen.*

[13] Hewlett-Packard 100-μl vials.
[14] Pasteur transfer pipets, Curtin Matheson Scientific.

Table II—Accuracy of Ibuprofen GLC Assay

Ibuprofen Concentration, μg/ml		
Actual[a]	Calculated	Percent Difference
0	0	0
20.0	19.7	−1.5
5.0	4.6	−8.0
0.5	0.6	+20.0
10.0	10.2	+2.0
2.5	2.8	+12.0
30.0	31.4	+4.7
40.0	39.1	−2.2

[a] Serum spiked with ibuprofen at the indicated concentrations.

RESULTS AND DISCUSSION

Figure 1 shows a chromatogram of an extract from 1 ml of serum spiked with ibuprofen. Peak shapes were good with only a small amount of tailing. Ibuprofen and the internal standard were well resolved from coextractives.

The precision of the assay is shown in Table I. Relative standard deviations ranged from 1.1 to 25.0%. Assay sensitivity was 0.5 μg/ml for a 1-ml sample volume, the lowest concentration of ibuprofen in serum that was accurately detected and integrated by the instrumentation used. The accuracy of this assay was estimated by analyzing eight spiked serum unknowns under blind conditions. These results (Table II) show excellent accuracy at 5 μg/ml and above. Satisfactory accuracy (12–20% error) was achieved at low ibuprofen concentrations (2.5 and 0.5 μg/ml).

Ibuprofen in serum can be assayed by this method in less than one-half the time required by a derivatization method (4). By using those recovery data as an estimate of assay precision, a relative standard deviation of 7.0% was calculated for standards between 2 and 80 μg/ml. The average relative standard deviation of this method is 3.4% (excluding the 0.5-μg/ml concentration). Both methods have a sensitivity of 0.5 μg of ibuprofen/ml.

This assay provides the precision and accuracy needed for pharmacokinetic and bioavailability studies in humans where serum ibuprofen concentrations range from 0.5 to 30 μg/ml.

REFERENCES

(1) S. S. Adams, K. F. McCullough, and J. S. Nicholson, *Arch. Int. Pharmacodyn. Ther.*, **178**, 115 (1969).

(2) C. D. Brooks, C. A. Schlagel, N. C. Sekhar, and J. T. Sobota, *Curr. Ther. Res.*, **15**, 180 (1973).

(3) E. F. Davies and G. S. Avery, *Drugs*, **2**, 416 (1971).

(4) D. G. Kaiser and G. J. VanGiessen, *J. Pharm. Sci.*, **63**, 219 (1974).

(5) I. C. Dijkhuis and E. Vervloet, *Pharm. Weekbl.*, **109**, 1 (1974).

ACKNOWLEDGMENTS AND ADDRESSES

Received March 22, 1976, from the *Pharmaceutical Products Division, Abbott Laboratories, North Chicago, IL 60064.*

Accepted for publication July 1, 1976.

The author thanks S. Kulkarni for technical assistance.

Liquid Chromatography in Pharmaceutical Analysis VII: Determination of Dantrolene Sodium in Biological Fluids

S. J. SAXENA, I. L. HONIGBERG ˣ, J. T. STEWART, and J. J. VALLNER

Abstract □ Dantrolene sodium can be determined in plasma and urine samples by high-pressure liquid chromatography without interference from its two major metabolites, the hydroxy and acetamido compounds. The minimum detectability of the drug using this procedure is 8 ng. The complete assay including extraction, evaporation, and separation steps can be performed in approximately 70 min with an accuracy of 1–3%.

Keyphrases □ Dantrolene sodium—high-pressure liquid chromatographic analysis, biological fluids □ High-pressure liquid chromatography—analysis, dantrolene sodium, biological fluids □ Relaxants, skeletal muscle—dantrolene sodium, high-pressure liquid chromatographic analysis, biological fluids

Dantrolene sodium, 1-[[5-(*p*-nitrophenyl)furfurylidene]amino]hydantoin sodium salt hydrate, first reported by Snyder *et al.* (1), is a peripherally acting skeletal muscle relaxant indicated in controlling the manifestations of clinical spasticity resulting from serious chronic disorders such as spinal cord injury, stroke, cerebral palsy, and multiple sclerosis (2).

Analytical methods previously reported for dantrolene sodium include spectrophotofluorometry (3, 4), differential pulse polarography (5), and a qualitative colorimetric procedure (6). In continuing efforts to apply high-pressure liquid chromatography (HPLC) in pharmaceutical analysis (7–9), an HPLC procedure for the determination of dantrolene sodium in a dosage form was reported (9). This procedure has been adapted to the determination of dantrolene sodium in human plasma and urine in the presence of its two major metabolites, the hydroxy and acetamido compounds (5, 10).

The HPLC procedure described here separates and simultaneously quantitates the drug with no interference from the metabolites. The fluorometric and the polarographic methods require a differential analytical technique to measure the metabolites in the presence of the drug. The complete HPLC assay can be performed in approximately 70 min, including denaturing the proteins, extraction of the drug and its metabolites, chromatographic separation, and quantification. Biological determinations by HPLC were compared with the spectrophotofluorometric method. A preliminary *in vitro* experiment to determine the amount of dantrolene sodium bound to blood cells was also performed.

EXPERIMENTAL

Reagents and Chemicals—Micronized dantrolene sodium[1] powder was used. Reagent grade solvents and chemicals were used as received; solvents constituting the mobile phase, carbon tetrachloride and dimethylformamide, were filtered through a 0.5-μm filter[2] prior to use. The pH of a 0.5 *M* aqueous solution of dimethylformamide was consistently 6.8 ± 0.1.

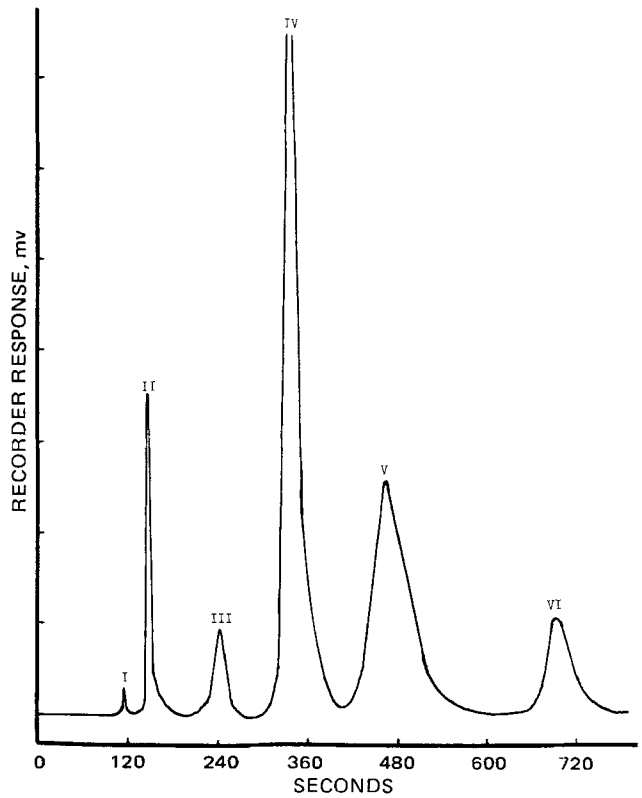

Figure 1—*Illustrative liquid chromatogram of dantrolene, its known metabolites, and furil (internal standard) in butanol–chloroform at a flow rate of 2.0 ml/min. The mobile phase was carbon tetrachloride–dimethylformamide (90:10). Key: I, solvent front; II, furil; III, impurity in dantrolene sodium; IV, dantrolene; V, hydroxy metabolite; and VI, acetamido metabolite.*

Mobile Phase—Carbon tetrachloride–dimethylformamide (90:10) was used as the mobile phase. The mixture was degassed before use.

Internal Standard Solution—Powdered furil[3] was dissolved in 1-butanol–chloroform (30:70) to give a stock internal standard solution of 400 μg/ml. This solution was filtered through a 0.5-μm filter[4] prior to use.

Standard Solution for Calibration Curve—A stock solution of dantrolene sodium (5 μg/ml) was prepared by dissolving powdered dantrolene sodium in 0.9% sodium chloride solution.

Calibration Curve—Into individual 60-ml separators were placed accurately pipetted volumes of 1.0, 2.0, 3.0, and 4.0 ml of the dantrolene sodium stock solution. The volume of each solution was adjusted to 7.0 ml with 0.9% sodium chloride solution. Then 40 ml of water-saturated 1-butanol–chloroform (30:70) and 2 ml of 0.1 *N* HCl were added. The solutions were shaken to partition the dantrolene acid into the organic layer. Then solid ammonium sulfate, about 1 g/ml of aqueous solution, was added in small portions to each solution and gently shaken for 5 min.

The solutions were set aside for 5 min, and then the organic layer (lower) was collected. The aqueous layer was shaken with another 40 ml of 1-butanol–chloroform, and the wash was combined with the previous

[1] Courtesy of Eaton Laboratories, Norwich, N.Y.
[2] Catalog No. FHLP04700, Millipore Corp., Bedford Mass.
[3] Catalog No. 2040, Eastman Organic Chemicals, Rochester, N.Y.
[4] Catalog No. LSWF01300, Millipore Corp., Bedford, Mass.

Table I—Calibration Data for Standard Drug Solutions

Initial Concentration of Dantrolene Sodium, μg/ml	Observed Results[a]
0.7143	2.0689 ± 0.0114
1.4286	3.9922 ± 0.0595
2.1429	6.1423 ± 0.0318
2.8571	8.0774 ± 0.0974
Slope = 0.4035	
Intercept = 0.0263	
$r \pm s_{yx}$[b] = 0.9998 ± 0.0495	

[a] D/IS ratio is based on three replicate injections of standard solution. Table value shows the mean ± *SD*. D/IS is the ratio of the integrated area of the drug at some concentration to the integrated area of furil at 50 μg/ml. [b] *r* is the correlation coefficient calculated from linear regression analysis, and s_{yx} is the sample standard deviation, also from regression analysis.

organic layer. The combined organic layer was evaporated to dryness in a hot water bath (~70°) under a stream of nitrogen. The residue was dissolved in 500 μl of 1-butanol–chloroform, and 500 μl of the internal standard solution was added. The solution was then filtered through a 0.5-μm filter, and 40 μl was injected into the liquid chromatograph.

Dantrolene Sodium in Human Plasma and Urine—To 3.0 ml of biological fluid was added 10 μg of dantrolene sodium. This solution was treated in the same manner as the standard solutions described under *Calibration Curve*. A control blank using 0.9% sodium chloride solution instead of the biological fluid was also included. Replicate injections of 40 μl were made for each sample.

***In Vitro* Binding of Dantrolene Sodium to Whole Blood Cells**—Dantrolene sodium (10 μg) was added to each of three 5-ml samples of whole blood; these samples were gently shaken and set aside for equilibration at room temperature for 5 min. The samples were then centrifuged at 1000 rpm for 20 min. The supernatant plasma from each tube was transferred to separate separators. A volume of 0.9% sodium chloride solution equal to the volume of the plasma removed was added to each packed cell sample, and the mixture was shaken gently and centrifuged again at 1000 rpm for 20 min.

The supernates from each tube were transferred to the respective separators, and the wash procedure was repeated once again. The plasma and washings in each separator were extracted and analyzed in the same manner as outlined under *Dantrolene Sodium in Human Plasma and Urine*. Injections of 40 μl were made.

Chromatographic Conditions—A liquid chromatograph equipped with a pump[5], a variable wavelength detector[6], an integrator with a digital printout[7], and a column containing a porous silica packing[8] was used. The degassed mobile phase was pumped through the column at 2.0 ml/min (1800 psig) at room temperature (23 ± 2°) until a stable baseline was obtained. Replicate 40-μl injections of samples and standard solutions were made using a 100-μl syringe[9]. A record of drug elution from the column as peaks on a chromatogram was provided by a chart recorder. The peaks were detected at 375 nm. The solute was measured by digital integration of the peak area in each case.

Determination of Dantrolene Sodium by Fluorescence—Spiked samples of urine and blood plasma, each containing 10 μg of dantrolene sodium, were assayed by a previously reported fluorometric method (9). The extraction procedure was identical to the one used for analysis by HPLC except that the final residue, after evaporation, was diluted to 10 ml with 1-butanol–chloroform (30:70). The fluorescence of each solution was measured in a spectrophotofluorometer[10] with the following operating parameters: excitation and emission slit widths, 5 nm; sensitivity, 3.0; excitation wavelength, 395 nm; and emission wavelength, 575 nm.

With the fine sensitivity control, the recorder was set to read full scale (100 units) for a 1-butanol–chloroform solution obtained from a 0.9% sodium chloride control containing 10 μg of dantrolene sodium, which was carried through the same extraction procedure as the biological fluids. Measurements for the biological fluid extracts were made relative to this arbitrary setting.

[5] Waters Associates liquid chromatograph, model ALC/GPC 201, equipped with an M-6000 pump.
[6] Perkin-Elmer model LC-55 variable wavelength UV–visible detector.
[7] Infotronics integrator model CRS-204.
[8] Waters packed <10-μm μPorasil column, 4 mm i.d. × 30 cm.
[9] Model B-110, Precision Sampling Corp., Baton Rouge, La.
[10] Perkin-Elmer fluorescence spectrophotometer model MPF-4.

Table II—Determination of Dantrolene Sodium in Human Plasma and Urine

Sample	Amount of Dantrolene Sodium Added, μg	HPLC, % Found[a]	Fluorometric, % Found[a]
Urine	10	91.27 ± 0.47[b]	90.94 ± 1.32[b]
Plasma	10	82.67 ± 1.09	81.68 ± 0.92

[a] Based on triplicate determinations of three individual samples. [b] Confidence limits at $p = 0.05$.

RESULTS AND DISCUSSION

Dantrolene sodium is converted to dantrolene acid in acidic media and can be extracted into an organic solvent (9). In biological fluids, an additional protein precipitation step was necessary. Precipitation was accomplished by the use of 1 g of ammonium sulfate/ml of aqueous solution. In addition, the smaller concentrations of dantrolene sodium in biological fluids necessitated the concentration of the organic extract from biological fluids prior to the HPLC analysis.

Dantrolene was eluted within 6 min (Fig. 1). Figure 1 illustrates the elution and separation of the two major metabolites of dantrolene, the hydroxy and acetamido compounds. These metabolites were well-separated from the parent drug and internal standard. The presence of the metabolites had no significant effect on the ratio of the drug to the internal standard (D/IS), even when present in equal concentrations. All components were detectable at the 375-nm wavelength used in this procedure. Figure 2 shows a typical chromatogram for dantrolene sodium from a spiked plasma sample.

The area under the curve for each peak on the chromatogram was digitally integrated. The D/IS ratio was calculated for each dantrolene concentration. A linear regression analysis of the data at the four standard concentrations of dantrolene sodium gave the results shown in Table I.

To determine the percent accuracy of the procedure, two known concentrations of dantrolene sodium were treated as unknowns and their

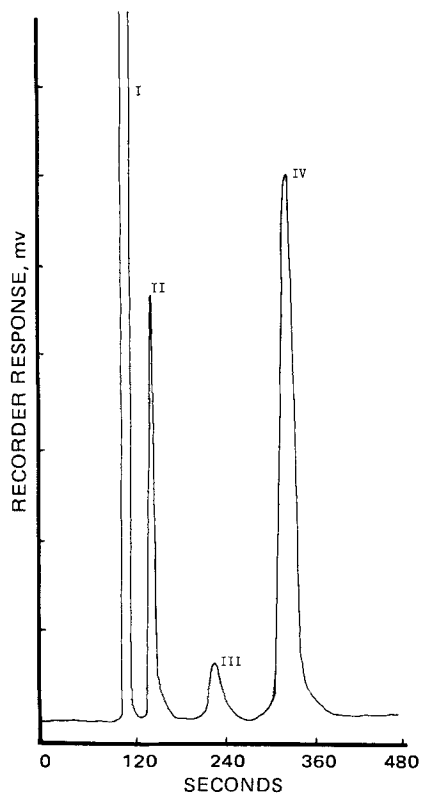

Figure 2—*Liquid chromatogram of dantrolene from a spiked plasma sample of dantrolene sodium at a flow rate of 2.0 ml/min. The mobile phase was carbon tetrachloride–dimethylformamide (90:10). Key: I, unidentified plasma components at solvent front; II, furil (internal standard); III, impurity in dantrolene sodium; and IV, dantrolene.*

Table III—Recovery Data of Dantrolene Sodium[a]

Sample	D/IS Ratio[b]	Recovery[c], %
Water	4.0368 ± 0.2148	99.4
Plasma	3.3620 ± 0.1916	82.7
Whole blood	2.7903 ± 0.0312	68.5

[a] Ten micrograms of dantrolene sodium was added to each sample. [b] Based on triplicate injections of three individual samples. [c] Calculated from linear regression analysis data.

concentrations were calculated from the constants (slope and intercept) obtained from the linear regression analysis. The concentration was calculated from the equation: D/IS = (slope × concentration) + intercept, using a programmable calculator[11]. Accuracy was 1–3% for the overall procedure.

The results for the spiked biological samples obtained from HPLC and fluorometry are shown in Table II. There was no significant difference between the values obtained by the two techniques at $p = 0.01$.

Recovery data of dantrolene sodium from water, plasma, and whole blood are shown in Table III. Extraction of the drug from spiked plasma accounted for approximately 82% of the added dantrolene. In the whole blood investigations, about 31.5% of the drug was not found in the plasma portion. Blood cells may account for about 15% binding of the dantrolene.

In summary, this procedure is useful for the determination of drug in the presence of its two major metabolites with a minimum detectability of 8 ng.

[11] Olivetti-Underwood Programma 101.

REFERENCES

(1) H. R. Snyder, Jr., C. S. Davis, R. K. Bickerton, and R. P. Halliday, *J. Med. Chem.*, **10**, 807 (1967).

(2) Package insert, Dantrium, Eaton Laboratories, Norwich, N.Y.

(3) R. D. Hollifield and J. D. Conklin, *Arch. Int. Pharmacodyn. Ther.*, **174**, 333 (1968).

(4) R. D. Hollifield and J. D. Conklin, *J. Pharm. Sci.*, **62**, 271 (1973).

(5) P. L. Cox, J. P. Heotis, D. Polin, and G. M. Rose, *ibid.*, **58**, 987 (1969).

(6) J. D. Conklin and R. J. Sobers, *ibid.*, **62**, 1024 (1973).

(7) I. L. Honigberg, J. T. Stewart, A. P. Smith, R. D. Plunkett, and E. L. Justice, *ibid.*, **64**, 1389 (1975).

(8) J. T. Stewart, I. L. Honigberg, J. P. Brant, W. A. Murray, J. L. Webb, and J. B. Smith, *ibid.*, **65**, 1536 (1976).

(9) S. J. Saxena, I. L. Honigberg, J. T. Stewart, G. R. Keene, and J. J. Vallner, *ibid.*, **66**, 286 (1977).

(10) R. L. White and T. J. Schwan, *ibid.*, **65**, 135 (1976).

ACKNOWLEDGMENTS AND ADDRESSES

Received April 27, 1976, from the *Department of Medicinal Chemistry and the Department of Pharmacy, School of Pharmacy, University of Georgia, Athens, GA 30602.*

Accepted for publication July 21, 1976.

The authors gratefully acknowledge the technical assistance of G. R. Keene and J. G. Washington.

[x] To whom inquiries should be directed.

Polynitro Aromatic Compounds in Analytical Chemistry I: Reaction with Ouabain and Digitoxin

L. B. BURNS, R. J. STEDMAN, and M. M. TUCKERMAN [x]

Abstract □ By the use of NMR spectroscopy, the highly colored reaction products formed by ouabain or digitoxin with 1,3,5-trinitrobenzene or 2,4,6-trinitroanisole in the presence of alkali (as used for the determination of these glycosides) are shown to be Meisenheimer complexes. The complexes are produced by attachment of a carbon of the butenolide ring to an aromatic carbon of the nitro compound with formation of a charge-delocalized cyclohexadienate anion.

Keyphrases □ Nitro aromatic compounds—1,3,5-trinitrobenzene and 2,4,6-trinitroanisole, NMR spectral characterization of products □ Ouabain—reaction with 1,3,5-trinitrobenzene or 2,4,6-trinitroanisole, NMR spectral characterization of products □ Digitoxin—reaction with 1,3,5-trinitrobenzene or 2,4,6-trinitroanisole, NMR spectral characterization of products □ NMR spectroscopy—characterization of products of reaction of ouabain and digitoxin with 1,3,5-trinitrobenzene or 2,4,6-trinitroanisole □ Cardiotonic agents—ouabain and digitoxin, reaction with 1,3,5-trinitrobenzene or 2,4,6-trinitroanisole, NMR spectral characterization of products

The most recent review article on the chemical estimation of ouabain and digitoxin was published in 1949 by Canbäck (1). In 1950, the same author (2) reported further results on the reaction of these cardiotonic glycosides with dinitro aromatic compounds in the presence of alkali. Canbäck attributed the intense color produced to the transfer of a proton from the butenolide ring of the glycoside to a ring carbon of the nitro compound. Later, Kimura (3) investigated the reaction between digitoxin and picric acid and proposed that the colored product resulted from the addition of the butenolide ring to one of the two unsubstituted carbons of the picric acid.

In the present work, NMR studies established that ouabain and digitoxin give Meisenheimer complexes (charge-delocalized cyclohexadienate anions) with both 1,3,5-trinitrobenzene and 2,4,6-trinitroanisole in dimethyl sulfoxide as the solvent. Comparison of the visible spectra of the products with those of materials produced in aqueous methanol (which more nearly approximates the normal assay medium) suggested that the colored components are the same in the two cases.

EXPERIMENTAL[1]

Visible Spectra—Approximately 3×10^{-5} *M* solutions of ouabain and digitoxin were used in a 1-cm cell. Excess 2,4,6-trinitroanisole and sodium hydroxide were added, and the spectra were measured against a reagent blank. The positions of the absorption maxima were: ouabain–trini-

[1] Visible spectra were obtained using a Cary model 15 UV-visible spectrophotometer. NMR spectra were run on a Jeolco MH-60-II spectrometer.

Table III—Recovery Data of Dantrolene Sodium[a]

Sample	D/IS Ratio[b]	Recovery[c], %
Water	4.0368 ± 0.2148	99.4
Plasma	3.3620 ± 0.1916	82.7
Whole blood	2.7903 ± 0.0312	68.5

[a] Ten micrograms of dantrolene sodium was added to each sample. [b] Based on triplicate injections of three individual samples. [c] Calculated from linear regression analysis data.

concentrations were calculated from the constants (slope and intercept) obtained from the linear regression analysis. The concentration was calculated from the equation: D/IS = (slope × concentration) + intercept, using a programmable calculator[11]. Accuracy was 1–3% for the overall procedure.

The results for the spiked biological samples obtained from HPLC and fluorometry are shown in Table II. There was no significant difference between the values obtained by the two techniques at $p = 0.01$.

Recovery data of dantrolene sodium from water, plasma, and whole blood are shown in Table III. Extraction of the drug from spiked plasma accounted for approximately 82% of the added dantrolene. In the whole blood investigations, about 31.5% of the drug was not found in the plasma portion. Blood cells may account for about 15% binding of the dantrolene.

In summary, this procedure is useful for the determination of drug in the presence of its two major metabolites with a minimum detectability of 8 ng.

[11] Olivetti-Underwood Programma 101.

REFERENCES

(1) H. R. Snyder, Jr., C. S. Davis, R. K. Bickerton, and R. P. Halliday, *J. Med. Chem.*, **10**, 807 (1967).

(2) Package insert, Dantrium, Eaton Laboratories, Norwich, N.Y.

(3) R. D. Hollifield and J. D. Conklin, *Arch. Int. Pharmacodyn. Ther.*, **174**, 333 (1968).

(4) R. D. Hollifield and J. D. Conklin, *J. Pharm. Sci.*, **62**, 271 (1973).

(5) P. L. Cox, J. P. Heotis, D. Polin, and G. M. Rose, *ibid.*, **58**, 987 (1969).

(6) J. D. Conklin and R. J. Sobers, *ibid.*, **62**, 1024 (1973).

(7) I. L. Honigberg, J. T. Stewart, A. P. Smith, R. D. Plunkett, and E. L. Justice, *ibid.*, **64**, 1389 (1975).

(8) J. T. Stewart, I. L. Honigberg, J. P. Brant, W. A. Murray, J. L. Webb, and J. B. Smith, *ibid.*, **65**, 1536 (1976).

(9) S. J. Saxena, I. L. Honigberg, J. T. Stewart, G. R. Keene, and J. J. Vallner, *ibid.*, **66**, 286 (1977).

(10) R. L. White and T. J. Schwan, *ibid.*, **65**, 135 (1976).

ACKNOWLEDGMENTS AND ADDRESSES

Received April 27, 1976, from the *Department of Medicinal Chemistry and the Department of Pharmacy, School of Pharmacy, University of Georgia, Athens, GA 30602.*

Accepted for publication July 21, 1976.

The authors gratefully acknowledge the technical assistance of G. R. Keene and J. G. Washington.

[x] To whom inquiries should be directed.

Polynitro Aromatic Compounds in Analytical Chemistry I: Reaction with Ouabain and Digitoxin

L. B. BURNS, R. J. STEDMAN, and M. M. TUCKERMAN [x]

Abstract □ By the use of NMR spectroscopy, the highly colored reaction products formed by ouabain or digitoxin with 1,3,5-trinitrobenzene or 2,4,6-trinitroanisole in the presence of alkali (as used for the determination of these glycosides) are shown to be Meisenheimer complexes. The complexes are produced by attachment of a carbon of the butenolide ring to an aromatic carbon of the nitro compound with formation of a charge-delocalized cyclohexadienate anion.

Keyphrases □ Nitro aromatic compounds—1,3,5-trinitrobenzene and 2,4,6-trinitroanisole, NMR spectral characterization of products □ Ouabain—reaction with 1,3,5-trinitrobenzene or 2,4,6-trinitroanisole, NMR spectral characterization of products □ Digitoxin—reaction with 1,3,5-trinitrobenzene or 2,4,6-trinitroanisole, NMR spectral characterization of products □ NMR spectroscopy—characterization of products of reaction of ouabain and digitoxin with 1,3,5-trinitrobenzene or 2,4,6-trinitroanisole □ Cardiotonic agents—ouabain and digitoxin, reaction with 1,3,5-trinitrobenzene or 2,4,6-trinitroanisole, NMR spectral characterization of products

The most recent review article on the chemical estimation of ouabain and digitoxin was published in 1949 by Canbäck (1). In 1950, the same author (2) reported further results on the reaction of these cardiotonic glycosides with dinitro aromatic compounds in the presence of alkali. Canbäck attributed the intense color produced to the transfer of a proton from the butenolide ring of the glycoside to a ring carbon of the nitro compound. Later, Kimura (3) investigated the reaction between digitoxin and picric acid and proposed that the colored product resulted from the addition of the butenolide ring to one of the two unsubstituted carbons of the picric acid.

In the present work, NMR studies established that ouabain and digitoxin give Meisenheimer complexes (charge-delocalized cyclohexadienate anions) with both 1,3,5-trinitrobenzene and 2,4,6-trinitroanisole in dimethyl sulfoxide as the solvent. Comparison of the visible spectra of the products with those of materials produced in aqueous methanol (which more nearly approximates the normal assay medium) suggested that the colored components are the same in the two cases.

EXPERIMENTAL[1]

Visible Spectra—Approximately 3×10^{-5} *M* solutions of ouabain and digitoxin were used in a 1-cm cell. Excess 2,4,6-trinitroanisole and sodium hydroxide were added, and the spectra were measured against a reagent blank. The positions of the absorption maxima were: ouabain–trini-

[1] Visible spectra were obtained using a Cary model 15 UV-visible spectrophotometer. NMR spectra were run on a Jeolco MH-60-II spectrometer.

Table I—Chemical Shifts (δ) of Protons of Trinitrobenzene and Trinitroanisole in Dimethyl Sulfoxide-d_6 as Affected by Base, Ouabain, and Digitoxin

Nitro Compound	Glycoside	Base	Chemical Shifts of Lowest Field Protons	Chemical Shift of Methoxyl Protons
Trinitrobenzene	None	None	9.04	—
Trinitrobenzene	None	Sodium hydroxide	7.68, 5.61[a,b]	—
Trinitrobenzene	Ouabain	None	9.04	—
Trinitrobenzene	Ouabain	Sodium hydroxide	8.17, 6.07[a,b]	—
Trinitrobenzene	Digitoxin	None	9.07	—
Trinitrobenzene	Digitoxin	Sodium hydroxide	8.23, 6.10[a,b]	—
Trinitroanisole	None	None	9.00	4.07
Trinitroanisole	None	Sodium hydroxide	8.56[a]	3.13
Trinitroanisole	Ouabain	None	9.00	4.07
Trinitroanisole	Ouabain	Sodium hydroxide	8.56[a]	3.30[c]
Trinitroanisole	Digitoxin	None	9.00	4.07
Trinitroanisole	Digitoxin	Sodium hydroxide	8.56[a]	3.30[c]

[a] Spectra also showed aromatic protons of the unchanged nitro compound. [b] Integrated areas of these peaks were in the ratio of 2:1. [c] Area around δ 3.30 was obscured by water peak unless concentration was carefully controlled. A solvent interaction peak at δ 3.13 also was present.

troanisole–base, λ_{max} 536 (aqueous methanol) and 545 (dimethyl sulfoxide) nm; and digitoxin–trinitroanisole–base, λ_{max} 536 (aqueous methanol) and 545 (dimethyl sulfoxide) nm.

NMR Spectra—The spectra of the nitro aromatic compounds were obtained in dimethyl sulfoxide-d_6, and then ouabain or digitoxin (presumably in excess) was added until the signals of the glycoside became visible. The colored products were formed by adding a small amount of sodium hydroxide in deuterium oxide, and the spectra were determined again (Table I). A reagent blank spectrum was obtained from a mixture of all components except the glycoside.

RESULTS AND DISCUSSION

The visible absorption peak developed by both glycosides with trinitroanisole in dimethyl sulfoxide was only 9 nm displaced from its position in aqueous methanol. Therefore, the colored complex in dimethyl sulfoxide probably has the same structure as that in aqueous methanol and corresponds to the species used in the chemical assay. Therefore, the NMR studies in dimethyl sulfoxide should help to elucidate the nature of the assay reaction.

The NMR spectra clearly showed that the nitro compounds did not undergo any reaction in the absence of base. Interpretation is complicated by the observation that there was complexation between the solvent and the aromatic nitro compound in the absence of a glycoside. Thus, the singlet from 1,3,5-trinitrobenzene at δ 9.04 in dimethyl sulfoxide alone was replaced by a pair of signals at δ 7.68 and 5.61 on the addition of base. When ouabain was present, the two new signals appeared at δ 8.17 and 6.07; clearly, a different complex was formed from that provided by the solvent.

The positions of the new peaks and their 2:1 intensity ratio were consistent with their representing the two protons on sp^2 hybridized carbon and the one proton on sp^3 hybridized carbon in a Meisenheimer complex (I) (4–11). Both peaks were moved upfield because of the loss of aromaticity of the ring. The chemical shift of the one-proton peak at δ 6.07 was consistent only with attachment of the new ligand at one unsubstituted carbon of the trinitrobenzene ring. Digitoxin with trinitrobenzene gave results almost identical to ouabain.

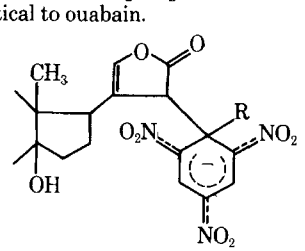

I: R = H or OCH_3

In the reactions of the glycosides with trinitroanisole and base, only one new low field peak, at δ 8.56, was seen. This finding strongly suggests attachment of the glycoside at the methoxylated carbon of the nitro compound. Since solvent and base gave a new peak also at δ 8.56, it could be argued that only solvent was involved in the complexation. However, the position of the trinitroanisole methoxyl peak proved that complexation with the glycosides was occurring; in the absence of the glycosides, it appeared at δ 3.13. When either glycoside was present, it was found at δ 3.30.

In summary, the evidence supports the view that the colored complexes formed by ouabain or digitoxin with the trinitroaromatic compounds in the presence of base may be formulated as Structure I. The butenolide ring is shown with its double bond shifted and the carbon next to the carbonyl group as the position reactive toward the nitro aromatic ring (2, 3). The present work does not provide any additional evidence about the condition of the butenolide ring.

REFERENCES

(1) T. Canbäck, *J. Pharm. Pharmacol.*, **1**, 201 (1949).
(2) T. Canbäck, *Sv. Farm. Tidskr.*, **54**, 201 (1950).
(3) M. Kimura, *Pharm. Bull. Jpn.*, **3**, 81 (1955).
(4) L. M. Jackman and S. Sternhell, "Applications of Nuclear Magnetic Resonance Spectroscopy in Organic Chemistry," Pergamon, New York, N.Y., 1969.
(5) "NMR Spectra Catalog," vol. I, Varian Associates, Palo Alto, Calif., 1962. *Ibid.*, vol. II, 1963.
(6) S. Gronowitz and R. A. Hoffman, *Acta Chem. Scand.*, **13**, 1687 (1959).
(7) P. R. Wells, *Aust. J. Chem.*, **16**, 165 (1963).
(8) B. Casu and M. Reggiani, *Tetrahedron Lett., No. 39*, **1964**, 2839.
(9) M. R. Crampton and V. Gold, *J. Chem. Soc.*, **1964**, 4293.
(10) M. R. Crampton and V. Gold, *Proc. Chem. Soc.*, **1964**, 298.
(11) M. R. Crampton, *J. Chem. Soc.*, **1969**, 211.

ACKNOWLEDGMENTS AND ADDRESSES

Received January 15, 1976, from the *School of Pharmacy, Health Sciences Center, Temple University, Philadelphia, PA 19140.*

Accepted for publication July 14, 1976.

Presented at the Pharmaceutical Analysis and Control Section, Poster Session, APhA Academy of Pharmaceutical Sciences, New Orleans meeting, April 1976.

Abstracted in part from a thesis submitted by Lorraine Burns to Temple University in partial fulfillment of the Doctor of Philosophy degree requirements.

[x] To whom inquiries should be directed.

In Vitro Estimates of Topical Bioavailability

Keyphrases □ Bioavailability, topical—quantitative skin model assuming inactive stratum corneum and viable, enzyme-containing epidermis □ Topical bioavailability—quantitative skin model assuming inactive stratum corneum and viable, enzyme-containing epidermis □ Metabolism, drug—topically applied, quantitative skin model assuming inactive stratum corneum and viable, enzyme-containing epidermis □ Absorption, percutaneous—quantitative skin model assuming inactive stratum corneum and viable, enzyme-containing epidermis □ Diffusion, drug—quantitative skin model assuming inactive stratum corneum and viable, enzyme-containing epidermis

To the Editor:

Many disease conditions of the skin are due to pathogens or aberrant metabolism of the epithelial layer. Cold sores, for example, are caused by the Herpes simplex type I virus (1) which forms intraepithelial vesicles as a result of successive rounds of infection and proliferation. Psoriasis, on the other hand, is due to the uncontrolled proliferation of the basal epithelial cells. This abnormal growth probably results from a metabolic defect of the basal cells.

Since the epidermis is the most metabolically active layer of the skin (2, 3), any topical dosage form that delivers active drug components to intraepithelial sites should be formulated realizing that the skin is an active metabolizing barrier. In the past, the passive permeability properties of the stratum corneum were shown to constitute the major diffusional resistance of the skin (4). Several studies (5–7) also examined the *in vivo* percutaneous absorption of topical dosage forms. However, since urine was usually assayed as the main excretory route of the drug, the degree of cutaneous metabolism could not be clearly established because the metabolism of other tissues was included in the data. In one human skin study on the *in vivo* catabolism of hydrocortisone (7), the conclusion drawn on the basis of urine data was that hydrocortisone was probably rapidly metabolized in the skin, thus becoming physiologically inactive before it reached its site of action.

Direct evidence of the cutaneous metabolism of adrenal steroids (8) and hydrocortisone (9) was obtained *in vitro* by incubating viable human skin in a medium containing the steroid and assaying the medium by chromatographic methods. In another study (10), the cutaneous conversion of fluorouracil (I) to 5-fluoro-2′-deoxyuridine 5′-monophosphate (II) was verified *in vitro*. The intraepithelial metabolism of I was important to verify, since II is considered to be the drug form with antitumor activity. Thus a "prodrug," I, penetrated the stratum corneum (II, being more polar, would be expected to penetrate less effectively) and was converted by the enzymes of the epithelial cells into II, the active drug form.

These considerations emphasize the need for a quantitative model of the skin that can assess the metabolic barrier of the skin concurrent with cutaneous transport. One model, which treats the skin as a bilayer (11), assumes that the stratum corneum is inactive metabolically and that the epidermis contains a homogeneous distribution of enzymes. Some preliminary experimental results based on the model are discussed here. It is hoped that these and future studies will provide the experimental framework for evaluating this and more complex models of the viable epidermis.

In this system, the viable epidermis contains an enzyme, adenosine deaminase, which can convert the antiviral drug vidarabine (9-β-D-arabinofuranosyladenine) (III) into 9-β-D-arabinofuranosylhypoxanthine (IV). Skin from a 3-month-old hairless mouse[1] containing both the dermis and epidermis was removed and placed between two 3-ml chambers of a dialysis cell[2] (Fig. 1). Both the stratum corneum and the dermis side of the diffusion chamber could be used as the donor compartment for III in Dulbecco's phosphate-buffered saline (12). Five-microliter samples were taken at different times using a disposable microliter pipet[3], spotted onto TLC plates[4], and developed in chloroform–methanol–3% acetic acid (3:2:1) (13). Both III and IV were assayed.

When this solution was placed on the stratum corneum side of the diffusion cell and saline was placed on the receptor side, no metabolism of III was observed on the epidermis side and no label was found on the dermis side for time intervals up to 24 hr. Similarly, when the dermis side was used as the donor compartment, no drug penetrated into the receptor compartment. However, in this latter situation, rapid metabolism was observed in the donor compartment; 50% of the original III was in the hypoxanthine form after 2 hr (Fig. 2).

One problem arose when the dermis side of the skin was used as the donor compartment. If samples from the donor compartment were taken at different times, stored in holding vials, and assayed 12 hr later, the amount of metabolism observed was greater than that found if the samples were assayed immediately. Evidently, adenosine deaminase, the enzyme that metabolized III, was leaching out of the skin into the donor compartment. Thus, the amount of metabolized drug in the donor compartment

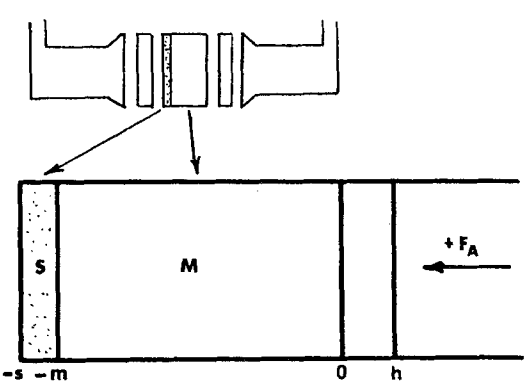

Figure 1—*Impermeable stratum corneum. Drug A moves in the negative* x *direction, first penetrating the aqueous diffusion* ($0 \leq x \leq h$) *and then the metabolizing epidermis* (M) *located at* $-m \leq x \leq 0$. *The stratum corneum* (S), located at $-s \leq x \leq -m$, *does not permit passage of A through it.*

[1] Jackson Laboratory, Bar Harbor, ME 04609.
[2] Karush-type dialysis chamber, Belco Glass Co., Vineland, NJ 08360.
[3] Drummon Scientific Co.; from A. H. Thomas, Philadelphia, PA 19105.
[4] Analtech, Newark, DE 19711.

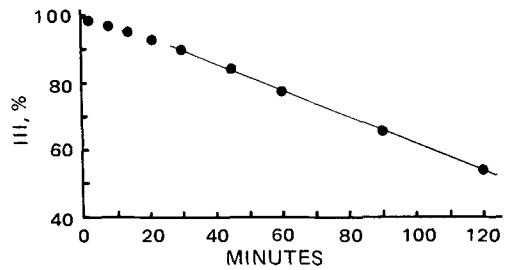

Figure 2—*Determination of* F_A. *Percent of III in the bulk solution was assayed with respect to time; the steady-state slope,* dC/dt, *was computed from the last five points. This value, −0.227, was corrected for bulk metabolism from Fig. 4 and was computed from* $F_A = (V/A)(dC/dt)$, *where* $V = 2.0\ cm^2$ *and* $A = 1.54\ cm^2$.

reflected not only the epidermal component but also a bulk phase metabolism due to leached enzyme. To correct for this bulk metabolism, a separate study was conducted.

Hairless mouse skin was prepared as already described, but only buffered saline was placed in both chambers of the diffusion cell. At 30-min intervals up to 2 hr, samples were taken from the dermis compartment. Compound III was immediately added to each sample, which was then assayed as a function of time for III metabolism. Figure 3 shows that the amount of enzyme in the bulk phase continuously increased with time. The slope of each curve was plotted in Fig. 4 as a function of sampling time to determine whether a linear relationship existed. Figure 4 shows that the slopes are highly linear with time so that:

$$\frac{dC_X(t)}{dt} = kt \qquad \text{(Eq. 1)}$$

or:

$$C_X(t) = C_X(0) + \frac{k}{2}t^2 \qquad \text{(Eq. 2)}$$

where C_X represents an upper bound to the amount of product, X, formed in the bulk aqueous phase, and k is the slope of the dC_X/dt *versus* time plot. The reason that $C_X(t)$ is an upper bound and not the actual amount of

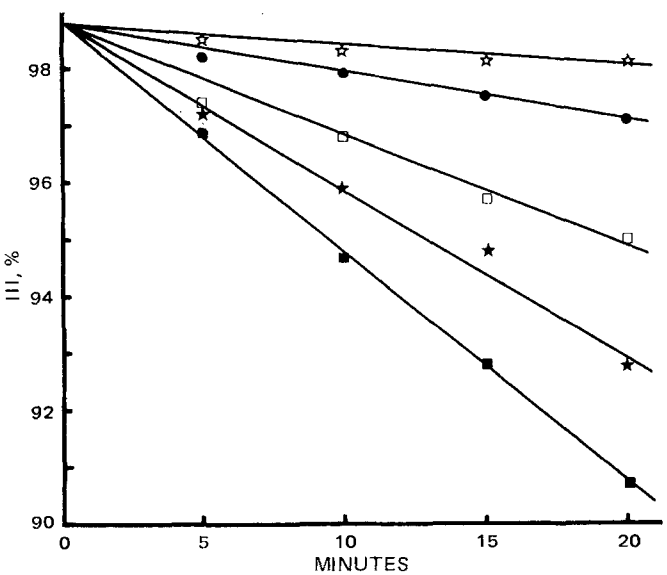

Figure 3—*Bulk phase metabolism. Metabolism of III in the bulk aqueous phase by enzymes leached out of the epidermal side of the diffusion cell at 5 (☆), 30 (●), 60 (□), 90 (★), and 120 (■) min. Solid lines were determined from linear regression fit forced through 98.8% purity for III.*

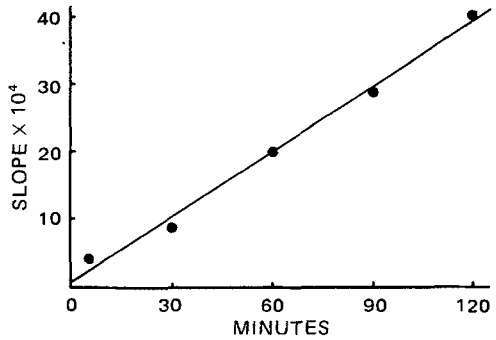

Figure 4—*Linearity of bulk phase metabolism slopes. Slopes determined from Fig. 3 are plotted against time to determine linearity. Linear regression gives an intercept of* $9.06 \times 10^{-5}\ min^{-1}$, *a slope of* $3.20 \times 10^{-5}\ min^{-2}$, *and a correlation coefficient of 0.996.*

product formed in the experiment of Fig. 2 is that the initial rate of enzyme reaction is usually faster than the reaction rate at later times. If the plots of Fig. 3 remained linear for times up to 2 hr, then $C_X(t)$ would represent the actual concentration of product formed, which would be reflected in Fig. 2. From Fig. 4, $k = 3.20 \times 10^{-5}\ min^{-2}$; therefore, at 20 min, $(k/2)t^2 = 0.0064$. The plots of Figs. 2 and 3 are linear up to 20 min, so that the flux determination from Fig. 2 can be corrected for bulk metabolism.

The model equation (11) that determines the loss of III from the bulk solution is:

$$\frac{1}{\kappa} = C_1 \tanh \kappa m \qquad \text{(Eq. 3)}$$

where:

$$C_1 = D_A\left[\frac{C_A(h)}{-F_A} - \frac{1}{P_{aqA}}\right] \qquad \text{(Eq. 4)}$$

and:

$$\kappa = \sqrt{\frac{k_m}{D_A}} \qquad \text{(Eq. 5)}$$

where m is the thickness of the skin sample, D_A is the diffusion coefficient of III in the skin, $C_A(h)$ is the concentration of III in the bulk solution, P_{aqA} is the permeability of III in the aqueous diffusion layer, and F_A is the flux of III into the skin. Since the flux of III from the bulk solution into the skin is considered negative, $-F_A$ is positive:

$$F_A = \frac{V}{A}\frac{dC_A}{dt} \qquad \text{(Eq. 6)}$$

where V is the volume of the bulk phase, and A is the area of the skin.

The initial flux of III can be estimated from Fig. 2 by using the steady-state slope of the last five points and correcting for the bulk metabolism using $(k/2)t^2$. The corrected slope is −0.227, so that F_A is 4.92×10^{-3}

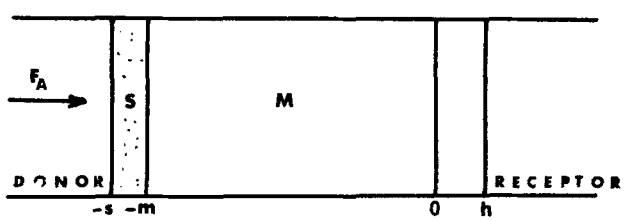

Figure 5—*Permeable stratum corneum. Drug A moves from left to right in the positive flux direction, first penetrating the stratum corneum* (S) *located at* $-s \leq x \leq -m$, *then the metabolizing epidermis* (M) *located at* $-m \leq x \leq 0$, *and then the aqueous diffusion layer at* $0 \leq x \leq h$.

amount/cm^2 sec, where $V = 2.0$ cm^3 and $A = 1.54$ cm^2. Because the full thick skin used also contained some subcutaneous tissue and dermis, there appeared to be a lag time of about 5 min (Fig. 1).

Using the value for F_A, we can compute that $C_A(h)/-F_A = 2.03 \times 10^4$ sec/cm, where $V = 2.0$ cm^3 and $A = 1.54$ cm^2. A reasonable upper limit for P_{aqA} might be estimated as $P_{aqA} \doteq 5 \times 10^{-4}$ cm/sec, which corresponds to a 200-μm aqueous diffusion layer with a diffusion coefficient for III of 10^{-5} cm^2/sec. When assuming a III epidermal diffusivity of 10^{-6} cm^2/sec, $C_1 \doteq 1.8 \times 10^{-2}$ cm.

Finally, plotting each side of Eq. 3 *versus* κ for an epidermis of 300 μm, we find that $\kappa = 82$ or $k_m \doteq 6.7 \times 10^{-3}$ sec^{-1} from the intersection of the two curves. This calculation for the linear enzyme parameter, k_m, assumed some typical values for the diffusion coefficient of III in the epidermis and aqueous diffusion layer and the thicknesses of these layers. Experiments are planned to determine these parameters directly. In addition, the validity of assuming a first-order enzyme reaction must be investigated.

The determination of the metabolic parameter, κ, can be used to predict to what degree metabolism affects the bioavailability of the drug when it is administered topically. Figure 5 shows an *in vitro* situation relevant to the clinical application of a topical dosage form. The drug passes from the topical vehicle through the stratum corneum, S, into the metabolizing epidermis, M, and then through the aqueous diffusion layer into the receptor compartment. Suppose that there is a virus lesion halfway through the epidermal layer of 100 μm. How might drug bioavailability be affected by the fact that the epidermis metabolizes the drug?

For the application of a topical drug, the relevant equations (11) are:

$$C_{AM}(x) = -\frac{P_{SA}(P_{aqA}\sinh\kappa S - D_A\kappa\cosh\kappa X)C_A(-s)}{D_A\kappa(P_{SA}+P_{aqA})\cosh\kappa M + [P_{SA}P_{aqA}+(D_A\kappa)^2]\sinh\kappa M} \quad \text{(Eq. 7)}$$

and:

$$C_{A0}(x) = -\frac{\left(\frac{1}{D_A/X}-\frac{1}{P_{aqA}}\right)C(-s)}{\frac{1}{P_{aqA}}+\frac{1}{P_{SA}}+\frac{1}{D_A/m}} \quad \text{(Eq. 8)}$$

where $C_A(-s)$ is the concentration of III in the vehicle at the stratum corneum boundary; $C_{AM}(x)$ and $C_{A0}(x)$ are the concentrations of III at the distance X for a metabolizing and a nonmetabolizing epidermis, respectively; and P_{SA} is the III permeability of the stratum corneum. For P_{SA} values of 10^{-6} and 10^{-7} cm/sec and for the computed κ:

$$\frac{C_{AM}(-m/2)}{C_{A0}(-m/2)} = 0.181 \quad \text{(Eq. 9)}$$

$$\frac{C_{AM}(-m/2)}{C_{A0}(-m/2)} = 0.183 \quad \text{(Eq. 10)}$$

These results show that, for a metabolizing membrane, the bioavailability of III due to metabolism does not depend strongly on the stratum corneum permeability and that the concentration of the active drug, III, is only 18% of the level that would have existed at the site of the lesion (halfway through the epidermis) had there been no metabolism.

(1) I. I. Ship, in "Proceedings of Symposium on Oral and Perioral Ulcerations," University of Michigan School of Dentistry, 1974, p. 20.
(2) O. D. Laerum, *J. Invest. Dermatol.*, **52**, 204 (1969).
(3) J. Bamshad, *ibid.*, **52**, 351 (1969).
(4) R. J. Scheuplein and I. H. Blank, *Physiol. Rev.*, **51**, 702 (1973).
(5) K. K. Wong, G. M. Wang, J. Dreyfuss, and E. C. Schreiher, *J. Invest. Dermatol.*, **56**, 44 (1971).
(6) M. J. Bartek, J. A. LaBudde, and H. I. Maibach, *ibid.*, **58**, 114 (1972).
(7) M. S. Gleanes, *ibid.*, **57**, 100 (1971).
(8) F. D. Malkinson, M. W. Lee, and I. Cutukovic, *ibid.*, **32**, 101 (1969).
(9) S. L. Hsia and Y. Hao, *Biochemistry*, **5**, 1469 (1966).
(10) J. L. Cohen and R. B. Stoughton, *J. Invest. Dermatol.*, **62**, 507 (1974).
(11) H. Y. Ando, N. F. H. Ho, and W. I. Higuchi, *J. Pharm. Sci.*, accepted for publication.
(12) D. J. Merchant, R. H. Kahn, and W. H. Murphy, Jr., "Handbook of Cell and Organ Culture," Burgess, Minneapolis, Minn., 1969.
(13) J. C. Drach and J. N. Novack, *Oral Biochem.*, **52**, 633 (1974).

H. Y. Ando
Philadelphia College of Pharmacy and Science
Philadelphia, PA 19104

N. F. H. Ho
W. I. Higuchi ˣ
College of Pharmacy
University of Michigan
Ann Arbor, MI 48109

Received December 18, 1975.
Accepted for publication January 14, 1977.

ˣ To whom inquiries should be directed.

Antineoplastic Agents L: Isolation and Characterization of Sphyrnastatins 1 and 2 from the Hammerhead Shark *Sphyrna lewini*

Keyphrases □ *Sphyrna lewini*—hammerhead shark, potential antineoplastic constituents isolated from body fluids, muscle tissue, and liver, identified □ Sphyrnastatins—isolated from hammerhead shark, preliminary evaluation of antineoplastic activity □ Antineoplastic activity—preliminary evaluation of sphyrnastatins isolated from hammerhead shark □ Marine antineoplastic agents, potential—sphyrnastatins isolated from hammerhead shark

To the Editor:

Hammerhead sharks of the Sphyrnidae family (cartilaginous fishes of the class Chondrichthyes) have inhabited the oceans for 181–350 million years (1) and represent a most successful evolutionary achievement. Sharks are rarely affected by diseases (2) and, to our knowledge, hammerhead sharks have not been found with cancer. In 1966, we began a long-term study (3) of marine animals for the purpose of developing cancer chemotherapeutic drugs (4). Early in this investigation, it was found that extracts of certain marine vertebrates exhibited a confirmed level of activity against the National Cancer Institute's PS (murine lymphocytic leukemia) screening system.

amount/cm^2 sec, where $V = 2.0$ cm^3 and $A = 1.54$ cm^2. Because the full thick skin used also contained some subcutaneous tissue and dermis, there appeared to be a lag time of about 5 min (Fig. 1).

Using the value for F_A, we can compute that $C_A(h)/-F_A = 2.03 \times 10^4$ sec/cm, where $V = 2.0$ cm^3 and $A = 1.54$ cm^2. A reasonable upper limit for P_{aqA} might be estimated as $P_{aqA} \doteq 5 \times 10^{-4}$ cm/sec, which corresponds to a 200-μm aqueous diffusion layer with a diffusion coefficient for III of 10^{-5} cm^2/sec. When assuming a III epidermal diffusivity of 10^{-6} cm^2/sec, $C_1 \doteq 1.8 \times 10^{-2}$ cm.

Finally, plotting each side of Eq. 3 *versus* κ for an epidermis of 300 μm, we find that $\kappa = 82$ or $k_m \doteq 6.7 \times 10^{-3}$ sec^{-1} from the intersection of the two curves. This calculation for the linear enzyme parameter, k_m, assumed some typical values for the diffusion coefficient of III in the epidermis and aqueous diffusion layer and the thicknesses of these layers. Experiments are planned to determine these parameters directly. In addition, the validity of assuming a first-order enzyme reaction must be investigated.

The determination of the metabolic parameter, κ, can be used to predict to what degree metabolism affects the bioavailability of the drug when it is administered topically. Figure 5 shows an *in vitro* situation relevant to the clinical application of a topical dosage form. The drug passes from the topical vehicle through the stratum corneum, S, into the metabolizing epidermis, M, and then through the aqueous diffusion layer into the receptor compartment. Suppose that there is a virus lesion halfway through the epidermal layer of 100 μm. How might drug bioavailability be affected by the fact that the epidermis metabolizes the drug?

For the application of a topical drug, the relevant equations (11) are:

$$C_{AM}(x) = -\frac{P_{SA}(P_{aqA}\sinh\kappa S - D_A\kappa\cosh\kappa X)C_A(-s)}{D_A\kappa(P_{SA}+P_{aqA})\cosh\kappa M + [P_{SA}P_{aqA}+(D_A\kappa)^2]\sinh\kappa M} \quad \text{(Eq. 7)}$$

and:

$$C_{A0}(x) = -\frac{\left(\frac{1}{D_A/X}-\frac{1}{P_{aqA}}\right)C(-s)}{\frac{1}{P_{aqA}}+\frac{1}{P_{SA}}+\frac{1}{D_A/m}} \quad \text{(Eq. 8)}$$

where $C_A(-s)$ is the concentration of III in the vehicle at the stratum corneum boundary; $C_{AM}(x)$ and $C_{A0}(x)$ are the concentrations of III at the distance X for a metabolizing and a nonmetabolizing epidermis, respectively; and P_{SA} is the III permeability of the stratum corneum. For P_{SA} values of 10^{-6} and 10^{-7} cm/sec and for the computed κ:

$$\frac{C_{AM}(-m/2)}{C_{A0}(-m/2)} = 0.181 \quad \text{(Eq. 9)}$$

$$\frac{C_{AM}(-m/2)}{C_{A0}(-m/2)} = 0.183 \quad \text{(Eq. 10)}$$

These results show that, for a metabolizing membrane, the bioavailability of III due to metabolism does not depend strongly on the stratum corneum permeability and that the concentration of the active drug, III, is only 18% of the level that would have existed at the site of the lesion (halfway through the epidermis) had there been no metabolism.

(1) I. I. Ship, in "Proceedings of Symposium on Oral and Perioral Ulcerations," University of Michigan School of Dentistry, 1974, p. 20.
(2) O. D. Laerum, *J. Invest. Dermatol.*, **52**, 204 (1969).
(3) J. Bamshad, *ibid.*, **52**, 351 (1969).
(4) R. J. Scheuplein and I. H. Blank, *Physiol. Rev.*, **51**, 702 (1973).
(5) K. K. Wong, G. M. Wang, J. Dreyfuss, and E. C. Schreiher, *J. Invest. Dermatol.*, **56**, 44 (1971).
(6) M. J. Bartek, J. A. LaBudde, and H. I. Maibach, *ibid.*, **58**, 114 (1972).
(7) M. S. Gleanes, *ibid.*, **57**, 100 (1971).
(8) F. D. Malkinson, M. W. Lee, and I. Cutukovic, *ibid.*, **32**, 101 (1969).
(9) S. L. Hsia and Y. Hao, *Biochemistry*, **5**, 1469 (1966).
(10) J. L. Cohen and R. B. Stoughton, *J. Invest. Dermatol.*, **62**, 507 (1974).
(11) H. Y. Ando, N. F. H. Ho, and W. I. Higuchi, *J. Pharm. Sci.*, accepted for publication.
(12) D. J. Merchant, R. H. Kahn, and W. H. Murphy, Jr., "Handbook of Cell and Organ Culture," Burgess, Minneapolis, Minn., 1969.
(13) J. C. Drach and J. N. Novack, *Oral Biochem.*, **52**, 633 (1974).

H. Y. Ando
Philadelphia College of Pharmacy and Science
Philadelphia, PA 19104

N. F. H. Ho
W. I. Higuchi ˣ
College of Pharmacy
University of Michigan
Ann Arbor, MI 48109

Received December 18, 1975.
Accepted for publication January 14, 1977.

ˣ To whom inquiries should be directed.

Antineoplastic Agents L: Isolation and Characterization of Sphyrnastatins 1 and 2 from the Hammerhead Shark *Sphyrna lewini*

Keyphrases □ *Sphyrna lewini*—hammerhead shark, potential antineoplastic constituents isolated from body fluids, muscle tissue, and liver, identified □ Sphyrnastatins—isolated from hammerhead shark, preliminary evaluation of antineoplastic activity □ Antineoplastic activity—preliminary evaluation of sphyrnastatins isolated from hammerhead shark □ Marine antineoplastic agents, potential—sphyrnastatins isolated from hammerhead shark

To the Editor:

Hammerhead sharks of the Sphyrnidae family (cartilaginous fishes of the class Chondrichthyes) have inhabited the oceans for 181–350 million years (1) and represent a most successful evolutionary achievement. Sharks are rarely affected by diseases (2) and, to our knowledge, hammerhead sharks have not been found with cancer. In 1966, we began a long-term study (3) of marine animals for the purpose of developing cancer chemotherapeutic drugs (4). Early in this investigation, it was found that extracts of certain marine vertebrates exhibited a confirmed level of activity against the National Cancer Institute's PS (murine lymphocytic leukemia) screening system.

Now we wish to report the first[1] isolation and characterization of a shark anticancer constituent. The hammerhead shark, *Sphyrna lewini*[2], was found to produce two new antineoplastic agents designated sphyrnastatin 1 and sphyrnastatin 2. These anticancer components were isolated from the blood (and other body fluids), the fins (and other muscle tissue), and the liver.

In a typical isolation sequence, the water extract of blood and body fluids was first chromatographed on macroreticular resin[3]. The aqueous fraction (20 → 13.5 g) was next subjected to gel[4] permeation chromatography (10 × 100-cm column). Following elution with 3.25 liters of water, the PS inhibitory fraction (0.6 g from 5.0 g) was finally purified by chromatographic separation[5] (5 × 69-cm column and elution with a mixture of 0.05 *M* tromethamine and 0.1 *M* potassium chloride). The two highest molecular weight fractions (0.076 and 0.34 g) represented the antineoplastic components.

Sphyrnastatins 1 and 2, isolated by this procedure, were glycoproteins [~22 and 26% carbohydrate, respectively (6)] with apparent molecular weights (7) of at least 40×10^6. Amino acid analyses indicated a minimum protein segment of 274 amino acid units for sphyrnastatin 1 and 380 amino acid units for sphyrnastatin 2. Upon preliminary biological evaluation, the sphyrnastatins produced a 30–40% (at 11–13 mg/kg) life extension in mice inoculated with the PS leukemia. More extensive antineoplastic evaluation of sphyrnastatins 1 and 2 in the National Cancer Institute's exploratory screening systems is in progress. Presently, we are attempting to isolate other shark and marine vertebrate anticancer constituents.

Perhaps the sphyrnastatins and other high molecular weight antineoplastic substances (4) act by stimulating the immune system to more effective action against invading neoplastic disease. If this hypothesis is valid, then immunotherapy approaches to cancer treatment with, for example, BCG might better be considered as just another facet of cancer chemotherapy.

(1) P. W. Gilbert and C. Gilbert, *Underwater J.*, **1973**, 69.
(2) L. E. Mawdesley-Thomas, *Nature*, **235**, 17 (1972).
(3) G. R. Pettit, J. F. Day, J. L. Hartwell, and H. B. Wood, Jr., *ibid.*, **227**, 962 (1970).
(4) G. R. Pettit, "Biosynthetic Products for Cancer Chemotherapy," vol. 1, Plenum, New York, N.Y., in press.
(5) E. H. Fyhn and B. Sullivan, *Comp. Biochem. Physiol.*, **50B**, 119 (1975).
(6) C. Francois, R. D. Marshall, and A. Newberger, *Biochem. J.*, **83**, 335 (1962).
(7) F. G. Lehmann, *Clin. Chim. Acta*, **28**, 335 (1970). J. Marrink and M. Graber, *FEBS Lett.*, **2**, 242 (1969).

George R. Pettit [x]
Richard H. Ode

Cancer Research Institute and
Department of Chemistry
Arizona State University
Tempe, AZ 85281

Received October 13, 1976.
Accepted for publication December 20, 1976.
Supported by the National Cancer Institute (performed pursuant to Contracts N01-CM-12308 and N01-CM-67048 with the Division of Cancer Treatment, Department of Health, Education and Welfare), Public Health Research Grants CA-16049-02 and CA-16049-03 from the National Cancer Institute, the Fannie E. Rippel Foundation, the J. W. Kieckhefer Foundation, Talley Industries, and the Phoenix Coca-Cola Bottling Co.
We thank Mr. L. D. Vanell, Mr. G. C. Bryan, Mr. J. F. Day, and Dr. W. C. Fleming for assistance with a number of experiments and Dr. J. Cronin and Mrs. S. Ode for assistance with the amino acid analysis. The contributions of Dr. Jonathan L. Hartwell are also recognized and appreciated.

[x] To whom inquiries should be directed.

[1] More broadly, this report represents the first isolation and characterization of a marine vertebrate antineoplastic agent.
[2] Specimens of *S. lewini* were collected off the coast of Florida from 1971 to 1974, and we thank Dr. C. Swift for the taxonomic identification. Except for inclusion in a recent study of elasmobranch hemoglobins, no prior assessment of *S. lewini* constituents has been made. See Ref. 5.
[3] XAD-2.
[4] G-50 Sephadex.
[5] Sepharose 2B.

BOOKS

REVIEWS

Drug Metabolism: Chemical and Biochemical Aspects. By BERNARD TESTA and PETER JENNER. Dekker, 270 Madison Ave., New York, NY 10016, 1976. xii + 500 pp. 18.5 × 26 cm. Price $47.50.

This is the fourth volume in the new "Drug and Pharmaceutical Sciences" series of textbooks and monographs edited by James Swarbrick. As stated by the editor, the purpose of the series is "to enable the pharmacist, and others in the health sciences field, to stay abreast of the changing trends, advances and innovations associated with drugs and the body of knowledge that has come to be known as the pharmaceutical sciences." According to the authors, the purpose of this volume is "to create a fundamental awareness of the basis of drug metabolic processes to those entering the subject or to those who have worked at higher levels of *in vivo* organization." Both purposes have been admirably met with this volume.

As promised in the title, the authors treat both the chemical and biochemical aspects of drug metabolism. The book is divided into these two major sections, with 60% of the text devoted to chemical considerations.

The five chapters devoted to chemical aspects include the major chapter of the book, phase I (biotransformation of chemical groupings) reactions, and a somewhat shorter chapter, phase II (conjugation) reactions. Together, these two chapters account for nearly one-half the total text. Having detailed the specific chemical reactions of drug metabolism, these chapters are brought together and placed in perspective in the third chapter of this section by presenting schematic views of the metabolism of 15 selected drugs. This is followed by a chapter concerning the stereochemical aspects of drug metabolism, a topic recently reviewed in some depth by the authors. The final chapter of this section deals with the influence of physiochemical factors on drug metabolism. This very short chapter (five pages) perhaps should have been expanded or eliminated.

The biochemical aspects of drug metabolism, primarily at the enzymatic level, are presented in four chapters of approximately equal length. The first describes the basic biochemical nature of the drug-metabolizing enzyme systems responsible for phase I and phase II reactions. The effects

Now we wish to report the first[1] isolation and characterization of a shark anticancer constituent. The hammerhead shark, *Sphyrna lewini*[2], was found to produce two new antineoplastic agents designated sphyrnastatin 1 and sphyrnastatin 2. These anticancer components were isolated from the blood (and other body fluids), the fins (and other muscle tissue), and the liver.

In a typical isolation sequence, the water extract of blood and body fluids was first chromatographed on macroreticular resin[3]. The aqueous fraction (20 → 13.5 g) was next subjected to gel[4] permeation chromatography (10 × 100-cm column). Following elution with 3.25 liters of water, the PS inhibitory fraction (0.6 g from 5.0 g) was finally purified by chromatographic separation[5] (5 × 69-cm column and elution with a mixture of 0.05 *M* tromethamine and 0.1 *M* potassium chloride). The two highest molecular weight fractions (0.076 and 0.34 g) represented the antineoplastic components.

Sphyrnastatins 1 and 2, isolated by this procedure, were glycoproteins [~22 and 26% carbohydrate, respectively (6)] with apparent molecular weights (7) of at least 40×10^6. Amino acid analyses indicated a minimum protein segment of 274 amino acid units for sphyrnastatin 1 and 380 amino acid units for sphyrnastatin 2. Upon preliminary biological evaluation, the sphyrnastatins produced a 30–40% (at 11–13 mg/kg) life extension in mice inoculated with the PS leukemia. More extensive antineoplastic evaluation of sphyrnastatins 1 and 2 in the National Cancer Institute's exploratory screening systems is in progress. Presently, we are attempting to isolate other shark and marine vertebrate anticancer constituents.

Perhaps the sphyrnastatins and other high molecular weight antineoplastic substances (4) act by stimulating the immune system to more effective action against invading neoplastic disease. If this hypothesis is valid, then immunotherapy approaches to cancer treatment with, for example, BCG might better be considered as just another facet of cancer chemotherapy.

(1) P. W. Gilbert and C. Gilbert, *Underwater J.*, **1973**, 69.
(2) L. E. Mawdesley-Thomas, *Nature*, **235**, 17 (1972).
(3) G. R. Pettit, J. F. Day, J. L. Hartwell, and H. B. Wood, Jr., *ibid.*, **227**, 962 (1970).
(4) G. R. Pettit, "Biosynthetic Products for Cancer Chemotherapy," vol. 1, Plenum, New York, N.Y., in press.
(5) E. H. Fyhn and B. Sullivan, *Comp. Biochem. Physiol.*, **50B**, 119 (1975).
(6) C. Francois, R. D. Marshall, and A. Newberger, *Biochem. J.*, **83**, 335 (1962).
(7) F. G. Lehmann, *Clin. Chim. Acta*, **28**, 335 (1970). J. Marrink and M. Graber, *FEBS Lett.*, **2**, 242 (1969).

George R. Pettit [x]
Richard H. Ode

Cancer Research Institute and
Department of Chemistry
Arizona State University
Tempe, AZ 85281

Received October 13, 1976.
Accepted for publication December 20, 1976.
Supported by the National Cancer Institute (performed pursuant to Contracts N01-CM-12308 and N01-CM-67048 with the Division of Cancer Treatment, Department of Health, Education and Welfare), Public Health Research Grants CA-16049-02 and CA-16049-03 from the National Cancer Institute, the Fannie E. Rippel Foundation, the J. W. Kieckhefer Foundation, Talley Industries, and the Phoenix Coca-Cola Bottling Co.
We thank Mr. L. D. Vanell, Mr. G. C. Bryan, Mr. J. F. Day, and Dr. W. C. Fleming for assistance with a number of experiments and Dr. J. Cronin and Mrs. S. Ode for assistance with the amino acid analysis. The contributions of Dr. Jonathan L. Hartwell are also recognized and appreciated.

[x] To whom inquiries should be directed.

[1] More broadly, this report represents the first isolation and characterization of a marine vertebrate antineoplastic agent.
[2] Specimens of *S. lewini* were collected off the coast of Florida from 1971 to 1974, and we thank Dr. C. Swift for the taxonomic identification. Except for inclusion in a recent study of elasmobranch hemoglobins, no prior assessment of *S. lewini* constituents has been made. See Ref. 5.
[3] XAD-2.
[4] G-50 Sephadex.
[5] Sepharose 2B.

BOOKS

REVIEWS

Drug Metabolism: Chemical and Biochemical Aspects. By BERNARD TESTA and PETER JENNER. Dekker, 270 Madison Ave., New York, NY 10016, 1976. xii + 500 pp. 18.5 × 26 cm. Price $47.50.

This is the fourth volume in the new "Drug and Pharmaceutical Sciences" series of textbooks and monographs edited by James Swarbrick. As stated by the editor, the purpose of the series is "to enable the pharmacist, and others in the health sciences field, to stay abreast of the changing trends, advances and innovations associated with drugs and the body of knowledge that has come to be known as the pharmaceutical sciences." According to the authors, the purpose of this volume is "to create a fundamental awareness of the basis of drug metabolic processes to those entering the subject or to those who have worked at higher levels of *in vivo* organization." Both purposes have been admirably met with this volume.

As promised in the title, the authors treat both the chemical and biochemical aspects of drug metabolism. The book is divided into these two major sections, with 60% of the text devoted to chemical considerations.

The five chapters devoted to chemical aspects include the major chapter of the book, phase I (biotransformation of chemical groupings) reactions, and a somewhat shorter chapter, phase II (conjugation) reactions. Together, these two chapters account for nearly one-half the total text. Having detailed the specific chemical reactions of drug metabolism, these chapters are brought together and placed in perspective in the third chapter of this section by presenting schematic views of the metabolism of 15 selected drugs. This is followed by a chapter concerning the stereochemical aspects of drug metabolism, a topic recently reviewed in some depth by the authors. The final chapter of this section deals with the influence of physiochemical factors on drug metabolism. This very short chapter (five pages) perhaps should have been expanded or eliminated.

The biochemical aspects of drug metabolism, primarily at the enzymatic level, are presented in four chapters of approximately equal length. The first describes the basic biochemical nature of the drug-metabolizing enzyme systems responsible for phase I and phase II reactions. The effects

of inducers and inhibitors of these enzymatic systems and the mechanisms of actions involved are treated in the next chapter. The third chapter of this section deals with the physiological factors influencing drug metabolism, including species, strain, sex, and age. The final chapter of the section, and the book, is devoted to a comparison of the biochemical aspects of extrahepatic drug metabolism.

This book deals with "drug metabolism" in the sense of biotransformation, not in the sense of the overall fate, of drugs. Commendably, it has not been diluted with pharmacokinetics, methodology, or extensive physiology. The authors selected, organized and wrote the material in such a manner that the text is entirely readable and instructive, yet valuable for reference. The many references are grouped so that pertinent ones usually are no more than five pages, and never more than 20 pages, away. The subject and author indexes should be useful. This book fills a need in the field for a definitive text relating the chemical and biochemical aspects of drug metabolism.

This reviewer highly recommends the book to anyone engaged in drug metabolism activities; it should be particularly valuable to those entering the field and to those whose experience has been primarily with *in vivo* systems. Unfortunately, its rather high price may prevent many from having a personal copy.

Reviewed by Richard C. Thomas
Research Laboratories
The Upjohn Company
Kalamazoo, MI 49001

Clinical Chemistry. Principles and Procedures. 4th Ed. By JOSEPH S. ANNINO and ROGER W. GIESE. Little, Brown, 34 Beacon St., Boston, MA 02106, 1976. 412 pp. 16 × 24 cm. Price $15.00.

The fourth edition of this book reflects the rapid growth in the field of clinical chemistry. Part I, which details fundamental information on basic analytical techniques, includes chapters on automation, separation techniques, and radioimmunoassay for the first time. In addition, quality control and spectrophotometry have been expanded and a section on atomic absorption has been added to the chapter dealing with emission spectrophotometry. The overall treatment in Part I is very basic and quite brief; however, most of the important techniques are appropriately referenced.

The majority of this book (Part II) is devoted to descriptions of analytical methods for most of the tests performed in a modern clinical chemistry laboratory. The authors attempted to limit the material presented to one or two established methods for each test, and specific automated procedures are omitted entirely. In addition to the experimental details, most chapters contain a brief discussion of the principle of the method as well as limitations and clinical significance of the results. A concise survey of other current methods with references is also included. One notable weakness is the expanded section on drugs and poisons. It is still quite short and details procedures that are useful in toxicology but not sensitive enough for therapeutic monitoring.

This book is generally well written and appears to be most useful as an inexpensive, concise reference source for the nonclinical chemist who requires access to the principles and details of a variety of clinical chemistry procedures.

Reviewed by Jordan L. Cohen
School of Pharmacy
University of Southern California
Los Angeles, CA 90033

Pharmacokinetics of Psychoactive Drugs: Blood Levels and Clinical Response. Edited by LOUIS A. GOTTSCHALK and SIDNEY MERLIS. Wiley, 605 Third Ave., New York, NY 10016, 1976. 255 pp. 16 × 23.5 cm. Price $20.00.

At the annual meeting of the American College of Neuropsychopharmacology held in December 1974 in Puerto Rico, a series of papers was presented at the first study group dealing with pharmacokinetics and clinical response. This book represents an organized compilation of those papers.

The book contains 16 chapters divided into two main sections: Methodological Problems and Approaches (six chapters, 114 pp) and Pharmacological–Clinical Response (10 chapters, 136 pp). A major contribution of the book is the emphasis on the critical evaluation of measurement techniques, analytical as well as behavioral. Particularly noteworthy are Chapters 4 and 6. Chapter 4 includes a limited quality control study (five laboratories) of the determination of chlorpromazine and three metabolites, and Chapter 6 involves comparisons of three types of psychological measurement procedures. The second section of the book illustrates well the challenges of establishing relationships between blood level and clinical response with predictive capabilities.

The references at the end of each chapter are generally adequate. Since the book is the result of contributions at a scientific meeting, the reader should expect a certain amount of discontinuity in content and style. However, the book illustrates the state of the art in this highly interdisciplinary field of research and represents the first attempt to draw attention to several problem areas.

Reviewed by René H. Levy
Schools of Pharmacy and Medicine
University of Washington
Seattle, WA 98195

Alicyclic Chemistry. Vol. 4. Edited by W. PARKER *et al.* The Chemical Society, Burlington House, London W1V OBN, England, 1976. 511 pp. 14 × 22 cm. Price $75.75.

The present volume is organized identically to Volume 2 [reviewed in *J. Pharm. Sci.*, **64**, 2032 (1975)], which dealt with the literature of alicyclic chemistry published during 1972. Four large chapters cover three- and four-membered rings, five- and six-membered rings (and related fused systems), medium- and large-ring compounds, and bridged carbocyclics. Each chapter is extensively subdivided and deals with ring characteristics of the systems, methods of synthesis, and reactions. The format is the same as in the earlier volumes. The general comments made by this reviewer about Volume 2 are equally applicable here.

As in all areas of chemistry (all science), the sheer quantity of information available each year continues to grow exponentially. For example, the number of publications dealing with three- and four-membered rings alone increased by 35% in 1974 over the previous year.

Each chapter in this book is prepared by different authors (reporters), with W. Parker serving as the senior reporter for this and previous volumes. Finally, I think it is fair to state that the price of this volume (obtainable through the American Chemical Society) is simply exorbitant. The price in England is considerably less (£27.50). This price differential is hard to understand.

Reviewed by Alex Gringauz
Arnold and Marie Schwartz College of Pharmacy and Health Sciences
Long Island University
Brooklyn, NY 11201

Drug Treatment. Principles and Practice of Clinical Pharmacology and Therapeutics. Edited by GRAEME S. AVERY. Publishing Sciences Group, 162 Great Neck Rd., Acton, MA 01720, 1976. 1048 pp. 18.5 × 27 cm. Price $25.00.

This text is composed of 28 chapters authored by 53 contributors from around the world. It is arranged in three sections: clinical pharmacology, therapeutics, and a section of five appendixes containing mostly tables of data on physiochemical and pharmacokinetic properties of drugs, adverse reactions to drugs, drug interactions, selection of systemic antibacterial agents, and a guide to dosage in renal failure.

Each chapter begins with a synopsis of important principles which itemizes generalities that should be understood and retained as residual information even after the smaller nitty-gritty facts in each chapter fade from one's mind.

The specific aim of the book is to aid the clinician in selecting a drug

of inducers and inhibitors of these enzymatic systems and the mechanisms of actions involved are treated in the next chapter. The third chapter of this section deals with the physiological factors influencing drug metabolism, including species, strain, sex, and age. The final chapter of the section, and the book, is devoted to a comparison of the biochemical aspects of extrahepatic drug metabolism.

This book deals with "drug metabolism" in the sense of biotransformation, not in the sense of the overall fate, of drugs. Commendably, it has not been diluted with pharmacokinetics, methodology, or extensive physiology. The authors selected, organized and wrote the material in such a manner that the text is entirely readable and instructive, yet valuable for reference. The many references are grouped so that pertinent ones usually are no more than five pages, and never more than 20 pages, away. The subject and author indexes should be useful. This book fills a need in the field for a definitive text relating the chemical and biochemical aspects of drug metabolism.

This reviewer highly recommends the book to anyone engaged in drug metabolism activities; it should be particularly valuable to those entering the field and to those whose experience has been primarily with *in vivo* systems. Unfortunately, its rather high price may prevent many from having a personal copy.

Reviewed by Richard C. Thomas
Research Laboratories
The Upjohn Company
Kalamazoo, MI 49001

Clinical Chemistry. Principles and Procedures. 4th Ed. By JOSEPH S. ANNINO and ROGER W. GIESE. Little, Brown, 34 Beacon St., Boston, MA 02106, 1976. 412 pp. 16 × 24 cm. Price $15.00.

The fourth edition of this book reflects the rapid growth in the field of clinical chemistry. Part I, which details fundamental information on basic analytical techniques, includes chapters on automation, separation techniques, and radioimmunoassay for the first time. In addition, quality control and spectrophotometry have been expanded and a section on atomic absorption has been added to the chapter dealing with emission spectrophotometry. The overall treatment in Part I is very basic and quite brief; however, most of the important techniques are appropriately referenced.

The majority of this book (Part II) is devoted to descriptions of analytical methods for most of the tests performed in a modern clinical chemistry laboratory. The authors attempted to limit the material presented to one or two established methods for each test, and specific automated procedures are omitted entirely. In addition to the experimental details, most chapters contain a brief discussion of the principle of the method as well as limitations and clinical significance of the results. A concise survey of other current methods with references is also included. One notable weakness is the expanded section on drugs and poisons. It is still quite short and details procedures that are useful in toxicology but not sensitive enough for therapeutic monitoring.

This book is generally well written and appears to be most useful as an inexpensive, concise reference source for the nonclinical chemist who requires access to the principles and details of a variety of clinical chemistry procedures.

Reviewed by Jordan L. Cohen
School of Pharmacy
University of Southern California
Los Angeles, CA 90033

Pharmacokinetics of Psychoactive Drugs: Blood Levels and Clinical Response. Edited by LOUIS A. GOTTSCHALK and SIDNEY MERLIS. Wiley, 605 Third Ave., New York, NY 10016, 1976. 255 pp. 16 × 23.5 cm. Price $20.00.

At the annual meeting of the American College of Neuropsychopharmacology held in December 1974 in Puerto Rico, a series of papers was presented at the first study group dealing with pharmacokinetics and clinical response. This book represents an organized compilation of those papers.

The book contains 16 chapters divided into two main sections: Methodological Problems and Approaches (six chapters, 114 pp) and Pharmacological–Clinical Response (10 chapters, 136 pp). A major contribution of the book is the emphasis on the critical evaluation of measurement techniques, analytical as well as behavioral. Particularly noteworthy are Chapters 4 and 6. Chapter 4 includes a limited quality control study (five laboratories) of the determination of chlorpromazine and three metabolites, and Chapter 6 involves comparisons of three types of psychological measurement procedures. The second section of the book illustrates well the challenges of establishing relationships between blood level and clinical response with predictive capabilities.

The references at the end of each chapter are generally adequate. Since the book is the result of contributions at a scientific meeting, the reader should expect a certain amount of discontinuity in content and style. However, the book illustrates the state of the art in this highly interdisciplinary field of research and represents the first attempt to draw attention to several problem areas.

Reviewed by René H. Levy
Schools of Pharmacy and Medicine
University of Washington
Seattle, WA 98195

Alicyclic Chemistry. Vol. 4. Edited by W. PARKER *et al.* The Chemical Society, Burlington House, London W1V OBN, England, 1976. 511 pp. 14 × 22 cm. Price $75.75.

The present volume is organized identically to Volume 2 [reviewed in *J. Pharm. Sci.*, **64**, 2032 (1975)], which dealt with the literature of alicyclic chemistry published during 1972. Four large chapters cover three- and four-membered rings, five- and six-membered rings (and related fused systems), medium- and large-ring compounds, and bridged carbocyclics. Each chapter is extensively subdivided and deals with ring characteristics of the systems, methods of synthesis, and reactions. The format is the same as in the earlier volumes. The general comments made by this reviewer about Volume 2 are equally applicable here.

As in all areas of chemistry (all science), the sheer quantity of information available each year continues to grow exponentially. For example, the number of publications dealing with three- and four-membered rings alone increased by 35% in 1974 over the previous year.

Each chapter in this book is prepared by different authors (reporters), with W. Parker serving as the senior reporter for this and previous volumes. Finally, I think it is fair to state that the price of this volume (obtainable through the American Chemical Society) is simply exorbitant. The price in England is considerably less (£27.50). This price differential is hard to understand.

Reviewed by Alex Gringauz
Arnold and Marie Schwartz College of Pharmacy and Health Sciences
Long Island University
Brooklyn, NY 11201

Drug Treatment. Principles and Practice of Clinical Pharmacology and Therapeutics. Edited by GRAEME S. AVERY. Publishing Sciences Group, 162 Great Neck Rd., Acton, MA 01720, 1976. 1048 pp. 18.5 × 27 cm. Price $25.00.

This text is composed of 28 chapters authored by 53 contributors from around the world. It is arranged in three sections: clinical pharmacology, therapeutics, and a section of five appendixes containing mostly tables of data on physiochemical and pharmacokinetic properties of drugs, adverse reactions to drugs, drug interactions, selection of systemic antibacterial agents, and a guide to dosage in renal failure.

Each chapter begins with a synopsis of important principles which itemizes generalities that should be understood and retained as residual information even after the smaller nitty-gritty facts in each chapter fade from one's mind.

The specific aim of the book is to aid the clinician in selecting a drug

of inducers and inhibitors of these enzymatic systems and the mechanisms of actions involved are treated in the next chapter. The third chapter of this section deals with the physiological factors influencing drug metabolism, including species, strain, sex, and age. The final chapter of the section, and the book, is devoted to a comparison of the biochemical aspects of extrahepatic drug metabolism.

This book deals with "drug metabolism" in the sense of biotransformation, not in the sense of the overall fate, of drugs. Commendably, it has not been diluted with pharmacokinetics, methodology, or extensive physiology. The authors selected, organized and wrote the material in such a manner that the text is entirely readable and instructive, yet valuable for reference. The many references are grouped so that pertinent ones usually are no more than five pages, and never more than 20 pages, away. The subject and author indexes should be useful. This book fills a need in the field for a definitive text relating the chemical and biochemical aspects of drug metabolism.

This reviewer highly recommends the book to anyone engaged in drug metabolism activities; it should be particularly valuable to those entering the field and to those whose experience has been primarily with *in vivo* systems. Unfortunately, its rather high price may prevent many from having a personal copy.

Reviewed by Richard C. Thomas
Research Laboratories
The Upjohn Company
Kalamazoo, MI 49001

Clinical Chemistry. Principles and Procedures. 4th Ed. By JOSEPH S. ANNINO and ROGER W. GIESE. Little, Brown, 34 Beacon St., Boston, MA 02106, 1976. 412 pp. 16 × 24 cm. Price $15.00.

The fourth edition of this book reflects the rapid growth in the field of clinical chemistry. Part I, which details fundamental information on basic analytical techniques, includes chapters on automation, separation techniques, and radioimmunoassay for the first time. In addition, quality control and spectrophotometry have been expanded and a section on atomic absorption has been added to the chapter dealing with emission spectrophotometry. The overall treatment in Part I is very basic and quite brief; however, most of the important techniques are appropriately referenced.

The majority of this book (Part II) is devoted to descriptions of analytical methods for most of the tests performed in a modern clinical chemistry laboratory. The authors attempted to limit the material presented to one or two established methods for each test, and specific automated procedures are omitted entirely. In addition to the experimental details, most chapters contain a brief discussion of the principle of the method as well as limitations and clinical significance of the results. A concise survey of other current methods with references is also included. One notable weakness is the expanded section on drugs and poisons. It is still quite short and details procedures that are useful in toxicology but not sensitive enough for therapeutic monitoring.

This book is generally well written and appears to be most useful as an inexpensive, concise reference source for the nonclinical chemist who requires access to the principles and details of a variety of clinical chemistry procedures.

Reviewed by Jordan L. Cohen
School of Pharmacy
University of Southern California
Los Angeles, CA 90033

Pharmacokinetics of Psychoactive Drugs: Blood Levels and Clinical Response. Edited by LOUIS A. GOTTSCHALK and SIDNEY MERLIS. Wiley, 605 Third Ave., New York, NY 10016, 1976. 255 pp. 16 × 23.5 cm. Price $20.00.

At the annual meeting of the American College of Neuropsychopharmacology held in December 1974 in Puerto Rico, a series of papers was presented at the first study group dealing with pharmacokinetics and clinical response. This book represents an organized compilation of those papers.

The book contains 16 chapters divided into two main sections: Methodological Problems and Approaches (six chapters, 114 pp) and Pharmacological–Clinical Response (10 chapters, 136 pp). A major contribution of the book is the emphasis on the critical evaluation of measurement techniques, analytical as well as behavioral. Particularly noteworthy are Chapters 4 and 6. Chapter 4 includes a limited quality control study (five laboratories) of the determination of chlorpromazine and three metabolites, and Chapter 6 involves comparisons of three types of psychological measurement procedures. The second section of the book illustrates well the challenges of establishing relationships between blood level and clinical response with predictive capabilities.

The references at the end of each chapter are generally adequate. Since the book is the result of contributions at a scientific meeting, the reader should expect a certain amount of discontinuity in content and style. However, the book illustrates the state of the art in this highly interdisciplinary field of research and represents the first attempt to draw attention to several problem areas.

Reviewed by René H. Levy
Schools of Pharmacy and Medicine
University of Washington
Seattle, WA 98195

Alicyclic Chemistry. Vol. 4. Edited by W. PARKER *et al.* The Chemical Society, Burlington House, London W1V OBN, England, 1976. 511 pp. 14 × 22 cm. Price $75.75.

The present volume is organized identically to Volume 2 [reviewed in *J. Pharm. Sci.*, **64**, 2032 (1975)], which dealt with the literature of alicyclic chemistry published during 1972. Four large chapters cover three- and four-membered rings, five- and six-membered rings (and related fused systems), medium- and large-ring compounds, and bridged carbocyclics. Each chapter is extensively subdivided and deals with ring characteristics of the systems, methods of synthesis, and reactions. The format is the same as in the earlier volumes. The general comments made by this reviewer about Volume 2 are equally applicable here.

As in all areas of chemistry (all science), the sheer quantity of information available each year continues to grow exponentially. For example, the number of publications dealing with three- and four-membered rings alone increased by 35% in 1974 over the previous year.

Each chapter in this book is prepared by different authors (reporters), with W. Parker serving as the senior reporter for this and previous volumes. Finally, I think it is fair to state that the price of this volume (obtainable through the American Chemical Society) is simply exorbitant. The price in England is considerably less (£27.50). This price differential is hard to understand.

Reviewed by Alex Gringauz
Arnold and Marie Schwartz College of Pharmacy and Health Sciences
Long Island University
Brooklyn, NY 11201

Drug Treatment. Principles and Practice of Clinical Pharmacology and Therapeutics. Edited by GRAEME S. AVERY. Publishing Sciences Group, 162 Great Neck Rd., Acton, MA 01720, 1976. 1048 pp. 18.5 × 27 cm. Price $25.00.

This text is composed of 28 chapters authored by 53 contributors from around the world. It is arranged in three sections: clinical pharmacology, therapeutics, and a section of five appendixes containing mostly tables of data on physiochemical and pharmacokinetic properties of drugs, adverse reactions to drugs, drug interactions, selection of systemic antibacterial agents, and a guide to dosage in renal failure.

Each chapter begins with a synopsis of important principles which itemizes generalities that should be understood and retained as residual information even after the smaller nitty-gritty facts in each chapter fade from one's mind.

The specific aim of the book is to aid the clinician in selecting a drug

of inducers and inhibitors of these enzymatic systems and the mechanisms of actions involved are treated in the next chapter. The third chapter of this section deals with the physiological factors influencing drug metabolism, including species, strain, sex, and age. The final chapter of the section, and the book, is devoted to a comparison of the biochemical aspects of extrahepatic drug metabolism.

This book deals with "drug metabolism" in the sense of biotransformation, not in the sense of the overall fate, of drugs. Commendably, it has not been diluted with pharmacokinetics, methodology, or extensive physiology. The authors selected, organized and wrote the material in such a manner that the text is entirely readable and instructive, yet valuable for reference. The many references are grouped so that pertinent ones usually are no more than five pages, and never more than 20 pages, away. The subject and author indexes should be useful. This book fills a need in the field for a definitive text relating the chemical and biochemical aspects of drug metabolism.

This reviewer highly recommends the book to anyone engaged in drug metabolism activities; it should be particularly valuable to those entering the field and to those whose experience has been primarily with *in vivo* systems. Unfortunately, its rather high price may prevent many from having a personal copy.

Reviewed by Richard C. Thomas
Research Laboratories
The Upjohn Company
Kalamazoo, MI 49001

Clinical Chemistry. Principles and Procedures. 4th Ed. By JOSEPH S. ANNINO and ROGER W. GIESE. Little, Brown, 34 Beacon St., Boston, MA 02106, 1976. 412 pp. 16 × 24 cm. Price $15.00.

The fourth edition of this book reflects the rapid growth in the field of clinical chemistry. Part I, which details fundamental information on basic analytical techniques, includes chapters on automation, separation techniques, and radioimmunoassay for the first time. In addition, quality control and spectrophotometry have been expanded and a section on atomic absorption has been added to the chapter dealing with emission spectrophotometry. The overall treatment in Part I is very basic and quite brief; however, most of the important techniques are appropriately referenced.

The majority of this book (Part II) is devoted to descriptions of analytical methods for most of the tests performed in a modern clinical chemistry laboratory. The authors attempted to limit the material presented to one or two established methods for each test, and specific automated procedures are omitted entirely. In addition to the experimental details, most chapters contain a brief discussion of the principle of the method as well as limitations and clinical significance of the results. A concise survey of other current methods with references is also included. One notable weakness is the expanded section on drugs and poisons. It is still quite short and details procedures that are useful in toxicology but not sensitive enough for therapeutic monitoring.

This book is generally well written and appears to be most useful as an inexpensive, concise reference source for the nonclinical chemist who requires access to the principles and details of a variety of clinical chemistry procedures.

Reviewed by Jordan L. Cohen
School of Pharmacy
University of Southern California
Los Angeles, CA 90033

Pharmacokinetics of Psychoactive Drugs: Blood Levels and Clinical Response. Edited by LOUIS A. GOTTSCHALK and SIDNEY MERLIS. Wiley, 605 Third Ave., New York, NY 10016, 1976. 255 pp. 16 × 23.5 cm. Price $20.00.

At the annual meeting of the American College of Neuropsychopharmacology held in December 1974 in Puerto Rico, a series of papers was presented at the first study group dealing with pharmacokinetics and clinical response. This book represents an organized compilation of those papers.

The book contains 16 chapters divided into two main sections: Methodological Problems and Approaches (six chapters, 114 pp) and Pharmacological–Clinical Response (10 chapters, 136 pp). A major contribution of the book is the emphasis on the critical evaluation of measurement techniques, analytical as well as behavioral. Particularly noteworthy are Chapters 4 and 6. Chapter 4 includes a limited quality control study (five laboratories) of the determination of chlorpromazine and three metabolites, and Chapter 6 involves comparisons of three types of psychological measurement procedures. The second section of the book illustrates well the challenges of establishing relationships between blood level and clinical response with predictive capabilities.

The references at the end of each chapter are generally adequate. Since the book is the result of contributions at a scientific meeting, the reader should expect a certain amount of discontinuity in content and style. However, the book illustrates the state of the art in this highly interdisciplinary field of research and represents the first attempt to draw attention to several problem areas.

Reviewed by René H. Levy
Schools of Pharmacy and Medicine
University of Washington
Seattle, WA 98195

Alicyclic Chemistry. Vol. 4. Edited by W. PARKER *et al.* The Chemical Society, Burlington House, London W1V OBN, England, 1976. 511 pp. 14 × 22 cm. Price $75.75.

The present volume is organized identically to Volume 2 [reviewed in *J. Pharm. Sci.*, **64**, 2032 (1975)], which dealt with the literature of alicyclic chemistry published during 1972. Four large chapters cover three- and four-membered rings, five- and six-membered rings (and related fused systems), medium- and large-ring compounds, and bridged carbocyclics. Each chapter is extensively subdivided and deals with ring characteristics of the systems, methods of synthesis, and reactions. The format is the same as in the earlier volumes. The general comments made by this reviewer about Volume 2 are equally applicable here.

As in all areas of chemistry (all science), the sheer quantity of information available each year continues to grow exponentially. For example, the number of publications dealing with three- and four-membered rings alone increased by 35% in 1974 over the previous year.

Each chapter in this book is prepared by different authors (reporters), with W. Parker serving as the senior reporter for this and previous volumes. Finally, I think it is fair to state that the price of this volume (obtainable through the American Chemical Society) is simply exorbitant. The price in England is considerably less (£27.50). This price differential is hard to understand.

Reviewed by Alex Gringauz
Arnold and Marie Schwartz College of Pharmacy and Health Sciences
Long Island University
Brooklyn, NY 11201

Drug Treatment. Principles and Practice of Clinical Pharmacology and Therapeutics. Edited by GRAEME S. AVERY. Publishing Sciences Group, 162 Great Neck Rd., Acton, MA 01720, 1976. 1048 pp. 18.5 × 27 cm. Price $25.00.

This text is composed of 28 chapters authored by 53 contributors from around the world. It is arranged in three sections: clinical pharmacology, therapeutics, and a section of five appendixes containing mostly tables of data on physiochemical and pharmacokinetic properties of drugs, adverse reactions to drugs, drug interactions, selection of systemic antibacterial agents, and a guide to dosage in renal failure.

Each chapter begins with a synopsis of important principles which itemizes generalities that should be understood and retained as residual information even after the smaller nitty-gritty facts in each chapter fade from one's mind.

The specific aim of the book is to aid the clinician in selecting a drug

of inducers and inhibitors of these enzymatic systems and the mechanisms of actions involved are treated in the next chapter. The third chapter of this section deals with the physiological factors influencing drug metabolism, including species, strain, sex, and age. The final chapter of the section, and the book, is devoted to a comparison of the biochemical aspects of extrahepatic drug metabolism.

This book deals with "drug metabolism" in the sense of biotransformation, not in the sense of the overall fate, of drugs. Commendably, it has not been diluted with pharmacokinetics, methodology, or extensive physiology. The authors selected, organized and wrote the material in such a manner that the text is entirely readable and instructive, yet valuable for reference. The many references are grouped so that pertinent ones usually are no more than five pages, and never more than 20 pages, away. The subject and author indexes should be useful. This book fills a need in the field for a definitive text relating the chemical and biochemical aspects of drug metabolism.

This reviewer highly recommends the book to anyone engaged in drug metabolism activities; it should be particularly valuable to those entering the field and to those whose experience has been primarily with *in vivo* systems. Unfortunately, its rather high price may prevent many from having a personal copy.

Reviewed by Richard C. Thomas
Research Laboratories
The Upjohn Company
Kalamazoo, MI 49001

Clinical Chemistry. Principles and Procedures. 4th Ed. By JOSEPH S. ANNINO and ROGER W. GIESE. Little, Brown, 34 Beacon St., Boston, MA 02106, 1976. 412 pp. 16 × 24 cm. Price $15.00.

The fourth edition of this book reflects the rapid growth in the field of clinical chemistry. Part I, which details fundamental information on basic analytical techniques, includes chapters on automation, separation techniques, and radioimmunoassay for the first time. In addition, quality control and spectrophotometry have been expanded and a section on atomic absorption has been added to the chapter dealing with emission spectrophotometry. The overall treatment in Part I is very basic and quite brief; however, most of the important techniques are appropriately referenced.

The majority of this book (Part II) is devoted to descriptions of analytical methods for most of the tests performed in a modern clinical chemistry laboratory. The authors attempted to limit the material presented to one or two established methods for each test, and specific automated procedures are omitted entirely. In addition to the experimental details, most chapters contain a brief discussion of the principle of the method as well as limitations and clinical significance of the results. A concise survey of other current methods with references is also included. One notable weakness is the expanded section on drugs and poisons. It is still quite short and details procedures that are useful in toxicology but not sensitive enough for therapeutic monitoring.

This book is generally well written and appears to be most useful as an inexpensive, concise reference source for the nonclinical chemist who requires access to the principles and details of a variety of clinical chemistry procedures.

Reviewed by Jordan L. Cohen
School of Pharmacy
University of Southern California
Los Angeles, CA 90033

Pharmacokinetics of Psychoactive Drugs: Blood Levels and Clinical Response. Edited by LOUIS A. GOTTSCHALK and SIDNEY MERLIS. Wiley, 605 Third Ave., New York, NY 10016, 1976. 255 pp. 16 × 23.5 cm. Price $20.00.

At the annual meeting of the American College of Neuropsychopharmacology held in December 1974 in Puerto Rico, a series of papers was presented at the first study group dealing with pharmacokinetics and clinical response. This book represents an organized compilation of those papers.

The book contains 16 chapters divided into two main sections: Methodological Problems and Approaches (six chapters, 114 pp) and Pharmacological–Clinical Response (10 chapters, 136 pp). A major contribution of the book is the emphasis on the critical evaluation of measurement techniques, analytical as well as behavioral. Particularly noteworthy are Chapters 4 and 6. Chapter 4 includes a limited quality control study (five laboratories) of the determination of chlorpromazine and three metabolites, and Chapter 6 involves comparisons of three types of psychological measurement procedures. The second section of the book illustrates well the challenges of establishing relationships between blood level and clinical response with predictive capabilities.

The references at the end of each chapter are generally adequate. Since the book is the result of contributions at a scientific meeting, the reader should expect a certain amount of discontinuity in content and style. However, the book illustrates the state of the art in this highly interdisciplinary field of research and represents the first attempt to draw attention to several problem areas.

Reviewed by René H. Levy
Schools of Pharmacy and Medicine
University of Washington
Seattle, WA 98195

Alicyclic Chemistry. Vol. 4. Edited by W. PARKER *et al.* The Chemical Society, Burlington House, London W1V OBN, England, 1976. 511 pp. 14 × 22 cm. Price $75.75.

The present volume is organized identically to Volume 2 [reviewed in *J. Pharm. Sci.*, **64**, 2032 (1975)], which dealt with the literature of alicyclic chemistry published during 1972. Four large chapters cover three- and four-membered rings, five- and six-membered rings (and related fused systems), medium- and large-ring compounds, and bridged carbocyclics. Each chapter is extensively subdivided and deals with ring characteristics of the systems, methods of synthesis, and reactions. The format is the same as in the earlier volumes. The general comments made by this reviewer about Volume 2 are equally applicable here.

As in all areas of chemistry (all science), the sheer quantity of information available each year continues to grow exponentially. For example, the number of publications dealing with three- and four-membered rings alone increased by 35% in 1974 over the previous year.

Each chapter in this book is prepared by different authors (reporters), with W. Parker serving as the senior reporter for this and previous volumes. Finally, I think it is fair to state that the price of this volume (obtainable through the American Chemical Society) is simply exorbitant. The price in England is considerably less (£27.50). This price differential is hard to understand.

Reviewed by Alex Gringauz
Arnold and Marie Schwartz College of Pharmacy and Health Sciences
Long Island University
Brooklyn, NY 11201

Drug Treatment. Principles and Practice of Clinical Pharmacology and Therapeutics. Edited by GRAEME S. AVERY. Publishing Sciences Group, 162 Great Neck Rd., Acton, MA 01720, 1976. 1048 pp. 18.5 × 27 cm. Price $25.00.

This text is composed of 28 chapters authored by 53 contributors from around the world. It is arranged in three sections: clinical pharmacology, therapeutics, and a section of five appendixes containing mostly tables of data on physiochemical and pharmacokinetic properties of drugs, adverse reactions to drugs, drug interactions, selection of systemic antibacterial agents, and a guide to dosage in renal failure.

Each chapter begins with a synopsis of important principles which itemizes generalities that should be understood and retained as residual information even after the smaller nitty-gritty facts in each chapter fade from one's mind.

The specific aim of the book is to aid the clinician in selecting a drug

and dose schedule by making it clear that one should first pay strict attention to the patient's particular disease conditions because these invariably affect the responses of the agents chosen. In this regard, it must be stated that no other text to date has done as good a job as this one. It truly succeeds as a bridge between classic pharmacology texts and those limited to therapeutics and medicine.

Through a close reading of any chapter, one is made aware of clinical pharmacology as it should be delineated; *i.e.*, as an area of concentration that deals with the understanding of the action of current drugs in patients with diseases, rather than simply the evaluation of new entities as they are synthesized and brought to the clinic for initial trials.

The handling of the reference material for books, tables, and figures is accomplished in such a way that if one is interested it can be found, but the descriptive material is not continuously interrupted with names, sources, and dates.

This work is recommended for anyone involved with the applied aspects of pharmacology including physicians, pharmacologists, pharmacists, and allied health professionals. It will make an excellent contribution to the literature and certainly fills a void that has developed as pharmacology and therapeutics have emerged as the foundations for a thorough understanding of the clinical implications of drug usage.

Reviewed by Ronald F. Gautieri
Department of Pharmacology
Temple University
School of Pharmacy
Philadelphia, PA 19140

Terpenoids and Steroids, Vol. 6. Edited by K. H. OVERTON *et al.* The Chemical Society, Burlington House, London W1V OBN, England, 1976. 363 pp. 15 × 22 cm. Price £20.50. (Available from Special Issues Sales, American Chemical Society, 1155 Sixteenth Street, N.W., Washington, DC 20036.)

This is the sixth volume on terpenoids and steroids in a valuable series first published 5 years ago. The aim of each series of Specialist Periodical Reports is to provide a systematic, comprehensive, and critical review of progress in the major areas of chemical research. The various series, which now total 35, are being published annually or bienially on such topics as Environmental Chemistry; Biosynthesis; Foreign Compound Metabolism in Mammals; The Alkaloids; Carbohydrate Chemistry; Amino-acids, Peptides, and Proteins; and Photochemistry.

This volume does not contain a subject index but is organized in a systematic manner which facilitates finding any information being sought. The six pages in the Table of Contents outline this volume in detail. The chapters are divided into many sections, which are identified in boldface type in the text as well as in the Table of Contents. These sections are further divided into subsections. Chapter titles are found at the top of every second page of the text. The author index of 3500 names is helpful to those following the research of a given individual.

This review is illustrated with drawings of 2100 chemical structures. It is documented with 1850 references, most of which are listed at the bottom of the first page of each chapter where cited.

Part I, which covers the terpenoids, is divided into chapters including Monoterpenoids, Sesquiterpenoids, Diterpenoids, Triterpenoids, Carotenoids and Polyterpenoids, and Biosynthesis of Terpenoids and Steroids. Part II, which covers steroids, is divided into two large chapters entitled Steroid Properties and Reactions, and Steroid Synthesis. No compilation of references to review articles on subjects related to terpenoids or steroids is included in this volume as in previous volumes.

The chapter on Steroid Properties and Reactions is divided into sections based upon more common functional groups, a section on Compounds of Nitrogen and Sulfur, and sections on such important subjects as Photochemical Reactions, Molecular Rearrangements, and Functionalization of Non-activated Positions. The chapter on Steroid Synthesis is divided into the following sections: Total Synthesis, Halogenosteroids, Oestranes, Androstanes, Pregnanes, Seco-steroids, Cholestane and Analogues, Steroidal Insect and Plant Hormones, Steroidal Alkaloids, Sapogenins, Cardenolides, and Bufadienolides.

The editor and 11 reporters who prepared this volume are to be commended for maintaining the high standards set by the previous volumes in this series. Everyone interested in the chemistry of terpenoids and/or steroids should have access to this volume and others in the series. They are great timesavers and sources of new ideas. I highly recommend this series.

Reviewed by Norman J. Doorenbos
School of Pharmacy
University of Mississippi
University, MS 38677

Progress in Toxicology. Special Topics. Vol. 2. By GERHARD ZBINDEN. Springer-Verlag, 175 Fifth Ave., New York, NY 10010, 1976. 117 pp. 18 × 26 cm. Price $7.40.

The cuisine of Zbinden's second book on special topics in toxicology is based on experience, sound reasoning, good common sense, a pinch of humor, and clear expression of realistic idealism. Is toxicology really too serious a matter to be left to the toxicologists? Read the book and answer the question yourself. Then read "How Safe is Safe?," available from the National Academy of Sciences. In a rather brief but informative manner, Zbinden covers in 93 pages (not including references and index) some of the most important problems confronting toxicology and related sciences but in a rather unusual manner. For example, he relates his son's experience with a gum ball machine, indicating that his son may put in two nickels and get nothing but doesn't give up until he finds out why or gets his two nickels back! "Why then does a negative response to a drug not elicit from us a similar anger?" More attention is paid to side-effects than negative medication responses. Zbinden then goes on to demonstrate the role of urinary pH as a factor in accelerated drug excretion and negative medication responses.

He discusses percutaneous drug permeation, hyperglycemia, the glutathione story, a new disease (pseudolupus), drug-induced lipidosis, the magnitude of drug combinations, drug interactions, and the growing problem (?) of health hazards from colors. In his discussion of food, drug, and cosmetic colors, he points out that the number of colors permitted in foods varies from country to country; *i.e.*, Australia permits seven synthetic and six natural dyes, and the United Kingdom permits 22 and 23, respectively. All other countries are somewhere inbetween. In this section, Zbinden also deletes expletives!

I personally enjoy reading anything that Zbinden writes (in English!) and don't hesitate to recommend this book to all concerned with toxicity, toxicology, and human health. I hope that Zbinden continues to write because what he says affords sound advice for those dealing with the naive.

Reviewed by Charles L. Winek
School of Pharmacy
Duquesne University
Pittsburgh, PA 15219

and dose schedule by making it clear that one should first pay strict attention to the patient's particular disease conditions because these invariably affect the responses of the agents chosen. In this regard, it must be stated that no other text to date has done as good a job as this one. It truly succeeds as a bridge between classic pharmacology texts and those limited to therapeutics and medicine.

Through a close reading of any chapter, one is made aware of clinical pharmacology as it should be delineated; *i.e.*, as an area of concentration that deals with the understanding of the action of current drugs in patients with diseases, rather than simply the evaluation of new entities as they are synthesized and brought to the clinic for initial trials.

The handling of the reference material for books, tables, and figures is accomplished in such a way that if one is interested it can be found, but the descriptive material is not continuously interrupted with names, sources, and dates.

This work is recommended for anyone involved with the applied aspects of pharmacology including physicians, pharmacologists, pharmacists, and allied health professionals. It will make an excellent contribution to the literature and certainly fills a void that has developed as pharmacology and therapeutics have emerged as the foundations for a thorough understanding of the clinical implications of drug usage.

Reviewed by Ronald F. Gautieri
Department of Pharmacology
Temple University
School of Pharmacy
Philadelphia, PA 19140

Terpenoids and Steroids, Vol. 6. Edited by K. H. OVERTON *et al.* The Chemical Society, Burlington House, London W1V OBN, England, 1976. 363 pp. 15 × 22 cm. Price £20.50. (Available from Special Issues Sales, American Chemical Society, 1155 Sixteenth Street, N.W., Washington, DC 20036.)

This is the sixth volume on terpenoids and steroids in a valuable series first published 5 years ago. The aim of each series of Specialist Periodical Reports is to provide a systematic, comprehensive, and critical review of progress in the major areas of chemical research. The various series, which now total 35, are being published annually or bienially on such topics as Environmental Chemistry; Biosynthesis; Foreign Compound Metabolism in Mammals; The Alkaloids; Carbohydrate Chemistry; Amino-acids, Peptides, and Proteins; and Photochemistry.

This volume does not contain a subject index but is organized in a systematic manner which facilitates finding any information being sought. The six pages in the Table of Contents outline this volume in detail. The chapters are divided into many sections, which are identified in boldface type in the text as well as in the Table of Contents. These sections are further divided into subsections. Chapter titles are found at the top of every second page of the text. The author index of 3500 names is helpful to those following the research of a given individual.

This review is illustrated with drawings of 2100 chemical structures. It is documented with 1850 references, most of which are listed at the bottom of the first page of each chapter where cited.

Part I, which covers the terpenoids, is divided into chapters including Monoterpenoids, Sesquiterpenoids, Diterpenoids, Triterpenoids, Carotenoids and Polyterpenoids, and Biosynthesis of Terpenoids and Steroids. Part II, which covers steroids, is divided into two large chapters entitled Steroid Properties and Reactions, and Steroid Synthesis. No compilation of references to review articles on subjects related to terpenoids or steroids is included in this volume as in previous volumes.

The chapter on Steroid Properties and Reactions is divided into sections based upon more common functional groups, a section on Compounds of Nitrogen and Sulfur, and sections on such important subjects as Photochemical Reactions, Molecular Rearrangements, and Functionalization of Non-activated Positions. The chapter on Steroid Synthesis is divided into the following sections: Total Synthesis, Halogenosteroids, Oestranes, Androstanes, Pregnanes, Seco-steroids, Cholestane and Analogues, Steroidal Insect and Plant Hormones, Steroidal Alkaloids, Sapogenins, Cardenolides, and Bufadienolides.

The editor and 11 reporters who prepared this volume are to be commended for maintaining the high standards set by the previous volumes in this series. Everyone interested in the chemistry of terpenoids and/or steroids should have access to this volume and others in the series. They are great timesavers and sources of new ideas. I highly recommend this series.

Reviewed by Norman J. Doorenbos
School of Pharmacy
University of Mississippi
University, MS 38677

Progress in Toxicology. Special Topics. Vol. 2. By GERHARD ZBINDEN. Springer-Verlag, 175 Fifth Ave., New York, NY 10010, 1976. 117 pp. 18 × 26 cm. Price $7.40.

The cuisine of Zbinden's second book on special topics in toxicology is based on experience, sound reasoning, good common sense, a pinch of humor, and clear expression of realistic idealism. Is toxicology really too serious a matter to be left to the toxicologists? Read the book and answer the question yourself. Then read "How Safe is Safe?," available from the National Academy of Sciences. In a rather brief but informative manner, Zbinden covers in 93 pages (not including references and index) some of the most important problems confronting toxicology and related sciences but in a rather unusual manner. For example, he relates his son's experience with a gum ball machine, indicating that his son may put in two nickels and get nothing but doesn't give up until he finds out why or gets his two nickels back! "Why then does a negative response to a drug not elicit from us a similar anger?" More attention is paid to side-effects than negative medication responses. Zbinden then goes on to demonstrate the role of urinary pH as a factor in accelerated drug excretion and negative medication responses.

He discusses percutaneous drug permeation, hyperglycemia, the glutathione story, a new disease (pseudolupus), drug-induced lipidosis, the magnitude of drug combinations, drug interactions, and the growing problem (?) of health hazards from colors. In his discussion of food, drug, and cosmetic colors, he points out that the number of colors permitted in foods varies from country to country; *i.e.*, Australia permits seven synthetic and six natural dyes, and the United Kingdom permits 22 and 23, respectively. All other countries are somewhere inbetween. In this section, Zbinden also deletes expletives!

I personally enjoy reading anything that Zbinden writes (in English!) and don't hesitate to recommend this book to all concerned with toxicity, toxicology, and human health. I hope that Zbinden continues to write because what he says affords sound advice for those dealing with the naive.

Reviewed by Charles L. Winek
School of Pharmacy
Duquesne University
Pittsburgh, PA 15219

and dose schedule by making it clear that one should first pay strict attention to the patient's particular disease conditions because these invariably affect the responses of the agents chosen. In this regard, it must be stated that no other text to date has done as good a job as this one. It truly succeeds as a bridge between classic pharmacology texts and those limited to therapeutics and medicine.

Through a close reading of any chapter, one is made aware of clinical pharmacology as it should be delineated; *i.e.*, as an area of concentration that deals with the understanding of the action of current drugs in patients with diseases, rather than simply the evaluation of new entities as they are synthesized and brought to the clinic for initial trials.

The handling of the reference material for books, tables, and figures is accomplished in such a way that if one is interested it can be found, but the descriptive material is not continuously interrupted with names, sources, and dates.

This work is recommended for anyone involved with the applied aspects of pharmacology including physicians, pharmacologists, pharmacists, and allied health professionals. It will make an excellent contribution to the literature and certainly fills a void that has developed as pharmacology and therapeutics have emerged as the foundations for a thorough understanding of the clinical implications of drug usage.

Reviewed by Ronald F. Gautieri
Department of Pharmacology
Temple University
School of Pharmacy
Philadelphia, PA 19140

Terpenoids and Steroids, Vol. 6. Edited by K. H. OVERTON *et al.* The Chemical Society, Burlington House, London W1V OBN, England, 1976. 363 pp. 15 × 22 cm. Price £20.50. (Available from Special Issues Sales, American Chemical Society, 1155 Sixteenth Street, N.W., Washington, DC 20036.)

This is the sixth volume on terpenoids and steroids in a valuable series first published 5 years ago. The aim of each series of Specialist Periodical Reports is to provide a systematic, comprehensive, and critical review of progress in the major areas of chemical research. The various series, which now total 35, are being published annually or bienially on such topics as Environmental Chemistry; Biosynthesis; Foreign Compound Metabolism in Mammals; The Alkaloids; Carbohydrate Chemistry; Amino-acids, Peptides, and Proteins; and Photochemistry.

This volume does not contain a subject index but is organized in a systematic manner which facilitates finding any information being sought. The six pages in the Table of Contents outline this volume in detail. The chapters are divided into many sections, which are identified in boldface type in the text as well as in the Table of Contents. These sections are further divided into subsections. Chapter titles are found at the top of every second page of the text. The author index of 3500 names is helpful to those following the research of a given individual.

This review is illustrated with drawings of 2100 chemical structures. It is documented with 1850 references, most of which are listed at the bottom of the first page of each chapter where cited.

Part I, which covers the terpenoids, is divided into chapters including Monoterpenoids, Sesquiterpenoids, Diterpenoids, Triterpenoids, Carotenoids and Polyterpenoids, and Biosynthesis of Terpenoids and Steroids. Part II, which covers steroids, is divided into two large chapters entitled Steroid Properties and Reactions, and Steroid Synthesis. No compilation of references to review articles on subjects related to terpenoids or steroids is included in this volume as in previous volumes.

The chapter on Steroid Properties and Reactions is divided into sections based upon more common functional groups, a section on Compounds of Nitrogen and Sulfur, and sections on such important subjects as Photochemical Reactions, Molecular Rearrangements, and Functionalization of Non-activated Positions. The chapter on Steroid Synthesis is divided into the following sections: Total Synthesis, Halogenosteroids, Oestranes, Androstanes, Pregnanes, Seco-steroids, Cholestane and Analogues, Steroidal Insect and Plant Hormones, Steroidal Alkaloids, Sapogenins, Cardenolides, and Bufadienolides.

The editor and 11 reporters who prepared this volume are to be commended for maintaining the high standards set by the previous volumes in this series. Everyone interested in the chemistry of terpenoids and/or steroids should have access to this volume and others in the series. They are great timesavers and sources of new ideas. I highly recommend this series.

Reviewed by Norman J. Doorenbos
School of Pharmacy
University of Mississippi
University, MS 38677

Progress in Toxicology. Special Topics. Vol. 2. By GERHARD ZBINDEN. Springer-Verlag, 175 Fifth Ave., New York, NY 10010, 1976. 117 pp. 18 × 26 cm. Price $7.40.

The cuisine of Zbinden's second book on special topics in toxicology is based on experience, sound reasoning, good common sense, a pinch of humor, and clear expression of realistic idealism. Is toxicology really too serious a matter to be left to the toxicologists? Read the book and answer the question yourself. Then read "How Safe is Safe?," available from the National Academy of Sciences. In a rather brief but informative manner, Zbinden covers in 93 pages (not including references and index) some of the most important problems confronting toxicology and related sciences but in a rather unusual manner. For example, he relates his son's experience with a gum ball machine, indicating that his son may put in two nickels and get nothing but doesn't give up until he finds out why or gets his two nickels back! "Why then does a negative response to a drug not elicit from us a similar anger?" More attention is paid to side-effects than negative medication responses. Zbinden then goes on to demonstrate the role of urinary pH as a factor in accelerated drug excretion and negative medication responses.

He discusses percutaneous drug permeation, hyperglycemia, the glutathione story, a new disease (pseudolupus), drug-induced lipidosis, the magnitude of drug combinations, drug interactions, and the growing problem (?) of health hazards from colors. In his discussion of food, drug, and cosmetic colors, he points out that the number of colors permitted in foods varies from country to country; *i.e.*, Australia permits seven synthetic and six natural dyes, and the United Kingdom permits 22 and 23, respectively. All other countries are somewhere inbetween. In this section, Zbinden also deletes expletives!

I personally enjoy reading anything that Zbinden writes (in English!) and don't hesitate to recommend this book to all concerned with toxicity, toxicology, and human health. I hope that Zbinden continues to write because what he says affords sound advice for those dealing with the naive.

Reviewed by Charles L. Winek
School of Pharmacy
Duquesne University
Pittsburgh, PA 15219

Journal of Pharmaceutical Sciences

MAY 1977

VOLUME 66 NUMBER 5

MARY H. FERGUSON
Editor

L. LUAN CORRIGAN
Assistant Editor

SHELLY ELLIOTT
Production Editor

JANET D. SHOFF
Copy Editor

EDWARD G. FELDMANN
Contributing Editor

SAMUEL W. GOLDSTEIN
Contributing Editor

EDITORIAL ADVISORY BOARD

JOHN AUTIAN	HARRY B. KOSTENBAUDER
NORMAN R. FARNSWORTH	HERBERT A. LIEBERMAN
WILLIAM O. FOYE	DAVID E. MANN, JR.
WILLIAM J. JUSKO	GERALD J. PAPARIELLO

The *Journal of Pharmaceutical Sciences* is published monthly by the American Pharmaceutical Association at 2215 Constitution Ave., N.W., Washington, DC 20037. Second-class postage paid at Washington, D.C., and at additional mailing office.

All expressions of opinion and statements of supposed fact appearing in articles or editorials carried in this journal are published on the authority of the writer over whose name they appear and are not to be regarded as necessarily expressing the policies or views of the American Pharmaceutical Association.

Offices—Editorial, Advertising, and Subscription Offices: 2215 Constitution Ave., N.W., Washington, DC 20037. Printing Offices: 20th & Northampton Streets, Easton, PA 18042.

Annual Subscriptions—United States and foreign, industrial and government institutions $50, educational institutions $50, individuals *for personal use only* $30; single copies $5. All foreign subscriptions add $5 for postage. Subscription rates are subject to change without notice. Members of the American Pharmaceutical Association may elect to receive the *Journal of Pharmaceutical Sciences* as a part of their annual $60 (foreign $65) APhA membership dues.

Claims—Missing numbers will not be supplied if dues or subscriptions are in arrears for more than 60 days or if claims are received more than 60 days after the date of the issue, or if loss was due to failure to give notice of change of address. The Association cannot accept responsibility for foreign delivery when its records indicate shipment has been made.

Change of Address—Members and subscribers should notify at once both the Post Office and the American Pharmaceutical Association, 2215 Constitution Ave., N.W., Washington, DC 20037, of any change of address.

© Copyright 1977, American Pharmaceutical Association, 2215 Constitution Ave., N.W., Washington, DC 20037; all rights reserved.

IMPEDING METRIC CONVERSION

For many years, this writer had served as a self-styled good will ambassador for the metric system. Whenever the subject happened to be discussed with family, friends, or professional acquaintances, we always talked up the merits of the system and the desirability of the United States converting *in toto* to its use.

Moreover, we felt very comfortable in doing so. The metric system is "the system" of the physical and biological sciences; it is "the system" of pharmacy; it is officially endorsed as "the system" by the American Pharmaceutical Association. Hence, by training, background, career, and affiliation, we were in concert with the metric theme. Indeed, we even had several occasions to participate as a witness in presenting testimony before U.S. Congressional committees which were hearing bills dealing with national conversion to the metric system.

On all these occasions, we have repeated what so many others have said in arguing the merits of such conversion; namely, we would be adopting a pure, uniform, and simple system which can be easily learned and, once learned, will remain unchanged forever.

But then some unsettling things began to happen. The first hint that all may not be quite as rosy as we thought was when the controversy arose over whether the preferred unit of volume was a "cubic centimeter" (cc) or a "milliliter" (ml). After what seemed to be a good deal of haggling, this was eventually settled with the result that much revising was necessary in style books, in texts, in calibrations on laboratory equipment, and in the labeling on numerous containers, particularly those of chemicals and drugs.

Then one day the local weather report began to give temperatures in terms of degrees celsius rather than the familiar degrees centigrade. And when we could not immediately explain the difference to our children, we suffered both embarrassment as well as a blow to our personal credibility.

We hardly had time to track this one down when we learned that the presses must be halted for our publications in order that the typesetters could scurry about changing all the "microns" to "micrometers" and the "millimicrons" to "nanometers"—along with corresponding changes in the symbols and abbreviations used in their stead.

What was happening? Why were these and other changes like them being made? Was no one else distressed and disturbed by what to us appeared to be a series of confusing, pointless, and disturbing disruptions?

Well, in the letters column of a recent issue of the American Chemical Society's publication, *Chemical and Engineering News*, we learned that there is at least one fellow sufferer. Dean W. Gibbons of Detroit wrote about his experience trying to keep up with such changes as those mentioned above, as well as a number of others including "torr" to honor Torricelli, the inventor of the barometer, and "kilopascals," presumably in honor of Pascal and his law of the pressure-volume relationship.

"There are better ways to honor our scientific forefathers than to rename familiar metric units," writes Gibbons. And he goes on to add: *"Public acceptance of the metric system will depend on whether the system is perceived as simple and logical, or regarded as a jumble of confusion. The use of long-established, descriptive units, instead of the latest fads, will aid the transition from the English to the metric system."*

His point is both well taken and well stated. Hopefully, the scientific community is more stable and sedate than the local town officials who will rename Main Street at the drop of a hat to honor—for political reasons—some celebrity or other public figure who is currently in the news.

Those of us who deal with measurement terms and their symbols on a daily basis have difficulty enough remembering which is what, and which is correct. For the general public to cope with such changes is simply asking too much. We hope that the scientists responsible for initiating such changes will recognize that they are doing a real disservice by needlessly impeding the process of metric conversion.

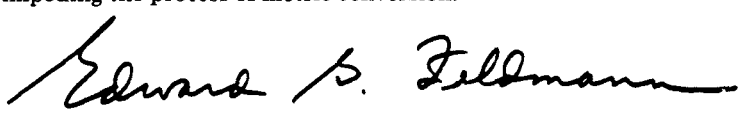

Journal of Pharmaceutical Sciences

JUNE 1977

VOLUME 66 NUMBER 6

MARY H. FERGUSON
Editor

SHELLY ELLIOTT
Production Editor

JANET D. SHOFF
Copy Editor

EDWARD G. FELDMANN
Contributing Editor

SAMUEL W. GOLDSTEIN
Contributing Editor

DAVID BOHARDT
Acting Director of Publications

L. LUAN CORRIGAN
Assistant Director of Publications

EDITORIAL ADVISORY BOARD

JOHN AUTIAN
NORMAN R. FARNSWORTH
WILLIAM O. FOYE
WILLIAM J. JUSKO
HARRY B. KOSTENBAUDER
HERBERT A. LIEBERMAN
DAVID E. MANN, JR.
GERALD J. PAPARIELLO

The *Journal of Pharmaceutical Sciences* is published monthly by the American Pharmaceutical Association at 2215 Constitution Ave., N.W., Washington, DC 20037. Second-class postage paid at Washington, D.C., and at additional mailing office.

All expressions of opinion and statements of supposed fact appearing in articles or editorials carried in this journal are published on the authority of the writer over whose name they appear and are not to be regarded as necessarily expressing the policies or views of the American Pharmaceutical Association.

Offices—Editorial, Advertising, and Subscription Offices: 2215 Constitution Ave., N.W., Washington, DC 20037. Printing Offices: 20th & Northampton Streets, Easton, PA 18042.

Annual Subscriptions—United States and foreign, industrial and government institutions $50, educational institutions $50, individuals *for personal use only* $30; single copies $5. All foreign subscriptions add $5 for postage. Subscription rates are subject to change without notice. Members of the American Pharmaceutical Association may elect to receive the *Journal of Pharmaceutical Sciences* as a part of their annual $60 (foreign $65) APhA membership dues.

Claims—Missing numbers will not be supplied if dues or subscriptions are in arrears for more than 60 days or if claims are received more than 60 days after the date of the issue, or if loss was due to failure to give notice of change of address. The Association cannot accept responsibility for foreign delivery when its records indicate shipment has been made.

Change of Address—Members and subscribers should notify at once both the Post Office and the American Pharmaceutical Association, 2215 Constitution Ave., N.W., Washington, DC 20037, of any change of address.

© Copyright 1977, American Pharmaceutical Association, 2215 Constitution Ave., N.W., Washington, DC 20037; all rights reserved.

HAS JUSTICE BEEN SERVED?

As this column is being written, the "blue ribbon" investigative body known as the HEW Review Panel on New Drug Regulation is in the last stages of winding down its two-year plus period of existence. At least, it appears to be approaching its final demise. The group has had a long history of twelfth-hour reprieves and extensions, each coming when the Panel's life previously seemed to be terminating.

From its inception, this Review Panel has been one of the most puzzling and curious activities to hit the Washington scene in a long time.

Its formation was originally announced by former HEW Secretary Caspar W. Weinberger on March 28, 1975, principally for the purpose of reviewing the allegations by a group of disgruntled Food and Drug Administration employees of FDA misconduct in the area of approval of New Drug Applications. These dissidents had publicly charged that NDA review procedures were improperly administered by agency officials sympathetic to the drug industry, and that any efforts by FDA staff members to be objective were met with abuse, retaliation, and harassment.

If such charges had been made by only a couple of employees, they might have been dismissed as nothing more than commonplace employee disenchantment and exaggeration. However, at least a score of medical scientists openly voiced such grievances. Hence, a full investigation was in order.

But immediately, even at its inception, the Panel got off to a peculiar start. Rather than confining its purpose to a review of the allegations of the dissident employees, the Panel embarked upon a broad scale review of the entire FDA operation, the entire concept of the drug approval process, the complete philosophy of FDA objectives and management, and more. The charge given the Panel was sufficiently broad that the Panel—rightly or wrongly—chose to interpret it as so sweeping as to encompass every aspect of FDA activity, involvement, and responsibility.

Subsequently, the Panel has had a turbulent and rocky history—within its own operation, in its relation with the HEW hierarchy, and in its purposeful adversary stance *versus* the FDA.

Its original Chairman drastically dissented from the views of the Panel majority and then resigned. The initial Executive Secretary resigned because of discord with the Panel, and several successors followed in as many months. Testimony presented during Panel hearings ranged from the bizarre to the incredulous and included a "true confessions" inside view of daily conduct in the FDA's Bureau of Drugs. Staff written reports were prepared in secret, circulated confidentially, discussed in open session, and then rejected by the Panel. The FDA Commissioner was obliged to prepare a defense in the form of a report running thirteen chapters and several hundred pages and which, in turn, was subjected by the Panel to a page-by-page, point-by-point dissection and rejection. A 765-page report prepared by the Panel's special legal counsel included a recommendation for both criminal and disciplinary actions against several former and present FDA officials.

But despite its sordid operation, the Panel has worked and produced. Full meetings have been held on a regular monthly basis, lengthy interim reports have been issued on each of the many subjects reviewed by the Panel, related documents such as announcements and meeting minutes have flowed promptly and consistently from the staff office, and a series of meaningful recommendations has ultimately emanated from the Panel's deliberations.

But now that the whole operation is about to conclude, we asked ourselves: Was it all worthwhile? What was accomplished? Were the complaints of the employees which triggered the entire operation adequately dealt with and satisfactorily resolved?

In all candor, we find it hard to say. And, judging by the ambivalence of virtually all other press reports we have read relating to the Panel, it appears that other observers of the Washington scene are experiencing similar difficulty in making judgments.

In many respects, this Review Panel operation reminds us of the various President Kennedy assassination inquiries which have been similarly intense, controversial, and, yet, unfulfilling in that few real answers have been provided. In fact, whatever satisfaction has been realized is probably the result of the catharsis effect derived from engaging in this lengthy and abrasive inquiry. Only time and history will ultimately determine if the result was worth the effort.

—EGF

Journal of Pharmaceutical Sciences

JUNE 1977

VOLUME 66 NUMBER 6

MARY H. FERGUSON
Editor

SHELLY ELLIOTT
Production Editor

JANET D. SHOFF
Copy Editor

EDWARD G. FELDMANN
Contributing Editor

SAMUEL W. GOLDSTEIN
Contributing Editor

DAVID BOHARDT
Acting Director of Publications

L. LUAN CORRIGAN
Assistant Director of Publications

EDITORIAL ADVISORY BOARD

JOHN AUTIAN
NORMAN R. FARNSWORTH
WILLIAM O. FOYE
WILLIAM J. JUSKO
HARRY B. KOSTENBAUDER
HERBERT A. LIEBERMAN
DAVID E. MANN, JR.
GERALD J. PAPARIELLO

The *Journal of Pharmaceutical Sciences* is published monthly by the American Pharmaceutical Association at 2215 Constitution Ave., N.W., Washington, DC 20037. Second-class postage paid at Washington, D.C., and at additional mailing office.

All expressions of opinion and statements of supposed fact appearing in articles or editorials carried in this journal are published on the authority of the writer over whose name they appear and are not to be regarded as necessarily expressing the policies or views of the American Pharmaceutical Association.

Offices—Editorial, Advertising, and Subscription Offices: 2215 Constitution Ave., N.W., Washington, DC 20037. Printing Offices: 20th & Northampton Streets, Easton, PA 18042.

Annual Subscriptions—United States and foreign, industrial and government institutions $50, educational institutions $50, individuals *for personal use only* $30; single copies $5. All foreign subscriptions add $5 for postage. Subscription rates are subject to change without notice. Members of the American Pharmaceutical Association may elect to receive the *Journal of Pharmaceutical Sciences* as a part of their annual $60 (foreign $65) APhA membership dues.

Claims—Missing numbers will not be supplied if dues or subscriptions are in arrears for more than 60 days or if claims are received more than 60 days after the date of the issue, or if loss was due to failure to give notice of change of address. The Association cannot accept responsibility for foreign delivery when its records indicate shipment has been made.

Change of Address—Members and subscribers should notify at once both the Post Office and the American Pharmaceutical Association, 2215 Constitution Ave., N.W., Washington, DC 20037, of any change of address.

© Copyright 1977, American Pharmaceutical Association, 2215 Constitution Ave., N.W., Washington, DC 20037; all rights reserved.

HAS JUSTICE BEEN SERVED?

As this column is being written, the "blue ribbon" investigative body known as the HEW Review Panel on New Drug Regulation is in the last stages of winding down its two-year plus period of existence. At least, it appears to be approaching its final demise. The group has had a long history of twelfth-hour reprieves and extensions, each coming when the Panel's life previously seemed to be terminating.

From its inception, this Review Panel has been one of the most puzzling and curious activities to hit the Washington scene in a long time.

Its formation was originally announced by former HEW Secretary Caspar W. Weinberger on March 28, 1975, principally for the purpose of reviewing the allegations by a group of disgruntled Food and Drug Administration employees of FDA misconduct in the area of approval of New Drug Applications. These dissidents had publicly charged that NDA review procedures were improperly administered by agency officials sympathetic to the drug industry, and that any efforts by FDA staff members to be objective were met with abuse, retaliation, and harassment.

If such charges had been made by only a couple of employees, they might have been dismissed as nothing more than commonplace employee disenchantment and exaggeration. However, at least a score of medical scientists openly voiced such grievances. Hence, a full investigation was in order.

But immediately, even at its inception, the Panel got off to a peculiar start. Rather than confining its purpose to a review of the allegations of the dissident employees, the Panel embarked upon a broad scale review of the entire FDA operation, the entire concept of the drug approval process, the complete philosophy of FDA objectives and management, and more. The charge given the Panel was sufficiently broad that the Panel—rightly or wrongly—chose to interpret it as so sweeping as to encompass every aspect of FDA activity, involvement, and responsibility.

Subsequently, the Panel has had a turbulent and rocky history—within its own operation, in its relation with the HEW hierarchy, and in its purposeful adversary stance *versus* the FDA.

Its original Chairman drastically dissented from the views of the Panel majority and then resigned. The initial Executive Secretary resigned because of discord with the Panel, and several successors followed in as many months. Testimony presented during Panel hearings ranged from the bizarre to the incredulous and included a "true confessions" inside view of daily conduct in the FDA's Bureau of Drugs. Staff written reports were prepared in secret, circulated confidentially, discussed in open session, and then rejected by the Panel. The FDA Commissioner was obliged to prepare a defense in the form of a report running thirteen chapters and several hundred pages and which, in turn, was subjected by the Panel to a page-by-page, point-by-point dissection and rejection. A 765-page report prepared by the Panel's special legal counsel included a recommendation for both criminal and disciplinary actions against several former and present FDA officials.

But despite its sordid operation, the Panel has worked and produced. Full meetings have been held on a regular monthly basis, lengthy interim reports have been issued on each of the many subjects reviewed by the Panel, related documents such as announcements and meeting minutes have flowed promptly and consistently from the staff office, and a series of meaningful recommendations has ultimately emanated from the Panel's deliberations.

But now that the whole operation is about to conclude, we asked ourselves: Was it all worthwhile? What was accomplished? Were the complaints of the employees which triggered the entire operation adequately dealt with and satisfactorily resolved?

In all candor, we find it hard to say. And, judging by the ambivalence of virtually all other press reports we have read relating to the Panel, it appears that other observers of the Washington scene are experiencing similar difficulty in making judgments.

In many respects, this Review Panel operation reminds us of the various President Kennedy assassination inquiries which have been similarly intense, controversial, and, yet, unfulfilling in that few real answers have been provided. In fact, whatever satisfaction has been realized is probably the result of the catharsis effect derived from engaging in this lengthy and abrasive inquiry. Only time and history will ultimately determine if the result was worth the effort.

—EGF

Journal of Pharmaceutical Sciences

JUNE 1977
VOLUME 66 NUMBER 6

RESEARCH ARTICLES

New Method for Characterizing Dissolution Properties of Drug Powders

PETER VENG PEDERSEN

Abstract □ Various multiparticulate dissolution models that assume a log-normal particle-size distribution are fitted by nonlinear least-squares regression to data from the dissolution of micronized glyburide. Estimates of parameters describing the effective initial particle-size distribution are obtained, together with estimates of the specific dissolution rate parameter. A dissolution equation based on an ideal, untruncated, log-normal distribution, with the single particles dissolving according to the Hixson–Crowell cube root law, is the best model. The dissolution behavior of glyburide can be well described by this model in terms of the specific dissolution rate parameter and one other parameter accounting for the distribution effect. The estimation of these two parameters represents a more exact way of describing the dissolution characteristics of drug powders than previous approaches. The method should be of interest in the quality control of drugs that may cause bioavailability problems because of dissolution rate-limited absorption.

Keyphrases □ Dissolution—micronized glyburide, various multiparticulate models fit to data, rate and size distribution parameters evaluated □ Powders—micronized glyburide, various multiparticulate models fit to dissolution data, rate and size distribution parameters evaluated □ Glyburide, micronized—dissolution, various multiparticulate models fit to data, rate and size distribution parameters evaluated

The dissolution behavior of a multiparticulate system is determined by the single-particle dissolution behavior and the particle-size distribution (1, 2). Dissolution profiles have been related to the initial particle-size distribution (3, 4). However, the mathematical models used to account for the size distribution effect were not exact but were based on empirical approximations.

A previous paper (5) showed good agreement between the theoretical dissolution profile based on a rigorous mathematical treatment and dissolution data for tolbutamide. The present paper evaluates some kinetic models for multiparticulate dissolution by fitting them to data from the dissolution of micronized glyburide. This method represents a new and better approach for characterizing the dissolution behavior of powders by evaluating both rate and size distribution parameters. The method should be of value in quality control measurements of slightly soluble pure drugs that can cause bioavailability problems.

THEORY

Consider a multiparticulate dissolution where the single particles dissolve according to the Hixson–Crowell (6) cube root law or the Niebergall *et al.* (7) square root law, which can be written in a common form as:

$$w^{1/m} = w_0^{1/m} - k_m t \qquad \text{(Eq. 1)}$$

where $m = 3$ for the cube root law and $m = 2$ for the square root law[1].

Let the initial effective particle diameters, a_0, be log normally distributed, *i.e.*, have a frequency distribution that is well approximated by the following density distribution (2):

$$\mu(\ln a_0) = \frac{N(\ln a_0,\mu,\sigma)}{\int_{\ln a_0=\mu-i\sigma}^{\ln a_0=\mu+j\sigma} N(\ln a_0,\mu,\sigma)d\ln a_0} \qquad \text{(Eq. 2)}$$

for $\mu - i\sigma \leq \ln a_0 \leq \mu + j\sigma$ where i and j are the lower and upper truncation parameters (Fig. 1), and N is the normal density function defined by:

$$N(x,\mu,\sigma) = \frac{1}{\sigma\sqrt{2\pi}} e^{-\frac{1}{2}\left(\frac{x-\mu}{\sigma}\right)^2} \qquad \text{(Eq. 3)}$$

The dissolution of such a multiparticulate powder is described by (2):

$$\frac{W}{W_0} = \sum_{n=0}^{m} \binom{m}{n} (-K_m t)^{(m-n)} \times \frac{F\left(\frac{T_2-\mu}{\sigma} - \frac{3n\sigma}{m}\right) - F\left(\frac{T_1-\mu}{\sigma} - \frac{3n\sigma}{m}\right)}{F(j-3\sigma) - F(-i-3\sigma)} e^{3(n-m)\{\mu+3(n+m)\sigma^2/2m\}/m} \qquad \text{(Eq. 4)}$$

[1] The positive constants k_3 ($m = 3$) and k_2 ($m = 2$) are used for simplicity to replace the coefficients of time that contain quantities such as density, the diffusion coefficient, and the shape factor, which are considered constant.

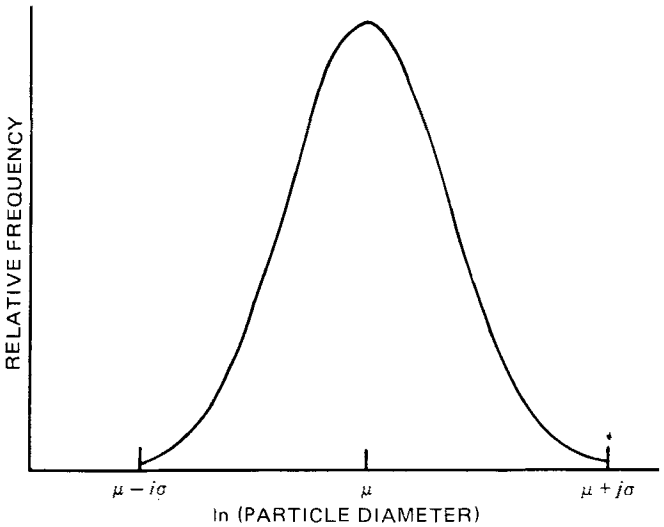

Figure 1—*Illustration of the initial (t = 0) particle-size distribution parameters, μ, σ, i, and j, of a log-normal powder. The approximating distribution function shown is defined in Eq. 2. The initial diameters, a_0, are diameters of hypothetical spherical particles that approximate the dissolution behavior of the real nonspherical particles. The dimensionless distribution shape parameters, i, j, and σ, can be estimated from the dissolution profile (Figs. 3–6) by nonlinear least-squares regression analysis (Table I). The scale parameter, μ, cannot be determined.*

where W/W_0 is the fraction of undissolved powder at time t, F is the cumulative standard normal distribution function defined by:

$$F(x) = \frac{1}{\sqrt{2\pi}} \int_{-\infty}^{x} e^{-x^2/2}\, dx \qquad \text{(Eq. 5)}$$

T_1 and T_2 are given by:

$$T_1 = \mu - i\sigma \qquad \text{for } \frac{m}{3}\ln(K_m t) < \mu - i\sigma \qquad \text{(Eq. 6)}$$

$$T_1 = \frac{m}{3}\ln(K_m t) \qquad \text{for } \frac{m}{3}\ln(K_m t) \geq \mu - i\sigma \qquad \text{(Eq. 7)}$$

$$T_2 = \mu + j\sigma \qquad \text{for } \frac{m}{3}\ln(K_m t) < \mu + j\sigma \qquad \text{(Eq. 8)}$$

$$T_2 = \frac{m}{3}\ln(K_m t) \qquad \text{for } \frac{m}{3}\ln(K_m t) \geq \mu + j\sigma \qquad \text{(Eq. 9)}$$

and:

$$\binom{m}{n} = \frac{m!}{(m-n)!n!} \qquad \text{(Eq. 10)}$$

If the particles are spherical, K_m is related to k_m by:

$$K_m = (6/\rho\pi)^{1/m} k_m \qquad \text{(Eq. 11)}$$

Equation 4 appears to contain five parameters, namely, σ, i, j, μ, and K_m, which define the dissolution profile (W/W_0 *versus* time). However, an attempt to obtain least-squares estimates of all five parameters from W/W_0 *versus* time data may fail, because μ and K_m can be fused into a single rate parameter:

$$K_m^* = e^{-3\mu/m} K_m \qquad \text{(Eq. 12)}$$

which will be called the specific dissolution rate parameter.

The uniqueness of these four parameters, σ, i, j, and K_m^*, in defining the dissolution profile can be seen by substituting $K_m = e^{3\mu/m}K_m^*$ into Eq. 4, resulting in total cancellation of μ, in full agreement with the theory discussed previously (2):

$$\frac{W}{W_0} = \sum_{n=0}^{m} \binom{m}{n} (-K_m^* t)^{(m-n)} \frac{F\left(j - \frac{3n\sigma}{m}\right) - A}{F(j - 3\sigma) - F(-i - 3\sigma)} e^{2[(n/m)^2 - 1]\sigma^2/9} \qquad \text{(Eq. 13)}$$

where:

$$A = F\left(-i - \frac{3n\sigma}{m}\right) \qquad \text{for } t < \frac{1}{K_m^*} e^{-3i\sigma/m} \qquad \text{(Eq. 14)}$$

and:

$$A = F\left[\frac{m}{3\sigma}\ln(K_m^* t) - \frac{3n\sigma}{m}\right] \qquad \text{for } \frac{1}{K_m^*} e^{3j\sigma/m} > t > \frac{1}{K_m^*} e^{-3i\sigma/m} \qquad \text{(Eq. 15)}$$

and:

$$\frac{W}{W_0} = 0 \qquad \text{for } t \geq \frac{1}{K_m^*} e^{3j\sigma/m} \qquad \text{(Eq. 16)}$$

The continuously recording flow-through dissolution apparatus used provides dissolution rate data. The fraction undissolved, W/W_0, *versus* time can be obtained by integrating these data (5). The parameters σ, i, j, and K_m^* can then be estimated by nonlinear least-squares regression analysis using Eq. 13. However, the integrated data contain integration errors. The integration also tends to "smooth" the original data, so estimates of the variability of the parameters will be less reliable than if the original rate data were used. Therefore, it is useful to derive an expression for the release rate to estimate the four parameters directly from the original (rate) data.

By applying Eq. 13*a* of Ref. 1, the following equation (similar to Eq. A2 in the same reference) is obtained:

$$\frac{W}{W_0} = \frac{\int_{R_1}^{R_2} (x^{3/m} - K_m t)^m x^{-1} N(\ln x, \mu, \sigma)\, dx}{\int_{d_0}^{D_0} x^2 N(\ln x, \mu, \sigma)\, dx} \qquad \text{(Eq. 17)}$$

where:

$$d_0 = e^{\mu - i\sigma} \qquad \text{(Eq. 18)}$$

$$D_0 = e^{\mu + j\sigma} \qquad \text{(Eq. 19)}$$

$$R_1 = d_0 \qquad \text{for } K_m t < d_0^{3/m} \qquad \text{(Eq. 20)}$$

$$R_1 = (K_m t)^{m/3} \qquad \text{for } K_m t \geq d_0^{3/m} \qquad \text{(Eq. 21)}$$

$$R_2 = D_0 \qquad \text{for } K_m t < D_0^{3/m} \qquad \text{(Eq. 22)}$$

$$R_2 = (K_m t)^{m/3} \qquad \text{for } K_m t \geq D_0^{3/m} \qquad \text{(Eq. 23)}$$

An expression for the dissolution rate of drug, $Q = -dW/dt$, can now be found by differentiating Eq. 17 with respect to time (using Leibnitz's rule). For abbreviation, let B denote the (constant) denominator of Eq. 17; differentiation then gives:

$$\frac{B}{W_0} Q = mK_m \int_{R_1}^{R_2} (x^{3/m} - Kt)^{(m-1)} x^{-1} N(\ln x, \mu, \sigma)\, dx - (R_2^{3/m} - K_m t)^m R_2^{-1} N(\ln R_2, \mu, \sigma) \frac{dR_2}{dt} + (R_1^{3/m} - K_m t)^m R_1^{-1} N(\ln R_1, \mu, \sigma) \frac{dR_1}{dt} \qquad \text{(Eq. 24a)}$$

Before the critical time[2], $R_1 = d_0$ and $R_2 = D_0$, so $dR_1/dt = dR_2 dt = 0$ and the last two terms of the right-hand side of Eq. 24*a* vanish. After the critical time, dR_2/dt is still zero, but $R_1 = (K_m t)^{m/3}$ (according to Eq. 21). Thus, the last term also vanishes because:

$$R_1^{3/m} - K_m t = [(K_m t)^{m/3}]^{3/m} - K_m t = 0 \qquad \text{(Eq. 24b)}$$

Equation 24*a* can be simplified to:

$$Q = mK_m W_0 \frac{\int_{R_1}^{R_2} (x^{3/m} - K_m t)^{(m-1)} x^{-1} N(\ln x, \mu, \sigma)\, dx}{\int_{d_0}^{D_0} x^2 N(\ln x, \mu, \sigma)\, dx} \qquad \text{(Eq. 25)}$$

The term $(x^{3/m} - K_m t)^{(m-1)} x^{-1}$ under the integral sign can be expanded:

$$(x^{3/m} - K_m t)^{(m-1)} x^{-1} = x - 2K_3 t + (K_3 t)^2 x^{-1} \qquad \text{(for } m = 3\text{)} \qquad \text{(Eq. 26)}$$

$$(x^{3/m} - K_m t)^{(m-1)} x^{-1} = x^{1/2} - K_2 t x^{-1} \qquad \text{(for } m = 2\text{)} \qquad \text{(Eq. 27)}$$

and a formula given previously (Eq. A3 of Ref. 1) can be applied to express the integrals in Eq. 25 in terms of the function F (Eq. 5). This process leads to the following expression for Q that can be evaluated more readily

[2] The critical time is the time when the first particles start disappearing in the dissolution process, *i.e.*, $t = (1/K_m)e^{3/m(\mu - i\sigma)}$.

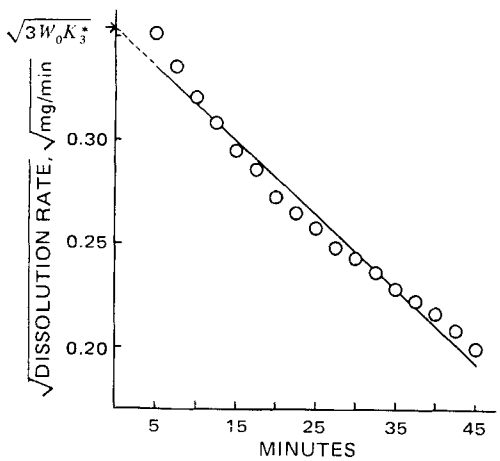

Figure 2—*Illustration of a graphic method for obtaining an initial estimate of the specific dissolution rate parameter, K_m^*, from rate data from the dissolution of 5 mg of micronized glyburide. Equation 39 predicts a linear relationship between $\sqrt{Q}$ and t for a monodisperse powder in which the single particles dissolve according to the cube root law (Eq. 1, m = 3). The deviation from linearity in the graph is caused by the particle-size distribution effect.*

and exactly than Eq. 25:

$$Q = mK_mW_0 \sum_{n=0}^{(m-1)} \binom{m-1}{n} (-K_mt)^{(m-n-1)} \times \frac{F\left(\frac{T_2-\mu}{\sigma} - \frac{3n\sigma}{m}\right) - F\left(\frac{T_1-\mu}{\sigma} - \frac{3n\sigma}{m}\right)}{F(j-3\sigma) - F(-i-3\sigma)} e^{3(n-m)[\mu+3(n+m)\sigma^2/2m]/m} \quad \text{(Eq. 28)}$$

where T_1 and T_2 are as defined previously (Eqs. 6–9).

This expression for the dissolution rate, Q, contains five parameters (σ, i, j, μ, and K_m). However, as before (Eq. 13), only four parameters (σ, i, j, and K_m^*) are needed to define uniquely the dissolution rate profile:

$$Q = mK_m^*W_0 \sum_{n=0}^{(m-1)} \binom{m-1}{n} (-K_m^*t)^{(m-n-1)} \times \frac{F\left(j - \frac{3n\sigma}{m}\right) - A}{F(j-3\sigma) - F(-i-3\sigma)} e^{9[(n/m)^2-1]\sigma^2/2} \quad \text{(Eq. 29)}$$

This equation is the differential form of Eq. 13.

The quantity A is as defined previously (Eqs. 14 and 15) and $Q = 0$ for $t \geq (1/K_m^*)\, e^{3j\sigma/m}$. This expression is valuable since it allows the effective initial particle-size distribution parameters, σ, i, and j, to be determined together with the specific dissolution rate parameter, K_m^*, by nonlinear regression analysis of the dissolution rate profile (dW/dt *versus* time).

It is also of interest to investigate how well the dissolution behavior can be described if the particle-size distribution is considered ideal, *i.e.*, if $i = j = \infty$. With $F(\infty) = 1$ and $F(-\infty) = 0$, Eq. 29 becomes, for an ideal distribution:

$$Q = mK_m^*W_0 \sum_{n=0}^{(m-1)} \binom{m-1}{n} (-K_m^*t)^{(m-n-1)} \times \left\{1 - F\left[\frac{m}{3\sigma}\ln(K_m^*t) - \frac{3n\sigma}{m}\right]\right\} e^{9[(n/m)^2-1]\sigma^2/2} \quad \text{(Eq. 30)}$$

If the distribution is considered ideal at the lower end ($i = \infty$) but truncated at the higher end, the expression becomes:

$$Q = mK_m^*W_0 \sum_{n=0}^{(m-1)} \binom{m-1}{n} (-K_m^*t)^{(m-n-1)} \times \frac{F\left(j - \frac{3n\sigma}{m}\right) - F\left[\frac{m}{3\sigma}\ln(K_m^*t) - \frac{3n\sigma}{m}\right]}{F(j-3\sigma)} e^{9[(n/m)^2-1]\sigma^2/2} \quad \text{(Eq. 31)}$$

and if it is considered truncated at the lower end but not at the higher end ($j = \infty$):

$$Q = mK_m^*W_0 \sum_{n=0}^{(m-1)} \binom{m-1}{n} (-K_m^*t)^{(m-n-1)} \times \frac{1-A}{1-F(-i-3\sigma)} e^{9[(n/m)^2-1]\sigma^2/2} \quad \text{(Eq. 32)}$$

Discussion of the limiting case where the particle-size distribution is infinitely narrow, *i.e.*, $\sigma = 0$, allows a better understanding of the specific dissolution rate parameter, K_m^*. It also provides a method of obtaining a suitable initial estimate of this parameter to use in nonlinear curve fitting.

When $\sigma = i = j = 0$, Eq. 29 becomes:

$$Q = mK_m^*W_0 \sum_{n=0}^{(m-1)} \binom{m-1}{n} (-K_m^*t)^{(m-n-1)} \quad \text{(Eq. 33)}$$

which can be written more simply as:

$$Q = -\frac{dW}{dt} = mK_m^*W_0(1 - K_m^*t)^{(m-1)} \quad \text{(Eq. 34)}$$

which, after integration, can be written:

$$\left(\frac{W}{W_0}\right)^{1/m} = 1 - K_m^*t \quad \text{(Eq. 35)}$$

As expected, since there is no size distribution effect (2), this equation predicts that the powder will dissolve strictly according to the cube root or square root law.

When the powder is monodisperse, $\mu = \ln a_0$ and Eq. 12 becomes:

$$K_m^* = e^{-(3/m)\ln a_0}K_m = a_0^{-3/m}K_m \quad \text{(Eq. 36)}$$

Equations 11 and 36 then give, for spherical particles[3]:

$$K_m^* = a_0^{-3/m}(6/\rho\pi)^{1/m}k_m = w_0^{-1/m}k_m \quad \text{(Eq. 37)}$$

When $k_m = w_0^{1/m} K_m^*$ (from Eq. 37) is inserted in Eq. 1:

$$\left(\frac{w}{w_0}\right)^{1/m} = 1 - K_m^*t \quad \text{(Eq. 38)}$$

A comparison of Eqs. 38 and 35 shows that, for a monodisperse powder, the specific dissolution rate parameter, K_m^*, is common to both multiparticulate (Eq. 35) and single-particle dissolutions (Eq. 38). It has the dimension of time^{-1} for both single-particle models ($m = 2$ and 3).

Equation 34 can be written:

$$Q^{1/(m-1)} = (mW_0K_m^*)^{1/(m-1)} - (mW_0)^{1/(m-1)}(K_m^*)^{m/(m-1)}t \quad \text{(Eq. 39)}$$

This equation can be used to obtain an initial estimate of K_m^* from the linear regression of $Q^{1/(m-1)}$ on t. In this way, the intercept value, $(mW_0K_m^*)^{1/(m-1)}$ ($t = 0$), divided by $(mW_0)^{1/(m-1)}$ gives $K_m^{*\,1/(m-1)}$ (Fig. 2).

EXPERIMENTAL

The high precision, flow-through, continuously recording dissolution apparatus used for the dissolution tests was described previously (5). Various amounts of micronized glyburide[4] were exposed in the dissolution cell to pH 7.25 phosphate buffer ($I = 0.05$) at a flow rate of 0.568 ml/sec (~ 0.149-cm/sec linear flow rate) and at a temperature of 37.5 ± 0.2°. Values of absorbance were read from the chart recording at 2.5-min intervals. The dissolution rate, Q, was then given as (volumetric flow rate) × (absorbance)/(absorption coefficient).

The accuracy of the rate data was checked by integration. The amount released, calculated in this way, agreed to within ±5% with the amount remaining in the dissolution cell at the end of the experiment (which was about 10% of the initial amount). The lower and upper limits for the nonlinear regression parameters used in the curve fitting were chosen as: σ = 0–1, K_m^* = 0–0.1, i = 0–10, and j = 0–10. The initial estimate for the rate parameter, K_m^*, was obtained graphically (Eq. 41 and Fig. 2).

RESULTS AND DISCUSSION

For a monodisperse powder, Eq. 39 predicts a linear relationship between $\sqrt{Q}$ and t when the single particles dissolve according to the cube root model ($m = 3$) and a linear relationship between Q and t when they dissolve according to the square root model ($m = 2$).

Significant deviations from linearity were observed when dissolution rate data for micronized glyburide were plotted in either of these ways (Figs. 2–6). Such deviations arise if the powder is not monodisperse or if the single particles do not dissolve according to the single-particle model (Eq. 1).

Under an electron microscope, the micronized glyburide used appeared to be considerably polydisperse. Therefore, the observed deviation from

[3] The derivation is also valid for nonspherical particles if the concept of spherical approximations (8) applies.

[4] Provided by Australian Hoechst Ltd., Sydney, Australia.

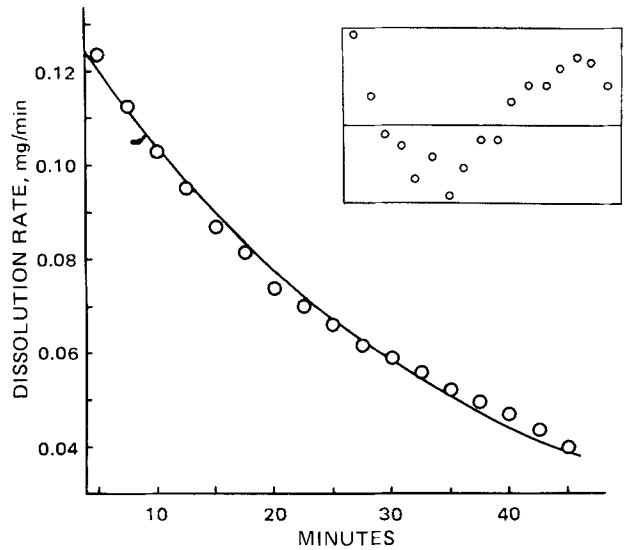

Figure 3—*Least-squares fit of the multiparticulate dissolution model (Eq. 30,* m = *3) to rate data from the dissolution of 5 mg of micronized glyburide. The model assumes that the effective initial particle-size distribution can be approximated by an ideal log-normal distribution* (i = j = ∞, *Fig. 1) and that the single particles dissolve according to the cube root model (Eq. 1,* m = *3). The inset graph shows a plot of the residuals* versus *time in arbitrary units.*

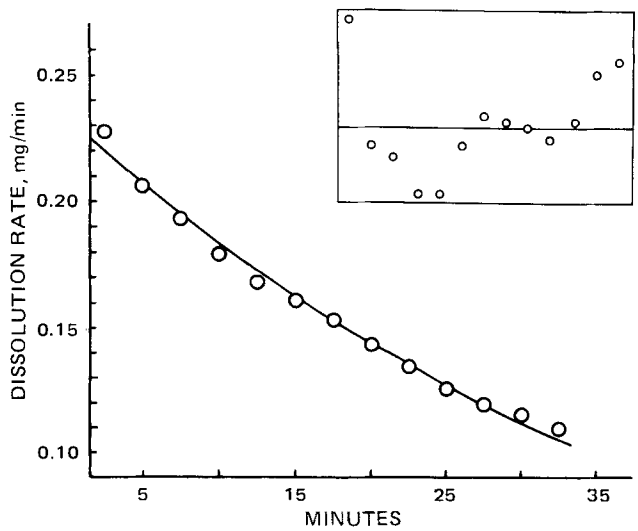

Figure 5—*Least-squares fit of the multiparticulate dissolution model (Eq. 30,* m = *3) to rate data from the dissolution of 10 mg of micronized glyburide. The model assumes that the effective initial particle-size distribution can be approximated by an ideal log-normal distribution* (i = j = ∞, *Fig. 1) and that the single particles dissolve according to the cube root model (Eq. 1,* m = *3). The inset graph shows a plot of the residuals* versus *time in arbitrary units.*

linearity in the rate plots can be explained as a particle-size distribution effect if Eq. 1 is assumed to be valid. However, the rate data can also be explained by other single-particle dissolution models in combination with a size distribution effect. Conclusions about the validity of a single-particle model can only be made when the size distribution effect is taken into account.

In a previous study (5) dealing with the dissolution of 60–85-mesh fraction tolbutamide in relation to its particle-size distribution, the dissolution of the single particles accorded well with the cube root model and nearly as well with the square root model. The distribution effect could be evaluated for tolbutamide because of the regular form of its particles. This was not possible for the much smaller micronized glyburide particles, which had very irregular shapes.

Effective Particle-Size Distribution—Spherical particles are assumed for the multiparticulate dissolution equations presented. Such particles are usually not encountered in pharmaceutical systems. However, the dissolution of a nonspherical particle can, in most cases, be well approximated by the dissolution of a hypothetical spherical particle (8), particularly under conditions of isotropic dissolution.

A previous paper showed how an equivalent spherical diameter can be calculated from the geometry of simple crystal forms (8). In this way, it is possible to obtain an effective particle-size distribution, *i.e.*, the shape of the distribution of hypothetical spherical particles that approximates the dissolution behavior of the real particles. For tolbutamide, the effective distribution was approximately log-normal (5). Because of the irregular particle shapes, it was not possible to make *a priori* conclusions about the effective particle-size distribution for glyburide. In these investigations, the distribution was assumed to be log-normal, consistent with previous results (5) and the fact that powders often have log-normal particle-size distribution (9, 10). Therefore, the distribution in Fig. 1 il-

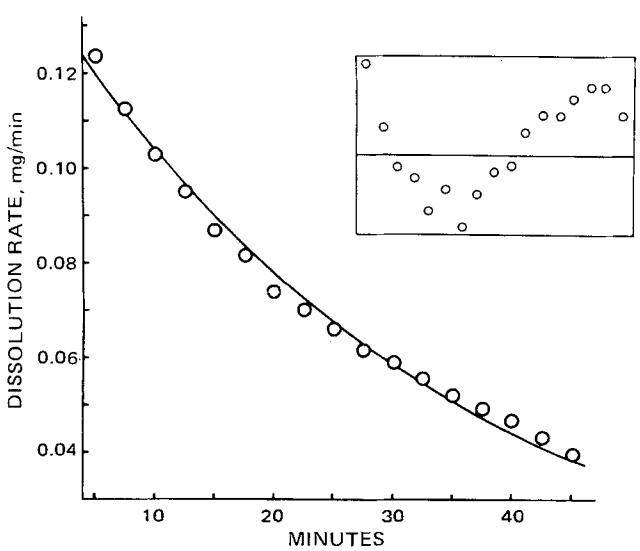

Figure 4—*Least-squares fit of the multiparticulate dissolution model (Eq. 29,* m = *3) to rate data from the dissolution of 5 mg of micronized glyburide. The model assumes that the effective initial particle-size distribution can be approximated by a log-normal distribution truncated at both ends (Fig. 1) and that the single particles dissolve according to the cube root model (Eq. 1,* m = *3). The inset graph shows a plot of the residuals* versus *time in arbitrary units.*

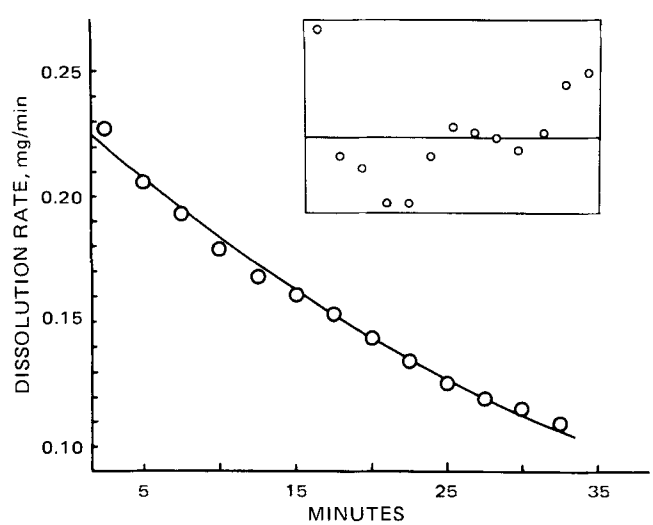

Figure 6—*Least-squares fit of the multiparticulate dissolution kinetic model (Eq. 29,* m = *3) to rate data from the dissolution of 10 mg of micronized glyburide. The model assumes that the effective initial particle-size distribution can be approximated by a log-normal distribution truncated at both ends (Fig. 1) and that the single particles dissolve according to the cube root model (Eq. 1,* m = *3). The inset graph shows a plot of the residuals* versus *time in arbitrary units.*

Table I—Least-Squares Estimates of Rate and Distribution Parameters Obtained from Nonlinear Regression Analysis of Data from the Dissolution of Micronized Glyburide, Using Various Models for Multiparticulate Dissolution Kinetics[a]

W_0, mg	Parameter	Square Root Model ($m = 2$)			Cube Root Model ($m = 3$)		
		Eq. 30[b]	Eq. 31[c]	Eq. 29[d]	Eq. 30[b]	Eq. 31[c]	Eq. 29[d]
5	K_m^*, min^{-1}	0.02858 (6.39)	0.02858 (5.12)	0.02859 (6.51)	0.02367 (4.55)	0.02367 (4.44)	0.02449 (3.96)
	σ	0.4759 (2.93)	0.4760 (2.70)	0.4760 (3.28)	0.6184 (2.47)	0.6184 (2.11)	0.6315 (1.71)
	i	∞	∞	5.136	∞	∞	2.364
	j	∞	5.299	5.655	∞	9.807	4.172
	r[e]	0.9935	0.9935	0.9935	0.9952	0.9952	0.9954
10	K_m^*, min^{-1}	0.02633 (7.18)	0.02633 (10.6)	0.02633 (9.35)	0.02147 (9.45)	0.02147 (4.74)	0.02176 (4.03)
	σ	0.4955 (3.20)	0.4956 (7.24)	0.4955 (5.14)	0.6374 (3.29)	0.6374 (2.03)	0.6446 (1.89)
	i	∞	∞	8.912	∞	∞	4.577
	j	∞	5.299	6.732	∞	7.060	4.200
	r[e]	0.9938	0.9938	0.9938	0.9957	0.9957	0.9958

[a] Values in parentheses are relative standard deviations (percent). [b] Initial size distribution is considered ideal ($i = j = \infty$, Fig. 1). [c] Initial size distribution is truncated at the upper end ($i = \infty$, $j < \infty$, Fig. 1). [d] Initial size distribution is truncated at both ends (Fig. 1). [e] Correlation coefficient.

lustrates a log-normal approximation to the effective particle-size distribution. The initial particle diameters, a_0 (Eq. 2), are the diameters of the hypothetical spherical particles that approximate the dissolution of the real nonspherical particles.

If the lower and upper truncation parameters, i or j, are finite, the log-distribution is said to be truncated; otherwise, it is ideal.

Regression Parameters—In a discussion of size distribution effects in multiparticulate dissolution, it was pointed out that the intrinsic dissolution profile does not depend on the actual size of the particles (a_0) but on the shape of their distribution (2). For the same reason, it is not possible to determine by regression analysis the scale parameter, μ, as might be erroneously expected from the appearance of Eq. 28. If, in fact, this equation is used to obtain least-squares estimates of μ and K_m, these values would not be unique. Any other of the infinite combinations of the two parameters that give the same value of K_m^* (Eq. 12) will, according to Eq. 13, result in the same fit (for the same values of σ, i, and j). Therefore, the regression analysis can only provide estimates of the dimensionless distribution parameters σ, i, and j, which define the shape of the initial distribution, and K_m^*. The scale or position of the distribution, given by μ, is hidden in the specific dissolution rate parameter, K_m^* (Eq. 12).

Curve Fitting—Equation 29 was fitted by least squares to dissolution rate data from dissolution of 5 and 10 mg of micronized glyburide[5]. The fitting was done using FUNFIT, an interactive time-sharing program for general nonlinear regression, written by the author[6].

The estimates obtained for the truncation parameters, i and j (Table I, Eq. 29), were all larger than 2 and usually exceeded 4, indicating that the effective initial particle-size distribution (Fig. 1) was close to ideal. It was shown earlier that the effect on the dissolution profile of the lower truncation parameter, i, is negligible (1). Simulation studies also show that the influence of an increase in the upper truncation parameter, j, becomes insignificant when j is larger than 2. Therefore, it is expected from the values of i and j obtained using Eq. 29 that the simpler model, Eq. 30, which assumes an ideal distribution ($i = j = \infty$), should fit the same data nearly as well.

The values in Table I and the curves fitted in Figs. 3–6 confirm this expectation. There does not seem to be any significant difference in the K_m^*, σ, or r values for the two models. The residual plots in Figs. 3–6 also seem to be very similar. Equation 31 (upper truncation) and Eq. 32 (lower truncation) also gave similar results (and, therefore, they have not been included).

Choice of Mathematical Model—In agreement with the general principles of mathematical modeling, Eq. 30 should be considered as the model that best describes the dissolution of the micronized glyburide. It is the simplest of the models, containing only the two parameters K_m^* and σ, and fits the dissolution data just as well as the other models that contain more parameters (i and j).

It also is clear (Table I) that the multiparticulate dissolution model based on the cube root model (Eq. 1, $m = 3$) agrees best with the dissolution data for either a truncated or ideal distribution using either 5 or 10 mg of powder (Table I). Of the eight multiparticulate models investigated, it can be concluded that the following equation:

$$\frac{dW}{dt} = -3K_3^* W_0 \sum_{n=0}^{2} \binom{2}{n} (-K_3^* t)^{(2-n)} \times \left\{1 - F\left[\frac{1}{\sigma}\ln(K_3^* t) - n\sigma\right]\right\} e^{(n^2-9)\sigma^2/2} \quad \text{(Eq. 40)}$$

which can be written in integrated form as:

$$\frac{W}{W_0} = \sum_{n=0}^{3} \binom{3}{n} (-K_3^* t)^{(3-n)} \times \left\{1 - F\left[\frac{1}{\sigma}\ln(K_3^* t) - n\sigma\right]\right\} e^{(n^2-9)\sigma^2/2} \quad \text{(Eq. 41)}$$

best describes the dissolution kinetics of the micronized glyburide. Either of these two equations uniquely characterizes the dissolution behavior in terms of the rate parameter, K_3^*, and the distribution parameter, σ.

It appears from the residual plots in Figs. 3–6 that there is a serial correlation between the residuals. The Durbin–Watson statistic indicates ($\alpha < 0.05$) that this correlation is significant (11). Systematic deviation can be caused by nonrandom experimental errors. It can also be caused by a significant departure from the assumed single-particle dissolution model (Eq. 1) or by a deviation from log-normality. The residual values are, however, so small in relation to the accuracy of the experimental technique that the correlation seems of little importance.

The specific dissolution rate parameter, K_3^*, theoretically should be independent of the initial amount used, W_0, but this condition was only approximately true. Values of the rate parameter, K_m^*, obtained for $W_0 = 10$ mg were consistently lower than for $W_0 = 5$ mg (Table I). The dissolution models consider dissolution under complete sink conditions, *i.e.*, conditions where there is no interaction between the dissolving particles. When using 10 mg of the very fine powder, it was not possible to load the dissolution cell with a single "layer" of particles in such a way that dissolved drug from any particle did not pass over other particles. The slightly larger K_m^* values observed when less powder was used in the cell agree with an expected smaller particle interaction.

Characterization and Quality Control of Drug Powders—Previous approaches to characterizing the dissolution properties of drug powders have been based on equations describing monodisperse systems. The so-called "dissolution rate constant" sometimes evaluated using such equations will often not characterize the dissolution behavior because the size distribution effect is not taken into account. This is particularly true for pharmaceutical systems, since these systems frequently involve fine, highly polydisperse powders.

The use of nonlinear regression analysis to evaluate the specific dissolution rate parameter, K_m^*, and the distribution parameter, σ, represents a more exact and meaningful approach.

The properties of K_m^* make its interpretation particularly useful. These properties are best understood in relation to the concepts of time scaling and the intrinsic dissolution profile (2) from which the following conclusion can be made:

If K_m^* is changed by a factor α, then the time for complete dissolution, or the time for any particular fraction to dissolve, is changed by a factor of $1/\alpha$[7].

The distribution parameter, σ, is a single measure of how polydisperse

[5] The initial data point(s) ($t = 0$ and 2.5 min) was not considered in the curve fitting because of irregularities due to initial adjustments of the solvent flow rate.

[6] The program is available on tape from the author together with a listing of the subroutines specifying the multiparticulate models (Eqs. 29–31).

[7] For example, if it takes x min for a powder to dissolve, *e.g.*, 30% for a given K_m^* value, then it will take the powder $x/2$ min to dissolve to the same extent if the value of K_m^* is doubled (see Fig. 1 in Ref. 2).

a powder is, or more exactly, how much the dissolution behavior deviates from what would be expected if the powder were completely monodisperse. A value close to zero characterizes a nearly monodisperse powder, while higher values indicate increasing "degrees of dispersion." Probably, the most important property of σ is that it is a measure of how long it takes the last fraction of a polydisperse powder to dissolve. For example, it is seen from Eq. 16 that the time for complete dissolution increases exponentially with σ. For this reason, a significant correlation probably exists between σ and systemic availability for very slightly soluble drugs that exhibit low systemic availability due to dissolution rate-limited absorption. Research in this area should be of considerable pharmaceutical interest.

Although the multiparticulate dissolution model (Eqs. 40 and 41) defining K_m^* and σ may seem complex, the interpretation of these parameters is simple and they can be readily obtained. The experimental technique used requires a high precision, flow-through dissolution apparatus that is easy to standardize [*e.g.*, the apparatus described in Ref. 5 or other suitable flow-through system (12)] in combination with a nonlinear regression program.

The method could well become established as a routine procedure in quality control, and further investigation could result in improved standards for drug dissolution.

REFERENCES

(1) P. Veng Pedersen and K. F. Brown, *J. Pharm. Sci.*, **64**, 1192 (1975).

(2) *Ibid.*, **64**, 1981 (1975).

(3) W. I. Higuchi, E. I. Rowe, and E. N. Hiestand, *J. Pharm. Sci.*, **52**, 162 (1963).

(4) J. T. Carstensen and M. Patel, *ibid.*, **64**, 1770 (1975).

(5) P. Veng Pedersen and K. F. Brown, *ibid.*, **65**, 1442 (1976).

(6) A. Hixson and J. Crowell, *Ind. Eng. Chem.*, **23**, 923 (1931).

(7) P. J. Niebergall, G. Milosovich, and J. E. Goyan, *J. Pharm. Sci.*, **52**, 236 (1963).

(8) P. Veng Pedersen and K. F. Brown, *ibid.*, **65**, 1437 (1976).

(9) G. Herdan and M. L. Smith, "Small Particle Statistics," Elsevier, New York, N.Y., 1953.

(10) T. Hatch and S. P. Choate, *J. Franklin Inst.*, **207**, 369 (1929).

(11) J. Durbin and G. S. Watson, *Biometrica*, **37**, 409 (1950).

(12) "Dissolution Technology," L. J. Leeson and J. T. Carstensen, Eds., Industrial Pharmaceutical Technology, APhA Academy of Pharmaceutical Sciences, Washington, D.C., 1974.

ACKNOWLEDGMENTS AND ADDRESSES

Received February 23, 1976, from the *Department of Pharmacy, University of Sydney, Sydney, N.S.W. 2006, Australia.*

Accepted for publication July 13, 1976.

Supported in part by Grant 7414244 from the National Health and Medical Research Council of Australia.

Present address: Department of Pharmacy, University of California, San Francisco, CA 94143.

Sensitive Assay Procedure for Ethambutol Hydrochloride *via* Charge Transfer Complex Formation

HENRY S. I. TAN ˣ, ERIC D. GERLACH, and ANTHONY S. DIMATTIO

Abstract □ The charge transfer complex formation between ethambutol and iodine was investigated and utilized as the basis for a sensitive spectrophotometric procedure for ethambutol and its dosage forms. The solutions exhibited blue-shifted iodine bands at 293 and 360 nm. A Job's plot of corrected absorbance against the mole ratio of ethambutol to iodine indicated a 1:2 drug–iodine ratio. At 293 nm, the absorbance was linear (r = 0.9998) over the 0.25–15-μg/ml concentration range, but the concentration range for best accuracy is 1.6–5.8 μg/ml. The method can be applied successfully to the analysis of commercially available ethambutol tablets.

Keyphrases □ Ethambutol—spectrophotometric analysis using charge transfer complex formation, prepared samples and commercial tablets □ Spectrophotometry—analysis using charge transfer complex formation, ethambutol in prepared samples and commercial tablets □ Charge transfer complex formation—spectrophotometric analysis of ethambutol in prepared samples and commercial tablets □ Antibacterials—ethambutol, spectrophotometric analysis using charge transfer complex formation, prepared samples and commercial tablets

Ethambutol is a new antitubercular drug included in USP XIX (1). Being a relatively new drug, few procedures have been reported for its determination as a drug substance or in commercial dosage forms. The official assay procedure involves a nonaqueous titration with perchloric acid titrant (1).

Quantitative analyses of small quantities of ethambutol have been based on the chelation properties of the drug with copper in aqueous or nonaqueous media (2, 3). A reineckate method and an acid–dye technique using bromthymol blue were also reported (4, 5). However, these procedures are not feasible for the analysis of microquantities of the drug in biological fluids.

Amines and alcohols are lone-pair (n) electron donors and can interact strongly with sacrificial electron acceptors such as iodine to form charge transfer complexes (6). Recently, a study on charge transfer complexes of iodine with alkaloids was reported (7). This paper reports the charge transfer complex formation of ethambutol with iodine and its application to drug assay.

EXPERIMENTAL

Apparatus—A UV–visible double-beam spectrophotometer[1] with 1-cm cells and dynode voltage of 500 v (slit width 0.80–0.85 mm) and an analytical balance[2] were used.

Materials and Reagents—Ethambutol hydrochloride[3] and 8×10^{-4} M iodine[4] (resublimed) in anhydrous chloroform[4] were used. Other reagents were analytical grade.

Ethambutol Base—Ethambutol hydrochloride (1 g) was dissolved

[1] Beckman Acta V, Beckman Instruments Inc., Fullerton, Calif.
[2] Mettler model H-18, Mettler Instruments Co., Princeton, N.J.
[3] Lederle Laboratories, Pearl River, N.Y.
[4] Fisher Scientific Co., Pittsburgh, Pa.

a powder is, or more exactly, how much the dissolution behavior deviates from what would be expected if the powder were completely monodisperse. A value close to zero characterizes a nearly monodisperse powder, while higher values indicate increasing "degrees of dispersion." Probably, the most important property of σ is that it is a measure of how long it takes the last fraction of a polydisperse powder to dissolve. For example, it is seen from Eq. 16 that the time for complete dissolution increases exponentially with σ. For this reason, a significant correlation probably exists between σ and systemic availability for very slightly soluble drugs that exhibit low systemic availability due to dissolution rate-limited absorption. Research in this area should be of considerable pharmaceutical interest.

Although the multiparticulate dissolution model (Eqs. 40 and 41) defining K_m^* and σ may seem complex, the interpretation of these parameters is simple and they can be readily obtained. The experimental technique used requires a high precision, flow-through dissolution apparatus that is easy to standardize [*e.g.*, the apparatus described in Ref. 5 or other suitable flow-through system (12)] in combination with a nonlinear regression program.

The method could well become established as a routine procedure in quality control, and further investigation could result in improved standards for drug dissolution.

REFERENCES

(1) P. Veng Pedersen and K. F. Brown, *J. Pharm. Sci.*, **64**, 1192 (1975).

(2) *Ibid.*, **64**, 1981 (1975).

(3) W. I. Higuchi, E. I. Rowe, and E. N. Hiestand, *J. Pharm. Sci.*, **52**, 162 (1963).

(4) J. T. Carstensen and M. Patel, *ibid.*, **64**, 1770 (1975).

(5) P. Veng Pedersen and K. F. Brown, *ibid.*, **65**, 1442 (1976).

(6) A. Hixson and J. Crowell, *Ind. Eng. Chem.*, **23**, 923 (1931).

(7) P. J. Niebergall, G. Milosovich, and J. E. Goyan, *J. Pharm. Sci.*, **52**, 236 (1963).

(8) P. Veng Pedersen and K. F. Brown, *ibid.*, **65**, 1437 (1976).

(9) G. Herdan and M. L. Smith, "Small Particle Statistics," Elsevier, New York, N.Y., 1953.

(10) T. Hatch and S. P. Choate, *J. Franklin Inst.*, **207**, 369 (1929).

(11) J. Durbin and G. S. Watson, *Biometrica*, **37**, 409 (1950).

(12) "Dissolution Technology," L. J. Leeson and J. T. Carstensen, Eds., Industrial Pharmaceutical Technology, APhA Academy of Pharmaceutical Sciences, Washington, D.C., 1974.

ACKNOWLEDGMENTS AND ADDRESSES

Received February 23, 1976, from the *Department of Pharmacy, University of Sydney, Sydney, N.S.W. 2006, Australia.*

Accepted for publication July 13, 1976.

Supported in part by Grant 7414244 from the National Health and Medical Research Council of Australia.

Present address: Department of Pharmacy, University of California, San Francisco, CA 94143.

Sensitive Assay Procedure for Ethambutol Hydrochloride *via* Charge Transfer Complex Formation

HENRY S. I. TAN ˣ, ERIC D. GERLACH, and ANTHONY S. DIMATTIO

Abstract □ The charge transfer complex formation between ethambutol and iodine was investigated and utilized as the basis for a sensitive spectrophotometric procedure for ethambutol and its dosage forms. The solutions exhibited blue-shifted iodine bands at 293 and 360 nm. A Job's plot of corrected absorbance against the mole ratio of ethambutol to iodine indicated a 1:2 drug–iodine ratio. At 293 nm, the absorbance was linear (r = 0.9998) over the 0.25–15-μg/ml concentration range, but the concentration range for best accuracy is 1.6–5.8 μg/ml. The method can be applied successfully to the analysis of commercially available ethambutol tablets.

Keyphrases □ Ethambutol—spectrophotometric analysis using charge transfer complex formation, prepared samples and commercial tablets □ Spectrophotometry—analysis using charge transfer complex formation, ethambutol in prepared samples and commercial tablets □ Charge transfer complex formation—spectrophotometric analysis of ethambutol in prepared samples and commercial tablets □ Antibacterials—ethambutol, spectrophotometric analysis using charge transfer complex formation, prepared samples and commercial tablets

Ethambutol is a new antitubercular drug included in USP XIX (1). Being a relatively new drug, few procedures have been reported for its determination as a drug substance or in commercial dosage forms. The official assay procedure involves a nonaqueous titration with perchloric acid titrant (1).

Quantitative analyses of small quantities of ethambutol have been based on the chelation properties of the drug with copper in aqueous or nonaqueous media (2, 3). A reineckate method and an acid–dye technique using bromthymol blue were also reported (4, 5). However, these procedures are not feasible for the analysis of microquantities of the drug in biological fluids.

Amines and alcohols are lone-pair (n) electron donors and can interact strongly with sacrificial electron acceptors such as iodine to form charge transfer complexes (6). Recently, a study on charge transfer complexes of iodine with alkaloids was reported (7). This paper reports the charge transfer complex formation of ethambutol with iodine and its application to drug assay.

EXPERIMENTAL

Apparatus—A UV–visible double-beam spectrophotometer[1] with 1-cm cells and dynode voltage of 500 v (slit width 0.80–0.85 mm) and an analytical balance[2] were used.

Materials and Reagents—Ethambutol hydrochloride[3] and 8×10^{-4} M iodine[4] (resublimed) in anhydrous chloroform[4] were used. Other reagents were analytical grade.

Ethambutol Base—Ethambutol hydrochloride (1 g) was dissolved

[1] Beckman Acta V, Beckman Instruments Inc., Fullerton, Calif.
[2] Mettler model H-18, Mettler Instruments Co., Princeton, N.J.
[3] Lederle Laboratories, Pearl River, N.Y.
[4] Fisher Scientific Co., Pittsburgh, Pa.

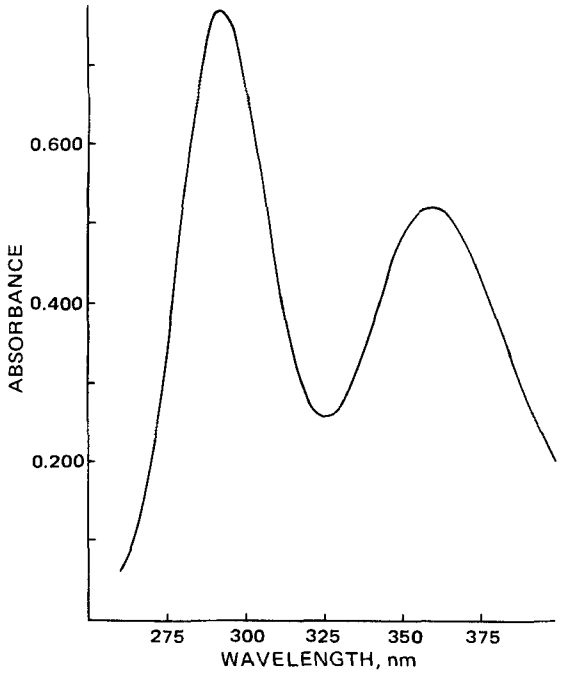

Figure 1—*Absorption spectrum of ethambutol–iodine complex.*

in 50 ml of aqueous sodium hydroxide solution (1:12) and extracted with five 30-ml portions of chloroform. The chloroform extracts were combined, dried with anhydrous sodium sulfate, and filtered, and the filtrate was evaporated to dryness under nitrogen. Recrystallization of the residue (yield 98.9%) from chloroform–hexane afforded white needles (mp 87–88°).

Standard Curve—A 25.0-mg portion of ethambutol base was weighed accurately and dissolved in 100.0 ml of anhydrous chloroform. Further dilutions were then made to prepare standard solutions containing 2.5–150 μg of ethambutol/ml. One milliliter of this solution was utilized for complex formation with the iodine reagent as described under *Assay Procedure for Ethambutol Hydrochloride,* beginning with: "Pipet 1.0 ml of this solution into a 10-ml volumetric flask . . . ."

Assay Procedure for Ethambutol Hydrochloride—*Powder*—Weigh accurately about 50.0 mg of ethambutol hydrochloride and transfer into a 60-ml separator. Dissolve the powder in 3 ml of sodium hydroxide solution (1:12) and extract with five 15-ml portions of anhydrous chloroform. Combine the chloroform extracts, dry them with anhydrous sodium sulfate (5 min), and filter through dry filter paper into a 100-ml volumetric flask. Rinse the sodium sulfate and filter with anhydrous chloroform, and use the washings to dilute the bulk solution to volume.

Measure 5.0 ml (buret or pipet) into a 50-ml volumetric flask and dilute to volume with anhydrous chloroform. Pipet 1.0 ml of this solution into a 10-ml volumetric flask, add 5.0 ml of iodine reagent, and dilute to volume with anhydrous chloroform. Allow the solution to stand in the dark for no less than 1 hr and measure the absorbance at 293 nm against a blank. Determine the concentration of ethambutol from the calibration curve or from the regression equation.

Tablets—Weigh and finely powder 20 ethambutol hydrochloride tablets. Transfer an accurately weighed portion of the powder, equivalent to about 50 mg of ethambutol hydrochloride, to a 60-ml separator. Then add 3 ml of sodium hydroxide solution (1:12) and proceed as described for the powder, beginning with: "extract with five 15-ml portions of anhydrous chloroform . . . ."

Stoichiometric Relationship—Master solutions of iodine (1.67×10^{-4} *M*) and ethambutol base (1.67×10^{-4} *M*) in anhydrous chloroform were prepared. A series of 10-ml quantities of mixtures containing a total of 10 ml of the master solution of ethambutol base and iodine in different complementary proportions (from 0:10 to 10:0 inclusive) were made up in 10-ml volumetric flasks. After the flasks were allowed to stand in a water bath at 25° for 60 min, absorbances were measured at 293 nm.

Association Constant and Molar Absorptivity—Ethambutol base solutions in anhydrous chloroform were prepared (1.5, 3.0, and 6.0×10^{-4} *M*), and these solutions and an iodine solution in anhydrous chloroform (8×10^{-5} *M*) were placed in a water bath at 25° for 30 min. Five milliliters of the iodine solution was mixed with the same volume of each ethambutol solution. After quick mixing, the absorbance of each solution was determined immediately at 293 nm.

Table I—Effect of Time on Absorbance of Ethambutol–Iodine Complex

Minutes after Mixing	Absorbance (293 nm)
0	0.823
10	0.930
20	0.923
30	0.917
40	0.908
50	0.896
60	0.881
70	0.880
80	0.879
90	0.880
120	0.878

RESULTS AND DISCUSSION

Charge transfer complex formation is distinguished from other slow oxidation or substitution reactions of iodine with amines by being practically instantaneous, analogous to ionic reactions. Upon reaction of ethambutol with a chloroform solution of iodine, the violet color of iodine is changed immediately to yellowish purple or yellow, depending on the amount of ethambutol present. Further confirmation of the charge transfer nature of the complex was obtained by extracting the drug from the complex by shaking with aqueous hydrochloric acid, whereby the violet color of iodine was restored in the chloroform layer. The regeneration of the drug from the charge transfer complex is easy, since the binding energy of charge transfer complexes is usually small; addition of a solvent of relatively high polarity causes complete decomposition (8).

Therefore, the chloroform used must be checked for its suitability. With some spectrograde samples of chloroform, no complex was formed, as evidenced by a lack of absorbance in the wavelength region studied. This result was due presumably to relatively high concentrations of water. Unfortunately, the water content levels in these spectrograde brands of chloroform were not furnished by the manufacturers. *Anhydrous* chloroform[4], which contains the same amount of ethanol preservative but a low water content of 0.02%, was suitable as a medium for the ethambutol–iodine complex formation.

The absorption spectrum of iodine in chloroform showed only one peak, with a maximum absorption at 515 nm. However, the charge transfer complex with ethambutol exhibited blue-shifted iodine bands at 293 and 360 nm, with the first peak being more intense than the second (Fig. 1). The absorption at these wavelengths is due solely to the complex because ethambutol itself is nonabsorbing.

Although the complex was formed rapidly, constant absorbance readings were obtained only after no less than 1 hr of standing in the dark (Table I). The readings remained constant for at least 1 additional hr.

At 293 nm, a linear relationship ($r = 0.9998$) was obtained between absorbance and concentration over the 0.25–15-μg/ml range. The regression equation[5] of the line was $A_{293} = 0.1648C - 0.0079$, where A_{293} is the absorbance at 293 nm, and C is the concentration of ethambutol base expressed in micrograms per milliliter. Conversion to the concentration (micrograms per milliliter) of ethambutol hydrochloride can be obtained by multiplying C by 1.357. The standard deviations ($n = 3$) of the slope and y-intercept were 4.1×10^{-3} and 5.5×10^{-3}, respectively.

The Ringbom plot (9) indicates that the concentration range for best accuracy is 1.6–5.8 μg of ethambutol base/ml in the final test solution (Fig. 2). Deviations from linearity in the Beer–Lambert plot result when the concentrations of donor and acceptor differ in magnitude (8, p. 171). For this reason, the concentration of iodine reagent was kept at the same order of magnitude as that of the ethambutol.

The determination of the mole ratio of reactants in the complex is based on the method of continuous variation (10). The plot (Fig. 3) shows a 1:2 molar ratio of ethambutol–iodine in the complex. No attempts were made to predict the orientation of the donor and acceptor moieties in the charge transfer complex.

In analogy to equations for the equilibria involved in a 1:1 charge

[5] Wang computer 700C and plotting output writer 2202.

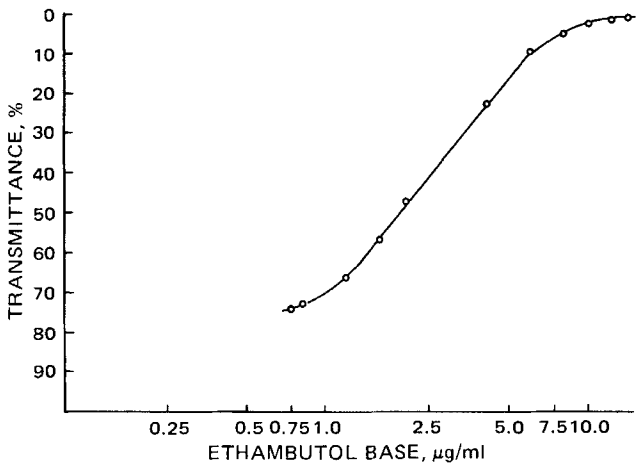

Figure 2—*Ringbom plot of ethambutol–iodine complex.*

transfer complex formation (8, 11, 12), it can be postulated that for a 1:2 ethambutol–iodine ratio the reaction for the equilibrium involved is shown in Scheme I:

$$E + 2I_2 \rightleftarrows E \cdot 2I_2$$

Scheme I

where E stands for ethambutol. Based on this equilibrium reaction, the association constant, K, for the complex $E \cdot 2I_2$ can be easily derived:

$$K = \frac{[E \cdot 2I_2]}{[E][I_2]^2} \qquad \text{(Eq. 1}a\text{)}$$

$$K = \frac{[E \cdot 2I_2]}{([E]_0 - [E \cdot 2I_2])([I]_0 - [E \cdot 2I_2])^2} \qquad \text{(Eq. 1}b\text{)}$$

where $[E]_0$ and $[I]_0$ indicate the total, *i.e.*, free and complexed, concentrations of ethambutol and iodine, respectively. Then:

$$\frac{1}{K} = \frac{[E]_0[I]_0^2}{[E \cdot 2I_2]} + [E \cdot 2I_2]([E]_0 + 2[I]_0) - [E \cdot 2I_2]^2 - [I]_0(2[E]_0 + [I]_0) \qquad \text{(Eq. 2)}$$

Since the absorbance, A, at 293 nm is due entirely to the complex, which obeys the Beer–Lambert law, in a 1-cm cell:

$$[E \cdot 2I_2] = \frac{A}{\epsilon} \qquad \text{(Eq. 3)}$$

where ϵ is the molar absorptivity of the complex. Substituting Eq. 3 into Eq. 2 yields:

$$\frac{1}{K} = \frac{[E]_0[I]_0^2\epsilon}{A} + \frac{A([E]_0 + 2[I]_0)}{\epsilon} - \frac{A^2}{\epsilon^2} - [I]_0(2[E]_0 + [I]_0) \qquad \text{(Eq. 4)}$$

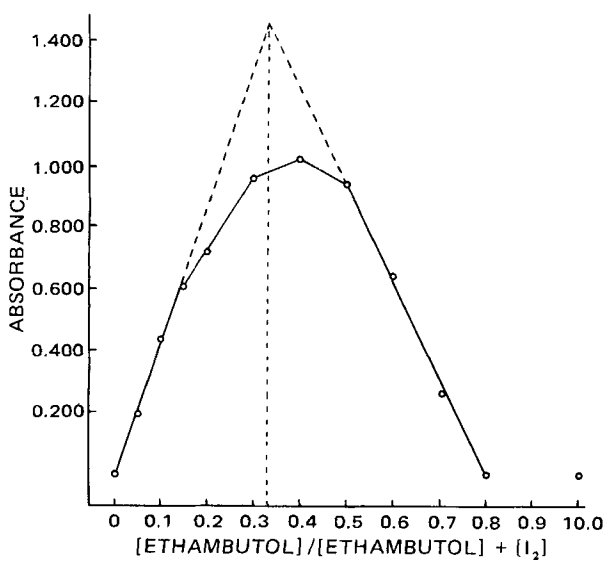

Figure 3—*Continuous variation plot obtained from solutions of ethambutol and iodine in chloroform (1.67×10^{-4} M).*

Table II—Precision Study of the Method at the 4.1-μg of Ethambutol Base/ml Concentration Level

Sample	Absorbance (293 nm)
1	0.630
2	0.611
3	0.614
4	0.629
5	0.631
6	0.618
7	0.618
8	0.619
9	0.624
10	0.624
11	0.626
12	0.633
13	0.616
Average	0.622
RSD	0.0112

Equation 4 contains two unknowns, K and ϵ. If two equations like Eq. 4 are set up, each representing different experimental trials (*i.e.*, $[E]_0$ and $[E]_0'$ and A and A'), an analytical solution can be derived specifically for ϵ. Because this expression was awkward to use, a graphical procedure was developed.

Evaluation of Eq. 4, which is a nonhomogeneous polynomial of the third order, by substituting random values of ϵ for a given set of experimental data generates corresponding values of K^{-1}. The values of K^{-1} and ϵ for *each* given set of experimental data are plotted. The intersect of the curves yields the association constant and molar absorptivity of the system. The results (Fig. 4) show that the association constant, K, for the ethambutol–iodine complex is $2.07 \pm 0.22 \times 10^8$ and that the molar absorptivity is $6.10 \pm 0.15 \times 10^3$.

The reproducibility of the procedure was determined by running 13 replicate samples, each containing 4.1 μg of ethambutol base/ml in the final test solution. At this concentration level, the relative standard deviation was 0.0112 (Table II).

Table III shows the accuracy of the proposed method. Recovery studies were performed on five different amounts of ethambutol hydrochloride,

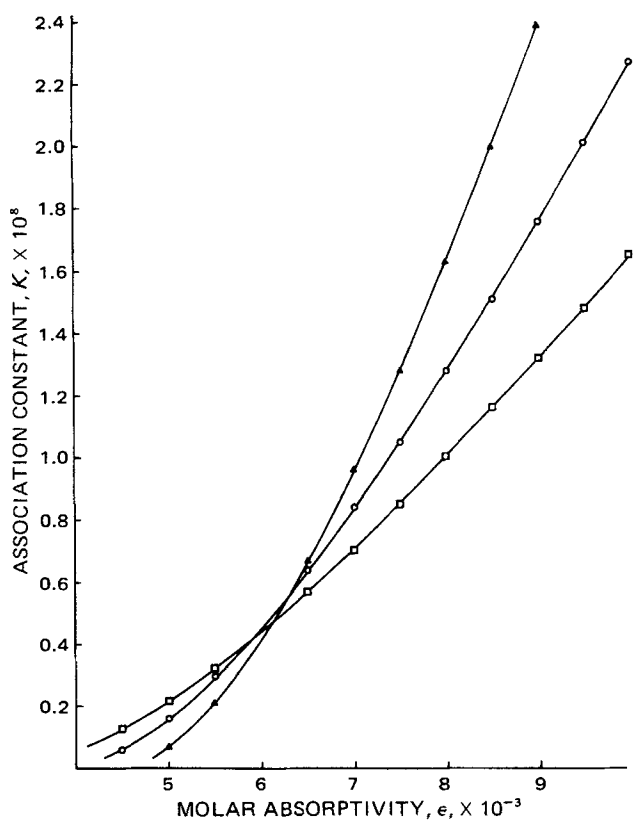

Figure 4—*Graphical solution of Eq. 4 for a series of ethambutol and 8×10^{-5} M iodine solutions in chloroform. Key: □, 1.5×10^{-4} M ethambutol; ○, 3.0×10^{-4} M ethambutol; and △, 6.0×10^{-4} M ethambutol.*

Table III—Recovery Studies of Known Ethambutol Hydrochloride Samples and Commercially Available Tablets

Amount Weighed, mg, or Claimed, mg/Tablet	Concentration Level, μg/ml	Amount Found, mg or mg/Tablet		Percent Recovery or Percent of Claim	
		Proposed Method	USP XIX Method	Proposed Method	USP XIX Method
		Known Samples			
42.1	3.10	42.6	—	101.2	—
46.4	3.42	46.2	—	99.6	—
50.6	1.86	48.7	—	96.2	—
50.7	3.74	50.2	—	99.0	—
63.8	9.40	62.8	—	98.4	—
201.6	—	—	192.8	—	95.6
203.1	—	—	195.3	—	96.2
Overall recovery, %				98.9	95.9
SEM				0.82	
		Commercial Tablets			
100.0	3.73	99.1	99.3	99.1	99.3
100.0	3.67	98.0	97.4	98.0	97.4
400.0	1.86	376.0	388.2	94.1	97.1
400.0	1.87	385.9	391.7	96.5	97.9

and each was analyzed at different concentration levels. The overall percent recovery of the five samples was 98.9% with a standard error of the mean of 0.82. Results obtained by applying the method to the analysis of commercially available ethambutol hydrochloride tablets are in agreement with those obtained by the compendial method.

REFERENCES

(1) "First Supplement to the United States Pharmacopeia," 19th rev., Mack Publishing Co., Easton, Pa., 1975, p. 20.

(2) H. Reutgen and M. Grunert, *Pharmazie*, **24**, 148 (1969).

(3) J. M. Burger, F. D. Pisano, and R. A. Nash, *J. Pharm. Sci.*, **58**, 110 (1969).

(4) P. Tarli, F. Lattanzi, and S. Benoci, *Farmaco, Ed. Prat.*, **24**, 707 (1969).

(5) E. H. Girgis, Z. Gad, and M. Maram, *J. Pharm. Sci.*, **63**, 1764 (1974).

(6) R. S. Mulliken, *J. Am. Chem. Soc.*, **72**, 600 (1950).

(7) A. M. Taha, A. K. S. Ahmad, C. S. Gomaa, and H. M. El-Fatatry, *J. Pharm. Sci.*, **63**, 1853 (1974).

(8) R. Foster, "Organic Charge-Transfer Complexes," Academic, London, England, 1969.

(9) G. H. Ayres, *Anal. Chem.*, **21**, 652 (1949).

(10) J. Rose, "Advanced Physico-Experiments," Pitman, London, England, 1964, p. 54.

(11) H. A. Benesi and J. H. Hildebrand, *J. Am. Chem. Soc.*, **71**, 2703 (1949).

(12) N. J. Rose and R. S. Drago, *ibid.*, **81**, 6138 (1959).

ACKNOWLEDGMENTS AND ADDRESSES

Received April 2, 1976, from the *College of Pharmacy, University of Cincinnati–Medical Center, Cincinnati, OH 45267.*

Accepted for publication June 30, 1976.

Presented at the Pharmaceutical Analysis and Control Section, APhA Academy of Pharmaceutical Sciences, New Orleans meeting, 1976.

The authors express their appreciation to Lederle Laboratories, a Division of American Cyanamid Co., Pearl River, N.Y., for supplying ethambutol hydrochloride.

[x] To whom inquiries should be directed.

GLC Determination of Lasalocid and Its Bromo Analog as Their Silyl Derivatives

GERALD MANIUS and V. VISWANATHAN [x]

Abstract □ A GLC method is presented for the determination of lasalocid and its bromo analog. The method is based on the quantitative trimethylsilylation of the compounds without any molecular cleavage, followed by chromatography on a nonpolar silicone column. Silylation was carried out directly without any extraction or prior cleanup, despite the complexity of the dosage forms. This procedure was used for the assay of pure substances, pellets, premixes, experimental ampul solutions, and mycelial filter cakes. The results were in good agreement with data obtained by microbiological procedures.

Keyphrases □ Lasalocid and bromo analog—GLC analysis, various preparations and dosage forms □ GLC—analysis, lasalocid and bromo analog, various preparations and dosage forms □ Coccidiostatic antibacterials—lasalocid and bromo analog, GLC analysis, various preparations and dosage forms

The isolation of lasalocid (I), an antibiotic, was reported by Berger *et al.* (1). The structural configuration and the existence of four homologs for this antibiotic were described subsequently (2–4). Recently, a microbiological cylinder-plate assay (5) and a spectrofluorometric procedure for the determination of lasalocid in premixes (6) were reported. A GLC procedure also was reported in which the antibiotic was assayed after thermal degradation to yield the retroaldol ketone (7).

The bioassay procedure is a good indicator of the mi-

Table III—Recovery Studies of Known Ethambutol Hydrochloride Samples and Commercially Available Tablets

Amount Weighed, mg, or Claimed, mg/Tablet	Concentration Level, μg/ml	Amount Found, mg or mg/Tablet		Percent Recovery or Percent of Claim	
		Proposed Method	USP XIX Method	Proposed Method	USP XIX Method
		Known Samples			
42.1	3.10	42.6	—	101.2	—
46.4	3.42	46.2	—	99.6	—
50.6	1.86	48.7	—	96.2	—
50.7	3.74	50.2	—	99.0	—
63.8	9.40	62.8	—	98.4	—
201.6	—	—	192.8	—	95.6
203.1	—	—	195.3	—	96.2
Overall recovery, %				98.9	95.9
SEM				0.82	
		Commercial Tablets			
100.0	3.73	99.1	99.3	99.1	99.3
100.0	3.67	98.0	97.4	98.0	97.4
400.0	1.86	376.0	388.2	94.1	97.1
400.0	1.87	385.9	391.7	96.5	97.9

and each was analyzed at different concentration levels. The overall percent recovery of the five samples was 98.9% with a standard error of the mean of 0.82. Results obtained by applying the method to the analysis of commercially available ethambutol hydrochloride tablets are in agreement with those obtained by the compendial method.

REFERENCES

(1) "First Supplement to the United States Pharmacopeia," 19th rev., Mack Publishing Co., Easton, Pa., 1975, p. 20.

(2) H. Reutgen and M. Grunert, *Pharmazie*, **24**, 148 (1969).

(3) J. M. Burger, F. D. Pisano, and R. A. Nash, *J. Pharm. Sci.*, **58**, 110 (1969).

(4) P. Tarli, F. Lattanzi, and S. Benoci, *Farmaco, Ed. Prat.*, **24**, 707 (1969).

(5) E. H. Girgis, Z. Gad, and M. Maram, *J. Pharm. Sci.*, **63**, 1764 (1974).

(6) R. S. Mulliken, *J. Am. Chem. Soc.*, **72**, 600 (1950).

(7) A. M. Taha, A. K. S. Ahmad, C. S. Gomaa, and H. M. El-Fatatry, *J. Pharm. Sci.*, **63**, 1853 (1974).

(8) R. Foster, "Organic Charge-Transfer Complexes," Academic, London, England, 1969.

(9) G. H. Ayres, *Anal. Chem.*, **21**, 652 (1949).

(10) J. Rose, "Advanced Physico-Experiments," Pitman, London, England, 1964, p. 54.

(11) H. A. Benesi and J. H. Hildebrand, *J. Am. Chem. Soc.*, **71**, 2703 (1949).

(12) N. J. Rose and R. S. Drago, *ibid.*, **81**, 6138 (1959).

ACKNOWLEDGMENTS AND ADDRESSES

Received April 2, 1976, from the *College of Pharmacy, University of Cincinnati–Medical Center, Cincinnati, OH 45267.*

Accepted for publication June 30, 1976.

Presented at the Pharmaceutical Analysis and Control Section, APhA Academy of Pharmaceutical Sciences, New Orleans meeting, 1976.

The authors express their appreciation to Lederle Laboratories, a Division of American Cyanamid Co., Pearl River, N.Y., for supplying ethambutol hydrochloride.

[x] To whom inquiries should be directed.

GLC Determination of Lasalocid and Its Bromo Analog as Their Silyl Derivatives

GERALD MANIUS and V. VISWANATHAN [x]

Abstract □ A GLC method is presented for the determination of lasalocid and its bromo analog. The method is based on the quantitative trimethylsilylation of the compounds without any molecular cleavage, followed by chromatography on a nonpolar silicone column. Silylation was carried out directly without any extraction or prior cleanup, despite the complexity of the dosage forms. This procedure was used for the assay of pure substances, pellets, premixes, experimental ampul solutions, and mycelial filter cakes. The results were in good agreement with data obtained by microbiological procedures.

Keyphrases □ Lasalocid and bromo analog—GLC analysis, various preparations and dosage forms □ GLC—analysis, lasalocid and bromo analog, various preparations and dosage forms □ Coccidiostatic antibacterials—lasalocid and bromo analog, GLC analysis, various preparations and dosage forms

The isolation of lasalocid (I), an antibiotic, was reported by Berger *et al.* (1). The structural configuration and the existence of four homologs for this antibiotic were described subsequently (2–4). Recently, a microbiological cylinder-plate assay (5) and a spectrofluorometric procedure for the determination of lasalocid in premixes (6) were reported. A GLC procedure also was reported in which the antibiotic was assayed after thermal degradation to yield the retroaldol ketone (7).

The bioassay procedure is a good indicator of the mi-

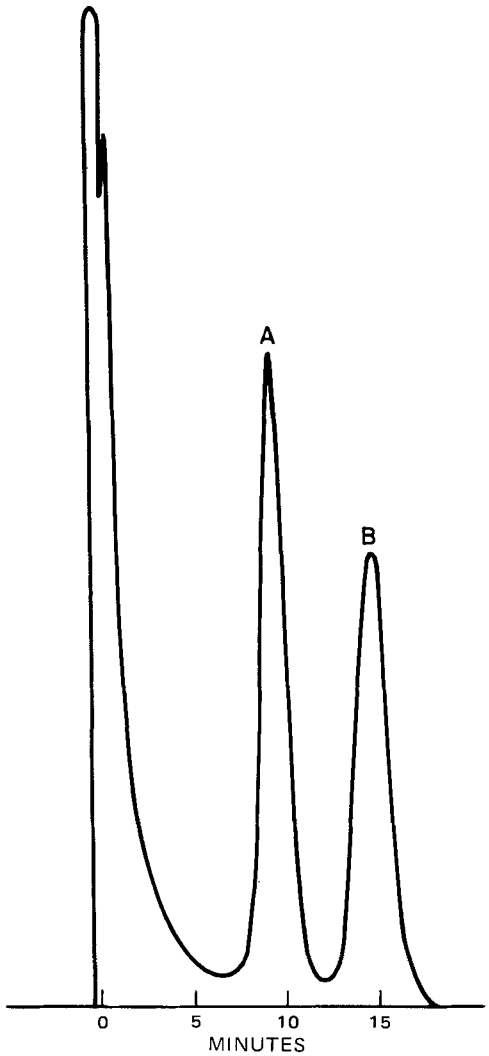

Figure 1—*Chromatogram of I (A) and II (B) trimethylsilyl derivatives.*

crobiological activity of the antibiotic. However, it is generally subject to interference from other antibiotics or biologically active degradation products and is very time consuming. Chemical methods such as the spectrofluorometric procedure require extraction and cleanup of the samples prior to analysis. GLC of the thermolysis product of lasalocid was reported to be quantitative; however, the degradation product of the antibiotic was assayed rather than the intact compound to establish sample purity. In most analytical applications, this approach is considered unsatisfactory, particularly for the assay of finished products for clinical use.

During this investigation, emphasis was placed on developing a specific assay procedure for the antibiotic in various dosage forms within a reasonably short time and with minimal sample preparation. Chromatographing the intact molecule in the form of a stable derivative appeared suitable, since this method would offer several advantages such as specificity for the antibiotic and the ability to resolve and quantitate the active ingredient in the presence of decomposition products and substances that interfere in other methods. In addition, a suitable derivative of the antibiotic would lend itself easily to confirmatory tests such as mass spectrometry when the intact antibiotic must be detected in complex media. Trimethylsilylation of the

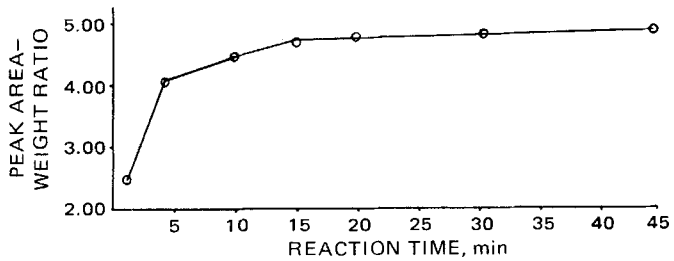

Figure 2—*Completeness of silylation reaction.*

carboxyl and secondary alcohol functions of the antibiotic was chosen, since this approach was used successfully for the assay of other antibiotics such as chloramphenicol, penicillin, erythromycin, neomycin, and lincomycin (8–14).

EXPERIMENTAL

Apparatus—A gas chromatograph equipped with a hydrogen flame-ionization detector was used. The chromatographic column was type 304 stainless steel, 61 cm in length and 3.2 mm o.d., fitted for on-column injections. The packing was 3% methyl silicone fluid on acid-washed, silane-treated diatomite support, which was sieved to specification before and after liquid phase coating. Data acquisition and quantitation were carried out using a computer system. All injections were made using a 10-μl syringe.

Reagents—*N,O*-Bis(trimethylsilyl)acetamide, *N*-trimethylsilylimidazole, trimethylchlorosilane, and tetrahydrofuran (reagent grade) were used as received. For the silylation reaction, a 3:3:2 (v/v) mixture of *N,O*-bis(trimethylsilyl)acetamide, *N*-trimethylsilylimidazole, and trimethylchlorosilane was made. To protect the stability of the reagent, mixtures were prepared fresh in small quantities and stored in tightly sealed containers under refrigeration.

Operational Parameters—For the chromatography of lasalocid and its bromo analog (II), the temperatures were: column, 260°, isothermal; injector port, 260°; and detector, 290°. The flow rate for the nitrogen carrier gas was 30 ml/min; the flow rates of hydrogen and air to the detector were set at 30 and 300 ml/min, respectively. The injection volume was 5 μl, and the attenuation was nominally set at 64× at a range setting of 10^{-11} amp/mv. Under these conditions, the trimethylsilyl derivatives of I and II eluted at retention times of 10 and 15 min, respectively.

Preparation of Solutions for Assay—*Reference Standard*—Approximately 20 mg of I or II reference material was accurately weighed into a 10-ml volumetric flask. One milliliter of the silylating reagent mixture was added, and the flask was capped and allowed to stand at ambient temperature for a minimum of 30 min. After the reaction was completed, the solution was diluted to 10 ml with tetrahydrofuran.

Sample Solutions—Pure substances were prepared in the same manner as the reference standard preparation. For premix pellets, final premixes, or mycelial cake materials, samples equivalent to approximately 20 mg of active ingredient were weighed into a 10-ml volumetric flask, silylated for 30 min or longer, and diluted as described. Small, accurately measured quantities of experimental ampul solutions equivalent to 2.0 mg of I were transferred into small vials, 2–3 drops of anhydrous methanol were added, and the mixture was evaporated to dryness under mild heat with a stream of nitrogen and reacted with exactly 1.0 ml of silylating reagent prior to chromatography.

Precautions were taken to exclude excessive heat, moisture, and metallic contact during the standard and sample preparations.

Table I—Statistical Evaluation of III Assay

Determination[a]	Assay, %
1	89.9
2	90.1
3	88.7
4	90.4
5	91.3
6	87.3
Mean	89.6
SD	±1.41

[a] Each determination represents individual silylation and assay.

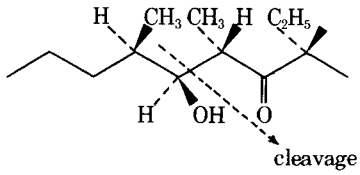

Ia

Prior to analyzing the samples, the chromatographic column was conditioned by making several 5.0-μl injections of appropriate reference standard solution until a constant response was obtained. The calculations were carried out in a conventional manner using standard and sample peak areas.

RESULTS AND DISCUSSION

Chemical Stability—High temperature causes cleavage of I at an apparent weak point (Ia) due to hydrogen bonding stress between the hydroxyl and carbonyl groups. Westley *et al.* (7) utilized this thermal degradation as the basis of a GLC assay wherein the retroaldol ketone formed during the degradation was assayed rather than the intact antibiotic.

Even though these authors utilized an injector port at 300° as an "on-site" pyrolytic chamber, experiments indicated that I in solutions would degrade with relative ease at a much lower temperature range. Due to the inherent nature of the compound to undergo cleavage at high temperatures, derivatization methods to chromatograph the intact molecule had to be carried out under ambient conditions. Attempts to silylate the compound at elevated temperatures did indeed result in multiple peaks, indicating degradation.

Silylation—*N,O*-Bis(trimethylsilyl)acetamide silylated the free acid to some extent at ambient temperatures but had no effect on the sodium salt of lasalocid (III). The addition of trimethylchlorosilane had the twofold effect of freeing I from its sodium chelate by acting as a Lewis acid and catalyzing the formation of more silylated derivative. This reagent combination, however, required 12 hr or longer to produce a quantitatively silylated product. The resulting derivative was unstable on standing (indicated by shoulder peaks), particularly after dilution with solvent, probably due to dissociation of the trimethylsilyl group from hindered sites.

The addition of the third ingredient, *N*-trimethylsilylimidazole, enhanced the reaction considerably. This reagent has the distinct advantage

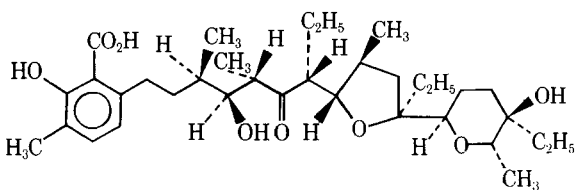

I

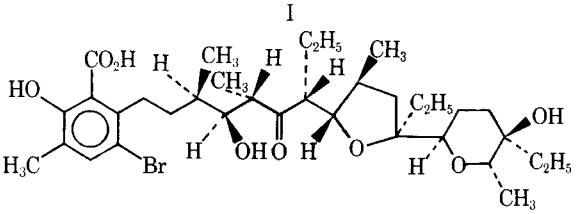

II

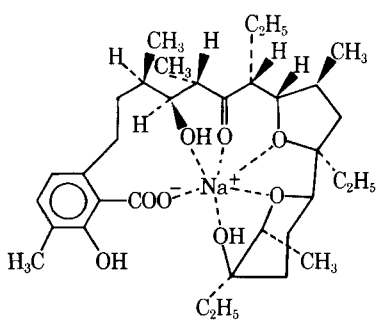

III

Table II—GLC Assay of Pure Substances

Sample	GLC Method, %	Alternative Method, %
I free acid	91.9	92.0[a]
I free acid	95.6	94.5[a]
II free acid	98.9	99.0[a]
III	89.8	88.8[b]
III	91.5	89.5[b]
III	90.8	89.5[b]

[a] Titration. [b] Microbiological.

of silylating the hindered hydroxyl groups due to its superior ability to accommodate a negative charge in the transition state (15). It also may act as a synergistic catalyst in the presence of trimethylchlorosilane to enhance the silylation of all active sites. The quantities of excess reagent present in sample solutions effectively prevented any dissociation of trimethylsilyl groups. The prepared solutions were stable during chromatography, as indicated by reproducible, well-resolved peaks for I and II derivatives (Fig. 1).

A time study was carried out on the silylation reaction at ambient temperature, and derivative formation reached equilibrium in about 30 min (Fig. 2). A time range of 30–45 min was satisfactory for the silylation of I in dosage forms. Due to the very reactive nature of the reagent mixture, contact with metallic surfaces such as aluminum cap liners was avoided throughout the study. Excess moisture in samples also was removed with mild heat and nitrogen prior to silylation to prevent an exothermic reaction with the reagent. Samples of I derivatives were subjected to GLC–mass spectrometric analysis, and the results confirmed the anticipated trimethylsilyl substitution of all carboxyl and alcohol functions, with the molecular ion observed at *m/e* 878.

Detector Response—The response of the flame-ionization detector to I and II derivatives was linear over a wide range. The II derivative was also chromatographed using scandium electron-capture detection, and the minimum detectable level was approximately 30 ng *versus* 300 ng for hydrogen flame-ionization detection.

An ideal internal standard could not be found, mainly due to solubility and elution characteristics associated with high molecular weight compounds. The external standard method used in the study yielded reproducible results.

Assay Results—A statistical analysis was carried out on the assay of III; the relative standard deviation was ±1.4%, significantly better than what is generally feasible in any microbiological assay method (Table I). Several samples of I and II pure substances also were assayed by this method, and the results were in good agreement with data obtained using other analytical techniques (Table II).

The procedure was used for the simultaneous assay of meglumine and active ingredients in I and II complexes with meglumine. The results were useful in establishing the molar concentrations of each component, depending upon the purity of materials used. However, the results could not be compared to other methods, since available chemical methodology was not reproducible for the assay of both chemical moieties of the complex (Table III). Other complex dosage forms such as ampuls (containing propylene glycol, preservative, and water), pellets, and feed premixes also were assayed with no special sample preparation. The chromatographic peak was free from interference, and the results are listed in Table IV.

All reported results are averages of duplicate determinations.

Specificity—During the assay of meglumine complexes, the chromatographic run was carried out at an initial column temperature of 160° for the elution of the meglumine trimethylsilyl derivative peak. Subse-

Table III—Assay of Experimental I and II Complexes with Meglumine

Sample	Percent Active by GLC	Percent Theory	Meglumine Percent by GLC	Meglumine Percent Theory[a]
I–monomeglumine	75.3	78	20.3	22
I–dimeglumine	52.5	62	39.8	38
I–dimeglumine	52.1	62	36.3	38
II–dimeglumine	64.8	65	35.6	35
II–dimeglumine	61.4	65	38.6	35

[a] Percent theory was calculated using molar ratios. Variations from the theoretical results were due to the presence of residual crystallization solvents, excess meglumine, and technical grade drug in the complexes.

Table IV—Assay of I in Other Matrixes

Sample	GLC Assay	Theoretical
Ampul solution 1	16.2 mg/2 ml[a]	20 mg/2 ml
Ampul solution 2	18.4 mg/2 ml[a]	20 mg/2 ml
Ampul solution 3	21.2 mg/2 ml	20 mg/2 ml
Premix pellets	2.53%	2.5%
Premix 1	14.8%	15.0%
Premix 2	16.1%	17.3%
Premix 3	16.4%	16.5%
Premix 4	16.2%	17.3%
Mycelial cake 1	6.3%	NA[b]
Mycelial cake 2	6.5%	NA
Mycelial cake 3	5.0%	NA
Mycelial cake 4[c] 1.1% excess	7.6%	7.4

[a] Decomposition of I in solution was indicated by the presence of an unknown GLC peak. [b] NA = not available. [c] Sample 1 to which had been added 1.1% of active ingredient to get an indication of recovery.

quently, the column temperature was raised to 260° to elute the I or II derivative peaks.

If any retroaldol ketone (known thermal degradation product) is present in the samples, it also would be silylated, resulting in a well-resolved peak suitable for quantitation. Samples of I and II complexes with meglumine were experimentally spiked with known amounts of retroaldol ketone and chromatographed after silylation. When the column temperature was programmed from 100 to 300°, trimethylsilyl derivatives of retroaldol ketone, meglumine, I, and II eluted at retention times of 7.5, 15, 30, and 35 min, respectively, clearly indicating the specificity and capability of the method for the assay of the antibiotic in multicomponent systems.

Furthermore, the I derivative peak area was approximately twice that of the retroaldol ketone when equal concentrations of I were subjected to the GLC–thermolysis method and the silylation procedure. This enhancement in peak response would be an added advantage in the analysis of low levels of I as a trimethylsilyl derivative.

The method presented has been applied to the assay of I in various solid and liquid preparations. It is specific for the antibiotic and does not require any extraction or pretreatment of the samples as in other reported methods.

REFERENCES

(1) J. Berger, A. I. Rachlin, W. E. Scott, L. H. Sternbach, and M. Goldberg, *J. Am. Chem. Soc.*, **73**, 5295 (1951).

(2) J. W. Westley, R. H. Evans, Jr., T. Williams, and A. Stempel, *Chem. Commun.*, **1970**, 71.

(3) S. M. Johnson, J. Herrin, S. J. Liu, and J. C. Paul, *ibid.*, **1970**, 72.

(4) J. W. Westley, W. Benz, J. Donahue, R. H. Evans, Jr., C. G. Scott, A. Stempel, and J. Berger, *J. Antibiot.*, **27** (10), 744 (1974).

(5) J. M. Scheiner, W. M. Cort, and J. Chen, *J. Assoc. Offic. Anal. Chem.*, **57**, 978 (1974).

(6) M. Osadca and M. Araujo, *ibid.*, **57**, 636 (1974).

(7) J. W. Westley, R. H. Evans, Jr., and A. Stempel, *Anal. Biochem.*, **59**, 574 (1974).

(8) P. D. Shaw, *Anal. Chem.*, **35**, 1581 (1963).

(9) M. Margosis, *J. Chromatogr.*, **47**, 341 (1970).

(10) C. Hishta, D. L. Mays, and M. Garafolo, *Anal. Chem.*, **43**, 1530 (1971).

(11) K. Tsuji and J. H. Robertson, *ibid.*, **43**, 918 (1971).

(12) *Ibid.*, **41**, 1332 (1969).

(13) M. Margosis, *J. Chromatogr.*, **37**, 46 (1968).

(14) R. L. Houtman, D. G. Kaiser, and A. J. Taraszka, *J. Pharm. Sci.*, **57**, 693 (1968).

(15) A. E. Pierce, "Silylation of Organic Compounds," Pierce Chemical Co., Rockford, Ill., pp. 19, 40–57.

ACKNOWLEDGMENTS AND ADDRESSES

Received April 16, 1976, from the *Analytical Research Laboratory, Quality Control Department, Hoffmann-La Roche Inc., Nutley, NJ 07110.*

Accepted for publication August 6, 1976.

The authors thank Dr. W. Cort for the microbiological assay results and Dr. C. G. Scott for the GLC–mass spectral data.

[x] To whom inquiries should be directed.

New Synthesis of 1,4,2-Dioxazoles and Their Pharmacological Properties

NED D. HEINDEL[*x], WILLIAM P. FIVES[*], and RICHARD A. CARRANO[‡§]

Abstract □ A series of 3-substituted 5-methoxycarbonyl-5-methoxycarbonylmethyl-1,4,2-dioxazoles was prepared by addition of hydroxamic acids to acetylene esters. Eleven of these previously unknown compounds were submitted to general pharmacological screening, and several displayed modest CNS depressant activity.

Keyphrases □ 1,4,2-Dioxazoles, substituted—synthesis, general pharmacological screening □ CNS activity—substituted 1,4,2-dioxazoles screened □ Structure-activity relationships—substituted 1,4,2-dioxazoles, general pharmacological screening

Most reported 1,4,2-dioxazoles are derived from the condensation of hydroxamic acids with phosgene (1, 2) or diethylacetals (3). Newer routes include a 1,3-dipolar addition method involving ketones and nitrile oxides (4) and a ring expansion of 2-acyloxaziridines (5). Except for some claims of antifungal activity in the 5-oxo derivatives (6) and of antibacterial potency in 5-benzenesulfonamido-substituted 1,4,2-dioxazoles (7), the possible pharmacological utility of this family of heterocyclics is still unknown.

CHEMISTRY

Reports from these laboratories noted the general utility of acetylenic esters in the synthesis of heterocyclic compounds generated by double nucleophilic additions to the same alkyne carbon (8, 9). In a similar fashion, hydroxamic acids, presumably in their enol tautomers (I) (10), reacted with dimethyl acetylenedicarboxylate (II*a*) and/or methyl propiolate (II*b*) (Schemes I and II) to produce high yields of 3-substituted 5-methoxycarbonyl-5-methoxycarbonylmethyl-1,4,2-dioxazoles (III*a*–III*j* and IV, Table I). In view of the paucity of information available on this heterocyclic family and the unique nature of this particular subclass, the general biological responses are now reported.

Available spectral evidence supported the assigned dioxazole structure.

Table IV—Assay of I in Other Matrixes

Sample	GLC Assay	Theoretical
Ampul solution 1	16.2 mg/2 ml[a]	20 mg/2 ml
Ampul solution 2	18.4 mg/2 ml[a]	20 mg/2 ml
Ampul solution 3	21.2 mg/2 ml	20 mg/2 ml
Premix pellets	2.53%	2.5%
Premix 1	14.8%	15.0%
Premix 2	16.1%	17.3%
Premix 3	16.4%	16.5%
Premix 4	16.2%	17.3%
Mycelial cake 1	6.3%	NA[b]
Mycelial cake 2	6.5%	NA
Mycelial cake 3	5.0%	NA
Mycelial cake 4[c] 1.1% excess	7.6%	7.4

[a] Decomposition of I in solution was indicated by the presence of an unknown GLC peak. [b] NA = not available. [c] Sample 1 to which had been added 1.1% of active ingredient to get an indication of recovery.

quently, the column temperature was raised to 260° to elute the I or II derivative peaks.

If any retroaldol ketone (known thermal degradation product) is present in the samples, it also would be silylated, resulting in a well-resolved peak suitable for quantitation. Samples of I and II complexes with meglumine were experimentally spiked with known amounts of retroaldol ketone and chromatographed after silylation. When the column temperature was programmed from 100 to 300°, trimethylsilyl derivatives of retroaldol ketone, meglumine, I, and II eluted at retention times of 7.5, 15, 30, and 35 min, respectively, clearly indicating the specificity and capability of the method for the assay of the antibiotic in multicomponent systems.

Furthermore, the I derivative peak area was approximately twice that of the retroaldol ketone when equal concentrations of I were subjected to the GLC–thermolysis method and the silylation procedure. This enhancement in peak response would be an added advantage in the analysis of low levels of I as a trimethylsilyl derivative.

The method presented has been applied to the assay of I in various solid and liquid preparations. It is specific for the antibiotic and does not require any extraction or pretreatment of the samples as in other reported methods.

REFERENCES

(1) J. Berger, A. I. Rachlin, W. E. Scott, L. H. Sternbach, and M. Goldberg, *J. Am. Chem. Soc.*, **73**, 5295 (1951).

(2) J. W. Westley, R. H. Evans, Jr., T. Williams, and A. Stempel, *Chem. Commun.*, **1970**, 71.

(3) S. M. Johnson, J. Herrin, S. J. Liu, and J. C. Paul, *ibid.*, **1970**, 72.

(4) J. W. Westley, W. Benz, J. Donahue, R. H. Evans, Jr., C. G. Scott, A. Stempel, and J. Berger, *J. Antibiot.*, **27** (10), 744 (1974).

(5) J. M. Scheiner, W. M. Cort, and J. Chen, *J. Assoc. Offic. Anal. Chem.*, **57**, 978 (1974).

(6) M. Osadca and M. Araujo, *ibid.*, **57**, 636 (1974).

(7) J. W. Westley, R. H. Evans, Jr., and A. Stempel, *Anal. Biochem.*, **59**, 574 (1974).

(8) P. D. Shaw, *Anal. Chem.*, **35**, 1581 (1963).

(9) M. Margosis, *J. Chromatogr.*, **47**, 341 (1970).

(10) C. Hishta, D. L. Mays, and M. Garafolo, *Anal. Chem.*, **43**, 1530 (1971).

(11) K. Tsuji and J. H. Robertson, *ibid.*, **43**, 918 (1971).

(12) *Ibid.*, **41**, 1332 (1969).

(13) M. Margosis, *J. Chromatogr.*, **37**, 46 (1968).

(14) R. L. Houtman, D. G. Kaiser, and A. J. Taraszka, *J. Pharm. Sci.*, **57**, 693 (1968).

(15) A. E. Pierce, "Silylation of Organic Compounds," Pierce Chemical Co., Rockford, Ill., pp. 19, 40–57.

ACKNOWLEDGMENTS AND ADDRESSES

Received April 16, 1976, from the *Analytical Research Laboratory, Quality Control Department, Hoffmann-La Roche Inc., Nutley, NJ 07110.*

Accepted for publication August 6, 1976.

The authors thank Dr. W. Cort for the microbiological assay results and Dr. C. G. Scott for the GLC–mass spectral data.

[x] To whom inquiries should be directed.

New Synthesis of 1,4,2-Dioxazoles and Their Pharmacological Properties

NED D. HEINDEL[*x], WILLIAM P. FIVES[*], and RICHARD A. CARRANO[‡§]

Abstract □ A series of 3-substituted 5-methoxycarbonyl-5-methoxycarbonylmethyl-1,4,2-dioxazoles was prepared by addition of hydroxamic acids to acetylene esters. Eleven of these previously unknown compounds were submitted to general pharmacological screening, and several displayed modest CNS depressant activity.

Keyphrases □ 1,4,2-Dioxazoles, substituted—synthesis, general pharmacological screening □ CNS activity—substituted 1,4,2-dioxazoles screened □ Structure-activity relationships—substituted 1,4,2-dioxazoles, general pharmacological screening

Most reported 1,4,2-dioxazoles are derived from the condensation of hydroxamic acids with phosgene (1, 2) or diethylacetals (3). Newer routes include a 1,3-dipolar addition method involving ketones and nitrile oxides (4) and a ring expansion of 2-acyloxaziridines (5). Except for some claims of antifungal activity in the 5-oxo derivatives (6) and of antibacterial potency in 5-benzenesulfonamido-substituted 1,4,2-dioxazoles (7), the possible pharmacological utility of this family of heterocyclics is still unknown.

CHEMISTRY

Reports from these laboratories noted the general utility of acetylenic esters in the synthesis of heterocyclic compounds generated by double nucleophilic additions to the same alkyne carbon (8, 9). In a similar fashion, hydroxamic acids, presumably in their enol tautomers (I) (10), reacted with dimethyl acetylenedicarboxylate (II*a*) and/or methyl propiolate (II*b*) (Schemes I and II) to produce high yields of 3-substituted 5-methoxycarbonyl-5-methoxycarbonylmethyl-1,4,2-dioxazoles (III*a*–III*j* and IV, Table I). In view of the paucity of information available on this heterocyclic family and the unique nature of this particular subclass, the general biological responses are now reported.

Available spectral evidence supported the assigned dioxazole structure.

Table I—Physical Data for 1,4,2-Dioxazoles

Compound	R_1	R_2	Yield, %	Melting Point (Boiling Point/ mm Hg)	n_D^{21}	Formula	Analysis, % Calc.	Found
III*a*	C_6H_5	$COOCH_3$	80	(154–156°/0.5)	1.5182	$C_{13}H_{13}NO_6$	C 55.91	55.81
							H 4.70	4.61
							N 5.02	4.97
III*b*	*p*-$CH_3OC_6H_4$	$COOCH_3$	90	50–51°	—	$C_{14}H_{15}NO_7$	C 54.37	54.65
							H 4.89	5.09
							N 4.53	4.72
III*c*	*m*-$CH_3OC_6H_4$	$COOCH_3$	66	(120–121°/0.1)	1.5221	$C_{14}H_{15}NO_7$	C 54.37	54.25
							H 4.89	4.80
							N 4.53	4.37
III*d*	*p*-BrC_6H_4	$COOCH_3$	83	—	1.5450	$C_{13}H_{12}BrNO_6$	C 43.60	43.78
							H 3.38	3.66
							N 3.91	4.01
III*e*	*m*-$NO_2C_6H_4$	$COOCH_3$	45	(145–148°/0.1)	1.5337	$C_{13}H_{12}N_2O_8$	C 48.15	48.29
							H 3.73	3.75
							N 8.64	8.60
III*f*	C_6H_{11}	$COOCH_3$	76	(123–135°/0.04)	1.4687	$C_{13}H_{19}NO_6$	C 54.73	54.58
							H 6.71	6.77
							N 4.91	4.93
III*g*	$C_6H_5CH_2$	$COOCH_3$	74	(161–163°/0.3)	—	$C_{14}H_{15}NO_6$	C 57.33	57.22
							H 5.16	5.35
							N 4.78	4.62
III*h*	$C_6H_5CH_2CH_2$	$COOCH_3$	79	—	1.5032	$C_{15}H_{17}NO_6$	C 58.63	58.56
							H 5.58	5.53
							N 4.56	4.73
III*i*	CH_3	$COOCH_3$	69	(77–79°/0.07)	—	$C_8H_{11}NO_6$	C 44.24	44.15
							H 5.11	5.22
							N 6.45	6.45
III*j*	C_6H_5	H	76	(134–136°/0.6)	1.5344	$C_{11}H_{11}NO_4$	C 59.72	59.94
							H 5.01	5.02
							N 6.33	6.52
IV	Terephthaloyl compound		58	112–114°	—	$C_{20}H_{20}N_2O_{12}$	C 50.00	49.94
							H 4.20	4.06
							N 5.83	5.74

In the IR spectrum, all NH and OH absorptions of the starting hydroxamic acid disappeared and the saturated ester carbonyls appeared between 1732 and 1752 cm^{-1}. The PMR spectrum revealed the ester methoxys between δ 3.65 and 3.86 ppm and, more significantly, the pendent methylene group by its characteristic geminally coupled *AB* quartet (J = 17 Hz) at δ 3.20 ± 0.20 ppm. This appearance of magnetically nonequivalent methylene protons adjacent to an asymmetric center is well known (11). Furthermore, the mass spectra of all 1,4,2-dioxazoles derived from dimethyl acetylenedicarboxylate showed the expected parent ion and fragments at P − 73 (loss of CH_2COOCH_3) and P − 59 (loss of $COOCH_3$), clearly indicating the nature of the two ester moieties attached at C-5 of the 1,4,2-dioxazoles.

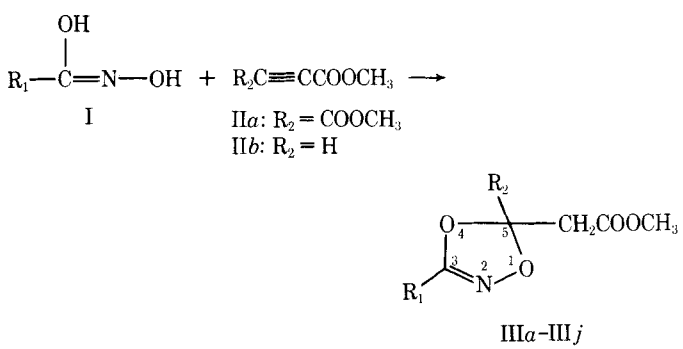

Scheme I

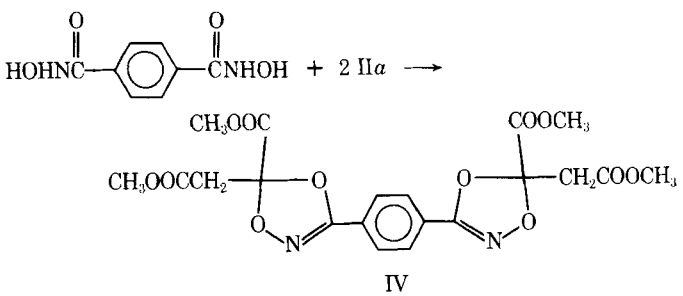

Scheme II

In accord with numerous citations in the patent literature claiming pyrolysis of 1,4,2-dioxazoles as a route to isocyanates (12, 13), distillation of the prepared liquid dioxazoles often produced a fraction containing the corresponding isocyanate (absorption at 2250 ± 15 cm^{-1}). Two dioxazoles (III*d* and III*h*) suffered such extensive thermal decomposition on refluxing that they could not be distilled. For these two particular materials, an extraction purification procedure was developed which yielded analytically pure product. This technique was also applicable to most other liquid dioxazoles.

Table I reports boiling points for the substances that could be vacuum distilled and refractive indexes for the dioxazoles purified by the extraction method. If an analytically pure product could be obtained by either route, then both boiling points and refractive index values are cited.

PHARMACOLOGY

General Rat Screening—All compounds were tested and the results were analyzed according to the methods described by Malone and Carrano (14) and employed previously (15). Nonfasted albino rats, 180–210 g, were used; injections were made intraperitoneally.

General Central Nervous System (CNS) Testing in Mice—Motor function and neurotoxicity were tested at 200 mg/kg ip by measuring the inability of trained animals to walk a rotating wooden rod (28 mm diameter at 6 rpm) for 1 min. Six 18–22-g nonfasted albino mice were used per group; dosing was done intraperitoneally. The animals were tested at 0, 15, 30, 60, 90, 120, 150, and 180 min postinjection.

If there was no neurotoxicity at 200 mg/kg ip, then that dose was used for subsequent work in the antistrychnine, antipentylenetetrazol, antielectroshock, and antioxotremorine tests. In these tests, the experimental drug was injected intraperitoneally into groups of six 18–22-g nonfasted albino mice; at 30 min postinjection, strychnine sulfate (1.1 mg/kg sc), pentylenetetrazol (70 mg/kg sc), oxotremorine (350 μg/kg sc), or a 50-amp, 0.2-sec shock was administered to each animal. The animals were observed for 30 min for tonic extensor seizures in the antistrychnine test and for clonic seizures in the antipentylenetetrazol test. In the antielectroshock test, they were observed for hindlimb tonic extensor seizures. In the antioxotremorine test, tremors were subjectively rated per

animal on a scale of 0–3 and the total response for the entire group was calculated and compared to that of a control group.

In each test, a group of animals receiving 0.9% NaCl (5 ml/kg) was run simultaneously with the experimental groups. In the acetylcholine writhing test, mice were injected orally with the experimental agent; 30 min later, they were challenged with 7.0 mg/kg ip of acetylcholine bromide. The number of animals in the experimental group that elicited a writhing response within 2 min was compared to a control group receiving 0.9% NaCl.

Selected drugs were tested for their ability to inhibit aggression induced in pairs of mice by subjecting them to an interrupted direct current foot shock of 0.8 mamp for 2 min.

Acute Anti-Inflammatory–Analgesic Testing—Nonfasted albino rats, 160–180 g, equally divided between sexes were used. The experimental drugs were administered orally. A modified Randall–Selitto (16) method was used; immediately following administration of the drug, 0.1 ml of a 1% carrageenan suspension was injected into the subplantar area of the right hindpaw, and the control foot volume was recorded by volume displacement. The control analgesic response was then estimated by placing the injected paw between two grooved disks, which were slowly forced together *via* air pressure. The amount of pressure required to cause the animal to vocalize or attempt to bite the disks was recorded. The analgesic response was again estimated at 45 min postinjection, and foot volume was measured at 4 hr postinjection. A control group that received 0.9% NaCl in place of the experimental drug was tested simultaneously.

RESULTS AND DISCUSSION

Table II lists the important observations in the general rat screening. The maximum sublethal dose is the highest dose administered at which no death occurred. Since no doses were made over 1.0 g/kg, the maximum sublethal dose was assumed to be greater than 1.0 g/kg in cases where there was no death at this dosage.

Also presented in Table II are scores that represent the extent of general autonomic nervous system (ANS) and general CNS depressant (CNSD) activity. The absolute values of these ANS and CNSD scores are not comparable. The significant symptomatology of the candidate dioxazoles is given. These data were subjected to a computer-matching operation against a library of 27 reference drugs. The symptomatology and ANS/CNSD scores for the drugs selected for comparison were reported previously (15).

Compounds III*a*, III*g*, and IV produced significant CNS depression in rats. The symptomatology exhibited by these drugs suggests that they have activity similar to tranquilizers, muscle relaxants, anticonvulsants, and other CNS depressants. On the basis of computerized matching, III*g* showed a particular similarity to chlorpromazine and chlordiazepoxide. Apparently, only the dioxazoles with phenyl moieties (lacking polar substituents such as methoxy, nitro, and bromo) attached directly to the hetero ring or in the α-position (*i.e.*, III*g*) displayed the depressant activity. The two pendent ester groupings are apparently necessary, since III*a* was one of the most active compounds tested while III*j* gave evidence of only very modest activity. On the basis of the primary rat screening, III*a*, III*g*, and IV were submitted for further evaluation in the CNS battery. The percent protection at the rotarod ED_{50} was evaluated.

Here again the benzyl derivative, III*g*, displayed the highest percentage protection (36%) against shock-induced aggression and did exhibit some antioxotremorine activity (14%). All compounds were tested at a considerably more elevated dose, 200 mg/kg ip, than the comparison drugs, and none was judged sufficiently active to warrant further study. Chlordiazepoxide hydrochloride, for example, at a dose of 32 mg/kg ip, provides 100% protection against shock-induced aggression and 75% protection in the antioxotremorine assay.

Some protection against acetylcholine writhing was observed with III*a* and IV, 33% in both cases, but they were rejected for advanced studies because of the elevated doses required (300 mg/kg po) and the lack of significant anti-inflammatory–analgesic activity in the Randall–Selitto assay (16).

Since both III*i* and III*j* displayed significant scores in the autonomic category of the general rat screen (Table II), they were selected for cardiovascular measurements in the anesthetized cat. Both compounds produced moderate to extreme transient falls in blood pressure at 1–25 mg/kg iv. Heart rate was not affected dramatically. Both drugs produced some potentiation of the responses to norepinephrine, a decrease in the pulse pressure response to isoproterenol, and an inhibition of the response to 1,1-dimethyl-4-phenylpiperazinium iodide. However, none of these actions was considered significant enough to merit further investigation.

Table II—*In Vivo* Rat Screening Data for 1,4,2-Dioxazoles

Compound[a]	ANS Score	CNSD Score	Significant Symptomatology
III*a*	0.53	4.78	Decreased body tone, body weight
III*b*	0	0	None
III*c*	2.01	1.23	Miosis, piloerection
III*d*	1.48	2.16	Miosis, piloerection, decreased body tone
III*e*	1.27	0	Miosis, piloerection, decreased body weight, fearfulness
III*g*[b]	1.06	11.88	Decreased motor activity, ataxia, decreased respiratory rate, piloerection, decreased rotarod ability, decreased body tone
III*i*	4.87	0.62	Miosis, decreased body weight
III*f*	0.74	2.93	Decreased motor activity, piloerection, increased body tone
III*j*	4.97	0.77	Miosis
IV	3.70	10.49	Decreased motor activity, ataxia, miosis, piloerection, decreased body weight, decreased body tone, decreased rotarod ability
III*h*	0.42	1.08	Decreased body weight

[a] The maximum sublethal dose was greater than 1000 mg/kg ip. [b] Similar to chlordiazepoxide and chlorpromazine.

In general, these 1,4,2-dioxazoles were water-insoluble viscous liquids that were difficult to manipulate and administer in the animal studies. Gross necropsy of rats at 48 hr after intraperitoneal injection revealed the presence of some unabsorbed drug in the peritoneal cavity.

EXPERIMENTAL[1]

Hydroxamic Acids—The required hydroxamic acids were either commercially available or prepared from the corresponding ester and hydroxylamine according to published procedures (17–22).

Compounds III*a*–III*i*—An equimolar mixture of the required hydroxamic acid and dimethyl acetylenedicarboxylate was prepared in anhydrous methanol at a concentration of 100 mmoles/100 ml of solvent. The solution was refluxed for 30–60 min and then allowed to stir at room temperature for 24 hr. Concentration *in vacuo* produced an oil, which solidified in the case of III*b* (recrystallized from methanol, mp 50–51°, 90%) but remained liquid in the other examples. Purification was effected by either fractional vacuum distillation or by the following solvent extraction procedure.

The oily dioxazole was dissolved in a minimum of carbon tetrachloride and washed four times with 50-ml portions of cold distilled water. The carbon tetrachloride layer was dried with magnesium sulfate and evaporated under vacuum with minimal heating to yield the product as a clear oil. Refractive indexes (n_D^{21}), yields, and analytical data are given in Table I for those dioxazoles purified by this method. If no refractive index is given, the purification was by vacuum distillation.

Compound III*j*—A solution of 73.0 mmoles of benzohydroxamic acid and methyl propiolate in 75 ml of methanol was heated at reflux for 24 hr, evaporated *in vacuo*, and purified by the solvent extraction procedure to return a 76% yield. The oil could also be vacuum distilled.

Compound IV—A methanol solution of 51.0 mmoles of terephthalohydroxamic acid, 102 mmoles of dimethyl acetylenedicarboxylate, and 200 ml of methanol was stirred at room temperature for 48 hr, during which time a white precipitate appeared. The reaction mixture was filtered, concentrated, and chilled to produce an additional crystal crop; the crude product was recrystallized from methanol to afford 14.2 g (58%) of white microneedles, mp 112–114° (Table I).

[1]Melting points were determined with a Fisher-Johns apparatus and are not corrected. IR spectra were obtained as hydrocarbon mulls or neat on a Perkin-Elmer model 257 spectrophotometer. PMR spectra were determined on a Hitachi Perkin-Elmer model R20A spectrometer in deuterochloroform, using tetramethylsilane as the internal reference.

REFERENCES

(1) G. Beck, *Chem. Ber.*, **84**, 688 (1951).

(2) S. Drabarek and S. Klimkiewicz, *Rocz. Chem.*, **44**, 919 (1970); through *Chem. Abstr.*, **74**, 3561 (1971).

(3) H. Nohira, K. Inoue, H. Hattori, T. Okawa, and T. Mukaiyama, *Bull. Chem. Soc. Jpn.*, **40**, 664 (1967).

(4) R. Huisgen and W. Mack, *Chem. Ber.*, **105**, 2805 (1972).

(5) E. Schmitz, R. Ohme, and S. Schramm, *Tetrahedron Lett.*, **1965**, 1857.

(6) K. Sasse and P. E. Frohberger, German pat. 2,059,990 (1972); through *Chem. Abstr.*, **77**, 110567n (1972).

(7) R. Neidlein and H. Kruell, *Arch. Pharm. (Weinheim)*, **304**, 763 (1971).

(8) N. D. Heindel and L. A. Schaeffer, *J. Med. Chem.*, **13**, 981 (1970).

(9) T. F. Lemke, H. W. Snady, Jr., and N. D. Heindel, *J. Org. Chem.*, **37**, 2337 (1972).

(10) R. E. Plapinger, *ibid.*, **24**, 802 (1959).

(11) D. J. Pasto and C. R. Johnson, "Organic Structure Determination," Prentice-Hall, Englewood Cliffs, N.J., 1969, p. 199.

(12) Sinclair Research, Netherlands pat. 6,615,003 (1967); through *Chem. Abstr.*, **67**, 63872 (1967).

(13) E. H. Burk, Jr., and D. D. Carlos, French pat. 1,505,468 (1967); through *Chem. Abstr.*, **70**, 11375 (1969).

(14) M. H. Malone and R. A. Carrano, "Hippocratic and Pharmacodynamic Screening," APhA Academy of Pharmaceutical Sciences, Washington, D.C. Meeting, Symposium on Advances in Screening Methodology, Nov. 1968.

(15) N. D. Heindel, W. P. Fives, T. F. Lemke, and R. A. Carrano, *J. Pharm. Sci.*, **60**, 703 (1971).

(16) L. O. Randall and I. I. Selitto, *Arch. Int. Pharmacodyn. Ther.*, **111**, 409 (1957).

(17) K. Buraczewski, E. Czerwinska, Z. Eckstein, E. Grochowski, R. Kowalik, and J. Plenkiewicz, *Przem. Chem.*, **43**, 626 (1964).

(18) N. Kornblum and R. A. Brown, *J. Am. Chem. Soc.*, **87**, 1742 (1965).

(19) O. Exner and W. Simon, *Collect. Czech. Chem. Commun.*, **30**, 4078 (1965).

(20) W. Cohen and B. F. Erlanger, *J. Am. Chem. Soc.*, **82**, 3928 (1960).

(21) J. Thiele and H. Pickard, *Ann. Chem.*, **309**, 197 (1899).

(22) W. Lossen, *ibid.*, **281**, 178 (1894).

ACKNOWLEDGMENTS AND ADDRESSES

Received May 17, 1976, from the *Center for Health Sciences, Lehigh University, Bethlehem, PA 18015, and the ‡Biomedical Research Department, ICI-United States, Inc., Wilmington, DE 19899.

Accepted for publication July 26, 1976.

Abstracted in part from a dissertation submitted by W. P. Fives to Lehigh University in partial fulfillment of the Doctor of Philosophy degree requirements.

Supported by a grant-in-aid to N. D. Heindel from the Stuart Pharmaceutical Division, ICI-United States.

The authors thank Dr. K. K. Kimura, Dr. J. W. LeMaistre, Dr. D. H. McCurdy, and Dr. A. D. Miller of ICI-United States for their support and suggestions.

§ Present address: Adria Laboratories, Inc., Wilmington, DE 19801.

x To whom inquiries should be directed.

Plasma Isosorbide Dinitrate Concentrations in Human Subjects after Administration of Standard and Sustained-Release Formulations

D. F. ASSINDER, L. F. CHASSEAUD[x], and T. TAYLOR

Abstract □ After sublingual administration of 5 mg of isosorbide dinitrate, mean plasma concentrations (± *SD*) peaked (8.9 ± 3.1 ng/ml) at 15 min after dosing and declined with a half-life of 30 min. After oral administration of 5 mg, mean concentrations peaked (3.1 ± 0.7 ng/ml) at 30 min and declined with a half-life of 40 min. After oral administration of 20 mg in a sustained-release tablet, mean concentrations initially peaked (1.4 ± 1.2 ng/ml) at 40 min, declining to 0.9 ± 0.5 ng/ml after 8 hr. Mean concentrations were maintained above half the mean peak level during 10 hr. Because of probable rapid first-pass metabolism, the bioavailability of isosorbide dinitrate after administration of the oral dose of the standard tablet was 58% of that from the sublingual dose, and the bioavailability from the sustained-release tablet was 47% of that from the sublingual dose of the standard tablet. The time course of mean plasma concentration data could be described by a one-compartment model; but a more complex model, taking the pass effect into account, probably is needed for a better description of the pharmacokinetics of isosorbide dinitrate.

Keyphrases □ Isosorbide dinitrate—pharmacokinetics, oral and sublingual administration compared, standard and sustained-release tablets compared, humans □ Pharmacokinetics—isosorbide dinitrate, oral and sublingual administration compared, standard and sustained-release tablets compared, humans □ Vasodilators—isosorbide dinitrate, pharmacokinetics, oral and sublingual administration compared, standard and sustained-release tablets compared, humans

The vasodilator isosorbide dinitrate has been in use for many years (1–9), but little has been reported regarding its pharmacokinetics in humans because, in part, of the difficulty in measuring small amounts of the drug in blood. Using a GLC method (10), peak plasma concentrations ranging between 10.5 and 34.5 ng/ml in different subjects were measured at 6 min following a 1.25-mg sublingual dose of isosorbide dinitrate. More detailed studies involving the oral administration of 5.4 mg of ^{14}C-isosorbide dinitrate (11) showed that peak levels of unchanged drug of about 5 ng/ml could be expected (12). However, higher concentrations of the respective mononitrate metabolites were present (12).

Isosorbide dinitrate and other organic nitrates are rapidly metabolized by the glutathione *S*-transferases (13, 14). From studies in animals, Needleman *et al.* (15) concluded that after oral administration of any one of the various organic nitrates, such as isosorbide dinitrate, essentially

REFERENCES

(1) G. Beck, *Chem. Ber.*, **84**, 688 (1951).

(2) S. Drabarek and S. Klimkiewicz, *Rocz. Chem.*, **44**, 919 (1970); through *Chem. Abstr.*, **74**, 3561 (1971).

(3) H. Nohira, K. Inoue, H. Hattori, T. Okawa, and T. Mukaiyama, *Bull. Chem. Soc. Jpn.*, **40**, 664 (1967).

(4) R. Huisgen and W. Mack, *Chem. Ber.*, **105**, 2805 (1972).

(5) E. Schmitz, R. Ohme, and S. Schramm, *Tetrahedron Lett.*, **1965**, 1857.

(6) K. Sasse and P. E. Frohberger, German pat. 2,059,990 (1972); through *Chem. Abstr.*, **77**, 110567n (1972).

(7) R. Neidlein and H. Kruell, *Arch. Pharm. (Weinheim)*, **304**, 763 (1971).

(8) N. D. Heindel and L. A. Schaeffer, *J. Med. Chem.*, **13**, 981 (1970).

(9) T. F. Lemke, H. W. Snady, Jr., and N. D. Heindel, *J. Org. Chem.*, **37**, 2337 (1972).

(10) R. E. Plapinger, *ibid.*, **24**, 802 (1959).

(11) D. J. Pasto and C. R. Johnson, "Organic Structure Determination," Prentice-Hall, Englewood Cliffs, N.J., 1969, p. 199.

(12) Sinclair Research, Netherlands pat. 6,615,003 (1967); through *Chem. Abstr.*, **67**, 63872 (1967).

(13) E. H. Burk, Jr., and D. D. Carlos, French pat. 1,505,468 (1967); through *Chem. Abstr.*, **70**, 11375 (1969).

(14) M. H. Malone and R. A. Carrano, "Hippocratic and Pharmacodynamic Screening," APhA Academy of Pharmaceutical Sciences, Washington, D.C. Meeting, Symposium on Advances in Screening Methodology, Nov. 1968.

(15) N. D. Heindel, W. P. Fives, T. F. Lemke, and R. A. Carrano, *J. Pharm. Sci.*, **60**, 703 (1971).

(16) L. O. Randall and I. I. Selitto, *Arch. Int. Pharmacodyn. Ther.*, **111**, 409 (1957).

(17) K. Buraczewski, E. Czerwinska, Z. Eckstein, E. Grochowski, R. Kowalik, and J. Plenkiewicz, *Przem. Chem.*, **43**, 626 (1964).

(18) N. Kornblum and R. A. Brown, *J. Am. Chem. Soc.*, **87**, 1742 (1965).

(19) O. Exner and W. Simon, *Collect. Czech. Chem. Commun.*, **30**, 4078 (1965).

(20) W. Cohen and B. F. Erlanger, *J. Am. Chem. Soc.*, **82**, 3928 (1960).

(21) J. Thiele and H. Pickard, *Ann. Chem.*, **309**, 197 (1899).

(22) W. Lossen, *ibid.*, **281**, 178 (1894).

ACKNOWLEDGMENTS AND ADDRESSES

Received May 17, 1976, from the *Center for Health Sciences, Lehigh University, Bethlehem, PA 18015, and the ‡Biomedical Research Department, ICI-United States, Inc., Wilmington, DE 19899.

Accepted for publication July 26, 1976.

Abstracted in part from a dissertation submitted by W. P. Fives to Lehigh University in partial fulfillment of the Doctor of Philosophy degree requirements.

Supported by a grant-in-aid to N. D. Heindel from the Stuart Pharmaceutical Division, ICI-United States.

The authors thank Dr. K. K. Kimura, Dr. J. W. LeMaistre, Dr. D. H. McCurdy, and Dr. A. D. Miller of ICI-United States for their support and suggestions.

§ Present address: Adria Laboratories, Inc., Wilmington, DE 19801.

x To whom inquiries should be directed.

Plasma Isosorbide Dinitrate Concentrations in Human Subjects after Administration of Standard and Sustained-Release Formulations

D. F. ASSINDER, L. F. CHASSEAUD[x], and T. TAYLOR

Abstract □ After sublingual administration of 5 mg of isosorbide dinitrate, mean plasma concentrations (± *SD*) peaked (8.9 ± 3.1 ng/ml) at 15 min after dosing and declined with a half-life of 30 min. After oral administration of 5 mg, mean concentrations peaked (3.1 ± 0.7 ng/ml) at 30 min and declined with a half-life of 40 min. After oral administration of 20 mg in a sustained-release tablet, mean concentrations initially peaked (1.4 ± 1.2 ng/ml) at 40 min, declining to 0.9 ± 0.5 ng/ml after 8 hr. Mean concentrations were maintained above half the mean peak level during 10 hr. Because of probable rapid first-pass metabolism, the bioavailability of isosorbide dinitrate after administration of the oral dose of the standard tablet was 58% of that from the sublingual dose, and the bioavailability from the sustained-release tablet was 47% of that from the sublingual dose of the standard tablet. The time course of mean plasma concentration data could be described by a one-compartment model; but a more complex model, taking the pass effect into account, probably is needed for a better description of the pharmacokinetics of isosorbide dinitrate.

Keyphrases □ Isosorbide dinitrate—pharmacokinetics, oral and sublingual administration compared, standard and sustained-release tablets compared, humans □ Pharmacokinetics—isosorbide dinitrate, oral and sublingual administration compared, standard and sustained-release tablets compared, humans □ Vasodilators—isosorbide dinitrate, pharmacokinetics, oral and sublingual administration compared, standard and sustained-release tablets compared, humans

The vasodilator isosorbide dinitrate has been in use for many years (1–9), but little has been reported regarding its pharmacokinetics in humans because, in part, of the difficulty in measuring small amounts of the drug in blood. Using a GLC method (10), peak plasma concentrations ranging between 10.5 and 34.5 ng/ml in different subjects were measured at 6 min following a 1.25-mg sublingual dose of isosorbide dinitrate. More detailed studies involving the oral administration of 5.4 mg of ^{14}C-isosorbide dinitrate (11) showed that peak levels of unchanged drug of about 5 ng/ml could be expected (12). However, higher concentrations of the respective mononitrate metabolites were present (12).

Isosorbide dinitrate and other organic nitrates are rapidly metabolized by the glutathione *S*-transferases (13, 14). From studies in animals, Needleman *et al.* (15) concluded that after oral administration of any one of the various organic nitrates, such as isosorbide dinitrate, essentially

none of the parent compound was present in the circulation to relax vascular smooth muscle. Previous work (11), however, showed that, in humans, orally administered isosorbide dinitrate does reach the peripheral circulation intact. Additional evidence is now presented, obtained from studies of standard and sustained-release formulations of the drug.

EXPERIMENTAL

Materials—Standard tablets[1] of isosorbide dinitrate for oral or sublingual administration each contained 5 mg of drug. Sustained-release tablets[1] for oral administration each contained 20 mg.

Drug Administration—Six male subjects[2], 22–39 years old and 57–89 kg, were given one tablet of each formulation of isosorbide dinitrate according to a randomized complete crossover treatment schedule, with about 1 week between dosing.

Following an overnight fast, the oral doses were taken with 100 ml of water and the sublingual doses were retained under the tongue until completely dissolved but were not swallowed deliberately. The subjects fasted for 4 hr following the dose. Blood samples were regularly withdrawn by venipuncture from the antecubital veins into heparinized tubes, and the plasma was immediately separated by centrifugation for rapid analysis.

The blood pressure of each subject was monitored for the first 2 hr after dosing. Decreases in blood pressure occurred after administration of all three formulations but particularly after the sublingual form. The subjects were under continual medical supervision.

Measurement of Drug—Concentrations of isosorbide dinitrate in plasma were measured by GLC using electron-capture detection by a modification[3] of the method of Rosseel and Bogaert (10). Glycerol trinitrate was used as the internal standard; under the conditions employed, it and isosorbide dinitrate were eluted as symmetrical peaks with retention times of 2 and 6 min, respectively. The limit of detection of isosorbide dinitrate in plasma was 0.5 ng/ml. The standard curves were prepared from known amounts of isosorbide dinitrate added to control plasma.

RESULTS

Plasma Concentrations—Fifteen minutes after administration of the standard tablet as a sublingual 5-mg dose, the peak of mean concentrations (±*SD*) was 8.9 ± 3.1 ng/ml (Table I and Fig. 1). Mean concentrations thereafter declined rapidly to 0.8 ± 0.3 ng/ml after 2 hr and were below the limit of detection (<0.5 ng/ml) at 4 hr after dosing. After administration of the standard tablet as an oral 5-mg dose, a peak of mean concentrations of 3.1 ± 0.7 ng/ml was reached at 30 min (Table I and Fig. 1). Mean concentrations declined to 0.7 ± 0.2 ng/ml at 2 hr and were below the limits of detection at 4 hr after dosing. After administration of 20 mg of isosorbide dinitrate as the sustained-release tablet, an initial peak of mean concentrations of 1.4 ± 1.2 ng/ml occurred at 40 min; concentrations remained at about this level during 1–6 hr (Table I and Fig. 1). Thereafter, mean concentrations declined to the limits of detection at about 12 hr after dosing.

After oral or sublingual doses, peak concentrations in individual subjects varied more than twofold. After administration of the 20-mg sustained-release tablet, at least two peak levels in the plasmas of five of the six subjects were measured (Table I). The first peak occurred at 1.5 hr after administration (0.9–3.1 ng/ml), and the second occurred between 4 and 6 hr (1.4–3.0 ng/ml). Three peak levels in the plasma of Subject 4 were measured: at 40 min, 2.2 ng/ml; at 2 hr, 2.1 ng/ml; and at 6 hr, 3.0 ng/ml. Plasma concentrations were maintained at a plateau during approximately 40 min–8 hr after dosing, and the average plateau (steady-state) plasma concentration during this time was 1.4 ng/ml (range of 1.3–1.9 ng/ml). Mean concentrations were maintained above a value of half the average plateau level during 10 hr after dosing; *i.e.*, the mean half-peak value duration time for this formulation was approximately 10 hr. In contrast, the mean half-peak value duration time for the oral dose of the standard tablet was approximately 1 hr, and the ratio, R_Δ, of the half-peak value duration times was 10. The R_c of peak mean concentrations after administration of the sustained-release tablet and the oral dose standard tablet was 1.4/3.1 = 0.45. The retard quotient (R_Δ, R_c) was (10.0, 0.45) for this pair of formulations; therefore, the *in vivo* performance of the sustained-release formulation was fairly good (16).

Table I—Plasma Isosorbide Dinitrate Concentrations (Nanograms per Milliliter ± *SD*, *n* = 6)

Minutes	Route of Administration: Sublingual	Oral	Oral Sustained Release
5	4.2 ± 2.2	—	—
10	8.7 ± 3.8	—	—
15	8.9 ± 3.1	2.4 ± 0.7	0.6 ± 0.5
30	6.5 ± 2.0	3.1 ± 0.7	1.0 ± 1.0
45	4.7 ± 1.5	2.6 ± 0.6	1.4 ± 1.2
60	3.3 ± 1.2	2.0 ± 0.6	1.3 ± 0.7
90	1.7 ± 0.5	1.1 ± 0.3	1.4 ± 0.5
120	0.8 ± 0.3	0.7 ± 0.2	1.4 ± 0.6
240	ND[a]	ND	1.3 ± 0.5
360	ND	ND	1.9 ± 0.8
480	—	—	0.9 ± 0.5
720	—	—	ND[b]

[a] ND = not detected (<0.5 ng/ml). [b] Concentrations (1.6 ng/ml) detected in one subject only.

Bioavailability—The bioavailability from the drug formulations was compared indirectly from the peak plasma concentrations and their times of occurrence. The first peak levels after administration of the sustained-release tablet were much lower (mean 1.8 ± 0.8 ng/ml) and occurred later (78 min) than those after administration of the sublingual dose (9.7 ± 2.1 ng/ml at 12.5 min) or the oral dose (3.3 ± 0.6 ng/ml at 27.5 min) (Table II and Fig. 1). The rates of bioavailability were obviously lowest after administration of the sustained-release tablet, and rates after administration of the oral dose were lower than those after administration of the sublingual dose of the standard tablet.

The extent of bioavailability was estimated by comparing the areas under the plasma concentration–time relationships (Fig. 1), taking the sublingual dose of the standard tablet as a reference. With the sublingual and oral doses of the standard tablet, plasma concentrations were below

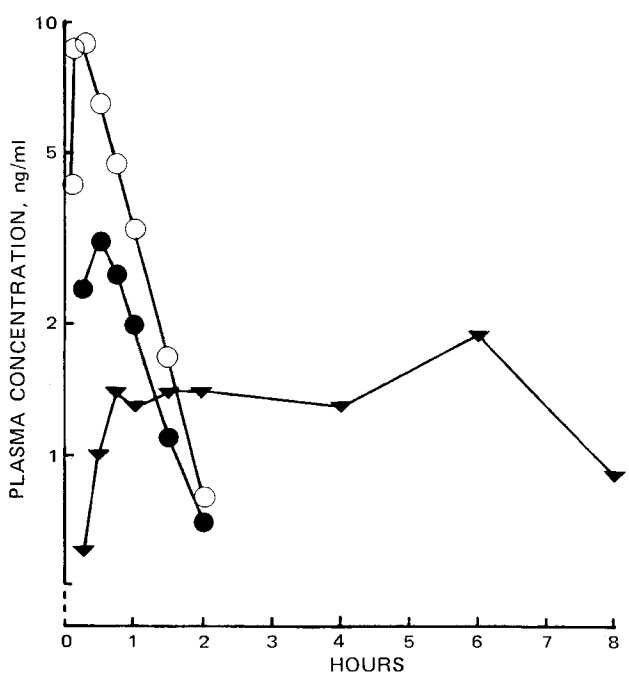

Figure 1—*Mean plasma concentrations of unchanged drug after administration of different formulations of isosorbide dinitrate to human subjects. Key:* ○, *5 mg sublingual;* ●, *5 mg oral; and* ▼, *20 mg oral sustained release.*

[1] Isoket, batches 10421 (standard) and 12463 (sustained release), provided by Pharma Schwarz GmbH, Monheim, Germany.

[2] The subjects were thoroughly screened medically and biochemically soon before and after the studies and were judged to be in good health. The subjects gave their consent to participate after the purpose of the studies and the nature of the drug had been explained.

[3] To be reported elsewhere.

Table II—Peak Isosorbide Dinitrate Concentrations and Their Times of Occurrence in Individual Subjects

Subject	Sublingual		Oral		Oral Sustained Release	
	Peak Level, ng/ml	Minutes	Peak Level, ng/ml	Minutes	Peak Level[a], ng/ml	Minutes[a]
1	7.2	15	3.2	30	3.1	40
2	9.5	10	3.5	45	1.3	90
3	6.9	15	4.1	30	1.7	120–240
4	9.6	10	3.4	15 and 30	2.2	40
5	10.0	10	2.2	30	1.3	30–60
6	15.0	15	3.3	30	0.9	60–90
Mean (±*SD*)	9.7 (±2.1)	12.5	3.3 (±0.6)	27.5	1.8 (±0.8)	78

[a] Initial peak level after administration of the sustained-release tablet containing 20 mg of drug. Several peak levels occurred in plasma of individual subjects.

the limits of detection 4 hr after administration, and areas to 4 hr were equivalent to "areas to infinite time," which are proportional to the fraction of the dose absorbed. With the sustained-release tablet, plasma concentrations were relatively high at the last time of sampling in one subject (12 hr), and comparison of areas to this time may have slightly underestimated the bioavailability from the formulation.

Measured areas under the concentration–time relationships were corrected for dose–body weight variations because unequal doses were administered (Table III). The ratios of corrected areas, with the area after administration of the sublingual dose as reference, provided an estimate of the relative fraction of the dose absorbed into the peripheral circulation and, hence, the bioavailability of isosorbide dinitrate from the standard tablet, oral dose, and the sustained-release tablet. The mean bioavailability from the standard tablet after oral administration was 58% of that from the standard tablet after sublingual administration. So calculated, the mean bioavailability of isosorbide dinitrate from the sustained-release tablet was 47% of that from the sublingual dose of the standard tablet. However, since comparison of areas to 12 hr after administration of the sustained-release tablet may have led to an underestimation of bioavailability, it was likely that a similar fraction of the dose was absorbed from both the sustained-release tablet and the standard tablet after oral administration.

Pharmacokinetics—The half-lives of drug elimination were calculated by least-squares regression analysis of $\log_e$ (concentration) against time from data points on the terminal linear section of the curve (Fig. 1). After sublingual doses, more than 96% of the total variance was accounted for by the regression, and half-lives were adequately estimated from the data. These half-lives were similar in individual subjects, with a mean of 0.5 hr (range of 0.47–0.53 hr; Fig. 1). After oral doses of the standard tablet, more than 93% of the variance was accounted for by the regression, and half-lives were again adequately estimated from the data. The mean half-life after these doses was 0.67 hr, with a wider range (0.47–1.05 hr) than after administration of the sublingual dose. A more prolonged absorptive phase after oral doses may have prolonged the half-lives after oral doses, although the difference in mean half-life after administration by these two routes was not statistically significant ($p > 0.05$).

Inspection of the mean plasma concentrations (Fig. 1) indicated that the data might be fitted to a one-compartment model (17). Accordingly, the rate constants for absorption were calculated by the method of Saunders and Natunen (18) assuming a one-compartment model. After sublingual and oral doses, the mean concentration–time relationships were described by the equations:

$$C_{\text{sublingual}} = 12.25(-e^{-0.2877t} + e^{-0.0229t}) \quad \text{(Eq. 1)}$$

$$C_{\text{oral}} = 5.40(-e^{-0.1093t} + e^{-0.0171t}) \quad \text{(Eq. 2)}$$

respectively. The calculated parameters of the model are given in Table IV; it was assumed that the dose was completely absorbed by the sublingual route and that 58% of the dose was absorbed after oral administration (see *Bioavailability* section).

This model requires a very large "unphysiological" volume of distribution and a high plasma clearance of 10 liters/min. The volume of distribution calculated from the mean data after oral administration (626 liters) was, however, larger than that calculated from data after sublingual administration (443 liters). After oral administration, the volume of distribution, V_D, was calculated for individual subjects both from the model parameters and from the expression V_D = clearance/k_e (where k_e is the elimination rate constant); good agreement was found between the two methods of calculation. The *in vivo* release rate of drug from the sustained-release tablet was calculated to be 1.2 mg/hr.

If the bioavailability of the drug from the sustained-release formulation was similar to that from the standard tablet after oral administration (see *Bioavailability* section), *i.e.*, 58% of the dose was absorbed, then the sustained-release tablet would be expected to supply drug over approximately 10 hr. Inspection of Fig. 1 indicated that plasma concentrations were maintained during 1–8 hr after dosing, in reasonable agreement with the calculated release rate.

Table III—Areas[a] under the Plasma Concentration–Time Relationship to 4 hr after Administration of Sublingual and Oral Doses of the Standard Tablet and to 12 hr after Administration of the Sustained-Release Tablet

Subject	Sublingual	Oral	Oral Sustained Release
1	71.6	62.2	59.0
2	132.7	75.5	50.9
3	87.3	53.9	38.0
4	86.2	59.2	59.2
5	129.7	62.0	44.7
6	190.3	46.0	27.3
Mean (±*SD*)	116.3 (±44.0)	59.8 (±9.8)	46.5 (±12.5)

[a] Corrected for dose–body weight variations. Units of ng × hr/ml/mg/kg.

DISCUSSION

Plasma concentrations of isosorbide dinitrate observed after oral doses (Table I) were in fairly good agreement with those measured using radiotracer methods (11). Concentrations observed after sublingual doses were somewhat lower than those reported by others (10). The plasma half-life of isosorbide dinitrate is short, probably too short to support the role of the drug as a relatively long-acting vasodilator. The pharmacologically active metabolites (19, 20), the two isosorbide mononitrates, also might contribute to drug action. These studies showed (Fig. 1) that the use of a sustained-release formulation may prolong the plasma drug concentrations and, probably, the pharmacological action.

Table IV—Parameters of a One-Compartment Open Model for the Pharmacokinetics of Isosorbide Dinitrate[a]

Parameter	Route of Administration	
	Sublingual	Oral
Absorption rate constant, min^{-1}	0.2877	0.1093
Absorption half-life, min	2.4	6.3
Elimination rate constant, min^{-1}	0.0229	0.0171
Elimination half-life, min	30.3	40.4
Volume of distribution, liters	443	626
Plasma clearance, liters/min	10.15	10.70

[a] Calculated from mean concentration data.

The one-compartment model appeared to describe adequately the data obtained after oral administration, but calculation of the absorption rate constant failed in computing with some sets of data from individual subjects after sublingual administration. It was likely, therefore, that after the absorption phase, a very rapid distribution phase preceded the linear elimination phase of the concentration–time relationships but that there were insufficient early sampling times to allow its detection. A simple one-compartment model, therefore, is probably not adequate to describe the pharmacokinetics of isosorbide dinitrate.

Moreover, isosorbide dinitrate is absorbed completely from the GI tract after oral doses (12). Although the reduced bioavailability of isosorbide dinitrate from the standard tablet after oral administration could have been formulation related, the decreased bioavailability after oral doses probably was due to rapid metabolism by the liver after absorption into the hepatoportal system, the drug being subjected to a considerable first-pass effect as occurs for certain other drugs (21–23). Rapid metabolism also explains the very large volumes of distribution and clearances of isosorbide dinitrate by applying a simple one-compartment model to the data. An adequate model of the pharmacokinetics of isosorbide dinitrate must include a pass effect and can be constructed only from a more intensive study of plasma concentrations of the drug and its metabolites after different routes of administration.

REFERENCES

(1) W. S. Aronow, in "Organic Nitrates," P. Needleman, Ed., Springer-Verlag, Berlin, Germany, 1975, p. 163.

(2) J. W. Berry, R. Carney, and H. Lankford, *Angiology*, **12**, 254 (1961).

(3) H. I. Russek, *Am. J. Med. Sci.*, **252**, 9 (1966).

(4) R. E. Goldstein, D. R. Rosing, D. R. Redwood, G. D. Beiser, and S. E. Epstein, *Circulation*, **43**, 629 (1971).

(5) T. Winsor, H. Kaye, and B. Mills, *Chest*, **62**, 407 (1972).

(6) M. Kaltenbach, J. Tiedemann, and W. Schellhorn, *Dtsch. Med. Wochenschr.*, **97**, 1479 (1972).

(7) J. A. Franciosa, E. Mikulic, J. N. Cohn, E. Jose, and A. Fabie, *Circulation*, **50**, 1020 (1974).

(8) A. A. Stipe and G. B. Fink, *J. Clin. Pharmacol.*, **13**, 244 (1973).

(9) Proceedings of the First Nitrate Symposium, Stockholm, Sweden, 1975.

(10) M. T. Rosseel and M. G. Bogaert, *J. Pharm. Sci.*, **62**, 754 (1973).

(11) W. H. Down, L. F. Chasseaud, and R. K. Grundy, *ibid.*, **63**, 1147 (1974).

(12) L. F. Chasseaud, W. H. Down, and R. K. Grundy, *Eur. J. Clin. Pharmacol.*, **8**, 157 (1975).

(13) W. H. Habig, J. H. Keen, and W. B. Jakoby, *Biochem. Biophys. Res. Commun.*, **64**, 501 (1975).

(14) L. F. Chasseaud, *Drug Metab. Rev.*, **2**, 185 (1973).

(15) P. Needleman, S. Lang, and E. M. Johnson, Jr., *J. Pharmacol. Exp. Ther.*, **181**, 489 (1972).

(16) J. Meier, E. Neusch, and R. Schmidt, *Eur. J. Clin. Pharmacol.*, **7**, 429 (1974).

(17) J. G. Wagner, "Biopharmaceutics and Relevant Pharmacokinetics," Drug Intelligence Publications, Hamilton, Ill., 1971.

(18) L. Saunders and T. Natunen, *J. Pharm. Pharmacol.*, **25**, 45P (1973).

(19) R. L. Wendt, *J. Pharmacol. Exp. Ther.*, **180**, 732 (1972).

(20) M. G. Bogaert and M. T. Rosseel, *Arch. Pharmacol.*, **275**, 339 (1972).

(21) M. Gibaldi and S. Feldman, *J. Pharm. Sci.*, **58**, 1477 (1969).

(22) M. Gibaldi, R. N. Boyes, and S. Feldman, *ibid.*, **60**, 1338 (1971).

(23) M. Rowland, *ibid.*, **61**, 70 (1972).

ACKNOWLEDGMENTS AND ADDRESSES

Received March 22, 1976, from the *Department of Metabolism and Pharmacokinetics, Huntingdon Research Centre, Huntingdon, United Kingdom.*

Accepted for publication July 22, 1976.

The authors thank Dr. A. Schrey of Sanol-Arzneimittel Dr. Schwarz GmbH, Monheim, Germany, for his help and interest. They also thank Dr. D. D. Cracknell for medical supervision of the subjects.

[x] To whom inquiries should be directed.

Systems Approach to Vaginal Delivery of Drugs IV: Methodology for Determination of Membrane Surface pH

S. HWANG, E. OWADA, L. SUHARDJA, N. F. H. HO, G. L. FLYNN, and W. I. HIGUCHI [x]

Abstract □ A physical model including a diffusional layer in series with the membrane was developed for studying the possible differences between the pH at the membrane surface and that in the bulk solution. Both the membrane-secreted substances (acids and bases) and buffer constituents in the bulk solutions are assumed to contribute to the surface pH. Equations derived for this situation, together with experimental determinations of the acidic dissociation constant of the secreted material, the total secretion flux, the flux of total secreted acidic species, and the diffusional layer thickness, allow estimates to be made of the pH at the membrane surface. With the rabbit vagina, the membrane surface pH was close to that of the bulk solution in most cases. These results were supported by the fact that the absorption of 1-alkanoic acids in pH 2.2 phosphate buffers was relatively constant over the buffer concentration range of 0.003–0.1 *M* phosphate.

Keyphrases □ Drug delivery, vaginal—membrane surface pH determined, compared to bulk solution pH, rabbits □ pH—membrane surface compared to bulk solution, vaginal drug delivery model, rabbits □ Vaginal drug delivery—model, membrane surface pH determined, compared to bulk solution pH, rabbits

The objectives of the present investigations were to develop suitable methodology in an appropriate animal system to obtain firm baseline data on vaginal absorption, to delineate the general barrier properties of the vaginal mucosa, and to develop quantitative integrated models describing both the release of drug from vaginal devices and the subsequent drug absorption.

The first paper (1) in this series described a method for evaluating drug absorption in the vagina, using the rabbit doe as a prototype animal. A rib-cage-type cell, which provided a closed absorptive compartment in the vaginal tract, was designed and surgically implanted in the rabbit. Drug absorption was determined by perfusing the drug solution through this system and following the time changes in drug concentration in the system. The study showed that the method generally affords good precision

The one-compartment model appeared to describe adequately the data obtained after oral administration, but calculation of the absorption rate constant failed in computing with some sets of data from individual subjects after sublingual administration. It was likely, therefore, that after the absorption phase, a very rapid distribution phase preceded the linear elimination phase of the concentration–time relationships but that there were insufficient early sampling times to allow its detection. A simple one-compartment model, therefore, is probably not adequate to describe the pharmacokinetics of isosorbide dinitrate.

Moreover, isosorbide dinitrate is absorbed completely from the GI tract after oral doses (12). Although the reduced bioavailability of isosorbide dinitrate from the standard tablet after oral administration could have been formulation related, the decreased bioavailability after oral doses probably was due to rapid metabolism by the liver after absorption into the hepatoportal system, the drug being subjected to a considerable first-pass effect as occurs for certain other drugs (21–23). Rapid metabolism also explains the very large volumes of distribution and clearances of isosorbide dinitrate by applying a simple one-compartment model to the data. An adequate model of the pharmacokinetics of isosorbide dinitrate must include a pass effect and can be constructed only from a more intensive study of plasma concentrations of the drug and its metabolites after different routes of administration.

REFERENCES

(1) W. S. Aronow, in "Organic Nitrates," P. Needleman, Ed., Springer-Verlag, Berlin, Germany, 1975, p. 163.

(2) J. W. Berry, R. Carney, and H. Lankford, *Angiology*, **12**, 254 (1961).

(3) H. I. Russek, *Am. J. Med. Sci.*, **252**, 9 (1966).

(4) R. E. Goldstein, D. R. Rosing, D. R. Redwood, G. D. Beiser, and S. E. Epstein, *Circulation*, **43**, 629 (1971).

(5) T. Winsor, H. Kaye, and B. Mills, *Chest*, **62**, 407 (1972).

(6) M. Kaltenbach, J. Tiedemann, and W. Schellhorn, *Dtsch. Med. Wochenschr.*, **97**, 1479 (1972).

(7) J. A. Franciosa, E. Mikulic, J. N. Cohn, E. Jose, and A. Fabie, *Circulation*, **50**, 1020 (1974).

(8) A. A. Stipe and G. B. Fink, *J. Clin. Pharmacol.*, **13**, 244 (1973).

(9) Proceedings of the First Nitrate Symposium, Stockholm, Sweden, 1975.

(10) M. T. Rosseel and M. G. Bogaert, *J. Pharm. Sci.*, **62**, 754 (1973).

(11) W. H. Down, L. F. Chasseaud, and R. K. Grundy, *ibid.*, **63**, 1147 (1974).

(12) L. F. Chasseaud, W. H. Down, and R. K. Grundy, *Eur. J. Clin. Pharmacol.*, **8**, 157 (1975).

(13) W. H. Habig, J. H. Keen, and W. B. Jakoby, *Biochem. Biophys. Res. Commun.*, **64**, 501 (1975).

(14) L. F. Chasseaud, *Drug Metab. Rev.*, **2**, 185 (1973).

(15) P. Needleman, S. Lang, and E. M. Johnson, Jr., *J. Pharmacol. Exp. Ther.*, **181**, 489 (1972).

(16) J. Meier, E. Neusch, and R. Schmidt, *Eur. J. Clin. Pharmacol.*, **7**, 429 (1974).

(17) J. G. Wagner, "Biopharmaceutics and Relevant Pharmacokinetics," Drug Intelligence Publications, Hamilton, Ill., 1971.

(18) L. Saunders and T. Natunen, *J. Pharm. Pharmacol.*, **25**, 45P (1973).

(19) R. L. Wendt, *J. Pharmacol. Exp. Ther.*, **180**, 732 (1972).

(20) M. G. Bogaert and M. T. Rosseel, *Arch. Pharmacol.*, **275**, 339 (1972).

(21) M. Gibaldi and S. Feldman, *J. Pharm. Sci.*, **58**, 1477 (1969).

(22) M. Gibaldi, R. N. Boyes, and S. Feldman, *ibid.*, **60**, 1338 (1971).

(23) M. Rowland, *ibid.*, **61**, 70 (1972).

ACKNOWLEDGMENTS AND ADDRESSES

Received March 22, 1976, from the *Department of Metabolism and Pharmacokinetics, Huntingdon Research Centre, Huntingdon, United Kingdom.*

Accepted for publication July 22, 1976.

The authors thank Dr. A. Schrey of Sanol-Arzneimittel Dr. Schwarz GmbH, Monheim, Germany, for his help and interest. They also thank Dr. D. D. Cracknell for medical supervision of the subjects.

[x] To whom inquiries should be directed.

Systems Approach to Vaginal Delivery of Drugs IV: Methodology for Determination of Membrane Surface pH

S. HWANG, E. OWADA, L. SUHARDJA, N. F. H. HO, G. L. FLYNN, and W. I. HIGUCHI [x]

Abstract □ A physical model including a diffusional layer in series with the membrane was developed for studying the possible differences between the pH at the membrane surface and that in the bulk solution. Both the membrane-secreted substances (acids and bases) and buffer constituents in the bulk solutions are assumed to contribute to the surface pH. Equations derived for this situation, together with experimental determinations of the acidic dissociation constant of the secreted material, the total secretion flux, the flux of total secreted acidic species, and the diffusional layer thickness, allow estimates to be made of the pH at the membrane surface. With the rabbit vagina, the membrane surface pH was close to that of the bulk solution in most cases. These results were supported by the fact that the absorption of 1-alkanoic acids in pH 2.2 phosphate buffers was relatively constant over the buffer concentration range of 0.003–0.1 *M* phosphate.

Keyphrases □ Drug delivery, vaginal—membrane surface pH determined, compared to bulk solution pH, rabbits □ pH—membrane surface compared to bulk solution, vaginal drug delivery model, rabbits □ Vaginal drug delivery—model, membrane surface pH determined, compared to bulk solution pH, rabbits

The objectives of the present investigations were to develop suitable methodology in an appropriate animal system to obtain firm baseline data on vaginal absorption, to delineate the general barrier properties of the vaginal mucosa, and to develop quantitative integrated models describing both the release of drug from vaginal devices and the subsequent drug absorption.

The first paper (1) in this series described a method for evaluating drug absorption in the vagina, using the rabbit doe as a prototype animal. A rib-cage-type cell, which provided a closed absorptive compartment in the vaginal tract, was designed and surgically implanted in the rabbit. Drug absorption was determined by perfusing the drug solution through this system and following the time changes in drug concentration in the system. The study showed that the method generally affords good precision

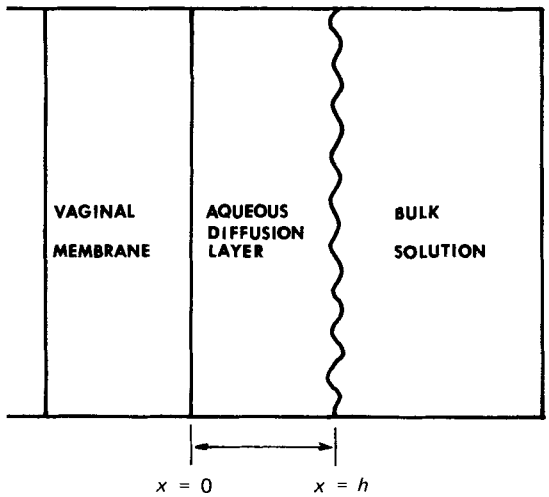

Figure 1—*Physical model for consideration of surface pH. Aqueous diffusion layer is in series with the membrane.*

and should provide a sound basis for meeting the objectives of this research.

The second paper (2) reported the results of the investigation of a physical model for the vaginal absorption barrier, utilizing experimental data on the absorption of the 1-alkanols from methanol to 1-octanol. The analysis of the data showed that experimental results were in reasonably good agreement with the model in which the absorption barrier consists of an aqueous diffusion layer in series with a membrane having two parallel pathways for solute transport—a lipoidal pathway and an aqueous pore pathway.

In the next phase, which is to explore the vaginal absorption behavior of ionizing solutes, it became apparent that an understanding of the membrane surface pH was necessary before a rational study of any physical model for the absorption of weakly ionized drugs (*e.g.*, weak acids and weak bases) could be undertaken. Therefore, the purposes of this study were to develop a method for evaluating the surface pH and to employ it to assess the possible importance of surface pH in analyzing the 1-alkanoic acid vaginal absorption data with the physical models.

THEORY

A schematic diagram of the physical model is shown in Fig. 1. There are the simultaneous fluxes of secretions from the membrane surface across the aqueous diffusion layer and fluxes of the buffer species in the aqueous diffusion layer.

It is assumed that the buffer species (*e.g.*, phosphate) are essentially conserved within the vagina, *i.e.*, there is little or no absorption of buffer species.

It is assumed that the membrane secretes two species, H_2X and HX^-, of a substance by some undefined mechanism. As shown later, the measured acid dissociation constant(s) of H_2X is very close to that for carbonic acid; therefore, H_2X and HX^- might be H_2CO_3 and HCO_3^-, respectively. However, it is unnecessary to specify the exact chemical nature of the secreted material in surface pH (pH_s) analysis.

For the present discussion, assume that phosphate is the buffer in the bulk solution and consider the bulk pH range of 2–8. Then the following six equations (steady state) may be written for the diffusion and chemical equilibrium reaction occurring in th aqueous diffusion layer:

$$K_1 = \frac{(H_2P)(H)}{(H_3P)} \quad \text{(Eq. 1)}$$

$$K_2 = \frac{(HP)(H)}{(H_2P)} \quad \text{(Eq. 2)}$$

$$K_X = \frac{(HX)(H)}{(H_2X)} \quad \text{(Eq. 3)}$$

$$D_{H_3P}\frac{d(H_3P)}{dx} + D_{H_2P}\frac{d(H_2P)}{dx} + D_{HP}\frac{d(HP)}{dx} + D_P\frac{d(P)}{dx} = 0 \quad \text{(Eq. 4)}$$

$$J_{TX} = D_{H_2X}\frac{d(H_2X)}{dx} + D_{HX}\frac{d(HX)}{dx} \quad \text{(Eq. 5)}$$

$$J_{TA} = D\frac{d(H_3P)}{dx} + D_{H_2P}\frac{d(H_2P)}{dx} + D_{HP}\frac{d(HP)}{dx} + D_H\frac{d(H)}{dx} + D_{H_2X}\frac{d(H_2X)}{dx} \quad \text{(Eq. 6)}$$

where (H_3P), (H_2P), (HP), and (P) = concentrations of phosphate buffer species, with the valence of the ions omitted for convenience; (H_2X) and (HX) = concentrations of secretion species of a diprotic acid, with the valence of the ions omitted for convenience; (H) = hydrogen-ion concentration; D = aqueous diffusion coefficient; K = dissociation constant; J_{TX} = total flux of the secretion buffer species per unit surface area; and J_{TA} = total flux of acidic species including drug solution buffer species and hydrogen ions per unit surface area.

The integration of Eqs. 4–6 yields:

$$(H_3P)_s + (H_2P)_s + (HP)_s + (P)_s = (H_3P)_b + (H_2P)_b + (HP)_b + (P)_b \quad \text{(Eq. 7)}$$

$$J_{TX} = \frac{D}{h}[(H_2X)_s - (H_2X)_b + (HX)_s - (HX)_b] \quad \text{(Eq. 8)}$$

$$J_{TA} = \frac{D}{h}[3(H_3P)_s - 3(H_3P)_b + 2(H_2P)_s - 2(H_2P)_b + (HP)_s - (HP)_b + (H_2X)_s - (H_2X)_b + (H)_s - R(H)_b] \quad \text{(Eq. 9)}$$

where h = effective thickness of the aqueous diffusion layer, and s and b = subscripts denoting the membrane surface and the bulk solution boundaries, respectively.

The aqueous diffusion coefficients of all buffer species have been taken to be equal to D, except for the hydrogen ions for which $R = D_H/D$. At low pH, <8, $(P)_b$ and $(P)_s$ are negligible. Then Eq. 7 is reduced to:

$$(H_3P)_s + (H_2P)_s + (HP)_s = (H_3P)_b + (H_2P)_b + (HP)_b \quad \text{(Eq. 10)}$$

Combining Eqs. 9 and 10 yields:

$$J_{TA} = \frac{D}{h}[2(H_3P)_s - 2(H_3P)_b + (H_2P)_s - (H_2P)_b + (H_2X)_s - (H_2X)_b + R(H)_s - R(H)_b] \quad \text{(Eq. 11)}$$

Equations 1–3, 8, 10, and 11 represent six independent equations. All bulk concentrations are known. The effective diffusion layer thickness, h, is 0.035 cm, as previously determined (2) from the alcohol absorption studies. The diffusion coefficients are taken to be 1×10^{-5} cm^2/sec, and R is in the order of 8 under swamping electrolyte conditions (3). The parameters K_X, J_{TX}, and J_{TA} are experimentally determined. Thus, there are six unknowns: $(H_3P)_s$, $(H_2P)_s$, $(P)_s$, $(H_2X)_s$, $(HX)_s$, and $(H)_s$. The J_{TX} and J_{TA} are determined for the experimental situations in which the phosphate buffer is perfused in the rabbit vagina. Subsequently, the surface concentrations of all buffer species and the hydrogen-ion concentration can be calculated. All of these results are examined in the light of the experimental aliphatic carboxylic acid absorption rates and bulk pH values.

EXPERIMENTAL

Materials and Apparatus—^{14}C-Labeled hexanoic acid[1] and tritium-labeled methanol[2] were used without further purification. The radioactivity of the sample was determined by a liquid scintillation counter[3], using a cocktail prepared as described previously (2). The pH was measured by a pH meter[4].

Absorption Procedure and Perfusion System—The absorption procedure and perfusion system were the same as described previously (2). Mature female New Zealand White rabbits, 3.5–5.5 kg, were used. The perfusion system consisted of a reservoir and a rib-cage cell surgically

[1] International Chemical & Nuclear Corp., Irvine, Calif.
[2] New England Nuclear Corp., Boston, Mass.
[3] Model LS 200, Beckman Instruments, Fullerton, Calif.
[4] Research pH meter, Beckman Instruments, Fullerton, Calif.

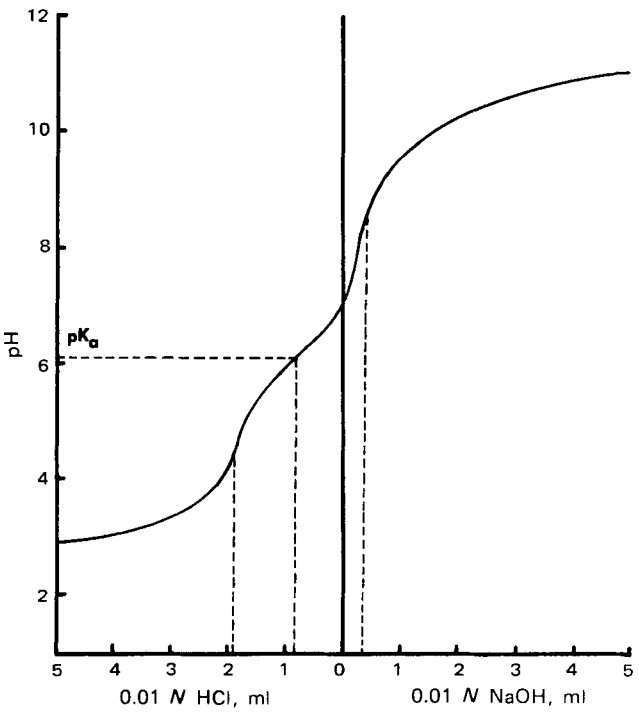

Figure 2—*Titration curve of the saline solution that was circulated in the rabbit vagina for 1 hr.*

implanted in the vagina. The entire path was made of glass and stainless steel, except a short connection [about a 2.54-cm (1-in.) polyethylene tube] between the rib-cage cell and the circuit.

Experiments were scheduled beginning 2 days after the surgical implantation of the rib-cage cell. Two or three experiments were carried out on each day, but the total time interval of an experiment did not exceed 2 hr. The rabbit was anesthetized with pentobarbital sodium (25 mg/kg), and the perfusion system was connected through the fenestra rotunda. The vagina was washed with normal saline solution for about 5 min at 35 ml/min and then with the buffer solution to be used in the experiment. Finally, the drug solution in the reservoir was introduced to the circuit, and the sample was taken periodically at 10-min intervals. The pH was measured before each sample was taken.

Determination of Acid Dissociation Constant, K_X, for Secreted Material—Thirty-five milliliters of 0.9% sodium chloride solution was circulated in the rabbit vagina for 1 hr. Two 10-ml samples were taken. One was titrated with 0.01 *N* NaOH and the other with 0.01 *N* HCl.

Determination of H_2X and HX^- Secretion Rates, J_{TX}—Thirty-five milliliters of phosphate buffer (0.001, 0.003, or 0.01 *M*) or 0.9% sodium chloride was circulated as usual in the system for 23, 43, and 63 min. The

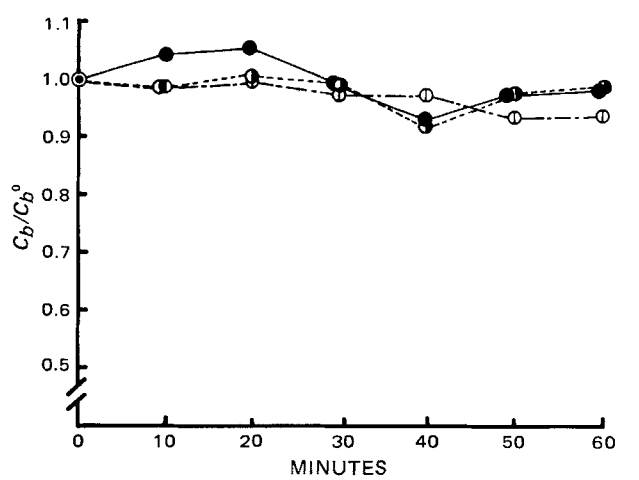

Figure 3—*Plots of phosphate concentration as a function of time. The* C_b *and* C_b^0 *represent the phosphate concentration at time* t *and 0, respectively. Key:* ●, *100 mM;* ◑, *10 mM; and* ⊙, *3 mM.*

Table I—Results of Typical Secretion Rate Determinations at Different Time Intervals

Solution Used	Secretion Rate, μEq/min/cm²		
	23 min	43 min	63 min
0.9% NaCl	0.13	0.11	0.10
3 m*M* Phosphate isotonic buffer (initial pH 3.0)	0.07	0.12	0.08

solutions were then titrated to determine the total acid and base content. The total phosphate concentration was determined by a colorimetric method (4). The difference between the total acid/base of the solution and the total acid/base calculated for the phosphate buffer was attributed to secretions.

Determination of Total Acid Flux, J_{TA}—Let *B* and *C* be the initial amounts of the acidic and basic species of the buffer (at pH close to 3, these will be H_3PO_4 and $H_2PO_4^-$, respectively). Let *Y* and *Z* be the amounts of H_2X and HX^-, respectively, secreted in the time interval, *t*. Then the reaction shown in Scheme I takes place at time *t*:

$$\underset{(B-\delta)}{H_3PO_4} + \underset{(Z-\delta)}{HX^-} \rightleftharpoons \underset{(C+\delta)}{H_2PO_4^-} + \underset{(Y+\delta)}{H_2X}$$

Scheme I

where δ is the amount of reaction taking place. Since the pH of the solution is known at time *t*:

$$K_X = \frac{(H)(Z-\delta)}{(Y+\delta)} \qquad \text{(Eq. 12)}$$

$$K_1 = \frac{(H)(C+\delta)}{(B-\delta)} \qquad \text{(Eq. 13)}$$

where (H) is the hydrogen-ion concentration, K_X is the acid dissociation constant for the secreted material, and K_1 is the first dissociation constant for phosphoric acid. The value of δ is determined by Eq. 13 because *B* and *C* are both known. Thus, *Y* (and *Z*) may be determined from Eq. 12 and the fact that $Y + Z$ is known from the J_{TX} determination discussed previously. The total acid flux, J_{TA}, can then be calculated from *Y*, *t*, and *A*, the surface area of the vaginal membrane, by:

$$J_{TA} = \frac{Y}{tA} \qquad \text{(Eq. 14)}$$

RESULTS AND DISCUSSION

A typical titration curve of the vaginal secretion obtained by perfusing normal saline solution in the vagina for 60 min is shown in Fig. 2. From five experiments, the effective pKa was 6.3 ± 0.1. These data also were used to estimate a second pKa of around 10. These pKa values are close to those for carbonic acid.

The absorption of the phosphate species over the concentration range of 0.003–0.10 *M* at pH 3 was insignificant during 1 hr (Fig. 3). Therefore, it was concluded that the total phosphate is essentially conserved within the usual experimental period.

The secretion rates were relatively constant during the experiments (Table I). The titratable secreted acid was essentially zero, and this value was determined by Eqs. 12 and 13.

The surface pH for the phosphate buffer at bulk pH 2 and 3 could then be calculated (Table II). The surface pH was not greatly different from the bulk pH in these instances over the buffer concentration range of 0.001–0.1 *M*. These results were supported by 1-hexanoic acid absorption studies where the absorption rate at pH 2.1 was independent of the buffer concentration (Fig. 4).

For most membrane transport studies of weak electrolytes conducted

Table II—Calculated Surface pH as a Function of Bulk pH and Total Phosphate Concentration

Bulk pH	Surface pH at Various Concentrations of Total Phosphate		
	100 m*M*	10 m*M*	1 m*M*
2.0	2.0	2.0	2.0
3.0	3.1	3.2	3.3

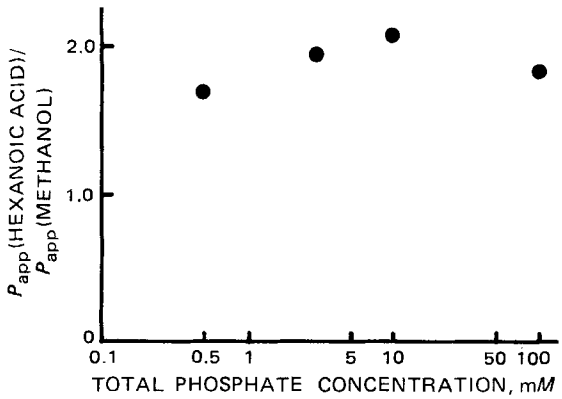

Figure 4—*Plot of the normalized permeability coefficient, P_{app} (hexanoic acid)/P_{app} (methanol), as a function of buffer concentration. The P_{app} is the apparent permeability coefficient.*

in these laboratories, the pH at the membrane surface was assumed to be the same as the pH in the bulk solution. This assumption has now been shown to be a reasonable approximation when the lumenal solution possesses a minimal modest buffer capacity in the case of the rabbit vagina because the rate of secretion (acids or bases) from the membrane is relatively small. In contrast, Desai (5) showed that the surface pH is significantly different from the bulk lumenal pH in *in situ* intestinal absorption experiments with *n*-butyric acid in the rat jejunum. In these studies with the rat intestine, wide ranges of initial buffer pH's (4.5–9.5), buffer capacities, and hydrodynamic conditions were employed in which the flux of buffer secretions across the aqueous diffusion layer was significant and the prevailing surface pH influenced the absorption of *n*-butyric acid.

REFERENCES

(1) T. Yotsuyanagi, A. Molokhia, S. Hwang, N. F. H. Ho, G. L. Flynn, and W. I. Higuchi, *J. Pharm. Sci.*, **64**, 71 (1975).

(2) S. Hwang, E. Owada, T. Yotsuyanagi, L. Suhardja, N. F. H. Ho, G. L. Flynn, and W. I. Higuchi, *ibid.*, **65**, 1574 (1976).

(3) J. R. Vinograd and J. W. McBain, *J. Am. Chem. Soc.*, **63**, 2008 (1941).

(4) A. Gee, L. P. Domingues, and V. R. Deitz, *Anal. Chem.*, **26**, 1487 (1954).

(5) K. Desai, Ph.D. thesis, University of Michigan, Ann Arbor, Mich., 1975.

ACKNOWLEDGMENTS AND ADDRESSES

Received December 12, 1975, from the *College of Pharmacy, University of Michigan, Ann Arbor, MI 48104.*

Accepted for publication July 23, 1976.

Supported by Contract N01-HD-3-2740, National Institute of Child Health and Human Development, National Institutes of Health, Bethesda, MD 20014.

[x] To whom inquiries should be directed.

Systems Approach to Vaginal Delivery of Drugs V: *In Situ* Vaginal Absorption of 1-Alkanoic Acids

S. HWANG, E. OWADA, L. SUHARDJA, N. F. H. HO, G. L. FLYNN, and W. I. HIGUCHI [x]

Abstract □ The vaginal absorption of a homologous series of ionizable compounds, the 1-alkanoic acids, was studied using a perfusion method with a rib-cage cell surgically implanted in the rabbit vagina. The absorption rates of these compounds followed first-order kinetics. The physical model previously used for the 1-alkanols, but accounting for the pKa and pH effects in the present case, was employed in the analysis of the carboxylic acid data. The aqueous diffusion layer thickness was 0.031 cm. The permeability coefficient for the lipoidal pathway increased 3.5-fold per methylene group. Both values agree reasonably well with those obtained in the alcohol study.

Keyphrases □ Drug delivery, vaginal—*in situ* absorption of 1-alkanoic acids, rabbits □ Absorption, vaginal—1-alkanoic acids, rabbits □ Acids, 1-alkanoic—vaginal absorption, rabbits

The first paper (1) of this series described a methodology for studying the absorption of solutes in the rabbit vagina. A rib-cage cell is implanted in the rabbit vagina, and an appropriate perfusion system is used. The absorption of a homologous series of 1-alkanols was studied (2) employing this technique. The data were analyzed by a physical model that involves a diffusion layer in series with a membrane consisting of two parallel pathways—a lipoidal and an aqueous pore pathway. Most recently (3), it was found that the surface pH of the rabbit vaginal membrane under experimental conditions was well approximated by the pH of the lumenal solution.

The general perfusion technique has now been used to study the permeability behavior of a homologous series of 1-alkanoic acids in the rabbit vaginal membrane. These compounds were expected to exhibit a lumen solution pH dependence for absorption and a chain length dependence. The same physical model as was used (2) with the 1-alkanols appeared to describe adequately the primary features of the absorption behavior of the 1-alkanoic acids in the rabbit vagina.

EXPERIMENTAL

Animals—Mature female New Zealand White rabbits, 3.5–5.0 kg, were maintained in a temperature-controlled animal room (25°) with free access to water and a regular diet.

Materials—^{14}C-Labeled acetic[1], butyric[1], octanoic[1], hexanoic[2], and decanoic[2] acids, ^{3}H-labeled polyethylene glycol[1] (mol. wt. ~4000), and ^{3}H-labeled methanol were used without further purification. Buffers of 0.1 *M* phosphate at pH 3, 6, and 8 were prepared (Table I).

[1] New England Nuclear Corp., Boston, Mass.
[2] International Chemical and Nuclear Corp., Irvine, Calif.

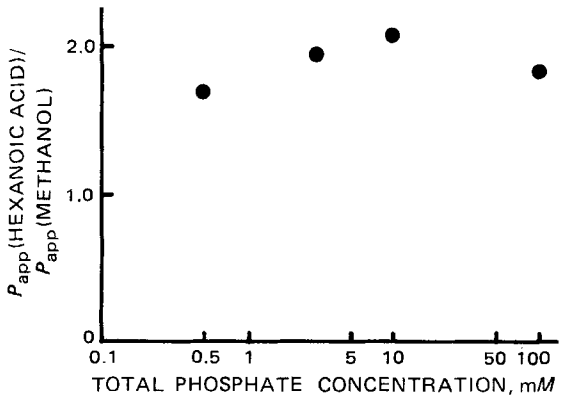

Figure 4—*Plot of the normalized permeability coefficient, P_{app} (hexanoic acid)/P_{app} (methanol), as a function of buffer concentration. The P_{app} is the apparent permeability coefficient.*

in these laboratories, the pH at the membrane surface was assumed to be the same as the pH in the bulk solution. This assumption has now been shown to be a reasonable approximation when the lumenal solution possesses a minimal modest buffer capacity in the case of the rabbit vagina because the rate of secretion (acids or bases) from the membrane is relatively small. In contrast, Desai (5) showed that the surface pH is significantly different from the bulk lumenal pH in *in situ* intestinal absorption experiments with *n*-butyric acid in the rat jejunum. In these studies with the rat intestine, wide ranges of initial buffer pH's (4.5–9.5), buffer capacities, and hydrodynamic conditions were employed in which the flux of buffer secretions across the aqueous diffusion layer was significant and the prevailing surface pH influenced the absorption of *n*-butyric acid.

REFERENCES

(1) T. Yotsuyanagi, A. Molokhia, S. Hwang, N. F. H. Ho, G. L. Flynn, and W. I. Higuchi, *J. Pharm. Sci.*, **64**, 71 (1975).

(2) S. Hwang, E. Owada, T. Yotsuyanagi, L. Suhardja, N. F. H. Ho, G. L. Flynn, and W. I. Higuchi, *ibid.*, **65**, 1574 (1976).

(3) J. R. Vinograd and J. W. McBain, *J. Am. Chem. Soc.*, **63**, 2008 (1941).

(4) A. Gee, L. P. Domingues, and V. R. Deitz, *Anal. Chem.*, **26**, 1487 (1954).

(5) K. Desai, Ph.D. thesis, University of Michigan, Ann Arbor, Mich., 1975.

ACKNOWLEDGMENTS AND ADDRESSES

Received December 12, 1975, from the *College of Pharmacy, University of Michigan, Ann Arbor, MI 48104.*

Accepted for publication July 23, 1976.

Supported by Contract N01-HD-3-2740, National Institute of Child Health and Human Development, National Institutes of Health, Bethesda, MD 20014.

[x] To whom inquiries should be directed.

Systems Approach to Vaginal Delivery of Drugs V: *In Situ* Vaginal Absorption of 1-Alkanoic Acids

S. HWANG, E. OWADA, L. SUHARDJA, N. F. H. HO, G. L. FLYNN, and W. I. HIGUCHI [x]

Abstract □ The vaginal absorption of a homologous series of ionizable compounds, the 1-alkanoic acids, was studied using a perfusion method with a rib-cage cell surgically implanted in the rabbit vagina. The absorption rates of these compounds followed first-order kinetics. The physical model previously used for the 1-alkanols, but accounting for the pKa and pH effects in the present case, was employed in the analysis of the carboxylic acid data. The aqueous diffusion layer thickness was 0.031 cm. The permeability coefficient for the lipoidal pathway increased 3.5-fold per methylene group. Both values agree reasonably well with those obtained in the alcohol study.

Keyphrases □ Drug delivery, vaginal—*in situ* absorption of 1-alkanoic acids, rabbits □ Absorption, vaginal—1-alkanoic acids, rabbits □ Acids, 1-alkanoic—vaginal absorption, rabbits

The first paper (1) of this series described a methodology for studying the absorption of solutes in the rabbit vagina. A rib-cage cell is implanted in the rabbit vagina, and an appropriate perfusion system is used. The absorption of a homologous series of 1-alkanols was studied (2) employing this technique. The data were analyzed by a physical model that involves a diffusion layer in series with a membrane consisting of two parallel pathways—a lipoidal and an aqueous pore pathway. Most recently (3), it was found that the surface pH of the rabbit vaginal membrane under experimental conditions was well approximated by the pH of the lumenal solution.

The general perfusion technique has now been used to study the permeability behavior of a homologous series of 1-alkanoic acids in the rabbit vaginal membrane. These compounds were expected to exhibit a lumen solution pH dependence for absorption and a chain length dependence. The same physical model as was used (2) with the 1-alkanols appeared to describe adequately the primary features of the absorption behavior of the 1-alkanoic acids in the rabbit vagina.

EXPERIMENTAL

Animals—Mature female New Zealand White rabbits, 3.5–5.0 kg, were maintained in a temperature-controlled animal room (25°) with free access to water and a regular diet.

Materials—^{14}C-Labeled acetic[1], butyric[1], octanoic[1], hexanoic[2], and decanoic[2] acids, ^{3}H-labeled polyethylene glycol[1] (mol. wt. ~4000), and ^{3}H-labeled methanol were used without further purification. Buffers of 0.1 *M* phosphate at pH 3, 6, and 8 were prepared (Table I).

[1] New England Nuclear Corp., Boston, Mass.
[2] International Chemical and Nuclear Corp., Irvine, Calif.

Table I—Compositions of 1 Liter of 0.1 *M* Buffer[a] at Designated pH

Component	pH 3	pH 6	pH 8
$NaH_2PO_4 \cdot H_2O$	13.8 g	13.8 g	0.69 g
Na_2HPO_4	—	—	13.5 g
1 *N* NaOH	—	16 ml	—
1 *N* HCl	12 ml	—	—

[a] Adjusted to isotonic by adding sodium chloride.

Perfusion System and Absorption Study Procedure—The perfusion system, as described previously (1, 2), consisted of an outside solution reservoir and a rib-cage cell surgically implanted in the vaginal tract. The entire perfusion path was made of glass tubing and stainless steel, except the short portion [about a 2.54-cm (1-in.) polyethylene tube] between the rib-cage cell and the fenestra rotunda. The rib-cage cell provided an interior volume of 8.1 cm^3 and a geometrical surface area of 22.5 cm^2. It was inserted through the wall of the upper part of the vaginal tract after an appropriate incision.

The procedure for an absorption experiment was essentially the same as described previously (2). Experiments were started 2 days after surgical implantation of the cell. For each rabbit, experiments were conducted on each day successively for 5 or 6 days. The rabbit was anesthetized with pentobarbital sodium, 25 mg/kg, and the perfusion system was connected through the fenestra rotunda. The vagina was first washed with normal saline solution for about 5 min at a flow rate of 35 ml/min and then for an additional 2 min with the buffer solution to be used in the experiment.

In all experiments (except that with polyethylene glycol 4000), ^3H-labeled methanol was run as a reference together with the acid of interest. After the vagina was washed with buffer, the drug solution was introduced by turning the three-way switch. The drug solution became well mixed with the buffer in the whole system after about 3 min (1). Then a zero-time sample was taken, and the experiment was continued for 1 hr during which samples were taken periodically and analyzed for both activities with a liquid scintillation counter[3] employing a dioxane cocktail[4].

RESULTS AND DISCUSSION

Water Flux in Rabbit Vagina—^3H-Labeled polyethylene glycol 4000 was used as a marker to determine the water flux with the three buffer systems (Table I) in the rabbit vagina. Three rabbits were used for each buffer. The water flux was not significant within the 1-hr experiment (Fig. 1 and Table II).

Permeability Coefficient of Methanol ($P_{app}^{methanol}$) with Three Buffers—Nine rabbits were equally divided into three groups for studying the permeability coefficient of methanol in the three buffers (pH 3, 6, and 8). Five experiments were carried out on 5 successive days for every rabbit (Table III). No significant differences in the permeability coefficient of methanol were found among the three buffers.

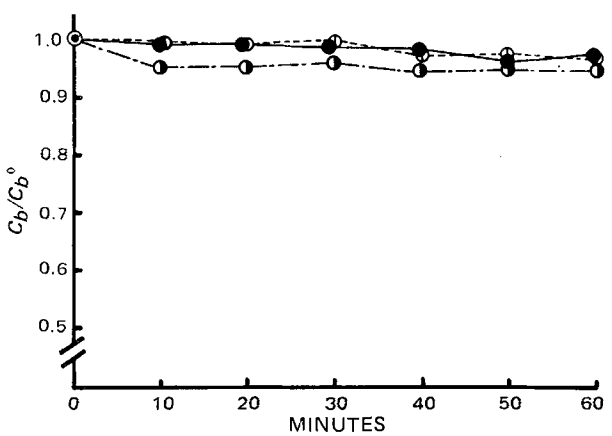

Figure 1—*Plots of polyethylene glycol 4000 concentration as a function of time. The C_b and C_b^0 represent the polyethylene glycol 4000 concentration at times t and 0, respectively. Key: ●, pH 3; ◑, pH 6; and ⊙, pH 8.*

[3] Model LS 200, Beckman Instruments, Fullerton, Calif.

[4] Prepared by dissolving 6 g of 2,5-diphenyloxazole and 100 g of naphthalene and diluting to 1000 ml with dioxane.

Table II—Percentage of Recovered Polyethylene Glycol after 1 hr of Circulation in the Rabbit Vagina

	pH 3	pH 6	pH 8
Rabbit 1	89	97	97
Rabbit 2	90	88	96
Rabbit 3	88	93	95
Mean	89	93	96

Table III—($P_{app}^{methanol} \pm SD$) × 10^4 cm/sec in Three Different Buffer Systems

	pH 3	pH 6	pH 8
	1.11 ± 0.32	1.07 ± 0.14	1.50 ± 0.21
	2.42 ± 0.28	2.26 ± 0.71	1.51 ± 0.19
	2.47 ± 0.30	1.31 ± 0.22	1.59 ± 0.43
Mean ± *SD*	2.00 ± 0.77	1.55 ± 0.63	1.53 ± 0.05

Absorption of 1-Alkanoic Acids—The absorption of the acids (from acetic to decanoic) was studied at pH 3, 6, and 8 in the same buffers. Three rabbits were used for each pH, and all acids were studied in each rabbit at the assigned pH. The order of the experiments was different for each rabbit in each pH group, but the same order combination was used for each pH group.

The data were plotted as log (C_b/C_b^0) *versus* time, where C_b^0 is the drug concentration at time zero. Without exception, the plots were linear for all acids (Fig. 2). This first-order pattern could be expressed by:

$$\frac{dC_b}{dt} = -K_u C_b \qquad \text{(Eq. 1)}$$

and:

$$K_u = P_{app}\left(\frac{A}{V}\right) \qquad \text{(Eq. 2)}$$

where C_b is the concentration of the drug in the bulk, K_u is the first-order rate constant, A is the effective surface area of the vaginal tract, V is the volume of the perfusion solution, and P_{app} is the apparent permeability coefficient.

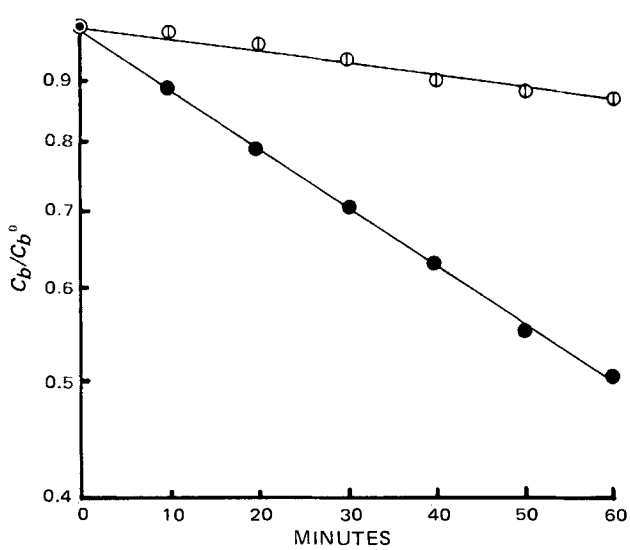

Figure 2—*Semilogarithmic plot of the acid concentration in solution as a function of time. Key: ⊙, acetic acid, pH 8; and ●, hexanoic acid, pH 3.*

Table IV—($P_{app} \pm SD$) × 10^4 cm/sec at Three Different pH Values[a]

Acid	pH 3	pH 6	pH 8
Acetic	2.39 ± 1.40	1.07 ± 0.20	0.49 ± 0.15
Butyric	3.31 ± 1.91	2.89 ± 0.95	0.48 ± 0.04
Hexanoic	3.68 ± 1.18	3.57 ± 0.59	1.15 ± 0.17
Octanoic	3.92 ± 1.48	3.57 ± 0.93	1.87 ± 0.18
Decanoic	—	—	1.89 ± 0.32

[a] Each value is a mean of three experiments involving three different rabbits.

The permeability coefficients of acids at various pH values calculated by Eq. 2 are summarized in Table IV. The ratio of $P_{app}/P_{app}^{methanol}$ is summarized in Table V. (The data for decanoic acid at pH 3 and 6 are not presented, because solute losses to the perfusion system were large for this compound under these conditions.) The relative standard deviations for the ratio were generally less than for the permeability coefficient itself, showing the value of having the reference solute, methanol, run simultaneously with the acid.

Figure 3 is a plot of the mean ratio as a function of the carbon number for the acids. For pH 3 and 6, the ratio reached a plateau between butyric and hexanoic acids. For pH 8, the ratio increased from acetic to decanoic acid.

Proposed Physical Model and Analysis of Acid Data—As previously reported (2), the rabbit vaginal absorption barrier may be considered to consist of two barriers in series, an effective aqueous barrier and a principal membrane barrier, with two parallel pathways: a lipoidal pathway and an aqueous pore pathway. The model is schematically illustrated in Fig. 4. Mathematically, the apparent permeability, $P_{app}(n,\text{pH})$, can be expressed as a function of the permeability coefficient for the aqueous barrier, $P_{aq}(n)$, and of the permeability coefficient for the membrane $P_m(n,\text{pH})$, where n is the number of carbon atoms in the compound of interest:

$$P_{app}(n,\text{pH}) = \frac{1}{\frac{1}{P_{aq}(n)} + \frac{1}{P_m(n,\text{pH})}} \qquad \text{(Eq. 3)}$$

The value of $P_{aq}(n)$ is assumed to be equal to $D_{aq}(n)/h$, where $D_{aq}(n)$ is the diffusion coefficient of the compound and h is the effective diffusion layer thickness. The Stokes–Einstein relationship was used to account for the difference in D_{aq} for the different compounds in the homologous series.

By assuming that the ionic form of the acid cannot be transported through the lipid pathway and that the undissociated acid molecule can go through both the pore and the lipid pathways, $P_m(n,\text{pH})$ can be expressed as a function of the fraction of undissociated acid, X, the permeability coefficient of the lipid pathway, P_l, and the permeability coefficient of the pore pathway, P_p:

$$P_m(n) = XP_l(n) + P_p(n) \qquad \text{(Eq. 4)}$$

$$X = \frac{(H)_s}{K_a(n) + (H)_s} \qquad \text{(Eq. 5)}$$

where $(H)_s$ is the membrane surface ($x = 0$) hydrogen-ion concentration, and $K_a(n)$ is the dissociation constant of the acid. The surface hydrogen-ion concentration in these experiments should be well approximated by the bulk hydrogen concentration, (H) (3).

Following the concept of incremental partition coefficient (4, 5) yields:

$$P_l(n) = P_l^0 \times 10^{\pi n} \qquad \text{(Eq. 6)}$$

where P_l^0 is the permeability coefficient of the lipoidal pathway for the hypothetical acid with zero carbon atoms.

The term $P_p(n)$ is a function of the diameter of the pore and the molecular size and shape of the permeant and its diffusion coefficient. However, it is assumed to be a constant in the present calculations since this approximation does not significantly affect our considerations. Thus, Eq. 3 may be rewritten as:

$$P_{app}(n,\text{pH}) = \frac{1}{\left[\frac{MV(n)}{125}\right]^{1/3}\frac{h}{D(6)} + \frac{1}{\frac{(H)}{K_a + (H)}P_l^0\,10^{\pi n} + P_p}} \qquad \text{(Eq. 7)}$$

where $MV(n)$ is the molar volume of the acid with n carbon atoms, 125 is the molar volume of hexanoic acid[5], and $D(6)$ is the diffusion coefficient of hexanoic acid at 37°[6].

By using the proposed model, the following assessments were made.

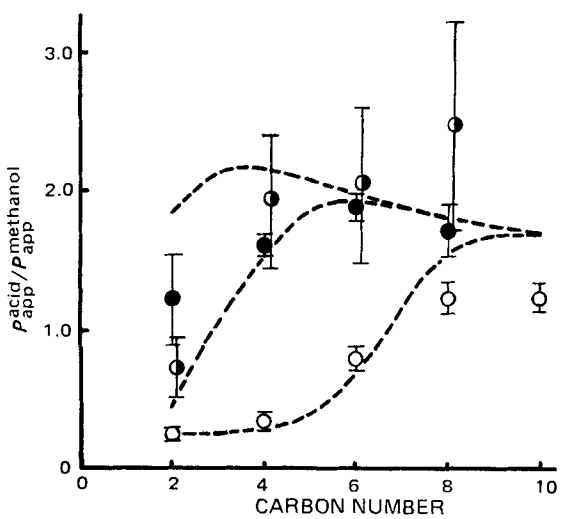

Figure 3—*Effect of carbon number on the normalized permeability coefficient,* $P_{app}^{acid}/P_{app}^{methanol}$, *at pH 3 (●), 6 (◑), and 8 (○).*

Table V—$P_{app}^{acid}/P^{methanol} \pm SD$ at Three Different pH Values[a]

Acid	pH 3	pH 6	pH 8
Acetic	1.22 ± 0.33	0.73 ± 0.23	0.25 ± 0.04
Butyric	1.62 ± 0.08	1.94 ± 0.48	0.34 ± 0.06
Hexanoic	1.89 ± 0.10	2.06 ± 0.56	0.81 ± 0.09
Octanoic	1.74 ± 0.18	2.49 ± 0.75	1.24 ± 0.12
Decanoic	—	—	1.26 0.10

[a] Each value is the mean of three experiments involving different rabbits.

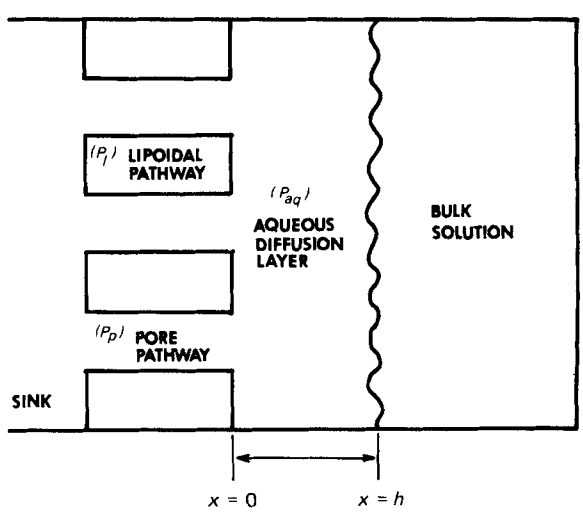

Figure 4—*Schematic model of the vaginal membrane as a transport barrier. Aqueous diffusion layer is in series with the membrane consisting of parallel lipoidal and aqueous pore pathways.*

[5] Hexanoic acid was arbitrarily chosen as a reference to allow for the Stokes–Einstein molar volume dependence for the diffusivity.

[6] It is calculated from the 25° value (6) by the Stokes–Einstein equation.

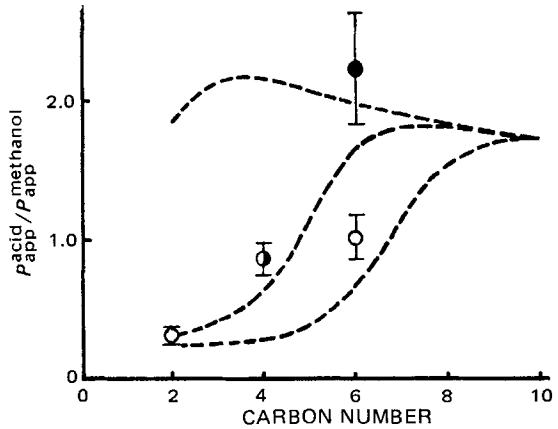

Figure 5—*Further test of the model. Theoretical curves are based on the results in Fig. 3. Key:* ●, *pH 3;* ◑, *pH 7; and* ○, *pH 8.*

At pH 3 and 6, the absorption rates for all acids (except acetic) were mainly controlled by the aqueous diffusion layer. At pH 8, the absorption rates of the lower acids were mainly controlled by the membrane. More specifically, both acetic and butyric acids were controlled by the pore pathway.

The best fit theoretical curves of $P_{app}/P_{app}^{methanol}$ *versus* n were deduced using Eq. 6 and by varying the parameters P_p, P_1^0, π, and h. A $P_{app}^{methanol}$ value of $(1.69 \pm 0.55) \times 10^{-4}$ cm/sec was used. This value, as mentioned earlier, was based on experiments with nine rabbits. The best fit set of curves is shown in Fig. 3, and these curves were based on the best parameter values $P_p = 4.6 \times 10^{-5}$ cm/sec, $P_1^0 = 6.8 \times 10^{-5}$ cm/sec, $\pi = 0.55$, and $h = 0.031$ cm.

The principal features of the proposed model are consistent with the experimental data (Fig. 3). The rather large standard deviations with the animal experiments preclude making a strong statement about the general quantitative validity of the proposed model. However, the π value of 0.55 ± 0.10 and the h value of 0.031 cm are believed to be physically significant.

Further Test of Model—Following the initial studies (Fig. 3), it was decided to pursue another study of limited scope to test the model. According to the theoretical predictions (Fig. 3), butyric acid at pH 7 was expected to be in a sensitive region of the $(P_{app}/P_{app}^{methanol})$ *versus* carbon number curve. Thus, an experiment involving butyric acid at pH 7 was expected to be a good further test of the model. Accordingly, a set of experiments involving three rabbits was designed and performed. Results of the new experiments were in good agreement with the predictions of the model based on the previous experiments (Fig. 5); these results were uniformly slightly higher but essentially within the experimental variations. Table VI shows that if only the results of the new experiments are used in the calculations with the model, a π value of 0.55 ± 0.06 is obtained, in excellent agreement with π values found with the first set of experiments (Fig. 3).

Table VI—Apparent Permeability Coefficient for the Acids and the Values of π for Three Rabbits

Acid	$P_{app} \times 10^4$ cm/sec		
Hexanoic acid, pH 3	4.69	6.24	6.71
Acetic acid, pH 8	0.46	0.50	0.54
Hexanoic acid, pH 8	1.13	1.64	1.97
Butyric acid, pH 7	1.05	1.32	1.32
Calculated π	0.50	0.54	0.62

Table VII—Physical Model Constants for the Aliphatic Acids and the Alcohols

Constant	Acid	Alcohol
P_p	4.6×10^{-5} cm/sec	1.9×10^{-4} cm/sec
P_1^0	6.8×10^{-5} cm/sec	1.5×10^{-6} cm/sec
h	0.031 cm	0.035 cm
π	0.55 ± 0.10	0.40 ± 0.15

Comparison of Results of Aliphatic Alcohols and Carboxylic Acids—These results with the acids compared favorably with those obtained with the alcohols. A summary of all physical constants for both series is presented in Table VII. The diffusion layer thickness, h, and the methylene group incremental constant, π, were in good agreement between these two homologous series. However, the permeability coefficient of the aqueous pore, P_p, for acids was significantly smaller than that for alcohols. This finding suggests two possibilities:

1. The "aqueous" pore phase may not be truly aqueous but somewhat semipolar in character and itself have a modest π value associated with it, or the aqueous pore may be negatively charged so that anions have more difficulty in being transported *via* this pathway.
2. As discussed previously (2), there may be an effective third parallel pathway in the membrane which may be characterized as being "lipoidal" but have a π value significantly less than that for the primary lipoidal pathway. This pathway may allow polar neutral species (*e.g.*, methanol) to go through with relative ease compared to ions like acetate or butyrate.

The methylene group incremental constant, π, had values close to that for the partition coefficient obtained in the 1-octanol–water system, $\pi = 0.5$, as reported by Hansch and Anderson (7). However, the difference in P_1^0 values between acid and alcohol was much larger than that expected by extrapolation of the octanol–water data for the alcohols and the fatty acids (8). Therefore, as might be expected, the similarity between the lipoidal pathway in rabbit vagina and octanol is not total.

REFERENCES

(1) T. Yotsuyanagi, A. Molokhia, S. Hwang, N. F. H. Ho, G. L. Flynn, and W. I. Higuchi, *J. Pharm. Sci.*, **64**, 71 (1975).

(2) S. Hwang, E. Owada, T. Yotsuyanagi, L. Suhardja, N. F. H. Ho, G. L. Flynn, and W. I. Higuchi, *ibid.*, **65**, 1574 (1976).

(3) S. Hwang, E. Owada, L. Suhardja, N. F. H. Ho, G. L. Flynn, and W. I. Higuchi, *ibid.*, **66**, 778 (1977).

(4) N. F. H. Ho and W. I. Higuchi, *ibid.*, **60**, 537 (1971).

(5) K. Vora, W. I. Higuchi, and N. F. H. Ho, *ibid.*, **61**, 1785 (1972).

(6) W. J. Albery, A. R. Greenwood, and R. F. Kibble, *Trans. Faraday Soc.*, **63**, 360 (1971).

(7) C. Hansch and S. M. Anderson, *J. Org. Chem.*, **32**, 2583 (1967).

(8) A. Leo, C. Hansch, and D. Elkins, *Chem. Rev.*, **71**, 525 (1971).

ACKNOWLEDGMENTS AND ADDRESSES

Received December 12, 1975, from the *College of Pharmacy, University of Michigan, Ann Arbor, MI 48104.*

Accepted for publication July 23, 1976.

Supported by Contract N01-HD-3-2740, National Institute of Child Health and Human Development, National Institutes of Health, Bethesda, MD 20014.

[x] To whom inquiries should be directed.

Simplified Method to Study Stability of Pharmaceutical Preparations

A. K. AMIRJAHED

Abstract □ Data simulating zero-, first-, and simple second- and third-order kinetic reactions are employed at four elevated temperatures. The existence of a linear relationship is established between the logarithm of $t_{0.9}$ (the time required for the concentration of the reactant remaining to decompose to reach 90% of its original value) and the reciprocal of the corresponding temperature in absolute degrees. The independence of the result from the order of the reaction is reconfirmed using literature data. The application of the linear relationship to predict the shelflife of dosage forms is discussed.

Keyphrases □ Stability—pharmaceutical preparations, linear relationship between log $t_{0.9}$ and reciprocal of absolute temperature related to shelflife □ Shelflife—pharmaceutical preparations, predicted using linear relationship between log $t_{0.9}$ and reciprocal of absolute temperature

The classical method of determining the shelflife of a pharmaceutical preparation was to store it under conditions similar to those of the normal market and to study its stability for the expected period of storage in the market. If the preparation was unstable and was subsequently modified, the same time-consuming process had to be repeated for the modified form (1). Later, high temperature accelerated stability studies were employed to predict the shelflife of the drug in a considerably shorter time. The application of such kinetic studies dates back to 1950 for consumer products in the food (2) and pharmaceutical (3, 4) industries.

BACKGROUND

In general, accelerated stability studies involve the determination of the concentration of drug remaining to decompose as a function of time. The concentration or a function of it is linearized with respect to time. The effect of relatively high temperatures on the slope of these straight lines (the specific rate constants) is determined and utilized for the preparation of an Arrhenius plot. Prediction of the time required for the drug to decompose to 90% of its original concentration at 25°—the shelflife—is based on the Arrhenius plot.

Many factors have to be investigated in such a study (5) including pH, moisture, light, oxidation, chelation, solubility, excipients, trace metals, compatibility, closures, containers, and sterilization. Other variables are the solvent, dielectric constant, ionic strength, substrate pKa, substrate reactive groups, nucleophiles, acids, and bases (4). All such studies employ the proper experimental design, a reliable assay procedure, and the appropriate statistical evaluation of the results. From the findings, the formulator determines a set of conditions that best keep the quality, purity, identity, and strength of the drug (6). Numerous articles and reviews deal with different aspects of such studies (4, 6–12). To ensure the safety and efficacy of medicaments, accelerated stability studies are now an essential part of the activities of the pharmaceutical formulator and the hospital and clinical pharmacist.

Most investigators emphasize the determination of the exact kinetic path followed by the degrading drug compound. However, some ignored such exact determinations and obtained shelflife predictions using reference decomposition models based on kinetic concepts (3) in an attempt to reduce the length of time required for stability studies. Clark and Hudson (13) suggested the use of a stability chart and explained it for first-order reactions. An experimental design and its proper statistical analysis were constructed to predict shelflife when imprecise assay methods have to be employed (14). The design provides for the minimum number of time–temperature combinations that can be used.

For first-order degradation, a stability chart was developed utilizing the Arrhenius equation, the specific rate of degradation at two elevated temperatures, and the heat of activation (15). The overall first-order rate of hydrolysis of procaine solutions was studied, and a linear relationship was found between the logarithm of the half-lives and the reciprocal of the corresponding temperatures in absolute degrees (16). As a corollary to the half-life concept, the time taken for the drug to decompose to 90% of its original concentration can be designated as $t_{0.9}$. The linear relationship between log $t_{0.9}$ and the reciprocal of the corresponding temperature in absolute degrees may be employed in the prediction of room temperature stability in a first-order reaction (6). The relationship between $t_{0.9}$ and the first-order specific rate constant was studied (17), and this concept was used for the prediction of stability of parenteral solutions from considerations of first-order reaction kinetics (18).

Lordi and Scott (15) indicated that, at less than 10% degradation and within the limits of the experimental error involved in stability studies, it is not possible to distinguish between first-, zero-, and simple second-order kinetics using curve-fitting techniques. Consequently, they felt confident that assuming first-order kinetics in their work should result

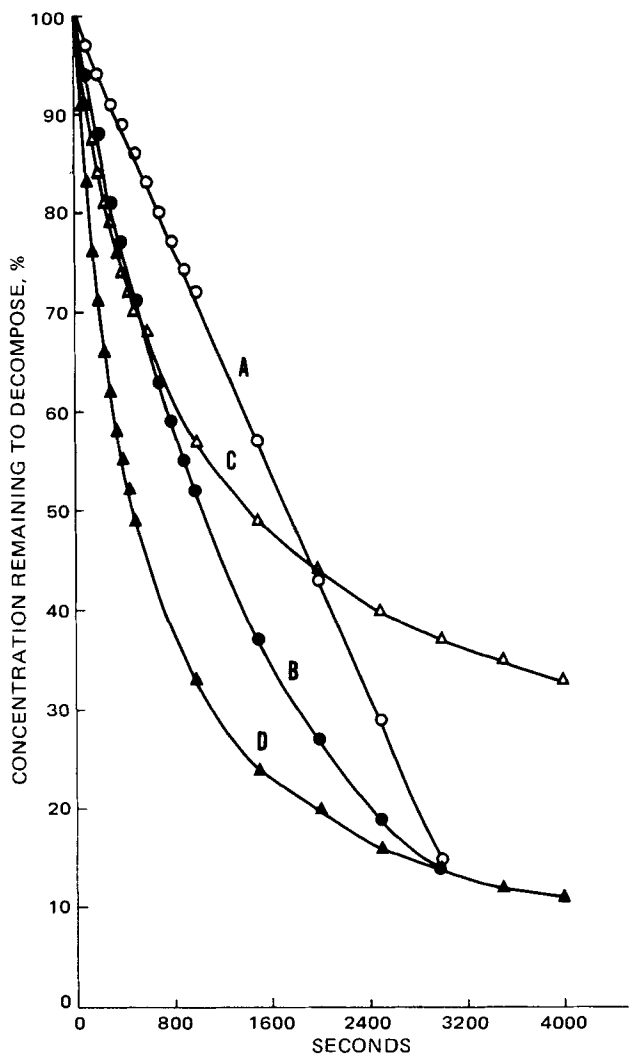

Figure 1—*Representative simulated concentration* versus *time data for zero-, first-, and simple second- and third-order reactions. Key: A, zero order; B, first order; C, third order; and D, second order.*

Table I—Straight Lines Obtained from Data Simulating a Zero-Order Kinetic Reaction[a]

Temperature[b]	Slope × 10^3	Intercept	Coefficient of Correlation[c]
40°	−3.64119	100.500	0.995915
	−4.00452	100.799	0.990657
50°	−8.03098	100.274	0.998321
	−8.03528	99.887	0.998078
60°	−14.39060	100.488	0.999175
	−14.21590	99.751	0.998575
70°	−28.75290	100.321	0.998592
	−28.53350	100.002	0.999313

[a] The dependent variable, Y, is the percent concentration remaining to decompose; the independent variable, X, is time in seconds. [b] The temperature is in centigrade degrees, and there are two replicates for each temperature. [c] All are significant at the 5% level of probability or higher.

in minimum error in the absence of a knowledge of the actual order of reaction.

The purpose of the present study was to investigate: (*a*) the presence of a linear relationship between log $t_{0.9}$ and the reciprocal of the corresponding temperature in absolute degrees regardless of the order of reaction and (*b*) the applicability of the results to the prediction of shelflife.

EXPERIMENTAL

In the first phase of this investigation, simulated concentration *versus* time data for zero-, first-, and simple second- and third-order reactions containing ±0.4–2% experimental error in the concentration terms were utilized (Fig. 1). Regression analysis of the data provided the formulas of the straight lines reported in Tables I–IV. For the different temperatures in each reaction order, the time required for the concentration to decrease to 90% of its value at zero time was determined from the respective straight-line equations. The logarithms of these values (log $t_{0.9}$) were plotted against the reciprocal of the corresponding temperatures in absolute degrees (Fig. 2).

Regression analysis provided the equations of the observed straight lines reported in Table V. The predicted $t_{0.9}$ at room temperature or the time required for the hypothetical substance to degrade at 25° to 90% of its original value was determined by substitution of the reciprocal of room temperature (in absolute degrees) multiplied by 10^3 for the independent variable. These values are also reported in Table V.

In the second phase of the investigation, available literature data were utilized to calculate log $t_{0.9}$ values. Standard kinetic equations for the particular order of reaction stated in the source were used for these calculations. The log $t_{0.9}$ values were plotted on the ordinate against the reciprocal of the corresponding temperatures (in absolute degrees multipled by 10^3 or 10^4) on the abscissa. The formula of the resultant straight line was obtained through least-squares regression analysis.

A simple substitution of the proper form of the room temperature similar to that performed in the first phase of the investigation provided the predicted value of $t_{0.9}$ at room temperature. This $t_{0.9}$ value was utilized in calculating the specific rate constant for the reaction at 25° (k_n). The k_n was subsequently compared with the equivalent specific rate constant value (k_0) reported in the source. The two specific rate constants are reported in Tables VI–VIII.

The literature sources were selected from kinetic studies reported since 1936. Many such studies could not be used in this particular investigation; only those that clearly indicated the order of reaction and provided enough data at different temperatures suitable for application of the standard kinetic equations were employed.

Table II—Straight Lines Obtained from Data Simulating a First-Order Kinetic Reaction[a]

Temperature[b]	Slope × 10^5	Intercept	Coefficient of Correlation[c]
40°	−3.52478	1.99909	0.995818
	−5.29083	2.00263	0.526871
50°	−8.11233	2.00302	0.998097
	−8.06925	1.99924	0.997575
60°	−14.42210	2.00130	0.997718
	−14.60200	2.00134	0.999469
70°	−29.12050	2.00471	0.998278
	−35.06620	1.99769	0.881244

[a] The dependent variable, Y, is the logarithm of the percent concentration remaining to decompose; the independent variable, X, is time in seconds. [b] The temperature is in centigrade degrees, and there are two replicates for each temperature. [c] All are significant at the 5% level of probability or higher.

Table III—Straight Lines Obtained from Data Simulating a Second-Order Kinetic Reaction[a]

Temperature[b]	Slope × 10^6	Intercept × 10^3	Coefficient of Correlation[c]
40°	3.64495	9.90145	0.996234
	3.57739	9.94983	0.996151
50°	6.92413	10.06870	0.997432
	6.93258	9.42949	0.986778
60°	11.80850	10.32450	0.983003
	13.80450	8.57760	0.996930
70°	21.09650	9.38233	0.994166
	19.00590	10.98070	0.993933

[a] The dependent variable, Y, is the reciprocal of the percent concentration remaining to decompose; the independent variable, X, is time in seconds. [b] The temperature is in centigrade degrees, and there are two replicates for each temperature. [c] All are significant at the 5% level of probability or higher.

RESULTS AND DISCUSSION

The nature and experimental error of the simulated data of Tables I–IV are representative of studies performed on simple degradation reactions. The number of concentration *versus* time data points (15–18) is also a practical and reasonable sample. Since kinetic studies utilizing greater than four elevated temperatures are not very common, four temperatures of 40, 50, 60, and 70° were selected as an acceptable range. Furthermore, there were two replicates for each temperature, providing a better basis for the determination of error. The values of the coefficients of correlation were all significant at least at the 95% level of probability.

Each set of data (concentration *versus* time pairs for a certain order

Table IV—Straight Lines Obtained from Data Simulating a Third-Order Kinetic Reaction[a]

Temperature[b]	Slope × 10^8	Intercept × 10^5	Coefficient of Correlation[c]
40°	3.44370	10.02760	0.995974
	3.76499	9.96291	0.997786
50°	6.60210	12.14580	0.947648
	6.86911	10.30320	0.997576
60°	6.19608	15.50950	0.666163
	11.99770	10.05600	0.996267
70°	19.03500	10.91040	0.997737
	21.54420	9.47549	0.995440

[a] The dependent variable, Y, is the reciprocal of the square of the percent concentration remaining to decompose; the independent variable, X, is time in seconds. [b] The temperature is in centigrade degrees, and there are two replicates for each temperature. [c] All are significant at the 5% level of probability or higher.

Table V—Straight Lines Obtained When the Logarithms of the $t_{0.9}$ Values (Dependent Variable Y) Calculated from the Simulated Data Are Plotted against the Reciprocals of the Corresponding Temperatures in Absolute Degrees [Independent Variable $X = (1/T) \times 10^3$]

Order of Reaction	Slope	Intercept	Coefficient of Correlation[a]	Predicted $t_{0.9}$[b] at 25°
Zero	3.15635	−6.64371	0.998177	8.76×10^3
First	3.24416	−7.26522	0.991399	4.12×10^3
Second	2.86193	−6.64283	0.910650	9.03×10^2
Third	2.58861	−5.48260	0.988905	1.58×10^3

[a] All are significant at the 1% level of probability. [b] Time in seconds.

Table VI—Zero-Order Reactions: Straight Lines Obtained When the Logarithm of the $t_{0.9}$ Values (Dependent Variable Y) Calculated from Data Reported in the Literature Is Plotted against the Reciprocal of the Corresponding Temperatures in Absolute Degrees [Independent Variable $X = (1/T) \times 10^3$]

Slope	Intercept	r^a	$k_n{}^b$	$k_0{}^c$	Reference
4.531751	−9.499254	0.999263	1.980×10^{-7}	2.210×10^{-7}	1
5.233304	−13.868966	0.998346	2.075×10^{-3}	2.054×10^{-3}	20
5.879029	−18.157259	0.999911	5.500×10^{-5}	5.620×10^{-5}	21
5.015686	−15.824473	0.998027	2.000×10^{-1}	2.000×10^{-1}	21
4.847425	−14.074462	0.999887	1.310×10^{-2}	1.180×10^{2}	21
6.918985	−17.625532	0.999577	3.160×10^{-4}	1.850×10^{-3}	22
6.978310	−17.818506	0.999259	3.110×10^{-4}	1.800×10^{-3}	22
5.825150	−14.216891	0.999886	5.740×10^{-4}	3.280×10^{-3}	22

[a] All values of the coefficient of correlation are significant at the 5% level of probability. [b] The k_n is the specific rate constant at 25° calculated from $t_{0.9}$ at 25°. The $t_{0.9}$ was predicted using the appropriate straight-line equation. [c] The k_0 is the specific rate constant reported in the reference.

of reaction and a specific temperature) provided one of the reported straight lines (Tables I–IV) and one $t_{0.9}$ value, so a total of eight log $t_{0.9}$ values was available for each order of reaction. Four elevated temperatures were employed for the same order, and each two of the log $t_{0.9}$ values corresponded to a different elevated temperature. The observed relationship between the log $t_{0.9}$ values and the reciprocal of the temperatures in absolute degrees was linear in all of the different orders of reaction (Fig. 2).

The slope, intercept, and coefficient of correlation for each line are reported in Table V. The coefficients of correlation were significant at least at the 1% level of probability. The linear relationship was used to predict the $t_{0.9}$ for the particular reaction at room temperature. In accelerated stability studies of pharmaceutical dosage forms, this time is the desired shelflife.

The establishment of the existence of the linear relationship between the log $t_{0.9}$ and the reciprocal of the absolute temperature regardless of the order of reaction led to the second phase of the investigation in which available data from selected literature sources were used to provide the same linear relationship (Tables VI–VIII). By utilizing the linear relationship, the specific rate constant at room temperature was calculated for the particular reaction. This calculated specific rate constant was compared with the specific rate constant for 25° reported in the source, using the Student t test (19). The difference between the two was not significant.

The existence of a linear relationship between the log $t_{0.9}$ and the reciprocal of the absolute temperature independent of the order of reaction is demonstrated by the simulated and experimental data. In practice, therefore, one may maintain the degradation reaction at several high temperatures, carrying on concentration determinations at predetermined time intervals. A plot of concentration remaining to decompose (on the ordinate) against time (on the abscissa) is constructed for each elevated temperature. The time taken for the concentration to decrease to 90% of the original value is read, and its logarithm is plotted against the reciprocal of the corresponding temperature in absolute degrees. The shelflife at the desirable temperature is predicted from the observed straight line. Before this new method is fully and solely employed, however, it should be applied to available data from a dosage form for which the shelflife has already been determined by other more elaborate means. Such a precaution will be of assistance in evaluating the accuracy of the simple technique.

The k and x of the general kinetic formula $-dC/dt = kC^x$ (C = concentration remaining to decompose, x = order of reaction, and k = specific reaction rate constant) can be determined using a suitable computer and program. The log k values (dependent variable Y) plotted against the reciprocal of the corresponding temperatures in absolute degrees (independent variable x) will provide an Arrhenius plot (based on $k = Ae^{-E_a/RT}$) from which the k value at room temperature can be predicted. Knowing the x and the predicted k, one can then calculate the $t_{0.9}$ at room temperature.

The present method does not depend on the x and k values, thus

Table VII—First-Order Reactions: Straight Lines Obtained When the Logarithm of the $t_{0.9}$ Values (Dependent Variable Y) Calculated from Data Reported in the Literature Is Plotted against the Reciprocal of the Corresponding Temperatures in Absolute Degrees [Independent Variable $X = (1/T) \times 10^3$]

Slope	Intercept	r^a	$k_n{}^b$	$k_0{}^c$	Reference
3.015920	−8.579299	0.999999	3.0687×10^{-3}	3.0684×10^{-3}	16
2.622350	−9.845875	0.999999	1.1845	1.1843	16
8.165610	−9.824702	0.996643	2.890×10^{-19}	3.420×10^{-19}	23
8.206471	−9.779591	0.994406	1.910×10^{-19}	2.060×10^{-19}	23
6.019405	−14.514888	0.999872	2.230×10^{-7}	2.218×10^{-7}	24
6.144731	−14.794646	0.997903	1.620×10^{-7}	1.587×10^{-7}	24
6.020490	−14.551780	0.999641	2.410×10^{-7}	2.349×10^{-7}	24
5.995196	−14.580394	0.999971	3.132×10^{-7}	3.134×10^{-7}	24
6.363474	−14.507285	0.999911	1.540×10^{-8}	1.566×10^{-8}	24
9.319568	−12.422928	0.997851	1.540×10^{-20}	1.650×10^{-20}	25
11.429101	−13.839593	0.999985	3.390×10^{-26}	3.400×10^{-26}	26
10.423916	−14.578298	0.999994	4.370×10^{-22}	4.380×10^{-22}	26
11.083506	−13.981022	0.999997	6.770×10^{-25}	6.930×10^{-25}	26
5.584305	−15.876697	0.997936	3.944×10^{-9}	3.867×10^{-4}	20
3.669914	−10.715582	0.999936	7.180×10^{-8}	7.300×10^{-8}	21
5.053777	−14.238390	0.998874	5.460×10^{-9}	5.600×10^{-9}	21
5.690677	−15.997422	0.999990	2.290×10^{-9}	2.310×10^{-9}	21
4.601365	−12.726488	0.999702	5.530×10^{-9}	5.730×10^{-9}	21
6.870275	−15.120840	0.999450	1.260×10^{-9}	1.420×10^{-9}	27
6.734594	−15.115829	0.998960	3.560×10^{-9}	4.770×10^{-9}	27
5.310601	−11.074757	0.960368	1.930×10^{-8}	1.490×10^{-8}	27
5.375524	−14.484671	0.998470	8.360×10^{-9}	8.110×10^{-9}	28
6.177557	−16.004070	0.999848	5.640×10^{-10}	7.920×10^{-10}	29
4.302462	−13.836206	0.999243	7.440×10^{-6}	7.920×10^{-6}	30
6.560143	−16.412022	0.998516	2.710×10^{-7}	2.750×10^{-7}	31
6.986699	−16.127803	0.999439	5.220×10^{-9}	7.570×10^{-9}	31
7.442154	−12.877465	0.998183	8.710×10^{-14}	5.180×10^{-14}	32

[a] All values of the coefficient of correlation are significant at the 5% level of probability. [b] The k_n is the specific rate constant at 25° calculated from $t_{0.9}$ at 25°. The $t_{0.9}$ was predicted using the appropriate straight-line equation. [c] The k_0 is the specific rate constant reported in the reference.

Table VIII—Second-Order Reactions: Straight Lines Obtained When the Logarithm of the $t_{0.9}$ Values (Dependent Variable Y) Calculated from Data Reported in the Literature Is Plotted against the Reciprocal of the Corresponding Temperatures in Absolute Degrees [Independent Variable $X = (1/T) \times 10^3$]

Slope	Intercept	r^a	$k_n{}^b$	$k_0{}^c$	Reference
1.400958	−15.418121[d]	0.999849	3.000×10^{-35}	4.510×10^{-35}	33
5.292292	−13.129828	0.999300	2.660×10^{-8}	3.989×10^{-8}	34
3.021353	−11.461445	0.996671	2.370×10^{-2}	1.090×10^{-2}	35
4.230676	−11.960942	0.999335	6.570×10^{-6}	5.320×10^{-6}	35
2.630486	−13.012160	0.999570	1.720×10^{4}	1.715×10^{4}	36
4.804216	−11.873939	0.996270	6.410×10^{-8}	6.760×10^{-8}	35
4.092603	−12.020604	0.999447	2.190×10^{-5}	2.010×10^{-5}	35

[a] All values of the coefficient of correlation are significant at the 5% level of probability. [b] The k_n is the specific rate constant at 25° calculated from $t_{0.9}$ at 25°. The $t_{0.9}$ was predicted using the appropriate straight-line equation. [c] The k_0 is the specific rate constant reported in the reference. [d] In this equation, X is $(1/T) \times 10^4$ instead of $(1/T) \times 10^3$.

minimizing the time and effort involved in accelerated stability studies without sacrificing scientific rigor. This approach is of particular advantage to small laboratories and hospital pharmacy manufacturing units where a suitable computer and program may not be available. The procedure is applicable only where the degradation reaction is a thermal process in which the use of an Arrhenius plot is justified.

The physicochemical properties of the particular medicinal substance and the possibilities available to the formulator dictate the range of elevated temperatures employed. The statistical reliability of the result can be increased by using a greater number of elevated temperatures. The reliability is also increased if the lower end of the temperature range is as close to the room temperature as possible. The accuracy of the result is indeed greater if the number of log $t_{0.9}$ and $1/T$ pairs is preferably about eight to 12. The procurement and analysis of the samples need not be carried beyond the point at which the concentration remaining to decompose becomes less than 80% of its original value. This possibility is particularly helpful in cases where the product of degradation is insoluble in the reaction mixture vehicle.

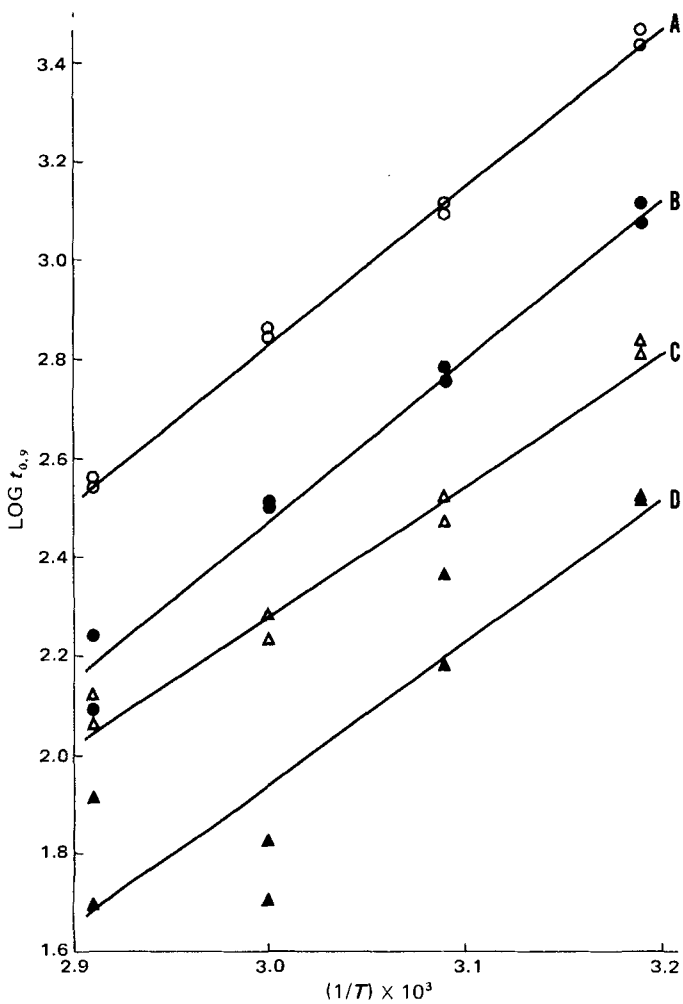

Figure 2—*Log $t_{0.9}$ values obtained from the simulated data and plotted against the reciprocal of corresponding temperatures (T in absolute degrees). Key: A, zero order; B, first order; C, third order; and D, second order.*

REFERENCES

(1) E. R. Garrett and R. F. Carper, *J. Am. Pharm. Assoc., Sci. Ed.*, **44**, 515 (1955).

(2) C. R. Oswin, *J. Soc. Chem. Ind.*, **64**, 67, 224 (1945).

(3) L. Kennon, *J. Pharm. Sci.*, **53**, 815 (1964).

(4) E. R. Garrett, *ibid.*, **51**, 811 (1962).

(5) "Guidelines: Manufacturing and Controls for IND's and NDA's," FDA 72-3013, FDA Papers, Food and Drug Administration, Bethesda, Md., 1971.

(6) "Stability and Expiration Dating of Drugs," FDA 72-3025, Division of Industry Liaison (BD-340), Food and Drug Administration, Bethesda, Md., 1972.

(7) L. Lachman and J. Cooper, *J. Am. Pharm. Assoc., Sci. Ed.*, **48**, 226 (1959).

(8) *Ibid.*, **48**, 233 (1959).

(9) L. Lachman, C. J. Swartz, and J. Cooper, *J. Am. Pharm. Assoc., Sci. Ed.*, **49**, 213 (1960).

(10) T. D. Whittet, *Am. J. Hosp. Pharm.*, **21**, 440 (1964).

(11) D. E. Guttman, *Proc. Am. Assoc. Colleges Pharm. Teachers' Seminar*, **13**, 77 (1961).

(12) J. W. Conine, *ibid.*, **13**, 77 (1961).

(13) C. J. Clark and H. E. Hudson, *Mfg. Chem. Aerosol News*, **39**, 25 (1968).

(14) J. P. R. Tootill, *J. Pharm. Pharmacol.*, **13**, 75T (1961).

(15) N. G. Lordi and M. W. Scott, *J. Pharm. Sci.*, **54**, 531 (1965).

(16) T. Higuchi, A. Havinga, and L. W. Busse, *J. Am. Pharm. Assoc., Sci. Ed.*, **39**, 405 (1950).

(17) L. Lachman, *Bull. Parenteral Drug Assoc.*, **13**, 8 (1959).

(18) N. F. H. Ho, in "Handbook of I.V. Additive Reviews," D. E. Francke, Ed., Drug Intelligence and Clinical Pharmacy, Washington, D.C., 1971, p. 27.

(19) H. C. Batson, "An Introduction to Statistics in the Medical Sciences," Chicago Medical Book Co., Chicago, Ill., 1956, p. 16.

(20) H. A. McLeod, O. Pelletier, and J. A. Campbell, *Can. Pharm. J.*, **91**, 173 (1958).

(21) E. R. Garrett, *J. Am. Pharm. Assoc., Sci. Ed.*, **45**, 171 (1956).

(22) S. M. Blaug and J. W. Wesolowski, *ibid.*, **48**, 691 (1959).

(23) G. P. Semeluk and R. B. Bernstein, *J. Am. Chem. Soc.*, **79**, 46 (1957).

(24) M. T. H. Liu and D. H. T. Chien, *J. Chem. Soc. Perkin Trans. II, No. 8*, **1974**, 937.

(25) N. Barroeta, V. DeSantis, and M. Rincon, *ibid.*, **1974**, 911.

(26) A. T. Blades and G. W. Murphy, *J. Am. Chem. Soc.*, **74**, 6219 (1952).

(27) E. R. Garrett, P. B. Chemburkar, and T. Suzuki, *Chem. Pharm. Bull.*, **13**, 1113 (1965).

(28) P. D. Gressel and J. F. Gallelli, *J. Pharm. Sci.*, **57**, 335 (1968).

(29) A. D. Marcus and J. L. Stanley, *ibid.*, **53**, 91 (1964).

(30) D. E. Guttman, *ibid.*, **51**, 1162 (1962).

(31) E. R. Garrett, *ibid.*, **53**, 42 (1964).

(32) M. Szware and J. Murawski, *Trans. Faraday Soc.*, **47**, 269 (1951).

(33) F. Kaufman and J. R. Kelso, *J. Chem. Phys.*, **23**, 1702 (1955).
(34) G. B. Kistiakowsky and W. W. Ramson, *ibid.*, **7**, 725 (1939).
(35) G. B. Kistiakowsky and J. R. Lacher, *J. Am. Chem. Soc.*, **58**, 123 (1936).
(36) J. W. L. Fordham and W. H. Leverne, *ibid.*, **73**, 1634 (1951).

ACKNOWLEDGMENTS AND ADDRESSES

Received February 3, 1976, from the *College of Pharmacy, University of Toledo, Toledo, OH 43606.*
Accepted for publication July 28, 1976.

Simple GLC Determination of Ethylene Oxide and Its Reaction Products in Drugs and Formulations

P. A. HARTMAN and P. B. BOWMAN ˣ

Abstract □ Convenient rapid GLC methods for the estimation of residual ethylene oxide, ethylene chlorohydrin, and ethylene glycol in ethylene oxide-sterilized bulk drugs and formulations prepared therefrom are described. Ethylene oxide was chromatographed using a porous polymer column; ethylene chlorohydrin and ethylene glycol were chromatographed using either polyethylene glycol 400 or a porous polymer column. All three residuals were determined from the same sample preparation for each type of drug or formulation examined. Recoveries of each of the three residuals were greater than 95% for all samples examined. Detection limits, at moderate electrometer sensitivities, were 2 μg/g or ml for ethylene oxide and ethylene chlorohydrin and 5 μg/g or ml for ethylene glycol. The most likely interferences are discussed.

Keyphrases □ Ethylene oxide—and reaction products, GLC analysis, sterilized bulk drugs and formulations □ GLC—analysis, ethylene oxide and reaction products in sterilized bulk drugs and formulations □ Sterilizers—ethylene oxide and reaction products, GLC analysis in bulk drugs and formulations

The determination of residual levels of ethylene oxide and its reaction products, ethylene chlorohydrin and ethylene glycol, has received a great deal of attention. However, most work has dealt with the estimation of the residual levels in plastic medical devices and foods (1, 2).

Essentially all recently published procedures depended on GLC for separation and quantitation. Differences in the methods were primarily in the sample preparations (3). Natural and synthetic polymers have the capacity to absorb large quantities of ethylene oxide, and various methods have been proposed to measure accurately ethylene oxide, ethylene chlorohydrin, and ethylene glycol in these materials (4). However, drugs and pharmaceutical formulations have received scant attention. A GLC procedure was described for the determination of residual ethylene oxide in steroids that involved distillation and thermal conductivity detection (5).

Recent work centered on the use of porous polymer packings (Chromosorb 101 or Porapak) for ethylene oxide and of polyethylene glycols for ethylene chlorohydrin and ethylene glycol.

To test large numbers of samples, a method was desired that would require minimal sample preparation and analyst time without compromising the requirements for quantitative results. Since the measurement of residual levels is more of a limits test than a precise quantitation for a potency measurement, simple sample preparations and minimum chromatographic time were desired. In this paper, procedures for water-insoluble bulk drugs, aqueous suspensions, aqueous solutions, and ointments are described. For each material or formulation discussed, a single sample preparation was suitable for the quantitation of ethylene oxide, ethylene chlorohydrin, and ethylene glycol.

For quantitation of ethylene oxide, a Porapak R column was employed; a polyethylene glycol 400 column was used for the other two compounds. The use of the two columns was advantageous, since both were operated at the same temperature. With a dual-column dual-electrometer instrument, all three residuals could be determined simultaneously.

EXPERIMENTAL

Instrument—A gas chromatograph[1] equipped with a flame-ionization detector and U-shaped glass columns, 180 cm × 3 mm i.d., was used. The column packings used were Porapak R[2] (80–100 mesh) for ethylene oxide determinations and 15% Carbowax 400 on 80–100-mesh Gas Chrom Q[3] for ethylene chlorohydrin and ethylene glycol measurements. The carrier gas was helium at a flow rate of approximately 60 ml/min, with hydrogen and air flows adjusted for maximum flame response.

The oven temperature was approximately 110° for both columns. A Porapak R column at 170° was also used for ethylene chlorohydrin and ethylene glycol. The flash heater and the detector were operated about 10 and 30° above the column temperature, respectively. The instrument sensitivity was range 10 and attenuation 1, 2, or 4, depending upon sample concentration.

Reagents and Chemicals—Distilled water, hexane[4], ethylene oxide[5] (liquid), ethylene chlorohydrin[5], and ethylene glycol[6] were used. The hexane was washed with distilled water prior to use.

Reference Preparations—The ethylene oxide reference solution was prepared by diluting an ethylene oxide stock solution with distilled water to a concentration of 30 μg/ml. The stock solution of ethylene oxide was prepared by adding about 0.5 ml of liquid ethylene oxide to a 50-ml volumetric flask containing about 25 ml of distilled water. The flask was weighed before and after addition of the ethylene oxide; the increase in weight was the amount of ethylene oxide dissolved. The ethylene oxide solution was diluted to volume and mixed prior to dilution.

A combined ethylene chlorohydrin and ethylene glycol reference solution was prepared by dilution of a stock solution containing both compounds to a concentration of 30 μg/ml each. The stock solution was

[1] Model 402, Hewlett-Packard Corp., Avondale, Pa.
[2] Waters Associates, Milford, Mass.
[3] Applied Science Labs, State College, Pa.
[4] Burdick and Jackson, Muskegon, Mich.
[5] Eastman Organic Chemicals, Rochester, N.Y.
[6] Matheson, Coleman and Bell, Norwood, Ohio.

(33) F. Kaufman and J. R. Kelso, *J. Chem. Phys.*, **23**, 1702 (1955).
(34) G. B. Kistiakowsky and W. W. Ramson, *ibid.*, **7**, 725 (1939).
(35) G. B. Kistiakowsky and J. R. Lacher, *J. Am. Chem. Soc.*, **58**, 123 (1936).
(36) J. W. L. Fordham and W. H. Leverne, *ibid.*, **73**, 1634 (1951).

ACKNOWLEDGMENTS AND ADDRESSES

Received February 3, 1976, from the *College of Pharmacy, University of Toledo, Toledo, OH 43606.*
Accepted for publication July 28, 1976.

Simple GLC Determination of Ethylene Oxide and Its Reaction Products in Drugs and Formulations

P. A. HARTMAN and P. B. BOWMAN ˣ

Abstract □ Convenient rapid GLC methods for the estimation of residual ethylene oxide, ethylene chlorohydrin, and ethylene glycol in ethylene oxide-sterilized bulk drugs and formulations prepared therefrom are described. Ethylene oxide was chromatographed using a porous polymer column; ethylene chlorohydrin and ethylene glycol were chromatographed using either polyethylene glycol 400 or a porous polymer column. All three residuals were determined from the same sample preparation for each type of drug or formulation examined. Recoveries of each of the three residuals were greater than 95% for all samples examined. Detection limits, at moderate electrometer sensitivities, were 2 μg/g or ml for ethylene oxide and ethylene chlorohydrin and 5 μg/g or ml for ethylene glycol. The most likely interferences are discussed.

Keyphrases □ Ethylene oxide—and reaction products, GLC analysis, sterilized bulk drugs and formulations □ GLC—analysis, ethylene oxide and reaction products in sterilized bulk drugs and formulations □ Sterilizers—ethylene oxide and reaction products, GLC analysis in bulk drugs and formulations

The determination of residual levels of ethylene oxide and its reaction products, ethylene chlorohydrin and ethylene glycol, has received a great deal of attention. However, most work has dealt with the estimation of the residual levels in plastic medical devices and foods (1, 2).

Essentially all recently published procedures depended on GLC for separation and quantitation. Differences in the methods were primarily in the sample preparations (3). Natural and synthetic polymers have the capacity to absorb large quantities of ethylene oxide, and various methods have been proposed to measure accurately ethylene oxide, ethylene chlorohydrin, and ethylene glycol in these materials (4). However, drugs and pharmaceutical formulations have received scant attention. A GLC procedure was described for the determination of residual ethylene oxide in steroids that involved distillation and thermal conductivity detection (5).

Recent work centered on the use of porous polymer packings (Chromosorb 101 or Porapak) for ethylene oxide and of polyethylene glycols for ethylene chlorohydrin and ethylene glycol.

To test large numbers of samples, a method was desired that would require minimal sample preparation and analyst time without compromising the requirements for quantitative results. Since the measurement of residual levels is more of a limits test than a precise quantitation for a potency measurement, simple sample preparations and minimum chromatographic time were desired. In this paper, procedures for water-insoluble bulk drugs, aqueous suspensions, aqueous solutions, and ointments are described. For each material or formulation discussed, a single sample preparation was suitable for the quantitation of ethylene oxide, ethylene chlorohydrin, and ethylene glycol.

For quantitation of ethylene oxide, a Porapak R column was employed; a polyethylene glycol 400 column was used for the other two compounds. The use of the two columns was advantageous, since both were operated at the same temperature. With a dual-column dual-electrometer instrument, all three residuals could be determined simultaneously.

EXPERIMENTAL

Instrument—A gas chromatograph[1] equipped with a flame-ionization detector and U-shaped glass columns, 180 cm × 3 mm i.d., was used. The column packings used were Porapak R[2] (80–100 mesh) for ethylene oxide determinations and 15% Carbowax 400 on 80–100-mesh Gas Chrom Q[3] for ethylene chlorohydrin and ethylene glycol measurements. The carrier gas was helium at a flow rate of approximately 60 ml/min, with hydrogen and air flows adjusted for maximum flame response.

The oven temperature was approximately 110° for both columns. A Porapak R column at 170° was also used for ethylene chlorohydrin and ethylene glycol. The flash heater and the detector were operated about 10 and 30° above the column temperature, respectively. The instrument sensitivity was range 10 and attenuation 1, 2, or 4, depending upon sample concentration.

Reagents and Chemicals—Distilled water, hexane[4], ethylene oxide[5] (liquid), ethylene chlorohydrin[5], and ethylene glycol[6] were used. The hexane was washed with distilled water prior to use.

Reference Preparations—The ethylene oxide reference solution was prepared by diluting an ethylene oxide stock solution with distilled water to a concentration of 30 μg/ml. The stock solution of ethylene oxide was prepared by adding about 0.5 ml of liquid ethylene oxide to a 50-ml volumetric flask containing about 25 ml of distilled water. The flask was weighed before and after addition of the ethylene oxide; the increase in weight was the amount of ethylene oxide dissolved. The ethylene oxide solution was diluted to volume and mixed prior to dilution.

A combined ethylene chlorohydrin and ethylene glycol reference solution was prepared by dilution of a stock solution containing both compounds to a concentration of 30 μg/ml each. The stock solution was

[1] Model 402, Hewlett-Packard Corp., Avondale, Pa.
[2] Waters Associates, Milford, Mass.
[3] Applied Science Labs, State College, Pa.
[4] Burdick and Jackson, Muskegon, Mich.
[5] Eastman Organic Chemicals, Rochester, N.Y.
[6] Matheson, Coleman and Bell, Norwood, Ohio.

Table I—Representative Recovery Data

Ethylene Oxide			Ethylene Chlorohydrin			Ethylene Glycol		
Added, μg/g	Found, μg/g	Recovery, %	Added, μg/g	Found, μg/g	Recovery, %	Added, μg/g	Found, μg/g	Recovery, %
				Bulk Drug				
0.0	0.0	—	0.0	0.0	—	0.0	0.0	—
8.7	8.9	102.3	20.5	19.5	95.1	18.8	20.6	109.6
17.4	17.2	98.9	41.2	38.9	94.5	37.6	30.5	81.1
34.9	30.1	86.2	82.4	79.1	96.0	75.6	79.3	104.9
Mean recovery		95.8			95.2			98.5
				Aqueous Suspension				
0.0	0.0	—	0.0	0.0	—	0.0	0.0	—
10.3	10.1	98.1	15.8	15.0	94.9	15.4	15.2	98.7
20.6	21.3	103.3	31.6	33.7	106.7	30.8	29.5	95.8
41.3	40.4	97.8	63.2	63.6	100.6	61.7	64.2	104.1
Mean recovery		99.7			100.7			99.5
				Ointment				
0.0	0.0	—	0.0	0.0	—	0.0	0.0	—
9.9	10.3	104.0	15.5	15.0	96.8	15.3	15.0	98.7
19.8	18.6	93.9	31.0	31.5	101.8	30.6	29.0	91.3
39.5	38.2	96.6	62.0	60.6	97.7	61.2	63.0	102.4
Mean recovery		98.2			98.8			97.5

prepared by combining about 0.3 g each, accurately weighed, of ethylene chlorohydrin and ethylene glycol in a 100-ml volumetric flask and diluting to volume with distilled water.

Sample Preparations—Aqueous solutions were chromatographed directly. Aqueous suspensions were centrifuged, and portions of the clear supernates were removed for chromatography.

One-gram samples of water-insoluble bulk drugs were placed in disposable vials, and 4.0 ml of distilled water was added. The samples were mixed thoroughly with a vortex mixer and shaken vigorously for at least 5 min. The samples were centrifuged, and portions of the clear supernates were withdrawn for chromatography.

Three-gram samples of ointments were placed into 35-ml centrifuge tubes and dissolved in 6.0 ml of water-washed hexane. Exactly 3.0 ml of distilled water was added, and the samples were mixed for 5 min with a vortex mixer and centrifuged. The upper organic layer was removed by aspiration, and the lower aqueous layer was retained for chromatography. A 3.0-ml portion of the ethylene oxide reference solution was washed with 6.0 ml of water-washed hexane before chromatography in this case.

Equal aliquots, usually 6.0 μl, of the sample preparations and the appropriate reference preparations were chromatographed using the specified conditions. It was necessary to equilibrate the columns by injecting two or three aliquots of the reference solutions prior to each day's analyses. Peak heights were determined directly from the chromatograms.

Calculations—The level of each residual, ethylene oxide, ethylene chlorohydrin, and ethylene glycol, was calculated by a peak height comparison with the corresponding reference.

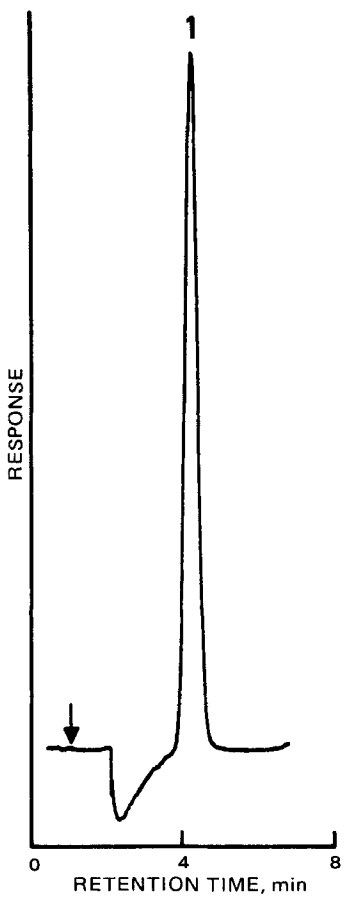

Figure 1—*Chromatogram of 40 μg/ml of ethylene oxide (1) added to an aqueous suspension of a steroid (Porapak R column). The arrow indicates the point of injection.*

RESULTS AND DISCUSSION

GLC—A representative chromatogram for ethylene oxide is shown in Fig. 1. Although water should not give a response in the flame-ionization detector, an apparent solvent front was observed, probably due to pertubation of flows by injection and vaporization. The shape of this solvent front varied from one sample type to another. Chromatographic response was linear over the 2–80-μg/ml range. The limit of detection was about 2 μg/ml for ethylene oxide.

Under the standard chromatographic conditions, ethylene oxide was not resolved from methanol. Methanol is a common recrystallization solvent for steroids and could be present in residual amounts. If a significant ethylene oxide response was observed, chromatography at 70° resolved the methanol. At a column temperature of 70°, ethylene oxide and methanol had retention times of 7 and 8 min, respectively. Acetone, another common recrystallization solvent, also was detected in some cases. This peak, which had a retention time of about 13 min at 110°, did not interfere with the ethylene oxide determination but did require extended chromatography time. No other interferences were observed.

Either of two sets of chromatographic conditions was used for the simultaneous determination of ethylene chlorohydrin and ethylene glycol. Typical chromatograms for the Carbowax 400 and Porapak R columns are shown in Figs. 2 and 3, respectively. Chromatographic response was linear for both columns over the 2–110-μg/ml range for ethylene chlorohydrin and the 5–200-μg/ml range for ethylene glycol. Limits of detection were estimated to be 2 μg/ml for ethylene chlorohydrin and 5 μg/ml for ethylene glycol.

Chromatography on the Carbowax 400 column was preferred over the Porapak R column because fewer extraneous peaks were observed and

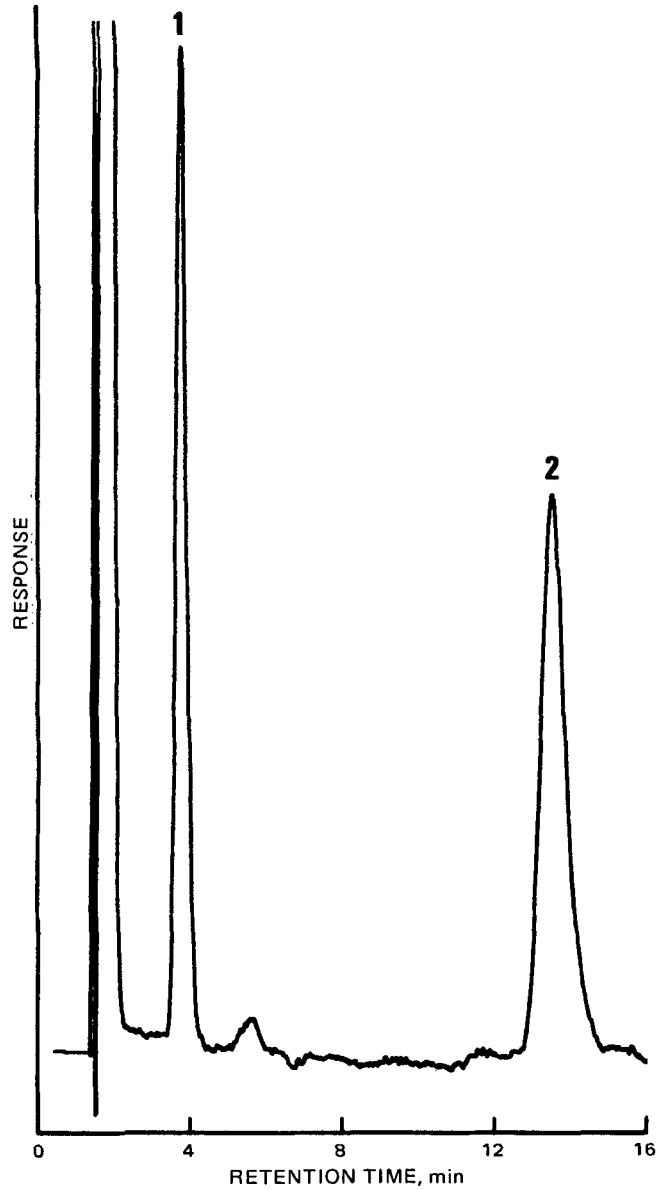

Figure 2—*Chromatogram of ethylene chlorohydrin and ethylene glycol added to an aqueous suspension of a steroid (polyethylene glycol 400 column). Key: 1, ethylene chlorohydrin (63 μg/ml); and 2, ethylene glycol (63 μg/ml).*

the resolution and shape of the peaks were superior. The Carbowax column was tried first in all cases. However, some aqueous suspensions and solutions were formulated with benzyl alcohol as a preservative, and the large benzyl alcohol peak masked the ethylene glycol peak when the Carbowax column was used. The retention time of benzyl alcohol on the Porapak R column was about 90 min at 170°, thus permitting several samples to be run before the benzyl alcohol eluted. It was necessary to chromatograph two or three aliquots of the reference solutions to establish a reproducible response, probably due to on-column adsorption of these compounds.

A buildup of components from the various sample formulations on the column packings was observed after extended use and caused a deterioration of the chromatographic performance. Original column efficiency was restored by replacing the front 4–5 cm of column packing and allowing the column to reequilibrate for at least 16 hr.

No attempt was made to identify extraneous peaks (other than those previously discussed) because they were always resolved from the peaks of interest. As a precautionary measure, the hexane was washed with distilled water prior to use to eliminate impurities that interfered.

Recovery—Recovery data were obtained for each of the 12 bulk drugs, 16 aqueous suspensions and solutions, and 11 ointments studied. Various spiking techniques were used to add three different levels each of ethylene oxide, ethylene chlorohydrin, and ethylene glycol to separate samples of every sample type studied.

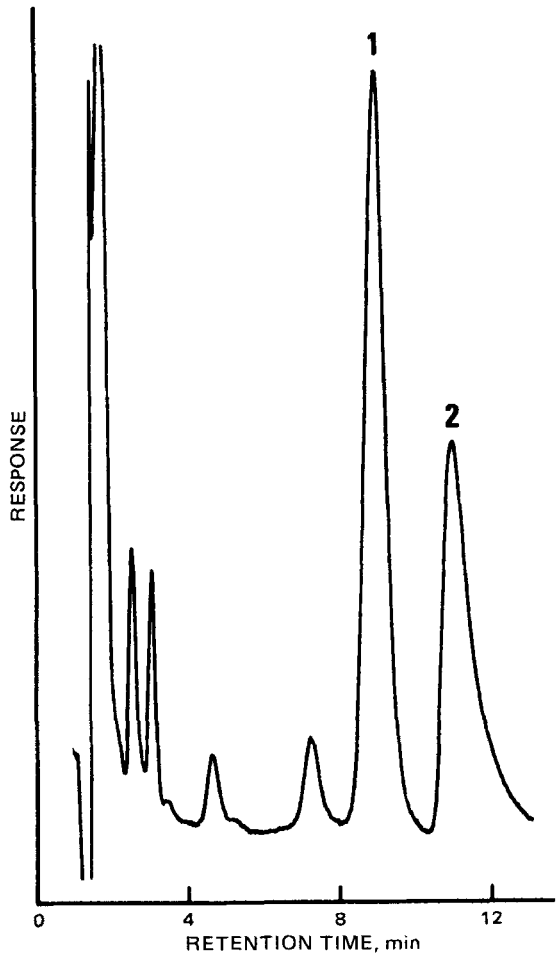

Figure 3—*Chromatogram of ethylene chlorohydrin and ethylene glycol added to a sterile infusion solution of a steroid (Porapak R column). Key: 1, ethylene chlorohydrin (61 μg/ml); and 2, ethylene glycol (62 μg/ml). Excipient peaks are not identified, and the benzyl alcohol peak is not shown.*

For bulk drugs, recovery samples were simulated by equilibrating aqueous solutions of the residuals with samples of non-ethylene-oxide-treated bulk drugs. The vortex mixer produced a homogeneous mixture of the bulk drug powder and the aqueous phase. This mixture was separated by centrifugation, and the clear supernates were chromatographed. Adler (5) found that the retention of ethylene oxide on steroids is due to sorption on the surface of the individual drug particles. Since ethylene oxide is highly water soluble and the drugs tested were generally micronized, the removal of this residual from the drug should have been highly efficient.

Aqueous suspensions and solutions for the recovery studies were prepared using vehicles containing non-ethylene-oxide-treated materials. Microliter aliquots of concentrated solutions of the residuals were added to produce the desired concentrations. The samples were mixed, centrifuged if necessary, and chromatographed under the appropriate conditions.

Recovery for the ointments was demonstrated by extracting hexane solutions of a nonsterilized formulation with aqueous solutions containing the residuals.

Typical recovery data are presented in Table I. In most cases, the recovery for individual samples was greater than 90%. The average recovery for each formulation or bulk material was greater than 95%. Due to the significant solubility of ethylene oxide in hexane, it was necessary to wash the ethylene oxide reference solution with hexane prior to analysis of ointments. Thus, the recoveries reported for ethylene oxide are actually apparent recovery.

The reference solutions were quite stable. The combined ethylene chlorohydrin and ethylene glycol reference preparation was retained for several weeks with no noticeable change in concentration. The ethylene

oxide reference solution was stable for about 1 week when prepared in distilled water. However, a change in pH or contamination with inorganic halide would induce rapid conversion of the ethylene oxide to ethylene glycol or ethylene halohydrin. The same concern existed for the sample preparations. Therefore, samples were always chromatographed on the same day that they were prepared.

Precision—Reproducibility of the chromatographic response was about 2% in each case, determined by replicate injections of reference solutions. The variation in results for actual samples was about 5%.

Simplicity—The measurement of the levels of residual ethylene oxide, ethylene chlorohydrin, and ethylene glycol present in pharmaceutical preparations is more of a limits test than a precise quantitation for potency determination. Thus, it is desirable to use rapid, simple, sensitive, and fairly accurate methods for these measurements. The procedures as described satisfy these requirements.

The sample preparation was as simple as possible. All three residuals were extracted simultaneously by a single aqueous extraction.

The chromatographic systems were ideal. Two columns in one dual column instrument provided the necessary instrumentation for estimating all three residuals without changing oven temperature.

Chromatographic time was held to a minimum. Since the highest precision was not required, internal standards were not employed which minimized chromatographic time and permitted a single sample preparation to be employed for all three residuals. Water proved to be the ideal solvent. It provided the highest extraction efficiency, yet did not respond in the flame-ionization detector. If an organic solvent had been required, it would probably have eluted after ethylene oxide and time would have been lost waiting for a large solvent peak to clear the column. With water, this delay was eliminated.

These procedures are versatile and applicable to a large number of aqueous suspensions, aqueous solutions, ointments, and water-insoluble bulk drugs.

REFERENCES

(1) C. W. Burch, in "Industrial Sterilization, International Symposium, 1972," G. Briggs and W. S. Miller, Eds., Duke University Press, Durham, N.C., 1973, p. 49.

(2) B. Berck, *J. Chromatogr. Sci.*, **13**, 256 (1975).

(3) S. J. Romano and J. A. Renner, *J. Pharm. Sci.*, **64**, 1412 (1975).

(4) H. D. Spitz and J. Weinburger, *ibid.*, **60**, 271 (1971).

(5) N. Adler, *ibid.*, **54**, 735 (1965).

ACKNOWLEDGMENTS AND ADDRESSES

Received May 13, 1976, from the *Control Analytical Research and Development Laboratories, The Upjohn Company, Kalamazoo, MI 49001.*

Accepted for publication July 28, 1976.

[x] To whom inquiries should be directed.

Enzymatic Activity of Pig Heart Mitochondrial Malate Dehydrogenase Monomolecular Films by Surface Exchange Technique

A. W. MALICK [*] and N. D. WEINER [x]

Abstract □ A technique for studying the catalytic activity of enzymes spread as a film at an air–water interface, by exchanging the subphase under the film to remove unspread enzyme molecules, was developed, and its effectiveness was studied using surface-spread mitochondrial malate dehydrogenase. Mitochondrial malate dehydrogenase formed stable films which gave reproducible π–A curves. The enzyme activity was measured by the oxidation rate of reduced nicotinamide adenine dinucleotide (NADH) in the presence of the substrate oxalacetic acid. Oxalacetic acid and NADH were injected into the subphase. The catalytic activity of the enzyme was dependent on the surface pressure of the film. The maximum catalytic activity was observed at a surface pressure of 4.4 dynes/cm. The activity was higher at intermediate surface pressures than at very low or very high surface pressures. A high bulk catalytic activity was observed in the unstable region, *i.e.*, at a high degree of compression, of the film. The catalytic activity of the surface-spread enzyme was only a fraction of an equivalent amount of enzyme in solution.

Keyphrases □ Catalytic activity—enzymes spread as a monomolecular film at an air–water interface, surface exchange technique developed □ Enzymes—mitochondrial malate dehydrogenase, spread as a monomolecular film at an air–water interface, surface exchange technique developed □ Malate dehydrogenase, mitochondrial—spread as a monomolecular film at an air–water interface, surface exchange technique developed □ Films, monomolecular—of enzymes at an air–water interface, surface exchange technique developed □ Surface exchange technique—enzymes spread as a monomolecular film at an air–water interface

Monomolecular films offer a useful model system for studying the behavior of membrane components at an air–water interface (1). The application of monomolecular films to the study of interactions that may occur at the membranes of cells and cell organelles is a flexible and versatile system whereby numerous effects can be observed. The relative simplicity of this system permits analysis and understanding of the effects that often cannot be observed in the extremely complex environment of living systems.

BACKGROUND

Modification of the film can be employed to gain further insight into cellular function. Since membrane-bound enzymes are situated at interfaces, it must be assumed that they are in a partially unfolded state and that the side chains are oriented in relation to the interface. Monolayer studies also afford a method to study the conformational change effects of proteins by monitoring the surface pressure, since the orientation of the side chains of surface-spread protein would be expected to vary with the surface pressure of the film. A dependence of the catalytic activity on surface pressure was reported for catalase and acetylcholinesterase films (2). The activity of surface-spread trypsin was dependent on the surface concentration of the enzyme (3).

Estimation of catalytic activity of surface-spread enzymes presents unique difficulties, because the fraction of the enzyme that escapes into the bulk phase must first be removed. Previously (4), an apparatus and technique for studying monomolecular films were reported; the subphase can be exchanged without disturbing the film, thereby removing any dissolved contaminants in the bulk phase. Data were presented to demonstrate the utility of this system for studying protein monolayers and its applicability to the study of ion-exchange properties of phospholipid monolayers.

In this study, the subphase exchange technique was used to investigate the enzymatic behavior of surface-spread pig heart mitochondrial malate

oxide reference solution was stable for about 1 week when prepared in distilled water. However, a change in pH or contamination with inorganic halide would induce rapid conversion of the ethylene oxide to ethylene glycol or ethylene halohydrin. The same concern existed for the sample preparations. Therefore, samples were always chromatographed on the same day that they were prepared.

Precision—Reproducibility of the chromatographic response was about 2% in each case, determined by replicate injections of reference solutions. The variation in results for actual samples was about 5%.

Simplicity—The measurement of the levels of residual ethylene oxide, ethylene chlorohydrin, and ethylene glycol present in pharmaceutical preparations is more of a limits test than a precise quantitation for potency determination. Thus, it is desirable to use rapid, simple, sensitive, and fairly accurate methods for these measurements. The procedures as described satisfy these requirements.

The sample preparation was as simple as possible. All three residuals were extracted simultaneously by a single aqueous extraction.

The chromatographic systems were ideal. Two columns in one dual column instrument provided the necessary instrumentation for estimating all three residuals without changing oven temperature.

Chromatographic time was held to a minimum. Since the highest precision was not required, internal standards were not employed which minimized chromatographic time and permitted a single sample preparation to be employed for all three residuals. Water proved to be the ideal solvent. It provided the highest extraction efficiency, yet did not respond in the flame-ionization detector. If an organic solvent had been required, it would probably have eluted after ethylene oxide and time would have been lost waiting for a large solvent peak to clear the column. With water, this delay was eliminated.

These procedures are versatile and applicable to a large number of aqueous suspensions, aqueous solutions, ointments, and water-insoluble bulk drugs.

REFERENCES

(1) C. W. Burch, in "Industrial Sterilization, International Symposium, 1972," G. Briggs and W. S. Miller, Eds., Duke University Press, Durham, N.C., 1973, p. 49.

(2) B. Berck, *J. Chromatogr. Sci.*, **13**, 256 (1975).

(3) S. J. Romano and J. A. Renner, *J. Pharm. Sci.*, **64**, 1412 (1975).

(4) H. D. Spitz and J. Weinburger, *ibid.*, **60**, 271 (1971).

(5) N. Adler, *ibid.*, **54**, 735 (1965).

ACKNOWLEDGMENTS AND ADDRESSES

Received May 13, 1976, from the *Control Analytical Research and Development Laboratories, The Upjohn Company, Kalamazoo, MI 49001.*

Accepted for publication July 28, 1976.

[x] To whom inquiries should be directed.

Enzymatic Activity of Pig Heart Mitochondrial Malate Dehydrogenase Monomolecular Films by Surface Exchange Technique

A. W. MALICK [*] and N. D. WEINER [x]

Abstract □ A technique for studying the catalytic activity of enzymes spread as a film at an air–water interface, by exchanging the subphase under the film to remove unspread enzyme molecules, was developed, and its effectiveness was studied using surface-spread mitochondrial malate dehydrogenase. Mitochondrial malate dehydrogenase formed stable films which gave reproducible π–A curves. The enzyme activity was measured by the oxidation rate of reduced nicotinamide adenine dinucleotide (NADH) in the presence of the substrate oxalacetic acid. Oxalacetic acid and NADH were injected into the subphase. The catalytic activity of the enzyme was dependent on the surface pressure of the film. The maximum catalytic activity was observed at a surface pressure of 4.4 dynes/cm. The activity was higher at intermediate surface pressures than at very low or very high surface pressures. A high bulk catalytic activity was observed in the unstable region, *i.e.*, at a high degree of compression, of the film. The catalytic activity of the surface-spread enzyme was only a fraction of an equivalent amount of enzyme in solution.

Keyphrases □ Catalytic activity—enzymes spread as a monomolecular film at an air–water interface, surface exchange technique developed □ Enzymes—mitochondrial malate dehydrogenase, spread as a monomolecular film at an air–water interface, surface exchange technique developed □ Malate dehydrogenase, mitochondrial—spread as a monomolecular film at an air–water interface, surface exchange technique developed □ Films, monomolecular—of enzymes at an air–water interface, surface exchange technique developed □ Surface exchange technique—enzymes spread as a monomolecular film at an air–water interface

Monomolecular films offer a useful model system for studying the behavior of membrane components at an air–water interface (1). The application of monomolecular films to the study of interactions that may occur at the membranes of cells and cell organelles is a flexible and versatile system whereby numerous effects can be observed. The relative simplicity of this system permits analysis and understanding of the effects that often cannot be observed in the extremely complex environment of living systems.

BACKGROUND

Modification of the film can be employed to gain further insight into cellular function. Since membrane-bound enzymes are situated at interfaces, it must be assumed that they are in a partially unfolded state and that the side chains are oriented in relation to the interface. Monolayer studies also afford a method to study the conformational change effects of proteins by monitoring the surface pressure, since the orientation of the side chains of surface-spread protein would be expected to vary with the surface pressure of the film. A dependence of the catalytic activity on surface pressure was reported for catalase and acetylcholinesterase films (2). The activity of surface-spread trypsin was dependent on the surface concentration of the enzyme (3).

Estimation of catalytic activity of surface-spread enzymes presents unique difficulties, because the fraction of the enzyme that escapes into the bulk phase must first be removed. Previously (4), an apparatus and technique for studying monomolecular films were reported; the subphase can be exchanged without disturbing the film, thereby removing any dissolved contaminants in the bulk phase. Data were presented to demonstrate the utility of this system for studying protein monolayers and its applicability to the study of ion-exchange properties of phospholipid monolayers.

In this study, the subphase exchange technique was used to investigate the enzymatic behavior of surface-spread pig heart mitochondrial malate

dehydrogenase. Mitochondrial malate dehydrogenase, an enzyme of the tricarboxylic acid cycle, catalyzes the oxidation of L-malate to oxalacetate (5). This enzyme requires relatively drastic isolation procedures, including an acetone-dried powder preparation of tissues and an ethanol fractionation (6). The difficulty in its isolation suggests that the enzyme is firmly bound to the mitochondrial framework. Aqueous solutions of mitochondrial malate dehydrogenase are quite unstable, and most of the catalytic activity is lost on standing for a few hours at room temperature (7). This instability of the enzyme is associated with the removal of the enzyme from its bound state, which also suggests that it is situated at a biological interface.

A previous article (4) discussed film studies of pig heart mitochondrial malate dehydrogenase at an air–water interface with and without subphase exchange. Malate dehydrogenase forms stable films, which give reproducible surface pressure–surface area (π–A) curves. Films of malate dehydrogenase that were formed using different amounts of this enzyme were studied after the buffered subphase was changed with a buffer solution of the same composition. The exchange of this subphase had no effect on the π–A plots of any malate dehydrogenase film studied.

The purposes of this phase of the study were to investigate the applicability of the subphase exchange technique for studying the catalytic activity of surface-spread malate dehydrogenase and to determine the effect of surface pressure on catalytic activity.

EXPERIMENTAL

Materials—Malate dehydrogenase[1] (porcine heart) was supplied as a suspension in 70% saturated ammonium sulfate solution. Oxalacetic acid[2] (*cis*-enol) and nicotinamide adenine dinucleotide, reduced[1] (NADH), 90%, were used to measure the activity of the enzyme. The inorganic chemicals used, all reagent grade, were checked for surface impurities. The water used was first deionized by passing distilled water through a mixed resin bed of a demineralizer[3] and then distilled twice from an all-glass still. All buffer solutions were passed through a column of activated charcoal.

Surface tension measurements were made by the Wilhelmy plate method (8), using a thin roughened platinum plate suspended from a torsion balance. The film balance[4] consisted of a 500-ml capacity Langmuir-type polytef[5] trough equipped with a polytef movable barrier and two ribbon screw polytef stirrers running along the two long edges of the trough. The stirring system was designed so that the motion at reasonable speeds did not disturb the film. For all experiments, the temperature of the trough was maintained at 27 ± 2° by circulating water from a bath in a jacket surrounding the trough.

Monolayer Methods—The apparatus and procedure for subphase exchange and for determining π–A isotherms for protein monolayers spread at the air–water interface were described previously (4). The π–A isotherms of proteins were obtained by film compression after the protein was spread by the Trurnit (9) method. Compression was initiated 25 min after the protein was spread, which allowed enough time for equilibration and subphase exchange. In the exchange process, 900 ml of subphase was exchanged (trough capacity = 500 ml) with a phosphate buffer solution of the same composition as the subphase.

Spreading solutions of malate dehydrogenase were prepared by diluting a suspension of malate dehydrogenase with sufficient 0.1 *M* phosphate buffer (pH 7.4) to yield a concentration of 1.36 mg/ml. The subphase in the surface balance trough also consisted of 0.1 *M* phosphate buffer (pH 7.4). The pH value of 7.4 was chosen because the highest activity of malate dehydrogenase occurs in the physiological range of pH 7.3–7.5 (10). Different volumes of spreading solution of the same concentration of enzyme were delivered to spread films of different protein surface concentrations. For each experiment, a fresh spreading solution of malate dehydrogenase was prepared.

To determine the amount of enzyme adsorbed at the air–water interface after subphase exchange, films were removed by negative pressure using a narrow glass tube and then analyzed for protein content by a modification of the Lowry (11) technique.

Enzyme Activity Methods—For enzyme activity studies, a fresh solution of oxalacetic acid was prepared for each experiment by dissolving 50 mg of oxalacetic acid in 50 ml of pH 7.4 phosphate buffer and adjusting to pH 7.2–7.4. The solution was stored at 0°. Solutions of NADH were prepared by dissolving 112 mg of NADH in 50 ml of the pH 7.4 phosphate buffer immediately before use. This solution was never frozen.

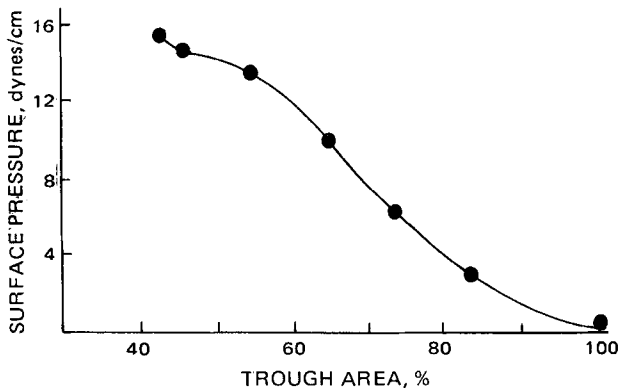

Figure 1—*The π–A curves of mitochondrial malate dehydrogenase films of 0.081 mg of enzyme spread on pH 7.4 phosphate buffer and the subphase was exchanged with 900 ml of buffered solution.*

The malate dehydrogenase film was first spread by the method described previously. Five minutes after the protein had been spread, the subphase exchange was started and continued for 15 min. In the process, 900 ml of the subphase was exchanged. After the exchange, the polytef barrier of the surface balance was moved to a position that gave the desired surface pressure at which the activity of the enzyme was to be measured.

Following compression, 40 ml of the NADH solution was injected under the film with two glass syringes attached to stainless steel needles previously placed at the midline of the trough 10 cm from each edge in the trough. Two injections were used instead of one to obtain a quicker mixing of the injected solution with the subphase. Injections were made at a slow, steady rate to avoid any disturbance of the film. The injection of air bubbles was also avoided.

Soon after injection of the NADH solution, the stirrers were started. The stirrer speed, at which there was no disturbance at the surface, was kept constant for all experiments. Seven minutes after the injection of NADH solution, oxalacetic acid solution was injected through the two syringes to initiate the reaction. The time at which the contents of the first syringe of oxalacetic acid solution was injected was taken as time zero for the reaction.

As soon as the oxalacetic acid solution was injected, a 4-ml sample of the subphase was pulled through one needle. Additional 4-ml samples were then pulled at specific intervals for UV analysis[6] at 340 nm. The UV absorbance of the subphase solution was independent of the part of the trough from which the sample was withdrawn. Throughout the experiment, the needles remained in place and the stirring was continued. The activity of the enzyme was measured spectrophotometrically by virtue of disappearance of NADH based on the characteristic absorption of NADH at 340 nm.

The slope of the absorbance–time curve, representing the rate of enzyme-induced oxidation of NADH to NAD, was used as a measure of malate dehydrogenase activity. Plots of NADH absorbance *versus* time were linear, and results were reproducible. Slopes were calculated using a linear regression computer program.

RESULTS AND DISCUSSION

The malate dehydrogenase films were spread on pH 7.4 phosphate buffer, and the subphase was exchanged with a buffer solution of the same composition. In all experiments, malate dehydrogenase formed stable films which gave reproducible π–A curves.

Figure 1 shows the π–A curve of 0.081 mg of malate dehydrogenase spread on buffer solution with the subphase exchanged. The π–A plot shows an inflection point at 15 dynes/cm. Beyond the inflection point, *i.e.*, at smaller surface areas, the film became less compressible and also less reproducible. This concentration of protein was chosen because it allowed observation of the catalytic activity of the enzyme film essentially from the gaseous state up to the point where the film became unstable, using the same trough without changing the amount of protein spread. The concentration of malate dehydrogenase at the surface must be

[1] P. L. Biochemicals, Milwaukee, Wis.
[2] Schwarz/Mann, Orangeburg, N.Y.
[3] Bantam.
[4] Frater Instrument Co., Corona, N.Y.
[5] Teflon (du Pont).
[6] Beckman DB spectrophotometer, Beckman Instruments, Fullerton, Calif.

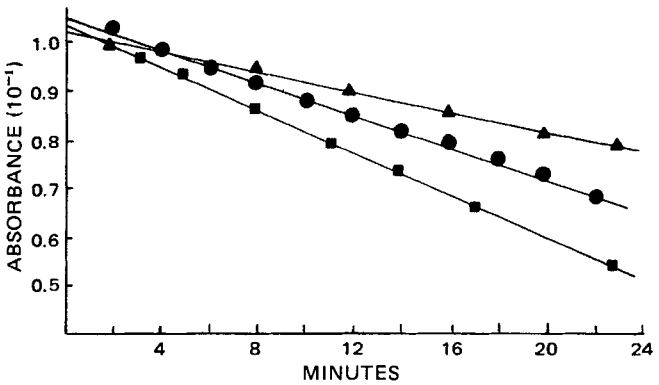

Figure 2—*Catalytic activity plots of surface-spread mitochondrial malate dehydrogenase (absorbance of NADH at 340 nm* versus *time) at full trough area. Key: ▲, 0.04 mg; ●, 0.06 mg; and ■, 0.08 mg.*

constant because the π–A plots using different concentrations of this protein are parallel but not superimposable (4). The π–A curves of higher malate dehydrogenase concentration films are condensed relative to those of lower concentrations.

Figure 2 shows some catalytic activity data of the surface-spread malate dehydrogenase. The plots of NADH absorbance *versus* time were linear and reproducible. The slopes of these plots were taken as a measure of malate dehydrogenase activity. The reactions were followed for about 20 min.

To investigate the effect of surface pressure on enzyme activity, compression of the enzyme film was necessary. The movement of the polytef barrier to compress the film resulted in a proportional decrease in area available to the enzyme at the surface. Since the reaction was carried out under zero-order saturated conditions, the available surface area of the enzyme at any given surface pressure should not have affected the reaction rate. To be certain that this was the case, different amounts of malate dehydrogenase were spread at the surface and the catalytic activity was studied at different available areas of the surface.

Figure 2 and Table I show the catalytic activity of different amounts of protein. Since the surface pressure of all films in this phase of the study was about zero, all of these films were gaseous in nature. First, 0.08 mg of protein was applied to the surface at full trough area and the enzyme activity of this film was recorded. The catalytic activity of 0.04 mg of enzyme spread at full trough area was then observed. In another experiment, 0.04 mg of enzyme was spread at full trough area and the area was then reduced to one-half the original trough area. The catalytic activity of this system was then studied. Similarly, the catalytic activity of 0.06 mg of enzyme was studied at full trough area and then after reduction to three-quarters trough area.

Table I shows that the activity of 0.04 mg of the enzyme, both at full trough area and at one-half trough area, was one-half of the catalytic activity observed for 0.08 mg of the enzyme. Similarly, the activity of 0.06 mg of the enzyme was about three-quarters of the activity observed for 0.08 mg of the enzyme both at full and three-quarters trough areas. These results indicate that the surface area available to the enzyme did not affect the catalytic activity when 0.08 mg or less of protein was spread as long as the surface pressure remained constant, *i.e.*, no conformational changes occurred. Thus, any changes of enzyme activity observed with compression of the film can be safely attributed to the change in surface pressure, *i.e.*, the conformational changes of the enzyme molecules associated with the change in surface pressure.

The orientation of the side chains of the surface-spread protein in relation to the surface may vary with the surface pressure (2). At film pressures close to zero, the side chains may lie flat in the surface. If the pressure is increased, the polar groups would be oriented into the aqueous phase while the nonpolar groups would be oriented toward the air phase. Therefore, it should be possible to vary the orientation of the protein molecules in a film by applying surface pressures of varying magnitudes.

Table I—Enzyme Activity of Malate Dehydrogenase Films

Amount of Enzyme Spread, mg	Surface Area Available to Enzyme	Enzyme Activity[a], Arbitrary Units
0.08	Full trough	2.2
0.06	Full trough	1.62
	Three-quarters trough	1.5
0.04	Full trough	0.98
	One-half trough	1.07

[a] Slope ($\times 10^2$) of absorbance of NADH at 340 nm *versus* time plot.

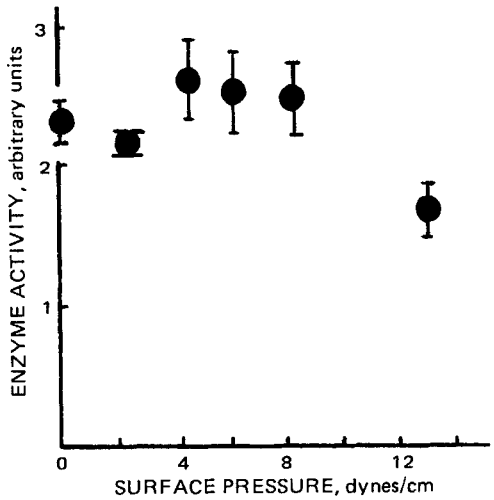

Figure 3—*Catalytic activity of mitochondrial malate dehydrogenase* versus *surface pressure plot of malate dehydrogenase films.*

In all subsequent experiments in this study, the same amount of enzyme, 0.081 mg, was spread each time. The concentration of the spreading solution was also kept constant.

Figure 3 shows the catalytic activity of surface-spread malate dehydrogenase at different surface pressures. A dependence of catalytic activity was observed with surface pressure. At intermediate film pressures, the activity of the enzyme was higher than at very low or very high surface pressures. The maximum activity was noted at 4.4 dynes/cm, and very small changes in catalytic activity were observed at surface pressures between 4 and 8 dynes/cm. Although not shown in Fig. 3, at a surface pressure of 18 dynes/cm, a point beyond the inflection point of malate dehydrogenase film (Fig. 1), a high bulk catalytic activity was observed.

The film studies of the enzyme showed that the π–A plots were not reproducible beyond 15 dynes/cm. This finding suggests that the enzyme film at this pressure becomes unstable and that some enzyme leaves the surface and diffuses to the bulk. This idea is borne out by the observation of significant catalytic activity in the subphase at a high surface pressure (18 dynes/cm).

These results show that the catalytic activity of malate dehydrogenase films is dependent on the surface pressure and, in turn, on the conformation of the enzyme molecules and suggest a mechanism by which the activity of enzymes may be regulated in membranes. A dependence of catalytic activity on surface pressure also was reported for surface-spread acetylcholinesterase and catalase (2). With acetylcholinesterase, maximum activity was attained at a surface pressure of 10 dynes/cm and decreased at both lower and higher pressures.

The results of the surface protein content analysis show that when 0.081 mg of enzyme was spread, 29.6% of the original protein spread was found at the surface after subphase exchange. This loss would be expected since, when a solution of protein is applied at the interface, some protein unfolds and anchors at the surface while the remainder escapes into the bulk in globular form. The amount of protein escaping to the bulk would be dependent on, among other factors, the amount of protein originally applied to the surface. When acetylcholinesterase was applied to the surface, 44–74% of the original protein applied anchored at the surface (2). In another study (3), 80% of the trypsin applied to the surface was lost to the subphase.

An amount of malate dehydrogenase equivalent to that present at the surface after exchange was used to compare enzyme activity in the bulk with that of surface-spread enzyme under similar conditions; *i.e.*, the final concentrations of the enzyme, oxalacetic acid, and NADH were kept the same as in the activity studies of the film. The enzyme activity at the surface was equal to 13% of the activity of the same amount of the enzyme in solution.

The loss of activity of enzyme adsorbed at an air–water interface has been shown by a number of workers. Catalase retained about 22% catalytic activity on adsorption at the air–water interface (12). The catalytic

activity was dependent on the surface pressure of a film of acetylcholinesterase, and the maximum activity observed was at a surface pressure of 10 dynes/cm (2). This activity was equal to 29% of the activity of the same amount of enzyme in solution. The fraction of the retained enzyme activity on adsorption at an air–water interface in the case of trypsin varied from 0.125 to 0.35, depending on the surface concentration of the enzyme (3).

This study demonstrated the effectiveness of the subphase exchange technique for investigating the catalytic activity of enzymes spread at an air–water interface, without interference of bulk reaction. Future reports will discuss the effects of various lipids on the catalytic activity of surface-spread malate dehydrogenase.

REFERENCES

(1) L. L. M. Van Deenen, in "The Molecular Basis of Membrane Function," D. C. Testeson, Ed., Prentice-Hall, Englewood Cliffs, N.J., 1969, p. 47.

(2) J. C. Skou, *Biochim. Biophys. Acta*, **31**, 1 (1959).

(3) L. Inbar and I. R. Miller, *ibid.*, **364**, 146 (1974).

(4) A. W. Malick, A. Felmeister, and N. D. Weiner, *J. Pharm. Sci.*, **62**, 1871 (1973).

(5) M. Dixon and E. C. Webb, "Enzymes," 2nd ed., Academic, New York, N.Y., 1964.

(6) R. G. Wolfe and J. B. Neiland, *J. Biol. Chem.*, **221**, 61 (1956).

(7) G. H. Dodd, *Eur. J. Biochem.*, **33**, 418 (1973).

(8) A. W. Adamson, "Physical Chemistry of Surfaces," 2nd ed., Interscience, New York, N.Y., 1967, p. 26.

(9) H. J. Trurnit, *J. Colloid Sci.*, **15**, 1 (1960).

(10) J. W. Callahan and G. W. Kosicki, *Can. J. Biochem.*, **45**, 839 (1967).

(11) O. H. Lowry, *J. Biol. Chem.*, **193**, 265 (1951).

(12) J. G. Kaplan, *J. Colloid Sci.*, **7**, 382 (1952).

ACKNOWLEDGMENTS AND ADDRESSES

Received May 6, 1976, from the *College of Pharmacy, University of Michigan, Ann Arbor, MI 48104.*

Accepted for publication August 5, 1976.

* College of Pharmacy and Allied Health Professions, Wayne State University, Detroit, MI 48202.

ˣ To whom inquiries should be directed.

Kinetics and Mechanisms of Hydrolysis of 1,4-Benzodiazepines III: Nitrazepam

WESLEY W. HAN *, GERALD J. YAKATAN ˣ, and DALE D. MANESS

Abstract □ The hydrolysis of nitrazepam involves a two-step sequential mechanism. The intermediate is the ring-opened compound resulting from scission of the azomethine bond. The final products are glycine and 2-amino-5-nitrobenzophenone. Recyclization of the intermediate to nitrazepam occurs at pH values above the pKa of the intermediate, in the pH region where the amino group of the intermediate is not protonated. As opposed to chlordiazepoxide and oxazepam, the initial hydrolysis step occurs at the 4,5-bond, not at the 1,2-amide linkage. This difference is attributed to a preferential activation for hydrolysis of the azomethine linkage by the nitro group. The hydrolysis involves an uncatalyzed reaction, specific acid–base catalysis, and general acid–base catalysis for acetate and phosphate buffers.

Keyphrases □ 1,4-Benzodiazepines—nitrazepam, kinetics and mechanisms of hydrolysis □ Nitrazepam—kinetics and mechanisms of hydrolysis □ Hydrolysis—nitrazepam, kinetics and mechanisms □ Anticonvulsants—nitrazepam, kinetics and mechanisms of hydrolysis

Nitrazepam, 1,3-dihydro-7-nitro-5-phenyl-2*H*-1,4-benzodiazepin-2-one, belongs to the 1,4-benzodiazepine class of tranquilizing agents. This compound is centrally active (1), surpassing diazepam, a popular benzodiazepine, in anticonvulsant activity (2).

Preceding publications (3, 4) in this series reported the hydrolysis kinetics of 7-chloro-1,4-benzodiazepines. The present study concerned the hydrolysis of the 7-nitro analog, nitrazepam.

EXPERIMENTAL

Materials—Compound purity was verified by TLC. Nitrazepam[1] and 2-amino-5-nitrobenzophenone[1] were used as received.

Buffer Solutions—All buffer solutions were made with deionized, distilled water. They were adjusted to an ionic strength of 1.0 with sodium chloride, except in ionic strength effect studies where they were adjusted to ionic strengths other than 1. The pH at the temperature of the runs was measured with a digital pH meter[2] equipped with high temperature electrodes.

The buffer systems used were: pH 1.0–3.0, hydrochloric acid; pH 3.2–5.6, acetate; pH 6.4–7.4, phosphate; pH 7.9–9.5, borate; and pH 10.1–11, sodium hydroxide.

Kinetic Measurements—The kinetic studies of the hydrolysis of nitrazepam were followed spectrophotometrically. Details of the specific procedures were given previously (3) and are summarized as follows.

A stock solution of nitrazepam (6.3×10^{-3} *M*) in ethanol was diluted in an appropriate buffer to a final concentration for the kinetic run of 2.4×10^{-5} *M*. The reaction flasks (light protected) were maintained in a constant-temperature oil bath[3] controlled within 0.1° at selected temperatures between 70 and 85°. Samples were withdrawn at suitable time intervals and cooled to room temperature by quenching in an ice water bath. Visible and UV spectrophotometric measurements were made with a double-beam spectrophotometer[4].

Isolation and Identification—Thin-layer chromatograms were made on 20 × 20-cm glass plates coated with a 250-μm layer of silica gel GF_{254}. After lyophilization, the samples were dissolved in chloroform, spotted, and developed in a closed tank for approximately 1 hr with dioxane–benzene–hexane–7.4 *M* NH_4OH (45:50:70:5). The solvent front was allowed to travel 17 cm from the origin. After drying, the plates were visualized using a short wavelength UV lamp and then sprayed with ninhydrin aerosol (0.5%) to produce visible spots. Nitrazepam, 2-amino-5-nitrobenzophenone, and glycine were spotted as reference standards. An intermediate was isolated by preparative TLC and characterized by its IR[5], NMR[6], and high-resolution mass[7] spectra.

[1] Hoffmann–La Roche, Nutley, N.J.

[2] Model 701, Orion Research, Cambridge, Mass.

[3] Sargent model SW equipped with Sargent thermonitor model ST, R. L. Sargent Co., Dallas, Tex.

[4] Model 124, Coleman Instruments Division, Perkin-Elmer Corp., Maywood, Ill.

[5] Model IR8, Beckman Instruments, Fullerton, Calif.

[6] Model C60HL, Jeol, Medford, Mass.

[7] CEC-21-110, DuPont Instruments, Wilmington, Del.

activity was dependent on the surface pressure of a film of acetylcholinesterase, and the maximum activity observed was at a surface pressure of 10 dynes/cm (2). This activity was equal to 29% of the activity of the same amount of enzyme in solution. The fraction of the retained enzyme activity on adsorption at an air–water interface in the case of trypsin varied from 0.125 to 0.35, depending on the surface concentration of the enzyme (3).

This study demonstrated the effectiveness of the subphase exchange technique for investigating the catalytic activity of enzymes spread at an air–water interface, without interference of bulk reaction. Future reports will discuss the effects of various lipids on the catalytic activity of surface-spread malate dehydrogenase.

REFERENCES

(1) L. L. M. Van Deenen, in "The Molecular Basis of Membrane Function," D. C. Testeson, Ed., Prentice-Hall, Englewood Cliffs, N.J., 1969, p. 47.

(2) J. C. Skou, *Biochim. Biophys. Acta*, **31**, 1 (1959).

(3) L. Inbar and I. R. Miller, *ibid.*, **364**, 146 (1974).

(4) A. W. Malick, A. Felmeister, and N. D. Weiner, *J. Pharm. Sci.*, **62**, 1871 (1973).

(5) M. Dixon and E. C. Webb, "Enzymes," 2nd ed., Academic, New York, N.Y., 1964.

(6) R. G. Wolfe and J. B. Neiland, *J. Biol. Chem.*, **221**, 61 (1956).

(7) G. H. Dodd, *Eur. J. Biochem.*, **33**, 418 (1973).

(8) A. W. Adamson, "Physical Chemistry of Surfaces," 2nd ed., Interscience, New York, N.Y., 1967, p. 26.

(9) H. J. Trurnit, *J. Colloid Sci.*, **15**, 1 (1960).

(10) J. W. Callahan and G. W. Kosicki, *Can. J. Biochem.*, **45**, 839 (1967).

(11) O. H. Lowry, *J. Biol. Chem.*, **193**, 265 (1951).

(12) J. G. Kaplan, *J. Colloid Sci.*, **7**, 382 (1952).

ACKNOWLEDGMENTS AND ADDRESSES

Received May 6, 1976, from the *College of Pharmacy, University of Michigan, Ann Arbor, MI 48104.*

Accepted for publication August 5, 1976.

* College of Pharmacy and Allied Health Professions, Wayne State University, Detroit, MI 48202.

ˣ To whom inquiries should be directed.

Kinetics and Mechanisms of Hydrolysis of 1,4-Benzodiazepines III: Nitrazepam

WESLEY W. HAN *, GERALD J. YAKATAN ˣ, and DALE D. MANESS

Abstract □ The hydrolysis of nitrazepam involves a two-step sequential mechanism. The intermediate is the ring-opened compound resulting from scission of the azomethine bond. The final products are glycine and 2-amino-5-nitrobenzophenone. Recyclization of the intermediate to nitrazepam occurs at pH values above the pKa of the intermediate, in the pH region where the amino group of the intermediate is not protonated. As opposed to chlordiazepoxide and oxazepam, the initial hydrolysis step occurs at the 4,5-bond, not at the 1,2-amide linkage. This difference is attributed to a preferential activation for hydrolysis of the azomethine linkage by the nitro group. The hydrolysis involves an uncatalyzed reaction, specific acid–base catalysis, and general acid–base catalysis for acetate and phosphate buffers.

Keyphrases □ 1,4-Benzodiazepines—nitrazepam, kinetics and mechanisms of hydrolysis □ Nitrazepam—kinetics and mechanisms of hydrolysis □ Hydrolysis—nitrazepam, kinetics and mechanisms □ Anticonvulsants—nitrazepam, kinetics and mechanisms of hydrolysis

Nitrazepam, 1,3-dihydro-7-nitro-5-phenyl-2*H*-1,4-benzodiazepin-2-one, belongs to the 1,4-benzodiazepine class of tranquilizing agents. This compound is centrally active (1), surpassing diazepam, a popular benzodiazepine, in anticonvulsant activity (2).

Preceding publications (3, 4) in this series reported the hydrolysis kinetics of 7-chloro-1,4-benzodiazepines. The present study concerned the hydrolysis of the 7-nitro analog, nitrazepam.

EXPERIMENTAL

Materials—Compound purity was verified by TLC. Nitrazepam[1] and 2-amino-5-nitrobenzophenone[1] were used as received.

Buffer Solutions—All buffer solutions were made with deionized, distilled water. They were adjusted to an ionic strength of 1.0 with sodium chloride, except in ionic strength effect studies where they were adjusted to ionic strengths other than 1. The pH at the temperature of the runs was measured with a digital pH meter[2] equipped with high temperature electrodes.

The buffer systems used were: pH 1.0–3.0, hydrochloric acid; pH 3.2–5.6, acetate; pH 6.4–7.4, phosphate; pH 7.9–9.5, borate; and pH 10.1–11, sodium hydroxide.

Kinetic Measurements—The kinetic studies of the hydrolysis of nitrazepam were followed spectrophotometrically. Details of the specific procedures were given previously (3) and are summarized as follows.

A stock solution of nitrazepam (6.3×10^{-3} *M*) in ethanol was diluted in an appropriate buffer to a final concentration for the kinetic run of 2.4×10^{-5} *M*. The reaction flasks (light protected) were maintained in a constant-temperature oil bath[3] controlled within 0.1° at selected temperatures between 70 and 85°. Samples were withdrawn at suitable time intervals and cooled to room temperature by quenching in an ice water bath. Visible and UV spectrophotometric measurements were made with a double-beam spectrophotometer[4].

Isolation and Identification—Thin-layer chromatograms were made on 20 × 20-cm glass plates coated with a 250-μm layer of silica gel GF_{254}. After lyophilization, the samples were dissolved in chloroform, spotted, and developed in a closed tank for approximately 1 hr with dioxane–benzene–hexane–7.4 *M* NH_4OH (45:50:70:5). The solvent front was allowed to travel 17 cm from the origin. After drying, the plates were visualized using a short wavelength UV lamp and then sprayed with ninhydrin aerosol (0.5%) to produce visible spots. Nitrazepam, 2-amino-5-nitrobenzophenone, and glycine were spotted as reference standards. An intermediate was isolated by preparative TLC and characterized by its IR[5], NMR[6], and high-resolution mass[7] spectra.

[1] Hoffmann–La Roche, Nutley, N.J.

[2] Model 701, Orion Research, Cambridge, Mass.

[3] Sargent model SW equipped with Sargent thermonitor model ST, R. L. Sargent Co., Dallas, Tex.

[4] Model 124, Coleman Instruments Division, Perkin-Elmer Corp., Maywood, Ill.

[5] Model IR8, Beckman Instruments, Fullerton, Calif.

[6] Model C60HL, Jeol, Medford, Mass.

[7] CEC-21-110, DuPont Instruments, Wilmington, Del.

Table I—Apparent First-Order Rate Constant, 10^4 k (in Minutes^{-1}), for Nitrazepam at 75°, μ = 1.0

pH	Buffer		k_1	k_2	r_1	r_2
		[HCl]				
0.93		0.1000	599 ± 13.5	9.04 ± 1.33	0.99	0.98
1.70		0.0158	499 ± 5.4	3.06 ± 0.03	0.99	0.99
2.60		0.0025	365 ± 6.4	1.70 ± 0.01	0.99	0.99
3.03		0.0010	363 ± 17.4	1.51 ± 0.07	0.99	0.99
	[CH_3COOH]	[CH_3COO^-]				
3.24	0.0957	0.0043	—	1.60 ± 0.05	—	0.99
4.00	0.0761	0.0239	—	0.88 ± 0.03	—	0.99
4.85	0.0322	0.0678	—	0.67 ± 0.01	—	0.99
5.64	0.0081	0.919	—	0.85 ± 0.10	—	0.96
	[$H_2PO_4^-$]	[HPO_4^{2-}]				
6.47	0.0275	0.0391	—	0.209 ± 0.09	—	0.99
7.40	0.0049	0.0617	—	19.47 ± 0.19	—	0.99
	[H_3BO_3]	[$H_2BO_3^-$]				
7.93	0.103	0.029	—	43 ± 0.18	—	0.99
8.52	0.061	0.110	—	196 ± 4.04	—	0.99
9.27	0.008	0.100	—	428 ± 12.16	—	0.99
9.53	0.003	0.100	—	458 ± 23.74	—	0.99
		[NaOH]				
10.18		0.01	—	1957 ± 210	—	0.98

RESULTS AND DISCUSSION

Spectral Changes and Rate Constant Determinations—The kinetics of hydrolysis of nitrazepam were monitored by following the change in absorbance, A, of the visible and/or UV chromophore as a function of time. The pKa values for nitrazepam are 3.2 and 10.8 (5). No pKa was found for 2-amino-5-nitrobenzophenone in the pH region of the present study. For pH values below the pKa of 3.2, two apparent reaction steps were observed. The first was characterized by an absorbance decrease at λ_{max} 278 nm with isosbestic points at 252 and 315 nm. The second showed an absorbance decrease at λ_{max} 265 nm with the formation of a new absorbance band with λ_{max} 364 nm.

For pH values intermediate to pKa_1 and pKa_2, only one reaction step was observed spectrally. The spectral changes were similar to those observed for the second hydrolysis step for pH values below pKa_1. For pH values above pKa_2, the single reaction step observed was characterized by a red shift from λ_{max} 364 to 380 nm. The spectrum at the time infinity point was identical to the spectrum of 2-amino-5-nitrobenzophenone throughout the entire pH region.

The logarithms of the difference in the final absorbance, A_∞, and the absorbance at any time, A_t, at the desired wavelength were plotted against time. The apparent first-order rate constants were calculated from the slopes of the linear segment according to:

$$\ln(A_t - A_\infty) = \ln(A_0 - A_\infty) - kt \qquad \text{(Eq. 1)}$$

where A_0 is the absorbance at zero time, and k is the apparent first-order rate constant. Absorbance changes in the visible region (370 nm) were used to calculate the apparent first-order rate constants for all pH values above the first pKa. For pH values below pKa_1, plots made according to Eq. 1 were biphasic, indicative of a two-step hydrolytic reaction in this pH region. For these data, the "feathering" technique was utilized to determine the sequential apparent first-order rate constants for the first and second reaction steps. Typical first-order plots for the hydrolysis of nitrazepam are shown in Fig. 1. The rate constants derived from these plots are presented in Table I.

Based on the observed spectral and kinetic behavior of nitrazepam (I), a two-step sequential hydrolysis pathway could be proposed (Scheme I). A reversible first-step hydrolytic ring opening of the benzodiazepine nucleus is followed by a second hydrolytic step, leading to the formation of glycine and a substituted benzophenone derivative.

Log k–pH Profiles—The log k–pH profile for nitrazepam was constructed at 75° with the data in Table I. For pH values below pKa_1, the first reaction step can be described by:

$$k_{obs} = k_{H_2O} f_{NH} \qquad \text{(Eq. 2)}$$

or by its kinetic equivalent:

$$k_{obs} = k_H[H^+]f_N \qquad \text{(Eq. 3)}$$

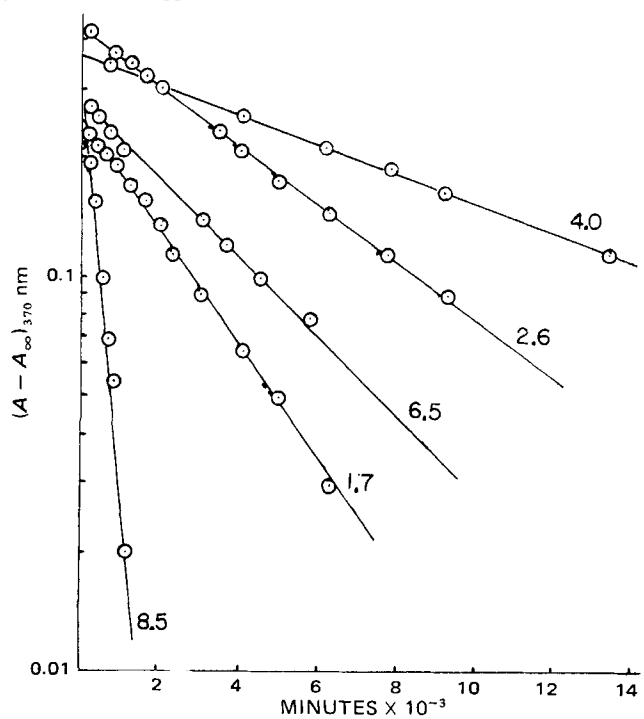

Figure 1—*Typical apparent first-order plots for the hydrolysis of 10^{-5} M nitrazepam as a function of pH.*

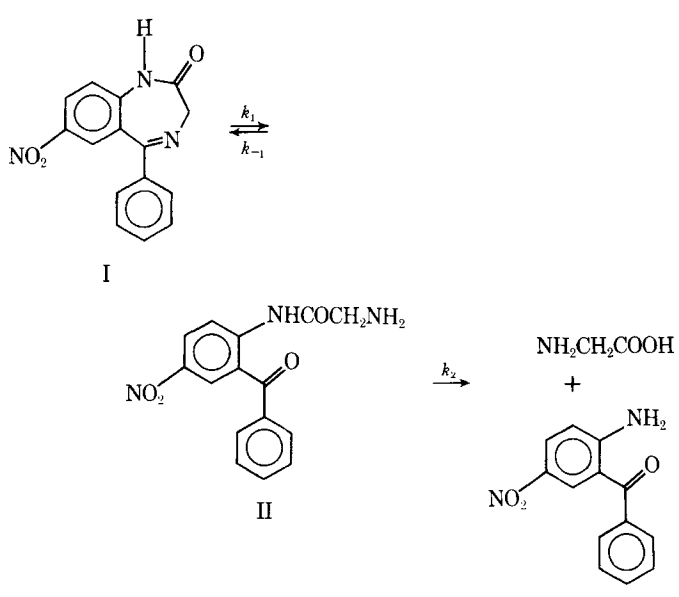

Scheme I

Table II—Apparent First-Order Rate Constants, 10^4 k (in Minutes^{-1}) for Hydrolysis of Nitrazepam at Various Buffer Concentrations

pH	Total Buffer Concentration in 1X	1X	2X	3X	4X	k_0
4.74	[CH_3COOH][CH_3COO^-] 0.100	0.63	0.74	1.0	1.17	0.41
6.37	[$H_2PO_4^-$][HPO_4^{2-}] 0.066	2.52	3.08	3.42	3.56	2.2

The terms f_{NH} and f_N are the fractions existing as protonated and deprotonated nitrazepam, respectively.

The rate constants that provided the best fit are $k_{H_2O} = 0.054$ min^{-1} and $k_H = 54$ min^{-1} M^{-1}. The kinetic pKa at 75° was 3.0, in agreement with the reported pKa_1 of nitrazepam at room temperature.

The log k–pH profile for the second reaction step exhibited five distinct components. At low pH values, the kinetics indicated hydrogen-ion catalysis on the protonated intermediate H_2S, followed by water attack on the neutral intermediate, HS. Uncatalyzed hydrolysis on the neutral intermediate, or the kinetic equivalent of hydroxide-ion attack on the protonated species, was observed over the neutral pH region.

The hydrolysis kinetics of nitrazepam in the basic pH region indicated hydroxide-ion catalysis on the double deprotonated intermediate, S, followed by water attack on the deprotonated species or its kinetic equivalent of hydroxide-ion catalysis on the neutral species. The apparent first-order rate constant at any pH can be quantitatively described by:

$$k_{obs} = k_H[H^+]f_{H_2S} + k_{H'}[H^+]f_{HS} + k_{H_2O}f_{HS} + k_{OH}[OH]f_{HS} + k_{OH'}[OH^-]f_S \quad \text{(Eq. 4)}$$

or the following substituted kinetic equivalents:

$$k_{H'}[H^+]f_{HS} = k_{H_2O}'f_{H_2S} \quad \text{(Eq. 5)}$$

$$k_{H_2O}f_{HS} = k_{OH''}[OH^-]f_{H_2S} \quad \text{(Eq. 6)}$$

$$k_{OH'}[OH^-]f_{HS} = k_{H_2O}''f_S \quad \text{(Eq. 7)}$$

The bimolecular rate constants that provided the best fit are $k_H = 0.0088$ min^{-1} M^{-1}, $k_{H'} = 1.88$ min^{-1} M^{-1}, $k_{H_2O} = 0.00015$ min^{-1}, $k_{OH} = 1.52 \times 10^5$ min^{-1} M^{-1}, and $k_{OH'} = 247$ min^{-1} M^{-1}.

From the log k–pH profile, the two kinetic pKa's were calculated as 4.1 and 8.8 and were assigned to the amino nitrogen and the amide group of the intermediate, respectively. The experimental data points with the theoretical curves calculated from Eqs. 2 and 4 are shown in Fig. 2.

Isolation and Identification—Samples withdrawn at appropriate times were subjected to TLC analysis. At pH values below the pKa_1 of nitrazepam, TLC showed an increase in intensity of the yellow 2-amino-5-nitrobenzophenone spot (R_f 0.43) and a decrease in the relative intensity of the nitrazepam spot (R_f 0.22). A compound (R_f 0.17) appeared transiently and was attributed to a reaction intermediate. For pH values above the pKa_1 of nitrazepam, no intermediate was observed by TLC. The spectral changes in this pH region also demonstrated a single isosbestic point, indicative of a one-to-one transformation.

The intermediate was isolated as a yellow solid by preparative TLC. Mass spectrometric analysis of the intermediate demonstrated a possible molecular ion at 18 mass units above the molecular weight of nitrazepam. A compound with this molecular weight could result from hydrolysis of either the 1,2-amide bond or the 4,5-azomethine bond. The NMR spectrum did not show a characteristic carboxylic acid absorption. Since the acid group would result from heterolysis of the amide, the structure resulting from hydrolysis of the azomethine bond was tentatively assigned as II in Scheme I.

Corroborating evidence for this structural assignment was obtained by studying the reversibility of the reaction leading to II. Prior reports (6, 7) showed that, in 1,4-benzodiazepin-2-one hydrolysis, the recyclization of the protonated opened-ring intermediate resulting from scission of the 1,2-amide linkage is quite facile. Additionally, the deprotonated form does not undergo recyclization (3). The opposite was found for recyclization of intermediate II. When heated at 75° for 5 min, the intermediate was shown spectrally to revert to nitrazepam at pH values greater than 5. At pH values below the first pKa of the intermediate, no recyclization was indicated. Indeed, at the higher pH values, II was not observable by either TLC or spectral measurements. If the intermediate is of the benzophenone structure (II), then protonation of the primary amine at pH values below 4 would decrease its nucleophilicity. This, in turn, would decrease the rate of recyclization, in agreement with the experimental results showing rapid recyclization only at pH values above 5.

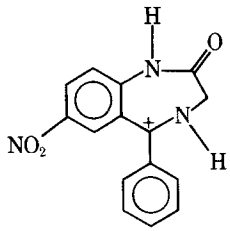

IV

Hydrolytic Mechanisms—The preceding kinetic and TLC data are mechanistically interpretable according to Scheme I. The first hydrolytic reaction step is only reversible at pH values above the pKa_1 of the intermediate. Initially, the 4,5-bond is hydrolyzed, leading to the ring-opened compound, intermediate II. Although models show that this bond is sterically hindered to nucleophilic attack relative to the amide bond, protonation of the azomethine nitrogen should electronically favor attack at the 5-position. This conclusion is based on possible resonance contribution shown as Structure IV.

However, the 7-chloro-1,4-benzodiazepines chlordiazepoxide (3) and oxazepam (4), also capable of 4-nitrogen protonation to lead to a positive charge resident on the 5-position by resonance, show initial 1,2-bond hydrolysis preferentially. The difference noted between these 7-substituted analogs can be interpreted using the Hammett relationship:

$$\log k/k_0 = \sigma\rho \quad \text{(Eq. 8)}$$

where k and k_0 are the rate constants for hydrolysis of the substituted and unsubstituted compounds, respectively; σ measures the electron-attracting ability of the substituents; and ρ is a parameter defined by the reaction type. The σ values for chloro and nitro substituents are σ_{Cl}^m 0.37 and $\sigma_{NO_2}^m$ 0.71 for *meta*-substitution and σ_{Cl}^p 0.23 and $\sigma_{NO_2}^p$ 0.78 for *para*-substitution (8). Upon substitution of these values into Eq. 8, the Hammett relationship can be written as:

$$\log (k_{Cl}^p/k_{Cl}^m) = -0.14\rho \quad \text{(Eq. 9)}$$

where k_{Cl}^p and k_{Cl}^m are the rate constants for the hydrolysis of *p*- and *m*-chloro-substituted positions, respectively. The equation indicates that the *m*-chloro-substituted position is less reactive than the *p*-chloro-substituted position, assuming a negative ρ value due to electronic requirements for acid-catalyzed hydrolysis. Thus, initial 1,2-bond hydrolysis would be favored. For the 7-nitro compound, the Hammett equation operable is:

$$\log (k_{NO_2}^p/k_{NO_2}^m) = 0.07\rho \quad \text{(Eq. 10)}$$

The *meta*-position (azomethine) hydrolysis would be slightly favored, again assuming a negative ρ.

Stability Parameters—To provide a complete profile of the stability of nitrazepam, hydrolysis kinetics as a function of buffer concentration, ionic strength, and temperature were investigated. Buffer catalysis was studied according to the relationship:

$$k_{obs} = k_0 + \left(\frac{k_{HA}[H^+]}{K_a} + k_A\right)[A^-] \quad \text{(Eq. 11)}$$

where K_a is the dissociation constant for the buffer species, k_0 is the hydrolysis rate constant in absence of buffer catalysis, and k_{HA} and k_A are the rate constants for buffer catalysis of the acid buffer species, HA, and its conjugate base, A^-, respectively. Buffer effects were investigated by changing the original buffer concentration fourfold in a gradient manner. Table II gives the results of these studies on the rate constants

Table III—Apparent First-Order Rate Constants, 10^4 k (in Minutes^{-1}) for Hydrolysis of Nitrazepam at Various Ionic Strengths.

pH	k_i	0.1	0.2	0.4	0.8	Q
0.98	k_1	973.5	1158.9	870.0	776.0	No relation
	k_2	6.06	7.3	8.05	9.04	0.37
4.8	k_2	0.52	0.52	0.61	0.58	No relation

Table IV—Apparent First-Order Rate Constants (10^4 k in Minutes^{-1}) and Thermodynamic Parameters for Hydrolysis of Nitrazepam at pH 0.93

	85°	80°	75°	70°	E_a	ln P	ΔH_a	ΔS_a	ΔF
k_1	1418.0	1166.5	599.5	550.3	17.0	22.0	16.3	−7.0	22.3
k_2	14.0	12.2	9.0	6.6	12.5	11.0	11.8	−38.9	25.5

for hydrolysis of nitrazepam. Both acetate and phosphate buffers catalyzed the hydrolysis.

The kinetics of hydrolysis were carried out for different ionic strengths from 0.1 to 1.0 at pH 0.98 and 4.80. The apparent first-order rate constants are given in Table III. No significant ionic strength effect was observed for the k_1 step at pH 0.98 and the k_2 step at pH 4.80. A positive ionic strength effect was observed for the k_2 step at pH 0.98. The use of the Bronsted–Bjerrum equation together with the extended Debye–Huckel equation yields:

$$\log k = \log k_0 + 2QZ_AZ_B \sqrt{\mu}/(1 + \sqrt{\mu}) \qquad \text{(Eq. 12)}$$

where k is the apparent first-order rate constant, k_0 is the rate constant at zero ionic strength, Q is a constant equal to 0.557 (9) at 80°, Z_A and Z_B are the charges of the reacting molecules, and μ is the ionic strength. The ionic strength effect plot for k_2 of pH 0.98 shows a Q value of 0.37. This result suggests that the hydrolysis at pH 0.98 involves a reaction between molecules of like univalent charge.

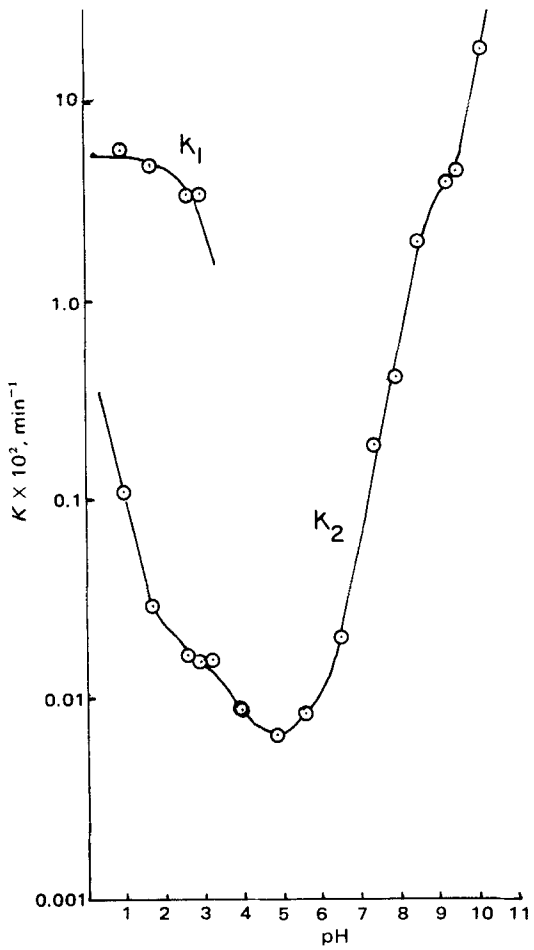

Figure 2—*Log* k–*pH profile for the hydrolysis of* 10^{-5} M *nitrazepam at 75°,* μ = *1.0. The* k_1 *and* k_2 *refer to the first and second reaction steps, respectively.*

The Arrhenius parameters for the hydrolysis of nitrazepam were obtained from the slope and intercept of a plot of the logarithm of the apparent first-order rate constant, k, *versus* the reciprocal of the absolute temperature, T, shown by:

$$\ln k = \ln P - E_a/RT \qquad \text{(Eq. 13)}$$

where R is the gas constant equal to 1.987 cal deg^{-1} mole^{-1}; ln P is related to the entropy of activation, ΔS_a, by:

$$\Delta S_a = R[\ln P - \ln (KT/h) - 1] \qquad \text{(Eq. 14)}$$

where h and K are the Planck and Boltzman constants, respectively; and E_a is related to the enthalpy of activation of the hydrolysis, ΔH_a, by:

$$\Delta H_a = E_a - RT \qquad \text{(Eq. 15)}$$

The Arrhenius parameters for the hydrolysis of nitrazepam at pH 0.93 are given in Table IV. These values will allow stability prediction in this pH region where degradation is rapid.

REFERENCES

(1) I. Haider, *Br. J. Psychiat.*, **114,** 337 (1968).

(2) J. W. Lance, *Med. J. Aust.*, **1,** 113 (1968).

(3) W. W. Han, G. J. Yakatan, and D. D. Maness, *J. Pharm. Sci.*, **65,** 1198 (1976).

(4) *Ibid.*, **66,** 573 (1977).

(5) J. Barrett, W. F. Smyth, and I. E. Davidson, *J. Pharm. Pharmacol.*, **25,** 387 (1973).

(6) L. H. Sternbach and E. Reeder, *J. Org. Chem.*, **26,** 4936 (1961).

(7) S. C. Bell, T. S. Sulkowski, C. Gochman, and S. J. Childress, *ibid.*, **27,** 562 (1962).

(8) H. H. Jaffe, *Chem. Rev.*, **53,** 191 (1953).

(9) J. T. Carstensen, *J. Pharm. Sci.*, **59,** 1140 (1970).

ACKNOWLEDGMENTS AND ADDRESSES

Received June 10, 1976, from the *College of Pharmacy, University of Texas at Austin, Austin, TX 78712.*

Accepted for publication August 4, 1976.

Presented in part at the Basic Pharmaceutics Section, APhA Academy of Pharmaceutical Sciences, San Francisco meeting, April 1975.

Abstracted in part from a dissertation submitted by W. W. Han to the University of Texas at Austin in partial fulfillment of the Doctor of Philosophy degree requirements.

Supported in part by a grant from the University Research Institute, University of Texas at Austin.

The authors express their gratitude to Dr. W. E. Scott of Hoffmann–La Roche Inc. for samples supplied and to Dr. Jay Nematollahi for helpful discussions.

* Present address: Searle Laboratories, Chicago, IL 60680.

ˣ To whom inquiries should be directed.

GLC Determinations of Plasma Acenocoumarol Levels

K. K. MIDHA ˣ and J. K. COOPER

Abstract □ A method for the quantitative estimation of acenocoumarol in plasma is described. Plasma containing acenocoumarol, to which a known amount of γ-oxo derivative of phenylbutazone is added as an internal standard, is acidified and extracted with ethylene dichloride. The drug and the internal standard are then back-extracted into alkali, which, in turn, is acidified and reextracted with ethylene dichloride. The organic extract is evaporated and treated with an ethereal solution of diazomethane (100 μl). The reacted mixture is evaporated, and the residue is dissolved in 25 μl of carbon disulfide. Aliquots (2–3 μl) are injected into a gas chromatograph equipped with a flame-ionization detector. The methyl derivatives of acenocoumarol and the internal standard give sharp, well-separated, symmetrical peaks. The method is of sufficient sensitivity to determine 0.25 μg/ml of the drug in plasma with a relative standard deviation of 4%.

Keyphrases □ Acenocoumarol—GLC analysis, human and dog plasma □ GLC—analysis, acenocoumarol, human and dog plasma □ Anticoagulants—acenocoumarol, GLC analysis, human and dog plasma

Acenocoumarol (I) is an oral anticoagulant with an onset of action similar to that of dicumarol. It is structurally related to warfarin, both drugs belonging to the coumarin class. Although GLC procedures for the quantitative determination of warfarin (1, 2) and phenprocoumon (3) and a high-pressure liquid chromatographic (HPLC) procedure for quantitating warfarin (4) from plasma have been reported, no GLC or HPLC procedures for quantitating acenocoumarol from biological fluids have been described.

The chromatographic behavior of I and its trimethylsilyl ether derivative was investigated using an aluminum column packed with silicone gum rubber on dimethyldichlorosilane-treated, flux-calcined diatomite support (5). However, this procedure was not applied to plasma level determinations. To facilitate study of the pharmacokinetics and potential interactions after single- and multiple-dose oral administration of I, a sensitive and apparently specific GLC procedure was developed for the measurement of the intact drug in plasma.

EXPERIMENTAL

Reagents—Ethylene dichloride[1] and ether[2] were glass distilled prior to use. Stock solutions containing 100 μg of I[3]/ml were prepared daily in 0.1 *N* NaOH and stored in the dark at 4°. Appropriate dilutions (0.25–4.0 μg/ml) were made immediately before use. Aqueous solutions containing 100 μg/ml of the internal standard, the γ-oxo derivative of phenylbutazone[4] (II), were prepared weekly in 0.1 *N* NaOH and diluted daily to 15 μg/ml with distilled water. An ethereal solution of diazomethane was synthesized from *N*-methyl-*N*-nitroso-*p*-toluenesulfonamide[5].

Plasma Level Study—Acenocoumarol was administered orally in gelatin capsules to two dogs. One dog, 35 kg, received 1 mg/kg of I; a second dog, 30 kg, was given 0.5 mg/kg of I. Blood samples (10 ml) were withdrawn from the cephalic vein of each dog, using heparinized evacuated tubes[6], at 14 appropriate time intervals for 96 hr. The blood samples

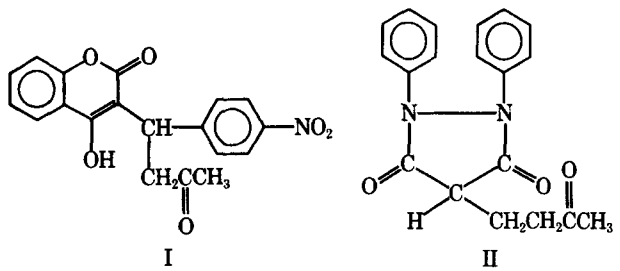

I II

were centrifuged, and the plasma was transferred to another tube before storage at −15°.

Extraction of Acenocoumarol—To a 2-ml human or canine plasma sample ("spiked" or from dosed animals) in a glass-stoppered centrifuge tube[7] (50 ml) were added 1 ml of the internal standard solution (II, 15 μg), 3 ml of 3 *N* HCl, and 20 ml of ethylene dichloride. The samples were stoppered and extracted by shaking at an angle of 30° for 30 min at 180 cpm on a flat-bed shaker[8]. After centrifugation at 3000 rpm for 10 min, the aqueous layer was removed by aspiration; 18 ml of the organic phase was then transferred into another glass-stoppered centrifuge tube[7] (50 ml) containing 10 ml of 1 *N* NaOH.

The extraction was repeated (shaking for 15 min and centrifuging for 10 min), and 9 ml of the aqueous phase was transferred to another glass-stoppered tube[7] (50 ml) containing 3 ml of 5 *N* HCl. The tube was

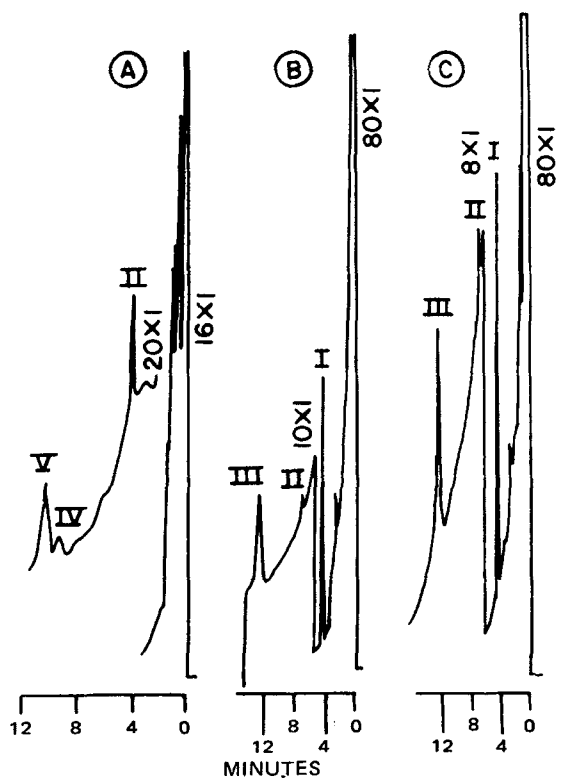

Figure 1—*Gas chromatograms of human plasma. Key: A, control plasma; B, plasma containing 1.0 μg/ml of I and 7.5 μg/ml of II; and C, plasma (7 hr) from a dog given 1 mg of I/kg po containing I (1.24 μg/ml) and II (7.5 μg/ml). Peak I is methylated II, and peak III is methylated I. Peaks II, IV, and V are due to endogenous materials in plasma.*

[1] Caledon Laboratories Ltd., Georgetown, Ontario, Canada.
[2] Mallinckrodt Chemical Works Ltd., Montreal, Quebec, Canada.
[3] Geigy Pharmaceuticals, Dorval, Quebec, Canada.
[4] United Pharmaceutical Works, Praha, Czechoslovakia.
[5] Diazald, Aldrich Chemical Co., Milwaukee, Wis.
[6] Vacutainers, Becton-Dickinson Co., Mississauga, Ontario, Canada.
[7] Fisher Scientific Co., Montreal, Quebec, Canada.
[8] Eberbach Corp., Ann Arbor, Mich.

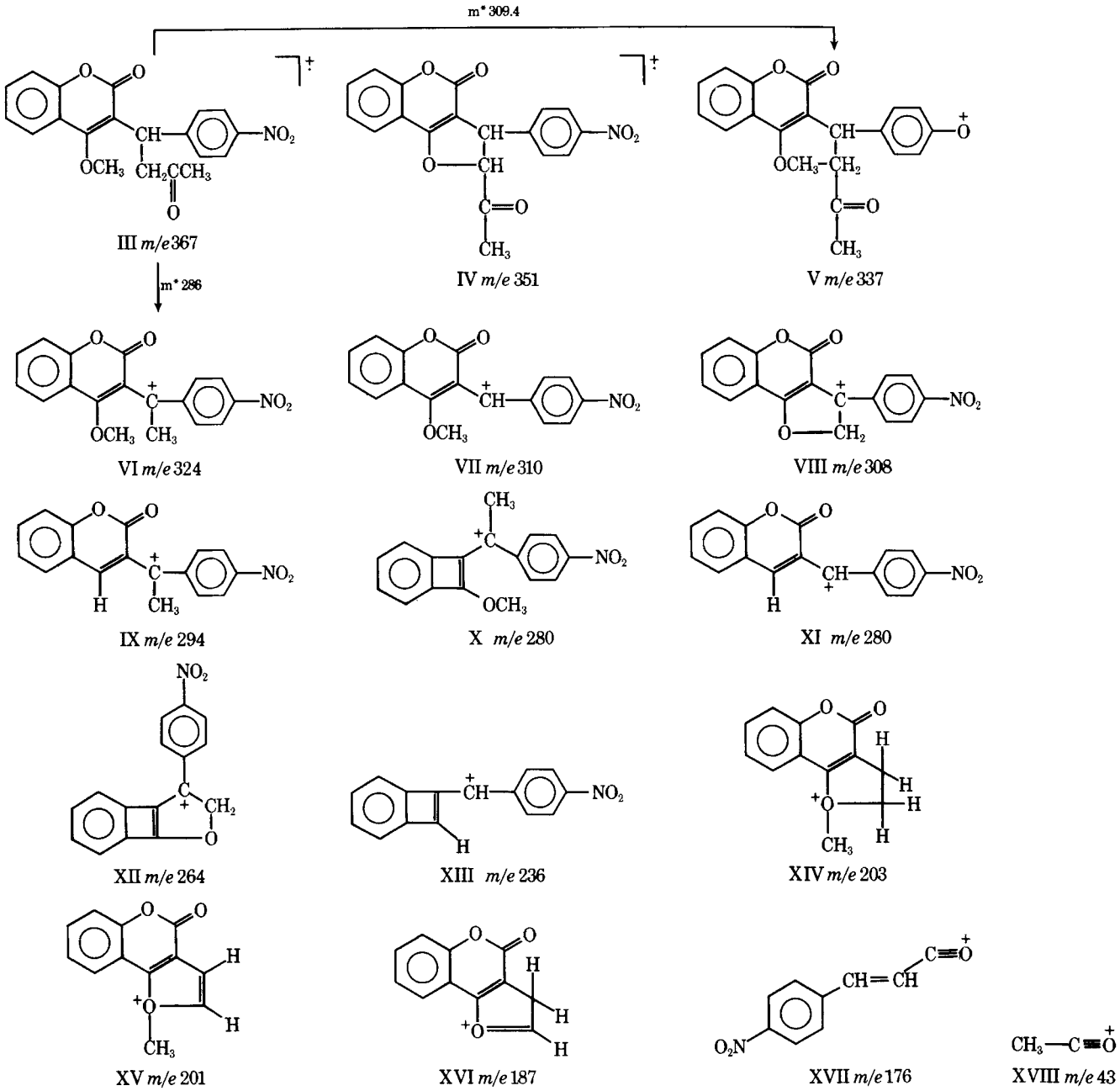

Scheme I

swirled gently, and the extraction was carried out with another 20 ml of ethylene dichloride for 20 min. The aqueous layer was removed by aspiration, and 18 ml of the organic phase was transferred to a glass-stoppered centrifuge tube[7] (50 ml).

The organic extract was evaporated[9] at 85° under a stream of dry nitrogen to a volume of approximately 4 ml. A crystal of anhydrous calcium chloride[7] was added, and the tube was swirled gently. The extract was transferred quantitatively into a custom-made evaporating tube (6) containing a small antibumping granule[10] and evaporated as before to dryness.

The tube was then allowed to cool to room temperature, and the residue was dissolved in 100 μl of ethereal diazomethane by mixing[11] for 30 sec. After the solution was left to incubate for 10 min, it was evaporated to dryness at room temperature. The evaporated extract was dissolved in 25 μl of carbon disulfide by mixing[11] for 30 sec, and aliquots (2–3 μl) were then injected into the gas chromatograph.

GLC—A gas chromatograph[12] equipped with a flame-ionization detector was employed. The column was a spiral glass tube[12], 180 × 0.25 cm i.d., packed with 3% phenyl methyl dimethyl silicone[13] coated on acid-washed, dimethylchlorosilane-treated, 80–100-mesh, high performance, flux-calcined diatomite support[14].

The column was conditioned by maintaining the column at 340° for 18 hr with a low nitrogen flow. In use, the injection port, detector, and column oven temperatures were 300, 310, and 285°, respectively. The nitrogen carrier gas was maintained at a flow rate of 70 ml/min. Hydrogen and compressed air flow rates were adjusted to give maximum response.

Calculations—Peak height ratios were calculated by dividing the height of the peak due to methylated I (7.1 min) by that of methylated II (2.6 min). Calibration curves were constructed from the results of

[9] Thermolyne Dri-Bath, Fisher Scientific Co., Montreal, Quebec, Canada.
[10] British Drug House, Toronto, Ontario, Canada.
[11] Vortex Genie, Fisher Scientific Co., Montreal, Quebec, Canada.
[12] Model 3920, Perkin-Elmer, Montreal, Quebec, Canada.
[13] OV-11, Chromatographic Specialties, Brockville, Ontario, Canada.
[14] Chromosorb W, Chromatographic Specialties, Brockville, Ontario, Canada.

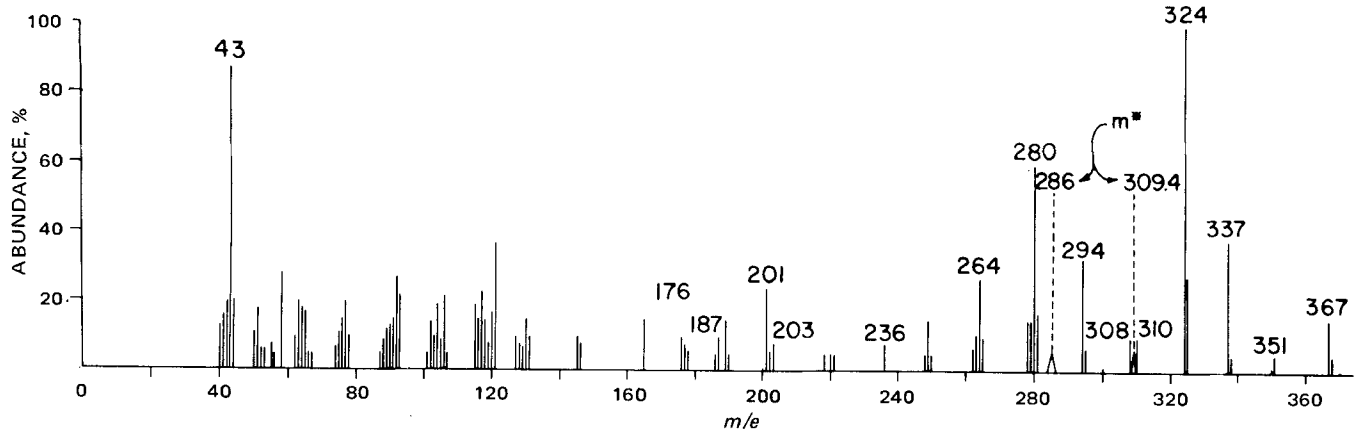

Figure 2—*GLC–mass spectrum (normalized) of methylated acenocoumarol.*

spiked control plasma samples by plotting the peak height ratios against the concentration of I (micrograms per milliliter of plasma).

RESULTS AND DISCUSSION

Methylation of I with diazomethane gave one peak on GLC analysis with a retention time of 7.1 min (peak III, Fig. 1B). Methylation of II with diazomethane also gave one peak on GLC with a retention time of 2.6 min (peak I, Fig. 1B). Combined GLC–mass spectrometric[15] analysis was carried out on the compound giving rise to peak III (Fig. 1B).

The mass spectrum (Fig. 2) showed a molecular ion at *m/e* 367 and abundant ions at *m/e* 351, 337, 324, 310, 308, 294, 280, 264, 236, 203, 201, 187, 176, and 43. Structures III–XVIII (Scheme I) are postulated for these ions. These fragmentations are in agreement with those reported for warfarin (2, 7) and phenprocoumon (3, 8, 9) and suggest that the methylated derivative of I has the structure 3-(α-acetonyl-*p*-nitrobenzyl)-4-methoxycoumarin. Combined GLC–mass spectral evidence for the structure of the internal standard (peak I, Fig. 1B, retention time of 2.6 min) indicated it to be 1,2-diphenyl-4-methyl-4-(2-butanone)-3,5-dioxopyrazoline (molecular ion at *m/e* 336 and other diagnostic ions at *m/e* 321, 308, 293, 279, 264, 202, 177, 160, 119, 77, 51, and 43).

Attempts to prepare a methyl derivative of I by the safer flash-heater methylation technique using trimethylanilinium hydroxide were unsuccessful. However, ethereal diazomethane was effective in the methylation of I and other coumarin derivatives such as phenprocoumon[16] and warfarin[17], the later two being investigated as possible internal standards for the assay of I. These derivatives gave sharp well-defined GLC peaks; however, phenprocoumon and warfarin could not be employed as internal standards because their methyl derivatives eluted too close to the solvent front. Since methylated II [a metabolite of phenylbutazone in humans (10)] gave a single GLC peak with the desired retention time and had similar partition characteristics to I, it was chosen as an internal standard for the assay of I.

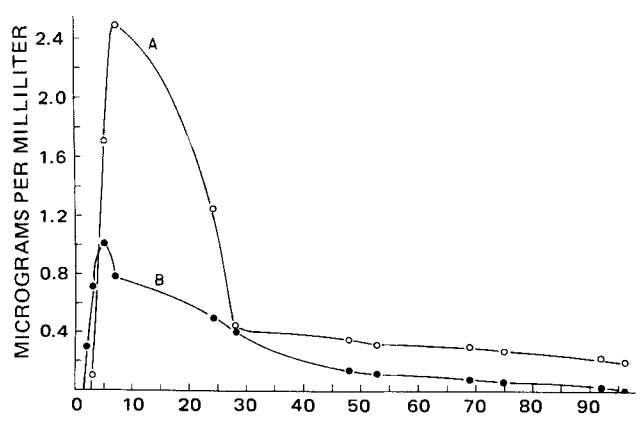

Figure 3—*Plasma profiles of acenocoumarol. Key: Dog A (35 kg), 1.0 mg/kg po; and Dog B (30 kg), 0.5 mg/kg po.*

Several other liquid phases such as saturated hydrocarbon lubricant[18], methyl silicone gum[19], phenyl methyl silicone fluid[20], and phenyl methyl dimethyl silicone fluid[21] were tested, but the peak for methylated I under these conditions was either not sharp or had interference from plasma constituents. When carbon disulfide was employed as the injection solvent, it rendered a very small solvent peak. Untreated plasma extracts were much less stable than those reacted immediately after extraction. The plasma extracts that had been reacted with diazomethane were stable up to 12 hr at room temperature.

Figure 1A shows a typical chromatogram obtained by processing fresh blank plasma from humans as described under *Experimental.* Extraneous peaks II, IV, and V were observed in chromatograms of all human plasma samples, but IV and V were not present in chromatograms of dog plasma samples. A chromatogram obtained when the method was applied to spiked plasma containing 1.0 μg of I/ml and 7.5 μg of II/ml is shown in Fig. 1B. Extraneous peaks II, IV, and V did not interfere with the peak from the internal standard (peak I, retention time of 2.6 min) or acenocoumarol (peak III, retention time of 7.1 min). Figure 1C shows a chromatogram obtained from a 7-hr sample (1 ml) of a 35-kg dog which received an extemporaneously prepared gelatin capsule containing 35 mg of I.

The overall recoveries of I and II from plasma were 99.90 ± 1.25 and 47.42 ± 1.64%, respectively (Table I). The accuracy and precision of the GLC assay are demonstrated in Table II. Results are based on at least five determinations of each acenocoumarol concentration (0.25–4.0 μg/ml), treated as described under *Experimental.* The overall relative standard deviation was 3.12%. The calibration curve obtained by plotting the peak height ratio of methylated I/II *versus* the concentration of I was linear ($y = mx$) over the concentration range of 0.25–4.0 μg of I/ml of plasma. A mean slope value of 0.0492 ± 0.0006 ($p = 0.05$; $r^2 = 0.998$) was obtained. The peak height ratio of the drug and the internal standard was used as the index of detector performance and overall efficiency of the analytical procedure.

The application of the method to plasma level determinations in dogs is demonstrated in Fig. 3. This figure shows the plasma profiles over 96 hr for Dogs A (35 kg) and B (30 kg), which received 1 and 0.5 mg/kg, respectively, of I orally in extemporaneously prepared capsules. The specificity of the analytical procedure was determined by pooling the remaining plasma from dosed dogs, extracting and derivatizing it as described under *Experimental.* A GLC–mass spectrum of the compound giving rise to the resultant peak for I was obtained and compared with that of authentic methylated I. No ions other than those for methylated I were observed in the mass spectrum of the peak from pooled plasma samples, indicating virtually no interference.

The described GLC procedure is sensitive for the determination of acenocoumarol, and large plasma samples are not required. It also offers

[15] Perkin-Elmer model 900 gas chromatograph attached to a Hitachi Perkin-Elmer model RMSU mass spectrometer through a jet separator.
[16] Marcumar, Hoffmann–La Roche Inc., Montreal, Quebec, Canada.
[17] Warfarin sodium, Warner-Lambert, Scarborough, Ontario, Canada.
[18] Apiezon-L, Chromatographic Specialties, Brockville, Ontario, Canada.
[19] SE-30, Chromatographic Specialties, Brockville, Ontario, Canada.
[20] OV-17, Chromatographic Specialties, Brockville, Ontario, Canada.
[21] OV-7, Chromatographic Specialties, Brockville, Ontario, Canada.

Table I—Recovery of I and II from Plasma (n = 4)

Compound	Micrograms Added to 1 ml of Plasma	Mean Micrograms Recovered	Mean Percent Recovery	*SD* of Percent Recovery
I	1.00	0.996	99.60	1.11
	2.00	2.04	100.20	1.37
	Mean = 99.90 ± 1.25%			
II	1.00	0.47	47.39	0.01
	2.00	0.95	47.46	0.01
	Mean = 47.42 ± 1.64%			

Table II—GLC Estimation of I Added to Plasma

Added I, μg	n	Mean Peak Height Ratio I/II	*SD*	*RSD*
0.25	7	0.012	0.001	3.98
0.50	6	0.024	0.001	3.13
1.00	7	0.048	0.002	3.19
2.00	6	0.095	0.002	1.76
4.00	5	0.200	0.001	4.14
			Mean *RSD*	3.12
$y = mx$, where $m = 0.0492 \pm 0.0006$; $r^2 = 0.998$				

the advantage that the intact drug is measured. The technique is being used for investigating single- and multiple-dose pharmacokinetics.

REFERENCES

(1) D. G. Kaiser and R. S. Martin, *J. Pharm. Sci.*, **63**, 1579 (1974).

(2) K. K. Midha, I. J. McGilveray, and J. K. Cooper, *ibid.*, **63**, 1725 (1974).

(3) K. K. Midha, J. W. Hubbard, J. K. Cooper, and I. J. McGilveray, *ibid.*, **65**, 387 (1976).

(4) E. S. Vessell and C. A. Shively, *Science*, **184**, 466 (1974).

(5) F. W. Deckert, *J. Chromatogr.*, **69**, 201 (1972).

(6) A. H. Beckett, *Dan. Tidssk. Farm.*, **40**, 197 (1966).

(7) W. F. Trager, R. J. Lewis, and W. A. Garland, *J. Med. Chem.*, **13**, 1196 (1970).

(8) L. R. Pohl, R. Haddock, W. A. Garland, and W. F. Trager, *ibid.*, **18**, 513 (1975).

(9) R. E. Haddock, W. F. Trager, and L. R. Pohl, *ibid.*, **18**, 519 (1975).

(10) I. J. McGilveray, K. K. Midha, and N. Mousseau, *Pharmacologist*, **16**, 218 (1974).

ACKNOWLEDGMENTS AND ADDRESSES

Received January 29, 1976, from the *Drug Research Laboratories, Health Protection Branch, Health and Welfare Canada, Tunney's Pasture, Ottawa, Ontario K1A 0L2, Canada.*

Accepted for publication August 3, 1976.

The authors thank Dr. I. J. McGilveray, Dr. J. W. Hubbard, and Mr. A. G. Butterfield for helpful discussions and Dr. A. By and Mr. J.-C. Ethier for running the mass spectra. Mr. J. Evans and Mr. L. Martin are acknowledged for veterinary assistance.

[x] To whom inquiries should be directed.

Binding of Codeine, Morphine, and Methadone to Human Serum Proteins

JOSEPH JUDIS

Abstract □ The binding properties of codeine, morphine (as representative opium alkaloids), and methadone (a synthetic pharmacologically similar compound) were studied with selected human serum proteins. The methodology involved equilibrium and dynamic dialysis using ^3H- and/or ^{14}C-labeled compounds. For estimation of the percent binding with equilibrium dialysis, concentrations of the ligand used were approximately therapeutic blood levels and another concentration 30–60 times higher. The percent binding to whole human serum ranged from about 20% for morphine to almost 60% for methadone. Of the human serum proteins investigated, the highest percent binding was found with albumin, except for methadone for which it was β-globulin III. The affinity for other serum proteins varied with the ligand. In studies with albumin using dynamic dialysis, the plots of nubar divided by free concentration *versus* nubar were similar for all three ligands studied and had positive slopes, unlike those reported for acidic compounds for which the slope is always negative. In studies of binding of one ligand in the presence of another, significant competition was demonstrated, suggesting that the same binding sites were involved.

Keyphrases □ Codeine—binding to human serum proteins □ Morphine—binding to human serum proteins □ Methadone—binding to human serum proteins □ Binding, protein—codeine, morphine, and methadone to human serum □ Protein binding—codeine, morphine, and methadone to human serum □ Analgesics, narcotic—codeine, morphine, and methadone, binding to human serum proteins □ Alkaloids, opium—codeine, morphine, and methadone, binding to human serum proteins

The binding of drugs to serum proteins is well established as a parameter in pharmacological and therapeutic activities of medicinal agents (1). Several reviews treated the methodology for studying protein binding and summarized the vast number of substances already investigated (2–5). Of the hundreds of compounds studied, the vast majority are acidic or nonpolar; few studies have

Table I—Binding of Methadone, Morphine, and Codeine to Various Human Serum Proteins[a]

Serum Protein Fraction	Concentration, mg/ml	Ligand, % Bound for Concentration Indicated: Methadone 9.3×10^{-8} Mole	Methadone 3.3×10^{-6} Mole	Morphine 5.5×10^{-8} Mole	Morphine 3.6×10^{-6} Mole	Codeine 5.6×10^{-8} Mole	Codeine 3.4×10^{-6} Mole
Albumin	40.0	31.16 (2.23)	21.84 (0.29)	23.24 (1.30)	16.56 (1.15)	14.26 (0.68)	28.50 (0.09)
α-Globulin IV-1	1.0	10.19 (1.28)	5.70 (0.51)	1.61 (0.07)	4.10 (0.98)	9.59 (1.46)	5.03 (0.21)
α-Globulin IV-4	5.0	12.53 (1.65)	4.58 (0.13)	6.42 (0.01)	7.56 (0.39)	12.34 (0.70)	17.05 (0.40)
β-Globulin III	7.0	37.75 (2.76)	10.90 (0.56)	7.39 (0.05)	3.16 (0.21)	7.98 (0.60)	3.68 (1.04)
γ-Globulin II	11.0	8.26 (0.72)	6.47 (0.40)	4.16 (0.20)	10.02 (2.72)	5.71 (0.72)	8.60 (1.16)
Human serum	—	59.78 (3.00)	39.54 (1.20)	24.02 (1.82)	20.08 (1.04)	29.01 (2.70)	22.35 (0.87)

[a] The number of moles of ligand added to each system is indicated as the concentration. Values in parentheses are standard deviations.

Table I—Recovery of I and II from Plasma (n = 4)

Compound	Micrograms Added to 1 ml of Plasma	Mean Micrograms Recovered	Mean Percent Recovery	*SD* of Percent Recovery
I	1.00	0.996	99.60	1.11
	2.00	2.04	100.20	1.37
	Mean = 99.90 ± 1.25%			
II	1.00	0.47	47.39	0.01
	2.00	0.95	47.46	0.01
	Mean = 47.42 ± 1.64%			

Table II—GLC Estimation of I Added to Plasma

Added I, μg	n	Mean Peak Height Ratio I/II	*SD*	*RSD*
0.25	7	0.012	0.001	3.98
0.50	6	0.024	0.001	3.13
1.00	7	0.048	0.002	3.19
2.00	6	0.095	0.002	1.76
4.00	5	0.200	0.001	4.14
			Mean *RSD*	3.12
$y = mx$, where $m = 0.0492 \pm 0.0006$; $r^2 = 0.998$				

the advantage that the intact drug is measured. The technique is being used for investigating single- and multiple-dose pharmacokinetics.

REFERENCES

(1) D. G. Kaiser and R. S. Martin, *J. Pharm. Sci.*, **63**, 1579 (1974).

(2) K. K. Midha, I. J. McGilveray, and J. K. Cooper, *ibid.*, **63**, 1725 (1974).

(3) K. K. Midha, J. W. Hubbard, J. K. Cooper, and I. J. McGilveray, *ibid.*, **65**, 387 (1976).

(4) E. S. Vessell and C. A. Shively, *Science*, **184**, 466 (1974).

(5) F. W. Deckert, *J. Chromatogr.*, **69**, 201 (1972).

(6) A. H. Beckett, *Dan. Tidssk. Farm.*, **40**, 197 (1966).

(7) W. F. Trager, R. J. Lewis, and W. A. Garland, *J. Med. Chem.*, **13**, 1196 (1970).

(8) L. R. Pohl, R. Haddock, W. A. Garland, and W. F. Trager, *ibid.*, **18**, 513 (1975).

(9) R. E. Haddock, W. F. Trager, and L. R. Pohl, *ibid.*, **18**, 519 (1975).

(10) I. J. McGilveray, K. K. Midha, and N. Mousseau, *Pharmacologist*, **16**, 218 (1974).

ACKNOWLEDGMENTS AND ADDRESSES

Received January 29, 1976, from the *Drug Research Laboratories, Health Protection Branch, Health and Welfare Canada, Tunney's Pasture, Ottawa, Ontario K1A 0L2, Canada.*

Accepted for publication August 3, 1976.

The authors thank Dr. I. J. McGilveray, Dr. J. W. Hubbard, and Mr. A. G. Butterfield for helpful discussions and Dr. A. By and Mr. J.-C. Ethier for running the mass spectra. Mr. J. Evans and Mr. L. Martin are acknowledged for veterinary assistance.

[x] To whom inquiries should be directed.

Binding of Codeine, Morphine, and Methadone to Human Serum Proteins

JOSEPH JUDIS

Abstract □ The binding properties of codeine, morphine (as representative opium alkaloids), and methadone (a synthetic pharmacologically similar compound) were studied with selected human serum proteins. The methodology involved equilibrium and dynamic dialysis using ^3H- and/or ^{14}C-labeled compounds. For estimation of the percent binding with equilibrium dialysis, concentrations of the ligand used were approximately therapeutic blood levels and another concentration 30–60 times higher. The percent binding to whole human serum ranged from about 20% for morphine to almost 60% for methadone. Of the human serum proteins investigated, the highest percent binding was found with albumin, except for methadone for which it was β-globulin III. The affinity for other serum proteins varied with the ligand. In studies with albumin using dynamic dialysis, the plots of nubar divided by free concentration *versus* nubar were similar for all three ligands studied and had positive slopes, unlike those reported for acidic compounds for which the slope is always negative. In studies of binding of one ligand in the presence of another, significant competition was demonstrated, suggesting that the same binding sites were involved.

Keyphrases □ Codeine—binding to human serum proteins □ Morphine—binding to human serum proteins □ Methadone—binding to human serum proteins □ Binding, protein—codeine, morphine, and methadone to human serum □ Protein binding—codeine, morphine, and methadone to human serum □ Analgesics, narcotic—codeine, morphine, and methadone, binding to human serum proteins □ Alkaloids, opium—codeine, morphine, and methadone, binding to human serum proteins

The binding of drugs to serum proteins is well established as a parameter in pharmacological and therapeutic activities of medicinal agents (1). Several reviews treated the methodology for studying protein binding and summarized the vast number of substances already investigated (2–5). Of the hundreds of compounds studied, the vast majority are acidic or nonpolar; few studies have

Table I—Binding of Methadone, Morphine, and Codeine to Various Human Serum Proteins[a]

Serum Protein Fraction	Concentration, mg/ml	Ligand, % Bound for Concentration Indicated: Methadone 9.3×10^{-8} Mole	Methadone 3.3×10^{-6} Mole	Morphine 5.5×10^{-8} Mole	Morphine 3.6×10^{-6} Mole	Codeine 5.6×10^{-8} Mole	Codeine 3.4×10^{-6} Mole
Albumin	40.0	31.16 (2.23)	21.84 (0.29)	23.24 (1.30)	16.56 (1.15)	14.26 (0.68)	28.50 (0.09)
α-Globulin IV-1	1.0	10.19 (1.28)	5.70 (0.51)	1.61 (0.07)	4.10 (0.98)	9.59 (1.46)	5.03 (0.21)
α-Globulin IV-4	5.0	12.53 (1.65)	4.58 (0.13)	6.42 (0.01)	7.56 (0.39)	12.34 (0.70)	17.05 (0.40)
β-Globulin III	7.0	37.75 (2.76)	10.90 (0.56)	7.39 (0.05)	3.16 (0.21)	7.98 (0.60)	3.68 (1.04)
γ-Globulin II	11.0	8.26 (0.72)	6.47 (0.40)	4.16 (0.20)	10.02 (2.72)	5.71 (0.72)	8.60 (1.16)
Human serum	—	59.78 (3.00)	39.54 (1.20)	24.02 (1.82)	20.08 (1.04)	29.01 (2.70)	22.35 (0.87)

[a] The number of moles of ligand added to each system is indicated as the concentration. Values in parentheses are standard deviations.

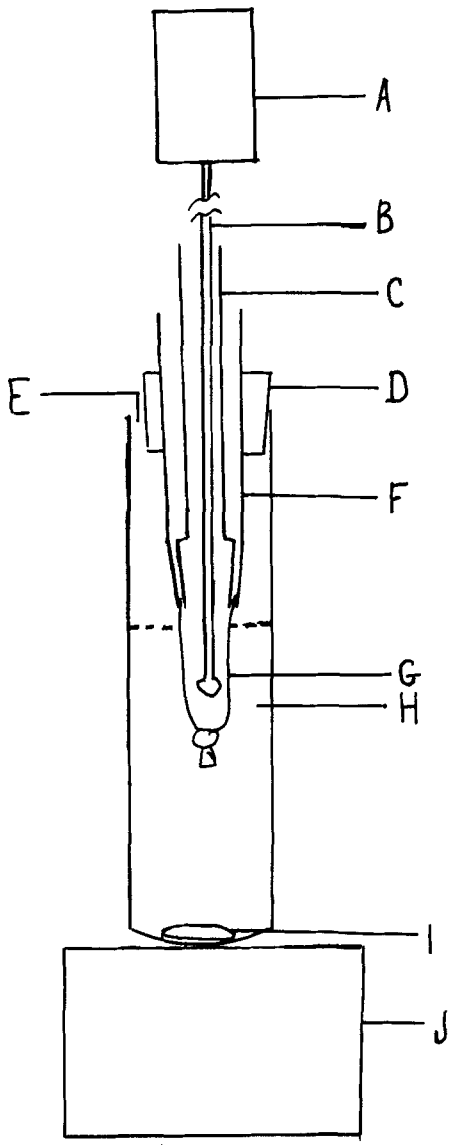

Figure 1—*Diagram of the apparatus used for dynamic equilibrium dialysis. Key: A, stirring motor; B, stirring rod; C, inner tube; D, rubber stopper; E, slot for withdrawing and adding buffer; F, middle tube; G, dialysis bag; H, 100 ml of buffer; I, stirring bar; and J, magnetic stirrer.*

concerned the serum protein binding properties of alkaloids and other basic organic compounds.

Only a handful of reports treated such widely used compounds as opium alkaloids or methadone. Morphine and methadone were shown to bind to serum proteins on the basis of decreased analgesic qualities resulting when the compounds were dissolved in serum prior to injection as compared to aqueous solutions (6). Several studies (7, 8) demonstrated the binding of morphine and methadone to human serum albumin and the binding of methadone to γ-globulin (9), but these studies involved nothing more quantitative than percent binding figures. In addition, the binding of morphine to α_1-globulin was demonstrated using electrophoresis (10), and the binding of papaverine to plasma proteins also was reported (11).

In view of the paucity of investigations of human serum protein binding of alkaloids, studies were conducted using codeine and morphine, as naturally occurring alkaloids, and methadone, as a synthetic organic base with pharmacological properties similar to the other two.

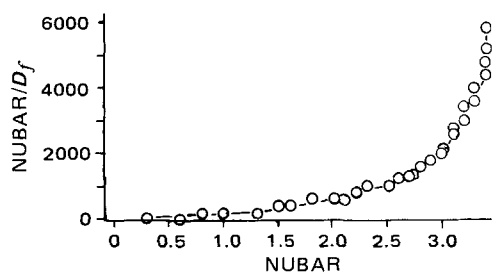

Figure 2—*Binding of codeine to human serum albumin determined by dynamic equilibrium dialysis. The plot is of nubar divided by free concentration* versus *nubar. A total of 3.368 × 10^{-5} mole of codeine was added at the beginning of the run, and the albumin concentration in the bag was 5.797 × 10^{-4}* M.

Table II—Binding of Methadone, Morphine, and Codeine to Various Human Serum Proteins[a] (Ranking in Order by Percent Binding)

	Methadone		Morphine		Codeine	
	9.3 × 10^{-8} Mole[b]	3.3 × 10^{-6} Mole	5.5 × 10^{-8} Mole	3.6 × 10^{-6} Mole	5.6 × 10^{-8} Mole	3.4 × 10^{-6} Mole
Rank 1	HS	HS	HS	HS	HS	ALB
Rank 2	B-III	ALB	ALB	ALB	ALB	HS
Rank 3	ALB	B-III	B-III	G-II	AG4	AG4
Rank 4	AG4	G-II	AG4	AG4	AG1	G-II
Rank 5	AG1	AG1	G-II	AG1	B-III	AG1
Rank 6	G-II	AG4	AG1	B-III	G-II	B-III

[a] Abbreviations for serum proteins are as follows: HS = human serum, ALB = human serum albumin, AG1 = α-globulin IV-1, AG4 = α-globulin IV-4, G-II = γ-globulin II, and B-III = β-globulin III. [b] Total concentration of ligand in cell.

EXPERIMENTAL

Materials—[^{14}C-*N*-Methyl]codeine hydrochloride[1], [^{14}C-*N*-methyl]morphine hydrochloride[1], and 1-^{3}H-*l*-methadone hydrobromide[2] had specific activities of 54, 57, and 135 mCi/mmole, respectively. Crystalline human serum albumin[3] and the other human serum proteins[3] were used as received. A liquid scintillation phosphor solution[4] was used in all radioactivity determinations. All other chemicals were reagent grade.

Methods—Equilibrium dialysis was employed for the estimation of the percent binding to specific proteins. However, to obtain more data efficiently for Scatchard-type plots, the dynamic equilibrium procedure was used. The procedure for the determination of protein binding using equilibrium dialysis was identical with that described previously (12, 13). All components of the system were dissolved in pH 7, 0.67 *M* phosphate

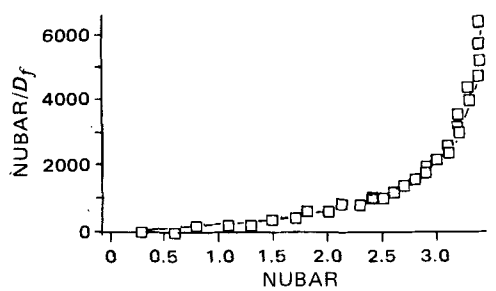

Figure 3—*Binding of morphine to human serum albumin determined by dynamic equilibrium dialysis. The plot is of nubar divided by free concentration* versus *nubar. A total of 3.527 × 10^{-5} mole of morphine was added at the beginning of the run, and the albumin concentration in the bag was 5.797 × 10^{-4}* M.

[1] Amersham/Searle Corp.
[2] New England Nuclear Corp.
[3] Nutritional Biochemicals Corp., Cleveland, Ohio.
[4] Aquasol, New England Nuclear Corp.

Table III—Binding Parameters for Codeine, Morphine, and Methadone and Human Serum Albumin Calculated from Plots[a] of D_b/D_f versus D_b

Ligand	K_1	n_1	K_2	n_2	K_3	n_3
Codeine	280.6	0.209	4380	2.5	12,568	2.998
Morphine	388.3	0.047	3633	2.379	15,539	3.043
Methadone	487.75	0.23	2488	1.092	6,828	1.457

[a] D_b is concentration of bound ligand (molar), and D_f is concentration of free ligand (molar).

Table IV—Inhibition of Binding of ^{14}C-Codeine to Human Serum Albumin by Unlabeled Morphine

Absence of Unlabeled Morphine			Presence of Unlabeled Morphine[a]				
Total Moles of Codeine in System $\times 10^{-4}$	Beta	Nubar	Total Moles of Codeine in System $\times 10^{-4}$	Beta	Percent Decrease in Beta	Nubar	Percent Decrease in Nubar
0.22867	0.228	1.8005	0.22898	0.0978	57.15	0.7725	57.10
0.1627	0.5167	2.8986	0.16383	0.22196	57.04	1.2462	57.01
0.14232	0.6598	3.2378	0.142995	0.28154	57.33	1.3882	57.12
0.13146	0.7541	3.4185	0.131904	0.32268	57.21	1.4677	57.07

[a] A total of 1.75×10^{-5} mole of morphine added to the dialysis bag.

Table V—Inhibition of Binding of ^{14}C-Morphine to Human Serum Albumin by Unlabeled Codeine

Absence of Unlabeled Codeine			Presence of Unlabeled Codeine[a]				
Total Moles of Morphine in System $\times 10^{-4}$	Beta	Nubar	Total Moles of Morphine in System $\times 10^{-4}$	Beta	Percent Decrease in Beta	Nubar	Percent Decrease in Nubar
0.28185	0.1111	1.0798	0.28099	0.07878	29.10	0.7633	29.31
0.20356	0.3237	2.2722	0.20372	0.22564	30.30	1.5851	30.24
0.15624	0.5555	2.9929	0.156634	0.38619	30.48	2.0859	30.31
0.13038	0.7533	3.3868	0.130796	0.52342	30.52	2.3607	30.30

[a] A total of 1.67×10^{-5} mole of codeine added to the dialysis bag.

buffer and incubated on a shaker in a 37° water bath for 24 hr, previously shown to be adequate for reaching equilibrium.

The dynamic equilibrium procedure used was a modification (14) of the Meyer and Guttman (15) procedure. The basic apparatus (Fig. 1) consisted of a collodion bag apparatus[5] modified by the attachment of dialysis tubing[6] (3.32 cm flat width), tied off at one end and held in the

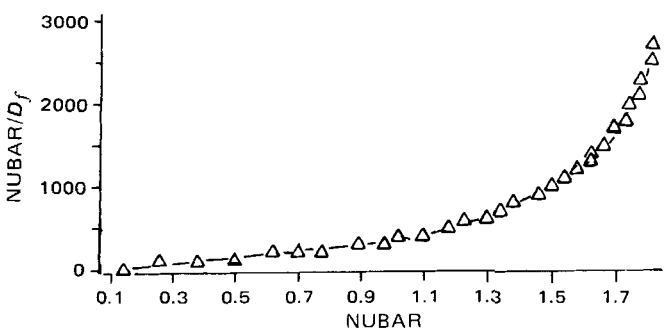

Figure 4—*Binding of methadone to human serum albumin determined by dynamic equilibrium dialysis. The plot is of nubar divided by free concentration* versus *nubar. A total of 2.589×10^{-5} mole of methadone was added at the beginning of the run, and the albumin concentration in the bag was 5.797×10^{-4}* M.

[5] No. 100/21, Schleicher and Schuell.
[6] Fisher Scientific Co.

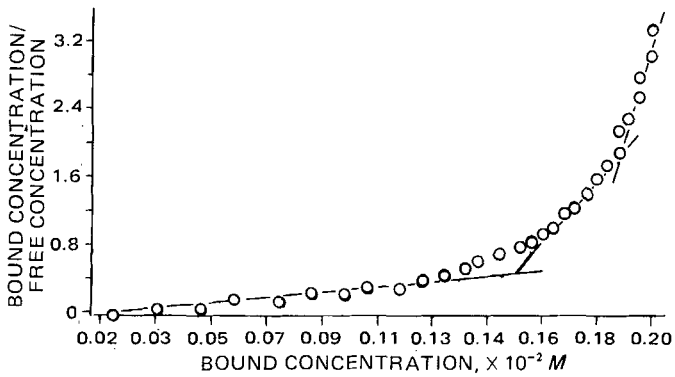

Figure 5—*Binding of codeine to human serum albumin determined by dynamic equilibrium dialysis. The plot is of bound concentration divided by free concentration* versus *bound concentration; amounts of albumin and codeine are the same as for Fig. 2.*

ground-glass joint at the end of the inner tubes of the collodion bag apparatus at the other end. The dialysis tubing was soaked overnight in phosphate buffer prior to use and cut to hold a volume of 5 ml.

Buffer was added through a slot cut in the rubber stopper at the top of the apparatus, and the contents of the bag were stirred with a motor-driven glass stirring rod. Incubation was at room temperature (24 ± 2°). The buffer was stirred with a polytef[7]-coated stirring bar driven by a magnetic stirrer. At the start of a run, protein and ligand solutions (total volume of 5 ml) were added to the bag and 100 ml of pH 7, 0.067 *M* phosphate buffer was added to the apparatus. At 30-min intervals for 3 hr, 50 ml of buffer was withdrawn with a syringe and replaced by 50 ml of fresh buffer.

Radioactivity was determined[8] in an aliquot of the withdrawn buffer. The amount of radioactivity added to the bag initially was determined from an aliquot of the stock solution of radioisotope and the counts per minute in the bag calculated for each sampling time. Free ligand counts per minute in the bag at each sampling time was calculated using the equation given by Meyer and Guttman (15) and the computer program developed by Dearden and Tomlinson (14). From the knowledge of the total and free concentrations of ligand, bound concentrations could be calculated; from the equation relating free concentrations and times of sampling, bound concentrations for intermediate time intervals could be calculated. Approximate estimates of binding parameters were calculated using the method of Sandberg *et al.* (16).

RESULTS AND DISCUSSION

Codeine, morphine, and methadone bound to the several human serum proteins to varying extents (Table I). The lower concentrations of the

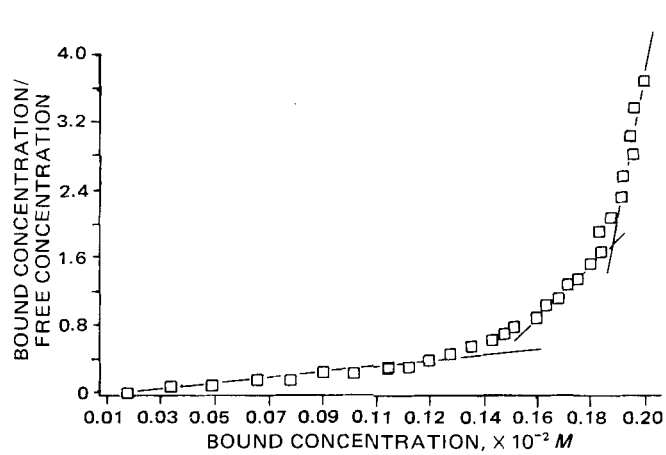

Figure 6—*Binding of morphine to human serum albumin determined by dynamic equilibrium dialysis. The plot is of bound concentration divided by free concentration* versus *bound concentration; amounts of albumin and morphine are the same as for Fig. 3.*

[7] Teflon, du Pont.
[8] Beckman model LS-133.

Table VI—Inhibition of Binding of ^{3}H-Methadone to Human Serum Albumin by Unlabeled Codeine

Absence of Unlabeled Codeine			Presence of Unlabeled Codeine[a]				
Total Moles of Methadone in System $\times 10^{-4}$	Beta	Nubar	Total Moles of Methadone in System $\times 10^{-4}$	Beta	Percent Decrease in Beta	Nubar	Percent Decrease in Nubar
0.25537	0.0868	0.76465	0.25722	0.04121	52.54	0.3655	52.20
0.20445	0.1859	1.3104	0.20475	0.09085	51.12	0.6414	51.05
0.14216	0.4035	1.9780	0.14196	0.19848	50.81	0.9716	50.88
0.11272	0.5900	2.2934	0.112692	0.28964	50.91	1.1255	50.92

[a] A total of 1.67×10^{-5} mole of codeine added to the dialysis bag.

Table VII—Inhibition of Binding of ^{3}H-Methadone to Human Serum Albumin by Unlabeled Morphine

Absence of Unlabeled Morphine			Presence of Unlabeled Morphine[a]				
Total Moles of Methadone in System $\times 10^{-4}$	Beta	Nubar	Total Moles of Methadone in System $\times 10^{-4}$	Beta	Percent Decrease in Beta	Nubar	Percent decrease in Nubar
0.26779	0.0684	0.63162	0.26536	0.02765	59.58	0.2530	59.95
0.20445	0.1859	1.3104	0.20312	0.07275	60.86	0.5096	61.11
0.15666	0.3374	1.8225	0.157693	0.12816	62.01	0.6969	61.76
0.11781	0.5511	2.2389	0.117747	0.21219	61.50	0.8616	61.52

[a] A total of 1.75×10^{-5} mole of morphine added to the dialysis bag.

ligands were approximately those indicated in the literature as therapeutic levels[9] (8, 17–20). When the concentrations were increased by a factor of 30–60, the percent binding did change, generally decreasing. When the ligands were arranged according to the percent binding in decreasing order, the greatest binding occurred with whole human serum with one exception (Table II) and with albumin next except for methadone at the lower concentration and codeine at the higher concentration. Otherwise, the order was different for the three ligands.

The conventional binding curves, Scatchard plots (2, 3, 21) in which moles bound per mole of protein (nubar) divided by free ligand concentration (D_f) is plotted against nubar, are shown in Figs. 2–4. For most ligands studied previously (22–27), the Scatchard plot curve has a negative slope and is a straight line unless more than one type of binding site is involved. In the latter situation, a curve is found. The plots in Figs. 2–4 all have positive slopes and are curves, indicating more than one type of binding site.

Positive slopes have been interpreted to indicate possible cooperativity (28) and do not lend themselves to the analyses generally performed with typical Scatchard curves in terms of the calculation of binding parameters. However, to obtain approximate estimates of the binding parameters, the Sandberg *et al.* (16) method was used. This method involves plots of bound concentration of ligand divided by free concentration *versus* bound concentration (Figs. 5–7). The y-intercept is equal to nKP, the x-intercept is equal to n, and the slope is equal to K (n refers to the number of binding sites, K refers to the association constant, and P refers to the molar protein concentration). Each curve had three distinct segments, and each segment was treated as a separate curve for calculation (Table III).

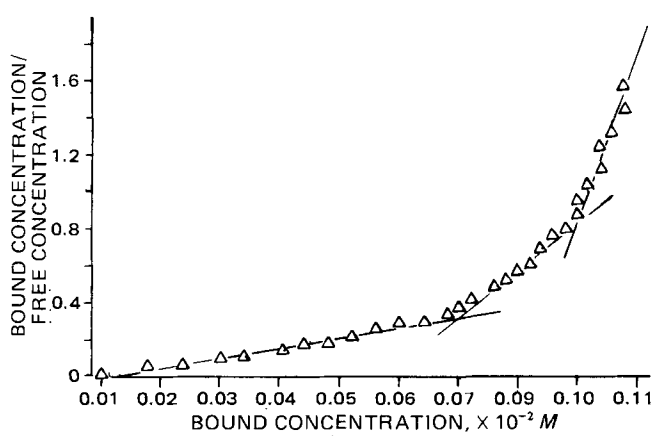

Figure 7—*Binding of methadone to human serum albumin determined by dynamic equilibrium dialysis. The plot is of bound concentration divided by free concentration* versus *bound concentration; amounts of albumin and methadone are the same as for Fig. 4.*

As an approach to determining whether the three ligands bind to the same sites on albumin, binding of one ligand was determined in the presence of another. Unlabeled morphine decreased significantly the binding of ^{14}C-codeine (Table IV), and codeine interfered with the binding of ^{14}C-morphine (Table V). Both codeine and morphine interfered with the binding of ^{3}H-methadone to human serum albumin (Tables VI and VII).

Codeine, morphine, and methadone apparently do bind significantly to human serum proteins, with all of the implications in terms of pharmacological action of drugs (1). Binding to albumin is greatest generally for the three ligands, which is characteristic of many molecules. The three compounds yielded binding plots (nubar divided by D_f *versus* nubar) that are clearly distinct from those of many anionic and nonpolar compounds. The curves for codeine, morphine, and methadone have positive slopes, and this feature may be characteristic of alkaloids and organic bases in general. The same types of plots were obtained in this laboratory in preliminary experiments with amphetamine, histamine, atropine, and epinephrine with human serum albumin as the protein. A curve with a positive slope (same type of plot) was found by Powis (29) in studies of the binding of tetracycline to albumin.

[9] Data on therapeutic serum levels for codeine were obtained from Carl W. Sigel, Burroughs Wellcome Co., Research Triangle Park, N.C.

REFERENCES

(1) A. Goth, "Medical Pharmacology," C. V. Mosby, St. Louis, Mo., 1974, pp. 20, 21, 698.

(2) A. Goldstein, *Pharmacol. Rev.*, **1**, 102 (1949).

(3) M. C. Meyer and D. E. Guttman, *J. Pharm. Sci.*, **57**, 895 (1968).

(4) C. F. Chignell, *Crit. Rev. Toxicol.*, **Oct. 1972**, 413.

(5) "Transport Function of Plasma Proteins," P. Desgrez, Ed., Elsevier, New York, N.Y., 1966.

(6) J. Knoll, E. Komlos, and L. Tardos, *Acta Physiol. Acad. Sci. Hung.*, **4**, 141 (1953).

(7) G. D. Olsen, *Science*, **176**, 525 (1972).

(8) G. D. Olsen, *Clin. Pharmacol. Ther.*, **17**, 31 (1975).

(9) *Ibid.*, **14**, 338 (1973).

(10) M. B. Drevon, C. Fournier, and R. Donikian, *Bull. Soc. Pharm. Bordeaux*, **94**, 177 (1955).

(11) J. Axelrod, R. Shofer, W. M. King, and J. D. Davidson, *J. Pharmacol. Exp. Ther.*, **15**, 485 (1956).

(12) J. Judis, *J. Pharm. Sci.*, **61**, 89 (1972).

(13) *Ibid.*, **62**, 232 (1973).
(14) J. C. Dearden and E. Tomlinson, *J. Pharm. Pharmacol.*, **22**, 53S (1970).
(15) M. C. Meyer and D. E. Guttman, *J. Pharm. Sci.*, **57**, 1627 (1968).
(16) A. A. Sandberg, H. Rosenthal, S. L. Schneider, and M. R. Slaunwhite, in "Steroid Dynamics," T. Nkro, G. Pincus, and J. F. Tait, Eds., Academic, New York, N.Y., 1966, pp. 33–41.
(17) S. Spector and E. S. Vesell, *Science*, **174**, 421 (1971).
(18) S. F. Brunk and M. Delle, *Clin. Pharmacol. Ther.*, **16**, 51 (1974).
(19) C. E. Inturrisi and K. Verebely, *ibid.*, **13**, 633 (1972).
(20) A. E. Robinson and F. M. Williams, *J. Pharm. Pharmacol.*, **23**, 353 (1971).
(21) G. Scatchard, *Ann. N.Y. Acad. Sci.*, **51**, 660 (1949).
(22) G. Scatchard, J. S. Coleman, and A. L. Shen, *J. Am. Chem. Soc.*, **79**, 12 (1957).
(23) D. S. Goodman, *ibid.*, **80**, 3892 (1958).
(24) C. Davison and P. K. Smith, *J. Pharmacol. Exp. Ther.*, **133**, 161 (1961).
(25) A. Agren and T. Back, *Acta Pharm. Suec.*, **10**, 223 (1973).
(26) S. Nilsson, A. Agren, J. Branstad, and U. Meresaar, *ibid.*, **10**, 455 (1973).
(27) D. Hultmark, K. O. Borg, R. Elofsson, and L. Palmer, *ibid.*, **12**, 259 (1975).
(28) J. E. Fletcher, D. Ashbrook, and A. A. Spector, *Ann. N.Y. Acad. Sci.*, 226 (1973).
(29) G. Powis, *J. Pharm. Pharmacol.*, **26**, 113 (1973).

ACKNOWLEDGMENTS AND ADDRESSES

Received April 30, 1976, from the *College of Pharmacy, University of Toledo, Toledo, OH 43606.*

Accepted for publication August 9, 1976.

The technical assistance of Mrs. Virginia Matusek is gratefully acknowledged.

Pharmacokinetics of β-Methyldigoxin in Healthy Humans IV: Comparisons of Radioimmunoassays, Total Radioactivity, and Specific Assays of β-Methyldigoxin and Digoxin in Plasma

EDWARD R. GARRETT ˣ and PETER H. HINDERLING *

Abstract □ A modified radioimmunoassay, using the displacement of the ^{125}I-digoxin derivative bound to antiserum, is presented. It permitted the monitoring of plasma for total glycosides up to 144 hr after oral and intravenous administrations of 0.3 and 0.6 mg of ^{3}H-β-methyldigoxin to healthy humans. In a specific plasma, the radioimmunoassay response of β-methyldigoxin was 86 ± 3% that of digoxin. Radioimmunoassay of plasma was highly correlated with liquid scintillation spectrometric analysis of total radioactivity, and plots of various studies showed intercepts not significantly different than zero. However, radioimmunoassay underestimated the radiolabeled plasma concentration by 12–38% and was dependent on the individual plasma. Since total radioactivity and radioimmunoassay can be expressed as a linear sum of the ^{3}H-digoxin and ^{3}H-β-methyldigoxin plasma concentrations, plots of ratios of total radioactivity to ^{3}H-digoxin concentration against ratios of ^{3}H-β-methyldigoxin to ^{3}H-digoxin plasma concentration were statistically evaluated to determine the specific activities of both glycosides in the two assays. The contributions of ^{3}H-β-methyldigoxin and its metabolite ^{3}H-digoxin were equivalent in liquid scintillation spectrometry, but the former ranged from 65 to 87% of the potency of the latter in the various radioimmunoassay studies. There was a significant difference in the estimated specific antigenicity of β-methyldigoxin at higher and lower plasma concentration ratios of β-methyldigoxin to digoxin, where the specific antigenicity was less at the higher ratios.

Keyphrases □ β-Methyldigoxin—oral and intravenous, pharmacokinetics, radioimmunoassay compared to radiochemical spectrometric assays, human plasma □ Pharmacokinetics—β-methyldigoxin, oral and intravenous, radioimmunoassay compared to radiochemical spectrometric assays, human plasma □ Radioimmunoassay—β-methyldigoxin, pharmacokinetic study after oral and intravenous administration, compared to radiochemical spectrometric assays, human plasma □ Cardiac glycosides—β-methyldigoxin, oral and intravenous, pharmacokinetics, radioimmunoassay compared to radiochemical spectrometric assays, human plasma

Radioimmunoassay has been applied to measure glycoside concentrations in biological fluids after administration of therapeutic dosages of digoxin and β-methyldigoxin (1–4). This radioimmunoassay of glycosides should be compared with other established methods, such as liquid scintillation spectrophotometry of labeled glycosides, to monitor total radioactivity or the specifically assigned radioactivity of separated parent drug and metabolites. Such comparisons should elucidate the specificity of such procedures.

Recent studies with radioimmuno- and ^{86}Rb-uptake assays investigated the mutual relationships between digoxin and its metabolites and quantified the fractional contributions of parent drug and metabolites (2, 5) to total activity. It was suggested that all cardioactive metabolites of digoxin and digitoxin also contribute to the total antigenicity and total uptake inhibition in the radioimmuno- and ^{86}Rb-uptake assays, respectively (2, 6). Potency differences were reported for different glycoside metabolites and derivatives in the radioimmunoassay (2). Equipotency can be assumed for the parent drug and metabolites when total radioactivity is monitored by liquid scintillation spectrophotometry.

This paper compares the radioimmunoassay and total and specific radioactivity methods used to monitor the glycoside ^{3}H-β-methyldigoxin (7, 8), which is about 50% metabolized, mainly to digoxin (7–9).

EXPERIMENTAL

Equipment—An automated-control γ-scintillation spectrometer[1] was used for determining the activity of the ^{125}I-digoxin derivative after addition to plasma in the radioimmunoassay procedure.

Materials and Methods—The ^{125}I-digoxin derivative, digoxin standard, buffer components, and antiserum used for the radioimmunoassay were obtained from the commercially available kit[2].

[1] Auto Gamma Counter, Packard Instruments Co., Downers Grove, Ill.
[2] ^{125}I-Digoxin derivative radioimmunoassay kit, Schwarz/Mann, Orangeburg, N.J.

(13) *Ibid.*, **62**, 232 (1973).
(14) J. C. Dearden and E. Tomlinson, *J. Pharm. Pharmacol.*, **22**, 53S (1970).
(15) M. C. Meyer and D. E. Guttman, *J. Pharm. Sci.*, **57**, 1627 (1968).
(16) A. A. Sandberg, H. Rosenthal, S. L. Schneider, and M. R. Slaunwhite, in "Steroid Dynamics," T. Nkro, G. Pincus, and J. F. Tait, Eds., Academic, New York, N.Y., 1966, pp. 33–41.
(17) S. Spector and E. S. Vesell, *Science*, **174**, 421 (1971).
(18) S. F. Brunk and M. Delle, *Clin. Pharmacol. Ther.*, **16**, 51 (1974).
(19) C. E. Inturrisi and K. Verebely, *ibid.*, **13**, 633 (1972).
(20) A. E. Robinson and F. M. Williams, *J. Pharm. Pharmacol.*, **23**, 353 (1971).
(21) G. Scatchard, *Ann. N.Y. Acad. Sci.*, **51**, 660 (1949).
(22) G. Scatchard, J. S. Coleman, and A. L. Shen, *J. Am. Chem. Soc.*, **79**, 12 (1957).
(23) D. S. Goodman, *ibid.*, **80**, 3892 (1958).
(24) C. Davison and P. K. Smith, *J. Pharmacol. Exp. Ther.*, **133**, 161 (1961).
(25) A. Agren and T. Back, *Acta Pharm. Suec.*, **10**, 223 (1973).
(26) S. Nilsson, A. Agren, J. Branstad, and U. Meresaar, *ibid.*, **10**, 455 (1973).
(27) D. Hultmark, K. O. Borg, R. Elofsson, and L. Palmer, *ibid.*, **12**, 259 (1975).
(28) J. E. Fletcher, D. Ashbrook, and A. A. Spector, *Ann. N.Y. Acad. Sci.*, 226 (1973).
(29) G. Powis, *J. Pharm. Pharmacol.*, **26**, 113 (1973).

ACKNOWLEDGMENTS AND ADDRESSES

Received April 30, 1976, from the *College of Pharmacy, University of Toledo, Toledo, OH 43606.*

Accepted for publication August 9, 1976.

The technical assistance of Mrs. Virginia Matusek is gratefully acknowledged.

Pharmacokinetics of β-Methyldigoxin in Healthy Humans IV: Comparisons of Radioimmunoassays, Total Radioactivity, and Specific Assays of β-Methyldigoxin and Digoxin in Plasma

EDWARD R. GARRETT ˣ and PETER H. HINDERLING *

Abstract □ A modified radioimmunoassay, using the displacement of the ^{125}I-digoxin derivative bound to antiserum, is presented. It permitted the monitoring of plasma for total glycosides up to 144 hr after oral and intravenous administrations of 0.3 and 0.6 mg of ^{3}H-β-methyldigoxin to healthy humans. In a specific plasma, the radioimmunoassay response of β-methyldigoxin was 86 ± 3% that of digoxin. Radioimmunoassay of plasma was highly correlated with liquid scintillation spectrometric analysis of total radioactivity, and plots of various studies showed intercepts not significantly different than zero. However, radioimmunoassay underestimated the radiolabeled plasma concentration by 12–38% and was dependent on the individual plasma. Since total radioactivity and radioimmunoassay can be expressed as a linear sum of the ^{3}H-digoxin and ^{3}H-β-methyldigoxin plasma concentrations, plots of ratios of total radioactivity to ^{3}H-digoxin concentration against ratios of ^{3}H-β-methyldigoxin to ^{3}H-digoxin plasma concentration were statistically evaluated to determine the specific activities of both glycosides in the two assays. The contributions of ^{3}H-β-methyldigoxin and its metabolite ^{3}H-digoxin were equivalent in liquid scintillation spectrometry, but the former ranged from 65 to 87% of the potency of the latter in the various radioimmunoassay studies. There was a significant difference in the estimated specific antigenicity of β-methyldigoxin at higher and lower plasma concentration ratios of β-methyldigoxin to digoxin, where the specific antigenicity was less at the higher ratios.

Keyphrases □ β-Methyldigoxin—oral and intravenous, pharmacokinetics, radioimmunoassay compared to radiochemical spectrometric assays, human plasma □ Pharmacokinetics—β-methyldigoxin, oral and intravenous, radioimmunoassay compared to radiochemical spectrometric assays, human plasma □ Radioimmunoassay—β-methyldigoxin, pharmacokinetic study after oral and intravenous administration, compared to radiochemical spectrometric assays, human plasma □ Cardiac glycosides—β-methyldigoxin, oral and intravenous, pharmacokinetics, radioimmunoassay compared to radiochemical spectrometric assays, human plasma

Radioimmunoassay has been applied to measure glycoside concentrations in biological fluids after administration of therapeutic dosages of digoxin and β-methyldigoxin (1–4). This radioimmunoassay of glycosides should be compared with other established methods, such as liquid scintillation spectrophotometry of labeled glycosides, to monitor total radioactivity or the specifically assigned radioactivity of separated parent drug and metabolites. Such comparisons should elucidate the specificity of such procedures.

Recent studies with radioimmuno- and ^{86}Rb-uptake assays investigated the mutual relationships between digoxin and its metabolites and quantified the fractional contributions of parent drug and metabolites (2, 5) to total activity. It was suggested that all cardioactive metabolites of digoxin and digitoxin also contribute to the total antigenicity and total uptake inhibition in the radioimmuno- and ^{86}Rb-uptake assays, respectively (2, 6). Potency differences were reported for different glycoside metabolites and derivatives in the radioimmunoassay (2). Equipotency can be assumed for the parent drug and metabolites when total radioactivity is monitored by liquid scintillation spectrophotometry.

This paper compares the radioimmunoassay and total and specific radioactivity methods used to monitor the glycoside ^{3}H-β-methyldigoxin (7, 8), which is about 50% metabolized, mainly to digoxin (7–9).

EXPERIMENTAL

Equipment—An automated-control γ-scintillation spectrometer[1] was used for determining the activity of the ^{125}I-digoxin derivative after addition to plasma in the radioimmunoassay procedure.

Materials and Methods—The ^{125}I-digoxin derivative, digoxin standard, buffer components, and antiserum used for the radioimmunoassay were obtained from the commercially available kit[2].

[1] Auto Gamma Counter, Packard Instruments Co., Downers Grove, Ill.
[2] ^{125}I-Digoxin derivative radioimmunoassay kit, Schwarz/Mann, Orangeburg, N.J.

Table I—Influence of Plasma Volume on Radioimmunoassay Efficiency[a]

Plasma Volume in 1 ml of Phosphate Buffer, μl	Replicate Measured Digoxin Concentrations by Radioimmunoassay, dpm/ml
50	1091, 1206
100	1183, 1218
200	1203, 1335
500	1162, 1248

[a] There was no statistically significant influence of the size of the assayed plasma on the radioimmunoassay ($F = 0.0052$; $df = 3, 4$; $p > 0.9$).

The seven volunteers received 0.3 and 0.6 mg of β-methyldigoxin orally and intravenously. Plasma glycoside concentrations were assayed by radioimmunoassay in five subjects (A, B, C, D, and G) (7, 8, 10) at the following times: 0, 1.5, 2, 2.5, 3.5, 7, 10, 15, 45, 60, and 90 min and 2, 3, 5, 7, 9, 11, 15, 20, 24, 36, 48, 60, 72, 84, 96, 120, and 144 hr after intravenous administration. Samples were assayed at the same times after oral administration except for 1.5, 2.5, and 3.5 min.

The methods and procedures for measurement of total plasma radioactivity and the radioactivity assignments to the separated drug and metabolite were described previously (7). The commercially available kit was modified in accordance with Stoll *et al.* (2) so that the wide glycoside concentration ranges found in plasma up to 144 hr after administration could be monitored by radioimmunoassay. The ^{125}I-digoxin derivative, rather than the ^{3}H-digoxin derivative, was used since the administered β-methyldigoxin was tritium labeled. This change alleviated the problem of quenching and led to increased sensitivity (11).

All plasma samples of a particular study were assayed at the same time. Individual calibration curves used the particular volunteer's blank plasma to which known concentrations of standard digoxin solutions were added.

Isotonic pH 7.4 phosphate buffer (1.0 ml) was added to 50–500 μl of plasma containing unknown concentrations of digoxin and/or β-methyldigoxin standard. Tracer, 10 μl, and 10 μl of antiserum were added to the mixtures. The mixtures were gently vortexed and incubated for 2 hr at 25° and then for an additional 16 hr at 4°. Equilibration was undoubtedly effected in the first 0.5 hr at room temperature but certainly was achieved by this procedure. The subsequent time under refrigeration was only to inhibit bacterial growth. Dextran-coated charcoal, 500 μl, was squirted into each mixture. Subsequently, at no more than 5 min, the samples were centrifuged at 1500 rpm for 10 min. The clear supernates were decanted and transferred to γ-counting tubes for measurement.

The influence of varied plasma volumes on the assay was studied since contradictions were reported (2, 12). Plasma blanks of 50, 100, 200, and 500 μl were spiked with digoxin standard so that the ultimate digoxin concentrations would be 2.0 ng/ml after dilution with phosphate buffer to the same 1.00-ml volume. Duplicate radioimmunoassays were performed (Table I), and no statistically significant difference was observed with decreasing fractions of plasma in the final solution.

Both the ^{3}H-digoxin and the ^{125}I-digoxin derivative radioimmunoassays were originally designed to measure unknown digoxin concentrations. However, these assays are not specific for digoxin but also respond to digoxin metabolites (2) and digoxin derivatives such as β-methyldigoxin (3, 4).

Since β-methyldigoxin is metabolized, mainly to digoxin (5, 9), the individual antigenic potencies of β-methyldigoxin and digoxin were evaluated in the radioimmunoassay over a significant concentration range. Plasma aliquots were spiked with either β-methyldigoxin or digoxin standards to give concentrations of 0.4, 1.0, 2.0, 3.0, 4.0, 5.0, and 10.0 ng/ml. Controls with blank plasma were run at the same time.

RESULTS AND DISCUSSION

Typical semilogarithmic plots of total plasma glycoside concentrations as determined by total radioactivity as measured by liquid scintillation spectrophotometry and by "total antigenicity," *i.e.*, the total antigenic effect resulting from the sum of antigenic effective glycosides, as measured by radioimmunoassay are given against time for intravenous and oral administrations (Fig. 1) of β-methyldigoxin. Both methods of analysis permitted the measurement of plasma glycoside concentrations from 40.0 to 0.2 ng/ml.

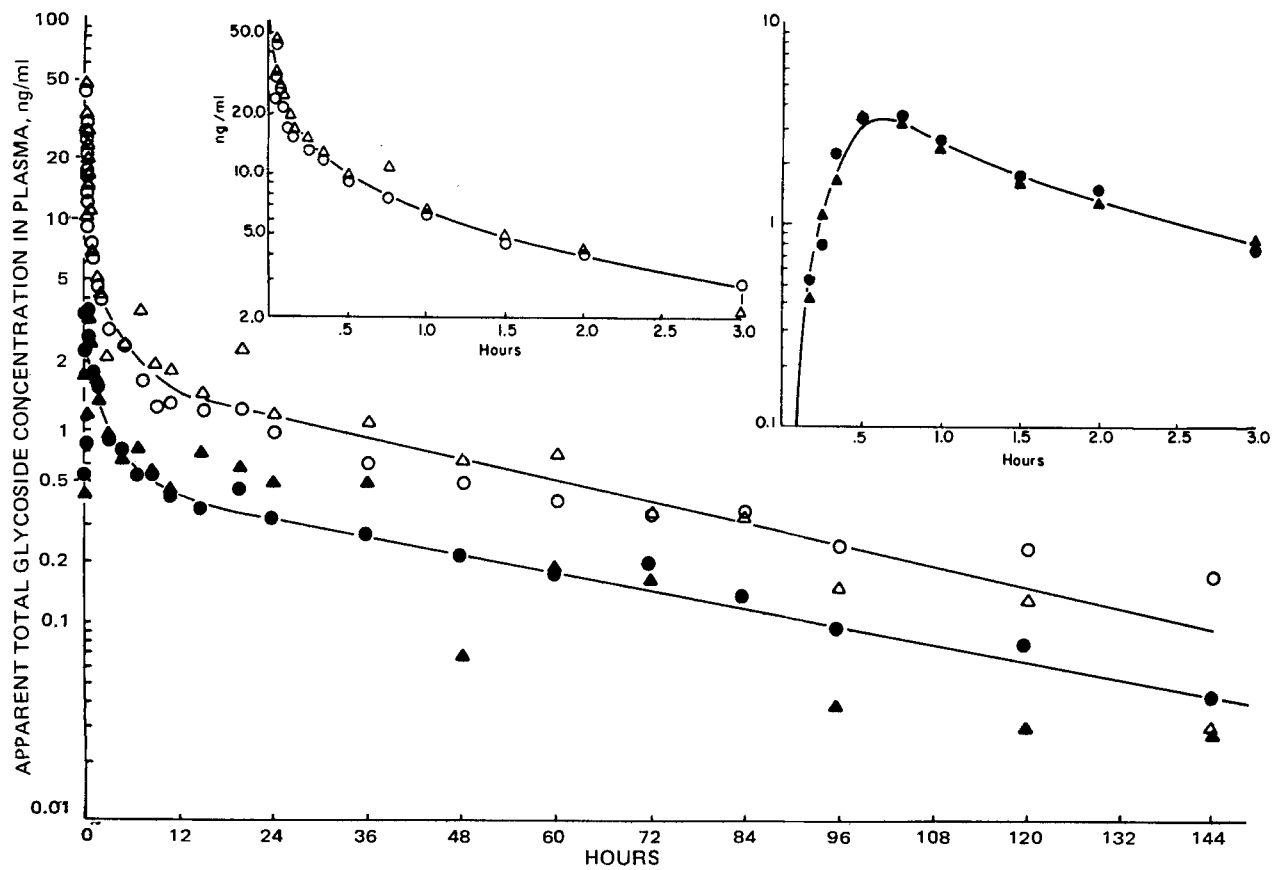

Figure 1—*Typical semilogarithmic plots of plasma concentrations of total glycosides against time by radioimmunoassay (▲, Subject B, 0.3-mg po dose; and △, Subject G, 0.6-mg iv dose) and liquid scintillation spectrometry (●, Subject B, 0.3-mg po dose; and ○, Subject G, 0.6-mg iv dose) after β-methyldigoxin administration. The insets expand the time axis over the initial period.*

Table II—Linear Regressions of Plasma Concentrations by Radioimmunoassay (RIA) on Concentration by Liquid Scintillation Spectrometry (LSC): RIA = mLSC + b

Subject	Dose, mg	Mode of Administration	Range, ng/ml	n[a]	$m \pm SE$	$b \pm SE$	r[b]	S_{RIA}[c]
A	0.6	Intravenous	0.10–20.0	29	0.858 ± 0.071	0.79 ± 0.51	0.919	1.97
A	0.6	Oral	0.16–6.2	23	0.731 ± 0.053	0.03 ± 0.14	0.949	0.48
B	0.6	Intravenous	0.10–32	29	0.618 ± 0.022	0.44 ± 0.24	0.983	1.05
B	0.3	Oral	0.03–3.6	24	0.893 ± 0.037	0.05 ± 0.05	0.982	0.18
C	0.6	Intravenous	0.20–88	27	0.850 ± 0.023	−1.11 ± 0.61	0.991	2.70
C	0.3	Oral	0.05–4.0	24	0.698 ± 0.081	0.27 ± 0.10	0.878	0.39
G	0.6	Intravenous	0.03–48	30	1.081 ± 0.017	0.34 ± 0.23	0.997	1.01
G	0.6	Oral	0.10–4.5	23	0.888 ± 0.043	0.12 ± 0.08	0.976	0.28

[a] Number of pairs. [b] Correlation coefficient. [c] Standard error of estimate of RIA by LSC.

Table III—Radioimmunoassays of Plasma β-Methyldigoxin in a System Calibrated against Digoxin

Concentration, ng/ml			Percent of Actual Concentrations	
Actual	Assayed			
0.40	0.40	0.30	100	75
1.00	0.80	0.85	80	85
2.00	1.60	2.10	80	105
3.00	2.40	2.75	80	71
5.00	4.00	4.70	80	94
10.00	>5.0	9.00	—	90
	Average ± SE		84 ± 4	87 ± 5
	Overall average			85.5 ± 3.2

Correlation of Plasma Concentrations of Glycosides by Radioimmunoassay and Liquid Scintillation Spectrophotometry of Total Radioactivity—Highly significant linear correlations existed between concentrations assayed by radioimmunoassay (RIA) and liquid scintillation spectrophotometry (LSC):

$$\text{RIA} = m\text{LSC} + b \qquad \text{(Eq. 1)}$$

The parameters of Eq. 1 and their variability are given in Table II for all studies conducted. Typical plots are given in Fig. 2.

The intercepts, b, in all cases were not significantly different from zero. The slopes, m, were significantly different among subjects and frequently within subjects, indicating that an individual plasma factor contributed to the variability in the radioimmunoassay response and that this plasma factor may vary within the individual.

In all cases except for Subject G, the slopes were significantly less than unity and indicated that the radioimmunoassay as established was not equivalent to the assay by liquid scintillation spectrophotometry. Radioimmunoassay alone would underestimate the radiolabeled material by 12–38% with Subject G excluded.

The radioimmunoassay was calibrated for digoxin by plotting the percent of added tracer bound to the antiserum against the added digoxin concentrations. Equivalent amounts of β-methyldigoxin were assayed at the same seven concentration levels between 0.40 and 10 ng/ml, and the experimental assay values were determined as digoxin-equivalent responses. β-Methyldigoxin was only 86% as responsive as digoxin in the plasma used for the radioimmunoassay (Table III).

Both of these compounds compete with ^{125}I-digoxin for binding sites. Since varying ratios of digoxin (DIG) and β-methyldigoxin (BMD) in plasma were assayed simultaneously, the presence of one could have modified the separate response of the other. Since:

$$\text{RIA} = m_R\text{BMD} + b_R\text{DIG} \qquad \text{(Eq. 2)}$$

it is possible that the factor m_R is not constant but varies as a function of the digoxin concentration.

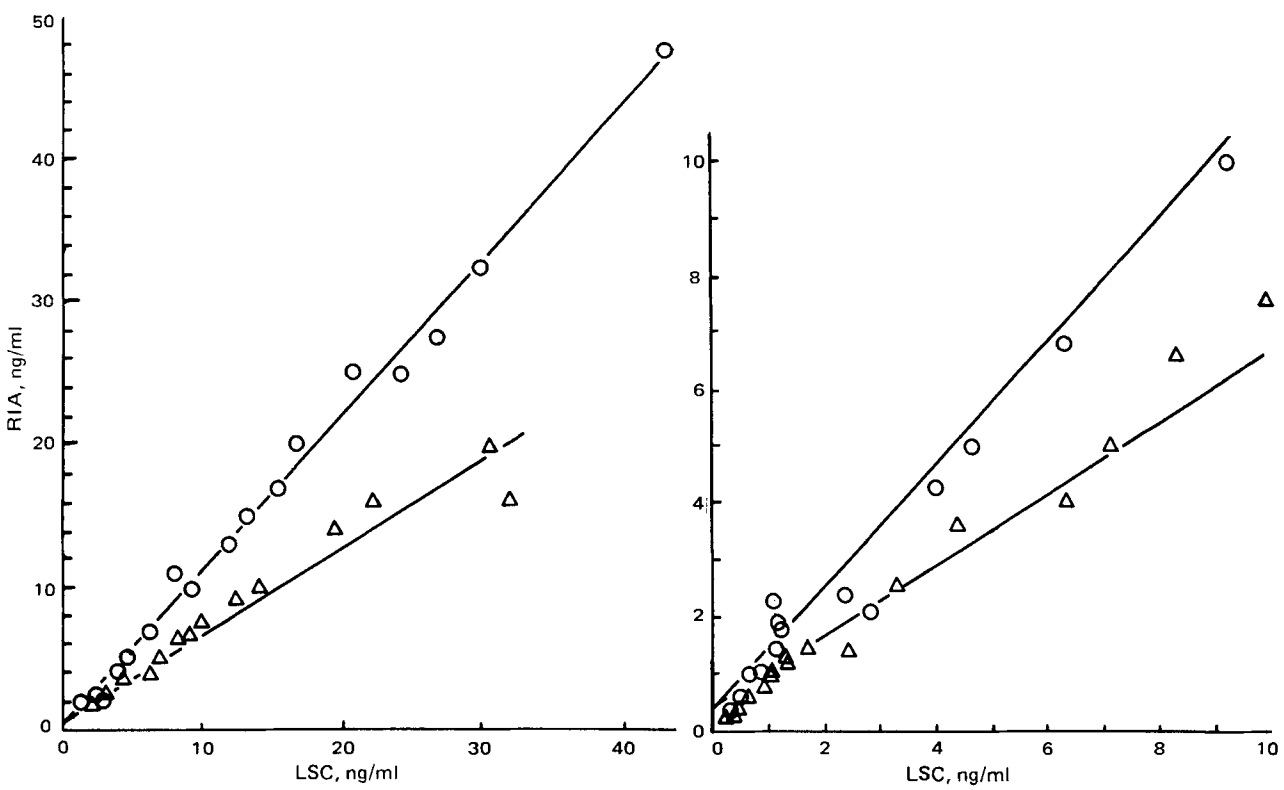

Figure 2—*Typical regressions of assays of total glycosides in plasma by radioimmunoassay (RIA) against assays by liquid scintillation spectrometry (LSC) for Subjects B (△) and G (○) given 0.6 mg iv of β-methyldigoxin. The lines drawn over the shorter range are the best fit over the longer range.*

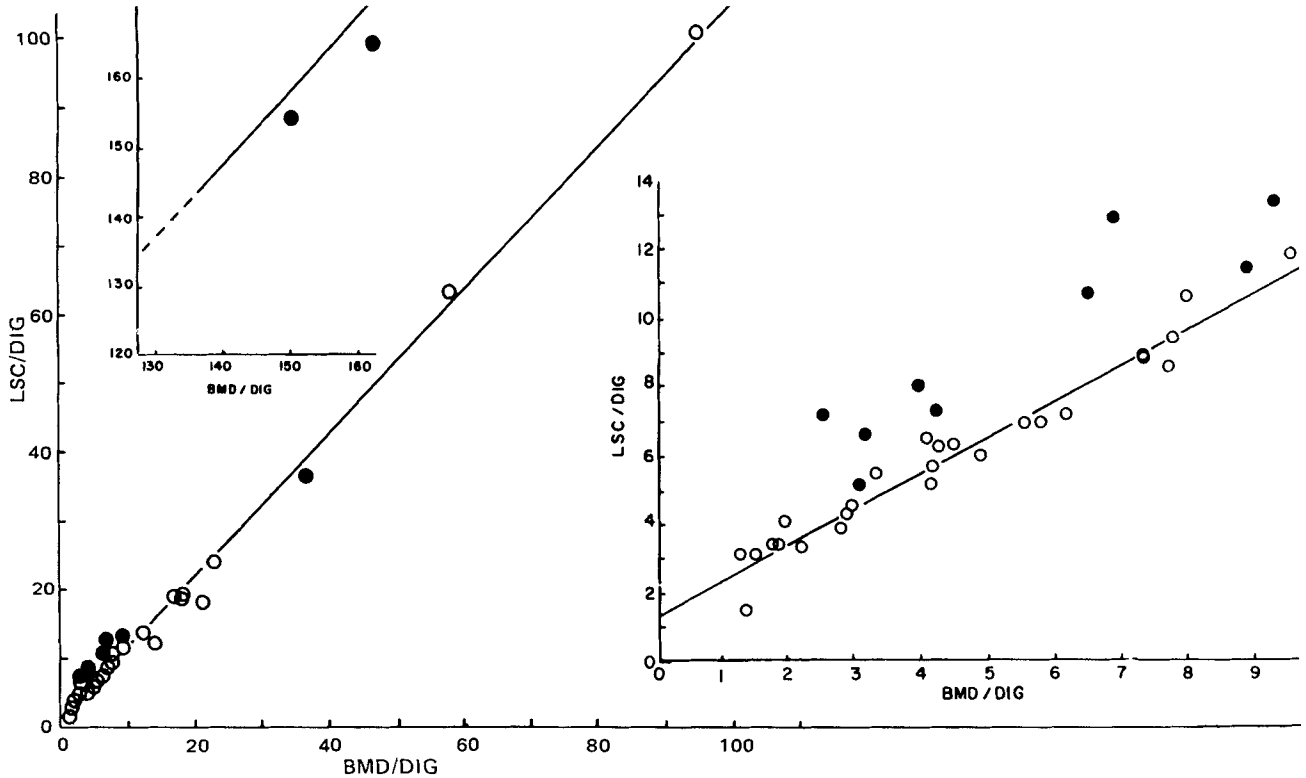

Figure 3—*Plots of the ratios of total glycoside plasma concentration by liquid scintillation spectrometry (LSC) to the plasma digoxin concentration (DIG) against the plasma concentration ratios of β-methyldigoxin (BMD) to digoxin (DIG) for the pooled available data from all subjects, oral and intravenous. The left inset shows the extrapolated regression line of best fit. The right inset is for the BMD/DIG range of 0–10 fitted separately. The dark symbols are for the data from Subject A, 0.6 mg po of β-methyldigoxin, which were excluded in fitting the shown regression line.*

It is also possible that the radiolabeled β-methyldigoxin metabolites or digoxin metabolites were monitored in the plasma by the liquid scintillation spectrometry but did not respond to the radioimmunoassay. However, studies on the TLC-separated β-methyldigoxin and digoxin from plasma did not show any significant amounts of other metabolites in plasma (7, 8).

Relative Potencies of β-Methyldigoxin and Digoxin in Several Plasma Assays after β-Methyldigoxin Administration—Total radioactivity (LSC) in a plasma aliquot can be expressed as the linear sum of the individual radioactivities of labeled β-methyldigoxin and digoxin:

$$\text{LSC} = m_L\text{BMD} + b_L\text{DIG} \qquad \text{(Eq. 3)}$$

where m_L and b_L reflect the relative potencies of β-methyldigoxin and digoxin, respectively, in the liquid scintillation spectrometric assay. The "total antigenicity" by the radioimmunoassay also can be expressed as a similar linear sum (Eq. 2) of the partial antigenicities.

Equation 3 can be rearranged to:

$$\text{LSC/DIG} = m_L\text{BMD/DIG} + b_L \qquad \text{(Eq. 4)}$$

and typical plots of one ratio against the other are given in Fig. 2 and for the pooled data in Fig. 3. Statistical evaluations of the regressions for the available studies are given in Table IV. As anticipated, the parameters m_L and b_L were not significantly different from unity, and the contributions of digoxin and β-methyldigoxin to the total radioactivity were equivalent except for b_L for Subject A at the 0.6-mg po dose. The anomalous discrepancy in this intercept is obvious from the plotted solid symbols in Fig. 3, where the regression line was fitted to the pooled data with the data from this particular study excluded. There were no significant differences between the parameters for β-methyldigoxin (Table IV). Plots of LSC/BMD *versus* DIG/BMD gave similar information; the intercepts, m_L, were unity in all studies.

Similarly, Eq. 2 can be rearranged to:

$$\text{RIA/DIG} = m_R\text{BMD/DIG} + b_R \qquad \text{(Eq. 5)}$$

Table IV—Typical Linear Regressions of Ratios of Plasma Concentrations of Glycosides by Liquid Scintillation Spectrometry (LSC) and by Radioimmunoassay (RIA) to Plasma Digoxin Concentration (DIG) against the Ratios of Concentrations of β-Methyldigoxin (BMD) to Digoxin (DIG) in Human Plasma: LSC/DIG = m_LBMD/DIG + b_L; RIA/DIG = m_RBMD/DIG + b_R

Subject	Dose, mg	Mode of Administration	Range, BMD/DIG	n^a	$m_L \pm SE$	$b_L \pm SE$	$r_L{}^b$	$m_R{}^c \pm SE$	$b_R \pm SE$	$r_R{}^b$
A	0.6	Intravenous	1.4–23	11	0.930 ± 0.052	1.12 ± 0.73	0.986	0.870 ± 0.035 (0.80–0.90)	1.31 ± 0.49	0.994
A	0.6	Oral	5–165	9	0.999 ± 0.009	3.30 ± 0.71	1.000	0.871 ± 0.054 (0.60–0.90)	0.75 ± 3.0	0.989
B	0.6	Intravenous	1.9–95	11	1.050 ± 0.006	1.32 ± 0.20	1.000	0.706 ± 0.018 (0.70)	1.62 ± 0.62	0.997
C	0.3	Oral	2.8–21	7	1.013 ± 0.032	1.16 ± 0.30	0.998	0.649 ± 0.036 (0.67)	2.3 ± 0.34	0.993
Pooled	0.3, 0.6	Oral, intravenous	1.4–165	49	1.012 ± 0.010	1.87 ± 0.36	0.998	0.829 ± 0.017	1.04 ± 0.52	0.991
Pooled[d]	0.3, 0.6	Oral, intravenous	1.4–165	40	1.016 ± 0.010	1.39 ± 0.39	0.998	0.716 ± 0.014	1.76 ± 0.30	0.994
Pooled[d]	0.3, 0.6	Oral, intravenous	1.4–10	26	1.052 ± 0.046	1.23 ± 0.23	0.978	0.825 ± 0.082	0.981 ± 0.41	0.903

[a] Numbers of pairs. [b] Respective correlation coefficients. [c] Parenthetical values are estimates of m_R from the intercepts of plots of RIA/BMD *versus* DIG/BMD. When given as a range, the initial data were too scattered by this plotting method to conclude anything other than that the value lay within this range. Similar plots of LSC/BMD *versus* DIG/BMD were conclusive of intercepts, m_R, of unity in all cases. [d] Data of Subject A at the 0.6-mg po doses were excluded because of an anomalous intercept, b_L.

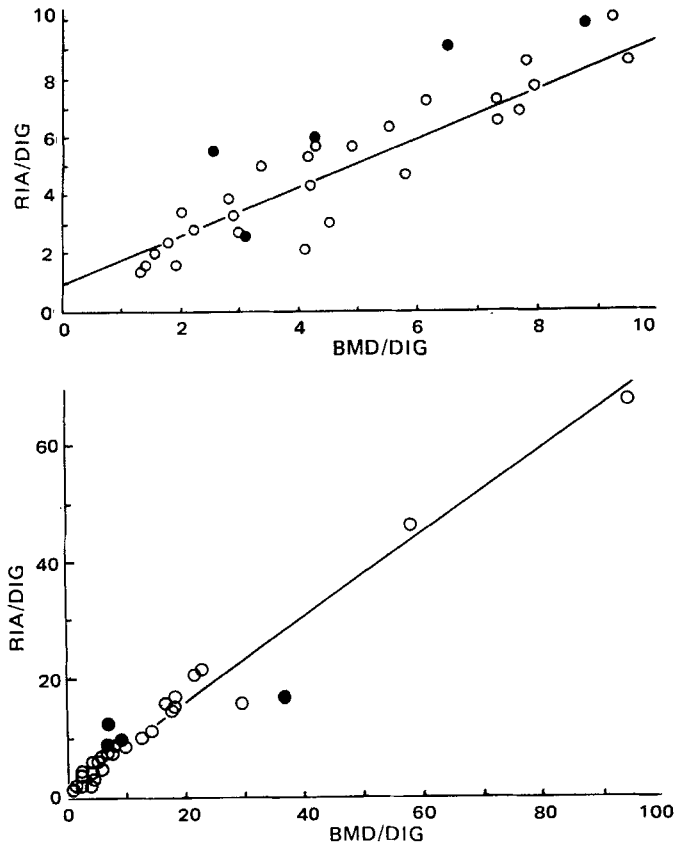

Figure 4—*Plots of the ratios of total glycoside plasma concentration by radioimmunoassay (RIA) to the plasma digoxin concentration (DIG) against the plasma concentration ratios of β-methyldigoxin (BMD) to digoxin (DIG) for the pooled available data from all subjects, oral and intravenous. The dark symbols are for the data from Subject A, 0.6 mg po of β-methyldigoxin, which were excluded in fitting the shown regression lines. Both ranges were fitted separately.*

and plots of the pooled data over several BMD/DIG ranges are given in Fig. 4. The regression lines were fitted for the particular ranges given where the anomalous data of Subject A at the 0.6-mg po dose were excluded. The statistical evaluations of the regressions for the pooled data over several ranges and for the available specific studies are given in Table IV. There were no significant differences among the various intercepts, b_R, which were not significantly different from unity. This result was a measure of the individual "antigenicity" of digoxin in the assay and was anticipated since the radioimmunoassay was calibrated for digoxin. However, individual m_R values, measures of antigenic potency of β-methyldigoxin in the assay, were significantly different for the separate studies. This finding was consistent with the previously discussed results for the regressions of RIA *versus* LSC (Table II).

The m_R values were significantly less than unity for the separate studies and for the pooled data of all available studies, consistent with the fact that the specific antigenicity of β-methyldigoxin was less than that of digoxin (Table III). The separate regressions for different ranges of β-methyldigoxin to digoxin ratios, BMD/DIG, showed significantly different slopes when the anomalous oral study for Subject A was excluded. The slope, 0.72 ± 0.014, for the longer range (1.4–165) or higher relative β-methyldigoxin concentrations was significantly less than the m_R = 0.03 ± 0.08 for the shorter range (1.4–10), indicative of higher specific potency for β-methyldigoxin in the presence of relatively large amounts of digoxin. This finding tends to confirm the previously stated possibility that the presence of one glycoside may modify the radioimmunoassay response of the other. Similar values for m_R were obtained (Table III) from the intercepts of RIA/BMD plots against DIG/BMD.

In summary, it can be stated that an *a priori* assumption of radioimmunoassay equivalency of glycosides with their derivatives and their cardioactive metabolites is unwarranted. The fundamental basis of a radioimmunoassay demands a competition for binding sites, and minor functional changes in a molecule can affect the binding constants. An assumption that the specific potency of an agonist in the presence of others is not modified by changes in their relative concentration is also unwarranted. These factors are further perturbed by interactions peculiar to an individual plasma.

REFERENCES

(1) V. P. Butler and J. P. Chen, *Proc. Nat. Acad. Sci. USA*, **57**, 71 (1967).

(2) R. G. Stoll, M. S. Christensen, E. Sakmar, D. Blair, and J. G. Wagner, *Commun. Chem. Pathol. Pharmacol.*, **4**, 503 (1972).

(3) D. Larbig and K. Kochsiek, *Dtsch. Med. Wochenschr.*, **97**, 1310 (1972).

(4) G. Härtel, V. Manninen, J. Melin, and A. Apajalahti, *Ann. Clin. Res.*, **5**, 87 (1973).

(5) J. M. Kaufman and F. M. Belpaire, *Eur. J. Clin. Pharmacol.*, **6**, 54 (1973).

(6) A. Kroneberg, *Arch. Exp. Pathol. Pharmakol.*, **237**, 222 (1959).

(7) P. H. Hinderling, E. R. Garrett, and R. C. Wester, *J. Pharm. Sci.*, **66**, 242 (1977).

(8) *Ibid.*, **66**, 314 (1977).

(9) H. Rennekamp, A. Rennekamp, U. Abshagen, K. V. Bergman, and N. Rietbrock, *Naunyn-Schmiedeberg's Arch. Pharmacol.*, **272**, 454 (1972).

(10) P. H. Hinderling and E. R. Garrett, *J. Pharm. Sci.*, **66**, 326 (1977).

(11) E. Cerceo and C. A. Elloso, *Clin. Chem.*, **18**, 539 (1972).

(12) P. R. Klink, R. I. Poust, J. L. Colaizzi, and R. H. McDonald, *J. Pharm. Sci.*, **63**, 1231 (1974).

ACKNOWLEDGMENTS AND ADDRESSES

Received January 12, 1976, from *The Beehive, College of Pharmacy, University of Florida, Gainesville, FL 32610.*

Accepted for publication July 23, 1976.

Supported in part by Grant NIH-RR-82 from the National Institutes of Health, Bethesda, Md., and by an unrestricted grant from Searle Laboratories, Skokie, Ill.

The authors thank R. Tilden and F. Deland of the Department of Nuclear Medicine, Veterans Administration Hospital, and the College of Medicine, University of Florida, for the performance of the radioimmunoassays.

* Present address: Department of Pharmacology, Der Universität Basel, Klingelbergstrasse 70, CH-4056 Basel, Switzerland.

ˣ To whom inquiries should be directed.

UV Spectrophotometric Determination of Aminophylline, Amobarbital, and Ephedrine Hydrochloride in an Antiasthma Capsule Preparation

FABRIZIO De FABRIZIO

Abstract □ A simple and rapid procedure for the determination of aminophylline, amobarbital, and ephedrine hydrochloride in a capsule preparation is described. Aminophylline and amobarbital are determined simultaneously using differential UV spectrophotometry; ephedrine hydrochloride is determined separately after elution from an alginic acid column with 0.1 *N* hydrochloric acid.

Keyphrases □ Aminophylline—UV spectrophotometric analysis, commercial capsule in combination with amobarbital and ephedrine hydrochloride □ Amobarbital—UV spectrophotometric analysis, commercial capsule in combination with aminophylline and ephedrine hydrochloride □ Ephedrine hydrochloride—UV spectrophotometric analysis, commercial capsule in combination with aminophylline and amobarbital □ UV spectrophotometry—analyses, aminophylline, amobarbital, and ephedrine hydrochloride in combination commercial capsule

The combination of aminophylline, ephedrine hydrochloride, and barbituric acid derivatives is frequently encountered in commercial and clinical preparations and in research situations. Procedures for the determination of these active ingredients alone or in combination in tablets, capsules, or syrups include gravimetric (1), titrimetric (2), spectrophotometric (3, 4), GLC (5), and IR (6) measurements.

The National Formulary (7) describes a method for the analysis of theophylline, phenobarbital, and ephedrine hydrochloride in a tablet formulation; the active components are separated using column partition chromatography and liquid–liquid extraction, followed by UV spectrophotometric determination of the isolated ingredients. However, this NF procedure is tedious and requires much care to obtain good results; the various steps are the largest sources of both systematic and random errors. Therefore, this work was planned to propose a uniform methodology that would reduce sample manipulation.

EXPERIMENTAL

Apparatus—A recording spectrophotometer[1] with matched 1- and 4-cm cells was used. The glass column was 50 × 2 cm and had a fine regulatory needle valve stopcock with a polytef insert[2].

Reagents—The following were used: alginic acid[3] cation-exchange resin, 40–100 mesh; 2 *N* hydrochloric acid in water; 0.1 *N* hydrochloric acid in water; 0.02 *N* sodium hydroxide in water; 50% ethanol in water; and 50% ethanol in 4% (v/v) acetic acid.

Standard Solutions—The following were used: ephedrine hydrochloride, 0.136 mg/ml in 0.1 *N* hydrochloric acid; aminophylline, 0.7 mg/ml in 50% ethanol in 0.4% (v/v) acetic acid; and amobarbital, 0.136 mg/ml in 50% ethanol in 0.4% (v/v) acetic acid. All standards were USP XVI, NF XIII, or BP 1973 quality[4].

Column Preparation—A slurry of about 4 g of alginic acid, previously soaked in water for 4 hr, was transferred to a chromatographic column and allowed to settle. The column was eluted with 2 *N* hydrochloric acid until the eluate gave an absorbance less than 0.005 between 230 and 330 nm. It was then washed with distilled water until the eluate was neutral to the litmus solution. Finally, a small pledget of glass wool was added to the column. After 20 ml of 50% ethanol in water was passed through the column, alginic acid was slightly tamped.

Sample Treatment—The average weight of not less than 20 capsules[5] was determined. An accurately weighed portion of powder, equivalent to about 67 mg of ephedrine hydrochloride, was transferred to a 50-ml volumetric flask, and 50% ethanol–acetic acid solution was added to the mark. A magnetic stirring bar was slipped into the flask, and the mixture was stirred for 10 min and then centrifuged for 2 min.

Determination—*Aminophylline and Amobarbital*—Pipet a 10-ml aliquot of the centrifuged sample onto the prepared alginic acid column. Place a 100-ml volumetric flask beneath the column and start collecting the eluate at a rate of 1 ml/min. Then add 50 ml of 50% ethanol (in water) in small portions, letting each drain through the column before successive additions. Remove the flask and dilute to volume with the same solvent. This solution contains aminophylline and amobarbital.

Transfer a 2-ml aliquot of the solution into each of two 50-ml volumetric flasks. Adjust the solution in one flask to pH 4 and the other to pH 10 by adding 0.02 *N* sodium hydroxide; then dilute to 50 ml with distilled water. Using the pH 4 solution as the reference and the pH 10 solution in the sample position, measure the absorbance at 285.5 and 240 nm (1-cm cells). Calculate the concentration of aminophylline and amobarbital in the tablets by determining the absorptivities at 285.5 and

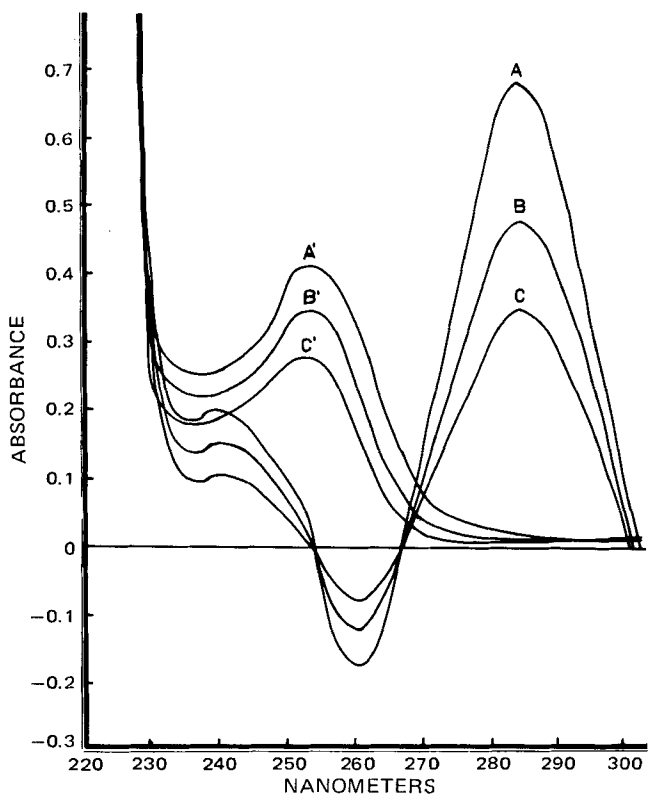

Figure 1—*Differential spectra of aminophylline (A, B, and C) and amobarbital (A′, B′, and C′).*

[1] Beckman DB.
[2] Brand, West Germany.
[3] British Drug Houses.
[4] E. Merck, Darmstadt, Germany.

[5] Capsules contained 130 mg of aminophylline, 25 mg of amobarbital, and 25 mg of ephedrine hydrochloride and are marketed as Emelasma.

Table I—Recovery of Aminophylline, Amobarbital, and Ephedrine Hydrochloride from Synthetic Mixtures in the Presence of an Excipient

Mixture	Aminophylline		Amobarbital		Ephedrine Hydrochloride	
	Added, mg	Recovery, %	Added, mg	Recovery, %	Added, mg	Recovery, %
1	351.0	97.9	67.5	101.3	68.3	98.7
2	349.5	98.6	68.0	99.2	67.5	100.0
3	350.3	98.0	67.9	98.8	67.3	99.0
4	349.4	99.3	66.8	97.9	67.0	98.4
5	349.9	99.1	67.5	98.2	67.4	98.8
6	350.7	97.5	69.3	99.6	66.5	98.7
7	348.8	99.7	67.3	98.1	67.4	99.6
8	348.7	98.2	66.9	98.8	68.0	98.3
9	347.2	98.6	66.9	97.9	66.9	98.7
10	350.2	98.6	67.4	98.5	67.1	98.5
Average, %		98.9		98.5		98.8
SD, %		±0.49		±0.44		±1.11

240 nm of both aminophylline and amobarbital standard solutions, taken individually, diluted as the sample, and adjusted to pH 4 (blank) and 10 (sample).

Ephedrine Hydrochloride—Wash the column with 20 ml of distilled water divided into two portions. Elute the column with 0.1 *N* hydrochloric acid at a rate of 2 ml/min, discarding the first 7 ml of the liquid. Collect the eluate in a volumetric flask to the 100-ml mark. Scan the sample and standard solutions between 330 and 230 nm, using 4-cm cells, against 0.1 *N* hydrochloric acid as the reference. Determine the absorptivity at the maximum (about 257 nm) for the ephedrine hydrochloride standard and calculate its concentration in the sample solution.

RESULTS AND DISCUSSION

A prepared column containing alginic acid retained ephedrine hydrochloride from an ethanolic solution and allowed aminophylline and amobarbital to pass through as washings. Subsequently, ephedrine hydrochloride was eluted with 0.1 *N* hydrochloric acid and determined spectrophotometrically at 257 nm. Aminophylline and amobarbital were volumetrically collected and quantitatively determined by UV differential spectrophotometry at 240 (maximum for amobarbital) and 285.5 (maximum for aminophylline) nm, using two aliquots of the same solution as the blank and sample at pH 4 and 10, respectively.

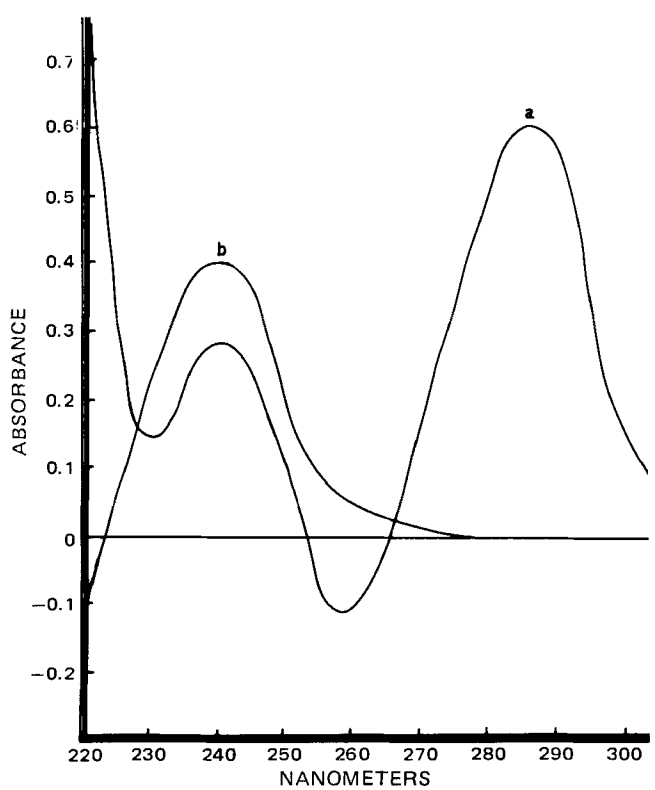

Figure 2—*Differential absorption spectra of aminophylline (a) and amobarbital (b) at pH 10.*

Synthetic mixtures of the three active ingredients in the presence of an excipient (light magnesium carbonate) were prepared and assayed by this method including the chromatographic step. Recovery results are given in Table I; analyses of commercial samples are reported in Table II.

The determination of aminophylline and amobarbital represented the main problem. An algebraic method for additive absorbances was not applicable, since the weight ratio of aminophylline to amobarbital was about 5:1. Therefore, the pH–chromophoric properties of the two compounds had to be considered. Both aminophylline and amobarbital are organic acids and have hydrogen atoms that can be ionized in alkaline media. When their absorption spectra are determined at different pH values that include molecular and ionic forms, isosbestic points are observed frequently. To find an eventual isosbestic point that might be employed as the baseline, differential absorption spectra of individually prepared solutions of aminophylline and amobarbital between pH 10 and 13 were examined.

A series of aminophylline solutions at pH 10, 11, 12, and 13 (using the same solutions at pH 4 as reference) showed two maxima at 240 and 285.5 nm and two isosbestic points at 253.5 and 263 nm. The differential curves determined at pH 11, 12, and 13 did not exhibit a significant change over those taken at pH 10, as would be expected from the pK value of aminophylline. When differential absorption spectra of amobarbital solutions were prepared following the same procedure, a gradual shift of the absorption maxima from 240 to about 254 nm was observed as the pH was increased from 10 to 13. Particular attention was focused on the absorption curves taken at pH 13, where the correlation between the isosbestic point at 253.5 nm for aminophylline and the maximum for amobarbital and the correspondence of the maximum for aminophylline at 285.5 nm with an insignificant absorbance for amobarbital seemed to be the ideal setup for the quantitative determination of the ingredients in the presence of one another.

Figure 1 illustrates the differential absorption spectra at pH 13 of three concentrations of aminophylline and three concentrations of amobarbital. Each solution contained the active ingredient in the weight ratio similar to that of the commercial preparation. However, while both compounds followed the Lambert–Beer law individually, their mixtures, over the same concentration range, did not. When these mixtures were scanned

Table II—Analyses of Commercial Product

Product	Aminophylline Found, % of Claim (130 mg)	Amobarbital Found, % of Claim (25 mg)	Ephedrine Hydrochloride Found, % of Claim (25 mg)
A	97.6	99.3	100.8
B	98.1	98.3	99.5
C	97.9	97.4	98.2
D	98.8	99.9	97.4
E	101.2	97.9	102.1
F	99.6	97.3	98.9
G	97.8	98.0	99.7

Table III—Recovery of Aminophylline and Amobarbital Mixed Standard in 50% Ethanol in 4% (v/v) Acetic Acid[a]

Mixture	Aminophylline		Amobarbital	
	Amount Taken, mg	Recovery, %	Amount Taken, mg	Recovery, %
A	350.0	100.7	67.0	97.4
B	350.0	98.9	67.0	98.6
C	360.0	99.3	69.0	99.1
D	340.0	97.5	65.0	99.4
E	300.0	97.9	57.5	101.3
F	350.0	98.6	67.0	100.6
G	360.0	99.1	69.0	99.8
H	350.0	97.7	67.0	97.8
I	350.0	98.6	67.0	98.9
J	340.0	98.9	65.0	99.4
Average, %	—	98.7	—	99.2
SD, %		±0.92		±1.67

[a] Synthetic mixes were prepared by dissolving an accurately weighed amount of both compounds in 50% ethanol in 4% acetic acid in a 50-ml volumetric flask. Each mixture was treated and diluted as the sample, excluding the chromatographic step.

between 320 and 220 nm, the absorption curves showed that the maximum at 285.5 nm remained unchanged and that the maximum at 254 nm was absent. The absorption at 240 nm increased significantly in intensity with respect to that of aminophylline determined individually at the same concentration.

The cause of this deviation at pH 13 may have been that the keto–enolic equilibrium of the doubly ionized form of amobarbital with the absorption maximum at 254 nm was probably shifted by a much larger concentration of the enolized aminophylline to exhibit an absorption maximum at 240 nm (singly ionized form). To eliminate such a possible keto–enolic equilibrium effect, a new approach was followed. The differential absorption curves at pH 10, previously plotted for the separated compounds, showed that aminophylline and amobarbital exhibited fairly strong maxima at about 240 nm and that there was a wide variation between the intensities of absorption of both components at 285.5 nm. Figure 2 shows the differential absorption spectra at pH 10 of aminophylline and amobarbital. These conditions seemed to be theoretically adequate for the quantitative determination of mixtures of aminophylline and amobarbital (8).

This hypothesis was verified experimentally when mixtures of the two substances, analyzed at pH 10, gave a positive response. The results in Table III show that the procedure is both accurate and precise. Compared to the NF procedure, the proposed method significantly shortens the time required for the analysis of aminophylline, amobarbital, and ephedrine hydrochloride, thus making possible the quantitative determination of more samples per day.

REFERENCES

(1) "British Pharmacopoeia," Pharmaceutical Press, London, England, 1973, p. 32.

(2) "The National Formulary," 13th ed., Mack Publishing Co., Easton, Pa., 1970, pp. 266, 267.

(3) R. J. Hyatt, *J. Assoc. Offic. Agr. Chem.*, **38**, 624 (1955).

(4) *Ibid.*, **36**, 673 (1954).

(5) C. G. Cunninghan and S. Barkan, *J. Assoc. Offic. Anal. Chem.*, **58**, 525 (1975).

(6) G. B. Pleat, J. H. Harley, and S. E. Wiberley, *J. Am. Pharm. Assoc., Sci. Ed.*, **40**, 107 (1951).

(7) "The National Formulary," 13th ed., Mack Publishing Co., Easton, Pa., 1970, pp. 695, 696.

(8) A. E. Gillam, "Electronic Absorption Spectroscopy," 2nd ed., Edward Arnold, London, England, 1962, p. 214.

ACKNOWLEDGMENTS AND ADDRESSES

Received October 14, 1975, from *Saphar Laboratories (PTY) Ltd., P.O. Box 2368, Industria West, Johannesburg, South Africa.*

Accepted for publication August 5, 1976.

Liquid Chromatography in Pharmaceutical Analysis VIII: Determination of Isoniazid and Acetyl Derivative in Plasma and Urine Samples

S. J. SAXENA, J. T. STEWART, I. L. HONIGBERG ˣ, J. G. WASHINGTON, and G. R. KEENE

Abstract □ Parameters are described for the qualitative and quantitative analysis of a mixture of isoniazid and its acetyl derivative. The compounds are chromatographed on an octadecylsilane column, using absolute methanol–distilled water (60:40) at pH 2.5 containing 0.01 *M* dioctyl sodium sulfosuccinate. The flow rate was 2.0 ml/min (2500 psig). The separation and quantification are applicable to plasma and urine samples. The determination in each biological fluid can be achieved in approximately 90 min with percentage accuracies for isoniazid of 5.25 and 7.45 and for the acetyl derivative of 4.47 and 1.56 in plasma and urine, respectively.

Keyphrases □ Isoniazid and acetyl derivative—high-pressure liquid chromatographic analyses, plasma and urine □ High-pressure liquid chromatography—analyses, isoniazid and acetyl derivative, plasma and urine □ Tuberculostatic antibacterials—isoniazid and acetyl derivative, high-pressure liquid chromatographic analyses, plasma and urine

Interest in high-pressure liquid chromatography (HPLC) for the determination of drugs and their metabolites in biological media led to the analysis of isoniazid (I) and its major metabolite, the acetyl derivative (II). Presently, I is very effective as an antituberculosis drug, and the determination of I and II is important in studies related to I disposition and metabolism. A review of analytical methodology concerning I and its metabolites is available (1).

This paper reports the HPLC separation of I and II and the application of the procedure to the quantification of these compounds in plasma and urine. The HPLC separation is effected utilizing ion-pair formation with dioctyl sodium sulfosuccinate on an octadecylsilane column. Generalities of ion-pair formation were reviewed extensively (2, 3). Some investigators (4–6) used ion-pair formation as a tool for effecting chromatographic analysis of selected organic ions. The mechanism for such a separation apparently depends upon the reversible formation of ion-pairs in the chromatographic system and the separa-

Table III—Recovery of Aminophylline and Amobarbital Mixed Standard in 50% Ethanol in 4% (v/v) Acetic Acid[a]

Mixture	Aminophylline		Amobarbital	
	Amount Taken, mg	Recovery, %	Amount Taken, mg	Recovery, %
A	350.0	100.7	67.0	97.4
B	350.0	98.9	67.0	98.6
C	360.0	99.3	69.0	99.1
D	340.0	97.5	65.0	99.4
E	300.0	97.9	57.5	101.3
F	350.0	98.6	67.0	100.6
G	360.0	99.1	69.0	99.8
H	350.0	97.7	67.0	97.8
I	350.0	98.6	67.0	98.9
J	340.0	98.9	65.0	99.4
Average, %	—	98.7	—	99.2
SD, %		±0.92		±1.67

[a] Synthetic mixes were prepared by dissolving an accurately weighed amount of both compounds in 50% ethanol in 4% acetic acid in a 50-ml volumetric flask. Each mixture was treated and diluted as the sample, excluding the chromatographic step.

between 320 and 220 nm, the absorption curves showed that the maximum at 285.5 nm remained unchanged and that the maximum at 254 nm was absent. The absorption at 240 nm increased significantly in intensity with respect to that of aminophylline determined individually at the same concentration.

The cause of this deviation at pH 13 may have been that the keto–enolic equilibrium of the doubly ionized form of amobarbital with the absorption maximum at 254 nm was probably shifted by a much larger concentration of the enolized aminophylline to exhibit an absorption maximum at 240 nm (singly ionized form). To eliminate such a possible keto–enolic equilibrium effect, a new approach was followed. The differential absorption curves at pH 10, previously plotted for the separated compounds, showed that aminophylline and amobarbital exhibited fairly strong maxima at about 240 nm and that there was a wide variation between the intensities of absorption of both components at 285.5 nm. Figure 2 shows the differential absorption spectra at pH 10 of aminophylline and amobarbital. These conditions seemed to be theoretically adequate for the quantitative determination of mixtures of aminophylline and amobarbital (8).

This hypothesis was verified experimentally when mixtures of the two substances, analyzed at pH 10, gave a positive response. The results in Table III show that the procedure is both accurate and precise. Compared to the NF procedure, the proposed method significantly shortens the time required for the analysis of aminophylline, amobarbital, and ephedrine hydrochloride, thus making possible the quantitative determination of more samples per day.

REFERENCES

(1) "British Pharmacopoeia," Pharmaceutical Press, London, England, 1973, p. 32.

(2) "The National Formulary," 13th ed., Mack Publishing Co., Easton, Pa., 1970, pp. 266, 267.

(3) R. J. Hyatt, *J. Assoc. Offic. Agr. Chem.*, **38**, 624 (1955).

(4) *Ibid.*, **36**, 673 (1954).

(5) C. G. Cunninghan and S. Barkan, *J. Assoc. Offic. Anal. Chem.*, **58**, 525 (1975).

(6) G. B. Pleat, J. H. Harley, and S. E. Wiberley, *J. Am. Pharm. Assoc., Sci. Ed.*, **40**, 107 (1951).

(7) "The National Formulary," 13th ed., Mack Publishing Co., Easton, Pa., 1970, pp. 695, 696.

(8) A. E. Gillam, "Electronic Absorption Spectroscopy," 2nd ed., Edward Arnold, London, England, 1962, p. 214.

ACKNOWLEDGMENTS AND ADDRESSES

Received October 14, 1975, from *Saphar Laboratories (PTY) Ltd., P.O. Box 2368, Industria West, Johannesburg, South Africa.*

Accepted for publication August 5, 1976.

Liquid Chromatography in Pharmaceutical Analysis VIII: Determination of Isoniazid and Acetyl Derivative in Plasma and Urine Samples

S. J. SAXENA, J. T. STEWART, I. L. HONIGBERG ˣ, J. G. WASHINGTON, and G. R. KEENE

Abstract □ Parameters are described for the qualitative and quantitative analysis of a mixture of isoniazid and its acetyl derivative. The compounds are chromatographed on an octadecylsilane column, using absolute methanol–distilled water (60:40) at pH 2.5 containing 0.01 *M* dioctyl sodium sulfosuccinate. The flow rate was 2.0 ml/min (2500 psig). The separation and quantification are applicable to plasma and urine samples. The determination in each biological fluid can be achieved in approximately 90 min with percentage accuracies for isoniazid of 5.25 and 7.45 and for the acetyl derivative of 4.47 and 1.56 in plasma and urine, respectively.

Keyphrases □ Isoniazid and acetyl derivative—high-pressure liquid chromatographic analyses, plasma and urine □ High-pressure liquid chromatography—analyses, isoniazid and acetyl derivative, plasma and urine □ Tuberculostatic antibacterials—isoniazid and acetyl derivative, high-pressure liquid chromatographic analyses, plasma and urine

Interest in high-pressure liquid chromatography (HPLC) for the determination of drugs and their metabolites in biological media led to the analysis of isoniazid (I) and its major metabolite, the acetyl derivative (II). Presently, I is very effective as an antituberculosis drug, and the determination of I and II is important in studies related to I disposition and metabolism. A review of analytical methodology concerning I and its metabolites is available (1).

This paper reports the HPLC separation of I and II and the application of the procedure to the quantification of these compounds in plasma and urine. The HPLC separation is effected utilizing ion-pair formation with dioctyl sodium sulfosuccinate on an octadecylsilane column. Generalities of ion-pair formation were reviewed extensively (2, 3). Some investigators (4–6) used ion-pair formation as a tool for effecting chromatographic analysis of selected organic ions. The mechanism for such a separation apparently depends upon the reversible formation of ion-pairs in the chromatographic system and the separa-

Table I—Calibration Data for Standard Drug Solutions

Compound	Initial Concentration, μg/ml[a]	D/IS Ratio[b]	Slope	Intercept	$r \pm s_{yx}$[c]
For plasma levels:					
I	10.0	0.2046 ± 0.0298[d]	0.0055	−0.0395	0.9873
	15.0	0.4248 ± 0.2268			±0.0326
	20.0	0.4858 ± 0.1166			
	30.0	0.7945 ± 0.0926			
II	13.3	0.2291 ± 0.0043	0.0041	0.0214	0.9999
	20.0	0.3332 ± 0.0096			±0.0019
	26.6	0.4321 ± 0.0096			
	40.0	0.6510 ± 0.0149			
For urine levels:					
I	60.0	0.2893 ± 0.0955	0.0009	0.0181	0.9970
	80.0	0.3841 ± 0.0530			±0.0112
	120.0	0.5748 ± 0.0585			
	140.0	0.6470 ± 0.1095			
II	186.6	0.7388 ± 0.0122	0.00089	0.1294	0.9977
	266.6	1.0425 ± 0.0000			±0.0157
	320.0	1.2086 ± 0.0342			
	373.3	1.3629 ± 0.0285			

[a] Based on a typical 3-ml biological sample. [b] Data represent three replicate injections of calibration solutions; D/IS is the ratio of the integrated area of the drug at some concentration divided by the integrated area of the internal standard. [c] The r is the correlation coefficient determined from linear regression analysis, and s_{yx} is the standard error of the estimated concentration. [d] Confidence limits at $p = 0.05$.

tion of the constituents on the basis of differences in the lipophilicity of the ion-pairs formed.

The analysis of an isoniazid–pyridoxine hydrochloride dosage form, using ion-pair formation with dioctyl sodium sulfosuccinate, was recently reported (7). The chromatographic separation described herein takes approximately 10 min. The overall analysis time is approximately 90 min, which includes extraction of the drug and metabolite from the biological fluid (8) followed by HPLC separation and quantification.

EXPERIMENTAL[1]

Reagents and Chemicals—Powdered samples of I[2] and II (9) were used in the analytical procedure, and dioctyl sodium sulfosuccinate[3] was used as a component of the mobile phase. All other chemicals and solvents were commercially available and were utilized as received.

Mobile Phase—The mobile phase, consisting of absolute methanol–distilled water (60:40), was prepared fresh daily. It was made 0.01 *M* with respect to dioctyl sodium sulfosuccinate (4.4 g/liter), and its pH was adjusted to 2.5 by dropwise addition of 2 *M* sulfuric acid (<1 ml).

Internal Standard Solution—The stock internal standard solution (8 mg/10 ml) was prepared by dissolving 1-benzoyl-2-isonicotinoylhydrazine in distilled water. The substituted hydrazine was originally synthesized by Kerr *et al.* (10). It was recrystallized from water (mp 232–234°) before use.

Standard Solutions for Calibration Curves—Stock solutions of I (6 mg/10 ml) and II (8 mg/10 ml) were prepared by dissolving weighed amounts of each powder in distilled water.

Determination of Calibration Curve—*For Plasma Levels*—Into individual 60-ml separators were placed accurately pipetted volumes[4] of 0.050, 0.075, 0.100, and 0.150 ml of both I and II standard solutions. A 0.200-ml volume of the internal standard solution was added to each separator, and the volume of each solution was adjusted to 6 ml with distilled water. Then 1 ml of 0.1 *N* sodium hydroxide solution and solid ammonium sulfate, about 1 g/ml of aqueous solution, were added. The latter was added in small portions to each solution followed by gentle shaking for 5 min. Each solution was then shaken for 5 min with 40 ml of water-saturated 1-butanol–chloroform (30:70).

The layers were allowed to separate, and 30 ml of the organic layer (bottom) from each separator was transferred to clean 45-ml stoppered conical centrifuge tubes. Four milliliters of 0.1 *N* sulfuric acid was added to each tube, and the contents were shaken for 5 min. The layers were allowed to separate, with centrifugation if necessary, and a 40-μl aliquot of the acidic layer (top) was injected into the liquid chromatograph. The concentrations of both I and II were subjected to a linear regression analysis, and the slope and intercept for each component were calculated (Table I).

For Urine Levels—Into individual 60-ml separators were placed the following accurately pipetted volumes of I and II standard solutions, respectively: 0.300 and 0.700 ml, 0.400 and 1.000 ml, 0.600 and 1.20 ml, and 0.700 and 1.40 ml. A 0.800-ml quantity of the internal standard solution was added to each separator, and the volume of each mixture was adjusted to 6 ml with distilled water. The solutions were then treated in the same manner as described for plasma levels.

Determination of I and II in Human Plasma and Urine—To 3.0 ml of human plasma in a 60-ml separator were added accurately pipetted quantities of 0.100 ml of both I and II standard solutions and 0.200 ml of the internal standard solution. To 3.0 ml of human urine in another separator were added 0.400 and 0.900 ml of I and II solutions, respectively, along with 0.800 ml of the internal standard solution. Each plasma and urine sample was then treated in the same manner as described for the standard solutions. Control blanks for each biological fluid were also included. Replicate 40-μl injections were made for each sample.

Chromatographic Separation and Quantification—The degassed mobile phase was pumped through an octadecylsilane column[5] at a flow rate of 2.0 ml/min (2500 psig) at room temperature until a stable baseline was obtained. Replicate 40-μl injections of sample and standard solutions were made using a 100-μl syringe[6]. The wavelength of the UV detector was set at 266 nm. The chart recorder provided a record of drug elution from the column as peaks on a chromatogram. In all cases, the solute was measured by digital integration of the peak area[1].

RESULTS AND DISCUSSION

The analysis of the I–II mixture and the application to plasma and urine extracts necessitated the examination of three separate problems: (*a*) the development of a set of HPLC operating parameters that would separate the two compounds without peak overlap, (*b*) the detection and quantification of each compound at the level found in biological fluids, and (*c*) the contribution of extracted plasma and urine blanks to the chromatograms.

Initially, the separation was achieved on a cation-exchange column using aqueous 0.01 *M* ammonium acetate (pH 3.5) as the mobile phase. However, this procedure was rejected due to the lack of reproducible

[1] A Waters Associates liquid chromatograph (model ALC/GPC 201), equipped with an M-6000 pump, a Perkin-Elmer model LC-55 variable wavelength UV–visible detector, an Infotronics integrator (model CRS-204) with digital printout, and a Waters packed column, 4 mm i.d. × 30 cm, was used.

[2] Matheson, Coleman and Bell, East Rutherford, N.J.

[3] Sigma Chemical Co., St. Louis, Mo.

[4] Volumes of standard drug solutions of ≤1.0 ml added to plasma and urine samples were pipetted using Eppendorf pipets (Brinkmann Instruments, Westbury, N.Y.). Quantities >1 ml were delivered using Class A graduated volumetric pipets.

[5] Micro-Bondapak/C_{18}, <10 μm, Waters Associates, Milford, Mass.

[6] Model B-110, Precision Sampling Corp., Baton Rouge, La.

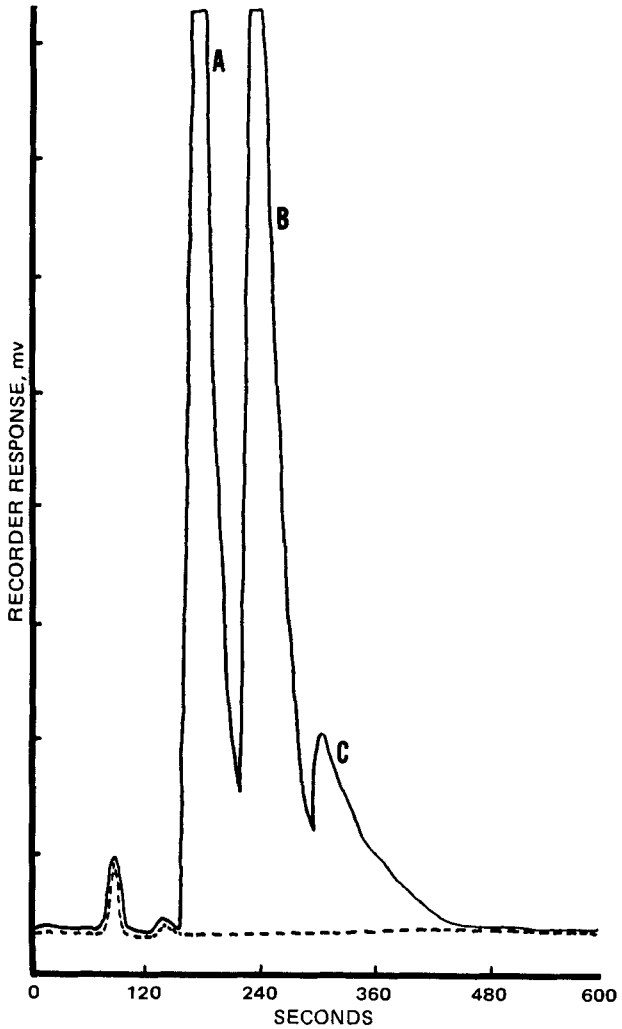

Figure 1—*Liquid chromatogram of I and II in plasma extract on octadecylsilane column using absolute methanol–distilled water (60:40) at pH 2.5 with 0.01* M *dioctyl sodium sulfosuccinate. Key: - - -, blank plasma extract; —, plasma extract containing drug and metabolite; A, II; B, 1-benzoyl-2-isonicotinoylhydrazine; and C, I.*

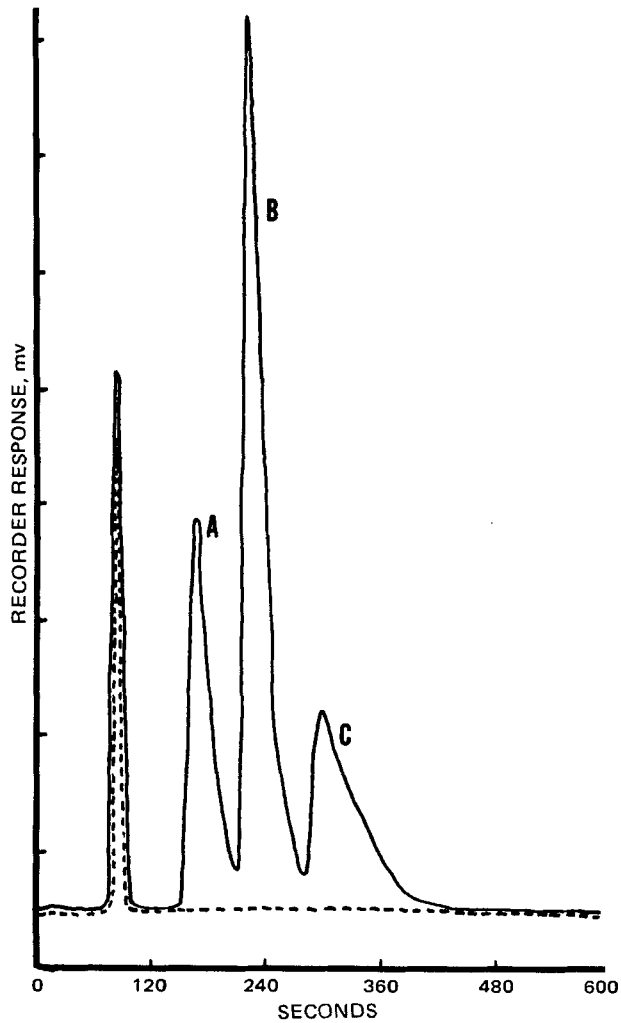

Figure 2—*Liquid chromatogram of I and II in urine extract on octadecylsilane column using absolute methanol–distilled water (60:40) at pH 2.5 with 0.01* M *dioctyl sodium sulfosuccinate. Key: - - -, blank urine extract; —, urine extract containing drug and metabolite; A, II; B, 1-benzoyl-2-isonicotinoylhydrazine; and C, I.*

resolution of the compounds from different batches of resin from the same supplier and due to a loss in resolution of I and II from plasma and urine extracts.

Attempts to separate I and II using conventional reversed-phase chromatography were also unsuccessful. Studies showed that the compounds were most propitiously separated on an octadecylsilane column using absolute methanol–distilled water (60:40) at pH 2.5 with 0.01 *M* dioctyl sodium sulfosuccinate. The mobile phase had been successfully employed for the determination of a I–pyridoxine hydrochloride mixture (7) and was readily adaptable to the I–II problem. Adequate separation was achieved between I and II in this solvent mixture as evidenced by an approximate resolution (R_s) value of 2.0 (11). Furthermore, use of this mobile phase allowed 1-benzoyl-2-isonicotinoylhydrazine to be used as a suitable internal standard.

A flow rate of 2.0 ml/min (2500 psig at room temperature) was the most satisfactory, since separations could be obtained in less than 10 min. The void volume of the column was 2.8 ml. UV detection at 266 nm was employed, since both I and II give maximum absorption at this wavelength and the detector would therefore provide maximum sensitivity for the low concentration levels present in biological fluids.

The solutions used in the determination of the standard curves as well as the plasma and urine samples were extracted according to a literature procedure for I (8). To make the sample compatible with the mobile phase, the extraction method was slightly modified with the use of 0.1 *N* sulfuric acid in the reextraction step. The internal standard was added to the original samples prior to extraction to improve precision. The drug concentrations used in the preparation of the standard curves and biological samples were in the range of those reported for plasma and urine levels (1, 12). Minimum detectability of I and II utilizing the chromatographic procedure described herein was 200 and 50 ng, respectively.

Calibration curves for both plasma and urine levels of I and II were obtained as follows. Digital integration of the area under the curve for each peak on the chromatograms was performed. The ratios of I and II peak areas to the area of the internal standard were calculated for each chromatogram. A linear regression analysis of these data at the four concentrations of each component gave the slope, intercept, and correlation coefficient for the plasma and urine calibration curves (Table I).

The liquid chromatograms of I–II from the spiked plasma and urine samples are shown in Figs. 1 and 2. No interferences from blank plasma and urine samples were noted. The ratios of drug peak areas/internal standard peak areas (D/IS) were calculated for I and II. The constants (slope and intercept) shown in Table I for the linear regression equations were used to solve for drug concentration in each biological sample: [D/IS

Table II—Analysis of I and II in Plasma and Urine

Biological Fluid	Compound	Initial Concentration Added, μg/ml	Amount Found[a], μg/ml	Accuracy, %
Plasma	I	20.0	18.9 ± 2.51[b]	5.25
	II	26.6	25.41 ± 0.36	4.47
Urine	I	80.0	74.04 ± 1.65	7.45
	II	240.0	243.74 ± 2.15	1.56

[a] Based on three replicate determinations of each solution. [b] Confidence limits at $p = 0.05$.

= (slope × concentration) + intercept]. Calculations were performed on a programmable calculator[7].

The data in Table II demonstrate the utility of HPLC in the analysis of I and II in biological fluids at plasma and urine concentration levels.

REFERENCES

(1) H. G. Boxenbaum and S. Riegelman, *J. Pharm. Sci.*, **63**, 1191 (1974).

(2) R. Modin, *Acta Pharm. Suec.*, **9**, 157 (1972).

(3) B. A. Perrson, *ibid.*, **8**, 217 (1971).

(4) B. L. Karger and B. A. Perrson, *J. Chromatogr. Sci.*, **12**, 521 (1974).

(5) B. L. Karger, S. C. Su, S. Marchese, and B. A. Perrson, *ibid.*, **12**, 678 (1974).

(6) D. P. Wittmer, N. O. Nuessle, and W. G. Haney, *Anal. Chem.*, **47**, 1422 (1975).

(7) J. T. Stewart, I. L. Honigberg, J. P. Brant, W. A. Murray, J. L. Webb, and J. B. Smith, *J. Pharm. Sci.*, **65**, 1536 (1976).

(8) "Manual of Analytical Toxicology," I. Sunshine, Ed., Chemical Rubber Co., Cleveland, Ohio, 1971, pp. 191, 192.

(9) H. H. Fox and J. T. Gibas, *J. Org. Chem.*, **18**, 1375 (1953).

(10) V. N. Kerr, D. G. Ott, and F. N. Hayes, *J. Am. Chem. Soc.*, **82**, 186 (1960).

(11) B. L. Karger, L. R. Snyder, and C. Horvath, "An Introduction to Separation Science," Wiley, New York, N.Y., 1973, pp. 146–150.

(12) J. H. Peters, *Am. Rev. Resp. Dis.*, **81**, 485 (1960).

[7] Olivetti-Underwood Programma 101.

ACKNOWLEDGMENTS AND ADDRESSES

Received October 9, 1975, from the *Department of Medicinal Chemistry, School of Pharmacy, University of Georgia, Athens, GA 30602.*

Accepted for publication August 5, 1976.

Presented at the Pharmaceutical Control and Analysis Section, APhA Academy of Pharmaceutical Sciences, Atlanta meeting, November 1975.

[x] To whom inquiries should be directed.

In Vitro and *In Vivo* Considerations of a Novel Matrix-Controlled Bovine Progesterone-Releasing Intravaginal Device

V. W. WINKLER [x], S. BORODKIN, S. K. WEBEL, and J. T. MANNEBACH

Abstract □ An *in vitro* system measuring progesterone release from silicone matrixes into serum is described. Drug release followed a matrix-controlled diffusion model in which the cumulative quantity released was linear with the square root of time. A bovine intravaginal device, consisting of a steel coil coated on both sides with a progesterone silicone matrix, was used as an *in vivo* drug delivery system. *In vivo* drug release also was matrix controlled, with rates comparable to those obtained *in vitro*. However, lag times of 1.7 and 4.2 days before reaching the steady-state rate were obtained for the outer and inner surfaces, respectively. The combination of effects resulted in a pseudo-zero-order drug-releasing device in which cumulative drug released was linear with time for at least 16 days.

Keyphrases □ Progesterone—release from silicone matrixes, *in vitro* system compared to bovine intravaginal device *in vivo* □ Silicone matrixes—release of progesterone, *in vitro* system compared to bovine intravaginal device *in vivo* □ Drug delivery—progesterone from silicone matrixes, *in vitro* system compared to bovine intravaginal device *in vivo* □ Vaginal devices, bovine—progesterone in silicone matrix, compared to *in vitro* system □ Hormones—progesterone, release from silicone matrixes, *in vitro* system compared to bovine intravaginal device *in vivo*

Intravaginal devices coated with a progesterone silicone matrix were used successfully (1–3) to control the bovine estrus cycle and to synchronize estrus by regulating pituitary release of gonadotropic hormones. Estrus occurs at a predictable time upon removal of the device developed in these laboratories 9–21 days after intravaginal implantation. The drug release rate profile of this device is defined in this report through correlation of *in vitro* and *in vivo* studies.

EXPERIMENTAL

Matrix Preparation—Progesterone silicone matrixes at various drug concentrations were prepared by first mixing the required amount of micronized drug into silicone fluid 360[1] and then adding Silastic elastomer 382[1]. The mixture was blended for 30 min to ensure random distribution of drug before adding the polymerizing catalyst, stannous octanoate[1].

***In Vitro* Study**—Matrixes used in the *in vitro* studies were prepared by streaking the silicone drug mixture containing catalyst onto fiber glass cloth and allowing it to cure. A template was used to obtain a uniform thickness of 1.5 mm. The cured matrixes were cut accurately into 2 × 2-cm pieces, mounted onto stainless steel plates with medical adhesive[1], and allowed to dry for 48 hr.

Two types of *in vitro* experiments were performed. The first followed the release of progesterone as a function of time from a silicone matrix containing 6.75% drug. The second concerned the release rate as a function of drug concentration using 5, 7.5, and 10% progesterone in silicone matrixes. The 6.75% matrix was prepared from a different lot of silicone liquid and elastomer, restricting direct comparison of the two *in vitro* experiments.

In both experiments, a specified number of matrixes mounted on stainless steel were individually placed in 25 × 150-mm glass tubes. To each tube, 15 ml of sheep serum[2] and 2 drops of toluene were added to retard microbial growth. Each tube was capped with a rubber stopper, placed on a shaker, and incubated at 37°. Serum changes at the end of Days 1, 2, 3, 4, 7, 11, 15, and 18 for one set of matrixes were matched with serum changes at the end of Days 0.1, 0.2, 0.3, 0.7, 1, 1.3, 2, 2.3, 3, 4, 5, 8, 12, 15, 18, and 20 for a duplicate set of matrixes.

The progesterone released in selected mounted matrixes was determined at various scheduled times by analyzing the amount of drug re-

[1] Dow Corning Corp., Midland, MI 48640.

[2] International Scientific Industries, Cary, IL 60013.

= (slope × concentration) + intercept]. Calculations were performed on a programmable calculator[7].

The data in Table II demonstrate the utility of HPLC in the analysis of I and II in biological fluids at plasma and urine concentration levels.

REFERENCES

(1) H. G. Boxenbaum and S. Riegelman, *J. Pharm. Sci.*, **63**, 1191 (1974).

(2) R. Modin, *Acta Pharm. Suec.*, **9**, 157 (1972).

(3) B. A. Perrson, *ibid.*, **8**, 217 (1971).

(4) B. L. Karger and B. A. Perrson, *J. Chromatogr. Sci.*, **12**, 521 (1974).

(5) B. L. Karger, S. C. Su, S. Marchese, and B. A. Perrson, *ibid.*, **12**, 678 (1974).

(6) D. P. Wittmer, N. O. Nuessle, and W. G. Haney, *Anal. Chem.*, **47**, 1422 (1975).

(7) J. T. Stewart, I. L. Honigberg, J. P. Brant, W. A. Murray, J. L. Webb, and J. B. Smith, *J. Pharm. Sci.*, **65**, 1536 (1976).

(8) "Manual of Analytical Toxicology," I. Sunshine, Ed., Chemical Rubber Co., Cleveland, Ohio, 1971, pp. 191, 192.

(9) H. H. Fox and J. T. Gibas, *J. Org. Chem.*, **18**, 1375 (1953).

(10) V. N. Kerr, D. G. Ott, and F. N. Hayes, *J. Am. Chem. Soc.*, **82**, 186 (1960).

(11) B. L. Karger, L. R. Snyder, and C. Horvath, "An Introduction to Separation Science," Wiley, New York, N.Y., 1973, pp. 146–150.

(12) J. H. Peters, *Am. Rev. Resp. Dis.*, **81**, 485 (1960).

[7] Olivetti-Underwood Programma 101.

ACKNOWLEDGMENTS AND ADDRESSES

Received October 9, 1975, from the *Department of Medicinal Chemistry, School of Pharmacy, University of Georgia, Athens, GA 30602.*

Accepted for publication August 5, 1976.

Presented at the Pharmaceutical Control and Analysis Section, APhA Academy of Pharmaceutical Sciences, Atlanta meeting, November 1975.

[x] To whom inquiries should be directed.

In Vitro and *In Vivo* Considerations of a Novel Matrix-Controlled Bovine Progesterone-Releasing Intravaginal Device

V. W. WINKLER [x], S. BORODKIN, S. K. WEBEL, and J. T. MANNEBACH

Abstract □ An *in vitro* system measuring progesterone release from silicone matrixes into serum is described. Drug release followed a matrix-controlled diffusion model in which the cumulative quantity released was linear with the square root of time. A bovine intravaginal device, consisting of a steel coil coated on both sides with a progesterone silicone matrix, was used as an *in vivo* drug delivery system. *In vivo* drug release also was matrix controlled, with rates comparable to those obtained *in vitro*. However, lag times of 1.7 and 4.2 days before reaching the steady-state rate were obtained for the outer and inner surfaces, respectively. The combination of effects resulted in a pseudo-zero-order drug-releasing device in which cumulative drug released was linear with time for at least 16 days.

Keyphrases □ Progesterone—release from silicone matrixes, *in vitro* system compared to bovine intravaginal device *in vivo* □ Silicone matrixes—release of progesterone, *in vitro* system compared to bovine intravaginal device *in vivo* □ Drug delivery—progesterone from silicone matrixes, *in vitro* system compared to bovine intravaginal device *in vivo* □ Vaginal devices, bovine—progesterone in silicone matrix, compared to *in vitro* system □ Hormones—progesterone, release from silicone matrixes, *in vitro* system compared to bovine intravaginal device *in vivo*

Intravaginal devices coated with a progesterone silicone matrix were used successfully (1–3) to control the bovine estrus cycle and to synchronize estrus by regulating pituitary release of gonadotropic hormones. Estrus occurs at a predictable time upon removal of the device developed in these laboratories 9–21 days after intravaginal implantation. The drug release rate profile of this device is defined in this report through correlation of *in vitro* and *in vivo* studies.

EXPERIMENTAL

Matrix Preparation—Progesterone silicone matrixes at various drug concentrations were prepared by first mixing the required amount of micronized drug into silicone fluid 360[1] and then adding Silastic elastomer 382[1]. The mixture was blended for 30 min to ensure random distribution of drug before adding the polymerizing catalyst, stannous octanoate[1].

***In Vitro* Study**—Matrixes used in the *in vitro* studies were prepared by streaking the silicone drug mixture containing catalyst onto fiber glass cloth and allowing it to cure. A template was used to obtain a uniform thickness of 1.5 mm. The cured matrixes were cut accurately into 2 × 2-cm pieces, mounted onto stainless steel plates with medical adhesive[1], and allowed to dry for 48 hr.

Two types of *in vitro* experiments were performed. The first followed the release of progesterone as a function of time from a silicone matrix containing 6.75% drug. The second concerned the release rate as a function of drug concentration using 5, 7.5, and 10% progesterone in silicone matrixes. The 6.75% matrix was prepared from a different lot of silicone liquid and elastomer, restricting direct comparison of the two *in vitro* experiments.

In both experiments, a specified number of matrixes mounted on stainless steel were individually placed in 25 × 150-mm glass tubes. To each tube, 15 ml of sheep serum[2] and 2 drops of toluene were added to retard microbial growth. Each tube was capped with a rubber stopper, placed on a shaker, and incubated at 37°. Serum changes at the end of Days 1, 2, 3, 4, 7, 11, 15, and 18 for one set of matrixes were matched with serum changes at the end of Days 0.1, 0.2, 0.3, 0.7, 1, 1.3, 2, 2.3, 3, 4, 5, 8, 12, 15, 18, and 20 for a duplicate set of matrixes.

The progesterone released in selected mounted matrixes was determined at various scheduled times by analyzing the amount of drug re-

[1] Dow Corning Corp., Midland, MI 48640.

[2] International Scientific Industries, Cary, IL 60013.

Table I—Comparative *In Vitro* Progesterone Release Rates from 5, 7.5, and 10% Silicone Matrixes Incubated 21 Days at 37° in Sheep Serum

Parameter	Progesterone Matrix Concentration		
	5%	7.5%	10%
Rate ($k = Q/t^{1/2}$ mg/cm day$^{1/2}$)	1.924	2.164	2.436
Confidence limit ($p < 0.05$), ±%	10.7	6.2	8.3
Extrapolated lag time, hr	5.0	4.5	5.0
Correlation coefficient (r)	0.969	0.987	0.980

maining and calculating the difference from the initial content (determined by percent progesterone of total matrix weight) of the particular mounted matrix analyzed. Since there were no significant differences in results between the two serum changing schedules and at no point did the released progesterone exceed 10% of its maximum solubility in serum, near perfect sink conditions existed throughout the experiment.

***In Vivo* Study**—Intravaginal devices were prepared by injection molding the silicone drug mixture containing catalyst around a 3.5 × 28.5 × 0.1-cm stainless steel strip set in a die such that both sides of the strip had 1.5 mm of matrix attached. The cured progesterone silicone device was then formed into a coil with a diameter of ~4 cm and a length of ~12 cm before intravaginal implantation into cows as described by Roche (1).

Devices were removed at the end of Days 2, 6, 9, 12, and 16. The silicone matrix of the inside and outside surfaces was peeled from the steel and analyzed for progesterone content. As was done in the *in vitro* studies, the progesterone released was determined by difference from the initial progesterone content of the device.

Analytical—Progesterone was extracted from the silicone matrixes by soaking in ethyl acetate, and the extracted drug was analyzed by flame-ionization GLC using bis(2-ethylhexyl) sebacate[3] as an internal standard. The column was a 0.31-cm × 1.22-m (0.125-in. × 4-ft) glass U-tube[4] containing 3% Dexsil on Chromosorb W Hp[3]. The flow rates (milliliters per minute) were: air, 300; hydrogen, 25; and nitrogen, 40. The temperatures were: injection, 250°; column, 240°; and detector, 250°.

The method described is accurate with 100% recovery on spiked samples and a coefficient of variation less than ±3%.

RESULTS AND DISCUSSION

The release rate of drugs suspended in a stationary matrix was described theoretically (4) to be a linear function of the square root of time. With the assumptions that (*a*) a quasi-steady state exists, (*b*) the drug particles are small compared to the average distance of diffusion, and (*c*) perfect sink conditions exist in the external media, the basic equation of interest for planar systems is:

$$Q = [D(2A - C_s)C_s t]^{1/2} \quad \text{(Eq. 1)}$$

where Q is the amount of drug released after time t per unit of exposed area, A is the initial drug concentration, C_s is the solubility of the drug in the matrix, and D is the effective diffusivity through the matrix.

For a given matrix system, D, A, and C_s remain constant; therefore, Eq. 1 can be expressed as:

$$Q = kt^{1/2} \quad \text{(Eq. 2)}$$

where the release rate constant:

$$k = [D(2A - C_s)C_s]^{1/2} \quad \text{(Eq. 3)}$$

Results of the first *in vitro* experiment (Fig. 1), using the 6.75% progesterone silicone matrix, dramatically demonstrate the relationship in Eq. 2, with a matrix-controlled rate constant, k, of 2.425 mg/cm^2 day$^{1/2}$ ± 4% ($p < 0.05$ and $r = 0.995$). Extrapolation to the x axis indicates a lag time of 6 hr before reaching steady state. This lag time is generally seen in systems of this type, and it has been attributed to drug release being controlled by a matrix-boundary diffusion layer model in the early stages (5).

The Higuchi equation describing matrix-controlled drug release (Eq. 1) also dictates that the rate constant should be proportional to the square root of drug concentration as long as $2A$ is much greater than C_s. This

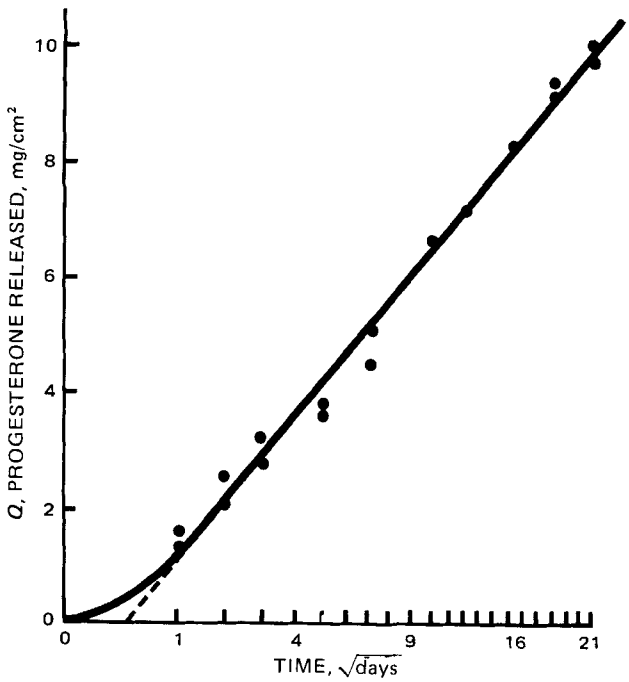

Figure 1—In vitro *progesterone release as a function of the square root of time from a silicone matrix containing 6.75% drug incubated at 37° in sheep serum. Matrix-controlled release rate* ($k = Q/t^{1/2}$ *mg/cm*^{2} *day*$^{1/2}$) *is 2.425 ± 4% (*$p < 0.05$ *and* $r = 0.995$*). Based on extrapolated intercepts, there is a 0.25-day lag time before reaching steady state.*

should be the case in the progesterone-silicone matrix system for which Roseman (6) reported a C_s value of 0.513 mg/ml. The relationship may be expressed as:

$$\frac{k_1}{k_2} = \frac{\sqrt{A_1}}{\sqrt{A_2}} \quad \text{(Eq. 4)}$$

Chien *et al.* (7) reported this relationship in a study of ethynodiol diacetate in silicone matrixes. Results of the second *in vitro* experiment, comparing progesterone release from matrixes containing 5, 7.5, and 10% drug, are shown in Table I. The rate constants show increasing values with drug concentration as predicted, although the magnitude of increase is somewhat less than that expected from Eq. 4. When using the 7.5% rate

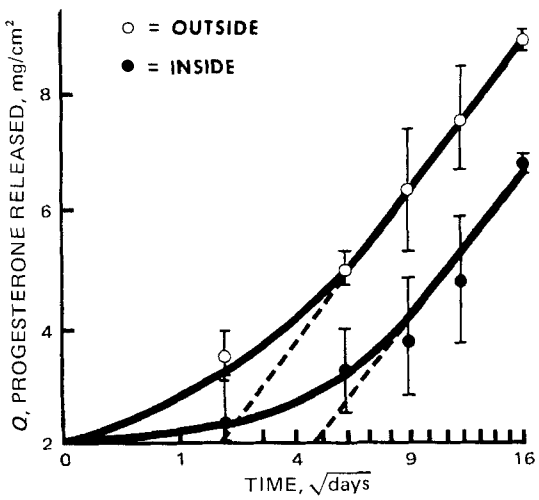

Figure 2—In vivo *cumulative progesterone release* ±SD *as a linear function of the square root of time from separate outside and inside surfaces of a silicone matrix intravaginal device containing 7.8% drug implanted in cows. The following matrix-controlled release rates (in milligrams per square centimeter day*$^{1/2}$*) were calculated from the 6-, 9-, 12-, and 16-day means shown in Table II: outside rate,* $k_o = 2.597 \pm 23\%$ ($p < 0.05$ *and* $r = 0.998$*); and inside rate,* $k_i = 2.359 \pm 87\%$ ($p < 0.05$ *and* $r = 0.959$*). Based on extrapolated intercepts, there are 1.7- and 4.2-day lag times before reaching steady state for the outside and inside surfaces, respectively.*

[3] Applied Science Laboratories, State College, PA 16801.
[4] Varian 2100.

Table II—*In Vivo* Progesterone Release from the Outside and Inside Surfaces of 7.8% Silicone Matrix Intravaginal Coils Implanted in Cows

Day	Device Section	Cumulative Progesterone Released per Unit of Exposed Area, mg/cm²						Mean	±SD
2	Outside	2.02	1.83	1.18	1.08	—	—	1.53	0.47
	Inside	1.23	0.36	0.56	−0.83[a]	—	—	0.33	0.86
	Total	1.62	1.10	1.37	0.13	—	—	1.06	0.75
6	Outside	3.42	3.06	2.66	3.01	—	—	3.04	0.31
	Inside	0.94	1.98	0.16	1.58	—	—	1.17	0.80
	Total	2.18	2.52	1.41	2.29	—	—	2.10	0.48
9	Outside	3.93	5.39	3.25	—	—	—	4.19	1.09
	Inside	1.16	2.79	1.03	—	—	—	1.66	0.98
	Total	2.55	4.09	2.14	—	—	—	2.93	1.03
12	Outside	5.46	5.10	5.67	7.25	5.71	4.33	5.59	0.96
	Inside	2.56	2.95	4.07	0.75	3.06	3.20	2.77	1.10
	Total	4.01	4.03	4.87	4.00	4.39	3.77	4.18	0.39
16	Outside	6.86	7.15	7.03	—	—	—	7.01	0.15
	Inside	4.68	5.08	4.74	—	—	—	4.83	0.21
	Total	5.77	6.12	5.89	—	—	—	5.92	0.18

[a] Negative value results from positive variation in actual progesterone content of individual implant from assumed initial progesterone content. Thus, percent drug remaining after a 2-day implantation was greater than the theoretical 7.8%. Since averages are used in determining drug release, the negative value must be included so as not to bias the final result.

as reference, the 5 and 10% rates are 108 and 97.9% of expected theory.

It is intriguing to speculate that an increase in drug concentration increases the diffusion pathway, thus decreasing the effective diffusion coefficient, D. Such a process is conceivable, because a "sponge effect" is created in the matrix as insoluble drug is removed by the matrix diffusion process. The higher the drug concentration, the more "holes" exist; consequently, there is an increased migration distance for soluble drug before passing into the external media. When using C_s at 0.513 (6), the effective diffusion coefficients are (Eq. 3) 0.0445, 0.0337, and 0.0285 cm²/day for the 5, 7.5, and 10% matrixes, respectively. The net result of such a decrease in the effective diffusion coefficients is a less than expected increase in rates with respect to increasing drug concentrations. There is no doubt, however, that the release of progesterone is matrix controlled.

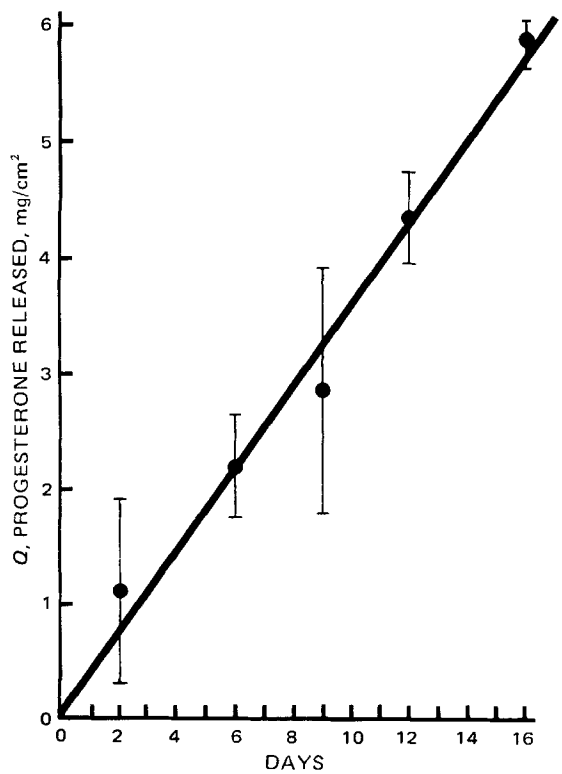

Figure 3—In vivo *cumulative progesterone release* ±SD *as a linear function of time from total outside and inside surfaces of a silicone matrix intravaginal device containing 7.8% drug implanted in cows. When using mean* Q *values shown in Table II including Day 0, the zero-order rate* (k_t = Q/t *mg/cm² day) is 0.357* ± *24%* ($p < 0.05$ *and* $r = 0.991$).

Results of the *in vivo* progesterone release from the outside and inside surfaces of 7.8% progesterone intravaginal devices implanted in cows are shown in Table II. The mean release values with respect to time (Q) are greater with less variation for the outer surface than for the inner surface of the coils at all time periods. The release rates as a function of the square root of time from the separate outside and inside surfaces are graphically shown in Fig. 2. When using the mean Q values from Days 6 through 16 in Table II, the following matrix-controlled release rates are calculated (in milligrams per square centimeter day$^{1/2}$): outside rate, $k_o = 2.597 \pm 23\%$ ($p < 0.05$ and $r = 0.998$); and inside rate, $k_i = 2.359 \pm 87\%$ ($p < 0.05$ and $r = 0.959$). These results are in excellent agreement with those obtained in the *in vitro* system and demonstrate progesterone release from the coils to be a matrix-controlled process *in vivo*.

Based on extrapolated intercepts, there are 1.7- and 4.2-day lag times before reaching steady state for the outside and inside surfaces, respectively. The shorter lag time for the outer surface accounts for its greater release values and less variation. The longer lag time for the inner surface likewise accounts for the smaller release values and greater variation. The difference between lag times may be attributed to physical phenomena such as wetting of the polymer surface, establishment of a steady-state diffusion gradient, and contact with the vaginal wall.

The most remarkable effect of the time lag difference between the two surfaces is the establishment of a pseudo-zero-order drug-releasing device. Indeed, as shown in Fig. 3, the amount of progesterone released per day is approximately uniform. When using the mean Q values including Day 0, the zero-order rate ($k_t = Q/t$ mg/cm² day) for 16 days is 0.357 ± 24% ($p < 0.05$ and $r = 0.991$). The net 16-day progesterone dose administered to the cow implanted with the described intravaginal device having a surface area of 224 cm² is 80 ± 19 mg/day ($p < 0.05$). This linear dose rate is achieved by superimposing *via* time lag the nonlinear matrix-controlled dose rate of the outer and inner surfaces of the implanted device.

REFERENCES

(1) J. F. Roche, *J. Reprod. Fert.*, **43**, 471 (1975).

(2) *Ibid.*, **40**, 433 (1974).

(3) R. E. Mauer, S. K. Webel, and M. D. Brown, *Ann. Biol. Anim. Biochim. Biophys.*, **15**, 291 (1975).

(4) T. Higuchi, *J. Pharm. Sci.*, **52**, 1145 (1963).

(5) T. J. Roseman and W. I. Higuchi, *ibid.*, **59**, 353 (1970).

(6) T. J. Roseman, *ibid.*, **61**, 46 (1972).

(7) Y. W. Chien, H. J. Lambert, and D. E. Grant, *ibid.*, **63**, 365 (1974).

ACKNOWLEDGMENTS AND ADDRESSES

Received December 29, 1975, from *Product Development, Agricultural and Veterinary Products Division, Abbott Laboratories, North Chicago, IL 60064.*

Accepted for publication August 9, 1976.

[x] To whom inquiries should be directed.

Stability of Aqueous Solutions of Pirbuterol

P. C. BANSAL * and D. C. MONKHOUSE ˣ

Abstract □ The hydrolytic degradation of pirbuterol was investigated under saturated oxygen conditions over a wide range of pH values and at different temperatures. Two of the five observed breakdown products were positively identified. The first-order decomposition rate appeared to depend on the rate constants of the four dissociated ionic species. The most stable region for the drug was pH 1–2, where the diprotonated molecule predominated; appropriate thermodynamic parameters were calculated.

Keyphrases □ Pirbuterol—aqueous solutions, stability, effect of pH and temperature □ Stability—pirbuterol, aqueous solutions, effect of pH and temperature □ Degradation, hydrolytic—pirbuterol, effect of pH and temperature □ Bronchodilators—pirbuterol, stability of aqueous solutions, effect of pH and temperature

Pirbuterol[1] (I) is a potent sympathomimetic bronchodilator that possesses high selectivity for pulmonary as opposed to cardiac adrenergic receptors. Exploratory studies indicated that satisfactory pirbuterol stability could be attained in acidic media, while degradation occurred under alkaline conditions. Since this bronchodilator will be manufactured in many liquid dosage forms (aerosol, oral spray, intravenous injection, and pediatric syrup), its solution stability profile should be well characterized and understood.

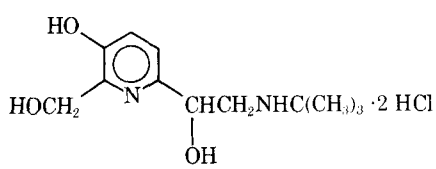

I

The stability of pirbuterol should be superior to that of the catecholamines, since intramolecular cyclization leading to indole derivatives can be excluded on mechanistic grounds. Its stability is more likely to compare with that of the more stable compounds terbutaline and phenylephrine. Upon oxidation, these compounds produce formaldehyde, which can further react with the intact molecule to form isoquinoline derivatives *via* the Pictet–Spengler reaction (1, 2).

The purpose of this study was to evaluate pirbuterol in the light of what has already been reported about structurally similar agents of contrasting stability behavior. The stability of pirbuterol's closest analog, albuterol, has not yet been reported.

EXPERIMENTAL

Quantitative TLC Assay—Pirbuterol[2] solutions (0.5–5.0 mg/ml) were spotted (5 μl) on scored precoated silica gel TLC plates[3] using capillary pipets[4]. Following each application, the pipet was rinsed with 5 μl of ethanol, which was applied to the respective spot to ensure complete transfer. Then the pipet was rinsed with the next solution to be spotted. The same pipet was used for each series. Standard samples containing known amounts of pirbuterol were spotted alternately with the unknown samples.

The chromatographic bath was prepared in a glass chamber (30 × 22 × 10 cm) by mixing 40 ml of acetic acid and 40 ml of water into 240 ml of methyl ethyl ketone. The chamber was lined on one side with filter paper, which was in contact with the mobile phase. The chamber was tightly sealed and allowed to equilibrate overnight.

After drying the applied spots thoroughly, chromatographic development was performed until the solvent front was 14–16 cm above the origin. The plates were removed from the chamber and dried in a stream of forced warm air. The reflectance of the pirbuterol spot (R_f 0.43) was measured on a double-beam spectrodensitometer[5] at 282 nm, using a slit width of 1 mm and a sensitivity of 0.4. Peak areas were measured with a computing integrator[6].

Kinetic Studies—Aqueous 5-mg/ml solutions of pirbuterol were prepared (initial pH ~3), and the pH was adjusted with 1 *N* HCl or NaOH to integral values of pH from 1 to 14. Since preliminary investigation showed that oxygen played a significant role in the degradation of pirbuterol, the oxygen tension was kept constant in the test solutions. Oxygen saturation was achieved by bubbling oxygen through each solution throughout the experiment. The apparatus used is shown in Fig. 1. Oxygen was bubbled into the solution at a rate of 6 ml/min and was allowed to escape through a condenser, which prevented loss of water vapor.

The test solution pH was adjusted periodically by the addition of 1 *N* NaOH or HCl, utilizing a pH meter equipped with an electrode[7] specially

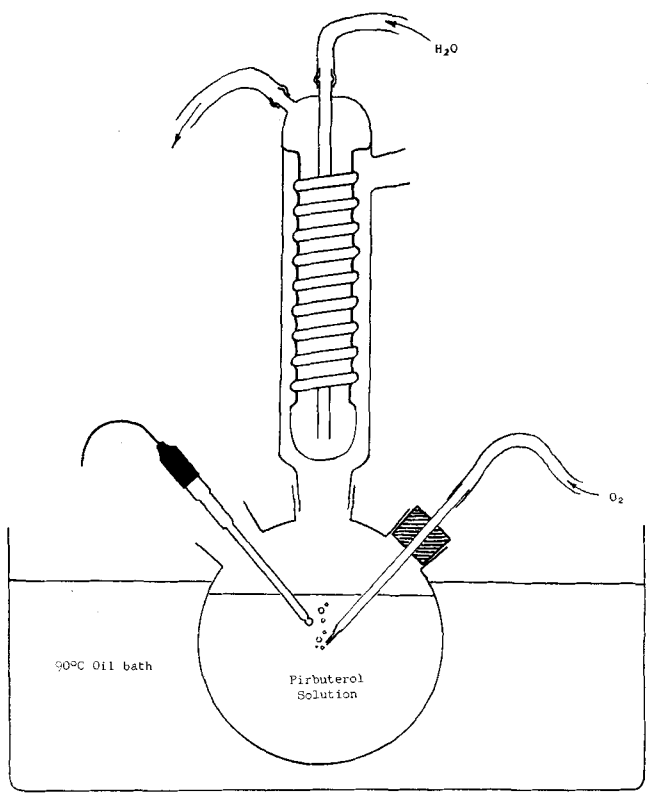

Figure 1—*Apparatus used for kinetic studies of pirbuterol degradation as a function of pH under stressed oxidative conditions.*

[1] α⁶-[[(1,1-Dimethylethyl)amino]methyl]-3-hydroxy-2,6-pyridinedimethanol dihydrochloride, CP-24,314-1, Pfizer Inc.
[2] Lot 8267-140-1.
[3] Silica gel GF, 20 × 20 × 0.025 cm, Uniplate, Analtech, Inc.
[4] SGA Co.
[5] Schoeffel model SD 3000.
[6] Spectra-Physics, Autolab System I.
[7] A pH meter 26 with GK2301C combined electrode, Radiometer, Copenhagen.

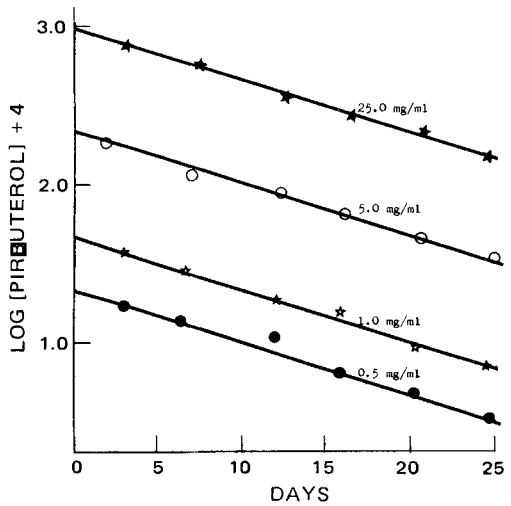

Figure 2—*Plot illustrating first-order dependence in pirbuterol concentration at pH 7 and 90°.*

prepared for use at high temperatures. To prevent aging and poisoning of the electrode, immersion in the actual reaction mixtures was kept to a minimum. At no time was the pH allowed to deviate more than 0.2 pH unit from the original settings. Only those solutions with pH >5 required periodic adjustment.

Temperature was controlled by immersing the solution flask into a constant-temperature oil bath. Loss of intact drug was monitored by TLC–densitometry.

Determination of Ionization Constants—The pKa's of pirbuterol were determined at 21 and 90°. A 0.25-mmole sample of drug was dissolved in freshly boiled double-distilled water and titrated with 1 *N* NaOH (carbon dioxide free). Change in pH as a function of the titrant delivered was monitored with a pH meter equipped with the high temperature electrode[7]. Confirmation of pKa's was achieved by titrating the structurally similar compounds 2,6-bis(hydroxymethyl)-3-hydroxypyridine and 2-(*tert*-butylamino)ethanol.

2-Hydroxymethyl-3-hydroxypyridine-6-carboxaldehyde (II)—An authentic sample of this compound[8] was prepared, and the structure was confirmed by NMR, IR, and elemental analyses. It exhibited an R_f value of 0.75 on the TLC system previously described.

RESULTS AND DISCUSSION

For the quantitative TLC procedure, the densitometric response for pirbuterol is linear and can be quantitated over a 0.5–5.0-mg/ml range when 5-μl spots are applied. The calibration plot (electronic peak area *versus* quantity spotted) for the assay had a correlation coefficient of 99.9% with a standard deviation of ±3.9%.

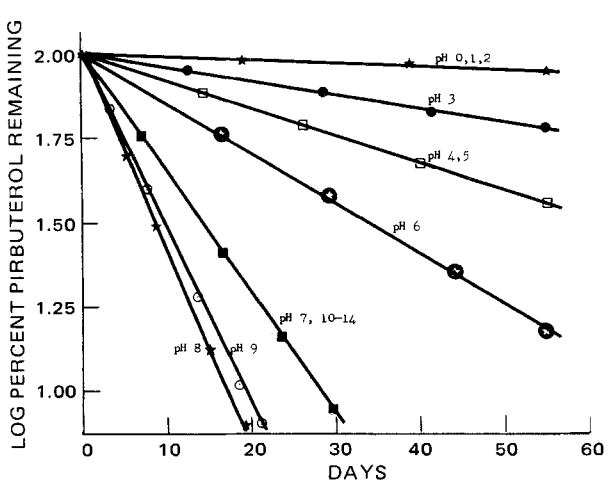

Figure 3—*First-order degradation of pirbuterol at 90° at various pH values.*

[8] CP-34,028, Pfizer Inc.

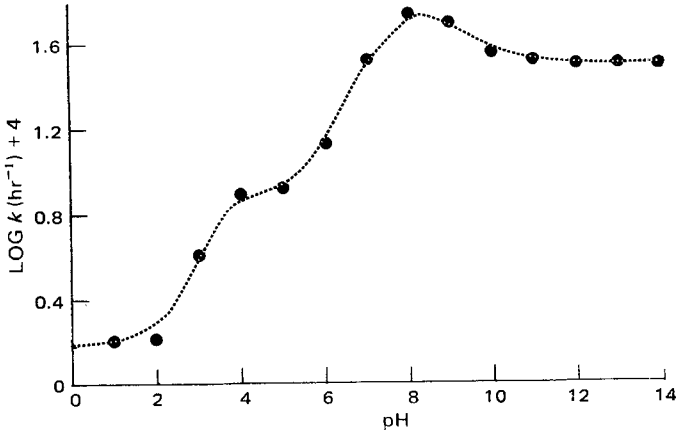

Figure 4—*The pH–rate profile of pirbuterol degradation at 90° as a function of pH.*

In the present study, the degradation of pirbuterol was investigated over a pH range of 1–14. These studies were conducted at 90° to accelerate the decomposition rates so that their measurement would be kinetically convenient. Preliminary studies indicated that the reaction rate was affected both by oxygen tension and by buffer catalysis but unaffected by ionic strength effects and light. Therefore, the study was designed so that constant oxygen tension was maintained (saturation conditions) and buffers *per se* were not used. Hence, it was assumed that only thermal phenomena and pH contributed to the rate constants obtained.

The reaction followed apparent first-order kinetics with respect to pirbuterol. Figure 2 shows that log concentration *versus* time plots were linear and parallel for each concentration studied (0.5–25 mg/ml) at pH 7. Similar results were also obtained at pH 1, 5, 8.5, and 11. The reaction was then treated as first order in pirbuterol over the entire pH range of 1–14. In Fig. 3, the log concentration of pirbuterol remaining is plotted as a function of time. The slopes of these lines were used to calculate the first-order rate constants (Table I). These log k values can be used to plot a log k–pH profile for the reaction (Fig. 4).

The pH of maximum stability was between 1 and 3. Another pH-independent region occurred between pH 10 and 14. The degradation rate

Table I—Rate Constants for Pirbuterol Degradation Varying as a Function of pH

pH	Experimental $k \times 10^4$, hr^{-1}	Experimental log $k + 4$	Theoretical[a] $k \times 10^4$, hr^{-1}	Theoretical[a] log $k + 4$
0	—	—	1.50	0.177
1	1.61	0.207	1.55	0.189
2	1.61	0.207	1.94	0.288
3	4.11	0.614	4.28	0.631
4	7.85	0.895	7.43	0.871
5	8.06	0.906	8.55	0.932
6	13.7	1.136	12.1	1.081
7	33.3	1.522	31.2	1.495
8	53.6	1.729	53.1	1.725
9	49.4	1.693	48.9	1.690
10	36.6	1.563	36.0	1.556
11	33.2	1.521	32.6	1.513
12	32.2	1.507	32.2	1.508
13	32.2	1.507	32.2	1.508
14	32.2	1.507	32.2	1.507

[a] Rate constants and equilibrium constants of individual species used in the rate equation for calculation of theoretical curve were: $k_A = 1.50 \times 10^{-4}\ hr^{-1}$, $k_B = 8.24 \times 10^{-4}\ hr^{-1}$, $k_C = 6.00 \times 10^{-3}\ hr^{-1}$, $k_D = 3.22 \times 10^{-3}\ hr^{-1}$, $K_1 = 7.0 \times 10^{-4}$, $K_2 = 8.0 \times 10^{-8}$, and $K_3 = 6.3 \times 10^{-10}$.

Table II—Ionization Constants of Pirbuterol

Functional Group		21°	90°
Pyridine	pKa_1 =	3.0	2.8
Pyridol	pKa_2 =	7.0	7.1
Secondary amine	pKa_3 =	10.3	9.2

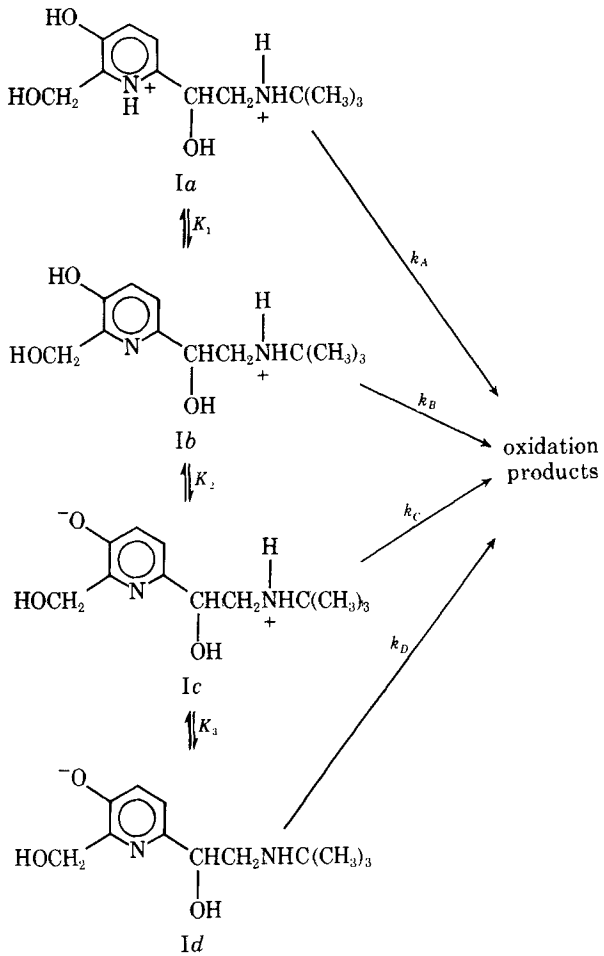

Scheme I

increased with pH between 3 and 6, reaching a pseudomaximum at pH 6, after which the rate rose again until minimum stability was observed at pH 8. This unusual profile can be explained by considering the degradation rates of the various ionic species of pirbuterol whose concentrations change with pH.

Pirbuterol exists as four ionic species. Their pKa's, determined by the titration method described under *Experimental*, are listed in Table II. The equilibria involved in the total reaction are shown in Scheme I.

From these pKa values, it was possible to calculate the degree to which each functional group ionizes as the pH varies (Fig. 5). Figure 6 shows the proportions of ionic species of pirbuterol that are expected to exist in aqueous solution, adjusted to any pH, at 90° [9].

The total rate equation for Scheme I is then:

$$k_{obs} = k_A f_A + k_B f_B + k_C f_C + k_D f_D \qquad \text{(Eq. 1)}$$

where:

$$f_A = \frac{[A]}{[A] + [B] + [C] + [D]} \qquad \text{(Eq. 2)}$$

$$f_A = \frac{1}{1 + \frac{[B]}{[A]} + \frac{[C]}{[A]} + \frac{[D]}{[A]}} \qquad \text{(Eq. 3)}$$

[9] Scheme I presents a simplified picture of the ionic equilibria involved. Many more ionic species could theoretically exist (3, 4), the most likely of which would be the totally unionized form. This species would be in equilibrium with species B and D as follows:

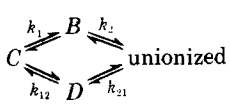

where $K_2 = k_1 + k_2$ and $(1/K_3) = (1/k_{12}) + (1/k_{21})$. Based on the relative pKa's of the pyridol and secondary amine, the proportion of unionized species to zwitterion is expected to be very small. Therefore, the mathematical treatment of experimental data neglects the formation of unionized species.

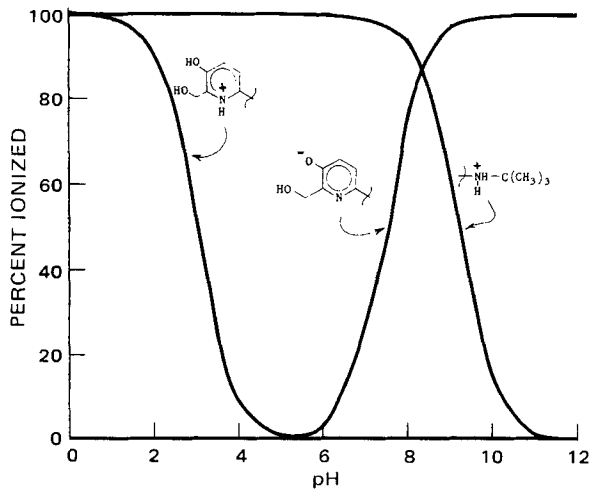

Figure 5—*Degree of ionization of pirbuterol at 90° as a function of pH.*

$$f_A = \frac{1}{1 + \frac{K_1}{[H^+]} + \frac{K_1K_2}{[H^+]^2} + \frac{K_1K_2K_3}{[H^+]^3}} \qquad \text{(Eq. 4)}$$

$$f_A = \frac{[H^+]^3}{[H^+]^3 + K_1[H^+]^2 + K_1K_2[H^+] + K_1K_2K_3} \qquad \text{(Eq. 5)}$$

Species B, C, and D can be treated similarly. Substituting the appropriate (f_i) equalities into Eq. 1 yields:

$$k_{obs} = \frac{k_A[H^+]^3 + k_BK_1[H^+]^2 + k_CK_1K_2[H^+] + k_DK_1K_2K_3}{[H^+]^3 + K_1[H^+]^2 + K_1K_2[H^+] + K_1K_2K_3} \qquad \text{(Eq. 6)}$$

In the pH 1–2 region, pirbuterol is diprotonated and $k_A \sim k_{obs}$. Similarly, in the pH 10–12 region, pirbuterol exists as the pyridinolate ion in which case $k_D \sim k_{obs}$. By using these two derived constants, k_A and k_D, Eq. 6 can be solved as two simultaneous equations at two pH's with two unknowns, k_B and k_C. The latter two rate constants were estimated and optimized in this manner (Table I), and the theoretical pH–rate profile was then plotted and compared with experimental data points (as indicated by the dashed line *versus* observed data points in Fig. 4). The goodness of fit suggests that this model is consistent with experimental data and can be used to explain the unusually shaped pH–rate profile.

The apparent energies of activation were determined at four pH's: 1, 5, 8.5, and 11. As indicated by Fig. 6, essentially one single ionic species exists at any of these pH's; therefore, the E_a's reflect the thermodynamic

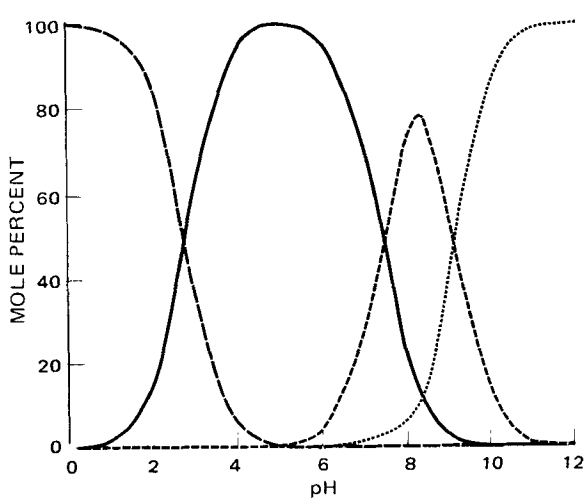

Figure 6—*Variation in concentration of pirbuterol species as a function of pH. Key: – –, Ia (diprotonated); —, Ib (monoprotonated); - - - -, Ic (zwitterion); and . . . . , Id (anion).*

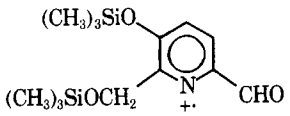

III (*m/e* 297)

behavior of the respective pirbuterol ion present in that solution. Arrhenius plots of kinetic data collected at 70, 80, and 90° yielded the apparent activation parameters listed in Table III.

As the profile indicates, drug stability is best at pH 2[10], a major factor to be considered in the formulation of liquid products. The relatively small value of the energies of activation indicates a low sensitivity of the reaction rate to temperature. The large negative value of the entropies reflects a significant requirement in molecular orientation for the reaction to occur, presumably imposed by the large bulky *tert*-butyl moiety.

A representative TLC plate of stressed oxidative degradation of pirbuterol is shown in Fig. 7. Five degradation products were observed. The spot migrating to R_f 0.75 (pH 7–12) had a GLC retention time of 2.4 min when derivatized on-column with bis(trimethylsilyl)trifluoroacetamide plus 1% trimethylchlorosilane. The mass spectra[11] of the trimethylsilyl derivative (III) of the degradation product and of II, prepared by unambiguous synthesis, were identical. The prominent peaks in the fragmentation pattern of III (Fig. 8) are listed in Table IV.

Another product resulting from the same reaction sequence is *tert*-butylamine. During the kinetic studies, vapors from the reaction vessels were passed through a saturated aqueous picric acid solution to confirm the presence of the volatile amine. A precipitate was collected in this manner and, upon drying, was analyzed. The melting point, IR spectrum, and elemental analysis corresponded to authentic *tert*-butylamine picrate.

Scheme II is proposed to describe the degradation in solution at pH 7–12 in accordance with the data. The degradation pattern observed at low pH (Fig. 7) indicates that an entirely different mechanism is operative in acidic media. Before a pathway of degradation can be proposed, further identification of degradation products is necessary. Any such mechanism should, however, accommodate the obvious dependence of the reaction rate on the ionization of the ring functionalities.

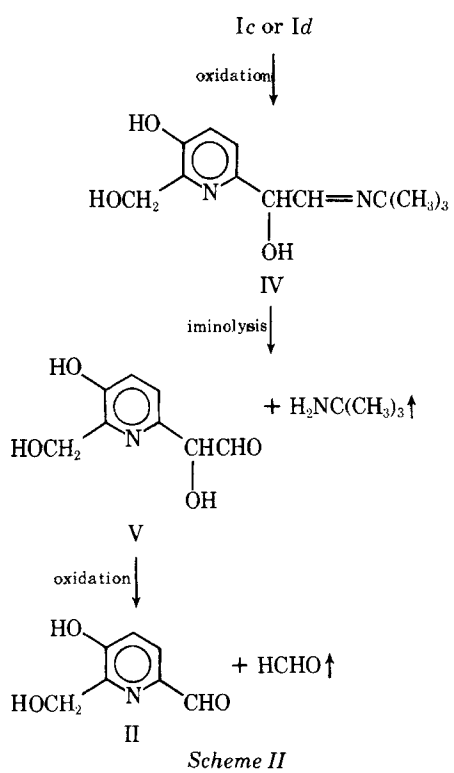

Scheme II

[10] Because E_a's were determined over a small temperature range, extrapolation involves considerable risk. Nevertheless, room temperature data obtained so far do suggest that the $t_{1/2}$ at pH 1–2 is consistent with the predicted value of ~5 years.

[11] LKB-9000 GC–mass spectrometer coupled with a PDP 8 data system.

Table III—Apparent Thermodynamic Activation Parameters for Pirbuterol Species

Ionic Species	Reaction pH	E_a, kcal/mole	$\Delta S^{\ddagger}_{298}$, eu
A	1	8.8	−67.5
B	5	11	−58
C	8.5	9.5	−59
D	11	11.9	−53.2

Table IV—Fragmentation Pattern for the Trimethylsilyl Derivative of II

m/e	Empirical Formula	Comment
297	$C_{13}H_{23}NO_3Si_2^+$	M^+ (molecular ion)
282	$C_{12}H_{20}NO_3Si_2^+$	$M^+ - 15$, loss of CH_3 from trimethylchlorosilane
253	$C_{11}H_{19}NO_2Si_2^+$	$M^+ - 44$, loss of both CH_3 and CHO
147	$C_5H_{15}OSi_2^+$	$M^+ - 150$, characteristic of trimethylchlorosilane
73, 75	$C_3H_9Si^+$	Characteristic of trimethylchlorosilane and its isotope

Formaldehyde, produced by oxidation of the secondary alcohol (V), can react with the parent amine in a Pictet–Spengler-type reaction to produce the corresponding isoquinoline derivative in the cases of phenylephrine and, to a lesser extent, terbutaline. The parallel reaction, if observed with pirbuterol, would be represented by I (Scheme II) reacting with formaldehyde produced during the formation of II to result in the corresponding pyrido[4,3-*b*]pyridine product. Upon the addition of excess formaldehyde to a solution of pirbuterol (pH ~6), TLC revealed a spot at R_f 0.30, which did not correspond to any observed in Fig. 7. Although this product may have been the cyclized adduct, it was concluded that such a reaction did not occur to any observable extent in the degradation of pirbuterol. This conclusion is likely, since the pyridine nucleus and hydroxyl substitution of pirbuterol should differ significantly in their directing properties from those of the isoquinoline precursors.

Identification of the spots at R_f 0, 0.12, 0.51, and 0.55 has not yet been achieved. Some possible degradation routes lead to *N*-oxide formation, self-condensation, 2,2′-pyridoin compound formation, polymerization of oxidation products, and oxidation of the primary alcohol.

CONCLUSIONS

The shape of the pH–rate profile (Fig. 4) indicates that each of the four ionic species of pirbuterol oxidizes at a rate independent of the other species present. The diprotonated species appears to be most stable to oxidation, as implied by the profile where optimum stability lies at pH 1–2. In accordance with the pH–rate profile, the rank order of the individual rate constants of the species was observed to be $k_A < k_B \ll k_D$

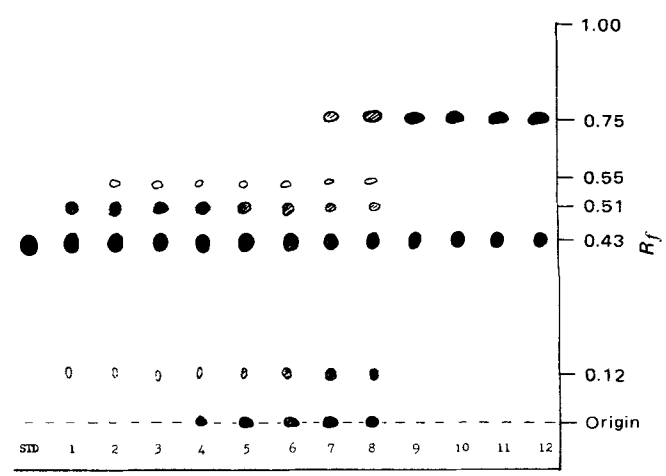

Figure 7—*Representative TLC plate showing degradation of pirbuterol at various pH values after* ~$t_{1/2}$.

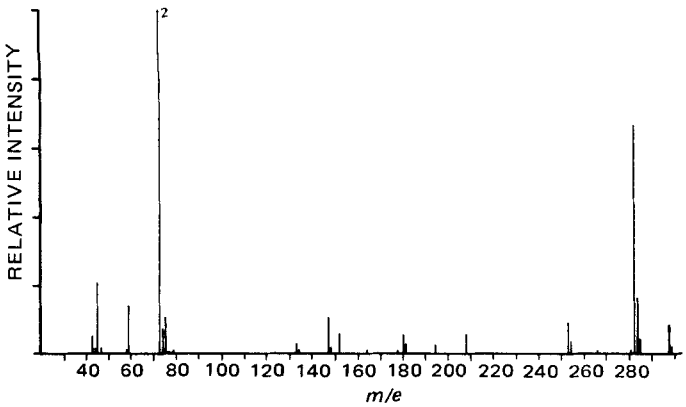

Figure 8—*Mass spectrum of the trimethylsilyl derivative of the degradation product from the oxidation of pirbuterol.*

$< k_C$. The experimental values were consistent with the derived rate equation. Arrhenius plots revealed low activation energies (~10 kcal/mole), which explain why conducting the experiments at 90° did not markedly accelerate the oxidation over that predicted (and observed) at room temperature.

REFERENCES

(1) L. Svensson, *Acta Pharm. Suec.*, **9**, 141 (1972).

(2) B. J. Millard, D. J. Priaulx, and E. Shotton, *J. Pharm. Pharmacol.*, **25**, 24P (1973).

(3) L. Z. Benet and J. E. Goyan, *J. Pharm. Sci.*, **56**, 665 (1967).

(4) P. J. Niebergall, R. L. Schnaare, and E. T. Sugita, *ibid.*, **61**, 232 (1972).

ACKNOWLEDGMENTS AND ADDRESSES

Received March 2, 1976, from *Central Research, Pfizer Inc., Groton, CT 06340.*

Accepted for publication August 5, 1976.

Presented at the Basic Pharmaceutics Section, APhA Academy of Pharmaceutical Sciences, New Orleans meeting, April 1976.

The authors acknowledge L. Van Campen for writing the programs necessary to the calculations and for technical assistance with the manuscript and also C. H. Huang for laboratory assistance.

* Present address: Ortho Pharmaceutical Corp., Raritan, NJ 08876.

[x] To whom inquiries should be directed.

Prostaglandin Monolayers II: Monomolecular Film Behavior of Dinoprost C-15 Alkyl Esters

BERNARD E. SIMS [x] and GLENFORD R. DERR

Abstract □ Monomolecular film compression–relaxation behavior was examined for select dinoprost C-15 alkyl esters. Higher homologs of the series such as palmitate and decanoate esters yielded stable expanded monolayers that exhibited minimal relaxation of surface pressure during noncompression. Their limiting molecular areas were consistent with a Hirschfelder model projection in which the prostaglandin moiety assumes a horizontal orientation at the interface with its alkyl ester chain oriented vertical to the surface plane. Shorter chain homologs such as hexanoate, valerate, butyrate, propionate, and acetate also formed expanded monolayers but exhibited increased instability with decreased alkyl chain length, as reflected in their lower surface pressure development during compression and significant relaxation of pressure during noncompression. Such instability can be tied to their increased solubility in the subphase solution and higher desorption rate from the interface.

Keyphrases □ Dinoprost C-15 alkyl esters, various—monomolecular film compression–relaxation behavior compared □ Films, monomolecular—various dinoprost C-15 alkyl esters, compression–relaxation behavior compared □ Prostaglandins—various dinoprost C-15 alkyl esters, monomolecular film compression–relaxation behavior compared

In recent years, much effort has been directed to elucidating the pharmacological and physiological properties of a new class of biological compounds termed prostaglandins (1–3). Very little attention, however, has been directed toward their possible surface-active properties, even though they have been implicated in various roles portending high surface activity (4–9).

The naturally occurring prostaglandins dinoprost ($F_{2\alpha}$), dinoprostone (E_2), A_1, and B_1 exhibited surface activity in the presence of spread insoluble monomolecular films (10). They in themselves, however, do not tend to form stable monolayers because of their high aqueous solubility. In this article, monolayer film behavior for some long chain alkyl derivatives of dinoprost that do form stable monolayers is reported. This basic and fundamental study should contribute to the limited information available on surface behavior of these ubiquitous and biologically important compounds.

The prostaglandin derivatives selected for monolayer investigation were long chain aliphatic esters of dinoprost attached at the C-15 hydroxyl group (I, R = alkyl). The numbering system generally accepted for prostaglandin-type compounds is with the upper chain carboxylic acid function as the 1-position.

EXPERIMENTAL

Materials—A TLC analysis of the synthesized[1] prostaglandin esters indicated a purity of 99+% for all compounds. Spectroscopic grade hexane–chloroform–methanol (20:2:1) was used as the spreading solvent. Subphase solutions consisted of 0.01 *M* HCl prepared with double-distilled water in an all-glass apparatus with alkaline permanganate.

Equipment—The monolayer balance consisted of a polytef[2]-covered

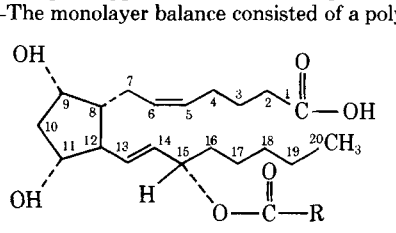

I

[1] By Dr. Walter Morozowich, The Upjohn Co.

[2] Teflon, du Pont.

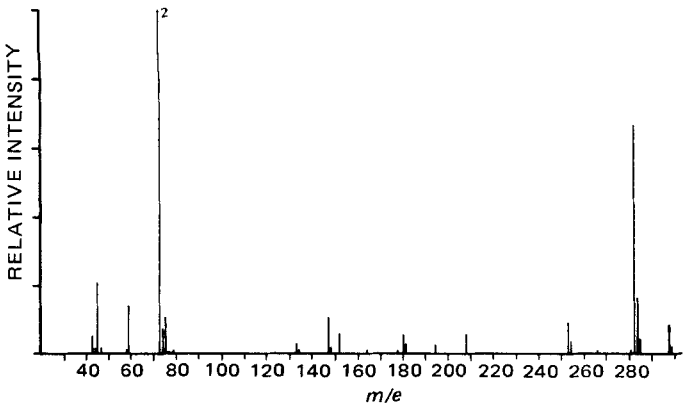

Figure 8—*Mass spectrum of the trimethylsilyl derivative of the degradation product from the oxidation of pirbuterol.*

$< k_C$. The experimental values were consistent with the derived rate equation. Arrhenius plots revealed low activation energies (~10 kcal/mole), which explain why conducting the experiments at 90° did not markedly accelerate the oxidation over that predicted (and observed) at room temperature.

REFERENCES

(1) L. Svensson, *Acta Pharm. Suec.*, **9**, 141 (1972).

(2) B. J. Millard, D. J. Priaulx, and E. Shotton, *J. Pharm. Pharmacol.*, **25**, 24P (1973).

(3) L. Z. Benet and J. E. Goyan, *J. Pharm. Sci.*, **56**, 665 (1967).

(4) P. J. Niebergall, R. L. Schnaare, and E. T. Sugita, *ibid.*, **61**, 232 (1972).

ACKNOWLEDGMENTS AND ADDRESSES

Received March 2, 1976, from *Central Research, Pfizer Inc., Groton, CT 06340.*

Accepted for publication August 5, 1976.

Presented at the Basic Pharmaceutics Section, APhA Academy of Pharmaceutical Sciences, New Orleans meeting, April 1976.

The authors acknowledge L. Van Campen for writing the programs necessary to the calculations and for technical assistance with the manuscript and also C. H. Huang for laboratory assistance.

* Present address: Ortho Pharmaceutical Corp., Raritan, NJ 08876.

[x] To whom inquiries should be directed.

Prostaglandin Monolayers II: Monomolecular Film Behavior of Dinoprost C-15 Alkyl Esters

BERNARD E. SIMS [x] and GLENFORD R. DERR

Abstract □ Monomolecular film compression–relaxation behavior was examined for select dinoprost C-15 alkyl esters. Higher homologs of the series such as palmitate and decanoate esters yielded stable expanded monolayers that exhibited minimal relaxation of surface pressure during noncompression. Their limiting molecular areas were consistent with a Hirschfelder model projection in which the prostaglandin moiety assumes a horizontal orientation at the interface with its alkyl ester chain oriented vertical to the surface plane. Shorter chain homologs such as hexanoate, valerate, butyrate, propionate, and acetate also formed expanded monolayers but exhibited increased instability with decreased alkyl chain length, as reflected in their lower surface pressure development during compression and significant relaxation of pressure during noncompression. Such instability can be tied to their increased solubility in the subphase solution and higher desorption rate from the interface.

Keyphrases □ Dinoprost C-15 alkyl esters, various—monomolecular film compression–relaxation behavior compared □ Films, monomolecular—various dinoprost C-15 alkyl esters, compression–relaxation behavior compared □ Prostaglandins—various dinoprost C-15 alkyl esters, monomolecular film compression–relaxation behavior compared

In recent years, much effort has been directed to elucidating the pharmacological and physiological properties of a new class of biological compounds termed prostaglandins (1–3). Very little attention, however, has been directed toward their possible surface-active properties, even though they have been implicated in various roles portending high surface activity (4–9).

The naturally occurring prostaglandins dinoprost ($F_{2\alpha}$), dinoprostone (E_2), A_1, and B_1 exhibited surface activity in the presence of spread insoluble monomolecular films (10). They in themselves, however, do not tend to form stable monolayers because of their high aqueous solubility. In this article, monolayer film behavior for some long chain alkyl derivatives of dinoprost that do form stable monolayers is reported. This basic and fundamental study should contribute to the limited information available on surface behavior of these ubiquitous and biologically important compounds.

The prostaglandin derivatives selected for monolayer investigation were long chain aliphatic esters of dinoprost attached at the C-15 hydroxyl group (I, R = alkyl). The numbering system generally accepted for prostaglandin-type compounds is with the upper chain carboxylic acid function as the 1-position.

EXPERIMENTAL

Materials—A TLC analysis of the synthesized[1] prostaglandin esters indicated a purity of 99+% for all compounds. Spectroscopic grade hexane–chloroform–methanol (20:2:1) was used as the spreading solvent. Subphase solutions consisted of 0.01 *M* HCl prepared with double-distilled water in an all-glass apparatus with alkaline permanganate.

Equipment—The monolayer balance consisted of a polytef[2]-covered

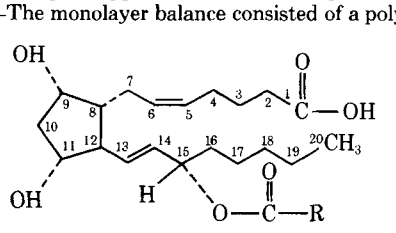

I

[1] By Dr. Walter Morozowich, The Upjohn Co.

[2] Teflon, du Pont.

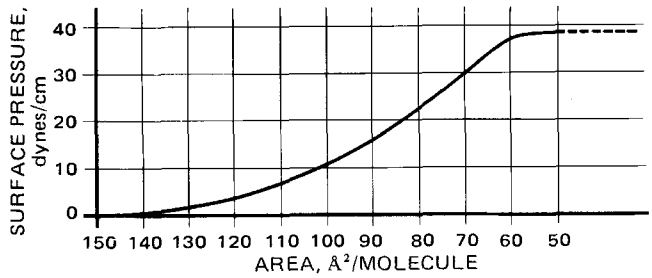

Figure 1—*Monolayer compression–relaxation isotherm generated by dinoprost palmitate ester on 0.01 M HCl subphase at 25° and* v_0 *= 5.17 Å²/molecule-min.*

trough having an area of 315 cm^2 and a width of 10.5 cm. The trough was hollowed out so that water at controlled temperatures could be circulated. This entire unit was enclosed in a large metallic box for protection against dust. The barrier mechanism was driven at controlled rates by means of constant revolutions per minute motors equipped with reversible drive and a positive clutch for an instant stop.

Surface pressure was measured using the Wilhelmy plate method, utilizing a 5-cm roughened platinum plate. Mass changes were measured with an electromagnetic balance[3] and recorded[4]. The balance was housed in a large metallic box above the trough unit and was situated on an elevating stand to facilitate placement of the plate into the subphase. Since vertical movement of the plate was negligible when the self-balancing unit was used (11, 12), it was possible to minimize any errors introduced by possible contact angle change.

General Procedure—Monolayers of the prostaglandins were spread from 1.0-mg/ml solutions of the particular component dissolved in the mixed solvent system. These solutions were added to the surface of the subphase by means of a micrometer syringe[5], which delivered 20–30 μg of material at an initially high area per molecule. After 15 min was allowed for complete spreading and equilibration, the film was subjected to compression at a constant velocity, followed by a period of noncompression to observe relaxation (12–14) and/or dissolution effects.

Each subphase was used only once, and each reported isotherm was reproduced from at least three different spreadings in which areas agreed within ±0.5 Å²/molecule. All experiments were conducted at 25 ± 0.2°.

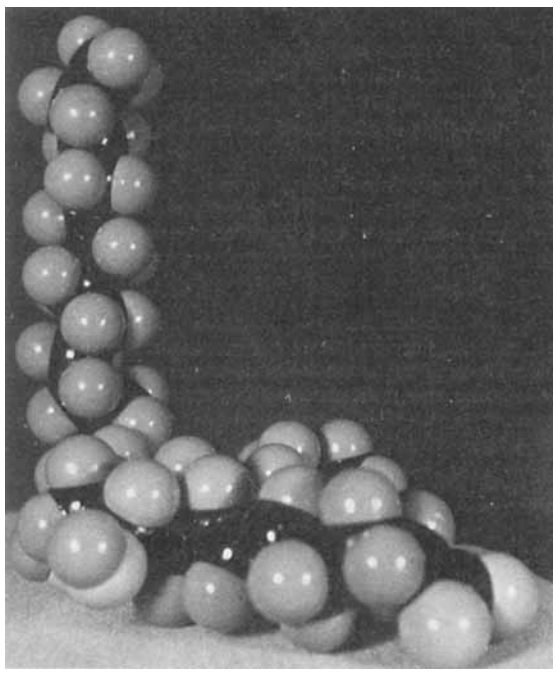

Figure 2—*Hirschfelder molecular model for dinoprost palmitate ester showing vertical orientation of the palmitoyl chain and horizontal orientation of dinoprost moiety in the surface plane (1 cm = 1 Å).*

[3] Cahn RG.
[4] Sargent Welch model SRLG.
[5] Agla, Burroughs-Wellcome.

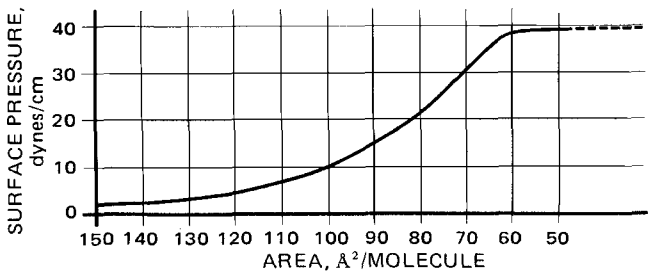

Figure 3—*Monolayer compression–relaxation isotherm generated by dinoprost decanoate ester on 0.01 M HCl subphase at 25° and* v_0 *= 5.17 Å²/molecule-min.*

No significant increment in surface pressure development (>0.2 dyne/cm) was observed upon manual advancement of the barrier over the subphase in the absence of spread film.

RESULTS AND DISCUSSION

The monolayer isotherm obtained for dinoprost palmitate is depicted in Fig. 1. The generally expanded character of the film exhibits surface pressure development at rather high areas per molecule. The isotherm begins to rise rather steeply around 120 Å²/molecule, until collapse is observed at a surface pressure of 40 dynes/cm. During the period of noncompression (dashed lines) immediately following collapse, no relaxation behavior is observed. Such film behavior suggests that lens formation occurs at collapse and that some degree of equilibrium is established between the collapsed bulk phase and monolayer molecules (15).

A limiting area per molecule of 108 Å² can be obtained by extrapolation of the upper linear portion of the curve preceding collapse. This area per molecule agrees very closely with that obtained from a Hirschfelder molecular model projection (Fig. 2). In this molecular configuration, the basic prostaglandin moiety assumes a horizontal orientation within the plane of the surface, with the palmitate chain extended upward and vertical to the surface. The model area projections for such an orientation are approximately 115–98 Å²/molecule. Again, these values appear to be in close agreement with the actual area per molecule of 108 Å² obtained from the π–A isotherm.

A test for this postulated configuration would be to examine another dinoprost C-15 alkyl ester having a significantly different chain length. If the alkyl portion is extended out of the surface, it should not contribute to the limiting area per molecule and both compounds should approximate the same limiting area.

Figure 3 depicts film compression behavior observed for dinoprost decanoate. The π–A compression character is similar to that observed for the palmitate monolayer. The isotherm is expanded at higher areas per molecule and exhibits a relatively rapid surface pressure development at intermediate areas. Collapse occurs at approximately 40 dynes/cm, with no evidence of relaxation during the noncompression period. The limiting area obtained by extrapolation to the area axis yields a value of 103 Å²/molecule. Hence, decreasing the ester chain length by six methylene groups appears to make no major contribution to the observed limiting area per molecule. This finding strongly supports the configuration previously postulated for these prostaglandin esters at the air–solution interface.

In Fig. 4, the monolayer isotherms obtained for dinoprost hexanoate and valerate are presented. Both shorter chained esters produce generally expanded monolayers, as observed with the palmitate and decanoate films. However, the period of noncompression here is characterized by

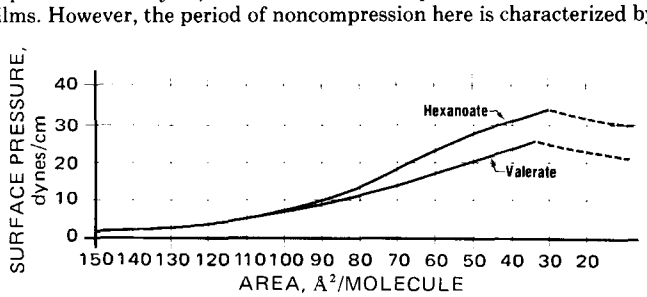

Figure 4—*Monolayer compression–relaxation isotherms generated by dinoprost hexanoate and valerate esters on 0.01 M HCl subphase at 25° and* v_0 *= 5.17 Å²/molecule-min.*

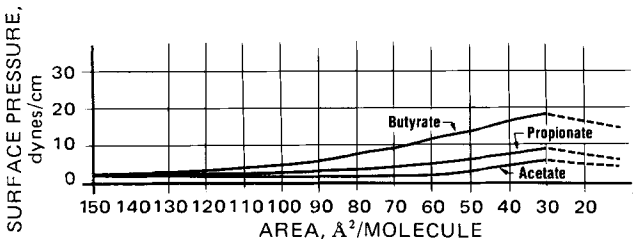

Figure 5—*Monolayer compression–relaxation isotherms generated by dinoprost butyrate, propionate, and acetate esters on 0.01* M *HCl subphase at 25° and* $v_0 = 5.17$ *Å²/molecule-min.*

significant surface pressure reduction, in contrast to the palmitate and decanoate. Another effect of chain length on the stability of these monolayers is seen in the maximum surface pressure developed during compression. The area per molecule at which compression is terminated in Fig. 4 is not a collapse area. Indeed, no collapse is observed for either film. However, under similar conditions of spreading, elapsed time before compression, and compression rate, the hexanoate film is the more stable, as evidenced by the higher surface pressure development throughout the compression sequence. At 32 Å²/molecule, where compression is terminated, the hexanoate film exhibits a maximum pressure of 35 dynes/cm compared to 26.5 dynes/cm for the valerate. The lower pressure of the valerate as well as the surface pressure reduction observed during the noncompression period can be attributed to the shorter chain length and faster dissolution rate from the interface. The hexanoate film is also somewhat soluble in the subphase but to a lesser degree.

Figure 5 presents monolayer behavior for three other members of this alkyl derivative series, butyrate, propionate, and acetate. All three esters tend to accentuate the film behavior previously observed with the hexanoate and valerate films. Monolayer stability is progressively decreased with decreasing alkyl chain length, as evidenced by reductions in surface pressure development during compression. All three compounds exhibit relaxation of surface pressure during noncompression, which appears to be tied directly to their decreased stability as a result of dissolution.

REFERENCES

(1) T. O. Oesterling, W. Morozowich, and T. J. Roseman, *J. Pharm. Sci.*, **61**, 1861 (1972).

(2) B. Samuelsson, E. Granström, K. Gréen, and M. Hamberg, *Ann. N.Y. Acad. Sci.*, **180**, 138 (1971).

(3) W. P. Schneider, in "Prostaglandins," S. M. Karim, Ed., Medical and Technical Publishing Co., Oxford, England, 1972, p. 294.

(4) M. B. Meyers and N. I. Swislocki, *Arch. Biochem. Biophys.*, **164**, 544 (1974).

(5) J. Eggenton, R. J. Flower, P. T. Hardcastle, P. A. Sanford, and D. H. Smyth, *J. Physiol.*, **238** (1), 79P (1974).

(6) B. F. Mize, W. C. Wu, and G. E. Whalen, *Gastroenterology*, **66** (4), 747 (1974).

(7) O. Al-Awqati and W. B. Greenough, *Nature New Biol.*, **238**, 26 (1972).

(8) S. J. Kirtland and H. Baum, *ibid.*, **236**, 47 (1972).

(9) J. B. Smith, C. Ingerman, J. J. Kocsis, and M. J. Silver, *J. Clin. Invest.*, **52**, 965 (1973).

(10) B. Sims and S. L. Holder, *J. Pharm. Sci.*, **63**, 1540 (1974).

(11) G. L. Gaines, Jr., "Insoluble Monolayers at Liquid-Gas Interfaces," Interscience, New York, N.Y., 1966, p. 347.

(12) W. Rabinovitch, R. F. Robertson, and S. G. Mason, *Can. J. Chem.*, **38**, 1881 (1960).

(13) B. E. Sims and G. Zografi, *Chem. Phys. Lipids*, **6**, 109 (1971).

(14) B. E. Sims and G. Zografi, *J. Colloid Interface Sci.*, **41**, 35 (1972).

(15) G. L. Gaines, Jr., "Insoluble Monolayers at Liquid–Gas Interfaces," Interscience, New York, N.Y., 1966, p. 144.

ACKNOWLEDGMENTS AND ADDRESSES

Received June 3, 1976, from *Pharmacy Research, The Upjohn Company, Kalamazoo, MI 49001.*

Accepted for publication August 10, 1976.

[x] To whom inquiries should be directed. Present address: Lederle Laboratories, Pearl River, NY 10965.

Effect of Primidone Concentration on Glass Transition Temperature and Dissolution of Solid Dispersion Systems Containing Primidone and Citric Acid

M. P. SUMMERS [x] and R. P. ENEVER

Abstract □ The glass transition temperatures of glasses containing various concentrations of primidone in citric acid were measured and found to increase as the primidone concentration increased. Dissolution studies of these systems and particle-size measurements of primidone precipitated during dissolution of devitrified glasses suggest that the increase in the dissolution rate of the devitrified systems is due to both the small size of the precipitated crystals and the excellent wettability of these systems.

Keyphrases □ Primidone—solid dispersion systems with citric acid, effect of concentration on glass transition temperature and dissolution □ Citric acid—solid dispersion systems with primidone, effect of primidone concentration on glass transition temperature and dissolution □ Glass transition temperature—primidone–citric acid solid dispersion systems, effect of primidone concentration □ Dissolution—primidone–citric acid solid dispersion systems, effect of primidone concentration □ Solid dispersion systems—primidone–citric acid, effect of primidone concentration on glass transition temperature and dissolution □ Anticonvulsants—primidone, solid dispersion systems with citric acid, effect of concentration on glass transition temperature and dissolution

The use of citric acid as a water-soluble carrier for sparingly soluble drugs was first investigated by Chiou and Riegelman (1). Recently, a study of a solid dispersion system containing primidone in citric acid was reported (2). The systems were prepared by fusing citric acid with primidone; immediately after preparation, they existed in the vitreous state. Both the viscosity of these glasses and their devitrification rate were dependent on the primidone concentration.

Dissolution studies conducted on the devitrified dispersions showed that they dissolved more rapidly than physical mixtures of primidone and citric acid. It was postulated that there was rapid depletion of citric acid from the solid dispersions, leaving a suspension of primi-

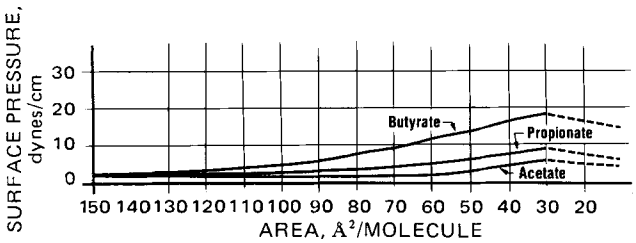

Figure 5—*Monolayer compression–relaxation isotherms generated by dinoprost butyrate, propionate, and acetate esters on 0.01* M *HCl subphase at 25° and* $v_0 = 5.17$ *Å²/molecule-min.*

significant surface pressure reduction, in contrast to the palmitate and decanoate. Another effect of chain length on the stability of these monolayers is seen in the maximum surface pressure developed during compression. The area per molecule at which compression is terminated in Fig. 4 is not a collapse area. Indeed, no collapse is observed for either film. However, under similar conditions of spreading, elapsed time before compression, and compression rate, the hexanoate film is the more stable, as evidenced by the higher surface pressure development throughout the compression sequence. At 32 Å²/molecule, where compression is terminated, the hexanoate film exhibits a maximum pressure of 35 dynes/cm compared to 26.5 dynes/cm for the valerate. The lower pressure of the valerate as well as the surface pressure reduction observed during the noncompression period can be attributed to the shorter chain length and faster dissolution rate from the interface. The hexanoate film is also somewhat soluble in the subphase but to a lesser degree.

Figure 5 presents monolayer behavior for three other members of this alkyl derivative series, butyrate, propionate, and acetate. All three esters tend to accentuate the film behavior previously observed with the hexanoate and valerate films. Monolayer stability is progressively decreased with decreasing alkyl chain length, as evidenced by reductions in surface pressure development during compression. All three compounds exhibit relaxation of surface pressure during noncompression, which appears to be tied directly to their decreased stability as a result of dissolution.

REFERENCES

(1) T. O. Oesterling, W. Morozowich, and T. J. Roseman, *J. Pharm. Sci.*, **61**, 1861 (1972).

(2) B. Samuelsson, E. Granström, K. Gréen, and M. Hamberg, *Ann. N.Y. Acad. Sci.*, **180**, 138 (1971).

(3) W. P. Schneider, in "Prostaglandins," S. M. Karim, Ed., Medical and Technical Publishing Co., Oxford, England, 1972, p. 294.

(4) M. B. Meyers and N. I. Swislocki, *Arch. Biochem. Biophys.*, **164**, 544 (1974).

(5) J. Eggenton, R. J. Flower, P. T. Hardcastle, P. A. Sanford, and D. H. Smyth, *J. Physiol.*, **238** (1), 79P (1974).

(6) B. F. Mize, W. C. Wu, and G. E. Whalen, *Gastroenterology*, **66** (4), 747 (1974).

(7) O. Al-Awqati and W. B. Greenough, *Nature New Biol.*, **238**, 26 (1972).

(8) S. J. Kirtland and H. Baum, *ibid.*, **236**, 47 (1972).

(9) J. B. Smith, C. Ingerman, J. J. Kocsis, and M. J. Silver, *J. Clin. Invest.*, **52**, 965 (1973).

(10) B. Sims and S. L. Holder, *J. Pharm. Sci.*, **63**, 1540 (1974).

(11) G. L. Gaines, Jr., "Insoluble Monolayers at Liquid-Gas Interfaces," Interscience, New York, N.Y., 1966, p. 347.

(12) W. Rabinovitch, R. F. Robertson, and S. G. Mason, *Can. J. Chem.*, **38**, 1881 (1960).

(13) B. E. Sims and G. Zografi, *Chem. Phys. Lipids*, **6**, 109 (1971).

(14) B. E. Sims and G. Zografi, *J. Colloid Interface Sci.*, **41**, 35 (1972).

(15) G. L. Gaines, Jr., "Insoluble Monolayers at Liquid–Gas Interfaces," Interscience, New York, N.Y., 1966, p. 144.

ACKNOWLEDGMENTS AND ADDRESSES

Received June 3, 1976, from *Pharmacy Research, The Upjohn Company, Kalamazoo, MI 49001.*

Accepted for publication August 10, 1976.

[x] To whom inquiries should be directed. Present address: Lederle Laboratories, Pearl River, NY 10965.

Effect of Primidone Concentration on Glass Transition Temperature and Dissolution of Solid Dispersion Systems Containing Primidone and Citric Acid

M. P. SUMMERS [x] and R. P. ENEVER

Abstract □ The glass transition temperatures of glasses containing various concentrations of primidone in citric acid were measured and found to increase as the primidone concentration increased. Dissolution studies of these systems and particle-size measurements of primidone precipitated during dissolution of devitrified glasses suggest that the increase in the dissolution rate of the devitrified systems is due to both the small size of the precipitated crystals and the excellent wettability of these systems.

Keyphrases □ Primidone—solid dispersion systems with citric acid, effect of concentration on glass transition temperature and dissolution □ Citric acid—solid dispersion systems with primidone, effect of primidone concentration on glass transition temperature and dissolution □ Glass transition temperature—primidone–citric acid solid dispersion systems, effect of primidone concentration □ Dissolution—primidone–citric acid solid dispersion systems, effect of primidone concentration □ Solid dispersion systems—primidone–citric acid, effect of primidone concentration on glass transition temperature and dissolution □ Anticonvulsants—primidone, solid dispersion systems with citric acid, effect of concentration on glass transition temperature and dissolution

The use of citric acid as a water-soluble carrier for sparingly soluble drugs was first investigated by Chiou and Riegelman (1). Recently, a study of a solid dispersion system containing primidone in citric acid was reported (2). The systems were prepared by fusing citric acid with primidone; immediately after preparation, they existed in the vitreous state. Both the viscosity of these glasses and their devitrification rate were dependent on the primidone concentration.

Dissolution studies conducted on the devitrified dispersions showed that they dissolved more rapidly than physical mixtures of primidone and citric acid. It was postulated that there was rapid depletion of citric acid from the solid dispersions, leaving a suspension of primi-

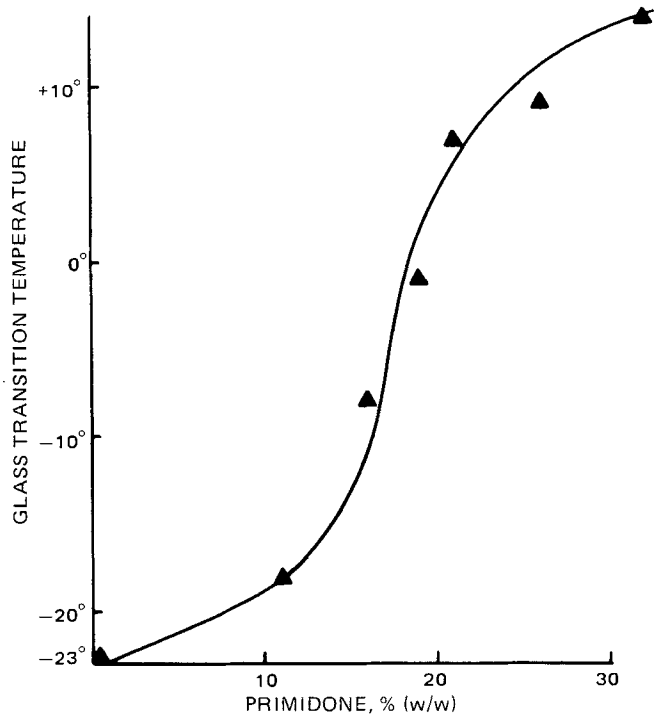

Figure 1—*Variation of the glass transition temperature with primidone concentration.*

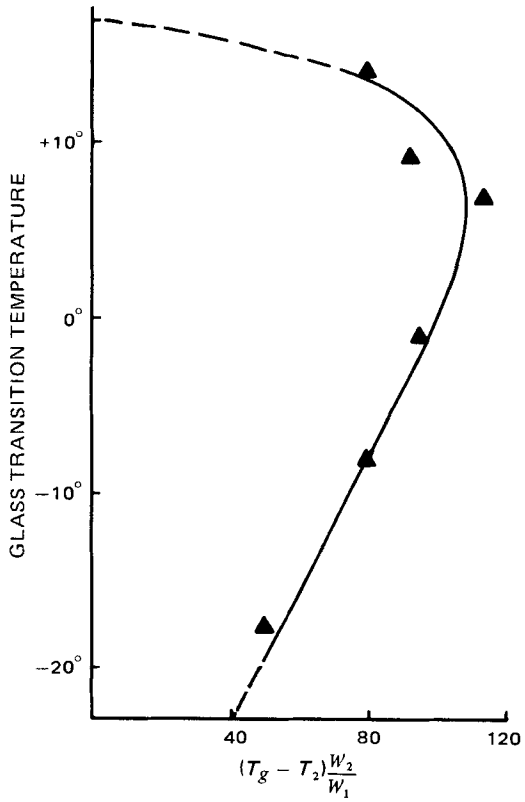

Figure 2—*Plot of the glass transition temperature against* $(T_g - T_2)$ W_2/W_1.

done crystals. The enhanced dissolution rate would then be due, in part, to the small size of these crystals.

The work now reported was conducted to examine the viscous nature of the glasses and to assess the importance of particle size of the precipitated primidone crystals on the dissolution rate of the devitrified systems.

EXPERIMENTAL

Solid Dispersion Systems—The method of preparation was described previously (2).

Glass Transition Temperatures—The glass transition temperatures, T_g, of the vitreous state of the dispersions were measured using a differential scanning calorimeter[1]. A marked shift in the baseline due to a change in the specific heat of the material indicated the transition.

Dispersions containing various concentrations of primidone in citric acid were prepared and poured directly into aluminum sample pans. An aluminum cover was placed on the sample before transferring the pan to the sample holder of the instrument. The sample holder was covered with the low temperature head containing liquid nitrogen to obtain starting temperatures of approximately −20°. A heating rate of 2°/min was used, and at least three determinations were performed on each system studied. The precision of the measurement was ±1°.

Isolation of Primidone Precipitated from Vitreous and Devitrified Dispersions—A 10-g sample of vitreous dispersion containing 16% (w/w) primidone was added to 100 ml of distilled water and shaken until the citric acid dissolved. The resulting suspension of primidone crystals was collected by filtering through a 0.45-μm membrane filter[2]. The crystals were subsequently dried at 50° overnight.

The process was repeated using 10 g of devitrified dispersion containing 16% (w/w) primidone.

The crystallinity and polymorphic form of the precipitated material were checked by X-ray diffraction[3] (2).

Dissolution Studies—Dissolution studies were performed on powdered material using the apparatus and methods previously described (2). The dissolution of 150–250-μm size samples of the following devitrified dispersions in distilled water at 37° was studied: (*a*) 700 mg of a dispersion containing 3% (w/w) primidone (21 mg of primidone), (*b*) 100 mg of a dispersion containing 21% (w/w) primidone (21 mg of primidone), (*c*) 200 mg of a dispersion containing 16% (w/w) primidone (32 mg of primidone), and (*d*) 400 mg of a dispersion containing 8% (w/w) primidone (32 mg of primidone).

The dissolution of physical mixtures produced by adding 150–250-μm size citric acid crystals to the precipitated primidone was also studied by using 200 mg of mixtures containing 16% (w/w) primidone.

Particle-Size Measurement of Primidone—The size distributions of the commercial primidone starting material and the primidone precipitated from the vitreous and devitrified dispersion systems were measured using an automated particle counter[4] fitted with a 50-μm orifice tube. The electrolyte was 0.9% (w/w) sodium chloride previously saturated with primidone at room temperature. The solution was filtered before use through a 0.45-μm membrane filter[2]. Two samples of each system were used, and two determinations were performed on each.

RESULTS AND DISCUSSION

Glass Transition Temperature of Vitreous State—The glass transition temperature may be defined as the temperature at which changes in physical properties such as specific heat and viscosity occur that indicate that the vitreous state is changing to the liquid state. Because of the differing bond lengths and bond strengths in the random structure, the point is ill defined (3, 4).

For a series of glasses containing the same constituents, at a fixed temperature above the transition points of all glasses, the glasses possessing the lowest transition temperatures will be the least viscous. Previous work with primidone–citric acid dispersions showed that the devitrification rate of the systems was dependent upon the primidone concentration and that the most rapidly devitrifying systems were the least viscous (2). The present glass transition data confirm this relationship. As Fig. 1 shows, the smaller the primidone concentration, the lower was the glass transition temperature and hence the lower was the viscosity of the system at ambient temperature.

The glass transition points of all dispersions were below ambient temperature (20°). Therefore, these systems, which previously were re-

[1] Perkin-Elmer DSC-1B, Perkin-Elmer, Beaconsfield, Bucks, United Kingdom.
[2] Oxoid Ltd., London, United Kingdom.
[3] Nonius Mk2 self-focusing Guinier diffractometer.
[4] Model A Coulter counter, Coulter Electronics Ltd., Dunstable, United Kingdom.

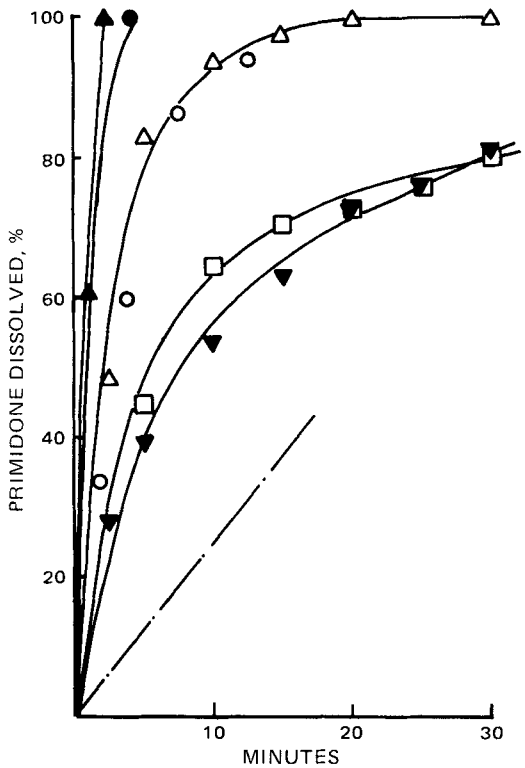

Figure 3—*Dissolution rate of primidone. Key: ▲, 3% (w/w) devitrified system; ●, 8% (w/w) devitrified system; △, 16% (w/w) devitrified system; ○, 21% (w/w) devitrified system; ▼, primidone from 16% (w/w) devitrified system (physical mixture); □, primidone from 16% (w/w) vitreous system (physical mixture); and — · —, 16% physical mixtures previously tested (2), primidone particle size of 150–250 μm.*

ferred to as glasses, are more correctly described as highly viscous supercooled liquids.

Gordon and Taylor (5) derived an equation to predict the variation of the glass transition temperature with composition for a copolymer system:

$$T_g = -k(T_g - T_2)\frac{W_2}{W_1} + T_1 \qquad \text{(Eq. 1)}$$

where T_1 and T_2 are the glass transition temperatures of pure Components 1 and 2, W_1 and W_2 are the weight fractions of the components, and k is a coefficient defined by:

$$k = \Delta B_1/\Delta B_2 \qquad \text{(Eq. 2)}$$

where ΔB is the difference between the coefficients of expansion of the vitreous and liquid states.

Equation 1 is valid provided the following relationship is obeyed (6):

$$A_{AB} = \frac{A_{AA} + A_{BB}}{2} \qquad \text{(Eq. 3)}$$

where A_{AA} and A_{BB} are the bonding energies between molecules of the individual components, and A_{AB} is the bonding energy between molecules in the mixture.

Figure 2 shows a plot of the citric acid–primidone data in accordance with Eq. 1. Since the graph is not a straight line, the system does not obey the ideal situation described by Eq. 1. Similar cases have been shown for copolymer systems (6). The bonding energy between citric acid and primidone molecules is not the arithmetic mean of the bonding energies of the pure components and may support the hypothesis previously advanced (2) that the concentration-dependent devitrification of these systems could be due to extensive formation of strong hydrogen bonds between the component molecules in the vitreous state.

Dissolution Studies of Devitrified Systems Containing Low Primidone Concentrations—Figure 3 shows a plot of the percentage primidone released against time for systems containing 3, 8, 16, and 21% (w/w) primidone. The dissolution profiles of the 16 and 21% (w/w) devitrified systems are the same as those previously published (2) and indicate that the percentage primidone released is independent of the

Table I—Particle-Size Data of Primidone Crystals

Source of Crystals	Mean Particle Diameter, μm	*SD*
3% (w/w) devitrified glass	5.2 ± 0.3	2.10
8% (w/w) devitrified glass	4.6 ± 0.2	1.91
16% (w/w) devitrified glass	4.7 ± 0.3	2.06
21% (w/w) devitrified glass	4.7 ± 0.3	1.91
32% (w/w) devitrified glass	4.5 ± 0.3	1.92
16% (w/w) glass	4.2 ± 0.2	1.95
Commercial material	6.2 ± 0.4	2.17

primidone content of the sample. However, the 3 and 8% (w/w) primidone systems do not follow this pattern, even though the quantities of primidone in the samples are equivalent to those in the 21 and 16% (w/w) systems, respectively.

Particle-Size Measurement of Precipitated Crystals—Table I shows the mean particle diameter of primidone precipitated from the solid dispersion systems, together with values for the standard deviations of the log-normal distributions. Prior to particle-size measurement, the crystals were well dispersed with an octylphenol–ethylene oxide polymer[5] so measurements were conducted on a suspension of individual particles.

The mean diameter and size distribution of the precipitated crystals did not vary significantly between systems containing different concentrations of primidone. The mean diameter of the commercial sample was, however, slightly larger than that of the precipitated crystals.

Dissolution Studies of Physical Mixtures of Precipitated Primidone and Citric Acid—The results of the dissolution studies of 16% (w/w) physical mixtures of primidone precipitated from the dispersion before and after devitrification are shown in Fig. 3. X-Ray diffraction studies confirmed that the precipitate was the crystalline Form II primidone polymorph. The data in Fig. 3 indicate that the smaller particle size of the primidone in these mixtures was responsible for an increased dissolution rate when compared with physical mixtures previously tested (containing primidone of 152–250-μm size) (2). The dissolution rates,

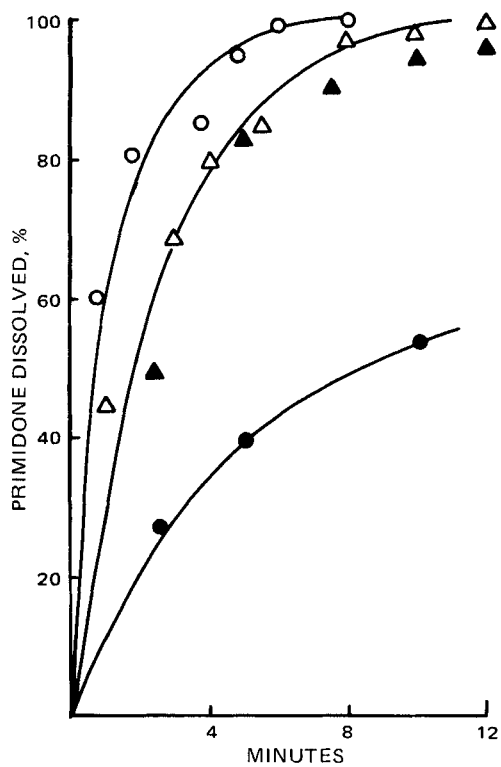

Figure 4—*Effect of dispersal with polyethylene glycol 300 on the dissolution rate of primidone. Key: ○, 16% (w/w) physical mixture (dispersed); ●, 16% (w/w) physical mixture (not dispersed); △, 16% (w/w) devitrified system (dispersed); and ▲, 16% (w/w) devitrified system (not dispersed).*

[5] Nonidet P40, British Drug Houses, Poole, Dorset, United Kingdom.

however, were not as rapid as those from the 16% (w/w) devitrified dispersion.

It is doubtful whether the increased solubility of primidone in the citric acid contained in the diffusion layer surrounding the dissolving devitrified dispersion could account for the differences in dissolution of the physical mixture and the devitrified dispersion. If it is assumed that the diffusion layer thickness is about 3×10^{-3} cm (7) and that the diffusion layer is saturated with citric acid, then calculations indicate that the maximum amount of primidone that could be in solution is 1–10% of the primidone content of the system (depending upon the primidone concentration in the dispersion). Thus, a gross excess of primidone is present in all cases.

The precipitated primidone crystals were very cohesive, and incomplete wetting could have inhibited dissolution from the physical mixtures. To test this possibility, the dissolution experiment was repeated using another 200-mg sample of the 16% (w/w) physical mixture of precipitated primidone and citric acid previously dispersed with 0.4 ml of polyethylene glycol 300[6]. A sample of the 16% (w/w) devitrified dispersion was also examined in the same manner. From the results (Fig. 4), it can be seen that the dissolution of the devitrified dispersion was not significantly affected by the addition of the polyethylene glycol. The dissolution of the physical mixture was, however, increased and was greater than that of the devitrified dispersion, even though complete dispersal of the mixture was not achieved.

These results indicate that the primidone particles precipitated during dissolution of the devitrified system remain as loose agglomerates during the dissolution process. The collection of these particles and their redispersal with polyethylene glycol in the mixture with citric acid probably result in the destruction of these agglomerates to produce individual particles. The resulting increase in the primidone surface area is responsible for the higher dissolution rate seen with these physical mixtures.

The enhanced dissolution rate of primidone in these devitrified systems (2) is thus confirmed to be due to the reduction in particle size of the primidone in the system and the improved wetting characteristics of the solid dispersion system. Nevertheless, the dissolution rate is impaired by the failure of the precipitated primidone particles to separate completely during dissolution. The enhanced dissolution rates of the 3 and 8% (w/w) devitrified glasses could be due to better particle separation during dissolution.

[6] Koch Light Laboratories, Colnbrook, Bucks, United Kingdom.

CONCLUSIONS

Interactions between primidone and citric acid occur when they are fused together, and viscous supercooled liquids are produced when the melt is cooled. The viscosity of the supercooled liquids increases with increasing primidone concentration, as reflected in an increased glass transition temperature.

During dissolution of the devitrified systems, primidone is precipitated in aggregates of fine particles. The relatively large surface area produced by this process results in the powdered devitrified dispersions (150–250-μm size) having a faster rate of dissolution than physical mixtures of primidone and citric acid of the same size.

The aggregation of primidone particles during dissolution appears to be dependent on the primidone concentration in the dispersion. At low concentrations (3% w/w), the aggregation is less than at 8–16% (w/w), resulting in a faster dissolution of primidone from the devitrified dispersion.

REFERENCES

(1) W. L. Chiou and S. Riegelman, *J. Pharm. Sci.*, **58**, 1505 (1969).

(2) M. P. Summers and R. P. Enever, *ibid.*, **65**, 1613 (1976).

(3) G. O. Jones, "Glass," Wiley, New York, N.Y., 1958, p. 46.

(4) J. M. Stevels, "Progress in the Theory of the Physical Properties of Glass," Elsevier, New York, N.Y., 1948, pp. 1–5.

(5) M. Gordon and J. S. Taylor, *J. Appl. Chem.*, **2**, 493 (1952).

(6) G. Kanig, *Kolloid-Z. Z.-Polym.*, **190**, 1 (1963). [Royal Aircraft Establishment Library Translation, No. 1135 (1965).]

(7) L. L. Bircumshaw and A. C. Riddiford, *Q. Rev.*, **6**, 157 (1952).

ACKNOWLEDGMENTS AND ADDRESSES

Received June 1, 1976, from the *Department of Pharmaceutics, School of Pharmacy, University of London, London, WC1N 1AX, England.*

Accepted for publication August 6, 1976.

[x] To whom inquiries should be directed.

Phytochemical Investigation of Xanthones of *Eustoma grandiflorum* (Raf.) Shinners

GERALD SULLIVAN [x], FRANCIS D. STILES, and KARL-HEINZ A. ROSLER *

Abstract □ Six polyoxygenated xanthones were isolated from the roots of *Eustoma grandiflorum* (Raf.) Shinners collected in Texas. Structural elucidation of five of these xanthones (1-hydroxy-3,7-dimethoxyxanthone, 1-hydroxy-3,5-dimethoxyxanthone, 1-hydroxy-3,5,6,7-tetramethoxyxanthone, 1-hydroxy-3,5,6,7,8-pentamethoxyxanthone, and 1-hydroxy-3,7,8-trimethoxyxanthone) was accomplished *via* UV, IR, NMR, and mass spectrometry; traditional physical–chemical methods; or direct comparison with a prepared derivative. The sixth xanthone derivative was characterized incompletely. The pentamethoxyxanthone is a new compound and has been designated generically as eustomin. The probable occurrence of these six xanthone compounds in the plant as glycosides is reported.

Keyphrases □ *Eustoma grandiflorum*—methanol extract of roots, six polyoxygenated xanthones isolated □ Xanthones, polyoxygenated—six isolated from methanol extract of roots of *Eustoma grandiflorum* □ Hydroxyxanthones—six isolated from methanol extract of roots of *Eustoma grandiflorum*

Eustoma grandiflorum (Raf.) Shinners (Gentianaceae), a plant primarily indigenous to the southwestern portion of the United States, is commonly referred to as the catchfly-gentian, Texas bluebell, and lira de San Pedro. It has a very showy, eye-catching flower, blooming in great profusion in several areas of Texas. A prominent taproot is evident, and even a cursory examination reveals a bright yellow pigment.

The Gentianaceae family is known to produce xanthone derivatives liberally, and several have been isolated from related genera such as *Canscora, Frasera, Gentiana,* and *Swertia* (1–5). Plant extracts obtained from these genera

however, were not as rapid as those from the 16% (w/w) devitrified dispersion.

It is doubtful whether the increased solubility of primidone in the citric acid contained in the diffusion layer surrounding the dissolving devitrified dispersion could account for the differences in dissolution of the physical mixture and the devitrified dispersion. If it is assumed that the diffusion layer thickness is about 3×10^{-3} cm (7) and that the diffusion layer is saturated with citric acid, then calculations indicate that the maximum amount of primidone that could be in solution is 1–10% of the primidone content of the system (depending upon the primidone concentration in the dispersion). Thus, a gross excess of primidone is present in all cases.

The precipitated primidone crystals were very cohesive, and incomplete wetting could have inhibited dissolution from the physical mixtures. To test this possibility, the dissolution experiment was repeated using another 200-mg sample of the 16% (w/w) physical mixture of precipitated primidone and citric acid previously dispersed with 0.4 ml of polyethylene glycol 300[6]. A sample of the 16% (w/w) devitrified dispersion was also examined in the same manner. From the results (Fig. 4), it can be seen that the dissolution of the devitrified dispersion was not significantly affected by the addition of the polyethylene glycol. The dissolution of the physical mixture was, however, increased and was greater than that of the devitrified dispersion, even though complete dispersal of the mixture was not achieved.

These results indicate that the primidone particles precipitated during dissolution of the devitrified system remain as loose agglomerates during the dissolution process. The collection of these particles and their redispersal with polyethylene glycol in the mixture with citric acid probably result in the destruction of these agglomerates to produce individual particles. The resulting increase in the primidone surface area is responsible for the higher dissolution rate seen with these physical mixtures.

The enhanced dissolution rate of primidone in these devitrified systems (2) is thus confirmed to be due to the reduction in particle size of the primidone in the system and the improved wetting characteristics of the solid dispersion system. Nevertheless, the dissolution rate is impaired by the failure of the precipitated primidone particles to separate completely during dissolution. The enhanced dissolution rates of the 3 and 8% (w/w) devitrified glasses could be due to better particle separation during dissolution.

[6] Koch Light Laboratories, Colnbrook, Bucks, United Kingdom.

CONCLUSIONS

Interactions between primidone and citric acid occur when they are fused together, and viscous supercooled liquids are produced when the melt is cooled. The viscosity of the supercooled liquids increases with increasing primidone concentration, as reflected in an increased glass transition temperature.

During dissolution of the devitrified systems, primidone is precipitated in aggregates of fine particles. The relatively large surface area produced by this process results in the powdered devitrified dispersions (150–250-μm size) having a faster rate of dissolution than physical mixtures of primidone and citric acid of the same size.

The aggregation of primidone particles during dissolution appears to be dependent on the primidone concentration in the dispersion. At low concentrations (3% w/w), the aggregation is less than at 8–16% (w/w), resulting in a faster dissolution of primidone from the devitrified dispersion.

REFERENCES

(1) W. L. Chiou and S. Riegelman, *J. Pharm. Sci.*, **58**, 1505 (1969).

(2) M. P. Summers and R. P. Enever, *ibid.*, **65**, 1613 (1976).

(3) G. O. Jones, "Glass," Wiley, New York, N.Y., 1958, p. 46.

(4) J. M. Stevels, "Progress in the Theory of the Physical Properties of Glass," Elsevier, New York, N.Y., 1948, pp. 1–5.

(5) M. Gordon and J. S. Taylor, *J. Appl. Chem.*, **2**, 493 (1952).

(6) G. Kanig, *Kolloid-Z. Z.-Polym.*, **190**, 1 (1963). [Royal Aircraft Establishment Library Translation, No. 1135 (1965).]

(7) L. L. Bircumshaw and A. C. Riddiford, *Q. Rev.*, **6**, 157 (1952).

ACKNOWLEDGMENTS AND ADDRESSES

Received June 1, 1976, from the *Department of Pharmaceutics, School of Pharmacy, University of London, London, WC1N 1AX, England.*

Accepted for publication August 6, 1976.

[x] To whom inquiries should be directed.

Phytochemical Investigation of Xanthones of *Eustoma grandiflorum* (Raf.) Shinners

GERALD SULLIVAN [x], FRANCIS D. STILES, and KARL-HEINZ A. ROSLER *

Abstract □ Six polyoxygenated xanthones were isolated from the roots of *Eustoma grandiflorum* (Raf.) Shinners collected in Texas. Structural elucidation of five of these xanthones (1-hydroxy-3,7-dimethoxyxanthone, 1-hydroxy-3,5-dimethoxyxanthone, 1-hydroxy-3,5,6,7-tetramethoxyxanthone, 1-hydroxy-3,5,6,7,8-pentamethoxyxanthone, and 1-hydroxy-3,7,8-trimethoxyxanthone) was accomplished *via* UV, IR, NMR, and mass spectrometry; traditional physical–chemical methods; or direct comparison with a prepared derivative. The sixth xanthone derivative was characterized incompletely. The pentamethoxyxanthone is a new compound and has been designated generically as eustomin. The probable occurrence of these six xanthone compounds in the plant as glycosides is reported.

Keyphrases □ *Eustoma grandiflorum*—methanol extract of roots, six polyoxygenated xanthones isolated □ Xanthones, polyoxygenated—six isolated from methanol extract of roots of *Eustoma grandiflorum* □ Hydroxyxanthones—six isolated from methanol extract of roots of *Eustoma grandiflorum*

Eustoma grandiflorum (Raf.) Shinners (Gentianaceae), a plant primarily indigenous to the southwestern portion of the United States, is commonly referred to as the catchfly-gentian, Texas bluebell, and lira de San Pedro. It has a very showy, eye-catching flower, blooming in great profusion in several areas of Texas. A prominent taproot is evident, and even a cursory examination reveals a bright yellow pigment.

The Gentianaceae family is known to produce xanthone derivatives liberally, and several have been isolated from related genera such as *Canscora, Frasera, Gentiana,* and *Swertia* (1–5). Plant extracts obtained from these genera

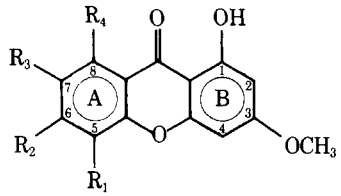

I: $R_1 = R_2 = R_4 = H$, $R_3 = OCH_3$
II: $R_1 = OCH_3$, $R_2 = R_3 = R_4 = H$
III: $R_1 = R_2 = R_3 = OCH_3$, $R_4 = H$
IV: $R_1 = R_2 = R_3 = R_4 = OCH_3$
V: $R_1 = R_2 = H$, $R_3 = R_4 = OCH_3$

are used to treat various ailments including constipation, nervous debility, tuberculosis, fever, and anorexia. Since certain chemotaxonomic relationships often occur among related genera and since results of a preliminary TLC examination of the root extract were promising, it was postulated that xanthones might be present in *E. grandiflorum*.

EXPERIMENTAL

Instrumentation—All NMR spectra[1] were determined in deuterated chloroform solutions in microcells unless otherwise stated. Tetramethylsilane served as an internal standard. IR spectra[2] were determined in potassium bromide pellets. Only significant bands are quoted. All molecular weights were obtained by mass spectrometry[3]. UV spectra were determined with a double-beam spectrophotometer[4] equipped with a recorder[5]. Determinations were made in 95% ethanol unless otherwise stated.

Melting points were determined on a Koffler hot-stage microscope and are uncorrected. Sublimation was performed in a sublimation tube fitted with a cold-finger condenser under vacuum and heat. Silicone fluid[6] was used as the heating medium. Liquid chromatography[7] was performed with Porasil A (37–75 μm) as the column packing and chloroform–methanol (5:1) as the mobile phase.

Plant Material—The plant material was collected near Brenham, Washington County, Tex., in late August of 1971[8]. The air-dried roots (705 g) were ground to a coarse powder in a Wiley mill and subjected to continuous soxhlet extraction with methanol for 60 hr.

TLC—Several investigators (1–5) used TLC procedures to separate xanthones, but none of these procedures was satisfactory for this investigation. Silica gel G plates, prepared according to Stahl (6) and developed in benzene–ethyl acetate–acetic acid (90:5:5), resulted in excellent separation of xanthone constituents. Examination of the methanol extract by this procedure indicated the possible presence of five xanthone constituents. These constituents were detected visually as discrete yellow spots or by UV light whereby the spots fluoresced a rust-red color. This system was employed in all preparative work unless otherwise stated.

Hydrolysis of Root Extract—The methanol was removed under reduced pressure, and the resulting dark-reddish-black extract was treated with four 500-ml portions of 3% aqueous hydrochloric acid. Each portion was boiled over steam for 1 hr, and finally all portions were combined and allowed to cool.

Partition of Hydrolyzed Root Extract—The cooled hydrolyzed root extract was partitioned with benzene. Initial partitions were deep red in color, but repeated partitionings were carried out until a colorless benzene fraction was obtained. The aqueous portions were discarded. The benzene portions were combined, filtered, and allowed to stand at room temperature for several hours. A lemon-yellow compound precipitated from the pooled benzene fractions and was removed by gravity filtration.

Isolation of Xanthone II—The lemon-yellow precipitate from the benzene fractions was purified by column chromatography[9], employing dichloromethane as the eluting solvent. It was crystallized from methanol as yellow needles and designated Xanthone II.

Benzene Partitions—The fraction containing benzene partitions from which Xanthone II had precipitated was placed on a chromatographic column and eluted with dichloromethane. Three major fractions, A-1, A-2, and A-3, were collected.

Xanthone I from Fraction A-1—Fraction A-1 was subjected to high-pressure liquid chromatography with a mobile phase of chloroform–methanol (5:1). One yellow compound was obtained and further purified by preparative TLC. The compound was recrystallized as fluffy, pale-yellow needles from methanol and designated Xanthone I.

Xanthone III from Fraction A-2—Preparative TLC of Fraction A-2, using benzene–ethyl acetate–acetic acid (90:5:5), yielded a yellow compound. Upon recrystallization from methanol, this compound was crystallized as pale-yellow needles and labeled Xanthone III.

Xanthones IV and V from Fraction A-3a—Fraction A-3 was placed on a column and again eluted with dichloromethane, resulting in the collection of two distinct fractions, A-3a and A-3b. Fraction A-3a was subjected to preparative TLC with carbon tetrachloride–methanol (25:1) as the solvent system. Two compounds, Xanthones IV and V, were obtained as pale-yellow needles from methanol.

Xanthone VI from Fraction A-3b—This fraction was evaporated to dryness and sublimed under reduced pressure. This procedure yielded a small amount of yellow material, which was recrystallized from methanol as yellow needles and designated Xanthone VI.

RESULTS AND DISCUSSION

Preliminary examination of the methanol extract of the root material of *E. grandiflorum* by TLC initially revealed the possible presence of five xanthone constituents. These constituents exhibited R_f values of 0.93, 0.86, 0.79, 0.63, and 0.49. It was later shown that six xanthone derivatives had actually been isolated, since two compounds exhibited identical migration patterns and resided at R_f 0.63. These two xanthones were easily separated by TLC procedures with a solvent system of carbon tetrachloride–methanol (25:1). These compounds then exhibited R_f values of 0.73 and 0.65.

The structural characterization of the isolated and purified compounds is discussed in the order in which they were isolated.

1-Hydroxy-3,5-dimethoxyxanthone (II)—This compound exhibited an R_f value of 0.86 and a melting point of 174°. Its UV absorption spectrum was characteristic of a 1,3,5-trioxygenated xanthone (7). Mass spectrometry revealed the parent ion and base peak to be *m/e* 272, corresponding to a xanthone derivative containing one hydroxyl and two methoxyl functions. The compound exhibited positive ferric chloride (8) and Wilson's boric acid (9) tests and was insoluble in aqueous sodium carbonate (1)[10].

These chemical and physical data indicated the presence of a free phenolic hydroxyl *ortho* to a carbonyl and also a methoxyl group at C-3 on the xanthone nucleus. Further confirmation of the hydroxyl function *ortho* to a carbonyl was accomplished utilizing IR spectrometry, since a strong band due to carbonyl absorption occurred near 1650 cm^{-1} (7, 8). Xanthone II exhibited a significant band at 1650 cm^{-1}. Final elucidation was accomplished utilizing NMR spectroscopy. Two singlets representing six protons at 6.17 and 6.03 τ accounted for the presence of two methyl group protons. From previous NMR studies, it was shown that a xanthone having substituents at C-1 and C-3 exhibited characteristic signals. In general, a pair of doublets occurred in the 3.2–3.7 τ region. The proton on C-2 always occurred at a higher field than the proton on C-4.

Furthermore, a signal far downfield may be attributed to a hydroxyl proton on C-1 (or the equivalent C-8 position) due to a deshielding effect of the adjacent carbonyl (2, 10). Thus, two doublets at 3.68 and 3.48 τ represented two aromatic protons, one at C-2 and the other at C-4. A signal far downfield at −2.31 τ represented a hydroxyl proton on C-1. Carbons 1 and 3 must be occupied by a hydroxyl and a methoxyl function, respectively. Since all positions on ring B were accounted for, only ring

[1] Japanese Electron Optics Lab. model C-60 HL or Varian A-60 spectrometer.
[2] Beckman IR 5A.
[3] DuPont Instruments model 214-91 spectrometer.
[4] Perkin-Elmer model 124.
[5] Rikka Denki model B-161.
[6] Dow Corning DC550.
[7] Waters Associates model ALC/GPC-202 liquid chromatograph.
[8] The plant material utilized was identified as *Eustoma grandiflorum* (Raf.) Shinners (Gentianaceae) by Dr. B. L. Turner, Department of Botany, University of Texas at Austin. A voucher specimen [Sullivan–S. N. (Acc. No. 298773)] representing material collected for this investigation is available for inspection at the Herbarium, Department of Botany, University of Texas at Austin.
[9] All separations by column chromatography were carried out by using 100–200-mesh Bio Sil A silicic acid.
[10] All test reagents were prepared immediately prior to use.

A could contain the remaining methoxyl function. A quartet at 2.20 τ was indicative of a proton on C-8 splitting with two protons exhibiting a multiplet at 2.68–3.03 τ on C-6 and C-7 (2). Thus, the second methoxyl group was placed at C-5.

NMR: −2.31 (s, OH), 3.68 (d, 2-H), 3.48 (d, 4-H), 2.68–3.03 (m, 6,7-H), 2.20 (q, 8-H), 6.17 (s, 3,5-OCH_3), and 6.03 (s) ppm [lit. (11) NMR ($CDCl_3$): 3.69 (d, 2-H), 3.51 (d, 4-H), 2.65–3.00 (m, 6,7-H), and 2.24 (q, 8H) ppm]; UV: λ_{max} (ethanol) 354 (log ϵ 3.53), 307 (4.10), and 244 (4.49) nm [lit. (11) UV: λ_{max} (ethanol) 355 (log ϵ 3.75), 306 (4.28), and 245 (4.60) nm; (1) 308 (4.27) and 245 (4.60) nm; (12) 355 (3.66), 335 sh (3.70), 310 (4.24), and 245 (4.59) nm]; mp 174° [lit. (1) mp 173–174°; (11) 174–175°; (12) 170–171°]; IR_{max}: 1650, 1613, and 1577 cm^{-1} [lit. (11) IR (mineral oil mull): 1662, 1610, and 1575 cm^{-1}].

1-Hydroxy-3,7-dimethoxyxanthone (I)—The second compound isolated and purified exhibited an R_f value of 0.93 and a melting point of 168–169°. Mass spectrometry revealed the parent ion and base peak to be *m/e* 272. This mass again corresponds to a xanthone derivative having one hydroxyl function and two methoxyl groups. It exhibited positive Wilson's boric acid and ferric chloride tests and was insoluble in aqueous sodium carbonate. These data similarly pointed to a compound having a free phenolic hydroxyl *ortho* to a carbonyl and the presence of a methoxyl group at C-3. IR spectrometry verified the presence of an *ortho*-hydroxyl, since a major band of absorption occurred at 1645 cm^{-1}.

By utilizing NMR spectroscopy, final structural elucidation was accomplished. Two singlets representing six protons at 6.10 and 6.11 τ corresponded to two methyl group protons, while two doublets at 3.69 and 3.60 τ occurred due to a proton at C-2 and C-4, respectively. A low field signal at −2.92 τ indicated the presence of a hydroxyl proton on C-1. These assignments placed a hydroxyl and a methoxyl function on ring B, thus leaving final placement of the second methoxyl on ring A. A multiplet at 2.68 τ was attributed to single protons on C-5 and C-6, while a quartet at 2.40 τ arose from a proton splitting with those on C-5 and C-6 and was assigned to C-8. Thus, the second methoxyl substituent must be located at C-7.

NMR: −2.92 (s, OH), 3.69 (d, 2-H), 3.60 (d, 4-H), 2.68 (m, 5,6-H), 2.40 (q, 8-H), 6.10 (s, 3,7-OCH_3), and 6.11 (s) ppm [lit. (2) NMR ($CDCl_3$): −2.94 (s, OH), 3.70 (d, 2-H), 3.58 (d, 4-H), 2.68 (m, 5,6-H), and 2.41 (q, 8H) ppm]; UV: λ_{max} (ethanol) 368 (log ϵ 3.76), 307 (4.12), 260 (4.58), and 232 (4.49) nm [lit. (13) UV: λ_{max} (ethanol) 311 (log ϵ 4.2), 261 (4.7), and 239 (4.5) nm; (14) (methanol) 369 (3.83), 292 (4.39), 259 (4.59), and 231 (4.54) nm; (2) (ethanol) 396 (4.80), 308 (4.14), 259 (4.59), and 238 (4.46) nm]; mp 168–169° [lit. (2) mp 167.5–169°; (15) 167°]; IR_{max}: 1645, 1608, and 1575 cm^{-1}.

As further proof of structure, a synthesis of I (methylgentisin) was accomplished by selective methylation of commercially available gentisin[11] (1,7-dihydroxy-3-methoxyxanthone) (11). Simultaneous development of I with methylgentisin on a TLC plate gave identical spots having an R_f value of 0.93. Chemical and physical test results were identical to those obtained for I. Furthermore, spectral data were also almost identical to those obtained for I.

NMR ($CDCl_3$): −2.94 (s, OH), 3.70 (d, 2-H), 3.58 (d, 4-H), 2.68 (m, 5,6-H), 2.41 (q, 8-H), 6.08 (s, 3,7-OCH_3), and 6.11 (s) ppm; UV: λ_{max} 234, 258, 306, and 368 nm; mp 168°; IR_{max}: 1645, 1610, and 1577 cm^{-1}.

1-Hydroxy-3,5,6,7-tetramethoxyxanthone (III)—Xanthone III exhibited an R_f value of 0.79 and a melting point of 178°. Mass spectrometry indicated a parent ion and base peak at *m/e* 332, corresponding to a xanthone compound having one hydroxyl group and four methoxyl functions. Chemical and physical test results were identical to those mentioned for the previous compounds, and an IR analysis showed a major band at 1653 cm^{-1}. NMR data indicated three singlets at 5.95, 6.04, and 6.15 τ, which were assigned to four methyl group protons. Two doublets at 3.64 and 3.47 τ were assigned to protons on C-2 and C-4, respectively.

From the preceding data, it could be ascertained that all positions on ring B were fully accounted for, with one hydroxyl group on C-1 and a methoxyl group on C-3. Therefore, the three methoxyl functions left to be assigned could only be on ring A. With three of four positions on ring A being occupied, only one singlet for an aromatic proton would be expected; indeed, this signal was observed at 2.70 τ. This signal was assigned to a proton on C-8, while another singlet far downfield at −2.93 τ was assigned to the hydroxyl proton on C-1. These assignments placed the remaining three methoxyl groups at C-5, C-6, and C-7.

NMR: −2.93 (s, OH), 3.64 (d, 2-H), 3.47 (d, 4-H), 2.70 (s, 8-H), 5.95 (s, 3,5,6,7-OCH_3), 6.04 (s), and 6.15 (s) ppm [lit. (3) NMR ($CDCl_3$): 3.76 (d, 2-H), 3.60 (d, 4-H), 2.70 (s, 8-H), 6.03 (s, 3,5,6,7-OCH_3), 6.13 (s), and 6.20 (s) ppm]; UV: λ_{max} (ethanol) 364 (log ϵ 4.03), 311 (4.44), 258 (4.74), and 239 (4.64) nm [lit. (3) UV: λ_{max} (methanol) 364 (log ϵ 3.81), 312 (4.18), 258 (4.49), and 240 (4.35) nm]; mp 178°; IR_{max}: 1653, 1608, and 1582 cm^{-1}.

1-Hydroxy-3,5,6,7,8-pentamethoxyxanthone (IV)—This compound exhibited an R_f value of 0.63 with benzene–ethyl acetate–acetic acid (90:5:5) as the solvent system and an R_f value of 0.73 with carbon tetrachloride–methanol (25:1). A melting point of 108–109° was observed. Mass spectrometry indicated the parent ion and base peak to be at *m/e* 362. This mass corresponds with a xanthone derivative having one hydroxyl and five methoxyl groups. It produced positive Wilson's boric acid and ferric chloride tests and was insoluble in aqueous sodium carbonate.

The IR spectrum exhibited a major band at 1653 cm^{-1}. NMR indicated four singlets at 6.05, 5.99, 5.93, and 5.80 τ, corresponding to five methyl group protons. Doublets at 3.58 and 3.43 τ were assigned to protons on C-2 and C-4, respectively. A single signal at −3.37 τ was indicative of a hydroxyl proton located on C-1. The characteristic pattern of doublets, the singlet far downfield, and data just mentioned indicated the presence of a hydroxyl group on C-1 and a methoxyl group on C-3. Thus, all positions on ring B were accounted for, leaving only ring A to accommodate the four remaining methoxyl groups. With only four positions available for substitution, no signal downfield would be anticipated if all four positions were occupied. This was indeed the case, as no downfield signal (other than that far downfield for the hydroxyl proton on C-1) was noted. Thus, the compound in question must be 1-hydroxy-3,5,6,7,8-pentamethoxyxanthone (IV). This compound has never been reported in the literature and has been named eustomin.

NMR: −3.37 (s, OH), 3.58 (d, 2-H), 3.43 (d, 4-H), 5.80 (s, 3,5,6,7,8-OCH_3), 5.93 (s), 5.99 (s), and 6.05 (s) ppm; UV: λ_{max} (ethanol) 350 sh (log ϵ 3.71), 312 (4.27), and 255 (4.55) nm; mp 108–109°; IR_{max}: 1653, 1595, and 1590 cm^{-1}.

1-Hydroxy-3,7,8-trimethoxyxanthone (V)—The fifth compound isolated exhibited an R_f value of 0.63 with benzene–ethyl acetate–acetic acid (90:5:5) as the solvent system and an R_f value of 0.65 with carbon tetrachloride–methanol (25:1). A melting point of 150–151° was noted. Mass spectrometry showed a parent ion and base peak at *m/e* 302. This mass corresponds to a xanthone compound having one hydroxyl and three methoxyl functions. Chemical and physical tests provided results identical to those mentioned for previous compounds, while the IR spectrum indicated a major band at 1642 cm^{-1}.

NMR analysis revealed two singlets at 6.15, 6.08, and 6.00 τ, representing three methyl group protons. A singlet at −3.10 τ represented a hydroxyl proton on C-1; a peak at 3.69 τ, which arose from two overlapping doublets, was assigned to protons on C-2 and C-4. Thus, once again a 1,3-dioxygenation pattern was evident with a hydroxyl group at C-1 and a methoxyl function at C-3. Therefore, only ring A was available to accommodate the two remaining methoxyl groups. Signals assigned to protons on C-5 and C-6 exhibited peaks at 2.83 and 2.74 τ, thus leaving only positions C-7 and C-8 to accommodate the methoxyl functions.

NMR: −3.10 (s, OH), 3.69 (d, 2-H), 3.69 (d, 4-H), 2.83 (s, 5-H), 2.74 (s, 6-H), 6.00 (s, 3,7,8-OCH_3), 6.08 (s), and 6.15 (s) ppm [lit. (4) NMR ($CDCl_3$): −3.30 (s, OH), 3.69 (d, 2-H), 3.69 (d, 4-H), 2.86 (s, 5H), 2.65 (s, 6-H), 5.99 (s, 3,7,8-OCH_3), 6.07, and 6.11 ppm]; UV: λ_{max} (ethanol) 373 (log ϵ 3.62), 312 (4.13), 261 (4.52), and 241 (4.44) nm [lit. (7) UV: λ_{max} (ethanol) 380 (log ϵ 3.7), 315 (4.1), 260 (4.6), and 242 (4.6) nm; (1) (ethanol) 313 (4.16), 362 (4.42), and 242 (4.29) nm]; mp 150–151° [lit. (5) mp 148–149°]; IR_{max}: 1642, 1603, and 1570 cm^{-1}.

Xanthone VI—This compound, collected in 1–2-mg yield, was not fully characterized. It exhibited an R_f value of 0.49. It did produce positive Wilson's boric acid and ferric chloride tests and was insoluble in aqueous sodium carbonate. The mass spectrometry was variable, as was an NMR analysis, undoubtedly due to impurities. UV scans indicated major bands at 237, 261, and 375 nm; its IR spectrum showed major bands at 1653, 1610, and 1580 cm^{-1}. Its NMR spectrum revealed the presence of two methyl group protons as singlets at 6.12 and 5.95 τ. A singlet far downfield at −3.78 τ represented a hydroxyl proton adjacent to a carbonyl function. This compound apparently contained the usual 1,3-dioxygenation pattern of ring B with a methyl group(s?) on ring A.

Yields of approximately 5, 10, 5, 6, 5, and 1 mg were obtained for Xanthones I, II, III, IV, V, and VI, respectively.

Glycosidic Studies—The solvent of the methanol extract of coarsely powdered root material was evaporated under vacuum. The resulting syrupy extract was solubilized in water and exhaustively partitioned with benzene. A final partitioning with chloroform left an extract in which no free xanthones (aglycones) could be detected when spotted on TLC and

[11] K and K Laboratories, Inc., Hollywood, Calif.

developed with either benzene–ethyl acetate–acetic acid or carbon tetrachloride–methanol. The developed plate was placed in an empty developing chamber. A 50-ml beaker of concentrated hydrochloric acid was placed in the chamber and then covered. The plate was thus exposed to concentrated hydrochloric acid fumes. Exposure was continued for 30 min.

After removal from the chamber, the plate was redeveloped in the solvent systems indicated. Six xanthone compounds, which corresponded on TLC with previously isolated material, were found. Also, by hydrolyzing the root extract from which all free xanthones had been removed with 3% aqueous hydrochloric acid and partitioning with benzene, the six xanthone (aglycone) derivatives could be detected. Thus, each of the six xanthones isolated from *E. grandiflorum* may exist in the plant as glycosides as well as free aglycones.

Phytochemical investigations of the various higher plants revealed the presence of xanthones in four primary families: Gentianaceae, Guttiferae, Moraceae, and Polygalaceae. The xanthones obtained from the Gentianaceae are limited to polyoxygenated derivatives, and the variation of substituents is restricted to hydroxyl and/or methoxyl groups (16). There are, however, exceptions to this general rule, as evidenced by the occurrence of mangiferin (a C-glucoside) in *Canscora decussata* Schult (1) and the presence of certain *O*-glucosides isolated from various members of this family (10, 17).

The oxygenation patterns of xanthones derived from higher plants indicate that they are formed by a mixed shikimate–acetate pathway (18). This approach suggests that ring A and the attached carbonyl group (C-7 unit) are provided *via* the shikimic acid pathway, whereas ring B (C-6 unit) originates through the acetate–malonate polyketide route. The C-7 and C-6 units thus generated form polyhydroxybenzophenones or benzophenone-like intermediates. The next step in biogenesis involves the intramolecular transformation of these intermediates into polyoxygenated xanthones (16, 18).

Various suggestions have been presented to account for the intramolecular transformation of the intermediates into xanthones. One method, direct phenolic oxidative coupling, is regarded as particularly valid. Carpenter *et al.* (18) emphasized that the observed oxygenation patterns of naturally occurring xanthones is precisely what would be expected for a phenoxyl radical coupling process in which the newly created carbon–oxygen bond would necessarily be located either *ortho* or *para* to oxygen functions in ring A. This could account for the frequently observed cooccurrence of pairs of corresponding oxygenated xanthones, *e.g.*, 5- and 7-monooxygenated xanthones, 1,5- and 1,7-dioxyxanthones, 1,5,6- and 1,6,7-trioxyxanthones, 1,3,5- and 1,3,7-trioxyxanthones, and 1,3,5,6- and 1,3,6,7-tetraoxyxanthones.

In support of the work just described, the xanthones isolated from *E. grandiflorum* were substituted with hydroxyl and methoxyl functions only. These substitutions closely parallel those of other members of the Gentianaceae. Also, the probable presence of glycosides was noted, and this observation coincided with previous reports concerning their presence in the Gentianaceae (10, 18).

This plant appears to follow the substitution pattern of some previously mentioned xanthones that contain corresponding oxygen pairs; that is, it contains 1,3,5- and 1,3,7-trioxygenated components as evidenced in II and I, respectively. Furthermore, it is interesting in that it produces a totally oxygenated and completely methoxylated A ring in IV.

No pharmacological or microbiological work was performed on these compounds, but other investigators noted such activity in total xanthone studies (19, 20). Compound II exhibited antitubercular activity, while V showed monoamine oxidase inhibiting activity devoid of pressor effects of tyramine and lacking in high toxicity. It would be interesting to note the actions of eustomin (IV) if subjected to similar studies due to its increased methoxylation. Increasing methoxylation may or may not enhance activity; however, it would perhaps be useful to determine if this activity is or is not related to the number of methoxyl groups in a xanthone compound.

REFERENCES

(1) R. K. Chaudhuri and S. Ghosal, *Phytochemistry*, **10,** 2425 (1971).

(2) G. H. Stout, E. N. Christensen, W. J. Balkenhol, and K. L. Stevens, *Tetrahedron*, **25,** 1961 (1969).

(3) A. J. Quillinan, *J. Chem. Soc. Perkins Trans.*, **1,** 1329 (1973).

(4) P. Rivaille, J. Massicot, M. Guyot, and V. Plouvier, *Phytochemistry*, **8,** 1533 (1969).

(5) S. Ghosal, P. V. Sharma, R. K. Chaudhuri, and S. K. Bhattacharya, *J. Pharm. Sci.*, **62,** 926 (1973).

(6) E. Stahl, "Thin-Layer Chromatography," Academic, New York, N.Y., 1965, pp. 31–41.

(7) J. C. Roberts, *Chem. Rev.*, **61,** 591 (1961).

(8) F. M. Dean, "Naturally Occurring Oxygen Ring Compounds," Butterworths, London, England, 1963, pp. 266–279.

(9) C. W. Wilson, *J. Am. Chem. Soc.*, **61,** 2303 (1939).

(10) G. H. Stout and W. J. Balkenhol, *Tetrahedron*, **25,** 1947 (1960).

(11) O. R. Gottlieb, M. Taveira Magalhaes, M. Camey, A. A. Lins Mesquita, and D. de Barros Correa, *ibid.*, **22,** 1777 (1966).

(12) T. R. Govindachari, B. R. Pai, P. S. Subramaniam, R. R. Rao, and N. Muthukumarawwamy, *ibid.*, **23,** 243 (1967).

(13) P. Yates and G. H. Stout, *J. Am. Chem. Soc.*, **80,** 1691 (1958).

(14) B. Jackson, H. D. Locksley, and F. Scheinmann, *J. Chem. Soc.*, **1967,** 2500.

(15) S. Bhanu, T. Saroja, and T. R. Seshadri, *Indian J. Chem.*, **10,** 577 (1972).

(16) W. D. Ollis, *An. Acad. Brasil. Cienc., Suplemento*, **42,** 9 (1970).

(17) S. Ghosal, P. V. Sharma, and R. K. Chaudhuri, *J. Pharm. Sci.*, **63,** 1286 (1974).

(18) I. Carpenter, H. D. Locksley, and F. Scheinmann, *Phytochemistry*, **8,** 2013 (1969).

(19) S. Ghosal, P. V. Sharma, R. K. Chaudhuri, and S. K. Bhattacharya, *J. Pharm. Sci.*, **64,** 80 (1975).

(20) S. J. Gabriel and O. R. Gottlieb, *An. Acad. Brasil. Cienc., Suplemento*, **42,** 115 (1970).

ACKNOWLEDGMENTS AND ADDRESSES

Received May 20, 1976, from the *College of Pharmacy, University of Texas at Austin, Austin, TX 78712.*

Accepted for publication August 11, 1976.

* Present address: School of Pharmacy, University of Maryland, Baltimore, MD 21201.

[x] To whom inquiries should be directed.

Quantitative Determination of Fenclorac in Serum

J. K. LEE ˣ, R. D. SMYTH *, A. POLK, T. HERCZEG, C. T. TSUEI, and N. H. REAVEY-CANTWELL

Abstract □ A spectrophotometric method for the analysis of fenclorac and its metabolite, 3-chloro-4-cyclohexylbenzeneglycolic acid, in human serum was developed. The parent compound represented at least 90% of the total species present in blood; the metabolite was present to the extent of about 10%, primarily in the elimination phase. The basic procedure consists of extraction of both compounds from serum, further extraction to remove interfering substances, alkaline conversion of fenclorac to the α-hydroxy acid metabolite, oxidation of this metabolite to the corresponding benzaldehyde derivative, and spectrophotometric measurement of the absorbance of the aldehyde at 252 nm. A comparison of serum concentrations obtained by this method with concentrations calculated from ^{14}C-data following oral administration of 1-^{14}C-fenclorac to eight normal adult volunteers indicated a 90% correlation between methodologies over a range of 1.4–25.5 μg of fenclorac/ml of serum.

Keyphrases □ Fenclorac and metabolite—spectrophotometric analysis, serum □ Spectrophotometry—analysis, fenclorac and metabolite in serum □ Anti-inflammatory agents—fenclorac and metabolite, spectrophotometric analysis in serum

Fenclorac (α,3-dichloro-4-cyclohexylbenzeneacetic acid) is a potent antiphlogistic, antinociceptive, and antipyretic agent (1, 2). Fenclorac is more potent than phenylbutazone or aspirin in the treatment of developing or established adjuvant arthritis and inhibition of carrageenan paw edema. Fenclorac is more potent than aspirin and indomethacin in reducing fever in rats rendered hyperthermic with brewer's yeast.

This paper describes the development of a quantitative assay for fenclorac (I) and its metabolite, 3-chloro-4-cyclohexylbenzene glycolic acid (II), in serum.

EXPERIMENTAL

Apparatus—A spectrophotometer[1], a recording spectrophotometer[2], and 1-cm quartz semimicro cells[3] were used.

Materials and Reagents—Methanol[4] (certified ACS grade), ceric ammonium sulfate dihydrate[4] (certified grade), sodium hydroxide[4] (certified ACS electrolytic pellets), chloroform[5] (spectrophotometric grade), sulfuric acid[5], hydrochloric acid[6] (analytical reagent grade), hexane[7] (distilled-in-glass UV grade), and normal human serum[8] were used as received.

Compounds I, II, 3-chloro-4-cyclohexylbenzaldehyde (III) and 1-^{14}C-carboxyl-labeled I and II were all synthesized[9].

Ceric reagent solution, 0.2 *M*, was prepared by the following procedure (3). Ceric ammonium sulfate, 126 g, was transferred to a 1-liter glass-stoppered volumetric flask containing a magnetic stirring bar. Approximately 700 ml of distilled water was added, followed by 30 ml of concentrated sulfuric acid. The mixture was stirred briefly, the volume was adjusted to 1 liter, and mixing was continued for about 2 hr. Insoluble material was allowed to settle overnight, and the clear supernate was used.

Serum Samples for Standard Curve—Standard solutions of I in serum were prepared by first mixing 3 ml of a 1.25-mg/ml methanolic solution of the diethylammonium salt of I with 97 ml of normal human serum to yield a stock serum standard equivalent to 30 μg of I/ml (factor for converting diethylammonium salt to free acid = 1.25). Dilutions of this stock serum standard were prepared to yield samples containing 2, 5, 10, 20, and 30 μg of I/ml of serum. Aliquots were dispensed into small tubes and frozen prior to use.

Analytical Procedure—The following procedure was a modification of the method of Cummins and Perry (4).

Methanol (5.0 ml) was added to a 35-ml ground-glass-stoppered conical centrifuge tube containing exactly 1.5 ml of serum sample or serum standard. The contents were mixed[10] during this addition, and the mixing was continued for another 10 sec. The tube was capped, and the contents were mixed[10] for 30 sec, followed by centrifugation for 5 min at 1500 rpm.

The methanol extract was quantitatively transferred to a second tube containing 1 ml of water, 0.2 ml of 8 *N* hydrochloric acid, and 5 ml of chloroform. The sample was mixed[10] for 1 min and centrifuged for 5 min. The lower phase (containing the chloroform extract) was quantitatively transferred to another tube containing exactly 8.5 ml of 1 *N* sodium hydroxide. The sample was again mixed for 1 min[10] and centrifuged for 5 min. Exactly 8 ml of the clear aqueous phase was transferred to a 40-ml glass-stoppered centrifuge tube, and the sample was reextracted with a second 8.5-ml aliquot of 1 *N* sodium hydroxide and centrifuged. The clear aqueous phase was transferred quantitatively to the second tube containing the first alkaline extract, and the combined extracts were mixed thoroughly.

The combined alkaline extract was heated in a boiling water bath for 15 min and then cooled to room temperature. Approximately 5 ml of hexane was added, and the sample was mixed for 30 sec[10] and centrifuged. The hexane phase was separated and discarded, and the sample was then reheated in boiling water for another 5 min to remove residual hexane.

After cooling to room temperature and acidification with 3 ml of 8 *N* hydrochloric acid, exactly 5 ml of ceric reagent was added and the contents were mixed briefly and allowed to stand for 30 min in the dark. Approximately 3 ml of 10 *N* sodium hydroxide was added, and the sample was mixed. The aqueous phase, containing the product of oxidation, was then extracted with 2.5 ml of hexane by mixing for 45 sec[10]. After centrifugation, the hexane phase was transferred to a semimicro UV cell. The absorbance was measured at 252 nm with hexane in the reference cell and then compared with the measurements obtained from the serum standard curve. Each standard curve was drawn from linear regression analysis of the individual data points.

Recovery Studies—Although II is a minor metabolite, its recovery from serum must approximate that of I so that the final extract is representative of the original serum sample.

Small aliquots of 1-^{14}C-I and/or 1-^{14}C-II were added to serum, and these samples were then carried through the assay procedure. Recoveries of carbon-14 were determined after each step, and the cumulative percent recovery was determined from these values. To minimize any effect due to volume changes upon sampling, no more than 10% of any extract was sampled for ^{14}C-analysis.

The radioactivity of all samples was determined in a liquid scintillation counter[11] using a modified Bray's solution cocktail (5). All counts were then corrected for background and quench by the external standard channels ratio method and converted to disintegrations per minute. The counting efficiency was 68%.

Extent of Oxidation—The oxidation of II, the final product obtained in the assay procedure just prior to oxidation, was studied by determining the disappearance of chloroform-extractable radioactivity from the acid medium of the ceric reaction mixture. Since the ^{14}C-label was on the carboxyl function of both I and II, its disappearance as ^{14}C-labeled carbon dioxide after oxidation served as an index of the extent of oxidation.

Identification of Oxidation Product—A serum sample containing added fenclorac and a serum sample from a subject who had received

[1] Model DB or DU, Beckman Instruments, Irvine, Calif.
[2] Cary 14, Cary Instruments, Monrovia, Calif.
[3] Precision Glass Products Co., Oreland, Pa.
[4] Fisher Scientific Co., Fair Lawn, N.J.
[5] J. T. Baker Chemical Co., Phillipsburg, N.J.
[6] Mallinckrodt, St. Louis, Mo.
[7] Burdick and Jackson Laboratories, Muskegon, Mich.
[8] Fox Chemical Co., Tucson, Ariz.
[9] Department of Medicinal Chemistry, William H. Rorer, Fort Washington, Pa.

[10] Vortex test tube mixer, Scientific Industries, Springfield, Mass.
[11] Model LS-350, Beckman Instruments, Irvine, Calif.

Table I—Recovery of I and II in the Extraction Procedure

Assay Step	Recovery, %		
	I[a]	II[b]	I[c] and II[c]
Methanol extraction	89.6	81.5	91.0
Chloroform extraction	100	100	100
Alkaline extraction	76.9	88.1	83.0
Cumulative	68.9	71.8	75.5

[a] Original serum sample contained 19.6 μg/ml. [b] Original serum sample contained 23.8 μg/ml. [c] Original serum sample contained 9.8 μg of I and 11.9 μg of II/ml.

Table II—Extent of Oxidation of II to III

Component in Original Serum Sample	Percent of Sample Unoxidized	Percent Oxidized
I[a]	2.4	97.6
II[b]	0.2	99.8
I and II[c]	1.4	98.6

[a] Serum sample contained 19.6 μg of I/ml. [b] Serum sample contained 23.8 μg of II/ml. [c] Serum sample contained 9.8 μg of I and 11.9 μg of II/ml.

fenclorac were carried through the entire procedure. The UV spectra were determined on the product of oxidation and compared with the spectrum of the authentic oxidation product, III.

Correlation with Radioactivity Data—Serum samples were obtained from eight normal adult volunteers following oral administration of 200 mg of 1-^{14}C-I (specific activity of 0.317 μCi/mg). One hundred and twenty samples, representing various time intervals after the administration of the radioactive compound to the eight subjects, were assayed (15 samples/subject).

The levels of I found were compared to those levels obtained from liquid scintillation counting. Since GLC–mass spectrometry studies (6, 7) had shown that I is the major serum component along with small amounts of II, a direct correlation was made between levels obtained by this spectrophotometric method and the ^{14}C-levels.

Reproducibility—Within-day reproducibility was determined by assaying, on the same day, 10 identical serum samples containing exactly 20 μg of I/ml.

Day-to-day reproducibility was determined on a series of standard curves obtained over 3 weeks.

RESULTS AND DISCUSSION

The principal reactions in this assay are (*a*) the conversion of I to II (8, 9) (Scheme I), which occurs at room temperature but is greatly accelerated in an alkaline medium at elevated temperatures (100°); and (*b*) the oxidation of II by ceric sulfate (10) (Scheme II).

Although small amounts of the methyl esters of both I and II are formed in acidified methanol, base-catalyzed hydrolysis at elevated temperatures converted the esters to 3-chloro-4-cyclohexylbenzeneglycolate and eliminated any interferences (11).

Recovery Studies—The cumulative percent recovery of I and/or II from serum was equivalent up to the step immediately prior to oxidation. Therefore, if a serum sample contained I and/or II, the final extract was representative of the composition of the original serum sample. This condition is necessary when two compounds are present in the same sample and when both must be assayed simultaneously. Table I summarizes the complete recovery study.

Extent of Oxidation—Less than 2.5% of radioactivity was recovered into chloroform from the ceric reaction mixture, indicating that the oxidation was essentially quantitative after 30 min (Table II).

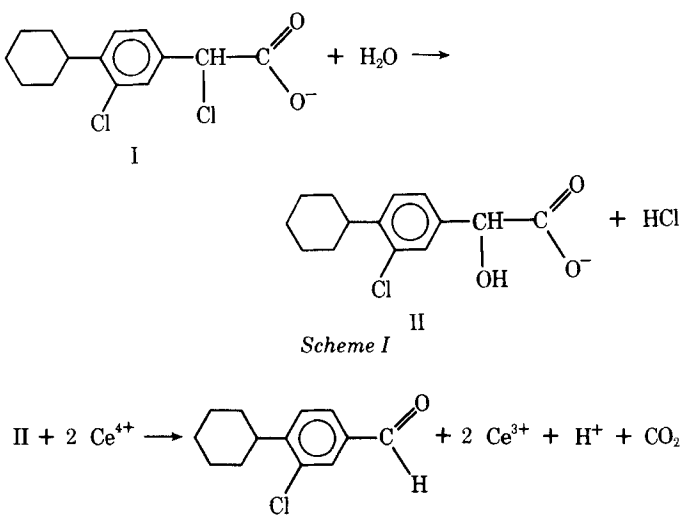

Scheme I

Scheme II

Identification of Oxidation Product—The product of ceric oxidation of II or extracts of serum samples from subjects who received I had the same UV spectral characteristics as the predicted product of oxidation, III (Fig. 1).

Correlation of Spectrophotometric and ^{14}C-Analyses—Linear regression analysis of serum concentrations of I determined by spectrophotometric (C_{sp}) or ^{14}C (C_{RI}) procedures indicated a 90% correlation between the two methods ($r^2 = 0.965$; $C_{sp} = 0.90C_{RI} - 0.46$) over a range of 1.4–25.5 μg of I/ml. There was no significant serum blank, and slight hemolysis in serum did not interfere.

GLC–mass spectrometric studies indicated that I was the major species present in serum after oral administration of fenclorac. Only small amounts (<10%) of II were present (6, 7). Also, due to the small difference in molecular weight between I and II (~7%), this assay gives a direct measure of the unchanged parent compound.

Figure 2 is a graphical comparison of the average values obtained on the serum samples of eight subjects by the spectrophotometric method with the ^{14}C-values obtained by liquid scintillation.

Reproducibility—The standard curves used for the radioisotope

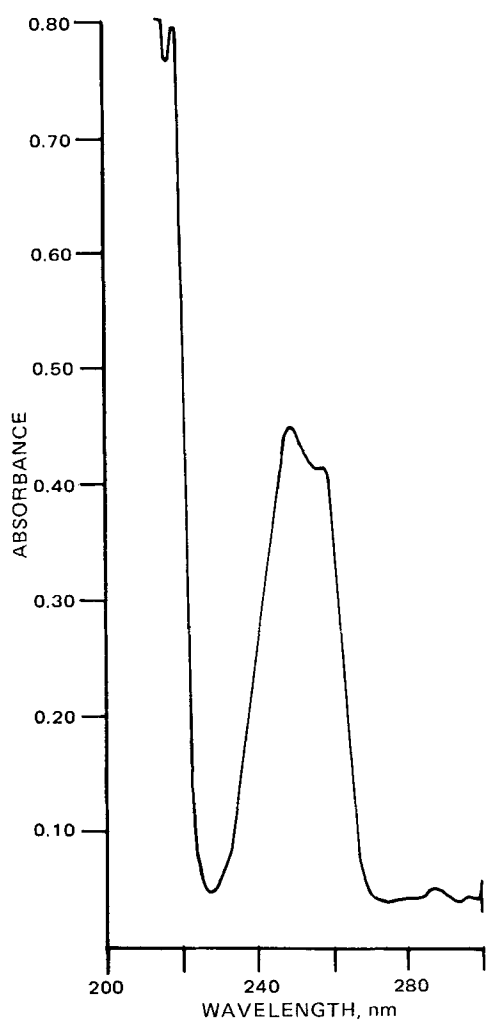

Figure 1—*UV spectrum of III in hexane.*

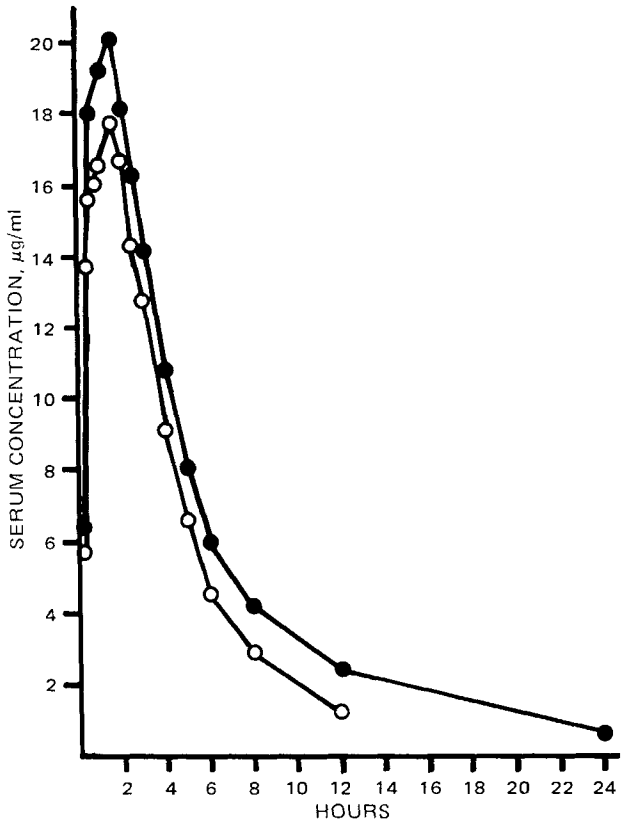

Figure 2—*Serum I concentration after oral administration of 200 mg of I in an aqueous medium. Key (mean values of eight subjects): ●, ^{14}C-assay; and ○, UV spectrophotometric assay.*

study indicated good day-to-day reproducibility on samples assayed over 3 weeks.

The composite linear regression standard curve had a y-intercept of 0.024 absorbance unit (blank), a slope of 0.018 absorbance unit/μg of I/ml, and $r^2 = 0.995$ ($y = 0.018x + 0.024$), where x is micrograms of I per milliliter of serum. The coefficient of variation was 5% with serum samples containing 2, 5, 10, 20, and 30 μg of I/ml on 12–14 determinations of each concentration over 3 weeks.

Replicate determinations of I in 10 identical serum standards, each containing 20 μg of I/ml, on the same day resulted in a coefficient of variation of 2.8% and a mean of 0.321 ± 0.009 absorbance unit at 252 nm.

Sensitivity—As mentioned previously, linear regression analysis of absorbance *versus* standard concentration data yielded a slope of 0.018 absorbance unit for 1 μg of I/ml of serum. When using 1.5 ml of serum per test, the minimum detectable quantity of I was approximately 1 μg/ml.

REFERENCES

(1) G. W. Nuss, R. D. Smyth, C. H. Breder, M. J. Hitchings, and N. H. Reavey-Cantwell, *Clin. Res.*, **23**(5), 584A (1975).

(2) G. W. Nuss, R. D. Smyth, C. H. Breder, M. J. Hitchings, G. N. Mir, and N. H. Reavey-Cantwell, *Fed. Proc.*, **35**(3), 774 (1976).

(3) L. Chafetz, *J. Pharm. Sci.*, **53**, 1192 (1964).

(4) L. M. Cummins and J. E. Perry, *ibid.*, **58**, 762 (1969).

(5) G. A. Bray, *Anal. Biochem.*, **1**, 279 (1960).

(6) R. D. Smyth, A. Polk, A. F. DeLong, R. K. Nayak, and N. H. Reavey-Cantwell, *Clin. Res.*, **23**(5), 585A (1975).

(7) A. F. DeLong, R. D. Smyth, A. Polk, R. K. Nayak, and N. H. Reavey-Cantwell, *Fed. Proc.*, **35**(3), 565 (1976).

(8) S. Wideqvist, *Arkiv. Kemi.*, **19**, 551 (1962).

(9) L. Fieser and M. Fieser, "Advanced Organic Chemistry," Reinhold, New York, N.Y., 1961, pp. 315, 316.

(10) L. Chafetz and C. A. Gaglia, *J. Pharm. Sci.*, **55**, 854 (1966).

(11) L. Fieser and M. Fieser, "Advanced Organic Chemistry," Reinhold, New York, N.Y., 1961, pp. 373, 374.

ACKNOWLEDGMENTS AND ADDRESSES

Received May 27, 1976, from the *Research Division, William H. Rorer, Inc., Fort Washington, PA 19034.*

Accepted for publication August 12, 1976.

The authors acknowledge the technical assistance of Ms. Kay Rush and Dr. R. K. Nayak.

* Present address: Department of Biochemistry and Biopharmaceutics, Bristol Laboratories, Syracuse, NY 13201.

ˣ To whom inquiries should be directed.

Quantitation of the Antimalarial Agent, Mefloquine, in Blood, Plasma, and Urine Using High-Pressure Liquid Chromatography

J. M. GRINDEL *ˣ, P. F. TILTON *, and R. D. SHAFFER ‡

Abstract □ Sensitive and specific assays are described for the quantitation of mefloquine in whole blood, plasma, and urine specimens using high-pressure liquid chromatography. Specimens were extracted with ethyl acetate and concentrated before chromatography. Whole blood and plasma extracts were chromatographed on a polar bonded phase partitioning column, and urine extracts were chromatographed on a bonded reversed-phase partitioning column. The sensitivity of the assays for mefloquine was 0.05 μg/ml of whole blood or plasma and 0.25 μg/ml of urine using 5-ml samples. The assays are suitable for studying mefloquine pharmacokinetics in humans.

Keyphrases □ Mefloquine—high-pressure liquid chromatographic analysis, whole blood, plasma, and urine □ High-pressure liquid chromatography—analysis, mefloquine in whole blood, plasma, and urine □ Antimalarial agents—mefloquine, high-pressure liquid chromatographic analysis in whole blood, plasma, and urine

Mefloquine hydrochloride[1] (I) is a radical curative agent for the treatment of drug-resistant falciparum malaria (1, 2). Mefloquine also provided suppressive prophylaxis against mosquito-induced infections with *Plasmodium vivax* and *P. falciparum* in human volunteers (3, 4). The disposition of mefloquine in rats was studied (5), but its fate in humans has not been determined due to the lack of

[1] DL-*erythro*-α-2-Piperidyl-2,8-bis(trifluoromethyl)-4-quinolinemethanol hydrochloride (WR 142,490 hydrochloride), Cordova Chemical, Sacramento, Calif.

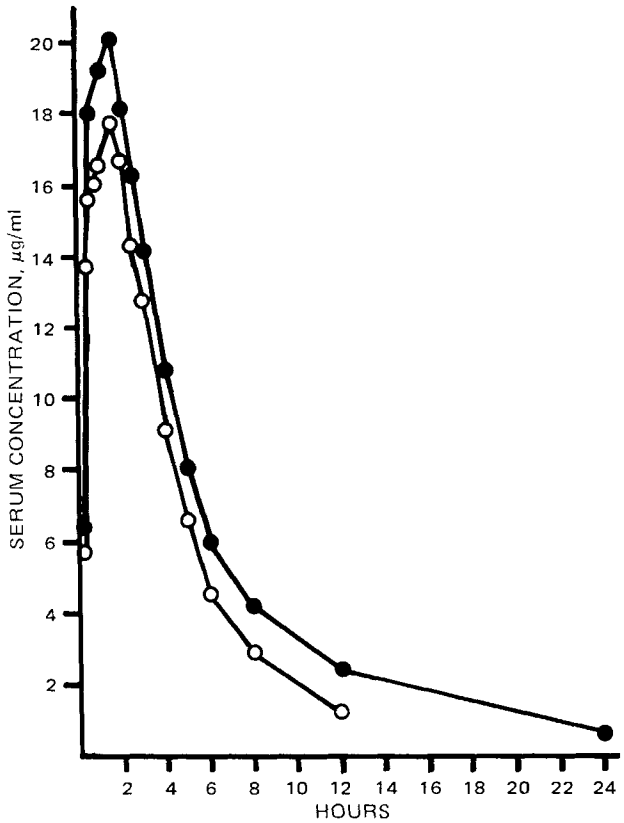

Figure 2—*Serum I concentration after oral administration of 200 mg of I in an aqueous medium. Key (mean values of eight subjects): ●, ^{14}C-assay; and ○, UV spectrophotometric assay.*

study indicated good day-to-day reproducibility on samples assayed over 3 weeks.

The composite linear regression standard curve had a y-intercept of 0.024 absorbance unit (blank), a slope of 0.018 absorbance unit/μg of I/ml, and $r^2 = 0.995$ ($y = 0.018x + 0.024$), where x is micrograms of I per milliliter of serum. The coefficient of variation was 5% with serum samples containing 2, 5, 10, 20, and 30 μg of I/ml on 12–14 determinations of each concentration over 3 weeks.

Replicate determinations of I in 10 identical serum standards, each containing 20 μg of I/ml, on the same day resulted in a coefficient of variation of 2.8% and a mean of 0.321 ± 0.009 absorbance unit at 252 nm.

Sensitivity—As mentioned previously, linear regression analysis of absorbance *versus* standard concentration data yielded a slope of 0.018 absorbance unit for 1 μg of I/ml of serum. When using 1.5 ml of serum per test, the minimum detectable quantity of I was approximately 1 μg/ml.

REFERENCES

(1) G. W. Nuss, R. D. Smyth, C. H. Breder, M. J. Hitchings, and N. H. Reavey-Cantwell, *Clin. Res.*, **23**(5), 584A (1975).

(2) G. W. Nuss, R. D. Smyth, C. H. Breder, M. J. Hitchings, G. N. Mir, and N. H. Reavey-Cantwell, *Fed. Proc.*, **35**(3), 774 (1976).

(3) L. Chafetz, *J. Pharm. Sci.*, **53**, 1192 (1964).

(4) L. M. Cummins and J. E. Perry, *ibid.*, **58**, 762 (1969).

(5) G. A. Bray, *Anal. Biochem.*, **1**, 279 (1960).

(6) R. D. Smyth, A. Polk, A. F. DeLong, R. K. Nayak, and N. H. Reavey-Cantwell, *Clin. Res.*, **23**(5), 585A (1975).

(7) A. F. DeLong, R. D. Smyth, A. Polk, R. K. Nayak, and N. H. Reavey-Cantwell, *Fed. Proc.*, **35**(3), 565 (1976).

(8) S. Wideqvist, *Arkiv. Kemi.*, **19**, 551 (1962).

(9) L. Fieser and M. Fieser, "Advanced Organic Chemistry," Reinhold, New York, N.Y., 1961, pp. 315, 316.

(10) L. Chafetz and C. A. Gaglia, *J. Pharm. Sci.*, **55**, 854 (1966).

(11) L. Fieser and M. Fieser, "Advanced Organic Chemistry," Reinhold, New York, N.Y., 1961, pp. 373, 374.

ACKNOWLEDGMENTS AND ADDRESSES

Received May 27, 1976, from the *Research Division, William H. Rorer, Inc., Fort Washington, PA 19034.*

Accepted for publication August 12, 1976.

The authors acknowledge the technical assistance of Ms. Kay Rush and Dr. R. K. Nayak.

* Present address: Department of Biochemistry and Biopharmaceutics, Bristol Laboratories, Syracuse, NY 13201.

ˣ To whom inquiries should be directed.

Quantitation of the Antimalarial Agent, Mefloquine, in Blood, Plasma, and Urine Using High-Pressure Liquid Chromatography

J. M. GRINDEL *ˣ, P. F. TILTON *, and R. D. SHAFFER ‡

Abstract □ Sensitive and specific assays are described for the quantitation of mefloquine in whole blood, plasma, and urine specimens using high-pressure liquid chromatography. Specimens were extracted with ethyl acetate and concentrated before chromatography. Whole blood and plasma extracts were chromatographed on a polar bonded phase partitioning column, and urine extracts were chromatographed on a bonded reversed-phase partitioning column. The sensitivity of the assays for mefloquine was 0.05 μg/ml of whole blood or plasma and 0.25 μg/ml of urine using 5-ml samples. The assays are suitable for studying mefloquine pharmacokinetics in humans.

Keyphrases □ Mefloquine—high-pressure liquid chromatographic analysis, whole blood, plasma, and urine □ High-pressure liquid chromatography—analysis, mefloquine in whole blood, plasma, and urine □ Antimalarial agents—mefloquine, high-pressure liquid chromatographic analysis in whole blood, plasma, and urine

Mefloquine hydrochloride[1] (I) is a radical curative agent for the treatment of drug-resistant falciparum malaria (1, 2). Mefloquine also provided suppressive prophylaxis against mosquito-induced infections with *Plasmodium vivax* and *P. falciparum* in human volunteers (3, 4). The disposition of mefloquine in rats was studied (5), but its fate in humans has not been determined due to the lack of

[1] DL-*erythro*-α-2-Piperidyl-2,8-bis(trifluoromethyl)-4-quinolinemethanol hydrochloride (WR 142,490 hydrochloride), Cordova Chemical, Sacramento, Calif.

Table I—Retention Volumes (V_R) for I and II on Reversed-Phase or Normal Phase Partition Chromatography

Mobile Phase	V_R, ml I	V_R, ml II
Bonded Reversed-Phase Partition Chromatography[a]		
Methanol–0.1 *M* NaH_2PO_4		
3:2 (v/v)	5.4	4.0
2:1 (v/v)	4.6	2.9
4:1 (v/v)	3.0	2.2
Polar Bonded Phase Partition Chromatography[b]		
Isopropyl ether–dioxane–acetic acid		
3:2 (v/v) + 0.5%	4.4	10.3
2:3 (v/v) + 0.5%	3.7	6.5
1:4 (v/v) + 0.5%	20.5	42.5

[a] μBondapak C_{18} column (4 mm i.d. × 30 cm). [b] μBondapak CN column (4 mm i.d. × 30 cm).

a sensitive and specific nonradioactive assay.

High-pressure liquid chromatography (HPLC) is a powerful analytical technique for the quantitative analysis of pharmaceuticals in biological fluids. Due to the low vapor pressure of mefloquine, GLC was not as applicable as HPLC. Thus, HPLC was utilized to effect a specific separation and quantitation of mefloquine from whole blood, plasma, and urine specimen extracts.

EXPERIMENTAL

Reagents—Mefloquine hydrochloride and the internal standard[2] (II) were assayed at >99 and 98% purity, respectively. All solvents used were spectroquality, and drug solutions were made with the appropriate salt form of the compound. All concentrations are expressed as the free base.

Standard Solutions—A solution of the internal standard was prepared in dioxane–methanol (7:3 v/v) (196 μg/ml). The internal standard solution was used as the solvent for the preparation of a stock solution of mefloquine (1028 μg/ml), from which dilutions were made with the internal standard solution to give solutions with concentrations of 10.2–205.6 μg of mefloquine/ml and 1.96 μg of II/ml.

Chromatographic Conditions—A high-pressure liquid chromatograph[3] equipped with a 280-nm absorbance monitor was utilized. Whole blood and plasma extracts were chromatographed on a column of 10-μm, fully porous silica, bonded with a monomolecular layer of cyanopropylsilane[4]. A mobile phase of isopropyl ether–dioxane–acetic acid (3:2 v/v + 0.5%) at 2 ml/min was used. Urine extracts were chromatographed on a column of 10-μm, fully porous silica, bonded with a monomolecular layer of octadecylsilane[5]. A mobile phase of methanol–0.1 *M* NaH_2PO_4 (3:2 v/v) at 2 ml/min was used.

General Assay Procedure—The internal standard solution (50 μl) containing 9.8 μg of II, 5 ml of whole blood, plasma, or urine, and 5 ml of pH 7.4 phosphate buffer (0.065 *M*) were placed in a 45-ml glass conical tube with a polytef[6]-lined screw cap and thoroughly mixed. Then 10 ml of ethyl acetate was added to each tube, and the samples were agitated at 100 strokes/min for 30 min on a reciprocating shaker bath[7] and centrifuged[8] at 2000 rpm for 10 min. The ethyl acetate layer was then pipetted carefully into a 45-ml glass conical tube with a polytef stopper.

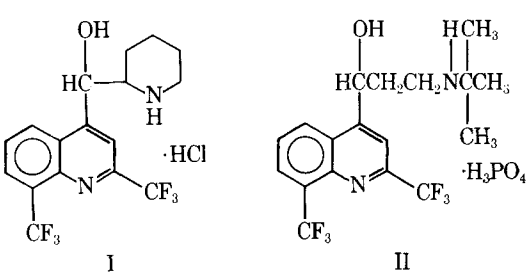

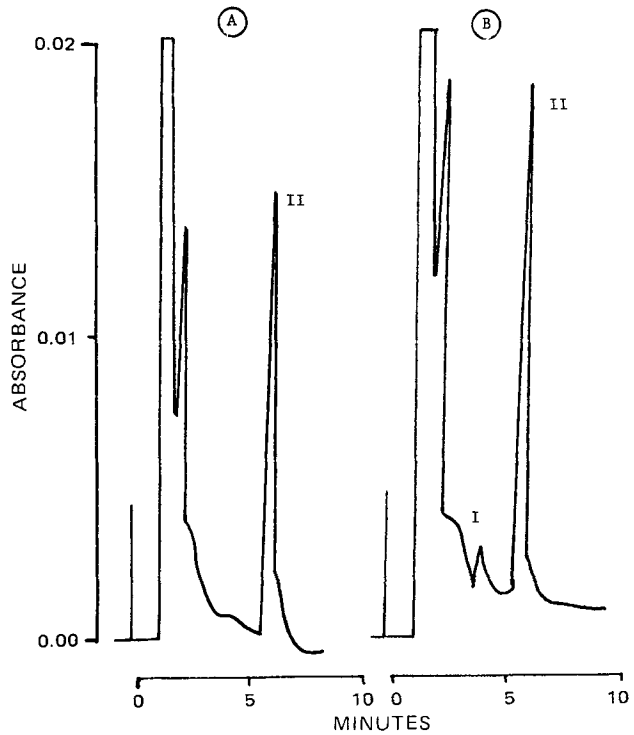

Figure 1—*Representative chromatograms of a whole blood extract containing 0.98 μg of II (A) and of a whole blood extract containing 0.05 μg of I plus 0.98 μg of II (B) after chromatography on a polar bonded phase column using isopropyl ether–dioxane–acetic acid (3:2 v/v +0.5%) as the mobile phase.*

The extraction procedure was repeated two more times, the combined ethyl acetate layers from each sample were evaporated to dryness under a gentle stream of nitrogen at 40° [9], and the residues were stored overnight in a vacuum desiccator. The sample residues were reconstituted with 500 μl of the appropriate mobile phase, and 50-μl aliquots were injected into the chromatograph. Quantitation was achieved by measuring peak area ratios for I/II and relating them to the least-squares linear regression curve of the peak area ratio for I/II *versus* the amount of mefloquine injected. Peak areas were obtained from the product of the maximum peak height (centimeters) × width at peak half-height (centimeters).

Spiked Samples—*Recovery of Mefloquine from Whole Blood*—Aliquots (25 ml) of human whole blood were spiked with a methanol solution of mefloquine (250 μg/ml) to give drug concentrations of 1.00, 0.50, and 0.10 μg/ml. The samples were thoroughly mixed for 30 min and treated as described under *General Assay Procedure*, except that the internal standard (II) was not added until the extraction was completed.

Recovery of II from Whole Blood—Aliquots (25 ml) of human whole blood were spiked with a methanol solution of II (250 μg/ml) to give drug concentrations of 1.00, 0.50, and 0.10 μg/ml. The spiked blood was thoroughly mixed for 30 min, and four 5-ml samples of each concentration level were placed in individual glass tubes along with 5 ml of pH 7.4 phosphate buffer (0.065 *M*). Each sample was extracted with 3 × 10 ml of ethyl acetate, the combined ethyl acetate extracts were evaporated under nitrogen, the residues were reconstituted with 500 μl of mobile phase, and 50-μl aliquots were injected into the chromatograph. Quan-

[2] DL-2,8-Bis(trifluoromethyl)-4-[1-hydroxy-3-(*N-tert*-butylamino)propyl]quinoline phosphate (WR 184,806 phosphate), Starks Associates, Buffalo, N.Y.

[3] A model 6000A solvent delivery system, a model U6K injector, and a model 440 UV absorbance monitor, Waters Associates, Milford, Mass.

[4] μBondapak CN column (4 mm i.d. × 30 cm), Waters Associates, Milford, Mass.

[5] μBondapak C_{18} column (4 mm i.d. × 30 cm), Waters Associates, Milford, Mass.

[6] Teflon, du Pont.

[7] Model 2156, American Optical Corp., Buffalo, N.Y. The tube holder assembly was fabricated by the Division of Instrumentation, Walter Reed Army Institute of Research, Washington, D.C.

[8] Model PR-2 refrigerated centrifuge, IEC, Needham Heights, Mass.

[9] Model 112 N-Evap, Organomation Associates, Northborough, Mass.

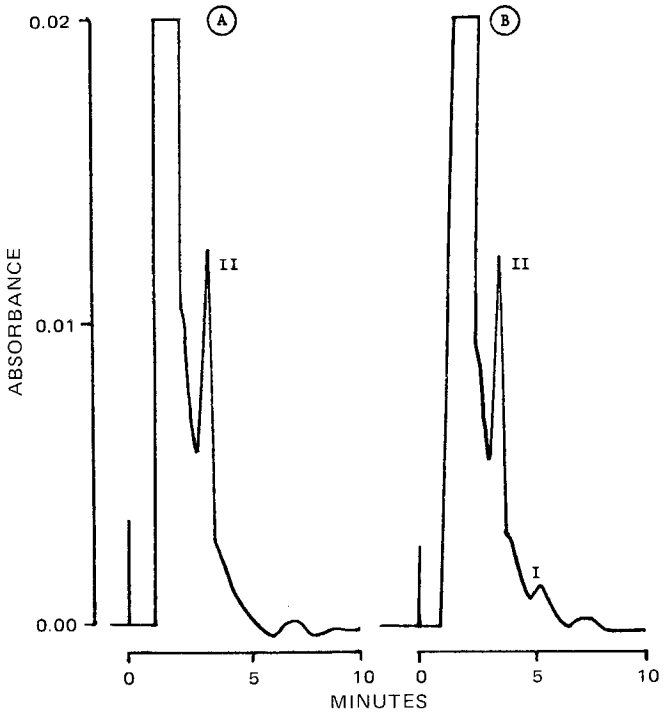

Figure 2—*Representative chromatograms of a urine extract containing 0.98 μg of II (A) and of a urine extract containing 0.125 μg of I plus 0.98 μg of II (B) after chromatography on a bonded reversed-phase column using methanol–0.1 M NaH_2PO_4 (3:2 v/v) as the mobile phase.*

titation was achieved by measuring the peak areas of II and relating them to the least-squares linear regression curve (n = 15) of the peak area of II *versus* the amount of II injected. Peak areas were measured as described previously.

Precision Determination for Mefloquine Assay—Aliquots (25 ml) of human whole blood and plasma were spiked with a methanol solution of mefloquine (250 μg/ml) to give drug concentrations of 5.00, 1.00, 0.50, and 0.05 μg/ml. Urine aliquots (25 ml) were spiked at 5.00, 1.00, 0.50, and 0.25 μg/ml. The samples were thoroughly mixed for 30 min and treated as described under *General Assay Procedure*.

Clinical Study—An adult male was given two 250-mg tablets of mefloquine hydrochloride. Whole blood and plasma samples were obtained at 0, 1, 2, 4, 8, and 12 hr and at 2, 3, 4, 7, 9, 14, 21, 31, and 57 days. A random urine sample was obtained on Days 1 and 2. All specimens were stored in glass tubes with polytef-lined screw caps at −10° until analyzed.

RESULTS AND DISCUSSION

Mefloquine and its analog II have similar physicochemical properties. Both compounds are extensively bound to plasma proteins and are concentrated in the erythrocytes (5, 6); they have nearly identical molar absorptivity at 280 nm, pKa's, solvent partition coefficients, and low aqueous solubility. Both compounds were well resolved from each other and from extracts of blood and urine under appropriate chromatographic conditions. For these reasons, II was chosen as the internal standard for the mefloquine assay.

The establishment of HPLC conditions was accomplished by examining the retention characteristics of mefloquine and II on polar bonded phase and bonded reversed-phase partitioning columns. Comparative retention volumes for mefloquine and II are presented in Table I. Optimal resolution of both compounds from each other and from ethyl acetate extracts of blood and plasma was accomplished using a polar bonded phase partitioning column with a mobile phase of isopropyl ether–dioxane–acetic acid (3:2 v/v + 0.5%). These conditions did not adequately resolve mefloquine and II from the urine extract peaks. Resolution of mefloquine and II from urine extracts was achieved on a bonded reversed-phase column utilizing a mobile phase of methanol–0.1 M NaH_2PO_4 (3:2 v/v). Representative chromatograms are presented in Figs. 1 and 2. No interfering peaks from blood, plasma, or urine extract components were detected in control samples.

Table II—Recovery of I and II from Spiked Whole Blood Specimens [a]

Mefloquine Added, μg/ml [b]	Recovery, % ± *SD*	
	I	II
1.00	95.4 ± 2.4	95.5 ± 1.3
0.50	99.1 ± 8.3	96.3 ± 4.9
0.10	105.2 ± 13.6	95.3 ± 9.3
Mean	99.9 ± 9.3	95.7 ± 5.4

[a] Chromatographic conditions are described under *Experimental*. [b] Four samples at each concentration level.

Table III—Precision Data for the Determination of Mefloquine in Spiked Whole Blood, Plasma, and Urine Specimens [a]

Mefloquine Added, μg/ml [b]	Assayed Mefloquine Concentration, μg/ml [c]		
	Whole Blood	Plasma	Urine
5.00	4.96 ± 0.25	5.20 ± 0.11	4.76 ± 0.14
1.00	1.04 ± 0.02	1.00 ± 0.06	0.97 ± 0.06
0.50	0.54 ± 0.04	0.47 ± 0.07	0.48 ± 0.05
0.25			0.25 ± 0.04
0.05	0.05 ± 0.004	0.05 ± 0.004	
Mean percent recovery ± *RSD*	102.9 ± 6.7	99.5 ± 9.5	97.1 ± 9.4

[a] Chromatographic conditions are described under *Experimental*. [b] The concentration of internal standard was 1.96 μg/ml. [c] Mean ± *SD* for four replicates at each level.

Recovery percentages for the individual extraction of mefloquine and II from whole blood using ethyl acetate as solvent are presented in Table II. The recoveries were greater than 95% for both compounds over the range studied with standard deviations less than 10%.

Linear calibration curves of the peak area ratio for I/II *versus* the amount of I were constructed each day utilizing 15 points at five concentration ratios. The data were analyzed using least-squares regression analysis. A family of curves over a 6-month period had a mean slope of 1.013 with a relative standard deviation of 3.9% and a correlation coefficient (r) of 0.9997.

Precision data utilizing optimal conditions for the assay of blood, plasma, and urine specimens spiked with known concentrations of mefloquine are presented in Table III. The relative accuracy was ±3% of the amount added with relative standard deviations less than 10% over the 0.05–5.00-μg/ml range for blood and plasma and over the 0.25–5.00-μg/ml range for urine. The lower limit of sensitivity for the assay was 0.05 μg/ml for blood and plasma samples and 0.25 μg/ml for urine samples.

Based on the results of these experiments, an adult male was given 500 mg of mefloquine hydrochloride, and serial blood and plasma specimens were assayed for 2 months for mefloquine concentrations (Figs. 3 and 4). Blood and plasma levels of mefloquine were readily quantitated 57 days after drug ingestion. Random urine specimens obtained on Days 1 and 2 were assayed for free mefloquine content (Table IV) and contained low, but quantifiable, levels of mefloquine.

The mefloquine blood and plasma level data from a single subject after oral administration indicated relatively rapid absorption, extensive distribution, and prolonged elimination phases. Partitioning of mefloquine into the erythrocytes in competition with extensive binding to

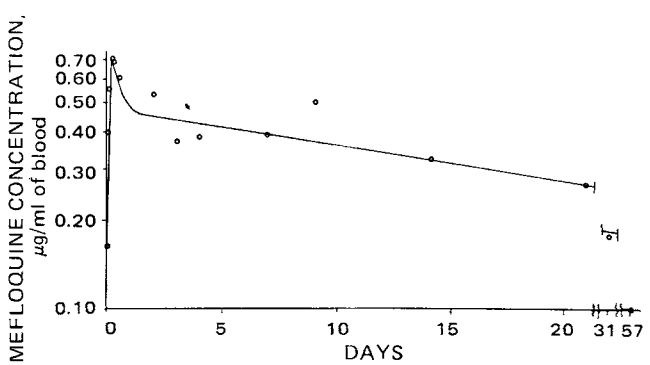

Figure 3—*Whole blood I concentrations in a male subject following a single oral dose of 500 mg of I.*

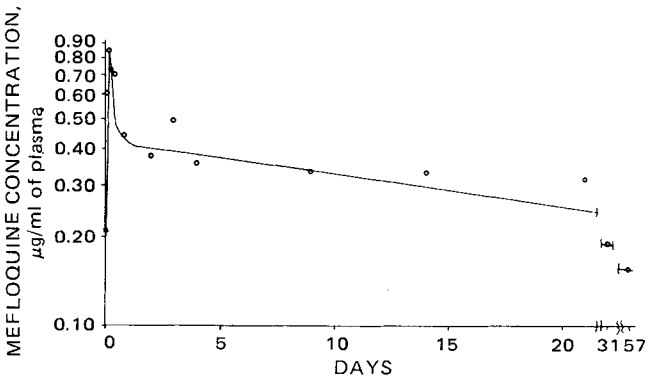

Figure 4—*Plasma I concentrations in a male subject following a single oral dose of 500 mg of I.*

plasma proteins probably caused the apparent disparities in the blood and plasma level data. Further data interpretation will be performed in conjunction with ongoing pharmacokinetic studies. The ability of the assay to follow blood and plasma levels of mefloquine for at least 57 days after a single oral administration of the drug established its utility for studying mefloquine's pharmacokinetic parameters in humans.

Table IV—Mefloquine Excretion in the Urine of an Adult Male after a Single Oral Dose of 500 mg of I [a]

	I Excretion		
Day[b]	μg/ml	μg/Sample	% Dose
1	3.03	527.92	0.12
2	0.76	127.01	0.03

[a] Chromatographic conditions are described under *Experimental.* [b] A random urine sample was obtained on each day.

REFERENCES

(1) C. J. Canfield and R. S. Rozman, *Bull. WHO,* **50,** 203 (1974).

(2) G. M. Trenholme, R. L. Williams, R. E. Desjardins, H. Frischer, P. E. Carson, K. H. Rieckman, and C. J. Canfield, *Science,* **190,** 792 (1975).

(3) K. H. Rieckman, G. M. Trenholme, R. L. Williams, P. E. Carson, H. Frischer, and R. E. Desjardins, *Bull. WHO,* **51,** 375 (1974).

(4) D. F. Clyde, V. C. McCarthy, R. M. Miller, and R. B. Hornick, *Antimicrob. Ag. Chemother.,* **9,** 384 (1976).

(5) J. Y. Mu, Z. H. Israili, and P. G. Dayton, *Drug Metab. Disp.,* **3,** 198 (1975).

(6) J. M. Grindel, R. S. Rozman, D. M. Leahy, N. A. Molek, and H. H. Gillum, *ibid.,* **4,** 133 (1976).

ACKNOWLEDGMENTS AND ADDRESSES

Received May 17, 1976, from the *Department of Pharmacology, Division of Medicinal Chemistry, Walter Reed Army Institute of Research, Washington, DC 20012 and [‡]INTERx Research Corporation, Lawrence, KS 66045.

Accepted for publication August 11, 1976.

Supported in part by Contract DAMD17-74-408 with the U.S. Army Medical Research and Development Command.

This report is Contribution 1410 of the Army Research Program on Malaria.

The authors thank Mr. Dave Skiles of Waters Associates for advice and support and Dr. C. J. Canfield and Dr. R. E. Desjardins for the clinical study.

[x] To whom inquiries should be directed. Present address: Biochemistry Department, McNeil Laboratories, Fort Washington, PA 19034.

Cytolysis of Neuroblastoma Cells *In Vitro* and Treatment of Neuronal Tumors *In Vivo* with Bromoacetylcholine

C. Y. CHIOU

Abstract □ The effect of bromoacetylcholine on mouse neuroblastoma C-1300 was investigated in cell culture as well as in A/J mice. *In vitro,* bromoacetylcholine (1×10^{-5} *M*) was a potent cytolytic agent and produced an additive effect in combination with vincristine (3×10^{-9} *M*). Since the choline acetyltransferase inhibitor, dimethylaminoethyl chloroacetate, does not inhibit neuroblastoma efficiently *in vitro,* the potent cytolytic action of bromoacetylcholine is probably not due to its choline acetyltransferase inhibitory action. Furthermore, the neuroblastoma inhibitory effect of bromoacetylcholine was not affected by atropine. Therefore, the inhibitory action is not related to the interaction of bromoacetylcholine with muscarinic receptors either. In *in vivo* experiments, 1, 10, or 30 mg/kg of bromoacetylcholine was injected directly into the tumors three times daily for 6 weeks. Bromoacetylcholine at 10 and 30 mg/kg gave significant protection of A/J mice from the death induced by neuroblastoma inoculation, and the lifespan was prolonged significantly with these bromoacetylcholine treatments.

Keyphrases □ Bromoacetylcholine—*in vitro* cytotoxic and *in vivo* antitumor activity, mice □ Cytotoxic activity—bromoacetylcholine evaluated, mouse neuroblastoma cell culture □ Antitumor activity—bromoacetylcholine evaluated, mouse neuroblastoma □ Cholinergic agents—bromoacetylcholine, *in vitro* cytotoxic and *in vivo* antitumor activity, mice

Many attempts have been made to treat the highly malignant neuroblastoma in children (1). However, no drug tested, including cyclophosphamide and vincristine, is satisfactory, mainly because the remission rate in neuroblastoma patients is quite low and the duration of drug effectiveness is fairly short (2–4).

The nature of neuroblastoma cells can be cholinergic, adrenergic, or inactive (5–8). Acetylcholinesterase is always present, and these cells possess membranes that respond to acetylcholine and are excitable electrically. These data indicate the existence of cholinergic receptors at the membrane site (7, 9). Attempts were made to destroy these

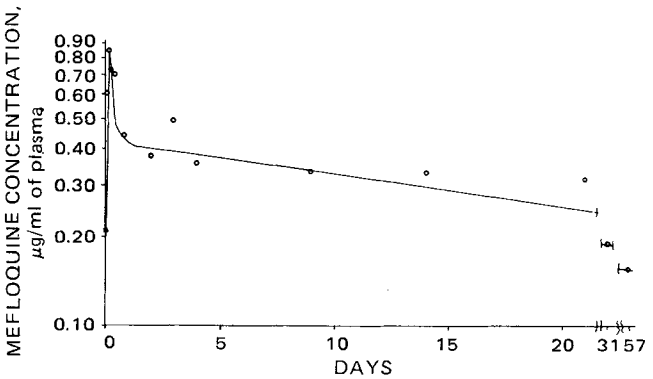

Figure 4—*Plasma I concentrations in a male subject following a single oral dose of 500 mg of I.*

plasma proteins probably caused the apparent disparities in the blood and plasma level data. Further data interpretation will be performed in conjunction with ongoing pharmacokinetic studies. The ability of the assay to follow blood and plasma levels of mefloquine for at least 57 days after a single oral administration of the drug established its utility for studying mefloquine's pharmacokinetic parameters in humans.

Table IV—Mefloquine Excretion in the Urine of an Adult Male after a Single Oral Dose of 500 mg of I [a]

	I Excretion		
Day[b]	μg/ml	μg/Sample	% Dose
1	3.03	527.92	0.12
2	0.76	127.01	0.03

[a] Chromatographic conditions are described under *Experimental.* [b] A random urine sample was obtained on each day.

REFERENCES

(1) C. J. Canfield and R. S. Rozman, *Bull. WHO,* **50,** 203 (1974).

(2) G. M. Trenholme, R. L. Williams, R. E. Desjardins, H. Frischer, P. E. Carson, K. H. Rieckman, and C. J. Canfield, *Science,* **190,** 792 (1975).

(3) K. H. Rieckman, G. M. Trenholme, R. L. Williams, P. E. Carson, H. Frischer, and R. E. Desjardins, *Bull. WHO,* **51,** 375 (1974).

(4) D. F. Clyde, V. C. McCarthy, R. M. Miller, and R. B. Hornick, *Antimicrob. Ag. Chemother.,* **9,** 384 (1976).

(5) J. Y. Mu, Z. H. Israili, and P. G. Dayton, *Drug Metab. Disp.,* **3,** 198 (1975).

(6) J. M. Grindel, R. S. Rozman, D. M. Leahy, N. A. Molek, and H. H. Gillum, *ibid.,* **4,** 133 (1976).

ACKNOWLEDGMENTS AND ADDRESSES

Received May 17, 1976, from the *Department of Pharmacology, Division of Medicinal Chemistry, Walter Reed Army Institute of Research, Washington, DC 20012 and [‡]INTERx Research Corporation, Lawrence, KS 66045.

Accepted for publication August 11, 1976.

Supported in part by Contract DAMD17-74-408 with the U.S. Army Medical Research and Development Command.

This report is Contribution 1410 of the Army Research Program on Malaria.

The authors thank Mr. Dave Skiles of Waters Associates for advice and support and Dr. C. J. Canfield and Dr. R. E. Desjardins for the clinical study.

[x] To whom inquiries should be directed. Present address: Biochemistry Department, McNeil Laboratories, Fort Washington, PA 19034.

Cytolysis of Neuroblastoma Cells *In Vitro* and Treatment of Neuronal Tumors *In Vivo* with Bromoacetylcholine

C. Y. CHIOU

Abstract □ The effect of bromoacetylcholine on mouse neuroblastoma C-1300 was investigated in cell culture as well as in A/J mice. *In vitro,* bromoacetylcholine (1×10^{-5} *M*) was a potent cytolytic agent and produced an additive effect in combination with vincristine (3×10^{-9} *M*). Since the choline acetyltransferase inhibitor, dimethylaminoethyl chloroacetate, does not inhibit neuroblastoma efficiently *in vitro,* the potent cytolytic action of bromoacetylcholine is probably not due to its choline acetyltransferase inhibitory action. Furthermore, the neuroblastoma inhibitory effect of bromoacetylcholine was not affected by atropine. Therefore, the inhibitory action is not related to the interaction of bromoacetylcholine with muscarinic receptors either. In *in vivo* experiments, 1, 10, or 30 mg/kg of bromoacetylcholine was injected directly into the tumors three times daily for 6 weeks. Bromoacetylcholine at 10 and 30 mg/kg gave significant protection of A/J mice from the death induced by neuroblastoma inoculation, and the lifespan was prolonged significantly with these bromoacetylcholine treatments.

Keyphrases □ Bromoacetylcholine—*in vitro* cytotoxic and *in vivo* antitumor activity, mice □ Cytotoxic activity—bromoacetylcholine evaluated, mouse neuroblastoma cell culture □ Antitumor activity—bromoacetylcholine evaluated, mouse neuroblastoma □ Cholinergic agents—bromoacetylcholine, *in vitro* cytotoxic and *in vivo* antitumor activity, mice

Many attempts have been made to treat the highly malignant neuroblastoma in children (1). However, no drug tested, including cyclophosphamide and vincristine, is satisfactory, mainly because the remission rate in neuroblastoma patients is quite low and the duration of drug effectiveness is fairly short (2–4).

The nature of neuroblastoma cells can be cholinergic, adrenergic, or inactive (5–8). Acetylcholinesterase is always present, and these cells possess membranes that respond to acetylcholine and are excitable electrically. These data indicate the existence of cholinergic receptors at the membrane site (7, 9). Attempts were made to destroy these

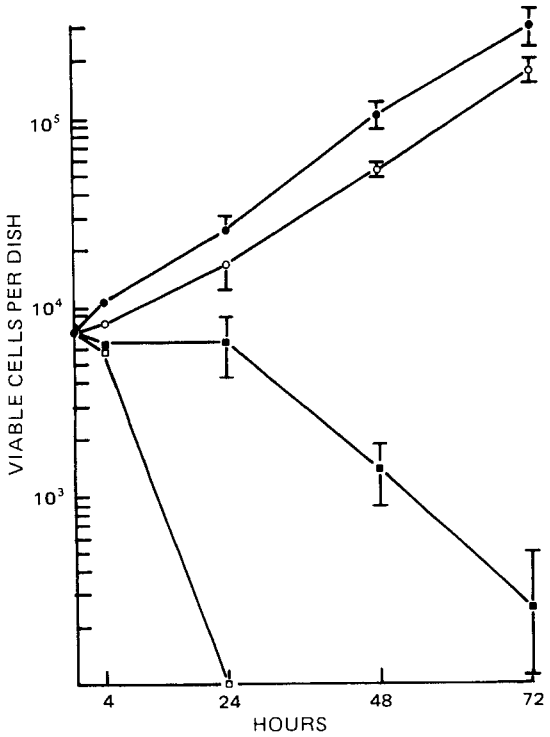

Figure 1—*Inhibition of neuroblastoma by various concentrations of bromoacetylcholine* in vitro. *Bromoacetylcholine was added to the culture medium at time zero and left in the medium throughout the experiment. Key:* ●, *control;* ○, *3 × 10^{-6}* M *bromoacetylcholine;* ■, *1 × 10^{-5}* M *bromoacetylcholine; and* □, *3 × 10^{-5}* M *bromoacetylcholine. Each point is a mean of four values, and bars represent* SEM.

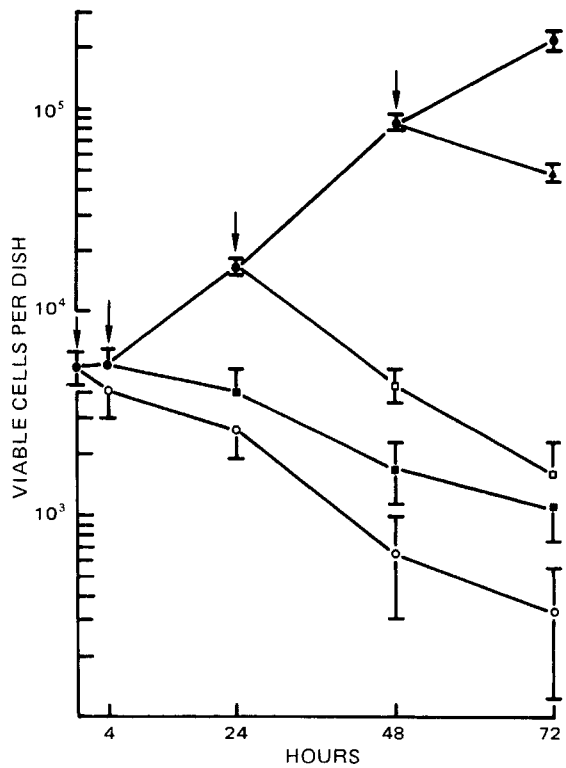

Figure 2—*Inhibition of neuroblastoma by bromoacetylcholine (3 × 10^{-5}* M*)* in vitro *after various stages of incubation. Bromoacetylcholine was added to the medium after 0 (○), 4 (■), 24 (□), or 48 (▲) hr of incubation time (indicated with arrows). Each point is a mean of four values, and bars represent* SEM.

neuronal tumors with an irreversible sympatholytic agent, 6-hydroxydopamine (10), resulting in a brief tumor regression only in the 1st week of treatment. The effectiveness of this treatment then decreased rapidly.

The ineffectiveness of 6-hydroxydopamine to maintain cytolysis of neuroblastoma was confirmed further by Finklestein *et al.* (11). Therefore, instead of an adrenolytic agent, an irreversible cholinolytic agent, bromoacetylcholine (12), was evaluated and is the subject of this report.

EXPERIMENTAL

Materials—Vincristine sulfate, 6-hydroxydopamine hydrochloride, and atropine sulfate were obtained commercially. Bromoacetylcholine perchlorate and dimethylaminoethyl chloroacetate were synthesized using previously published methods (13, 14).

Culture Medium—Mouse neuroblastoma C-1300 was cultivated in Dulbecco modified Eagle medium[1] supplemented with 10% fetal calf serum[2], 200 m*M* L-glutamine, 30 m*M* $NaHCO_3$, 50 units of penicillin/ml, and 50 μg of streptomycin/ml (7). The cells were grown at 37° under 95% air–5% CO_2 with 100% humidity.

For the culture experiments, 1×10^6 cells were placed in a tissue culture flask[3] (75 cm^2) for 3–5 days until the cells were in the logarithmic growth phase. They were then removed from the surface by a 15-min exposure to 0.25% trypsin in modified D_1 solution[4] (7, 15). The cells were then tapped off in fresh medium containing 10% fetal calf serum. Aliquots of the cell suspension were incubated for 5 min with 0.4% trypan blue, and the number of viable and nonviable cells was counted with a hemocytometer.

Appropriate dilution was made, and the cell suspension was plated at

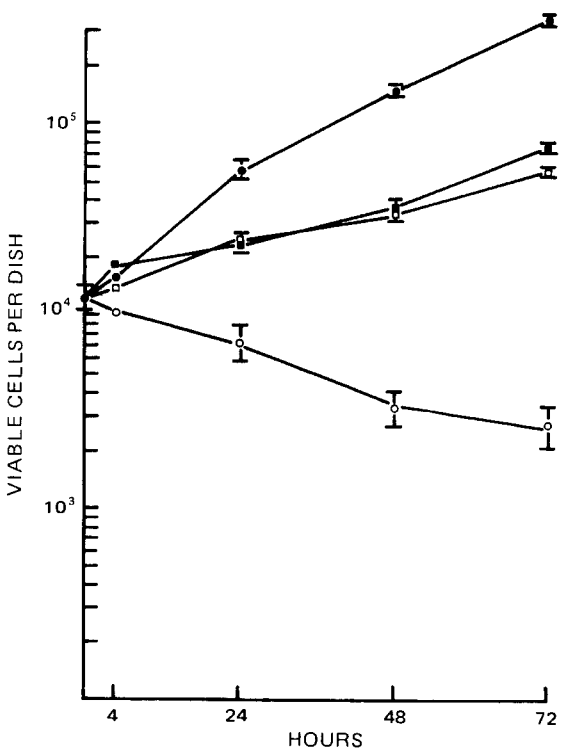

Figure 3—*Additive action of bromoacetylcholine and vincristine to inhibit neuroblastoma. Key:* ●, *control;* ■, *1 × 10^{-5}* M *bromoacetylcholine;* □, *3.2 × 10^{-9}* M *vincristine; and* ○, *1 × 10^{-5}* M *bromoacetylcholine plus 3.2 × 10^{-9}* M *vincristine. Each point is a mean of four values, and bars represent* SEM.

[1] MEM, Earle's Powder, Catalog No. F-11, Grand Island Biological Co., Grand Island, N.Y.

[2] Catalog No. 614, Grand Island Biological Co., Grand Island, N.Y.

[3] Falcon.

[4] Modified D_1 solution contained 1.2 mg of phenolsulfonphthalein, 8 g of sodium chloride, 0.4 g of potassium chloride, 45 mg of dibasic sodium phosphate heptahydrate, 30 mg of monobasic potassium phosphate, 2 g of glucose, 20.2 g of sucrose, 5×10^4 units of penicillin, and 50 mg of streptomycin in 1 liter of double-distilled water.

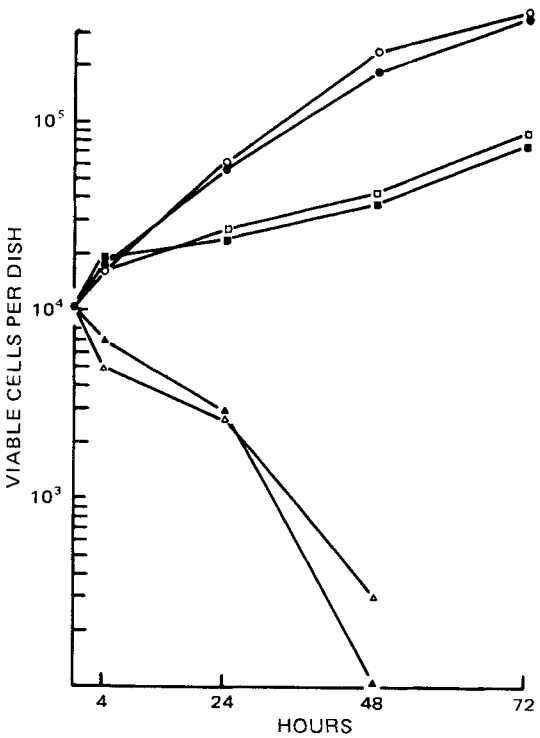

Figure 4—*Effect of atropine (1×10^{-7} M) on the control growth of neuroblastoma and inhibitory action of bromoacetylcholine* in vitro. *Key: ●, control; ○, 1×10^{-7} M atropine; ■, 1×10^{-5} M bromoacetylcholine; □, 1×10^{-5} M bromoacetylcholine plus 1×10^{-7} M atropine; ▲, 3×10^{-5} M bromoacetylcholine; and △, 3×10^{-5} M bromoacetylcholine plus 1×10^{-7} M atropine. Each point is a mean of four experiments.*

5×10^4 cells/dish (tissue culture dishes[3] of 35-mm diameter) and grown for 24 hr. Various concentrations of drugs were added to the medium, and these cultures were incubated further for 72 hr. The cultures were removed at intervals (4, 24, 48, and 72 hr) for cell count.

Inhibition of Neuroblastoma *In Vitro*—Various concentrations of bromoacetylcholine, dimethylaminoethyl chloroacetate, 6-hydroxydopamine, and vincristine were added to the cell culture to determine the potency of these drugs and drug combinations to inhibit neuroblastoma. Drug concentrations required to reduce the initial control viable cells (at zero time) by 50% after 72 hr of incubation were termed CD_{50} (50% cytolytic dose). Bromoacetylcholine (3×10^{-5} *M*) also was added to the culture medium after various incubation times (0, 4, 24, and 48 hr) to study its inhibitory ability at various stages of neuroblastoma culture.

To determine whether the inhibitory action of bromoacetylcholine is mediated through its interaction with the muscarinic site, atropine was added to the medium.

Treatment of Neuroblastoma *In Vivo*—The cell suspension of mouse neuroblastoma C-1300 was injected (1×10^6 cells/mouse) subcutaneously to the interscapular area of A/J mice[5], 16–18 g (11, 16). Ten days later, the animals were divided into tumor-control and tumor-treated groups. The control group was injected three times daily, except Saturdays and Sundays, with saline; the treated groups were injected similarly with bromoacetylcholine at 1, 10, or 30 mg/kg. Injections were made directly into the tumors. The size and body weight were recorded every other day.

Figure 5—*Control A/J mouse inoculated with 10^6 cells of neuroblastoma for 5 weeks.*

[5] Jackson Lab., Bar Harbor, Me.

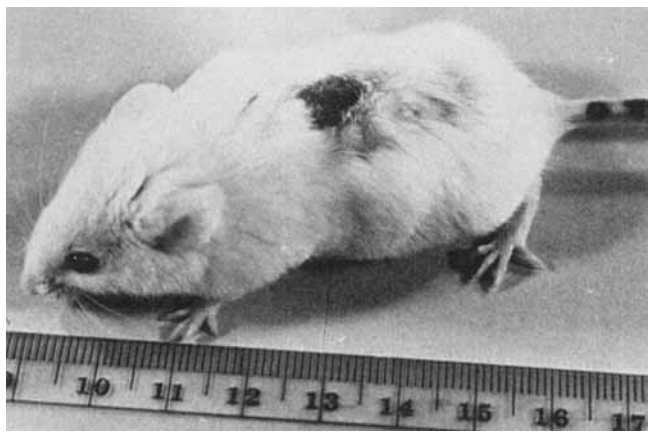

Figure 6—*Treatment of neuroblastoma-inoculated A/J mouse with 30 mg of bromoacetylcholine/kg three times daily for 6 weeks.*

RESULTS

Figure 1 shows a potent cytolytic effect of bromoacetylcholine on neuroblastoma cells at a concentration of 1×10^{-5} *M*. The neuroblastoma cells could be inhibited by bromoacetylcholine (3×10^{-5} *M*) at any stage of the incubation period (0, 4, 24, and 48 hr) (Fig. 2). The CD_{50} of bromoacetylcholine was 5.8×10^{-6} *M*.

Bromoacetylcholine is a potent inhibitor of choline acetyltransferase in cell-free choline acetyltransferase preparations (17). Although bromoacetylcholine does not cross the cell membrane efficiently because of its positive charge in the molecule, it is possible to accumulate enough bromoacetylcholine in the intracellular site to inhibit choline acetyltransferase after prolonged incubation. To determine whether the cytolytic action of bromoacetylcholine is related to its inhibition of choline acetyltransferase in the intracellular site, dimethylaminoethyl chloroacetate was used because it can get into the intracellular site efficiently. Although dimethylaminoethyl chloroacetate inhibited choline acetyltransferase in the intact cellular preparation with an I_{50} of 1.29×10^{-4} *M* (14), it took 1.3×10^{-3} *M* to inhibit the growth of neuroblastoma, indicating that the cytolytic action of dimethylaminoethyl chloroacetate

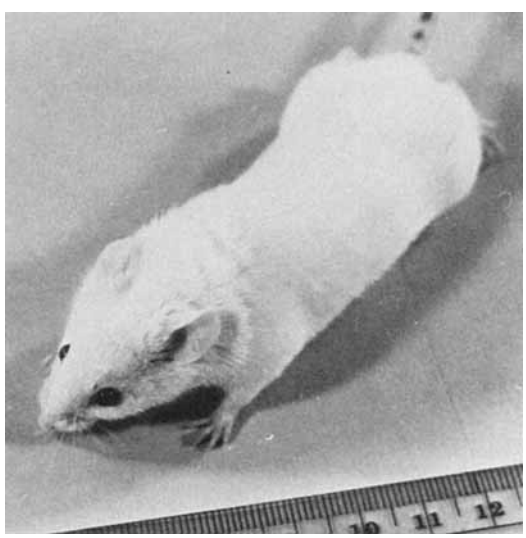

Figure 7—*Complete recovery of neuroblastoma-inoculated A/J mouse. The mouse was treated with 30 mg of bromoacetylcholine/kg three times daily for 6 weeks. Drug treatment was stopped thereafter, and the picture was taken 7 weeks after the drug treatment was stopped.*

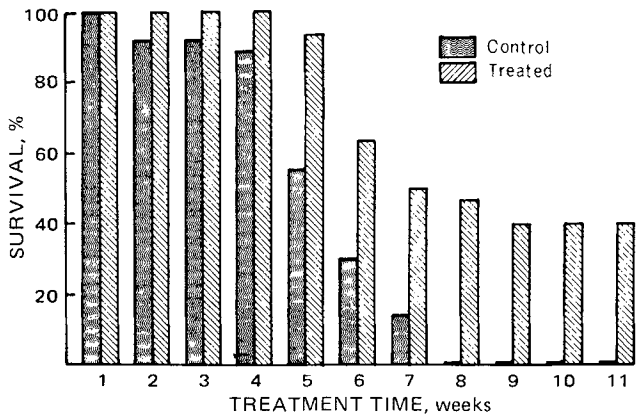

Figure 8—*Comparison of survival rate between treated (bromoacetylcholine, 30 mg/kg) and untreated (control) neuroblastoma-inoculated A/J mice.*

on neuroblastoma is either unrelated to the inhibition of choline acetyltransferase or due to a rise in concentration needed in cancer cells to inhibit choline acetyltransferase.

The sympatholytic, 6-hydroxydopamine, had a CD_{50} of 2.0×10^{-5} *M*. Vincristine, a cellular mitotic arresting agent used clinically to treat neuroblastoma, was very potent, inhibiting neuroblastoma *in vitro* with a CD_{50} of 8.5×10^{-9} *M*. Combined use of bromoacetylcholine (1×10^{-5} *M*) and vincristine (3×10^{-9} *M*) produced an additive effect, which was equivalent to the higher concentration of bromoacetylcholine or vincristine given individually (Fig. 3).

Atropine (1×10^{-7}–1×10^{-5} *M*) did not affect the cytolytic action of bromoacetylcholine on neuroblastoma (Fig. 4), indicating that bromoacetylcholine does not act *via* muscarinic sites to inhibit neuroblastoma. The CD_{50} of atropine was greater than 1.0×10^{-4} *M*.

In *in vivo* experiments, a dramatic difference between control and treated neuroblastoma mice was noted (Figs. 5–8). Marked tumor regression was noted 3 weeks after bromoacetylcholine treatment at doses of 10 and 30 mg/kg (Figs. 5 and 6). The area of tumor became hard, flattened, and necrotic after 6 weeks of treatment. Finally, the fur grew back and looked healthy 3 months after the treatment was initiated (Fig. 7). Treatments were stopped after 6 weeks.

The survival time increased significantly with mice treated with 10 and 30 mg/kg of bromoacetylcholine (Table I and Fig. 8). Although the body weight of the control group was only slightly lower than that of treated ones (Fig. 9), subtraction of tumor weight from the total body weight would make the net body weight of control mice be even lighter than the treated ones.

DISCUSSION

Bromoacetylcholine is promising as a cancer chemotherapeutic agent for metastatic neuroblastoma, because it inhibits effectively the growth

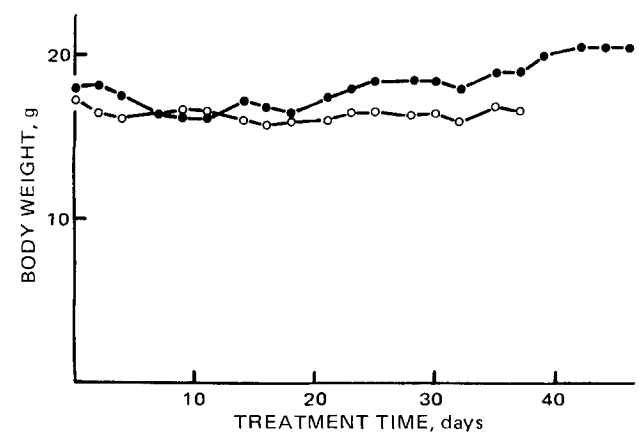

Figure 9—*Comparison of body weights of treated (bromoacetylcholine, 30 mg/kg) and untreated (control) neuroblastoma-inoculated A/J mice. Key: ●, treated; and ○, control.*

Table I—Treatment of Neuroblastoma with Bromoacetylcholine in Adult A/J Mice on Subcutaneously Inoculated Tumors

Treatment	*n*	Survival Time: Range, days	Survival Time: Mean, days	CLS[a], %
Control	12	10–47	34.3 ± 2.9	—
Bromoacetylcholine, 1 mg/kg[b]	7	27–39	33.4 ± 1.7	−2.6
Bromoacetylcholine, 10 mg/kg[b]	7	31–120[c]	56.9 ± 11.7[d]	+65.8
Bromoacetylcholine, 30 mg/kg[b]	10	30–120[c]	64.3 ± 12.6[d]	+87.5

[a] Percent change in lifespan (CLS) of treated over control mice. [b] These doses were administered three times daily, except Saturday and Sunday, for 6 weeks (40 days). [c] The 120 days is not the upper range of survival time, because some mice survived longer; 120 days was chosen arbitrarily as a cutoff date for the purpose of statistical analysis. [d] Statistically different from control ($p < 0.05$).

of neuroblastoma at 5.8×10^{-6} *M* or higher *in vitro* (12).

One major obstacle of using anticancer drugs is toxicity. The main side effect anticipated with the use of bromoacetylcholine is the muscarinic (parasympathomimetic) action, which can be eliminated with atropine and its analogs. Bromoacetylcholine is a cholinergic agonist and stimulates both nicotinic and muscarinic receptors directly (18–20). However, when it is incubated with cells for 15 min or longer, it binds irreversibly to the cholinergic receptor at the nicotinic site but not at the muscarinic site (18, 21).

Atropine (up to 1×10^{-5} *M*) did not affect the cytolytic actions of bromoacetylcholine on neuroblastoma. Therefore, it is possible that bromoacetylcholine can be used along with muscarinic blocking agents as a safe and potent drug to treat neuronal tumors.

Alternatively, reduced doses of more than one cancer chemotherapeutic agent with different action mechanisms can be used in combination. In this way, the chemotherapeutic actions of these drugs can be enhanced while their side effects can be minimized.

Among several agents tested, vincristine was the most potent neuroblastoma inhibitor. When combined with bromoacetylcholine, it showed additive effects, indicating that reduced quantities of bromoacetylcholine (1×10^{-5} *M*) and vincristine (3×10^{-9} *M*) can be used together to get an effect that requires higher concentrations of bromoacetylcholine (3×10^{-5} *M*) or vincristine (1×10^{-8} *M*) when given individually.

Results obtained from *in vivo* experiments are very encouraging, because 50% of the neuronal tumor mice that were treated with bromoacetylcholine at the 30-mg/kg dose injected three times daily for 6 weeks survived after all untreated control mice were dead. Certainly, the dose regimens and the administration route in this study are not ideal, and the combined use of bromoacetylcholine with atropine and/or vincristine should be tried[6].

Since the murine neuroblastoma system used is reported to be a model of human disease (16), the effectiveness of bromoacetylcholine for treating neuroblastoma *in vivo* in this study makes it promising for treating neuroblastoma in children.

REFERENCES

(1) H. W. Dargeon, *J. Pediatr.*, **61**, 456 (1962).

(2) A. E. Evans, R. M. Heyn, W. A. Newton, Jr., and S. L. Leiken, *J. Am. Med. Assoc.*, **207**, 1325 (1969).

(3) D. H. James, Jr., O. Histu, E. L. Wrenn, and D. Pinkel, *ibid.*, **194**, 123 (1965).

(4) M. P. Sullivan, A. H. Nora, P. Kulapongs, D. M. Lane, J. Windmiller, and W. G. Thurman, *Pediatrics*, **44**, 685 (1969).

(5) T. Amano, E. Richelson, and M. Nirenberg, *Proc. Natl. Acad. Sci. USA*, **69**, 258 (1972).

(6) G. Augusti-Tocco and G. Sato, *ibid.*, **64**, 311 (1969).

(7) A. Blume, F. Gilbert, S. Wilson, J. Farbes, R. Rosenberg, and M. Nirenberg, *ibid.*, **67**, 786 (1970).

(8) D. Schubert, S. Humphreys, C. Baroni, and M. Cohn, *ibid.*, **64**, 316 (1969).

(9) N. W. Seeds, *ibid.*, **68**, 1858 (1971).

(10) P. M. Angeletti and R. Levi-Montalcini, *Cancer Res.*, **30**, 2863 (1972).

[6] Details of these studies will be published shortly.

(11) J. Z. Finklestein, K. Tittle, R. Meshnik, and J. Weiner, *Cancer Chemother. Rep.*, **59**, 571 (1975).
(12) C. Y. Chiou, *J. Pharm. Sci.*, **64**, 469 (1975).
(13) C. Y. Chiou and B. V. R. Sastry, *Biochem. Pharmacol.*, **17**, 805 (1968).
(14) P. P. Rowell and C. Y. Chiou, *ibid.*, **25**, 1093 (1976).
(15) G. R. Ham and T. T. Tuck, in "Methods in Enzymology," vol. 5, S. P. Colowick and N. O. Kaplan, Eds., Academic, New York, N.Y., 1962, pp. 90–119.
(16) J. Z. Finklestein, E. Arima, P. E. Byfield, J. E. Byfield, and E. W. Fonkalsrud, *Cancer Chemother. Rep.*, **57**, 405 (1973).
(17) R. C. Speth and D. E. Schmidt, *Fed. Proc.*, **33**, 477 (1974).
(18) C. Y. Chiou, *Eur. J. Pharmacol.*, **13**, 367 (1971).
(19) C. Y. Chiou and B. V. R. Sastry, *Arch. Int. Pharmacodyn. Ther.*, **181**, 94 (1969).
(20) C. Y. Chiou and B. V. R. Sastry, *J. Pharmacol. Exp. Ther.*, **172**, 351 (1970).
(21) C. Y. Chiou, *Eur. J. Pharmacol.*, **26**, 268 (1974).

ACKNOWLEDGMENTS AND ADDRESSES

Received June 30, 1976, from the *Department of Pharmacology and Therapeutics, College of Medicine, University of Florida, Gainesville, FL 32610.*

Accepted for publication August 11, 1976.

Supported in part by Grant CA-17584, National Cancer Institute, Department of Health, Education, and Welfare, and Grant CH-81, American Cancer Society.

The author is grateful for the dedication and technical assistance of Ms. Marilyn Martin.

Determination of Triprolidine in Human Plasma by Quantitative TLC

R. L. DeANGELIS, M. F. KEARNEY, and R. M. WELCH ˣ

Abstract □ A chromatographic thin-layer fluorescence procedure, with a sensitivity limit of 0.8 ng/ml, is described for the quantitative analysis of triprolidine in human and rat plasma. Following the intravenous administration of 1 mg/kg of triprolidine to rats, the drug distributed rapidly into tissues and was eliminated from plasma with a half-life of 53 min. The method was used to determine the plasma triprolidine levels in 16 normal human volunteers following oral administration of 3.75 mg of triprolidine hydrochloride in 15 ml of a syrup. The drug obtained a mean peak plasma level of 8.2 ng/ml in 2 hr and was eliminated from the plasma with a half-life of 5 hr. Considerable individual variation was observed in the area under the plasma triprolidine level–time curve; values ranged from 19 to 163 ng hr/ml with a mean value of 75 ng hr/ml.

Keyphrases □ Triprolidine—TLC analysis, human and rat plasma, pharmacokinetic profile □ TLC—analysis, triprolidine, human and rat plasma □ Pharmacokinetics—triprolidine, humans and rats □ Antihistamines—triprolidine, TLC analysis, human and rat plasma, pharmacokinetic profile

Triprolidine hydrochloride [(*E*)-2-[3-(1-pyrrolidinyl)-1-*p*-tolylpropenyl]pyridine hydrochloride] is an unusually potent antihistaminic agent used for the treatment of various allergic conditions. Although animal data (1–3) and several clinical reports (4–8) substantiate the efficacy of triprolidine, its disposition is unknown. One report indicated that triprolidine had a duration of action of approximately 4–6 hr (5), but no confirming plasma level data were given.

In another study on the *in vitro* metabolism of ^{14}C-triprolidine by guinea pig liver, the drug was extensively metabolized (9). Other reports described the TLC (10) and GC (11) properties of triprolidine, but no attempt was made to quantitate the drug in tissues. Considering the extensive clinical use of this antihistamine, alone and in combination with other drugs, a sensitive quantitative analysis in biological fluids is needed.

This report describes a sensitive analytical method for quantitating triprolidine in plasma following oral administration of a therapeutic dose to human subjects. The method was used to determine the pharmacokinetic profile of the drug in animals and humans.

EXPERIMENTAL

Materials—The organic solvents utilized to develop the thin-layer plates were reagent grade and were used as received; the solvents employed for the extraction of triprolidine from plasma were glass distilled[1]. A 0.01% stock solution of triprolidine hydrochloride was prepared by dissolving the drug in 1–2 ml of methanol and then adding an appropriate volume of chloroform. From this solution, a working standard of 1 μg/ml was prepared in chloroform. A spray reagent of 2 *M* ammonium bisulfate, prepared every 2 weeks, was employed to induce the fluorescence of the drug on the TLC plate.

Analytical Procedure—Plasma, 1 ml, and 6 ml of dichloroethane were added to a 15-ml conical glass centrifuge tube, mechanically shaken for 15 min, and centrifuged (1000×*g*). Five milliliters of the organic phase was placed in a disposable glass culture tube, the tube was immersed in a water bath at 45°, and the solvent was evaporated to dryness under a nitrogen stream. The residue was redissolved in 0.1 ml of chloroform, and a suitable aliquot (50–80 μl) was spotted on a prescored silica gel plate[2]. Samples were applied to a thin-layer plate with an automatic spotter[3], while the standards (1–5 ng) were spotted by hand using a 10-μl syringe.

Prior to use, each TLC plate was channeled (scored) into 20 units 1 cm wide. The plate was developed to a height of 15 cm in methanol–ammonium hydroxide–chloroform (10:1:89). The solvent system was prepared fresh each day and allowed to equilibrate for 30 min prior to use. After development, the plate was allowed to air dry for 15 min and then sprayed with a 2 *M* aqueous solution of ammonium bisulfate until shiny. After the plate was air dried for about 1 hr, each channel was scanned, and the fluorescent spot representing triprolidine was quantitated.

Instrumentation—Fluorescence measurements were determined by scanning the TLC plate with a spectrodensitometer[4] in the reflectance mode, utilizing only the sample beam that had been passed through a secondary cutoff filter of 405 nm. The fluorophore was excited at 300 nm, and the total emission above 405 nm was read using a density computer[5].

[1] Burdick and Jackson Laboratories.
[2] Siliplate-22, 20 × 20 cm, 0.25 mm, E. M. Laboratories.
[3] Analytical Instrument Specialties multispotter.
[4] Schoeffel SD3000 with reflectance-mode assembly.
[5] Schoeffel SD 30.

(11) J. Z. Finklestein, K. Tittle, R. Meshnik, and J. Weiner, *Cancer Chemother. Rep.*, **59**, 571 (1975).
(12) C. Y. Chiou, *J. Pharm. Sci.*, **64**, 469 (1975).
(13) C. Y. Chiou and B. V. R. Sastry, *Biochem. Pharmacol.*, **17**, 805 (1968).
(14) P. P. Rowell and C. Y. Chiou, *ibid.*, **25**, 1093 (1976).
(15) G. R. Ham and T. T. Tuck, in "Methods in Enzymology," vol. 5, S. P. Colowick and N. O. Kaplan, Eds., Academic, New York, N.Y., 1962, pp. 90–119.
(16) J. Z. Finklestein, E. Arima, P. E. Byfield, J. E. Byfield, and E. W. Fonkalsrud, *Cancer Chemother. Rep.*, **57**, 405 (1973).
(17) R. C. Speth and D. E. Schmidt, *Fed. Proc.*, **33**, 477 (1974).
(18) C. Y. Chiou, *Eur. J. Pharmacol.*, **13**, 367 (1971).
(19) C. Y. Chiou and B. V. R. Sastry, *Arch. Int. Pharmacodyn. Ther.*, **181**, 94 (1969).
(20) C. Y. Chiou and B. V. R. Sastry, *J. Pharmacol. Exp. Ther.*, **172**, 351 (1970).
(21) C. Y. Chiou, *Eur. J. Pharmacol.*, **26**, 268 (1974).

ACKNOWLEDGMENTS AND ADDRESSES

Received June 30, 1976, from the *Department of Pharmacology and Therapeutics, College of Medicine, University of Florida, Gainesville, FL 32610.*

Accepted for publication August 11, 1976.

Supported in part by Grant CA-17584, National Cancer Institute, Department of Health, Education, and Welfare, and Grant CH-81, American Cancer Society.

The author is grateful for the dedication and technical assistance of Ms. Marilyn Martin.

Determination of Triprolidine in Human Plasma by Quantitative TLC

R. L. DeANGELIS, M. F. KEARNEY, and R. M. WELCH ˣ

Abstract □ A chromatographic thin-layer fluorescence procedure, with a sensitivity limit of 0.8 ng/ml, is described for the quantitative analysis of triprolidine in human and rat plasma. Following the intravenous administration of 1 mg/kg of triprolidine to rats, the drug distributed rapidly into tissues and was eliminated from plasma with a half-life of 53 min. The method was used to determine the plasma triprolidine levels in 16 normal human volunteers following oral administration of 3.75 mg of triprolidine hydrochloride in 15 ml of a syrup. The drug obtained a mean peak plasma level of 8.2 ng/ml in 2 hr and was eliminated from the plasma with a half-life of 5 hr. Considerable individual variation was observed in the area under the plasma triprolidine level–time curve; values ranged from 19 to 163 ng hr/ml with a mean value of 75 ng hr/ml.

Keyphrases □ Triprolidine—TLC analysis, human and rat plasma, pharmacokinetic profile □ TLC—analysis, triprolidine, human and rat plasma □ Pharmacokinetics—triprolidine, humans and rats □ Antihistamines—triprolidine, TLC analysis, human and rat plasma, pharmacokinetic profile

Triprolidine hydrochloride [(*E*)-2-[3-(1-pyrrolidinyl)-1-*p*-tolylpropenyl]pyridine hydrochloride] is an unusually potent antihistaminic agent used for the treatment of various allergic conditions. Although animal data (1–3) and several clinical reports (4–8) substantiate the efficacy of triprolidine, its disposition is unknown. One report indicated that triprolidine had a duration of action of approximately 4–6 hr (5), but no confirming plasma level data were given.

In another study on the *in vitro* metabolism of ^{14}C-triprolidine by guinea pig liver, the drug was extensively metabolized (9). Other reports described the TLC (10) and GC (11) properties of triprolidine, but no attempt was made to quantitate the drug in tissues. Considering the extensive clinical use of this antihistamine, alone and in combination with other drugs, a sensitive quantitative analysis in biological fluids is needed.

This report describes a sensitive analytical method for quantitating triprolidine in plasma following oral administration of a therapeutic dose to human subjects. The method was used to determine the pharmacokinetic profile of the drug in animals and humans.

EXPERIMENTAL

Materials—The organic solvents utilized to develop the thin-layer plates were reagent grade and were used as received; the solvents employed for the extraction of triprolidine from plasma were glass distilled[1]. A 0.01% stock solution of triprolidine hydrochloride was prepared by dissolving the drug in 1–2 ml of methanol and then adding an appropriate volume of chloroform. From this solution, a working standard of 1 μg/ml was prepared in chloroform. A spray reagent of 2 *M* ammonium bisulfate, prepared every 2 weeks, was employed to induce the fluorescence of the drug on the TLC plate.

Analytical Procedure—Plasma, 1 ml, and 6 ml of dichloroethane were added to a 15-ml conical glass centrifuge tube, mechanically shaken for 15 min, and centrifuged (1000×*g*). Five milliliters of the organic phase was placed in a disposable glass culture tube, the tube was immersed in a water bath at 45°, and the solvent was evaporated to dryness under a nitrogen stream. The residue was redissolved in 0.1 ml of chloroform, and a suitable aliquot (50–80 μl) was spotted on a prescored silica gel plate[2]. Samples were applied to a thin-layer plate with an automatic spotter[3], while the standards (1–5 ng) were spotted by hand using a 10-μl syringe.

Prior to use, each TLC plate was channeled (scored) into 20 units 1 cm wide. The plate was developed to a height of 15 cm in methanol–ammonium hydroxide–chloroform (10:1:89). The solvent system was prepared fresh each day and allowed to equilibrate for 30 min prior to use. After development, the plate was allowed to air dry for 15 min and then sprayed with a 2 *M* aqueous solution of ammonium bisulfate until shiny. After the plate was air dried for about 1 hr, each channel was scanned, and the fluorescent spot representing triprolidine was quantitated.

Instrumentation—Fluorescence measurements were determined by scanning the TLC plate with a spectrodensitometer[4] in the reflectance mode, utilizing only the sample beam that had been passed through a secondary cutoff filter of 405 nm. The fluorophore was excited at 300 nm, and the total emission above 405 nm was read using a density computer[5].

[1] Burdick and Jackson Laboratories.
[2] Siliplate-22, 20 × 20 cm, 0.25 mm, E. M. Laboratories.
[3] Analytical Instrument Specialties multispotter.
[4] Schoeffel SD3000 with reflectance-mode assembly.
[5] Schoeffel SD 30.

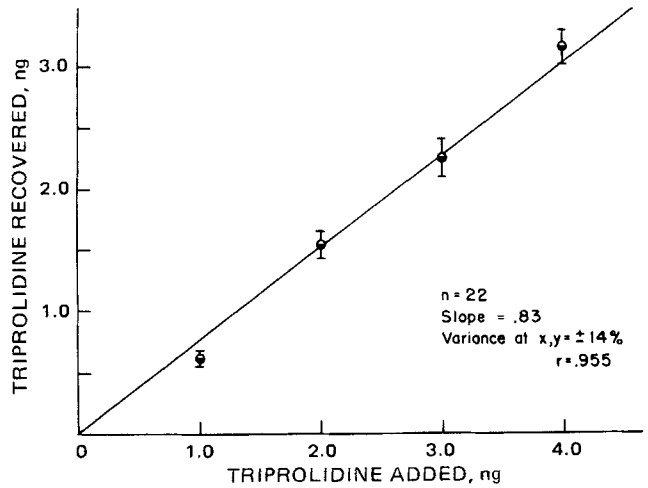

Figure 1—*Recovery of triprolidine from human plasma.*

The area of each peak was simultaneously integrated[6] while recorded on a strip-chart recorder.

Subjects and Protocol—Sixteen male volunteers, with an average age of 23 years and an average weight of 72.5 kg (160 lb), were studied. A complete medical history was taken to eliminate individuals with a history of kidney, liver, or cardiovascular disease. All subjects were fasted 12 hr before and 2 hr after dosing and were free of other medication for 2 weeks prior to triprolidine administration.

Each subject received 15 ml of a syrup[7] containing 3.75 mg of triprolidine hydrochloride followed by 240 ml of water. The syrup was given orally by syringe to ensure complete drug delivery. Seven milliliters of blood was drawn at 0, 0.5, 1, 2, 4, 6, 12, and 24 hr and placed into a Vacutainer containing edetate disodium as the anticoagulant. These samples were centrifuged, and the resulting plasmas were stored in a refrigerator for no more than 24–36 hr before analysis.

RESULTS AND DISCUSSION

Since the pKa of triprolidine is approximately 6.5, it can be extracted quantitatively from plasma into dichloroethane at a physiological pH of 7.4. As shown in Fig. 1, the recovery of 1–4 ng of triprolidine from human plasma was 83% with a variance of 14% at the mean of the linear regression based on 22 determinations. A similar recovery was obtained (n = 29) when higher amounts (5–35 ng) of triprolidine were added to plasma and extracted. The stability of triprolidine was reduced considerably in the presence of a strong base, and the recovery data indicate

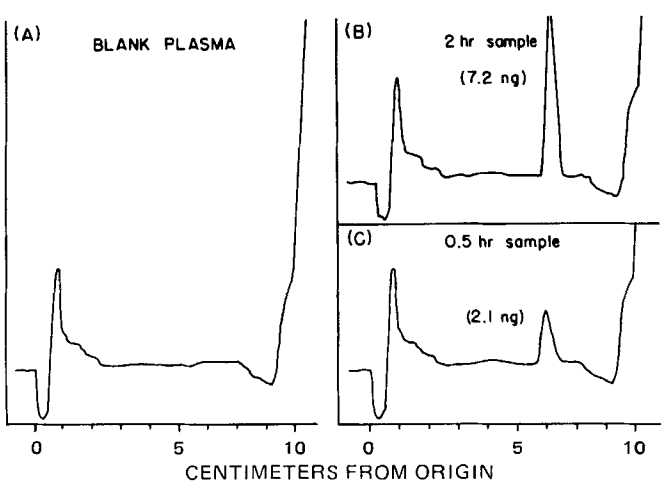

Figure 2—*TLC scan of triprolidine extracted from human plasma. Key: A, control plasma; B, 2.0-hr plasma sample; and C, 0.5-hr plasma sample.*

[6] Autolab System IV.
[7] Actifed Syrup, lot 170-N, Burroughs Wellcome Co.

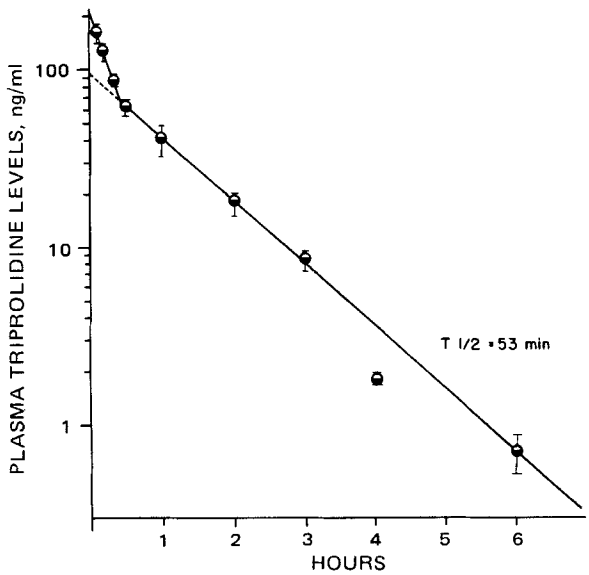

Figure 3—*Disappearance of triprolidine from plasma following intravenous administration of 1 mg of triprolidine hydrochloride/kg to male Sprague–Dawley rats. Results represent the mean ±SE from four rats at each time interval.*

that increasing the pH of plasma above the physiological range is not necessary for good recovery.

Although the exact chemical nature of the fluorophore formed on the plate after spraying triprolidine with ammonium bisulfate is unknown, it is relatively stable to UV irradiation; repeated scans over several hours or direct exposure to irradiation for several minutes did not change the intensity of the fluorescence. However, after 2–3 days of exposure to air, the fluorophore changed its original excitation (300 nm) and emission (>405 nm) wavelengths to 285 and 350 nm, respectively.

A chromatogram of plasma from a human subject prior to and after an oral dose of triprolidine hydrochloride is shown in Fig. 2. Since there was no interfering material in normal human plasma in the region of triprolidine, it was possible to quantitate as little as 0.4 ng of triprolidine spotted on the plate or as little as 0.8 ng of triprolidine/ml of human plasma.

The described procedure was used to determine plasma triprolidine levels in male Sprague–Dawley rats at various times after the administration of 1 mg/kg iv of triprolidine hydrochloride (Fig. 3). The observed plasma concentration (C_p) *versus* time (t) data were fitted to the biexponential equation $C_p = Ae^{-\alpha t} + Be^{-\beta t}$ by least-squares regression analysis, as shown by the solid line. The parameters A and B are zero time intercepts, and α and β are disposition slope constants. The apparent volume of distribution (V_d) of triprolidine was calculated by dividing the

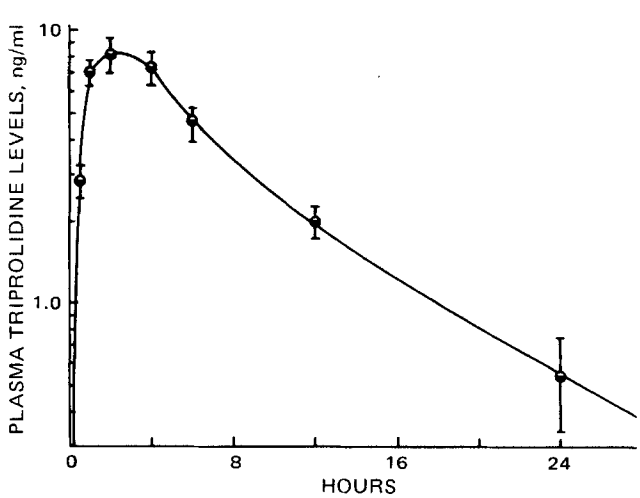

Figure 4—*Plasma triprolidine levels in human subjects following oral administration of a syrup containing 3.75 mg of triprolidine hydrochloride. Results represent the mean ±SE from 16 male volunteers.*

Table I—Plasma Triprolidine Levels in Human Male Subjects following Oral Administration of 15 ml of Syrup Containing 3.75 mg of Triprolidine Hydrochloride

Subject	Age	Weight, kg	Plasma Triprolidine Levels, ng/ml							*AUC*, ng hr/ml
			0.5 hr	1 hr	2 hr	4 hr	6 hr	12 hr	24 hr	
R.J.	27	68	3.3	6.8	6.4	4.2	3.7	3.2	2.0	80
J.H.	26	68	1.6	5.1	4.8	1.8	0.0[a]	0.0[a]	0.0[a]	19
R.F.	20	73	2.0	5.7	8.2	9.7	7.2	2.0	0.0[a]	85
P.D.	18	84	4.5	5.6	4.8	3.8	2.1	0.0[a]	0.0[a]	32
B.J.	18	75	2.9	5.9	6.9	6.5	3.2	0.8	0.0[a]	50
B.S.	20	77	1.3	6.7	11.5	12.5	6.1	1.8	0.0[a]	89
A.O.	21	71	4.2	13.5	14.2	13.3	10.5	5.7	1.7	163
W.K.	25	68	4.0	10.2	16.6	14.1	6.8	1.6	0.0[a]	105
A.L.	23	73	2.1	4.3	5.2	2.8	1.8	0.85	0.0[a]	33
D.G.	29	72	4.4	10.5	17.4	12.7	10.5	7.3	2.2	182
W.S.	21	68	1.3	4.2	3.0	2.3	1.3	0.0[a]	0.0[a]	21
W.L.	29	82	4.8	6.2	6.0	6.5	5.3	2.54	0.0[a]	76
K.W.	21	101	0.0[a]	6.1	8.1	8.8	6.5	4.1	1.6	107
M.D.	21	95	0.0[a]	5.5	5.3	4.9	1.8	0.0[a]	0.0[a]	32
B.S.	20	98	3.5	5.0	3.8	3.5	2.1	0.0[a]	0.0[a]	29
M.G.	20	105	5.2	10.7	9.2	9.5	5.8	2.3	0.0[a]	91

[a] Not detectable; value was considered below the sensitivity of the method and recorded as zero.

intravenous dose by $(AUC)(\beta)$, and the areas under the plasma triprolidine–time curve (AUC) were calculated by applying the trapezoidal rule.

The calculated pharmacokinetic parameters for the rat are: A, 132 ng/ml; α, 0.1 min^{-1}; B, 95 ng/ml; β, 0.0131 min^{-1}; V_d, 9.6 liters/kg; area, 133.5 ng hr/ml; and $T_{1/2}$, 53 min. Following a rapid distribution phase, triprolidine was eliminated from rat plasma with a half-life of 53 min. The large volume of distribution (9.6 liters/kg) indicates the extensive diffusion of this antihistamine into tissues, which is similar to the distribution reported for other antihistamines (12, 13).

Plasma Levels of Triprolidine in Humans—Although triprolidine is used extensively for the treatment of various congestive diseases associated with the release of histamine, plasma drug levels following a therapeutic dose to humans are unknown. Therefore, plasma triprolidine levels were determined in 16 healthy male volunteers following oral administration of 15 ml of a syrup containing 3.75 mg of triprolidine hydrochloride. Individual plasma triprolidine levels at various intervals over 24 hr and the area under the triprolidine plasma–time curve for each subject are shown in Table I. In addition, an average plasma curve for all subjects is shown in Fig. 4.

Plasma triprolidine levels less than 0.8 ng/ml were considered below the sensitivity of the method and were included as zero in calculating the areas under the curves. Of the 16 subjects studied, five individuals had peak plasma levels exceeding 10 ng/ml and only one subject had a peak plasma level below 5 ng/ml. The low plasma levels of this antihistamine in humans are not only related to the low dose administered but are consistent with the data showing a large volume of tissue distribution in rats.

The area under the triprolidine plasma–time curve ranged between 19 and 182 ng hr/ml with a mean value of 75 ng hr/ml. Although triprolidine was detected in plasma within 30 min after its oral administration, the average time required to achieve peak plasma levels was 2 hr. Also, the mean oral plasma half-life of triprolidine was 5.0 hr, but the between-subject variation ranged from 1.5 (Subject J.H.) to 20 (Subject R.J.) hr. Similarly, the mean peak plasma triprolidine level was 8.2 ng/ml but varied from 3 to 17.4 ng/ml. These variations may reflect genetic and environmental factors that influence drug metabolism in humans (14). Also to be considered are individual differences in absorption rates, which are always a problem in an oral study with humans. However, the plasma triprolidine levels obtained following a therapeutic dose of the drug are the lowest reported in humans for any antihistamine.

REFERENCES

(1) P. Armitage, H. Herxheimer, and L. Rosa, *Br. J. Pharmacol.*, **7**, 625 (1952).

(2) A. F. Green, *ibid.*, **8**, 171 (1953).

(3) E. L. Becker, I. Mota, and D. Wong, *ibid.*, **34**, 330 (1968).

(4) R. P. Warm, *Br. Med. J.*, **1**, 1066 (1954).

(5) F. Glassow, *ibid.*, **1**, 217 (1970).

(6) I. G. Popescu, V. Stroescu, and O. Banescu, *Rev. Roum. Med. Int.*, **6**, 291 (1969).

(7) H. P. Wassermann, *Dermatologica*, **130**, 201 (1965).

(8) A. S. E. Fowle, D. T. D. Hughes, and G. J. Knight, *Eur. J. Clin. Pharmacol.*, **3**, 215 (1971).

(9) R. Kuntzman, E. Sernatinger, I. Tsai, and A. Klutch, in "Importance of Fundamental Principles in Drug Evaluation," D. Tedeschi and R. Tedeschi, Eds., Raven, New York, N.Y., 1968, p. 87.

(10) W. W. Fike and I. Sunshine, *Anal. Chem.*, **37**, 127 (1965).

(11) C. R. Fontan, W. C. Smith, and P. L. Kirk, *ibid.*, **35**, 591 (1963).

(12) A. J. Glasko, D. A. McGinty, W. A. Dill, M. L. Wilson, and C. S. Ward, *J. Biol. Chem.*, **179**, 409 (1949).

(13) R. Kuntzman, A. Klutch, I. Tsai, and J. J. Burns, *J. Pharmacol. Exp. Ther.*, **149**, 29 (1965).

(14) J. J. Burns, in "Fundamentals of Drug Metabolism and Disposition," B. LaDu, H. Mandel, and E. Way, Eds., Williams & Wilkins, Baltimore, Md., 1971, p. 340.

ACKNOWLEDGMENTS AND ADDRESSES

Received May 19, 1976, from the *Department of Medicinal Biochemistry, The Wellcome Research Laboratories, Burroughs Wellcome Co., Durham, NC 27709.*

Accepted for publication August 13, 1976.

The authors thank Miss Claudia Taylor for her assistance in the preparation of this manuscript.

[x] To whom inquiries should be directed.

Probiotics: Antistaphylococcal Activity of 4-Aminocyclohexanecarboxylic Acid, Aminobenzoic Acid, and Their Derivatives and Structure–Activity Relationships

AKIRA FUJII *, JAMES H. BUSH ‡§, KENNETH E. SHORES ‡¶, ROBERT G. JOHNSON ‡, RICHARD J. GARASCIA ‡, and ELTON S. COOK *x

Abstract □ Derivatives of 4-aminocyclohexanecarboxylic acid and aminobenzoic acid were prepared and tested against experimentally induced *Staphylococcus aureus* infections in mice. *cis*- and *trans*-Guanidinocyclohexanecarboxylic acid, *trans*-4-aminomethylcyclohexanecarboxylic acid, *trans*-4-guanidinomethylcyclohexanecarboxylic acid, 4-aminomethylbenzoic acid, 4-guanidinomethylbenzoic acid, 4-(2-aminoethyl)benzoic acid, 4-(2-guanidinoethyl)benzoic acid, and most of the ω-aminoacyl-4-aminobenzoic acids possessed antistaphylococcal activity. The R_m values of these compounds were determined by a reversed-phase TLC system. Experimental R_m values of several additional series of probiotics (ω-amino acids, ω-aminoacyl-L-histidines, ω-guanidino acids, ω-guanidinoacyl-L-histidines, and ω-aminoalkanesulfonic acids) were also obtained. A regular relationship was observed between the constitution of the mobile phases and the R_m values; the optimal mobile phase was 70% acetone in water on silica gel G TLC plates. In all series, relationships were obtained between the biological response (antistaphylococcal activity per millimole) and the R_m values, with an increased R_m value paralleling an increased antistaphylococcal activity.

Keyphrases □ 4-Aminocyclohexanecarboxylic acid and derivatives—synthesized, evaluated for antistaphylococcal activity *in vivo*, mice □ Aminobenzoic acid and derivatives—synthesized, evaluated for antistaphylococcal activity *in vivo*, mice □ Structure–activity relationships—4-aminocyclohexanecarboxylic acid, aminobenzoic acid, and various derivatives evaluated for antistaphylococcal activity □ Antistaphylococcal activity—4-aminocyclohexanecarboxylic acid, aminobenzoic acid, and various derivatives evaluated

The term probiotics was proposed to designate compounds that build resistance to infection in the host but do not inhibit the growth of microorganisms *in vitro* (1). Investigations of probiotics (1–5) provided several series of compounds active against experimentally induced *Staphylococcus aureus* infections in mice. A relationship was indicated between the degree of protection afforded by the compounds against staphylococcal infections and the distance separating the functional groups, *i.e.*, between the ω-amino and carboxyl groups of ω-amino acids (2) and their dipeptides (2–4), between ω-guanidino and carboxyl groups of ω-guanidino acids and their dipeptides (1), and between ω-amino, ω-guanidino, and sulfonyl groups of ω-amino- and ω-guanidinoalkanesulfonic acids (5). The relationship between antifibrinolytic activity and the distance separating functional groups of ω-amino acids and related compounds was demonstrated (6–13). A possible relationship between the biological response and R_m values of probiotics also was reported (5).

The present report describes the synthesis and antistaphylococcal activity of derivatives of 4-aminocyclohexanecarboxylic acid (I*a*), aminobenzoic acid (II*a*), and ω-aminoacyl-4-aminobenzoic acids (III*a*–III*e*) and discusses the relationship between biological response of probiotics and R_m values.

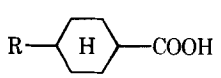

I*a*: R = NH_2
I*b*: R = $NHC(=NH)NH_2$
I*c*: R = CH_2NH_2
I*d*: R = $CH_2NHC(=NH)NH_2$

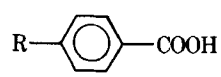

II*a*: R = NH_2
II*b*: R = $NHC(=NH)NH_2$
II*c*: R = CH_2NH_2
II*d*: R = $CH_2NHC(=NH)NH_2$
II*e*: R = $(CH_2)_2NH_2$
II*f*: R = $(CH_2)_2NHC(=NH)NH_2$

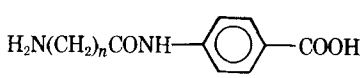

III*a*: *n* = 1
III*b*: *n* = 2
III*c*: *n* = 3
III*d*: *n* = 4
III*e*: *n* = 5

BACKGROUND

Compound I*a* was prepared by a modification of the method described by Pearlman (14) by hydrogenation of II*a* with hydrogen in the presence of 10% rhodium–0.1% palladium-on-carbon. Compound I*a* was also prepared by the method of Takagi *et al.* (15–18), using platinum dioxide in the presence of hydrogen gas. Compounds I*b*, I*d*, II*d*, and II*f* were prepared from I*a*, I*c*, II*c*, and II*e*, respectively, by a modification of the method reported by Morrison *et al.* (19). Compound II*b* was prepared from II*a* by a method described by Beyerman and Bontekoe (20). Compounds II*c* and II*e* were prepared from 4-bromomethylbenzoic acid and 4-(2-bromoethyl)benzoic acid, respectively, by treatment with concentrated ammonium hydroxide. Compounds III*a*–III*e* were prepared from the appropriate benzyloxycarbonyl-ω-amino acid by a reported method (2) that was modified using several literature methods (21–23).

To investigate a possible relationship between biological response and physicochemical character, R_m values of probiotics also were determined. The lipophilic–hydrophilic balance of a compound, which can be expressed by a partition coefficient, is critical for drug transport. The theoretical relationship between the partition coefficient, P, and R_f values was deduced (24–26) for liquid–liquid partition chromatography, and this relationship was simplified (27) to:

$$R_m = \log\left(\frac{1}{R_f} - 1\right) \qquad \text{(Eq. 1)}$$

Since R_m values are free-energy-based constants related to the π values of the Hansch approach, it is possible in principle to correlate the biological action of a drug with R_m values (28–32).

The optimal mobile phase constitution was first determined using silica gel G plates impregnated with paraffin oil white for ω-amino acids (IV*a*–IV*e*) and ω-aminoacyl-L-histidines (V*a*–V*e*), which possess antistaphylococcal activity (2). The optimal mobile phase was 70% acetone in water. The R_m values of derivatives of I*a* and II*a*, III*a*–III*e*, and additional series of probiotics, ω-guanidino acids (VI*a*–VI*e*), ω-guanidinoacyl-L-histidines (VII*a*–VII*e*), and ω-aminoalkanesulfonic acids (VIII*a*–VIII*e*), were then determined, using the optimal mobile phase, to investigate structure–activity relationships.

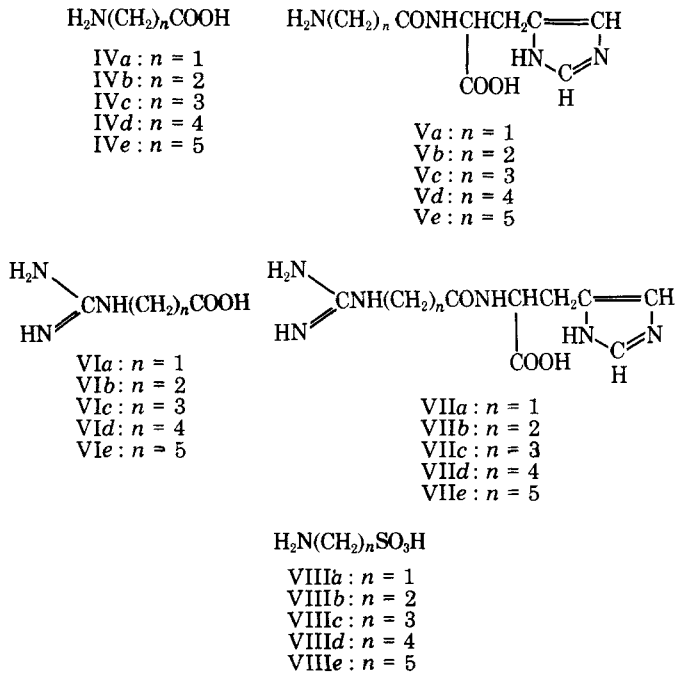

EXPERIMENTAL[1]

10% Rhodium–0.1% Palladium-on-Carbon—This catalyst was prepared by the method of Pearlman (14), using a mixture of 40 g of rhodium chloride trihydrate[2], 0.26 g of palladium chloride[2], 13.7 g of carbon[3], and 200 ml of water. The yield was 15.8 g.

***cis*- and *trans*-4-Aminocyclohexanecarboxylic Acid (Ia)**—*Method A*—A mixture of 27.4 g (0.200 mole) of IIa[4], 200 ml of water, and 4 g of 10% rhodium–0.1% palladium-on-carbon was placed in an autoclave[5] and hydrogenated at 3.52 kg/cm^2. When 0.26 mole of hydrogen gas was absorbed, the mixture was filtered and concentrated *in vacuo* until crystals started to form. Then the mixture was diluted with 200 ml of dimethylformamide and cooled to 5°. The precipitate was filtered, washed first with dimethylformamide and then cold methanol, and dried. The yield was 5.3 g (18.5%) [lit. (14) yield 68–71%], mp 271–275° dec. [lit. (14) mp 292–296°].

Method B—The compound was also prepared by the method of Takagi *et al.* (15–18) by pressure hydrogenation for 6 days in an autoclave[5] of a mixture of 20.0 g (0.146 mole) of IIa, 300 ml of water, and 2.0 g (0.085 mole) of platinum dioxide[3]. The yield was 6.6 g (32.0%), mp 269–270° dec. [lit. (14) mp 292–296°].

***cis*- and *trans*-4-Guanidinocyclohexanecarboxylic Acid (Ib)**—A mixture of 2.9 g (0.021 mole) of Ia and 4.5 g (0.053 mole) of *S*-methylisothiourea hemisulfate[6] in 30 ml of concentrated ammonium hydroxide was refluxed until all reactants were dissolved. After filtration, the solution was concentrated *in vacuo*.

The resulting syrup was diluted with pH 2.2 pyridine–formic acid buffer for purification by ion-exchange chromatography[7]. The sample was eluted with 250 ml of water, 250 ml of 0.5 *M* pyridine, 450 ml of 2 *M* pyridine, and then 200 ml of 2 *M* pyridine–2 *N* NH_4OH (50:50 v/v). Fractions containing Ib were pooled and concentrated *in vacuo* and crystallized from hot water. The yield was 0.6 g (20.0%), mp > 370°.

Anal.—Calc. for $C_8H_{15}N_3O_2$: C, 51.88; H, 8.16; N, 22.69. Found: C, 51.76; H, 8.10; N, 22.55.

***trans*-4-Guanidinomethylcyclohexanecarboxylic Acid (Id)**—A mixture of 2.0 g (0.013 mole) of Ic[8], 2.36 g (0.017 mole) of *S*-methylisothiourea hemisulfate[6], and 10 ml of concentrated ammonium hydroxide was treated in the same way as for Ib. The yield was 2.0 g (78.5%), mp 353–354° dec. [lit. (33) mp 349° dec.].

4-Guanidinomethylbenzoic Acid (IId)—A mixture of 1.43 g (0.0095 mole) of IIc, 2.1 g (0.0145 mole) of *S*-methylisothiourea hemisulfate[6], and 25 ml of concentrated ammonium hydroxide was allowed to react in the same way as already described. The yield was 1.32 g (72.0%), mp 303–304° dec.

Anal.—Calc. for $C_9H_{11}N_3O_2 \cdot H_2O$: C, 51.18; H, 6.20; N, 19.89. Found: C, 51.66; H, 6.10; N, 19.89.

4-(2-Guanidinoethyl)benzoic Acid (IIf)—A mixture of 5.0 g (0.030 mole) of IIe, 5.95 g (0.046 mole) of *S*-methylisothiourea hemisulfate[6], and 40 ml of concentrated ammonium hydroxide was allowed to react in the same way as for IId. The yield was 5.7 g (91.0%), mp 328–330° dec.

Anal.—Calc. for $C_{10}H_{13}N_3O_2$: C, 57.95; H, 6.32; N, 20.28. Found: C, 57.80; H, 6.20; N, 20.15.

4-Guanidinobenzoic Acid (IIb)—By using the method of Beyerman and Bontekoe (20), thioureidobenzoic acid was prepared from 15.8 g (0.115 mole) of IIa and 12.1 g (0.160 mole) of ammonium thiocyanate in 42 ml of concentrated hydrochloric acid and 75 ml of water. Thioureidobenzoic acid (10.65 g, 0.057 mole) and 8.1 g (0.057 mole) of methyl iodide in 82 ml of absolute ethanol[9] gave *S*-methylisoureidobenzoic acid. Compound IIb was obtained by refluxing 10.0 g (0.030 mole) of *S*-methylisoureidobenzoic acid with concentrated ammonium hydroxide. The yield was 4.26 g (62.0%), mp 300–302° dec. [lit. (20) mp ~310° for the free base and 268° dec. for the hydrochloride].

4-Aminomethylbenzoic Acid (IIc)—4-Bromomethylbenzoic acid[10] (14.0 g, 0.070 mole) was dissolved in 2100 ml of concentrated ammonium hydroxide and allowed to stand at room temperature for 2 weeks. The solution was concentrated to dryness *in vacuo*, and the residue was crystallized from water after the addition of absolute ethanol[9]–ether. The crystals were then filtered and subjected to ion-exchange chromatography using a 3 × 35-cm column[7] and the same eluents as in the preparation of Ib.

The elution of IIc was detected by the ninhydrin reaction and appeared in 500–700 ml of the effluent. These fractions were concentrated to dryness *in vacuo*. The residue was crystallized from water after the addition of absolute ethanol[9]–ether; yield, 6.92 g (70.7%); mp 351–353° dec. [lit. (34) mp 346–348° dec.].

4-(2-Aminoethyl)benzoic Acid (IIe)—4-(2-Bromoethyl)benzoic acid[10] (5.0 g, 0.0218 mole) and 675 ml of concentrated ammonium hydroxide were treated in the same way as for IIc, except that the ion-exchange purification was omitted. The residue, after concentration and the addition of absolute ethanol[9]–ether, was crystallized from water. The yield was 1.65 g (46.0%), mp >370°.

Anal.—Calc. for $C_9H_{11}NO_2$: C, 65.44; H, 6.71; N, 8.48. Found: C, 65.32; H, 6.60; N, 8.49.

4-(Glycylamino)benzoic Acid (IIIa)—To a solution of 10.5 g (0.050 mole) of benzyloxycarbonylglycine[11] in 250 ml of dichloromethane was added 7.0 ml of triethylamine. After the resulting solution had been chilled to −5°, 4.8 ml of ethyl chloroformate was added and the mixture was kept at this temperature for 10 min. To this solution was added rapidly a solution of ethyl 4-aminobenzoate[12] (8.3 g, 0.050 mole) in 100 ml of dichloromethane, which had been chilled to 0°.

The resulting mixture was stored at room temperature for 3 days. It was then washed with 200 ml of water and 200 ml of 1 *N* $NaHCO_3$, dried over sodium sulfate, and concentrated to a syrup. The concentrate was dissolved in 100 ml of methanol, and insoluble material (unreacted benzyloxycarbonylglycine) was filtered off. To the filtrate was added 50 ml of 1 *N* NaOH, and the mixture was kept at room temperature for 3 hr. The reaction mixture was adjusted to pH 5 with 4 *N* H_2SO_4 and concentrated to dryness *in vacuo*. The residue was extracted with two portions of 50 ml each of hot absolute ethanol[9], and 50 ml of water was added to the extract.

After the addition of 1.0 g of 10% palladium-on-carbon, the mixture was hydrogenated in an autoclave at atmospheric pressure and room temperature for 6 hr. The reaction mixture was then filtered and concentrated *in vacuo*. Ion-exchange chromatography, with a 2.0 × 30-cm column[7], was used to purify the product. The fractions containing IIIa were pooled, concentrated *in vacuo*, and then treated with absolute ethanol[9] to obtain white needle crystals. The yield was 1.55 g (15.0%), mp 237–238° dec.

---

[1] IR spectra (potassium bromide) were taken of all compounds with a Perkin-Elmer IR spectrophotometer, model 337, and were in accord with the assigned structures. Elemental analyses were made of all compounds by Galbraith Laboratories, Inc., Knoxville, Tenn., but analyses and melting points are reported only for new compounds. Solvents and chemicals, except where indicated, were purchased from Fisher Scientific Co. and Matheson, Coleman and Bell.

[2] Alfa Products.

[3] Darco G-60.

[4] Aldrich Chemical Co.

[5] Parr Instrument Co., series 450.

[6] Sigma Chemical Co.

[7] Amberlite CG 120, 200–400 mesh, pyridine form.

[8] A gift from Daiichi Seiyaku Co., Ltd., Tokyo, Japan.

[9] Commercial Solvents Corp.

[10] ICN Pharmaceuticals, Inc. (K&K Laboratories).

[11] Carbobenzoxyglycine, ICN Pharmaceuticals, Inc.

[12] Eastman Kodak Co.

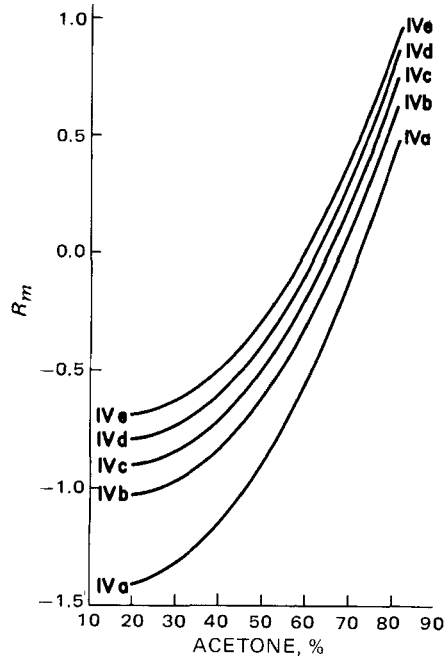

Figure 1—*Relationship between* R_m *values of ω-amino acids (series IV) and percent acetone in mobile phase.*

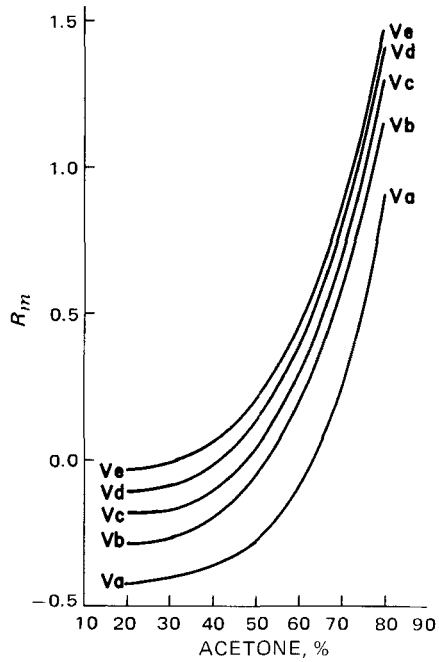

Figure 2—*Relationship between* R_m *values of ω-aminoacyl-L-histidines (series V) and percent acetone in mobile phase.*

Anal.—Calc. for $C_9H_{10}N_2O_3 \cdot H_2O$: C, 50.94; H, 5.70; N, 13.20. Found: C, 50.72; H, 5.48; N, 13.20.

After hydrolysis (6 *N* HCl, 105° for 24 hr), III*a* gave glycine and II*a* as confirmed on TLC.

4-(β-Alanylamino)benzoic Acid (III*b*)—Benzyloxycarbonyl-β-alanine[13] (4.4 g, 0.020 mole) and 3.3 g (0.020 mole) of ethyl 4-aminobenzoate[12] were treated in the same way as for III*a*. The yield was 2.1 g (47.4%), mp 256–257° dec.

Anal.—Calc. for $C_{10}H_{12}N_2O_3 \cdot \frac{1}{2}H_2O$: C, 55.29; H, 6.03; N, 12.90. Found: C, 55.04; H, 6.17; N, 12.80.

Acid hydrolysis gave β-alanine and II*a*.

4-(4-Aminobutyrylamino)benzoic Acid (III*c*)—4-(Benzyloxycarbonylamino)butyric acid[14] (12.0 g, 0.050 mole) and 8.3 g (0.050 mole) of ethyl 4-aminobenzoate[12] were treated in the same manner as for III*a*. The yield was 5.2 g (44.2%), mp 214–215° dec.

Anal.—Calc. for $C_{11}H_{14}N_2O_3$: C, 59.45; H, 6.35; N, 12.61. Found: C, 59.20; H, 6.50; N, 12.43.

Acid hydrolysis gave 4-aminobutyric acid and II*a*.

4-(5-Aminovalerylamino)benzoic Acid (III*d*)—5-(Benzyloxycarbonylamino)valeric acid[15] (12.5 g, 0.050 mole) and 8.3 g (0.050 mole) of ethyl 4-aminobenzoate[12] were treated in the same manner as for III*a*. The yield was 5.0 g (40.0%), mp 203–204°.

Anal.—Calc. for $C_{12}H_{16}N_2O_3$: C, 61.00; H, 6.83; N, 11.86. Found: C, 60.82; H, 6.96; N, 11.73.

Acid hydrolysis gave 5-aminovaleric acid and II*a*.

4-(6-Aminohexanoylamino)benzoic Acid (III*e*)—6-(Benzyloxycarbonylamino)hexanoic acid[16] (2.65 g, 0.010 mole) and 1.65 g (0.010 mole) of ethyl 4-aminobenzoate were treated in the same way as for III*a*. The yield was 1.20 g (45.4%), mp 258–259° dec.

Anal.—Calc. for $C_{13}H_{18}N_2O_3$: C, 62.38; H, 7.25; N, 11.19. Found: C, 62.19; H, 7.32; N, 11.05.

Acid hydrolysis gave 6-aminohexanoic acid and II*a*.

Reversed-Phase TLC—The R_m values were obtained by the method described by Boyce and Milborrow (28) using silica gel G TLC plates. Chromatography was carried out on glass plates[17] (10 × 20 cm) coated with a 250-μm layer of silica gel G. After activation at 105° for 10 min, the plates were impregnated by allowing a 5% (v/v) solution of paraffin oil white in hexane to cover the plate; the solvent was evaporated at 40°.

Optimal Solvent—The optimal mobile phase composition was determined using the mobile phases of 80, 70, 60, 50, 40, and 20% (v/v) acetone in water. Solutions that contained 1% of IV*a*–IV*e*, V*a*–V*e*, and L-alanine dissolved in 10% (w/v) 2-propanol were spotted and then developed[18] with each different mobile phase. The spots were located by the ninhydrin reaction. The relationship between R_m values of series IV and V and the composition of the mobile phases is shown in Figs. 1 and 2. The optimal solvent ratio, which produced maximum increments of R_m values (28, 29), was obtained from the most linear region of the curves: 70% (v/v) acetone in water.

Determination of R_m Values with Optimal Solvent System—With the optimal composition of the mobile phase, TLC plates were developed after spotting with series I–VIII; L-alanine and L-arginine were used as standards. The spots were located by the ninhydrin reaction, the Sakaguchi reaction, or iodine treatment. Figure 3 summarizes the relationship between biological response and R_m values of series IV–VIII.

Biological Testing Procedure—*In vivo* antistaphylococcal activity was determined by the method described previously (1–5), except that BDF mice, 9–13 weeks old and weighing 12–19 (male) and 18–24 (female) g, were used instead of Swiss albino mice. Because of the low solubility of some compounds, 1 mg of each sample (I*a*–I*d*, II*a*–II*f*, and III*a*–III*e*) was given in equally divided doses subcutaneously 2 hr before and 4 hr after the injection of *S. aureus*[19]. 5-Aminovaleryl-L-histidine (V*d*) was

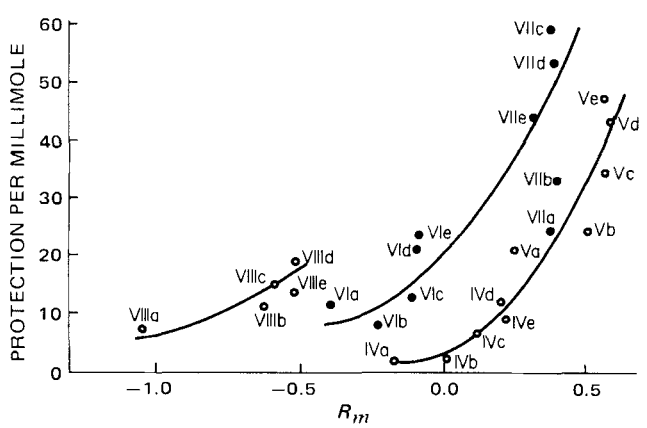

Figure 3—*Relationship between antistaphylococcal activity* in vivo *(protection per millimole) and* R_m *values of series IV–VIII.*

[13] Carbobenzoxy-β-alanine, Sigma Chemical Co.
[14] Carbobenzoxy-γ-aminobutyric acid, ICN Pharmaceuticals, Inc.
[15] Carbobenzoxy-δ-aminovaleric acid, prepared in this laboratory (2).
[16] Carbobenzoxy-ε-aminohexanoic acid, Sigma Chemical Co.
[17] Analtech, Inc.
[18] Polyethylene chamber (Analtech, Inc.).
[19] A clinical isolate, from a tonsilitis patient, carried in this laboratory since 1955 in the lyophilized state; see Ref. 35 for description.

Table I—R_f Values of Derivatives of Ia and IIa and of ω-Aminoacyl-4-aminobenzoic Acids on TLC [a] ($R_f \times 100$)

Compound	Solvent 1	Solvent 2	Solvent 3	Solvent 4	Solvent 5
Ia	66	87	86	—	92
Ib	45	62	79	33	61
Ic	41	65	76	63	91
Id	47	64	80	28	62
IIa	48	67	75	49	49
IIb	52	68	81	37	54
IIc	43	55	69	32	65
IId	52	67	81	32	55
IIe	37	59	71	31	68
IIf	55	66	80	34	60
IIIa	38	73	64	70	82
IIIb	38	69	61	40	79
IIIc	43	70	60	24	77
IIId	46	70	59	19	74
IIIe	49	72	61	14	77
L-Alanine [b]	35	40	52	47	71
L-Arginine [c]	13	22	36	4	25

[a] The plates were silica gel G (Merck), 250 μm, from Analtech, Inc. Solvent 1 = phenol–water (75:25 w/v), pH 2.0. Solvent 2 = 1-butanol–acetic acid–water (60:20:20), pH 2.4. Solvent 3 = 2-propanol–formic acid–water (77:4:19), pH 2.7. Solvent 4 = 1-methylpropanol–methyl ethyl ketone–dicyclohexylamine–water (55:15:10:20), pH 10.0. Solvent 5 = chloroform–methanol–17% NH_4OH (40:40:20), pH 11.4. [b] Spots were identified by ninhydrin reaction for Ia, Ic, IIa, IIc, IIe, and IIIa–IIIe, and L-alanine was the standard. [c] Spots were identified by Sakaguchi reaction for Ib, Id, IIb, IId, and IIf, and L-arginine was the standard.

used as the positive control. Compounds Ia, Ic, IIa, IIc, and IIe also were tested at 5 mg with a positive control of 4-aminobutyryl-L-histidine (Vc). Guanidino derivatives Ib, Id, IIb, IId, and IIf were poorly soluble in water. To provide a high dose of a compound of low water solubility, a fine suspension of IIf in cottonseed oil (20 mg/ml, dose of 0.25 ml) was also investigated.

Antistaphylococcal activity *in vivo* (ASA) is expressed as:

$$\text{ASA} = [(M_c - M_e)/M_c]/C \qquad \text{(Eq. 2)}$$

where M_c is the mortality of untreated negative control, M_e is the mortality of the experimental (treated), and C is the dose (millimoles). Previously (1–5), percent protection, $(M_c - M_e)100/M_c$, was used for comparison of activity. The relationship between antistaphylococcal activity and the R_m value of series I–III is summarized in Fig. 4. Antistaphylococcal activity *in vitro* was determined in the same manner as before (1).

RESULTS AND DISCUSSION

Compounds Ia–Id, IIa–IIe, and IIIa–IIIe were homogeneous on TLC with five different solvent systems (Table I). Single spots were given with the ninhydrin reaction, iodine treatment, and potassium dichromate–sulfuric acid. Compounds Ia, Ic, IIa, IIc, IIe, and IIIa–IIIe were positive to the phenol–calcium hypochlorite color reaction (2).

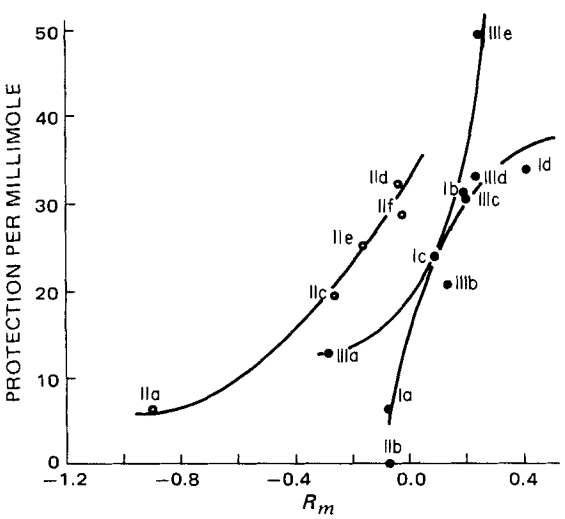

Figure 4—*Relationship between antistaphylococcal activity* in vivo *(protection per millimole) and* R_m *values of series I–III.*

Table II—Antistaphylococcal Activity *In Vivo* (ASA) and R_m Values of Probiotics

Compound [a]	ASA [b]	R_m [c]
Ia	6.44	−0.07 ± 0.11
Ib	31.53	0.19 ± 0.12
Ic	24.22	0.10 ± 0.08
Id	33.70	0.41 ± 0.14
IIa	6.17	−0.90 ± 0.10
IIb	0.00	−0.07 ± 0.12
IIc	19.53	−0.26 ± 0.11
IId	32.11	−0.04 ± 0.13
IIe	25.11	−0.16 ± 0.10
IIf	28.78	0.02 ± 0.14
IIIa	12.71	−0.29 ± 0.07
IIIb	20.72	0.14 ± 0.07
IIIc	29.66	0.21 ± 0.11
IIId	31.53	0.24 ± 0.08
IIIe	49.47	0.25 ± 0.09
IVa	1.80	−0.18 ± 0.07
IVb	2.32	0.01 ± 0.09
IVc	6.60	0.12 ± 0.09
IVd	13.12	0.20 ± 0.10
IVe	8.92	0.22 ± 0.10
Va	21.22	0.26 ± 0.11
Vb	23.98	0.51 ± 0.12
Vc	35.08	0.57 ± 0.13
Vd	43.57	0.59 ± 0.13
Ve	46.69	0.57 ± 0.08
VIa	11.71	−0.39 ± 0.10
VIb	8.39	−0.23 ± 0.06
VIc	12.77	−0.11 ± 0.07
VId	21.01	−0.09 ± 0.05
VIe	23.90	−0.08 ± 0.07
VIIa	24.50	0.38 ± 0.09
VIIb	33.21	0.40 ± 0.09
VIIc	59.34	0.38 ± 0.11
VIId	53.61	0.39 ± 0.10
VIIe	44.07	0.32 ± 0.10
VIIIa	7.11	−1.05 ± 0.10
VIIIb	11.26	−0.63 ± 0.11
VIIIc	15.31	−0.59 ± 0.10
VIIId	19.30	−0.52 ± 0.12
VIIIe	13.71	−0.52 ± 0.10

[a] L-Alanine was used as a positive control with an average R_m value of −0.30 ± 0.06 for ninhydrin-positive compounds Ia, Ic, IIa, IIc, IIe, and series III–VIII. L-Arginine was used as a positive control with an average R_m value of 1.32 ± 0.37 for Sakaguchi-reaction-positive compounds Ib, Id, IIb, IId, IIf, and series VI and VII. [b] ASA is defined by Eq. 2. [c] Silica gel G (Merck), 250-μm plates (Analtech, Inc.), were used. The stationary and mobile phases were 5% paraffin oil white in hexane (v/v) and 70% acetone in water (v/v), respectively.

The effectiveness of protection was calculated using the χ^2-test. All series I–III compounds, except Ia, IIa, IIb, and IIIa, were significantly effective as compared with the untreated negative control (>95% confidence level) at 1 mg. All of the compounds tested at 5 mg (Ia, Ic, IIa, IIc, and IIe) were significantly more effective than the untreated negative control (>95% confidence level). With a 5-mg dose as an oil suspension, IIf provided significant effectiveness at greater than the 99.5% confidence level. Antistaphylococcal activities *in vivo* obtained with two different dosages, 1 and 5 mg, were essentially identical (percent deviation <5.0), except for Ia which gave 31.1% deviation. None of the compounds had antistaphylococcal activity *in vitro*, as was true of the previously reported probiotics.

A regular relationship was obtained between the composition of the mobile phases and the R_m values (Figs. 1 and 2). The optimal mobile phase was determined to be 70% acetone in water, and it was used in the study of the correlation between structure and biological response. Antistaphylococcal activity *in vivo* and R_m values of series I–VIII compounds are summarized in Table II. In general, increased R_m values paralleled a corresponding increase in biological response to experimentally induced *S. aureus* infections in mice for each group of compounds investigated (Figs. 3 and 4). The histidine dipeptides of both ω-amino acids (series V) and ω-guanidino acids (series VII) showed higher R_m values and also higher antistaphylococcal activity than the corresponding parent acids.

The ω-amino acids have partition coefficients in 1-octanol–water of

the order of 10^{-3} [20]. The partition coefficient of IIa in the same system was reported as 4.8 (uncorrected) (36) or 2.9 (corrected) (37). It was hoped that the lipophilicity of the ω-amino acids would be enhanced by forming the ω-aminoacyl-4-aminobenzoic acids. The results on reversed-phase TLC indicate that no increase in lipophilicity of ω-amino acids resulted from forming IIa derivatives.

While there was a significant relationship between biological response and R_m values in each series of compounds, this was not true when all series I–VIII compounds were considered together. This finding suggests that the modifications of functions from amino (NH_2) to guanidino [$NCH(=NH)NH_2$], from carboxylic acid (COOH) to sulfonic acid (SO_3H), and from straight-chain polymethylene [$-(CH_2)_n-$] to ring (C_6H_6 or C_6H_{10}) gave a considerable change in partitioning. Therefore, each of the groups (series I–VIII) should be viewed independently.

REFERENCES

(1) A. Fujii and E. S. Cook, *J. Med. Chem.*, **16,** 1409 (1973).

(2) A. Fujii, K. Tanaka, Y. Tsuchiya, and E. S. Cook, *ibid.*, **14,** 354 (1971).

(3) A. Fujii, K. Tanaka, and E. S. Cook, *ibid.*, **15,** 378 (1972).

(4) A. Fujii and E. S. Cook, "Abstracts, 3rd Central Regional Meeting of the American Chemical Society," Cincinnati, Ohio, May 1971, Abstract 186.

(5) A. Fujii and E. S. Cook, *J. Med. Chem.*, **18,** 502 (1975).

(6) S. Okamoto and U. Okamoto, *Keio J. Med.*, **11,** 105 (1962).

(7) S. Okamoto, *Jpn. J. Brain Physiol.*, **No. 40,** 1617 (1963).

(8) S. Okamoto, S. Sato, Y. Takada, and U. Okamoto, *Keio J. Med.*, **13,** 177 (1964).

(9) M. Mangyo, *Seikagaku*, **36,** 735 (1964).

(10) S. Okamoto, S. Oshiba, H. Mihara, and U. Okamoto, *Ann. N.Y. Acad. Sci.*, **146,** 414 (1968).

(11) K. Lohmann, F. Markwardt, and H. Landmann, *Thromb. Diath. Haemorrh.*, **10,** 424 (1964).

(12) W. Baumgarten, L. I. Priester, D. W. Stiller, A. E. W. Duncan, J. L. Ciminera, and L. J. Loeffler, *ibid.*, **22,** 263 (1969).

(13) L. J. Loeffler, S. F. Britcher, and W. Baumgarten, *J. Med. Chem.*, **13,** 926 (1970).

(14) W. M. Pearlman, *Org. Synth.*, **49,** 75 (1969).

(15) E. Takagi, Y. Yokoi, and M. Mangyo, Japanese pat. 7327 (1957); through *Chem. Abstr.*, **52,** 12903i (1958).

(16) E. Takagi, Y. Yokoi, and M. Mangyo, Japanese pat. 7331 (1957); through *Chem. Abstr.*, **52,** 12903f (1958).

(17) E. Takagi, Y. Yokoi, and M. Mangyo, Japanese pat. 9073 (1957); through *Chem. Abstr.*, **52,** 14672h (1958).

(18) E. Takagi, Y. Yokoi, and M. Mangyo, Japanese pat. 27 (1958); through *Chem. Abstr.*, **52,** 19983g (1958).

(19) J. F. Morrison, A. H. Ennor, and D. E. Griffiths, *Biochem. J.*, **68,** 477 (1958).

(20) H. C. Beyerman and J. S. Bontekoe, *Rev. Trav. Chim.*, **72,** 262 (1953).

(21) M. Bergmann and L. Zervas, *Chem. Ber.*, **65,** 1192 (1932).

(22) R. H. Sifferd and V. du Vigneaud, *J. Biol. Chem.*, **108,** 753 (1935).

(23) J. J. Pisano, J. D. Wilson, L. Cohen, D. Abraham, and S. Udenfriend, *ibid.*, **236,** 499 (1961).

(24) A. J. P. Martin, *Biochem. Soc. Symp. Camb.*, **3,** 4 (1949).

(25) A. J. P. Martin and R. L. M. Synge, *Biochem. J.*, **35,** 1358 (1941).

(26) R. Consden, A. H. Gordon, and A. J. P. Martin, *ibid.*, **38,** 224 (1944).

(27) E. C. Bate-Smith and R. G. Westall, *Biochim. Biophys. Acta*, **4,** 427 (1950).

(28) C. B. C. Boyce and B. V. Milborrow, *Nature*, **208,** 537 (1965).

(29) G. L. Biagi, A. M. Barbaro, and M. C. Guerra, "Biological Correlations—The Hansch Approach," Advances in Chemistry Series No. 114, American Chemical Society, Washington, D.C., 1972, chap. 5.

(30) B. F. Cain, R. N. Seelye, and G. L. Atwell, *J. Med. Chem.*, **17,** 922 (1974).

(31) A. N. Tischler, F. M. Thompson, L. J. Libertini, and M. Calvin, *ibid.*, **17,** 948 (1974).

(32) G. L. Biagi, O. Gandolfi, M. C. Guerra, A. M. Barbaro, and G. Cantelli-Forti, *ibid.*, **18,** 868 (1975).

(33) A. Okano, M. Imaoka, S. Funabashi, M. Iwamoto, S. Isoda, R. Moroi, Y. Abiko, and M. Hirata, *ibid.*, **15,** 247 (1972).

(34) E. Takagi and M. Mangyo, Japanese pat. 421 (1959); through *Chem. Abstr.*, **54,** 6651f (1960).

(35) Y. Tsuchiya, K. Tanaka, E. S. Cook, and L. G. Nutini, *Appl. Microbiol.*, **19,** 813 (1970).

(36) A. Leo, C. Hansch, and D. Elkins, *Chem. Rev.*, **71,** 525 (1971).

(37) H. Terada, *Chem. Pharm. Bull.*, **20,** 765 (1972).

ACKNOWLEDGMENTS AND ADDRESSES

Received April 23, 1976, from the *Division of Chemistry and Biochemistry, St. Thomas Institute, Cincinnati, OH 45206, and the ‡Department of Chemistry, Xavier University, Cincinnati, OH 45207.

Accepted for publication August 13, 1976.

Presented in part at the 168th National Meeting of the American Chemical Society, Atlantic City, N.J., September 1974 (Abstract No. MEDI 69); the 169th National Meeting of the American Chemical Society, Philadelphia, Pa., April 1975 (Abstract No. MEDI 42); and the 170th National Meeting of the American Chemical Society, Chicago, Ill., August 1975 (Abstract No. MEDI 59).

Abstracted in part from dissertations submitted by J. H. Bush and K. E. Shores to the Graduate School, Xavier University, in partial fulfillment of the Master of Science degree requirements.

Supported by a grant from Stanley Drug Products, Inc., Division of Sperti Drug Products, Inc.

The authors thank Dr. George S. Sperti, Dr. Leo G. Nutini, Dr. Kinji Tanaka, and Dr. Harvey A. Dube for their helpful suggestions. They also thank the Daiichi Seiyaku Co., Ltd., Tokyo, Japan, for a gift of *trans*-4-aminomethylcyclohexanecarboxylic acid.

§ Present address: Department of Chemistry, University of Wyoming, Laramie, WY 82070.

¶ Present address: Department of Biological Chemistry, College of Medicine, University of Cincinnati, Cincinnati, OH 45267.

x To whom inquiries should be directed.

[20] A. Fujii, M. L. Woebkenberg, H. A. Dube, and E. S. Cook, 1975, unpublished data.

Potential Antitumor Agents: Procarbazine Analogs and Other Methylhydrazine Derivatives

JOHN A. BEISLER ˣ, GEOFFREY W. PENG *, and JOHN S. DRISCOLL

Abstract □ With the objective of developing new antitumor agents, two groups of hydrazine compounds, having structural features in common with the antitumor agents procarbazine and 1-acetyl-2-picolinoylhydrazine, were synthesized. The L-1210 leukemia system was used to evaluate compounds of both groups. The aliphatic procarbazines also were screened for antitumor activity as bis(benzyloxycarbonyl) derivatives and as derivatives having a phthalazine nucleus. No L-1210 antitumor activity was exhibited by these compounds.

Keyphrases □ Hydrazines, substituted—synthesized, antitumor activity evaluated □ Procarbazine analogs—synthesized, antitumor activity evaluated □ Phthalazines, substituted—synthesized, antitumor activity evaluated □ Antitumor activity—evaluated in substituted hydrazines and phthalazines □ Structure-activity relationships—substituted hydrazines and phthalazines evaluated for antitumor activity

Hydrazine derivatives interact with biological systems to produce a wide range of responses. For example, isoniazid is a well-established tuberculostatic agent (1), and isocarboxazid finds clinical utility as a monoamine oxidase inhibitor (2). A recent survey (3) listed 19 hydrazine derivatives that are tumorigenic in animals, although hydrazine sulfate inhibited tumor growth in rats (4).

Procarbazine (I), a methylhydrazine derivative, displayed antitumor effects in a spectrum of animal neoplasms and is used clinically in the treatment of Hodgkin's disease (5). Although hydrazine and benzylhydrazine have considerable toxicity, they selectively inhibited Ehrlich ascites carcinoma in mice (6). The corresponding methyl derivatives (methylhydrazine and 1-methyl-2-benzylhydrazine) retained toxicity but exhibited an increased antitumor effect, apparently because the *N*-methyl groups metabolized to formaldehyde, which contributed an added cytotoxic effect. Thus, the *N*-normethyl analog of procarbazine was much less effective against Ehrlich ascites than procarbazine itself; however, both showed a diminished toxicity with respect to 1-methyl-2-benzylhydrazine.

A series of acylhydrazines and 1,2-diacylhydrazines showed activity in the Walker 256 carcinosarcoma test system with moderate toxicities in some instances, giving favorable therapeutic indexes (7). One member of the series, 1-acetyl-2-picolinoylhydrazine (II), was selected for clinical trials (8–10).

As part of a continuing interest in the development of new antitumor agents (11), a study was initiated to synthesize methylhydrazine derivatives for potential antitumor activity. Two groups of compounds were selected for

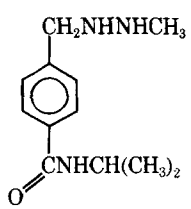

I

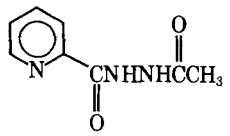

II

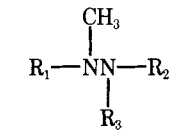

III: $R_1 = R_2 = H$, $R_3 = CH_2CH_3$
IV: $R_1 = CH_3CO$, $R_2 = R_3 = H$
V: $R_1 = R_2 = CH_3CO$, $R_3 = H$
VI: $R_1 = R_2 = C_6H_5CH_2OCO$, $R_3 = H$
VII: $R_1 = R_2 = C_6H_5CO$, $R_3 = H$

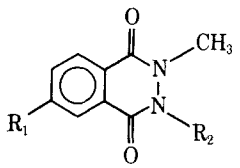

VIII: $R_1 = R_2 = H$
IX: $R_1 = CO_2H$, $R_2 = CH_3$

synthesis and antitumor evaluation against L-1210 leukemia. The first group consisted of simple methylhydrazines (III–IX), having structural attributes of both I and II. Accordingly, these hydrazines were provided with *N*-methyl groups in the hope of augmenting any emergent antitumor activity and acyl functions to moderate toxicity. In the second group, the structural importance of the phenylene group of I for antitumor activity was explored by replacing it with straight-chain aliphatic moieties. As in the first group, the methylhydrazine substructure was incorporated into the aliphatic procarbazine derivatives (Scheme I, XVI–XVIII), and provisions were made in the synthetic scheme to prepare acylated derivatives for antitumor testing.

RESULTS AND DISCUSSION

Chemistry—Compound III was synthesized using a modification of a literature procedure (12). Compounds IV–VIII were made according to established procedures (13–16, Table I).

The synthetic route to the aliphatic procarbazine derivatives (XVI–XVIII) utilized the approach developed by Zeller *et al.* (17), wherein the doubly blocked methylhydrazine (VI) served as a starting material. Thus, condensation of VI with the requisite bromo ester (Scheme I) gave the fully substituted hydrazines (X–XII). These compounds were converted to the *N*-isopropyl-substituted amides (XIII–XV) using a standard three-step synthetic sequence. As an inadvertant result, the lower homolog in the series (XIII) quantitatively lost a benzyloxycarbonyl substituent. The loss was probably due to the presence of the terminal carboxyl function, which is favorably disposed toward participation in a six-membered cyclic intermediate with the carbonyl of the near benzyloxycarbonyl group. Based on this reasoning, Structure XIII was assigned to this compound.

Hydrogenolysis smoothly removed the benzyloxycarbonyl-protecting groups to provide the substituted methylhydrazines, which were isolated as the semicrystalline hygroscopic dihydrochloride salts. Water solutions of the latter, when passed through an anion-exchange column (oxalate form), yielded oxalate salts after lyophilization as analytically pure, white solids (XVI–XVIII), which were not hygroscopic. Attempted recrystallization of the oxalates led to decomposition.

Reaction of the hydrazines, either as the oxalate or dihydrochloride salts, formed phthalazine derivatives (XIX–XXI). The three phthalazine

Table I—Experimental Data

Compound	Boiling Point (mm Hg) or Melting Point (Solvent)	Yield, %	Formula[a]	Analysis, %		Preparation Reference Number
				Calc.	Found	
III	149–150° (ethanol–acetone) [lit. (12) mp 141–143°]	52	$C_3H_{10}N_2 \cdot 2HCl$	C 24.50 H 8.22 Cl 48.22 N 19.05	24.64 8.33 48.20 18.71	—
IV	75° (2) [lit. (13) bp 103° (8)]	60	$C_3H_8N_2O$	C 40.90 H 9.15 N 31.79	40.50 9.15 31.97	13
V	120–125° (0.1) [lit. (14) bp 280° (760)]	70	$C_5H_{10}N_2O_2$	C 46.17 H 7.70 N 21.54	46.16 7.95 21.50	14
VI	72–73° (ether–cyclohexane) [lit. (15) mp 67–68°]	80	$C_{17}H_{18}N_2O_4$	C 64.95 H 5.77 N 8.91	65.13 6.01 9.01	15
VII	141–143° (ethanol) [lit.(14) mp 145°]	81	$C_{15}H_{14}N_2O_2$	C 70.85 H 5.55 N 11.01	71.04 5.67 10.67	14
VIII	239–240.5° (ethanol) [lit. (16) mp 238.5–240°]	58	$C_9H_8N_2O_2$	C 61.36 H 4.58 N 15.90	61.21 4.65 16.06	16
IX	282–285° (methanol)	52	$C_{11}H_{10}N_2O_4$	C 56.41 H 4.30 N 11.96	56.14 4.41 11.89	—
X	178° (0.005)[b]	77	$C_{22}H_{26}N_2O_6$	C 63.75 H 6.32 N 6.76	63.55 6.27 6.98	—
XI	182° (0.01)[b]	78	$C_{21}H_{24}N_2O_6$	C 64.46 H 6.59 N 6.54	64.27 6.44 6.66	—
XII	183° (0.01)[b]	78	$C_{24}H_{30}N_2O_6$	C 65.14 H 6.83 N 6.33	65.19 6.75 6.50	—
XIII	Oil[c]	43[d]	$C_{15}H_{23}N_3O_3$[e]	C 61.41 H 7.90 N 14.33	61.38 7.96 14.50	—
XIV	Oil[c]	62[d]	$C_{24}H_{31}N_3O_5$	C 65.28 H 7.08 N 9.52	64.99 7.00 9.45	—
XV	77–78° (ether–hexane)	69[d]	$C_{25}H_{33}N_3O_5$	C 65.91 H 7.30 N 9.23	65.92 7.23 9.23	—
XVI	Lyophilizate[f]	67	$C_7H_{17}N_3O \cdot (CO_2H)_2$	C 43.36 H 7.68 N 16.86 O 32.09	43.17 7.81 16.96 31.90	—
XVII	Lyophilizate[f]	82	$C_8H_{19}N_3O \cdot (CO_2H)_2$	C 45.62 H 8.04 N 15.96 O 30.38	45.52 8.04 16.11 30.41	—
XVIII	Lyophilizate[f]	99	$C_9H_{21}N_3O \cdot (CO_2H)_2$	C 47.64 H 8.36 N 15.15 O 28.85	47.44 8.59 15.18 28.68	—
XIX	146–147° (benzene–cyclohexane)	32	$C_{15}H_{19}N_3O_3$	C 62.26 H 6.62 N 14.52	62.53 6.84 14.61	—
XX	121–122° (benzene–cyclohexane)	35	$C_{16}H_{21}N_3O_3$	C 63.35 H 6.98 N 13.85	63.20 6.84 14.08	—
XXI	118–118.5° (benzene–cyclohexane)	31	$C_{17}H_{23}N_3O_3$	C 64.33 H 7.30 N 13.24	64.28 7.38 13.28	—

[a] NMR and IR spectra were consistent with structure assignments. [b] The temperature indicated is that of the heating block of a short path distillation apparatus. The recorded temperatures are not corrected. [c] The analytical sample was prepared by condensing the necessary amount on a cold finger under high vacuum. [d] Percentage yield over three synthetic steps. [e] One benzyloxycarbonyl blocking group was lost (NMR) using the general synthetic procedure. [f] The melting points of the lyophilized oxalates were broad and variable, although the compounds were spectrally and analytically pure.

homologs gave mass spectra (Table II) characterized by three common ions at m/e 189 $[C_6H_4(CON)_2CH_3(CH_2)]^+$, 162 $[C_6H_4(CO)_2NHCH_3]^+$, and 89 $[CONHC_3H_7]^+$. The balance of the fragmentation patterns for each phthalazine could be readily interpreted in terms of stepwise scissions of the respective side-chain elements.

Biology—The synthesized compounds, including synthetic intermediates, were evaluated for antitumor activity in the mouse L-1210 leukemia system according to established protocols (18). Compounds III–XXI showed no significant activity (Table III), as indicated by the ratio of the mean survival time of the test animals over that of the control animals expressed as a percentage (%T/C). A %T/C value greater than 125 is considered indicative of activity in this test system.

The murine tumor systems used to evaluate I and II, as well as their respective analogs, were Ehrlich carcinoma, Sarcoma 180, and Walker carcinosarcoma 256 (6, 7). However, the L-1210 system was chosen for screening the present series of compounds because of its greater predictive value for clinically useful drugs (19).

The nonacylated methylhydrazine, 1-ethyl-2-methylhydrazine (III), exerted a general toxicity on L-1210 tumor-bearing mice (Table III). Addition of acyl groups to methylhydrazine (IV–VII) neither ameliorated toxicity nor elicited antitumor activity. Compounds VIII and IX were both nontoxic and inactive.

The more fully elaborated methylhydrazines (XVI–XVIII) patterned after procarbazine demonstrated a nonselective toxicity, which was

Table II—Mass Spectral Data for the Phthalazines[a]

Compound	M+	M − 28	M − 29	M − 58	M − 100	189	Base	M − 175	89
XIX	289 (7.8)	261 (20.3)	260 (16.6)	231 (4.4)	189 (6.9)		162 (100)	114 (19)	89 (9.4)
XX	303 (81.7)	275 (9.4)	274 (8.7)	245 (12.2)	203 (10)	189 (8.5)	162 (100)	128 (93)	89 (76)
XXI	317 (7.1)	289 (6.9)	288 (7.5)	259 (14)	217 (0.7)	189 (10.7)	162 (100)	142 (63)	89 (15.7)

[a] The tabulated values are mass-charge ratios *(m/e)* followed by the relative intensities (indicated in parentheses) as percentages of the base peak.

eliminated when they were tested as bis(benzyloxycarbonyl) derivatives (XIV and XV) but without a concomitant appearance of antitumor effects. Methylhydrazine XVIII has a calculated partition coefficient that is nearly identical to the measured value (20) of procarbazine (log P = 0.06, octanol). The lack of activity shown by XVIII and its derivatives (XV and XXI) was, therefore, particularly disappointing.

Derivatizing the aliphatic procarbazine analogs with phthalic anhydride gave water-soluble phthalazines (XIX–XXI), which were nontoxic and inactive.

EXPERIMENTAL[1]

1-Ethyl-2-methylhydrazine Dihydrochloride (III)—A procedure (12) for the synthesis of 1,2-dimethylhydrazine dihydrochloride was modified for the preparation of III. Accordingly, a twofold excess of ethyl bromide was reacted with 7.6 g (0.03 mole) of VII in ethanolic potassium hydroxide solution.

6-Carboxy-2,3-dihydro-2-methyl-1,4-phthalazinedione (IX)—1,2,4-Benzenetricarboxylic anhydride (9.6 g, 0.05 mole) and 1,2-dimethylhydrazine dihydrochloride (6.6 g, 0.05 mole) were refluxed in a mixture of 100 ml each of triethylamine and dimethylformamide for 18 hr. After solvent evaporation, the residue was treated with dilute hydrochloric acid and the product was extracted with ether–ethyl acetate (1:1). Evaporation of the dried extracts gave 6.1 g of IX after recrystallization.

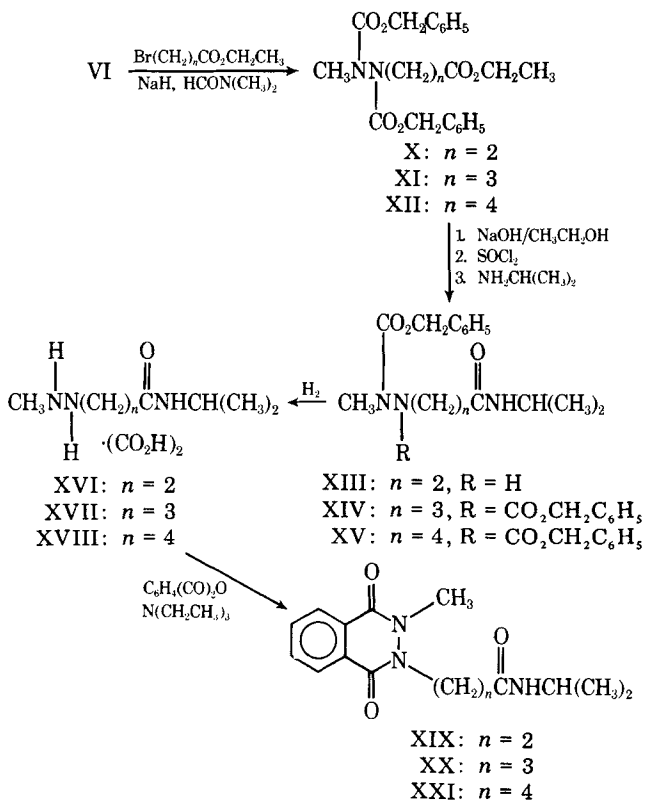

Scheme I

Bis(phenylmethyl) 1-(5-Ethoxy-5-oxopentyl)-2-methyl-1,2-hydrazinedicarboxylate (XII): General Preparation for X and XI—To a stirring suspension of 0.72 g (30 mmoles) of sodium hydride in 70 ml of dry dimethylformamide was added, in parts, 9.42 g (30 mmoles) of VI. The reaction mixture was protected with a calcium sulfate drying tube and stirred for 30 min after the addition. A solution of 6.27 g (30 mmoles) of ethyl 5-bromovalerate in 20 ml of dry dimethylformamide was added dropwise to the reaction solution over 10 min, producing a mild exothermicity. After the reaction solution was stirred for 20 hr, it was poured into 500 ml of saline and the product was removed by extraction with ether. The dried extracts were evaporated, and the residual oil was vacuum distilled in a short path apparatus to give 11.46 g of XII.

Bis(phenylmethyl) 1-Methyl-2-[5-[(1-methylethyl)amino]-5-oxopentyl]-1,2-hydrazinedicarboxylate (XV): General Preparation for XIII and XIV—A solution of XII (11.3 g, 25.5 mmoles) in 100 ml of 95% ethanol was treated with 35 ml of 2 N sodium hydroxide solution, stirred at room temperature for 4 hr, and then poured into 500 ml of cold saline. Neutral materials were removed by extracting twice with ether. Ice chips were added to the aqueous solution, the solution was acidified with concentrated hydrochloric acid, and the acidic product was collected by three ether extractions. The combined extracts were dried and evaporated to yield quantitatively the carboxylic acid.

The carboxylic acid (10.1 g) was stirred with 50 ml of thionyl chloride for 30 min at room temperature and subsequently refluxed for 30 min. Excess thionyl chloride was removed under vacuum, and the residue was dissolved in 100 ml of dry tetrahydrofuran. While the latter solution was stirred, protected with a drying tube and cooled with an ice bath, a solution of 10 ml of isopropylamine in 100 ml of dry tetrahydrofuran was added dropwise over 20 min. The resulting solution mixed with a copious precipitate was stirred 1 hr at ice temperature and 1 hr at room temperature and was then poured into saline made basic with sodium hydroxide solution. The product was removed by three ether extractions. The combined dried extracts were concentrated to about 100 ml on a steam bath, and 150 ml of hexane was slowly added to give a saturated solution at a boil. Allowing the solution to crystallize at room temperature gave 8.02 g of XV in two crops.

Compounds XIII and XIV could not be induced to crystallize and were purified by column chromatography on alumina. After eluting with benzene, the pure product was obtained by eluting with benzene–ethyl acetate (4:1).

***N*-(1-Methylethyl)-5-(2-methylhydrazino)pentanamide Ethanedioate (1:1) (XVIII): General Preparation for XVI and XVII**—A solution of 4.56 g (10 mmoles) of XV in 50 ml of 95% ethanol was placed in a 500-ml pressure bottle containing 0.5 g of 10% palladium-on-charcoal catalyst and hydrogenated at 2.67 kg/cm^2 (38 lb/in.^{2}) pressure with shaking for 18 hr. Immediately after venting the apparatus, the reaction mixture was treated with 10 ml of 10% hydrochloric acid. The catalyst was removed by filtering through a pad of diatomaceous silica[2].

The filtrate was concentrated under vacuum, and the residue was partitioned between 140 ml of distilled water and 100 ml of ether and separated. The ether layer was washed once with 10 ml of distilled water, and the combined aqueous layers were lyophilized to give the dihydrochloride as a partially crystalline, hygroscopic glass. The glass in 10 ml of water was applied to a strongly basic, 20–50-mesh, anion-exchange column[3] (3.5 × 20 cm, oxalate form) and eluted with 400 ml of water to give 2.76 g of XVIII as a white nonhygroscopic cake after lyophilization of the fractions.

The oxalate (XVIII, XVI, and XVII) lyophilizates were analytically pure. Attempts to recrystallize them resulted in decomposition.

1-[3,4-Dihydro-3-methyl-1,4-dioxo-2(1*H*)-phthalazinyl]-*N*-(1-

[1] NMR spectra were determined with a Varian T-60 spectrometer. IR spectra were recorded with a Perkin-Elmer model 621 spectrometer in chloroform. Mass spectra were obtained by direct probe insertion with a DuPont 21-492 spectrometer with a 75-ev ionizing voltage. Combustion analyses were performed by the National Institute of Arthritis, Metabolism, and Digestive Diseases, National Institutes of Health, Bethesda, Md., and by Galbraith Laboratories, Knoxville, Tenn. All melting points are uncorrected and were determined with a Thomas-Hoover capillary melting-point apparatus. Organic extracts were dried over anhydrous sodium sulfate in all cases. The alumina for column chromatography was neutral alumina, 100–200 mesh, Brockmann Activity III.

[2] Celite, Johns-Manville Co.

[3] Amberlite IRA-401S, Rohm & Haas Co., Philadelphia, Pa.

Table III—Mouse L-1210 Antitumor Evaluation

Compound[a]	%T/C (Dose)[b]	T − C[c]	NSC Number
III	108 (200)[d]	−1.1	237649
IV	105 (200)[d]	0.5	235817
V	120 (200)[e]	−0.3	235818
VI	110 (400)	−1.5	235821
VII	126 (200)[d,e]	0.3	235819
VIII	103 (400)	1.2	235820
IX	98 (400)	0.0	237651
X	100 (400)	−0.5	264080
XI	101 (400)	0.1	249986
XII	97 (400)	−1.0	249988
XIV	95 (400)	0.5	264081
XV	95 (400)	−1.1	264082
XVI	91 (200)[d]	−3.0	266768
XVII	112 (200)[d]	−4.4	266767
XVIII	101 (100)[f]	0.1	266769
XIX	101 (400)	−0.9	267970
XX	98 (400)	−0.8	267971
XXI	104 (400)	−0.8	267972

[a] Test compounds were administered intraperitoneally on Days 1, 5, and 9 following intraperitoneal tumor implantation. [b] The tabulated dose (milligrams per kilogram) was the highest dose given producing the indicated %T/C in a dose–response assay. [c] The difference of the average body weight change in grams of the test group (T) and the control group (C) measured on Day 5. [d] Toxic at 400 mg/kg. [e] Activity could not be reproduced. [f] Toxic at 200 mg/kg.

methylethyl)pentanamide (XXI): General Preparation for XIX and XX—A mixture of XVIII (0.77 g, 2.96 mmoles) as the crude dihydrochloride salt (use of the oxalate salt gave similar results) and phthalic anhydride (0.48 g, 3.26 mmoles) was combined with 50 ml of triethylamine and refluxed with stirring for 4 hr. Most of the triethylamine was removed by flash distillation (bath 45°), and the residue was partitioned between 50 ml of 10% hydrochloric acid and 100 ml of chloroform and separated. The aqueous layer was extracted twice with chloroform; the organic layers were combined, dried, and evaporated, yielding 0.69 g of a yellow syrup, which crystallized. The crystals in 5 ml of chloroform were chromatographed on 37 g of alumina. Elution with 200 ml of chloroform gave 290 mg of white crystals of XXI after recrystallization.

REFERENCES

(1) A. Lewis and R. G. Shepherd, in "Medicinal Chemistry," A. Burger, Ed., Wiley–Interscience, New York, N.Y., 1970, p. 435.

(2) C. Kaiser and C. L. Zirkle, in *ibid.*, p. 1483.

(3) B. Toth, *Cancer Res.*, **35**, 3693 (1975).

(4) J. Gold, *Oncology*, **25**, 66 (1971).

(5) D. J. Reed, in "Antineoplastic and Immunosuppressive Agents," part II, A. C. Sartorelli and D. G. Johns, Eds., Springer-Verlag, Berlin, Germany, 1975, p. 747.

(6) G. Weitzel, F. Schneider, A. Fretzdorff, J. Durst, and W. D. Hirschman, *Hoppe Seyler Z. Physiol. Chem.*, **348**, 433 (1967).

(7) H. Rutner, N. Lewin, E. C. Woodbury, T. J. McBride, and K. V. Rao, *Cancer Chemother. Rep.*, **58**, 803 (1974).

(8) A. M. Vandermerwe, H. C. Falkson, and G. Falkson, *S. Afr. Cancer Bull.*, **14**, 75 (1970).

(9) J. Laszlo, J. Durant, and V. Loeb, *Cancer Chemother. Rep.*, **53**, 131 (1969).

(10) K. B. Olson, J. Horton, K. L. Pratt, W. J. Paladine, Jr., T. Cunningham, J. Sullivan, H. Hosely, and D. H. Treble, *ibid.*, **53**, 291 (1969).

(11) J. A. Beisler and S. S. Hillery, *J. Pharm. Sci.*, **64**, 84 (1975).

(12) F. E. Condon, *J. Org. Chem.*, **37**, 3615 (1972).

(13) *Ibid.*, **37**, 3608 (1972).

(14) A. Michaelis and E. Hadanck, *Chem. Ber.*, **41**, 3285 (1908).

(15) K. A. Jensen, U. Anthoni, B. Kagi, C. Larsen, and C. T. Pedersen, *Acta Chem. Scand.*, **22**, 1 (1968).

(16) E. H. White, D. F. Roswell, and O. C. Zafiriou, *J. Org. Chem.*, **34**, 2462 (1969).

(17) P. Zeller, H. Gutmann, B. Hegedus, A. Kaiser, A. Langemann, and M. Muller, *Experientia*, **19**, 129 (1963).

(18) R. I. Geran, N. H. Greenberg, M. M. Macdonald, A. M. Schumacher, and B. J. Abbott, *Cancer Chemother. Rep., Part 3*, **3**, 1 (1972).

(19) A. Goldin, A. A. Serpick, and N. Mantel, *Cancer Chemother. Rep.*, **50**, 173 (1966).

(20) A. Leo, C. Hansch, and D. Elkins, *Chem. Rev.*, **71**, 525 (1971).

ACKNOWLEDGMENTS AND ADDRESSES

Received July 23, 1976, from the *Drug Design & Chemistry Section, Laboratory of Medicinal Chemistry and Biology, Drug Research and Development Program, Division of Cancer Treatment, National Cancer Institute, National Institutes of Health, Bethesda, MD 20014.*

Accepted for publication August 17, 1976.

The authors thank Dr. J. A. Kelley of this laboratory for mass spectrometric data and Mr. Leo Dudeck and Mr. George Congleton, Hazleton Laboratories, Vienna, Va., for conducting the antitumor assays.

* National Institutes of Health Visiting Postdoctoral Fellow 1972–1974. Present address: University of Illinois Medical Center, Chicago, IL 60612.

[x] To whom inquiries should be directed.

Formulation Factors Affecting Strength and Dissolution of Uncoated Oxytetracycline Tablets

S. ESEZOBO and N. PILPEL [x]

Abstract □ The effect of various formulation and processing factors on the properties of 300-mg oxytetracycline tablets was studied. At a constant moisture level and packing fraction, an increase in gelatin concentration resulted in increased tensile strength, increased disintegration and dissolution times, and reduced capping tendency. The Wagner theory of dissolution applied satisfactorily to tablets containing up to 5% (w/w) gelatin but was less applicable at higher gelatin levels. Dissolution rate constants were calculated, and their values depended on the gelatin content and packing fraction of the tablets.

Keyphrases □ Oxytetracycline tablets—tensile strength and dissolution, effect of various formulation and processing factors □ Tablets, oxytetracycline—tensile strength and dissolution, effect of various formulation and processing factors □ Tensile strength—oxytetracycline tablets, effect of various formulation and processing factors □ Dissolution—oxytetracycline tablets, effect of various formulation and processing factors □ Dosage forms—oxytetracycline tablets, tensile strength and dissolution, effect of various formulation and processing factors

Recently, various investigators (1, 2) reported that commercial oxytetracycline hydrochloride capsules, nominally containing the same dose but produced by different manufacturers, are not biologically equivalent. Brice and Hammer (1) performed disintegration and dissolution tests and found that, in general, batches that gave poor

Table III—Mouse L-1210 Antitumor Evaluation

Compound[a]	%T/C (Dose)[b]	T − C[c]	NSC Number
III	108 (200)[d]	−1.1	237649
IV	105 (200)[d]	0.5	235817
V	120 (200)[e]	−0.3	235818
VI	110 (400)	−1.5	235821
VII	126 (200)[d,e]	0.3	235819
VIII	103 (400)	1.2	235820
IX	98 (400)	0.0	237651
X	100 (400)	−0.5	264080
XI	101 (400)	0.1	249986
XII	97 (400)	−1.0	249988
XIV	95 (400)	0.5	264081
XV	95 (400)	−1.1	264082
XVI	91 (200)[d]	−3.0	266768
XVII	112 (200)[d]	−4.4	266767
XVIII	101 (100)[f]	0.1	266769
XIX	101 (400)	−0.9	267970
XX	98 (400)	−0.8	267971
XXI	104 (400)	−0.8	267972

[a] Test compounds were administered intraperitoneally on Days 1, 5, and 9 following intraperitoneal tumor implantation. [b] The tabulated dose (milligrams per kilogram) was the highest dose given producing the indicated %T/C in a dose–response assay. [c] The difference of the average body weight change in grams of the test group (T) and the control group (C) measured on Day 5. [d] Toxic at 400 mg/kg. [e] Activity could not be reproduced. [f] Toxic at 200 mg/kg.

methylethyl)pentanamide (XXI): General Preparation for XIX and XX—A mixture of XVIII (0.77 g, 2.96 mmoles) as the crude dihydrochloride salt (use of the oxalate salt gave similar results) and phthalic anhydride (0.48 g, 3.26 mmoles) was combined with 50 ml of triethylamine and refluxed with stirring for 4 hr. Most of the triethylamine was removed by flash distillation (bath 45°), and the residue was partitioned between 50 ml of 10% hydrochloric acid and 100 ml of chloroform and separated. The aqueous layer was extracted twice with chloroform; the organic layers were combined, dried, and evaporated, yielding 0.69 g of a yellow syrup, which crystallized. The crystals in 5 ml of chloroform were chromatographed on 37 g of alumina. Elution with 200 ml of chloroform gave 290 mg of white crystals of XXI after recrystallization.

REFERENCES

(1) A. Lewis and R. G. Shepherd, in "Medicinal Chemistry," A. Burger, Ed., Wiley–Interscience, New York, N.Y., 1970, p. 435.

(2) C. Kaiser and C. L. Zirkle, in *ibid.*, p. 1483.

(3) B. Toth, *Cancer Res.*, **35**, 3693 (1975).

(4) J. Gold, *Oncology*, **25**, 66 (1971).

(5) D. J. Reed, in "Antineoplastic and Immunosuppressive Agents," part II, A. C. Sartorelli and D. G. Johns, Eds., Springer-Verlag, Berlin, Germany, 1975, p. 747.

(6) G. Weitzel, F. Schneider, A. Fretzdorff, J. Durst, and W. D. Hirschman, *Hoppe Seyler Z. Physiol. Chem.*, **348**, 433 (1967).

(7) H. Rutner, N. Lewin, E. C. Woodbury, T. J. McBride, and K. V. Rao, *Cancer Chemother. Rep.*, **58**, 803 (1974).

(8) A. M. Vandermerwe, H. C. Falkson, and G. Falkson, *S. Afr. Cancer Bull.*, **14**, 75 (1970).

(9) J. Laszlo, J. Durant, and V. Loeb, *Cancer Chemother. Rep.*, **53**, 131 (1969).

(10) K. B. Olson, J. Horton, K. L. Pratt, W. J. Paladine, Jr., T. Cunningham, J. Sullivan, H. Hosely, and D. H. Treble, *ibid.*, **53**, 291 (1969).

(11) J. A. Beisler and S. S. Hillery, *J. Pharm. Sci.*, **64**, 84 (1975).

(12) F. E. Condon, *J. Org. Chem.*, **37**, 3615 (1972).

(13) *Ibid.*, **37**, 3608 (1972).

(14) A. Michaelis and E. Hadanck, *Chem. Ber.*, **41**, 3285 (1908).

(15) K. A. Jensen, U. Anthoni, B. Kagi, C. Larsen, and C. T. Pedersen, *Acta Chem. Scand.*, **22**, 1 (1968).

(16) E. H. White, D. F. Roswell, and O. C. Zafiriou, *J. Org. Chem.*, **34**, 2462 (1969).

(17) P. Zeller, H. Gutmann, B. Hegedus, A. Kaiser, A. Langemann, and M. Muller, *Experientia*, **19**, 129 (1963).

(18) R. I. Geran, N. H. Greenberg, M. M. Macdonald, A. M. Schumacher, and B. J. Abbott, *Cancer Chemother. Rep., Part 3*, **3**, 1 (1972).

(19) A. Goldin, A. A. Serpick, and N. Mantel, *Cancer Chemother. Rep.*, **50**, 173 (1966).

(20) A. Leo, C. Hansch, and D. Elkins, *Chem. Rev.*, **71**, 525 (1971).

ACKNOWLEDGMENTS AND ADDRESSES

Received July 23, 1976, from the *Drug Design & Chemistry Section, Laboratory of Medicinal Chemistry and Biology, Drug Research and Development Program, Division of Cancer Treatment, National Cancer Institute, National Institutes of Health, Bethesda, MD 20014.*

Accepted for publication August 17, 1976.

The authors thank Dr. J. A. Kelley of this laboratory for mass spectrometric data and Mr. Leo Dudeck and Mr. George Congleton, Hazleton Laboratories, Vienna, Va., for conducting the antitumor assays.

* National Institutes of Health Visiting Postdoctoral Fellow 1972–1974. Present address: University of Illinois Medical Center, Chicago, IL 60612.

[x] To whom inquiries should be directed.

Formulation Factors Affecting Strength and Dissolution of Uncoated Oxytetracycline Tablets

S. ESEZOBO and N. PILPEL [x]

Abstract □ The effect of various formulation and processing factors on the properties of 300-mg oxytetracycline tablets was studied. At a constant moisture level and packing fraction, an increase in gelatin concentration resulted in increased tensile strength, increased disintegration and dissolution times, and reduced capping tendency. The Wagner theory of dissolution applied satisfactorily to tablets containing up to 5% (w/w) gelatin but was less applicable at higher gelatin levels. Dissolution rate constants were calculated, and their values depended on the gelatin content and packing fraction of the tablets.

Keyphrases □ Oxytetracycline tablets—tensile strength and dissolution, effect of various formulation and processing factors □ Tablets, oxytetracycline—tensile strength and dissolution, effect of various formulation and processing factors □ Tensile strength—oxytetracycline tablets, effect of various formulation and processing factors □ Dissolution—oxytetracycline tablets, effect of various formulation and processing factors □ Dosage forms—oxytetracycline tablets, tensile strength and dissolution, effect of various formulation and processing factors

Recently, various investigators (1, 2) reported that commercial oxytetracycline hydrochloride capsules, nominally containing the same dose but produced by different manufacturers, are not biologically equivalent. Brice and Hammer (1) performed disintegration and dissolution tests and found that, in general, batches that gave poor

Table I—Values of Tensile Strength for the Oxytetracycline Flat-Faced Tablets[a] Prepared with a Single-Punch Machine at a Packing Fraction of 0.85–0.87

Gelatin Concentration, % (w/w)	Log Tensile Strength, MNm^{-2}	Tensile Strength, MNm^{-2}
0	0.15	1.41
2.50	0.25	1.77
3.75	0.33	2.17
5.00	0.41	2.57
6.25	0.43	2.72
7.50	0.51	3.20

[a] Tablets weighed 325 mg and had a moisture content range of 2.4–3.2% (w/w).

serum levels also had slower *in vitro* dissolution rates.

Further investigations (3, 4) on several samples of commercial 250-mg oxytetracycline dihydrate tablets BP showed that the dissolution rate profiles varied between generic brands obtained from different manufacturers and also between and within batches from one source. More recently, Chalmers and Elworthy (5) conducted studies on a particular oxytetracycline formulation (similar in some respects to the one used in the present investigations but with povidone as the binding agent). Their work was concerned primarily with the effects of particle size, binder concentration, binder volume, and massing time on the tensile strength and disintegration and dissolution times of the resulting granules and tablets.

Preliminary work was reported (6) on the effects of moisture, gelatin binding agent, and packing fraction on the properties of certain oxytetracycline tablets prepared with a hand press. It was considered necessary to extend the work along two lines: (*a*) to see whether any correlation existed between the properties of tablets made in a hand press and in high speed tableting machines, and (*b*) to analyze in detail the dissolution results obtained on all of the tablets to arrive at a better understanding of the mechanisms of dissolution in typical oxytetracycline tablet formulations.

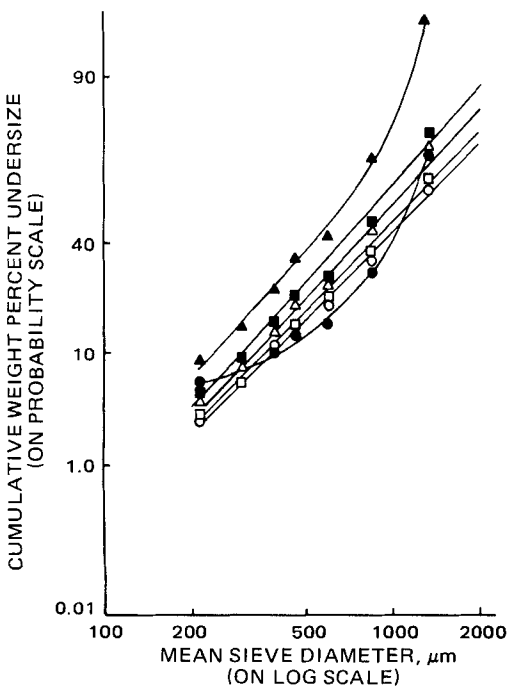

Figure 1—*Sieve analysis of granules on a log probability plot. Key (% w/w gelatin): ●, 0; ▲, 2.50; ■, 3.75; △, 5.00; □, 6.25; and ○, 7.50.*

Table II—Effect of Gelatin Concentration on the Capping Pressure of 300-mg Deep Biconvex Tablets Using a Hand-Operated Hydraulic Press

Gelatin Concentration, % (w/w)	Capping Pressure, MNm^{-2}	Packing Fraction (ρ_f)
0	29.8	0.74
2.50	59.5	0.81
3.75	89.3	0.83
5.00	119.1	0.85
6.25	119.1	0.87
7.50	148.9	0.88

Two methods of analysis were employed. The first involved using the equation of Wagner (7):

$$\text{\% dissolved by time } t = \frac{W}{W^\infty} \times 100 = \frac{\int_0^t s(t)\,dt}{\int_0^\infty s(t)\,dt}$$

$$\times 100 = \text{\% surface area generated by time } t \text{ of total surface generated} \quad \text{(Eq. 1)}$$

in which it is assumed that the surface area of the drug available for dissolution is initially zero, then increases to a maximum as disintegration occurs, and then falls off progressively to zero when dissolution is complete. The W and W^∞ are the amounts of drug dissolved at time t and at infinite time, respectively; the integrals represent the cumulative surface areas, S, that have been made available for dissolution from time zero to the particular time t and infinity, respectively.

The applicability of Eq. 1 can be tested by plotting values of cumulative percent drug dissolved on a probability scale (ordinate) *versus* the corresponding time values on a logarithmic scale (abscissa) and seeing whether straight-line graphs are obtained.

The second method of analysis was the equation proposed by Kitazawa *et al.* (8):

$$\ln \frac{C_s}{C_s - C} = kt \quad \text{(Eq. 2)}$$

where k is the dissolution rate constant, C_s is the concentration of the solute at saturation, and C is the actual solute concentration in solution at time t. Equation 2 was derived from a study of the dissolution of uncoated caffeine tablets and showed that a change in the dissolution rate at a cer-

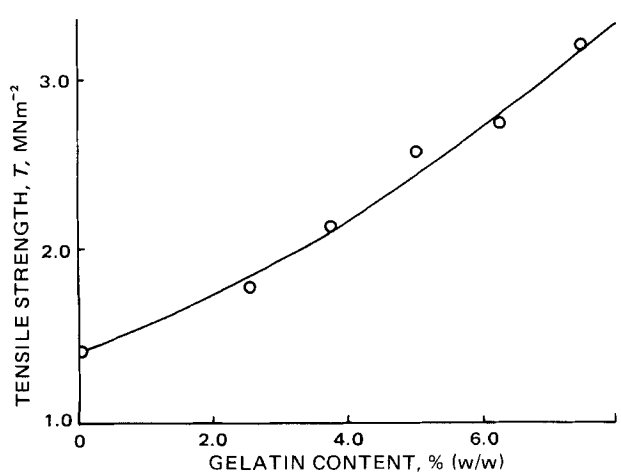

Figure 2—*Tensile strength* versus *gelatin content of flat-faced tablets prepared with a single-punch machine. The range of ρ_f was 0.85–0.87, and the range of moisture content was 2.4–3.2% (w/w).*

Table III—Influence of Gelatin Content on the Dissolution and Disintegration of Biconvex Tablets at $\rho_f \simeq 0.80$

Gelatin Concentration, % (w/w)	Moisture Content, % (w/w)	Mean Packing Fraction (ρ_f)	Dissolution Time, min[a]			Disintegration Time, min[b]	
			$t_{25\%}$	$t_{50\%}$	$t_{75\%}$	Mean Packing Fraction (ρ_f)	Mean Disintegration Time, min
		Tablets Prepared with Single-Punch Machine					
0	2.70	0.79	1.88	3.13	4.50	0.79	1.54
2.50	2.40	0.80	2.25	3.25	5.25	0.79	1.62
3.75	2.70	0.80	3.75	5.75	8.75	0.79	2.79
5.00	3.60	0.80	15.50	25.00	35.50	0.78	6.46
6.25	3.20	0.80	50.00	101.00	141.00	0.80	31.38
		Tablets Prepared with Multipunch Machine					
0	2.70	0.79	2.00	3.38	6.00	0.79	1.05
2.50	2.40	0.79	2.13	3.25	5.25	0.78	1.48
3.75	2.70	0.80	3.50	5.38	8.75	0.78	2.75
5.00	3.60	0.78	10.00	17.50	30.50	0.77	7.07
6.25	3.20	0.79	62.00	144.00	—[c]	0.79	30.74

[a] Mean of four tablets. [b] Mean of 20 tablets. [c] Sixty-one percent released after 180 min.

tain time, t, represented a change in the surface area of the tablet due to it breaking into small particles.

EXPERIMENTAL

Materials—The basic formulation employed was 90.2% (w/w) oxytetracycline dihydrate[1] EP, 7.2% (w/w) microcrystalline cellulose BPC[2], and 3.6% (w/w) alginic acid HED[3] BPC.

Granule Preparation—Granules were prepared using gelatin[4] as previously reported (6).

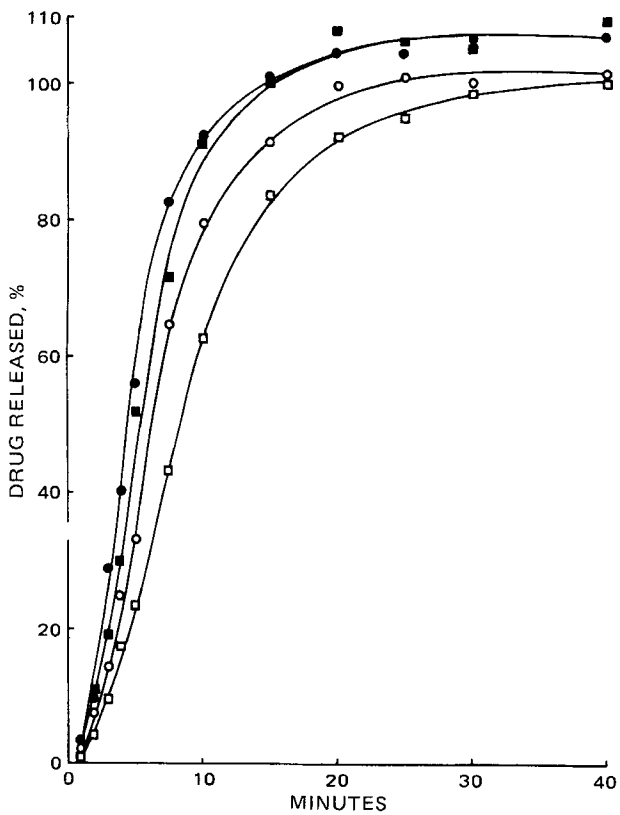

Figure 3—*Drug release* versus *time for tablets containing 3.75% (w/w) gelatin prepared with a single-punch machine of a constant pressure setting. Key (packing fraction, ρ_f): ●, 0.79; ■, 0.80; ○, 0.81; and □, 0.82.*

Tableting Procedure—A hand-operated hydraulic press[5] (6) and single-punch[6] and rotary-punch[7] tableting machines equipped with flat-faced or deep concave punches, 1.03 cm in diameter, were used to compress the granules. The granules had been lubricated with 1% (w/w) magnesium stearate. The compression speed of the single-punch machine was adjusted to 70 strokes/min. The multipunch machine was modified by blocking off 14 stations so that only two compression stations, fitted with deep concave punches on opposite sides of the revolving turret, were used. It was operated at 30 rpm.

The setting on each machine was adjusted to produce tablets (about 400–500) from each batch of granules with predetermined weights and packing fractions. The following tablets were prepared (all contained approximately 250 mg of oxytetracycline):

type of machine	shape	total weight, mg	tablets packing fraction (ρ_f)
hand press	deep biconvex	300 ± 10	0.69–0.90
single punch	flat faced	325 ± 10	0.85 ± 0.05
	deep biconvex	300 ± 10	0.80 ± 0.05
rotary punch	deep biconvex	300 ± 10	0.80 ± 0.05

Tests on Tablets—*Tensile Strength*—The tensile strengths of 325-mg flat-faced tablets were determined using the diametral compression test (6, 9, 10) on 20 tablets of each batch, and the means were calculated. The measurements were made in a room having a relative humidity of 50%.

Capping Pressure—Capping pressure was determined by subjecting the 300-mg biconvex tablets, which had been compressed to different packing fractions with the hand press, to the diametral test. The packing fraction at which each batch of tablets capped was noted, and the corresponding pressure employed to achieve tablets of this packing fraction was regarded as the capping pressure. The determination was made on at least 20 tablets per packing fraction in each batch, and capping was said to occur at a particular packing fraction when at least 50% of tablets tested capped.

Disintegration—The disintegration times of the 300-mg deep biconvex tablets were measured individually on 20 tablets by the BP method in a disintegration apparatus[8], and a mean time was calculated. Distilled water was used as the disintegration fluid (6).

Dissolution—The dissolution times of the 300-mg deep biconvex tablets were measured in an apparatus similar in principle to the "beaker method" of Levy and Hayes (6, 11). Individual tablets were placed in a pH 2 dissolution buffer solution and stirred at 100 rpm. Samples were removed at known time intervals and assayed in a spectrophotometer[9] for oxytetracycline content. The mean of four tablets was calculated at each gelatin concentration and packing fraction.

RESULTS

The size distributions of the granules used for preparing the tablets are shown in Fig. 1 as a log-probability plot.

[1] ICI Ltd., Pharmaceuticals Division, Macclesfield, Cheshire, United Kingdom.
[2] Avicel PH101, Honeywell and Stein Ltd., London, United Kingdom.
[3] Alginate Industries Ltd., London, United Kingdom.
[4] Bloom No. 300, acid-treated hide, Richard Hodgson and Sons Ltd., Beverley, Yorkshire, United Kingdom.
[5] Research and Industrial Instrument Co., Ltd., London, United Kingdom.
[6] Model F3, Manesty Machines Ltd., Liverpool, United Kingdom.
[7] Model D3B, Manesty Machines Ltd., Liverpool, United Kingdom.
[8] Manesty disintegration tester, Manesty Machines Ltd., Liverpool, United Kingdom.
[9] CE202, Cecil Instruments Ltd., Cambridge, United Kingdom.

Table IV—Combined Effects of Gelatin Content and Packing Fraction on the Dissolution Rates of Biconvex Tablets at $\rho_f \simeq 0.80$ Using Eq. 2

Gelatin Content, % (w/w)	Packing Fraction (ρ_f)	t_1, min	k_1, min^{-1}	k_2, min^{-1}
0	0.73	5.0	0.280	0.152
	0.81	—[a]	0.320	—[a]
	0.86	—[a]	0.490	—[a]
	0.87	—[a]	0.358	—[a]
	0.92	5.0	0.180	0.139
2.50	0.72	—[a]	0.253	—[a]
	0.80	—[a]	0.270	—[a]
	0.81	—[a]	0.313	—[a]
	0.85	—[a]	0.256	—[a]
	0.88	10.4	0.160	0.132
3.75	0.69	42.5	0.047	0.018
	0.78	30.0	0.109	0.200
	0.84	36.0	0.065	0.040
	0.86	17.0	0.024	0.078
	0.90	30.5	0.022	0.040
5.00	0.70	25.0	0.031	0.018
	0.79	49.0	0.035	0.017
	0.83	82.0	0.007	0.019
	0.86	113.0	0.007	0.019
6.25	0.69	124.0	0.017	0.028
	0.78	85.0	0.013	0.023
	0.83	145.0	0.009	0.021

[a] A single straight regression line with slope = k was obtained.

The calculated values of the tensile strengths in Table I are for the 325-mg flat-faced tablets, prepared at packing fractions between 0.85 and 0.87 and containing moisture levels between 2.4 and 3.2% (w/w) with the single-punch tableting machine. The tensile strength is plotted *versus* percent (w/w) of gelatin in Fig. 2.

The information on the effects of gelatin concentration on the capping tendency of the 300-mg biconvex tablets is presented in Table II.

Table III lists the mean dissolution times for 25, 50, and 75% of drug released from the tablets (having packing fractions of approximately 0.80) prepared with both single-punch and multipunch machines. Table III also includes the mean disintegration times for these tablets.

Figure 3 shows a representative graph of the variation in dissolution profiles for tablets containing 3.75% (w/w) gelatin prepared with the single-punch machine at the same pressure settings. Similar variations were also obtained for tablets prepared with the multipunch machine at a fixed pressure setting.

The marked effect of gelatin concentration on the dissolution profiles of the tablets prepared with the single-punch machine at a packing fraction of approximately 0.80 is illustrated in Fig. 4. To test whether the data given in Table III and plotted in Fig. 4 were amenable to the Wagner (7) type of analysis, the values of percentage drug dissolved were plotted against time on a log–probability graph (Fig. 5). In general, straight lines could be drawn through the points for the tablets containing 0, 2.5, and 3.75% (w/w) gelatin. For tablets made with 5.0 and 6.25% (w/w) gelatin, curved lines were obtained.

The apparent pseudo-first-order plots corresponding to curves A and B in Fig. 5, together with similar curves obtained for tablets prepared (at the same packing fraction) with a hand-operated press and multipunch machine, are shown in Fig. 6. The Kitazawa *et al.* (8) types of plot of $\ln [C_s/(C_s - C)]$ *versus* time are shown in Figs. 7 and 8 for tablets compressed with the hand-operated press to different packing fractions and containing 0 and 5% (w/w) gelatin, respectively. Similar plots were obtained for tablets made (at approximately the 0.80 packing fraction) with the single-punch machine (Fig. 9). Depending on the packing fraction and gelatin content, either a single straight line or two intersecting straight lines were obtained for each formulation. For those with two straight lines, the time at which the lines intersect is termed t_1, the slope of the first is designated k_1, and the slope of the second is designated k_2. Additional relevant data showing the effects of both packing fraction and gelatin content on these values are listed in Tables IV and V.

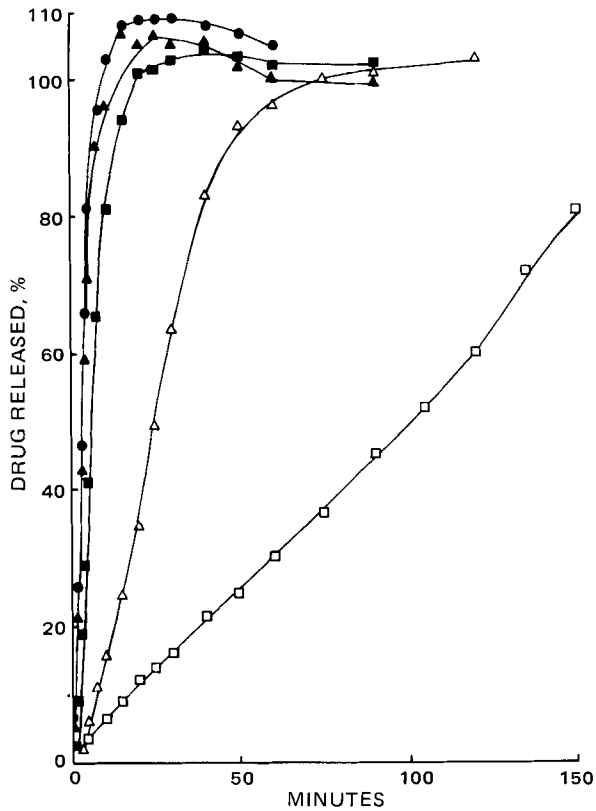

Figure 4—*Effect of gelatin content on the dissolution of tablets prepared with a single-punch machine at $\rho_f \simeq 0.80$. Key: ●, 0% (w/w) gelatin and 0.79 mean ρ_f; ▲, 2.50% (w/w) gelatin and 0.80 mean ρ_f; ■, 3.75% (w/w) gelatin and 0.80 mean ρ_f; △, 5.00% (w/w) gelatin and 0.80 mean ρ_f; and □, 6.25% (w/w) gelatin and 0.80 mean ρ_f.*

DISCUSSION

With some formulations, variations in granule size (Fig. 1) may cause significant changes in the disintegration and dissolution rates of the tablets (12, 13). However, these changes were small for two oxytetracycline formulations, one containing gelatin (14) and the other povidone (5) as the binding agent.

Increasing the gelatin concentration increased the tensile strengths of the tablets (Fig. 2). Therefore, the result was similar to that obtained on loosely packed beds (15) on tablets prepared with a hand-operated press (6) and when povidone was used as the binding agent (5). This result could be attributed to the considerable amount of heat generated during the tableting of powders or granules, producing overall temperature rises of about 5–30° and still higher rises of the contact points between the asperities on the particles (16, 17). This temperature increase could cause

Table V—Effects of Gelatin Content on the Dissolution Rates of Biconvex Tablets at $\rho_f \simeq 0.80$ Using Eq. 2

Gelatin Content, % w/w	Tablets Prepared with Single-Punch Machine, ρ_f Range = 0.79–0.80			Tablets Prepared with Multipunch Machine, ρ_f Range = 0.78–0.80		
	t_1, min	k_1, min^{-1}	k_2, min^{-1}	t_1, min	k_1, min^{-1}	k_2, min^{-1}
0	—[a]	0.271	—[a]	—[a]	0.274	—[a]
2.50	—[a]	0.217	—[a]	—[a]	0.250	—[a]
3.75	—[a]	0.150	—[a]	—[a]	0.150	—[a]
5.00	20	0.020	0.056	36	0.042	0.076
6.25	115	0.008	0.033	114	0.008	0.025

[a] A single straight regression line with slope = k was obtained.

melting of asperities and, in the present systems, of the gelatin binding agent; on cooling, they would solidify to form strong bonds between the particles (18). The amount of bonding that would take place and, therefore, the strength of the tablet would be expected to depend *in part* on the amount of gelatin present.

As observed previously (6), the 300-mg deep biconvex tablets spontaneously capped when subjected to the diametral compression test, presumably because of their very thin edges. These tablets are known to be subject to capping in production. However, the higher the gelatin concentration in the formulations, the higher was the packing fraction to which the tablets could be compressed before capping occurred (Table II). Therefore, to overcome the tendency of the 300-mg biconvex oxytetracycline tablets to cap during production, a reasonably high concentration of gelatin should be incorporated into the formulation.

Small changes in the packing fraction of oxytetracycline tablets containing the same gelatin concentration and prepared at the same nominal pressure setting of the machine produced wide variations in their dissolution profiles (Fig. 3). This effect could also account for the reported variations in the dissolution rates of oxytetracycline tablets from different manufacturers and between or within batches obtained from one manufacturer (3, 4).

Besides bond formation, another mechanism that might contribute to the observed increases in both the disintegration and dissolution times of the tablets with an increase in gelatin content (Table III and Fig. 4) might be the formation of a thin film of gelatin around the powder particles or granules; its thickness would depend on the quantity of gelatin employed. This thin film could subsequently be converted into a mucilaginous viscous barrier when the tablets and breakup fragments contacted the test media (19), which would increase their disintegration and dissolution times. The greater rate of disintegration than of dissolution (Table III) was as expected, since the disintegration tests only measured the time for the tablets to break into granules or particles that could pass through a No. 10 mesh screen while dissolution tests measured the time for the oxytetracycline particles to dissolve from the intact tablets, fragments, granules, or aggregates.

Analysis of the dissolution results showed that the oxytetracycline tablets containing less than 5% (w/w) gelatin conformed satisfactorily to Wagner's (7) concept of a log-normal distribution plot, since linear graphs were obtained for these samples (Fig. 5). [Wagner (7) obtained linear plots on results obtained by various other workers using, for example, tablets of buffered aspirin, griseofulvin, and potassium chloride.] When more than 5% (w/w) gelatin was present, the graphs became curved and exhibited kinks when linearized by the first-order method of plotting (Fig. 6).

The value of a Wagner plot (Fig. 5) (7) is that it enables a dissolution rate to be described in terms of two parameters: the medium $t_{50\%}$ and the standard deviation. One can also obtain values of $t_{20\%}$, $t_{90\%}$, *etc.*, from these plots. Under theoretically ideal circumstances, when a tablet disintegrates and liberates the primary particles of drug, the dissolution rate is limited by the effective surface area of the particles. On this basis, Wagner (7) suggested that both the $t_{50\%}$ and standard deviation values might provide information on the likely behavior of tablets in *in vivo* tests, but this suggestion has not yet been confirmed.

Analysis by the Kitazawa *et al.* (8) method showed that tablets compressed to a packing fraction of approximately 0.80 and containing less than 5% (w/w) gelatin yielded straight lines, with one dissolution rate constant, k, in each case (Fig. 9). These tablets broke up rapidly into small particles as soon as they were in contact with the dissolution medium, resulting in a sudden increase in surface area and a subsequent constant decrease as the granules dissolved.

However, for tablets containing 5 and 6.25% (w/w) gelatin, the dissolution rate constants changed from k_1 to k_2 at certain times, t_1, at all packing fractions (Figs. 8 and 9). Similar observations were obtained with tablets containing less than 5% (w/w) gelatin when their packing fractions were either below 0.75 or above 0.85 (Fig. 7). This change in the dissolution rate constant is ascribed to an increase in surface area due to break-up of the tablets into large and small fragments at time t_1. The changes in the dissolution rate profile with packing fraction (Fig. 7 and Table IV) showed that the dissolution rate was a maximum (6) at packing

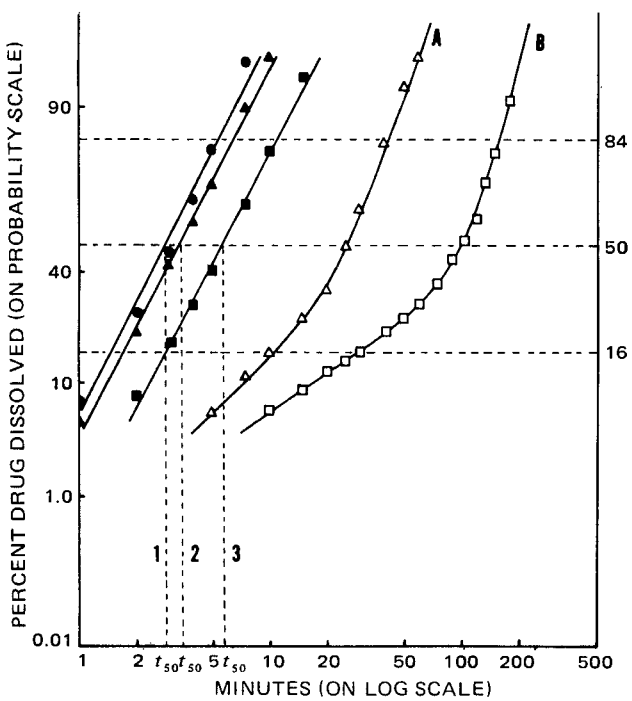

Figure 5—*Wagner plot of dissolution results on tablets ($\rho_f \doteq 0.80$) prepared with a single-punch machine.*

key	gelatin content, % (w/w)	mean (ρ_f)	t_{50}, min	σ
●	0	0.79	2.8	1.93
▲	2.50	0.80	3.3	1.94
■	3.75	0.80	5.6	1.93
△	5.00	0.80	—	—
□	6.25	0.80	—	—

1, σ = 1.93; 2, σ = 1.94; 3, σ = 1.93

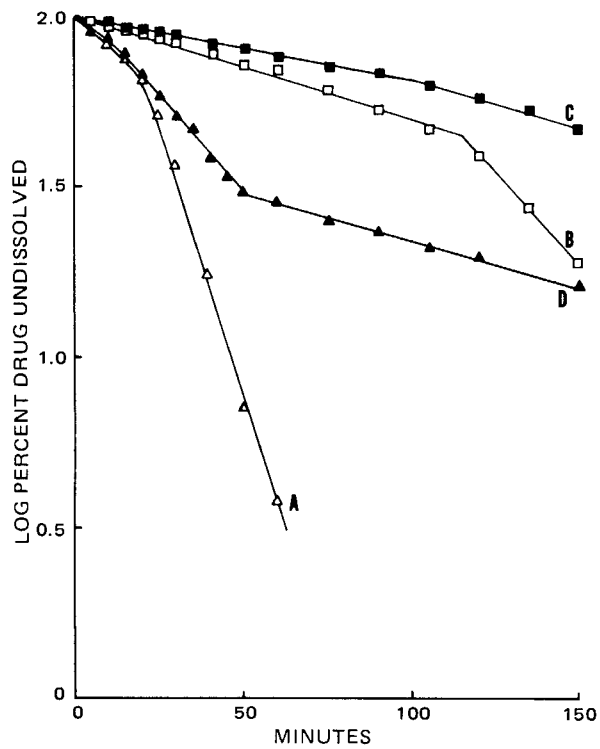

Figure 6—*Apparent pseudo-first-order plot for tablets that did not conform to the Wagner plot.*

key	machine used for preparing tablets	gelatin content, % (w/w)	k value of first section, min^{-1}	k value of second section, min^{-1}
A	single punch	5.00	0.069	—
B	single punch	6.25	0.007	0.025
C	multipunch	6.25	0.004	0.007
D	hydraulic press	5.00	0.026	0.006

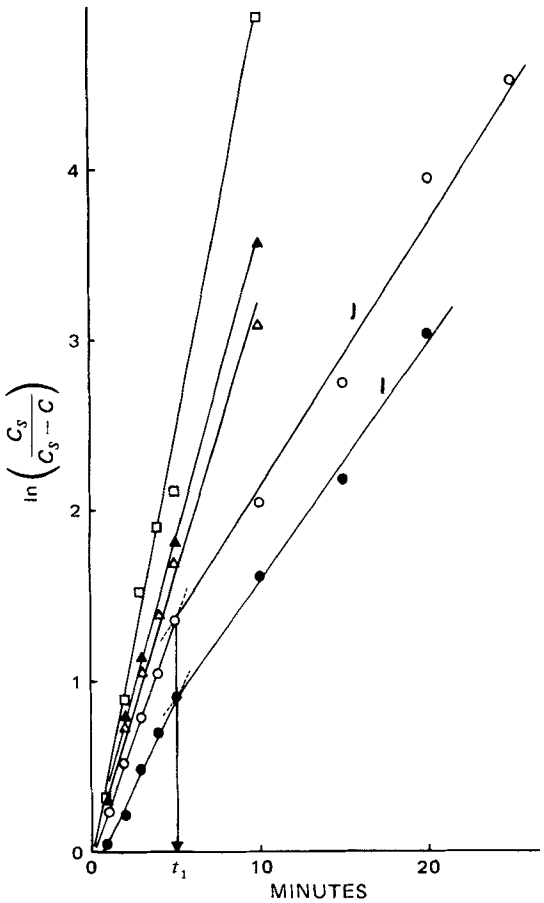

Figure 7—*Determination of dissolution rate constants of oxytetracycline tablets using Eq. 2. The tablets had 0% (w/w) gelatin and were prepared at different packing fractions with the hydraulic press. Key (packing fraction, ρ_f): ○, 0.73; △, 0.81; □, 0.86; ▲, 0.87; and ●, 0.92.*

fractions between 0.75 and 0.85. This maximum was not observed for the formulation containing povidone as the binding agent (5), illustrating the need for a detailed reinvestigation each time a tablet formulation is

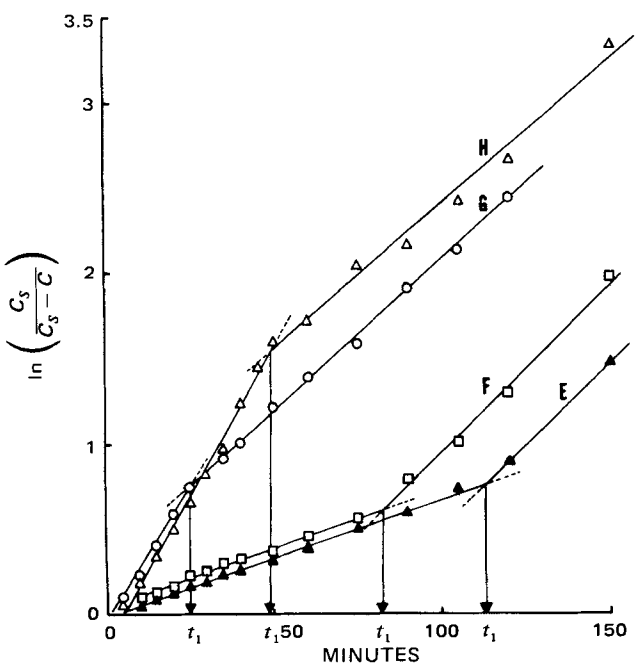

Figure 8—*Determination of dissolution rate constants of oxytetracycline tablets using Eq. 2. The tablets had 5% (w/w) gelatin and were prepared at different packing fractions with the hydraulic press. Key (packing fraction, ρ_f): ○, 0.70; △, 0.79; □, 0.83; and ▲, 0.86.*

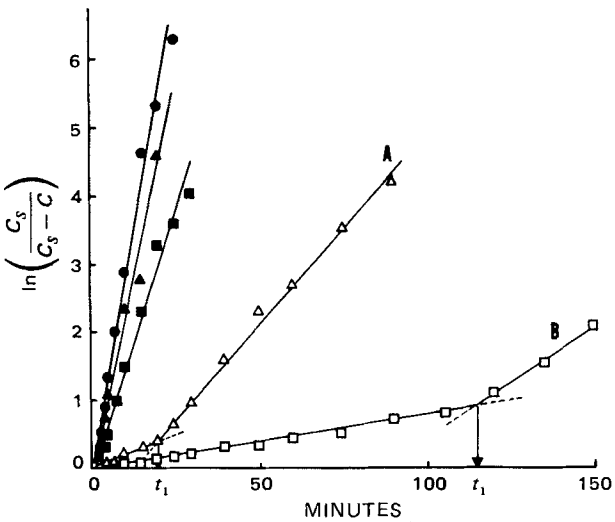

Figure 9—*Effect of gelatin content on the determination of dissolution rate constants using Eq. 2 for oxytetracycline tablets prepared with a single-punch machine at ρ_f 0.80. Key: ●, 0% (w/w) gelatin and 0.79 mean ρ_f; ▲, 2.50% (w/w) gelatin and 0.80 mean ρ_f; ■, 3.75% (w/w) gelatin and 0.80 mean ρ_f; △, 5.00% (w/w) gelatin and 0.80 mean ρ_f; and □, 6.25% (w/w) gelatin and 0.80 mean ρ_f.*

altered. The times corresponding to the kinks in Fig. 6 were identical with the t_1 values obtained from Figs. 8 and 9 because Eqs. 1 and 2 were both derived from the same basic equation of Noyes and Whitney (20):

$$\frac{dC}{dt} = k(C_s - C) \qquad \text{(Eq. 3)}$$

where the symbols are as defined for Eq. 2.

Visual observations during the tests confirmed that in the first sections (*i.e.*, up to times t_1) in graphs A–C in Figs. 6 and 9 and in graphs E and F in Fig. 8, dissolution was occurring from intact tablets; the second sections (*i.e.*, after times t_1) represented dissolution from broken fragments of the tablets. The tablets whose results are shown in graph D of Fig. 6 and in graphs G–J of Figs. 7 and 8 initially broke up quite rapidly into fairly large fragments, and these fragments then broke up into smaller fragments very slowly. Similar conclusions were reached by Kitazawa *et al.* (8).

In contrast to their results (8) on caffeine tablets, no good correlation was obtained between the values of t_1 and disintegration time or between k_1 and k_2 for the oxytetracycline tablets investigated. The disintegration times of these tablets were less than the t_1 values, possibly because in the present work [in contrast to that of Kitazawa *et al.* (8)] more vigorous agitation was employed in the disintegration test than in the dissolution test.

Irrespective of the tableting equipment employed, the values of k for

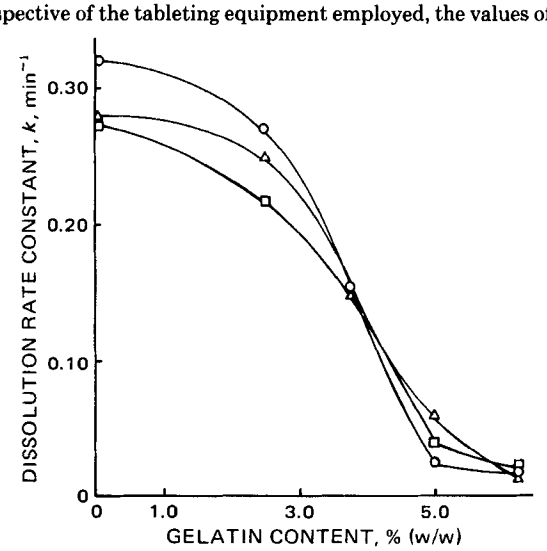

Figure 10—*Effect of gelatin content on the k values calculated using Eq. 2 for tablets prepared with the three types of machines at $\rho_f \simeq 0.80$. Key: ○, hydraulic press; □, single punch; and △, multipunch.*

all tablets decreased with their binding agent content (Fig. 10). Although this finding is similar to a previous one where povidone was substituted for gelatin (5), it is also clear that the nature of the binding agent has a profound effect on the dissolution characteristics of a formulation.

REFERENCES

(1) G. W. Brice and H. F. Hammer, *J. Am. Med. Assoc.*, **208**, 1189 (1969).

(2) D. C. Blair, R. W. Barnes, E. L. Wilder, and W. J. Murray, *ibid.*, **215** (2), 251 (1971).

(3) M. J. Groves, *Pharm. J.*, **Apr.**, 318 (1973).

(4) T. M. Jones, P. C. Risdall, and M. Frier, *J. Pharm. Pharmacol., Suppl.*, **26**, 116P (1974).

(5) A. A. Chalmers and P. H. Elworthy, *J. Pharm. Pharmacol.*, **28**, 228 (1976).

(6) S. Esezobo and N. Pilpel, *ibid.*, **28**, 8 (1976).

(7) J. G. Wagner, *J. Pharm. Sci.*, **58**, 1253 (1969).

(8) S. Kitazawa, I. Johno, Y. Ito, S. Teramura, and I. Okeda, *J. Pharm. Pharmacol.*, **27**, 765 (1975).

(9) J. T. Fell and J. M. Newton, *J. Pharm. Sci.*, **59**, 688 (1970).

(10) P. York and N. Pilpel, *J. Pharm. Pharmacol., Suppl.*, **25**, 1 (1973).

(11) G. Levy and B. A. Hayes, *N. Engl. J. Med.*, **262**, 1053 (1960).

(12) G. Levy, J. M. Antkowiak, J. A. Procknal, and D. C. White, *J. Pharm. Sci.*, **52**, 1047 (1963).

(13) J. K. C. Yen, *Can. Pharm. J.*, **97**, 439 (1964).

(14) S. Esezobo, Ph.D. thesis, University of London, London, England, (1976).

(15) S. Esezobo and N. Pilpel, *J. Pharm. Pharmacol., Suppl.*, **26**, 47P (1974).

(16) E. Nelson, L. W. Busse, and T. Higuchi, *J. Am. Pharm. Assoc., Sci. Ed.*, **44**, 223 (1955).

(17) E. J. Hanus and L. D. King, *J. Pharm. Sci.*, **57**, 677 (1968).

(18) P. York and N. Pilpel, *Mater. Sci. Eng.*, **12**, 295 (1973).

(19) H. E. Huber, L. B. Dale, and G. L. Christenson, *J. Pharm. Sci.*, **55**, 974 (1966).

(20) A. A. Noyes and W. R. Whitney, *J. Am. Chem. Soc.*, **19**, 930 (1897).

ACKNOWLEDGMENTS AND ADDRESSES

Received May 24, 1976, from the *Department of Pharmacy, Chelsea College of Science, University of London, Manresa Road, London, SW3 6LX, United Kingdom.*

Accepted for publication August 13, 1976.

The award to S. Esezobo of a scholarship by the Bendel State of Nigeria and financial support from ICI Pharmaceuticals Division are gratefully acknowledged.

* To whom inquiries should be directed.

Micellar Distribution Equilibria: Ultracentrifugal Study of Apparent Partition Coefficients

JUNG Y. PARK * and EDWARD G. RIPPIE *

Abstract □ Ultracentrifugation was used for the partial isolation of polysorbate 80 micelles in aqueous media to determine the apparent partition coefficients of various drug species between water and the micellar pseudophase. The ratio of solute concentration in the micelles to that in water was measured for procaine, salicylic acid, sulfapyridine, sulfisoxazole, and sodium 2-naphthalenesulfonate over ranges of pH, surfactant concentration, drug concentration, and micelle sedimentation. Apparent partition coefficients for the systems investigated were independent of both drug concentration and surfactant concentration, indicating that the mode(s) of surfactant–drug interaction are essentially invariant over the ranges of systematic variables studied. The method provides a relatively simple and rapid means of quantitatively evaluating drug–surfactant interactions above the CMC, when surfactant and solute can be assayed in mixtures without interference.

Keyphrases □ Micellar distribution—ultracentrifugal study of apparent partition coefficients of various drugs between water and micellar pseudophase □ Partition coefficients, apparent—various drugs between water and micellar pseudophase, ultracentrifugal study □ Ultracentrifugation—determination of apparent partition coefficients of various drugs between water and micellar pseudophase □ Solute–micelle interactions—ultracentrifugal study of apparent partition coefficients of various drugs between water and micellar pseudophase

Much experimental evidence relating to the mechanisms of interactions between secondary solutes and surfactant micelles is obtained from measurements of the magnitude of solute–micelle interactions and their dependence on variables such as concentration, ionic strength, temperature, and pH. Experimental techniques often introduce inherent systematic errors. Methods such as dialysis, gel filtration, and ultrafiltration, which are based on the mechanical or physicochemical isolation of the micellar pseudophase from the aqueous phase (1, 2), require the use of semipermeable membranes, selectively permeable gels, or other materials that may interact with various components and perturb the system beyond the desired separation.

The micellar isolation or separation process also may result in the destruction of the micellar structure of the surfactant system by concentrating the surfactant until it separates as a true second phase. Solute–micelle interactions also were studied extensively through the solubilization resulting from such interactions (3–6). While this latter method overcomes the problems previously mentioned, it is limited to a single thermodynamic activity for a given solute.

The analytical ultracentrifuge was used to determine the molecular weight, size, and molecular interactions of micelles (7, 8) and to determine the partition coefficients of drugs between liquid and liquid crystalline phases (9) that have been caused to separate. Ultracentrifugation offers the capability of either complete or partial micellar isolation without membranes or other added components within a reasonably short experiment time. The present paper investigates the feasibility of determining solute–micelle interactions, over a range of both solute and surfactant concentrations, using a moderate partial micelle separation by ultracentrifugation. Previously studied systems of aqueous polysorbate 80 solutions containing

all tablets decreased with their binding agent content (Fig. 10). Although this finding is similar to a previous one where povidone was substituted for gelatin (5), it is also clear that the nature of the binding agent has a profound effect on the dissolution characteristics of a formulation.

REFERENCES

(1) G. W. Brice and H. F. Hammer, *J. Am. Med. Assoc.*, **208**, 1189 (1969).

(2) D. C. Blair, R. W. Barnes, E. L. Wilder, and W. J. Murray, *ibid.*, **215** (2), 251 (1971).

(3) M. J. Groves, *Pharm. J.*, **Apr.**, 318 (1973).

(4) T. M. Jones, P. C. Risdall, and M. Frier, *J. Pharm. Pharmacol., Suppl.*, **26**, 116P (1974).

(5) A. A. Chalmers and P. H. Elworthy, *J. Pharm. Pharmacol.*, **28**, 228 (1976).

(6) S. Esezobo and N. Pilpel, *ibid.*, **28**, 8 (1976).

(7) J. G. Wagner, *J. Pharm. Sci.*, **58**, 1253 (1969).

(8) S. Kitazawa, I. Johno, Y. Ito, S. Teramura, and I. Okeda, *J. Pharm. Pharmacol.*, **27**, 765 (1975).

(9) J. T. Fell and J. M. Newton, *J. Pharm. Sci.*, **59**, 688 (1970).

(10) P. York and N. Pilpel, *J. Pharm. Pharmacol., Suppl.*, **25**, 1 (1973).

(11) G. Levy and B. A. Hayes, *N. Engl. J. Med.*, **262**, 1053 (1960).

(12) G. Levy, J. M. Antkowiak, J. A. Procknal, and D. C. White, *J. Pharm. Sci.*, **52**, 1047 (1963).

(13) J. K. C. Yen, *Can. Pharm. J.*, **97**, 439 (1964).

(14) S. Esezobo, Ph.D. thesis, University of London, London, England, (1976).

(15) S. Esezobo and N. Pilpel, *J. Pharm. Pharmacol., Suppl.*, **26**, 47P (1974).

(16) E. Nelson, L. W. Busse, and T. Higuchi, *J. Am. Pharm. Assoc., Sci. Ed.*, **44**, 223 (1955).

(17) E. J. Hanus and L. D. King, *J. Pharm. Sci.*, **57**, 677 (1968).

(18) P. York and N. Pilpel, *Mater. Sci. Eng.*, **12**, 295 (1973).

(19) H. E. Huber, L. B. Dale, and G. L. Christenson, *J. Pharm. Sci.*, **55**, 974 (1966).

(20) A. A. Noyes and W. R. Whitney, *J. Am. Chem. Soc.*, **19**, 930 (1897).

ACKNOWLEDGMENTS AND ADDRESSES

Received May 24, 1976, from the *Department of Pharmacy, Chelsea College of Science, University of London, Manresa Road, London, SW3 6LX, United Kingdom.*

Accepted for publication August 13, 1976.

The award to S. Esezobo of a scholarship by the Bendel State of Nigeria and financial support from ICI Pharmaceuticals Division are gratefully acknowledged.

* To whom inquiries should be directed.

Micellar Distribution Equilibria: Ultracentrifugal Study of Apparent Partition Coefficients

JUNG Y. PARK * and EDWARD G. RIPPIE *

Abstract □ Ultracentrifugation was used for the partial isolation of polysorbate 80 micelles in aqueous media to determine the apparent partition coefficients of various drug species between water and the micellar pseudophase. The ratio of solute concentration in the micelles to that in water was measured for procaine, salicylic acid, sulfapyridine, sulfisoxazole, and sodium 2-naphthalenesulfonate over ranges of pH, surfactant concentration, drug concentration, and micelle sedimentation. Apparent partition coefficients for the systems investigated were independent of both drug concentration and surfactant concentration, indicating that the mode(s) of surfactant–drug interaction are essentially invariant over the ranges of systematic variables studied. The method provides a relatively simple and rapid means of quantitatively evaluating drug–surfactant interactions above the CMC, when surfactant and solute can be assayed in mixtures without interference.

Keyphrases □ Micellar distribution—ultracentrifugal study of apparent partition coefficients of various drugs between water and micellar pseudophase □ Partition coefficients, apparent—various drugs between water and micellar pseudophase, ultracentrifugal study □ Ultracentrifugation—determination of apparent partition coefficients of various drugs between water and micellar pseudophase □ Solute–micelle interactions—ultracentrifugal study of apparent partition coefficients of various drugs between water and micellar pseudophase

Much experimental evidence relating to the mechanisms of interactions between secondary solutes and surfactant micelles is obtained from measurements of the magnitude of solute–micelle interactions and their dependence on variables such as concentration, ionic strength, temperature, and pH. Experimental techniques often introduce inherent systematic errors. Methods such as dialysis, gel filtration, and ultrafiltration, which are based on the mechanical or physicochemical isolation of the micellar pseudophase from the aqueous phase (1, 2), require the use of semipermeable membranes, selectively permeable gels, or other materials that may interact with various components and perturb the system beyond the desired separation.

The micellar isolation or separation process also may result in the destruction of the micellar structure of the surfactant system by concentrating the surfactant until it separates as a true second phase. Solute–micelle interactions also were studied extensively through the solubilization resulting from such interactions (3–6). While this latter method overcomes the problems previously mentioned, it is limited to a single thermodynamic activity for a given solute.

The analytical ultracentrifuge was used to determine the molecular weight, size, and molecular interactions of micelles (7, 8) and to determine the partition coefficients of drugs between liquid and liquid crystalline phases (9) that have been caused to separate. Ultracentrifugation offers the capability of either complete or partial micellar isolation without membranes or other added components within a reasonably short experiment time. The present paper investigates the feasibility of determining solute–micelle interactions, over a range of both solute and surfactant concentrations, using a moderate partial micelle separation by ultracentrifugation. Previously studied systems of aqueous polysorbate 80 solutions containing

Table I—pH Values and Mean Concentrations of Solute and Polysorbate 80 in Solutions Studied

Solute	Concentration of Solute, % (w/w)	Concentration of Polysorbate 80, % (w/w)	pH
Procaine	0.1, 0.01	1, 2, 4	7.7, 7.9, 8.2, 8.7, 9.5
Salicylic acid	0.1, 0.01	1, 2, 4	2.0, 2.2, 2.6, 3.6, 3.8
Sulfapyridine	0.01, 0.001	1, 2, 4	7.7, 7.9, 8.2, 8.7, 9.5
Sulfisoxazole	0.01, 0.001	1, 2, 4	4.7, 4.9, 5.2, 5.7, 6.5
Sodium naphthalenesulfonate	0.2, 0.02, 0.002	1, 2, 4	7.0

procaine, salicylic acid, sulfapyridine, sulfisoxazole, and sodium 2-naphthalenesulfonate were selected.

DATA TREATMENT

Various separate and distinct modes of solute–micelle interaction occur, including adsorption onto the micelle surface, penetration into the palisade layer of nonionic micelles, and dissolution in the fluid hydrocarbon central core. No attempt is made here to imply or otherwise define the particular mechanisms operating, but the solute–micelle association is treated as a partition phenomenon having an associated apparent partition coefficient. The appropriateness of this simple pseudophase model was discussed (1), and it serves as a useful approximation if contributions to micellar free energy from changes in solvent are small and if the micelles are essentially noninteracting. That these conditions are met is evidenced by the independence of the apparent partition coefficients on surfactant concentration. Further assumptions and approximations implicit in the pseudophase model were discussed by Mukerjee (10).

Consider an aqueous micellar solution of a nonionic surfactant containing a second solute partitioned between the water and the micellar pseudophase. After a suitable period of ultracentrifugation, a higher concentration of the more dense micelles exists in the lower (outer) portion of the centrifuge tube as opposed to the upper portion. By assuming that there is no change in the system other than the induced micellar concentration gradient, a resultant concentration gradient of the associated partitioning solute can be predicted.

If, following centrifugation, the contents of the centrifuge tube are separated into upper and lower portions, which are subsequently mixed individually to ensure their homogeneity, the following expressions can be written for X and Y, which are solute concentrations in grams per milliliter in the upper and lower portions, respectively:

$$X = (U/\rho)[(HA) + (A^-)] + (1 - U/\rho)[[HA] + [A^-]] \quad \text{(Eq. 1)}$$

$$Y = (L/\rho)[(HA) + (A^-)] + (1 - L/\rho)[[HA] + [A^-]] \quad \text{(Eq. 2)}$$

where U and L represent surfactant concentrations in grams per milliliter in the upper and lower portions, respectively, and ρ is the micellar density in grams per milliliter. The equations are derived for weakly acidic solutes whose free acid, HA, and conjugate base, A^-, concentrations in grams per milliliter are denoted by ( ) and [ ] in the micellar and aqueous pseudophases, respectively. The first terms on the right in Eqs. 1 and 2 represent the micelle associated solute in 1 ml of aqueous micellar solution, whereas the second terms represent the aqueous solute in the same 1 ml of solution. These expressions can be written in terms of the apparent acid dissociation constant of the solute, K_a, and the solute's apparent partition coefficients, $K_1 = (HA)/[HA]$ and $K_2 = (A^-)/[A^-]$, in its free acid and conjugate base forms:

$$[H^+]\rho X = U[HA][K_1[H^+] + K_2K_a] + (\rho - U)[HA][[H^+] + K_a] \quad \text{(Eq. 3)}$$

$$[H^+]\rho Y = L[HA][K_1[H^+] + K_2K_a] + (\rho - L)[HA][[H^+] + K_a] \quad \text{(Eq. 4)}$$

Combining Eqs. 3 and 4 to eliminate [HA] yields the following expression relating K_1 and K_2 to experimentally measurable quantities:

$$[H^+]K_1 + K_2K_a = ([H^+] + K_a)\left[1 - \frac{\rho(X - Y)}{(XL - YU)}\right] \quad \text{(Eq. 5)}$$

A plot of the expression on the right of Eq. 5 *versus* $[H^+]$ yields a straight line with slope K_1 and intercept K_2K_a. For weakly basic drugs, the following definitions apply to Eq. 5: $K_a = K_w/K_b$, $K_1 = (BH^+)/[BH^+]$, and $K_2 = (B)/[B]$.

Application of Eq. 5 requires that the stoichiometric concentrations of both the surfactant and the partitioning solute be determined. The concentration of micellar surfactant was taken to be equal to its stoichiometric concentration since the critical micelle concentration (CMC) of polysorbate 80 is approximately $1.0–6.2 \times 10^{-3}$% (w/v) (3, 11–14) and can be neglected at the surfactant concentrations studied. The density, ρ, of the polysorbate 80 micelles was taken as 1.11 (11), and the K_a values (moles per liter) employed are: procaine, 1.40×10^{-9}; salicylic acid, 1.06×10^{-3}; sulfapyridine, 3.60×10^{-9}; and sulfisoxazole, 7.60×10^{-6}. Slopes and intercepts of data plotted in accordance with Eq. 5 were obtained by the method of least squares, and their standard deviations were estimated from an analysis of variance of the experimental data points.

EXPERIMENTAL

Centrifugation—Aliquots, 10 ml, of aqueous solutions containing the desired concentrations of polysorbate 80[1] and the secondary solutes were centrifuged at 25° for 10 hr in an ultracentrifuge[2] at 40,000 rpm in cellulose nitrate tubes. The tubes were then cut in half with a tube slicer, and the upper and lower samples were assayed to determine the polysorbate 80 and partitioning solute concentrations. The period of centrifugation was selected to give an approximately 40% separation of micelles and was a fraction of the time required to reach sedimentation equilibrium. This degree of separation was sufficient to provide suitable sensitivity for the method and yet not great enough to alter micellar properties significantly.

The solutes investigated were procaine hydrochloride[3], salicylic acid[4], sulfapyridine[5], sulfisoxazole[5], and sodium 2-naphthalenesulfonate[6]. All other chemicals were reagent grade and were used as received without further purification. Solutions were prepared by dissolving measured quantities of polysorbate 80 and the various drugs in double-distilled water, diluting to 90% of volume, adjusting the pH to the desired values with either hydrochloric acid or sodium hydroxide solutions, and diluting to volume. The pH's were checked in all cases following centrifugation and did not change.

Polysorbate 80 Assay—Polysorbate 80 was assayed in the presence of the solubilized drugs by the method of Cucakovich (15), based on the formation of a complex between the amylose fraction of potato starch and polysorbate 80. That portion of the starch added in excess and not complexed with polysorbate combined quantitatively with iodine to form a blue amylose–iodine complex. The blue color was determined spectrophotometrically[7] at 680 nm, and the procedure gave good results without interference by the solubilized drugs present.

Secondary Solute Assays—Following centrifugation of the micellar polysorbate 80–drug solutions, samples of the upper and lower fractions were diluted with 95% ethyl alcohol to appropriate concentrations of drug and assayed spectrophotometrically[7] for drug content. The presence of polysorbate 80 did not interfere with the assays conducted at the following wavelength maxima: procaine, 288 nm; salicylic acid, 298 nm; and sulfapyridine and sulfisoxazole, 260 nm.

The assay for sodium 2-naphthalenesulfonate was performed fluorometrically[8] at an excitation wavelength of 280 nm and an emission wavelength of 340 nm following dilution of the centrifuged samples with water to a concentration of approximately 1 μg/ml at pH 7. No interference by polysorbate 80 was observed, and the same calibration curve was used with all surfactant concentrations.

RESULTS AND DISCUSSION

Distribution measurements were made at several concentrations of the surfactant and of the various drugs at a number of pH values. Table I summarizes the scope of these experimental variables. The good linearity of data plotted in accordance with Eq. 5 is apparent from Fig. 1, for 0.01% solutions of procaine and sulfapyridine in 1% polysorbate 80, and is typical of all systems studied.

[1] Polyoxyethylene (20) sorbitan monooleate, Tween 80, Atlas Chemical Industries, Wilmington, Del.
[2] Model L2-65B, Beckman Instruments, Palo Alto, Calif.
[3] Matheson, Coleman and Bell, Milwaukee, Wis.
[4] Fisher Scientific Co., Pittsburgh, Pa.
[5] Sigma Chemical Co., St. Louis, Mo.
[6] Eastman Chemical Co., Rochester, N.Y.
[7] Hitachi model 139 spectrophotometer.
[8] Aminco-Bowman spectrophotofluorometer.

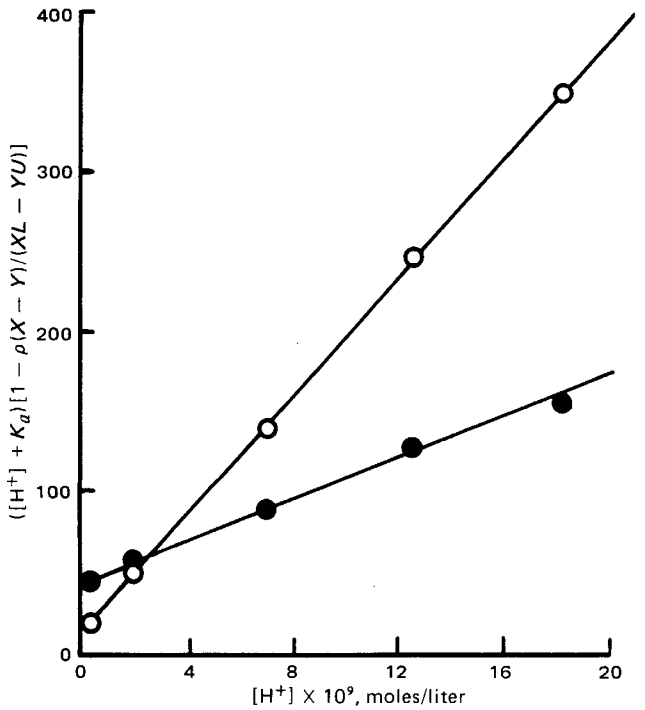

Figure 1—*Relationship of solute distribution data to hydrogen-ion concentration for 0.01% (w/w) procaine and sulfapyridine in 1% (w/w) polysorbate 80 plotted according to Eq. 5. Key: ●, procaine; and ○, sulfapyridine.*

Apparent partition coefficients for the weakly acidic and basic drugs and their conjugate forms are listed in Table II together with their estimated standard deviations and the corresponding linear correlation coefficients, r, of the various plots. No significant difference was found between the apparent partition coefficients of any given drug or its conjugate acid or base over the range of drug or surfactant concentrations studied. This observation is consistent with the assumption, made in deriving Eq. 5, that the nature of the micelles would not be measurably altered by the concentration differences induced by centrifugation.

Apparent partition coefficients of the free drugs reported here are approximately 50–60% of those previously reported or estimated from the literature (5, 6, 16). Also, micellar association with procaine ion (5) and with salicylate ion (2, 6) occurred, in contrast to previous reports. However, these findings should be considered in light of the rather large drug concentration differences and temperature and ionic strength differences used in these methods.

Implicit in the present method is the assumption that ultracentrifugation does not significantly alter the chemical potential of molecular solutes at various levels within the centrifuge tube. For incompressible solutions of neutral molecules, the chemical potential at equilibrium, u_i, is given as a function of angular velocity, ω, radial distance, r, and molecular weight, M_i (17), as:

$$d\bar{u}_i/dr = du_i/dr - M_i\omega^2 r = 0 \qquad \text{(Eq. 6)}$$

The magnitude of centrifugal effects is small for low molecular weight solutes. Furthermore, the apparent average molecular weight of association colloids can be assumed to be a function only of the monomer activity; therefore, the apparent average molecular weight *versus* monomer concentration curve is independent of the rotor speeds and solution depths at which various monomer concentrations occur.

A Donnan effect may occur when a concentration gradient is induced in a charged species in a solution where no such gradient is induced in other diffusible ions. While this effect is commonly observed when a polyelectrolyte in solution is excluded from a second solution by a semipermeable membrane, it also results from the centrifugal induction of a concentration gradient of micelles containing associated charged species. The expression:

$$K_2 = \frac{\rho([A^-]_u^2 - [A^-]_l^2)}{L[A^-]_u^2 - U[A^-]_l^2} \qquad \text{(Eq. 7)}$$

holds for the apparent partition coefficient of a negatively charged species, A^-, between water and nonionic surfactant micelles where subscripts u and l denote upper and lower fractions of the centrifuged solution. Equation 7 requires that $[A^-]_u < [A^-]_l$, a condition not assumed in the derivation of Eq. 5. Neglect of the Donnan effect will diminish the magnitude of the calculated value of K_2.

The effect of a swamping electrolyte on the apparent partition coefficient, K, of sodium 2-naphthalenesulfonate between water and polysorbate 80 micelles was determined by the addition of potassium chloride to the micellar solutions prior to centrifugation. Results of measurements at several concentration combinations of polysorbate and naphthalenesulfonate are presented in Table III. Calculations of K were made with the use of:

$$K = 1 - \frac{\rho(X - Y)}{(XL - YU)} \qquad \text{(Eq. 8)}$$

which is a limiting form of Eq. 5 and applies where only charged solute species exist. Results compare favorably with those reported using dialysis (2). No attempts were made to adjust K_2 values for Donnan effects, since such calculations would require an exact knowledge of the micellar concentration profile within the centrifuge tube.

Table II—Apparent Partition Coefficients of Solutes between Polysorbate 80 Micelles and Water

Solute, % (w/w)	Polysorbate 80, % (w/w)	$K_1 \pm SD$	$K_2 \pm SD$	r
		Procaine		
0.1	1	7.0 ± 0.2	29.2 ± 1.5	0.9988
0.1	2	7.0 ± 0.1	28.9 ± 0.7	0.9997
0.1	4	7.0 ± 0.1	28.8 ± 0.9	0.9995
0.01	1	6.4 ± 0.3	30.2 ± 2.2	0.9969
0.01	2	6.6 ± 0.3	29.2 ± 1.9	0.9977
0.01	4	6.9 ± 0.2	28.9 ± 1.1	0.9993
		Salicylic Acid		
0.1	1	57.3 ± 2.9	24.0 ± 14.7	0.9924
0.1	2	57.6 ± 2.7	23.6 ± 13.9	0.9967
0.1	4	57.6 ± 2.8	24.0 ± 14.3	0.9964
0.01	1	56.3 ± 3.8	21.6 ± 19.5	0.9932
0.01	2	56.4 ± 3.2	26.6 ± 16.4	0.9952
0.01	4	56.4 ± 2.5	33.8 ± 12.6	0.9972
		Sulfapyridine		
0.01	1	18.5 ± 0.4	4.0 ± 1.2	0.9992
0.01	2	18.6 ± 0.5	3.8 ± 1.4	0.9991
0.01	4	19.0 ± 0.6	3.2 ± 1.8	0.9984
0.001	1	18.9 ± 0.6	2.8 ± 1.9	0.9983
0.001	2	18.8 ± 0.6	3.6 ± 1.7	0.9985
0.001	4	18.8 ± 0.6	3.6 ± 1.7	0.9986
		Sulfisoxazole		
0.01	1	79.0 ± 2.0	14.5 ± 2.7	0.9991
0.01	2	79.4 ± 2.3	13.8 ± 3.2	0.9987
0.01	4	79.2 ± 2.2	14.3 ± 3.0	0.9989
0.001	1	78.5 ± 2.0	15.0 ± 2.7	0.9991
0.001	2	77.8 ± 2.1	15.2 ± 2.9	0.9989
0.001	4	78.9 ± 1.7	15.6 ± 2.3	0.9993

Table III—Apparent Partition Coefficients of Sodium 2-Naphthalenesulfonate between Polysorbate 80 Micelles and Water[a]

Sulfonate, % (w/w)	Polysorbate 80, % (w/w)	Potassium Chloride, moles/liter	K
0.2	1	0	4.1
0.2	1	0.1	8.8
0.2	1	0.2	13.9
0.2	2	0	4.6
0.2	2	0.1	8.5
0.2	2	0.2	13.4
0.2	4	0	4.6
0.2	4	0.1	8.6
0.2	4	0.2	13.5
0.02	2	0	4.3
0.02	2	0.1	8.8
0.02	2	0.2	13.1
0.002	2	0	4.4
0.002	2	0.1	8.7
0.002	2	0.2	12.8

[a] All solutions were adjusted to pH 7.

SUMMARY

The study of micelle–solute interactions by means of partial ultracentrifugal separations of the micellar components offers some possible advantages over other procedures. It permits relatively rapid separations, which are advantageous when solutes are unstable chemically, and avoids the use of membranes or other added materials for the purpose of micelle isolation. Moreover, flexibility in the choice of systems is essentially limited only by the need to assay both the micellar and secondary solute components. While the data were treated in terms of a nonspecific partitioning model in the present paper, the general approach is equally compatible with various adsorption, specific site, or other models of micelle–solute interactions.

REFERENCES

(1) S. J. Dougherty and J. C. Berg, *J. Colloid Interface Sci.*, **48**, 110 (1974).

(2) A. R. Hurwitz, P. P. DeLuca, and H. B. Kostenbauder, *J. Pharm. Sci.*, **52**, 893 (1963).

(3) M. J. Schick, "Nonionic Surfactants," Dekker, New York, N.Y., 1967.

(4) C. J. Kern and T. Antoshkiw, *Ind. Eng. Chem.*, **42**, 709 (1950).

(5) E. G. Rippie, D. J. Lamb, and P. W. Romig, *J. Pharm. Sci.*, **53**, 1346 (1964).

(6) J. H. Collett and R. Withington, *J. Pharm. Pharmacol.*, **24**, 211 (1972).

(7) J. Kirschbaum, *J. Pharm. Sci.*, **63**, 981 (1974).

(8) A. J. Richard, *ibid.*, **64**, 873 (1975).

(9) S. Friberg and L. Larsson, *ibid.*, **64**, 822 (1975).

(10) P. Mukerjee, *ibid.*, **63**, 972 (1974).

(11) B. Farhadieh, *ibid.*, **62**, 1685 (1973).

(12) S. G. Bjaastad, N. A. Hall, and A. L. Thakkar, *ibid.*, **54**, 1529 (1965).

(13) L. S. C. Wan and P. F. S. Lee, *ibid.*, **63**, 136 (1974).

(14) M. R. U. Paruta and L. D. King, *ibid.*, **53**, 1217 (1964).

(15) N. B. Cucakovich, *Anal. Biochem.*, **40**, 183 (1971).

(16) A. A. Ismail, M. W. Gouda, and M. M. Motawi, *J. Pharm. Sci.*, **59**, 220 (1970).

(17) J. W. Williams, "Ultracentrifugation of Macromolecules," Academic, New York, N.Y., 1972, pp. 41, 83.

ACKNOWLEDGMENTS AND ADDRESSES

Received June 14, 1976, from the *Department of Pharmaceutics, College of Pharmacy, University of Minnesota, Minneapolis, MN 55455.*

Accepted for publication August 17, 1976.

Abstracted from a thesis submitted by J. Y. Park to the University of Minnesota in partial fulfillment of the Master of Science degree requirements.

* Present address: College of Pharmacy, University of Michigan, Ann Arbor, MI 48104.

[x] To whom inquiries should be directed.

Physicochemical Properties of β-Lactam Antibacterials: Deuterium Solvent Isotope Effect on Penicillin G Degradation Rate

TSUKINAKA YAMANA [x], AKIRA TSUJI, EMI KIYA, and ETSUKO MIYAMOTO

Abstract □ To obtain kinetic evidence on the degradation mechanism of penicillin in aqueous solution, degradation rates of penicillin G in water and deuterium oxide were measured in the pH (pD) range of 4–10. The solvent isotope effect (k^{H_2O}/k^{D_2O}) of 1.53 below pH (pD) 6 supports the mechanism of water-catalyzed rearrangement of undissociated penicillin G to benzylpenicillenic acid. The spontaneous degradation at neutral pH (pD) and the hydroxide-ion-catalyzed degradation in the alkaline pH (pD) range progress with a deuterium solvent isotope effect (k^{H_2O}/k^{D_2O}) of 4.5 and 0.59, respectively. This finding indicates the mechanisms of general base-catalyzed hydrolysis by water in the neutral pH range and of nucleophilic attack of the hydroxide ion on the β-lactam in the alkaline pH range. No significant side-chain dependency was observed in the reaction of penicillins with bases. The solvent isotope studies led to the conclusion that penicillin degradation is catalyzed by a series of bases *via* general base-catalyzed and nucleophilic mechanisms, depending on their basicity.

Keyphrases □ Penicillin G—degradation in aqueous solution, deuterium solvent isotope effect, pH 4–10 □ Degradation—penicillin G in aqueous solution, deuterium solvent isotope effect, pH 4–10 □ Deuterium oxide—solvent isotope effect on penicillin G degradation in aqueous solution, pH 4–10 □ Antibacterials—penicillin G, degradation in aqueous solution, deuterium solvent isotope effect, pH 4–10

Although the stability of penicillins in aqueous solution has been studied (1–14), little work has been done on their mechanism of degradation.

Interest in the degradation of penicillin in acid and neutral solutions has been stimulated by the suggestion that its degradative product, penicillenic acid, rather than penicillin itself, may be responsible for allergic reactions[1]. During the degradation of penicillin G at a physiological pH of 7.5, the solution slowly gave rise to both benzylpenicilloic acid and benzylpenicillenic acid (15, 16). Levine (15, 16) suggested that the formation of benzylpenicilloic acid proceeded by way of benzylpenicillenic acid as an intermediate, because the latter compound was converted rapidly into the former with a half-life of 6.5 min at pH 7.5 and 37° (17).

Furthermore, some investigators (18, 19) assumed that higher sensitivity of the β-lactam ring in penicillin molecules relative to that of simple β-lactams to hydroxide-ion-catalyzed degradation can be attributed in part to the intramolecular attack of the side-chain amide on the β-lactam moiety. These two hypotheses (15–19) recently were criticized (13, 20) on the basis of kinetic observations, although the mechanism of degradation in neutral and alkaline solutions is not completely understood.

The present study was undertaken to obtain kinetic

[1] The chemical aspects involved in penicillin allergy were reviewed by M. A. Schwartz, *J. Pharm. Sci.*, **58**, 643 (1969).

SUMMARY

The study of micelle–solute interactions by means of partial ultracentrifugal separations of the micellar components offers some possible advantages over other procedures. It permits relatively rapid separations, which are advantageous when solutes are unstable chemically, and avoids the use of membranes or other added materials for the purpose of micelle isolation. Moreover, flexibility in the choice of systems is essentially limited only by the need to assay both the micellar and secondary solute components. While the data were treated in terms of a nonspecific partitioning model in the present paper, the general approach is equally compatible with various adsorption, specific site, or other models of micelle–solute interactions.

REFERENCES

(1) S. J. Dougherty and J. C. Berg, *J. Colloid Interface Sci.*, **48**, 110 (1974).

(2) A. R. Hurwitz, P. P. DeLuca, and H. B. Kostenbauder, *J. Pharm. Sci.*, **52**, 893 (1963).

(3) M. J. Schick, "Nonionic Surfactants," Dekker, New York, N.Y., 1967.

(4) C. J. Kern and T. Antoshkiw, *Ind. Eng. Chem.*, **42**, 709 (1950).

(5) E. G. Rippie, D. J. Lamb, and P. W. Romig, *J. Pharm. Sci.*, **53**, 1346 (1964).

(6) J. H. Collett and R. Withington, *J. Pharm. Pharmacol.*, **24**, 211 (1972).

(7) J. Kirschbaum, *J. Pharm. Sci.*, **63**, 981 (1974).

(8) A. J. Richard, *ibid.*, **64**, 873 (1975).

(9) S. Friberg and L. Larsson, *ibid.*, **64**, 822 (1975).

(10) P. Mukerjee, *ibid.*, **63**, 972 (1974).

(11) B. Farhadieh, *ibid.*, **62**, 1685 (1973).

(12) S. G. Bjaastad, N. A. Hall, and A. L. Thakkar, *ibid.*, **54**, 1529 (1965).

(13) L. S. C. Wan and P. F. S. Lee, *ibid.*, **63**, 136 (1974).

(14) M. R. U. Paruta and L. D. King, *ibid.*, **53**, 1217 (1964).

(15) N. B. Cucakovich, *Anal. Biochem.*, **40**, 183 (1971).

(16) A. A. Ismail, M. W. Gouda, and M. M. Motawi, *J. Pharm. Sci.*, **59**, 220 (1970).

(17) J. W. Williams, "Ultracentrifugation of Macromolecules," Academic, New York, N.Y., 1972, pp. 41, 83.

ACKNOWLEDGMENTS AND ADDRESSES

Received June 14, 1976, from the *Department of Pharmaceutics, College of Pharmacy, University of Minnesota, Minneapolis, MN 55455.*

Accepted for publication August 17, 1976.

Abstracted from a thesis submitted by J. Y. Park to the University of Minnesota in partial fulfillment of the Master of Science degree requirements.

* Present address: College of Pharmacy, University of Michigan, Ann Arbor, MI 48104.

[x] To whom inquiries should be directed.

Physicochemical Properties of β-Lactam Antibacterials: Deuterium Solvent Isotope Effect on Penicillin G Degradation Rate

TSUKINAKA YAMANA [x], AKIRA TSUJI, EMI KIYA, and ETSUKO MIYAMOTO

Abstract □ To obtain kinetic evidence on the degradation mechanism of penicillin in aqueous solution, degradation rates of penicillin G in water and deuterium oxide were measured in the pH (pD) range of 4–10. The solvent isotope effect (k^{H_2O}/k^{D_2O}) of 1.53 below pH (pD) 6 supports the mechanism of water-catalyzed rearrangement of undissociated penicillin G to benzylpenicillenic acid. The spontaneous degradation at neutral pH (pD) and the hydroxide-ion-catalyzed degradation in the alkaline pH (pD) range progress with a deuterium solvent isotope effect (k^{H_2O}/k^{D_2O}) of 4.5 and 0.59, respectively. This finding indicates the mechanisms of general base-catalyzed hydrolysis by water in the neutral pH range and of nucleophilic attack of the hydroxide ion on the β-lactam in the alkaline pH range. No significant side-chain dependency was observed in the reaction of penicillins with bases. The solvent isotope studies led to the conclusion that penicillin degradation is catalyzed by a series of bases *via* general base-catalyzed and nucleophilic mechanisms, depending on their basicity.

Keyphrases □ Penicillin G—degradation in aqueous solution, deuterium solvent isotope effect, pH 4–10 □ Degradation—penicillin G in aqueous solution, deuterium solvent isotope effect, pH 4–10 □ Deuterium oxide—solvent isotope effect on penicillin G degradation in aqueous solution, pH 4–10 □ Antibacterials—penicillin G, degradation in aqueous solution, deuterium solvent isotope effect, pH 4–10

Although the stability of penicillins in aqueous solution has been studied (1–14), little work has been done on their mechanism of degradation.

Interest in the degradation of penicillin in acid and neutral solutions has been stimulated by the suggestion that its degradative product, penicillenic acid, rather than penicillin itself, may be responsible for allergic reactions[1]. During the degradation of penicillin G at a physiological pH of 7.5, the solution slowly gave rise to both benzylpenicilloic acid and benzylpenicillenic acid (15, 16). Levine (15, 16) suggested that the formation of benzylpenicilloic acid proceeded by way of benzylpenicillenic acid as an intermediate, because the latter compound was converted rapidly into the former with a half-life of 6.5 min at pH 7.5 and 37° (17).

Furthermore, some investigators (18, 19) assumed that higher sensitivity of the β-lactam ring in penicillin molecules relative to that of simple β-lactams to hydroxide-ion-catalyzed degradation can be attributed in part to the intramolecular attack of the side-chain amide on the β-lactam moiety. These two hypotheses (15–19) recently were criticized (13, 20) on the basis of kinetic observations, although the mechanism of degradation in neutral and alkaline solutions is not completely understood.

The present study was undertaken to obtain kinetic

[1] The chemical aspects involved in penicillin allergy were reviewed by M. A. Schwartz, *J. Pharm. Sci.*, **58**, 643 (1969).

Table I—Rate Constants [a] and pKa Values Determined for the Degradation of Penicillin G in Water and Deuterium Oxide at 0.5 Ionic Strength

Solvent	Temperature	k_0, hr^{-1}	$10^3 k_0'$, hr^{-1}	$10^{-3} k'_{OH}$ [b], $M^{-1} hr^{-1}$	pKa
Water	35°	3.41	0.90	1.19	2.80[c]
Water	60°	37.4	7.20	5.39	2.78[d]
Deuterium oxide	60°	24.5	1.60	9.12	3.24[c]

[a] Based on the kinetic expression of Eq. 1. [b] Calculated using the autoprotolytic constant: $K_w = 2.09 \times 10^{-14}$ at 35° and $K_w = 9.61 \times 10^{-14}$ at 60° (31); $K_{D2O} = 1.36 \times 10^{-14}$ at 60°, which was extrapolated from the data of Corington *et al.* (32) by the least-squares curve-fitting method. [c] Determined potentiometrically. [d] Reference 7.

evidence on the degradation mechanism of penicillin and to consider possible ways of stabilizing penicillins in aqueous solution. The rates of degradation of penicillin G as a model penicillin were measured in buffered and unbuffered deuterium oxide solutions.

EXPERIMENTAL

Materials—Penicillin G potassium[2], cloxacillin sodium[2], ampicillin sodium[3], and cyclacillin[3] were used as supplied. All other chemicals were the highest commercial grades available. Double-distilled water was used.

Kinetic Procedures—Degradation was initiated by the addition of a known weight of penicillin to a buffer solution preheated to the desired temperature. Aliquots of the solution were withdrawn at suitable time intervals. Unless otherwise stated, the residual penicillin concentration was analyzed by the modified iodometric method (7). In most cases, the initial concentration of penicillin was 5×10^{-3} *M*. The pseudo-first-order rate constants, k_{obs}, were calculated by linear regression analysis of a plot of the logarithm of the penicillin concentration against time.

The rate constants of penicillin G corresponding to those in unbuffered solution of water (k_{pH}) and deuterium oxide (k_{pD}) were determined by the two methods: (*a*) by extrapolation of a plot of k_{obs} *versus* buffer total concentration to zero concentration at constant pH (pD) or by direct determination from analysis of the solution whose pH was maintained constant with the aid of a pH-stat[4], and (*b*) by following the rate of acid formation on a pH-stat. The rate constants were calculated from Guggenheim plots of recorded curves of the volume of titrant [standard 0.01–0.1 *N* NaOH (NaOD) solution whose ionic strength was adjusted to 0.5 with potassium chloride] as a function of time.

In the pH-stat experiments, edetate disodium was added to a final concentration of 5×10^{-4} *M* to avoid occasional erratic results, apparently due to heavy metal-catalyzed decomposition. The concentration of penicillin G was in the range of $5–10 \times 10^{-3}$ *M*.

Unless otherwise stated, kinetic experiments were conducted at 35 or 60° and at a constant ionic strength of 0.5 adjusted with potassium chloride. The pH (pD) of a kinetic solution was measured[5] both before and at the end of the experiments. Where the buffer capacity was too low, constant pH was maintained by a pH-stat. When using deuterium oxide as a solvent, the pD values were taken as the pH meter reading plus the electrode correction of 0.25 at 60° (21).

pKa Determination—The pKa of penicillin G in deuterium oxide at 60° and $\mu = 0.5$ was determined in the manner described by Finholt *et al.* (7). The pKa values of conjugated acids of oxygen bases and amines were determined by the method of half-neutralization.

RESULTS AND DISCUSSION

Degradation Pathway and Mechanism—Figure 1 shows the rate constants, k_{pH}, of penicillin G degradation at 35 and 60° as a function of pH in water. Above pH 4, this degradation is known to obey the following rate law (5, 7, 13):

$$k_{pH} = k_0 \frac{a_{H^+}}{K_a + a_{H^+}} + (k_0' + k'_{OH}\text{-}K_w/a_{H^+}) \frac{K_a}{K_a + a_{H^+}} \quad \text{(Eq. 1)}$$

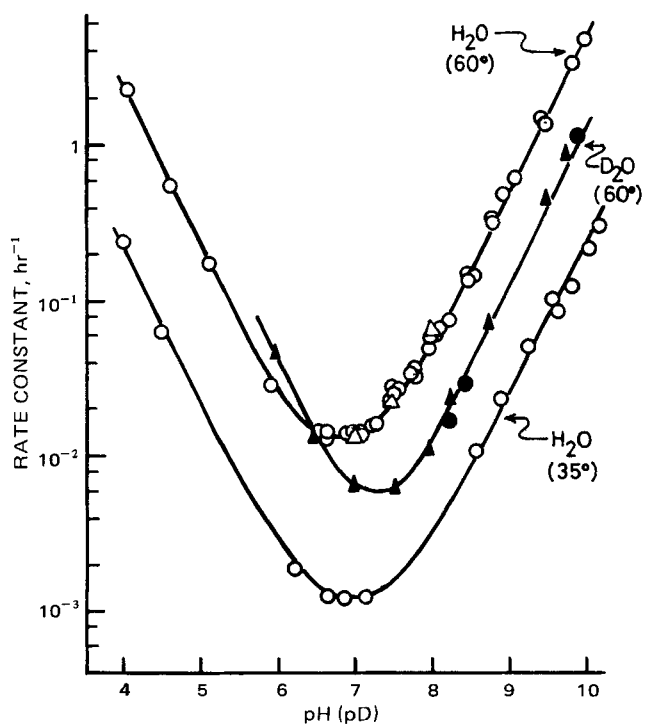

Figure 1—*Log k–pH (pD) profiles for the degradation of penicillin G in water (○, △) and in deuterium oxide (●, ▲) at 35 and 60° and 0.5 ionic strength. Triangles and circles refer to the data determined by the pH-stat alkalimetric titration and iodometric methods, respectively.*

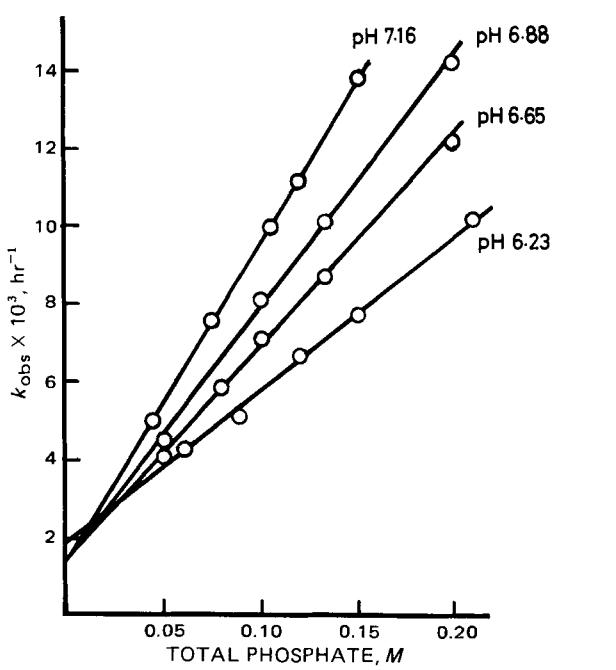

Figure 2—*Plots of pseudo-first-order rate constants* versus *total phosphate concentration for the degradation of penicillin G in aqueous solution at 35° and 0.5 ionic strength.*

[2] Meiji Seika Kaisha, Ltd., Tokyo, Japan.
[3] Takeda Chemical Ind., Ltd., Osaka, Japan.

[4] Radiometer pH-stat titrimeter assembly consisting of TTT2 titrator, SBR3 titrigraph, and ABU12b autoburet or TTT11 titrator, PHM26 pH meter, SBR3 titrigraph, and ABU12b autoburet.
[5] Radiometer PHM26 pH meter or TTT2 titrator.

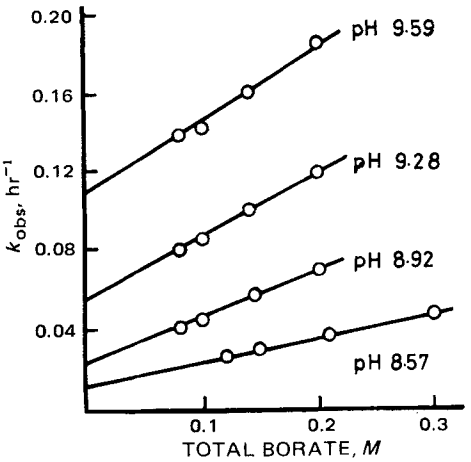

Figure 3—*Plots of pseudo-first-order rate constants* versus *total borate concentration for the degradation of penicillin G in aqueous solution at 35° and 0.5 ionic strength.*

where K_a is the dissociation constant of penicillin G; K_w is the autoprotolysis constant for water; a_{H^+} is the hydrogen-ion activity as determined by the glass electrode; k_0 and k_0' represent the spontaneous or water-catalyzed degradation rate of undissociated and ionized penicillin G, respectively; and k'_{OH^-} is the second-order rate constant for the hydroxide-ion-catalyzed degradation of ionized penicillin G. In the experimental pH region, acid-catalyzed degradation of undissociated penicillin G can be neglected, since such a reaction is only significant below pH 2 (1, 5). The specific rate constants and the dissociation constant are listed in Table I. These values at 60° are in good agreement with those reported by Finholt *et al.* (7).

The rates in deuterium oxide were also determined in the same way as in water. The log k_{pD}–pD profile at 60° is shown in Fig. 1, and the various specific rate constants corresponding to those in water and the pKa value are given in Table I. Above pH (pD) 7, the rates in water were about five times faster than those in deuterium oxide; below pH (pD) 6, the rates in deuterium oxide were about twice those in water.

The k'_{OH^-}/k'_{OD^-} ratio (Table I) was 0.59, consistent with the expected kinetic isotope effect for the reaction involving nucleophilic attack of OH^- and OD^- on the carbonyl carbon of carboxylic acid derivatives (22). The lack of a significant side-chain dependency on k'_{OH^-} (13, 23–25) and the present results led to the conclusion that the 10^4-fold higher reactivity of penicillins toward hydroxide-ion attack compared with that of monocyclic β-lactam and ordinary amides is not primarily due to an intramolecular participation effect as suggested (18, 19) but exclusively due to the strained fused-ring β-lactam and/or to a suppression of the usual amide resonance resulting from the nonplanarity of the β-lactam nitrogen atom.

The reaction below pH 6 is attributed to the spontaneous degradation of unionized penicillin G or the kinetically equivalent hydrogen-ion-

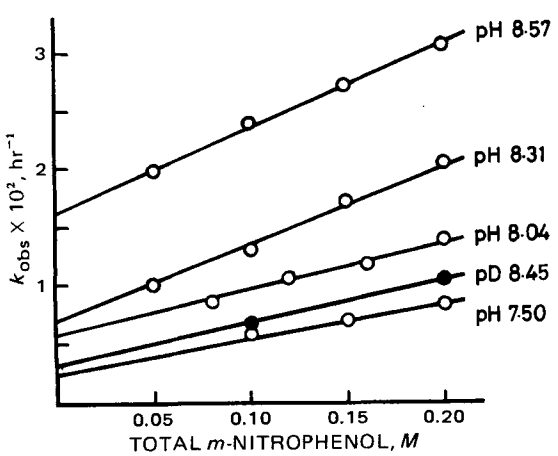

Figure 4—*Plots of pseudo-first-order rate constants* versus *total m-nitrophenol concentration for the degradation of penicillin G in water (○) and deuterium oxide (●, 50% free base) at 60° and 0.5 ionic strength.*

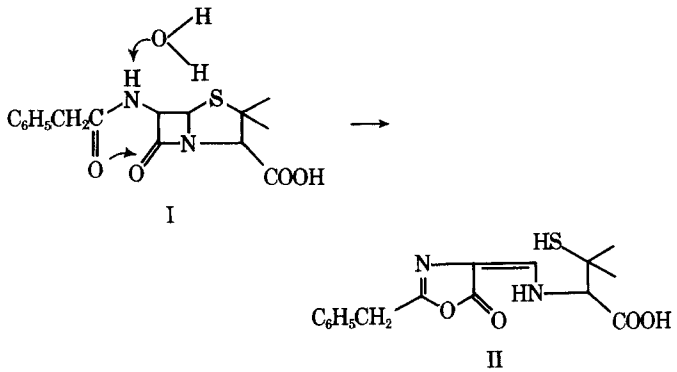

Scheme I

catalyzed degradation of its ionized form. The observed solvent isotope effect of 1.53 for $k_0^{H_2O}/k_0^{D_2O}$ is consistent with the former reaction mechanism favored by Finholt *et al.* (7) and Yamana *et al.* (13) on the basis of the kinetic observation of little ionic strength effect in the pH 4–6 region. However, a more plausible mechanism would be water-catalyzed rearrangement of undissociated penicillin G (I) to benzylpenicillenic acid (II) (Scheme I).

The proposed mechanism should give the expected solvent isotope effect of $1 < k^{H_2O}/k^{D_2O} < 2.5$. A value of 1.53 is not totally consistent with water attack on the β-lactam ring to afford the penicilloic acid (III) (Scheme II, k^{H_2O}/k^{D_2O} expected to be >2.2) or with direct attack of the neighboring acylamide oxygen on the β-lactam ring to produce the penicillenic acid (II) (Scheme III, expected isotope effect of 1.0). The other two kinetically undistinguishable mechanisms, hydrogen-ion-catalyzed rearrangement of ionized penicillin G to benzylpenicillenic acid (Scheme IV) and attack of water on the protonated β-lactam moiety (Scheme V),

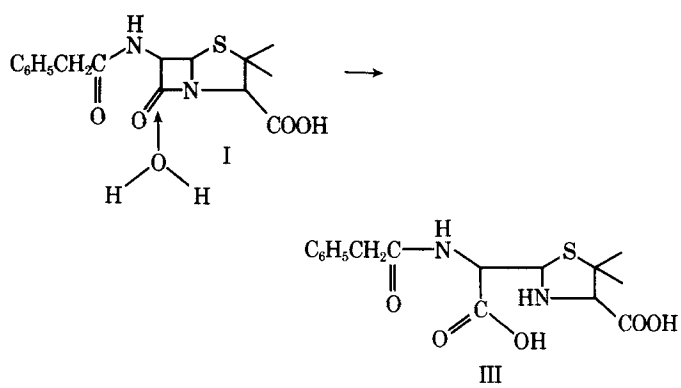

Scheme II

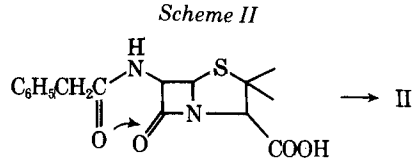

Scheme III

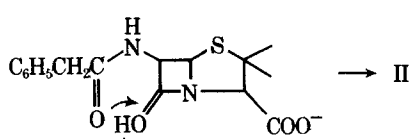

Scheme IV

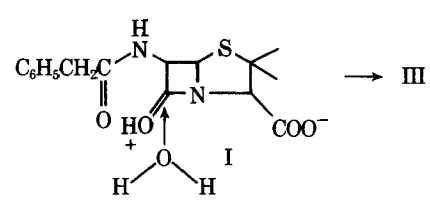

Scheme V

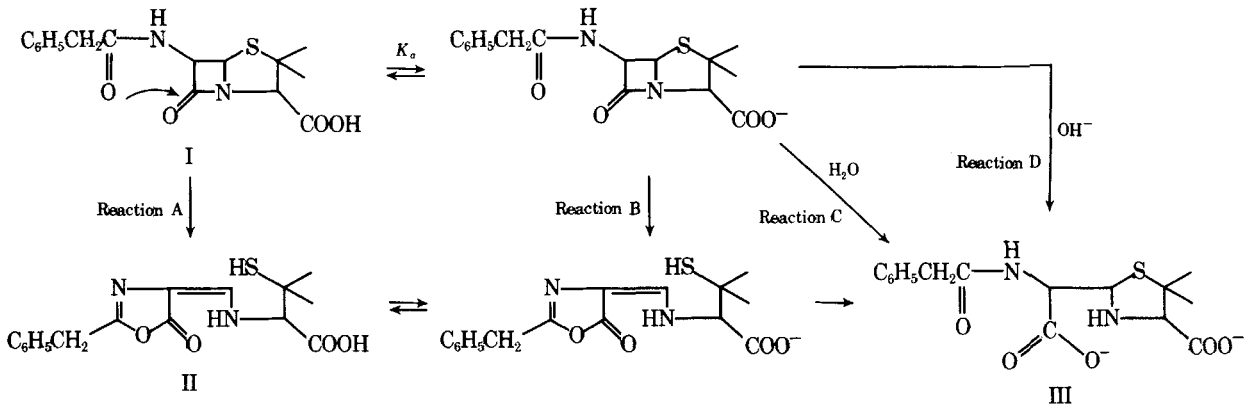

Scheme VI

can probably both be excluded because k^{H_2O}/k^{D_2O} should be[6] <1.

The production of unstable benzylpenicillenic acid as the reaction intermediate under the conditions below pH (pD) 6 was confirmed by the increase in absorbance at 325 nm of the reaction solution in both water and deuterium oxide. Based on these facts, Scheme I would be the most reasonable to account for the k_0 reaction.

The unique feature of the pH–rate profile for the degradation of penicillin G is the plateau in the neutral pH region. Remarkably broad plateaus have been observed in the degradation of penicillins such as ampicillin (9), cyclacillin (13), phenethicillin (4), and cloxacillin (10), which have characteristically lower k_0 values than penicillin G. The spontaneous rate, k_0', may be due to (*a*) intramolecular attack of the side-chain amide carbonyl on the β-lactam of ionized penicillin (Scheme VI) to produce the penicillenic acid (II) (Reaction B) and/or (*b*) a water-catalyzed β-lactam cleavage to give the penicilloic acid (III) (Reaction C).

Levine (15, 16) postulated that the degradation of penicillin G at pH 7.5 proceeds through benzylpenicillenic acid (II) (*via* Reaction B, Scheme VI), which can be rapidly converted to benzylpenicilloic acid (III) (17). The intramolecularly catalyzed mechanism is an unlikely explanation for the plateau rates, since the large deuterium solvent isotope effect on k_0' ($k_0'^{H_2O}/k_0'^{D_2O}$ = 4.5, Table I) and largely negative entropies of activation ($\Delta S^{\ddagger}$ = −30 eu)[7] are inconsistent with Reaction B (Scheme VI). The most logical possibility for the pH-independent degradation (k_0' reaction) of penicillin G at neutral pH is spontaneous hydrolysis involving nucleophilic attack at the β-lactam ring by a water molecule facilitated (general base) by neighboring water molecules to produce benzylpenicilloic acid (III) directly (Reaction C, Scheme VI). Two possible transition states (I*a* and I*b*) for Reaction C might explain the extremely large solvent isotope effect of 4.5.

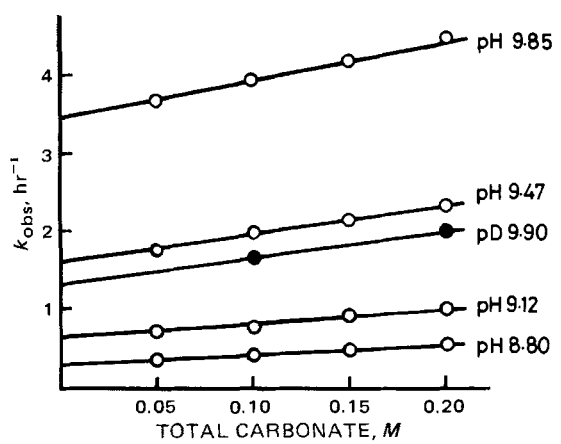

Figure 5—*Plots of pseudo-first-order rate constants* versus *total carbonate concentration for the degradation of penicillin G in water* (○) *and deuterium oxide* (●, *50% free base) at 60° and 0.5 ionic strength.*

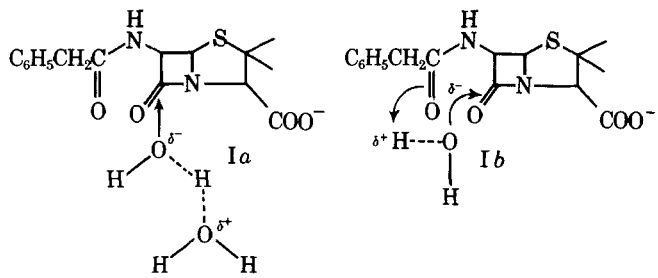

Although Reaction C rather than Reaction B has widely been believed to proceed in neutral degradation of penicillins, no reliable evidence sufficiently supports Reaction C and differentiates these reactions. Yamana *et al.* (13) and Butler *et al.* (20) reached the same conclusion from the absence of significant side-chain dependency on k_0' values and by following the benzylpenicillenic acid formation rate, respectively.

Reaction Mechanism with General Base—Previous work on penicillin aminolysis (26, 27) showed that the reaction of penicillin G with various primary and secondary amines proceeds exclusively through a nucleophilic attack pathway to produce the corresponding benzylpenicilloylamides. In the present work, the reactions of penicillin G with oxygen bases were studied. A linear relationship between k_{obs} and total oxygen-compound concentration was observed (Figs. 2–5).

The second-order rate constants, k_B, thus determined at 35 and 60° from the relationship between ($k_{obs} - k_{pH}$) values and base concentrations are recorded in Table II, together with values reported by Finholt *et al.* (7).

Figure 6 shows a plot of log k_B against pKa of the conjugated acid of an oxygen base. The solid line corresponds to the Brønsted equation, log k_B = 0.56pKa − 4.41, for the unassisted nucleophilic reaction of an amine with penicillin G at 60° and μ = 0.5 (26).

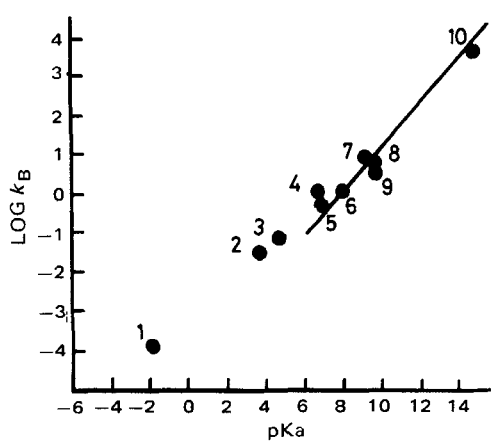

Figure 6—*Brønsted plots for the reaction of penicillin G with oxygen bases in aqueous solution at 60° and 0.5 ionic strength. The numbers refer to the bases in Table II. The solid line corresponds to the Brønsted equation, log* k_B = 0.56pKa − 4.41, *for the unassisted nucleophilic reaction of amines with penicillin G at 60° and 0.5 ionic strength (26).*

[6] R. L. Schowen University of Kansas, Lawrence, Kans., personal communication.

[7] Where $\Delta S^{\ddagger} = 2.303R[\log k_0' - \log(\kappa T/h)] + \Delta H^{\ddagger}/T$ at 35°. The k_0' value in Table I and that at 45° from Ref. 12 gave a $\Delta H^{\ddagger}$ value of 16.8 kcal/mole at 35°.

Table II—Second-Order Rate Constants for the Reactions of Penicillin G, Cloxacillin, Ampicillin, and Cyclacillin with Oxygen Bases and Nitrogen Bases at 35 or 60° and 0.5 Ionic Strength [a]

				k_B, M^{-1} hr^{-1}				
		pKa[b]		Penicillin G				
Number	Base	60°	35°	60°	35°	Cloxacillin, 35°	Ampicillin, 35°	Cyclacillin, 35°
Oxygen bases								
1	Water[c]	−1.74	−1.74	1.30×10^{-4}	1.62×10^{-5}	1.69×10^{-5} [d]	1.35×10^{-5} [e]	4.49×10^{-5}
2	HCO_2^- [f]	3.60	—	3.20×10^{-2}	—	—	—	—
3	$CH_3CO_2^-$ [f]	4.58	—	8.00×10^{2}	—	—	—	—
4	HPO_4^{2-}	6.54	6.59	0.87	7.80×10^{-2}	9.20×10^{-2} [d]	0.17[e]	—
5	p-$NO_2C_6H_4O^-$	6.80	—	0.50	—	—	—	—
6	m-$NO_2C_6H_4O^-$	8.04	—	1.00	—	—	—	—
	in deuterium oxide	8.45	—	0.75	—	—	—	—
7	$H_2BO_3^-$	8.75[g]	8.92	9.30[g]	0.47	0.92[d]	—	—
8	CO_3^{2-}	9.47	9.67	7.00	0.90	0.59	—	1.50
	in deuterium oxide	9.90	—	7.00	—	—	—	—
9	$C_6H_5O^-$	9.51	—	3.45	—	—	—	—
10	OH^-	14.76	15.42	5.39×10^{3}	1.19×10^{3}	1.34×10^{3} [d]	2.57×10^{3} [e]	1.10×10^{3}
Nitrogen bases								
11	Imidazole	6.65	6.96	0.25[h]	3.50×10^{-2} [h]	6.00×10^{-2}	0.10	3.00×10^{-2}
12	Glycine	8.87	9.41	2.50[h]	0.40	—	0.40	0.40

[a] All rates were determined by the iodometric titration method. Each reaction was carried out at three or more different buffer concentrations at each of three or more different pH values. [b] Determined by the half-neutralization method. [c] $k_0'/55.5$. [d] Reference 10. [e] Reference 9. [f] The reactions were carried out at pH 7.0 and 7.5. The pH of the reaction solution was maintained by means of a pH-stat. [g] Reference 7. [h] Reference 26.

The reactions of penicillin G with oxygen bases, except acetate, formate, and water, appear to represent a nucleophilic displacement reaction rather than a general base-catalyzed degradation, because the rate constants, k_B, for m-nitrophenol (Fig. 4) and carbonate (Fig. 5) showed only a small deuterium solvent isotope effect, with a $k_B^{H_2O}/k_B^{D_2O}$ ratio of approximately 1.0 in both cases. Nucleophilic reaction did not lead to a deuterium solvent isotope effect appreciably greater than unity (28). Water, however, probably acts as a general base catalyst as discussed on the basis of a large solvent isotope effect. The formate and acetate ions, having relatively low pKa values, also probably participate as general bases in the degradation of penicillin G, in view of the general principle (28) that a change in the mechanism from a general base-catalyzed path to a nucleophilic reaction may occur as the pKa value of the reacting base becomes greater than that for the leaving group (imino group in β-lactam in this case), as was found for an ester (29) and an amide (30).

Table II also includes k_B values from the literature (7, 9, 10, 13) and from the present study for the reaction of other penicillins with some bases. Figure 7 shows a plot of log k_B of penicillin G *versus* log k_B of other penicillins for the reaction of the same series of bases with penicillin G at 35° and $\mu = 0.5$. The solid line drawn has slope 1.0 and passes through zero. All points almost fall on this line, suggesting that alteration of the side chain of penicillins gives no significant change in the rates of their base-catalyzed degradation.

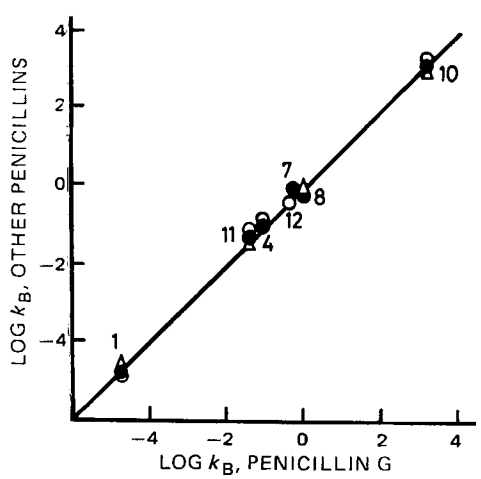

Figure 7—*Double logarithmic plots of second-order rate constants for the reaction of penicillin G with bases* versus *second-order rate constants for the reaction of other penicillins with the same bases. The numbers refer to the bases in Table II.*

REFERENCES

(1) R. Broderson, *Trans. Faraday Soc.*, **43**, 351 (1947).
(2) R. Broderson, *Acta Pharmacol.*, **3**, 345 (1947).
(3) D. W. Dennen and W. W. Davis, *Antimicrob. Ag. Chemother.*, **1961**, 531.
(4) M. A. Schwartz, A. P. Granatek, and F. H. Buckwalter, *J. Pharm. Sci.*, **51**, 523 (1962).
(5) M. A. Schwartz, *ibid.*, **54**, 472 (1965).
(6) M. A. Schwartz, E. Bara, I. Rubycz, and A. P. Granatek, *ibid.*, **54**, 149 (1965).
(7) P. Finholt, G. Jürgensen, and H. Kristiansen, *ibid.*, **54**, 387 (1965).
(8) N. C. Hsi, F. S. Chao, and Y. S. Feng, *Yao Hsueh Hsueh Pao*, **12**, 615 (1965).
(9) J. P. Hou and J. W. Poole, *J. Pharm. Sci.*, **58**, 447 (1969).
(10) H. Bundgaard and K. Ilver, *Dan. Tidsskr. Farm.*, **44**, 365 (1970).
(11) H. Bundgaard, *J. Pharm. Sci.*, **60**, 1273 (1971).
(12) R. E. Lindsay and S. L. Hem, *ibid.*, **61**, 202 (1972).
(13) T. Yamana, A. Tsuji, and Y. Mizukami, *Chem. Pharm. Bull.*, **22**, 1186 (1974).
(14) J. T. H. Ong and H. B. Kostenbauder, *J. Pharm. Sci.*, **64**, 1378 (1975).
(15) B. B. Levine, *Nature*, **187**, 939 (1960).
(16) B. B. Levine, *J. Exp. Med.*, **112**, 1131 (1960).
(17) B. B. Levine, *Arch. Biochem. Biophys.*, **93**, 50 (1961).
(18) F. P. Doyle and J. H. C. Nayler, in "Advances in Drug Research," vol. 1, N. J. Harper and A. B. Simmonds, Eds., Academic, New York, N.Y., 1964, p. 1.
(19) F. Moll, *Arch. Pharm.*, **301**, 272 (1968).
(20) T. C. Butler, K. H. Dudley, and D. Johnson, *J. Pharmacol. Exp. Ther.*, **181**, 201 (1972).
(21) T. H. Fife and T. C. Bruice, *J. Phys. Chem.*, **65**, 1079 (1961).
(22) T. C. Bruice, T. H. Fife, J. J. Bruno, and P. Benkovic, *J. Am. Chem. Soc.*, **84**, 3012 (1962).
(23) M. A. Schwartz and G.-M. Wu, *J. Pharm. Sci.*, **55**, 550 (1966).
(24) R. D. Kinget and M. A. Schwartz, *ibid.*, **58**, 1102 (1969).
(25) H. Bundgaard, *Dan. Tidsskr. Farm.*, **46**, 85 (1972).
(26) A. Tsuji, T. Yamana, E. Miyamoto, and E. Kiya, *J. Pharm. Pharmacol.*, **27**, 580 (1975).
(27) T. Yamana, A. Tsuji, E. Miyamoto, and E. Kiya, *ibid.*, **27**, 283 (1975).
(28) S. L. Johnson, in "Advances in Physical Organic Chemistry," vol. 5, V. Gold, Ed., Academic, New York, N.Y., 1967, p. 237.
(29) W. P. Jencks and J. Carriuolo, *J. Am. Chem. Soc.*, **83**, 1743 (1961).
(30) D. G. Oakenful and W. P. Jencks, *ibid.*, **93**, 178 (1971).
(31) H. S. Harned and W. J. Hamer, *ibid.*, **55**, 2194 (1933).

(32) A. K. Corington, R. A. Robinson, and R. G. Bates, *J. Phys. Chem.*, **70**, 3820 (1966).

ACKNOWLEDGMENTS AND ADDRESSES

Received January 26, 1976, from the *Faculty of Pharmaceutical Sciences, Kanazawa University, Takara-machi, Kanazawa 920, Japan.*

Accepted for publication August 11, 1976.

The authors express their appreciation to Dr. V. Stella of the University of Kansas for many helpful suggestions. They also acknowledge the gifts of penicillins from Meiji Seika Kaisha, Ltd., and Takeda Chemical Ind., Ltd.

[x] To whom inquiries should be directed.

Pharmacokinetics of Methylphenidate in the Rat Using Single-Ion Monitoring GLC–Mass Spectrometry

J. GAL [x], B. J. HODSHON, C. PINTAURO, B. L. FLAMM, and A. K. CHO

Abstract □ A GLC–mass spectrometric assay for methylphenidate in biological fluids was developed using the ethyl ester homolog of the drug as the internal standard. The procedure has a lower level of sensitivity of 1.2 ng/ml and is based on GLC–mass spectrometic monitoring of the *m/e* 180 ion common to the mass spectra of the *N*-trifluoroacetyl derivatives of the drug and internal standard. The brain and plasma levels of methylphenidate in rats were determined after intravenous administration of 0.5 mg/kg of the drug. The two-compartment open pharmacokinetic model fit the data.

Keyphrases □ Methylphenidate—GLC–mass spectrometric analysis in biological fluids, pharmacokinetics in rats □ GLC–mass spectrometry—analysis, methylphenidate in biological fluids, pharmacokinetic study in rats □ Pharmacokinetics—methylphenidate, GLC–mass spectrometric study in rats □ Stimulants, central—methylphenidate, GLC–mass spectrometric analysis in biological fluids, pharmacokinetics in rats

Methylphenidate [(±)-*threo*-methyl α-phenyl-2-piperidineacetate, I] has pharmacological properties similar to those of dextroamphetamine (1). It is used to treat depressed states of various origins and hyperkinesis in children (2). In addition, I has become a drug of abuse in many countries (3–5).

The metabolic fate of I in humans and several other species was studied by Faraj *et al.* (6), who also reviewed previously published work. The main urinary metabolite in humans, accounting for 30% of the dose, is the hydrolysis product of I, ritalinic acid (II).

BACKGROUND

Studies on the disposition of radioactive I in the rat were reported (7), as was information on plasma I levels in humans (6, 8). While the drug appears to be essentially completely absorbed after oral administration, the concentration of I after a 20-mg oral dose of I hydrochloride was reported not to exceed 20 ng/ml of plasma (6). Plasma I levels in humans were 10–60 ng/ml 1–3 hr after a 0.4-mg/kg oral dose of I hydrochloride (8). Such low levels of I achieved after therapeutic doses may partially explain the paucity of I pharmacokinetic data.

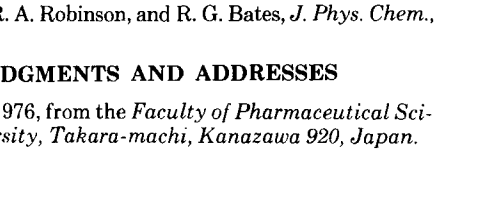

I: $R_1 = CH_3$, $R_2 = H$
II: $R_1 = R_2 = H$
III: $R_1 = CH_2CH_3$, $R_2 = H$
IV: $R_1 = CH_3$, $R_2 = COCF_3$
V: $R_1 = CH_2CH_3$, $R_2 = COCF_3$

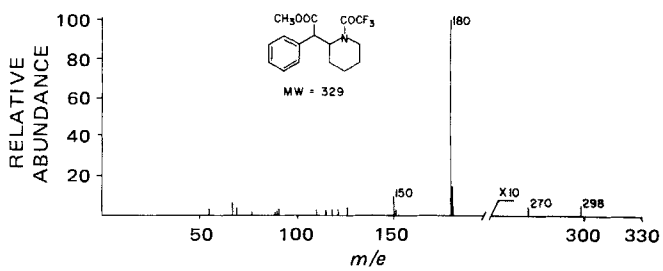

Figure 1—*Mass spectrum of IV obtained by GLC–mass spectrometry under the described conditions.*

Several analytical methods for I were reported (6–10), but none appears capable of measuring I reliably and routinely at the low levels required. *N*-Acylation of I with trichloroacetyl chloride followed by electron-capture GLC gave (9) a lower limit of detection of 9 ng/ml in plasma. Another procedure (10), also using electron-capture GLC, involved reduction of the methoxycarbonyl function of I to $-CH_2OH$ using lithium aluminum hydride, followed by derivatization with pentafluoropropionic anhydride. The sensitivity of the assay was 2 ng of I/ml of plasma. Recently, an analytical procedure for I based on GLC–mass spectrometry, with a sensitivity limit of 1.5 ng/ml in plasma, was described (8).

None of these methods (8–10) included an internal standard. A further difficulty with the published (8) GLC–mass spectrometric assay is that the procedure involved the GLC of underivatized I. Underivatized I may undergo extensive and variable decomposition in the injection port of the gas chromatograph, making quantitative determination difficult at best (11).

A new GLC–mass spectrometric assay for I in biological fluids and tissues is now described. The procedure involves the addition of the ethyl ester homolog of I, Compound III (12), to the biological medium, extraction of the drug and internal standard under mildly basic conditions, concentration of the extract, and derivatization with trifluoroacetic anhydride. GLC–mass spectrometric analysis was then performed with the mass spectrometer focused on an ion common to the spectra of both I and the internal standard. The lower limit of sensitivity of the assay is 1.2 ng of I/ml of plasma. The procedure was applied to the study of the pharmacokinetics of I in the rat, and the data obtained were examined in terms of classical pharmacokinetic models.

EXPERIMENTAL

Materials—Internal standard III was prepared *via* two different methods. A solution of II[1] (0.5 g) in 55 ml of absolute ethanol containing

[1] Ciba-Geigy Corp.

(32) A. K. Corington, R. A. Robinson, and R. G. Bates, *J. Phys. Chem.*, **70**, 3820 (1966).

ACKNOWLEDGMENTS AND ADDRESSES

Received January 26, 1976, from the *Faculty of Pharmaceutical Sciences, Kanazawa University, Takara-machi, Kanazawa 920, Japan.*

Accepted for publication August 11, 1976.

The authors express their appreciation to Dr. V. Stella of the University of Kansas for many helpful suggestions. They also acknowledge the gifts of penicillins from Meiji Seika Kaisha, Ltd., and Takeda Chemical Ind., Ltd.

[x] To whom inquiries should be directed.

Pharmacokinetics of Methylphenidate in the Rat Using Single-Ion Monitoring GLC–Mass Spectrometry

J. GAL [x], B. J. HODSHON, C. PINTAURO, B. L. FLAMM, and A. K. CHO

Abstract □ A GLC–mass spectrometric assay for methylphenidate in biological fluids was developed using the ethyl ester homolog of the drug as the internal standard. The procedure has a lower level of sensitivity of 1.2 ng/ml and is based on GLC–mass spectrometic monitoring of the *m/e* 180 ion common to the mass spectra of the *N*-trifluoroacetyl derivatives of the drug and internal standard. The brain and plasma levels of methylphenidate in rats were determined after intravenous administration of 0.5 mg/kg of the drug. The two-compartment open pharmacokinetic model fit the data.

Keyphrases □ Methylphenidate—GLC–mass spectrometric analysis in biological fluids, pharmacokinetics in rats □ GLC–mass spectrometry—analysis, methylphenidate in biological fluids, pharmacokinetic study in rats □ Pharmacokinetics—methylphenidate, GLC–mass spectrometric study in rats □ Stimulants, central—methylphenidate, GLC–mass spectrometric analysis in biological fluids, pharmacokinetics in rats

Methylphenidate [(±)-*threo*-methyl α-phenyl-2-piperidineacetate, I] has pharmacological properties similar to those of dextroamphetamine (1). It is used to treat depressed states of various origins and hyperkinesis in children (2). In addition, I has become a drug of abuse in many countries (3–5).

The metabolic fate of I in humans and several other species was studied by Faraj *et al.* (6), who also reviewed previously published work. The main urinary metabolite in humans, accounting for 30% of the dose, is the hydrolysis product of I, ritalinic acid (II).

BACKGROUND

Studies on the disposition of radioactive I in the rat were reported (7), as was information on plasma I levels in humans (6, 8). While the drug appears to be essentially completely absorbed after oral administration, the concentration of I after a 20-mg oral dose of I hydrochloride was reported not to exceed 20 ng/ml of plasma (6). Plasma I levels in humans were 10–60 ng/ml 1–3 hr after a 0.4-mg/kg oral dose of I hydrochloride (8). Such low levels of I achieved after therapeutic doses may partially explain the paucity of I pharmacokinetic data.

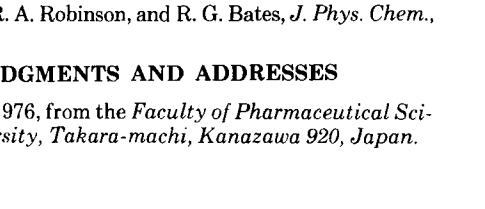

I: $R_1 = CH_3$, $R_2 = H$
II: $R_1 = R_2 = H$
III: $R_1 = CH_2CH_3$, $R_2 = H$
IV: $R_1 = CH_3$, $R_2 = COCF_3$
V: $R_1 = CH_2CH_3$, $R_2 = COCF_3$

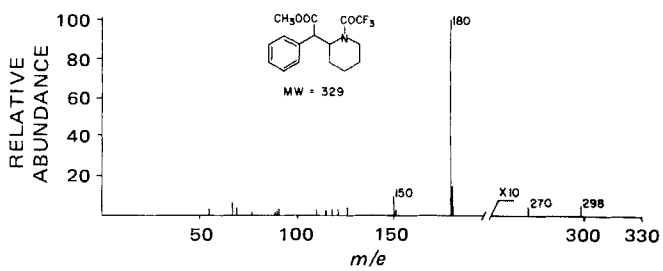

Figure 1—*Mass spectrum of IV obtained by GLC–mass spectrometry under the described conditions.*

Several analytical methods for I were reported (6–10), but none appears capable of measuring I reliably and routinely at the low levels required. *N*-Acylation of I with trichloroacetyl chloride followed by electron-capture GLC gave (9) a lower limit of detection of 9 ng/ml in plasma. Another procedure (10), also using electron-capture GLC, involved reduction of the methoxycarbonyl function of I to $-CH_2OH$ using lithium aluminum hydride, followed by derivatization with pentafluoropropionic anhydride. The sensitivity of the assay was 2 ng of I/ml of plasma. Recently, an analytical procedure for I based on GLC–mass spectrometry, with a sensitivity limit of 1.5 ng/ml in plasma, was described (8).

None of these methods (8–10) included an internal standard. A further difficulty with the published (8) GLC–mass spectrometric assay is that the procedure involved the GLC of underivatized I. Underivatized I may undergo extensive and variable decomposition in the injection port of the gas chromatograph, making quantitative determination difficult at best (11).

A new GLC–mass spectrometric assay for I in biological fluids and tissues is now described. The procedure involves the addition of the ethyl ester homolog of I, Compound III (12), to the biological medium, extraction of the drug and internal standard under mildly basic conditions, concentration of the extract, and derivatization with trifluoroacetic anhydride. GLC–mass spectrometric analysis was then performed with the mass spectrometer focused on an ion common to the spectra of both I and the internal standard. The lower limit of sensitivity of the assay is 1.2 ng of I/ml of plasma. The procedure was applied to the study of the pharmacokinetics of I in the rat, and the data obtained were examined in terms of classical pharmacokinetic models.

EXPERIMENTAL

Materials—Internal standard III was prepared *via* two different methods. A solution of II[1] (0.5 g) in 55 ml of absolute ethanol containing

[1] Ciba-Geigy Corp.

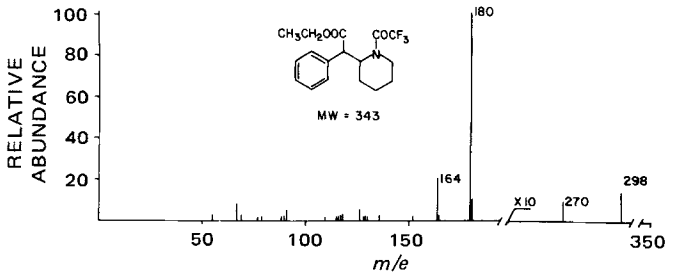

Figure 2—*Mass spectrum of V obtained by GLC–mass spectrometry under the described conditions.*

dry 10% (w/w) HCl was refluxed overnight. The solvent was then evaporated, and the residue was recrystallized from ethanol–ether to give III hydrochloride, mp 171–173° [lit. (12) mp 172–173°]. In the second method, I hydrochloride[1] (0.2 g) was treated in the same way, but the reflux time was 3 weeks. Stock solutions of I hydrochloride in methanol and III hydrochloride in ethanol were used in the described analytical procedures.

Animal Procedures—Male Sprague–Dawley rats, 200–250 g, were given an intravenous injection of I hydrochloride in normal saline equivalent to 0.5 mg of free base/kg; 0.5 ml of solution/100 g of animal weight was used. At the appropriate times, the animals were lightly anesthetized with ether, and blood was collected by cardiac puncture with a heparinized syringe. The brains were removed and immediately frozen. The whole blood was centrifuged (3000×*g*), and aliquots of plasma were taken for analysis.

Extraction and Sample Preparation—The brain was homogenized in twice the volume of saturated ammonium carbonate solution containing 500 pmoles of internal standard, and the homogenate was extracted as described for the plasma samples. To a 2-ml aliquot of plasma were added 500 pmoles of the internal standard and 0.6 g of ammonium carbonate, and the mixture was extracted with 6 ml of hexane by shaking[2] for 15 min. The mixture was then centrifuged for 10 min, 4.5 ml of the organic layer was transferred to a 5-ml microcentrifuge tube[3], and the solvent was evaporated in a nitrogen stream.

The residue in each tube was treated with 50 μl of acetonitrile and 50 μl of trifluoroacetic anhydride, and the solution was swirled on a mixer and then heated at 70° for 15 min. The solvent and excess derivatizing agent were evaporated in a nitrogen stream. The residue was treated with 50 μl of acetonitrile and swirled[4]. Analysis by GLC–mass spectrometry was then performed.

A standard curve was routinely obtained by adding 0–2000 pmoles of I to a series of extraction tubes containing 2 ml of a solution of plasma proteins[5] and 500 pmoles of the internal standard. These tubes were then carried through the assay procedure.

GLC–Mass Spectrometry—A quadrupole GLC–mass spectrometry system[6] was used under the following conditions: helium carrier gas, 35 ml/min; injector temperature, 250°; and column temperature, 170°. The 0.9-m × 2-mm i.d. glass column was packed with 3% phenyl methyl silicone[7] coated on acid-washed dimethylchlorosilane-treated diatomite[8] support. The temperature of the membrane separator was 170°, and that of the transfer line was 250°. The ionizing energy was 70 ev.

A digital selected-ion monitor (13) was used to monitor the ion current at *m/e* 180. The retention times of the *N*-trifluoroacetyl derivatives IV and V were 2.8 and 3.4 min, respectively. No interfering peaks were observed when brain and plasma samples from animals not given the drug were analyzed without adding the internal standard.

RESULTS AND DISCUSSION

Since I may decompose when injected directly into a gas chromatograph (11), the assay developed involved the derivatization of I with trifluoroacetic anhydride before GLC. The mass spectrum of the *N*-trifluoroacetyl derivative IV of I is shown in Fig. 1. The molecular ion is not discernible. Weak ions are seen at *m/e* 298 and 270 with relative intensities of 0.5 and 0.4%, respectively.

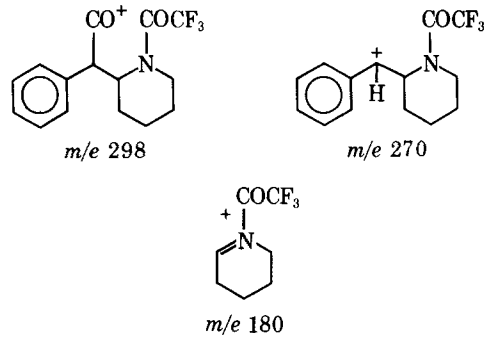

The *m/e* 298 ion likely results from the loss of the methoxyl radical from the molecular ion, while the *m/e* 270 ion arises from the loss of the entire methoxycarbonyl group. The ion of *m/e* 150 (8%) appears to be formed *via* the McLafferty rearrangement, frequently occurring during the fragmentation of carbonyl-containing compounds (Scheme I). The base peak in the spectrum is the *m/e* 180 ion, arising *via* β-cleavage to nitrogen. All other ions in the spectrum are weak, <5%.

The mass spectrum of the *N*-trifluoroacetyl derivative V of the ethyl ester homolog III is shown in Fig. 2. The spectrum is similar to that of IV (Fig. 1). The molecular ion is not seen, the base peak is at *m/e* 180, and the ions of *m/e* 270 and 298 are present. The ion arising *via* the McLafferty rearrangement appears, as expected, at *m/e* 164.

The ethyl ester III was selected to serve as the internal standard in the assay for I. This homolog is readily obtained by esterification of amino acid II or by transesterification of I in ethanolic hydrochloric acid. Homologs, rather than stable-isotope-labeled analogs, were used as internal standards in some selected-ion monitoring GLC–mass spectrometric assays (14, 15), and the two approaches were critically compared (16). In the present case, III proved highly suitable as an internal standard due to its chemical similarity to I and the similarity of the mass spectrum of its *N*-trifluoroacetyl derivative (V) (Fig. 2) to that of IV (Fig. 1). The ion of *m/e* 180 is the base peak in the spectra of both compounds and was chosen for selected-ion monitoring. The mass spectrometer could thus be used in the *single*-ion monitoring mode, serving as a sensitive and selective GLC detector. The two trifluoroacetyl derivatives are sufficiently resolved under the GLC conditions used (Fig. 3).

Compounds I and III were extracted with hexane from plasma or rat brain homogenate after saturation with ammonium carbonate (pH 8.8–9.0) (17) since these esters rapidly hydrolyze (18) under the strongly basic conditions often used to extract basic drugs (19). The overall recovery of I from plasma was 96% at 117 ng/ml and 101% at 23 ng/ml. The relative standard deviation of the slopes of three calibration curves was 4.2%. The coefficient of variation in the determination of five 2-ml plasma samples containing 1.2 ng of I/ml was 14%. This concentration is considered to be the lower limit of sensitivity of the assay; attempted determination of three samples of 0.6 ng of I/ml gave an average value of 0.3 ng/ml with a coefficient of variation of 100%.

Concentrations of I in rat plasma and brain are plotted in Fig. 4. The concentration in plasma (C_p) declined biexponentially, and the two-compartment open model (20) (Scheme II) fit the data. In Scheme II, V_1

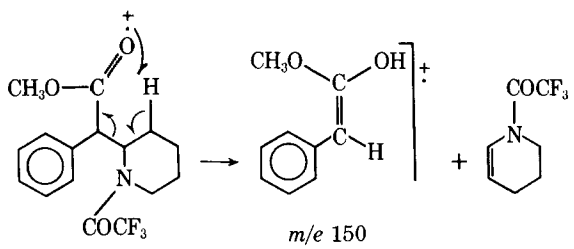

Scheme I

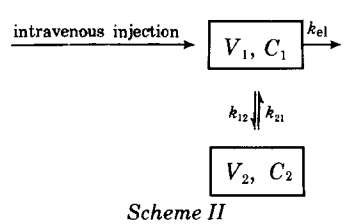

Scheme II

[2] International bottle shaker, International Equipment Co., Boston, Mass.
[3] Microflex tube, Kontes Glass Co., Vineland, N.J.
[4] Vortex Genie, Scientific Industries, Springfield, Mass.
[5] Plasmanate, Cutter Laboratories, Berkeley, Calif.
[6] Model 5981A, Hewlett-Packard, Palo Alto, Calif.
[7] OV-17, Applied Science Laboratories, State College, Pa.
[8] Gas Chrom Q, Applied Science Laboratories, State College, Pa.

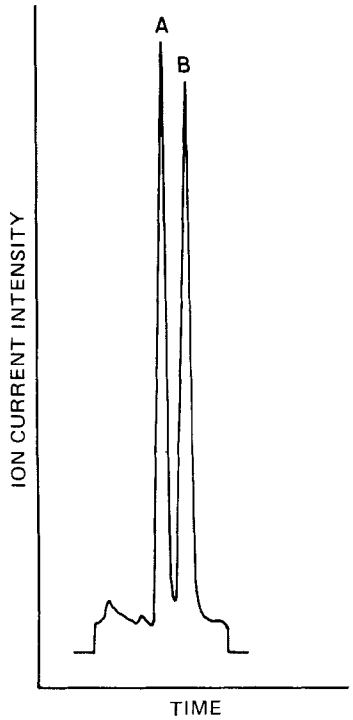

Figure 3—*Tracing of the ion current at* m/e *180 monitored by the GLC–mass spectrometer. Key: A, IV; and B, V.*

and V_2 are the volumes of the central and second compartments, respectively, and the k's are the rate constants for the movement of the drug as indicated by the arrows. A desk calculator[9] using a nonlinear regression program was employed to determine the four parameters A, B, α, and β of the equation $C_p = Ae^{-\alpha t} + Be^{-\beta t}$ that best fits the experimentally determined plasma I concentrations.

Analysis of the plasma data in terms of this model gave the results shown in Table I. The initial decline in plasma concentration is rapid and the β-phase is reached within a few minutes. Thus, transfer of I from plasma to tissues is rapid and distribution is extensive, as indicated by the ratio $C_p{}^0/B$, which was as high as 3.5. The volume of the central compartment (1.18 liters/kg) is about twice the volume of body water.

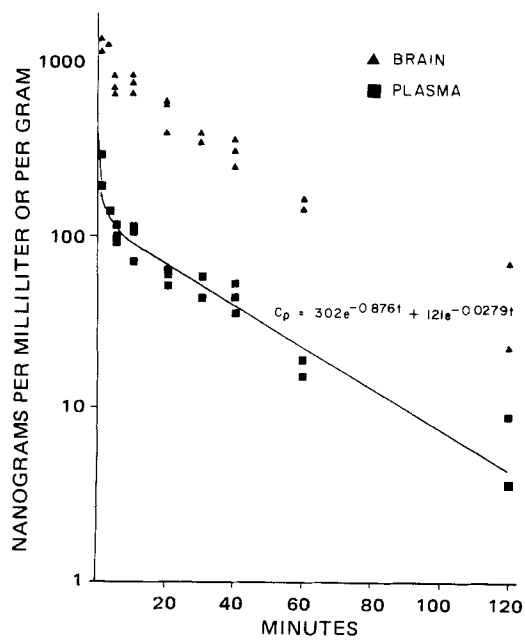

Figure 4—*Plasma and brain I levels. The line superimposed on the plasma data points was obtained by nonlinear regression analysis as described. The correlation coefficient for the plasma data on the calculated curve was 0.959.*

[9] Wang 600, Wang Laboratories, Tewksbury, Mass.

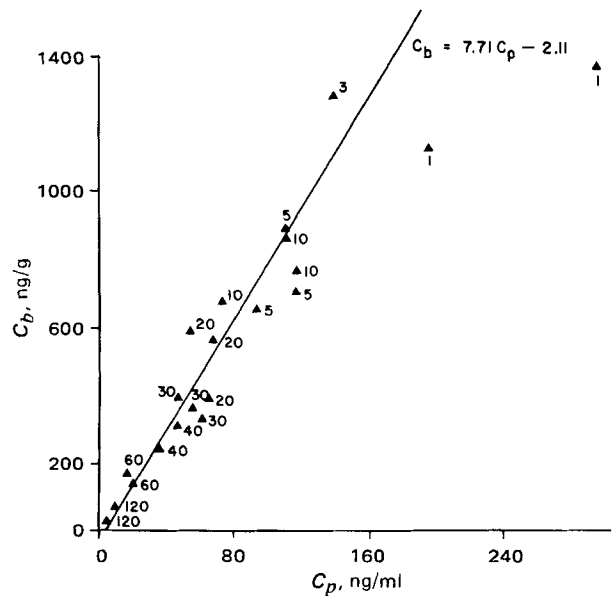

Figure 5—*Relationship of brain and plasma I concentrations* (C_b *and* C_p, *respectively). The number next to each data point is the time of sampling in minutes. The equation of the line was determined by least-squares linear regression analysis without the 1-min time points. (See text for explanation.) The correlation coefficient is 0.947.*

Compound I is metabolized extensively in the rat; less than 1% unchanged I was found in the 48-hr urine (6). The major route of metabolism in this species appears to be initial *para*-hydroxylation, and the resulting metabolite may undergo further transformations. In humans, the predominant route is hydrolysis of the ester portion of the molecule without *para*-hydroxylation (6). This difference between humans and rats in the metabolism of I is similar to the differences in the metabolism of amphetamine by the two species. The major route of *in vivo* biotransformation of amphetamine in the rat is *para*-hydroxylation; this pathway is minor in humans, however, with deamination and side-chain degradation being the predominant transformations (22). It was suggested (6) that metabolism of I is very rapid, in agreement with the rapid clearance of the drug from rat plasma (Table I). Compound I has been found to be poorly bound to human plasma proteins (6).

The concentration of I in rat brain was higher than the plasma concentration and declined parallel with the plasma concentration after the 1-min sampling point (Fig. 5), with a brain/plasma ratio of 7.7. The rapid entry of I into the brain is in agreement with its rapid and extensive tissue distribution and with its organic–aqueous partitioning characteristics (6). The brain appears to be part of the central compartment. The deviation in the 1-min sampling points (Fig. 5) may be the result of the delay caused by the mixing time of the bolus with the blood or of inaccurate measurement at the early time point when the change in concentration is very rapid.

Segal *et al.* (7) recently published a study on the disposition of ^{14}C-I in the rat, with emphasis on the time course of entry and distribution of the drug in the brain. In agreement with the present report, the concentration of I in rat plasma declined biexponentially. However, a detailed pharmacokinetic analysis in terms of an appropriate model was not described. The biological half-life (β-phase) was given (7) as 105 min, a value considerably larger than the finding (24.8 min) of the present report. The origin of this discrepancy is not clear. The assay of ^{14}C-labeled I used (7) was based on extraction of the biological medium with methylene chloride, and no further purification was performed. A metabolite could interfere in such determinations, since at least one lipid-soluble metabolite of I has been found in the rat (6). The rapid entry of I into rat brain after intravenous administration of the drug reported by Segal *et al.* (7) is in qualitative agreement with the findings of the present report, although significant quantitative differences in the half-life of I in the brain between the two studies exist.

The half-life of I in the rat is 24.8 min (Table I), while that of dextroamphetamine is 86.7 min (23), reflecting the faster metabolism of I.

Table I—Pharmacokinetic Analysis of Plasma Methylphenidate Concentrations[a]

Parameter	Value
C_p^0, ng/ml	424
V_1, liters/kg	1.18
V_2, liters/kg	2.35
$V_{d_{ss}}$, liters/kg	3.53
k_{12}, min^{-1}	0.542
k_{21}, min^{-1}	0.272
k_{el}, min^{-1}	0.090
Total body clearance, ml/min/kg	107.2
$t_{1/2}$, min	24.8

[a] The plasma levels were analyzed by nonlinear regression to the two-exponential function describing the two-compartment model (20). The volume of distribution at steady state, $V_{d_{ss}}$, is that defined by Riegelman *et al.* (21).

The volume of distribution of dextroamphetamine is 6.04 liters/kg (23), considerably larger than the value obtained for I, 3.53 liters/kg (Table I). The pKa values of I and dextroamphetamine are 8.8 (24) and 9.9 (25), respectively. The apparent heptane–water partition coefficient of I at pH 7.4 was determined (6) to be 0.63, while that of dextroamphetamine may be computed from published data (25) as 0.00593. Thus, I is ionized at physiological pH to a lesser extent than dextroamphetamine and is considerably more lipid soluble. The larger volume of distribution of amphetamine may be a reflection of the greater concentration of this compound, a stronger base than I, in the intracellular water of tissues, the pH of which is lower than that of extracellular water (26).

REFERENCES

(1) "Drill's Pharmacology in Medicine," 3rd ed., J. R. DiPalma, Ed., McGraw Hill, New York, N.Y., 1965, p. 369.

(2) R. L. Sprague and E. K. Sleator, *Pediatr. Clin. North Am.*, **20,** 719 (1973).

(3) R. F. Willey, *N. Engl. J. Med.*, **285,** 464 (1971).

(4) E. S. Perman, *ibid.*, **283,** 760 (1971).

(5) B. Schubert, *Acta Chem. Scand.*, **24,** 433 (1970).

(6) B. A. Faraj, Z. H. Israili, J. M. Perel, M. L. Jenkins, S. G. Holtzman, S. A. Cucinell, and P. G. Dayton, *J. Pharmacol. Exp. Ther.*, **191,** 535 (1974).

(7) J. L. Segal, R. F. Cunningham, P. G. Dayton, and Z. H. Israili, *Drug Metab. Disp.*, **4,** 140 (1976).

(8) R. M. Milberg, K. L. Rinehart, Jr., R. L. Sprague, and E. K. Sleator, *Biomed. Mass Spectrom.*, **2,** 2 (1975).

(9) R. S. Ray, J. S. Noonan, P. W. Murdick, and V. L. Tharp, *Am. J. Vet. Res.*, **33,** 27 (1972).

(10) R. Huffman, J. W. Blake, R. Ray, J. Noonan, and P. W. Murdick, *J. Chromatogr. Sci.*, **12,** 382 (1974).

(11) B. L. Flamm and J. Gal, *Biomed. Mass Spectrom.*, **2,** 281 (1975).

(12) L. Panizzon, *Helv. Chim. Acta*, **27,** 1748 (1944).

(13) R. W. Silverman and D. J. Jenden, Proceedings of the 2nd International Conference on Stable Isotopes, Oak Brook, Ill., Oct. 1975.

(14) A. K. Cho, *Res. Commun. Chem. Pathol. Pharmacol.*, **7,** 67 (1974).

(15) J. N. T. Gilbert and J. W. Powell, *Biomed. Mass Spectrom.*, **1,** 142 (1974).

(16) M. G. Lee and B. J. Millard, *ibid.*, **2,** 78 (1975).

(17) M. G. Horning, P. Gregory, J. Nowlin, M. Stafford, K. Lertratannangkoon, C. Butler, W. G. Stillwell, and R. M. Hill, *Clin. Chem.*, **20,** 282 (1974).

(18) F. T. Delbeke and M. Debackere, *J. Chromatogr.*, **106,** 412 (1975).

(19) A. K. Cho, B. Lindeke, B. J. Hodshon, and D. J. Jenden, *Anal. Chem.*, **45,** 570 (1973).

(20) S. Riegelman, J. C. K. Loo, and M. Rowland, *J. Pharm. Sci.*, **57,** 117 (1968).

(21) *Ibid.*, **57,** 128 (1968).

(22) L. G. Dring, R. L. Smith, and R. T. Williams, *Biochem. J.*, **116,** 425 (1970).

(23) A. K. Cho, B. J. Hodshon, B. Lindeke, and G. T. Miwa, *J. Pharm. Sci.*, **62,** 1491 (1973).

(24) S. Siegel, L. Lachman, and L. Malspeis, *J. Am. Pharm. Assoc., Sci. Ed.*, **48,** 431 (1959).

(25) T. B. Vree, A. T. J. M. Muskens, and J. M. van Rossum, *J. Pharm. Pharmacol.*, **21,** 774 (1969).

(26) W. J. Waddell and R. G. Bates, *Physiol. Rev.*, **49,** 285 (1969).

ACKNOWLEDGMENTS AND ADDRESSES

Received May 24, 1976, from the *Department of Pharmacology, School of Medicine, Center for the Health Sciences, University of California, Los Angeles, CA 90024.*

Accepted for publication August 18, 1976.

Presented in part at the 24th Annual Conference on Mass Spectrometry and Allied Topics, American Society for Mass Spectrometry, San Diego, Calif., May 1976.

Supported by U.S. Public Health Service Grant DAO-1057 and Contract ADM-45-74-178.

The authors are grateful to Ms. Mary Judin for excellent assistance in the preparation of the manuscript. Thanks are also due to Dr. J. Steinborn for helpful discussions.

[x] To whom inquiries should be directed. Present address: School of Pharmacy, University of Wisconsin, Madison, WI 53706.

Stannous-Ion Quantitation in Pyrophosphate and Polyphosphate Radiopharmaceutical Kits Using Differential Pulse Polarography

MARTIN H. D. McBRIDE, ROBERT E. GEORGE, WAYNE V. KESSLER, and STANLEY M. SHAW ˣ

Abstract □ Stannous salts are used as reducing agents in many radiopharmaceutical kits. Differential pulse polarography, with 1 *M* sulfuric acid as the supporting electrolyte, is a relatively simple and effective technique for stannous quantitation and can be used in the quality assurance testing of pyrophosphate and polyphosphate radiopharmaceutical kits.

Keyphrases □ Stannous ion—differential pulse polarographic analysis in pyrophosphate and polyphosphate radiopharmaceutical kits □ Polarography, differential pulse—analysis, stannous ion in pyrophosphate and polyphosphate radiopharmaceutical kits □ Radiopharmaceutical kits—pyrophosphate and polyphosphate types, differential pulse polarographic analysis of stannous content □ Tin—stannous ion, differential pulse polarographic analysis in pyrophosphate and polyphosphate radiopharmaceutical kits

Stannous ion, Sn(II), is the most effective and widely used reducing agent in radiopharmaceutical kits. However, Sn(II) is unstable in the presence of oxygen. Even in the crystalline state, stannous chloride can react with oxygen to form insoluble oxychlorides (1) and stannic, Sn(IV), "material" (2). In aqueous solution, Sn(II) can be precipitated as an insoluble basic chloride (3) or oxidized to Sn(IV) (4) by dissolved oxygen.

A quantitative test for Sn(II) content during the manufacture and storage of various radiopharmaceutical kits would be a very desirable quality assurance procedure. This Sn(II) test must be highly sensitive, because many kits contain much less than 1 mg of stannous salt. Furthermore, the test must be accurate in the presence of Sn(IV) contamination.

Differential pulse polarography was studied as a method for measuring the Sn(II) content of pyrophosphate and polyphosphate kits. Measured Sn(II) levels, 10^{-3}–10^{-4} *M*, were in the range of those found in many reconstituted commercial kits.

EXPERIMENTAL

The relationship between polarographic peak height and Sn(II) content of pyrophosphate and polyphosphate kits was studied by assaying a series of each kit type. The total tin concentration of each pyrophosphate kit was 8.3×10^{-4} *M* (equivalent to the tin supplied by 0.49 mg of stannous chloride dihydrate in a kit). The total tin concentration in each polyphosphate kit was 2.8×10^{-3} *M* (equivalent to 1.3 mg of stannous chloride dihydrate). The fraction of total tin as Sn(II) was varied among the kits from 0 to 1.0 in steps of 0.1 to illustrate the sensitivity range of differential pulse polarographic Sn(II) analysis and to demonstrate any polarographic interference produced by the presence of Sn(IV).

Tin Solutions—Sn(II) stock solutions were prepared by dissolving stannous chloride dihydrate[1] in concentrated reagent grade hydrochloric acid and diluting to volume with distilled water. The Sn(IV) stock solutions were prepared in a similar manner with anhydrous stannic chloride[2]. Tin concentrations in these stock solutions were 1.4×10^{-3} *M* for use with pyrophosphate kits and 5.5×10^{-3} *M* for use with the polyphosphate kits. The hydrochloric acid concentration in all tin stock solutions was 2 *M*. To reduce the chance of Sn(II) deterioration, Sn(II) stock solutions were placed in 20-ml multiple-dose vials, purged with nitrogen, and stored under 2.4 atm of nitrogen.

Radiopharmaceutical Kits—Pyrophosphate kits were prepared in 10-ml vials by combining 1.1 ml of an aqueous solution containing 17 mg of tetrasodium pyrophosphate[3] with an appropriate aliquot of Sn(IV) stock solution. Polyphosphate kits were prepared in 10-ml vials by combining 1.0 ml of an aqueous solution containing 67 mg of polyphosphate, prepared by the method of Subramanian *et al.* (5), with an appropriate aliquot of Sn(IV) stock solution. All vials were sealed, nitrogen purged, and stored under a positive nitrogen pressure for a maximum of 8 hr.

An appropriate amount of Sn(II) stock solution was added to the kits just prior to the polarographic analysis (*i.e.*, during the sulfuric acid outgassing in the cell). The combined volume of Sn(II) and Sn(IV) stock solutions added to each pyrophosphate kit was 1.5 ml. The combined volume of tin stock solutions added to each polyphosphate kit was 1.0 ml.

Instrumentation and Analyses—An unmodified, commercially available polarographic analyzer[4] was used for the differential pulse polarographic analysis as follows. Nine milliliters of 1 *M* H_2SO_4 was placed in the polarographic cell, and the cell was outgassed with nitrogen (prepurified grade, scrubbed with vanadous chloride) for 1 min. A 1-ml portion of the kit was then added through the cell top with a 1-ml disposable syringe, and the cell solution was outgassed for 1 additional min. The nitrogen was then diverted over the solution, and a differential pulse polarographic scan was made from −0.30 to −1.00 v with a saturated calomel electrode (SCE) as reference. The following parameters were used: drop time, 0.5 sec; modulation amplitude, 25 mv/pulse; and scan rate, 5 mv/sec.

The peak heights and peak potentials of the scans were calculated and recorded. Peak heights were measured from the baseline of the peak. Each kit analysis required approximately 3.5 min.

RESULTS

Differential pulse polarographic peaks corresponding to Sn(II) reduction were found at peak potentials of −0.44 v for pyrophosphate kits (Fig. 1) and −0.48 v for polyphosphate kits. Standard curves of peak height *versus* Sn(II) concentration were prepared and were linear. The slope of the curves was 0.14 μamp/10^{-4} *M* for polyphosphate kits (correlation coefficient of 0.9962) and 0.17 μamp/10^{-4} *M* for pyrophosphate kits (correlation coefficient of 0.9994). Peak heights for individual kits, especially those with low Sn(II) concentrations, varied with maximum standard deviations of 7% for pyrophosphate and 17% for polyphosphate over four calibration runs.

The polyphosphate Sn(II) peaks were somewhat asymmetric, suggesting the presence of maxima. Ordinary pulse polarography scans confirmed the maxima. The larger standard deviation for the polyphosphate kits as well as the shift in peak potential may be attributed

[1] Analytical reagent grade, Fisher Scientific Co.

[2] Baker analyzed reagent.

[3] Sigma Chemical Co.

[4] Princeton Applied Research polarographic analyzer model 174 with cell and drop timer.

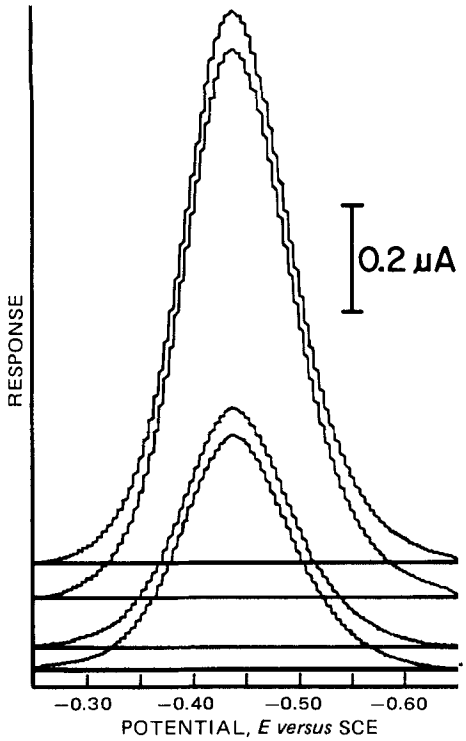

Figure 1—*Differential pulse polarographic scans of two pyrophosphate kits (8.3 × 10⁻⁴ M total tin). The top two scans are of a kit containing 70% of the tin as Sn(II) and 30% as Sn(IV). The lower two scans are of a kit containing 30% Sn(II) and 70% Sn(IV). The peaks occurred at −0.44 v. The vertical positioning of the scans is unimportant, since peak height was measured from the baseline of each peak.*

to the maxima. However, the potential shift could also be an indication of the differences between the Sn(II)–pyrophosphate and Sn(II)–polyphosphate complexes. Nothing was done to suppress the maxima because the polyphosphate variability was not so great to warrant an added step, namely the addition of a surfactant to the supporting electrolyte prior to each analysis.

Several supporting electrolytes were used, but only 1 *M* H_2SO_4 was satisfactory. Since Sn(IV) is not soluble in this electrolyte (6), it does not produce a reduction peak that could interfere with the Sn(II) peak.

Sn(II) solutions in 0.12 *M* HCl were tested by the differential pulse polarographic technique. The method was effective in quantitating Sn(II) at concentrations as low as 8×10^{-6} *M* (2 μg of stannous chloride dihydrate in 1 ml). Sn(IV) interference was not examined at these low Sn(II) concentrations.

DISCUSSION

Classical dc polarography, electrolysis on a microscale in which the magnitude of current flow is proportional to the sample concentration, is useful in tin analysis (6). Differential pulse polarography is a relatively new, highly sensitive version of this technique (7) and is a convenient and effective method for the quantitation of Sn(II) in pyrophosphate and polyphosphate radiopharmaceutical kits. One should not assume that simple Sn(II)–hydrochloric acid solutions can be used as standards, since different peak potentials and slopes can be expected for different kit types as the result of different matrixes. This Sn(II) analytical technique is currently being studied for its value in the qualitative control testing of other radiopharmaceutical products.

REFERENCES

(1) "The Merck Index," 8th ed., Merck & Co., Rahway, N.J., 1968, p. 978.

(2) J. D. Donaldson and W. Moser, *J. Chem. Soc.*, **1960**, 4000.

(3) "Mellor's Modern Inorganic Chemistry," G. D. Parkes, Ed., Wiley, New York, N.Y., 1967, pp. 790, 791.

(4) F. A. Cotton and G. Wilkinson, "Advanced Inorganic Chemistry," 3rd ed., Interscience, New York, N.Y., 1972, p. 331.

(5) G. Subramanian, J. G. McAfee, E. G. Bell, R. J. Blair, R. E. O'Mara, and P. H. Ralston, *Radiology*, **102**, 701 (1972).

(6) J. J. Lingane, *Anal. Chem.*, **18**, 429 (1946).

(7) J. B. Flato, *ibid.*, **44**, 75A (1972).

ACKNOWLEDGMENTS AND ADDRESSES

Received March 17, 1976, from the *Bionucleonics Department, School of Pharmacy and Pharmacal Sciences, Purdue University, West Lafayette, IN 47907.*

Accepted for publication July 21, 1976.

Supported in part by U.S. Public Health Service Training Grant 5-T01-ES00076 from the National Institute for Environmental Health Sciences.

The authors thank Dr. A. M. Knevel for making available the polarographic equipment.

[x] To whom inquiries should be directed.

GI Absorption of Niacin in Humans

HELLE BECHGAARD [x] and S. JESPERSEN

Abstract □ By using the GI tube technique, niacin was shown to be equally well absorbed from the stomach and the upper small intestine. The maximum plasma niacin concentrations occurred 10–20 and 5–10 min, respectively, after instillation. Thus, the physiological prerequisites for a physically retarded niacin preparation were established.

Keyphrases □ Absorption, GI—niacin, stomach and small intestine compared, humans □ Niacin—absorption from stomach and small intestine compared, humans □ Vitamins—niacin, absorption from stomach and small intestine compared, humans

It is generally accepted that weak organic acids or bases are absorbed primarily by penetration of the unionized form of the drug through a lipoidal barrier (1). Niacin (nicotinic acid) (pKa 4.8) should theoretically be better absorbed from the stomach than from the small intestine. However, salicylic acid (pKa 3.0) is reportedly well absorbed even at pH values where it is predominantly ionized (2).

Limited data are available concerning the GI absorption of niacin in humans. In a steady-state situation, about 85% of an orally administered dose (3 g/day) of niacin was recovered from the urine, and it was concluded that absorption was nearly complete (3).

In a comparative study of plain and enteric-coated niacin tablets (4), niacin was absorbed from the small intestine to only a small extent. Based on this finding, in-

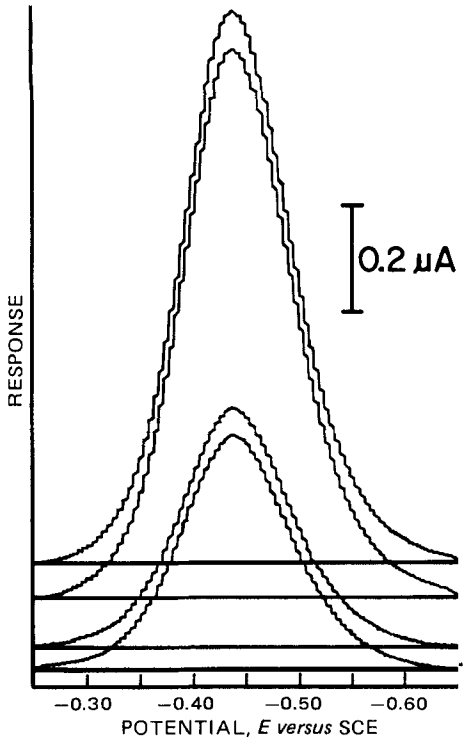

Figure 1—*Differential pulse polarographic scans of two pyrophosphate kits (8.3 × 10⁻⁴ M total tin). The top two scans are of a kit containing 70% of the tin as Sn(II) and 30% as Sn(IV). The lower two scans are of a kit containing 30% Sn(II) and 70% Sn(IV). The peaks occurred at −0.44 v. The vertical positioning of the scans is unimportant, since peak height was measured from the baseline of each peak.*

to the maxima. However, the potential shift could also be an indication of the differences between the Sn(II)–pyrophosphate and Sn(II)–polyphosphate complexes. Nothing was done to suppress the maxima because the polyphosphate variability was not so great to warrant an added step, namely the addition of a surfactant to the supporting electrolyte prior to each analysis.

Several supporting electrolytes were used, but only 1 *M* H_2SO_4 was satisfactory. Since Sn(IV) is not soluble in this electrolyte (6), it does not produce a reduction peak that could interfere with the Sn(II) peak.

Sn(II) solutions in 0.12 *M* HCl were tested by the differential pulse polarographic technique. The method was effective in quantitating Sn(II) at concentrations as low as 8×10^{-6} *M* (2 μg of stannous chloride dihydrate in 1 ml). Sn(IV) interference was not examined at these low Sn(II) concentrations.

DISCUSSION

Classical dc polarography, electrolysis on a microscale in which the magnitude of current flow is proportional to the sample concentration, is useful in tin analysis (6). Differential pulse polarography is a relatively new, highly sensitive version of this technique (7) and is a convenient and effective method for the quantitation of Sn(II) in pyrophosphate and polyphosphate radiopharmaceutical kits. One should not assume that simple Sn(II)–hydrochloric acid solutions can be used as standards, since different peak potentials and slopes can be expected for different kit types as the result of different matrixes. This Sn(II) analytical technique is currently being studied for its value in the qualitative control testing of other radiopharmaceutical products.

REFERENCES

(1) "The Merck Index," 8th ed., Merck & Co., Rahway, N.J., 1968, p. 978.

(2) J. D. Donaldson and W. Moser, *J. Chem. Soc.*, **1960**, 4000.

(3) "Mellor's Modern Inorganic Chemistry," G. D. Parkes, Ed., Wiley, New York, N.Y., 1967, pp. 790, 791.

(4) F. A. Cotton and G. Wilkinson, "Advanced Inorganic Chemistry," 3rd ed., Interscience, New York, N.Y., 1972, p. 331.

(5) G. Subramanian, J. G. McAfee, E. G. Bell, R. J. Blair, R. E. O'Mara, and P. H. Ralston, *Radiology*, **102**, 701 (1972).

(6) J. J. Lingane, *Anal. Chem.*, **18**, 429 (1946).

(7) J. B. Flato, *ibid.*, **44**, 75A (1972).

ACKNOWLEDGMENTS AND ADDRESSES

Received March 17, 1976, from the *Bionucleonics Department, School of Pharmacy and Pharmacal Sciences, Purdue University, West Lafayette, IN 47907.*

Accepted for publication July 21, 1976.

Supported in part by U.S. Public Health Service Training Grant 5-T01-ES00076 from the National Institute for Environmental Health Sciences.

The authors thank Dr. A. M. Knevel for making available the polarographic equipment.

[x] To whom inquiries should be directed.

GI Absorption of Niacin in Humans

HELLE BECHGAARD [x] and S. JESPERSEN

Abstract □ By using the GI tube technique, niacin was shown to be equally well absorbed from the stomach and the upper small intestine. The maximum plasma niacin concentrations occurred 10–20 and 5–10 min, respectively, after instillation. Thus, the physiological prerequisites for a physically retarded niacin preparation were established.

Keyphrases □ Absorption, GI—niacin, stomach and small intestine compared, humans □ Niacin—absorption from stomach and small intestine compared, humans □ Vitamins—niacin, absorption from stomach and small intestine compared, humans

It is generally accepted that weak organic acids or bases are absorbed primarily by penetration of the unionized form of the drug through a lipoidal barrier (1). Niacin (nicotinic acid) (pKa 4.8) should theoretically be better absorbed from the stomach than from the small intestine. However, salicylic acid (pKa 3.0) is reportedly well absorbed even at pH values where it is predominantly ionized (2).

Limited data are available concerning the GI absorption of niacin in humans. In a steady-state situation, about 85% of an orally administered dose (3 g/day) of niacin was recovered from the urine, and it was concluded that absorption was nearly complete (3).

In a comparative study of plain and enteric-coated niacin tablets (4), niacin was absorbed from the small intestine to only a small extent. Based on this finding, in-

Table I—Mean (Range) Plasma Niacin Concentrations (Micrograms per Milliliter) after Instillation of 200 mg of Niacin, $n = 3$

	Minutes						
	5	10	20	40	80	160	320
Stomach[a]	1.6(0.5–1.0)	2.7(1.2–4.5)	2.7(2.4–3.3)	1.4(1.0–1.6)	0.8(0.6–0.9)	0.6(0.4–1.0)	0.5(0.3–0.6)
Stomach[b]	0.4(0.3–0.5)	2.4(1.6–3.6)	3.9(2.9–4.9)	2.2(1.9–2.6)	1.0(0.9–1.1)	0.8(0.5–0.9)	0.5(0.4–0.7)
Small intestine[a]	5.3(3.5–6.5)	5.7(3.0–8.9)	4.8(2.8–6.1)	1.3(0.5–2.8)	0.6(0.4–0.9)	0.9(0.3–1.4)	0.4(0.1–0.5)

[a] Thirty minutes after ingestion of a standard meal. [b] Without ingestion of a standard meal.

vestigators suggested that the physiological prerequisites for a sustained-release niacin preparation are absent (4, 5). In general, however, absorption from enteric-coated tablets is known to be unreliable and often incomplete.

In the present study, absorption of niacin from the human stomach and the upper intestinal tract was compared by means of the GI tube technique.

EXPERIMENTAL

Three healthy, young, male volunteers with normal GI function were the test subjects. No medicine or alcohol consumption was allowed during the 24 hr preceding the tests, and only water was allowed during the 12 hr preceding the tests. In each subject, niacin absorption was studied after instillation of the drug under the following three conditions: (*a*) in the empty stomach, (*b*) in the stomach 30 min after a standard meal, and (*c*) in the small intestine 30 min after a standard meal. An interval of at least 2 weeks was allowed between two consecutive tests.

When niacin absorption from the small intestine was studied, the subjects were admitted to a hospital ward on the day before the test and the stomach tube (weighted with lead shot at the distal opening) was applied. During the night, peristalsis moved the tube into the intestinal tract. The localization of the tube was estimated by an X-ray check and by the measured distance from the nose. In all cases, the distal opening of the tube was located 1–1.5 m from the pylorus.

Niacin (200 mg) dissolved in water (25 ml) was instilled over 15–30 sec, immediately followed by two rinses with water (totaling 50 ml). Venous blood samples were drawn from the supine experimental subject before the test and at fixed time intervals after drug instillation. Blood pressure and pulse rate were registered simultaneously.

Free niacin in plasma was analyzed by the colorimetric technique of Carlson (6). Considering the high levels of niacin involved and the fact that each individual's basal values for König-positive substances before instillation of the drug were used for correction, the well-known relative unspecificity of the analytical method did not compromise the significance of the results obtained (7–9). The coefficient of variation for the analytical procedure was 5%.

RESULTS AND DISCUSSION

The highest level of niacin in plasma was found 5–10 min after instillation into the upper small intestine (Table I). During instillation into the stomach, the maximum plasma niacin concentration occurred 10–20 min after drug administration. Evidently, food did not influence niacin absorption, as evidenced by the peak plasma concentrations with and without a standard meal (Table I).

Immediately after drug instillation, an increase in pulse rate (maximum 45%) and blood pressure (maximum 20%) appeared, indicating rapid absorption. The pulse rate was normalized after 20 min. The increase in blood pressure, however, was ultimately followed by a decrease and normalized after 20–50 min.

CONCLUSION

After instillation into the small intestine of an aqueous niacin solution, the drug appears faster in the plasma and reaches higher levels than after instillation into the stomach. This finding indicates that the compound is absorbed at least as readily from the small intestine as from the stomach. Thus, the physiological basis for the development of a sustained-release niacin preparation is established.

REFERENCES

(1) L. S. Schanker, in "Concepts in Biochemical Pharmacology," B. B. Brodie and J. R. Gillette, Eds., "Handbook of Experiment Pharmacology," vol. XXVIII/1, Springer-Verlag, Heidelberg, Germany, 1971, pp. 9–24.

(2) J. T. Doluisio, N. F. Billups, L. W. Dittert, E. T. Sugita, and J. V. Swintosky, *J. Pharm. Sci.*, **58,** 1196 (1969).

(3) O. N. Miller, J. G. Hamilton, and G. A. Goldsmith, *Am. J. Clin. Nutr.*, **8,** 480 (1960).

(4) N. Svedmyr and L. Harthon, *Acta Pharmacol. Toxicol.*, **28,** 66 (1970).

(5) N. Svedmyr and G. Åberg, *Läkartidningen*, **68,** 1753 (1971).

(6) L. A. Carlson, *Clin. Chim. Acta*, **13,** 349 (1966).

(7) N. Svedmyr, L. Harthon, and L. Lundholm, *Clin. Pharmacol. Ther.*, **10,** 559 (1969).

(8) R. Brattsand and L. Harthon, *Acta Pharmacol. Toxicol.*, **36,** 203 (1975).

(9) G. Brenner, *Arzneim.-Forsch.*, **25,** 237 (1975).

ACKNOWLEDGMENTS AND ADDRESSES

Received June 1, 1976, from the *Pharmacological Department, A/S Alfred Benzon, 29, Halmtorvet, DK-1700 Copenhagen V, Denmark.*

Accepted for publication July 26, 1976.

The authors thank J. Lyngsøe and Mrs. B. Steffensen for assistance.

[x] To whom inquiries should be directed.

Alkaloids of *Glaucium flavum* Grantz, Populations Isfahan and Kazerun

A. SHAFIEE [x], I. LALEZARI, S. LAJEVARDI, and F. KHALAFI

Abstract □ *Glaucium flavum* Grantz, population Isfahan, contained four major alkaloids: dicentrine (0.8%), bulbocapnine (0.42%), protopine (0.35%), and salutaridine (0.2%). *G. flavum* Grantz, population Kazerun, contained four major alkaloids: dicentrine (1.4%), bulbocapnine (0.5%), *O*-methylflavinantine (0.5%), and salutaridine (0.3%); it also contained two minor alkaloids, protopine and α-allocryptonine. *O*-Methylflavinantine was found for the first time in the Papaveraceae.

Keyphrases □ *Glaucium flavum* Grantz—populations Isfahan and Kazerun, major alkaloids identified □ Alkaloids—identified in *Glaucium flavum* Grantz, populations Isfahan and Kazerun

Recently, in a continuation of a research program dealing with the chemotaxonomic studies of Iranian wild Papaveraceae (1–4), the major alkaloids of *Glaucium flavum* Grantz, population Ghom, were reported (5). In this work, the alkaloids of *G. flavum* Grantz, populations Isfahan (south) and Kazerun[1] (southwest of Iran), are reported. Although *Glaucium* species growing in Ghom, Isfahan, and Kazerun are morphologically similar and were identified as *G. flavum* Grantz, careful chemical studies revealed that they are independent chemotypes.

EXPERIMENTAL[2]

Plant Material—The whole aerial parts were collected during May, air dried in the shade, further dried at 60° to a constant weight, and powdered so that all material passed a mesh not greater than 0.5 mm.

Extraction—Powdered plant material, 200 g, was moistened with 200 ml of 15% ammonium hydroxide solution, stirred with 600 ml of chloroform at room temperature for 1 hr, and filtered. The extraction was repeated four times. After the evaporation of the solvent, the residue was extracted with 100 ml of 5% sulfuric acid. The solution was filtered and extracted with petroleum ether (3 × 20 ml) to remove the colored material. The aqueous layer was made alkaline with 15% ammonium hydroxide solution and extracted with chloroform (4 × 50 ml).

Evaporation of the solvent gave a residue of crude alkaloids. The crude extract was subjected to preparative TLC (silica gel $HF_{254+366}$, thickness 1 mm, plate size 20 × 20 cm). Two solvent systems were used for the separation of alkaloids: A, ethyl acetate–methanol–ammonia (85:10:5); and B, petroleum ether–chloroform–diethylamine (70:20:10). Resolved components were detected under 254-nm UV light. Appropriate zones were removed from the plates, and the components were extracted with chloroform–methanol (80:20). The solvent was evaporated under reduced pressure, and the alkaloids were crystallized from an appropriate solvent and characterized.

RESULTS AND DISCUSSION

The following alkaloids were isolated from *G. flavum* population Isfahan:

1. Dicentrine, R_f 0.6 (Solvent System A) and 0.44 (Solvent System B); yield 1.6 g (0.8%); mp 166–169° [lit. (5) mp 166–169°].

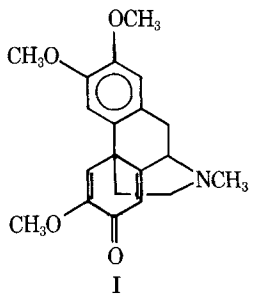

I

2. Bulbocapnine, R_f 0.65 (Solvent System A) and 0.32 (Solvent System B); yield 0.8 g (0.4%); mp 199–200° [lit. (5) mp 199–200°].

3. Salutaridine, R_f 0.42 (Solvent System A) and 0.15 (Solvent System B); yield 0.4 g (0.2%); mp 197–199° [lit. (5) mp 197–199°].

[The melting points, mixed melting points, IR, UV, NMR, and mass spectral data of these alkaloids were identical with those reported (5).]

4. Protopine, R_f 0.71 (Solvent System A) and 0.5 (Solvent System B); yield 0.7 g (0.35%), mp 205–207° [lit. (6) mp 207°]; mixed melting point with an authentic sample 205–207°. Its NMR spectrum was identical with that reported previously (7).

From *G. flavum* population Kazerun, in addition to dicentrine (1.5%), bulbocapnine (0.5%), salutaridine (0.3%), and protopine (minor alkaloid), the following alkaloid was also isolated:

α-Allocryptonine, R_f 0.59 (Solvent System A) and 0.47 (Solvent System B); mp 160–161° [lit. (8) mp 160–161°]; mixed melting point with an authentic sample 160–161°. Its spectral data were similar to those reported previously (9, 10).

In addition, another alkaloid was also isolated [R_f 0.35 (Solvent System A) and 0.15 (Solvent System B)]. This alkaloid was an oil; UV: λ_{max} (ethanol) 282 and 238 nm; IR ($CHCl_3$): 1666 (C=O), 1642, and 1621 cm^{-1}; NMR ($CDCl_3$): δ 1.93 (m, 2H), 2.44 (s, 3H, NCH_3), 2.49–3.66 (m, 5H), 3.82 (s, 3H, OCH_3), 3.87 (s, 3H, OCH_3), 3.90 (s, 3H, OCH_3), 6.30 (s, 1H), 6.53 (s, 1H), 6.70 (s, 1H), and 6.95 (s, 1H); mass spectrum: *m/e* 341 (M^+), 326 ($M^+ - 15$), 313 ($M^+ - 28$), 298 ($M^+ - 43$), 282, and 149.

Anal.—Calc. for $C_{20}H_{23}NO_4$: C, 70.38; H, 6.74; N, 4.11. Found: C, 70.45; H, 6.83; N, 4.26.

The hydrochloride had a melting point of 195–196° (ethanol). The methiodide had a melting point of 223–225° (methanol) [lit. (11) mp 223–225°].

The spectral data (UV, IR, NMR, and mass) as well as the TLC data of this alkaloid (I) were identical with an authentic sample of *O*-methylflavinantine.

The alkaloid profiles of *G. flavum* Grantz, populations Ghom, Isfahan, and Kazerun, indicate that they are independent chemotypes. The major alkaloids of Ghom are dicentrine, bulbocapnine, and salutaridine. *G. flavum* population Isfahan also has protopine as a major alkaloid. Protopine could not be detected in *G. flavum* population Ghom. Finally, *G. flavum* population Kazerun also has *O*-methylflavinantine, which was not present in the other populations. A literature survey revealed that *O*-methylflavinantine was found in *Nemuaron vieillardii* (Monimiaceae) (12) and *Rhigiocarja racemifera* Miers (Menispermaceae) (13).

REFERENCES

(1) N. Sharghi and I. Lalezari, *Nature*, **213**, 1244 (1967).

(2) I. Lalezari, A. Shafiee, and P. Nasseri-Nouri, *J. Pharm. Sci.*, **62**, 1718 (1973).

(3) I. Lalezari, P. Nasseri-Nouri, and R. Asgharian, *ibid.*, **63**, 1331 (1974).

(4) A. Shafiee, I. Lalezari, P. Nasseri-Nouri, and R. Asgharian, *ibid.*, **64**, 1570 (1975).

(5) I. Lalezari, A. Shafiee, and M. Mahjour, *ibid.*, **65**, 923 (1976).

(6) W. H. Perkin, *J. Chem. Soc.*, **109**, 1023 (1916).

(7) F. A. L. Anet and B. A. Brown, *Tetrahedron Lett.*, **1967**, 4881.

[1] The plants were identified by Professor K. Hummel, Tubingen University. Herbarium samples were deposited in the Herbarium of the College of Pharmacy, Tehran University.

[2] Melting points were taken with a Koffler hot-stage microscope and are uncorrected. UV spectra were recorded on a Varian Techtron 635 instrument. NMR spectra were taken with a Varian T 60A instrument, using tetramethylsilane as the internal standard. Mass spectra were recorded on CH5 spectrometer at Arya-Mehr University. IR spectra were obtained with a Leitz model III spectrograph. Protopine and α-allocryptonine were obtained from Koch-Light Laboratories, Colnbrook SL3 OBZ, Buckinghamshire, England.

(8) R. D. Haworth and W. H. Perkin, *J. Chem. Soc.*, **1926**, 445.
(9) C. E. Redemann, B. B. Wisegarver, and G. A. Alles, *J. Am. Chem. Soc.*, **71**, 1030 (1941).
(10) L. Dolejs, V. Hanus, and J. Slavik, *Collect. Czech. Chem. Commun.*, **29**, 2479 (1964).
(11) T. Kametani, K. Fukumoto, F. Satoh, and H. Yagi, *J. Chem. Soc. C*, **1969**, 520.
(12) I. R. C. Bick, H. M. Leow, N. W. Preston, and J. J. Wright, *Aust. J. Chem.*, **26**, 455 (1973).
(13) A. N. Tackie, D. Dwuma-Badu, J. E. Knapp, D. J. Slatkin, and P. L. Schiff, Jr., *Phytochemistry*, **13**, 2884 (1974).

ACKNOWLEDGMENTS AND ADDRESSES

Received January 2, 1976, from the *Institute of Medical Plants, College of Pharmacy, Tehran University, Tehran, Iran.*

Accepted for publication July 21, 1976.

Supported by Grant 13 of the International Foundation for Science and a grant from the Ministry of Science Research Council.

The authors are grateful to Dr. J. E. Knapp of the Department of Pharmacognosy, University of Pittsburgh, for a sample of *O*-methylflavinantine.

[x] To whom inquiries should be directed.

Rapid Determination of Procainamide and Its *N*-Acetyl Derivative in Human Plasma by High-Pressure Liquid Chromatography

ORVILLE H. WEDDLE and WILLIAM D. MASON [x]

Abstract □ A rapid, specific, high-pressure liquid chromatographic method for the determination of procainamide and its *N*-acetyl derivative in plasma was developed. The procedure is fast enough (15 min from receipt of blood to reporting value) to be used for emergency determinations. The sensitivity, precision, and accuracy are sufficient for routine monitoring of therapeutic levels in patients. The assay is specific enough to be valid in the presence of a number of drugs and dietary substances present in clinical samples.

Keyphrases □ Procainamide and *N*-acetyl derivative—high-pressure liquid chromatographic analyses, human plasma □ High-pressure liquid chromatography—analyses, procainamide and *N*-acetyl derivative, human plasma □ Cardiac depressants—procainamide and *N*-acetyl derivative, high-pressure liquid chromatographic analyses, human plasma

Procainamide (I) is an antiarrhythmic compound which demonstrates marked intersubject variability in absorption and elimination (1). Its *N*-acetyl metabolite (II) in humans (2) has antiarrhythmic activity comparable to that of I (3) but demonstrates an even greater variability in plasma concentration with a given I dosage schedule. Methods of monitoring plasma I concentrations that do not also determine II are not adequate.

Recently, several methods for the simultaneous determination of I and II were reported. A fluorometric method required more than 4 ml of blood for a duplicate determination and involved reextraction into acid, addition of alkali, and two fluorescence measurements (4). No mention was made of the possible interference of the fluorescent base quinidine, which would be extracted under these conditions and might be present in patients receiving procainamide.

A GLC method was reported for I and II determinations in urine samples (5), but no mention was made of its application to blood samples. Another GLC method for the determination of both I and II in blood, urine, and saliva samples was reported (6). However, each duplicate analysis probably required 1 hr or more because of a three-stage acid–base extraction, evaporation, and the 23.5-min retention time for II.

A quantitative TLC approach to the problem was developed (2). The reported standard deviations of 9% for I and 11% for II reflect a well-known difficulty of quantitative TLC.

None of the reported methods claimed the combination of small sample size, rapidity, specificity, and precision desirable for routine patient monitoring. This paper describes a method for performing a duplicate analysis in 16 min on as little as 300 μl of whole blood with sufficient accuracy, precision, and specificity for clinical samples.

EXPERIMENTAL

Materials—UV grade hexane, 2-propanol, methanol, 1-butanol, and chloroform[1] and reagent grade concentrated ammonium hydroxide[2] were used as obtained. High purity samples of I and II[3] were used in the preparation of standards.

Apparatus—A high-pressure liquid chromatograph[4] was equipped with a septumless injection port[5] and a fixed wavelength (280 nm) UV absorption detector[6]. The detector was operated at 0.005 and 0.01 absorbance unit full scale.

Chromatographic Parameters—The mobile phase was prepared by diluting concentrated ammonium hydroxide 10:1 with distilled water. One milliliter of this solution was added to 1 liter of 2-propanol and 1 liter of hexane, and the solution was diluted to 5 liters with methanol. The mobile phase was pumped at 5.0 ml/min (3500 psi) through a stainless steel column (4 mm i.d. × 30 cm) packed with a high efficiency bonded-phase absorption packing[7].

Analytical Procedure—Two 50-μl aliquots of each plasma sample were placed in 1.5-ml disposable centrifuge tubes[8]. To each tube was added 10 μl of 5 *N* NaOH solution and 600 μl of an organic extraction solution containing 20% 1-butanol, 20% chloroform, and 60% hexane by volume. The two tubes, together with any other samples being run at the same time, were shaken for 30 sec at 1350 oscillations/sec[9] and then centrifuged for 30 sec at 15,000 rpm[10].

[1] Burdick and Jackson Laboratories, Muskegon, Mich.
[2] Mallinckrodt Chemical Works, St. Louis, Mo.
[3] E. R. Squibb & Sons.
[4] Model 6000A, Waters Associates, Milford, Mass.
[5] Model U6K, Waters Associates, Milford, Mass.
[6] Model 440, Waters Associates, Milford, Mass.
[7] μBondapak CN, Waters Associates, Milford, Mass.
[8] Brinkmann Instruments, Westbury, N.Y.
[9] Eppendorf Micro Shaker, Brinkmann Instruments, Westbury, N.Y.
[10] Eppendorf Micro Centrifuge, Model 3200, Brinkmann Instruments, Westbury, N.Y.

(8) R. D. Haworth and W. H. Perkin, *J. Chem. Soc.*, **1926**, 445.
(9) C. E. Redemann, B. B. Wisegarver, and G. A. Alles, *J. Am. Chem. Soc.*, **71**, 1030 (1941).
(10) L. Dolejs, V. Hanus, and J. Slavik, *Collect. Czech. Chem. Commun.*, **29**, 2479 (1964).
(11) T. Kametani, K. Fukumoto, F. Satoh, and H. Yagi, *J. Chem. Soc. C*, **1969**, 520.
(12) I. R. C. Bick, H. M. Leow, N. W. Preston, and J. J. Wright, *Aust. J. Chem.*, **26**, 455 (1973).
(13) A. N. Tackie, D. Dwuma-Badu, J. E. Knapp, D. J. Slatkin, and P. L. Schiff, Jr., *Phytochemistry*, **13**, 2884 (1974).

ACKNOWLEDGMENTS AND ADDRESSES

Received January 2, 1976, from the *Institute of Medical Plants, College of Pharmacy, Tehran University, Tehran, Iran.*

Accepted for publication July 21, 1976.

Supported by Grant 13 of the International Foundation for Science and a grant from the Ministry of Science Research Council.

The authors are grateful to Dr. J. E. Knapp of the Department of Pharmacognosy, University of Pittsburgh, for a sample of *O*-methylflavinantine.

[x] To whom inquiries should be directed.

Rapid Determination of Procainamide and Its *N*-Acetyl Derivative in Human Plasma by High-Pressure Liquid Chromatography

ORVILLE H. WEDDLE and WILLIAM D. MASON [x]

Abstract □ A rapid, specific, high-pressure liquid chromatographic method for the determination of procainamide and its *N*-acetyl derivative in plasma was developed. The procedure is fast enough (15 min from receipt of blood to reporting value) to be used for emergency determinations. The sensitivity, precision, and accuracy are sufficient for routine monitoring of therapeutic levels in patients. The assay is specific enough to be valid in the presence of a number of drugs and dietary substances present in clinical samples.

Keyphrases □ Procainamide and *N*-acetyl derivative—high-pressure liquid chromatographic analyses, human plasma □ High-pressure liquid chromatography—analyses, procainamide and *N*-acetyl derivative, human plasma □ Cardiac depressants—procainamide and *N*-acetyl derivative, high-pressure liquid chromatographic analyses, human plasma

Procainamide (I) is an antiarrhythmic compound which demonstrates marked intersubject variability in absorption and elimination (1). Its *N*-acetyl metabolite (II) in humans (2) has antiarrhythmic activity comparable to that of I (3) but demonstrates an even greater variability in plasma concentration with a given I dosage schedule. Methods of monitoring plasma I concentrations that do not also determine II are not adequate.

Recently, several methods for the simultaneous determination of I and II were reported. A fluorometric method required more than 4 ml of blood for a duplicate determination and involved reextraction into acid, addition of alkali, and two fluorescence measurements (4). No mention was made of the possible interference of the fluorescent base quinidine, which would be extracted under these conditions and might be present in patients receiving procainamide.

A GLC method was reported for I and II determinations in urine samples (5), but no mention was made of its application to blood samples. Another GLC method for the determination of both I and II in blood, urine, and saliva samples was reported (6). However, each duplicate analysis probably required 1 hr or more because of a three-stage acid–base extraction, evaporation, and the 23.5-min retention time for II.

A quantitative TLC approach to the problem was developed (2). The reported standard deviations of 9% for I and 11% for II reflect a well-known difficulty of quantitative TLC.

None of the reported methods claimed the combination of small sample size, rapidity, specificity, and precision desirable for routine patient monitoring. This paper describes a method for performing a duplicate analysis in 16 min on as little as 300 μl of whole blood with sufficient accuracy, precision, and specificity for clinical samples.

EXPERIMENTAL

Materials—UV grade hexane, 2-propanol, methanol, 1-butanol, and chloroform[1] and reagent grade concentrated ammonium hydroxide[2] were used as obtained. High purity samples of I and II[3] were used in the preparation of standards.

Apparatus—A high-pressure liquid chromatograph[4] was equipped with a septumless injection port[5] and a fixed wavelength (280 nm) UV absorption detector[6]. The detector was operated at 0.005 and 0.01 absorbance unit full scale.

Chromatographic Parameters—The mobile phase was prepared by diluting concentrated ammonium hydroxide 10:1 with distilled water. One milliliter of this solution was added to 1 liter of 2-propanol and 1 liter of hexane, and the solution was diluted to 5 liters with methanol. The mobile phase was pumped at 5.0 ml/min (3500 psi) through a stainless steel column (4 mm i.d. × 30 cm) packed with a high efficiency bonded-phase absorption packing[7].

Analytical Procedure—Two 50-μl aliquots of each plasma sample were placed in 1.5-ml disposable centrifuge tubes[8]. To each tube was added 10 μl of 5 *N* NaOH solution and 600 μl of an organic extraction solution containing 20% 1-butanol, 20% chloroform, and 60% hexane by volume. The two tubes, together with any other samples being run at the same time, were shaken for 30 sec at 1350 oscillations/sec[9] and then centrifuged for 30 sec at 15,000 rpm[10].

[1] Burdick and Jackson Laboratories, Muskegon, Mich.
[2] Mallinckrodt Chemical Works, St. Louis, Mo.
[3] E. R. Squibb & Sons.
[4] Model 6000A, Waters Associates, Milford, Mass.
[5] Model U6K, Waters Associates, Milford, Mass.
[6] Model 440, Waters Associates, Milford, Mass.
[7] μBondapak CN, Waters Associates, Milford, Mass.
[8] Brinkmann Instruments, Westbury, N.Y.
[9] Eppendorf Micro Shaker, Brinkmann Instruments, Westbury, N.Y.
[10] Eppendorf Micro Centrifuge, Model 3200, Brinkmann Instruments, Westbury, N.Y.

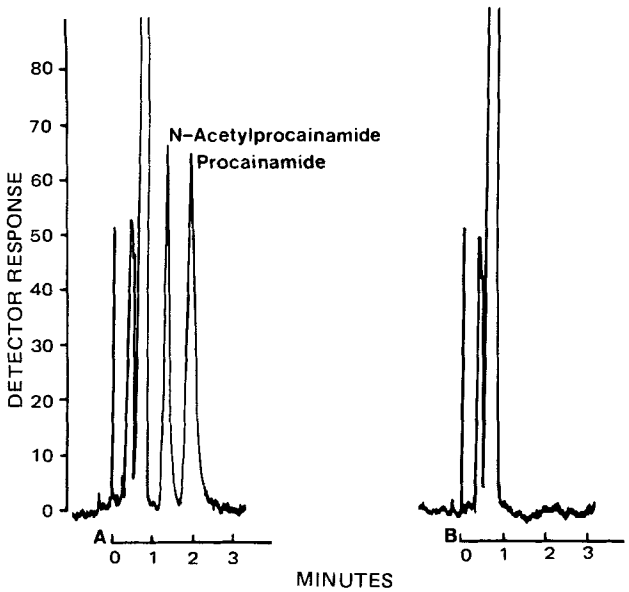

Figure 1—*High-pressure liquid chromatograms of human plasma extracts. Key: A, plasma containing 5 μg of I/ml and 5 μg of II/ml; amd B, control plasma.*

After centrifugation, exactly 100 μl of the supernate from the first tube was measured accurately with a syringe[11] and injected into the chromatograph. Three minutes after the first injection, 100 μl from the second tube was injected. Three minutes after the second injection, the chromatogram was removed and the peak heights were measured in millimeters. The peak heights were converted to plasma I and II concentrations by comparison to a standard curve.

Standard Curve—Stock solutions of 0.10 mg of I/ml and 0.10 mg of II/ml were prepared by dissolving weighed drug samples in methanol. Appropriate aliquots of these standards were added to conical centrifuge tubes and evaporated under nitrogen. Sufficient pooled human plasma was added to each tube to produce final concentrations of 2, 4, 6, 8, 10, 15, and 20 μg/ml. The tubes were vortexed to dissolve the drugs, and then 100-μl aliquots were removed for analysis by the described procedure.

Eight analyses were done at each concentration. The heights of the chromatographic peaks were measured in millimeters. A straight-line fit of the data was made by linear regression analysis, and the correlation coefficient was determined.

Accuracy and Precision—The accuracy and precision of the method were evaluated by performing 48 duplicate analyses on spiked samples of human plasma. Twelve duplicate analyses were performed at each of the following concentrations: 2, 4, 6, and 8 μg/ml. The spiked samples were prepared by adding appropriate aliquots of the 0.10-mg/ml stock solution to centrifuge tubes, evaporating the methanol in a nitrogen stream, and then dissolving I and II in 100-μl aliquots from selected plasma samples.

The 48 plasma samples used were left over from blood samples originally drawn for analyses of other drugs from patients known not to be receiving I or II. After preparation, the spiked samples were analyzed as described; the mean and standard deviation of the measured values were determined.

Evaluation of Interferences—Samples of caffeine, theobromine, theophylline, 3-methylxanthine, quinidine, and propranolol were dissolved in the extraction solution. Aliquots (100 μl) of these solutions were injected into the chromatograph, and the retention times of the drugs were determined. The possibility of interferences also was tested by performing the analysis on a series of plasma samples from patients receiving drugs other than procainamide. Any interferences from quinidine, primidone, phenobarbital, phenytoin, and their metabolites were detected in this way.

RESULTS AND DISCUSSION

Figure 1A shows the chromatogram obtained by injecting 100 μl of the extract of the plasma sample spiked with 5 μg of I/ml and 5 μg of II/ml. The method of analysis described under *Analytical Procedure* was used.

[11] Precision Sampling Corp.

Table I—Accuracy and Precision of HPLC Assay for I and II

I Added, μg/ml	II Added, μg/ml	I Found, μg/ml	*SD* of I Found, %	II Found, μg/ml	*SD* of II Found, %
4	4	3.95	3.0	3.93	2.4
6	6	5.94	2.2	5.96	2.2
8	8	8.04	2.1	7.92	1.4
10	10	10.13	1.2	10.06	1.4

Figure 1B shows the chromatogram of a 100-μl injection of a plasma sample extracted in exactly the same way but with no added I or II. Figure 1B shows that all significant artifact peaks and baseline variations due to the injection of 100 μl of extraction solvent plus components extracted from plasma were complete within about 1 min after injection. Figure 1A shows that the I and II peaks were well separated from each other and from the artifact peaks.

The I and II peak heights (in millimeters) measured on the chromatograms were plotted against the concentrations (in micrograms per milliliter) of I and II in the plasma standard solutions to prepare a standard curve. Twelve plasma samples were assayed at each concentration: 2, 4, 6, 8, 10, 15, and 20 μg/ml of both I and II. The curves obtained by linear regression analyses of these data were $y = 22.8x - 4.76$ for I and $y = 22.5x - 4.6$ for II. The regression coefficients were 0.9999 for I and 0.9996 for II.

The method is sufficiently accurate and precise for routine analysis of clinical samples (Table I). The time required for a duplicate analysis, from centrifugation of the blood to final calculations, is only 16 min. In this laboratory, all routine I and II analyses are run once a day along with external standards. The stat samples are run as soon as received and are checked by external standards, which are run after the values are reported. It has never proven necessary to recall a stat value.

Several drugs that might be taken by patients also taking procainamide were tested for interference with the procainamide assay. Plasma samples from patients having therapeutic levels of quinidine, primidone, phenobarbital, and phenytoin but no procainamide were analyzed. The samples were extracted and chromatographed in exactly the same way as for a I and II analysis. In none of these cases was there a peak giving a false I or II level. In some cases, this result was probably due to the fact that the drug or its metabolites did not extract under the assay conditions. Injection of solutions of caffeine, theobromine, theophylline, 3-methylxanthine, quinidine, and propranolol made up in the extraction solvent failed to reveal any interferences. Only quinidine gave a peak, with a retention time of about 1 min, and it was well resolved from II.

A total of 37 clinical samples have been run by this method. In all of these samples as well as in all controls, no significant peaks with retention times longer than the procainamide have been observed. This result is perhaps due partly to the fact that substances more polar than procainamide tend to be left behind in the aqueous phase during extraction. An important conclusion is that the extractions into less polar solvents followed by normal phase liquid chromatography can lead to short chromatographic runs and short analysis times.

REFERENCES

(1) J. Koch-Weser and S. W. Klein, *J. Am. Med. Assoc.*, **215**, 1454 (1971).

(2) M. M. Reidenberg, D. E. Drayer, M. Levy, and H. Warner, *Clin. Pharmacol. Ther.*, **17**, 722 (1975).

(3) J. Elson, J. M. Strong, W.-K. Lee, and A. J. Atkinson, Jr., *ibid.*, **17**, 134 (1975).

(4) E. Matusik and T. P. Gibson, *Clin. Chem.*, **21**, 1899 (1975).

(5) T. P. Gibson, J. Matusik, E. Matusik, H. A. Nelson, J. Wilkinson, and W. A. Briggs, *Clin. Pharmacol. Ther.*, **17**, 395 (1975).

(6) R. L. Galeazzi, L. B. Sheiner, T. Lackwood, and L. Z. Benet, *ibid.*, **19**, 55 (1976).

ACKNOWLEDGMENTS AND ADDRESSES

Received June 1, 1976, from the *School of Pharmacy, University of Missouri–Kansas City, Kansas City, MO 64108.*

Accepted for publication July 28, 1976.

Supported in part by Grant D08PE05146-01 from the Department of Health, Education, and Welfare.

The authors thank the Clinical Pharmacy Faculty of the University of Missouri–Kansas City for their assistance in this project.

[x] To whom inquiries should be directed.

Lipid–Protein Interactions: Detergent Binding to L-Glutamic Acid Dehydrogenase

DAVID H. KEMPNER and BRIAN J. JOHNSON ˣ

Abstract □ A nonionic detergent was found to bind to the enzyme L-glutamic acid dehydrogenase [L-glutamate:nicotinamide adenine dinucleotide phosphate oxidoreductase (deaminating) EC1.4.1.3]. The amount bound was 17 moles of detergent/mole of enzyme, which, however, was not sufficient for the enzyme to be included in a detergent micelle.

Keyphrases □ L-Glutamic acid dehydrogenase—binding of nonionic detergent □ Detergents, nonionic—binding to L-glutamic acid dehydrogenase □ Binding—L-glutamic acid dehydrogenase to nonionic detergent □ Enzymes—L-glutamic acid dehydrogenase, binding to nonionic detergent

It has been reported (1) that the enzyme activity of L-glutamic acid dehydrogenase [L-glutamate:nicotinamide adenine dinucleotide phosphate oxidoreductase (deaminating) EC 1.4.1.3] changes in the presence of nonionic detergents. It was suggested that this change was due to some conformational event being produced in the enzyme by the detergent. Such a supposition implies that the detergent is bound to the enzyme. This paper reports an investigation of this hypothesis.

EXPERIMENTAL

The concentration of L-glutamic acid dehydrogenase solutions was determined using an $E^{1\%}_{280}$ of 10.0 (2). Quantitation of the enzyme in detergent solution and of ovalbumin was determined by fluorescamine (3).

Synthesis of ^{125}I-L-Glutamic Acid Dehydrogenase—The labeled compound was prepared by the method of Marchalonis (4) as modified by David and Reisfeld (5). To 600 μl of a 0.5% solution of enzyme in phosphate-buffered saline (1×10^{-4} *M* ethylenediaminetetraacetic acid, 0.1 *M* NaCl, and 0.04 *M* sodium phosphate, pH 7.4) were added 11 μg of lactoperoxidase coupled to 40 mg of wet Sepharose 4B[1] and 1 mCi of carrier-free ^{125}I-labeled sodium iodide. The reaction was initiated by addition of 20 μl of a 1×10^{-2} *M* solution of hydrogen peroxide in water.

The reaction mixture was shaken for a total of 10 min, but the shaking was stopped at 2-min intervals so that additional 20-μl aliquots of the hydrogen peroxide solution could be added. At the completion of the reaction, the radioiodinated enzyme was collected by centrifugation at 6000×*g* for 2 min. The supernate containing the enzyme was decanted off, and the beads were washed once with 0.5 ml of phosphate Buffer A (1×10^{-4} *M* ethylenediaminetetraacetic acid and 0.04 *M* sodium phosphate, pH 7.4) and centrifuged to extract any residual iodinated enzyme. The combined solutions were dialyzed overnight at 4° against 2 × 300-ml changes of phosphate Buffer A.

An equal volume of 2 *M* ammonium sulfate was added to the dialysate, and the solution was allowed to stand overnight at 4°. The precipitated protein was collected by centrifugation at 5000×*g* for 10 min, and the pellet was washed once with approximately 2 ml of chilled 2 *M* ammonium sulfate and recentrifuged. The pellet was dissolved in approximately 1 ml of phosphate Buffer A and dialyzed overnight at 4° against 2 × 300-ml changes of the same phosphate buffer.

The final traces of unbound iodine were removed by gel filtration on a column (2.3 × 9 cm) of Sephadex G-200. Fractions of 1 ml were collected and counted for radioactivity. Alternate fractions were assayed for protein by fluorescamine. Appropriate fractions, as determined by the ratio of radioactive counts to fluorescence, were pooled such that the specific activity of a preparation was typically 34,000 cpm/μg of enzyme.

Synthesis of ^{125}I-Nonionic Detergent—To 600 μl of a 10% solution of the detergent[2] in phosphate Buffer A were added 11 μg of lactoperoxidase coupled to 40 mg of wet Sepharose 4B and 1 mCi of carrier-free ^{125}I-labeled sodium iodide[3]. The reaction was initiated by addition of a 20-μl aliquot of a 1×10^{-2} *M* solution of hydrogen peroxide in deionized water. The reaction mixture was shaken for a total of 10 min, but shaking was interrupted at 2-min intervals so that additional 20-μl aliquots of the hydrogen peroxide solution could be added. A control was performed in an identical manner, except that 0.1 mCi of ^{125}I-labeled sodium iodide was used without lactoperoxidase or hydrogen peroxide.

After the iodination of the nonionic detergent, the entire reaction mixture was passed through a column (2.3 × 9 cm) of Sephadex G-15 to remove the unbound iodine. Fractions of 0.8 ml were collected and counted for radioactivity. The absorbance at 275 nm of alternate fractions was obtained; those fractions, as determined by the ratio of radioactive counts to absorption at 275 nm, were pooled such that a typical preparation with a specific activity of 8×10^9 cpm/mmole was obtained.

Micelle Formation and Binding of Nonionic Detergent to L-Glutamic Acid Dehydrogenase—*Sephadex G-75 Chromatography*—Samples (3.5–0.35%) of enzyme in phosphate Buffer A were mixed with equal volumes of radioiodinated nonionic detergent. The mixtures were incubated at 4° overnight and then passed through a column (0.9 × 14 cm) of Sephadex G-75 at 4°. The sample was eluted from the column using the phosphate buffer as eluant at a flow rate of 7 ml/hr. Each fraction of 0.3 ml was counted for radioactivity. A control consisting of only radioiodinated detergent was also run.

Bio-Gel A-15m Chromatography—A 50-μl aliquot of a 100-μg/ml solution of ^{125}I-labeled enzyme (specific activity of 7000 cpm/μg) was added to 100 μl of a 7% solution of enzyme in phosphate Buffer A. To this mixture was added 50 μl of detergent. A control was prepared in the same way, except that 50 μl of deionized water was substituted for the detergent.

The samples were then incubated at 37° for 15 min and then at 4° overnight. All samples were layered onto a column (0.9 × 14 cm) and eluted with phosphate Buffer B (0.2 *M* NaCl, 1×10^{-4} *M* ethylenediaminetetraacetic acid, and 0.04 *M* sodium phosphate, pH 7.4), which also contained 1% by volume of the nonionic detergent. Fractions of 0.2 ml were collected and counted for radioactivity.

Sephadex G-200 Chromatography—The molecular weight markers, L-glutamic acid dehydrogenase, and ovalbumin, each dissolved in Buffer B, were run through their respective columns (0.9 × 29 cm) to determine their elution volumes. The void volume of the columns also was determined with Blue Dextran 2000 with every column run. A 50-μl aliquot of a 60-μg/ml solution of ^{125}I-labeled enzyme (specific activity of 3.7×10^4 cpm/μg) in phosphate Buffer B was added to 100 μl of a 7% solution of enzyme in phosphate Buffer A. To this mixture was added 50 μl of the nonionic detergent. For the control, run under identical conditions, 50 μl of deionized water was added to the enzyme sample. For samples of radioiodinated enzyme containing the nonionic detergent, the eluting buffer also contained 1% by volume of the detergent. Fractions of 0.4 ml were collected and counted for radioactivity. Each peak was pooled and assayed for protein by the use of fluorescamine.

RESULTS AND DISCUSSION

The binding of a nonionic detergent to the enzyme L-glutamic acid dehydrogenase was investigated because such detergents previously enhanced the activity of the enzyme to an appreciable extent (1). This investigation necessitated the preparation of the radioiodinated detergent and the enzyme. Enzyme synthesis was achieved by the use of insolubilized lactoperoxidase (4, 5).

The interaction of the enzyme and detergent was studied using gel

[1] Worthington Biochemical Corp., Freehold, N.J.

[2] Triton X-102, Sigma Chemical Co., St. Louis, Mo. This detergent possessed a hydrophilic portion in the form of a polyoxyethylene moiety and a lipophilic portion consisting of octylphenyl. These data were obtained from Rohm and Haas Surfactants Technical Bulletin, Rohm and Haas Co., Philadelphia, Pa.

[3] New England Nuclear Corp., Boston, Mass.

filtration. The results of this procedure have been shown to be in good agreement with those obtained by equilibrium dialysis (6). However, this technique will not determine accurately the binding parameters of any rapidly equilibrating system; under such circumstances, an overestimation of binding is observed.

In the present studies, it was possible to separate the detergent bound to the enzyme from that unbound and to estimate the amount of interaction between the two moieties. The enzyme, at a 4–5% concentration dissolved in a 0.9% solution of radioiodinated detergent, was chromatographed on Sephadex G-75. It was found that 1.4×10^{-5} mmole (mol. wt. 744) of the detergent was associated with 825 μg of the enzyme. This result indicates that 17 moles of detergent bound per mole of enzyme, calculated on the latter having a molecular weight of 1×10^6. This ratio of detergent to enzyme nearly corresponds to one binding site per 55,000 molecular weight subunit of the enzyme (7). This calculation presupposes detergent that is bound rather than in the micellar form. Such binding has occurred when ligand and protein were present in relatively low concentrations (8–10).

One interesting aspect of the interactions between proteins and detergents is the inclusion of several protein molecules in one detergent micelle (11). To test whether the enzyme could be included in detergent micelles, solutions of the radioiodinated enzyme in detergent were prepared and passed through a column of Bio-Gel A-15m. The results indicated that the enzyme could not be aggregated in detergent micelles, because no sample of L-glutamic acid dehydrogenase in detergent had an elution volume less than the native enzyme, even when the eluting buffer contained 1% by volume of the detergent.

While this experiment on agarose showed that the enzyme was not measurably aggregated in detergent micelles, it was not clear whether the enzyme was dissociating into its 55,000 subunits (7). Therefore, gel filtration on Sephadex G-200 was performed. The enzyme buffer only eluted as a single peak, whereas the enzyme in detergent gave a chromatograph of two peaks. In this latter case, the first peak eluted with the void volume whereas the position of the second peak indicated a molecular weight of 55,000. However, the amount of dissociation into these small subunits was never more than 5% of the total amount applied to the column.

The results indicate that the nonionic detergent can bind to the enzyme L-glutamic acid dehydrogenase. This binding is only in the order of approximately 17 moles of detergent/mole of enzyme, hardly sufficient to allow the enzyme to be included in a detergent micelle. However, it obviously is sufficient to cause enhancement of the activity of this enzyme (1).

These results suggest a possible avenue for enhancement of the biological activities of other proteins and drugs.

REFERENCES

(1) D. H. Kempner and B. J. Johnson, *J. Pharm. Sci.*, **65,** 1799 (1976).

(2) M. W. Bitensky, K. L. Yielding, and G. M. Tomkins, *J. Biol. Chem.*, **240,** 668 (1965).

(3) S. Udenfriend, S. Stein, P. Bohlen, W. Dairman, W. Leimgruber, and W. Weigle, *Science*, **178,** 871 (1972).

(4) J. J. Marchalonis, *Biochem. J.*, **113,** 299 (1969).

(5) G. S. David and R. A. Reisfeld, *Biochemistry*, **13,** 1014 (1974).

(6) P. F. Cooper and G. C. Wood, *J. Pharm. Pharmacol., Suppl.*, **20,** 150S (1968).

(7) N. Tatal, G. M. Tomkins, J. F. Muchinski, and K. L. Yielding, *J. Mol. Biol.*, **8,** 46 (1964).

(8) S. Makino, J. A. Reynolds, and C. Tanford, *J. Biol. Chem.*, **248,** 4926 (1973).

(9) J. A. Reynolds and C. Tanford, *Proc. Nat. Acad. Sci. USA*, **66,** 1002 (1970).

(10) Y. Nozaki, J. A. Reynolds, and C. Tanford, *J. Biol. Chem.*, **249,** 4452 (1974).

(11) J. N. Umbreit and J. L. Strominger, *ibid.*, **248,** 6759 (1973).

ACKNOWLEDGMENTS AND ADDRESSES

Received April 7, 1976, from the *Department of Microbiology, University of Alabama Medical School, Birmingham, AL 35294.*

Accepted for publication July 28, 1976.

Supported in part by Grant AI 11970 from the National Institutes of Health.

[x] To whom inquiries should be directed.

Separation and Quantitative Determination of 2,4-Disulfamyl-5-trifluoromethylaniline in Hydroflumethiazide Using High-Pressure Liquid Chromatography

B. J. OWEN [x] and S. V. WILKIE

Abstract □ A high-pressure liquid chromatographic method was developed to quantify 2,4-disulfamyl-5-trifluoromethylaniline in hydroflumethiazide using a bonded pellicular packing. An internal standard was added to the samples to ensure reproducibility. The results were compared with methods currently in use.

Keyphrases □ 2,4-Disulfamyl-5-trifluoromethylaniline—high-pressure liquid chromatographic analysis in hydroflumethiazide samples and tablets □ Hydroflumethiazide—prepared samples and tablets, high-pressure liquid chromatographic analysis of its precursor 2,4-disulfamyl-5-trifluoromethylaniline □ High-pressure liquid chromatography—analysis, 2,4-disulfamyl-5-trifluoromethylaniline in hydroflumethiazide prepared samples and tablets □ Antihypertensives—hydroflumethiazide prepared samples and tablets, high-pressure liquid chromatographic analysis of its precursor 2,4-disulfamyl-5-trifluoromethylaniline

The hydroflumethiazide monographs in the National Formulary (1) and the British Pharmacopoeia (2) include assays for free amine in the form of its precursor 2,4-disulfamyl-5-trifluoromethylaniline (I) (3–6). In the BP method, the free amine in the sample is compared visually with a standard of I using TLC for the separation. A diazotization is performed in the NF method, and the solution absorbance is read spectrophotometrically and compared with a standard preparation.

This paper describes a high-pressure liquid chromatographic (HPLC) method for the separation of I from hydroflumethiazide, and the results are compared with those from the compendial methods.

EXPERIMENTAL

Materials—Standard solutions containing 0.02, 0.04, 0.06, and 0.08 mg of I[1]/ml of reagent grade methanol were prepared. Hydroflumethia-

[1] E. R. Squibb standard substance.

filtration. The results of this procedure have been shown to be in good agreement with those obtained by equilibrium dialysis (6). However, this technique will not determine accurately the binding parameters of any rapidly equilibrating system; under such circumstances, an overestimation of binding is observed.

In the present studies, it was possible to separate the detergent bound to the enzyme from that unbound and to estimate the amount of interaction between the two moieties. The enzyme, at a 4–5% concentration dissolved in a 0.9% solution of radioiodinated detergent, was chromatographed on Sephadex G-75. It was found that 1.4×10^{-5} mmole (mol. wt. 744) of the detergent was associated with 825 μg of the enzyme. This result indicates that 17 moles of detergent bound per mole of enzyme, calculated on the latter having a molecular weight of 1×10^6. This ratio of detergent to enzyme nearly corresponds to one binding site per 55,000 molecular weight subunit of the enzyme (7). This calculation presupposes detergent that is bound rather than in the micellar form. Such binding has occurred when ligand and protein were present in relatively low concentrations (8–10).

One interesting aspect of the interactions between proteins and detergents is the inclusion of several protein molecules in one detergent micelle (11). To test whether the enzyme could be included in detergent micelles, solutions of the radioiodinated enzyme in detergent were prepared and passed through a column of Bio-Gel A-15m. The results indicated that the enzyme could not be aggregated in detergent micelles, because no sample of L-glutamic acid dehydrogenase in detergent had an elution volume less than the native enzyme, even when the eluting buffer contained 1% by volume of the detergent.

While this experiment on agarose showed that the enzyme was not measurably aggregated in detergent micelles, it was not clear whether the enzyme was dissociating into its 55,000 subunits (7). Therefore, gel filtration on Sephadex G-200 was performed. The enzyme buffer only eluted as a single peak, whereas the enzyme in detergent gave a chromatograph of two peaks. In this latter case, the first peak eluted with the void volume whereas the position of the second peak indicated a molecular weight of 55,000. However, the amount of dissociation into these small subunits was never more than 5% of the total amount applied to the column.

The results indicate that the nonionic detergent can bind to the enzyme L-glutamic acid dehydrogenase. This binding is only in the order of approximately 17 moles of detergent/mole of enzyme, hardly sufficient to allow the enzyme to be included in a detergent micelle. However, it obviously is sufficient to cause enhancement of the activity of this enzyme (1).

These results suggest a possible avenue for enhancement of the biological activities of other proteins and drugs.

REFERENCES

(1) D. H. Kempner and B. J. Johnson, *J. Pharm. Sci.*, **65,** 1799 (1976).

(2) M. W. Bitensky, K. L. Yielding, and G. M. Tomkins, *J. Biol. Chem.*, **240,** 668 (1965).

(3) S. Udenfriend, S. Stein, P. Bohlen, W. Dairman, W. Leimgruber, and W. Weigle, *Science*, **178,** 871 (1972).

(4) J. J. Marchalonis, *Biochem. J.*, **113,** 299 (1969).

(5) G. S. David and R. A. Reisfeld, *Biochemistry*, **13,** 1014 (1974).

(6) P. F. Cooper and G. C. Wood, *J. Pharm. Pharmacol., Suppl.*, **20,** 150S (1968).

(7) N. Tatal, G. M. Tomkins, J. F. Muchinski, and K. L. Yielding, *J. Mol. Biol.*, **8,** 46 (1964).

(8) S. Makino, J. A. Reynolds, and C. Tanford, *J. Biol. Chem.*, **248,** 4926 (1973).

(9) J. A. Reynolds and C. Tanford, *Proc. Nat. Acad. Sci. USA*, **66,** 1002 (1970).

(10) Y. Nozaki, J. A. Reynolds, and C. Tanford, *J. Biol. Chem.*, **249,** 4452 (1974).

(11) J. N. Umbreit and J. L. Strominger, *ibid.*, **248,** 6759 (1973).

ACKNOWLEDGMENTS AND ADDRESSES

Received April 7, 1976, from the *Department of Microbiology, University of Alabama Medical School, Birmingham, AL 35294.*

Accepted for publication July 28, 1976.

Supported in part by Grant AI 11970 from the National Institutes of Health.

[x] To whom inquiries should be directed.

Separation and Quantitative Determination of 2,4-Disulfamyl-5-trifluoromethylaniline in Hydroflumethiazide Using High-Pressure Liquid Chromatography

B. J. OWEN [x] and S. V. WILKIE

Abstract □ A high-pressure liquid chromatographic method was developed to quantify 2,4-disulfamyl-5-trifluoromethylaniline in hydroflumethiazide using a bonded pellicular packing. An internal standard was added to the samples to ensure reproducibility. The results were compared with methods currently in use.

Keyphrases □ 2,4-Disulfamyl-5-trifluoromethylaniline—high-pressure liquid chromatographic analysis in hydroflumethiazide samples and tablets □ Hydroflumethiazide—prepared samples and tablets, high-pressure liquid chromatographic analysis of its precursor 2,4-disulfamyl-5-trifluoromethylaniline □ High-pressure liquid chromatography—analysis, 2,4-disulfamyl-5-trifluoromethylaniline in hydroflumethiazide prepared samples and tablets □ Antihypertensives—hydroflumethiazide prepared samples and tablets, high-pressure liquid chromatographic analysis of its precursor 2,4-disulfamyl-5-trifluoromethylaniline

The hydroflumethiazide monographs in the National Formulary (1) and the British Pharmacopoeia (2) include assays for free amine in the form of its precursor 2,4-disulfamyl-5-trifluoromethylaniline (I) (3–6). In the BP method, the free amine in the sample is compared visually with a standard of I using TLC for the separation. A diazotization is performed in the NF method, and the solution absorbance is read spectrophotometrically and compared with a standard preparation.

This paper describes a high-pressure liquid chromatographic (HPLC) method for the separation of I from hydroflumethiazide, and the results are compared with those from the compendial methods.

EXPERIMENTAL

Materials—Standard solutions containing 0.02, 0.04, 0.06, and 0.08 mg of I[1]/ml of reagent grade methanol were prepared. Hydroflumethia-

[1] E. R. Squibb standard substance.

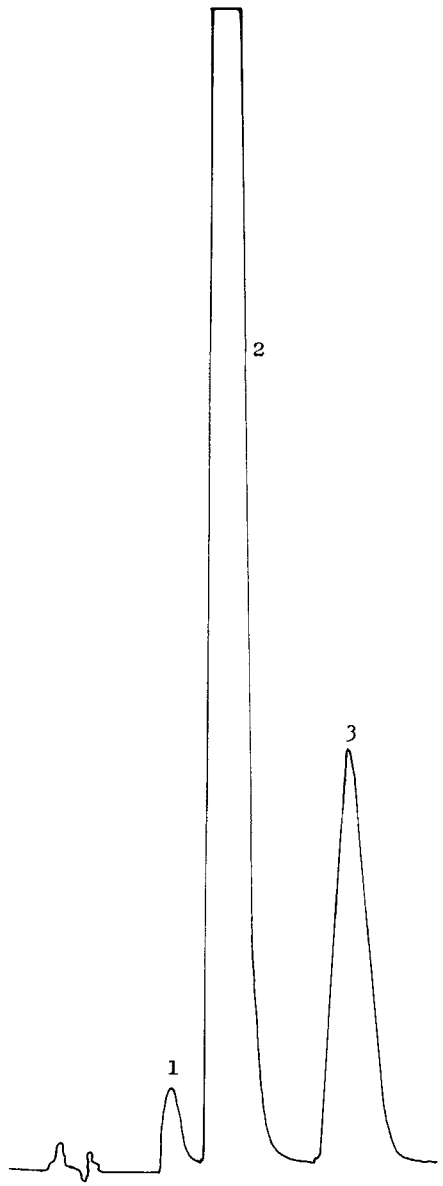

Figure 1—*HPLC separation of I (1), hydroflumethiazide (2), and sulfathiazole (3).*

zide samples were diluted to 4 mg/ml in methanol. Hydroflumethiazide tablets were made up to the same concentration; the solutions were filtered before injection. Sulfathiazole, 0.4 mg/ml, was added to both standard and sample solutions as an internal standard.

Apparatus—A high-pressure liquid chromatograph[2] with a double-beam UV detector operating at 254 nm was used in conjunction with a 10-mv recorder. The columns were 0.5 m long stainless steel (2.6 mm i.d.) packed with an octadecyl hydrocarbon bonded to a deactivated silica[3].

Separation Conditions—The eluting solvent was 5% methanol (reagent grade) in distilled water flowing at 1.5 ml/min, and the temperature of the column oven was 35°. Three microliters of each solution was chromatographed, and the time for complete elution of the sample was approximately 15 min. Each sample was run once, and the calculations were based on peak height. The response for I in the sample was compared with that of the standard solutions. The separation is shown in Fig. 1.

[2] Perkin-Elmer, Norwalk, Conn.
[3] O.D.S. Sil-X-I, Perkin-Elmer, Norwalk, Conn.

Table I—Comparison of Assay Methods for the Estimation of Free Amine in Hydroflumethiazide

Sample	HPLC, %	TLC, %	Diazotizable Substances Assay, %
1	0.97	~1	1.14
2	0.83	<1	0.88
3	0.55	<1	0.83
4	0.30	<1	0.51
5	0.45	<1	0.57
6	0.29	<1	0.57
7	0.55	<1	0.74
8	0.56	<1	0.57
9	0.51	<1	0.55
10	0.58	<1	0.70
11	0.71	<1	0.69
Tablet 1	0.44	<1	—
Tablet 2	0.46	<1	—
Tablet 3	0.40	<1	—
Tablet 4	0.46	<1	—
Tablet 5	0.41	<1	—

Table II—Recovery of Free Amine Added to 4.000-mg/ml Samples of Hydroflumethiazide

Weight of Free Amine Added, mg/ml	Free Amine Added, %	Free Amine Determined, %	Free Amine Recovered, %
0.000	0.00	0.495	—
0.008	0.2	0.696	0.201
0.016	0.4	0.897	0.402
0.024	0.6	1.125	0.630
0.032	0.8	1.304	0.809

RESULTS AND DISCUSSION

The primary goal in developing this assay was to provide a fast precise method for the estimation of I in hydroflumethiazide and hydroflumethiazide tablets. The assay described met these criteria. This HPLC assay gave better precision than TLC and similar results to the diazotizable substance assay (Table I). The linearity of the detector response for 0.02, 0.04, 0.06, and 0.08 mg of I/ml of methanol was satisfactory. From one sample of hydroflumethiazide, 10 weighings produced assays giving a mean result for free amine content of 0.971 ± 0.0281% (*SD*). The recovery of free amine added to a sample of hydroflumethiazide was also checked (Table II).

REFERENCES

(1) "The National Formulary," 14th ed., Mack Publishing Co., Easton, Pa., 1975, p. 329.

(2) "The British Pharmacopoeia," Pharmaceutical Press, London, England, 1973, p. 232.

(3) C. T. Holdrege, R. B. Babel, and L. C. Cheney, *J. Am. Chem. Soc.*, **81**, 4807 (1959).

(4) W. J. Close, L. R. Swett, L. E. Brady, J. H. Short, and M. Vernsten, *ibid.*, **82**, 1132 (1960).

(5) H. L. Yale, K. Losee, and J. Bernstein, *ibid.*, **82**, 2042 (1960).

(6) F. C. Novello, S. C. Bell, L. A. Abrams, C. Ziegler, and J. M. Sprague, *J. Org. Chem.*, **25**, 970 (1960).

ACKNOWLEDGMENTS AND ADDRESSES

Received January 2, 1976, from *Linson Limited, Swords, Dublin, Ireland.*

Accepted for publication July 28, 1976.

[x] To whom inquiries should be directed.

Enhancement of Intestinal Glucose Transport following Chronic Parathion Poisoning

CASEY P. ROBINSON ˣ, JUNGJA J. CHOI, and J. THOMAS PENTO

Abstract □ Chronic administration of parathion to male rats stimulated glucose ($p < 0.05$) but not calcium ($p > 0.05$) transport in the everted duodenal gut sac preparation. Chronic parathion stimulation was not reduced by concurrent administration of atropine. Acutely applied parathion or paraoxon, its active metabolite, did not increase glucose transport in this preparation.

Keyphrases □ Parathion—chronic administration, effect on intestinal glucose and calcium transport, rats □ Paraoxon—chronic administration, effect on intestinal glucose and calcium transport, rats □ Glucose transport, intestinal—effect of chronic administration of parathion or paraoxon, rats □ Calcium transport, intestinal—effect of chronic administration of parathion or paraoxon, rats □ Insecticides—parathion and paraoxon, chronic administration, effect on intestinal glucose and calcium transport, rats

Parathion (*O,O*-diethyl *O*-*p*-nitrophenyl phosphorothioate), a widely used insecticide, is toxic to both insects and mammals only after conversion to the active metabolite paraoxon (*O,O*-diethyl *O*-*p*-nitrophenyl phosphate), which is a potent inhibitor of cholinesterases. The toxicity observed after parathion poisoning results from an accumulation of acetylcholine at certain critical sites subsequent to cholinesterase inhibition. Other effects not clearly associated with cholinesterase inhibition also have been reported for organophosphates. Two organophosphate cholinesterase-inhibiting insecticides (azinphosmethyl and dimethoate) reduced glucose penetration across the isolated mouse intestine (1). Dimethoate resembles parathion in that it requires activation to an active metabolite before becoming a cholinesterase inhibitor; azinphosmethyl does not require activation. The reduction of glucose penetration observed (1) in the presence of parathion was not significant ($p > 0.05$).

It is unlikely that a large portion of an organophosphate that requires activation would be activated in the isolated intestine. Thus, any change in intestinal glucose transport occurring after the addition of such an organophosphate would probably result from a direct effect of the unactivated organophosphate or from an effect of a very small quantity of active metabolite. Therefore, it was of interest to determine the effects of acute exposure to parathion and its active metabolite paraoxon and of chronic parathion poisoning on intestinal glucose transport. The mechanism and specificity of these effects on glucose transport were also examined.

EXPERIMENTAL

Two experiments were undertaken to examine the effects of parathion or paraoxon on intestinal transport of glucose and calcium. One experiment concerned the effects of the acute addition of the insecticides *in vitro*. Male Holtzman rats were initially placed on a diet of ground rat chow[1] and tap water for 7 days and then on a ground, low calcium diet[2] (0.02% calcium) and distilled water for 7 days. Each animal was given vitamin D (200 units po) every 3rd day. The mean weight of the rats at the time of sacrifice was 81 ± 10 g. The low calcium diet and vitamin D were used to optimize calcium transport.

Rats were fasted overnight before the intestinal segments were removed. Upon removal of the segments, they were placed into one of three types of incubation media: with parathion (0.1 m*M*), with paraoxon (0.1 m*M*), or with no insecticide. Each of the three solutions contained polysorbate 80[3] (0.03%), used to solubilize the insecticides. The organophosphate was in the media both inside and outside the gut sacs.

In the other experiment, the effects of chronic parathion poisoning on intestinal transport were investigated. Rats, 60–80 g (mean of 69 g), were randomly divided into four groups. One group received rat chow containing 20 ppm of parathion, a second group received rat chow containing 20 ppm each of parathion and atropine, and a third group was fed rat chow containing no parathion as a control. Each group was allowed free access to food. In another control group, rats were pair-fed with the parathion-poisoned rats.

Rats were poisoned for 14 days. Vitamin D was administered to these rats as described in the previous experiment; during the last 7 days of the poisoning period, the poisons were administered in the low calcium diet previously described. Animals were fasted overnight before removal of the intestinal segments. Thus, poisoning was discontinued 15–18 hr before removal of the intestinal segments. The mean weight of the control rats at the time of sacrifice was 108 ± 10 g.

Glucose and calcium transport were measured by a modification of the everted gut sac technique of Wiseman (2). The animals were lightly anesthetized with ether, bled by cardiac puncture, and killed by cervical fracture. Blood was collected in heparinized syringes, and the plasma was separated immediately. The upper intestine was quickly removed, everted, and washed in saline. Duodenal segments, 5 cm in length, were filled with 0.5 ml of an oxygenated phosphate buffer and placed into 25-ml erlenmeyer flasks containing 3 ml of the same solution, which was sufficient to cover the gut sac.

The phosphate buffer contained 2.4 m*M* dibasic sodium phosphate, 1.6 m*M* monobasic sodium phosphate, 150 m*M* sodium chloride, 5.6 m*M* glucose, and 0.045 μCi/ml of calcium-45. The buffer pH was adjusted to 7.4. The duodenal segments were incubated under an atmosphere of 95% O_2–5% CO_2 for 1 hr at 37° on a gyrorotary metabolic shaker[4]. The ratio of the final concentration of glucose and calcium-45 in the serosal medium (solution inside the gut sac) to the concentration in the mucosal medium (solution bathing the gut sac) was used as an index of transport.

Calcium-45 in the mucosal and serosal media was measured by counting 0.1-ml aliquots of the media on a liquid scintillation counter[5]. Plasma calcium was determined by the method of Baginski *et al.* (3). Plasma and incubation medium glucose was measured by the method of Feteris (4).

In the parathion and control groups of the chronic study, a 2-cm section of intestine immediately adjacent to that used in each transport study was removed, washed, blotted dry, weighed, and frozen for the later determination of cholinesterase activity. This assay was accomplished by the automated colorimetric method of Fowler and McKenzie (5).

Statistical comparisons were made using the Student *t* test for unpaired data.

RESULTS

Both glucose and calcium were actively transported in the rat everted duodenal sac from calcium-deprived rats (Table I). Neither parathion nor paraoxon affected ($p > 0.05$) the transport of either of these substances when the toxins were added to the incubation media.

Rats chronically poisoned with parathion had diarrhea and other signs of parasympathetic stimulation. These signs tended to become less severe

[1] Purina Laboratory Chow, Ralston Purina Co., St. Louis, Mo.
[2] General Biochemicals, Chagrin Falls, Ohio.
[3] Tween 80, Atlas Chemical Co., Wilmington, Del.
[4] New Brunswick Scientific, New Brunswick, N.J.
[5] Beckman model LS-100, Beckman Instruments, Fullerton, Calif.

Table I—Effects of Acute Exposure to Parathion or Paraoxon on Glucose and Calcium Transport in Duodenal Segments

Treatment	Transport, Serosal/Mucosal[a]	
	Glucose	Calcium
Control	3.9 ± 0.80	4.2 ± 0.42
Parathion, 0.1 m*M*	3.4 ± 0.48	4.2 ± 0.44
Paraoxon, 0.1 m*M*	4.2 ± 1.02	4.8 ± 0.88

[a] After 60-min incubation. Each value is the mean ± *SEM* of one segment from each of five or six rats.

with time and, in some cases, disappeared toward the end of the 14-day poisoning period. Rats receiving atropine and parathion exhibited few, if any, signs of parasympathetic stimulation.

Cholinesterase activities were lower ($p < 0.05$) in segments from parathion-poisoned rats (7.16 ± 0.95 m*M* of acetylcholine hydrolyzed/min/g of tissue) than in segments from control rats (10.49 ± 0.89).

Chronic parathion poisoning enhanced intestinal glucose transport ($p < 0.05$) without affecting calcium transport in calcium-deprived rats (Table II). Glucose and calcium transport in the control group was lower than in the acute experiment. At the time of sacrifice, these rats averaged 27 g more than those in the acute experiment. A decreasing rate of active intestinal transport with maturing may have accounted for some, or perhaps all, of the differences in control transport rates between the two experiments. Rats weighing less than 100 g have a faster rate of intestinal glucose transport than heavier rats (6), and the rate of intestinal transport of calcium in rats decreases with maturing (7). However, treatment-induced changes in transport should not be influenced by differences in baseline values in the control groups.

Addition of the muscarinic blocking drug atropine did not decrease the parathion-induced enhancement of glucose transport. Thus, if increased glucose transport results from acetylcholine accumulation following cholinesterase inhibition, it is unlikely that it is mediated through stimulation of muscarinic receptors.

Reduction in food intake by parathion-poisoned rats apparently was not involved in the enhanced glucose absorption, judging from the glucose transport values observed in intestinal segments from control rats pair-fed with poisoned rats and from control rats allowed to eat *ad libitum* (Table II).

Neither plasma glucose nor plasma calcium levels were different ($p > 0.05$) in chronically parathion-poisoned rats (glucose, 125.4 ± 17.2 mg %; calcium, 11.7 ± 0.5 mg %) than in control rats (glucose, 128.3 ± 11.4 mg %; calcium, 11.3 ± 0.4 mg %).

DISCUSSION

Although acute *in vitro* exposure of duodenal segments to parathion or its active metabolite paraoxon did not alter glucose transport, chronic poisoning with parathion enhanced it. Concurrent administration of atropine did not alter the parathion effect. However, since both atropine and parathion were discontinued 15 or more hr prior to obtaining the duodenal segments, neither atropine, free paraoxon, nor parathion should have been present in the duodenum at the time of the transport study. However, partial inhibition of cholinesterase (30%) was still observable at this time. Thus, if the enhancemnt of glucose transport results from the accumulation of acetylcholine, either it does not involve chronic stimulation of muscarinic receptors or the period of time after the bioremoval of atropine was sufficient to allow this effect to develop.

One model of glucose transport across the intestinal epithelial cell has glucose transferred across the brush border coupled with a sodium ion (8, 9) by a membrane carrier system allowing coupled facilitated diffusion. The model requires that the sodium concentration be lower inside the cell than in the lumen. This concentration gradient is maintained by a sodium pump (10). Thus, stimulation of movement of sodium ions into the cells should increase the rate of glucose transport. One means of accomplishing this is by stimulating the extrusion of sodium from epithelial cells. Phenytoin stimulated extrusion of sodium ions in brain (11) and muscle (12) cells and also enhanced intestinal glucose absorption in the rat isolated jejunal loop (13). Sodium transport by the acetylcholine receptor in cultured muscle cells has been observed (14). If acetylcholine stimulates a receptor to enhance coupled sodium and glucose transport, it should probably also do so on acute exposure. However, enhanced glucose transport on acute exposure to cholinesterase inhibitors was not observed. Also, acute applications of acetylcholine in isolated human ileal strips did not affect sodium transport (15).

This effect may be unrelated to cholinesterase inhibition. Whatever the mechanism, the results of this study indicate that sublethal chronic exposure to parathion stimulates glucose transport in the rat duodenum. Furthermore, this enhancement shows some specificity, since the rate of calcium transport was not significantly altered.

Table II—Effects of Chronic Poisoning with Parathion or Parathion and Atropine on Glucose and Calcium Transport in Duodenal Segments

Treatment[a]	Transport, Serosal/Mucosal[b]	
	Glucose	Calcium
Control	2.6 ± 0.69	2.4 ± 0.50
Control (paired with parathion)	2.6 ± 0.57	2.1 ± 0.37
Parathion, 20 ppm	4.4[c] ± 0.38	3.1 ± 0.37
Parathion, 20 ppm, and atropine, 20 ppm	4.5 ± 0.97	3.2 ± 0.60

[a] In rat chow for 14 days. [b] After 60-min incubation. Each value is the mean ± *SEM* of one segment from each of four or five rats. [c] Significantly different from control-paired ($p < 0.05$) and control ($p = 0.05$).

REFERENCES

(1) F. E. Guthrie, P. V. Shah, and D. E. Moreland, *J. Agr. Food Chem.*, **22**, 713 (1974).

(2) G. Wiseman, *Methods Med. Res.*, **9**, 287 (1961).

(3) E. C. Baginski, S. S. Marie, and W. L. Clark, *Clin. Chim. Acta*, **46**, 46 (1973).

(4) W. A. Feteris, *Am. J. Med. Technol.*, **31**, 17 (1965).

(5) P. R. Fowler and J. M. McKenzie, "Symposium: Automation in Analytical Chemistry," Mediad, New York, N.Y., 1967, pp. 155, 159.

(6) R. O. Scow and V. G. Foglia, *Am. J. Physiol.*, **166**, 541 (1951).

(7) H. E. Harrison and H. C. Harrison, *J. Biol. Chem.*, **188**, 83 (1951).

(8) R. K. Crane, *Fed. Proc.*, **24**, 1000 (1965).

(9) R. K. Crane, in "Handbook of Physiology," section 6, "Alimentary Canal," vol. 3, American Physiological Society, Washington, D.C., 1968, pp. 1323–1351.

(10) S. G. Schultz and P. F. Curran, *Physiol. Rev.*, **50**, 637 (1970).

(11) D. M. Woodbury, *J. Pharmacol. Exp. Ther.*, **115**, 74 (1955).

(12) I. Bihler and P. C. Sawh, *Biochim. Biophys. Acta*, **249**, 250 (1971).

(13) H. Van Rees, F. A. DeWolff, and E. L. Noach, *Eur. J. Pharmacol.*, **28**, 310 (1974).

(14) W. A. Catterall, *J. Biol. Chem.*, **250**, 1776 (1975).

(15) P. E. T. Isaacs, C. L. Corbett, and A. Riley, *Gut*, **16**, 398 (1975).

ACKNOWLEDGMENTS AND ADDRESSES

Received June 4, 1976, from the *College of Pharmacy, University of Oklahoma, Oklahoma City, OK 73190.*

Accepted for publication July 28, 1976.

[x] To whom inquiries should be directed.

Metabolic Studies with the Nonnutritive Sweetener Cycloheptylsulfamate

G. ANTHONY BENSON and WILLIAM J. SPILLANE ˣ

Abstract □ The nonnutritive sweetener cycloheptylsulfamate was administered orally to rabbits and rats. The urine of each species was separately collected for 3 days and examined for the metabolites cycloheptylamine, cycloheptanone, and cycloheptanol and for cycloheptylsulfamate. A previously tested GLC method was adapted for the determination of the metabolites. Cycloheptylsulfamate was assayed by hydrolysis and subsequent measurement of the absorbance of the product formed (λ_{max} = 489 nm) by the liberated amine with *p*-benzoquinone. The conversions to the metabolites were 0.276, 0.390, and 0.170%, respectively, in rabbits and 0.064, 0.022, and 0.017%, respectively, in rats.

Keyphrases □ Cycloheptylsulfamate—metabolism, rabbits and rats □ Metabolism—cycloheptylsulfamate, rabbits and rats □ Excretion, urinary—cycloheptylsulfamate and metabolites, rabbits and rats □ Sweeteners—cycloheptylsulfamate, metabolism, rabbits and rats

Cyclamates (sodium and calcium salts of cyclohexylsulfamic acid) have been the subject of considerable investigation over the past few years. This research involved metabolic studies in humans (1–5) and other species (6–12) to determine the metabolites and toxicity of the cyclamates. Further work involved the search for the metabolic site of cyclamate breakdown and the possible microorganisms involved (13–19).

It also seemed worthwhile to evaluate other sulfamates that have a reduced ring and are sweet. Since enzymatic action has been implicated in the breakdown of cyclamate, other sweet sulfamates might be resistant to enzyme action and not be metabolized. Metabolic experiments involving cyclopentylsulfamate were carried out previously (20). Since cycloheptylsulfamate is also sweet (21, 22), in fact, almost as sweet as cyclamate sodium (23), it was tested in rabbits and rats. The results of these metabolic experiments are presented in this paper.

EXPERIMENTAL

Reagents and Chemicals—Sodium cycloheptylsulfamate was synthesized by the reaction of cycloheptylamine in dry chloroform with chlorosulfonic acid (24) and recrystallized twice from ethanol. It was administered orally as an approximately 1% aqueous solution to rats and as an approximately 1.7% aqueous solution to rabbits at doses of 1250 and 349 mg/kg, respectively.

Anal.—Calc. for $C_7H_{14}NNaO_3S$: C, 39.07; H, 6.51; N, 6.51. Found: C, 38.89; H, 6.43; N, 6.56.

Cycloheptylamide[1], cycloheptanone[1], cycloheptanol[1], and dichloromethane[2] were redistilled before use. *p*-Benzoquinone was sublimed. *n*-Dodecane[3], sulfosalicylic acid[2] (Analar), chloroform, ethanol, and 1,4-dioxane (reagent grade) were used as obtained.

Metabolism Experiments—Female New Zealand White rabbits, 3.1–3.6 kg, were kept on solid food and water in metabolism cages[4]. Female Wistar albino rats, approximately 400 g, were kept on solid food and water in smaller metabolism cages[5].

GLC and Visible Spectrophotometry—Cycloheptylamine, cycloheptanol, and cycloheptanone excreted in the urine of both rats and rabbits receiving cycloheptylsulfamate were determined by the GLC method described previously (20) except for the following changes. The column temperature was 130° and the gas flow rates were: nitrogen (carrier), 75 ml/min; hydrogen, 60 ml/min; and overall, 500 ml/min. Under these conditions, the retention times of *n*-dodecane, cycloheptylamine, cycloheptanone, and cycloheptanol were 4.6, 6.3, 8.4, and 13 min, respectively (Fig. 1).

For the purpose of estimating the percent recovery, varying amounts of amine, ketone, and alcohol were determined (Table I). The unmetabolized cycloheptylsulfamate excreted in the urine was determined by visible spectrophotometry (20). Samples of control urine of both species were monitored using both detection methods.

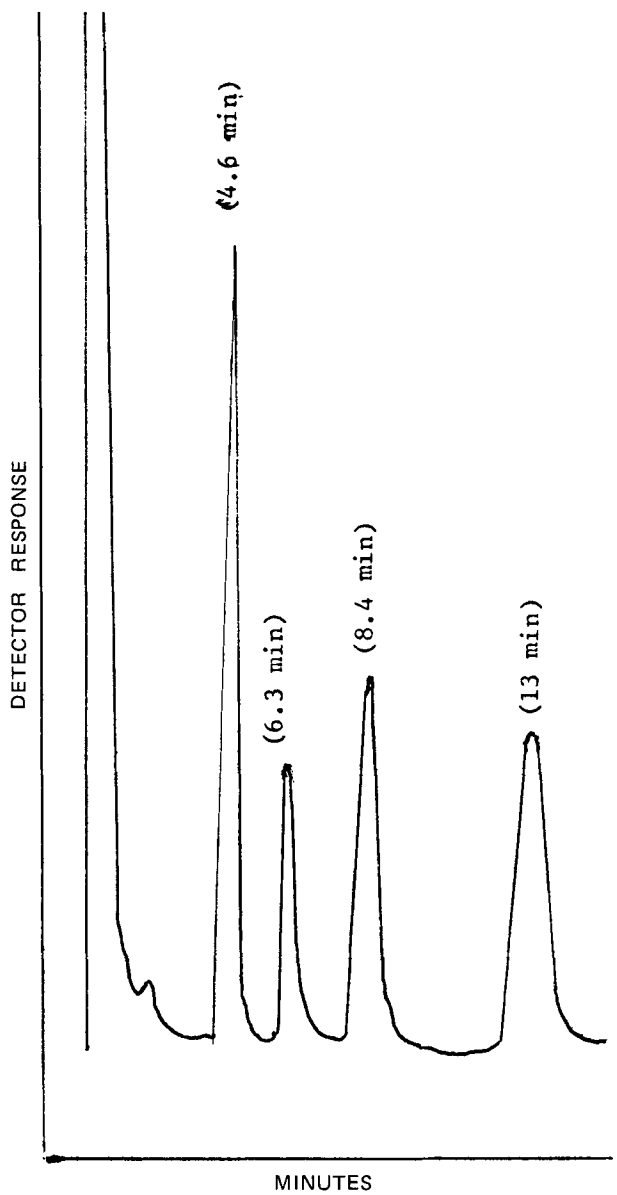

Figure 1—*Gas chromatogram of the urine metabolites of cycloheptylsulfamate (left to right):* n-*dodecane, cycloheptylamine, cycloheptanone, and cycloheptanol.*

[1] Aldrich Chemical Co.
[2] May and Baker.
[3] British Drug Houses.
[4] Bowman Accessories, London, England.
[5] NKP cages, Kent, England.

Table I—Percent Recovery of Cycloheptylamine, Cycloheptanone, and Cycloheptanol from Urine

Amine		Ketone		Alcohol	
μg	%	μg	%	μg	%
60.9	92.69	67.8	90.41	67.5	96.17
121.3	90.90	135.6	98.01	135.0	96.03
151.3	101.33	175.3	87.84	166.2	93.86
225.0	105.87	254.3	101.08	249.0	106.49
303.6	94.90	338.7	97.77	333.0	111.11
456.1	109.25	508.1	115.55	499.8	115.55
874.8	104.2	950.7	99.97	947.8	—[a]
874.8	99.4	950.7	96.97	947.8	97.6
1020.6	103.4	1109.2	98.44	1105.8	84.5
1020.6	98.7	1109.2	99.52	1105.8	—[a]
1166.4	94.6	1267.6	95.42	1263.2	94.9
1166.4	94.6	1267.6	104.91	1263.2	—[a]
Mean ± *SE*	99.15 ± 4.75		98.82 ± 4.48		99.57 ± 7.64

[a] Not determined.

Table II—Metabolism of Sodium Cycloheptylsulfamate in Rabbits

	Parent Drug[a]		Cycloheptanol[b]		Cycloheptanone[b]		Cycloheptylamine[b]		Total Metabolites,
Animal	mg	%	mg	%	mg	%	mg	%	%
1	1141.5	92.72	0.553	0.084	0.779	0.121	2.214	0.342	0.547
2	671.6	54.55	0.186	0.028	0.542	0.084	0.341	0.052	0.167
3	395.4	34.26	0.350	0.057	0.812	0.135	0.225	0.037	0.229
4	1167.3	89.44	4.160	0.599	9.664	1.418	6.016	0.875	2.887
5	656.2	60.92	0.469	0.082	1.105	0.196	0.435	0.076	0.354
Mean ± *SE*	806.4 ± 278.4	66.37 ± 19.76	1.143 ± 1.206	0.170 ± 0.171	2.58 ± 2.95	0.390 ± 0.415	0.289 ± 0.277	0.276 ± 0.265	0.836 ± 0.819

[a] Determined using visible spectrophotometry. [b] Determined by GLC.

Table III—Metabolism of Sodium Cycloheptylsulfamate in Rats

	Parent Drug[a]		Cycloheptanol[b]		Cycloheptanone[b]		Cycloheptylamine[b]		Total Metabolites,
Animal	mg	%	mg	%	mg	%	mg	%	%
1	56.38	11.27	None	—	None	—	0.034	0.012	0.012
2	43.58	8.71	None	—	None	—	Trace	—	—
3	160.12	32.02	0.046	0.017	0.073	0.028	0.519	0.197	0.242
4	322.07	64.41	None	—	Trace	—	0.066	0.025	0.025
5	294.60	58.92	None	—	0.042	0.016	0.061	0.023	0.039
Mean ± *SE*	175.35 ± 106.38	35.06 ± 21.27	0.046	0.017	0.057 ± 0.015	0.022 ± 0.006	0.136 ± 0.126	0.064 ± 0.06	0.079 ± 0.07

[a] Determined using visible spectrophotometry. [b] Determined by GLC.

RESULTS AND DISCUSSION

The results from the analysis of the urine of rabbits and rats for unchanged cycloheptylsulfamate and various metabolites are given in Tables II and III, respectively. The average percentage for unchanged cycloheptylsulfamate excreted in the urine for rats was 35%; for rabbits, it was 66%. In metabolic studies with cyclopentylsulfamate (20), rats excreted 15% unchanged cyclopentylsulfamate in the urine and rabbits excreted 56%. U-^{14}C-Cyclamate sodium also was extensively excreted in the urine by rabbits, whereas the average level of excretion for rats was 40% in the urine (2). In rats that had received a level of cyclamate similar to that used in the present study, about 17% cyclamate was excreted in the urine and about 70% in the feces (25). Thus, the main excretory pathways for these administered sulfamates apparently are the urine for rabbits and the feces for rats.

The average conversion of cycloheptylsulfamate by rabbits to cycloheptylamine, cycloheptanone, and cycloheptanol was 0.276, 0.390, and 0.170%, respectively (Table II). Comparison of these results with those for cyclopentylsulfamate (20) showed that they were slightly higher. The conversion results of Ichibagase *et al.* (14) and Suenaga *et al.* (16) for cyclamate also were lower than the present results for cycloheptylsulfamate in rabbits. Renwick and Williams (2) also found a lower conversion in rabbits for cyclamate.

In the five rats studied, the level of cycloheptylamine found (Table III) was similar to the level of cyclopentylamine found (20) and higher than the level of cyclohexylamine obtained (14, 16) in metabolic studies with cyclopentylsulfamate and cyclamate, respectively. Only one rat excreted cycloheptanol in urine, and only two rats excreted cycloheptanone (Table III).

It appears that cycloheptyl- and cyclopentylsulfamates are cleaved to the same extent in rats, but in rabbits the conversion of cycloheptylsulfamate is higher. Metabolic studies with other sweet sulfamates are necessary to assess the breakdown pattern, if any, and the effect of prolonged administration on metabolite levels.

REFERENCES

(1) A. G. Renwick and R. T. Williams, *Biochem. J.*, **129,** 857 (1972).

(2) *Ibid.*, **129,** 869 (1972).

(3) M. Asahina, T. Yamaha, K. Watanabe, and G. Sarrazin, *Chem. Pharm. Bull.*, **19,** 628 (1971) and references therein.

(4) J. S. Leahy, T. Taylor, and C. J. Rudd, *Food Cosmet. Toxicol.*, **5,** 595 (1967).

(5) S. Kojima and H. Ichibagase, *Chem. Pharm. Bull.*, **17,** 2620 (1969).

(6) M. Asahina, T. Yamaha, K. Watanabe, and G. Sarrazin, *ibid.*, **20,** 102 (1972).

(7) B. L. Oser, S. Carson, E. E. Vogin, and R. C. Sonders, *Nature,* **220,** 178 (1968).

(8) G. T. Bryan and E. Erturk, *Science,* **167,** 996 (1970).

(9) P. G. Branton, I. F. Gaunt, and P. Grasso, *Food Cosmet. Toxicol.*, **11,** 735 (1973).

(10) J. M. Price, C. G. Biava, B. L. Oser, E. E. Vogin, J. Steinfeld, and H. L. Ley, *Science,* **167,** 1131 (1970).

(11) F. J. C. Roe, L. S. Levy, and R. L. Carter, *Food Cosmet. Toxicol.*, **87,** 135 (1970).

(12) C. Parekh, E. K. Goldberg, and L. Goldberg, *Toxicol. Appl.*

Pharmacol., **17**, 282 (1970).
(13) B. S. Draser, A. G. Renwick, and R. T. Williams, *Biochem. J.*, **129**, 881 (1972).
(14) H. Ichibagase, S. Kojima, K. Inoue, and A. Suenaga, *Chem. Pharm. Bull.*, **20**, 175 (1972).
(15) *Ibid.*, **20**, 1093 (1972).
(16) A. Suenaga, S. Kojima, and H. Ichibagase, *Chem. Pharm. Bull.*, **20**, 1357 (1972).
(17) T. Nimura, T. Tokieda, and T. Yamaha, *J. Biochem. (Tokyo)*, **75**, 407 (1974).
(18) J. J. Roxon and A. A. Tesorio, *Aust. J. Pharm. Sci.*, **NS3**, 26 (1974).
(19) J. J. Roxon and A. A. Tesorio, *Xenobiotica*, **5**, 25 (1975).
(20) G. A. Benson and W. J. Spillane, *J. Pharm. Sci.*, **65**, 1841 (1976).
(21) F. F. Blick, H. E. Millson, Jr., and N. J. Doorenbos, *J. Am. Chem. Soc.*, **76**, 2498 (1954).
(22) B. Unterhalt and L. Böschemeyer, *Z. Lebensm.-Unters.-Forsch.*, **145**, 93 (1971).
(23) W. J. Spillane and G. A. Benson, *J. Med. Chem.*, **19**, 869 (1976).
(24) L. F. Audrieth and M. Sveda, *J. Org. Chem.*, **9**, 89 (1944).
(25) P. H. Derse and R. J. Daun, *J. Assoc. Offic. Anal. Chem.*, **49**, 1090 (1966).

ACKNOWLEDGMENTS AND ADDRESSES

Received March 26, 1976, from the *Department of Chemistry, University College, Galway, Ireland.*
Accepted for publication August 3, 1976.
The authors thank the Department of Education (Ireland) for a grant to G. A. Benson.
[x] To whom inquiries should be directed.

Cytotoxic Agents from *Michelia champaca* and *Talauma ovata*: Parthenolide and Costunolide

JOSEPH J. HOFFMANN, STERLING J. TORRANCE, RICHARD M. WIEDHOPF, and JACK R. COLE [x]

Abstract □ The ethanol extract of *Michelia champaca* and the petroleum ether extract of *Talauma ovata* showed activity toward the human epidermoid carcinoma of the nasopharynx test system. The active constituents were sesquiterpene lactones, identified as parthenolide ($C_{15}H_{20}O_3$) and costunolide ($C_{15}H_{20}O_2$). Their identities were proven by elemental analyses, PMR, IR, and mass spectral data, melting-point and mixed melting-point determinations, and comparisons with authentic samples and spectra.

Keyphrases □ Parthenolide—isolated from ethanol extract of bark of *Michelia champaca*, cytotoxic activity evaluated □ Costunolide—isolated from ethanol extract of bark of *Michelia champaca* and petroleum ether extract of roots of *Talauma ovata*, cytotoxic activity evaluated □ *Michelia champaca*—parthenolide and costunolide isolated from ethanol extract of bark, cytotoxic activity evaluated □ *Talauma ovata*—costunolide isolated from petroleum ether extract of roots, cytotoxic activity evaluated □ Cytotoxic activity—plant constituents parthenolide and costunolide evaluated

As a result of the continuing search for plants having tumor inhibitory constituents, it was found that the ethanol extract of the stem bark of *Michelia champaca* L.[1] (Magnoliaceae) and the petroleum ether extract of the roots of *Talauma ovata* A. St. Hil.[2] (Magnoliaceae) showed cytotoxic activity toward the human epidermoid carcinoma of the nasopharynx test system[3] (KB).

DISCUSSION

The cytotoxic agents were found to be parthenolide (from *M. champaca*) and costunolide (from *M. champaca* and *T. ovata*). Parthenolide previously was isolated from several Magnoliaceae plants, including *Magnolia grandiflora* (1) and *M. champaca* (2), and also from *Chrysanthemum parthenium* (Asteraceae) (3). Costunolide has been found mainly in Asteraceae plants, *e.g.*, the "costus root," *Saussurea lappa* (4). Identification of parthenolide and costunolide was achieved by IR, PMR, and mass spectral data and by comparison with authentic spectra and samples.

Parthenolide demonstrated an activity of 2.3 μg/ml, and costunolide showed an activity of 2.8 μg/ml. Activity in the KB test system is defined as $ED_{50} \leq 20$ μg/ml (5).

EXPERIMENTAL[4]

Isolation Procedure—The ground stem of *M. champaca* (7 kg) was extracted exhaustively with ethanol in a Lloyd-type extractor. The air-dried residue was partitioned between chloroform and water. The air-dried chloroform phase (11.8 g) was extracted twice with benzene (500 ml), and the benzene-soluble fraction (8 g) was subjected to silica gel 60 (200 g) column (4 × 46 cm) chromatography. The column was eluted with benzene (1000 ml), chloroform (1000 ml), chloroform–methanol [(95:5) six fractions, 500 ml each], acetone, and methanol.

The dried and ground roots of *T. ovata* (1.0 kg) were extracted by maceration with 3 liters of petroleum ether (bp 30–60°) overnight. After filtration and removal of the solvent from the extract, crude crystals of costunolide formed.

Isolation of Parthenolide—Parthenolide was isolated from the first chloroform–methanol (95:5) fraction by preparative TLC using benzene–dichloromethane–ethyl acetate (3:6:1). Crystallization from ether resulted in colorless plates, mp 115° [lit. (2) mp 115°]. The PMR spectrum was identical to the previously reported spectrum (2). The IR

[1] The plant was collected in India in March 1974. Identification was confirmed by Dr. Robert E. Perdue, Jr., Medicinal Plant Resources Laboratory, U.S. Department of Agriculture, Beltsville, Md. A reference specimen was deposited in that herbarium.
[2] The plant was collected in Brazil in June 1974. Identification was confirmed by Dr. Robert E. Perdue, Jr., Medicinal Plant Resources Laboratory, U.S. Department of Agriculture, Beltsville, Md. A reference specimen was deposited in that herbarium.
[3] Of the Drug Evaluation Branch, Drug Research and Development, Division of Cancer Treatment, National Cancer Institute, National Institutes of Health, Department of Health, Education, and Welfare, Bethesda, Md.
[4] Carbon and hydrogen analyses were performed by Chemalytics, Inc., Tempe, Ariz. PMR, IR, and mass spectra were determined using a Varian T-60 spectrophotometer, a Beckman IR-33, and a Hitachi Perkin-Elmer double-focusing spectrometer (model RMU-6E), respectively. Melting points were determined on a Kofler hot-stage apparatus and are uncorrected.

Pharmacol., **17**, 282 (1970).
(13) B. S. Draser, A. G. Renwick, and R. T. Williams, *Biochem. J.*, **129**, 881 (1972).
(14) H. Ichibagase, S. Kojima, K. Inoue, and A. Suenaga, *Chem. Pharm. Bull.*, **20**, 175 (1972).
(15) *Ibid.*, **20**, 1093 (1972).
(16) A. Suenaga, S. Kojima, and H. Ichibagase, *Chem. Pharm. Bull.*, **20**, 1357 (1972).
(17) T. Nimura, T. Tokieda, and T. Yamaha, *J. Biochem. (Tokyo)*, **75**, 407 (1974).
(18) J. J. Roxon and A. A. Tesorio, *Aust. J. Pharm. Sci.*, **NS3**, 26 (1974).
(19) J. J. Roxon and A. A. Tesorio, *Xenobiotica*, **5**, 25 (1975).
(20) G. A. Benson and W. J. Spillane, *J. Pharm. Sci.*, **65**, 1841 (1976).
(21) F. F. Blick, H. E. Millson, Jr., and N. J. Doorenbos, *J. Am. Chem. Soc.*, **76**, 2498 (1954).
(22) B. Unterhalt and L. Böschemeyer, *Z. Lebensm.-Unters.-Forsch.*, **145**, 93 (1971).
(23) W. J. Spillane and G. A. Benson, *J. Med. Chem.*, **19**, 869 (1976).
(24) L. F. Audrieth and M. Sveda, *J. Org. Chem.*, **9**, 89 (1944).
(25) P. H. Derse and R. J. Daun, *J. Assoc. Offic. Anal. Chem.*, **49**, 1090 (1966).

ACKNOWLEDGMENTS AND ADDRESSES

Received March 26, 1976, from the *Department of Chemistry, University College, Galway, Ireland.*
Accepted for publication August 3, 1976.
The authors thank the Department of Education (Ireland) for a grant to G. A. Benson.
[x] To whom inquiries should be directed.

Cytotoxic Agents from *Michelia champaca* and *Talauma ovata*: Parthenolide and Costunolide

JOSEPH J. HOFFMANN, STERLING J. TORRANCE, RICHARD M. WIEDHOPF, and JACK R. COLE [x]

Abstract □ The ethanol extract of *Michelia champaca* and the petroleum ether extract of *Talauma ovata* showed activity toward the human epidermoid carcinoma of the nasopharynx test system. The active constituents were sesquiterpene lactones, identified as parthenolide ($C_{15}H_{20}O_3$) and costunolide ($C_{15}H_{20}O_2$). Their identities were proven by elemental analyses, PMR, IR, and mass spectral data, melting-point and mixed melting-point determinations, and comparisons with authentic samples and spectra.

Keyphrases □ Parthenolide—isolated from ethanol extract of bark of *Michelia champaca*, cytotoxic activity evaluated □ Costunolide—isolated from ethanol extract of bark of *Michelia champaca* and petroleum ether extract of roots of *Talauma ovata*, cytotoxic activity evaluated □ *Michelia champaca*—parthenolide and costunolide isolated from ethanol extract of bark, cytotoxic activity evaluated □ *Talauma ovata*—costunolide isolated from petroleum ether extract of roots, cytotoxic activity evaluated □ Cytotoxic activity—plant constituents parthenolide and costunolide evaluated

As a result of the continuing search for plants having tumor inhibitory constituents, it was found that the ethanol extract of the stem bark of *Michelia champaca* L.[1] (Magnoliaceae) and the petroleum ether extract of the roots of *Talauma ovata* A. St. Hil.[2] (Magnoliaceae) showed cytotoxic activity toward the human epidermoid carcinoma of the nasopharynx test system[3] (KB).

DISCUSSION

The cytotoxic agents were found to be parthenolide (from *M. champaca*) and costunolide (from *M. champaca* and *T. ovata*). Parthenolide previously was isolated from several Magnoliaceae plants, including *Magnolia grandiflora* (1) and *M. champaca* (2), and also from *Chrysanthemum parthenium* (Asteraceae) (3). Costunolide has been found mainly in Asteraceae plants, *e.g.*, the "costus root," *Saussurea lappa* (4). Identification of parthenolide and costunolide was achieved by IR, PMR, and mass spectral data and by comparison with authentic spectra and samples.

Parthenolide demonstrated an activity of 2.3 μg/ml, and costunolide showed an activity of 2.8 μg/ml. Activity in the KB test system is defined as $ED_{50} \leq 20$ μg/ml (5).

EXPERIMENTAL[4]

Isolation Procedure—The ground stem of *M. champaca* (7 kg) was extracted exhaustively with ethanol in a Lloyd-type extractor. The air-dried residue was partitioned between chloroform and water. The air-dried chloroform phase (11.8 g) was extracted twice with benzene (500 ml), and the benzene-soluble fraction (8 g) was subjected to silica gel 60 (200 g) column (4 × 46 cm) chromatography. The column was eluted with benzene (1000 ml), chloroform (1000 ml), chloroform–methanol [(95:5) six fractions, 500 ml each], acetone, and methanol.

The dried and ground roots of *T. ovata* (1.0 kg) were extracted by maceration with 3 liters of petroleum ether (bp 30–60°) overnight. After filtration and removal of the solvent from the extract, crude crystals of costunolide formed.

Isolation of Parthenolide—Parthenolide was isolated from the first chloroform–methanol (95:5) fraction by preparative TLC using benzene–dichloromethane–ethyl acetate (3:6:1). Crystallization from ether resulted in colorless plates, mp 115° [lit. (2) mp 115°]. The PMR spectrum was identical to the previously reported spectrum (2). The IR

[1] The plant was collected in India in March 1974. Identification was confirmed by Dr. Robert E. Perdue, Jr., Medicinal Plant Resources Laboratory, U.S. Department of Agriculture, Beltsville, Md. A reference specimen was deposited in that herbarium.
[2] The plant was collected in Brazil in June 1974. Identification was confirmed by Dr. Robert E. Perdue, Jr., Medicinal Plant Resources Laboratory, U.S. Department of Agriculture, Beltsville, Md. A reference specimen was deposited in that herbarium.
[3] Of the Drug Evaluation Branch, Drug Research and Development, Division of Cancer Treatment, National Cancer Institute, National Institutes of Health, Department of Health, Education, and Welfare, Bethesda, Md.
[4] Carbon and hydrogen analyses were performed by Chemalytics, Inc., Tempe, Ariz. PMR, IR, and mass spectra were determined using a Varian T-60 spectrophotometer, a Beckman IR-33, and a Hitachi Perkin-Elmer double-focusing spectrometer (model RMU-6E), respectively. Melting points were determined on a Kofler hot-stage apparatus and are uncorrected.

spectrum was superimposable with the IR spectrum of an authentic sample. The mixed melting point obtained showed no depression.

Anal.—Calc. for $C_{15}H_{20}O_3$: C, 72.17; H, 8.06; mol. wt. 248. Found: C, 72.38; H, 8.26; *m/e* 248.

Isolation of Costunolide—Costunolide was isolated from the chloroform fraction of *M. champaca* by crystallization from hexane–benzene, and the crude crystals from *T. ovata* were purified by recrystallization from hexane–benzene to give 352 mg of colorless spears, mp 106–107° [lit. (4) mp 106–107°]. The IR and PMR spectra were identical to the authentic spectra.

Anal.—Calc. for $C_{15}H_{20}O_2$: C, 77.54; H, 8.67; mol. wt. 232. Found: C, 77.32; H, 8.84; *m/e* 232.

REFERENCES

(1) R. M. Wiedhopf, M. Young, E. Bianchi, and J. R. Cole, *J. Pharm. Sci.*, **62**, 345 (1973).

(2) T. R. Govindachari, B. S. Joshi, and V. N. Kamat, *Tetrahedron*, **21**, 1509 (1965).

(3) V. Herout and F. Sŏrm, *Chem. Ind.*, **1959**, 1067.

(4) S. C. Bhattacharyya, G. R. Kelkar, and A. S. Rao, *ibid.*, **1959**, 1069.

(5) R. I. Geran, N. H. Greenberg, M. N. MacDonald, A. M. Schumacher, and B. J. Abbott, *Cancer Chemother. Rep.*, **3** (3), 17 (1972).

ACKNOWLEDGMENTS AND ADDRESSES

Received April 2, 1976, from the *Division of Pharmaceutical Chemistry, College of Pharmacy, University of Arizona, Tucson, AZ 85721.*

Accepted for publication July 28, 1976.

Supported by Contract N0I-CM-33750 from the Division of Cancer Treatment, National Cancer Institute, National Institutes of Health, Department of Health, Education, and Welfare, Bethesda, MD 20014, and the Elsa U. Pardee Foundation, Midland, MI 48640.

The authors are indebted to Dr. B. S. Joshi, Ciba of India Ltd., Goregaon Bombay, India, for providing the authentic sample of parthenolide, and to Professor Raymond W. Doskotch, Ohio State University, Columbus, Ohio, for providing authentic spectra (IR and NMR) of costunolide. A specimen was unavailable because of prior decomposition.

[x] To whom inquiries should be directed.

NMR Solvent Shift Data for Methoxylated Xanthones

R. A. FINNEGAN [x] and K. E. MERKEL

Abstract □ The NMR spectra of 1-, 2-, 3-, and 4-hydroxyxanthones, 1,3-, 1,5-, 1,6-, 1,7-, 1,8-, 2,5-, 3,4-, 3,5-, 3,6-, and 4,5-dihydroxyxanthones, 1,3,6- and 1,3,8-trihydroxyxanthones, and 1,3,6,8-tetrahydroxyxanthone, as well as those of the corresponding methyl ethers and acetates, were recorded. The spectra of the methyl ethers were measured in deuterochloroform, benzene, trifluoroacetic acid, and 3% trifluoroacetic acid in benzene. The solvent shift parameters for the methoxyl resonances are tabulated and discussed.

Keyphrases □ Methoxyxanthones, various—NMR spectra and solvent shift data □ NMR—spectra and solvent shift data, various methoxyxanthones □ Xanthones, methoxy substituted—NMR spectra and solvent shift data

Recently, the isolation of four simple hydroxylated xanthones from seed extracts of *Mammea americana* L. was reported (1). They were identified as the 2- and 4-monohydroxy derivatives and the 1,7- and 1,5-dihydroxy derivatives by a combination of spectroscopic studies and syntheses of authentic materials (1). The last substance, in fact, was prepared for the first time. The 2,5- and 4,5-dihydroxy isomers were also prepared (2). During this work, other hydroxylated xanthones (3, 4) were prepared, not only for comparison purposes but also for inclusion in a preliminary antitumor screen (5).

The chemical shifts of methoxy resonances in some methoxyxanthone derivatives were dependent on the position of substitution (3). The magnitude of the benzene-induced solvent shift for the methyl group in substituted anisoles was dependent on the nature and orientation of the substituents (6). These facts suggested that benzene-induced shifts of methoxyl resonances in methoxyxanthones also might be position dependent and, therefore, might be helpful in elucidating the structures of naturally occurring hydroxyxanthones and methoxyxanthones.

While this work was in progress, benzene-induced shifts of methoxyl resonances in flavonoids (7–11) and substituted xanthones (12, 13) were reported and, indeed, found to be of use in structure determination. Useful solvent shift correlations were previously derived for steroidal ketones (14, 15) and substituted coumarins (16). In addition, trifluoroacetic acid (I) was found to be a useful adjunct to the

Table I—Chemical Shifts (Parts per Million) for Methoxyl Resonances of Various Methoxyxanthones in Various Solvents

Xanthone	Trifluoroacetic Acid	Deuterochloroform	Benzene	Benzene–Trifluoroacetic Acid
1-Methoxy	4.50	4.05	3.43	3.39
2-Methoxy	4.12	3.94	3.29	3.43
3-Methoxy	4.18	3.95	3.18	3.16
4-Methoxy	4.27	4.05	3.33	3.32
1,8-Dimethoxy	4.37	3.99	3.42	3.40
3,6-Dimethoxy	4.18	3.95	3.19	3.20
4,5-Dimethoxy	4.22	4.08	3.34	3.30
1,3-Dimethoxy	4.42	4.00	3.38	3.37
	4.23	3.92	3.22	3.22
1,5-Dimethoxy	4.50	4.03	3.41	3.36
	4.28	4.03	3.34	3.30
1,6-Dimethoxy	4.44	4.03	3.45	3.45
	4.20	3.92	3.16	3.15
1,7-Dimethoxy	4.48	4.04	3.44	3.41
	4.13	3.92	3.27	3.33
2,5-Dimethoxy	4.27	4.05	3.38	3.40
	4.12	3.95	3.29	3.33
3,4-Dimethoxy	4.30	4.05	3.84	3.75
	4.22	4.03	3.25	3.22
3,5-Dimethoxy	4.29	4.06	3.38	3.35
	4.17	3.94	3.11	3.12
1,3,6-Trimethoxy	4.38	3.99	3.44	3.42
	4.18	3.91	3.28	3.33
	4.18	3.91	3.22	3.25
1,3,8-Trimethoxy	4.34	3.98	3.43	3.45
	4.25	3.95	3.37	3.38
	4.17	3.89	3.22	3.26
1,3,6,8-Tetramethoxy	4.26	3.94	3.42	3.38
	4.15	3.88	3.26	3.38

spectrum was superimposable with the IR spectrum of an authentic sample. The mixed melting point obtained showed no depression.

Anal.—Calc. for $C_{15}H_{20}O_3$: C, 72.17; H, 8.06; mol. wt. 248. Found: C, 72.38; H, 8.26; *m/e* 248.

Isolation of Costunolide—Costunolide was isolated from the chloroform fraction of *M. champaca* by crystallization from hexane–benzene, and the crude crystals from *T. ovata* were purified by recrystallization from hexane–benzene to give 352 mg of colorless spears, mp 106–107° [lit. (4) mp 106–107°]. The IR and PMR spectra were identical to the authentic spectra.

Anal.—Calc. for $C_{15}H_{20}O_2$: C, 77.54; H, 8.67; mol. wt. 232. Found: C, 77.32; H, 8.84; *m/e* 232.

REFERENCES

(1) R. M. Wiedhopf, M. Young, E. Bianchi, and J. R. Cole, *J. Pharm. Sci.*, **62**, 345 (1973).

(2) T. R. Govindachari, B. S. Joshi, and V. N. Kamat, *Tetrahedron*, **21**, 1509 (1965).

(3) V. Herout and F. Sŏrm, *Chem. Ind.*, **1959**, 1067.

(4) S. C. Bhattacharyya, G. R. Kelkar, and A. S. Rao, *ibid.*, **1959**, 1069.

(5) R. I. Geran, N. H. Greenberg, M. N. MacDonald, A. M. Schumacher, and B. J. Abbott, *Cancer Chemother. Rep.*, **3** (3), 17 (1972).

ACKNOWLEDGMENTS AND ADDRESSES

Received April 2, 1976, from the *Division of Pharmaceutical Chemistry, College of Pharmacy, University of Arizona, Tucson, AZ 85721.*

Accepted for publication July 28, 1976.

Supported by Contract N0I-CM-33750 from the Division of Cancer Treatment, National Cancer Institute, National Institutes of Health, Department of Health, Education, and Welfare, Bethesda, MD 20014, and the Elsa U. Pardee Foundation, Midland, MI 48640.

The authors are indebted to Dr. B. S. Joshi, Ciba of India Ltd., Goregaon Bombay, India, for providing the authentic sample of parthenolide, and to Professor Raymond W. Doskotch, Ohio State University, Columbus, Ohio, for providing authentic spectra (IR and NMR) of costunolide. A specimen was unavailable because of prior decomposition.

[x] To whom inquiries should be directed.

NMR Solvent Shift Data for Methoxylated Xanthones

R. A. FINNEGAN [x] and K. E. MERKEL

Abstract □ The NMR spectra of 1-, 2-, 3-, and 4-hydroxyxanthones, 1,3-, 1,5-, 1,6-, 1,7-, 1,8-, 2,5-, 3,4-, 3,5-, 3,6-, and 4,5-dihydroxyxanthones, 1,3,6- and 1,3,8-trihydroxyxanthones, and 1,3,6,8-tetrahydroxyxanthone, as well as those of the corresponding methyl ethers and acetates, were recorded. The spectra of the methyl ethers were measured in deuterochloroform, benzene, trifluoroacetic acid, and 3% trifluoroacetic acid in benzene. The solvent shift parameters for the methoxyl resonances are tabulated and discussed.

Keyphrases □ Methoxyxanthones, various—NMR spectra and solvent shift data □ NMR—spectra and solvent shift data, various methoxyxanthones □ Xanthones, methoxy substituted—NMR spectra and solvent shift data

Recently, the isolation of four simple hydroxylated xanthones from seed extracts of *Mammea americana* L. was reported (1). They were identified as the 2- and 4-monohydroxy derivatives and the 1,7- and 1,5-dihydroxy derivatives by a combination of spectroscopic studies and syntheses of authentic materials (1). The last substance, in fact, was prepared for the first time. The 2,5- and 4,5-dihydroxy isomers were also prepared (2). During this work, other hydroxylated xanthones (3, 4) were prepared, not only for comparison purposes but also for inclusion in a preliminary antitumor screen (5).

The chemical shifts of methoxy resonances in some methoxyxanthone derivatives were dependent on the position of substitution (3). The magnitude of the benzene-induced solvent shift for the methyl group in substituted anisoles was dependent on the nature and orientation of the substituents (6). These facts suggested that benzene-induced shifts of methoxyl resonances in methoxyxanthones also might be position dependent and, therefore, might be helpful in elucidating the structures of naturally occurring hydroxyxanthones and methoxyxanthones.

While this work was in progress, benzene-induced shifts of methoxyl resonances in flavonoids (7–11) and substituted xanthones (12, 13) were reported and, indeed, found to be of use in structure determination. Useful solvent shift correlations were previously derived for steroidal ketones (14, 15) and substituted coumarins (16). In addition, trifluoroacetic acid (I) was found to be a useful adjunct to the

Table I—Chemical Shifts (Parts per Million) for Methoxyl Resonances of Various Methoxyxanthones in Various Solvents

Xanthone	Trifluoroacetic Acid	Deuterochloroform	Benzene	Benzene–Trifluoroacetic Acid
1-Methoxy	4.50	4.05	3.43	3.39
2-Methoxy	4.12	3.94	3.29	3.43
3-Methoxy	4.18	3.95	3.18	3.16
4-Methoxy	4.27	4.05	3.33	3.32
1,8-Dimethoxy	4.37	3.99	3.42	3.40
3,6-Dimethoxy	4.18	3.95	3.19	3.20
4,5-Dimethoxy	4.22	4.08	3.34	3.30
1,3-Dimethoxy	4.42	4.00	3.38	3.37
	4.23	3.92	3.22	3.22
1,5-Dimethoxy	4.50	4.03	3.41	3.36
	4.28	4.03	3.34	3.30
1,6-Dimethoxy	4.44	4.03	3.45	3.45
	4.20	3.92	3.16	3.15
1,7-Dimethoxy	4.48	4.04	3.44	3.41
	4.13	3.92	3.27	3.33
2,5-Dimethoxy	4.27	4.05	3.38	3.40
	4.12	3.95	3.29	3.33
3,4-Dimethoxy	4.30	4.05	3.84	3.75
	4.22	4.03	3.25	3.22
3,5-Dimethoxy	4.29	4.06	3.38	3.35
	4.17	3.94	3.11	3.12
1,3,6-Trimethoxy	4.38	3.99	3.44	3.42
	4.18	3.91	3.28	3.33
	4.18	3.91	3.22	3.25
1,3,8-Trimethoxy	4.34	3.98	3.43	3.45
	4.25	3.95	3.37	3.38
	4.17	3.89	3.22	3.26
1,3,6,8-Tetramethoxy	4.26	3.94	3.42	3.38
	4.15	3.88	3.26	3.38

Table II—Solvent Shift Data for Monomethoxyxanthones and Selected Dimethoxyxanthones

Xanthone	Methoxyl Position	Δ Deuterochloroform–Benzene	Δ Trifluoroacetic Acid–Benzene	Δ Trifluoroacetic Acid–Deuterochloroform
1-Methoxy	1	0.62	1.07	0.45
2-Methoxy	2	0.65	0.83	0.18
3-Methoxy	3	0.77	1.00	0.23
4-Methoxy	4	0.72	0.94	0.22
1,8-Dimethoxy	1(8)	0.57	0.95	0.38
3,6-Dimethoxy	3(6)	0.76	0.99	0.23
4,5-Dimethoxy	4(5)	0.74	0.88	0.14
1,5-Dimethoxy	1	0.62	1.09	0.47
	5	0.69	0.94	0.25
1,6-Dimethoxy	1	0.58	1.04	0.41
	6	0.76	0.99	0.28
1,7-Dimethoxy	1	0.60	1.04	0.44
	7	0.65	0.86	0.21
2,5-Dimethoxy	2	0.66	0.83	0.17
	5	0.67	0.89	0.22
3,5-Dimethoxy	3	0.83	1.06	0.23
	5	0.68	0.91	0.23

Table III—Average Solvent Shift Values for Each Position of the Xanthone Ring

Position	Average Δ Deuterochloroform–Benzene	Average Δ Trifluoroacetic Acid–Benzene	Average Δ Trifluoroacetic Acid–Deuterochloroform
1(8)	0.59 (0.57–0.62)	1.02 (0.95–1.09)	0.42 (0.38–0.47)
2(7)	0.65 (0.65–0.66)	0.84 (0.83–0.86)	0.20 (0.18–0.22)
3(6)	0.78 (0.76–0.83)	1.01 (0.99–1.06)	0.24 (0.23–0.28)
4(5)	0.71 (0.67–0.74)	0.91 (0.88–0.94)	0.20 (0.14–0.25)

use of benzene (II) and deuterochloroform (III) as shift-inducing solvents (9, 10, 17) and was included in the present study.

EXPERIMENTAL

The preparation of the compounds used (1–4) and their complete NMR, IR, and UV data and those of their related phenols and corresponding acetates were presented previously (4). All spectra were determined using a 60-mHz spectrometer. Tetramethylsilane (2%) was employed as the internal reference in all solvents. The concentration of the solute was not greater than 3% (w/v), and the benzene–trifluoroacetic acid solvent contained 3% (v/v) of the latter. The chemical shifts for the methyl groups in the various methoxyxanthones are listed in Table I.

RESULTS AND DISCUSSION

Table II lists the Δ values ($\Delta = \delta_{\text{Solvent 1}} - \delta_{\text{Solvent 2}}$) for the four monomethoxyxanthones and for eight (of the 10 possible) dimethoxyxanthones that do not have the methoxyl groups in the same ring. For Table III, the data from Table II were retabulated and averaged according to the methoxyl positions on the xanthone nucleus. (For the purposes of averaging, the symmetrical xanthones were counted twice. The range of values found is also included in the table.)

Since the 3(6)-position is *para* to the electron-withdrawing carbonyl group, it showed the largest benzene-induced shift, Δ (III–II), in line with the indications of Bowie *et al.* (6) for simple anisole derivatives. The magnitude of Δ (III–II) decreased in the order of C-3(6) > C-4(5) > C-2(7) > C-1(8), and the differences in magnitudes were large enough to distinguish among the closely related isomeric pairs listed in Table II. The introduction of the second methoxyl group into the unsubstituted ring of monomethoxyxanthone seemed to have little effect on the Δ (III–II) value for the first methoxyl. A possible exception was seen for 3,5-dimethoxyxanthone, where the shift for the 3-methoxyl group was somewhat enhanced. This exception could have been a reflection of the fact that the 5-methoxyl group, being *meta* to the carbonyl group, increased its electron-withdrawing power.

Methoxyl resonances appeared at relatively low field in trifluoroacetic acid, so relatively large solvent shifts were obtained in combination with benzene. These shifts again showed a dependence on the position of substitution; their magnitude decreased in the order C-1(8) ≅ C-3(6) > C-4(5) > C-2(7). The 1(8)- and 3(6)-positions (*ortho* and *para* to the

Table IV—Solvent Shift Data for Some Methoxyxanthones Having More than One Methoxyl Group on the Same Ring

Xanthone	Methoxyl Position	Δ Deuterochloroform–Benzene	Δ Trifluoroacetic Acid–Benzene	Δ Trifluoroacetic Acid–Deuterochloroform
1,3-Dimethoxy	1	0.62	1.04	0.42
	3	0.70	1.01	0.31
3,4-Dimethoxy	3	0.78	0.97	0.25
	4	0.21	0.46	0.19
1,3,6-Trimethoxy	1	0.55	0.94	0.39
	3(6)	0.63	0.90	0.27
	6(3)	0.69	0.96	0.27
1,3,8-Trimethoxy	1(8)	0.55	0.91	0.36
	3	0.67	0.88	0.28
	8(1)	0.58	0.95	0.30
1,3,6,8-Tetramethoxy	1(8)	0.52	0.84	0.32
	3(6)	0.62	0.89	0.27
Average	1(8)	0.56	0.90	0.35
	3(6)	0.68	0.93	0.27
Average (12, 13)	2(7)	0.55		
	3(6)	0.64		
	4(5)	0.67		

carbonyl group) were those from which the electron pairs on the methoxyl groups were most efficiently delocalized and, therefore, were the least basic positions. The fact that they showed enhanced rather than reduced values for Δ (I–II) suggests that protonation occurred on the carbonyl oxygen rather than on the ether oxygens.

Tables II and III also list the Δ (I–III) values, which also showed positional dependence, in this case mainly for the 1(8)-position where the shift was about twice that for the other three positions. This pattern was similar to that found (9) for methoxyflavones, where the shift for the 5-methoxyl (*ortho* to the carbonyl) was larger and easily distinguished from those for methoxyls at the 6-, 7-, or 8-position. Values of 0.37 and 0.15 ppm were reported (10) for the 1- and 7-methoxyls of 1,7-dimethoxyxanthone, and the deviations from the presently reported measurements of 0.44 and 0.21 ppm probably resulted from the slightly different experimental conditions.

Table IV gives shift data for a few xanthones having two methoxyls in the same ring. The abnormally low value of Δ (III–II) for the 4-methoxyl in 3,4-dimethoxyxanthone is consistent with values reported for similarly situated methoxyls flanked by two *ortho*-substituents (6, 12, 13, 16, 18). This apparent decrease in the ability of the benzene solvent to shield the methoxyl group in question has been ascribed to steric hindrance. This effect is also apparent in the corresponding value of Δ (I–II) for the 4-methoxyl in this compound. The Δ (I–III) value (0.19 ppm), however, is quite normal for a methoxyl in this position (*cf.*, the value 0.20 ppm in Table III), although it was suggested (9, 17) that such a methoxyl ought to show an enhanced shift because of its increased basicity.

Although the data in Table IV are limited, they suggest that polyoxygenation tends to increase the Δ values by a small amount. This decrease can also be noted in the values reported (12, 13) for a series of 1,3,5,6- and 1,3,6,7-tetraoxygenated xanthones (further substituted by saturated or unsaturated alkyl groups), which are included (as average values) in Table IV.

Finally, the trifluoroacetic acid addition shifts, Δ (II–II/I), were extremely small (*cf.*, Table I), mostly within the experimental error of 1–2 Hz. Therefore, they are of little help in distinguishing the positions of methoxylation, at least in these simple xanthones. This finding is in contrast to their potential usefulness in the methoxyflavone series (9).

REFERENCES

(1) R. A. Finnegan and J. K. Patel, *J. Chem. Soc. Perkin I*, **1972,** 1896.

(2) R. A. Finnegan and K. E. Merkel, *J. Org. Chem.*, **37,** 2986 (1972).

(3) J. K. Patel, M.S. thesis, State University of New York at Buffalo, Buffalo, N.Y., 1967.

(4) K. E. Merkel, Ph.D. thesis, State University of New York at Buffalo, Buffalo, N.Y., 1970.

(5) R. A. Finnegan, K. E. Merkel, and J. K. Patel, *J. Pharm. Sci.*, **62,** 483 (1973). *Cf.* also: R. A. Finnegan, K. E. Merkel, and N. Back, *ibid.*, **61,** 1599 (1972).

(6) J. H. Bowie, J. Ronayne, and D. H. Williams, *J. Chem. Soc. B*, **1966,** 785.

(7) R. G. Wilson, J. H. Bowie, and D. H. Williams, *Tetrahedron*, **24,** 1407 (1968).

(8) P. J. Garrat, F. Scheinmann, and F. Sondheimer, *ibid.*, **23,** 2413 (1967).

(9) R. G. Wilson and D. H. Williams, *J. Chem. Soc. C*, **1968,** 2477.

(10) D. Anker, C. Mercier, M. Baran-Marszak, and J. Massicot, *Tetrahedron*, **25,** 5027 (1969).

(11) A. Pelter, R. Warren, J. N. Usmani, M. Ilyas, and W. Rahman, *Tetrahedron Lett.*, **1969,** 4259.

(12) B. Jackson, H. D. Locksley, and F. Scheinmann, *J. Chem. Soc. C*, **1967,** 2500.

(13) F. Scheinmann, *Chem. Commun.*, **1967,** 1015.

(14) J. D. Connolly and R. McCrindle, *Chem. Ind. (London)*, **1965,** 379.

(15) D. H. Williams and N. S. Bhacca, *Tetrahedron*, **21,** 2021 (1965).

(16) R. Grigg, J. A. Knight, and P. Roffey, *ibid.*, **22,** 3301 (1966).

(17) R. G. Wilson and D. H. Williams, *J. Chem. Soc. C*, **1968,** 2475.

(18) H. M. Fales and K. S. Warren, *J. Org. Chem.*, **32,** 501 (1967).

ACKNOWLEDGMENTS AND ADDRESSES

Received July 1, 1976, from the *Department of Medicinal Chemistry, School of Pharmacy, State University of New York at Buffalo, Buffalo, NY 14214.*

Accepted for publication August 13, 1976.

Abstracted in part from a thesis submitted by K. E. Merkel to the Department of Medicinal Chemistry, State University of New York at Buffalo, in partial fulfillment of the Doctor of Philosophy degree requirements.

Supported by Grant GM-11412 from the National Institutes of Health, U.S. Public Health Service, Bethesda, MD 20014.

This article was written while R. A. Finnegan was a Guest Professor at the Institut für Pharmazeutische Arzneimittellehre der Universität München and he wishes to thank the Directors of the Institute for their hospitality.

This article is considered Part XIII in the series "Constituents of *Mammea americana* L." For Part XII, see Ref. 5.

ˣ To whom inquiries should be directed.

Synthesis of 5-Substituted 2-Oxazolidinethiones and Their Antagonism to Uterotropic Effect of Diethylstilbestrol

A. K. AGRAWAL *, S. S. PARMAR *, C. DWIVEDI ‡§, and R. D. HARBISON ‡x

Abstract □ 5-(4-Aminophenoxymethyl)-2-oxazolidinethiones were synthesized by the cyclization of 1-(4-aminophenoxy)-3-amino-2-propanol in the presence of potassium hydroxide and carbon disulfide. This oxazolidinethione, on reaction with suitable isothiocyanates, yielded 5-[4-(substituted thiocarbamido)phenoxymethyl]-2-oxazolidinethiones. These compounds antagonized the uterotropic effects of diethylstilbestrol in female rats and possessed approximate LD_{50} values of 400–>800 mg/kg.

Keyphrases □ 2-Oxazolidinethiones, 5-substituted—synthesized, evaluated for antagonism to diethylstilbestrol effects, rats □ Diethylstilbestrol effects—antagonism by 5-substituted 2-oxazolidinethiones evaluated, rats □ Structure–activity relationships—5-substituted 2-oxazolidinethiones evaluated for antagonism to diethylstilbestrol effects, rats

Significant anti-implantation effects in rats after oral or subcutaneous administration of oxazolidinethiones suggested an antifertility property for these compounds (1). Oxazolidinethiones also lack androgenic and antigonadotropic activity (2). These observations led to the synthesis of substituted 2-oxazolidinethiones and the evaluation of their ability to antagonize the uterotropic effects of diethylstilbestrol in female rats. The various oxazolidinethiones were synthesized according to Scheme I.

EXPERIMENTAL

Melting points were taken in open capillary tubes with a partial immersion thermometer. The compounds were characterized by their sharp melting points and elemental analyses. All compounds were analyzed for carbon, hydrogen, and nitrogen.

Chemistry—*p*-Acetylaminophenol, on reaction with epichlorohydrin, gave 1-(4-acetylaminophenoxy)-2,3-epoxypropane (I). On treatment with succinimide, I yielded 1-(4-acetylaminophenoxy)-2-hydroxypropylsuccinimide (II). Compound II, on hydrolysis, yielded 1-(4-aminophenoxy)-3-amino-2-propanol (III), which cyclized in the presence of carbon disulfide and potassium hydroxide to 5-(4-aminophenoxymethyl)-2-oxazolidinethione (IV). This oxazolidinethione, on reaction with appropriate isothiocyanates, yielded corresponding thiocarbamide derivatives (V–XIII).

1-(4-Acetylaminophenoxy)-2,3-epoxypropane (I)—A mixture of *p*-acetylaminophenol (0.2 mole), epichlorohydrin (0.6 mole), and pyridine (3 ml) was stirred at 100° for 17 hr. The excess epichlorohydrin was distilled off under reduced pressure. The residue was added to a solution of 23 g of sodium hydroxide in 150 ml of water, and the mixture was stirred at room temperature for 24 hr and then extracted with ether. The ethereal extract was washed with water (200 ml), dried over anhydrous calcium chloride, and filtered. Excess ether from the filtrate was removed by distillation under reduced pressure. The solid mass thus obtained was recrystallized from ethanol (70% yield), mp 103–104°.

Anal.—Calc. for $C_{11}H_{13}NO_3$: C, 63.76; H, 6.28; N, 6.76. Found: C, 63.97; H, 6.01; N, 6.58.

1-(4-Acetylaminophenoxy)-2-hydroxypropylsuccinimide (II)—A mixture of I (0.1 mole), succinimide (0.1 mole), 100 ml of ethanol, and 4 drops of pyridine was refluxed on a steam bath for 20 hr and then poured over 500 ml of cold water. The separated solid mass was filtered, washed with water, and recrystallized from methanol (80% yield), mp 152–153°.

Anal.—Calc. for $C_{15}H_{18}N_2O_5$: C, 58.82; H, 5.88; N, 9.15. Found: C, 59.12; H, 5.68; N, 8.92.

1-(4-Aminophenoxy)-3-amino-2-propanol (III)—A mixture of II (0.1 mole), 33 g of sodium hydroxide, and 120 ml of ethanol was refluxed on a steam bath for 20 hr. Excess ethanol was distilled off under reduced pressure, and 90 ml of cold water was added to the residue. The separated solid mass was collected by filtration, washed thoroughly with water, and recrystallized from ethanol (75% yield), mp 184°.

Anal.—Calc. for $C_9H_{14}N_2O_2$: C, 59.39; H, 7.63; N, 15.38. Found: C, 59.67; H, 7.53; N, 15.00.

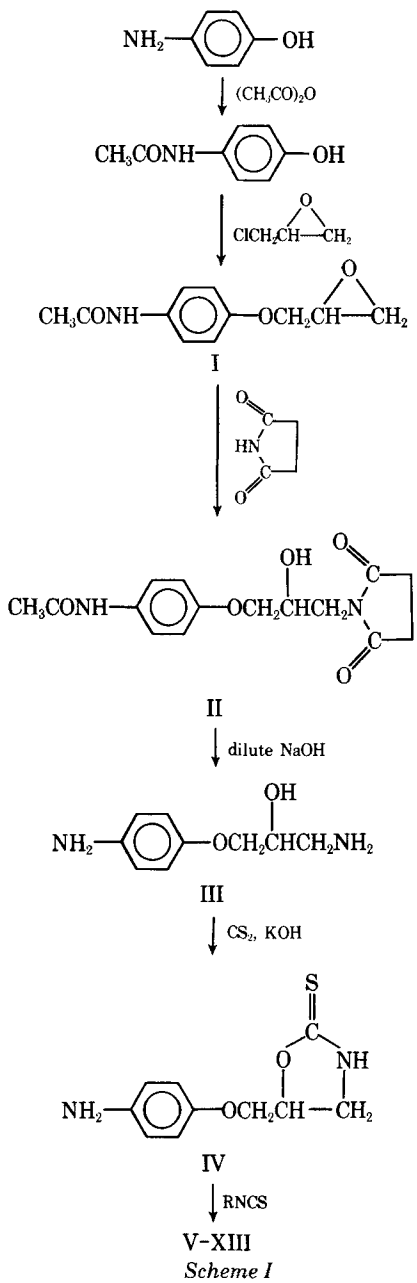

Scheme I

Table I—5-Substituted 2-Oxazolidinethiones and Their Antiestrogenic Activity

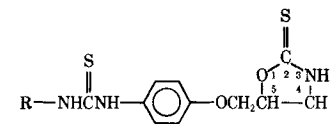

Compound	R	Melting Point	Yield, %	Formula		Analysis, % Calc.	Found
V	C_6H_5	242°	60	$C_{17}H_{17}N_3O_2S_2$	C	56.82	57.05
					H	4.73	4.62
					N	11.69	11.88
VI	2-$CH_3C_6H_4$	237°	60	$C_{18}H_{19}N_3O_2S_2$	C	57.90	58.29
					H	5.09	5.23
					N	11.26	11.00
VII	3-$CH_3C_6H_4$	248°	65	$C_{18}H_{19}N_3O_2S_2$	C	57.90	58.10
					H	5.09	5.18
					N	11.26	10.99
VIII	4-$CH_3C_6H_4$	244°	50	$C_{18}H_{19}N_3O_2S_2$	C	57.90	58.12
					H	5.09	4.77
					N	11.26	10.91
IX	2-$OCH_3C_6H_4$	241°	55	$C_{18}H_{19}N_3O_3S_2$	C	55.52	55.82
					H	4.88	4.77
					N	10.79	10.53
X	4-$OCH_3C_6H_4$	245°	60	$C_{18}H_{19}N_3O_3S_2$	C	55.52	55.23
					H	4.88	4.54
					N	10.79	11.09
XI	4-ClC_6H_4	95°	65	$C_{17}H_{16}ClN_3O_2S_2$	C	51.83	52.10
					H	4.06	4.04
					N	10.67	10.83
XII	4-BrC_6H_4	258°	80	$C_{17}H_{16}BrN_3O_2S_2$	C	46.57	46.67
					H	3.65	3.72
					N	9.58	9.55
XIII	C_2H_5	245°	85	$C_{13}H_{17}N_3O_2S_2$	C	50.16	50.00
					H	5.48	5.53
					N	13.50	13.29

5-(4-Aminophenoxymethyl)-2-oxazolidinethione (IV)—A cold solution of potassium hydroxide (0.2 mole) in 30 ml of water containing 20 ml of ethanol was added to a mixture of III (0.1 mole) and carbon disulfide (0.1 mole). The mixture was refluxed on a steam bath for 4 hr. Excess ethanol was distilled off under reduced pressure. The residue was diluted with 300 ml of water, cooled in an ice bath, and acidified with 6 *N* hydrochloric acid. The separated solid mass was filtered, washed with water, and recrystallized from acetone (60% yield), mp 230°.

Anal.—Calc. for $C_{10}H_{11}N_2O_2S$: C, 53.57; H, 5.35; N, 12.28. Found: C, 53.89; H, 5.45; N, 12.55.

5-[4-(Substituted Thiocarbamido)phenoxymethyl]-2-oxazolidinethiones (V–XIII)—A mixture of IV (0.01 mole) and the appropriate alkyl or aryl isothiocyanate (0.01 mole) in 40 ml of absolute ethanol was refluxed on a steam bath for 5 hr. Excess ethanol was removed by distillation. The solid mass thus obtained was filtered, washed thoroughly with water and ether, and recrystallized from ethanol. The various substituted 2-oxazolidinethiones (Table I) gave characteristic bands of C=S at 1051–1100 cm^{-1} and >NH at 3300–3340 cm^{-1} in their IR spectra.

Biological Methods—The ability of V–XIII to antagonize the uterotropic effect of diethylstilbestrol was determined using immature healthy female rats (3). The compounds were dissolved in propylene glycol (100%) and administered to 10 rats at a dose of 80 mg/kg ip every 24 hr for 3 days. The control group received an equivalent amount of propylene glycol. Diethylstilbestrol, 2 mg/kg sc, was administered on the 3rd day 6 hr after the last dose of the test compound or propylene glycol.

The decrease in the dry weight of the uterus caused by the test compounds in diethylstilbestrol-treated rats was recorded to evaluate the antiestrogenic activity of the oxazolidinethiones. The results were analyzed statistically using the Student *t* test. The approximate LD_{50} values were determined in mice by intraperitoneal administration of substituted oxazolidinethiones (4).

RESULTS AND DISCUSSION

The ability of V–XIII to antagonize the uterotropic effect of diethylstilbestrol at a dose of 80 mg/kg is recorded in Table II. Diethylstilbestrol treatment significantly increased the dry weight of the uterus to 22.9 ± 2.61 mg as compared to 8.4 ± 1.62 mg in the control rats ($p < 0.001$). All compounds reduced the diethylstilbestrol-induced increase in the dry weight of the uterus of rats. Most of these compounds produced statistically significant reductions in the dry weight of the uterus increased by diethylstilbestrol treatment; maximum reduction was observed with VIII and IX ($p < 0.05$), which possess a methyl or methoxy substituent at the 4-position of the phenyl moiety. Compounds with a 2-methylphenyl (VI) or alkyl (XIII) group showed considerably lower reduction. The introduction of an aromatic nucleus (V and VII–XII) in place of an alkyl substituent (XIII) increased the effectiveness, with the exception of VI where a decrease was observed.

These results failed to provide a definite structure–activity relationship of substituted 2-oxazolidinethiones. The decrease in the uterotropic effects of diethylstilbestrol provided evidence for the greater affinity of substituted 2-oxazolidinethiones without appreciable intrinsic activity toward estrogen receptors in the rat uterus. However, the ability of these compounds to alter the estrogen and progesterone balance, which may lead to the termination of pregnancy, could presumably permit their use as postcoital antifertility agents. Because of the low toxicity, as reflected by their approximate LD_{50} values of 400–>800 mg/kg, further study to

Table II—Antagonism to the Uterotropic Effect of Diethylstilbestrol by 5-Substituted 2-Oxazolidinethiones

Treatment	Weight of Uterus[a], mg	Approximate LD_{50}, mg/kg
Control	8.4 ± 1.62	—
Diethylstilbestrol	22.9 ± 2.61[b]	—
V	10.8 ± 1.20[c]	400
VI	20.0 ± 1.40	>800
VII	12.2 ± 1.42[c]	>800
VIII	8.6 ± 1.28[c]	800
IX	11.4 ± 1.31[c]	600
X	8.5 ± 0.83[c]	600
XI	15.5 ± 1.31	400
XII	14.5 ± 1.18[c]	>800
XIII	16.5 ± 1.00	>800

[a] Screening procedures are as indicated in the text. The values are the mean (± *SE*) of the dry weight of the uteri after administration of diethylstilbestrol in 5-substituted 2-oxazolidinethione-treated rats. [b] Significant difference ($p < 0.001$) from control. [c] Significant difference ($p < 0.05$) from only diethylstilbestrol treated.

determine the antifertility effects of 5-[4-(substituted thiocarbamido)-phenoxymethyl]-2-oxazolidinethiones is warranted.

REFERENCES

(1) G. A. Youngdale, G. W. Duncan, D. E. Emmert, and D. Lednicer, *J. Med. Chem.*, **9**, 155 (1966).

(2) G. W. Duncan, R. L. Johnston, and S. C. Lyster, *J. Reprod. Fertil.*, **11**, 85 (1966).

(3) V. K. Rastogi, A. K. Agrawal, S. S. Parmar, and S. J. Brumleve, *Res. Commun. Chem. Pathol. Pharmacol.*, **7**, 763 (1974).

(4) C. C. Smith, *J. Pharmacol. Exp. Ther.*, **100**, 408 (1950).

ACKNOWLEDGMENTS AND ADDRESSES

Received June 3, 1976, from the *Department of Pharmacology, King George's Medical College, Lucknow 226003, India, and the ‡Department of Pharmacology and Center in Toxicology, Vanderbilt University School of Medicine, Nashville, TN 37232.

Accepted for publication July 28, 1976.

Supported in part by U.S. Public Health Service Grant ES 00267.

The authors thank Professor K. P. Bhargava and Professor Carl D. Chambers for advice and encouragement and Dr. Nitya Nand, Central Drug Research Institute, Lucknow, Uttar Pradesh, India, for elemental analyses. Grateful acknowledgment is made to the State Medical Research Council of Uttar Pradesh, Lucknow, India, and the Indian Council of Medical Research, New Delhi, India, for providing a research fellowship to A. K. Agrawal.

§ Present address: Department of Pediatrics, Meharry Medical College, Nashville, TN 37208.

ˣ To whom inquiries should be directed.

Cytotoxic Agents from *Bursera klugii* (Burseraceae) I: Isolation of Sapelins A and B

S. D. JOLAD, R. M. WIEDHOPF, and J. R. COLE ˣ

Abstract □ A crude chloroform-soluble fraction of the ethanol extract of the leaves of *Bursera klugii* showed activity against two test systems, the P-388 lymphocytic leukemia (3PS) and the human epidermoid carcinoma of the nasopharynx (9KB). The PS activity was due to two constituents, sapelins A and B.

Keyphrases □ Sapelins A and B—isolated from ethanol extract of leaves of *Bursera klugii*, cytotoxic activity evaluated □ *Bursera klugii*—sapelins A and B isolated from ethanol extract of leaves, cytotoxic activity evaluated □ Cytotoxic activity—sapelins A and B evaluated

During a continuing search for plants having tumor inhibitory constituents, the chloroform-soluble fraction of the ethanol extract of the leaves of *Bursera klugii* Macbr (Burseraceae[1]) was shown to be active against the P-388 lymphocytic leukemia test system (3PS) and the human epidermoid carcinoma of the nasopharynx test system[2] (9KB). The activity against the PS test system was due to two constituents of the crude chloroform-soluble fraction.

DISCUSSION

The two major constituents of the chloroform-soluble fraction were triterpenes, sapelin A (I) and sapelin B (II). These compounds were isolated previously from commercial sapele, *Entandrophragma cylindricum* Sprague (1). Isolation of these triterpenes was effected by solvent extraction followed by column chromatography and crystallization. Identification was made by elemental analysis; IR, NMR, and mass spectral data; and direct comparison with an authentic specimen.

Sapelin A demonstrated activities of 130, 136, 127, and 130% test/control (T/C) at 10.0, 5.0, 2.5, and 1.25 mg/kg, respectively. Sapelin B demonstrated activities of 136, 136, 130, and 138% T/C at the same doses, respectively. Activity in the PS system is defined as an increase in the survival of treated animals over that of control animals resulting in a T/C ≥ 125% (2).

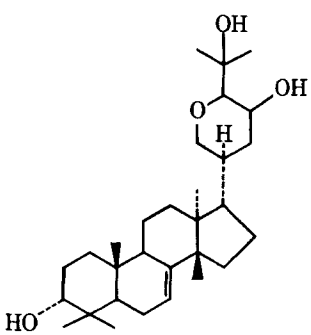

I

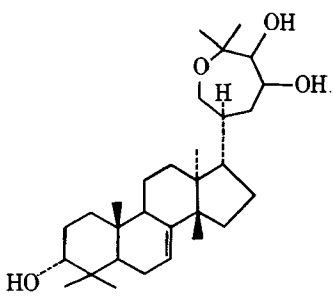

II

EXPERIMENTAL[3]

The leaves of *B. klugii*, collected in Peru during August 1975, were ground and stored at −10° prior to extraction.

The ground material (7.72 kg) was extracted exhaustively in a Lloyd-type extractor with petroleum ether followed by 95% ethanol. The air-dried ethanol extract was subjected to partitioning between chloroform and water. The chloroform phase was first air dried and then vacuum dried. A 300-g portion of the residue was extracted with 5 liters of *n*-hexane in three portions by mechanical stirring. The hexane-insoluble residue was then extracted with 5 liters of ether in three portions using a magnetic stirrer.

The combined ether-soluble fraction, on concentration under vacuum followed by cooling in a freezer overnight, yielded a residue. TLC of this residue showed two spots as major constituents, one corresponding to sapelin A and the other to sapelin B. A 4-g portion of this residue was subjected to alumina (grade III, 160 g) dry column chromatography. Elution with ethyl acetate–benzene (1:1) afforded nearly pure sapelins

[1] Identification was confirmed by Dr. Robert E. Perdue, Medicinal Plant Resources Laboratory, Plant Genetics and Germ Plasm Institute, Beltsville, Md. A reference specimen was deposited in that herbarium.

[2] Division of Cancer Treatment, National Cancer Institute, National Institutes of Health, Bethesda, Md.

[3] Carbon and hydrogen analyses were carried out by Chemalytics, Inc., Tempe, Ariz. Melting points were determined on a Kofler hot-stage apparatus and are uncorrected. IR spectra were run on a Beckman IR-33. NMR and mass spectra were run using a Varian T-60 spectrometer and a Hewlett-Packard quadrupole spectrometer (model 5930), respectively.

determine the antifertility effects of 5-[4-(substituted thiocarbamido)-phenoxymethyl]-2-oxazolidinethiones is warranted.

REFERENCES

(1) G. A. Youngdale, G. W. Duncan, D. E. Emmert, and D. Lednicer, *J. Med. Chem.*, **9**, 155 (1966).

(2) G. W. Duncan, R. L. Johnston, and S. C. Lyster, *J. Reprod. Fertil.*, **11**, 85 (1966).

(3) V. K. Rastogi, A. K. Agrawal, S. S. Parmar, and S. J. Brumleve, *Res. Commun. Chem. Pathol. Pharmacol.*, **7**, 763 (1974).

(4) C. C. Smith, *J. Pharmacol. Exp. Ther.*, **100**, 408 (1950).

ACKNOWLEDGMENTS AND ADDRESSES

Received June 3, 1976, from the *Department of Pharmacology, King George's Medical College, Lucknow 226003, India, and the ‡Department of Pharmacology and Center in Toxicology, Vanderbilt University School of Medicine, Nashville, TN 37232.

Accepted for publication July 28, 1976.

Supported in part by U.S. Public Health Service Grant ES 00267.

The authors thank Professor K. P. Bhargava and Professor Carl D. Chambers for advice and encouragement and Dr. Nitya Nand, Central Drug Research Institute, Lucknow, Uttar Pradesh, India, for elemental analyses. Grateful acknowledgment is made to the State Medical Research Council of Uttar Pradesh, Lucknow, India, and the Indian Council of Medical Research, New Delhi, India, for providing a research fellowship to A. K. Agrawal.

§ Present address: Department of Pediatrics, Meharry Medical College, Nashville, TN 37208.

ˣ To whom inquiries should be directed.

Cytotoxic Agents from *Bursera klugii* (Burseraceae) I: Isolation of Sapelins A and B

S. D. JOLAD, R. M. WIEDHOPF, and J. R. COLE ˣ

Abstract □ A crude chloroform-soluble fraction of the ethanol extract of the leaves of *Bursera klugii* showed activity against two test systems, the P-388 lymphocytic leukemia (3PS) and the human epidermoid carcinoma of the nasopharynx (9KB). The PS activity was due to two constituents, sapelins A and B.

Keyphrases □ Sapelins A and B—isolated from ethanol extract of leaves of *Bursera klugii*, cytotoxic activity evaluated □ *Bursera klugii*—sapelins A and B isolated from ethanol extract of leaves, cytotoxic activity evaluated □ Cytotoxic activity—sapelins A and B evaluated

During a continuing search for plants having tumor inhibitory constituents, the chloroform-soluble fraction of the ethanol extract of the leaves of *Bursera klugii* Macbr (Burseraceae[1]) was shown to be active against the P-388 lymphocytic leukemia test system (3PS) and the human epidermoid carcinoma of the nasopharynx test system[2] (9KB). The activity against the PS test system was due to two constituents of the crude chloroform-soluble fraction.

DISCUSSION

The two major constituents of the chloroform-soluble fraction were triterpenes, sapelin A (I) and sapelin B (II). These compounds were isolated previously from commercial sapele, *Entandrophragma cylindricum* Sprague (1). Isolation of these triterpenes was effected by solvent extraction followed by column chromatography and crystallization. Identification was made by elemental analysis; IR, NMR, and mass spectral data; and direct comparison with an authentic specimen.

Sapelin A demonstrated activities of 130, 136, 127, and 130% test/control (T/C) at 10.0, 5.0, 2.5, and 1.25 mg/kg, respectively. Sapelin B demonstrated activities of 136, 136, 130, and 138% T/C at the same doses, respectively. Activity in the PS system is defined as an increase in the survival of treated animals over that of control animals resulting in a T/C ≥ 125% (2).

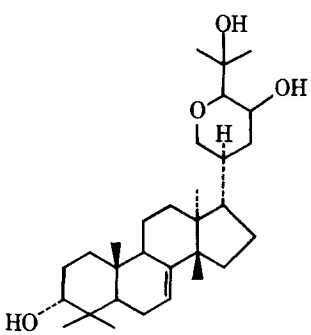

I

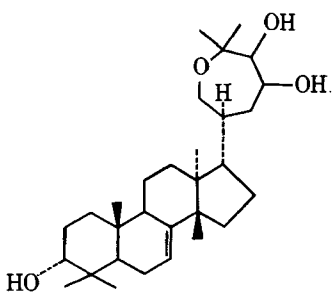

II

EXPERIMENTAL[3]

The leaves of *B. klugii*, collected in Peru during August 1975, were ground and stored at −10° prior to extraction.

The ground material (7.72 kg) was extracted exhaustively in a Lloyd-type extractor with petroleum ether followed by 95% ethanol. The air-dried ethanol extract was subjected to partitioning between chloroform and water. The chloroform phase was first air dried and then vacuum dried. A 300-g portion of the residue was extracted with 5 liters of *n*-hexane in three portions by mechanical stirring. The hexane-insoluble residue was then extracted with 5 liters of ether in three portions using a magnetic stirrer.

The combined ether-soluble fraction, on concentration under vacuum followed by cooling in a freezer overnight, yielded a residue. TLC of this residue showed two spots as major constituents, one corresponding to sapelin A and the other to sapelin B. A 4-g portion of this residue was subjected to alumina (grade III, 160 g) dry column chromatography. Elution with ethyl acetate–benzene (1:1) afforded nearly pure sapelins

[1] Identification was confirmed by Dr. Robert E. Perdue, Medicinal Plant Resources Laboratory, Plant Genetics and Germ Plasm Institute, Beltsville, Md. A reference specimen was deposited in that herbarium.

[2] Division of Cancer Treatment, National Cancer Institute, National Institutes of Health, Bethesda, Md.

[3] Carbon and hydrogen analyses were carried out by Chemalytics, Inc., Tempe, Ariz. Melting points were determined on a Kofler hot-stage apparatus and are uncorrected. IR spectra were run on a Beckman IR-33. NMR and mass spectra were run using a Varian T-60 spectrometer and a Hewlett-Packard quadrupole spectrometer (model 5930), respectively.

A and B, which were further purified by decolorization followed by crystallization.

Sapelin A was obtained as long colorless thick needles from methanol, mp 219–220° with initial sweating. It was identical in all respects with the authentic specimen[3].

Anal.—Calc. for $C_{30}H_{50}O_4$: C, 75.9; H, 10.6; mol. wt. 474. Found: C, 75.31; H, 10.10; *m/e* 474 (M^+).

Sapelin B was obtained as tiny colorless needles from ethyl acetate–petroleum ether, mp 174–176° with initial sweating. It was identical in all respects with the authentic specimen.

Anal.—Calc. for $C_{30}H_{50}O_4$: C, 75.9; H, 10.6; mol. wt. 474. Found: C, 75.32; H, 10.13; *m/e* 474 (M^+).

REFERENCES

(1) W. R. Chan, D. R. Taylor, and T. Yee, *J. Chem. Soc. C*, **1970**, 311.

(2) R. I. Geran, N. H. Greenberg, M. N. MacDonald, A. M. Schumacher, and B. J. Abbott, *Cancer Chemother. Rep.*, 3(3), 9 (1972).

ACKNOWLEDGMENTS AND ADDRESSES

Received June 28, 1976, from the *Division of Pharmaceutical Chemistry, College of Pharmacy, University of Arizona, Tucson, AZ 85721.*

Accepted for publication August 2, 1976.

Supported by Contract NOI-CM-33750 from the Division of Cancer Treatment, National Cancer Institute, National Institutes of Health, Department of Health, Education, and Welfare, Bethesda, MD 20014, and the Elsa U. Pardee Foundation, Midland, MI 48640.

The authors are indebted to Dr. D. R. Taylor, Department of Chemistry, University of Alberta, Edmonton, Alberta, Canada, for providing the authentic samples of sapelins A and B and their NMR spectra.

[x] To whom inquiries should be directed.

Quinuclidine Chemistry: Autocondensation Reactions of 3-Quinuclidinone

R. A. SANDMANN [x] and W. C. McHUGH, Jr.

Abstract □ During the synthesis of 3-hydroxy-3-ethinylquinuclidine (I), two additional products were isolated and identified as (*E*)-3-[2-(3-oxoquinuclidine)]quinuclidylidene (III) and (*E*)-3-[2-(3-hydroxy-3-ethinylquinuclidine)]quinuclidylidene (V). The base-catalyzed autocondensation of 3-quinuclidinone resulted in the α,β-unsaturated ketone dimer (III) as a single isomer. The geometric configuration was deduced by examination of the NMR spectra of the methyl iodide salt. Compound V was thus the result of attack on the carbonyl carbon of III by the acetylide anion. The isolation and identification of these compounds clarified the reported differences in the physical properties of I and its analogs.

Keyphrases □ Quinuclidines, substituted—synthesized, structures, stereoisomers, and physical properties identified □ Autocondensation—3-quinuclidinone, products identified

It was necessary to synthesize significant quantities of 3-hydroxy-3-ethinylquinuclidine (I) as an intermediate in preparing a series of potential antidepressant agents. However, there was a disparity in the physical properties of I prepared by two different methods (1, 2). The synthetic method employed by Ernest (2) gave a compound melting at 192°, and that of Clemo and Hoggarth (1) gave a compound melting at 159°.

A clarification of these discrepancies by the synthesis of I and (*E*)-3-[2-(3-oxoquinuclidine)]quinuclidylidene (III) (mp 159°) is now reported.

DISCUSSION

The preparation of I involved dispersing acetylene gas through a tetrahydrofuran solution of 3-quinuclidinone and sodium amide. Three products were isolated, the major compound being I and having the same characteristics as demonstrated by Ernest (2). Mass spectra of the remaining two compounds indicated masses of 258 and 232. The difference in masses was 26, the molecular weight of acetylene. IR analysis of the 258 compound indicated a terminal acetylene (ν_{max} at 3240 and 2095 cm^{-1}). The IR spectrum for the 232 compound showed an α,β-unsaturated ketone (ν_{max} 1685 and 1615 cm^{-1}).

3-Quinuclidinone condenses with aldehydes under basic conditions (3–5); autocondensation under similar conditions and by the same aldol-type mechanism can now be demonstrated (Scheme I). A base such as sodium amide generates the enolate, which condenses by nucleophilic attack with another molecule of 3-quinuclidinone. The resultant dimer alkoxide is protonated, and dehydration of the ketol should result in a mixture of α,β-unsaturated ketone isomers, III and IV, its (*Z*)-isomer.

Conventional synthesis of III employed the use of potassium *tert*-butoxide in *tert*-butyl alcohol as the condensing agent for 3-quinuclidinone. The product (mol. wt. 232) proved to be identical with the one isolated from the acetylene–sodium amide reaction. Thus, the reaction between III and the acetylide ion gave (*E*)-3-[2-(3-hydroxy-3-ethinylquinuclidine)]quinuclidylidene (V, mol. wt. 258).

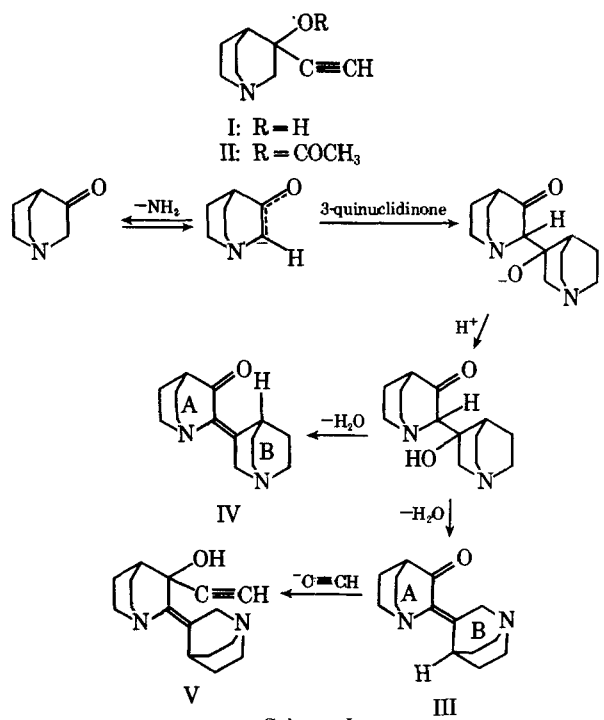

Scheme I

A and B, which were further purified by decolorization followed by crystallization.

Sapelin A was obtained as long colorless thick needles from methanol, mp 219–220° with initial sweating. It was identical in all respects with the authentic specimen[3].

Anal.—Calc. for $C_{30}H_{50}O_4$: C, 75.9; H, 10.6; mol. wt. 474. Found: C, 75.31; H, 10.10; *m/e* 474 (M^+).

Sapelin B was obtained as tiny colorless needles from ethyl acetate–petroleum ether, mp 174–176° with initial sweating. It was identical in all respects with the authentic specimen.

Anal.—Calc. for $C_{30}H_{50}O_4$: C, 75.9; H, 10.6; mol. wt. 474. Found: C, 75.32; H, 10.13; *m/e* 474 (M^+).

REFERENCES

(1) W. R. Chan, D. R. Taylor, and T. Yee, *J. Chem. Soc. C*, **1970**, 311.

(2) R. I. Geran, N. H. Greenberg, M. N. MacDonald, A. M. Schumacher, and B. J. Abbott, *Cancer Chemother. Rep.*, 3(3), 9 (1972).

ACKNOWLEDGMENTS AND ADDRESSES

Received June 28, 1976, from the *Division of Pharmaceutical Chemistry, College of Pharmacy, University of Arizona, Tucson, AZ 85721.*

Accepted for publication August 2, 1976.

Supported by Contract NOI-CM-33750 from the Division of Cancer Treatment, National Cancer Institute, National Institutes of Health, Department of Health, Education, and Welfare, Bethesda, MD 20014, and the Elsa U. Pardee Foundation, Midland, MI 48640.

The authors are indebted to Dr. D. R. Taylor, Department of Chemistry, University of Alberta, Edmonton, Alberta, Canada, for providing the authentic samples of sapelins A and B and their NMR spectra.

[x] To whom inquiries should be directed.

Quinuclidine Chemistry: Autocondensation Reactions of 3-Quinuclidinone

R. A. SANDMANN [x] and W. C. McHUGH, Jr.

Abstract □ During the synthesis of 3-hydroxy-3-ethinylquinuclidine (I), two additional products were isolated and identified as (*E*)-3-[2-(3-oxoquinuclidine)]quinuclidylidene (III) and (*E*)-3-[2-(3-hydroxy-3-ethinylquinuclidine)]quinuclidylidene (V). The base-catalyzed autocondensation of 3-quinuclidinone resulted in the α,β-unsaturated ketone dimer (III) as a single isomer. The geometric configuration was deduced by examination of the NMR spectra of the methyl iodide salt. Compound V was thus the result of attack on the carbonyl carbon of III by the acetylide anion. The isolation and identification of these compounds clarified the reported differences in the physical properties of I and its analogs.

Keyphrases □ Quinuclidines, substituted—synthesized, structures, stereoisomers, and physical properties identified □ Autocondensation—3-quinuclidinone, products identified

It was necessary to synthesize significant quantities of 3-hydroxy-3-ethinylquinuclidine (I) as an intermediate in preparing a series of potential antidepressant agents. However, there was a disparity in the physical properties of I prepared by two different methods (1, 2). The synthetic method employed by Ernest (2) gave a compound melting at 192°, and that of Clemo and Hoggarth (1) gave a compound melting at 159°.

A clarification of these discrepancies by the synthesis of I and (*E*)-3-[2-(3-oxoquinuclidine)]quinuclidylidene (III) (mp 159°) is now reported.

DISCUSSION

The preparation of I involved dispersing acetylene gas through a tetrahydrofuran solution of 3-quinuclidinone and sodium amide. Three products were isolated, the major compound being I and having the same characteristics as demonstrated by Ernest (2). Mass spectra of the remaining two compounds indicated masses of 258 and 232. The difference in masses was 26, the molecular weight of acetylene. IR analysis of the 258 compound indicated a terminal acetylene (ν_{max} at 3240 and 2095 cm^{-1}). The IR spectrum for the 232 compound showed an α,β-unsaturated ketone (ν_{max} 1685 and 1615 cm^{-1}).

3-Quinuclidinone condenses with aldehydes under basic conditions (3–5); autocondensation under similar conditions and by the same aldol-type mechanism can now be demonstrated (Scheme I). A base such as sodium amide generates the enolate, which condenses by nucleophilic attack with another molecule of 3-quinuclidinone. The resultant dimer alkoxide is protonated, and dehydration of the ketol should result in a mixture of α,β-unsaturated ketone isomers, III and IV, its (*Z*)-isomer.

Conventional synthesis of III employed the use of potassium *tert*-butoxide in *tert*-butyl alcohol as the condensing agent for 3-quinuclidinone. The product (mol. wt. 232) proved to be identical with the one isolated from the acetylene–sodium amide reaction. Thus, the reaction between III and the acetylide ion gave (*E*)-3-[2-(3-hydroxy-3-ethinylquinuclidine)]quinuclidylidene (V, mol. wt. 258).

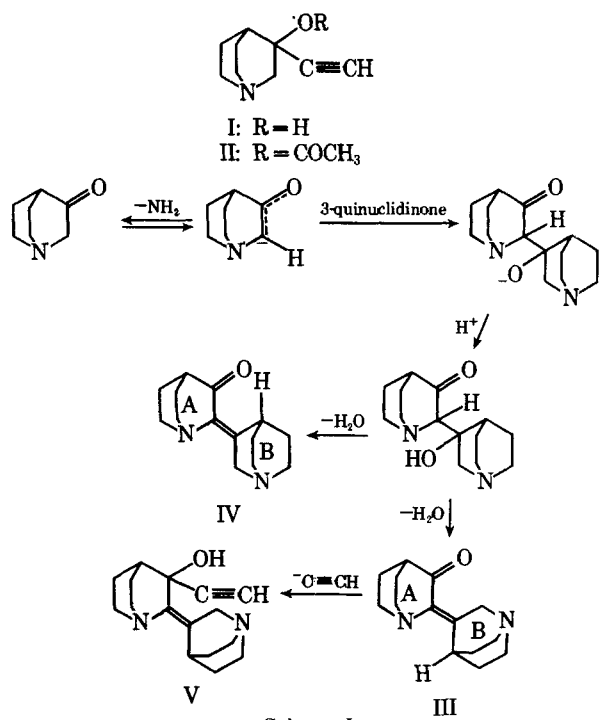

Scheme I

Basic conditions need not necessarily be employed in obtaining III. While attempting to make a dioxolone quinuclidine by reacting 3-quinuclidinone with glycolic acid and a catalytic amount of *p*-toluenesulfonic acid, a small amount of III was isolated.

Since only one isomer (III) was isolated, comparative spectral data between the (*E*)- and (*Z*)-configurations were not available to substantiate their geometry. However, inspection of molecular models of the two isomers indicated that the nitrogen in ring A (the ring containing the carbonyl) was sterically hindered by the bridgehead proton in ring B for the (*E*)-isomer. If this configuration was correct for the (*E*)-isomer, only the monomethyl iodide salt could be formed, since the formation of the dimethyl iodide salt would be impeded. NMR and elemental analysis confirmed that just one methyl iodide added, indicating the (*E*)-isomer.

Thermal and chemical techniques were employed to induce isomerization of the (*E*)-form. These attempts failed, as indicated by no significant changes in the NMR spectra. Again, models help to explain why the (*E*)-isomer would be favored over the (*Z*)-form. The model of the (*Z*)-isomer indicates very unfavorable steric interactions between the carbonyl oxygen in ring A and the bridgehead hydrogen on ring B. The space-filling models actually show that the valence orbitals of the bridgehead hydrogen and the oxygen overlap and that considerable twisting of the carbonyl is necessary to prevent this interaction. The rigidity of the quinuclidine cage maintains the bridgehead hydrogen in a fixed position. Thus, the carbonyl is forced out of its normal plane, increasing strain in the quinuclidine ring and causing a loss of conjugation with the exocyclic double bond. The (*Z*)-isomer is definitely the thermodynamically less stable configuration.

The rate of dimer formation is fairly rapid. Clemo and Hoggarth (1) used potassium metal in *tert*-amyl alcohol to generate the acetylide anion *in situ*. The result was the condensation product III, incorrectly identified as I. Ernest (2) generated the acetylide anion in liquid ammonia and then added 3-quinuclidinone, obtaining the expected product I. The formation of the (*E*)-isomer is stereoselective, and its formation should be considered in reactions using 3-quinuclidinone and base, especially in solvents that enhance aldol condensations.

The hydrochloride salt of 3-acetoxy-3-ethinylquinuclidine (II) was previously reported (6). Since the method of Clemo and Hoggarth (1) was used in obtaining I, the values are suspect. The results of Grob *et al.* (6) would not be corroborated, since they did not report the free base. Also, their melting points for the hydrochloride (234–240°) and the picrate (181–183°) were dissimilar to those found.

EXPERIMENTAL

3-Hydroxy-3-ethinylquinuclidine (I)—Sodium amide (10.5 g, 0.26 mole) was suspended in 90 ml of tetrahydrofuran, which had been dried over potassium hydroxide pellets and distilled. Dry acetylene gas was bubbled into the suspension; positive pressure was maintained using a mercury trap. 3-Quinuclidinone (32.3 g, 0.26 mole), which had been recrystallized from petroleum ether, was dissolved in 90 ml of dry tetrahydrofuran and dropped into the mixture over 4 hr. The reaction was allowed to continue for another 19 hr. After that time, most solvent was removed *in vacuo*. Ice and then ice water were added to the residue. The precipitate that resulted was filtered and dried, giving 25.47 g. It was recrystallized from ethanol–water, giving 13.52 g (34.76%), mp 191–193°; IR (KBr): 3225 (≡C—H) and 2090 (C≡C) cm^{-1}.

Anal.—Calc. for $C_9H_{13}NO$: C, 71.52; H, 8.60; N, 9.27. Found: C, 71.49; H, 8.86; N, 9.23.

The hydrochloride salt, recrystallized from 2-propanol, gave a melting point of 198–199°.

(*E*)-3-[2-(3-Oxoquinuclidine)]quinuclidylidene (III)—*Method A: Dihydrochloride*—The basic solution from which I was filtered was extracted with methylene chloride, decolorized with activated charcoal, and dried over magnesium sulfate. Hydrogen chloride gas was bubbled into the methylene chloride, and the solvent was removed *in vacuo*. The residue was recrystallized from water–methanol–2-propanol, yielding 2 g of white needle crystals, mp 275–276°. The IR spectrum indicated a hydrate, as was confirmed by Karl Fischer titration.

Anal.—Calc. for $C_{14}H_{22}Cl_2N_2O{\cdot}H_2O$: C, 52.05; H, 7.49; N, 8.67. Found: C, 51.99; H, 7.58; N, 8.37.

Method A: Free Base—The dihydrochloride was dissolved in water and made basic with 10% NaOH solution. This solution was extracted with methylene chloride and dried over magnesium sulfate. The solvent was removed *in vacuo*, and the residue was recrystallized from absolute ether (mp 159–160°).

Method B—3-Quinuclidinone (50 g, 0.4 mole) was dissolved in 200 ml of *tert*-butyl alcohol containing 23 g (0.205 mole) of potassium *tert*-butoxide. This mixture was stirred under a nitrogen atmosphere for 4 hr, giving a red-brown solution. After that time, the solvent was removed *in vacuo*. Water was added to the residue, this solution was extracted with hot benzene, and the benzene was dried over magnesium sulfate. The solvent was removed *in vacuo*, giving 42.7 g (92%) of a light-yellow powder, mp 148–157°, soften 138°. Recrystallization in absolute ether gave prism crystals having a green tint, mp 159–160°; IR (KBr): 1685 (C=O) and 1615 (conjugated C=C) cm^{-1}; NMR ($CDCl_3$): δ 1.90 [m, 8H, $(CH_2)_2C$], 2.5 (quintet, 1H, bridgehead hydrogen, ring A), 2.87 [t, 8H, $(CH_2)_2N$], 3.33 (quintet, 1H, bridgehead hydrogen, ring B), and 3.83 (s, 2H, $=CCH_2N$) ppm.

Anal.—Calc. for $C_{14}H_{20}N_2O$: C, 72.38; H, 8.68; N, 12.06. Found: C, 72.45; H, 8.96; N, 11.87.

The methyl iodide salt was recrystallized from methanol–acetone–absolute ether, mp 225–226°.

Anal.—Calc. for $C_{15}H_{23}IN_2O$: C, 48.14; H, 6.19; N, 7.48. Found: C, 47.20; H, 6.29; N, 7.48.

The picrate was recrystallized from ethanol, mp 207–208°.

(*E*)-3-[2-(3-Hydroxy-3-ethinylquinuclidine)]quinuclidylidene (V)—From the ethanol–water solution from which I was recrystallized, V was isolated by a number of selective recrystallizations using methanol until TLC indicated one component [silica gel developed with chloroform–methanol–ammonium hydroxide (85:15:1)]. The yield was 550 mg, mp 245–247°; IR (KBr): 3240 (≡CH) and 2090 (C≡C) cm^{-1}. Preparation of the hydrochloride salt of V was accomplished by preparing a solution in hot tetrahydrofuran and treating with hydrogen chloride gas. The solvent was removed *in vacuo*, and the solid was recrystallized from methanol–2-propanol, mp 259–260°.

Anal.—Calc. for $C_{16}H_{24}Cl_2N_2O$: C, 58.04; H, 7.25; N, 8.46. Found: C, 57.82; H, 7.35; N, 8.12.

3-Acetoxy-3-ethinylquinuclidine (II)—To 7.85 g (0.52 mole) of I was added 85 ml of acetic anhydride and 550 mg of zinc chloride. This mixture was refluxed for 2 hr. After that time, the excess acetic anhydride was distilled off under reduced pressure to a volume of approximately 15 ml. Ice was then added. The pH was adjusted to 12 with cold saturated potassium carbonate, and the solution was extracted with chloroform. The chloroform was dried over magnesium sulfate, and the solvent was removed *in vacuo*. An oil resulted and then crystallized upon scratching. Absolute ether–acetone was used for recrystallization. Large colorless prisms resulted, 4.61 g (46%), mp 89–91°; IR (KBr): 3250 (≡CH), 2100 (C≡C), and 1730 (C=O) cm^{-1}.

Anal.—Calc. for $C_{11}H_{15}NO_2$: C, 68.39; H, 7.77; N, 7.25. Found: C, 68.49; H, 7.99; N, 7.10.

The hydrochloride had a melting point of 217–219° dec., and the picrate had a melting point of 149°.

REFERENCES

(1) G. R. Clemo and E. Hoggarth, *J. Chem. Soc.*, **1941**, 476.

(2) J. Ernest, *Collect. Czech. Chem. Commun.*, **15**, 322 (1950).

(3) A. T. Nielsen, *J. Org. Chem.*, **31**, 1053 (1966).

(4) L. Stermbach and S. Kaiser, *J. Am. Chem. Soc.*, **74**, 2215 (1952).

(5) E. J. Warawa, N. J. Mueller, and R. Jules, *J. Med. Chem.*, **17**, 497 (1974).

(6) C. A. Grob, A. Kaiser, and E. Renk, *Helv. Chim. Acta*, **40**, 2170 (1957).

ACKNOWLEDGMENTS AND ADDRESSES

Received May 27, 1976, from the *School of Pharmacy, University of Missouri-Kansas City, Kansas City, MO 64110.*

Accepted for publication August 3, 1976.

Presented in part at the Medicinal Chemistry Section, APhA Academy of Pharmaceutical Sciences, New Orleans meeting, April 1976.

[x] To whom inquiries should be directed.

Cytotoxic Agents from *Bursera morelensis* (Burseraceae): Deoxypodophyllotoxin and a New Lignan, 5′-Desmethoxydeoxypodophyllotoxin

S. D. JOLAD, R. M. WIEDHOPF, and J. R. COLE ˣ

Abstract □ The isolation and identification of deoxypodophyllotoxin and a new lignan, 5′-desmethoxydeoxypodophyllotoxin, from the dried exudate of *Bursera morelensis* (Burseraceae) are reported. Deoxypodophyllotoxin showed high activity in the KB and PS test systems; the new lignan, although highly active against the KB test system, demonstrated only marginal activity against the PS test system. A structure is suggested for the new lignan, which was named morelensin.

Keyphrases □ Deoxypodophyllotoxin—and 5′-desmethoxy derivative, isolated from dried exudate of *Bursera morelensis*, cytotoxic activity evaluated □ *Bursera morelensis*—deoxypodophyllotoxin and 5′-desmethoxy derivative isolated from dried exudate, cytotoxic activity evaluated □ Cytotoxic activity—deoxypodophyllotoxin and 5′-desmethoxy derivative evaluated

During a continuing search for plants having tumor-inhibitory constituents, the ethanol extract of the dried exudate of the Mexican plant *Bursera morelensis* (Burseraceae[1]) demonstrated biological activity against two test systems, the P-388 lymphocytic leukemia (PS) and the human epidermoid carcinoma of the nasopharynx[2] (KB). The activity against these two test systems was due to two constituents, deoxypodophyllotoxin (I) and a new lignan, 5′-desmethoxydeoxypodophyllotoxin (II), which was named morelensin.

RESULTS AND DISCUSSION

Exhaustive extraction of the dried exudate of *B. morelensis* with ethanol, followed by partition of the ethanol extract between chloroform and water, yielded a chloroform-soluble syrup. The syrup was separated into methanol-soluble and methanol-insoluble fractions. The methanol-insoluble fraction was dissolved in ether, and precipitation with isopropyl ether yielded a gum. Extraction of the gum with ether afforded almost a single-component residue. On crystallization, this residue yielded a known lignan, I, mp 167°. Compound I [$C_{22}H_{22}O_7$, *m/e* 398 (M^+)] was identified by its IR, NMR, and mass spectral properties and by direct comparison with an authentic specimen.

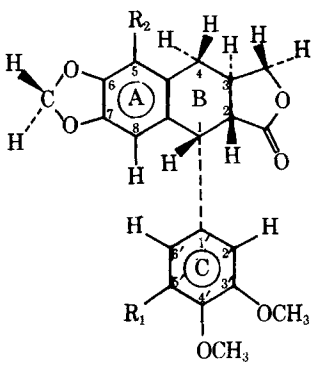

I: $R_1 = OCH_3, R_2 = H$ III: $R_1 = H, R_2 = OCH_3$
II: $R_1 = R_2 = H$

The ether-soluble fraction was essentially a mixture of two components. Separation of these two components by silica gel column chromatography and subsequent crystallization yielded, in addition to I, a new lignan, II, mp 181°. This new compound was 1-(3′,4′-dimethoxyphenyl)-3-hydroxymethyl-6,7-methylenedioxy-1,2,3,4-tetrahydronaphthalene-2-carboxylic acid lactone.

The molecular formula of II ($C_{21}H_{20}O_6$) was established by carbon and hydrogen analysis and mass spectrometry. The intense molecular ion peak (*m/e* 368) in the mass spectrum of II immediately suggested that the new lignan was desmethoxy-I. Biogenetically, the 5′-desmethoxy compound (*i.e.*, Structure II) is most favorable. Support of this hypothesis was found in the spectra of this new lignan. The IR spectrum indicated the absence of hydroxyl groups and the presence of methoxy (2840 cm^{-1}), methylenedioxy (2780 cm^{-1}), and γ-lactone (1775 cm^{-1}) groups. The NMR spectrum supported these findings, exhibiting signals for two methoxy groups (δ 3.79 and 3.86, both three-proton singlets) and one methelenedioxy group (δ 5.90, two-proton singlet). A comparison of the NMR signals contributed by the tetrahydronaphthalene-γ-lactone moiety of Compounds I and II indicated that the A, B, and lactone rings of both compounds were identical.

The proposed substitution pattern in ring C of II is identical to the pattern of 5′-desmethoxy-β-peltatin-A methyl ether (III), previously isolated from *B. fagaroides* (Burseraceae) (1). Indeed, a comparison of the aromatic region of the NMR spectra of II and III (subtracting A-ring signals) showed nearly identical signals for C-ring protons. This proposed C-ring substitution in II was supported by its mass spectrum. The significant peak at *m/e* 77 can be visualized as having arisen from the dimethoxybenzene ion (*m/e* 138) *via* the protonated oxepin ion (*m/e* 95) followed by the expulsion of a molecule of water. Among the three isomeric dimethoxybenzenes, only the *o*-isomer displays a mass spectrum with this fragmentation pattern (2). Morelensin (II) was optically active, $[\alpha]_D^{24}$ −125°, indicating one A-type isomer (*cis*, 1/2; *trans*, 2/3). Since the absolute configuration of III was established previously by X-ray crystallography (3), the stereochemistry of II was assumed to be identical to that of III.

Compound I demonstrated activities of 194 (one cure) and 161% test/control (T/C) at 12.50 and 6.25 mg/kg, respectively. Compound II demonstrated activity of 127% test/control (T/C) at 50 mg/kg. Activity in the PS test system is defined as an increase in the survival of treated animals over that of control animals resulting in a T/C ≥ 125% (4).

In the KB test system, I and II demonstrated activities of 2.48×10^{-4} and 3.99×10^{-4} μg/ml, respectively. Activity in the KB test system is defined as $ED_{50} \leq 20$ μg/ml (5).

EXPERIMENTAL[3]

The dried exudate of *B. morelensis*, collected in Mexico during October 1974, was stored at −10° prior to extraction.

The exudate (0.68 kg) was extracted exhaustively with 95% ethanol. The air-dried chloroform-soluble fraction (syrup) was dried further as much as possible under vacuum to a total of 80 g and then dissolved in a minimum amount of methanol. The solution was left in a freezer for 2 days, and the resulting residue was separated by decanting the supernate. The residue was then dissolved in a minimum amount of ether, and isopropyl ether was added until the solution was slightly turbid. The mixture was left in a freezer overnight, and the gummy residue that separated was removed by decantation. Trituration of the residue with ether followed by stirring with a magnetic stirrer gave a colorless residue, which was filtered. The residue (2.13 g), which on TLC showed essentially

[1] Identification was confirmed by Dr. Robert E. Purdue, Medicinal Plant Resources Laboratory, Plant Genetics and Germ Plasma Institute, Beltsville, Md. A reference specimen was deposited in that herbarium.

[2] Division of Cancer Treatment, National Cancer Institute, National Institutes of Health, Bethesda, Md.

[3] Carbon and hydrogen analyses were carried out by Chemalytics, Inc., Tempe, Ariz. Melting points were determined on a Kofler hot-stage apparatus and are uncorrected. IR spectra were run on a Beckman IR-33 instrument. NMR and mass spectra were run using a Varian T-60 spectrometer and Hewlett-Packard model 5930 spectrometer, respectively.

a single spot corresponding to I, was further purified by crystallization.

Solvent was removed under vacuum from the ether-soluble fraction (13 g), which on TLC showed two major spots corresponding to I and II. It was then subjected to silica gel 60 (500 g) column chromatography. Elution with dichloromethane with increasing concentration of ethyl acetate yielded fractions containing pure I and pure II, which were further purified by crystallization.

Deoxypodophyllotoxin (I)—This compound was obtained as colorless prisms, mp 167° (ether–dichloromethane). It was identical in all respects with the authentic specimen.

Anal.—Calc. for $C_{22}H_{22}O_7$: C, 66.32; H, 5.57; mol. wt. 398. Found: C, 66.49; H, 5.68; *m/e* 398 (M^+).

5′-Desmethoxydeoxypodophyllotoxin (II)—This compound was obtained as colorless needles, mp 181° (ether–dichloromethane). The IR ($CHCl_3$: 3000, 2900, 2840, 2780, 1775, and 930 cm^{-1}), NMR [$CDCl_3$: δ 2.9 (3H, m), 3.79 (3H, s), 3.86 (3H, s), 3.9 (2H, m), 4.5 (2H, m), 5.90 (2H, s), 6.37 (1H, dd, J = 8 and 2 Hz), 6.49 (1H, s), 6.66 (1H, s), 6.67 (1H, d, J = 8 Hz), and 6.90 (1H, d, J = 2 Hz)], and mass [*m/e* 368 (M^+, base), 353, 340, 338, 337, 323, 309, 308, 253, 230, 212, 185, 151, 138, 95, and 77] spectra were in accord with Structure II. This compound was optically active, $[\alpha]_D^{24}$ − 125° (c 0.014 in chloroform).

Anal.—Calc. for $C_{21}H_{20}O_6$: C, 68.47; H, 5.77; mol. wt. 368. Found: C, 68.47; H, 5.47; *m/e* 368 (M^+).

REFERENCES

(1) E. Bianchi, K. Sheth, and J. R. Cole, *Tetrahedron Lett.*, **1969**, 2759.

(2) C. S. Barnes and J. L. Occolowitz, *Aust. J. Chem.*, **16**, 219 (1963).

(3) R. B. Bates and J. B. Wood, III, *J. Org. Chem.*, **37**, 562 (1972).

(4) R. I. Geran, N. H. Greenberg, M. N. MacDonald, A. M. Schumancher, and B. J. Abbott, *Cancer Chemother. Rep.*, **3** (3), 9 (1972).

(5) *Ibid.*, **3** (3), 17 (1972).

ACKNOWLEDGMENTS AND ADDRESSES

Received June 28, 1976, from the *Division of Pharmaceutical Chemistry, College of Pharmacy, University of Arizona, Tucson, AZ 85721.*

Accepted for publication August 2, 1976.

Supported in part by Contract N01-CM-3-3750 from the Division of Cancer Treatment, National Cancer Institute, National Institutes of Health, Bethesda, MD 20014, and the Elsa U. Pardee Foundation, Midland, MI 48640.

The authors are grateful to Drug Research and Development, Chemotherapy, National Cancer Institute, for supplying authentic samples of deoxypodophyllotoxin.

[x] To whom inquiries should be directed.

Modified Electron-Capture GLC Assay for Salsolinol in Brain Tissue

PATRICK J. O'NEILL [*] and RALF G. RAHWAN [x]

Abstract □ A modified assay for a neuroamine-derived tetrahydroisoquinoline, salsolinol, is presented. It combines the ease and rapidity of solvent extraction from brain tissue with the sensitivity of electron-capture GLC. Detection of salsolinol (1,2,3,4-tetrahydro-1-methyl-6,7-isoquinolinediol), the alkaloid derived from condensation of dopamine and acetaldehyde, at levels of 5–10 ng/g of brain tissue is possible. The advantages afforded by the modifications are discussed in relation to existing procedures.

Keyphrases □ Salsolinol—electron-capture GLC analysis, mouse brain tissue □ GLC, electron capture—analysis, salsolinol in mouse brain tissue □ Tetrahydroisoquinolines, substituted—salsolinol, electron-capture GLC analysis in mouse brain tissue □ Alkaloids—salsolinol, electron-capture GLC analysis in mouse brain tissue

The *in vivo* formation of tetrahydroisoquinoline alkaloids from aldehydes and endogenous biogenic amines has been suggested to mediate some effects of alcohol (1, 2). These alkaloids possess a variety of pharmacological actions *in vitro* and *in vivo* (3). Tetrahydropapaveroline (the condensation product of dopamine with dopaldehyde) and salsolinol (1,2,3,4-tetrahydro-1-methyl-6,7-isoquinolinediol) (the condensation product of acetaldehyde with dopamine) were detected in the urine of humans (4) and in rat brain (5, 6). Likewise, tetrahydroprotoberberines (the cyclization derivatives of tetrahydropapaveroline) were recovered from human urine (7).

The analyses used in some of these studies (4, 5, 7) involved costly mass fragmentography. Recently, a sensitive electron-capture GLC assay was reported for salsolinol in rat brain (8). However, the tissue extraction method was time consuming (adsorption onto and elution from alumina, followed by overnight lyophilization) and presented additional problems such as inadequate buffering of the extract prior to alumina adsorption and incomplete removal of the derivatizing reagent prior to injection into the chromatograph. Even with appropriate modifications to eliminate the latter problems, the long extraction procedure still proved undesirable.

The present report describes a more rapid and convenient method for the detection of salsolinol in mouse brain using a simplified solvent extraction and electron-capture GLC system. Detection of salsolinol at levels of 5–10 ng/g of brain tissue [approximately 1% of the endogenous dopamine level (9)] is possible with this method.

EXPERIMENTAL

Extraction—The extraction method from tissue is essentially that of Maruyama and Takemori (9) with some modifications. A single mouse brain was added to an all-glass grinding vessel[1] containing 1 ml of 0.05 *N* oxalic acid, saturated with sodium chloride, and 3.5 ml of 25% 1-butanol in 2-propanol and was homogenized. Standards were added at this point and mixed by passing the pestle through the homogenate.

The homogenate was transferred to a conical test tube and centrifuged at 3000×*g* for 5 min in a clinical centrifuge. The lower phase was discarded, and a 3-ml aliquot of the upper solvent phase was removed. Hexane, 3 ml, and 0.5 ml of 0.5 *M* sodium phosphate buffer (pH 6.5) were added to this aliquot, and the mixture was shaken for 5 min, followed by a 5-min centrifugation. The upper phase was discarded, and a 0.5-ml

[1] Size 22, Kontes Glass Co., Vineland, N.J.

a single spot corresponding to I, was further purified by crystallization.

Solvent was removed under vacuum from the ether-soluble fraction (13 g), which on TLC showed two major spots corresponding to I and II. It was then subjected to silica gel 60 (500 g) column chromatography. Elution with dichloromethane with increasing concentration of ethyl acetate yielded fractions containing pure I and pure II, which were further purified by crystallization.

Deoxypodophyllotoxin (I)—This compound was obtained as colorless prisms, mp 167° (ether–dichloromethane). It was identical in all respects with the authentic specimen.

Anal.—Calc. for $C_{22}H_{22}O_7$: C, 66.32; H, 5.57; mol. wt. 398. Found: C, 66.49; H, 5.68; *m/e* 398 (M^+).

5′-Desmethoxydeoxypodophyllotoxin (II)—This compound was obtained as colorless needles, mp 181° (ether–dichloromethane). The IR ($CHCl_3$: 3000, 2900, 2840, 2780, 1775, and 930 cm^{-1}), NMR [$CDCl_3$: δ 2.9 (3H, m), 3.79 (3H, s), 3.86 (3H, s), 3.9 (2H, m), 4.5 (2H, m), 5.90 (2H, s), 6.37 (1H, dd, J = 8 and 2 Hz), 6.49 (1H, s), 6.66 (1H, s), 6.67 (1H, d, J = 8 Hz), and 6.90 (1H, d, J = 2 Hz)], and mass [*m/e* 368 (M^+, base), 353, 340, 338, 337, 323, 309, 308, 253, 230, 212, 185, 151, 138, 95, and 77] spectra were in accord with Structure II. This compound was optically active, $[\alpha]_D^{24}$ − 125° (c 0.014 in chloroform).

Anal.—Calc. for $C_{21}H_{20}O_6$: C, 68.47; H, 5.77; mol. wt. 368. Found: C, 68.47; H, 5.47; *m/e* 368 (M^+).

REFERENCES

(1) E. Bianchi, K. Sheth, and J. R. Cole, *Tetrahedron Lett.*, **1969**, 2759.

(2) C. S. Barnes and J. L. Occolowitz, *Aust. J. Chem.*, **16**, 219 (1963).

(3) R. B. Bates and J. B. Wood, III, *J. Org. Chem.*, **37**, 562 (1972).

(4) R. I. Geran, N. H. Greenberg, M. N. MacDonald, A. M. Schumancher, and B. J. Abbott, *Cancer Chemother. Rep.*, **3** (3), 9 (1972).

(5) *Ibid.*, **3** (3), 17 (1972).

ACKNOWLEDGMENTS AND ADDRESSES

Received June 28, 1976, from the *Division of Pharmaceutical Chemistry, College of Pharmacy, University of Arizona, Tucson, AZ 85721.*

Accepted for publication August 2, 1976.

Supported in part by Contract N01-CM-3-3750 from the Division of Cancer Treatment, National Cancer Institute, National Institutes of Health, Bethesda, MD 20014, and the Elsa U. Pardee Foundation, Midland, MI 48640.

The authors are grateful to Drug Research and Development, Chemotherapy, National Cancer Institute, for supplying authentic samples of deoxypodophyllotoxin.

[x] To whom inquiries should be directed.

Modified Electron-Capture GLC Assay for Salsolinol in Brain Tissue

PATRICK J. O'NEILL [*] and RALF G. RAHWAN [x]

Abstract □ A modified assay for a neuroamine-derived tetrahydroisoquinoline, salsolinol, is presented. It combines the ease and rapidity of solvent extraction from brain tissue with the sensitivity of electron-capture GLC. Detection of salsolinol (1,2,3,4-tetrahydro-1-methyl-6,7-isoquinolinediol), the alkaloid derived from condensation of dopamine and acetaldehyde, at levels of 5–10 ng/g of brain tissue is possible. The advantages afforded by the modifications are discussed in relation to existing procedures.

Keyphrases □ Salsolinol—electron-capture GLC analysis, mouse brain tissue □ GLC, electron capture—analysis, salsolinol in mouse brain tissue □ Tetrahydroisoquinolines, substituted—salsolinol, electron-capture GLC analysis in mouse brain tissue □ Alkaloids—salsolinol, electron-capture GLC analysis in mouse brain tissue

The *in vivo* formation of tetrahydroisoquinoline alkaloids from aldehydes and endogenous biogenic amines has been suggested to mediate some effects of alcohol (1, 2). These alkaloids possess a variety of pharmacological actions *in vitro* and *in vivo* (3). Tetrahydropapaveroline (the condensation product of dopamine with dopaldehyde) and salsolinol (1,2,3,4-tetrahydro-1-methyl-6,7-isoquinolinediol) (the condensation product of acetaldehyde with dopamine) were detected in the urine of humans (4) and in rat brain (5, 6). Likewise, tetrahydroprotoberberines (the cyclization derivatives of tetrahydropapaveroline) were recovered from human urine (7).

The analyses used in some of these studies (4, 5, 7) involved costly mass fragmentography. Recently, a sensitive electron-capture GLC assay was reported for salsolinol in rat brain (8). However, the tissue extraction method was time consuming (adsorption onto and elution from alumina, followed by overnight lyophilization) and presented additional problems such as inadequate buffering of the extract prior to alumina adsorption and incomplete removal of the derivatizing reagent prior to injection into the chromatograph. Even with appropriate modifications to eliminate the latter problems, the long extraction procedure still proved undesirable.

The present report describes a more rapid and convenient method for the detection of salsolinol in mouse brain using a simplified solvent extraction and electron-capture GLC system. Detection of salsolinol at levels of 5–10 ng/g of brain tissue [approximately 1% of the endogenous dopamine level (9)] is possible with this method.

EXPERIMENTAL

Extraction—The extraction method from tissue is essentially that of Maruyama and Takemori (9) with some modifications. A single mouse brain was added to an all-glass grinding vessel[1] containing 1 ml of 0.05 *N* oxalic acid, saturated with sodium chloride, and 3.5 ml of 25% 1-butanol in 2-propanol and was homogenized. Standards were added at this point and mixed by passing the pestle through the homogenate.

The homogenate was transferred to a conical test tube and centrifuged at 3000×*g* for 5 min in a clinical centrifuge. The lower phase was discarded, and a 3-ml aliquot of the upper solvent phase was removed. Hexane, 3 ml, and 0.5 ml of 0.5 *M* sodium phosphate buffer (pH 6.5) were added to this aliquot, and the mixture was shaken for 5 min, followed by a 5-min centrifugation. The upper phase was discarded, and a 0.5-ml

[1] Size 22, Kontes Glass Co., Vineland, N.J.

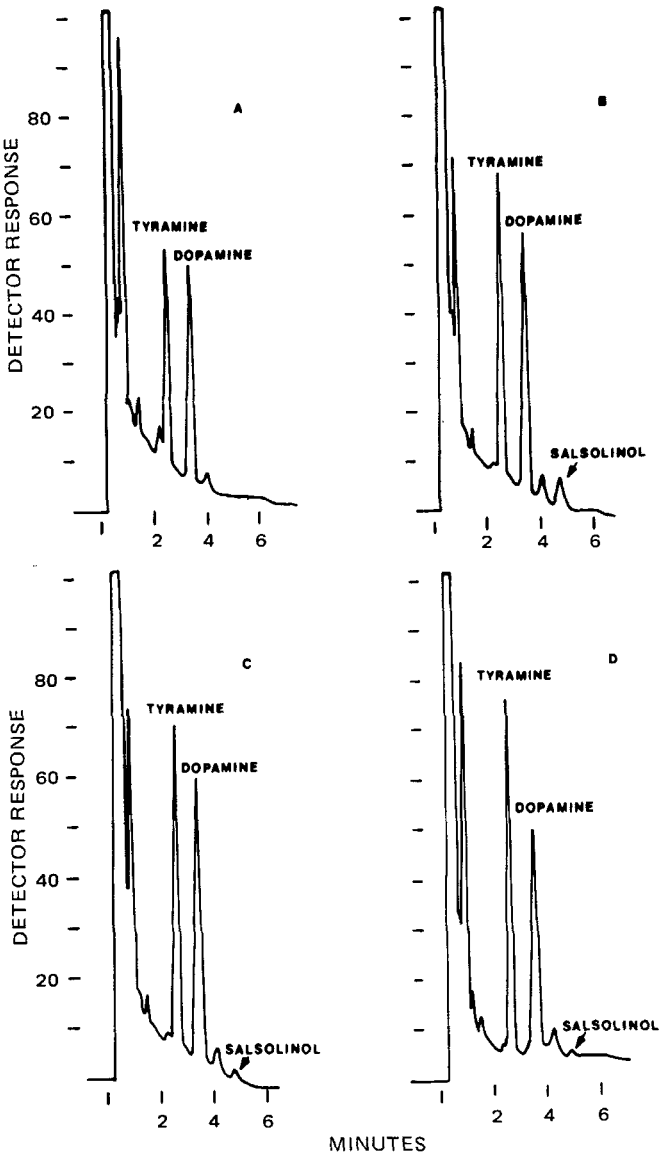

Figure 1—*Chromatograms of mouse brain extracts. Key: A, single mouse brain with 500 ng of tyramine added; B, single mouse brain with 500 ng of tyramine and 40 ng of salsolinol added; C, single mouse brain with 500 ng of tyramine and 10 ng of salsolinol added; and D, single mouse brain with 500 ng of tyramine and 4 ng of salsolinol added. Samples of 5 μl were injected at attenuation 512; attenuation was changed to 256 after tyramine appeared. See text for conditions. The peak immediately preceding tyramine corresponds to norepinephrine.*

aliquot of the aqueous lower phase was saturated with sodium chloride and reextracted with 0.5 ml of 25% 1-butanol in 2-propanol. The lower phase was discarded, and 0.5 ml of the upper solvent phase was transferred to another tube and evaporated to dryness under nitrogen; the residue was used for derivatization.

Derivatization—Derivatization of the compounds was carried out using a modification of the method of Bigdeli and Collins (8). Acetonitrile, 0.2 ml, and 0.05 ml of heptafluorobutyric anhydride[2] were added to the nitrogen-dried residue and allowed to react at room temperature for 30 min. The samples were evaporated to dryness under nitrogen, and the residue was dissolved in 1 ml of benzene. Immediately prior to assay, each sample was washed with 5 ml of a saturated solution of sodium borate (10) by shaking, followed by a brief centrifugation to separate the aqueous and organic phases. A portion (2–5 μl) of the upper benzene layer was injected into the chromatograph.

[2] Eastman Kodak Co., Rochester, N.Y.

Table I—Retention Times and Recoveries for Tyramine, Dopamine, and Salsolinol

Compound	Retention Time, min	Recovery[a], % ± *SEM*
Tyramine	2.6	38.8 ± 1.13[b]
Dopamine	3.5	68.5 ± 5.07[c]
Salsolinol	4.8	62.3 ± 2.14[d]

[a] Mean of six to 16 determinations. [b] Recovery was calculated from 500 ng of added tyramine. [c] Dopamine recovery was estimated on the basis of an average whole brain content of 350 ng (9). [d] Recovery was calculated from 10–100 ng of added salsolinol. Recovery was linear over the range of 4–400 ng of added salsolinol.

Instrumentation—A gas chromatograph[3] with a ^{63}Ni-electron-capture detector was used for the analyses. A 1.83-m (6-ft) glass column (2 mm i.d.) packed with 3% OV-17 on 100–120-mesh Gas Chrom Q[4] was used. Temperatures were: injector, 250°; oven, 150°; and detector, 300°. The mobile phase was argon–methane (95:5) at a flow rate of 20 ml/min.

Quantitation—The peak height ratio method (11) was employed to estimate quantities of salsolinol. Tyramine[2] (500 ng) was added to each homogenate as the internal standard; various amounts of authentic salsolinol[5] (4–400 ng) were also added. A standard curve was constructed by plotting the ratio of the relative peak height of salsolinol to the relative peak height of tyramine *versus* the quantity of authentic salsolinol in the sample. Regression lines were fitted by computer analysis using the method of least squares.

RESULTS AND DISCUSSION

Chromatograms obtained are shown in Fig. 1. Figure 1A represents a brain extracted as described under *Experimental* but with no salsolinol added. Figures 1B, 1C, and 1D represent single brains with 40, 10, and 4 ng of salsolinol added, respectively. The on-column lower limit of detection sensitivity for salsolinol under the conditions of the assay (attenuation = 256) was approximately 10 pg. Identity of the peaks was confirmed by comparison of retention times of derivatized authentic standards or by addition of derivatized authentic standards to the injection solution.

Recoveries and retention times for tyramine, dopamine, and salsolinol are shown in Table I; recoveries were slightly higher than those reported by Bigdeli and Collins (8) for dopamine and salsolinol. Regression analysis indicated that the method was linear over the tested range of 4–400 ng of added salsolinol. Norepinephrine was neither well extracted nor sensitive to detection by this method.

The assay described in this report differs in several respects from the extraction and assay procedures previously reported (8, 9). Maruyama and Takemori (9) suggested adjusting the aqueous phase (after separation from hexane) to pH 2 with hydrochloric acid prior to saturation with sodium chloride and extraction with 25% 1-butanol in 2-propanol. However, preliminary experiments using this method gave low recoveries. Furthermore, adding no acid gave the maximum recovery for salsolinol and dopamine, the compounds of major interest for *in vivo* studies conducted in this laboratory (12). The entire extraction procedure described here takes approximately 3 hr to bring as many as 16 samples to the derivatizing step; the alumina adsorption method of Bigdeli and Collins (8) involves an extensive time period, even including overnight lyophilization to reach this point.

Bigdeli and Collins (8) suggested a ratio of 0.2 ml of acetonitrile to 0.4 ml of heptafluorobutyric anhydride during derivatization. In the present method, the quantity of heptafluorobutyric anhydride can be reduced to 0.05 ml without any decrease in efficiency while derivatizing as much as 1 mg of any of the amines. Therefore, a significant saving of an expensive reagent is realized, and the amount of unreacted heptafluorobutyric anhydride that must be removed prior to the electron-capture GLC assay is substantially reduced.

In this respect, the use of benzene as a solvent [rather than ethyl acetate (8)] allows a significant improvement. Any traces of unreacted heptafluorobutyric anhydride left in the GLC injection solution make it virtually impossible to obtain meaningful results. "Washing" the sample with a saturated solution of sodium borate (see *Experimental*) removes

[3] Model 5713A, Hewlett-Packard, Palo Alto, Calif.
[4] Applied Science Laboratories, State College, Pa.
[5] Aldrich Chemical Co., Milwaukee, Wis.

any traces of the derivatizing reagent (10), thus removing the interfering contaminant; however, this washing is not possible with ethyl acetate as the injection solvent (8), since the latter is miscible with the sodium borate solution. Therefore, benzene was selected since the derivatized compounds are freely soluble in it, it is not miscible with aqueous solutions, and no significant loss occurs from this organic layer by washing with the saturated solution of sodium borate.

The sensitivity achieved for salsolinol in the present method is comparable to that for tetrahydropapaveroline using GC–mass spectrometry (5). Sandler *et al.* (4) also used a GC–mass spectrometric method for salsolinol, but they did not report the absolute sensitivity of their method.

Preliminary *in vivo* experiments utilizing this method to investigate the role of salsolinol in the effects of alcohol were reported elsewhere (12).

REFERENCES

(1) G. Cohen and M. Collins, *Science*, **167**, 1749 (1970).

(2) V. E. Davis, M. J. Walsh, and Y. Yamanaka, *J. Pharmacol. Exp. Ther.*, **174**, 401 (1970).

(3) R. G. Rahwan, *Toxicol. Appl. Pharmacol.*, **34**, 3 (1975).

(4) M. Sandler, S. B. Carter, K. R. Hunter, and G. M. Stern, *Nature (London)*, **241**, 439 (1973).

(5) A. J. Turner, K. M. Baker, S. Algeri, A. Frigerio, and S. Garattini, *Life Sci.*, **14**, 2247 (1974).

(6) M. A. Collins and M. G. Bigdeli, *ibid.*, **16**, 585 (1975).

(7) J. L. Cashaw, K. D. McMurtrey, H. Brown, and V. E. Davis, *J. Chromatogr.*, **99**, 567 (1974).

(8) M. G. Bigdeli and M. A. Collins, *Biochem. Med.*, **12**, 55 (1975).

(9) Y. Maruyama and A. E. Takemori, *Anal. Biochem.*, **49**, 240 (1972).

(10) R. A. Sams and L. Malspeis, *J. Chromatogr.*, **125**, 409 (1976).

(11) E. L. Arnold and R. Ford, *Anal. Chem.*, **45**, 85 (1973).

(12) R. G. Rahwan and P. J. O'Neill, *Pharmacologist*, **18**, 190 (1976).

ACKNOWLEDGMENTS AND ADDRESSES

Received May 10, 1976, from the *Division of Pharmacology, College of Pharmacy, Ohio State University, Columbus, OH 43210.*

Accepted for publication August 6, 1976.

Supported by National Institute of Mental Health Grant 1 R01 AA02466-01 (R. G. Rahwan). P. J. O'Neill is the Abe Plough Citation Fellow of the American Foundation for Pharmaceutical Education.

The authors are grateful to Dr. Rafik H. Bishara for helpful suggestions.

* Present address: Department of Biochemistry, McNeil Laboratories, Fort Washington, PA 19034.

ˣ To whom inquiries should be directed.

Quantitative Determinations of Codeine Phosphate, Guaifenesin, Pheniramine Maleate, Phenylpropanolamine Hydrochloride, and Pyrilamine Maleate in an Expectorant by High-Pressure Liquid Chromatography

V. DAS GUPTA ˣ and A. G. GHANEKAR

Abstract □ The quantitative determinations of codeine phosphate, guaifenesin, pheniramine maleate, phenylpropanolamine hydrochloride, and pyrilamine maleate in a liquid dosage form are described. All active and inactive ingredients (sodium benzoate and FD&C Yellow No. 5 dye) can be separated with high-pressure liquid chromatography except the two antihistamines, pheniramine maleate and pyrilamine maleate. Pheniramine maleate is determined colorimetrically, and pyrilamine maleate is determined either by difference or spectrophotometrically. The methods are simple, short, accurate, and precise. The standard deviations are reported.

Keyphrases □ Codeine phosphate—high-pressure liquid chromatographic analysis, cough syrup □ Guaifenesin—high-pressure liquid chromatographic analysis, cough syrup □ Phenylpropanolamine hydrochloride—high-pressure liquid chromatographic analysis, cough syrup □ Pheniramine maleate—colorimetric analysis, cough syrup □ Pyrilamine maleate—spectrophotometric analysis, cough syrup □ High-pressure liquid chromatography—analyses, codeine phosphate, guaifenesin, and phenylpropanolamine hydrochloride, cough syrup □ Colorimetry—analysis, pheniramine maleate, cough syrup □ Spectrophotometry—analysis, pyrilamine maleate, cough syrup □ Antitussives—cough syrup ingredients analyzed by high-pressure liquid chromatography, colorimetry, and spectrophotometry

A commonly used cough syrup contains an antitussive agent, codeine phosphate, an expectorant, guaifenesin, two antihistamines, pheniramine maleate and pyrilamine maleate, and a decongestant, phenylpropanolamine hydrochloride. In addition to active ingredients, most cough syrups contain dye(s), preservative(s), flavor(s), and sweetening agent(s). Due to interferences, no easy methods are available for the quantitative determinations of various ingredients in such a cough syrup. The purpose of these investigations was to develop easy, simple, short, and accurate methods for the quantitative determinations of various ingredients in such a cough syrup by high-pressure liquid chromatography (HPLC).

EXPERIMENTAL

Chemicals and Reagents—All chemicals and reagents including codeine phosphate (I), guaifenesin (II), pheniramine maleate (III), phenylpropanolamine hydrochloride (IV), and pyrilamine maleate (V) were ACS, USP, or NF grade and were used without further purification.

Apparatus—A high-pressure liquid chromatograph[1] equipped with a fixed wavelength (254 nm) detector and recorder[2] was used.

Column—A nonpolar column[3] consisting of a monomolecular layer of octadecyltrichlorosilane permanently bonded to Si–C (30 cm long and 4 mm i.d.) was used.

Chromatographic Conditions—The chromatographic solvent was 0.05 *M* KH_2PO_4 in water containing 13% (v/v) methanol. The temperature was ambient, and the solvent flow rate was 2.0 ml/min (at an inlet

[1] Waters ALC 202 equipped with a U6K universal injector.
[2] Omniscribe 5213-12 equipped with an integrator.
[3] Waters μ-Bondapak/C_{18}, Catalog No. 27324 (prepacked column).

any traces of the derivatizing reagent (10), thus removing the interfering contaminant; however, this washing is not possible with ethyl acetate as the injection solvent (8), since the latter is miscible with the sodium borate solution. Therefore, benzene was selected since the derivatized compounds are freely soluble in it, it is not miscible with aqueous solutions, and no significant loss occurs from this organic layer by washing with the saturated solution of sodium borate.

The sensitivity achieved for salsolinol in the present method is comparable to that for tetrahydropapaveroline using GC–mass spectrometry (5). Sandler *et al.* (4) also used a GC–mass spectrometric method for salsolinol, but they did not report the absolute sensitivity of their method.

Preliminary *in vivo* experiments utilizing this method to investigate the role of salsolinol in the effects of alcohol were reported elsewhere (12).

REFERENCES

(1) G. Cohen and M. Collins, *Science*, **167**, 1749 (1970).

(2) V. E. Davis, M. J. Walsh, and Y. Yamanaka, *J. Pharmacol. Exp. Ther.*, **174**, 401 (1970).

(3) R. G. Rahwan, *Toxicol. Appl. Pharmacol.*, **34**, 3 (1975).

(4) M. Sandler, S. B. Carter, K. R. Hunter, and G. M. Stern, *Nature (London)*, **241**, 439 (1973).

(5) A. J. Turner, K. M. Baker, S. Algeri, A. Frigerio, and S. Garattini, *Life Sci.*, **14**, 2247 (1974).

(6) M. A. Collins and M. G. Bigdeli, *ibid.*, **16**, 585 (1975).

(7) J. L. Cashaw, K. D. McMurtrey, H. Brown, and V. E. Davis, *J. Chromatogr.*, **99**, 567 (1974).

(8) M. G. Bigdeli and M. A. Collins, *Biochem. Med.*, **12**, 55 (1975).

(9) Y. Maruyama and A. E. Takemori, *Anal. Biochem.*, **49**, 240 (1972).

(10) R. A. Sams and L. Malspeis, *J. Chromatogr.*, **125**, 409 (1976).

(11) E. L. Arnold and R. Ford, *Anal. Chem.*, **45**, 85 (1973).

(12) R. G. Rahwan and P. J. O'Neill, *Pharmacologist*, **18**, 190 (1976).

ACKNOWLEDGMENTS AND ADDRESSES

Received May 10, 1976, from the *Division of Pharmacology, College of Pharmacy, Ohio State University, Columbus, OH 43210.*

Accepted for publication August 6, 1976.

Supported by National Institute of Mental Health Grant 1 R01 AA02466-01 (R. G. Rahwan). P. J. O'Neill is the Abe Plough Citation Fellow of the American Foundation for Pharmaceutical Education.

The authors are grateful to Dr. Rafik H. Bishara for helpful suggestions.

* Present address: Department of Biochemistry, McNeil Laboratories, Fort Washington, PA 19034.

ˣ To whom inquiries should be directed.

Quantitative Determinations of Codeine Phosphate, Guaifenesin, Pheniramine Maleate, Phenylpropanolamine Hydrochloride, and Pyrilamine Maleate in an Expectorant by High-Pressure Liquid Chromatography

V. DAS GUPTA ˣ and A. G. GHANEKAR

Abstract □ The quantitative determinations of codeine phosphate, guaifenesin, pheniramine maleate, phenylpropanolamine hydrochloride, and pyrilamine maleate in a liquid dosage form are described. All active and inactive ingredients (sodium benzoate and FD&C Yellow No. 5 dye) can be separated with high-pressure liquid chromatography except the two antihistamines, pheniramine maleate and pyrilamine maleate. Pheniramine maleate is determined colorimetrically, and pyrilamine maleate is determined either by difference or spectrophotometrically. The methods are simple, short, accurate, and precise. The standard deviations are reported.

Keyphrases □ Codeine phosphate—high-pressure liquid chromatographic analysis, cough syrup □ Guaifenesin—high-pressure liquid chromatographic analysis, cough syrup □ Phenylpropanolamine hydrochloride—high-pressure liquid chromatographic analysis, cough syrup □ Pheniramine maleate—colorimetric analysis, cough syrup □ Pyrilamine maleate—spectrophotometric analysis, cough syrup □ High-pressure liquid chromatography—analyses, codeine phosphate, guaifenesin, and phenylpropanolamine hydrochloride, cough syrup □ Colorimetry—analysis, pheniramine maleate, cough syrup □ Spectrophotometry—analysis, pyrilamine maleate, cough syrup □ Antitussives—cough syrup ingredients analyzed by high-pressure liquid chromatography, colorimetry, and spectrophotometry

A commonly used cough syrup contains an antitussive agent, codeine phosphate, an expectorant, guaifenesin, two antihistamines, pheniramine maleate and pyrilamine maleate, and a decongestant, phenylpropanolamine hydrochloride. In addition to active ingredients, most cough syrups contain dye(s), preservative(s), flavor(s), and sweetening agent(s). Due to interferences, no easy methods are available for the quantitative determinations of various ingredients in such a cough syrup. The purpose of these investigations was to develop easy, simple, short, and accurate methods for the quantitative determinations of various ingredients in such a cough syrup by high-pressure liquid chromatography (HPLC).

EXPERIMENTAL

Chemicals and Reagents—All chemicals and reagents including codeine phosphate (I), guaifenesin (II), pheniramine maleate (III), phenylpropanolamine hydrochloride (IV), and pyrilamine maleate (V) were ACS, USP, or NF grade and were used without further purification.

Apparatus—A high-pressure liquid chromatograph[1] equipped with a fixed wavelength (254 nm) detector and recorder[2] was used.

Column—A nonpolar column[3] consisting of a monomolecular layer of octadecyltrichlorosilane permanently bonded to Si–C (30 cm long and 4 mm i.d.) was used.

Chromatographic Conditions—The chromatographic solvent was 0.05 *M* KH_2PO_4 in water containing 13% (v/v) methanol. The temperature was ambient, and the solvent flow rate was 2.0 ml/min (at an inlet

[1] Waters ALC 202 equipped with a U6K universal injector.
[2] Omniscribe 5213-12 equipped with an integrator.
[3] Waters μ-Bondapak/C_{18}, Catalog No. 27324 (prepacked column).

Table I—Assay Results on Various Ingredients Using High-Pressure Liquid Chromatography

Syrup	Percent of Label Claim Found			
	I	II	III + V Combination	IV
Lot A	99.8	101.3	99.2	100.8
SD^a	1.96	1.08	1.24	2.32
Commercial sample	—[b]	106.9	104.3	55.3

[a] Based on four readings. [b] Had no codeine; *i.e.*, the manufacturer did not claim any on the label.

pressure of approximately 2000 psig). The chart speed was 30.5 cm/hr; the attenuation unit for full scale deflection was 0.04, which was changed to 0.08 after 10 min.

Solutions for HPLC—A standard solution containing 20 mg of I, 200 mg of II, 12.5 mg each of III and V, and 25 mg of IV/100 ml of chromatographic solvent was prepared using a simple solution method. Solutions of sodium benzoate (50 μg/ml) and FD&C No. 5 (4 μg/ml) in the chromatographic solvent also were prepared.

Solutions for Colorimetric Analysis of Pheniramine Maleate—A standard solution containing 50 μg/ml of pheniramine maleate in approximately 0.25 *N* HCl was prepared. Cyanogen bromide, 4 g/100 ml of water, also was prepared. A buffer was prepared according to a reported procedure (1).

Solution for Spectrophotometric Analysis of Pyrilamine Maleate—A standard solution containing 20 μg/ml of pyrilamine maleate in approximately 0.1 *N* HCl was prepared. Other solutions were prepared as needed.

Cough Syrup—Lot A cough syrup was prepared containing the following: 200 mg of codeine phosphate, 2 g of guaifenesin, 125 mg of pheniramine maleate, 250 mg of phenylpropanolamine hydrochloride, 125 mg of pyrilamine maleate, 1 ml of dye solution (0.8% FD&C Yellow No. 5 in water), 1 drop of flavor[4], 50 g of sugar, 5 mg of methylparaben, 2 mg of propylparaben, and 5 ml of alcohol.

The flavor was dissolved in alcohol. In 40 ml of water, sugar and guaifenesin were dissolved with the aid of heat and then cooled to room temperature. Then the remaining ingredients were added. The aqueous and alcoholic solutions were mixed and diluted to 100 ml with water.

Two additional lots, B (without pheniramine maleate) and C (without pyrilamine maleate), were prepared.

Assay Procedure for Cough Syrup—First 10.0 ml of the cough syrup (Lot A) was diluted to 100 ml with the chromatographic solvent, and then 10 μl was injected. For purposes of comparison, an identical volume of the standard solution was injected after the assay was eluted.

Since preliminary investigations indicated that the peak area of each ingredient was directly related to the concentration (range for I was 1.4–4 μg, range for II was 10–30 μg, range for III and V in combination was 1.25–5 μg, and range for IV was 1.25–5 μg), the results were calculated by direct comparison of the peak areas as follows:

$$\frac{A_a}{A_s} = \text{percent of label claim found} \qquad \text{(Eq. 1)}$$

where A_a = peak area of the assay sample, and A_s = peak area of the standard solution. The detector's response is presented in Fig. 1, and the results are presented in Table I.

A commercial sample was assayed according to the described procedure. The detector's response is presented in Fig. 2, and the results are presented in Table I.

To identify the additional peaks in the commercial sample, 10 μl each of the dye solution and of the sodium benzoate solution was injected. The detector's response is presented in Fig. 3.

Colorimetric Assay Procedure for Pheniramine Maleate—First 4.0 ml of the cough syrup (Lot A) was diluted to 100 ml with 0.25 *N* HCl and then to 1.0 ml of this dilution were added 7.0 ml of the buffer and 3.0 ml of the cyanogen bromide solution. Immediately after 13 min[5], the absorbance value of the color developed at 480 nm was measured against a blank prepared by substituting 3.0 ml of water for the cyanogen bromide solution. Concurrently, the absorbance value of the standard solution of pheniramine maleate (50 μg/ml) was determined.

Since preliminary investigations indicated that Beer's law was followed

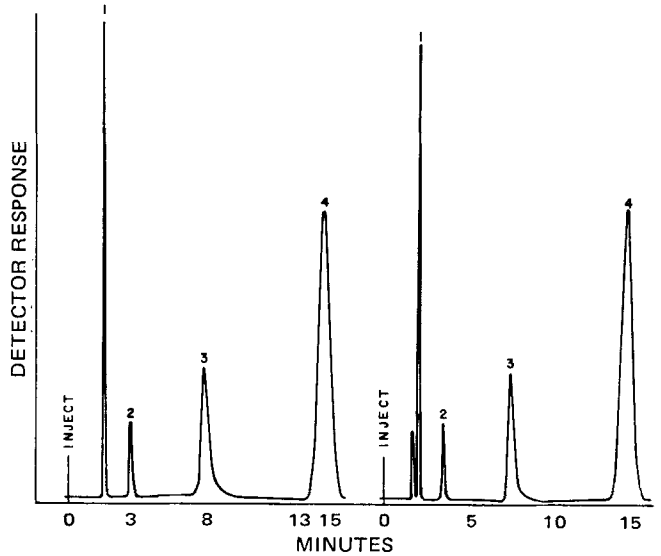

Figure 1—*HPLC analysis of Lot A cough syrup (for chromatographic conditions, see text). Peaks 1, 2, 3, and 4 are two antihistamines in combination (pheniramine maleate and pyrilamine maleate), phenylpropanolamine hydrochloride, codeine phosphate, and guaifenesin, respectively, from a standard solution (first injection) and cough syrup Lot A (second injection).*

(range of 30–80 μg/ml of the standard solution) and that there was no interference from other active and inactive ingredients, the results were calculated by a direct comparison of the absorbance values:

$$\frac{(A_{480})_a}{(A_{480})_s} = \text{percent of label claim} \qquad \text{(Eq. 2)}$$

where $(A_{480})_a$ = absorbance value of the assay sample, and $(A_{480})_s$ = absorbance value of the standard solution.

A commercial sample was also assayed according to the procedure reported (Table II).

Assay Procedure for Pyrilamine Maleate—First 2.0 ml of the syrup (Lot A) was diluted to 100 ml with approximately 0.1 *N* HCl solution and then the absorbance value at 315 nm was determined against 0.1 *N* HCl as the blank. A small interference from the dye may be corrected by either: (*a*) using Lot C syrup (2.0 ml diluted to 100.0 ml with 0.1 *N* HCl solution) as the blank or (*b*) measuring the absorbance values of the diluted Lot C syrup at 315 and 365 nm against 0.1 *N* HCl solution as the blank and determining the correction factor using:

$$\text{factor} = \frac{A_{315}}{A_{365}} \qquad \text{(Eq. 3)}$$

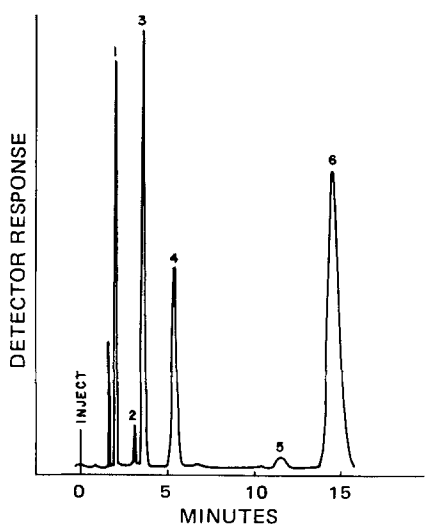

Figure 2—*HPLC analysis of a commercial cough syrup. Peaks 1, 2, and 6 are two antihistamines in combination, phenylpropanolamine hydrochloride, and guaifenesin, respectively. Peak 4 is sodium benzoate, and other peaks are unidentified.*

[4] Dolco Cherry, No. 5225, Dodge & Olcott, Inc., New York, N.Y.

[5] Time required for the maximum sensitivity in the assay procedure as determined in this laboratory.

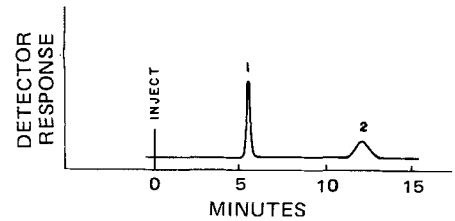

Figure 3—*HPLC analysis of some inactive ingredients used in cough syrups. Peaks 1 and 2 are sodium benzoate and FD&C Yellow No. 5, respectively.*

and:

$$\text{corrected } A_{315} = A_{315} - A_{365} \times \text{factor} \qquad \text{(Eq. 4)}$$

Since preliminary investigations indicated that Beer's law was followed, the results were calculated by direct comparison of the absorbance values at 315 nm:

$$\frac{\text{corrected } A_{315}}{(A_{315})_s} = \text{percent of label claim} \qquad \text{(Eq. 5)}$$

where corrected A_{315} is the absorbance value of the assay sample from Eq. 4, and $(A_{315})_s$ is the absorbance value of the standard solution containing 20 μg/ml of pyrilamine maleate in 0.1 *N* HCl solution against 0.1 *N* HCl as the blank. The results are presented in Table II.

DISCUSSION

The results (Tables I and II) indicate that a complex mixture of five active ingredients and two inactive ingredients (Figs. 2 and 3) can be separated and assayed quantitatively using HPLC. HPLC always has additional advantages such as the identification of the compounds from their retention times and separation of some inactive ingredients. In these investigations, it was possible to separate the preservative (sodium benzoate) and to identify it in the commercial sample (Figs. 2 and 3). Moreover, HPLC is usually short and often stability indicating.

The developed method is easy, accurate, and precise (for standard deviations, see Table I). It was not possible to separate pheniramine maleate from pyrilamine maleate, even by using many other solvents such as: (*a*) 0.05 *M* KH_2PO_4 in water containing 10% (v/v) methanol with the pH adjusted to 3.5 using acetic acid; (*b*) 0.05 *M* KH_2PO_4 in water containing 10, 15, 17, 20, and 45% (v/v) methanol; (*c*) 0.05 *M* KH_2PO_4 in water containing 13% (v/v) methanol with the pH adjusted to 6.5 using 0.2 *N* NaOH; (*d*) 0.05 *M* KH_2PO_4 in water containing 20% (v/v) acetonitrile; (*e*) 0.05 *M* NH_4HCO_3 in water containing 10% (v/v) methanol; and (*f*) 1-heptanesulfonic acid for paired-ion chromatography (2) in water containing 1% (v/v) acetic acid and 13% (v/v) methanol and filtered through a 0.45-μm filter.

Table II—Assay Results on Pheniramine Maleate and Pyrilamine Maleate by Spectrophotometric Methods

	Percent of Label Claim Found		
Syrup	III	V (by Difference)[a]	V (by Spectrophotometry)
Lot A	98.6	99.8	99.5
Commercial sample	105.2	103.4	—[b]

[a] Since preliminary investigations indicated that the combined peak area of III and V was equal to the sum of the separate peak areas of III and V and that, after determining the exact concentration of III by the cyanogen bromide method, it was possible to determine the peak area due to III, the peak area due to V could be determined by difference. This area was directly compared with the peak area of the standard solution of V (125.0 μg/ml in the chromatographic solvent). [b] Not determined since the authors did not know what dyes were used in the commercial sample.

Due to problems in separating III and V, spectrophotometric methods were used to determine the two antihistamines separately (Table II). However, if the concentration of one is known, the concentration of the other may be determined by difference (Table II, footnote *a*).

In these studies, it was possible to determine the concentration of pyrilamine maleate by difference after the quantitative analysis of pheniramine maleate with cyanogen bromide, which opens the pyridine ring (1) and imparts color to the solution. Whenever new prepacked columns are purchased, the percent of methanol in the chromatographic solvent may have to be changed slightly to accomplish the same separation.

REFERENCES

(1) H. Hudanick, *J. Pharm. Sci.*, **53**, 332 (1964).

(2) "Paired Ion Chromatography," Bulletin D61, Waters Associates, Milford, Mass., Dec. 1975.

ACKNOWLEDGMENTS AND ADDRESSES

Received May 28, 1976, from the *College of Pharmacy, University of Houston, Houston, TX 77004.*

Accepted for publication August 6, 1976.

[x] To whom inquiries should be directed.

Quantitative Determinations of Antipyrine and Benzocaine in Ear Drops by High-Pressure Liquid Chromatography

V. DAS GUPTA [x] and S. SACHANANDANI

Abstract □ Antipyrine and benzocaine were determined quantitatively in ear drops by high-pressure liquid chromatography on an octadecyltrichlorosilane permanently bonded to a Si–C column, using 0.02 *M* KH_2PO_4 in methanol–water as the mobile phase. Both compounds can be assayed in combination directly without interference from each other or from oxyquinoline sulfate (the preservative). The method is accurate, precise (estimated universe standard deviations of 0.68% for antipyrine and 1.18% for benzocaine), simple, and short (requires 30 min *versus* 2–3 hr by the NF method). The method was tried on a commercial product with excellent results and can be used in the presence of decomposition products.

Keyphrases □ Antipyrine—high-pressure liquid chromatographic analysis, commercial combination with benzocaine □ Benzocaine—high-pressure liquid chromatographic analysis, commercial combination with antipyrine □ High-pressure liquid chromatography—analyses, antipyrine and benzocaine in commercial combination

An antipyrine and benzocaine mixture is used extensively for earache. The NF methods (1) for the quantitative determinations of antipyrine and benzocaine are lengthy and tedious. The purpose of these investigations was to develop a simple, short, accurate, precise, and stability-indicating assay method for the quantitative determina-

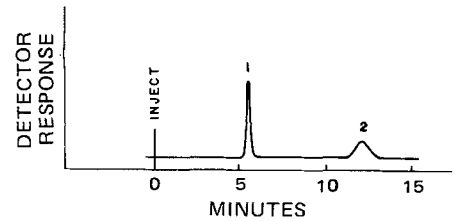

Figure 3—*HPLC analysis of some inactive ingredients used in cough syrups. Peaks 1 and 2 are sodium benzoate and FD&C Yellow No. 5, respectively.*

and:

$$\text{corrected } A_{315} = A_{315} - A_{365} \times \text{factor} \qquad \text{(Eq. 4)}$$

Since preliminary investigations indicated that Beer's law was followed, the results were calculated by direct comparison of the absorbance values at 315 nm:

$$\frac{\text{corrected } A_{315}}{(A_{315})_s} = \text{percent of label claim} \qquad \text{(Eq. 5)}$$

where corrected A_{315} is the absorbance value of the assay sample from Eq. 4, and $(A_{315})_s$ is the absorbance value of the standard solution containing 20 μg/ml of pyrilamine maleate in 0.1 *N* HCl solution against 0.1 *N* HCl as the blank. The results are presented in Table II.

DISCUSSION

The results (Tables I and II) indicate that a complex mixture of five active ingredients and two inactive ingredients (Figs. 2 and 3) can be separated and assayed quantitatively using HPLC. HPLC always has additional advantages such as the identification of the compounds from their retention times and separation of some inactive ingredients. In these investigations, it was possible to separate the preservative (sodium benzoate) and to identify it in the commercial sample (Figs. 2 and 3). Moreover, HPLC is usually short and often stability indicating.

The developed method is easy, accurate, and precise (for standard deviations, see Table I). It was not possible to separate pheniramine maleate from pyrilamine maleate, even by using many other solvents such as: (*a*) 0.05 *M* KH_2PO_4 in water containing 10% (v/v) methanol with the pH adjusted to 3.5 using acetic acid; (*b*) 0.05 *M* KH_2PO_4 in water containing 10, 15, 17, 20, and 45% (v/v) methanol; (*c*) 0.05 *M* KH_2PO_4 in water containing 13% (v/v) methanol with the pH adjusted to 6.5 using 0.2 *N* NaOH; (*d*) 0.05 *M* KH_2PO_4 in water containing 20% (v/v) acetonitrile; (*e*) 0.05 *M* NH_4HCO_3 in water containing 10% (v/v) methanol; and (*f*) 1-heptanesulfonic acid for paired-ion chromatography (2) in water containing 1% (v/v) acetic acid and 13% (v/v) methanol and filtered through a 0.45-μm filter.

Table II—Assay Results on Pheniramine Maleate and Pyrilamine Maleate by Spectrophotometric Methods

	Percent of Label Claim Found		
Syrup	III	V (by Difference)[a]	V (by Spectrophotometry)
Lot A	98.6	99.8	99.5
Commercial sample	105.2	103.4	—[b]

[a] Since preliminary investigations indicated that the combined peak area of III and V was equal to the sum of the separate peak areas of III and V and that, after determining the exact concentration of III by the cyanogen bromide method, it was possible to determine the peak area due to III, the peak area due to V could be determined by difference. This area was directly compared with the peak area of the standard solution of V (125.0 μg/ml in the chromatographic solvent). [b] Not determined since the authors did not know what dyes were used in the commercial sample.

Due to problems in separating III and V, spectrophotometric methods were used to determine the two antihistamines separately (Table II). However, if the concentration of one is known, the concentration of the other may be determined by difference (Table II, footnote *a*).

In these studies, it was possible to determine the concentration of pyrilamine maleate by difference after the quantitative analysis of pheniramine maleate with cyanogen bromide, which opens the pyridine ring (1) and imparts color to the solution. Whenever new prepacked columns are purchased, the percent of methanol in the chromatographic solvent may have to be changed slightly to accomplish the same separation.

REFERENCES

(1) H. Hudanick, *J. Pharm. Sci.*, **53**, 332 (1964).

(2) "Paired Ion Chromatography," Bulletin D61, Waters Associates, Milford, Mass., Dec. 1975.

ACKNOWLEDGMENTS AND ADDRESSES

Received May 28, 1976, from the *College of Pharmacy, University of Houston, Houston, TX 77004.*

Accepted for publication August 6, 1976.

[x] To whom inquiries should be directed.

Quantitative Determinations of Antipyrine and Benzocaine in Ear Drops by High-Pressure Liquid Chromatography

V. DAS GUPTA [x] and S. SACHANANDANI

Abstract □ Antipyrine and benzocaine were determined quantitatively in ear drops by high-pressure liquid chromatography on an octadecyltrichlorosilane permanently bonded to a Si–C column, using 0.02 *M* KH_2PO_4 in methanol–water as the mobile phase. Both compounds can be assayed in combination directly without interference from each other or from oxyquinoline sulfate (the preservative). The method is accurate, precise (estimated universe standard deviations of 0.68% for antipyrine and 1.18% for benzocaine), simple, and short (requires 30 min *versus* 2–3 hr by the NF method). The method was tried on a commercial product with excellent results and can be used in the presence of decomposition products.

Keyphrases □ Antipyrine—high-pressure liquid chromatographic analysis, commercial combination with benzocaine □ Benzocaine—high-pressure liquid chromatographic analysis, commercial combination with antipyrine □ High-pressure liquid chromatography—analyses, antipyrine and benzocaine in commercial combination

An antipyrine and benzocaine mixture is used extensively for earache. The NF methods (1) for the quantitative determinations of antipyrine and benzocaine are lengthy and tedious. The purpose of these investigations was to develop a simple, short, accurate, precise, and stability-indicating assay method for the quantitative determina-

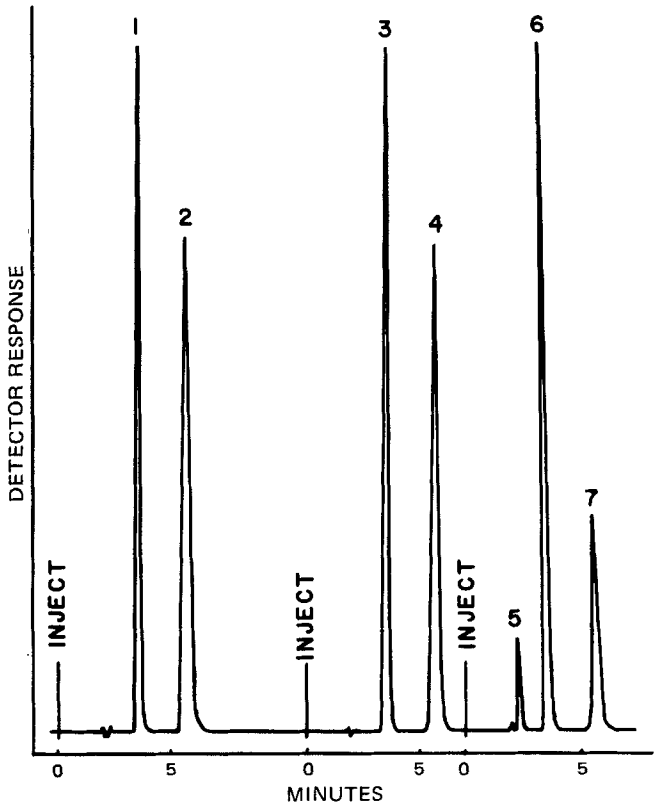

Figure 1—*HPLC analysis of antipyrine and benzocaine in combination (for chromatographic conditions, see text). Peaks 1 and 2 are antipyrine and benzocaine, respectively, from a standard solution; peaks 3 and 4 are antipyrine and benzocaine, respectively, from a commercial sample. Peaks 5, 6, and 7 are from the decomposed standard solution.*

tions of antipyrine and benzocaine in combination in the NF solution (1) using high-pressure liquid chromatography (HPLC).

EXPERIMENTAL

Chemicals and Reagents—All chemicals and reagents were ACS, USP, or NF grade and were used without further purification.

Apparatus—A high-pressure liquid chromatograph[1] equipped with a fixed wavelength (254 nm) detector and recorder[2] was used.

Column—A nonpolar column[3] consisting of a monomolecular layer of octadecyltrichlorosilane permanently bonded to Si–C (30 cm long and 4 mm i.d.) was used.

Chromatographic Conditions—The chromatographic solvent was 0.02 *M* KH_2PO_4 in water containing 40% (v/v) methanol. The temperature was ambient, and the solvent flow rate was 1.6 ml/min (at an inlet pressure of approximately 2200 psig). The chart speed was 30.5 cm/hr, and the absorbance units for full scale deflection were 0.08 for benzocaine and 0.64 for antipyrine.

Standard Solutions—The following standard solutions were prepared in water containing 0.5% (v/v) glycerin: A, 0.027% antipyrine alone; B, 0.007% benzocaine alone; C, 0.027% antipyrine plus 0.007% benzocaine in combination; and D, 0.027% antipyrine, 0.007% benzocaine, and 0.002% oxyquinoline sulfate in combination. Solutions E–G were the same as Solutions A–C, respectively, except that pH 9 borate buffer USP (2) was substituted for water.

[1] Waters ALC 202 equipped with a U6K universal injector.
[2] Omniscribe 5213-12 equipped with an integrator.
[3] Waters μ-Bondapak/C_{18}, Catalog No. 27324.

Table I—Assay Results on Antipyrine and Benzocaine

Solution	Assay Results, % of Claim	
	Antipyrine	Benzocaine
Prepared NF solution	99.52[a]	99.43[a]
Universe standard deviation (estimated)	0.68	1.18
Commercial sample	99.23[b]	99.13[b]
NF solution after decomposition	99.42[c]	52.86

[a] Average of four. The statistical data are based on four results. [b] The assay results by the NF method (1) as supplied by the manufacturer were 98.52% for antipyrine and 99.29% for benzocaine. [c] A small difference in the assay result from the undecomposed sample may be an experimental error.

Assay Procedure for NF Solution or Commercial Product—First 0.5 ml of the solution is diluted to 100.0 ml with water and then 10 μl is injected. For comparison, an identical volume of the appropriate standard solution is injected after the assay sample is eluted.

Calculations—Since preliminary investigations indicated that the peak area of each ingredient was directly related to the concentration (range of 1.35–4.05 μg for antipyrine and of 0.35–1.40 μg for benzocaine), the results were calculated by direct comparison of the peak areas:

$$\frac{A_a}{A_s} = \text{percent of label claim} \qquad \text{(Eq. 1)}$$

where A_a = peak area of the assay sample, and A_s = peak area of the standard solution. The detector's response is presented in Fig. 1, and the assay results are presented in Table I.

Procedure for Decomposition of Solution—For decomposition studies, 25.0 ml of the standard solution containing both antipyrine and benzocaine in pH 9 borate buffer [with 0.5% (v/v) glycerin] was heated on a hot plate until the volume was reduced to approximately 5 ml. The solution was cooled and brought to the original volume (25.0 ml) with water. A 10-μl aliquot of this solution was injected for quantitative determinations of antipyrine and benzocaine as described. Since preliminary investigations indicated that borate buffer does not interfere with the quantitative determinations of the active ingredients, the results were calculated using Eq. 1. The detector's response is presented in Fig. 1, and the results are presented in Table I.

DISCUSSION

The results (Table I) indicate that antipyrine and benzocaine can be easily separated (Fig. 1) and assayed by HPLC. The method developed is simple, accurate, precise, and short (requires only about 30 min *versus* 2–3 hr by the NF method). However, the developed method requires a high-pressure liquid chromatograph, costing about three times more than the equipment required for NF methods. Since the proposed method appears to be stability indicating (Fig. 1), it may be preferred by those who already have a high-pressure liquid chromatograph available.

In the decomposed sample, the assay results on benzocaine were 52.86 *versus* 99.43% in the undecomposed sample. In the process used for the decomposition, benzocaine appears to have hydrolyzed. The hydrolyzed sample showed an additional peak (Fig. 1, peak 5). There was no interference from the preservative, oxyquinoline sulfate.

REFERENCES

(1) "The National Formulary," 13th ed., Mack Publishing Co., Easton, Pa., 1970, p. 60.

(2) "The United States Pharmacopeia," 19th rev., Mack Publishing Co., Easton, Pa., 1975, p. 654.

ACKNOWLEDGMENTS AND ADDRESSES

Received May 24, 1976, from the *College of Pharmacy, University of Houston, Houston, TX 77004.*

Accepted for publication August 6, 1976.

[x] To whom inquiries should be directed.

GI Pharmacology of Polyethyleneimine I: Effects on Gastric Emptying in Rats

SIDNEY MELAMED *, GLENN R. CARLSON *, JACK N. MOSS *, ERNEST J. BELAIR *, and MARTIN F. TANSY ‡x

Abstract □ Experiments were conducted to determine the effect of ingested polyethyleneimine upon gastric emptying of the fasted rat. Emptying was evaluated by the phenolsulfonphthalein and resin bead methods. The two techniques gave comparable results; both showed that this agent inhibited gastric emptying. A delay in gastric emptying could be detected within 15 min of intubation. The effect was dose related, quite long lasting (~4 hr), and reversible. Commercially available, branched polyethyleneimines were highly active, but the linear polyethyleneimine was without observable effect. A branched polyethyleneimine derivative with all primary amine sites selectively acetylated also was inactive.

Keyphrases □ Polyethyleneimines, various—effect on gastric emptying, phenolsulfonphthalein and resin bead methods compared, rats □ Gastric emptying—effect of various polyethyleneimines, phenolsulfonphthalein and resin bead methods compared, rats □ Polyamines—various polyethyleneimines, effect on gastric emptying, phenolsulfonphthalein and resin bead methods compared, rats

Commercial polyethyleneimines are used as fungicides in shampoo (1), as bactericides (2), as antiviral and antitumor agents (3), and as mucolytic agents in mouthwash (4). They are extensively used in industry as wet strength paper additives, flocculants, and modifiers for adhesives and coatings (5).

Polyethyleneimine is a water-soluble polyamine formed by the acid-catalyzed polymerization of ethyleneimine (6). Polyethyleneimine prepared in this manner contains primary, secondary, and tertiary amine nitrogens in a 1:2:1 ratio (5). The result is a highly branched spheroid-shaped molecule such as Structures I and II. A linear polymer (IV) of polyethyleneimine is also available *via* a two-step synthesis (7) and contains essentially only the secondary amine functionality if n is large. This linear polymer is crystalline and essentially insoluble in water at 25°.

In view of the therapeutic and hygienic usefulness of the commercial polyethyleneimines and the lack of literature

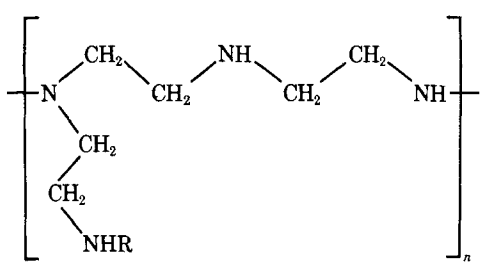

I: R = H, mol. wt. 40,000–60,000
II: R = H, mol. wt. 600
III: R = $COCH_3$, mol. wt. 40,000–60,000

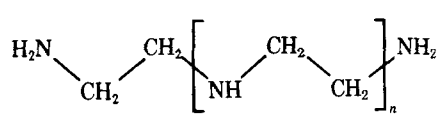

IV

Table I—Milligrams of Dye Retained (per Group of Three Rats[a]) *versus* Dose of I

Dose, mg/kg	Hours after Dosing 1[b]	2[c]	4[d]
250	7.50	5.50	3.98
	7.70	5.35	3.32
Average	7.60	5.43	3.65
125	4.67	3.05	1.08
	5.34	2.85	1.21
Average	5.01	2.95	1.15
62.5	5.55	1.28	0.65
	4.13	1.38	0.92
Average	4.84	1.33	0.79
31.2	2.35	0.73	0.10
	2.22	0.78	0.34
Average	2.29	0.76	0.22
15.7	1.07	0.68	0.38
	1.02	0.85	0.14
Average	1.05	0.77	0.26
0	1.17	0.40	0.08
	1.07	0.35	0.04
Average	1.12	0.38	0.06

[a] Six rats were used at each dosage level. Tabulated data refer to pooled values of these levels with two sets of three rats per level. [b] Zero-time control values: 5.75 and 7.25 (mean = 6.50). [c] Zero-time control values: 6.95 and 7.75 (mean = 7.35). [d] Zero-time control values: 5.70 and 6.70 (mean = 6.20).

Table II—Effect of Various Doses of I on Gastric Emptying Using the Phenolsulfonphthalein Method at Three Posttreatment Times[a]

Dose, mg/kg	Gastric Inhibition, % 1 hr	2 hr	4 hr
250	99.7 ± 1.5[b]	68.6 ± 1.0[b]	57.9 ± 5.3[c]
125	59.8 ± 5.2[c]	35.0 ± 1.4[b]	17.5 ± 1.0[b]
62.5	57.2 ± 1.1[d]	12.9 ± 0.7[b]	11.7 ± 2.2[d]
31.2	17.9 ± 1.0[c]	4.8 ± 0.3[c]	2.6 ± 1.9
15.7	−1.0 ± 0.4	5.2 ± 1.2[d]	3.2 ± 1.9
0.0	0.0 ± 0.0	0.0 ± 0.0	0.0 ± 0.0

[a] The samples consisted of two groups of three rats in each instance. Values are expressed as the mean ± *SE* of the mean. [b] $p < 0.005$ when compared to control groups. [c] $p < 0.025$ when compared to control groups. [d] $p < 0.05$ when compared to control groups.

reports concerning their effects on the gut, a study was conducted to determine the effects of ingestion of these polymers upon GI motor activity.

EXPERIMENTAL

Methods—Three hundred and twenty-four female Wistar rats, 144–155 g, were used. The first series of experiments was designed to determine the influence of polyethyleneimine mol. wt. 40,000–60,000[1] (I) upon gastric emptying; the phenolsulfonphthalein method (8) was used. Essentially, overnight fasted rats were intubated in groups of six with a predetermined dosage of I (adjusted to pH 7.0 with dilute hydrochloric acid) for each group along with 3 mg of phenolsulfonphthalein, a nontoxic, nonabsorbable dye.

Compound I and the dye were given in 1.5 ml of aqueous solution. At fixed time intervals, the animals were sacrificed and the residual phenolsulfonphthalein stomach content was determined by spectrophotometry. Control groups of animals received only dye and were sacrificed

[1] PEI 600, Dow Chemical Co., Midland, Mich.

Table III—Evaluation of the Rate of Onset of the Gastric Emptying Inhibitory Effect of I

Treatment	Time of Sacrifice after Phenol-sulfonphthalein Dosing, min	Gastric Dye Content in Milligrams at Time of Sacrifice; Dye Dosed at Indicated Times after Water (Control) or I (Treatment)[a]		
		0 min	15 min	30 min
Control (water)	0	5.8	7.75	7.05
	60	0.90	1.55	1.30
% Retention (60 min)	$= \frac{\text{mg (60)}}{\text{mg (0)}} = A$	15.5 ± 4.3	20.0 ± 1.0	18.4 ± 3.9
I (125 mg/kg)	0	7.65	8.40	8.40
	60	6.15	6.70	5.30
% Retention	$= \frac{\text{mg (60)}}{\text{mg (0)}} = B$	80.4 ± 7.2[b]	79.8 ± 1.2[c]	63.1 ± 3.6[b]
% Inhibition	= % retention with drug − % retention with water = B − A	64.9 ± 8.4	59.8 ± 1.5	44.7 ± 5.3

[a] Values are expressed as the mean for two groups of three animals. Retention and inhibition values are expressed as the mean ± *SE* of the mean. [b] $p < 0.025$ when compared to control group. [c] $p < 0.005$ when compared to control group.

similarly. Each group of six rats, including the control group, was divided into two sets of three rats each. The milligrams of dye was determined for each pooled set of three rats, and the group average was determined from the two sets of three rats in each group. Thus, group means were compared.

Zero-time controls also received only dye but were sacrificed immediately after dosing (t_0). This number is important since some dye is forced mechanically past the pyloric sphincter on dosing. Therefore, the actual dye at zero time must be determined. This phenomenon was confirmed by injecting laparotomized, anesthetized rats and observing the dye passage. Animals should be dosed gently. Stomach retention and percent inhibition of stomach emptying were calculated as follows:

$$\% \text{ retention } (t_1) = \frac{\text{mg of dye at } t_1 \text{ (treated)}}{\text{mg of dye at } t_0 \text{ (zero-time control)}} \times 100 \quad \text{(Eq. 1)}$$

$$\% \text{ inhibition } (t_1) = \% \text{ retention } (t_1) - \frac{\text{mg of dye at } t_1 \text{ (control)}}{\text{mg of dye at } t_0 \text{ (zero-time control)}} \times 100 \quad \text{(Eq. 2)}$$

The percent inhibition is the percent retention corrected for the percent of dye that remains at time t_1 in untreated, control animals. Table I provides the actual amount of dye determined at each dosage level, including zero-time and timed controls. These data show the reproducibility of the data and provide a basis for calculating the retention and inhibition values reported in Table II.

In the second series of experiments, designed to compare the phenolsulfonphthalein method with a bead method (9), 1.0 ml of the polyamine solution, again adjusted to pH 7.0, was administered to rats by intubation. This time, however, the polymer dose was immediately followed by a second solution (0.5 ml) containing a suspension of 30 very small resin beads of uniform diameter (0.5 mm) and shape. Each dosage group consisted of six animals. For the bead studies, the bead content was determined for each animal and was averaged for each group of six. The phenolsulfonphthalein comparison groups were analyzed as described.

The animals were sacrificed after fixed time periods (t_1), and the locations of the beads were noted. The number of beads leaving the stomach in a specified time was assumed to be a measure of stomach emptying. The percent retention and inhibition were calculated after referring to the appropriate control groups in a manner similar to that used in the phenolsulfonphthalein method:

$$\% \text{ retention } (t_1) = \frac{\text{number of beads at } t_1 \text{ (treated)}}{\text{number of beads at } t_0 \text{ (zero-time control)}} \times 100 \quad \text{(Eq. 3)}$$

$$\% \text{ inhibition } (t_1) = \% \text{ retention } (t_1) - \frac{\text{number of beads at } t_1 \text{ (control)}}{\text{number of beads at } t_0 \text{ (zero-time control)}} \times 100 \quad \text{(Eq. 4)}$$

Table IV—Comparison of Phenolsulfonphthalein and Bead Methods of Estimating the Effect of Various Doses of I on Gastric Emptying at 4 hr Posttreatment

Dose, mg/kg	Inhibition (Phenol-sulfonphthalein), %	Inhibition (Beads)[a], %
250	60.7 ± 5.0[b]	93.2 ± 4.8[c]
125	17.0 ± 1.1[c]	45.2 ± 12.2[b]
62.5	12.4 ± 1.9	29.3 ± 12.9
31.2	5.4 ± 1.9	15.8 ± 11.3
15.7	4.6 ± 1.6	22.0 ± 7.0[b]
0	0.0 ± 0.0	0.0 ± 0.0

[a] The samples consisted of six rats in each instance. Phenolsulfonphthalein samples were pooled as before, $n = 2$. Values are expressed as the mean ± *SE* of the mean. [b] $p < 0.025$ when compared to control groups. [c] $p < 0.005$ when compared to control groups.

In the next series of experiments, designed to determine the rate of onset of gastroinhibitory effects, 12 sets of three female rats were fasted for 24 hr. Zero-time (treated) animals were given 1.5 ml of a solution containing 125 mg of I/kg (pH 7) plus 3 mg of phenolsulfonphthalein. Fifteen- and thirty-minute animals were first given I at time zero in 0.75 ml of water and then, after the appropriate time, were given an additional 0.75 ml of a second solution containing 3 mg of the dye. Control groups of animals at 0, 15, and 30 min were treated in the same way except that they received pure water instead of the polymer solution.

All animals in this experiment were sacrificed 1 hr after dye administration, and the dye content of the stomachs was determined. The stomach contents of each group of three rats were pooled; that is, each group of three rats received a total of 9 mg of phenolsulfonphthalein. The results in Table III indicate the milligrams of dye remaining for each pooled set of three rats.

The next series of experiments was designed to evaluate the duration of the effect of I. Sets of six rats were each dosed with 125 mg/kg of the polymer and the dye marker. The same analytical techniques as already described were used; the groups were sacrificed at various time periods up to 6 hr after dosing.

Materials—Compound I was dialyzed for 30 hr in regenerated cellulose tubing[2] (molecular weight cutoff of 12,000) prior to use. A change of tubing was made after approximately 15 hr. Polyethyleneimine mol. wt. 600[3] (II) was used without dialysis. $\text{Acetyl}_{0.25}$ polyethyleneimine (III) was prepared from I and acetic anhydride (0.33 equivalent) in water at 35° according to literature procedures (6). It was dialyzed for 48 hr prior to use. Analysis by NMR spectroscopy in deuterium oxide indicated only primary amine acetylation: a broad singlet at 1.9 ppm ($NHCOCH_3$) and no signal at 2.1 ppm ($NRCOCH_3$). Linear polyethyleneimine mol. wt. 10,000[4] (IV) was used without dialysis.

RESULTS AND DISCUSSION

Dosages of 15–250 mg of I/kg to fasted rats gave dose-related, long lasting, but reversible, inhibition of stomach emptying. The effect of I on gastric emptying performance was defined by the time-dependent percentage loss of either inert beads or phenolsulfonphthalein from the stomachs of rats dosed orally with the polyamine (Tables II and IV).

These data indicate that the two techniques gave qualitatively com-

[2] A. H. Thomas Co., Philadelphia, Pa.
[3] PEI 6, Dow Chemical Co., Midland, Mich.
[4] Supplied by Dow Chemical Co.

Table V—Duration of the Delay of Gastric Emptying by I

Dosage	Retention[a] of Phenolsulfonphthalein in Rat Stomachs at Predetermined Posttreatment Times, %			
	1 hr	2 hr	4 hr	6 hr
Control	17.2 ± 0.7	4.1 ± 0.7	2.0 ± 1.1	0.1 ± 0.1
125 mg/kg	99.0 ± 1.5[b]	67.6 ± 1.9[b]	22.3 ± 3.4[c]	9.5 ± 3.0

[a] Calculations: (mg of dye remaining in stomach × 100)/(mg of dye initially administered). Samples consisted of two groups of three rats. Values are expressed as the mean ± *SE* of the mean. [b] $p < 0.005$ when compared with control groups. [c] $p < 0.05$ when compared with control groups.

parable results. The phenolsulfonphthalein method was quicker, easier, and more reproducible, and it gave lower values than the bead method. With the phenolsulfonphthalein method of estimating gastric emptying, an experiment was done to determine the onset of gastric inhibition, as indicated under *Experimental* (Table III).

In addition to the actual amounts of dye remaining at each of the three dosing times, Table III shows the percent retention and inhibition. Within the limits of the method, the percent inhibition at zero time after dosing was as great as at 15 min. At 30 min, the effect of the drug began to decrease. Thus, the data indicate that the onset of the effect of I must occur fairly rapidly following oral administration. The results in Table V indicate the duration of action of I at a dosage level of 125 mg/kg. Some effect was still observable 6 hr after dosing.

The LD_{50} for oral administration of I (pH 7) to the rat is approximately 2 g/kg[5]. At the dosages used for stomach retention, no signs of overt toxicity or pathology were observed over a pH range of 2–12.

In a recent article (10), it was reported that chemical trauma to the small intestinal mucosa prevents gastric emptying. Histopathological examination of the small intestine of rats treated with I showed normal tissue.

Preliminary retention experiments with a lower molecular weight branched polymer (II) suggest that the activity of this agent in producing a delay in gastric emptying may depend on molecular weight. A 250-mg/kg dose of II produced an inhibition of 82 ± 0.7% at 2 hr, in contrast with the value of 68.6 ± 1.0% observed for I.

Compound III did not inhibit gastric emptying in the rat as measured by the phenolsulfonphthalein method (inhibition of 2.0 ± 0.9%, 250 mg/kg, 4-hr evaluation). Likewise, IV had no observable effect when administered in the range of dosages that proved to be effective for I. These results suggest that large numbers of primary amine sites per molecule are required for optimum activity.

In summary, these results indicate that orally administered branched-chain polyethyleneimine is associated with delayed gastric emptying in fasted rats. With the method used, a dosage of 125 mg of I/kg produced this effect as early as 15 min following administration, and the effect could be detected up to 6 hr later.

[5] Unpublished data.

REFERENCES

(1) T. T. Hewitt, U.S. pat. 3,740,422 (May 25, 1970).

(2) V. S. Zalesov, A. L. Friedman, A. N. Plaksina, E. P. Ketov, and N. S. Churilova, *Nauchn. Ir. Perm. Farm. Inst.*, **4**, 31 (1971).

(3) R. A. Perlmutter and E. D. Holyoke, *J. Med. (Basel)*, **2**, 112 (1971).

(4) W. Schmitt, R. Purrmann, P. Jochum, and W. D. Zahler, U.S. pat. 3,862,308 (Jan. 21, 1975).

(5) PEI Polymers Product Bulletin, 192-328-74, Dow Chemical Co., Midland, Mich., 1974.

(6) T. W. Johnson and I. M. Klotz, *Macromolecules*, **7**, 149 (1974).

(7) T. Saegusa, H. Ikeda, and H. Fujii, *ibid.*, **5**, 108 (1972).

(8) T. C. Reynell and G. H. Spray, *J. Physiol.*, **131**, 452 (1956).

(9) D. A. Brodie, *Gastroenterology*, **50**, 45 (1966).

(10) T. H. Kent, B. Cannon, J. Reynolds, and J. W. Osborne, *ibid.*, **69**, 1246 (1975).

ACKNOWLEDGMENTS AND ADDRESSES

Received September 29, 1975, from the *Research Laboratories, Rohm and Haas Company, Spring House, PA 19477, and the ‡Department of Physiology and Biophysics, Health Sciences Center, Temple University, Philadelphia, PA 19140.

Accepted for publication October 6, 1976.

The authors are indebted to Mr. H. Mathason, Mr. A. Sambuca, Mr. H. Tomlinson, and Mr. M. Watts for technical assistance. They also thank Dr. D. Drees for histopathological support and Mr. J. Ritts for statistical data treatment.

x To whom inquiries should be directed.

GI Pharmacology of Polyethyleneimine II: Motor Activity in Anesthetized Dogs

MARTIN F. TANSY *x, JOHN S. MARTIN *, DAVID L. INNES *, FRANK M. KENDALL *, SIDNEY MELAMED ‡, and JACK N. MOSS ‡

Abstract □ The effects of orally and intravenously administered doses of polyethyleneimine were observed in 18 chloralose–urethan-anesthetized dogs. Polyethyleneimine produced an initial augmentation of rhythmic segmenting gastric antral contractions, a copious flow of gastric mucus, increased segmenting and propulsive activities of the small and large intestines, and occasional micturition and defecation. The gastric corpus and fundic regions became relaxed and enlarged. These events were associated with the prompt appearance of retching. The retching response to oral administration could only be abolished by bilateral vagotomy or bilateral sympathectomy. The skeletal muscle component of retching was blocked by tubocurarine. Intravenous administration of chlorpromazine blocked the retching response and gastric corporal atonia to either intravenous or oral doses of polyethyleneimine. Either oral or intravenous administration of polyethyleneimine produced no detectable changes in the lead II ECG but was associated with marked transient reductions in both mean and pulsatile arterial blood pressures. These depressor effects showed clear tachyphylaxis. In all cases where GI effects were noted, respiration was augmented and erratic in a manner associated with the retching responses.

Keyphrases □ Polyethyleneimine—GI and cardiopulmonary effects, oral and intravenous administrations compared, dogs □ GI effects—polyethyleneimine, oral and intravenous administrations compared, dogs □ Cardiopulmonary effects—polyethyleneimine, oral and intravenous administrations compared, dogs □ Polyamines—polyethyleneimine, GI and cardiopulmonary effects, oral and intravenous administrations compared, dogs

The naturally occurring polyamines putrescine, spermidine, and spermine have attracted considerable attention with regard to their biological functions (1). However, there have been no studies to determine the effects of either the naturally occurring or synthetic polyethyleneimines on GI functions.

Recent experimental data indicated that a high molecular weight polyethyleneimine polymer produced delayed gastric emptying when orally administered to fasted rats (2). It might be possible to utilize this effect to prolong orally administered drug action or as an appetite suppressant (3). The objective of the present experiments was to determine those GI secreto-motor effects associated with the oral administration of the polyamine as well as any cardiopulmonary effects.

EXPERIMENTAL

Methods—Eighteen mongrel dogs of both sexes were used. Following an overnight fast with water *ad libitum*, all animals were anesthetized with a mixture of 5% α-chloralose dissolved in polyethylene glycol 200 and 50% urethan in 0.9% saline. Each animal was individually titrated to a surgical plane of anesthesia using this mixture. Anesthesia was maintained by individual subsequent administration of the same mixture.

In all cases, the following procedures were used. A tracheal cannula was inserted to ensure patency of the airway and to permit monitoring of respiratory frequency. The femoral artery was cannulated for the purpose of recording blood pressure. The ipsilateral vein was cannulated to permit either bolus or infusion administration of drugs. The standard lead II ECG was continuously monitored throughout each experiment.

The following specific procedures were employed depending on the design of the particular experiment. Motor activities of the small and large intestines were monitored by surgically placed intraluminal water-filled balloons. Gastric motor activity was monitored by oral intubation with a water-filled balloon. Gastric secretion was collected by continuous drainage from a Thomas cannula surgically placed into the corpus of the stomach, as previously described (4).

Biliary and pancreatic flows were monitored by drop counters connected *via* polyethylene cannulas to the extramural pancreatic and common bile ducts. Portal venous pressure was monitored *via* a cannula placed in a splenic vein. The vagus nerves were exposed cervically, and either the splanchnic nerves or the sympathetic chains were exposed at the T-9–T-10 level.

In some experiments, the vagi were sectioned and the peripheral ends were electrically stimulated using bipolar electrodes. Square-wave stimuli ranged from 12 to 30 v at 30 Hz with a 2-msec duration. Monitored parameters were recorded on a strip-chart recorder. Increases in GI motor activities were directly visualized and photographed so that the resulting pressure wave forms could be interpreted in terms of the type of activity represented.

Materials—The test agent employed was the high molecular weight (40,000–60,000) branched polyethyleneimine[1] (I) in saline, 10–200 mg/kg iv depending on the experiment. Tubocurarine (1.0 mg/kg) and 2.0 mg of chlorpromazine hydrochloride[2]/kg were also used.

RESULTS AND DISCUSSION

In all 18 dogs, the intravenous administration of I was immediately associated with a marked reduction in arterial blood pressure (Fig. 1). This response showed marked tachyphylaxis to an extent that it had disappeared completely by the beginning of the third trial in each dog (Fig. 1). Other than reflex changes in heart rate, the morphology of the ECG showed no suggestive changes. Respiratory rate was augmented with substantially complete tachyphylaxis by the beginning of the third dose.

Portal venous pressure promptly and consistently rose following intravenous administration of I (Fig. 1). These responses also showed tachyphylaxis (Fig. 1). All doses were consistently associated with transient decreases in extrahepatic bile flow. Pancreatic flow was not influenced by any dose employed. The entire small and large intestines exhibited increased motor activities. Gastric motor activity took the form of an initial augmentation followed by a marked depression within 2–3 min of I administration. In all 18 animals, exaggerated respiratory movements were noted; in some cases, they progressed to violent cyclic retching (Fig. 1), frequently accompanied by micturition and defecation. Fatalities in six dogs occurred at total cumulative intravenous dosages of 25–31 mg/kg.

The described effects also were noted in eight dogs when doses of 200 mg/kg were administered by gastric or duodenal intubation. The only differences were the latencies of the responses, which were uniformly longer (Fig. 2).

The fatal total oral dose in three dogs was estimated by average to be about 1.8 g/kg. The retching observed subsequent to oral administration could be abolished by bilateral cervical vagotomy. This procedure did not abolish the retching responses to intravenous administration.

The first task resulting from the previous observations was to determine the exact changes of gastric motor activity that resulted from I administration. In these four experiments, the intravenous dosage was 1 mg/kg and the intragastric dosage was reduced to 50 mg/kg.

Direct visualization of the stomach following I administration revealed that the gastric antrum, defined as the region below the incisura angularis, exhibited protracted, rhythmic, propulsive contractile activity, which

[1] PEI 600, Dow Chemical Co., Midland, Mich.

[2] Thorazine Injectable, Smith Kline and French Laboratories, Philadelphia, Pa.

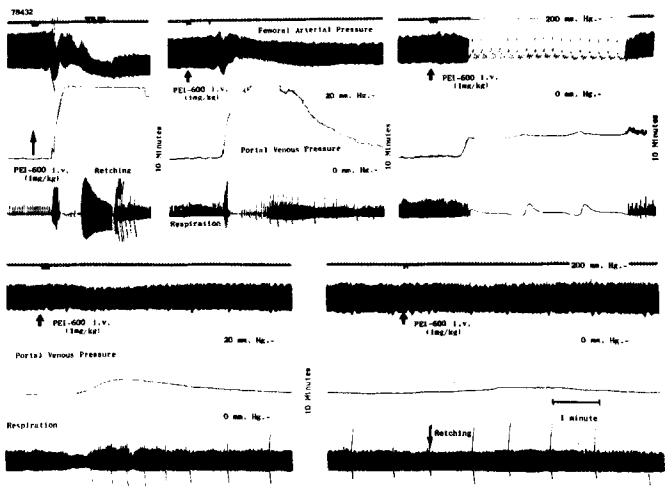

Figure 1—*Polygrams depicting the time course of femoral arterial pressure (top trace), portal venous pressure (center trace), and respiratory movements (bottom trace). The panels are ordered sequentially. This figure shows that tachyphylaxis was noticeably present with respect to all parameters upon the third intravenous administration of I (PEI-600). Tachyphylaxis was essentially complete following the fifth dose. The sharp spikes on the respiration trace show that retching movements were present during the entire period depicted.*

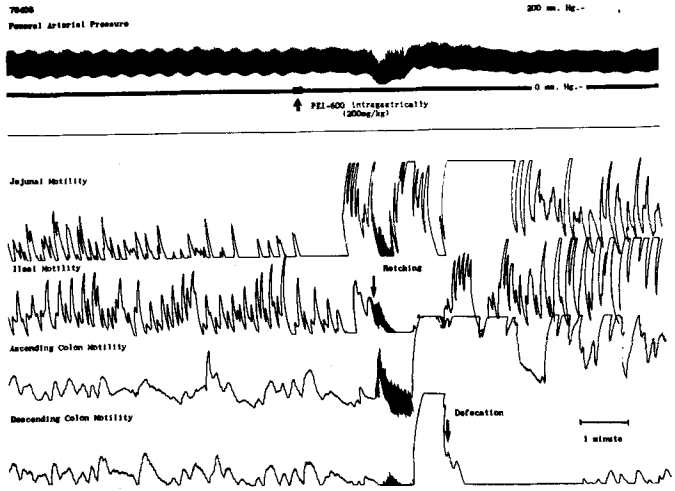

Figure 2—*Polygram depicting the time course of arterial blood pressure and jejunal, ileal, ascending colon, and descending colon motilities following the intragastric administration of 200 mg/kg of I (PEI-600). The latency of the responses was about 1.5 min. Arterial blood pressure was transiently affected. Jejunal, ileal, and ascending colonic movements underwent protracted augmentation. In this particular recording, the abrupt decrease in activity of the descending colon was associated with spontaneous defecation. The blurring of the motility traces was an artifact associated with gross retching movements.*

was coincident with increased propulsive activity of the small intestine. As additional drug was administered, a progressive enlargement of the corpus and fundic regions occurred to an extent that the total volume occupied by the stomach became greatly enlarged. During repeated administrations, exaggerated respiratory movements and retching appeared. Electrical stimulation of the peripheral vagi augmented the propulsive movements of both the gastric antrum and the small intestine.

A gastric pH electrode was introduced orally into the stomachs of three dogs. The gastric pH rose continuously during 2 hr of intravenous I administration. At the end of 2 hr, the gastric pH was 8.0. A single gastric fistula dog was then prepared to determine the effect of intravenous I administration on gastric acid secretion following an overnight fast. The repeated intravenous administration of 1.0 mg/kg markedly increased the amount of gastric mucus produced during the 15-min collection periods. Tachyphylaxis was not noted.

The latter observations suggested that a sympathetic component might be responsible for the motor effects and the secretion of gastric mucus (4). Accordingly, in another series of four dogs, the sympathetic chains were surgically interrupted prior to intravenous I administration. Gastric enlargement was not seen in these animals, but they all had cyclic bouts of retching. One dog retched continuously. Retching was abolished in the four dogs by intravenous tubocurarine administration.

A final experimental series utilized two dogs and was designed to determine whether the prior intravenous administration of 2 mg/kg of chlorpromazine could modify the observed GI effects of oral or intravenous I. Oral dosages ranged from 50 to 200 mg/kg, and intravenous dosages ranged from 1.0 to 5.0 mg/kg. In no case was either retching or gastric enlargement observed.

During the first canine experiments, it was immediately noted that the classic physiological responses (5) included in the description of retching were produced by I. The 1.0-mg/kg iv dose appears to be near the threshold for this response because the responses were variable. One animal retched each time the drug was administered, while another dog retched unpredictably with no apparent relationship between total accumulated dosage and prediction of the response.

The responses themselves were of unpredictable duration. One dog might retch continuously during the entire experiment following the initial dosage while another retched for a short time following a dosage that happened to produce the response. At the higher intragastric and intravenous dosages, retching was more predictable and of longer duration.

An analysis of the retching responses indicates the following. The skeletal muscle component was blocked by curare, indicating that the classical voluntary skeletal muscle component of the response was present. The gastric response consisted of increased secretion of mucus, relaxation of the corpus and fundus, and marked antral contractions. Interruption of the sympathetic chains and sectioning of the splanchnic nerves abolished relaxation and increased mucus secretion. This response indicates that a characteristic sympathetic component of the retch reflex was present.

The immediate sympathetic and parasympathetic responses to gastric or duodenal administration could be blocked by bilateral vagotomy (Fig. 3), indicating that the reflex can be subserved by vagal afferent pathways (6). Furthermore, the observation that retching produced by intravenous administration of I could be blocked by prior treatment with chlorpromazine (7) indicates that the agent or one or more of its metabolites can directly stimulate the chemoreceptor trigger zone. Thus, the emetic action of I (emesis did occur in the nonfasted dog) appears to be similar to that of ipecac (7).

The most pronounced effects of I upon systems other than the GI are upon the circulation. The marked decreases in arterial pressure were

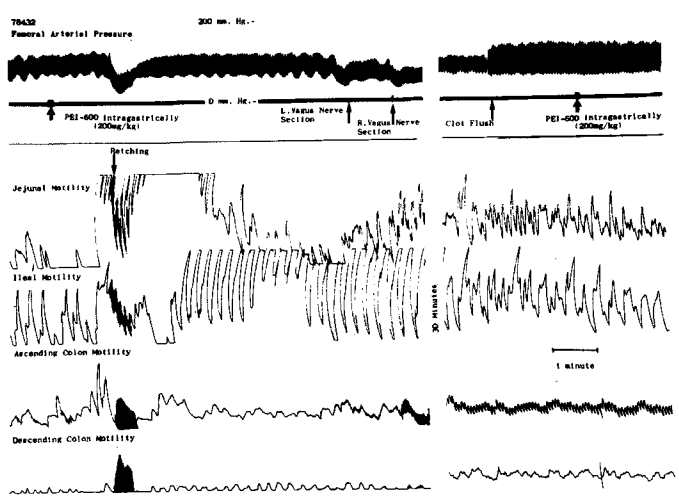

Figure 3—*Polygram depicting the time course of femoral arterial pressure and motor activities of the jejunum, ileum, and ascending and descending colons of a dog subsequent to the intragastric administrations of 200 mg/kg of I (PEI-600) prior to and following bilateral cervical vagotomy. The pressure artifacts produced by gross retching movements were absent following vagotomy.*

associated with reductions in pulse pressures and rises in portal venous pressures. These changes appeared to exhibit rapid and complete tachyphylaxis. The lack of apparent changes in the morphology of the lead II ECG indicates that the effects of the agent did not produce arrhythmias or ectopic foci of excitation. A determination of whether minor local changes in excitation occurred secondary to such effects as regional changes in myocardial circulation cannot be inferred from these limited data.

Experiments with lower dosages or apparently ineffective 1.0-mg/kg iv and 50-mg/kg intragastric dosages indicated that the individual components of the retch response (increased frequency of respiration, gastric mucus secretion, antral contractions, and corporal-fundal atonia) were invariably present but of such small intensity that the composite response was decidedly less than that constituting frank retching.

A similar set of sequelae is also present in humans who report feelings of nausea but who do not visibly retch. It is impossible to make this judgment with dogs, particularly anesthetized dogs. But these observations furnish an adequate physiological basis to suspect that the gastric or intravenous administration of dosages that are insufficient to produce frank retching might be accompanied by sensations of nausea.

It is concluded that the high molecular weight, branched polyethyleneimine, whether administered to dogs by gastric intubation or intravenously, produces an emetic response similar to ipecac in that it can act reflexly or by direct stimulation of the chemoreceptor trigger zone.

REFERENCES

(1) A. Raina and J. Jänne, *Med. Biol.*, **53**, 121 (1975).

(2) S. Melamed, G. R. Carlson, J. N. Moss, E. J. Belair, and M. F. Tansy, *J. Pharm. Sci.*, **66**, 899 (1977).

(3) S. Lepkovsky, M. K. Dimick, F. Furuta, S. E. Feldman, and R. Park, *J. Nutr.*, **105**, 1491 (1975).

(4) M. F. Tansy, R. C. Mackowiak, and M. H. F. Friedman, *Surg. Gynecol. Obstet.*, **127**, 259 (1968).

(5) H. L. Borison and S. C. Wang, *Pharmacol. Rev.*, **5**, 193 (1953).

(6) J. Zabara, R. B. Chaffee, Jr., and M. F. Tansy, *Space Life Sci.*, **3**, 282 (1972).

(7) J. E. Weaver and J. F. Griffith, *Toxicol. Appl. Pharmacol.*, **14**, 214 (1969).

ACKNOWLEDGMENTS AND ADDRESSES

Received September 29, 1975, from the *Department of Physiology and Biophysics, Health Sciences Center, Temple University, Philadelphia, PA 19140, and the ‡Research Laboratories, Rohm and Haas Co., Spring House, PA 19477.

Accepted for publication June 23, 1976.

The authors are indebted to Mr. Harold Perrong and Mr. Wendell Landin for technical assistance.

ˣ To whom inquiries should be directed.

New Compounds: Potential Antituberculous Agents I: Alkylaryl 4-Arylformamidinothiosemicarbazones

P. K. SRIVASTAVA ˣ and J. S. UPADHYAYA

Abstract □ A series of alkylaryl 4-arylformamidinothiosemicarbazones was synthesized for evaluation as antituberculous agents. The synthesis was effected by the condensation of different arylcyanamides with various thiosemicarbazones. The required intermediates also are described.

Keyphrases □ Thiosemicarbazones, various—synthesized for evaluation as antituberculous agents □ Antituberculous agents, potential—various thiosemicarbazones synthesized

Interest in the synthesis and biological evaluation of thiosemicarbazone derivatives was renewed by the fact that tibione (*p*-acetylaminobenzaldehyde thiosemicarbazone) (1–3) possesses antituberculous activity. Many reports (4–13) discussed the change of activity due to variations in the structure of the parent compound.

DISCUSSION

The present report deals with the synthesis of acetophenone 4-arylformamidinothiosemicarbazones (V*a*–V*m*, Table I) and 1-acetonaphthone 4-arylformamidinothiosemicarbazones (VI*a*–VI*m*, Table II) by the condensation of corresponding arylcyanamide hydrochlorides (I, Scheme I) with the appropriate thiosemicarbazones (II or III, Scheme II). Although the monosulfides (IV) could not be isolated, this intermediate stage was confirmed previously in analogous reactions (14–17).

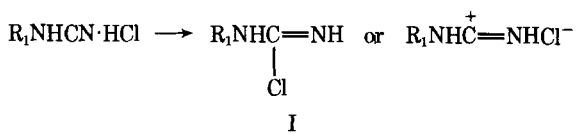

Scheme I

Precursors (I) were obtained by the desulfurization of related thioureas by lead hydroxide and conversion to related hydrochlorides (18). The synthesized thiosemicarbazones (Tables I and II) are white crystalline compounds soluble in polar solvents. Since these compounds could not be crystallized without decomposition, purification was achieved by repeated washings with several solvents. It was hoped that these potential antituberculous agents would have low toxicity to normal cells and have a good chemotherapeutic index[1].

EXPERIMENTAL[2]

Phenylcyanamide (18)—A mixture of phenylthiourea (15.2 g, 0.1 mole) dissolved in sodium hydroxide (3 g in 200 ml of water) and freshly prepared lead hydroxide (24.12 g, 0.1 mole) was heated on a water bath for 4 hr. It then was cooled and filtered, and the filtrate was acidified with acetic acid. The fluffy precipitate of phenylcyanamide was dissolved in ether and dried by adding anhydrous sodium sulfate. The hydrochloride of phenylcyanamide was prepared by passing dry hydrogen chloride gas through the ethereal solution.

By adopting a similar procedure, the following cyanamides were prepared: 2-methylphenyl, 3-methylphenyl, 4-methylphenyl, 2-methoxyphenyl, 4-methoxyphenyl, 4-ethoxyphenyl, 2-chlorophenyl, 3-chlorophenyl, 4-chlorophenyl, 4-bromophenyl, 2,5-dimethylphenyl, and 1-naphthyl.

Acetophenone Thiosemicarbazone (II) (12, 13)—Acetophenone (12.0 g, 0.1 mole) was dissolved in ethanol (50%, 100 ml) and acetic acid (2.0 ml), and thiosemicarbazide (9.10 g, 0.1 mole) was added. The solution was warmed with occasional swirling until the thiosemicarbazide dissolved, and then the solution was refluxed for 1 hr. After cooling, crys-

[1] These compounds have been submitted for testing, and the results will be reported elsewhere.

[2] Melting points were determined with a Kofler hot-stage apparatus and are uncorrected.

associated with reductions in pulse pressures and rises in portal venous pressures. These changes appeared to exhibit rapid and complete tachyphylaxis. The lack of apparent changes in the morphology of the lead II ECG indicates that the effects of the agent did not produce arrhythmias or ectopic foci of excitation. A determination of whether minor local changes in excitation occurred secondary to such effects as regional changes in myocardial circulation cannot be inferred from these limited data.

Experiments with lower dosages or apparently ineffective 1.0-mg/kg iv and 50-mg/kg intragastric dosages indicated that the individual components of the retch response (increased frequency of respiration, gastric mucus secretion, antral contractions, and corporal-fundal atonia) were invariably present but of such small intensity that the composite response was decidedly less than that constituting frank retching.

A similar set of sequelae is also present in humans who report feelings of nausea but who do not visibly retch. It is impossible to make this judgment with dogs, particularly anesthetized dogs. But these observations furnish an adequate physiological basis to suspect that the gastric or intravenous administration of dosages that are insufficient to produce frank retching might be accompanied by sensations of nausea.

It is concluded that the high molecular weight, branched polyethyleneimine, whether administered to dogs by gastric intubation or intravenously, produces an emetic response similar to ipecac in that it can act reflexly or by direct stimulation of the chemoreceptor trigger zone.

REFERENCES

(1) A. Raina and J. Jänne, *Med. Biol.*, **53**, 121 (1975).

(2) S. Melamed, G. R. Carlson, J. N. Moss, E. J. Belair, and M. F. Tansy, *J. Pharm. Sci.*, **66**, 899 (1977).

(3) S. Lepkovsky, M. K. Dimick, F. Furuta, S. E. Feldman, and R. Park, *J. Nutr.*, **105**, 1491 (1975).

(4) M. F. Tansy, R. C. Mackowiak, and M. H. F. Friedman, *Surg. Gynecol. Obstet.*, **127**, 259 (1968).

(5) H. L. Borison and S. C. Wang, *Pharmacol. Rev.*, **5**, 193 (1953).

(6) J. Zabara, R. B. Chaffee, Jr., and M. F. Tansy, *Space Life Sci.*, **3**, 282 (1972).

(7) J. E. Weaver and J. F. Griffith, *Toxicol. Appl. Pharmacol.*, **14**, 214 (1969).

ACKNOWLEDGMENTS AND ADDRESSES

Received September 29, 1975, from the *Department of Physiology and Biophysics, Health Sciences Center, Temple University, Philadelphia, PA 19140, and the ‡Research Laboratories, Rohm and Haas Co., Spring House, PA 19477.

Accepted for publication June 23, 1976.

The authors are indebted to Mr. Harold Perrong and Mr. Wendell Landin for technical assistance.

ˣ To whom inquiries should be directed.

New Compounds: Potential Antituberculous Agents I: Alkylaryl 4-Arylformamidinothiosemicarbazones

P. K. SRIVASTAVA ˣ and J. S. UPADHYAYA

Abstract □ A series of alkylaryl 4-arylformamidinothiosemicarbazones was synthesized for evaluation as antituberculous agents. The synthesis was effected by the condensation of different arylcyanamides with various thiosemicarbazones. The required intermediates also are described.

Keyphrases □ Thiosemicarbazones, various—synthesized for evaluation as antituberculous agents □ Antituberculous agents, potential—various thiosemicarbazones synthesized

Interest in the synthesis and biological evaluation of thiosemicarbazone derivatives was renewed by the fact that tibione (*p*-acetylaminobenzaldehyde thiosemicarbazone) (1–3) possesses antituberculous activity. Many reports (4–13) discussed the change of activity due to variations in the structure of the parent compound.

DISCUSSION

The present report deals with the synthesis of acetophenone 4-arylformamidinothiosemicarbazones (V*a*–V*m*, Table I) and 1-acetonaphthone 4-arylformamidinothiosemicarbazones (VI*a*–VI*m*, Table II) by the condensation of corresponding arylcyanamide hydrochlorides (I, Scheme I) with the appropriate thiosemicarbazones (II or III, Scheme II). Although the monosulfides (IV) could not be isolated, this intermediate stage was confirmed previously in analogous reactions (14–17).

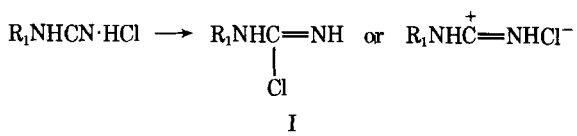

Scheme I

Precursors (I) were obtained by the desulfurization of related thioureas by lead hydroxide and conversion to related hydrochlorides (18). The synthesized thiosemicarbazones (Tables I and II) are white crystalline compounds soluble in polar solvents. Since these compounds could not be crystallized without decomposition, purification was achieved by repeated washings with several solvents. It was hoped that these potential antituberculous agents would have low toxicity to normal cells and have a good chemotherapeutic index[1].

EXPERIMENTAL[2]

Phenylcyanamide (18)—A mixture of phenylthiourea (15.2 g, 0.1 mole) dissolved in sodium hydroxide (3 g in 200 ml of water) and freshly prepared lead hydroxide (24.12 g, 0.1 mole) was heated on a water bath for 4 hr. It then was cooled and filtered, and the filtrate was acidified with acetic acid. The fluffy precipitate of phenylcyanamide was dissolved in ether and dried by adding anhydrous sodium sulfate. The hydrochloride of phenylcyanamide was prepared by passing dry hydrogen chloride gas through the ethereal solution.

By adopting a similar procedure, the following cyanamides were prepared: 2-methylphenyl, 3-methylphenyl, 4-methylphenyl, 2-methoxyphenyl, 4-methoxyphenyl, 4-ethoxyphenyl, 2-chlorophenyl, 3-chlorophenyl, 4-chlorophenyl, 4-bromophenyl, 2,5-dimethylphenyl, and 1-naphthyl.

Acetophenone Thiosemicarbazone (II) (12, 13)—Acetophenone (12.0 g, 0.1 mole) was dissolved in ethanol (50%, 100 ml) and acetic acid (2.0 ml), and thiosemicarbazide (9.10 g, 0.1 mole) was added. The solution was warmed with occasional swirling until the thiosemicarbazide dissolved, and then the solution was refluxed for 1 hr. After cooling, crys-

[1] These compounds have been submitted for testing, and the results will be reported elsewhere.

[2] Melting points were determined with a Kofler hot-stage apparatus and are uncorrected.

Table I—Physical Constants of Acetophenone 4-Arylformamidinothiosemicarbazone Hydrochlorides

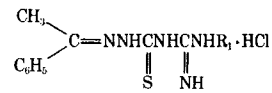

Compound	R_1	Yield, %	Melting Point	Molecular Formula	Analysis, %	
					Calc.	Found
V*a*	C_6H_5	75	208–209°	$C_{16}H_{18}ClN_5S$	C 55.25	55.08
					H 5.18	5.06
					N 20.14	20.06
					S 9.20	9.15
V*b*	2-$CH_3C_6H_4$	78	210–212°	$C_{17}H_{20}ClN_5S$	C 56.43	56.38
					H 5.53	5.51
					N 19.36	19.27
					S 8.85	8.81
V*c*	3-$CH_3C_6H_4$	65	157–158°	$C_{17}H_{20}ClN_5S$	C 56.43	56.37
					H 5.53	5.48
					N 19.36	19.27
					S 8.85	8.78
V*d*	4-$CH_3C_6H_4$	70	207–208°	$C_{17}H_{20}ClN_5S$	C 56.43	56.40
					H 5.53	5.50
					N 19.36	19.24
					S 8.85	8.77
V*e*	2-$CH_3OC_6H_4$	68	200–201°	$C_{17}H_{20}ClN_5OS$	C 54.04	53.88
					H 5.29	5.18
					N 18.54	18.46
					S 8.47	8.42
V*f*	4-$CH_3OC_6H_4$	60	160–162°	$C_{17}H_{20}ClN_5OS$	C 54.04	53.96
					H 5.29	5.24
					N 18.54	18.47
					S 8.47	8.39
V*g*	4-$C_2H_5OC_6H_4$	72	187–188°	$C_{18}H_{22}ClN_5OS$	C 55.17	55.10
					H 5.61	5.54
					N 17.88	17.81
					S 8.17	8.11
V*h*	2-ClC_6H_4	70	145–146°	$C_{16}H_{17}Cl_2N_5S$	C 50.26	50.18
					H 4.45	4.40
					N 18.32	18.28
					S 8.37	8.33
V*i*	3-ClC_6H_4	66	132–133°	$C_{16}H_{17}Cl_2N_5S$	C 50.26	50.20
					H 4.45	4.42
					N 18.32	18.25
					S 8.37	8.31
V*j*	4-ClC_6H_4	74	151–152°	$C_{16}H_{17}Cl_2N_5S$	C 50.26	50.22
					H 4.45	4.39
					N 18.32	18.27
					S 8.37	8.32
V*k*	4-BrC_6H_4	65	171–172°	$C_{16}H_{17}BrClN_5S$	C 45.01	44.78
					H 3.98	3.86
					N 16.41	16.34
					S 7.50	7.46
V*l*	2,5-$(CH_3)_2C_6H_3$	68	209–210°	$C_{18}H_{22}ClN_5S$	C 57.52	57.47
					H 5.85	5.78
					N 18.64	18.60
					S 8.52	8.49
V*m*	1-$C_{10}H_7$	72	203–204°	$C_{20}H_{20}ClN_5S$	C 60.37	60.22
					H 5.03	4.98
					N 17.61	17.29
					S 8.08	8.01

talline II was collected and recrystallized from 50% ethanol as white needles, 18.9 g (90%), mp 116–117° [lit. (19) mp 118–119°].

1-Acetonaphthone thiosemicarbazone (III) was prepared similarly.

Acetophenone 4-Phenylformamidinothiosemicarbazone Hydrochloride (V*a*)—Compound II (3.0 g, 0.015 mole) was dissolved in acetone (20.0 ml), and the solution was cooled in a freezing mixture. To this cooled solution, phenylcyanamide hydrochloride (2.4 g, 0.015 mole) dissolved in acetone (10.0 ml) was gradually added with constant shaking. After this solution was in the freezing mixture for 1 hr, crystalline pure V*a* was separated, filtered, and washed with acetone and petroleum ether to remove any unreacted material, 4.15 g (18%), mp 208–209°.

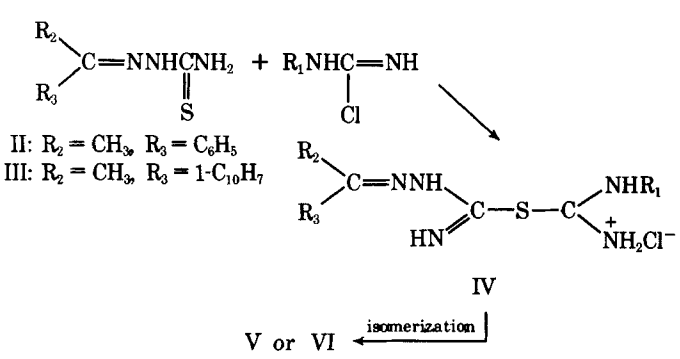

Scheme II

Anal.—Calc. for $C_{16}H_{18}ClN_5S$: C, 55.25; H, 5.18; N, 20.14; S, 9.20. Found: C, 55.08; H, 5.06; N, 20.06; S, 9.15.

Compounds V*b*–V*m* (Table I) were prepared by condensing II with the appropriate I.

With a similar procedure, VI*a*–VI*m* (Table II) were obtained.

These thiosemicarbazone hydrochlorides were characterized by elemental analyses and the presence of characteristic bands at 1520 (N=C=S), 1625 (C=N), and 3400 (NH) cm^{-1} and a substituted benzene ring (760 cm^{-1}) in their IR spectra.

REFERENCES

(1) G. Domagk, R. Behnisch, F. Mietzsch, and H. Schmidt, *Naturwissenschaften*, **33**, 315 (1946).

(2) R. Behnisch, F. Mietzsch, and H. Schmidt, *Angew. Chem.*, **60**, 113 (1948).

Table II—Physical Constants of 1-Acetonaphthone 4-Arylformamidinothiosemicarbazone Hydrochlorides

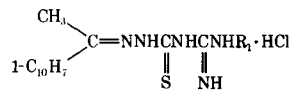

Compound	R_1	Yield, %	Melting Point	Molecular Formula	Analysis, %	
					Calc.	Found
VI*a*	C_6H_5	67	197–198°	$C_{20}H_{20}ClN_5S$	C 60.37	60.22
					H 5.03	4.98
					N 17.61	17.29
					S 8.05	8.00
VI*b*	2-$CH_3C_6H_4$	65	200–201°	$C_{21}H_{22}ClN_5S$	C 61.23	61.12
					H 5.34	5.28
					N 17.01	16.92
					S 7.77	7.68
VI*c*	3-$CH_3C_6H_4$	60	148–149°	$C_{21}H_{22}ClN_5S$	C 61.23	61.14
					H 5.34	5.30
					N 17.01	16.96
					S 7.77	7.70
VI*d*	4-$CH_3C_6H_4$	75	208–210°	$C_{21}H_{22}ClN_5S$	C 61.23	61.19
					H 5.34	5.27
					N 17.01	16.99
					S 7.77	7.66
VI*e*	2-$CH_3OC_6H_4$	65	195–196°	$C_{21}H_{22}ClN_5OS$	C 58.94	58.82
					H 5.14	5.08
					N 16.37	16.22
					S 7.48	7.42
VI*f*	4-$CH_3OC_6H_4$	70	203–204°	$C_{21}H_{22}ClN_5OS$	C 58.94	58.84
					H 5.14	5.12
					N 16.37	16.24
					S 7.48	7.40
VI*g*	4-$C_2H_5OC_6H_4$	60	155–156°	$C_{22}H_{24}ClN_5OS$	C 59.79	59.68
					H 5.43	5.39
					N 15.85	15.78
					S 7.24	7.16
VI*h*	2-ClC_6H_4	72	146–147°	$C_{20}H_{19}Cl_2N_5S$	C 55.55	55.48
					H 4.39	4.28
					N 16.20	16.12
					S 7.40	7.22
VI*i*	3-ClC_6H_4	64	141–142°	$C_{20}H_{19}Cl_2N_5S$	C 55.55	55.47
					H 4.39	4.32
					N 16.20	16.14
					S 7.40	7.32
VI*j*	4-ClC_6H_4	72	152–153°	$C_{20}H_{19}Cl_2N_5S$	C 55.55	55.50
					H 4.39	4.27
					N 16.20	16.18
					S 7.40	7.34
VI*k*	4-BrC_6H_4	62	167–168°	$C_{20}H_{19}BrClN_5S$	C 50.36	50.24
					H 3.98	3.82
					N 14.69	14.62
					S 6.71	6.65
VI*l*	2,5-$(CH_3)_2C_6H_3$	64	206–207°	$C_{22}H_{24}ClN_5S$	C 62.04	61.98
					H 5.64	5.59
					N 16.45	16.40
					S 7.52	7.48
VI*m*	1-$C_{10}H_7$	69	202–204°	$C_{24}H_{22}ClN_5S$	C 64.35	64.22
					H 4.91	4.80
					N 15.64	15.49
					S 7.15	7.02

(3) R. Behnisch, F. Mietzsch, and H. Schmidt, *Am. Rev. Tuberc.*, **61**, 1 (1950).

(4) E. Hoggarth, A. R. Martin, N. E. Storey, and F. H. P. Young, *Br. J. Pharmacol.*, **4**, 248 (1949).

(5) W. B. Stillmann and A. B. Scott, U.S. pat. 2,416,239 (Feb. 18, 1947).

(6) J. Bernstein, H. L. Yale, K. Losee, M. Holsing, J. Martius, and W. A. Lott, *J. Am. Chem. Soc.*, **73**, 906 (1951).

(7) C. J. Duca, M. V. Rothlauf, and J. V. Scudi, *Antibiot. Chemother.*, **2**, 16 (1952).

(8) R. Donovick, F. Pansy, G. Stryker, and J. Bernstein, *J. Bacteriol.*, **59**, 667 (1950).

(9) D. Hamre, J. Bernstein, and R. Donovick, *Proc. Soc. Exp. Biol. Med.*, **73**, 275 (1950).

(10) K. A. Brownlee and D. Hamre, *J. Bacteriol.*, **61**, 127 (1951).

(11) R. L. Thompson, M. L. Price, and S. A. Minton, Jr., *Proc. Soc. Exp. Biol. Med.*, **78**, 11 (1951).

(12) E. Campaigne, P. A. Monroe, B. Arnwine, and W. L. Archer, *J. Am. Chem. Soc.*, **75**, 988 (1953).

(13) F. E. Anderson, C. J. Duca, and J. V. Scudi, *ibid.*, **73**, 4967 (1951).

(14) P. K. Srivastava and M. Saleem, *Tetrahedron Lett.*, **23**, 2725 (1968).

(15) S. N. Pandeya, *Indian. J. Chem.*, **1**, 525 (1963).

(16) P. K. Srivastava, *J. Indian Chem. Soc.*, **2**, 154 (1963).

(17) P. K. Srivastava and Y. R. Rao, *ibid.*, **40**, 803 (1963).

(18) R. M. Sahasrabudhey and H. Krall, *ibid.*, **19**, 345 (1942).

(19) "Dictionary of Organic Compounds," vol. I, Eyre and Spottiswood, London, England, 1965, p. 13.

ACKNOWLEDGMENTS AND ADDRESSES

Received June 8, 1975, from the *Surgical Research Laboratory, Institute of Medical Sciences, Banaras Hindu University, Varanasi-221005, India.*

Accepted for publication June 30, 1976.

The authors are grateful to Prof. K. N. Udupa, Institute of Medical Sciences, Banaras Hindu University, and Prof. W. U. Malik, Department of Chemistry, Roorkee University, Roorkee, India, for providing necessary facilities and to C.S.I.R., New Delhi (India), for a Junior Research Fellowship (held by J. S. Upadhyaya).

[x] To whom inquiries should be directed.

Perfluorooctyl Bromide: A Potential Antiobesity Compound

Keyphrases □ Perfluorooctyl bromide—coated on GI tract, effect on food absorption and weight gain, rats □ Absorption, food—effect of perfluorooctyl bromide coated on GI tract, rats □ GI absorption—effect of coating with perfluorooctyl bromide, rats □ Antiobesity agents, potential—perfluorooctyl bromide, coated on GI tract, effect on food absorption and weight gain, rats

To the Editor:

Perfluorooctyl bromide (I) is a chemically and biologically inert, high molecular weight fluorocarbon used as a radiopaque contrast medium (1, 2). Although this compound is immiscible with water, its low surface tension renders it easily spreadable over mucous membranes. This property led to our investigation of its possible use in retarding food absorption and, therefore, as an agent for the treatment of obesity.

The radiopaque nature of I allowed direct observation of its transit through the GI tract using whole body X-ray imaging (Fig. 1). After administration of 2 ml of I[1] *via* an oral intubation needle to a rat weighing about 450 g, an instantaneous coating of the stomach was obtained. It took about 1.5 hr to clear the GI tract of the fluorocarbon, which uniformly coated the walls of the stomach and intestine. Since I serves as a poor solvent for most chemical structures (3), the coating of the stomach and intestines forms a temporary barrier to the absorption of ingested food.

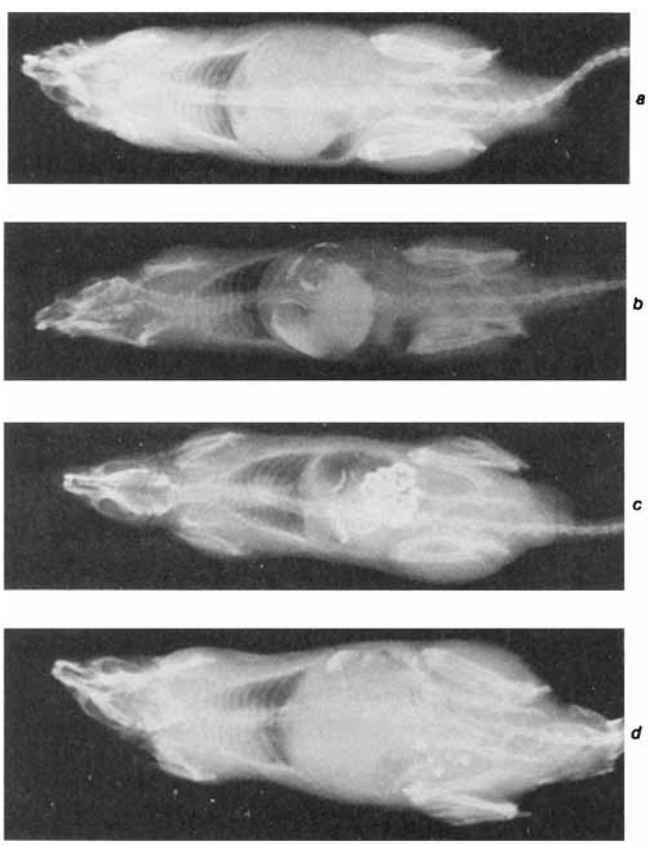

Figure 1—*Whole body X-ray images of rat before* (a) *and 7* (b), *30* (c), *and 75* (d) *min following administration of 2 ml of I.*

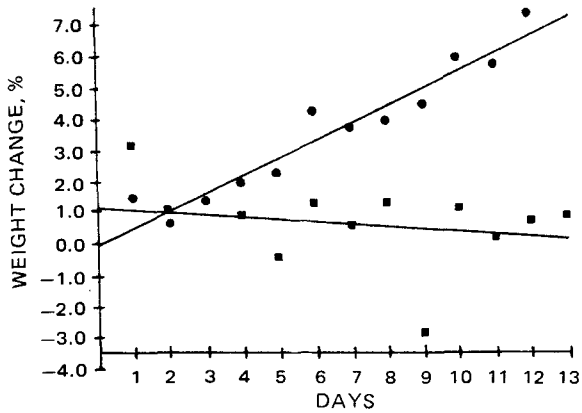

Figure 2—*Comparison of rate of growth of rats given I* (■) *and water* (●) *during their feeding cycle* (n = *19*).

To test this hypothesis, Sprague–Dawley male rats, 400–500 g, were conditioned for 2 weeks by allowing food[2] for only 3 hr/day and water for 14 hr/day, commencing with the food intake cycle. All rats were weighed before the feeding cycle. A crossover study was performed where the test group was given 1 ml of I at 1.5 and 2.0 hr of their 3-hr food intake cycle. The control group was given water instead, and the study was continued for 14 days. The control group showed a net increase in weight whereas the treated group showed a slight decrease (Fig. 2). The weight gain difference between the groups was statistically significant at the 95% confidence level, proving the definite effect of I on food absorption in rats.

The schedule of I administration was chosen to allow at least 1 hr for the coating of the stomach and almost 2 hr of residence time in the GI tract. Variations in this schedule may result in greater or lesser effects of the fluorocarbon on food absorption, and studies in this area are in progress.

The suitability of I for reducing food absorption is due to its complete inertness, lack of absorption from the GI tract, and physical properties that allow its uniform distribution throughout the GI tract. Also, the small quantity of fluorocarbon administered does not result in any apparent change in the bowel movement (diarrhea).

At present, we are designing dosage forms of I that can be tested in humans, and these findings will be reported soon.

(1) D. M. Long and M. S. Liu, *Radiology*, **10S**, 323 (1972).
(2) C. L. Clark, F. Becatlini, and S. Kaplan, *Triangle*, **2**, 115 (1972).
(3) D. M. Long, M. S. Liu, D. Dobben, P. S. Szanto, and A. S. Arambulo, in "Biochemistry Involving Carbon–Fluorine Bonds," R. Filler, Ed., American Chemical Society, Washington, D.C., 1976, pp. 171–189.

[1] Supplied by 3M Co., St. Paul, Minn.

[2] Purina rat chow.

M. Hussain
S. Niazi [x]
A. Arambulo
Department of Pharmacy
College of Pharmacy
University of Illinois at the
Medical Center
Chicago, IL 60612

D. M. Long
Department of Radiology
University of California
San Diego, Calif.

Received March 28, 1977.
Accepted for publication April 19, 1977.
[x] To whom inquiries should be directed.

Cudranone: A Novel Benzophenone Derivative from *Cudrania chochinchinensis* var. *gerontogea*

Keyphrases □ Cudranone—isolated and identified from stems and roots of *Cudrania chochinchinensis*, antimicrobial activity evaluated □ Benzophenone derivative—cudranone isolated and identified from stems and roots of *Cudrania chochinchinensis*, antimicrobial activity evaluated □ Antimicrobial agents, potential—cudranone, isolated and identified from stems and roots of *Cudrania chochinchinensis*

To the Editor:

In a largescale program for screening higher plants for antimicrobial activity, an ethanolic extract of the stems and roots of the Chinese plant[1] *Cudrania chochinchinensis* (Lour.) Kudo & Masam. var. *gerontogea* (Sieb. & Zucc.) Kudo & Masam. (Moraceae) exhibited strong activity against a wide range of microorganisms. Partitioning the alcohol extract between water and chloroform concentrated the antimicrobial activity in the chloroform phase. This fraction was then chromatographed over silica gel, using increasing amounts of ether (4–40%) in benzene as the solvent system. Several known crystalline compounds[2] were isolated from the column fractions.

The 4% ether in benzene fraction yielded, upon crystallization from *n*-hexane–ethyl acetate, a novel crystalline substance which was named cudranone (I). This new compound occurred in the form of bright-yellow needles, mp 172–173°, and had a molecular formula of $C_{19}H_{20}O_5$, as supported by elemental analysis and high-resolution mass spectral data.

The 60-MHz ^{1}H-NMR spectrum (taken in acetone-d_6 with tetramethylsilane as the internal standard) provided information on most functional groups of this compound. It revealed the presence of a β,β-dimethylallyl group (two vinylic three-proton singlets at δ 1.53 and 1.50; a broad one-proton triplet at δ 5.23, J = 8 Hz; and a two-proton doublet at δ 3.37, J = 8 Hz). It also exhibited a methoxy singlet at δ 3.83 and three exchangeable phenolic protons as a broad signal at δ 10.17. The aromatic region of the

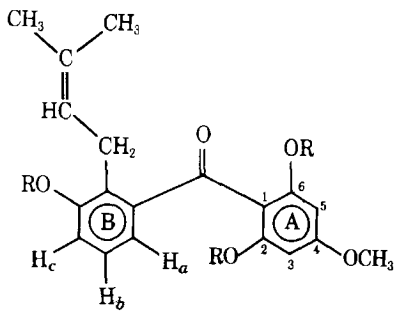

I: R = H
II: R = CH_3
III: R = CCH_3 (=O)

NMR spectrum showed a two-proton singlet at δ 6.00 and a three-proton group of signals forming a complex *ABC* system centered at δ 6.91. The IR spectrum confirmed the phenolic nature of the compound and showed a carbonyl absorption band at λ_{max} (potassium bromide) 6.06 μm, assigned to a hydrogen-bonded ketonic carbonyl function. Thus, by assuming that the compound had two aromatic rings, it was concluded that it must have a benzophenone skeleton rather than a xanthone skeleton like some reported constituents of the *Cudrania* species (1, 2).

The nature of ring A was revealed when the compound gave, in low yields, phloroglucinol monomethyl ether[3] by heating with solid potassium hydroxide at 245–250°. This finding indicated that the rest of the benzophenone moiety must be substituting ring A at C-1 rather than at C-3 or C-5 to account for the equivalency of the two aromatic protons of ring A appearing in the NMR spectrum as a sharp singlet at δ 6.00. This finding also indicated that the β,β-dimethylallyl group and the remaining hydroxyl group should be substituting ring B.

Compound I yielded the trimethyl ether (II) as white needles, mp 126–127°, by treatment with dimethyl sulfate and aqueous sodium hydroxide. The NMR spectrum of II taken in deuterochloroform still showed the complex *ABC* three-proton system in the aromatic region. However, this system was simplified and showed first-order splitting when benzene-d_6 (100%) was used as the solvent. It showed a one-proton doublet[4] at δ 7.23, J = 8 Hz; a one-proton triplet at δ 6.80, J = 8 Hz; and another one-proton doublet[4]

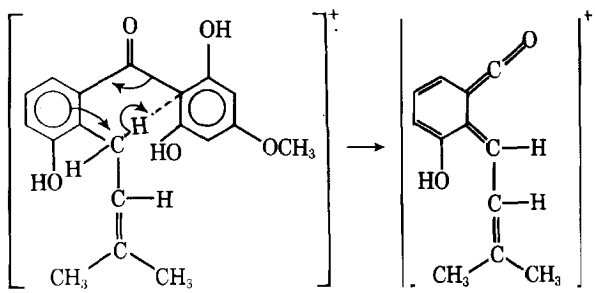

m/e 328 (10%) IV *m/e* 188 (100%)

Scheme I

[1] The plant material was collected in Chia-Yi, Taiwan, in 1974. Its identity was confirmed by Dr. Ping C. Cheng, Taipei Medical College. A voucher specimen is deposited in the herbarium of the Department of Pharmacognosy, School of Pharmacy, University of Mississippi.
[2] To be reported later.
[3] Characterized by direct comparison with an authentic sample (superimposable IR, NMR, and mass spectra and identical R_f values on TLC and retention times on GLC).
[4] The doublets due to H_a and H_c were slightly split (J = 2 Hz) due to *meta*-coupling to each other.

M. Hussain
S. Niazi [x]
A. Arambulo
Department of Pharmacy
College of Pharmacy
University of Illinois at the
Medical Center
Chicago, IL 60612

D. M. Long
Department of Radiology
University of California
San Diego, Calif.

Received March 28, 1977.
Accepted for publication April 19, 1977.
[x] To whom inquiries should be directed.

Cudranone: A Novel Benzophenone Derivative from *Cudrania chochinchinensis* var. *gerontogea*

Keyphrases □ Cudranone—isolated and identified from stems and roots of *Cudrania chochinchinensis*, antimicrobial activity evaluated □ Benzophenone derivative—cudranone isolated and identified from stems and roots of *Cudrania chochinchinensis*, antimicrobial activity evaluated □ Antimicrobial agents, potential—cudranone, isolated and identified from stems and roots of *Cudrania chochinchinensis*

To the Editor:

In a largescale program for screening higher plants for antimicrobial activity, an ethanolic extract of the stems and roots of the Chinese plant[1] *Cudrania chochinchinensis* (Lour.) Kudo & Masam. var. *gerontogea* (Sieb. & Zucc.) Kudo & Masam. (Moraceae) exhibited strong activity against a wide range of microorganisms. Partitioning the alcohol extract between water and chloroform concentrated the antimicrobial activity in the chloroform phase. This fraction was then chromatographed over silica gel, using increasing amounts of ether (4–40%) in benzene as the solvent system. Several known crystalline compounds[2] were isolated from the column fractions.

The 4% ether in benzene fraction yielded, upon crystallization from *n*-hexane–ethyl acetate, a novel crystalline substance which was named cudranone (I). This new compound occurred in the form of bright-yellow needles, mp 172–173°, and had a molecular formula of $C_{19}H_{20}O_5$, as supported by elemental analysis and high-resolution mass spectral data.

The 60-MHz ^{1}H-NMR spectrum (taken in acetone-d_6 with tetramethylsilane as the internal standard) provided information on most functional groups of this compound. It revealed the presence of a β,β-dimethylallyl group (two vinylic three-proton singlets at δ 1.53 and 1.50; a broad one-proton triplet at δ 5.23, J = 8 Hz; and a two-proton doublet at δ 3.37, J = 8 Hz). It also exhibited a methoxy singlet at δ 3.83 and three exchangeable phenolic protons as a broad signal at δ 10.17. The aromatic region of the

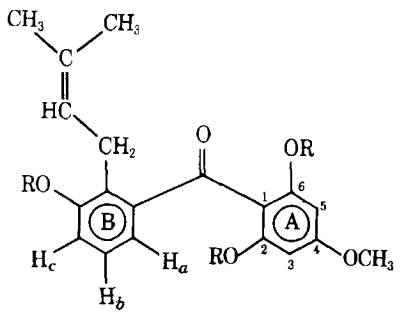

I: R = H
II: R = CH_3
III: R = CCH_3 (=O)

NMR spectrum showed a two-proton singlet at δ 6.00 and a three-proton group of signals forming a complex *ABC* system centered at δ 6.91. The IR spectrum confirmed the phenolic nature of the compound and showed a carbonyl absorption band at λ_{max} (potassium bromide) 6.06 μm, assigned to a hydrogen-bonded ketonic carbonyl function. Thus, by assuming that the compound had two aromatic rings, it was concluded that it must have a benzophenone skeleton rather than a xanthone skeleton like some reported constituents of the *Cudrania* species (1, 2).

The nature of ring A was revealed when the compound gave, in low yields, phloroglucinol monomethyl ether[3] by heating with solid potassium hydroxide at 245–250°. This finding indicated that the rest of the benzophenone moiety must be substituting ring A at C-1 rather than at C-3 or C-5 to account for the equivalency of the two aromatic protons of ring A appearing in the NMR spectrum as a sharp singlet at δ 6.00. This finding also indicated that the β,β-dimethylallyl group and the remaining hydroxyl group should be substituting ring B.

Compound I yielded the trimethyl ether (II) as white needles, mp 126–127°, by treatment with dimethyl sulfate and aqueous sodium hydroxide. The NMR spectrum of II taken in deuterochloroform still showed the complex *ABC* three-proton system in the aromatic region. However, this system was simplified and showed first-order splitting when benzene-d_6 (100%) was used as the solvent. It showed a one-proton doublet[4] at δ 7.23, J = 8 Hz; a one-proton triplet at δ 6.80, J = 8 Hz; and another one-proton doublet[4]

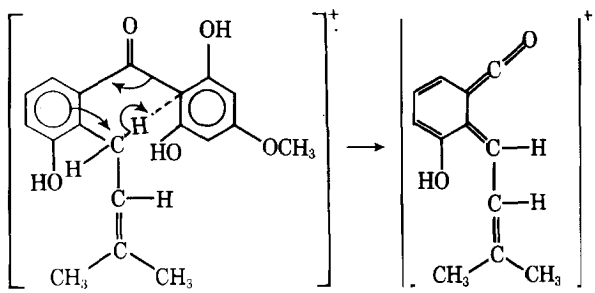

m/e 328 (10%) IV *m/e* 188 (100%)

Scheme I

[1] The plant material was collected in Chia-Yi, Taiwan, in 1974. Its identity was confirmed by Dr. Ping C. Cheng, Taipei Medical College. A voucher specimen is deposited in the herbarium of the Department of Pharmacognosy, School of Pharmacy, University of Mississippi.
[2] To be reported later.
[3] Characterized by direct comparison with an authentic sample (superimposable IR, NMR, and mass spectra and identical R_f values on TLC and retention times on GLC).
[4] The doublets due to H_a and H_c were slightly split (J = 2 Hz) due to *meta*-coupling to each other.

at δ 6.42, J = 8 Hz. This pattern indicated that the three remaining aromatic protons in I must be located on three successive carbon atoms in ring B with the one most downfield (H_a) *ortho* to the ketone group, the one most upfield (H_c) *ortho* to the phenolic hydroxyl group, and the one in between (H_b) on the middle of these three carbons. This finding was further confirmed by the presence in the mass spectrum of the base peak IV, derived by acyl cleavage associated by hydrogen migration to ring A (3) (Scheme I). The highly conjugated nature of this fragment accounts for its abundance in the mass spectrum. The formation of fragment IV is favorable only if the β,β-dimethylallyl group is located *ortho* to the ketone group.

Although the evidence that I is the structure of cudranone was convincing, it was uncertain why the NMR signal of H_a was never as far downfield as expected for a proton *ortho* to a carbonyl group. This position was found not only for the H_a signal in I but also its trimethyl ether (II) and triacetate[5] (III) when taken in acetone-d_6 or deuterochloroform. A possible explanation for the shielding of H_a can be provided by assuming that I adopts a conformation that leads to the placing of H_a in the shielding zone of ring A. The assigned structure was confirmed by X-ray crystallographic analysis[6].

The structure of cudranone proves that biogenetic isoprenylation of xanthones does not take place after the cyclization of the corresponding benzophenones as suggested previously (4).

Cudranone exhibited significant activity against *Staphylococcus aureus* (MIC 25 μg/ml) and *Bacillus subtilis* (MIC 12.5 μg/ml) and even greater activity against *Mycobacterium smegmatis* (MIC 1.6 μg/ml)[7]. Further evaluation of antimicrobial activity of I is in progress.

(1) J. E. Knapp and P. L. Schiff, Jr., *J. Pharm. Sci.*, **60**, 1729 (1971).

(2) V. V. S. Murti, T. R. Seshadri, and S. Sivakuman, *Phytochemistry*, **11**, 2089 (1972).

(3) J. A. Ballantine and C. T. Pillinger, *Org. Mass Spectrom.*, **1**, 425 (1968).

(4) I. Carpenter, H. D. Locksley, and F. Scheinmann, *Phytochemistry*, **8**, 2013 (1969).

Bee-Lian Chang
Farouk S. El-Feraly
Norman J. Doorenbos [x]
Department of Pharmacognosy
School of Pharmacy
University of Mississippi
University, MS 38677

Received October 8, 1976.

Accepted for publication February 4, 1977.

Supported by the Research Institute of Pharmaceutical Sciences, School of Pharmacy, University of Mississippi.

Appreciation is expressed to Ms. Elaine Wallace for the antimicrobial data and to Dr. Stephen Billets for the mass spectral data.

[x] To whom inquiries should be directed.

[5] Prepared by treating cudranone with acetic anhydride in pyridine at room temperature overnight. It crystallized from methanol as prisms, mp 100–101°.

[6] The details will be published.

[7] The minimum inhibitory concentration against these microorganisms was determined by the serial dilution method using streptomycin as a positive control. The results were read after incubation at 37° for 24 hr.

BOOKS

REVIEWS

Marihuana: An Annotated Bibliography. By COY W. WALLER, JACQUELINE J. JOHNSON, JUDY BUELKE, and CARLTON E. TURNER. Macmillan, 866 Third Ave., New York, NY 10022, 1976. 560 pp. 18.5 × 25.5 cm. Price $13.95.

This handbook will be most appreciated by those interested in the world literature on any aspect of marihuana (*Cannabis* species), its constituents, pharmacology, metabolism, toxicology, chemistry, synthesis, botany, *etc.* Every conceivable type of citation is found, ranging from reviews and books to original research reports, notes, communications, letters to the editor, rebuttals, book reviews, patents, dissertations, UN documents, introductory remarks to symposia, and the like.

The compilation was assembled by the Waller–Turner group, who have been actively engaged in *Cannabis* research for several years at the Research Institute of Pharmaceutical Sciences, University of Mississippi, under sponsorship of the National Institute of Mental Health. Literature coverage is stated to be from the beginning of 1964 through 1974, and "3045 entries covering the international scientific publications" are included (all entries are definitely not "scientific"). In all cases, the full citation of each entry is given, *i.e.*, all author names, journal title, volume, issue number, full pagination (in most, but not all, cases), and year of publication. Foreign language titles are given with parenthetical English translations in some cases.

Articles are entered alphabetically by senior author name. Most citations are followed by a brief abstract prepared by the editors. Author and subject indexes are included, as well as a summary table, the Biological Actions of Marihuana in Various Animals. The structure, molecular formula, and molecular weight of each known "natural" cannabinoid are given. Also, all of the names and structures of the metabolities of Δ^9-tetrahydrocannabinol, Δ^8-tetrahydrocannabinol, cannabinol, and cannabidiol are given, with an indication of those that are "active," although the term "active" is undefined.

Although this useful handbook represents a monumental effort on the part of the Mississippi group and was apparently prepared without governmental support (no acknowledgment was found to this effect), a number of minor deficiencies, as judged by this reviewer, and errors should be pointed out so that the user may be forewarned.

There is no statement concerning where the citations were obtained and how systematic the literature coverage may have been. For example, were "Chemical Abstracts" and "Biological Abstracts" covered completely for the stated time period? Were the brief abstracts derived from abstracts or from reading the original papers or books? Since the entries covered range from citations of introductory remarks to *Cannabis* symposia through entries in "Encyclopedia Britannica," one must wonder where the literature coverage started and ceased. For example, the authoritative book by H. Wagner, "Rauschgift-Drogen" (Springer-Verlag, Berlin, Germany, 1969), most surely should have been included in the handbook.

A useful addition to each citation would have been either the mailing address of the senior author and/or the secondary source, since the articles in some obscure journals would have to be verified before obtaining an interlibrary loan of the journal.

To this reviewer, the subject index was difficult to use. For example, no major heading concerning Isolation of Constituents was found. A major heading "Trigonelline (isolation from *Cannabis*)" was found, but no major headings for "Friedelin," "Epifriedelanol," "Sitosterol," "Stigmasterol," "Campesterol," and most other noncannabinoids isolated from *Cannabis* were entered. The major subject heading "Biochemistry" lists

at δ 6.42, J = 8 Hz. This pattern indicated that the three remaining aromatic protons in I must be located on three successive carbon atoms in ring B with the one most downfield (H_a) *ortho* to the ketone group, the one most upfield (H_c) *ortho* to the phenolic hydroxyl group, and the one in between (H_b) on the middle of these three carbons. This finding was further confirmed by the presence in the mass spectrum of the base peak IV, derived by acyl cleavage associated by hydrogen migration to ring A (3) (Scheme I). The highly conjugated nature of this fragment accounts for its abundance in the mass spectrum. The formation of fragment IV is favorable only if the β,β-dimethylallyl group is located *ortho* to the ketone group.

Although the evidence that I is the structure of cudranone was convincing, it was uncertain why the NMR signal of H_a was never as far downfield as expected for a proton *ortho* to a carbonyl group. This position was found not only for the H_a signal in I but also its trimethyl ether (II) and triacetate[5] (III) when taken in acetone-d_6 or deuterochloroform. A possible explanation for the shielding of H_a can be provided by assuming that I adopts a conformation that leads to the placing of H_a in the shielding zone of ring A. The assigned structure was confirmed by X-ray crystallographic analysis[6].

The structure of cudranone proves that biogenetic isoprenylation of xanthones does not take place after the cyclization of the corresponding benzophenones as suggested previously (4).

Cudranone exhibited significant activity against *Staphylococcus aureus* (MIC 25 μg/ml) and *Bacillus subtilis* (MIC 12.5 μg/ml) and even greater activity against *Mycobacterium smegmatis* (MIC 1.6 μg/ml)[7]. Further evaluation of antimicrobial activity of I is in progress.

(1) J. E. Knapp and P. L. Schiff, Jr., *J. Pharm. Sci.*, **60**, 1729 (1971).

(2) V. V. S. Murti, T. R. Seshadri, and S. Sivakuman, *Phytochemistry*, **11**, 2089 (1972).

(3) J. A. Ballantine and C. T. Pillinger, *Org. Mass Spectrom.*, **1**, 425 (1968).

(4) I. Carpenter, H. D. Locksley, and F. Scheinmann, *Phytochemistry*, **8**, 2013 (1969).

Bee-Lian Chang
Farouk S. El-Feraly
Norman J. Doorenbos [x]
Department of Pharmacognosy
School of Pharmacy
University of Mississippi
University, MS 38677

Received October 8, 1976.

Accepted for publication February 4, 1977.

Supported by the Research Institute of Pharmaceutical Sciences, School of Pharmacy, University of Mississippi.

Appreciation is expressed to Ms. Elaine Wallace for the antimicrobial data and to Dr. Stephen Billets for the mass spectral data.

[x] To whom inquiries should be directed.

[5] Prepared by treating cudranone with acetic anhydride in pyridine at room temperature overnight. It crystallized from methanol as prisms, mp 100–101°.

[6] The details will be published.

[7] The minimum inhibitory concentration against these microorganisms was determined by the serial dilution method using streptomycin as a positive control. The results were read after incubation at 37° for 24 hr.

BOOKS

REVIEWS

Marihuana: An Annotated Bibliography. By COY W. WALLER, JACQUELINE J. JOHNSON, JUDY BUELKE, and CARLTON E. TURNER. Macmillan, 866 Third Ave., New York, NY 10022, 1976. 560 pp. 18.5 × 25.5 cm. Price $13.95.

This handbook will be most appreciated by those interested in the world literature on any aspect of marihuana (*Cannabis* species), its constituents, pharmacology, metabolism, toxicology, chemistry, synthesis, botany, *etc.* Every conceivable type of citation is found, ranging from reviews and books to original research reports, notes, communications, letters to the editor, rebuttals, book reviews, patents, dissertations, UN documents, introductory remarks to symposia, and the like.

The compilation was assembled by the Waller–Turner group, who have been actively engaged in *Cannabis* research for several years at the Research Institute of Pharmaceutical Sciences, University of Mississippi, under sponsorship of the National Institute of Mental Health. Literature coverage is stated to be from the beginning of 1964 through 1974, and "3045 entries covering the international scientific publications" are included (all entries are definitely not "scientific"). In all cases, the full citation of each entry is given, *i.e.*, all author names, journal title, volume, issue number, full pagination (in most, but not all, cases), and year of publication. Foreign language titles are given with parenthetical English translations in some cases.

Articles are entered alphabetically by senior author name. Most citations are followed by a brief abstract prepared by the editors. Author and subject indexes are included, as well as a summary table, the Biological Actions of Marihuana in Various Animals. The structure, molecular formula, and molecular weight of each known "natural" cannabinoid are given. Also, all of the names and structures of the metabolities of Δ^9-tetrahydrocannabinol, Δ^8-tetrahydrocannabinol, cannabinol, and cannabidiol are given, with an indication of those that are "active," although the term "active" is undefined.

Although this useful handbook represents a monumental effort on the part of the Mississippi group and was apparently prepared without governmental support (no acknowledgment was found to this effect), a number of minor deficiencies, as judged by this reviewer, and errors should be pointed out so that the user may be forewarned.

There is no statement concerning where the citations were obtained and how systematic the literature coverage may have been. For example, were "Chemical Abstracts" and "Biological Abstracts" covered completely for the stated time period? Were the brief abstracts derived from abstracts or from reading the original papers or books? Since the entries covered range from citations of introductory remarks to *Cannabis* symposia through entries in "Encyclopedia Britannica," one must wonder where the literature coverage started and ceased. For example, the authoritative book by H. Wagner, "Rauschgift-Drogen" (Springer-Verlag, Berlin, Germany, 1969), most surely should have been included in the handbook.

A useful addition to each citation would have been either the mailing address of the senior author and/or the secondary source, since the articles in some obscure journals would have to be verified before obtaining an interlibrary loan of the journal.

To this reviewer, the subject index was difficult to use. For example, no major heading concerning Isolation of Constituents was found. A major heading "Trigonelline (isolation from *Cannabis*)" was found, but no major headings for "Friedelin," "Epifriedelanol," "Sitosterol," "Stigmasterol," "Campesterol," and most other noncannabinoids isolated from *Cannabis* were entered. The major subject heading "Biochemistry" lists

under it "Edestin from hemp seed," "Edestinase from hemp seed," and "Quaternary bases in *Cannabis*" only. For the amount of biochemical studies published on the cannabinoids, the biochemists will be disturbed with this type of index coverage.

A large number of incorrect spellings of common and technical words are found in the abstracts. These errors are self-evident for the most part but confusing in cases such as, for example, citation 2914 where "Cannabidivarian" appears in the title of the article and "Cannabidivarin" in the abstract, the latter presumably correct. In a few cases, words and/or phrases are apparently missing in titles of articles or in the abstracts. These omissions are usually not too much of a problem as in citations 368, 431, 474, 740, 1290, 1321, 1679, 1905, 1927, 2058, 2480, 2493, 2708, 2722, and 2914. The journal citation in 301 is confusing, and citation 2212 does not refer to the journal cited.

When abstracts are given, there is a great degree of inconsistency regarding content. Also, the summary table on p. XXII hardly can be considered complete.

However, even though these minor problems were found, the book at a very reasonable price of $13.95 is a bargain. It will be an indispensable, and much used addition to the personal library of anyone having even a remote interest in *Cannabis*. It will be of special interest to researchers in the field of *Cannabis*, to students in the medical professions and social sciences, to the pharmaceutical industry, and to reporters in the media and should be available in every library.

Reviewed by Norman R. Farnsworth
Department of Pharmacognosy and Pharmacology
College of Pharmacy
University of Illinois at the Medical Center
Chicago, IL 60612

Essentials of Medicinal Chemistry. By ANDREJUS KOROLKOVAS and JOSEPH H. BURCKHALTER. Wiley, 605 Third Ave., New York, N Y 10016, 1976. 697 pp. 16 × 23.5 cm. Price $22.50.

The book is designed as an undergraduate text in medicinal chemistry as well as a resource work for the chemist and biologist interested in several aspects of drugs. The composition of the book is built around succinctly stated facts and theories, which the authors hope are presented in a palatable, yet useful, form for the student. The authors have in mind the role of the pharmacist as an information source helping the physician and patient.

The book is in eight parts and generally follows pharmacological or therapeutic categories. These are Introduction: Basics, Drug Development and Theories; CNS Drugs; Drugs Acting at the Peripheral Nervous System; Cardiovascular, Blood and Renal Systems; Chemotherapeutics; Vitamins; Hormones; and Miscellaneous Agents including Diagnostics. The appendix lists drugs in the USP and NF.

Each part consists of several chapters dealing with discrete topics. They are concisely written along the lines of precis or compendia. The highlights of drug structure and action, as well as side effects and dosage, are recorded. Structural formulas and tables are utilized to illustrate structure–activity relationships in some cases. Useful references are appended to each chapter and are divided into general background and specific citations by class of agents.

The book should prove useful as a compendium of information in medicinal chemistry. This book plus a text organized in depth over the same topics should provide the student with a good background in course work, for board exams, and for professional practice.

Reviewed by Lemont B. Kier
Massachusetts College of Pharmacy
Boston, MA 02115

Manual of Clinical Immunology. Edited by NOEL R. ROSE and HERMAN FRIEDMAN. American Society for Microbiology, 1913 I St. N.W., Washington, DC, 20006, 1976. 932 pp. 17.5 × 26 cm. Price $16.00, flexible binding; $20.00, cloth binding.

This much needed volume, written by 180 authorities in various aspects of the rapidly expanding field of immunology, presents the latest information. The book is directed mainly to laboratory directors and technologists but should prove extremely useful to graduate students, medical students, postdoctoral fellows, residents, and clinicians. The greatest value of this book is the presentation of methodologies, allowing a stepwise approach to various procedures currently used in both clinical and research immunology. Of particular importance is the discussion of the pros and cons of each procedure with emphasis on the pitfalls encountered. Suggestions as to sources of materials and equipment required for each test can save time when setting up a new method.

The arrangement of the book in sections covering different aspects of the components involved in immunological responses and the cross-referencing between chapters allow the investigator to understand not only his or her own area but also the influence of cellular *versus* humoral aspects of immunology. Of particular importance are the chapters covering delayed hypersensitivity, lymphocyte subpopulations, and lymphocyte transformation.

The principles of radioimmunoassay are well presented, and the methods for determining various hormones in body fluids have general applicability not only in the clinic but also in the research laboratory.

Coverage of the immunological aspects of bacterial, mycotic, parasitic, viral, rickettsial, and chlamydial diseases will assist the clinician in more accurate diagnosis. The disadvantages of immunofluorescence and radioimmunoassays in immunodiagnosis of viral diseases are discussed, and suggestions for the use of microplate enzyme methods are given. The main advantages of the latter are a long shelflife, cheap simple equipment, and the same degree of sensitivity as the other procedures.

In the immunohematology section, the chapters on autoimmune and drug immune hemolytic anemia and the immunology of clotting factors point out the importance of modern immulogical methods in the diagnosis of often fatal diseases. Allergic disease testing is well covered, but the importance of testing for drug hypersensitivity is not adequate, being confined almost entirely to penicillin. The subject of autoimmune diseases receives full treatment, including tests for antibodies to tissue-specific antigens. The section on tumor immunology covers the present state of the art and indicates the necessity for further research to improve early tumor diagnosis. The section on transplantation immunology presents the immunological aspects of tissue transplantation, particularly the rejection phenomenon. The last section is of importance to clinical laboratories because it covers legal requirements, quality control, standardization of materials and methods, and proficiency testing of laboratory personnel.

This volume should be available to clinical and research workers in immunology and, because the field is expanding so rapidly, it should be updated more often than most such manuals.

Reviewed by Thomas J. Haley
National Center for Toxicological Research
Jefferson, AK 72079

Aliphatic Chemistry. Vol. 4. A Specialist Periodical Report. Edited by A. McKILLOP *et al.* The Chemical Society, Burlington House, London, W1V 0BN, England, 1976. 281 pp. 14 × 22.5 cm. Price $49.50.

The fourth volume of the Specialist Periodical Reports on aliphatic chemistry is comprised of four chapters which summarize developments reported during 1974 in each of the chosen areas. Chapter 1, on the chemistry of acetylenes, alkanes, allenes, and alkenes, was contributed by D. W. Dunwell, J. C. Saunders, and B. P. Swann. The second chapter, which deals with aliphatic compounds having other functional groups (carboxylic acids and their derivatives, amino acids, aldehydes and ketones, alcohols, amines, alkyl halides, ethers, sulfur compounds, and miscellaneous aliphatic compounds) was prepared by E. W. Colvin, who also contributed the analogous reviews in all of the preceding volumes of this series.

The remainder of the volume is devoted to surveys of the literature dealing with naturally occurring polyolefinic and polyacetylenic compounds (Chapter 3) and with the chemistry of prostaglandins (Chapter 4). Both of these chapters were written by G. Pattenden, as were the corresponding chapters of Volumes 2 and 3. The reviews of Chapter 3 include, in addition to other topics, summaries of new work on polyolefinic antibiotics (*e.g.*, ansamycins) and other microbial metabolites, a variety of plant-product structures, polyolefins and polyacetylenes of marine origin, and insect pheromones. The fact that the chapter on prostaglandins is less than one-third of the length of the same chapter in Volume 3 is cogent testimony to the author's opening assertion of the

under it "Edestin from hemp seed," "Edestinase from hemp seed," and "Quaternary bases in *Cannabis*" only. For the amount of biochemical studies published on the cannabinoids, the biochemists will be disturbed with this type of index coverage.

A large number of incorrect spellings of common and technical words are found in the abstracts. These errors are self-evident for the most part but confusing in cases such as, for example, citation 2914 where "Cannabidivarian" appears in the title of the article and "Cannabidivarin" in the abstract, the latter presumably correct. In a few cases, words and/or phrases are apparently missing in titles of articles or in the abstracts. These omissions are usually not too much of a problem as in citations 368, 431, 474, 740, 1290, 1321, 1679, 1905, 1927, 2058, 2480, 2493, 2708, 2722, and 2914. The journal citation in 301 is confusing, and citation 2212 does not refer to the journal cited.

When abstracts are given, there is a great degree of inconsistency regarding content. Also, the summary table on p. XXII hardly can be considered complete.

However, even though these minor problems were found, the book at a very reasonable price of $13.95 is a bargain. It will be an indispensable, and much used addition to the personal library of anyone having even a remote interest in *Cannabis*. It will be of special interest to researchers in the field of *Cannabis*, to students in the medical professions and social sciences, to the pharmaceutical industry, and to reporters in the media and should be available in every library.

Reviewed by Norman R. Farnsworth
Department of Pharmacognosy and Pharmacology
College of Pharmacy
University of Illinois at the Medical Center
Chicago, IL 60612

Essentials of Medicinal Chemistry. By ANDREJUS KOROLKOVAS and JOSEPH H. BURCKHALTER. Wiley, 605 Third Ave., New York, N Y 10016, 1976. 697 pp. 16 × 23.5 cm. Price $22.50.

The book is designed as an undergraduate text in medicinal chemistry as well as a resource work for the chemist and biologist interested in several aspects of drugs. The composition of the book is built around succinctly stated facts and theories, which the authors hope are presented in a palatable, yet useful, form for the student. The authors have in mind the role of the pharmacist as an information source helping the physician and patient.

The book is in eight parts and generally follows pharmacological or therapeutic categories. These are Introduction: Basics, Drug Development and Theories; CNS Drugs; Drugs Acting at the Peripheral Nervous System; Cardiovascular, Blood and Renal Systems; Chemotherapeutics; Vitamins; Hormones; and Miscellaneous Agents including Diagnostics. The appendix lists drugs in the USP and NF.

Each part consists of several chapters dealing with discrete topics. They are concisely written along the lines of precis or compendia. The highlights of drug structure and action, as well as side effects and dosage, are recorded. Structural formulas and tables are utilized to illustrate structure–activity relationships in some cases. Useful references are appended to each chapter and are divided into general background and specific citations by class of agents.

The book should prove useful as a compendium of information in medicinal chemistry. This book plus a text organized in depth over the same topics should provide the student with a good background in course work, for board exams, and for professional practice.

Reviewed by Lemont B. Kier
Massachusetts College of Pharmacy
Boston, MA 02115

Manual of Clinical Immunology. Edited by NOEL R. ROSE and HERMAN FRIEDMAN. American Society for Microbiology, 1913 I St. N.W., Washington, DC, 20006, 1976. 932 pp. 17.5 × 26 cm. Price $16.00, flexible binding; $20.00, cloth binding.

This much needed volume, written by 180 authorities in various aspects of the rapidly expanding field of immunology, presents the latest information. The book is directed mainly to laboratory directors and technologists but should prove extremely useful to graduate students, medical students, postdoctoral fellows, residents, and clinicians. The greatest value of this book is the presentation of methodologies, allowing a stepwise approach to various procedures currently used in both clinical and research immunology. Of particular importance is the discussion of the pros and cons of each procedure with emphasis on the pitfalls encountered. Suggestions as to sources of materials and equipment required for each test can save time when setting up a new method.

The arrangement of the book in sections covering different aspects of the components involved in immunological responses and the cross-referencing between chapters allow the investigator to understand not only his or her own area but also the influence of cellular *versus* humoral aspects of immunology. Of particular importance are the chapters covering delayed hypersensitivity, lymphocyte subpopulations, and lymphocyte transformation.

The principles of radioimmunoassay are well presented, and the methods for determining various hormones in body fluids have general applicability not only in the clinic but also in the research laboratory.

Coverage of the immunological aspects of bacterial, mycotic, parasitic, viral, rickettsial, and chlamydial diseases will assist the clinician in more accurate diagnosis. The disadvantages of immunofluorescence and radioimmunoassays in immunodiagnosis of viral diseases are discussed, and suggestions for the use of microplate enzyme methods are given. The main advantages of the latter are a long shelflife, cheap simple equipment, and the same degree of sensitivity as the other procedures.

In the immunohematology section, the chapters on autoimmune and drug immune hemolytic anemia and the immunology of clotting factors point out the importance of modern immulogical methods in the diagnosis of often fatal diseases. Allergic disease testing is well covered, but the importance of testing for drug hypersensitivity is not adequate, being confined almost entirely to penicillin. The subject of autoimmune diseases receives full treatment, including tests for antibodies to tissue-specific antigens. The section on tumor immunology covers the present state of the art and indicates the necessity for further research to improve early tumor diagnosis. The section on transplantation immunology presents the immunological aspects of tissue transplantation, particularly the rejection phenomenon. The last section is of importance to clinical laboratories because it covers legal requirements, quality control, standardization of materials and methods, and proficiency testing of laboratory personnel.

This volume should be available to clinical and research workers in immunology and, because the field is expanding so rapidly, it should be updated more often than most such manuals.

Reviewed by Thomas J. Haley
National Center for Toxicological Research
Jefferson, AK 72079

Aliphatic Chemistry. Vol. 4. A Specialist Periodical Report. Edited by A. McKILLOP *et al.* The Chemical Society, Burlington House, London, W1V 0BN, England, 1976. 281 pp. 14 × 22.5 cm. Price $49.50.

The fourth volume of the Specialist Periodical Reports on aliphatic chemistry is comprised of four chapters which summarize developments reported during 1974 in each of the chosen areas. Chapter 1, on the chemistry of acetylenes, alkanes, allenes, and alkenes, was contributed by D. W. Dunwell, J. C. Saunders, and B. P. Swann. The second chapter, which deals with aliphatic compounds having other functional groups (carboxylic acids and their derivatives, amino acids, aldehydes and ketones, alcohols, amines, alkyl halides, ethers, sulfur compounds, and miscellaneous aliphatic compounds) was prepared by E. W. Colvin, who also contributed the analogous reviews in all of the preceding volumes of this series.

The remainder of the volume is devoted to surveys of the literature dealing with naturally occurring polyolefinic and polyacetylenic compounds (Chapter 3) and with the chemistry of prostaglandins (Chapter 4). Both of these chapters were written by G. Pattenden, as were the corresponding chapters of Volumes 2 and 3. The reviews of Chapter 3 include, in addition to other topics, summaries of new work on polyolefinic antibiotics (*e.g.*, ansamycins) and other microbial metabolites, a variety of plant-product structures, polyolefins and polyacetylenes of marine origin, and insect pheromones. The fact that the chapter on prostaglandins is less than one-third of the length of the same chapter in Volume 3 is cogent testimony to the author's opening assertion of the

under it "Edestin from hemp seed," "Edestinase from hemp seed," and "Quaternary bases in *Cannabis*" only. For the amount of biochemical studies published on the cannabinoids, the biochemists will be disturbed with this type of index coverage.

A large number of incorrect spellings of common and technical words are found in the abstracts. These errors are self-evident for the most part but confusing in cases such as, for example, citation 2914 where "Cannabidivarian" appears in the title of the article and "Cannabidivarin" in the abstract, the latter presumably correct. In a few cases, words and/or phrases are apparently missing in titles of articles or in the abstracts. These omissions are usually not too much of a problem as in citations 368, 431, 474, 740, 1290, 1321, 1679, 1905, 1927, 2058, 2480, 2493, 2708, 2722, and 2914. The journal citation in 301 is confusing, and citation 2212 does not refer to the journal cited.

When abstracts are given, there is a great degree of inconsistency regarding content. Also, the summary table on p. XXII hardly can be considered complete.

However, even though these minor problems were found, the book at a very reasonable price of $13.95 is a bargain. It will be an indispensable, and much used addition to the personal library of anyone having even a remote interest in *Cannabis*. It will be of special interest to researchers in the field of *Cannabis*, to students in the medical professions and social sciences, to the pharmaceutical industry, and to reporters in the media and should be available in every library.

Reviewed by Norman R. Farnsworth
Department of Pharmacognosy and Pharmacology
College of Pharmacy
University of Illinois at the Medical Center
Chicago, IL 60612

Essentials of Medicinal Chemistry. By ANDREJUS KOROLKOVAS and JOSEPH H. BURCKHALTER. Wiley, 605 Third Ave., New York, N Y 10016, 1976. 697 pp. 16 × 23.5 cm. Price $22.50.

The book is designed as an undergraduate text in medicinal chemistry as well as a resource work for the chemist and biologist interested in several aspects of drugs. The composition of the book is built around succinctly stated facts and theories, which the authors hope are presented in a palatable, yet useful, form for the student. The authors have in mind the role of the pharmacist as an information source helping the physician and patient.

The book is in eight parts and generally follows pharmacological or therapeutic categories. These are Introduction: Basics, Drug Development and Theories; CNS Drugs; Drugs Acting at the Peripheral Nervous System; Cardiovascular, Blood and Renal Systems; Chemotherapeutics; Vitamins; Hormones; and Miscellaneous Agents including Diagnostics. The appendix lists drugs in the USP and NF.

Each part consists of several chapters dealing with discrete topics. They are concisely written along the lines of precis or compendia. The highlights of drug structure and action, as well as side effects and dosage, are recorded. Structural formulas and tables are utilized to illustrate structure–activity relationships in some cases. Useful references are appended to each chapter and are divided into general background and specific citations by class of agents.

The book should prove useful as a compendium of information in medicinal chemistry. This book plus a text organized in depth over the same topics should provide the student with a good background in course work, for board exams, and for professional practice.

Reviewed by Lemont B. Kier
Massachusetts College of Pharmacy
Boston, MA 02115

Manual of Clinical Immunology. Edited by NOEL R. ROSE and HERMAN FRIEDMAN. American Society for Microbiology, 1913 I St. N.W., Washington, DC, 20006, 1976. 932 pp. 17.5 × 26 cm. Price $16.00, flexible binding; $20.00, cloth binding.

This much needed volume, written by 180 authorities in various aspects of the rapidly expanding field of immunology, presents the latest information. The book is directed mainly to laboratory directors and technologists but should prove extremely useful to graduate students, medical students, postdoctoral fellows, residents, and clinicians. The greatest value of this book is the presentation of methodologies, allowing a stepwise approach to various procedures currently used in both clinical and research immunology. Of particular importance is the discussion of the pros and cons of each procedure with emphasis on the pitfalls encountered. Suggestions as to sources of materials and equipment required for each test can save time when setting up a new method.

The arrangement of the book in sections covering different aspects of the components involved in immunological responses and the cross-referencing between chapters allow the investigator to understand not only his or her own area but also the influence of cellular *versus* humoral aspects of immunology. Of particular importance are the chapters covering delayed hypersensitivity, lymphocyte subpopulations, and lymphocyte transformation.

The principles of radioimmunoassay are well presented, and the methods for determining various hormones in body fluids have general applicability not only in the clinic but also in the research laboratory.

Coverage of the immunological aspects of bacterial, mycotic, parasitic, viral, rickettsial, and chlamydial diseases will assist the clinician in more accurate diagnosis. The disadvantages of immunofluorescence and radioimmunoassays in immunodiagnosis of viral diseases are discussed, and suggestions for the use of microplate enzyme methods are given. The main advantages of the latter are a long shelflife, cheap simple equipment, and the same degree of sensitivity as the other procedures.

In the immunohematology section, the chapters on autoimmune and drug immune hemolytic anemia and the immunology of clotting factors point out the importance of modern immulogical methods in the diagnosis of often fatal diseases. Allergic disease testing is well covered, but the importance of testing for drug hypersensitivity is not adequate, being confined almost entirely to penicillin. The subject of autoimmune diseases receives full treatment, including tests for antibodies to tissue-specific antigens. The section on tumor immunology covers the present state of the art and indicates the necessity for further research to improve early tumor diagnosis. The section on transplantation immunology presents the immunological aspects of tissue transplantation, particularly the rejection phenomenon. The last section is of importance to clinical laboratories because it covers legal requirements, quality control, standardization of materials and methods, and proficiency testing of laboratory personnel.

This volume should be available to clinical and research workers in immunology and, because the field is expanding so rapidly, it should be updated more often than most such manuals.

Reviewed by Thomas J. Haley
National Center for Toxicological Research
Jefferson, AK 72079

Aliphatic Chemistry. Vol. 4. A Specialist Periodical Report. Edited by A. McKILLOP *et al.* The Chemical Society, Burlington House, London, W1V 0BN, England, 1976. 281 pp. 14 × 22.5 cm. Price $49.50.

The fourth volume of the Specialist Periodical Reports on aliphatic chemistry is comprised of four chapters which summarize developments reported during 1974 in each of the chosen areas. Chapter 1, on the chemistry of acetylenes, alkanes, allenes, and alkenes, was contributed by D. W. Dunwell, J. C. Saunders, and B. P. Swann. The second chapter, which deals with aliphatic compounds having other functional groups (carboxylic acids and their derivatives, amino acids, aldehydes and ketones, alcohols, amines, alkyl halides, ethers, sulfur compounds, and miscellaneous aliphatic compounds) was prepared by E. W. Colvin, who also contributed the analogous reviews in all of the preceding volumes of this series.

The remainder of the volume is devoted to surveys of the literature dealing with naturally occurring polyolefinic and polyacetylenic compounds (Chapter 3) and with the chemistry of prostaglandins (Chapter 4). Both of these chapters were written by G. Pattenden, as were the corresponding chapters of Volumes 2 and 3. The reviews of Chapter 3 include, in addition to other topics, summaries of new work on polyolefinic antibiotics (*e.g.*, ansamycins) and other microbial metabolites, a variety of plant-product structures, polyolefins and polyacetylenes of marine origin, and insect pheromones. The fact that the chapter on prostaglandins is less than one-third of the length of the same chapter in Volume 3 is cogent testimony to the author's opening assertion of the

decrease in the chemical literature in this area.

As in the preceding volumes, the emphasis is on syntheses and reactions of the various classes of compounds. The liberal use of structural formulas and reaction schemes is an invaluable aid to the user of these volumes. Like its predecessors, this volume serves as a well-organized source of much valuable information on general aliphatic chemistry and on aliphatic natural products.

Reviewed by Y. Fulmer Shealy
Medicinal Chemistry Division
Southern Research Institute
Birmingham, AL 35205

Physiologic Disposition of Drugs of Abuse. By LOUIS LEMBERGER and ALAN RUBIN. Halsted, 605 Third Ave., New York, NY 10016, 1976. 401 pp. 16 × 23.5 cm. Price $29.50.

This book contains 10 chapters. The first chapter describes the fundamental principles of drug disposition. The absorption, distribution, and *in vivo* and *in vitro* metabolism of drugs of abuse are described in Chapters 2–9. The 10th chapter deals with the phenomenon and mechanism of tolerance.

The drugs of abuse discussed include amphetamine, mescaline and related phenylalkylamines, LSD and related indolealkylamines, morphine, morphine substitutes, barbiturates, methaqualone, caffeine, nicotine, alcohol, the cannabinoids, cocaine, and miscellaneous drugs including volatile solvents.

Numerous scattered papers and reviews concerning the physiologic disposition of drugs of abuse are summarized in the book. Chemical structural illustrations are used to demonstrate the metabolic pathways of drugs. These illustrations help readers to understand the process of biotransformation of the drug. There is no doubt in the reviewer's mind that this book will be of value and benefit to pharmacologists, psychiatrists, psychologists, and those in basic and clinical fields, especially graduate students and research associates beginning research in fields related to drugs of abuse. The extensive, up-to-date bibliography is very helpful.

It would be nice if a chapter on tranquilizers, especially benzodiazepams, was incorporated in this book.

Reviewed by S. Y. Yeh
National Institute on Drug Abuse
Division of Research
Addiction Research Center
Lexington, KY 40511

Drug Regulation and Innovation: Empirical Evidence and Policy Options. By HENRY G. GRABOWSKI. American Enterprise Institute for Public Policy Research, 1150 17th Street, N. W., Washington, DC 20036, 1976. 82 pp. 15 × 23 cm. Price $3.00.

This book sets out to prove that there is a drug lag in the United States due to governmental regulation of the pharmaceutical industry. It must be seen as an attempt to convince readers of this lag by citing portions of several economic studies. The first five chapters examine various aspects of the effects of regulation on the pharmaceutical industry, and the final chapter presents some suggested policy modifications to rectify the supposed "drug lag."

The book, which is very one-sided, failed to convince the reviewer of the seriousness, or even existence, of the problem. There is a citation that U.S. doctors sent patients abroad for treatment in order to use a drug not available here. This statement is supported by a single citation indicating TWO such examples,

The tone of the work is evident in a quotation from the forward, written by Professor Yale Brozen: "A small step in this direction would be to eliminate the FDA's power to require substantial evidence of effectiveness" (p. 7). Essentially, the argument is made that the United States is falling behind in the number of new chemical entities first developed and/or introduced in this country and that this problem is related to the 1962 amendments to the Federal, Food, Drug, and Cosmetics Act. Arguments for the value of some drugs include their sales and market share abroad. The market test is hardly a valid indicator of the value of a product, and it is perplexing that economists choose to use this argument. No one would deny that each of 80 different penicillin derivatives could be useful individually, but more subject to controversy is whether we have a "drug lag" at all if analogs of existing products are not on the U.S. market.

It is argued that the 1962 amendments will decrease U.S. prestige, harm our foreign balance of payments, and decrease support of academic pharmacology. Yet these arguments are unsupported. Surely the author must have considered factors encouraging foreign research such as the corporate tax structure, foreign profit repatriation rules, and relative labor costs. We come across the statement that the pharmaceutical industry is of above-average riskiness (p. 40). While this may be so for individual products, Barges and Hickey and others have refuted this argument. Easing of FDA regulation and earlier releasing of drugs with greater surveillance after marketing are proposed.

It is no great shock to this reviewer to see that researchers and investors in foreign lands have had successes as we have had. Also, one might argue that the availability of fewer new products is less potentially confusing to prescribers and that competition from products having expired patent protection should help to reduce prices. It seems that in this book conclusions are made repeatedly that are far broader than merited by the findings. The author dismisses arguments about decreases in the number of new product introductions in other countries and points made by government officials if they do not coincide with his hypothesis. This reviewer was expecting a much more even-handed treatment of the subject than he found.

Reviewed by Albert I. Wertheimer
College of Pharmacy
University of Minnesota
Minneapolis, MN 55414

Antibiotics. A Critical Review. Edited by W. KURYLOWICZ. Polish Medical Publishers, Warsaw, Poland. Distributed by the American Society for Microbiology, 1913 I St., N.W., Washington, DC 20006, 1976. 204 pp. 17 × 24.5 cm. Price $6.00.

This book by four Polish authorities in the field attempts to compress the subject of antibiotics into about 200 pages. There is a short introduction as well as a brief section on classification, but the bulk of the book is devoted to two sections. Antibiotics in Microbial Metabolism deals with the biosynthesis and mode of action of antibiotics, and Antibiotics as Therapeutic Agents discusses the pharmacology and therapeutics. A great deal of condensed information is included in this book, which is both its strength and its weakness.

The section Antibiotics in Microbial Metabolism is the most useful. Structural formulas and diagrams are plentifully used in a valuable overview of this complex area. The section Antibiotics as Therapeutic Agents is less successful. Here the abridgement combined with the desire to be comprehensive, even to the point of presenting the principles of drug–protein binding and pharmacokinetics, each in a few pages, creates significant problems. A large number of drugs, some of only minor clinical interest in the United States, are dealt with summarily and important omissions occur. There is no mention, for instance, of colitis as a toxic side effect of clindamycin or of cardiomyopathy as a toxicity of the anthracycline antibiotics.

The book contains a substantial number of misprints, most of which are trivial, but some are more problematic; for instance, on page 97 there is a reference to Table 1 which, I think, though I cannot be sure, is a reference to Table 4–3.

In summary, I feel that these authors have made an admirable attempt to review an enormous amount of information in a small book. The result is a valuable introduction to the subject of antibiotics and a useful adjunct to other texts, but it would be unwise to rely on it as a sole source of information about these compounds.

Reviewed by Patrick J. Creaven
Department of Experimental Therapeutics and Department of Medicine A
Roswell Park Memorial Institute
Buffalo, NY 14263

Lipid Chromatographic Analysis. Vol. 2. Edited by GUIDO V. MARINETTI. Dekker, 270 Madison Avenue, New York, NY 10016, 1976. 400 pp. 15 × 23.5 cm. Price $34.50.

This text contains five chapters covering compounds that, in the broadest sense, can be considered as lipids. The chapters cover TLC of sterols and steroids, GLC of bile acids, chromatography of prostaglandins,

decrease in the chemical literature in this area.

As in the preceding volumes, the emphasis is on syntheses and reactions of the various classes of compounds. The liberal use of structural formulas and reaction schemes is an invaluable aid to the user of these volumes. Like its predecessors, this volume serves as a well-organized source of much valuable information on general aliphatic chemistry and on aliphatic natural products.

Reviewed by Y. Fulmer Shealy
Medicinal Chemistry Division
Southern Research Institute
Birmingham, AL 35205

Physiologic Disposition of Drugs of Abuse. By LOUIS LEMBERGER and ALAN RUBIN. Halsted, 605 Third Ave., New York, NY 10016, 1976. 401 pp. 16 × 23.5 cm. Price $29.50.

This book contains 10 chapters. The first chapter describes the fundamental principles of drug disposition. The absorption, distribution, and *in vivo* and *in vitro* metabolism of drugs of abuse are described in Chapters 2–9. The 10th chapter deals with the phenomenon and mechanism of tolerance.

The drugs of abuse discussed include amphetamine, mescaline and related phenylalkylamines, LSD and related indolealkylamines, morphine, morphine substitutes, barbiturates, methaqualone, caffeine, nicotine, alcohol, the cannabinoids, cocaine, and miscellaneous drugs including volatile solvents.

Numerous scattered papers and reviews concerning the physiologic disposition of drugs of abuse are summarized in the book. Chemical structural illustrations are used to demonstrate the metabolic pathways of drugs. These illustrations help readers to understand the process of biotransformation of the drug. There is no doubt in the reviewer's mind that this book will be of value and benefit to pharmacologists, psychiatrists, psychologists, and those in basic and clinical fields, especially graduate students and research associates beginning research in fields related to drugs of abuse. The extensive, up-to-date bibliography is very helpful.

It would be nice if a chapter on tranquilizers, especially benzodiazepams, was incorporated in this book.

Reviewed by S. Y. Yeh
National Institute on Drug Abuse
Division of Research
Addiction Research Center
Lexington, KY 40511

Drug Regulation and Innovation: Empirical Evidence and Policy Options. By HENRY G. GRABOWSKI. American Enterprise Institute for Public Policy Research, 1150 17th Street, N. W., Washington, DC 20036, 1976. 82 pp. 15 × 23 cm. Price $3.00.

This book sets out to prove that there is a drug lag in the United States due to governmental regulation of the pharmaceutical industry. It must be seen as an attempt to convince readers of this lag by citing portions of several economic studies. The first five chapters examine various aspects of the effects of regulation on the pharmaceutical industry, and the final chapter presents some suggested policy modifications to rectify the supposed "drug lag."

The book, which is very one-sided, failed to convince the reviewer of the seriousness, or even existence, of the problem. There is a citation that U.S. doctors sent patients abroad for treatment in order to use a drug not available here. This statement is supported by a single citation indicating TWO such examples,

The tone of the work is evident in a quotation from the forward, written by Professor Yale Brozen: "A small step in this direction would be to eliminate the FDA's power to require substantial evidence of effectiveness" (p. 7). Essentially, the argument is made that the United States is falling behind in the number of new chemical entities first developed and/or introduced in this country and that this problem is related to the 1962 amendments to the Federal, Food, Drug, and Cosmetics Act. Arguments for the value of some drugs include their sales and market share abroad. The market test is hardly a valid indicator of the value of a product, and it is perplexing that economists choose to use this argument. No one would deny that each of 80 different penicillin derivatives could be useful individually, but more subject to controversy is whether we have a "drug lag" at all if analogs of existing products are not on the U.S. market.

It is argued that the 1962 amendments will decrease U.S. prestige, harm our foreign balance of payments, and decrease support of academic pharmacology. Yet these arguments are unsupported. Surely the author must have considered factors encouraging foreign research such as the corporate tax structure, foreign profit repatriation rules, and relative labor costs. We come across the statement that the pharmaceutical industry is of above-average riskiness (p. 40). While this may be so for individual products, Barges and Hickey and others have refuted this argument. Easing of FDA regulation and earlier releasing of drugs with greater surveillance after marketing are proposed.

It is no great shock to this reviewer to see that researchers and investors in foreign lands have had successes as we have had. Also, one might argue that the availability of fewer new products is less potentially confusing to prescribers and that competition from products having expired patent protection should help to reduce prices. It seems that in this book conclusions are made repeatedly that are far broader than merited by the findings. The author dismisses arguments about decreases in the number of new product introductions in other countries and points made by government officials if they do not coincide with his hypothesis. This reviewer was expecting a much more even-handed treatment of the subject than he found.

Reviewed by Albert I. Wertheimer
College of Pharmacy
University of Minnesota
Minneapolis, MN 55414

Antibiotics. A Critical Review. Edited by W. KURYLOWICZ. Polish Medical Publishers, Warsaw, Poland. Distributed by the American Society for Microbiology, 1913 I St., N.W., Washington, DC 20006, 1976. 204 pp. 17 × 24.5 cm. Price $6.00.

This book by four Polish authorities in the field attempts to compress the subject of antibiotics into about 200 pages. There is a short introduction as well as a brief section on classification, but the bulk of the book is devoted to two sections. Antibiotics in Microbial Metabolism deals with the biosynthesis and mode of action of antibiotics, and Antibiotics as Therapeutic Agents discusses the pharmacology and therapeutics. A great deal of condensed information is included in this book, which is both its strength and its weakness.

The section Antibiotics in Microbial Metabolism is the most useful. Structural formulas and diagrams are plentifully used in a valuable overview of this complex area. The section Antibiotics as Therapeutic Agents is less successful. Here the abridgement combined with the desire to be comprehensive, even to the point of presenting the principles of drug–protein binding and pharmacokinetics, each in a few pages, creates significant problems. A large number of drugs, some of only minor clinical interest in the United States, are dealt with summarily and important omissions occur. There is no mention, for instance, of colitis as a toxic side effect of clindamycin or of cardiomyopathy as a toxicity of the anthracycline antibiotics.

The book contains a substantial number of misprints, most of which are trivial, but some are more problematic; for instance, on page 97 there is a reference to Table 1 which, I think, though I cannot be sure, is a reference to Table 4–3.

In summary, I feel that these authors have made an admirable attempt to review an enormous amount of information in a small book. The result is a valuable introduction to the subject of antibiotics and a useful adjunct to other texts, but it would be unwise to rely on it as a sole source of information about these compounds.

Reviewed by Patrick J. Creaven
Department of Experimental Therapeutics and Department of Medicine A
Roswell Park Memorial Institute
Buffalo, NY 14263

Lipid Chromatographic Analysis. Vol. 2. Edited by GUIDO V. MARINETTI. Dekker, 270 Madison Avenue, New York, NY 10016, 1976. 400 pp. 15 × 23.5 cm. Price $34.50.

This text contains five chapters covering compounds that, in the broadest sense, can be considered as lipids. The chapters cover TLC of sterols and steroids, GLC of bile acids, chromatography of prostaglandins,

decrease in the chemical literature in this area.

As in the preceding volumes, the emphasis is on syntheses and reactions of the various classes of compounds. The liberal use of structural formulas and reaction schemes is an invaluable aid to the user of these volumes. Like its predecessors, this volume serves as a well-organized source of much valuable information on general aliphatic chemistry and on aliphatic natural products.

Reviewed by Y. Fulmer Shealy
Medicinal Chemistry Division
Southern Research Institute
Birmingham, AL 35205

Physiologic Disposition of Drugs of Abuse. By LOUIS LEMBERGER and ALAN RUBIN. Halsted, 605 Third Ave., New York, NY 10016, 1976. 401 pp. 16 × 23.5 cm. Price $29.50.

This book contains 10 chapters. The first chapter describes the fundamental principles of drug disposition. The absorption, distribution, and *in vivo* and *in vitro* metabolism of drugs of abuse are described in Chapters 2–9. The 10th chapter deals with the phenomenon and mechanism of tolerance.

The drugs of abuse discussed include amphetamine, mescaline and related phenylalkylamines, LSD and related indolealkylamines, morphine, morphine substitutes, barbiturates, methaqualone, caffeine, nicotine, alcohol, the cannabinoids, cocaine, and miscellaneous drugs including volatile solvents.

Numerous scattered papers and reviews concerning the physiologic disposition of drugs of abuse are summarized in the book. Chemical structural illustrations are used to demonstrate the metabolic pathways of drugs. These illustrations help readers to understand the process of biotransformation of the drug. There is no doubt in the reviewer's mind that this book will be of value and benefit to pharmacologists, psychiatrists, psychologists, and those in basic and clinical fields, especially graduate students and research associates beginning research in fields related to drugs of abuse. The extensive, up-to-date bibliography is very helpful.

It would be nice if a chapter on tranquilizers, especially benzodiazepams, was incorporated in this book.

Reviewed by S. Y. Yeh
National Institute on Drug Abuse
Division of Research
Addiction Research Center
Lexington, KY 40511

Drug Regulation and Innovation: Empirical Evidence and Policy Options. By HENRY G. GRABOWSKI. American Enterprise Institute for Public Policy Research, 1150 17th Street, N. W., Washington, DC 20036, 1976. 82 pp. 15 × 23 cm. Price $3.00.

This book sets out to prove that there is a drug lag in the United States due to governmental regulation of the pharmaceutical industry. It must be seen as an attempt to convince readers of this lag by citing portions of several economic studies. The first five chapters examine various aspects of the effects of regulation on the pharmaceutical industry, and the final chapter presents some suggested policy modifications to rectify the supposed "drug lag."

The book, which is very one-sided, failed to convince the reviewer of the seriousness, or even existence, of the problem. There is a citation that U.S. doctors sent patients abroad for treatment in order to use a drug not available here. This statement is supported by a single citation indicating TWO such examples,

The tone of the work is evident in a quotation from the forward, written by Professor Yale Brozen: "A small step in this direction would be to eliminate the FDA's power to require substantial evidence of effectiveness" (p. 7). Essentially, the argument is made that the United States is falling behind in the number of new chemical entities first developed and/or introduced in this country and that this problem is related to the 1962 amendments to the Federal, Food, Drug, and Cosmetics Act. Arguments for the value of some drugs include their sales and market share abroad. The market test is hardly a valid indicator of the value of a product, and it is perplexing that economists choose to use this argument. No one would deny that each of 80 different penicillin derivatives could be useful individually, but more subject to controversy is whether we have a "drug lag" at all if analogs of existing products are not on the U.S. market.

It is argued that the 1962 amendments will decrease U.S. prestige, harm our foreign balance of payments, and decrease support of academic pharmacology. Yet these arguments are unsupported. Surely the author must have considered factors encouraging foreign research such as the corporate tax structure, foreign profit repatriation rules, and relative labor costs. We come across the statement that the pharmaceutical industry is of above-average riskiness (p. 40). While this may be so for individual products, Barges and Hickey and others have refuted this argument. Easing of FDA regulation and earlier releasing of drugs with greater surveillance after marketing are proposed.

It is no great shock to this reviewer to see that researchers and investors in foreign lands have had successes as we have had. Also, one might argue that the availability of fewer new products is less potentially confusing to prescribers and that competition from products having expired patent protection should help to reduce prices. It seems that in this book conclusions are made repeatedly that are far broader than merited by the findings. The author dismisses arguments about decreases in the number of new product introductions in other countries and points made by government officials if they do not coincide with his hypothesis. This reviewer was expecting a much more even-handed treatment of the subject than he found.

Reviewed by Albert I. Wertheimer
College of Pharmacy
University of Minnesota
Minneapolis, MN 55414

Antibiotics. A Critical Review. Edited by W. KURYLOWICZ. Polish Medical Publishers, Warsaw, Poland. Distributed by the American Society for Microbiology, 1913 I St., N.W., Washington, DC 20006, 1976. 204 pp. 17 × 24.5 cm. Price $6.00.

This book by four Polish authorities in the field attempts to compress the subject of antibiotics into about 200 pages. There is a short introduction as well as a brief section on classification, but the bulk of the book is devoted to two sections. Antibiotics in Microbial Metabolism deals with the biosynthesis and mode of action of antibiotics, and Antibiotics as Therapeutic Agents discusses the pharmacology and therapeutics. A great deal of condensed information is included in this book, which is both its strength and its weakness.

The section Antibiotics in Microbial Metabolism is the most useful. Structural formulas and diagrams are plentifully used in a valuable overview of this complex area. The section Antibiotics as Therapeutic Agents is less successful. Here the abridgement combined with the desire to be comprehensive, even to the point of presenting the principles of drug–protein binding and pharmacokinetics, each in a few pages, creates significant problems. A large number of drugs, some of only minor clinical interest in the United States, are dealt with summarily and important omissions occur. There is no mention, for instance, of colitis as a toxic side effect of clindamycin or of cardiomyopathy as a toxicity of the anthracycline antibiotics.

The book contains a substantial number of misprints, most of which are trivial, but some are more problematic; for instance, on page 97 there is a reference to Table 1 which, I think, though I cannot be sure, is a reference to Table 4–3.

In summary, I feel that these authors have made an admirable attempt to review an enormous amount of information in a small book. The result is a valuable introduction to the subject of antibiotics and a useful adjunct to other texts, but it would be unwise to rely on it as a sole source of information about these compounds.

Reviewed by Patrick J. Creaven
Department of Experimental Therapeutics and Department of Medicine A
Roswell Park Memorial Institute
Buffalo, NY 14263

Lipid Chromatographic Analysis. Vol. 2. Edited by GUIDO V. MARINETTI. Dekker, 270 Madison Avenue, New York, NY 10016, 1976. 400 pp. 15 × 23.5 cm. Price $34.50.

This text contains five chapters covering compounds that, in the broadest sense, can be considered as lipids. The chapters cover TLC of sterols and steroids, GLC of bile acids, chromatography of prostaglandins,

decrease in the chemical literature in this area.

As in the preceding volumes, the emphasis is on syntheses and reactions of the various classes of compounds. The liberal use of structural formulas and reaction schemes is an invaluable aid to the user of these volumes. Like its predecessors, this volume serves as a well-organized source of much valuable information on general aliphatic chemistry and on aliphatic natural products.

Reviewed by Y. Fulmer Shealy
Medicinal Chemistry Division
Southern Research Institute
Birmingham, AL 35205

Physiologic Disposition of Drugs of Abuse. By LOUIS LEMBERGER and ALAN RUBIN. Halsted, 605 Third Ave., New York, NY 10016, 1976. 401 pp. 16 × 23.5 cm. Price $29.50.

This book contains 10 chapters. The first chapter describes the fundamental principles of drug disposition. The absorption, distribution, and *in vivo* and *in vitro* metabolism of drugs of abuse are described in Chapters 2–9. The 10th chapter deals with the phenomenon and mechanism of tolerance.

The drugs of abuse discussed include amphetamine, mescaline and related phenylalkylamines, LSD and related indolealkylamines, morphine, morphine substitutes, barbiturates, methaqualone, caffeine, nicotine, alcohol, the cannabinoids, cocaine, and miscellaneous drugs including volatile solvents.

Numerous scattered papers and reviews concerning the physiologic disposition of drugs of abuse are summarized in the book. Chemical structural illustrations are used to demonstrate the metabolic pathways of drugs. These illustrations help readers to understand the process of biotransformation of the drug. There is no doubt in the reviewer's mind that this book will be of value and benefit to pharmacologists, psychiatrists, psychologists, and those in basic and clinical fields, especially graduate students and research associates beginning research in fields related to drugs of abuse. The extensive, up-to-date bibliography is very helpful.

It would be nice if a chapter on tranquilizers, especially benzodiazepams, was incorporated in this book.

Reviewed by S. Y. Yeh
National Institute on Drug Abuse
Division of Research
Addiction Research Center
Lexington, KY 40511

Drug Regulation and Innovation: Empirical Evidence and Policy Options. By HENRY G. GRABOWSKI. American Enterprise Institute for Public Policy Research, 1150 17th Street, N. W., Washington, DC 20036, 1976. 82 pp. 15 × 23 cm. Price $3.00.

This book sets out to prove that there is a drug lag in the United States due to governmental regulation of the pharmaceutical industry. It must be seen as an attempt to convince readers of this lag by citing portions of several economic studies. The first five chapters examine various aspects of the effects of regulation on the pharmaceutical industry, and the final chapter presents some suggested policy modifications to rectify the supposed "drug lag."

The book, which is very one-sided, failed to convince the reviewer of the seriousness, or even existence, of the problem. There is a citation that U.S. doctors sent patients abroad for treatment in order to use a drug not available here. This statement is supported by a single citation indicating TWO such examples,

The tone of the work is evident in a quotation from the forward, written by Professor Yale Brozen: "A small step in this direction would be to eliminate the FDA's power to require substantial evidence of effectiveness" (p. 7). Essentially, the argument is made that the United States is falling behind in the number of new chemical entities first developed and/or introduced in this country and that this problem is related to the 1962 amendments to the Federal, Food, Drug, and Cosmetics Act. Arguments for the value of some drugs include their sales and market share abroad. The market test is hardly a valid indicator of the value of a product, and it is perplexing that economists choose to use this argument. No one would deny that each of 80 different penicillin derivatives could be useful individually, but more subject to controversy is whether we have a "drug lag" at all if analogs of existing products are not on the U.S. market.

It is argued that the 1962 amendments will decrease U.S. prestige, harm our foreign balance of payments, and decrease support of academic pharmacology. Yet these arguments are unsupported. Surely the author must have considered factors encouraging foreign research such as the corporate tax structure, foreign profit repatriation rules, and relative labor costs. We come across the statement that the pharmaceutical industry is of above-average riskiness (p. 40). While this may be so for individual products, Barges and Hickey and others have refuted this argument. Easing of FDA regulation and earlier releasing of drugs with greater surveillance after marketing are proposed.

It is no great shock to this reviewer to see that researchers and investors in foreign lands have had successes as we have had. Also, one might argue that the availability of fewer new products is less potentially confusing to prescribers and that competition from products having expired patent protection should help to reduce prices. It seems that in this book conclusions are made repeatedly that are far broader than merited by the findings. The author dismisses arguments about decreases in the number of new product introductions in other countries and points made by government officials if they do not coincide with his hypothesis. This reviewer was expecting a much more even-handed treatment of the subject than he found.

Reviewed by Albert I. Wertheimer
College of Pharmacy
University of Minnesota
Minneapolis, MN 55414

Antibiotics. A Critical Review. Edited by W. KURYLOWICZ. Polish Medical Publishers, Warsaw, Poland. Distributed by the American Society for Microbiology, 1913 I St., N.W., Washington, DC 20006, 1976. 204 pp. 17 × 24.5 cm. Price $6.00.

This book by four Polish authorities in the field attempts to compress the subject of antibiotics into about 200 pages. There is a short introduction as well as a brief section on classification, but the bulk of the book is devoted to two sections. Antibiotics in Microbial Metabolism deals with the biosynthesis and mode of action of antibiotics, and Antibiotics as Therapeutic Agents discusses the pharmacology and therapeutics. A great deal of condensed information is included in this book, which is both its strength and its weakness.

The section Antibiotics in Microbial Metabolism is the most useful. Structural formulas and diagrams are plentifully used in a valuable overview of this complex area. The section Antibiotics as Therapeutic Agents is less successful. Here the abridgement combined with the desire to be comprehensive, even to the point of presenting the principles of drug–protein binding and pharmacokinetics, each in a few pages, creates significant problems. A large number of drugs, some of only minor clinical interest in the United States, are dealt with summarily and important omissions occur. There is no mention, for instance, of colitis as a toxic side effect of clindamycin or of cardiomyopathy as a toxicity of the anthracycline antibiotics.

The book contains a substantial number of misprints, most of which are trivial, but some are more problematic; for instance, on page 97 there is a reference to Table 1 which, I think, though I cannot be sure, is a reference to Table 4–3.

In summary, I feel that these authors have made an admirable attempt to review an enormous amount of information in a small book. The result is a valuable introduction to the subject of antibiotics and a useful adjunct to other texts, but it would be unwise to rely on it as a sole source of information about these compounds.

Reviewed by Patrick J. Creaven
Department of Experimental Therapeutics and Department of Medicine A
Roswell Park Memorial Institute
Buffalo, NY 14263

Lipid Chromatographic Analysis. Vol. 2. Edited by GUIDO V. MARINETTI. Dekker, 270 Madison Avenue, New York, NY 10016, 1976. 400 pp. 15 × 23.5 cm. Price $34.50.

This text contains five chapters covering compounds that, in the broadest sense, can be considered as lipids. The chapters cover TLC of sterols and steroids, GLC of bile acids, chromatography of prostaglandins,

decrease in the chemical literature in this area.

As in the preceding volumes, the emphasis is on syntheses and reactions of the various classes of compounds. The liberal use of structural formulas and reaction schemes is an invaluable aid to the user of these volumes. Like its predecessors, this volume serves as a well-organized source of much valuable information on general aliphatic chemistry and on aliphatic natural products.

Reviewed by Y. Fulmer Shealy
Medicinal Chemistry Division
Southern Research Institute
Birmingham, AL 35205

Physiologic Disposition of Drugs of Abuse. By LOUIS LEMBERGER and ALAN RUBIN. Halsted, 605 Third Ave., New York, NY 10016, 1976. 401 pp. 16 × 23.5 cm. Price $29.50.

This book contains 10 chapters. The first chapter describes the fundamental principles of drug disposition. The absorption, distribution, and *in vivo* and *in vitro* metabolism of drugs of abuse are described in Chapters 2–9. The 10th chapter deals with the phenomenon and mechanism of tolerance.

The drugs of abuse discussed include amphetamine, mescaline and related phenylalkylamines, LSD and related indolealkylamines, morphine, morphine substitutes, barbiturates, methaqualone, caffeine, nicotine, alcohol, the cannabinoids, cocaine, and miscellaneous drugs including volatile solvents.

Numerous scattered papers and reviews concerning the physiologic disposition of drugs of abuse are summarized in the book. Chemical structural illustrations are used to demonstrate the metabolic pathways of drugs. These illustrations help readers to understand the process of biotransformation of the drug. There is no doubt in the reviewer's mind that this book will be of value and benefit to pharmacologists, psychiatrists, psychologists, and those in basic and clinical fields, especially graduate students and research associates beginning research in fields related to drugs of abuse. The extensive, up-to-date bibliography is very helpful.

It would be nice if a chapter on tranquilizers, especially benzodiazepams, was incorporated in this book.

Reviewed by S. Y. Yeh
National Institute on Drug Abuse
Division of Research
Addiction Research Center
Lexington, KY 40511

Drug Regulation and Innovation: Empirical Evidence and Policy Options. By HENRY G. GRABOWSKI. American Enterprise Institute for Public Policy Research, 1150 17th Street, N. W., Washington, DC 20036, 1976. 82 pp. 15 × 23 cm. Price $3.00.

This book sets out to prove that there is a drug lag in the United States due to governmental regulation of the pharmaceutical industry. It must be seen as an attempt to convince readers of this lag by citing portions of several economic studies. The first five chapters examine various aspects of the effects of regulation on the pharmaceutical industry, and the final chapter presents some suggested policy modifications to rectify the supposed "drug lag."

The book, which is very one-sided, failed to convince the reviewer of the seriousness, or even existence, of the problem. There is a citation that U.S. doctors sent patients abroad for treatment in order to use a drug not available here. This statement is supported by a single citation indicating TWO such examples,

The tone of the work is evident in a quotation from the forward, written by Professor Yale Brozen: "A small step in this direction would be to eliminate the FDA's power to require substantial evidence of effectiveness" (p. 7). Essentially, the argument is made that the United States is falling behind in the number of new chemical entities first developed and/or introduced in this country and that this problem is related to the 1962 amendments to the Federal, Food, Drug, and Cosmetics Act. Arguments for the value of some drugs include their sales and market share abroad. The market test is hardly a valid indicator of the value of a product, and it is perplexing that economists choose to use this argument. No one would deny that each of 80 different penicillin derivatives could be useful individually, but more subject to controversy is whether we have a "drug lag" at all if analogs of existing products are not on the U.S. market.

It is argued that the 1962 amendments will decrease U.S. prestige, harm our foreign balance of payments, and decrease support of academic pharmacology. Yet these arguments are unsupported. Surely the author must have considered factors encouraging foreign research such as the corporate tax structure, foreign profit repatriation rules, and relative labor costs. We come across the statement that the pharmaceutical industry is of above-average riskiness (p. 40). While this may be so for individual products, Barges and Hickey and others have refuted this argument. Easing of FDA regulation and earlier releasing of drugs with greater surveillance after marketing are proposed.

It is no great shock to this reviewer to see that researchers and investors in foreign lands have had successes as we have had. Also, one might argue that the availability of fewer new products is less potentially confusing to prescribers and that competition from products having expired patent protection should help to reduce prices. It seems that in this book conclusions are made repeatedly that are far broader than merited by the findings. The author dismisses arguments about decreases in the number of new product introductions in other countries and points made by government officials if they do not coincide with his hypothesis. This reviewer was expecting a much more even-handed treatment of the subject than he found.

Reviewed by Albert I. Wertheimer
College of Pharmacy
University of Minnesota
Minneapolis, MN 55414

Antibiotics. A Critical Review. Edited by W. KURYLOWICZ. Polish Medical Publishers, Warsaw, Poland. Distributed by the American Society for Microbiology, 1913 I St., N.W., Washington, DC 20006, 1976. 204 pp. 17 × 24.5 cm. Price $6.00.

This book by four Polish authorities in the field attempts to compress the subject of antibiotics into about 200 pages. There is a short introduction as well as a brief section on classification, but the bulk of the book is devoted to two sections. Antibiotics in Microbial Metabolism deals with the biosynthesis and mode of action of antibiotics, and Antibiotics as Therapeutic Agents discusses the pharmacology and therapeutics. A great deal of condensed information is included in this book, which is both its strength and its weakness.

The section Antibiotics in Microbial Metabolism is the most useful. Structural formulas and diagrams are plentifully used in a valuable overview of this complex area. The section Antibiotics as Therapeutic Agents is less successful. Here the abridgement combined with the desire to be comprehensive, even to the point of presenting the principles of drug–protein binding and pharmacokinetics, each in a few pages, creates significant problems. A large number of drugs, some of only minor clinical interest in the United States, are dealt with summarily and important omissions occur. There is no mention, for instance, of colitis as a toxic side effect of clindamycin or of cardiomyopathy as a toxicity of the anthracycline antibiotics.

The book contains a substantial number of misprints, most of which are trivial, but some are more problematic; for instance, on page 97 there is a reference to Table 1 which, I think, though I cannot be sure, is a reference to Table 4–3.

In summary, I feel that these authors have made an admirable attempt to review an enormous amount of information in a small book. The result is a valuable introduction to the subject of antibiotics and a useful adjunct to other texts, but it would be unwise to rely on it as a sole source of information about these compounds.

Reviewed by Patrick J. Creaven
Department of Experimental Therapeutics and Department of Medicine A
Roswell Park Memorial Institute
Buffalo, NY 14263

Lipid Chromatographic Analysis. Vol. 2. Edited by GUIDO V. MARINETTI. Dekker, 270 Madison Avenue, New York, NY 10016, 1976. 400 pp. 15 × 23.5 cm. Price $34.50.

This text contains five chapters covering compounds that, in the broadest sense, can be considered as lipids. The chapters cover TLC of sterols and steroids, GLC of bile acids, chromatography of prostaglandins,

GLC of carbohydrate glycolipids, and GLC of long chain nitrogen bases.

The chapter on sterols and steroids (139 pages) deals primarily with TLC, and data are presented clearly in tabular form for a most comprehensive list including many steroids currently on the market. The chapter on bile acids (130 pages) provides a highly detailed description of GLC methodology including experimental methodology for "Filling of Columns" and "Formation of Derivatives." The chapter on prostaglandins (51 pages) succinctly covers all chromatographic methods with emphasis on metabolites and extraction. The section on carbohydrate glycolipid GLC (37 pages) includes many common sugars as well as detailed methodology for synthesizing derivatives. The section on long chain nitrogen bases (11 pages) provides detailed procedures for cleavage, derivative formation, and GLC.

Knowledge of chromatographic methodology is often critical in many pharmaceutical, biological, and synthetic research projects. The detailed information and experimental methodology presented in this book should provide a most useful source to the pharmaceutical scientist. It is highly recommended to those involved in research as well as development of compounds in the classes covered.

Reviewed by Walter Morozowich
Pharmacy Research
The Upjohn Company
Kalamazoo, MI 49001

Pharmacology of Marihuana. Vols. 1 and 2. Edited by MONIQUE C. BRAUDE and STEPHEN SZARA. Raven, 1140 Avenue of the Americas, New York, NY 10036, 1976. 458 pp. 16.5 × 24.5 cm. Price $50.00 (two volumes).

This two-volume set represents the proceedings of the International Conference sponsored by the National Institute on Drug Abuse in Savannah, Ga., December 3–6, 1974.

These books contain a total of nine parts. The first part offers general background information, and the last part deals with the therapeutic potential. In the remaining seven parts, comprehensive research data are presented, including chemical and metabolic aspects; cellular, immunological, hormonal, autonomic, and neuropharmacological effects; behavioral pharmacology; related drug interactions; effects on genetics and reproduction; and the long-term effects of marihuana.

The data from both preclinical and clinical research are presented. Respiratory and cardiovascular effects are discussed in Part IV under Autonomic Effects. It is rather surprising that only a small portion of the text is devoted to these aspects, considering the complex effects of Δ^9-tetrahydrocannabinol on the cardiovascular and respiratory systems, including interference with the reflexogenic mechanisms. The discussion on p. 287, Cardiovascular Effects, has very little to do with the cardiovascular system and deals mostly with bronchodilator effects.

The primary means of self-administration of marihuana is by inhalation, but little information is presented in these texts concerning its acute and/or chronic effects on pulmonary hemodynamics. Such information would have been useful, especially since therapeutic value has been implicated for marihuana in bronchial asthma. These limitations perhaps emphasize the urgent need for further research in these areas. In this respect, these books serve a useful purpose in documenting what is known and what is not.

Marihuana and its constituents are highly complex and possess numerous pharmacological properties; the National Institute on Drug Abuse performed an extremely useful service in comprehensively presenting this material. Dr. Braude and Dr. Szara should be commended for excellence in designing the symposium and editing the proceedings. These books will be extremely useful for researchers and clinicians concerned with research on marihuana.

Reviewed by B. S. Jandhyala
College of Pharmacy
University of Houston
Houston, TX 77004

NOTICES

Kremers and Urdang's History of Pharmacy. Fourth Ed. Revised by GLENN SONNEDECKER. J. B. Lippincott, East Washington Square, Philadelphia, PA 19105, 1976. 571 pp. 19.5 × 24 cm. Price $24.00.

Methods in Receptor Research. Part 1. Edited by MELVIN BLECHER. Dekker, 270 Madison Ave., New York, NY 10016, 1976. 383 pp. 15.5 × 23.5 cm. Price $36.50.

Drugs and Therapy. A Psychotherapist's Handbook of Psychotropic Drugs. By ALVIN K. SWONGER and LARRY L. CONSTANTINE. Little, Brown, 34 Beacon St., Boston, MA 02106, 1976. 292 pp. 14.5 × 22 cm. Price $8.95.

Fluorocarbon and Related Chemistry. Vol. 3. Edited by R. E. BANKS, M.G. BARLOW, *et al.* The Chemical Society, Burlington House, London W1V OBN, England, 1976. 491 pp. 14.5 × 22.5 cm. Price £35.00.

Stylebook/Editorial Manual of the AMA. 6th Ed. By the Scientific Publications Division, American Medical Assn. Publishing Sciences Group, 162 Great Rd., Acton, MA 01720, 1976. 161 pp. 13.5 × 21.5 cm. Price $6.50.

Handbook of Basic Pharmacokinetics. By W. A. RITSCHEL. Drug Intelligence Publications, Hamilton, IL 62341, 1976. 370 pp. 11.5 × 19.5 cm. Price $16.00.

Aminergic Hypotheses of Behavior: Reality or Cliche? National Institute on Drug Abuse Research Monograph Series 3. Edited by BRUCE K. BERNARD. National Institute on Drug Abuse, 11400 Rockville Pike, Rockville, MD 20852, 1975. 148 pp. 20.5 × 27 cm. Price $6.75.

Handbook of Intermediary Metabolism of Aromatic Compounds. By B. L. GOODWIN. Halsted, 605 Third Ave., New York, NY 10016, 1976. 25.5 × 20 cm. Price $75.00.

Frontiers of Pharmacology. Journal of Pharmacy and Pharmacology: Special Supplement. Edited by B. A. CALLINGHAM, M. A. SIMMONDS, and D. W. STRAUGHAN. The Pharmaceutical Press, 17 Bloomsbury Square, London, WC1A 2NN, England, 1976. 405 pp. 18 × 25.5 cm. Price £2.50.

Dimethyl Sulphoxide. By DIETER MARTIN and HERMANN G. HAUTHAL. Halsted, 605 Third Ave., New York, NY 10016, 1975. 500 pp. 16 × 25 cm.

Organic Chemistry, Series Two. Vol. 3: Aromatic Compounds. Edited by H. ZOLLINGER. Butterworth, Borough Green, NR Sevenoaks, Kent, England, 1976. 350 pp. 16 × 24 cm. Price £13.45.

Organic Chemistry, Series Two. Vol. 4: Heterocyclic Compounds. Edited by K. SCHOFIELD. Butterworth, Borough Green, NR Sevenoaks, Kent, England, 1976. 392 pp. 16 × 24 cm. Price £13.45.

Lung Liquids. Ciba Foundation Symposium 38 (new series). CIBA Pharmaceutical Co. Elsevier, 52 Vanderbilt Ave., New York, NY 10017, 1976. 330 pp. 17 × 24.5 cm.

Narcolepsy. (Advances in Sleep Research. Vol. 3) Edited by C. GUILLEMINAULT, C. DEMENT, and P. PASSOUANT. Halsted, 605 Third Ave., New York, NY 10016, 1976. 689 pp. 16 × 23.5 cm. Price $40.00.

Organophosphorus Chemistry. Vol. 7. Edited by S. TRIPPETT *et al.* The Chemical Society, Burlington House, London, W1V OBN, England, 1976. 285 pp. 14.5 × 22.5 cm. Price $55.00.

Pharmacology of Behavior and Memory. By R. YU. Il'YUCHENOK. Halsted, 605 Third Ave., New York, NY 10016, 1976. 216 pp. 16 × 23.5 cm. Price $22.50.

Photochemistry. Vol. 7. Edited by D. BRYCE-SMITH *et al.* The Chemical Society, Burlington House, London, W1V OBN, England, 1976. 617 pp. 14.5 × 22.5 cm. Price £32.00.

Psychotropic Action of Hormones. Edited by T. M. ITIL, G. LAUDAHN, and W. M. HERRMANN. Halsted, 605 Third Ave., New York, NY 10016, 1976. 248 pp. 16 × 23.5 cm. Price $25.00.

Separation and Purification Methods. Vol. 4. Edited by E. S. PERRY, C. J. van OSS, and E. GRUSHKA. Dekker, 270 Madison Ave., New York, NY 10016, 1976. 413 pp. 16 × 23.5 cm. Price $32.50.

Drug Misuse . . . Human Abuse. By HELEN I. GREEN and MICHAEL H. LEVY. Dekker, 270 Madison Ave., New York, NY 10016, 1976. 566 pp. 18.5 × 26 cm. Price $19.75.

Basic Neurochemistry. Second Ed. Edited by GEORGE J. SIEGEL *et al.* Little, Brown, 34 Beacon St., Boston, MA 02106, 1976. 825 pp. 15.5 × 23.5 cm. Price $15.00.

Genetic and Biochemical Aspects of the Development of Datura. Monographs in Developmental Biology. Vol. 12. By MARIE E. CONKLIN. S. Karger AG., Arnold-Bocklin-Strasse 25, CH-4011 Basel, Switzerland, 1976. 170 pp. 15.5 × 22.5 cm. Price $30.50.

GLC of carbohydrate glycolipids, and GLC of long chain nitrogen bases.

The chapter on sterols and steroids (139 pages) deals primarily with TLC, and data are presented clearly in tabular form for a most comprehensive list including many steroids currently on the market. The chapter on bile acids (130 pages) provides a highly detailed description of GLC methodology including experimental methodology for "Filling of Columns" and "Formation of Derivatives." The chapter on prostaglandins (51 pages) succinctly covers all chromatographic methods with emphasis on metabolites and extraction. The section on carbohydrate glycolipid GLC (37 pages) includes many common sugars as well as detailed methodology for synthesizing derivatives. The section on long chain nitrogen bases (11 pages) provides detailed procedures for cleavage, derivative formation, and GLC.

Knowledge of chromatographic methodology is often critical in many pharmaceutical, biological, and synthetic research projects. The detailed information and experimental methodology presented in this book should provide a most useful source to the pharmaceutical scientist. It is highly recommended to those involved in research as well as development of compounds in the classes covered.

Reviewed by Walter Morozowich
Pharmacy Research
The Upjohn Company
Kalamazoo, MI 49001

Pharmacology of Marihuana. Vols. 1 and 2. Edited by MONIQUE C. BRAUDE and STEPHEN SZARA. Raven, 1140 Avenue of the Americas, New York, NY 10036, 1976. 458 pp. 16.5 × 24.5 cm. Price $50.00 (two volumes).

This two-volume set represents the proceedings of the International Conference sponsored by the National Institute on Drug Abuse in Savannah, Ga., December 3–6, 1974.

These books contain a total of nine parts. The first part offers general background information, and the last part deals with the therapeutic potential. In the remaining seven parts, comprehensive research data are presented, including chemical and metabolic aspects; cellular, immunological, hormonal, autonomic, and neuropharmacological effects; behavioral pharmacology; related drug interactions; effects on genetics and reproduction; and the long-term effects of marihuana.

The data from both preclinical and clinical research are presented. Respiratory and cardiovascular effects are discussed in Part IV under Autonomic Effects. It is rather surprising that only a small portion of the text is devoted to these aspects, considering the complex effects of Δ^9-tetrahydrocannabinol on the cardiovascular and respiratory systems, including interference with the reflexogenic mechanisms. The discussion on p. 287, Cardiovascular Effects, has very little to do with the cardiovascular system and deals mostly with bronchodilator effects.

The primary means of self-administration of marihuana is by inhalation, but little information is presented in these texts concerning its acute and/or chronic effects on pulmonary hemodynamics. Such information would have been useful, especially since therapeutic value has been implicated for marihuana in bronchial asthma. These limitations perhaps emphasize the urgent need for further research in these areas. In this respect, these books serve a useful purpose in documenting what is known and what is not.

Marihuana and its constituents are highly complex and possess numerous pharmacological properties; the National Institute on Drug Abuse performed an extremely useful service in comprehensively presenting this material. Dr. Braude and Dr. Szara should be commended for excellence in designing the symposium and editing the proceedings. These books will be extremely useful for researchers and clinicians concerned with research on marihuana.

Reviewed by B. S. Jandhyala
College of Pharmacy
University of Houston
Houston, TX 77004

NOTICES

Kremers and Urdang's History of Pharmacy. Fourth Ed. Revised by GLENN SONNEDECKER. J. B. Lippincott, East Washington Square, Philadelphia, PA 19105, 1976. 571 pp. 19.5 × 24 cm. Price $24.00.

Methods in Receptor Research. Part 1. Edited by MELVIN BLECHER. Dekker, 270 Madison Ave., New York, NY 10016, 1976. 383 pp. 15.5 × 23.5 cm. Price $36.50.

Drugs and Therapy. A Psychotherapist's Handbook of Psychotropic Drugs. By ALVIN K. SWONGER and LARRY L. CONSTANTINE. Little, Brown, 34 Beacon St., Boston, MA 02106, 1976. 292 pp. 14.5 × 22 cm. Price $8.95.

Fluorocarbon and Related Chemistry. Vol. 3. Edited by R. E. BANKS, M.G. BARLOW, *et al.* The Chemical Society, Burlington House, London W1V OBN, England, 1976. 491 pp. 14.5 × 22.5 cm. Price £35.00.

Stylebook/Editorial Manual of the AMA. 6th Ed. By the Scientific Publications Division, American Medical Assn. Publishing Sciences Group, 162 Great Rd., Acton, MA 01720, 1976. 161 pp. 13.5 × 21.5 cm. Price $6.50.

Handbook of Basic Pharmacokinetics. By W. A. RITSCHEL. Drug Intelligence Publications, Hamilton, IL 62341, 1976. 370 pp. 11.5 × 19.5 cm. Price $16.00.

Aminergic Hypotheses of Behavior: Reality or Cliche? National Institute on Drug Abuse Research Monograph Series 3. Edited by BRUCE K. BERNARD. National Institute on Drug Abuse, 11400 Rockville Pike, Rockville, MD 20852, 1975. 148 pp. 20.5 × 27 cm. Price $6.75.

Handbook of Intermediary Metabolism of Aromatic Compounds. By B. L. GOODWIN. Halsted, 605 Third Ave., New York, NY 10016, 1976. 25.5 × 20 cm. Price $75.00.

Frontiers of Pharmacology. Journal of Pharmacy and Pharmacology: Special Supplement. Edited by B. A. CALLINGHAM, M. A. SIMMONDS, and D. W. STRAUGHAN. The Pharmaceutical Press, 17 Bloomsbury Square, London, WC1A 2NN, England, 1976. 405 pp. 18 × 25.5 cm. Price £2.50.

Dimethyl Sulphoxide. By DIETER MARTIN and HERMANN G. HAUTHAL. Halsted, 605 Third Ave., New York, NY 10016, 1975. 500 pp. 16 × 25 cm.

Organic Chemistry, Series Two. Vol. 3: Aromatic Compounds. Edited by H. ZOLLINGER. Butterworth, Borough Green, NR Sevenoaks, Kent, England, 1976. 350 pp. 16 × 24 cm. Price £13.45.

Organic Chemistry, Series Two. Vol. 4: Heterocyclic Compounds. Edited by K. SCHOFIELD. Butterworth, Borough Green, NR Sevenoaks, Kent, England, 1976. 392 pp. 16 × 24 cm. Price £13.45.

Lung Liquids. Ciba Foundation Symposium 38 (new series). CIBA Pharmaceutical Co. Elsevier, 52 Vanderbilt Ave., New York, NY 10017, 1976. 330 pp. 17 × 24.5 cm.

Narcolepsy. (Advances in Sleep Research. Vol. 3) Edited by C. GUILLEMINAULT, C. DEMENT, and P. PASSOUANT. Halsted, 605 Third Ave., New York, NY 10016, 1976. 689 pp. 16 × 23.5 cm. Price $40.00.

Organophosphorus Chemistry. Vol. 7. Edited by S. TRIPPETT *et al.* The Chemical Society, Burlington House, London, W1V OBN, England, 1976. 285 pp. 14.5 × 22.5 cm. Price $55.00.

Pharmacology of Behavior and Memory. By R. YU. Il'YUCHENOK. Halsted, 605 Third Ave., New York, NY 10016, 1976. 216 pp. 16 × 23.5 cm. Price $22.50.

Photochemistry. Vol. 7. Edited by D. BRYCE-SMITH *et al.* The Chemical Society, Burlington House, London, W1V OBN, England, 1976. 617 pp. 14.5 × 22.5 cm. Price £32.00.

Psychotropic Action of Hormones. Edited by T. M. ITIL, G. LAUDAHN, and W. M. HERRMANN. Halsted, 605 Third Ave., New York, NY 10016, 1976. 248 pp. 16 × 23.5 cm. Price $25.00.

Separation and Purification Methods. Vol. 4. Edited by E. S. PERRY, C. J. van OSS, and E. GRUSHKA. Dekker, 270 Madison Ave., New York, NY 10016, 1976. 413 pp. 16 × 23.5 cm. Price $32.50.

Drug Misuse . . . Human Abuse. By HELEN I. GREEN and MICHAEL H. LEVY. Dekker, 270 Madison Ave., New York, NY 10016, 1976. 566 pp. 18.5 × 26 cm. Price $19.75.

Basic Neurochemistry. Second Ed. Edited by GEORGE J. SIEGEL *et al.* Little, Brown, 34 Beacon St., Boston, MA 02106, 1976. 825 pp. 15.5 × 23.5 cm. Price $15.00.

Genetic and Biochemical Aspects of the Development of Datura. Monographs in Developmental Biology. Vol. 12. By MARIE E. CONKLIN. S. Karger AG., Arnold-Bocklin-Strasse 25, CH-4011 Basel, Switzerland, 1976. 170 pp. 15.5 × 22.5 cm. Price $30.50.

GLC of carbohydrate glycolipids, and GLC of long chain nitrogen bases.

The chapter on sterols and steroids (139 pages) deals primarily with TLC, and data are presented clearly in tabular form for a most comprehensive list including many steroids currently on the market. The chapter on bile acids (130 pages) provides a highly detailed description of GLC methodology including experimental methodology for "Filling of Columns" and "Formation of Derivatives." The chapter on prostaglandins (51 pages) succinctly covers all chromatographic methods with emphasis on metabolites and extraction. The section on carbohydrate glycolipid GLC (37 pages) includes many common sugars as well as detailed methodology for synthesizing derivatives. The section on long chain nitrogen bases (11 pages) provides detailed procedures for cleavage, derivative formation, and GLC.

Knowledge of chromatographic methodology is often critical in many pharmaceutical, biological, and synthetic research projects. The detailed information and experimental methodology presented in this book should provide a most useful source to the pharmaceutical scientist. It is highly recommended to those involved in research as well as development of compounds in the classes covered.

Reviewed by Walter Morozowich
Pharmacy Research
The Upjohn Company
Kalamazoo, MI 49001

Pharmacology of Marihuana. Vols. 1 and 2. Edited by MONIQUE C. BRAUDE and STEPHEN SZARA. Raven, 1140 Avenue of the Americas, New York, NY 10036, 1976. 458 pp. 16.5 × 24.5 cm. Price $50.00 (two volumes).

This two-volume set represents the proceedings of the International Conference sponsored by the National Institute on Drug Abuse in Savannah, Ga., December 3–6, 1974.

These books contain a total of nine parts. The first part offers general background information, and the last part deals with the therapeutic potential. In the remaining seven parts, comprehensive research data are presented, including chemical and metabolic aspects; cellular, immunological, hormonal, autonomic, and neuropharmacological effects; behavioral pharmacology; related drug interactions; effects on genetics and reproduction; and the long-term effects of marihuana.

The data from both preclinical and clinical research are presented. Respiratory and cardiovascular effects are discussed in Part IV under Autonomic Effects. It is rather surprising that only a small portion of the text is devoted to these aspects, considering the complex effects of Δ^9-tetrahydrocannabinol on the cardiovascular and respiratory systems, including interference with the reflexogenic mechanisms. The discussion on p. 287, Cardiovascular Effects, has very little to do with the cardiovascular system and deals mostly with bronchodilator effects.

The primary means of self-administration of marihuana is by inhalation, but little information is presented in these texts concerning its acute and/or chronic effects on pulmonary hemodynamics. Such information would have been useful, especially since therapeutic value has been implicated for marihuana in bronchial asthma. These limitations perhaps emphasize the urgent need for further research in these areas. In this respect, these books serve a useful purpose in documenting what is known and what is not.

Marihuana and its constituents are highly complex and possess numerous pharmacological properties; the National Institute on Drug Abuse performed an extremely useful service in comprehensively presenting this material. Dr. Braude and Dr. Szara should be commended for excellence in designing the symposium and editing the proceedings. These books will be extremely useful for researchers and clinicians concerned with research on marihuana.

Reviewed by B. S. Jandhyala
College of Pharmacy
University of Houston
Houston, TX 77004

NOTICES

Kremers and Urdang's History of Pharmacy. Fourth Ed. Revised by GLENN SONNEDECKER. J. B. Lippincott, East Washington Square, Philadelphia, PA 19105, 1976. 571 pp. 19.5 × 24 cm. Price $24.00.

Methods in Receptor Research. Part 1. Edited by MELVIN BLECHER. Dekker, 270 Madison Ave., New York, NY 10016, 1976. 383 pp. 15.5 × 23.5 cm. Price $36.50.

Drugs and Therapy. A Psychotherapist's Handbook of Psychotropic Drugs. By ALVIN K. SWONGER and LARRY L. CONSTANTINE. Little, Brown, 34 Beacon St., Boston, MA 02106, 1976. 292 pp. 14.5 × 22 cm. Price $8.95.

Fluorocarbon and Related Chemistry. Vol. 3. Edited by R. E. BANKS, M.G. BARLOW, *et al.* The Chemical Society, Burlington House, London W1V OBN, England, 1976. 491 pp. 14.5 × 22.5 cm. Price £35.00.

Stylebook/Editorial Manual of the AMA. 6th Ed. By the Scientific Publications Division, American Medical Assn. Publishing Sciences Group, 162 Great Rd., Acton, MA 01720, 1976. 161 pp. 13.5 × 21.5 cm. Price $6.50.

Handbook of Basic Pharmacokinetics. By W. A. RITSCHEL. Drug Intelligence Publications, Hamilton, IL 62341, 1976. 370 pp. 11.5 × 19.5 cm. Price $16.00.

Aminergic Hypotheses of Behavior: Reality or Cliche? National Institute on Drug Abuse Research Monograph Series 3. Edited by BRUCE K. BERNARD. National Institute on Drug Abuse, 11400 Rockville Pike, Rockville, MD 20852, 1975. 148 pp. 20.5 × 27 cm. Price $6.75.

Handbook of Intermediary Metabolism of Aromatic Compounds. By B. L. GOODWIN. Halsted, 605 Third Ave., New York, NY 10016, 1976. 25.5 × 20 cm. Price $75.00.

Frontiers of Pharmacology. Journal of Pharmacy and Pharmacology: Special Supplement. Edited by B. A. CALLINGHAM, M. A. SIMMONDS, and D. W. STRAUGHAN. The Pharmaceutical Press, 17 Bloomsbury Square, London, WC1A 2NN, England, 1976. 405 pp. 18 × 25.5 cm. Price £2.50.

Dimethyl Sulphoxide. By DIETER MARTIN and HERMANN G. HAUTHAL. Halsted, 605 Third Ave., New York, NY 10016, 1975. 500 pp. 16 × 25 cm.

Organic Chemistry, Series Two. Vol. 3: Aromatic Compounds. Edited by H. ZOLLINGER. Butterworth, Borough Green, NR Sevenoaks, Kent, England, 1976. 350 pp. 16 × 24 cm. Price £13.45.

Organic Chemistry, Series Two. Vol. 4: Heterocyclic Compounds. Edited by K. SCHOFIELD. Butterworth, Borough Green, NR Sevenoaks, Kent, England, 1976. 392 pp. 16 × 24 cm. Price £13.45.

Lung Liquids. Ciba Foundation Symposium 38 (new series). CIBA Pharmaceutical Co. Elsevier, 52 Vanderbilt Ave., New York, NY 10017, 1976. 330 pp. 17 × 24.5 cm.

Narcolepsy. (Advances in Sleep Research. Vol. 3) Edited by C. GUILLEMINAULT, C. DEMENT, and P. PASSOUANT. Halsted, 605 Third Ave., New York, NY 10016, 1976. 689 pp. 16 × 23.5 cm. Price $40.00.

Organophosphorus Chemistry. Vol. 7. Edited by S. TRIPPETT *et al.* The Chemical Society, Burlington House, London, W1V OBN, England, 1976. 285 pp. 14.5 × 22.5 cm. Price $55.00.

Pharmacology of Behavior and Memory. By R. YU. Il'YUCHENOK. Halsted, 605 Third Ave., New York, NY 10016, 1976. 216 pp. 16 × 23.5 cm. Price $22.50.

Photochemistry. Vol. 7. Edited by D. BRYCE-SMITH *et al.* The Chemical Society, Burlington House, London, W1V OBN, England, 1976. 617 pp. 14.5 × 22.5 cm. Price £32.00.

Psychotropic Action of Hormones. Edited by T. M. ITIL, G. LAUDAHN, and W. M. HERRMANN. Halsted, 605 Third Ave., New York, NY 10016, 1976. 248 pp. 16 × 23.5 cm. Price $25.00.

Separation and Purification Methods. Vol. 4. Edited by E. S. PERRY, C. J. van OSS, and E. GRUSHKA. Dekker, 270 Madison Ave., New York, NY 10016, 1976. 413 pp. 16 × 23.5 cm. Price $32.50.

Drug Misuse . . . Human Abuse. By HELEN I. GREEN and MICHAEL H. LEVY. Dekker, 270 Madison Ave., New York, NY 10016, 1976. 566 pp. 18.5 × 26 cm. Price $19.75.

Basic Neurochemistry. Second Ed. Edited by GEORGE J. SIEGEL *et al.* Little, Brown, 34 Beacon St., Boston, MA 02106, 1976. 825 pp. 15.5 × 23.5 cm. Price $15.00.

Genetic and Biochemical Aspects of the Development of Datura. Monographs in Developmental Biology. Vol. 12. By MARIE E. CONKLIN. S. Karger AG., Arnold-Bocklin-Strasse 25, CH-4011 Basel, Switzerland, 1976. 170 pp. 15.5 × 22.5 cm. Price $30.50.

Journal of Pharmaceutical Sciences

JULY 1977

VOLUME 66 NUMBER 7

MARY H. FERGUSON
Editor

SHELLY ELLIOTT
Production Editor

JANET D. SHOFF
Copy Editor

EDWARD G. FELDMANN
Contributing Editor

SAMUEL W. GOLDSTEIN
Contributing Editor

DAVID BOHARDT
Acting Director of Publications

L. LUAN CORRIGAN
Assistant Director of Publications

EDITORIAL ADVISORY BOARD

JOHN AUTIAN — HARRY B. KOSTENBAUDER

NORMAN R. FARNSWORTH — HERBERT A. LIEBERMAN

WILLIAM O. FOYE — DAVID E. MANN, JR.

WILLIAM J. JUSKO — GERALD J. PAPARIELLO

The *Journal of Pharmaceutical Sciences* is published monthly by the American Pharmaceutical Association at 2215 Constitution Ave., N.W., Washington, DC 20037. Second-class postage paid at Washington, D.C., and at additional mailing office.

All expressions of opinion and statements of supposed fact appearing in articles or editorials carried in this journal are published on the authority of the writer over whose name they appear and are not to be regarded as necessarily expressing the policies or views of the American Pharmaceutical Association.

Offices—Editorial, Advertising, and Subscription Offices: 2215 Constitution Ave., N.W., Washington, DC 20037. Printing Offices: 20th & Northampton Streets, Easton, PA 18042.

Annual Subscriptions—United States and foreign, industrial and government institutions $50, educational institutions $50, individuals *for personal use only* $30; single copies $5. All foreign subscriptions add $5 for postage. Subscription rates are subject to change without notice. Members of the American Pharmaceutical Association may elect to receive the *Journal of Pharmaceutical Sciences* as a part of their annual $60 (foreign $65) APhA membership dues.

Claims—Missing numbers will not be supplied if dues or subscriptions are in arrears for more than 60 days or if claims are received more than 60 days after the date of the issue, or if loss was due to failure to give notice of change of address. The Association cannot accept responsibility for foreign delivery when its records indicate shipment has been made.

Change of Address—Members and subscribers should notify at once both the Post Office and the American Pharmaceutical Association, 2215 Constitution Ave., N.W., Washington, DC 20037, of any change of address.

© Copyright 1977, American Pharmaceutical Association, 2215 Constitution Ave., N.W., Washington, DC 20037; all rights reserved.

A NEW KIND OF "DRUG LAG"

Much has been said and written about the purported "drug lag" in the United States. Although we are certain that most of our readers are quite familiar with this issue, for the sake of those who are not, a brief description would be in order.

Basically, the present drug laws in this country require a demonstration of both safety and effectiveness before the marketing of a new drug is permitted. Moreover, the implementing regulations spell out in more precise terms and in greater detail the types of testing and test data that must be compiled in support of the claims made in the application submitted for approval. For example, controlled, double-blind clinical studies generally are considered essential in the effort to document the effectiveness claimed for a new drug.

The documentation required, both in a qualitative and a quantitative sense, coupled with the administrative procedures utilized generally results in new drugs appearing on the U.S. market at a later date than in most countries abroad. Depending upon the interests and politics of the person commenting, this situation is depicted as ranging from a very serious problem in which desperate patients are denied lifesaving therapy for years on end, to a blessing in which the public is guarded and shielded from inadequately tested, dangerous agents that are promiscuously marketed in other countries.

The drugs involved are new chemical entities which are patentable and, therefore, the firm submitting the New Drug Application would retain exclusive property rights—except, of course, for possible licensing and royalty agreements—to that agent for the life of the patent. Hence, there is a strong profit motive which greatly encourages the interested company to actively pursue its efforts toward obtaining government approval for marketing the new drug discovery.

Indeed, various allegations have been made that certain firms and certain drug industry representatives have pursued this objective too vigorously to the point of bringing improper pressures to bear upon the government agency's medical scientists in a zealous effort to win such approval for their new drugs.

The purpose of this editorial, however, is not to enter this familiar "drug lag" controversy. Rather, it is to call attention to the neglected compounds that have great potential as useful drugs, but which are shunned by drug companies simply because they are unpatentable. For all its benefits and advantages, the free enterprise and patent system discourages private industry from investigating the potential therapeutic value of such unpatentable compounds.

Consequently, a "research lag" exists because research and development relating to these compounds—which happen to be in this category of known compounds or naturally occurring substances—simply are not conducted. A rather dramatic illustration is the drug lithium carbonate. The value of lithium in treating manic-depression was suggested many years ago; indeed, reports of its effectiveness appeared in the late 1940's. However, as recent as 1965, no commercial firm was sufficiently interested in pursuing these leads because lithium and its common salts are naturally occurring substances which are not patentable.

Eventually, we understand that the American College of Neuropsychopharmacology, in a move that would have been without precedent, seriously considered submitting a New Drug Application in its own name in order to win government approval for the agent as a drug. What abruptly changed this situation and prompted industry interest in the mid-1960's was a recognition that the clinical usefulness of lithium is dependent upon its formulation as a slow-release dosage form and that such timed-release products are patentable.

We are not suggesting that the drug industry was negligent or derelict in failing to devote research dollars to study lithium or any other such unprofitable entity. But we are suggesting that a void exists in our present system, which results in potentially useful drugs being neglected.

Various possible remedies are available to fill this research gap, including private foundations, academic institutions, and various public facilities such as hospitals operated by the Public Health Service or Veterans Administration. However, it would appear that the most logical central facility to assume this role is the National Institutes of Health and, specifically, the National Institute of General Medical Sciences. Moreover, it strikes us that federal research dollars—which often are spent in such questionable pursuits as to merit U.S. Senator William Proxmire's celebrated "Golden Fleece Award"—would be well utilized if expended for this purpose.

—EGF

Journal of Pharmaceutical Sciences

JULY 1977

VOLUME 66 NUMBER 7

MARY H. FERGUSON
Editor

SHELLY ELLIOTT
Production Editor

JANET D. SHOFF
Copy Editor

EDWARD G. FELDMANN
Contributing Editor

SAMUEL W. GOLDSTEIN
Contributing Editor

DAVID BOHARDT
Acting Director of Publications

L. LUAN CORRIGAN
Assistant Director of Publications

EDITORIAL ADVISORY BOARD

JOHN AUTIAN — HARRY B. KOSTENBAUDER

NORMAN R. FARNSWORTH — HERBERT A. LIEBERMAN

WILLIAM O. FOYE — DAVID E. MANN, JR.

WILLIAM J. JUSKO — GERALD J. PAPARIELLO

The *Journal of Pharmaceutical Sciences* is published monthly by the American Pharmaceutical Association at 2215 Constitution Ave., N.W., Washington, DC 20037. Second-class postage paid at Washington, D.C., and at additional mailing office.

All expressions of opinion and statements of supposed fact appearing in articles or editorials carried in this journal are published on the authority of the writer over whose name they appear and are not to be regarded as necessarily expressing the policies or views of the American Pharmaceutical Association.

Offices—Editorial, Advertising, and Subscription Offices: 2215 Constitution Ave., N.W., Washington, DC 20037. Printing Offices: 20th & Northampton Streets, Easton, PA 18042.

Annual Subscriptions—United States and foreign, industrial and government institutions $50, educational institutions $50, individuals *for personal use only* $30; single copies $5. All foreign subscriptions add $5 for postage. Subscription rates are subject to change without notice. Members of the American Pharmaceutical Association may elect to receive the *Journal of Pharmaceutical Sciences* as a part of their annual $60 (foreign $65) APhA membership dues.

Claims—Missing numbers will not be supplied if dues or subscriptions are in arrears for more than 60 days or if claims are received more than 60 days after the date of the issue, or if loss was due to failure to give notice of change of address. The Association cannot accept responsibility for foreign delivery when its records indicate shipment has been made.

Change of Address—Members and subscribers should notify at once both the Post Office and the American Pharmaceutical Association, 2215 Constitution Ave., N.W., Washington, DC 20037, of any change of address.

© Copyright 1977, American Pharmaceutical Association, 2215 Constitution Ave., N.W., Washington, DC 20037; all rights reserved.

A NEW KIND OF "DRUG LAG"

Much has been said and written about the purported "drug lag" in the United States. Although we are certain that most of our readers are quite familiar with this issue, for the sake of those who are not, a brief description would be in order.

Basically, the present drug laws in this country require a demonstration of both safety and effectiveness before the marketing of a new drug is permitted. Moreover, the implementing regulations spell out in more precise terms and in greater detail the types of testing and test data that must be compiled in support of the claims made in the application submitted for approval. For example, controlled, double-blind clinical studies generally are considered essential in the effort to document the effectiveness claimed for a new drug.

The documentation required, both in a qualitative and a quantitative sense, coupled with the administrative procedures utilized generally results in new drugs appearing on the U.S. market at a later date than in most countries abroad. Depending upon the interests and politics of the person commenting, this situation is depicted as ranging from a very serious problem in which desperate patients are denied lifesaving therapy for years on end, to a blessing in which the public is guarded and shielded from inadequately tested, dangerous agents that are promiscuously marketed in other countries.

The drugs involved are new chemical entities which are patentable and, therefore, the firm submitting the New Drug Application would retain exclusive property rights—except, of course, for possible licensing and royalty agreements—to that agent for the life of the patent. Hence, there is a strong profit motive which greatly encourages the interested company to actively pursue its efforts toward obtaining government approval for marketing the new drug discovery.

Indeed, various allegations have been made that certain firms and certain drug industry representatives have pursued this objective too vigorously to the point of bringing improper pressures to bear upon the government agency's medical scientists in a zealous effort to win such approval for their new drugs.

The purpose of this editorial, however, is not to enter this familiar "drug lag" controversy. Rather, it is to call attention to the neglected compounds that have great potential as useful drugs, but which are shunned by drug companies simply because they are unpatentable. For all its benefits and advantages, the free enterprise and patent system discourages private industry from investigating the potential therapeutic value of such unpatentable compounds.

Consequently, a "research lag" exists because research and development relating to these compounds—which happen to be in this category of known compounds or naturally occurring substances—simply are not conducted. A rather dramatic illustration is the drug lithium carbonate. The value of lithium in treating manic-depression was suggested many years ago; indeed, reports of its effectiveness appeared in the late 1940's. However, as recent as 1965, no commercial firm was sufficiently interested in pursuing these leads because lithium and its common salts are naturally occurring substances which are not patentable.

Eventually, we understand that the American College of Neuropsychopharmacology, in a move that would have been without precedent, seriously considered submitting a New Drug Application in its own name in order to win government approval for the agent as a drug. What abruptly changed this situation and prompted industry interest in the mid-1960's was a recognition that the clinical usefulness of lithium is dependent upon its formulation as a slow-release dosage form and that such timed-release products are patentable.

We are not suggesting that the drug industry was negligent or derelict in failing to devote research dollars to study lithium or any other such unprofitable entity. But we are suggesting that a void exists in our present system, which results in potentially useful drugs being neglected.

Various possible remedies are available to fill this research gap, including private foundations, academic institutions, and various public facilities such as hospitals operated by the Public Health Service or Veterans Administration. However, it would appear that the most logical central facility to assume this role is the National Institutes of Health and, specifically, the National Institute of General Medical Sciences. Moreover, it strikes us that federal research dollars—which often are spent in such questionable pursuits as to merit U.S. Senator William Proxmire's celebrated "Golden Fleece Award"—would be well utilized if expended for this purpose.

—EGF

Journal of Pharmaceutical Sciences

JULY 1977
VOLUME 66 NUMBER 7

REVIEW ARTICLE

Electrophysiological and Pharmacological Properties of Skeletal Muscle in Culture

A. L. HARVEY and W. F. DRYDEN ˣ

Keyphrases □ Skeletal muscle in culture—electrophysiological and pharmacological properties, chemosensitivity, review □ Tissue culture—skeletal muscle, electrophysiological and pharmacological properties, chemosensitivity, review □ Electrophysiology—skeletal muscle in culture, review □ Chemosensitivity—skeletal muscle in culture, review

Tissue culture is the maintenance or growth of biological tissues in an artificial medium. Techniques in use include: (*a*) organ culture, which uses a complete organ in isolation from the body; (*b*) explant culture, in which a small portion of tissue is excised and maintained as a discrete piece; (*c*) cell culture, which involves dissociation of the explant to a suspension of separate cells; and (*d*) continuous cell lines, which can be maintained in culture conditions by continuous multiplication.

Tissue culture has several advantages over conventional *in vivo* or *in vitro* experimental systems. Blood flow, hormones, nerve trophic factors, and other body influences no longer affect the functions of the tissue; the cultures are in a controlled environment which is easy to alter for experimental purposes. The amount of tissue disintegration can be selected by the choice of technique, for example, by using explants or cell lines. Monolayer cultures of dissociated cells are usually more accessible than tissues *in situ*, thus enabling cells to be studied throughout development and allowing prolonged experiments. In addition, human tissue from biopsies or embryos can be readily studied using culture techniques.

Many cell types have been grown in tissue culture, but skeletal muscle appears to be particularly suitable. It remains remarkably similar in physiology and biochemistry to skeletal muscle *in situ* (1). Skeletal muscle from various species, including chick, rat, mouse, and human, has been grown as explants, cell cultures, or cell lines (2–7).

Skeletal muscle in culture is especially useful in pharmacological studies, because it provides a simple system of only muscle fibers without nerves. The effects of neurons on muscle function can, however, be studied in culture (8, 9).

Early studies on skeletal muscle in culture used organ culture or explants of muscle from embryos or adult animals. Often such tissue suffered from "dedifferentiation"—loss of characteristic structures of the tissue and reappearence of cytological features typical of an earlier state of differentiation. Advances were made rapidly after studies that led to a method of growing consistent cell cultures of skeletal muscle fibers (2, 10).

For cell cultures, tissue is ideally obtained from embryos or neonates. Muscle is dissected and broken down to a suspension of individual cells, either mechanically or by using enzymes such as trypsin or collagenase. The cell suspension contains myoblasts, the mononuclear precursors of muscle fibers, and connective tissue cells, the fibroblasts.

Cultures can easily be grown in plastic petri dishes that have been coated with collagen; collagen appears to be a necessary substrate during the early stages of muscle differentiation (10). The cells are maintained at 37° in a standard tissue culture medium supplemented with serum and embryo extract.

The sequence of events during differentiation of skeletal muscle in culture has been studied in some detail. After trypsin dissociation, the cultures consist of spherical mononuclear cells. These cells settle onto the surface of the culture dish, and different types can be distinguished after a few hours. Some cells appear extremely flattened and have an irregular multipolar shape; these cells are usually regarded as fibroblasts. Other cells have a marked bipolar

shape with a prominent central nucleus and scanty cytoplasm; these cells, thought to be myogenic in origin, are termed "myoblasts" (11).

The mononuclear cell population goes through a period of replication. After a time, some cells stop dividing, line up in parallel arrays, and fuse to form multinucleated cells called "myotubes." This fusion, taking 4–8 hr, occurs sooner in cultures with a higher initial cell density (12). The multinuclear myotubes are often highly branched (especially chick muscle), and the cell nuclei are in a central position. These myotube cells continue to grow and develop in culture, forming mature cross-striated muscle fibers with nuclei aligned along the cell membrane.

The fibroblasts continually divide in culture and eventually can overgrow the muscle fibers, thus making experiments difficult. After the formation of myotubes, the cultures can be treated with a DNA synthesis inhibitor, such as cytarabine (cytosine arabinoside), to remove the actively replicating fibroblasts. Since DNA synthesis in muscle ceases after cell fusion, this treatment does not hinder the development of the muscle fibers (13, 14).

The studies on skeletal muscle in culture that are dealt with in detail in this review are grouped for convenience into three separate areas: electrophysiological properties, development of chemosensitivity, and pharmacological properties. Nevertheless, there is considerable overlap among these sections.

ELECTROPHYSIOLOGY

Passive Electrophysiological Properties—In directing the techniques of conventional electrophysiology toward recording from cells in culture, a few refinements are necessary. While normal electronic amplification and glass microelectrodes of resistance 5–50 megohms may be used with ease, the nature of the test material requires a microscope, preferably of the inverted type, with phase contrast or Nomarski interference optics. Furthermore, the scale of the work dictates that the utmost stability in micromanipulators and worktop be sought.

Embryonic chick skeletal muscle fibers explanted into tissue culture retained a resting membrane potential between −60 and −75 mv (15), although Harris *et al.* (5) noted a drop from −63.8 (mean) to a mean of −51.0 mv over a 10-day culture period. No difference was noted between explants from chick anterior latissimus dorsi (slow muscle) and posterior latissimus dorsi (fast muscle) (16).

In muscle fibers developed from the fusion of disaggregated primary myoblasts obtained from chick embryos or neonatal rodents, the resting membrane potential changed from a value around −10 mv before fusion and immediately afterward, rising steadily as fiber length and diameter increased to about −50 or −60 mv (4, 6, 14, 17–20). Thereafter, little change in the resting membrane potential was observed. Higher values, between −70 and −95 mv, were reported by some workers but were less common (21–23).

The increase in membrane potential was correlated with numbers of nuclei in the fiber (4), with fiber thickness (14), and with fiber length (6, 18). Fibers of 1000 μm in length usually have attained their maximum resting membrane potential, although the morphology of multiply branched myotubes in culture presents formidable difficulties in measuring fiber length. However, Hooisma *et al.* (23) were unable to note any correlation between the resting membrane potential and the fiber age or size in their cultures.

With respect to membrane potential, the development of muscle in culture resembled closely the development followed by embryonic muscle *in situ* (24); the highest membrane potentials recorded were similar to the values reported for isolated chicken muscle (25) and rodent muscle (26–28). Human muscle, developing in culture from fetal myoblasts, showed a similar increase in membrane potential[1]. The progressive increase in the resting membrane potential was apparently achieved by changes in the ratio of the permeabilities of the principal cations, sodium and potassium. Intracellular potassium remained constant at about 140 m*M* throughout muscle development in culture. In chick muscle, intracellular sodium fell from 56 to 22 m*M* over a period when the resting membrane potential rose from −10 to −21 mv (14). Catterall (29) estimated the internal sodium concentration of 5–9-day chick myotubes to be 13 m*M*; Ritchie and Fambrough (20) reported the same value for rat myotubes, although no change during development was observed.

Both chick and rat myoblasts and myotubes of low resting membrane potential are relatively insensitive to alterations in external potassium. As the resting membrane potential increases, however, the sensitivity to changes in $[K]_0$ increases until there is a virtual linear relationship between log $[K]_0$ and membrane potential (14, 20, 30). The curves obtained with rat myotubes closely followed the theoretical line derived from the Goldman equation and derived values for the internal ion concentrations (20). This correlation was interpreted as an increase in membrane potassium permeability during development, while sodium permeability remained low. However, since the resting membrane potential never attained the level of the potassium equilibrium potential, it must be assumed that sodium permeability remains a significant factor in determining the final resting membrane potential.

Chloride distribution across the cell membrane is such that the Nernst equilibrium potential (E_{Cl}) is the same as the resting membrane potential[2]. Chloride permeability, however, appears to be low, since changes in external chloride concentration caused no alteration in membrane potential or input resistance (20). The ionic composition of the cell is maintained by a ouabain-sensitive ion pump. Electrogenic pumping is not a significant contribution to the maintenance of membrane potential, at least in chick myotubes, although it can be identified during recovery from prolonged exposure to low temperature or acetylcholine. Presumably, the increased sodium within the myotube acts as the stimulus to such electrogenic pumping.

The input resistance of muscle fibers in culture was shown to fall from relatively high values of 30–40 megohms to about 1 megohm or less as the cells increased in size (5, 18). This change in input resistance was not apparently caused by changes in the specific resistance of the membrane, which remained constant. Fischbach *et al.* (18) were

[1] A. L. Harvey and W. F. Dryden, unpublished observations.
[2] W. F. Dryden, unpublished observations.

Table I—Physical Constants of Muscle Fibers in Culture

	Specific Resistance of Membrane (R_m), ohm cm^2	Resistance of Cytoplasm (R_i), ohm cm	Membrane Time Constant (T_m), msec	Membrane Capacitance (C_m), μF/cm^2	Length Constant (λ), μm
		Steady-State Analysis			
Chick (Ref. 5)	720	—	5	—	—
Mouse (Ref. 6)	694 ± 75	109 ± 19	5.4 ± 0.9	8.4 ± 1.2	609 ± 50
Rat (5 day) (Ref. 20)	1000 ± 94	—	3.1 ± 0.1	3.0 ± 0.3	—
		Transient Analysis			
Chick (Ref. 18)	2639 ± 1166	220 ± 190	9.95 ± 5.45	3.9 ± 1.45	639 ± 299
Mouse (Ref. 6)	2089 ± 343	132 ± 41	6.9 ± 1.6	4.6 ± 2	912 ± 158

unable to demonstrate any correlation between the specific resistance of the myotube membrane and the resting membrane potential. The values obtained for the membrane constants depended on the method of analysis after passing a current of known intensity through the membrane and recording the change in electrotonic potential.

Powell and Fambrough (6), using cultures of mouse muscle where the myotubes were relatively unbranched, preferred to base their calculations on the steady state of the electrotonic potential rather than on an analysis of transient potentials, since the inconstancy of potassium conductance and possible low resistance coupling between myotubes and other cells introduced indeterminate variables. The values reported (Table I) for mouse and chick showed no significant difference, whereas there was an appreciable difference in the results obtained by each method. The values showed similarities to values quoted for adult muscle preparations, but they appeared to occupy a position intermediate between the values quoted for innervated and denervated muscle, suggesting that they can be further modified after the establishment of neural control at innervation.

In contrast to muscle fibers developing from primary myoblasts, the myogenic cell line L6 shows little developmental change in passive electrical properties during the formation of myotubes. Line L6 was first reported by Richter and Yaffe (31), and a number of reports have appeared on its electrophysiological properties. The individual myoblasts, prior to fusion, showed an unusually high resting membrane potential of between −60 and −80 mv (32–34). After fusion, no significant change in the resting membrane potential was detectable. A linear relationship existed between membrane potential and the logarithm of the external potassium concentration, suggesting that the membranes of both myoblasts and myotubes were permeable to K^+ ions. Little Na^+ or Cl^- permeability, however, was measurable.

The specific membrane resistance and capacitance for L6 myoblasts were 8 kilohms cm^2 and 1 μF/cm^2; for myotubes, the values were 12 kilohms cm^2 and 5 μF/cm^2. These values differed significantly from those reported in Table I and probably reflected the altered ion permeability found in this cell line. Myoblasts did not show delayed rectification, which was demonstrable in myotubes. Clearly, therefore, a change in the nature of ionic channels in the membrane did occur at fusion of the L6 myoblast.

Active Electrophysiological Properties—Active changes in membrane potential of muscle fibers in culture have been observed. In general, they can be classified as either action potentials or as oscillations of membrane potential, often associated with twitching or fibrillation of the fibers. The latter activity was first detected by Li *et al.* (15), who noted that a discharge of an action potential ensued in fibers developing from explants when the oscillations in membrane potential caused it to fall below a threshold of about −50 mv. The origins of these fibrillation potentials were suggested to be metabolic (35).

Although action potentials do occur spontaneously in muscle in culture (6, 18), they are seen most frequently after extraneous stimulation. A much slower depolarization, described as a plateau, sometimes with a train of spike discharges superimposed, may also be observed (15, 22). Mainly, the response of a cell to a rapid depolarization from around −70 to below −50 mv is the discharge of an action potential with overshoot. Where the resting potential of the myotubes is less than −50 mv, it is usually necessary first to hyperpolarize the cell by passing an inward current (5, 6, 18).

Unlike the passive properties, the active responses of myotubes of both primary cultures and myogenic clones differ little. Catterall and Nirenberg (36) demonstrated that in both primary chick myotubes and a cloned line of muscle, the sodium channels which open transiently during the action potential, can be activated by veratridine. This activation was antagonized by tetrodotoxin. The fast spike potentials seen in discharging cultured muscle cells can be abolished by removing external sodium or by adding tetrodotoxin to the medium (5, 22, 37). Therefore, the fast spike component is caused by an inward sodium current and resembles that found in normal vertebrate muscle and nerve. The threshold potential necessary to initiate the fast sodium spike was about −45 mv (37).

A study of the currents flowing during voltage clamp suggested that the depolarization necessary to evoke the sodium spike was greater than that necessary to initiate a sodium current. This condition was also true of the peak or reversal potential at which the sodium current ceased to be inward. These differences were ascribed to the cable properties of myotubes, which permitted membrane currents to flow in restricted areas of the membrane during voltage clamp but necessitated a greater depolarization of the membrane for a propagated action potential in an unclamped fiber. To overcome such problems, the cable properties of myotubes of indeterminate length were eliminated by exposing the cultures of 10^{-8} *M* colchicine after 3–4 days of development (38). The destruction of microtubules that this procedure caused resulted in the formation of "myosacs," nearly spherical structures rather than the normal cylindrical shape. Contractile elements were present in such structures, and membrane potentials (−48 mv), action potentials, depolarization in response to acetylcholine, and contractions induced by various agents suggested that the properties of myosacs were comparable

with those of myotubes. An extensive t-tubular system was considered as a possible cause of slight deviations from the predicted response during the initial stages of constant current hyperpolarization. The cytoplasm of these cells was at the isopotential with respect to ground, so good membrane clamping could be achieved. Under these conditions, threshold and peak potentials for both current depolarization and current flow during clamping were in close agreement.

The slow potential was more difficult to characterize. It could be absent, present alone, or present in combination with a fast tetrodotoxin-sensitive spike. Where it occurred, the slow potential was insensitive to tetrodotoxin (37, 39), its amplitude and duration were increased by elevating the concentration of calcium in the bathing medium (40), and it could be abolished by the addition of 2 m*M* manganese chloride (39) or lanthanum chloride (41) to the bath. Removal of the external sodium from the medium also abolished the slow potential (33). Barium was apparently able to substitute for calcium in the bathing solution. The conclusion was that the slow potential was attributable to an inward current of both sodium and calcium. The time course of the tetrodotoxin-resistant slow potential resembled that found in neonatal muscle and denervated muscle (42); the slow channel may be a feature of incomplete development, which is eliminated once full tropic control is established after innervation.

A third type of depolarizing response was noted by Fukuda *et al.* (37, 43), when the membrane potential of the cells was hyperpolarized by passing an appropriate current through electrodes. After the fast spike and the slow potential had been elicited by a short depolarizing pulse superimposed on the hyperpolarizing current, a prolonged depolarization was seen and lasted for several seconds. The amount of depolarization was increased when the external chloride was reduced in concentration, and substitution of potassium chloride in the current passing electrode with the more impermeant potassium acetate resulted in a decrease in amplitude and duration. It appeared, therefore, that the prolonged depolarization of the fibers was attributable to an outward flow of chloride ions supplied to the cytoplasm from the hyperpolarizing electrode, which followed a post spike increase in chloride conductance.

In myosacs (44), prolonged depolarizations of up to 10 sec were associated with a late inward current, attributed to an outflow of chloride ions. This late current and the late chloride spike previously reported were attributed to the same mechanism, which operated in response to changes in membrane potential; chloride redistributed itself during a change in conductance, which was at a maximum around −50 mv. Under normal conditions, such a change in chloride conductance would not be manifested, since active fluctuations and action potentials have a much more rapid time course.

DEVELOPMENT OF CHEMOSENSITIVITY

Acetylcholine Receptor—Much of the relevance of skeletal muscle as a pharmacological preparation hinges on the presence and properties of specialized structures associated with chemosensitivity in the intact fiber, the acetylcholine receptor, and acetylcholinesterase. A detailed review of the developmental biology of membrane cholinoceptors is contained in a recent series of publications (30, 45, 46).

The presence of sensitivity to acetylcholine in muscle in culture was confirmed by Dryden (47) by direct application of acetylcholine from a micropipet to individual fibers in culture. The response was simple contractions of the fiber, but this response was dependent on the possession by the fiber of an intact contractile mechanism. Noncontractile cells and myoblasts cannot be expected to respond mechanically, and intracellular electrophysiological methods are required to investigate fully the properties of the acetylcholine receptor in cultured muscle. The receptor was found in myoblasts insofar as an electrophysiological response could be evoked from myoblasts, especially more developed ones (4, 14), but not in myoblasts of the L6 clone (48). Instead, a slow hyperpolarization of some L6 myoblasts from −25 to −60 mv was observed after acetylcholine iontophoresis. This response was not susceptible to α-neurotoxin or tubocurarine blockade and was not comparable with the rapid hyperpolarization to the reversal potential seen in primary chick myoblasts of low membrane potential exposed to acetylcholine (14). It probably represents an interaction with a membrane component other than the conventionally recognized nicotinic receptor and serves to distinguish clone L6 myoblasts from primary cells.

The rapid rate of acetylcholine receptor formation that occurs at fusion is not apparently dependent on fusion itself, since it also occurs when fusion is prevented by lowering the calcium content of the bathing medium. Indeed, fusion appears to be incidental to the acquisition of differentiated characteristics, since myofilaments, acetylcholinesterase activity, and adenylate cyclase activity all were greatly increased at the time of normal fusion (4, 49). A functioning receptor was not apparently required for fusion of myotubes, since this process proceeded in the presence of tubocurarine, acetylcholine (4), or α-bungarotoxin (50).

The use of ^{125}I-labeled α-bungarotoxin has greatly aided research into receptor distribution and incorporation in view of the virtual irreversibility of the reaction between the two. Autoradiographic investigation of cells and fibers thus labeled confirmed the presence of receptors on the occasional myoblast; on young myotubes, the label appeared to be uniformly distributed over the surface (51, 52), corresponding to a receptor density between 1500 and 2000/μm^2 (53). The uniformity of receptor distribution was a feature only of young myotubes; as development proceeded, clusters of greater receptor density were noted with increasing frequency. The average cluster was 125 μm^2 in area and ovoid and occurred predominantly at the fiber margin. No correlation between the occurrence of clusters and cytological features of the fibers could be found (52, 53).

Electrophysiological confirmation of nonuniform sensitivity along the muscle fibers was provided by a number of reports. Initially, fibers when formed exhibited uniform sensitivity to the transmitter along their length (5, 14, 54). The iontophoretic sensitivities were between 4 and 400 mv/nC. Close application of acetylcholine from an iontophoretic pipet revealed variations in sensitivity ranging from 10 to 1000 mv/nC (55). The areas of greatest sensitivity coincided with the areas of greatest density of

^{125}I-labeled α-bungarotoxin. Furthermore, the areas of greatest sensitivity were thought to be associated with prominent muscle nuclei, although no great significance has been attached to this observation. Such "hot spots" of acetylcholine sensitivity also were noted in myosacs (38). Fetal skeletal muscle prior to innervation, denervated muscle, and adult muscle maintained in organ culture were all sensitive to acetylcholine over the whole muscle surface (56–58), although the sensitivity was not necessarily uniform. The original end-plate membrane retained a much higher receptor density than surrounding areas (59, 60). The muscle in cell culture, therefore, had properties similar to other muscle preparations devoid of nervous control.

The accumulation of receptors, at least at points of innervation in nerve–clonal muscle cultures, was not inhibited by blockade of muscle activity by long-term depolarization in a high K^+ growth medium (61) or by exposure to cobra α-neurotoxin (62). However, the overall sensitivity of muscle fibers was lower if they were repeatedly stimulated by field current depolarization during development (63). The mechanism relating electrical properties of the membrane and receptor incorporation remains to be demonstrated.

The dynamic aspects of receptor biosynthesis and degradation have been studied. Work with fluorescent labeled antimuscle antibody revealed a fair degree of mobility in the surface molecules of membranes of cells in culture (64). It was supposed that the acetylcholine receptor in the absence of innervation was no exception and that a fluid to rigid transformation occurred at synaptogenesis to provide the lattice of receptors found in normal adult end-plates (30).

The binding of ^{125}I-α-bungarotoxin to myotubes was biphasic with a rapid and a slow component (53). The slow component was attributed to the appearance of new receptors, since it could be abolished by inhibitors of RNA synthesis such as cycloheximide and dactinomycin. There was, however, a delay in the reduction in the appearance of new receptors after inhibitor treatment, which suggested that there existed within the myotube a pool of newly synthesized receptors available for incorporation into the membrane. The rate of new receptor incorporation was 90 receptors/μm^2/hr, although the increase in density was only 35/μm^2/hr. This difference was explained by the fact that the surface area in the developing myotubes was also increasing by about 4–5%/hr.

Further work (65) revealed a proteolytic degradation of receptors which required energy and was not affected by prior binding of ^{125}I-α-bungarotoxin. The degradation of the receptors followed first-order kinetics and was, therefore, presumably random. The half-life of receptors in both chick and rat myotubes was about 22 hr. Proteolysis was apparently a cytoplasmic event requiring prior internalization of the receptor. Whether this sequence of events occurs in innervated muscle, which is susceptible to the trophic regulation of the neuron, is a question of considerable interest.

The interactions of receptors with both agonist and antagonist drugs are considered in the following section, but the ionic parameters associated with the activation of the receptor in cultured muscle are discussed here. In myotubes, including clone L6 myotubes (48), exposure of the cell to cholinomimetic agonists resulted in a rapid depolarization of the cell membrane as in "normal" muscle. The action of carbachol was associated with a substantial increase in the rate of sodium entry into a fiber (29). The time course of this entry was not constant throughout equilibration in the presence of carbachol but fell after an initial rapid influx. The fall in influx was attributed to desensitization of the receptors by the agonist. By reducing the temperature to 2°, the rapid initial sodium influx could be studied. The maximum influx (V_{max}) under these conditions was 2×10^7 min^{-1} ions/ionophore. This value compared well with the value of $4–12 \times 10^8$ min^{-1} at 35° computed from the membrane noise measurements of Sachs and Lecar (66) in cultured muscle. Their value for the elementary conductance of a single channel was 0.8×10^{-10} mho which was close to values obtained in frog sartorius muscle (67, 68).

When activated by a cholinomimetic agonist drug, the acetylcholine receptor in cultured muscle fibers apparently opens a sodium permeable ionophore in a manner similar, if not identical, to that taking place in the normal muscle end-plate. Within the ion channel, there is apparently a sodium binding site or energy barrier, possibly analogous to those proposed for the transient tetrodotoxin-sensitive sodium channels of nerve (69).

More recent work (70) on acetylcholine current noise in cultured muscle cells that had fused but had been prevented from elongating (myosacs or "myoballs") showed reasonable agreement with Sachs and Lecar (single-channel conductance = 0.3×10^{-10} mho) and provided evidence that the conformational freedom of the acetylcholine channel is limited by the fluidity of membrane lipids. Since these membrane lipids undergo a phase transition to a more rigid state at about 20° in homeothermic animals, the degree of channel opening is restricted below this temperature. The channel is not apparently specific for sodium, since potassium permeability too is increased on activation (and also trivalent ions, if present) but chloride remains impermeant (71). The behavior of the two permeant ions is interesting in that potential changes attributable to potassium can be predicted from the Goldman equation, *i.e.*, ion flow is through channels of fixed conductance and dependent on ion concentration on each side of the membrane. Sodium-dependent potential changes are described by:

$$E_r = E_K + \frac{(\Delta g_{Na}/\Delta g_K)E_{Na}}{1 + \Delta g_{Na}/\Delta g_K} \qquad \text{(Eq. 1)}$$

where the conductance of the channels is variable. The precise mechanism of ion transfer through the ionophore is clearly complex and awaits further work.

The reversal potential of the activated receptor was described as from 0 to +10 mv for chick embryo muscle explants (5), between −20 and +10 mv (55) and −7 mv (14) in dissociated chick embryo muscle cultures, from +5 to +10 mv in dissociated rat muscle cultures (4), and −2.5 mv in clone L6 myotubes (48). Ritchie and Fambrough (71) reported a mean reversal potential of −2.6 mv, which remained constant despite the increase in the resting membrane potential (30). This result was obtained using rat tissue, which the same authors had shown to retain an unchanged internal ion composition during this period (20). Where the internal sodium concentration fell, a change in reversal potential was expected. The reversal

potential of L6 myoblasts was the same at 22° as at 35° (48). Reduction in $[K]_0$ or $[Na]_0$ caused the reversal potential to be more negative, reversing at between −30 and −40 mv in sodium-free solution. Chloride movement was not apparently involved in determining this value, so suspicion fell on Ca^{2+} as a possible participant in the receptor activated current. No experimental evidence was available, however, to substantiate this view.

Acetylcholinesterase—The enzyme responsible for the hydrolysis of acetylcholine is found in close association with the cholinoceptor in intact muscle, and similar activity was found in muscle in culture (72, 73). Choline acetyltransferase activity was predictably absent in cultures of muscle cells (74). Although acetylcholinesterase was present in myoblasts, a substantial increase in enzymic activity occurred at the time of fusion (75–77). This association of activity and myoblast fusion was also noted for a number of other enzymes (78). The cholinesterase was specific for acetylcholine, since butyrylcholinesterase activity remained at a low level throughout the culture period (76, 77). However, a number of different isozymic forms were present, comparable with those found in embryonic muscle *in situ*.

Harvey and Dryden (77) identified soluble and membrane-bound fractions of total activity and showed that the soluble activity reached a plateau after 4 days of culture while the membrane-bound fraction continued to increase. Little of the enzyme activity was found at the cell surface, most being associated with intracellular membranes (79). The distribution of the enzyme in the myotube showed developmental changes reminiscent of those noted with the cholinoceptor. Enzyme could be histochemically demonstrated in a uniform distribution in the cytoplasm of young myotubes; but, as the cultures aged, the enzyme was apparently localized into areas of greater activity than the surrounding cytoplasm. No correlation between the distribution of receptors and enzyme activity has been shown, and the factors that influence this development remain a matter of speculation.

The sequence of enzyme synthesis in 14-day myotubes was studied by Wilson and Walker (80) after inhibition of existing enzyme with isoflurophate (diisopropyl fluorophosphate). Within 4 hr, 78% of the original activity was restored. The newly synthesized enzyme was of low molecular weight and was not stained by traditional cytochemical methods. The low molecular weight isozymes were readily released from the cell and could be detected in the medium after 4 hr. About this time, the first cytochemically identifiable enzyme appeared around the myotube nuclei. This enzyme was associated with the polymerization of the low molecular weight isozymes and their incorporation into membranous structures. The process continued with a reduction in the proportion of the low molecular weight form present.

The physiological function of acetylcholinesterase in cultured muscle is not obvious. Pharmacological studies, discussed in the following section, suggest that the developmental process in cultures of muscle alone is incomplete.

PHARMACOLOGICAL PROPERTIES

Receptor Specificity—The close similarity of some physiological properties of skeletal muscle in culture to muscle *in vivo* led to the assumption that the pharmacological characteristics would also be similar. Indeed, the response of cultured muscle to acetylcholine was blocked by tubocurarine (4, 47, 54). In the last few years, more detailed studies have shown the faith of muscle physiologists to be justified.

Obata (81), Steinbach (48), and Harvey and Dryden (82) considered the possibility that the development of muscle in the artificial environment of culture may cause the appearance of unusual receptor types. Obata tested cell cultures prepared from the diaphragms of 1-day-old rats. Depolarization responses were obtained with acetylcholine added iontophoretically or directly to the bath, but levarterenol, γ-aminobutyric acid, and glutamic acid had no effect on membrane potential. Steinbach applied methacholine, choline, and levarterenol iontophoretically to L6 myotubes without success. Harvey and Dryden tested a series of compounds (epinephrine, levarterenol, histamine, 5-hydroxytryptamine, dopamine, and γ-aminobutyric acid) for agonist and antagonist activities on cultured chick embryonic muscle. None of these substances produced a significant change in membrane potential. However, epinephrine (but not levarterenol) and 5-hydroxytryptamine reduced responses to the test agonist, carbachol; the mechanism of this depressant activity is unknown and requires further investigation.

Three muscarinic receptor stimulants, methacholine, bethanechol, and pilocarpine, were tested on cultures of chick embryo leg muscle (14, 80). Since no response could be obtained, it is likely that skeletal muscle in culture does not have muscarinic receptor sites.

All nicotinic cholinoceptor stimulant drugs that have been tested on skeletal muscle in culture produced a response. The drugs used included acetylcholine, carbachol (83), decamethonium, tetramethylammonium, nicotine, succinylcholine, and dimethylphenylpiperazinium (82).

From the results of such studies, it is concluded that skeletal muscle in culture responds to agonists that normally activate nicotinic cholinoceptors at the neuromuscular junction but not to agonists that do not normally act on skeletal muscle.

The reversal potential of the acetylcholine response in cultured muscle is between +10 and −20 mv. Feltz and Mallart (84) reported that the reversal potential in junctional areas of frog skeletal muscle was −16 mv, whereas it was −42 mv in extrajunctional areas. This finding suggested that the receptors in muscle in culture behave in a manner more closely resembling junctional rather than extrajunctional cholinoceptors.

The specificity of receptors on cultured skeletal muscle was examined using antagonist drugs. Muscarinic receptor antagonists in high concentrations blocked the response to acetylcholine of normal rat and frog skeletal muscle preparations (85, 86). Similar results were found with cultured muscle. A low concentration of atropine was without effect on responses of cultured skeletal muscle to acetylcholine (81), but responses were inhibited by concentrations of 10^{-4}–10^{-2} *M* atropine (5, 29, 55, 82) and hyoscine (82). Similarly, high concentrations of atropine inhibited end-plate potentials in combined chick muscle–ciliary ganglia cultures (23). Acetylcholine responses of primary mouse cultures and of rat cell line cultures were blocked by both tubocurarine and atropine (40).

All of these studies indicated that the concentrations of atropine have to be 100–1000 times greater than the effective concentrations of tubocurarine. A similar ratio was seen in other skeletal muscle preparations (85, 86).

The reduction of acetylcholine-induced responses by the nicotinic antagonist tubocurarine was demonstrated in several culture systems (13, 47, 48, 53, 81, 83). The concentration–effect curves to carbachol were shifted in a parallel fashion to the right by increasing concentrations of tubocurarine. Similar results were obtained with other nicotinic antagonists, *e.g.*, gallamine (82) and chandonium iodide (87). Affinity constants were calculated to be around 10^7 for tubocurarine, about $2–5 \times 10^6$ for gallamine, and between 10^7 and 10^8 for chandonium iodide. From the half-blocking concentrations of tubocurarine on miniature end-plate potentials in combined spinal cord–rat muscle cell line cultures, the affinity constant would be 0.25×10^7 (88). These values were of the same order as reported from experiments on other more conventional skeletal muscle preparations.

Acetylcholine-induced depolarization can be antagonized by neurotoxins from snake venoms. Such toxins were reported to be highly specific for nicotinic receptors in skeletal muscle preparations (89). Cobra neurotoxin blocked responses in a rat cell line (90) and in explants of chick embryo skeletal muscle (5); α-bungarotoxin blocked responses in primary cultures of rat (53, 81) and chick muscle (55, 91, 92). Dose–response curves to carbachol in the presence of increasing concentrations of α-bungarotoxin showed a reduction in maximal response, as would be expected with a noncompetitive antagonist. Blockade with α-bungarotoxin was essentially irreversible (53, 91). Moreover, β-type bungarotoxins that are selective prejunctional antagonists (93) were without effect on skeletal muscle fibers in nerve-free cultures (92).

The results of experiments with antagonists further substantiated the postulate that cultured skeletal muscle fibers possess one main receptor type that resembles the nicotinic cholinoceptor. There is evidence that the receptor in denervated skeletal muscle has different affinities for antagonists from those of the receptor at the normal motor end-plate (85, 94). While it was suggested (40) that the receptors on cultured muscle resembled more closely those of denervated muscle, available evidence does not support this proposal.

The nicotinic cholinoceptor was suggested to be a protein with an easily reducible disulfide bond near the acetylcholine binding site, and reduction of the disulfide bond was thought to alter the conformation of the receptor protein and its specificity (95). Treatment of electroplax with the disulfide bond reducing agent, 1,4-dithiothreitol, decreased the effects of carbachol and acetylcholine and converted the action of hexamethonium from that of an antagonist to that of an agonist; these changes could be reversed by oxidation (96, 97). Similar results were obtained with several skeletal muscle preparations including frog rectus abdominis (98) and sartorius muscles (99–101), denervated rat skeletal muscle (102), chick biventer cervicis muscle (103), and leech dorsal muscle (104). Despite some species variation (101, 104), 1,4-dithiothreitol appeared to affect the properties of the nicotinic receptor in skeletal muscle.

Harvey and Dryden (105) examined the effects of 1,4-dithiothreitol treatment on chick embryo skeletal muscle grown in cell culture and compared the behavior of the receptors present in cultured muscle to that of the receptors in adult muscle. The receptors on cultured chick embryonic skeletal muscle underwent the characteristic changes in properties following disulfide bond reduction. The concentrations of 1,4-dithiothreitol and exposure times required to produce these effects were similar to the conditions employed in other studies. The changes after 1,4-dithiothreitol (decrease in response to carbachol and conversion of the action of hexamethonium from antagonist to agonist) were as readily reversed by oxidation in cultured muscle as in other systems (96, 97, 103). Membrane depolarization by K^+ ions was not affected by 1,4-dithiothreitol treatment, suggesting that the action of 1,4-dithiothreitol is related to the receptor itself rather than to a nonspecific membrane effect. The actions of 1,4-dithiothreitol were also distinguished from receptor desensitization effects. Harvey and Dryden (105) concluded that the receptors in cultured aneural muscle and in normal muscle were affected similarly by disulfide bond reduction.

Effects of Anticholinesterase Drugs—At the adult neuromuscular junction, the transmitter action of acetylcholine is terminated by hydrolysis by the enzyme acetylcholinesterase. The activity of this enzyme can be affected by anticholinesterase drugs (106). The actions of acetylcholine are generally potentiated and prolonged after administration of an anticholinesterase. The actions of anticholinesterases have been tested on responses to acetylcholine applied directly to cultured muscle cells and on cholinergic end-plate potentials found in combined cultures of nerve and muscle. Physostigmine or neostigmine in concentrations between 0.1 and 100 μg/ml did not affect the size or time course of end-plate potentials in cultures of chick embryo muscle and spinal cord (13, 21). Physostigmine (5–20 μg/ml) did not increase the duration of end-plate potentials in combined cultures of chick embryo muscle and ciliary ganglia; however, 20 μg of physostigmine/ml decreased the amplitude of the end-plate potentials (23). Edrophonium (3.8×10^{-6}–10^{-4} M) did not increase amplitude, time to peak, or half decay time of miniature end-plate potentials recorded in cultures of the muscle cell line L6 and fetal rat spinal cord (88).

Physostigmine and edrophonium did not potentiate the response of cultured chick embryo muscle to iontophoretically applied acetylcholine, and high concentrations of both anticholinesterase drugs inhibited the response to acetylcholine (5, 79). The response of cultured chick embryo muscle to bath application of 10^{-6} M acetylcholine was not increased in the presence of 0.5 μg of neostigmine or physostigmine/ml; the responses to 10^{-3} M acetylcholine and carbachol were inhibited slightly (83). Higher concentrations of anticholinesterase produced depolarization and reduced subsequent acetylcholine responses.

An extension of this study showed that concentration–effect curves to acetylcholine were not altered by 10^{-8}–10^{-7} M physostigmine or neostigmine or by pretreatment of the cultures with 5.4×10^{-6} M of the irreversible anticholinesterase isoflurophate (107).

Although anticholinesterase treatment potentiates the action of acetylcholine in normal muscle, it has little effect on chronically denervated muscle (57). In this respect,

muscle in culture is similar to denervated muscle. A recent electron microscope study of the subcellular distribution of cholinesterase in cultured muscle indicated that little enzyme is on the surface membrane, most being located in the cytoplasm, over myofilaments, or associated with internal membranes (79). The localization of acetylcholinesterase on the external surface of the muscle and the assumption of its physiological function probably occur later in development and are regulated by a "trophic" influence from nerves. Presumably, the lack of effect of anticholinesterases on end-plate potentials in combined nerve and muscle cultures is due to the immaturity of the functional contacts.

Direct effects of the anticholinesterases on membrane potential have also been tested. At concentrations above 10^{-7} *M*, both neostigmine and physostigmine produced a concentration-dependent depolarization of myotubes (107). The depolarization induced by neostigmine, but not that by physostigmine, was inhibited by tubocurarine (107). Isoflurophate at 5.4×10^{-6} *M* had no effect on membrane potential but reduced responses to both acetylcholine and carbachol (107). It was postulated that the antagonism by isoflurophate and the inhibitory actions of high concentrations of other anticholinesterases on acetylcholine responses in culture (5, 79, 83) may be caused by receptor desensitization induced by the anticholinesterase.

Owing to its lack of physiologically functional acetylcholinesterase, nerve-free muscle cultures were the preparation of choice in a study of the site of action of nicotinic agonists (108). It had been postulated that certain agonists other than acetylcholine act at the neuromuscular junction by releasing endogenous acetylcholine (109). This postulate was based on the findings that triethylcholine, tetraethylammonium, and hexamethonium, drugs assumed to block choline and cholinomimetic uptake by the nerve terminal, inhibited responses to carbachol, nicotine, tetramethylammonium, decamethonium, and dimethylphenylpiperazinium but not to acetylcholine (109, 110). However, these effects may result from a combination of two postjunctional actions of these drugs: a curare-like blocking action and an anticholinesterase action (111).

When tested in cultured skeletal muscle at concentrations used previously to eliminate neural acetylcholine release (109, 110, 112), hemicholinium, triethylcholine, tetraethylammonium, and hexamethonium blocked responses to all agonists, and acetylcholine responses were affected as much as those of other cholinomimetics (108). This finding confirms previous work (111, 113) and lends support to the belief that the lack of effect of these blocking drugs on acetylcholine responses in whole muscle was because of their anticholinesterase activity. The results obtained with cultured muscle support the classical theory that nicotinic agonists act directly on receptors on the muscle itself and not by releasing endogenous acetylcholine.

Receptor Desensitization—In many skeletal muscle preparations, cholinomimetic-induced depolarization is not maintained despite a constant drug concentration. This phenomenon, termed "desensitization" (114), is equivalent to a progressive decrease of the response during prolonged contact with cholinomimetics. Desensitization in skeletal muscle has several characteristic features: it is specific for cholinoceptors, it increases with agonist concentration and contact time, and it is reversible.

In explant cultures of chick embryo muscle, the response to iontophoretic pulses of acetylcholine declined if the frequency of stimulation was above 6/min (5). Since the responses did not recover fully after rest, the decline in sensitivity may have represented desensitization or a gradual deterioration of the preparation. Desensitization was, however, evident in rat muscle cultures when acetylcholine pulses were given during a maintained acetylcholine-induced depolarization (81). A similar phenomenon occurred with repeated or prolonged application of acetylcholine or carbachol to L6 myotubes (48). The responses to the brief acetylcholine pulses recovered to control level after the desensitizing exposure was stopped.

The response of cultured chick embryo muscle to prolonged exposure to acetylcholine and carbachol was not maintained, and the membrane gradually repolarized (83). This fading response was suggested to reflect desensitization, and evidence was presented that the desensitization affected cholinoceptors specifically and depended on the concentration of the agonist. Cross-desensitization between acetylcholine and carbachol was also reported. Desensitization in cultured chick embryo muscle was reversible, although the recovery rate was much slower than the recovery rate of other muscle preparations (83). Recovery of cultured muscle appeared to be a two-component process, with an initial phase of rapid recovery followed by a very slow recovery rate (115).

Ritchie and Fambrough (20) found a marked difference in the response of rat and chick myotubes to prolonged application of acetylcholine. Chick myotubes repolarized rapidly in the presence of 10^{-5} *M* acetylcholine, but the depolarization of rat myotubes could be maintained for as long as 100 min. The reason for this difference is unknown.

Desensitization was reported to be more pronounced in older cultures (115). Catterall (29) thought that desensitization increased with the morphological maturity of the myotubes, being more rapid in myotubes possessing cross-striations and hypolemmal nuclei. However, it is possible that the increased rate of desensitization reflects the increased resting membrane potential of the more developed cells (116).

Different agonists have differing abilities to produce desensitization in cultured chick embryo muscle. Concentrations of drugs that produced the same depolarization had markedly different rates of repolarization (117). Succinylcholine produced rapid desensitization, while nicotine caused slow desensitization; acetylcholine and carbachol were intermediate in activity.

Certain drugs increased the rate of repolarization in the presence of a cholinomimetic. Isoflurophate (107), atropine, and hyoscine (115) produced this effect, which is equivalent to an increase in rate of desensitization. Isoflurophate increased the rate of decay of the end-plate current of frog sciatic nerve–sartorius muscle preparations (118). Isoflurophate was thought to be affecting the receptor–ionic conductance modulator complex. Atropine shortened the time that an acetylcholine molecule opened the ionic channels in the muscle membrane (119). This action seems to indicate an enhancement by atropine of desensitization by acetylcholine. The results obtained with

cultured muscle suggest that these drugs (isoflurophate, atropine, and hyoscine) may operate similar mechanisms in cultured muscle fibers.

Desensitization protected cholinoceptors of frog sartorius muscle preparations from binding of snake venom neurotoxins (120, 121). In a similar study with cultured chick embryo muscle, α-bungarotoxin was ineffective in blocking agonist responses after receptor desensitization (122). These results provide further evidence that the nicotinic receptors present in cultured skeletal muscle are similar in properties to the receptors of normal muscle. The finding that desensitization prevents α-bungarotoxin from blocking receptors suggests that desensitization involves a change in the conformation of the receptor so that the toxin-binding sites are no longer operational.

Recent studies showed that binding of labeled snake venom toxins to cultured muscle was reduced in the presence of cholinomimetics (51, 90, 123). Desensitization, rather than physical occlusion, of receptor sites may account for some part of this protective effect.

CONCLUSION

Much has been written on the suitability of some cells in culture for pharmacological investigation. The evidence presented in this review supports the inclusion of skeletal muscle in this category. Most of the pharmacology so far investigated involved electrophysiological changes occurring at the sarcolemma. T-Tubule and sarcoplasmic reticulum sensitivities have not yet been investigated, nor have phenomena involving the contractile element itself. There are formidable technical problems in measuring tension generated by single muscle fibers, and little additional information would be added to existing information achieved using conventional methods.

Yet the increasing availability of sophisticated techniques involving ion-sensitive electrodes, fluorescent probes, and other physical and physicochemical tools will undoubtedly add cell culture to the list of preparations available for the study of all aspects of pharmacology in muscle. The development of membrane noise analysis together with the easy availability of receptor sites gives promise of answers to some fundamental questions concerning the reaction of a drug molecule with a single receptor.

REFERENCES

(1) M. R. Murray, in "The Structure and Function of Muscle," vol. 1, G. H. Bourne, Ed., Academic, New York, N.Y., 1972, p. 237.

(2) I. R. Konigsberg, N. McElvain, M. Tootle, and H. Herrmann, *J. Biophys. Biochem. Cytol.*, **8**, 333 (1960).

(3) D. Yaffe, *Proc. Nat. Acad. Sci. USA*, **61**, 477 (1968).

(4) D. Fambrough and J. E. Rash, *Dev. Biol.*, **26**, 55 (1971).

(5) J. B. Harris, M. W. Marshall, and P. Wilson, *J. Physiol. (London)*, **229**, 751 (1973).

(6) J. A. Powell and D. M. Fambrough, *J. Cell. Physiol.*, **82**, 21 (1973).

(7) S. D. Hauschka, *Dev. Biol.*, **37**, 329 (1974).

(8) Y. Shimada and D. A. Fischman, *ibid.*, **31**, 200 (1973).

(9) P. G. Nelson, *Physiol. Rev.*, **55**, 1 (1975).

(10) S. D. Hauschka and I. R. Konigsberg, *Proc. Nat. Acad. Sci. USA*, **55**, 119 (1966).

(11) I. R. Konigsberg, *Science*, **140**, 1273 (1963).

(12) J. A. Powell, *Exp. Cell Res.*, **80**, 251 (1973).

(13) G. D. Fischbach, *Dev. Biol.*, **28**, 407 (1972).

(14) W. F. Dryden, S. D. Erulkar, and G. de la Haba, *Clin. Exp. Pharmacol. Physiol.*, **1**, 369 (1974).

(15) C. L. Li, K. Engel, and I. Klatzo, *J. Cell. Comp. Physiol.*, **53**, 421 (1959).

(16) R. D. Purves and G. Vrbova, *J. Cell. Physiol.*, **84**, 97 (1974).

(17) G. D. Fischbach, M. Nameroff, and P. G. Nelson, *Biophys. J.*, **10**, 76a (1970).

(18) G. D. Fischbach, M. Nameroff, and P. G. Nelson, *J. Cell. Physiol.*, **78**, 289 (1971).

(19) W. F. Dryden, S. D. Erulkar, and G. de la Haba, *J. Pharm. Pharmacol.*, **23**, 228S (1971).

(20) A. K. Ritchie and D. M. Fambrough, *J. Gen. Physiol.*, **66**, 327 (1975).

(21) M. Kano and Y. Shimada, *J. Cell. Physiol.*, **78**, 233 (1971).

(22) M. Kano, Y. Shimada, and K. Ishikawa, *ibid.*, **79**, 363 (1972).

(23) J. Hooisma, D. W. Slaaf, E. Meetzer, and W. F. Stevens, *Brain Res.*, **85**, 79 (1975).

(24) J. Boethius and E. Knutsson, *Acta Physiol. Scand., Suppl. 277*, **68**, 27 (1966).

(25) M. R. Fedde, *J. Gen. Physiol.*, **53**, 624 (1969).

(26) J. Boëthius, *Acta Physiol. Scand.*, **75**, 253 (1969).

(27) *Ibid.*, **81**, 692 (1971).

(28) J. B. Harris and A. R. Luff, *Comp. Biochem. Physiol.*, **33**, 923 (1970).

(29) W. A. Catterall, *J. Biol. Chem.*, **250**, 1776 (1975).

(30) D. Fambrough, H. C. Hartzell, J. E. Rash, and A. K. Ritchie, *Ann. N.Y. Acad. Sci.*, **228**, 47 (1974).

(31) C. Richter and D. Yaffe, *Dev. Biol.*, **23**, 1 (1970).

(32) A. J. Harris, S. Heinemann, D. Schubert, and H. Tarakis, *Nature*, **231**, 269 (1971).

(33) Y. Kidokoro, *ibid.*, **241**, 158 (1973).

(34) Y. Kidokoro, *J. Physiol. (London)*, **244**, 129 (1975).

(35) C. L. Li, *Science*, **132**, 1889 (1960).

(36) W. A. Catterall and M. Nirenberg, *Proc. Nat. Acad. Sci. USA*, **70**, 3759 (1973).

(37) J. Fukuda, G. D. Fischbach, and T. G. Smith, *Dev. Biol.*, **49**, 412 (1976).

(38) J. Fukuda, M. P. Henkart, G. D. Fischbach, and T. G. Smith, *ibid.*, **49**, 395 (1976).

(39) M. Kano and Y. Shimada, *J. Cell. Physiol.*, **81**, 85 (1973).

(40) B. R. Land, A. Sastre, and T. R. Podleski, *ibid.*, **82**, 497 (1973).

(41) Y. Kidokoro, *J. Physiol. (London)*, **244**, 145 (1975).

(42) J. B. Harris and M. W. Marshall, *Nature New Biol.*, **234**, 191 (1973).

(43) J. Fukuda, *Science*, **185**, 76 (1974).

(44) J. Fukuda, *Nature*, **257**, 408 (1975).

(45) D. M. Fambrough, in "Neurochemistry of Cholinergic Receptors," E. de Robertis and J. Schacht, Eds., Raven, New York, N.Y., 1974, p. 85.

(46) D. M. Fambrough, H. C. Hartzell, J. A. Powell, J. E. Rash, and N. Joseph, in "Synaptic Transmission and Neuronal Interaction," M. V. L. Bennett, Ed., Raven, New York, N.Y., 1974, p. 285.

(47) W. F. Dryden, *Experientia*, **26**, 984 (1970).

(48) J. H. Steinbach, *J. Physiol. (London)*, **247**, 393 (1975).

(49) J. M. Prives and B. M. Paterson, *Proc. Nat. Acad. Sci. USA*, **71**, 3208 (1974).

(50) A. L. Harvey and W. F. Dryden, *Experientia*, **30**, 613 (1974).

(51) Z. Vogel, A. J. Sytkowski, and M. W. Nirenberg, *Proc. Nat. Acad. Sci. USA*, **69**, 3180 (1972).

(52) A. J. Sytkowski, Z. Vogel, and M. W. Nirenberg, *ibid.*, **70**, 270 (1973).

(53) H. C. Hartzell and D. M. Fambrough, *Dev. Biol.*, **30**, 153 (1973).

(54) M. Kano, Y. Shimada, and K. Ishikawa, *Brain Res.*, **25**, 216 (1971).

(55) G. D. Fischbach and S. A. Cohen, *Dev. Biol.*, **31**, 147 (1973).

(56) J. Diamond and R. Miledi, *J. Physiol. (London)*, **162**, 393 (1962).

(57) J. Axelsson and S. Thesleff, *ibid.*, **147**, 178 (1959).

(58) R. Miledi and O. A. Trowell, *Nature*, **194**, 981 (1962).

(59) H. C. Hartzell and D. M. Fambrough, *J. Gen. Physiol.*, **60**, 248 (1972).

(60) D. M. Fambrough, *ibid.*, **64**, 468 (1974).

(61) J. H. Steinbach, *Nature*, **248**, 70 (1974).

(62) J. H. Steinbach, A. J. Harris, J. Patrick, D. Schubert, and S. Heinemann, *J. Gen. Physiol.*, **62**, 255 (1973).

(63) S. A. Cohen and G. D. Fischbach, *Science*, **181**, 76 (1973).

(64) M. Edidin and D. Fambrough, *J. Cell Biol.*, **57**, 27 (1973).

(65) P. N. Devreotes and D. M. Fambrough, *ibid.*, **65,** 335 (1975).
(66) F. Sachs and H. Lecar, *Nature New Biol.*, **246,** 214 (1973).
(67) B. Katz and R. Miledi, *J. Physiol. (London)*, **230,** 707 (1973).
(68) C. R. Anderson and C. F. Stevens, *ibid.*, **235,** 655 (1973).
(69) B. Hille, *J. Gen. Physiol.*, **66,** 535 (1975).
(70) Y. Lass and G. D. Fischbach, in "The Synapse: Scottish Electrophysiological Society Symposium," G. Cottrell, Ed., Blackie & Sons, Glasgow, Scotland, 1976, p. C14.
(71) A. K. Ritchie and D. M. Fambrough, *J. Gen. Physiol.*, **65,** 751 (1975).
(72) W. K. Engel, *J. Histochem. Cytochem.*, **9,** 66 (1961).
(73) B. C. Goodwin and I. W. Sizer, *Dev. Biol.*, **11,** 136 (1965).
(74) E. L. Giller, S. K. Schrier, A. Shainberg, H. R. Fisk, and P. G. Nelson, *Science*, **182,** 588 (1973).
(75) R. A. Fluck and R. C. Strohman, *Dev. Biol.*, **33,** 417 (1973).
(76) B. W. Wilson, P. S. Nieberg, C. R. Walker, T. A. Linkhart, and M. D. Fry, *ibid.*, **33,** 285 (1973).
(77) A. L. Harvey and W. F. Dryden, *Differentiation*, **2,** 237 (1974).
(78) A. Shainberg, G. Yagil, and D. Yaffe, *Dev. Biol.*, **25,** 1 (1971).
(79) G. D. Fischbach, S. A. Cohen, and M. P. Henkart, *Ann. N.Y. Acad. Sci.*, **228,** 35 (1974).
(80) B. W. Wilson and C. R. Walker, *Proc. Nat. Acad. Sci. USA*, **71,** 3194 (1974).
(81) K. Obata, *Brain Res.*, **73,** 71 (1974).
(82) A. L. Harvey and W. F. Dryden, *Eur. J. Pharmacol.*, **28,** 125 (1974).
(83) *Ibid.*, **27,** 5 (1974).
(84) A. Feltz and A. Mallart, *J. Physiol. (London)*, **218,** 101 (1971).
(85) R. Beranek and F. Vyskocil, *ibid.*, **188,** 53 (1967).
(86) *Ibid.*, **195,** 493 (1968).
(87) A. L. Harvey, D. Paul, and H. Singh, *J. Pharm. Pharmacol.*, **27,** 62P (1975).
(88) Y. Kidokoro and S. Heinemann, *Nature*, **252,** 593 (1974).
(89) C. Y. Lee, *Ann. Rev. Pharmacol.*, **12,** 265 (1972).
(90) J. Patrick, S. F. Heinemann, J. Lindstrom, D. Schubert, and J. H. Steinbach, *Proc. Nat. Acad. Sci. USA*, **69,** 2762 (1972).
(91) A. L. Harvey, W. F. Dryden, and I. G. Marshall, *J. Pharm. Pharmacol.*, **25,** 126P (1973).
(92) W. F. Dryden, A. L. Harvey, and I. G. Marshall, *Eur. J. Pharmacol.*, **26,** 262 (1974).
(93) *Ibid.*, **26,** 256 (1974).
(94) A. J. Lapa, E. X. Albuquerque, and J. Daly, *Exp. Neurol.*, **43,** 375 (1974).
(95) A. Karlin, *Fed. Proc.*, **32,** 1847 (1973).
(96) A. Karlin and E. Bartels, *Biochim. Biophys. Acta*, **126,** 525 (1966).
(97) A. Karlin and M. Winnik, *Proc. Nat. Acad. Sci. USA*, **60,** 668 (1968).
(98) T. W. Mittag and A. Tormay, *Fed. Proc.*, **29,** 547 (1970).
(99) D. H. Lambert, *Experientia*, **29,** 668 (1973).
(100) J. M. Lindstrom, S. J. Singer, and E. S. Lennox, *J. Membr. Biol.*, **11,** 217 (1973).
(101) D. Ben-Haim, E. M. Landau, and I. Silman, *J. Physiol. (London)*, **234,** 305 (1973).
(102) E. X. Albuquerque, M. D. Sokoll, B. Sonesson, and S. Thesleff, *Eur. J. Pharmacol.*, **4,** 40 (1968).
(103) H. P. Rang and J. M. Ritter, *Mol. Pharmacol.*, **7,** 620 (1971).
(104) D. H. Ross and D. J. Triggle, *Biochem. Pharmacol.*, **21,** 2532 (1972).
(105) A. L. Harvey and W. F. Dryden, *ibid.*, **23,** 3093 (1974).
(106) W. C. Bowman and S. N. Webb, in "International Encyclopedia of Pharmacology and Therapeutics," section 14, vol. 2., J. Cheymol, Ed., Pergamon, Oxford, England, 1972, p. 427.
(107) A. L. Harvey and W. F. Dryden, *J. Pharm. Pharmacol.*, **26,** 865 (1974).
(108) A. L. Harvey and W. F. Dryden, *Eur. J. Pharmacol.*, **28,** 131 (1974).
(109) C. Y. Chiou and J. P. Long, *Proc. Soc. Exp. Biol. Med.*, **132,** 732 (1969).
(110) C. Y. Chiou, *Eur. J. Pharmacol.*, **12,** 342 (1970).
(111) I. G. Marshall, *Br. J. Pharmacol.*, **42,** 462 (1971).
(112) I. G. Marshall, *Eur. J. Pharmacol.*, **8,** 204 (1969).
(113) A. Gandiha, A. L. Green, and I. G. Marshall, *ibid.*, **18,** 174 (1972).
(114) B. Katz and S. Thesleff, *J. Physiol. (London)*, **138,** 63 (1957).
(115) A. L. Harvey, Ph.D. thesis, University of Strathclyde, Glasgow, Scotland, 1974.
(116) L. G. Magazanik and F. Vyskocil, *J. Physiol. (London)*, **210,** 507 (1970).
(117) A. L. Harvey and W. F. Dryden, Abstracts Sixth International Congress Pharmacology, No. 464, Helsinki, Finland, 1975.
(118) K. Kuba, E. X. Albuquerque, and E. A. Barnard, *Science*, **181,** 853 (1973).
(119) B. Katz and R. Miledi, *Proc. Roy. Soc., B*, **184,** 221 (1973).
(120) R. Miledi and L. T. Potter, *Nature*, **233,** 599 (1971).
(121) H. A. Lester, *Mol. Pharmacol.*, **8,** 632 (1972).
(122) W. F. Dryden and A. L. Harvey, *Br. J. Pharmacol.*, **51,** 456 (1974).
(123) B. Paterson and J. Prives, *J. Cell Biol.*, **59,** 241 (1973).

ACKNOWLEDGMENTS AND ADDRESSES

Received from the *Department of Physiology and Pharmacology, University of Strathclyde, Glasgow G1 1XW, Scotland.*

[x] To whom inquiries should be directed. Present address: Department of Pharmacology, University of Alberta, Edmonton, Alberta T6G 2E1, Canada.

Sulfur-Containing Derivatives of Amphetamine: Thioureas, Methanesulfonamides, and Trifluoromethanesulfonamides

WILLIAM O. FOYE ˣ and JAYANT N. SANE

Abstract □ *N*-Methylthiourea, methanesulfonamide, and trifluoromethanesulfonamide derivatives of amphetamine, 4-nitroamphetamine, and 4-aminoamphetamine were synthesized. The *N*-methylthiourea derivative of amphetamine, as well as the triethylammonium salt of the dithiocarbamate, produced significant depressor effects in normotensive dogs. *N,N'*-Bis(methanesulfonyl)-1-methyl-2-(4-aminophenyl)ethylamine and *N*-trifluoromethanesulfonyl-1-methyl-2-phenylethylamine, but not *N*-methanesulfonyl-1-methyl-2-phenylethylamine and *N*-trifluoroacetyl-1-methyl-2-(4-trifluoromethanesulfonamidophenyl)ethylamine, showed significant antiobesity effects in rats.

Keyphrases □ Amphetamine analogs—various sulfur-containing derivatives synthesized, evaluated for central stimulant and anorexic effects, rats □ 2-Phenylethylamines, substituted—various sulfur-containing amphetamine derivatives synthesized, evaluated for central stimulant and anorexic effects, rats □ Stimulant activity—various sulfur-containing amphetamine derivatives evaluated □ Anorexic activity—various sulfur-containing amphetamine derivatives evaluated □ Structure–activity relationships—various sulfur-containing amphetamine derivatives evaluated for central stimulant and anorexic activity

Conversion of the amino group of the 2-phenylethylamine structure to dithiocarbamate and thiourea groups, with the intention of providing copper-binding ligands to inhibit dopamine β-hydroxylase, resulted in compounds with blood pressure lowering effects (1). Similarly, conversion of the 2-phenylethylamine structure to methanesulfonamides, both of the aliphatic nitrogen and in the *para*-position of the ring, also gave compounds that lowered blood pressure in hypertensive rats and dogs (2). The methanesulfonamide of dextroamphetamine produced a similar result (2). Previously, inclusion of the alkanesulfonamide group in the aromatic ring of phenylethanolamines was shown to confer either adrenergic stimulant or blocking activity, the latter generally in conjunction with an isopropyl or larger group on the aliphatic nitrogen (3, 4).

To investigate further the effect of converting the aliphatic amino group of 2-phenylethylamines, particularly the amphetamine structure, to an acidic function, methanesulfonamido, trifluoromethanesulfonamido, and trifluoroacetyl derivatives of amphetamine, 4-nitroamphetamine, and 4-aminoamphetamine were prepared. Thiourea derivatives also were prepared, since a number of thiourea derivatives have shown inhibitory activity against dopamine β-hydroxylase (5) and the aliphatic amino is converted to an acidic function. Several corresponding derivatives of 2-phenylethylamine also were obtained.

Since both tyramine and the 4-hydroxy derivative of amphetamine are better substrates for dopamine β-hydroxylase than the nonhydroxylated compounds (6), the inclusion of the *para*-substituents in the amphetamine structure should provide compounds with potential for activity as inhibitors of dopamine β-hydroxylase. Larsen and Lish (7) pointed out that methanesulfonamides may be considered bioisosteres of the phenolic function.

The possibility exists that by conversion of the basic nitrogen of the amphetamine structure to an acidic function or by introduction of an essentially acidic function into the *para*-position of amphetamine, some of the characteristic pharmacological effects of amphetamine might be lost and others retained. Some ring substitutions in 2-phenylethylamine dithiocarbamates resulted in a loss of behavioral effects (8). Several pharmacological activities to be expected from amphetamine, including blood pressure effects, central nervous system (CNS) stimulation, behavioral effects, and antiobesity effects, have been observed in animals on treatment with these compounds.

DISCUSSION

Chemistry—Ammonium (+)-1-methyl-2-phenylethyldithiocarbamate was prepared previously and showed behavioral effects somewhat different from those of amphetamine (8). Since the compound was rather unstable, the triethylammonium salt was obtained to provide a product of greater stability. Nitration of amphetamine was carried out by the procedure of Holland *et al.* (9), in which the *para*-isomer was separated by fractional crystallization of the trifluoroacetyl derivative. Hydrogenation of the *para*-nitro group was achieved with either the *N*-trifluoroacetyl derivative (9) or 4-nitroamphetamine obtained by hydrolysis of the *N*-trifluoroacetyl derivative, using platinum oxide as the catalyst.

The methanesulfonamide and trifluoroacetamide derivatives were readily obtained from methanesulfonyl chloride and trifluoroacetic anhydride. Preparation of the trifluoromethanesulfonamides proved to be more difficult, but they were obtained by use of trifluoromethanesulfonic anhydride in dry ether. Vacuum distillation of the resulting liquids generally gave low melting solids. Methylthiourea derivatives were obtained from methyl isothiocyanate; many of these products were extremely hygroscopic and had to be stored under dry nitrogen and *in vacuo*.

Attempts also were made to obtain 4-trifluoroacetamido-2-phenylethylamine, 4-trifluoromethanesulfonamido-2-phenylethylamine, and 4-methanesulfonamido-2-phenylethylamine from the respective benzyl cyanide derivatives; catalytic hydrogenation with various catalysts and such reducing agents as lithium aluminum hydride, diborane, and sodium borohydride failed to provide pure products. The compounds prepared are listed in Table I.

Biological Results[1]—Behavioral effects in rats were observed continuously for 6 hr and daily for 7 days after dosing with *N,N'*-bis(methanesulfonyl)-1-methyl-2-(4-aminophenyl)ethylamine (XI). An oral dose of 25 mg/kg in three rats caused low body posture (2/3), moderately decreased spontaneous motor activity (2/3), and slight (1/3) or moderate

[1] The behavioral observations and antiobesity tests were carried out at Smith Kline & French Laboratories. Results were made available through the courtesy of Dr. J. W. Wilson.

Table I—Derivatives of Amphetamine and Related Compounds

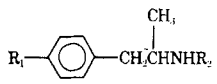

Compound	R_1	R_2	Formula	Yield, %	Melting Point	Analysis, % Calc.	Found
I(+)	H	$CS_2^-(C_2H_5)_3NH^+$	$C_{16}H_{28}N_2S_2$	46	—	C 61.54	61.3
						H 8.87	9.0
						N 8.97	8.3
						S 20.51	20.2
II(±)	H	$C(=S)NHCH_3$	$C_{11}H_{16}N_2S$	65	—	C 63.46	63.7
						H 7.69	7.8
						N 13.46	13.4
III(+)	H	SO_2CF_3	$C_{10}H_{12}F_3NO_2S$	40	75–78°	C 44.94	44.8
						H 4.49	4.46
						N 5.24	5.22
						S 11.98	12.36
IV(±)	NO_2	$C(=S)NHCH_3$	$C_{11}H_{15}N_3O_2S$	69	41–43°	C 52.17	52.0
						H 5.93	6.1
						N 16.60	16.3
V(+)	NO_2	SO_2CF_3	$C_{10}H_{11}F_3N_2O_4S$	25	42–45°	C 38.46	38.7
						H 3.53	3.8
						N 8.97	9.2
						S 10.26	10.3
VI(+)	NO_2	SO_2CH_3	$C_{10}H_{14}N_2O_4S$	79	95–98°	C 46.51	46.53
						H 5.43	5.41
						N 10.81	10.65
						S 12.40	12.32
VII(±)	CF_3CONH	$C(=S)NHCH_3$	$C_{13}H_{16}F_3N_3OS$	66	147–149°	C 48.90	49.2
						H 5.02	5.1
						N 13.17	12.7
						S 10.03	9.8
VIII(±)	CF_3CONH	$COCF_3$	$C_{13}H_{12}F_6N_2O_2$	76	173–176°	C 45.61	45.34
						H 3.51	3.72
						F 33.33	32.9
						N 8.19	7.98
IX(±)	CF_3SO_2NH	$COCF_3$	$C_{12}H_{12}F_6N_2O_3S$	37	121–123°	C 38.10	38.22
						H 3.17	3.24
						N 7.41	7.50
X(±)	$CH_3NHC(=S)NH$	$C(=S)NHCH_3$	$C_{13}H_{20}N_4S_2$	67	99–102°	C 52.70	52.62
						H 6.76	7.21
						N 18.92	18.90
XI(±)	CH_3SO_2NH	SO_2CH_3	$C_{11}H_{18}N_2O_4S_2$	50	105–108°	C 43.14	42.7
						H 5.88	5.5
						N 9.15	8.8
XII(±)	CF_3CONH	SO_2CH_3	$C_{12}H_{15}F_3N_2O_3S$	20	157–160°	C 44.44	44.7
						H 4.63	4.7
						N 8.64	8.8
XIII(±)	CH_3SO_2NH	$C(=S)NHCH_3$	$C_{12}H_{19}N_3O_2S_2$	—	45–50°	C 47.84	48.3
						H 6.31	6.4
						N 13.95	13.6
XIV(+)	CF_3CONH	SO_2CF_3	$C_{12}H_{12}F_6N_2O_3S$	26	143–145°	C 38.10	38.2
						H 3.17	3.2
						N 7.41	7.7
						S 8.47	8.1
		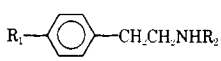					
XV	H	SO_2CF_3	$C_9H_{10}F_3NO_2S$	35	35–38°	C 42.29	42.06
						H 3.95	3.87
						N 5.54	5.34
						S 13.00	12.85
XVI	CF_3CONH	$COCF_3$	$C_{12}H_{10}F_6N_2O_2$	51	210–212°	C 43.90	44.06
						H 3.05	2.96
						N 8.54	8.53
XVII	CF_3SO_2NH	SO_2CF_3	$C_{10}H_{10}F_6N_2O_4S_2$	33	143–145°	C 30.00	30.2
						H 2.50	2.6
						N 7.00	6.8
		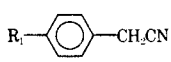					
XVIII	CF_3CONH	—	$C_{10}H_7F_3N_2O$	70	153–156°	C 52.63	52.56
						H 3.07	3.27
						N 12.28	12.20
XIX	CF_3SO_2NH	—	$C_9H_7F_3N_2O_2S$	18	105–108°	C 40.91	40.8
						H 2.65	2.7
						N 10.61	10.5
						S 12.12	12.1

(1/3) hypothermia. The bis(trifluoroacetyl) derivative (VIII), however, showed most of the behavioral effects of amphetamine, whereas IX had no overt effects at the same dose level.

In antiobesity tests, oral administration of 25 mg/kg of the same compound to rats daily for 5 days significantly reduced 1-hr food consumption as well as 5-hr food consumption over the 5-day period. There was also a significant change in body weight gain compared to controls during the 5-day test period.

Oral administration of 25 mg/kg of III to rats in the antiobesity test significantly reduced both 1- and 5-hr food consumptions over the 5-day period. There was also a significant change in body weight gain compared to controls during this period. However, oral administration of 25 mg/kg of *N*-methanesulfonyl-1-methyl-2-phenylethylamine, previously prepared (2), to rats significantly reduced 1-hr food consumption only on Day 4 and failed to reduce 5-hr food consumption significantly. There was no significant change in body weight gain for this compound compared to controls over the 5-day period. Oral administration of 25 mg/kg of *N*-trifluoroacetyl-1-methyl-2-(4-trifluoromethanesulfonamidophenyl)ethylamine (IX) to rats failed to produce a significant reduction in either 1- or 5-hr food consumption. There was, however, a significant reduction in body weight compared to controls over the 5-day test period.

The following cardiovascular effects were observed[2]. The triethylammonium salt of the dithiocarbamate of amphetamine (I) and the *N*-methylthiourea of amphetamine (II) both produced significant depressor effects at doses of 4 mg/kg in normotensive dogs anesthetized with urethan–chloralose, with I being the most potent (10). Both compounds caused CNS stimulation, significantly reduced the effects of ephedrine in rats, and reduced hexobarbital sleeping time in mice. In addition, the typical stereotyped behavior of amphetamine was observed in mice, along with increased motor activity and mydriasis.

Whereas the dithiocarbamate and methylthiourea of amphetamine retained much of the behavioral pattern of amphetamine, the more negatively *N*-substituted bis(methanesulfonyl) derivative (XI) lost most of these behavioral effects while retaining the ability to suppress appetite. Conversion of the nitrogen of amphetamine to a negatively substituted amide was not the sole requirement for this combination of effects, however, since the *N*-methanesulfonyl derivative of amphetamine (2) and IX showed no significant appetite suppressant effects.

EXPERIMENTAL[3]

The following procedures are representative.

Triethylammonium (+)-1-Methyl-2-phenylethyldithiocarbamate (I)—To a cooled solution of 5.44 g (0.04 mole) of dextroamphetamine in 25 ml of absolute ethanol was added, with stirring, 6.06 g (0.06 mole) of triethylamine. To this solution was added dropwise 4.56 g (0.06 mole) of carbon disulfide. Stirring was continued for 24 hr, and the dark-yellow liquid was evaporated in a rotary evaporator, leaving a sticky, yellow residue. This residue was washed with dry ether and dried *in vacuo*, giving 5.8 g (46%) of yellow oil; IR (film): 3220 (NH), 2620 (NH^+), 1300 (C=S), and 970 (C=S) cm^{-1}; $[\alpha]_D^{29}$ +32.1° (c = 1, ethyl acetate); n_D^{22} 1.6011.

Anal.—Calc. for $C_{16}H_{28}N_2S_2$: C, 61.54; H, 8.97; N, 8.97; S, 20.51. Found: C, 61.3; H, 9.0; N, 8.5; S, 20.2.

(±)-1-Methyl-3-(1-methyl-2-phenylethyl)thiourea (II)—To a solution of 2.72 g (0.02 mole) of dextroamphetamine in 25 ml of absolute ethanol was added dropwise, with stirring, 1.125 g (0.025 mole) of methyl isothiocyanate in 10 ml of absolute ethanol. The mixture was refluxed for 12 hr and was allowed to cool, and the solvent was removed in a rotary evaporator. The sticky residue was washed with petroleum ether and dried *in vacuo*. A 65% yield of brown oil was obtained; IR (film): 3220 (NH), 1250 (C=S), and 970 (C=S) cm^{-1}; n_D^{22} 1.6042.

Anal.—Calc. for $C_{11}H_{16}N_2S$: C, 63.46; H, 7.69; N, 13.46. Found: C, 63.7; H, 7.8; N, 13.4.

(+) - *N* - Trifluoromethanesulfonyl-1-methyl-2-phenylethylamine (III)—To a cooled solution of 2.72 g (0.02 mole) of dextroamphetamine in 25 ml of ether was added, with stirring, 7.05 g (0.025 mole) of trifluoromethanesulfonic anhydride (8) in 25 ml of ether. The mixture was stirred for 3 hr, refrigerated overnight, and filtered; the solvent was removed in a rotary evaporator. The white solid was recrystallized from petroleum ether (bp 30–60°), giving 2.1 g (40%), mp 75–78°; IR (potassium bromide): 3300 (NH), 1600 (NH), and 1175–1225 (SO_2) cm^{-1}; $[\alpha]_D^{29}$ +21.0° (c = 1, ethyl acetate).

Anal.—Calc. for $C_{10}H_{12}F_3NO_2S$: C, 44.94; H, 4.49; N, 5.24; S, 11.98. Found: C, 44.8; H, 4.46; N, 5.22; S, 12.36.

(+)-1-Methyl-2-(4-nitrophenyl)ethylamine—A mixture of 11.0 g (0.04 mole) of (+)-*N*-trifluoroacetyl-1-methyl-2-(4-nitrophenyl)ethylamine (9) and 120 ml of 1 *N* sodium hydroxide in 180 ml of dimethoxyethane was stirred at 25° for 3 hr under nitrogen. The dimethoxyethane was removed *in vacuo*, and the aqueous portion was extracted three times with 70-ml portions of methylene chloride. The combined extracts were washed three times with 50-ml portions of water and dried over anhydrous sodium sulfate. The solvent was removed in a rotary evaporator, leaving 5 g (95%) of residual oil. This oil was converted to the hydrochloride, mp 195–199° [lit. (11) mp 197–199°]; $[\alpha]_D^{29}$ +30.0° (c = 4, ethyl acetate).

(+) - *N* - Methanesulfonyl-1-methyl-2-(4-nitrophenyl)ethylamine (VI)—To a cooled solution of 9.0 g (0.05 mole) of (+)-1-methyl-2-(4-nitrophenyl)ethylamine in 50 ml of methylene chloride were added dropwise, with stirring, 5.92 g (0.052 mole) of methanesulfonyl chloride in 40 ml of methylene chloride and 5.25 g (0.052 mole) of triethylamine in 40 ml of methylene chloride. The mixture was then allowed to reach room temperature and was stirred for 12 hr. The resulting solution was washed with 1 *N* hydrochloric acid and water, dried over anhydrous sodium sulfate, and evaporated in a rotary evaporator. The brown residue was dissolved in hot benzene, treated with charcoal, and filtered. The cooled filtrate gave 10 g (79%) of the desired product, mp 95–98°; IR (potassium bromide): 3270 (NH), 1500 (NO_2), and 1145 (SO_2) cm^{-1}; $[\alpha]_D^{29}$ +30.0° (c = 1, ethyl acetate).

Anal.—Calc. for $C_{10}H_{14}N_2O_4S$: C, 46.51; H, 5.43; N, 10.81; S, 12.40. Found: C, 46.53; H, 5.41; N, 10.65; S, 12.32.

(+)-1-Methyl-2-(4-aminophenyl)ethylamine—(+)-1-Methyl-2-(4-nitrophenyl)ethylamine (18 g, 0.1 mole) in 200 ml of tetrahydrofuran with 0.3 g of platinum dioxide was hydrogenated at 4 atm. After the theoretical amount of hydrogen had been taken up, the catalyst was filtered and the solvent was removed in a rotary evaporator. A yield of 14.2 g (95%) of compound was obtained; the dihydrochloride melted at 255–260° [lit. (12) mp 258–260°]; $[\alpha]_D^{29}$ +15.8° (c = 1, ethyl acetate).

(±)-*N,N'*-Bis(trifluoroacetyl)-1-methyl-2 - (4 - aminophenyl)ethylamine (VIII)—To a cooled solution of 2.46 g (0.01 mole) of (±)-1-methyl-2-(4-aminophenyl)ethyltrifluoroacetamide (9) in 50 ml of benzene was added 2.94 g (0.014 mole) of trifluoroacetic anhydride dropwise over 10 min. The mixture was brought to room temperature and refluxed for 3 hr. It was refrigerated overnight, and the white solid was filtered, washed with dilute hydrochloric acid and water, and dried in a vacuum desiccator. The product was recrystallized from chloroform, giving 2.6 g (76%) of white solid, mp 173–176°; IR (potassium bromide): 3300 (NH), 1700 (C=O), 1550 (amide), and 1150 (CF_3) cm^{-1}.

Anal.—Calc. for $C_{13}H_{12}F_6N_2O_2$: C, 45.61; H, 3.51; F, 33.33; N, 8.19. Found: C, 45.34; H, 3.72; F, 32.9; N, 7.98.

(±)-*N*-Methanesulfonyl-1-methyl-2-(4 - trifluoroacetylaminophenyl)ethylamine (XII)—A solution of 2.28 g (0.01 mole) of VI in 200 ml of absolute ethanol with 0.65 g of 5% platinum-on-charcoal was hydrogenated at 3 atm. After 48 hr, the mixture was filtered and the solvent was removed *in vacuo*. The residual viscous liquid was dissolved in 250 ml of benzene, and trifluoroacetic anhydride (2.1 g, 0.015 mole) was added with stirring. The mixture was refluxed for 3 hr, allowed to cool, and refrigerated overnight. The resulting solid was filtered, washed with water, and dried *in vacuo*. It was recrystallized from ethanol–water, giving 0.5 g, mp 157–160°; IR (potassium bromide): 3270 (NH) and 1700 (C=O) cm^{-1}.

Anal.—Calc. for $C_{12}H_{15}F_3N_2O_3S$: C, 44.44; H, 4.63; N, 8.64. Found: C, 44.7; H, 4.7; N, 8.8.

(±)-1-Methyl-3-[1-methyl-2-(4-methanesulfonamidophenyl)ethyl]thiourea (XIII)—A solution of 2.28 g (0.01 mole) of VI in 200 ml of absolute ethanol with 0.65 g of 5% platinum-on-charcoal was hydrogenated at 3 atm. After 48 hr, the mixture was filtered and the solvent was removed *in vacuo*. The residual viscous liquid was dissolved in 50 ml of absolute ethanol, and 0.85 g (0.008 mole) of methyl isothiocyanate was added. The mixture was refluxed for 3 hr, the solvent was removed *in vacuo*, and the residue was washed with dry ether and dried *in vacuo*, mp 45–50°; IR (film): 3350 (NH), 1300–1335 (SO_2), and 1135–1165 (SO_2) cm^{-1}.

Anal.—Calc. for $C_{12}H_{19}N_3O_2S_2$: C, 47.84; H, 6.31; N, 13.95. Found: C, 48.2; H, 6.4; N, 13.6.

(+)-*N*-Trifluoromethanesulfonyl-1-methyl-2 - (4 - nitrophenyl)ethylamine (V)—To a cooled solution of 9.0 g (0.05 mole) of (+)-1-methyl-2-(4-nitrophenyl)ethylamine in 30 ml of anhydrous ether was added, with stirring, 14.6 g (0.052 mole) of trifluoromethanesulfonic anhydride in 20 ml of anhydrous ether. The resulting mixture was stirred

[2] C. S. Venugopalan, Pharmacology Department, Massachusetts College of Pharmacy.

[3] Melting points were determined in capillaries with a Mel-Temp melting-point block and are uncorrected. IR absorption spectra were obtained with a Perkin-Elmer model 137B spectrophotometer. Optical rotations were obtained with a Carl Zeiss polarimeter. NMR spectra were determined with a Varian T60 spectrometer using tetramethylsilane as the internal standard. Elemental analyses were performed by Dr. F. B. Strauss, Oxford, England, or by Dr. Carol K. Fitz of Carlisle, Mass. TLC was carried out using silica gel, and products were detected by exposure to iodine vapor. Dextroamphetamine, 4-aminobenzyl cyanide, 4-amino-2-phenylethylamine, trifluoroacetic anhydride, methyl isothiocyanate, and methanesulfonyl chloride were obtained from Aldrich Chemical Co. Trifluoromethanesulfonic acid was obtained from the 3M Co.

for 12 hr and refrigerated overnight. The precipitate was filtered and washed with dry ether, and the filtrate was evaporated *in vacuo*, leaving an oil. This oil was distilled at 165–170°/0.2 mm, giving 3.8 g (25%) of a solid, mp 42–45°; IR (potassium bromide): 3300 (NH), 1520 (NO_2), 1335–1375, and 1125–1150 (SO_2) cm^{-1}; $[\alpha]_D^{30}$ +37.0° (c = 1, ethyl acetate).

Anal.—Calc. for $C_{10}H_{11}F_3N_2O_4S$: C, 38.46; H, 3.53; N, 8.97; S, 10.26. Found: C, 38.7; H, 3.8; N, 9.2; S, 10.3.

(+)-*N*-Trifluoromethanesulfonyl-1-methyl-2 - (4 - trifluoroacetylaminophenyl)ethylamine (XIV)—A solution of 3.12 g (0.01 mole) of V in 150 ml of tetrahydrofuran with 0.4 g of platinum dioxide was hydrogenated at 3 atm. After 48 hr, the solution was filtered and the solvent was removed *in vacuo*. The residual viscous liquid was dissolved in 250 ml of benzene; to this solution was added, with stirring, 2.1 g (0.015 mole) of trifluoroacetic anhydride. The mixture was refluxed for 3 hr, allowed to cool, and refrigerated overnight. The resulting solid was filtered, washed with water, and dried *in vacuo*. Recrystallization from aqueous ethanol gave 0.8 g, mp 143–145°; IR (potassium bromide): 3350, 3230 (NH), 1700 (C=O), 1200, and 1150 (SO_2) cm^{-1}; $[\alpha]_D^{29}$ +20° (c = 1, ethyl acetate).

Anal.—Calc. for $C_{12}H_{12}F_6N_2O_3S$: C, 38.10; H, 3.17; N, 7.41; S, 8.47. Found: C, 38.2; H, 3.2; N, 7.7; S, 8.1.

Antiobesity Test—Rats were trained over 2 weeks to eat their daily food ration[4] in only 5 hr. After training, either vehicle (controls) or drug was administered orally by gastric intubation daily for 5 days. One hour after drug, tared food cups containing the food ration were presented. The cups were weighed after 1 hr of feeding and again after 5 hr of feeding. Water was available *ad libitum*. Rats were weighed daily before drug administration.

[4] Ground Purina Laboratory Chow.

REFERENCES

(1) W. O. Foye and J. C. Anderson, *J. Pharm. Sci.*, **58**, 1558 (1969).

(2) W. O. Foye, J. C. Anderson, and J. N. Sane, *ibid.*, **60**, 1095 (1971).

(3) R. H. Uloth, J. R. Kirk, W. A. Gould, and A. A. Larsen, *J. Med. Chem.*, **9**, 88 (1966).

(4) A. A. Larsen, W. A. Gould, H. R. Roth, W. J. Comer, R. H. Uloth, K. W. Dungan, and P. M. Lish, *ibid.*, **10**, 462 (1967).

(5) G. A. Johnson, S. J. Boukma, and E. G. Kim, *J. Pharmacol. Exp. Ther.*, **168**, 229 (1969).

(6) C. R. Creveling, J. W. Daly, B. Witkop, and S. Udenfriend, *Biochim. Biophys. Acta*, **64**, 125 (1962).

(7) A. A. Larsen and P. M. Lish, *Nature*, **203**, 1283 (1964).

(8) W. O. Foye and J. P. Speranza, *Eur. J. Med. Chem.*, **9**, 177 (1974).

(9) G. F. Holland, C. J. Buck, and A. Weissman, *J. Med. Chem.*, **6**, 519 (1963).

(10) C. S. Venugopalan, M.S. thesis, Massachusetts College of Pharmacy, Boston, Mass., 1975.

(11) W. Grauber and I. C. Gunsalus, *J. Org. Chem.*, **21**, 1024 (1956).

(12) T. Satoh, S. Suzuki, Y. Suzuki, Y. Miyaji, and Z. Imai, *Tetrahedron Lett.*, **1969**, 4555.

ACKNOWLEDGMENTS AND ADDRESSES

Received July 8, 1976, from the *Samuel M. Best Research Laboratory, Massachusetts College of Pharmacy, Boston, MA 02115.*

Accepted for publication August 18, 1976.

Abstracted from a thesis submitted by J. N. Sane to the Massachusetts College of Pharmacy in partial fulfillment of the Doctor of Philosophy degree requirements.

The authors are indebted to Mr. Edward Macko, Dr. Arnold B. Davidson, and their colleagues in the Pharmacology Department of Smith Kline & French Laboratories, Philadelphia, Pa., for the behavioral observations and antiobesity test results.

[x] To whom inquiries should be directed.

Release of Drugs from Ointment Bases II: *In Vitro* Release of Benzocaine from Suspension-Type Aqueous Gels

F. BOTTARI, G. DI COLO [x], E. NANNIPIERI, M. F. SAETTONE, and M. F. SERAFINI

Abstract □ The *in vitro* release of benzocaine, suspended in an aqueous gel, through silicone rubber membranes was studied to test an extension of existing mathematical models. The theoretical treatment proposed is intended for experimental systems involving release, through a nonporous membrane, of a drug whose concentration is a few times (≥3) greater than its solubility in the vehicle. For either micronized (2 μm) or macrosize (125 μm) drug, the Q (amount released) *versus* $t^{1/2}$ (time$^{1/2}$) plots were not linear until substantial time had elapsed. Excellent agreement was found between the experimental points and theoretical plots, generated by a computer fit to experimental data of an equation derived from a reported vehicle-boundary diffusion layer model. The values of the solubility and of the diffusion coefficient of benzocaine in the gel, calculated by the present mathematical treatment from release data, were in agreement with literature data. The particle size of released benzocaine did not influence the release pattern, thus confirming release in the present conditions to be diffusion rather than dissolution controlled. The present method is applicable for determining the solubility and diffusion coefficient of drugs in vehicles in cases not contemplated in current release theories.

Keyphrases □ Drug release—benzocaine from aqueous gels through silicone rubber membranes *in vitro*, mathematical models extended □ Benzocaine—release from aqueous gels through silicone rubber membranes *in vitro*, mathematical models extended □ Models, mathematical—extended to fit *in vitro* drug release system where drug concentration is greater than solubility in vehicle □ Solubility—benzocaine in aqueous gel vehicle, calculations derived from mathematical drug release models □ Diffusion coefficients—benzocaine in aqueous gel vehicle, calculations derived from mathematical drug release models

The *in vitro* release of drugs from topical vehicles, in spite of its limited correlations with *in vivo* absorption, may offer useful information on some physicochemical factors involved in the latter process. Such important parameters as the diffusion coefficient and the solubility of a drug in a vehicle can be calculated by relatively simple equations, derived from mathematical models describing the process of *in vitro* release of drugs dissolved (1–3) or

for 12 hr and refrigerated overnight. The precipitate was filtered and washed with dry ether, and the filtrate was evaporated *in vacuo*, leaving an oil. This oil was distilled at 165–170°/0.2 mm, giving 3.8 g (25%) of a solid, mp 42–45°; IR (potassium bromide): 3300 (NH), 1520 (NO_2), 1335–1375, and 1125–1150 (SO_2) cm^{-1}; $[\alpha]_D^{30}$ +37.0° (c = 1, ethyl acetate).

Anal.—Calc. for $C_{10}H_{11}F_3N_2O_4S$: C, 38.46; H, 3.53; N, 8.97; S, 10.26. Found: C, 38.7; H, 3.8; N, 9.2; S, 10.3.

(+)-*N*-Trifluoromethanesulfonyl-1-methyl-2 - (4 - trifluoroacetylaminophenyl)ethylamine (XIV)—A solution of 3.12 g (0.01 mole) of V in 150 ml of tetrahydrofuran with 0.4 g of platinum dioxide was hydrogenated at 3 atm. After 48 hr, the solution was filtered and the solvent was removed *in vacuo*. The residual viscous liquid was dissolved in 250 ml of benzene; to this solution was added, with stirring, 2.1 g (0.015 mole) of trifluoroacetic anhydride. The mixture was refluxed for 3 hr, allowed to cool, and refrigerated overnight. The resulting solid was filtered, washed with water, and dried *in vacuo*. Recrystallization from aqueous ethanol gave 0.8 g, mp 143–145°; IR (potassium bromide): 3350, 3230 (NH), 1700 (C=O), 1200, and 1150 (SO_2) cm^{-1}; $[\alpha]_D^{29}$ +20° (c = 1, ethyl acetate).

Anal.—Calc. for $C_{12}H_{12}F_6N_2O_3S$: C, 38.10; H, 3.17; N, 7.41; S, 8.47. Found: C, 38.2; H, 3.2; N, 7.7; S, 8.1.

Antiobesity Test—Rats were trained over 2 weeks to eat their daily food ration[4] in only 5 hr. After training, either vehicle (controls) or drug was administered orally by gastric intubation daily for 5 days. One hour after drug, tared food cups containing the food ration were presented. The cups were weighed after 1 hr of feeding and again after 5 hr of feeding. Water was available *ad libitum*. Rats were weighed daily before drug administration.

[4] Ground Purina Laboratory Chow.

REFERENCES

(1) W. O. Foye and J. C. Anderson, *J. Pharm. Sci.*, **58**, 1558 (1969).

(2) W. O. Foye, J. C. Anderson, and J. N. Sane, *ibid.*, **60**, 1095 (1971).

(3) R. H. Uloth, J. R. Kirk, W. A. Gould, and A. A. Larsen, *J. Med. Chem.*, **9**, 88 (1966).

(4) A. A. Larsen, W. A. Gould, H. R. Roth, W. J. Comer, R. H. Uloth, K. W. Dungan, and P. M. Lish, *ibid.*, **10**, 462 (1967).

(5) G. A. Johnson, S. J. Boukma, and E. G. Kim, *J. Pharmacol. Exp. Ther.*, **168**, 229 (1969).

(6) C. R. Creveling, J. W. Daly, B. Witkop, and S. Udenfriend, *Biochim. Biophys. Acta*, **64**, 125 (1962).

(7) A. A. Larsen and P. M. Lish, *Nature*, **203**, 1283 (1964).

(8) W. O. Foye and J. P. Speranza, *Eur. J. Med. Chem.*, **9**, 177 (1974).

(9) G. F. Holland, C. J. Buck, and A. Weissman, *J. Med. Chem.*, **6**, 519 (1963).

(10) C. S. Venugopalan, M.S. thesis, Massachusetts College of Pharmacy, Boston, Mass., 1975.

(11) W. Grauber and I. C. Gunsalus, *J. Org. Chem.*, **21**, 1024 (1956).

(12) T. Satoh, S. Suzuki, Y. Suzuki, Y. Miyaji, and Z. Imai, *Tetrahedron Lett.*, **1969**, 4555.

ACKNOWLEDGMENTS AND ADDRESSES

Received July 8, 1976, from the *Samuel M. Best Research Laboratory, Massachusetts College of Pharmacy, Boston, MA 02115.*

Accepted for publication August 18, 1976.

Abstracted from a thesis submitted by J. N. Sane to the Massachusetts College of Pharmacy in partial fulfillment of the Doctor of Philosophy degree requirements.

The authors are indebted to Mr. Edward Macko, Dr. Arnold B. Davidson, and their colleagues in the Pharmacology Department of Smith Kline & French Laboratories, Philadelphia, Pa., for the behavioral observations and antiobesity test results.

[x] To whom inquiries should be directed.

Release of Drugs from Ointment Bases II: *In Vitro* Release of Benzocaine from Suspension-Type Aqueous Gels

F. BOTTARI, G. DI COLO [x], E. NANNIPIERI, M. F. SAETTONE, and M. F. SERAFINI

Abstract □ The *in vitro* release of benzocaine, suspended in an aqueous gel, through silicone rubber membranes was studied to test an extension of existing mathematical models. The theoretical treatment proposed is intended for experimental systems involving release, through a nonporous membrane, of a drug whose concentration is a few times (≥3) greater than its solubility in the vehicle. For either micronized (2 μm) or macrosize (125 μm) drug, the Q (amount released) *versus* $t^{1/2}$ (time$^{1/2}$) plots were not linear until substantial time had elapsed. Excellent agreement was found between the experimental points and theoretical plots, generated by a computer fit to experimental data of an equation derived from a reported vehicle-boundary diffusion layer model. The values of the solubility and of the diffusion coefficient of benzocaine in the gel, calculated by the present mathematical treatment from release data, were in agreement with literature data. The particle size of released benzocaine did not influence the release pattern, thus confirming release in the present conditions to be diffusion rather than dissolution controlled. The present method is applicable for determining the solubility and diffusion coefficient of drugs in vehicles in cases not contemplated in current release theories.

Keyphrases □ Drug release—benzocaine from aqueous gels through silicone rubber membranes *in vitro*, mathematical models extended □ Benzocaine—release from aqueous gels through silicone rubber membranes *in vitro*, mathematical models extended □ Models, mathematical—extended to fit *in vitro* drug release system where drug concentration is greater than solubility in vehicle □ Solubility—benzocaine in aqueous gel vehicle, calculations derived from mathematical drug release models □ Diffusion coefficients—benzocaine in aqueous gel vehicle, calculations derived from mathematical drug release models

The *in vitro* release of drugs from topical vehicles, in spite of its limited correlations with *in vivo* absorption, may offer useful information on some physicochemical factors involved in the latter process. Such important parameters as the diffusion coefficient and the solubility of a drug in a vehicle can be calculated by relatively simple equations, derived from mathematical models describing the process of *in vitro* release of drugs dissolved (1–3) or

suspended (1, 4–7) in ointment bases. In practice, these equations are used rarely, since their use is restricted by theoretical requirements whose fulfillment is difficult to realize and to verify in most experimental systems (3, 8–10).

For suspended systems, zero concentration of the drug at the interface separating the donor and the receiving phase is required in the vehicle-controlled model proposed by Higuchi (4), while Roseman and Higuchi's (6) vehicle–interfacial barrier-controlled model applies only to systems where the solubility of the drug is negligible with respect to the concentration in the vehicle. Neither model adequately fits some common experimental systems such as those involving release through a nonporous membrane of a drug whose concentration is only a few times greater than its solubility in an ointment.

The purposes of the present work are to describe and to assess an extension of the existing quantitative treatments that might be useful in similar cases. As a practical test of the theory, the release of benzocaine from suspension-type aqueous gels through silicone rubber membranes was investigated.

THEORETICAL

The matrix–boundary layer model proposed by Roseman and Higuchi (6) for the release of drugs suspended in planar matrixes may be extended to any homogeneous solid or semisolid vehicle separated from a receptor sink by a planar diffusional barrier. Accordingly, the following equation describing the pattern of the amount of drug released *versus* time can be derived:

$$Q^2 + 2D_vRAQ = 2D_vAC_st \qquad \text{(Eq. 1)}$$

where Q is the amount of drug released per unit area; D_v is the effective diffusivity of drug in the vehicle; A and C_s are the total concentration and the solubility, respectively, of drug in the vehicle; and R is the diffusional resistance of the barrier interposed between the vehicle and the receiving phase[1].

The following assumptions were made in the derivation of Eq. 1: (*a*) a quasi-steady state (11) exists, (*b*) the drug particles are small when compared to the average distance of diffusion, (*c*) the concentration of drug in the vehicle is much greater than its solubility in the vehicle ($A \gg C_s$), (*d*) the diffusion coefficients in the vehicle and in the barrier are constant, (*e*) diffusion rather than dissolution is the rate-controlling step, (*f*) the diffusion process occurs through the continuous phase rather than through pores or channels within the medium, and (*g*) the receiving solution is a perfect sink.

Equation 1 is essentially valid for all times in which the suspended phase is present, less than the initial lag time, corresponding to the time necessary for establishment of a quasi-stationary state and for the average distance of diffusion to overwhelm particle dimension [see conditions (*a*) and (*b*)].

When $Q^2 \gg 2D_vRAQ$, *i.e.*, when $Q/A \gg 2D_vR$, Eq. 1 reduces to Eq. 2, previously derived by Higuchi (4) for the entirely vehicle-controlled process:

$$Q = \sqrt{2AC_sD_vt} \qquad \text{(Eq. 2)}$$

Under these conditions, any appreciable resistance to diffusion at the vehicle-receiving phase interface, where the drug concentration drops to negligible values, no longer exists.

Where C_s is not negligible with respect to A, the vehicle-controlled model is described by (3):

$$Q = \sqrt{(2A - C_s)C_sD_vt} \qquad \text{(Eq. 3)}$$

The conditions for validity of Eq. 3 are the same as for Eq. 2, except that the total drug concentration (A) is only a few (3–4) times greater than the solubility in the vehicle (C_s). The application of Eq. 3 to the determination of the diffusivity and solubility of drugs in solid or semisolid vehicles was reported previously (12). However, Eq. 3 is only applicable when zero concentration exists at the vehicle-receiving phase interface. This condition is well approximated only in cases of very little diffusional resistance of the interfacial barrier compared with that of the vehicle. The more general Eq. 1, although not limited by this condition, is only valid when C_s is negligible with respect to A [condition (*c*)], so its use for the determination of D_v and C_s is limited in cases of high C_s values due to considerable experimental difficulties in attaining the $A \gg C_s$ condition.

The applicability of Eq. 1 can be extended to experimental systems in which A is but a few times (≥ 3) greater than C_s if it is modified as follows:

$$Q^2 + 2D_vRA^*Q = 2D_vA^*C_st \qquad \text{(Eq. 4)}$$

where:

$$A^* = A - \frac{(C_s + C_v)}{2} \qquad \text{(Eq. 5)}$$

and C_v represents the concentration of drug in the vehicle at the interface with the barrier. According to the assumptions made in the *Appendix*, where details of the derivation of Eq. 4 are discussed, A^* seems to be comparatively little influenced by the variation of C_v with time and may be considered as constant. For small values of R and/or large values of time, Eq. 5 reduces to $A^* = A - C_s/2$ (*cf.*, Eq. 8) and Eq. 4 reduces to Eq. 3.

Equation 4 should lend itself to the determination of the solubility and diffusivity of drugs in ointments through release data when either Eq. 1 or 3 is inapplicable. Therefore, it is convenient to put Eq. 4 in the form:

$$Q = -a + \sqrt{a^2 + b(t - q)} \qquad \text{(Eq. 6)}$$

where $a = D_vRA^*$, $b = 2D_vC_sA^*$, and q is a correction term which depends on the lag time.

The values of a, b, and q can be obtained through a least-squares fit of Eq. 6 to experimental release data. By recalling Eq. 5, the following relationship between the parameter b and $(A - C_v/2)$ can be written:

$$b = 2D_vC_s\left(A - \frac{C_v}{2}\right) - D_vC_s^2 \qquad \text{(Eq. 7)}$$

For the same reasons indicated for Eqs. 4 and 5, Eq. 7 is supposed to hold with sufficient approximation for any value assumed by C_v in the time interval under study. Since linear concentration gradients are assumed, the value of C_v at any point of this interval can be obtained, once the diffusional resistance, R, is experimentally determined (*e.g.*, by steady- or quasi-steady-state permeation experiments), from the relationship (11):

$$C_v = R\frac{dQ}{dt} \qquad \text{(Eq. 8)}$$

where dQ/dt, the instantaneous release rate, can be obtained from Eq. 6 by differentiation. According to Eq. 7, it should be possible to construct a linear plot of b *versus* $(A - C_v/2)$ by carrying out experiments with varying drug concentrations ($A \geq 3C_s$) and calculating a single C_v value for each A at any time in the interval studied. The value of C_s equals twice the abscissa intercept of this plot.

Alternatively, C_s can be obtained from the averaged ratio of parameter b to parameter a (Eq. 6) once R is known:

$$C_s = (R/2)\overline{(b/a)} \qquad \text{(Eq. 9)}$$

Following the calculation of C_s, D_v can be calculated from the slope of the b *versus* $(A - C_v/2)$ plot utilizing Eq. 7. The accuracy of the results and its dependence on the C_v values used in the calculations will be evaluated later.

EXPERIMENTAL

Materials—Carbomer 934P, a carboxyvinyl polymer[2], was used as received; its sodium salt was prepared as described in the literature (13). Benzocaine[3] was crystallized to a constant melting point of 91.5°. Particles with an average diameter of 125 μm (geometric) were obtained using 100–140-mesh ASTM sieves. A sample was micronized[4], and the average diameter of the particles (microscopic analysis) was 2.0 μm (geometric).

[1] When more than one barrier is involved (*e.g.*, a membrane and the adjacent hydrodynamic layer), the resistance is the sum of the resistances of the individual barriers.

[2] Carbopol 934, B. F. Goodrich Chemical Corp., Cleveland, Ohio.
[3] Carlo Erba, Milano, Italy.
[4] Jet mill model JMRS-80, Fryma Maschinen AG, Rheinfelden, Switzerland.

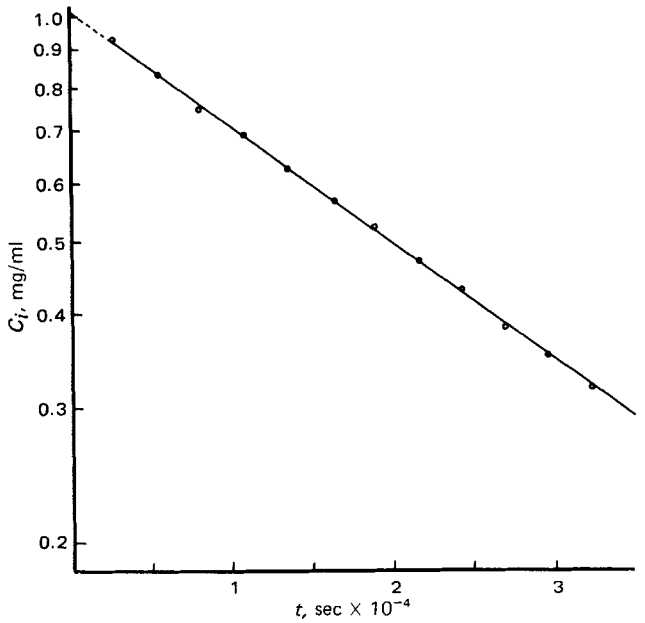

Figure 1—*Quasi-steady-state permeation plot of benzocaine through a silicone rubber membrane from an aqueous solution. Initial concentration* C_{i0} = *1.0 mg/ml.*

Silicone rubber[5] sheeting, labeled thickness of approximately 127 μm, was used as the membrane material.

Solubility Determinations—The water solubility of benzocaine at 30°, determined spectrophotometrically[6] (286 nm) on a sample equilibrated for 3 days, was 1.31 g/liter. The solubility in the gel was presumed to be the same, since gels containing 1.31 mg of benzocaine/ml were perfectly clear on microscopic[7] examination while suspended particles were visible in the gel kept at 30° several days after addition of 5% excess drug over the water solubility value.

Gel Preparation—The following procedure allowed preparation of homogeneous, air-free, suspension-type gels. To 100 ml of a saturated solution of benzocaine (0.13% w/v) in distilled water at 30° was added portionwise, while stirring, the sodium salt of the carboxyvinyl polymer (1.0 g, or 2.0 g in one case) together with the appropriate amount of either micronized or macrosize benzocaine. After the addition, the vessel was connected to a water pump; thorough stirring was continued until a bubble-free, clear gel formed.

After preparation, all gels were stored at 30° for future use. The benzocaine contents of the gels used, determined spectrophotometrically after appropriate dilution with water, were 2.59, 3.03, 3.70, 4.60, 5.10, and 10.90 mg/ml for micronized drug and 3.05, 4.12, and 4.92 mg/ml for macrosize drug.

Release Experiments—The release of benzocaine from the gels through silicone rubber membranes was investigated using a previously described apparatus (14) with minor modifications. A new cell, made entirely of polymethyl methacrylate[8], was used in place of the metal cell. The metal cell released, to the acidic (0.1 *N* HCl) receiving solution, substances interfering with the spectrophotometric assays. The only metal parts were the screw shanks (*cf.*, Ref. 14, Fig. 1), whose contact with the external solution was prevented by polymethyl methacrylate cap nuts and silicone rubber gaskets. The transparent material also allowed inspection of the cell contents, so the development of a sharply defined depletion zone in the gels could be observed during the experiments.

The capacity of the cell was 19.60 ml, and the diameter of the available area for diffusion was 5.0 cm. The cell was filled with the gel, the excess was removed with a spatula to produce an even surface, and the membrane, which had been presoaked in water for at least 24 hr, was carefully placed and pressed on the gel. The upper part of the cell was then assembled. All of these operations were performed in a conditioned atmosphere (30° and 100% relative humidity). The cell was then placed into a jacketed beaker (full capacity of 1.5 liters) connected to a constant-temperature bath (30 ± 0.1°) and circulator.

[5] Silastic, Medical Products Division, Dow Corning Corp., Midland, Mich.
[6] Beckman DU spectrophotometer.
[7] Zeiss Zoom III stereomicroscope.
[8] Plexiglas, Rohm & Haas Co., Philadelphia, Pa.

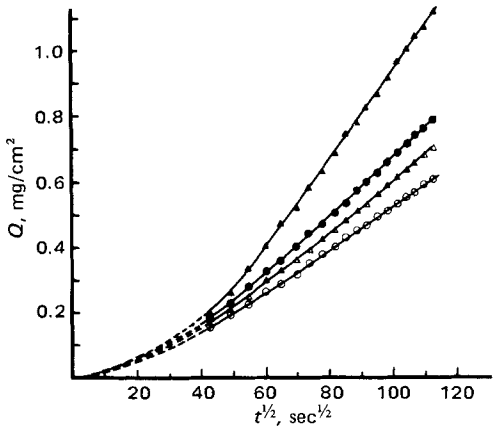

Figure 2—*Amount of benzocaine released from suspension-type gels prepared with micronized drug as a function of the square root of time. Key:* ▲, *10.9 mg/ml;* ●, *4.6 mg/ml;* △, *3.7 mg/ml; and* ○, *2.59 mg/ml. Two plots (5.10 and 3.03 mg/ml) were omitted for clarity.*

At t = 0, prewarmed 0.1 *N* HCl (0.5–1.0 liter, depending on the gel concentration) was introduced into the beaker, and stirring was immediately initiated using a two-blade propeller connected to a 300-rpm synchronous motor[9]. At appropriate intervals, measured volumes of the receiving phase were removed, diluted, if necessary, with 0.1 *N* HCl, and analyzed spectrophotometrically for benzocaine hydrochloride (227 nm). Blank runs demonstrated the absence in the external solution of materials that might interfere with the measurements.

Diffusional Resistance of Membrane—This value was determined by allowing benzocaine to permeate through the membrane under quasi-steady-state conditions. The experimental technique was described previously (15, 16). The permeation cell used had polymethyl methacrylate parts, instead of the stainless steel parts of the original cell, in contact with the external solution. The membranes were of the same type as in the release experiments and were presoaked in water for at least 24 hr. Both the internal and external stirring was performed by 300-rpm synchronous motors[9].

The available area for diffusion was 7.55 cm^2; the volume of the internal solution (benzocaine in distilled water, 0.1% w/v) was 25.0 ml. The experiments were carried out at 30°. Aqueous 0.1 *N* HCl (500 ml) was used as the external solution; the permeant content of this solution was determined at appropriate intervals, as in the release experiments. The concentration of the internal solution (C_i) at different times was calculated from the final drug concentration inside the cell and the amount that had appeared in the external solution. Blank runs demonstrated the absence, in the external solution, of materials that might interfere with the measurements.

Data Treatment—Each release and permeation experiment was performed at least four times, and the averaged data were used to draw the individual plots. With the linear plots, the data were fed to a desk electronic computer[10] fitted with a program for the computation of regression parameters and statistics. All linear regressions were highly significant ($p < 0.005$). Least-squares fits of Eq. 6 to release data were done with the aid of a digital computer, using an appropriate program[11].

RESULTS AND DISCUSSION

Diffusional Resistance of Membrane—In the present system, the diffusional resistance of the interfacial barrier, R, was only due to the silicone rubber membrane, since the diffusant was completely converted to a different species (its salt form) immediately after crossing the membrane. To obtain a more realistic value, R was determined by quasi-steady-state rather than by steady-state experiments. The conditions were thought to reproduce more closely those existing during release experiments, *i.e.*, a varying drug concentration at the membrane–donor phase interface.

If sink conditions are assured, the permeation of a drug from a stirred

[9] Crouzet SA, Paris, France.
[10] Olivetti Programma 101.
[11] IBM 370/158; Nonlinear Least-Squares Regression Program BMDX85 (W. J. Dixon, "Biomedical Computer Program, X-Series Supplement," University of California Press, Berkeley, Calif., 1970).

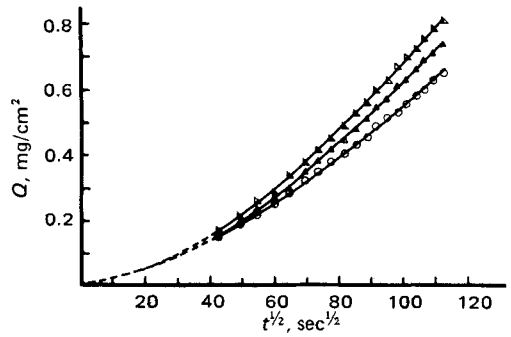

Figure 3—*Amount of benzocaine released from suspension-type gels prepared with macrosize drug as a function of the square root of time. Key: ◺, 4.92 mg/ml; △, 4.12 mg/ml; and ○, 3.05 mg/ml.*

solution across a membrane under quasi-steady-state conditions is described by (11):

$$\ln C_i/C_{i0} = \frac{S}{R'V_i}t \qquad \text{(Eq. 10)}$$

where C_i and C_{i0} are the concentrations of the donor solution at finite time t and at $t = 0$, respectively; V_i is the volume of the donor solution; S is the area of the membrane; and R' is the diffusional resistance of the membrane if contributions from nonstirred liquid layers adjacent to both sides of the membrane are insignificant, as assumed for the present experimental system.

The value of R (in release experiments) is related to R' (calculated from permeation experiments) through the following equation, which takes into account the difference existing between the donor phases in release and permeation experiments:

$$R = \frac{K_{m/w}}{K_{m/g}}R' \qquad \text{(Eq. 11)}$$

where $K_{m/w}$ and $K_{m/g}$ are the membrane–water and membrane–gel partition coefficients, respectively. In the present case, the drug solubility

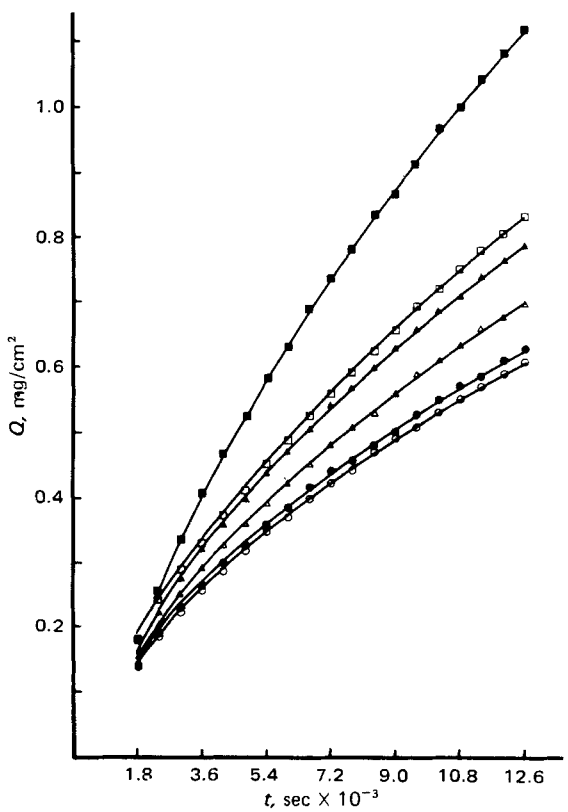

Figure 4—*Amount of benzocaine released from suspension-type gels containing different concentrations of micronized drug as a function of time. Symbols represent experimental data; curves are based on theoretical calculations. Key: ■, 10.9 mg/ml; □, 5.1 mg/ml; ▲, 4.6 mg/ml; △, 3.7 mg/ml; ●, 3.03 mg/ml; and ○, 2.59 mg/ml.*

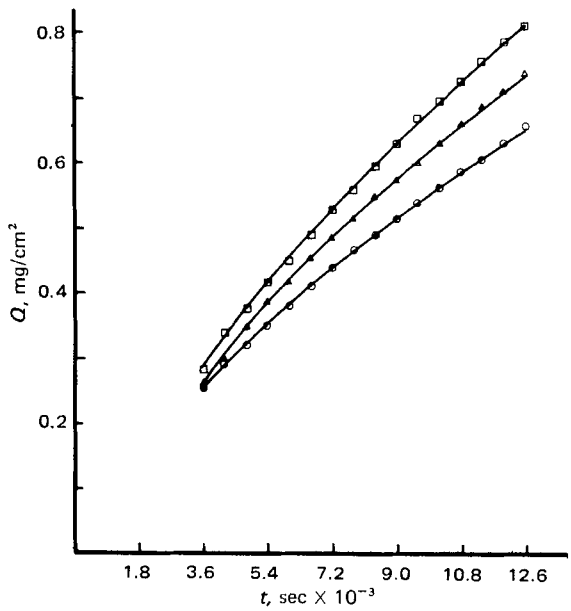

Figure 5—*Amount of benzocaine released from suspension-type gels containing different concentrations of macrosize drug as a function of time. Symbols represent experimental data; curves are based on theoretical calculations. Key: □, 4.92 mg/ml; △, 4.12 mg/ml; and ○, 3.05 mg/ml.*

in the gel was the same as in water. Therefore, $K_{m/w} = K_{m/g}$, and R could be calculated directly from the slope of the permeation plot according to Eq. 10. Figure 1 illustrates a typical permeation (log C_i/C_{i0} *versus* t) plot, whose linearity demonstrates the adherence of the experimental system to Eq. 10. An average value of 8.3×10^3 sec/cm resulted for R from the permeation experiments.

Release Experiments—Figures 2 and 3 illustrate the results of release experiments with micronized and macrosize benzocaine, respectively. The experiments were carried out over 3.5 hr at concentrations ranging from 2.59 to 10.9 mg/ml for micronized drug and from 3.05 to 4.92 mg/ml for macrosize drug. In no case was a linear relationship between Q and $t^{1/2}$ observed, at least until a substantial amount of time elapsed. Thus, the nonlinearity of the graphs appears to rule out the vehicle-controlled model described by Eq. 3. Since Eqs. 1 and 4 predict the presence of a nonlinear region during early release times, it is reasonable to assume that the vehicle–membrane-controlled model was operative in this case.

This assumption is confirmed by the graphs in Figs. 4 and 5, in which the experimental release plots of benzocaine (micronized and macrosize, respectively) are compared with theoretical plots, generated by a least-squares fit of Eq. 6 to experimental data, obtained with the aid of a digital computer. Since, as pointed out in the theoretical section, Eq. 6 is valid after the lag time, all data used for the interpretation were taken 30 min after the beginning of release experiments with micronized drug (60 min with macrosize drug). After these lapses of time, the thickness of the depletion zone, l, approximately estimated for each concentration from the amount of released drug ($l = Q/A$), was sufficiently great with respect to particle size and interparticulate distance for micronized and macrosize particles. The time required for establishment of a linear concentration gradient in the membrane should be negligible, as shown by the quasi-steady-state permeation graph in Fig. 1, whose ordinate intercept closely approaches the theoretical value, 1.00 mg/ml. Thus, it can be safely assumed that conditions (*a*) and (*b*) for the validity of Eq. 1 (and 6) were attained. The excellent agreement between calculated and experimental points indicates that Eq. 6 is well suited for describing the release pattern of micronized and macrosize drug.

The values of a, b, and q, estimated for each release experiment by the computer fit of Eq. 6 to release data, and the corresponding values of the concentration at the gel–membrane interface, calculated by Eqs. 6 and 8, at the lower (C_v^i) and the upper (C_v^f) ends of each time interval, are listed in Table I. The values of C_v^i and C_v^f are approximately 47–80 and 18–40%, respectively, of C_s, the solubility of benzocaine in the gel (1.31 mg/ml, see *Experimental*). These comparatively high values possibly account for the curvature of the Q *versus* $t^{1/2}$ plots (Figs. 2 and 3) and further support the application of Eq. 4, rather than of Eq. 3, to the present experimental system.

Table I—Values of Parameters *a*, *b*, and *q* (Eq. 6) and of C_v (Eq. 8) Calculated at the Lower ($C_v{}^i$) and Upper ($C_v{}^f$) Ends of the Time Interval for Each Release Experiment

Particle Size, μm	*A*, mg/ml	*a*	$b \times 10^4$	*q*	$C_v{}^i$, mg/ml	$C_v{}^f$, mg/ml
2.0	2.59	0.140	0.441	297	0.62	0.24
2.0	3.03	0.170	0.485	163	0.61	0.25
125.0	3.05	0.173	0.550	990	0.55	0.28
2.0	3.70	0.208	0.640	396	0.73	0.29
125.0	4.12	0.254	0.797	1170	0.65	0.33
2.0	4.60	0.260	0.852	378	0.81	0.34
125.0	4.92	0.325	0.995	945	0.68	0.37
2.0	5.10	0.330	1.005	360	0.83	0.36
2.0	10.90	0.720	2.330	405	1.05	0.53

Determination of Diffusion Coefficient and Solubility—In Fig. 6, *b* was plotted *versus* $(A - C_v{}^i/2)$ and $(A - C_v{}^f/2)$ (*cf.*, Eq. 7 and Table I). Since all points fell, within the range of experimental error, on the same line, all data were grouped to build up the regression line. The nonperfect alignment of the points in the line is due to wide variations of the parameter *b* with experimental error. However, the high value of the correlation coefficient (0.998) points to a significant linear relationship between *b* and $(A - C_v/2)$ as predicted by Eq. 7.

The value for the solubility of benzocaine in the gel, C_s, calculated from the abscissa intercept of the plot in Fig. 6, was 1.18 mg/ml; the value of C_s calculated by Eq. 9 was 1.29 mg/ml. Both values are in satisfactory agreement with the directly determined solubility value at 30°, 1.31 mg/ml. The values of the diffusion coefficient of benzocaine in the gel, calculated from the slope of the plot reported in Fig. 5 according to Eq. 7, are 1.00×10^{-5} and 9.14×10^{-6} cm²/sec, assuming $C_s = 1.18$ and 1.29 mg/ml, respectively. The agreement with the literature (17) value for the diffusion coefficient of benzocaine in water at 30° (9.9×10^{-6} cm²/sec) is satisfactory. This finding is indicative of the absence of interactions, mechanical and/or chemical, between diffusant and gel. Indeed, the pores in the gel network should be much larger than the molecular diameter of the diffusing drug, as indicated also by the observation that the rate of release of benzocaine was unaffected when the concentration of carboxyvinyl polymer in the gels was doubled. The occurrence of chemical interactions appears unlikely in view of the chemical nature of benzocaine and the carboxyvinyl polymer and because the solubility of benzocaine in the gel was the same as in water.

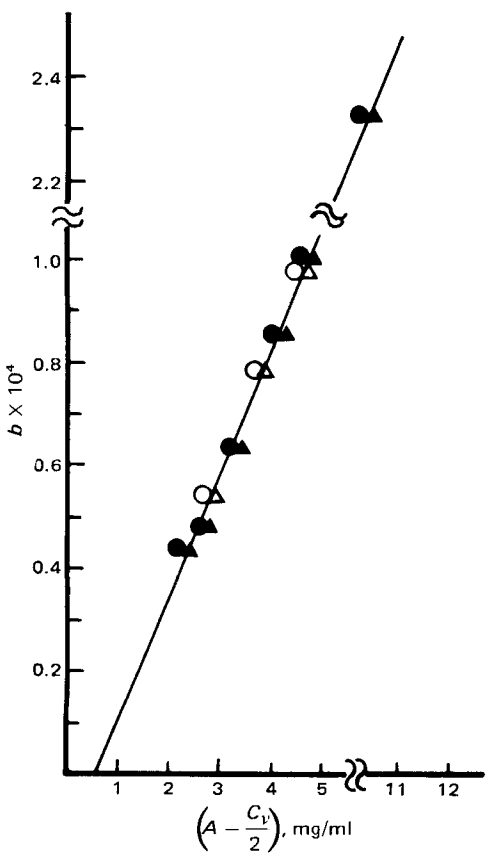

Figure 6—*Relationship between parameter* b *and* $(A - C_v/2)$. *Key:* ●, $(A - C_v{}^i/2)$, *micronized;* ○, $(A - C_v{}^i/2)$, *macrosize;* ▲, $(A - C_v{}^f/2)$, *micronized; and* △, $(A - C_v{}^f/2)$, *macrosize. See text for details.*

Influence of Particle Size—As stated earlier, the release pattern of benzocaine was unaffected by particle size; both micronized and macrosize drug were released according to Eq. 4 after a finite time from the beginning of the experiments. Indeed, the surface area of undissolved drug should not influence the release rate beyond the lag time, since Eq. 4 requires release to be diffusion rather than dissolution controlled. However, the lag time itself should be highly influenced by particle size insofar as it depends on the time necessary for the thickness of the depletion zone to overwhelm particle diameter. In effect, the correction factor *q* (Eq. 6), which is directly related to the lag time, was greater for macrosize than for micronized drug (Table I).

The observations do not disagree with the assumptions of Haleblian *et al.* (10), who found that the surface area greatly influenced the release rate of chlormadinone acetate from silicone elastomer matrixes. They attributed this effect to a dissolution-influenced release. Indeed, the thickness of the depletion zone of their experimental system, estimated (as the Q/A ratio) from the reported data, was at most about 100 μm, while the diameters of the macrocrystals used were in the 100–300-μm range.

CONCLUSIONS

Equation 1, applied previously to the release of drugs from solid matrixes at concentrations largely exceeding solubility, is valid in a modified form (Eq. 4) for the release of benzocaine from an aqueous gel at drug concentrations only a few times greater than solubility. Equation 4 lends itself to the determination of the solubility as well as of the diffusion coefficient of drug in a vehicle. The determined values are satisfactorily accurate, at least for practical purposes.

The present results are indicative of a method of potential utility for the study of the above parameters, particularly where the application of Eq. 3 is ruled out by the influence on release of the diffusional resistance of the barrier separating the donor and receiving phase and where the use of Eq. 1 is prevented by the practical impossibility of attaining the $A \gg C_s$ condition because of a high drug solubility in the ointment.

The size of suspended particles is particularly important. Since the time necessary for attainment of the conditions of applicability of Eq. 4 is remarkably dependent on particle dimension, the use of macrosize powder might waste both time and materials.

APPENDIX

Equation 1 was derived by equating the rate of release and the rate of quasi-steady-state diffusion through the vehicle and the interfacial barrier. For the $A \gg C_s$ condition, the first parameter is directly proportional to the rate of increase of the thickness of the depletion zone, *l* (6):

$$dQ/dt = A\, dl/dt \qquad \text{(Eq. A1)}$$

When C_s is not negligible with respect to *A*, the proportionality fails as long as the time-dependent concentration at the interface with the barrier, C_v, must also be taken into account in the expression of the released amount per unit area and of the release rate:

$$Q = [A - (C_s + C_v)/2]l \qquad \text{(Eq. A2)}$$

$$dQ/dt = [A - (C_s + C_v)/2]\, dl/dt - 1/2l\, dC_v/dt \qquad \text{(Eq. A3)}$$

However, if the second term in the rate expression is negligible when compared with the first, the factor within brackets in Eq. A3 can be as-

sumed by approximation to be constant (*cf.*, Eq. 5). The consequent proportionality between dQ/dt and dl/dt should enable derivation of Eq. 4 in complete analogy with Eq. 1. That the condition for proportionality is generally satisfied also for values of A as little as $3C_s$ can be verified by expressing this condition through the ratio of the first to the second term in the expression of the release rate (Eq. A3):

$$\left|\frac{2A - C_s - C_v}{l} dl/dC_v\right| \gg 1 \qquad \text{(Eq. A4)}$$

and further substituting into this relationship the following expressions of C_v, dC_v, l, and dl:

$$C_v = R\, dQ/dt \qquad \text{(Eq. A5)}$$

$$dC_v = (R\, d^2Q/dt^2)\, dt \qquad \text{(Eq. A6)}$$

$$l = Q/(n - 1/2)C_s \qquad \text{(Eq. A7)}$$

$$dl = [1/(n - 1/2)C_s]\, dQ \qquad \text{(Eq. A8)}$$

where $n = A/C_s$. Equation 1, where $(n - 1/2)C_s$ is used in place of A, can be employed to obtain approximate expressions of Q, dQ, and d^2Q/dt^2.

Following calculation, the condition for proportionality between the release rate and the rate of increase of the thickness of the depletion zone can be written as follows:

$$\frac{2x^2(n - 1/2) - x}{x - 1} \gg 1 \qquad \text{(Eq. A9)}$$

where $x = \sqrt{1 + [2/(n - 1/2)D_vR^2]t}$.

It can be readily verified that the minimum value of the ratio is 18 for $n = 3$, while it increases with increasing n.

REFERENCES

(1) T. Higuchi, *J. Soc. Cosmet. Chem.*, **11**, 85 (1960).

(2) W. I. Higuchi, *J. Pharm. Sci.*, **51**, 802 (1962).

(3) *Ibid.*, **56**, 315 (1967).

(4) *Ibid.*, **50**, 874 (1961).

(5) *Ibid.*, **52**, 1145 (1963).

(6) T. J. Roseman and W. I. Higuchi, *J. Pharm. Sci.*, **59**, 353 (1970).

(7) T. J. Roseman, *ibid.*, **61**, 46 (1972).

(8) A. L. Weiss and B. J. Sciarrone, *ibid.*, **58**, 980 (1969).

(9) C. W. Whitworth and R. E. Stephenson, *ibid.*, **60**, 48 (1971).

(10) J. Haleblian, R. Runkel, N. Mueller, J. Christopherson, and K. Ng, *ibid.*, **60**, 541 (1971).

(11) G. L. Flynn, S. H. Yalkowsky, and T. J. Roseman, *ibid.*, **63**, 487 (1974).

(12) "Proceedings of the Post-Graduate School on Diffusion in Pharmaceutical Formulation and Packaging," The Pharmaceutical Society of Great Britain, London, England, Apr. 1975, pp. 186–193.

(13) A. G. Perotti, *Farmaco, Ed. Prat.*, **25**, 651 (1970).

(14) F. Bottari, G. Di Colo, E. Nannipieri, M. F. Saettone, and M. F. Serafini, *J. Pharm. Sci.*, **63**, 1779 (1974).

(15) *Ibid.*, **64**, 946 (1975).

(16) F. Bottari, G. Di Colo, E. Nannipieri, M. F. Saettone, and M. F. Serafini, *Boll. Chim. Farm.*, **115**, 113 (1976).

(17) P. Singh, S. J. Desai, D. R. Flanagen, A. P. Simonelli, and W. I. Higuchi, *J. Pharm. Sci.*, **57**, 959 (1968).

ACKNOWLEDGMENTS AND ADDRESSES

Received February 5, 1976, from the *Pharmaceutical Technology Laboratory, Institute of Pharmaceutical Chemistry, University of Pisa, 56100, Pisa, Italy.*

Accepted for publication August 10, 1976.

Supported in part by a grant from Consiglio Nazionale delle Ricerche.

Reference 14 is considered Part I of this series.

The authors thank Prof. Olga Dun De Finamore for assistance.

[x] To whom inquiries should be directed.

Metabolism of *N*-Ethyl-3-piperidyl Benzilate in Rats

CHING-HSIU CHEN [*], MAHMOUD M. ABDEL-MONEM [*x], and THOMAS P. KRICK [‡]

Abstract □ The metabolic fate of *N*-ethyl-3-piperidyl benzilate (I) and its potential metabolites 3-piperidyl benzilate (II), *N*-ethyl-3-hydroxypiperidine (III), and 3-hydroxypiperidine (IV) was studied. Incubation of I with rat liver homogenates resulted in the formation of II and III. Only a trace of unchanged drug appeared in urine after intraperitoneal injection of I. Approximately 9% of the injected dose of I was excreted in urine as III and 2% in the form of metabolites that produced III after acid hydrolysis. After intraperitoneal injection of II in rats, 18% of the dose was excreted in urine as IV. Approximately 26% of the injected dose of III was present in urine as the unchanged drug, and 63% of the dose was excreted in the urine in the form of conjugates that produced III on acid hydrolysis. Urine of rats injected with IV contained approximately 50% of the injected dose as the unchanged drug and 50% of the dose in the form of a conjugate that produced IV on acid hydrolysis. The identity of the metabolites in extracts from urine was established by GLC–mass spectrometry. It is concluded that hydrolysis was one metabolic pathway for I and II. The major routes of elimination of these compounds are not yet known and may include excretion in feces or metabolic transformations resulting in the degradation of the piperidine ring.

Keyphrases □ *N*-Ethyl-3-piperidyl benzilate—metabolism in rats □ Metabolism—*N*-ethyl-3-piperidyl benzilate in rats □ Benzilates—*N*-ethyl-3-piperidyl ester, metabolism in rats

During studies to develop potent and selectively acting atropine substituents for the treatment of GI disturbances, numerous compounds were synthesized that were superior to atropine with respect to anticholinergic potency, antisecretory effects, and reduced incidence of side effects (1). Most of these compounds are glycolate esters of heterocyclic imino alcohols. In experimental animals, these drugs produced potent central nervous system (CNS) stimulation, as indicated by hyperactivity and other behavioral disturbance tests (2). In humans, they were potent and long-lasting hallucinogenic and psychotomimetic agents (3).

Some human subjects manifested a marked change in their basic mood and drive 1 or 2 days following a single

sumed by approximation to be constant (*cf.*, Eq. 5). The consequent proportionality between dQ/dt and dl/dt should enable derivation of Eq. 4 in complete analogy with Eq. 1. That the condition for proportionality is generally satisfied also for values of A as little as $3C_s$ can be verified by expressing this condition through the ratio of the first to the second term in the expression of the release rate (Eq. A3):

$$\left|\frac{2A - C_s - C_v}{l} dl/dC_v\right| \gg 1 \qquad \text{(Eq. A4)}$$

and further substituting into this relationship the following expressions of C_v, dC_v, l, and dl:

$$C_v = R\, dQ/dt \qquad \text{(Eq. A5)}$$

$$dC_v = (R\, d^2Q/dt^2)\, dt \qquad \text{(Eq. A6)}$$

$$l = Q/(n - 1/2)C_s \qquad \text{(Eq. A7)}$$

$$dl = [1/(n - 1/2)C_s]\, dQ \qquad \text{(Eq. A8)}$$

where $n = A/C_s$. Equation 1, where $(n - 1/2)C_s$ is used in place of A, can be employed to obtain approximate expressions of Q, dQ, and d^2Q/dt^2.

Following calculation, the condition for proportionality between the release rate and the rate of increase of the thickness of the depletion zone can be written as follows:

$$\frac{2x^2(n - 1/2) - x}{x - 1} \gg 1 \qquad \text{(Eq. A9)}$$

where $x = \sqrt{1 + [2/(n - 1/2)D_vR^2]t}$.

It can be readily verified that the minimum value of the ratio is 18 for $n = 3$, while it increases with increasing n.

REFERENCES

(1) T. Higuchi, *J. Soc. Cosmet. Chem.*, **11**, 85 (1960).

(2) W. I. Higuchi, *J. Pharm. Sci.*, **51**, 802 (1962).

(3) *Ibid.*, **56**, 315 (1967).

(4) *Ibid.*, **50**, 874 (1961).

(5) *Ibid.*, **52**, 1145 (1963).

(6) T. J. Roseman and W. I. Higuchi, *J. Pharm. Sci.*, **59**, 353 (1970).

(7) T. J. Roseman, *ibid.*, **61**, 46 (1972).

(8) A. L. Weiss and B. J. Sciarrone, *ibid.*, **58**, 980 (1969).

(9) C. W. Whitworth and R. E. Stephenson, *ibid.*, **60**, 48 (1971).

(10) J. Haleblian, R. Runkel, N. Mueller, J. Christopherson, and K. Ng, *ibid.*, **60**, 541 (1971).

(11) G. L. Flynn, S. H. Yalkowsky, and T. J. Roseman, *ibid.*, **63**, 487 (1974).

(12) "Proceedings of the Post-Graduate School on Diffusion in Pharmaceutical Formulation and Packaging," The Pharmaceutical Society of Great Britain, London, England, Apr. 1975, pp. 186–193.

(13) A. G. Perotti, *Farmaco, Ed. Prat.*, **25**, 651 (1970).

(14) F. Bottari, G. Di Colo, E. Nannipieri, M. F. Saettone, and M. F. Serafini, *J. Pharm. Sci.*, **63**, 1779 (1974).

(15) *Ibid.*, **64**, 946 (1975).

(16) F. Bottari, G. Di Colo, E. Nannipieri, M. F. Saettone, and M. F. Serafini, *Boll. Chim. Farm.*, **115**, 113 (1976).

(17) P. Singh, S. J. Desai, D. R. Flanagen, A. P. Simonelli, and W. I. Higuchi, *J. Pharm. Sci.*, **57**, 959 (1968).

ACKNOWLEDGMENTS AND ADDRESSES

Received February 5, 1976, from the *Pharmaceutical Technology Laboratory, Institute of Pharmaceutical Chemistry, University of Pisa, 56100, Pisa, Italy.*

Accepted for publication August 10, 1976.

Supported in part by a grant from Consiglio Nazionale delle Ricerche.

Reference 14 is considered Part I of this series.

The authors thank Prof. Olga Dun De Finamore for assistance.

[x] To whom inquiries should be directed.

Metabolism of *N*-Ethyl-3-piperidyl Benzilate in Rats

CHING-HSIU CHEN [*], MAHMOUD M. ABDEL-MONEM [*x], and THOMAS P. KRICK [‡]

Abstract □ The metabolic fate of *N*-ethyl-3-piperidyl benzilate (I) and its potential metabolites 3-piperidyl benzilate (II), *N*-ethyl-3-hydroxypiperidine (III), and 3-hydroxypiperidine (IV) was studied. Incubation of I with rat liver homogenates resulted in the formation of II and III. Only a trace of unchanged drug appeared in urine after intraperitoneal injection of I. Approximately 9% of the injected dose of I was excreted in urine as III and 2% in the form of metabolites that produced III after acid hydrolysis. After intraperitoneal injection of II in rats, 18% of the dose was excreted in urine as IV. Approximately 26% of the injected dose of III was present in urine as the unchanged drug, and 63% of the dose was excreted in the urine in the form of conjugates that produced III on acid hydrolysis. Urine of rats injected with IV contained approximately 50% of the injected dose as the unchanged drug and 50% of the dose in the form of a conjugate that produced IV on acid hydrolysis. The identity of the metabolites in extracts from urine was established by GLC–mass spectrometry. It is concluded that hydrolysis was one metabolic pathway for I and II. The major routes of elimination of these compounds are not yet known and may include excretion in feces or metabolic transformations resulting in the degradation of the piperidine ring.

Keyphrases □ *N*-Ethyl-3-piperidyl benzilate—metabolism in rats □ Metabolism—*N*-ethyl-3-piperidyl benzilate in rats □ Benzilates—*N*-ethyl-3-piperidyl ester, metabolism in rats

During studies to develop potent and selectively acting atropine substituents for the treatment of GI disturbances, numerous compounds were synthesized that were superior to atropine with respect to anticholinergic potency, antisecretory effects, and reduced incidence of side effects (1). Most of these compounds are glycolate esters of heterocyclic imino alcohols. In experimental animals, these drugs produced potent central nervous system (CNS) stimulation, as indicated by hyperactivity and other behavioral disturbance tests (2). In humans, they were potent and long-lasting hallucinogenic and psychotomimetic agents (3).

Some human subjects manifested a marked change in their basic mood and drive 1 or 2 days following a single

dose of these drugs (4). Clinical trials of one compound[1] in psychiatric patients revealed that it was a safe and effective antidepressant agent (5). The delayed onset of the mood enhancement effects of the glycolate esters in humans might be attributed to the formation of active metabolites. Therefore, the metabolic fate of these compounds in rats was studied as a prelude to metabolic studies in humans.

The metabolic fate of glycolate esters has received little attention, and the few reported studies provide somewhat contradictory results. The metabolism of ^{3}H-*N*-ethyl-3-piperidyl benzilate (I) was studied in rats; 75% of the injected dose was present in urine as the unchanged drug at 2 hr after intraperitoneal injection, and 96% was excreted after 12 hr (6). However, the unchanged drug was not detected in urine of rats during 48 hr after intraperitoneal injection of I and the only metabolites detected were benzilic acid, *N*-ethyl-3-hydroxypiperidine (III), and a small amount of conjugate(s) that produced III after acid hydrolysis (7). Another study (8) found that I produced acetaldehyde when incubated *in vitro* with microsomes from rat liver. The present paper reports the identification of the metabolites produced from the incubation of I with rat liver homogenate *in vitro* and the urinary metabolites of I after intraperitoneal injection in rats.

RESULTS AND DISCUSSION

Synthesis and Identification of Potential Metabolites—The hydrochloride of I was synthesized from III and methyl benzilate as described by Biel *et al.* (1). 3-Piperidyl benzilate (II) hydrochloride was obtained by catalytic hydrogenolysis of *N*-benzyl-3-piperidyl benzilate. The latter was obtained by reacting *N*-benzyl-3-chloropiperidine with benzilic acid. The hydrochlorides of III and 3-hydroxypiperidine (IV) were obtained from commercially available III and IV.

***In Vitro* Studies**—Compound I hydrochloride was incubated with rat liver homogenate. The metabolites were extracted from the incubation mixture and examined by two-dimensional TLC on silica gel plates. Spots with chromatographic mobilities similar to authentic samples of I–III were observed on the TLC plates. No spot corresponding in position to IV was observed.

To confirm the identity of the metabolites produced, areas of the TLC plates corresponding to the positions of I–III were scraped and the adsorbent was extracted with methanol. The methanol extracts were evaporated to dryness, and the residues were submitted for mass spectral analysis. The mass spectrum of an authentic sample of I and that of the substance recovered from the incubation mixture were virtually identical, confirming the identity of the latter. The mass spectrum for I showed the molecular ion at *m/e* 339. The base peak appeared at *m/e* 111 and was tentatively assigned to the $C_7H_{13}N^+$ fragment. A plausible fragmentation pathway accounting for the major fragments in the mass spectrum of I is shown in Scheme I.

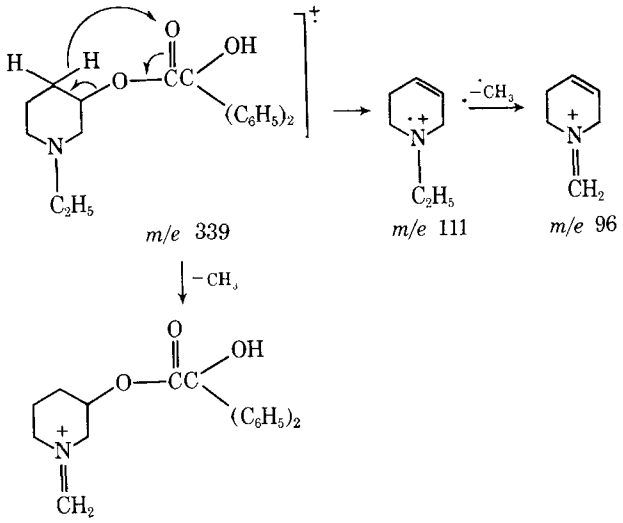

Scheme I

The mass spectrum of authentic II was not identical to that of the metabolite believed to be II. Evidently, the fragmentation pattern of II by electron impact was dependent on the concentration of the compound and/or the temperature in the ionization chamber, since recording consecutive spectra after the introduction of the sample in the ionization chamber of the mass spectrometer resulted in vastly different spectra. To confirm the identity of the metabolite, the IR spectrum of the residue eluted from the TLC plate was recorded and was identical to that of an authentic sample of II.

The crude extract from the incubation mixture was examined by GLC–mass spectrometry to detect the presence of III and IV. The chromatographic separation was performed on a 12% Carbowax 20M column, and the mass spectrum for the peaks eluted with the same retention time as III and IV were recorded. No peak with the same retention time and mass spectrum as IV was detected in the crude extract of the incubation mixture. A peak with the same retention time as III was present in this extract, and the mass spectrum of this peak was virtually identical to that obtained for an authentic sample of III. The mass spectrum of III showed the molecular ion at *m/e* 129 and the base peak at *m/e* 114 and was similar to the spectrum previously reported for this compound (9).

The possibility that III was produced by the nonenzymatic hydrolysis of I also was explored. Incubation of I under the same conditions as for the enzymatic studies, except for the absence of liver homogenate, resulted in the formation of only a trace of III, if at all. This result indicated that the hydrolysis of I to III in the previous studies was indeed enzyme catalyzed, undoubtedly by esterases present in liver homogenates. It was of interest to determine the site of these esterases in the different fractions of liver homogenates and whether these esterases were present in rat blood.

Compound I was incubated with the microsomal and the supernatant fractions of the rat liver homogenate and with rat blood. The incubation conditions and the workup of the incubation mixture were the same as described for the experiments using liver homogenates. Incubation of I with the microsomal fraction of the rat liver homogenates resulted in a metabolite profile qualitatively and quantitatively (as determined by comparison of the relative intensities of the spots on the TLC plate) similar to that obtained with the rat liver homogenates. On the other hand, incubation of I with the 105,000×*g* supernate of rat liver homogenates resulted only in the formation of traces of III. The formation of III by incubation with the 105,000×*g* supernate may be attributed to the presence of residual microsomes or the presence of esterase enzymes in this fraction. Incubation of I with rat blood resulted in the formation of traces of III. These results indicated that the enzymes responsible for the metabolism of I *in vitro* were mainly localized in the microsomal fraction of the liver homogenates. The blood showed only a very low esterase activity for this compound.

The absence of IV in the products of the metabolism of I was not expected, since the incubation conditions resulted in the accumulation of II and III in the incubation mixture. The latter two metabolites would be expected to be substrates for the liver enzymes and would be further metabolized to IV. Therefore, II and III were investigated as substrates

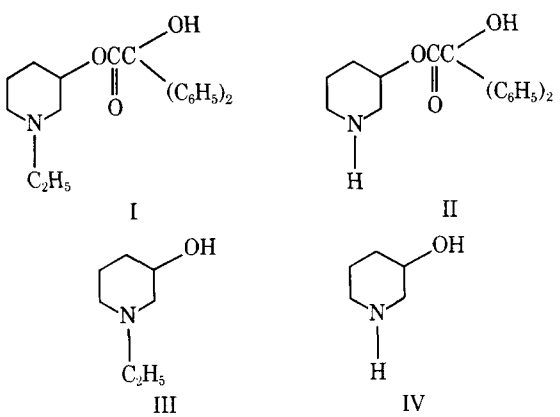

[1] Ditran.

for the rat liver homogenate enzymes. Compounds II and III were incubated with the rat liver homogenates using the same incubation conditions and workup procedures described for I. These studies indicated that II was not hydrolyzed to IV by the microsomal esterases. Likewise, III was not *N*-deethylated to IV.

Urinary Metabolites of I in Rats—The urinary excretion of I and its potential metabolites after intraperitoneal injection in rats also was studied. Several methods for the isolation of the metabolites from urine were investigated, including extraction of urine with solvents, adsorption of the metabolites on activated charcoal (10), use of cation-exchange resins to retain the basic metabolites, and partition column chromatography as described by Egli (7). The use of activated charcoal for the adsorption of the metabolites from urine was most satisfactory. The recovery of metabolites from urine was high, and there was minimum interference from other urinary constituents.

Extracts from urine of rats injected with I hydrochloride were examined by GLC–mass spectrometry using a 3% OV-1 column and monitoring *m/e* 339 and 129. A peak of *m/e* 339, at a column temperature of 220°, with the same retention time as I was observed in the urine extracts, indicating the urinary excretion of unchanged drug. The identity of this substance was further established by recording the spectrum of this peak between *m/e* 400 and 10. This spectrum was virtually identical to that obtained for an authentic sample of I treated in the same way as the metabolite sample. The amount of unchanged drug in urine was very small, and quantitation was not practical. This finding indicated that only a trace amount of the unchanged drug was excreted in urine after intraperitoneal injection in rats.

The extracts from urine also showed a peak with *m/e* 129, at a column temperature of 120°, with a retention time equal to that of an authentic sample of III. The identity of this substance was further established by recording its mass spectrum between *m/e* 200 and 10. The mass spectrum obtained was virtually identical to that of an authentic sample of this compound. Compound III was present in a considerably larger amount than the unchanged drug.

The chromatographic separation of IV using the described conditions was not satisfactory. However, the separation of the silyl derivatives of III and IV was acceptable. Extracts from urine were silylated with *N,O*-bis(trimethylsilyl)acetamide to form the monosilyl derivative of III (mol. wt. 201) and the disilyl derivative of IV (mol. wt. 245). The silylated extract was examined by GLC–mass spectrometry using a 3% OV-1 column at 65° and monitoring *m/e* 201 (monosilyl derivative of III) and at 80° and monitoring *m/e* 245 (disilyl derivative of IV).

A peak of *m/e* 201 was observed, confirming the presence of III in urine. The quantitation of III in urine was achieved by comparing the absolute intensity of *m/e* 201 at the peak maximum with the intensities obtained by adding different known concentrations of the standard compound to rat urine and subjecting these samples to exactly the same processes as the experimental samples. Estimation of III in urine indicated that approximately 9% of the injected dose was excreted as this metabolite. No peak of *m/e* 245 (the disilylated derivative of IV) was detected in urine.

Since it was not possible to develop a GLC procedure for the detection and quantitation of II in urine, it was imperative to use an indirect method for its determination. This method involved the acid hydrolysis of urine and measurement of the increase in the amount of IV. Conjugated metabolites that may be excreted in urine after the intraperitoneal injection of I would produce III and IV on acid hydrolysis. Urine was subjected to acid hydrolysis and extracted in the same way as previously described. The GLC–mass spectrometric examination of these extracts directly and after silylation indicated the presence of only III. The amount of III in urine after acid hydrolysis was 11% of the injected dose, indicating that 2% of the injected dose was excreted in urine in the form of a conjugate of I or III and/or unchanged I. The absence of IV in the hydrolyzed urine indicated that neither II nor conjugates of II and IV were excreted in urine.

These findings are in agreement with those of Egli (7), who reported that approximately 9% of injected I was recovered in the 48-hr urine of rats as III and that 2% was recovered as conjugates that produced III on acid hydrolysis. Egli (7) was not able to detect the presence of the unchanged drug in urine.

However, these findings are in contradiction with the findings of Abood and Rinaldi (6), who reported that 96% of the injected dose of I was excreted unchanged in rat urine within 48 hr after intraperitoneal injection in rats. These investigators used tritium-labeled I with no provision to establish the position of the label in the molecule. The radioactivity they measured in rat urine may have been due to some metabolite not detected with the present analytical methods.

The absence of II and its hydrolysis product IV from urine was unexpected since II was a major metabolite of I *in vitro*. Also, it was disturbing that about 90% of the injected dose was not accounted for. Consequently, the metabolism of the potential metabolites, II–IV, was studied to determine whether they are terminal metabolites or may be further metabolized to other products.

Extracts from urine of rats injected with II hydrochloride contained the disilyl derivative of IV in an amount approximately 18% of the injected dose. The amount of IV in urine after hydrolysis was approximately the same as before hydrolysis, indicating that no unchanged II or a conjugate that produced IV on acid hydrolysis was present.

These findings indicated that hydrolysis was one metabolic pathway for II. However, the major route of elimination of this compound as well as I is not as yet known. The presence of IV in urine of rats injected with II and its absence in the urine of rats injected with I indicated that II is probably not a major metabolite of I.

Approximately 26% of the injected dose of III hydrochloride was present in urine as the unchanged drug. The amount of III in urine after acid hydrolysis was 89% of the injected dose, indicating that 63% of the injected dose was excreted in urine in the form of conjugates that produced III on acid hydrolysis. The extracts from urine did not contain the potential metabolite IV.

Extracts from urine of rats injected with IV hydrochloride contained approximately 50% of the injected dose as the unchanged drug. The amount of IV in urine after acid hydrolysis was approximately 100% of the injected dose, indicating that 50% of the injected dose was excreted in urine in the form of conjugates that produced IV on acid hydrolysis.

EXPERIMENTAL[2]

Compound I Hydrochloride—The title compound was obtained in 72% yield from III and methyl benzilate as described by Biel *et al.* (1). Recrystallization from absolute ethanol gave pure I hydrochloride, mp 190–192° [lit. (1) mp 191–192°].

Anal.—Calc. for $C_{21}H_{25}ClNO_3$: C, 67.11; H, 6.92; Cl, 9.45; N, 3.72. Found: C, 66.89; H, 7.16; Cl, 9.84; N, 3.54.

Compound II Hydrochloride—*N*-Benzyl-3-chloropiperidine (6.7 g, 30 mmoles) was dissolved in dry isopropyl alcohol (30 ml). To this solution was added benzilic acid (10.29 g, 45 mmoles) in dry isopropyl alcohol (90 ml), and the mixture was heated under reflux for 24 hr. Isopropyl alcohol was then removed by evaporation under reduced pressure. The precipitate was partitioned between 5% potassium carbonate aqueous solution and ether (60 ml). The ether layer was evaporated to dryness, and the residue was dissolved in a minimum volume of isopropyl alcohol; hydrogen chloride-saturated ether was added to precipitate the hydrochloride salt.

The resulting *N*-benzyl-3-piperidyl benzilate hydrochloride was filtered and recrystallized from absolute ethanol. It weighed 5.3 g (40.4% yield), mp 204.5° dec. *N*-Benzyl-3-piperidyl benzilate (4.6 mmoles) was dissolved in methanol (60 ml) containing acetic acid (0.4 ml), and 5% palladium-on-charcoal (900 mg) was added. The mixture was shaken under 46.5 psi of hydrogen for 90 min and filtered. The filtrate was concentrated to about one-third of its volume under reduced pressure. Hydrogen chloride-saturated ether (40 ml) was added and evaporated to dryness.

The residue was dissolved in methanol, and sufficient ether was added to effect complete precipitation. The precipitate was filtered, washed with ether, and dried *in vacuo* to provide 1.435 g (90% yield). Recrystallization from absolute ethanol gave 1.435 g of II hydrochloride (71% yield), mp 179.5–182°; NMR ($CDCl_3$): δ 7.25 (m, 10H), 4.8 (m, 1H), 3.4 (m, 2H), 2.5 (m, 4H), and 1.5 (m, 4H); mass spectrum: *m/e* (relative intensity), 312 (0.2), 212 (0.3), 183 (42.4), 105 (68.1), 84 (20.8), 83 (100), and 76 (1.7).

Compound III Hydrochloride—The hydrochloride was prepared by dissolving III[3] in methanol and adding hydrogen chloride-saturated ether. The precipitate was collected and recrystallized from isopropyl alcohol–ether, mp 159–162°; NMR (free base in $CDCl_3$): δ 3.0 (s, 1H), 3.6 (m, 1H), 1.1 (t, 3H, J = 7 Hz), 2.35 (q, 2H, J = 7 Hz), 2.35 (m, 4H), and

[2] Melting points were determined in open capillary tubes and are *uncorrected*. IR spectra were obtained with a Perkin-Elmer 237B spectrophotometer in potassium bromide disks. NMR spectra were obtained in deuterochloroform with a Varian A-60D spectrometer, using tetramethylsilane as the internal standard. Microanalyses were performed by M-H-W Laboratories, Garden City, Mich. Mass spectra were obtained with an AEI MS-30 mass spectrometer. GLC analyses were carried out on a Perkin-Elmer 900 instrument equipped with a flame-ionization detector. GLC–mass spectral analyses were performed on an LKB 9000 instrument equipped with a PDP 8E data processing system.

[3] Aldrich Chemical Co., Milwaukee, Wis.

1.68 (m, 4H); mass spectrum: *m/e* (relative intensity) 129 (17.39), 114 (100), 199 (6.77), 84 (9.16), 72 (32.71), 58 (14.91), 57 (40.37), 44 (21.74), 43 (20.91), 42 (58.18), and 41 (18.63).

Compound IV Hydrochloride—Compound IV[3] was dissolved in methanol and treated with hydrogen chloride-saturated ether until complete precipitation of the hydrochloride salt was observed. The precipitate was recrystallized from isopropyl alcohol–ether, mp 193–196°; NMR (free base in $CDCl_3$): δ 3.7 (m, H), 3.45 (s, H), 2.96 (m, H), 2.75 (m, 4H), and 1.65 (m, 4H); mass spectrum: *m/e* (relative intensity) 101 (42.61), 83 (2.20), 57 (65.25), 56 (35.85), 55 (12.74), 44 (100), 43 (32.23), 42 (24.06), and 41 (16.35).

***In Vitro* Studies**—*Tissue Preparations*—Livers from male Sprague–Dawley rats, 150–200 g, were used as the source of liver homogenates and microsomal preparations. Blood from the same rats was used for measurement of blood esterase activity. The animals were allowed food and water *ad libitum*. They were stunned by a blow on the head and decapitated, and the blood was collected in heparinized beakers.

The livers were removed rapidly and placed in ice-cold 1.15% KCl solution. All further preparations were conducted at 0–4°. The livers were mixed with three times their weight of 1.15% KCl and homogenized[4], and the homogenate was centrifuged in a refrigerated centrifuge[5] at 10,000×*g* for 30 min. The supernate was withdrawn, and half of it was used in studies with liver homogenates. The other half was centrifuged[6] at 105,000×*g* for 60 min. The high-speed supernatant layer was used as the "supernatant fraction of liver homogenate," and the precipitate, the microsomal pellet, was resuspended in 1.15% KCl solution.

Incubation Conditions—All solutions for enzyme preparation and incubation mixtures were prepared in water double distilled from glass. The incubation mixture contained 10 ml of 10 m*M* substrate (I, II, or III), 10 ml of enzyme preparation (liver homogenate, microsomal fraction, supernate of liver homogenate, or blood), 5 ml of cofactors solution (2.25 μmoles of NADP and 25 μmoles of glucose 6-phosphate in 1.15% KCl), 20 ml of buffer (prepared from 10 μmoles of nicotinamide, 5 μmoles of magnesium chloride, 1.63 g of dibasic sodium phosphate/100 ml, and 0.53 g of monobasic potassium phosphate/100 ml and adjusted to pH 7.4 with sodium hydroxide), and 5 ml of 1.15% KCl solution. The total volume was 50 ml.

Incubations were conducted at 37° in an open atmosphere for 2 hr in 250-ml conical flasks placed in a water bath shaker[7]. The reactions were terminated by the addition of 10 ml of 0.6 *N* perchloric acid. The incubation mixtures used in the zero-time studies were identical to the described mixtures without the enzyme preparation. Addition of the enzyme preparation was carried out in the last step, after the addition of perchloric acid. The mixtures were centrifuged, and the supernate was used for the identification of metabolites.

Identification of Metabolites—The supernate was extracted with an equal volume of benzene to remove lipids. The aqueous phase was adjusted to pH >10 with dilute ammonium hydroxide and extracted first with methylene chloride (75 ml) and then with 75 ml of chloroform–isopropyl alcohol (3:1). The extracts were combined and evaporated to dryness in a nitrogen stream, and the residues were dissolved in 0.1-ml portions of methylene chloride.

The residues obtained from each incubation were applied onto 10 silica gel GF TLC plates[8] (20 × 20 cm, 250 μm). The plates were developed in acetonitrile–chloroform–methanol–ammonium hydroxide (50:40:29:1) in one dimension and then in ethyl acetate–methanol–ammonium hydroxide (100:100:1) in a second dimension. The dry plates were examined under a UV lamp for the detection of I and II, and one plate was sprayed with 0.5% $KMnO_4$ to locate the metabolites. Areas of the plates corresponding to the positions of the authentic samples were scraped off the remaining nine plates.

The adsorbent fractions obtained from the same area on different plates were combined and extracted with methanol. The methanol extracts were dried in a nitrogen stream, and the residues were submitted for mass spectral analysis. The residue obtained from the area on the TLC plates corresponding in position to that of an authentic sample of II was dissolved in 0.1 ml of chloroform and mixed with 200 mg of potassium bromide (IR grade). The dried mixture was used for the preparation of a pellet for IR spectroscopy.

The residues obtained by evaporation of the extracts from the incubation mixtures (before application to the TLC plates) also were examined by GLC–mass spectrometry, using a 12% Carbowax 20M column at 120° to detect metabolites III and IV. The mass spectrum of the peak eluted with the same retention time as authentic III was recorded. No chromatographic peaks with the same retention times as authentic IV were observed in any extract.

***In Vivo* Studies**—Three male Sprague–Dawley rats, 500 g, were used for each experiment. The rats were placed individually in metabolism cages and allowed food and water *ad libitum;* urine (control) was collected for 24 hr. The rats were injected intraperitoneally with solutions of the hydrochloride salts of I, II, III, or IV in normal saline at 80 mg/kg in four equal injections for I, III, and IV or at 60 mg/kg in five equal injections for II. The urine was collected under toluene for 72 hr after injection. Urine samples were removed from the metabolism cage periodically and stored at −25° until analyzed.

Preparation of Correlation Curves—A 30-, 20-, 10-, or 7.5-mg portion of authentic III hydrochloride was added to separate 10-ml aliquots of control urine. The solutions were made alkaline (pH 8.0) by the addition of dilute ammonium hydroxide. A 20-ml aliquot of 0.2 *M* carbonate buffer (pH 11) and 5 ml of the basic charcoal suspension were added to each urine sample. The basic charcoal suspension was prepared by adding 15 g of charcoal[9] to 400 ml of carbonate buffer (sodium carbonate–sodium bicarbonate, pH 11) and mixing thoroughly, allowing the charcoal to settle overnight, and then aspirating as much as possible of the supernatant buffer.

The mixtures were mixed thoroughly by repeated gentle shaking for 30 min and then centrifuged at 4000×*g* for 15 min. The clear supernatant layers were discarded, and the charcoal precipitates were shaken with 150 ml of methanol. The methanol extracts were filtered and evaporated to dryness in a nitrogen stream. The residues were each treated with 235 mg of *N,O*-bis(trimethylsilyl)acetamide to form the monosilyl derivative of III. The mixtures were examined by computer-equipped GLC–mass spectrometry on 3% OV-1 at 65°, using the mass spectrometer as a specific ion detector. A correlation curve was obtained by plotting the concentration of authentic III *versus* the absolute intensity of the ions of *m/e* 201 at the peak maximum for the monosilyl derivative of III. Regression analysis[10] was used to determine the line of the best fit for the data points.

A 7.5-mg portion of authentic IV hydrochloride was added to a 10-ml aliquot of urine. The standard sample was then extracted as described. The residue after silylation was examined by computer-equipped GLC–mass spectrometry using a 3% OV-1 column at 80°.

Examination of Urine for I, III, and IV—An aliquot of urine (one-third to one-fourth the urine sample) was adjusted to pH 11.0 and treated with a suspension of charcoal, and the charcoal was extracted with methanol as previously described. The methanol extract was evaporated in a nitrogen stream, and the residue was dissolved in methylene chloride. The detection of I in urine was achieved by examining the solution by computer-equipped GLC–mass spectrometry using a 3% OV-1 column at 220°. The mass spectrometer was used in the specific ion detector mode to monitor the peaks with *m/e* 339.

The methylene chloride solution was evaporated to dryness in a nitrogen stream, and the residue was treated with 609 mg of *N,O*-bis(trimethylsilyl)acetamide. The solution was examined again by computer-equipped GLC–mass spectrometry using a 3% OV-1 column at 65° and monitoring the ions with *m/e* 201 for the monosilyl derivative of III. The column temperature was raised to 80°, and the sample was reinjected; the mass spectrometer was set to monitor ions with *m/e* 245 for the detection and quantitation of the disilyl derivative of IV.

Examination of Urine for Compounds that Produce III or IV after Acid Hydrolysis—An aliquot of the urine sample was mixed with an equal volume of 12 *N* HCl and heated at 118° for 16 hr. The mixture was adjusted to pH 11.0 and treated with a suspension of charcoal, and the charcoal was extracted with methanol as previously described. The methanol extract was evaporated in a nitrogen stream, and the residue was treated with 609 mg of *N,O*-bis(trimethylsilyl)acetamide. The solution was examined for the presence of the monosilyl derivative of III and the disilyl derivative of IV by computer-equipped GLC–mass spectrometry as previously described.

REFERENCES

(1) J. H. Biel, L. G. Abood, W. K. Hoya, H. H. Leiser, P. A. Nuhfer, and E. Kluchesky, *J. Org. Chem.*, **26**, 4096 (1961).

[4] Polytron ultrasonic homogenizer, Brinkmann Instruments, Westbury, N.Y.
[5] Beckman J-21, Beckman Instruments, Fullerton, Calif.
[6] Beckman L2-65B ultracentrifuge, Beckman Instruments, Fullerton, Calif.
[7] Eberbach Corp., Ann Arbor, Mich.
[8] Analtech, Newark, Del.
[9] Merck and Co.
[10] Hewlett-Packard 9100A calculator.

(2) L. G. Abood and J. H. Biel, *Int. Rev. Neurobiol.*, **4**, 218 (1962).
(3) L. G. Abood, A. Astfeld, and J. H. Biel, *Arch. Int. Pharmacodyn. Ther.*, **120**, 186 (1959).
(4) L. G. Abood and L. J. Meduna, *J. Nerv. Ment. Dis.*, **127**, 546 (1958).
(5) D. C. English, *J. Neuropsychiat.*, **3**, 304 (1962).
(6) L. G. Abood and F. Rinaldi, *Psychopharmacologia*, **1**, 117 (1959).
(7) K. Egli, Master's thesis, University of Minnesota, Minneapolis, Minn., 1973.
(8) M. W. Anders and G. J. Mannering, *Mol. Pharmacol.*, **2**, 219 (1966).
(9) L. F. Zerilli, A. Cometti, N. Rimorini, and G. G. Gallo, in "Proceedings of the International Symposium on Gas Chromatography Mass Spectrometry," A. Frigerio, Ed., Elba, Italy, 1972.
(10) J. M. Meola and M. Vanko, *Clin. Chem.*, **20**, 184 (1974).

ACKNOWLEDGMENTS AND ADDRESSES

Received May 20, 1976, from the *College of Pharmacy and the ‡College of Biological Sciences, University of Minnesota, Minneapolis, MN 55455.

Accepted for publication August 18, 1976.

Supported in part by a grant from the research funds provided by the Graduate School of the University of Minnesota.

The authors also thank the Samuel W. Melendy Summer Fellowship for financial support to C.-H. Chen.

ˣ To whom inquiries should be directed.

Effects of Agitation on Size Distribution of Particulate Matter in Large-Volume Parenterals

JAMES BLANCHARD ˣ, JOHN A. SCHWARTZ, and DALE M. BYRNE *

Abstract □ The particle-size distributions of six types of large-volume parenterals subjected to different degrees of agitation were determined using an automatic particle counter. Data acquired from each solution, which had been maintained in a stored condition, subjected to agitation by inverting 20 times, and then mechanically shaken for 30 min, produced a linear relationship between log $N_{>D}$ and log D. Both the slope (K) and the number of particles per milliliter exceeding 1 μm in diameter ($N_{>1}$) exhibited a dependence on the degree of agitation. Their combined effect indicates that agitation by 20 hand inversions removed particulate matter from the surface of the container, which increased the total number of particles in solution (>1 μm) but did not significantly alter the relative size distribution. Agitation for 30 min, however, disintegrated agglomerates and produced a particle-size distribution with a greatly increased number of particles whose diameters were less than 1 μm and a corresponding decrease in the number of particles exceeding 1 μm in diameter. The particle-size distribution of a parenteral solution determined by this *in situ* instrumental method was, therefore, dependent upon the degree of agitation to which the parenteral was subjected prior to examination.

Keyphrases □ Particle-size distribution—various large-volume parenterals, effect of different degrees of agitation □ Parenterals, large volume—particle-size distribution, effect of different degrees of agitation □ Dosage forms—various large-volume parenterals, particle-size distribution, effect of different degrees of agitation □ Agitation—effect on particle-size distribution of various large-volume parenterals

Particulate matter was defined as "extraneous, mobile, undissolved substances, other than gas bubbles, unintentionally present in parenteral solutions" (1). In a previous report, efforts to compare and contrast the ability of five methods to monitor the levels of particulate matter were described (2). During this investigation, it became apparent that the automatic particle counter was suitable for the rapid determination and sizing of particulate matter. This instrument's ability to provide a reasonably accurate determination of the particle-size distributions present in large-volume parenterals was comparable[1] to the membrane filtration and microscopic examination technique utilized in the recently adopted USP–NF standard (1).

Some difficulties previously were noted in determining the actual levels of particulate matter of a given size present in parenterals. Ernerot *et al.* (3), who utilized a destructive counting procedure, reported that the particle-size distribution in a parenteral solution at a given time was largely dependent upon the degree of agitation the solution had previously received. By its very nature, a destructive counting technique introduces a certain amount of shear force upon the particles in the solution, thereby altering the initial distribution of particles. This shear force introduced by the measuring technique itself would be eliminated by a nondestructive technique, since it would not be necessary to remove the solution from its container. Therefore, a nondestructive *in situ* technique that does not impose any additional shear force on the particles in a solution would be ideally suited for characterizing the effects of agitation on particle-size distributions in parenteral solutions.

Some recent reports gave conflicting accounts of the importance of the effects of agitation. Groves (4) attributed the increase in particle counts observed (3) to the presence of air bubbles generated during the agitation procedure. Ernerot (5) refuted this argument and identified the disintegration and flocculation of particles as the true sources of the variation in particle counts following agitation. Blaug and Sarabia (6) noted that the particle counts recorded using an electronic particle counter were the same for samples taken from intravenous bottles at rest or from the same bottles shaken immediately prior to sampling. Since destructive particle counting techniques were used in these investigations, it is difficult to draw definitive conclusions regarding the actual effects of agitation. Therefore, a major goal of this study was to examine more definitively the effects of agitation on the particle-size distribution in large-volume parenterals utilizing a nondestructive instrumental technique.

[1] J. Blanchard, J. A. Schwartz, and D. M. Byrne, to be published.

(2) L. G. Abood and J. H. Biel, *Int. Rev. Neurobiol.*, **4**, 218 (1962).
(3) L. G. Abood, A. Astfeld, and J. H. Biel, *Arch. Int. Pharmacodyn. Ther.*, **120**, 186 (1959).
(4) L. G. Abood and L. J. Meduna, *J. Nerv. Ment. Dis.*, **127**, 546 (1958).
(5) D. C. English, *J. Neuropsychiat.*, **3**, 304 (1962).
(6) L. G. Abood and F. Rinaldi, *Psychopharmacologia*, **1**, 117 (1959).
(7) K. Egli, Master's thesis, University of Minnesota, Minneapolis, Minn., 1973.
(8) M. W. Anders and G. J. Mannering, *Mol. Pharmacol.*, **2**, 219 (1966).
(9) L. F. Zerilli, A. Cometti, N. Rimorini, and G. G. Gallo, in "Proceedings of the International Symposium on Gas Chromatography Mass Spectrometry," A. Frigerio, Ed., Elba, Italy, 1972.
(10) J. M. Meola and M. Vanko, *Clin. Chem.*, **20**, 184 (1974).

ACKNOWLEDGMENTS AND ADDRESSES

Received May 20, 1976, from the *College of Pharmacy and the ‡College of Biological Sciences, University of Minnesota, Minneapolis, MN 55455.

Accepted for publication August 18, 1976.

Supported in part by a grant from the research funds provided by the Graduate School of the University of Minnesota.

The authors also thank the Samuel W. Melendy Summer Fellowship for financial support to C.-H. Chen.

ˣ To whom inquiries should be directed.

Effects of Agitation on Size Distribution of Particulate Matter in Large-Volume Parenterals

JAMES BLANCHARD ˣ, JOHN A. SCHWARTZ, and DALE M. BYRNE *

Abstract □ The particle-size distributions of six types of large-volume parenterals subjected to different degrees of agitation were determined using an automatic particle counter. Data acquired from each solution, which had been maintained in a stored condition, subjected to agitation by inverting 20 times, and then mechanically shaken for 30 min, produced a linear relationship between log $N_{>D}$ and log D. Both the slope (K) and the number of particles per milliliter exceeding 1 μm in diameter ($N_{>1}$) exhibited a dependence on the degree of agitation. Their combined effect indicates that agitation by 20 hand inversions removed particulate matter from the surface of the container, which increased the total number of particles in solution (>1 μm) but did not significantly alter the relative size distribution. Agitation for 30 min, however, disintegrated agglomerates and produced a particle-size distribution with a greatly increased number of particles whose diameters were less than 1 μm and a corresponding decrease in the number of particles exceeding 1 μm in diameter. The particle-size distribution of a parenteral solution determined by this *in situ* instrumental method was, therefore, dependent upon the degree of agitation to which the parenteral was subjected prior to examination.

Keyphrases □ Particle-size distribution—various large-volume parenterals, effect of different degrees of agitation □ Parenterals, large volume—particle-size distribution, effect of different degrees of agitation □ Dosage forms—various large-volume parenterals, particle-size distribution, effect of different degrees of agitation □ Agitation—effect on particle-size distribution of various large-volume parenterals

Particulate matter was defined as "extraneous, mobile, undissolved substances, other than gas bubbles, unintentionally present in parenteral solutions" (1). In a previous report, efforts to compare and contrast the ability of five methods to monitor the levels of particulate matter were described (2). During this investigation, it became apparent that the automatic particle counter was suitable for the rapid determination and sizing of particulate matter. This instrument's ability to provide a reasonably accurate determination of the particle-size distributions present in large-volume parenterals was comparable[1] to the membrane filtration and microscopic examination technique utilized in the recently adopted USP–NF standard (1).

Some difficulties previously were noted in determining the actual levels of particulate matter of a given size present in parenterals. Ernerot *et al.* (3), who utilized a destructive counting procedure, reported that the particle-size distribution in a parenteral solution at a given time was largely dependent upon the degree of agitation the solution had previously received. By its very nature, a destructive counting technique introduces a certain amount of shear force upon the particles in the solution, thereby altering the initial distribution of particles. This shear force introduced by the measuring technique itself would be eliminated by a nondestructive technique, since it would not be necessary to remove the solution from its container. Therefore, a nondestructive *in situ* technique that does not impose any additional shear force on the particles in a solution would be ideally suited for characterizing the effects of agitation on particle-size distributions in parenteral solutions.

Some recent reports gave conflicting accounts of the importance of the effects of agitation. Groves (4) attributed the increase in particle counts observed (3) to the presence of air bubbles generated during the agitation procedure. Ernerot (5) refuted this argument and identified the disintegration and flocculation of particles as the true sources of the variation in particle counts following agitation. Blaug and Sarabia (6) noted that the particle counts recorded using an electronic particle counter were the same for samples taken from intravenous bottles at rest or from the same bottles shaken immediately prior to sampling. Since destructive particle counting techniques were used in these investigations, it is difficult to draw definitive conclusions regarding the actual effects of agitation. Therefore, a major goal of this study was to examine more definitively the effects of agitation on the particle-size distribution in large-volume parenterals utilizing a nondestructive instrumental technique.

[1] J. Blanchard, J. A. Schwartz, and D. M. Byrne, to be published.

Table I—Effect of Agitation on the Average Size Distribution Characteristics of Large-Volume Parenteral Solutions

Type of Solution	Degree of Agitation	Average[a] Number of Particles per Milliliter >1 μm	Average Slope (K) of log–log Plot ± SE
Dextrose, 5% in half-strength normal saline[b]	Storage	235.5	−3.1445 ± 0.8328
	20 inversions	495.2	−2.9704 ± 0.1111
	30-min shake	336.1	−3.2988 ± 0.8381
Normal saline[c]	Storage	559.5	−3.3050 ± 0.4240
	20 inversions	686.6	−2.7139 ± 0.4143
	30-min shake	454.5	−3.7144 ± 1.0690
Dextrose, 5% in multiple electrolyte solution[d]	Storage	1022.4	−3.1047 ± 0.7970
	20 inversions	1710.1	−2.4779 ± 0.5774
	30-min shake	867.4	−3.1315 ± 0.9748
Dextrose, 5% in normal saline[e]	Storage	838.0	−3.1239 ± 0.1581
	20 inversions	784.2	−3.5116 ± 0.2869
	30-min shake	808.5	−3.8292 ± 0.2384
Dextrose, 5% in water[f]	Storage	869.0	−2.8606 ± 0.4505
	20 inversions	1090.0	−2.8929 ± 0.3545
	30-min shake	1025.2	−3.0351 ± 0.5778
Dextrose, 5% in lactated Ringer's solution[g]	Storage	590.5	−2.7193 ± 0.2445
	20 inversions	813.5	−2.9037 ± 0.2166
	30-min shake	737.8	−2.9229 ± 0.4822

[a] Average of three bottles. [b] Lot A4N265A. [c] Lot A5A130B. [d] Dextrose, 5% in Isolyte M, Lot A5E302C. [e] Lot A5C047C. [f] Lot A5C239B. [g] Lot A5E483B.

EXPERIMENTAL

Large-volume parenteral solutions[2] (1000 ml) were inspected using an automatic particle counter[3]. The six types of commercially available solutions examined were chosen on the basis of their extensive use in clinical practice (Table I).

The particle counter utilized is capable of detecting particles as small as 1 μm in diameter. Solutions were examined by the automatic particle counter in the manner previously described (2). The number of particles per milliliter exceeding the following diameters was determined: 1.000, 1.259, 1.585, 1.995, 2.512, 3.162, 3.981, 5.012, and 6.310 μm. These diameters were chosen to facilitate data analysis since their logarithms are equally spaced. Starting at 1 μm, particle counts were recorded at successively increasing threshold settings until a given setting produced 10 readings whose average was less than 10 particles/ml. This value was chosen to ensure statistical accuracy and to limit the instrumental error resulting from the fact that this instrument displays the truncated, rather than the rounded, version of the number of particles counted (2).

Triplicate samples of each of the six types of large-volume parenterals, stored in an undisturbed condition for 65 days, were gently placed in position on the instrument for counting. After completion of the readings on the stored solutions, each bottle was agitated by being inverted, end-over-end, 20 times. This degree of agitation was chosen to conform with the degree of agitation used in the recently instituted compendial standard technique (1). These inversions were performed by the same individual to obtain a uniform degree of agitation from bottle to bottle.

Upon completion of this set of readings, each bottle was then shaken for 30 min at 140 excursions/min on a mechanical agitator[4]. After each agitation procedure, the bottles sat undisturbed on the measuring platform of the instrument for a *minimum* of 45–60 sec before any readings were recorded. This time period was reported to be adequate to ensure that air bubbles introduced even under "severe" agitation conditions would not be counted by this instrument (7, 8). The present data support these observations.

RESULTS AND DISCUSSION

The particle-size distributions in parenteral solutions often can be described[1] by a straight-line equation of the form:

$$\log N_{>D} = K \log D + \log N_{>1} \qquad \text{(Eq. 1)}$$

where $N_{>D}$ is the number of particles per milliliter with a diameter larger than D, $N_{>1}$ is the number of particles per milliliter with a diameter larger than 1 μm, D is the particle diameter in micrometers, and K is equal to the slope of a plot of log $N_{>D}$ *versus* log D. This equation was used to characterize the particle-size distributions of the parenteral solutions to determine the effects of agitation on particle-size distributions.

The effects of different degrees of agitation on the measured particle counts in a typical solution are shown in Table II; only the particle counts with diameters greater than 1.000, 1.585, and 2.512 μm are represented. Values for K, $N_{>1}$, and correlation coefficients were calculated from *all* results, provided that at least 10 particles/ml exceeding a given diameter were counted.

The data in Table II for the stored solutions illustrate how the particle-size distribution characteristics varied considerably among individual samples, as previously noted[1]. In addition, the effects of agitation on the measured particle-size distributions varied from sample to sample. For example, 20 inversions of a stored solution caused the particles counted, exceeding 1 μm in diameter, to *decrease* in Solutions C and K and to *increase* in Solution G relative to the stored condition. When these same solutions were subsequently shaken for 30 min, $N_{>1}$ *decreased* for Solutions C and G and *increased* for Solution K relative to the condition in these same solutions following 20 hand inversions.

The effects of these different degrees of agitation on the slopes of the log–log plots also varied between individual samples. For example, 20 inversions of a stored solution *increased* the absolute magnitude of the slopes for Solutions C and K relative to the stored condition, but that for Solution G *decreased*. When these same solutions were subjected to 30 min of shaking, the slopes for Solutions G and K *increased* (*i.e.*, became steeper) while the slope for Solution C *decreased* relative to the condition in these same solutions following 20 hand inversions. A close adherence to Eq. 1 (indicative of a linear relationship between log $N_{>D}$ and log D) is apparent for all three individual solutions shown in Table II regardless of the degree of agitation since the poorest correlation coefficient is −0.9815.

Due to the variable effects of agitation on particle-size distributions among individual solutions (Table II), the data for each solution type were averaged. The averaging of triplicate samples of a given type of solution facilitated the discrimination of the effects of agitation on their particle-size distributions. The data in Table I clearly indicate certain trends. First, the average number of particles per milliliter exceeding 1.000 μm in diameter *increased* upon 20 inversions of a stored solution and then *decreased* when the solution was subsequently shaken for 30 min. Only the 5% dextrose in normal saline solution deviated from this trend. However, individual samples of 5% dextrose in normal saline exhibited some of these trends (Table II). Second, the average slopes of the log–log plots varied throughout the six solution types. Upon 20 inversions of the stored solutions, the slopes for three solution types *increased* while three decreased. However, the subsequent 30 min of shaking resulted in an *increase* in all slopes of the log–log plots.

Finally, the correlation coefficients between log $N_{>D}$ and log D for any type of solution were very high, regardless of the degree of agitation, and ranged from −0.9257 to −0.9998. These high correlation coefficients show that neither the type of solution nor the degree of agitation had any significant effect upon the linearity of the log–log plots. These observations differ from those of Ernerot (5) who reported a bend in the log–log plots of the particle-size distributions of stored parenterals.

Since these results and those in another study[1] indicated that the effects of agitation upon the particle-size distributions and the particle-size distributions themselves were independent of the type of solution, the data were analyzed without regard to solution type. When the 18 stored

[2] McGaw Laboratories, Glendale, CA 91201.
[3] Prototron, model ILI 1000, Spectrex Corp., Redwood City, CA 94063.
[4] Eberbach model 6000, Eberbach Corp., Ann Arbor, MI 48106.

Table II—Effect of Agitation on the Size Distribution Characteristics of Individual Large-Volume Parenteral Solutions

Dextrose, 5% in Normal Saline Solutions[a]	Degree of Agitation	Number[b] of Particles per Milliliter			Slope (K) of log–log Plot	Correlation Coefficient between log $N_{>D}$ and log D
		>1.000 μm	>1.585 μm	>2.512 μm		
Sample C	Storage	599.3	122.9	<10	−3.2137	−0.9998
	20 inversions	524.5	147.9	<10	−4.0791	−0.9939
	30-min shake	444.8	141.9	<10	−3.4268	−0.9963
Sample G	Storage	1105.1	150.6	65.5	−3.3415	−0.9815
	20 inversions	1158.5	274.9	<10	−3.3020	−0.9946
	30-min shake	1123.3	121.3	23.4	−4.2520	−0.9948
Sample K	Storage	968.6	300.5	55.6	−2.8165	−0.9985
	20 inversions	828.7	165.9	43.7	−3.1538	−0.9981
	30-min shake	1126.9	151.6	41.6	−3.8088	−0.9982

[a] Lot A5C047C. [b] Average of 10 readings.

samples were inverted 20 times, the slopes of the log–log plots of nine of the samples *increased* while the other nine *decreased*. The values of the individual slopes were analyzed by the Student t-test, and no significant difference ($p > 0.5$) was observed between the slopes corresponding to these two degrees of agitation. When these bottles that had been inverted 20 times were subjected to an additional 30 min of shaking, 13 of the 18 individual slopes *increased*. This increase was significant ($p < 0.01$) by the Student t-test.

A similar analysis of the number of particles exceeding 1 μm in diameter indicated that, when a stored solution was inverted 20 times, 15 of the 18 individual intercepts (log $N_{>1}$) *increased;* the subsequent 30 min of shaking caused 12 of the 18 individual intercepts to *decrease*. A Student t-test revealed that these trends were significant at the $p < 0.005$ and $p < 0.05$ levels, respectively.

Figure 1 illustrates the effects of agitation on K and $N_{>1}$. Since the particle-size distribution was independent of the type of solution, the data in Fig. 1 represent the average values of these two parameters for the 18 solutions.

When a stored solution was inverted 20 times, two effects were evident (Fig. 1). As previously noted, there was no statistically significant change in the slope of the log–log plot whereas the intercept *increased* significantly. These simultaneous effects can be interpreted to mean that there is an increase in the number of particles at all size ranges measured. The origin of these additional particles is most likely particles that are dislodged from the inner surface of the container (9) by the relatively mild agitation produced by 20 inversions (10).

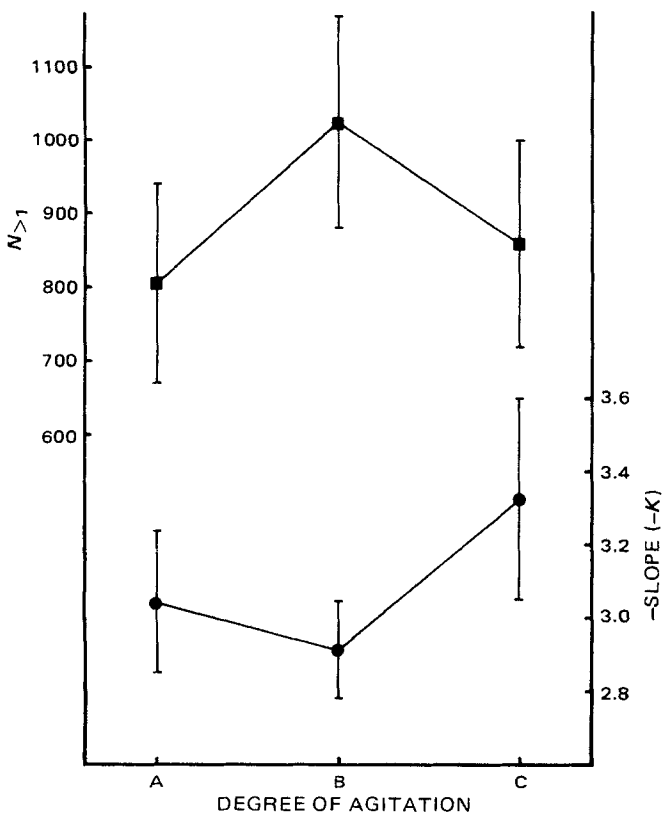

Figure 1—*Effects of degree of agitation on the slopes and intercepts of the log–log plots. Key: A, storage for 65 days; B, 20 hand inversions; and C, 30-min shake.*

However, Ernerot *et al.* (3) previously noted that one effect of agitation on a parenteral solution was a disintegration of large agglomerates into smaller sized particles. This effect would result in an increase in the intercept and a steeper slope. Since no significant increase in the slope was observed at this degree of agitation, the predominant effect appeared to be the dislodging of particles from the surface of the container whose size distribution was similar to those already present in solution. An alternative possibility is that only the larger particles were resuspended by the 20 hand inversions and that the process, in addition to resuspending these particles, also supplied sufficient shear force to disintegrate them into smaller particles whose resulting distribution was similar to the existing distribution.

When the solutions previously subjected to 20 inversions were subsequently shaken for 30 min, there was a significant *increase* in the slope of the log–log plot coupled with a significant *decrease* in the intercept. This decrease in the intercept is obviously indicative of the reduction of the total number of particles greater than 1 μm in diameter. The increased slope of the log–log plot represents a greater reduction in the number of larger sized, relative to smaller sized, particles following 30 min of shaking. A logical explanation for these concurrent effects is that the reduction in the number of larger sized particles is due to their disintegration caused by the high degree of agitation. This agitation, in turn, reduces these smaller particles to a size less than 1 μm in diameter, which is below the minimum size detectable by the automatic particle counter, causing a reduction in the observed intercept value. Since the disintegration of particles is the predominant event at this degree of agitation, the slope increases and the intercept decreases concurrently.

The health-related implications of these observations are difficult to state unequivocally, since the clinical significance of the very presence of particulate matter in a parenteral solution has not been proven conclusively. There is some controversy as to the most harmful size of particles (9), although one would intuitively suspect that a given number of larger sized particles would be potentially more harmful than a like number of smaller particles. The comment by Groves (11) that a container of parenteral fluid should not be subjected to violent shaking prior to injection is therefore somewhat difficult to reconcile. One point that is clear is that particle counting procedures should be carried out under well-controlled and reproducible conditions utilizing measuring techniques that do not impose a shear force upon the particles.

REFERENCES

(1) "First Supplement to USP XIX–NF XIV," Mack Publishing Co., Easton, Pa., July 1975, pp. 56, 57.

(2) J. Blanchard, C. M. Thompson, and J. A. Schwartz, *Am. J. Hosp. Pharm.*, **33**, 144 (1976).

(3) L. Ernerot, I. Helmstein, and E. Sandell, *Acta Pharm. Suec.*, **7**, 501 (1970).

(4) M. J. Groves, *Proc. Soc. Anal. Chem.*, 8, 271 (1971).

(5) L. Ernerot, *Acta Pharm. Suec.*, **11**, 1 (1974).

(6) S. M. Blaug and R. E. Sarabia, *Bull. Parenteral Drug Assoc.*, **29**, 74 (1975).

(7) M. Porter, *ibid.*, **29**, 169 (1975).

(8) "Instruction Manual, Prototron In Situ Liquid Inspection Station, Model ILI 1000," Spectrex Corp., Redwood City, Calif., 1974.

(9) W. H. Thomas and Y. K. Lee, *N. Z. Med. J.*, **80**, 170 (1974).

(10) R. A. Runkel, K. Ng, and L. Palagyi, *Bull. Parenteral Drug Assoc.*, **26**, 114 (1972).

(11) M. J. Groves, "Parenteral Products," William Heinemann Medical Books, London, England, 1973, p. 243.

ACKNOWLEDGMENTS AND ADDRESSES

Received March 11, 1976, from the *Department of Pharmaceutical Sciences, College of Pharmacy, University of Arizona, Tucson, AZ 85721.*

Accepted for publication August 17, 1976.

The authors thank Mr. William T. Fink and Mr. Donald Speray for their constructive criticism of the manuscript and Mr. John Hoyte for the use of the Prototron. Financial support from the University of Arizona Foundation and the University of Arizona Alumni Association is gratefully acknowledged.

* Present address: Optical Sciences Center, University of Arizona, Tucson, AZ 85721.

ˣ To whom inquiries should be directed.

Actions of Mescaline on Isolated Rat Atria

PETER K. S. SIEGL and RAYMOND F. ORZECHOWSKI ˣ

Abstract □ Mescaline, in concentrations of 5×10^{-4} and 1×10^{-3} *M*, produced negative chronotropic and positive inotropic responses in isolated, spontaneously beating rat atria. In tissues driven at a constant rate, the inotropic response was diminished greatly, indicating that the increment in the force of contraction was secondary to the reduction in rate. These chronotropic and inotropic responses were not altered consistently by pretreatment with the histamine antagonists chlorpheniramine and metiamide.

Keyphrases □ Mescaline—chronotropic and inotropic effects on isolated rat atria □ Chronotropic effects—mescaline on isolated rat atria □ Inotropic effects—mescaline on isolated rat atria □ Phenethylamines—mescaline, chronotropic and inotropic effects on isolated rat atria □ Cardiovascular effects—mescaline on isolated rat atria □ Psychotomimetics—mescaline, chronotropic and inotropic effects on isolated rat atria

In this study, the effects of mescaline (3,4,5-trimethoxyphenethylamine) on isolated rat atria were examined to reveal its possible actions directly on the pacemaker and atrial tissue. By the use of histamine antagonists, the involvement of histamine receptors (both H_1 and H_2) was examined as a possible mechanism of the *in vitro* cardiac action of mescaline.

BACKGROUND

The cardiovascular actions of the psychotomimetic amine mescaline were reported previously (1–8). Mescaline consistently evoked bradycardia in several species of animals. Mescaline-induced slowing of the frog heart was first observed by Dixon (1); others confirmed this action in the dog (2), rabbit, and cat (3). The bradycardia was inhibited by vagotomy or pretreatment with atropine (3); however, other published data (1, 2, 4) challenged these findings. Most evidence favors the conclusion that mescaline does not produce an effect on the heart by a vagal reflex or cholinergic stimulation.

Competition for epinephrine receptors by mescaline was proposed (5) because both mescaline-induced bradycardia and hypoglycemia in rats were reduced upon pretreatment with epinephrine. In another study (6), mescaline showed no propranolol-like antagonism of isoproterenol-induced relaxation of spontaneously contracting rat uterus. Mescaline failed to antagonize isoproterenol-induced positive chronotropism and hypotension (4) or to reverse an ethylnorepinephrine depressor response (6) in anesthetized dogs. From these data, β-adrenergic receptor blockade by mescaline or one of its metabolites was an unlikely explanation.

Histamine release or direct stimulation of histamine receptors by mescaline might account for the observed bradycardia. Potentiation of the hypotensive response to histamine in rats (7) was attributed to inhibition of the histaminolytic action of diamine oxidase by mescaline. Dogs receiving an intravenous infusion of mescaline showed (4) increased plasma histamine levels and a hypotensive response similar to that produced by compound 48/80, a known histamine-liberating substance (9). Alteration of respiratory dynamics and elevated right ventricular pressure, resembling responses to histamine, were observed in the guinea pig (8). Attempts to block these effects of mescaline with the antihistamine diphenhydramine were unsuccessful (4, 8).

More recent evidence suggested that histamine produced bradycardia by a stimulation of histamine receptor subtypes (H_2-receptors), which were not blocked by conventional antihistaminic agents such as diphenhydramine (10). The possible interaction of mescaline or mescaline-released histamine with H_2-receptors in the myocardium could be evaluated with an H_2-blocker, such as metiamide, in an attempt to confirm or refute this hypothesis.

EXPERIMENTAL

Sprague–Dawley rats of both sexes, 250–400 g, were sacrificed by cervical fracture and the hearts were rapidly removed. Paired atria were sectioned from the ventricles with a bridge of tissue joining the two atria. For examination of inotropic responses, left atria were electrically driven by paired platinum electrodes. Monophasic square wave pulses of 1-msec duration were delivered by a stimulator[1]. Tissues were suspended in a 10-ml glass tissue bath filled with Krebs–Henseleit solution (11) at a constant temperature of 35° and equilibrated with 95% O_2–5% CO_2. The solution pH was adjusted to 7.3.

A constant resting tension of 1.0 g was maintained throughout each experiment. All preparations were allowed to equilibrate for a minimum of 50 min with washes at 10-min intervals prior to drug challenge. Isometric contractions were measured with a force-displacement transducer[2] and recorded on a polygraph[3]. A linear tachometer[4] was used to record changes in heart rate. All drug solutions were prepared daily in Krebs–Henseleit solution and expressed as molar concentration of base.

Dose–Response Curves with Mescaline—To observe chronotropic and inotropic responses to mescaline, concentrations of 1×10^{-4}, 5×10^{-4}, and 1×10^{-3} *M* mescaline base were generated in a tissue bath containing spontaneously beating, paired atria. Heart rate and developed tension were recorded as maximum responses within 5 min. To minimize possible tachyphylaxis, only two drug challenges per preparation were employed. The challenges were separated by three washes and a 15-min reequilibration period. Sixteen atrial preparations were tested in this manner. All data were reported as the percent change from the pretreatment period and analyzed by Duncan's New Multiple Range Test (12).

The effects of mescaline were studied on separated left and right atria of the same heart to determine differences in inotropic responses in both the presence and absence of chronotropic responses. Right atria were allowed to contract spontaneously, while left atria were electrically driven (150% threshold voltage). After a 1-hr equilibration period, the rate of electrical stimulation was adjusted to equal the heart rate of the spontaneously contracting right atrium. At 5 min after the addition of mescaline to the tissue bath, changes in the developed tension for both atria

[1] Grass model S48.
[2] Grass model FT-03.
[3] Grass model 7B.
[4] Grass model 7P4-D.

ACKNOWLEDGMENTS AND ADDRESSES

Received March 11, 1976, from the *Department of Pharmaceutical Sciences, College of Pharmacy, University of Arizona, Tucson, AZ 85721.*

Accepted for publication August 17, 1976.

The authors thank Mr. William T. Fink and Mr. Donald Speray for their constructive criticism of the manuscript and Mr. John Hoyte for the use of the Prototron. Financial support from the University of Arizona Foundation and the University of Arizona Alumni Association is gratefully acknowledged.

* Present address: Optical Sciences Center, University of Arizona, Tucson, AZ 85721.

ˣ To whom inquiries should be directed.

Actions of Mescaline on Isolated Rat Atria

PETER K. S. SIEGL and RAYMOND F. ORZECHOWSKI ˣ

Abstract □ Mescaline, in concentrations of 5×10^{-4} and 1×10^{-3} *M*, produced negative chronotropic and positive inotropic responses in isolated, spontaneously beating rat atria. In tissues driven at a constant rate, the inotropic response was diminished greatly, indicating that the increment in the force of contraction was secondary to the reduction in rate. These chronotropic and inotropic responses were not altered consistently by pretreatment with the histamine antagonists chlorpheniramine and metiamide.

Keyphrases □ Mescaline—chronotropic and inotropic effects on isolated rat atria □ Chronotropic effects—mescaline on isolated rat atria □ Inotropic effects—mescaline on isolated rat atria □ Phenethylamines—mescaline, chronotropic and inotropic effects on isolated rat atria □ Cardiovascular effects—mescaline on isolated rat atria □ Psychotomimetics—mescaline, chronotropic and inotropic effects on isolated rat atria

In this study, the effects of mescaline (3,4,5-trimethoxyphenethylamine) on isolated rat atria were examined to reveal its possible actions directly on the pacemaker and atrial tissue. By the use of histamine antagonists, the involvement of histamine receptors (both H_1 and H_2) was examined as a possible mechanism of the *in vitro* cardiac action of mescaline.

BACKGROUND

The cardiovascular actions of the psychotomimetic amine mescaline were reported previously (1–8). Mescaline consistently evoked bradycardia in several species of animals. Mescaline-induced slowing of the frog heart was first observed by Dixon (1); others confirmed this action in the dog (2), rabbit, and cat (3). The bradycardia was inhibited by vagotomy or pretreatment with atropine (3); however, other published data (1, 2, 4) challenged these findings. Most evidence favors the conclusion that mescaline does not produce an effect on the heart by a vagal reflex or cholinergic stimulation.

Competition for epinephrine receptors by mescaline was proposed (5) because both mescaline-induced bradycardia and hypoglycemia in rats were reduced upon pretreatment with epinephrine. In another study (6), mescaline showed no propranolol-like antagonism of isoproterenol-induced relaxation of spontaneously contracting rat uterus. Mescaline failed to antagonize isoproterenol-induced positive chronotropism and hypotension (4) or to reverse an ethylnorepinephrine depressor response (6) in anesthetized dogs. From these data, β-adrenergic receptor blockade by mescaline or one of its metabolites was an unlikely explanation.

Histamine release or direct stimulation of histamine receptors by mescaline might account for the observed bradycardia. Potentiation of the hypotensive response to histamine in rats (7) was attributed to inhibition of the histaminolytic action of diamine oxidase by mescaline. Dogs receiving an intravenous infusion of mescaline showed (4) increased plasma histamine levels and a hypotensive response similar to that produced by compound 48/80, a known histamine-liberating substance (9). Alteration of respiratory dynamics and elevated right ventricular pressure, resembling responses to histamine, were observed in the guinea pig (8). Attempts to block these effects of mescaline with the antihistamine diphenhydramine were unsuccessful (4, 8).

More recent evidence suggested that histamine produced bradycardia by a stimulation of histamine receptor subtypes (H_2-receptors), which were not blocked by conventional antihistaminic agents such as diphenhydramine (10). The possible interaction of mescaline or mescaline-released histamine with H_2-receptors in the myocardium could be evaluated with an H_2-blocker, such as metiamide, in an attempt to confirm or refute this hypothesis.

EXPERIMENTAL

Sprague–Dawley rats of both sexes, 250–400 g, were sacrificed by cervical fracture and the hearts were rapidly removed. Paired atria were sectioned from the ventricles with a bridge of tissue joining the two atria. For examination of inotropic responses, left atria were electrically driven by paired platinum electrodes. Monophasic square wave pulses of 1-msec duration were delivered by a stimulator[1]. Tissues were suspended in a 10-ml glass tissue bath filled with Krebs–Henseleit solution (11) at a constant temperature of 35° and equilibrated with 95% O_2–5% CO_2. The solution pH was adjusted to 7.3.

A constant resting tension of 1.0 g was maintained throughout each experiment. All preparations were allowed to equilibrate for a minimum of 50 min with washes at 10-min intervals prior to drug challenge. Isometric contractions were measured with a force-displacement transducer[2] and recorded on a polygraph[3]. A linear tachometer[4] was used to record changes in heart rate. All drug solutions were prepared daily in Krebs–Henseleit solution and expressed as molar concentration of base.

Dose–Response Curves with Mescaline—To observe chronotropic and inotropic responses to mescaline, concentrations of 1×10^{-4}, 5×10^{-4}, and 1×10^{-3} *M* mescaline base were generated in a tissue bath containing spontaneously beating, paired atria. Heart rate and developed tension were recorded as maximum responses within 5 min. To minimize possible tachyphylaxis, only two drug challenges per preparation were employed. The challenges were separated by three washes and a 15-min reequilibration period. Sixteen atrial preparations were tested in this manner. All data were reported as the percent change from the pretreatment period and analyzed by Duncan's New Multiple Range Test (12).

The effects of mescaline were studied on separated left and right atria of the same heart to determine differences in inotropic responses in both the presence and absence of chronotropic responses. Right atria were allowed to contract spontaneously, while left atria were electrically driven (150% threshold voltage). After a 1-hr equilibration period, the rate of electrical stimulation was adjusted to equal the heart rate of the spontaneously contracting right atrium. At 5 min after the addition of mescaline to the tissue bath, changes in the developed tension for both atria

[1] Grass model S48.
[2] Grass model FT-03.
[3] Grass model 7B.
[4] Grass model 7P4-D.

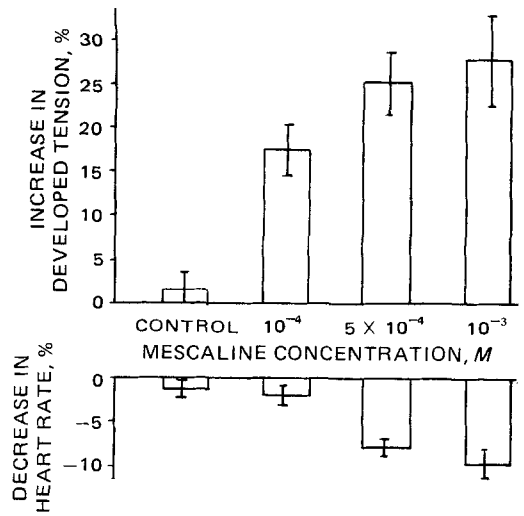

Figure 1—*Responses to mescaline challenge in spontaneously contracting paired rat atria. All bars indicate mean* ± SEM; n = *8.*

and the heart rate for the right atria were recorded. Twelve preparations were studied (*i.e.*, six hearts), each challenged with 1×10^{-4}, 5×10^{-4}, and 1×10^{-3} *M* mescaline base. Inotropic responses of left *versus* right atria were treated as paired data and tested by the Student *t* test (13).

To establish the relationship between rate and tension for rat atria and to allow interpretation of the effects obtained with mescaline, a Bowditch or rate–tension curve was constructed. Four left atria were electrically driven at 150% of threshold voltage and at various rates of stimulation. The maximum developed tension was recorded 5 min after the rate was altered. Results were graphed as the average developed tension (grams) *versus* the rate of stimulation (Hertz and beats per minute).

Histaminic Mechanism Study: Pretreatment with Antihistamines—Two concentrations of an H_1-antagonist (chlorpheniramine maleate, 1×10^{-6} and 1×10^{-5} *M*) and an H_2-antagonist (metiamide, 3×10^{-6} and 3×10^{-5} *M*) were each employed to pretreat six spontaneously contracting, paired atria 8 min prior to challenge with mescaline. Twelve control preparations were pretreated with 0.1 ml of Krebs–Henseleit solution. Pretreatments were randomized by the use of a table of random numbers.

Concentrations of mescaline were log spaced, and each challenge was separated by three washes and 8 min of incubation with the antagonist. Chronotropic and inotropic responses were measured before and 5 min after the addition of mescaline. Results were reported as the percent change from pretreatment values. Tukey's multiple range procedure for

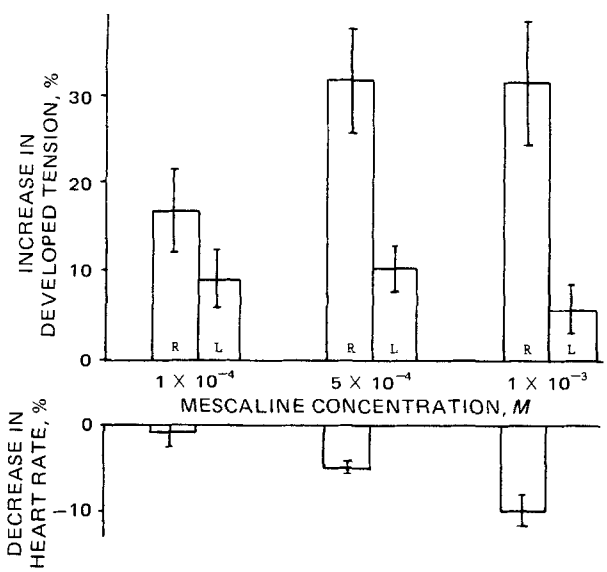

Figure 2—*Comparison of inotropic responses of electrically driven left atrium (L) and spontaneously contracting right atrium (R) to challenge with mescaline. All bars indicate mean* ± SEM; n = *6.*

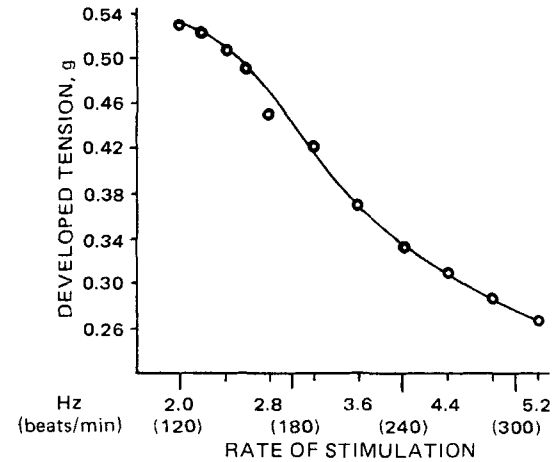

Figure 3—*Bowditch (rate–tension) curve for electrically stimulated left rat atrium.*

unequal subclass numbers[5] was used to test for statistical significance.

RESULTS

Dose–Response Curves with Mescaline—Dose-related positive inotropic and negative chronotropic responses were observed when spontaneously beating, paired rat atria were challenged with 1×10^{-4}, 5×10^{-4}, and 1×10^{-3} *M* mescaline (Fig. 1). All inotropic responses were significantly different from the control; however, only the two highest concentrations of mescaline produced a chronotropic response significantly different ($p < 0.05$) from the control.

Positive inotropic responses in electrically driven left atria challenged with 5×10^{-4} and 1×10^{-3} *M* mescaline were significantly less in the absence of a negative chronotropic response (Fig. 2). Since 10^{-4} *M* mescaline produced no significant change in heart rate, a difference in inotropic responses between spontaneously beating and electrically driven preparations was neither anticipated nor seen. Responses of spontaneously beating right atria were similar to those of spontaneously beating paired atria.

Since data from electrically driven atria suggested that a major component of the positive inotropic response was related to the negative chronotropic effect of mescaline, it was important to examine the effects of heart rate upon the developed tension in the control atria. A Bowditch or rate–tension curve for the electrically stimulated left rat atrium (Fig. 3) indicated that a positive inotropic response accompanied a decrease in heart rate. This relationship between rate and tension also was reported for rat papillary muscle (14, 15) and rat arterially perfused septal (16) preparations.

Histaminic Mechanism Study: Effects of Pretreatment with Antihistaminic Agents—Negative chronotropic responses to mescaline

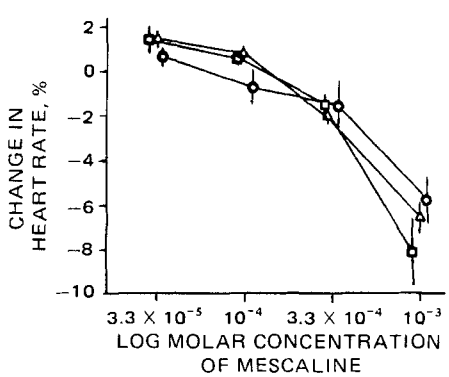

Figure 4—*Effect of pretreatment with chlorpheniramine upon the negative chronotropic response to mescaline challenge. Key: △, control,* n = *12;* □, *1* × *10^{-6}* M *chlorpheniramine,* n = *6; and* ○, *1* × *10^{-5}* M *chlorpheniramine,* n = *6.*

[5] J. L. Ciminera, Merck Institute for Therapeutic Research, West Point, Pa., personal communication.

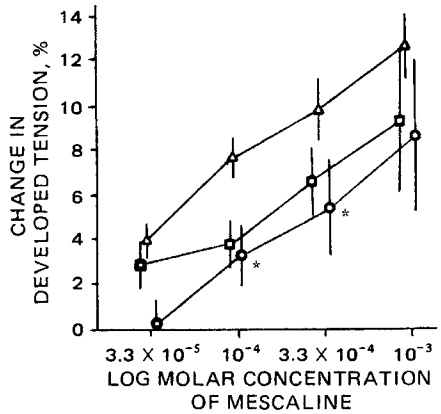

Figure 5—*Effect of pretreatment with chlorpheniramine upon the positive inotropic response to mescaline challenge. Key: same as Fig. 4; and *, p < 0.05.*

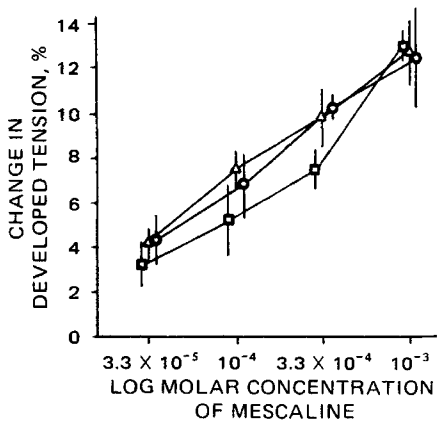

Figure 7—*Effect of pretreatment with metiamide upon the positive inotropic response to mescaline challenge. Key: same as Fig. 6.*

were unaltered by pretreatment with 1×10^{-5} or 1×10^{-6} *M* chlorpheniramine (Fig. 4). Both concentrations of chlorpheniramine produced a dose-related shift of the percent change in developed tension *versus* the log concentration of mescaline (Fig. 5); however, only responses to 1×10^{-4} and 3.3×10^{-4} *M* mescaline were reduced significantly by 1×10^{-5} *M* chlorpheniramine.

Metiamide, 3×10^{-5} and 3×10^{-6} *M*, failed to show a significant blockade of the negative chronotropic response, except at 1×10^{-3} *M* mescaline with 3×10^{-5} *M* metiamide (Fig. 6). Positive inotropic responses also were unchanged following pretreatment with metiamide (Fig. 7).

DISCUSSION

A significant role of endogenous histamine in the regulation of cardiac dynamics was proposed previously (17–19). The presence of histamine in rat atrial tissue (17) and evidence of the histamine-releasing activity of mescaline in vascular tissue (4) suggested that the cardiac actions of mescaline might involve activation of a histaminergic mechanism. Recent studies (10, 20, 21) indicated that separate receptors may mediate the chronotropic and inotropic responses to histamine in guinea pig atria. Positive chronotropic responses blocked by metiamide or burimamide, but not by promethazine or tripelennamine, suggested involvement of histamine H_2-receptor subtypes, whereas positive inotropic responses were altered only by promethazine and tripelennamine, histamine H_1-receptor blocking agents.

Exogenous histamine effects a negative chronotropic response in the isolated rat heart (17, 22). Based on the situation in the guinea pig heart, stimulation of H_2-receptors in rat atria by mescaline, either directly or *via* a release of endogenous histamine, could be responsible for the observed bradycardia (10, 20). That direct stimulation of histamine receptors could not account for the cardiac effects of mescaline was indicated by failure of histamine receptor blockers of the H_1 and H_2 type to obtund the response to mescaline. This explanation of mescaline-induced bradycardia in species other than the rat is untenable, since exogenous histamine evokes positive chronotropic responses in most species (22–27).

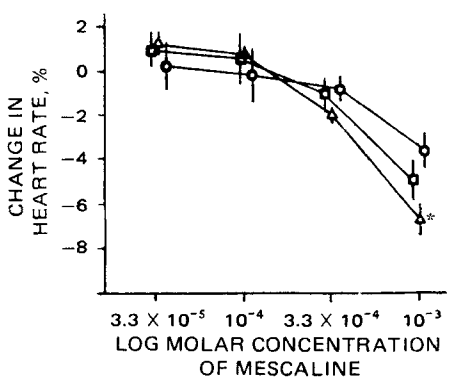

Figure 6—*Effect of pretreatment with metiamide upon the negative chronotropic response to mescaline challenge. Key: △, control,* n = *12;* □, *3 × 10⁻⁶* M *metiamide,* n = *6; and* ○, *3 × 10⁻⁵* M *metiamide,* n = *6.*

An inverse relationship existed between atrial rate and peak muscle tension in control rat atria; *i.e.*, the Bowditch curve showed that a decrease in atrial rate was associated with an increase in peak tension development (Fig. 3). Thus, it was of interest to determine whether the positive inotropic effect of mescaline would persist in atrial preparations electrically driven at a constant rate. The data indicated that a major component of the observed increase in tension development following mescaline was directly attributable to the slowing effect of the drug on atrial rate, since only slight increases in contractile force were seen in electrically driven tissues when the rate was held constant (Fig. 2).

A central action of mescaline might account for the bradycardia reported to occur in *in vivo* preparations. α-Adrenergic agonists injected into certain brain sites produced bradycardia and hypotension, due apparently to a reduction in sympathetic nervous tone (28). Mescaline penetrated into the central nervous system (29) and also evidenced α-adrenergic agonist properties in *in vitro* systems (30). Bradycardia was observed 1 min following injections of mescaline into the lateral brain ventricle of the mouse (31). Further investigation into the central mechanism appears to be warranted.

Finally, the concentrations of mescaline required to evoke alterations in myocardial rate in this study were relatively high (3.3×10^{-5}–1×10^{-3} *M*). Such concentrations, if extrapolated to the *in vivo* situation, would probably represent toxic concentrations of the drug (5).

REFERENCES

(1) A. F. Dixon, *J. Physiol.*, **25**, 69 (1899).

(2) Raymond-Hamet, *Arch. Exp. Pathol. Pharmakol.*, **169**, 97 (1932).

(3) G. S. Grace, *J. Pharmacol. Exp. Ther.*, **50**, 359 (1934).

(4) R. F. Orzechowski and F. J. Goldstein, *Toxicol. Appl. Pharmacol.*, **25**, 525 (1973).

(5) L. B. Speck, *J. Pharmacol. Exp. Ther.*, **119**, 78 (1956).

(6) J. J. P. Morton and M. H. Malone, *J. Pharm. Sci.*, **58**, 1169 (1969).

(7) E. A. Carlini, M. Santos, and M. R. P. Sampaio, *Experientia*, **21**, 72 (1965).

(8) V. de P. Lynch, E. Clemente, and S. Carson, *J. Pharm. Sci.*, **56**, 477 (1967).

(9) P. B. Dews, A. L. Wnuck, R. V. Fanelli, A. E. Light, J. A. Tornaben, S. Norton, C. H. Ellis, and E. J. de Beer, *J. Pharmacol. Exp. Ther.*, **107**, 1 (1957).

(10) M. I. Steinberg and D. R. Holland, *Eur. J. Pharmacol.*, **34**, 95 (1975).

(11) J. V. Levy, in, "Methods in Pharmacology," vol. 1, A. Schwartz, Ed., Meredith, New York, N.Y., 1971, p. 77.

(12) O. B. Duncan, *Biometrics*, **11**, 1 (1959).

(13) G. W. Snedecor and W. G. Cochran, "Statistical Methods," 6th ed., Iowa State University Press, Ames, Iowa, 1973, p. 91.

(14) B. F. Hoffman and J. J. Kelly, *Am. J. Physiol.*, **197**(6), 1199 (1959).

(15) A. H. Henderson, D. L. Brutsaert, W. W. Parmley, and E. H. Sonnenblick, *ibid.*, **215**(5), 1273 (1969).

(16) E. S. Blesa, G. A. Langer, A. J. Brady, and S. D. Serena, *ibid.*, **219**(3), 747 (1970).
(17) P. F. Mannaioni, *Arch. Int. Pharmacodyn. Ther.*, **196**, 64 (1972).
(18) M. J. Hughes and I. A. Coret, *Am. J. Physiol.*, **223**(5), 1257 (1972).
(19) J. H. McNeill and J. D. Muschek, *J. Mol. Cell. Cardiol.*, **4**, 611 (1972).
(20) D. Reinhardt, J. Wagner, and H. J. Schumann, *Agents Actions*, **4**, 217 (1974).
(21) F. Ledda, R. Fantozzi, A. Mugelli, F. Moroni, and P. F. Mannaioni, *ibid.*, **4**, 193 (1974).
(22) A. L. Bartlet, *Br. J. Pharmacol.*, **21**, 450 (1963).
(23) H. H. Dale and P. P. Laidlaw, *J. Physiol.*, **41**, 318 (1910).
(24) P. M. Dean, *Br. J. Pharmacol.*, **32**, 65 (1968).
(25) P. F. Mannaioni, *ibid.*, **15**, 500 (1960).
(26) P. F. Mannaioni, R. Levi, F. Ledda, and A. Giothi, *Life Sci.*, **7**, 777 (1968).
(27) U. Trendelenburg, *J. Pharmacol. Exp. Ther.*, **130**, 450 (1960).
(28) W. Kobinger and L. Pichler, *Eur. J. Pharmacol.*, **27**, 151 (1974).
(29) J. Cochin, L. A. Woods, and M. H. Seevers, *J. Pharmacol. Exp. Ther.*, **101**, 205 (1951).
(30) E. Clemente and V. de P. Lynch, *J. Pharm. Sci.*, **57**, 72 (1968).
(31) E. Lehr and G. Werner, *Arzneim.-Forsch.*, **20**, 901 (1970).

ACKNOWLEDGMENTS AND ADDRESSES

Received July 1, 1976, from the *Department of Biological Sciences, Philadelphia College of Pharmacy and Science, Philadelphia, PA 19104.*

Accepted for publication August 23, 1976.

[x] To whom inquiries should be directed.

Comparative Pharmacokinetics of Coumarin Anticoagulants XXIV: Effect of Treatment with Phenobarbital on Serum Protein Binding of Warfarin and Dicumarol in Rats

AVRAHAM YACOBI, JOHN T. SLATTERY, and GERHARD LEVY [x]

Abstract □ Rats were treated with the enzyme inducer phenobarbital to determine if it would affect the serum protein binding of warfarin and dicumarol, possibly by changing the rate of formation or elimination of endogenous inhibitor(s). Daily administration of phenobarbital, 75 mg/kg, for 4 days increased relative liver size (a concomitant of enzyme induction) but had no apparent effect on the serum protein binding of warfarin and dicumarol.

Keyphrases □ Phenobarbital—effects on serum protein binding of warfarin and dicumarol, rats □ Protein binding, serum—warfarin and dicumarol, effect of phenobarbital, rats □ Binding, serum protein—warfarin and dicumarol, effect of phenobarbital, rats □ Warfarin—serum protein binding, effect of phenobarbital, rats □ Dicumarol—serum protein binding, effect of phenobarbital, rats □ Anticoagulants—warfarin and dicumarol, serum protein binding, effect of phenobarbital, rats □ Enzyme inducers—phenobarbital, effect on serum protein binding of warfarin and dicumarol, rats

The total clearance of warfarin by the body is directly proportional to the free fraction of this drug in serum of rats (1, 2) and humans (3). There are pronounced interindividual differences in free fraction values of warfarin (4) and corresponding differences in the total clearance of this drug by the body (2, 3). Ongoing studies in rats[1] indicate that this is true also for the other major coumarin anticoagulant, dicumarol. There is no relationship between the free fraction values of either warfarin (2) or dicumarol (data in this report) and the concentration of albumin in serum.

Recent studies showed that endogenous inhibitors in uremic as well as in normal human serum cause a decrease in the protein binding of warfarin and other drugs (5). Therefore, interindividual differences in the serum protein binding of warfarin and dicumarol may be caused by corresponding differences in the serum concentration of such inhibitors. Treatment with an enzyme inducer such as phenobarbital may change the serum protein binding of warfarin, dicumarol, and other drugs by changing the concentration of endogenous inhibitors in serum. This situation could result from a change in the formation or elimination kinetics of the inhibitors due to increased activity of certain enzyme systems. Accordingly, a study was initiated to determine the effect of treatment with phenobarbital on the protein binding of warfarin and dicumarol in the serum of rats.

EXPERIMENTAL

Forty-eight adult male Sprague–Dawley rats, ~350 g, were used for an initial screening study. About 3 ml of blood was obtained from the tail artery of each animal, and serum was separated. The free fraction of racemic warfarin in these serum samples was determined by equilibrium dialysis as described previously (2). Based on the results of this screening study, 20 rats were selected and classified into 10 pairs with very small intrapair and large interpair differences in the warfarin free fraction value.

Four days later, one member of each pair received phenobarbital, 75 mg/kg/day ip, for 4 days while the other member received injections of normal saline solution. One day later, the animals were sacrificed by removing all blood from the aorta under ether anesthesia. The liver was also removed, compressed slightly between paper tissue to remove remaining blood, and weighed. Serum was separated and used to determine the free fraction values for warfarin (2) and dicumarol (6) by equilibrium dialysis. The concentration of total protein in serum was determined by the method of Gornall *et al.* (7) with crystalline rat albumin as the standard, and the fraction of albumin was determined by electrophoresis using a commercial[2] serum protein electrophoresis system.

[1] To be published.

[2] Gelman Instrument Co., Ann Arbor, Mich.

(16) E. S. Blesa, G. A. Langer, A. J. Brady, and S. D. Serena, *ibid.*, **219**(3), 747 (1970).
(17) P. F. Mannaioni, *Arch. Int. Pharmacodyn. Ther.*, **196**, 64 (1972).
(18) M. J. Hughes and I. A. Coret, *Am. J. Physiol.*, **223**(5), 1257 (1972).
(19) J. H. McNeill and J. D. Muschek, *J. Mol. Cell. Cardiol.*, **4**, 611 (1972).
(20) D. Reinhardt, J. Wagner, and H. J. Schumann, *Agents Actions*, **4**, 217 (1974).
(21) F. Ledda, R. Fantozzi, A. Mugelli, F. Moroni, and P. F. Mannaioni, *ibid.*, **4**, 193 (1974).
(22) A. L. Bartlet, *Br. J. Pharmacol.*, **21**, 450 (1963).
(23) H. H. Dale and P. P. Laidlaw, *J. Physiol.*, **41**, 318 (1910).
(24) P. M. Dean, *Br. J. Pharmacol.*, **32**, 65 (1968).
(25) P. F. Mannaioni, *ibid.*, **15**, 500 (1960).
(26) P. F. Mannaioni, R. Levi, F. Ledda, and A. Giothi, *Life Sci.*, **7**, 777 (1968).
(27) U. Trendelenburg, *J. Pharmacol. Exp. Ther.*, **130**, 450 (1960).
(28) W. Kobinger and L. Pichler, *Eur. J. Pharmacol.*, **27**, 151 (1974).
(29) J. Cochin, L. A. Woods, and M. H. Seevers, *J. Pharmacol. Exp. Ther.*, **101**, 205 (1951).
(30) E. Clemente and V. de P. Lynch, *J. Pharm. Sci.*, **57**, 72 (1968).
(31) E. Lehr and G. Werner, *Arzneim.-Forsch.*, **20**, 901 (1970).

ACKNOWLEDGMENTS AND ADDRESSES

Received July 1, 1976, from the *Department of Biological Sciences, Philadelphia College of Pharmacy and Science, Philadelphia, PA 19104.*

Accepted for publication August 23, 1976.

[x] To whom inquiries should be directed.

Comparative Pharmacokinetics of Coumarin Anticoagulants XXIV: Effect of Treatment with Phenobarbital on Serum Protein Binding of Warfarin and Dicumarol in Rats

AVRAHAM YACOBI, JOHN T. SLATTERY, and GERHARD LEVY [x]

Abstract □ Rats were treated with the enzyme inducer phenobarbital to determine if it would affect the serum protein binding of warfarin and dicumarol, possibly by changing the rate of formation or elimination of endogenous inhibitor(s). Daily administration of phenobarbital, 75 mg/kg, for 4 days increased relative liver size (a concomitant of enzyme induction) but had no apparent effect on the serum protein binding of warfarin and dicumarol.

Keyphrases □ Phenobarbital—effects on serum protein binding of warfarin and dicumarol, rats □ Protein binding, serum—warfarin and dicumarol, effect of phenobarbital, rats □ Binding, serum protein—warfarin and dicumarol, effect of phenobarbital, rats □ Warfarin—serum protein binding, effect of phenobarbital, rats □ Dicumarol—serum protein binding, effect of phenobarbital, rats □ Anticoagulants—warfarin and dicumarol, serum protein binding, effect of phenobarbital, rats □ Enzyme inducers—phenobarbital, effect on serum protein binding of warfarin and dicumarol, rats

The total clearance of warfarin by the body is directly proportional to the free fraction of this drug in serum of rats (1, 2) and humans (3). There are pronounced interindividual differences in free fraction values of warfarin (4) and corresponding differences in the total clearance of this drug by the body (2, 3). Ongoing studies in rats[1] indicate that this is true also for the other major coumarin anticoagulant, dicumarol. There is no relationship between the free fraction values of either warfarin (2) or dicumarol (data in this report) and the concentration of albumin in serum.

Recent studies showed that endogenous inhibitors in uremic as well as in normal human serum cause a decrease in the protein binding of warfarin and other drugs (5). Therefore, interindividual differences in the serum protein binding of warfarin and dicumarol may be caused by corresponding differences in the serum concentration of such inhibitors. Treatment with an enzyme inducer such as phenobarbital may change the serum protein binding of warfarin, dicumarol, and other drugs by changing the concentration of endogenous inhibitors in serum. This situation could result from a change in the formation or elimination kinetics of the inhibitors due to increased activity of certain enzyme systems. Accordingly, a study was initiated to determine the effect of treatment with phenobarbital on the protein binding of warfarin and dicumarol in the serum of rats.

EXPERIMENTAL

Forty-eight adult male Sprague–Dawley rats, ~350 g, were used for an initial screening study. About 3 ml of blood was obtained from the tail artery of each animal, and serum was separated. The free fraction of racemic warfarin in these serum samples was determined by equilibrium dialysis as described previously (2). Based on the results of this screening study, 20 rats were selected and classified into 10 pairs with very small intrapair and large interpair differences in the warfarin free fraction value.

Four days later, one member of each pair received phenobarbital, 75 mg/kg/day ip, for 4 days while the other member received injections of normal saline solution. One day later, the animals were sacrificed by removing all blood from the aorta under ether anesthesia. The liver was also removed, compressed slightly between paper tissue to remove remaining blood, and weighed. Serum was separated and used to determine the free fraction values for warfarin (2) and dicumarol (6) by equilibrium dialysis. The concentration of total protein in serum was determined by the method of Gornall *et al.* (7) with crystalline rat albumin as the standard, and the fraction of albumin was determined by electrophoresis using a commercial[2] serum protein electrophoresis system.

[1] To be published.

[2] Gelman Instrument Co., Ann Arbor, Mich.

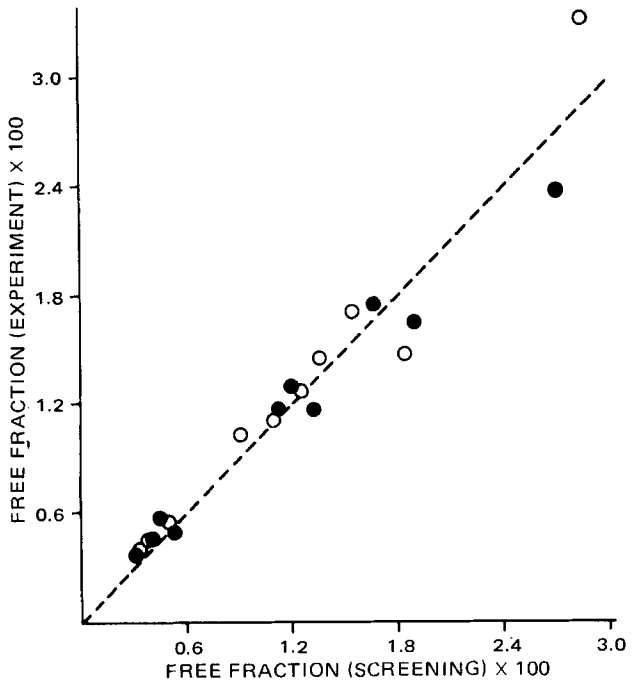

Figure 1—*Effect of phenobarbital treatment (75 mg/kg/day for 4 days) on the free fraction of warfarin in the serum of individual rats. Shown is a plot of free fraction values determined in a screening study preceding the experiment against the free fraction values in the same animals 1 day after the treatment period. Key: ●, animals treated with phenobarbital; and ○, control animals that received only saline solution. The stippled line has a slope of unity.*

RESULTS AND DISCUSSION

The warfarin free fraction value in the serum of the 20 selected rats ranged from 0.00344 to 0.0286 in the screening experiment. The percentage difference in the free fraction value within the 10 matched pairs was 3.9 ± 2.5 (mean ± *SD*). The correlation of free fraction values between the members of the 10 pairs was strong and highly statistically

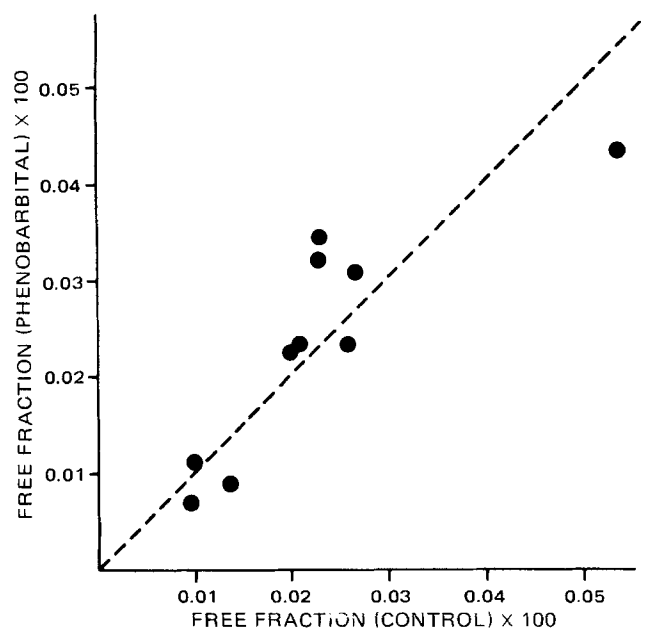

Figure 2—*Effect of phenobarbital treatment on the free fraction of dicumarol in the serum of rats. Plotted are the free fraction values in 10 control rats against the free fraction values in 10 phenobarbital-treated rats (r = 0.863, p < 0.001). The 10 pairs of rats were matched on the basis of nearly identical warfarin free fraction values in a preceding screening experiment. The stippled line has a slope of unity.*

Table I—Effect of Treatment with Phenobarbital on the Serum Protein Binding of Racemic Warfarin in Male Sprague–Dawley Rats

Group	Free Fraction × 100[a] Before	After	Ratio, After/Before[b]
Control	1.22 (0.344–2.86)	1.28 (0.389–3.34)	1.06 ± 0.107
Phenobarbital treated	1.17 (0.315–2.72)	1.14 (0.350–2.38)	1.03 ± 0.122[c]

[a] Mean (range) for 10 animals per group, 4 days before and 1 day after daily injections of phenobarbital (75 mg/kg) for 4 days. [b] Mean ± *SD*. [c] Not statistically significantly different from control ratio values.

significant ($r = 0.997$, $p < 0.001$). The group treated with phenobarbital had a significantly higher relative liver weight than the control group (37.0 ± 3.5 *versus* 30.9 ± 1.6 g/kg, $p < 0.001$), but there was no significant difference in serum albumin concentration (3.30 ± 0.20 *versus* 3.49 ± 0.20 g/100 ml, $p > 0.1$).

Treatment with phenobarbital had no apparent effect on the serum protein binding of warfarin (Table I). There was a strong correlation between the pretreatment and posttreatment free fraction values for individual animals (Fig. 1). The correlation coefficients for the data from control and phenobarbital-treated animals were 0.957 ($p < 0.001$) and 0.906 ($p < 0.001$), respectively.

It was not possible to obtain enough blood in the screening study to determine the free fraction values for dicumarol in addition to those for warfarin. However, in view of the previously documented strong correlation between the free fraction values for warfarin and dicumarol in individual rats (6), the warfarin free fraction values serve also to characterize and classify the animals with respect to serum protein binding of dicumarol. Therefore, it is possible to compare the posttreatment free fraction values for dicumarol in serum of phenobarbital-treated rats with the free fraction values of control animals. These values were 0.000238 (range of 0.000070–0.000432) for the phenobarbital group and 0.000225 (range of 0.000099–0.000540) for the control group and did not differ

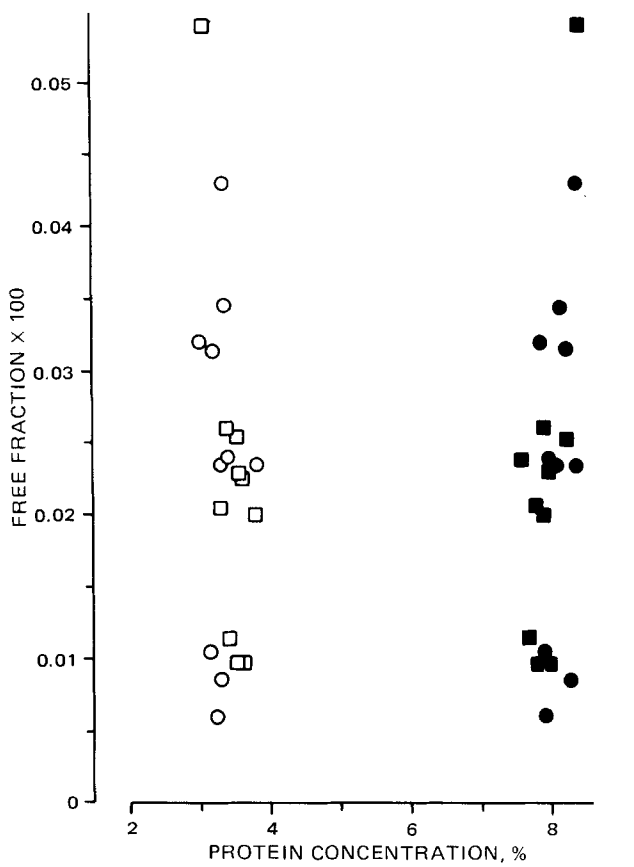

Figure 3—*Relationship between free fraction of dicumarol and the concentrations of albumin (open symbols) or total protein (closed symbols) in the serum of control rats (squares) and phenobarbital-treated rats (circles).*

significantly from one another. The ratio of free fraction values (treated/control) for the 10 matched pairs was 1.06 ± 0.27 (mean ± *SD*), and the correlation of these values between members of each pair was strong (Fig. 2).

Figure 3 is a plot of dicumarol free fraction values in serum against the serum concentration of albumin or total protein. The pronounced interindividual differences in serum protein binding of dicumarol were not related to corresponding differences in the concentration of serum proteins. Similar results were obtained previously for warfarin (2). Also consistent with previous observations (6) was the strong correlation between the free fraction values for dicumarol and warfarin in individual animals ($r = 0.937$, $p < 0.001$, $n = 20$ in this study).

The phenobarbital treatment regimen used is sufficient to cause pronounced enzyme induction, as reflected by the increased total clearance of warfarin[1] and dicumarol (8) and by the increase in relative liver weight. This treatment had no significant effect on the serum protein binding of warfarin and dicumarol. This result could mean that the concentrations of endogenous inhibitors in serum were not affected by enzyme induction or that the interindividual differences in serum protein binding of the coumarin anticoagulants are due to conformational differences of albumin, with enzyme induction having no effect on the steady-state concentration of that particular protein.

REFERENCES

(1) G. Levy and A. Yacobi, *J. Pharm. Sci.*, **63**, 805 (1974).

(2) A. Yacobi and G. Levy, *ibid.*, **64**, 1660 (1975).

(3) A Yacobi, J. A. Udall, and G. Levy, *Clin. Pharmacol. Ther.*, **19**, 552 (1976).

(4) J. T. Slattery, A. Yacobi, and G. Levy, *Life Sci.*, **19**, 447 (1976).

(5) I. Sjöholm, A. Kober, I. Odar-Cederlöf, and O. Borgå, *Biochem. Pharmacol.*, **25**, 1205 (1976).

(6) A. Yacobi, C.-M. Lai, and G. Levy, *J. Pharm. Sci.*, **64**, 1995 (1975).

(7) A. G. Gornall, C. J. Bardawill, and M. M. Davis, *J. Biol. Chem.*, **177**, 751 (1949).

(8) C.-M. Lai, A. Yacobi, and G. Levy, *J. Pharmacol. Exp. Ther.*, **199**, 74 (1976).

ACKNOWLEDGMENTS AND ADDRESSES

Received July 6, 1976, from the *Department of Pharmaceutics, School of Pharmacy, State University of New York at Buffalo, Buffalo, NY 14214.*

Accepted for publication August 13, 1976.

Supported in part by Grant GM 20852 from the National Institute of General Medical Sciences, National Institutes of Health, Bethesda, MD 20014.

Previous paper in this series: A. Yacobi, R. G. Stoll, A. R. DiSanto, and G. Levy, *Res. Commun. Chem. Pathol. Pharmacol.*, **14**, 743 (1976).

[x] To whom inquiries should be directed.

Comparative Pharmacokinetics of Coumarin Anticoagulants XXV: Warfarin–Ibuprofen Interaction in Rats

JOHN T. SLATTERY, AVRAHAM YACOBI, and GERHARD LEVY [x]

Abstract □ The effect of ibuprofen on the pharmacokinetics and anticoagulant action of racemic warfarin was determined in a crossover study on male Sprague–Dawley rats. At average plasma concentrations of 24–83 mg/liter, ibuprofen decreased the biological half-life and increased the total clearance of warfarin. It also increased the anticoagulant effect produced by a given plasma concentration of total (free and protein-bound) warfarin. These effects of ibuprofen appear to be a consequence of its displacing effect on warfarin in plasma.

Keyphrases □ Ibuprofen—effect on pharmacokinetics and anticoagulant action of warfarin, rats □ Pharmacokinetics—warfarin, effect of ibuprofen, rats □ Anticoagulant action—warfarin, effect of ibuprofen, rats □ Warfarin—pharmacokinetics and anticoagulant action, effect of ibuprofen, rats □ Anti-inflammatory agents—ibuprofen, effect on pharmacokinetics and anticoagulant action of warfarin, rats

The widely used nonsteroidal anti-inflammatory agent ibuprofen is a weak acid extensively bound to plasma proteins (1). As such, it may be expected to displace coumarin anticoagulants such as warfarin from plasma protein binding sites. This type of drug interaction can modify the distribution and elimination kinetics of warfarin and produce transient potentiation of its anticoagulant effect (2–4). Nevertheless, several clinical investigations failed to detect any effect of ibuprofen, in doses of up to 2.4 g/day, on the anticoagulant action of the coumarin drugs phenprocoumon and warfarin (5–8).

In view of the recent tendency to use doses of ibuprofen larger than 2.4 g/day for the treatment of inflammatory disease, it is important to determine *in principle* if ibuprofen interacts with warfarin under appropriate conditions (*i.e.*, at plasma ibuprofen concentrations sufficient to displace warfarin from protein binding sites). Such an investigation was carried out on rats dosed with ibuprofen at a rate producing ibuprofen concentrations moderately higher than those commonly encountered clinically.

EXPERIMENTAL

Male Sprague–Dawley rats[1], 250–300 g at screening time and 350–450 g during the interaction study, were maintained on a standard diet[2] with unrestricted access to water.

To determine the *in vitro* effect of ibuprofen on warfarin binding to rat serum protein, blood was obtained from the abdominal aorta of 11 ether-anesthetized rats and the serum was separated. To serum samples from individual rats were added 0.7–0.8 μg/ml of racemic ^{14}C-warfarin[3], 76 μCi/mg, and 0–150 μg/ml of racemic ibuprofen[4]. The free fraction of warfarin in serum (free/total warfarin concentration) was determined by equilibrium dialysis (9).

Sixty-three rats were screened for the *in vivo* interaction study by collecting 3 ml of blood from the tail artery under light ether anesthesia, separating the serum, and determining the free fraction of warfarin by equilibrium dialysis. Fourteen rats with widely differing warfarin free fraction values (0.0023–0.0157) were selected from this group for the

[1] Blue Spruce Farms, Altamont, N.Y.
[2] Charles River Formula 4RF.
[3] Amersham/Searle Corp., Arlington Heights, Ill.
[4] Supplied by The Upjohn Co., Kalamazoo, Mich.

significantly from one another. The ratio of free fraction values (treated/control) for the 10 matched pairs was 1.06 ± 0.27 (mean ± *SD*), and the correlation of these values between members of each pair was strong (Fig. 2).

Figure 3 is a plot of dicumarol free fraction values in serum against the serum concentration of albumin or total protein. The pronounced interindividual differences in serum protein binding of dicumarol were not related to corresponding differences in the concentration of serum proteins. Similar results were obtained previously for warfarin (2). Also consistent with previous observations (6) was the strong correlation between the free fraction values for dicumarol and warfarin in individual animals ($r = 0.937$, $p < 0.001$, $n = 20$ in this study).

The phenobarbital treatment regimen used is sufficient to cause pronounced enzyme induction, as reflected by the increased total clearance of warfarin[1] and dicumarol (8) and by the increase in relative liver weight. This treatment had no significant effect on the serum protein binding of warfarin and dicumarol. This result could mean that the concentrations of endogenous inhibitors in serum were not affected by enzyme induction or that the interindividual differences in serum protein binding of the coumarin anticoagulants are due to conformational differences of albumin, with enzyme induction having no effect on the steady-state concentration of that particular protein.

REFERENCES

(1) G. Levy and A. Yacobi, *J. Pharm. Sci.*, **63**, 805 (1974).

(2) A. Yacobi and G. Levy, *ibid.*, **64**, 1660 (1975).

(3) A Yacobi, J. A. Udall, and G. Levy, *Clin. Pharmacol. Ther.*, **19**, 552 (1976).

(4) J. T. Slattery, A. Yacobi, and G. Levy, *Life Sci.*, **19**, 447 (1976).

(5) I. Sjöholm, A. Kober, I. Odar-Cederlöf, and O. Borgå, *Biochem. Pharmacol.*, **25**, 1205 (1976).

(6) A. Yacobi, C.-M. Lai, and G. Levy, *J. Pharm. Sci.*, **64**, 1995 (1975).

(7) A. G. Gornall, C. J. Bardawill, and M. M. Davis, *J. Biol. Chem.*, **177**, 751 (1949).

(8) C.-M. Lai, A. Yacobi, and G. Levy, *J. Pharmacol. Exp. Ther.*, **199**, 74 (1976).

ACKNOWLEDGMENTS AND ADDRESSES

Received July 6, 1976, from the *Department of Pharmaceutics, School of Pharmacy, State University of New York at Buffalo, Buffalo, NY 14214.*

Accepted for publication August 13, 1976.

Supported in part by Grant GM 20852 from the National Institute of General Medical Sciences, National Institutes of Health, Bethesda, MD 20014.

Previous paper in this series: A. Yacobi, R. G. Stoll, A. R. DiSanto, and G. Levy, *Res. Commun. Chem. Pathol. Pharmacol.*, **14**, 743 (1976).

[x] To whom inquiries should be directed.

Comparative Pharmacokinetics of Coumarin Anticoagulants XXV: Warfarin–Ibuprofen Interaction in Rats

JOHN T. SLATTERY, AVRAHAM YACOBI, and GERHARD LEVY [x]

Abstract □ The effect of ibuprofen on the pharmacokinetics and anticoagulant action of racemic warfarin was determined in a crossover study on male Sprague–Dawley rats. At average plasma concentrations of 24–83 mg/liter, ibuprofen decreased the biological half-life and increased the total clearance of warfarin. It also increased the anticoagulant effect produced by a given plasma concentration of total (free and protein-bound) warfarin. These effects of ibuprofen appear to be a consequence of its displacing effect on warfarin in plasma.

Keyphrases □ Ibuprofen—effect on pharmacokinetics and anticoagulant action of warfarin, rats □ Pharmacokinetics—warfarin, effect of ibuprofen, rats □ Anticoagulant action—warfarin, effect of ibuprofen, rats □ Warfarin—pharmacokinetics and anticoagulant action, effect of ibuprofen, rats □ Anti-inflammatory agents—ibuprofen, effect on pharmacokinetics and anticoagulant action of warfarin, rats

The widely used nonsteroidal anti-inflammatory agent ibuprofen is a weak acid extensively bound to plasma proteins (1). As such, it may be expected to displace coumarin anticoagulants such as warfarin from plasma protein binding sites. This type of drug interaction can modify the distribution and elimination kinetics of warfarin and produce transient potentiation of its anticoagulant effect (2–4). Nevertheless, several clinical investigations failed to detect any effect of ibuprofen, in doses of up to 2.4 g/day, on the anticoagulant action of the coumarin drugs phenprocoumon and warfarin (5–8).

In view of the recent tendency to use doses of ibuprofen larger than 2.4 g/day for the treatment of inflammatory disease, it is important to determine *in principle* if ibuprofen interacts with warfarin under appropriate conditions (*i.e.*, at plasma ibuprofen concentrations sufficient to displace warfarin from protein binding sites). Such an investigation was carried out on rats dosed with ibuprofen at a rate producing ibuprofen concentrations moderately higher than those commonly encountered clinically.

EXPERIMENTAL

Male Sprague–Dawley rats[1], 250–300 g at screening time and 350–450 g during the interaction study, were maintained on a standard diet[2] with unrestricted access to water.

To determine the *in vitro* effect of ibuprofen on warfarin binding to rat serum protein, blood was obtained from the abdominal aorta of 11 ether-anesthetized rats and the serum was separated. To serum samples from individual rats were added 0.7–0.8 μg/ml of racemic ^{14}C-warfarin[3], 76 μCi/mg, and 0–150 μg/ml of racemic ibuprofen[4]. The free fraction of warfarin in serum (free/total warfarin concentration) was determined by equilibrium dialysis (9).

Sixty-three rats were screened for the *in vivo* interaction study by collecting 3 ml of blood from the tail artery under light ether anesthesia, separating the serum, and determining the free fraction of warfarin by equilibrium dialysis. Fourteen rats with widely differing warfarin free fraction values (0.0023–0.0157) were selected from this group for the

[1] Blue Spruce Farms, Altamont, N.Y.
[2] Charles River Formula 4RF.
[3] Amersham/Searle Corp., Arlington Heights, Ill.
[4] Supplied by The Upjohn Co., Kalamazoo, Mich.

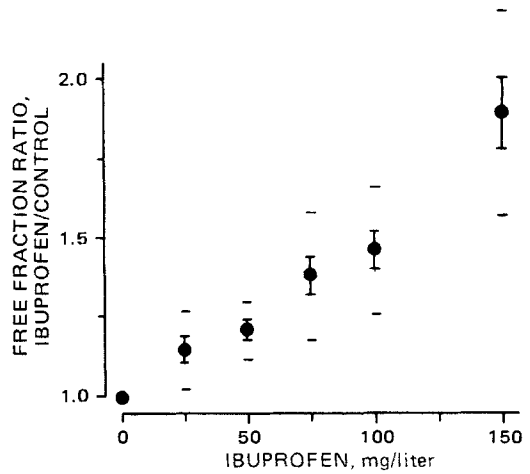

Figure 1—*Effect of ibuprofen on protein binding of warfarin in rat serum. Shown is the relationship between the warfarin free fraction ratio (with ibuprofen/control) and the ibuprofen concentration. Each point is the mean of the free fraction values in individual serum samples from 11 animals. Bars = ±1 SE; dashes = ±1 SD. The concentration of racemic warfarin was 0.718 ± 0.095 mg/liter, and the control free fraction value ranged from 0.00482 to 0.0149.*

interaction study, which was initiated 30 days after the screening experiment.

All animals received racemic ^{14}C-warfarin, 0.45 mg/kg iv. Some animals also received ibuprofen, 40 mg/kg ip at −1 hr and 20 mg/kg ip every 3 hr thereafter; the others received injections of normal saline solution at the same intervals. A crossover experiment was carried out 3 weeks later. The warfarin and ibuprofen injection solutions were freshly prepared by dissolving the drugs in a small amount of sodium hydroxide solution and diluting to the desired volume with isotonic pH 7.4 phosphate buffer.

Blood samples (0.20–0.45 ml) were obtained at frequent intervals from the tail artery (10). Plasma was separated and used for determination of prothrombin complex activity (10), warfarin concentration (11), and ibuprofen concentration (12). Ibuprofen was separated from the plasma extract during TLC separation of warfarin. Ibuprofen reference spots were located on the TLC plate after development by spraying the appropriate region with 0.1% bromocresol purple in water (13). A band of silica coating corresponding to the R_f of ibuprofen[5] was then scraped off,

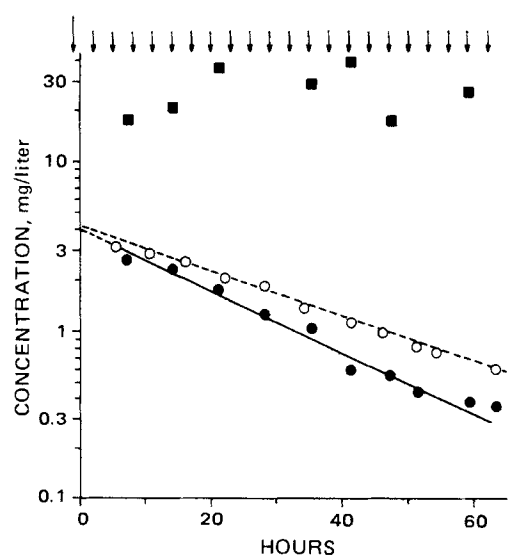

Figure 2—*Effect of ibuprofen administration on the elimination of warfarin in Rat 11. Shown are the warfarin concentrations in serum during the control experiment (○) and during ibuprofen administration (●) 3 weeks later. The ibuprofen concentrations in serum (■) were produced by an initial injection of 40 mg/kg at −1 hr (long arrow) followed by 20 mg/kg every 3 hr (short arrows).*

[5] The R_f of ibuprofen in this system is about 0.35; that of warfarin is about 0.7.

Table I—Concentrations of Ibuprofen in Plasma of Rats Used in the Warfarin Interaction Study[a]

Rat Number	Average Concentration (± *SD*), mg/liter	Number of Determinations
1	71.6 (±32.9)	7
2	68.1 (±27.8)	7
3	33.6 (±26.0)	12
4	38.7 (±31.9)	10
5	78.4 (±43.7)	5
6	71.6 (±27.2)	3
7	60.5 (±31.7)	6
8	48.8 (±28.6)	8
9	47.4 (±38.8)	9
10	82.7 (±40.3)	10
11	23.8 (±9.69)	7
12	42.9 (±32.9)	11
13	39.2 (±26.2)	8
14	54.8 (±28.3)	8
Mean	54.4	

[a] The rats received an initial ibuprofen dose of 40 mg/kg and 20 mg/kg every 3 hr thereafter.

placed in a glass centrifuge tube with 2.5 ml of 0.1 *N* sodium hydroxide, shaken for 20 min, and centrifuged. A 2-ml aliquot of the supernate was acidified with 0.5 ml of 6 *N* hydrochloric acid and extracted (20 min of shaking) into 5 ml of benzene, which was then separated by centrifugation; 4 ml of the benzene phase was used for GLC analysis (12). The recovery of ibuprofen was 90 ± 7.5% (mean ± *SD*, n = 14) and was independent of concentration in the 2–120-μg/ml range.

The effect of ibuprofen on the prothrombin complex activity (PCA) in the serum of otherwise untreated rats was determined by administering ibuprofen, 25 mg/kg ip, every 4 hr to six rats and obtaining blood samples at 12, 24, and 36 hr. The effect of ibuprofen on the rate constant for degradation of prothrombin complex activity, k_{deg}, was determined by administering a prothrombin complex activity synthesis blocking dose (12 mg/kg) of warfarin to 12 rats. Six received ibuprofen, 25 mg/kg ip, every 4 hr from −36 hr to the end of the experiment while the other six received normal saline injections at the same intervals. Blood samples for prothrombin complex activity determination were obtained every 3 hr for 9–12 hr after warfarin administration.

RESULTS

Ibuprofen, at concentrations of 25 mg/liter and above, significantly ($p < 0.001$) decreased the protein binding of warfarin in the serum of rats (Fig. 1). There was a statistically significant ($p < 0.001$) correlation between the control free fraction value and the free fraction value of warfarin at each ibuprofen concentration in individual animals.

Figure 2 shows the effect of ibuprofen administration on the pharmacokinetics of warfarin in a rat. The average plasma ibuprofen con-

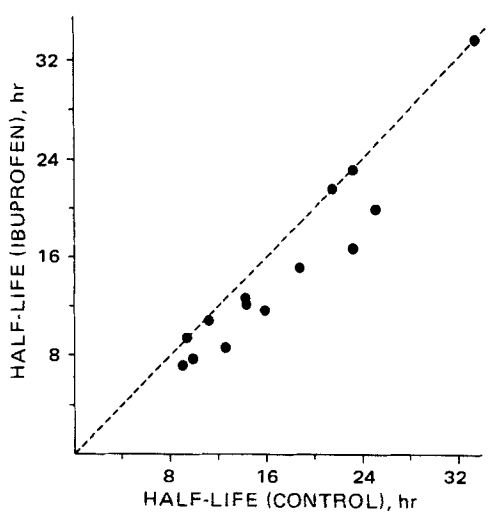

Figure 3—*Relationship between half-life of warfarin in the same animals in a control experiment and during ibuprofen administration in a crossover study. The stippled line has a slope of unity.*

Table II—Effect of Ibuprofen Administration on the Pharmacokinetics of Warfarin in Rats

Parameter	Control Experiment (C)	With Ibuprofen (I)	Ratio, C:I
Half-life, hr	17.3 (9.13–33.5)[a]	15.0 (7.17–33.5)[b]	1.19 (1.00–1.47)
Apparent volume of distribution, ml/kg	155 (98–212)	154 (118–197)[c]	1.01 (0.824–1.21)
Body clearance, ml/hr/kg	7.62 (2.36–13.4)	8.99 (2.56–16.2)[b]	0.851 (0.592–1.00)

[a] Mean (n = 14) and range of individual values. [b] Significantly different from control value by paired t-test ($p < 0.01$). [c] Not significantly different from control value.

centrations observed during the study ranged from 23.8 to 82.7 mg/liter in the 14 animals (Table I). Preliminary studies on six other rats yielded ibuprofen total clearance values from 139 to 220 ml/hr/kg and a half-life of 1.5–3.6 hr after a single 75-mg/kg iv dose. The effect of ibuprofen on the pharmacokinetics of warfarin in all 14 rats is summarized in Table II. Ibuprofen caused a small but statistically significant ($p < 0.01$) decrease in the biological half-life and increase in total body clearance ($p < 0.001$) of warfarin but had no apparent effect on the volume of distribution of the anticoagulant. There was a highly statistically significant correlation between the control and ibuprofen treatment values of half-life ($r = 0.957$, $p < 0.001$; Fig. 3), the apparent volume of distribution ($r = 0.980$, $p < 0.001$; Fig. 4), and the total body clearance ($r = 0.980$, $p < 0.001$; Fig. 5) for warfarin in individual animals.

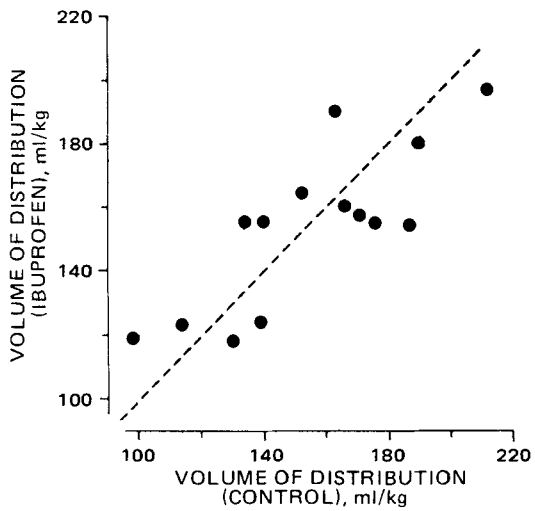

Figure 4—*Relationship between apparent volume of distribution of warfarin in a control experiment and during ibuprofen administration to the same animals in a crossover study. The stippled line has a slope of unity.*

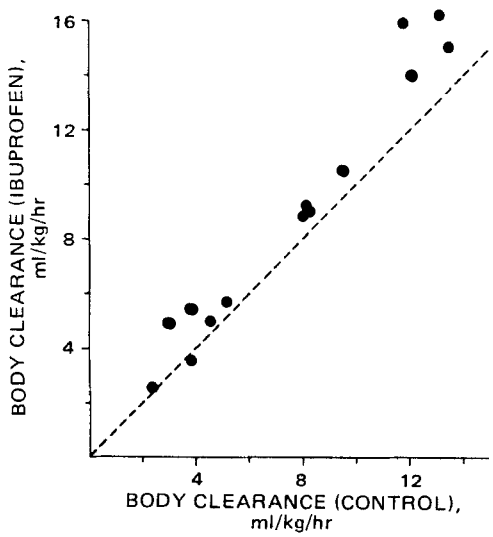

Figure 5—*Relationship between body clearance of warfarin in a control experiment and during ibuprofen administration to the same animals in a crossover study. The stippled line has a slope of unity.*

Table III—Effect of Ibuprofen Treatment[a] on Clotting Time of Plasma in Rats

Duration of Treatment, hr	Clotting Time, sec[b]
0	28.9 ± 0.88
0[c]	28.6 ± 0.66
12	29.3 ± 0.84[d]
24	29.6 ± 1.7[d]
36	28.9 ± 2.3[d]

[a] 25 mg/kg ip every 4 hr. [b] Mean ± SD, n = 8, except at 36 hr when n = 5 (three animals died). [c] Ibuprofen, 0.1 mg/ml, added *in vitro*. [d] Not statistically significantly different from zero-time value.

Ibuprofen, when added to plasma *in vitro* or when administered to the rats, had no apparent effect on the prothrombin complex activity, as reflected by a lack of significant change in the clotting time of plasma (Table III). Ibuprofen administration also had no statistically significant effect on the degradation kinetics of prothrombin complex activity (k_{deg} = 5.48 ± 0.42 days^{-1} in control animals and 5.99 ± 0.63 days^{-1} in ibuprofen-treated animals).

Figure 6 shows the effect of ibuprofen treatment on the relationship between the relative synthesis rate of prothrombin complex activity and the plasma warfarin concentration in one rat. The linear logarithmic regression line can be characterized by its slope and by the concentration required to decrease the relative synthesis rate to one-half of normal (designated as the "effective concentration"). The results obtained in all animals are summarized in Table IV. Ibuprofen caused a significant decrease in the effective concentration and increase in the absolute slope value. There was a statistically significant correlation ($r = 0.974$, $p < 0.001$) between the effective concentrations of warfarin for individual animals in the control experiment and during ibuprofen administration (Fig. 7).

DISCUSSION

Ibuprofen can displace warfarin from serum protein binding sites. Since the total clearance of warfarin by the body is proportional to the free fraction of the drug in serum or plasma (14, 15) and since the anticoagulant action of warfarin is a function of the concentration of free drug

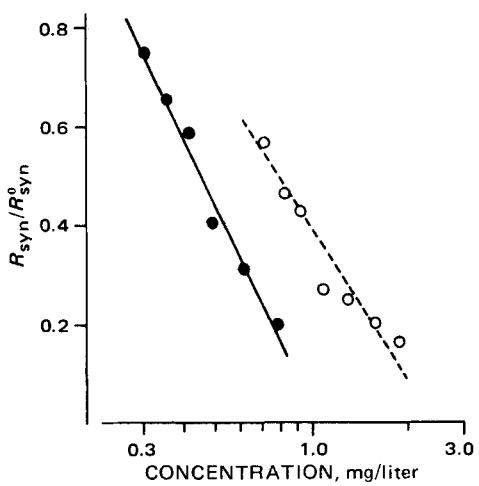

Figure 6—*Effect of ibuprofen administration on the relationship between the relative synthesis rate of prothrombin complex activity (R_{syn}/R^0_{syn}) and warfarin concentration in plasma. Data are from Rat 11 during a control experiment (○) and during ibuprofen administration (●).*

Table IV—Effect of Ibuprofen Treatment on the Relationship between Anticoagulant Effect and Plasma Concentration of Warfarin in Rats[a]

Parameter	Control (C)	Ibuprofen (I)	Ratio, C:I
Effective concentration (concentration when $R_{syn} = 0.5\ R^0_{syn}$), mg/liter	0.598 (0.146–2.03)[b]	0.414 (0.042–1.38)[c]	1.65 (0.730–3.48)
Slope of regression line for R_{syn}/R^0_{syn} *versus* log concentration	−1.01 (−0.455 to −1.69)	−1.31 (−0.851 to −2.06)[d]	0.830 (0.452–1.70)

[a] Crossover study on 13 rats (data on the 14th animal could not be obtained for technical reasons). [b] Mean (range). [c] $p < 0.005$ *versus* control (paired t-test). [d] $p < 0.05$ *versus* control (paired t-test).

(16), it follows that, all else being equal, displacement of warfarin from plasma proteins by ibuprofen should increase the total clearance of the anticoagulant and decrease the plasma concentration required to produce a given degree of anticoagulation. The results of this investigation are consistent with these considerations; ibuprofen treatment caused an increase in the total clearance of warfarin and a decrease in its effective concentration. Since ibuprofen has no apparent inductive effect on drug-metabolizing enzyme systems (1, 17), it is unlikely that the increased total clearance of warfarin was due to enzyme induction.

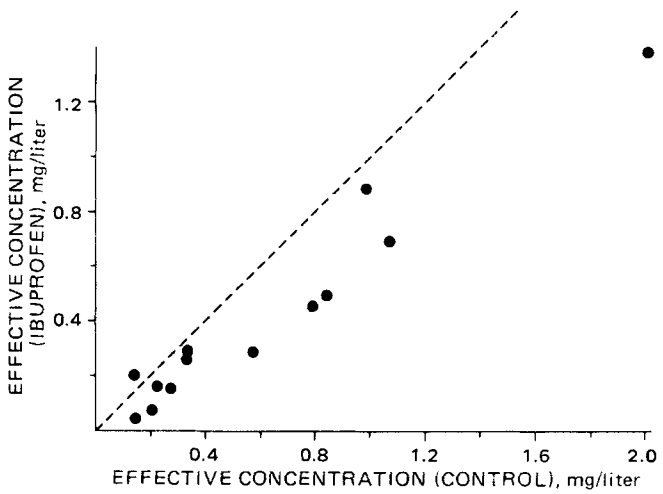

Figure 7—*Relationship between the effective plasma warfarin concentration in rats in a control experiment and during ibuprofen administration to the same animals in a crossover study. The effective concentration is the concentration of total (free and protein-bound) warfarin required to decrease* R_{syn} *to one-half of normal* (i.e., $R_{syn}/R^0_{syn} = 0.5$). *The stippled line has a slope of unity.*

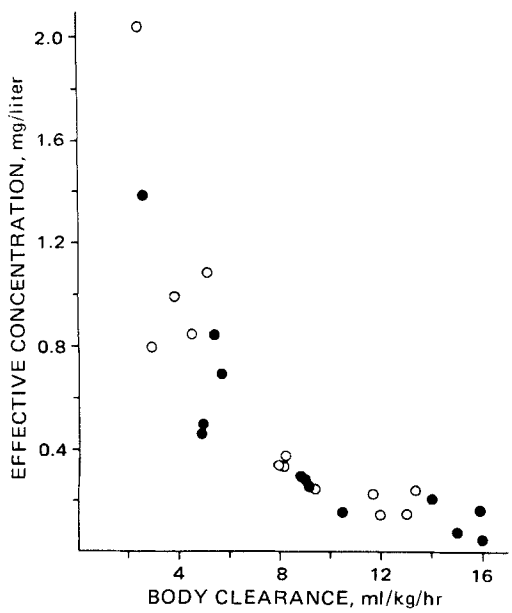

Figure 8—*Relationship between the effective plasma warfarin concentration and the body clearance of warfarin in individual rats in a crossover study. Key:* ○, *control experiment; and* ●, *during ibuprofen administration.*

Due to the short half-life of ibuprofen in rats, the concentrations of this drug fluctuated significantly during the 3-hr interval between injections. The timing of blood sample withdrawals was dictated primarily by the need to characterize the pharmacokinetics and time course of the anticoagulant effect of warfarin. Consequently, blood samples were not obtained at constant times after ibuprofen injection, and this magnified the intra- and intersubject variations in the observed plasma ibuprofen concentrations. For the same reason, the free fraction value of warfarin fluctuated within ibuprofen dosing intervals. These complexities and the need to keep the animals in good condition for the crossover experiment made it impossible to determine the time course of concentrations of free (not protein-bound) warfarin in serum during the *in vivo* interaction study.

It is feasible, however, to determine indirectly if displacement of warfarin from serum proteins is the sole or predominant mechanism of the observed warfarin–ibuprofen interaction or if additional factors contribute significantly to the interaction. Since both the body clearance and anticoagulant effect of warfarin are functions of the free fraction of drug in plasma, the relationship between body clearance and effective concentration should be the same in control and ibuprofen experiments if the interaction is due only to displacement of the protein-bound anticoagulant. As evident in Fig. 8, this appears to be the case. In support of this conclusion are the observations that ibuprofen has no apparent effect on the synthesis and degradation of prothrombin complex activity and that the average increase in total clearance of warfarin (Table II) is of similar magnitude as the increase in warfarin free fraction produced by the observed average ibuprofen concentrations (Table I and Fig. 1).

Based on pharmacokinetic data from humans (12), the steady-state plasma concentration of ibuprofen produced by a daily dose of 2.4 g is estimated to be 30–40 mg/liter. Peak concentrations of ibuprofen during a dosing interval will be appreciably higher, and an increase in the dosing rate will produce a corresponding increase in the steady-state concentration. It was estimated that the binding capacity of albumin in human plasma for ibuprofen is only 120 mg/liter (1). Inflammatory disease is often associated with hypoalbuminemia (18), resulting in a decreased binding capacity of plasma. For these reasons, it is desirable to determine the effect of various concentrations of ibuprofen on warfarin binding in normal and hypoalbuminemic human plasma.

This investigation showed that ibuprofen can, in principle, modify the elimination kinetics and anticoagulant activity of warfarin. These effects appear to be the consequence of decreased serum protein binding of warfarin in the presence of ibuprofen. Since this displacing effect of ibuprofen is concentration dependent, the clinical significance of these findings can only be assessed by determining the effect of therapeutic concentrations of the agent on the plasma protein binding of warfarin (19). Such determinations are in order also for other nonsteroidal anti-inflammatory agents that have recently come into clinical use (20).

REFERENCES

(1) R. F. N. Mills, S. S. Adams, E. E. Cliffe, W. Dickinson, and J. S. Nicholson, *Xenobiotica*, **3**, 589 (1973).

(2) R. A. O'Reilly and P. M. Aggeler, *Pharmacol. Rev.*, **22**, 35 (1970).

(3) J. Koch-Weser and E. M. Sellers, *N. Engl. J. Med.*, **285**, 487, 547 (1971).

(4) R. A. O'Reilly and G. Levy, *J. Pharm. Sci.*, **59**, 1258 (1970).

(5) L. Concalves, *J. Int. Med. Res.*, **1**, 180 (1973).

(6) D. Thilo, D. Nyman, and F. Duckert, *ibid.*, **2**, 27 (1974).

(7) M. J. Bockhout-Mussert and E. A. Loeliger, *ibid.*, **2**, 279 (1974).

(8) J. A. Penner and P. H. Abbrecht, *Curr. Ther. Res.*, **18**, 862 (1975).

(9) A. Yacobi and G. Levy, *J. Pharm. Sci.*, **64**, 1660 (1975).

(10) L. B. Wingard, Jr., and G. Levy, *J. Pharmacol. Exp. Ther.*, **184**, 253 (1973).

(11) A. Yacobi, L. B. Wingard, Jr., and G. Levy, *J. Pharm. Sci.*, **63**, 868 (1974).
(12) D. G. Kaiser and G. J. VanGiessen, *ibid.*, **63**, 219 (1974).
(13) S. S. Adams and E. E. Cliffe, *J. Pharm. Pharmacol.*, **17**, 173 (1965).
(14) G. Levy and A. Yacobi, *J. Pharm. Sci.*, **63**, 805 (1974).
(15) A. Yacobi, J. A. Udall, and G. Levy, *Clin. Pharmacol. Ther.*, **19**, 552 (1976).
(16) A. Yacobi and G. Levy, *Res. Commun. Chem. Pathol. Pharmacol.*, **12**, 405 (1975).
(17) C. Reinicke and W. Klinger, *Biochem. Pharmacol.*, **24**, 145 (1975).
(18) J. Allerhand, *Am. J. Med. Sci.*, **274**, 431 (1964).
(19) J. T. Slattery and G. Levy, *J. Pharm. Sci.*, **66**, 1060 (1977).
(20) A. Yacobi and G. Levy, *Res. Commun. Chem. Pathol. Pharmacol.*, **15**, 369 (1976).

ACKNOWLEDGMENTS AND ADDRESSES

Received July 6, 1976, from the *Department of Pharmaceutics, School of Pharmacy, State University of New York at Buffalo, Buffalo, NY 14214.*

Accepted for publication August 13, 1976.

Supported in part by Grant GM 20852 from the National Institute of General Medical Sciences, National Institutes of Health, Bethesda, MD 20014.

[x] To whom inquiries should be directed.

Interrelation between Two Anticomplement Cobra Venom Factors Isolated from Crude *Naja naja* Cobra Venom

BRIAN J. JOHNSON [x] and UMBERTO N. KUCICH [x]

Abstract □ Two moieties occurring in crude *Naja naja* cobra venom were found to possess anticomplement activity. Both materials possessed similar molecular weights and specific activities but dissimilar elution profiles upon ion-exchange chromatography. The anticomplement activities of these materials were maintained upon digestion with neuraminidase, and their elution profiles from cation-exchange chromatography became identical after this treatment. It was concluded that the differences between the two anticomplement materials were due to their different sialic acid contents.

Keyphrases □ Cobra venom—two anticomplement factors isolated by ion-exchange chromatography, effect of neuraminidase digestion □ Ion-exchange chromatography—isolation, two anticomplement factors from cobra venom □ Anticomplement activity—two factors isolated by ion-exchange chromatography from cobra venom, effect of neuraminidase digestion

Purified cobra venom factor is probably the single most valuable substance for lowering complement levels *in vivo*. The mechanism of action of cobra venom factor *via* one pathway was described previously (1). When the factor is administered in small doses to minimize the lysis of red blood cells, complement activity is depressed; this depression can be maintained for 3–4 days (1). However, an antibody eventually develops against the cobra venom factor, inhibiting its anticomplement activity.

The possible clinical usefulness of cobra venom factor in reducing the amount of infarcted tissue following coronary occlusion was reported previously (2). In experimental animals, the myocardium that can be salvaged is substantial, and the treatment may be started a number of hours following the occlusion and still be effective. Since acute myocardial infarction constitutes the most common cause of death in this country, any procedure that can salvage substantial quantities of the patient's myocardium after the patient's arrival at the hospital should be investigated. Animal studies showed that cobra venom factor diminishes the inflammatory response following ischemic damage and thus reduces the size of myocardial infarcts after coronary occlusion (3, 4). These conclusions were reached using various electrophysiological, biochemical, histological, histochemical, and electron microscope techniques.

During an investigation on the purification of cobra venom factor from crude *Naja naja* cobra venom, two anticomplement factors were obtained. This report concerns the identification of these materials and their interrelationship.

EXPERIMENTAL

All buffers were prepared from reagent grade materials according to American Chemical Society standards. Gel filtration media were equilibrated with starting buffer for 2 days or heated to 80° for 6 hr prior to column preparation. All absorbance measurements were made at 280 nm. Freshly drawn human blood was allowed to clot, and the resulting serum served as the complement source.

Anticomplement Activity—*Qualitative Assay*—The assay was based on previously reported methods (5–7). For scanning column runs, sensitized sheep erythrocytes, EA (8), were labeled by incubation with ^{51}Cr-labeled sodium chromate in barbital buffer, pH 7.4 (50 μCi/1 × 10^9 cells), at 37° for 45 min with constant agitation. The cells were washed (5 × 10 ml of barbital buffer at 4°), resuspended in buffer, and then standardized to a concentration of 1 × 10^9 cells/ml.

To a series of wells in a microtiter test plate was added 20 μl of human complement, C. To each well was added 20 μl of cobra venom factor or column sample, and the plate was incubated at 37° for 1 hr. Another 100 μl of buffer was added to each well, followed by 20 μl of the ^{51}Cr-primed sensitized sheep erythrocytes, EA, with constant agitation. The samples were incubated at 37° for 1 hr and centrifuged, and aliquots of 50 μl were removed from each well.

The amount of lysis was obtained by measuring the amount of ^{51}Cr-label released with a γ-counter. Controls consisting of sensitized cells alone, sensitized cells plus complement, and cells plus water were run concurrently with the described assay. The percentage of inhibition (I) of lysis was calculated from:

$$\%I = 100\left[1 - \frac{\text{cpm released by EA, sample, and C} - \text{cpm released by EA alone}}{\text{cpm released by EA and C} - \text{cpm released by EA alone}}\right] \quad \text{(Eq. 1)}$$

(11) A. Yacobi, L. B. Wingard, Jr., and G. Levy, *J. Pharm. Sci.*, **63**, 868 (1974).
(12) D. G. Kaiser and G. J. VanGiessen, *ibid.*, **63**, 219 (1974).
(13) S. S. Adams and E. E. Cliffe, *J. Pharm. Pharmacol.*, **17**, 173 (1965).
(14) G. Levy and A. Yacobi, *J. Pharm. Sci.*, **63**, 805 (1974).
(15) A. Yacobi, J. A. Udall, and G. Levy, *Clin. Pharmacol. Ther.*, **19**, 552 (1976).
(16) A. Yacobi and G. Levy, *Res. Commun. Chem. Pathol. Pharmacol.*, **12**, 405 (1975).
(17) C. Reinicke and W. Klinger, *Biochem. Pharmacol.*, **24**, 145 (1975).
(18) J. Allerhand, *Am. J. Med. Sci.*, **274**, 431 (1964).
(19) J. T. Slattery and G. Levy, *J. Pharm. Sci.*, **66**, 1060 (1977).
(20) A. Yacobi and G. Levy, *Res. Commun. Chem. Pathol. Pharmacol.*, **15**, 369 (1976).

ACKNOWLEDGMENTS AND ADDRESSES

Received July 6, 1976, from the *Department of Pharmaceutics, School of Pharmacy, State University of New York at Buffalo, Buffalo, NY 14214.*

Accepted for publication August 13, 1976.

Supported in part by Grant GM 20852 from the National Institute of General Medical Sciences, National Institutes of Health, Bethesda, MD 20014.

[x] To whom inquiries should be directed.

Interrelation between Two Anticomplement Cobra Venom Factors Isolated from Crude *Naja naja* Cobra Venom

BRIAN J. JOHNSON [x] and UMBERTO N. KUCICH [x]

Abstract □ Two moieties occurring in crude *Naja naja* cobra venom were found to possess anticomplement activity. Both materials possessed similar molecular weights and specific activities but dissimilar elution profiles upon ion-exchange chromatography. The anticomplement activities of these materials were maintained upon digestion with neuraminidase, and their elution profiles from cation-exchange chromatography became identical after this treatment. It was concluded that the differences between the two anticomplement materials were due to their different sialic acid contents.

Keyphrases □ Cobra venom—two anticomplement factors isolated by ion-exchange chromatography, effect of neuraminidase digestion □ Ion-exchange chromatography—isolation, two anticomplement factors from cobra venom □ Anticomplement activity—two factors isolated by ion-exchange chromatography from cobra venom, effect of neuraminidase digestion

Purified cobra venom factor is probably the single most valuable substance for lowering complement levels *in vivo*. The mechanism of action of cobra venom factor *via* one pathway was described previously (1). When the factor is administered in small doses to minimize the lysis of red blood cells, complement activity is depressed; this depression can be maintained for 3–4 days (1). However, an antibody eventually develops against the cobra venom factor, inhibiting its anticomplement activity.

The possible clinical usefulness of cobra venom factor in reducing the amount of infarcted tissue following coronary occlusion was reported previously (2). In experimental animals, the myocardium that can be salvaged is substantial, and the treatment may be started a number of hours following the occlusion and still be effective. Since acute myocardial infarction constitutes the most common cause of death in this country, any procedure that can salvage substantial quantities of the patient's myocardium after the patient's arrival at the hospital should be investigated. Animal studies showed that cobra venom factor diminishes the inflammatory response following ischemic damage and thus reduces the size of myocardial infarcts after coronary occlusion (3, 4). These conclusions were reached using various electrophysiological, biochemical, histological, histochemical, and electron microscope techniques.

During an investigation on the purification of cobra venom factor from crude *Naja naja* cobra venom, two anticomplement factors were obtained. This report concerns the identification of these materials and their interrelationship.

EXPERIMENTAL

All buffers were prepared from reagent grade materials according to American Chemical Society standards. Gel filtration media were equilibrated with starting buffer for 2 days or heated to 80° for 6 hr prior to column preparation. All absorbance measurements were made at 280 nm. Freshly drawn human blood was allowed to clot, and the resulting serum served as the complement source.

Anticomplement Activity—*Qualitative Assay*—The assay was based on previously reported methods (5–7). For scanning column runs, sensitized sheep erythrocytes, EA (8), were labeled by incubation with ^{51}Cr-labeled sodium chromate in barbital buffer, pH 7.4 (50 μCi/1 × 10^9 cells), at 37° for 45 min with constant agitation. The cells were washed (5 × 10 ml of barbital buffer at 4°), resuspended in buffer, and then standardized to a concentration of 1 × 10^9 cells/ml.

To a series of wells in a microtiter test plate was added 20 μl of human complement, C. To each well was added 20 μl of cobra venom factor or column sample, and the plate was incubated at 37° for 1 hr. Another 100 μl of buffer was added to each well, followed by 20 μl of the ^{51}Cr-primed sensitized sheep erythrocytes, EA, with constant agitation. The samples were incubated at 37° for 1 hr and centrifuged, and aliquots of 50 μl were removed from each well.

The amount of lysis was obtained by measuring the amount of ^{51}Cr-label released with a γ-counter. Controls consisting of sensitized cells alone, sensitized cells plus complement, and cells plus water were run concurrently with the described assay. The percentage of inhibition (I) of lysis was calculated from:

$$\%I = 100\left[1 - \frac{\text{cpm released by EA, sample, and C} - \text{cpm released by EA alone}}{\text{cpm released by EA and C} - \text{cpm released by EA alone}}\right] \quad \text{(Eq. 1)}$$

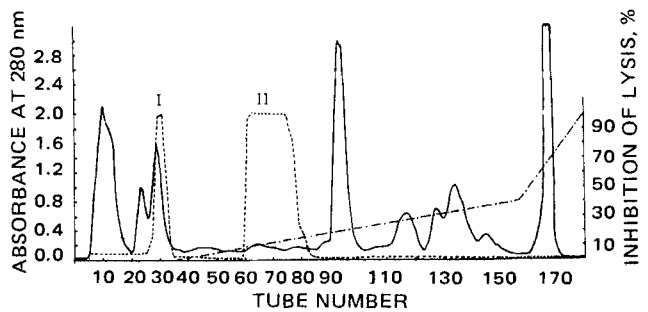

Figure 1—*Carboxymethylcellulose cation-exchange chromatography of dialyzed crude* N. naja *cobra venom. Key: —, optical density; - - -, anticomplement activity; and — · —, sodium chloride gradient (0.0 → 0.2 → 0.5 M).*

Quantitative Assay—The method was essentially the same as the qualitative one, except that serial dilutions of the anticomplement samples were assayed. To a series of wells in a microtiter plate was added 20 μl of human complement, to each of these was added the serially diluted sample, and the plate was incubated at 37° for 1 hr. Each well was diluted with 100 μl of buffer, and the microtiter plate was agitated during these additions. After incubation at 37° for 1 hr, the samples were centrifuged, aliquots of 50 μl were removed from each well, and the amount of lysis was ascertained by the ^{51}Cr-label released. Identical controls to those described were run concurrently.

The percentage of inhibition of lysis was calculated from Eq. 1 and was plotted against the dilution of the complement-consuming material. The dilution of material that produced 50% inhibition of lysis was considered equal to the number of cobra venom factor units in the original 20-μl aliquot of material. By this means, comparison could be made of the purification and activity of the various complement-consuming materials.

Isolation of Cobra Venom Factor—*Carboxymethylcellulose Chromatography*—One gram of lyophilized cobra venom[1] was suspended in 15 ml of 0.05 *M* sodium acetate buffer, pH 5.5, containing 0.02% sodium azide and then dialyzed overnight against two changes of 1 liter each of the same buffer. A column (1.5 × 25.0 cm) of CM-52 carboxymethylcellulose[2] was equilibrated with 0.05 *M* sodium acetate buffer, pH 5.5. The crude dialyzed cobra venom mixture, typically containing 560–760 absorbance units, was applied to the column; elution was performed using 0.05 *M* sodium acetate, pH 5.5.

When no further material was eluted from the column, as shown by absorbance measurements, a sodium chloride gradient was applied. The flow rate of the column was 20 ml/hr, and 4-ml fractions were collected. Each tube was assayed for anticomplement activity. The elution profile and the peaks of activity, I and II, are shown in Fig. 1.

Gel Filtration Chromatography—Lyophilized peak II, obtained from carboxymethylcellulose chromatography, was suspended in 3.5 ml of 0.015 *M* tris(hydroxymethyl)aminomethane–0.15 *M* sodium chloride buffer, pH 8.5, containing 0.02% sodium azide. This sample, containing 28 absorbance units, was applied to a column (1.5 × 85 cm) of Sephadex G-200 equilibrated in the same buffer.

The flow rate was adjusted to 15 ml/hr, and 2.5-ml fractions were collected. Three well-defined protein peaks were obtained (Fig. 2A). The major peak, containing all of the anticomplement activity eluted, possessed a molecular weight slightly less than 150,000, as shown by using human IgG1 as a molecular weight marker. The fraction containing the biological activity was pooled and then lyophilized.

Peak I, obtained from carboxymethylcellulose chromatography was treated in an identical manner as peak II. The elution and anticomplement activity profiles are shown in Fig. 2B.

Diethylaminoethylcellulose Chromatography—One gram of lyophilized cobra venom was suspended in 10.6 ml of 0.05 *M* barbital sodium buffer, pH 8.6, containing 0.05% sodium azide. This solution, containing 967 absorbance units, was filtered through a filtration membrane[3], 1 × 10^5 mol. wt. exclusion limit, and washed thoroughly with 0.05 *M* barbital sodium buffer, pH 8.6. The solution was then concentrated to 15.5 ml, and it possessed 688 absorbance units.

The material was charged on a column (2.5 × 40 cm) of DE-52 diethylaminoethylcellulose[2] equilibrated with 0.05 *M* barbital sodium buffer, pH 8.6. The flow rate of the column was 35 ml/hr, and 5-ml fractions were collected. After the initial protein was eluted from the column, a sodium chloride gradient was applied. The elution and anticomplement activity profiles are shown in Fig. 3.

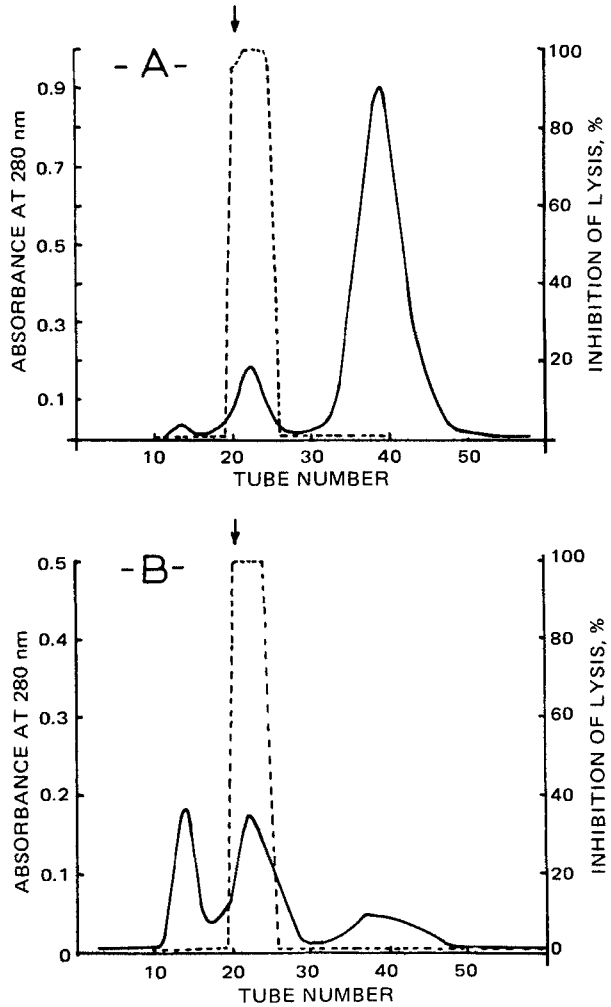

Figure 2—*Sephadex G-200 chromatography of peaks I and II obtained from cation-exchange chromatography (Fig. 1). Figure 2A corresponds to peak I and Fig. 2B to peak II. The molecular weight marker, human IgG1, is indicated by an arrow. Key: —, optical density; and - - -, anticomplement activity.*

Neuraminidase Digestion A—In separate but concurrent experiments, 4.2 ml of anticomplement active peak I, 5.46 absorbance units, and 4.4 ml of anticomplement active peak II, 2.66 absorbance units, obtained from the procedure described under *Carboxymethylcellulose Chromatography* were digested with insolubilized neuraminidase. To each sample in 0.05 *M* sodium acetate–0.02% sodium azide, pH 5.5, was added 1.7 units of insolubilized neuraminidase. Each mixture was incubated at 37° for 1 hr with shaking. At the end of the digestion, the solutions were cleared by centrifugation and the supernates were removed by decantation. Control samples of peaks I and II were treated identically except that buffer was substituted for neuraminidase.

Quantitative anticomplement assays of each peak after neuraminidase treatment and its appropriate control were performed. Peak I possessed 680 cobra venom factor units per absorbance unit without neuraminidase digestion and 640 after digestion. Peak II possessed 695 cobra venom factor units per absorbance unit without neuraminidase digestion and 642 after digestion. A further control to investigate the activity of the insolubilized neuraminidase was also performed. To 0.4 ml of a 4% solution of bovine mucin in 0.05 *M* sodium acetate–0.02% sodium azide buffer, pH 5.5, was added 1.7 units of insolubilized neuraminidase. The digestion was conducted for 1 hr at 37° with mixing and was arrested by removal of the insolubilized enzyme by centrifugation. The presence of sialic acid was determined using 2-thiobarbituric acid as reported by Warren (9) and modified by Aminoff (10).

[1] Ross Allen Reptile Farm, Silver Springs, Fla.
[2] Whatman, Maidstone, Kent, England.
[3] Diaflo.

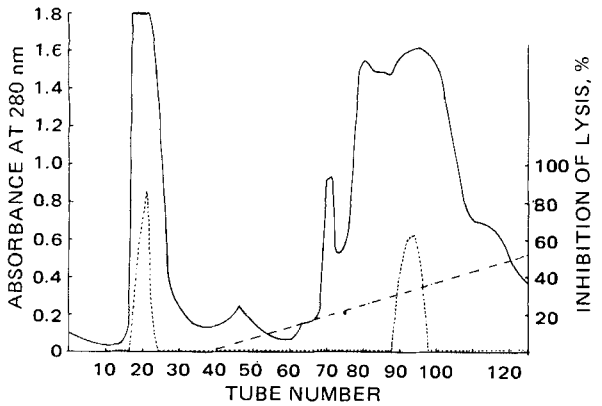

Figure 3—*Diethylaminoethylcellulose anion chromatography of crude* N. naja *cobra venom. Key: —, optical density; - - - , anticomplement activity; and — · —, sodium chloride gradient (0.0 → 0.25* M*).*

Neuraminidase Digestion B—Peaks I and II obtained from the carboxymethylcellulose ion-exchange chromatography were combined. The solution was concentrated using a filtration membrane[3], 30,000 mol. wt. exclusion limit, and then was dialyzed overnight against 1000 ml of 0.05 *M* sodium acetate–0.05% sodium azide buffer, pH 5.5. The solution was centrifuged to give 13.5 ml containing 13.5 absorbance units of material. This material was incubated with 3.4 units of previously calibrated insolubilized neuraminidase for 1 hr at 37° with agitation.

After this digestion period, the enzyme was removed by centrifugation. The supernate, 14.0 ml, 10.4 absorbance units, was chromatographed on a column (2.0 × 37.5 cm) of CM-52 carboxymethylcellulose. The flow rate of the column was 40 ml/hr, and 5.5-ml fractions were collected. Each fraction was assayed for anticomplement activity. Only one peak of anticomplement activity was detected, and it eluted from the column in an identical position to that of peak II before neuraminidase digestion.

RESULTS AND DISCUSSION

The complement fixation assays utilized the quantitation of ^{51}Cr-release by the action of complement on sensitized erythrocytes (5–7). The anticomplement activity of a pertinent sample was ascertained by its prior incubation with human serum and then quantitation of the unconsumed complement (8).

Dialysis of crude *N. naja* venom usually removed up to 25% of the available optical density. Chromatography of the dialyzed cobra venom through a carboxymethylcellulose column gave two peaks, I and II (Fig. 1), of anticomplement activity. Similarly, chromatography of crude *N. naja* cobra venom on diethylaminoethylcellulose gave two peaks of anticomplement activity. Other investigators reported the presence of only a single material with anticomplement activity (11, 12), mol. wt. 144,000 (12).

Each anticomplement material from cation-exchange chromatography (Fig. 1) was subjected to gel filtration chromatography on Sephadex G-200. Both materials eluted in identical positions (Fig. 2), and both had apparent molecular weights of slightly under 150,000. Furthermore, the specific anticomplement activities of each peak were very similar. The interrelationship between peaks I and II (Fig. 1) was shown using neuraminidase digestion.

In separate experiments, peaks I and II were digested with insolubilized neuraminidase (Digestion A); within experimental error, there was no change in the specific activity of either peak. In another experiment (Digestion B), fresh samples of peaks I and II were combined and then treated with insolubilized neuraminidase. Only one peak of anticomplement activity was detected when this digest was subjected to cation-exchange chromatography.

Neuraminidase cleaves sialic acid (*N*-acetyl- and *O*-acetylneuraminic acids) from suitable substrates. However, sterically hindered sialic acids are resistant (13). Neuraminidase did not cause either cobra venom factor I or II to lose anticomplement activity. However, it did change the elution profile of peak I on cation-exchange chromatography such that it eluted in an identical position to that of peak II. These results indicate that these anticomplement materials, peaks I and II, probably differ in their sialic acid compositions.

REFERENCES

(1) R. A. Nelson, *Surv. Ophthalmol.*, **11**, 498 (1966).
(2) P. R. Moroko and C. B. Carpenter, *Clin. Res.*, **21**, 950 (1973).
(3) E. Braunwald and P. R. Maroko, *Circulation*, **50**, 206 (1974).
(4) E. Braunwald, *N. Engl. J. Med.*, **291**, 525 (1974).
(5) N. R. Cooper and H. J. Müller-Eberhard, *J. Exp. Med.*, **132**, 775 (1970).
(6) U. N. Kucich, J. C. Bennett, and B. J. Johnson, *J. Immunol.*, **115**, 626 (1975).
(7) B. J. Johnson, U. N. Kucich, and A. T. Maurelli, *ibid.*, **116**, 1669 (1976).
(8) E. A. Kabat and M. M. Mayer, "Experimental Immunochemistry," 2nd ed., Charles C Thomas, Springfield, Ill., 1967.
(9) L. Warren, *J. Biol. Chem.*, **234**, 1971 (1959).
(10) D. Aminoff, *Biochem. J.*, **81**, 384 (1961).
(11) M. Ballow and L. G. Cochrane, *J. Immunol.*, **103**, 944 (1969).
(12) H. J. Müller-Eberhard and K. Fjellström, *ibid.*, **107**, 1666 (1971).
(13) J. T. Cassidy, G. W. Jourdian, and S. Roseman, *J. Biol. Chem.*, **240**, 3501 (1965).

ACKNOWLEDGMENTS AND ADDRESSES

Received July 2, 1976, from the *Department of Microbiology, University of Alabama Medical School, Birmingham, AL 35294.*

Accepted for publication August 25, 1976.

Supported by Grant AI 11970 from the National Institutes of Health.

* Recipient of an Institutional Research Fellowship, Award T32-AM07069, from the National Institute of Arthritis, Metabolism, and Digestive Diseases.

ˣ To whom inquiries should be directed.

Functional Modification of Indole Binding Site with Indomethacin Congeners

E. M. K. LUI *, P. S. FARMER ˣ, and C. R. DEAN *

Abstract □ Indomethacin and four congeners were shown by equilibrium dialysis to interfere with the binding of L-tryptophan at the primary indole binding site on defatted human serum albumin. Incubation of albumin with 1-(*p*-bromoacetamidobenzoyl)- and 1-(*m*-bromoacetamidobenzoyl)-5-methoxy-2-methyl-3-indolylacetic acids functionally modified this site, decreasing the availability of the site for the binding of L-tryptophan. Incubation in the presence of a large excess of L-tryptophan resulted in the partial protection of the site from modification by 1-(*m*-bromoacetamidobenzoyl)-5-methoxy-2-methyl-3-indolylacetic acid.

Keyphrases □ Indomethacin and congeners—effect on binding of L-tryptophan by defatted human serum albumin □ L-Tryptophan—binding by defatted human serum albumin, effect of indomethacin and congeners □ Binding, protein—L-tryptophan binding by defatted human serum albumin, effect of indomethacin and congeners □ Protein binding—L-tryptophan binding by defatted human serum albumin, effect of indomethacin and congeners □ Indole binding site—on defatted human serum albumin, functional modification with indomethacin and congeners □ Anti-inflammatory agents—indomethacin and congeners, effect on binding of L-tryptophan by defatted human serum albumin

The nonsteroidal anti-inflammatory agents exert various pharmacological effects. There are several currently prevailing theories regarding their mode(s) of action, and a single biochemical mechanism for the anti-inflammatory and antirheumatic actions of these drugs has not yet been identified. Furthermore, the mechanisms so far proposed are not necessarily mutually exclusive. These agents are bound strongly with serum proteins, and at various concentrations they inhibit numerous enzyme systems implicated in the inflammatory process. The clinical effects of these drugs may possibly result from action at several sites rather than from a specific action on a single enzyme system.

Nevertheless, it is desirable to determine the extent to which any one enzyme or other protein is involved in inflammation and to evaluate the importance of inhibiting or interfering with that involvement. One approach is to design agents to bind selectively and irreversibly with one protein of interest. Functional modification of an implicated protein *in vivo* by such an agent and the evaluation of the anti-inflammatory effect achieved by such modification would provide a measure of the significance of interference with that protein by the drug.

In the present investigation, the object was to obtain a chemical agent that selectively alkylates the serum albumin binding sites of the anti-inflammatory agent indomethacin (I) while leaving its other receptors intact.

BACKGROUND

Indomethacin and other nonsteroidal anti-inflammatory agents are strongly bound by human serum albumin. The protein-bound rather than the unbound forms of these drugs may be responsible for their chronic antirheumatic effects (1). The drugs compete with endogenous biologically active small molecules for their binding sites on albumin. Among those substances displaced by these drugs are L-tryptophan (1–4) and certain dipeptides (1–3). Measurement of the displacement of tryptophan from human serum albumin was proposed as a new assay for screening drugs for potential anti-inflammatory activity (5).

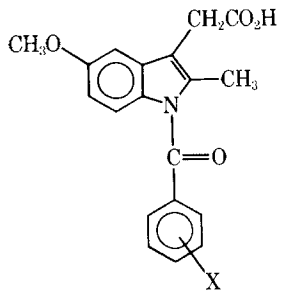

I: X = *p*-Cl
II: X = *p*-NHCOCH$_2$Br
III: X = *p*-NHCOCH$_3$
IV: X = *m*-NHCOCH$_2$Br
V: X = *m*-NHCOCH$_3$

Several forms of human serum albumin are believed to exist and to have different affinities and binding capacities for L-tryptophan and other small molecules (6–8). Rheumatoid arthritis patients may have an abnormal ratio of one form of albumin to another (8). Thus, rheumatoid arthritis and related diseases may be due to an abnormal serum protein binding of certain endogenous anti-inflammatory peptide-like small molecules, leading to a decrease in the free concentration of these substances for protection against chronic inflammatory insult (1, 8–10). Anti-inflammatory agents may act by displacing these endogenous factors from their binding sites on albumin, thereby redressing the bound–free ratio to that found in normal subjects.

The binding of L-tryptophan and its displacement may parallel those of the postulated protective peptides; thus, L-tryptophan could be used as an indicator of the extent of binding of the peptides. L-Tryptophan and some other indole derivatives combine tightly with albumin at a specific primary binding site (11–14) but are displaced by anti-inflammatory agents. L-Tryptophan is not displaced from albumin by other drugs that resemble the commonly used antirheumatic drugs in being administered over long periods and being equivalently bound to plasma proteins (3).

These observations and hypotheses lend themselves quite conveniently to examination by an affinity labeling technique. The proteins under scrutiny, namely serum albumins from humans and other species, are

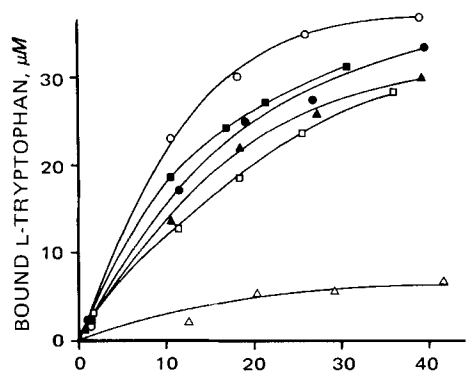

Figure 1—*Binding of L-tryptophan by defatted human serum albumin (0.4%) in 67 mM phosphate buffer at pH 7.4 and 3° and effect of competitors. Key: ○, no competitor (control); △, in presence of I (40 μM); □, in presence of II (40 μM); ●, in presence of III (40 μM); ▲, in presence of IV (40 μM); and ■, in presence of V (40 μM). In this and subsequent figures, each data point represents a single determination.*

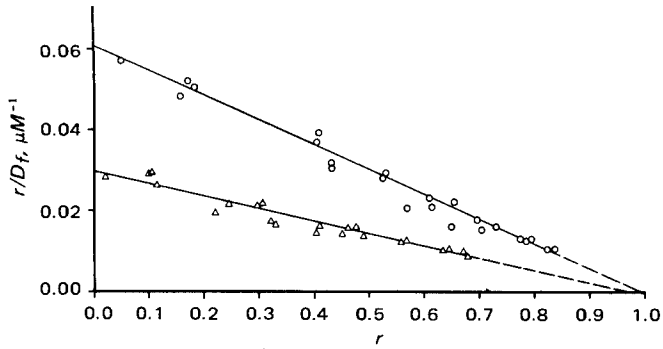

Figure 2—*Scatchard plots for the binding of* L-*tryptophan by defatted human serum albumin (0.4%) in 67 mM phosphate buffer at pH 7.4 and 3°. Key:* O, *control; and* Δ, *presence of II (40 μM).*

readily isolated for *in vitro* screening. More importantly, serum albumin is accessible in the intact animal. *In vivo* affinity labeling and active-site-directed irreversible enzyme inhibition usually require the reagent to reach the target site by a random-walk process, avoiding premature reaction with a bewildering array of tissue constituents (15). In contrast, for the present proposal, the reagent is required to alkylate specifically a major constituent of the compartment into which it is administered—albumin of the serum. Thus, the danger of alkylating other tissue components is mainly circumvented.

Gambhir and McMenamy (16) demonstrated site-specific covalent binding at the indole binding site by *N*-bromoacetyl-L-tryptophan and by two other reagents. They used these affinity labels to locate the site in the albumin molecule. Their results, however, cannot be extrapolated to nonsteroidal anti-inflammatory agents.

Therefore, it was decided to investigate the influence of indomethacin and four congeners (II–V) on L-tryptophan binding by human serum albumin. Compounds II and IV are potential affinity-labeling reagents for indomethacin receptors, since these compounds bear the electrophilic bromoacetamido moiety. Indomethacin was chosen as the pharmacophoric structure from which to design an irreversible protein binder, because it has a high displacement potency of L-tryptophan from its binding site and the indole ring and general similarity of the indomethacin structure to that of L-tryptophan may increase the specificity of its binding to albumin. (It is not certain whether indomethacin and L-tryptophan share the same binding site on albumin or whether the indole moiety of both compounds has a similar orientation in the binding site.)

The indolic nature of I suggests the possibility of displacement of active molecules from albumin as a major mode of action for I, with inhibition of various enzymes such as the prostaglandin synthetase system playing more minor roles in its action; other drugs may act predominantly by the latter mechanisms, with specific albumin binding being secondary. Such differences in the relative importance of their component actions could account for the different spectra of pharmacological activities of these drugs.

The alkylating function required placement in such a position that it would not interfere with the initial reversible binding of the agents to the protein site. Since the benzoyl group of I constitutes a considerable change in gross dimensions from those of L-tryptophan, it was selected as the most logical area on which to substitute the bromoacetamido

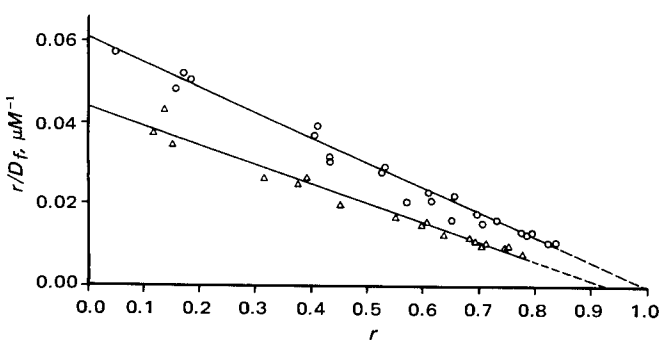

Figure 3—*Scatchard plots for the binding of* L-*tryptophan by defatted human serum albumin (0.4%) in 67 mM phosphate buffer at pH 7.4 and 3°. Key:* O, *control; and* Δ, *presence of III (40 μM).*

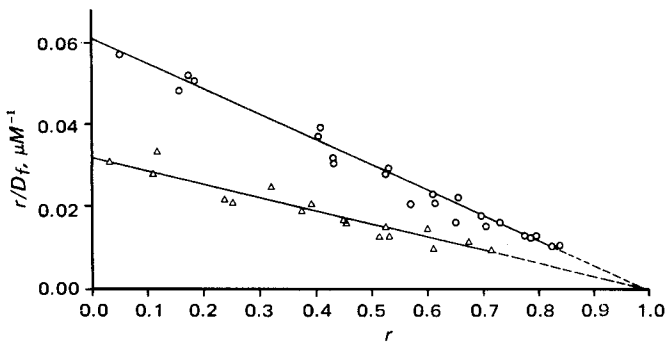

Figure 4—*Scatchard plots for the binding of* L-*tryptophan by defatted human serum albumin (0.4%) in 67 mM phosphate buffer at pH 7.4 and 3°. Key:* O, *control; and* Δ, *presence of IV (40 μM).*

moiety. Furthermore, the benzoyl group may act as a "bridge" between the site-directing group and the covalent bond-forming group, thereby enhancing the probability of alkylation of the indomethacin-binding site by the exo mechanism (17).

RESULTS AND DISCUSSION

L-Tryptophan was extensively bound by its primary binding site on albumin. The maximum number of binding sites, n, was 0.98, in good agreement with previous reports (10–12); the association constant, K_d, was $6.11 \times 10^4\ M^{-1}$. As reported previously (1–4), this binding of L-tryptophan was greatly inhibited in the presence of indomethacin; apparent n and K_d values could not be estimated.

The new indole compounds also inhibited the binding of L-tryptophan by albumin (Fig. 1). The order of decreasing L-tryptophan-displacement potency was: I ≫ II > IV > III > V. Scatchard plots for the binding of L-tryptophan in the presence of each indomethacin congener are illustrated in Figs. 2–5, and apparent binding parameters for L-tryptophan are listed in Table I. That these compounds probably inhibit albumin binding of L-tryptophan by a competitive mechanism at 3° is indicated by the constant value of n ($p < 0.01$)[1] while K_d changes significantly ($p > 0.01$)[1]. These findings are significant, since they show that the L-tryptophan binding site on human serum albumin has the bulk tolerance necessary to accommodate an acetamido or bromoacetamido group in the 3′- or 4′-position of the 1-benzoylindole system.

Once it was established that the indomethacin congeners did compete with L-tryptophan for its albumin binding site, a series of experiments was carried out to determine their ability to block or modify the binding site irreversibly at physiological temperature. The increased temperature was expected to promote covalent bond formation. An analogous situation was reported wherein acetylation of a lysine residue of albumin occurred readily at 37° but not at 0° (18). Thus, L-tryptophan binding was measured after incubation of the albumin at 37° for 24 hr in the presence of the respective competitors (Table II).

Defatted human serum albumin, incubated as a control in the absence of an indole compound, exhibited a slightly enhanced affinity for L-tryptophan. Incubation of albumin alone at 37° similarly increased its affinity for phenylbutazone, flufenamic acid, and dicumarol (19).

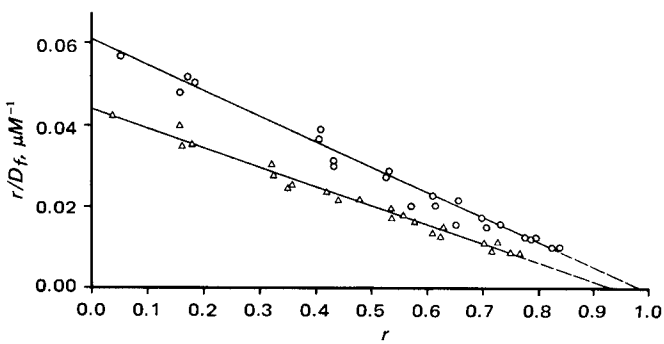

Figure 5—*Scatchard plots for the binding of* L-*tryptophan by defatted human serum albumin (0.4%) in 67 mM phosphate buffer at pH 7.4 and 3°. Key:* O, *control; and* Δ, *presence of V (40 μM).*

[1] Significance tested at 1% level with a Fortran analysis of variance program.

Table I—Binding of L-Tryptophan by 0.4% Defatted Human Serum Albumin and Effect of Competitors[a]

Competitor	$K_d \times 10^{-4}$, M^{-1}	n	Linear Correlation Coefficient
None (control)	6.11	0.98	−0.988
I	—[b]	—[b]	—
II	3.07[c]	0.95[d]	−0.967
III	4.64[c]	0.94[d]	−0.981
IV	3.52[c]	0.96[d]	−0.960
V	4.73[c]	0.93[d]	−0.990

[a] Determined in 67 m*M* phosphate buffer at pH 7.4 and 3°; L-tryptophan concentration was varied from 5 to 100 μ*M*; competitors were used with single initial concentration of 40 μ*M*. [b] Not measurable; no correlation was found between r and r/D_f. [c] Significantly different from control value at $p > 0.01$. [d] No significant difference from control value at $p < 0.01$.

Incubation with II decreased the availability of the primary L-tryptophan-binding site by about 26% and also decreased the affinity slightly (Fig. 6). That is, functional modification of the primary L-tryptophan-binding site was observed. The slight decrease in K_d was probably due to competitive binding of residual noncovalently bound II, in spite of dialysis against four changes of sodium chloride. The presence of L-tryptophan during incubation with II in another experiment did not protect significantly against the modification (Fig. 6). The K_d was returned to the control value, however, indicating that L-tryptophan successfully competed with II for the site under these conditions. [L-Tryptophan is more effectively removed than II by sodium chloride. Chloride ion is an acknowledged competitive inhibitor of tryptophan binding (13).] These observations suggest that the functional modification by II is not dependent on the initial formation of a reversible complex with the primary indole-binding site.

Figure 7 shows the effects of incubation with IV. When incubated without L-tryptophan, the indole-binding site is more extensively modified by IV than by II, with only about 30% of the original site left unblocked. Unlike the observations with II, the presence of L-tryptophan during incubation of albumin with IV provided approximately 60% protection to the site, allowing modification of only about 28%. Protection at secondary sites would not be expected since, at a total concentration of 250 μ*M*, L-tryptophan is not bound appreciably by secondary sites on human serum albumin[2].

That the protection achieved was by competition and not by chemical inactivation of IV was evidenced by the lack of reaction between IV and L-tryptophan in the absence of albumin (*cf., Experimental*). These experiments provide evidence for site specificity in the functional modification by IV of the L-tryptophan primary binding site on albumin. They do not preclude additional *nonselective* reaction of IV at other sites on the protein molecule.

A second feature obvious from Fig. 7 is the generation or exposure by

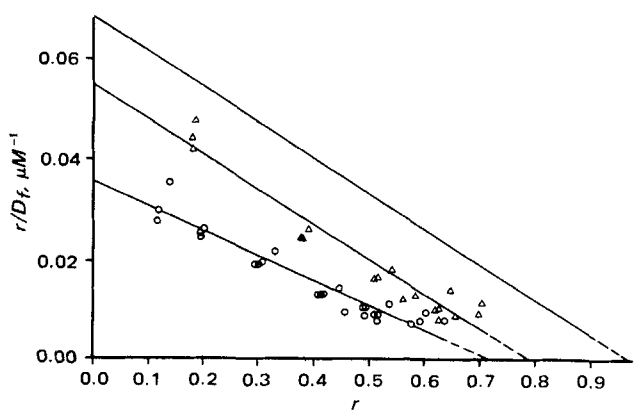

Figure 6—*Scatchard plots for the binding of L-tryptophan by defatted human serum albumin (0.4%) in 67 m*M *phosphate buffer at pH 7.4 and 3° after incubation at 37° for 24 hr. Key: top line without data points, albumin incubated in buffer alone (control); ○, albumin incubated in presence of II (290 μ*M*); and △, albumin incubated in presence of both II (290 μ*M*) and L-tryptophan (250 μ*M*).*

[2] This laboratory, unpublished data.

Table II—Binding of L-Tryptophan by 0.4% Defatted Human Serum Albumin after Incubation with Indole Compounds

Compound Incubated with	$K_d \times 10^{-4}$, M^{-1}	n	Linear Correlation Coefficient
None (control)	7.20	0.96	−0.987
I	4.22[a]	0.91[b]	−0.967
II	4.96[a]	0.71[a,c]	−1.002
II + 250 μ*M* L-tryptophan	6.91[b]	0.77[c]	−0.990
III	5.93[a]	0.89[b]	−0.995
IV	5.21[a,d]	0.29[a,d,e]	−0.982
IV + 250 μ*M* L-tryptophan	7.19[b]	0.69[e]	−0.993
V	4.86[a]	0.98[b]	−0.996

[a] Significantly different from control value at $p > 0.01$. [b] No significant difference from control value at $p < 0.01$. [c] No significant difference between the two values at $p < 0.01$. [d] Estimates for the first class of binding sites; insufficient data were available for determination of parameters for the second class by nonlinear least-squares fit. [e] These two values are significantly different at $p > 0.01$.

IV of a second class of L-tryptophan-binding sites. Visual inspection of the Scatchard plot of the "tryptophan-protection" experiment (Fig. 7) similarly reveals a possible break in the curve at higher r values, although a linear regression line was obtained with a correlation coefficient of −0.993 (*cf.*, Table II). Two possible explanations for this phenomenon were considered: (*a*) additional sites on the albumin molecule may be modified by IV, generating by an allosteric effect a new L-tryptophan-binding site; and (*b*) partial blocking or modification of the primary site on some albumin molecules may result in decreased, but measurable, affinity (K_d) at those sites. The unconvincing protection by L-tryptophan against the formation of the new class of sites discredits the latter explanation.

To establish that site modification was a function of the electrophilic bromoacetyl moieties of II and IV, albumin was incubated under the same conditions with I and with the nonalkylating congeners III and V separately. These compounds had no significant effect on r, the availability of the primary indole-binding site (Fig. 8). These compounds, like II and IV, decreased the association constant slightly.

Acetylation of albumin by aspirin modified binding of phenylbutazone and flufenamic acid, while acylation by other reagents had no measurable effect (19). Site protection experiments were not carried out, however, and the investigators were unable to state that all three drugs were bound at the same or proximal sites on the albumin.

EXPERIMENTAL

Biological—*Measurement of L-Tryptophan Binding by Albumin*—Protein binding was measured by equilibrium dialysis at 3°, using Visking dialysis bags[3]. Essentially fatty acid-free human serum albumin[4] (0.4%) in 2.0 ml of 67 m*M* phosphate buffer (pH 7.4) was used after dialysis overnight against the buffer at 3°. Diffusate solutions contained 15 ml of 3-^{14}C-L-tryptophan with initial concentrations of 5–100 μ*M* and activities of at least 4000 cpm.

3-^{14}C-L-Tryptophan was assayed as free (diffusate) and total (retentate) L-tryptophan by single-channel liquid scintillation counting[5] at 6–8°, with a counting time of 10 min and a counting efficiency of 97.36%. The scintillation fluid consisted of a commercial fluor[6]–toluene–ethylene glycol monomethyl ether (1:175:75) and was used to dilute 0.2 ml of dialysate to 10 ml. The protein concentration of the retentate after equilibrium dialysis was determined by the method of Lowry *et al.* (20).

The extent of binding was computed by the Scatchard method (21):

$$r/D_f = nK_d - rK_d \qquad \text{(Eq. 1)}$$

where r is the number of moles of L-tryptophan bound per mole of human serum albumin, D_f is the molar concentration of free L-tryptophan at equilibrium, n is the maximum number of binding sites of a single class, and K_d is the association constant for the binding of L-tryptophan by sites in that class.

A regression line for each set of experiments was generated using the

[3] Dialysis tubing, 0.63-cm (0.1251-in.) diameter (Union Carbide Corp.), was prepared for use as described by Gambhir and McMenamy (16).
[4] Sigma Chemical Co., St. Louis, Mo.
[5] Unilux II scintillation spectrometer, Nuclear Chicago, Des Plaines, Ill.
[6] OmniFluor, New England Nuclear, Boston, Mass.

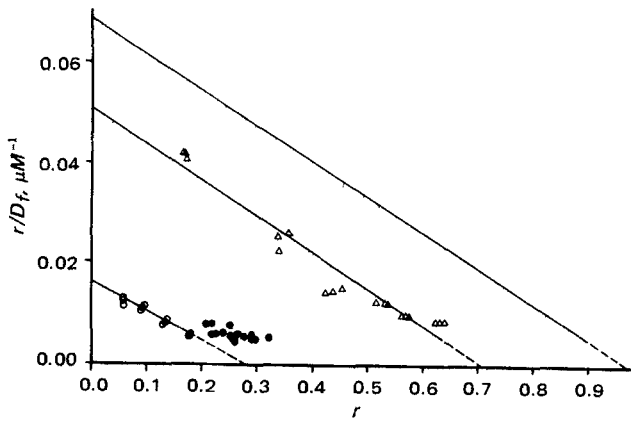

Figure 7—*Scatchard plots for the binding of L-tryptophan by defatted human serum albumin (0.4%) in 67 mM phosphate buffer at pH 7.4 and 3° after incubation at 37° for 24 hr. Key: top line without data points, albumin incubated in buffer alone (control); ○, albumin incubated in presence of IV (290 μM), data points used for estimation of regression line and binding parameters; ●, albumin incubated in presence of IV (290 μM), data points excluded for estimation of binding parameters; and △, albumin incubated in presence of both IV (290 μM) and L-tryptophan (250 μM).*

program BMDO3R[7] with a digital computer[8]. The slopes and elevations of replicated lines were compared ($p = 0.01$), using a Fortran analysis of covariance program (22). The homogeneous data were pooled for the estimation of a single regression line. Where the correlations between r/D_f and r were nonlinear, indicating binding at secondary binding sites, a second Fortran program[9] was used to compute binding parameters for both classes of binding sites.

Estimation of Competition by Indomethacin and Congeners—L-Tryptophan binding by 0.4% defatted human serum albumin in the presence of I–V was similarly measured. The diffusate solutions initially contained 5–100 μ*M* L-tryptophan and one test compound (I–V) in a single concentration of 40 μ*M*. Preliminary experiments showed I–V to have no appreciable quenching effect.

Affinity Labeling—Essentially fatty acid-free human serum albumin (0.4%) was incubated at 37° for 24 hr with each test compound (I–V) (290 μ*M*) in 67 m*M* phosphate buffer (pH 7.4). The incubated albumin solutions were then dialyzed at 3° for 48 hr against four changes of 0.15 *M* NaCl solution and finally against four changes of distilled water (19). A control experiment was run in which the albumin was incubated without an indole compound. L-Tryptophan binding by the albumin was measured as already described.

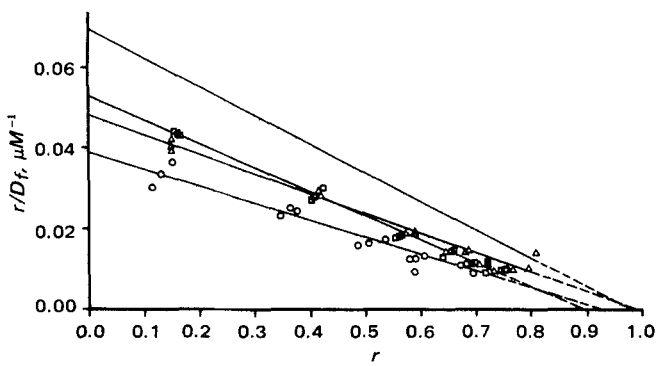

Figure 8—*Scatchard plots for the binding of L-tryptophan by defatted human serum albumin (0.4%) in 67 mM phosphate buffer at pH 7.4 and 3° after incubation at 37° for 24 hr. Key: top line without data points, albumin incubated in buffer alone (control); ○, albumin incubated in presence of I (290 μM); △, albumin incubated in presence of III (290 μM); and □, albumin incubated in presence of V (290 μM).*

Site Protection—Solutions of essentially fatty acid-free human serum albumin (0.4%), which had been equilibrated at 37° with 250 μ*M* L-tryptophan, were incubated with II or IV and subsequently treated as described. The L-tryptophan solution used for the preliminary equilibration carried the same specific activity (3-^{14}C) as the stock solution used in the binding studies.

Determination of Ionization Constants[10]—A spectrophotometric method (23) was used for the determination of pKa values for I and III. The absorbance of 1×10^{-4} *M* solutions of I was measured at 259 nm in 1.0 *M* HCl, 0.1 *M* NaOH, and seven formate buffers (0.01 *M*, pH 3.55–4.36), giving pKa 3.96 ± 0.03. When 3.85×10^{-5} *M* solutions of III were measured at 244 and 272 nm, they had a pKa of 4.11 ± 0.07. No suitable wavelength was found for differentiating between the acid and anion forms of V; their absorbances did not differ by greater than 10% in any part of the spectrum. The pKa of V was not determined.

The compounds are too insoluble in water or even in 50% methanol for potentiometric determination of their ionization constants.

Chemistry[11]—A modified Fischer indole synthesis, such as that de-

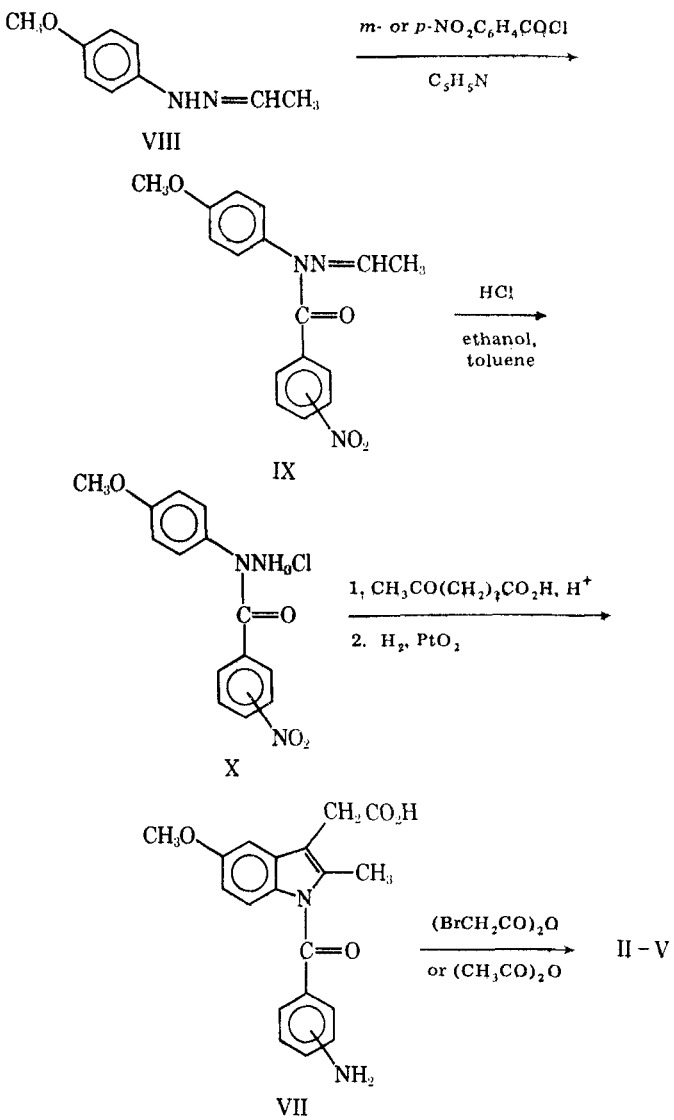

Scheme I

[7] One of the BMD series of programs available from the health sciences computing facility of the University of California at Los Angeles.

[8] Model 6400, Control Data Corp.

[9] This program for nonlinear least-squares fit was made available by Dr. R. F. Mais, Midwest Research Support Center, Veterans Administration Hospital, Hines, Ill.

[10] For the determination of acid dissociation constants, a Fisher Accumet model 220 pH meter was used with a standard combination electrode; spectra were obtained with a Zeiss model PMQ II spectrophotometer, using matched 1.0-cm quartz cells.

[11] Melting points were determined with a Thomas–Hoover capillary melting-point apparatus and are uncorrected. IR spectra were recorded with a Perkin-Elmer model 237B spectrophotometer. NMR spectra were recorded, using tetramethylsilane as the internal reference, with a Varian model T-60 spectrometer and, where indicated, with a Varian model HR-220 spectrometer, the latter at the 220 MHz NMR Center, Ontario Research Foundation, Sheridan Park, Ontario. Microanalyses were carried out by Dr. G. I. Robertson, Jr., Robertson Laboratory, Florham Park, N.J., and by Dr. H. Bieler, Organisch-Chemisches Institut, Vienna, Austria.

scribed for I (24, 25) and for certain 1-heteroaroyl analogs (25, 26), was used (Scheme I). The nitrobenzoylindoles (VI) so obtained were easily hydrogenated in the presence of platinum dioxide in tetrahydrofuran, giving the corresponding amines (VII). Hydrogenation did not proceed in anhydrous ether or dimethyl formamide. The amines were acylated in anhydrous acetone by bromoacetic anhydride or acetic anhydride to yield II–V.

Acetaldehyde p-*Methoxyphenylhydrazone* (*VIII*)—Compound VIII was prepared from *p*-methoxyphenylhydrazine hydrochloride (14 g, 80 moles) and acetaldehyde (6.6 g, 150 mmoles) by the method of Yamamoto (27). The yield was 10.1 g (76%), bp 120–124°/0.2 mm [lit. (27) bp 119–125°/0.2 mm]; IR (film): 3300, 1500, 1235, 1030, and 820 cm^{-1}.

Acetaldehyde N^1-p-*Nitrobenzoyl*-N^1-p-*methoxyphenylhydrazone* (*IX*a)—Powdered *p*-nitrobenzoyl chloride (9.6 g, 50 mmoles) was added in portions to a solution of VIII (7 g, 45 mmoles) in 60 ml of pyridine at 0–5° for 1.5 hr. After being stirred at ice-bath temperature for an additional 2.5 hr, the reaction mixture was poured into 500 ml of cold water. On standing overnight at 2–5°, precipitation occurred. The orange precipitate was isolated, washed with 100 ml of cold water, and dried *in vacuo* overnight. The product was obtained from ethylene glycol monomethyl ether as yellow crystals (12 g, 91%), mp 126–127.5°; IR (KBr): 1650 (C=O, tertiary amide), 1520, and 1340 (NO_2, aromatic) cm^{-1}; NMR (60 MHz) (dimethyl sulfoxide-d_6): δ 1.70 (d, 3, J = 5 Hz, CH_3CH), 3.75 (s, 3, CH_3O), 6.73 (q, 1, J = 5 Hz, CH_3CH), 7.18 (*AB*q, 4, J = 9 Hz, ArH), and 8.08 (*AB*q, 4, J = 9 Hz, benzoyl ArH) ppm.

Anal.—Calc. for $C_{16}H_{15}N_3O_4$: C, 61.34; H, 4.83; N, 13.41. Found: C, 61.37; H, 5.00; N, 13.29.

Acetaldehyde N^1-m-*Nitrobenzoyl*-N^1-p-*methoxyphenylhydrazone* (*IX*b)—Compound IX*b* was prepared in 90% yield by the method described for IX*a*. Recrystallized from 95% ethanol, the product had a melting point of 106°; IR (KBr): 1650 (C=O, tertiary amide), 1520, and 1340 (NO_2, aromatic) cm^{-1}; NMR (60 MHz) (dimethyl sulfoxide-d_6): δ 1.70 (d, 3, J = 5 Hz, CH_3CH), 3.76 (s, 3, CH_3O), 6.76 (q, 1, J = 5 Hz, CH_3CH), 7.20 (*AB*q, 4, J = 9 Hz, ArH), and 7.7–8.52 (m, 4, benzoyl ArH) ppm.

Anal.—Calc. for $C_{16}H_{15}N_3O_4$: C, 61.34; H, 4.83; N, 13.41. Found: C, 61.50; H, 5.00; N, 13.29.

N^1-p-*Nitrobenzoyl*-N^1-p-*methoxyphenylhydrazine Hydrochloride* (*X*a)—Gaseous hydrogen chloride was bubbled through a solution of IX*a* (5 g, 16 mmoles) in 99% ethanol (2 ml) and 27 ml of toluene below 5° for 15 min with stirring. Stirring was continued for an additional 2 hr at 0–5°. The precipitate was collected by filtration, washed with ether, and dried *in vacuo* overnight. The product was obtained from absolute ethanol as white needles (4.8 g, 92.8%), mp 183.5°; IR (KBr): 3000–2250 (NH^+), 1665 (tertiary amide), 1520, and 1340 (NO_2, aromatic) cm^{-1}; NMR (60 MHz) (dimethyl sulfoxide-d_6): δ 3.75 (s, 3, CH_3O), 7.22 (*AB*q, 4, J = 9 Hz, ArH), 7.92 (*AB*q, 4, J = 9 Hz, benzoyl ArH), and 9.77 (s, 3, NH_3^+) ppm.

Anal.—Calc. for $C_{14}H_{14}ClN_3O_4$: C, 51.94; H, 4.36; Cl, 10.95; N, 12.98. Found: C, 51.98; H, 4.50; Cl, 10.88; N, 13.01.

N^1-m-*Nitrobenzoyl*-N^1-p-*methoxyphenylhydrazine Hydrochloride* (*X*b)—Compound X*b* was prepared in 99% yield by the method described for X*a*. Recrystallized from absolute ethanol, the product had a melting point of 178–178.4°; IR (KBr): 3000–2250 (NH^+), 1665 (tertiary amide), 1520, and 1340 (NO_2, aromatic) cm^{-1}; NMR (60 MHz) (dimethyl sulfoxide-d_6): δ 3.80 (s, 3, CH_3O), 5.25 (H_2O), 7.26 (q, 4, J = 9 Hz, ArH), and 7.63–8.37 (m, 4, benzoyl ArH) ppm.

Anal.—Calc. for $C_{14}H_{14}ClN_3O_4$: C, 51.94; H, 4.36; Cl, 10.95; N, 12.98. Found: C, 52.19; H, 4.54; Cl, 10.79; N, 13.02.

5-Methoxy-2-methyl-1-(p-*nitrobenzoyl*)-*3-indolylacetic Acid* (*VI*a)—Compound X*a* (9.4 g, 29 mmoles) and levulinic acid (4.3 g, 37 mmoles) were stirred in 17 ml of acetic acid at 65° for 2 hr. The reaction mixture was allowed to stand at room temperature overnight, and the precipitate was collected by filtration. Then the precipitate was washed with 100 ml of water in three portions and dried *in vacuo* overnight. It was recrystallized from a solution of acetone and water. The greenish-yellow powder (8.1 g, 77%) had a melting point of 180–181°; IR (KBr): 1700 (CO_2H), 1670 (C=O, tertiary amide), 1520, and 1350 (NO_2, aromatic) cm^{-1}; NMR (60 MHz) (dimethyl sulfoxide-d_6): δ 2.13 (s, 3, indole-CH_3), 3.60 (s, 2, CH_2CO_2H), 3.73 (s, 3, CH_3O), 6.63 (split d, *ABC*, 1, J = 2.5, 9.0 Hz, indole-6-H), 6.95–7.15 (m, *ABC*, 2, indole-4, 7-H), and 8.11 (*AB*q, 4, J = 9 Hz, benzoyl ArH) ppm.

Anal.—Calc. for $C_{19}H_{16}N_2O_6$: C, 61.95; H, 4.38; N, 7.61. Found: C, 62.04; H, 4.61; N, 7.57.

5-Methoxy-2-methyl-1-(m-*nitrobenzoyl*)-*3-indolylacetic Acid* (*VI*b)—Compound VI*b* was prepared in 76% yield by the method described for VI*a*. The product was recrystallized from acetone in the form of a greenish-yellow powder, mp 191–191.7°; IR (KBr): 1700 (CO_2H), 1670 (C=O, tertiary amide), 1520, and 1350 (NO_2, aromatic) cm^{-1}; NMR (60 MHz) (dimethyl sulfoxide-d_6): 2.23 (s, 3, indole-CH_3), 3.70 (s, 2, CH_2CO_2H), 3.78 (s, 3, CH_3O), 6.72 (split d, *ABC*, 1, J = 2.5, 9.0 Hz, indole-6H), 7.07 (d, *ABC*, 1, J = 9.0 Hz, indole-7H), 7.10 (d, *ABC*, 1, J = 2.5 Hz, indole-4-H), and 7.70–8.67 (m, 4, benzoyl ArH) ppm.

Anal.—Calc. for $C_{19}H_{16}N_2O_6$: C, 61.95; H, 4.38; N, 7.61. Found: C, 62.15; H, 4.65; N, 7.50.

1-(p-*Aminobenzoyl*)-*5-methoxy-2-methyl-3-indolylacetic Acid* (*VII*a)—By means of a Parr hydrogenator, VI*a* (15.0 g, 41 mmoles) in 100 ml of tetrahydrofuran was hydrogenated in the presence of platinum oxide (0.28 g) at 25° for 24 hr. The reaction mixture was filtered with the use of a filtering aid[12], and the solvent was removed by evaporation under reduced pressure. A light-yellow powder was obtained and recrystallized from 95% ethanol. The product was in the form of a milky-colored powder (14.0 g, 94.1%), mp 193.5–194.5°; IR (KBr): 3420, 3340 (NH stretching), 1700 (CO_2H), 1670 (C=O, tertiary amide), and 1650 (NH bending) cm^{-1}; NMR (220 MHz) (dimethyl sulfoxide-d_6): δ 2.28 (s, 3, indole-CH_3), 3.66 (s, 2, CH_2CO_2H), 3.75 (s, 3, CH_3O), 6.3 (s, 2, NH_2), 6.36 (d, 2, J = 9 Hz, benzoyl-*m*-H), 6.43 (split d, *ABC*, 1, J = 2.5, 9.0 Hz, indole-6-H), 6.85 (d, *ABC*, 1, J = 9 Hz, indole-7-H), 6.98 (d, *ABC*, 1, J = 2.5 Hz, indole-4H), and 7.36 (d, 2, J = 9 Hz, benzoyl-*o*-H) ppm.

Anal.—Calc. for $C_{19}H_{18}N_2O_4$: C, 67.44; H, 5.36; N, 8.28. Found: C, 67.32; H, 4.95; N, 8.02.

1-(m-*Aminobenzoyl*)-*5-methoxy-2-methyl-3-indolylacetic Acid* (*VII*b)—Compound VII*b* was obtained in 92.0% yield by the method described for VII*a*. The product was recrystallized from benzene–chloroform in the form of yellowish-white crystals, mp 164–165°; IR (KBr): 3430, 3330 (NH stretching), 1705 (CO_2H), 1665 (C=O, tertiary amide), and 1650 (NH bending) cm^{-1}; NMR (60 MHz) (dimethyl sulfoxide-d_6): δ 2.30 (s, 3, indole-CH_3), 3.66 (s, 2, CH_2CO_2H), 3.78 (s, CH_3O), and 6.60–7.38 (m, 9, NH_2, ArH) ppm.

Anal.—Calc. for $C_{19}H_{18}N_2O_4$: C, 67.44; H, 5.36; N, 8.28. Found: C, 67.05; H, 5.36; N, 7.93.

1-(p-*Bromoacetamidobenzoyl*)-*5-methoxy-2-methyl-3-indolylacetic Acid* (*II*) (*Method A*)—Bromoacetic anhydride (0.80 g, 2.9 mmoles) in 20 ml of anhydrous acetone was added all at once to a solution of VII*a* (1.0 g, 2.9 mmoles) in 80 ml of anhydrous acetone. The reaction mixture was stirred at room temperature for 20 hr. On evaporating the solvent under reduced pressure, a milky-colored solid was collected. The product was obtained from aqueous ethanol as a white powder (1.2 g, 90%), mp 208°; IR (KBr): 3440 (NH), 1710 (CO_2H), 1680 (C=O, secondary amide), and 1670 (C=O, tertiary amide) cm^{-1}; NMR (220 MHz) (dimethyl sulfoxide-d_6): δ 2.25 (s, 3, indole-CH_3), 3.66 (s, 2, CH_2CO_2H), 3.75 (s, 3, CH_3O), 4.08 (s, 2, $COCH_2Br$), 6.70 (split d, *ABC*, 1, J = 2.5, 9.0 Hz, indole-6-H), 6.85 (d, *ABC*, 1, J = 9.0 Hz, indole-7-H), 7.01 (d, *ABC*, 1, J = 2.5 Hz, indole-4-H), and 7.70 (*AB*q, 4, J = 9.0 Hz, benzoyl ArH) ppm.

Anal.—Calc. for $C_{21}H_{19}BrN_2O_5$: C, 54.91; H, 4.17; Br, 17.40; N, 6.10. Found: C, 54.78; H, 4.36; Br, 17.00; N, 5.87.

1-(p-*Bromoacetamidobenzoyl*)-*5-methoxy-2-methyl-3-indolylacetic Acid* (*II*) (*Method B*)—Bromoacetyl bromide was used in place of the anhydride, giving II identical with that obtained by Method A but in lower yield. A considerable quantity of the hydrobromide salt of VII*a* formed, from which VII*a* was recovered on treatment with potassium bicarbonate followed by extraction with chloroform. Attempts to protect VII*a* from salt formation by carrying out the reaction in the presence of triethylamine failed to yield any II.

1-(m-*Bromoacetamidobenzoyl*)-*5-methoxy-2-methyl-3-indolylacetic Acid* (*IV*)—Compound IV was prepared in 77.6% yield from VII*b* by Method A. The product was recrystallized from benzene–chloroform in the form of a milky-colored powder, mp 130°; IR (KBr): 3440 (NH), 1710 (CO_2H), 1680 (C=O, secondary amide), and 1670 (C=O, tertiary amide) cm^{-1}; NMR (60 MHz) (dimethyl sulfoxide-d_6): δ 2.25 (s, 3, indole-CH_3), 3.67 (s, 2, CH_2CO_2H), 3.78 (s, 3, CH_3O), 4.05 (s, 2, $COCH_2Br$), 6.77–7.13 (m, 3, indole-H), and 7.40–7.95 (m, 4, benzoyl ArH) ppm.

Anal.—Calc. for $C_{21}H_{19}BrN_2O_5$: C, 54.91; H, 4.17; N, 6.10. Found: C, 54.73; H, 4.37; N, 5.93.

1-(p-*Acetamidobenzoyl*)-*5-methoxy-2-methyl-3-indolylacetic Acid* (*III*)—Compound III was prepared in 87.5% yield from VII*a* and acetic anhydride by Method A. Recrystallized from benzene–chloroform, the product had a melting point of 210°; IR (KBr): 3440 (NH), 1710 (CO_2H), 1670 (C=O, secondary amide), and 1650 (C=O, tertiary amide) cm^{-1}; NMR (60 MHz) (dimethyl sulfoxide-d_6): δ 2.05 (s, 3, $COCH_3$), 2.20 (s, 3, indole-CH_3), 3.64 (s, 2, CH_2CO_2H), 3.75 (s, 3, CH_3O), 6.67 (m, 1, indole-

[12] Hyflo Super Cel, Fisher Scientific Co., Fair Lawn, N.J.

6-H), 6.77 (m, 1, indole-7-H), 6.93 (m, 1, indole-4-H), and 7.65 (*AB*q, 4, benzoyl ArH) ppm; pKa 4.11.

Anal.—Calc. for $C_{21}H_{20}N_2O_5$: C, 66.30; H, 5.30; N, 7.37. Found: C, 66.25; H, 5.38; N, 7.31.

1-(m-Acetamidobenzoyl)-5-methoxy-2-methyl-3-indolylacetic Acid (V)—Compound V was prepared in 77.8% yield from VII*b* and acetic anhydride by Method A. Recrystallized from benzene–chloroform, the product had a melting point of 135°; IR (KBr): 3440 (NH), 1710 (CO_2H), 1670 (C=O, secondary amide), and 1650 (C=O, tertiary amide) cm^{-1}; NMR (60 MHz) (dimethyl sulfoxide-d_6): δ 2.07 (s, 3, $COCH_3$), 2.25 (s, 3, indole-CH_3), 3.67 (s, 2, CH_2CO_2H), 3.80 (s, 3, CH_3O), 6.63–7.13 (m, 3, indole-H), and 7.33–7.97 (m, 4, benzoyl ArH) ppm.

Anal.—Calc. for $C_{21}H_{20}N_2O_5$: C, 66.30; H, 5.30; N, 7.37. Found: C, 65.80; H, 5.34; N, 7.29.

Reactivity of II and IV toward L-Tryptophan—L-Tryptophan was shaken at 37° for 24 hr with an equimolar quantity of II or IV in 67 m*M* phosphate buffer (pH 7.4). TLC revealed no products of reaction between either II or IV and L-tryptophan.

REFERENCES

(1) J. N. McArthur, P. D. Dawkins, M. J. H. Smith, and E. B. D. Hamilton, *Br. Med. J.*, **2**, 677 (1971).

(2) J. N. McArthur, P. D. Dawkins, and M. J. H. Smith, *J. Pharm. Pharmacol.*, **23**, 393 (1971).

(3) *Ibid.*, **23**, 451 (1971).

(4) M. Aylward and J. Maddock, *J. Pharm. Pharmacol.*, **25**, 570 (1973).

(5) M. Aylward and J. Maddock, *IRCS Libr. Compend.*, **2**, 1143 (1974); through *Chem. Abstr.*, **82**, 51374a (1975).

(6) C. W. Denko, D. B. Purser, and R. M. Johnson, *Arthritis Rheum.*, **13**, 311 (1970).

(7) C. W. Denko, D. B. Purser, and R. M. Johnson, *Clin. Chem.*, **16**, 54 (1970).

(8) J. N. McArthur, *J. Rheumatol.*, **1**, 241 (1974).

(9) J. N. McArthur, M. J. H. Smith, and E. B. D. Hamilton, *Br. Med. J.*, **4**, 230 (1971).

(10) J. N. McArthur, M. J. H. Smith, and P. C. Freeman, *J. Pharm. Pharmacol.*, **24**, 669 (1972).

(11) R. H. McMenamy and J. L. Oncley, *J. Biol. Chem.*, **233**, 1436 (1958).

(12) R. H. McMenamy and R. H. Seder, *ibid.*, **238**, 3241 (1963).

(13) J. Krasner and R. H. McMenamy, *ibid.*, **241**, 4186 (1966).

(14) J. Steinhardt and J. A. Reynolds, "Multiple Equilibria in Proteins," Academic, New York, N.Y., 1969, p. 46.

(15) B. R. Baker, "Design of Active-Site-Directed Irreversible Enzyme Inhibitors," Wiley, New York, N.Y., 1967, p. 190.

(16) K. K. Gambhir and R. H. McMenamy, *J. Biol. Chem.*, **248**, 1956 (1973).

(17) B. R. Baker, "Design of Active-Site-Directed Irreversible Enzyme Inhibitors," Wiley, New York, N.Y., 1967, p. 20.

(18) R. N. Pinckard, D. Hawkins, and R. S. Farr, *Arthritis Rheum.*, **13**, 361 (1970).

(19) C. F. Chignell and D. K. Starkweather, *Mol. Pharmacol.*, **7**, 229 (1971).

(20) O. H. Lowry, N. J. Rosebrough, L. Farr, and R. J. Randall, *J. Biol. Chem.*, **193**, 265 (1951).

(21) G. Scatchard, *Ann. N.Y. Acad. Sci.*, **51**, 660 (1949).

(22) G. W. Snedecor and W. G. Cochran, "Statistical Methods," Iowa State University Press, Ames, Iowa, 1967, pp. 432–435.

(23) A. Albert and E. P. Serjeant, "Ionization Constants of Acids and Bases," Wiley, New York, N.Y., 1962, pp. 16–42.

(24) H. Yamamoto, *Chem. Pharm. Bull.*, **16**, 17 (1968).

(25) H. Yamamoto, Nishinomiya-shi, and M. Nakao, U.S. pat. 3,629,284 (1971).

(26) H. Yamamoto, M. Nakao, and T. Okamoto, *Chem. Pharm. Bull.*, **16**, 1927 (1968).

(27) H. Yamamoto, *J. Org. Chem.*, **32**, 3693 (1967).

ACKNOWLEDGMENTS AND ADDRESSES

Received October 6, 1975, from the *College of Pharmacy, Dalhousie University, Halifax, Nova Scotia, Canada B3H 3J5.*

Accepted for publication September 1, 1976.

Presented at the Canadian Federation of Biological Societies, 17th Annual Meeting, Hamilton, Ontario, June 1974.

Abstracted from a thesis submitted by E. M. K. Lui to Dalhousie University in partial fulfillment of the Master of Science degree requirements.

Grateful acknowledgment is made to Geigy (Canada) Ltd. and to Warner–Lambert Canada Ltd. for graduate research scholarships to E. M. K. Lui and to Merck Sharp and Dohme Canada Ltd. for indomethacin.

* Present address: Department of Pharmacology, Faculty of Medicine, Dalhousie University, Halifax, Nova Scotia, Canada B3H 3J5.

ˣ To whom inquiries should be directed.

Rectal Absorption of Nitrofurantoin

EUGENE L. PARROTT ˣ and LLOYD E. MATHESON, Jr.

Abstract □ The absorption in humans of nitrofurantoin from seven suppository bases was studied using urinary excretion measurements. Rectal absorption was poorer than GI absorption. The administration of 400 mg of nitrofurantoin in a polyethylene glycol–polysorbate 80 suppository base and in a polyethylene glycol–silica suppository base provided an adequate urinary concentration of nitrofurantoin. Persons who cannot tolerate orally administered nitrofurantoin due to gastric upset could receive nitrofurantoin therapy rectally.

Keyphrases □ Nitrofurantoin—rectal absorption, effect of various suppository bases, humans □ Absorption, rectal—nitrofurantoin, effect of various suppository bases, humans □ Antibacterials, urinary—nitrofurantoin, rectal absorption, effect of various suppository bases, humans

Nitrofurantoin is an antibacterial agent used widely in the treatment of urinary tract infections (1). Between 30 and 50% of an oral or intravenous dose can be recovered intact from the urine (2). The efficacy of nitrofurantoin depends on attaining an adequate concentration of drug in the urine.

Patients receiving nitrofurantoin may exhibit emesis and be deprived of an effective medication. Macrocrystals of nitrofurantoin improved GI tolerance without interfering with clinical efficacy (3). An optimal average crystal size of 150 mesh (80–200-mesh size fraction) reduced the incidence of emesis while still permitting ample urinary excretion for efficacy (4). The larger crystals dissolved more slowly than the smaller crystals and, since dissolution is the rate-limiting step for slightly soluble drugs, nitrofurantoin absorption was slower.

The purpose of this study was to investigate the rectal absorption of nitrofurantoin and to determine if nitrofurantoin could be administered in a suppository to per-

6-H), 6.77 (m, 1, indole-7-H), 6.93 (m, 1, indole-4-H), and 7.65 (*AB*q, 4, benzoyl ArH) ppm; pKa 4.11.

Anal.—Calc. for $C_{21}H_{20}N_2O_5$: C, 66.30; H, 5.30; N, 7.37. Found: C, 66.25; H, 5.38; N, 7.31.

1-(m-Acetamidobenzoyl)-5-methoxy-2-methyl-3-indolylacetic Acid (V)—Compound V was prepared in 77.8% yield from VII*b* and acetic anhydride by Method A. Recrystallized from benzene–chloroform, the product had a melting point of 135°; IR (KBr): 3440 (NH), 1710 (CO_2H), 1670 (C=O, secondary amide), and 1650 (C=O, tertiary amide) cm^{-1}; NMR (60 MHz) (dimethyl sulfoxide-d_6): δ 2.07 (s, 3, $COCH_3$), 2.25 (s, 3, indole-CH_3), 3.67 (s, 2, CH_2CO_2H), 3.80 (s, 3, CH_3O), 6.63–7.13 (m, 3, indole-H), and 7.33–7.97 (m, 4, benzoyl ArH) ppm.

Anal.—Calc. for $C_{21}H_{20}N_2O_5$: C, 66.30; H, 5.30; N, 7.37. Found: C, 65.80; H, 5.34; N, 7.29.

Reactivity of II and IV toward L-Tryptophan—L-Tryptophan was shaken at 37° for 24 hr with an equimolar quantity of II or IV in 67 m*M* phosphate buffer (pH 7.4). TLC revealed no products of reaction between either II or IV and L-tryptophan.

REFERENCES

(1) J. N. McArthur, P. D. Dawkins, M. J. H. Smith, and E. B. D. Hamilton, *Br. Med. J.*, **2**, 677 (1971).

(2) J. N. McArthur, P. D. Dawkins, and M. J. H. Smith, *J. Pharm. Pharmacol.*, **23**, 393 (1971).

(3) *Ibid.*, **23**, 451 (1971).

(4) M. Aylward and J. Maddock, *J. Pharm. Pharmacol.*, **25**, 570 (1973).

(5) M. Aylward and J. Maddock, *IRCS Libr. Compend.*, **2**, 1143 (1974); through *Chem. Abstr.*, **82**, 51374a (1975).

(6) C. W. Denko, D. B. Purser, and R. M. Johnson, *Arthritis Rheum.*, **13**, 311 (1970).

(7) C. W. Denko, D. B. Purser, and R. M. Johnson, *Clin. Chem.*, **16**, 54 (1970).

(8) J. N. McArthur, *J. Rheumatol.*, **1**, 241 (1974).

(9) J. N. McArthur, M. J. H. Smith, and E. B. D. Hamilton, *Br. Med. J.*, **4**, 230 (1971).

(10) J. N. McArthur, M. J. H. Smith, and P. C. Freeman, *J. Pharm. Pharmacol.*, **24**, 669 (1972).

(11) R. H. McMenamy and J. L. Oncley, *J. Biol. Chem.*, **233**, 1436 (1958).

(12) R. H. McMenamy and R. H. Seder, *ibid.*, **238**, 3241 (1963).

(13) J. Krasner and R. H. McMenamy, *ibid.*, **241**, 4186 (1966).

(14) J. Steinhardt and J. A. Reynolds, "Multiple Equilibria in Proteins," Academic, New York, N.Y., 1969, p. 46.

(15) B. R. Baker, "Design of Active-Site-Directed Irreversible Enzyme Inhibitors," Wiley, New York, N.Y., 1967, p. 190.

(16) K. K. Gambhir and R. H. McMenamy, *J. Biol. Chem.*, **248**, 1956 (1973).

(17) B. R. Baker, "Design of Active-Site-Directed Irreversible Enzyme Inhibitors," Wiley, New York, N.Y., 1967, p. 20.

(18) R. N. Pinckard, D. Hawkins, and R. S. Farr, *Arthritis Rheum.*, **13**, 361 (1970).

(19) C. F. Chignell and D. K. Starkweather, *Mol. Pharmacol.*, **7**, 229 (1971).

(20) O. H. Lowry, N. J. Rosebrough, L. Farr, and R. J. Randall, *J. Biol. Chem.*, **193**, 265 (1951).

(21) G. Scatchard, *Ann. N.Y. Acad. Sci.*, **51**, 660 (1949).

(22) G. W. Snedecor and W. G. Cochran, "Statistical Methods," Iowa State University Press, Ames, Iowa, 1967, pp. 432–435.

(23) A. Albert and E. P. Serjeant, "Ionization Constants of Acids and Bases," Wiley, New York, N.Y., 1962, pp. 16–42.

(24) H. Yamamoto, *Chem. Pharm. Bull.*, **16**, 17 (1968).

(25) H. Yamamoto, Nishinomiya-shi, and M. Nakao, U.S. pat. 3,629,284 (1971).

(26) H. Yamamoto, M. Nakao, and T. Okamoto, *Chem. Pharm. Bull.*, **16**, 1927 (1968).

(27) H. Yamamoto, *J. Org. Chem.*, **32**, 3693 (1967).

ACKNOWLEDGMENTS AND ADDRESSES

Received October 6, 1975, from the *College of Pharmacy, Dalhousie University, Halifax, Nova Scotia, Canada B3H 3J5.*

Accepted for publication September 1, 1976.

Presented at the Canadian Federation of Biological Societies, 17th Annual Meeting, Hamilton, Ontario, June 1974.

Abstracted from a thesis submitted by E. M. K. Lui to Dalhousie University in partial fulfillment of the Master of Science degree requirements.

Grateful acknowledgment is made to Geigy (Canada) Ltd. and to Warner–Lambert Canada Ltd. for graduate research scholarships to E. M. K. Lui and to Merck Sharp and Dohme Canada Ltd. for indomethacin.

* Present address: Department of Pharmacology, Faculty of Medicine, Dalhousie University, Halifax, Nova Scotia, Canada B3H 3J5.

ˣ To whom inquiries should be directed.

Rectal Absorption of Nitrofurantoin

EUGENE L. PARROTT ˣ and LLOYD E. MATHESON, Jr.

Abstract □ The absorption in humans of nitrofurantoin from seven suppository bases was studied using urinary excretion measurements. Rectal absorption was poorer than GI absorption. The administration of 400 mg of nitrofurantoin in a polyethylene glycol–polysorbate 80 suppository base and in a polyethylene glycol–silica suppository base provided an adequate urinary concentration of nitrofurantoin. Persons who cannot tolerate orally administered nitrofurantoin due to gastric upset could receive nitrofurantoin therapy rectally.

Keyphrases □ Nitrofurantoin—rectal absorption, effect of various suppository bases, humans □ Absorption, rectal—nitrofurantoin, effect of various suppository bases, humans □ Antibacterials, urinary—nitrofurantoin, rectal absorption, effect of various suppository bases, humans

Nitrofurantoin is an antibacterial agent used widely in the treatment of urinary tract infections (1). Between 30 and 50% of an oral or intravenous dose can be recovered intact from the urine (2). The efficacy of nitrofurantoin depends on attaining an adequate concentration of drug in the urine.

Patients receiving nitrofurantoin may exhibit emesis and be deprived of an effective medication. Macrocrystals of nitrofurantoin improved GI tolerance without interfering with clinical efficacy (3). An optimal average crystal size of 150 mesh (80–200-mesh size fraction) reduced the incidence of emesis while still permitting ample urinary excretion for efficacy (4). The larger crystals dissolved more slowly than the smaller crystals and, since dissolution is the rate-limiting step for slightly soluble drugs, nitrofurantoin absorption was slower.

The purpose of this study was to investigate the rectal absorption of nitrofurantoin and to determine if nitrofurantoin could be administered in a suppository to per-

Table I—Formulas for Suppositories Containing 400 mg of Nitrofurantoin

Formula	Ingredient	Amount, g
B	Theobroma oil[a]	1.40
K	Lecithin and dried whey[b]	0.50
	Theobroma oil	1.00
D	Polyoxyethylene 4 sorbitan monostearate[c]	1.57
	Glyceryl monolaurate[d]	0.17
B-7	Polyethylene glycol 1540[e]	0.70
	Polyethylene glycol 6000	0.97
	Polyethylene glycol 400	0.42
C	Polyethylene glycol 1540	0.66
	Polyethylene glycol 6000	0.92
	Polyethylene glycol 400	0.40
	Sodium bicarbonate	0.14
L	Polyethylene glycol 1540	0.66
	Polyethylene glycol 6000	0.92
	Polyethylene glycol 400	0.40
	Colloidal silica[f]	
T	Polyethylene glycol 1540	0.66
	Polyethylene glycol 6000	0.92
	Polyethylene glycol 400	0.40
	Polysorbate 80[g]	0.20

[a] Hershey's. [b] Leciflow, Kraftco Corp. [c] Tween 61, ICI United States Inc. [d] Aldo MLD, Glyco Chemicals. [e] Carbowax, Union Carbide Chemicals. [f] Cab-O-Sil, G.L. Cabot Corp. [g] Tween 80, ICI United States Inc.

sons who otherwise would be deprived of nitrofurantoin therapy because of GI intolerance.

EXPERIMENTAL

Dosage Forms—Nitrofurantoin[1] was classified by a sonic sifter[2], and the 230–325-mesh size fraction (53 μm) was used throughout the experiment. Two hundred milligrams of nitrofurantoin without excipients was placed in a No. 2 gelatin capsule.

The formulations for the suppositories are given in Table I. The suppositories were prepared by the cold compress method[3] when feasible; suppositories containing polyethylene glycols were prepared by the fusion method. For Formula L, the powder to be incorporated into the suppository base was prepared by dissolving the nitrofurantoin in alcohol, suspending the silica in the liquid, and evaporating the solvent in a stream of air. The solid, which consisted of 20% silica and 80% nitrofurantoin, was then passed through a 100-mesh screen (5).

The percent of nitrofurantoin dissolved from the dosage form was determined using the USP disintegration apparatus. The dosage form was placed in the apparatus and held in a single glass cylinder by means of plastic tubing bent in the upper end of the cylinder to prevent the escape of the dosage form. The disintegration apparatus operated in 16 liters of distilled water at 37° contained in a 30 × 30-cm cylindrical jar. Samples were removed by a pipet fitted with a sintered-glass filter. The samples were analyzed, and the percent dissolved at each interval of time was calculated (Fig. 1).

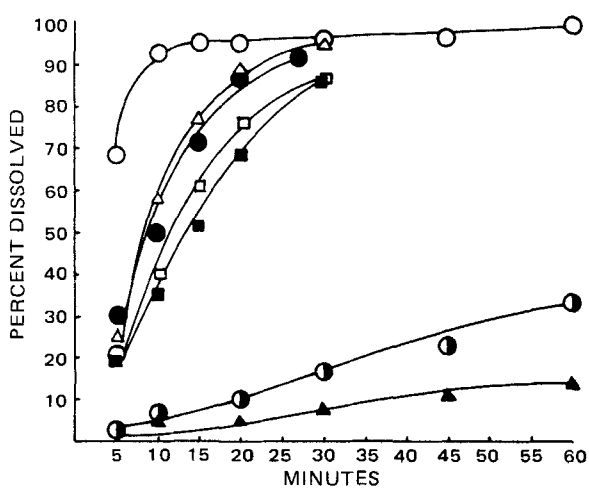

Figure 1—*Dissolution profiles in 16 liters of water at 37° of 400 mg of nitrofurantoin from several dosage forms. Key: ○, gelatin capsule; △, polyethylene glycol–sodium bicarbonate; ●, polyethylene glycol; □, polyethylene glycol–polysorbate 80; ■, polyethylene glycol–silica; ◑, lecithin and dried whey; and ▲, theobroma oil.*

[1] Sigma lot 43C-1550.
[2] Allen-Bradley.
[3] Apfelbaum machine.

Table II—Dosage Forms Administered to Subjects

Subject	Dosage
EP	400 mg po; 400 mg in five suppository bases (T, L, C, B, and D); 65 mg po
RW	400 mg po; 400 mg in two suppository bases (T and B-7)
SB	400 mg po; 400 mg in two suppository bases (T and B-7)
MS	400 mg po; 400 mg in two suppository bases (T and B)
SK	400 mg po; 400 mg in two suppository bases (K and B)
KS	400 mg po; 400 mg in two suppository bases (L and B-7)
TI	400 mg po; 400 mg in two suppository bases (L and B)

Analytical Method—The analysis of the urine samples was carried out by the method of Conklin and Hollifield (6) on the day of collection. To protect the nitrofurantoin from light, amber glassware was used.

Protocol—Seven healthy male human subjects, 25–51 years old and 62–77 kg, were studied. Four hundred milligrams of nitrofurantoin in gelatin capsules was administered orally after arising and voiding the bladder. Subjects were ambulatory and ingested food as desired. It was recommended that a minimum of 150 ml of water be ingested hourly.

Urine samples were collected at 1-hr intervals for 14 hr. Volumes were measured, and aliquots were retained in amber vials for analysis. The pH of the urine was determined at the time of each sample collection and ranged from 5 to 7.5. No attempt was made to control the urinary pH.

After 1 week, a suppository containing the same dose of nitrofurantoin was administered rectally, and the urine samples were collected according to the protocol. All suppositories were identified by code, and the drug was not identified for the subjects. After another week, a suppository containing the same dose of nitrofurantoin in a different suppository base was administered rectally, and the urine samples were collected according to the protocol. Each subject served as his control in the comparison of the urinary excretion of the drug from the oral and rectal administrations. Subjects received nitrofurantoin according to the schedule of dosage forms given in Table II.

RESULTS AND DISCUSSION

For the seven subjects, the fraction of the 400-mg oral dose of nitrofurantoin recovered in the urine in 24 hr ranged from 0.22 to 0.54, with

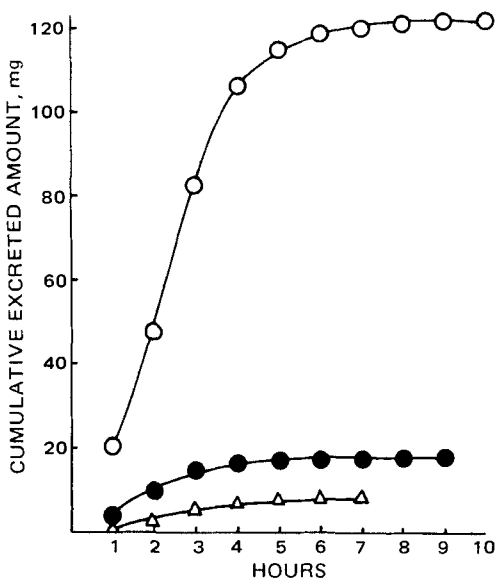

Figure 2—*Cumulative amount of nitrofurantoin excreted in the urine after oral and rectal administrations as a function of time. Key: ○, 400 mg po in a capsule; ●, 65 mg po in a capsule; and △, 400 mg rectally in theobroma oil.*

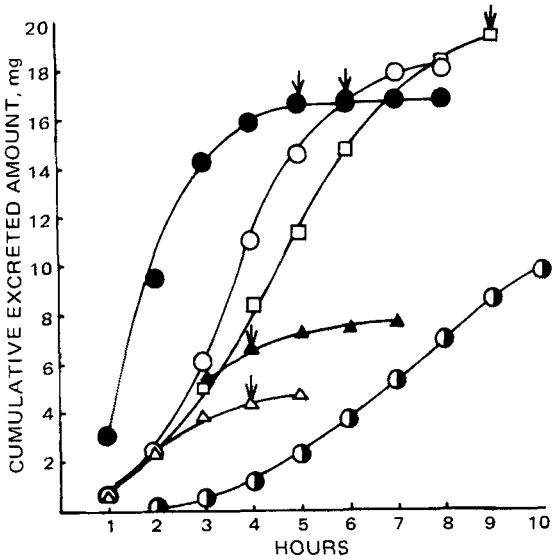

Figure 3—*Cumulative amount of nitrofurantoin excreted in the urine of Subject EP after oral and rectal administrations as a function of time. Key: ↓, latest urine sample having a concentration exceeding 1:100,000; ●, 65 mg po in a capsule; ○, polyethylene glycol–polysorbate 80; □, polyethylene glycol–silica; △, polyethylene glycol–sodium bicarbonate; ▲, theobroma oil; and ◑, sorbitan monostearate–glyceryl monolaurate.*

an average of 0.39. Nitrofurantoin is bacteriostatic in concentrations as low as 1:100,000–1:200,000 (7). A nitrofurantoin concentration of approximately 30 μg/ml (1:40,000) reportedly will eradicate at least 90% of the strains of *Escherichia coli* (8). In the seven subjects studied, the concentration of nitrofurantoin exceeded 1:40,000 for 7–9 hr, with an average of 8.6 hr, after a single oral administration of 400 mg of nitrofurantoin.

Nitrofurantoin frequently causes nausea and/or emesis. In this study, the administration of a single oral 400-mg dose of nitrofurantoin caused gastric upset in four of eight subjects (one subject withdrew). Rectal administration of 400 mg of nitrofurantoin provided poor absorption (Fig. 2); however, even though the fraction of the dose recovered in the urine was 0.02, the concentration of the nitrofurantoin in the urine exceeded 1:100,000 for 4 hr after insertion of the suppository. This result suggested that the administration of a large dose (400 mg) in a suitable suppository base might provide an adequate bacteriostatic concentration in the urine without gastric upset from three or four daily insertions.

In the preliminary stage, five suppository bases were used to administer 400 mg of nitrofurantoin rectally to Subject EP. The cumulative amount excreted and the concentration in the urine were compared to the amount

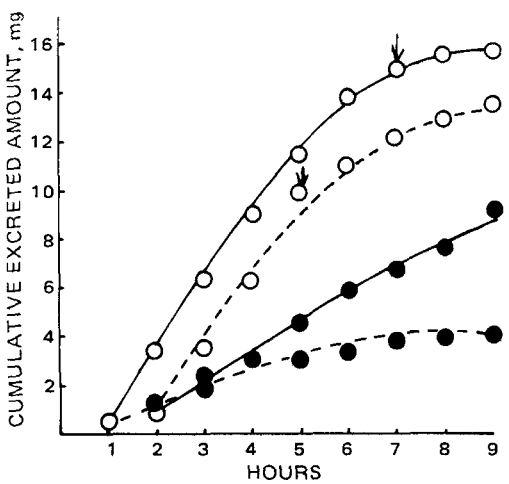

Figure 4—*Comparison of effect of suppository formulation on cumulative amount of nitrofurantoin excreted. Key: ↓, latest urine sample having a concentration exceeding 1:100,000; ○, polyethylene glycol–polysorbate 80; ●, polyethylene glycol; —, Subject RW; and - - -, Subject SB.*

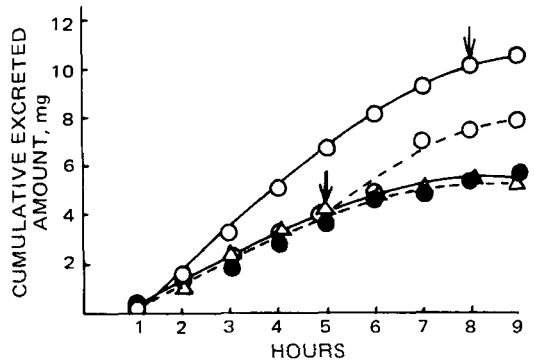

Figure 5—*Comparison of effect of suppository formulation on cumulative amount of nitrofurantoin excreted. Key: ↓, latest urine sample having a concentration exceeding 1:100,000; ○, polyethylene glycol–silica; ●, polyethylene glycol; △, theobroma oil; —, Subject KS; and - - -, Subject TI.*

and concentration after the administration of 65 mg of nitrofurantoin orally (Fig. 3). Formulas B, C, and D were unsatisfactory. Formulas L and T provided approximately 5% recovery of the administered dose in the urine, with the maximum amount released in the 4th hr of urine collection. The concentration of nitrofurantoin in the urine was 1:32,000 in the 6-hr collection with the polyethylene glycol–polysorbate 80 base (Formula T) and 1:34,000 in the 9-hr collection with the polyethylene glycol–silica base (Formula L).

For Subjects RW and SB 9 hr after administration, 1.7 and 3.3 times as much nitrofurantoin were eliminated in the urine from Formula T as from the polyethylene glycol base (Formula B-7) (Fig. 4), respectively. The amount of nitrofurantoin absorbed from the polyethylene glycol base was not sufficient to provide a bacteriostatic concentration. The amount of nitrofurantoin absorbed from the polyethylene glycol–polysorbate 80 base provided a concentration exceeding 1:100,000 until at least the 5th hr after insertion in Subjects EP, RW, and SB.

The volume of fluid in the rectum is only several milliliters. As a consequence of the limited fluid and the very slight solubility of nitrofurantoin, only a small part of the 400 mg administered rectally is dissolved. Thus, the apparently poor rectal absorption of nitrofurantoin is probably due to the severe restrictions on dissolution of the drug from the suppository base. The addition of a surface-active agent to a dosage form containing a hydrophobic drug often increases dissolution (9–12). With Formula T, polysorbate 80 reduced interfacial tension and thereby promoted wetting and/or deaggregation of nitrofurantoin.

For Subject KS 9 hr after administration, 1.8 times as much nitrofurantoin was eliminated in the urine from the polyethylene glycol–silica base (Formula L) as from the polyethylene glycol base (Formula B-7) (Fig. 5). With the latter, the concentration of nitrofurantoin in the urine exceeded 1:40,000 for only 1 hr. The concentration exceeded 1:40,000 for 6 hr after the insertion of a polyethylene glycol–silica base suppository. A similar elimination pattern is shown in Fig. 3. For Subject TI 9 hr after administration, 1.5 times as much nitrofurantoin was eliminated in the urine from Formula L as from the theobroma oil base (Formula B) suppository (Fig. 5).

If a hydrophobic drug is dispersed by means of a volatile organic solvent onto the surface of fumed silicon dioxide and then the mixture is dried, the resulting small size of the drug and the concomitant increase in surface area greatly increase the surface available for contact with the dissolution medium. Thus, adsorbents facilitate the dissolution process of relatively insoluble drugs (5).

In Subject MS, the amount of nitrofurantoin eliminated in the urine

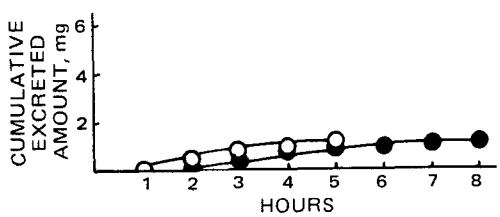

Figure 6—*Comparison of effect of suppository formulation on cumulative amount of nitrofurantoin excreted in Subject MS. Key: ○, polyethylene glycol–polysorbate 80; and ●, theobroma oil.*

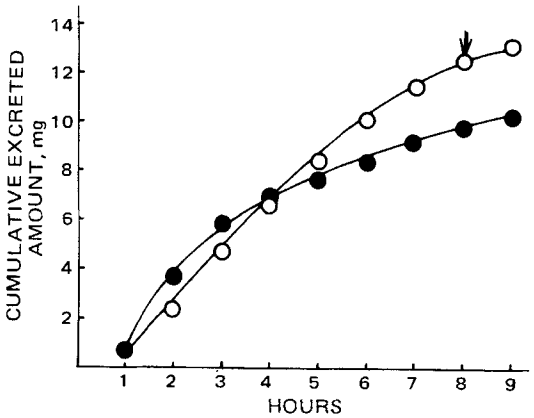

Figure 7—*Comparison of effect of suppository formulation of cumulative amount of nitrofurantoin excreted in Subject SK. Key: ○, lecithin and dried whey product; and ●, theobroma oil.*

from Formula T was greater than that from Formula B (Fig. 6); however, in this subject, both bases provided an adequate bacteriostatic concentration in the urine.

The amount of nitrofurantoin released from Formula D (Fig. 3) was so small that further investigation was not attempted.

Formula K provided a slightly greater amount of nitrofurantoin in the urine than the theobroma oil base suppository (Fig. 7). The dissolution profile of the theobroma oil base suppository suggested poor bioavailability, which was confirmed by *in vivo* data. In water at body temperature, the nitrofurantoin–theobroma oil suppository melted and formed a tacky mass from which the nitrofurantoin was slowly dissolved. With the limited fluid in the rectum, dissolution of the nitrofurantoin from the tacky mass was a very slow process. By mixing a lecithin and dried whey product with theobroma oil, it was hoped that the surface activity of the lecithin and the water solubility of the whey might enhance nitrofurantoin release. In measuring the dissolution profile, it was noticed that the mass was not tacky and that the release was slightly faster. Similarly, in the *in vivo* test, the amount of nitrofurantoin eliminated in the urine was slightly greater than that from the theobroma oil base.

SUMMARY

The usual adult dose of nitrofurantoin is 50–100 mg four times a day. If doses of nitrofurantoin several times the usual oral dose are administered with the same frequency rectally, adequate concentration of nitrofurantoin in the urine is attained. In this preliminary investigation, 400 mg of nitrofurantoin administered in a polyethylene glycol–polysorbate 80 suppository base and in a polyethylene glycol–silica suppository base provided an adequate concentration in the urine. Persons who exhibit nausea and emesis after oral administration of nitrofurantoin possibly could receive nitrofurantoin therapy by the rectal route.

REFERENCES

(1) D. E. Cadwallader, *J. Am. Pharm. Assoc.*, **NS15**, 409 (1975).

(2) H. E. Paul and M. F. Paul, "Experimental Chemotherapy," vol. II, Academic, New York, N.Y., 1964, pp. 307–370.

(3) F. J. Halley and H. W. Gloscock, *Curr. Ther. Res.*, **9**, 600 (1967).

(4) H. E. Paul, J. J. Hayes, M. F. Paul, and A. R. Borgmann, *J. Pharm. Sci.*, **56**, 882 (1967).

(5) D. C. Monkhouse and J. L. Lach, *ibid.*, **61**, 1430 (1972).

(6) J. D. Conklin and R. D. Hollifield, *Clin. Chem.*, **11**, 925 (1965).

(7) "Physicians' Desk Reference," 29th ed., B. B. Huff, Ed., Medical Economics Co., Oradell, N.J., 1976, p. 768.

(8) M. R. Turck, A. R. Ronald, and R. G. Peterdorf, *Antimicrob. Ag. Chemother.*, **1967**, 446.

(9) P. Finholt and S. Solvang, *J. Pharm. Sci.*, **57**, 1322 (1968).

(10) S. Solvang and P. Finholt, *Medd. Norsk. Farm. Selsk.*, **31**, 101 (1969).

(11) H. Weintraub and M. Gibaldi, *J. Pharm. Sci.*, **58**, 1368 (1969).

(12) J. M. Newton, G. Rowley, and J. Thornblom, *J. Pharm. Pharmacol.*, **23**, 156S (1971).

ACKNOWLEDGMENTS AND ADDRESSES

Received June 7, 1976, from the *College of Pharmacy, University of Iowa, Iowa City, IA 52242.*

Accepted for publication August 27, 1976.

[x] To whom inquiries should be directed.

Electronic Absorption Spectra and Protolytic Equilibria of Doxorubicin: Direct Spectrophotometric Determination of Microconstants

ROY J. STURGEON [*] and STEPHEN G. SCHULMAN [*x]

Abstract □ The ground- and excited-state dissociation constants and the electronic absorption and fluorescence spectra of doxorubicin were investigated by spectrophotometry. A general method for the direct calculation of individual microscopic dissociation constants was derived using the spectrophotometric data obtained. It was concluded that the protonated amino sugar group is slightly more acidic than the phenolic group. The spectrophotometric data were analyzed, and the macro- and microconstants for the various equilibria are reported.

Keyphrases □ Doxorubicin—electronic absorption and fluorescence spectrophotometric determination of dissociation constants and protolytic equilibria □ Spectrophotometry, electronic absorption and fluorescence—determination, doxorubicin dissociation constants and protolytic equilibria □ Dissociation constants—doxorubicin, electronic absorption and fluorescence spectrophotometric determination □ Protolytic equilibria—doxorubicin, electronic absorption and fluorescence spectrophotometric determination □ Antineoplastic agents—doxorubicin, electronic absorption and fluorescence spectrophotometric determination of dissociation constants and protolytic equilibria

Molecules containing a quinone moiety have been widely employed in trace analysis, dye manufacturing, and metal–ligand binding. In pharmaceutical applications, molecules such as the naphthoquinones (1) and the anthraquinones have shown promise as antifungal and antibacterial agents. Of more recent importance is the use of

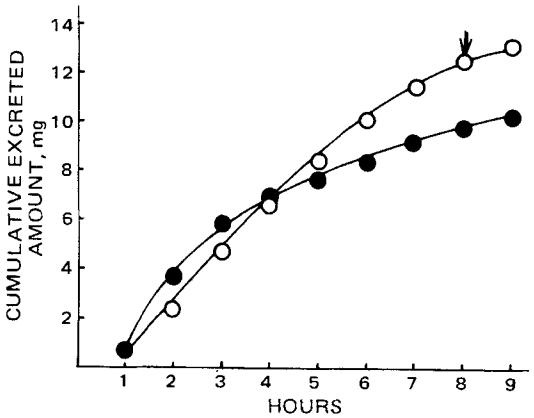

Figure 7—*Comparison of effect of suppository formulation of cumulative amount of nitrofurantoin excreted in Subject SK. Key: ○, lecithin and dried whey product; and ●, theobroma oil.*

from Formula T was greater than that from Formula B (Fig. 6); however, in this subject, both bases provided an adequate bacteriostatic concentration in the urine.

The amount of nitrofurantoin released from Formula D (Fig. 3) was so small that further investigation was not attempted.

Formula K provided a slightly greater amount of nitrofurantoin in the urine than the theobroma oil base suppository (Fig. 7). The dissolution profile of the theobroma oil base suppository suggested poor bioavailability, which was confirmed by *in vivo* data. In water at body temperature, the nitrofurantoin–theobroma oil suppository melted and formed a tacky mass from which the nitrofurantoin was slowly dissolved. With the limited fluid in the rectum, dissolution of the nitrofurantoin from the tacky mass was a very slow process. By mixing a lecithin and dried whey product with theobroma oil, it was hoped that the surface activity of the lecithin and the water solubility of the whey might enhance nitrofurantoin release. In measuring the dissolution profile, it was noticed that the mass was not tacky and that the release was slightly faster. Similarly, in the *in vivo* test, the amount of nitrofurantoin eliminated in the urine was slightly greater than that from the theobroma oil base.

SUMMARY

The usual adult dose of nitrofurantoin is 50–100 mg four times a day. If doses of nitrofurantoin several times the usual oral dose are administered with the same frequency rectally, adequate concentration of nitrofurantoin in the urine is attained. In this preliminary investigation, 400 mg of nitrofurantoin administered in a polyethylene glycol–polysorbate 80 suppository base and in a polyethylene glycol–silica suppository base provided an adequate concentration in the urine. Persons who exhibit nausea and emesis after oral administration of nitrofurantoin possibly could receive nitrofurantoin therapy by the rectal route.

REFERENCES

(1) D. E. Cadwallader, *J. Am. Pharm. Assoc.*, **NS15**, 409 (1975).

(2) H. E. Paul and M. F. Paul, "Experimental Chemotherapy," vol. II, Academic, New York, N.Y., 1964, pp. 307–370.

(3) F. J. Halley and H. W. Gloscock, *Curr. Ther. Res.*, **9**, 600 (1967).

(4) H. E. Paul, J. J. Hayes, M. F. Paul, and A. R. Borgmann, *J. Pharm. Sci.*, **56**, 882 (1967).

(5) D. C. Monkhouse and J. L. Lach, *ibid.*, **61**, 1430 (1972).

(6) J. D. Conklin and R. D. Hollifield, *Clin. Chem.*, **11**, 925 (1965).

(7) "Physicians' Desk Reference," 29th ed., B. B. Huff, Ed., Medical Economics Co., Oradell, N.J., 1976, p. 768.

(8) M. R. Turck, A. R. Ronald, and R. G. Peterdorf, *Antimicrob. Ag. Chemother.*, **1967**, 446.

(9) P. Finholt and S. Solvang, *J. Pharm. Sci.*, **57**, 1322 (1968).

(10) S. Solvang and P. Finholt, *Medd. Norsk. Farm. Selsk.*, **31**, 101 (1969).

(11) H. Weintraub and M. Gibaldi, *J. Pharm. Sci.*, **58**, 1368 (1969).

(12) J. M. Newton, G. Rowley, and J. Thornblom, *J. Pharm. Pharmacol.*, **23**, 156S (1971).

ACKNOWLEDGMENTS AND ADDRESSES

Received June 7, 1976, from the *College of Pharmacy, University of Iowa, Iowa City, IA 52242.*

Accepted for publication August 27, 1976.

[x] To whom inquiries should be directed.

Electronic Absorption Spectra and Protolytic Equilibria of Doxorubicin: Direct Spectrophotometric Determination of Microconstants

ROY J. STURGEON [*] and STEPHEN G. SCHULMAN [*x]

Abstract □ The ground- and excited-state dissociation constants and the electronic absorption and fluorescence spectra of doxorubicin were investigated by spectrophotometry. A general method for the direct calculation of individual microscopic dissociation constants was derived using the spectrophotometric data obtained. It was concluded that the protonated amino sugar group is slightly more acidic than the phenolic group. The spectrophotometric data were analyzed, and the macro- and microconstants for the various equilibria are reported.

Keyphrases □ Doxorubicin—electronic absorption and fluorescence spectrophotometric determination of dissociation constants and protolytic equilibria □ Spectrophotometry, electronic absorption and fluorescence—determination, doxorubicin dissociation constants and protolytic equilibria □ Dissociation constants—doxorubicin, electronic absorption and fluorescence spectrophotometric determination □ Protolytic equilibria—doxorubicin, electronic absorption and fluorescence spectrophotometric determination □ Antineoplastic agents—doxorubicin, electronic absorption and fluorescence spectrophotometric determination of dissociation constants and protolytic equilibria

Molecules containing a quinone moiety have been widely employed in trace analysis, dye manufacturing, and metal–ligand binding. In pharmaceutical applications, molecules such as the naphthoquinones (1) and the anthraquinones have shown promise as antifungal and antibacterial agents. Of more recent importance is the use of

Table I—Electronic Absorption (λ_{max}) and Fluorescence (λ_f) Maxima of the Prototropic Species of Doxorubicin in Water

Doxorubicin	λ_{max}, nm	log ϵ	λ_f, nm
Doubly charged cation	580	4.35	596
Monocation	495	4.00	552
Singly charged anion	550	3.81	588
Doubly charged anion	612	3.53	—

anthracycline antibiotics to treat carcinomas (2–4). The anthracyclines contain the anthraquinone nucleus linearly fused to a saturated six-membered ring.

Several fluorometric procedures for the analysis of doxorubicin have been reported (5–7), but little information is available about its acid–base properties and electronic absorption spectra. To obtain information of analytical, biological, and photochemical interest, it is desirable to know accurately in what prototropic form doxorubicin occurs in various media. Such studies are a necessary prerequisite to the spectrometric interpretation of the interactions of doxorubicin with biologically significant macromolecules such as proteins and nucleic acids.

EXPERIMENTAL

Reagents—Doxorubicin[1] was used without further purification.

Analytical reagent grade sulfuric acid[2] was diluted with distilled, deionized water for the solutions used to study the Hammett acidity region (8). Solutions in the pH range were citrate and phosphate buffers and sodium hydroxide solutions in distilled, deionized water.

Each sulfuric acid or buffer solution, in a 10-ml volumetric flask, was injected with 100 μl of a 4.4×10^{-4} *M* stock solution of doxorubicin in a mixed solvent of 10% (v/v) ethanol and 90% distilled, deionized water immediately prior to the taking of spectra to minimize decomposition errors. The tendency of doxorubicin to self-aggregate at higher concentrations dictated the low concentrations ($\sim 4 \times 10^{-6}$ *M*) employed.

Apparatus—Absorption spectra were taken on a spectrophotometer[3]. Fluorescence spectra were taken on a fluorescence spectrophotometer[4] whose monochromators were calibrated against the emission spectrum from a low-pressure mercury lamp and whose output was uncorrected for wavelength variable instrumental response. The pH measurements were made on a pH meter[5] employing a silver–silver chloride–glass combination electrode[6].

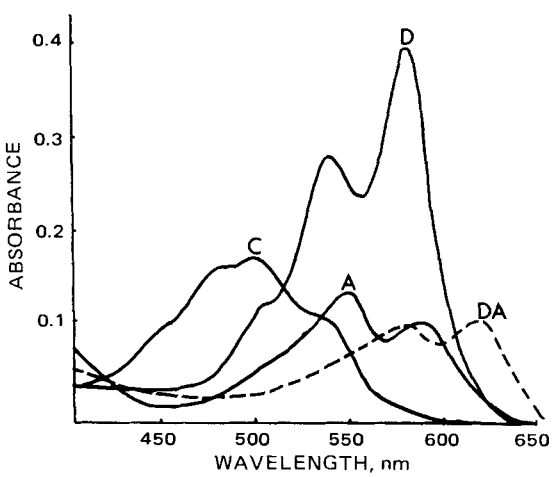

Figure 1—*Electronic absorption spectra of 1.6 × 10⁻⁵ M doxorubicin as the monocation (C), doubly charged cation (D), singly charged anion (A), and doubly charged anion (DA).*

[1] Adriamycin, courtesy of Adria Laboratories, Wilmington, Del.
[2] Mallinckrodt Chemical Works, St. Louis, Mo.
[3] Aminco DW-2.
[4] Aminco–Bowman SPF-1.
[5] Markson Electromark.
[6] Markson 888.

Table II—Negative Logarithms of Dissociation Constants of Doxorubicin

Constant	Value
pK_1	-5.9 ± 0.05
pK_2	8.15 ± 0.07
pK_3	10.16 ± 0.09
pK_{CN}	8.22
pK_{CZ}	9.01
pK_{ZA^-}	9.36
pK_{NA}	10.10
$\frac{[N]}{[Z]}$	6.27 ± 0.02
pK_4	13.2 ± 0.2

Calculations of macro- and microconstants were made employing three analytical wavelengths in the 465–495-nm region, where the molar absorptivity of the phenolate form is minimal compared to the undissociated phenolic form. Within experimental error, the results reported are independent of the wavelength selected.

RESULTS AND DISCUSSION

The electronic absorption and fluorescence spectra of doxorubicin and its various prototropic forms are shown in Figs. 1 and 2, respectively. The maxima along with the corresponding molar absorptivities (log ϵ) of the various species are presented in Table I.

To establish the optimal pH region for the analysis of aqueous solutions of doxorubicin, the ground-state dissociation constants (pKa) for the various prototropic species must be known. The pKa values (Table II) were determined for the dissociation in concentrated sulfuric acid of a proton from a protonated carbonyl group and for the dissociations in alkaline media of a protonated alkyl amino group and two phenolic groups, as shown in Scheme I. The pK_{CN} corresponds to the equilibrium between the singly charged cation and the neutral species; pK_{CZ} corresponds to the equilibrium between the singly charged cation and the zwitterionic species; pK_{AZ} corresponds to the equilibrium between the zwitterion and the singly charged anion, and pK_{NA} corresponds to the equilibrium between the neutral species and the singly charged anion.

In concentrated sulfuric acid, one of the three carbonyl groups of doxorubicin is protonated, the molecule existing as a dication (D). Dissociation of the protonated carbonyl group results in a blue shift of the long wavelength absorption maximum, from which the pKa of −5.9 may be calculated. The only species significantly present in the region between Hammett acidity −4.0 and pH 7.0 is the singly charged species with the positive charge at the amino sugar group. However, at a pH greater than 7.0, this monocation (C) can lose a proton either from a phenolic group to form a zwitterion (Z) or from the amino sugar group to form the neutral species (N). Either may then lose a proton to form the singly charged anion (A^-).

Doxorubicin, like numerous other drugs, contains several ionizable functions, including some of similar acidity. Therefore, overlapping

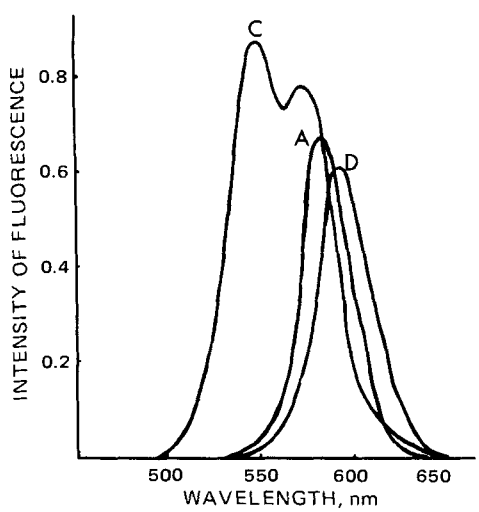

Figure 2—*Fluorescence spectra of doxorubicin as the monocation (C), doubly charged cation (D), and singly charged anion (A).*

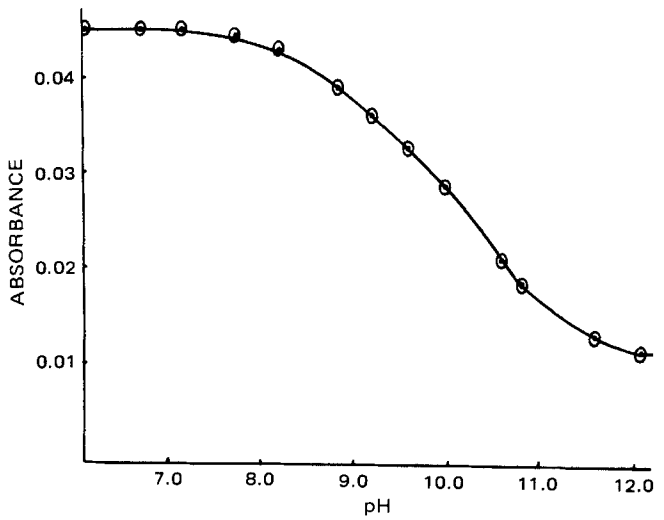

Figure 3—*Plot of absorbance at 495 nm* versus *pH for* 4.4×10^{-6} M *doxorubicin in the pH 7–12 range.*

protolytic equilibria are possible. In doxorubicin, the amino sugar group and a phenolic group both ionized in the pH region from 8 to 13. To calculate accurately the corresponding dissociation constants, the effects of the dissociations on the electronic absorption spectra must be followed carefully. Because the amino group of the amino sugar moiety is several atoms removed from the aromatic chromophore of doxorubicin, electrometric or inductive influences, due to the free or protonated amino group, upon the electronic spectrum of doxorubicin are negligible. Thus, only the dissociation of the phenolic group affects the spectrometric properties of the molecule in alkaline solutions. However, the competing protolytic equilibria involving the amino sugar group affect the rate of appearance of the various spectrometric species of doxorubicin during the pH titration.

While following the spectrometric changes resulting from variations in pH of solutions of doxorubicin in the pH 7–12 region, no distinct isosbestic point was observed. The lack of an isosbestic point is indicative of three or more absorbing species present in the solutions. The overlapping successive protolytic equilibria also result in a wider titration interval than would normally be expected if no competition was observed. Figure 3 shows a plot of absorbance *versus* pH for the titration of doxorubicin in the pH 6.0–12.5 range.

Since dissociation of the zwitterion to form the singly charged anion is spectrometrically undetectable, the molar absorptivities (ϵ_λ) of the monocation and neutral species are equal and those of the zwitterion and anion are equal at the analytical wavelength. The total absorbance (A_T) at the analytical wavelength may be written as the sum of the absorbances of the various species present:

$$A_T = A_C + A_Z + A_N + A_{A^-} = \epsilon_C[C]1 + \epsilon_Z[Z]1 + \epsilon_N[N]1 + \epsilon_{A^-}[A^-]1 \quad \text{(Eq. 1)}$$

The individual stages of ionization have microscopic dissociation constants, denoted as K_{CN}, K_{CZ}, K_{ZA^-}, and K_{NA^-} in Scheme I. The macroscopic constants, K_2 and K_3, have the following relation to the microscopic constants:

$$K_2 = K_{CN} + K_{CZ} \quad \text{(Eq. 2)}$$

$$K_3^{-1} = K_{ZA}^{-1} + K_{NA}^{-1} \quad \text{(Eq. 3)}$$

and since the free energy change in going from C to A^- is the same regardless of whether path C → N → A^- or C → Z → A^- is taken:

$$K_2K_3 = K_{CN}K_{NA} = K_{CZ}K_{ZA} \quad \text{(Eq. 4)}$$

By letting the sum of the concentrations of the neutral species and zwitterion equal [N′], Eqs. 2–4 may be written as:

$$K_2 = \frac{[H^+][N']}{[C]} \quad \text{(Eq. 5)}$$

$$K_3 = \frac{[A^-][H^+]}{[N']} \quad \text{(Eq. 6)}$$

$$K_2K_3 = \frac{[H^+]^2[A^-]}{[C]} \quad \text{(Eq. 7)}$$

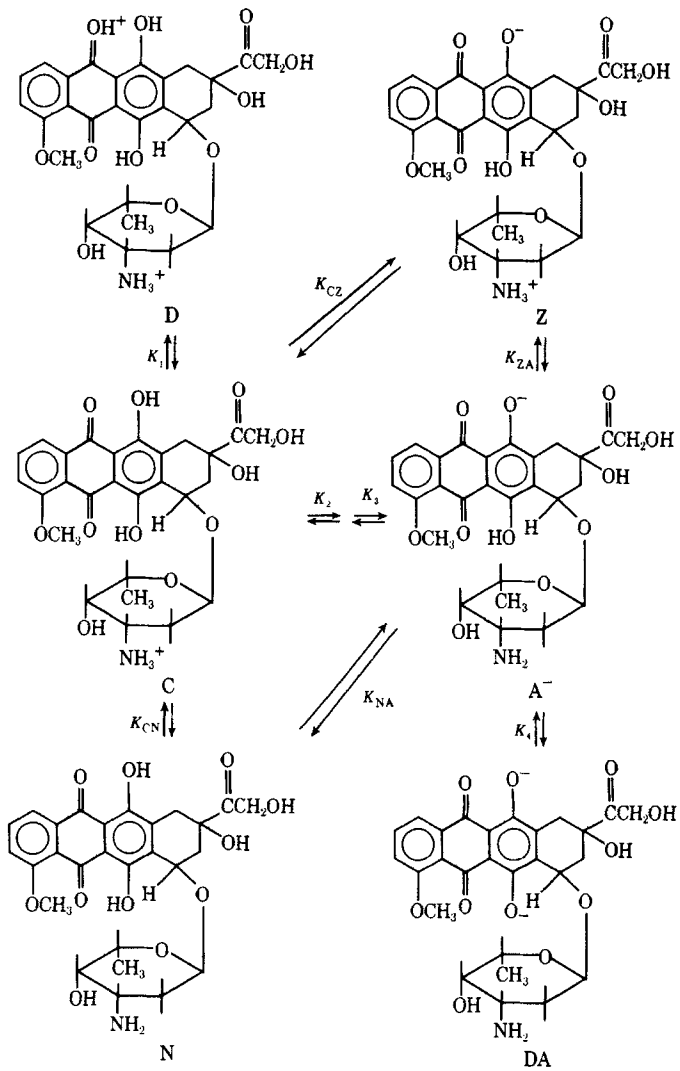

Scheme I

At equilibrium, the mass balance equation states that the sum of the concentrations of all species must equal the total analytical concentration of doxorubicin (C_T):

$$C_T = [C] + [N'] + [A^-] \quad \text{(Eq. 8)}$$

By combining the mass balance equations and the equilibrium expressions, the concentrations of the cation, [C], zwitterion, [Z], neutral, [N], and anion, [A^-], may be written as:

$$[C] = \frac{C_T[H^+]^2}{[H^+]^2 + K_2[H^+] + K_2K_3} \quad \text{(Eq. 9)}$$

$$[N'] = \frac{C_TK_2[H^+]}{[H^+]^2 + K_2[H^+] + K_2K_3} \quad \text{(Eq. 10)}$$

$$[A^-] = \frac{C_TK_2K_3}{[H^+]^2 + K_2[H^+] + K_2K_3} \quad \text{(Eq. 11)}$$

Equation 1 can be rewritten as:

$$A_T = \epsilon_C[C]1 + \epsilon_{N'}[N']1 + \epsilon_{A^-}[A^-]1 \quad \text{(Eq. 12)}$$

Since [N′] is the sum of the concentrations of the neutral and zwitterionic species, $\epsilon_{N'}$ is the expedient molar absorptivity of N′. This ϵ value is essentially a weighted sum of the neutral and zwitterionic molar absorptivities with respect to the fraction of each uncharged species present.

By substituting Eqs. 9–11 into Eq. 12, the following equation results:

$$(A_T - \epsilon_CC_T)[H^+]^2 + (A_T - \epsilon_{N'}C_T)K_2[H^+] + (A_T - \epsilon_{A^-}C_T)K_2K_3 = 0 \quad \text{(Eq. 13)}$$

Equation 13 may now be solved at three different points in the titration

for the values of $\epsilon_{N'}$, K_2, and K_3 (9). With these values (Table II), the microconstants may then be determined. The K_{NZ}, the ratio of the concentration of the neutral species to that of the zwitterionic species, is a constant independent of pH. Since:

$$\epsilon_C[N] + \epsilon_A[Z] = \epsilon_{N'}[N'] \qquad \text{(Eq. 14)}$$

and at 495 nm $\epsilon_{N'}$ is equal to 9.10×10^3 cm^{-1} M^{-1}, the following equation can be used to evaluate K_{NZ}:

$$K_{NZ} = \frac{[N]}{[Z]} = \frac{\epsilon_{N'} - \epsilon_A}{\epsilon_C - \epsilon_{N'}} \qquad \text{(Eq. 15)}$$

Since [N] = 6.27 [Z], Eq. 2 may be solved for K_{CZ} and K_{CN} as follows:

$$K_2 = \frac{6.27[H^+][Z]}{[C]} + \frac{[H^+][Z]}{[C]} = 7.27\,K_{CZ} \qquad \text{(Eq. 16)}$$

Similar substitution into Eq. 3 allows both K_{NA} and K_{ZA} to be calculated.

A similar method for the spectrophotometric evaluation of microconstants involving overlapping equilibria, in which the dissociation of one group affects the absorption spectrum and the other does not, was developed by Edsall *et al.* (10) in studies of the dissociations of tyrosine. This method was applied to the dissociation equilibria of alkanolamines (11). However, the latter approach is somewhat more complicated algebraically than the present one. Moreover, the macroconstants in Edsall's method are calculated from the microconstants. In the present approach, the preliminary evaluation of macroconstants from spectrophotometric data can be checked independently by potentiometry if solubility permits.

The fluorescence spectrum of doxorubicin in the pH region follows the same changes observed in the pH dependence of the absorption spectrum, indicating that protolytic reaction in the excited state is too slow to compete with fluorescence. However, in the Hammett acidity region the fluorescence spectrum of doxorubicin red shifts with increasing acidity in acid solutions more dilute than those in which the corresponding absorption spectral changes occur. This shift is indicative of protonation in the lowest excited singlet state, with the inflection point in the fluorometric titration representing the excited-state dissociation constant (pK*) of −3.1. Doxorubicin becomes more basic in the excited state due to the transfer of charge to a carbonyl group upon excitation.

The method allows the direct calculation of microconstants when overlapping dissociation equilibria are present in a system under spectrometric study. This method is general for any molecule with overlapping equilibria in which dissociation of only one functional group affects the electronic spectral properties of the molecule. The values of the microconstants show that the protonated amino sugar group is slightly more acidic than the phenolic group.

In developing or using any method of analysis for doxorubicin, careful choice of the pH and the analytical wavelength is necessary. The prevalence of only one absorbing species having intense, long wavelength absorption in the pH 4–7 region and one emitting species having intense fluorescence in the pH 1–7 region suggests that the spectrometric analysis of doxorubicin in aqueous solutions be carried out in dilute acidic solutions.

REFERENCES

(1) H. Gershon and L. Shanks, *Can. J. Microbiol.*, **21**, 1317 (1975).

(2) R. K. Oldham and T. C. Pomeroy, *Cancer Chemother. Rep., No. 5*, **1972**, 56.

(3) A. M. Casazza, C. Gambarucci, and R. Silvestrini, *Rev. Eur. Etudes Clin. Biol. XVII*, **1972**, 622.

(4) D. H. Huffman, R. S. Benjamin, and N. R. Bachur, *Clin. Pharmacol. Ther.*, **13**, 895 (1972).

(5) J. M. Finkel, K. T. Knapp, and L. T. Mulligan, *Cancer Chemother. Rep.*, **53**, 159 (1969).

(6) H. S. Schwartz, *Biochem. Med.*, **7**, 396 (1973).

(7) R. Rosso, C. Rauazzoni, M. Esposito, R. Sala, and L. Santi, *Eur. J. Cancer*, **8**, 455 (1972).

(8) M. J. Jorgenson and D. R. Hartter, *J. Am. Chem. Soc.*, **85**, 878 (1963).

(9) R. A. Robinson and A. I. Biggs, *Aust. J. Chem.*, **10**, 128 (1957).

(10) J. T. Edsall, R. B. Martin, and B. R. Hollingworth, *Proc. Natl. Acad. Sci. USA*, **44**, 505 (1958).

(11) S. Riegelman, L. A. Strait, and E. T. Fischer, *J. Pharm. Sci.*, **51**, 129 (1962).

ACKNOWLEDGMENTS AND ADDRESSES

Received March 29, 1976, from the *College of Pharmacy, University of Kentucky, Lexington, KY 40506.*

Accepted for publication August 25, 1976.

* Present address: College of Pharmacy, University of Florida, Gainesville, FL 32610.

ˣ To whom inquiries should be directed.

Determination of Energy Change Associated with Dissolution of a Solid

DAVID C. HSIA *, CHONG-KOOK KIM, and DANE O. KILDSIG ˣ

Abstract □ The dissolution of a solid immersed in a solvent was considered as a consecutive process, consisting of a primary surface interaction leading to the production of a new surface at the solid–liquid interface, solvation of the solid at the interface, and transfer of the solvated solid into the bulk of the solution. The energy changes involved in each step were studied for the dissolution of *m*-tolylacetamide in hexane and heptane. An energy diagram was constructed according to the proposed dissolution mechanism. The heats of dissolution determined from the energy diagram agreed well with those obtained experimentally.

Keyphrases □ Solids—dissolution in a solvent, energy changes determined □ Dissolution—solid in a solvent, energy changes determined □ Energy changes—determined for dissolution of a solid in a solvent

Several recent investigations concerned the energy changes involved in the dissolution process. Wadke and Reier (1) presented a rate equation, based on previously published results (2–4), involving both the heat of solution of the solid and the activation energy for diffusion. Szinai and coworkers (5, 6), after reviewing several articles on dissolution, proposed a rate equation incorporating an energy term comprised of the energy required to remove a solute molecule from the solid surface, the energy of solvation, and the activation energy for diffusion. A numerical study of the three energy terms was not reported.

The purpose of this study was to quantify the energy associated with initial solvent–solid interaction, the solvation of the solute, and the mass transfer steps of the dissolution process.

for the values of $\epsilon_{N'}$, K_2, and K_3 (9). With these values (Table II), the microconstants may then be determined. The K_{NZ}, the ratio of the concentration of the neutral species to that of the zwitterionic species, is a constant independent of pH. Since:

$$\epsilon_C[N] + \epsilon_A[Z] = \epsilon_{N'}[N'] \quad \text{(Eq. 14)}$$

and at 495 nm $\epsilon_{N'}$ is equal to 9.10×10^3 cm^{-1} M^{-1}, the following equation can be used to evaluate K_{NZ}:

$$K_{NZ} = \frac{[N]}{[Z]} = \frac{\epsilon_{N'} - \epsilon_A}{\epsilon_C - \epsilon_{N'}} \quad \text{(Eq. 15)}$$

Since [N] = 6.27 [Z], Eq. 2 may be solved for K_{CZ} and K_{CN} as follows:

$$K_2 = \frac{6.27[H^+][Z]}{[C]} + \frac{[H^+][Z]}{[C]} = 7.27\,K_{CZ} \quad \text{(Eq. 16)}$$

Similar substitution into Eq. 3 allows both K_{NA} and K_{ZA} to be calculated.

A similar method for the spectrophotometric evaluation of microconstants involving overlapping equilibria, in which the dissociation of one group affects the absorption spectrum and the other does not, was developed by Edsall *et al.* (10) in studies of the dissociations of tyrosine. This method was applied to the dissociation equilibria of alkanolamines (11). However, the latter approach is somewhat more complicated algebraically than the present one. Moreover, the macroconstants in Edsall's method are calculated from the microconstants. In the present approach, the preliminary evaluation of macroconstants from spectrophotometric data can be checked independently by potentiometry if solubility permits.

The fluorescence spectrum of doxorubicin in the pH region follows the same changes observed in the pH dependence of the absorption spectrum, indicating that protolytic reaction in the excited state is too slow to compete with fluorescence. However, in the Hammett acidity region the fluorescence spectrum of doxorubicin red shifts with increasing acidity in acid solutions more dilute than those in which the corresponding absorption spectral changes occur. This shift is indicative of protonation in the lowest excited singlet state, with the inflection point in the fluorometric titration representing the excited-state dissociation constant (pK*) of −3.1. Doxorubicin becomes more basic in the excited state due to the transfer of charge to a carbonyl group upon excitation.

The method allows the direct calculation of microconstants when overlapping dissociation equilibria are present in a system under spectrometric study. This method is general for any molecule with overlapping equilibria in which dissociation of only one functional group affects the electronic spectral properties of the molecule. The values of the microconstants show that the protonated amino sugar group is slightly more acidic than the phenolic group.

In developing or using any method of analysis for doxorubicin, careful choice of the pH and the analytical wavelength is necessary. The prevalence of only one absorbing species having intense, long wavelength absorption in the pH 4–7 region and one emitting species having intense fluorescence in the pH 1–7 region suggests that the spectrometric analysis of doxorubicin in aqueous solutions be carried out in dilute acidic solutions.

REFERENCES

(1) H. Gershon and L. Shanks, *Can. J. Microbiol.*, **21**, 1317 (1975).

(2) R. K. Oldham and T. C. Pomeroy, *Cancer Chemother. Rep., No. 5*, **1972**, 56.

(3) A. M. Casazza, C. Gambarucci, and R. Silvestrini, *Rev. Eur. Etudes Clin. Biol. XVII*, **1972**, 622.

(4) D. H. Huffman, R. S. Benjamin, and N. R. Bachur, *Clin. Pharmacol. Ther.*, **13**, 895 (1972).

(5) J. M. Finkel, K. T. Knapp, and L. T. Mulligan, *Cancer Chemother. Rep.*, **53**, 159 (1969).

(6) H. S. Schwartz, *Biochem. Med.*, **7**, 396 (1973).

(7) R. Rosso, C. Rauazzoni, M. Esposito, R. Sala, and L. Santi, *Eur. J. Cancer*, **8**, 455 (1972).

(8) M. J. Jorgenson and D. R. Hartter, *J. Am. Chem. Soc.*, **85**, 878 (1963).

(9) R. A. Robinson and A. I. Biggs, *Aust. J. Chem.*, **10**, 128 (1957).

(10) J. T. Edsall, R. B. Martin, and B. R. Hollingworth, *Proc. Natl. Acad. Sci. USA*, **44**, 505 (1958).

(11) S. Riegelman, L. A. Strait, and E. T. Fischer, *J. Pharm. Sci.*, **51**, 129 (1962).

ACKNOWLEDGMENTS AND ADDRESSES

Received March 29, 1976, from the *College of Pharmacy, University of Kentucky, Lexington, KY 40506.*

Accepted for publication August 25, 1976.

* Present address: College of Pharmacy, University of Florida, Gainesville, FL 32610.

ˣ To whom inquiries should be directed.

Determination of Energy Change Associated with Dissolution of a Solid

DAVID C. HSIA *, CHONG-KOOK KIM, and DANE O. KILDSIG ˣ

Abstract □ The dissolution of a solid immersed in a solvent was considered as a consecutive process, consisting of a primary surface interaction leading to the production of a new surface at the solid–liquid interface, solvation of the solid at the interface, and transfer of the solvated solid into the bulk of the solution. The energy changes involved in each step were studied for the dissolution of *m*-tolylacetamide in hexane and heptane. An energy diagram was constructed according to the proposed dissolution mechanism. The heats of dissolution determined from the energy diagram agreed well with those obtained experimentally.

Keyphrases □ Solids—dissolution in a solvent, energy changes determined □ Dissolution—solid in a solvent, energy changes determined □ Energy changes—determined for dissolution of a solid in a solvent

Several recent investigations concerned the energy changes involved in the dissolution process. Wadke and Reier (1) presented a rate equation, based on previously published results (2–4), involving both the heat of solution of the solid and the activation energy for diffusion. Szinai and coworkers (5, 6), after reviewing several articles on dissolution, proposed a rate equation incorporating an energy term comprised of the energy required to remove a solute molecule from the solid surface, the energy of solvation, and the activation energy for diffusion. A numerical study of the three energy terms was not reported.

The purpose of this study was to quantify the energy associated with initial solvent–solid interaction, the solvation of the solute, and the mass transfer steps of the dissolution process.

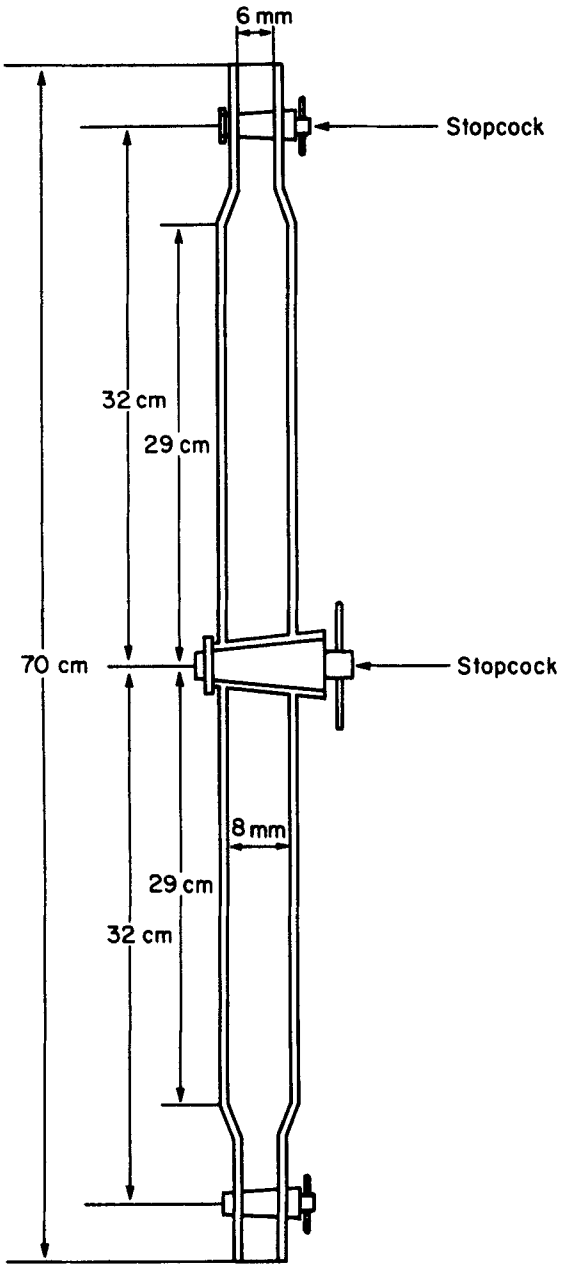

Figure 1—*Diagram of glass dispersion column.*

EXPERIMENTAL

Materials—The solid was *m*-tolylacetamide[1] (I). The solvents used were spectral quality.

Temperature Dependence of Solubility of I—The solubility of I in hexane and heptane was determined at 14.3–39.9 ± 0.01°. A 300-ml, three-necked, round-bottom flask, containing approximately 20 g of I powder, was put in a constant-temperature water bath at 14.3 ± 0.01°. A stirrer was mounted in the flask, 200 ml of hexane or heptane was added, and the stirring speed was set at 150 rpm.

After 24 hr, a 10-ml sample was taken from the flask and quickly filtered through a 0.45-μm filter. Five milliliters of the filtered solution was diluted in a 250-ml volumetric flask with anhydrous methanol. Duplicate samples were taken each time. The temperature of the water bath was then increased about 5°. After temperature equilibrium was reached in the water bath for 24 hr, another sample was removed, filtered, and diluted as previously described.

The absorbance of each sample was determined at 242 nm with a 1:50 dilution of hexane or heptane in methanol as the reference. A blank was run each time to ensure that the baseline was straight. The absorbance at 242 nm was recorded and converted into concentration through an appropriate calibration curve. The solubility of I in hexane and heptane at the different temperatures was then calculated.

[1] Eastman Kodak Co., Rochester, NY 14605.

Table I—Molecular Structure of *m*-Tolylacetamide

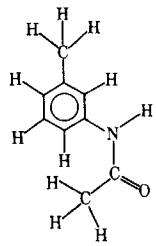

Bond	Bond Length	Group	Geometry	Angle
C=O	1.162	Carbonyl	Planar	120°
C—H	1.09	Methyl	Tetrahedral	109°
C—C	1.54	Alkane	Tetrahedral	109°
N—H	1.038	Amide	Tetrahedral	109°
C=C in benzene	1.39	Benzene	Planar	120°
C—N	1.329	Amide	Tetrahedral	109°

Temperature Dependence of Dissolution Rate of I—The dissolution rate of I in hexane and heptane was determined at 25.0, 29.9, 33.1, and 35.5 ± 0.05° in a constant-temperature chamber (7).

Glass tubes, 45 cm long × 1.65 cm i.d., were flat sealed on one end and employed as dissolution vessels. A stainless steel tablet holder was constructed to fit easily into the dissolution tube without causing bubble formation.

A small amount of I was placed in a casserole, which was then warmed in a water bath at 75°. After the compound was melted, it was poured into a 1.11-cm (7/16-in.) tablet die with a polished, flat-faced punch in place. The cast tablets were removed after solidification, and mottled or chipped tablets were discarded. The punch face was cleaned with anhydrous methanol.

A mixture containing 40% polyethylene glycol 4000 and 60% polyethylene glycol 400 was prepared and carefully applied to the cylindrical surface of the tablet. Care was taken to prevent any of the mixture from contacting the flat surface of the tablet. Solvent, 85 ml, was placed in the dissolution tube and allowed to equilibrate for 8 hr in the controlled temperature chamber. The dissolution tubes were held in a perfect vertical position using a suitable supporting device (8). The tablet was wrapped with aluminum foil and pushed into the tablet holder, which was put through the center of a stopper that sealed the open end of the dissolution tube.

A dissolution run was begun by gently immersing the tablet surface just below the solvent surface. Dissolution was timed for 3 min. The run was stopped by gently removing the tablet holder from the dissolution tube, and the amount dissolved was then determined. Dissolution rate determination was made in triplicate, using a new tablet for each determination. The temperature of the chamber was then increased by 5°, and the dissolution rate was determined at this temperature in the same manner.

Determination of Dispersion Rate—A Pyrex glass column (70 cm long × 8 mm i.d.) was used to measure the dispersion rate of solutions of I in hexane and heptane into the pure solvent (Fig. 1). The column had stopcocks of 2-mm bore at each end and a stopcock with a straight 8-mm bore in the middle.

Dispersion experiments were conducted at 30° in the constant-temperature chamber. The solvent, solution, and column were placed inside the chamber and allowed to equilibrate. The lower stopcock was then closed, and the lower half of the column was filled with solvent to a point above the middle stopcock. Suction was then applied to remove any entrapped air bubbles in the lower column. The middle stopcock was then closed, and the solvent remaining in the upper column was removed. The upper column was then dried with a stream of air.

A series of I solutions in hexane and in heptane were prepared ranging in concentration from 30 to 300 mg/liter. A solution of I was transferred into the upper column while the middle stopcock was still in a closed position. The upper stopcock was then closed, and the entire column was inspected to be certain that no air bubbles were present. Two hours after

Table II—Temperature Dependence of the Solubility of *m*-Tolylacetamide in Hexane and Heptane

Temperature	Solubility in Hexane, mg/liter	Solubility in Heptane, mg/liter
14.3°	294.8	—
19.8°	449.5	—
24.5°	562.4	—
25.7°	—	527.5
29.8°	666.1	—
30.3°	—	688.4
33.8°	758.1	—
35.2°	—	901.0
39.9°	—	1066.9

the column was filled, the middle stopcock was turned to the open position for 3 min and then closed. The upper column was first drained and rinsed with 10 ml of solvent five times. After the upper column was air dried, the middle stopcock was opened to let the liquid inside the stopcock mix with the liquid in the lower column. The solution in the lower column was then removed for assay.

The volumes of the upper and lower (including the stopcock) columns were calibrated with a 50-ml buret and found to be 19.1 ± 0.05 and 20.25 ± 0.05 ml, respectively. From the volume and the final solution concentration in the lower column, the amount of I transferred from the upper column to the lower column and the dispersion rate of I in hexane and heptane were calculated.

Temperature Dependence of Dispersion Rate—The dispersion rates of solutions of I in hexane and heptane into their respective pure solvents were determined at four different temperatures using the same dispersion column and the described method. The concentration of I used in the upper column was that concentration which, during dispersion, transferred to the lower column approximately the same amount of solute as was dissolved from the solid I during the same time period. This concentration was 44.2 mg/liter in hexane and 32.6 mg/liter in heptane. A second concentration, 240 mg/liter in hexane and 265 mg/liter in heptane, was also used to determine if the temperature dependence of the dispersion rate was a function of concentration.

The temperature dependence of the dispersion rate was independent of concentration for the concentrations used. The rates of dispersion, expressed as the amount of solute transferred per minute, were determined by assaying for the amount of I transferred to the lower section of the column.

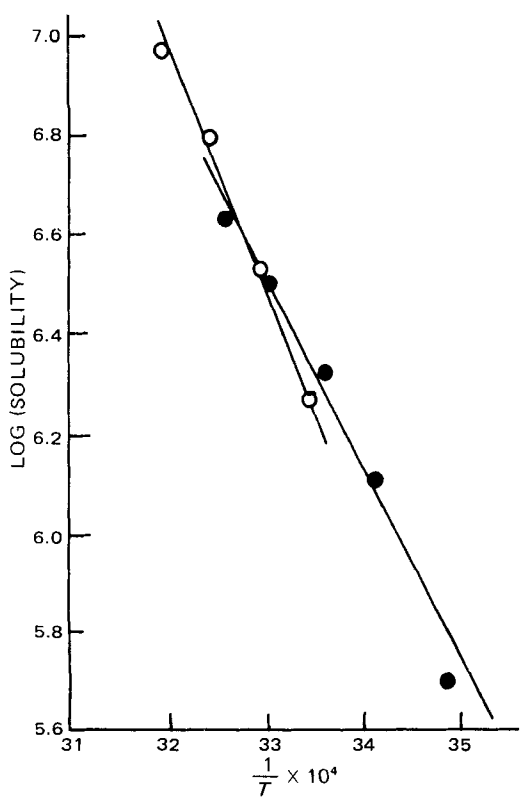

Figure 2—*Temperature dependence of the solubility of I in hexane* (●) *and heptane* (○).

Table III—Temperature Dependence of the Dispersion Rate of *m*-Tolylacetamide in Hexane and Heptane

Temperature	Dispersion Rate in Hexane, μg/min	Dispersion Rate in Heptane, μg/min
27.9°	34.2	23.6
30.0°	36.2	26.4
33.1°	37.9	28.0
35.4°	41.1	29.5

Heat of Fusion—The heat of fusion of I was determined in a differential scanning calorimeter[2] with indium as the standard. Approximately 3 mg of I was weighed to the nearest 0.01 mg on a microbalance[3] into each of five sample holders, which were then sealed. Empty sample holders were used as reference. An indium sample weighing 6.22 mg was used as a standard. The temperature was scanned from 416 to 430 °K for indium and from 316 to 338 °K for I at a rate of 2.5 °C/min. Sharp and symmetric peaks were obtained in each case. The area under the curves was measured with a planimeter.

The calculation of the heat of fusion of I was based on the following equation:

$$\Delta H_1 = \frac{\Delta H_2 A_1 W_2}{A_2 W_1} \qquad \text{(Eq. 1)}$$

where ΔH_1 is the heat of fusion of I, ΔH_2 is the heat of fusion of indium, A_1 is the area under the curve of the sample, A_2 is the area under the curve of indium, W_1 is the weight of the sample, and W_2 is the weight of indium.

RESULTS AND DISCUSSION

Determination of Energy Involved in Each Dissolution Step—Three fundamental processes contribute to the dissolution of a solid immersed in a solvent, regardless of the mechanism by which dissolution is thought to occur (Scheme I). The three processes are: (*a*) the primary surface interaction leading to the continual production of a new surface at the solid–liquid interface, (*b*) solvation of the solid at the solid surface or solid–liquid interface, and (*c*) mass transfer of the dissolved solid into the bulk of the solution. The slowest process determines the dissolution mechanism. The first two steps are interfacial interactions between the solid and the solvent, which are related to interfacial energy and the solid lattice energy. In Step 3, the mass transfer process, solvated solid is brought into the bulk of the solution by diffusion and/or convection.

$$\text{solid} \xrightarrow[\Delta E_1]{\text{surface interaction}} \text{solvent} \cdots \text{solid} \xrightarrow[\Delta E_2]{\text{solvation}} \text{solvated solid at solid surface} \xrightarrow[\Delta E_4]{\text{mass transfer}} \text{solution}$$

Scheme I

The energy required to produce a new surface or to remove a molecule from the surface of a solid, ΔE_1, is equal to the product of the interfacial tension between the solid and the solvent and the surface area of the solid or:

$$\Delta E_1 = \gamma_{SL}\, \Delta A \qquad \text{(Eq. 2)}$$

where ΔA represents the exposed surface area of a mole of solid, and γ_{SL} is the interfacial tension. The literature values of γ_{SL} for I in hexane and heptane are 3.9 and 7.6 dynes/cm, respectively. The value of ΔA for I can be calculated from its molecular structure. The calculation is made possible through a knowledge of the bond lengths and bond angles (Table I), the fact that the benzene ring and acetyl group are planar, and the assumption that the methyl group is spherical. The surface area of I calculated from the molecular structure, based on a two-dimensional planar projection and the assumption that both sides of the molecule interact with the solvent, is 47.08 A^2 or 2.83 × 10^9 cm^2/mole. The ΔE_1 values for I in hexane and heptane calculated from Eq. 2 are 0.26 and 0.51 kcal/mole, respectively.

The heat of solvation consists of two energy terms. The first, ΔE_2, is the energy required to break the solid lattice energy and is equal to the

[2] Model 1B, Perkin-Elmer, Norwalk, Conn.
[3] Cahn R. G. electrobalance, Cahn Instrument Co., St. Paramount, CA 90723.

Table IV—Energy Terms Involved in Each Step of the Dissolution of *m*-Tolylacetamide in Hexane and Heptane

Solvent	ΔE_1 ($\Delta E_{wetting}$), kcal/mole	ΔE_2 (ΔE_{fusion}), kcal/mole	ΔE_3 ($\Delta E_{solvation}$), kcal/mole	ΔE_4 ($\Delta E_{disperson}$), kcal/mole	ΔH_S ($\Delta H_{solution}$), kcal/mole	ΔE_d ($\Delta E_{dissolution}$), kcal/mole (exp)	ΔE_d ($E_{dissolution}$), kcal/mole (calc. from Eq. 7)
Hexane	0.26	4.15	5.61	4.17	10.0	15.9	14.2
Heptane	0.51	4.15	4.63	5.25	9.30	15.3	14.6

heat of fusion of the solid, ΔH_f. The heat of fusion for I determined by differential scanning calorimetry was 4.15 kcal/mole.

The second energy term, ΔE_3, is the energy released or required during solvation. If the interaction energy between the solid and solvent is larger than that between solid molecules, energy is released; if the interaction energy is less than that existing between solid molecules, energy is required. Although ΔE_3 cannot be determined experimentally, it can be calculated from ΔE_1, ΔE_2, and the heat of solution, ΔH_S.

Since the amount of I in the saturated solution in hexane and heptane is relatively small, 602 and 646 mg/liter, respectively, at 30°, the volume change during dissolution may be considered negligible. From the equation:

$$\Delta H_S = \Delta E_S + P\,\Delta V \qquad \text{(Eq. 3)}$$

it can be seen that at constant pressure the heat of solution, ΔH_S, is equal to the energy change in solution, ΔE_S. Then:

$$\Delta H_S = \Delta E_S = \Delta E_1 + \Delta E_2 + \Delta E_3 \qquad \text{(Eq. 4)}$$

The heat of solution, ΔH_S, is the energy difference between two equilibrium states, *i.e.*, the energy of the system before and after the solid is dissolved. This energy term can be obtained from a Van't Hoff plot of the I solubility data (Table II). Figure 2 shows a plot of log (I solubility) as a function of the reciprocal of temperature. From the slope of the line, values of 10.0 and 9.30 kcal/mole were calculated for the heat of solution of I in hexane and heptane, respectively.

From the experimental results of ΔH_S, ΔE_1, and ΔE_2 and Eq. 4, the term ΔE_3 can be obtained such that:

$$\Delta E_3 = \Delta H_S - \Delta E_1 - \Delta E_2 \qquad \text{(Eq. 5)}$$

which yields ΔE_3 = 5.60 kcal/mole for I in hexane and 4.63 kcal/mole for I in heptane. The fact that ΔE_3 has a positive sign shows that energy is required for the solvation step in addition to the heat of fusion.

The activation energy for mass transfer or dispersion is the energy required to transfer the solvated solid from the interfacial region to the bulk of the solution. This energy, ΔE_4, can be determined from the temperature dependence of the liquid–liquid dispersion rate of the I solution into pure solvent (Table III). If it is assumed that the dispersion coefficient is related to temperature in the same manner as the diffusion coefficient, then:

$$D = D_0 e^{-\Delta E_4/RT} \qquad \text{(Eq. 6)}$$

where D is the dispersion coefficient, D_0 is a constant related to the molecular dimensions of the solute, ΔE_4 is the activation energy for dispersion, R is the gas constant, and T is the absolute temperature. Since the dispersion rate is proportional to the dispersion coefficient, an Arrhenius plot may be made of the dispersion rate data as a function of the reciprocal of temperature. Arrhenius-type plots are shown in Fig. 3. From the slope of the lines, values of 4.17 and 5.25 kcal/mole were calculated for ΔE_4 for the systems of I in hexane and heptane, respectively.

The heat of dissolution, ΔE_d, is the energy of activation associated with solid dissolution. This term may also be determined from an Arrhenius plot using the dissolution rate in place of the dispersion rate constant. Figure 4 shows a plot of log (dissolution rate) *versus* the reciprocal of absolute temperature for the dissolution of I in both hexane and heptane. The energies of activation determined from the slope of the lines in Fig. 4, along with the energy terms discussed, are listed in Table IV.

Based on these energy terms, an energy diagram (Fig. 5) can be constructed. From the energy diagram, it can be seen that:

$$\Delta E_d = \Delta E_1 + \Delta E_2 + \Delta E_3 + \Delta E_4 \qquad \text{(Eq. 7)}$$

The activation energy of dissolution, ΔE_d, can then be calculated from Eq. 7 and compared with the value of ΔE_d determined experimentally. This comparison is shown in Table IV.

The comparison between the experimental value of ΔE_d and the value

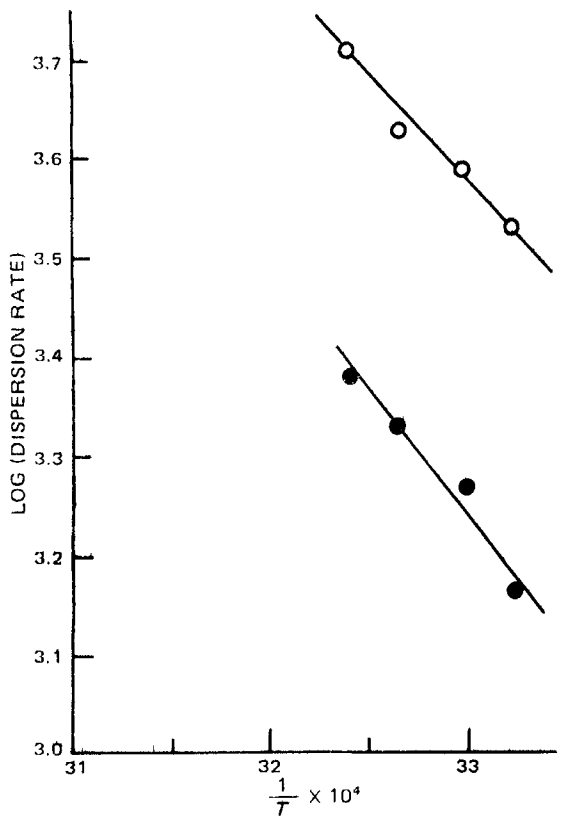

Figure 3—*Temperature dependence of the dispersion rate of I in hexane* (○) *and heptane* (●).

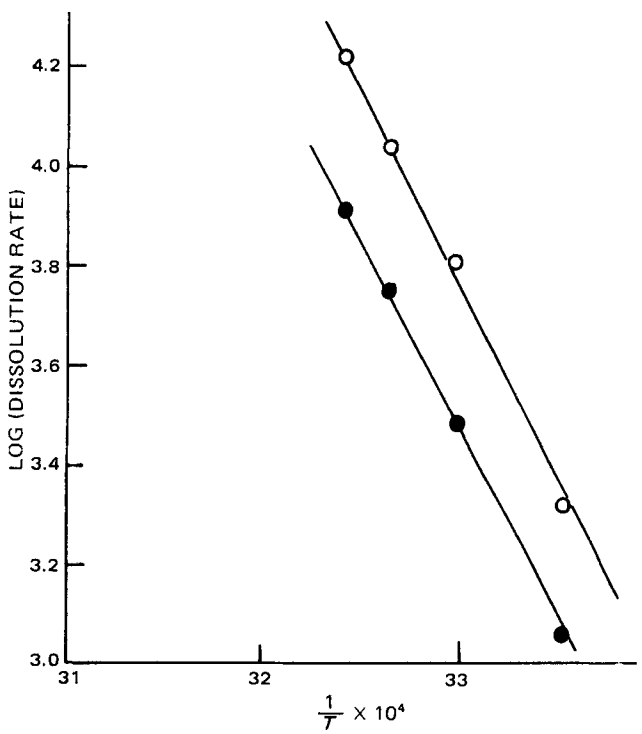

Figure 4—*Temperature dependence of the dissolution rate of I in hexane* (○) *and heptane* (●).

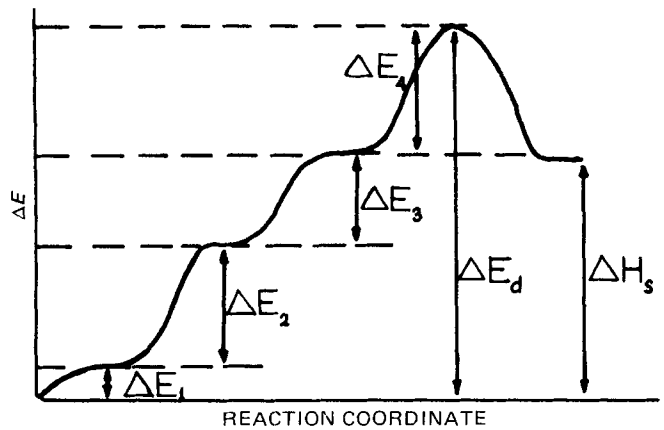

Figure 5—*Energy diagram for the dissolution of I.*

of ΔE_d based on the proposed energy diagram is quite good, considering the errors inherent in the graphical determination of energy values. This finding indicates that the proposed scheme of dissolution should reflect accurately the overall mechanism of the dissolution process. The sum of the energy terms of ΔE_1, ΔE_2, and ΔE_3, all of which are related to the process at the interface between the solid and solvent, is larger than ΔE_4, which is related to the dispersion process. This finding may also indicate that the energy barrier for dissolution of I is the interaction between the solvent and solid at the interface and not the mass transfer of solute into the bulk solution.

REFERENCES

(1) D. A. Wadke and G. E. Reier, *J. Pharm. Sci.*, **61**, 868 (1972).
(2) E. Shefter and T. Higuchi, *ibid.*, **52**, 781 (1963).
(3) J. W. Poole and C. K. Bahal, *ibid.*, **57**, 1945 (1968).
(4) A. J. Aguir and J. E. Zelmar, *ibid.*, **58**, 983 (1969).
(5) S. S. Szinai and A. Hunt, *Can. J. Pharm. Sci.*, **7**, 78 (1972).
(6) S. S. Szinai and N. Szinai, *ibid.*, **7**, 82 (1972).
(7) R. L. Nedich and D. O. Kildsig, *J. Pharm. Sci.*, **61**, 214 (1972).
(8) P. D. Krause and D. O. Kildsig, *ibid.*, **61**, 1478 (1972).

ACKNOWLEDGMENTS AND ADDRESSES

Received April 2, 1976, from the *Department of Industrial and Physical Pharmacy, School of Pharmacy and Pharmacal Sciences, Purdue University, West Lafayette, IN 47907.*

Accepted for publication August 30, 1976.

* David Ross Fellow. Present address: G.D. Searle Co., Chicago, Ill.

ˣ To whom inquiries should be directed.

Effect of Laboratory Light on Tetrazolium Reaction and on Stability of Formazans in Various Solvents

ROBERT E. GRAHAM *ˣ, EDWARD R. BIEHL ‡, and CHARLES T. KENNER ‡

Abstract □ Studies on purified formazans of blue tetrazolium and triphenyltetrazolium showed that ordinary laboratory fluorescent light of about 52-foot-candle intensity provided sufficient energy for phototransformation in certain nonpolar solvents. Slow reoxidation of formazan to tetrazolium was observed in all solvents tested in the presence or absence of light. Water greatly inhibited the oxidation of the red formazan of blue tetrazolium. The blue formazan of blue tetrazolium isomerized to the red formazan in protic solvents in the presence and absence of light. The photochromic phenomena for the blue formazan of blue tetrazolium and the formazan of triphenyltetrazolium in cyclohexane were completely reversible when exposed to alternate periods of intense light and darkness. Under irradiation, the formazans of blue tetrazolium and triphenyltetrazolium in chloroform solution formed their respective photoformazans; darkness reversed the process, and continued exposure of the same solutions for extended times or at a higher light intensity created a solution whose spectrum was no longer reversibly affected by the presence or absence of light. When alcohol USP is used as the solvent for the quantitative determination of corticosteroids, no light precautions need be observed, although reagent blanks have higher absorbances than light-protected solutions. Exact compensation is made by running samples and standards *versus* the reagent blank as recommended by the USP. When other solvents and/or tetrazolium reagents are used, special precautions may be required to keep the reagents, developing solutions, and final formazans protected from light to ensure a quantitative reaction.

Keyphrases □ Tetrazolium reagents—effect of laboratory light, various solvents □ Formazans—of blue tetrazolium and triphenyltetrazolium, stability, effect of laboratory light, various solvents □ Phototransformation—formazans of blue tetrazolium and triphenyltetrazolium, effect of various solvents □ Stability—formazans of blue tetrazolium and triphenyltetrazolium, effect of laboratory light, various solvents

The blue tetrazolium reaction is widely used for the analysis of corticosteroids. USP XIX (1) and NF XIV (2) indicate a slightly modified Mader and Bück procedure (3) for corticosteroid analysis. Blue tetrazolium (I) [3,3′-(3,3′-dimethoxy -4,4′- biphenylylene)bis(2,5-diphenyl-2*H*-tetrazolium chloride)] and triphenyltetrazolium (II) (2,3,5-triphenyl-2*H*-tetrazolium chloride) oxidize the α-keto moiety of the C_{17} side chain in strongly alkaline solution and are reduced quantitatively to highly colored formazans, which are measured spectrophotometrically.

The analytical procedure is subject to several variables such as temperature (4–6), solvent (1–3, 7–13), and concentrations of base (14), water (6, 14), and tetrazolium (6), as well as the steric configuration of the corticosteroid molecule (15). The effect of these variables is minimized by analyzing reagent blanks, standards, and samples concurrently.

Light may or may not influence the tetrazolium reaction. For example, both II (16, 17) and II formazan (10, 12, 16–19) were reported to be light sensitive. Photochemical reoxidation of II formazan to the tetrazolium salt in the presence of intermittent UV irradiation was observed (20). The I formazan was reported (21) to be photosensitive in chloroform solution, and the sensitivity of I to light in 60% chloroform was observed (11) to present problems in the assay. The use of actinic glassware was recommended in

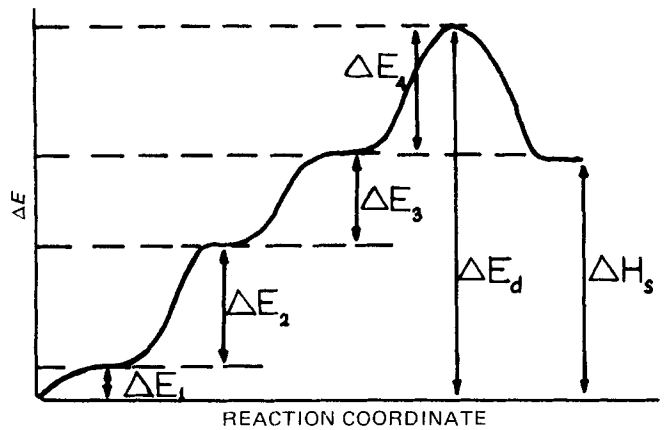

Figure 5—*Energy diagram for the dissolution of I.*

of ΔE_d based on the proposed energy diagram is quite good, considering the errors inherent in the graphical determination of energy values. This finding indicates that the proposed scheme of dissolution should reflect accurately the overall mechanism of the dissolution process. The sum of the energy terms of ΔE_1, ΔE_2, and ΔE_3, all of which are related to the process at the interface between the solid and solvent, is larger than ΔE_4, which is related to the dispersion process. This finding may also indicate that the energy barrier for dissolution of I is the interaction between the solvent and solid at the interface and not the mass transfer of solute into the bulk solution.

REFERENCES

(1) D. A. Wadke and G. E. Reier, *J. Pharm. Sci.*, **61**, 868 (1972).
(2) E. Shefter and T. Higuchi, *ibid.*, **52**, 781 (1963).
(3) J. W. Poole and C. K. Bahal, *ibid.*, **57**, 1945 (1968).
(4) A. J. Aguir and J. E. Zelmar, *ibid.*, **58**, 983 (1969).
(5) S. S. Szinai and A. Hunt, *Can. J. Pharm. Sci.*, **7**, 78 (1972).
(6) S. S. Szinai and N. Szinai, *ibid.*, **7**, 82 (1972).
(7) R. L. Nedich and D. O. Kildsig, *J. Pharm. Sci.*, **61**, 214 (1972).
(8) P. D. Krause and D. O. Kildsig, *ibid.*, **61**, 1478 (1972).

ACKNOWLEDGMENTS AND ADDRESSES

Received April 2, 1976, from the *Department of Industrial and Physical Pharmacy, School of Pharmacy and Pharmacal Sciences, Purdue University, West Lafayette, IN 47907.*

Accepted for publication August 30, 1976.

* David Ross Fellow. Present address: G.D. Searle Co., Chicago, Ill.

ˣ To whom inquiries should be directed.

Effect of Laboratory Light on Tetrazolium Reaction and on Stability of Formazans in Various Solvents

ROBERT E. GRAHAM *ˣ, EDWARD R. BIEHL ‡, and CHARLES T. KENNER ‡

Abstract □ Studies on purified formazans of blue tetrazolium and triphenyltetrazolium showed that ordinary laboratory fluorescent light of about 52-foot-candle intensity provided sufficient energy for phototransformation in certain nonpolar solvents. Slow reoxidation of formazan to tetrazolium was observed in all solvents tested in the presence or absence of light. Water greatly inhibited the oxidation of the red formazan of blue tetrazolium. The blue formazan of blue tetrazolium isomerized to the red formazan in protic solvents in the presence and absence of light. The photochromic phenomena for the blue formazan of blue tetrazolium and the formazan of triphenyltetrazolium in cyclohexane were completely reversible when exposed to alternate periods of intense light and darkness. Under irradiation, the formazans of blue tetrazolium and triphenyltetrazolium in chloroform solution formed their respective photoformazans; darkness reversed the process, and continued exposure of the same solutions for extended times or at a higher light intensity created a solution whose spectrum was no longer reversibly affected by the presence or absence of light. When alcohol USP is used as the solvent for the quantitative determination of corticosteroids, no light precautions need be observed, although reagent blanks have higher absorbances than light-protected solutions. Exact compensation is made by running samples and standards *versus* the reagent blank as recommended by the USP. When other solvents and/or tetrazolium reagents are used, special precautions may be required to keep the reagents, developing solutions, and final formazans protected from light to ensure a quantitative reaction.

Keyphrases □ Tetrazolium reagents—effect of laboratory light, various solvents □ Formazans—of blue tetrazolium and triphenyltetrazolium, stability, effect of laboratory light, various solvents □ Phototransformation—formazans of blue tetrazolium and triphenyltetrazolium, effect of various solvents □ Stability—formazans of blue tetrazolium and triphenyltetrazolium, effect of laboratory light, various solvents

The blue tetrazolium reaction is widely used for the analysis of corticosteroids. USP XIX (1) and NF XIV (2) indicate a slightly modified Mader and Bück procedure (3) for corticosteroid analysis. Blue tetrazolium (I) [3,3′-(3,3′-dimethoxy -4,4′- biphenylylene)bis(2,5-diphenyl-2*H*-tetrazolium chloride)] and triphenyltetrazolium (II) (2,3,5-triphenyl-2*H*-tetrazolium chloride) oxidize the α-keto moiety of the C_{17} side chain in strongly alkaline solution and are reduced quantitatively to highly colored formazans, which are measured spectrophotometrically.

The analytical procedure is subject to several variables such as temperature (4–6), solvent (1–3, 7–13), and concentrations of base (14), water (6, 14), and tetrazolium (6), as well as the steric configuration of the corticosteroid molecule (15). The effect of these variables is minimized by analyzing reagent blanks, standards, and samples concurrently.

Light may or may not influence the tetrazolium reaction. For example, both II (16, 17) and II formazan (10, 12, 16–19) were reported to be light sensitive. Photochemical reoxidation of II formazan to the tetrazolium salt in the presence of intermittent UV irradiation was observed (20). The I formazan was reported (21) to be photosensitive in chloroform solution, and the sensitivity of I to light in 60% chloroform was observed (11) to present problems in the assay. The use of actinic glassware was recommended in

Table I—Effect of Light on Reaction of I with Hydrocortisone

Sample	Net Absorbance at 90 min Light[a]	Dark[b]
1	0.577	0.578
2	0.579	0.579
3	0.580	0.579
4	0.578	0.579
5	0.578	0.577
6	0.578	0.579
7	0.579	0.578
8	0.579	0.576
9	0.579	0.579
10	0.581	0.579
Blank[c] (90 min)	0.066	0.044
Blank[c] (130 min)	0.076	0.051
Mean[d]	0.579	0.578
$SD^{d,e}$	0.001	0.001

[a] Exposed to laboratory fluorescent light of 52 ft-c. [b] Aluminum foil wrapped. [c] Measured against alcohol as reference. [d] Values for blanks are not included in mean and standard deviation figures reported. [e] Calculated by the method of Dean and Dixon (23).

a study of the effect of light and other parameters on the reaction of II with corticosteroids (12). In contrast, several studies (6, 22) found that the reaction of I with corticosteroids was not sensitive to light.

This paper reports the effect of laboratory fluorescent lighting on the compendial (1, 2) reaction of I with corticosteroids. The effect of fluorescent and incandescent light on I and II formazans in various solvents also is discussed.

EXPERIMENTAL

Apparatus—The following were used: UV–visible recording spectrophotometers[1] with 1-cm stoppered quartz matched cells, an electrobalance[2], a TLC apparatus[3], a light meter[4], an IR instrument[5], and a microscope light[6] equipped with a transformer.

Materials—The following solvents were used: distilled-in-glass acetone, acetonitrile, absolute methanol, chloroform, and cyclohexane; analytical reagent grade absolute ethanol, cyclohexanol, cyclohexene, carbon tetrachloride, dimethylformamide, dimethyl sulfoxide, *n*-hexane, and methylene chloride; alcohol USP; sodium borohydride[7], 0.8-cm (0.3-in.) pellets; blue tetrazolium[8]; triphenyltetrazolium[9]; 10% aqueous tetramethylammonium hydroxide[9]; and USP reference standard hydrocortisone and prednisone.

Reagents—Tetramethylammonium hydroxide (1%) was prepared by diluting 5.00 ml of 10% aqueous reagent to 50.0 ml with alcohol USP. Blue tetrazolium (5 mg/ml) was prepared by dissolving 250.0 mg of I in 50.0 ml of alcohol USP. A standard solution containing 0.010 mg of hydrocortisone/ml of alcohol USP was prepared.

General Procedure—All studies were performed in 25-ml glass-stoppered flasks, which were placed on white paper during irradiation. Unless otherwise indicated, the solutions were irradiated with laboratory fluorescent light of 52-foot-candle (ft-c) intensity. Spectrophotometric scans were made from 720 to 250 nm *versus* the same solvent as the blank unless otherwise noted.

Formazan Isolation—Actinic glassware and aluminum foil-wrapped columns were used to protect the formazans from light during the isolation procedures.

I Blue Formazan—One pellet of sodium borohydride was added to a solution containing 53 mg of I in 100 ml of absolute ethanol, and this mixture was placed in the dark for several days. The precipitate was filtered, washed with absolute ethanol, dissolved in chloroform, and evaporated to dryness to obtain the blue formazan.

I Red Formazan—Three milliliters of 10% tetramethylammonium hydroxide was added to a solution containing 75 mg of prednisone and 1.53 g of I in 300 ml of alcohol USP. The mixture was placed in the dark for 30 min and then transferred to a separator containing 600 ml of water and 100 ml of chloroform. This solution was shaken vigorously for 1 min, the layers were allowed to separate, and the chloroform layer was filtered through a 12-cm length of sodium sulfate. An additional 50-ml portion of chloroform was used to complete the extraction and to wash the formazan from the sodium sulfate column. The chloroform extracts were combined and evaporated to obtain the red formazan.

II Formazan—One pellet of sodium borohydride was added to a solution of 100 mg of II in 20 ml of absolute ethanol. The solution was kept in the dark for 24 hr; it was then transferred to a separator containing 80 ml of water and extracted repeatedly with chloroform until the aqueous phase became colorless. The combined chloroform extracts were filtered through chloroform-washed cotton and evaporated to dryness to obtain a pure crystalline formazan.

Effect of Light on I–Hydrocortisone Reaction—Ten 20.0-ml aliquots, each containing 0.200 mg of USP reference standard hydrocortisone in alcohol USP plus a reagent blank, were treated in accordance with the official procedure (1). Each of the 10 hydrocortisone standard solutions was scanned *versus* the reagent blank from 720 to 490 nm exactly 90 min after addition of the tetramethylammonium hydroxide reagent. The reagent blank was scanned *versus* alcohol USP exactly 90 and 130 min after addition of the tetramethylammonium hydroxide. All reagents and solutions were protected from light at all times. The experiment was repeated with the exception that all reagents and solutions were exposed to laboratory fluorescent lighting during the entire study.

Photochemical Effect of Laboratory Lighting on Tetrazolium Formazans—For each experiment involving formazans, aliquots of chloroform stock solutions were taken to dryness carefully, and these residues were dissolved in an appropriate volume of solvent. Care was taken to protect all solutions from light before the experiment was initiated.

Solutions of I blue formazan (0.0086 mg/ml), I red formazan (0.0647 mg/ml), and II formazan (0.0103 mg/ml) in each of several different solvents were exposed to laboratory lighting for 1 hr and to office lighting (78 candle power) for 19 hr, with spectra being obtained after 0, 20, and 60 min and 20 hr. These solutions were then exposed to intense incandescent light of approximately 1×10^4-ft-c intensity for 90 min and rescanned. Certain red formazan solutions were exposed to laboratory lighting for an additional 11 days. These solutions were then scanned and evaporated to dryness. Each residue was dissolved in alcohol USP, a pellet of sodium borohydride was added, and the absorption spectrum of the resulting solution was obtained.

Reversibility of Photoeffect on I and II Formazans—*I Blue Formazan in Chloroform*—Duplicate solutions containing 0.0687 mg of I blue formazan in 10.0 ml of chloroform were prepared; one solution was placed in the light and the other was kept in the dark for 24 hr. During this period, absorption spectra were determined periodically on each solution. Both solutions were subsequently exposed to alternating periods of laboratory lighting and darkness, and their visible absorption spectra were obtained periodically for an additional 976 hr. The solutions were then evaporated to dryness; each residue was dissolved in alcohol USP, a pellet of sodium borohydride was added, and the absorption spectrum of the resulting solution was obtained.

I Blue Formazan in Cyclohexane—A solution containing 0.0687 mg of I blue formazan in 10.0 ml of cyclohexane was exposed alternately to light and darkness for 960 hr, and absorption spectra were obtained during this time.

I Red Formazan in Chloroform—A solution containing 0.496 mg of

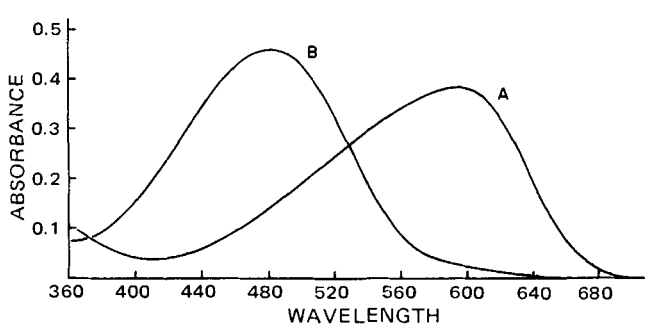

Figure 1—*Spectra of I blue formazan (A) and its photoformazan (B) in cyclohexane.*

[1] Cary models 15 and 17.
[2] Cahn model G-2.
[3] Eastman No. 6060 silica gel.
[4] Weston model 703-60.
[5] Perkin-Elmer model 337.
[6] Bausch & Lomb model 282.
[7] Alpha Products.
[8] Dajac Laboratories.
[9] Eastman Organic Chemicals.

Table II—Effect of Extent of Exposure on the λ_{max} and Absorbance Values of I Blue Formazan in Selected Solvents

Solvent	Minutes at 52 ft-c			19 hr at 78 ft-c	90 min at 1×10^4 ft-c
	0	20	60		
Absolute ethanol[a]	595 (0.140)[b]	595 (0.139)	595 (0.136)	575 (0.120)	570 (0.302)
Absolute methanol[a]	590 (0.055)	585 (0.051)	585 (0.045)	530 (0.108)	530 (0.150)
Acetone	594 (0.619)	594 (0.617)	593 (0.615)	590 (0.592)	573 (0.436)
Acetonitrile[a]	592 (0.340)	590 (0.350)	590 (0.350)	585 (0.340)	560 (0.365)
Alcohol USP[a]	580 (0.060)	580 (0.068)	575 (0.069)	550 (0.087)	550 (0.236)
Chloroform	595 (0.590)	592 (0.584)	588 (0.573)	592 (0.582)	575 (0.401)
Cyclohexane[a]	590 (0.176)	580 (0.149)	578 (0.123)	463 (0.360)	460 (0.470)
Dimethyl-formamide	602 (0.621)	602 (0.625)	602 (0.624)	602 (0.598)	595 (0.511)
Dimethyl sulfoxide	605 (0.518)	605 (0.577)	605 (0.584)	605 (0.573)	602 (0.525)
n-Hexane[a]	575 (0.114)	570 (0.112)	570 (0.105)	460 (0.195)	453 (0.463)

[a] The amount of I blue formazan taken was not completely dissolved in the volume of solvent used. [b] Values are the λ_{max}, nanometers, with the absorbance in parentheses.

I red formazan in 10.0 ml of chloroform was exposed to laboratory light and scanned periodically for 485 min. It was then treated as follows, with the absorption spectrum taken at the end of each step: dark, 88 hr; light, 24 hr; dark, 168 hr; light days and dark nights, 5 days; 78-ft-c light, 24 hr; dark, 48 hr; and the same light intensity, 18 hr.

Two additional solutions containing 0.496 mg of I red formazan in 8.0 and 10.0 ml of chloroform were prepared. The former solution was scanned, exposed to incandescent light of approximately 1×10^4 ft-c for 65 min, and scanned immediately after being exposed to light. The volume was adjusted to 8.0 ml after light exposure before scanning. The latter solution was kept in the dark for 23 days, and absorption spectra were obtained periodically during this time.

II Formazan in Chloroform—Ten milliliters of chloroform containing 0.161 mg of II formazan was exposed for 34 days to several cycles of laboratory light and darkness, and the absorption spectrum was obtained after each cycle. The experiment was repeated with a duplicate aliquot irradiated with approximately 1×10^4 ft-c of light intensity.

II Formazan in Cyclohexane—Ten milliliters of cyclohexane was pipetted into each of two flasks containing 0.161 mg of II formazan. One solution was exposed to laboratory lighting continuously for 53 hr; the other was wrapped in aluminum foil for the first 5 hr before exposure to light for 48 hr. Nine absorption spectra were made of these samples during this time. These solutions were then exposed to a light of approximately 1×10^4-ft-c intensity for short periods, scanned, placed in the dark overnight, and rescanned. This latter procedure was repeated through several cycles of light and darkness.

Rate Studies—*Light Effect*—A 10.0-ml chloroform solution containing 0.496 mg of I red formazan was exposed to laboratory light, and absorption spectra were obtained periodically during 485 min to follow the conversion of I red formazan to its photoformazan.

Dark Effect—A 4.0-ml chloroform solution containing 0.496 mg of I red formazan was exposed to laboratory fluorescent light of 78 ft-c intensity until the maximum amount of its yellow photoform was generated. The solution was placed in a stoppered spectrophotometric cell in the dark, and absorption spectra were made every 15 min for 8 hr.

Correlation of Phototransformation of Formazans to Photoformazans—Chloroform solutions of I red, I blue, and II formazans were scanned, irradiated with light to complete the conversion to their respective photoformazans, and then rescanned. The wavelength of the absorption maximum for each species was determined.

Photochemical Effect of Laboratory Lighting on Tetrazoliums—*Blue Tetrazolium*—A saturated solution of I in absolute ethanol and a concentration of 5 mg of I/ml of alcohol USP were exposed to laboratory fluorescent lighting for 4 days, after which time the absorption spectrum of each solution was taken.

Triphenyltetrazolium—A colorless solution of II in absolute ethanol and another in alcohol USP (both 5 mg/ml) were exposed for 24 hr to laboratory lighting and then scanned. The absolute ethanol solution was then divided into two parts; one part was used as a control, and enough water was added to the other to change it to the equivalent of alcohol USP. These solutions were exposed to light for 1 additional week and rescanned.

RESULTS AND DISCUSSION

The effect of laboratory fluorescent light upon the reaction of I with hydrocortisone is shown in Table I. The average net absorbance (0.578 ± 0.001 *SD*) of 10 determinations of hydrocortisone not exposed to light by the USP XIX (1) method was essentially the same as that (0.579 ± 0.001 *SD*) obtained for the same number of hydrocortisone determinations exposed to laboratory lighting. These results indicate that the net absorbance of this reaction is not affected by ordinary laboratory light. The reagent blank of I was found previously (10, 21) to be affected by light. This study found that the absorbance of the light-exposed blanks was approximately 1.5 times as great as the blank protected from light at 90 and 130 min from the start of the reaction. However, the procedure of running sample *versus* blank compensated for any deviation in the reagent blank caused by light.

The influence of light on the stability of I and II formazans in various solvents is listed in Tables II–IV. In general, the formazans were converted to photoderivatives in nonpolar solvents such as cyclohexane, *n*-hexane, and chloroform. Exposure of these solutions to laboratory lighting resulted in hypsochromic shifts of the absorption maxima. Figures 1 and 2 show typical absorption spectra of I blue and red formazans

Table III—Effect of Extent of Exposure on the λ_{max} and Absorbance Values of I Red Formazan to Light

Solvent	Minutes at 52 ft-c			19 hr at 78 ft-c	90 min at 1×10^4 ft-c
	0	20	60		
Absolute ethanol	522 (0.532)[a]	523 (0.529)	523 (0.546)	523 (0.480)	525 (0.426)
Absolute methanol	517 (0.521)	517 (0.526)	517 (0.522)	518 (0.521)	518 (0.490)
Acetone	525 (0.511)	520 (0.513)	520 (0.510)	520 (0.480)	ND[b]
Acetonitrile	515 (0.517)	515 (0.504)	512 (0.499)	512 (0.476)	500 (0.380)
Alcohol USP	522 (0.520)	522 (0.513)	522 (0.513)	525 (0.512)	520 (0.482)
Chloroform	525 (0.497)	500 (0.438)	465 (0.451)	440 (0.854)	525 (0.660)
Cyclohexane			Insoluble		
Dimethyl-formamide	535 (0.466)	535 (0.459)	535 (0.456)	535 (0.433)	535 (0.322)
Dimethyl sulfoxide	542 (0.486)	542 (0.483)	542 (0.483)	542 (0.482)	542 (0.452)
n-Hexane			Insoluble		

[a] Values are the λ_{max}, nanometers, with the absorbance in parentheses. [b] ND = not determined.

Table IV—Effect of Extent of Exposure on the λ_{max} and Absorbance Values of II Formazan in Selected Solvents

Solvent	Minutes at 52 ft-c			19 hr at 78 ft-c	90 min at 1×10^4 ft-c
	0	20	60		
Absolute ethanol	483 (0.566)[a]	483 (0.569)	483 (0.570)	483 (0.564)	483 (0.535)
Absolute methanol	480 (0.513)	480 (0.551)	480 (0.553)	480 (0.525)	480 (0.472)
Acetone	482 (0.572)	482 (0.533)	482 (0.573)	480 (0.492)[b]	480 (0.276)
Acetonitrile	480 (0.560)	480 (0.560)	478 (0.530)	405 (0.570)[b]	480 (0.302)
Alcohol USP	483 (0.558)	483 (0.569)	482 (0.561)	482 (0.560)	483 (0.510)
Carbon tetrachloride	490 (0.555)	488 (0.411)[b]	415 (0.470)[b]	489 (0.370)[b]	483 (0.070)
Chloroform	485 (0.540)	433 (0.414)[b]	406 (0.751)[b]	404 (0.749)[b]	486 (0.400)
Cyclohexane	487 (0.573)	486 (0.486)[b]	486 (0.496)[b]	487 (0.556)	400 (0.665)[b]
Cyclohexanol	488 (0.572)	487 (0.564)	487 (0.567)	487 (0.550)	486 (0.380)
Cyclohexene	490 (0.569)	490 (0.553)	489 (0.542)	489 (0.532)	489 (0.552)[c]
Dimethylformamide	485 (0.487)	485 (0.492)	483 (0.490)	483 (0.450)	484 (0.350)
Dimethyl sulfoxide	485 (0.496)	485 (0.495)	485 (0.496)	485 (0.469)	485 (0.367)
n-Hexane	478 (0.567)	480 (0.558)	480 (0.551)	413 (0.421)[b]	480 (0.235)
Methylene chloride	490 (0.561)	483 (0.465)[b]	403 (0.659)[b]	403 (1.007)[b]	482 (0.393)[b]

[a] Values are the λ_{max}, nanometers, with the absorbance in parentheses. [b] A second λ_{max} was observed in these solvents. [c] The yellow photosolution reverted completely to orange before the spectrum could be obtained.

and their corresponding yellow derivatives. The conversion of II formazan to its photoderivative was accompanied by a change in the color of the solution from orange to yellow. Small amounts of the three formazans were converted to the corresponding photoformazans in acetonitrile. The insolubility of I red formazan in cyclohexane and *n*-hexane prevented the investigation of the effect of light in these systems.

In the protic solvents, absolute methanol, absolute ethanol, and alcohol USP, I blue formazan was partially converted to I red formazan in the presence or absence of light. During this process, a gradual diminution in the absorption maxima at about 585 nm and a corresponding increase at approximately 525 nm were observed. The amount of conversion of the blue form to the red form decreased as the solvent was varied from absolute methanol to alcohol USP to absolute ethanol. These results are consistent with the conclusion of Graham *et al.* (13) that water and methanol stabilize the *trans-anti*-configuration of I red formazan to a larger extent than ethanol due to the smaller size and greater hydrogen-bonding ability of methanol and water.

Of all solvents studied, I red formazan was the most stable in absolute methanol in the presence of light, even though methanol inhibits the formation of I formazan in the reaction of I with corticosteroids. By using the procedure described previously (13), the formazans were reoxidized to tetrazolium in varying degrees in all solvents listed in Tables II–IV.

To study the influence of water on the stability of I red formazan toward light, selected solutions of this formazan were exposed to laboratory light for 12 days. After this time, the absorbance of the absolute ethanol solution was reduced to 47% of its original value; the absorbance of the alcohol USP solution was reduced to only 93%. Construction of Dreiding models revealed that the *trans-syn*-configuration, III, of I blue formazan would be more readily reoxidized to I than the *trans-anti*-configuration, IV, of I red formazan. Water stabilizes I red formazan (13) and thus acts to prevent the rearrangement of IV to III and the subsequent oxidation of III to I.

The reversibility of the photoeffect observed in solutions of I and II formazans was studied by exposing these solutions to alternating periods of light and darkness and obtaining spectra at appropriate times during each cycle. In cyclohexane, I blue formazan (λ_{max} 595 nm) and its photoderivative (λ_{max} 487 nm) were completely interconverted by the action of light and darkness during 960 hr. During this time, a small portion (21%) of I blue formazan was reoxidized to tetrazolium, as shown by a decrease in absorbance.

An immediate scan of II formazan in cyclohexane yielded an absorption spectrum of typical shape with a maximum at 486 nm. Further scans of the solution during light exposure produced time-related curves in which an absorption maximum of the photoderivative appeared at about 400 nm. The absorbance of this wavelength increased with time and reached a maximum after 30 min of light exposure. However, further scans during 53 hr of continued light exposure produced curves in which the photoderivative absorption maximum gradually disappeared to yield a spectrum similar to that of the original II formazan. The absorption spectrum of II formazan in a duplicate cyclohexane solution that was not exposed to light exhibited no change during 5 hr; however, when this solution was exposed to light for an additional 48 hr, periodic scans yielded spectra similar to those observed for the first solution. Figure 3 shows spectra typical of those obtained for II formazan in cyclohexane when irradiated with laboratory light.

Irradiation of a solution of II formazan in cyclohexane with approximately 1×10^4 ft-c of light intensity produced a light-stable yellow photoderivative (λ_{max} 400 nm), which could be converted to the original II formazan by darkness. These two species were readily interconvertible over several cycles of alternating intense light and darkness.

Five alternate periods of exposure of I blue formazan in chloroform to laboratory light and darkness during 1000 hr showed partial reversibility of the photoformazan. The wavelength and absorbance at the maximum returned to the starting value after each period of darkness, but there was less conversion to the photoform with each period of light exposure, as shown by decreased absorbance at 487 nm. This result indicates that two forms of I blue formazan exist and have similar absorbance maxima in chloroform. One form apparently is photolabile and converts gradually to the other, which is not further affected by light.

Spectra of the aliquot exposed to light in the initial 24 hr revealed that I blue formazan was converted mainly to its yellow photoform. A dupli-

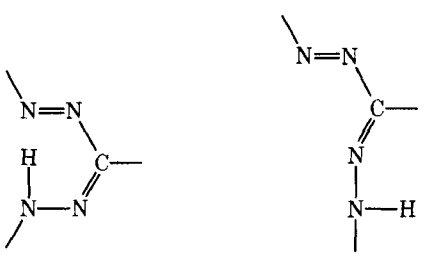

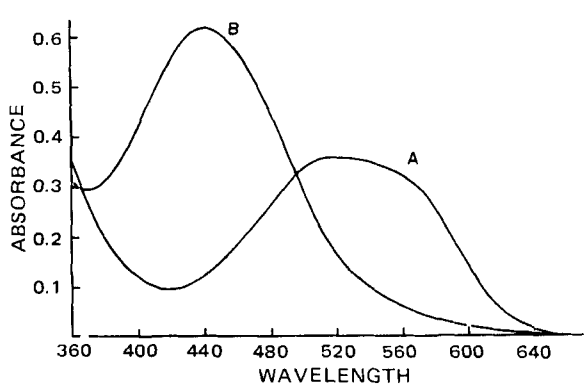

Figure 2—*Spectra of I red formazan (A) and its photoformazan (B) in chloroform.*

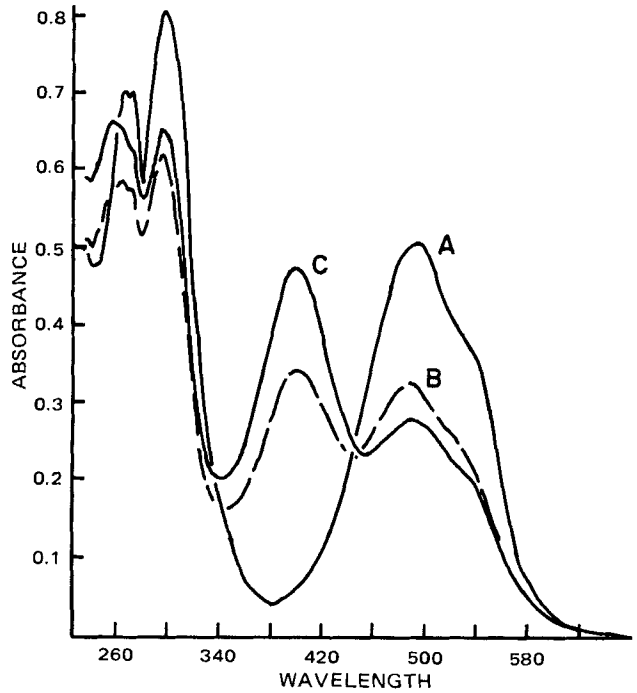

Figure 3—*Spectral changes of II formazan exposed to laboratory lighting. Key: A, identical spectra of II formazan and of II orange photoformazan; and B and C, intermediate spectra of the yellow photoderivative of II after different exposure periods.*

cate aliquot kept in the dark during the same period showed no spectral changes. However, when the latter solution was exposed to light, a similar photoeffect was observed. During the observation period, the absorbances of both solutions gradually decreased until they were free of color and contained only I. The addition of a sodium borohydride pellet to an alcoholic solution of the final tetrazolium residue yielded a mixture of I red and blue formazans (λ_{max} 555 nm). TLC confirmed the presence of both colored formazans in these solutions.

Exposure of a chloroform solution of I red formazan (λ_{max} 525 nm) to ordinary laboratory fluorescent lighting of approximately 52-ft-c intensity produced the corresponding yellow photoform (λ_{max} 440 nm). This photoform readily interconverted to I red formazan by exposure to alternating periods of light and darkness. Evaporation of the yellow photoform solution afforded the crystalline I red formazan, as determined by TLC, IR, and its reconversion to the yellow photoform derivative upon being redissolved in chloroform and exposed to laboratory light. During the evaporation process, the color of the solution changed from yellow to red immediately before dryness.

Exposure of a chloroform solution of the yellow photoform of I red

Table V—Change of Absorbance at 525 nm of I Red Formazan when Exposed to Laboratory Lighting

Minutes	Observed Absorbance[a]	Absorbance of Yellow Photoformazan[b]	Net Absorbance of Red Photoformazan
0	0.357	0.000	0.357
10	0.342	0.005	0.337
28	0.304	0.014	0.290
50	0.271	0.024	0.247
70	0.251	0.034	0.217
105	0.210	0.051	0.159
130	0.190	0.063	0.127
160	0.180	0.078	0.102
190	0.164	0.092	0.072
220	0.155	0.107	0.048
250	0.149	0.121	0.028
280[c]	0.136	0.136	0.000
310	0.136	0.136	0.000
485	0.136	0.136	0.000

[a] Includes the absorbance of I red formazan plus its photoformazan. [b] Absorbance due to the yellow photoformazan of I red formazan calculated from maximum absorbance (0.136), assuming that the rate of formation of the photoformazan is constant. [c] Complete conversion to photoformazan occurs by this time.

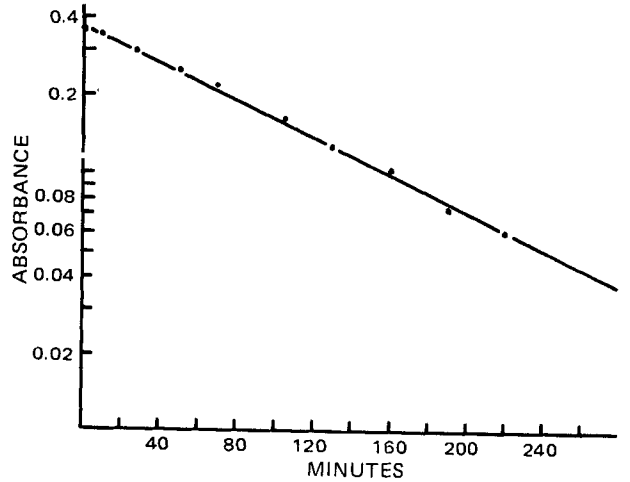

Figure 4—*Rate of change of I red formazan to its yellow photoform in chloroform when exposed to laboratory lighting.*

formazan to ordinary office light of approximately 72 ft-c for about 16 hr converted it to a red color with a spectrum like the original. This spectrum does not change upon further exposure to alternate periods of light and darkness. Exposure of a chloroform solution of I red formazan to intense incandescent light of approximately 1×10^4 ft-c produced a yellow color within 2 min, which remained unchanged for 1 hr under continuous irradiation and then quickly turned (5 min) to red. The spectrum of the final red solution was similar to the original, but the absorbance was 44% higher in the final solution as compared to the original. The higher absorbances and the lack of response of this photoform to successive periods of light and darkness indicate that it may be a different high energy conformer than the original I red formazan. A chloroform solution of the I red formazan that was kept in the dark and scanned periodically showed no change in the spectrum during 23 days.

The II formazan in chloroform demonstrated a photoeffect during the first 2 hr of exposure to laboratory fluorescent lighting, as shown by a change in color from orange to yellow and by a hypsochromic shift of the maximum from 487 to 406 nm. Within the next 5 hr of exposure, the solution returned to an orange color with a spectrum similar to the original and a bathochromic shift of the maximum back to 487 nm. No change was observed in the spectra following successive exposures of the solution to light and dark during the next 33 days, except for a gradual reduction in the intensity of the color due to the oxidation of the orange photoformazan back to II. A chloroform solution of II formazan, when irradiated with approximately 1×10^4 ft-c, changed to a yellow color within 1 min and back to orange within 5 min. The spectrum of the latter color was similar in absorbance and shape to the original formazan but was not reversible when exposed to additional periods of light and dark.

Table V lists the spectral data obtained from the rate study of the conversion of I red formazan to its photoderivative in chloroform in the presence of laboratory light. The observed absorbance values at 525 nm had to be corrected for a small amount of overlap of the absorption maximum of the yellow photoform of I red formazan (Fig. 2). From the graph of the corrected absorbance *versus* time (Fig. 4), the rate of conversion of I red formazan to its photoderivative in chloroform was found to be 1.4×10^{-3} absorbance unit/min.

A sequence of spectrophotometric scans of the regeneration of I red formazan from its yellow photoformazan in chloroform in the dark was taken at 15-min intervals over 8 hr. These scans revealed isosbestic points at 370 and 490 nm, indicating that these two species were in equilibrium with each other. The rate for the regeneration process calculated either from the decrease in absorbance of the yellow form or from the increase in absorbance of the red form corrected for overlap by the yellow form yielded the same value, 2.5×10^{-3} absorbance unit/min.

The difference in energy of the transformation of a formazan to its photoderivative may be calculated from:

$$\Delta E = \frac{hc(\lambda_2 - \lambda_1)}{\lambda_2 \lambda_1} \qquad \text{(Eq. 1)}$$

where ΔE is the difference in energy in ergs at the longer wavelength (λ_2) of absorption of the formazan and the shorter wavelength (λ_1) of the photoform, h is Planck's constant, and c is the speed of light. By using

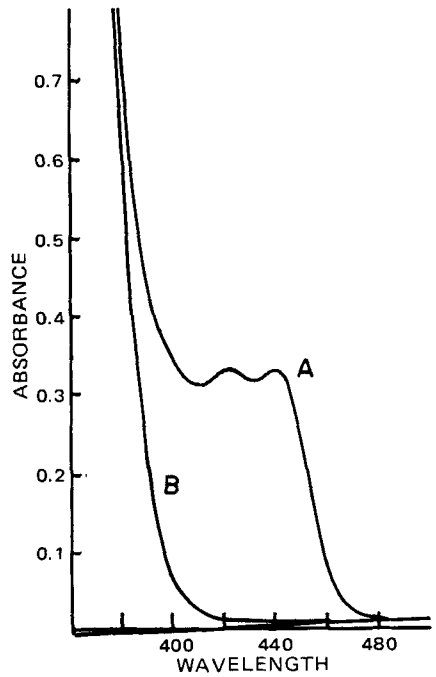

Figure 5—*Spectra of II (B) and its photoderivative (A) in absolute ethanol.*

the maximum absorption values for the hypsochromic shifts observed in chloroform solutions of 595–487 nm for I blue formazan, 525–440 nm for I red formazan, and 487–407 nm for II formazan, the following ΔE values were calculated: 7.31×10^{-13} erg for the I blue formazan transformation, 7.40×10^{-13} erg for the I red formazan transformation, and 8.02×10^{-13} erg for the II formazan transformation. These calculated values indicate that the transformation process is similar for all three formazans.

A possible mechanism for the phototransformation of I blue and red formazans is suggested in Scheme I. The *trans–syn*-configuration, III, of I blue formazan is isomerized to the *cis–syn*-configuration, V, and the *trans–anti*-configuration, IV, of I red formazan is isomerized to the *cis–anti*-configuration, VI, by absorption of light by the N=N moiety. Construction of Dreiding models revealed that steric effects prevent coplanarity of the conjugated π electronic system in the photoderivatives, V and VI, which would account for the hypsochromic shifts observed in these phototransformations.

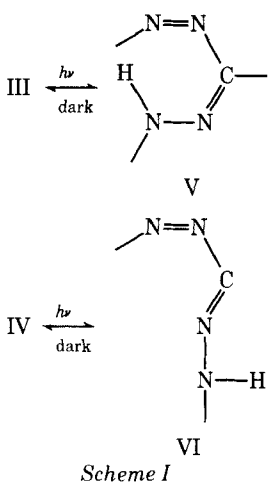

Scheme I

Finally, the stability of I and II in the presence of light was studied. Solutions of I in absolute ethanol and alcohol USP showed no apparent change in their absorption spectra after extended exposure to laboratory light. However, when II reagent in absolute alcohol was exposed to laboratory lighting, the solution changed from colorless to yellow within a few hours. The absorption spectrum of this solution (Fig. 5) shows the presence of two additional peaks with maxima at 420 and 440 nm. Addition of water to a portion of the yellow photosolution of II sufficient to make a 95% ethanol–water mixture (USP) caused the solution to become colorless within 1 week of continuous light exposure. The other portion of the absolute ethanol solution remained yellow. A control solution of II in absolute ethanol kept in the dark as well as a similar concentration of II in alcohol USP exposed to laboratory light for the same period remained colorless.

These experiments showed that ordinary laboratory fluorescent lighting of approximately 52–74 ft-c provided sufficient energy for phototransformations of the formazans studied to take place in certain nonpolar solvents. Alcohol USP, recommended by the compendia (1, 2), is the solvent of choice for both the tetrazolium reagent and the I reaction with corticosteroids since no special light precautions need be observed, although reagent blanks have higher absorbances than light-protected ones. Exact compensation is made by running samples and standards *versus* the blanks in accordance with the official procedure. If other solvents and/or tetrazolium reagents are used, special precautions may be required to keep the reagents, developing solutions, and final formazans protected from light to ensure a quantitative reaction.

REFERENCES

(1) "The United States Pharmacopeia," 19th rev., Mack Publishing Co., Easton, Pa., 1975, p. 622.

(2) "The National Formulary," 14th ed., Mack Publishing Co., Easton, Pa., 1975, p. 976.

(3) W. J. Mader and R. R. Buck, *Anal. Chem.*, **24**, 666 (1952).

(4) T. E. Weichselbaum and H. Margraf, *J. Clin. Endocrinol. Metab.*, **15**, 970 (1955).

(5) W. Nowaczynski, M. Goldner, and J. Genest, *J. Lab. Clin. Med.*, **45**, 818 (1955).

(6) R. O. Rechnagel and M. Litteria, *ibid.*, **48**, 463 (1956).

(7) D. E. Guttman, *J. Pharm. Sci.*, **55**, 919 (1966).

(8) P. E. Manni and J. E. Sinsheimer, *Anal. Chem.*, **33**, 1900 (1961).

(9) J. E. Sinsheimer and E. F. Salim, *ibid.*, **37**, 29 (1965).

(10) C. A. Johnson, R. King, and C. Vikers, *Analyst*, **85**, 714 (1960).

(11) P. Ascione and C. Fogelin, *J. Pharm. Sci.*, **52**, 709 (1963).

(12) J. J. Callahan, F. Litterio, E. Britt, B. D. Rosen, and J. Owens, *ibid.*, **51**, 333 (1962).

(13) R. E. Graham, E. R. Biehl, and C. T. Kenner, *ibid.*, **65**, 1048 (1976).

(14) R. E. Graham and C. T. Kenner, *ibid.*, **62**, 103 (1973).

(15) R. E. Graham, E. R. Biehl, C. T. Kenner, G. H. Luttrell, and D. L. Middleton, *ibid.*, **64**, 226 (1975).

(16) A. W. Nineham, *Chem. Rev.*, **55**, 355 (1955).

(17) B. Jambor, *Nature*, **173**, 774 (1954).

(18) "The United States Pharmacopeia," 16th rev., Mack Publishing Co., Easton, Pa., 1960, p. 569.

(19) R. Kuhn and H. M. Weitz, *Chem. Ber.*, **86**, 1199 (1953).

(20) V. P. Moekel, *Z. Chem.*, **11**, 421 (1963).

(21) A. M. Rutenberg, R. Gofstein, and A. M. Seligman, *Cancer Res.*, **10**, 113 (1950).

(22) F. M. Kunze and J. S. Davis, *J. Pharm. Sci.*, **53**, 1259 (1964).

(23) R. B. Dean and W. J. Dixon, *Anal. Chem.*, **23**, 636 (1951).

ACKNOWLEDGMENTS AND ADDRESSES

Received July 15, 1976, from the [*]*Dallas District, Food and Drug Administration, Dallas, TX 75204*, and the [‡]*Department of Chemistry, Southern Methodist University, Dallas, TX 75275.*

Accepted for publication September 7, 1976.

[x] To whom inquiries should be directed.

Anticonvulsant Activity and Selective Inhibition of NAD-Dependent Oxidations in Rat Brain Homogenates by Newer Mercaptotriazoles

SURENDRA S. PARMAR *‡ˣ, MAHIMA CHAUDHARY *, SUNIL K. CHAUDHARY *, SUSHIL KUMAR *, and HERZL R. SPIRO ‡

Abstract □ Eight 1-(2,6-dimethylphenoxyacetyl)-4-(substituted phenyl)thiosemicarbazides were cyclized to the corresponding 5-(2,6-dimethylphenoxymethyl)-4-(substituted phenyl)-3-mercapto-1,2,-4(4*H*)-triazoles and 5-(2,6-dimethylphenoxymethyl)-4-(substituted phenyl)-3-[1,2,4(4*H*)-triazolethioglycolic] acids. These compounds were characterized by their sharp melting points, elemental analyses, and IR spectra and were evaluated for anticonvulsant activity. The degree of protection (range) provided by these thiosemicarbazides, triazoles, and triazolethioglycolic acids at a dose of 100 mg/kg ip against pentylenetetrazol (90 mg/kg sc)-induced convulsions in mice was 10–50, 20–80, and 10–70%, respectively, where cyclization to triazoles increased anticonvulsant activity of the precursor thiosemicarbazides. Increased protection by these compounds against convulsions was generally associated with decreased 24-hr pentylenetetrazol-induced mortality. These compounds exhibited selective *in vitro* inhibition of nicotinamide adenine dinucleotide (NAD)-dependent oxidation of pyruvate, α-ketoglutarate, and NADH by rat brain homogenates while NAD-independent oxidation of succinate remained unaltered. The presence of added NAD to the reaction mixture during *in vitro* oxidation of pyruvic acid not only increased the respiratory activity of rat brain homogenates but also decreased the inhibitory effectiveness of thiosemicarbazides, triazoles, and triazolethioglycolic acids. The degree of selective inhibition of NAD-dependent oxidations was unrelated to their anticonvulsant activity.

Keyphrases □ Thiosemicarbazides, various—synthesized, evaluated for anticonvulsant activity and effect on NAD-dependent oxidations, rats □ Mercaptotriazoles, various—synthesized, evaluated for anticonvulsant activity and effect on NAD-dependent oxidations, rats □ Triazolethioglycolic acids, various—synthesized, evaluated for anticonvulsant activity and effect on NAD-dependent oxidations, rats □ Anticonvulsant activity—evaluated in various thiosemicarbazides, mercaptotriazoles, and triazolethioglycolic acids, rats □ NAD-dependent oxidations—effect of various thiosemicarbazides, mercaptotriazoles, and triazolethioglycolic acids, rat brain homogenates □ Oxidations, NAD dependent—effect of various thiosemicarbazides, mercaptotriazoles, and triazolethioglycolic acids, rat brain homogenates □ Structure–activity relationships—various thiosemicarbazides, mercaptotriazoles, and triazolethioglycolic acids evaluated for anticonvulsant activity and effect on NAD-dependent oxidations, rats

Interest has been focused on the pharmacology of 1-phenyl-1,2,4-triazoles and 4-phenyl-1,2,4-triazoles (1). Earlier studies indicated central nervous system depressant (2), analgesic (3), and anti-inflammatory (4, 5) properties of 1,2,4(4*H*)-triazoles. Furthermore, 1,4-disubstituted thiosemicarbazides, the precursors for the synthesis of cyclized triazoles, possess a broad spectrum of biological activities (6, 7). Anticonvulsant compounds also cause selective inhibition of nicotinamide adenine dinucleotide (NAD)-dependent oxidations (8).

These observations prompted synthesis of eight 1-(2,6-dimethylphenoxyacetyl)-4-(substituted phenyl)-thiosemicarbazides and their corresponding cyclized 5-(2,6-dimethylphenoxymethyl)-4-(substituted phenyl)-3-mercapto-1,2,4(4*H*)-triazoles. The substituted triazoles were further converted into 5-(2,6-dimethylphenoxymethyl)-4-(substituted phenyl)-3-[1,2,4(4*H*)-triazolethioglycolic] acids. The effects of all compounds were determined on the respiratory activity of rat brain homogenates in an attempt to elucidate the biochemical basis for their anticonvulsant activity.

CHEMISTRY

The various substituted 1,2,4(4*H*)-triazoles were synthesized by following the reactions outlined in Scheme I. Conversion of 2,6-dimethylphenol (I) to ethyl 2,6-dimethylphenoxyacetate (II) was carried out to synthesize 2,6-dimethylphenoxyacetohydrazide (III) through refluxing in ethanol with 99–100% hydrazine hydrate. Substituted thiosemicarbazides (IV–XI, Table I), prepared by the reaction of III with the appropriate aryl isothiocyanate, were cyclized to the corresponding mercaptotriazoles (XII–XIX, Table II) in 2 *N* NaOH. Condensation of the substituted triazoles with monochloroacetic acid resulted in the formation of substituted 3-triazolethioglycolic acids (XX–XXVII, Table III). All compounds were characterized by their sharp melting points, elemental analyses, and IR spectra.

EXPERIMENTAL[1]

Ethyl 2,6-Dimethylphenoxyacetate (II)—Equimolar quantities of I (0.2 mole), ethyl chloroacetate (0.2 mole), and potassium carbonate (0.25 mole) in dry acetone (60 ml) were refluxed under anhydrous conditions for 12 hr. The reaction mixture was filtered, and the filtrate was poured over 100 ml of ice-cold water. The separated ester was extracted with ether and dried over anhydrous magnesium sulfate. Excess ether was removed by distillation, the remaining liquid fraction was subjected to fractional distillation, and the fraction boiling at 270° was collected, yield 33.3 g (80%).

2,6-Dimethylphenoxyacetohydrazide (III)—To a solution of 0.15 mole (31.2 g) of II in absolute ethanol (50 ml) was added 10 g of 99–100% hydrazine hydrate, and the mixture was refluxed under anhydrous conditions on a water bath for 4 hr. A white solid mass, which separated on cooling, was collected by filtration and recrystallized from ethanol into white crystalline solid, mp 92°, yield 17.4 g (60%).

Anal.—Calc. for $C_{10}H_{14}N_2O_2$: C, 61.85; H, 7.21; N, 14.63. Found: C, 61.40; H, 7.36; N, 14.98.

1-(2,6-Dimethylphenoxyacetyl)-4-(substituted Phenyl)-thiosemicarbazides (IV–XI)—Equimolar quantities of III (0.02 mole) and the appropriate aryl isothiocyanate (0.02 mole) were mixed in dry benzene, and the mixture was refluxed on a steam bath for 2 hr. Excess benzene was removed by distillation. The separated solid was collected by filtration, washed with a cold ethanol–water mixture, dried, and recrystallized from ethanol. The various substituted thiosemicarbazides (Table I) were characterized by their sharp melting points and elemental analyses.

5-(2,6-Dimethylphenoxymethyl)-4-(substituted Phenyl)-3-mercapto-1,2,4(4*H*)-triazole (XII–XIX)—A solution of 1-(2,6-dimethylphenoxyacetyl)-4-(substituted phenyl)thiosemicarbazide (0.01 mole) in 2 *N* NaOH was refluxed over a free flame for 2–3 hr. After cooling, the mixture was filtered; the filtrate was acidified with dilute hydrochloric acid until complete precipitation occurred (9, 10). The separated solid was collected by filtration, washed with water, dried, and recrystallized from ethanol. Various substituted mercaptotriazoles were characterized by their sharp melting points and elemental analyses (Table II).

[1] All compounds were analyzed for their carbon, hydrogen, and nitrogen content. Melting points were taken in open capillary tubes with a partial immersion thermometer and are corrected. IR spectra provided support for the structures of these compounds.

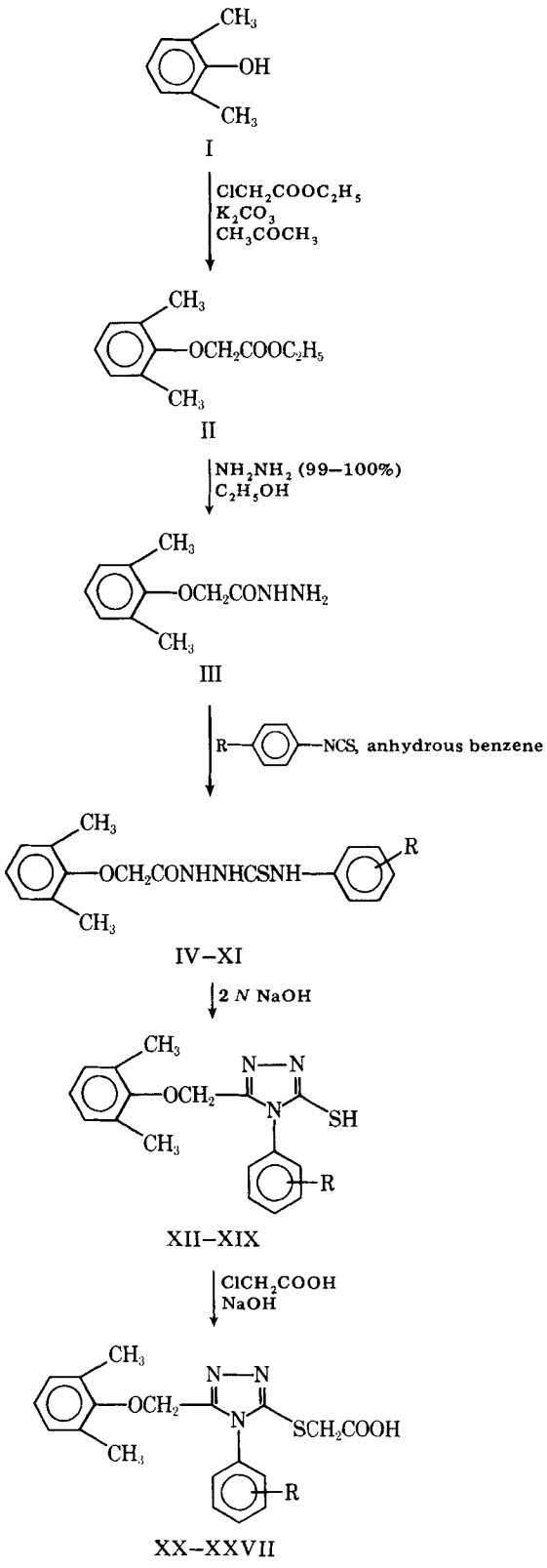

Scheme I

5-(2,6-Dimethylphenoxymethyl)-4-(substituted Phenyl)-3-[1,2,4(4*H*)-triazolethioglycolic] Acids (XX–XXVII)—A mixture of the appropriate substituted mercaptotriazole (0.005 mole), chloroacetic acid (0.005 mole), and sodium hydroxide (0.01 mole) was refluxed for 3 hr. The mixture was cooled and acidified with dilute hydrochloric acid. The solid mass, which separated slowly from the acid solution, was collected by filtration and recrystallized from ethanol (11) (Table III).

Determination of Respiratory Activity of Rat Brain Homogenates[2]—Male albino rats, 100–150 g, were kept on an *ad libitum* diet until they were sacrificed by decapitation. The brains were removed immediately and homogenized[3] in ice-cold 0.25 *M* sucrose in a ratio of 1:9 (w/v). All incubations were carried out at 37° in the conventional Warburg manometric apparatus, using air as the gas phase (12). The oxygen uptake was measured at 10-min intervals.

Fresh brain homogenate (1 ml) equivalent to 100 mg wet brain weight was added to the chilled Warburg vessels containing 6.7 m*M* magnesium sulfate, 20 m*M* dibasic sodium phosphate buffer solution (pH 7.4), 1 m*M* adenosine monophosphate (sodium salt), 33 m*M* potassium chloride, and 500 μg of cytochrome c in a final volume of 3 ml unless otherwise stated. The central well contained 0.2 ml of 20% KOH solution. Pyruvate, α-ketoglutarate, and succinate were used at a final concentration of 10 m*M*; NAD and NADH were used at 0.5 m*M*. It was presumed that the endogenous NAD, present in brain homogenates, was sufficient for the cellular respiratory activity of rat brain homogenates.

All test compounds were dissolved in propylene glycol (100%) and were used at a final concentration of 2 m*M*. An equal volume of propylene glycol was added to the control vessels.

Determination of Anticonvulsant Activity—Anticonvulsant activity was determined (13) in mice of both sexes weighing 25–30 g. The mice were divided into groups of 10, keeping the group weights as near the same as possible. The test compounds were suspended in 5% aqueous gum acacia (1% w/v) and injected in a group of 10 mice each at a dose of 100 mg/kg ip. Four hours after the administration of the test compound, the mice were injected with 90 mg/kg sc of pentylenetetrazol. This dose of pentylenetetrazol not only produced convulsions in almost all untreated mice but also caused 100% mortality during the 24-hr period. No mortality was found in mice treated with 100 mg/kg alone of the test compounds, and the animals were devoid of any behavioral effects.

The occurrence of seizures was observed for 60 min. An episode of clonic spasm that persisted for a minimum of 5 sec after administration of pentylenetetrazol was considered a threshold convulsion. Transient intermittent jerks and tremulousness were not counted. Animals devoid of threshold convulsions during 60 min were considered protected. The number of animals protected in each group was recorded, and the anticonvulsant activity of the test compounds was represented as the percent protection. The mice were then observed for 24 hr, and their mortality was recorded.

RESULTS AND DISCUSSION

In the present study, the anticonvulsant activity possessed by thiosemicarbazides, triazoles, and triazolethioglycolic acids was reflected by their ability to provide 10–50% (Table I), 20–80% (Table II), and 10–70% (Table III) protection, respectively, against pentylenetetrazol (90 mg/kg sc)-induced convulsions in mice at a dose of 100 mg/kg ip. Compounds V, X, and XXII were devoid of anticonvulsant activity, since no protection was observed at 100 mg/kg. These results indicated an increase in anticonvulsant activity by cyclization of the precursor thiosemicarbazides into the corresponding triazoles. Further conversion of the triazoles into the corresponding triazolethioglycolic acids in most cases caused a decrease in their anticonvulsant activity; however, XXIV and XXV provided greater protection than their precursors (XVI and XVII).

These results did not provide any specific requirements in the molecular structure of these compounds to warrant structure–activity relationships with respect to the anticonvulsant activity. In addition, the anticonvulsant activity of some substituted mercaptotriazoles alone was comparable to that of methaqualone and meprobamate, which provided 60 and 80% protection, respectively, at 100 mg/kg ip against pentylenetetrazol-induced convulsions in mice under similar experimental conditions (14).

All thiosemicarbazides, triazoles, and triazolethioglycolic acids selectivity inhibited NAD-dependent oxidation of pyruvate, α-ketoglutarate, and NADH by rat brain homogenates at 2 m*M* (Table IV). The degree of inhibition of pyruvic acid oxidation ranged from 35.4 to 93.7, from 18.5 to 62.3, and from 30.5 to 90.8% with thiosemicarbazides, triazoles, and triazolethioglycolic acids, respectively. Similar inhibition of the oxidation of α-ketoglutarate was 30.5–54.2, 14.4–46, and 37.2–64.7%, respectively. Of NADH, it was 36.2–60.2, 14.1–89.2, and 45.6–67.5% by thiosemicarbazides, triazoles, and triazolethioglycolic acids, respectively. Oxidation of succinate remained unaltered in the presence of these compounds.

[2] Commercial chemicals were used. Sodium pyruvate, sodium α-ketoglutarate, NADH, sodium succinate, adenosine monophosphate (sodium salt), and cytochrome c were obtained from Sigma Chemical Co., St. Louis, Mo.

[3] Potter–Elvehjem.

Table I—1-(2,6-Dimethylphenoxyacetyl)-4-(substituted Phenyl)thiosemicarbazides and Their Anticonvulsant Activity

Compound	R	Melting Point	Yield, %	Molecular Formula	Analysis, %	Calc.	Found	Anticonvulsant Activity[a], % Protection	Pentylenetetrazol Mortality[b], %
IV	H	166°	73	$C_{17}H_{19}N_3O_2S$	C	62.00	62.20	30	50
					H	5.77	5.78		
					N	12.76	12.60		
V	2-CH_3	150°	70	$C_{18}H_{21}N_3O_2S$	C	62.97	62.80	Nil	90
					H	6.12	6.32		
					N	12.24	12.13		
VI	4-CH_3[c]	168°	68	$C_{18}H_{21}N_3O_2S$	C	62.97	62.86	50	70
					H	6.12	6.32		
					N	12.24	12.25		
VII	2,4-$(CH_3)_2$	108°	81	$C_{19}H_{23}N_3O_2S$	C	63.86	63.72	30	50
					H	6.44	6.54		
					N	11.76	11.80		
VIII	2,6-$(CH_3)_2$	170°	60	$C_{19}H_{23}N_3O_2S$	C	63.86	63.72	10	100
					H	6.44	6.46		
					N	11.76	11.60		
IX	2-OCH_3	144°	68	$C_{18}H_{21}N_3O_3S$	C	60.16	60.20	50	50
					H	5.84	5.60		
					N	11.69	11.70		
X	4-OCH_3	142°	66	$C_{18}H_{21}N_3O_3S$	C	60.16	60.26	Nil	90
					H	5.84	5.76		
					N	11.69	11.72		
XI	4-Cl	174°	65	$C_{17}H_{18}ClN_3O_2S$	C	56.12	56.29	30	10
					H	4.95	5.02		
					N	11.55	11.64		

[a] Anticonvulsant activity was determined at 100 mg/kg ip as described under *Experimental*. [b] Represents mortality over 24 hr in each group of animals administered pentylenetetrazol (90 mg/kg sc). [c] The presence of characteristic bands of C=O (attached to nitrogen), C=S (flanked by nitrogen), and NH groups at 1695, 1538, and 3344 cm^{-1}, respectively, in the IR spectrum of VI provided further support for the structure of substituted thiosemicarbazides.

Addition of NAD during the oxidation of pyruvate not only increased the respiratory activity of rat brain homogenates but also decreased the ability of these compounds to inhibit pyruvate oxidation, as reported earlier with quinazolones (15), β-aminoketones (12), and thiazolidones (16). The degree of inhibition of 35.4–93.7, 18.5–62.3, and 30.5–90.8% observed during the oxidation of pyruvate by thiosemicarbazides, triazoles, and triazolethioglycolic acids was reduced to 26.2–82.3, 10.7–52.7, and 25.5–79.3%, respectively, in the presence of added NAD. These results provided evidence for a possible competition between thiosemicarbazides, triazoles, and triazolethioglycolic acids and NAD for the active site(s) on the enzyme molecule. Cyclization to triazoles caused a significant decrease in the ability of triazoles to inhibit NAD-dependent oxidations as compared to precursor thiosemicarbazides. Further conversion of triazoles into triazolethioglycolic acids increased the inhibitory effectiveness of the latter compounds to inhibit respiratory activity of rat brain homogenates with pyruvate, α-ketoglutarate, and NADH as the substrates.

As was observed with the anticonvulsant activity possessed by these compounds, their selective inhibition of NAD-dependent oxidations was unrelated to their structure; a definite structure–activity relationship was not exhibited (Table IV). The ability of these thiosemicarbazides, triazoles, and triazolethioglycolic acids to inhibit oxidation of pyruvate, α-ketoglutarate, and NADH provides evidence regarding the possible inactivation of the electron-transfer process in the electron-transport chain by their actions presumably at the site of transfer of electrons from NADH to flavine adenine dinucleotide.

Contrary to the increase in the anticonvulsant activity observed after cyclization of thiosemicarbazides into triazoles, the results indicated a decrease in the ability of triazoles to inhibit NAD-dependent oxidations by rat brain homogenates. Thus, selective inhibition of the respiratory

Table II—5-(2,6-Dimethylphenoxymethyl)-4-(substituted Phenyl)-3-mercapto-1,2,4(4*H*)-triazoles and Their Anticonvulsant Activity

Compound	R	Melting Point	Yield, %	Molecular Formula	Analysis, %	Calc.	Found	Anticonvulsant Activity[a], % Protection	Pentylenetetrazol Mortality[a], %
XII	H	246°	77	$C_{17}H_{17}N_3OS$	C	65.59	65.40	80	20
					H	5.46	5.23		
					N	13.50	13.26		
XIII	2-CH_3	201°	80	$C_{18}H_{19}N_3OS$	C	66.46	66.72	60	40
					H	5.84	5.76		
					N	12.92	12.90		
XIV	4-CH_3[b]	182°	58	$C_{18}H_{19}N_3OS$	C	66.46	66.42	50	50
					H	5.84	5.62		
					N	12.92	12.96		
XV	2,4-$(CH_3)_2$	204°	70	$C_{19}H_{21}N_3OS$	C	67.25	66.96	70	20
					H	6.19	6.32		
					N	12.39	12.50		
XVI	2,6-$(CH_3)_2$	220°	56	$C_{19}H_{21}N_3OS$	C	67.25	67.50	50	60
					H	6.19	6.38		
					N	12.39	12.40		
XVII	2-OCH_3	198°	64	$C_{18}H_{19}N_3O_2S$	C	63.34	63.50	40	70
					H	5.57	5.60		
					N	12.31	12.56		
XVIII	4-OCH_3	184°	67	$C_{18}H_{19}N_3O_2S$	C	63.34	63.24	50	70
					H	5.57	5.60		
					N	12.31	12.52		
XIX	4-Cl	194°	68	$C_{17}H_{16}ClN_3OS$	C	59.04	58.96	20	60
					H	4.63	4.72		
					N	12.15	12.25		

[a] Screening procedures were as indicated in Table I. [b] The presence of the characteristic band of C=N (1610 cm^{-1}) and the absence of the C=O stretching band in the IR spectrum of XIV provided further support for the structure of substituted mercaptotriazoles.

Table III—5-(2,6-Dimethylphenoxymethyl)-4-(substituted Phenyl)-1,2,4(4*H*)triazole-3-yl-thioglycolic Acids and Their Anticonvulsant Activity

Compound	R	Melting Point	Yield, %	Molecular Formula	Analysis, %	Calc.	Found	Anticonvulsant Activity[a], % Protection	Pentylenetetrazol Mortality[a], %
XX	H	152°	60	$C_{19}H_{19}N_3O_3S$	C	61.79	61.60	10	70
					H	5.14	5.20		
					N	11.38	11.42		
XXI	2-CH_3[b]	200°	65	$C_{20}H_{21}N_3O_3S$	C	62.66	62.40	30	70
					H	5.48	5.60		
					N	10.96	11.20		
XXII	4-CH_3	172°	70	$C_{20}N_{21}N_3O_3S$	C	62.66	62.44	Nil	50
					H	5.48	5.30		
					N	10.96	10.68		
XXIII	2,4-$(CH_3)_2$	144°	65	$C_{21}H_{23}N_3O_3S$	C	63.47	63.27	10	70
					H	5.79	5.82		
					N	10.57	10.60		
XXIV	2,6-$(CH_3)_2$	218°	60	$C_{21}H_{23}N_3O_4S$	C	63.47	63.30	70	Nil
					H	5.79	5.82		
					N	10.57	10.62		
XXV	2-OCH_3	168°	62	$C_{20}H_{21}N_3O_4S$	C	60.15	60.25	50	10
					H	5.26	5.40		
					N	10.52	10.72		
XXVI	4-OCH_3	150°	55	$C_{20}H_{21}N_3O_4S$	C	60.15	60.28	10	50
					H	5.26	5.30		
					N	10.52	10.40		
XXVII	4-Cl	138°	68	$C_{19}H_{18}ClN_3O_3S$	C	56.50	56.40	10	50
					H	4.46	4.52		
					N	10.40	10.60		

[a] Screening procedures were as indicated in Table I. [b] The presence of characteristic bands of C=O and C=N groups at 1739 and 1600 cm^{-1}, respectively, in the IR spectrum of XXI provided further support for the structure of substituted triazolethioglycolic acids.

Table IV—Selective Inhibition (Percent) of Respiratory Activity of Rat Brain Homogenates by Thiosemicarbazides, Triazoles, and Triazolethioglycolic Acids[a]

Compound	Pyruvate Oxidation: Absence of NAD	Pyruvate Oxidation: Presence of NAD	α-Ketoglutarate Oxidation	NADH Oxidation
		Thiosemicarbazides		
IV	55.2 ± 1.3	43.8 ± 0.9	54.2 ± 1.2	54.9 ± 1.5
V	82.7 ± 0.9	72.9 ± 1.3	43.1 ± 1.4	44.1 ± 1.7
VI	93.7 ± 0.9	82.3 ± 1.4	41.7 ± 0.9	36.2 ± 0.9
VII	83.9 ± 1.3	69.5 ± 1.1	33.4 ± 1.5	39.4 ± 1.0
VIII	73.3 ± 1.3	61.3 ± 1.8	44.9 ± 1.1	46.1 ± 1.2
IX	64.1 ± 0.8	58.3 ± 1.4	51.3 ± 1.3	60.2 ± 1.1
X	35.4 ± 1.0	26.2 ± 0.9	30.5 ± 1.4	38.6 ± 0.7
XI	64.3 ± 0.8	52.4 ± 1.3	44.3 ± 1.1	50.5 ± 1.5
		Triazoles		
XII	51.1 ± 1.5	34.3 ± 0.8	20.5 ± 0.3	16.5 ± 0.5
XIII	18.5 ± 0.8	10.7 ± 1.4	14.4 ± 0.9	29.1 ± 1.1
XIV	63.6 ± 1.3	52.7 ± 0.8	37.3 ± 1.2	89.2 ± 1.5
XV	40.2 ± 0.9	29.1 ± 1.3	46.0 ± 1.0	57.5 ± 1.2
XVI	26.2 ± 0.6	18.4 ± 1.3	23.0 ± 1.3	14.1 ± 0.5
XVII	62.3 ± 1.7	50.5 ± 1.5	41.5 ± 1.3	59.5 ± 1.4
XVIII	29.1 ± 0.6	17.6 ± 1.2	16.3 ± 1.0	26.5 ± 1.3
XIX	48.1 ± 1.2	30.5 ± 0.9	30.4 ± 1.3	67.4 ± 1.6
		Triazolethioglycolic Acids		
XX	64.0 ± 1.3	50.9 ± 1.2	55.1 ± 1.5	66.2 ± 1.4
XXI	75.0 ± 1.3	64.4 ± 1.3	64.7 ± 1.2	50.3 ± 1.3
XXII	90.0 ± 0.8	70.5 ± 1.4	59.5 ± 1.4	59.8 ± 1.5
XXIII	87.5 ± 1.4	72.4 ± 1.3	59.5 ± 1.2	67.5 ± 1.2
XXIV	90.8 ± 2.2	79.3 ± 1.9	46.4 ± 1.3	57.2 ± 1.3
XXV	56.1 ± 1.4	40.8 ± 1.5	62.1 ± 1.4	49.2 ± 1.5
XXVI	30.5 ± 0.3	25.5 ± 1.0	58.2 ± 1.8	59.9 ± 1.3
XXVII	67.7 ± 1.4	46.5 ± 0.4	37.2 ± 1.3	45.6 ± 1.4

[a] Vessel contents and assay procedures were as described in the test. All values are the mean of three duplicate experiments. The percent inhibition and standard errors (*SE*) were calculated from the decrease in the oxygen uptake per 100 mg of wet brain weight per hour. The final concentration of pyruvate, α-ketoglutarate, and succinate was 10 m*M*; the final concentration of NAD and NADH was 0.5 m*M*. All thiosemicarbazides, triazoles, and triazolethioglycolic acids were used at 2 m*M*. The values of oxygen uptake in the control experiments during oxidation of pyruvate, pyruvate plus NAD, α-ketoglutarate, NADH, and succinate were 71.6 ± 1.3, 83 ± 2.2, 96 ± 1.8, 63.3 ± 1.1, and 163 ± 2.8 μl, respectively. The inhibition of the oxidation of succinate by these compounds was nil.

activity cannot account for the biochemical basis of the anticonvulsant activity of thiosemicarbazides, triazoles, and triazolethioglycolic acids.

REFERENCES

(1) W. R. Gibson, E. E. Swanson, and D. B. Meyers, *J. Am. Pharm. Assoc., Sci. Ed.*, **47**, 778 (1958).

(2) S. S. Parmar, A. K. Gupta, H. H. Singh, and T. K. Gupta, *J. Med. Chem.*, **15**, 999 (1972).

(3) P. G. Gold-Aubert, D. Melkonian, and R. Y. Mauvernay, *Neth. Appl.*, **6**, 504 (1965); through *Chem. Abstr.*, **64**, 8198g (1966).

(4) T. George, D. V. Mehta, R. Tahilramani, J. David, and P. K. Talwalker, *J. Med. Chem.*, **14**, 335 (1971).

(5) S. S. Parmar, V. Kishore, and B. Ali, *Agents Actions*, **3**, 386 (1973).

(6) A. K. Bhat, R. P. Bhamaria, R. A. Bellare, and C. V. Deliwala, *Indian J. Chem.*, **5**, 397 (1967).

(7) T. Zsolnai, *Biochem. Pharmacol.*, **11**, 271 (1962).

(8) S. S. Parmar, C. Dwivedi, and B. Ali, *J. Pharm. Sci.*, **61**, 1366 (1972).
(9) J. S. Shukla, H. H. Singh, and S. S. Parmer, *J. Prakt. Chem.*, **311**, 523 (1969).
(10) M. H. Shah, M. Y. Mhasalkar, M. N. Varaya, R. A. Bellare, and C. V. Deliwala, *Indian J. Chem.*, **5**, 391 (1967).
(11) H. L. Yale and J. J. Piala, *J. Med. Chem.*, **9**, 42 (1966).
(12) R. S. Verma, B. Ali, S. S. Parmar, and W. L. Noble, *ibid.*, **13**, 147 (1970).
(13) A. K. Chaturvedi, J. P. Barthwal, S. S. Parmar, and V. I. Stenberg, *J. Pharm. Sci.*, **64**, 454 (1975).
(14) S. P. Singh, A. Chaudhari, V. I. Stenberg, and S. S. Parmar, *ibid.*, **65**, 1678 (1976).
(15) S. Parmar and P. K. Seth, *Can. J. Biochem.*, **43**, 1179 (1965).
(16) S. S. Parmar, C. Dwivedi, A. Chaudhari, and T. K. Gupta, *J. Med. Chem.*, **15**, 99 (1972).

ACKNOWLEDGMENTS AND ADDRESSES

Received June 1, 1976, from the **Jawahar Lal Nehru Research Laboratory of Molecular Biology, Department of Pharmacology and Therapeutics, King George's Medical College, Lucknow University, Lucknow 226003, India,* and the ‡*Department of Psychiatry and Mental Health Sciences, Medical College of Wisconsin, Milwaukee, WI 53226.*

Accepted for publication August 23, 1976.

Supported in part by the Department of Atomic Energy, Government of India, Bombay, India, the State Council of Scientific and Industrial Research of Uttar Pradesh, Lucknow, India, and the National Institute on Drug Abuse (Grant 1-R01-DA00996-01).

The authors thank Professor K. P. Bhargava and Dr. J. P. Barthwal for their advice and encouragement. Grateful acknowledgment is made to the Department of Atomic Energy, Government of India, Bombay, India, and the State Council of Scientific and Industrial Research of Uttar Pradesh, Lucknow, India, for providing research fellowships to S. K. Chaudhary and S. Kumar, respectively.

ˣ To whom inquiries should be directed. Present address: Department of Physiology and Pharmacology, University of North Dakota School of Medicine, Grand Forks, ND 58202.

Interaction of Hydrocortisone with Model Membranes Containing Phospholipid and Cholesterol

GARY W. CLEARY * and JOEL L. ZATZ ˣ

Abstract □ Pure and mixed monolayers of lecithin and cholesterol were spread on substrates of dissolved hydrocortisone at 25 and 37°. The presence of hydrocortisone increased the surface pressure of dipalmitoyl and egg lecithin films that were in head contact. The increase in surface pressure was dependent on steroid concentration. There were no significant interactions with coherent cholesterol monolayers. Penetration of hydrocortisone was decreased by the addition of cholesterol to the monolayer system. These model membrane systems indicate that hydrocortisone interacts with the hydrated polar head group of the phospholipid and not with films whose molecules are in hydrocarbon tail contact.

Keyphrases □ Hydrocortisone—interaction with pure and mixed monolayers of lecithin and cholesterol □ Monolayers—lecithin and cholesterol, pure and mixed, interaction with hydrocortisone □ Lecithin—monolayers, pure and mixed with cholesterol, interaction with hydrocortisone □ Cholesterol—monolayers, pure and mixed with lecithin, interaction with hydrocortisone □ Membranes, model—pure and mixed monolayers of lecithin and cholesterol, interaction with hydrocortisone

Several literature reports have drawn attention to the possibility that the biological activity of certain steroids is due to an interaction with biological membranes (1–5). In a review of steroids and cell surfaces, Willmer (1) proposed a mechanism of steroid activity based on the penetration of steroid molecules between the hydrocarbon tails of membrane phospholipids. Erythrocytes were more resistant to lysis in hypotonic solution when steroids were present in low concentration (2). In high concentration, the steroids themselves caused lysis or precipitation. Another study (3) showed that the corticosteroids tended to stabilize lysosomes at pharmacological concentration (10^{-4}–10^{-6} *M*) but to lyse them at higher concentrations. Cortisone and hydrocortisone exerted a protective effect on the membranes of erythrocytes (4) and rat liver cells (5).

BACKGROUND

One approach to an understanding of steroid–membrane interactions is through model membrane systems. Monomolecular films provide an organized interfacial structure believed to be similar to that found in biological membranes. Studies of drug penetration into monolayers containing components of natural membranes have been useful in explaining the mode of action of many drugs (6, 7).

Current concepts of cellular membranes suggest the existence of a fluid mosaic structure of globular proteins embedded in, and partially protruding from, an organized but discontinuous lipid layer (8). The site of attachment for membrane-active steroids might be protein or lipid. But membrane proteins have not been well characterized. Because of the availability of pure lipid substances known to be components of biological membranes and in view of Willmer's hypothesis (1), it was decided to use monolayers containing lecithins and cholesterol as membrane models.

Few studies on the effect of steroids on monolayers have been reported. Progesterone penetrated monolayers of cholesterol and dipalmitoyl lecithin to some extent (9). Cortisone had little effect on monolayers of stearic acid or cholesterol (10), and the properties of stearyl alcohol monolayers were not affected by the presence of dissolved steroids (11).

Progesterone, testosterone, etiocholanolone, and androsterone had little effect on the surface pressure of lipid monolayers in the condensed state (12), but the surface potential of every monolayer was lowered by the same amount in the presence of a given steroid regardless of the nature of the polar group. This finding was attributed to alteration of the structure of water beneath the monolayers by the steroids. Similar changes in surface potential were caused by hydrocortisone in the presence of lecithin and cholesterol monolayers (13). However, the observed changes were an artifact of the experimental procedure and not a result of changes in water structure.

This report describes the effect of hydrocortisone (I) on model membranes composed of monolayers containing dipalmitoyl (II) and egg (III) lecithins and cholesterol (IV). The molecular weights (in daltons) used

(8) S. S. Parmar, C. Dwivedi, and B. Ali, *J. Pharm. Sci.*, **61**, 1366 (1972).
(9) J. S. Shukla, H. H. Singh, and S. S. Parmer, *J. Prakt. Chem.*, **311**, 523 (1969).
(10) M. H. Shah, M. Y. Mhasalkar, M. N. Varaya, R. A. Bellare, and C. V. Deliwala, *Indian J. Chem.*, **5**, 391 (1967).
(11) H. L. Yale and J. J. Piala, *J. Med. Chem.*, **9**, 42 (1966).
(12) R. S. Verma, B. Ali, S. S. Parmar, and W. L. Noble, *ibid.*, **13**, 147 (1970).
(13) A. K. Chaturvedi, J. P. Barthwal, S. S. Parmar, and V. I. Stenberg, *J. Pharm. Sci.*, **64**, 454 (1975).
(14) S. P. Singh, A. Chaudhari, V. I. Stenberg, and S. S. Parmar, *ibid.*, **65**, 1678 (1976).
(15) S. Parmar and P. K. Seth, *Can. J. Biochem.*, **43**, 1179 (1965).
(16) S. S. Parmar, C. Dwivedi, A. Chaudhari, and T. K. Gupta, *J. Med. Chem.*, **15**, 99 (1972).

ACKNOWLEDGMENTS AND ADDRESSES

Received June 1, 1976, from the **Jawahar Lal Nehru Research Laboratory of Molecular Biology, Department of Pharmacology and Therapeutics, King George's Medical College, Lucknow University, Lucknow 226003, India,* and the ‡*Department of Psychiatry and Mental Health Sciences, Medical College of Wisconsin, Milwaukee, WI 53226.*

Accepted for publication August 23, 1976.

Supported in part by the Department of Atomic Energy, Government of India, Bombay, India, the State Council of Scientific and Industrial Research of Uttar Pradesh, Lucknow, India, and the National Institute on Drug Abuse (Grant 1-R01-DA00996-01).

The authors thank Professor K. P. Bhargava and Dr. J. P. Barthwal for their advice and encouragement. Grateful acknowledgment is made to the Department of Atomic Energy, Government of India, Bombay, India, and the State Council of Scientific and Industrial Research of Uttar Pradesh, Lucknow, India, for providing research fellowships to S. K. Chaudhary and S. Kumar, respectively.

ˣ To whom inquiries should be directed. Present address: Department of Physiology and Pharmacology, University of North Dakota School of Medicine, Grand Forks, ND 58202.

Interaction of Hydrocortisone with Model Membranes Containing Phospholipid and Cholesterol

GARY W. CLEARY * and JOEL L. ZATZ ˣ

Abstract □ Pure and mixed monolayers of lecithin and cholesterol were spread on substrates of dissolved hydrocortisone at 25 and 37°. The presence of hydrocortisone increased the surface pressure of dipalmitoyl and egg lecithin films that were in head contact. The increase in surface pressure was dependent on steroid concentration. There were no significant interactions with coherent cholesterol monolayers. Penetration of hydrocortisone was decreased by the addition of cholesterol to the monolayer system. These model membrane systems indicate that hydrocortisone interacts with the hydrated polar head group of the phospholipid and not with films whose molecules are in hydrocarbon tail contact.

Keyphrases □ Hydrocortisone—interaction with pure and mixed monolayers of lecithin and cholesterol □ Monolayers—lecithin and cholesterol, pure and mixed, interaction with hydrocortisone □ Lecithin—monolayers, pure and mixed with cholesterol, interaction with hydrocortisone □ Cholesterol—monolayers, pure and mixed with lecithin, interaction with hydrocortisone □ Membranes, model—pure and mixed monolayers of lecithin and cholesterol, interaction with hydrocortisone

Several literature reports have drawn attention to the possibility that the biological activity of certain steroids is due to an interaction with biological membranes (1–5). In a review of steroids and cell surfaces, Willmer (1) proposed a mechanism of steroid activity based on the penetration of steroid molecules between the hydrocarbon tails of membrane phospholipids. Erythrocytes were more resistant to lysis in hypotonic solution when steroids were present in low concentration (2). In high concentration, the steroids themselves caused lysis or precipitation. Another study (3) showed that the corticosteroids tended to stabilize lysosomes at pharmacological concentration (10^{-4}–10^{-6} *M*) but to lyse them at higher concentrations. Cortisone and hydrocortisone exerted a protective effect on the membranes of erythrocytes (4) and rat liver cells (5).

BACKGROUND

One approach to an understanding of steroid–membrane interactions is through model membrane systems. Monomolecular films provide an organized interfacial structure believed to be similar to that found in biological membranes. Studies of drug penetration into monolayers containing components of natural membranes have been useful in explaining the mode of action of many drugs (6, 7).

Current concepts of cellular membranes suggest the existence of a fluid mosaic structure of globular proteins embedded in, and partially protruding from, an organized but discontinuous lipid layer (8). The site of attachment for membrane-active steroids might be protein or lipid. But membrane proteins have not been well characterized. Because of the availability of pure lipid substances known to be components of biological membranes and in view of Willmer's hypothesis (1), it was decided to use monolayers containing lecithins and cholesterol as membrane models.

Few studies on the effect of steroids on monolayers have been reported. Progesterone penetrated monolayers of cholesterol and dipalmitoyl lecithin to some extent (9). Cortisone had little effect on monolayers of stearic acid or cholesterol (10), and the properties of stearyl alcohol monolayers were not affected by the presence of dissolved steroids (11).

Progesterone, testosterone, etiocholanolone, and androsterone had little effect on the surface pressure of lipid monolayers in the condensed state (12), but the surface potential of every monolayer was lowered by the same amount in the presence of a given steroid regardless of the nature of the polar group. This finding was attributed to alteration of the structure of water beneath the monolayers by the steroids. Similar changes in surface potential were caused by hydrocortisone in the presence of lecithin and cholesterol monolayers (13). However, the observed changes were an artifact of the experimental procedure and not a result of changes in water structure.

This report describes the effect of hydrocortisone (I) on model membranes composed of monolayers containing dipalmitoyl (II) and egg (III) lecithins and cholesterol (IV). The molecular weights (in daltons) used

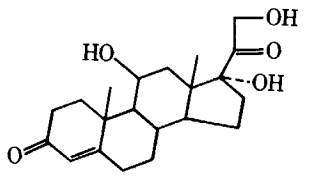

I

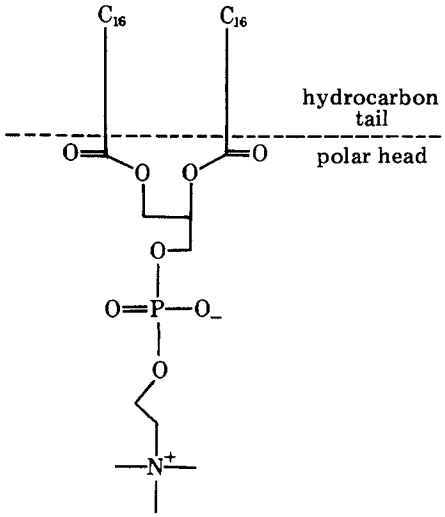

II

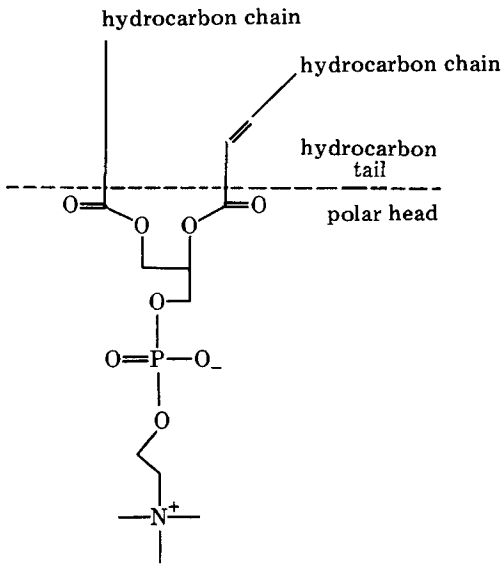

III

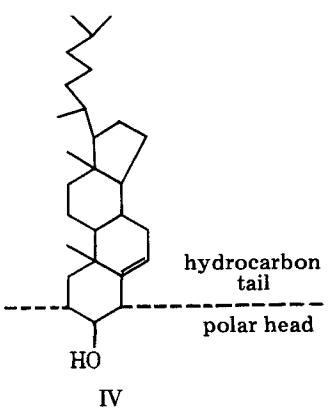

IV

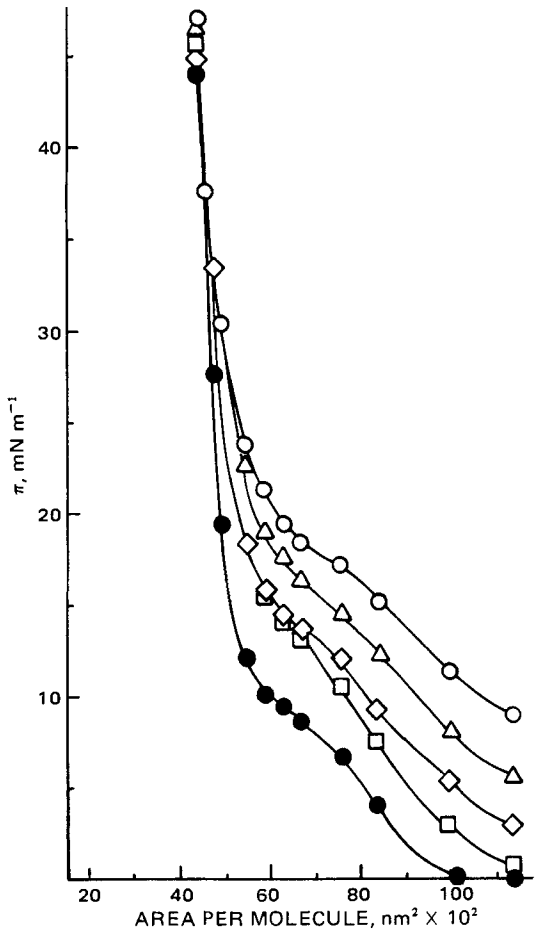

Figure 1—*The π–A curves of dipalmitoyl lecithin monolayers on a subphase containing dissolved hydrocortisone at 25°. Key: ●, no hydrocortisone; □, 2.98 × 10⁻⁵ M hydrocortisone; ◊, 8.20 × 10⁻⁵ M hydrocortisone; △, 13.7 × 10⁻⁵ M hydrocortisone; and ○, 19.7 × 10⁻⁵ M hydrocortisone.*

in the calculation of surface area per molecule of the monolayer-forming substances were: I, 362; II, 752; III, 790; and IV, 387.

EXPERIMENTAL

Hydrocortisone[1] was used as received. Its identity and purity were checked by melting point, optical rotation, paper chromatography, TLC, and IR spectroscopy. Cholesterol[2], dipalmitoyl lecithin[2], and egg lecithin[3] were reported as 99% pure by the suppliers. Organic solvents, spectrograde, were free of surface-active impurities (14). Sodium chloride was reagent grade. Water was double distilled with the final distillation in an all-glass still.

Surface pressure, π, measurements were made by the Wilhelmy plate method using a thin platinum plate suspended from a torsion balance[4] (15). The polytef[5] surface balance was similar to one described previously (16).

The hydrocortisone was dissolved in the subphase consisting of 0.9% sodium chloride solution prior to spreading the monolayer. Hexane was the spreading solvent for cholesterol. The lecithins and all mixed lipid systems were spread from solution in hexane–ethanol (4:1). The lipid solutions were spread on the subphase with a micrometer syringe[6]. Subphase temperature was controlled to within 0.1° with a thermostat[7]. The reproducibility of each π reading in replicate experiments at the 95% confidence interval was ±0.5 mN m^{-1} at all areas.

[1] Merck Sharp and Dohme Research Laboratories, West Point, Pa.
[2] Schwarz/Mann, New York, N.Y.
[3] Sylvana Co., Milburn, N.J.
[4] Rosano surface tensiometer, Newark, N.J.
[5] Teflon (du Pont).
[6] Agla, Burroughs-Wellcome, Sheffield, England.
[7] Lauda K-2/R circulator, Westbury, N.Y.

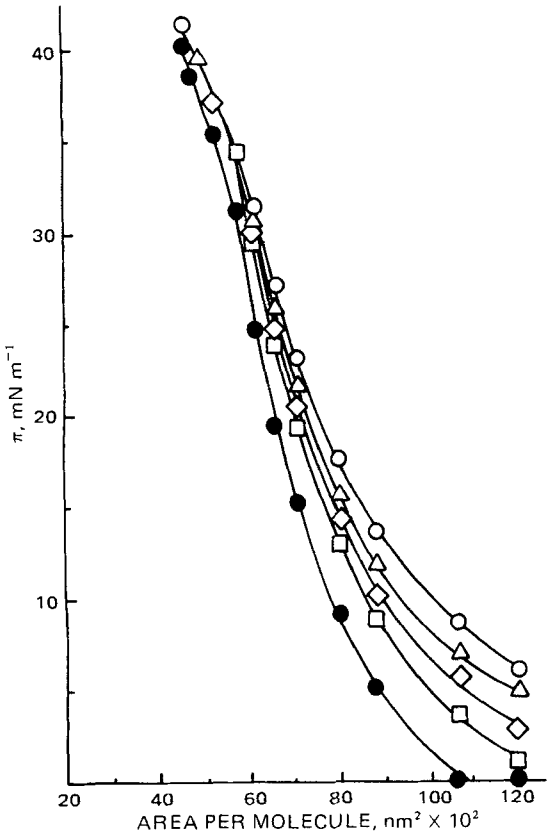

Figure 2—*The π–A curves of dipalmitoyl lecithin monolayers spread on a subphase containing dissolved hydrocortisone at 37°. Key: ●, no hydrocortisone; □, 2.98 × 10⁻⁵ M hydrocortisone; ◊, 8.20 × 10⁻⁵ M hydrocortisone; △, 13.7 × 10⁻⁵ M hydrocortisone; and ○, 19.7 × 10⁻⁵ M hydrocortisone.*

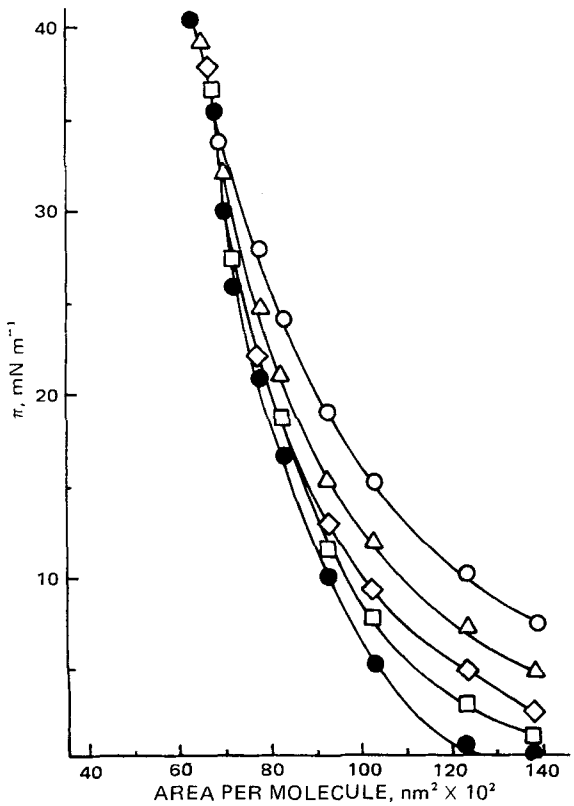

Figure 3—*The π–A curves of egg lecithin monolayers on a subphase containing dissolved hydrocortisone at 25°. Key: ●, no hydrocortisone; □, 2.98 × 10⁻⁵ M hydrocortisone; ◊, 8.20 × 10⁻⁵ M hydrocortisone; △, 13.7 × 10⁻⁵ M hydrocortisone; and ○, 19.7 × 10⁻⁵ M hydrocortisone.*

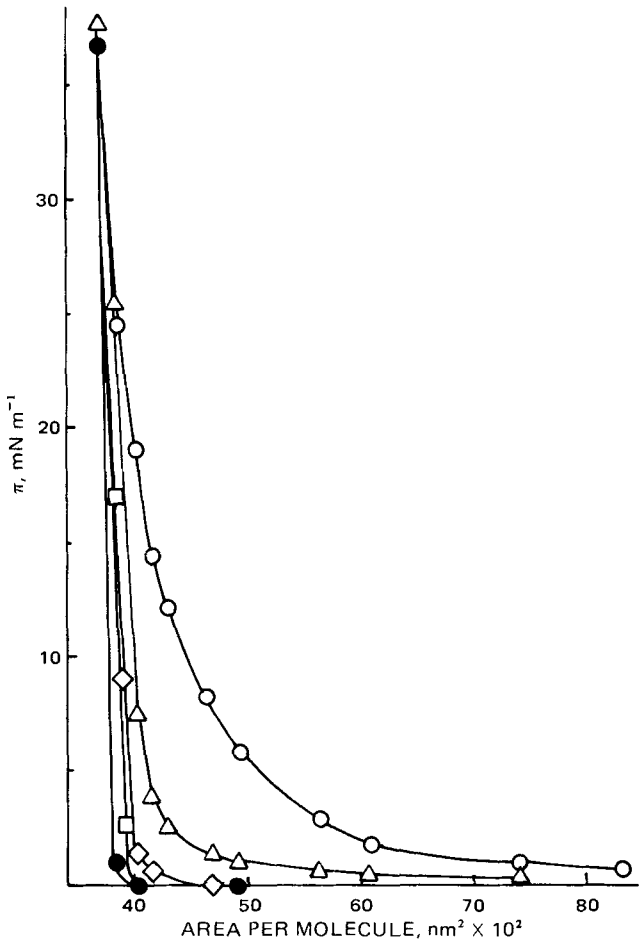

Figure 4—*The π–A curves of cholesterol monolayers on a subphase containing dissolved hydrocortisone at 25°. Key: ●, no hydrocortisone; □, 2.98 × 10⁻⁵ M hydrocortisone; ◊, 8.20 × 10⁻⁵ M hydrocortisone; △, 13.7 × 10⁻⁵ M hydrocortisone; and ○, 19.7 × 10⁻⁵ M hydrocortisone.*

RESULTS AND DISCUSSION

Single-Component Monolayers—The properties of dipalmitoyl lecithin monolayers were described previously (17). Surface pressure–surface area (π–A) curves for dipalmitoyl lecithin monolayers on a subphase containing dissolved hydrocortisone at 25° are shown in Fig. 1. The surface pressure of the monolayer was increased in the presence of hydrocortisone if the area per molecule of dipalmitoyl lecithin was greater than about 0.5 nm^2. Under these conditions, the lecithin molecules had their hydrated polar groups in close contact while the hydrocarbon "tails" were not tightly packed (17).

The increase in surface pressure that occurred when hydrocortisone was in the subphase was indicative of surface penetration by hydrocortisone molecules. The magnitude of the change in surface pressure was a function of hydrocortisone concentration. As the monolayers were compressed to surface areas smaller than 0.50 nm^2/molecule of dipalmitoyl lecithin, the π–A curves for the systems containing hydrocortisone approached the curve obtained in the absence of the steroid. This finding was interpreted as an expulsion of steroid molecules from the monolayers. The removal of hydrocortisone from the surface coincided with a change in monolayer structure in which the lecithin polar groups underwent a change in hydration and the vertically oriented hydrocarbon tails became closely associated (17). The presence of hydrocortisone did not prevent this transition or alter the surface area at which it took place.

At a subphase temperature of 37°, the transition from an arrangement involving head contact to one of tail contact in dipalmitoyl lecithin monolayers (Fig. 2) took place at a much higher surface pressure than at 25° (17). Penetration of the monolayers by hydrocortisone was, again, a function of subphase concentration of the steroid. As the monolayers were compressed to smaller values of surface area available to the lecithin, the π–A curves obtained with hydrocortisone present (Fig. 2) were shifted closer to the curve for lecithin alone, suggesting that hydrocortisone molecules were being forced from the surface in response to the change to a state of tail contact in the monolayer.

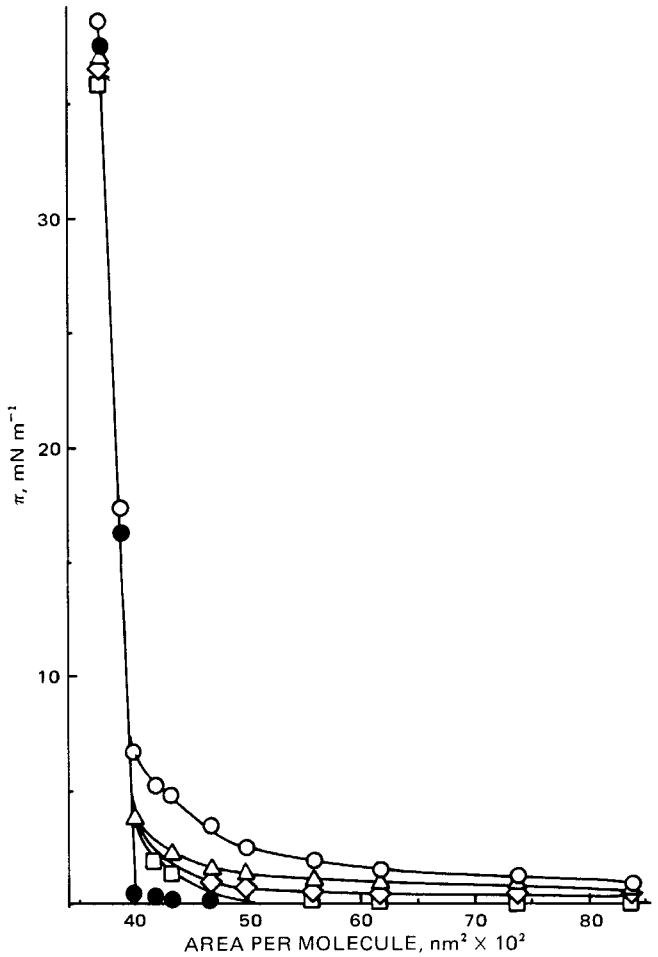

Figure 5—*The π–A curves of cholesterol monolayers spread on a subphase containing dissolved hydrocortisone at 37°. Key: ●, no hydrocortisone; □, 2.98 × 10⁻⁵ M hydrocortisone; ◇, 8.20 × 10⁻⁵ M hydrocortisone; △, 13.7 × 10⁻⁵ M hydrocortisone; and ○, 19.7 × 10⁻⁵ M hydrocortisone.*

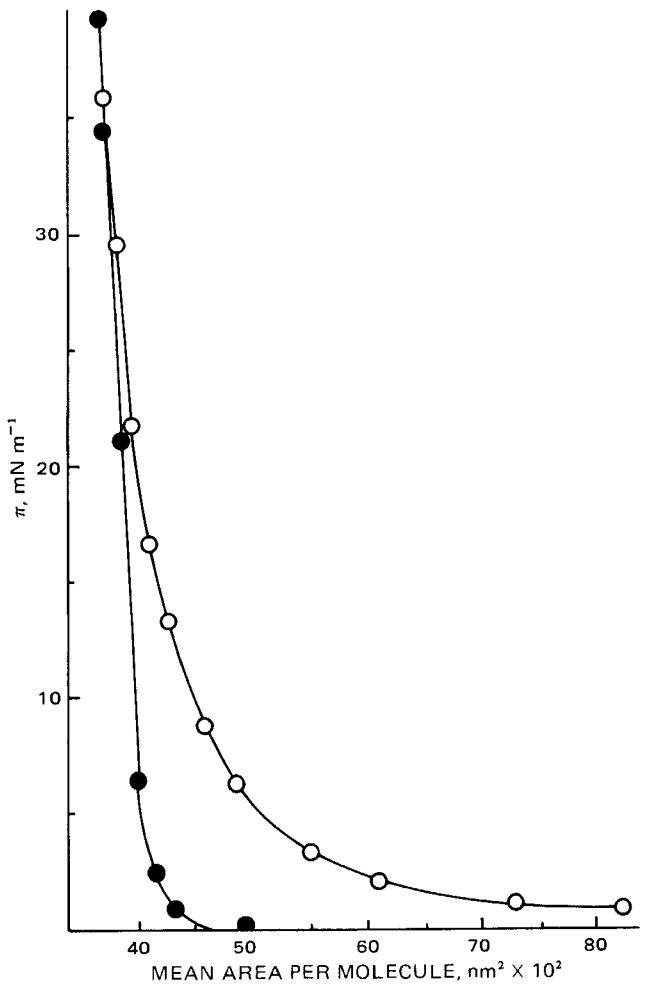

Figure 6—*The π–A curves of monolayers of dipalmitoyl lecithin and cholesterol in a 1:2 molar ratio on a subphase containing dissolved hydrocortisone at 25°. Key: ●, no hydrocortisone; and ○, 19.7 × 10⁻⁵ M hydrocortisone.*

Egg lecithin contains a mixture of phosphatidyl cholines. Approximately 53% of the fatty tails are unsaturated (18). The *π–A* curve (Fig. 3) was of the expanded type, and compression of the monolayer did not force the hydrocarbon groups together until near the collapse point (19). As with dipalmitoyl lecithin, the extent of monolayer penetration by hydrocortisone depended on subphase concentration. Compression caused the *π–A* curves for the systems containing steroid to approach the curve for egg lecithin alone, and all curves merged just before the collapse pressure was reached.

Figure 4 demonstrates the effect of hydrocortisone on cholesterol monolayers at 25°. At the lower concentrations, hydrocortisone caused little change in the *π–A* curve; but at a subphase concentration of 19.7 × 10^{-5} *M* hydrocortisone, the surface pressure of the cholesterol monolayer increased significantly. However, this effect may have been due to physical entrapment of hydrocortisone molecules during compression of the cholesterol surface films. Surface potential work showed that some adsorption of hydrocortisone takes place at the air–water interface (13). If desorption were slow relative to compression, some hydrocortisone might remain at the surface even in the absence of an appreciable interaction with the monolayer. The cholesterol monolayers were unstable in the sense that when the surface area per cholesterol molecule was held constant, surface pressure readings dropped with time. In contrast, the surface pressure measurements made on the lecithin monolayers remained stable for at least 20 min whether or not hydrocortisone was present.

At a subphase temperature of 37°, hydrocortisone caused a small increase in surface pressure when the area per cholesterol molecule exceeded 0.40 nm^2 (Fig. 5). The condensed portion of the *π–A* curve was unaffected, indicating that hydrocortisone was not retained in the monolayer. These results are in agreement with the report of Gershfeld and Heftmann (10). When the molecular area of cholesterol is greater than 0.40 nm^2, the cholesterol molecules exist as individual units or clusters, leaving some aqueous surface available for adsorption of hydrocortisone. Compression forces the cholesterol molecules together (the monolayer becomes coherent) and causes desorption of hydrocortisone.

The incorporation of hydrocortisone into monolayers can be thought of as a distribution phenomenon in which the surface concentration depends on the characteristics of the surface film as well as the bulk concentration of steroid. With a monolayer in a condensed state (with close packed vertical hydrophobic groups), hydrocortisone cannot penetrate between the fatty tails. Hydrophobic interactions between hydrocortisone and the film molecules cannot compete successfully with the interactions between film molecules.

In earlier work on monolayers in which no penetration by steroids was observed (10, 11), the surface films studied were condensed. With expanded monolayers, hydrocortisone can enter the surface under two sets of conditions. First, adsorption occurs at monolayer-free aqueous interfaces so it should also take place when monolayer molecules are widely separated at the surface. Such simple adsorption does not require any interaction with film molecules but can occur only when the monolayer is gaseous, *i.e.*, at surface areas where the monolayer without hydrocortisone is less than 1–2 mN m^{-1}. This mechanism appears to be operative in cholesterol monolayers.

The second condition involves penetration of a monolayer in which the film molecules are in contact without tight packing of hydrocarbon tails. The effective molecular area of film molecules is determined by the size of the hydrated polar group. With this arrangement, steroid molecules might displace water of hydration and associate with film molecules. This mechanism appears to be operative in the penetration of lecithin monolayers by hydrocortisone.

Mixed Monolayers—Cholesterol causes changes in the molecular organization of dipalmitoyl lecithin monolayers (17). Since the pene-

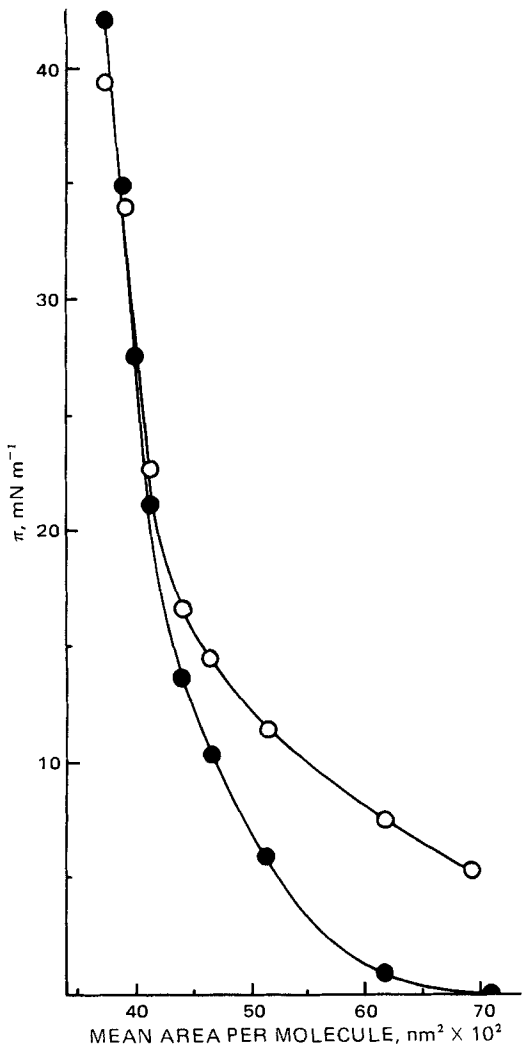

Figure 7—*The π–A curves of monolayers of dipalmitoyl lecithin and cholesterol in a 2:1 molar ratio on a subphase containing dissolved hydrocortisone at 25°. Key: ●, no hydrocortisone; and ○, 19.7 × 10^{-5} M hydrocortisone.*

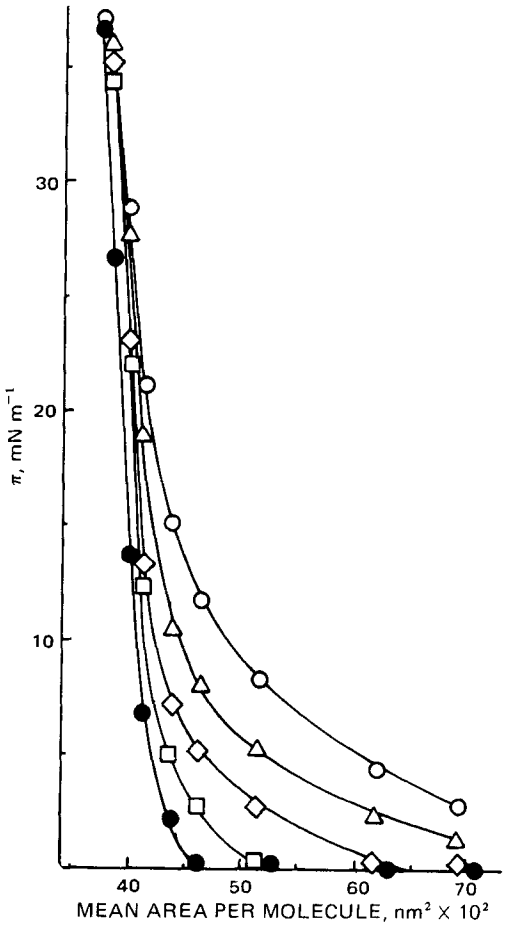

Figure 8—*The π–A curves of monolayers of dipalmitoyl lecithin and cholesterol in a 1:1 molar ratio on a subphase containing dissolved hydrocortisone at 25°. Key: ●, no hydrocortisone; □, 2.98 × 10^{-5} M hydrocortisone; ◇, 8.20 × 10^{-5} M hydrocortisone; △, 13.7 × 10^{-5} M hydrocortisone; and ○, 19.7 × 10^{-5} M hydrocortisone.*

tration of monolayers by hydrocortisone depends on the monolayer state, it was of interest to see whether the inclusion of cholesterol in surface films of lecithin influences interactions of the model system with hydrocortisone. Accordingly, some experiments were conducted in which mixed dipalmitoyl lecithin–cholesterol monolayers were spread on subphases containing hydrocortisone (Figs. 6–9). Only one subphase concentration was used with the dipalmitoyl lecithin–cholesterol mixed monolayer in a 1:2 molar ratio (Fig. 6). The *π–A* curve obtained with hydrocortisone present was the same as the one produced when the monolayer contained only cholesterol. The influence of the lecithin seemed to be completely swamped.

A single subphase concentration of hydrocortisone was used with the dipalmitoyl lecithin–cholesterol mixed monolayer in a 2:1 molar ratio (Fig. 7). The change in surface pressure due to hydrocortisone was smaller than with a monolayer of pure dipalmitoyl lecithin. The equimolar mixed systems at 25° (Fig. 8) and 37° (Fig. 9) were similar in structure (17). At 25° (Fig. 8), hydrocortisone increased the surface pressure only at mean molecular areas corresponding to a gaseous monolayer, one in which the film molecules are separated from one another. In a coherent system, such as a membrane, no space would be available to steroid molecules. At 37° (Fig. 9), the situation was quite similar, although there was a small region of head contact in the *π–A* curves. All curves met at about 15 mN m^{-1}.

Comparison of these results for mixed monolayers with the experiments on single-component lecithin monolayers shows that monolayer penetration by hydrocortisone was diminished effectively in the presence of cholesterol. Previously (20), the addition of cholesterol to lipid dispersions decreased the uptake of hydrocortisone and other steroids by the membranes.

Application of the heads-or-tails model (17, 19) provides an explanation for the effect of cholesterol. In mixed monolayers containing cholesterol and dipalmitoyl lecithin, cholesterol molecules change the packing in the monolayer under conditions where the cholesterol molecules become interspersed among the hydrocarbon tails of the dipalmitoyl lecithin molecules. The molecular assembly is more compact, and the molecular area is determined by the cross-sectional area of the hydrocarbon portion.

The extent of this change in packing depends on the cholesterol content. When cholesterol is the principal component of the mixed systems, all molecules are in tail contact. In the 1:1 mixed system, all molecules are in tail contact over most of the surface pressure range. When dipalmitoyl lecithin is the principal component, some lecithin molecules are in tail contact while a portion are in the same state as they would be in a monolayer of pure dipalmitoyl lecithin at the same surface pressure. Conversion of lecithin molecules from a head contact situation to one of tail contact blocks possible sites of hydrocortisone penetration, making it more difficult for hydrocortisone to enter the monolayer.

Extrapolation to Biological Membranes—Although extrapolation from a simple model system to a complex biological system is always hazardous, some general statements seem justified. The ability of hydrocortisone to penetrate lecithin monolayers at 37° that are coherent (but in head contact) suggests that hydrocortisone can associate with lecithin molecules in biological membranes. The uptake by membranes is expected to be dependent on the bulk concentration. Cholesterol monolayers must be in the gaseous state to interact with hydrocortisone. This is not likely in membranes. In mixed monolayers, cholesterol reduces monolayer penetration by hydrocortisone. Membranes containing cholesterol should admit fewer hydrocortisone molecules into the plane of the membrane than those that are free of cholesterol.

Orientation of Hydrocortisone in Penetrated Monolayers—The inability of hydrocortisone to be accommodated between hydrocarbon chains in lecithin monolayers whose molecules are in a state of tail contact

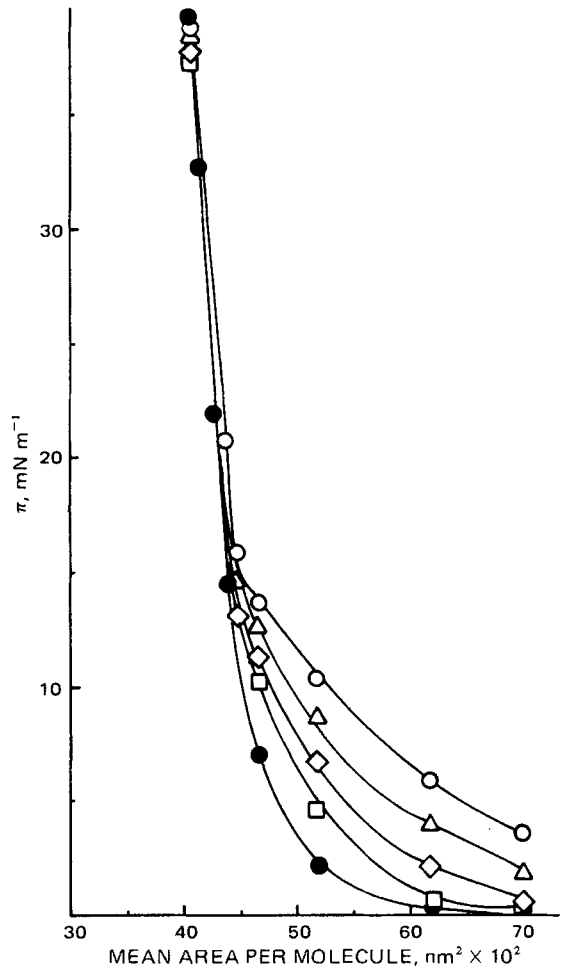

Figure 9—*The π–A curves of monolayers of dipalmitoyl lecithin and cholesterol in a 1:1 molar ratio on a subphase containing dissolved hydrocortisone at 37°. Key: ●, no hydrocortisone; □, 2.98 × 10⁻⁵ M hydrocortisone; ◇, 8.20 × 10⁻⁵ M hydrocortisone; △, 13.7 × 10⁻⁵ M hydrocortisone; and ○, 19.7 × 10⁻⁵ M hydrocortisone.*

is in marked contrast to the behavior of cholesterol, which is completely miscible (17). The difference is most likely due to the location of polar groups on the hydrocortisone molecule. Cholesterol has a single polar group at one end of the molecule, allowing orientation at the interface so that the polar group is in contact with water while the hydrophobic portion of the molecule protrudes from the surface. Hydrocortisone has polar groups at both ends of the molecule, thus favoring a horizontal orientation so that all polar groups can remain hydrated. Support for this orientation comes from spin label studies showing that corticosteroids do not orient in the hydrocarbon tail region of lipid bilayers (21). Willmer's theory of steroid hormone activity (1) was based on the notion that steroid molecules would be retained between the phospholipid fatty chains so that the long axis of the steroid molecule would be normal to the surface. The results of this study, therefore, contradict Willmer's hypothesis.

REFERENCES

(1) E. N. Willmer, *Biol. Rev.*, **36**, 368 (1961).

(2) P. M. Seeman, *Biochem. Pharmacol.*, **15**, 1632 (1966).

(3) D. A. Lewis, A. M. Symons, and R. J. Ancill, *J. Pharm. Pharmacol.*, **22**, 902 (1970).

(4) J. F. Jennings and G. Taylor, *Nature (London)*, **203**, 661 (1964).

(5) Y. Takeda, A. Ichihara, H. Tanioka, and H. Inoue, *J. Biol. Chem.*, **239**, 3590 (1964).

(6) A. W. Cuthbert, *Pharmacol. Rev.*, **19**, 59 (1967).

(7) A. Felmeister, *J. Pharm. Sci.*, **61**, 151 (1972).

(8) S. J. Singer and G. L. Nicolson, *Science*, **175**, 720 (1972).

(9) J. L. Taylor and D. A. Haydon, *Biochim. Biophys. Acta*, **94**, 488 (1965).

(10) N. L. Gershfeld and E. Heftmann, *Experientia*, **19**, 2 (1963).

(11) C. Y. C. Pak and N. L. Gershfeld, *Nature*, **214**, 888 (1967).

(12) N. L. Gershfeld and M. Muramatsu, *J. Gen. Physiol.*, **58**, 650 (1971).

(13) G. W. Cleary and J. L. Zatz, *J. Colloid Interface Sci.*, **45**, 507 (1973).

(14) J. L. Zatz, *J. Pharm. Sci.*, **59**, 117 (1970).

(15) A. W. Adamson, "Physical Chemistry of Surfaces," 2nd ed., Interscience, New York, N.Y., 1967, p. 26.

(16) A. Felmeister, M. Amanat, and N. D. Weiner, *Environ. Sci. Technol.*, **2**, 40 (1968).

(17) J. L. Zatz and G. W. Cleary, *J. Pharm. Sci.*, **64**, 1534 (1975).

(18) D. O. Shah and J. H. Schulman, *J. Colloid Interface Sci.*, **25**, 107 (1967).

(19) J. L. Zatz, *J. Pharm. Sci.*, **63**, 858 (1974).

(20) R. S. Snart and M. J. Wilson, *Nature*, **215**, 964 (1967).

(21) K. W. Butler, I. C. P. Smith, and H. Schneider, *Biochim. Biophys. Acta*, **219**, 514 (1970).

ACKNOWLEDGMENTS AND ADDRESSES

Received May 24, 1976, from the *College of Pharmacy, Rutgers—the State University, New Brunswick, NJ 08903.*

Accepted for publication November 10, 1976.

Supported by a Merck Grant for Faculty Development to J. L. Zatz.

G. W. Cleary expresses thanks for the support of a Johnson and Johnson Fellowship.

* Present address: Alza Research, Palo Alto, CA 94304.

ˣ To whom inquiries should be directed.

Absorption Kinetics of Procainamide in Humans

CARL V. MANION ×, DAVID LALKA *,
DENISE T. BAER, and MELVIN B. MEYER

Abstract □ Plasma procainamide concentrations following the administration of 500 mg of procainamide hydrochloride *via* intravenous infusion, conventional capsules, and sustained-release tablets were compared in 11 healthy male volunteers. Two-compartment open modeling of the plasma levels from the intravenous infusion experiments yielded mean K_{el}, k_{12}, and k_{21} values of 0.0162, 0.0542, and 0.0233 min^{-1}, respectively. The bioavailability of the oral preparations (*versus* intravenous) averaged 83% for the capsule and 79% for the sustained-release tablet. Calculations using a previously reported method suggested that absorption was a first-order process with mean k_a's of 0.0336 and 0.0039 min^{-1} for the capsule and sustained-release tablet, respectively. The sustained-release formulation exhibited delayed release and adequate bioavailability.

Keyphrases □ Procainamide—bioavailability of intravenous infusion, capsules, and sustained-release tablets, absorption of oral forms compared, humans □ Bioavailability—procainamide, intravenous infusion, capsules, and sustained-release tablets compared, humans □ Absorption, GI—procainamide, capsules and sustained-release tablets compared, humans □ Antiarrhythmic agents—procainamide, bioavailability of intravenous infusion, capsules, and sustained-release tablets, absorption of oral forms compared, humans

Procainamide, a widely used antiarrhythmic agent, has a log-linear phase plasma disappearance half-life of about 3 hr (1). This short half-life can lead to subtherapeutic plasma levels 4 hr after oral administration of conventional formulations. Therefore, a 3-hr dosing interval was recommended for maintenance of a therapeutic plasma concentration (2).

More recently, several attempts to prolong the apparent half-life of plasma procainamide utilized formulation techniques to produce sustained release (3–5). Studies with these formulations generally suggested some advantages. The present study was undertaken to measure the absorption rate and bioavailability of an experimental sustained-release tablet and to document its plasma concentration–time curve.

EXPERIMENTAL

Subjects and Dosing—Eleven male subjects participated after giving written informed consent. They were healthy as judged by history, physical examination, and laboratory tests. Their ages ranged between 21 and 28 years with a mean of 21.8, and their weights ranged between 73.6 and 94 kg (Table I).

Procainamide hydrochloride for intravenous use[1] was administered by intravenous infusion over 16 min at a constant rate of 27.1 mg of base/min. Each of the other two dosage forms, the capsule[2] or sustained-release tablet[3], was given with 100 ml of water after an overnight fast. The schedule of administration of dosage forms was randomly determined for each volunteer. Each dosage form was administered at intervals of 1 week or more.

Sample Collection—Blood specimens were collected at −0.25, 0.25, 0.5, 0.75, 1, 1.5, 2, 3, 4, 5, 6, 8, 12, and 24 hr for both oral preparations. Blood specimens were collected during and after the intravenous infusion at −5, 3.5, 7, 10.5, 14, 17.5, 20, 24, 28, 32, 38, 44, 50, and 60 min and 1.5, 2, 3, 4, 5, 6, 8, 12, and 24 hr. A pretreatment urine sample as well as 0–8- and 8–24-hr specimens was collected for drug determination. For the first eight single studies, 24–48-hr urine specimens were collected.

Analysis of Procainamide and Apparent *N*-Acetylprocainamide in Plasma and Urine—Plasma procainamide levels were measured spectrophotometrically by the method of Mark *et al.* (6) as modified by Sitar *et al.* (7). In some studies, conjugates of procainamide (presumably *N*-acetylprocainamide) were approximated by the same method after acid hydrolysis of the methylene chloride extract (evaporated to dryness, dissolved in 1 *N* hydrochloric acid, and heated to 100° for 1 hr) of the plasma specimen. Urine samples were assayed as described but were also analyzed by a modification of a reported GLC procedure (8), again with and without hydrolysis.

The sensitivity of the spectrophotometric method was approximately 0.10 μg/ml with a concentration-independent recovery of 98% during this study; the sensitivity of the GLC method was 1–5 μg/ml with a recovery of 97% over a similar concentration range (urine contained an interfering peak). The coefficient of variation for the spectrophotometric method throughout this study was 3% as measured by quality control specimens run daily. The GLC method yielded an 8% coefficient of variation measured from deviation of slopes of the standard curves. These measurements were similar to previous estimates of precision, sensitivity, and recovery (1, 6–9).

Plasma specimens were frozen to −20° and stored at that temperature until the analysis was performed, except as noted below. Since artifactual procainamide could be generated from *N*-acetylprocainamide (a known metabolite) by hydrolysis, a blank plasma sample to which *N*-acetylprocainamide (10 μg/ml) had been added was also carried through the assay procedure. Furthermore, several sets of samples were assayed within 48 hr or less of the time they were drawn or received and were reanalyzed 6–8 weeks later. These studies were all performed in an effort to ensure that the procainamide plasma and urine levels were not artifactual.

Pharmacokinetics—Plasma concentrations, C_p, following intravenous infusion declined biexponentially in accordance with:

$$C_p = Ae^{-\alpha t} + Be^{-\beta t} \qquad \text{(Eq. 1)}$$

The values of A and B were corrected by the method of Loo and Riegelman (10) for the infusion time of 16 min using:

$$A_i = \frac{k_i \tau}{(1 - e^{-k_i \tau})} A_i' \qquad \text{(Eq. 2)}$$

where τ is the duration of the constant-rate infusion, the A_i's are the $t = \tau$ intercepts of the two exponential phases, and the k_i's are the disposition slope constants (*i.e.*, α and β). The data were fitted to a two-compartment open model (Scheme I), and the values for K_{el}, k_{12}, k_{21}, and V_c were estimated by utilizing the nonlinear least-squares regression analysis program NONLIN (11) on a time-share computer. Each plasma concentration was weighted as its reciprocal.

The computer fit values for K_{el}, k_{12}, k_{21}, and V_c from each individual were then further utilized for the calculation of the apparent absorption rate constant, k_a, by the method of Loo and Riegelman (12). Percent unabsorbed estimations were made at various times, and least-squares

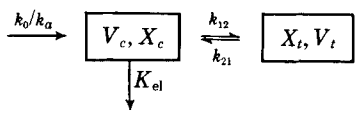

Scheme I—Representation of transfer and elimination in a two-compartment open model; k_{12} *and* k_{21} *are first-order transfer rate constants between the central and peripheral compartments as indicated;* K_{el} *is the first-order elimination rate constant from the central compartment;* k_0 *is a zero-order infusion rate constant;* k_a *is the first-order rate constant for drug absorption;* V_c *and* V_t *are the apparent volumes of the central and tissue compartments, respectively; and* X_c *and* X_t *are the masses of drug contained in these compartments.*

[1] Lot 4J825, Squibb.
[2] Lot 4D302, Squibb.
[3] Lot H7426-5, Hässle.

Table I—Characteristics of Volunteers

Subject	Age, years	Weight, kg	Dose, mg/kg
G.B.	28	78.6	6.36
P.Gt.	21	73.6	6.79
L.D.	22	85.0	5.88
F.N.	21	77.2	6.47
P.Ga.	21	76.3	6.55
B.M.	21	88.6	5.64
P.R.	21	74.0	6.75
S.R.	21	75.0	6.67
C.H.	21	81.8	6.11
C.F.	21	77.2	6.47
T.C.	22	94.0	5.31
Mean ± *SD*	21.8	80.1 ± 6.5	6.27 ± .48

fits were performed to estimate k_a. Plasma level simulations from mean data were performed by the method of superposition as described by Westlake (13). Individual curves were described by:

$$C_p = \frac{k_a DF}{V_c}\left[\frac{(\alpha - k_{21})}{(\alpha - \beta)(k_a - \alpha)}e^{-\alpha t} + \frac{(k_{21} - \beta)}{(\alpha - \beta)(k_a - \beta)}e^{-\beta t} - \frac{(k_a - k_{21})}{(k_a - \alpha)(k_a - \beta)}e^{-k_a t}\right] \quad \text{(Eq. 3)}$$

RESULTS

Intravenous Infusion Experiments—After a brief infusion of procainamide, the plasma concentration declined biexponentially with a $t_{1/2\alpha}$ = 8.8 ± 1.2 min and a $t_{1/2\beta}$ = 204 ± 14 min (Table II). Fitting of these data to a two-compartment open model (Scheme I) yielded mean K_{el}, k_{12}, and k_{21} values of 0.0162, 0.0542, and 0.0233 min^{-1}, respectively (Table III). The apparent volume of the immediately equilibrating space, V_c, was 0.79 liter/kg, and $V_{d\beta}$ was 2.74 liters/kg. Renal clearance, Cl_R, and total body clearance, Cl_B, averaged 400 and 749 ml/min, respectively.

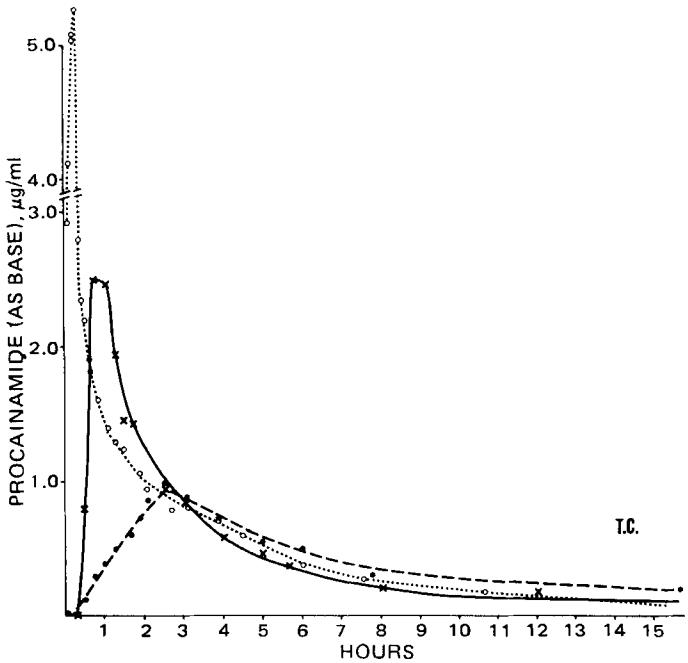

Figure 1—*Plasma concentration–time curves in Subject T.C. following the administration of 500 mg of procainamide hydrochloride as a 16-min constant-rate intravenous infusion (○), a sustained-release tablet (●), and a conventional capsule (×).*

Oral Dose Experiments—The plasma concentration–time curves observed following the administration of an intravenous infusion, a sustained-release tablet, and a conventional capsule to a volunteer who exhibited nearly equal areas under the curve (*AUC*) values following

Table II—Coefficients of the Biexponential Equation Describing the Decline of Plasma Concentration following the Intravenous Administration of 500 mg of Procainamide Hydrochloride to Normal Volunteers[a]

Subject	A, μ/ml	α, min^{-1}	$t_{1/2\alpha}$, min	B, μg/ml	β, min^{-1}	$t_{1/2\beta}$, min
G.B.	5.1	0.066	10.5	1.8	0.0034	204
P.Gt.	2.8	0.031	22.4	1.5	0.0029	239
L.D.	4.6	0.097	7.1	1.8	0.0037	187
F.N.	9.8	0.106	6.5	1.3	0.0044	158
P.Ga.	5.6	0.094	7.4	1.9	0.0042	165
B.M.	5.7	0.073	9.5	0.8	0.0032	217
P.R.	1.6	0.114	6.1	2.1	0.0045	154
S.R.	5.4	0.116	6.0	2.0	0.0043	161
C.H.	16.4	0.138	5.0	1.3	0.0025	277
C.F.	9.0	0.067	10.3	1.0	0.0025	277
T.C.	8.0	0.084	8.3	1.3	0.0033	210
Mean	6.7	0.090	8.8	1.5	0.0035	204
SEM	1.2	0.009	1.2	0.13	0.0002	14

[a] Infusion data corrected to instantaneous input by method of Loo and Riegelman (10).

Table III—Derived Pharmacokinetic Parameters for Procainamide in Normal Volunteers: Constants Characterizing the Two-Compartment Open Model

Subject	k_{12}[a], min^{-1}	k_{21}[a], min^{-1}	K_{el}[a], min^{-1}	V_c[a], liters/kg	$V_{d\beta}$[b], liters/kg	Cl_R[c], ml/min	Cl_B[d], ml/min
G.B.	0.0382	0.0194	0.0116	0.81	2.32	314 (380)[e]	619
P.Gt.	0.0133	0.0128	0.0079	1.35	2.98	407 (349)	635
L.D.	0.0588	0.0301	0.0117	0.79	2.01	297 (303)	633
F.N.	0.0660	0.0161	0.0281	0.51	3.00	464 (548)	1020
P.Ga.	0.0562	0.0272	0.0149	0.76	2.35	533 (537)	752
B.M.	0.0463	0.0135	0.0160	0.73	3.32	214 (457)	942
P.R.	0.0435	0.0670	0.0075	1.57	2.06	393 (485)	687
S.R.	0.0718	0.0345	0.0139	0.78	1.99	320 (406)	641
C.H.	0.0982	0.0123	0.0303	0.30	3.82	458 (433)	781
C.F.	0.0429	0.0087	0.0173	0.56	3.64	541 (447)	702
T.C.	0.0613	0.0145	0.0194	0.49	2.66	454 (269)	825
Mean	0.0542	0.0233	0.0162	0.79	2.74	400 (419)	749
±*SEM*	0.0065	0.0050	0.0022	0.11	0.20	31 (27)	40

[a] Defined in Scheme I. [b] Calculated from $V_{d\beta}$ = dose/$\beta(AUC)$. [c] Calculated from $Cl_R = PA_u^{24hr}/\int_0^{24hr} C_p\,dt$. [d] Calculated from $Cl_B = dose_{iv}/\int_0^{\infty} C_p\,dt$. [e] Numbers in parentheses are the mean renal clearance values for the three experiments in each volunteer; the numbers outside the parentheses are the renal clearances observed from the intravenous experiments.

Table IV—Procainamide Bioavailability in Normal Volunteers

Subject	Bioavailability[a]			
	Conventional Capsule		Sustained-Release Tablet	
	$AUC_{po}^{\alpha}/AUC_{iv}^{\alpha}$	$PA_{u,po}^{\alpha}/PA_{u,iv}^{\alpha}$	$AUC_{po}^{\alpha}/AUC_{iv}^{\alpha}$	$PA_{u,po}^{\alpha}/PA_{u,iv}^{\alpha}$
P.Gt.	71	86	69	25
P.Ga.	113	—	94	96
G.B.	83	77	54	93
L.D.	84	99	70	62
F.N.	73	120	91	82
B.M.	69	207[b]	86	210[b]
P.R.	91	108	65	99
S.R.	66	112	73	81
C.H.	66	69	84	67
C.F.	107	82	86	61
T.C.	88	20	94	52
Mean ± *SEM*	83 ± 4.9	86 ± 5.1	79 ± 4.0	71 ± 18

[a] All ratios ×100. [b] This value was excluded from bioavailability calculations because it is believed that the volunteer lost some urine containing drug following his intravenous dose.

administration of the two oral preparations are shown in Fig. 1. The plasma procainamide levels following the conventional capsule were higher during the first 3 hr of the experiment; at later time points, the sustained-release tablet yielded higher levels.

Bioavailability was estimated by two methods: the ratio of the areas under the plasma concentration–time curves ($AUC_{po}^{24hr}/AUC_{iv}^{24hr}$) and the ratio of the total urinary excretion of procainamide ($PA_{u,po}^{24hr}/PA_{u,iv}^{24hr}$). The *AUC* estimates suggest that the two preparations (conventional capsule and sustained-release tablet) possess nearly equal bioavailability, while the urinary excretion data indicate that procainamide is absorbed more completely from the conventional capsule (86.0 *versus* 71.0%, Table IV).

The plasma levels from each subject were further analyzed by the method of Loo and Riegelman (12) to estimate the apparent absorption rate constant from each formulation (Fig. 2). The results of these estimations for all subjects (assuming first-order absorption) as well as the Loo–Riegelman approximation of the known intravenous infusion rate are shown in Table V. The k_a for the sustained-release tablet averaged almost an order of magnitude slower than the k_a of procainamide from the conventional capsule.

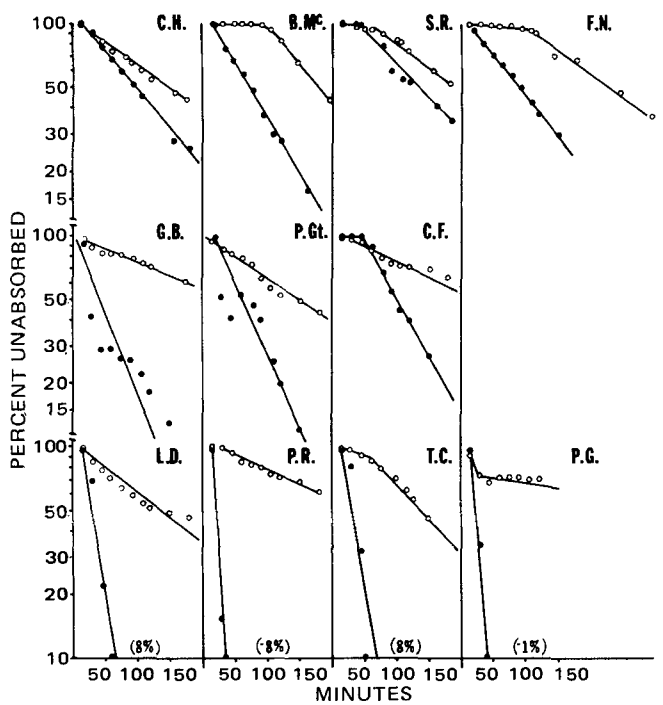

Figure 2—*Loo–Riegelman plots of percent unabsorbed* versus *time following the administration of 500 mg of procainamide hydrochloride as a sustained-release tablet (○) and a conventional capsule (●) for volunteers.*

DISCUSSION

Intravenous Studies—A two-compartment open model adequately described the plasma levels following intravenous infusion of procainamide. The value of V_c was 0.79 ± 0.11 liter/kg, substantially greater than a previously reported value (5). That report (5), however, contained a fixed recording error of elapsed time for the intravenous procainamide doses, which, if corrected, yields a V_c of 0.48 liter/kg[4]. The V_{dB} (2.74 liters/kg) was approximately equal to the previous literature value (5). Other differences in pharmacokinetic constants are, therefore, explained by this correction in V_c.

Concern in this study regarding the potential hydrolysis of *N*-acetylprocainamide to procainamide as a general source of error appears answered by the small coefficient of variation observed for the assay, the absence of hydrolysis as measured under the assay conditions utilized, and the relative agreement of infusion rate prediction (Loo–Riegelman) with the known infusion rate. These observations are supported by a recent report suggesting that the various procainamide assay procedures yield similar results (13). If any method is subject to interference from *N*-acetylprocainamide, it appears to be the fluorometric procedure (14).

Bioavailability—The sustained-release preparation, whose characteristics this study was to determine, appears to have satisfactory bioavailability. First-pass metabolic effect considerations (15) suggest that the bioavailability of both oral preparations approaches the maximum possible for procainamide in humans if nonrenal clearance ($Cl_{NR} = Cl_B - Cl_R$) is presumed to represent hepatic clearance. The difference in the ($PA_{u,po}^{24hr}/PA_{u,iv}^{24hr}$) bioavailability calculation suggests that the sustained-release tablet is less available than the conventional capsule. However, the urinary procainamide excretion from any administration is subject to the problem of the completeness of urine collection, and the urinary recovery ratio method may be less reliable (footnote *a*, Table IV). Indeed, incomplete urinary recovery from Subject B.M. following his intravenous dose is perhaps the most plausible explanation for his high bioavailability when calculated from urinary excretion data. The overall variability in the urinary excretion data is sufficiently great to limit the capacity to suggest a bioavailability difference.

Absorption Rate—A principal objective of this study was to compare the absorption rate of procainamide from a sustained-release tablet to that from a conventional capsule. The calculation of an absorption rate constant further requires that the individual percent unabsorbed *versus* time data points be fitted to an equation. This approach assumes that oral absorption can be adequately described as a simple function of time (which is not necessarily accurate). Since the Loo–Riegelman plots did show good linearity on semilogarithmic coordinates when the initial "lag time" and the postabsorptive phase were ignored, it seems that apparent first-order kinetics were operative. Furthermore, the relative agreement of the known intravenous infusion rate with that calculated by the method of Loo and Riegelman supports this approach for the approximation of the k_a's (at least for the study of procainamide in humans). Based on these data, a substantial alteration has been achieved in k_a that may be clinically meaningful (16).

[4] C. Graffner, A. B. Hässle, Mölndal, Sweden, personal communication.

Table V—Apparent Absorption Rate of Procainamide in Normal Volunteers

Subject	K_a, Capsule, min^{-1}	K_a, Sustained Release, min^{-1}	k_0, Intravenous Infusion, mg/min
S.R.	0.0045	0.0034	29.3
C.H.	0.0077	0.0046	37.6
B.M.	0.0107	0.0058	33.1
F.N.	0.0092	0.0045	29.9
P.Gt.	0.0198	0.0040	42.0
C.F.	0.0173	0.0036	31.1
G.B.	0.0116	0.0022	60.1[a]
P.R.	0.0866	0.0027	28.6
T.C.	0.0693	0.0051	30.8
P.Ga.	0.0866	0.0026	42
L.D.	0.0462	0.0041	27.0
Mean	0.0336	0.0039	33.1
SEM	0.0098	0.0003	1.7

[a] This value was not used in the calculation of the mean k_0 since when it was deleted it fell more than 5 *SD* above the mean.

CONCLUSIONS

1. It seems to be possible to delay the *in vivo* absorption rate of procainamide in humans at least an order of magnitude and still achieve satisfactory bioavailability.
2. The method of Loo and Riegelman seems to be satisfactory for the estimation of absorption rate constants for procainamide in humans.
3. Plasma procainamide levels following a brief intravenous infusion were well described by a biexponential equation.
4. Therapeutic blood levels may be achieved with the sustained-release tablet with doses of approximately 1–2 g (four tablets) every 6–8 hr.

REFERENCES

(1) J. Koch-Weser and S. W. Klein, *J. Am. Med. Assoc.*, **215**, 1454 (1971).

(2) J. Koch-Weser, *Ann. N.Y. Acad. Sci.*, **179**, 370 (1971).

(3) M. Arstila, M. Katila, H. Sundquist, M. Anttila, E. Pere, and R. Tikkamen, *Acta Med. Scand.*, **195**, 217 (1974).

(4) D. Fremstand, S. Dahl, S. Jacobsen, P. K. M. Lunde, K. J. Nadland, A. A. Marthinsen, T. Waaler, and K. H. Landmark, *Eur. J. Clin. Pharmacol.*, **6**, 251 (1973).

(5) C. Graffner, G. Johnsson, and J. Sjogren, *Clin. Pharmacol. Ther.*, **17**, 414 (1975).

(6) L. C. Mark, J. J. Kayden, J. M. Steele, J. R. Cooper, I. Berlin, E. A. Rovenstine, and B. B. Brodie, *J. Pharmacol. Exp. Ther.*, **102**, 5 (1951).

(7) D. S. Sitar, D. N. Graham, R. E. Rangno, L. Dufresne, and R. I. Ogilvie, *Pharmacologist*, **16**, 175 (1974).

(8) A. J. Atkinson, M. Parker, and J. Strong, *Clin. Chem.*, **18**, 643 (1972).

(9) S. Sterling, S. Cox, and W. G. Haney, *J. Pharm. Sci.*, **63**, 1744 (1974).

(10) J. C. K. Loo and S. Riegelman, *ibid.*, **59**, 53 (1970).

(11) C. M. Metzler, NONLIN, Tech. Rept. 7292/69/7293/005, Upjohn Co., Kalamazoo, Mich., 1969.

(12) J. C. K. Loo and S. Riegelman, *J. Pharm. Sci.*, **57**, 918 (1968).

(13) W. J. Westlake, *ibid.*, **60**, 882 (1971).

(14) T. P. Gibson, D. T. Lowenthal, H. A. Nelson, and W. A. Briggs, *Clin. Pharmacol. Ther.*, **17**, 321 (1975).

(15) M. Gibaldi, R. N. Boyes, and S. Feldman, *J. Pharm. Sci.*, **60**, 1338 (1971).

(16) J. Birkhead, T. Evans, P. Mumford, E. Martinez, and D. Jewett, *Br. Heart J.*, **38**, 77 (1976).

ACKNOWLEDGMENTS AND ADDRESSES

Received January 12, 1976, from the *Research Laboratories, Astra Pharmaceutical Products, Inc., Framingham, MA 01701*, and the *Clinical Pharmacology Unit, St. Vincent Hospital, Worcester, MA 01606.*

Accepted for publication September 2, 1976.

The authors acknowledge the excellent help and assistance of Susan Wolshin, June Lufkin, and Susan Manion.

* Present address: Department of Pharmaceutics, School of Pharmacy, State University of New York at Buffalo, Buffalo, NY, 14214.

[x] To whom inquiries should be directed.

Liposomal Entrapment of Floxuridine

STEPHEN P. SIMMONS and PAUL A. KRAMER [x]

Abstract □ Floxuridine was found to have an apparent initial entrapment within negatively charged sphingomyelin liposomes about three times higher than its parent, fluorouracil. The drug also diffused out of the liposomes at a much lower rate than fluorouracil. Substitution of lecithin for sphingomyelin destroyed the effect. Liposomal entrapment may provide enhanced stability and decreased toxicity of floxuridine, permitting wider therapeutic utilization of pyrimidine nucleosides.

Keyphrases □ Floxuridine—entrapment within sphingomyelin and lecithin liposomes, compared to fluorouracil □ Liposomes, sphingomyelin and lecithin—entrapment of floxuridine, compared to fluorouracil □ Antitumor agents—floxuridine, entrapment within sphingomyelin and lecithin liposomes, compared to fluorouracil

The actual inhibitor of thymidylate synthetase and, hence, DNA biosynthesis in tumor growth inhibition by fluorouracil (I) is 2′-deoxy-5-fluorouridine 5′-monophosphate (II) (1). Floxuridine (2′-deoxy-5-fluorouridine) (III) is a better precursor of II than I, as evidenced by the fact that it is 10^3 times as effective in inhibiting DNA thymine synthesis in Ehrlich ascites cells *in vitro* (2) and is a more effective carcinostatic agent against both Ehrlich ascites and Sarcoma-180 *in vivo* (3). This increased intrinsic activity is not translated into increased effectiveness in humans, because III is degraded to its constituent pyrimidine and sugar moieties by nucleoside phosphorylases in serum and tissues (4). Attempts at stabilization have included chemical modification of the drug itself as well as the addition of deoxyribose donors and enzyme inhibitors to suppress the degradation reaction (5, 6).

One might expect the encapsulation of III within the aqueous compartments of phospholipid vesicles (liposomes) to be of utility in this regard. The protective lipid sheath might prevent enzymatic degradation in serum and reduce the toxicity of the drug by excluding it from regions such as the GI tract. Previous workers reported difficulty

Table V—Apparent Absorption Rate of Procainamide in Normal Volunteers

Subject	K_a, Capsule, min^{-1}	K_a, Sustained Release, min^{-1}	k_0, Intravenous Infusion, mg/min
S.R.	0.0045	0.0034	29.3
C.H.	0.0077	0.0046	37.6
B.M.	0.0107	0.0058	33.1
F.N.	0.0092	0.0045	29.9
P.Gt.	0.0198	0.0040	42.0
C.F.	0.0173	0.0036	31.1
G.B.	0.0116	0.0022	60.1[a]
P.R.	0.0866	0.0027	28.6
T.C.	0.0693	0.0051	30.8
P.Ga.	0.0866	0.0026	42
L.D.	0.0462	0.0041	27.0
Mean	0.0336	0.0039	33.1
SEM	0.0098	0.0003	1.7

[a] This value was not used in the calculation of the mean k_0 since when it was deleted it fell more than 5 *SD* above the mean.

CONCLUSIONS

1. It seems to be possible to delay the *in vivo* absorption rate of procainamide in humans at least an order of magnitude and still achieve satisfactory bioavailability.
2. The method of Loo and Riegelman seems to be satisfactory for the estimation of absorption rate constants for procainamide in humans.
3. Plasma procainamide levels following a brief intravenous infusion were well described by a biexponential equation.
4. Therapeutic blood levels may be achieved with the sustained-release tablet with doses of approximately 1–2 g (four tablets) every 6–8 hr.

REFERENCES

(1) J. Koch-Weser and S. W. Klein, *J. Am. Med. Assoc.*, **215**, 1454 (1971).

(2) J. Koch-Weser, *Ann. N.Y. Acad. Sci.*, **179**, 370 (1971).

(3) M. Arstila, M. Katila, H. Sundquist, M. Anttila, E. Pere, and R. Tikkamen, *Acta Med. Scand.*, **195**, 217 (1974).

(4) D. Fremstand, S. Dahl, S. Jacobsen, P. K. M. Lunde, K. J. Nadland, A. A. Marthinsen, T. Waaler, and K. H. Landmark, *Eur. J. Clin. Pharmacol.*, **6**, 251 (1973).

(5) C. Graffner, G. Johnsson, and J. Sjogren, *Clin. Pharmacol. Ther.*, **17**, 414 (1975).

(6) L. C. Mark, J. J. Kayden, J. M. Steele, J. R. Cooper, I. Berlin, E. A. Rovenstine, and B. B. Brodie, *J. Pharmacol. Exp. Ther.*, **102**, 5 (1951).

(7) D. S. Sitar, D. N. Graham, R. E. Rangno, L. Dufresne, and R. I. Ogilvie, *Pharmacologist*, **16**, 175 (1974).

(8) A. J. Atkinson, M. Parker, and J. Strong, *Clin. Chem.*, **18**, 643 (1972).

(9) S. Sterling, S. Cox, and W. G. Haney, *J. Pharm. Sci.*, **63**, 1744 (1974).

(10) J. C. K. Loo and S. Riegelman, *ibid.*, **59**, 53 (1970).

(11) C. M. Metzler, NONLIN, Tech. Rept. 7292/69/7293/005, Upjohn Co., Kalamazoo, Mich., 1969.

(12) J. C. K. Loo and S. Riegelman, *J. Pharm. Sci.*, **57**, 918 (1968).

(13) W. J. Westlake, *ibid.*, **60**, 882 (1971).

(14) T. P. Gibson, D. T. Lowenthal, H. A. Nelson, and W. A. Briggs, *Clin. Pharmacol. Ther.*, **17**, 321 (1975).

(15) M. Gibaldi, R. N. Boyes, and S. Feldman, *J. Pharm. Sci.*, **60**, 1338 (1971).

(16) J. Birkhead, T. Evans, P. Mumford, E. Martinez, and D. Jewett, *Br. Heart J.*, **38**, 77 (1976).

ACKNOWLEDGMENTS AND ADDRESSES

Received January 12, 1976, from the *Research Laboratories, Astra Pharmaceutical Products, Inc., Framingham, MA 01701*, and the *Clinical Pharmacology Unit, St. Vincent Hospital, Worcester, MA 01606.*

Accepted for publication September 2, 1976.

The authors acknowledge the excellent help and assistance of Susan Wolshin, June Lufkin, and Susan Manion.

* Present address: Department of Pharmaceutics, School of Pharmacy, State University of New York at Buffalo, Buffalo, NY, 14214.

[x] To whom inquiries should be directed.

Liposomal Entrapment of Floxuridine

STEPHEN P. SIMMONS and PAUL A. KRAMER [x]

Abstract □ Floxuridine was found to have an apparent initial entrapment within negatively charged sphingomyelin liposomes about three times higher than its parent, fluorouracil. The drug also diffused out of the liposomes at a much lower rate than fluorouracil. Substitution of lecithin for sphingomyelin destroyed the effect. Liposomal entrapment may provide enhanced stability and decreased toxicity of floxuridine, permitting wider therapeutic utilization of pyrimidine nucleosides.

Keyphrases □ Floxuridine—entrapment within sphingomyelin and lecithin liposomes, compared to fluorouracil □ Liposomes, sphingomyelin and lecithin—entrapment of floxuridine, compared to fluorouracil □ Antitumor agents—floxuridine, entrapment within sphingomyelin and lecithin liposomes, compared to fluorouracil

The actual inhibitor of thymidylate synthetase and, hence, DNA biosynthesis in tumor growth inhibition by fluorouracil (I) is 2′-deoxy-5-fluorouridine 5′-monophosphate (II) (1). Floxuridine (2′-deoxy-5-fluorouridine) (III) is a better precursor of II than I, as evidenced by the fact that it is 10^3 times as effective in inhibiting DNA thymine synthesis in Ehrlich ascites cells *in vitro* (2) and is a more effective carcinostatic agent against both Ehrlich ascites and Sarcoma-180 *in vivo* (3). This increased intrinsic activity is not translated into increased effectiveness in humans, because III is degraded to its constituent pyrimidine and sugar moieties by nucleoside phosphorylases in serum and tissues (4). Attempts at stabilization have included chemical modification of the drug itself as well as the addition of deoxyribose donors and enzyme inhibitors to suppress the degradation reaction (5, 6).

One might expect the encapsulation of III within the aqueous compartments of phospholipid vesicles (liposomes) to be of utility in this regard. The protective lipid sheath might prevent enzymatic degradation in serum and reduce the toxicity of the drug by excluding it from regions such as the GI tract. Previous workers reported difficulty

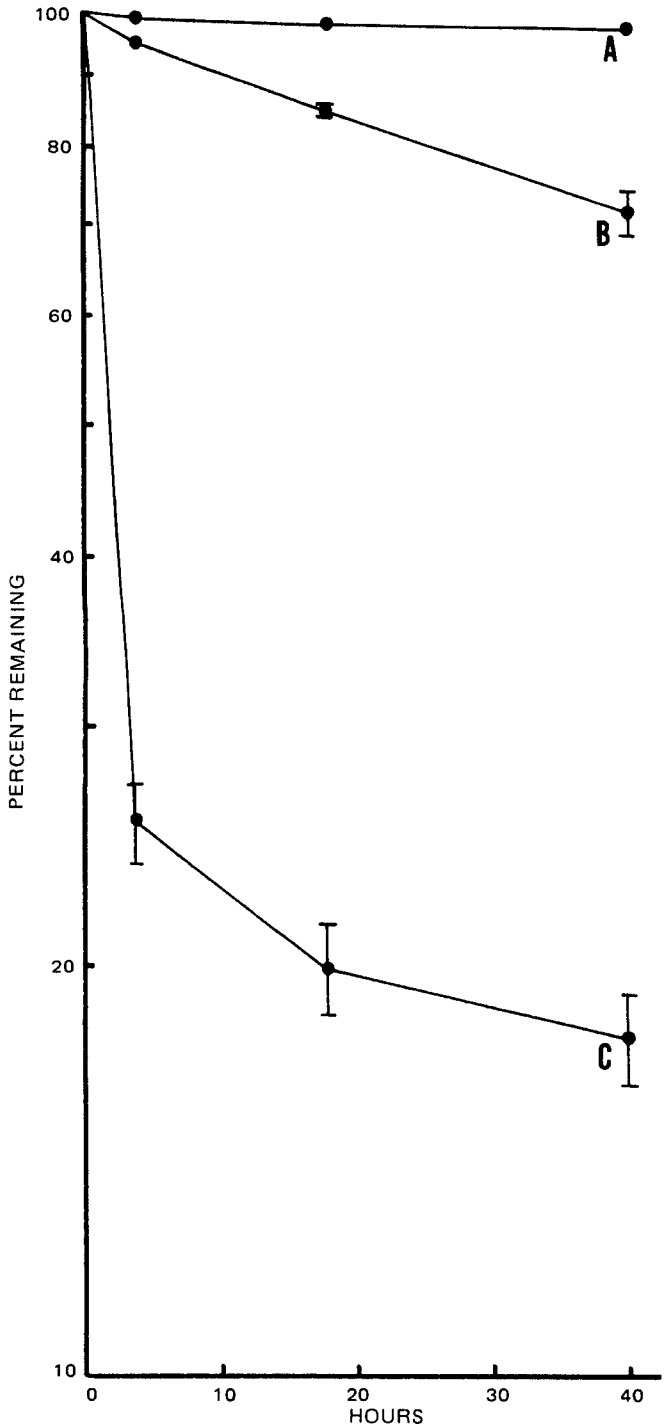

Figure 1—*Diffusion of sucrose (A), floxuridine (B), and fluorouracil (C) from sphingomyelin liposomes. The sphingomyelin–cholesterol–dicetyl phosphate ratio was 4.8:2.8:1.0, and the lipid–aqueous phase ratio was 70:1. The zero-time value of 100% represents initial entrapment after 4 hr of swelling at 25° plus 15 min of sonication. All other values are percentages of this initial quantity that remained entrapped after incubation of the liposomes for various times at 25°. Plotted points are mean ±SEM for three determinations.*

retaining I within liposomes (7, 8). The distribution of I in the rat was favorably altered toward exclusion of the drug from GI tissues, even though there was pronounced diffusion of drug from liposomes to plasma (8). The present studies were undertaken to determine if the more hydrophilic deoxyribose derivative might be a better candidate for liposomal delivery.

EXPERIMENTAL

Materials—Sphingomyelin[1] (bovine brain), egg lecithin[2], and dicetyl phosphate[3] were used as received. Fluorouracil[4], floxuridine[5], sucrose[6], and cholesterol[5] were mixed with 6-^{3}H-fluorouracil[7] (26 Ci/mmole), 6-^{3}H-floxuridine[7] (2.3 Ci/mmole), 6,6′(*n*)-^{3}H-sucrose[7] (3.6 Ci/mmole), and 4-^{14}C-cholesterol[7] (47.2 mCi/mmole) (5 μCi/ml), respectively, prior to use. Spectral grade chloroform was used to dissolve the lipids, and all water was double distilled in an all-glass system.

Liposome Preparation—Liposomes were prepared from chloroform solutions of phospholipid (egg lecithin or sphingomyelin), cholesterol (sometimes 4-^{14}C-labeled), and dicetyl phosphate in molar ratios of 7:2:1 or 4.8:2.8:1. The lipids were evaporated under vacuum to a thin film on a 10-ml pear-shaped flask, and an isotonic, buffered (pH 6.0, 0.01 *M* phosphate) solution of tritiated sucrose, fluorouracil, or floxuridine (0.077 *M*) was added. The lipid–aqueous phase ratios used were 50 and 70 μmoles of lipid/ml of buffer.

A small number of 0.5-mm glass beads was added, and the lipids were dispersed by vortexing[8] for 2 min. After a 2-hr "swelling period" at 25°, the vesicles were sonicated in a bath sonicator[9] for 15 min at 15°. They were held at 25° for an additional 2 hr and then separated from unentrapped drug by chromatography on a 1.5 × 16-cm column[10]. The liposomal eluate was pooled, and the drug content was taken as a measure of "initial" entrapment. The liposomes obtained had a diameter range of 0.5–5.0 μm.

Quantitative determination of drugs and liposomal cholesterol was accomplished by liquid scintillation counting[11]. Drug release kinetics were determined by removing aliquots of liposomes from the pool at various sampling times, rechromatographing to remove released drug, and counting the liposome fractions upon elution from the column.

RESULTS AND DISCUSSION

Table I shows the initial entrapment percentages as a function of drug and lipid composition of the liposome. These percentages depend upon lipid–aqueous phase ratios and molar ratios of constituents of the vesicle as expected. Sucrose was used as a nearly nondiffusable marker to indicate liposome integrity. Increasing the total lipid content and the relative quantity of cholesterol enhanced entrapment of both floxuridine and sucrose. These materials were entrapped to about the same extent when sphingomyelin was the phospholipid, but the entrapment of floxuridine relative to sucrose decreased dramatically when lecithin was substituted.

Increased unsaturation and melting of the acyl side chains were reported to increase the rate of diffusion of both charged and uncharged solutes through phospholipid membranes (9). The fact that sphingomyelin has a gel–liquid crystalline phase transition temperature of 40° (10) while egg lecithin vesicles "melt" at −15° (11) may account for the observed results. Fluorouracil was apparently entrapped within sphingomyelin liposomes about three times less extensively than floxuridine, but this finding could be an anomalous result produced by the arbitrary definition of "initial" entrapment.

Figure 1 depicts the release of sucrose, floxuridine, and fluorouracil from sphingomyelin liposomes at 25° over nearly 2 days. The liposomal preparation used was that providing the best initial entrapment (Table I). Sucrose was nearly completely retained, as expected. Fluorouracil diffused out with a very high initial rate, high enough to perhaps account for the apparently lower initial entrapment which was actually measured more than 4 hr after swelling began. At least for sphingomyelin liposomes, the hydrogen-bonding hydroxyl groups on the deoxyribose moiety of floxuridine prevent its rapid diffusional loss, as evidenced by the improved retention of floxuridine within sphingomyelin liposomes. This effect is in accord with previous observations by Cohen (12), who concluded that retention of materials within the aqueous interstices of liposomes was directly related to the ability of the material to hydrogen bond. The kinetics of diffusion of drug from these multiconcentric spheres

[1] Pierce Chemical Co., Rockford, Ill.
[2] Grand Island Biological Co., Grand Island, N.Y.
[3] K & K Labs, Plainview, N.Y.
[4] Aldrich Chemical Co., Milwaukee, Wis.
[5] Sigma Chemical Co., St. Louis, Mo.
[6] Mallinckrodt Chemical Works.
[7] Schwartz-Mann, Orangeburg, N.Y.
[8] Vortex-Genie, Scientific Industries, Springfield, Mass.
[9] Eighty watts, 60 Hz, Heat Systems Ultrasonics, Plainview, N.Y.
[10] Sephadex G-50 (coarse), Pharmacia Fine Chemicals, Piscataway, N.J.
[11] Beckman model LS-250.

Table I—Initial Entrapment of Floxuridine in Liposomes

Vesicle Composition	Lipid Ratio	Percent Entrapped[a]		
		Sucrose	Floxuridine	Fluorouracil
Sphingomyelin–cholesterol–dicetyl phosphate	4.8:2.8:1.0[b]	14.3 ± 1.1[c]	11.9 ± 2.5[c]	3.6 ± 0.3[c]
Lecithin–cholesterol–dicetyl phosphate	4.8:2.8:1.0[b]	8.0	0.87	1.0
Sphingomyelin–cholesterol–dicetyl phosphate	7.0:2.0:1.0[d]	4.3[e]	3.0[e]	—
Lecithin–cholesterol–dicetyl phosphate	7.0:2.0:1.0[d]	4.1[e]	0.34[e]	—

[a] Measured after 2 min of vortexing, 2 hr of swelling at 25°, 15 min of sonication, and a second 2 hr of swelling at 25°. [b] Seventy micromoles of lipid/ml of aqueous phase. [c] Mean ± *SEM* (three determinations). [d] Fifty micromoles of lipid/ml of aqueous phase. [e] Average of two determinations.

are complex and not first order. The data are plotted on a semilogarithmic plot only as a convenient method for visualizing the relative differences observed.

There is considerable rationale for the entrapment of fluorouracil within liposomes and, as mentioned, retention has been a problem. The present results indicate that floxuridine is retained far better when sphingomyelin liposomes are used, and several other benefits, such as higher intrinsic activity against some cancers, favor the nucleoside. Preliminary results in these laboratories indicate that, after intraperitoneal administration to mice bearing L-1210 leukemia in the ascites form, the liposomes and their floxuridine content are avidly engulfed by the L-1210 cells, with large quantities of floxuridine concentrating in the cells. Further studies are in progress to ascertain the effect of such administrations on the survival times of tumor-bearing mice.

REFERENCES

(1) S. S. Cohen, J. G. Flaks, H. D. Barner, M. R. Loeb, and J. Lichtenstein, *Proc. Nat. Acad. Sci. USA*, **44**, 1004 (1958).

(2) K. L. Mukherjee and C. Heidelberger, *Cancer Res.*, **22**, 815 (1962).

(3) C. Heidelberger, L. Griesbach, O. Cruz, R. J. Schnitzer, and E. Grunberg, *Proc. Soc. Exp. Biol. Med.*, **97**, 470 (1958).

(4) C. Heidelberger, "Cancer Medicine," E. Frei and J. F. Holland, Eds., Lea & Febiger, Philadelphia, Pa., 1973, p. 776.

(5) J. J. Windheuser and J. Jato, *J. Pharm. Sci.*, **61**, 1669 (1972).

(6) G. D. Birnie, H. Kroeger, and C. Heidelberger, *Biochemistry*, **2**, 566 (1963).

(7) L. J. Lesko and R. Ganapathi, presented at the APhA Academy of Pharmaceutical Sciences, Atlanta meeting, Nov. 1975.

(8) G. Gregoriadis, *Biochem. Soc. Trans.*, **2**, 117 (1974).

(9) D. Papahadjopoulous and H. K. Kimelberg, *Prog. Surf. Sci.*, **4**, 141 (1973).

(10) E. Oldfield and D. Chapman, *FEBS Lett.*, **21**, 303 (1972).

(11) B. D. Ladbrooke and D. Chapman, *Chem. Phys. Lipids*, **3**, 304 (1969).

(12) B. E. Cohen, *J. Membr. Biol.*, **20**, 205 (1975).

ACKNOWLEDGMENTS AND ADDRESSES

Received July 23, 1976, from the *Industrial and Physical Pharmacy Department, School of Pharmacy and Pharmacal Sciences, Purdue University, West Lafayette, IN 47907.*

Accepted for publication August 18, 1976.

Supported by Grant 17866 from the National Cancer Institute, National Institutes of Health, Bethesda, MD 20014.

[x] To whom inquiries should be directed. Present address: Pharmacy Department, University of Connecticut Health Center, Farmington, CT 06032.

Inhibition of Catechol *O*-Methyltransferase and Transfer RNA Methyltransferases by Coralyne, Nitidine, and Related Compounds

JOHN W. LEE, JOHN O. MacFARLANE, ROBERT K. Y. ZEE-CHENG, and C. C. CHENG [x]

Abstract □ Inhibitory activity against both catechol *O*-methyltransferase and transfer RNA methyltransferases was observed among the antileukemic alkaloids coralyne, nitidine, and related synthetic alkoxy analogs. Inhibition of both classes of enzymes seems to have a similar profile. The role of water solubility of these compounds with regard to their enzyme inhibitory activity was noted.

Keyphrases □ Catechol *O*-methyltransferase—activity, effect of coralyne, nitidine, and related compounds, rat liver homogenate □ tRNA methyltransferase—activity, effect of coralyne, nitidine, and related compounds, rat liver homogenate □ Enzyme activity—catechol *O*-methyltransferase and tRNA methyltransferase, effect of coralyne, nitidine, and related compounds, rat liver homogenate □ Coralyne—effect on catechol *O*-methyltransferase and tRNA methyltransferase activity, rat liver homogenate □ Nitidine—effect on catechol *O*-methyltransferase and tRNA methyltransferase activity, rat liver homogenate □ Alkaloids, antileukemic—coralyne, nitidine, and related compounds, effect on catechol *O*-methyltransferase and tRNA methyltransferase activity, rat liver homogenate □ Structure–activity relationships—effect of coralyne, nitidine, and related compounds on catechol *O*-methyltransferase and tRNA methyltransferase activity, rat liver homogenate

Experimental evidence (1–9) has substantiated the observation of higher transfer RNA (tRNA) methyltransferase activity in fetal or malignant tumor tissue than in normal or benign tumor tissue. Also, certain chemical carcinogens increased tRNA methyltransferase activity (10, 11). These aberrant methylating enzymes may differ qualitatively from the regular tRNA methyltransferase in their specificity of action (12, 13). Certain oxygen-containing compounds possessing antileukemic activity may be tRNA 2′-*O*-methyltransferase inhibitors, and this

Table I—Initial Entrapment of Floxuridine in Liposomes

Vesicle Composition	Lipid Ratio	Percent Entrapped[a]		
		Sucrose	Floxuridine	Fluorouracil
Sphingomyelin–cholesterol–dicetyl phosphate	4.8:2.8:1.0[b]	14.3 ± 1.1[c]	11.9 ± 2.5[c]	3.6 ± 0.3[c]
Lecithin–cholesterol–dicetyl phosphate	4.8:2.8:1.0[b]	8.0	0.87	1.0
Sphingomyelin–cholesterol–dicetyl phosphate	7.0:2.0:1.0[d]	4.3[e]	3.0[e]	—
Lecithin–cholesterol–dicetyl phosphate	7.0:2.0:1.0[d]	4.1[e]	0.34[e]	—

[a] Measured after 2 min of vortexing, 2 hr of swelling at 25°, 15 min of sonication, and a second 2 hr of swelling at 25°. [b] Seventy micromoles of lipid/ml of aqueous phase. [c] Mean ± *SEM* (three determinations). [d] Fifty micromoles of lipid/ml of aqueous phase. [e] Average of two determinations.

are complex and not first order. The data are plotted on a semilogarithmic plot only as a convenient method for visualizing the relative differences observed.

There is considerable rationale for the entrapment of fluorouracil within liposomes and, as mentioned, retention has been a problem. The present results indicate that floxuridine is retained far better when sphingomyelin liposomes are used, and several other benefits, such as higher intrinsic activity against some cancers, favor the nucleoside. Preliminary results in these laboratories indicate that, after intraperitoneal administration to mice bearing L-1210 leukemia in the ascites form, the liposomes and their floxuridine content are avidly engulfed by the L-1210 cells, with large quantities of floxuridine concentrating in the cells. Further studies are in progress to ascertain the effect of such administrations on the survival times of tumor-bearing mice.

REFERENCES

(1) S. S. Cohen, J. G. Flaks, H. D. Barner, M. R. Loeb, and J. Lichtenstein, *Proc. Nat. Acad. Sci. USA*, **44**, 1004 (1958).

(2) K. L. Mukherjee and C. Heidelberger, *Cancer Res.*, **22**, 815 (1962).

(3) C. Heidelberger, L. Griesbach, O. Cruz, R. J. Schnitzer, and E. Grunberg, *Proc. Soc. Exp. Biol. Med.*, **97**, 470 (1958).

(4) C. Heidelberger, "Cancer Medicine," E. Frei and J. F. Holland, Eds., Lea & Febiger, Philadelphia, Pa., 1973, p. 776.

(5) J. J. Windheuser and J. Jato, *J. Pharm. Sci.*, **61**, 1669 (1972).

(6) G. D. Birnie, H. Kroeger, and C. Heidelberger, *Biochemistry*, **2**, 566 (1963).

(7) L. J. Lesko and R. Ganapathi, presented at the APhA Academy of Pharmaceutical Sciences, Atlanta meeting, Nov. 1975.

(8) G. Gregoriadis, *Biochem. Soc. Trans.*, **2**, 117 (1974).

(9) D. Papahadjopoulous and H. K. Kimelberg, *Prog. Surf. Sci.*, **4**, 141 (1973).

(10) E. Oldfield and D. Chapman, *FEBS Lett.*, **21**, 303 (1972).

(11) B. D. Ladbrooke and D. Chapman, *Chem. Phys. Lipids*, **3**, 304 (1969).

(12) B. E. Cohen, *J. Membr. Biol.*, **20**, 205 (1975).

ACKNOWLEDGMENTS AND ADDRESSES

Received July 23, 1976, from the *Industrial and Physical Pharmacy Department, School of Pharmacy and Pharmacal Sciences, Purdue University, West Lafayette, IN 47907.*

Accepted for publication August 18, 1976.

Supported by Grant 17866 from the National Cancer Institute, National Institutes of Health, Bethesda, MD 20014.

[x] To whom inquiries should be directed. Present address: Pharmacy Department, University of Connecticut Health Center, Farmington, CT 06032.

Inhibition of Catechol *O*-Methyltransferase and Transfer RNA Methyltransferases by Coralyne, Nitidine, and Related Compounds

JOHN W. LEE, JOHN O. MacFARLANE, ROBERT K. Y. ZEE-CHENG, and C. C. CHENG [x]

Abstract □ Inhibitory activity against both catechol *O*-methyltransferase and transfer RNA methyltransferases was observed among the antileukemic alkaloids coralyne, nitidine, and related synthetic alkoxy analogs. Inhibition of both classes of enzymes seems to have a similar profile. The role of water solubility of these compounds with regard to their enzyme inhibitory activity was noted.

Keyphrases □ Catechol *O*-methyltransferase—activity, effect of coralyne, nitidine, and related compounds, rat liver homogenate □ tRNA methyltransferase—activity, effect of coralyne, nitidine, and related compounds, rat liver homogenate □ Enzyme activity—catechol *O*-methyltransferase and tRNA methyltransferase, effect of coralyne, nitidine, and related compounds, rat liver homogenate □ Coralyne—effect on catechol *O*-methyltransferase and tRNA methyltransferase activity, rat liver homogenate □ Nitidine—effect on catechol *O*-methyltransferase and tRNA methyltransferase activity, rat liver homogenate □ Alkaloids, antileukemic—coralyne, nitidine, and related compounds, effect on catechol *O*-methyltransferase and tRNA methyltransferase activity, rat liver homogenate □ Structure–activity relationships—effect of coralyne, nitidine, and related compounds on catechol *O*-methyltransferase and tRNA methyltransferase activity, rat liver homogenate

Experimental evidence (1–9) has substantiated the observation of higher transfer RNA (tRNA) methyltransferase activity in fetal or malignant tumor tissue than in normal or benign tumor tissue. Also, certain chemical carcinogens increased tRNA methyltransferase activity (10, 11). These aberrant methylating enzymes may differ qualitatively from the regular tRNA methyltransferase in their specificity of action (12, 13). Certain oxygen-containing compounds possessing antileukemic activity may be tRNA 2′-*O*-methyltransferase inhibitors, and this

methylating enzyme may act *via* a complex analogous to that known for catechol *O*-methyltransferase (COMT) (14).

Therefore, preliminary enzyme inhibitory activity tests of the antileukemic alkaloids coralyne, nitidine, and related compounds (15–19) against catechol *O*-methyltransferase and tRNA methyltransferases were conducted. A number of antitumor purine nucleosides (20), the tubercidin analog of *S*-adenosylhomocysteine (21), and polyinosinate (22) have already been reported as inhibitors of tRNA (and rRNA) methyltransferases.

EXPERIMENTAL

Assay of Catechol *O*-Methyltransferase—The colorimetric assay method used was based on that reported by Herblin (23). The catechol *O*-methyltransferase enzyme extract was prepared according to the method of Axelrod and Tomchick (24) with some modification (all procedures performed at 0–5°). Male adult rat liver, 100 g, was homogenized in 400 ml of 0.15 *M* isotonic potassium chloride. The solution was centrifuged at 41,000×*g* for 30 min. The supernate was drained through cheesecloth, adjusted to pH 5.3 with 1 *N* acetic acid, and centrifuged at 800×*g* for 10 min. The precipitate was discarded, and ammonium sulfate was added to achieve 30% saturation.

This solution was again centrifuged (800×*g* for 10 min), and ammonium sulfate was added to the supernate to achieve 50% saturation. The resulting solution was centrifuged at 6600×*g* for 15 min. The precipitate was collected and dissolved in 40 ml of water and dialyzed against 0.001 *M* phosphate buffer at pH 7 for 4 hr. The enzyme preparation was then dispensed into small (1–5-ml) aliquots and frozen at −60°. The partially purified enzyme preparations used for these tests contained approximately 40–50 mg of protein/ml and 0.05–0.1 unit of enzyme/mg of protein, or approximately 0.75–1.5 units of enzyme per test.

Based upon a series of preliminary titrations and experimental studies, the following procedure was used. Reagents were added to the reaction tubes at 0–5° (ice bath) in the following quantities and order: 0.25 μmole of pH 7 tris(hydroxymethyl)aminomethane buffer, 2.5 μmoles of magnesium chloride hexahydrate, 0.5 ml of the prepared catechol *O*-methyltransferase enzyme extract, 0.1 μmole of *S*-adenosylmethionine (SAM), and 0.13 μmole of 2.68×10^{-4} *M* 4-nitrocatechol as the methyl acceptor. Distilled water was added to tubes as needed to give a final total volume of 2.5 ml.

For the inhibition test, 0.5 ml of the inhibitor solution was allowed to react with 0.5 ml of the enzyme preparation at 0–5° for 5 min and then was added to the reaction mixture. This solution was allowed to remain in a 37° water bath for 45 min, followed by the addition of 2 ml of 6 *N* NaOH to terminate the enzyme reaction. Tubes containing the reaction mixture were centrifuged at 800×*g* at 5° for 10 min. The absorbance of the supernate was measured at 520 nm in a UV spectrophotometer (cell had 10-mm light path). Since at pH ≥ 9, 4-nitrocatechol exhibits a red color whereas its methylated product does not, methylation of catechol *O*-methyltransferase activity can be measured as a decrease in absorbance at 520 nm.

To determine enzyme activity, a reaction mixture was run as a control against the mixture with enzyme. The difference in the absorbance of these two mixtures was then the measure of enzyme activity. Inhibitors were generally tested at three different concentrations. The concentration of an inhibitor was calculated as the final concentration after dilution of the reaction mixture (0.5 ml in 2.5 ml or 1:5). The level of inhibition was determined by measuring the absorbance of a reaction mixture with the inhibitor and subtracting that of a reaction mixture with both the inhibitor and the enzyme.

The percent of enzyme inhibition was then calculated as:

$$\% \text{ inhibition} = \frac{\Delta \text{ absorbance (reflecting enzyme activity with inhibitor)}}{\Delta \text{ absorbance (reflecting enzyme activity without inhibitor)}} \times 100 \quad \text{(Eq. 1)}$$

As a control of the entire procedure, a known inhibitor of catechol *O*-methyltransferase, pyrogallol, was run to achieve a "standard" curve of inhibition (100, 45, and 12% inhibition at 10^{-3}, 10^{-4}, and 10^{-5} *M*, respectively). Pyrogallol was run periodically to check that the assay was producing consistent results.

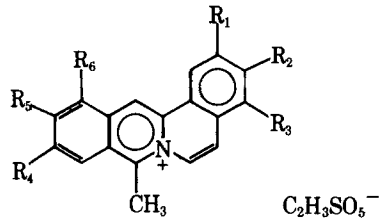

I: $R_1 = R_2 = R_4 = R_5 = OCH_3$, $R_3 = R_6 = H$
II: $R_1 = R_2 = R_5 = R_6 = OCH_3$, $R_3 = R_4 = H$
III: $R_2 = R_3 = R_4 = R_5 = OCH_3$, $R_1 = R_6 = H$

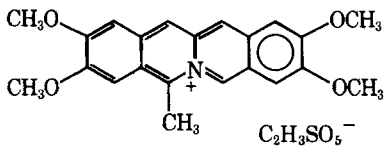

IV

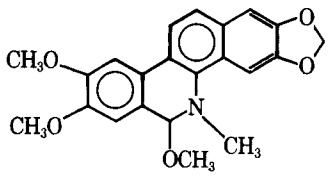

VIII

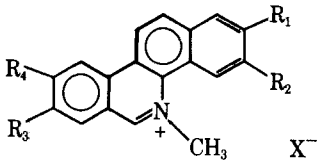

V: $R_1 R_2 = OCH_2O$, $R_3 = R_4 = OCH_3$, X = Cl
VI: $R_1 R_2 = OCH_2O$, $R_3 = R_4 = OCH_3$, $X = CH_3SO_4$
VII: $R_1 R_2 = OCH_2O$, $R_3 = R_4 = OCH_3$, $X = BrCH_2CO_2$
IX: $R_1 = R_2 = R_3 = R_4 = OCH_3$, $X = SO_3F$
X: $R_1 = R_2 = R_3 = R_4 = OCOCH_3$, $X = SO_3F$
XI: $R_1 = R_2 = R_3 = R_4 = OH$, X = Cl

Assay of tRNA Methyltransferases—The activity of tRNA methyltransferases was measured by the amount of ^{14}C-methyl groups incorporated into the tRNA using the procedure of Waalkes *et al.* (25) with slight modification. The tRNA methyltransferase enzyme extraction was prepared according to the method of Kerr (26) with some modification. Male adult rat liver, 50 g, was homogenized in 200 ml of isotonic potassium chloride, and the mixture was centrifuged at 60,000×*g* for 60 min.

The supernate was drained through cheesecloth, adjusted to pH 5.3 with 1 *N* acetic acid, and centrifuged for 10 min at 6600×*g*. The precipitate was collected and dissolved in 20 ml of 0.1 *M* tris(hydroxymethyl)aminomethane hydrochloride buffer (pH 8). This solution was then stored in small aliquots at −60° and used as the source of inhibitor-free enzyme. Since this extract contained some catechol *O*-methyltransferase activity, pyrogallol was added to the reaction mixture to suppress this activity.

The following procedure was used as the basis of a series of titrations and experimental studies. Reagents were added to the reaction tubes at 0–5° in the following order and quantities: 70 μmoles of ammonium acetate, 0.3 μmole of dithiothreitol[1], 0.3 μmole of tetrasodium ethylenediaminetetraacetate, 25 μmoles of pH 9 tris(hydroxymethyl)aminomethane hydrochloride, 0.5 μmole of magnesium chloride, 0.5 μmole of pyrogallol, enzyme extract (200 μg of protein), 100 μg of undermethylated *Escherichia coli* B tRNA[2], and 5 pmoles of ^{14}C-*S*-adenosyl-L-methionine (58 mCi/mole). The final volume of each tube was 0.5 ml.

For the inhibition test, 0.05 ml of the inhibitor solution was mixed with the enzyme extract in an ice bath (0–5°) for 5 min and then added to the reaction mixture, which was placed in a 37° water bath for 30 min. The reaction was terminated by placing the tube in an ice bath and adding 2.5 ml of 10% trichloroacetic acid. After 20 min, the reaction mixture was

[1] Calbiochem.
[2] Sigma.

Table I—Enzyme Inhibition Test Results

	Compound	COMT Inhibition, %			tRNA Methyltransferase Inhibition, %		
		10^{-3} *M*	10^{-4} *M*	10^{-5} *M*	10^{-3} *M*	10^{-4} *M*	10^{-5} *M*
I	(coralyne acetosulfate)	100	80	43	48	10	0
II	(isocoralyne acetosulfate)	(75)[a]	15	0	56	10	0
III	(neocoralyne acetosulfate)	73	35	0	64	49	33
IV	(stracoralyne acetosulfate)	—[b]	7	0	20	5	0
V	(nitidine chloride)	60	0	0	37	32	21
VI	(nitidine methosulfate)	70	0	0	46	35	11
VII	(nitidine bromoacetate)	13	10	8	58	31	5
VIII	(methoxydihydronitidine)	(100)	71	0	73	33	0
IX	(*O*-methylfagaronine fluorosulfonate)	100	34	8	100	96	18
X		100	71	0	100	94	11
XI		(74)	54	34	87	15	0
XII		6	2	0	0	0	0
XIII		6	3	0	18	2	0
XIV		0	0	0	15	0	0

[a] Values in parentheses denote those obtained by graph extrapolation. [b] Insoluble.

filtered through a type HA individual filter (0.45-μm pore size) and washed with 20 ml of 5% trichloroacetic acid. The residue was then air dried and placed into vials with 10 ml of a mixture of 91% of 2,5-diphenyloxazole and 9% of 1,4-bis[2-(4-methyl-5-phenyloxazolyl)]benzene. Radioactivity was measured in a liquid scintillation counter.

To determine enzyme activity, a reaction mixture without tRNA was run as a control against a reaction mixture with tRNA. The difference in ^{14}C-incorporation, measured in counts per minute between these two mixtures, is a measure of enzyme activity (*A*).

Inhibitors were generally tested at three different concentrations. The concentration of an inhibitor was calculated as the final concentration after dilution of the reaction mixture. The level of inhibition was determined by subtracting the counts per minute of a reaction mixture with the inhibitor only from that of a reaction mixture with both the inhibitor and the enzyme (*B*). The percent of inhibition was then calculated as $[(A - B)/A] \times 100$.

An ideal standard for inhibition of tRNA methyltransferases is yet to be found. Nicotinamide (27, 28) and ascorbic acid (40 and 51% inhibition, respectively, at 10^{-3} *M*) were used as controls throughout the tRNA methyltransferase inhibitory tests.

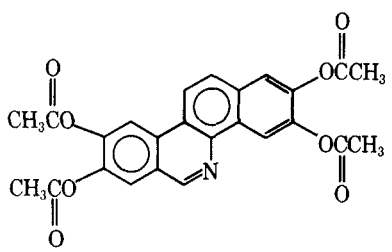

XII

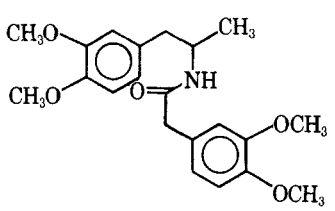

XIII

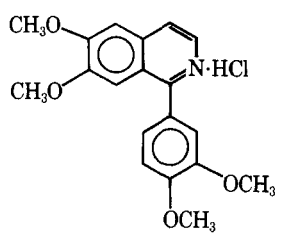

XIV

RESULTS AND DISCUSSION

Preliminary enzyme inhibitory results are given in Table I. The first nine compounds (I–IX) were active against leukemias P-388 and L-1210 (15–19), whereas the last five compounds (X–XIV) were inactive. Although no definite conclusion should be drawn at this stage, the results suggest that there is a parallel correlation between the antileukemic activity of these alkoxy compounds and their inhibitory activity against both classes of enzyme. In addition, inhibition against both enzymes seems to have a similar profile.

Solubility characteristics of these compounds in water play an important role in enzyme inhibition. Compound IV (stracoralyne acetosulfate), for example, is quite insoluble in water. Thus, the observed activity may not reflect the true value.

Although X showed high inhibitory activity against both enzymes, it was without effect against leukemias P-388 and L-1210. This finding is probably due to the relative ease of hydrolysis of the acetoxy groups *in vivo;* the resulting phenolic compounds may not be readily transported to the proper biological site to achieve the desired antineoplastic action. (The fact that the tetrahydroxy compound, XI, possessed enzyme inhibitory activity but was inactive against leukemias P-388 and L-1210 further substantiates the proposition.) The corresponding uncharged compound, XII, which is much less soluble in water, was inactive against both enzyme and leukemia systems.

Since the presently studied tRNA methyltransferases are composed of a mixture of methylating enzymes and since purified enzymes such as tRNA *O*-methyltransferase and tRNA *N*-methyltransferase could not be realized, a definite relationship could not be drawn as to whether the inhibitory action against tRNA methylating enzymes is directed to any specific portion of the macromolecule. The original tRNA 2′-*O*-methylation hypothesis (14) thus remains to be examined. Therefore, single tRNA methyltransferases that specifically methylate oxygen, nitrogen, or other atoms should be isolated and purified before further study.

REFERENCES

(1) S. J. Kerr, *J. Biol. Chem.*, **247,** 4248 (1972).

(2) S. E. Wright, R. E. Gallagher, R. C. Ting, and R. C. Gallo, *Cancer Res.*, **33,** 2513 (1973).

(3) B. Sheid, T. Lu, and J. H. Nelson, Jr., *ibid.*, **33,** 2518 (1973).

(4) T. P. Waalkes, S. R. Dinsmore, and J. E. Mrochek, *J. Natl. Cancer Inst.*, **51,** 271 (1973).

(5) B. Sheid, T. Lu, and J. H. Nelson, Jr., *Cancer Res.*, **34,** 2416 (1974).

(6) N. P. Trifunac and A. I. Krasna, *Biochemistry,* **13,** 2403 (1974).

(7) M. Hayashi and A. C. Griffin, *Cancer Res.*, **34,** 3311 (1974).

(8) J. E. Heady and S. J. Kerr, *ibid.*, **35,** 640 (1975).

(9) R. Gantt, G. H. Smith, and B. T. Julian, *ibid.*, **35,** 1847 (1975).

(10) R. L. Hancock, *Biochim. Biophys. Acta,* **281,** 472 (1972).

(11) R. L. Hancock and P. I. Forrester, *Cancer Res.*, **33,** 1747 (1973).

(12) F. Nau, F. Garbit, and J.-M. Dubert, *Biochim. Biophys. Acta,* **277,** 80 (1972).

(13) M. C. Liau, C. M. O'Rourke, and R. B. Hurlbert, *Biochemistry,* **111,** 629 (1972).

(14) C. C. Cheng, *J. Pharm. Sci.*, **61**, 645 (1972).
(15) K. Y. Zee-Cheng and C. C. Cheng, *ibid.*, **61**, 969 (1972).
(16) K. Y. Zee-Cheng and C. C. Cheng, *J. Heterocycl. Chem.*, **10**, 85, 867 (1973).
(17) K. Y. Zee-Cheng, K. D. Paull, and C. C. Cheng, *J. Med. Chem.*, **17**, 347 (1974).
(18) R. K. Y. Zee-Cheng and C. C. Cheng, *ibid.*, **18**, 66 (1975).
(19) *Ibid.*, **19**, 882 (1976).
(20) E. Wainfan and B. Landsberg, *Biochem. Pharmacol.*, **22**, 493 (1973).
(21) J. K. Coward, D. O. Bussolotti, and C.-D. Chang, *J. Med. Chem.*, **17**, 1286 (1974).
(22) M. C. Liau, J. B. Hunt, D. W. Smith, and R. B. Hurlbert, *Cancer Res.*, **33**, 323 (1973).
(23) W. F. Herblin, *Anal. Biochem.*, **51**, 19 (1973).
(24) J. Axelrod and R. Tomchick, *J. Biol. Chem.*, **233**, 702 (1958).
(25) T. P. Waalkes,.R. H. Adamson, D. Riddick, and R. C. Gallo, *Arch. Int. Pharmacodyn. Ther.*, **196**, 345 (1972).
(26) S. J. Kerr, *Biochemistry*, **9**, 690 (1970).
(27) R. M. Halpern, S. Q. Chaney, B. C. Halpern, and R. A. Smith, *Biochem. Biophys. Res. Commun.*, **42**, 602 (1971).
(28) L. Buch, D. Streeter, R. M. Halpern, L. N. Simon, M. G. Stout, and R. A. Smith, *Biochemistry*, **11**, 393 (1972).

ACKNOWLEDGMENTS AND ADDRESSES

Received May 14, 1976, from the *Midwest Research Institute, Kansas City, MO 64110.*

Accepted for publication September 15, 1976.

Supported by Contract N01-CM-33743 from the Division of Cancer Treatment, National Cancer Institute, National Institutes of Health, Department of Health, Education, and Welfare.

The authors thank Dr. Harry B. Wood, Jr., for interest and encouragement.

[x] To whom inquiries should be directed.

Pharmaceutical Applications of Solid Dispersion Systems: X-Ray Diffraction and Aqueous Solubility Studies on Griseofulvin–Polyethylene Glycol 6000 Systems

WIN L. CHIOU

Abstract □ The X-ray diffraction method was used to characterize physicochemical properties of griseofulvin dispersed in polyethylene glycol 4000 and 6000. Results indicate a negligible or very limited solid solubility of griseofulvin in the pulverized solid dispersions. Pulverization and aging had pronounced effects on the X-ray diffraction spectrum. Results from aqueous solubility studies of griseofulvin in various concentrations of polyethylene glycol 6000 further indicate weak or insignificant interactions between the drug and the carrier. Mechanisms are postulated to account for the reported marked enhancement of dissolution rates and oral absorption of griseofulvin dispersed in these carriers.

Keyphrases □ Griseofulvin—dispersed in polyethylene glycol 6000, X-ray diffraction study, aqueous solubility, effects of pulverization and aging □ Polyethylene glycol 6000—dispersions with griseofulvin, X-ray diffraction study, aqueous solubility, effects of pulverization and aging □ Solid dispersions—griseofulvin–polyethylene glycol 6000, X-ray diffraction study, aqueous solubility, effects of pulverization and aging □ Dispersions, solid—griseofulvin–polyethylene glycol 6000, X-ray diffraction study, aqueous solubility, effects of pulverization and aging □ Solubility, aqueous—griseofulvin–polyethylene glycol 6000 dispersions, X-ray diffraction study □ X-ray diffraction—study, griseofulvin–polyethylene glycol 6000 dispersion, effects of pulverization and aging □ Antifungal agents—griseofulvin dispersed in polyethylene glycol 6000, X-ray diffraction study, aqueous solubility

The *in vitro* dissolution and oral absorption of griseofulvin in dogs and humans were markedly enhanced by the formation of solid dispersions in polyethylene glycol 6000 (1–3). Recently, these results were confirmed with a newly introduced commercial product[1] in single- (4) and multiple- (5) dose studies using larger numbers of test subjects. The new product requires only half of the dose recommended for conventional micronized products. Furthermore, the incidence of side effects decreased with this new formulation (5).

Although it was proposed that the enhancement of dissolution and absorption of griseofulvin dispersed in the polymer was primarily due to the molecular and colloidal dispersion of the drug in the highly water-soluble carrier (1–3), no extensive experimental data regarding physicochemical properties of such a dispersed system have been reported.

This paper reports the detailed results of X-ray diffraction and aqueous solubility studies on such a system. The X-ray diffraction data do not support the previous postulate regarding the extensive formation of a solid solution of griseofulvin in polyethylene glycol polymers. The aqueous solubility study was performed to investigate the possible interaction between the drug and the polymer in an aqueous medium. Findings from the present study should be valuable to the development of solid dispersion dosage forms of other poorly water-soluble drugs utilizing the same type of carriers. Some preliminary results were discussed in a review article (6).

Although different average molecular weights of polyethylene glycol polymers can be used as dispersion carriers (1–3), only polymer 6000 was studied in detail in the present investigation. This polymer has much less absorption in the UV and visible region than polymer 20,000 and thus interferes less with the direct spectrophotometric analysis of drugs (1). Furthermore, based on the author's experience, the solid dispersions prepared with this polymer were generally much easier to pulverize than those prepared with other molecular weights of the polymer.

[1] Gris-PEG, Dorsey Laboratories, Lincoln, Neb.

(14) C. C. Cheng, *J. Pharm. Sci.*, **61**, 645 (1972).
(15) K. Y. Zee-Cheng and C. C. Cheng, *ibid.*, **61**, 969 (1972).
(16) K. Y. Zee-Cheng and C. C. Cheng, *J. Heterocycl. Chem.*, **10**, 85, 867 (1973).
(17) K. Y. Zee-Cheng, K. D. Paull, and C. C. Cheng, *J. Med. Chem.*, **17**, 347 (1974).
(18) R. K. Y. Zee-Cheng and C. C. Cheng, *ibid.*, **18**, 66 (1975).
(19) *Ibid.*, **19**, 882 (1976).
(20) E. Wainfan and B. Landsberg, *Biochem. Pharmacol.*, **22**, 493 (1973).
(21) J. K. Coward, D. O. Bussolotti, and C.-D. Chang, *J. Med. Chem.*, **17**, 1286 (1974).
(22) M. C. Liau, J. B. Hunt, D. W. Smith, and R. B. Hurlbert, *Cancer Res.*, **33**, 323 (1973).
(23) W. F. Herblin, *Anal. Biochem.*, **51**, 19 (1973).
(24) J. Axelrod and R. Tomchick, *J. Biol. Chem.*, **233**, 702 (1958).
(25) T. P. Waalkes,.R. H. Adamson, D. Riddick, and R. C. Gallo, *Arch. Int. Pharmacodyn. Ther.*, **196**, 345 (1972).
(26) S. J. Kerr, *Biochemistry*, **9**, 690 (1970).
(27) R. M. Halpern, S. Q. Chaney, B. C. Halpern, and R. A. Smith, *Biochem. Biophys. Res. Commun.*, **42**, 602 (1971).
(28) L. Buch, D. Streeter, R. M. Halpern, L. N. Simon, M. G. Stout, and R. A. Smith, *Biochemistry*, **11**, 393 (1972).

ACKNOWLEDGMENTS AND ADDRESSES

Received May 14, 1976, from the *Midwest Research Institute, Kansas City, MO 64110.*

Accepted for publication September 15, 1976.

Supported by Contract N01-CM-33743 from the Division of Cancer Treatment, National Cancer Institute, National Institutes of Health, Department of Health, Education, and Welfare.

The authors thank Dr. Harry B. Wood, Jr., for interest and encouragement.

[x] To whom inquiries should be directed.

Pharmaceutical Applications of Solid Dispersion Systems: X-Ray Diffraction and Aqueous Solubility Studies on Griseofulvin–Polyethylene Glycol 6000 Systems

WIN L. CHIOU

Abstract □ The X-ray diffraction method was used to characterize physicochemical properties of griseofulvin dispersed in polyethylene glycol 4000 and 6000. Results indicate a negligible or very limited solid solubility of griseofulvin in the pulverized solid dispersions. Pulverization and aging had pronounced effects on the X-ray diffraction spectrum. Results from aqueous solubility studies of griseofulvin in various concentrations of polyethylene glycol 6000 further indicate weak or insignificant interactions between the drug and the carrier. Mechanisms are postulated to account for the reported marked enhancement of dissolution rates and oral absorption of griseofulvin dispersed in these carriers.

Keyphrases □ Griseofulvin—dispersed in polyethylene glycol 6000, X-ray diffraction study, aqueous solubility, effects of pulverization and aging □ Polyethylene glycol 6000—dispersions with griseofulvin, X-ray diffraction study, aqueous solubility, effects of pulverization and aging □ Solid dispersions—griseofulvin–polyethylene glycol 6000, X-ray diffraction study, aqueous solubility, effects of pulverization and aging □ Dispersions, solid—griseofulvin–polyethylene glycol 6000, X-ray diffraction study, aqueous solubility, effects of pulverization and aging □ Solubility, aqueous—griseofulvin–polyethylene glycol 6000 dispersions, X-ray diffraction study □ X-ray diffraction—study, griseofulvin–polyethylene glycol 6000 dispersion, effects of pulverization and aging □ Antifungal agents—griseofulvin dispersed in polyethylene glycol 6000, X-ray diffraction study, aqueous solubility

The *in vitro* dissolution and oral absorption of griseofulvin in dogs and humans were markedly enhanced by the formation of solid dispersions in polyethylene glycol 6000 (1–3). Recently, these results were confirmed with a newly introduced commercial product[1] in single- (4) and multiple- (5) dose studies using larger numbers of test subjects. The new product requires only half of the dose recommended for conventional micronized products. Furthermore, the incidence of side effects decreased with this new formulation (5).

Although it was proposed that the enhancement of dissolution and absorption of griseofulvin dispersed in the polymer was primarily due to the molecular and colloidal dispersion of the drug in the highly water-soluble carrier (1–3), no extensive experimental data regarding physicochemical properties of such a dispersed system have been reported.

This paper reports the detailed results of X-ray diffraction and aqueous solubility studies on such a system. The X-ray diffraction data do not support the previous postulate regarding the extensive formation of a solid solution of griseofulvin in polyethylene glycol polymers. The aqueous solubility study was performed to investigate the possible interaction between the drug and the polymer in an aqueous medium. Findings from the present study should be valuable to the development of solid dispersion dosage forms of other poorly water-soluble drugs utilizing the same type of carriers. Some preliminary results were discussed in a review article (6).

Although different average molecular weights of polyethylene glycol polymers can be used as dispersion carriers (1–3), only polymer 6000 was studied in detail in the present investigation. This polymer has much less absorption in the UV and visible region than polymer 20,000 and thus interferes less with the direct spectrophotometric analysis of drugs (1). Furthermore, based on the author's experience, the solid dispersions prepared with this polymer were generally much easier to pulverize than those prepared with other molecular weights of the polymer.

[1] Gris-PEG, Dorsey Laboratories, Lincoln, Neb.

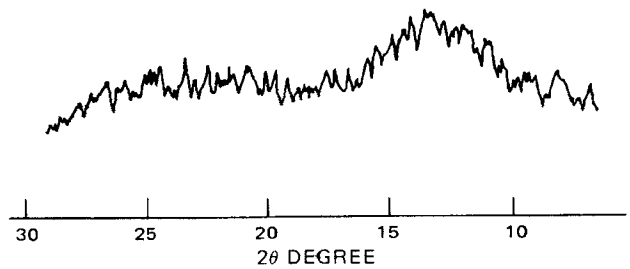

Figure 1—*X-ray diffraction spectrum of the unpulverized resolidified melt of griseofulvin.*

EXPERIMENTAL

Solid Dispersions—Griseofulvin[2]–polyethylene glycol 6000[3] solid dispersions containing 5, 10, 25, and 50% (w/w) griseofulvin were prepared by the melting method (1). After hardening, the melt was pulverized to a fine powder with a mortar and pestle. To study the effect of powdering on the X-ray diffraction pattern of the sample, some melts were poured directly into the sample holder used for the X-ray diffraction studies.

X-Ray Diffraction Studies—The procedure used was described previously (7, 8). The samples studied included the pure and resolidified griseofulvin and the polymers, solid dispersions and their physical mixtures.

Solubility Studies—Micronized griseofulvin, 10 mg, was evenly suspended in 15 ml of 0–10% (w/v) aqueous solutions of polyethylene glycol 6000 in screw-topped extraction tubes and equilibrated by shaking for 48 hr (a preliminary study indicated essentially a constant solubility value after 48 hr) in a constant-temperature water bath maintained at 22 ± 0.5°. The suspensions were then filtered through a 0.22-μm filter[4]. The first 10 ml of the filtrate was discarded to saturate the adsorption sites for griseofulvin on the filter (9); the last 5 ml of the filtrate was analyzed for the concentration of griseofulvin at 295 nm[5]. All experiments were performed at least in duplicate. The UV absorption, due to the presence of the polymer, was corrected in griseofulvin concentration determinations.

RESULTS AND DISCUSSION

X-ray diffraction spectra of the untreated griseofulvin and polyethylene glycol 6000 were previously reported (6). In the present study, essentially identical spectra were also obtained after they were melted, solidified, and pulverized. This, however, was not the case for the unpulverized resolidified griseofulvin melt (Fig. 1). The absence of major griseofulvin diffraction peaks indicates that an amorphous form existed in the unpulverized melt; this amorphous form is thought to convert to the crystalline form after pulverization. The observed glassy and brittle property of the melt and the appearance of an exothermic transition peak below the melting point when the melt was rerun in a differential thermal analyzer[6] are also in accordance with the postulate of the amorphous state of the melt sample. This effect of pulverization on the crystallinity was not observed for polyethylene glycol 4000 and 6000.

Major X-ray diffraction peaks of griseofulvin, particularly at 10.8, 13.3, and 16.6° (8), were all present in the pulverized dispersion samples containing 5–50% griseofulvin. A typical spectrum is shown in Fig. 2. The diffraction spectra of the 5% griseofulvin system were previously reported (6). The similarity of heights of the major diffraction peaks of griseofulvin in the physical mixture and dispersion samples with the same composition indicates the limited or negligible solid solubility of griseofulvin in the polymer. This result is obviously different from the previous postulation of the extensive solid solution formulation (1). Similar findings were also obtained for the griseofulvin–polyethylene 4000 system. Based on these findings and analyses, the (pulverized) dispersed systems of griseofulvin in polyethylene glycol 4000 or 6000 should be classified as simple eutectic mixtures with negligible or limited solid solubility. This result is similar to the findings with chloramphenicol–urea (10) and griseofulvin–succinic acid (8) binary systems and different from the finding on sulfathiazole–urea binary system (7).

[2] Griseofulvin USP, McNeil Laboratories, Fort Washington, Pa.
[3] Carbowax, Union Carbide Corp., New York, N.Y.
[4] Millipore.
[5] Beckman DBG spectrophotometer, Beckman Instruments, Inc., Fullerton, Calif.
[6] DuPont 900 thermal analyzer, DuPont Instruments Co., Wilmington, Del.

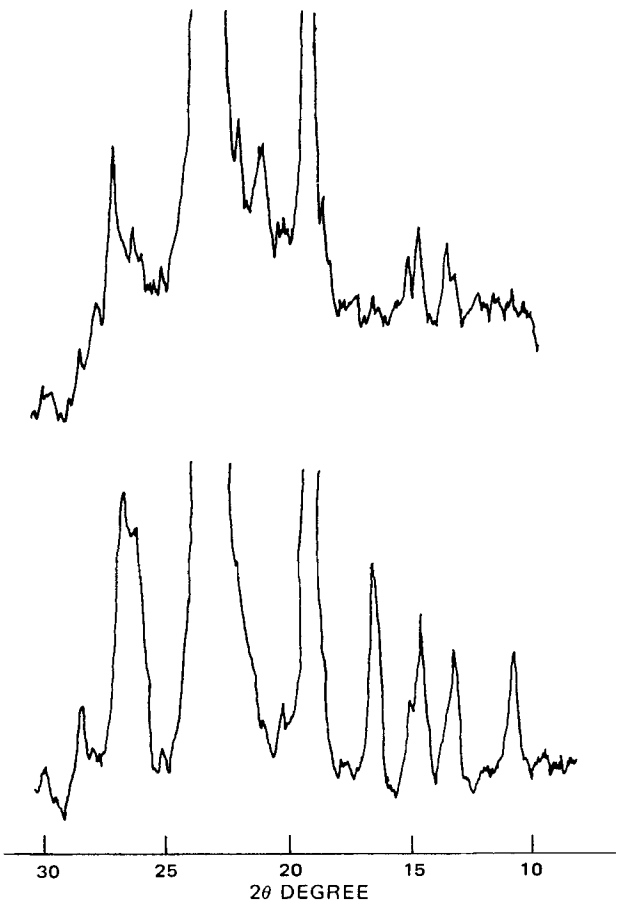

Figure 2—*X-ray diffraction spectra of 20% griseofulvin solid dispersion in polyethylene glycol 6000. Key: top spectrum, unpulverized sample; and bottom spectrum, pulverized sample.*

X-ray diffraction spectra of the freshly prepared (within 2 hr) unpulverized solid dispersions were quite different from those of freshly prepared or aged pulverized samples (Figs. 2 and 3). All major diffraction peaks of griseofulvin were absent. The most logical explanation is that the amorphous form of griseofulvin was precipitated from the melt after cooling, which is consistent with the observed formation of the amorphous form after resolidification of the pure griseofulvin melt, as discussed. The viscous property of the melt of the polymer also might retard the orderly crystallization of griseofulvin during the resolidification process.

The absence of those diffraction peaks, particularly in samples con-

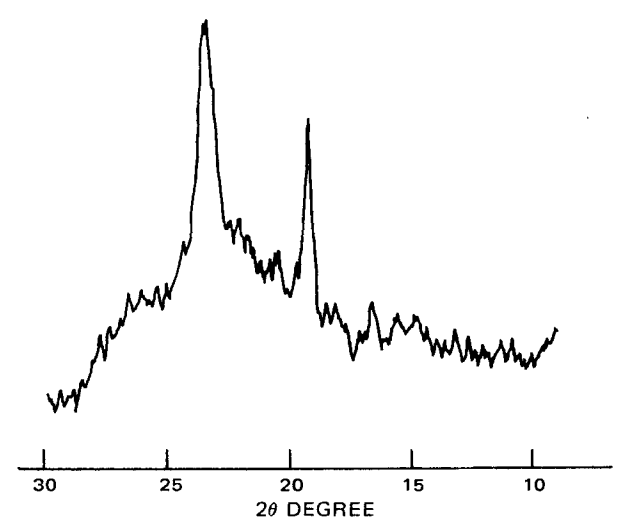

Figure 3—*X-ray diffraction spectrum of the freshly prepared unpulverized sample of 50% griseofulvin solid dispersion in polyethylene glycol 6000.*

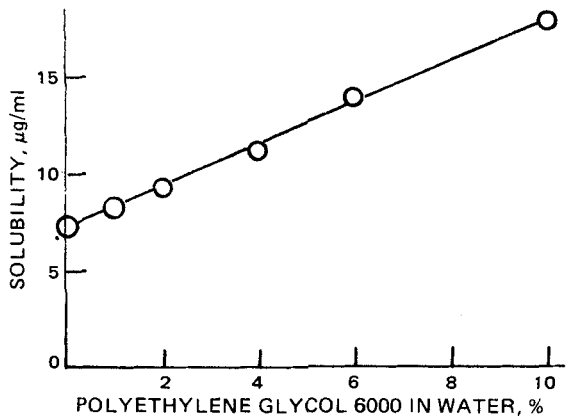

Figure 4—*Solubilities of griseofulvin in the presence of polyethylene glycol 6000.*

taining smaller fractions of griseofulvin, may also be attributed to the supersaturation of griseofulvin in the polymer caused by the retardation of the viscous polymer on the precipitation of griseofulvin (1, 6) and/or the colloidal or ultrafine crystallization. When X-ray diffraction studies were repeated several days later, major diffraction peaks of griseofulvin appeared in all samples except for the 5% griseofulvin system. Identical results for the latter system were obtained even after 3 months of storage at room temperature.

Intensive diffraction peaks of polyethylene glycol 6000 were present in all unpulverized, freshly prepared solid dispersions except for the 50% griseofulvin sample. It was soft and somewhat sticky 1 hr after preparation, and the hardness increased with time. The hardness of freshly solidified melts increased with the increase in griseofulvin concentration. This phenomenon is somewhat similar to that observed in the eutectic mixture of the sulfathiazole–urea system (7).

The effects of pulverization and aging on the X-ray diffraction pattern and hardness of the solid dispersions reported in this paper may also have some pronounced effect on their dissolution and absorption characteristics. The dissolution rate of sulfathiazole dispersed in urea with the eutectic composition decreased after storage (7). However, it is possible that no further changes in physical properties may occur after initial pulverization or a short period of storage. Identical dissolution profiles of griseofulvin were obtained for the pulverized samples of the 10% griseofulvin–90% succinic acid system and from its 10–20% dispersion in polyethylene glycol 4000 and 6000 even after 1 year of storage at ambient temperature. These original dissolution studies (not on samples aged for 1 year) were reported previously (1).

The absence of any X-ray diffraction peaks, other than those attributed to pure griseofulvin and the polymers in all solid dispersion samples, also indicates a lack of definite chemical complexation between the drug and the carrier polymer in their solid state. However, some interaction could be detected in their aqueous solutions, as shown by a moderate increase in the aqueous glycol 6000 (Fig. 4). Based on these data, the ratio for the number of molecules of the polymer required to solubilize one molecule of griseofulvin is 555. Since the ratio is so high, it is difficult to visualize the existence of any strong complexation between the two components. The high ratio can, however, be rationalized by the formation of a very weak complex with a high dissociation constant. The slight enhancement in the polymer solution can be equally well explained by the cosolvent effect of the polymer rather than by invoking complexation theory.

Based on the results of the X-ray diffraction and aqueous solubility studies, the previously reported marked enhancement of dissolution and absorption rates of griseofulvin dispersed in the polyethylene glycol polymers was primarily due to the reduction of the size of griseofulvin crystals rather than to the formation of solid solution, complexation, or metastable polymorphic forms. The generally observed decrease in the dissolution rate as the fraction of griseofulvin in solid dispersions increased (1) can be rationalized by the formation of larger crystals of griseofulvin due to the presence of relatively less carrier. This approach is in analogy to the griseofulvin–succinic acid solid dispersion system (11).

Other factors (6, 7, 11) such as increased wettability, reduction or absence of aggregation, and agglomeration and solubilization of the drug by the carrier at the diffusion layer of particles may also partially contribute to the enhancement of dissolution and absorption rates of griseofulvin dispersed in the polyethylene glycol polymers.

REFERENCES

(1) W. L. Chiou and S. Riegelman, *J. Pharm. Sci.*, **58**, 1505 (1969).
(2) *Ibid.*, **59**, 937 (1970).
(3) *Ibid.*, **60**, 1376 (1971).
(4) W. E. Barrett and J. Bianchine, *Curr. Ther. Res.*, **18**, 501 (1975).
(5) W. E. Barrett and J. J. Hanigan, *ibid.*, **18**, 491 (1975).
(6) W. L. Chiou and S. Riegelman, *J. Pharm. Sci.*, **60**, 1281 (1971).
(7) W. L. Chiou and S. Niazi, *ibid.*, **60**, 1331 (1971).
(8) *Ibid.*, **62**, 498 (1973).
(9) W. L. Chiou and L. D. Smith, *J. Pharm. Sci.*, **59**, 843 (1970).
(10) W. L. Chiou, *ibid.*, **60**, 1406 (1971).
(11) W. L. Chiou and S. Niazi, *ibid.*, **65**, 1212 (1976).

ACKNOWLEDGMENTS AND ADDRESSES

Received January 12, 1976, from the *Department of Pharmacy and the Clinical Pharmacokinetics Laboratory, College of Pharmacy, University of Illinois at the Medical Center, Chicago, IL 60612,* and the *College of Pharmacy, Washington State University, Pullman, WA 99163.*

Accepted for publication August 11, 1976.

Present address: College of Pharmacy, University of Illinois.

GLC Determination of Ethinamate and Its Hydroxy Derivative in Biological Fluids

J. W. KLEBER [x], L. D. BECHTOL, M. K. BRUNSON, and S. M. CHERNISH

Abstract □ A sensitive, specific GLC assay was developed for the determination of ethinamate in plasma and its major metabolite, *trans*-4-hydroxyethinamate, in urine. The assay uses a mass internal standard of dimethylethinamate. Ethinamate is extracted from alkalinized plasma with dichloromethane. Urine samples require β-glucuronidase hydrolysis prior to extraction of hydroxyethinamate. The dichloromethane is removed by evaporation, and the compounds are measured by GLC using a flame-ionization detector. By using GLC–chemical-ionization mass spectrometry, the compounds measured were identified as the intact ethinamates. Plasma and urine data are presented from a bioavailability study to demonstrate the utility of this method. From these data, the ethinamate plasma half-life was calculated as 1.9 ± 0.3 hr.

Keyphrases □ Ethinamate and hydroxy derivative—GLC analysis in biological fluids, bioavailability from tablets and capsules, humans □ GLC—analysis, ethinamate and hydroxy derivative in biological fluids □ Sedatives—ethinamate and hydroxy derivative, GLC analysis in biological fluids, bioavailability from tablets and capsules, humans

GLC of acetylenic hypnotic agents was first described in 1960 (1) and later applied to biological samples (2). A method also was developed[1] for the determination of ethinamate[2] in human plasma by GLC. This method was improved (3) by using benzene instead of carbon disulfide as the extracting solvent. None of the foregoing methods utilized a mass internal standard.

This paper describes a method for the assay of ethinamate (I) in plasma and of *trans*-4-hydroxyethinamate (III) (4) in urine; it employs a mass internal standard.

EXPERIMENTAL

Reagents—Ethinamate and dimethylethinamate (II) were synthesized[3]. Compound II was used as the internal standard for GLC analysis. Compound III was obtained from the urine of human subjects given ethinamate. All solvents were spectroquality. The GLC packing material was 2% OV-17 on 80–100-mesh Chromosorb G[4].

Apparatus—The gas–liquid chromatograph[5] was equipped with a flame-ionization detector and 1-mv recorder[6]. Disposable 15-ml centrifuge tubes[7] were used for the extractions. Tapered 15-ml glass centrifuge tubes[8], previously silanized, were used for evaporating dichloromethane (IV).

Chromatographic Conditions—The recorder was operated at a chart speed of 0.63 cm/min. Helium carrier gas (flow rate of 60 ml/min) was filtered through a sieve, which had been preconditioned overnight at 200° with dry nitrogen. A glass column (0.61 m × 3 mm i.d.) containing the packing material was heated isothermally at 140° for 4 min followed by 16°/min programming to 240° during the analysis to clear the column of late emerging peaks. The detector temperature was maintained at 250°. The oxygen and hydrogen flow rates were 240 and 60 ml/min, respectively.

Under these conditions, the following retention times were observed: I, 170 sec; II, 240 sec; and III, 420 sec (Fig. 1). The chromatogram obtained when a urinary extract was evaluated by GLC looked similar but was devoid of the ethinamate peak.

Table I—Precision and Accuracy in Measurement of Ethinamate Added to Plasma and *trans*-4-Hydroxyethinamate Added to Urine

Added, μg/ml	Measured μg/ml	*RSD*, %	*RE*, %
	Plasma		
1.0	0.91 (0.76–1.09)[a]	14.3	−9.0
4.0	3.76 (3.60–3.98)	3.5	−6.0
8.0	7.97 (7.38–8.51)	5.1	−0.4
	Urine		
300	310 (290–322)[b]	4.7	+3.3
600	616 (605–645)	3.1	+2.7

[a] Mean of eight replicate samples with range. [b] Mean of four replicate samples with range.

Procedure—The 15-ml tapered centrifuge tubes were washed with chromic acid cleaning solution, rinsed with water, dried, and then silanized using a 1% solution of dimethyldichlorosilane in toluene[9]. A standard solution of ethinamate in chloroform was added to 2 ml of blank plasma to give calibration concentrations of 0, 0.5, 2, 4, and 8 μg of drug/ml. To each tube was added 30 μl (6 μg) of the internal standard solution and 1 ml of 0.1 *N* NaOH. The mixture was then vortexed to ensure uniform distribution of the compounds in the plasma.

With a pipet[10], 10 ml of IV was added to each tube. The samples were shaken for 2 min and then centrifuged at 2000 rpm for 4 min. The upper aqueous phase was aspirated and discarded. The IV phase was transferred to a 15-ml silanized, tapered centrifuge tube and was evaporated to dryness at room temperature under a gentle stream of dry nitrogen. The residue was dissolved in 20 μl of carbon disulfide–chloroform (1:1) with the aid of a vortex mixer, and 2 μl of each sample solution was injected onto the GLC column.

Urine was assayed for III by the following procedure. A standard solution of III in chloroform was added to 0.1 ml of blank urine to give calibration concentrations of 100, 200, 400, and 800 μg of drug/ml. This solution was buffered with 1 ml of 0.2 *N* sodium acetate buffer (pH 5.5)

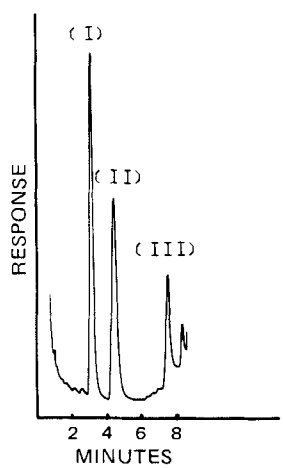

Figure 1—*Gas–liquid chromatogram of extract of plasma spiked with 4 μg/ml of I, 6 μg/ml of II, and 4 μg/ml of III.*

[1] D. M. Fuller, Lilly Research Center, Erl Wood, England, personal communication.
[2] Valmid, Eli Lilly and Co., Indianapolis, Ind.
[3] At the Lilly Research Laboratories, Eli Lilly and Co., Indianapolis, Ind.
[4] Ohio Valley Specialty Chemical, Marietta, Ohio.
[5] Model 5700A, Hewlett-Packard, Avondale, Pa.
[6] Model 7127A, Hewlett-Packard, Avondale, Pa.
[7] Corning Glass Co., Corning, N.Y.
[8] Matheson Scientific Co., Chicago, Ill.
[9] This treatment appears to prevent adsorption of the ethinamates to the glassware.
[10] Repipet, Labindustries, Berkeley, Calif.

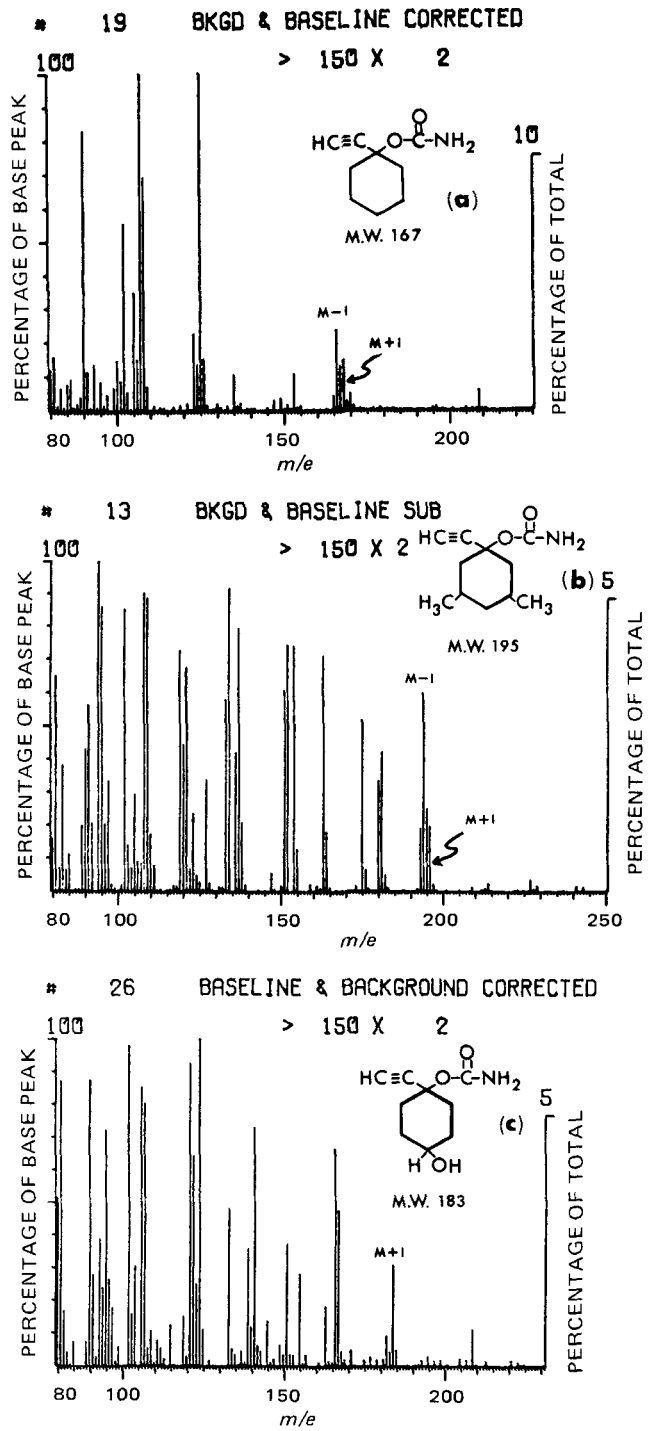

Figure 2—*Chemical-ionization mass spectra of I (a), II (b), and III (c) obtained after GLC. Methane was used as the reagent gas.*

and incubated overnight at 37° with 50 μl of β-glucuronidase solution[11]. The next day, 30 μl (6 μg) of the internal standard solution was added, and the procedure used for plasma was followed.

Following chromatography of the calibration standards, peak height ratios[12] of I and III to the internal standard were calculated. These ratios, plotted against concentrations in the 0.50–8.0-μg/ml range for I in plasma and in the 200–800-μg/ml range for III in urine, gave straight lines passing through the origin ($r = 1.0$). Mean slope values of 0.39 ± 0.02 and 0.012 ± 0.0007 were obtained for I and III, respectively.

A bioavailability study of different dosage forms of ethinamate dem-

[11] Glusulase, Endo Laboratories, Garden City, N.Y.

[12] Results were virtually unaffected when relative peak areas were used instead of relative peak heights.

Table II—Dissolution Profiles of Ethinamate Tablets and Capsules[a]

Minutes	Ethinamate in Solution, $\bar{X}$% (Range, *RSD*) Tablet	Capsule
5	58.6 (9.3, 6.2)	41.9 (21.4, 18.8)
15	78.0 (11.6, 5.7)	74.3 (29.2, 14.2)
20	84.7 (6.2, 3.4)	89.4 (26.4, 19.4)
60	94.1 (9.5, 3.6)	101.9 (15.4, 5.6)

[a] Mean of six tablets or capsules.

Table III—Ethinamate in Plasma Data

Data Set	Mean ± *SE* Tablets	Capsules	Mean Difference[a]
Area under curves, 0–24 hr, μg hr/ml	23.63 ± 12.57	25.24 ± 12.84	−1.61
Mean peak plasma concentrations, μg/ml	9.60 ± 4.17	9.12 ± 4.60	+0.48
Mean peak times, hr	0.60 ± 0.38	0.75 ± 0.57	−0.15

[a] Not significant at $p < 0.05$.

onstrated the utility of this method. Ethinamate tablets and capsules[13], 500 mg each, were administered to 12 subjects in a two-way crossover study. Each subject fasted for 8 hr before receiving a therapeutic dose of two ethinamate tablets or capsules. Blood samples were drawn at 0, 0.25, 0.5, 1, 1.5, 2, 4, 6, 8, 10, 12, and 24 hr. Urine was collected for 24 hr.

Dissolution characteristics of the ethinamate tablets and capsules were determined using the USP–NF apparatus. Tablets or capsules were placed in 500 ml of pH 1.2 buffer at 37° and stirred at 50 rpm. The ethinamate content of the buffer solution was assayed colorimetrically[14] using an automated analysis system.

RESULTS AND DISCUSSION

To estimate the precision and accuracy of the assay, plasma samples with known amounts of I and urine samples with known amounts of III were assayed. The results are summarized in Table I.

Chemical-ionization mass spectra[15] of I–III were obtained after GLC (Figs. 2*a*–2*c*). These spectra verify that these compounds pass through the chromatographic column intact and are the compounds measured by the detector.

The dissolution profiles (Table II) show that I is rapidly made available for absorption from both the tablet and capsule formulations.

The mean plasma ethinamate concentrations after administration of tablets and capsules are shown in Fig. 3. These plasma data were evaluated by an analysis of variance on the basis of the area under the plasma concentration–time curves, peak times, and the peak plasma concentrations (Table III). All parameters showed the tablets and capsules to be similar. The mean recoveries of the metabolite in the 24-hr urines were 359.6 ± 119.1 mg (32.8% recovery) for the tablets and 490.4 ± 193.5 mg

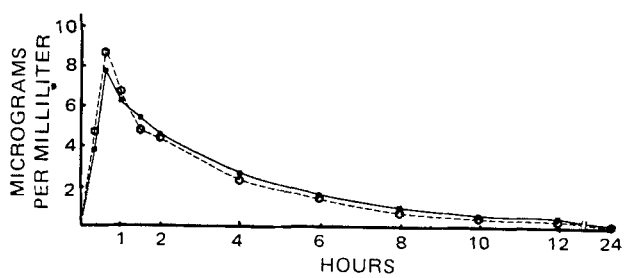

Figure 3—*Plasma ethinamate concentrations after administration of two 500-mg tablets (○) or two 500-mg capsules (■) of ethinamate to 12 subjects.*

[13] Valmid (ethinamate, Dista), Pulvules 399, 500 mg.

[14] Sulfuric acid is used to hydrolyze the amide portion of the molecule. The liberated ammonia is complexed with sodium phenolate. This complex is oxidized with sodium hypochlorite to yield a chromophore absorbing at 590 nm.

[15] A Finnigan model 3100 Quadrupole mass spectrometer (Sunnyvale, Calif.) was used with the column and conditions used in this procedure. Methane was the reagent gas.

(44.6% recovery) for the capsules. The mean difference of 130.8 mg of hydroxyethinamate in the 24-hr urine from the tablets and capsules was significant. However, this significant difference can be explained largely by the unusually low recovery of 77 mg of III from one subject. Without this subject, the average 24-hr urine recovery of III was 385 mg for the other 11 subjects. The mean difference of 105 mg of III recovered in the 24-hr urine from the two dosage forms was not significant.

The half-life of ethinamate in plasma was determined from a semilogarithmic regression analysis. The $t_{1/2}$ of ethinamate in plasma from these products was 1.9 ± 0.3 hr.

REFERENCES

(1) W. J. Cadman and T. Johns, *J. Forensic Sci.*, **5**, 369 (1960).

(2) M. K. Linturi-Laurila, *Acta Chem. Scand.*, **18**, 415 (1964).

(3) C. J. Parli, N. Wang, and R. E. McMahon, *J. Pharmacol. Exp. Ther.*, **180**, 719 (1972).

(4) R. E. McMahon, *J. Org. Chem.*, **24**, 1834 (1959).

ACKNOWLEDGMENTS AND ADDRESSES

Received October 28, 1975, from the *Lilly Research Laboratories, Indianapolis, IN 46206.*

Accepted for publication September 1, 1976.

Presented in part at the Pharmaceutical Analysis and Control Section, APhA Academy of Pharmaceutical Sciences, San Diego meeting, November 1973.

The authors thank Mr. T. Collins for collecting the samples, Dr. R. Wolen for the GLC–chemical-ionization mass spectral data, Mr. L. D. Bechtel for the dissolution data, and Mr. P. Page for analysis of the samples. Dr. R. E. McMahon supplied III.

[x] To whom inquiries should be directed.

Solubility and Ionization Characteristics of Phenytoin

PETER A. SCHWARTZ [*], C. T. RHODES [*x], and J. W. COOPER, Jr.[‡]

Abstract □ The solubility of phenytoin was determined in pH 7.4 and 5.4 phosphate buffers at five temperatures; in hydroalcoholic solutions, 0–4% methanol; and in pH 4.8–8.4 buffer solutions. From the temperature data, the enthalpy and entropy of solution of this nonideal system were calculated and were similar at both pH values. The data obtained from the buffer solutions were used to calculate the apparent dissociation constant, pKa′, of phenytoin as 8.06. A GLC method with on-column methylation was used to quantitate phenytoin with 5-(*p*-methylphenyl)-5-phenylhydantoin as an internal standard. The assay uses chloroform for extraction of the drug from aqueous solutions. The ratio of peak heights was adjusted for weights of aqueous and organic layers, and results were calculated in micrograms per gram of sample and mole fraction of phenytoin. Although hydroalcoholic solutions enhanced drug solubility, there is a potentially significant disadvantage in using alcohol for clinical studies.

Keyphrases □ Phenytoin—solubility and ionization characteristics in various buffers and hydroalcoholic solutions □ Solubility—phenytoin in various buffers and hydroalcoholic solutions □ Ionization characteristics—phenytoin in various buffers and hydroalcoholic solutions □ Anticonvulsants—phenytoin, solubility and ionization characteristics in various buffers and hydroalcoholic solutions

Because of its regulating effect on the bioelectric activity of the nervous system, phenytoin is used widely as an anticonvulsant and cardiac antiarrhythmic (1). The therapeutic activity of the drug appears to be related to the concentration of free unbound drug in the plasma (2, 3). The present paper reports some fundamental physicochemical properties of the drug which have considerable relevance for pharmacokinetic studies. A GLC method was devised to achieve acceptable sensitivity (<5% error) from 0.5 to 100 μg of phenytoin/ml.

The apparent dissociation constant, pKa′, was 8.31 when determined by UV spectrophotometry and 8.33 when determined by potentiometric titration in hydroalcoholic solutions (4). A graph of pKa′ values as a function of the ethanol concentrations yields the apparent pKa′ value in water (0% alcohol). A pKa′ of 9.2 was determined by titration in 50% methanol (5), in good agreement with that for 50% ethanol (4).

Phenytoin is very slightly soluble in alkali at 26° (5), *e.g.*, 165 μg/ml at pH 9.1 (borate buffer) and 1.52 mg/ml at pH 10, but it is practically insoluble in water, *e.g.*, 14 μg/ml at pH 7 and 20 μg/ml at pH 7.4 at 24° (6). However, it is sparingly soluble in alcohol, 19.4 mg/g (7) or 1 g in about 60 ml, and about one part in 30 ml of acetone (8). It is only slightly soluble in ether and chloroform (9).

Shortly after the introduction of phenytoin as an anticonvulsant in 1937 (10), the first analytical method, a titrimetric procedure, was developed for the determination of quantitative plasma phenytoin levels (11, 12), but this method lacked sensitivity in the clinical microgram range. Several spectrophotometric procedures (13–18) had considerably improved sensitivity.

The most recent development in phenytoin assay procedures involves the application of GLC, a highly specific and sensitive analytical technique (19, 20). A procedure using trimethylsilyl derivatives of phenytoin and its metabolic products is sensitive, but these products are unstable in the presence of moisture (21, 22). The quaternary ammonium base, trimethylanilinium hydroxide (I), was used successfully as a methylating agent (23) to convert the hydantoins to nonpolar, volatile derivatives, using the injection port of a gas chromatograph as the reaction chamber. This flash-heater methylation reaction is complete; the 1,3-dimethylhydantoin products are stable (24) and were identified by mass spectrometry as the sole products of this reaction (25).

EXPERIMENTAL

Materials—Phenytoin (5,5-diphenylhydantoin) and 5-(*p*-methylphenyl)-5-phenylhydantoin (II) were used as obtained (99+%)[1]. The melting point and IR spectrum of phenytoin were determined as an index of purity (9). Chloroform[2] and all other chemicals employed were reagent grade.

[1] Aldrich Chemical Co., Milwaukee, WI 53233.

[2] J. T. Baker Chemical Co., Phillipsburg, N.J.

(44.6% recovery) for the capsules. The mean difference of 130.8 mg of hydroxyethinamate in the 24-hr urine from the tablets and capsules was significant. However, this significant difference can be explained largely by the unusually low recovery of 77 mg of III from one subject. Without this subject, the average 24-hr urine recovery of III was 385 mg for the other 11 subjects. The mean difference of 105 mg of III recovered in the 24-hr urine from the two dosage forms was not significant.

The half-life of ethinamate in plasma was determined from a semilogarithmic regression analysis. The $t_{1/2}$ of ethinamate in plasma from these products was 1.9 ± 0.3 hr.

REFERENCES

(1) W. J. Cadman and T. Johns, *J. Forensic Sci.*, **5**, 369 (1960).

(2) M. K. Linturi-Laurila, *Acta Chem. Scand.*, **18**, 415 (1964).

(3) C. J. Parli, N. Wang, and R. E. McMahon, *J. Pharmacol. Exp. Ther.*, **180**, 719 (1972).

(4) R. E. McMahon, *J. Org. Chem.*, **24**, 1834 (1959).

ACKNOWLEDGMENTS AND ADDRESSES

Received October 28, 1975, from the *Lilly Research Laboratories, Indianapolis, IN 46206.*

Accepted for publication September 1, 1976.

Presented in part at the Pharmaceutical Analysis and Control Section, APhA Academy of Pharmaceutical Sciences, San Diego meeting, November 1973.

The authors thank Mr. T. Collins for collecting the samples, Dr. R. Wolen for the GLC–chemical-ionization mass spectral data, Mr. L. D. Bechtel for the dissolution data, and Mr. P. Page for analysis of the samples. Dr. R. E. McMahon supplied III.

[x] To whom inquiries should be directed.

Solubility and Ionization Characteristics of Phenytoin

PETER A. SCHWARTZ [*], C. T. RHODES [*x], and J. W. COOPER, Jr.[‡]

Abstract □ The solubility of phenytoin was determined in pH 7.4 and 5.4 phosphate buffers at five temperatures; in hydroalcoholic solutions, 0–4% methanol; and in pH 4.8–8.4 buffer solutions. From the temperature data, the enthalpy and entropy of solution of this nonideal system were calculated and were similar at both pH values. The data obtained from the buffer solutions were used to calculate the apparent dissociation constant, pKa′, of phenytoin as 8.06. A GLC method with on-column methylation was used to quantitate phenytoin with 5-(*p*-methylphenyl)-5-phenylhydantoin as an internal standard. The assay uses chloroform for extraction of the drug from aqueous solutions. The ratio of peak heights was adjusted for weights of aqueous and organic layers, and results were calculated in micrograms per gram of sample and mole fraction of phenytoin. Although hydroalcoholic solutions enhanced drug solubility, there is a potentially significant disadvantage in using alcohol for clinical studies.

Keyphrases □ Phenytoin—solubility and ionization characteristics in various buffers and hydroalcoholic solutions □ Solubility—phenytoin in various buffers and hydroalcoholic solutions □ Ionization characteristics—phenytoin in various buffers and hydroalcoholic solutions □ Anticonvulsants—phenytoin, solubility and ionization characteristics in various buffers and hydroalcoholic solutions

Because of its regulating effect on the bioelectric activity of the nervous system, phenytoin is used widely as an anticonvulsant and cardiac antiarrhythmic (1). The therapeutic activity of the drug appears to be related to the concentration of free unbound drug in the plasma (2, 3). The present paper reports some fundamental physicochemical properties of the drug which have considerable relevance for pharmacokinetic studies. A GLC method was devised to achieve acceptable sensitivity (<5% error) from 0.5 to 100 μg of phenytoin/ml.

The apparent dissociation constant, pKa′, was 8.31 when determined by UV spectrophotometry and 8.33 when determined by potentiometric titration in hydroalcoholic solutions (4). A graph of pKa′ values as a function of the ethanol concentrations yields the apparent pKa′ value in water (0% alcohol). A pKa′ of 9.2 was determined by titration in 50% methanol (5), in good agreement with that for 50% ethanol (4).

Phenytoin is very slightly soluble in alkali at 26° (5), *e.g.*, 165 μg/ml at pH 9.1 (borate buffer) and 1.52 mg/ml at pH 10, but it is practically insoluble in water, *e.g.*, 14 μg/ml at pH 7 and 20 μg/ml at pH 7.4 at 24° (6). However, it is sparingly soluble in alcohol, 19.4 mg/g (7) or 1 g in about 60 ml, and about one part in 30 ml of acetone (8). It is only slightly soluble in ether and chloroform (9).

Shortly after the introduction of phenytoin as an anticonvulsant in 1937 (10), the first analytical method, a titrimetric procedure, was developed for the determination of quantitative plasma phenytoin levels (11, 12), but this method lacked sensitivity in the clinical microgram range. Several spectrophotometric procedures (13–18) had considerably improved sensitivity.

The most recent development in phenytoin assay procedures involves the application of GLC, a highly specific and sensitive analytical technique (19, 20). A procedure using trimethylsilyl derivatives of phenytoin and its metabolic products is sensitive, but these products are unstable in the presence of moisture (21, 22). The quaternary ammonium base, trimethylanilinium hydroxide (I), was used successfully as a methylating agent (23) to convert the hydantoins to nonpolar, volatile derivatives, using the injection port of a gas chromatograph as the reaction chamber. This flash-heater methylation reaction is complete; the 1,3-dimethylhydantoin products are stable (24) and were identified by mass spectrometry as the sole products of this reaction (25).

EXPERIMENTAL

Materials—Phenytoin (5,5-diphenylhydantoin) and 5-(*p*-methylphenyl)-5-phenylhydantoin (II) were used as obtained (99+%)[1]. The melting point and IR spectrum of phenytoin were determined as an index of purity (9). Chloroform[2] and all other chemicals employed were reagent grade.

[1] Aldrich Chemical Co., Milwaukee, WI 53233.

[2] J. T. Baker Chemical Co., Phillipsburg, N.J.

Table I—Average Solubility for Six Samples of Phenytoin in Buffers at 25°

pH	Solubility, μg/ml (SD)	S/S^0
8.3	56.8 (2.8)	3.08
8.2	44.7 (2.2)	2.43
8.0	32.4 (2.0)	1.76
7.8	27.6 (1.8)	1.50
7.5	21.9 (1.4)	1.19
7.1	20.3 (0.9)	1.10
4.9	18.4 (0.8)	—

Phenytoin Extraction—Phenytoin and II, as an internal standard, were extracted from aqueous samples in chloroform and measured by a modification of several methods using flash-heater methylation (24, 26, 27). To 1 ml of an aqueous sample in a 50-ml glass-stoppered centrifuge tube was added 5 ml of chloroform containing 2 μg of II/ml. The mixture was shaken[3] for 15 min and centrifuged[4] at 1000 rpm for 6 min to break any emulsion. As much of the organic (lower) phase as possible was removed by pipet and placed in a 15-ml ground-glass-stoppered centrifuge tube.

This mixture was dried under a nitrogen stream on a 60° water bath. Twenty-five microliters[5] of a solution of I, 0.5 *M* in methanol[6], was added to the dry residue, and 1 μl of the extract was injected into the gas chromatograph. The centrifuge tubes and aqueous and organic solvents were weighed[7] to permit calculation of mole fractions from the microgram per gram concentrations.

Phenytoin Analysis—A gas chromatograph[8] fitted with dual hydrogen flame-ionization detectors was used. Each U-shaped borosilicate glass column (183 cm × 2 mm i.d.) was packed with 3% phenyl methyl silicone[9] coated on acid-washed, dimethyldichlorosilane-treated, high performance flux-calcined diatomite support[10], 100–200 mesh. Small silanized glass wool plugs were inserted in both ends of the columns after packing by the vibrator method.

Heat conditioning was accomplished by connecting the columns to the injector inlet only with a nitrogen purge of about 20 ml/min and maintaining a temperature of 325° for at least 24 hr (the recommended maximum is 350° for the packing). During periods of inactivity, the column oven was set at 160° with a small nitrogen flow of about 5–10 ml/min.

For routine analysis of phenytoin, the on-column injectors were sealed with high temperature septa[11] and maintained at 250°. The same temperature was chosen for the detectors. The column was operated isothermally at 230° using a nitrogen carrier gas flow rate of about 30 ml/min (65 psi) and a hydrogen and air flame, 30 ml/min (20 psi) and 300 ml/min (40 psi), respectively. The electrometer output was monitored with a 1-mv recorder[12] with a chart speed of 0.254 cm (0.1 in.)/min at a range of 10^{-11} amp/mv, and the signal was usually attenuated by a factor of 2–64.

Under these operating conditions, a 1-μl injection[5] of an extracted standard solution of 10 μg/ml each of phenytoin and II produced peak height responses of about one-half to three-fourths full scale. Retention times of the methylated phenytoin and II were 8 and 12 min, respectively. There was no trap for any trimethylamine eluted from the GLC column since the entire effluent passed through the flame detector.

Calibration—Standard solutions were prepared from dry chemicals without further purification. The melting point and IR spectra[13] were determined for phenytoin and were acceptable evidence of purity. Stock solutions of phenytoin, 1 mg/ml, and II, 250 μg/ml, were prepared in anhydrous methanol and maintained in a freezer at −15° for no more than 6 months. No apparent loss of activity was noted over this time.

Standard solutions of phenytoin were freshly prepared from aliquots of the stock solution and were evaporated to dryness under nitrogen at room temperature. These samples were redissolved in 1% (w/v) methanol in pH 7.4 aqueous buffer, so that the ionic strength of the final solution was 0.16. Multiple samples were extracted in less than 1 hr. A 2-μg/ml solution of II in chloroform, the extracting solvent for phenytoin, was maintained at −15°; unused portions were discarded after 30 days.

[3] Wrist-action shaker, Burrell Corp., Pittsburgh, Pa.
[4] Damon/IEC HT centrifuge, Damon Corp., Needham Heights, Mass.
[5] Hamilton Co., Reno, Nev.
[6] Southwestern Analytical Chem., Austin, Tex.
[7] H5 Mettler balance, Mettler Instrument Corp., Hightstown, N.J.
[8] Model 2100, Varian Aerograph, Los Altos, CA 94002.
[9] OV-17, Varian Aerograph, Los Altos, CA 94002.
[10] HP Chromosorb W, Varian Aerograph, Los Altos, CA 94002.
[11] HT9, Applied Science Laboratories, State College, Pa.
[12] Model A-25, Varian Aerograph, Los Altos, CA 94002.
[13] Model 457 grating IR spectrophotometer, Beckman Instruments, Fullerton, Calif.

Table II—Average Solubility[a] for Six Samples of Phenytoin in Buffered (pH 7.4) Methanol at 25 and 37°

Temperature	Methanol, % (w/v)				
	0	0.5	1.0	2.0	4.0
25°	20.6 (1.3)	21.2 (1.0)	21.8 (0.8)	24.2 (0.5)	27.7 (0.3)
37°	30.6 (0.9)	32.2 (0.8)	34.2 (0.6)	36.4 (0.3)	38.6 (0.3)

[a] Values are micrograms per milliliter with the standard deviation given in parentheses.

A series of standard solutions, 1–50 μg/ml, were extracted, completely dried, and kept in stoppered centrifuge tubes at room temperature for up to 6 months without any apparent loss of sample activity. These dried standards permitted ready calibration of the gas chromatograph. Several sets of standard solutions were analyzed; the chromatograms were linear with respect to peak height ratios of phenytoin to II up to 100 μg/ml, with reproducibility of less than 5% error. A single 5-ml extraction of a 100-μg/ml phenytoin solution was examined for completeness of the extraction procedure. Samples of the separate aqueous and chloroform layers were evaporated to dryness, and direct comparison demonstrated a >99% extraction.

Solubility—Methanolic solutions for the determination of phenytoin solubility were prepared using pH 7.4 phosphate buffer with an ionic strength of 0.16. Determination of the apparent pH values[14] for these 0.5, 1, 2, and 4% methanol solutions demonstrated no significant pH shifts from the pH measured in the buffer alone.

A series of pH 5.6–8.4 phosphate buffers with an ionic strength of 0.16 were prepared for the determination of the solubility and the dissociation constant of phenytoin at 25°. Similarly prepared solutions at pH 5.4 and 7.4 were used to determine the change in phenytoin solubility with temperature over 25–50°.

The saturated solubility of phenytoin in alcohols and buffers was attained using a previously described procedure (28). The solute, in an amount in excess of its solubility (about 100 mg), was placed in polytef[15]-lined screw-capped glass vials with each solvent system. The vials were closed tightly and rotated at 28 rpm in a large constant-temperature (±0.2°) water bath[16] maintained successively at 50, 44, 37, 30, and 25°. After at least 24 hr of continuous rotation, a time sufficient to obtain saturated solutions at 25°, each sample vial was removed in succession for assay.

The exterior of the vial was quickly dried, and the cap was unscrewed carefully to prevent water contamination. A 2-ml sample of the saturated solution was drawn into a glass syringe and filtered into a small glass vial through a cellulose acetate filter with a pore size of 0.22 μm[17]. A 1-ml sample of this filtrate was placed in a tared 50-ml centrifuge tube, the total weight was recorded, and the filtrate was extracted. All glass syringes, pipets, and filter apparatus was prewarmed to prevent drug precipitation.

Calculations—Peak height ratios were calculated by dividing the height of the peak due to phenytoin by the height of the peak due to II. A peak height adjustment was made using the weights of the aqueous and chloroform layers. Calibration curves were constructed from the results of extracted standards by plotting the concentration of phenytoin in micrograms per gram against the respective adjusted peak height ratios.

RESULTS AND DISCUSSION

Phenytoin is more soluble in alkaline solutions (Table I). The total solubility, S, can be expressed as a function of the hydrogen-ion concentration, solubility of the unionized form, S^0, and the dissociation constant, K_a:

$$S = S^0 + P^- = S^0 + K_a S^0/[H^+] \quad \text{(Eq. 1)}$$

Krebs and Speakman (29, 30) transformed this equation into the more customary pH and pKa notation:

$$\log(S/S^0 - 1) = \text{pH} - \text{pKa} \quad \text{(Eq. 2)}$$

[14] Expandomatic SS-2, Beckman Instruments, Fullerton, Calif.
[15] Teflon (du Pont).
[16] Portatemp, Precision Scientific, Chicago, Ill.
[17] Millipore Corp., Bedford, Mass.

Table III—Average Solubility for Six Samples of Phenytoin as a Function of Temperature

pH	Temperature °C	Temperature °K	$1/T$, °K^{-1}	Solubility, μg/g (*SD*)	Mole Fraction × 10^6
5.4	25.4	298.5	0.00335	19.4 (1.0)	1.4
	30.2	303.3	0.00330	23.9 (1.7)	1.7
	37.2	310.3	0.00323	30.1 (2.1)	2.2
	44.7	317.8	0.00315	43.4 (2.3)	3.1
	50.3	323.4	0.00309	50.4 (2.8)	3.6
7.4	25.2	298.3	0.00335	20.5 (1.1)	1.5
	30.1	303.2	0.00330	24.6 (1.7)	1.8
	37.1	310.2	0.00322	31.0 (2.2)	2.2
	44.1	317.2	0.00315	45.6 (2.5)	3.3
	49.7	322.8	0.00310	55.1 (3.0)	4.0

so that a plot of pH against the logarithmic term gives a straight line intersecting the pH axis at the pKa. The value of the pKa is described by this method as an apparent dissociation constant, pKa′, since the activity coefficients are unknown. From the data plotted in Fig. 1, a value of 8.06 for the pKa′ was obtained. This pKa′ differs slightly (8.3) from that reported by Agarwal and Blake (4), but their methods and materials differed and the temperature was not specified.

Table II contains the data for the solubility of phenytoin in methanolic solutions at 25 and 37° and shows the increase in phenytoin solubility with increasing alcohol concentration. The data also show the expected increase in solubility with temperature for all concentrations in methanol. The phenytoin could not be redissolved easily or quickly after extraction without using methanol. The reasons for this finding are not fully apparent, but one possible mechanism is solvate formation by phenytoin and methanol. A 1% (w/v) methanol solution in buffer was chosen for all studies to ensure a phenytoin concentration in the range of up to 20 μg/ml.

The solubility of phenytoin is quite low in aqueous buffered solutions ($\mu = 0.16$), and the results at 25° (Table I) agree with those of Glazko and Chang (6). Several studies with phenytoin, *e.g.*, protein binding, reported concentrations of the drug exceeding the aqueous solubility and, in fact, used hydroalcoholic solutions of the drug without considering the effects of the alcohol on the binding process (31–33).

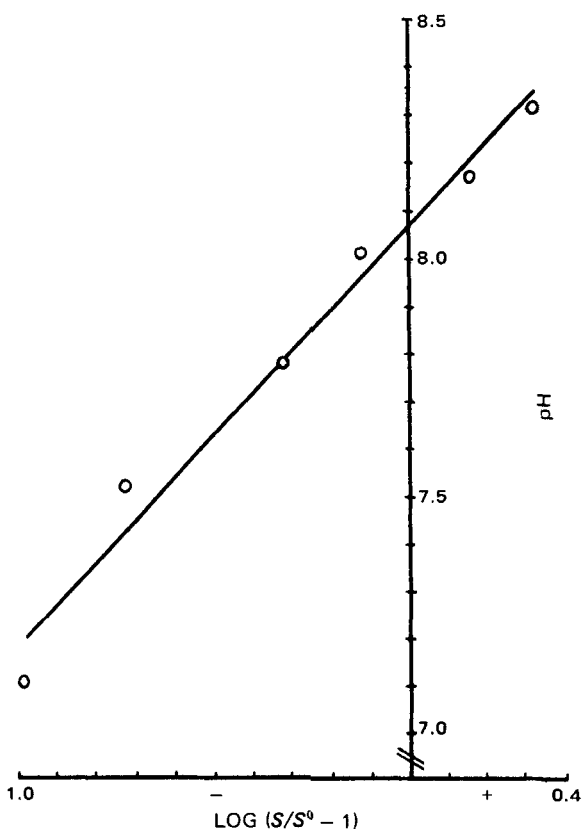

Figure 1—*Plot of log(S/S⁰ − 1) for phenytoin as a function of pH, r = 0.977. The intercept on the pH axis is the apparent pKa.*

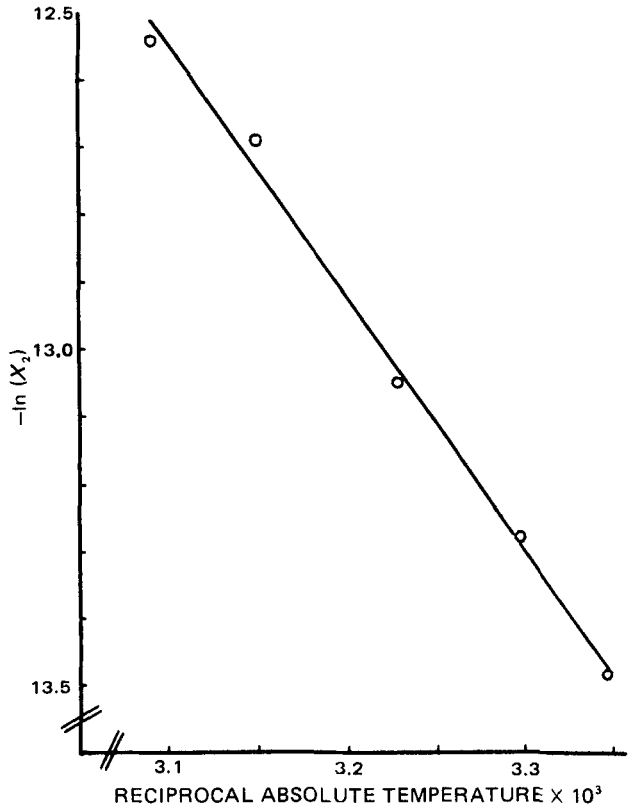

Figure 2—*Van't Hoff plot for solubility of phenytoin at pH 5.4, r = 0.995.*

The data for the phenytoin solubilities at pH 5.4 and 7.4 at five temperatures (Table III) are expressed as micrograms per gram and were converted to mole fractions from the appropriate specific gravity of the solutions. Specific gravities were determined by a pycnometer; in all cases, the difference in weight per milliliter between samples and reference was less than 1%. This procedure allowed for the determination of thermodynamic relationships that do not require corrections for the cratic effect, *i.e.*, volume changes on mixing (34). Values for the enthalpy and entropy of solution were determined from the slope and intercept of the plot of log mole fraction solubility against the reciprocal absolute temperature, as shown in Fig. 2 for pH 5.4 (35).

The literature does not apparently contain any previous reports on the thermodynamic functions for phenytoin. The enthalpy of fusion was determined[18], using samples of phenytoin from this laboratory, to be approximately 47.5 kjoules/mole (11.3 kcal/mole) by differential scanning calorimetry. The entropy of fusion was calculated as 84 joules/kelvin (20 cal/mole kelvin) using the melting point of 294° found for this sample.

The enthalpy of solution is positive, as would be expected for nonelectrolytes with low aqueous solubility. The entropy of solution is negative, since the highly ordered crystal is dispensed into smaller (disordered) units in solution, a process accompanied by an entropy increase. However, the nonpolar phenyl groups of the drug may change the structure of water surrounding these groups (36) into a more ordered arrangement, accounting for a negative entropic effect that outweighs the positive entropy associated with the breakdown of the crystal lattice. Thermodynamic functions derived from the system at pH 5.4 and 7.4 are: enthalpy, 31.3 (7.5) and 33.6 (9.0) kjoules/mole (kcal/mole), respectively; and entropy, −7.1 (−1.7) and −1.4 (−0.3) joules/mole kelvin (cal/mole kelvin), respectively. The acid was essentially unionized (>99%) at pH 5.4, while the data at pH 7.4 (>80% unionized) represent both ionized and unionized species.

Investigators must have a clear understanding of the physicochemical characteristics of phenytoin. Because of its limited solubility, hydroalcoholic solutions have been used in the past to broaden the experimental range of concentrations. Alcohol would affect *in vitro* binding experiments; studies intended to be of clinical relevance should be conducted at physiologic temperature, pH, and ionic strength in aqueous buffer.

[18] At Upjohn Laboratories.

REFERENCES

(1) S. Bogoch and J. Dreyfus, "The Broad Range of Use of Diphenylhydantoin," Dreyfus Medical Foundation, New York, N.Y., 1970.

(2) R. R. Levine, "Pharmacology," Little, Brown, Boston, Mass., 1973, p. 103.

(3) B. B. Brodie, *Proc. Roy. Soc. Med.*, **58**, 946 (1965).

(4) S. P. Agarwal and M. I. Blake, *J. Pharm. Sci.*, **57**, 1434 (1968).

(5) W. A. Dill, A. Kazenko, L. M. Wolf, and A. J. Glazko, *J. Pharmacol. Exp. Ther.*, **118**, 270 (1956).

(6) A. J. Glazko and T. Chang, in "Antiepileptic Drugs," D. M. Woodbury, J. K. Penry, and R. P. Schmidt, Eds., Raven, New York, N.Y., 1970.

(7) L. T. Grady, S. E. Hays, R. O. King, H. R. Klein, W. J. Mader, D. K. Wyatt, and R. C. Zimmerer, Jr., *J. Pharm. Sci.*, **62**, 456 (1973).

(8) "The Merck Index," 8th ed., Merck & Co., Rahway, N.J., 1968.

(9) E. G. C. Clarke, "Isolation and Identification of Drugs," Pharmaceutical Press, London, England, 1969.

(10) H. H. Merritt and T. J. Putnam, *J. Am. Med. Assoc.*, **111**, 1068, (1938).

(11) C. H. Hine and F. L. Kozelka, *J. Pharmacol. Exp. Ther.*, **69**, (1940).

(12) F. L. Kozelka and C. H. Hine, *ibid.*, **72**, 276 (1941).

(13) G. L. Plaa and C. H. Hine, *J. Lab. Clin. Med.*, **47**, 649 (1956).

(14) W. A. Dill, A. Kazenko, L. M. Wolf, and A. J. Glazko, *J. Pharmacol. Exp. Ther.*, **118**, 270 (1956).

(15) J. Wallace, J. Biggs, and E. V. Dahl, *Anal. Chem.*, **37**, 410 (1965).

(16) J. Wallace, *J. Forensic Sci.*, **11**, 552 (1966).

(17) J. Wallace, *Anal. Chem.*, **40**, 978 (1968).

(18) S. I. Lee and N. H. Bass, *Neurology*, **20**, 115 (1970).

(19) S. Ahuja, *J. Pharm. Sci.*, **65**, 163 (1976).

(20) E. Brochmann-Hanssen, *ibid.*, **51**, 1017 (1962).

(21) T. Chang and A. J. Glazko, *Clin. Res.*, **16**, 339 (1968).

(22) T. Chang and A. J. Glazko, *J. Lab. Clin. Med.*, **75**, 145 (1970).

(23) E. Brochmann-Hanssen and T. O. Oke, *J. Pharm. Sci.*, **58**, 370 (1969).

(24) J. MacGee, *Anal. Chem.*, **42**, 421 (1970).

(25) K. Sabih and K. S. Sabih, *J. Pharm. Sci.*, **60**, 1216 (1971).

(26) H. J. Kupferberg, *Clin. Chim. Acta*, **29**, 283 (1970).

(27) M. J. Barrett, *Clin. Chem. Newslett.*, **3**, 16 (1971).

(28) P. A. Schwartz and A. N. Paruta, *J. Pharm. Sci.*, **65**, 252 (1976).

(29) H. A. Krebs and J. C. Speakman, *J. Chem. Soc.*, **2**, 593 (1945).

(30) H. A. Krebs and J. C. Speakman, *Br. Med. J.*, **47**, (1946).

(31) P. K. M. Lunde, A. Rane, S. J. Yaffe, L. Lund, and F. Sjoqvist, *Clin. Pharmacol. Ther.*, **11**, 846 (1970).

(32) R. J. Porter and R. B. Layzer, *Arch. Neurol.*, **32**, 298 (1975).

(33) I. Odar-Cederlof and O. Borga, *Clin. Pharmacol. Ther.*, **20**, 36 (1976).

(34) K. W. Kauzmann, *Adv. Protein Chem.*, **14**, 1 (1959).

(35) M. A. Lauffer, "Entropy-Driven Processes in Biology," Springer-Verlag, New York, N.Y., 1975, p. 1.

(36) G. Nemethy and H. A. Scheraga, *J. Phys. Chem.*, **66**, 1773 (1962).

ACKNOWLEDGMENTS AND ADDRESSES

Received April 26, 1976, from the *Department of Pharmacy, University of Rhode Island, Kingston, RI 02881, and the ‡School of Pharmacy, University of Georgia, Athens, GA 30602.

Accepted for publication September 9, 1976.

Presented at the Pharmaceutical Analysis and Control Section, APhA Academy of Pharmaceutical Sciences, New Orleans meeting, April 1976.

The authors thank Dr. Samuel Yalkowsky and The Upjohn Laboratories, Kalamazoo, Mich., for analyzing the sample of phenytoin by differential scanning calorimetry. Thanks are also expressed to Dr. Sut Ahuja and Ciba-Geigy Corp., Ardsley, N.Y., for financial assistance.

ˣ To whom inquiries should be directed.

Determination of Acenocoumarol in Plasma and Urine by Double Radioisotope Derivative Analysis

Y. Le ROUX ˣ and J. RICHARD

Abstract □ Acenocoumarol, to which a ^{14}C-labeled internal standard has been added, is extracted at pH 4 into ethyl acetate–heptane (20:80 v/v), back-extracted into aqueous sodium hydroxide solution after solvent washing with a pH 7 buffer, and reextracted after acidification in the solvent mixture. It is then acetylated with ^{3}H-acetic anhydride. The acenocoumarol acetyl derivative is separated from the metabolite derivatives by TLC, and its radioactivity is measured. The method is specific and sensitive to a concentration of 8 ng/ml.

Keyphrases □ Acenocoumarol—double radioisotope derivative analysis, plasma and urine □ Radiochemistry—double radioisotope derivative analysis of acenocoumarol in plasma and urine □ Anticoagulants—acenocoumarol, double radioisotope derivative analysis in plasma and urine

Acenocoumarol (I) is an oral coumarin anticoagulant[1]. It is analyzed in biological fluids using the O'Reilly *et al.* (1) method. This technique was originally developed for the determination of another coumarin anticoagulant, warfarin, which was then administered in much higher doses than acenocoumarol. It is a simple UV absorption assay, performed after solvent extraction; its sensitivity is limited to 1 μg/ml, and its specificity has not been verified. Nevertheless, it has been used for the determination of acenocoumarol (2). Two other methods, neither of which is more sensitive, also were reported (3, 4). Recently, a fluorometric assay after TLC was reported that is more sensitive (0.2 μg/ml) (5).

The metabolism of acenocoumarol was only recently elucidated[2]. Several metabolites were found: 3-[α-(4′-aminophenyl)-β-acetylethyl]-4-hydroxycoumarin (III), 3-[α-(4′-acetamidophenyl) -β- acetylethyl] -4- hydroxycoumarin (IV), two diastereoisomers of the alcohol 3-[α-(4′-nitrophenyl)-γ-hydroxybutyl]-4-hydroxycoumarin (V), 3-[α-(4′-nitrophenyl)-β-acetylethyl] -4,7- dihydroxycoumarin (VI), and 3-[α-(4′-nitrophenyl)-β-acetylethyl]-4,6-dihydroxycoumarin (VII).

All attempts to elaborate a GLC procedure for aceno-

[1] Sintrom, Ciba-Geigy.

[2] W. Dieterle *et al.*, to be published.

REFERENCES

(1) S. Bogoch and J. Dreyfus, "The Broad Range of Use of Diphenylhydantoin," Dreyfus Medical Foundation, New York, N.Y., 1970.

(2) R. R. Levine, "Pharmacology," Little, Brown, Boston, Mass., 1973, p. 103.

(3) B. B. Brodie, *Proc. Roy. Soc. Med.*, **58**, 946 (1965).

(4) S. P. Agarwal and M. I. Blake, *J. Pharm. Sci.*, **57**, 1434 (1968).

(5) W. A. Dill, A. Kazenko, L. M. Wolf, and A. J. Glazko, *J. Pharmacol. Exp. Ther.*, **118**, 270 (1956).

(6) A. J. Glazko and T. Chang, in "Antiepileptic Drugs," D. M. Woodbury, J. K. Penry, and R. P. Schmidt, Eds., Raven, New York, N.Y., 1970.

(7) L. T. Grady, S. E. Hays, R. O. King, H. R. Klein, W. J. Mader, D. K. Wyatt, and R. C. Zimmerer, Jr., *J. Pharm. Sci.*, **62**, 456 (1973).

(8) "The Merck Index," 8th ed., Merck & Co., Rahway, N.J., 1968.

(9) E. G. C. Clarke, "Isolation and Identification of Drugs," Pharmaceutical Press, London, England, 1969.

(10) H. H. Merritt and T. J. Putnam, *J. Am. Med. Assoc.*, **111**, 1068, (1938).

(11) C. H. Hine and F. L. Kozelka, *J. Pharmacol. Exp. Ther.*, **69**, (1940).

(12) F. L. Kozelka and C. H. Hine, *ibid.*, **72**, 276 (1941).

(13) G. L. Plaa and C. H. Hine, *J. Lab. Clin. Med.*, **47**, 649 (1956).

(14) W. A. Dill, A. Kazenko, L. M. Wolf, and A. J. Glazko, *J. Pharmacol. Exp. Ther.*, **118**, 270 (1956).

(15) J. Wallace, J. Biggs, and E. V. Dahl, *Anal. Chem.*, **37**, 410 (1965).

(16) J. Wallace, *J. Forensic Sci.*, **11**, 552 (1966).

(17) J. Wallace, *Anal. Chem.*, **40**, 978 (1968).

(18) S. I. Lee and N. H. Bass, *Neurology*, **20**, 115 (1970).

(19) S. Ahuja, *J. Pharm. Sci.*, **65**, 163 (1976).

(20) E. Brochmann-Hanssen, *ibid.*, **51**, 1017 (1962).

(21) T. Chang and A. J. Glazko, *Clin. Res.*, **16**, 339 (1968).

(22) T. Chang and A. J. Glazko, *J. Lab. Clin. Med.*, **75**, 145 (1970).

(23) E. Brochmann-Hanssen and T. O. Oke, *J. Pharm. Sci.*, **58**, 370 (1969).

(24) J. MacGee, *Anal. Chem.*, **42**, 421 (1970).

(25) K. Sabih and K. S. Sabih, *J. Pharm. Sci.*, **60**, 1216 (1971).

(26) H. J. Kupferberg, *Clin. Chim. Acta*, **29**, 283 (1970).

(27) M. J. Barrett, *Clin. Chem. Newslett.*, **3**, 16 (1971).

(28) P. A. Schwartz and A. N. Paruta, *J. Pharm. Sci.*, **65**, 252 (1976).

(29) H. A. Krebs and J. C. Speakman, *J. Chem. Soc.*, **2**, 593 (1945).

(30) H. A. Krebs and J. C. Speakman, *Br. Med. J.*, **47**, (1946).

(31) P. K. M. Lunde, A. Rane, S. J. Yaffe, L. Lund, and F. Sjoqvist, *Clin. Pharmacol. Ther.*, **11**, 846 (1970).

(32) R. J. Porter and R. B. Layzer, *Arch. Neurol.*, **32**, 298 (1975).

(33) I. Odar-Cederlof and O. Borga, *Clin. Pharmacol. Ther.*, **20**, 36 (1976).

(34) K. W. Kauzmann, *Adv. Protein Chem.*, **14**, 1 (1959).

(35) M. A. Lauffer, "Entropy-Driven Processes in Biology," Springer-Verlag, New York, N.Y., 1975, p. 1.

(36) G. Nemethy and H. A. Scheraga, *J. Phys. Chem.*, **66**, 1773 (1962).

ACKNOWLEDGMENTS AND ADDRESSES

Received April 26, 1976, from the *Department of Pharmacy, University of Rhode Island, Kingston, RI 02881, and the ‡School of Pharmacy, University of Georgia, Athens, GA 30602.

Accepted for publication September 9, 1976.

Presented at the Pharmaceutical Analysis and Control Section, APhA Academy of Pharmaceutical Sciences, New Orleans meeting, April 1976.

The authors thank Dr. Samuel Yalkowsky and The Upjohn Laboratories, Kalamazoo, Mich., for analyzing the sample of phenytoin by differential scanning calorimetry. Thanks are also expressed to Dr. Sut Ahuja and Ciba-Geigy Corp., Ardsley, N.Y., for financial assistance.

ˣ To whom inquiries should be directed.

Determination of Acenocoumarol in Plasma and Urine by Double Radioisotope Derivative Analysis

Y. Le ROUX ˣ and J. RICHARD

Abstract □ Acenocoumarol, to which a ^{14}C-labeled internal standard has been added, is extracted at pH 4 into ethyl acetate–heptane (20:80 v/v), back-extracted into aqueous sodium hydroxide solution after solvent washing with a pH 7 buffer, and reextracted after acidification in the solvent mixture. It is then acetylated with ^{3}H-acetic anhydride. The acenocoumarol acetyl derivative is separated from the metabolite derivatives by TLC, and its radioactivity is measured. The method is specific and sensitive to a concentration of 8 ng/ml.

Keyphrases □ Acenocoumarol—double radioisotope derivative analysis, plasma and urine □ Radiochemistry—double radioisotope derivative analysis of acenocoumarol in plasma and urine □ Anticoagulants—acenocoumarol, double radioisotope derivative analysis in plasma and urine

Acenocoumarol (I) is an oral coumarin anticoagulant[1]. It is analyzed in biological fluids using the O'Reilly *et al.* (1) method. This technique was originally developed for the determination of another coumarin anticoagulant, warfarin, which was then administered in much higher doses than acenocoumarol. It is a simple UV absorption assay, performed after solvent extraction; its sensitivity is limited to 1 μg/ml, and its specificity has not been verified. Nevertheless, it has been used for the determination of acenocoumarol (2). Two other methods, neither of which is more sensitive, also were reported (3, 4). Recently, a fluorometric assay after TLC was reported that is more sensitive (0.2 μg/ml) (5).

The metabolism of acenocoumarol was only recently elucidated[2]. Several metabolites were found: 3-[α-(4′-aminophenyl)-β-acetylethyl]-4-hydroxycoumarin (III), 3-[α-(4′-acetamidophenyl) -β- acetylethyl] -4- hydroxycoumarin (IV), two diastereoisomers of the alcohol 3-[α-(4′-nitrophenyl)-γ-hydroxybutyl]-4-hydroxycoumarin (V), 3-[α-(4′-nitrophenyl)-β-acetylethyl] -4,7- dihydroxycoumarin (VI), and 3-[α-(4′-nitrophenyl)-β-acetylethyl]-4,6-dihydroxycoumarin (VII).

All attempts to elaborate a GLC procedure for aceno-

[1] Sintrom, Ciba-Geigy.

[2] W. Dieterle *et al.*, to be published.

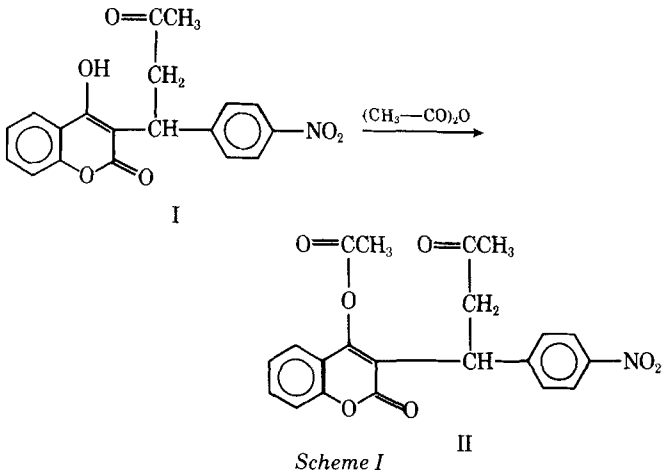

Scheme I

coumarol were unsuccessful; one of the two alcohol metabolites (V) could never be separated from the unchanged drug. Therefore, a specific method of determination was developed based on the principle of double radioisotope derivative analysis (6). After the addition of ^{14}C-labeled internal standard, acenocoumarol was extracted and then acetylated with ^{3}H-acetic anhydride (Scheme I). The acetyl derivative (II) was separated from the acetyl derivatives of the metabolites by TLC, and its radioactivity was measured.

EXPERIMENTAL

Reagents—Sodium hydroxide (2×10^{-3} *N*, 11.76 μg/ml) and a methanolic solution of ^{14}C-acenocoumarol[3] (20 μCi/mg) were used. ^{3}H-Acetic anhydride[4] (100 mCi/mmole) was diluted in freshly dried heptane to give a concentration of 1 μmole/50 μl.

This solution was stored in 2-ml portions in sealed glass ampuls at 4°. ^{3}H-Maprotiline[3] (65 μCi/mg) methanolic solution (944 ng/ml) was used to determine the ^{3}H-channel ratio.

Dioxane was distilled over lithium aluminum hydride and stored in glass ampuls sealed under nitrogen at 4°.

All other reagents were analytical grade[5,6]. Buffers, pH 4 and 7[6], were used in fourfold concentrations.

Materials—Radiochemical measurement was performed by means of a liquid scintillation spectrometer[7]; the scintillator used was 2-(4-*tert*-butylphenyl)-5-(4-biphenyl)-1,3,4-oxadiazole[3] (0.8% toluene solution).

Extraction—Plasma or urine (2 ml), 1 ml of aqueous ^{14}C-acenocoumarol (58.8 ng/ml), 2 ml of pH 4[8] citrate buffer, and 10 ml of solvent mixture [ethyl acetate–heptane (20:80 v/v)] were introduced into conical polypropylene tubes with screw caps. These tubes were vigorously shaken for 15 min and then centrifuged at 3500 rpm for 10 min. The organic phase was transferred with a Pasteur pipet into 10-ml glass ampuls containing 1 ml of pH 7[8] phosphate buffer. Each ampul was closed with a polyethylene cap, shaken for 15 min, and centrifuged at 2000 rpm for 10 min.

The organic phase was transferred into 10-ml glass ampuls containing 0.5 ml of 1 *N* NaOH; these ampuls were then closed, shaken, and centrifuged. The organic phase was discarded, and 0.7 ml of 1 *N* H_2SO_4 and 5 ml of solvent mixture were added to the basic phase. Again the ampuls were closed, shaken, and centrifuged. The organic phase was then transferred into 5-ml glass ampuls, which were closed with polyethylene caps and stored overnight at 4°. On the following day, the ampuls were placed in a thermostat bath at 40°, and the solvent was removed with a nitrogen flow. Thereafter, they were kept in a vacuum desiccator for 1 hr.

Acetylation—Dioxane (100 μl) and 50 μl of ^{3}H-acetic anhydride (1 μmole or 100 μCi) in heptane solution were added to the evaporation residue. The ampuls were closed with polyethylene caps, heated at 60° for 1 hr, and then opened. The acetic anhydride, dioxane, and heptane were evaporated by heating at 50° for 10 min and sucking off the vapors with a water aspirator (the aspirated air was passed through two wash bottles containing concentrated sodium hydroxide). Then 2 ml of heptane–ethyl acetate (80:20 v/v) and 1 ml of pH 4 buffer were added, and the ampuls were shaken for 15 min and then centrifuged at 2000 rpm for 10 min. The organic phase was transferred into 2-ml glass ampuls, and the solvent was removed at 40° with a nitrogen flow. The ampuls were kept in a vacuum desiccator overnight.

TLC Purification—A diluted solution (50 μl) of unlabeled acenocoumarol acetyl derivative and unlabeled V acetyl derivatives in chloroform were added to the residue and spotted on a silica gel F254[6] thin-

Table I—Assay of Unknown Solutions

Acenocoumarol Introduced, ng/ml		Concentration Found, ng/ml	*SD*	95% Confidence Interval	*SE*, %
Plasma	4.02	3.7 (n = 6)	0.97	2.63–4.69	10.9
	8.04	8.4 (n = 7)	0.99	7.52–9.36	4.45
	40.24	41.5 (n = 3)	1.97	36.62–46.43	2.74
	80.48	82.7 (n = 3)	1.64	78.65–86.71	1.14
Urine	30.18	32.0 (n = 6)	2.68	29.24–34.78	3.36
	50.30	53.5 (n = 7)	2.56	51.15–55.90	1.80
Aqueous solution	30.18	33.2 (n = 5)	1.43	31.45–35.02	1.93
	60.36	61.1 (n = 6)	1.47	59.58–62.68	0.98

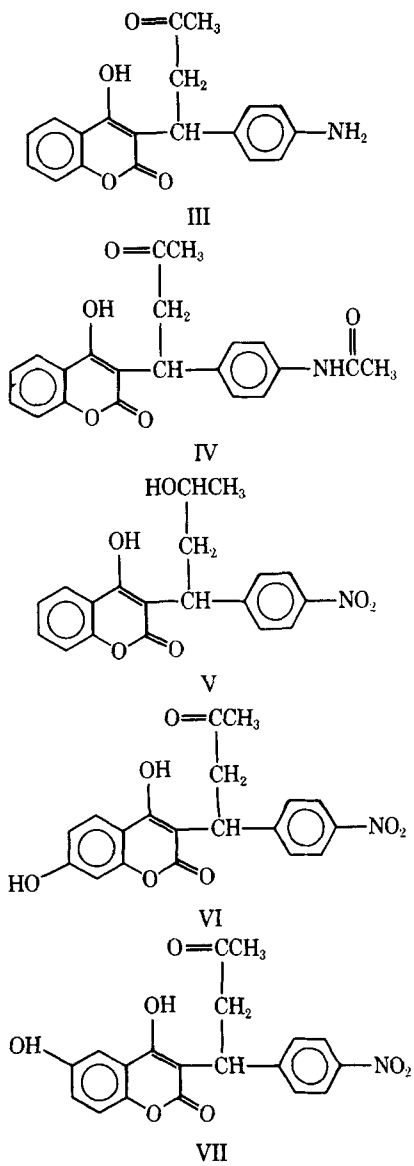

[3] Ciba-Geigy, Basle, Switzerland.
[4] Commissariat a l'Energie Atomique, Gif-sur-Yvette, France.
[5] Mallinckrodt, Wesel, West Germany.
[6] Merck A. G., Darmstadt, West Germany.
[7] Model 3385, Packard Instrument Co.
[8] Titrisol, Merck.

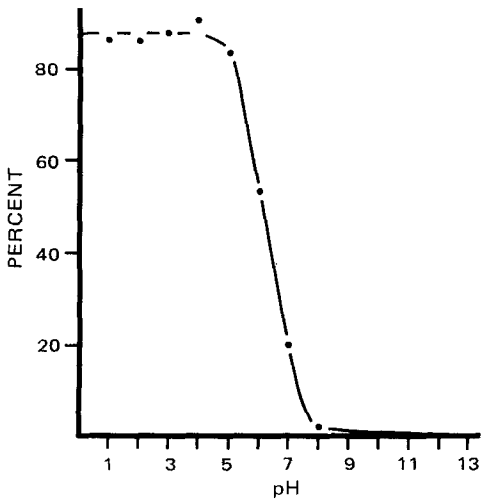

Figure 1—*Extraction of acenocoumarol from 2 ml of its plasma solution (117.6 ng/ml) into 10 ml of heptane–ethyl acetate (80:20) at different pH's.*

layer plate. Each ampul was rinsed with 50 μl of chloroform, which also was spotted on the plate. The chromatogram was developed in the first dimension with petroleum ether–acetone (140:60 v/v) and then in the second dimension with benzene–ethyl acetate (140:60 v/v) to about 2 cm from the edge of the plate.

Radiochemistry—Each plate was examined under a UV lamp (254 nm), and the spots were outlined with a pencil. The plate was cut close to the spot of acetylated acenocoumarol, which was scraped into a counting vial. Then 200 μl of methanol and 20 ml of scintillator solution were added. Four "blank" counting samples, four ^{3}H-standard samples (125.9 ng of ^{3}H-maprotiline in methanol), and four ^{14}C-standard samples (58.8 ng of ^{14}C-acenocoumarol in methanol) were counted together in a liquid scintillator spectrometer with a discriminator setting for simultaneous counting of tritium and carbon-14.

Data Processing—The calculation program subtracted the plasma or urine blanks from the ^{3}H-counts and then calculated a linear regression from the known concentrations and g (^{3}H − 100% cpm/ml of plasma or urine) (6, 7) before calculating the unknown concentrations from the linear regression.

The linear regression must be checked for each series of analyses from several concentrations (4 × 4) in the range expected for the study.

RESULTS AND DISCUSSION

Extraction—Acenocoumarol (I) was extracted only at acid pH (Fig. 1). After extraction, the solvent was washed to remove some plasma impurities extracted from the acid solution. It was then very important to have 1 ml of pH 7 buffer and 10 ml of organic phase (volume of organic phase/total volume = 10/11 = 0.9), because at pH 7 the solubility of I in the organic phase depended on the relative volumes of the organic and aqueous phases. When the ratio decreased, the solubility of I in the organic phase also decreased.

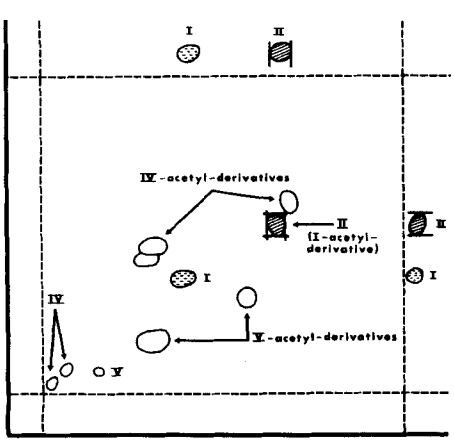

Figure 2—*TLC purification of II.*

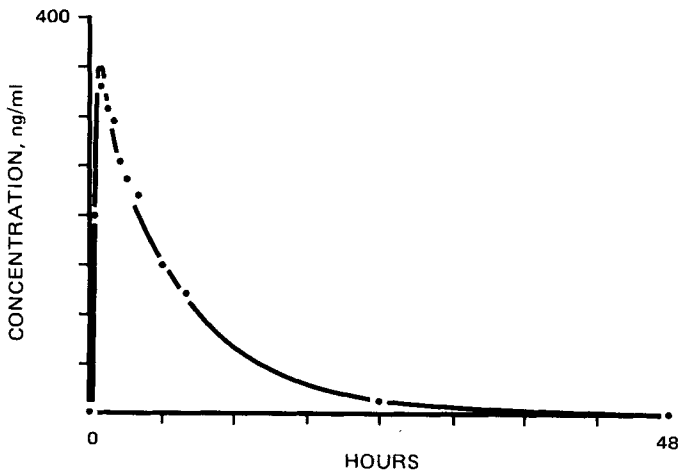

Figure 3—*Plasma concentrations of acenocoumarol as a function of time after the oral administration of a single dose of 8 mg to humans.*

Under the described conditions, I was satisfactorily extracted from plasma over a large range of concentrations (70–75% extraction).

Acetylation—Acenocoumarol was acetylated under the same experimental conditions as maprotiline (6). The overall yield (≃ 20–30% after thin-layer purification) was not improved by the addition of pyridine. The elemental analysis and mass spectrum of II corresponded to those of the monoacetylated compound.

Calibration Curves—Several known concentrations of I were prepared in plasma, urine, or water. After extraction and derivatization, the values of g (^{3}H − 100% cpm/ml) were calculated, and a linear regression was obtained from known concentrations and g. For plasma:

$$^3\text{H} - 100\%\ \text{cpm/ml} = 107.72 \times \text{concentration (ng/ml)} + 2{,}871.4 \qquad r = 0.999 \qquad \text{(Eq. 1)}$$

For urine:

$$^3\text{H} - 100\%\ \text{cpm/ml} = 83.33 \times \text{concentration (ng/ml)} + 2{,}662.6 \qquad r = 0.997 \qquad \text{(Eq. 2)}$$

For the aqueous solution:

$$^3\text{H} - 100\%\ \text{cpm/ml} = 88.43 \times \text{concentration (ng/ml)} + 2{,}024.6 \qquad r = 0.997 \qquad \text{(Eq. 3)}$$

The slopes of the calibration curves were different because the ^{3}H-acetic anhydride solutions were not the same for plasma as for urine and the aqueous solution.

Sensitivity and Accuracy—Good determinations could be obtained in plasma to 8 ng/ml with a 95% confidence interval from 7.5 to 9.4 (± 11%) and a standard error percent of 4.45 for n = 7 (Table I).

Specificity—TLC purification of II was elaborated to avoid any interference of metabolites and their acetyl derivatives. Figure 2 shows that a satisfactory separation was achieved. The described method was verified in the presence of each metabolite except VII, which was not available. None of these metabolites interfered. Owing to their close structural relationship, VII should behave similarly to VI and should also not interfere with II. Therefore, the method can be considered specific for the analysis of plasma samples.

It also can be considered specific for urine, after verification for VII, but practically no further acenocoumarol was found in urine after administration of a 12-mg dose[2].

Application in Pharmacokinetic Study[9]—Acenocoumarol (8 mg) was administered to one healthy volunteer. Before administration and at specified times after administration (0.5, 1, 1.5, 2, 2.5, 3, 4, 6, 8, 24, and 48 hr), 10-ml blood samples were collected in heparinized tubes. After centrifugation, the plasma was immediately deep frozen and kept at −20° until analysis. The determinations were made in duplicate (Fig. 3).

REFERENCES

(1) R. A. O'Reilly, P. M. Aggeler, M. S. Hoag, and G. L. Leong, *Thromb. Diath. Haemorrh.*, 8, 82 (1962).

[9] To be published.

(2) J. P. Tillement, S. R. Charonnat, and C. Blatrix, *Therapie*, **20**, 1311 (1965).
(3) E. Fidelius, *Z. Anal. Chem.*, **256**, 131 (1971).
(4) F. W. Deckert, *J. Chromatogr.*, **64**, 355 (1972).
(5) F. A. De Wolf, A. A. M. Kassenaar, E. A. Loeliger, and W. Van der Slik, *Ann. Biol. Clin.*, **33**, 224 (1975).
(6) W. Riess, *Anal. Chim. Acta*, **68**, 363 (1974).
(7) G. T. Okita, J. J. Kabara, F. Richardson, and G. L. Leroy, *Nucleonics*, **15**, 111 (1957).

ACKNOWLEDGMENTS AND ADDRESSES

Received April 13, 1976, from *Ciba-Geigy Biopharmaceutical Research Center, B. P. 130, 92505 Rueil-Malmaison, France.*

Accepted for publication September 1, 1976.

The authors are grateful to Dr. J. W. Faigle and Dr. W. Dieterle for helpful discussions and encouragement and to Dr. W. Küng for synthesis of ^{14}C-acenocoumarol.

[x] To whom inquiries should be directed.

Effect of Sleep on Bioavailability of Tetracycline

JOSEPH ADIR [x] and WILLIAM H. BARR [*]

Abstract □ The effect of sleep on the bioavailability of tetracycline was studied using 250-mg tetracycline hydrochloride capsules from two commercial sources. One capsule of each brand was given to each of 12 healthy volunteers on two separate occasions. On one occasion, the subject ingested the drug upon arising in the morning and remained ambulatory (ambulatory trial). On the other, the subject awakened during the night, ingested the capsule, and resumed sleep (sleep trial). Bioavailability was assessed from the cumulative amount of drug excreted in the urine during the 96 hr following drug intake. While there was no significant difference in the bioavailability of one brand between the ambulatory and sleep trials, the bioavailability of the other decreased an average 27% ($p < 0.01$) in the sleep trial. Also, the difference between the bioavailability of the two preparations was not discernible in ambulatory subjects, but it was statistically significant ($p < 0.05$) in the sleep trial. The impaired bioavailability appears to result from decreased dissolution of one brand in the high gastric pH occurring at night. These findings raise questions as to the predictability of bioavailability studies in ambulatory subjects relative to the actual use of drug products, which are frequently administered during conditions of bed rest or sleep.

Keyphrases □ Tetracycline—bioavailability, different commercial capsules, effect of sleep, humans □ Bioavailability—tetracycline, different commercial capsules, effect of sleep, humans □ Sleep—effect on bioavailability of tetracycline, different commercial capsules, humans □ Antibacterials—tetracycline, bioavailability, different commercial capsules, effect of sleep, humans

The pharmacokinetics and pharmacodynamics of several drugs including sulfonamides, penicillin, streptomycin, griseofulvin, minocycline, indomethacin, and levodopa (1–8) may be subject to diurnal variations and may display considerable dependency on changes in the posture and state of wakefulness. Observed changes in blood drug levels, urinary excretion, and pharmacological effects generally were attributed to changes in distribution or elimination. However, decreased systemic availability would also provide a reasonable explanation for some observed results.

Gastric pH increases at night (9), and body position may greatly affect gastric emptying (10). These changes might significantly affect the absorption of some drugs, such as tetracycline, whose dissolution is pH dependent. Absorption of tetracycline from solid dosage forms is dependent upon rapid dissolution in acidic gastric fluids and subsequent gastric emptying of dissolved drug into the upper small intestine where absorption occurs (11–15).

The solubility and dissolution rate of tetracycline are much smaller at duodenal pH (4–5) than gastric pH (1–3), which would result in the decreased absorption of products that are incompletely dissolved in gastric fluids when emptying occurs (14, 15). Furthermore, decreased absorption of tetracycline from solid dosage forms occurs when gastric pH is increased. Concomitant administration of sufficient sodium bicarbonate to increase the gastric pH to 4–5 resulted in a 50% decrease in the bioavailability of tetracycline (14). In this study, tetracycline absorption in one individual who returned to sleep after drug ingestion was dramatically less than in all other subjects (14).

These considerations prompted this study on the bioavailability of two tetracycline products in ambulatory and sleeping individuals.

EXPERIMENTAL

Twelve apparently healthy volunteers (11 males and one female) participated. Each subject was administered one capsule containing 250 mg (labeled amount) of tetracycline hydrochloride with 200 ml of water either upon arising in the morning (ambulatory trial) or during the night (sleep trial). Two preparations, Brands A[1] and B[2], containing the same labeled amount of the drug[3], were used in each ambulatory and sleep trial, so that each subject participated in four separate trials. Brand A was tested first, and the trial condition was assigned randomly to the subjects by drawing lots. Then Brand B was ingested by all subjects in the sleep trial, followed by its administration to the subjects while ambulatory. At least 2 weeks separated each trial.

In the ambulatory trial, the drug was ingested in the morning between 8:00 and 9:00 am following an overnight fast. No food was allowed for at least the next 4 hr, and the subjects remained ambulatory for the rest of the day. In the sleep trial, the subjects were instructed to awaken at about the midpoint of their sleeping time, ingest the capsule, and directly resume sleep. Breakfast was taken upon arising in the morning, after which the subjects remained ambulatory. The average sleeping time was 6–8 hr, and the drug was ingested at about 4:00 am. Therefore, in both trials, food was withheld for at least 4 hr before and after drug ingestion.

No attempt was made to control the composition of the meal of the evening before or the day after drug administration, except that milk and dairy products were strictly forbidden on the 1st day of the study. No other medication was allowed for at least 7 days before and throughout the study. Immediately before taking the drug, the subjects voided completely, and this sample was saved and used as the urine blank sample. Urine was collected every hour for the first 8 hr after drug ingestion in the ambulatory trial or upon arising in the sleep trial and then

[1] Lot 202-101, Lederle Labs, Pearl River, N.Y.
[2] Lot 23/G, Gyma Lab., Forest Hills, N.Y.
[3] Chemical assay indicated that the amounts of drug present in Brands A and B were 262 and 258 mg, respectively.

(2) J. P. Tillement, S. R. Charonnat, and C. Blatrix, *Therapie*, **20**, 1311 (1965).
(3) E. Fidelius, *Z. Anal. Chem.*, **256**, 131 (1971).
(4) F. W. Deckert, *J. Chromatogr.*, **64**, 355 (1972).
(5) F. A. De Wolf, A. A. M. Kassenaar, E. A. Loeliger, and W. Van der Slik, *Ann. Biol. Clin.*, **33**, 224 (1975).
(6) W. Riess, *Anal. Chim. Acta*, **68**, 363 (1974).
(7) G. T. Okita, J. J. Kabara, F. Richardson, and G. L. Leroy, *Nucleonics*, **15**, 111 (1957).

ACKNOWLEDGMENTS AND ADDRESSES

Received April 13, 1976, from *Ciba-Geigy Biopharmaceutical Research Center, B. P. 130, 92505 Rueil-Malmaison, France.*

Accepted for publication September 1, 1976.

The authors are grateful to Dr. J. W. Faigle and Dr. W. Dieterle for helpful discussions and encouragement and to Dr. W. Küng for synthesis of ^{14}C-acenocoumarol.

[x] To whom inquiries should be directed.

Effect of Sleep on Bioavailability of Tetracycline

JOSEPH ADIR [x] and WILLIAM H. BARR [*]

Abstract □ The effect of sleep on the bioavailability of tetracycline was studied using 250-mg tetracycline hydrochloride capsules from two commercial sources. One capsule of each brand was given to each of 12 healthy volunteers on two separate occasions. On one occasion, the subject ingested the drug upon arising in the morning and remained ambulatory (ambulatory trial). On the other, the subject awakened during the night, ingested the capsule, and resumed sleep (sleep trial). Bioavailability was assessed from the cumulative amount of drug excreted in the urine during the 96 hr following drug intake. While there was no significant difference in the bioavailability of one brand between the ambulatory and sleep trials, the bioavailability of the other decreased an average 27% ($p < 0.01$) in the sleep trial. Also, the difference between the bioavailability of the two preparations was not discernible in ambulatory subjects, but it was statistically significant ($p < 0.05$) in the sleep trial. The impaired bioavailability appears to result from decreased dissolution of one brand in the high gastric pH occurring at night. These findings raise questions as to the predictability of bioavailability studies in ambulatory subjects relative to the actual use of drug products, which are frequently administered during conditions of bed rest or sleep.

Keyphrases □ Tetracycline—bioavailability, different commercial capsules, effect of sleep, humans □ Bioavailability—tetracycline, different commercial capsules, effect of sleep, humans □ Sleep—effect on bioavailability of tetracycline, different commercial capsules, humans □ Antibacterials—tetracycline, bioavailability, different commercial capsules, effect of sleep, humans

The pharmacokinetics and pharmacodynamics of several drugs including sulfonamides, penicillin, streptomycin, griseofulvin, minocycline, indomethacin, and levodopa (1–8) may be subject to diurnal variations and may display considerable dependency on changes in the posture and state of wakefulness. Observed changes in blood drug levels, urinary excretion, and pharmacological effects generally were attributed to changes in distribution or elimination. However, decreased systemic availability would also provide a reasonable explanation for some observed results.

Gastric pH increases at night (9), and body position may greatly affect gastric emptying (10). These changes might significantly affect the absorption of some drugs, such as tetracycline, whose dissolution is pH dependent. Absorption of tetracycline from solid dosage forms is dependent upon rapid dissolution in acidic gastric fluids and subsequent gastric emptying of dissolved drug into the upper small intestine where absorption occurs (11–15).

The solubility and dissolution rate of tetracycline are much smaller at duodenal pH (4–5) than gastric pH (1–3), which would result in the decreased absorption of products that are incompletely dissolved in gastric fluids when emptying occurs (14, 15). Furthermore, decreased absorption of tetracycline from solid dosage forms occurs when gastric pH is increased. Concomitant administration of sufficient sodium bicarbonate to increase the gastric pH to 4–5 resulted in a 50% decrease in the bioavailability of tetracycline (14). In this study, tetracycline absorption in one individual who returned to sleep after drug ingestion was dramatically less than in all other subjects (14).

These considerations prompted this study on the bioavailability of two tetracycline products in ambulatory and sleeping individuals.

EXPERIMENTAL

Twelve apparently healthy volunteers (11 males and one female) participated. Each subject was administered one capsule containing 250 mg (labeled amount) of tetracycline hydrochloride with 200 ml of water either upon arising in the morning (ambulatory trial) or during the night (sleep trial). Two preparations, Brands A[1] and B[2], containing the same labeled amount of the drug[3], were used in each ambulatory and sleep trial, so that each subject participated in four separate trials. Brand A was tested first, and the trial condition was assigned randomly to the subjects by drawing lots. Then Brand B was ingested by all subjects in the sleep trial, followed by its administration to the subjects while ambulatory. At least 2 weeks separated each trial.

In the ambulatory trial, the drug was ingested in the morning between 8:00 and 9:00 am following an overnight fast. No food was allowed for at least the next 4 hr, and the subjects remained ambulatory for the rest of the day. In the sleep trial, the subjects were instructed to awaken at about the midpoint of their sleeping time, ingest the capsule, and directly resume sleep. Breakfast was taken upon arising in the morning, after which the subjects remained ambulatory. The average sleeping time was 6–8 hr, and the drug was ingested at about 4:00 am. Therefore, in both trials, food was withheld for at least 4 hr before and after drug ingestion.

No attempt was made to control the composition of the meal of the evening before or the day after drug administration, except that milk and dairy products were strictly forbidden on the 1st day of the study. No other medication was allowed for at least 7 days before and throughout the study. Immediately before taking the drug, the subjects voided completely, and this sample was saved and used as the urine blank sample. Urine was collected every hour for the first 8 hr after drug ingestion in the ambulatory trial or upon arising in the sleep trial and then

[1] Lot 202-101, Lederle Labs, Pearl River, N.Y.
[2] Lot 23/G, Gyma Lab., Forest Hills, N.Y.
[3] Chemical assay indicated that the amounts of drug present in Brands A and B were 262 and 258 mg, respectively.

Table I—Cumulative Amounts (Milligrams) of Tetracycline Excreted in Urine in 4 Days

Subject	Sex	Age	Weight, kg	Height, m	Brand A		Brand B	
					Ambulatory	Sleep	Ambulatory	Sleep
A	M	24	109	1.72	194.6	50.2	121.3	97.1
B	M	34	84	1.73	197.9	164.8	165.1	169.0
C	M	24	66	1.75	92.3	112.4	109.9	107.0
D	M	23	61.3	1.62	154.6	91.0	120.0	108.8
E	M	22	60	1.7	122.8	128.0	65.7	61.5
F	M	22	70.3	1.72	160.0	100.7	156.3	53.0
G	M	24	63.5	1.7	145.2	133.8	78.4	73.8
H	F	25	64.4	1.62	147.2	131.3	177.1	120.0
I	M	24	63.5	1.73	125.2	152.4	154.9	124.3
J	M	25	77.2	2.6	171.4	119.8	171.2	104.3
K	M	23	68.1	2.67	97.5	133.0	98.3	22.7
L	M	31	72.1	1.72	126.8	84.0	52.2	26.4
Mean					144.6	116.8	122.5	89.0
SD					33.7	31.5	42.9	42.8

ad libitum for a total of 96 hr. The volume of each sample was measured and an aliquot was frozen until analyzed.

The amount of tetracycline in the two preparations and the unchanged drug excreted in urine were assayed spectrophotofluorometrically[4] by the method of Kohn (16). This assay is specific for tetracycline and has a high degree of precision, as indicated by the 3–6% variations in replicate determinations of biological samples (16).

The results were analyzed according to the analysis of variance of split-plot in time design (17). Differences between the means of the four trials were tested for significance by Duncan's new multiple-range analysis (18).

RESULTS

The cumulative amounts of intact tetracycline excreted in urine in 96 hr (Qu^{∞}) in the four trials are reported in Table I. Large inter- and intrasubject variations were seen in the urinary recoveries. Six subjects (A, B, D, F, H, and J) of the 12 ingesting Brand A in the sleep trial had between an 11 and 74% decrease in Qu^{∞} compared with the ambulatory trial of the same brand. However, in four other subjects (C, I, K, and L), a 22–36% increase in Qu^{∞} in the sleep trial was observed. Subjects E and G excreted essentially the same amount of tetracycline in the sleep and ambulatory trials.

When Brand B was taken in the sleep trial, eight subjects (A, D, F, H, I, J, K, and L) showed a 10–77% decrease in Qu^{∞} compared with drug ingestion while ambulatory. The other four subjects excreted virtually the same amount of tetracycline in the sleep and ambulatory trials. Unlike with Brand A, no increase in Qu^{∞} was observed when Brand B was taken in the sleep trial.

The overall mean and standard deviation of the Qu^{∞} obtained with Brand A in the ambulatory and sleep trials were 144.6 ± 33.7 and 116.8 ± 31.5 mg, respectively. The mean Qu^{∞} and standard deviation of Brand B were 122.5 ± 42.9 mg in ambulatory subjects compared to 89.0 ± 42.8 mg in the same subjects taking the drug in the sleep trial, representing a decrease of about 27%.

Analysis of variance of these data and the multiple-range comparison between means are shown in Table II. Sleep had a differential effect on the two brands of tetracycline. Whereas no statistically significant difference in the mean Qu^{∞} was observed between the sleep and ambulatory trials of Brand A, the average urinary recovery of Brand B in the sleep trial was significantly reduced ($p < 0.01$) compared with its mean Qu^{∞} in the ambulatory subjects. Most importantly, in spite of the lack of significant difference between the two preparations in the ambulatory subjects, the difference between their mean Qu^{∞} in the sleep trials was statistically significant ($p < 0.05$).

If urinary recovery from Brand A during the ambulatory trial is taken as a standard, then Brand B administered at night during sleep showed a highly significant ($p < 0.01$), almost 39% decrease in the cumulative amount of tetracycline excreted in urine (Fig. 1).

Figure 2 shows a representative plot (Subject J) of urinary excretion rates of tetracycline as a function of time in the sleep and ambulatory trials. The inset figure indicates that the elimination kinetics of the drugs in the postabsorptive-distributive phase were essentially identical for both brands in these trials. Similar results were observed in all other subjects.

DISCUSSION

Generally, a decrease in urinary recovery of a drug under different experimental conditions may result from changes in several events involved in its absorption and/or disposition[5] including: (*a*) decreased renal excretion, (*b*) increased extrarenal elimination from the systemic circulation such as hepatic metabolism and biliary or other clearances, and (*c*) a decrease in the amount of drug reaching the systemic circulation (bioavailability).

A decrease in bioavailability may be characterized further as resulting from a decrease in the fraction of drug available for absorption from the luminal contents or an increase in the fraction of drug metabolized, stored in intestinal tissue, or cleared by biliary secretion during the initial transit through the hepatoportal system (first-pass effect).

Decrease in Elimination—The parallel slopes of the urinary excretion rate–time plots (Fig. 2) rule out the occurrence of changes in elimination kinetics during the postabsorptive-distributive phase (~8–10 hr after drug administration). However, this finding does not rule out the possibility of changes occurring in the elimination of tetracycline from the systemic circulation during the first few hours following its administration when the subjects were either sleeping or ambulatory. Since urinary excretion parameters were employed in the present study, it is logical to consider the possibility of decreased renal elimination at night during sleep as a result of alteration in urine pH or renal function.

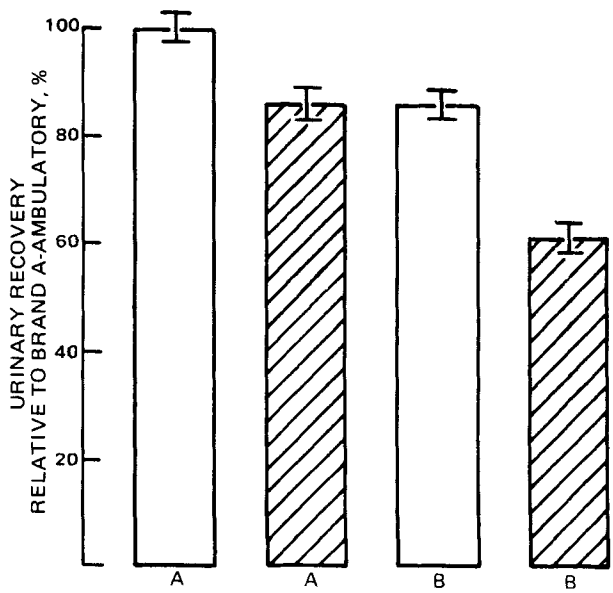

Figure 1—*Percent mean urinary recovery relative to Brand A administered to ambulatory subject when Brands A and B were administered to ambulatory subjects (open bars) and during sleep (hatched bars). The standard errors of the mean are indicated by the horizontal lines.*

[4] Aminco-Bowman model 4-8202, American Instrument Co., Silver Spring, Md.

[5] Changes in distribution are excluded from this discussion because of the obvious lack of reference to its parameters in the urinary excretion data.

Table II—Analysis of Variance[a] of the Cumulative Amounts of Tetracycline Excreted in Urine in 4 Days

Source of Variation	Degrees of Freedom	Sums of Squares	Mean Sums of Squares	F	p
Subjects	11	34,601.9	3,145.6	3.27	<0.10
Conditions[b]	1	11,303.7	11,303.7	11.74	<0.05
Residual error	11	10,586.8	962.4		
Total	23	56,492.4			
Brands	1	7,465.0	7,465.0	8.49	<0.05
Brands × subjects	11	9,036.3	821.5	0.93	>0.10
Conditions[b] × brands	1	97.5	97.5	0.11	>0.10
Residual error	11	9,669.3	879.0		
Total	47	82,760.5			

Comparison of Trial Means[c]

$A_{ambulatory}$ *versus* A_{sleep}	Not significant at 0.05 level
$A_{ambulatory}$ *versus* $B_{ambulatory}$	Not significant at 0.05 level
$A_{ambulatory}$ *versus* B_{sleep}	Significant at 0.01 level
A_{sleep} *versus* $B_{ambulatory}$	Not significant at 0.05 level
A_{sleep} *versus* B_{sleep}	Significant at 0.05 level
$B_{ambulatory}$ *versus* B_{sleep}	Significant at 0.01 level

[a] Split-plot in time design (17). [b] Refers to ambulatory and sleep conditions. [c] Duncan's new multiple-range test (18).

Elliot *et al.* (19) observed a 0.77–2.48 unit rise in urinary pH in 12 of 18 normal subjects after awakening in the morning compared with urinary pH at night. This rise in pH, termed the morning tide, lasted 2–3 hr after arising (19), occurred irrespective of food intake (20), and was part of the diurnal variation in urinary pH, which appeared to follow a pattern characteristic for a given individual (21). A similar increase in urinary pH was observed in humans upon assuming a recumbent posture (22).

Alkalinization of urine pH (~7.5) over 48 hr significantly increased the cumulative amount of tetracycline excreted in urine (23). Based on this study and the presumed occurrence of high urinary pH in the morning, subjects who ingest the tetracycline capsules at 4:00 am should show an *increase* in urinary recovery of the drug compared with the ambulatory trials in which the drug is taken at 8:00–9:00 am. This assumption is made because the sleep trial drug absorption, which lasts between 3 and 4 hr (24), is essentially complete upon awakening and the presumably high urinary pH enhances tetracycline excretion in urine; the ambulatory subjects, who take the drug upon arising, cannot absorb significant amounts during the time their urinary pH remains alkaline.

The results shown in Table I do not support this logical corollary. Only four subjects (C, I, K, and L) displayed an increase in Qu^{∞} in the sleep trial of Brand A that was not manifested in the sleep trial of Brand B as would be expected from the consistency of the urinary pH profile of individuals (21). In fact, three of these subjects (I, K, and L) had a 20–77% decrease in the urinary recovery of Brand B and the fourth showed a meager 3% reduction. In addition, comparison between the means of the four trials indicates that sleep caused a significant differential reduction in Qu^{∞} of Brand B (Table II). These facts are difficult to reconcile with the notion that the observed decreases in urinary recovery of the drug in the sleep trials are due to its reduced renal excretion as a result of changes occurring in urinary pH.

The other factor that would account for the decreased urinary excretion of tetracycline in the sleep trial is the physiological alterations of kidney function. Little information is available on the effect of sleep, bed rest, or recumbent posture on the function of this organ. In a recent study employing seven catheterized sleeping patients, within 2 min of the onset of rapid eye movement (REM) epochs, there was a marked decrease in the urine flow rate; however, the glomerular filtration rate in these patients remained unaffected (25). At the termination of the REM state, the urine flow rate increased even beyond the baseline value.

In a study of renal function in 18 normal male subjects at 4-hr intervals over 24 hr (26), there was no change in renal plasma flow during sleep at night as compared to bed rest during the day. There was a slight, but statistically significant, drop in the glomerular filtration rates during the REM sleep between 12:00 midnight and 4:00 am, after which the glomerular filtration rate achieved a normal value. The urine flow rate, however, was diminished significantly during sleep, with the greatest drop occurring during the REM periods. This drop in the urine flow rate was attributed to increased tubular reabsorption of water (26). In another study, prolonged bed rest had no effect on the urine flow rate or kidney function (27).

These findings indicate that while the glomerular filtration rate of the subjects ingesting tetracycline at about 4:00 am could be considered reasonably similar to that of the ambulatory subjects, a comparison between their urine flow rates is difficult to make. It is particularly difficult to conjecture the effect of arising to ingest the drug and then resuming sleep on the urine flow rate. Nevertheless, other investigators found that changes in the urine flow rate had no effect on the renal clearance of tetracycline and three other analogs (28, 29). Although no information is available on the effect of this parameter on the fraction of tetracycline ultimately excreted in urine, it is inconceivable that such an effect would be demonstrated in the sleep trial of only one brand of the drug and not the other.

Increase in Extrarenal Elimination—The tetracyclines are not appreciably metabolized (30). In addition, biliary excretion of tetracycline in the rat does not constitute a major route of elimination, since 95% of the amount excreted *via* the bile is absorbed from the small intestine (31). Rather, excretion in the lower part of the small intestine and colon is believed to account for the extrarenal elimination, as stipulated for another analog of this antibiotic (32). If this is also the other extrarenal route of elimination of tetracycline in humans, then, to account for the observed decrease in Qu^{∞}, a compensatory increase in its elimination *via* this route must be expected. Although this possibility cannot be ruled out, some physiological modalities of sleep provide no support for its occurrence. For instance, blood pressure, which may affect organ perfusion, drops and intestinal function proceeds normally during sleep (33).

On the other hand, if extrarenal elimination of tetracycline in humans occurs *via* biliary excretion, this route of elimination may actually be diminished at night. Bile collected through a fistula in humans was lower at night, with a minimum between 1:00 and 5:00 am (34); the same was true for rabbits which are more active at night (35).

An increase in any other extrarenal route of elimination of tetracycline during sleep is unlikely because of the difficulty to explain its differential occurrence with two preparations of the same drug.

Decrease in Bioavailability—Previously (15) in ambulatory subjects, urinary excretion rates of tetracycline were proportional to serum concentrations, and the cumulative amount excreted in urine, Qu^{∞}, was proportional to the total amount absorbed as assessed by the area under the serum concentration–time curve (AUC). In both of these relationships, the proportionality constant, as predicted by theory, was equal to the renal clearance of the drug, namely 80–90 ml/min. Since changes in the glomerular filtration rate, urine pH, and renal and extrarenal elimination have been ruled out implicitly, the observed decrease in Qu^{∞} when tetracycline capsules are taken during sleep more likely represents a decrease in the bioavailability of the drug relative to its administration to ambulatory subjects.

Sleep reportedly causes a decrease in gastric, salivary, and lacrimal secretion, but it has no effect on intestinal function (33). The decrease in gastric acidity is likely to affect the dissolution of a drug such as tetracycline (14), which is favored by low pH, thereby causing a decrease in the extent of its bioavailability during sleep[6]. No information is available on the effect of sleep on gastric emptying, and its contribution to the decreased bioavailability at night cannot be ruled out. However, an increase in the fraction eliminated during the first pass through the hepatoportal system may be rejected on the basis of a lack of evidence

[6] Because of the inherent limitations of urinary excretion studies, alteration in the absorption rate of tetracycline at sleep cannot be established.

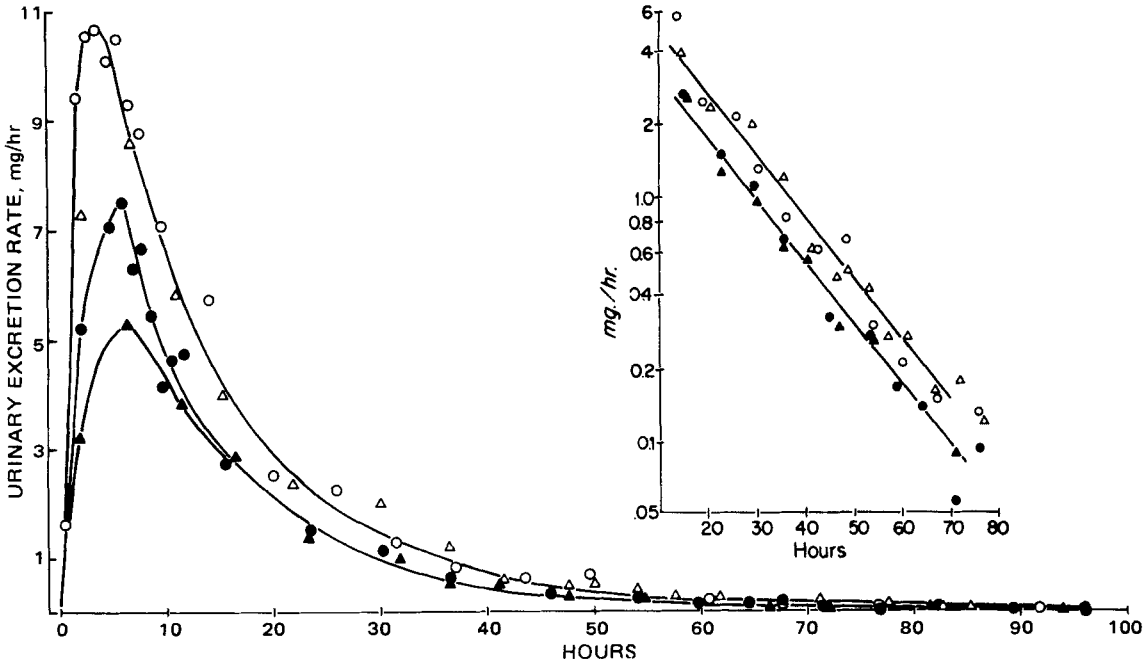

Figure 2—*Representative urinary excretion rates* versus *time plots for Subject J ingesting a tetracycline hydrochloride capsule while ambulatory (open symbols) and during sleep (closed symbols). Data for Brand A are designated by circles; Brand B by triangles. The excretion rates of the two brands in the ambulatory phase (open symbols) are superimposable.*

for the hepatic or biliary clearances of tetracycline (30–32).

In addition to dissolution, other important considerations suggest and possibly contribute to the decreased bioavailability of tetracycline during sleep. While the difference in the mean Qu^{∞} between the two brands in the 12 ambulatory subjects was not large enough to be statistically significant, the difference between them in the sleep trials was significant (Table II). In other words, differences between the bioavailability of the two brands conceivably could have been demonstrated in a larger number of *ambulatory* subjects, but only 12 *sleeping* subjects were needed to detect these bioavailability differences.

In addition, the bioavailability of Brand A in the ambulatory subjects was statistically similar to its bioavailability in the sleep trial, but it was almost 39% greater ($p < 0.01$) than the bioavailability of Brand B in the sleep trial (Fig. 1). Poor formulation, coupled with the sleep effect, could have produced the marked impairment in the bioavailability of Brand B. This situation is implied also by the lack of interaction between brands and conditions (Table II), which may characterize an additive effect between two factors (36).

The difference in formulation is illustrated also by the intersubject variability of the two brands. In general, this variability was smaller in Brand A than B. The coefficients of variation for A in the ambulatory and sleep trials were 23.3 and 27%, respectively; the coefficient of variation of B in ambulatory subjects was 35%, compared with 48% in the same subjects ingesting the drug during sleep. This increased variability is characteristic of products with low bioavailability (37).

CONCLUSIONS

The results of the present study involving two brands of tetracycline under the specific conditions of the trials indicate that the ingestion of one brand of tetracycline hydrochloride capsule during sleep resulted in a decrease in the bioavailability of the drug compared with its administration to ambulatory subjects. Obviously, these results cannot be extrapolated to other drugs or even other brands or lots of the same drug. In addition, although it was previously shown that differences between tetracycline products observed in single-dose studies are quantitatively predictive of multiple-dose plasma levels in ambulatory subjects (15), further studies are needed to determine whether the effect of sleep also is observed upon multiple-dose administration.

These findings, however, provide one example of an interaction between physiological and formulation variables which must be considered in the design and interpretation of bioavailability studies. Questions are raised as to the predictability of ambulatory studies relative to the actual clinical use of drug products frequently administered during conditions of bed rest or sleep. Most important is the fact that differences in products that were not statistically demonstrable in the usual ambulatory subjects were evident in the more clinically realistic situation involving sleep.

REFERENCES

(1) L. Dettli and P. S. Spring, *Helv. Med. Acta*, **33**, 191 (1966).

(2) H. Schmidt and K. Roholt, *Acta Pathol. Microbiol. Scand.*, **68**, 396 (1966).

(3) G. Levy, *J. Pharm. Sci.*, **56**, 928 (1967).

(4) H. R. C. Riches, *Lancet*, **1**, 540 (1954).

(5) P. Kabasakalian, M. Katz, B. Rosenkrantz, and E. Townley, *J. Pharm. Sci.*, **59**, 595 (1970).

(6) B. Bernard, E. J. Ying, and H. J. Simon, *J. Clin. Pharmacol.*, **11**, 332 (1971).

(7) E. C. Huskisson and F. D. Hart, *Practitioner*, **208**, 248 (1972).

(8) G. Aguggini, M. Meucci, and G. Reina, *Curr. Ther. Res.*, **14**, 749 (1972).

(9) H. W. Davenport, "Physiology of the Digestive Tract," 2nd ed., Year Book Medical Publishers, Chicago, Ill., 1966, p. 104.

(10) T. R. Bates and M. Gibaldi, in "Current Concepts in the Pharmaceutical Sciences: Biopharmaceutics," J. Swarbrick, Ed., Lea & Febiger, Philadelphia, Pa., 1970, p. 74.

(11) W. C. Barringer, W. Schultz, G. M. Sieger, and R. A. Nash, *Am. J. Pharm.*, **146**, 179 (1974).

(12) J. L. Colaizzi and P. R. Klink, *J. Pharm. Sci.*, **58**, 1184 (1969).

(13) M. H. Pindel, K. M. Cull, K. M. Doran, and H. L. Dickison, *J. Pharmacol. Exp. Ther.*, **125**, 287 (1959).

(14) W. H. Barr, J. Adir, and L. K. Garrettson, *Clin. Pharmacol. Ther.*, **12**, 779 (1971).

(15) W. H. Barr, L. M. Gerbracht, K. Letcher, M. Plant, and N. Strahl, *ibid.*, **13**, 97 (1972).

(16) K. W. Kohn, *Anal. Chem.*, **33**, 862 (1961).

(17) R. G. D. Steel and J. H. Torrie, "Principles and Procedures of Statistics," McGraw-Hill, New York, N.Y., 1960, p. 242.

(18) D. B. Duncan, *Biometrics*, **11**, 1 (1955).

(19) J. S. Elliot, R. F. Sharp, and L. Lewis, *J. Urol.*, **81**, 339 (1959).

(20) G. D. Barnett and F. E. Blume, *J. Clin. Invest.*, **17**, 159 (1938).

(21) M. A. Bridges and M. R. Mattice, *Am. J. Med. Sci.*, **200**, 84 (1940).

(22) P. R. Steinmetz and N. Bank, *J. Clin. Invest.*, **42**, 1142 (1963).

(23) J. M. Jaffe, J. L. Colaizzi, R. I. Poust, and R. H. McDonald, Jr., *J. Pharmacokinet. Biopharm.*, **1**, 267 (1973).

(24) J. T. Doluisio and L. W. Dittert, *Clin. Pharmacol. Ther.*, **10**, 690 (1969).

(25) A. J. Mandell, B. Chaffey, P. Brill, M. P. Mandell, J. Rodnick, R. T. Rubin, and R. Sheff, *Science*, **151**, 1558 (1966).
(26) J. H. Sirota, D. S. Baldwin, and H. Villarreal, *J. Clin. Invest.*, **29**, 187 (1950).
(27) M. Epstein, *J. Appl. Physiol.*, **30**, 366 (1971).
(28) C. M. Kunin, A. C. Dornbush, and M. Finland, *J. Clin. Invest.*, **38**, 1950 (1959).
(29) J. H. Sirota and A. Saltzman, *J. Pharmacol. Exp. Ther.*, **100**, 210 (1950).
(30) R. G. Kelly and D. A. Buyske, *ibid.*, **130**, 144 (1960).
(31) J. Adir, *J. Pharm. Sci.*, **64**, 1847 (1975).
(32) M. S. von Wittenan, T. M. Twomey, and A. C. Swindell, *Chemotherapy*, **17**, 26 (1972).
(33) J. G. Wagner, "Fundamentals of Clinical Pharmacokinetics," Drug Intelligence Publications, Hamilton, Ill., 1975, p. 372.
(34) B. Josephson and H. Larsson, *Scand. Arch. Physiol.*, **69**, 227 (1934).
(35) E. Forsgren, *Acta Med. Scand., Suppl.*, **59**, 95 (1934).
(36) G. W. Snedecor and W. G. Cochran, "Statistical Methods," Iowa State University Press, Ames, Iowa, 1974, p. 345.
(37) W. H. Barr, in "Current Concepts in the Pharmaceutical Sciences: Dosage Form Design and Bioavailability," J. Swarbrick, Ed., Lea & Febiger, Philadelphia, Pa., 1973, p. 58.

ACKNOWLEDGMENTS AND ADDRESSES

Received June 16, 1976, from the *Department of Pharmaceutics, School of Pharmacy, State University of New York at Buffalo, Buffalo, NY 14214.*

Accepted for publication September 14, 1976.

Presented at the Basic Pharmaceutics Section, APhA Academy of Pharmaceutical Sciences, Houston meeting, April 1972.

Supported in part by National Institutes of Health Grant IROICM 17068.

The authors are grateful to Dr. Richard P. Miller for suggestions in the statistical analysis of the data.

* Present address: Department of Pharmacy and Pharmaceutics, School of Pharmacy, Medical College of Virginia, Virginia Commonwealth University, Richmond, VA 23211.

[x] To whom inquiries should be directed. Present address: Departments of Pharmacy and Pharmacology-Toxicology, School of Pharmacy, University of Maryland, Baltimore, MD 21201.

Hydrolysis and Epimerization Kinetics of Hetacillin in Aqueous Solution

AKIRA TSUJI, YOSHITAKA ITATANI, and TSUKINAKA YAMANA [x]

Abstract □ Methods were developed for quantitating epimerization to epihetacillin and hydrolysis to ampicillin in the alkaline degradation of hetacillin, and both rates in deuterium oxide at 35° and in water at various temperatures were determined. In each case, plots of log k for the epimerization against pH or pD yielded straight lines with a positive slope, which verified the first-order dependence on the hydroxide ion or deuteroxide ion. The activation energy of the epimerization process was 21.2 kcal/mole. In aqueous solution at high pH, epimerization rather than conversion to ampicillin represents a major pathway of hetacillin degradation, although the β-lactam ring of the hetacillin molecule is highly resistant to attack by the hydroxide ion.

Keyphrases □ Hetacillin—epimerization and hydrolysis in aqueous solution, effect of pH and temperature □ Epimerization—hetacillin in aqueous solution, effect of pH and temperature □ Hydrolysis—hetacillin in aqueous solution, effect of pH and temperature □ Antibacterials—hetacillin, epimerization and hydrolysis in aqueous solution, effect of pH and temperature

Hetacillin, which was developed to improve the aqueous stability of concentrated ampicillin solutions and to increase oral absorption of ampicillin, is a condensation product of ampicillin and acetone (1) and is often used instead of ampicillin.

In the degradation of hetacillin (I) in aqueous solution, at least two reactions are possible: hydrolytic interconversion to ampicillin (II) (2, 3) and epimerization to 6-epihetacillin (III) (4), which produces inactive 6-epiampicillin (5). The rates of both hydrolysis (2, 3, 6) and epimerization (7) depend on pH and occur simultaneously (Scheme I). Although detailed kinetics of the hydrolysis of hetacillin to ampicillin were reported (2, 3, 6, 8–10), much less is known about the kinetic behavior of the C-6 epimerization reaction.

The present investigation was undertaken to develop methods for quantitating epimerization of hetacillin and to determine the rates of hydrolysis and epimerization of hetacillin in aqueous basic solution by utilizing NMR and optical rotatory dispersion spectroscopy. The preliminary NMR observations were reported previously (7).

EXPERIMENTAL

Materials—Hetacillin potassium[1] and ampicillin sodium[2] were used as supplied.

Epihetacillin was synthesized by a reported procedure (4). Two grams of hetacillin potassium was placed in 20 ml of distilled water, and the

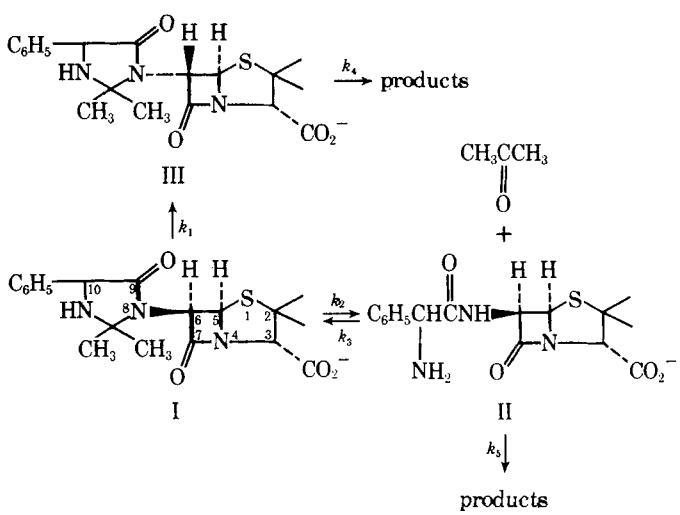

Scheme I

[1] Banyu Pharmaceutical Co., Tokyo, Japan.
[2] Takeda Chemical Ind., Osaka, Japan.

(25) A. J. Mandell, B. Chaffey, P. Brill, M. P. Mandell, J. Rodnick, R. T. Rubin, and R. Sheff, *Science*, **151**, 1558 (1966).
(26) J. H. Sirota, D. S. Baldwin, and H. Villarreal, *J. Clin. Invest.*, **29**, 187 (1950).
(27) M. Epstein, *J. Appl. Physiol.*, **30**, 366 (1971).
(28) C. M. Kunin, A. C. Dornbush, and M. Finland, *J. Clin. Invest.*, **38**, 1950 (1959).
(29) J. H. Sirota and A. Saltzman, *J. Pharmacol. Exp. Ther.*, **100**, 210 (1950).
(30) R. G. Kelly and D. A. Buyske, *ibid.*, **130**, 144 (1960).
(31) J. Adir, *J. Pharm. Sci.*, **64**, 1847 (1975).
(32) M. S. von Wittenan, T. M. Twomey, and A. C. Swindell, *Chemotherapy*, **17**, 26 (1972).
(33) J. G. Wagner, "Fundamentals of Clinical Pharmacokinetics," Drug Intelligence Publications, Hamilton, Ill., 1975, p. 372.
(34) B. Josephson and H. Larsson, *Scand. Arch. Physiol.*, **69**, 227 (1934).
(35) E. Forsgren, *Acta Med. Scand., Suppl.*, **59**, 95 (1934).
(36) G. W. Snedecor and W. G. Cochran, "Statistical Methods," Iowa State University Press, Ames, Iowa, 1974, p. 345.
(37) W. H. Barr, in "Current Concepts in the Pharmaceutical Sciences: Dosage Form Design and Bioavailability," J. Swarbrick, Ed., Lea & Febiger, Philadelphia, Pa., 1973, p. 58.

ACKNOWLEDGMENTS AND ADDRESSES

Received June 16, 1976, from the *Department of Pharmaceutics, School of Pharmacy, State University of New York at Buffalo, Buffalo, NY 14214.*

Accepted for publication September 14, 1976.

Presented at the Basic Pharmaceutics Section, APhA Academy of Pharmaceutical Sciences, Houston meeting, April 1972.

Supported in part by National Institutes of Health Grant IROICM 17068.

The authors are grateful to Dr. Richard P. Miller for suggestions in the statistical analysis of the data.

* Present address: Department of Pharmacy and Pharmaceutics, School of Pharmacy, Medical College of Virginia, Virginia Commonwealth University, Richmond, VA 23211.

[x] To whom inquiries should be directed. Present address: Departments of Pharmacy and Pharmacology-Toxicology, School of Pharmacy, University of Maryland, Baltimore, MD 21201.

Hydrolysis and Epimerization Kinetics of Hetacillin in Aqueous Solution

AKIRA TSUJI, YOSHITAKA ITATANI, and TSUKINAKA YAMANA [x]

Abstract □ Methods were developed for quantitating epimerization to epihetacillin and hydrolysis to ampicillin in the alkaline degradation of hetacillin, and both rates in deuterium oxide at 35° and in water at various temperatures were determined. In each case, plots of log k for the epimerization against pH or pD yielded straight lines with a positive slope, which verified the first-order dependence on the hydroxide ion or deuteroxide ion. The activation energy of the epimerization process was 21.2 kcal/mole. In aqueous solution at high pH, epimerization rather than conversion to ampicillin represents a major pathway of hetacillin degradation, although the β-lactam ring of the hetacillin molecule is highly resistant to attack by the hydroxide ion.

Keyphrases □ Hetacillin—epimerization and hydrolysis in aqueous solution, effect of pH and temperature □ Epimerization—hetacillin in aqueous solution, effect of pH and temperature □ Hydrolysis—hetacillin in aqueous solution, effect of pH and temperature □ Antibacterials—hetacillin, epimerization and hydrolysis in aqueous solution, effect of pH and temperature

Hetacillin, which was developed to improve the aqueous stability of concentrated ampicillin solutions and to increase oral absorption of ampicillin, is a condensation product of ampicillin and acetone (1) and is often used instead of ampicillin.

In the degradation of hetacillin (I) in aqueous solution, at least two reactions are possible: hydrolytic interconversion to ampicillin (II) (2, 3) and epimerization to 6-epihetacillin (III) (4), which produces inactive 6-epiampicillin (5). The rates of both hydrolysis (2, 3, 6) and epimerization (7) depend on pH and occur simultaneously (Scheme I). Although detailed kinetics of the hydrolysis of hetacillin to ampicillin were reported (2, 3, 6, 8–10), much less is known about the kinetic behavior of the C-6 epimerization reaction.

The present investigation was undertaken to develop methods for quantitating epimerization of hetacillin and to determine the rates of hydrolysis and epimerization of hetacillin in aqueous basic solution by utilizing NMR and optical rotatory dispersion spectroscopy. The preliminary NMR observations were reported previously (7).

EXPERIMENTAL

Materials—Hetacillin potassium[1] and ampicillin sodium[2] were used as supplied.

Epihetacillin was synthesized by a reported procedure (4). Two grams of hetacillin potassium was placed in 20 ml of distilled water, and the

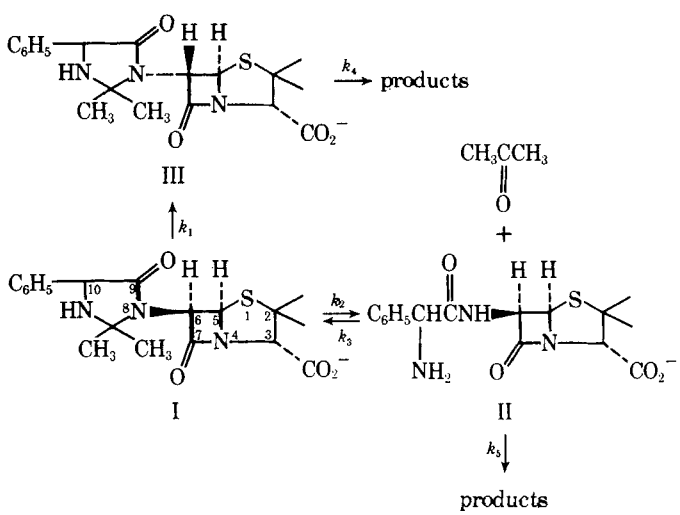

Scheme I

[1] Banyu Pharmaceutical Co., Tokyo, Japan.
[2] Takeda Chemical Ind., Osaka, Japan.

Table I—Chemical Shifts[a] (Parts per Million) of Protons of Hetacillin, Epihetacillin, and Ampicillin at 35°

Penicillin	Solvent	Proton								
		Phenyl	C-10	C-6	C-5	C-3	CCH_3			
Hetacillin potassium	Deuterium oxide[b]	7.48 m	4.76	5.08 d (4.0)	5.58 d (4.0)	4.30	1.67	1.55	1.51	1.46
Epihetacillin	Deuterium oxide[b]	7.44 m	4.85	4.74 d (2.0)	5.53 d (2.0)	4.39	1.61	1.56	1.52	1.48
	Dimethyl sulfoxide-d_6[c,d]	7.40 m	4.68	4.58 d (2.0)	5.38 d (2.0)	4.41	1.54	1.45	1.40	1.38
Ampicillin sodium	Deuterium oxide[b,e]	7.40	—[f]	5.46 s	5.46 s	4.19	1.51	1.47	—	—

[a] J values in Hertz in parentheses. [b] Relative to sodium 2,2,3,3-tetradeutero-3-(trimethylsilyl)propionate as internal standard. [c] Relative to tetramethylsilane as internal standard. [d] Assignments from Ref. 4. [e] Assignments from Ref. 13. [f] Not observable under water peak.

solution pH was maintained at 11.50 for 90 min at 25° with the aid of a pH-stat. The reaction solution was acidified to pH 4.5 with 1 N HCl at 0° to precipitate epihetacillin as a white powder. The collected crystals were washed exhaustively with cold water and dried over phosphorus pentoxide, mp 163° [lit. (4) mp 164–165°]. The identity was confirmed by elemental analysis, IR and NMR spectroscopy, and TLC.

Deuterium oxide (99.75%)[3], deuterium chloride (20% in deuterium oxide)[3], and sodium deuteroxide (40% in deuterium oxide)[3] were used for the preparation of the deuterium solvent buffer. All other chemicals were analytical reagent grade.

Apparatus—NMR spectra were recorded on a 100-MHz spectrometer[4] operating in a field sweep mode. Optical rotatory dispersion measurements were made on a recording spectropolarimeter[5], using thermostated 1-cm cells. The apparent pH values of the reaction solution were measured using microelectrodes and a pH meter[6], both before and at the end of the reaction. When no buffer or a low buffer capacity was used, a constant pH was maintained during the reaction by a pH-stat[7]. The pD values in deuterium solvent were obtained by proper correction (11) to the pH meter reading.

Kinetic Procedure—*NMR Study*—Hetacillin potassium (80 mg) was dissolved in 2 ml of deuterium oxide buffer at 35°. The time was recorded when the pH of the reaction buffer was corrected to the desired pD values by addition of 1 N NaOD by a pH-stat. As soon as possible after the pH adjustment, 1 ml of the reaction solution was placed in the NMR sample tube and left in the probe of the instrument[4].

The spectra were recorded at suitable time intervals, with sodium 2,2,3,3-tetradeutero-3-(trimethylsilyl)propionate as the internal reference. The temperature was maintained at 35 ± 0.5° by a variable-temperature probe unit[4]. The NMR spectra of the phenyl groups and C-3 protons were recorded with a twofold-scale expansion, and their signals were integrated on a spectrometer. The same procedure was used for epihetacillin and ampicillin sodium.

Optical Rotatory Dispersion Study—The reaction was initiated by dissolving exactly weighed hetacillin potassium or epihetacillin into a buffer preheated to a suitable temperature (±0.05°) to give a final concentration of 6×10^{-4} M. The 3 ml was replaced in a cell, which was thermally equilibrated (±0.05°) in the thermostated compartment of the spectrometer, and the optical rotatory dispersion change at 240 nm as the function of time was recorded. The reactions in deuterium solvent were also carried out in a similar manner as in water.

The buffers used in NMR and optical rotatory dispersion studies were NaD_2PO_4–Na_2DPO_4, $NaDCO_3$–Na_2CO_3, Na_2DPO_4–Na_3PO_4, H_3BO_3–$Na_2B_2O_7$, $NaHCO_3$–Na_2CO_3, and Na_2HPO_4–Na_3PO_4. The ionic strength of each solution was adjusted to 0.5 by the addition of potassium chloride. The pH and pD drifts during the reaction were within ±0.02 and ±0.05 unit for optical rotatory dispersion and NMR studies, respectively.

TLC Study—TLC was also employed to identify the degradation products and to verify the NMR and optical rotatory dispersion results. Aliquots, 10 μl, of the degradation solution ($\sim 1 \times 10^{-2}$ M) were applied to silica gel G precoated glass plates[3] (5 × 20 cm) of 250-μm thickness. Chromatograms were run for 15 cm in acetone–acetic acid (95:5). Spots were visualized by spraying 0.5% aqueous permanganate reagent or by exposure of the plates to iodine vapor.

Hetacillin, epihetacillin, ampicillin, and epiampicillin showed R_f values of 0.32, 0.45, 0.13, and 0.25, respectively. TLC of the standard solutions of the penicilloic acids of ampicillin and epihetacillin, synthesized by the method similar to that described by Schwartz and Delduce (12) for benzylpenicilloic acid, revealed virtually single spots with R_f values of 0.05 and 0.17, respectively. All spots, except for epiampicillin, were detected by TLC of the degradation solution of hetacillin at high pH.

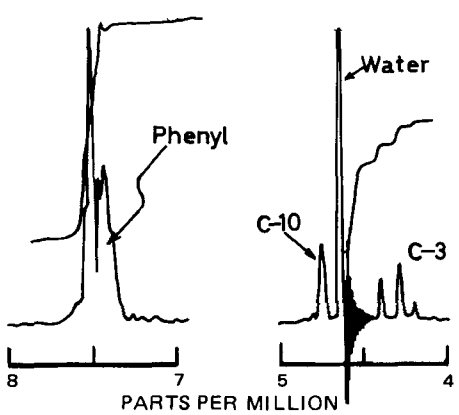

Figure 1—*NMR spectrum (100 MHz) of a synthetic mixture of hetacillin (50%), epihetacillin (40%), and ampicillin (10%) in 0.2* M *$NaDCO_3$–Na_2CO_3 buffer at pD 10.6.*

RESULTS AND DISCUSSION

Kinetic Study by NMR Spectroscopy—Table I summarizes the 100-MHz spectral data of hetacillin, epihetacillin, and ampicillin in deuterium oxide and dimethyl sulfoxide-d_6. Assignments were made on the basis of previous results (4, 13). Although the principal differences in the spectra of the two epimers were due to the characteristic protons at C-5 and C-6 (J = 4.0 Hz in hetacillin and J = 2.0 Hz in epihetacillin), these signal areas were unsuitable for monitoring the kinetics of hetacillin degradation because of considerable interference of other proton signals.

The chemical shifts for the C-3 methine groups differed by 0.1 ppm

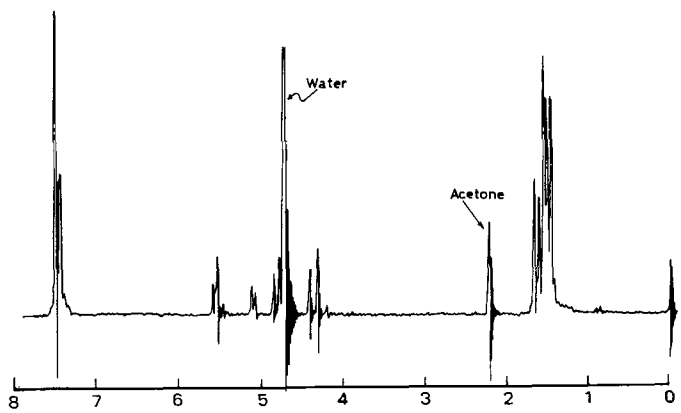

Figure 2—*NMR spectrum (100 MHz) of a reaction mixture of hetacillin after 40 min in 0.2* M *$NaDCO_3$–Na_2CO_3 buffer at pD 10.6 and 35°.*

[3] E. Merck AG, Darmstadt, West Germany.
[4] JNM-PS-100 NMR spectrometer, Tokyo, Japan.
[5] JASCO ORD-UV-CD-5 optical rotatory dispersion recorder, Tokyo, Japan.
[6] Model PHM-26, Radiometer, Copenhagen, Denmark.
[7] Radiometer pH-stat titrimeter assembly consisting of a PHM-26 pH meter, a TTT11 titrator, an SBR3 titrigraph, and an ABU12b autoburet.

Table II—Recovery of Hetacillin, Epihetacillin, and Ampicillin from Synthetic Mixtures by NMR Spectroscopic Method

Sample	Quantities Added, %			Quantities Found, %[a]		
	Hetacillin	Epihetacillin	Ampicillin	Hetacillin	Epihetacillin	Ampicillin
1	95	0	5	93	0	6
2	75	0	25	75	0	25
3	50	50	0	50	52	0
4	45	55	0	44	56	0
5	50	40	10	48	42	10
6	25	60	15	26	62	15

[a] Calculated using Eq. 1.

among these β-lactam compounds and their β-lactam cleavage products and provided the best means for quantifying epimerization and also hydrolysis of hetacillin. A typical NMR spectrum of a synthetic mixture of hetacillin (50%), epihetacillin (40%), and ampicillin (10%) in 0.2 *M* carbonate buffer at pD 10.6 is depicted in Fig. 1. Signals due to the phenyl groups in these compounds all fell in the area of 7.40–7.50 ppm. If the total integration values for the range represent 100% of the phenyl groups present, then the amount of the three compounds may be calculated from each integrated value of the respective C-3 proton as follows:

$$\text{percent compound} = (5I/I_T) \times 100 \qquad \text{(Eq. 1)}$$

where I_T = total integral value of the phenyl groups in the area of 7.40–7.50 ppm, and I = integral value of the C-3 methine proton for hetacillin, epihetacillin, or ampicillin.

The recovery of known synthetic mixtures of the three compounds at lower pD than 10.6 was satisfactory, with standard deviation of less than ±2% (Table II). Although such tests at a more alkaline pD gave relatively poor recovery for hetacillin and epihetacillin because of rapid epimerization and for ampicillin because of facile β-lactam cleavage, each concentration in the kinetic solutions at the desired time after hetacillin dissolution in such a high alkaline buffer at the kinetic temperature might be determined reasonably by this analytical method.

NMR spectra of the degradation solution of hetacillin in alkaline deuterium oxide solution showed that each proton for hetacillin at 4.30 (C-3), 5.08 (C-6), and 4.76 (C-10) ppm decreased in intensity, accompanied by an increase and then a decrease in intensity of proton resonance at 4.39 ppm due to the C-3 proton and at 4.85 ppm due to the C-10 proton of epihetacillin and at 4.19 ppm due to the C-3 proton of ampicillin. Two signals also appeared at 3.30 and 3.52 ppm, assigned to the C-3 protons of the β-lactam ring opening products, probably the penicilloic acids, of ampicillin and epiampicillin. However, there were no detectable signals corresponding to intact epiampicillin. During the reaction processes studied, the total integrated values for the phenyl proton area were constant and gave an I_T value corresponding to five protons. The typical NMR spectrum for the degradation after 40 min in 0.2 *M* carbonate buffer at pD 10.6 and 35° is illustrated in Fig. 2.

Figures 3, 4, and 5 give typical plots of the mole percents for hetacillin, epihetacillin, and ampicillin, calculated from the integral value of the C-3 proton for each compound using Eq. 1, as a function of time for the degradation of hetacillin at pD 9.8, 10.6, and 11.4, respectively. The completed curves were generated from an analog computer[8] according to Scheme I. The kinetic parameters used are listed in Table III; the rate constants, k_4 and k_5, were determined directly from the degradation of epihetacillin and ampicillin under the same conditions, and the k_3 value was assumed to be zero. In all cases, reasonably good agreement was found between the experimental values for each species and the computer-drawn curves (Figs. 3–5). These results indicate that the present NMR method is sufficiently accurate for simultaneous determination of hetacillin, epihetacillin, and ampicillin from a kinetic solution.

The reaction of epihetacillin at pD 9.8, 10.6, and 11.4 gave no detectable amount of hetacillin. This result is consistent with the previous report (5) of the irreversible conversion of hetacillin into epihetacillin. The degradation products from hetacillin in deuterium oxide at high pD were also confirmed by TLC studies to be in accordance with the NMR observations. These results strongly support the assumption that the degradation of hetacillin, in the pD ranges examined, follows the reaction route illustrated in Scheme I. The reversible reaction of ampicillin and acetone to form hetacillin gave only a negligible contribution under the present experimental conditions.

Kinetic Study by Optical Rotatory Dispersion Spectroscopy—By utilizing the large difference in optical rotatory dispersion maxima near 240 nm between hetacillin ($[\Phi]_{240\,nm} = 3.40 \times 10^3$) and epihetacillin ($[\Phi]_{238\,nm} = 2.12 \times 10^3$), Mitscher *et al.* (14) proposed a useful method for monitoring the kinetics of epimerization of hetacillin in aqueous solution. Loss of the 238-nm optical rotatory dispersion peak with time in glycine buffer at pH 11 and 23.8° followed a biexponential process in accordance with the following general equation (14):

$$\text{rotation} = Ae^{-\alpha t} + Be^{-\beta t} \qquad \text{(Eq. 2)}$$

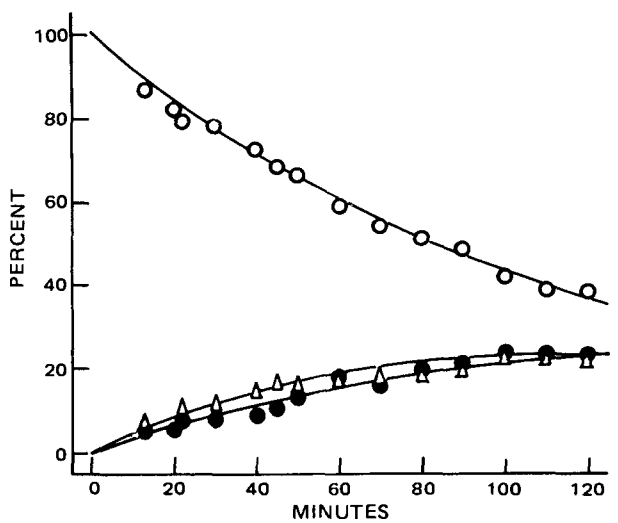

Figure 3—*Time course for hetacillin (○), epihetacillin (●), and ampicillin (△) determined by NMR spectroscopy during the degradation of hetacillin in 0.1 M $NaDCO_3$–Na_2CO_3 buffer at pD 9.8 and 35°. Curves were generated by the analog computer simulation according to Scheme I and the kinetic parameters listed in Table III.*

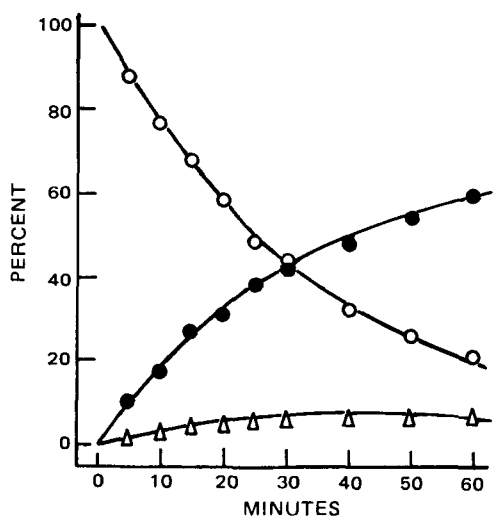

Figure 4—*Time course for hetacillin (○), epihetacillin (●), and ampicillin (△) determined by NMR spectroscopy during the degradation of hetacillin in 0.2 M $NaDCO_3$–Na_2CO_3 buffer at pD 10.6 and 35°. Curves were generated by the analog computer simulation according to Scheme I and the kinetic parameters listed in Table III.*

[8] Hitachi ALS-250, Hitachi Ltd., Tokyo, Japan.

Table III—Various Rate Constants[a] for the Degradation of Hetacillin, Epihetacillin, and Ampicillin Determined by NMR and Optical Rotatory Dispersion (ORD) Spectroscopic Methods in Water and Deuterium Oxide under Various Conditions at μ = 0.5.

Buffer	Solvent	pH or pD	Temperature	Rate Constants, hr^{-1}				Analytical Method
				k_1[b]	k_2	k_4	k_5	
0.1 *M* Phosphate	Deuterium oxide	6.0	35°	—	1.60	—	—	NMR
0.1 *M* Phosphate	Deuterium oxide	6.0	35°	—	—	0.53	—	NMR
0.1 *M* Borate	Water	9.7	35°	0.88	—	0.08	—	ORD
0.1 *M* Carbonate	Deuterium oxide	9.8	35°	0.20	0.30	0.10	0.42	NMR
0.1 *M* Carbonate	Water	9.9	35°	1.10	—	0.09	—	ORD
0.1 *M* Carbonate	Water	10.3	35°	1.80	—	0.12	—	ORD
0.2 *M* Carbonate	Deuterium oxide	10.6	35°	1.30	0.30	0.11	1.20	NMR
0.2 *M* Carbonate	Deuterium oxide	10.6	35°	1.55	—	0.10	—	ORD
0.1 *M* Carbonate	Water	10.7	35°	3.30	—	0.14	—	ORD
0.1 *M* Phosphate	Water	11.1	35°	7.18	—	0.20	—	ORD
0.1 *M* Phosphate	Deuterium oxide	11.4	35°	8.00	0.30	0.12	7.00	NMR
0.1 *M* Phosphate	Deuterium oxide	11.4	35°	8.38	—	0.10	—	ORD
0.025 *M* Phosphate	Water	11.4	35°	22.3	—	0.25	—	ORD
0.05 *M* Phosphate	Water	11.4	35°	22.0	—	0.27	—	ORD
0.1 *M* Phosphate	Water	11.4	35°	22.3	—	0.38	—	ORD
Sodium hydroxide	Water	11.4	35°	22.1	—	0.23	—	ORD
Sodium hydroxide	Water	11.6	35°	—	—	0.27	—	ORD
Sodium hydroxide	Water	12.0	35°	—	—	0.65	—	ORD
Sodium hydroxide	Water	12.3	35°	—	—	1.54	—	ORD
Sodium deuteroxide	Deuterium oxide	12.4	35°	—	—	0.69	—	NMR
Sodium deuteroxide	Deuterium oxide	12.4	35°	—	—	0.65	—	ORD
Sodium hydroxide	Water	12.5	35°	—	—	1.65	—	ORD
0.1 *M* Phosphate	Water	11.0	30°	2.80	—	0.08	—	ORD
0.1 *M* Phosphate	Water	11.4	30°	7.90	—	0.15	—	ORD
0.1 *M* Phosphate	Water	11.5	30°	11.0	—	0.16	—	ORD
0.1 *M* Phosphate	Water	11.2	25°	2.00	—	0.05	—	ORD
0.1 *M* Phosphate	Water	11.4	25°	4.20	—	0.08	—	ORD
0.1 *M* Phosphate	Water	11.6	25°	5.90	—	0.09	—	ORD

[a] Rate constants are defined in Scheme I. [b] The value was obtained from the assumption that ($k_1 + k_2$) values determined by the optical rotatory dispersion method would be almost equal to k_1 values (see text).

where A, B, α, and β are constants. Although Mitscher *et al.* (14) suggested that the results of rotation change reflect epimerization followed by hydrolysis, theoretical implications of Eq. 2 or detailed kinetics of epimerization of hetacillin by means of the optical rotatory dispersion method have not been reported.

The rotation at any time during the reaction of hetacillin, R_t, may be the sum of the rotation of the individual species of hetacillin (I), ampicillin (II), epihetacillin (III), epiampicillin (IV), and penicilloic acids of the last three compounds, V–VII, as follows:

$$R_t = \Phi_I[I] + \Phi_{II}[II] + \Phi_{III}[III] + \Phi_{IV}[IV] + \Phi_V[V] + \Phi_{VI}[VI] + \Phi_{VII}[VII] \quad \text{(Eq. 3)}$$

where Φ_i refers to the molar rotation coefficient of the ith species. In aqueous solution at pH >10, the amount of intact β-lactam compounds II and IV may be negligible because of their slow formation rate and the fast degradation rate of the β-lactam rings. These speculations were confirmed using TLC for the degradation of hetacillin at pH >10 and 35°. Equation 3 can be reduced to:

$$R_t = \Phi_I[I] + \Phi_{III}[III] + \Phi_V[V] + \Phi_{VI}[VI] + \Phi_{VII}[VII] \quad \text{(Eq. 4)}$$

and the following approximate relationship can be derived:

$$[V] + [VI] + [VII] = C_0 - ([I] + [III]) \quad \text{(Eq. 5)}$$

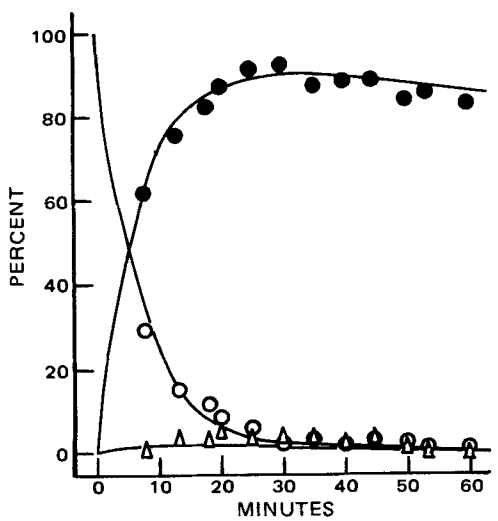

Figure 5—*Time course for hetacillin (○), epihetacillin (●), and ampicillin (△) determined by NMR spectroscopy during the degradation of hetacillin in 0.1 M Na_2DPO_4–Na_3PO_4 buffer at pD 11.4 and 35°. Curves were generated by the analog computer simulation according to Scheme I and the kinetic parameters listed in Table III.*

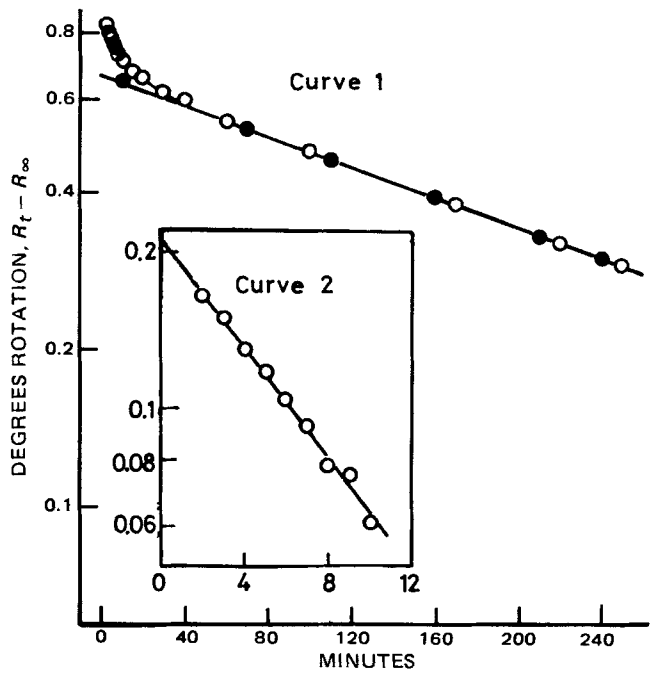

Figure 6—*First-order plot for the decrease in optical rotatory dispersion at 240 nm for the degradation of hetacillin (○, 6×10^{-4} M) and epihetacillin (●, 6×10^{-4} M) in 0.1 M Na_2HPO_4–Na_3PO_4 buffer at pH 11.1 and 35°. Curve 2 is a first-order plot for epimerization and hydrolysis.*

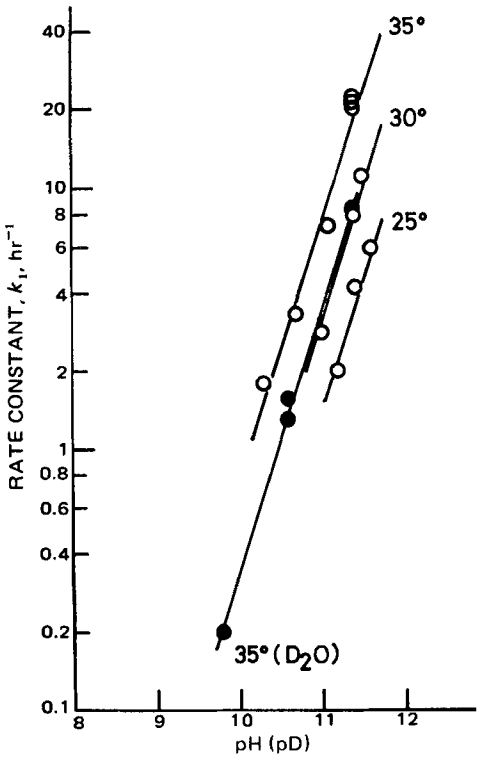

Figure 7—*Log* k-*pH (pD) profiles for the epimerization of hetacillin in water (○) at various temperatures and in deuterium oxide (●) at 35°.*

where C_0 represents the initial concentration of hetacillin. Results from the degradation of epihetacillin and ampicillin at pH >10 gave, within the experimental error, an approximate and simple relationship at 240 nm:

$$\Phi_V C_0 = \Phi_{VI} C_0 = \Phi_{VII} C_0 = R_\infty \qquad \text{(Eq. 6)}$$

Since the reversed reaction from ampicillin and acetone to hetacillin may be negligible in a sufficiently dilute solution of hetacillin, the time dependence of [I] and [III] can be given by the following equations from Scheme I:

$$[I] = C_0 e^{-(k_1+k_2)t} \qquad \text{(Eq. 7)}$$

$$[III] = \frac{k_1}{(k_1+k_2)-k_4} C_0 [e^{-k_4 t} - e^{-(k_1+k_2)t}] \qquad \text{(Eq. 8)}$$

These specific situations in a highly basic solution can lead to Eq. 9 for the R_t change at 240 nm:

$$R_t - R_\infty = A e^{-(k_1+k_2)t} + B e^{-k_4 t} \qquad \text{(Eq. 9)}$$

where:

$$A = (\Phi_I C_0 - R_\infty) - (\Phi_{III} C_0 - R_\infty) \frac{k_1}{(k_1+k_2)-k_4} \qquad \text{(Eq. 10)}$$

$$B = (\Phi_{III} C_0 - R_\infty) \frac{k_1}{(k_1+k_2)-k_4} \qquad \text{(Eq. 11)}$$

Equation 9 is essentially in agreement with that found by Mitscher *et al.* (14).

Figure 6 shows a typical plot of log $(R_t - R_\infty)$ *versus* time for the degradation of hetacillin and epihetacillin in 0.1 *M* phosphate buffer (μ = 0.5) at pH 11.1 and 35°. Since $k_1 + k_2$ is faster than k_4, $e^{-(k_1+k_2)t}$ approaches zero at some time point. There will remain a term in $e^{-k_4 t}$, and the plot of log $(R_t - R_\infty)$ *versus* time will be linear with a slope of $-k_4/2.303$. This linear portion of the curve may be extrapolated to zero time, and the value of $(R_t - R_\infty)$ along this portion of the line represents the contribution of the term in $e^{-k_4 t}$ to the overall value. Thus, subtraction of this term from the observed $(R_t - R_\infty)$ leaves only the term $e^{-(k_1+k_2)t}$. Then a plot of the logarithm of these residuals against time should be linear with a slope of $-(k_1 + k_2)/2.303$ (curve 2 in Fig. 6). The linear portions corresponding to $Be^{-k_4 t}$ were essentially identical at pH > 10 to the portion for epihetacillin itself, obtained from independent measurements at the same concentration under the same conditions as shown in Fig. 6, indicating the validity of Eq. 9 and suggesting the relation of $k_1 \gg k_2, k_4$.

Table IV—Epimerization Rate Constants of Hetacillin at Various Temperatures and μ = 0.5

Solvent	Temperature	k_{ep}, M^{-1} hr^{-1}
Water	25°	1.29×10^3
Water	30°	2.05×10^3
Water	35°	3.84×10^3
Deuterium oxide	35°	1.04×10^4

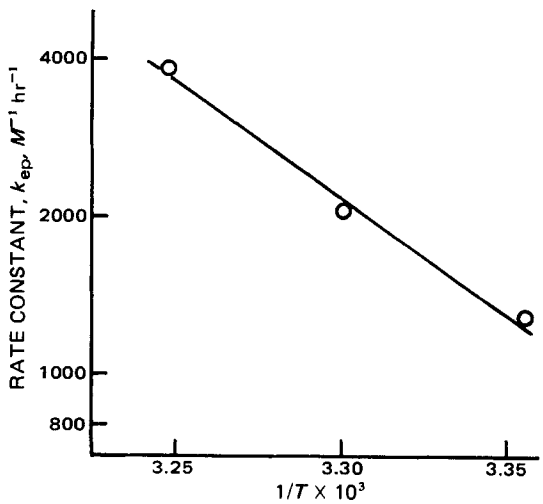

Figure 8—*Arrhenius plot of the second-order epimerization rate constant,* k_{ep}, *of hetacillin.*

Calculation of each value of k_1 and k_2 is theoretically possible from the intercept value of A or B. However, when taking into account the experimental error and large contribution of k_1 in the $(k_1 + k_2)$ value, it seems reasonable to assume for the data at pH > 10 that the $(k_1 + k_2)$ values thus determined are approximately equal to the epimerization rate constant, k_1. These rate constants are summarized in Table III. The k_1 and k_4 values determined at pD 10.6 and 11.4 by optical rotatory dispersion spectroscopy are in satisfactory agreement with those determined by NMR spectroscopy.

The results in phosphate buffer and sodium hydroxide solution at pH 11.4 (Table III) revealed that the apparent epimerization rate constants, k_1, were almost independent of the buffer concentration used. Since the C-6 epimerization of penicillin is known to proceed by general base catalysis (15, 16), the present results indicate that the general base-catalyzed epimerization rate of hetacillin may be negligible compared with the hydroxide-ion-catalyzed process in the experimental pH range.

pH–Rate Profile and Temperature Dependence for Epimerization of Hetacillin—Plots of log k_1 against pH (pH > 10) or pD for various temperatures in water and in deuterium oxide are illustrated in Fig. 7 and yielded straight lines with a slope of unity in each case, verifying a first-order dependence on the hydroxide ion. The rate law may be written as:

$$k_1 = k_{ep} a_{OH^-} \qquad \text{(Eq. 12)}$$

$$k_1 = k_{ep}(a_{H^+}/K_w) \qquad \text{(Eq. 13)}$$

where k_{ep} represents the second-order rate constant for hydroxide-ion-catalyzed epimerization; and a_{OH^-} and a_{H^+} refer to the activity of the hydroxide ion and hydrogen ion, respectively, which were calculated from pH measurements and the autoprotolytic constant in water (17) and deuterium oxide (18). The rate constants, k_{ep}, consistent with the experimental results in water and deuterium oxide are shown in Table IV.

Since the epimerization of hetacillin was suggested (5, 15) to occur through a rate-limiting formation of an enolate intermediate resulting from the proton subtraction of the acidic C-6 proton by a hydroxide ion, the ratio $k_{ep}^{D_2O}/k_{ep}^{H_2O}$ = 2.7 may be attributed to the difference in base strength between deuteroxide and hydroxide ions. Subsequent reprotonation gives the thermodynamically more stable epihetacillin; then epimerization proceeds irreversibly, as noted previously (5).

An Arrhenius plot for k_{ep} is illustrated in Fig. 8. By applying the method of least squares to the plots, the energy of activation for epimerization to epihetacillin was 21.2 kcal/mole.

In plots of log k_1 *versus* pH at 35° in water, slight positive deviation from the first-order dependence on the hydroxide ion was observed at alkaline pH < 10 (not presented in Fig. 7). This result may have been due to the considerable contribution of the hydrolysis rate, k_2, to the k_1 value estimated from the optical rotatory dispersion method. This result would occur because of the pH-dependent degradation behavior of hetacillin in which the epimerization process is a major pathway in a highly basic solution, whereas hydrolysis to ampicillin becomes increasingly significant in medium basic and neutral solutions (2, 3, 6).

No significant β-lactam cleavage reaction probably would take place in hetacillin itself, since the disappearance of hetacillin was virtually accompanied, even in highly basic solutions, with two competing reactions, the formation of epihetacillin (k_1 reaction) and the conversion to ampicillin (k_2 reaction), as verified by quantitative NMR studies (Figs. 3–5). The extreme stability of the β-lactam in the hetacillin molecule was also revealed in epihetacillin degradation. The k_4 reaction concerned with the disappearance of epihetacillin is controlled by hydrolysis of the β-lactam ring and conversion to epiampicillin. The pH dependency of k_4 at 35° (Table III) indicates that the hydroxide-ion-catalyzed hydrolysis of the β-lactam moiety of epihetacillin is predominant above pH 11.5, and conversion to epiampicillin seems to be significant below this pH.

The second-order rate constant for the β-lactam hydrolysis of epihetacillin was calculated to be 65.8 M^{-1} hr^{-1} at 35°, one-twentieth of the value for the hydrolysis of ampicillin β-lactam (19). The remarkable stability of both β-lactam rings of hetacillin and its epimer may be attributed to the steric hindrance of *gem*-dimethyl groups of the imidazolidine rings toward the attack by a hydroxide ion.

REFERENCES

(1) G. A. Hardcastle, Jr., D. A. Johnson, C. A. Panetta, A. I. Scott, and S. A. Sutherland, *J. Org. Chem.*, **31**, 897 (1966).

(2) J. T. Smith and J. M. T. Hamilton-Miller, *Chemotherapy*, **15**, 366 (1970).

(3) L. Magni, B. Ortengren, B. Sjoberg, and S. Wahlqvist, *Scand. J. Clin. Lab. Invest.*, **20**, 195 (1967).

(4) D. A. Johnson, D. Mania, C. A. Panetta, and H. H. Silvestri, *Tetrahedron Lett.*, **1968**, 1903.

(5) J. P. Clayton, J. H. C. Nayler, R. Southgate, and E. R. Stove, *Chem. Commun.*, **1969**, 129.

(6) A. Tsuji and T. Yamana, *Chem. Pharm. Bull.*, **22**, 2434 (1974).

(7) T. Yamana, A. Tsuji, and Y. Itatani, *J. Antibiot.*, **28**, 242 (1975).

(8) A. K. Durbin and H. N. Rydon, *Chem. Commun.*, **1970**, 1249.

(9) M. A. Schwartz and W. L. Hayton, *J. Pharm. Sci.*, **61**, 906 (1972).

(10) G. N. Levy, J. V. Ioia, and E. J. Kuchinskas, *ibid.*, **63**, 1197 (1974).

(11) T. H. Fife and T. C. Bruice, *J. Phys. Chem.*, **65**, 1079 (1961).

(12) M. A. Schwartz and A. J. Delduce, *J. Pharm. Sci.*, **58**, 1137 (1969).

(13) J. M. Padfield and I. W. Kellaway, *ibid.*, **63**, 143 (1974).

(14) L. A. Mitscher, P. W. Howison, and T. D. Sokoloski, *J. Antibiot.*, **27**, 215 (1974).

(15) S. Wolfe, W. S. Lee, and R. Misra, *Chem. Commun.*, **1970**, 1067.

(16) B. G. Ramsay and R. J. Stoodley, *ibid.*, **1971**, 450.

(17) H. S. Harned and W. J. Hammer, *J. Am. Chem. Soc.*, **55**, 2194 (1933).

(18) A. K. Corigton, R. A. Robinson, and R. G. Bates, *J. Phys. Chem.*, **70**, 3820 (1966).

(19) J. P. Hou and J. W. Poole, *J. Pharm. Sci.*, **58**, 447 (1969).

ACKNOWLEDGMENTS AND ADDRESSES

Received April 5, 1976, from the *Faculty of Pharmaceutical Sciences, Kanazawa University, Takara-machi, Kanazawa 920, Japan.*

Accepted for publication September 7, 1976.

The authors are grateful to Banyu Pharmaceutical Co. and Takeda Chemical Ind. for supplies of hetacillin potassium and ampicillin sodium, respectively. They also acknowledge the excellent technical assistance of Mr. O. Kubo and Miss E. Kiya.

[x] To whom inquiries should be directed.

Reactions of Benzenesulfonohydrazides and Benzenesulfonamides with Hydrogen Chloride or Hydrogen Bromide in Acetic Acid

D. K. YUNG [*x], T. P. FORREST [‡], A. R. MANZER [*], and M. L. GILROY [*]

Abstract □ Benzenesulfonohydrazides capable of yielding a sulfinic acid intermediate by virtue of a basic nitrogen atom in the second position of the hydrazide moiety produced thiosulfonates when treated with 1 *N* hydrogen chloride in acetic acid and produced disulfides when treated with 1 *N* hydrogen bromide in the same solvent. In two cases, a crystalline mixture of *p*-nitrophenyl *p*-nitrobenzenethiosulfonate and bis(*p*-nitrophenyl) disulfide was isolated from the hydrogen chloride reactions. No reaction product was obtained from either the hydrogen chloride or hydrogen bromide reaction with benzenesulfonohydrazides that were unable to form a sulfinic acid intermediate. Reduction of benzenesulfonamides to disulfides appeared to be possible only with hydrogen bromide in acetic acid. No thiosulfonate was isolated from the treatments of benzenesulfonamides with 1 *N* hydrogen chloride in acetic acid. *p*-Nitrophenyl *p*-nitrobenzenethiosulfonate and *p*-bromophenyl *p*-bromobenzenethiosulfonate exhibited some antimicrobial activities against Gram-positive bacteria. The latter compound also showed analgesic properties in the phenylquinone test.

Keyphrases □ Benzenesulfonohydrazides and benzenesulfonamides—reaction with hydrogen chloride or bromide in acetic acid, pharmacological activity of thiosulfonates formed □ Thiosulfonates—formed by reaction of benzenesulfonohydrazides and benzenesulfonamides with hydrogen chloride in acetic acid, pharmacological activity screened □ Antimicrobial activity—screened in thiosulfonates formed by reaction of benzenesulfonohydrazides and benzenesulfonamides with hydrogen chloride in acetic acid

While preparing some potential antimicrobial unsymmetrical piperazine compounds, it was necessary to synthesize 1-(*p*-acetamidobenzenesulfonamido)piperazine from 1-(*p*-acetamidobenzenesulfonamido)-4-ethoxycarbonylpiperazine (Ia, Table I). Removal of ethoxycarbonyl groups of piperazine derivatives is usually accomplished by either acidic or alkaline hydrolysis (1, 2).

A nonhydrolytic method utilizing dry hydrogen bromide

An Arrhenius plot for k_{ep} is illustrated in Fig. 8. By applying the method of least squares to the plots, the energy of activation for epimerization to epihetacillin was 21.2 kcal/mole.

In plots of log k_1 *versus* pH at 35° in water, slight positive deviation from the first-order dependence on the hydroxide ion was observed at alkaline pH < 10 (not presented in Fig. 7). This result may have been due to the considerable contribution of the hydrolysis rate, k_2, to the k_1 value estimated from the optical rotatory dispersion method. This result would occur because of the pH-dependent degradation behavior of hetacillin in which the epimerization process is a major pathway in a highly basic solution, whereas hydrolysis to ampicillin becomes increasingly significant in medium basic and neutral solutions (2, 3, 6).

No significant β-lactam cleavage reaction probably would take place in hetacillin itself, since the disappearance of hetacillin was virtually accompanied, even in highly basic solutions, with two competing reactions, the formation of epihetacillin (k_1 reaction) and the conversion to ampicillin (k_2 reaction), as verified by quantitative NMR studies (Figs. 3–5). The extreme stability of the β-lactam in the hetacillin molecule was also revealed in epihetacillin degradation. The k_4 reaction concerned with the disappearance of epihetacillin is controlled by hydrolysis of the β-lactam ring and conversion to epiampicillin. The pH dependency of k_4 at 35° (Table III) indicates that the hydroxide-ion-catalyzed hydrolysis of the β-lactam moiety of epihetacillin is predominant above pH 11.5, and conversion to epiampicillin seems to be significant below this pH.

The second-order rate constant for the β-lactam hydrolysis of epihetacillin was calculated to be 65.8 M^{-1} hr^{-1} at 35°, one-twentieth of the value for the hydrolysis of ampicillin β-lactam (19). The remarkable stability of both β-lactam rings of hetacillin and its epimer may be attributed to the steric hindrance of *gem*-dimethyl groups of the imidazolidine rings toward the attack by a hydroxide ion.

REFERENCES

(1) G. A. Hardcastle, Jr., D. A. Johnson, C. A. Panetta, A. I. Scott, and S. A. Sutherland, *J. Org. Chem.*, **31**, 897 (1966).

(2) J. T. Smith and J. M. T. Hamilton-Miller, *Chemotherapy*, **15**, 366 (1970).

(3) L. Magni, B. Ortengren, B. Sjoberg, and S. Wahlqvist, *Scand. J. Clin. Lab. Invest.*, **20**, 195 (1967).

(4) D. A. Johnson, D. Mania, C. A. Panetta, and H. H. Silvestri, *Tetrahedron Lett.*, **1968**, 1903.

(5) J. P. Clayton, J. H. C. Nayler, R. Southgate, and E. R. Stove, *Chem. Commun.*, **1969**, 129.

(6) A. Tsuji and T. Yamana, *Chem. Pharm. Bull.*, **22**, 2434 (1974).

(7) T. Yamana, A. Tsuji, and Y. Itatani, *J. Antibiot.*, **28**, 242 (1975).

(8) A. K. Durbin and H. N. Rydon, *Chem. Commun.*, **1970**, 1249.

(9) M. A. Schwartz and W. L. Hayton, *J. Pharm. Sci.*, **61**, 906 (1972).

(10) G. N. Levy, J. V. Ioia, and E. J. Kuchinskas, *ibid.*, **63**, 1197 (1974).

(11) T. H. Fife and T. C. Bruice, *J. Phys. Chem.*, **65**, 1079 (1961).

(12) M. A. Schwartz and A. J. Delduce, *J. Pharm. Sci.*, **58**, 1137 (1969).

(13) J. M. Padfield and I. W. Kellaway, *ibid.*, **63**, 143 (1974).

(14) L. A. Mitscher, P. W. Howison, and T. D. Sokoloski, *J. Antibiot.*, **27**, 215 (1974).

(15) S. Wolfe, W. S. Lee, and R. Misra, *Chem. Commun.*, **1970**, 1067.

(16) B. G. Ramsay and R. J. Stoodley, *ibid.*, **1971**, 450.

(17) H. S. Harned and W. J. Hammer, *J. Am. Chem. Soc.*, **55**, 2194 (1933).

(18) A. K. Corigton, R. A. Robinson, and R. G. Bates, *J. Phys. Chem.*, **70**, 3820 (1966).

(19) J. P. Hou and J. W. Poole, *J. Pharm. Sci.*, **58**, 447 (1969).

ACKNOWLEDGMENTS AND ADDRESSES

Received April 5, 1976, from the *Faculty of Pharmaceutical Sciences, Kanazawa University, Takara-machi, Kanazawa 920, Japan.*

Accepted for publication September 7, 1976.

The authors are grateful to Banyu Pharmaceutical Co. and Takeda Chemical Ind. for supplies of hetacillin potassium and ampicillin sodium, respectively. They also acknowledge the excellent technical assistance of Mr. O. Kubo and Miss E. Kiya.

[x] To whom inquiries should be directed.

Reactions of Benzenesulfonohydrazides and Benzenesulfonamides with Hydrogen Chloride or Hydrogen Bromide in Acetic Acid

D. K. YUNG [*x], T. P. FORREST [‡], A. R. MANZER [*], and M. L. GILROY [*]

Abstract □ Benzenesulfonohydrazides capable of yielding a sulfinic acid intermediate by virtue of a basic nitrogen atom in the second position of the hydrazide moiety produced thiosulfonates when treated with 1 *N* hydrogen chloride in acetic acid and produced disulfides when treated with 1 *N* hydrogen bromide in the same solvent. In two cases, a crystalline mixture of *p*-nitrophenyl *p*-nitrobenzenethiosulfonate and bis(*p*-nitrophenyl) disulfide was isolated from the hydrogen chloride reactions. No reaction product was obtained from either the hydrogen chloride or hydrogen bromide reaction with benzenesulfonohydrazides that were unable to form a sulfinic acid intermediate. Reduction of benzenesulfonamides to disulfides appeared to be possible only with hydrogen bromide in acetic acid. No thiosulfonate was isolated from the treatments of benzenesulfonamides with 1 *N* hydrogen chloride in acetic acid. *p*-Nitrophenyl *p*-nitrobenzenethiosulfonate and *p*-bromophenyl *p*-bromobenzenethiosulfonate exhibited some antimicrobial activities against Gram-positive bacteria. The latter compound also showed analgesic properties in the phenylquinone test.

Keyphrases □ Benzenesulfonohydrazides and benzenesulfonamides—reaction with hydrogen chloride or bromide in acetic acid, pharmacological activity of thiosulfonates formed □ Thiosulfonates—formed by reaction of benzenesulfonohydrazides and benzenesulfonamides with hydrogen chloride in acetic acid, pharmacological activity screened □ Antimicrobial activity—screened in thiosulfonates formed by reaction of benzenesulfonohydrazides and benzenesulfonamides with hydrogen chloride in acetic acid

While preparing some potential antimicrobial unsymmetrical piperazine compounds, it was necessary to synthesize 1-(*p*-acetamidobenzenesulfonamido)piperazine from 1-(*p*-acetamidobenzenesulfonamido)-4-ethoxycarbonylpiperazine (Ia, Table I). Removal of ethoxycarbonyl groups of piperazine derivatives is usually accomplished by either acidic or alkaline hydrolysis (1, 2).

A nonhydrolytic method utilizing dry hydrogen bromide

Table I—Benzenesulfonohydrazides

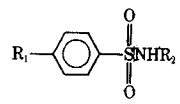

Compound	R_1	R_2	Yield, %	Melting Point	Formula	Analysis, % Calc.	Found
Ia	$NHCOCH_3$	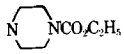	54	173.5–174.5° dec.	$C_{15}H_{22}N_4O_5S$	C 48.63 H 5.99 N 15.12 S 8.66	48.62 6.10 15.18 8.42
Ib	Br	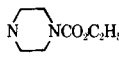	61	148–150°	$C_{13}H_{18}BrN_3O_4S$	C 39.80 H 4.62 Br 20.37 N 10.71 S 8.18	39.69 4.58 20.76 10.39 7.96
Ic	NO_2	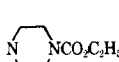	67	154–155°	$C_{13}H_{18}N_4O_6S$	C 43.56 H 5.07 N 15.64 S 8.95	43.73 5.00 15.79 8.90
IIa	Br		46	143.5–144.5°	$C_{11}H_{15}BrN_2O_2S$	C 41.38 H 4.74 Br 25.03	41.25 4.77 25.12
IIb	NO_2		74	155–157° dec.	$C_{11}H_{15}N_3O_4S$	C 46.30 H 5.30 N 14.73 S 11.24	46.65 5.32 14.88 11.50
IIIa	Br		43	161–162°	$C_{10}H_{13}BrN_2O_3S$	C 37.39 H 4.08 Br 24.88	37.40 4.17 25.11
IIIb	NO_2		85	182–184°[a]	$C_{10}H_{13}N_3O_5S$	—	—
IVa	Br	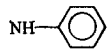	74	139–140°	$C_{12}H_{11}BrN_2O_2S$	C 44.05 H 3.39 Br 24.42	43.80 3.37 24.62
IVb	NO_2	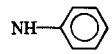	91	147–148.5° dec.[b]	$C_{12}H_{11}N_3O_4S$	—	—
Va	Br	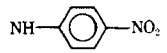	81	175.5–176°	$C_{12}H_{10}BrN_3O_4S$	C 38.72 H 2.71 Br 21.47 S 8.62	38.88 2.90 21.75 8.58
Vb	NO_2	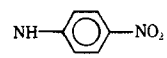	50	170.5–171°[c]	$C_{12}H_{10}N_4O_6S$	—	—
VIa	Br	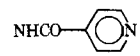	64	198–198.5°	$C_{12}H_{10}BrN_3O_3S \cdot H_2O$	C 38.51 H 3.23 Br 21.36	38.61 3.29 21.47
VIb	NO_2	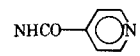	93	211–212°	$C_{10}H_{10}N_4O_5S$	C 44.72 H 3.13 N 17.39	45.03 3.25 17.21

[a] Lit. (19) mp 180.5–181°. [b] Lit. (20) mp 150°. [c] Lit. (20) mp 172–173°.

in acetic acid for 1-alkyl-4-ethoxycarbonylpiperazines and 1-ethylsulfonyl-4-ethoxycarbonylpiperazine was reported (3). Similarly, other studies (4, 5) used dry hydrogen bromide or dry hydrogen chloride in acetic acid to remove benzoxycarbonyl groups from the nitrogen atoms in peptides. This paper describes the products isolated from the reactions of Ia and other structurally related compounds with dry hydrogen chloride in acetic acid and with dry hydrogen bromide in acetic acid.

RESULTS AND DISCUSSION

In the original attempt to remove the ethoxycarbonyl group of Ia, two problems were envisioned. First, the generally useful hydrolytic methods were considered unsuitable because of another vulnerable acetamido substituent in the molecule. Second, treatment of Ia with dry hydrogen bromide in acetic acid could result in the cleavage of the sulfonamide linkage, giving bis(*p*-acetamidophenyl) disulfide (XIIa) (6, 7) instead of the desired product.

However, in view of reported success with 1-ethylsulfonyl-4-ethoxycarbonylpiperazine (3), Ia was treated with 1 *N* hydrogen bromide in acetic acid. The desired product was not obtained; only XIIa in a 48% yield was isolated. Since it was reported that cleavage of sulfonamide with hydrogen bromide in acetic acid was a reduction process (8), it was decided to replace the dry hydrogen bromide with hydrogen chloride, a less active reducing agent. The reaction of Ia with 1 *N* hydrogen chloride in acetic acid produced a product characterized by IR, NMR, and elemental analysis to be the thiosulfonate XIa in about an 80% yield. No other products could be isolated from the reaction mixture.

In view of these results, two other piperazine compounds (Ib and Ic) were examined. In each instance, the corresponding thiosulfonates (XIb and XIc) were obtained in good yield on reaction with hydrogen chloride in acetic acid. However, treatment of Ib and Ic with 1 *N* hydrogen bromide in acetic acid resulted in the formation of disulfides (XIIb and XIIc).

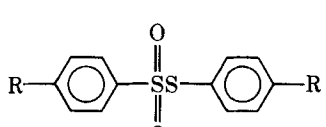

XIa: R = $NHCOCH_3$
XIb: R = Br
XIc: R = NO_2

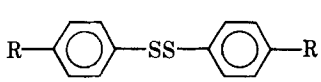

XIIa: R = $NHCOCH_3$
XIIb: R = Br
XIIc: R = NO_2

Table II—Major Reaction Products of Benzenesulfonohydrazides (I–VI) and Benzenesulfonamides (VII–X) with 1 *N* Hydrogen Chloride and/or 1 *N* Hydrogen Bromide in Acetic Acid

Compound	Reaction Product with 1 *N* Hydrogen Chloride in Acetic Acid	Yield, %	Recovery of Starting Compound %	Reaction Product with 1 *N* Hydrogen Bromide in Acetic Acid	Yield, %	Recovery of Starting Compound, %
I*a*	*p*-Acetamidophenyl *p*-acetamidobenzenethiosulfonate	82	—	Bis(*p*-acetamidophenyl) disulfide monohydrate	48	—
I*b*	*p*-Bromophenyl *p*-bromobenzenethiosulfonate	77	—	Bis(*p*-bromophenyl) disulfide	60	—
I*c*	*p*-Nitrophenyl *p*-nitrobenzenethiosulfonate	72	—	Bis(*p*-nitrophenyl) disulfide	84	—
II*a*	*p*-Bromophenyl *p*-bromobenzenethiosulfonate	50	—	—	—	—
II*b*	Mixture of *p*-nitrophenyl *p*-nitrobenzenethiosulfonate and bis(*p*-nitrophenyl) disulfide	—	—	Bis(*p*-nitrophenyl) disulfide	62	—
III*a*	*p*-Bromophenyl *p*-bromobenzenethiosulfonate	68	—	Bis(*p*-bromophenyl) disulfide	56	—
III*b*	*p*-Nitrophenyl *p*-nitrobenzenethiosulfonate	94	—	Bis(*p*-nitrophenyl) disulfide	42	—
IV*a*	*p*-Bromophenyl *p*-bromobenzenethiosulfonate	70	—	—	—	—
IV*b*	Mixture of *p*-nitrophenyl *p*-nitrobenzenethiosulfonate and bis(*p*-nitrophenyl) disulfide	—	—	Bis(*p*-nitrophenyl) disulfide	90	—
V*a*	None isolated	—	33	—	—	—
V*b*	None isolated	—	45	—	—	—
VI*a*	None isolated	—	88	None isolated	—	95
VI*b*	None isolated	—	84	None isolated	—	99
VII*a*	None isolated	—	76	Bis(*p*-nitrophenyl) disulfide	91[a]	35
VIII*a*	None isolated	—	65	—	—	—
VIII*b*	None isolated	—	70	Bis(*p*-nitrophenyl) disulfide	99[a]	33
IX*a*	None isolated	—	85	Bis(*p*-nitrophenyl) disulfide	98[a]	30
X*a*	None isolated	—	70	—		
X*b*	None isolated	—	73	—		

[a] Yield is calculated on the basis of unrecovered starting compound.

To determine the scope of the reaction involving 1 *N* hydrogen chloride in acetic acid, 10 other benzenesulfonohydrazides without the piperazine ring (Table I) were investigated. As indicated in Table II, thiosulfonates were obtained from II*a*, III*a*, III*b*, and IV*a*. The hydrazides II*b* and IV*b*, however, produced the disulfide (XII*c*) in addition to the thiosulfonate (XI*c*). The two products were isolated as a crystalline solid (mp 157–158°), which consisted of an equimolar mixture of the two, as indicated by the proton NMR spectrum. Recrystallizations from common organic solvents failed to separate the two compounds; however, they could be separated by TLC (silica gel) using carbon tetrachloride–benzene (4:1) as the eluant. The melting point and IR spectrum of the mixture were identical to those of the authentic mixture (1:1) of XI*c* and XII*c*.

The other four benzenesulfonohydrazides (V*a*, V*b*, VI*a*, and VI*b*) do not have a basic nitrogen in the second position and did not yield any isolatable products in the reaction with hydrogen chloride in acetic acid. A significant amount of unreacted starting compound was recovered in each instance when the acid was removed *in vacuo*. Thus, the formation of thiosulfonates in the reactions with hydrogen chloride in acetic acid apparently depends on the availability of a basic nitrogen atom in the second position of the benzenesulfonohydrazides. Such a postulation is supported by the fact that none of the benzenesulfonamides (Table III) produced any thiosulfonates under similar conditions.

Thiosulfonates and sulfonic acids are known to result from disproportionation of sulfinic acids. In the acid-catalyzed hydrolysis of toluenesulfonohydrazides, sulfinic acids were formed as intermediates (9). Kice and coworkers (10, 11) proposed that the mechanism for the disproportionation of sulfinic acids involved an initial equilibrium between benzenesulfinic acid (XIII) and a sulfinyl sulfone intermediate (XIV), followed by the rearrangement of XIV to a sulfenyl sulfonate (XV). Reaction of XV with an additional molecule of XIII led to thiosulfonate and sulfonic acid as final products. Sulfonohydrazides are also reported to undergo a pyrolytic disproportionation, presumably *via* sulfinic acids, to yield a mixture of disulfide and thiosulfonate (12).

In the present study, all those benzenesulfonohydrazides that yielded thiosulfonates when treated with hydrogen chloride in acetic acid are capable of forming a sulfinic acid by electron shift from the basic nitrogen atom in the second position to the SO_2 group (Scheme I). Thus, the formation of thiosulfonates from these hydrazides probably proceeds *via* a sulfinic acid intermediate. When the same benzenesulfonohydrazides were allowed to react with 1 *N* hydrogen bromide in acetic acid, only the

Table III—Benzenesulfonamides

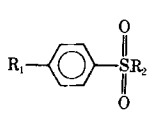

Compound	R_1	R_2	Yield, %	Melting Point	Formula	Analysis, % Calc.	Analysis, % Found
VII*a*	NO_2	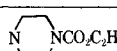	70	157–159°	$C_{13}H_{17}N_3O_6S$	C 45.47 H 4.99 N 12.24 S 9.34	45.27 5.14 12.17 9.15
VIII*a*	Br		52	90–91°[a]	$C_{11}H_{14}BrNO_2S$	—	—
VIII*b*	NO_2		74	170.5–171°	$C_{11}H_{14}N_2O_4S$	C 48.87 H 5.22 N 10.37	48.84 5.38 10.33
IX*a*	NO_2		89	172.5–173°	$C_{10}H_{12}N_2O_5S$	C 44.11 H 4.44 N 10.29	44.05 4.44 10.09
X*a*	Br	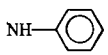	64	117.5–118.5°[b]	$C_{12}H_{10}BrNO_2S$	—	—
X*b*	NO_2	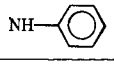	68	168–170.5°[c]	$C_{12}H_{10}N_2O_4S$	—	—

[a] Lit. (21) mp 91–91.5°. [b] Lit. (22) mp 116–117°. [c] Lit. (23) mp 168–169°.

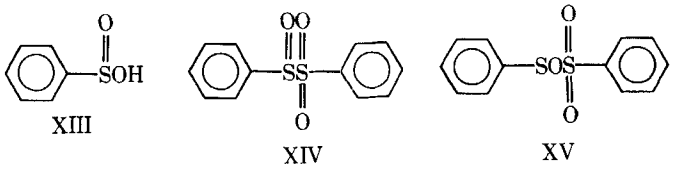

XIII XIV XV

disulfides were formed. This finding is in contrast to reported results for the reactions of toluenesulfonohydrazides and aqueous hydrobromic acid, in which the thiosulfonates were the major products (9). A plausible explanation for the exclusive disulfide formation could be that the bromide ions attack the sulfinyl sulfur in XIV to give sulfinyl bromide (XVI) and XIII before the sulfenyl sulfonate (XV) is formed. In dioxane–water (60:40), the bromide ion was about five times more active a nucleophile than chloride ion toward the sulfinyl sulfur atom in XIV (13). Reduction of XVI by hydrogen bromide would yield the sulfenyl bromide (XVII), which has been suggested to be an intermediate for disulfide formation in the cleavage of sulfonamide with aqueous hydrogen bromide (7).

The fact that the sulfonamides (VII*a*, VIII*b*, and IX*a*) are not capable of producing the sulfinic acid intermediate and are still reduced to the disulfides suggests that the benzenesulfonohydrazides might react in a similar manner with hydrogen bromide to form the disulfides. However, the almost quantitative recovery of VI*a* and VI*b* from the reactions with hydrogen bromide in acetic acid does not support this suggestion.

Although thiosulfonates are not novel compounds, information on their biological properties is lacking. For this reason, a general screening of the pharmacological activities was performed on XI*b* and XI*c*. Preliminary results indicated that none of the compounds showed any significant antidepressant, cardiovascular, anti-inflammatory, antidiabetic, antihistaminic, or antiallergic activities. However, both compounds did exhibit some antimicrobial activities against Gram-positive bacteria such as *Bacillus subtilis* (ATCC 6633), *Staphylococcus aureus* (ATCC 8030), *Streptococcus pyogenes* (ATCC 6538), *Streptococcus faecalis* (a clinical isolate), and *Diplococcus pneumoniae* (ATCC 6303) but not against Gram-negative bacteria. In addition, XI*b* showed some analgesic activity in the phenylquinone test[1].

EXPERIMENTAL[2]

The benzenesulfonohydrazides and benzenesulfonamides were prepared from the amine and the corresponding benzenesulfonyl chloride in pyridine and were purified by recrystallization from ethanol or aqueous ethanol. With the exception of 1-amino-4-ethoxycarbonylpiperazine, all amines and benzenesulfonyl chlorides were obtained commercially. 1-Amino-4-ethoxycarbonylpiperazine was prepared by a previously reported method (14). The physical data of the benzenesulfonohydrazides and benzenesulfonamides are listed in Tables I and III, respectively.

p-Acetamidophenyl p-Acetamidobenzenethiosulfonate (XI*a*)—In a flask fitted with a gas-absorption trap were placed 0.8 g (0.0022 mole) of I*a* and 70 ml of 1 *N* hydrogen chloride in acetic acid, prepared by adding acetic acid to 10–15% hydrogen chloride in acetic acid. The mixture was warmed in a steam bath for 25 min and at 60° for 3 hr. The solution was allowed to stand at room temperature overnight and then filtered. About 0.2 g of crystalline XI*a* was collected and washed with ether. The filtrate was concentrated *in vacuo* to give a residue which, upon mixing with a small amount of ethanol, yielded an additional 0.12 g of XI*a*. Removal of the ethanol gave an unmanageable tar-like material. The total yield of XI*a* was 82%, mp 227–228°, after recrystallization from aqueous ethanol.

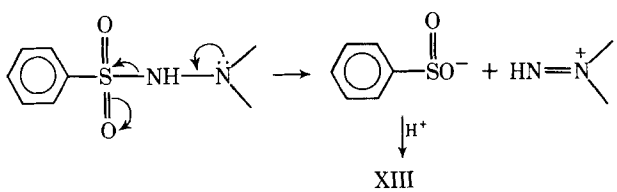

XIII

Scheme I

[1] The preliminary biological data were supplied by the Bio-Research Laboratories Ltd., Montreal, Quebec, Canada.

[2] Melting points were determined on a Thomas-Hoover capillary melting-point apparatus and are uncorrected. Elemental analyses were performed by Robertson Laboratory, Florham Park, N.J. IR spectra were recorded on a Perkin-Elmer model 237B spectrophotometer in potassium bromide. A Varian model T-60 spectrometer was used to record the NMR spectra, with deuterochloroform as the solvent and tetramethylsilane as the internal reference.

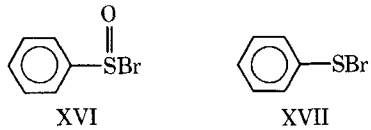

XVI XVII

Anal.—Calc. for $C_{16}H_{16}N_2O_3S$: C, 52.73; H, 4.43; N, 7.69; S, 17.60. Found: C, 52.36; H, 4.77; N, 7.72; S, 17.98.

p-Bromophenyl *p*-bromobenzenethiosulfonate (XI*b*), mp 157–158° [lit. (15) mp 160–161°], and *p*-nitrophenyl *p*-nitrobenzenethiosulfonate (XI*c*), mp 181–181.5° [lit. (16) mp 180–181°], were similarly prepared. The yields of these thiosulfonates are listed in Table II.

Bis(*p*-acetamidophenyl) Disulfide (XII*a*)—The procedure described for XI*a* was followed to synthesize this compound from the reaction of I*a* with 1 *N* hydrogen bromide in acetic acid, prepared by adding acetic acid to 30–32% hydrogen bromide in acetic acid. Compound XII*a* was recrystallized from aqueous ethanol, mp 217.5–219°. The yield was 48%.

Anal.—Calc. for $C_{16}H_{16}N_2O_2S_2 \cdot H_2O$: C, 54.83; H, 5.18; N, 8.00; S, 18.30. Found: C, 54.79; H, 5.14; N, 8.13; S, 18.54.

Bis(*p*-bromophenyl) disulfide (XII*b*), mp 92–93° [lit. (17) mp 95–96°], and bis(*p*-nitrophenyl) disulfide (XII*c*), mp 181–182.5° [lit. (18) mp 182°], were similarly prepared. The yields of these disulfides are shown in Table II.

REFERENCES

(1) T. S. Moore, M. Boyle, and V. M. Thorne, *J. Chem. Soc.*, **1929**, 39.

(2) M. Harfenist, *J. Am. Chem. Soc.*, **76**, 4991 (1954).

(3) W. O. Foye, L. Chafetz, and E. G. Feldmann, *J. Org. Chem.*, **22**, 713 (1957).

(4) D. Ben-Ishai and A. Berger, *ibid.*, **17**, 1564 (1952).

(5) G. W. Anderson, J. Blodinger, and A. D. Welcher, *J. Am. Chem. Soc.*, **74**, 5309 (1952).

(6) H. R. Snyder and R. E. Heckert, *ibid.*, **74**, 2006 (1952).

(7) H. R. Snyder and H. C. Geller, *ibid.*, **74**, 4864 (1952).

(8) R. L. Shriner, R. C. Fuson, and D. Y. Curtin, "The Systematic Identification of Organic Compounds," 5th ed., Wiley, New York, N.Y., 1964, p. 120.

(9) S. Wawzonek and W. McKillip, *J. Org. Chem.*, **27**, 3946 (1962).

(10) J. L. Kice and K. W. Bowers, *J. Am. Chem. Soc.*, **84**, 605 (1962).

(11) J. L. Kice, G. Guaraldi, and C. G. Venier, *J. Org. Chem.*, **31**, 3561 (1966).

(12) F. Muth, in "Methoden Der Organischen Chemie," vol. 9, E. Müller, Ed., Georg Thieme Verlag, Stuttgart, Germany, 1955, p. 650.

(13) J. L. Kice and G. Guaraldi, *Tetrahedron Lett.*, **1966**, 6135.

(14) S. Kushner, L. M. Brancone, R. I. Hewitt, W. C. McEwen, Y. Subbarow, H. W. Stewart, R. J. Turner, and J. J. Denton, *J. Org. Chem.*, **13**, 144 (1948).

(15) U. Lerch and J. G. Moffatt, *ibid.*, **36**, 3861 (1971).

(16) S. Oae, O. Yamada, and T. Maeda, *Bull. Chem. Soc. Jpn.*, **47**, 166 (1974).

(17) D. Walker and J. Leib, U.S. pat. 3,296,308 (1967); through *Chem. Abstr.*, **68**, 12695x (1968).

(18) "Handbook of Chemistry and Physics," 52nd ed., R. C. Weast, Ed., Chemical Rubber Co., Cleveland, Ohio, 1971, p. C-273.

(19) R. Lehmann and E. Grivsky, *Bull. Soc. Chim. Belges*, **55**, 52 (1946); through *Chem. Abstr.*, **41**, 5477a (1947).

(20) A. A. M. Witte, *Rec. Trav. Chim.*, **51**, 299 (1932).

(21) P. T. Paul, U.S. pat. 2,373,335 (1945); through *Chem. Abstr.*, **40**, 1056[6] (1946).

(22) T. A. Mastryukova, Y. N. Sheinker, and I. K. Kabachnik, *Tetrahedron*, **19**, 357 (1963).

(23) E. V. Chechegoeva, L. K. Vinograd, and V. A. Izmail'skii, *Zh. Org. Khim.*, **2**, 1321 (1966); through *Chem. Abstr.*, **66**, 65225j (1967).

ACKNOWLEDGMENTS AND ADDRESSES

Received June 17, 1976, from the *College of Pharmacy, Faculty of Health Professions, and the [1]Department of Chemistry, Faculty of Arts and Science, Dalhousie University, Halifax, Nova Scotia, Canada.

Accepted for publication September 7, 1976.

Supported in part by Smith Kline and French Canada Ltd.

[x] To whom inquiries should be directed.

Mechanism of Methacholine-Induced Rise in Intraocular Pressure in the Dog

EUGENE R. BAIZMAN and HOWARD J. JENKINS ˣ

Abstract □ The mechanism of the methacholine-induced rise in intraocular pressure in the dog was studied to determine the basis of the relationship, if any, between lens thickness and intraocular pressure. The results rule out a vasodilator component in methacholine intraocular pressure elevation, and the tonometric recording of the elevation makes unlikely the involvement of methacholine stimulation of the rectus muscles of the eye. Thus, indirect evidence points to methacholine stimulation of ciliary muscle contraction with consequent thickening of the lens as responsible for its intraocular pressure-elevating effect and, hence, the ability of the response under investigation to specify the cycloplegic liability of a neurotropic antispasmodic agent.

Keyphrases □ Methacholine—mechanism of induced rise in intraocular pressure, effect of phenylephrine, dogs □ Intraocular pressure—mechanism of methacholine-induced rise, effect of phenylephrine, dogs □ Phenylephrine—effect on methacholine-induced rise in intraocular pressure, dogs □ Cholinergic agents—methacholine, mechanism of induced rise in intraocular pressure, effect of phenylephrine, dogs □ Adrenergic agents—phenylephrine, effect on methacholine-induced rise in intraocular pressure, dogs

During studies to determine the relative response of a number of parameters to intravenously administered methacholine chloride, intraocular pressure, as measured with an applanation tonometer, increased during a brief postinjection period and then decreased to normal (1). In contrast, parasympathomimetic agents in general, when applied topically to the cornea, were reported (2, 3) to lower intraocular pressure. It became apparent that the increase in intraocular pressure in response to methacholine is dose dependent and that it can be offset by the prior administration of an anticholinergic compound such as atropine if the dose of the latter is adequate. Moreover, if the dose of the anticholinergic be such as to effect a partial block of established extent of the cholinergic receptors, the magnitude of the dose of methacholine that will elicit a 50% increase (half of the maximal response) in intraocular pressure (Me_{50}) is an index of the affinity of the anticholinergic agent for cholinergic receptors associated with the response.

EXPERIMENTAL

Mongrel, male dogs, 12–17 kg, were fed once a day at approximately the same time each day and allowed water *ad libitum*. Each dog was anesthetized with 10 mg of thiopental sodium/kg and 90 mg of α-chloralose/kg iv, mixed in the calculated amounts and heated in an aqueous solution to 40–45° to increase solubility just prior to injection.

Blood pressure was recorded directly by femoral artery puncture and pressure transducer. Changes in intraocular pressure during a determination were transmitted to a pressure preamplifier by an applanation pressure transducer, the pressure-sensitive metallic core of which was positioned directly over the pupil on the corneal surface. A short piece of glass tubing, flanged at its point of contact with the eyeball, was used to support the base of the tonometer so that the core of the tapered end made unobstructed contact with the corneal surface.

The dosage regimen employed in the initial portion of this study was identical with that used previously (1). The first standard dose of 5.55 μg of methacholine/kg iv was injected and subsequently flushed into the circulatory system of the animal with 3 ml of saline. Intraocular pressure responses to methacholine were read at their respective peaks. Blood pressure responses were read twice for each dose of methacholine administered. The first reading was made just prior to drug administration, and the second was made at the nadir of the depressor response.

The second standard dose of methacholine (5.55 μg/kg) was administered in the same manner as the first. If the response to either of these two drug administrations differed by much more than 10% from the average of the two, a third standard dose of methacholine was given. Then the three responses were averaged for use in subsequent calculations to determine the degree of inhibition of the response occasioned by the anticholinergic agent.

When the effect of the last preanticholinergic dose of methacholine had terminated, a 6.5-μg/kg iv dose of the anticholinergic agent, glycopyrrolate bromide, was administered. During the following 30 min, the anticholinergic compound was allowed to exert its full effect. Then the preanticholinergic dose of methacholine (5.55 μg/kg) was repeated, and the responses of the two parameters to this dose were read in the same manner as described previously. After ensuring that all records had returned to their respective baselines, a second dose of methacholine was administered 15 min after the administration of the initial postanticholinergic dose; similarly, a third dose of this drug was administered 15 min following the second dose.

In all determinations, the quantities of the postanticholinergic doses of methacholine were equivalent to: (*a*) the preanticholinergic dose, (*b*) twice the preanticholinergic dose, and (*c*) three times the preanticholinergic dose. This series was chosen in an attempt to elicit responses such that one would be approximately 50% of the (average) preanticholinergic response, one would be greater than 50% of this (average) response, and one would be less than 50%.

Each postanticholinergic response to methacholine was expressed as the percent inhibition of the (average) preanticholinergic response. An Me_{50} was then obtained for each parameter whose responses lent themselves to quantitative treatment (intraocular pressure and arterial blood pressure) by plotting dose–response data on logarithmic–probability paper, with the percent inhibition as the ordinate and the dose of methacholine as the abscissa (single dose of anticholinergic per determination). The fit of the line to the plotted points was determined both by visual inspection and by the method of least squares. The Me_{50}'s so obtained were averaged, and their standard deviations were determined.

The first modification of the described drug dosage regimen was the substitution of an intravenous dose of phenylephrine hydrochloride for glycopyrrolate. Doses of 10, 20, and 30 μg/kg of the latter were administered 15 min apart, beginning 15 min after the last prephenylephrine dose of methacholine had been injected. Responses were recorded in the usual manner.

Exactly 60 sec after the injection of the first dose of phenylephrine, at the peak of the response to this pressor agent, a dose of methacholine equivalent to the prephenylephrine dose (5.55 μg/kg) was administered and the responses were recorded. After both intraocular pressure and blood pressure parameters had again returned to their respective baselines, the second phenylephrine dose was administered, followed 1 min later by a dose of methacholine identical to the one previously administered. The third and largest dose of phenylephrine was then given, again followed precisely 1 min later by 5.55 μg/kg of methacholine. By means of the prior systemic administration of phenylephrine, a potent vasoconstrictor and pressor agent, it was possible to obtain pharmacological opposition to the depressor and vasodilator effects of methacholine which might be involved in the intraocular pressure rise.

RESULTS AND DISCUSSION

Variations in such physiological phenomena as respiration and arterial blood pressure can affect intraocular pressure (4), and intraocular pressure elevated as a result of such variations has been reported. Carballo (4) stated that acetylcholine and anticholinesterases elevate ocular tension by producing vasodilation in the eye and by stimulating the contraction of the external rectus muscles. This finding was substantiated

Table I—Methacholine-Induced Responses of Intraocular Pressure and Arterial Blood Pressure after Injection of Phenylephrine Hydrochloride in a 16.0-kg Dog

Time	Drug	Pupil Size, mm	Intraocular Pressure, mm Hg	Arterial Blood Pressure, mm Hg
2:45	Thiopental, 10 mg/kg iv, and chloralose, 90 mg/kg iv	—	—	—
3:00	Chloralose, 45 mg/kg sc	—	—	—
3:10		3	—	170/105
3:20		3	—	182/115
3:22	Methacholine, 55 μg/kg iv	4	13.0	70/50
3:32		3	—	198/120
3:37	Phenylephrine, 10 μg/kg iv	4	—	240/180
3:38	Methacholine, 5.55 μg/kg iv	4	14.0	150/80
3:48		3	—	200/122
3:53	Phenylephrine, 20 μg/kg iv	4	—	250/180
3:54	Methacholine, 5.55 μg/kg iv	3	12.5	182/120
4:04		4	—	200/130
4:09	Phenylephrine, 30 μg/kg iv	4	—	250/90
4:10	Methacholine, 5.55 μg/kg iv	4	13.0	170/120

by Colle *et al.* (5), who observed that administration of large doses of acetylcholine produced a rapid rise in intraocular pressure of the perfused dog head, with a rise in systemic blood pressure. Here also vasodilation of intraocular vessels and contraction of the rectus muscle were implicated in the response. Methacholine, certain anticholinesterases, and pilocarpine have all caused a vasodilation of the conjunctival and intraocular vessels as well as increased permeability of their walls (6). The volume of blood contained in the vessels of the choroid and of the ciliary body constitutes a large part of the total volume of the eye. Hence, any agent affecting the filling of these vessels may affect intraocular pressure (7).

Cholinergic agents, especially echothiophate iodide and pilocarpine, may produce a shallowing of the anterior chamber, which could result from an anterior displacement of the lens with relaxation of the suspensory ligaments following contraction of the ciliary muscle (8). The thrust of the anterior lenticular displacement may cause a bowing of the iris in the direction of the cornea, narrowing the chamber angle and increasing resistance to drainage. As the thickening lens pushes anteriorly against the iris, its more spherical anterior surface may achieve a pupil block, which prevents dissipation of a pressure rise through this avenue of escape.

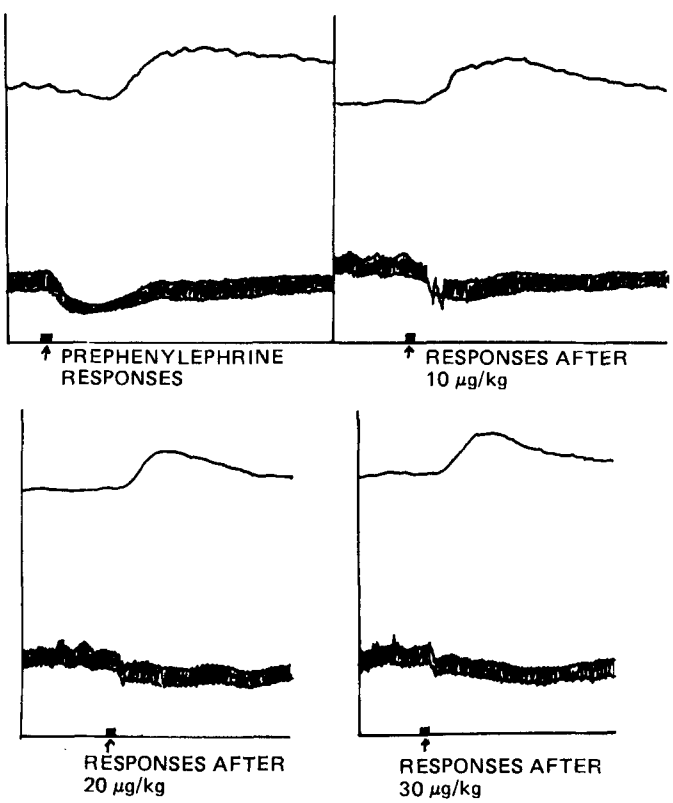

Figure 1—*Intraocular and arterial blood pressure responses to methacholine chloride (5.55 μg/kg) in an anesthetized dog before and after injection of 10, 20, and 30 μg of phenylephrine hydrochloride/kg iv. (Time: 1 mm = 1 sec; arterial blood pressure: 1 mm = 10 mm Hg; intraocular pressure: 1 mm = 1 mm Hg.)*

Thus, there are three (chief) mechanisms by which parasympathetic stimulation and parasympathomimetic agents may increase intraocular pressure such as is obtained in the intravenous administration of methacholine chloride in the dog:

1. Increased aqueous humor production through vasodilation and increased permeability of ciliary vessels.
2. Anterior thickening of the crystalline lens pushing the iris toward the rigid cornea, thereby decreasing the drainage angle of the anterior chamber and the chamber volume. (A combination of 1 and 2 is possible.)
3. Contraction of the external rectus muscle with consequent reduction in intrachamber volume.

In light of results obtained when phenylephrine was injected intravenously, vasodilation probably does not play a significant role in the methacholine-induced rise in intraocular pressure in the intact dog (Table I and Fig. 1). Little, if any, change occurred in the elevation of intraocular pressure after methacholine injection when phenylephrine was administered intravenously beforehand and was acting systemically to constrict intraocular vessels or was applied topically, directly upon the corneal surface (not shown). Phenylephrine was used to eliminate the possibility that intraocular vessel changes elicited by methacholine are responsible for the rise in intraocular pressure. This sympathomimetic mydriatic agent is reported to lower significantly an elevated intraocular pressure by decreasing aqueous humor formation through constriction of the intraocular vessels of the ciliary body and the choroid coat. Furthermore, it induces no significant changes in the aqueous humor outflow, the ciliary muscle, or the crystalline lens (9–11).

A comparison of the mean and standard deviation of the mean blood pressure Me_{50} values with the mean and standard deviation of the intraocular pressure Me_{50} values for glycopyrrolate shows a significant difference ($p = 0.005$) between the affinities of vascular and ciliary cholinergic receptors for this anticholinergic agent (Table II). This difference indicates that the rise in intraocular pressure elicited by methacholine is not secondary to the fall in arterial blood pressure, *i.e.*, to vasodilation and the subsequent increase in aqueous humor production. Thus, the two responses do not appear to represent the same basic phenomenon and might be separable on an experimental basis. Moreover, the rapidity of the rise of intraocular pressure in response to methacholine makes increased aqueous humor production an unlikely etiologic factor. Besides, the contraction of ciliary muscle in response to methacholine reduces muscle volume, with a resultant constriction of ciliary blood vessels, each of which tends to lower intraocular pressure. On the other hand, the reduction in the diameter of the ciliary circle, which attends contraction of the ciliary muscle, itself reduces the size of the anterior chamber and favors a pressure rise. In the early work of Armaly (8), the latter effect predominated in the cat eye after parasympathetic stimulation.

Because of the nature of the intraocular pressure determination (employing an applanation tonometer), any contraction of the external rectus muscle would manifest itself as a decrease in intraocular pressure and would be thus detectable.

By deduction, then, it appears that a thickening of the crystalline lens

Table II—Determination of Me_{50} Values for Glycopyrrolate (6.5 μg/kg iv)

	Intraocular Pressure, mm Hg	Inhibition, %	Arterial Blood Pressure, mm Hg	Inhibition, %
Mean preantispasmodic	12.0		85.00	
Methacholine, 5.55 μg/kg iv	4.0	66.66	35.02	58.80
Methacholine, 11.10 μg/kg iv	6.0	50.00	49.98	41.20
Methacholine, 16.65 μg/kg iv	7.5	37.50	57.46	32.40
Me_{50} value (from graphs)	10.08 μg/kg			8.10 μg/kg
Me_{50} mean	9.95 + 2.14 (n = 9)			5.79 ± 1.61 (n = 16)
t = 5.489				

with a resultant thrust of the iris in the direction of the cornea, decreasing the chamber volume and drainage angle, together with a (possible) block of the pupillary opening preventing the dissipation of increasing chamber pressure is responsible for the methacholine-induced rise in intraocular pressure. This rise probably occurs only after intravenous injection of methacholine when the rapid forward thrust of the iris by the thickening of the lens, which appears responsible for it, is able to overcome for a time the tendency of the drainage system to offset it, a tendency soon realized in the speedy return of pressure to baseline following the postinjection rise. Subsequent investigation might involve another route of methacholine administration in an effort to determine the influence of the administration route on the response. It should also attempt to determine whether a dose of methacholine that is threshold for blood pressure reduction has any effect on intraocular pressure or, conversely, the extent to which methacholine might reduce blood pressure before it effects an increase in intraocular pressure.

The significance of this study involves the use of the parameter of intraocular pressure to determine the liability of a neurotropic antispasmodic (parasympatholytic) agent to induce cycloplegia. If a direct relationship exists between intraocular pressure and lens thickness, as this study indicates, then the extent to which the neurotropic antispasmodic interferes with a cholinergic-induced rise in intraocular pressure is a measure of its tendency to produce cycloplegia or blurring of vision. Hence, neurotropic antispasmodic compounds with relatively high intraocular pressure Me_{50}'s (in relation to their antimotility or antisecretory Me_{50}'s) should have a high liability with respect to the side effect of cycloplegia.

The study reported is a facet of a comprehensive investigation conducted over years. Numerous determinations of the effect of neurotropic antispasmodic agents on the intraocular pressure response to methacholine in the dog were made, and the data reported here are representative.

REFERENCES

(1) W. H. Stigelman, M.S. thesis, Massachusetts College of Pharmacy, Boston, Mass., 1969.

(2) W. M. Grant, *Annu. Rev. Pharmacol.*, **9**, 85 (1969).

(3) W. M. Grant, *Pharmacol. Rev.*, **7**, 143 (1955).

(4) A. S. Carballo, *Can. Anaesth. Soc. J.*, **12**, 486 (1965).

(5) J. C. Colle, P. M. Duke-Elder, and W. S. Duke-Elder, *J. Physiol. (London)*, **71**, 1 (1931).

(6) W. S. Duke-Elder, "System of Ophthalmology," vol. 11, Mosby, St. Louis, Mo., 1969.

(7) A. K. Adams and K. C. Barrett, *Anaesthesia*, **21**, 202 (1966).

(8) M. F. Armaly, *Arch. Ophthalmol.*, **61**, 14 (1958).

(9) P. F. Lee, *ibid.*, **60**, 863 (1958).

(10) B. Becker, T. Gage, A. E. Kolker, and A. J. Gay, *Am. J. Ophthalmol.*, **48**, 313 (1959).

(11) B. Becker and J. S. Friedenwald, *Arch. Ophthalmol.*, **50**, 557 (1953).

ACKNOWLEDGMENTS AND ADDRESSES

Received May 24, 1976, from the *Massachusetts College of Pharmacy, Boston, MA 02115.*

Accepted for publication September 16, 1976.

[x] To whom inquiries should be directed.

Impurities in Drugs I: Imipramine, Desipramine, and Their Formulations

K. M. McERLANE [x], N. M. CURRAN, and E. G. LOVERING

Abstract □ Nineteen lots of imipramine tablets and four lots of desipramine tablets were examined for impurities by TLC. Iminodibenzyl, desipramine, and 10,11-dihydro-5-[3-(methylamino-3′-dimethylaminopropyl)propyl]-5*H*-dibenz[*b,f*]azepine dihydrobromide (I) were found in some imipramine tablets, and iminodibenzyl and imipramine were found in some desipramine tablets, all at levels of less than 0.3% of label claim of the drug. Except for I, the identity of the impurities was established by comparison with known standards; I was synthesized and its composition was established by elemental analysis. All impurities, including I, were characterized by TLC, GLC, and mass spectrometry.

Keyphrases □ Imipramine tablets—impurities, TLC, GLC, and mass spectral analysis □ Desipramine tablets—impurities, TLC, GLC, and mass spectral analysis □ Impurities—in imipramine and desipramine tablets, TLC, GLC, and mass spectral analysis □ Tablets—imipramine and desipramine, TLC, GLC, and mass spectral analysis of impurities □ Dosage forms—tablets, imipramine and desipramine, TLC, GLC, and mass spectral analysis of impurities □ Antidepressants—imipramine and desipramine tablets, TLC, GLC, and mass spectral analysis of impurities

Organic compounds found as impurities in drugs and drug formulations may be intermediates or by-products of the drug synthesis, products of drug or excipient degradation, products of drug–excipient interaction, or the result of contamination. The nature of the impurities in a drug may depend on the synthetic process and the source of materials used in manufacture or the nature and source of the excipients. Impurities may be toxic, and their

Table II—Determination of Me_{50} Values for Glycopyrrolate (6.5 μg/kg iv)

	Intraocular Pressure, mm Hg	Inhibition, %	Arterial Blood Pressure, mm Hg	Inhibition, %
Mean preantispasmodic	12.0		85.00	
Methacholine, 5.55 μg/kg iv	4.0	66.66	35.02	58.80
Methacholine, 11.10 μg/kg iv	6.0	50.00	49.98	41.20
Methacholine, 16.65 μg/kg iv	7.5	37.50	57.46	32.40
Me_{50} value (from graphs)	10.08 μg/kg			8.10 μg/kg
Me_{50} mean	9.95 + 2.14 (n = 9)			5.79 ± 1.61 (n = 16)
t = 5.489				

with a resultant thrust of the iris in the direction of the cornea, decreasing the chamber volume and drainage angle, together with a (possible) block of the pupillary opening preventing the dissipation of increasing chamber pressure is responsible for the methacholine-induced rise in intraocular pressure. This rise probably occurs only after intravenous injection of methacholine when the rapid forward thrust of the iris by the thickening of the lens, which appears responsible for it, is able to overcome for a time the tendency of the drainage system to offset it, a tendency soon realized in the speedy return of pressure to baseline following the postinjection rise. Subsequent investigation might involve another route of methacholine administration in an effort to determine the influence of the administration route on the response. It should also attempt to determine whether a dose of methacholine that is threshold for blood pressure reduction has any effect on intraocular pressure or, conversely, the extent to which methacholine might reduce blood pressure before it effects an increase in intraocular pressure.

The significance of this study involves the use of the parameter of intraocular pressure to determine the liability of a neurotropic antispasmodic (parasympatholytic) agent to induce cycloplegia. If a direct relationship exists between intraocular pressure and lens thickness, as this study indicates, then the extent to which the neurotropic antispasmodic interferes with a cholinergic-induced rise in intraocular pressure is a measure of its tendency to produce cycloplegia or blurring of vision. Hence, neurotropic antispasmodic compounds with relatively high intraocular pressure Me_{50}'s (in relation to their antimotility or antisecretory Me_{50}'s) should have a high liability with respect to the side effect of cycloplegia.

The study reported is a facet of a comprehensive investigation conducted over years. Numerous determinations of the effect of neurotropic antispasmodic agents on the intraocular pressure response to methacholine in the dog were made, and the data reported here are representative.

REFERENCES

(1) W. H. Stigelman, M.S. thesis, Massachusetts College of Pharmacy, Boston, Mass., 1969.

(2) W. M. Grant, *Annu. Rev. Pharmacol.*, **9**, 85 (1969).

(3) W. M. Grant, *Pharmacol. Rev.*, **7**, 143 (1955).

(4) A. S. Carballo, *Can. Anaesth. Soc. J.*, **12**, 486 (1965).

(5) J. C. Colle, P. M. Duke-Elder, and W. S. Duke-Elder, *J. Physiol. (London)*, **71**, 1 (1931).

(6) W. S. Duke-Elder, "System of Ophthalmology," vol. 11, Mosby, St. Louis, Mo., 1969.

(7) A. K. Adams and K. C. Barrett, *Anaesthesia*, **21**, 202 (1966).

(8) M. F. Armaly, *Arch. Ophthalmol.*, **61**, 14 (1958).

(9) P. F. Lee, *ibid.*, **60**, 863 (1958).

(10) B. Becker, T. Gage, A. E. Kolker, and A. J. Gay, *Am. J. Ophthalmol.*, **48**, 313 (1959).

(11) B. Becker and J. S. Friedenwald, *Arch. Ophthalmol.*, **50**, 557 (1953).

ACKNOWLEDGMENTS AND ADDRESSES

Received May 24, 1976, from the *Massachusetts College of Pharmacy, Boston, MA 02115.*

Accepted for publication September 16, 1976.

[x] To whom inquiries should be directed.

Impurities in Drugs I: Imipramine, Desipramine, and Their Formulations

K. M. McERLANE [x], N. M. CURRAN, and E. G. LOVERING

Abstract □ Nineteen lots of imipramine tablets and four lots of desipramine tablets were examined for impurities by TLC. Iminodibenzyl, desipramine, and 10,11-dihydro-5-[3-(methylamino-3′-dimethylaminopropyl)propyl]-5*H*-dibenz[*b,f*]azepine dihydrobromide (I) were found in some imipramine tablets, and iminodibenzyl and imipramine were found in some desipramine tablets, all at levels of less than 0.3% of label claim of the drug. Except for I, the identity of the impurities was established by comparison with known standards; I was synthesized and its composition was established by elemental analysis. All impurities, including I, were characterized by TLC, GLC, and mass spectrometry.

Keyphrases □ Imipramine tablets—impurities, TLC, GLC, and mass spectral analysis □ Desipramine tablets—impurities, TLC, GLC, and mass spectral analysis □ Impurities—in imipramine and desipramine tablets, TLC, GLC, and mass spectral analysis □ Tablets—imipramine and desipramine, TLC, GLC, and mass spectral analysis of impurities □ Dosage forms—tablets, imipramine and desipramine, TLC, GLC, and mass spectral analysis of impurities □ Antidepressants—imipramine and desipramine tablets, TLC, GLC, and mass spectral analysis of impurities

Organic compounds found as impurities in drugs and drug formulations may be intermediates or by-products of the drug synthesis, products of drug or excipient degradation, products of drug–excipient interaction, or the result of contamination. The nature of the impurities in a drug may depend on the synthetic process and the source of materials used in manufacture or the nature and source of the excipients. Impurities may be toxic, and their

Table I—Chromatographic Characteristics

Compound	TLC R_f	TLC Detectability Limit[a], μg	GLC Retention Time, min
Iminodibenzyl	0.81	0.06	3
Imipramine[b]	0.67	0.03	6.5
I	0.26	0.03	23
Desipramine[c]	0.36	0.03	8

[a] Applied with 200 μg of the drug. [b] As an impurity in desipramine. [c] As an impurity in imipramine.

presence may be indicative of inadequately controlled manufacturing or storage conditions.

To obtain a broadly based perspective of impurity levels and the potential problems associated with them, drug products and formulations from many different sources should be examined. This paper, the first of a series reporting the occurrence of impurities in drugs, describes a study of imipramine and desipramine formulations.

Imipramine hydrochloride is official in USP XIX (1) and BP 1973 (2, 3). Limits for iminodibenzyl, one of the starting materials, are set at 0.1% by the USP and at 0.2% by the BP. Tablets and injections are described in the USP, and tablets are described in the BP, but only the latter specifies a limit for iminodibenzyl (0.3%) in tablet formulations.

Desipramine hydrochloride is official in NF XIV (4) and in BP 1973 (2). The limits specified for iminodibenzyl are 0.1 and 0.2%, respectively. Tablets and capsules are described in the NF, and tablets are described in the BP. The latter sets a limit of 0.3% for the content of iminodibenzyl in tablets.

EXPERIMENTAL

Materials—Imipramine hydrochloride and desipramine hydrochloride were the respective USP and NF reference standard materials. Nineteen lots of seven brands of imipramine tablets and four lots of two brands of desipramine tablets were obtained from the manufacturers. The other reagents used were redistilled chloroform[1], benzene[1], ethyl acetate[1], absolute ethanol[2], and dimethylaminopropyl chloride[3]. Macherey–Nagel TLC plates[4] were precoated with 0.25-mm silica gel G containing a 254-nm fluorescent indicator.

Standard Solutions—For imipramine studies, 56.5 mg of imipramine hydrochloride was dissolved in 2.0 ml of 0.1 *N* hydrochloric acid, made basic with 0.1 ml of concentrated ammonium hydroxide, and extracted by shaking into 5.0 ml of chloroform containing 0.15 mg of iminodibenzyl, 0.17 mg of desipramine hydrochloride, and 0.22 mg of 10,11-dihydro-5-[3-(methylamino-3′-dimethylaminopropyl)propyl] - 5*H* - dibenz[*b,f*]-azepine dihydrobromide (I, Scheme I). The standard solution in chloroform was separated from the aqueous layer. The desipramine standard solution was prepared in a similar way by extracting 57.9 mg of desipramine hydrochloride into 5 ml of chloroform containing 0.15 mg of iminodibenzyl and 0.17 mg of imipramine hydrochloride.

Both reference standard drugs were shown, by the TLC system described in this paper, to be free of detectable impurities. Each standard solution contained 10 mg/ml of the free base form of the drug with the remaining compounds, also as the free bases, at 0.3% with respect to the drug.

TLC Solvent Systems—For imipramine, a system of benzene–ethyl acetate–absolute ethanol–concentrated ammonium hydroxide (50:50:15:3) was used. For desipramine, the proportions were 50:50:20:3, respectively. Both solutions were placed in filter paper-lined chromatographic tanks and allowed to equilibrate for 1 hr prior to use.

Tablet Extraction—Twenty tablets were weighed and finely powdered. An amount of drug equivalent to 50 mg of the free base was weighed into a 10-ml polytef-lined, screw-capped centrifuge tube. Then 2 ml of 0.1 *N* hydrochloric acid was added, and the tube was shaken vigorously for 15 min on a horizontal shaker. Concentrated ammonium hydroxide, 0.1 ml, and 5 ml of redistilled chloroform were added, and the tube was shaken for 20 min. A portion of the chloroform layer, containing the drug and impurities, was removed for analysis.

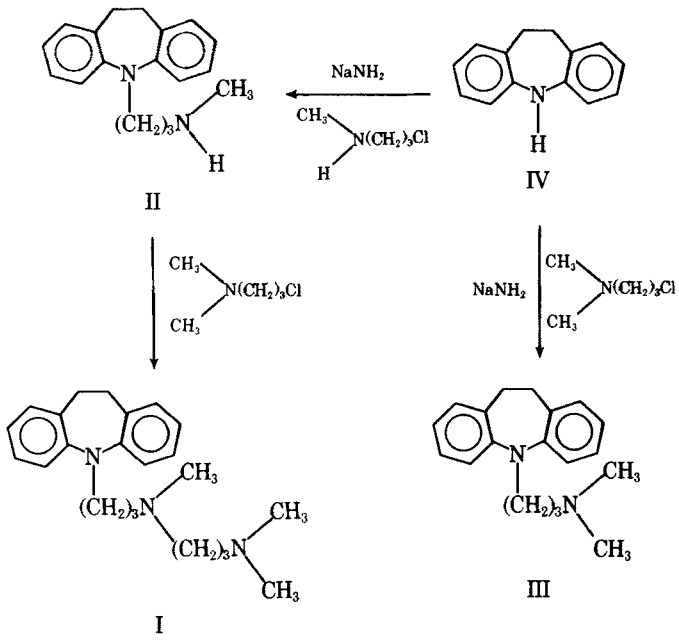

Scheme I

Screening for Impurities—The R_f of each drug and impurity in chloroform solution was determined in the appropriate TLC system. To check for possible decomposition, each compound was scraped from the plate and subjected to GLC and mass spectrometry. A portion of the eluate recovered from the gas chromatograph was rerun in the TLC system. The lower detection limit of each impurity was established by spotting serial dilutions of the appropriate stock solution.

Aliquots of 10 and 20 μl (100 and 200 μg) of the tablet extract in chloroform for each formulation were spotted beside 10- and 20-μl (100- and 200-μg) aliquots of the appropriate standard solution. Plates were developed, and the compounds were visualized using UV light at 254 nm and subsequently spraying with 0.5% (w/v) potassium dichromate in 20% (v/v) sulfuric acid. The concentration of impurities was approximated by comparison of the spot diameters and intensities with the corresponding spots due to the standard solutions.

Isolation of Impurities—A tablet extract containing 40 mg of drug as the hydrochloride in 1.0 ml of chloroform was applied in a narrow band to a 0.25-mm TLC plate, 20 × 20 cm, and developed in the appropriate solvent system. Four such plates were prepared. Impurities were visualized by UV light at 254 nm and by spraying a 1-cm band along each side of the plate with 0.5% (w/v) potassium dichromate in 20% (v/v) sulfuric acid.

To reduce the possibility of decomposition during manipulation, the impurities were converted to the more stable hydrochloride form by spraying lightly with ethanolic hydrochloric acid, and the bands were scraped from the TLC plates. The scrapings were stirred with 25 ml of absolute ethanol for 60 min and then filtered, and the ethanol solution was evaporated to dryness on a rotary evaporator at room temperature. The purity of the isolated compounds was checked by TLC and GLC.

Samples of impurities for mass spectral analysis were isolated by GLC using a column of 5% OV-25 on 100–120-mesh Chromosorb W (HP). The injection port, detector block, and column temperatures were 250, 250, and 240°, respectively. The flow rates of nitrogen, hydrogen, and air were 40, 50, and 400 ml/min, respectively. Approximately 50 μg of drug from the TLC plate extract was injected into the chromatographic column.

Fractions were collected in dry ice-cooled capillary tubes held over the flame tip of the chromatograph. The hydrogen flame was extinguished just prior to elution of the required fraction and reignited after collection to burn off material condensed on the flame tip. TLC showed that each fraction consisted of a single component, was free from decomposition products, and was identical to the material originally removed from the TLC plate.

[1] Caledon Laboratories Ltd., Georgetown, Ontario, Canada.
[2] Consolidated Alcohols Ltd., Toronto, Ontario, Canada.
[3] Aldrich Chemical Co., Milwaukee, Wis.
[4] Brinkmann Instruments, Toronto, Ontario, Canada.

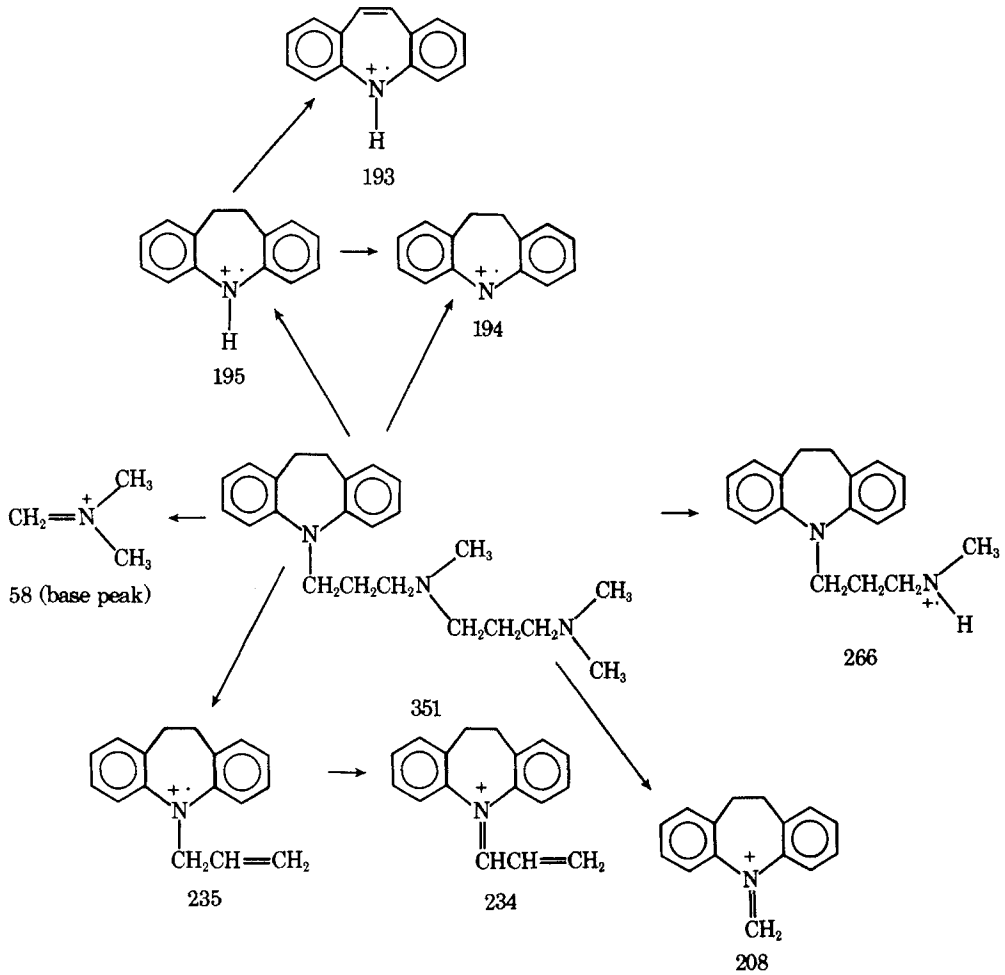

Scheme II

Synthesis—Dimethylaminopropyl chloride was obtained from its hydrochloride salt by triturating 16.0 g of the latter with 8.0 g of flaked sodium hydroxide (5). The free amine was decanted from the solid phase and distilled at 124–128°/160 mm Hg through a 5-cm vigreaux column.

Compound I was prepared by refluxing a mixture of 7.5 g of freshly distilled dimethylaminopropyl chloride and 0.83 g of desipramine (II) in 20.0 ml of dry acetone for 18 hr (Scheme I). The acetone and excess dimethylaminopropyl chloride were removed on a rotary evaporator. The residue was taken up in 10 ml of 0.1 *N* hydrochloric acid, washed twice with 50 ml of ether, made basic with 1.0 ml of concentrated ammonium hydroxide, and extracted with two 50-ml portions of chloroform. The chloroform was removed on a rotary evaporator at room temperature, and ethanolic hydrogen bromide was added to the residue. The resulting salt was crystallized by the addition of ether and dried at 56°/1 mm Hg. The crystalline melting point[5] was 218–221° (uncorrected).

Anal.—Calc. for $C_{23}H_{33}N_3 \cdot 2HBr$: C, 53.81; H, 6.87; N, 8.19. Found: C, 53.95; H, 6.97; N, 8.05.

The PMR[6] spectrum (1% in deuterochloroform, 40°) exhibited distinctive signals downfield from trimethylsilane at 131 Hz due to the three-proton *N*-methyl singlet and at 138 Hz due to the six-proton *N,N*-dimethyl singlet, but the signal at 73.5 Hz due to the NH proton in desipramine was not observed. The mass spectrum[7] was obtained by direct probe in the electron-impact mode at 70 ev and 160°. Attempts to prepare the crystalline hydrochloride salt were unsuccessful.

RESULTS AND DISCUSSION

A single chloroform extraction was sufficient for complete removal of imipramine and desipramine from aqueous tablet powder mixtures. No drug was found in the chloroform fraction following a second extraction of the aqueous tablet powder mixture. In addition, the diameters and intensities of the TLC spots from tablet extracts were identical to those from standard solutions of the hydrochlorides at corresponding concentrations. No degradation of the drug or its impurities was observed when the free bases were applied at 0.5-hr intervals over 3 hr. The TLC solvent system was chosen to maximize separation of the impurities. The toluene–methanol (95:5) system described in BP 1973 (2) is adequate only for iminodibenzyl.

The identity of iminodibenzyl, imipramine, and desipramine found in tablet formulations was established by comparison of the TLC R_f values, GLC retention times, and mass spectral fragmentation patterns with those of known samples. Tablet impurities for GLC were recovered from TLC plates, and GLC eluates were collected for mass spectrometry and TLC, as previously described. The purity of the standard compounds was authenticated by subjecting them to the TLC, GLC, and mass spectral treatment.

The structure postulated for I is in agreement with the elemental analysis and the PMR spectrum. It is further supported by the mass spectral results, which conformed to the fragmentation scheme presented

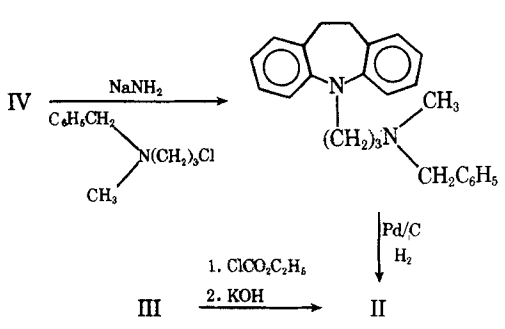

Scheme III

[5] Thomas-Hoover capillary melting-point apparatus.
[6] Varian A-60A NMR spectrometer.
[7] Hitachi Perkin-Elmer RMU 6L mass spectrometer.

Table II—Impurities in Imipramine Tablets

Brand	Dose, mg	Impurities[a], %			
		Iminodibenzyl	Desipramine	I	Other
A	10	0.2	0.3	0.25	ND[b]
	25	0.05	0.1	0.10	ND
B	10	0.1	0.1	0.05	R_f 0.15; Tr[c]
	25	0.2	0.1	0.1	R_f 0.15; Tr
	50	0.2	0.2	0.2	ND
C	10	0.2	0.2	0.1	R_f 0.30; Tr
	25	0.05	0.05	0.05	ND
	50	0.05	0.1	0.1	R_f 0.30; 0.3%
	75	0.1	0.1	0.1	R_f 0.30; Tr
	150	0.2	0.1	ND	ND
D	25	ND	0.1	0.05	ND
	50	0.1	0.25	ND	ND
E	10	0.1	0.2	ND	R_f 0.30; 0.3%
	25	ND	0.2	ND	R_f 0.30; 0.2%
	50	0.1	0.15	ND	ND
F	10	0.1	0.2	0.2	ND
	25	0.1	0.2	0.2	ND
G	10	0.1	0.3	0.1	ND
	25	0.1	0.3	0.3	ND

[a] Expressed as percentage of the label claim of drug in the free base form. [b] None detected. [c] Trace.

in Scheme II. Detectability limits and R_f values by TLC and retention times by GLC for imipramine, desipramine, iminodibenzyl, and I are given in Table I.

Nineteen lots of imipramine tablets from seven manufacturers were tested for impurities (Table II). All lots contained desipramine at levels from 0.1 to 0.3%, and all but two contained iminodibenzyl at levels from 0.05 to 0.2%. Compound I was found in 14 lots in amounts to 0.3%. The occurrence of desipramine (II) and I in imipramine (III) formulations may be due to the presence of monomethylaminopropyl chloride in the dimethylaminopropyl chloride used as a starting material in at least one synthetic process (6) (Scheme I). Iminodibenzyl (IV) is used as a starting material, but its presence may also result from decomposition of the drug (7).

An impurity at R_f 0.30 was observed in five lots at levels from trace to 0.3%, on the basis of the sensitivity established for imipramine. This impurity may be the 10-hydroxy analog of imipramine suggested by Adank and Hammerschmidt (7), but attempts to isolate and identify the compound were unsuccessful. Trace amounts of an impurity at R_f 0.15 were observed in two lots, but no attempt at isolation and identification was made.

Each of four lots of two brands of desipramine contained iminodibenzyl, and three of the four contained imipramine, all at levels below 0.15% (Table III). Iminodibenzyl is a synthetic precursor (8) (Scheme III) and may also result from breakdown of the drug (9); the source of imipramine may be due to the residual material remaining if imipramine is demethylated *via* the chloroformate ester to produce desipramine (10). The level of iminodibenzyl in all formulations tested was below the limit of 0.3% specified for tablets in BP 1973, even though some formulations were manufactured to specifications other than those of the BP.

Table III—Impurities in Desipramine Tablets

Brand	Dose, mg	Impurities[a], %	
		Iminodibenzyl	Imipramine
A	10	0.15	0.15
A	25	0.15	0.15
A	50	0.15	0.15
B	25	0.1	ND[b]

[a] Expressed as a percentage of the label claim of drug in the free base form. [b] None detected.

REFERENCES

(1) "The United States Pharmacopeia," 19th rev., Mack Publishing Co., Easton, Pa., 1975.

(2) "British Pharmacopoeia 1973," Her Majesty's Stationery Office, London, England, 1973.

(3) "European Pharmacopoeia 1971," Maisonneuve, France, 1971.

(4) "The National Formulary," 14th ed., Mack Publishing Co., Easton, Pa., 1975.

(5) R. R. Burtner, *J. Am. Chem. Soc.*, **71**, 2578 (1949).

(6) W. Schindler and F. Haefliger, *Helv. Chim. Acta*, **37**, 472 (1954).

(7) K. Adank and W. Hammerschmidt, *Chimia*, **18**, 361 (1964).

(8) J. H. Biel and C. I. Judd, British pat. 980,231 (1965); through *Chem. Abstr.*, **63**, 14830 (1965).

(9) K. Adank and T. Schmidt, *Chimia*, **23**, 299 (1969).

(10) J. R. Geigy Co., Belgium pat. 614,616 (1966); through *Chem. Abstr.*, **58**, 11337c (1963).

ACKNOWLEDGMENTS AND ADDRESSES

Received June 9, 1976, from the *Drug Research Laboratory, Health Protection Branch, Tunney's Pasture, Ottawa, Ontario, K1A 0L2, Canada.*

Accepted for publication September 14, 1976.

The assistance of Mr. H. Avdovich and Dr. A. By in obtaining the PMR and mass spectra is gratefully acknowledged.

[x] To whom inquiries should be directed.

Chemical and Spectroscopic Analysis of a Phenobarbital–Ephedrine Complex

MARSHA B. MRTEK ˣ, JAMES E. GEARIEN, and MARTIN I. BLAKE

Abstract □ A complex of phenobarbital and ephedrine was prepared and characterized. The complex was differentiated from physical mixtures of the two drugs by TLC and IR spectroscopy. NMR spectroscopy was used to verify the proportion of each drug in the complex and to confirm the existence of intermolecular binding. Mass spectrometry was employed to establish that all fragments characteristic of the individual drug entities could be isolated from the complex. Elemental analysis confirmed the chemical composition of the complex. A possible chemical structure for the complex was hypothesized on the basis of the chemical and spectroscopic data.

Keyphrases □ Phenobarbital—complex with ephedrine prepared, chemical and spectroscopic analysis □ Ephedrine—complex with phenobarbital prepared, chemical and spectroscopic analysis □ Complexes—phenobarbital with ephedrine, preparation, chemical and spectroscopic analysis

One widely used method to measure complexation has been to monitor a change in the curve produced for some additive property such as spectrophotometric absorbance. Titration techniques have been used whenever a change in pH accompanied the complexation reaction. The change in absolute solubility in a given solvent was used to measure quantitatively the production of caffeine complexes (1), and a phase solubility technique was used to study the formation of complex salts of triamterene with several acids (2).

The color reaction of local anesthetics with 1,3,5-trinitrobenzene was utilized to study the stoichiometry of complex formation (3). NMR spectroscopy was used (4) to study the structure of the caffeine–sodium benzoate complex, and differential thermal analysis was used (5) to follow the interaction of aminopyrine and barbital. A combination of NMR and IR spectroscopy was employed to investigate the extent of hydrogen bonding resulting in increased solubility of paraben combinations (6).

A number of molecular phenobarbital complexes were investigated. Phase solubility studies of phenobarbital and polyethylene glycol complexes (7), an IR study of phenobarbital association with purines (8), and IR studies of phenobarbital complexes with quinine, quinidine, and hydroquinidine (9) were reported. The isolation of a 1:1 phenobarbital–ephedrine complex formed by acid–base neutralization in ether also was reported (10).

The objective of this study was to apply chemical and spectroscopic analytical techniques to determine the nature and structure of a phenobarbital–ephedrine complex.

EXPERIMENTAL

Phenobarbital was recrystallized from boiling water, and the melting point of the recrystallized and dried product was determined by differential thermal analysis to be 174–176°. Ephedrine hemihydrate was made anhydrous by azeotroping with benzene, and the resulting solid was dried and stored under vacuum. The melting point determined by differential thermal analysis was 33–36°. Spectral grade chloroform was used for the IR analysis. All other reagents were analytical grade. The recrystallized complex was subjected to elemental analysis[1].

Table I—R_f Values for Ephedrine, Phenobarbital, and Complex

Solvent System	Plates	R_f Ephedrine	R_f Phenobarbital	R_f Complex
50% Ethanol	Alumina	0.38	0.75	0.70
Anhydrous methanol	Alumina	0.57	0.31	0.23
50% Ethanol	Silica	0.10	0.80	0.80
				0.03
Anhydrous methanol	Silica	0.18	0.71	0.71
				0.11

Synthesis of Complex—Exactly 1.65 g (10 mmoles) of anhydrous ephedrine was added to 2.70 g (12 mmoles) of phenobarbital. The mixture was dissolved in approximately 15 ml of anhydrous ether, which had been stored over metallic sodium. Any excess phenobarbital was removed by filtration. The resulting solution was crystallized by chilling in an acetone–dry ice bath. The sides of the flask were scratched with a sharp glass rod to induce crystallization.

A "dry box" was prepared from an air-tight glove box containing phosphorus pentoxide under an atmosphere of nitrogen and was fitted with a suction hose for filtration. A specially prepared funnel was made by cutting a hole for a 9-cm büchner funnel in a 15-cm polyethylene büchner funnel. The holes in the outer funnel were sealed with a resin, and the space between the two funnels was filled with crushed dry ice. The funnel and filter paper were allowed to equilibrate in the dry box for at least 0.5 hr prior to filtration.

The crystals were collected in the central filter, and the ether was removed as rapidly as possible by vigorous suction aided by a positive pressure from nitrogen gas being introduced into the box. The filter system, including the dry ice and the crystalline material, was rapidly removed to a vacuum desiccator containing sulfuric acid and phosphorus pentoxide. The desiccator was immediately evacuated, and the crystals were left to dry for not less than 24 hr.

TLC—TLC was performed on both silica[2] and alumina[3] fluorescent plates for phenobarbital, ephedrine, and the complex. The plates were spotted with an ether solution of each compound, and spots were visualized with a UV lamp and iodine vapors. The following solvents were used: anhydrous methanol, 95% ethanol, 70% ethanol, anhydrous ether, 75% benzene–25% ethyl acetate, and 50% benzene–50% ethyl acetate.

IR Spectroscopy—IR spectra were obtained[4] for ephedrine, phenobarbital, and the complex using approximately 10% (w/v) samples dissolved in spectral grade chloroform.

NMR Spectroscopy—NMR spectroscopy[5] was used to examine the proton resonance structures of ephedrine, phenobarbital, the complex, ephedrine acetate, and phenobarbital triethylamine solutions in deuterochloroform (approximately 5% w/v). The spectra were determined in the field-sweep mode using an internal tetramethylsilane standard.

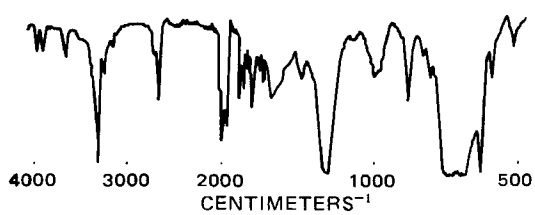

Figure 1—*IR spectrum of phenobarbital.*

[1] Carbon and hydrogen analyses were performed by Micro-Tech Laboratories, Skokie, Ill. Nitrogen analysis was obtained using a Coleman nitrogen analyzer.
[2] Merck silica gel 60 F254.
[3] Merck aluminum oxide type T F254.
[4] Perkin-Elmer 337 grating spectrophotometer.
[5] Varian T-60A NMR spectrometer equipped with Fourier transform.

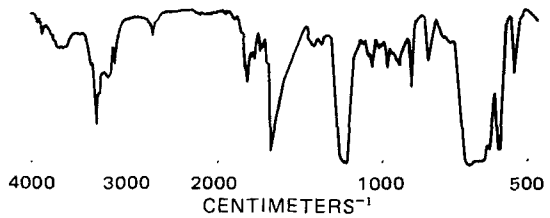

Figure 2—*IR spectrum of ephedrine.*

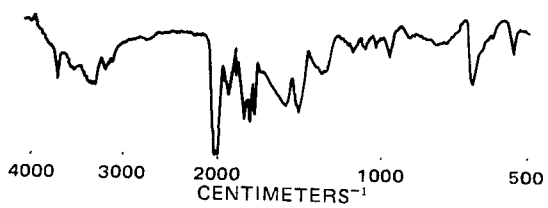

Figure 3—*IR spectrum of complex.*

Mass Spectrometry—Mass spectrograms for ephedrine, phenobarbital, and the complex were obtained[6].

RESULTS AND DISCUSSION

The results of Babin and Coustou (10) for the preparation of the complex by titration could not be duplicated in this laboratory. Only by removing all sources of water from the reagents and from the atmosphere surrounding them could a crystalline substance be isolated. It was then necessary to dry the crystals in a chilled, evacuated vessel to prevent further absorption of water and subsequent liquefaction. Once the crystals were completely free of solvent, they exhibited no further hygroscopic tendency. Differential thermal analysis showed the complex to have a wide melting range, centering at approximately 70°.

The results of TLC studies performed on the complex are summarized in Table I. Since the manufacturer's plates were used without subsequent activation, hydration of the silica plates cannot be ruled out as a cause of the decomposition of the complex that occurred on the silica plates but not on the alumina plates.

IR spectroscopy of phenobarbital in spectral grade chloroform yielded values of 3690 and 3630 cm^{-1} for NH and of 1750 and 1730 cm^{-1} for CO (Fig. 1). Ephedrine yielded peaks at 3670 and 3620 cm^{-1} for the phenolic hydrogen and a broad peak between 3500 and 3300 cm^{-1} for the hydrogen-bonded COH group (Fig. 2). The IR spectrum of the complex differed greatly from spectra of the individual compounds. An NH peak was found at approximately 3375 cm^{-1} with broad and ill-defined peaks surrounding it, indicating that hydrogen bonding existed in this area of the molecular complex (Fig. 3). The 3600–2600-cm^{-1} region for the complex more closely resembled that of the salts of ephedrine than of the alkaloid itself. A CO peak was found at 1750 cm^{-1}, as in the spectrum of phenobarbital.

To gain further evidence of complex formation, the NMR spectra of ephedrine, phenobarbital, and the product of their reaction were examined. The formation of a complex (Structure I) might be expected to affect the magnetic environment of the hydrogens of the aromatic rings of both compounds and the protons on the carbon atom of ephedrine adjacent to the methylamino group. It is assumed that the reaction proceeds first with salt formation, followed by the formation of a hydrogen bond between phenobarbital and the hydroxyl group of ephedrine and an alignment of the phenyl groups one on top of the other.

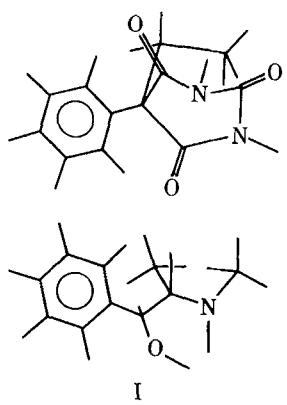

I

The NMR spectra of phenobarbital and ephedrine are shown in Figs. 4 and 5, respectively. The spectrum of the product of the reaction between phenobarbital and ephedrine (Fig. 6) appears to exist as a superimposition of one spectrum on another. A closer examination indicates an appreciable change in the chemical shift of the protons of the aromatic ring of phenobarbital, the benzylic proton of ephedrine, and the methine proton adjacent to the methylamino group of ephedrine (Table II). Since these shifts might result from the protonation of ephedrine by phenobarbital or the formation of the anion of phenobarbital, the spectra of these species were examined. The anion was formed by treating a solution of phenobarbital in deuterochloroform with excess triethylamine (Fig. 7). The spectrum of the protonated species of ephedrine (Fig. 8) was obtained by treating a deuterochloroform solution of ephedrine with excess acetic acid. The significant chemical shifts of these species are summarized in Table II.

In the complex, the aromatic protons of ephedrine and phenobarbital overlapped, representing an upfield shift of the aromatic protons of phenobarbital to 7.28 ppm. Formation of the anion of phenobarbital caused a downfield shift of the aromatic protons to 7.41 ppm. Protonation of ephedrine caused a downfield shift of the aromatic protons. The benzylic proton of ephedrine appeared as a doublet at 4.65 ppm. When protonated with excess acetic acid, it was slightly shifted downfield to 4.83 ppm. In the complex, this proton gave a doublet at 5.14 ppm. Protonation of the hydrogen adjacent to the methylamino group of ephedrine caused a downfield shift from 2.69 to 3.15 ppm. In the complex, this multiplet was found at 2.78 ppm.

The chemical shifts reported in Table II represent several spectral examinations and did not result from concentration differences. The findings indicate that the product of the reaction of phenobarbital and ephedrine is held together by weak intermolecular forces as well as an ionic bond. The changes in chemical shifts of aliphatic protons between ephedrine, the complex, and the protonated species were all to a lower magnetic field, and the complex was shifted the most. In the case of the aromatic protons of phenobarbital, however, the aromatic protons of the anion were shifted downfield from phenobarbital while those of the complex were shifted upfield. Integration of the NMR signal as well as

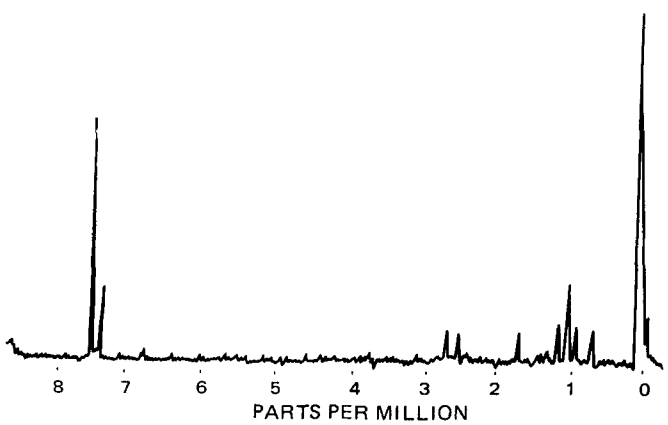

Figure 4—*NMR spectrum of phenobarbital.*

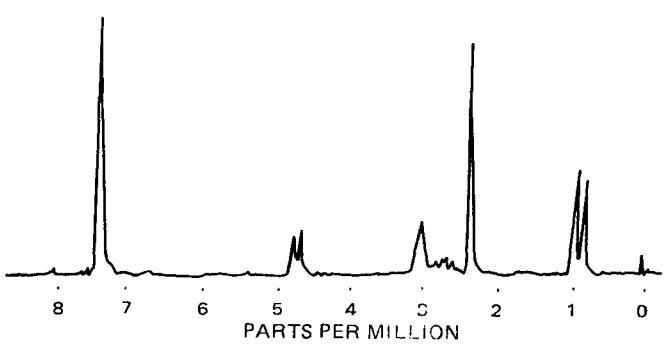

Figure 5—*NMR spectrum of ephedrine.*

[6] Hitachi Perkin-Elmer RMU-60 spectrometer.

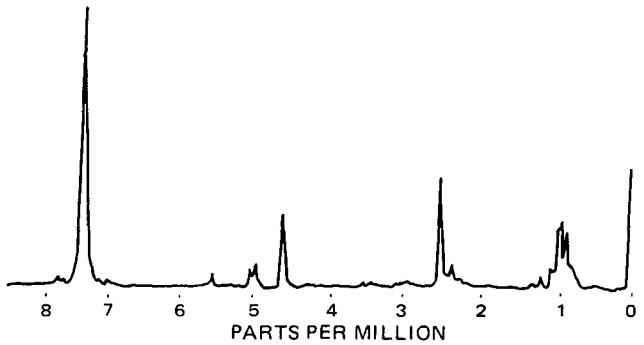

Figure 6—*NMR spectrum of complex.*

elemental analysis suggests that the complex is composed of equimolecular quantities of phenobarbital and ephedrine.

While it is not possible to elucidate completely the structure of the complex, the spectral data suggest the protonation of ephedrine by phenobarbital followed by the formation of a hydrogen bond between the alcoholic hydroxyl of ephedrine and a suitable group of phenobarbital. A structure resembling I would place the phenyl groups of one molecule above the other and provide an opportunity for hydrophobic bonding. Such an arrangement might provide a conformational change in phenobarbital, which would account for the change in chemical shift of the aromatic protons.

The observed fragmentation pattern for phenobarbital as determined by mass spectrometry yielded two different primary fragments: one from the loss of an NH group, which had an *m/e* ratio of 217, and another from the loss of a CO group with an *m/e* of 204. Both gave rise to a secondary fragment of *m/e* 189 in which both a CO and an NH were missing. This fragment was broken down further by loss of a second CO to give an ion with *m/e* 161. A second NH was then lost to produce a fragment of *m/e* 146. The mass spectrometry data show that ephedrine broke down into four primary fragments with *m/e* ratios of 132, 105, 91, and 58. Furthermore, the fragment at 105 split to produce an ion with an *m/e* ratio of 77. The fragmentation pattern observed from the mass spectrometry of the complex was the combination of the two patterns for phenobarbital and ephedrine.

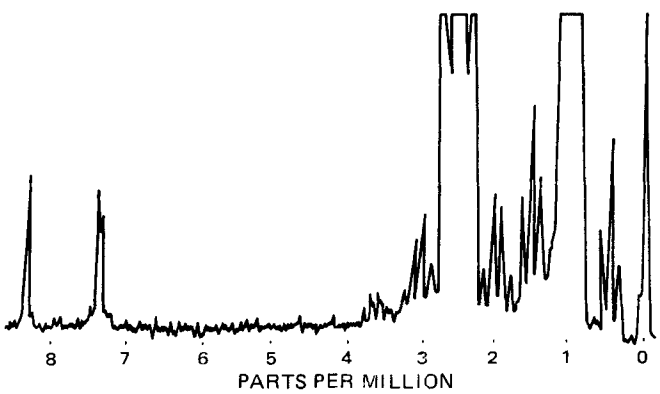

Figure 7—*NMR spectrum of phenobarbital plus triethylamine.*

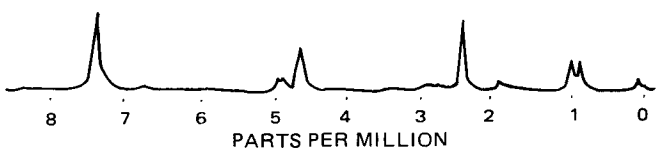

Figure 8—*NMR spectrum of ephedrine plus acetic acid.*

Table II—Pertinent Chemical Shifts from NMR Spectra

Compound	Chemical Shifts, ppm: Aromatic Proton	Benzylic Proton of Ephedrine	Methine Proton Adjacent to Nitrogen of Ephedrine
Phenobarbital	7.33	—	—
Phenobarbital triethylamine	7.41	—	—
Complex	7.28	5.14	2.78
Ephedrine acetate	7.32	4.83	3.15
Ephedrine	7.28	4.65	2.69

Anal.—Calc. for 1:1 complex: C, 67.37; H, 7.18; N, 10.27. Found: C, 66.99; H, 7.23; N, 10.25.

CONCLUSIONS

A complex of phenobarbital and ephedrine was isolated and demonstrated to have different physical and chemical properties from the individual drugs or from simple admixtures of the drugs. It is postulated that the phenobarbital–ephedrine complex forms through a combination of bonding types rather than simply being a salt formed as the product of a neutralization reaction between an acid and a base. The complex does, however, exhibit some characteristics of a salt, and salt formation is proposed as one bonding mechanism involved.

Other types of bonds are proposed as an explanation for some of its unique properties. Face-to-face stacking of the aromatic rings may occur and allow π forces to interact between the rings. Hydrogen bonding may also occur at several sites. In addition to dimer formation, it is also possible that trimers, tetramers, and higher aggregates such as base-stacked tetramers, spirals, and indefinite linear aggregates may occur.

REFERENCES

(1) T. Higuchi and J. L. Lach, *J. Am. Pharm. Assoc., Sci. Ed.*, **43**, 349 (1954).

(2) L. W. Dittert, T. Higuchi, and D. R. Reese, *J. Pharm. Sci.*, **53**, 1325 (1964).

(3) W. A. Strickland and L. Robertson, *ibid.*, **54**, 452 (1965).

(4) P. Rohdewald and H. Wellmann, *Acta Pharm. Suec.*, **10**, 532 (1973).

(5) K. Sekiguchi, T. Yotsuyanagi, and S. Mikami, *Chem. Pharm. Bull.*, **12**, 994 (1964).

(6) F. Shihab, J. Sprowls, and J. Nematollahi, *J. Pharm. Sci.*, **60**, 622 (1971).

(7) P. Singh, J. K. Guillory, T. D. Sokoloski, L. Z. Benet, and V. N. Bhatia, *ibid.*, **55**, 63 (1966).

(8) J. C. Smith, J. W. Clitherow, and W. Marlow, *J. Pharm. Pharmacol.*, **24**, 111P (1972).

(9) W. N. French and J. C. Morrison, *J. Pharm. Sci.*, **54**, 1133 (1965).

(10) R. Babin and F. Coustou, *Bull. Soc. Pharm. Bordeaux*, **105**, 77 (1966).

ACKNOWLEDGMENTS AND ADDRESSES

Received April 30, 1976, from the *College of Pharmacy, University of Illinois at the Medical Center, Chicago, IL 60612.*

Accepted for publication September 2, 1976.

Presented at the Pharmaceutical Analysis and Control Section, APhA Academy of Pharmaceutical Sciences, New Orleans meeting, April 1976.

Abstracted in part from a thesis submitted by M. B. Mrtek to the University of Illinois at the Medical Center in partial fulfillment of the Doctor of Philosophy degree requirements.

[x] To whom inquiries should be directed.

Synthesis and Cytotoxic Activity of Latentiated Derivatives of 3-Methyleneoxindole

M. J. KORNET ˣ, A. P. THIO, and J. H. THORSTENSON

Abstract □ Several latentiated derivatives of 3-methyleneoxindole were synthesized and examined for cytotoxic activity. The latentiated forms are represented by three general types which differ in leaving and cleaved groups. All are expected to be converted into 3-methyleneoxindole by bioactivation processes normally occurring in the cell. Two compounds were tested against L-1210 lymphoid leukemia, and six were tested against P-388 lymphocytic leukemia; all were inactive.

Keyphrases □ 3-Methyleneoxindole—latentiated derivatives synthesized and evaluated for cytotoxic activity □ Oxindoles, substituted—latentiated derivatives synthesized and evaluated for cytotoxic activity □ Cytotoxic activity—evaluated in latentiated derivatives of 3-methyleneoxindole □ Structure–activity relationships—latentiated derivatives of 3-methyleneoxindole evaluated for cytotoxic activity

Beneficial effects were reported when several cancer patients were treated with 3-indoleacetic acid for extended periods (1). Other studies found that certain esters of 3-indoleacetic acid prolonged the survival time of white mice (2) implanted with Ehrlich ascites carcinoma. The similarity of the effect on cell growth of 3-indoleacetic acid and 3-methyleneoxindole (I) (3) and the demonstrated oxidative conversion of 3-indoleacetic acid into I (4) strongly suggest that I may be the actual pharmacological agent in the action of 3-indoleacetic acid on cancer growth.

BACKGROUND

Compound I was first synthesized in 1964 (5) and is unstable. It possesses an activated ethylenic double bond and is very reactive toward the sulfhydryl group. It reacts smoothly with thiophenol (5), glutathione, and other biologically important thiol compounds (6) to give stable adducts. A sulfhydryl reagent such as I may exhibit selective cytotoxicity toward cancer cells, not only because rapidly proliferating cells reportedly expose more sulfhydryl groups (7) but also because I–sulfhydryl adducts should be more resistant toward dissociation (6) in the more acidic tumor cells (8), resulting in a slower rate of detoxification of I (9).

Finally, I bears a marked similarity to a number of anticancer substances including the antibiotic enzyme inhibitor sarkomycin (II) (10–12) and the antiascites substance primocarcin (III) (13, 14).

The pronounced instability and reactivity of this compound and the marked concentration dependency of its biological action (3, 15) make it impractical to apply I itself as a drug. This report is concerned with the synthesis and evaluation of latentiated forms of I, which can be converted into the active I by processes known to occur *in vivo*, *e.g.*, hydrolysis, oxidation, and reduction (16).

Immediate precursors of I that may be expected to undergo spontaneous conversion into the active compound can be represented by the three general types, A, B, and C (17), illustrated in Structures I*a*, I*b*, and I*c*, respectively. In these structures, X represents leaving groups (*e.g.*, halogens, hydroxyl, acyloxy, and amino), while Y stands for cleaved groups capable of being cleaved off from the electron pair that binds them to the rest of the molecule (*e.g.*, carboxylate and immomium). In most cases, these immediate precursors are too unstable to be useful as drugs and need to be latentiated.

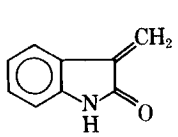

I

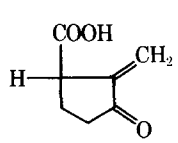

II

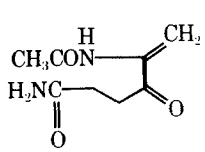

III

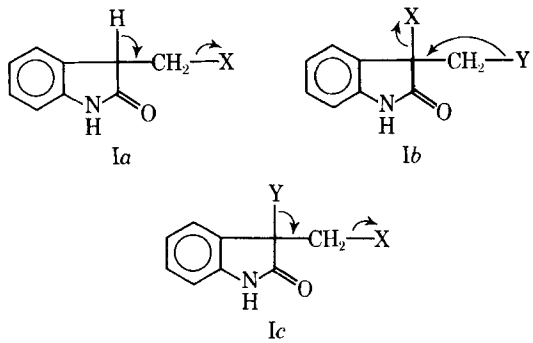

Ia Ib Ic

RESULTS AND DISCUSSION

Synthesis—Two examples of compounds of Type A were prepared (VI*a* and VI*b*, Scheme I). Compound VI*a* was obtained in four steps from oxindole (18, 19). Compound VI*b* was analogously prepared, except that acylation in the next to the last step involved ethyl chloroformate.

Three latentiated 3-methyleneoxindole derivatives of Type B were prepared. Ethyl 2,3-dioxindolyl-3-acetate (VII) (20) was synthesized from isatin and ethyl bromoacetate. Compound VII is a close relative of 3-bromo-3-oxindoleacetic acid (VIII); the latter is transformed into I almost immediately by dissolving it in water (5). For this reason, VIII (21) also was prepared for biological evaluation.

In addition, the preparation of the spirolactone X (Scheme II), which represents a third Type B compound, was attempted. 5-Bromo-2,3-dioxindole-3-butyric lactone (IX) was obtained by the *N*-bromosuccinimide oxidation of 4-indolebutyric acid according to a previous method

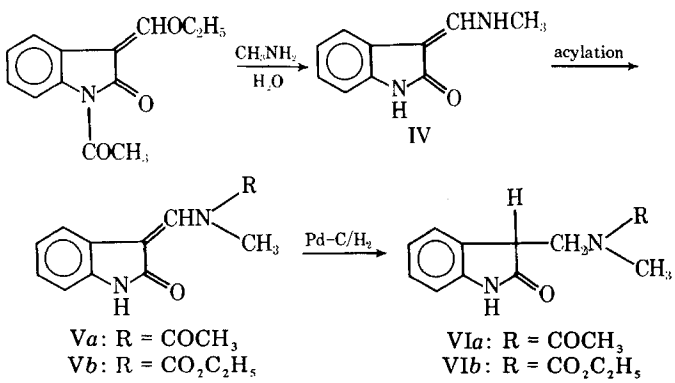

Va: R = $COCH_3$
Vb: R = $CO_2C_2H_5$

VI*a*: R = $COCH_3$
VI*b*: R = $CO_2C_2H_5$

Scheme I

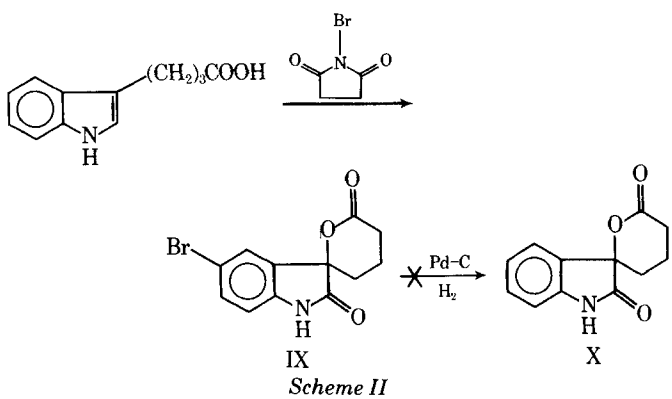

IX X

Scheme II

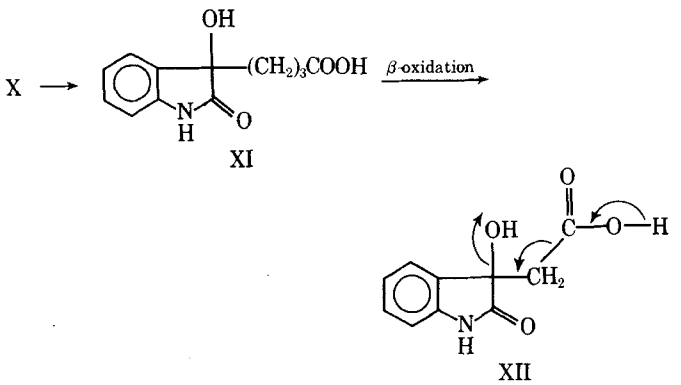

Scheme III

(22) for the corresponding propionic lactone. However, debromination of IX failed to give X. Bioactivation of X would necessitate lactone hydrolysis followed by β-oxidation (Scheme III). 2,3-Dioxindole-3-acetic acid (XII) has been proposed as the intermediate in the enzymatic oxidation of the plant growth hormone 3-indoleacetic acid to I (23).

Compounds of Type C include XIV–XVI (Scheme IV). Treatment of oxindole with diethyl carbonate in the presence of sodium ethoxide provided 3-ethoxycarbonyloxindole (XIII). The latter readily added formaldehyde and gave the adduct XIV. Tosylation of XIV afforded the corresponding tosyl derivative XV. Compound XVI was synthesized in good yield from XIII and *N*-chloromethylphthalimide (Scheme IV).

Biological Activity—Compounds VI*a*, VI*b*, VII–IX, and XIV–XVI[1] were screened according to standard protocols[2] (24). Compounds VI*b* and VIII were evaluated against L-1210 lymphoid leukemia and were inactive at doses of 100, 200, and 400 mg/kg. The remaining six compounds were tested against P-388 lymphocytic leukemia and were inactive at 50, 100, and 200 mg/kg.

One interpretation of the data is that I is devoid of antitumor activity. Other possible explanations include: (*a*) unfavorable distribution of the latentiated forms chosen, (*b*) inappropriate biological test systems, and (*c*) bioactivation before reaching the tumor site. Further investigation is required to determine which, if any, of these explanations is correct.

EXPERIMENTAL[3]

3-Bromo-3-oxindoleacetic Acid (VIII)—This compound was prepared according to Hinman and Bauman (21) and recrystallized from acetonitrile, mp 153.5–155.5° [lit. (21) mp 152–153°].

3-Methylaminomethyleneoxindole (IV)—A mixture of 1.0 g (4.34 mmoles) of 1-acetyl-3-ethoxymethyleneoxindole (18) in 20 ml of 30% aqueous methylamine was stirred at ambient temperature for 2.5 hr (Scheme I). The resulting precipitate was filtered and dried and amounted to 690 mg of solid, mp 230–232° [lit. (19) mp 235°]. Its IR and UV spectra agreed with the reported (19) spectra.

3-[(*N*-Methylacetamido)methyl]oxindole (VI*a*)—This compound was obtained by hydrogenation of V*a* (Scheme I) according to the recorded procedure (19), mp 134–136° [lit. (19) mp 135°]; NMR ($CDCl_3$): δ 1.92, 2.09 (2 s, 3H, CH_3C=O), 3.02, 3.05 (2 s, 3H, NCH_3), 3.58–4.17 (m, 3H, CH_2 and aliphatic CH), 6.75–7.50 (m, 4H, ArH), 9.36, and 9.67 (2 broad s, 1H, NH) ppm.

3-[(*N*-Ethoxycarbonyl-*N*-methylamino)methylene]oxindole (V*b*)—To a stirred, cooled solution of 4.0 g (0.023 mole) of IV in 32 ml of dry pyridine was added dropwise 12 ml of ethyl chloroformate (Scheme I). The solution was then warmed on the steam bath for 15 min and poured onto ice. The pale-yellow solid was filtered and washed well with cold water. The dried product, 5.24 g (93%), was recrystallized from 95% ethanol, mp 201–203°; IR ($CHCl_3$): 1710 (C=O) cm^{-1}; NMR (dimethyl sulfoxide-d_6): δ 1.28 (t, 3H, CCH_3), 3.43 (s, 3H, NCH_3), 4.30 (q, 2H, OCH_2), 6.73–7.68 (m, 4H, ArH), 7.90 (s, 1H, =CHN), and 10.47 (broad s, 1H, NH) ppm.

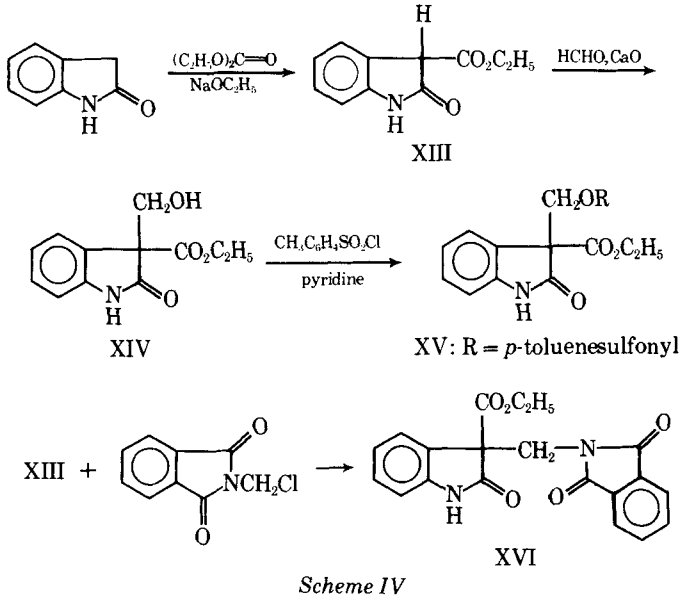

Scheme IV

Anal.—Calc. for $C_{13}H_{14}N_2O_3$: C, 63.40; H, 5.73; N, 11.38. Found: C, 63.14; H, 5.84; N, 11.20.

3 - [(*N* - Ethoxycarbonyl - *N* - methylamino)methyl]oxindole (VI*b*)—A slurry of 2.5 g (0.0102 mole) of V*b* in 200 ml of 95% ethanol containing 250 mg of 10% palladium-on-carbon catalyst was hydrogenated in a Parr apparatus (Scheme I). Hydrogen uptake stopped after 30 min, and the solution was filtered and evaporated under reduced pressure to give a colorless oil in quantitative yield. The oil was dried over phosphorus pentoxide in a drying pistol at 0.1 mm Hg for 2 hr. TLC on silica gel (ethyl acetate) exhibited a single spot, R_f 0.52; IR ($CHCl_3$): 1700 (C=O) cm^{-1}; NMR ($CDCl_3$): δ 1.18, 1.23 (overlapping t, 3H, CCH_3), 3.0 (s, 3H, NCH_3), 3.50–4.35 (m, 5H, OCH_2, CCH_2, and CH), 6.78–7.44 (m, 4H, ArH), and 9.70 (broad s, 1H, NH) ppm.

Anal.—Calc. for $C_{13}H_{16}N_2O_3$: C, 62.89; H, 6.50; N, 11.28. Found: C, 62.93; H, 6.54; N, 11.34.

Ethyl 2,3-Dioxindolyl-3-acetate (VII)—Compound VII was obtained *via* a Reformatsky reaction between isatin and ethyl bromoacetate by the method of Hallmann (20). The product was recrystallized from benzene and yielded colorless crystals, mp 111–111.5° [lit. (20) mp 102°]; mass spectrum: *m/e* 235 (M^+); NMR ($CDCl_3$): δ 1.13 (t, 3H, CCH_3), 2.98 (s, 2H, CH_2C=O), 4.08 (q, 2H, OCH_2), 4.82 (s, 1H, OH), 6.76–7.56 (m, 4H, ArH), and 9.02 (broad s, 1H, NH) ppm.

5-Bromo-2,3-dioxindole-3-butyric Lactone (IX)—This compound was prepared according to a previous procedure (22) (Scheme II) for the preparation of the propionic lactone analog. The pale-yellow solid obtained from filtration was air dried overnight and amounted to 2.15 g, mp 198–203°. From the ether extraction, an additional 0.33 g was obtained, mp 204–208°, giving a total of 2.48 g (79%). Recrystallization from aqueous methanol afforded white crystals, mp 208–211°; IR (KBr): 1720 and 1750 (C=O) cm^{-1}; NMR (dimethyl sulfoxide-d_6): δ 1.42–2.94 (m, 6H, $CH_2CH_2CH_2$) and 6.75–7.92 (m, 3H, ArH) ppm.

Anal.—Calc. for $C_{12}H_{10}BrNO_3$: C, 48.67; H, 3.40; N, 4.73. Found: C, 48.48; H, 3.60; N, 4.66.

Attempted Debromination of IX—A mixture of 1.0 g (3.37 mmoles) of IX, 350 mg of 5% palladium-on-charcoal catalyst, 4 ml of dry triethylamine, and 75 ml of absolute ethanol was hydrogenated in a Parr apparatus for 2 hr (Scheme II). Workup gave 100 mg of crystals, mp 160.5–163.5°. A second crop of 65 mg, mp 164.5–168°, was also obtained. Spectroscopic evidence indicated that this compound was a carboxylic acid and it was not investigated further.

3-Ethoxycarbonyloxindole (XIII)—To a hot solution containing 10.5 g (0.079 mole) of oxindole, 40 ml of diethyl carbonate (~0.32 mole), and 50 ml of dry toluene was added dropwise an ethanolic solution of sodium ethoxide [from 1.97 g (0.085 g-atom) of sodium in 30 ml of absolute ethanol] (Scheme IV). The flask contained a mechanical stirrer and was equipped for distillation. Moisture was excluded by means of a drying tube. The rate of addition was controlled to allow a smooth rate of distillation of the ethanol–toluene azeotrope (bp 76.7°).

Near the end of the addition, a heavy precipitate appeared and an additional 75 ml of toluene was added. Heating was continued until the boiling point of the distillate fell below 76°. The resulting solid was fil-

[1] NSC 246030–246037, respectively.

[2] National Cancer Institute.

[3] Melting points were determined with a Fisher-Johns melting-point apparatus and are uncorrected. The structures of the products were confirmed by their IR and NMR spectra. IR spectra were obtained on a Beckman IR-8 spectrophotometer. NMR spectra were determined on a Varian A-60A spectrometer, using tetramethylsilane as the internal reference. Microanalysis were performed by Dr. Kurt Eder, Geneva, Switzerland.

tered, washed with toluene, slurried in water, and acidified in the cold to pH 3–4. The mixture was extracted three times with 100-ml portions of ether, and the combined extract was dried over magnesium sulfate. Concentration of the solution gave 11.5 g (71%) of an oil that slowly solidified.

Trituration with ligroin and recrystallization from cyclohexane–benzene gave crystals, mp 91–93°. A second recrystallization from the same solvent system afforded the analytically pure product, mp 93–94°; IR ($CHCl_3$): 1725 (C=O) cm^{-1}; NMR ($CDCl_3$ containing D_2O and Na_2CO_3): δ 1.27 (t, 3H, CH_3), 4.25 (q, 2H, OCH_2), and 6.75–7.60 (m, 4H, ArH) ppm. Both the NH and 3-H exchange under these conditions.

Anal.—Calc. for $C_{11}H_{11}NO_3$: C, 64.38; H, 5.40; N, 6.83. Found: C, 64.50; H, 5.44; N, 6.87.

3-Ethoxycarbonyl-3-hydroxymethyloxindole (XIV)—To a cooled solution containing 5.7 g (0.0278 mole) of 3-ethoxycarbonyloxindole and 100 mg of calcium oxide in 150 ml of 70% aqueous ethanol was added dropwise a mixture of 2.26 ml of 40% aqueous formaldehyde in 5 ml of water (Scheme IV). The resulting solution was kept at room temperature overnight. The mixture was acidified with 6.5 ml of 5% aqueous hydrochloric acid, followed by addition of 50 ml of 95% ethanol. The solution was filtered and evaporated under reduced pressure at 35° to give a solid. Recrystallization from acetonitrile afforded 2.5 g (38%) of crystals, mp 149–152° dec. (with evolution of formaldehyde); IR (KBr): 1720 (C=O) cm^{-1}; mass spectrum: *m/e* 235 (M^+); NMR (dimethyl sulfoxide-d_6): δ 1.08 (t, 3H, CH_3), 3.74 (m, 4H, 2 CH_2), 5.05 (t, 1H, OH), and 6.85–7.53 (m, 4H, ArH) ppm.

Anal.—Calc. for $C_{12}H_{13}NO_4$: C, 61.27; H, 5.57; N, 5.95. Found: C, 61.15; H, 5.65; N, 6.00.

3 - Ethoxycarbonyl - 3 - *p* - toluenesulfonyloxymethyloxindole (XV)—A mixture of 2.11 g (0.00897 mole) of XIV and 3.43 g (0.018 mole) of *p*-toluenesulfonyl chloride in 75 ml of pyridine was stored at 0° for 46 hr. The rose-colored solution was poured onto 100 g of ice and stirred; a pink solid was collected by filtration. After drying *in vacuo*, 1.65 g (47%) of the tosylate was obtained, mp 155–157°. Recrystallization from 95% ethanol gave colorless crystals, mp 163–164.5°; IR ($CHCl_3$): 1730 (C=O) cm^{-1}; NMR ($CDCl_3$): δ 1.14 (t, 3H, $OCCH_3$), 2.42 (s, 3H, $ArCH_3$), 4.18 (q, 2H, O=$COCH_2$), 4.58 (d, 1H, J = 10 Hz, SO_2OCH_2), 4.83 (d, 1H, J = 10 Hz, SO_2OCH_2), 6.78–7.85 (m, 8H, ArH), and 8.93 (broad s, 1H, NH) ppm.

Anal.—Calc. for $C_{19}H_{19}NO_6S$: C, 58.61; H, 4.92; N, 3.60. Found: C, 58.74; H, 4.99; N, 3.61.

3-Ethoxycarbonyl-3-phthalimidomethyloxindole (XVI)—To a slurry of 368 mg (7.68 mmoles) of a 50% sodium hydride dispersion in mineral oil in 40 ml of dimethylformamide was added 1.28 g (6.25 mmoles) of XII portionwise at room temperature (Scheme IV). After stirring for 15 min, 1.22 g (6.26 mmoles) of *N*-chloromethylphthalimide (25) was added. The dark-red color of the mixture was slowly discharged upon stirring at room temperature overnight. Then the solution was poured onto 100 g of ice, and the precipitate was filtered. After drying, 1.95 g (85%) of solid was obtained, which was recrystallized from benzene–carbon tetrachloride, mp 202–203°; IR ($CHCl_3$): 1720 and 1770 (C=O) cm^{-1}; mass spectrum: *m/e* 364 (M^+); NMR ($CDCl_3$): δ 1.19 (t, 3H, CH_3), 4.25 (q, 2H, OCH_2), 4.50 (d, 1H, J = 14.5 Hz, NCH_2), 4.83 (d, 1H, J = 14.5 Hz, NCH_2), 6.75–7.93 (m, 8H, ArH), and 8.72 (broad s, 1H, NH) ppm.

Anal.—Calc. for $C_{20}H_{16}N_2O_5$: C, 65.93; H, 4.43; N, 7.69. Found: C, 65.95; H, 4.39; N, 7.82.

REFERENCES

(1) A. C. Boranao, *Rev. Argent. Cancerol.*, **4**, 84 (1962).

(2) D. Norman and R. D. Schultz, *Nature (London)*, **206**, 477 (1965).

(3) P. S. Basu and V. Tuli, *Plant Physiol.*, **50**, 507 (1972), and papers cited therein.

(4) R. L. Hinman and J. Lang, *Biochemistry*, **4**, 144 (1965).

(5) R. L. Hinman and C. P. Bauman, *J. Org. Chem.*, **29**, 2431 (1964).

(6) C. C. Still, T. T. Fukuyama, and H. S. Moyed, *J. Biol. Chem.*, **240**, 2612 (1965).

(7) P. Emmelot, in "Molecular Pharmacology," vol. 2, E. J. Ariens, Ed., Academic, New York, N.Y., 1964, part III, pp. 100, 144.

(8) *Ibid.*, pp. 127, 134, 149.

(9) W. C. J. Ross, "Biological Alkylating Agents," Butterworths, London, England, 1962, chap. 8.

(10) N. Neuss, M. Gorman, and I. S. Johnson, in "Methods in Cancer Research," vol. III, H. Busch, Ed., Academic, New York, N.Y., 1967, pp. 657, 660–662.

(11) J. A. Stock, in "Experimental Chemotherapy," vol. IV, R. J. Schmitzer and F. Hawking, Eds., Academic, New York, N.Y., 1966, pp. 300–305.

(12) P. Emmelot, in "Molecular Pharmacology," vol. 2, E. J. Ariens, Ed., Academic, New York, N.Y., 1964, part III, pp. 125–127.

(13) Y. Sumiki, K. Isono, J. Nagatsu, and T. Takanuchi, *J. Antibiot. (Tokyo), Ser. A*, **13**, 416 (1960).

(14) R. E. Bowman, M. D. Closier, and P. V. Islip, *J. Chem. Soc.*, **1965**, 470.

(15) V. Tuli and H. S. Moyed, *J. Biol. Chem.*, **241**, 4564 (1966).

(16) J. N. Smith, in "Comparative Biochemistry," vol. VI, M. Florkin and H. S. Mason, Eds., Academic, New York, N.Y., 1964, pp. 403–457.

(17) J. A. Jonker, *Chem. Tech. (Amsterdam)*, **25**, 349 (1970).

(18) H. Behringer and H. Weissauer, *Chem. Ber.*, **85**, 774 (1952).

(19) E. Wenkert, J. H. Udelhofen, and N. K. Bhattacharyya, *J. Am. Chem. Soc.*, **81**, 3763 (1959).

(20) G. Hallmann, *Chem. Ber.*, **95**, 1138 (1962).

(21) R. L. Hinman and C. P. Bauman, *J. Org. Chem.*, **29**, 1206 (1964).

(22) W. B. Lawson, A. Patchornik, and B. Witkop, *J. Am. Chem. Soc.*, **82**, 5918 (1960).

(23) R. L. Hinman, C. P. Bauman, and J. Lang, *Biochem. Biophys. Res. Commun.*, **5**, 250 (1961).

(24) J. M. Venditti, *Cancer Chemother. Rep.*, **3**, 1 (1972).

(25) H. Bohmer, *Chem. Ber.*, **92**, 1258 (1959).

ACKNOWLEDGMENTS AND ADDRESSES

Received June 21, 1976, from the *College of Pharmacy, University of Kentucky, Lexington, KY 40506.*

Accepted for publication September 16, 1976.

[x] To whom inquiries should be directed.

Relationship between Protein Binding of Bilirubin, Salicylic Acid, and Sulfisoxazole in Serum of Unmedicated and Phenobarbital-Treated Rats

AVRAHAM YACOBI, SVEIN ØIE, and GERHARD LEVY ˣ

Abstract □ The relationship between the protein binding of bilirubin, salicylic acid, and sulfisoxazole in the serum of phenobarbital-treated and untreated rats was studied. The free fraction of bilirubin in serum varied about threefold between animals but was not related to the albumin concentration, the free fraction of salicylate, or the free fraction of sulfisoxazole. However, there was a strong positive correlation between the free fraction values of salicylate and sulfisoxazole. The free fraction value for each of these drugs showed a significant negative correlation with the serum albumin concentration. Treatment of the animals with phenobarbital had no apparent effect on the serum protein binding of bilirubin, salicylic acid, and sulfisoxazole.

Keyphrases □ Bilirubin—protein binding, relationship to binding of salicylic acid and sulfisoxazole, effect of phenobarbital, rat serum □ Salicylic acid—protein binding, relationship to binding of bilirubin and sulfisoxazole, effect of phenobarbital, rat serum □ Sulfisoxazole—protein binding, relationship to binding of salicylic acid and bilirubin, effect of phenobarbital, rat serum □ Protein binding—bilirubin, salicylic acid, and sulfisoxazole, effect of phenobarbital, rat serum □ Binding, protein—bilirubin, salicylic acid, and sulfisoxazole, effect of phenobarbital, rat serum □ Phenobarbital—effect on protein binding of bilirubin, salicylic acid and sulfisoxazole, rat serum

Drugs that displace bilirubin from plasma protein binding sites can cause brain damage and death in premature infants with neonatal jaundice (1–3). Classical bilirubin displacing agents, in terms of clinical experience and experimental interest, are sulfisoxazole and salicylic acid. Administration of these drugs to humans and animals during hyperbilirubinemia causes a redistribution of bilirubin from plasma to extravascular tissues, including the brain (4–9).

The rat has been used in this laboratory as a model for investigating the pharmacokinetics of the interaction of salicylic acid and sulfisoxazole with bilirubin. As an extension of this research, the relationship between the protein binding of bilirubin, salicylic acid, and sulfisoxazole in the serum of individual rats has been determined. A previous study revealed that there are pronounced interindividual differences in the serum protein binding of bilirubin in rats (10).

Neonatal unconjugated hyperbilirubinemia is treated sometimes with the enzyme inducer phenobarbital (11, 12). *In vitro* addition of phenobarbital to hyperbilirubinemic serum does not change the total binding capacity of albumin (13), but it remains to be determined if enzyme induction *per se* affects the serum protein binding of bilirubin, perhaps by changing the formation and/or elimination kinetics of endogenous inhibitors of bilirubin binding. Accordingly, protein binding studies were carried out with serum from unmedicated and phenobarbital-pretreated rats.

EXPERIMENTAL

Twenty adult male Sprague–Dawley rats, ~350 g, were divided into two groups. One group received daily injections of phenobarbital, 75 mg/kg ip, for 4 days; the other group received daily injections of normal saline solution. On the 5th day, all blood was removed from the aorta under light ether anesthesia and the liver was excised and weighed. Serum was separated and assayed for total protein (14), using crystalline rat albumin as the standard. The fraction of albumin was determined by electrophoresis[1].

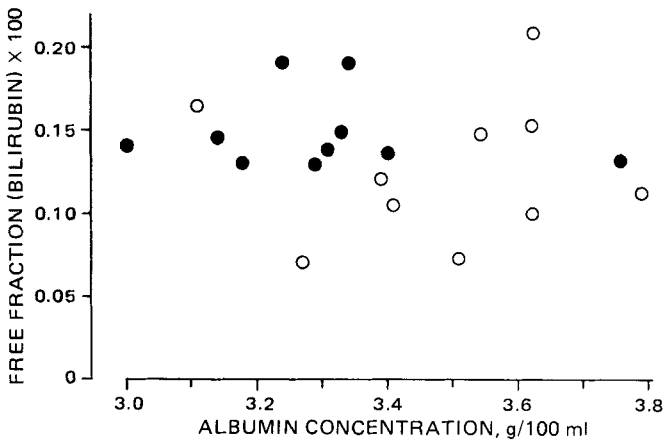

Figure 1—*Relationship between free fraction of bilirubin and albumin concentration in serum of phenobarbital-treated (●) and control (○) rats. Correlation coefficient = 0.36 (not significant) for combined data.*

The protein binding of salicylic acid and sulfisoxazole was determined by equilibrium dialysis at 37° as previously described (15). The buffer solution contained an initial concentration of 30 mg of salicylic acid or 10 mg of sulfisoxazole/100 ml. The protein binding of bilirubin was determined by measuring the rate of the peroxidase-catalyzed degradation of the pigment by peroxide (16). Since only unbound bilirubin reacts with peroxide, the reaction rate is proportional to the free bilirubin concentration.

Bilirubin solution[2], 10 μl, was added to 0.5 ml of serum from a rat to

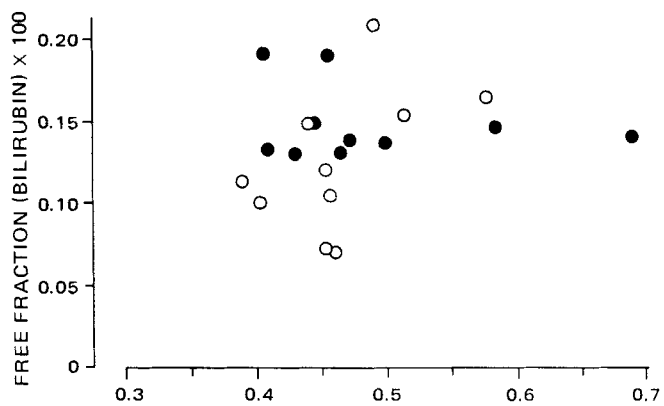

Figure 2—*Relationship between free fraction values of bilirubin and salicylic acid in serum of phenobarbital-treated (●) and control (○) rats. Correlation coefficient is 0.185 (not significant) for combined data and 0.518 (not significant) for control data.*

[1] Gelman serum protein electrophoresis system.

[2] Crystalline bilirubin (Sigma) dissolved in water with the aid of a small quantity of 2 *M* sodium hydroxide.

Table I—Effect of Treatment with Phenobarbital on Total Protein and Albumin Concentrations[a] in Serum of Rats

	Before Treatment		After Treatment	
	Control	Phenobarbital	Control	Phenobarbital
Total protein, g/100 ml	8.10 ± 0.24	8.01 ± 0.35	7.94 ± 0.26	8.13 ± 0.20
Albumin, g/100 ml	3.96 ± 0.22	3.77 ± 0.21	3.49 ± 0.20	3.30 ± 0.20
	N.S.		N.S.	
	$p < 0.001$			
		$p < 0.001$		

[a] Mean ± *SD*, $n = 10$.

obtain a serum bilirubin concentration of 8.7–9.5 mg/100 ml. A 0.1-ml aliquot of 0.1 *M* phosphate buffer, pH 7.4, containing 0.01 *M* edetate disodium was evaporated to dryness in a 10-ml centrifuge tube. Plasma, 0.1 ml, was added, and the dried buffer was dissolved in it by vortexing. Peroxidase solution, 10 μl (8 purpurogallin units of horseradish peroxidase[3]/ml of 0.1 *M* phosphate buffer, pH 7.4), was then added.

The reaction was started by adding 5 μl of peroxide solution (0.2% ethyl hydrogen peroxide in 0.1 *M* phosphate buffer, pH 7.4) and stopped after 1–2 min by addition of 1 ml of 6% ascorbic acid in 0.2 *M* phosphate buffer, pH 8.2. The entire reaction was carried out in a water bath at 37°. The concentration of total unconjugated bilirubin before and after the reaction was determined spectrophotometrically after chloroform extraction (17), using a commercial bilirubin control[4] as the standard.

All protein binding data are expressed as free fraction values, *i.e.*, the concentration of free (unbound) divided by the concentration of total (free and protein bound) drug or bilirubin in serum.

RESULTS

Treatment with phenobarbital caused a significant increase in liver weight (3.70 ± 0.35 *versus* 3.09 ± 0.16 g/100 g of body weight, $p < 0.001$) but had no apparent effect on the concentrations of total protein and albumin in serum (Table I). There was a small but statistically significant decrease in the serum albumin concentration in both the control and phenobarbital-treated groups during the treatment period. Treatment with phenobarbital had no statistically significant effect on the serum protein binding of bilirubin, sulfisoxazole, and salicylic acid (Table II).

There were appreciable intersubject differences in the binding of bilirubin and the concentration of albumin in serum but no apparent correlation between the free fraction values of bilirubin and the albumin concentration in serum (Fig. 1). There was also no apparent correlation between the free fraction values of bilirubin and those of salicylic acid (Fig. 2) or sulfisoxazole (Fig. 3). On the other hand, a strong and statistically highly significant correlation existed between the free fraction values of salicylic acid and sulfisoxazole in individual animals (Fig. 4). There was also a statistically significant negative correlation between

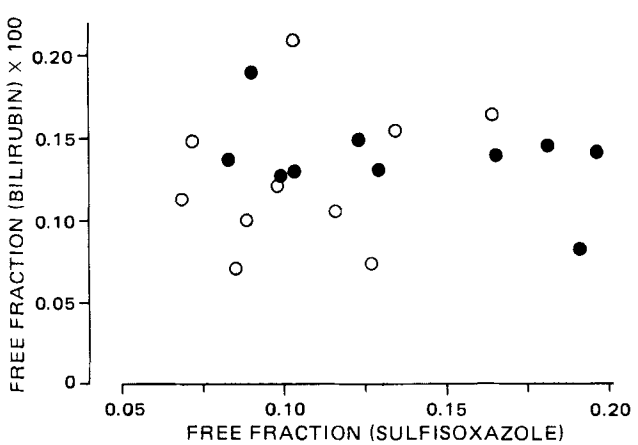

Figure 3—*Relationship between free fraction values of bilirubin and sulfisoxazole in serum of phenobarbital-treated (●) and control (○) rats. Correlation coefficient is 0.074 (not significant) for combined data.*

[3] Sigma type I.
[4] Dade Division, American Hospital Supply Corp., Miami, Fla.

Table II—Effect of Treatment with Phenobarbital on Protein Binding of Bilirubin, Salicylic Acid, and Sulfisoxazole in Serum of Rats

	Free Fraction[a]	
	Control	Phenobarbital
Bilirubin	0.00126 ± 0.00043 (0.00071–0.00209)	0.00149 ± 0.00023[b] (0.00131–0.00191)
Sulfisoxazole	0.106 ± 0.030 (0.0717–0.164)	0.125 ± 0.042[b] (0.0816–0.196)
Salicylic acid	0.463 ± 0.053 (0.390–0.573)	0.484 ± 0.088[b] (0.405–0.690)

[a] Mean ± *SD* (range), $n = 10$. [b] Not significantly different from control value (Student *t* test).

the serum albumin concentration and the free fraction of salicylic acid ($r = -0.635$, $p < 0.005$) and sulfisoxazole ($r = -0.600$, $p < 0.005$).

DISCUSSION

Binding of bilirubin to albumin in serum, which is technically difficult to determine because it is so extensive (>99%), cannot be predicted by the extent of serum protein binding of two other weak acids, salicylic acid and sulfisoxazole, at least in the rat. There are significant intersubject differences in the protein binding of bilirubin, salicylic acid, sulfisoxazole, and other drugs in the rat and also in humans (10, 15, 18, 19, and unpublished data). This fact must be considered in the design and interpretation of studies on species differences in serum protein binding of drugs.

No apparent relationship between the concentration of albumin and the free fraction of bilirubin in serum of rats was found. A similar lack of correlation was observed previously with two other extensively albumin-bound compounds, warfarin (18) and dicumarol (20). However, the

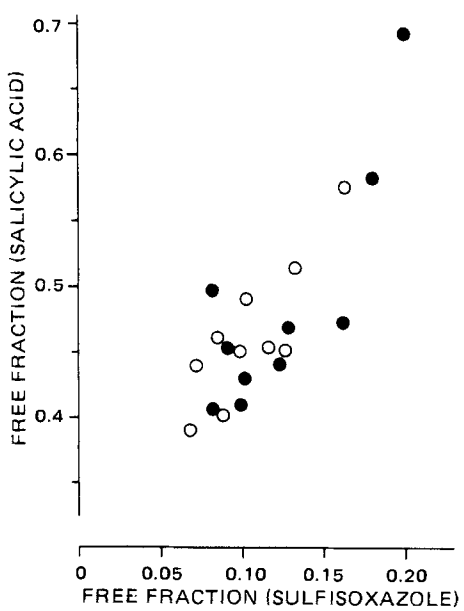

Figure 4—*Relationship between free fraction values of salicylic acid and sulfisoxazole in serum of phenobarbital-treated (●) and control (○) rats. Correlation coefficient is 0.818, p < 0.001, for combined data.*

free fraction values of salicylic acid and sulfisoxazole, which are much less extensively protein bound, exhibited a statistically significant negative correlation with the concentration of albumin in rat serum.

Phenobarbital treatment, which is an effective means of lowering the serum bilirubin concentration in certain types of unconjugated hyperbilirubinemia (11, 12), has no apparent effect on the serum protein binding of bilirubin in rats. This information will facilitate the interpretation of results of phenobarbital–bilirubin interaction studies in normal rats. It remains to be determined if phenobarbital treatment affects bilirubin binding in the Gunn rat, the most important animal model of physiological unconjugated hyperbilirubinemia.

REFERENCES

(1) W. A. Silverman, D. H. Anderson, W. A. Blanc, and D. N. Crozier, *Pediatrics*, **18**, 614 (1956).

(2) R. C. Harris, J. F. Lucey, and J. R. MacLean, *ibid.*, **20**, 875 (1958).

(3) J. D. Johnson, *N. Engl. J. Med.*, **292**, 194 (1975).

(4) L. Johnson, M. L. Garcia, E. Fegueroa, and F. Sarmiento, *Am. J. Dis. Child.*, **101**, 322 (1961).

(5) D. Watson, *Clin. Sci.*, **22**, 435 (1962).

(6) R. Schmid, I. Diamond, L. Hawmaker, and C. B. Gundersen, *Nature*, **206**, 1041 (1965).

(7) I. Diamond and R. Schmid, *J. Clin. Invest.*, **45**, 678 (1966).

(8) J. C. Topham and R. D. Broad, *Biochem. Pharmacol.*, **20**, 718 (1971).

(9) R. A. Yeary and D. R. Davis, *Toxicol. Appl. Pharmacol.*, **28**, 283 (1974).

(10) S. Øie and G. Levy, *J. Pharm. Sci.*, **64**, 1433 (1975).

(11) S. J. Yaffe, G. Levy, T. Matsuzawa, and T. Baliah, *N. Engl. J. Med.*, **275**, 1461 (1966).

(12) L. Stern, N. N. Khanna, G. Levy, and S. J. Yaffe, *Am. J. Dis. Child.*, **120**, 26 (1970).

(13) W. C. Griffiths, I. Diamond, and P. Dextraze, *Clin. Biochem.*, **8**, 254 (1975).

(14) A. C. Gornall, C. J. Bardawill, and M. M. Davis, *J. Biol. Chem.*, **177**, 751 (1949).

(15) G. Levy, T. Baliah, and J. A. Procknal, *Clin. Pharmacol. Ther.*, **20**, 512 (1976).

(16) J. Jacobsen and O. Fedders, *Scand. J. Clin. Lab. Invest.*, **26**, 237 (1970).

(17) R. Brodersen and I. Vind, *ibid.*, **15**, 107 (1963).

(18) A. Yacobi and G. Levy, *J. Pharm. Sci.*, **64**, 1660 (1975).

(19) A. Yacobi, J. A. Udall, and G. Levy, *Clin. Pharmacol. Ther.*, **19**, 552 (1976).

(20) A. Yacobi, J. T. Slattery, and G. Levy, *J. Pharm. Sci.*, **66**, 941 (1977).

ACKNOWLEDGMENTS AND ADDRESSES

Received August 13, 1976, from the *Department of Pharmaceutics, School of Pharmacy, State University of New York at Buffalo, Buffalo, NY 14214.*

Accepted for publication September 17, 1976.

Supported in part by Grant GM 19568 from the National Institute of General Medical Sciences, National Institutes of Health.

[x] To whom inquiries should be directed.

Rapid GLC Determination of Therapeutic Plasma Glycerin Levels

THOMAS J. GOEHL [x], WILLIAM H. PITLICK, GERALD K. SHIU, and PICHAI PIRAKITIKULR

Abstract □ A new rapid and inexpensive method for the determination of therapeutic plasma glycerin concentrations is described. In this method, acetic anhydride and pyridine are added to 15 μl of plasma. After brief incubation and centrifugation, an aliquot of the supernate is injected directly onto the 3% OV-1 column. A linear calibration curve was found in the 0.05–3-mg/ml range, with the precision of the assay estimated to be ±5.5% (*RSD*). The method was used in determining preliminary pharmacokinetic data in the rabbit.

Keyphrases □ Glycerin—GLC analysis, plasma □ GLC—analysis, glycerin in plasma □ Hyperosmolar dehydrating agents—glycerin, GLC analysis in plasma

Cerebral edema, or swelling of brain tissue, increases intracranial pressure, which, if not medically corrected, leads to herniation of brain tissue with irreversible brain damage and subsequent death. Deterioration of brain function and progressive deepening of coma in acute neurologic emergencies are often results of increased intracranial pressure due to cerebral edema. Medical management is a triad composed of hypothermia, hypocapnea, and hyperosmolar dehydration of cerebral tissues (1). Glycerin has been particularly useful for the treatment of cerebral edema by hyperosmolar dehydration because of its physical properties, but a lack of clinical knowledge has hindered its maximum use (2, 3).

At present, empirical relationships govern the use of glycerin in life-threatening situations. The efficacy of treatment with glycerin probably could be improved with quantitative assessment of glycerin therapy, including monitoring of plasma levels. It is now possible, and preferable, to individualize the dosage regimen for each patient based on a desired therapeutic plasma concentration range known to produce a desired response. In life-threatening situations, such as increased intracranial pressure, it is imperative to have rapid assessment of plasma glycerin levels for effective therapy.

Currently, the most commonly used methods for the determination of plasma glycerin levels are enzymatic (4–11). The first such method (4) was developed for determining endogenous glycerin levels, normally in the 5–17-μg/ml range. For assaying therapeutic plasma glycerin levels (milligram per milliliter range) with enzymatic methods, it is necessary to find the proper dilution factor for each sample, which is both time consuming and expensive. Thus, another method was needed that would be

free fraction values of salicylic acid and sulfisoxazole, which are much less extensively protein bound, exhibited a statistically significant negative correlation with the concentration of albumin in rat serum.

Phenobarbital treatment, which is an effective means of lowering the serum bilirubin concentration in certain types of unconjugated hyperbilirubinemia (11, 12), has no apparent effect on the serum protein binding of bilirubin in rats. This information will facilitate the interpretation of results of phenobarbital–bilirubin interaction studies in normal rats. It remains to be determined if phenobarbital treatment affects bilirubin binding in the Gunn rat, the most important animal model of physiological unconjugated hyperbilirubinemia.

REFERENCES

(1) W. A. Silverman, D. H. Anderson, W. A. Blanc, and D. N. Crozier, *Pediatrics*, **18**, 614 (1956).

(2) R. C. Harris, J. F. Lucey, and J. R. MacLean, *ibid.*, **20**, 875 (1958).

(3) J. D. Johnson, *N. Engl. J. Med.*, **292**, 194 (1975).

(4) L. Johnson, M. L. Garcia, E. Fegueroa, and F. Sarmiento, *Am. J. Dis. Child.*, **101**, 322 (1961).

(5) D. Watson, *Clin. Sci.*, **22**, 435 (1962).

(6) R. Schmid, I. Diamond, L. Hawmaker, and C. B. Gundersen, *Nature*, **206**, 1041 (1965).

(7) I. Diamond and R. Schmid, *J. Clin. Invest.*, **45**, 678 (1966).

(8) J. C. Topham and R. D. Broad, *Biochem. Pharmacol.*, **20**, 718 (1971).

(9) R. A. Yeary and D. R. Davis, *Toxicol. Appl. Pharmacol.*, **28**, 283 (1974).

(10) S. Øie and G. Levy, *J. Pharm. Sci.*, **64**, 1433 (1975).

(11) S. J. Yaffe, G. Levy, T. Matsuzawa, and T. Baliah, *N. Engl. J. Med.*, **275**, 1461 (1966).

(12) L. Stern, N. N. Khanna, G. Levy, and S. J. Yaffe, *Am. J. Dis. Child.*, **120**, 26 (1970).

(13) W. C. Griffiths, I. Diamond, and P. Dextraze, *Clin. Biochem.*, **8**, 254 (1975).

(14) A. C. Gornall, C. J. Bardawill, and M. M. Davis, *J. Biol. Chem.*, **177**, 751 (1949).

(15) G. Levy, T. Baliah, and J. A. Procknal, *Clin. Pharmacol. Ther.*, **20**, 512 (1976).

(16) J. Jacobsen and O. Fedders, *Scand. J. Clin. Lab. Invest.*, **26**, 237 (1970).

(17) R. Brodersen and I. Vind, *ibid.*, **15**, 107 (1963).

(18) A. Yacobi and G. Levy, *J. Pharm. Sci.*, **64**, 1660 (1975).

(19) A. Yacobi, J. A. Udall, and G. Levy, *Clin. Pharmacol. Ther.*, **19**, 552 (1976).

(20) A. Yacobi, J. T. Slattery, and G. Levy, *J. Pharm. Sci.*, **66**, 941 (1977).

ACKNOWLEDGMENTS AND ADDRESSES

Received August 13, 1976, from the *Department of Pharmaceutics, School of Pharmacy, State University of New York at Buffalo, Buffalo, NY 14214.*

Accepted for publication September 17, 1976.

Supported in part by Grant GM 19568 from the National Institute of General Medical Sciences, National Institutes of Health.

[x] To whom inquiries should be directed.

Rapid GLC Determination of Therapeutic Plasma Glycerin Levels

THOMAS J. GOEHL [x], WILLIAM H. PITLICK, GERALD K. SHIU, and PICHAI PIRAKITIKULR

Abstract □ A new rapid and inexpensive method for the determination of therapeutic plasma glycerin concentrations is described. In this method, acetic anhydride and pyridine are added to 15 μl of plasma. After brief incubation and centrifugation, an aliquot of the supernate is injected directly onto the 3% OV-1 column. A linear calibration curve was found in the 0.05–3-mg/ml range, with the precision of the assay estimated to be ±5.5% (*RSD*). The method was used in determining preliminary pharmacokinetic data in the rabbit.

Keyphrases □ Glycerin—GLC analysis, plasma □ GLC—analysis, glycerin in plasma □ Hyperosmolar dehydrating agents—glycerin, GLC analysis in plasma

Cerebral edema, or swelling of brain tissue, increases intracranial pressure, which, if not medically corrected, leads to herniation of brain tissue with irreversible brain damage and subsequent death. Deterioration of brain function and progressive deepening of coma in acute neurologic emergencies are often results of increased intracranial pressure due to cerebral edema. Medical management is a triad composed of hypothermia, hypocapnea, and hyperosmolar dehydration of cerebral tissues (1). Glycerin has been particularly useful for the treatment of cerebral edema by hyperosmolar dehydration because of its physical properties, but a lack of clinical knowledge has hindered its maximum use (2, 3).

At present, empirical relationships govern the use of glycerin in life-threatening situations. The efficacy of treatment with glycerin probably could be improved with quantitative assessment of glycerin therapy, including monitoring of plasma levels. It is now possible, and preferable, to individualize the dosage regimen for each patient based on a desired therapeutic plasma concentration range known to produce a desired response. In life-threatening situations, such as increased intracranial pressure, it is imperative to have rapid assessment of plasma glycerin levels for effective therapy.

Currently, the most commonly used methods for the determination of plasma glycerin levels are enzymatic (4–11). The first such method (4) was developed for determining endogenous glycerin levels, normally in the 5–17-μg/ml range. For assaying therapeutic plasma glycerin levels (milligram per milliliter range) with enzymatic methods, it is necessary to find the proper dilution factor for each sample, which is both time consuming and expensive. Thus, another method was needed that would be

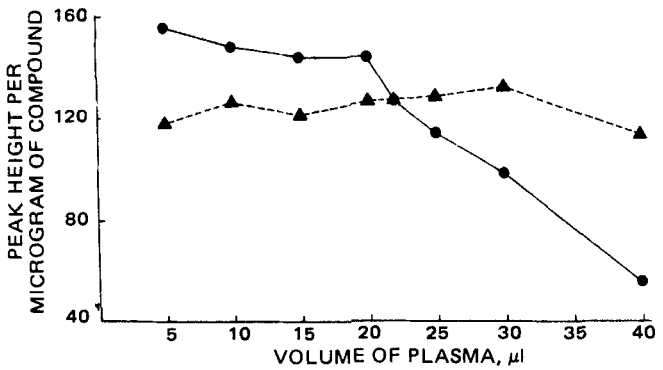

Figure 1—*Effect of plasma volume on acetylation of glycerin* (●) *and 1,6-hexanediol* (▲).

applicable over a wide range of plasma glycerin concentrations. In addition, it was highly desirable to reduce the cost of each assay by eliminating the use of relatively expensive enzymes. Consequently, a rapid, specific, and inexpensive method for the determination of glycerin in microliter volumes of plasma was developed.

EXPERIMENTAL

Apparatus—A gas chromatograph, equipped with a flame-ionization detector[1] and a 2-mm i.d. × 180-cm coiled glass column packed with 3% OV-1 on 80–100-mesh Supelcoport[2], was used. Prior to packing, the column was thoroughly rinsed with methanol and acetone, dried, and conditioned for 1 hr with 5% dimethyldichlorosilane[3] in toluene. Then the column was rinsed with toluene and acetone and dried. A silane-treated glass wool[3] plug was placed in the exit end of the column, but none was used in the injection port side. Prior to use, the column was conditioned by injecting 30 μl of a trimethylsilylating mixture[4].

Chromatographic Conditions—The column oven, injection port, and detector were maintained at 120, 250, and 250°, respectively. Nitrogen, the carrier gas, was maintained at 60 ml/min, with hydrogen and air at 20 and 240 ml/min, respectively.

Reagents—Glycerin[5], the internal standard 1,6-hexanediol[6], pyridine[7], and acetic anhydride[5] were of reagent grade and were used without further purification. Stock solutions containing 1 and 2 mg of 1,6-hexanediol/ml of pyridine were prepared. Small aliquots of stock aqueous solutions of glycerin were added to control citrated plasma to prepare plasma standards.

GLC Assay Procedure—To 15 μl of plasma in a 12-ml Pyrex glass-stoppered centrifuge tube were added 100 μl of acetic anhydride and 10 μl of the stock pyridine solution of 1,6-hexanediol. The glass stoppers were then inserted, and the test tubes were mixed well and heated for 15 min at 80°. After centrifugation at about 3000 rpm for 5 min, 4 μl of the supernate was injected onto the GLC column.

Enzymatic Assay Procedure—This newly developed GLC method was compared to an established enzymatic method. A commercial glycerin assay kit[8], which had been developed based on the Bucolo and David method (10), was used.

Calculations—Peak height ratios were calculated by dividing the peak height corresponding to the acetylated glycerin by the peak height corresponding to the acetylated 1,6-hexanediol. Calibration curves were constructed daily from results of spiked control plasma samples by plotting peak height ratios *versus* concentrations of glycerin.

RESULTS AND DISCUSSION

Quantification of glycerin in lipids by GLC was reported previously (12–14); glycerin was methylated (12), silylated (13), or acetylated (14) prior to chromatography. However, these methods do not lend themselves to an easy direct adaptation to the assay of glycerin in plasma.

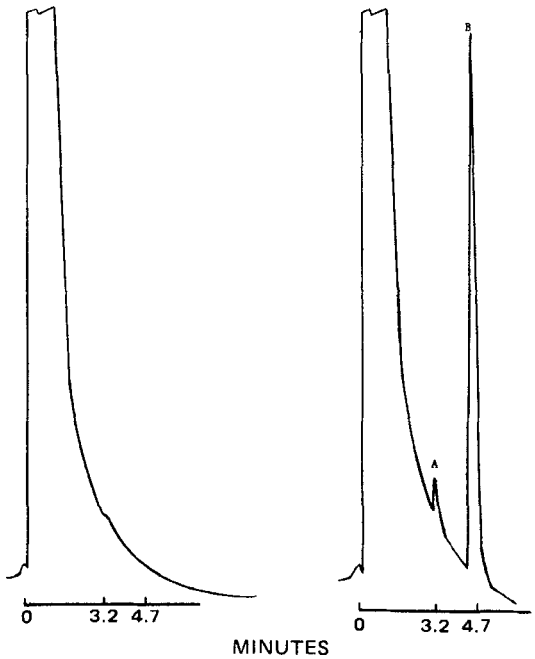

Figure 2—*Chromatograms showing peaks from glycerin analysis. Key: left, control plasma; and right, plasma containing 0.09 mg of glycerin/ml and 2.0 mg of 1,6-hexanediol/ml.*

Since removal of the glycerin from its aqueous environment in plasma proved to be difficult without a lengthy procedure, an attempt was made to derivatize the glycerin in plasma directly. A major factor that would seem to make this approach feasible was the high plasma glycerin concentrations found when glycerin was used to produce hyperosmolar dehydration of cerebral tissue. With such high concentrations, only small volumes of plasma are needed.

Acetylation of glycerin and 1,6-hexanediol, the internal standard, was accomplished with acetic anhydride in the presence of pyridine. Within 15 min at 80°, the reaction was complete. The effect of plasma volume on the acetylation was then studied. Various aliquots (5–40 μl) of plasma spiked with 1.15 mg of glycerin/ml were transferred to glass-stoppered test tubes. To each test tube were added 100 μl of acetic anhydride and 10 μl of a pyridine solution of the internal standard. Then these test tubes were incubated at 80° for 15 min.

After GLC analysis, the peak heights were measured and divided by the absolute amount of compound injected onto the column. A plot of peak height (millimeters) per microgram of compound *versus* plasma volume (microliters) was constructed (Fig. 1). The reaction with glycerin was minimally affected with up to 20 μl of plasma; with 1,6-hexanediol, up to 30 μl of plasma was tolerated. As a precaution, it is recommended that 15 μl of plasma be used. Acetic anhydride serves as an acetylating agent for the glycerin and 1,6-hexanediol and also as a precipitating agent of the plasma protein.

The recovery of glycerin and 1,6-hexanediol in this direct derivatization method was virtually 100%. In a stability study, glycerin was added to control plasma; aliquots were frozen and assayed periodically. Glycerin was stable in frozen plasma for at least 1 month.

Chromatograms of control human plasma and human plasma containing 0.09 mg of glycerin/ml are shown in Fig. 2. The chromatogram of control plasma shows no interfering peaks. In the other chromatogram, two peaks with retention times of 3.2 and 4.7 min correspond to the derivatives of glycerin and 1,6-hexanediol, respectively.

Since glycerin is often given in a glucose solution, the effect of high concentration of glucose in plasma was studied. Blood glucose levels as high as 500 mg % did not interfere with the glycerin determination.

The standard curve for the assay of glycerin in human plasma was linear and showed good reproducibility.

Table I shows a comparison of the precision and accuracy of the GLC and enzymatic assays. The enzymatic assay includes a series of reactions. First, glycerin in the sample solution is phosphorylated by adenosine triphosphate in a reaction catalyzed by glycerin kinase forming adenosine diphosphate and glycerin phosphate. Second, adenosine diphosphate reacts with phosphoenol pyruvate in a reaction mediated by pyruvate

[1] Model 5720A, Hewlett-Packard, Avondale, Pa.
[2] Supelco, Bellefonte, PA 16823.
[3] Applied Science Laboratories, State College, Pa.
[4] Pierce Chemical Co., Rockford, IL 61105.
[5] Mallinckrodt, St. Louis, Mo.
[6] Eastman-Kodak, Rochester, NY 14650.
[7] Fisher Scientific, Fair Lawn, NJ 07410.
[8] Calbiochem, La Jolla, CA 92037.

Table I—Comparison of the Precision and Accuracy of GLC and Enzymatic Assays for Glycerin

Actual Concentration, mg/ml	GLC Assay		Enzymatic Assay	
	Concentration, mg/ml ± % *RSD*	Error, %	Concentration, mg/ml ± % *RSD*	Error, %
Control	—[a]	—	—[b]	—
0.052	0.052 ± 5.8	0	0.052 ± 0	0
0.073	0.075 ± 10.7	+2.7	0.086 ± 0	+18
0.100	0.10 ± 8.0	0	0.12 ± 0	+18
0.17	0.17 ± 4.7	0	0.20 ± 2.0	+18
0.37	0.38 ± 6.6	+2.7	0.36 ± 0	−2.8
0.73	0.74 ± 5.0	+1.4	0.73 ± 1.1	0
1.3	1.2 ± 2.7	−7.7	1.2 ± 0.7	7.7
1.7	1.6 ± 0.9	−5.9	1.5 ± 0.8	−12
2.0	2.0 ± 5.5	0	2.0 ± 0.4	0
2.5	2.7 ± 3.2	+8.0	2.2 ± 1.1	−12
3.2	3.1 ± 2.4	−3.1	3.2 ± 0.9	0
Mean *RSD*, %	5.5		0.6	
Mean error, %	2.9		7.1	

[a] Not detectable. [b] Values of 0.0009 and 0.0005 mg/ml were obtained in the low and high range validation runs, respectively.

kinase, forming pyruvate and regenerating adenosine triphosphate. Third, pyruvate is reduced to lactate by lactate dehydrogenase. The concomitant oxidation of NADH to NAD^+ results in an absorbance change at 340 nm proportional to the glycerin content of the sample.

Two validation runs were made; one covered the 0.05–0.20-mg/ml range, and the other covered the 0.2–3.5-mg/ml range. The amount of internal standard used for the higher concentration range was twice that of the lower range. With the GLC assay, a mean percent *RSD* of 5.5 was found with a mean percent error of 2.9. These results compared favorably with the mean percent *RSD* of 0.6 and mean percent error of 7.1 for the enzyme assay.

A problem of sample carryover was encountered in the chromatography of these samples. This carryover could not be eliminated by on-column silylation or by increasing the injection port temperature, but it could be eliminated by removing the glass wool from the injection end of the column. In practice, a very small plug of silane-treated glass wool was used, and 5 μl of solvent was injected between samples to flush the system.

The method was used to monitor glycerin in clinical situations and to study glycerin pharmacokinetics in the rabbit. Glycerin, 10% (w/v), in normal saline solution was infused intravenously into the marginal ear vein of three rabbits (1 g/kg). Blood samples were withdrawn from the opposite marginal ear vein into small heparinized capillary tubes. After centrifugation, 15 μl of plasma was transferred into a glass-stoppered test tube and derivatized by the direct acetylation method.

A standard curve was prepared by assaying control plasma to which had been added known amounts of glycerin. A linear plot of peak height ratio *versus* concentration was prepared and used to determine the concentration of glycerin in the rabbit plasma. A semilogarithmic plot of the plasma concentration–time profile for three rabbits is shown in Fig. 3. From the mean concentration values, the half-life of glycerin in the rabbit was about 41 min with a volume of distribution of about 0.6 liter/kg, corresponding to a clearance ($K_E V_d$) of about 9 ml/kg/min.

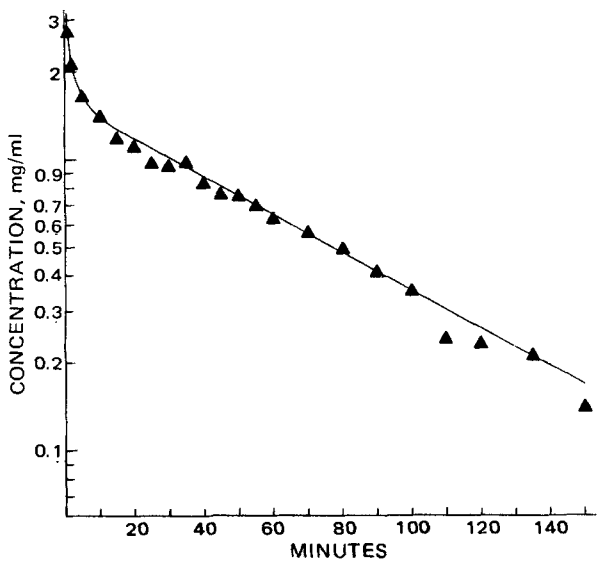

Figure 3—*Plot of plasma glycerin levels* versus *time in rabbits after intravenous medication (1 g/kg).*

REFERENCES

(1) J. R. Saper and S. Yosselson, *Postgrad. Med.*, **57**, 89 (1975).

(2) T. A. Newkirk, W. W. Tourtelotte, and J. L. Reinglass, *Arch. Neurol.*, **27**, 95 (1972).

(3) J. L. Reinglass, *Neurology*, **27**, 743 (1974).

(4) O. Wieland, *Biochem. Z.*, **329**, 313 (1957).

(5) J. Himms-Hagan and P. B. Hogen, *Can. J. Biochem. Physiol.*, **40**, 1129 (1962).

(6) F. H. Kreutz, *Klin. Wochenschr.*, **40**, 362 (1962).

(7) P. B. Garland and P. J. Randle, *Nature (London)*, **196**, 987 (1962).

(8) S. Laurell and G. Tibbling, *Clin. Chim. Acta*, **13**, 317 (1966).

(9) C. Spinella and M. Mager, *J. Lipid Res.*, **7**, 167 (1966).

(10) G. Bucolo and H. David, *Clin. Chem.*, **19**, 476 (1973).

(11) F. Moller and M. W. Roomi, *Anal. Biochem.*, **59**, 248 (1974).

(12) M. E. Massan, M. E. Eager, and G. R. Waller, *Anal. Chem.*, **36**, 587 (1964).

(13) A. Rajiah, M. R. Subbaram, and K. T. Achaya, *J. Chromatogr.*, **38**, 35 (1968).

(14) L. A. Horrocks and D. G. Cornwell, *J. Lipid Res.*, **3**, 165 (1962).

ACKNOWLEDGMENTS AND ADDRESSES

Received July 19, 1976, from the *Departments of Medicinal Chemistry and Pharmaceutics, School of Pharmacy, University of Pittsburgh, Pittsburgh, PA 15261.*

Accepted for publication September 9, 1976.

[x] To whom inquiries should be directed.

Pharmacokinetics of the Anti-Inflammatory Tiaprofenic Acid in Humans, Mice, Rats, Rabbits, and Dogs

J. POTTIER ˣ, D. BERLIN, and J. P. RAYNAUD

Abstract □ The pharmacokinetics of tiaprofenic acid were studied in rats, dogs, mice, and rabbits using the ^{14}C-labeled compound and in humans using the radioinert compound. Its absorption was partially gastric but mainly intestinal and was total in all species. Its apparent volume of distribution was small; it was bound markedly to albumin, and its plasma clearance was high in all species. Absence of retention was confirmed in rats by the very low tissue radioactivity levels 24 hr after oral dosing. In humans, identical maximum plasma concentrations and elimination rates were recorded after the first and 40th dose during a 2-week treatment with 200 mg three times daily. During this period, constant residual levels were recorded before the first dose of the day. These results indicate that, for a dose in the therapeutic range, a steady state was reached as early as the end of the 1st day of treatment and that tiaprofenic acid did not inhibit or induce its own biotransformation. Urinary excretion accounted for one-half of the dose in rats and from 0.6 to 0.9 in humans, dogs, mice, and rabbits. Two metabolites were formed, one resulting from the reduction of the ketone group to an alcohol and the other from oxidation generating a phenol in the benzene ring in the *para*-position to the ketone group. These two metabolites were common to all species, but the latter was present in minute amounts only in dogs. Tiaprofenic acid was conjugated as an amide in dogs and as an acylglucuronide in the other species. In rats, phenobarbital induced the oxidative, but not the reductive, pathway.

Keyphrases □ Tiaprofenic acid—pharmacokinetics in humans, rats, dogs, mice, and rabbits □ Pharmacokinetics—tiaprofenic acid in humans, rats, dogs, mice, and rabbits □ Anti-inflammatory agents—tiaprofenic acid, pharmacokinetics in humans, rats, dogs, mice, and rabbits

Tiaprofenic acid[1], 5-benzoyl-α-methyl-2-thiopheneacetic acid (I) (Table I), is a highly potent anti-inflammatory and nonnarcotic analgesic agent as demonstrated both in animal (1) and in human (2–4) studies. In the present study, its animal pharmacokinetics were studied in rats and dogs—the species used to evaluate its pharmacological activity and tolerance—and, in less detail, in rabbits and mice—the species used to establish the absence of teratogenicity[2]. The absorption, distribution, excretion, and biotransformations of tiaprofenic acid were compared in these species and in humans after oral and parenteral administrations.

EXPERIMENTAL

Radiolabeled Compound—Tiaprofenic acid was labeled[3] with carbon-14 in the carbonyl group (Table I) with a specific activity of 54 mCi/mmole and a radiochemical purity of 95% as checked by TLC.

Animal and Human Studies—Male adult animals were used: Swiss mice (22 g), Sprague-Dawley rats (200 g), "Normandy" rabbits (2.4 kg), and beagle dogs (15 kg). Clinical pharmacology studies were carried out in adult subjects of both sexes. Prior to oral administration, animals and humans were fasted overnight. Unless otherwise indicated, the pharmacological dose of 5 mg/kg was administered to animals. In humans, the dosage varied from 1.5 to 3.0 mg/kg in a single administration. For the steady-state study, a daily dose of 600 mg (8.5 mg/kg), divided into three equal doses to be taken at 9:00 am, 2:00 pm, and 8:00 pm was administered for 13 days. A 40th dose of 200 mg was administered on the morning of the 14th day.

The drug was administered either as a suspension in 0.25% carboxymethylcellulose with 0.2% polysorbate 80, a solution after addition of lysine or tromethamine, capsules, or tablets. The stability of formulations containing ^{14}C-I was checked by TLC and scanning.

Blood samples were collected in dry heparin sodium in animals and with or without an anticoagulant in humans. Tissue samples were deposited on dry ice and stored at −25°. Bile was collected by catheterization of the common bile duct under prolonged anesthesia with urethan (1 g/kg ip). For intraduodenal administration, the pylorus was ligatured to avoid gastric reflux. Gastric absorption was studied in rats treated 1 hr after recovery from ligation of the pylorus under mild ether anesthesia. Pulmonary carbon dioxide was trapped in an aqueous solution of 4 *N* ethanolamine. Enzymatic induction was obtained with daily subcutaneous injections of 100 mg of phenobarbital sodium/kg for 3 days.

Hydrolysis of Conjugates—Biliary and urinary conjugates were hydrolyzed either enzymatically by leaving the material for 24 hr at 37° in a buffered acetate medium (pH 5.2) containing *Helix pomatia* juice[4] or at alkaline pH by slowly adding 0.2 *N* NaOH at 0°, away from light and under argon. In some excreta, polar products persisting after hydrolysis at alkaline pH were separated by TLC and, after elution, hydrolyzed with 1 or 6 *N* HCl for 1 hr at 100°.

Extraction and Chromatography—Plasma samples were acidified to pH ≃ 5 with 1 *M* KH_2PO_4. Urine and bile samples were acidified to pH 5 (extraction of I and II) or 2 (extraction of III) with 1 *N* HCl and then extracted twice with ethyl acetate. Extracts were chromatographed on silica gel plates[5] in various solvent systems (Table I). When ^{14}C-tiaprofenic acid was administered, the radioinert reference compounds were added before TLC to enable detection at 254 nm. Relevant areas were eluted either with methanol–acetic acid (1:1) (radiochemical assay) or with acetone or ethyl acetate–acetic acid (98:2) (spectrophotometric assay).

Radiochemical Assay—A solution of either scintillator[6] alone (0.4% w/v) in toluene or of scintillator (0.4% w/v) and naphthalene (8% w/v) in methoxyethanol–toluene (2:3) was added to the samples. Carbon dioxide formed after combustion of tissues[7] was trapped in a solution of scintillator (0.7% w/v) in toluene–phenylethylamine–methanol–water (40:33:22:5). Radioactivity was measured in a liquid scintillation spectrometer[8]. Quenching was corrected by the channel ratio method. Certain measurements were obtained by integration of the chromatographic curves with a scanner[9].

Spectrophotometric Assay—Chromatographic eluates were taken up by aqueous 1 *M* sodium acetate–ethanol (1:9). Absorbances were determined at 313 nm for I (ϵ = 15,400 M^{-1} cm^{-1}), at 248 nm for II (ϵ = 10,300 M^{-1} cm^{-1}), and at 319 nm for III (ϵ = 19,400 M^{-1} cm^{-1}). Optical interferences were eliminated by assaying control samples obtained before treatment or from untreated subjects.

For the determination of I, corrections for losses were made by the addition of labeled compound to the samples prior to analysis. Because the absorption of II is negligible above 280 nm, the determination of I is possible after chromatography in System B (Table I) even though this system does not separate I from II. This approach was checked on dog plasma, which contained relatively large quantities of II. The coefficient of correlation between radiochemical and spectrophotometric determinations of I was 0.997 (12 pairs of plasma concentrations from 3 to 100 mg/liter).

The method for the determination of I and its two metabolites in human urine after separation in System C (Table I) was checked by the analysis of control samples with compounds added *in vitro* (10 mg/liter

[1] Surgam, Laboratoires Roussel.
[2] R. Glomot, Toxicology Department, Roussel-Uclaf Research Center.
[3] Synthesized by A. Jouquey, Roussel-Uclaf Research Center.
[4] I. B. F., Gennevilliers, France.
[5] Merck, Darmstadt, 60F 254.
[6] 2-(4′-*tert*-Butylphenyl)-5-(4″-biphenyl)-1,3,4-oxadiazole, Ciba.
[7] Oxymat Intertechnique.
[8] Packard model 3385.
[9] Berthold, Wiedbad, West Germany.

Table I—Structures and R_f Values of Tiaprofenic Acid and Its Derivatives Found in Biological Media

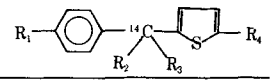

Compound	Substituent R_1	R_2	R_3	R_4	R_f of System: Solvent System A[a]	Solvent System B[b]	Solvent System C[c]
I	H	=O		$CH(CH_3)CO_2H$	0.35	0.50	0.70
II[d]	H	H	OH	$CH(CH_3)CO_2H$	0.25	0.50	0.60
III[e]	OH	=O		$CH(CH_3)CO_2H$	0.05	0.40	0.30
IV[f]	H	=O		$COCH_3$	0.45	0.60	0.80
V[g]	H	=O		CH_2CH_3	0.70	0.80	0.85

[a] Toluene–acetic acid (88:12). [b] Benzene–dioxane–acetic acid (10:5:1). [c] Benzene–dioxane–acetic acid (9:1:1); two migrations. [d] 5-(α-Hydroxybenzyl)-α-methyl-2-thiopheneacetic acid. [e] 5-(4-Hydroxybenzoyl)-α-methyl-2-thiopheneacetic acid. [f] (2-Acetyl-5-thienyl)phenylmethanone. [g] (2-Ethyl-5-thienyl)phenylmethanone.

of each). The recovery of I [88.2 ± 2.6% (mean ± *SD*, $n = 8$)] was total when radiochemical corrections were applied (100.2 ± 2.6%). Recoveries of II and III were 94.5 ± 3.7 and 95.3 ± 1.7% ($n = 8$), respectively, and no correction was applied in these cases.

For a 5-ml sample, the limits of sensitivity were 0.1 mg/liter for I, whatever the mode of separation, 0.1 mg/liter for III, and 0.3 mg/liter for II.

Plasma Protein Binding—Binding to nondiluted plasma or to human albumin[10] in 0.1 *M* phosphate buffer (pH 7.4) was determined by ultrafiltration[11] to avoid the degradations occurring during long contact (equilibrium dialysis). Protein solutions were ultrafiltered at room temperature under a nitrogen pressure of 0.5 kg/cm^2 and magnetic stirring. In 5 min, 10% of the total volume was collected.

RESULTS

Structures of Free Compounds Found in Biological Media—The ^{14}C-label was stable; during 24 hr after intravenous administration, less than 0.01% of the radioactivity in the rat and less than 0.1% in the mouse were excreted by the lungs as ^{14}C-carbon dioxide.

Apart from tiaprofenic acid, which was found in all media studied and which was characterized by the similarity between its chromatographic properties, UV spectrum, and mass spectrum and those of a reference sample, four products were identified (II–V, Table I). Their presence was established both in humans and in the four animal species.

Compound II arises from the reduction of the ketone group of I to an alcohol. Absence of absorption in the UV spectrum around 300 nm indicated the loss of the ketone group. Its mass spectrum with a molecular peak at 262 corresponded to the introduction of two hydrogen atoms, and the fragmentation pattern was in agreement with the proposed formula.

Compound III results from an oxidation process introducing a phenol function in the benzene ring in a *para*-position to the ketone group. The maximum of absorption at 319 nm in its UV spectrum established the presence of the ketone group. Its mass spectrum revealed the introduction of an oxygen atom (molecular peak at 276) in the benzene ring (fragmentation pattern). The position of the phenol group was established by the NMR spectrum, which indicated that the proton in the *para*-position to the ketone group was absent.

Compounds II and III were identified conclusively by comparison with reference substances (1).

Compounds IV and V result from substitution of the methylacetic radical by acetyl and ethyl radicals, respectively, with the loss of one carbon atom. They were first isolated from an aqueous solution of I as degradation products; their structures were established by mass spectrometry (molecular peaks at 230 and 216, respectively, and fragmentation patterns in agreement). They were also found in small quantities *in vivo*.

In the plasma of the four animal species studied, IV and V accounted for about 5% of the total radioactivity measured after treatment with ^{14}C-I, and this proportion did not change significantly with time. Likewise, they accounted for 2–5% of the excreted radioactivity, the amount depending on the conditions of hydrolysis. Too strong alkalinization considerably increased the quantities of IV at the expense of free and conjugated I. Unlike II and III, which exist only *in vivo*, IV and V result from degradation and not from enzymatic biotransformations. Therefore, they cannot be considered as metabolites.

Animal Plasma Kinetics—Total radioactivity kinetic curves after oral and intravenous administrations of ^{14}C-I (Fig. 1) showed that absorption was rapid in the rat for the oral route and slightly slower in the dog; plasma clearance of I and its metabolites, 24 hr after administration, was almost complete in the rat but not in the dog. Tiaprofenic acid was the major constituent. Compound II was present in small quantities in rat plasma (not shown) but in appreciable quantities in dog plasma. In the plasma of both species, III was not detectable.

The kinetics of I after intravenous administration can be depicted according to a two-compartment open model. The apparent initial volumes of distribution, V_c, were calculated from biexponential plasma curves ($C = Ae^{-\alpha t} + Be^{-\beta t}$). The value of V_c is given by $V_c = \chi_0/C_0$, where χ_0 is the intravenous dose and C_0 is the plasma concentration at time $t = 0$ ($C_0 = A + B$) (5). The V_c was 17% of body weight in the rat and

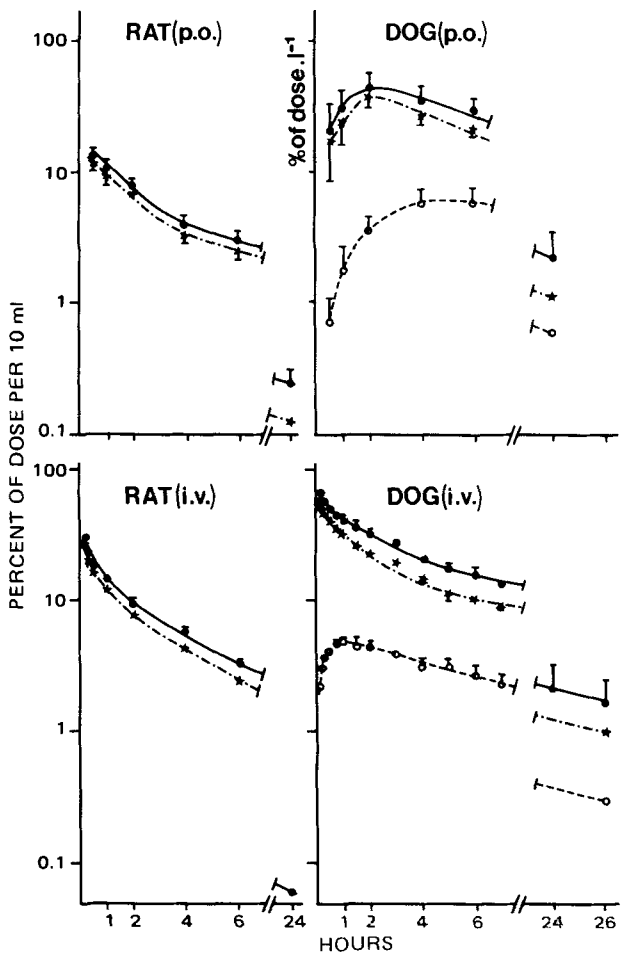

Figure 1—*Plasma kinetics in the rat and dog. Key:* ●, *total radioactivity;* ★, *tiaprofenic acid; and* ○, *II (mean* ± SE; n = *5, rat;* n = *4, dog, oral;* n = *2, dog, intravenous).*

[10] Centre National de Transfusion Sanguine, Paris, France.
[11] Pellicon Carrousel, Millipore-Diaflo Amicon P.M. 30 membranes.

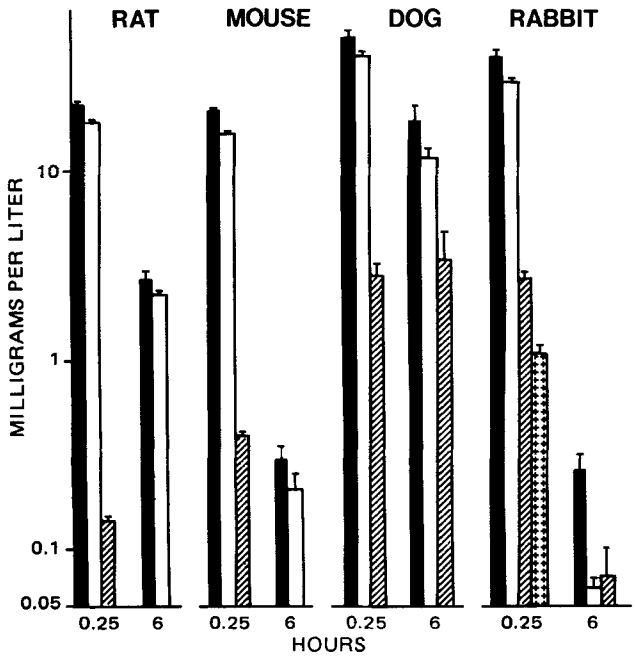

Figure 2—*Plasma levels in four animal species 0.25 and 6 hr after intravenous administration, expressed in tiaprofenic acid equivalent. Key:* ■, *total radioactivity;* □, *I;* ▨, *II; and* ⊞, *III (mean* ± SE; n = 5, *rat and rabbit;* n = 3, *dog;* n = 5, *pools of four plasmas, mouse).*

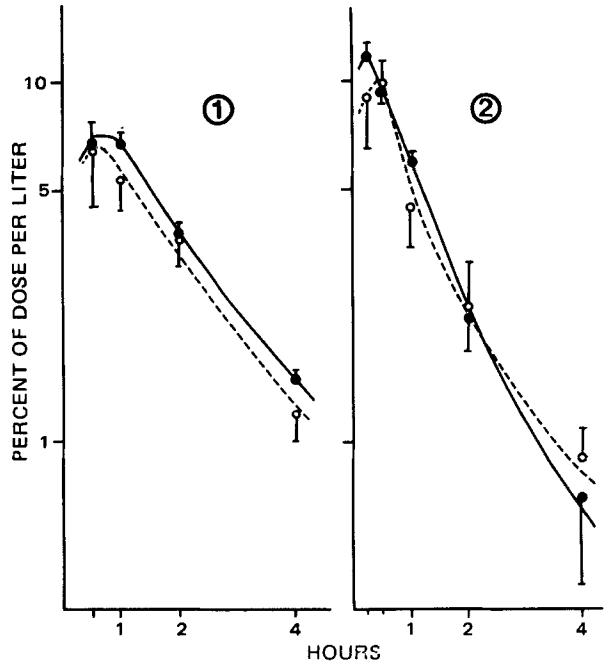

Figure 3—*Serum kinetics of tiaprofenic acid in humans after oral (1) or intramuscular (2) administration. Key:* ●, *100 mg; and* ○, *200 mg (mean* ● SE, n = *17, oral, 100 mg;* n = 5, *oral, 200 mg;* n = 5, *intramuscular, 100 mg;* n = 4, *intramuscular, 200 mg).*

8% in the dog. The extravascular diffusion space was thus smaller in the dog. The plasma clearance of I [$Cl_p = \chi_0/\int_0^\infty C\,dt = \chi_0\alpha\beta/(A\beta + B\alpha)$] per kilogram was 27 ml/hr in the dog and 96 ml/hr in the rat.

Absorption was estimated (6) from the ratio of areas under plasma curves after oral and intravenous administrations. In the rat and dog, the area ratios based on total radioactivity were 0.78 and 1.01; based on tiaprofenic acid, they were 0.87 and 1.12, indicating both a good rate of absorption and no first-pass effect.

Total plasma radioactivity and the radioactivities due to the different compounds were determined 0.25 and 6 hr after intravenous administration of ^{14}C-I in all four animal species (Fig. 2). The decrease in total radioactivity was much faster in the rabbit and mouse than in the rat and, particularly, the dog. Six hours after the injection, tiaprofenic acid represented the major fraction in all species except the rabbit. Metabolite II concentrations were very low in the rat, a little higher in the mouse, and considerably higher in the dog and rabbit. Metabolite III was detected in the rabbit only—in limited quantities and only 0.25 hr after the injection.

On the basis of a simplified one-compartment open model, $C = Ae^{-\alpha t}$, defined by the concentrations at 0.25 and 6 hr, the clearance of I ($Cl_p = \chi_0\alpha/A$) was 91 ml/hr/kg in the rat and 25 ml/hr/kg in the dog. These values are similar to those calculated in the preceding assay. Its clearance was 140 ml/hr/kg in the rabbit and 196 ml/hr/kg in the mouse. The V_c values were calculated according to this same model and enabled the classification of the animal species into two groups with V_c values equivalent to 12 and 13% (dog and rabbit, respectively) and to 24 and 26% (rat and mouse, respectively) of body weight.

Human Serum or Plasma Kinetics—The concentrations of I were assayed spectrophotometrically. Although the UV absorption of II was detected in some samples, this metabolite was present only in weak concentrations and was not measured. The presence of III could not be confirmed in serum, since a meaningful UV spectrum could not be obtained after elution.

After a single oral dose of 100 or 200 mg, peak concentrations were achieved in 0.5–1 hr. Within 4 hr of administration, the level had dropped to one-fifth of the peak value, indicating both rapid absorption and disappearance of the compound (Fig. 3). After a single intramuscular injection of the same dosages (Fig. 3), a rapid decrease in plasma levels established satisfactory diffusion from the injection site and confirmed the fast elimination rate. The V_c of I, calculated according to a one-compartment open model, was about 10% of body weight, and its clearance was 6 liters/hr.

In the steady-state study, the plasma kinetics of tiaprofenic acid after the first dose on Day 1 and after the 40th and last dose on Day 14 were similar (Fig. 4), with mean peaks of 17 mg/liter and equal elimination rate constants (0.50 and 0.46 hr^{-1}, respectively). The areas under individual curves, calculated from 0 to 5 hr by the trapezoidal rule, were not significantly different (paired t test). From Days 2 to 11, mean plasma concentrations fluctuated from 0.6 to 0.8 mg/liter. After the end of treatment (Day 14), from Days 15 to 18, concentrations were equal to or below the limit of sensitivity of the method (0.1 mg/liter).

Absorption by Stomach—The importance of gastric absorption was evaluated in rats by comparing the plasma radioactivity of a group of animals with a ligated pylorus to that of a sham group 0.5 hr after oral administration of ^{14}C-I. Plasma concentrations in control animals were close to those found previously at 0.5 hr (11.7 *versus* 13.9% of dose/10 ml). Therefore, anesthesia and laparotomy did not influence absorption. After ligature of the pylorus, the plasma concentration was only halved, 5.07 ± 0.82 (n = 10) *versus* 11.7 ± 1.08 (n = 7), indicating that the gastric mucosa absorbs tiaprofenic acid.

Tissue Distribution in Rats—Figure 5 represents plasma and tissue concentrations of total radioactivity in the rat 24 hr after ingestion of ^{14}C-I. Tissue levels were all very low and generally lower than plasma levels. Levels in central nervous system tissues were particularly low. The only tissues with concentrations higher than in the plasma were those involved in metabolism and excretion (liver and kidney) or in contact with excreta (bladder). On the basis of the tissue composition of the rat (7), the total concentrations in the whole animal, excluding the GI tract, accounted for about 2% of the dose. This very low residual fraction indicated that I and its metabolites were almost totally eliminated 24 hr after ingestion.

Excretion Routes in Animals—Renal excretion of I and its metabolites was high in all of the animal species (Table II). The total radioactivity excreted in 24 hr accounted for one-half of the dose in the rat and two-thirds of the dose in the dog after ingestion of 5 mg/kg. It accounted for three-fourths of the dose in the mouse and about nine-tenths in the rabbit after ingestion of 50 mg/kg. These high excretion levels recorded after administration of such a suprapharmacological dose are indicative of excellent absorption.

Recovery of about one-half of the dose in rat feces implies significant biliary excretion, since absorption is good in this species. This biliary excretion was measured in anesthetized rats after intravenous administration of ^{14}C-I (Fig. 6). Under conditions where bile collection prevented enterohepatic recirculation, 70% of the dose was excreted in 6 hr and 80% in 24 hr. These results confirmed the importance of biliary excretion of I and/or its metabolites.

Reabsorption of products excreted in the bile was evaluated by comparing the quantity absorbed after administration of bile of control rats

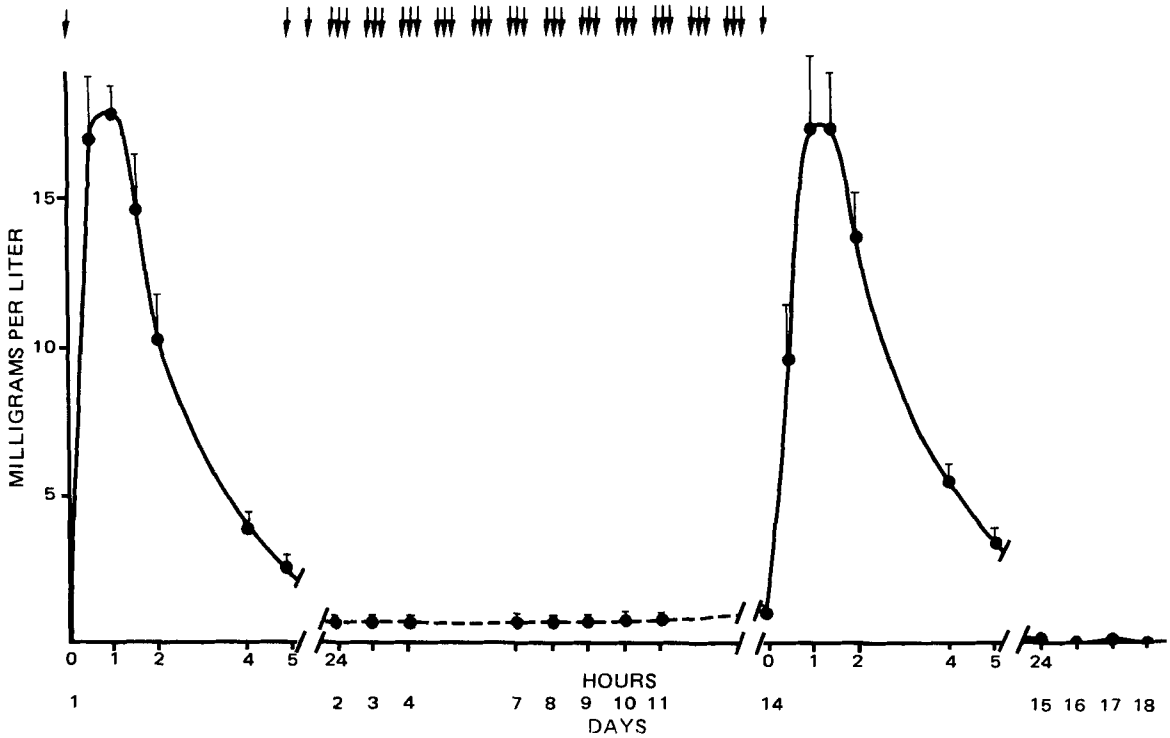

Figure 4—*Plasma concentrations of tiaprofenic acid during and after a chronic treatment with 600 mg/day. Key: ↓: dose of 200 mg (mean ± SE, n = 12).*

with ^{14}C-I added *in vitro* or of bile collected after intravenous injection of ^{14}C-I. These two types of bile samples were administered either orally to conscious rats or intraduodenally to anesthetized rats after catheterization of the common bile duct. Reabsorption, when given by the ratio of the areas under plasma radioactivity curves, was 32% (Fig. 7, top); when given by the ratio of the excreted radioactivity in the collected bile samples, it was 56% (Fig. 7, bottom). Thus, in the rat, there is a significant enterohepatic cycle.

Tiaprofenic acid was much more rapidly absorbed than its biliary metabolites, as indicated by a comparison of plasma kinetics in the first assay and of biliary excretion kinetics in the second assay.

Nature of Excreted Radioactivity in Animals—In the rat, after intravenous administration of ^{14}C-I, the percentage of radioactivity excreted within 6 hr was 29.0 ± 1.1 (n = 5) in urine (conscious animals) and 74.1 ± 2.5 (n = 4) in bile (anesthetized animals). Compounds I and II were mainly free in urine, whereas almost nine-tenths was conjugated in bile. In both fluids, the yields obtained after hydrolysis at alkaline pH were greater than those liberated by enzymatic lysis. Conjugates of I and II were consequently acylglucuronides. Their hydrolysis during collection due to their instability explains the presence of a larger free fraction in urine than in bile under the experimental conditions used.

Compound III was mainly conjugated in urine and bile. Since significant quantities of free III were liberated after enzymatic hydrolysis only, it was conjugated as an ether glucuronide or sulfate ester of the phenol group, although, in addition, an acylglucuronide with the carboxyl group could not be excluded. Tiaprofenic acid and its two metabolites represented three-fourths of the urinary radioactivity and two-thirds of the biliary radioactivity, I being the major fraction in both cases (Fig. 8). The two metabolites were excreted mainly *via* the urine. The remaining ra-

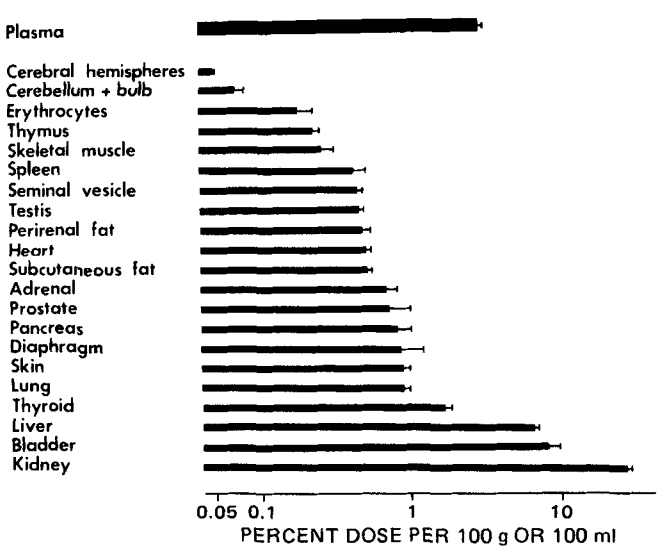

Figure 5—*Tissue distribution of total radioactivity in the rat 24 hr after oral administration (mean ± SE, n = 5).*

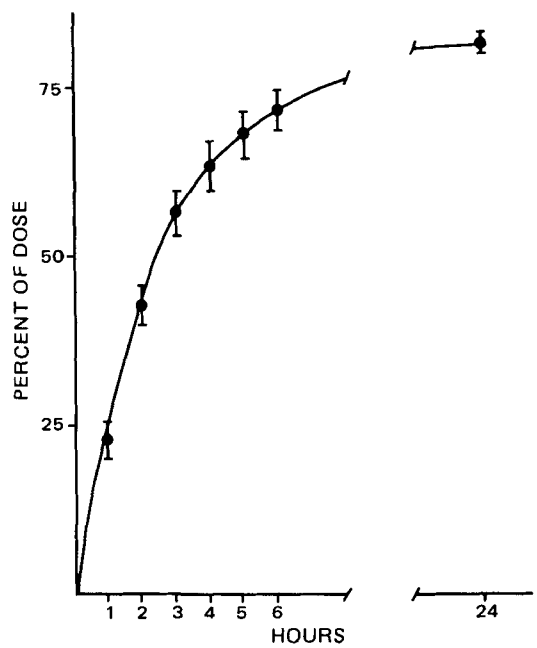

Figure 6—*Cumulative biliary excretion of total radioactivity in the rat (mean ± SE, n = 8).*

Table II—Urinary and Fecal Excretion [a] of Radioactivity in the Rat and Urinary Excretion in the Dog, Rabbit, and Mouse after Oral Administration of ^{14}C-I

	Hours	Rat (5)[b], 5 mg/kg Urine	Rat (5)[b], 5 mg/kg Feces	Dog (3), 5 mg/kg, Urine	Rabbit (3), 50 mg/kg, Urine	Mouse (2), 50 mg/kg, Urine
	0–24	46.9 ± 2.6	41.8 ± 2.9	59.3 ± 2.5	85.8 ± 4.6	73.4 ± 3.6
	24–48	1.2 ± 0.2	4.0 ± 1.3	5.2 ± 2.0	—	—
	48–72	0.3 ± —[c]	0.4 ± 0.2	—	—	—
Total	0–48			64.5 ± 0.6	—	—
Total	0–72	48.4 ± 2.7	46.2 ± 2.2	—	—	—
Grand total	0–72	94.6 ± 1.3				

[a] Expressed as means ± *SE* of percent administered radioactivity. [b] Number of animals or of groups of 10 mice. [c] *SE* < 0.05.

dioactivity was due to the noncarboxylic degradation products IV and V and primarily to polar products(s), possibly nonhydrolyzed conjugate(s). More vigorous hydrolytic methods yielded no further information because of degradation.

In the dog, the percentage of the dose excreted in the urine 6 hr after an intravenous injection of ^{14}C-I was 42.8 ± 9.4 (n = 3). Free II accounted for one-third of the total excretion (15.1 ± 6.2%, n = 3). A small quantity of free tiaprofenic acid (0.5% of dose) was unchanged after hydrolysis by enzymes or by alkaline pH. On the other hand, the residual polar fraction, after isolation by chromatography and hydrolysis by hot 6 N HCl, released a significant quantity of I (7.3 ± 1.3%, n = 3). Considering the easy degradation of I under these severe conditions, this quantity was only a minimum. The conjugate of I excreted in the urine of the dog was consequently not an acylglucuronide. Its characteristics suggest that it was an amide conjugate. Compound III was identified by its mass spectrum after hydrochloric acid hydrolysis of this same polar fraction from the urine of dogs treated orally by 100 mg of ^{14}C-I/kg. It was present in very small quantities.

In rabbit and mouse urine, collected for 24 hr after oral administration of 50 mg of ^{14}C-I/kg, tiaprofenic acid was excreted partially conjugated and accounted for most of the radioactivity, *i.e.*, 60% in rabbits and 57% in mice. Its conjugate, because it was hydrolyzed by β-glucuronidase and with a better yield at an alkaline pH, was an acylglucuronide. Compounds II and III occurred mainly in free form and accounted for 5% each of total excretion in the rabbit and 5 and 10%, respectively, in the mouse.

Urinary Excretion in Humans—Tiaprofenic acid was assayed spectrophotometrically in 24-hr urine samples. Its free form and the acylglucuronide, which was the main form, accounted for 45.2 ± 4.9 (n = 17) and 51.4 ± 3.5% (n = 5) of the dose 24 hr after oral administration of 100 and 200 mg, respectively. They accounted for 50.3 ± 3.4 (n = 5) and 39.7 ± 7.9% (n = 3) after intramuscular administration of the same doses, respectively. Metabolites II and III were also excreted partly as acylglucuronides, but the presence of an ether glucuronide or sulfate ester of the alcoholic or phenol groups cannot be excluded completely. Tiaprofenic acid and its two metabolites accounted for 60% of an oral 100-mg dose (Table III); I accounted for nine-tenths of the total excretion. The excretion of II was about double that of III.

Biotransformations of tiaprofenic acid in humans and in the four animal species studied are summarized in Scheme I.

Induction with Phenobarbital—Enzymatic induction was studied by comparing the plasma levels of I and its metabolites and their urinary excretions after intravenous injection of ^{14}C-I in rats, with or without phenobarbital pretreatment.

Compound I and its metabolites were cleared more rapidly from plasma in phenobarbital-induced rats, since plasma radioactivity was about the same 0.25 hr after the injection but was reduced by nearly 50% compared

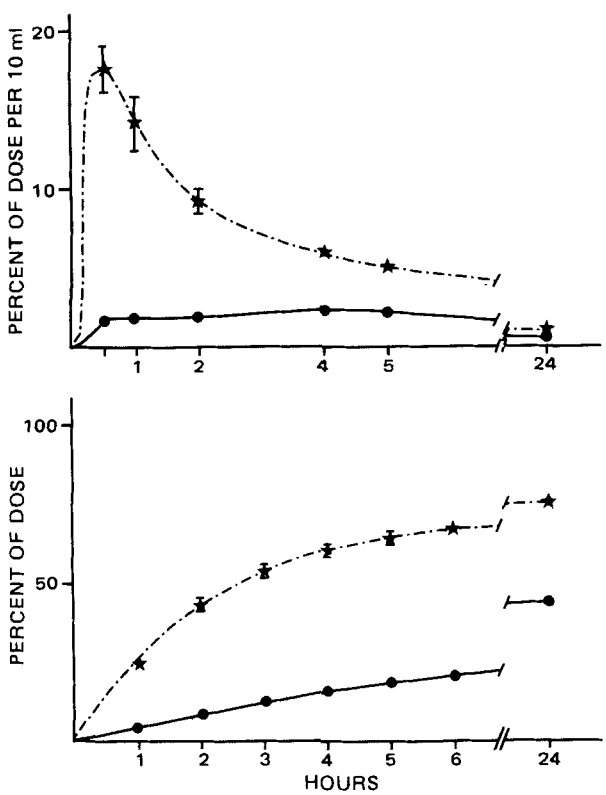

Figure 7—*Enterohepatic cycle in the rat. Top: plasma concentrations of radioactivity after oral administration of I or its biliary metabolites to conscious rats. Bottom: biliary excretion of radioactivity after intraduodenal administration of I or its biliary metabolites to anesthetized rats. Key: ★, control bile with ^{14}C-I added in vitro; and ●, bile from treated rats containing I and its metabolites. In both cases, the dose was 5 mg of I/kg or its equivalent calculated from radioactivity (mean ± SE, n = 5).*

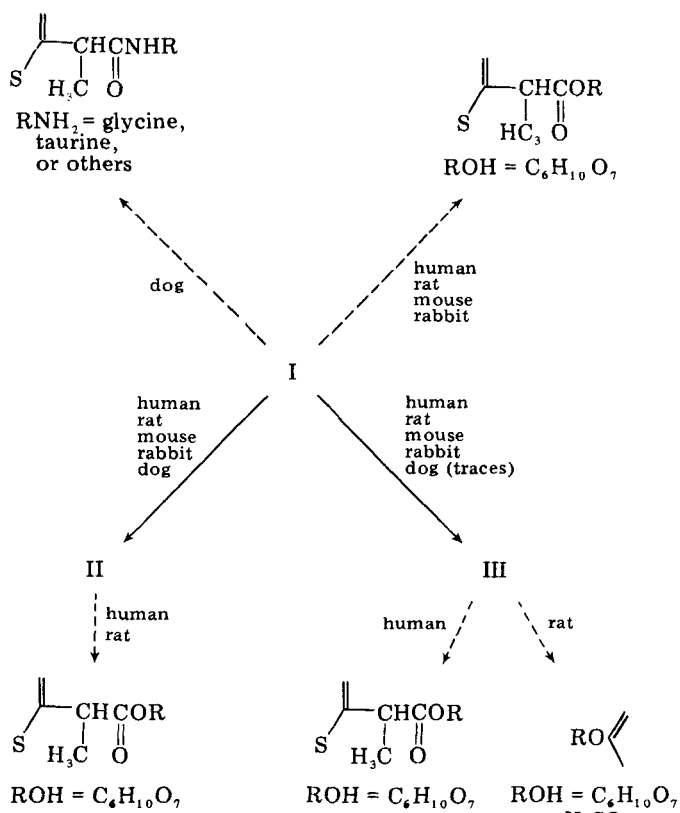

Scheme I—Metabolic pathway of tiaprofenic acid in humans and animal species studied. Key: →, phase I biotransformations; and ⇢, phase II biotransformations (conjugations).

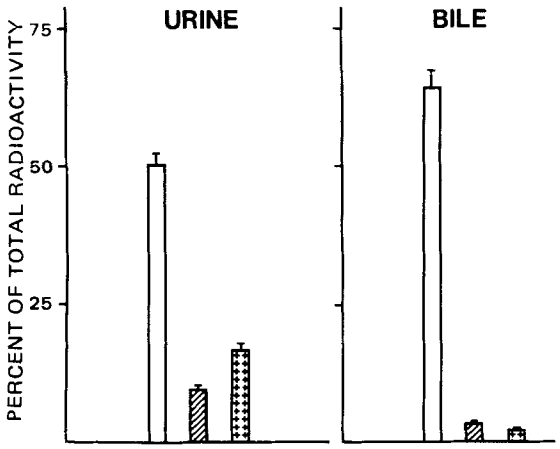

Figure 8—*Urinary and biliary levels of I and its metabolites (after deconjugation) in the rat 6 hr after intravenous administration. Key:* □, *tiaprofenic acid;* ▨, *II; and* ⊞, *III (mean* ± SE, n = 5, *urine;* n = 4, *bile).*

to controls 6 hr after the injection (Fig. 9, top). Plasma levels of I also were reduced; its plasma clearance, calculated with a one-compartment open model, was increased by 58% (139 compared to 88 ml/hr/kg in control animals). There were no significant changes in the quantities of II and III, which remained very low.

After induction by phenobarbital, the urinary excretion of radioactivity 6 hr after injection was slightly increased: 30.1 ± 1.5 *versus* 27.5 ± 2.5% (n = 5). However, the quantities of I and II were lowered, whereas the quantity of III was increased (Fig. 9, bottom). The radioactivity from other origins, mainly composed of polar products, was increased ($0.05 > p > 0.02$).

The enzymes that hydroxylate I and probably those that conjugate I and its metabolites are induced by phenobarbital. On the contrary, the enzymes that reduce I are not induced by phenobarbital, leading to a decrease in the excretion of II.

Protein Binding—The amount of radioactivity bound from a nondiluted plasma pool from rats 0.5 hr after oral administration of ^{14}C-I was 98.2 ± 0.2% (n = 5). As shown previously, 85% of the plasma radioactivity was due to I under these conditions. A similar result, 97.6 ± 0.1% (n = 3), was obtained from a plasma pool taken from control animals with identical concentrations of ^{14}C-I added *in vitro*. Similarly, 97.9 ± 0.3% (n = 3) of radioactivity was bound when I was added to a solution of human albumin (0.5 m*M*). This concentration was close to that of albumin in normal plasma.

DISCUSSION

The absorption of tiaprofenic acid was very good in all species studied, as shown by a comparison of its plasma kinetics after oral administration and after intravenous or intramuscular injection in rats, dogs, and humans, as well as by its very high urinary excretion after oral administration of a large dose in rabbits and mice.

The gastric mucosa plays a role in this absorption. In the rat, gastric absorption occurs by passive diffusion of undissociated compounds (8), and I is certainly weakly dissociated at gastric pH. Plasma radioactivity in rats with a ligated pylorus 0.5 hr after ingestion was 43% of that observed in controls, a percentage close to that obtained, under identical conditions after ingestion of ^{3}H-water, ^{14}C-ethanol, or ^{14}C-sodium acetate (50–70%). Acetic acid, like I, is only weakly dissociated at gastric pH. For

Table III—Urinary Excretion[a] of Tiaprofenic Acid (I) and Its Metabolites (II and III) in Humans for 24 hr following Oral Administration of 100 mg of I

I	II	III
43.7	1.7	0.9
81.3	2.9	0.2
50.4	4.5	2.5
51.3	2.9	1.5
43.7	2.0	3.2
54.1 ± 7.0[b]	2.8 ± 0.5	1.7 ± 0.5

[a] Expressed as percent of dose. [b] Mean ± *SE*.

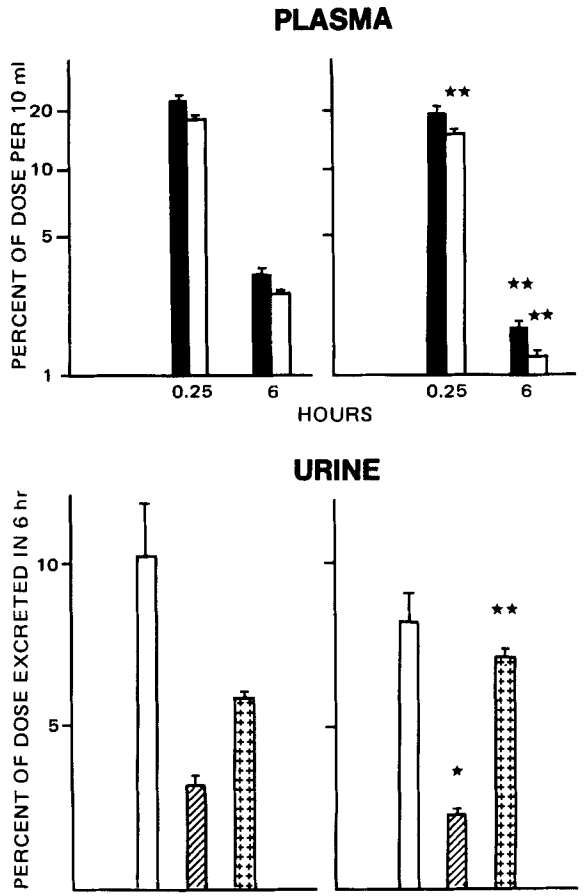

Figure 9—*Influence of phenobarbital on plasma concentrations and urine excretion in the rat. Left: control animals; right, induced animals. Key:* ■, *total radioactivity;* □, *tiaprofenic acid;* ▨, *II; and* ⊞, *III (mean* ± SE, n = 5; *significance according to Student* t *test:* ★, $0.02 > p > 0.01$; *and* ★★, $p < 0.01$).

a highly dissociated product, such as floctafenine (9), a very low (1%) percentage was recorded. Human gastric mucosa probably also absorbs I since the absorption mechanisms are qualitatively and quantitatively identical in both humans and rats (10). Absorption speed and capacity were considerable in the rat duodenum after *in situ* administration. The duodenum is certainly the main site of absorption, since, under normal conditions, residence time and the area of contact are higher in it than in the stomach.

The very high plasma concentrations recorded shortly after injection indicated that the extravascular diffusion space of tiaprofenic acid was small in all species. The V_c varied, however, according to species. In rats and mice, it was about twice that in dogs, rabbits, and humans. Like other anionic molecules such as indomethacin (11), fenoprofen (12), and tolmetin (13), tiaprofenic acid was extensively bound to the many available sites of plasma albumin.

Radioactivity was almost entirely cleared from the plasma 24 hr after administration in all species studied, including the dog where disappearance was slowest. The clearance of tiaprofenic acid in humans, 6 liters/hr, was close to that of indomethacin, 7.8 liters/hr (14). These values are relatively high, about twice those obtained for fenoprofen (15) and ketoprofen (calculated from Ref. 16) and much higher than the clearance of naproxen, 0.4 liter/hr (calculated from Ref. 17), and phenylbutazone, 0.1 liter/hr (calculated from Ref. 18). In relation to body weight, human clearance of tiaprofenic acid was of the same order as in the rat and rabbit, half that in the mouse, and four times that in the dog.

The chronic study in humans confirmed rapid elimination, since the steady state was reached as early as the end of the 1st treatment day and the concentrations were down to zero 24 hr after the last ingestion. The maximum concentrations, the areas under curves, and the elimination rate constants, which were identical after the first and 40th ingestion, showed that tiaprofenic acid cannot inhibit or induce its own biotransformations.

Renal excretion, which in rats was equal to fecal excretion, was preponderant in humans and in the other species studied. A significant en-

terohepatic cycle was demonstrated in the rat. Biliary metabolites were absorbed slower than I, since most of them were conjugated, with polarities unfavorable to intestinal absorption (19). Progressive hydrolysis of acylglucuronides by the weakly alkaline pH in the distal part of the duodenum and of all types of conjugates by bacterial enzymes (20) accounts for this difference.

Metabolites II and III were common to all species. In the dog, however, II was present in large quantities and III was present in very small quantities. They are pharmacologically less active than I (1).

In the rat, the clearance of I was greatly increased by phenobarbital, partly because of enzymatic induction of hydroxylation. This result is in agreement with the location of hydroxylase(s) in the hepatic endoplasmic reticulum, which is stimulated by phenobarbital (21). The approximately 50% increase in biliary flow induced by phenobarbital (22) increases the importance of this route of excretion and, together with enzymatic induction, accounts for the large increase in plasma clearance as opposed to the small increase in urinary radioactivity excretion. On the other hand, the enzymes that reduce the ketone group were not induced, in agreement with the location of several keto reductases in the soluble fraction from rabbit (23), rat, and human (24) liver and kidney.

No reduction of the ketone group was observed for two compounds whose structures, like I, are formed by a ring with a carboxylic radical linked to another ring by a carbonyl group: tolmetin [1-methyl-5-(4-methylbenzoyl)-2-[1*H*]-pyrroleacetic acid] (25) and ketoprofen [2-(3-benzoylphenyl)propanoic acid] (16).

For tolmetin, the only metabolite identified in rats, monkeys, and humans was the diacid formed by oxidation of the 4-methyl group. For ketoprofen, the two metabolites partially identified in rats, dogs, rabbits, and humans resulted from hydroxylation in different positions of the benzene ring not substituted by a propanoic radical.

On the other hand, Lan *et al.* (26) found that, after administration of a similar structure, 4-cyclopropylcarbonylbenzeneacetic acid[12] (VI), the alcohol derivative was excreted in low quantities in the urine of rats and monkeys but in much higher quantities in the urine of dogs. This result is parallel to the present observation of a higher urinary excretion of II in the dog than in the rat.

Regarding secondary biotransformations, a ketoprofen acylglucuronide was found in all species, including the dog (16), whereas VI was excreted in this species conjugated with taurine (26). Like VI, tiaprofenic acid was also excreted as an amide conjugate in the dog but as an acylglucuronide in the other species.

[12] S.Q. 20650.

REFERENCES

(1) F. Clémence, O. Le Martret, R. Fournex, G. Plassard, and M. Dagnaux, *Eur. J. Med. Chem.*, **9**, 390 (1974).

(2) A. V. Camp, "8th European Congress of Rheumatology," Helsinki, Finland, June 1975.

(3) J. Soullard, *G. M. France*, **83**, 149 (1976).

(4) J. Mine, *ibid.*, **83**, 249 (1976).

(5) M. Gibaldi and D. Perrier, "Pharmacokinetics," in "Drugs and the Pharmaceutical Sciences," vol. 1, J. Swarbrick, Ed., Dekker, New York, N.Y., 1975, p. 48.

(6) F. H. Dost, "Grundlagen der Pharmakokinetik," 2nd ed., G. Thieme Verlag, Stuttgart, Germany, 1968.

(7) W. O. Caster, J. Poncelet, A. B. Simon, and W. D. Armstrong, *Proc. Soc. Exp. Biol. Med.*, **91**, 122 (1956).

(8) L. S. Shanker, P. A. Shore, B. B. Brodie, and C. A. M. Hogben, *J. Pharmacol. Exp. Ther.*, **120**, 528 (1957).

(9) J. Pottier, M. Busigny, and J. P. Raynaud, *Drug. Metab. Disp.*, **3**, 133 (1975).

(10) C. A. M. Hogben, L. S. Shanker, D. J. Tocco, and B. B. Brodie, *J. Pharmacol. Exp. Ther.*, **120**, 540 (1957).

(11) H. B. Hucker, A. G. Zacchei, S. V. Cox, D. A. Brodie, and N. H. R. Cantwell, *ibid.*, **153**, 237 (1966).

(12) A. Rubin, P. Warrick, R. L. Wolen, S. M. Chernish, A. S. Ridolfo, and C. M. Gruber, Jr., *ibid.*, **183**, 449 (1972).

(13) M. M. Selley, J. Glass, E. J. Triggs, and J. Thomas, *Clin. Pharmacol. Ther.*, **17**, 599 (1975).

(14) D. E. Duggan, A. F. Hogans, K. C. Kwan, and F. G. McMahon, *J. Pharmacol. Exp. Ther.*, **181**, 563 (1972).

(15) A. Rubin, B. E. Rodda, P. Warrick, A. S. Ridolfo, and C. M. Gruber, Jr., *J. Pharm. Sci.*, **61**, 739 (1972).

(16) P. Populaire, B. Terlain, S. Pascal, B. Decouvelaere, A. Renard, and J. P. Thomas, *Ann. Pharm. fr.*, **31**, 735 (1973).

(17) G. Boost, *Arzneim.-Forsch.*, **25**, 281 (1975).

(18) J. J. Burns, T. F. Yu, P. G. Dayton, A. B. Gutman, and B. B. Brodie, *Ann. N.Y. Acad. Sci.*, **86**, 253 (1960).

(19) R. L. Smith and R. T. Williams, in "Glucuronic Acid: Free and Combined Chemistry, Biochemistry, Pharmacology and Medicine," G. J. Dutton, Ed., Academic, New York, N.Y., 1966, p. 457.

(20) R. R. Scheline, *Pharmacol. Rev.*, **25**, 451 (1973).

(21) J. R. Gillette, *Ann. N.Y. Acad. Sci.*, **179**, 43 (1971).

(22) C. D. Klaassen, *J. Pharmacol. Exp. Ther.*, **168**, 218 (1969).

(23) H. W. Culp and R. E. McMahon, *J. Biol. Chem.*, **243**, 848 (1968).

(24) T. A. Moreland and D. S. Hewick, *Biochem. Pharmacol.*, **24**, 1953 (1975).

(25) D. D. Sumner, P. G. Dayton, S. A. Cucinell, and J. Plostnieks, *Drug Metab. Disp.*, **3**, 283 (1975).

(26) S. J. Lan, A. M. El-Hawey, A. V. Dean, and E. C. Schreiber, *ibid.*, **3**, 171 (1975).

ACKNOWLEDGMENTS AND ADDRESSES

Received July 13, 1976, from the *Centre de Recherches Roussel-Uclaf, 111, Route de Noisy, 93230 Romainville, France.*

Accepted for publication September 16, 1976.

The authors thank R. Deraedt and S. Jouquey for their valued collaboration, N. O. Eve for conducting the clinical portion, and V. Delaroff for the physical analysis. The technical assistance of M. J. Fontana, M. Fortin, and M. Rainbeaud is gratefully acknowledged.

Part of this work was reported briefly in a preliminary communication to the 12th meeting of the French Association of Pharmacologists, Paris, France, October 1974; abstracted in *J. Pharmacol.*, **6**, 106 (1975).

[x] To whom inquiries should be directed.

Colorimetric Assay of Benzocaine and Some Dosage Forms

HENRY S. I. TAN ˣ, GARY A. BRUEMMER, and DAVID SHELTON *

Abstract □ A colorimetric procedure for benzocaine and a number of its dosage forms was developed; it offers improvement in ease, speed, and sensitivity over the official method. The method is based on the formation of a red Schiff base between benzocaine and *p*-dimethylaminocinnamaldehyde in a nonaqueous acidic medium. At the maximum absorption of 544 nm, the Beer–Lambert law was adhered to over the 0.025–2.5-μg/ml range. Best accuracy can be obtained for solutions containing 0.25–1.25 μg/ml. The color was stable for at least 2 hr. Analysis of benzocaine in the dosage forms studied can be directly performed without prior drug extraction.

Keyphrases □ Benzocaine—colorimetric analysis, bulk drug and commercial dosage forms □ Colorimetry—analysis, benzocaine bulk drug and commercial dosage forms □ Anesthetics, topical—benzocaine, colorimetric analysis, bulk drug and commercial dosage forms

Benzocaine (ethyl *p*-aminobenzoate) is an extensively used local anesthetic in various products for the relief of pain and pruritis. A significantly large number of products are readily available as nonprescription drugs, varying in benzocaine concentration from 0.5 to 20.0%.

The NF XIV (1) method for benzocaine is based on the known diazotization or nitritometric titration (2–7). This tedious and time-consuming titration utilizes standard sodium nitrite at low temperatures with starch iodide paper as an external indicator. The official assay procedures (1) for benzocaine creams and ointments also are based on the same diazotization titration where the endpoint is determined potentiometrically. In ointments having water-insoluble bases, the drug must be isolated by solvent extraction prior to the diazotization titration. Furthermore, in formulations with antipyrine in glycerin or propylene glycol bases, the benzocaine is analyzed by UV spectrophotometry after it is separated from antipyrine by column partition chromatography using three different columns assembled serially (8, 9).

Colorimetric methods for the analysis of benzocaine based on the formation of Schiff bases were performed using *p*-dimethylaminobenzaldehyde (10) and vanillin (11) in acidic hydroalcoholic solutions, and the products obtained were yellow. *p*-Dimethylaminocinnamaldehyde was utilized as a colorimetric agent for primary aromatic amines (12–14). This reagent is advantageously employed in place of *p*-dimethylaminobenzaldehyde and vanillin, since the resulting Schiff bases are red. This paper presents a simple, sensitive, and accurate method for the analysis of benzocaine and some of its dosage forms.

EXPERIMENTAL

Instruments—A UV–visible double-beam spectrophotometer[1] with 1-cm cells and a dynode voltage of 500 v (slit width 0.35–0.55 mm) and an analytical balance[2] were used.

Materials and Reagents—The following were used: benzocaine[3], acetone-free absolute methanol containing 0.05% water[4], a 0.1% (w/v) solution of *p*-dimethylaminocinnamaldehyde[5] (mp 137–139°) in methanol (stable for at least 3 weeks if refrigerated), and a 50% (w/v) solution of trichloroacetic acid (ACS grade) in methanol.

Standard Curve—A stock solution of benzocaine was prepared by dissolving 50.0 mg of the drug in methanol. Further dilutions were made to prepare standard solutions containing 0.25–25.0 μg of benzocaine/ml. One milliliter of each solution was utilized for color development as described under *Assay Procedure for Benzocaine*. The stock and standard solutions were freshly prepared.

Assay Procedure for Benzocaine—Pipet 1.0 ml of a methanolic solution containing 2.5–12.5 μg of benzocaine into a 10-ml volumetric flask. To this solution, add exactly 2.00 ml of *p*-dimethylaminocinnamaldehyde reagent followed by 1.0 ml of trichloroacetic acid reagent and wait for 10 min. Dilute to volume with methanol, and measure the absorbance at 544 nm against a blank prepared similarly but omitting the benzocaine.

Assay Procedure for Benzocaine Dosage Forms—*Creams, Ointments with Water-Soluble Bases, and Otic Drops*—Weigh or pipet accurately an amount equivalent to 15–50 mg of benzocaine, transfer into a 100-ml volumetric flask, and dissolve or suspend in methanol. Dilute to volume with methanol. Filter through dry filter paper, if necessary, and discard the first 5 ml of filtrate. Pipet 1.0 ml of the filtrate into a 50-ml volumetric flask, and dilute to volume with methanol. Pipet 1.0 ml of the resulting solution into a 10-ml volumetric flask and proceed as described under *Assay Procedure for Benzocaine*, beginning with: "To this solution, add exactly . . . ."

Ointments and Suppositories with Water-Insoluble Bases—Weigh accurately an amount equivalent to 15–50 mg of benzocaine in a beaker, dissolve in 14 ml of cyclohexane, and transfer quantitatively into a 100-ml volumetric flask. Rinse the beaker three times with 2-ml portions of cyclohexane, and combine the washings with the cyclohexane solution in the volumetric flask. Shake the solution vigorously, and slowly add methanol to the mark. Proceed as described for creams, beginning with: "Filter through dry filter paper . . . ."

Lozenges—Weigh and grind 20 lozenges to a very fine powder. Add slowly an accurately weighed amount of the powder, equivalent to 15–50 mg of benzocaine, to about 75 ml of methanol in a 100-ml volumetric flask with shaking. Place the stoppered volumetric flask in an ultrasonic bath for 30 min to enhance dissolution of the benzocaine, and dilute to volume with methanol. Proceed as described for creams, beginning with: "Filter through dry filter paper . . . ."

Table I—Effect of Time on Absorbance of Benzocaine–*p*-Dimethylaminocinnamaldehyde Colored Product [a]

Minutes after Reaction	Absorbance at 544 nm
2	0.433
5	0.443
10	0.445
20	0.445
50	0.446
70	0.445
90	0.447
100	0.445
120	0.446

[a] Concentration of 0.75 μg of benzocaine/ml.

RESULTS AND DISCUSSION

The red Schiff base produced by the interaction of benzocaine and *p*-dimethylaminocinnamaldehyde in an acidic anhydrous medium exhibited a maximum absorption at 544 nm (Fig. 1). This reaction resulted in a more sensitive and deep coloration than the yellow color obtained

[1] Acta V, Beckman Instruments, Fullerton, Calif.
[2] Mettler H-18, Mettler Instruments Corp., Princeton, N.J.
[3] Eastman Kodak Co., Rochester, N.Y.
[4] Fisher Scientific Co., Pittsburgh, Pa.
[5] Aldrich Chemical Co., Milwaukee, Wis.

Table II—Reproducibility of Color Development of Replicate 0.5-μg/ml Samples of Benzocaine

Sample	Absorbance at 544 nm
1	0.301
2	0.303
3	0.302
4	0.302
5	0.300
6	0.300
7	0.303
8	0.295
9	0.295
Average	0.300
SD	0.0031
RSD	0.0103

from the reaction of benzocaine with the commonly used aldehydes such as *p*-dimethylaminobenzaldehyde (10) and vanillin (11). This bathochromic shift was expected since the structure of the Schiff base (I) formed with *p*-dimethylaminocinnamaldehyde showed greater conjugation than, for example, II, that formed with *p*-dimethylaminobenzaldehyde. The red color of the product was stable for at least 120 min (Table I).

The effect of reagents on color development was investigated by adding varying volumes of 0.1% *p*-dimethylaminocinnamaldehyde in methanol to 10-ml volumetric flasks, each containing 1.0 ml of 16 μg of benzocaine/ml and 1.0 ml of 50% trichloroacetic acid in methanol. The absorbance of each solution was measured at 544 nm against a blank[6] after each solution was diluted to volume with methanol. The absorbance readings increased with increasing amounts of *p*-dimethylaminocinnamaldehyde up to a concentration of about 250 μg/ml in the final solution.

However, blank solutions containing more than 200 μg of *p*-dimethylaminocinnamaldehyde/ml were dark colored. This condition limits the range of usable concentrations and makes the method less sensitive, because wider slit widths must be used to maintain the dynode voltage on the spectrophotometer at 500 v. Based on these considerations, exactly 2.0 ml of the 0.1% *p*-dimethylaminocinnamaldehyde reagent was used for color development. Changing the volumes of 50% trichloroacetic acid did not appreciably affect absorbance readings; 1.0 ml of this acid reagent was used for the assay.

As in a previous study (14), the color formed was instable in the presence of water. Therefore, the methanol used must be as anhydrous as possible. The use of methanol containing 0.05% water appeared to be satisfactory for the benzocaine assay.

Under the proposed experimental conditions, a linear response between absorbance and concentration was demonstrated over the concentration range of 0.025–2.5 μg/ml (r = 0.9997). The linear regression line[7] was $A_{544} = 0.5974C - 0.0059$, where A_{544} is the absorbance at 544 nm and C is the concentration expressed in micrograms per milliliter in the final test solution. The standard deviations of the slope and y intercept were 0.0121 and 0.0076, respectively (n = 4). The calculated molar absorptivity, ϵ, was 9.87×10^4 liter mole^{-1} cm^{-1}.

Determination of the concentration range for maximum accuracy was done by constructing the Ringbom plot (15, 16). The plot (Fig. 2) indicates an optimum range for solutions containing 0.25–1.25 μg of benzocaine/ml in the final test solution. The curve also shows an inflection at 37% transmittance, indicating that the system follows the Beer–Lambert law.

The limit of detection, as determined on 20 samples by the procedure of Kaiser (17), at the 95% confidence level is 5.5×10^{-7} M or 0.090 μg of benzocaine/ml in the test solution.

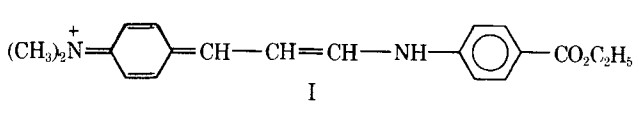

I

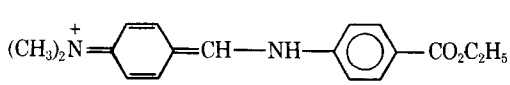

II

[6] Each blank contained the same amount of *p*-dimethylaminocinnamaldehyde and trichloroacetic acid as in the solution studied but contained no benzocaine.

[7] Wang computer 700 C and plotting output writer 2202.

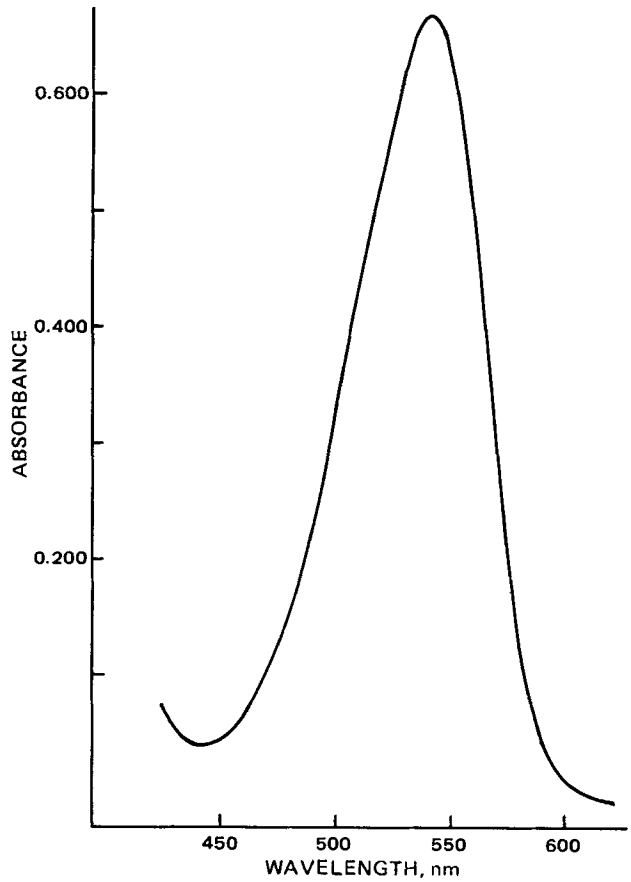

Figure 1—*Absorption spectrum of the benzocaine–*p*-dimethylaminocinnamaldehyde reaction product.*

The reproducibility of the proposed color development was determined by analyzing nine replicate samples of benzocaine solutions in methanol, each containing 0.5 μg/ml. The precision at this concentration level showed a relative standard deviation of 0.0103 (Table II).

The data in Table III show the accuracy of the procedure. These studies were performed on four different, but accurately known, amounts of benzocaine. Each sample was dissolved in 100.0 ml of methanol. Appropriate dilutions were then made to give different concentration levels (Table III), which were analyzed by the proposed method. The results

Table III—Assay of Solutions of Known Concentrations of Benzocaine at Different Levels

Amount Weighed, mg	Analyzed at Concentration Level, μg/ml	Amount Found, mg (Proposed Method)	Percent Found (Proposed Method)	
			Individual Samples	Average
54.0	0.5	53.7	99.4	
	1.6	53.0	98.1	98.5
	2.2	53.0	98.1	
54.5	0.5	54.9	100.7	
	1.6	54.7	100.4	100.4
	2.2	54.6	100.2	
150.0	0.6	149.8	99.9	
	1.2	152.1	101.4	100.8
	1.8	151.6	101.1	
154.5	0.6	154.0	99.7	
	1.2	153.1	99.1	98.8
	1.9	150.7	97.5	
300.0		302.0[a]	100.7[a]	
300.0		301.5[a]	100.5[a]	
Overall percent found				99.6
SD				1.14

[a] Analyzed by NF XIV method.

Table IV—Assay of Some Commerically Available Benzocaine Formulations

Formulation	Amount Benzocaine Claimed, mg/g or mg/ml	Amount Found, mg/g or mg/ml		Average Percent Label Claim	
		Proposed Method	NF XIV Method	Proposed Method	NF XIV Method
Ointment (water-insoluble base	20.0	19.9 20.2	19.7 20.0	100.3	99.3
Ointment (water-soluble base)[a]	200.0	199.6 202.2	199.4 202.0	100.5	100.4
Cream[b]	10.0	9.67 9.65	10.8 11.1	96.6	109.5
Suppository[c]	130.0[d]	126.0 126.8	124.5 127.3	97.3	96.2
Otic drops[a]	200.0	229.0 228.0	230.4 229.5	114.3	115.0
Otic drops[e]	14.0	13.9 14.1	14.2 14.4	100.0	102.2
Lozenges	10.0[f]	9.80 9.88	9.72 9.89	98.4	98.1

[a] Contains benzethonium chloride. [b] Contains menthol, camphor, and triclosan. [c] Contains oxyquinoline sulfate, zinc oxide, menthol, and Peru balsam. [d] Milligrams per suppository. [e] Contains antipyrine. [f] Milligrams per lozenge.

were in agreement with those obtained by the compendial method. An average of 99.6% of the original amount weighed was found. In comparison, an average of 100.6% was obtained for two benzocaine samples analyzed by the NF XIV method.

Results of analyses of different benzocaine dosage forms by the proposed method are presented in Table IV. The recovery data showed good correlation with those of the NF XIV procedure. The results also indicated that benzocaine in ointments or suppositories with water-insoluble bases need not be isolated by solvent extraction prior to analysis as required by the official method. This difference shortens the analysis time considerably.

The concentration of cyclohexane used to dissolve the ointment or suppository in the final test solution was 0.04% (w/v). Increasing the cyclohexane concentration to 0.06% (w/v), which corresponded to an initial volume of 30 ml, did not affect color intensity or stability. Furthermore, active ingredients normally present in the benzocaine formulations studied, such as antipyrine, menthol, camphor, triclosan, benzethonium chloride, and oxyquinoline sulfate, do not interfere with the reaction and do not have to be removed; these compounds lack the primary aromatic amino functional group necessary for the reaction with *p*-dimethylaminocinnamaldehyde to form a red Schiff base. On the other hand, *p*-aminobenzoic acid, a degradation product of benzocaine, reacts under the proposed experimental conditions, producing a red color with λ_{max} of 541 nm.

In the analysis of lozenges, the lozenges must be ground to a very fine powder, and care must be taken when suspending the powder in methanol. The powder must be added slowly with frequent shaking to prevent the formation of lumps. The undissolved particles must flow freely upon shaking. The use of an ultrasonic bath facilitates the disintegration of lumps and enhances the dissolution of benzocaine. The pink dye present in the lozenges did not interfere with the analysis.

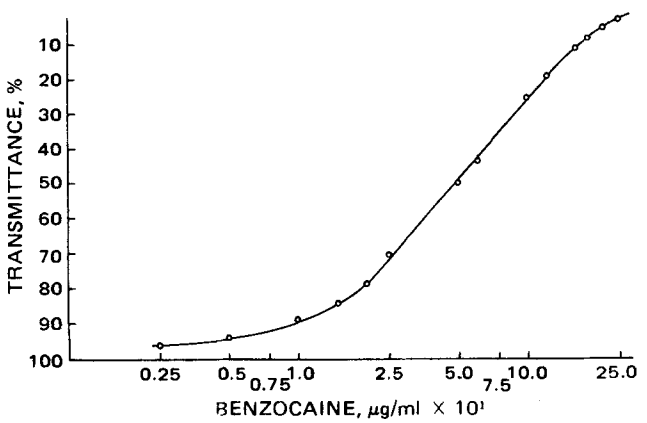

Figure 2—*Ringbom plot for the benzocaine–p-dimethylaminocinnamaldehyde reaction product.*

REFERENCES

(1) "The National Formulary," 14th ed., Mack Publishing Co., Easton, Pa., 1975, p. 70.

(2) P. J. Levine and B. F. Allen, *Drug Stand.*, **27**, 60 (1959).

(3) G. Di Bacco, *Boll. Chim. Farm.*, **99**, 208 (1960).

(4) V. S. Eremeeva, L. N. Poroikova, R. I. Petrova, Z. S. Morunova, and O. K. Sivitskaya, *Aptechn. Delo*, **9**, 60 (1960); through *Chem. Abstr.*, **60**, 15680 (1964).

(5) S. Kh. Dzottsoti, *Azerbaidzhan Khim. Zhur.*, **3**, 137 (1961); through *Chem. Abstr.*, **56**, 8843 (1962).

(6) L. N. Guseva, *Aptechn. Delo*, **12**, 62 (1963); through *Chem. Abstr.*, **61**, 11850 (1964).

(7) S. Ebel and S. Kalb, *Arch. Pharm.*, **307**, 2 (1974).

(8) R. Krause, *J. Assoc. Offic. Anal. Chem.*, **50**, 685 (1967).

(9) *Ibid.*, **51**, 624 (1968).

(10) H. W. Unterman and E. Constantin, *Farmacia*, **12**, 301 (1964); through *Chem. Abstr.*, **62**, 1515 (1965).

(11) G. I. Lukyanchikova and V. N. Bernstein, *Peredovye Methody Khim. Tekhnol. i Kontrolya Proizvod. Sb.*, **1964**, 257; through *Chem. Abstr.*, **62**, 12977 (1965).

(12) S. Sakai, K. Suzuki, H. Mori, and M. Fujino, *Jpn. Anal.*, **9**, 862 (1960).

(13) M. Pesez and J. Bartos, *Bull. Soc. Chim. Fr.*, **1966**, 3802.

(14) H. S. I. Tan and D. Shelton, *J. Pharm. Sci.*, **63**, 916 (1974).

(15) A. Ringbom, *Z. Anal. Chem.*, **115**, 332 (1939).

(16) G. H. Ayres, *Anal. Chem.*, **21**, 652 (1949).

(17) H. Kaiser, *Z. Anal. Chem.*, **209**, 1 (1965).

ACKNOWLEDGMENTS AND ADDRESSES

Received March 31, 1976, from the *College of Pharmacy, University of Cincinnati–Medical Center, Cincinnati, OH 45267.*

Accepted for publication September 17, 1976.

Presented at the Pharmaceutical Analysis and Control Section, APhA Academy of Pharmaceutical Sciences, New Orleans meeting, April 1976.

The authors thank Mr. Christopher Kiel for technical assistance in performing the assay of some formulations.

* Present address: Winton Hill Technical Center, Procter and Gamble Co., Cincinnati, OH 45224.

ˣ To whom inquiries should be directed.

Solvent-Dependent Conformational System of Hydroxyureas in Octanol–Water and in Inhibition of Ribonucleotide Reductase

GEORGE R. PARKER ˣ and E. COLLEEN MOORE *

Abstract □ The carbonyl nitrogen IR absorption region of selected hydroxyureas was examined in octanol. The spectra indicated appreciably different absorptions prior to and after equilibration with water. Stability studies on the hydroxyureas indicated that the absorption differences were not due to chemical decomposition in the equilibration process but were due to solvent conformational and/or tautomeric dependency of the system. Preliminary *in vitro* inhibition of the enzyme ribonucleoside diphosphate reductase by selected hydroxyureas also indicated an apparent solvent dependency, which may involve the conformational and/or tautomeric properties of these agents. The implications of the solvent-dependent conformational–tautomeric system observed are discussed in relation to this property in the biological action of these agents.

Keyphrases □ Hydroxyureas, various—solvent-dependent conformation in octanol–water, effect on ribonucleotide reductase activity *in vitro* □ Conformation—various hydroxyureas in octanol–water, effect of solvent equilibration □ Ribonucleotide reductase—activity, effect of various hydroxyureas *in vitro* □ Enzymes—ribonucleotide reductase, effect of various hydroxyureas on activity *in vitro* □ Structure–activity relationships—various hydroxyureas, solvent-dependent conformation in octanol–water, effect on ribonucleotide reductase activity *in vitro*

A solvent-dependent conformational system in substituted hydroxyureas was reported (1) utilizing solvents such as acetone, pyridine, and tetrachloroethane in the presence and absence of water. The conformational aspects of hydroxyureas were investigated, since this property may influence their transport, stability *in vivo*, and mechanism of action. Since there is no accepted explanation for the low anticancer activity of substituted hydroxyurea analogs compared to the parent antileukemia agent hydroxyurea, the conformational properties of hydroxyureas were examined.

In this study, the properties of the carbonyl–nitrogen system of substituted hydroxyureas were examined in the solvent 1-octanol before and after equilibration with water (pH 7.4); this system closely simulates the environment of *in vitro* and *in vivo* systems. The findings further substantiate conformational properties of hydroxyureas as detected by IR spectroscopy in 1-octanol. Initial biological data on the action of hydroxyureas on the enzyme ribonucleoside diphosphate reductase, the proposed site of anticancer action, indicate that the solvent plays a role in the *in vitro* inhibition of the enzyme, which may be due to the solvent-dependent conformation of certain hydroxyureas.

EXPERIMENTAL

Compounds—The 3-substituted analogs were synthesized according to a literature method (2) with modifications (3, 4). Hydroxyurea and the 1-substituted analogs were used as received[1].

IR Spectra—The IR spectra were obtained[2] using liquid cells. The solvent was 1-octanol[3] dried over anhydrous sodium sulfate. Spectra were taken immediately after dissolution, after equilibration with glass-distilled water (adjusted to pH 7.4) for 24 hr, and after 2 weeks.

After equilibration, the solvents were separated; the octanol layer was dried over sodium sulfate prior to recording the IR spectra. All spectra were taken with the following instrument settings: gain, 2; period, 1 sec; balance, 0; chart expansion, 1×; sensitivity, 3; ordinate scale, 100%; scan speed, 600 (8 min); and baseline transmission, 90%. All spectra were taken with dry octanol as the blank.

Stability Studies—The stability and decomposition of hydroxyureas in aqueous solutions were examined *via* the method of Harmon *et al.* (3). The solution of the hydroxyurea in a reaction vessel was connected to a gas dispersion tube immersed in anhydrous ether. Any gas evolved in the hydroxyurea decomposition was observed visually or in the IR spectrum of the ether solution after bubbling through the ether. IR spectra of the ether solutions after standing in water (pH 7.4), in acidic solutions at pH 1.5, and with ferric chloride added (in a ratio of 2 moles of hydroxyurea to 1 mole of ferric chloride) were recorded at intervals (up to 1 week for water at pH 7.4) using a double-beam instrument[4] and liquid cells with ether as the blank. The pH values were determined on a standard pH meter[5]. The pH of the aqueous layers in the equilibration experiments was also checked after 24 hr and 2 weeks and was in all cases 7.4 ± 0.2, indicating that no appreciable pH change occurred in the equilibration process. Water layers were removed by freeze drying[6] (at 20 mm Hg) to afford solids identical to starting materials, as verified by melting points and IR spectra.

Ribonucleotide Reductase Assay—The enzyme ribonucleoside diphosphate reductase was isolated from Novikoff ascites hepatoma of rats and purified according to the method of Moore (5). The assay included 8.3 m*M* phosphate buffer (pH 7), 2.1 m*M* adenosine triphosphate, 4.2 m*M* magnesium acetate, 0.04 m*M* $Fe(NH_4)_2(SO_4)_2$, 0.17 m*M* cytidine ^{32}P-diphosphate, 6.3 m*M* dithiothreitol, 1.0 μl of thioredoxin, and approximately 0.2 mg of partially purified ribonucleotide reductase in a total volume of 0.12 ml. Inhibitors were present in the reaction mixture (in an ice bath) when the enzyme was added; the mixture was then moved to a water bath at 37° and incubated for 30 min. The reaction was stopped with perchloric acid (1 *M*), and the products were hydrolyzed, separated on a cation-exchange resin[7], and analyzed according to the method of Reichard (6).

The hydroxyureas were tested five times over 6 months; each compound was evaluated at four different concentrations with two tests at each concentration. The enzyme activity was plotted *versus* the inhibitor concentration and extrapolated to determine the concentration required to inhibit 50% of the enzyme activity (ID_{50}). The control activities for the enzyme system in the five determinations were 2.28, 0.75, 4.16, 2.20, and 1.50 nmoles/30 min/tube.

RESULTS

The IR spectra of the carbonyl nitrogen region of the hydroxyureas in 1-octanol (with 1-octanol as blank) are shown in Fig. 1. The spectra labeled A were taken immediately after dissolving each compound in dried solvent; those labeled B and C were taken after equilibration with water (pH 7.4) for 24 hr and 2 weeks, respectively. In each case, octanol was separated from the water layer and dried over sodium sulfate, and the IR spectra were taken in the same manner as A.

Since B and C spectra were appreciably different from A spectra in every case except hydroxyurea, the stability of the compounds was examined using the method of Harmon *et al.* (3) to determine if chemical decomposition had occurred in the pH 7.4 water layer compared to so-

[1] Squibb Institute for Medical Research.
[2] Beckman IR 4250 double-beam instrument.
[3] Matheson, Coleman and Bell.
[4] Model 700 Perkin-Elmer IR spectrophotometer.
[5] Model 7, Corning.
[6] Virtis freeze-drying apparatus.
[7] Dowex 50.

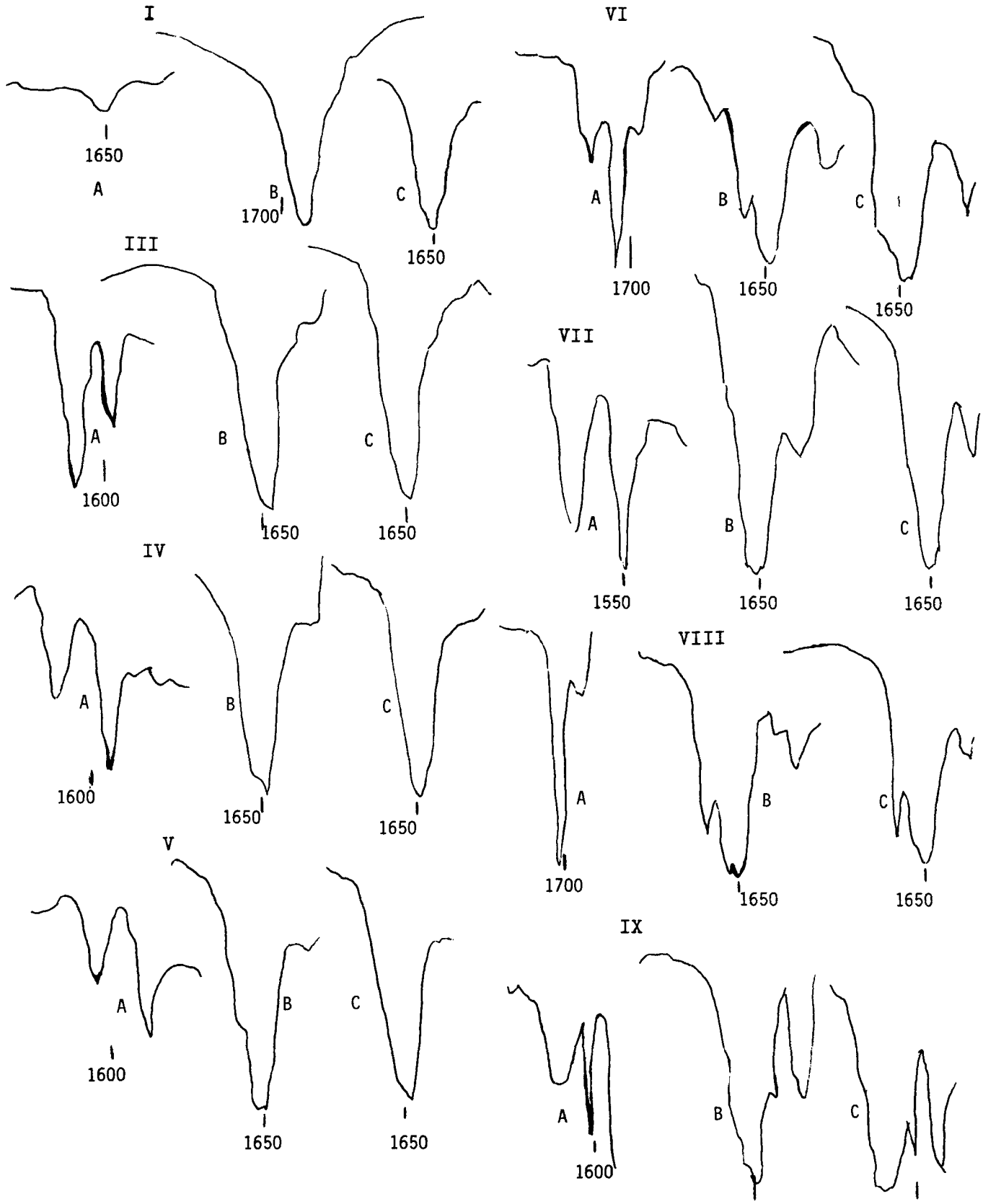

Figure 1—*The C=O and C=N regions in IR spectra of hydroxyureas. Spectra were taken in dry octanol after dissolution (A), after 24 hr of equilibration (B), and after 2 weeks of equilibration (C).*

lutions of pH 1.5 or in solution with ferric chloride (pH 1.5) (Table I). All compounds were stable in pH 7.4 water, whereas only I was stable in pH 1.5 water, with gas evolution observed for the other compounds.

The relative inhibitory concentrations of selected substituted hydroxyureas compared to hydroxyurea are shown in Table II. By using the method of Moore (5) for the purification of the enzyme and the method of Reichard (6) for the evaluation of the inhibitory concentration of the hydroxyureas, the concentration required for 50% enzyme inhibition was

Table I—Stability[a] of Hydroxyureas in Ferric Chloride Solution (pH 1.5)

$$R_1NHC(=O)NOH\text{-}R_2$$

Compound	R_1	R_2	Stability in Ferric Chloride Solution
I	H	H	Gas[b] plus blue color
II	H	CH_3	Gas plus blue color
III	H	C_2H_5	Gas plus blue color
IV	C_2H_5	H	Gas plus blue color
V	n-C_3H_7	H	Gas plus blue color
VI	iso-C_3H_7	H	Gas plus black color
VII	n-C_4H_9	H	Gas plus blue color
VIII	$tert$-C_4H_9	H	Gas plus brown color
IX	p-ClC_6H_4	H	Gas and no color change

[a] All compounds were stable in pH 7.4 solutions; only I was stable in pH 1.5 solutions, with gas evolution observed for the other compounds. Reaction vessels were connected to gas dispersion tube in ether; no signals were detected in IR spectra of ether solutions after 1 week. [b] Gas was detected according to method of Harmon *et al.* (3); signals were observed in the 2350–2200- and 600–700-cm^{-1} regions for all compounds where gas was observed. In most cases, gas was evolved immediately.

determined. Hydroxyurea and the 1-substituted analogs were dissolved in distilled water for all determinations. The 3-*n*-propyl analog (V) was dissolved in water and the 3-*n*-butyl analog (VII) was dissolved in 1 ml of 95% ethanol and diluted with water to 1% for the first determination. For the second, third, and fourth determinations, V and VII were dissolved in 6 and 10% dimethyl sulfoxide, respectively, and diluted to 1% with water. Ethanol and dimethyl sulfoxide were not inhibitory to the enzyme system at 1% concentrations.

A general trend in relative inhibitory activity was observed in all but the first determination (especially for V) where a different solvent was used. A fifth determination was performed with water as the solvent, and again a higher relative concentration was required for V to produce 50% enzyme inhibition compared to the concentration required when the solvent was 1% dimethyl sulfoxide.

DISCUSSION

For a drug molecule to exhibit its biological action at its molecular site of action in an *in vivo* system, it must first be transported from its original entry site to its target site. To simplify the dynamics of drugs in biological fluids (the biophase), various model systems attempt to approximate the biophase (an aqueous system with a nonpolar component present similar to a colloidal suspension) with, for example, the octanol–water system (7–9). The octanol–water system used in determining drug dynamics in complex *in vivo* biophases is a simplification of the actual occurrences but has been accepted as suitable for determining relative membrane *versus* water solubilities. It is the most extensively studied system depicting *in vitro* partitioning between polar and nonpolar biological components (10, 11).

The octanol–water system was selected as a model to evaluate the effect of lipophilicity or hydrophobicity in the biological action of substituted hydroxyureas. Surprisingly, the properties of the substituted hydroxyureas, as observed by their IR carbonyl nitrogen absorption (1720–1550 cm^{-1}), were different in octanol after equilibration with pH 7.4 water compared to spectra taken immediately after dissolving the substituted hydroxyurea in octanol (Fig. 1). This spectral change (C spectra compared to A spectra) after extended equilibration with water (2–4 weeks) occurred after 24 hr of equilibration with water (B spectra), and this process proceeded without a change of pH in the aqueous system. In spectra of all hydroxyureas except hydroxyurea itself, a change occurred in the carbonyl nitrogen region after water equilibration from two distinct peaks at around 1550–1580 and 1650–1690 cm^{-1} [1720 and 1780 cm^{-1} for the isopropyl analog (VI) and 1660 and 1710 cm^{-1} for the *tert*-butyl analog (VIII)] to a broad band centered around 1650 cm^{-1}. The spectra of VI–VIII also had additional shoulders in the broad band at 1650 cm^{-1}.

To determine if a chemical reaction occurred in the aqueous solvents during water equilibration, the compounds were allowed to stand in water (pH 7.4 at room temperature) in sealed flasks. These flasks were attached *via* polyethylene tubing to a gas dispersion apparatus in anhydrous ether. With this method, a gas could be detected immediately after the solution was acidified to pH 1.5 or after ferric chloride was added (with a corresponding color change to blue) for most hydroxyureas (Table I). IR spectra of the ether solutions (using a double-beam instrument with ether as the blank) also indicated the presence of decomposition gases after treatment with acid or ferric chloride. For the hydroxyureas in pH 7.4 water at room temperature, no decomposition gases were observed over 4 weeks, and no absorption could be detected in the ether solution spectra (taken at intervals) in which the gas dispersion tube had been immersed.

Table II—Relative Concentrations Required to Inhibit 50% Enzyme Activity (ID_{50}) of Ribonucleoside Diphosphate Reductase

Compound	Determination 1	2	3	4	5	Inhibitor Concentration Range, m*M*	Average Concentration
I	1.0	1.0	1.0	1.0	1.0	0.055–0.27	0.12
II	2.7	1.7	0.7	0.7	—	0.07–0.15	0.09
III	4.9	2.0	0.9	1.1	1.0	0.11–0.27	0.17
V	15.5	4.2	3.6	3.6	13.3	0.23–0.85	0.48
VII	9.1	6.4	5.8	7.0	7.5	0.35–2.0	0.84
VI	—		—	—	19.0	0.80	—
VIII	—		—	—	9.5	0.40	—

The solutes (hydroxyureas) also were examined for possible decomposition during the equilibration process. Attempts to remove octanol by evaporation under vacuum were unsuccessful (hydroxyurea slowly decomposed) due to the high boiling point of 1-octanol (194–195°), but the water layer could be removed by freeze drying under vacuum. The solids obtained from solutions treated by freeze drying (I and IV–VIII) were identical to starting material (melting points) and showed IR spectra in dry octanol identical to those obtained for the initial solution (*i.e.*, A spectra in Fig. 1). Identical solid materials also could be obtained when the octanol layer was washed with water and the water was removed by freeze drying under vacuum, indicating that chemical decomposition was not the cause of the IR spectral changes in octanol after water equilibration.

Various reactions of the hydroxyureas with water could account for the IR spectra, and the function of water in each reaction is different (Scheme I). Scheme I depicts the conformational system of hydroxyureas (I*e*, I*f*, I*j*, and I*k*) produced by interconversion through canonical forms I*g* and I*h*. Water could: (*a*) catalyze the tautomerization (as could the solvent) of the N-1 or N-3 proton to form tautomers I*a*–I*d* and I*l*–I*o*; (*b*) react with a form similar to canonical form I*h* to produce a diol (I*i*) by addition to the carbonyl function; or (*c*) react with a form that is not internally hydrogen bonded, such as conformer I*k*, *via* hydrogen bonding to form a solvated form of the hydroxyurea (I*p*).

In B and C spectras (Fig. 1) for all substituted hydroxyureas, there is an absence of absorption similar to that observed in A spectra, indicating that the chemical process that caused the new signals had proceeded to 100% completion. The presence of water in the original samples of hydroxyureas could account for different spectra after equilibration and drying due to the removal of all water. This possibility was eliminated when spectra taken after initial solution and those taken after drying over anhydrous sodium sulfate (for 1 and 24 hr) were identical (Fig. 2).

Of the three possible products that can form with water in octanol, the diol (I*i*) is the least likely and would be the most unstable. For diol formation to occur, the carbonyl carbon would have to possess a strong $\delta+$ charge ($\delta+CO^{\delta-}$); therefore, the canonical form I*h* would represent the form of hydroxyurea present. This form would require minimal double bond character between N^1C and N^2C bonds, which is unlikely since any positive charge that forms at the carbonyl carbon causes electron flow

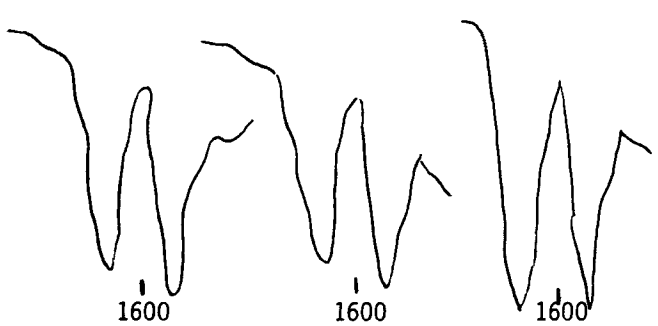

Figure 2—*Carbonyl nitrogen region of IR spectra of VII after dissolution in dry octanol (left) and after drying over anhydrous sodium sulfate for 1 (middle) and 24 (right) hr.*

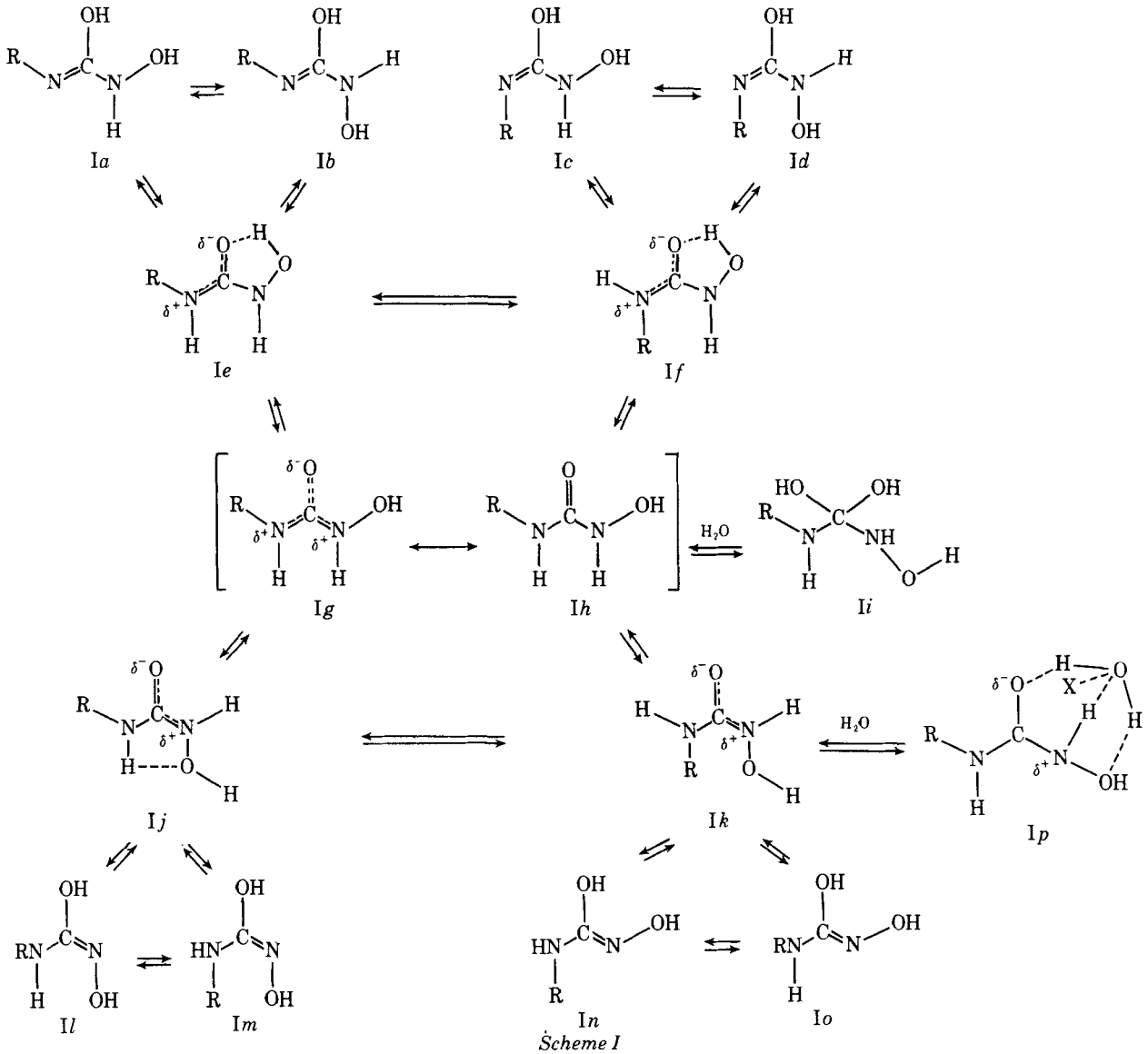

Scheme I

from the nitrogens toward the δ+C=O to stabilize the carbonyl group. Since the carbonyl absorption completely disappears, it is highly unlikely that it is due to a 100% conversion to diol I*i*, which could not have a C=N system, and it would be hard to rationalize the strong absorption at 1650 cm^{-1}, which is probably due to C=N in the molecules.

The reaction of the hydroxyurea with water in the other two cases involves tautomerization catalyzed by water or the solvent to form tautomers I*a*–I*d* and I*l*–I*o* and the solvate formation with water to form I*p* (Scheme I). In tautomerization, water does not add to the molecule, but rather bond breaking and bond making are promoted by water or by the solvent. The spectral phenomenon observed in octanol also occurred in ether. Upon initial solution, two signals were observed; after water equilibration and drying, a single signal (also around 1650 cm^{-1}) was detected. Attempts to reproduce the spectral changes in a solvent without the addition of water were performed by allowing VII to stand for 3 days in dry solvents with proton affinity closer to water [proton affinities in kilocalories per mole (12) are: water, 164; 1-octanol, 202; and ether and tetrahydrofuran, 187]. Tests with tetrahydrofuran and ether were unsuccessful, indicating that the process observed when water was present did not occur in the dry solvent and that the molecular species in the dry solvents were probably the same.

Therefore, the spectral changes observed in octanol after equilibration with water are due to conformational and/or tautomeric changes similar to those reported in other solvents (1). The conformational and/or tautomeric changes are the result of the stabilization or destabilization of conformational isomers in each solvent system (Scheme I). This type of conformational system would be sensitive to the presence of water or other polar solvents or molecules (allowing hydrogen bonding to water or other polar groups rather than internal hydrogen bonding). The IR spectra of the hydroxyureas taken in dry solvents immediately after solution most likely depict conformers I*e* and I*f*, which are stabilized by OH···O=C hydrogen bonding, and conformer I*j*, which is stabilized by weaker NH···OH hydrogen bonds (Scheme I). All conformers (I*e*, I*f*, I*j*, and I*k*) are formed by interconversion through some intermediate. This intermediate may be similar to canonical form I*g*, where rotation around the NC bonds is restricted due to the C=N character, or the canonical form I*h*, which allows rapid rotation and interconversion.

In dry octanol, the internal hydrogen bonding may exist in preference to hydrogen bonding with the solvent. This effect would be observed in the IR spectra as complex signals due to conformers I*e*, I*f*, and I*j* and the canonical form present during interconversion. Conformer I*k* should not be an important contributor in the IR absorption, since it is not stabilized by internal hydrogen bonding and it would be quickly interconverted to the other conformers through canonical forms I*g* and I*h*. After equilibration with water, a form similar to I*k* is present. This form is stabilized by solvate formation with water, which does not allow it to interconvert back to the other forms due to hydrogen bonding with water. Since I*k* or its solvate form would be stabilized, it would not be able to interconvert into a canonical form, which would have a carbonyl absorption and would primarily possess a C=N absorption observed as strong absorptions at 1650 cm^{-1}.

The implications of these data are relevant to drug action if different forms of the hydroxyurea conformational system are present in preference to others, depending on whether the system is in a polar or a non-

polar environment and whether internal hydrogen bonding is stabilized or whether hydrogen bonding to a solvent or to other biochemical entities has occurred. Hydroxyurea appears to possess the same type of carbonyl nitrogen character before and after equilibration with water. Therefore, no conformational preference may exist in hydroxyurea in solutions where conformational preference may be conferred to substituted hydroxyureas by their bulk or steric hindrance or to some electronic stabilization factor. The crystal structure of hydroxyurea indicates that intermolecular hydrogen bonding exists between the hydroxyl group of one molecule and the carbonyl oxygen of another molecule rather than intramolecular hydrogen bonding (13), and internal hydrogen bonding may not be preferred in solution.

The *in vitro* inhibition of ribonucleotide reductase by selected hydroxyureas (Table II) relative to hydroxyurea seems to indicate a solvent dependency. Although the enzyme system is quite complex and its activity is dependent on many variables (14), its inhibition by hydroxyureas followed a general trend, except for the 3-*n*-propyl analog (V) in the first determination. The solvent for hydroxyurea and the 1-analogs (II and III) was water for all determinations, and water was used for V in the first determination. The solvent for all other determinations for V and VII was 1% dimethyl sulfoxide.

The inhibitory concentration required to obtain 50% enzyme activity with V was much higher in the first determination than in the other determinations (2–4 in Table II), and this result was due to some error in the enzyme determination or to the different solvent. To verify which factor was the determinant in the inhibition study, another analysis was performed (5 in Table II) in which water was the solvent for all compounds. Again the concentration required for 50% enzyme inhibition for V was appreciably higher than in determinations where dimethyl sulfoxide was the solvent. This result implicates the solvent as a potential variable in the ability of hydroxyureas to function in the *in vitro* inhibition of ribonucleoside diphosphate reductase, and this property should be considered in the elucidation of the biodynamics of drugs in the hydroxyurea class.

Although it is not possible to determine whether the solvent-dependent conformational system observed in substituted hydroxyureas is the actual cause of the poor inhibition of the enzyme, with V the conformation and solvent have an interdependence that may affect the biological action of the drug. The transport and partitioning properties of hydroxyureas in octanol–water are currently being investigated to determine whether predicted and actual partition coefficients support the solvent-dependent conformation and the importance of this property in drug transport *in vivo*.

REFERENCES

(1) G. R. Parker, N. K. Hilgendorf, and J. G. Lindberg, *J. Pharm. Sci.*, **65**, 585 (1976).

(2) W. Dresler and R. Stein, *Justus Liebigs Ann. Chem.*, **150**, 242 (1869).

(3) R. E. Harmon, J. C. Dabrowiak, D. J. Brown, S. K. Gupta, M. Herbert, and D. Chitharanjan, *J. Med. Chem.*, **13**, 577 (1970).

(4) G. Clifton, S. R. Bryant, and C. G. Skinner, *ibid.*, **13**, 377 (1970).

(5) E. C. Moore, in "Methods in Enzymology," vol. 12, S. P. Colowick and N. D. Kaplan, Eds., Academic, New York, N.Y., 1967, pp. 155–174.

(6) P. Reichard, *J. Biol. Chem.*, **237**, 3513 (1962).

(7) C. Hansch and S. M. Anderson, *J. Org. Chem.*, **32**, 2583 (1967).

(8) J. Iwasa, T. Fujita, and C. Hansch, *J. Med. Chem.*, **8**, 150 (1965).

(9) T. Fujita, J. Iwasa, and C. Hansch, *J. Am. Chem. Soc.*, **86**, 5175 (1964).

(10) C. Hansch, R. M. Muir, T. Fujita, P. P. Maloney, F. Geiger, and M. Streich, *ibid.*, **85**, 817 (1963).

(11) A. Leo, C. Hansch, and D. Elkins, *Chem. Rev.*, **71**, 525 (1971).

(12) J. E. Huheey, "Inorganic Chemistry: Structure and Reactivity," Harper and Row, New York, N.Y., 1972, pp. 220, 221.

(13) N. Armagan, J. P. G. Richards, and A. A. Uraz, *Acta Crystallogr.*, **B32**, 1042 (1976).

(14) H. P. C. Hogenkamp and G. N. Sando, in "Structure and Bonding," vol. 20, J. D. Dunitz, Ed., Springer-Verlag, Berlin, Germany, 1974, pp. 23–58.

ACKNOWLEDGMENTS AND ADDRESSES

Received June 14, 1976, from the *Department of Medicinal Chemistry and Pharmacognosy, College of Pharmacy, University of Houston, Houston, TX 77004.*

Accepted for publication September 16, 1976.

Presented in part at the 3rd Annual Southcentral Medicinal Chemistry Meeting in Miniature (ALTO), Monroe, La., May 1976.

Supported in part by National Institutes of Health Grant CAO-4464.

The authors thank Miss Barbara Stearns, Squibb Institute of Medical Research, for supplying hydroxyurea and the 1-substituted analogs.

* Present address: Department of Biochemistry, M. D. Anderson Hospital and Tumor Institute, Houston, TX 77025.

ˣ To whom inquiries should be directed.

NOTES

Improved Recovery of Morphine from Biological Tissues Using Siliconized Glassware

HEMENDRA N. BHARGAVA

Abstract □ The adsorption of morphine onto glassware during analysis in aqueous solutions and biological tissues is a common problem, resulting in lower recoveries than expected. The problem can be remedied by siliconization of all glassware involved. The same glassware cannot be used repeatedly without incurring a significant loss of morphine.

Keyphrases □ Morphine—adsorption onto glassware during fluorometric analysis, effect of siliconization □ Adsorption—morphine onto glassware during fluorometric analysis, effect of siliconization □ Siliconization—of glassware, effect on adsorption of morphine during fluorometric analysis □ Narcotic analgesics—morphine, adsorption onto glassware during fluorometric analysis, effect of siliconization

Several methods including fluorometric (1, 2), flame-ionization (3) and electron-capture (4) GLC, and radioimmunoassay (5) have been used to measure morphine levels in biological tissues. The fluorometric procedure is still the most widely used method because of its simplicity and rapidity.

polar environment and whether internal hydrogen bonding is stabilized or whether hydrogen bonding to a solvent or to other biochemical entities has occurred. Hydroxyurea appears to possess the same type of carbonyl nitrogen character before and after equilibration with water. Therefore, no conformational preference may exist in hydroxyurea in solutions where conformational preference may be conferred to substituted hydroxyureas by their bulk or steric hindrance or to some electronic stabilization factor. The crystal structure of hydroxyurea indicates that intermolecular hydrogen bonding exists between the hydroxyl group of one molecule and the carbonyl oxygen of another molecule rather than intramolecular hydrogen bonding (13), and internal hydrogen bonding may not be preferred in solution.

The *in vitro* inhibition of ribonucleotide reductase by selected hydroxyureas (Table II) relative to hydroxyurea seems to indicate a solvent dependency. Although the enzyme system is quite complex and its activity is dependent on many variables (14), its inhibition by hydroxyureas followed a general trend, except for the 3-*n*-propyl analog (V) in the first determination. The solvent for hydroxyurea and the 1-analogs (II and III) was water for all determinations, and water was used for V in the first determination. The solvent for all other determinations for V and VII was 1% dimethyl sulfoxide.

The inhibitory concentration required to obtain 50% enzyme activity with V was much higher in the first determination than in the other determinations (2–4 in Table II), and this result was due to some error in the enzyme determination or to the different solvent. To verify which factor was the determinant in the inhibition study, another analysis was performed (5 in Table II) in which water was the solvent for all compounds. Again the concentration required for 50% enzyme inhibition for V was appreciably higher than in determinations where dimethyl sulfoxide was the solvent. This result implicates the solvent as a potential variable in the ability of hydroxyureas to function in the *in vitro* inhibition of ribonucleoside diphosphate reductase, and this property should be considered in the elucidation of the biodynamics of drugs in the hydroxyurea class.

Although it is not possible to determine whether the solvent-dependent conformational system observed in substituted hydroxyureas is the actual cause of the poor inhibition of the enzyme, with V the conformation and solvent have an interdependence that may affect the biological action of the drug. The transport and partitioning properties of hydroxyureas in octanol–water are currently being investigated to determine whether predicted and actual partition coefficients support the solvent-dependent conformation and the importance of this property in drug transport *in vivo*.

REFERENCES

(1) G. R. Parker, N. K. Hilgendorf, and J. G. Lindberg, *J. Pharm. Sci.*, **65**, 585 (1976).

(2) W. Dresler and R. Stein, *Justus Liebigs Ann. Chem.*, **150**, 242 (1869).

(3) R. E. Harmon, J. C. Dabrowiak, D. J. Brown, S. K. Gupta, M. Herbert, and D. Chitharanjan, *J. Med. Chem.*, **13**, 577 (1970).

(4) G. Clifton, S. R. Bryant, and C. G. Skinner, *ibid.*, **13**, 377 (1970).

(5) E. C. Moore, in "Methods in Enzymology," vol. 12, S. P. Colowick and N. D. Kaplan, Eds., Academic, New York, N.Y., 1967, pp. 155–174.

(6) P. Reichard, *J. Biol. Chem.*, **237**, 3513 (1962).

(7) C. Hansch and S. M. Anderson, *J. Org. Chem.*, **32**, 2583 (1967).

(8) J. Iwasa, T. Fujita, and C. Hansch, *J. Med. Chem.*, **8**, 150 (1965).

(9) T. Fujita, J. Iwasa, and C. Hansch, *J. Am. Chem. Soc.*, **86**, 5175 (1964).

(10) C. Hansch, R. M. Muir, T. Fujita, P. P. Maloney, F. Geiger, and M. Streich, *ibid.*, **85**, 817 (1963).

(11) A. Leo, C. Hansch, and D. Elkins, *Chem. Rev.*, **71**, 525 (1971).

(12) J. E. Huheey, "Inorganic Chemistry: Structure and Reactivity," Harper and Row, New York, N.Y., 1972, pp. 220, 221.

(13) N. Armagan, J. P. G. Richards, and A. A. Uraz, *Acta Crystallogr.*, **B32**, 1042 (1976).

(14) H. P. C. Hogenkamp and G. N. Sando, in "Structure and Bonding," vol. 20, J. D. Dunitz, Ed., Springer-Verlag, Berlin, Germany, 1974, pp. 23–58.

ACKNOWLEDGMENTS AND ADDRESSES

Received June 14, 1976, from the *Department of Medicinal Chemistry and Pharmacognosy, College of Pharmacy, University of Houston, Houston, TX 77004.*

Accepted for publication September 16, 1976.

Presented in part at the 3rd Annual Southcentral Medicinal Chemistry Meeting in Miniature (ALTO), Monroe, La., May 1976.

Supported in part by National Institutes of Health Grant CAO-4464.

The authors thank Miss Barbara Stearns, Squibb Institute of Medical Research, for supplying hydroxyurea and the 1-substituted analogs.

* Present address: Department of Biochemistry, M. D. Anderson Hospital and Tumor Institute, Houston, TX 77025.

ˣ To whom inquiries should be directed.

NOTES

Improved Recovery of Morphine from Biological Tissues Using Siliconized Glassware

HEMENDRA N. BHARGAVA

Abstract □ The adsorption of morphine onto glassware during analysis in aqueous solutions and biological tissues is a common problem, resulting in lower recoveries than expected. The problem can be remedied by siliconization of all glassware involved. The same glassware cannot be used repeatedly without incurring a significant loss of morphine.

Keyphrases □ Morphine—adsorption onto glassware during fluorometric analysis, effect of siliconization □ Adsorption—morphine onto glassware during fluorometric analysis, effect of siliconization □ Siliconization—of glassware, effect on adsorption of morphine during fluorometric analysis □ Narcotic analgesics—morphine, adsorption onto glassware during fluorometric analysis, effect of siliconization

Several methods including fluorometric (1, 2), flame-ionization (3) and electron-capture (4) GLC, and radioimmunoassay (5) have been used to measure morphine levels in biological tissues. The fluorometric procedure is still the most widely used method because of its simplicity and rapidity.

A major problem in the extraction of morphine from aqueous solutions and biological tissues has been adsorption of the drug onto detergent-cleaned glassware. Wilkinson and Way (3) were unsuccessful in circumventing this problem since they siliconized only the centrifuge tubes. The present paper reports that siliconization of all glassware that comes in contact with aqueous solutions of morphine reduces the loss of morphine by adsorption and thus significantly increases its recovery from aqueous solutions and from biological tissues.

EXPERIMENTAL

Chemicals—1-Butanol[1], chloroform[2], sodium bicarbonate[3], monobasic sodium phosphate[3], dibasic sodium phosphate[3], potassium ferricyanide[3], and potassium ferrocyanide[3] were the highest quality commercially available.

Siliconization of Glassware—The glassware was siliconized by using a water-soluble silicone concentrate[4] and was dried at 100° for 10 min according to the directions on the container.

Procedures—*Recovery of Morphine from Rat Brain*—The procedure of Kupferberg *et al.* (2), slightly modified, was used. Individual rat brain samples were homogenized[5] for 30 sec with 1.5 ml of isotonic saline in a 50-ml polyethylene tube. The shaft of the homogenizer was then washed with 0.5 ml of saline into the centrifuge tube. Different amounts (0.125–0.5 μg) of morphine sulfate contained in equal volumes (50 μl) were added to the homogenate. Each concentration was run in duplicate.

Sodium bicarbonate (0.5 g) and 10% 1-butanol in chloroform (10 ml) were added to the homogenate. The mixture was shaken on a mechanical shaker for 10 min at 200 oscillations/min and then centrifuged at 28,000×*g* for 30 min at 4°. The aqueous layer was aspirated, and the matted tissue was removed with a spatula. A 7-ml aliquot of the organic phase (butanol–chloroform) was transferred to a 15-ml glass-stoppered centrifuge tube containing 1.2 ml of 0.01 *M* hydrochloric acid; the tube was gently inverted 30 times and then centrifuged for 10 min at 2000 rpm at 4°.

One milliliter of the acid phase was removed and added to 1 ml of phosphate buffer (pH 8.5), and this mixture was oxidized with 0.1 ml of potassium ferricyanide–ferrocyanide reagent (2). The fluorescence of the solution was measured at 440 nm after excitation at 250 nm on a spectrophotofluorometer[6].

Recovery of Morphine from Aqueous Solution—The assay procedure used for the brain tissue was also used to determine recovery of morphine sulfate (0.125–0.5 μg) from aqueous solutions.

RESULTS AND DISCUSSION

A linear relationship existed between the amount (0.125–0.5 μg in the original sample) of morphine sulfate used and the relative fluorescence intensity. A similar relationship existed after morphine was extracted from aqueous solutions or rat brain homogenates to which morphine sulfate had been added. When all glassware was siliconized, the average recoveries of morphine from the water standards and brain tissues, excluding aliquot losses, were 52.6 ± 1.9 (n = 5) and 46.5 ± 2.0% (SE) (n = 4), respectively (Table I). Similarly, the recoveries of morphine, including aliquot losses, were 90.0 and 79.4%, respectively. When none of the glassware was siliconized, the recovery from the rat brain, including aliquot losses, was only 26.3%.

The major loss of morphine occurred when the volumetric flasks used to prepare stock solutions and dilutions of morphine were not siliconized.

[1] Merck and Co., Rahway, N.J.
[2] Mallinckrodt Chemical Co., St. Louis, Mo.
[3] Fisher Scientific Co., Fair Lawn, N.J.
[4] Siliclad, Clay Adams, Division of Becton, Dickinson and Co., Parsippany, N.J.
[5] Polytron homogenizer, Brinkmann Instruments.
[6] Model 8202G, American Instrument Co.

Table I—Effect of Siliconization on Recovery of Morphine[a]

Number of Times Glassware Was Used	Fluorescence Intensity for 0.5 μg of Morphine		Recovery from Water, %	Recovery from Rat Brain, %
	Absolute	%		
1	140	100.0	47.0	39.5
2	125	89.2	47.3	38.6
3	110	78.4	46.2	36.5
4	82	58.4	46.9	32.9
0[b]	225	—	52.6	46.5

[a] All glassware was siliconized except for the volumetric flasks used for making stock solutions of morphine. [b] Represents values when all glassware was siliconized.

The absolute fluorescence units for 0.5 μg of morphine fell from 225 to 140, a decrease of 38% (Table I).

Repeated use of glassware also decreased the absolute fluorescence intensity of morphine. The silicone coating is probably lost during the cleaning procedure, resulting in a loss of morphine due to its adsorption to the glass. Table I shows the fluorescence intensities for morphine recovered from aqueous solutions and from brain homogenates when glassware was used four consecutive times after siliconization. The glassware was cleaned with laboratory detergents and deionized water prior to each experimental run.

The recovery of morphine from the water standard or aqueous solution was not affected significantly by repeated use of glassware, but it was lower than when all glassware was siliconized before use. The recovery of morphine from rat brain samples decreased with each successive use of the glassware. Thus, both the absolute recovery and the extraction recovery were reduced when all glassware was not siliconized. This result could be seen by the decrease in the slope of the calibration curves (Table I). A net loss of 10, 20, and 40% of morphine was observed during the second, third, and fourth use, respectively, of the same glassware. No loss of morphine was observed when nonsiliconized pipets were used to transfer butanol–chloroform extract containing morphine, indicating that adsorption losses occurred only when morphine was present in the aqueous solution.

In conclusion, the present study shows that significant loss of morphine onto glassware can occur. This adsorption loss can be minimized by siliconization of all glassware that comes in contact with aqueous solutions of morphine. Since the slope of the calibration curve declines with successive use of the glassware, the sensitivity of the method decreases. Therefore, to minimize adsorption losses, all glassware should be siliconized each time morphine is to be analyzed in aqueous solutions and tissue samples.

REFERENCES

(1) J. M. Fujimoto, E. L. Way, and C. H. Hine, *J. Lab. Clin. Med.*, **44**, 627 (1954).

(2) H. Kupferberg, A. Burkhalter, and E. L. Way, *J. Pharmacol. Exp. Ther.*, **145**, 247 (1964).

(3) G. R. Wilkinson and E. L. Way, *Biochem. Pharmacol.*, **18**, 1435 (1969).

(4) J. E. Wallace, H. E. Hamilton, K. Blum, and C. Petty, *Anal. Chem.*, **46**, 2107 (1974).

(5) S. Spector and C. W. Parker, *Science*, **168**, 1347 (1970).

ACKNOWLEDGMENTS AND ADDRESSES

Received July 6, 1976, from the *Department of Pharmacognosy and Pharmacology, College of Pharmacy, University of Illinois at the Medical Center, Chicago, IL 60612.*

Accepted for publication August 18, 1976.

Supported in part by a grant from the Graduate College Research Board, University of Illinois at the Medical Center, Chicago, IL 60612.

The author thanks Dr. Norman R. Farnsworth for interest and encouragement and Mr. George Matwyshyn for technical assistance.

Binding of Pyridine Derivatives to Cytochrome P-450

JERRY L. BORN ˣ and DAVID VAUGHN *

Abstract □ The spectral binding constants, K_s, of pyridine, methylpyridine, and dimethylpyridines were determined. The K_s values of the compounds were discussed in terms of mechanisms of possible bonding to cytochrome P-450.

Keyphrases □ Pyridine and derivatives—spectral binding to cytochrome P-450, constants determined □ Spectral binding—pyridine and derivatives to cytochrome P-450, constants determined □ Binding, spectral—pyridine and derivatives to cytochrome P-450, constants determined □ Cytochrome P-450—spectral binding to pyridine and derivatives, constants determined

Cytochrome P-450, a terminal oxidase responsible for the hydroxylation of many drugs and organic compounds (1, 2), exhibits two distinct types of spectral binding curves when the difference spectra are recorded in the presence of "substrates." Type I binding curves are thought to result from the interaction of a substrate with the enzyme at a site associated with hydroxylation (3), resulting in a perturbation of the enzyme that produces a difference spectrum with a peak in the 390-nm region and a trough in the 420-nm region (4). The binding of type II substrates involves the interaction of nonbonding electrons with the heme site (5–8), producing difference spectra with a peak in the 420-nm region and a trough at approximately 390 nm (4).

Many type II binding compounds have been identified including aliphatic alcohols, primary aliphatic and aromatic amines, pyridine, and metyrapone[1], the potent inhibitor of cytochrome P-450 (2). Water recently was proposed as the sixth ligand of the heme site with four ligands from the porphyrin ring and the other ligand from a sulfhydryl group (5). The nonbonding electrons of pyridine are thought to result in the displacement of water from the heme site, resulting in a pyridine-coordinated cytochrome P-450. This work describes the determination of the spectral binding constants for a series of methylpyridines.

EXPERIMENTAL

Adult male rats were injected with 80 mg/kg ip of phenobarbital sodium for 3 consecutive days, fasted for 24 hr, and then sacrificed by decapitation. The liver was removed, washed with 0.25 *M* sucrose, and then homogenized in 10 volumes of 0.25 *M* sucrose using a Potter–Elvehjem glass tube and a polytef [2] pestle. The homogenized material was centrifuged for 15 min at 10,000×*g*, and the supernate was removed and centrifuged at 100,000×*g* for 1 hr to produce a microsomal pellet. The microsomal pellet was resuspended in 0.15 *M* KCl and recentrifuged at 100,000×*g*. This microsomal pellet was then resuspended in 0.05 *M* tromethamine buffer (pH 7.4), and the protein was adjusted to 1 mg/ml by the method of Lowry (9).

Difference spectra were recorded by placing 3 ml of the protein solution in both the sample and reference cells and then recording the baseline using a double-beam spectrophotometer[3] equipped with a scattered transmission accessory. After the baseline was established, 3-μl portions of substrate dissolved in tromethamine buffer were added to the sample cell and successive spectra were recorded. When the solubility of the substrate in tromethamine buffer was low, spectroanalyzed methanol was utilized to dissolve the compounds in the buffer.

The spectral binding constant, K_s, was determined by substituting the difference between the maximum and minimum absorbance in the spectrum for initial velocity in the classical enzyme substrate models (10).

The pyridine compounds were distilled prior to use, and their purity was checked by GLC.

Table I—Comparison of Spectral Binding Constants (K_s) for Pyridine and Methylpyridines

Compound	K_s	Relative Activities	pKa of Conjugate Acid[a]
Pyridine	1.46×10^{-3}	1	5.3
2-Methylpyridine	6.15×10^{-3}	0.24	5.95
3-Methylpyridine	0.353×10^{-3}	4.14	5.85
4-Methylpyridine	0.166×10^{-3}	8.8	6.10
2,6-Dimethylpyridine	1.95×10^{-3}	0.75	6.72
2,4-Dimethylpyridine	0.945×10^{-3}	1.54	6.8
2,5-Dimethylpyridine	3.7×10^{-3}	0.39	6.55
3,4-Dimethylpyridine	0.089×10^{-3}	16.4	6.61
3,5-Dimethylpyridine	0.16×10^{-3}	9.13	6.34

[a] N. Ikekana, Y. Sato, and T. Maeda, *Pharm. Bull.*, 2, 205 (1954).

RESULTS AND DISCUSSION

Three distinct factors should influence the binding of methylpyridines to the heme site: the basicity of the compound, the steric factors involved with the approach of the methylpyridines to the heme site, and the hydrophobic bonding of the methyl groups to the site as proposed by Jefcoate *et al.* (7). The instability of 2-methylpyridine and 2,6-dimethylpyridine complexes with formyl-substituted hemins (11) was attributed to steric inhibition of bonding, as was the instability of the boron trifluoride–2-methylpyridine complex (12). If the nonbonding electrons of pyridine are involved with coordination with the heme site of cytochrome P-450, introduction of a methyl group on the 2-position of pyridine should result in less binding of the compound to the heme site.

Table I shows the spectral binding constants for some methyl-substituted pyridines, the relative activities of the compounds as binders to cytochrome P-450, and the pKa values. The results support the concept of the nonbonding electrons of pyridine interacting with the heme site. In each case investigated, the activity of 2-methylpyridines was uniformly low. 2-Methylpyridine was approximately one-fourth as active as pyridine, and the activities of 2,4-dimethylpyridine and 2,5-dimethylpyridine were significantly lower than those of their parent compounds, 4-methylpyridine and 3-methylpyridine, respectively, indicating the importance of having an unsubstituted 2-position on the pyridine ring for maximal binding.

The discovery that 2,6-dimethylpyridine had a greater activity than 2-methylpyridine was unexpected and may be due to its basicity (pKa 6.72). The activity of 2,6-dimethylpyridine cannot be explained by a direct interaction between the nonbonding electrons and the heme site and may result from the transfer of electrons from the nitrogen to the heme site through a molecule of water.

A plot of log K_s for the 3- and 4-substituted pyridines against the pKa for the compounds shows a linear relationship between pKa and the binding activity ($r = 0.9817$). While this information cannot preclude the possibility of hydrophobic bonding, it strongly suggests that the basicity of the nitrogen is the dominant binding force in this series of compounds.

The consistently high activities of 4-methylpyridines suggests that appropriately substituted 4-pyridines may be potent binders of cytochrome P-450, a possibility now under investigation in these laboratories.

[1] Metopirone, Ciba-Geigy.
[2] Teflon (du Pont).
[3] Beckman M6 Acta.

REFERENCES

(1) J. R. Gillette, *Adv. Pharmacol.*, **4**, 219 (1966).

(2) G. J. Mannering, in "Fundamentals of Drug Metabolism and Drug Disposition," B. N. LaDue, H. G. Mandel, and E. L. Way, Eds., Williams & Wilkins, Baltimore, Md., chap. 12.

(3) K. J. Netter, G. F. Hall, and M. P. Nagnussen, *Arch. Exp. Pathol. Pharmakol.*, **265**, 205 (1969).

(4) J. B. Schenkman, H. Remmer, and R. W. Estabrook, *Mol. Pharmacol.*, **3**, 113 (1967).

(5) B. W. Griffin, J. A. Peterson, J. Werringloer, and R. W. Estabrook, *Ann. N.Y. Acad. Sci.*, **244**, 107 (1975).

(6) Y. Imai and R. Sato, *J. Biochem.*, **62**, 239 (1967).

(7) C. R. E. Jefcoate, J. L. Gaylor, and R. Calabrese, *Biochemistry*, **8**, 3455 (1969).

(8) J. B. Schenkman, *ibid.*, **9**, 2081 (1970).

(9) G. H. Lowry, N. J. Rosenbrough, A. L. Farr, and R. J. Randall, *J. Biol. Chem.*, **193**, 265 (1951).

(10) K. C. Leibman, A. G. Hildebrandt, and R. W. Estabrook, *Biochem. Biophys. Res. Commun.*, **36**, 789 (1969).

(11) R. Lemberg and A. Velins, *Biochim. Biophys. Acta*, **104**, 487 (1965).

(12) H. C. Brown and G. K. Barbaras, *J. Am. Chem. Soc.*, **69**, 1137 (1947).

ACKNOWLEDGMENTS AND ADDRESSES

Received March 26, 1976, from the *College of Pharmacy, Butler University, Indianapolis, IN 46208.*

Accepted for publication August 26, 1976.

The authors thank the Riley Tar and Chemical Co., Indianapolis, Ind., for the gift of methylpyridines and dimethylpyridines.

* Project SEED student, summer 1975.

[x] To whom inquiries should be directed. Present address: College of Pharmacy, University of New Mexico, Albuquerque, NM 87131.

Determination of Dextrorphan in Plasma and Evaluation of Bioavailability of Dextromethorphan Hydrobromide in Humans

GOLLAMUDI RAMACHANDER [x], FLORENCE D. WILLIAMS, and JANE FRANCES EMELE

Abstract □ A method is described for the estimation of dextrorphan, a metabolite of dextromethorphan, in plasma. The bioavailability of dextromethorphan hydrobromide after 30 mg po, as measured by the concentration of total (free and conjugated) dextrorphan in the plasma, was determined in six human volunteers with this procedure.

Keyphrases □ Dextrorphan—fluorometric analysis, human plasma □ Dextromethorphan hydrobromide—bioavailability evaluated using fluorometric analysis of dextrorphan in human plasma □ Fluorometry—analysis, dextrorphan in human plasma □ Bioavailability—dextromethorphan hydrobromide evaluated using fluorometric analysis of dextrorphan in human plasma □ Antitussives—dextromethorphan hydrobromide, bioavailability evaluated using fluorometric analysis of dextrorphan in human plasma

Dextromethorphan hydrobromide, a widely accepted, nonnarcotic antitussive agent, is a common ingredient in many cough–cold preparations. Despite its clinical use for over two decades, a method for estimating its plasma levels in humans has not been published. Presently available analytical methods lack the sensitivity needed to determine its plasma levels after oral administration of the maximum permissible over-the-counter dose of 30 mg[1] (1).

The metabolism of dextromethorphan has been studied in several species (2–6). Following oral administration, this drug is rapidly metabolized; the principal metabolites are the *O*-demethylated product dextrorphan and its glucuronide and sulfate ester conjugates. In humans, dextrorphan [(+)-3-hydroxy-*N*-methylmorphinan], (+)-3-hydroxymorphinan, and traces of the unmetabolized drug were found in urine after oral administration of the drug (6). Enzymatic hydrolysis of urines from patients administered dextromethorphan yielded 40–50% of the drug and metabolites, mostly in the form of glucuronide and sulfate conjugates[1].

Because the blood levels of unmetabolized dextromethorphan were low, another approach was to measure the levels of the major metabolites. Dextrorphan was estimated in plasma and urine by paper chromatography (7), colorimetric determination of the methyl orange complex (8), and radiotracer techniques (9). These methods suffer from inherent disadvantages such as a lack of sensitivity and cumbersome operation. This report describes a sensitive and more convenient method for the determination of plasma levels of dextrorphan and its conjugates. Its applicability to bioavailability studies in humans also is demonstrated.

EXPERIMENTAL

Plasma Levels of Dextrorphan and Its Conjugates—Plasma (3.0 ml) was transferred into a glass-stoppered erlenmeyer flask (25 ml). The pH was adjusted to 5.5 with 3.0 *N* acetic acid, and an enzyme solution[2] (0.2 ml) containing 30,000 units of β-glucuronidase and 10,000 units of arylsulfatase was added. The flask was stoppered and incubated at 37° for 2 hr. The incubate was brought to room temperature, and the pH of the contents was adjusted to 9.5 by the addition of a saturated solution of sodium carbonate (0.6 ml).

Spectroscopically pure ethyl acetate (15 ml) was then pipetted into the flask, and the contents were shaken for 20 min on a mechanical shaker. The mixture was transferred quantitatively into a 30-ml centrifuge tube, and the extract was separated by centrifuging at 3000 rpm for 15 min. Then an aliquot (12 ml) of the supernate was transferred into a stoppered 50-ml erlenmeyer flask containing 3.0 ml of 1.0 *N* HCl, and

[1] B. A. Koechlin and F. Rubio, work cited in Ref. 1.

[2] Glusulase, Endo Laboratories, Garden City, NY 11530.

REFERENCES

(1) J. R. Gillette, *Adv. Pharmacol.*, **4**, 219 (1966).

(2) G. J. Mannering, in "Fundamentals of Drug Metabolism and Drug Disposition," B. N. LaDue, H. G. Mandel, and E. L. Way, Eds., Williams & Wilkins, Baltimore, Md., chap. 12.

(3) K. J. Netter, G. F. Hall, and M. P. Nagnussen, *Arch. Exp. Pathol. Pharmakol.*, **265**, 205 (1969).

(4) J. B. Schenkman, H. Remmer, and R. W. Estabrook, *Mol. Pharmacol.*, **3**, 113 (1967).

(5) B. W. Griffin, J. A. Peterson, J. Werringloer, and R. W. Estabrook, *Ann. N.Y. Acad. Sci.*, **244**, 107 (1975).

(6) Y. Imai and R. Sato, *J. Biochem.*, **62**, 239 (1967).

(7) C. R. E. Jefcoate, J. L. Gaylor, and R. Calabrese, *Biochemistry*, **8**, 3455 (1969).

(8) J. B. Schenkman, *ibid.*, **9**, 2081 (1970).

(9) G. H. Lowry, N. J. Rosenbrough, A. L. Farr, and R. J. Randall, *J. Biol. Chem.*, **193**, 265 (1951).

(10) K. C. Leibman, A. G. Hildebrandt, and R. W. Estabrook, *Biochem. Biophys. Res. Commun.*, **36**, 789 (1969).

(11) R. Lemberg and A. Velins, *Biochim. Biophys. Acta*, **104**, 487 (1965).

(12) H. C. Brown and G. K. Barbaras, *J. Am. Chem. Soc.*, **69**, 1137 (1947).

ACKNOWLEDGMENTS AND ADDRESSES

Received March 26, 1976, from the *College of Pharmacy, Butler University, Indianapolis, IN 46208.*

Accepted for publication August 26, 1976.

The authors thank the Riley Tar and Chemical Co., Indianapolis, Ind., for the gift of methylpyridines and dimethylpyridines.

* Project SEED student, summer 1975.

[x] To whom inquiries should be directed. Present address: College of Pharmacy, University of New Mexico, Albuquerque, NM 87131.

Determination of Dextrorphan in Plasma and Evaluation of Bioavailability of Dextromethorphan Hydrobromide in Humans

GOLLAMUDI RAMACHANDER [x], FLORENCE D. WILLIAMS, and JANE FRANCES EMELE

Abstract □ A method is described for the estimation of dextrorphan, a metabolite of dextromethorphan, in plasma. The bioavailability of dextromethorphan hydrobromide after 30 mg po, as measured by the concentration of total (free and conjugated) dextrorphan in the plasma, was determined in six human volunteers with this procedure.

Keyphrases □ Dextrorphan—fluorometric analysis, human plasma □ Dextromethorphan hydrobromide—bioavailability evaluated using fluorometric analysis of dextrorphan in human plasma □ Fluorometry—analysis, dextrorphan in human plasma □ Bioavailability—dextromethorphan hydrobromide evaluated using fluorometric analysis of dextrorphan in human plasma □ Antitussives—dextromethorphan hydrobromide, bioavailability evaluated using fluorometric analysis of dextrorphan in human plasma

Dextromethorphan hydrobromide, a widely accepted, nonnarcotic antitussive agent, is a common ingredient in many cough–cold preparations. Despite its clinical use for over two decades, a method for estimating its plasma levels in humans has not been published. Presently available analytical methods lack the sensitivity needed to determine its plasma levels after oral administration of the maximum permissible over-the-counter dose of 30 mg[1] (1).

The metabolism of dextromethorphan has been studied in several species (2–6). Following oral administration, this drug is rapidly metabolized; the principal metabolites are the *O*-demethylated product dextrorphan and its glucuronide and sulfate ester conjugates. In humans, dextrorphan [(+)-3-hydroxy-*N*-methylmorphinan], (+)-3-hydroxymorphinan, and traces of the unmetabolized drug were found in urine after oral administration of the drug (6). Enzymatic hydrolysis of urines from patients administered dextromethorphan yielded 40–50% of the drug and metabolites, mostly in the form of glucuronide and sulfate conjugates[1].

Because the blood levels of unmetabolized dextromethorphan were low, another approach was to measure the levels of the major metabolites. Dextrorphan was estimated in plasma and urine by paper chromatography (7), colorimetric determination of the methyl orange complex (8), and radiotracer techniques (9). These methods suffer from inherent disadvantages such as a lack of sensitivity and cumbersome operation. This report describes a sensitive and more convenient method for the determination of plasma levels of dextrorphan and its conjugates. Its applicability to bioavailability studies in humans also is demonstrated.

EXPERIMENTAL

Plasma Levels of Dextrorphan and Its Conjugates—Plasma (3.0 ml) was transferred into a glass-stoppered erlenmeyer flask (25 ml). The pH was adjusted to 5.5 with 3.0 *N* acetic acid, and an enzyme solution[2] (0.2 ml) containing 30,000 units of β-glucuronidase and 10,000 units of arylsulfatase was added. The flask was stoppered and incubated at 37° for 2 hr. The incubate was brought to room temperature, and the pH of the contents was adjusted to 9.5 by the addition of a saturated solution of sodium carbonate (0.6 ml).

Spectroscopically pure ethyl acetate (15 ml) was then pipetted into the flask, and the contents were shaken for 20 min on a mechanical shaker. The mixture was transferred quantitatively into a 30-ml centrifuge tube, and the extract was separated by centrifuging at 3000 rpm for 15 min. Then an aliquot (12 ml) of the supernate was transferred into a stoppered 50-ml erlenmeyer flask containing 3.0 ml of 1.0 *N* HCl, and

[1] B. A. Koechlin and F. Rubio, work cited in Ref. 1.

[2] Glusulase, Endo Laboratories, Garden City, NY 11530.

the drug and its metabolites were extracted into the acid by shaking the mixture for 20 min.

The aqueous layer was separated using a 50-ml separator, and its fluorescence was measured in a fluorescence spectrophotometer[3]. The fluorescence and excitation wavelengths were 310 and 280 nm, respectively, and the slit dials were set to give a bandpass of 8 nm for excitation and of 5 nm for fluorescence. The concentrations of the drug and its metabolites in the sample were read from a calibration curve whose validity was determined by including three or four known concentrations of dextrorphan added to normal human plasma with each series of unknowns.

Bioavailability Studies in Humans—Six healthy male volunteers, 27–32 years old, received 30 mg po of dextromethorphan hydrobromide in a syrup (10 ml) after an overnight fast. Blood samples were drawn from the antecubetal vein into heparinized tubes immediately prior to and at 15 and 30 min and 1, 2, and 4 hr after drug administration. Plasma was separated by centrifuging at 3000 rpm for 20 min, and an aliquot was assayed by the described procedure.

RESULTS AND DISCUSSION

A calibration curve was constructed by plotting the fluorescence intensity against the concentration of dextrorphan added to drug-free plasma. Regression analysis of the least-squares line fitting the data points provided an equation for the curve as $y = 0.2658x + 3.728$ ($r = 0.9956$), where y represents fluorescence units and x is nanograms of dextrorphan per milliliter of plasma. The recovery of known amounts of dextrorphan added to human plasma was 70%. To determine the precision of the method, eight plasma samples spiked with 400 ng of dextrorphan/ml and four samples containing 600 ng of dextrorphan/ml were analyzed in duplicate over 6 months. The coefficients of variation at these two concentrations were 8 and 4%, respectively.

The fluorescence characteristics of dextrorphan and dextromethorphan in 1.0 *N* hydrochloric acid are rather similar. The fluorescence and excitation wavelengths of dextrorphan are 310 and 280 nm, respectively; for dextromethorphan, they are 305 and 270 nm, respectively.

The fluorescence spectrum of dextrorphan extracted from plasma was identical with that of dextrorphan in 1.0 *N* HCl. Some interference by the unmetabolized drug and possibly other minor metabolites could be expected in the measurement of dextrorphan levels. However, the contribution to fluorescence by the unmetabolized drug would be negligible in this method because extracts from plasma of humans administered dextromethorphan hydrobromide exhibited fluorescence spectra characteristic of dextrorphan but not dextromethorphan. Furthermore, since dextromethorphan is metabolized rapidly and extensively upon oral administration, the amount present in the extracts would be very low.

Plasma Levels in Humans—The average plasma levels ($\pm SE$) of dextrorphan and its conjugates following 30 mg po of dextromethorphan hydrobromide to six volunteers at 15, 30, and 60 min were 21.3 ± 6.7, 107.3 ± 44.6, and 368.0 ± 71.2 ng/ml, respectively. The peak level was 381.3 ± 56.9 ng/ml at 2 hr and it declined thereafter, reaching 262.7 ± 43.3 ng/ml at 4 hr. Almost all of the dextrorphan was present in the form of conjugates. This finding was confirmed by analyzing the plasma samples from one of the six volunteers, with and without enzymatic hydrolysis. Whereas hydrolysis gave rise to concentrations ranging from 26 to 380 ng/ml, none of the unhydrolyzed samples contained measurable levels of the unconjugated drug or metabolites.

It may be concluded that this method is applicable to the determination of the bioavailability of dextromethorphan hydrobromide in humans.

[3] Perkin-Elmer model MPF-3.

REFERENCES

(1) J. A. F. de Silva and L. D'Arconte, *J. Forensic Sci.*, **14**, 184 (1969).

(2) J. Axelrod, *J. Pharmacol. Exp. Ther.*, **117**, 322 (1956).

(3) C. Elison and H. Elliott, *ibid.*, **144**, 265 (1964).

(4) J. Kamm, A. Taddeo, and E. Van Loon, *ibid.*, **158**, 437 (1967).

(5) A. Brossi, O. Haffliger, and O. Schneider, *Arzneim.-Forsch.*, **5**, 62 (1955).

(6) K. Willner, *ibid.*, **13**, 20 (1963).

(7) H. Kaiser and H. Jori, *Arch. Pharm.*, **287**, 224 (1954).

(8) P. A. Shore, J. Axelrod, C. A. M. Hogben, and B. B. Brodie, *J. Pharmacol. Exp. Ther.* **113**, 192 (1955).

(9) K. D. Wuepper, S. Y. Yeh, and L. A. Woods, *Proc. Soc. Exp. Biol. Med.*, **124**, 1146 (1967).

ACKNOWLEDGMENTS AND ADDRESSES

Received April 10, 1974, from the *Warner–Lambert Research Institute, Morris Plains, NJ 07950.*

Accepted for publication August 18, 1976.

Presented at the 57th Annual Meeting of the Federation of the American Societies for Experimental Biology, Atlantic City, N.J., April 1973.

[x] To whom inquiries should be directed. Present address: Division of Drug Metabolism and Biopharmaceutics, Department of Medicinal Chemistry, College of Pharmacy, University of Tennessee Center for the Health Sciences, Memphis, TN 38163.

Effects of 3,4-Dimethoxyphenethylamine Derivatives on Monoamine Oxidase

WILLIAM J. KELLER [x] and GARY G. FERGUSON

Abstract □ The cactus alkaloid 3,4-dimethoxyphenethylamine and its naturally occurring *N*-methylated homologs inhibited the deamination of tyramine and tryptamine by rat brain monoamine oxidase. In contrast, the β-hydroxylated derivatives of this series failed to inhibit the action of monoamine oxidase on both tyramine and tryptamine.

Keyphrases □ 3,4-Dimethoxyphenethylamine and *N*-methyl homologs—effect on monoamine oxidase-catalyzed deamination of tyramine and tryptamine □ Monoamine oxidase—deamination of tyramine and tryptamine, effect of 3,4-dimethoxyphenethylamine and *N*-methyl homologs □ Tyramine—monoamine oxidase-catalyzed oxidative deamination, effect of 3,4-dimethoxyphenethylamine and *N*-methyl homologs □ Tryptamine—monoamine oxidase-catalyzed deamination, effect of 3,4-dimethoxyphenethylamine and *N*-methyl homologs □ Enzymes—monoamine oxidase, deamination of tyramine and tryptamine, effect of 3,4-dimethoxyphenethylamine and *N*-methyl homologs □ Structure–activity relationships—3,4-dimethoxyphenethylamine and *N*-methyl homologs, effect on monoamine oxidase-catalyzed deamination of tyramine and tryptamine

The present study was directed at observing the effects of 3,4-dimethoxyphenethylamine (I) and its *N*-methyl homologs on rat brain monoamine oxidase, using both tyramine and tryptamine as substrates. The results of these experiments were contrasted with those obtained with the β-hydroxy derivatives of the same series. The al-

the drug and its metabolites were extracted into the acid by shaking the mixture for 20 min.

The aqueous layer was separated using a 50-ml separator, and its fluorescence was measured in a fluorescence spectrophotometer[3]. The fluorescence and excitation wavelengths were 310 and 280 nm, respectively, and the slit dials were set to give a bandpass of 8 nm for excitation and of 5 nm for fluorescence. The concentrations of the drug and its metabolites in the sample were read from a calibration curve whose validity was determined by including three or four known concentrations of dextrorphan added to normal human plasma with each series of unknowns.

Bioavailability Studies in Humans—Six healthy male volunteers, 27–32 years old, received 30 mg po of dextromethorphan hydrobromide in a syrup (10 ml) after an overnight fast. Blood samples were drawn from the antecubetal vein into heparinized tubes immediately prior to and at 15 and 30 min and 1, 2, and 4 hr after drug administration. Plasma was separated by centrifuging at 3000 rpm for 20 min, and an aliquot was assayed by the described procedure.

RESULTS AND DISCUSSION

A calibration curve was constructed by plotting the fluorescence intensity against the concentration of dextrorphan added to drug-free plasma. Regression analysis of the least-squares line fitting the data points provided an equation for the curve as $y = 0.2658x + 3.728$ ($r = 0.9956$), where y represents fluorescence units and x is nanograms of dextrorphan per milliliter of plasma. The recovery of known amounts of dextrorphan added to human plasma was 70%. To determine the precision of the method, eight plasma samples spiked with 400 ng of dextrorphan/ml and four samples containing 600 ng of dextrorphan/ml were analyzed in duplicate over 6 months. The coefficients of variation at these two concentrations were 8 and 4%, respectively.

The fluorescence characteristics of dextrorphan and dextromethorphan in 1.0 *N* hydrochloric acid are rather similar. The fluorescence and excitation wavelengths of dextrorphan are 310 and 280 nm, respectively; for dextromethorphan, they are 305 and 270 nm, respectively.

The fluorescence spectrum of dextrorphan extracted from plasma was identical with that of dextrorphan in 1.0 *N* HCl. Some interference by the unmetabolized drug and possibly other minor metabolites could be expected in the measurement of dextrorphan levels. However, the contribution to fluorescence by the unmetabolized drug would be negligible in this method because extracts from plasma of humans administered dextromethorphan hydrobromide exhibited fluorescence spectra characteristic of dextrorphan but not dextromethorphan. Furthermore, since dextromethorphan is metabolized rapidly and extensively upon oral administration, the amount present in the extracts would be very low.

Plasma Levels in Humans—The average plasma levels ($\pm SE$) of dextrorphan and its conjugates following 30 mg po of dextromethorphan hydrobromide to six volunteers at 15, 30, and 60 min were 21.3 ± 6.7, 107.3 ± 44.6, and 368.0 ± 71.2 ng/ml, respectively. The peak level was 381.3 ± 56.9 ng/ml at 2 hr and it declined thereafter, reaching 262.7 ± 43.3 ng/ml at 4 hr. Almost all of the dextrorphan was present in the form of conjugates. This finding was confirmed by analyzing the plasma samples from one of the six volunteers, with and without enzymatic hydrolysis. Whereas hydrolysis gave rise to concentrations ranging from 26 to 380 ng/ml, none of the unhydrolyzed samples contained measurable levels of the unconjugated drug or metabolites.

It may be concluded that this method is applicable to the determination of the bioavailability of dextromethorphan hydrobromide in humans.

[3] Perkin-Elmer model MPF-3.

REFERENCES

(1) J. A. F. de Silva and L. D'Arconte, *J. Forensic Sci.*, **14**, 184 (1969).

(2) J. Axelrod, *J. Pharmacol. Exp. Ther.*, **117**, 322 (1956).

(3) C. Elison and H. Elliott, *ibid.*, **144**, 265 (1964).

(4) J. Kamm, A. Taddeo, and E. Van Loon, *ibid.*, **158**, 437 (1967).

(5) A. Brossi, O. Haffliger, and O. Schneider, *Arzneim.-Forsch.*, **5**, 62 (1955).

(6) K. Willner, *ibid.*, **13**, 20 (1963).

(7) H. Kaiser and H. Jori, *Arch. Pharm.*, **287**, 224 (1954).

(8) P. A. Shore, J. Axelrod, C. A. M. Hogben, and B. B. Brodie, *J. Pharmacol. Exp. Ther.* **113**, 192 (1955).

(9) K. D. Wuepper, S. Y. Yeh, and L. A. Woods, *Proc. Soc. Exp. Biol. Med.*, **124**, 1146 (1967).

ACKNOWLEDGMENTS AND ADDRESSES

Received April 10, 1974, from the *Warner–Lambert Research Institute, Morris Plains, NJ 07950.*

Accepted for publication August 18, 1976.

Presented at the 57th Annual Meeting of the Federation of the American Societies for Experimental Biology, Atlantic City, N.J., April 1973.

[x] To whom inquiries should be directed. Present address: Division of Drug Metabolism and Biopharmaceutics, Department of Medicinal Chemistry, College of Pharmacy, University of Tennessee Center for the Health Sciences, Memphis, TN 38163.

Effects of 3,4-Dimethoxyphenethylamine Derivatives on Monoamine Oxidase

WILLIAM J. KELLER [x] and GARY G. FERGUSON

Abstract □ The cactus alkaloid 3,4-dimethoxyphenethylamine and its naturally occurring *N*-methylated homologs inhibited the deamination of tyramine and tryptamine by rat brain monoamine oxidase. In contrast, the β-hydroxylated derivatives of this series failed to inhibit the action of monoamine oxidase on both tyramine and tryptamine.

Keyphrases □ 3,4-Dimethoxyphenethylamine and *N*-methyl homologs—effect on monoamine oxidase-catalyzed deamination of tyramine and tryptamine □ Monoamine oxidase—deamination of tyramine and tryptamine, effect of 3,4-dimethoxyphenethylamine and *N*-methyl homologs □ Tyramine—monoamine oxidase-catalyzed oxidative deamination, effect of 3,4-dimethoxyphenethylamine and *N*-methyl homologs □ Tryptamine—monoamine oxidase-catalyzed deamination, effect of 3,4-dimethoxyphenethylamine and *N*-methyl homologs □ Enzymes—monoamine oxidase, deamination of tyramine and tryptamine, effect of 3,4-dimethoxyphenethylamine and *N*-methyl homologs □ Structure–activity relationships—3,4-dimethoxyphenethylamine and *N*-methyl homologs, effect on monoamine oxidase-catalyzed deamination of tyramine and tryptamine

The present study was directed at observing the effects of 3,4-dimethoxyphenethylamine (I) and its *N*-methyl homologs on rat brain monoamine oxidase, using both tyramine and tryptamine as substrates. The results of these experiments were contrasted with those obtained with the β-hydroxy derivatives of the same series. The al-

Table I—Inhibiting Effects of Compounds on Oxidation of Tyramine Hydrochloride and Tryptamine Hydrochloride by Rat Brain Mitochondria [a]

Compound	Inhibition, %	Tyramine Hydrochloride Significance	Tyramine Hydrochloride SD	Tryptamine Hydrochloride Inhibition, %	Tryptamine Hydrochloride Significance	Tryptamine Hydrochloride SD
I	32	+	1.3	27	+	0.7
II	49	+	1.3	27	+	1.3
III	33	+	1.1	37	+	1.3
IV	7	−	2.6	19	−	2.3
V	7	−	2.6	19	−	3.2
VI	0	−	2.8	16	−	2.9
Isocarboxazid [b]	100	+	1.5	67	+	1.0

[a] Each value represents the results obtained using three or more flasks per compound for each substrate. Percent inhibition was calculated by comparing control and experimental values for each compound with each substrate. [b] Reference.

leged mind-altering effects produced by ingesting cacti containing one or more of the test compounds could be partially explained by data generated from this investigation.

BACKGROUND

Many members of the Cactaceae produce and accumulate various derivatives of I. Compound I was detected in several species of *Trichocereus* (1–3), *Echinocereus merkeri* Hildm. (4), *Pelecyphora aselliformis* Ehrenberg (5), *Stetsonia coryne* (SD.)-Br. and R. (3), and *Lophophora williamsii* (Lem.) Coult. (6). *N*-Methyl-3,4-dimethoxyphenethylamine (II) was identified as a natural product (2) and was isolated from numerous cacti (4, 5, 7–15). The *N,N*-dimethyl derivative of I has a more restricted distribution in nature, having been originally isolated from extracts of *E. merkeri* (4) and subsequently found to be present in *Coryphantha greenwoodii* H. Bravo (14) and *Ariocarpus scapharostrus* Bodeker (15).

N-Methylated homologs of 3,4-dimethoxy-β-hydroxyphenethylamine are particularly abundant in the cactus genus *Coryphantha*. Macromerine [2-hydroxy-2-(3,4-dimethoxyphenyl)-*N,N*-dimethylethylamine] occurs naturally in *C. macromeris* (Engelm.) Lem. (16) and several other *Coryphantha* species (10, 11, 17).

Normacromerine [2-hydroxy-2-(3,4-dimethoxyphenyl)-*N*-methylethylamine] was isolated from *C. macromeris* (Engelm.) Br. and R. var. *runyonii* L. Benson (18) and two other *Coryphantha* species (13, 14), *Dolichothele longimamma* (DC.) Br. and R. (19), and a legume, *Desmodium tiliaefolium* G. Don. (20). The parent compound of this series is not a natural product.

L. williamsii and the various *Trichocereus* species are hallucinogenic because of their mescaline content. The other previously mentioned cacti are suspected of containing psychoactive substances because of various folkloric tales. Recently, the monoamine oxidase inhibitory activity of 4-methoxylated phenethylamines was used in an attempt to explain the purported pharmacological activity of cactus plants containing these compounds (21). The hypothesis was expanded when a series of β-hydroxylated 4-methoxyphenethylamines was observed to inhibit selectively enzymatic oxidative deamination of tyramine but not tryptamine (22).

EXPERIMENTAL

Synthesis—Compound I hydrochloride[1] was available commercially and served as the starting point for the *N*-methylation reactions that yielded the other two members of this series. Compound II hydrochloride, mp 132–134° [lit. (4) mp 134–136°], was synthesized by reacting I with 36% formaldehyde[2] followed by a sodium borohydride reduction of the Schiff-base intermediate. Refluxing equimolar quantities of II, 36% formaldehyde, and 88% formic acid[3] gave *N,N*-dimethyl-3,4-dimethoxyphenethylamine (III) hydrochloride, mp 193–194° [lit. (4) mp 193–196°].

Racemic 3,4-dimethoxy-β-hydroxyphenethylamine (IV) hydrochloride, mp 170–171° [lit. (23) mp 170–171°], *N*-methyl-3,4-dimethoxy-β-hydroxyphenethylamine (V) hydrochloride, mp 115–116° [lit. (18) mp 115–117°], and *N,N*-dimethyl-3,4-dimethoxy-β-hydroxyphenethylamine (VI) hydrochloride, mp 161–162° [lit. (23) mp 161–162°], were produced by a Houben–Hoesch condensation of veratrole[3] with aminoacetonitrile hydrochloride[4], *N*-methylaminoacetonitrile hydrochloride[4], and *N,N*-dimethylaminoacetonitrile hydrochloride[4], respectively, followed by a reduction of the ketone intermediate with sodium borohydride.

Warburg Studies—As an evaluation of possible monoamine oxidase inhibition, the effects of the compounds on the oxidation of tyramine and tryptamine hydrochlorides by rat brain mitochondria were investigated. Brain mitochondria (containing monoamine oxidase) were prepared from albino Wistar female rats, 150–200 g, according to the method of Brody and Bain (24). Monoamine oxidase activity was determined in the presence and absence of the respective compounds by conventional manometric techniques (25)[5].

In the manometric determinations, the main compartment of the Warburg flasks contained 0.8 ml of a 0.1 *M* buffered solution of the compound studied (or buffer), 1 ml of mitochondrial suspension (representing 500 mg wet weight of original brain tissue), and sufficient 0.01 *M* phosphate buffer (pH 7.4) to make a total volume of 2.7 ml. All aliquots for a given run were taken from the same mitochondrial preparation. The side arm of each flask contained 0.3 ml of 0.1 *M* tyramine or tryptamine hydrochloride. After the flasks were allowed to equilibrate for 15 min at 37°, the manometer valves were closed and the side arm contents of each were tipped in.

Manometers were set at 150 mm, and readings were taken at 15-min intervals for 90 min. Values for the 90-min reaction period were obtained for each flask and were multiplied by the respective flask constants after adjusting for changes in the thermobarometer. The total microliters of oxygen uptake for each flask was thus obtained.

Reference flasks, using 0.05 *M* isocarboxazid (0.8 ml) as the monoamine oxidase inhibitor, were employed as already described and were used for comparison.

Statistical Analysis—The mean and standard error were determined for each control or treated group. Values thus obtained were compared, using the difference between the means and the standard error of the difference between the means for the respective control-treated pairs of groups. The Student *t* test was applied to the results, and the probability was determined (p values of less than 0.05 were considered significant).

RESULTS AND DISCUSSION

Data from Warburg studies revealed that I–III produced significant ($p < 0.05$) inhibition of rat brain monoamine oxidase when tyramine and tryptamine were used as substrates. Conversely, the β-hydroxylated derivatives of this series (IV–VI) had little effect on the enzymatic oxidative deamination of tyramine and tryptamine. These results were validated by the activity exhibited by reference isocarboxazid (Table I).

Substrate selectivity was observed with an *N*-methylated series of 4-methoxy-β-hydroxyphenethylamines, with each member inhibiting the action of monoamine oxidase on tyramine but not on tryptamine (22). The same series of compounds without the β-hydroxy group inhibited monoamine oxidase with respect to both tyramine and tryptamine. Johnston (26) found that there are at least two forms of monoamine oxidase in rat brain, while Tabakoff *et al.* (27) suggested that separate interacting sites exist in brain monoamine oxidase for the binding of phenethylamines and for compounds possessing an indole nucleus. With this information, it was proposed that the presence of a β-hydroxy group in the 4-methoxyphenethylamine moiety interferes with the binding of

[1] Calbiochem.
[2] Fisher Scientific Co.
[3] Aldrich Chemical Co.
[4] K and K Laboratories.
[5] Precision Warburg apparatus, Precision Scientific Co.

these derivatives with the active site and/or isozyme responsible for the oxidation of tryptamine (22). From these suppositions, it appears that a 3,4-dimethoxyphenethylamine nucleus with a β-hydroxy group cannot properly bind with the active site and/or isozyme associated with both tyramine and tryptamine oxidation.

The monoamine oxidase inhibitory activity of 4-methoxyphenethylamine derivatives has been used to explain the folkloric uses of *D. longimamma* as a psychoactive "peyote" cactus (19). Macromerine and normacromerine are the major alkaloids in *C. macromeris* var. *runyonii* (11), and this cactus was reported to be psychoactive (16, 28). Vogel *et al.* (29) concluded that macromerine and normacromerine were not responsible for the psychoactivity, since they produced no effects on the conditioned avoidance response in rats. Since macromerine and normacromerine are devoid of monoamine oxidase inhibitory activity, there appears to be no correlation between the presence of these compounds and the purported psychoactivity of *C. macromeris* var. *runyonii*.

Harley-Mason (30) predicted that an abnormal methylation of dopamine and/or norepinephrine *in vivo* could produce I or IV. Of these compounds, I received wide attention because of its detection in the urine of schizophrenics (31). Later studies revealed that urinary excretion of I is not unique to schizophrenia (32) and that administration of this compound to humans produces no psychological changes (33, 34). However, the ingestion of cacti containing I and/or its *N*-methyl derivatives together with indirectly acting amines such as synephrine could alter behavior by inhibiting monoamine oxidase and thus potentiating the effects of the indirectly acting amines. This may be the case with the supposedly psychoactive *C. macromeris* var. *runyonii*. Although the major alkaloids do not inhibit monoamine oxidase, this cactus does contain two known monoamine oxidase inhibitors, *N*-methyl-4-methoxyphenethylamine and II, together with several indirectly acting amines (11). This situation may also contribute to the well-documented hallucinogenic activity of the mescaline-containing cacti.

REFERENCES

(1) S. Agurell, *Lloydia*, **32**, 40 (1969).

(2) *Ibid.*, **32**, 206 (1969).

(3) S. Agurell, J. G. Bruhn, J. Lundstrom, and U. Svensson, *Lloydia*, **34**, 183 (1971).

(4) S. Agurell, J. Lundstrom, and A. Masoud, *J. Pharm. Sci.*, **58**, 1413 (1969).

(5) J. M. Neal, P. T. Sato, W. N. Howald, and J. L. McLaughlin, *Science*, **176**, 1131 (1972).

(6) J. Lundstrom and S. Agurell, *J. Chromatogr.*, **36**, 105 (1968).

(7) D. G. Norquist and J. L. McLaughlin, *J. Pharm. Sci.*, **59**, 1840 (1970).

(8) W. W. Speir, V. Mihranian, and J. L. McLaughlin, *Lloydia*, **33**, 15 (1970).

(9) J. M. Neal and J. L. McLaughlin, *ibid.*, **33**, 395 (1970).

(10) K. M. K. Hornemann, J. M. Neal, and J. L. McLaughlin, *J. Pharm. Sci.*, **61**, 41 (1972).

(11) W. J. Keller, J. L. McLaughlin, and L. R. Brady, *ibid.*, **62**, 408 (1973).

(12) J. G. Bruhn and C. Bruhn, *Econ. Bot.*, **27**, 241 (1973).

(13) J. G. Bruhn and S. Agurell, *J. Pharm. Sci.*, **63**, 574 (1974).

(14) J. G. Bruhn, S. Agurell, and J. E. Lindgren, *Acta Pharm. Suec.*, **12**, 199 (1975).

(15) J. G. Bruhn, *Phytochemistry*, **14**, 2509 (1975).

(16) J. E. Hodgkins, S. D. Brown, and J. L. Massingill, *Tetrahedron Lett.*, **14**, 1321 (1967).

(17) L. E. Below, A. Y. Leung, J. L. McLaughlin, and A. G. Paul, *J. Pharm. Sci.*, **57**, 515 (1968).

(18) W. J. Keller and J. L. McLaughlin, *ibid.*, **61**, 147 (1972).

(19) R. L. Ranieri and J. L. McLaughlin, *J. Org. Chem.*, **41**, 319 (1976).

(20) S. Ghosal and R. S. Srivastava, *Phytochemistry*, **12**, 193 (1973).

(21) G. G. Ferguson and W. J. Keller, *J. Pharm. Sci.*, **64**, 1431 (1975).

(22) W. J. Keller and G. G. Ferguson, *ibid.*, **65**, 1539 (1976).

(23) W. J. Keller, Ph.D. dissertation, University of Washington, Seattle, Wash., 1972.

(24) T. M. Brody and J. A. Bain, *J. Biol. Chem.*, **195**, 685 (1952).

(25) W. W. Umbreit, R. H. Burris, and J. F. Stauffer, "Manometric Techniques," 4th ed., Burgess, Minneapolis, Minn., 1964, pp. 61, 76.

(26) J. P. Johnston, *Biochem. Pharmacol.*, **17**, 1285 (1968).

(27) B. Tabakoff, L. R. Meyerson, and S. G. A. Alivisatos, *Brain Res.*, **66**, 491 (1974).

(28) M. J. Superweed, "Herbal Highs," Stone Kingdom Syndicate, San Francisco, Calif., 1970, p. 5.

(29) W. H. Vogel, B. D. Evans, E. M. Bonnem, J. F. Fischer, and J. L. McLaughlin, *Psychopharmacologia*, **30**, 145 (1973).

(30) J. Harley-Mason, *J. Ment. Sci.*, **98**, 313 (1952).

(31) A. J. Friedhoff and E. Van Winkle, *Nature*, **194**, 897 (1962).

(32) A. A. Boulton, *Nature*, **231**, 22 (1971).

(33) L. E. Hollister and A. J. Friedhoff, *ibid.*, **210**, 1377 (1966).

(34) A. T. Shulgin, T. Sargent, and C. Naranjo, *ibid.*, **212**, 1606 (1966).

ACKNOWLEDGMENTS AND ADDRESSES

Received July 29, 1976, from the *School of Pharmacy, Northeast Louisiana University, Monroe, LA 71209.*

Accepted for publication August 18, 1976.

[x] To whom inquiries should be directed.

Alkaloids of *Papaver orientale* L.

A. SHAFIEE [x], I. LALEZARI, F. ASSADI, and F. KHALAFI

Abstract □ According to the alkaloid profiles, five different chemotypes (A, B, C, D, and E) were classified in *Papaver orientale* L. with haploid chromosome number $n = 14$. Chemotype A had only oripavine; chemotype B contained oripavine and thebaine; chemotype C had isothebaine in addition to oripavine; chemotype D contained oripavine and alpinigenine; and chemotype E had oripavine, thebaine, and alpinigenine. In all chemotypes, oripavine was either the sole alkaloid or the single major alkaloid.

Keyphrases □ *Papaver orientale* L.—chloroform extract of seed capsules, alkaloids isolated and identified, five chemotypes classified □ Alkaloids—isolated and identified, chloroform extract of seed capsules of *Papaver orientale* L., five chemotypes classified

In continuation of a broad study of the Iranian wild Papaveraceae (1–5), alkaloids of *Papaver pseudo-orientale* Fedde. and preliminary results on the alkaloids of *P. orientale* L. were reported (4). In this work, qualitative and

these derivatives with the active site and/or isozyme responsible for the oxidation of tryptamine (22). From these suppositions, it appears that a 3,4-dimethoxyphenethylamine nucleus with a β-hydroxy group cannot properly bind with the active site and/or isozyme associated with both tyramine and tryptamine oxidation.

The monoamine oxidase inhibitory activity of 4-methoxyphenethylamine derivatives has been used to explain the folkloric uses of *D. longimamma* as a psychoactive "peyote" cactus (19). Macromerine and normacromerine are the major alkaloids in *C. macromeris* var. *runyonii* (11), and this cactus was reported to be psychoactive (16, 28). Vogel *et al.* (29) concluded that macromerine and normacromerine were not responsible for the psychoactivity, since they produced no effects on the conditioned avoidance response in rats. Since macromerine and normacromerine are devoid of monoamine oxidase inhibitory activity, there appears to be no correlation between the presence of these compounds and the purported psychoactivity of *C. macromeris* var. *runyonii*.

Harley-Mason (30) predicted that an abnormal methylation of dopamine and/or norepinephrine *in vivo* could produce I or IV. Of these compounds, I received wide attention because of its detection in the urine of schizophrenics (31). Later studies revealed that urinary excretion of I is not unique to schizophrenia (32) and that administration of this compound to humans produces no psychological changes (33, 34). However, the ingestion of cacti containing I and/or its *N*-methyl derivatives together with indirectly acting amines such as synephrine could alter behavior by inhibiting monoamine oxidase and thus potentiating the effects of the indirectly acting amines. This may be the case with the supposedly psychoactive *C. macromeris* var. *runyonii*. Although the major alkaloids do not inhibit monoamine oxidase, this cactus does contain two known monoamine oxidase inhibitors, *N*-methyl-4-methoxyphenethylamine and II, together with several indirectly acting amines (11). This situation may also contribute to the well-documented hallucinogenic activity of the mescaline-containing cacti.

REFERENCES

(1) S. Agurell, *Lloydia*, **32**, 40 (1969).

(2) *Ibid.*, **32**, 206 (1969).

(3) S. Agurell, J. G. Bruhn, J. Lundstrom, and U. Svensson, *Lloydia*, **34**, 183 (1971).

(4) S. Agurell, J. Lundstrom, and A. Masoud, *J. Pharm. Sci.*, **58**, 1413 (1969).

(5) J. M. Neal, P. T. Sato, W. N. Howald, and J. L. McLaughlin, *Science*, **176**, 1131 (1972).

(6) J. Lundstrom and S. Agurell, *J. Chromatogr.*, **36**, 105 (1968).

(7) D. G. Norquist and J. L. McLaughlin, *J. Pharm. Sci.*, **59**, 1840 (1970).

(8) W. W. Speir, V. Mihranian, and J. L. McLaughlin, *Lloydia*, **33**, 15 (1970).

(9) J. M. Neal and J. L. McLaughlin, *ibid.*, **33**, 395 (1970).

(10) K. M. K. Hornemann, J. M. Neal, and J. L. McLaughlin, *J. Pharm. Sci.*, **61**, 41 (1972).

(11) W. J. Keller, J. L. McLaughlin, and L. R. Brady, *ibid.*, **62**, 408 (1973).

(12) J. G. Bruhn and C. Bruhn, *Econ. Bot.*, **27**, 241 (1973).

(13) J. G. Bruhn and S. Agurell, *J. Pharm. Sci.*, **63**, 574 (1974).

(14) J. G. Bruhn, S. Agurell, and J. E. Lindgren, *Acta Pharm. Suec.*, **12**, 199 (1975).

(15) J. G. Bruhn, *Phytochemistry*, **14**, 2509 (1975).

(16) J. E. Hodgkins, S. D. Brown, and J. L. Massingill, *Tetrahedron Lett.*, **14**, 1321 (1967).

(17) L. E. Below, A. Y. Leung, J. L. McLaughlin, and A. G. Paul, *J. Pharm. Sci.*, **57**, 515 (1968).

(18) W. J. Keller and J. L. McLaughlin, *ibid.*, **61**, 147 (1972).

(19) R. L. Ranieri and J. L. McLaughlin, *J. Org. Chem.*, **41**, 319 (1976).

(20) S. Ghosal and R. S. Srivastava, *Phytochemistry*, **12**, 193 (1973).

(21) G. G. Ferguson and W. J. Keller, *J. Pharm. Sci.*, **64**, 1431 (1975).

(22) W. J. Keller and G. G. Ferguson, *ibid.*, **65**, 1539 (1976).

(23) W. J. Keller, Ph.D. dissertation, University of Washington, Seattle, Wash., 1972.

(24) T. M. Brody and J. A. Bain, *J. Biol. Chem.*, **195**, 685 (1952).

(25) W. W. Umbreit, R. H. Burris, and J. F. Stauffer, "Manometric Techniques," 4th ed., Burgess, Minneapolis, Minn., 1964, pp. 61, 76.

(26) J. P. Johnston, *Biochem. Pharmacol.*, **17**, 1285 (1968).

(27) B. Tabakoff, L. R. Meyerson, and S. G. A. Alivisatos, *Brain Res.*, **66**, 491 (1974).

(28) M. J. Superweed, "Herbal Highs," Stone Kingdom Syndicate, San Francisco, Calif., 1970, p. 5.

(29) W. H. Vogel, B. D. Evans, E. M. Bonnem, J. F. Fischer, and J. L. McLaughlin, *Psychopharmacologia*, **30**, 145 (1973).

(30) J. Harley-Mason, *J. Ment. Sci.*, **98**, 313 (1952).

(31) A. J. Friedhoff and E. Van Winkle, *Nature*, **194**, 897 (1962).

(32) A. A. Boulton, *Nature*, **231**, 22 (1971).

(33) L. E. Hollister and A. J. Friedhoff, *ibid.*, **210**, 1377 (1966).

(34) A. T. Shulgin, T. Sargent, and C. Naranjo, *ibid.*, **212**, 1606 (1966).

ACKNOWLEDGMENTS AND ADDRESSES

Received July 29, 1976, from the *School of Pharmacy, Northeast Louisiana University, Monroe, LA 71209.*

Accepted for publication August 18, 1976.

[x] To whom inquiries should be directed.

Alkaloids of *Papaver orientale* L.

A. SHAFIEE [x], I. LALEZARI, F. ASSADI, and F. KHALAFI

Abstract □ According to the alkaloid profiles, five different chemotypes (A, B, C, D, and E) were classified in *Papaver orientale* L. with haploid chromosome number $n = 14$. Chemotype A had only oripavine; chemotype B contained oripavine and thebaine; chemotype C had isothebaine in addition to oripavine; chemotype D contained oripavine and alpinigenine; and chemotype E had oripavine, thebaine, and alpinigenine. In all chemotypes, oripavine was either the sole alkaloid or the single major alkaloid.

Keyphrases □ *Papaver orientale* L.—chloroform extract of seed capsules, alkaloids isolated and identified, five chemotypes classified □ Alkaloids—isolated and identified, chloroform extract of seed capsules of *Papaver orientale* L., five chemotypes classified

In continuation of a broad study of the Iranian wild Papaveraceae (1–5), alkaloids of *Papaver pseudo-orientale* Fedde. and preliminary results on the alkaloids of *P. orientale* L. were reported (4). In this work, qualitative and

Table I—Classification of *P. orientale* L.

Population	Chemotype	Oripavine[a], %	Thebaine[a], %	Isothebaine[a], %	Alpinigenine[a], %
Khalkhal	A	1.15	None	None	None
	B	0.85	0.15	None	None
	C	0.5	None	0.3	None
Siah Cheshmeh	A	1	None	None	None
	B	0.8	0.1	None	None
	D	0.5	None	None	0.3
Guleh Khaneh	A	1.2	None	None	None
	B	0.88	0.4	None	None
	E	0.8	0.35	None	0.05
Shuran	A	1.25	None	None	None
	E	1.2	0.3	None	0.05

[a] The percentages of the alkaloids were based on the dried seedless capsules.

quantitative results on the alkaloid content of *P. orientale* L.[1] are reported.

BACKGROUND

P. orientale L. is a perennial wild poppy growing in the north and northwest of Iran at 2000–2500 m above sea level. The height of the plant is 30–70 cm (occasionally 1 m), bearing one to four flowering stems and usually four, rarely six, pale-orange petals with no marking above the base. The petals distinguish *P. orientale* L. from *P. bracteatum* Lindl. and *P. pseudo-orientale* Fedde. In addition, *P. orientale* L. lacks bracts while the other two species have bracts.

P. orientale L. is the only species in section oxytona that can be regarded as truly alpine, though it also grows at low altitudes with *P. pseudo-orientale* Fedde. in moist, sheltered areas. It blooms in late June at low elevations, but flowering continues until early September at high altitudes and on open slopes.

Three species of section oxytona were classified according to their haploid chromosome numbers: *P. bracteatum* Lindl., $n = 7$; *P. orientale* L., $n = 14$; and *P. pseudo-orientale* Fedde., $n = 21$ (6).

Extensive chemical studies in section oxytona revealed that *P. bracteatum* Lindl. contained thebaine (1, 3) or thebaine along with alpinigenine (2, 7, 8). *P. pseudo-orientale* Fedde. contained isothebaine as a major alkaloid and orientalidine, bracteolin, salutaridine, Or_1, Or_2, PO-4, alborine (PO-5), and aryapavine as minor alkaloids (4). Some workers found oripavine in *P. orientale* L. (9, 10), while others reported the same alkaloid in *P. bracteatum* Lindl. (11). These results suggest that the previous alkaloid accounts are unreliable with respect to species determination (6).

To clarify present uncertainties, the alkaloid contents of the capsules of *P. orientale* L., collected from Shuran, Zinjinab, Siah Cheshmeh, Khalkhal, and Guleh Khaneh, were isolated and studied.

EXPERIMENTAL[2]

A small portion (about 100 mg) of individual capsules collected from each region was ground, moistened with ammonia, and extracted exhaustively with chloroform (5 × 5 ml) at room temperature. The solvent was evaporated, and the residue was chromatographed [TLC, silica gel, ethyl acetate–methanol–ammonia (85:10:5)]. The spots were detected first under the UV lamp and then were developed with Dragendorf reagent.

For semiquantitative analysis, the remaining individual capsules, which were chemically similar by TLC and were collected from the same geographical source, were mixed to obtain about 50 g of dried material. These capsules were powdered so that all of the material possessed a mesh size not greater than 0.5 mm. The powder was moistened with ammonia, macerated with 200 ml of chloroform overnight at room temperature, and filtered. This procedure was repeated three more times. The chloroform was evaporated under reduced pressure, and the residue was treated with dilute acetic acid (20%, 20 ml) and filtered. The residue was then washed with water (20 ml).

The combined aqueous solutions were made alkaline with ammonia and extracted with chloroform (4 × 25 ml). The organic layer was dried (sodium sulfate), filtered, and evaporated to give the crude total alkaloids. The crude extract was subjected to preparative TLC [silica gel, ethyl acetate–methanol–ammonia (85:10:5)], and each alkaloid was eluted with chloroform–methanol (80:20). The solvent was evaporated and weighed to determine the percentage of alkaloid. The residue was crystallized from an appropriate solvent and characterized (see *Results and Discussion* and Table I).

RESULTS AND DISCUSSION

The following alkaloids were isolated by TLC and characterized.

1. Oripavine (I): R_f 0.36, mp 201–203° (ethanol) [lit. (4, 9) mp 201–203°], mixed melting point with an authentic sample 201–203°; NMR (deuterochloroform): δ 6.50 (broad s, 2H, aromatic), 5.90–5.63 (broad s, 1H, OH), 5.50 (d, 1H, H-7 or 8), 5.23 (s, 1H, H-5), 5.0 (d, 1H, H-8 or 7), 3.56 (s, 3H, CH_3O), and 2.43 (s, 3H, NCH_3) ppm; $[\alpha]_D^{20}$ −216.9° (c = 3.44, $CHCl_3$) [lit. (9) $[\alpha]_D^{20}$ −211.8°]; UV_{max} (ethanol): 283 (log ε 3.90) nm; *m/e*: 297 (M^+).

Anal.—Calc. for $C_{18}H_{19}NO_3$: C, 72.73; H, 6.39; N, 4.71. Found: C, 72.85; H, 6.41; N, 4.65.

The reaction of oripavine with diazomethane in methanol–ether afforded, in quantitative yield, thebaine (II), mp 193° (ethanol), mixed melting point with an authentic sample 193° (1). The spectral data (IR, UV, NMR, and mass) were identical with an authentic sample.

2. Thebaine (II): R_f 0.36, mp 193° (ethanol) [lit. (1) mp 193°], mixed melting point with an authentic sample 193°. The spectral data (IR, UV, NMR, and mass) were identical with an authentic sample.

3. Isothebaine: R_f 0.43, mp 203–204° [lit. (4, 12) mp 203–204°], mixed melting point with an authentic sample 203–204°; NMR ($CDCl_3$): δ 7.63 (broad s, 1H, OH), 7.30–6.70 (m, 3H, aromatic), 6.53 (s, 1H, H-3), 3.88 (s, 3H, OCH_3), 3.82 (s, 3H, OCH_3), and 2.47 (s, 3H, NCH_3) ppm (13); $[\alpha]_D^{20}$ +275° (c = 1.47, $CHCl_3$) [lit. (14) $[\alpha]_D^{21}$ 281 ± 10°]; UV_{max} (methanol): 270

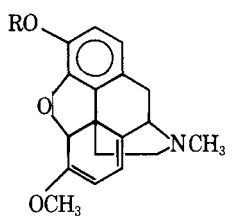

I: R = H
II: R = CH_3

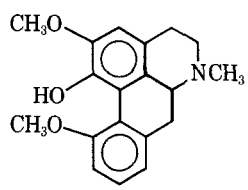

III

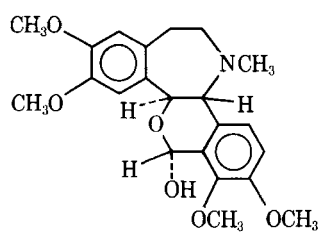

IV

[1] The plant was identified by P. Goldblatt, Missouri Botanical Garden, St. Louis, Mo. Herbarium samples were deposited in the Missouri Botanical Garden. (Also see Ref. 6.)

[2] Melting points were taken with a Koffler hot-stage microscope and are uncorrected. UV spectra were recorded on a Varian Techtron 635 instrument. NMR spectra were taken with a Varian A60A instrument. Mass spectra were recorded on a CH5 spectrometer at Aryamehr Technical University. IR spectra were obtained with a Leitz Model III spectrograph. The optical rotation was measured with a Perkin-Elmer polarimeter model 241 instrument. For qualitative detection of alkaloids, the silica gel was DC-Karten SI F from Riedel (West Germany).

(log ϵ 4.16) nm; *m/e*: 311 (M^+).

Anal.—Calc. for $C_{19}H_{21}NO_3$: C, 73.31; H, 6.75; N, 4.50. Found: C, 73.21; H, 6.81; N, 4.58.

4. Alpinigenine: R_f 0.68, mp 185–186° [lit. (2) mp 185–186°], mixed melting point with an authentic sample 185–186°; $[\alpha]_D^{20}$ +230.2° (c = 1.59, $CHCl_3$) [lit. (15) $[\alpha]_D^{20}$ +286°]. The spectral data (IR, UV, NMR, and mass) were identical with an authentic sample (2).

The alkaloid profiles of *P. orientale* L. from different geographical areas suggested classification according to five different chemotypes (Table I). Oripavine was either a sole alkaloid of the poppy (chemotype A) or a single major alkaloid (chemotypes B, C, D, and E).

A literature survey (16) revealed that alpinigenine was not found previously in *P. orientale* L.

REFERENCES

(1) N. Sharghi and I. Lalezari, *Nature*, **213**, 1244 (1967).

(2) I. Lalezari, A. Shafiee, and P. Nasseri-Nouri, *J. Pharm. Sci.*, **62**, 1718 (1973).

(3) I. Lalezari, P. Nasseri-Nouri, and R. Asgharian, *ibid.*, **63**, 1331 (1974).

(4) A. Shafiee, I. Lalezari, P. Nasseri-Nouri, and R. Asgharian, *ibid.*, **64**, 1570 (1975).

(5) I. Lalezari, A. Shafiee, and M. Mahjour, *ibid.*, **65**, 923 (1976).

(6) P. Goldblatt, *Ann. Mo. Bot. Gard.*, **61**, 264 (1974).

(7) H. Boehm and H. Roensch, *Z. Naturforsch. B*, **23**, 1552 (1968).

(8) H. Boehm, *Biochem. Physiol. Pflanz.*, **162**, 476 (1971).

(9) R. Konowalowa, S. Yunussoff, and A. Orechoff, *Chem. Ber.*, **68**, 2158 (1935).

(10) G. Sonja and R. F. Dawson, *Biochemistry*, **2**, 186 (1963).

(11) V. V. Kisselev and R. A. Konovalova, *J. Gen. Chem., USSR*, **18**, 142 (1048); through *Chem. Abstr.*, **42**, 5037 (1948).

(12) D. K. Keydenreich and S. Pfeifer, *Pharmazie*, **24**, 635 (1969).

(13) V. Precninger, J. Hrbeh, Jr., Z. Samek, and F. Santavy, *Arch. Pharm.*, **302**, 808 (1969).

(14) A. R. Battersby, T. H. Brown, and J. H. Clements, *J. Chem. Soc.*, **1965**, 4550.

(15) M. Maturova, D. Pavlaskova, and F. Santavy, *Planta Med.*, **14**, 22 (1966).

(16) F. Santavy, in "The Alkaloids," vol. XII, Maraske, Ed., Academic, New York, N.Y., 1970, p. 337.

ACKNOWLEDGMENTS AND ADDRESSES

Received March 22, 1976, from the *Institute of Medicinal Plants, College of Pharmacy, Tehran University, Tehran, Iran.*

Accepted for publication August 25, 1976.

Supported by the Iranian Ministry of Science and Higher Education Research Development Center.

[x] To whom inquiries should be directed.

Physiologically Active Substances from Marine Sponges IV: Heterocyclic Compounds

JOGINDER S. CHIB [x], MARTIN F. STEMPIEN, Jr., JACK T. CECIL, GEORGE D. RUGGIERI, and ROSS F. NIGRELLI

Abstract □ Several guanidine compounds were synthesized by the reaction of acid chlorides of thiophene and furan with guanidines. Some of these compounds showed antibiotic and cytotoxic activities. Series of pyrrole compounds were synthesized and found to have significant antibiotic activity.

Keyphrases □ Pyrroles, various—synthesized, evaluated for antibacterial activity □ Furans, various—synthesized, evaluated for antibacterial and cytotoxic activity □ Thiophenes, various—synthesized, evaluated for antibacterial and cytotoxic activity □ Heterocycles—various pyrroles, furans, and thiophenes synthesized, evaluated for antibacterial and cytotoxic activity □ Antibacterial activity—various pyrroles, furans, and thiophenes evaluated □ Cytotoxic activity—various furans and thiophenes evaluated □ Structure–activity relationships—various pyrroles, furans, and thiophenes evaluated for antibacterial and cytotoxic activity

Several biologically significant pyrrole (1) and indole (2, 3) derivatives have been isolated from marine sources. Most of these compounds show pronounced antibiotic activity. During the present investigation of the sponge *Agelas* sp. (JC-6), a new brominated pyrrole derivative incorporating the guanidine moiety was isolated and showed significant activity against *Escherichia coli* (4). This natural product also showed cytotoxicity against KB carcinoma cells (5). This report describes the synthesis of several pyrrole, furan, and thiophene analogs and their physiological activities.

Table I—Antibiotic Activity of Pyrrole Derivatives

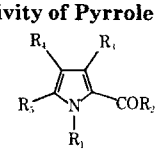

Compound	R_1	R_2	R_3	R_4	R_5	Activity against *E. coli*[a]
XII*a*	H	OCH_3	H	H	H	+++
XII*b*	H	NH_2	H	H	H	++++
XII*c*	CH_3	OCH_3	H	H	H	+++
XII*d*	CH_3	NH_2	H	H	H	++++
XII*e*	H	H	H	Br	H	++++
XII*f*	H	OCH_3	H	Br	H	++++
XII*g*	H	OCH_3	H	Br	Br	++
XII*h*	H	OCH_3	Br	Br	Br	+

[a] After paper disk incubation, zones of bacterial inhibition were measured: +, <15 mm; ++, 15–18 mm; +++, 18–22 mm; and ++++, >22 mm.

EXPERIMENTAL[1]

Chemistry—Since 2-aminopyrimidine (I*a*) and guanidine (II*a*) have a common structural unit, it was considered desirable to synthesize furan, thiophene, and pyrrole derivatives incorporating this structural feature.

[1] All melting points are uncorrected. Microanalyses were performed by Schwarzkopf Microanalytical Laboratories, Woodside, N.Y. IR spectra were recorded on a Perkin-Elmer 421 grating IR spectrometer, NMR spectra were recorded on a Varian A-60A spectrometer, and mass spectra were recorded on a Hitachi Perkin-Elmer spectrometer 107.

(log ϵ 4.16) nm; *m/e*: 311 (M^+).

Anal.—Calc. for $C_{19}H_{21}NO_3$: C, 73.31; H, 6.75; N, 4.50. Found: C, 73.21; H, 6.81; N, 4.58.

4. Alpinigenine: R_f 0.68, mp 185–186° [lit. (2) mp 185–186°], mixed melting point with an authentic sample 185–186°; $[\alpha]_D^{20}$ +230.2° (c = 1.59, $CHCl_3$) [lit. (15) $[\alpha]_D^{20}$ +286°]. The spectral data (IR, UV, NMR, and mass) were identical with an authentic sample (2).

The alkaloid profiles of *P. orientale* L. from different geographical areas suggested classification according to five different chemotypes (Table I). Oripavine was either a sole alkaloid of the poppy (chemotype A) or a single major alkaloid (chemotypes B, C, D, and E).

A literature survey (16) revealed that alpinigenine was not found previously in *P. orientale* L.

REFERENCES

(1) N. Sharghi and I. Lalezari, *Nature*, **213**, 1244 (1967).

(2) I. Lalezari, A. Shafiee, and P. Nasseri-Nouri, *J. Pharm. Sci.*, **62**, 1718 (1973).

(3) I. Lalezari, P. Nasseri-Nouri, and R. Asgharian, *ibid.*, **63**, 1331 (1974).

(4) A. Shafiee, I. Lalezari, P. Nasseri-Nouri, and R. Asgharian, *ibid.*, **64**, 1570 (1975).

(5) I. Lalezari, A. Shafiee, and M. Mahjour, *ibid.*, **65**, 923 (1976).

(6) P. Goldblatt, *Ann. Mo. Bot. Gard.*, **61**, 264 (1974).

(7) H. Boehm and H. Roensch, *Z. Naturforsch. B*, **23**, 1552 (1968).

(8) H. Boehm, *Biochem. Physiol. Pflanz.*, **162**, 476 (1971).

(9) R. Konowalowa, S. Yunussoff, and A. Orechoff, *Chem. Ber.*, **68**, 2158 (1935).

(10) G. Sonja and R. F. Dawson, *Biochemistry*, **2**, 186 (1963).

(11) V. V. Kisselev and R. A. Konovalova, *J. Gen. Chem., USSR*, **18**, 142 (1048); through *Chem. Abstr.*, **42**, 5037 (1948).

(12) D. K. Keydenreich and S. Pfeifer, *Pharmazie*, **24**, 635 (1969).

(13) V. Precninger, J. Hrbeh, Jr., Z. Samek, and F. Santavy, *Arch. Pharm.*, **302**, 808 (1969).

(14) A. R. Battersby, T. H. Brown, and J. H. Clements, *J. Chem. Soc.*, **1965**, 4550.

(15) M. Maturova, D. Pavlaskova, and F. Santavy, *Planta Med.*, **14**, 22 (1966).

(16) F. Santavy, in "The Alkaloids," vol. XII, Maraske, Ed., Academic, New York, N.Y., 1970, p. 337.

ACKNOWLEDGMENTS AND ADDRESSES

Received March 22, 1976, from the *Institute of Medicinal Plants, College of Pharmacy, Tehran University, Tehran, Iran.*

Accepted for publication August 25, 1976.

Supported by the Iranian Ministry of Science and Higher Education Research Development Center.

[x] To whom inquiries should be directed.

Physiologically Active Substances from Marine Sponges IV: Heterocyclic Compounds

JOGINDER S. CHIB [x], MARTIN F. STEMPIEN, Jr., JACK T. CECIL, GEORGE D. RUGGIERI, and ROSS F. NIGRELLI

Abstract □ Several guanidine compounds were synthesized by the reaction of acid chlorides of thiophene and furan with guanidines. Some of these compounds showed antibiotic and cytotoxic activities. Series of pyrrole compounds were synthesized and found to have significant antibiotic activity.

Keyphrases □ Pyrroles, various—synthesized, evaluated for antibacterial activity □ Furans, various—synthesized, evaluated for antibacterial and cytotoxic activity □ Thiophenes, various—synthesized, evaluated for antibacterial and cytotoxic activity □ Heterocycles—various pyrroles, furans, and thiophenes synthesized, evaluated for antibacterial and cytotoxic activity □ Antibacterial activity—various pyrroles, furans, and thiophenes evaluated □ Cytotoxic activity—various furans and thiophenes evaluated □ Structure–activity relationships—various pyrroles, furans, and thiophenes evaluated for antibacterial and cytotoxic activity

Several biologically significant pyrrole (1) and indole (2, 3) derivatives have been isolated from marine sources. Most of these compounds show pronounced antibiotic activity. During the present investigation of the sponge *Agelas* sp. (JC-6), a new brominated pyrrole derivative incorporating the guanidine moiety was isolated and showed significant activity against *Escherichia coli* (4). This natural product also showed cytotoxicity against KB carcinoma cells (5). This report describes the synthesis of several pyrrole, furan, and thiophene analogs and their physiological activities.

Table I—Antibiotic Activity of Pyrrole Derivatives

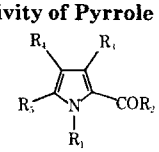

Compound	R_1	R_2	R_3	R_4	R_5	Activity against *E. coli*[a]
XII*a*	H	OCH_3	H	H	H	+++
XII*b*	H	NH_2	H	H	H	++++
XII*c*	CH_3	OCH_3	H	H	H	+++
XII*d*	CH_3	NH_2	H	H	H	++++
XII*e*	H	H	H	Br	H	++++
XII*f*	H	OCH_3	H	Br	H	++++
XII*g*	H	OCH_3	H	Br	Br	++
XII*h*	H	OCH_3	Br	Br	Br	+

[a] After paper disk incubation, zones of bacterial inhibition were measured: +, <15 mm; ++, 15–18 mm; +++, 18–22 mm; and ++++, >22 mm.

EXPERIMENTAL[1]

Chemistry—Since 2-aminopyrimidine (I*a*) and guanidine (II*a*) have a common structural unit, it was considered desirable to synthesize furan, thiophene, and pyrrole derivatives incorporating this structural feature.

[1] All melting points are uncorrected. Microanalyses were performed by Schwarzkopf Microanalytical Laboratories, Woodside, N.Y. IR spectra were recorded on a Perkin-Elmer 421 grating IR spectrometer, NMR spectra were recorded on a Varian A-60A spectrometer, and mass spectra were recorded on a Hitachi Perkin-Elmer spectrometer 107.

Table II—Analytical and Spectral Data

Compound	Melting Point	Yield, %	Formula		Analysis, % Calc.	Found	Spectral Data
V	290–293°	18	$C_8H_{11}N_3O_2 \cdot H_2O$	C	48.23	47.87	IR (KBr): 1680 (CO) cm^{-1}; NMR (CD_3OD): δ 3.03 (s, 6H), 6.43 (m, 1H), 6.85 (m, 1H), and 7.47 (m, 1H)
				H	6.58	6.45	
				N	21.09	20.82	
VII	124–127°	25	$C_9H_7N_3O_2$	C	57.14	57.20	IR (mineral oil): 3420 (NH) and 1680 (CO) cm^{-1}; NMR ($CDCl_3$): δ 7.1 (m, 3H), 7.6 (m, 3H), and 8.7 (m, 2H); mass spectrum (M^+): *m/e* 189
				H	3.73	3.96	
				N	22.21	22.23	
VIII	183–185°	20	$C_{11}H_{11}N_3O_2$	C	60.82	60.77	IR (KBr): 3450 (NH) and 1680 (CO) cm^{-1}; NMR ($CDCl_3$): δ 2.45 (s, 6H), 6.55 (m, 1H), 6.78 (s, 1H), 7.3 (m, 1H), and 7.51 (m, 1H); mass spectrum (M^+): *m/e* 217
				H	5.10	5.09	
				N	19.34	19.05	
VI	269–270°	19	$C_8H_{11}N_3O_2S \cdot 2H_2O$	C	41.20	41.67	IR (KBr): 3340 and 3290 (NH, H_2O) cm^{-1}; mass spectrum (M^+): *m/e* 215
				H	6.24	5.94	
				N	18.02	18.30	
				S	13.44	13.72	
IX	160–161°	35	$C_9H_7N_3OS$	C	52.69	52.99	IR (KBr): 3450 (NH) and 1670 (CO) cm^{-1}; NMR ($CDCl_3$): δ 7.1 (m, 3H), 7.65 (m, 3H), and 8.96 (m, 2H); mass spectrum (M^+): *m/e* 205
				H	3.44	3.35	
				N	20.48	20.73	
				S	15.59	15.71	
X	168–169°	37	$C_{11}H_{11}N_3OS$	C	56.65	56.49	IR (KBr): 3450 (NH) and 1670 (CO) cm^{-1}; NMR ($CDCl_3$): δ 7.1 (m, 3H) and 7.5 (m, 2H); mass spectrum (M^+): *m/e* 233
				H	4.75	4.80	
				N	18.02	18.10	
				S	13.72	13.89	
XI	153–154°	5	$C_{14}H_9N_3O_2S$	C	53.34	53.59	IR (KBr): 3450 (NH) and 1670 (CO) cm^{-1}; NMR ($CDCl_3$): δ 8.75 (m, 2H), 7.6 (m, 4H), and 7.05 (m, 3H); mass spectrum (M^+): *m/e* 283
				H	2.88	2.79	
				N	13.34	13.60	
				S	20.20	19.90	

The reaction of guanidine (II*a*) with 2-furoyl chloride (III) and 2-thiophenecarbonyl chloride (IV) afforded intractable mixtures. However, the reaction of *N,N*-dimethylguanidine (II*b*) with these two carbonyl chlorides yielded crystalline derivatives V and VI.

2-Aminopyrimidine (I*a*) and 2-amino 4,6-dimethylpyrimidine (I*b*), on similar treatment with these acid chlorides, resulted in products VII–X. The 5-acylated derivative (XI) was also isolated as a minor component from the reaction of 2-aminopyrimidine (I*a*) and thiophene carbonyl chloride (IV). This product resulted from the nucleophilic substitution at C-5 of the pyrimidine ring. Attempts to synthesize similar derivatives from pyrrole were unsuccessful.

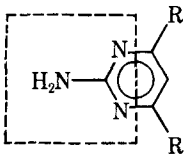

I*a*: R = H
I*b*: R = CH_3

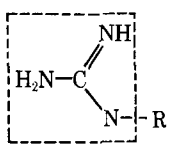

II*a*: R = H_2
II*b*: R = $(CH_3)_2$

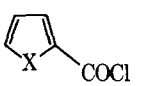

III: X = O
IV: X = S

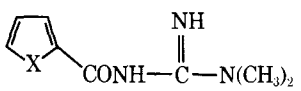

V: X = O
VI: X = S

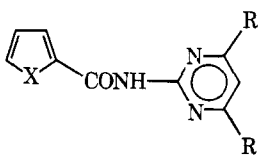

VII: X = O, R = H
VIII: X = O, R = CH_3
IX: X = S, R = H
X: X = S, R = CH_3

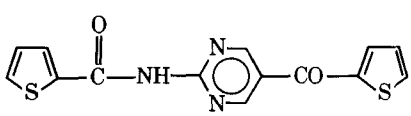

XI

Biological Activity—The thiophene and furan derivatives were tested for antibacterial (4) and cytotoxic activities (6).

In testing the activity against *Escherichia coli*[2] (ATCC 4157), 0.005 g of the compound was applied to a paper disk and incubated for 18 hr at 35°. Zones of bacterial inhibition were measured. Compounds IX and X showed 15–18-mm inhibition zones; VI showed an 18–22-mm zone.

Cytotoxic activity was tested against human oral epidermoid carcinoma KB cells (ATCC CCL 17) by adding 25–50 μg/ml of the test compound to the growth medium. Compounds V and VI showed 50% cytotoxicity.

Furan derivatives V, VII, and VIII were inactive against *E. coli*, but V was fairly cytotoxic. Thiophene derivatives VI, IX, and X showed moderate activity against *E. coli.*, but only VI exhibited cytotoxic activity.

Several pyrrole derivatives were also examined for antibacterial activity (Table I) and were considerably more potent as antibacterial agents than the corresponding thiophene and furan compounds. Although it is difficult to establish rigorously any structure–activity relationship, the introduction of halogen progressively decreased the antibiotic activity in this series.

General Method for Synthesis of Furan and Thiophene Derivatives—A solution of 2-furoyl chloride (III) (3.92 g, 0.03 mole) was added dropwise, at room temperature over 2 hr, to a suspension of 2-amino-4,6-dimethylpyrimidine (I*b*) (3.69 g, 0.03 mole) and triethylamine (3.03 g, 0.03 mole) in 150 ml of acetonitrile. The reaction mixture was heated to 65° for 0.5 hr and then kept overnight at room temperature. The precipitated triethylamine hydrochloride was filtered off, and the filtrate was evaporated under reduced pressure.

The residue was dissolved in chloroform (150 ml), washed with sodium bicarbonate solution (50 ml, 1 *N*) and water (2 × 100 ml), and dried over magnesium sulfate. Removal of the solvent afforded a dark viscous material. Repeated crystallization from ethyl acetate gave VIII.

Analytical and spectral data for these compounds are given in Table II.

Pyrrole derivatives were synthesized by literature methods (7–9).

REFERENCES

(1) G. Cimino, S. De Sefano, and L. Minale, *Comp. Biochem. Physiol.*, **47B**, 895 (1974).

[2] From NCTC 86 (original Escherich strain). Contains both smooth and rough colonies.

(2) J. T. Baker and M. D. Sutherland, *Tetrahedron Lett.*, **1968**, 43.
(3) P. Friedlander, *Chem. Ber.*, **42**, 765 (1909).
(4) M. F. Stempien, Jr., R. F. Nigrelli, and J. S. Chib, presented at the 164th American Chemical Society National Meeting, New York, Aug. 27–Sept. 1, 1972, MEDI 21.
(5) M. F. Stempien, Jr., G. D. Ruggieri, R. F. Nigrelli, and J. T. Cecil, in "Food-Drugs from the Sea Proceeding, Marine Technology Society," H. W. Youngken, Jr., Ed., Marine Technology Society, Washington, D.C., 1969, p. 295.
(6) J. T. Cecil, M. F. Stempien, Jr., G. D. Ruggieri, and R. F. Nigrelli, in "Aspects of Sponge Biology," R. W. Harrison and R. R. Cowdèn, Eds., Academic, New York, N.Y., 1976, p. 171.
(7) P. Hodge and R. W. Rickards, *J. Chem. Soc.*, **1963**, 2543.
(8) *Ibid.*, **1965**, 459.
(9) H. J. Anderson and S. F. Lee, *Can. J. Chem.*, **43**, 409 (1965).

ACKNOWLEDGMENTS AND ADDRESSES

Received May 10, 1976, from the *Osborn Laboratories of Marine Sciences, New York Aquarium, New York Zoological Society, Brooklyn, NY 11224.*

Accepted for publication August 27, 1976.

Supported by Sea Grant Project Grant 1-35263 to the New York Zoological Society.

The authors thank Professor A. K. Bose of Stevens Institute of Technology, Hoboken, N.J., for helpful discussions and for providing facilities for the recording of mass and NMR spectra.

[x] To whom inquiries should be directed.

Preparation of Spin-Labeled Opiates: Morphine and Codeine

JAMES A. CELLA [x] and JAMES A. KELLEY

Abstract □ The preparation of 6-spin-labeled codeine and morphine is described. Treatment of either 6-chlorocodide or 8-bromocodide with 4-amino-2,2,6,6-tetramethylpiperidino-1-oxyl free radical in dimethylformamide afforded 6-spin-labeled codeine. Similar treatment of 6-chloromorphide afforded 6-spin-labeled morphine. Exclusive formation of the 6-isomer in these reactions is explained by halide-ion-catalyzed isomerization of the 6-halo opiate to the 8-halo isomer followed by a normal S_N2' displacement of the halogen. Both spin-labeled compounds displayed weak *in vivo* analgesic activity and did not bind appreciably to receptors in brain homogenate.

Keyphrases □ Spin-labeled opiates—morphine and codeine labeled in 6-position, effect on binding to brain receptors and analgesic activity □ Morphine—spin labeled in 6-position, effect on binding to brain receptors and analgesic activity □ Codeine—spin labeled in 6-position, effect on binding to brain receptors and analgesic activity □ Opiates—morphine and codeine, spin labeled in 6-position, effect on binding to brain receptors and analgesic activity □ Analgesics, narcotic—morphine and codeine, spin labeled in 6-position, effect on binding to brain receptors and analgesic activity

In numerous attempts to identify and characterize the opiate receptor (1–4), the binding characteristics of pharmacologically active and inactive isomers were compared or the reduced agonist binding in the presence of antagonists was noted using radiolabeled opiates with high specific activity. The spin label method (5, 6) is an attractive alternative to the radioisotope method for studying this drug–receptor interaction *in vitro*, since it obviates the need for separating bound from unbound drug. A preliminary report demonstrated the feasibility of this method (7).

DISCUSSION

Essential to the success of this approach is the requirement that the nitroxide label not constitute a significant perturbation to the interaction of the drug with its receptor. As such, the label should be attached to a pharmacologically unimportant position in the drug molecule. For purposes of stability, the label should be covalently attached to the drug *via* a linkage resistant to hydrolytic enzymes and inert to aqueous media at physiological pH. Finally, it is desirable, although not essential, that the labeled drug possess biological activity similar to that of the parent drug.

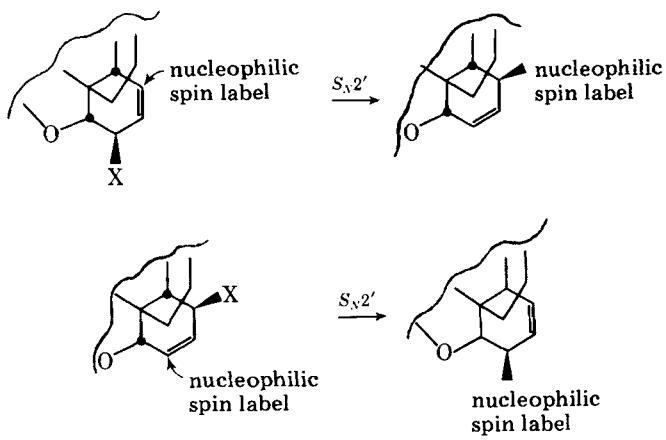

Scheme I

With these requirements in mind, the preparation of spin-labeled derivatives of morphine and codeine suitable for the *in vitro* study of the interaction of these drugs with possible receptors was attempted.

The hydroxyl group at the 6-position of morphine and codeine appeared to offer a suitable point for attachment for the spin label, particularly in view of the relative unimportance of this position in the pharmacological activity of these drugs (8, 9). However, the steric inaccessibility of this alcohol (10, 11) precluded all attempts to alkylate at this position[1]. Consequently, the mode of reaction was reversed by using a nucleophilic spin label to displace halogen from a 6- or 8-halo opiate (Scheme I). In the isomeric halocodides and morphides, the halogen atom has a beta configuration (*syn* to the ethylamino bridge) and is displaced by nucleophiles exclusively from the beta side in an S_N2' fashion (13). Following this precedent, the reaction of the isomeric halocodides and morphides with 4-amino-2,2,6,6-tetramethylpiperidino-1-oxyl free radical (I) as a route to spin-labeled morphine and codeine was investigated.

Reaction of I with 8-bromocodide (IIa) in dimethylformamide afforded the expected 6-spin-labeled codeine (IIIa) in 23% yield (Scheme II).

[1] A recent report (12) described the selective methylation of morphine at the 6-position *via* its dipotassium salt. A similar approach to introduce a spin label at the 6-position was attempted; however, with alkylating agents much larger than methyl, reaction occurred exclusively at the 3-position.

(2) J. T. Baker and M. D. Sutherland, *Tetrahedron Lett.*, **1968**, 43.
(3) P. Friedlander, *Chem. Ber.*, **42**, 765 (1909).
(4) M. F. Stempien, Jr., R. F. Nigrelli, and J. S. Chib, presented at the 164th American Chemical Society National Meeting, New York, Aug. 27–Sept. 1, 1972, MEDI 21.
(5) M. F. Stempien, Jr., G. D. Ruggieri, R. F. Nigrelli, and J. T. Cecil, in "Food-Drugs from the Sea Proceeding, Marine Technology Society," H. W. Youngken, Jr., Ed., Marine Technology Society, Washington, D.C., 1969, p. 295.
(6) J. T. Cecil, M. F. Stempien, Jr., G. D. Ruggieri, and R. F. Nigrelli, in "Aspects of Sponge Biology," R. W. Harrison and R. R. Cowdèn, Eds., Academic, New York, N.Y., 1976, p. 171.
(7) P. Hodge and R. W. Rickards, *J. Chem. Soc.*, **1963**, 2543.
(8) *Ibid.*, **1965**, 459.
(9) H. J. Anderson and S. F. Lee, *Can. J. Chem.*, **43**, 409 (1965).

ACKNOWLEDGMENTS AND ADDRESSES

Received May 10, 1976, from the *Osborn Laboratories of Marine Sciences, New York Aquarium, New York Zoological Society, Brooklyn, NY 11224.*

Accepted for publication August 27, 1976.

Supported by Sea Grant Project Grant 1-35263 to the New York Zoological Society.

The authors thank Professor A. K. Bose of Stevens Institute of Technology, Hoboken, N.J., for helpful discussions and for providing facilities for the recording of mass and NMR spectra.

[x] To whom inquiries should be directed.

Preparation of Spin-Labeled Opiates: Morphine and Codeine

JAMES A. CELLA [x] and JAMES A. KELLEY

Abstract □ The preparation of 6-spin-labeled codeine and morphine is described. Treatment of either 6-chlorocodide or 8-bromocodide with 4-amino-2,2,6,6-tetramethylpiperidino-1-oxyl free radical in dimethylformamide afforded 6-spin-labeled codeine. Similar treatment of 6-chloromorphide afforded 6-spin-labeled morphine. Exclusive formation of the 6-isomer in these reactions is explained by halide-ion-catalyzed isomerization of the 6-halo opiate to the 8-halo isomer followed by a normal S_N2' displacement of the halogen. Both spin-labeled compounds displayed weak *in vivo* analgesic activity and did not bind appreciably to receptors in brain homogenate.

Keyphrases □ Spin-labeled opiates—morphine and codeine labeled in 6-position, effect on binding to brain receptors and analgesic activity □ Morphine—spin labeled in 6-position, effect on binding to brain receptors and analgesic activity □ Codeine—spin labeled in 6-position, effect on binding to brain receptors and analgesic activity □ Opiates—morphine and codeine, spin labeled in 6-position, effect on binding to brain receptors and analgesic activity □ Analgesics, narcotic—morphine and codeine, spin labeled in 6-position, effect on binding to brain receptors and analgesic activity

In numerous attempts to identify and characterize the opiate receptor (1–4), the binding characteristics of pharmacologically active and inactive isomers were compared or the reduced agonist binding in the presence of antagonists was noted using radiolabeled opiates with high specific activity. The spin label method (5, 6) is an attractive alternative to the radioisotope method for studying this drug–receptor interaction *in vitro*, since it obviates the need for separating bound from unbound drug. A preliminary report demonstrated the feasibility of this method (7).

DISCUSSION

Essential to the success of this approach is the requirement that the nitroxide label not constitute a significant perturbation to the interaction of the drug with its receptor. As such, the label should be attached to a pharmacologically unimportant position in the drug molecule. For purposes of stability, the label should be covalently attached to the drug *via* a linkage resistant to hydrolytic enzymes and inert to aqueous media at physiological pH. Finally, it is desirable, although not essential, that the labeled drug possess biological activity similar to that of the parent drug.

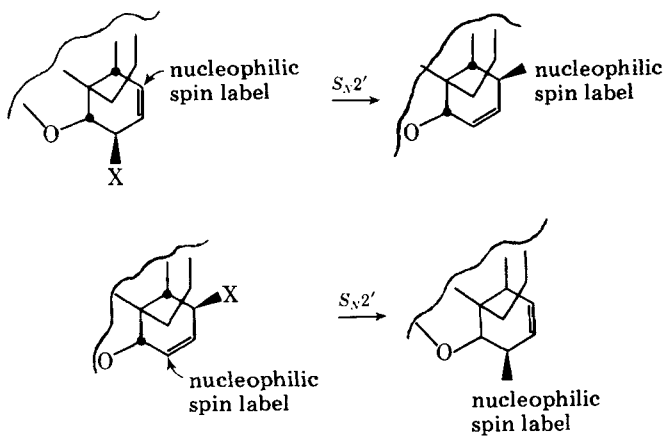

Scheme I

With these requirements in mind, the preparation of spin-labeled derivatives of morphine and codeine suitable for the *in vitro* study of the interaction of these drugs with possible receptors was attempted.

The hydroxyl group at the 6-position of morphine and codeine appeared to offer a suitable point for attachment for the spin label, particularly in view of the relative unimportance of this position in the pharmacological activity of these drugs (8, 9). However, the steric inaccessibility of this alcohol (10, 11) precluded all attempts to alkylate at this position[1]. Consequently, the mode of reaction was reversed by using a nucleophilic spin label to displace halogen from a 6- or 8-halo opiate (Scheme I). In the isomeric halocodides and morphides, the halogen atom has a beta configuration (*syn* to the ethylamino bridge) and is displaced by nucleophiles exclusively from the beta side in an S_N2' fashion (13). Following this precedent, the reaction of the isomeric halocodides and morphides with 4-amino-2,2,6,6-tetramethylpiperidino-1-oxyl free radical (I) as a route to spin-labeled morphine and codeine was investigated.

Reaction of I with 8-bromocodide (IIa) in dimethylformamide afforded the expected 6-spin-labeled codeine (IIIa) in 23% yield (Scheme II).

[1] A recent report (12) described the selective methylation of morphine at the 6-position *via* its dipotassium salt. A similar approach to introduce a spin label at the 6-position was attempted; however, with alkylating agents much larger than methyl, reaction occurred exclusively at the 3-position.

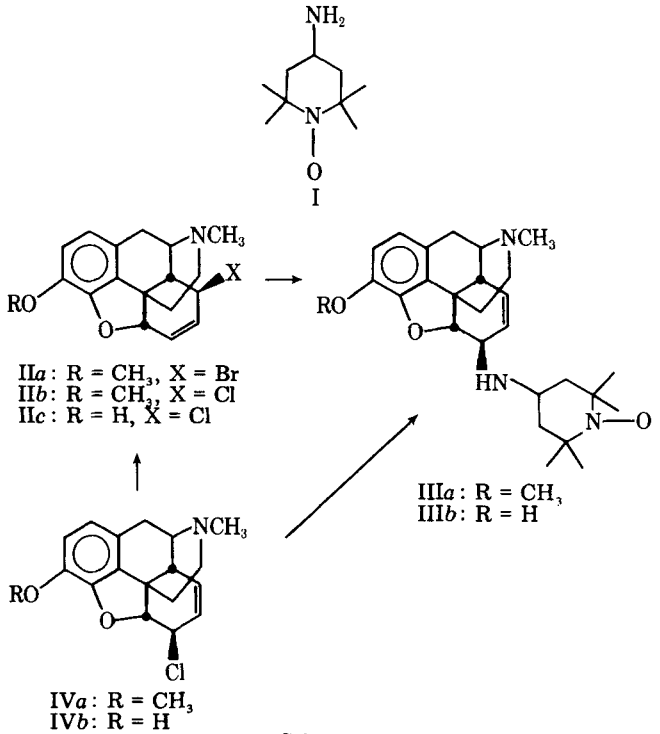

Scheme II

Similar reaction of I with 6-chlorocodide (IV*a*) produced a spin-labeled codeine in 10% yield identical in all respects to III*a* (see *Experimental*). This apparently anomalous result is accounted for by the fact that isomerization of IV*a* to the more stable 8-chlorocodide (II*b*) occurred more rapidly than did the reaction with the spin label[2]. While IV*a* did not isomerize to II*b* under the reaction conditions in the absence of added nucleophile, addition of a small amount of chloride ion to the mixture resulted in rapid conversion of IV*a* to II*b*. Thus, chloride ion generated from the initial reaction of I with IV*a* catalyzed the isomerization of the halogen to the 8-position. The 8-chlorocodide thus produced underwent a normal S_N2' reaction to produce III*a*.

In an analogous fashion, 6-chloromorphide (IV*b*) reacted with I to yield 22% of 6-spin-labeled morphine (III*b*). The structure of III*b* was confirmed by elemental and spectral analyses (see *Experimental*) and its conversion to III*a* on methylation with diazomethane. Interestingly, the chloromorphide recovered from this reaction was exclusively the 8-isomer, II*c*, verifying that halogen migration occurred during the reaction.

The low yields of spin-labeled products were due mostly to low conversions (yields based on recovered starting materials were substantially higher). An evident side reaction was the elimination of hydrogen halide from the halo opiates to produce dehydromorphine and codeine derivatives. No attempt was made to ascertain whether the dehydro derivatives were the 5,7- or 6,8-diene isomers.

The spin-labeled derivatives prepared in this study showed only marginal *in vivo* analgesic activity in the Eddy hot plate test (14, 15) and displayed weak *in vitro* binding to receptors in brain homogenate (P_2 fraction) by the method of Klee and Streaty (16). There was a small but noticeably greater potency of the labeled morphine over the labeled codeine[3]. These results, while disappointing, do not preclude the use of these compounds for studying *in vitro* binding to receptors in brain homogenate or subfractions thereof by the spin label method.

EXPERIMENTAL[4]

General—When reaction mixtures were to be separated and analyzed, a 1.9-m (6-ft), 2-mm i.d. glass column packed with 3% OV-17 on 60–80-mesh Gas Chrom Q[5] was operated in the 200–240° range with a helium carrier gas flow of 25 ml/min. The gas chromatograph was interfaced to the mass spectrometer by a permeable silicone rubber membrane separator maintained at 240°. Samples that were pure or not amenable to GLC–mass spectrometry were introduced directly into the mass spectrometer ion source *via* a direct insertion probe with a sample heater, which was varied from ambient to 250° depending on the compound.

For electron-impact ionization, the following conditions were employed: ion source, 180°; ionizing current, 0.15 mamp; and electron energy, 70 ev. Chemical-ionization mass spectra were obtained with an ion source pressure of 0.35 torr methane[6] (instrument grade, 99.7%), an ionizing current of 0.15 mamp, and an electron energy of 75 ev.

4-Amino-2,2,6,6-tetramethylpiperidino-1-oxyl (I) was obtained commercially[7]. 6-Chlorocodide, 8-bromocodide, and 6-chloromorphide were prepared as described previously (17, 18).

Preparation of 6-Spin-Labeled Codeine (III*a*)—*Reaction of I with II*a—A mixture of 2.8 g (7.8 mmoles) of II*a*, 1.5 g (9.0 mmoles) of I, and 1.1 g (8.0 mmoles) of solid potassium carbonate in dimethylformamide (20 ml) was heated in an oil bath at 90–95° for 4.5 hr. The cooled mixture was diluted with an equal volume of water, and the resulting suspension was extracted with 3 × 50 ml of ether. The combined ether extracts were washed with brine and then dried (sodium sulfate). Evaporation of solvent afforded 2.2 g of a residue, which was chromatographed on 75 g of silica gel[8] (100–200 mesh) and eluted with a chloroform–methanol gradient. Fractions were monitored by TLC [silica gel, chloroform–methanol (10:1)].

The first component eluted was a dehydrocodeine derivative; mass spectrum: *m/e* 281 (M^+, 100), 280 (67.3), 266 (45.0), 264 (11.9), 238 (14.9), 223 (11.4), 220 (11.9), 165 (17.8), 152 (19.3), and 41 (13.4). The second component eluted was III*a*, which was obtained as an oil. The oil crystallized from ether–petroleum ether as a tan solid, 970 mg (27%), mp 66–70°; mass spectrum: *m/e* 150, 453 (M + H[9], 15.3), 452 (M, 1.0), 437 (2.9), 420 (2.3), 379 (51.0), 366 (9.3), 323 (7.9), 308 (15.0), 282 (100), 266 (10.9), 192 (36.7), and 154 (25.4); methane chemical-ionization mass spectrum: *m/e* 250, 454 (M + 2H, 68.5), 453 (M + H, 100), 438 (8.3), 436 (13.4), 379 (13.2), and 282 (10.9). The electron spin resonance spectrum of III*a* exhibited the usual three-line pattern for a nitroxide derived from tetramethylpiperidine.

Anal.—Calc. for $C_{27}H_{38}N_3O_3$: C, 71.65; H, 8.46; N, 9.28. Found: C, 71.44; H, 8.51; N, 9.31.

*Reaction of I with IV*a—A mixture of 2.5 g (7.8 mmoles) of IV*a*, 1.5 g (9.0 mmoles) of I, and 1.1 g (8.0 mmoles) of potassium carbonate in dimethylformamide (20 ml) was heated in an oil bath at 110° for 8 hr. By using the same workup and chromatographic procedures described in the preceding experiment, 383 mg (10%) of III*a* was obtained as a tan solid, mp 65–68°. That this substance was indeed III*a* was ascertained by the following comparisons. The IR and mass spectra were superimposable on the spectra obtained for III*a*. TLC on silica gel using six different solvent systems demonstrated identical R_f values for this substance and III*a*. Finally, the melting point of this substance was not depressed on admixture with III*a*.

Isomerization of IV*a* to II*b*—A solution of 50 mg of IV*a* in 1 ml of dimethylformamide was heated at 90° for 1.5 hr. The IR spectrum of the recovered material was identical to that of the starting material. This experiment was repeated except that 20 mg of sodium chloride was added to the mixture. The IR spectrum of the recovered material indicated that 50% of IV*a* had isomerized to II*b*.

Preparation of 6-Spin-Labeled Morphine (III*b*)—A solution of 700 mg (2.4 mmoles) of IV*b* and 855 mg (5 mmoles) of I in dimethylformamide (10 ml) was stirred in an oil bath at 90–100° for 20 hr. The cooled solution was diluted with 25 ml of chloroform, and the resultant solution was extracted with 3 × 25 ml of 3 *N* NaOH. The combined aqueous extracts were adjusted to pH 8.5 by the slow addition of cold, concentrated hydrochloric acid, and the resultant slurry was extracted with 3 × 50 ml of chloroform. The combined chloroform extracts were dried (sodium sulfate), and the solvent was removed to afford 2.6 g of a residue containing dimethylformamide.

The residue was chromatographed on 75 g of silica gel (100–200 mesh) using a chloroform–methanol gradient. Fractions were monitored by TLC

[2] Piperidine displaces halide ion from the haloopiates much more rapidly than I (13).

[3] In the *in vitro* assay (16), III*a* was about 1/500th and III*b* about 1/350th as potent as morphine.

[4] Melting points were determined on a Thomas-Hoover melting-point apparatus. IR spectra were recorded on a Beckman IR-5A spectrophotometer using potassium chloride pellets or sodium chloride solution cells. Mass spectra were obtained on a Hewlett-Packard 5982 A gas chromatograph–mass spectrometer system. Electron spin resonance spectra were recorded on a Varian E-9 spectrometer.

[5] Applied Science Laboratories, State College, Pa.

[6] Air Products and Chemicals, Allentown, Pa.

[7] Aldrich.

[8] W. R. Grace.

[9] The much more intense than expected M + 1 peak was probably due to hydrogen radical abstraction from water adsorbed in the ion source or glass capillary sample holder by the even electron molecular ion species (19, 20).

[silica gel, chloroform–methanol (4:1)]. Compound III*b*, 960 mg (22%), was obtained as tan flakes from ether–petroleum ether, mp 212–215° dec.; mass spectrum: *m/e* >150, 439 (M + H, 18.9), 438 (M^+, 1.8), 406 (3.8), 365 (74.8), 352 (27.9), 309 (15.3), 268 (100), 266 (12.8), 178 (33.5), and 154 (27.3); methane chemical-ionization mass spectrum: *m/e* >250, 440 (M + 2H, 100), 439 (M + H, 71.1), 424 (27.1), 422 (22.6), 365 (8.3), and 268 (24.0). The electron spin resonance spectrum of III*b* exhibited the usual three-line pattern for a nitroxide derived from tetramethylpiperidine.

Anal.—Calc. for $C_{26}H_{37}N_3O_3$: C, 71.20; H, 8.27; N, 9.58. Found; C, 71.12; H, 8.11; N, 9.81.

A small portion of this material was treated with excess ethereal diazomethane. Evaporation of solvent and excess diazomethane afforded a crystalline residue identical to III*a* in all respects (melting point, IR, TLC, and mass spectral data).

Also isolated from column chromatography of this reaction mixture was a component having an R_f similar to that of IV*b*. This substance was identified as II*c* by its melting point and IR and mass spectra. No IV*b* was eluted from the column.

REFERENCES

(1) S. H. Snyder, C. B. Pert, and G. W. Pasternak, *Ann. Intern. Med.*, **81**, 534 (1974).

(2) A. Goldstein, *Life Sci.*, **14**, 615 (1974).

(3) H. H. Loh, T. M. Cho, Y. C. Wu, and E. L. Way, *ibid.*, **14**, 2231 (1974).

(4) L. I. Lowney, K. Schulz, P. J. Lowery, and A. Goldstein, *Science*, **183**, 749 (1974).

(5) C. L. Hamilton and H. M. McConnell, in "Structural Chemistry and Molecular Biology," A. Rich and N. Davidson, Eds., Freeman, San Francisco, Calif., 1968, p. 115.

(6) O. H. Griffith and A. S. Waggoner, *Acc. Chem. Res.*, **2**, 17 (1969).

(7) E. S. Copeland, M. E. Boykin, J. A. Kelley, and M. P. Kullberg, *Biophys. J.*, **15**, 1125 (1975).

(8) A. H. Beckett and A. F. Casey, *J. Pharm. Pharmacol.*, **6**, 986 (1954).

(9) P. S. Portoghese, *J. Pharm. Sci.*, **55**, 865 (1966).

(10) G. Stork, in "The Alkaloids," vol. II, R. H. F. Manske and H. L. Holmes, Eds., Academic, New York, N.Y., 1952, p. 176.

(11) *Ibid.*, vol. VI, 1960, chap. 7, p. 219.

(12) R. B. Barber and H. Rapoport, *J. Med. Chem.*, **18**, 1074 (1975).

(13) G. Stork and F. H. Clarke, *J. Am. Chem. Soc.*, **78**, 4619 (1956).

(14) N. B. Eddy and D. Leimtach, *J. Pharmacol. Exp. Ther.*, **107**, 385 (1953).

(15) A. E. Jacobsen and E. L. May, *J. Med. Chem.*, **8**, 563 (1965).

(16) W. A. Klee and R. A. Streaty, *Nature*, **248**, 61 (1974).

(17) H. Wieland and P. Kappelmeir, *Ann.*, **382**, 306 (1911).

(18) S. B. Schryver and F. H. Lees, *J. Chem. Soc.*, **79**, 563 (1901).

(19) A. Morrison and A. P. Davies, *Org. Mass Spectrom.*, **3**, 353 (1970).

(20) A. P. Davies, A. Morrison, and M. D. Barratt, *ibid.*, **8**, 43 (1974).

ACKNOWLEDGMENTS AND ADDRESSES

Received February 5, 1976, from the *Division of Biochemistry, Walter Reed Army Institute of Research, Washington, DC 20012.*

Accepted for publication September 2, 1976.

The authors are grateful to Dr. Kenner C. Rice, Dr. Werner Klee, and Mrs. Louise Atwell of the National Institutes of Health, Bethesda, Md., for the biological activity tests, and Dr. Edmund S. Copeland of Walter Reed for determination of the electron spin resonance spectra.

[x] To whom inquiries should be directed. Present address: Corporate Research and Development Center, General Electric Co., Schenectady, NY 12301.

Radiochemical GLC Assay for Nortriptyline in Human Plasma

ARTHUR LOH, FRANCIS R. ZULESKI, and FREDERICK J. Di CARLO [x]

Abstract □ A novel method was developed for the assay of nortriptyline in plasma. After nortriptyline was extracted, it was acetylated with ^{3}H-acetic anhydride; the quantity of ^{3}H-acetylnortriptyline in the extract was determined by radiochemical GLC. The method is capable of assaying 5 ng of nortriptyline/ml of plasma. The instrumentation was assembled from commercially available components.

Keyphrases □ Nortriptyline—radiochemical GLC analysis, human plasma □ Radiochemical GLC- -analysis, nortriptyline in human plasma □ GLC, radiochemical—analysis, nortriptyline in human plasma □ Antidepressants—nortriptyline, radiochemical GLC analysis in human plasma

The assay of nortriptyline in plasma is important because its clinical activity is related to plasma levels (1, 2), which vary remarkably among individuals even at steady state (3, 4). GLC methods for nortriptyline assay (5–7), although capable of detecting 10–20 ng of compound/ml of plasma, are frequently inadequately sensitive for measuring the levels attained after a single dose. A recently published TLC assay is considerably less sensitive, having a lower limit of 50 ng/ml (8).

Zuleski *et al.* (9) developed a nortriptyline assay method which involved extracting the compound from plasma by a modification of the method of Hammer and Brodie (10), acetylating it with ^{14}C-acetic anhydride, separating acetylnortriptyline by TLC, locating this derivative by radiochromatogram scanning, removing it from the plate, and counting it by scintillation spectrometry. The present approach was more direct. Radiochemical GLC was performed directly following derivatization with ^{3}H-acetic anhydride. Thus, ^{3}H-acetylnortriptyline was resolved and counted simultaneously. Despite the wide applicability of radiochemical GLC to drug metabolism studies, this method has been developed only in a few laboratories (11–13). The present investigation shows that the method can be developed using commercially available components.

EXPERIMENTAL

Reagents—^{3}H-Acetic anhydride (50 mCi/4.36 mg in 5 ml of dry benzene) was received[1] in a sealed ampul. A 0.05-ml aliquot of this so-

[1] New England Nuclear, Boston, Mass.

[silica gel, chloroform–methanol (4:1)]. Compound III*b*, 960 mg (22%), was obtained as tan flakes from ether–petroleum ether, mp 212–215° dec.; mass spectrum: *m/e* >150, 439 (M + H, 18.9), 438 (M^+, 1.8), 406 (3.8), 365 (74.8), 352 (27.9), 309 (15.3), 268 (100), 266 (12.8), 178 (33.5), and 154 (27.3); methane chemical-ionization mass spectrum: *m/e* >250, 440 (M + 2H, 100), 439 (M + H, 71.1), 424 (27.1), 422 (22.6), 365 (8.3), and 268 (24.0). The electron spin resonance spectrum of III*b* exhibited the usual three-line pattern for a nitroxide derived from tetramethylpiperidine.

Anal.—Calc. for $C_{26}H_{37}N_3O_3$: C, 71.20; H, 8.27; N, 9.58. Found; C, 71.12; H, 8.11; N, 9.81.

A small portion of this material was treated with excess ethereal diazomethane. Evaporation of solvent and excess diazomethane afforded a crystalline residue identical to III*a* in all respects (melting point, IR, TLC, and mass spectral data).

Also isolated from column chromatography of this reaction mixture was a component having an R_f similar to that of IV*b*. This substance was identified as II*c* by its melting point and IR and mass spectra. No IV*b* was eluted from the column.

REFERENCES

(1) S. H. Snyder, C. B. Pert, and G. W. Pasternak, *Ann. Intern. Med.*, **81**, 534 (1974).

(2) A. Goldstein, *Life Sci.*, **14**, 615 (1974).

(3) H. H. Loh, T. M. Cho, Y. C. Wu, and E. L. Way, *ibid.*, **14**, 2231 (1974).

(4) L. I. Lowney, K. Schulz, P. J. Lowery, and A. Goldstein, *Science*, **183**, 749 (1974).

(5) C. L. Hamilton and H. M. McConnell, in "Structural Chemistry and Molecular Biology," A. Rich and N. Davidson, Eds., Freeman, San Francisco, Calif., 1968, p. 115.

(6) O. H. Griffith and A. S. Waggoner, *Acc. Chem. Res.*, **2**, 17 (1969).

(7) E. S. Copeland, M. E. Boykin, J. A. Kelley, and M. P. Kullberg, *Biophys. J.*, **15**, 1125 (1975).

(8) A. H. Beckett and A. F. Casey, *J. Pharm. Pharmacol.*, **6**, 986 (1954).

(9) P. S. Portoghese, *J. Pharm. Sci.*, **55**, 865 (1966).

(10) G. Stork, in "The Alkaloids," vol. II, R. H. F. Manske and H. L. Holmes, Eds., Academic, New York, N.Y., 1952, p. 176.

(11) *Ibid.*, vol. VI, 1960, chap. 7, p. 219.

(12) R. B. Barber and H. Rapoport, *J. Med. Chem.*, **18**, 1074 (1975).

(13) G. Stork and F. H. Clarke, *J. Am. Chem. Soc.*, **78**, 4619 (1956).

(14) N. B. Eddy and D. Leimtach, *J. Pharmacol. Exp. Ther.*, **107**, 385 (1953).

(15) A. E. Jacobsen and E. L. May, *J. Med. Chem.*, **8**, 563 (1965).

(16) W. A. Klee and R. A. Streaty, *Nature*, **248**, 61 (1974).

(17) H. Wieland and P. Kappelmeir, *Ann.*, **382**, 306 (1911).

(18) S. B. Schryver and F. H. Lees, *J. Chem. Soc.*, **79**, 563 (1901).

(19) A. Morrison and A. P. Davies, *Org. Mass Spectrom.*, **3**, 353 (1970).

(20) A. P. Davies, A. Morrison, and M. D. Barratt, *ibid.*, **8**, 43 (1974).

ACKNOWLEDGMENTS AND ADDRESSES

Received February 5, 1976, from the *Division of Biochemistry, Walter Reed Army Institute of Research, Washington, DC 20012.*

Accepted for publication September 2, 1976.

The authors are grateful to Dr. Kenner C. Rice, Dr. Werner Klee, and Mrs. Louise Atwell of the National Institutes of Health, Bethesda, Md., for the biological activity tests, and Dr. Edmund S. Copeland of Walter Reed for determination of the electron spin resonance spectra.

[x] To whom inquiries should be directed. Present address: Corporate Research and Development Center, General Electric Co., Schenectady, NY 12301.

Radiochemical GLC Assay for Nortriptyline in Human Plasma

ARTHUR LOH, FRANCIS R. ZULESKI, and FREDERICK J. Di CARLO [x]

Abstract □ A novel method was developed for the assay of nortriptyline in plasma. After nortriptyline was extracted, it was acetylated with ^{3}H-acetic anhydride; the quantity of ^{3}H-acetylnortriptyline in the extract was determined by radiochemical GLC. The method is capable of assaying 5 ng of nortriptyline/ml of plasma. The instrumentation was assembled from commercially available components.

Keyphrases □ Nortriptyline—radiochemical GLC analysis, human plasma □ Radiochemical GLC- -analysis, nortriptyline in human plasma □ GLC, radiochemical—analysis, nortriptyline in human plasma □ Antidepressants—nortriptyline, radiochemical GLC analysis in human plasma

The assay of nortriptyline in plasma is important because its clinical activity is related to plasma levels (1, 2), which vary remarkably among individuals even at steady state (3, 4). GLC methods for nortriptyline assay (5–7), although capable of detecting 10–20 ng of compound/ml of plasma, are frequently inadequately sensitive for measuring the levels attained after a single dose. A recently published TLC assay is considerably less sensitive, having a lower limit of 50 ng/ml (8).

Zuleski *et al.* (9) developed a nortriptyline assay method which involved extracting the compound from plasma by a modification of the method of Hammer and Brodie (10), acetylating it with ^{14}C-acetic anhydride, separating acetylnortriptyline by TLC, locating this derivative by radiochromatogram scanning, removing it from the plate, and counting it by scintillation spectrometry. The present approach was more direct. Radiochemical GLC was performed directly following derivatization with ^{3}H-acetic anhydride. Thus, ^{3}H-acetylnortriptyline was resolved and counted simultaneously. Despite the wide applicability of radiochemical GLC to drug metabolism studies, this method has been developed only in a few laboratories (11–13). The present investigation shows that the method can be developed using commercially available components.

EXPERIMENTAL

Reagents—^{3}H-Acetic anhydride (50 mCi/4.36 mg in 5 ml of dry benzene) was received[1] in a sealed ampul. A 0.05-ml aliquot of this so-

[1] New England Nuclear, Boston, Mass.

lution was transferred quantitatively to a 50-ml volumetric flask with benzene, which had been dried over metallic sodium and then diluted to volume with the same solvent. Air in the neck of the flask was displaced gently with dry nitrogen; the flask was stoppered, sealed with tape, and stored under refrigeration in a bottle containing desiccant (calcium sulfate). The bottle and its contents were allowed to equilibrate to room temperature before opening. After using a portion of the ^{3}H-acetic anhydride solution, the flask was prepared for storage as described.

Nortriptyline hydrochloride was used as received[2]. Reagent grade solvents were used in this study.

Radiochemical GLC—An oven and proportioning temperature controller[3] were connected to a gas proportional counter[4] by a heated glass-lined metal tube. The gas chromatograph was fitted with a 1.83-m × 2-mm i.d. coiled-glass column packed with 20% SE-30 on 80–100-mesh Gas Chrom Q. Oven and injector temperatures were set at 215 and 245°, respectively.

Helium was used as carrier gas at a flow rate of 50 ml/min. The transfer line to the gas proportional counter was maintained at 237°. The hydrogen and propane (quench gas) flow rates were 10 and 2.5 ml/min, respectively. The temperature of the oxidizer and reduction furnace was 750°.

Standard Nortriptyline Solutions—Nortriptyline hydrochloride (11.35 mg) was dissolved in 10 ml of distilled water to produce a free base concentration of 1.0 mg/ml. From this solution, others were prepared in duplicate concentrations of 100, 50, 25, 12.5, and 6.25 ng/ml.

Nortriptyline Extracts and Derivatization—Twelve 2.0-ml aliquots of normal human plasma were placed into 15-ml polyethylene-stoppered conical test tubes. Duplicate standard nortriptyline solutions (1.0 ml) were added to 10 of these tubes, and water (1.0 ml) was added to the other two tubes to serve as blanks. Then 0.5 ml of 1 *N* NaOH was mixed with the contents of each tube.

Each plasma specimen was extracted twice with 5.0 ml of *n*-hexane. Any emulsion was broken by placing the tube into a dry ice–acetone mixture followed by thawing and recentrifugation. The hexane layer was transferred to another tube with an isopentyl alcohol-pretreated pipet (10). The combined hexane extracts were evaporated to dryness with nitrogen, and the residue was dissolved in 0.65 ml of dry benzene. ^{3}H-Acetic anhydride solution, 100 μl, and 0.25 ml of pyridine were added to the benzene solution, which was then mixed thoroughly and incubated at 60° for 1 hr.

After the solvent was evaporated in a water bath at 90°, 2.0 ml of 0.1 *N* NaOH was added and the tube was shaken for a few seconds. Then the solution was placed in a water bath at 95° for 15 min. The solution was cooled to room temperature, and acetylnortriptyline was extracted with two 5.0-ml aliquots of heptane. The combined heptane extracts were evaporated under nitrogen. Then the inner wall of the tube was washed down with heptane, and the solvent was evaporated to dryness. Each residue was dissolved in 50 μl of heptane.

Measurement of ^{3}H-Acetylnortriptyline—Aliquots (10 μl) of each plasma blank and ^{3}H-acetylnortriptyline solution in heptane were injected into the gas chromatograph. The area under each radioactive peak on the chromatograms was measured by planimetry. A standard curve was constructed by plotting mean areas against quantities of nortriptyline (expressed as free base) per milliliter of human plasma.

RESULTS

No peak appeared on chromatograms of "blanks" consisting of plasma and ^{3}H-acetic anhydride. Under the described operating conditions, radiochemical GLC yielded a single peak representing ^{3}H-acetylnortriptyline (Fig. 1). The retention time of this compound was 31.8 min from each plasma extract. A linear standard curve resulted from plotting peak areas against human plasma concentrations of nortriptyline ranging from 3.125 to 50.0 ng/ml. This curve passed through the intercept of the ordinate and abscissa; the peak area per nanogram of nortriptyline was 0.658 cm^2. By preparing the extracted acetylnortriptyline concentrate as described and using only one-fifth of it for assay, the radiochemical GLC method was reliable for levels of nortriptyline down to 5 ng/ml of plasma.

DISCUSSION

The radiochemical GLC assay has advantages over other methodology for nortriptyline in plasma. It is more sensitive than the TLC (8) and GLC (5–7) methods that do not employ radioactivity. Although the radiochemical GLC procedure is no more sensitive than the radiochemical TLC assay (9), it is shorter and more direct. As presently developed, both radioassays can measure nortriptyline levels as low as 5 ng/ml. However, the sensitivity of these and other radioacetylation methods probably can be increased by using acetic anhydride of higher specific activity. The major expansion of radiochemical derivatization assays probably will be in the direction of broadening their application by employing other radiolabeled reagents.

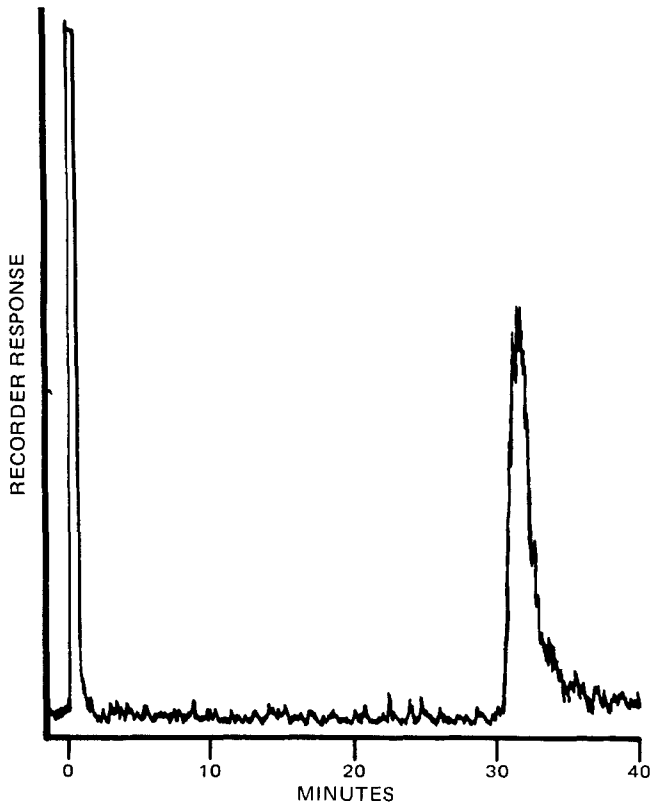

Figure 1—*Radiochemical gas chromatogram of ^{3}H-acetylnortriptyline representing 10 ng of nortriptyline extracted from human blood plasma.*

REFERENCES

(1) W. Hammer and F. Sjöqvist, *Life Sci.*, **6**, 1895 (1967).

(2) M. B. Ashberg, B. Cronholm, F. Sjöqvist, and D. Tuck, *Br. Med. J.*, **4**, 18 (1970).

(3) W. Hammer, S. Martens, and F. Sjöqvist, *Clin. Pharmacol. Ther.*, **10**, 44 (1969).

(4) B. Alexanderson and F. Sjöqvist, *Ann. N.Y. Acad. Sci.*, **179**, 739 (1971).

(5) R. A. Braithwaite and B. Widdop, *Clin. Chim. Acta*, **35**, 461 (1971).

(6) H. B. Hucker and S. C. Stauffer, *J. Pharm. Sci.*, **63**, 296 (1974).

(7) A. Jorgensen, *Acta Pharmacol. Toxicol.*, **36**, 79 (1975).

(8) D. B. Faber, C. Mulder, and W. A. Man In't. Veld, *J. Chromatogr.*, **100**, 55 (1974).

(9) F. R. Zuleski, A. Loh, and F. J. Di Carlo, *ibid.*, **132**, 45 (1977).

(10) W. M. Hammer and B. B. Brodie, *J. Pharmacol. Exp. Ther.*, **157**, 503 (1967).

(11) H.-G. Neumann and J. Schenk, *Xenobiotica*, **3**, 435 (1973).

(12) J. R. L. Smith, B. A. J. Shaw, and D. M. Foulkes, *ibid.*, **2**, 215 (1972).

(13) A. Kuksis, N. Kovacevic, D. Lau, and M. Vranic, *Fed. Proc.*, **34**, 2238 (1975).

ACKNOWLEDGMENTS AND ADDRESSES

Received July 6, 1976, from the *Department of Drug Metabolism,*

[2] Eli Lilly, Indianapolis, Ind.
[3] Warner-Chilcott, Morris Plains, N.J.
[4] Model 894, Packard Instrument Co., Downers Grove, Ill.

Warner–Lambert Research Institute, Morris Plains, NJ 07950.

Accepted for publication August 30, 1976.

The authors are indebted to Mr. E. J. Merrill of this Institute for furnishing a stock solution of ^{3}H-acetic anhydride in dry benzene and for advice on the storage of this material. They also thank Mr. Roger Warner, Packard Instrument Co., for technical assistance in setting up the gas proportional counter.

[x] To whom inquiries should be directed.

Pharmacokinetic Evidence for Improved Ophthalmic Drug Delivery by Reduction of Instilled Volume

THOMAS F. PATTON

Abstract □ The bioavailability of topically applied pilocarpine nitrate was studied as a function of instilled volume. As the instilled volume decreased, the fraction of dose absorbed increased. The relationship between fraction absorbed and instilled volume was not direct, but appropriate adjustment of instilled volume and concentration should permit substantial dosage reductions without sacrifice of drug concentration in the eye. The implications of these findings from both a therapeutic and toxicity standpoint are discussed.

Keyphrases □ Pilocarpine nitrate—bioavailability, effect of instilled volume □ Bioavailability—pilocarpine nitrate, effect of instilled volume □ Ophthalmic cholinergics—pilocarpine nitrate, bioavailability, effect of instilled volume

The drainage of an instilled drug solution away from the eye is considerable and can affect its biological activity (1). This drainage is dependent upon the volume instilled and increases linearly with instilled volume over a large range (1). This fact (2, 3) has been incorporated into experimental design. However, the concept of reducing drop size to improve ophthalmic drug delivery has not become widespread, perhaps because the pharmacokinetic advantages of such an approach have not been emphasized.

A study of the dynamics of instilled fluid drainage (1) showed that the miotic activity of pilocarpine was enhanced by administering the same amount of pilocarpine in decreasing volumes. No actual measurements of drug penetration to the interior of the eye were made. More recent studies showed that the bioavailability of ophthalmic drugs was improved by slowing the rate of drainage of instilled drug solutions (4–8). The measurement of drug concentration in the eye following the reduction of instilled volume and the resultant pharmacokinetic parameters were not reported previously.

In a recent study (9), the aqueous chamber drug distribution volume for ophthalmic drugs was calculated, thereby making it possible to define more precisely the pharmacokinetics of topically applied ophthalmic drugs. Therefore, the purpose of the present study is to show that, as the instilled volume of pilocarpine nitrate is decreased, the fraction of dose absorbed increases. As a result, the parameters of instilled volume and drug concentration can be quantitated to provide a desired level of drug in the eye.

EXPERIMENTAL

Pilocarpine Solutions—Pilocarpine nitrate was used as received[1]. Tritiated pilocarpine[2], specific activity 4.1 Ci/mmole, was purified prior to use by evaporation as recommended previously (10). The concentration of pilocarpine nitrate used was 1×10^{-2} *M* in all studies. Solutions were prepared in isotonic pH 6.24 Sorensen phosphate buffer and were filtered but not sterile. Procedures for the preparation of the tritiated solutions were described previously (10).

Methods—Male, New Zealand, albino rabbits, 60–67 days old, were used. Prior to experimentation, the animals were maintained in standard laboratory animal cages and allowed food and water *ad libitum*. During the experiments, all test animals were kept in restraining boxes in the normal upright position. The head was unencumbered so that all normal eye movements were maintained. The animals were unanesthetized in all cases.

The volumes of instilled solutions administered were 5, 10, 15, and 25 μl and were delivered accurately with a microliter syringe[3]. At various times postinstillation (5, 10, 15, 20, 30, 45, 60, 90, and 120 min), rabbits were sacrificed with an overdose of pentobarbital sodium injected into a marginal ear vein. Eyes were immediately rinsed and blotted, and aqueous humor (at least 100 μl) was aspirated from the anterior chamber.

One hundred microliters of aqueous humor was quantitatively transferred[4] to scintillation counting vials[5] containing 5 ml of prerefrigerated liquid scintillation cocktail[6]. After storage in the dark at room temperature for at least 24 hr, samples were counted[7]. These counts were converted to micrograms of pilocarpine per milliliter of aqueous humor using suitable standard and blank corrections.

RESULTS

Aqueous humor concentration–time profiles of pilocarpine for the four instilled volumes are shown in Table I. These data were plotted semilogarithmically, and the terminal slopes were calculated *via* linear regression analysis. From these slopes, the elimination rate constants were calculated. By using the trapezoidal rule with extrapolation to infinity, the areas under the aqueous humor concentration–time profiles were calculated (Table II). The apparent maximum in area under the curve with an instilled volume of 15 μl is currently unexplained. This maximum also was observed in other experiments and will be discussed in more detail later.

Using rabbits of similar size and age, Conrad and Robinson (9) calculated the aqueous humor distribution volume of pilocarpine to be 0.575

[1] Sigma Chemical Co., St. Louis, Mo.
[2] New England Nuclear, Boston, Mass.
[3] Hamilton Co., Reno, Nev.
[4] Biopette, Schwarz/Mann, Orangeburg, N.Y.
[5] Mini-vial, ICN Isotope and Nuclear Division, Cleveland, Ohio.
[6] Aquasol, New England Nuclear, Boston, Mass.
[7] Model LS-150 liquid scintillation counter, Beckman Instruments, Fullerton, Calif.

Warner–Lambert Research Institute, Morris Plains, NJ 07950.

Accepted for publication August 30, 1976.

The authors are indebted to Mr. E. J. Merrill of this Institute for furnishing a stock solution of ^{3}H-acetic anhydride in dry benzene and for advice on the storage of this material. They also thank Mr. Roger Warner, Packard Instrument Co., for technical assistance in setting up the gas proportional counter.

[x] To whom inquiries should be directed.

Pharmacokinetic Evidence for Improved Ophthalmic Drug Delivery by Reduction of Instilled Volume

THOMAS F. PATTON

Abstract □ The bioavailability of topically applied pilocarpine nitrate was studied as a function of instilled volume. As the instilled volume decreased, the fraction of dose absorbed increased. The relationship between fraction absorbed and instilled volume was not direct, but appropriate adjustment of instilled volume and concentration should permit substantial dosage reductions without sacrifice of drug concentration in the eye. The implications of these findings from both a therapeutic and toxicity standpoint are discussed.

Keyphrases □ Pilocarpine nitrate—bioavailability, effect of instilled volume □ Bioavailability—pilocarpine nitrate, effect of instilled volume □ Ophthalmic cholinergics—pilocarpine nitrate, bioavailability, effect of instilled volume

The drainage of an instilled drug solution away from the eye is considerable and can affect its biological activity (1). This drainage is dependent upon the volume instilled and increases linearly with instilled volume over a large range (1). This fact (2, 3) has been incorporated into experimental design. However, the concept of reducing drop size to improve ophthalmic drug delivery has not become widespread, perhaps because the pharmacokinetic advantages of such an approach have not been emphasized.

A study of the dynamics of instilled fluid drainage (1) showed that the miotic activity of pilocarpine was enhanced by administering the same amount of pilocarpine in decreasing volumes. No actual measurements of drug penetration to the interior of the eye were made. More recent studies showed that the bioavailability of ophthalmic drugs was improved by slowing the rate of drainage of instilled drug solutions (4–8). The measurement of drug concentration in the eye following the reduction of instilled volume and the resultant pharmacokinetic parameters were not reported previously.

In a recent study (9), the aqueous chamber drug distribution volume for ophthalmic drugs was calculated, thereby making it possible to define more precisely the pharmacokinetics of topically applied ophthalmic drugs. Therefore, the purpose of the present study is to show that, as the instilled volume of pilocarpine nitrate is decreased, the fraction of dose absorbed increases. As a result, the parameters of instilled volume and drug concentration can be quantitated to provide a desired level of drug in the eye.

EXPERIMENTAL

Pilocarpine Solutions—Pilocarpine nitrate was used as received[1]. Tritiated pilocarpine[2], specific activity 4.1 Ci/mmole, was purified prior to use by evaporation as recommended previously (10). The concentration of pilocarpine nitrate used was 1×10^{-2} *M* in all studies. Solutions were prepared in isotonic pH 6.24 Sorensen phosphate buffer and were filtered but not sterile. Procedures for the preparation of the tritiated solutions were described previously (10).

Methods—Male, New Zealand, albino rabbits, 60–67 days old, were used. Prior to experimentation, the animals were maintained in standard laboratory animal cages and allowed food and water *ad libitum*. During the experiments, all test animals were kept in restraining boxes in the normal upright position. The head was unencumbered so that all normal eye movements were maintained. The animals were unanesthetized in all cases.

The volumes of instilled solutions administered were 5, 10, 15, and 25 μl and were delivered accurately with a microliter syringe[3]. At various times postinstillation (5, 10, 15, 20, 30, 45, 60, 90, and 120 min), rabbits were sacrificed with an overdose of pentobarbital sodium injected into a marginal ear vein. Eyes were immediately rinsed and blotted, and aqueous humor (at least 100 μl) was aspirated from the anterior chamber.

One hundred microliters of aqueous humor was quantitatively transferred[4] to scintillation counting vials[5] containing 5 ml of prerefrigerated liquid scintillation cocktail[6]. After storage in the dark at room temperature for at least 24 hr, samples were counted[7]. These counts were converted to micrograms of pilocarpine per milliliter of aqueous humor using suitable standard and blank corrections.

RESULTS

Aqueous humor concentration–time profiles of pilocarpine for the four instilled volumes are shown in Table I. These data were plotted semilogarithmically, and the terminal slopes were calculated *via* linear regression analysis. From these slopes, the elimination rate constants were calculated. By using the trapezoidal rule with extrapolation to infinity, the areas under the aqueous humor concentration–time profiles were calculated (Table II). The apparent maximum in area under the curve with an instilled volume of 15 μl is currently unexplained. This maximum also was observed in other experiments and will be discussed in more detail later.

Using rabbits of similar size and age, Conrad and Robinson (9) calculated the aqueous humor distribution volume of pilocarpine to be 0.575

[1] Sigma Chemical Co., St. Louis, Mo.
[2] New England Nuclear, Boston, Mass.
[3] Hamilton Co., Reno, Nev.
[4] Biopette, Schwarz/Mann, Orangeburg, N.Y.
[5] Mini-vial, ICN Isotope and Nuclear Division, Cleveland, Ohio.
[6] Aquasol, New England Nuclear, Boston, Mass.
[7] Model LS-150 liquid scintillation counter, Beckman Instruments, Fullerton, Calif.

Table I—Aqueous Humor Concentration [a] (Micrograms per Milliliter)–Time Profiles following Instillation of Various Volumes of 1×10^{-2} *M* Pilocarpine Nitrate in Rabbits

Minutes	Volume Instilled, μl			
	5	10	15	25 [b]
5	0.17 (0.03)	0.29 (0.03)	0.29 (0.03)	0.55 (0.06)
10	0.47 (0.05)	0.44 (0.02)	0.79 (0.10)	1.03 (0.14)
15	0.48 (0.07)	0.65 (0.04)	1.03 (0.09)	1.11 (0.11)
20	0.51 (0.05)	0.88 (0.11)	1.16 (0.12)	0.98 (0.12)
30	0.50 (0.03)	0.74 (0.11)	0.92 (0.18)	0.93 (0.12)
45	0.38 (0.05)	0.49 (0.05)	0.67 (0.10)	0.42 (0.04)
60	0.26 (0.03)	0.36 (0.05)	0.33 (0.04)	0.44 (0.04)
90	0.17 (0.02)	0.22 (0.02)	0.21 (0.03)	0.19 (0.02)
120	0.08 (0.01)	0.11 (0.02)	0.15 (0.03)	0.11 (0.01)

[a] Mean with standard error in parentheses. Each point is the mean of at least seven determinations. [b] Data taken from Ref. 11.

ml. When this volume was applied to the data reported here, the fraction of dose absorbed (*F*) for each volume studied, 5, 10, 15, and 25 μl, was 3.01×10^{-2}, 2.23×10^{-2}, 1.92×10^{-2}, and 1.16×10^{-2}, respectively.

DISCUSSION

The smaller the instilled volume, the greater is the fraction of applied dose absorbed. These results were implied previously (1) but were not demonstrated pharmacokinetically. Drainage rate is linear with instilled volume over a fairly wide range (1), but the relationship between fraction absorbed and volume is more complex due to other complicating factors. For example, decreases in the drainage rate (*i.e.*, increasing drug contact time) did not result in proportional increases in aqueous humor levels of drug (7, 8).

This result is true also with the fraction of dose absorbed, as seen from the calculated values. A fivefold decrease in volume results in approximately a threefold increase in fraction absorbed, possibly due to competing routes of drug absorption. For a topically applied drug to reach the aqueous humor, it must penetrate the cornea, but conjunctival or nonproductive absorption also occurs and competes with the cornea for drug uptake (8). Drug absorbed by this nonproductive route is not thought to reach the anterior chamber.

What is apparent from this study is that a considerable decrease in instilled volume coupled with a slight increase in instilled concentration should result in the same amount of drug reaching the interior of the eye as if much larger volumes were administered. A simple calculation illustrates this point. Twenty-five microliters of a 1×10^{-2} *M* pilocarpine nitrate solution resulted in an area under the curve of 60.9 μg min ml^{-1}. The dose administered was 67.82 μg, and the fraction absorbed was 1.16×10^{-2} *M*. If one wishes to match this area with a dose of 5 μl, the following equation allows the calculation to be made:

$$A = \frac{FD}{VK} \qquad \text{(Eq. 1)}$$

or, rearranged:

$$D = \frac{AVK}{F} \qquad \text{(Eq. 2)}$$

The value of *F* for the 5-μl case is 3.01×10^{-2}, and $K = 1.88 \times 10^{-2}$ min^{-1}. The area desired is 60.9 μg min ml^{-1}, and the value for *V* is 0.575 ml (9). The calculated value for *D* is 21.87 μg, which corresponds to a concentration of 1.61×10^{-2} *M*. A 5-μl dose of 1.61×10^{-2} *M* pilocarpine nitrate should result in the same area under the curve as a 25-μl dose of 1.00×10^{-2} *M* pilocarpine nitrate.

Therapeutically, it should be possible, by reducing the instilled volume by a factor of five, to reduce the dose administered by approximately a factor of three without altering drug concentration at the active site. This finding is significant and shows that the doses currently used for ophthalmic drugs are generally much larger than required. Potentially more important, however, are the implications from a toxicity standpoint. In both the 5- and 25-μl cases, only a small fraction of the dose is absorbed into the eye, the remainder being lost by various routes and potentially available to act systemically. By reducing the instilled volume and, hence, substantially decreasing the applied dose, the potential for toxic effects is reduced while drug concentration in the eye is maintained.

By using the data presented here, other combinations of volume and concentration adjustments are possible. Studies are currently in progress to confirm these findings and determine any complicating factors. Any rational approach to the development of ophthalmic dosage regimens should consider the excessive volumes currently used and the advantages from the development of better, small volume delivery systems.

Table II—Elimination Rate Constants and Areas under the Aqueous Humor Concentration–Time Profiles following Instillation of Various Volumes of 1×10^{-2} *M* Pilocarpine Nitrate in Rabbits

Volume Instilled, μl	Dose, μg	*K*, min^{-1}	Area, μg min ml^{-1}
5	13.56	1.88×10^{-2}	37.8
10	27.13	2.05×10^{-2}	51.3
15	40.69	2.13×10^{-2}	63.8
25	67.82	2.25×10^{-2}	60.9

REFERENCES

(1) S. S. Chrai, T. F. Patton, A. Mehta, and J. R. Robinson, *J. Pharm. Sci.*, **62,** 1112 (1973).

(2) L. Sendelbeck, D. Moore, and J. Urquhart, *Am. J. Ophthalmol.*, **80,** 274 (1975).

(3) D. A. Benedetto, D. O. Shah, and H. E. Kaufman, *Invest. Ophthalmol.*, **14,** 887 (1975).

(4) S. S. Chrai and J. R. Robinson, *J. Pharm. Sci.*, **63,** 1218 (1974).

(5) T. F. Patton, M.S. thesis, University of Wisconsin, Madison, Wis., 1973.

(6) T. F. Patton and J. R. Robinson, *J. Pharm. Sci.*, **64,** 267 (1975).

(7) *Ibid.*, **64,** 1312 (1975).

(8) T. F. Patton, Ph.D. thesis, University of Wisconsin, Madison, Wis., 1975.

(9) J. M. Conrad and J. R. Robinson, *J. Pharm. Sci.*, **66,** 219 (1977).

(10) S. S. Chrai and J. R. Robinson, *Am. J. Ophthalmol.*, **77,** 735 (1974).

(11) T. S. Friedman and T. F. Patton, *J. Pharm. Sci.*, **65,** 1095 (1976).

ACKNOWLEDGMENTS AND ADDRESSES

Received July 9, 1976, from the *Department of Pharmaceutical Chemistry, School of Pharmacy, University of Kansas, Lawrence, KS 66044.*

Accepted for publication August 30, 1976.

Supported by a grant from the University of Kansas General Research Fund.

The author thanks Mr. T. S. Friedman for assistance in determining the concentration–time profiles and Dr. T. J. Mikkelson for helpful suggestions in the preparation of this manuscript.

Effect of Ibuprofen on Protein Binding of Warfarin in Human Serum

Keyphrases □ Ibuprofen—effect on protein binding of warfarin, human serum □ Binding—warfarin to serum protein, effect of ibuprofen, humans □ Warfarin—serum protein binding, effect of ibuprofen, humans □ Anti-inflammatory agents—ibuprofen, effect on protein binding of warfarin, human serum □ Anticoagulants—warfarin, serum protein binding, effect of ibuprofen, humans

To the Editor:

Ibuprofen is a widely used anti-inflammatory, which is extensively bound to plasma proteins (1). Studies in rats showed that ibuprofen can displace warfarin from serum protein binding sites and that this displacement causes an increase in the total body clearance of warfarin and in the anticoagulant effect produced by a given concentration of total (free and protein-bound) drug (2).

Theoretical considerations indicate that the displacement of a drug from protein binding sites should be associated with a transient and intermittent increase in the pharmacological effect (3, 4). However, no such potentiation was observed in humans with respect to the anticoagulant effect of warfarin when ibuprofen was administered in doses of up to 2.4 g/day (5). In view of the recent tendency to use even larger doses of ibuprofen for the treatment of inflammatory disease, it was considered advisable to determine the relationship between ibuprofen concentration and protein binding of warfarin in human serum.

Blood was obtained from five healthy adult females who were taking no drugs other than oral contraceptives. Serum was separated and pooled. Racemic ^{14}C-warfarin (1.34 μg/ml) and ibuprofen (0–200 μg/ml) were added, and the free fraction of warfarin was determined in duplicate by equilibrium dialysis (6).

The pooled serum contained 4.18% albumin and 8.46% total protein. The free fraction of warfarin in the absence of ibuprofen was 0.00978, equivalent to 99.022% protein binding. The free fraction increased continuously with the increasing ibuprofen concentration (Fig. 1). At the highest concentration of ibuprofen (about 200 μg/ml), the warfarin free fraction was 0.0198, *i.e.*, twice as large as in the absence of ibuprofen.

It is estimated that the steady-state serum concentration of ibuprofen produced by administration of 600 mg every 6 hr to adult patients is about 30–40 μg/ml (2). At this concentration, ibuprofen increases the warfarin free fraction in human serum by only about 10% so that no significant potentiation of anticoagulant effect should be apparent. However, a doubling of the dose will cause an appreciable displacement of warfarin and may be expected to produce a measurable potentiation of anticoagulant effect.

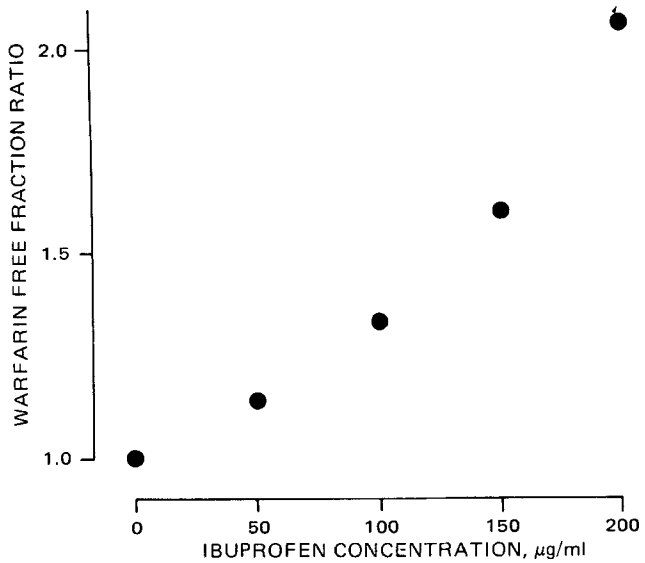

Figure 1—*Effect of ibuprofen on protein binding of warfarin in pooled human serum. Shown is the relationship between the warfarin free fraction ratio (with ibuprofen/control) and the ibuprofen concentration.*

(1) R. F. N. Mills, S. S. Adams, E. E. Cliffe, W. Dickinson, and J. S. Nicholson, *Xenobiotica*, **3**, 589 (1973).

(2) J. T. Slattery, A. Yacobi, and G. Levy, *J. Pharm. Sci.*, **66**, 943 (1977).

(3) G. Levy, *ibid.*, **65**, 1264 (1976).

(4) G. Levy, in "The Effect of Disease States on Drug Pharmacokinetics," L. Z. Benet, Ed., APhA Academy of Pharmaceutical Sciences, Washington, D.C., 1976.

(5) J. A. Penner and P. H. Abbrecht, *Curr. Ther. Res.*, **18**, 862 (1975).

(6) A. Yacobi and G. Levy, *J. Pharm. Sci.*, **64**, 1660 (1975).

John T. Slattery
Gerhard Levy [x]
Department of Pharmaceutics
School of Pharmacy
State University of New York at Buffalo
Buffalo, NY 14214

Received September 17, 1976.
Accepted for publication November 15, 1976.
Supported in part by Grant GM 20852 from the National Institute of General Medical Sciences, National Institutes of Health, Bethesda, MD 20014.

[x] To whom inquiries should be directed.

REVIEWS

Introduction to Pharmaceutical Dosage Forms. By HOWARD C. ANSEL. Lea & Febiger, Washington Square, Philadelphia, PA 19106, 1976. 415 pp. 18.5 × 26 cm. Price $22.50.

In this second edition, the organization and content have been extensively revised. References have been updated and take into account the current literature. The purpose of the book still remains to present to "the beginning student introductory concepts of dosage form design, manufacture, and utilization" of drugs, with emphasis given to the drug entities listed in the official compendia. By selecting the route of administration as the framework, the author has succeeded admirably in meeting this purpose.

The content of the revised edition reflects accurately the changes in curricula taking place in schools of pharmacy and in the practice of pharmacy. It will enable the student to integrate easily basic scientific pharmaceutic concepts with current concepts in patient care, thus presenting a refreshing view in a basic pharmaceutics textbook. The book's value is increased by the discussion of such topics as drug standards and good manufacturing practices and by the new appendix chapter which addresses information vital to the beginning pharmacy student.

While the author extends his appreciation to many who have cooperated in this effort, one strong point of the second edition, as of the first, is its uniformity of style.

This reviewer feels somewhat disappointed in the complete exclusion of a discussion of contact lens solutions, which probably differ in dosage form design and use sufficiently from ophthalmic solutions to deserve some recognition. Also somewhat disappointing is the all too brief discussion of radiopharmaceuticals. Nevertheless, it is easy to recommend adoption of this book by those responsible for teaching basic pharmaceutics courses. Furthermore, the book can serve well as a reference source for those in industry and research.

Reviewed by Peter P. Lamy
School of Pharmacy
University of Maryland
Baltimore, MD 21201

Dispensing of Medication. 8th Ed. Edited by JOHN E. HOOVER. Mack Publishing Co., Easton, PA 18042, 1976. 654 pp. 18 × 26 cm.

This book represents a modern approach to the subject as evidenced by the omission of many chapters dealing solely with the compounding of medications on the industrial level or the type of material presented in "Preparations" courses. Most authors have presented information concerned not only with the fabrication of dosage forms but also with the anatomy and physiology of the body organ systems as well as drug absorption from the various sites. This approach is entirely in keeping with the announced intention of the editor to "aid the patient-oriented pharmacist."

Keeping this intent in mind while reading the text reveals a lapse from time to time. Thus, while an excellent review of bioavailability is presented, one wonders if the dispensing pharmacist who is deeply involved in patient care should expect to receive some direct pointers regarding bioequivalent evaluation of specific products. The chapter on dermatologicals could have presented a clearer description of the effect of ointment bases in percutaneous absorption and the extent that the clinical symptoms determine the selection of dosage form or base in the treatment of dermatologic conditions. One wonders if it is still necessary to belabor the "ideal monodisperse" suspension or to cover the subject of pills.

An excellent balanced approach makes the chapter on parenterals useful to both hospital and industrial pharmacists. If the pharmacist is to monitor parenteral therapy in a rational manner, as suggested by the authors, should not criteria for the use of intravenous administration be provided?

The last chapter, Compounding and Dispensing Information, is over 300 pages and contains a wealth of information on drug interactions and incompatibilities. Unfortunately, a portion of this chapter is not presented in a format that allows the reader to utilize this information to the best advantage. The last 170 pages of this chapter, entitled Specific Compounding and Dispensing Information, is an extremely valuable tool. It presents physical–chemical properties of drugs and drug products by nonproprietary and/or trade names and gives data including incompatibilities, stability, choice of bases, information the pharmacist must consider when dispensing the drug, and information to be given the patient. This type of information should be at every pharmacist's fingertips.

This book represents a valuable addition to the library of the practicing pharmacist, especially one who is interested in ensuring that patients receive proper and optimal pharmaceutical care. The majority of it is well written, concise, and explicit while covering the necessary subjects and should serve the student well as a text.

Reviewed by Noel O. Nuessle
School of Pharmacy
University of Missouri–Kansas City
Kansas City, MO 64110

Pharmacognosy. 7th Ed. By VARRO E. TYLER, LYNN R. BRADY, and JAMES E. ROBBERS. Lea & Febiger, Washington Square, Philadelphia, PA 19106, 1976. 537 pp. 18.5 × 26 cm. Price $21.50.

This book is a revised and updated edition of the single standard textbook for pharmacognosy. It is the only reference suitable for general use by students in pharmacognosy in the United States. The unique position it holds attests to the usefulness of older editions over the past years but precludes comparisons with other books on the same subject.

Most of the book is unchanged from the last edition; new chapters mainly represent rearrangement of material (*e.g.*, Steroids and Peptide Hormones) taken from other sections. Other chapters have been updated, but none is totally rewritten. The drugs included are divided into chapters based upon the chemical (*e.g.*, volatile oils and alkaloids) or therapeutic category (*e.g.*, antibiotics and immunizing agents) classifications. Three chapters at the end contain introductory information on subjects difficult to find in other pharmacy books: Allergens, Poisonous Plants, and Pesticides.

The book has been revised with the expectation of making it more applicable to the "patient-oriented pharmacist." This approach can be detected in the information given regarding cardiac glycosides, in the immunization schedule, and in the list of diseases caused by various microorganisms. This aspect of the revision could have been expanded, because the use given for colchicine is simply "suppressant for gout" and the only use listed for caffeine is "central stimulant," even though the caffeine-containing prescription specialties listed are all used as analgesics. A few misleading statements have remained such as ephedrine "depressing . . . cardiac muscle action" and dextrose as a "fluid . . . replenisher."

The book is recommended as a textbook for all undergraduate pharmacognosy students.

Reviewed by C. Dwayne Ogzewalla
College of Pharmacy
University of Cincinnati
Cincinnati, OH 45267

Analytical Profiles of Drug Substances, Vol. 5. Edited by KLAUS FLOREY. Academic, 111 Fifth Ave., New York, NY 10003, 1976. xi + 560 pp. 16 × 23.5 cm. Price $22.50.

This is the fifth in a series of compilations under the sponsorship of the Pharmaceutical Analysis and Control Section of the APhA Academy of Pharmaceutical Sciences. It is the intent of these volumes to make available in a single source important information about drug substances which is scattered through the scientific literature or which may be filed

away in the laboratories of pharmaceutical scientists. Each drug profile provides useful information and data in the following general areas: description, physical properties, synthesis, stability and degradation, metabolism, analysis (for the drug substance, in its dosage forms, and in biological fluids), pharmacokinetics, and literature references. Physical properties include IR, NMR, UV, and mass spectral data, melting point, solubility data, crystal properties, and pK values where applicable. Analytical methods encompass titrimetry, chromatography, colorimetry, spectrophotometry, elemental analysis, and related techniques.

Each profile is presented in a well-organized and systematic manner. Each is introduced by a table of contents, followed in an orderly sequence by individual categories of specifications, and concluded by an extensive listing of quoted references. This compendium is printed clearly and is replete with tables and graphical presentations. Data are readily located and concisely presented with only a minimum of descriptive information. Maximum utilization is made of the available space.

This volume brings to a total of 97 the number of drugs for which profiles have thus far been prepared, including the 18 in Volume 5. These volumes serve well as companion books to the official compendia by presenting a wealth of data that supplement and are not duplicative of material found in the compendia. As noted in the Forward to Volume 1 of this series, the delegates to the 1970 meeting of the United States Pharmacopeial Convention adopted a resolution that consideration be given to the publication of just such a companion compendium. While the USPC did not undertake this project, it is worthy of note that a number of contributors to this series, including its esteemed editor, are, in fact, members of the USP Committee of Revision.

In view of the fact that fewer than 100 drug profiles have appeared in the first five volumes of this series, and with the mandate for USP XX to include all drugs currently official in USP XIX and NF XIV, all drugs added in their annual supplements, some 600 nonofficial drugs selected by the outgoing Subcommittee on Scope of the USP at its final meeting in January 1975, and new drugs marketed since that date, it is obvious that pharmaceutical scientists have their work cut out for them. It is worth repeating here the editor's invitation that: "All those who have found the profiles useful are earnestly requested to contribute a monograph of their own. The editors stand ready to receive such contributions." Hopefully, there will be an overwhelming response to this invitation.

This burgeoning library of "Analytical Profiles" is a must for all who are engaged in pharmaceutical research.

Reviewed by Martin I. Blake
College of Pharmacy
University of Illinois
Chicago, IL 60612

Aromatic and Heteroaromatic Chemistry. Vol. 4. A Specialist Periodical Report. Edited by C. W. BIRD, G. W. H. CHEESEMAN, *et al.* The Chemical Society, Burlington House, London W1V OBN, England, 1976. 513 pp. 14.5 × 22.5 cm. Price £28.00.

This volume comprises an in-depth review of the literature abstracted between July 1974 and June 1975 and covered by volumes 81 and 82 of "Chemical Abstracts." The organization of the report follows the established pattern of previous volumes.

There are 14 chapters written by 15 international scientists who are specialists in their fields. Most of the chapters include an introduction indicating the parameters established by the author(s) and the reviews on the subject published during the time period. A particularly helpful feature is that all literature citations are included as footnotes on the page that contains the abstract, thus eliminating the time consuming and thought-interrupting process of turning to the end of the chapter when a specific reference is desired. Another helpful feature is a complete author index.

The chapter titles include: Ring Systems of Topical Interest, Intermolecular and Intramolecular Cyclization Reactions in Ring Synthesis, Cycloaddition Reactions, Ring Transformations, Electrophilic Substitution on Carbon, Electrophilic Substitution on Heteroatoms, Nucleophilic Substitution, Aromatic Substitution by Free Radicals, Carbenes and Nitrenes, Addition Reactions, Ring Cleavage Reactions, Reactions of Substituents, Porphyrins and Related Compounds, Naturally Occurring Oxygen-ring Compounds, and Other Naturally Occurring Compounds. The volume comprises 513 pages and includes 2750 literature citations.

The book is well illustrated with many chemical structures and reaction mechanisms. These illustrations are numbered sequentially and placed in close proximity to their text reference, thus affording a free flowing continuity which contributes to the overall excellent readability of the material.

This treatise is an extremely well-organized and readable volume and should serve to stimulate fresh approaches in the ever more sophisticated areas of aromatic and heteroaromatic synthetic chemistry. It is recommended to all chemists who are actively involved in synthetic organic chemistry or who wish to be up to date and informed about research activity in aromatic and heteroaromatic chemistry.

Reviewed by Edward F. LaSala
Massachusetts College of Pharmacy
Boston, MA 02115

Handbook of Analysis of Organic Solvents. By VÁCLAV ŠEDIVEC and JAN FLEK. Halsted, 605 Third Ave., New York, NY 10016, 1976. 455 pp. 16 × 23.5 cm. Price $42.50.

Within this volume the authors have compiled an extensive aggregate of information concerning the chemical and physical properties and the analysis of organic solvents. Following a brief discussion of sampling and drying techniques, procedures are described for the determination of the physical properties and quantitative identification of unknown samples. After a presentation of methods for the analysis of two- and three-component mixtures by physicochemical methods, the basics of GC are described using a general procedure. Relative retention times are given for many common solvents using six different stationary phases.

The second part of the book deals with solvents as individual classes of organic compounds. The most frequently encountered solvents are described in depth, listing synonyms, chemical properties, usual impurities, and azeotropes. Tables containing extensive physical data are included. Detection methods, derivatives, and quantitative procedures are described in detail with corresponding literature references. Three appendixes covering 80 pages include a listing of the boiling points of solvents and their azeotropic mixtures, the major physical properties, and an alphabetical listing of universally used trade names.

This handbook represents a valuable accumulation of a myriad of facts and procedures which will be of use to the analyst, the chromatographer, and the synthetic organic chemist, all of whom frequently require data or techniques to utilize or analyze organic solvents.

Reviewed by Allen L. Jacobs
Pharmacy and Analytical Research Department
Sandoz, Inc.
East Hanover, NJ 07936

The National Formulary and the USP Guide to Select Drugs. Edited by W. M. HELLER, G. K. WURSTER, C. A. DICKIE, and J. W. WHEATLEY. U.S. Pharmacopeial Convention, 12601 Twinbrook Parkway, Rockville, MD 20852, 1976. 295 pp. 10 × 14.5 cm. Price $3.00.

This convenient pocket-size book is intended to be a companion to the official compendia and the USAN Dictionary and is the first compilation of its kind subsequent to the consolidation of the USP and NF. Its purpose is "to highlight those drugs that should receive attention and be used as preferred drugs."

The book contains an alphabetical list of both generic and brand names of effective and useful drugs, with the preferred drugs in boldface type. The entries also contain dosage forms and strength; indication of whether prescription, nonprescription, or DEA controlled; and the pharmacological classification. In addition, there is a cross-index by therapeutic classification.

This book should be useful as a personal prescribing and dispensing guide and as a basic list of preferred drugs for health facilities and various organizations.

Staff Review

REVIEWS

Introduction to Pharmaceutical Dosage Forms. By HOWARD C. ANSEL. Lea & Febiger, Washington Square, Philadelphia, PA 19106, 1976. 415 pp. 18.5 × 26 cm. Price $22.50.

In this second edition, the organization and content have been extensively revised. References have been updated and take into account the current literature. The purpose of the book still remains to present to "the beginning student introductory concepts of dosage form design, manufacture, and utilization" of drugs, with emphasis given to the drug entities listed in the official compendia. By selecting the route of administration as the framework, the author has succeeded admirably in meeting this purpose.

The content of the revised edition reflects accurately the changes in curricula taking place in schools of pharmacy and in the practice of pharmacy. It will enable the student to integrate easily basic scientific pharmaceutic concepts with current concepts in patient care, thus presenting a refreshing view in a basic pharmaceutics textbook. The book's value is increased by the discussion of such topics as drug standards and good manufacturing practices and by the new appendix chapter which addresses information vital to the beginning pharmacy student.

While the author extends his appreciation to many who have cooperated in this effort, one strong point of the second edition, as of the first, is its uniformity of style.

This reviewer feels somewhat disappointed in the complete exclusion of a discussion of contact lens solutions, which probably differ in dosage form design and use sufficiently from ophthalmic solutions to deserve some recognition. Also somewhat disappointing is the all too brief discussion of radiopharmaceuticals. Nevertheless, it is easy to recommend adoption of this book by those responsible for teaching basic pharmaceutics courses. Furthermore, the book can serve well as a reference source for those in industry and research.

Reviewed by Peter P. Lamy
School of Pharmacy
University of Maryland
Baltimore, MD 21201

Dispensing of Medication. 8th Ed. Edited by JOHN E. HOOVER. Mack Publishing Co., Easton, PA 18042, 1976. 654 pp. 18 × 26 cm.

This book represents a modern approach to the subject as evidenced by the omission of many chapters dealing solely with the compounding of medications on the industrial level or the type of material presented in "Preparations" courses. Most authors have presented information concerned not only with the fabrication of dosage forms but also with the anatomy and physiology of the body organ systems as well as drug absorption from the various sites. This approach is entirely in keeping with the announced intention of the editor to "aid the patient-oriented pharmacist."

Keeping this intent in mind while reading the text reveals a lapse from time to time. Thus, while an excellent review of bioavailability is presented, one wonders if the dispensing pharmacist who is deeply involved in patient care should expect to receive some direct pointers regarding bioequivalent evaluation of specific products. The chapter on dermatologicals could have presented a clearer description of the effect of ointment bases in percutaneous absorption and the extent that the clinical symptoms determine the selection of dosage form or base in the treatment of dermatologic conditions. One wonders if it is still necessary to belabor the "ideal monodisperse" suspension or to cover the subject of pills.

An excellent balanced approach makes the chapter on parenterals useful to both hospital and industrial pharmacists. If the pharmacist is to monitor parenteral therapy in a rational manner, as suggested by the authors, should not criteria for the use of intravenous administration be provided?

The last chapter, Compounding and Dispensing Information, is over 300 pages and contains a wealth of information on drug interactions and incompatibilities. Unfortunately, a portion of this chapter is not presented in a format that allows the reader to utilize this information to the best advantage. The last 170 pages of this chapter, entitled Specific Compounding and Dispensing Information, is an extremely valuable tool. It presents physical–chemical properties of drugs and drug products by nonproprietary and/or trade names and gives data including incompatibilities, stability, choice of bases, information the pharmacist must consider when dispensing the drug, and information to be given the patient. This type of information should be at every pharmacist's fingertips.

This book represents a valuable addition to the library of the practicing pharmacist, especially one who is interested in ensuring that patients receive proper and optimal pharmaceutical care. The majority of it is well written, concise, and explicit while covering the necessary subjects and should serve the student well as a text.

Reviewed by Noel O. Nuessle
School of Pharmacy
University of Missouri–Kansas City
Kansas City, MO 64110

Pharmacognosy. 7th Ed. By VARRO E. TYLER, LYNN R. BRADY, and JAMES E. ROBBERS. Lea & Febiger, Washington Square, Philadelphia, PA 19106, 1976. 537 pp. 18.5 × 26 cm. Price $21.50.

This book is a revised and updated edition of the single standard textbook for pharmacognosy. It is the only reference suitable for general use by students in pharmacognosy in the United States. The unique position it holds attests to the usefulness of older editions over the past years but precludes comparisons with other books on the same subject.

Most of the book is unchanged from the last edition; new chapters mainly represent rearrangement of material (*e.g.*, Steroids and Peptide Hormones) taken from other sections. Other chapters have been updated, but none is totally rewritten. The drugs included are divided into chapters based upon the chemical (*e.g.*, volatile oils and alkaloids) or therapeutic category (*e.g.*, antibiotics and immunizing agents) classifications. Three chapters at the end contain introductory information on subjects difficult to find in other pharmacy books: Allergens, Poisonous Plants, and Pesticides.

The book has been revised with the expectation of making it more applicable to the "patient-oriented pharmacist." This approach can be detected in the information given regarding cardiac glycosides, in the immunization schedule, and in the list of diseases caused by various microorganisms. This aspect of the revision could have been expanded, because the use given for colchicine is simply "suppressant for gout" and the only use listed for caffeine is "central stimulant," even though the caffeine-containing prescription specialties listed are all used as analgesics. A few misleading statements have remained such as ephedrine "depressing . . . cardiac muscle action" and dextrose as a "fluid . . . replenisher."

The book is recommended as a textbook for all undergraduate pharmacognosy students.

Reviewed by C. Dwayne Ogzewalla
College of Pharmacy
University of Cincinnati
Cincinnati, OH 45267

Analytical Profiles of Drug Substances, Vol. 5. Edited by KLAUS FLOREY. Academic, 111 Fifth Ave., New York, NY 10003, 1976. xi + 560 pp. 16 × 23.5 cm. Price $22.50.

This is the fifth in a series of compilations under the sponsorship of the Pharmaceutical Analysis and Control Section of the APhA Academy of Pharmaceutical Sciences. It is the intent of these volumes to make available in a single source important information about drug substances which is scattered through the scientific literature or which may be filed

REVIEWS

Introduction to Pharmaceutical Dosage Forms. By HOWARD C. ANSEL. Lea & Febiger, Washington Square, Philadelphia, PA 19106, 1976. 415 pp. 18.5 × 26 cm. Price $22.50.

In this second edition, the organization and content have been extensively revised. References have been updated and take into account the current literature. The purpose of the book still remains to present to "the beginning student introductory concepts of dosage form design, manufacture, and utilization" of drugs, with emphasis given to the drug entities listed in the official compendia. By selecting the route of administration as the framework, the author has succeeded admirably in meeting this purpose.

The content of the revised edition reflects accurately the changes in curricula taking place in schools of pharmacy and in the practice of pharmacy. It will enable the student to integrate easily basic scientific pharmaceutic concepts with current concepts in patient care, thus presenting a refreshing view in a basic pharmaceutics textbook. The book's value is increased by the discussion of such topics as drug standards and good manufacturing practices and by the new appendix chapter which addresses information vital to the beginning pharmacy student.

While the author extends his appreciation to many who have cooperated in this effort, one strong point of the second edition, as of the first, is its uniformity of style.

This reviewer feels somewhat disappointed in the complete exclusion of a discussion of contact lens solutions, which probably differ in dosage form design and use sufficiently from ophthalmic solutions to deserve some recognition. Also somewhat disappointing is the all too brief discussion of radiopharmaceuticals. Nevertheless, it is easy to recommend adoption of this book by those responsible for teaching basic pharmaceutics courses. Furthermore, the book can serve well as a reference source for those in industry and research.

Reviewed by Peter P. Lamy
School of Pharmacy
University of Maryland
Baltimore, MD 21201

Dispensing of Medication. 8th Ed. Edited by JOHN E. HOOVER. Mack Publishing Co., Easton, PA 18042, 1976. 654 pp. 18 × 26 cm.

This book represents a modern approach to the subject as evidenced by the omission of many chapters dealing solely with the compounding of medications on the industrial level or the type of material presented in "Preparations" courses. Most authors have presented information concerned not only with the fabrication of dosage forms but also with the anatomy and physiology of the body organ systems as well as drug absorption from the various sites. This approach is entirely in keeping with the announced intention of the editor to "aid the patient-oriented pharmacist."

Keeping this intent in mind while reading the text reveals a lapse from time to time. Thus, while an excellent review of bioavailability is presented, one wonders if the dispensing pharmacist who is deeply involved in patient care should expect to receive some direct pointers regarding bioequivalent evaluation of specific products. The chapter on dermatologicals could have presented a clearer description of the effect of ointment bases in percutaneous absorption and the extent that the clinical symptoms determine the selection of dosage form or base in the treatment of dermatologic conditions. One wonders if it is still necessary to belabor the "ideal monodisperse" suspension or to cover the subject of pills.

An excellent balanced approach makes the chapter on parenterals useful to both hospital and industrial pharmacists. If the pharmacist is to monitor parenteral therapy in a rational manner, as suggested by the authors, should not criteria for the use of intravenous administration be provided?

The last chapter, Compounding and Dispensing Information, is over 300 pages and contains a wealth of information on drug interactions and incompatibilities. Unfortunately, a portion of this chapter is not presented in a format that allows the reader to utilize this information to the best advantage. The last 170 pages of this chapter, entitled Specific Compounding and Dispensing Information, is an extremely valuable tool. It presents physical–chemical properties of drugs and drug products by nonproprietary and/or trade names and gives data including incompatibilities, stability, choice of bases, information the pharmacist must consider when dispensing the drug, and information to be given the patient. This type of information should be at every pharmacist's fingertips.

This book represents a valuable addition to the library of the practicing pharmacist, especially one who is interested in ensuring that patients receive proper and optimal pharmaceutical care. The majority of it is well written, concise, and explicit while covering the necessary subjects and should serve the student well as a text.

Reviewed by Noel O. Nuessle
School of Pharmacy
University of Missouri–Kansas City
Kansas City, MO 64110

Pharmacognosy. 7th Ed. By VARRO E. TYLER, LYNN R. BRADY, and JAMES E. ROBBERS. Lea & Febiger, Washington Square, Philadelphia, PA 19106, 1976. 537 pp. 18.5 × 26 cm. Price $21.50.

This book is a revised and updated edition of the single standard textbook for pharmacognosy. It is the only reference suitable for general use by students in pharmacognosy in the United States. The unique position it holds attests to the usefulness of older editions over the past years but precludes comparisons with other books on the same subject.

Most of the book is unchanged from the last edition; new chapters mainly represent rearrangement of material (*e.g.*, Steroids and Peptide Hormones) taken from other sections. Other chapters have been updated, but none is totally rewritten. The drugs included are divided into chapters based upon the chemical (*e.g.*, volatile oils and alkaloids) or therapeutic category (*e.g.*, antibiotics and immunizing agents) classifications. Three chapters at the end contain introductory information on subjects difficult to find in other pharmacy books: Allergens, Poisonous Plants, and Pesticides.

The book has been revised with the expectation of making it more applicable to the "patient-oriented pharmacist." This approach can be detected in the information given regarding cardiac glycosides, in the immunization schedule, and in the list of diseases caused by various microorganisms. This aspect of the revision could have been expanded, because the use given for colchicine is simply "suppressant for gout" and the only use listed for caffeine is "central stimulant," even though the caffeine-containing prescription specialties listed are all used as analgesics. A few misleading statements have remained such as ephedrine "depressing . . . cardiac muscle action" and dextrose as a "fluid . . . replenisher."

The book is recommended as a textbook for all undergraduate pharmacognosy students.

Reviewed by C. Dwayne Ogzewalla
College of Pharmacy
University of Cincinnati
Cincinnati, OH 45267

Analytical Profiles of Drug Substances, Vol. 5. Edited by KLAUS FLOREY. Academic, 111 Fifth Ave., New York, NY 10003, 1976. xi + 560 pp. 16 × 23.5 cm. Price $22.50.

This is the fifth in a series of compilations under the sponsorship of the Pharmaceutical Analysis and Control Section of the APhA Academy of Pharmaceutical Sciences. It is the intent of these volumes to make available in a single source important information about drug substances which is scattered through the scientific literature or which may be filed

REVIEWS

Introduction to Pharmaceutical Dosage Forms. By HOWARD C. ANSEL. Lea & Febiger, Washington Square, Philadelphia, PA 19106, 1976. 415 pp. 18.5 × 26 cm. Price $22.50.

In this second edition, the organization and content have been extensively revised. References have been updated and take into account the current literature. The purpose of the book still remains to present to "the beginning student introductory concepts of dosage form design, manufacture, and utilization" of drugs, with emphasis given to the drug entities listed in the official compendia. By selecting the route of administration as the framework, the author has succeeded admirably in meeting this purpose.

The content of the revised edition reflects accurately the changes in curricula taking place in schools of pharmacy and in the practice of pharmacy. It will enable the student to integrate easily basic scientific pharmaceutic concepts with current concepts in patient care, thus presenting a refreshing view in a basic pharmaceutics textbook. The book's value is increased by the discussion of such topics as drug standards and good manufacturing practices and by the new appendix chapter which addresses information vital to the beginning pharmacy student.

While the author extends his appreciation to many who have cooperated in this effort, one strong point of the second edition, as of the first, is its uniformity of style.

This reviewer feels somewhat disappointed in the complete exclusion of a discussion of contact lens solutions, which probably differ in dosage form design and use sufficiently from ophthalmic solutions to deserve some recognition. Also somewhat disappointing is the all too brief discussion of radiopharmaceuticals. Nevertheless, it is easy to recommend adoption of this book by those responsible for teaching basic pharmaceutics courses. Furthermore, the book can serve well as a reference source for those in industry and research.

Reviewed by Peter P. Lamy
School of Pharmacy
University of Maryland
Baltimore, MD 21201

Dispensing of Medication. 8th Ed. Edited by JOHN E. HOOVER. Mack Publishing Co., Easton, PA 18042, 1976. 654 pp. 18 × 26 cm.

This book represents a modern approach to the subject as evidenced by the omission of many chapters dealing solely with the compounding of medications on the industrial level or the type of material presented in "Preparations" courses. Most authors have presented information concerned not only with the fabrication of dosage forms but also with the anatomy and physiology of the body organ systems as well as drug absorption from the various sites. This approach is entirely in keeping with the announced intention of the editor to "aid the patient-oriented pharmacist."

Keeping this intent in mind while reading the text reveals a lapse from time to time. Thus, while an excellent review of bioavailability is presented, one wonders if the dispensing pharmacist who is deeply involved in patient care should expect to receive some direct pointers regarding bioequivalent evaluation of specific products. The chapter on dermatologicals could have presented a clearer description of the effect of ointment bases in percutaneous absorption and the extent that the clinical symptoms determine the selection of dosage form or base in the treatment of dermatologic conditions. One wonders if it is still necessary to belabor the "ideal monodisperse" suspension or to cover the subject of pills.

An excellent balanced approach makes the chapter on parenterals useful to both hospital and industrial pharmacists. If the pharmacist is to monitor parenteral therapy in a rational manner, as suggested by the authors, should not criteria for the use of intravenous administration be provided?

The last chapter, Compounding and Dispensing Information, is over 300 pages and contains a wealth of information on drug interactions and incompatibilities. Unfortunately, a portion of this chapter is not presented in a format that allows the reader to utilize this information to the best advantage. The last 170 pages of this chapter, entitled Specific Compounding and Dispensing Information, is an extremely valuable tool. It presents physical–chemical properties of drugs and drug products by nonproprietary and/or trade names and gives data including incompatibilities, stability, choice of bases, information the pharmacist must consider when dispensing the drug, and information to be given the patient. This type of information should be at every pharmacist's fingertips.

This book represents a valuable addition to the library of the practicing pharmacist, especially one who is interested in ensuring that patients receive proper and optimal pharmaceutical care. The majority of it is well written, concise, and explicit while covering the necessary subjects and should serve the student well as a text.

Reviewed by Noel O. Nuessle
School of Pharmacy
University of Missouri–Kansas City
Kansas City, MO 64110

Pharmacognosy. 7th Ed. By VARRO E. TYLER, LYNN R. BRADY, and JAMES E. ROBBERS. Lea & Febiger, Washington Square, Philadelphia, PA 19106, 1976. 537 pp. 18.5 × 26 cm. Price $21.50.

This book is a revised and updated edition of the single standard textbook for pharmacognosy. It is the only reference suitable for general use by students in pharmacognosy in the United States. The unique position it holds attests to the usefulness of older editions over the past years but precludes comparisons with other books on the same subject.

Most of the book is unchanged from the last edition; new chapters mainly represent rearrangement of material (*e.g.*, Steroids and Peptide Hormones) taken from other sections. Other chapters have been updated, but none is totally rewritten. The drugs included are divided into chapters based upon the chemical (*e.g.*, volatile oils and alkaloids) or therapeutic category (*e.g.*, antibiotics and immunizing agents) classifications. Three chapters at the end contain introductory information on subjects difficult to find in other pharmacy books: Allergens, Poisonous Plants, and Pesticides.

The book has been revised with the expectation of making it more applicable to the "patient-oriented pharmacist." This approach can be detected in the information given regarding cardiac glycosides, in the immunization schedule, and in the list of diseases caused by various microorganisms. This aspect of the revision could have been expanded, because the use given for colchicine is simply "suppressant for gout" and the only use listed for caffeine is "central stimulant," even though the caffeine-containing prescription specialties listed are all used as analgesics. A few misleading statements have remained such as ephedrine "depressing . . . cardiac muscle action" and dextrose as a "fluid . . . replenisher."

The book is recommended as a textbook for all undergraduate pharmacognosy students.

Reviewed by C. Dwayne Ogzewalla
College of Pharmacy
University of Cincinnati
Cincinnati, OH 45267

Analytical Profiles of Drug Substances, Vol. 5. Edited by KLAUS FLOREY. Academic, 111 Fifth Ave., New York, NY 10003, 1976. xi + 560 pp. 16 × 23.5 cm. Price $22.50.

This is the fifth in a series of compilations under the sponsorship of the Pharmaceutical Analysis and Control Section of the APhA Academy of Pharmaceutical Sciences. It is the intent of these volumes to make available in a single source important information about drug substances which is scattered through the scientific literature or which may be filed

away in the laboratories of pharmaceutical scientists. Each drug profile provides useful information and data in the following general areas: description, physical properties, synthesis, stability and degradation, metabolism, analysis (for the drug substance, in its dosage forms, and in biological fluids), pharmacokinetics, and literature references. Physical properties include IR, NMR, UV, and mass spectral data, melting point, solubility data, crystal properties, and pK values where applicable. Analytical methods encompass titrimetry, chromatography, colorimetry, spectrophotometry, elemental analysis, and related techniques.

Each profile is presented in a well-organized and systematic manner. Each is introduced by a table of contents, followed in an orderly sequence by individual categories of specifications, and concluded by an extensive listing of quoted references. This compendium is printed clearly and is replete with tables and graphical presentations. Data are readily located and concisely presented with only a minimum of descriptive information. Maximum utilization is made of the available space.

This volume brings to a total of 97 the number of drugs for which profiles have thus far been prepared, including the 18 in Volume 5. These volumes serve well as companion books to the official compendia by presenting a wealth of data that supplement and are not duplicative of material found in the compendia. As noted in the Forward to Volume 1 of this series, the delegates to the 1970 meeting of the United States Pharmacopeial Convention adopted a resolution that consideration be given to the publication of just such a companion compendium. While the USPC did not undertake this project, it is worthy of note that a number of contributors to this series, including its esteemed editor, are, in fact, members of the USP Committee of Revision.

In view of the fact that fewer than 100 drug profiles have appeared in the first five volumes of this series, and with the mandate for USP XX to include all drugs currently official in USP XIX and NF XIV, all drugs added in their annual supplements, some 600 nonofficial drugs selected by the outgoing Subcommittee on Scope of the USP at its final meeting in January 1975, and new drugs marketed since that date, it is obvious that pharmaceutical scientists have their work cut out for them. It is worth repeating here the editor's invitation that: "All those who have found the profiles useful are earnestly requested to contribute a monograph of their own. The editors stand ready to receive such contributions." Hopefully, there will be an overwhelming response to this invitation.

This burgeoning library of "Analytical Profiles" is a must for all who are engaged in pharmaceutical research.

Reviewed by Martin I. Blake
College of Pharmacy
University of Illinois
Chicago, IL 60612

Aromatic and Heteroaromatic Chemistry. Vol. 4. A Specialist Periodical Report. Edited by C. W. BIRD, G. W. H. CHEESEMAN, *et al.* The Chemical Society, Burlington House, London W1V OBN, England, 1976. 513 pp. 14.5 × 22.5 cm. Price £28.00.

This volume comprises an in-depth review of the literature abstracted between July 1974 and June 1975 and covered by volumes 81 and 82 of "Chemical Abstracts." The organization of the report follows the established pattern of previous volumes.

There are 14 chapters written by 15 international scientists who are specialists in their fields. Most of the chapters include an introduction indicating the parameters established by the author(s) and the reviews on the subject published during the time period. A particularly helpful feature is that all literature citations are included as footnotes on the page that contains the abstract, thus eliminating the time consuming and thought-interrupting process of turning to the end of the chapter when a specific reference is desired. Another helpful feature is a complete author index.

The chapter titles include: Ring Systems of Topical Interest, Intermolecular and Intramolecular Cyclization Reactions in Ring Synthesis, Cycloaddition Reactions, Ring Transformations, Electrophilic Substitution on Carbon, Electrophilic Substitution on Heteroatoms, Nucleophilic Substitution, Aromatic Substitution by Free Radicals, Carbenes and Nitrenes, Addition Reactions, Ring Cleavage Reactions, Reactions of Substituents, Porphyrins and Related Compounds, Naturally Occurring Oxygen-ring Compounds, and Other Naturally Occurring Compounds. The volume comprises 513 pages and includes 2750 literature citations.

The book is well illustrated with many chemical structures and reaction mechanisms. These illustrations are numbered sequentially and placed in close proximity to their text reference, thus affording a free flowing continuity which contributes to the overall excellent readability of the material.

This treatise is an extremely well-organized and readable volume and should serve to stimulate fresh approaches in the ever more sophisticated areas of aromatic and heteroaromatic synthetic chemistry. It is recommended to all chemists who are actively involved in synthetic organic chemistry or who wish to be up to date and informed about research activity in aromatic and heteroaromatic chemistry.

Reviewed by Edward F. LaSala
Massachusetts College of Pharmacy
Boston, MA 02115

Handbook of Analysis of Organic Solvents. By VÁCLAV ŠEDIVEC and JAN FLEK. Halsted, 605 Third Ave., New York, NY 10016, 1976. 455 pp. 16 × 23.5 cm. Price $42.50.

Within this volume the authors have compiled an extensive aggregate of information concerning the chemical and physical properties and the analysis of organic solvents. Following a brief discussion of sampling and drying techniques, procedures are described for the determination of the physical properties and quantitative identification of unknown samples. After a presentation of methods for the analysis of two- and three-component mixtures by physicochemical methods, the basics of GC are described using a general procedure. Relative retention times are given for many common solvents using six different stationary phases.

The second part of the book deals with solvents as individual classes of organic compounds. The most frequently encountered solvents are described in depth, listing synonyms, chemical properties, usual impurities, and azeotropes. Tables containing extensive physical data are included. Detection methods, derivatives, and quantitative procedures are described in detail with corresponding literature references. Three appendixes covering 80 pages include a listing of the boiling points of solvents and their azeotropic mixtures, the major physical properties, and an alphabetical listing of universally used trade names.

This handbook represents a valuable accumulation of a myriad of facts and procedures which will be of use to the analyst, the chromatographer, and the synthetic organic chemist, all of whom frequently require data or techniques to utilize or analyze organic solvents.

Reviewed by Allen L. Jacobs
Pharmacy and Analytical Research Department
Sandoz, Inc.
East Hanover, NJ 07936

The National Formulary and the USP Guide to Select Drugs. Edited by W. M. HELLER, G. K. WURSTER, C. A. DICKIE, and J. W. WHEATLEY. U.S. Pharmacopeial Convention, 12601 Twinbrook Parkway, Rockville, MD 20852, 1976. 295 pp. 10 × 14.5 cm. Price $3.00.

This convenient pocket-size book is intended to be a companion to the official compendia and the USAN Dictionary and is the first compilation of its kind subsequent to the consolidation of the USP and NF. Its purpose is "to highlight those drugs that should receive attention and be used as preferred drugs."

The book contains an alphabetical list of both generic and brand names of effective and useful drugs, with the preferred drugs in boldface type. The entries also contain dosage forms and strength; indication of whether prescription, nonprescription, or DEA controlled; and the pharmacological classification. In addition, there is a cross-index by therapeutic classification.

This book should be useful as a personal prescribing and dispensing guide and as a basic list of preferred drugs for health facilities and various organizations.

Staff Review

away in the laboratories of pharmaceutical scientists. Each drug profile provides useful information and data in the following general areas: description, physical properties, synthesis, stability and degradation, metabolism, analysis (for the drug substance, in its dosage forms, and in biological fluids), pharmacokinetics, and literature references. Physical properties include IR, NMR, UV, and mass spectral data, melting point, solubility data, crystal properties, and pK values where applicable. Analytical methods encompass titrimetry, chromatography, colorimetry, spectrophotometry, elemental analysis, and related techniques.

Each profile is presented in a well-organized and systematic manner. Each is introduced by a table of contents, followed in an orderly sequence by individual categories of specifications, and concluded by an extensive listing of quoted references. This compendium is printed clearly and is replete with tables and graphical presentations. Data are readily located and concisely presented with only a minimum of descriptive information. Maximum utilization is made of the available space.

This volume brings to a total of 97 the number of drugs for which profiles have thus far been prepared, including the 18 in Volume 5. These volumes serve well as companion books to the official compendia by presenting a wealth of data that supplement and are not duplicative of material found in the compendia. As noted in the Forward to Volume 1 of this series, the delegates to the 1970 meeting of the United States Pharmacopeial Convention adopted a resolution that consideration be given to the publication of just such a companion compendium. While the USPC did not undertake this project, it is worthy of note that a number of contributors to this series, including its esteemed editor, are, in fact, members of the USP Committee of Revision.

In view of the fact that fewer than 100 drug profiles have appeared in the first five volumes of this series, and with the mandate for USP XX to include all drugs currently official in USP XIX and NF XIV, all drugs added in their annual supplements, some 600 nonofficial drugs selected by the outgoing Subcommittee on Scope of the USP at its final meeting in January 1975, and new drugs marketed since that date, it is obvious that pharmaceutical scientists have their work cut out for them. It is worth repeating here the editor's invitation that: "All those who have found the profiles useful are earnestly requested to contribute a monograph of their own. The editors stand ready to receive such contributions." Hopefully, there will be an overwhelming response to this invitation.

This burgeoning library of "Analytical Profiles" is a must for all who are engaged in pharmaceutical research.

Reviewed by Martin I. Blake
College of Pharmacy
University of Illinois
Chicago, IL 60612

Aromatic and Heteroaromatic Chemistry. Vol. 4. A Specialist Periodical Report. Edited by C. W. BIRD, G. W. H. CHEESEMAN, *et al.* The Chemical Society, Burlington House, London W1V OBN, England, 1976. 513 pp. 14.5 × 22.5 cm. Price £28.00.

This volume comprises an in-depth review of the literature abstracted between July 1974 and June 1975 and covered by volumes 81 and 82 of "Chemical Abstracts." The organization of the report follows the established pattern of previous volumes.

There are 14 chapters written by 15 international scientists who are specialists in their fields. Most of the chapters include an introduction indicating the parameters established by the author(s) and the reviews on the subject published during the time period. A particularly helpful feature is that all literature citations are included as footnotes on the page that contains the abstract, thus eliminating the time consuming and thought-interrupting process of turning to the end of the chapter when a specific reference is desired. Another helpful feature is a complete author index.

The chapter titles include: Ring Systems of Topical Interest, Intermolecular and Intramolecular Cyclization Reactions in Ring Synthesis, Cycloaddition Reactions, Ring Transformations, Electrophilic Substitution on Carbon, Electrophilic Substitution on Heteroatoms, Nucleophilic Substitution, Aromatic Substitution by Free Radicals, Carbenes and Nitrenes, Addition Reactions, Ring Cleavage Reactions, Reactions of Substituents, Porphyrins and Related Compounds, Naturally Occurring Oxygen-ring Compounds, and Other Naturally Occurring Compounds. The volume comprises 513 pages and includes 2750 literature citations.

The book is well illustrated with many chemical structures and reaction mechanisms. These illustrations are numbered sequentially and placed in close proximity to their text reference, thus affording a free flowing continuity which contributes to the overall excellent readability of the material.

This treatise is an extremely well-organized and readable volume and should serve to stimulate fresh approaches in the ever more sophisticated areas of aromatic and heteroaromatic synthetic chemistry. It is recommended to all chemists who are actively involved in synthetic organic chemistry or who wish to be up to date and informed about research activity in aromatic and heteroaromatic chemistry.

Reviewed by Edward F. LaSala
Massachusetts College of Pharmacy
Boston, MA 02115

Handbook of Analysis of Organic Solvents. By VÁCLAV ŠEDIVEC and JAN FLEK. Halsted, 605 Third Ave., New York, NY 10016, 1976. 455 pp. 16 × 23.5 cm. Price $42.50.

Within this volume the authors have compiled an extensive aggregate of information concerning the chemical and physical properties and the analysis of organic solvents. Following a brief discussion of sampling and drying techniques, procedures are described for the determination of the physical properties and quantitative identification of unknown samples. After a presentation of methods for the analysis of two- and three-component mixtures by physicochemical methods, the basics of GC are described using a general procedure. Relative retention times are given for many common solvents using six different stationary phases.

The second part of the book deals with solvents as individual classes of organic compounds. The most frequently encountered solvents are described in depth, listing synonyms, chemical properties, usual impurities, and azeotropes. Tables containing extensive physical data are included. Detection methods, derivatives, and quantitative procedures are described in detail with corresponding literature references. Three appendixes covering 80 pages include a listing of the boiling points of solvents and their azeotropic mixtures, the major physical properties, and an alphabetical listing of universally used trade names.

This handbook represents a valuable accumulation of a myriad of facts and procedures which will be of use to the analyst, the chromatographer, and the synthetic organic chemist, all of whom frequently require data or techniques to utilize or analyze organic solvents.

Reviewed by Allen L. Jacobs
Pharmacy and Analytical Research Department
Sandoz, Inc.
East Hanover, NJ 07936

The National Formulary and the USP Guide to Select Drugs. Edited by W. M. HELLER, G. K. WURSTER, C. A. DICKIE, and J. W. WHEATLEY. U.S. Pharmacopeial Convention, 12601 Twinbrook Parkway, Rockville, MD 20852, 1976. 295 pp. 10 × 14.5 cm. Price $3.00.

This convenient pocket-size book is intended to be a companion to the official compendia and the USAN Dictionary and is the first compilation of its kind subsequent to the consolidation of the USP and NF. Its purpose is "to highlight those drugs that should receive attention and be used as preferred drugs."

The book contains an alphabetical list of both generic and brand names of effective and useful drugs, with the preferred drugs in boldface type. The entries also contain dosage forms and strength; indication of whether prescription, nonprescription, or DEA controlled; and the pharmacological classification. In addition, there is a cross-index by therapeutic classification.

This book should be useful as a personal prescribing and dispensing guide and as a basic list of preferred drugs for health facilities and various organizations.

Staff Review

away in the laboratories of pharmaceutical scientists. Each drug profile provides useful information and data in the following general areas: description, physical properties, synthesis, stability and degradation, metabolism, analysis (for the drug substance, in its dosage forms, and in biological fluids), pharmacokinetics, and literature references. Physical properties include IR, NMR, UV, and mass spectral data, melting point, solubility data, crystal properties, and pK values where applicable. Analytical methods encompass titrimetry, chromatography, colorimetry, spectrophotometry, elemental analysis, and related techniques.

Each profile is presented in a well-organized and systematic manner. Each is introduced by a table of contents, followed in an orderly sequence by individual categories of specifications, and concluded by an extensive listing of quoted references. This compendium is printed clearly and is replete with tables and graphical presentations. Data are readily located and concisely presented with only a minimum of descriptive information. Maximum utilization is made of the available space.

This volume brings to a total of 97 the number of drugs for which profiles have thus far been prepared, including the 18 in Volume 5. These volumes serve well as companion books to the official compendia by presenting a wealth of data that supplement and are not duplicative of material found in the compendia. As noted in the Forward to Volume 1 of this series, the delegates to the 1970 meeting of the United States Pharmacopeial Convention adopted a resolution that consideration be given to the publication of just such a companion compendium. While the USPC did not undertake this project, it is worthy of note that a number of contributors to this series, including its esteemed editor, are, in fact, members of the USP Committee of Revision.

In view of the fact that fewer than 100 drug profiles have appeared in the first five volumes of this series, and with the mandate for USP XX to include all drugs currently official in USP XIX and NF XIV, all drugs added in their annual supplements, some 600 nonofficial drugs selected by the outgoing Subcommittee on Scope of the USP at its final meeting in January 1975, and new drugs marketed since that date, it is obvious that pharmaceutical scientists have their work cut out for them. It is worth repeating here the editor's invitation that: "All those who have found the profiles useful are earnestly requested to contribute a monograph of their own. The editors stand ready to receive such contributions." Hopefully, there will be an overwhelming response to this invitation.

This burgeoning library of "Analytical Profiles" is a must for all who are engaged in pharmaceutical research.

Reviewed by Martin I. Blake
College of Pharmacy
University of Illinois
Chicago, IL 60612

Aromatic and Heteroaromatic Chemistry. Vol. 4. A Specialist Periodical Report. Edited by C. W. BIRD, G. W. H. CHEESEMAN, *et al.* The Chemical Society, Burlington House, London W1V OBN, England, 1976. 513 pp. 14.5 × 22.5 cm. Price £28.00.

This volume comprises an in-depth review of the literature abstracted between July 1974 and June 1975 and covered by volumes 81 and 82 of "Chemical Abstracts." The organization of the report follows the established pattern of previous volumes.

There are 14 chapters written by 15 international scientists who are specialists in their fields. Most of the chapters include an introduction indicating the parameters established by the author(s) and the reviews on the subject published during the time period. A particularly helpful feature is that all literature citations are included as footnotes on the page that contains the abstract, thus eliminating the time consuming and thought-interrupting process of turning to the end of the chapter when a specific reference is desired. Another helpful feature is a complete author index.

The chapter titles include: Ring Systems of Topical Interest, Intermolecular and Intramolecular Cyclization Reactions in Ring Synthesis, Cycloaddition Reactions, Ring Transformations, Electrophilic Substitution on Carbon, Electrophilic Substitution on Heteroatoms, Nucleophilic Substitution, Aromatic Substitution by Free Radicals, Carbenes and Nitrenes, Addition Reactions, Ring Cleavage Reactions, Reactions of Substituents, Porphyrins and Related Compounds, Naturally Occurring Oxygen-ring Compounds, and Other Naturally Occurring Compounds. The volume comprises 513 pages and includes 2750 literature citations.

The book is well illustrated with many chemical structures and reaction mechanisms. These illustrations are numbered sequentially and placed in close proximity to their text reference, thus affording a free flowing continuity which contributes to the overall excellent readability of the material.

This treatise is an extremely well-organized and readable volume and should serve to stimulate fresh approaches in the ever more sophisticated areas of aromatic and heteroaromatic synthetic chemistry. It is recommended to all chemists who are actively involved in synthetic organic chemistry or who wish to be up to date and informed about research activity in aromatic and heteroaromatic chemistry.

Reviewed by Edward F. LaSala
Massachusetts College of Pharmacy
Boston, MA 02115

Handbook of Analysis of Organic Solvents. By VÁCLAV ŠEDIVEC and JAN FLEK. Halsted, 605 Third Ave., New York, NY 10016, 1976. 455 pp. 16 × 23.5 cm. Price $42.50.

Within this volume the authors have compiled an extensive aggregate of information concerning the chemical and physical properties and the analysis of organic solvents. Following a brief discussion of sampling and drying techniques, procedures are described for the determination of the physical properties and quantitative identification of unknown samples. After a presentation of methods for the analysis of two- and three-component mixtures by physicochemical methods, the basics of GC are described using a general procedure. Relative retention times are given for many common solvents using six different stationary phases.

The second part of the book deals with solvents as individual classes of organic compounds. The most frequently encountered solvents are described in depth, listing synonyms, chemical properties, usual impurities, and azeotropes. Tables containing extensive physical data are included. Detection methods, derivatives, and quantitative procedures are described in detail with corresponding literature references. Three appendixes covering 80 pages include a listing of the boiling points of solvents and their azeotropic mixtures, the major physical properties, and an alphabetical listing of universally used trade names.

This handbook represents a valuable accumulation of a myriad of facts and procedures which will be of use to the analyst, the chromatographer, and the synthetic organic chemist, all of whom frequently require data or techniques to utilize or analyze organic solvents.

Reviewed by Allen L. Jacobs
Pharmacy and Analytical Research Department
Sandoz, Inc.
East Hanover, NJ 07936

The National Formulary and the USP Guide to Select Drugs. Edited by W. M. HELLER, G. K. WURSTER, C. A. DICKIE, and J. W. WHEATLEY. U.S. Pharmacopeial Convention, 12601 Twinbrook Parkway, Rockville, MD 20852, 1976. 295 pp. 10 × 14.5 cm. Price $3.00.

This convenient pocket-size book is intended to be a companion to the official compendia and the USAN Dictionary and is the first compilation of its kind subsequent to the consolidation of the USP and NF. Its purpose is "to highlight those drugs that should receive attention and be used as preferred drugs."

The book contains an alphabetical list of both generic and brand names of effective and useful drugs, with the preferred drugs in boldface type. The entries also contain dosage forms and strength; indication of whether prescription, nonprescription, or DEA controlled; and the pharmacological classification. In addition, there is a cross-index by therapeutic classification.

This book should be useful as a personal prescribing and dispensing guide and as a basic list of preferred drugs for health facilities and various organizations.

Staff Review

away in the laboratories of pharmaceutical scientists. Each drug profile provides useful information and data in the following general areas: description, physical properties, synthesis, stability and degradation, metabolism, analysis (for the drug substance, in its dosage forms, and in biological fluids), pharmacokinetics, and literature references. Physical properties include IR, NMR, UV, and mass spectral data, melting point, solubility data, crystal properties, and pK values where applicable. Analytical methods encompass titrimetry, chromatography, colorimetry, spectrophotometry, elemental analysis, and related techniques.

Each profile is presented in a well-organized and systematic manner. Each is introduced by a table of contents, followed in an orderly sequence by individual categories of specifications, and concluded by an extensive listing of quoted references. This compendium is printed clearly and is replete with tables and graphical presentations. Data are readily located and concisely presented with only a minimum of descriptive information. Maximum utilization is made of the available space.

This volume brings to a total of 97 the number of drugs for which profiles have thus far been prepared, including the 18 in Volume 5. These volumes serve well as companion books to the official compendia by presenting a wealth of data that supplement and are not duplicative of material found in the compendia. As noted in the Forward to Volume 1 of this series, the delegates to the 1970 meeting of the United States Pharmacopeial Convention adopted a resolution that consideration be given to the publication of just such a companion compendium. While the USPC did not undertake this project, it is worthy of note that a number of contributors to this series, including its esteemed editor, are, in fact, members of the USP Committee of Revision.

In view of the fact that fewer than 100 drug profiles have appeared in the first five volumes of this series, and with the mandate for USP XX to include all drugs currently official in USP XIX and NF XIV, all drugs added in their annual supplements, some 600 nonofficial drugs selected by the outgoing Subcommittee on Scope of the USP at its final meeting in January 1975, and new drugs marketed since that date, it is obvious that pharmaceutical scientists have their work cut out for them. It is worth repeating here the editor's invitation that: "All those who have found the profiles useful are earnestly requested to contribute a monograph of their own. The editors stand ready to receive such contributions." Hopefully, there will be an overwhelming response to this invitation.

This burgeoning library of "Analytical Profiles" is a must for all who are engaged in pharmaceutical research.

Reviewed by Martin I. Blake
College of Pharmacy
University of Illinois
Chicago, IL 60612

Aromatic and Heteroaromatic Chemistry. Vol. 4. A Specialist Periodical Report. Edited by C. W. BIRD, G. W. H. CHEESEMAN, *et al.* The Chemical Society, Burlington House, London W1V OBN, England, 1976. 513 pp. 14.5 × 22.5 cm. Price £28.00.

This volume comprises an in-depth review of the literature abstracted between July 1974 and June 1975 and covered by volumes 81 and 82 of "Chemical Abstracts." The organization of the report follows the established pattern of previous volumes.

There are 14 chapters written by 15 international scientists who are specialists in their fields. Most of the chapters include an introduction indicating the parameters established by the author(s) and the reviews on the subject published during the time period. A particularly helpful feature is that all literature citations are included as footnotes on the page that contains the abstract, thus eliminating the time consuming and thought-interrupting process of turning to the end of the chapter when a specific reference is desired. Another helpful feature is a complete author index.

The chapter titles include: Ring Systems of Topical Interest, Intermolecular and Intramolecular Cyclization Reactions in Ring Synthesis, Cycloaddition Reactions, Ring Transformations, Electrophilic Substitution on Carbon, Electrophilic Substitution on Heteroatoms, Nucleophilic Substitution, Aromatic Substitution by Free Radicals, Carbenes and Nitrenes, Addition Reactions, Ring Cleavage Reactions, Reactions of Substituents, Porphyrins and Related Compounds, Naturally Occurring Oxygen-ring Compounds, and Other Naturally Occurring Compounds. The volume comprises 513 pages and includes 2750 literature citations.

The book is well illustrated with many chemical structures and reaction mechanisms. These illustrations are numbered sequentially and placed in close proximity to their text reference, thus affording a free flowing continuity which contributes to the overall excellent readability of the material.

This treatise is an extremely well-organized and readable volume and should serve to stimulate fresh approaches in the ever more sophisticated areas of aromatic and heteroaromatic synthetic chemistry. It is recommended to all chemists who are actively involved in synthetic organic chemistry or who wish to be up to date and informed about research activity in aromatic and heteroaromatic chemistry.

Reviewed by Edward F. LaSala
Massachusetts College of Pharmacy
Boston, MA 02115

Handbook of Analysis of Organic Solvents. By VÁCLAV ŠEDIVEC and JAN FLEK. Halsted, 605 Third Ave., New York, NY 10016, 1976. 455 pp. 16 × 23.5 cm. Price $42.50.

Within this volume the authors have compiled an extensive aggregate of information concerning the chemical and physical properties and the analysis of organic solvents. Following a brief discussion of sampling and drying techniques, procedures are described for the determination of the physical properties and quantitative identification of unknown samples. After a presentation of methods for the analysis of two- and three-component mixtures by physicochemical methods, the basics of GC are described using a general procedure. Relative retention times are given for many common solvents using six different stationary phases.

The second part of the book deals with solvents as individual classes of organic compounds. The most frequently encountered solvents are described in depth, listing synonyms, chemical properties, usual impurities, and azeotropes. Tables containing extensive physical data are included. Detection methods, derivatives, and quantitative procedures are described in detail with corresponding literature references. Three appendixes covering 80 pages include a listing of the boiling points of solvents and their azeotropic mixtures, the major physical properties, and an alphabetical listing of universally used trade names.

This handbook represents a valuable accumulation of a myriad of facts and procedures which will be of use to the analyst, the chromatographer, and the synthetic organic chemist, all of whom frequently require data or techniques to utilize or analyze organic solvents.

Reviewed by Allen L. Jacobs
Pharmacy and Analytical Research Department
Sandoz, Inc.
East Hanover, NJ 07936

The National Formulary and the USP Guide to Select Drugs. Edited by W. M. HELLER, G. K. WURSTER, C. A. DICKIE, and J. W. WHEATLEY. U.S. Pharmacopeial Convention, 12601 Twinbrook Parkway, Rockville, MD 20852, 1976. 295 pp. 10 × 14.5 cm. Price $3.00.

This convenient pocket-size book is intended to be a companion to the official compendia and the USAN Dictionary and is the first compilation of its kind subsequent to the consolidation of the USP and NF. Its purpose is "to highlight those drugs that should receive attention and be used as preferred drugs."

The book contains an alphabetical list of both generic and brand names of effective and useful drugs, with the preferred drugs in boldface type. The entries also contain dosage forms and strength; indication of whether prescription, nonprescription, or DEA controlled; and the pharmacological classification. In addition, there is a cross-index by therapeutic classification.

This book should be useful as a personal prescribing and dispensing guide and as a basic list of preferred drugs for health facilities and various organizations.

Staff Review

Journal of Pharmaceutical Sciences

AUGUST 1977

VOLUME 66 NUMBER 8

MARY H. FERGUSON
Editor

SHELLY ELLIOTT
Production Editor

JANET D. SHOFF
Copy Editor

EDWARD G. FELDMANN
Contributing Editor

SAMUEL W. GOLDSTEIN
Contributing Editor

DAVID BOHARDT
Acting Director of Publications

L. LUAN CORRIGAN
Assistant Director of Publications

EDITORIAL ADVISORY BOARD

JOHN AUTIAN
NORMAN R. FARNSWORTH
WILLIAM O. FOYE
WILLIAM J. JUSKO
HARRY B. KOSTENBAUDER
HERBERT A. LIEBERMAN
DAVID E. MANN, JR.
GERALD J. PAPARIELLO

The *Journal of Pharmaceutical Sciences* is published monthly by the American Pharmaceutical Association at 2215 Constitution Ave., N.W., Washington, DC 20037. Second-class postage paid at Washington, D.C., and at additional mailing office.

All expressions of opinion and statements of supposed fact appearing in articles or editorials carried in this journal are published on the authority of the writer over whose name they appear and are not to be regarded as necessarily expressing the policies or views of the American Pharmaceutical Association.

Offices—Editorial, Advertising, and Subscription Offices: 2215 Constitution Ave., N.W., Washington, DC 20037. Printing Offices: 20th & Northampton Streets, Easton, PA 18042.

Annual Subscriptions—United States and foreign, industrial and government institutions $50, educational institutions $50, individuals *for personal use only* $30; single copies $5. All foreign subscriptions add $5 for postage. Subscription rates are subject to change without notice. Members of the American Pharmaceutical Association may elect to receive the *Journal of Pharmaceutical Sciences* as a part of their annual $60 (foreign $65) APhA membership dues.

Claims—Missing numbers will not be supplied if dues or subscriptions are in arrears for more than 60 days or if claims are received more than 60 days after the date of the issue, or if loss was due to failure to give notice of change of address. The Association cannot accept responsibility for foreign delivery when its records indicate shipment has been made.

Change of Address—Members and subscribers should notify at once both the Post Office and the American Pharmaceutical Association, 2215 Constitution Ave., N.W., Washington, DC 20037, of any change of address.

Microfilm—Microfilm volumes are available from University Microfilms International, 300 N. Zeeb Road, Ann Arbor, MI 48106.

© Copyright 1977, American Pharmaceutical Association, 2215 Constitution Ave., N.W., Washington, DC 20037; all rights reserved.

CANCER IN THE KITCHEN?

Pundits claim that television brought violence and sensationalism into the American living room. Perhaps this is true. By analogy, we are prompted to suggest that saccharin has brought science and toxicity into the American kitchen and dining room.

The conflicting arguments concerning this chemical substance have dramatically brought home to the average citizen the harsh reality of benefit-to-risk, of informed choice, of the fallacy of absolute safety, and of a host of other scientific issues, in a way that no other controversy before it has ever done.

In recent years, the public has been generally puzzled by the apparent inability of health professionals and medical scientists to agree that this drug or that drug should or should not be permitted to be used in therapy. Similar confusion has surrounded the questions raised about food additives such as monosodium glutamate, diagnostic techniques such as X-rays and mammography, environmental pollutants such as aerosol fluorocarbons, and various other items which have come to be regarded as a part of everyday life.

But in all these cases, it seemed that the hazards were relatively remote, and the perceived reliance upon—or need for—the item involved was not critical or even very important to a great number of people. Hence, few people got very excited over these matters, except to express impatience with the apparent inability of "the experts" to agree one way or the other in terms that were clearly black or white.

Regrettably, the inability of scientists to arrive at such unequivocal answers created an attitude of suspicion and distrust on the part of much of the public. For example, sinister motives frequently have been ascribed to fluoridation of drinking water, to controls on purported health cures such as krebiozan and laetrile, to the establishment of automobile exhaust standards, and to the regulation of flights of supersonic aircraft.

At best, these issues have been publicly perceived as selfish policies by a profit hungry industry. At worst, they have been branded as subversive political plots designed to destroy the physical and mental well-being of the general population. And always there were cries of interference with personal freedom and constitutional rights. No wonder, then, that science has lost its luster and scientists are no longer accorded the hero worship so common just a generation ago.

But for all its problems, headaches, and general nuisance effect, the saccharin controversy has proven to have considerable educational value. Even the average lay person seems to have a reasonable understanding of the questions involved, the uncertainty of the hazard, and the hard choices to be made.

Moreover, saccharin is something with which the consumer readily identifies. It is in the low calorie soft drinks, the diet foods on the supermarket shelves, the packets of sweetener on restaurant tables. People of all ages are weight and calorie conscious; artificial sweeteners are felt to provide a convenient, economical, and taste-satisfying answer to this problem.

However, only one generally acceptable artificial sweetener is currently available, and fuzzy questions have now been raised as to just how safe it is. People are very unhappy with this situation; nevertheless, they are able to comprehend and understand the dilemma it poses. It is also one that, at least for the moment, they are being forced to decide for themselves—does one push the button for the diet cola in the vending machine, or the button for the sugar-sweetened version? The choice is there, and the person is thirsty now. And the answer isn't easy.

Consequently, although the pharmaceutical world is primarily taken up with what impact the proposed saccharin ban will have on drug formulations and related products such as dentifrices and mouthwash, this far-reaching proposal has brought the general public face-to-face with the type of hard decision-making common to many contemporary scientific issues. Hopefully, this experience will provide the public with a better comprehension of the difficulty involved—even for "the experts"—in making the best choice when these kinds of situations arise in the future.

—EGF

Journal of Pharmaceutical Sciences

AUGUST 1977

VOLUME 66 NUMBER 8

MARY H. FERGUSON
Editor

SHELLY ELLIOTT
Production Editor

JANET D. SHOFF
Copy Editor

EDWARD G. FELDMANN
Contributing Editor

SAMUEL W. GOLDSTEIN
Contributing Editor

DAVID BOHARDT
Acting Director of Publications

L. LUAN CORRIGAN
Assistant Director of Publications

EDITORIAL ADVISORY BOARD

JOHN AUTIAN
NORMAN R. FARNSWORTH
WILLIAM O. FOYE
WILLIAM J. JUSKO
HARRY B. KOSTENBAUDER
HERBERT A. LIEBERMAN
DAVID E. MANN, JR.
GERALD J. PAPARIELLO

The *Journal of Pharmaceutical Sciences* is published monthly by the American Pharmaceutical Association at 2215 Constitution Ave., N.W., Washington, DC 20037. Second-class postage paid at Washington, D.C., and at additional mailing office.

All expressions of opinion and statements of supposed fact appearing in articles or editorials carried in this journal are published on the authority of the writer over whose name they appear and are not to be regarded as necessarily expressing the policies or views of the American Pharmaceutical Association.

Offices—Editorial, Advertising, and Subscription Offices: 2215 Constitution Ave., N.W., Washington, DC 20037. Printing Offices: 20th & Northampton Streets, Easton, PA 18042.

Annual Subscriptions—United States and foreign, industrial and government institutions $50, educational institutions $50, individuals *for personal use only* $30; single copies $5. All foreign subscriptions add $5 for postage. Subscription rates are subject to change without notice. Members of the American Pharmaceutical Association may elect to receive the *Journal of Pharmaceutical Sciences* as a part of their annual $60 (foreign $65) APhA membership dues.

Claims—Missing numbers will not be supplied if dues or subscriptions are in arrears for more than 60 days or if claims are received more than 60 days after the date of the issue, or if loss was due to failure to give notice of change of address. The Association cannot accept responsibility for foreign delivery when its records indicate shipment has been made.

Change of Address—Members and subscribers should notify at once both the Post Office and the American Pharmaceutical Association, 2215 Constitution Ave., N.W., Washington, DC 20037, of any change of address.

Microfilm—Microfilm volumes are available from University Microfilms International, 300 N. Zeeb Road, Ann Arbor, MI 48106.

© Copyright 1977, American Pharmaceutical Association, 2215 Constitution Ave., N.W., Washington, DC 20037; all rights reserved.

CANCER IN THE KITCHEN?

Pundits claim that television brought violence and sensationalism into the American living room. Perhaps this is true. By analogy, we are prompted to suggest that saccharin has brought science and toxicity into the American kitchen and dining room.

The conflicting arguments concerning this chemical substance have dramatically brought home to the average citizen the harsh reality of benefit-to-risk, of informed choice, of the fallacy of absolute safety, and of a host of other scientific issues, in a way that no other controversy before it has ever done.

In recent years, the public has been generally puzzled by the apparent inability of health professionals and medical scientists to agree that this drug or that drug should or should not be permitted to be used in therapy. Similar confusion has surrounded the questions raised about food additives such as monosodium glutamate, diagnostic techniques such as X-rays and mammography, environmental pollutants such as aerosol fluorocarbons, and various other items which have come to be regarded as a part of everyday life.

But in all these cases, it seemed that the hazards were relatively remote, and the perceived reliance upon—or need for—the item involved was not critical or even very important to a great number of people. Hence, few people got very excited over these matters, except to express impatience with the apparent inability of "the experts" to agree one way or the other in terms that were clearly black or white.

Regrettably, the inability of scientists to arrive at such unequivocal answers created an attitude of suspicion and distrust on the part of much of the public. For example, sinister motives frequently have been ascribed to fluoridation of drinking water, to controls on purported health cures such as krebiozan and laetrile, to the establishment of automobile exhaust standards, and to the regulation of flights of supersonic aircraft.

At best, these issues have been publicly perceived as selfish policies by a profit hungry industry. At worst, they have been branded as subversive political plots designed to destroy the physical and mental well-being of the general population. And always there were cries of interference with personal freedom and constitutional rights. No wonder, then, that science has lost its luster and scientists are no longer accorded the hero worship so common just a generation ago.

But for all its problems, headaches, and general nuisance effect, the saccharin controversy has proven to have considerable educational value. Even the average lay person seems to have a reasonable understanding of the questions involved, the uncertainty of the hazard, and the hard choices to be made.

Moreover, saccharin is something with which the consumer readily identifies. It is in the low calorie soft drinks, the diet foods on the supermarket shelves, the packets of sweetener on restaurant tables. People of all ages are weight and calorie conscious; artificial sweeteners are felt to provide a convenient, economical, and taste-satisfying answer to this problem.

However, only one generally acceptable artificial sweetener is currently available, and fuzzy questions have now been raised as to just how safe it is. People are very unhappy with this situation; nevertheless, they are able to comprehend and understand the dilemma it poses. It is also one that, at least for the moment, they are being forced to decide for themselves—does one push the button for the diet cola in the vending machine, or the button for the sugar-sweetened version? The choice is there, and the person is thirsty now. And the answer isn't easy.

Consequently, although the pharmaceutical world is primarily taken up with what impact the proposed saccharin ban will have on drug formulations and related products such as dentifrices and mouthwash, this far-reaching proposal has brought the general public face-to-face with the type of hard decision-making common to many contemporary scientific issues. Hopefully, this experience will provide the public with a better comprehension of the difficulty involved—even for "the experts"—in making the best choice when these kinds of situations arise in the future.

—EGF

Journal of Pharmaceutical Sciences

AUGUST 1977
VOLUME 66 NUMBER 8

RESEARCH ARTICLES

Kinetics of Drug–Drug Interactions in Sheep: Tolbutamide and Sulfadimethoxine

J. J. THIESSEN *x and M. ROWLAND ‡

Abstract □ The interaction between sulfadimethoxine and tolbutamide in sheep involving displacement from protein binding sites was investigated quantitatively. A 52% increase in the unbound plasma concentration of tolbutamide was observed *in vitro* at 37° after the addition of sulfadimethoxine (100 μg/ml) to sheep plasma containing tolbutamide (50 μg/ml). Transient changes in tolbutamide's unbound and total plasma concentrations were noted after acute intravenous administration of sulfadimethoxine to sheep receiving a constant intravenous infusion of tolbutamide. These observations were consistent with displacement of tolbutamide from plasma and tissue binding sites and redistribution of the displaced tolbutamide into body water spaces. The steady state of both agents featured little change in the total plasma tolbutamide concentration, a 150% increase in the unbound plasma tolbutamide concentration, and an inhibition of tolbutamide oxidation by sulfadimethoxine. A model is presented and mathematical relationships are derived that permit a quantitation of the interaction and that indicate that sulfadimethoxine's constant of metabolic inhibition (K_I) for tolbutamide metabolism is 65 μg/ml.

Keyphrases □ Tolbutamide—interaction with sulfadimethoxine, kinetic analysis, sheep □ Sulfadimethoxine—interaction with tolbutamide, kinetic analysis, sheep □ Drug interactions—tolbutamide and sulfadimethoxine, kinetic analysis, sheep □ Interactions, drug—tolbutamide and sulfadimethoxine, kinetic analysis, sheep □ Kinetics—analysis of tolbutamide–sulfadimethoxine interaction, sheep □ Antidiabetic agents—tolbutamide, interaction with sulfadimethoxine, kinetic analysis, sheep □ Antibacterials—sulfadimethoxine, interaction with tolbutamide, kinetic analysis, sheep

The coadministration of two or more drugs may produce ineffective therapy, exaggerated therapeutic responses, or even toxic responses. While numerous reports on such drug interactions have appeared in review articles (1–7) and books (8–10), they generally provide little more than a compilation of observed events. In one publication (11), attempts were made to discuss and relate the molecular events underlying various drug interactions.

The application of pharmacokinetic principles to the quantitation of drug–drug interactions has been limited but successful in the interpretation of the data. Kinetic analysis of the metabolic interaction of tolbutamide and sulfaphenazole explained observed clinical adverse effects and permitted a prediction of plasma levels of both agents when coadministered (12). Kinetic evaluation of the interaction between warfarin and phenylbutazone demonstrated the complexities that may be involved in metabolic interactions (13, 14). By using a perfusion-limited pharmacokinetic model (15), it was possible to assess contributions of enzyme induction and increased hepatic blood flow in mixed enzymatic–hemodynamic drug interactions (16).

Displacement of one drug by another from protein binding sites has frequently been suggested as the cause of an enhanced pharmacological response, but no reports exist quantitating the kinetics of these displacement interactions. The purpose of this investigation was to examine critically the pharmacokinetic aspects of an interaction between two agents, tolbutamide and sulfadimethoxine, that exhibit a displacement phenomenon *in vitro* (17). This report, describing experiments with sheep, demonstrates the involved complexities and the approaches that can be taken to quantitate drug interactions.

EXPERIMENTAL

Animal Preparation—Vascular catheters, 2.3-mm o.d. Tygon flexible tubing[1], were inserted into either the saphenous vein and the femoral artery or the jugular vein and the carotid artery of 40–50-kg sheep. Between experiments, the catheters were kept patent by filling with heparin[2] and flushing with normal saline periodically. A foley 20 FR catheter[3] was

[1] Type S-54-HL, Port Plastics Inc.
[2] Lipo-Hepin, 1000 units/ml, Riker.
[3] Bardex, 165V.

introduced into the bladder *via* its fundus after ventral midline abdominal incision. Both vascular and bladder catheters were externalized in a pocket attached to the side of the animal to permit ease of chronic sampling.

The sheep diet consisted of alfalfa pellets and water. Throughout all studies, food and water were permitted *ad libitum*.

Arterial blood samples were collected in heparinized or fluoridated Vacutainer tubes. Plasma was separated immediately by centrifugation and either used immediately for analysis or stored at −4° for subsequent analysis. All urine samples were either analyzed immediately or stored in scintillation vials at −4° for subsequent analysis.

Materials—All reagents were of analytical reagent grade. Solvents were generally redistilled prior to use. Tolbutamide[4], ^{14}C-tolbutamide[5], hydroxytolbutamide[4], ^{3}H-tolbutamide, and sulfadimethoxine[6] were administered as sodium salt solutions, diluted with normal saline where appropriate. All solutions were filtered[7] prior to intravenous administration[8].

Analytical Methods—Tolbutamide, hydroxytolbutamide, and carboxytolbutamide were determined in plasma, plasma water, or urine by the analytical method of Matin and Rowland (18).

Sulfadimethoxine and its N^4-conjugated metabolite were determined by the Bratton–Marshall method (19).

Glucose was measured[9] in plasma by the enzymatic glucose oxidase method (20).

Nonesterified (free) fatty acids were determined using the method of Dole (21).

Total plasma protein was measured, using automated equipment[10], by the biuret procedure (22) or the Lowry *et al.* method (23). Plasma electrophoresis was performed on cellulose acetate[11].

Plasma Protein Binding—All three methods were performed at 37°. Equilibrium dialysis was carried out for 6 hr using the dialyzing system[12] and the method of Weder *et al.* (24). Krebs–Henseleit buffer, pH 7.4, was used as the dialyzing fluid. Ultracentrifugation[13] was conducted at 55,000 rpm for 24 hr, after which 0.5–1.0 ml of supernate was removed for analysis. Ultrafiltration was carried out using membrane cones[14]; centrifuging[15] at 2000 rpm for 4 min provided a filtrate that was 10% of the initial plasma volume.

Radioactivity Measurements—Radioactivity was quantitated in biological fluids by scintillation counting[16] using the method of automatic external standardization and employing appropriate quench correction curves.

RESULTS AND DISCUSSION

Intravenous Tolbutamide Bolus—The intravenous bolus administration of tolbutamide in sheep served to determine its metabolic fate, characterize its disposition kinetics, and allow an appraisal of a pharmacological response, namely plasma glucose depression. In an experiment utilizing ^{3}H-tolbutamide (2.0 μCi/mg), 67.8% of the dose (100 mg, 2.9×10^7 dpm) was recovered in urine collected for 9 hr. Of this recovered radioactivity, 86.5% could be removed by exhaustive extraction of acidified urine with 0.5% isoamyl alcohol in dichloromethane. By using the separation method of Matin and Rowland (18), all extracted radioactivity was accounted for as tolbutamide, carboxytolbutamide, and hydroxytolbutamide in a ratio of 2:9:89. In subsequent experiments using unlabeled tolbutamide, 66–80% of the administered dose could be accounted for as the cumulative urinary excretion of these three compounds.

Since carboxytolbutamide represented only 10% of the detectable oxidation products excreted, it was included as part of the hydroxytolbutamide estimate in subsequent analyses of urine collected during the interaction studies. Sheep thus join rats, guinea pigs, rabbits, and humans as species that predominantly eliminate hydroxy- and carboxytolbutamide after tolbutamide administration (25–27). The tolbutamide excretion product(s) unaccounted for remain uncharacterized.

[4] Orinase Diagnostic, The Upjohn Co.
[5] Farbwerke Hoechst AG, Germany.
[6] Hoffmann-La Roche Inc.
[7] Millipore filter, 0.45 μm, 13 mm, Millipore Corp.
[8] Compact infusion pump, Harvard Apparatus Co.
[9] Beckman glucose analyzer, Beckman Instruments.
[10] Technicon, two channel.
[11] Beckman Instruments.
[12] Dianorm, Inno Med, Switzerland.
[13] L2-65B, Beckman Instruments.
[14] Centriflo (CF50A), Amicon Corp.
[15] International model UV
[16] Packard Tri-Carb, Packard Instrument Co.

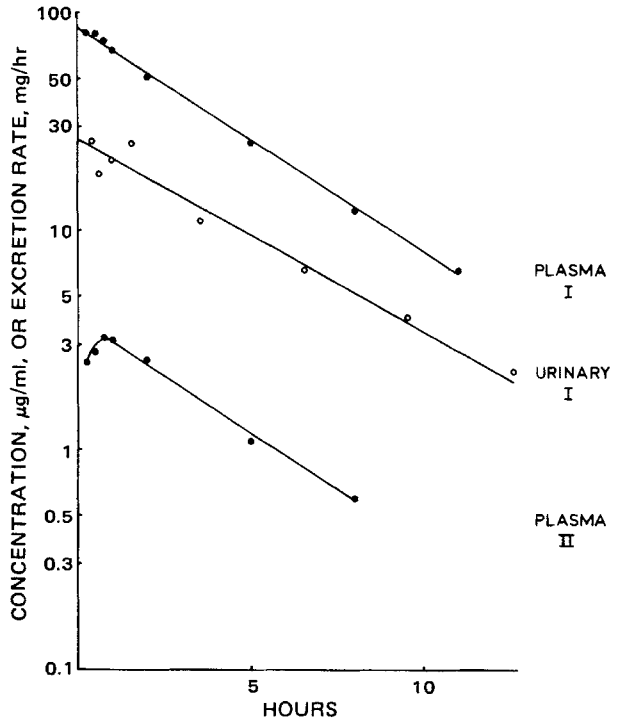

Figure 1—*Plasma concentration and urinary excretion rate of tolbutamide (I) and plasma concentration of hydroxytolbutamide (II) after an intravenous tolbutamide bolus (865 mg).*

Plasma tolbutamide and hydroxytolbutamide levels and the excretion rate of tolbutamide after an intravenous bolus dose of tolbutamide (865 mg) can be seen in Fig. 1. Tolbutamide is removed quickly from the sheep, and the data suggest that the disappearance of hydroxytolbutamide is rate limited by its formation. During some bolus experiments, a distribution phase was occasionally detected. When visible, however, its contribution was always less than 10% of the total area; therefore, less than 10% of the dose was eliminated during the distribution phase. Accordingly, as a reasonable approximation, the elimination of tolbutamide was characterized as occurring from a single compartment.

Repeated intravenous bolus administration of tolbutamide in a single sheep over 4 months provided half-lives, apparent volumes of distribution, and total body clearances (±*SD*) of 3.6 (±0.5) hr, 11.2 (±1.0) liters, and 37.5 (±2.1) ml/min, respectively. Excluded from these values are the results of an experiment that yielded a prolonged half-life of 10.6 hr, a similar apparent volume of distribution (11.7 liters), and a reduced total body clearance (12.7 ml/min). These abnormal kinetic parameters coincided with an infection. The differences could not be explained by changes in total or fractional plasma protein content or by changes in the fraction of tolbutamide bound to plasma proteins. The infectious state apparently decreased the metabolic activity of the liver.

The plasma glucose depression observed after an intravenous tolbutamide bolus (900 mg) can be seen in Fig. 2. A depression occurs shortly after administration, with a rapid return to baseline values within 2 hr. These observations made with sheep are similar to those reported for humans (28).

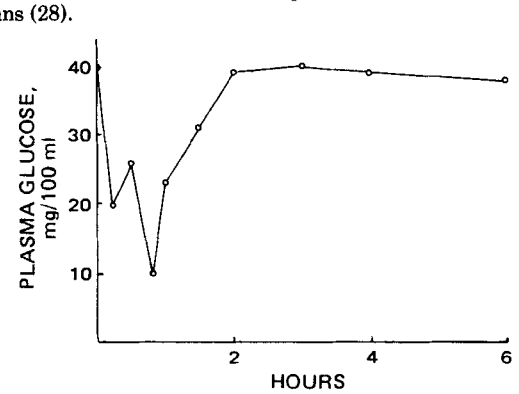

Figure 2—*Plasma glucose concentration in sheep after an intravenous tolbutamide bolus (900 mg).*

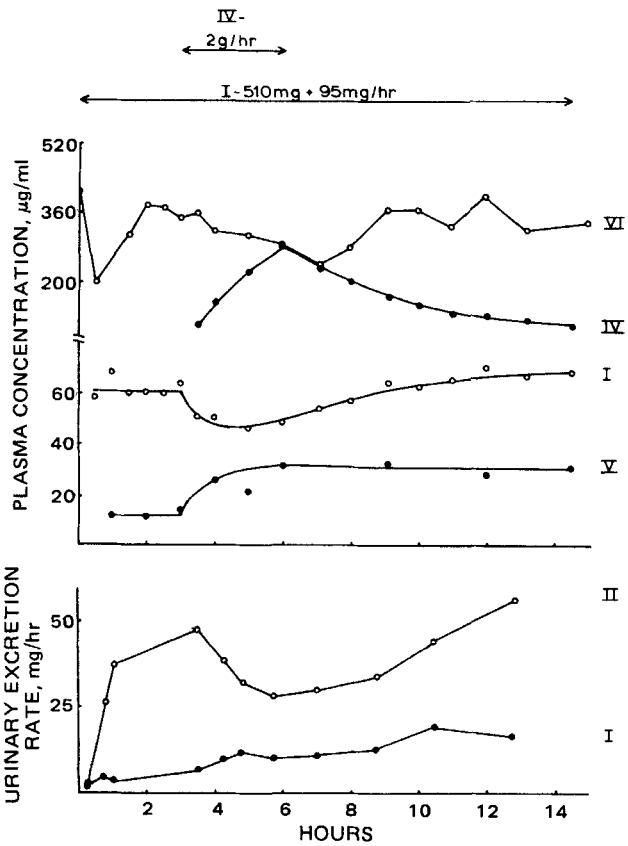

Figure 3—*Interaction Study 1 of tolbutamide and sulfadimethoxine in sheep. Tolbutamide (I) was given as a bolus (510 mg) followed by an infusion (95 mg/hr), while sulfadimethoxine (IV) was administered for 3 hr as an infusion (2 g/hr). The resultant plasma concentrations of glucose (VI), sulfadimethoxine (IV), tolbutamide (I), and unbound tolbutamide (V) and urinary excretion rates of hydroxytolbutamide (II) and tolbutamide (I) are displayed.*

Intravenous Hydroxytolbutamide Bolus—Hydroxytolbutamide is eliminated very rapidly from sheep. An intravenous bolus dose (250 mg) in two sheep provided terminal plasma half-lives of 13.5 and 26 min, apparent volumes of distribution of 15.8 and 26.5 liters, and total body clearances of 1.0 and 1.5 liters/min. These observations confirm the previous suggestion that the rate of removal of hydroxytolbutamide from the plasma after tolbutamide administration is rate limited by its formation (Fig. 1). The entire dose of hydroxytolbutamide was recovered in the urine, 90% as unchanged drug and the remainder as carboxytolbutamide. A 250-mg intravenous bolus dose failed to depress the plasma glucose level. Thus, hydroxytolbutamide appears to lack significant hypoglycemic activity.

Intravenous Sulfadimethoxine Bolus—Sulfadimethoxine exhibited biexponential kinetics, with the distribution and elimination phases having half-lives of 1 and 7.4 hr, respectively. The latter value is similar to a reported half-life of 8.4 hr in sheep (29). Further, the low total body clearance (31.8 ml/min) of sulfadimethoxine was similar to that noted for tolbutamide. However, a 4-g bolus dose failed to produce a significant hypoglycemic effect.

***In Vitro* Plasma Protein Binding**—When using ultracentrifugation, ultrafiltration, and equilibrium dialysis, tolbutamide (100 μg/ml) was bound 85.1, 85.4, and 85.6%, respectively, to sheep plasma at 37°. In light of these similar results, ultrafiltration was used almost exclusively in subsequent *in vivo* studies due to its short analysis time. While all experiments were conducted at 37°, a change to 25° resulted in a maximal mean increase in binding of only 0.7% over the tolbutamide concentration range of 10–100 μg/ml of plasma. At 100, 200, 300, and 400 μg/ml, sulfadimethoxine was bound to the extent of 88.2, 81.2, 73.4, and 66.8%, respectively, in sheep plasma.

Sulfadimethoxine displaces tolbutamide from binding sites in sheep plasma. At a tolbutamide concentration of 50 μg/ml, sulfadimethoxine concentrations of 100, 200, 300, and 400 μg/ml increased the unbound tolbutamide concentration by 52, 102, 128, and 150%, respectively. These observations confirmed the reported effectiveness of sulfadimethoxine

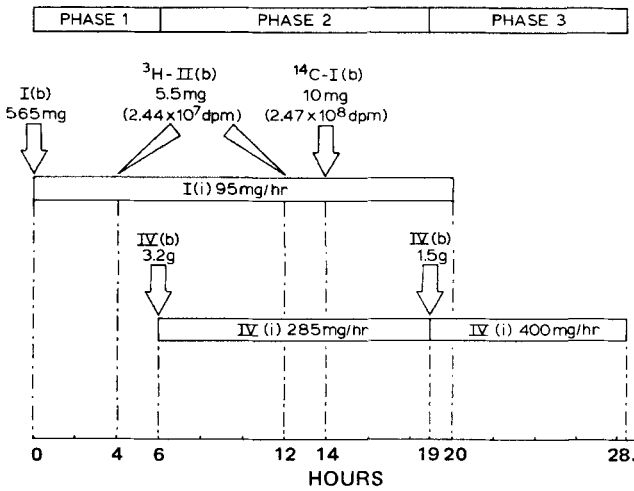

Figure 4—*Flow diagram indicating the times of administration of tolbutamide (I), hydroxytolbutamide (II), and sulfadimethoxine (IV) in Interaction Study 2. All compounds were administered in the form of an intravenous bolus (b) or infusion (i).*

as a displacer of tolbutamide from plasma proteins (17) and made this sulfonamide a logical choice for the investigation of the kinetics of drug interactions involving displacement of drugs from protein binding sites.

Tolbutamide–Sulfadimethoxine Interaction Studies—Significant displacement of tolbutamide from plasma binding sites *in vivo* was ensured by producing the same plasma concentrations of tolbutamide and sulfadimethoxine in the sheep as were used *in vitro*. By utilizing the intravenous bolus data, an infusion rate of tolbutamide was chosen to maintain its plasma concentration at approximately 50 μg/ml and a regimen of sulfadimethoxine was chosen to produce plasma concentrations up to 600 μg/ml. All interaction studies were conducted in a single animal.

In the initial experiment (Interaction Study 1), tolbutamide was administered as a bolus dose followed by a constant infusion for 14.5 hr. Sulfadimethoxine was coadministered for 3 hr by constant infusion. During its infusion, sulfadimethoxine caused a rise in the unbound concentration and a drop in the total plasma tolbutamide concentration (Fig. 3). These observations are in keeping with displacement of tolbutamide from plasma binding sites and redistribution of the unbound drug extravascularly.

At the peak plasma sulfadimethoxine concentration, the unbound tolbutamide concentration increased maximally by 160% (from 12.3 to 31.6 μg/ml). Thereafter, although the plasma sulfadimethoxine concentration fell and the total tolbutamide concentration rose eventually to exceed the presulfonamide steady-state level, the unbound tolbutamide level remained virtually unchanged for the remainder of the experiment. Meanwhile, whereas the urinary excretion rate of hydroxytolbutamide fell and rose during and after the sulfadimethoxine infusion, the tolbutamide excretion rate remained elevated despite a decrease in the plasma sulfadimethoxine concentration. Immediately after the bolus of tolbutamide, plasma glucose levels fell sharply, but they returned to the control value within 2 hr. They fell, albeit more slowly, during sulfadimethoxine administration, reaching a minimum which appeared coincident with the attainment of the maximal unbound plasma tolbutamide concentration.

The interaction study was repeated to examine the kinetics of interactions under steady-state tolbutamide levels in the absence and presence of a steady-state plasma sulfadimethoxine concentration (Interaction Study 2). Figure 4 contains a flow diagram indicating all aspects of drug administration during this study. Generally, the results in Fig. 5 confirm the observations seen during Interaction Study 1. By earlier sampling after an initial sulfadimethoxine bolus (6 hr after initiating tolbutamide administration), the early transient changes in unbound and total plasma tolbutamide concentrations were examined in greater detail. Again they reflected displacement from plasma proteins and rapid extravascular redistribution; similar events were noted in sheep (30) immediately following the displacement of sulfadoxine from binding sites by phenylbutazone.

By the end of phase 2 (19 hr), both unbound and total tolbutamide levels appeared to approach steady state. By then, the unbound tolbu-

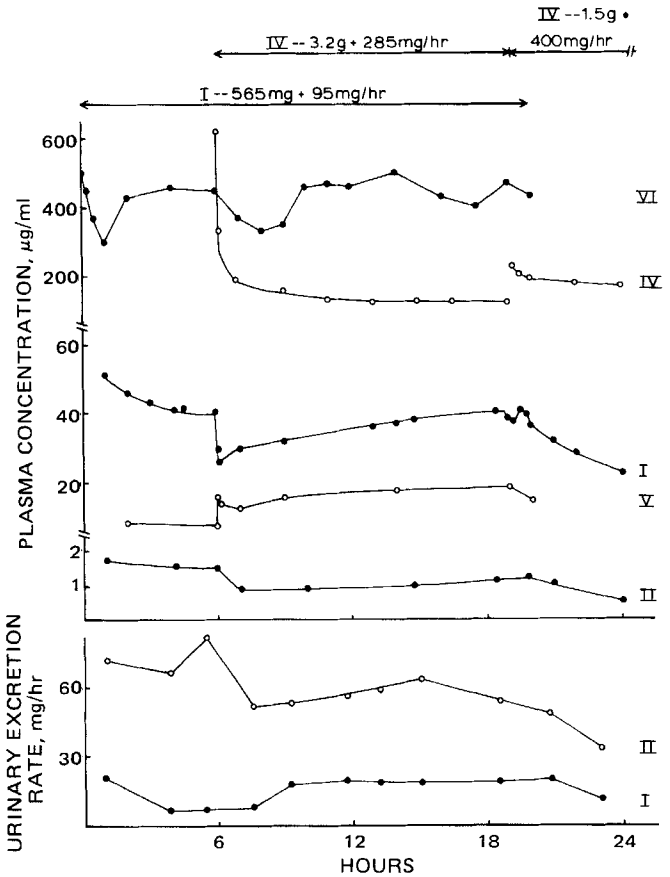

Figure 5—*Interaction Study 2 of tolbutamide and sulfadimethoxine in sheep. Tolbutamide (I) was given as a bolus (565 mg) followed by an infusion (95 mg/hr) until 20 hr. Sulfadimethoxine (IV) was coadministered as a bolus (3.2 g) at 6 hr followed by an infusion (285 mg/hr) until 19 hr, after which an additional bolus (1.5 g) was given followed by a new infusion rate (400 mg/hr) until 28.5 hr. The resultant plasma concentrations of glucose (VI), sulfadimethoxine (IV), tolbutamide (I), unbound tolbutamide (V), and hydroxytolbutamide (II), as well as the urinary excretion rates of hydroxytolbutamide (II) and tolbutamide (I), are exhibited.*

tamide level had increased twofold over the levels seen at the end of phase 1, while total tolbutamide had returned to the preexisting level. An additional bolus and increased infusion rate at the outset of phase 3 produced only minor changes in the total plasma tolbutamide concentration. The half-lives of ^{14}C-tolbutamide and nonradioactive tolbutamide during phase 3 (Figs. 6 and 5, respectively) were both 5.2 hr. This value was longer than the half-life of 3.8 hr observed following a 900-mg intravenous bolus dose of tolbutamide 2 days prior to this interaction study and longer than the ^{14}C-tolbutamide half-life (3.8 hr) observed during phase 2 of this study (Fig. 6).

Plasma hydroxytolbutamide decreased noticeably after the administration of sulfadimethoxine and then gradually increased, approaching a new steady state at 19 hr (Fig. 7). The urinary excretion rate of hydroxytolbutamide decreased temporarily and then increased, while that of tolbutamide remained notably elevated during sulfadimethoxine coadministration. The pattern of changes in plasma glucose was analogous to that seen in Fig. 3; levels were depressed after the first bolus of tolbutamide and sulfadimethoxine, but each time the glucose level returned to the control value.

Displacement of Tolbutamide by Sulfadimethoxine *In Vivo*—The magnitude of the initial changes and the subsequent levels of unbound tolbutamide as seen in Figs. 3 and 5 were greater than anticipated had only displacement from plasma protein sites occurred. By using a mean apparent volume of distribution of 11.2 liters (bolus data), a plasma volume of 1.8 liters, and 85% binding in plasma, it was calculated that only 14% of the drug in the body is bound to plasma proteins. Even if all of this plasma-bound drug had been displaced, to be redistributed throughout the rest of the body, it would fail to increase the unbound concentration to anything like the observed 110% within 1 hr following sulfadimethoxine administration. Therefore, sulfadimethoxine must also displace tolbutamide from an extensive extravascularly bound pool. The early maintenance of these elevated levels of unbound tolbutamide suggests that the distribution space of the unbound drug may, in fact, be limited. A similar explanation was suggested by Jähnchen *et al.* (31) who reported no statistically significant increase in the apparent volume of distribution of dicumarol in the rat, despite extensive displacement of this anticoagulant by phenylbutazone.

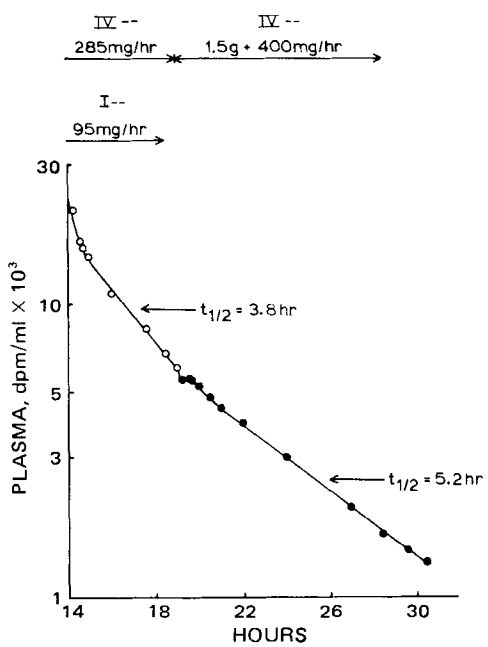

Figure 6—*Total plasma radioactivity after intravenous administration of a pulse of ^{14}C-tolbutamide (2.47×10^8 dpm) during Interaction Study 2.*

The unbound fraction of tolbutamide in plasma (α) depends on several factors, including the total plasma concentrations of the interacting drugs and binding protein(s), as well as the affinities of the binding species for the protein(s). To examine the altered binding during the interaction study, not entirely accounted for by changes in the plasma concentrations of tolbutamide and sulfadimethoxine, the following test was performed. A comparison was made between the values of α determined in samples obtained during Interaction Study 2 with those determined in samples prepared by placing the same concentrations of tolbutamide and sulfadimethoxine into control plasma collected from the animal 2 hr prior to the study.

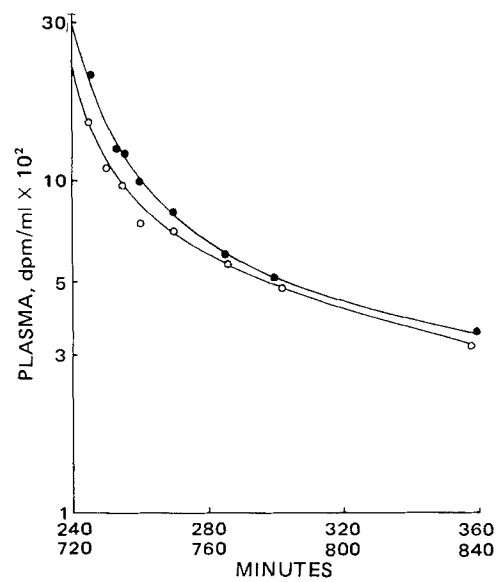

Figure 7—*Total plasma radioactivity determined after intravenous administration of a pulse of ^{3}H-hydroxytolbutamide (2.44×10^7 dpm) before (●) and after (○) sulfadimethoxine administration during Interaction Study 2.*

Table I—Evaluation of Nonesterified Fatty Acid (FFA) and Plasma Proteins in Sheep 1494 Prior or During Interaction Study 2

Hours	α[a] Found	α[a] Expected	FFA, μg/ml	Plasma Proteins, g/100 ml Total	Albumin	α_1-Globulin	α_2-Globulin	β-Globulin	γ-Globulin
Control-a[b]	—	—	—	9.2	2.7	0.5	0.9	2.6	2.5
Control-b[c]	—	—	—	9.2	2.3	0.4	1.1	3.7	1.7
0	—	—	0.66	—	—	—	—	—	—
2.0	0.18	—	0.51	—	—	—	—	—	—
6.0	0.19	—	0.42	—	—	—	—	—	—
7.0	0.43	0.39	0.33	—	—	—	—	—	—
9.0	0.48	0.36	0.44	—	—	—	—	—	—
13.0	—	—	—	9.2	2.7	0.4	1.0	2.4	2.7
14.0	0.47	0.34	—	—	—	—	—	—	—
18.5	—	—	0.52	—	—	—	—	—	—

[a] Unbound tolbutamide fraction in plasma. [b] Sample from the infectious state during which time the tolbutamide kinetics were altered. [c] Sample from the animal 2 months prior to Interaction Study 2.

As seen in Fig. 8, major differences in the value of α between the paired samples were noted throughout most of the interaction study. Measurement of 9-, 11-, and 14-hr samples also showed a similar elevation in the α values for sulfadimethoxine. The possibility that decreases in plasma proteins [*e.g.*, albumin (32–34)] or changes in free fatty acids (35, 36) during the interaction study might have caused the exaggerated unbound fraction was excluded. No significant differences were noted between samples obtained during the study and control samples prior to the study (Table I). The possibility of additional displacement caused by the excessive accumulation of a highly bound N^4-conjugated sulfadimethoxine metabolite (37) also was excluded. No significant increase was noted in the samples between the free and total sulfonamides. The question of the differences remains unresolved.

Tolbutamide Binding and Tolbutamide Renal Clearance—By using total and unbound plasma tolbutamide concentrations, along with the urinary data of Interaction Study 2, the renal clearance of tolbutamide was evaluated. Comparing the data at the end of phases 1 and 2 resulted in renal clearances, based upon total plasma tolbutamide concentrations, of 3.0 and 7.6 ml/min, respectively; the renal clearances based upon unbound tolbutamide levels were 16.2 and 16.5 ml/min, respectively. The similarities of the latter values suggested that the unbound plasma tolbutamide concentration dictated the urinary excretion rate.

Regression analysis on all data of Interaction Study 2 was performed to evaluate the correlation between the rate of urinary tolbutamide excretion and either the total or unbound tolbutamide concentration. As seen in Fig. 9, the correlation coefficient using the unbound data ($r = 0.90$) was higher than when total tolbutamide levels were used ($r = 0.59$). Unfortunately, the unbound tolbutamide data were primarily clustered at two points so the results in Fig. 9 are not conclusive. Nevertheless, the preceding results suggest that a linear relationship exists between the urinary excretion rate of tolbutamide and the unbound plasma tolbutamide concentration. These experiments point out the usefulness of drug interactions in perturbing the normal disposition of an agent in order to evaluate its mode of elimination kinetically.

Hydroxytolbutamide Renal Clearance—The hydroxytolbutamide urinary excretion results observed in Interaction Study 1 (Fig. 3) suggested that sulfadimethoxine possibly reduced the renal clearance of hydroxytolbutamide. This potential interaction was investigated in a separate experiment. The results did not show any significant effect by sulfadimethoxine on the renal clearance of hydroxytolbutamide (738 ml/min) (Fig. 10), and this finding was confirmed in Interaction Study 2. A pulse of ^{3}H-hydroxytolbutamide (5.5 mg, 2.44×10^7 dpm) was administered in the absence (4 hr) and presence (12 hr) of sulfadimethoxine, and the plasma was monitored for radioactivity. No significant change was found in the disposition of the radioactivity (Fig. 7). Since hydroxytolbutamide is cleared almost exclusively by renal excretion, these foregoing investigations indicate that any changes in its urinary excretion rate during the tolbutamide–sulfadimethoxine interaction must have been due to changes in its formation.

Inhibition of Tolbutamide Oxidation—The total plasma clearance of tolbutamide is much lower than the combined flow to the two organs, liver and kidney, responsible for tolbutamide elimination. It is anticipated that the elimination rate of drugs like tolbutamide, which are poorly extracted by the eliminating organs, is dependent on its unbound plasma concentration (35, 38). Certainly the dependence of the renal clearance of tolbutamide on α supports this hypothesis. If this hypothesis is extended to the metabolism of tolbutamide, the sustained elevation of unbound plasma tolbutamide and changes in its total plasma concentration favor a mechanism whereby sulfadimethoxine not only displaces tolbutamide from binding sites but also inhibits its metabolism. Scheme I is the simplest model consistent with the observations. Sulfadimethoxine is depicted as displacing tolbutamide from plasma and tissue binding sites and inhibiting tolbutamide's elimination by nonrenal (metabolic) routes. The basis for these conclusions follows.

In cases where the elimination rate of a drug is proportional to its unbound concentration (Cu), the steady-state unbound concentration (Cu_{ss}) depends only on the infusion rate (R^0) and the clearance based upon the unbound drug (CLu) (35):

$$Cu_{ss} = \frac{R^0}{CLu} \qquad \text{(Eq. 1)}$$

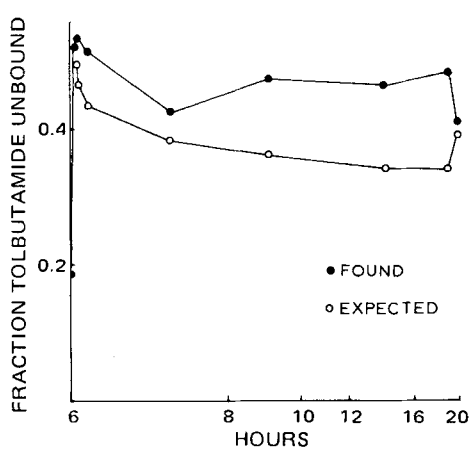

Figure 8—*Comparison of the unbound plasma tolbutamide fraction observed in Interaction Study 2, Fig. 5 (●), with the fraction anticipated (O) based upon* in vitro *displacement experiments using the same total plasma tolbutamide and sulfadimethoxine concentrations.*

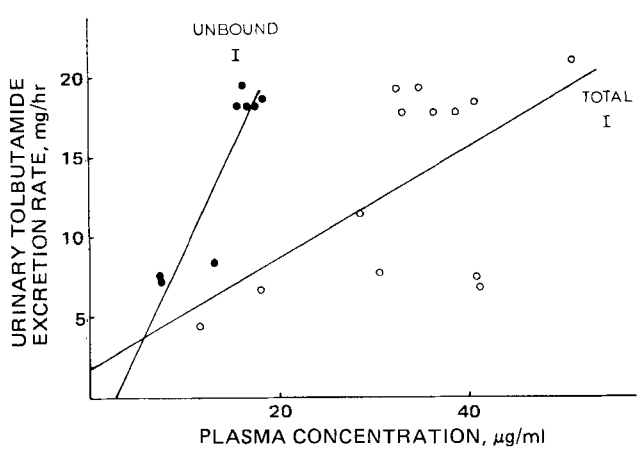

Figure 9—*Regression analysis of the rate of urinary excretion of tolbutamide on the total (O) and unbound (●) plasma tolbutamide (I) concentrations from Interaction Study 2. Correlation coefficients are 0.59 ($0.025 < p < 0.050$) and 0.90 ($p < 0.005$), respectively.*

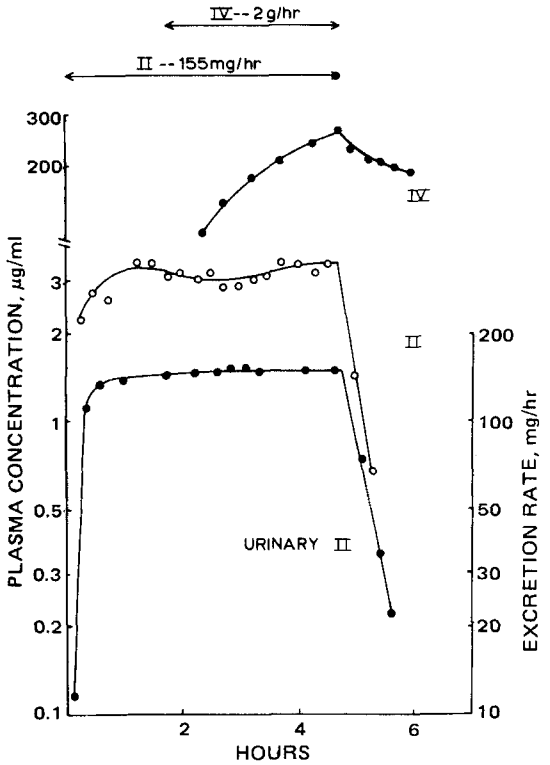

Figure 10—*Interaction of hydroxytolbutamide and sulfadimethoxine in sheep. Hydroxytolbutamide (II) was administered as an infusion (155 mg/hr) for 5 hr while sulfadimethoxine (IV) was coadministered from 2 to 5 hr as an infusion (2 g/hr). The resultant plasma concentrations of sulfadimethoxine (IV) and hydroxytolbutamide (II), as well as the urinary excretion rate of hydroxytolbutamide (II), are displayed.*

By definition, CLu is related to the clearance based on the total plasma concentration (CL) by:

$$CL = \alpha CLu \qquad \text{(Eq. 2)}$$

Thus, CLu, a measure of the inherent ability of an organ to clear a drug, may be regarded as the clearance when all drug has been displaced (α = 1). According to Eq. 1, if a compound acts only as a displacer (α increases), the steady-state unbound concentration of the displaced drug, being independent of α, remains unchanged. But, in the presence of sulfadimethoxine, the Cu_{ss} of tolbutamide rose (Fig. 5). As the infusion rate was fixed, CLu must, therefore, have decreased, with the cause being primarily the inhibition of tolbutamide metabolism.

The kinetics of competitive inhibition for a single metabolic step were described by Gillette (36):

$$\text{rate of metabolism} = \frac{V_{max}[S]}{[S] + K_m(1 + [I]/K_I)} \qquad \text{(Eq. 3)}$$

where V_{max} is the maximal velocity of the reaction, K_m is the Michaelis–Menten constant, $[S]$ is the substrate concentration, $[I]$ is the inhibitor concentration, and K_I is the concentration of inhibitor required to reduce the apparent K_m by 50%. For a compound eliminated by various routes, the rate of metabolism may alternatively be described in terms of its metabolic clearance (CLm) and when $[S] \ll K_m$:

$$\text{rate of metabolism} = \frac{CLm[S]}{1 + [I]/K_I} \qquad \text{(Eq. 4)}$$

This relationship, however, suggests that the metabolism rate is proportional to the total plasma concentration. From Eqs. 1 and 4, a general relationship is derived for the steady-state unbound plasma concentration of an agent during inhibition whose CLu takes place *via* a single metabolic step:

$$Cu_{ss} = \frac{R^0}{CLu}(1 + [I]/K_I) \qquad \text{(Eq. 5)}$$

By denoting $Cu_{ss}{}^1$ and $Cu_{ss}{}^2$ as the unbound steady-state concentration in the absence and presence of an inhibitor, respectively, Eq. 6 applies:

$$Cu_{ss}{}^2 = Cu_{ss}{}^1(1 + [I]/K_I) \qquad \text{(Eq. 6)}$$

When a compound is eliminated by various routes, the metabolic clearance based on unbound drug in the presence of inhibitor (CLu,m^2) can be predicted from the metabolic clearance in the absence of inhibitor (CLu,m^1) and the degree of inhibition:

$$CLu,m^2 = \frac{CLu,m^1}{1 + [I]/K_I} \qquad \text{(Eq. 7)}$$

Rearranging Eq. 7 yields an analytical solution for K_I:

$$K_I = \frac{[I]}{\frac{CLu,m^1}{CLu,m^2} - 1} \qquad \text{(Eq. 8)}$$

Table II—Evaluation of Tolbutamide Kinetics in Sheep 1494

Source	Parameter	Formula	Value				
Intravenous cold tolbutamide bolus data (means)	CL, ml/min	$\frac{\text{dose}}{\int_0^\infty C_p\,dt}$	37.5				
	α	—	0.18[a]				
	CLu, ml/min	CL/α	208				
	$t_{1/2}$, hr	—	3.6				
	V_d, liters	$(1.44CL)(t_{1/2})$	11.2				
			Value				
			Phase 1	Phase 2		Phase 3	
			Cold	Cold	^{14}C	Cold	^{14}C
Interaction Study 2	CL, ml/min	R^0/Ct_{ss}	40.7	38.7	45[b]	32.4[c]	34[d]
	α	Cu_{ss}/Ct_{ss}	0.19	0.45	—	0.45[c]	—
	CLu, ml/min	R^0/Cu_{ss}	214	86	—	72[c]	—
	$t_{1/2}$, hr	—	—	(3.8)	3.8	5.2	5.2
	V_d, liters	$(1.44CL)(t_{1/2})$	—	(12.7)	14.8	14.6	15.3

[a] 50 μg of tolbutamide/ml (*in vitro* determination). [b] Formula: $\text{dose}/[\int_{14}^{19} C_p\,dt + (C_p{}^{19}/K)]$. [c] Assumed or predicted values. [d] Formula:

$$\frac{\text{dose}\left[1 - \frac{\int_{14}^{19} C_p\,dt}{\int_{14}^{19} C_p\,dt + \frac{C_p{}^{19}}{K^2}}\right]}{\frac{C_p{}^{19}}{K^3}}$$

where K^2 and K^3 are the first-order rate constants for elimination during phases 2 and 3, respectively.

Table III—Results Found and Parameters Calculated from the Data of Interaction Study 2 [a]

Parameter	Formula	Phase 1	Phase 2	Phase 3
CLu, ml/min	R^0/Cu_{ss}	214	86	17 + 55 = 72[b]
CLu,r, ml/min	$\frac{\Delta Te}{\Delta t} / Cu_{ss}$	16	17	17[b]
CLu,m, ml/min	*CLu* − *CLu,r* or Eq. 7	198	70	55[b]
[*I*], μg/ml	—	—	120	168
K_I, μg/ml	Eq. 8	—	65	65
α	Cu_{ss}/Ct_{ss}	0.19	0.45	0.45[b]
V_d, liters	—	—	13.8	15.0
$t_{1/2}$ obs., hr	—	—	3.8	5.2
$t_{1/2}$ calc., hr	Eq. 9	—	—	4.9

[a] See text for explanation of abbreviations and equations. [b] Assumed or predicted values.

The elimination kinetics of tolbutamide can be characterized as occurring from a single compartment. Although the half-life in the presence of the displacer–inhibitor ($t_{1/2}^2$) is a function of the half-life in the absence of inhibitor ($t_{1/2}^1$), it also depends on the changes in overall clearance based upon the unbound drug, the apparent volumes of distribution (V_d), and the fractions of the compound in the unbound form according to:

$$t_{1/2}^2 = \frac{t_{1/2}^1 CLu^1 V_d^2 \alpha^1}{CLu^2 V_d^1 \alpha^2} \qquad \text{(Eq. 9)}$$

The superscripts 1 and 2 denote the situation in the absence and presence, respectively, of the displacer–inhibitor. Alternatively, they denote the situation at two levels of the displacer–inhibitor.

In Interaction Study 2, following the simplest model (Scheme I), the metabolic clearance based on unbound drug (*CLu,m*) was estimated by subtracting the renal clearance based on unbound drug (*CLu,r*), obtained by dividing the steady-state rate of renal tolbutamide excretion by its steady-state unbound plasma concentration, from the *CLu*, estimated from Eq. 1. The clearance associated with the oxidation of tolbutamide to hydroxytolbutamide, based on unbound drug, was estimated by dividing the steady-state hydroxytolbutamide excretion rate by the steady-state unbound plasma tolbutamide concentration.

Three phases were present in Interaction Study 2 (Figs. 4 and 5). A quantitative explanation for the tolbutamide–sulfadimethoxine interaction might be possible by accounting for tolbutamide's half-life during phase 3. The results of Figs. 5 and 6 revealed a prolongation in the half-life from 3.8 hr in phase 2 to 5.2 hr in phase 3. Table II summarizes the tolbutamide kinetics observed in Sheep 1494 during three nonradioactive (cold) tolbutamide intravenous bolus experiments and during Interaction Study 2. There is close agreement between the bolus results and those observed during phase 1 of Interaction Study 2. The transition from phase 1 to phases 2 and 3 was notably marked by a large reduction in the overall inherent clearance (*CLu*). The cold and ^{14}C-tolbutamide results of phases 2 and 3 are in agreement, providing mean total body clearances (*CL*), half-lives, and apparent volumes of distribution of 41.9 ml/min, 3.8 hr, and 13.8 liters, respectively, during phase 2 and of 33.2 ml/min, 5.2 hr, and 15.0 liters, respectively, during phase 3.

Table III summarizes the calculations made with the model depicted in Scheme I. From the data in phases 1 and 2, the K_I for sulfadimethoxine was calculated to be 65 μg/ml. Substituting this value of K_I and other data into the appropriate equations yielded a predicted half-life of tolbutamide in phase 3 of 4.9 hr. The close proximity between the predicted and observed half-life (5.2 hr) tends to favor the proposed interaction model. The data permitted the investigation of certain modifications in the proposed displacement–inhibition model. Inhibition by sulfadimethoxine at point a (Scheme I) or b and c independently failed to predict tolbutamide's half-life in phase 3 as well as that for the model evaluated. Consideration was also given to a model in which the renal clearance of tolbutamide was dictated by the unbound plasma concentration while the metabolic clearance was linearly related to tolbutamide's total plasma concentration. This model, however, failed to predict any change in tolbutamide's half-life in phase 3.

Tolbutamide Binding and Glucose Depression—The influence of the unbound tolbutamide concentration on glucose depression remains somewhat speculative. *In vitro* studies with pancreatic β-cells demonstrated a decreased islet uptake of tolbutamide in the presence of albumin (39). A sudden increase in unbound tolbutamide *in vivo* might, therefore, evoke an increased insulin release, resulting in a depression of plasma glucose. Indeed, the results of the interaction studies suggest such a possibility.

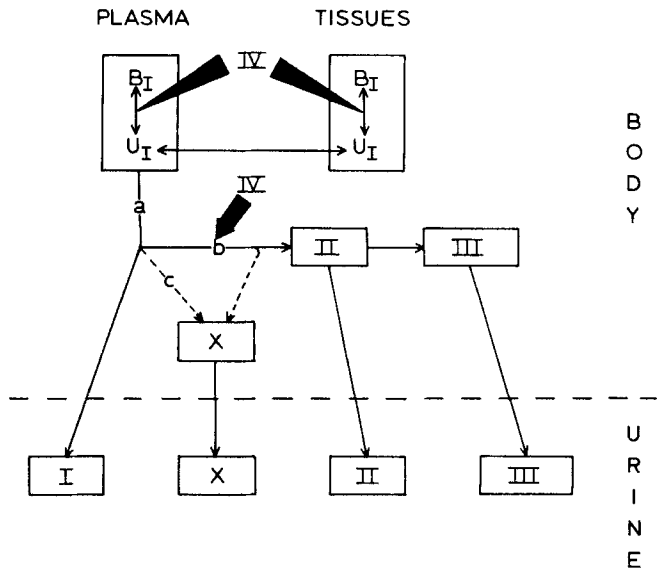

Scheme I—Sulfadimethoxine (IV) is depicted as altering the bound (B) to unbound (U) ratio of tolbutamide (I) in plasma and tissues. Further, it inhibits the metabolism of tolbutamide (at b) to hydroxytolbutamide (II) and an unknown metabolic product (X). A small portion of hydroxytolbutamide is oxidized to carboxytolbutamide (III).

Insulin release may involve occupancy of tolbutamide on the membrane of the β-cell (39) followed by release of part of the insulin in the labile pool (38). Maximum insulin release might follow the attainment of maximum unbound tolbutamide concentrations, leading to maximum glucose depression. After attainment of maximal unbound levels (maximum β-cell binding), no further stimulus for insulin release would exist. This hypothesis could explain the transient insulin release and glucose depression observed after an intravenous tolbutamide bolus (28).

SUMMARY

The results of the coadministration of sulfadimethoxine and tolbutamide in the sheep point to an interaction not only involving displacement of tolbutamide from proteins, which increases its renal clearance, but also inhibition of its metabolism. This explanation accounts for the changes in the total and unbound plasma tolbutamide concentrations and adequately predicts tolbutamide's half-life during phase 3 in Interaction Study 2. The observation of a simultaneous displacement–inhibition phenomenon in the interaction between tolbutamide and sulfadimethoxine is similar to that reported for the interaction between phenylbutazone and warfarin in humans (14).

This report illustrates some of the complexities of drug–drug interactions. Although gross changes in total plasma drug concentrations during the coadministration of highly plasma protein-bound agents may be absent, their absence may be due to compensative reactions. Considerable coincidental changes in unbound plasma drug concentrations may occur, however, and may provoke exaggerated therapeutic responses during chronic drug coadministration.

This report also presents a steady-state approach for investigating mechanisms of drug interactions and demonstrates that the coadministration of agents may permit investigators to scrutinize mechanisms of drug disposition. Knowledge thus obtained will help to evaluate and predict rationally the clinical significance of drug–drug interactions in humans.

REFERENCES

(1) A. G. MacGregor, *Proc. Roy. Soc. Med.*, **58**, 143 (1965).

(2) K. Melmon, H. F. Morrelli, J. A. Oates, A. H. Conney, T. N. Tozer, B. P. Harpole, and T. H. Clark, *Patient Care*, **1967**, 1.

(3) E. A. Hartshorn, *Drug Intell.*, **2**, 174 (1968).

(4) D. L. Azarnoff and A. Hurwitz, *Pharmacol. Physicians*, **4**, 1 (1970).

(5) D. W. Yesair, F. J. Bullock, and J. J. Coffey, *Drug Metab. Rev.*, **1**, 35 (1972).

(6) V. M. Rosenoer and G. M. Gill, *Med. Clin. N. Am.*, **56**, 585 (1972).
(7) S. S. Brown, *Foreign Compd. Metab. Mamm.*, **2**, 456 (1972).
(8) P. D. Hansten, "Drug Interactions," 2nd ed., Lea & Febiger, Philadelphia, Pa., 1971.
(9) E. W. Martin, "Hazards of Medication," Lippincott, Philadelphia, Pa., 1971.
(10) "Evaluations of Drug Interactions," 2nd ed., American Pharmaceutical Association, Washington, D.C., 1976.
(11) P. L. Morselli, S. Garattini, and S. N. Cohen, "Drug Interactions," Raven, New York, N.Y., 1974.
(12) M. Rowland and S. B. Matin, *J. Pharmacokinet. Biopharm.*, **1**, 553 (1973).
(13) R. J. Lewis, W. F. Trager, K. K. Chan, A. Breckenridge, M. Orme, M. Rowland, and W. Schary, *J. Clin. Invest.*, **53**, 1607 (1974).
(14) W. L. Schary, R. J. Lewis, and M. Rowland, *Res. Commun. Chem. Pathol. Pharmacol.*, **10**, 663 (1975).
(15) M. Rowland, L. Z. Benet, and G. G. Graham, *J. Pharmacokinet. Biopharm.*, **1**, 123 (1973).
(16) R. A. Branch, D. G. Shand, G. R. Wilkinson, and A. S. Nies, *J. Clin. Invest.*, **53**, 1101 (1974).
(17) M. Kristensen and L. K. Christensen, in "Pharmacokinetics and Mode of Action of Oral Hypoglycemic Agents," A. Loubatieres and A. E. Reynolds, Eds., III Capri Conference, Casa Editrice, Milan, Italy, 1969, p. 116.
(18) S. B. Matin and M. Rowland, *Anal. Lett.*, **6**, 865 (1973).
(19) A. C. Bratton and E. K. Marshall, *J. Biol. Chem.*, **128**, 537 (1939).
(20) P. H. Lenz and A. J. Passannante, *Clin. Chem.*, **16**, 426 (1970).
(21) V. P. Dole, *J. Clin. Invest.*, **35**, 150 (1956).
(22) S. P. Colowick and N. O. Kaplan, "Methods in Enzymology," vol. III, Academic, New York, N.Y., 1957, p. 450.
(23) O. H. Lowry, N. J. Rosebrough, A. L. Farr, and R. J. Randall, *J. Biol. Chem.*, **193**, 265 (1951).
(24) H. G. Weder, J. Schildknecht, and A. Kessekring, *Am. Lab.*, **10**, 15 (1971).
(25) G. Wittenhagen, G. Mohnike, and W. Langenbeck, *Z. Physiol. Chem.*, **316**, 157 (1959).
(26) R. C. Thomas and G. J. Ikeda, *J. Med. Chem.*, **9**, 507 (1966).
(27) J. Tagg, D. M. Yasula, M. Tanabe, and C. Mitoma, *Biochem. Pharmacol.*, **16**, 143 (1967).
(28) R. J. Mahler and O. Szabo, *Horm. Metab. Res.*, **2**, 9 (1970).
(29) W. H. Linkenheimer and S. J. Stolzenberg, *Am. J. Vet. Res.*, **26**, 1095 (1965).
(30) E. G. McQueen and W. M. Wardell, *Br. J. Pharmacol.*, **43**, 312 (1971).
(31) E. Jähnchen, L. B. Wingard, and G. Levy, *J. Pharmacol. Exp. Ther.*, **184**, 176 (1973).
(32) M. C. Meyer and D. E. Guttman, *J. Pharm. Sci.*, **57**, 895 (1968).
(33) W. D. Wosilait, *Res. Commun. Chem. Pathol. Pharmacol.*, **9**, 681 (1974).
(34) R. J. Porter and R. B. Layzer, *Arch. Neurol.*, **32**, 298 (1975).
(35) M. Rowland, S. B. Matin, J. Thiessen, and J. Karam, in "Drug Interactions," P. L. Morselli, S. Garattini, and S. N. Cohen, Eds., Raven, New York, N.Y., 1974, p. 199.
(36) J. R. Gillette, in "Fundamentals of Drug Metabolism," B. N. La Du, H. G. Mandel, and E. L. Way, Eds., Williams & Wilkins, Baltimore, Md., 1971, p. 400.
(37) T. Fujita, *J. Med. Chem.*, **15**, 1049 (1972).
(38) G. M. Grodsky, D. L. Curry, L. L. Bennett, and J. J. Rodrigo, *Acta Diabetol. Lat., Suppl. 1*, **5**, 140 (1968).
(39) J. Sehlin, *Acta Diabetol. Lat.*, **10**, 1052 (1973).

ACKNOWLEDGMENTS AND ADDRESSES

Received April 12, 1976, from the *School of Pharmacy, University of California, San Francisco, CA 94143.*

Accepted for publication August 25, 1976.

Presented in part at the Basic Pharmaceutics Section, APhA Academy of Pharmaceutical Sciences, San Diego meeting, November 1973.

Abstracted in part from a dissertation submitted by J. J. Thiessen to the University of California, San Francisco, in partial fulfillment of the Doctor of Philosophy degree requirements.

The authors thank Dr. S. Matin for gifts of ^{3}H-tolbutamide and ^{3}H-hydroxytolbutamide, Hoffmann-La Roche, Inc., for a gift of sulfadimethoxine, and Farbwerke Hoechst AG, Germany, for gifts of hydroxytolbutamide and ^{14}C-tolbutamide. They also thank Dr. Noel Fishman for assistance in the animal surgery.

* Supported by U.S. Public Health Service Grant GM 00728.

‡ Present address: Department of Pharmacy, University of Manchester, Manchester M13 9PL, England.

ˣ To whom inquiries should be directed. Present address: Faculty of Pharmacy, University of Toronto, Toronto, Canada, M5S 1A1.

Mathematical Model for Enteric Film Coating of Tablets

SALIH DINÇER *ˣ and SEZA ÖZDURMUŞ ‡

Abstract □ The enteric film coating of placebo tablets, using a methacrylic acid–methyl methacrylate copolymer as the film former in the coating solution, was studied by statistical techniques. The effects of four independent formulation and process variables on the disintegration time of the coated film in simulated intestinal fluid and on the resistance to disintegration of the coated film in simulated gastric fluid were studied. The results of a statistically designed set of experiments were used as the input data. Regression analysis of these data resulted in two first-order polynomial equations. The linear model obtained for the disintegration time of the coating in the simulated intestinal fluid was analyzed by the steepest descent method to determine the most suitable combination of the independent variables.

Keyphrases □ Tablets—enteric film coating with methacrylic acid–methyl methacrylate copolymer, disintegration time, mathematical model □ Film coating, enteric—with methacrylic acid–methyl methacrylate copolymer, tablet disintegration time, mathematical model □ Models, mathematical—disintegration time of tablets with enteric film coating of methacrylic acid–methyl methacrylate copolymer □ Disintegration time—tablets with enteric film coating of methacrylic acid–methyl methacrylate copolymer, mathematical model □ Methacrylic acid–methyl methacrylate copolymer—enteric film coating of tablets, disintegration time, mathematical model □ Dosage forms—tablets with enteric film coating of methacrylic acid–methyl methacrylate copolymer, disintegration time, mathematical model

Much research in pharmaceutics has concerned the relationship between the controllable formulation and process (independent) variables and the characteristics of the resultant system (response). An empirical relationship can be developed with data from statistically designed experiments. The relationship between the independent

(6) V. M. Rosenoer and G. M. Gill, *Med. Clin. N. Am.*, **56**, 585 (1972).
(7) S. S. Brown, *Foreign Compd. Metab. Mamm.*, **2**, 456 (1972).
(8) P. D. Hansten, "Drug Interactions," 2nd ed., Lea & Febiger, Philadelphia, Pa., 1971.
(9) E. W. Martin, "Hazards of Medication," Lippincott, Philadelphia, Pa., 1971.
(10) "Evaluations of Drug Interactions," 2nd ed., American Pharmaceutical Association, Washington, D.C., 1976.
(11) P. L. Morselli, S. Garattini, and S. N. Cohen, "Drug Interactions," Raven, New York, N.Y., 1974.
(12) M. Rowland and S. B. Matin, *J. Pharmacokinet. Biopharm.*, **1**, 553 (1973).
(13) R. J. Lewis, W. F. Trager, K. K. Chan, A. Breckenridge, M. Orme, M. Rowland, and W. Schary, *J. Clin. Invest.*, **53**, 1607 (1974).
(14) W. L. Schary, R. J. Lewis, and M. Rowland, *Res. Commun. Chem. Pathol. Pharmacol.*, **10**, 663 (1975).
(15) M. Rowland, L. Z. Benet, and G. G. Graham, *J. Pharmacokinet. Biopharm.*, **1**, 123 (1973).
(16) R. A. Branch, D. G. Shand, G. R. Wilkinson, and A. S. Nies, *J. Clin. Invest.*, **53**, 1101 (1974).
(17) M. Kristensen and L. K. Christensen, in "Pharmacokinetics and Mode of Action of Oral Hypoglycemic Agents," A. Loubatieres and A. E. Reynolds, Eds., III Capri Conference, Casa Editrice, Milan, Italy, 1969, p. 116.
(18) S. B. Matin and M. Rowland, *Anal. Lett.*, **6**, 865 (1973).
(19) A. C. Bratton and E. K. Marshall, *J. Biol. Chem.*, **128**, 537 (1939).
(20) P. H. Lenz and A. J. Passannante, *Clin. Chem.*, **16**, 426 (1970).
(21) V. P. Dole, *J. Clin. Invest.*, **35**, 150 (1956).
(22) S. P. Colowick and N. O. Kaplan, "Methods in Enzymology," vol. III, Academic, New York, N.Y., 1957, p. 450.
(23) O. H. Lowry, N. J. Rosebrough, A. L. Farr, and R. J. Randall, *J. Biol. Chem.*, **193**, 265 (1951).
(24) H. G. Weder, J. Schildknecht, and A. Kessekring, *Am. Lab.*, **10**, 15 (1971).
(25) G. Wittenhagen, G. Mohnike, and W. Langenbeck, *Z. Physiol. Chem.*, **316**, 157 (1959).
(26) R. C. Thomas and G. J. Ikeda, *J. Med. Chem.*, **9**, 507 (1966).
(27) J. Tagg, D. M. Yasula, M. Tanabe, and C. Mitoma, *Biochem. Pharmacol.*, **16**, 143 (1967).
(28) R. J. Mahler and O. Szabo, *Horm. Metab. Res.*, **2**, 9 (1970).
(29) W. H. Linkenheimer and S. J. Stolzenberg, *Am. J. Vet. Res.*, **26**, 1095 (1965).
(30) E. G. McQueen and W. M. Wardell, *Br. J. Pharmacol.*, **43**, 312 (1971).
(31) E. Jähnchen, L. B. Wingard, and G. Levy, *J. Pharmacol. Exp. Ther.*, **184**, 176 (1973).
(32) M. C. Meyer and D. E. Guttman, *J. Pharm. Sci.*, **57**, 895 (1968).
(33) W. D. Wosilait, *Res. Commun. Chem. Pathol. Pharmacol.*, **9**, 681 (1974).
(34) R. J. Porter and R. B. Layzer, *Arch. Neurol.*, **32**, 298 (1975).
(35) M. Rowland, S. B. Matin, J. Thiessen, and J. Karam, in "Drug Interactions," P. L. Morselli, S. Garattini, and S. N. Cohen, Eds., Raven, New York, N.Y., 1974, p. 199.
(36) J. R. Gillette, in "Fundamentals of Drug Metabolism," B. N. La Du, H. G. Mandel, and E. L. Way, Eds., Williams & Wilkins, Baltimore, Md., 1971, p. 400.
(37) T. Fujita, *J. Med. Chem.*, **15**, 1049 (1972).
(38) G. M. Grodsky, D. L. Curry, L. L. Bennett, and J. J. Rodrigo, *Acta Diabetol. Lat., Suppl. 1*, **5**, 140 (1968).
(39) J. Sehlin, *Acta Diabetol. Lat.*, **10**, 1052 (1973).

ACKNOWLEDGMENTS AND ADDRESSES

Received April 12, 1976, from the *School of Pharmacy, University of California, San Francisco, CA 94143.*

Accepted for publication August 25, 1976.

Presented in part at the Basic Pharmaceutics Section, APhA Academy of Pharmaceutical Sciences, San Diego meeting, November 1973.

Abstracted in part from a dissertation submitted by J. J. Thiessen to the University of California, San Francisco, in partial fulfillment of the Doctor of Philosophy degree requirements.

The authors thank Dr. S. Matin for gifts of ^{3}H-tolbutamide and ^{3}H-hydroxytolbutamide, Hoffmann-La Roche, Inc., for a gift of sulfadimethoxine, and Farbwerke Hoechst AG, Germany, for gifts of hydroxytolbutamide and ^{14}C-tolbutamide. They also thank Dr. Noel Fishman for assistance in the animal surgery.

* Supported by U.S. Public Health Service Grant GM 00728.

‡ Present address: Department of Pharmacy, University of Manchester, Manchester M13 9PL, England.

ˣ To whom inquiries should be directed. Present address: Faculty of Pharmacy, University of Toronto, Toronto, Canada, M5S 1A1.

Mathematical Model for Enteric Film Coating of Tablets

SALIH DINÇER *ˣ and SEZA ÖZDURMUŞ ‡

Abstract □ The enteric film coating of placebo tablets, using a methacrylic acid–methyl methacrylate copolymer as the film former in the coating solution, was studied by statistical techniques. The effects of four independent formulation and process variables on the disintegration time of the coated film in simulated intestinal fluid and on the resistance to disintegration of the coated film in simulated gastric fluid were studied. The results of a statistically designed set of experiments were used as the input data. Regression analysis of these data resulted in two first-order polynomial equations. The linear model obtained for the disintegration time of the coating in the simulated intestinal fluid was analyzed by the steepest descent method to determine the most suitable combination of the independent variables.

Keyphrases □ Tablets—enteric film coating with methacrylic acid–methyl methacrylate copolymer, disintegration time, mathematical model □ Film coating, enteric—with methacrylic acid–methyl methacrylate copolymer, tablet disintegration time, mathematical model □ Models, mathematical—disintegration time of tablets with enteric film coating of methacrylic acid–methyl methacrylate copolymer □ Disintegration time—tablets with enteric film coating of methacrylic acid–methyl methacrylate copolymer, mathematical model □ Methacrylic acid–methyl methacrylate copolymer—enteric film coating of tablets, disintegration time, mathematical model □ Dosage forms—tablets with enteric film coating of methacrylic acid–methyl methacrylate copolymer, disintegration time, mathematical model

Much research in pharmaceutics has concerned the relationship between the controllable formulation and process (independent) variables and the characteristics of the resultant system (response). An empirical relationship can be developed with data from statistically designed experiments. The relationship between the independent

Table I—Levels of Formulation and Process Variables in Physical Units

Variable	Lower Level, −1	Base Level, 0	Higher Level, +1
x_1 = film-former concentration (one experimental unit = 1%)	4.4	5.4	6.4
x_2 = plasticizer concentration (one experimental unit = 0.5%)	1.0	1.5	2.0
x_3 = total spraying time of coating solution (one experimental unit = 20 min)	40	60	80
x_4 = length of drying interval (one experimental unit = 5 sec)	10	15	20

variables can be optimized to obtain the best combination of formulation and process variables. Mathematical models for optimization of pharmaceutical formulation and processing were reported previously (1–3).

The purpose of this study was to develop a mathematical model for the enteric film coating of tablets with a widely used film former, a copolymer[1] based on methacrylic acid and methyl methacrylate, using a spray gun, a drier, and the conventional coating pan.

THEORY

Statistically designed experiments[2] were performed to derive a mathematical model for the optimization of the film-coating technique. The experimental design is dependent on the number of variables. For four independent formulation and process variables (Table I) (4), a half-factorial orthogonal design at two levels with four replicated center points requires 12 experiments (Table II).

The first eight experiments represent a half-factorial design for four factors at two levels resulting in eight (0.5×2^4) trials. The additional four trials represent the replicated center points. The two levels here are represented as +1 and −1. Level zero represents the base level. Experiments 9–12 are included to calculate the experimental error.

The type of predictor equation resulting from such a study was a first-order polynomial having the form:

$$y_j = b_0 + b_1x_1 + b_2x_2 + b_3x_3 + b_4x_4 \qquad \text{(Eq. 1)}$$

where y_j = response variable, b_i = regression coefficients for first-order polynomial, and x_i = independent variable. Such an equation can be generated for each dependent variable, relating it to the set of four independent variables.

To estimate the path of steepest descent, the gradient of the linear relation given by Eq. 1 can be written as:

$$\nabla y(x_1, x_2, \ldots, x_k) = \left(\frac{\partial y}{\partial x_1}, \frac{\partial y}{\partial x_2}, \ldots, \frac{\partial y}{\partial x_k}\right) = (b_1, b_2, \ldots, b_k) = b_i \qquad \text{(Eq. 2)}$$

where $i = 1, 2, \ldots, k$. Thus, the change in x_i in the path of steepest descent is proportional to $-b_i$, because it moves in the direction $-\nabla y(x_1, x_2, \ldots, x_k)$. In computations, one variable was selected as a standard and the changes in the other variables corresponding to a λ change in the standard variable (λ is the step size) were computed.

EXPERIMENTAL

The four independent formulation and process variables selected are defined in Table I. The length of the drying interval, x_4, was measured as the time interval the coated tablets were dried in the pan by the drier. The film former was a methacrylic acid–methyl methacrylate copolymer; the plasticizer was dibutyl phthalate[3]. Apart from the film former and the plasticizer, the coating solution consisted of isopropyl alcohol (its percentage was changed with the amounts of film former and plasticizer added), acetone (40% w/w), water (1.50% w/w), and a soluble dye (D&C Orange No. 4, 0.01% w/w).

The placebo tablets were composed of lactose, starch, gelatin solution, and magnesium stearate. The tablets were compressed on 2.65-mm deep concave punches and had an average thickness of 7.50 mm. The tablets were nonfriable with an average weight of 760 mg and an average hardness of 8.0 kg. The coating apparatus consisted of a conventional bench-type copper coating pan with 25-cm diameter and 30-rpm rotational speed.

The spraying unit consisted of a compressed air, hand-operated spray gun, but compressed nitrogen gas was used instead of compressed air. The nitrogen pressure was maintained at 0.4–0.5 atm in all experiments. The spray unit was arranged so that the spray jet met the falling cores in the upper part of the pan. It was fixed rigidly by means of clamps on a stand at the side of the pan opening approximately 20 cm from the surface of the rotating tablet bed. The drying unit consisted of a hair drier giving warm air at approximately 50°. The duration of the spraying and drying cycles was adjusted manually with the help of a stopwatch.

Since the main objective of the coating operation was to envelop the core tablets in a polymeric film, it was decided to determine the quantity of solution that would render the process inoperative. The amount of film-coating solution for a single application of the spray gun that a given weight of tablets could tolerate was determined. The amount of solution was measured as the length of spraying in seconds. The spray rate was kept constant (2.30 g/min) by adjusting the nitrogen gas pressure and

Table II—0.5×2^4 Fractional Factorial Orthogonal Design

Experiment	Levels of Controlled Variables in Coded Form			
	x_1	x_2	x_3	x_4
1	−1	−1	−1	−1
2	+1	+1	−1	−1
3	+1	−1	+1	−1
4	−1	+1	+1	−1
5	+1	−1	−1	+1
6	−1	+1	−1	+1
7	−1	−1	+1	+1
8	+1	+1	+1	+1
9	0	0	0	0
10	0	0	0	0
11	0	0	0	0
12	0	0	0	0

[a] Replicated center points.

Table III—Liquid Tolerance of Tablets with Solutions Having Different Concentrations of Film Former and Plasticizer

Formula	Concentrations in Solutions, %		Tolerance, sec/500 g of Tablets	Visual Inspection
	Film Former	Plasticizer		
A	5	1	20	Smooth
B	10	1	25	Not smooth
C	5	2	20	Smooth
D	10	2	25	Not smooth

Table IV—Disintegration Time Results of the Film Coat

Experiment[a]	Disintegration in Simulated Intestinal Fluid, min		Resistance to Disintegration in Simulated Gastric Fluid, min	
	Mean Time	*SD*	Mean Time	*SD*
1	6	0.447	50	8.165
2	14	1.080	175	10.165
3	20	0.913	200	11.402
4	15	0.533	280	9.661
5	13	0.632	180	5.477
6	8	0.730	120	17.512
7	16	0.447	250	12.780
8	28	1.414	420	0.000
9	14	0.913	180	11.547
10	14	0.775	200	10.488
11	15	1.169	220	14.491
12	17	0.816	240	18.074

[a] For each experiment, 16 tablets were tested.

[1] Eudragit L, Rohm Pharma GmbH, Darmstadt, Germany.

[2] A discussion of statistical design methods can be found in W. G. Cochran and G. M. Cox, "Experimental Designs," Wiley, New York, N.Y., 1957.

[3] This plasticizer is recommended in "Eudragit Lacquers for Tablet Coating," Rohm Pharma GmbH, Darmstadt, Germany.

Table V—Path of Steepest Descent and Predicted Responses

Level on Path	Levels of Variables in Units				Coded Levels of Variables				Predicted Responses	
	x_1, %	x_2, %	x_3, min	x_4, sec	x_1	x_2	x_3	x_4	y_1, min	y_2, min
0	5.4	1.5	60	15	0	0	0	0	15.00	209.583
1	5.3	1.483	57.467	14.833	−0.1	−0.034	−0.127	−0.033	13.938	193.791
2	5.2	1.466	54.934	14.666	−0.2	−0.068	−0.254	−0.067	12.874	177.967
3	5.1	1.449	52.401	14.499	−0.3	−0.102	−0.381	−0.100	11.812	i62.175
4	5.0	1.432	49.868	14.332	−0.4	−0.136	−0.508	−0.134	10.749	146.351
5	4.9	1.415	47.335	14.165	−0.5	−0.170	−0.635	−0.167	9.687	130.560
6	4.8	1.398	44.802	13.998	−0.6	−0.204	−0.762	−0.200	8.625	114.769
7	4.7	1.381	42.269	13.831	−0.7	−0.238	−0.889	−0.234	7.561	98.945
8	4.6	1.364	39.736	13.664	−0.8	−0.272	−1.016	−0.267	6.500	83.154
9	4.5	1.347	37.203	13.497	−0.9	−0.306	−1.143	−0.301	5.437	67.328
10	4.4	1.330	34.670	13.330	−1.0	−0.340	−1.270	−0.334	4.374	51.537

the controls of the spray gun. Coating solutions with different compositions were applied to the tablets in the rotating pan until the tablets adhered to the pan and to one another and could not be separated without breaking the deposited film. The length of the spraying interval at this point was taken as the liquid tolerance.

The results of these experiments (Table III) showed that the concentration of film former in the coating solution affected the appearance of the coated tablets greatly. Smooth coatings were obtained with a film-former concentration of 5% but not 10%; a 7% concentration was selected as the maximum. A study of the plasticization of the polymeric materials led to the selection of the 1–2% range for the dibutyl phthalate concentration (5, 6). The total spraying time of the coating solution was varied between 40 and 80 min.

During the liquid tolerance experiments, it was observed that the residual film on the tablets dried between 10 and 20 sec. The length of drying was shorter for solutions with low film-former concentrations and longer for solutions with high film-former concentrations. Therefore, the levels chosen for study were 10 and 20 sec (Table I).

In each experiment, a batch size of approximately 500 g of placebo tablets was coated. The coating solution was sprayed onto the tumbling tablets for 20 sec and then dried with warm air according to the length specified in each experiment. This spray–dry cycle was repeated several times until the total spraying time specified was reached.

Other process and formulation conditions including the spray rate, the temperature of the coating solution and tablet bed, the solvent system, and the amount of additives in the solution were the same for each trial.

After each experiment, samples of coated tablets were evaluated for disintegration in the USP disintegration apparatus (7) by placing the tablets into simulated intestinal fluid (7) and simulated gastric fluid (7). The end-point was taken when the first distinct signs of film disintegration, rupture, separation, or softening were evident.

RESULTS AND DISCUSSION

The mean values of the disintegration time in the simulated intestinal fluid and the resistance time to disintegration in the simulated gastric fluid were taken as the true values of the corresponding response at that experimental point. These values were then used in the statistical analysis to determine the regression equation for each response. The mean disintegration times and the standard deviations of the experiments are shown in Table IV.

Model for Disintegration of Film Coat in Simulated Intestinal Fluid—The fitted first-order polynomial model obtained as a result of the 0.5×2^4 fractional factorial design is:

$$y_1 = 15.000 + 3.750x_1 + 1.250x_2 + 4.750x_3 + 1.250x_4 \quad \text{(Eq. 3)}$$

where y_1 is the disintegration time of the film coat in the simulated intestinal fluid. A lack of fit test assuming a 95% F distribution led to the conclusion that the fitted model was adequate to represent the response function. The hypothesis that $b_i = 0$ for all four independent variables assuming a 95% F distribution was rejected. The ANOVA results showed that all regression coefficients were significant, assuming a 95% F distribution. The model had $R^2 = 94.64\%$, measuring the percent fit of the model.

Model for Resistance of Film Coat to Disintegration in Simulated Gastric Fluid—The fitted first-order polynomial model for this response is:

$$y_2 = 209.583 + 34.375x_1 + 39.375x_2 + 78.125x_3 + 33.125x_4 \quad \text{(Eq. 4)}$$

where y_2 is the resistance time to disintegration of the film coat in the simulated gastric fluid. A lack of fit test assuming a 95% F distribution led to the conclusion that the fitted model was adequate to represent the response function. The hypothesis that $b_i = 0$ for all four independent variables assuming a 95% F distribution was rejected. The ANOVA results showed that all regression coefficients were significant, assuming a 95% F distribution. The model had $R^2 = 89.76\%$.

Determination of Optimum Combination of Factor Levels—After obtaining the first-order regression equations for the two responses, one had to find the optimum combination of factor levels that satisfied the following constraints:

1. The film coat should disintegrate in the simulated intestinal fluid within 10 min ($y_1 < 10$ min). Past experience showed that with this choice, when the active material is inserted into the tablets, the tablets as a whole disintegrate within the desired time limit.
2. The film coat should resist disintegration in the simulated gastric fluid for at least 1 hr (7) ($y_2 > 60$ min). To satisfy these constraints, rather than selecting random values for the x's and finding the corresponding y's, the steepest descent method was employed.

When the coded base levels of the four independent variables (0, 0, 0, and 0) were inserted into the response functions, $y_1 = 15.000$ min and $y_2 = 209.583$ min. Response y_1 had to be decreased to satisfy the constraint of $y_1 < 10$ min. The value of y_2 at the base levels of the x's satisfied the constraint set on y_2.

The steepest descent procedure was applied on the regression equation of y_1. A step size of a 0.1% change in the film-former concentration, x_1, was used. Then the respective x_1, x_2, x_3, and x_4 values were obtained. By inserting the coded values of the x's into the two regression equations, corresponding y_1 and y_2 values at those points were predicted (Table V).

More than one combination of variables satisfied the restrictions set on y_1 and y_2 within the experimental region (Table V). The factor levels on the eighth trial were selected as the most suitable combination, giving the lowest predicted value for y_1 and satisfying the restriction set on y_2 within the experimental region, although the level of x_3 was negligibly below the lower limit (40 min) in the experimental design. An experiment was carried out using the selected levels in the same manner as previous experiments. The values of x_3 and x_4 were rounded to 40 min and 14 sec, respectively, since measuring the time in fractions was quite impossible. The experimental results, as the mean values for the disintegration measurements, were $y_1 = 6.375$ min and $y_2 = 80.000$ min. The predicted values for the two responses were $y_1 = 6.660$ min and $y_2 = 86.623$ min. Applying a two-tailed t test at the 5% significance level to the disintegration in the simulated intestinal fluid, with $n = 16$ and $s = 0.587$, and to the resistance to disintegration in the simulated gastric fluid, with $n = 16$ and $s = 12.712$, showed that experimental and predicted results were in good agreement.

REFERENCES

(1) J. R. Buck, G. E. Peck, and G. S. Banker, *Drug Dev. Commun.*, **1**, 89 (1975).

(2) D. E. Fonner, Jr., J. R. Buck, and G. S. Banker, *J. Pharm. Sci.*, **59**, 1587 (1970).

(3) J. B. Schwartz, J. R. Flamholz, and R. H. Press, *ibid.*, **62**, 1165 (1973).
(4) S. Özdurmuş, M.S. thesis, Boğaziçi University, Istanbul, Turkey, 1975.
(5) K. Lehmann, *Manuf. Chem. Aerosol News*, **May 1973**, 36.
(6) *Ibid.*, **June 1973**, 39.
(7) "The United States Pharmacopeia," 18th rev., Mack Publishing Co., Easton, Pa., 1970, pp. 932–934, 1026, 1027.

ACKNOWLEDGMENTS AND ADDRESSES

Received March 17, 1976, from the *Chemical Engineering Department, Boğaziçi University, Bebek, Istanbul, Turkey, and ‡Eczacibaşi A. Ş., Levent, Istanbul, Turkey.

Accepted for publication August 27, 1976.

* To whom inquiries should be directed.

Degradation of Carmustine in Aqueous Media

PAUL A. LASKAR * and JAMES W. AYRES

Abstract □ The degradation rate of carmustine was investigated in buffered aqueous media at several pH values. The buffering agents studied were those with potential use in parenteral formulations of this drug: acetate, citrate, and phosphate. The apparent first-order degradation rate constants were calculated using a linear regression procedure. A pH range over which minimum degradation occurred was ascertained. General acid and specific base catalysis was demonstrated for the degradation of carmustine. From the data at 5, 22, and 37°, the apparent activation energies for carmustine degradation in buffered aqueous media were computed and were strongly pH dependent.

Keyphrases □ Carmustine—degradation rate in aqueous media, effect of pH and temperature □ Degradation rate—carmustine in aqueous media, effect of pH and temperature □ Antineoplastic agents—carmustine, degradation rate in aqueous media, effect of pH and temperature □ Stability—carmustine in aqueous media, effect of pH and temperature

Drugs for the treatment of neoplastic disease have received a great deal of attention. Several thousand chemical agents are systematically screened each year for antineoplastic activity, but only a small percentage exhibit activity and are tested further for clinical utility. Carmustine [1,3-bis(2-chloroethyl)-1-nitrosourea; NSC 409962] (I) was effective in treating L-1210 leukemia, including cases where the central nervous system was involved (1–4).

Prior to the interest in I as a therapeutic agent, a study indicated that 1-methyl-1-nitrosourea (NSC 23909) (II) was unstable in aqueous solution (5), as was a nitrosamide-containing antibiotic, streptozocin, (6). The kinetics of I degradation were considered, and this compound also was unstable in aqueous media (4, 7).

Because I is often administered *via* intravenous solution (8, 9), further consideration of its stability in various aqueous media suitable for intravenous use is desirable. In addition, knowledge of the temperature dependence of the degradation of I is needed to obtain useful shelflife data and to determine desirable storage criteria. Furthermore, knowledge of acid or base catalysis also may be of value in formulating I.

The few published studies directed toward optimizing a parenteral formulation for I emphasized technological considerations such as lyophilization of drug solutions and dry filling with sterile solids (10–12). A formulation for clinical use was prepared by dry filling vials with sterile solid I and sterile, screened mannitol (11, 12). Alternatively, a solution of I in absolute ethanol was filtered through a 0.25-μm membrane and lyophilized (10, 11). These formulations should be used within 1 and 2 hr, respectively, following reconstitution with ethanol and dilution with saline (10, 12).

The purpose of this investigation was to perform accelerated stability studies on I in various aqueous media suitable for injection.

EXPERIMENTAL

Reagents—Carmustine, an investigational new drug, was obtained[1] as a lyophilized powder. All other chemicals were reagent grade.

Materials and Methods—All buffers and other solutions were prepared in volumetric flasks. Distilled water used for dissolving the basic component of the buffer systems was freshly boiled and cooled. Unless noted otherwise, solutions were stored at ambient temperature. Compound I, 0.025 g (stored at −19 ± 1°), was dissolved in sufficient cold (0°) ethanol to make 25 ml of stock solution. The stock solutions were stored at −19 ± 1° for not longer than 7 days.

Buffer solutions were prepared using published procedures (13, 14). All buffer solutions were checked for conformance to the desired pH using a pH meter calibrated at ambient temperature (20–22°) with a pH standard. When necessary, the pH was adjusted to within 0.05 pH unit of the nominal value with either the acidic or basic component of the buffer.

Degradation Experiments—All solvent systems were preequilibrated to the experiment temperature. For ambient (22 ± 1°) and physiological (37.0 ± 0.5°, forced-air oven) temperature experiments, the media were first allowed to equilibrate for at least 16 hr. For experiments at reduced temperature, the media were first chilled in a ice bath (1.0 ± 0.5°) for at least 15 min.

To a volume (~40–45 ml) of preequilibrated media was added 1.0 ml of I stock solution (1 μg/ml). Then the volume was brought rapidly to 50 ml with the appropriate medium, the mixture was shaken, and the time was recorded. A zero-time sample (0.2 ml) was taken for analysis, and the experimental solution was stored at the appropriate temperature. At designated time intervals, a sample volume (0.2, 0.5, 1.0, or 2.0 ml) was removed for analysis.

The criterion used to determine the sample size was that the apparent concentration should not fall below 1.0 μg/ml or exceed 5.0 μg/ml; the optimum range was 2–4 μg/ml to be well within the linear portion of the calibration curve. The sampling time interval depended in part on a previously observed or expected degradation rate.

Analytical Method—The colorimetric method of Loo and Dion (15) was utilized. The use of any substance that might interfere with the analytical method was scrupulously avoided.

An experimental sample volume not greater than 2.0 ml or estimated to contain between 1 and 5 μg of I/ml was added to a 17 × 150-mm Pyrex test tube. If necessary, sufficient distilled water was added to yield a total

[1] Merck Chemical Co. (through the National Cancer Institute).

(3) J. B. Schwartz, J. R. Flamholz, and R. H. Press, *ibid.*, **62**, 1165 (1973).
(4) S. Özdurmuş, M.S. thesis, Boğaziçi University, Istanbul, Turkey, 1975.
(5) K. Lehmann, *Manuf. Chem. Aerosol News*, **May 1973**, 36.
(6) *Ibid.*, **June 1973**, 39.
(7) "The United States Pharmacopeia," 18th rev., Mack Publishing Co., Easton, Pa., 1970, pp. 932–934, 1026, 1027.

ACKNOWLEDGMENTS AND ADDRESSES

Received March 17, 1976, from the *Chemical Engineering Department, Boğaziçi University, Bebek, Istanbul, Turkey, and ‡Eczacibaşi A. Ş., Levent, Istanbul, Turkey.

Accepted for publication August 27, 1976.

* To whom inquiries should be directed.

Degradation of Carmustine in Aqueous Media

PAUL A. LASKAR * and JAMES W. AYRES

Abstract □ The degradation rate of carmustine was investigated in buffered aqueous media at several pH values. The buffering agents studied were those with potential use in parenteral formulations of this drug: acetate, citrate, and phosphate. The apparent first-order degradation rate constants were calculated using a linear regression procedure. A pH range over which minimum degradation occurred was ascertained. General acid and specific base catalysis was demonstrated for the degradation of carmustine. From the data at 5, 22, and 37°, the apparent activation energies for carmustine degradation in buffered aqueous media were computed and were strongly pH dependent.

Keyphrases □ Carmustine—degradation rate in aqueous media, effect of pH and temperature □ Degradation rate—carmustine in aqueous media, effect of pH and temperature □ Antineoplastic agents—carmustine, degradation rate in aqueous media, effect of pH and temperature □ Stability—carmustine in aqueous media, effect of pH and temperature

Drugs for the treatment of neoplastic disease have received a great deal of attention. Several thousand chemical agents are systematically screened each year for antineoplastic activity, but only a small percentage exhibit activity and are tested further for clinical utility. Carmustine [1,3-bis(2-chloroethyl)-1-nitrosourea; NSC 409962] (I) was effective in treating L-1210 leukemia, including cases where the central nervous system was involved (1–4).

Prior to the interest in I as a therapeutic agent, a study indicated that 1-methyl-1-nitrosourea (NSC 23909) (II) was unstable in aqueous solution (5), as was a nitrosamide-containing antibiotic, streptozocin, (6). The kinetics of I degradation were considered, and this compound also was unstable in aqueous media (4, 7).

Because I is often administered *via* intravenous solution (8, 9), further consideration of its stability in various aqueous media suitable for intravenous use is desirable. In addition, knowledge of the temperature dependence of the degradation of I is needed to obtain useful shelflife data and to determine desirable storage criteria. Furthermore, knowledge of acid or base catalysis also may be of value in formulating I.

The few published studies directed toward optimizing a parenteral formulation for I emphasized technological considerations such as lyophilization of drug solutions and dry filling with sterile solids (10–12). A formulation for clinical use was prepared by dry filling vials with sterile solid I and sterile, screened mannitol (11, 12). Alternatively, a solution of I in absolute ethanol was filtered through a 0.25-μm membrane and lyophilized (10, 11). These formulations should be used within 1 and 2 hr, respectively, following reconstitution with ethanol and dilution with saline (10, 12).

The purpose of this investigation was to perform accelerated stability studies on I in various aqueous media suitable for injection.

EXPERIMENTAL

Reagents—Carmustine, an investigational new drug, was obtained[1] as a lyophilized powder. All other chemicals were reagent grade.

Materials and Methods—All buffers and other solutions were prepared in volumetric flasks. Distilled water used for dissolving the basic component of the buffer systems was freshly boiled and cooled. Unless noted otherwise, solutions were stored at ambient temperature. Compound I, 0.025 g (stored at −19 ± 1°), was dissolved in sufficient cold (0°) ethanol to make 25 ml of stock solution. The stock solutions were stored at −19 ± 1° for not longer than 7 days.

Buffer solutions were prepared using published procedures (13, 14). All buffer solutions were checked for conformance to the desired pH using a pH meter calibrated at ambient temperature (20–22°) with a pH standard. When necessary, the pH was adjusted to within 0.05 pH unit of the nominal value with either the acidic or basic component of the buffer.

Degradation Experiments—All solvent systems were preequilibrated to the experiment temperature. For ambient (22 ± 1°) and physiological (37.0 ± 0.5°, forced-air oven) temperature experiments, the media were first allowed to equilibrate for at least 16 hr. For experiments at reduced temperature, the media were first chilled in a ice bath (1.0 ± 0.5°) for at least 15 min.

To a volume (~40–45 ml) of preequilibrated media was added 1.0 ml of I stock solution (1 μg/ml). Then the volume was brought rapidly to 50 ml with the appropriate medium, the mixture was shaken, and the time was recorded. A zero-time sample (0.2 ml) was taken for analysis, and the experimental solution was stored at the appropriate temperature. At designated time intervals, a sample volume (0.2, 0.5, 1.0, or 2.0 ml) was removed for analysis.

The criterion used to determine the sample size was that the apparent concentration should not fall below 1.0 μg/ml or exceed 5.0 μg/ml; the optimum range was 2–4 μg/ml to be well within the linear portion of the calibration curve. The sampling time interval depended in part on a previously observed or expected degradation rate.

Analytical Method—The colorimetric method of Loo and Dion (15) was utilized. The use of any substance that might interfere with the analytical method was scrupulously avoided.

An experimental sample volume not greater than 2.0 ml or estimated to contain between 1 and 5 μg of I/ml was added to a 17 × 150-mm Pyrex test tube. If necessary, sufficient distilled water was added to yield a total

[1] Merck Chemical Co. (through the National Cancer Institute).

Table I—Parameter Values for Linear Regressions of Logarithm of Apparent Degradation Rate Constants for I on pH

pH Condition	Temperature (°K)	Regression Coefficient (*SE*)	Intercept
Citrate buffer (pH 3.0, 4.0, and 5.0) and acetate buffer (pH 3.6, 4.0, and 5.0)	278	−0.106 (0.026)	0.001
Citrate buffer (pH 6.0); phosphate buffer (pH 6.0, 6.6, and 7.6); barbital buffer (pH 7.4 and 8.0)	295	1.27 (0.07)	8.86×10^{-6}
Phosphate buffer (pH 6.0, 6.6, and 7.6)	278	1.01 (0.04)	2.91×10^{-6}
	295	1.07 (0.05)	3.26×10^{-5}
	310	0.93 (0.13)	5.46×10^{-4}

volume of 2.0 ml and the contents were mixed. To this solution was added 1.0 ml of 0.5% (w/v) sulfanilamide in 2 *N* HCl, and the solution was mixed and incubated in a water bath with a shaker at 50 ± 0.01° for 45 min. The position in the water bath was randomized to minimize any position-dependent effects on the analytical results.

After 45 min, the solution in the tubes was rapidly chilled in an ice–water mixture. To the cooled solution was added 0.2 ml of 0.3% (w/v) *N*-(1-naphthyl)ethylenediamine dihydrochloride, and the mixture was agitated. The color was allowed to develop for 10 min, after which the percent transmittance was determined using a spectrophotometer[2] at 540 nm calibrated with a reagent blank. The order of percent transmittance determination of samples was randomized, and the amount of I remaining was determined with a calibration curve.

An initial experiment to determine the reliability of the standard curve used the following nominal concentrations prepared from the I stock solutions: 0, 0.01, 0.05, 0.1, 0.5, 1.0, 2.0, 5.0, 10.0, and 50.0 μg/ml. The conformance of the colorimeter as well as the reagents to the calibration curve was checked at periodic intervals throughout the study using an abbreviated set of standards.

RESULTS AND DISCUSSION

The colorimetric method of Loo and Dion (15) was utilized to quantify I, and the calibration curve generated from pooled data was linear from about 0.5 to 7 μg/ml. When subsequent batches of reagent solutions were used, neither batch- nor time-dependent variation was detectable.

The effect of solvents and other adjuvants on drug degradation under some constant conditions can often be described according to the apparent first power of the drug concentration (16). A nitroso-containing compound related to the nitrosoureas, as well as several nitrosoureas, demonstrated first-order rate dependency (4, 6, 7, 17, 18). Therefore, the apparent first-order degradation rate constants for I in several buffer systems at three temperatures were computed from a linear regression of the logarithm of I remaining on time.

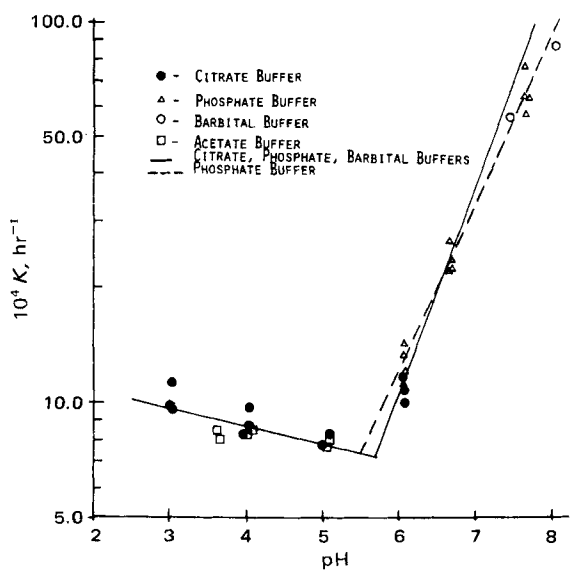

Figure 1—*Logarithm rate constant–pH profile at 278 °K.*

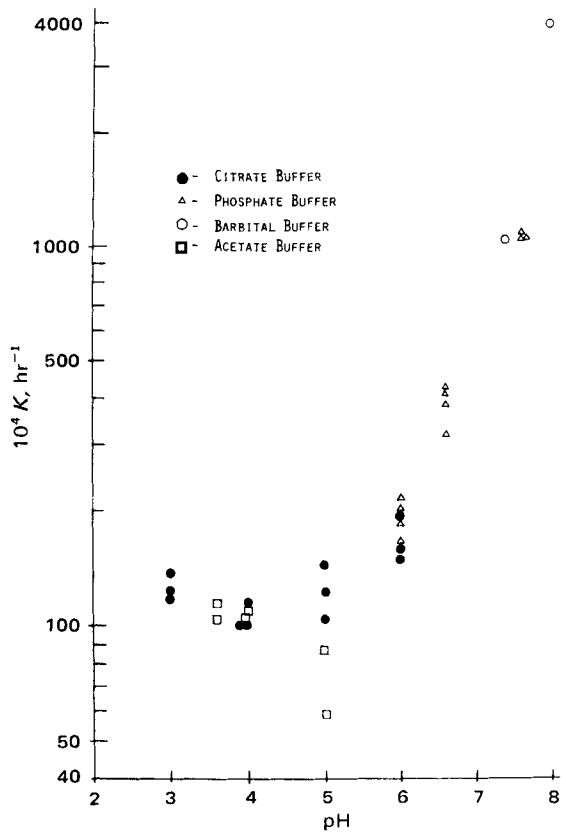

Figure 2—*Logarithm rate constant–pH profile at 295 °K.*

Examination of the linear regression lines for quadratic and cubic curvature revealed no significant departures from linearity for the data, indicating that the assumption of apparent first-order degradation is justified. When the rate constants for degradation in the various buffer solutions were plotted as the logarithm of the observed rate constants *versus* pH, the degradation rate minimum appeared between pH 5.2 and 5.5 (Fig. 1). The rate constants computed at a particular pH, regardless of the buffer system, remained similar, indicating the absence of catalytic effects by any one buffer species.

The results of regression of the logarithm of the degradation rate constants for I on pH in acetate and citrate buffers in the pH 3–5 range are summarized in Table I. The regression coefficient was nonzero and not equal to −1 at the 95% confidence level. Therefore, there is no reason to expect specific acid catalysis. Because the regression coefficient was significantly nonzero, the presence of only solvolysis was also ruled out and general acid catalysis was likely.

Determination of catalysis by base is also possible by examining Fig. 1 in the basic pH region.

The results of the regression of the logarithm of the apparent degradation rate constant for I on pH for citrate, phosphate, and barbital buffers in the pH 6–7.6 range appear in Table I and are illustrated in Figs. 1 and 2. The slope of the line was significantly nonzero but also significantly different than 1 at the 95% confidence level. This result indicates general base catalysis, which is disconcerting since the regression coefficient was nonzero and not significantly different than 1 at the 95% confidence level when only the phosphate buffers were used. The results are also shown in Table I.

The slope with combined citrate, phosphate, and barbital buffers increased with temperature, but the slope for the phosphate buffers showed no such tendency. If the degradation rate constant in a particular buffer was inordinately low at a low pH or high at a high pH, this result could be expected. The rate constants for I were lower in citrate buffer than in phosphate buffer at comparable pH values, and this difference increased with increasing temperature. While the difference at 5° was consistent but not great, the difference at 37° amounted to a factor of about 2. It is not likely that this result was anomalous, since it was consistent over all replications of both buffers.

[2] Bausch & Lomb Spectronic 20.

Table II—Effect of Total Phosphate Concentration on Apparent Degradation Rate Constant of I in Phosphate Buffer at Several pH Values

Ionic Strength	pH	Rate Constant, 10^4 hr^{-1} (*SE*) 5°	22°	37°
0.2	6.0	12.6 (0.30)	197.2 (3.11)	1281.5 (83.98)
	6.6	22.8 (0.45)	353.3 (24.20)	2818.4 (85.51)
	7.6	58.9 (2.82)	1069.0 (24.34)	5428.9 (549.29)
0.05	6.0	12.9 (0.22)	179.4 (24.89)	1395.2 (31.18)
	6.6	24.5 (0.45)	397.2 (11.48)	2922.4 (81.61)
	7.6	68.2 (1.17)	1053.3 (20.98)	7431.1 (384.5)

These data indicate that at pH 6 citrate seems to have a stabilizing effect on I. While the converse, that phosphate has a catalytic effect on nitrosourea degradation, was asserted (7, 18) and denied (4), the data in this experiment do not support the hypothesis of phosphate catalysis, primarily because the degradation of I in phosphate buffers was independent of phosphate concentration (Table II). Although the monohydrogen phosphate anion is said to be the catalytic species (7, 18), degradation rate determinations for I at differing total phosphate concentrations, and thus differing monohydrogen phosphate anion concentrations, provide a measure of such an effect. Since the rate constants at any particular pH and temperature with different ionic strength of phosphate buffers were the same within replication error, evidence for phosphate catalysis is lacking.

The observation that the slope of the logarithm of the apparent degradation rate constant *versus* pH for the phosphate buffers was not significantly different than 1 supports the view of no catalytic effect by phosphate. Finally, from examination of Figs. 1 and 2, it can be seen that the degradation rate constants for I in barbital buffer at pH 7.4 and for phosphate at pH 7.6 were similar, which suggests that no catalytic effect by phosphate or barbital was taking place. These observations tend to rule out the likelihood of specific phosphate catalysis for degradation of I.

The temperature dependence of the degradation rate constants for I in the various buffer systems provides data useful in performing accelerated stability analyses. The activation energies for the degradation of I in the various buffer systems were calculated by transforming the coefficient obtained for the regression of the logarithm of the apparent degradation rate constants on the reciprocal of absolute temperature (Table III). The activation energy appears to be proportional to the pH at which the activation energy was calculated.

To examine this possibility, the hypothesis that the activation energies are the same was tested using analysis of variance techniques (19) (Table IV); results indicated that this hypothesis should be rejected. To examine the possibility that there is a relationship between the activation energy and pH, a regression of the activation energy on pH was calculated (Table IV). While the regression of activation energy on pH was highly significant, the deviations from linear regression were also highly significant (Fig. 3). This relationship, however, seems linearized using a graph of the logarithm of the activation energy *versus* pH (Table IV and Fig. 4).

This effect of pH on the activation energy and linear relationship of the logarithm of the activation energy *versus* pH might be explicable if specific base catalysis is assumed. The rate constant used in determining the activation energy is the apparent rate constant or microscopic ex-

Table III—Activation Energies of I in Buffered Aqueous Media

Buffer	pH	Activation Energy, kcal/mole (*SE*)
Citrate	3.0	13.63 (1.56)
	4.0	15.40 (1.14)
	5.0	18.94 (1.43)
	6.0	20.17 (1.34)
Acetate	3.6	17.29 (1.98)
	4.0	19.88 (1.20)
	5.0	19.14 (0.74)
Phosphate (I^a = 0.2)	6.0	19.25 (2.02)
	6.6	25.55 (0.79)
	7.6	24.75 (0.81)
Phosphate (I = 0.05)	6.0	25.30 (0.37)
	6.6	25.95 (0.35)
	7.6	25.14 (0.39)
Barbital	7.4	25.92 (0.02)
	8.0	27.31 (0.12)

[a] I = ionic strength.

Table IV—Examination of Homogeneity of Slope of Activation Energy of I at Several pH Values and Regression [a] of Activation Energy on pH

Source of Variation	*df*	*SS*	*MS*
Homogeneity of Slope			
Among regression coefficients	9	6.8×10^5	7.6×10^4
Within regression (weighted mean of deviations)	14	2.4×10^2	1.7×10^1
Regression of Logarithm Activation Energy on pH			
Linear regression	1	0.525	0.525
Deviation from linear regression	8	0.069	0.008
Within pH groups	5	0.048	0.009

[a] The regression equation was ln $\Delta H^{\ddagger}$ (kcal/mole) = ln 10.51 + 0.12 (±0.016) pH.

perimental degradation rate constant, which includes contributions of all catalytic species. Since the macroscopic rate constant for the hydroxide anion has the greatest magnitude of the catalytic constants, the apparent degradation rate constant for which the activation energy is calculated is (20):

$$K_{app} = K_0 + K_{OH}[OH^-] \qquad \text{(Eq. 1)}$$

where K_{app}, K_0, and K_{OH} are the rate constants observed for the uncatalyzed reaction and for the hydroxide-ion contribution and $[OH^-]$ is the hydroxide-ion concentration.

The apparent activation energy computed from the slope of the graph is a function of the activation energy for K_0 as well as that for K_{OH}. Aside from demonstrating that there is a marked temperature dependence of the hydroxide-anion rate constant, the results indicate that the temperature dependence of the uncatalyzed solvolytic rate constant for I is not particularly strong.

The results indicate a minimum degradation rate between about pH 5.2 and 5.5. Examination of the degradation rate constants obtained in

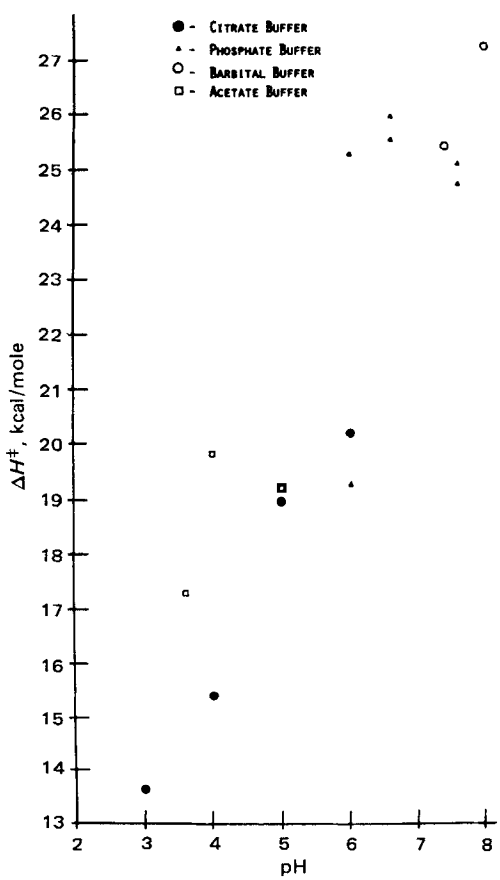

Figure 3—*Activation energy–pH profile for buffered aqueous systems.*

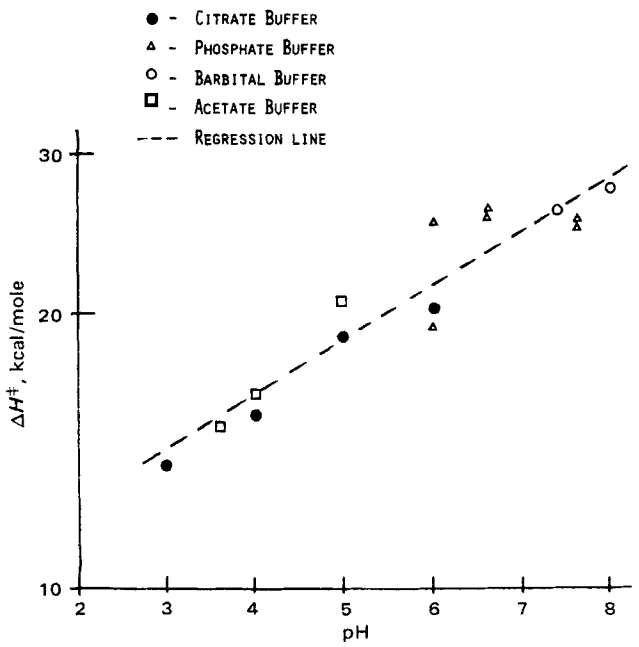

Figure 4—*Logarithm activation energy–pH profile for buffered aqueous systems.*

the accelerated stability analysis studies (Table I) indicates that I would have a short useful life at room temperature in the buffer systems studied. Ten percent degradation would occur in about 14 hr in the citrate buffer at pH 5.0. However, storage in the refrigerator (~5°) would prolong the time for 10% degradation to about 5.5 days.

These preliminary results indicate that it may be feasible to reconstitute I in some intravenous solutions at pH 5.2–5.5, to store the mixture at 5° for a few days, if necessary, and then to administer I parenterally. Further work is underway to determine the effect of certain electrolytes, commonly found in intravenous solutions, on the stability of I.

REFERENCES

(1) F. M. Schabel, Jr., T. P. Johnston, G. S. McCaleb, J. A. Montgomery, W. R. Laster, and H. E. Skipper, *Cancer Res.*, **23**, 725 (1963).

(2) D. P. Rall, D. M. McCarthy, and M. Ben, *Proc. Am. Assoc. Cancer Res.*, **4**, 55 (1963).

(3) M. D. Walker and B. S. Hurwitz, *Cancer Chemother. Rep.*, **54**, 263 (1970).

(4) T. L. Loo, R. L. Dion, R. L. Dixon, and D. P. Rall, *J. Pharm. Sci.*, **55**, 492 (1966).

(5) J. L. Boivin and P. A. Boivin, *Can. J. Chem.*, **29**, 478 (1954).

(6) E. R. Garrett, *J. Am. Pharm. Assoc., Sci. Ed.*, **49**, 767 (1960).

(7) J. A. Montgomery, R. James, G. S. McCaleb, and T. P. Johnston, *J. Med. Chem.*, **10**, 668 (1967).

(8) V. T. DeVita, P. D. Carbone, A. Owens, Jr., G. L. Gold, M. J. Krant, and J. Edmonson, *Cancer Res.*, **25**, 1876 (1965).

(9) S. K. Carter, F. M. Schabel, Jr., L. E. Broder, and T. P. Johnston, *Adv. Cancer Res.*, **16**, 273 (1972).

(10) J. P. Davignon, K. W. Yang, H. B. Wood, Jr., and J. C. Cradock, *Cancer Chemother. Rep., Part 3*, **4**, 7 (1973).

(11) D. W. Flamberg, D. L. Francis, S. L. Morgan, and G. F. Wickes, *Bull. Parenter. Drug Assoc.*, **24**, 209 (1970).

(12) J. P. Davigon, *ibid.*, **23**, 83 (1969).

(13) "Biochemists Handbook," C. Long, Ed., Van Nostrand, Princeton, N.J. 1961, p. 30ff.

(14) "Documenta Geigy Scientific Tables," 7th ed., K. Diem, Ed., Geigy Pharmaceuticals, Ardsley, N.Y., 1970, p. 280ff.

(15) T. L. Loo and R. L. Dion, *J. Pharm. Sci.*, **54**, 809 (1965).

(16) E. R. Garrett, *ibid.*, **51**, 811 (1962).

(17) E. R. Garrett, S. Goto, and J. F. Stubbins, *ibid.*, **54**, 119 (1965).

(18) E. R. Garrett and S. Goto, *Chem. Pharm. Bull.*, **182**, 973 (1973).

(19) R. R. Sokal and F. J. Rohlf, "Biometry," Freeman, San Francisco, Calif., 1969, p. 468ff.

(20) J. T. Carstensen, "Theory of Pharmaceutical Systems," vol. I, Academic, New York, N.Y., 1972, p. 181.

ACKNOWLEDGMENTS AND ADDRESSES

Received December 9, 1975, from the *Department of Pharmaceutical Science, School of Pharmacy, Oregon State University, Corvallis, OR 97331.*

Accepted for publication August 23, 1976.

Abstracted in part from a thesis submitted by P. A. Laskar to the Graduate School, Oregon State University, in partial fulfillment of the Doctor of Philosophy degree requirements.

[x] To whom inquiries should be directed. Present address: Department of Pharmacy, College of Pharmacy, University of Illinois at the Medical Center, Chicago, IL 60612.

Degradation of Carmustine in Mixed Solvent and Nonaqueous Media

PAUL A. LASKAR [x] and JAMES W. AYRES

Abstract □ The degradation rate of carmustine in several solvent mixtures and in mannitol solution was investigated at 5, 22, and 37°. The solvents chosen were those utilized as parenteral diluents. The apparent first-order degradation rate constants were computed using a linear regression procedure. The most nonaqueous solvent mixtures demonstrated minimum apparent degradation rates. The apparent degradation rate constant decreased with a decrease in the macroscopic dielectric constant. From the data at several temperatures, the apparent activation energies for carmustine degradation in the several solvent mixtures were calculated. There was no evidence for a relationship between the apparent activation energy and the dielectric constant.

Keyphrases □ Carmustine—degradation rate in mixed solvents and nonaqueous media, effect of temperature □ Degradation rate—carmustine in mixed solvents and nonaqueous media, effect of temperature □ Antineoplastic agents—carmustine, degradation rate in mixed solvents and nonaqueous media, effect of temperature □ Stability—carmustine in mixed solvents and nonaqueous media, effect of temperature

Numerous chemotherapeutic agents, including the nitrosoureas, show promise in the treatment of neoplastic diseases. The formulation of these agents into clinically useful dosage forms has, however, been slow. Carmustine [1,3-bis(2-chloroethyl)-1-nitrosourea; NSC 409962] (I), like many other nitrosoureas, has relatively poor aqueous sol-

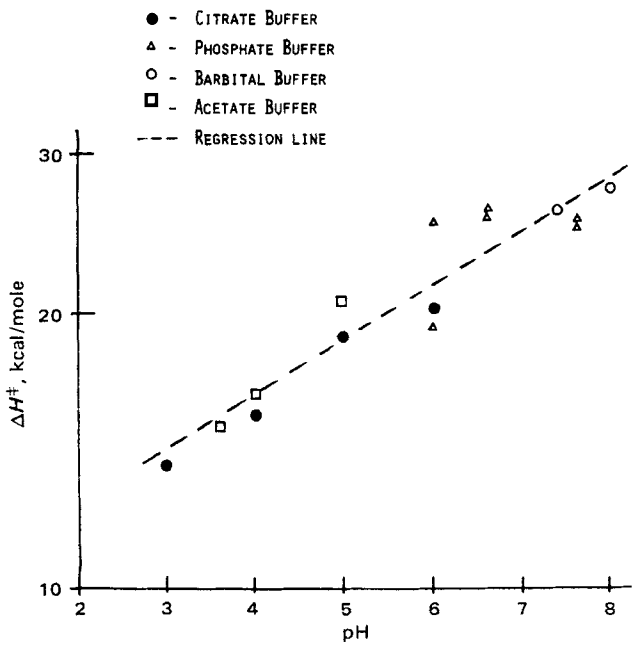

Figure 4—*Logarithm activation energy–pH profile for buffered aqueous systems.*

the accelerated stability analysis studies (Table I) indicates that I would have a short useful life at room temperature in the buffer systems studied. Ten percent degradation would occur in about 14 hr in the citrate buffer at pH 5.0. However, storage in the refrigerator (~5°) would prolong the time for 10% degradation to about 5.5 days.

These preliminary results indicate that it may be feasible to reconstitute I in some intravenous solutions at pH 5.2–5.5, to store the mixture at 5° for a few days, if necessary, and then to administer I parenterally. Further work is underway to determine the effect of certain electrolytes, commonly found in intravenous solutions, on the stability of I.

REFERENCES

(1) F. M. Schabel, Jr., T. P. Johnston, G. S. McCaleb, J. A. Montgomery, W. R. Laster, and H. E. Skipper, *Cancer Res.*, **23**, 725 (1963).

(2) D. P. Rall, D. M. McCarthy, and M. Ben, *Proc. Am. Assoc. Cancer Res.*, **4**, 55 (1963).

(3) M. D. Walker and B. S. Hurwitz, *Cancer Chemother. Rep.*, **54**, 263 (1970).

(4) T. L. Loo, R. L. Dion, R. L. Dixon, and D. P. Rall, *J. Pharm. Sci.*, **55**, 492 (1966).

(5) J. L. Boivin and P. A. Boivin, *Can. J. Chem.*, **29**, 478 (1954).

(6) E. R. Garrett, *J. Am. Pharm. Assoc., Sci. Ed.*, **49**, 767 (1960).

(7) J. A. Montgomery, R. James, G. S. McCaleb, and T. P. Johnston, *J. Med. Chem.*, **10**, 668 (1967).

(8) V. T. DeVita, P. D. Carbone, A. Owens, Jr., G. L. Gold, M. J. Krant, and J. Edmonson, *Cancer Res.*, **25**, 1876 (1965).

(9) S. K. Carter, F. M. Schabel, Jr., L. E. Broder, and T. P. Johnston, *Adv. Cancer Res.*, **16**, 273 (1972).

(10) J. P. Davignon, K. W. Yang, H. B. Wood, Jr., and J. C. Cradock, *Cancer Chemother. Rep., Part 3*, **4**, 7 (1973).

(11) D. W. Flamberg, D. L. Francis, S. L. Morgan, and G. F. Wickes, *Bull. Parenter. Drug Assoc.*, **24**, 209 (1970).

(12) J. P. Davigon, *ibid.*, **23**, 83 (1969).

(13) "Biochemists Handbook," C. Long, Ed., Van Nostrand, Princeton, N.J. 1961, p. 30ff.

(14) "Documenta Geigy Scientific Tables," 7th ed., K. Diem, Ed., Geigy Pharmaceuticals, Ardsley, N.Y., 1970, p. 280ff.

(15) T. L. Loo and R. L. Dion, *J. Pharm. Sci.*, **54**, 809 (1965).

(16) E. R. Garrett, *ibid.*, **51**, 811 (1962).

(17) E. R. Garrett, S. Goto, and J. F. Stubbins, *ibid.*, **54**, 119 (1965).

(18) E. R. Garrett and S. Goto, *Chem. Pharm. Bull.*, **182**, 973 (1973).

(19) R. R. Sokal and F. J. Rohlf, "Biometry," Freeman, San Francisco, Calif., 1969, p. 468ff.

(20) J. T. Carstensen, "Theory of Pharmaceutical Systems," vol. I, Academic, New York, N.Y., 1972, p. 181.

ACKNOWLEDGMENTS AND ADDRESSES

Received December 9, 1975, from the *Department of Pharmaceutical Science, School of Pharmacy, Oregon State University, Corvallis, OR 97331.*

Accepted for publication August 23, 1976.

Abstracted in part from a thesis submitted by P. A. Laskar to the Graduate School, Oregon State University, in partial fulfillment of the Doctor of Philosophy degree requirements.

[x] To whom inquiries should be directed. Present address: Department of Pharmacy, College of Pharmacy, University of Illinois at the Medical Center, Chicago, IL 60612.

Degradation of Carmustine in Mixed Solvent and Nonaqueous Media

PAUL A. LASKAR [x] and JAMES W. AYRES

Abstract □ The degradation rate of carmustine in several solvent mixtures and in mannitol solution was investigated at 5, 22, and 37°. The solvents chosen were those utilized as parenteral diluents. The apparent first-order degradation rate constants were computed using a linear regression procedure. The most nonaqueous solvent mixtures demonstrated minimum apparent degradation rates. The apparent degradation rate constant decreased with a decrease in the macroscopic dielectric constant. From the data at several temperatures, the apparent activation energies for carmustine degradation in the several solvent mixtures were calculated. There was no evidence for a relationship between the apparent activation energy and the dielectric constant.

Keyphrases □ Carmustine—degradation rate in mixed solvents and nonaqueous media, effect of temperature □ Degradation rate—carmustine in mixed solvents and nonaqueous media, effect of temperature □ Antineoplastic agents—carmustine, degradation rate in mixed solvents and nonaqueous media, effect of temperature □ Stability—carmustine in mixed solvents and nonaqueous media, effect of temperature

Numerous chemotherapeutic agents, including the nitrosoureas, show promise in the treatment of neoplastic diseases. The formulation of these agents into clinically useful dosage forms has, however, been slow. Carmustine [1,3-bis(2-chloroethyl)-1-nitrosourea; NSC 409962] (I), like many other nitrosoureas, has relatively poor aqueous sol-

Table I—Degradation Rate Constants of Carmustine in Mixed Solvents

Solvent in Water	Concentration, %	Rate Constant, 10^4 hr^{-1} (*SE*) 5°	22°	37°
Ethanol	2	13.9 (0.43)	220.4 (12.80)	707.3 (29.30)
	25	7.9 (0.13)	192.6 (4.54)	406.0 (13.36)
	50	2.4 (0.12)	25.6 (0.56)	149.1 (5.57)
	95	0.6 (0.18)	2.2 (0.34)	10.9 (0.33)
Propylene glycol	25	9.709 (0.20)	194.9 (6.01)	151.9 (11.50)
	50	4.572 (0.16)	89.7 (3.80)	275.1 (5.72)
	100	1.314 (0.22)	8.5 (0.46)	49.2 (1.80)
Dimethyl sulfoxide	2	13.7 (0.45)	389.1 (16.49)	1864.9 (46.30)
	25	7.5 (0.16)	240.4 (15.69)	1551.2 (110.70)
	50	5.1 (0.16)	74.5 (1.90)	366.8 (10,92)
	100		12.2 (0.28)	74.1 (1.83)
Mannitol	5		147.3 (1.92)	
	10		130.3 (1.22)	
	20		124.4 (2.49)	

ubility and is quite unstable in aqueous media (1–4). Therefore, in efforts to obtain a desirable dosage form, preformulation studies with I in aqueous, mixed solvent, and nonaqueous media are appropriate. Studies with I in aqueous media were reported previously (5). The mixed solvent and nonaqueous media chosen are those generally utilized in the parenteral administration of various drug agents including nitrosoureas (3).

Little work has been reported on optimizing a parenteral dosage form of I. To date, studies have emphasized technological considerations in the delivery of I as well as other antineoplastic nitrosoureas (3, 6–8).

The present investigation was undertaken at several temperatures to obtain useful shelflife and storage data *via* accelerated stability studies.

EXPERIMENTAL

Materials and Methods—All chemicals and solvents were reagent or USP grade except where noted. Solutions of I were prepared and analyzed as described previously (5).

Degradation Experiments—For ambient (22 ± 1°) and physiological (37.0 ± 0.5°, forced-air oven) temperature experiments, the media were first allowed to equilibrate for at least 16 hr. For experiments at reduced temperature, the media were first chilled in an ice bath (1.0 ± 0.5°) for at least 15 min.

To a volume (~40–45 ml) of temperature-equilibrated media was added 1.0 ml of I stock solution (1 μg/ml). Then the volume was brought rapidly to 50 ml with the appropriate medium, the mixture was shaken, and the time was recorded. A zero-time sample (0.2 ml) was taken for analysis, and the experimental solution was stored at the appropriate temperature. At designated time intervals, a sample volume (0.2, 0.5, 1.0, or 2.0 ml) was removed for analysis.

The criterion used to determine the sample size was that the apparent concentration should not fall below 1.0 μg/ml or exceed 5.0 μg/ml; the optimum range was 2–4 μg/ml. The sampling time interval depended in part on a previously observed or expected degradation rate.

Table II—Dielectric Constants for Solvents Utilized

Solvent	Concentration, %	Dielectric Constant 5°	22°	37°
Ethanol	25	71.10	65.20	60.50
	50	54.50	49.80	41.00
	90	29.75	26.75	23.40
Propylene glycol	25	75.09	67.56	61.54
	50	61.91	58.33	50.74
	100	34.80	31.31	28.52
Dimethyl sulfoxide	2	81.53	80.90	79.13
	25	81.13	80.50	78.73
	50	79.03	78.40	76.63
	100	—	48.75	47.63
Water		86.04	79.60	74.20
Mannitol	5	—	78.80	—
	10	—	78.50	—
	20	—	71.80	—

RESULTS AND DISCUSSION

The applicability of this analytical method to I was reported previously (5). Several nitrosoureas and compounds containing nitroso groups exhibit an apparent first-order degradation dependency (1, 4, 9, 10). Therefore, degradation exhibiting apparent first-order kinetics was hypothesized, and the collected data were tested for adherence to this model.

The suitability of the apparent first-order model was initially estimated visually from the graph of the logarithm of the concentration of I remaining (micrograms per milliliter) *versus* time. Since the data did not negate the assumption of apparent first-order dependence, a least-squares regression of the natural logarithm of I concentration on time was calculated and the linear parameters were estimated using a standard computer program (11). The standard error of the linear parameters, the slope, and the intercept were also calculated.

Curvilinearity was estimated qualitatively by examining residuals as well as more quantitatively by utilizing a multiple regression of the natural logarithm of I concentration on a third-degree polynomial in time (12, 13). The multiple regression was performed in a forward stepwise manner, and an analysis of variance (ANOVA) was calculated at each step to enable visualization of the individual variance contribution of the linear, quadratic, and cubic components (13). The results did not negate the assumption of an apparent first-order degradation of I in the several solvent mixtures.

The dependency of the degradation rate constant on the reciprocal dielectric constant and temperature was determined using a least-squares regression of the natural logarithm of the rate constant on the appropriate independent variable, and the regression coefficient(s) were computed. Homogeneity of the activation energy in buffered aqueous systems and solvent systems was evaluated using covariance analysis (14).

From the data calculated for I in the solvent mixtures, the apparent stability increased with an increasing nonaqueous solvent concentration (Table I). The apparent degradation rate constant in optimally buffered aqueous media was about 8×10^{-4} hr^{-1} at 5° (5). The apparent rate constants in solvent mixtures were of this magnitude or less in ethanol, propylene glycol, or dimethyl sulfoxide concentrations of 25% or greater at 5°. The solvent mixture demonstrating minimum degradation (95% ethanol at 5°) had a rate constant more than an order of magnitude less than the buffered aqueous system, thereby providing a t_{90} of about 78 days [*cf.*, about 5.5 days in the buffered aqueous media (5)].

A disadvantage of 95% ethanol as a solvent for direct parenteral administration of I is its irritation potential; this problem would necessitate dilution to a concentration at which irritation is sufficiently reduced. Propylene glycol does not have this irritation potential, although the minimum apparent degradation rate is about twice that for ethanol.

Table III—Regression of Logarithm of Apparent Rate Constant for Degradation of Carmustine on Reciprocal Dielectric Constant of Solvent

Solvent	Regression Coefficient (*SE*) 5°	22°	37°
Ethanol	−180.7 (84.8)	−193.2 (31.0)	−141.0 (2.8)
Propylene glycol	−130.6 (19.9)	−176.4 (12.4)	−101.6 (39.3)
Dimethyl sulfoxide	−355.8 (2740.3)	−350.6 (112.1)	−326.3 (115.2)
Mannitol	—	−180.2 (263.4)	—

Table IV—Activation Energies of Carmustine Degradation in Solvent Mixtures

Solvent	Concentration, %	Activation Energy, kcal/mole (*SE*)
Ethanol	2	21.43 (1.61)
	25	21.53 (3.22)
	50	22.08 (0.23)
	95	15.76 (0.94)
Propylene glycol	25	15.32 (4.73)
	50	22.21 (2.23)
	100	19.33 (0.50)
Dimethyl sulfoxide	2	26.56 (1.95)
	25	28.77 (1.59)
	50	22.97 (0.94)
	100	21.91 (——)

However, due to its high viscosity, propylene glycol presents potential difficulty for use in a syringe.

Dimethyl sulfoxide is not currently approved for use as a parenteral solvent, although it has been used in some animal studies. The results in this solvent and its mixtures were generally similar to those found for ethanol and propylene glycol. Degradation of I in 100% dimethyl sulfoxide was not followed at 5° since the mixture is solid at this temperature, presenting sampling difficulties. More important, interpretation of results might be compromised due to the "freezing out" of I, thus considerably altering the microscopic solvent environment for the degradation of I. While this occurrence has not been demonstrated for the nitrosoureas, it has been shown for other substances (15).

The results obtained for the solvent mixtures suggest that a proportionality exists between the apparent degradation rate constant and the macroscopic dielectric constant. The dielectric constants for the various solvent mixtures were obtained from the literature and adjusted for temperature (16–18) (Table II). The apparent degradation rate constant of I in a given solvent was regressed on the reciprocal dielectric constant of the solvent, and the results were tabulated (Table III). These computed data indicate a significant decrease in the rate constant with a decrease in the dielectric constant. There is likely to be disparity between the macroscopic tabulated dielectric constants and the microscopic dielectric constant existing in the immediate vicinity of the reacting species (19, 20), particularly in mixtures of solvents with disparate dielectric constants as a result of microscopic dielectric constants reflecting selective solvation (21). Therefore, these regression coefficients computed for I should be considered as qualitative rather than quantitative; they reflect the dielectric constant effect on the degradation rate constant for I.

Mannitol is used as a soluble diluent for I in dry filling vials for reconstitution. Several concentrations of mannitol were utilized to examine the effect of an altered dielectric constant on the apparent degradation rate constant of I. The effect of an increasing mannitol concentration, and thus a decreasing dielectric constant, was comparable to that for the solvent mixtures.

The temperature dependence of the apparent degradation rate constant for I in the solvent mixtures was examined using the Arrhenius equation. The activation energies were computed from the parameters estimated from the least-squares regression equation (Table IV). The regression coefficients were tested for common slope using ANOVA. The results (Table V) do not cause rejection of the hypothesis of a common slope for the temperature dependence of the degradation rate constant in the several solvent mixtures. Therefore, the activation energies may be regarded as constant and parallel. Since the degradation rate constants vary significantly for the solvent mixtures, the frequency factor term in the Arrhenius equation must vary.

Such variation in the frequency factor, and thus the degradation rates, results from the extent of solvation of the reactants and the transition state and affects the entropy of activation (20, 21). Following this reasoning, these data suggest that the differences in the degradation rate constants for I in the solvent mixtures are attributable to these factors relating to solvation.

Table V—Examination of Homogeneity of Slope of Activation Energy of Carmustine Degradation at Several Dielectric Constants

Source of Variation	*df*	*SS*	*MS*
Among regression coefficients	9	3.80	0.42
Within regression (weighted mean of deviations)	12	48.5	3.46
Common slope = 23.29 kcal/mole			

Solutions of I in concentrated ethanol or propylene glycol possessed t_{90} values at room temperature of about 2.5 and 1 week, respectively. Under refrigerated temperatures, the t_{90} values increased to about 2.5 and 1 month, respectively. The useful lifespans in these solvent mixtures permit reconstitution and refrigerated storage for reasonable time periods. Prior to parenteral administration, the reconstituted ethanol or propylene glycol solution of I would be diluted in a suitable parenteral vehicle.

Mannitol in solutions of I also stabilized I to some extent when compared to an approximately pure aqueous system. This finding may be attributable to the effect on the dielectric constant and to solvation effects. The extended timespans in solvent mixtures were significantly longer than those in buffered aqueous media, possibly attributable, at least in part, to the altered solvation of reactants and intermediates.

REFERENCES

(1) E. R. Garrett, S. Goto, and J. F. Stubbins, *J. Pharm. Sci.*, **54**, 119 (1965).

(2) T. L. Loo, R. L. Dion, R. L. Dixon, and D. P. Rall, *ibid.*, **55**, 492 (1966).

(3) J. P. Davignon, K. W. Yang, H. B. Wood, Jr., and J. C. Cradock, *Cancer Chemother. Rep., Part 3*, **4**, 7 (1973).

(4) J. A. Montgomery, R. James, G. S. McCaleb, and T. P. Johnson, *J. Med. Chem.*, **10**, 668 (1967).

(5) P. A. Laskar and J. W. Ayres, *J. Pharm. Sci.*, **66**, 1073 (1977).

(6) D. W. Flamberg, D. L. Francis, S. L. Morgan, and G. F. Wickes, *Bull. Parenter. Drug Assoc.*, **24**, 209 (1970).

(7) J. P. Davignon, *ibid.*, **24**, 88 (1969).

(8) C. L. Fortner, W. R. Grove, D. Bowie, and M. D. Walker, *Am. J. Hosp. Pharm.*, **32**, 582 (1975).

(9) E. R. Garrett, *J. Amer. Pharm. Assoc., Sci. Ed.*, **49**, 767 (1960).

(10) E. R. Garrett and S. Goto, *Chem. Pharm. Bull.*, **21**, 1811 (1973).

(11) D. Guthrie, C. A. Avery, and K. R. Avery, "Statistical Interactive Programming System: Preliminary Users' Guide," Department of Statistics, Oregon State University, Corvallis, Oreg., Sept. 1972.

(12) N. R. Draper and H. Smith, "Applied Regression Analysis," Wiley, New York, N.Y., 1966, p. 62.

(13) R. R. Sokal and F. J. Rohlf, "Biometry," Freeman, San Francisco, Calif., 1969, pp. 468ff.

(14) *Ibid.*, p. 450.

(15) W. P. Jencks, "Catalysis in Chemistry and Enzymology," McGraw-Hill, New York, N.Y., 1969, pp. 35, 36.

(16) G. Akerlöf, *J. Am. Chem. Soc.*, **54**, 4125 (1932).

(17) "Handbook of Chemistry and Physics," 54th ed., R. C. Weast, Ed., CRC Press, Cleveland, Ohio, 1973, p. E-45.

(18) Y. Doucet, F. Calmes-Perreault, and M. T. Durand, *C.R.*, **260**, 1878 (1965).

(19) W. P. Jencks, "Catalysis in Chemistry and Enzymology," McGraw-Hill, New York, N.Y., 1969, p. 585.

(20) K. J. Laidler, "Chemical Kinetics," 2nd ed., McGraw-Hill, New York, N.Y., 1965, p. 228.

(21) E. S. Amis, "Solvent Effects on Reaction Rates and Mechanisms," Academic, New York, N.Y., 1966, pp. 20, 21.

ACKNOWLEDGMENTS AND ADDRESSES

Received December 9, 1975, from the *Department of Pharmaceutical Science, School of Pharmacy, Oregon State University, Corvallis, OR 97331.*

Accepted for publication August 23, 1976.

Abstracted in part from a thesis submitted by P. A. Laskar to the Graduate School, Oregon State University, in partial fulfillment of the Doctor of Philosophy degree requirements.

x To whom inquiries should be directed. Present address: Department of Pharmacy, College of Pharmacy, University of Illinois at the Medical Center, Chicago, IL 60612.

Application of Proton and ^{13}C-NMR Spectroscopy to Estimation of Diastereoisomer Ratio in Phenethicillin

W. L. WILSON *x, H. W. AVDOVICH *,
D. W. HUGHES *, and G. W. BUCHANAN ‡

Abstract □ A procedure for the determination of the diastereoisomer ratio in phenethicillin potassium and its formulations is described. The method utilizes analyses of PMR and ^{13}C-NMR data. Assignments of ^{13}C-chemical shifts in D- and L-phenethicillin potassium also are included.

Keyphrases □ Phenethicillin—proton and ^{13}C-NMR spectral analysis of diastereoisomer ratio, bulk drug and commercial formulations □ NMR spectroscopy, proton and ^{13}C—analysis, diastereoisomer ratio of phenethicillin, bulk drug and commercial formulations □ Diastereoisomers—phenethicillin, proton and ^{13}C-NMR spectral analysis of ratio, bulk drug and commercial formulations □ Antibacterials—phenethicillin, proton and ^{13}C-NMR spectral analysis of diastereoisomer ratio, bulk drug and commercial formulations

The semisynthetic penicillin, phenethicillin potassium (I), is prepared by *N*-acylation of 6-aminopenicillanic acid with racemic α-phenoxypropionyl chloride (1). This condensation introduces another center of asymmetry into the molecule, and the resulting two diastereoisomers have different physical properties. The isomer composition of the product varies depending upon the solvent extraction and crystallization procedures. The two isomers show differences in their antibacterial spectra, thereby placing certain limitations on the interpretation of results of microbiological assay but also indicating that products from different manufacturers may vary in antibiotic effectiveness.

The L-phenethicillin potassium content of phenethicillin potassium NF is determined in the "Code of Federal Regulations" (2) by a microbiological assay. Limits of between 55 and 75% of this more active L-isomer are specified. The BP (3) allows optical rotation limits of $[\alpha]_D$ +215 to +240°, corresponding to isomer compositions of 100–34% of the L-isomer. This optical rotation measurement, however, sums the effect at all five asymmetric centers and is not as precise, although it is less tedious, than the microbiological procedure. In addition, none of the pharmacopeias specifies tests for monitoring this isomer ratio in pharmaceutical dosage forms, a control that would be useful from a regulatory standpoint.

In an earlier publication (4) on the NMR spectra of penicillins and cephalosporins, differences in the splitting patterns of the β-lactam protons in the D- and L-isomers of phenethicillin were noted. Since the area or intensity of an absorption band in an NMR spectrum is directly proportional to the number of nuclei that absorb energy at that particular frequency, an NMR assay should be possible provided that at least one resonance band from each component of a mixture is free from extensive overlap by other absorptions. Therefore, the applicability of proton (PMR) and ^{13}C- (CMR) magnetic resonance spectroscopy as a means of monitoring this isomer ratio was examined.

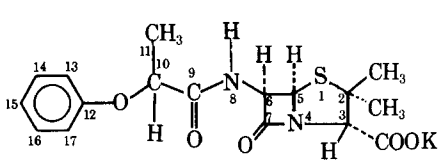

I

EXPERIMENTAL

Materials—Potassium 6-[L-(+)-α-phenoxypropionamido]penicillanate and potassium 6-[D-(+)-α-phenoxypropionamido]penicillinate were FDA reference standards. A sample of DL-phenethicillin potassium[1] contained 100% of the calculated amount of $C_{17}H_{19}KN_2O_5S$ with reference to the dried substance when determined by iodometric assay and had a microbiological potency of 880 μg/mg. The L-isomer content of this material as determined by the Code of Federal Regulations method (2) was 55.6%; by the BP (3) optical rotation method, it was 55.2%. A value of 55% was assigned to this material, which was used as a working standard. Phenethicillin potassium tablets were obtained locally.

Synthetic mixtures of varying L-isomer content were prepared by adding known amounts of the pure D- and L-isomers to a weighed amount of the DL-phenethicillin working standard. This approach was necessary because of the limited quantities of pure isomers available.

Sample Preparation—*Powders*—An amount of powder equivalent to about 50 mg of phenethicillin potassium was dissolved in 0.50 ml of deuterium oxide (99.8% D minimum isotopic purity) in a small glass vial. The solution was agitated for about 1 min and then transferred to a 5-mm diameter NMR tube.

Tablets—After grinding in a mortar and pestle, a weighed portion of the powder equivalent to about 250 mg of phenethicillin potassium was placed in a 15-ml centrifuge tube, and 2.5 ml of deuterium oxide was added. After mixing, the sample was centrifuged. Then 0.50 ml of the supernate was transferred to a 5-mm diameter NMR tube.

PMR—Spectra were recorded on a 60-MHz NMR spectrometer[2] at ambient probe temperature (40 ± 2°) using a sweep width of 500 Hz and a 250-sec sweep time. For quantitative purposes, the portion of the spectrum between 5 and 6 ppm (β-lactam protons) was rerecorded at a sweep width of 250 Hz and carefully integrated five times. A radio frequency power of 0.25 milligauss (normal dial setting) gave maximum integral amplitude and was used for integrations. Tetramethylsilane in deuterochloroform was the external reference. Chemical shifts were measured in parts per million downfield from tetramethylsilane.

The percent of L-phenethicillin in a sample was calculated by dividing the peak areas attributed to the *AB* quartet of L-phenethicillin by the total integral value (combination of D- and L-phenethicillins).

CMR—Spectra were recorded on a 25.2-MHz spectrometer[3].

The "standard condition" spectra were recorded using a 5000-Hz sweep width, 8192 data points, a pulse angle of 60° (20-μsec pulse duration), and a pulse interval of 1 sec. Good quality spectra were obtained from samples of 50 mg/0.50 ml with about 20,000 transients (approximately 5-hr accumulation time). To remove the effects of ^{13}C–H coupling, complete noise decoupling conditions were used. For integration, the area near δ 32 ppm was expanded to a width of 200 Hz and was electronically integrated five times.

Peak height ratios were determined from the 2-β-methyl resonances on the standard condition spectra. Probe temperature was 32°, and the deuterium of the solvent was employed for a field-frequency lock. Chemical shifts quoted are in parts per million downfield from tetramethylsilane; a methanol capillary served as an internal reference point.

[1] Courtesy of Bristol Laboratories of Canada.
[2] Varian A-60A.
[3] Varian XL-100-12.

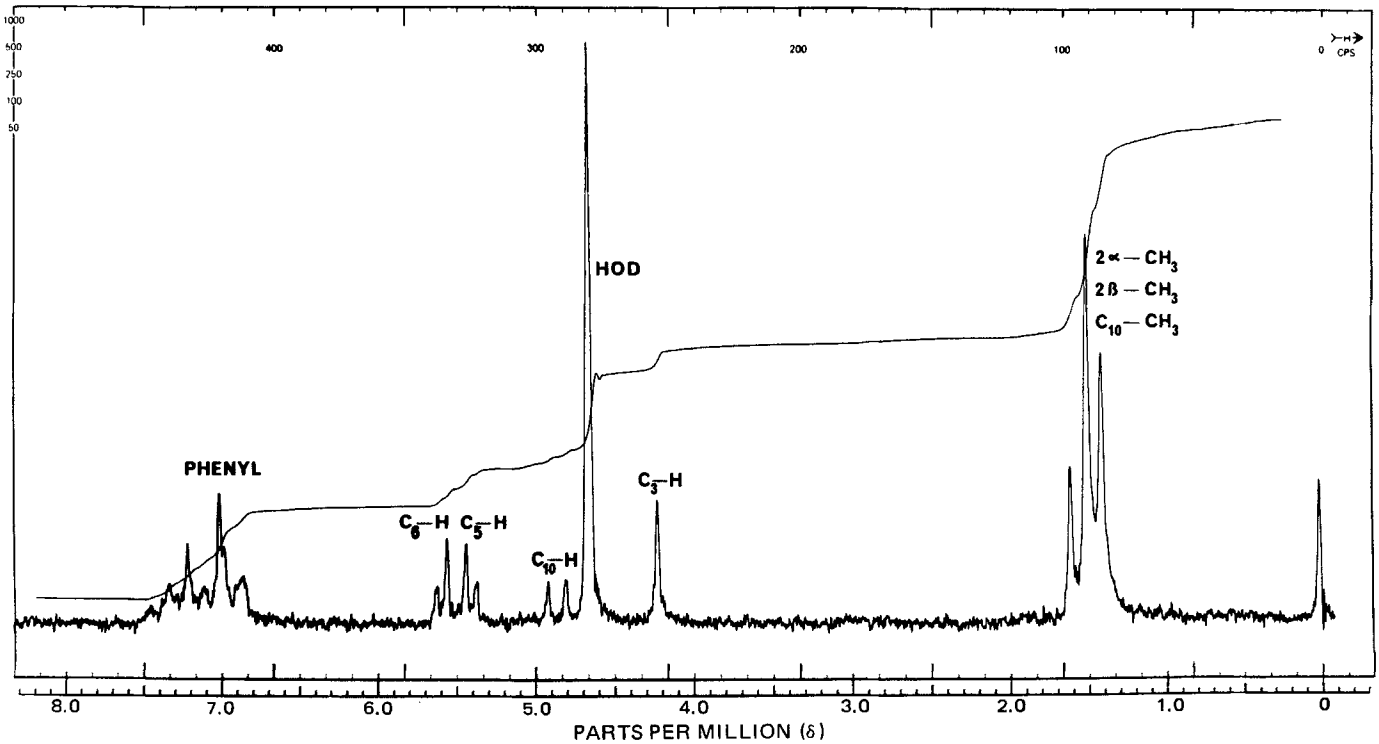

Figure 1—*PMR spectrum of* L-*phenethicillin potassium in deuterium oxide.*

The T_1 relaxation experiments, employing the kinetically inert paramagnetic metal complex tris(acetylacetonato)chromium, were conducted in the presence of 2×10^{-2} molar equivalents of the relaxation reagent. In the gated decoupling experiments, the ^{1}H-decoupler was "gated on" only during data acquisition periods, which were typically 0.5 sec. For the off-resonance decoupling experiments, the proton decoupling frequency was offset by 500 Hz from its optimum value. The selective decoupling experiments were conducted using low decoupler power in the absence of noise modulation.

RESULTS AND DISCUSSION

PMR—The PMR spectra of penicillins would be expected to have a characteristic single proton doublet arising from the C-5 hydrogen and a single proton doublet of doublets at the lower field for hydrogen at C-6. In spectra obtained from deuterium oxide solutions, these β-lactam proton signals should appear as an *AB* quartet (5).

Figure 1 illustrates the PMR spectrum of L-phenethicillin with the expected *AB* splitting pattern for the β-lactam proton signals ($J_{5,6}$ = 4 Hz; ν_5 = 5.4 and ν_6 = 5.6 ppm). The assignments of the other resonances were reported earlier (4). In the PMR spectrum of D-phenethicillin (Fig. 2), these β-lactam protons appeared as a singlet at 5.5 ppm. The β-lactam protons of ampicillin sodium also have given a two-proton singlet in deuterium oxide, possibly due to accidental equivalence of chemical shifts (6).

These spectra were recorded using a concentration of approximately 100 mg/ml. Under more dilute conditions (<60 mg/ml), broadening of the singlet in D-phenethicillin occurred, indicating that it too was splitting into an *AB* pattern.

The PMR spectrum of a typical sample of DL-phenethicillin is shown in Fig. 3. The β-lactam region was expanded and integrated (Fig. 3, inset). PMR spectra of mixtures containing varying amounts of D- and L-phenethicillins as well as commercial bulk drug powder and tablet formulations were analyzed by this method, and the percentage of the L-isomer was calculated from an average of five integrations. The results (Table I) indicated that the accuracy of this PMR quantitative method decreased as the proportion of D- and L-isomers deviated from a near equal mixture. As the relative amount of the L-isomer increased, the method led to an underestimation of its content. However, excellent correlation with calculated values was obtained in the region normally expected with commercial samples, *i.e.*, 55–75% L-isomer. Sample 9 (Table I) illustrates that results can also be obtained directly from tablets, which is particularly useful from a quality control and regulatory standpoint.

The high precision of this PMR assay method is indicated by the standard deviation and coefficient of variation of 0.6 and 1.1%, respectively, found for Sample 9 (Table I) when two separate determinations were each integrated five times. Because of broadening of the β-lactam proton signal in D-phenethicillin with dilute solutions (as mentioned previously) and the need for concentrated solutions to obtain large and,

Table I—Percent L-Phenethicillin Potassium Content by PMR and CMR Assay Methods

Sample	L-Phenethicillin Potassium, %			
	Actual[a]	By PMR[b]	By CMR	
			Integration[b]	Peak Height
1. Synthetic mixture	87	—	85.8 (±0.9)[c]	83
2. Synthetic mixture	78	73.3 (±0.7)	—	—
3. Synthetic mixture	64	63.5 (±0.6)	—	—
4. Working standard	55[d,e]	55.2 (±0.7)	57.0 (±0.6)	54
5. Synthetic mixture	53	53.8 (±0.1)	—	—
6. Synthetic mixture	44	48.7 (±0.3)	—	—
7. Synthetic mixture	28	—	25.6 (±0.2)	27
8. Tablet	64[d]	63.7 (±0.6)	—	—
9. Tablet	55[d]	57.6 (±0.6, 1.1%)[f]	54.9 (±0.2)	54

[a] Calculated for synthetic mixtures by adding known amounts of pure D- and L-isomers to working standard. [b] Average of five integrations. [c] Standard deviation from five integrations of one weighing. [d] Value from microbiological assay. [e] Value from optical rotation assay. [f] Standard deviation and coefficient of variation from five integrations of each of two weighings.

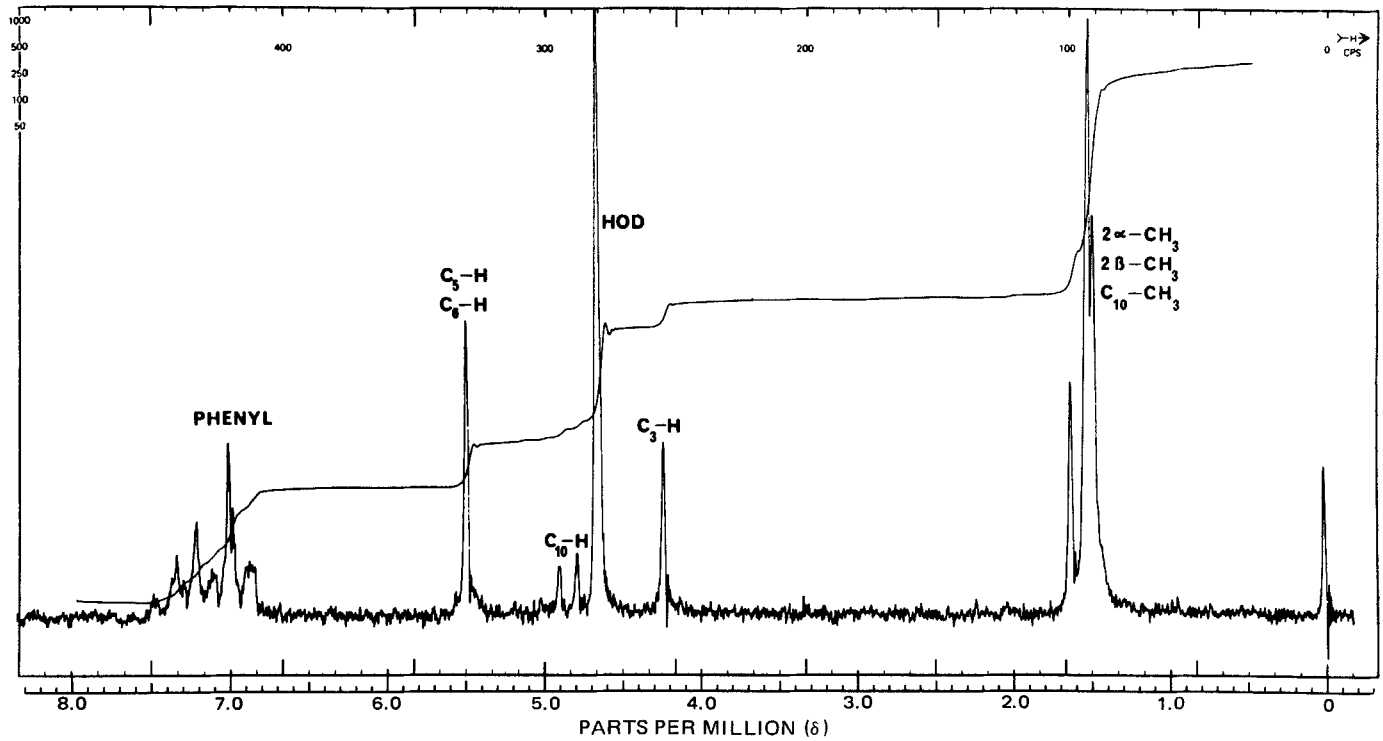

Figure 2—*PMR spectrum of* D*-phenethicillin potassium in deuterium oxide.*

therefore, more precise integrals, DL-phenethicillin potassium concentrations of 80–120 mg/ml were optimum for reproducible and precise quantitative results. Higher concentrations led to ill-defined separation of the *AB* quartet because of the concentration dependence of the chemical shift of protons at C-5 and C-6 (7).

CMR—The variation in carbon shieldings in neutral organic compounds is approximately 20-fold greater than that of protons, *i.e.*, approximately 200 ppm. These ^{13}C-shifts are also sensitive to steric, conformational, and electronic changes in a molecule. Because of the greater peak resolution of CMR, its application to this phenethicillin diastereoisomer study also was investigated. The CMR spectrum of DL-phenethicillin potassium is illustrated in Fig. 4. Since peaks were not assigned previously, they are listed in Table II.

Spectra of pure D- and pure L-phenethicillin potassium salts were recorded, which greatly facilitated the assignments for the diastereoisomeric mixture. To date, the only CMR data available for related systems are those for the methyl- and phenoxymethylpenicillins (8). Only assignment procedures for the L-isomer will be discussed, since completely

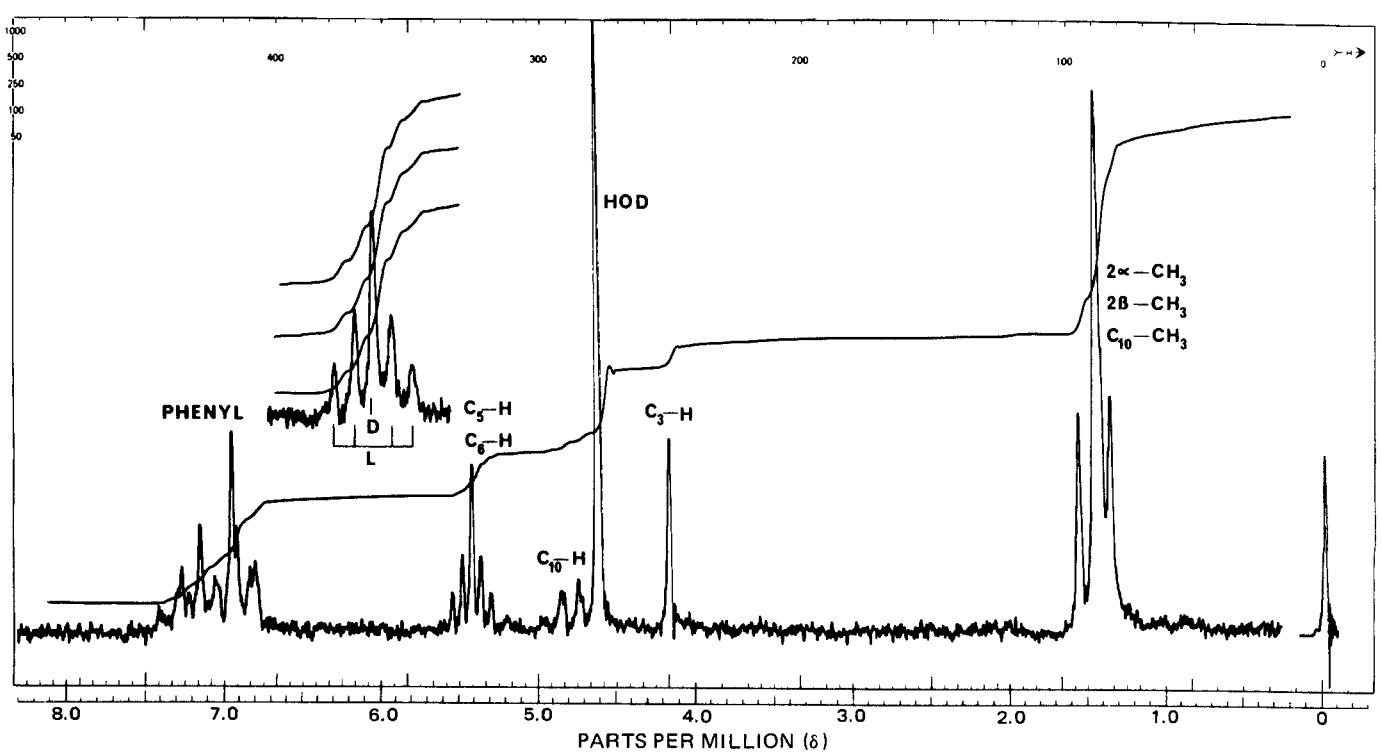

Figure 3—*PMR spectrum of commercial* DL*-phenethicillin potassium in deuterium oxide. Inset shows the β-lactam proton resonances recorded with a 250-Hz sweep width. Peaks labeled D and L refer to β-lactam protons of* D*- and* L*-phenethicillins, respectively.*

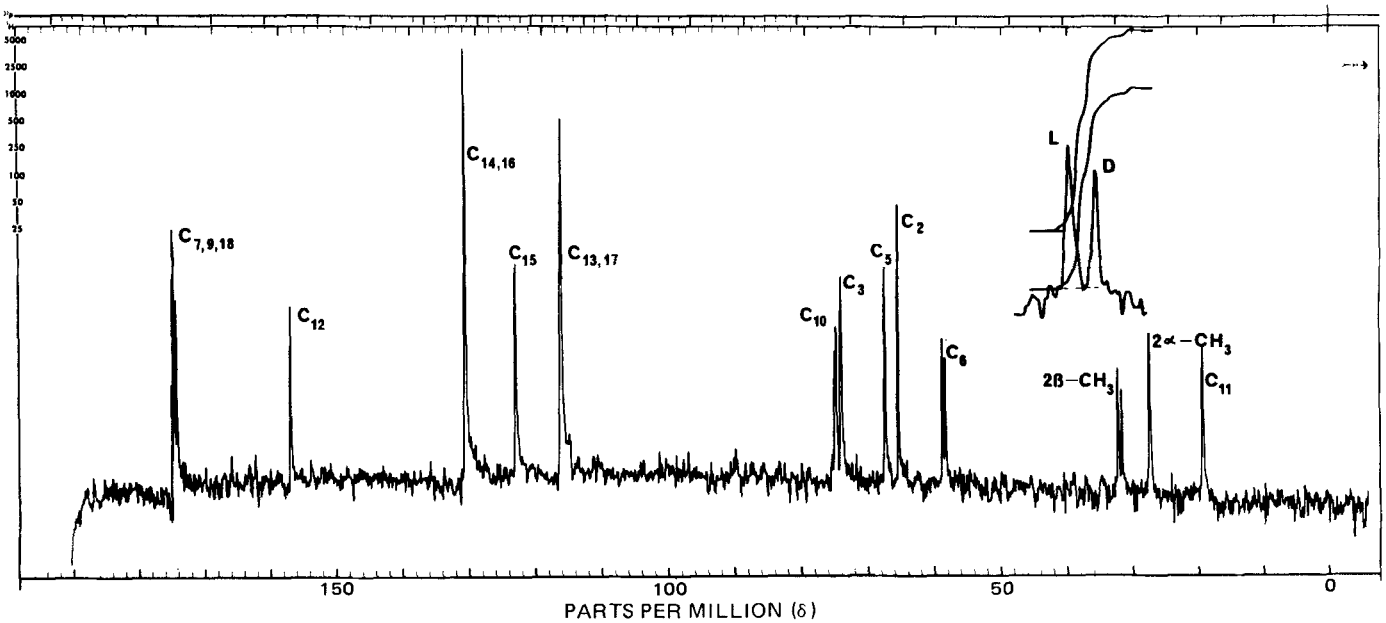

Figure 4—*CMR spectrum of commercial* DL*-phenethicillin potassium in deuterium oxide. Inset shows the 2-β-methyl carbon of* D*- and* L*-phenethicillins recorded with a 200-Hz sweep width.*

analogous techniques were used for the D-spectrum.

Initially, nonprotonated carbons were identified by their retention of singlet structure in the off-resonance decoupling experiment (9), whereas CH and CH_3 carbons yielded quartets and doublets, respectively. The three high field (lowest δ) resonances were due to the methyl groups, with that designated as C-11 being most shielded at δ 19.6 ppm. The 2-α and 2-β-methyl carbons were less shielded, which was consistent with their *gem*-dimethyl character. The 2-α group, being *cis* to the CO_2^- K^+ function, appeared 4.8 ppm upfield from its 2-β-counterpart. This shielding phenomenon at the 2-α-position presumably resulted from the γ steric interaction (10) between this function and the carboxylate moiety. The shift difference between signals from the epimeric methyls was very similar to that found in phenoxymethylpenicillin (8), although a strict comparison was not possible since the present data were recorded in deuterium oxide solutions as opposed to dimethyl sulfoxide-d_6 in the earlier work (8).

The C-2 resonance at δ 65.8 was similar to the C-2 of phenoxymethylpenicillin (δ 64.0). Distinction between the CH resonances at δ 74.3 and 75.1 was accomplished using selective ^1H-decoupling, since the corresponding proton shifts were known. Accordingly, C-3 was associated with the resonance at δ 74.3, and C-10 was associated with the δ 75.1 absorption. For the lactam ring carbons C-5 and C-6, phenoxymethylpenicillin again was a useful model compound, since the C-5 and C-6 resonances were at δ 67.4 and 58.4 ppm, respectively (8).

Assignment of the aromatic ring carbons C-12 to C-17 was straightforward, since it is well known that conjugative electron release by the ethereal oxygen shields the *ortho*- and *para*-carbons relative to the *meta*-position in anisoles and diphenyl ethers (11). Finally, the three carbonyl carbons were the most deshielded; however, unambiguous assignments were not possible.

For quantitative analysis of the diastereoisomeric mixtures, the 2-β-methyl resonances proved to be most useful since the chemical shift difference between them was the largest (0.6 ppm) and was essentially independent of the ratio of D- and L-phenethicillin potassium salts present in solution. In ^{13}C-Fourier transform NMR spectroscopy (12), great care must be taken in quantitative interpretation of data due to possible differences in spin lattice relaxation time (T_1's) and nuclear Overhauser enhancements between carbons of interest. In this study, the ratios of D- to L-forms as determined from two types of experiments were compared to verify that valid quantitative measurements were made.

Initially, the relaxation reagent tris(acetylacetonato)chromium (13) was used; no change was noted in the relative intensity of the 2-β-methyl resonances as compared to the standard condition spectrum, indicating that similar Overhauser enhancements and T_1's existed for the diastereomeric 2-β-methyl resonances. Subsequently, spectra were recorded using a gated decoupling technique (14), and again no alteration in the relative intensities of these resonances was noted. This result verified that essentially identical Overhauser enhancements operate for the diastereomeric 2-β-methyl resonances.

These experiments support the claim that the quantitative assessments are valid, and the close agreement between the CMR findings and the results from other techniques substantiates this claim. The CMR method is as accurate and as precise as the PMR assay but over a wider range of D to L ratios (Table I). Peak height measurement can be used instead without sacrificing accuracy. If more concentrated samples are used in the analysis, data accumulation time by the CMR method can be further reduced, giving reliable spectra within 2 hr.

Table II—^{13}C-Shift Assignments for D- and L-Phenethicillin Potassium in Parts per Million Downfield from Tetramethylsilane

L-Isomer	Assignment	D-Isomer
175.8	$C_{7,9,18}$	175.7
175.4	$C_{7,9,18}$	175.4 (2)
175.9	$C_{7,9,18}$	—
157.7	C_{12}	157.8
131.3	$C_{14,16}$	131.3
123.7	C_{15}	123.7
116.7	$C_{13,17}$	116.8
75.1	C_{10}	75.3
74.3	C_3	74.5
67.8	C_5	67.7
65.8	C_2	65.7
59.2	C_6	58.7
32.4	2-β-CH_3	31.8
27.6	2-α-CH_3	27.7
19.6	C_{11}	19.7

REFERENCES

(1) Y. G. Perron, L. B. Crast, W. J. Gottstein, W. F. Minor, and L. C. Cheney, "Antibiotics Annual 1959–1960," Antibiotica, Inc., New York, N.Y., 1960, p. 107.

(2) "Code of Federal Regulations," Title 21 440.82, U.S. Government Printing Office, Washington, D.C., 1975.

(3) "British Pharmacopoeia 1973," Her Majesty's Stationery Office, London, England, 1973, p. 353.

(4) W. L. Wilson, H. W. Avdovich, and D. W. Hughes, *J. Assoc. Offic. Anal. Chem.*, **57**, 1300 (1974).

(5) G. F. H. Green, J. E. Page, and S. Staniforth, *J. Chem. Soc.*, **1965**, 1595.

(6) J. M. Padfield and I. W. Kellaway, *J. Pharm. Sci.*, **63**, 143 (1974).

(7) A. L. Thakkar and W. L. Wilham, *Chem. Commun.*, **1971**, 320.

(8) R. A. Archer, R. D. G. Cooper, P. V. Demarco, and L. F. Johnson, *ibid.*, **1970**, 1291.
(9) J. B. Stothers, "Carbon-13 N.M.R. Spectroscopy," Academic, New York, N.Y., 1972, p. 38.
(10) W. R. Woolfenden and D. M. Grant, *J. Am. Chem. Soc.*, **88**, 1496 (1966).
(11) G. W. Buchanan, G. Montaudo, and P. Finocchiaro, *Can. J. Chem.*, **52**, 767 (1974).
(12) G. C. Levy and U. Edlund, *J. Am. Chem. Soc.*, **97**, 4482 (1975).
(13) O. A. Gansow, A. R. Burke, and W. D. Vernon, *ibid.*, **94**, 2550 (1972).
(14) G. C. Levy, "Topics in Carbon-13 NMR Spectroscopy," vol. 1, Wiley, New York, N.Y., 1974, p. 105.

ACKNOWLEDGMENTS AND ADDRESSES

Received July 26, 1976, from the *Drug Research Laboratories, Health Protection Branch, Department of National Health and Welfare, Ottawa, Canada, and the [1]Department of Chemistry, Carleton University, Ottawa, Canada.

Accepted for publication September 21, 1976.

[x] To whom inquiries should be directed.

Parameter for Assessing Parenteral Cleanliness Based on Particle-Size Distributions

JAMES BLANCHARD [x], JOHN A. SCHWARTZ, and DALE M. BYRNE *

Abstract □ A new parameter for assessing the particulate matter content of large-volume parenteral solutions was developed and tested. Some problems and shortcomings associated with previously proposed standards are discussed, together with the potential advantages of employing the proposed parameter. Cleanliness factors were compared with another parameter and were less susceptible to changes resulting from the method of measurement utilized and the premeasurement conditions encountered by the solution. The use of these cleanliness factors in conjunction with an automatic particle counter is proposed as a worthwhile supplement to the USP–NF standard for monitoring the quality of large-volume parenteral solutions.

Keyphrases □ Particle-size distributions—characterized in large-volume parenteral solutions, cleanliness factor developed □ Parenterals, large volume—particle-size distributions characterized, cleanliness factor developed □ Dosage forms—large-volume parenterals, particle-size distributions characterized, cleanliness factor developed

Particulate matter is defined as "extraneous, mobile, undissolved substances other than gas bubbles, unintentionally present in parenteral solutions" (1) and has been long recognized as a problem. Recently, official standards specified the allowable levels of particulate contamination (1, 2).

To aid in the evaluation of the cleanliness[1] of a parenteral solution, an auxiliary parameter that would describe accurately the contamination level is needed. Several desirable characteristics of this parameter were described previously (3, 4); it should provide a true measurement of particulate cleanliness that is not affected by the premeasurement handling conditions, and it should indicate the correct degree of particulate cleanliness using various instrumental techniques. The method also should be rapid, nondestructive, nonsubjective, simple, inexpensive, easy to standardize, and, preferably, not require the use of a clean room.

The present study was undertaken to develop such a parameter for the objective assessment of the relative particulate cleanliness of parenteral solutions.

[1] Throughout this article, the term "cleanliness" is used to denote the level of particulate matter.

BACKGROUND

Single-Point Standards—One early standard was proposed in 1966 (5). The initial proposal was revised and formed the basis of the first provisional Australian standard (6), which stated that a parenteral solution should not contain more than 250 particles/ml exceeding 3.5 μm in diameter. In the same year, another suggested single-point standard stated that a parenteral solution should not contain more than 50 particles/ml exceeding 5 μm in diameter (7).

Single-point standards are validly subject to criticism on the basis that the particles counted exceeding a given diameter are not necessarily indicative of the number of particles exceeding another diameter. Single-point standards were based on the observation that log–log plots of $N_{>D}$ (the particle concentration exceeding the diameter, D) *versus* D (the particle diameter) were essentially linear and parallel to one another among the individual solutions examined (5). However the slopes of the log–log plots vary among individual solutions[2] (6, 8), thereby invalidating the use of single-point standards.

Multiple-Point Standards—Recent attempts to establish standards focused on multiple-point determinations. As Kendall (9) noted, a standard should ideally be based upon the determination of the particle-size distribution over a broad size range. This consideration formed the basis for an Australian standard proposed in 1966 (5), which limited the allowable levels of particles exceeding four particle diameters. This and other recently proposed multiple-point standards are shown in Table I.

Multiple-point standards (as well as single-point standards) can be criticized on the grounds that the particle-size distribution may vary with the degree of agitation to which the solution is subjected (8, 10–12). Another potential criticism is that the measurement of particle concentrations may not be obtainable using a single technique (*i.e.*, instrumental, microscopic, *etc.*). If the particle diameters specified in the standard require measurement by more than one technique, the counts provided by each technique would have to correlate extremely well with one another. Besides introducing unnecessary uncertainty, this requirement would necessitate proficiency in more than one technique.

The USP–NF standard (Table I) suggests the use of a membrane filtration and microscopic examination technique. In a practical sense, it is only suitable for counting particles larger than 10 μm in diameter (3, 6). The Australian and British Pharmacopoeia standards do not prescribe a specific measuring technique. However, an electrical resistance counter or a light-scattering or light-blocking device is required, since these standards specify the counting of particles smaller than 10 μm in diameter. A recent version of the Australian standard (Table I), soon to become effective[3], specifies the use of an instrumental particle counter operating

[2] J. Blanchard, J. A. Schwartz, and D. M. Byrne, *J. Pharm. Sci.*, in press.
[3] C. E. Kendall, National Biological Standards Laboratory, Canberra, Australia, personal communication.

(8) R. A. Archer, R. D. G. Cooper, P. V. Demarco, and L. F. Johnson, *ibid.*, **1970**, 1291.
(9) J. B. Stothers, "Carbon-13 N.M.R. Spectroscopy," Academic, New York, N.Y., 1972, p. 38.
(10) W. R. Woolfenden and D. M. Grant, *J. Am. Chem. Soc.*, **88**, 1496 (1966).
(11) G. W. Buchanan, G. Montaudo, and P. Finocchiaro, *Can. J. Chem.*, **52**, 767 (1974).
(12) G. C. Levy and U. Edlund, *J. Am. Chem. Soc.*, **97**, 4482 (1975).
(13) O. A. Gansow, A. R. Burke, and W. D. Vernon, *ibid.*, **94**, 2550 (1972).
(14) G. C. Levy, "Topics in Carbon-13 NMR Spectroscopy," vol. 1, Wiley, New York, N.Y., 1974, p. 105.

ACKNOWLEDGMENTS AND ADDRESSES

Received July 26, 1976, from the *Drug Research Laboratories, Health Protection Branch, Department of National Health and Welfare, Ottawa, Canada, and the [1]Department of Chemistry, Carleton University, Ottawa, Canada.

Accepted for publication September 21, 1976.

[x] To whom inquiries should be directed.

Parameter for Assessing Parenteral Cleanliness Based on Particle-Size Distributions

JAMES BLANCHARD [x], JOHN A. SCHWARTZ, and DALE M. BYRNE *

Abstract □ A new parameter for assessing the particulate matter content of large-volume parenteral solutions was developed and tested. Some problems and shortcomings associated with previously proposed standards are discussed, together with the potential advantages of employing the proposed parameter. Cleanliness factors were compared with another parameter and were less susceptible to changes resulting from the method of measurement utilized and the premeasurement conditions encountered by the solution. The use of these cleanliness factors in conjunction with an automatic particle counter is proposed as a worthwhile supplement to the USP–NF standard for monitoring the quality of large-volume parenteral solutions.

Keyphrases □ Particle-size distributions—characterized in large-volume parenteral solutions, cleanliness factor developed □ Parenterals, large volume—particle-size distributions characterized, cleanliness factor developed □ Dosage forms—large-volume parenterals, particle-size distributions characterized, cleanliness factor developed

Particulate matter is defined as "extraneous, mobile, undissolved substances other than gas bubbles, unintentionally present in parenteral solutions" (1) and has been long recognized as a problem. Recently, official standards specified the allowable levels of particulate contamination (1, 2).

To aid in the evaluation of the cleanliness[1] of a parenteral solution, an auxiliary parameter that would describe accurately the contamination level is needed. Several desirable characteristics of this parameter were described previously (3, 4); it should provide a true measurement of particulate cleanliness that is not affected by the premeasurement handling conditions, and it should indicate the correct degree of particulate cleanliness using various instrumental techniques. The method also should be rapid, nondestructive, nonsubjective, simple, inexpensive, easy to standardize, and, preferably, not require the use of a clean room.

The present study was undertaken to develop such a parameter for the objective assessment of the relative particulate cleanliness of parenteral solutions.

[1] Throughout this article, the term "cleanliness" is used to denote the level of particulate matter.

BACKGROUND

Single-Point Standards—One early standard was proposed in 1966 (5). The initial proposal was revised and formed the basis of the first provisional Australian standard (6), which stated that a parenteral solution should not contain more than 250 particles/ml exceeding 3.5 μm in diameter. In the same year, another suggested single-point standard stated that a parenteral solution should not contain more than 50 particles/ml exceeding 5 μm in diameter (7).

Single-point standards are validly subject to criticism on the basis that the particles counted exceeding a given diameter are not necessarily indicative of the number of particles exceeding another diameter. Single-point standards were based on the observation that log–log plots of $N_{>D}$ (the particle concentration exceeding the diameter, D) *versus* D (the particle diameter) were essentially linear and parallel to one another among the individual solutions examined (5). However the slopes of the log–log plots vary among individual solutions[2] (6, 8), thereby invalidating the use of single-point standards.

Multiple-Point Standards—Recent attempts to establish standards focused on multiple-point determinations. As Kendall (9) noted, a standard should ideally be based upon the determination of the particle-size distribution over a broad size range. This consideration formed the basis for an Australian standard proposed in 1966 (5), which limited the allowable levels of particles exceeding four particle diameters. This and other recently proposed multiple-point standards are shown in Table I.

Multiple-point standards (as well as single-point standards) can be criticized on the grounds that the particle-size distribution may vary with the degree of agitation to which the solution is subjected (8, 10–12). Another potential criticism is that the measurement of particle concentrations may not be obtainable using a single technique (*i.e.*, instrumental, microscopic, *etc.*). If the particle diameters specified in the standard require measurement by more than one technique, the counts provided by each technique would have to correlate extremely well with one another. Besides introducing unnecessary uncertainty, this requirement would necessitate proficiency in more than one technique.

The USP–NF standard (Table I) suggests the use of a membrane filtration and microscopic examination technique. In a practical sense, it is only suitable for counting particles larger than 10 μm in diameter (3, 6). The Australian and British Pharmacopoeia standards do not prescribe a specific measuring technique. However, an electrical resistance counter or a light-scattering or light-blocking device is required, since these standards specify the counting of particles smaller than 10 μm in diameter. A recent version of the Australian standard (Table I), soon to become effective[3], specifies the use of an instrumental particle counter operating

[2] J. Blanchard, J. A. Schwartz, and D. M. Byrne, *J. Pharm. Sci.*, in press.
[3] C. E. Kendall, National Biological Standards Laboratory, Canberra, Australia, personal communication.

Table I—Some Standards for Particulate Contamination Levels

Standard Test	Maximum Allowable Number of Particles per Milliliter of Various Sizes					
	2.0 μm	3.5 μm	5 μm	10 μm	20 μm	25 μm
USP–NF	—	—	—	50	—	5
Australian I[a]	1000	250	100	25	—	—
Australian II[b]	—	—	100	—	2	—
BP_1[c]	2000	—	200	—	—	—
BP_5[c]	100	—	100	—	—	—

[a] See Ref. 3. [b] See footnote 2. [c] The BP_1 test refers to readings taken on one container, whereas the BP_5 test refers to the average reading of five containers.

on the light-blockage principle and the counting of particles exceeding two diameters.

Complex Standards—Ernerot (13) suggested the silting index determination as an alternative to particle counting for evaluating particulate contamination in large-volume parenterals. However, this method is not simple, either in theory or practice. While it offers certain advantages over other methods, it appears to be far from ideal because of the numerous assumptions involved. Further definitive studies might resolve some of these uncertainties.

To alleviate some shortcomings of the single- and multiple-point standards, the particle-size distribution of the contaminants should be examined over as broad a size range as practical to ascertain the correct relationship describing the particle-size distribution. In previous studies[2] (3, 12), many samples (both individually and when averaged) closely adhered to a linear equation of the form:

$$\log N_{>D} = K \log D + \log N_{>1} \qquad \text{(Eq. 1)}$$

where $N_{>D}$ is the number of particles per milliliter with a diameter larger than D, $N_{>1}$ is the number of particles per milliliter with a diameter larger than 1 μm, D is the particle diameter in micrometers, and K is equal to the slope of the plot of $\log N_{>D}$ *versus* $\log D$. This equation previously was utilized to describe the particle-size distribution of contaminants in parenterals (6). Recently (12), the effects of agitation on the particle-size distribution of particulate contamination of parenterals were determined. An unequivocal characterization of the effects of agitation on the particle-size distribution of a parenteral solution must be obtained by simultaneously examining both parameters that describe the distribution (*i.e.*, the slope *and* the intercept of the $\log N_{>D}$ *versus* $\log D$ plot). A single parameter based upon the slope and the intercept of the log–log plot would specify accurately the degree of cleanliness of a parenteral solution.

EXPERIMENTAL

The particle-size distribution data of large-volume parenteral solutions[4] (1000 ml) were obtained by two methods: a nondestructive instrumental technique, using an automatic particle counter[5], and a membrane filtration and microscopic method similar to the USP–NF technique, which is a destructive method. The exact procedures followed and the method of data analysis are described elsewhere[2] (3, 12).

The six types of parenteral solutions examined were: (*a*) 5% dextrose in 0.45% sodium chloride, (*b*) normal saline, (*c*) 5% dextrose in multiple-electrolyte solution[6], (*d*) 5% dextrose in normal saline, (*e*) 5% dextrose in water, and (*f*) 5% dextrose in lactated Ringer's solution. These solutions were chosen on the basis of their extensive clinical use.

RESULTS AND DISCUSSION

Groves (6) attempted to relate the slopes and intercepts of the $\log N_{>D}$ *versus* $\log D$ plots, which characterize the particle-size distribution of parenteral solutions, to their relative cleanliness. The form of Groves' postulated relationship is:

$$\frac{\log N_{>1} - 2.5}{-K} = \text{specific value } (S) \qquad \text{(Eq. 2)}$$

The S value was based upon the empirical observation that most parenteral solutions examined that passed a provisional Australian

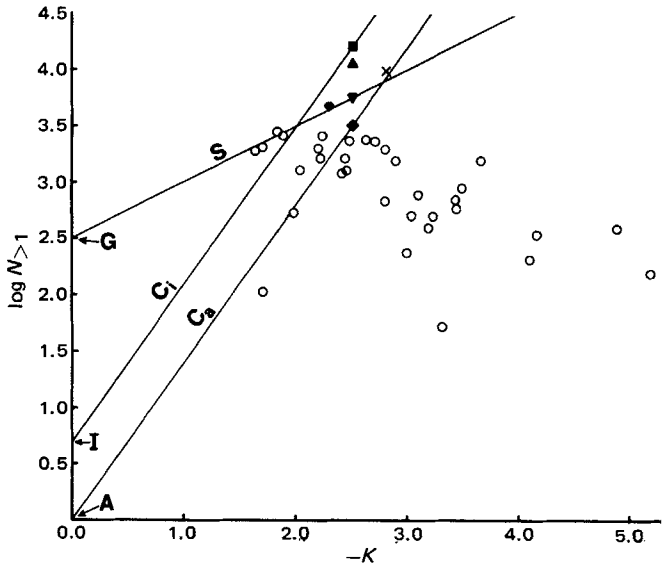

Figure 1—*Relationship between cleanliness factors and official standards. Key:* ■, *USP–NF standard;* ♦, *fivefold reduction of USP–NF standard;* ▲, *BP_1 standard;* ▼, *BP_5 standard;* ⧫, *Australian I standard;* ×, *Australian II standard; and* ○, *individual parenteral solutions. Points represent values of the slopes and intercepts of the particle-size distributions determined by a least-squares fitting procedure of the log–log plots of* $N_{>D}$ versus D.

standard (≯250 particles/ml > 3.5 μm) would lie below an arbitrarily drawn line (S) having a slope of 0.5 and a y intercept (point G) of 2.5 when $\log N_{>1}$ was plotted *versus* $-K$. Conversely, most solutions that failed this standard would lie above the line. This line (S) in Fig. 1 represents a family of straight lines on the log–log plot of $N_{>D}$ *versus* D (Fig. 2), all passing through the common point S' corresponding to 316 particles/ml >3.16 μm. Due to the arbitrary manner in which Groves admittedly developed the S value and because some solutions examined in this study would have failed the Australian standard and yet passed the S value, and vice versa, the suitability of using another parameter to assess parenteral cleanliness was investigated.

The recently developed USP–NF standard (Table I) was examined in this context. If the values listed in this standard exhibit the linear relationship described by Eq. 1, then the slope and the y intercept of this line shown in Fig. 2 are −2.5126 and 16,280 ($\log N_{>1} = 4.2116$), respectively. These values are the coordinates of the point shown as the filled square (■) in Fig. 1. This point (■) was plotted and connected to point I, which represents a hypothetical particle-size distribution such that the log–log plot of $N_{>D}$ *versus* D (Fig. 2) has a slope of zero and a y intercept of 5 ($\log N_{>1} = 0.6990$). The resultant line, C_i, in Fig. 1 can be described by:

$$C_i = \frac{\log N_{>1} - 0.6990}{-K} \qquad \text{(Eq. 3)}$$

This line represents a family of straight lines on the log–log plot of $N_{>D}$ *versus* D, all passing through the common point C_i' in Fig. 2 corresponding to five particles/ml >25 μm. This point was selected since it is representative of the USP–NF standard.

Practically all commercially manufactured solutions examined would have passed a more stringent standard (3). Since the most contaminated of these solutions contained approximately one-fifth of the level of particulate matter allowed by the USP–NF standard, the possibility of using a cleanliness factor based upon a fivefold reduction of this standard was investigated. A more stringent standard for evaluating parenteral cleanliness based upon averaged data is currently used in the BP (Table I and Fig. 2). This standard specifies a twofold reduction in allowable particles when averaging data from five solutions in contrast to data from individual solutions. Increased stringency for evaluating parenteral cleanliness when averaging data is reasonable, since the mean of a set of samples exhibits much less variability than individual samples.

When this fivefold reduction of the USP–NF standard was plotted in Fig. 2, the slope and the y intercept of the line were −2.5126 and 3255 ($\log N_{>1} = 3.5126$), respectively. These values are the coordinates of the point (♦) plotted in Fig. 1 and connected to point A, which represents a hypothetical particle-size distribution in Fig. 2 with a slope of zero and a

[4] McGaw Laboratories, Glendale, CA 91201.
[5] Prototron, model ILI 1000, Spectrex Corp., Redwood City, CA 94063.
[6] Isolyte M Maintenance with 5% Dextrose, McGaw Laboratories, Glendale, CA 91201.

Table II—Effect of Method of Measurement on the Cleanliness Factors

Cleanliness Factor (CF) ± SE[a]	Critical Value	Method of Measurement		Differences in Cleanliness Factor, %
		Microscope	Prototron	
$\frac{\log N_{>1}}{-K} = C_a$	1.3979	0.8905 ± 0.0456	1.1354 ± 0.0742	27.5
$\frac{\log N_{>1} - 0.6990}{-K} = C_i$	1.3979	0.5582 ± 0.0571	0.8694 ± 0.0619	55.8
$\frac{\log N_{>1} - 2.5}{-K} = S$	0.5000	−0.2978 ± 0.0913	0.1842 ± 0.0349	161.9

[a] Although the parameters C_i and S were developed to evaluate individual solutions, the data shown were based upon an average of 36 individually calculated cleanliness factors to demonstrate clearly the overall effects of the method of measurement.

y intercept of 1 ($\log N_{>1} = 0$). Line C_a in Fig. 1 can be described by:

$$C_a = \frac{\log N_{>1}}{-K} \qquad \text{(Eq. 4)}$$

This line represents a family of straight lines on the log–log plot of $N_{>D}$ *versus* D, all passing through the common point C_a' in Fig. 2 corresponding to one particle/ml >25 μm. It is proposed that this cleanliness factor, C_a, be used to evaluate the cleanliness of parenterals based upon *averaged* data for several solutions.

Equations 3 and 4 describe the two lines shown in Fig. 1 denoted by C_i and C_a, respectively, whose slopes are both numerically equal to 1.3979. This number represents the critical value, *i.e.*, the maximum allowable value of the cleanliness factors. Therefore, any individual solution whose C_i exceeds 1.3979 or a representative sample of a batch of solutions whose C_a exceeds this critical value would fail the respective standard. Effectively, this approach means that any line joining point I in Fig. 1 with a point depicting an individual parenteral solution, or point A with a point depicting the average of several parenteral solutions, whose slope exceeds that of the C_i or C_a lines would fail the respective standard. Since the relative distribution of particles is largely independent of the composition of the solution (3, 10), the cleanliness factors for the solutions were averaged without regard to solution type.

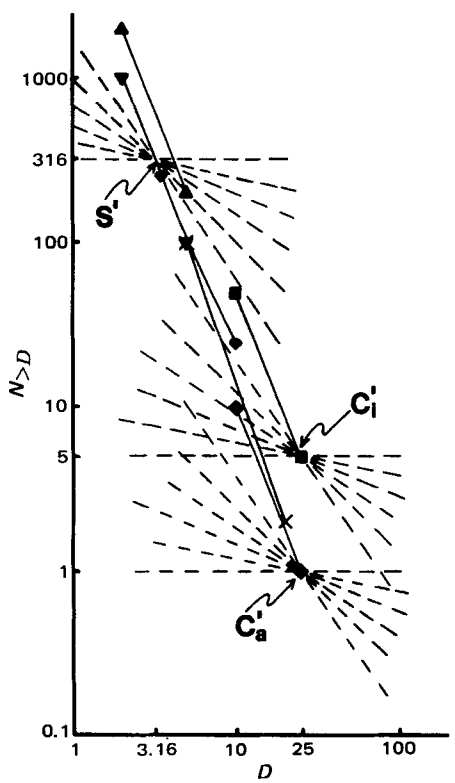

Figure 2—*Particle-size distributions of the official standards and of the critical values of the cleanliness factors. Key: -■—■-, USP–NF standard; -♦—♦-, fivefold reduction of USP–NF standard; -▲—▲-, BP_1 standard; -▼—▼-, BP_5 standard; -●—●-, Australian I standard; -×—×-, Australian II standard; and - - -, particle-size distribution of the critical value of the respective cleanliness factor.*

The cleanliness factors were calculated as follows. A particle-size distribution for a given solution was obtained by measuring the particle counts exceeding several diameters (1.000, 1.259, 1.585, 1.995, 2.512, 3.162, 3.981, 5.012, and 6.310 μm). These diameters were chosen to facilitate data analysis, since their logarithms are equally spaced. Equation 1 was fitted to the data points by means of a least-squares procedure. The slope (K) and the intercept ($\log N_{>1}$) were determined and used to calculate the cleanliness factors described by Eqs. 2–4. The cleanliness factors were then compared with the critical values of the respective standards to determine whether the solution(s) examined passed or failed.

As previously noted, one desirable feature of a parameter for assessing parenteral cleanliness is that it should be relatively independent of the method of measurement. Values for the two cleanliness factors, CF, proposed here (*i.e.*, C_i and C_a) were calculated using both microscopic and instrumental counting data based upon an average of 36 samples (Table II). The percentage differences in the CF values due to the measuring techniques employed varied considerably and were calculated as follows:

$$\% \text{ difference} = \left|\frac{\overline{CF^I} - \overline{CF^M}}{\overline{CF^M}}\right| \times 100 \qquad \text{(Eq. 5)}$$

where CF^I and CF^M refer to the CF values based upon data obtained using the instrumental and microscopic methods of measurement, respectively. This method of calculation was used since it was desirable to compare differences resulting from the method of measurement with the accepted compendial (microscopic) technique (1). Both C_i and C_a clearly exhibited much lower percentage differences resulting from a change in the method of measurement than did Groves' S value.

These observations, together with the standard error values reported in Table II, clearly indicate that the cleanliness factor utilized by Groves is much more susceptible to variations resulting from different methods of measurement than either C_i or C_a. Also, all cleanliness factors calculated for the average of 36 solutions were less than their respective critical value. Thus, the data shown in Table II are indicative of solutions whose average cleanliness factor value would have been passed by all three parameters (S, C_i, and C_a) using either microscopic or instrumental counting techniques.

Another consideration in selecting a cleanliness factor is that it should be relatively independent of the conditions to which the parenteral is subjected prior to measurement (8, 10, 12). Table III shows the effect of various degrees of agitation on the three cleanliness factors based upon averaged data for 18 parenteral solutions. The percentage change in the three CF values resulting from different degrees of agitation also varied considerably and was calculated as follows:

$$\% \text{ change} = \left|\frac{\overline{CF^A} - \overline{CF^B}}{\overline{CF^B}}\right| \times 100 \qquad \text{(Eq. 6a)}$$

or:

$$\% \text{ change} = \left|\frac{\overline{CF^C} - \overline{CF^B}}{\overline{CF^B}}\right| \times 100 \qquad \text{(Eq. 6b)}$$

where A refers to solutions stored in an undisturbed condition for 65 days, B refers to readings taken after these same solutions were inverted 20 times by hand, and C refers to the same solutions subsequently shaken for 30 min at 140 excursions/min on a mechanical agitator[7]. This method of calculation was used since it was desirable to compare the differences resulting from the effects of agitation to the degree of agitation recommended in the compendial standard technique (*i.e.*, 20 hand inversions).

[7] Model 6000, Eberbach Corp., Ann Arbor, MI 48106.

Table III—Effect of Agitation on the Cleanliness Factors

Cleanliness Factor (CF) ± SE[a]	Degree of Agitation: Stored (A)	Degree of Agitation: 20 Inversions (B)	Degree of Agitation: 30-min Shake (C)	Change of Cleanliness Factor, %: Stored (A) *versus* 20 Inversions (B)	Change of Cleanliness Factor, %: 30-min Shake (C) *versus* 20 Inversions (B)
$\frac{\log N_{>1}}{-K} = C_a$	0.9829 ± 0.0715	1.0566 ± 0.0685	0.9647 ± 0.0918	7.0	8.7
$\frac{\log N_{>1} - 0.6990}{-K} = C_i$	0.7402 ± 0.0588	0.7722 ± 0.0500	0.7285 ± 0.0735	4.1	6.3
$\frac{\log N_{>1} - 2.5}{-K} = S$	0.0981 ± 0.0447	0.1635 ± 0.0295	0.1040 ± 0.0407	40.0	36.4

[a] Although the parameters C_i and S were developed to evaluate individual solutions, the data shown were based upon an average of 18 individually calculated cleanliness factors to demonstrate clearly the overall effects of agitation.

Once again, the two cleanliness factors proposed here (*i.e.*, C_i and C_a) exhibited less variability (as indicated by the standard error values shown in Table III) and significantly lower percentage changes due to agitation effects than did Groves' S value. This finding indicates that the S value is also much more affected by the degree of agitation (*i.e.*, the manner in which the solution is handled prior to measurement) than either C_i or C_a. The CF values calculated for the average of 18 solutions were all less than the critical values dictated by the respective standard, *i.e.*, 1.3979 for C_i and C_a and 0.5 for S. Thus, the values shown in Table III are indicative of solutions whose average cleanliness factor value would have been passed by all three parameters when subjected to any of the three agitation conditions. These findings indicate that the large-volume parenterals tested here contained considerably fewer particles than the USP–NF standard allows.

For the 179 tests performed on parenteral solutions, perfect agreement was observed between the ability of a fivefold reduction of the USP–NF standard and the cleanliness factor for averaged data (C_a) to pass or fail parenteral solutions correctly. A perfect agreement was also observed between the USP–NF standard and the cleanliness factor for individual solutions (C_i). In contrast, five solutions failed the provisional Australian standard from which Groves' S value was developed, whereas the S value failed only one of these solutions. Furthermore, the S value failed one solution that would have passed this standard. This apparent inadequacy of the S value was likely related to the arbitrary manner in which Groves selected it. The C_i and C_a values suggested here were based upon the USP–NF standard and a fivefold reduction of it, respectively. Thus, the correlation (observed here) between the cleanliness factors and the standard would be anticipated.

The ability to obtain nondestructive readings in a short time would be advantageous when monitoring the cleanliness of batches of parenteral solutions, since a relatively large number of individual bottles could be averaged to obtain a representative sampling of the batch. However, the appropriate number of samples that should be averaged to ensure statistical accuracy is difficult to state unequivocally, since the operational factors involved in the manufacturing process may vary from batch to batch.

SUMMARY

To characterize a particle-size distribution as accurately as possible, it is advantageous to obtain counts over a broad range of particle sizes. This method enables the particle-size distribution to be determined by statistical weighting procedures so that any unusual variation in counts at one particle diameter can be effectively "smoothed out" by using a least-squares fitting procedure of the entire particle-size distribution. When utilizing these techniques, a particle-size distribution can best be described by specifying both the slope and the intercept of the log $N_{>D}$ *versus* log D plot (12). A parameter based upon both of these particle-size distribution characteristics was developed and is referred to as the cleanliness factor. The cleanliness factor for *individual* solutions (C_i) was based upon the present USP–NF standard; the cleanliness factor for an *average* of solutions (C_a) was based upon a fivefold reduction of this standard.

An ideal cleanliness factor would not be affected by differences in the measuring technique employed or by the degree of agitation experienced by the solution prior to measurement. When the cleanliness factors developed here were compared to Groves' S value, C_i and C_a were indeed affected much less by both the degree of agitation and the measuring technique.

A parameter based upon the total distribution of the particulate matter would reflect more accurately the true nature of a parenteral solution's cleanliness than mere statements of the allowable concentration of particles exceeding certain sizes. Since C_i and C_a appear to be relatively independent of the measuring technique utilized, it is desirable that these cleanliness factors be used in conjunction with a rapid, nondestructive, and easy to operate instrument such as the one described here. The proposed cleanliness factors can be regarded as complementary, more effective, means of applying the USP–NF standard.

REFERENCES

(1) "First Supplement to USP XIX–NF XIV," Mack Publishing Co., Easton, Pa., July 1975, pp. 56, 57.

(2) "British Pharmacopoeia 1973," Her Majesty's Stationery Office, London, England, 1973, p. A123.

(3) J. Blanchard, C. M. Thompson, and J. A. Schwartz, *Am. J. Hosp. Pharm.*, **33**, 144 (1976).

(4) M. J. Groves, "Parenteral Products," William Heinemann Medical Books, London, England, 1973, p. 248.

(5) I. Vessey and C. E. Kendall, *Analyst*, **91**, 273 (1966).

(6) M. J. Groves, *ibid.*, **94**, 992 (1969).

(7) M. J. Groves, *J. Pharm. Pharmacol.*, **18**, 161 (1966).

(8) L. Ernerot, *Acta Pharm. Suec.*, **11**, 1 (1974).

(9) C. E. Kendall, *Ann. N.Y. Acad. Sci.*, **158**, 640 (1969).

(10) L. Ernerot, I. Helmstein, and E. Sandell, *Acta Pharm. Suec.*, **7**, 501 (1970).

(11) M. J. Groves, *Proc. Soc. Anal. Chem.*, **8**, 271 (1971).

(12) J. Blanchard, J. A. Schwartz, and D. M. Byrne, *J. Pharm. Sci.*, **66**, 935 (1977).

(13) L. Ernerot, *Acta Pharm. Suec.*, **11**, 15 (1974).

ACKNOWLEDGMENTS AND ADDRESSES

Received May 10, 1976, from the *Department of Pharmaceutical Sciences, College of Pharmacy, University of Arizona, Tucson, AZ 85721.*

Accepted for publication September 17, 1976.

Supported by the University of Arizona Foundation and the University of Arizona Alumni Association.

The authors thank Mr. William T. Fink for constructive criticism of the manuscript.

* Present address: Optical Sciences Center, University of Arizona, Tucson, AZ 85721.

[x] To whom inquiries should be directed.

Factors Influencing Decomposition Rate of Amitriptyline Hydrochloride in Aqueous Solution

R. P. ENEVER ˣ, A. LI WAN PO, and E. SHOTTON

Abstract □ The degradation rate of amitriptyline hydrochloride in buffered aqueous solution containing various additives was determined. The oxidation was a free radical-mediated process, and the rate was accelerated by the presence of metal-ion contaminants. Glass ampuls, particularly amber ones, in which the solutions were stored were the major source of these contaminants. Edetate disodium stabilized the solution, but the primary antioxidants propyl gallate and hydroquinone were less effective. Sodium metabisulfite accelerated the decomposition, and it is postulated that there was direct attack by metabisulfite at the olefinic double bond in the drug molecule.

Keyphrases □ Amitriptyline hydrochloride—degradation in aqueous solution, effect of metal-ion contaminants, edetate disodium, and antioxidants □ Degradation—amitriptyline hydrochloride in aqueous solution, effect of metal-ion contaminants, edetate disodium, and antioxidants □ Metal-ion contaminants—effect on degradation of amitriptyline hydrochloride in aqueous solution □ Edetate disodium—effect on degradation of amitriptyline hydrochloride in aqueous solution □ Antioxidants, various—effect on degradation of amitriptyline hydrochloride in aqueous solution

A previous study (1) showed that amitriptyline hydrochloride decomposes in aqueous solution, with the production of dibenzocycloheptanone, 3-(propa-1,3-dienyl)-1,2:4,5-dibenzocyclohepta-1,4-diene, and 3-(2-oxoethylidene)-1,2:4,5-dibenzocyclohepta-1,4-diene. Subsequent work concerned the identification of factors influencing the rate of this oxidative process. The present report outlines this work and describes the use of chelating agents and antioxidants in stabilizing the system.

EXPERIMENTAL

Materials—The following chemicals were used: amitriptyline hydrochloride[1], citric acid[2], dibasic sodium phosphate dihydrate[2], potassium chloride[2], sodium hydroxide[2], hydroquinone[2], edetate disodium[2], ferric chloride[2], ether[2], propyl gallate[2], sodium metabisulfite[2], and chlorpromazine hydrochloride[3].

The purity of amitriptyline hydrochloride was checked by the British Pharmacopoeia (BP) method (2), and the drug was used without further purification. The pH 3.0 and 5.0 McIlvaine citric acid–phosphate buffers[4] (3) were prepared with double-distilled water and adjusted to an ionic strength of 0.5 with potassium chloride.

Assay of Amitriptyline Hydrochloride Solutions—The drug concentration was determined by GLC[5] using a 1.5-m (5-ft) × 0.6-cm (0.25-in.) i.d. glass column packed with 3% (w/w) SE-30[6] on 80–100-mesh Chromosorb W AW/DCMS[6]. The column temperature was 250° (injection port setting 6.5); the flow rates of hydrogen, air, and nitrogen were 80, 300, and 50 ml/min, respectively.

To produce a calibration curve for the assay, 1 ml of a 2-mg/ml solution of amitriptyline hydrochloride in the appropriate pH 3.0 or 5.0 buffer was pipetted into a 10-ml volumetric flask and 1 ml of a 2-mg/ml chlorpromazine hydrochloride solution (internal standard) was added. One milliliter of a 0.5-g/ml sodium hydroxide solution was added to liberate the bases, and the mixture was allowed to equilibrate with 7 ml of ether overnight in a stoppered flask previously flushed with nitrogen. Subsequently, 2 μl of the ethereal extract was injected into the chromatograph.

The procedure was repeated with amitriptyline hydrochloride solutions of 0.2, 0.4, 0.6, 0.8, 1.2, 1.4, 1.6, and 1.8 mg/ml. A linear response (slope 1.635) was obtained when the peak height ratio of amitriptyline to chlorpromazine was plotted against amitriptyline hydrochloride concentration. The test solutions of amitriptyline hydrochloride were assayed in a similar manner.

Assay of Iron in Aqueous Solution—The ferric content of the aqueous solutions was determined by atomic absorption spectroscopy[7] using an iron lamp and a wavelength of 2483 nm. A calibration curve was produced using freshly prepared solutions containing 1, 2, 3, 4, and 5 ppm of ferric ions in double-distilled water. Test solutions were assayed without further dilution.

Degradation of Amitriptyline Hydrochloride Solutions—Aliquots of 2 ml of 0.2% (w/v) solutions of amitriptyline hydrochloride in pH 3.0 or 5.0 buffer containing the appropriate additive were distributed into 10-ml clear and amber glass ampuls[8] and stored at 80° in constant-temperature water baths[9] in the dark. Samples were withdrawn at intervals up to 30 days and assayed for amitriptyline hydrochloride content.

RESULTS AND DISCUSSION

Figure 1 shows the results obtained for an amitriptyline solution sealed

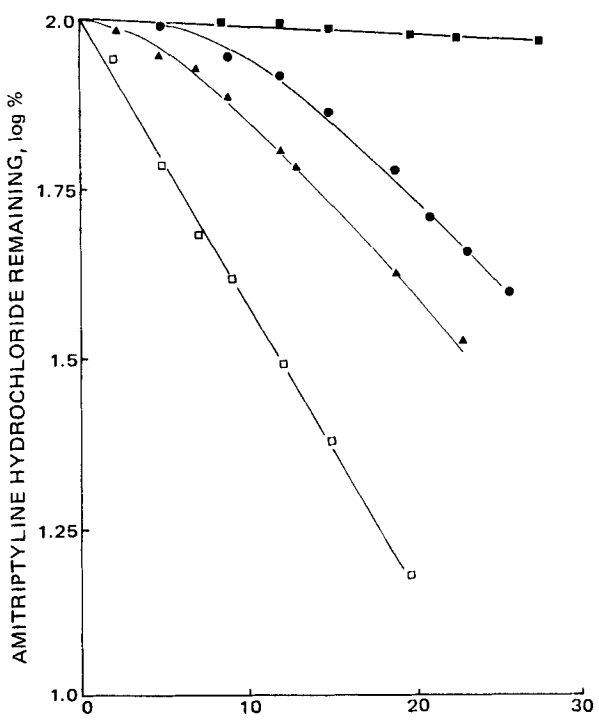

Figure 1—*Influence of metallic ions and edetate disodium on the decomposition rate of 0.2% (w/v) amitriptyline hydrochloride in pH 3.0 buffer at 80°. Key:* □, *containing* 2×10^{-4} *M ferric ions;* ■, *containing 0.1% (w/v) edetate disodium;* ▲, *containing* 2×10^{-4} *M cupric ions; and* ●, *control solution in amber ampuls (Batch BB242).*

[1] Merck Sharp and Dohme, Hoddesdon, Herts, England.
[2] Analar grade reagents, B.D.H. Chemicals Ltd., Poole, Dorset, England.
[3] May and Baker Ltd., Dagenham, Essex, England.
[4] The pH was checked with a model 290 Mk. 2 pH meter, Pye Unicam, Cambridge, England.
[5] Model 105 gas chromatograph equipped with flame-ionization detector, Pye Unicam, Cambridge, England.
[6] Perkin-Elmer Ltd., Beaconsfield, Bucks, England.
[7] Model 103 atomic absorption spectrometer, Perkin-Elmer, Beaconsfield, Bucks, England.
[8] Neutral glass, type Q (B.S.795:1961), Adelphi Tubes Ltd., London, England.
[9] SX 10, Grant Instruments, Cambridge, England.

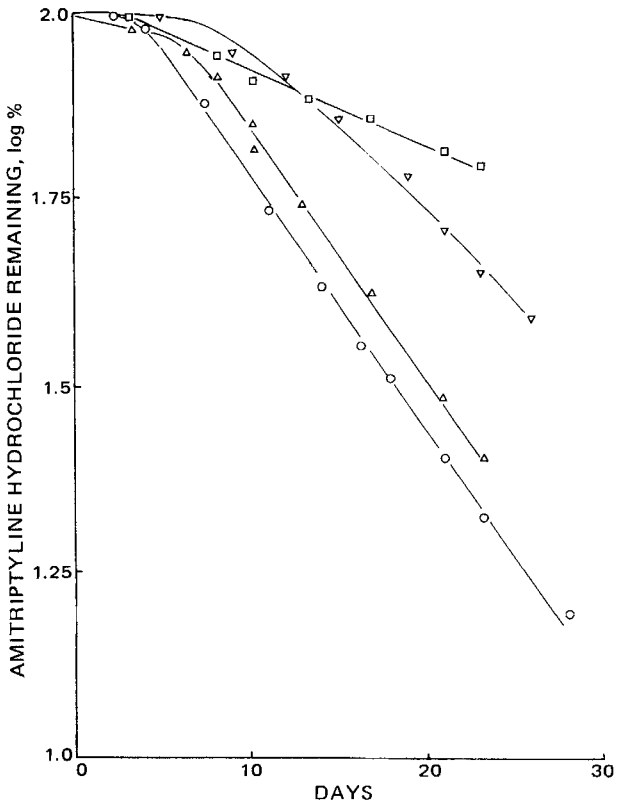

Figure 2—*Influence of glass type and batch of ampuls on decomposition of 0.2% (w/v) amitriptyline hydrochloride in pH 3.0 buffer at 80°. Key: □, clear glass ampuls (Batch 5018/10R); ○, amber glass ampuls (Batch HP65); △, amber glass ampuls (Batch HP67); and ▽, amber glass ampuls (Batch BB242).*

under air in amber ampuls. An initial slow decomposition rate was followed by a relatively faster rate ($k \sim 4.99 \times 10^{-2}$ day^{-1}). Decomposition was not measurable when a similar solution was sealed under nitrogen. Thus, the data are consistent with a free radical oxidation mechanism, since such a reaction normally exhibits an initial lag phase during which free radicals accumulate. To confirm the process, the sensitivity of the reaction to catalysts and inhibitors was investigated.

Addition of cupric acetate or ferric chloride (2×10^{-4} *M*) to amitriptyline hydrochloride solutions accelerated the decomposition rate (Fig. 1). The lag phase was removed with the ferric ions and greatly reduced with the cupric ions. The rate constants for the rapid phase of the reaction were increased to 0.0564 and 0.0854 day^{-1} with cupric and ferric ions, respectively. A reduction in the apparent activation energy of autoxidation processes by metal ions is well known (4), and such a positive catalytic effect on the decomposition of pharmaceutical compounds also was reported (5, 6).

The decomposition rate of amitriptyline hydrochloride solutions was reduced significantly by the addition of 0.1% (w/v) edetate disodium prior to storage (Fig. 1). The results obtained with this chelating agent confirm that metallic-ion impurities are a major cause of degradation. The source of impurities was at first thought to be the buffer salts, since they can contain significant amounts of metallic-ion contaminants (6). However, in the present work, metallic impurities leached from the containers were more important.

The iron content of amber glass ampuls is probably considerably greater than that of clear ampuls (7). Since amitriptyline is photolabile (8), however, such solutions probably would be stored in amber containers. The effect of different batches of such ampuls on the degradation rate is shown in Fig. 2; the rate was much greater in amber ampuls than in clear glass and there was considerable batch-to-batch variation. The amounts of iron leached from one batch[10] of amber ampuls into a 0.2% (w/v) amitriptyline hydrochloride solution in pH 3.0 buffer at 80° after 1, 8, 16, 19, 23, and 30 days were 0.8, 1.10, 1.35, 1.40, 1.58, and 1.80 ppm, respectively. There was a linear increase in iron concentration with time (rate of 0.034 ppm/day).

[10] Batch HP65.

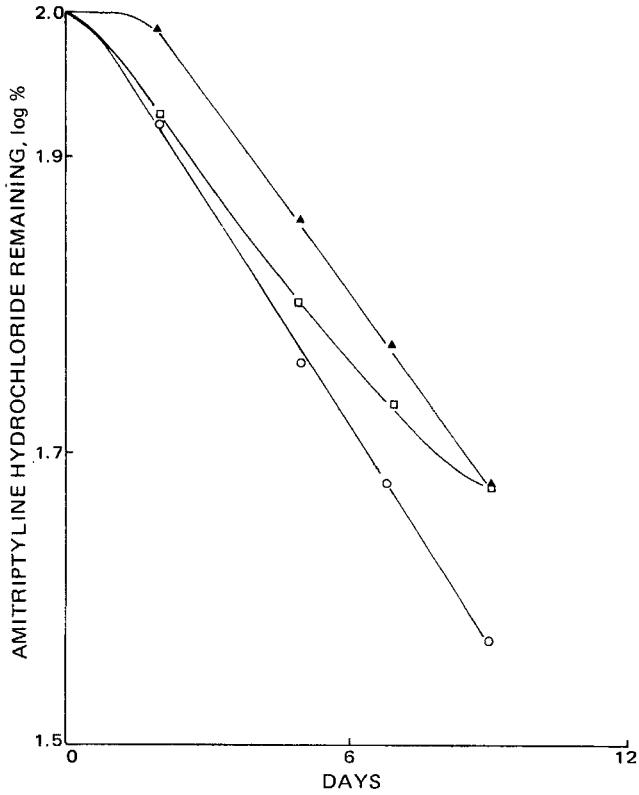

Figure 3—*Influence of addition of a decomposing solution or hydrogen peroxide to 0.2% (w/v) amitriptyline hydrochloride in pH 5.0 buffer at 80° in amber ampuls (Batch HP65). Key: ▲, 2 ml of 0.2% (w/v) amitriptyline hydrochloride solution; □, 2 ml of solution prepared by adding 1 ml of decomposing solution to 99 ml of fresh 0.2% (w/v) amitriptyline hydrochloride solution; and ○, 2 ml of solution prepared by adding 5 μl of 30% (w/w) hydrogen peroxide to 100 ml of fresh 0.2% (w/v) amitriptyline hydrochloride solution.*

Further support for the postulated free radical oxidation was obtained by adding a small volume of a partially decomposed solution to a fresh amitriptyline hydrochloride solution. Figure 3 shows that the lag phase was removed, although the chain propagation rate changed little. A similar result was obtained by adding 5 μl of a 30% (w/w) hydrogen per-

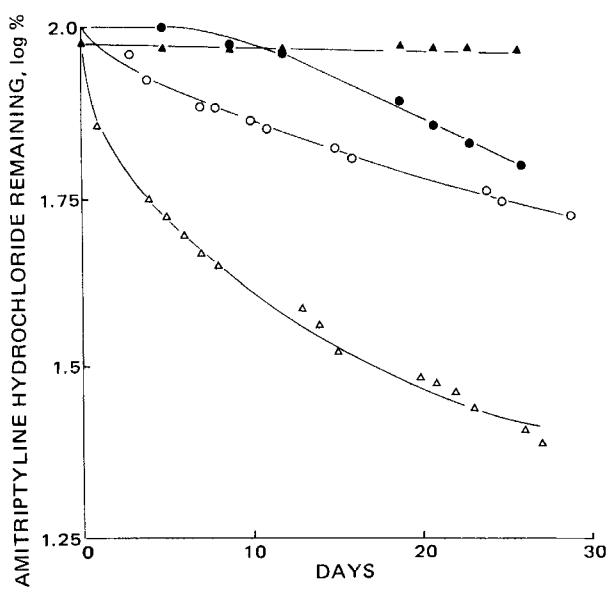

Figure 4—*Effect of antioxidants and sodium metabisulfite on the decomposition rate of 0.2% (w/v) amitriptyline hydrochloride in pH 3.0 buffer at 80°. Key: ●, control solution; ▲, containing 0.05% (w/v) propyl gallate; ○, containing 0.01% (w/v) hydroquinone; and △, containing 0.121% (w/v) sodium metabisulfite.*

oxide solution to 100 ml of fresh 0.2% (w/v) amitriptyline hydrochloride solution. The hydrogen peroxide content was insufficient to cause this marked degree of decomposition by direct oxidation.

Addition of 0.05% (w/v) of the antioxidant propyl gallate to an amitriptyline hydrochloride solution initially caused a 10% fall in drug concentration but subsequently completely stabilized the solution (Fig. 4). Hydroquinone, 0.01% (w/v), was less effective, since it abolished the lag phase and only appeared to slow the reaction after 15 days. The antioxidants appeared to break the chain reaction. With propyl gallate at least, however, there was evidence of a direct reaction with amitriptyline hydrochloride.

The reducing agent sodium metabisulfite was not effective in stabilizing the solution. Figure 4 shows that 0.121% (w/v) sodium metabisulfite produced an immediate fall in the drug concentration and a subsequent acceleration in the decomposition rate. This process did not follow first-order kinetics at any stage. The concentration of sodium metabisulfite was equimolar with amitriptyline hydrochloride (6.37×10^{-3} *M*), and the data fit a simple second-order kinetic plot.

Bisulfite-mediated reactions were reported previously (9–13), and a reaction mechanism similar to the thiamine cleavage shown previously (14, 15) is possible in the drug's side chain. However, using the isolation and identification techniques outlined previously (1), dibenzocycloheptanone was the only decomposition product present, suggesting that direct attack at the olefinic double bond in the molecule is more likely. Such an affinity for these bonds by sodium bisulfite was demonstrated and explained (16) on the basis of a free radical mechanism.

REFERENCES

(1) R. P. Enever, A. Li Wan Po, B. J. Millard, and E. Shotton, *J. Pharm. Sci.*, **64**, 1497 (1975).

(2) "British Pharmacopoeia, 1973", 1973, Her Majesty's Stationery Office, London, England, p. 26.

(3) "Documenta Geigy", 7th ed., edited by K. Diem and C. Lentner, J. R. Geigy, Basel, Switzerland, 1970, p. 280.

(4) G. Scott, "Atmospheric Oxidation and Antioxidants," Elsevier, London, England, 1965, p. 88.

(5) D. E. Griffith, *J. Pharm. Sci.*, **56**, 1197 (1967).

(6) T. O. Oesterling and D. E. Guttman, *ibid.*, **53**, 1189 (1964).

(7) V. Dimbleby, *J. Pharm. Pharmacol.*, **5**, 969 (1953).

(8) K. W. Blessel, B. C. Rudy, and B. Z. Senkowski, in "Analytical Profiles of Drug Substances," vol. 3, K. Florey, Ed., Academic, New York, N.Y., p. 127.

(9) L. C. Schroeter, T. Higuchi, and E. E. Schuler, *J. Am. Pharm. Assoc., Sci. Ed.*, **47**, 723 (1958).

(10) T. Higuchi and L. C. Schroeter, *ibid.*, **48**, 535 (1959).

(11) T. Higuchi and L. C. Schroeter, *J. Am. Chem. Soc.*, **82**, 904, (1960).

(12) S. Riegelman and E. Z. Fischer, *J. Pharm. Sci.*, **51**, 206 (1962).

(13) R. R. Williams, R. E. Waterman, J. C. Keresztesy, and E. R. Buckman, *J. Am. Chem. Soc.*, **57**, 536 (1935).

(14) K. Fry, L. L. Ingraham, and F. H. Westheimer, *ibid.*, **79**, 5225 (1957).

(15) D. F. DeTar and F. H. Westheimer, *ibid.*, **81**, 175 (1959).

(16) M. S. Kharasch, E. M. May, and F. R. Mayo, *J. Org. Chem.*, **3**, 175 (1938).

ACKNOWLEDGMENTS AND ADDRESSES

Received August 6, 1976, from the *Department of Pharmaceutics, School of Pharmacy, University of London, London, WC1N 1AX, England.*

Accepted for publication September 17, 1976.

The authors are grateful to Merck Sharp and Dohme for the gift of amitriptyline hydrochloride.

[x] To whom inquiries should be directed.

Polyamine Metabolism I: Synthesis of Dansyl Derivatives of *N*-(Monoaminoalkyl)- and *N*-(Polyaminoalkyl)acetamides and Elucidation in Urine of a Cancer Patient

MAHMOUD M. ABDEL-MONEM [x] and KOSEI OHNO

Abstract □ The dansyl derivatives of *N*-(monoaminoalkyl)- and *N*-(polyaminoalkyl)acetamides were synthesized and unequivocally characterized. TLC of the dansyl derivatives obtained from human urine indicated the presence of *N*-[3-[(4-aminobutyl)amino]propyl]acetamide (N^1-acetylspermidine), *N*-[4-[(3-aminopropyl)amino]butyl]acetamide (N^8-acetylspermidine), and *N*-(4-aminobutyl)acetamide (*N*-acetylputrescine) in appreciable amounts. The dansyl derivatives of N^1-acetylspermidine, N^8-acetylspermidine, and *N*-acetylputrescine were isolated and purified using various chromatographic methods. The mass spectra of these compounds were similar to those of authentic samples, which confirmed the identity of these compounds and established the presence of N^8-acetylspermidine as well as N^1-acetylspermidine and *N*-acetylputrescine in human urine.

Keyphrases □ Polyamines—*N*-(monoaminoalkyl)- and *N*-(polyaminoalkyl)acetamides, determined in human urine, dansyl derivatives synthesized □ *N*-(Aminoalkyl)acetamides—determined in human urine, dansyl derivatives synthesized □ Dansyl derivatives—of *N*-(monoaminoalkyl)- and *N*-(polyaminoalkyl)acetamides synthesized □ TLC—determination, dansyl derivatives of *N*-(monoaminoalkyl)- and *N*-(polyaminoalkyl)acetamides, human urine □ High-pressure liquid chromatography—determination, dansyl derivatives of *N*-(monoaminoalkyl)- and *N*-(polyaminoalkyl)acetamides, human urine

The diamine 1,4-butanediamine (putrescine) (I) and the polyamines *N*-(3-aminopropyl)-1,4-butanediamine (spermidine) (II) and *N,N'*-bis(3-aminopropyl)-1,4-butanediamine (spermine) (III) are present in all animal and plant tissues, and at least one of these is present in all microorganisms (1). Studies of both normal and neoplastic rapid growth systems indicate that the synthesis and accumulation of polyamines are elevated shortly after a stimulus inducing proliferation. Furthermore, the levels of these amines were elevated in the urine of cancer patients (2–10). These amines are excreted in human urine mainly as conjugates, which yield the free amines after hydrolysis (2).

Although several studies determined the levels of total

oxide solution to 100 ml of fresh 0.2% (w/v) amitriptyline hydrochloride solution. The hydrogen peroxide content was insufficient to cause this marked degree of decomposition by direct oxidation.

Addition of 0.05% (w/v) of the antioxidant propyl gallate to an amitriptyline hydrochloride solution initially caused a 10% fall in drug concentration but subsequently completely stabilized the solution (Fig. 4). Hydroquinone, 0.01% (w/v), was less effective, since it abolished the lag phase and only appeared to slow the reaction after 15 days. The antioxidants appeared to break the chain reaction. With propyl gallate at least, however, there was evidence of a direct reaction with amitriptyline hydrochloride.

The reducing agent sodium metabisulfite was not effective in stabilizing the solution. Figure 4 shows that 0.121% (w/v) sodium metabisulfite produced an immediate fall in the drug concentration and a subsequent acceleration in the decomposition rate. This process did not follow first-order kinetics at any stage. The concentration of sodium metabisulfite was equimolar with amitriptyline hydrochloride (6.37×10^{-3} *M*), and the data fit a simple second-order kinetic plot.

Bisulfite-mediated reactions were reported previously (9–13), and a reaction mechanism similar to the thiamine cleavage shown previously (14, 15) is possible in the drug's side chain. However, using the isolation and identification techniques outlined previously (1), dibenzocycloheptanone was the only decomposition product present, suggesting that direct attack at the olefinic double bond in the molecule is more likely. Such an affinity for these bonds by sodium bisulfite was demonstrated and explained (16) on the basis of a free radical mechanism.

REFERENCES

(1) R. P. Enever, A. Li Wan Po, B. J. Millard, and E. Shotton, *J. Pharm. Sci.*, **64**, 1497 (1975).

(2) "British Pharmacopoeia, 1973", 1973, Her Majesty's Stationery Office, London, England, p. 26.

(3) "Documenta Geigy", 7th ed., edited by K. Diem and C. Lentner, J. R. Geigy, Basel, Switzerland, 1970, p. 280.

(4) G. Scott, "Atmospheric Oxidation and Antioxidants," Elsevier, London, England, 1965, p. 88.

(5) D. E. Griffith, *J. Pharm. Sci.*, **56**, 1197 (1967).

(6) T. O. Oesterling and D. E. Guttman, *ibid.*, **53**, 1189 (1964).

(7) V. Dimbleby, *J. Pharm. Pharmacol.*, **5**, 969 (1953).

(8) K. W. Blessel, B. C. Rudy, and B. Z. Senkowski, in "Analytical Profiles of Drug Substances," vol. 3, K. Florey, Ed., Academic, New York, N.Y., p. 127.

(9) L. C. Schroeter, T. Higuchi, and E. E. Schuler, *J. Am. Pharm. Assoc., Sci. Ed.*, **47**, 723 (1958).

(10) T. Higuchi and L. C. Schroeter, *ibid.*, **48**, 535 (1959).

(11) T. Higuchi and L. C. Schroeter, *J. Am. Chem. Soc.*, **82**, 904, (1960).

(12) S. Riegelman and E. Z. Fischer, *J. Pharm. Sci.*, **51**, 206 (1962).

(13) R. R. Williams, R. E. Waterman, J. C. Keresztesy, and E. R. Buckman, *J. Am. Chem. Soc.*, **57**, 536 (1935).

(14) K. Fry, L. L. Ingraham, and F. H. Westheimer, *ibid.*, **79**, 5225 (1957).

(15) D. F. DeTar and F. H. Westheimer, *ibid.*, **81**, 175 (1959).

(16) M. S. Kharasch, E. M. May, and F. R. Mayo, *J. Org. Chem.*, **3**, 175 (1938).

ACKNOWLEDGMENTS AND ADDRESSES

Received August 6, 1976, from the *Department of Pharmaceutics, School of Pharmacy, University of London, London, WC1N 1AX, England.*

Accepted for publication September 17, 1976.

The authors are grateful to Merck Sharp and Dohme for the gift of amitriptyline hydrochloride.

[x] To whom inquiries should be directed.

Polyamine Metabolism I: Synthesis of Dansyl Derivatives of *N*-(Monoaminoalkyl)- and *N*-(Polyaminoalkyl)acetamides and Elucidation in Urine of a Cancer Patient

MAHMOUD M. ABDEL-MONEM [x] and KOSEI OHNO

Abstract □ The dansyl derivatives of *N*-(monoaminoalkyl)- and *N*-(polyaminoalkyl)acetamides were synthesized and unequivocally characterized. TLC of the dansyl derivatives obtained from human urine indicated the presence of *N*-[3-[(4-aminobutyl)amino]propyl]acetamide (N^1-acetylspermidine), *N*-[4-[(3-aminopropyl)amino]butyl]acetamide (N^8-acetylspermidine), and *N*-(4-aminobutyl)acetamide (*N*-acetylputrescine) in appreciable amounts. The dansyl derivatives of N^1-acetylspermidine, N^8-acetylspermidine, and *N*-acetylputrescine were isolated and purified using various chromatographic methods. The mass spectra of these compounds were similar to those of authentic samples, which confirmed the identity of these compounds and established the presence of N^8-acetylspermidine as well as N^1-acetylspermidine and *N*-acetylputrescine in human urine.

Keyphrases □ Polyamines—*N*-(monoaminoalkyl)- and *N*-(polyaminoalkyl)acetamides, determined in human urine, dansyl derivatives synthesized □ *N*-(Aminoalkyl)acetamides—determined in human urine, dansyl derivatives synthesized □ Dansyl derivatives—of *N*-(monoaminoalkyl)- and *N*-(polyaminoalkyl)acetamides synthesized □ TLC—determination, dansyl derivatives of *N*-(monoaminoalkyl)- and *N*-(polyaminoalkyl)acetamides, human urine □ High-pressure liquid chromatography—determination, dansyl derivatives of *N*-(monoaminoalkyl)- and *N*-(polyaminoalkyl)acetamides, human urine

The diamine 1,4-butanediamine (putrescine) (I) and the polyamines *N*-(3-aminopropyl)-1,4-butanediamine (spermidine) (II) and *N,N'*-bis(3-aminopropyl)-1,4-butanediamine (spermine) (III) are present in all animal and plant tissues, and at least one of these is present in all microorganisms (1). Studies of both normal and neoplastic rapid growth systems indicate that the synthesis and accumulation of polyamines are elevated shortly after a stimulus inducing proliferation. Furthermore, the levels of these amines were elevated in the urine of cancer patients (2–10). These amines are excreted in human urine mainly as conjugates, which yield the free amines after hydrolysis (2).

Although several studies determined the levels of total

$H_2N(CH_2)_4NH_2$ (I)

$H_2N(CH_2)_3NH(CH_2)_4NH_2$ (II)

$H_2N(CH_2)_3NH(CH_2)_4NH(CH_2)_3NH_2$ (III)

$CH_3COHN(CH_2)_nNH_2$ IV: $n = 4$; V: $n = 5$

$CH_3COHN(CH_2)_3NH(CH_2)_4NH_2$ (VI)

$CH_3COHN(CH_2)_4NH(CH_2)_3NH_2$ (VII)

polyamines in urine of normal subjects, cancer patients, and noncancer patients after hydrolysis, few studies addressed the identification of the polyamine conjugates present in urine. *N*-(4-Aminobutyl)acetamide (*N*-acetylputrescine) (IV) was identified in the urine of normal subjects (11), and *N*-(5-aminopentyl)acetamide (*N*-acetylcadaverine) (V) was found in the urine of schizophrenic patients (12). *N*-[3-[(4-Aminobutyl)amino]propyl]acetamide (N^1-acetylspermidine) (VI), but not *N*-[4-[(3-aminopropyl)amino]butyl]acetamide (N^8-acetylspermidine) (VII), also was detected in urine of healthy children (13) and a patient with acute myelocytic leukemia (14). Both VI and VII were formed in *Escherichia coli* on storage of a culture in the cold or growth in medium containing high concentrations of spermidine (15).

The present paper reports the synthesis and unequivocal characterization of the dansyl [5-(dimethylamino)-1-naphthalenesulfonyl] derivatives of *N*-(monoaminoalkyl)- and *N*-(polyaminoalkyl)acetamides and the isolation and unambiguous elucidation of the *N*-(monoaminoalkyl)- and *N*-(polyaminoalkyl)acetamides from the urine of one cancer patient who had not received therapy. The approach used in identifying the polyamine conjugates in human urine involved the separation and identification of their dansyl derivatives. This approach has several advantages: (*a*) the dansyl derivatives of the polyamines and their conjugates are fluorescent, which permits the detection of minor components; (*b*) chromatographic separation of the dansyl derivatives of polyamines is easier than the separation of the free amines; and (*c*) the use of the dansyl derivatives permits the quantitation of the identified polyamines.

EXPERIMENTAL

Synthesis of Dansyl Derivatives of *N*-(Monoaminoalkyl)acetamides (VIII–XI)—The diamines were treated with dansyl chloride according to the method of Nilsson *et al.* (16) to provide the monodansyl derivatives in 60–80% yields (Scheme I).

A solution of the monodansyl derivative in a mixture of chloroform (10 ml) and pyridine (2 ml) was cooled in an ice bath and treated dropwise with acetic anhydride (1.5 molar equivalents) in chloroform (8 ml) and pyridine (2 ml). The reaction mixture was stirred for 1 hr at room temperature and then treated with ice water. The chloroform layer was separated, washed with water, dried, and evaporated *in vacuo*. The yellow residue was purified by column chromatography on silica gel with chloroform–ethanol (97:3) to provide pure VIII–XI in 90–95% yields. The products were recrystallized from benzene–chloroform.

$$H_2N(CH_2)_nNH_2 \xrightarrow{(CH_3)_2NC_{10}H_6SO_2Cl} (CH_3)_2NC_{10}H_6SO_2HN(CH_2)_nNH_2$$

$$\xrightarrow{(CH_3CO)_2O} (CH_3)_2NC_{10}H_6SO_2HN(CH_2)_nNHCOCH_3$$

VIII: $n = 2$; IX: $n = 3$; X: $n = 4$; XI: $n = 5$

Scheme I

$$I + CH_2{=}CHCN \longrightarrow H_2N(CH_2)_4NHCH_2CH_2CN \xrightarrow{(CH_3)_2NC_{10}H_6SO_2Cl}$$

XII

$$(CH_3)_2NC_{10}H_6SO_2HN(CH_2)_4NCH_2CH_2CN \xrightarrow{B_2H_6}$$

$$\big|$$

$$SO_2C_{10}H_6N(CH_3)_2$$

XIII

$$(CH_3)_2NC_{10}H_6SO_2HN(CH_2)_4N(CH_2)_3NH_2 \xrightarrow{(CH_3CO)_2O}$$

$$\big|$$

$$SO_2C_{10}H_6N(CH_3)_2$$

XIV

$$(CH_3)_2NC_{10}H_6SO_2HN(CH_2)_4N(CH_2)_3NHCOCH_3$$

$$\big|$$

$$SO_2C_{10}H_6N(CH_3)_2$$

XV

Scheme II

Synthesis of Dansyl Derivative of *N*-[3-[(4-Aminobutyl)amino]propyl]acetamide (XV)—*N*-2-Cyanoethylbutane-1,4-diamine (XII) was prepared according to the method of Israel *et al.* (17) (Scheme II). The mixture of products was fractionally distilled three times *in vacuo* to provide XII, bp 87–92°/0.01 mm Hg [lit. (17) bp 88°/0.02 mm Hg]. A solution of triethylamine (10 mmoles) and XII (0.688 g, 4.88 mmoles) in chloroform (15 ml) was treated with a solution of dansyl chloride (2.69 g, 10.0 mmoles) in chloroform (25 ml), and the reaction mixture was stirred at room temperature for 4 hr. The usual workup of the reaction mixture provided a yellow oil (3.7 g), which was purified by column chromatography on silica gel. Elution with chloroform–benzene (7:3) gave an uncharacterized oil (0.21 g), and elution with chloroform provided 2.58 g (yield 87%) of XIII. The nitrile group of XIII was reduced with diborane using the method of Brown *et al.* (18).

A solution of crude XIV (0.6 g, 1.13 mmoles) in a mixture of chloroform (10 ml) and triethylamine (2 ml) was treated dropwise with acetic anhydride (1.5 ml) in chloroform (10 ml) and stirred for 2 hr. The usual workup of the reaction mixture provided a crude product, which was purified by column chromatography on silica gel using chloroform–ethanol (98:2). The first fraction provided XV as a yellow oil, 63% yield based on the amount of XIII used.

Synthesis of Dansyl Derivative of *N*-[4-[(3-Aminopropyl)amino]butyl]acetamide (XIX)—*N*-(4-Aminobutyl)acetamide hydrochloride (IV) was obtained using the method of Tabor *et al.* (19), mp 135–138° [lit. (19) mp 136–139° and (20) 140–141°]. TLC of the product on silica gel plates, using 1-butanol–acetic acid–pyridine–water (4:1:1:2) and visualization with ceric sulfate, indicated two major products in a 2:1 ratio. A solution of the crystalline product (10 g) in water was adjusted to pH 8.0 with ammonium hydroxide and added to an ion-exchange column[1]. The water eluate was evaporated to dryness *in vacuo* to provide diacetylputrescine (2.39 g), mp 137–138°. The column was washed with 1 *M* ammonium hydroxide, the eluate was concentrated and treated with ethanolic hydrochloric acid, and the product was recrystallized from 2-propanol to provide IV (5.0 g), mp 141–143° [lit. (20) mp 140–141° and (19) 135–138°].

N-[4-[(2-Cyanoethyl)amino]butyl]acetamide (XVI) was obtained from crude IV using the method of Tabor *et al.* (19) (Scheme III). The crude product, XVI hydrochloride, was dissolved in water, made basic with sodium bicarbonate, and extracted with chloroform. The chloroform extract was concentrated to dryness, and the residue was applied to a silica gel column and eluted with chloroform containing different amounts of ethanol. A fraction eluted with 2–5% ethanol in chloroform contained 5.4 g of *N*-[4-[bis(2-cyanoethyl)amino]butyl]acetamide, mp 55–58°. The second fraction, eluted with 5–15% ethanol in chloroform, contained a mixture of diacetylputrescine and XVI. The crude fraction was extracted with hot benzene; the benzene solution, on concentration, provided XVI, mp 35–37°. The benzene-insoluble solid was recrystallized from chloroform to provide diacetylputrescine, mp 137–138°.

A solution of XVI (1.83 g, 10 mmoles) and triethylamine (1.8 g, 17.8 mmoles) in chloroform (30 ml) was treated with a solution of dansyl chloride (2.8 g, 10.4 mmoles) in chloroform (20 ml), and the mixture was

[1] Amberlite IR-120 (H^+).

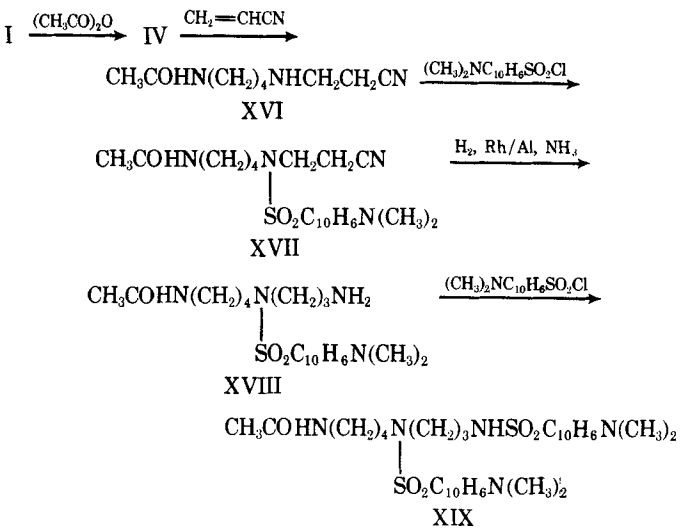

Scheme III

stirred at room temperature for 2 hr (Scheme III). The reaction mixture was filtered, the filtrate was washed with saturated sodium carbonate and then brine, dried over anhydrous sodium sulfate, and concentrated to dryness. The residue was purified by column chromatography on silica gel with chloroform to afford *N*-[4-[*N'*-(2-cyanoethyl)-*N'*-dansylamino]butyl]acetamide (XVII), 0.12 g (yield 99%).

Compound XVII was catalytically reduced using the method of Freifelder (21) (Scheme III). A solution of XVII (2.08 g, 5 mmoles) in ethanol (30 ml) containing ammonia (1.5 g) was hydrogenated with rhodium-on-alumina (10 g) catalyst. The catalyst was removed by filtration, and the filtrate was concentrated to dryness *in vacuo* to provide crude XVIII. A solution of crude XVIII (2.1 g, 5 mmoles) in triethylamine (2 ml) and chloroform (25 ml) was treated with a solution of dansyl chloride (1.35 g, 5 mmoles) in chloroform (15 ml), and the mixture was stirred at room temperature overnight. The usual workup of the reaction mixture provided a residue. This residue was purified by column chromatography on silica gel with chloroform–ethanol (97:3) to provide 2.55 g of pure XIX (yield 78%).

Preparation of Dansyl Derivatives of N^1-, N^8-, and N^4-Acetylspermidines (XV, XIX, and XX)—Spermidine (II) (1.45 g, 10 mmoles) was acetylated according to the method of Tabor *et al.* (19). The crude mixture of products was dissolved in triethylamine (5 ml) and chloroform (50 ml) and treated dropwise at room temperature with a solution of dansyl chloride (4.5 g, 17 mmoles) in chloroform (30 ml). Then the mixture was stirred at room temperature for 2 hr and concentrated *in vacuo*. The residue was treated with water (30 ml) and extracted with chloroform (3 × 50 ml). The chloroform solution was washed, dried, and evaporated to dryness.

The fluorescent oil obtained was purified by column (45 × 4.0 cm i.d.) chromatography on silica gel[2]. Elution with chloroform (containing 0.75% ethanol)–ethanol (99:1) provided tridansylspermidine (0.64 g, 5.4% yield). Elution with chloroform–ethanol (97:3) provided the mixture of the three

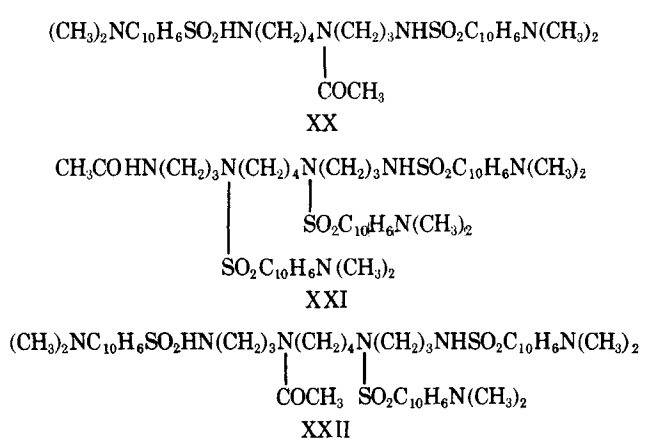

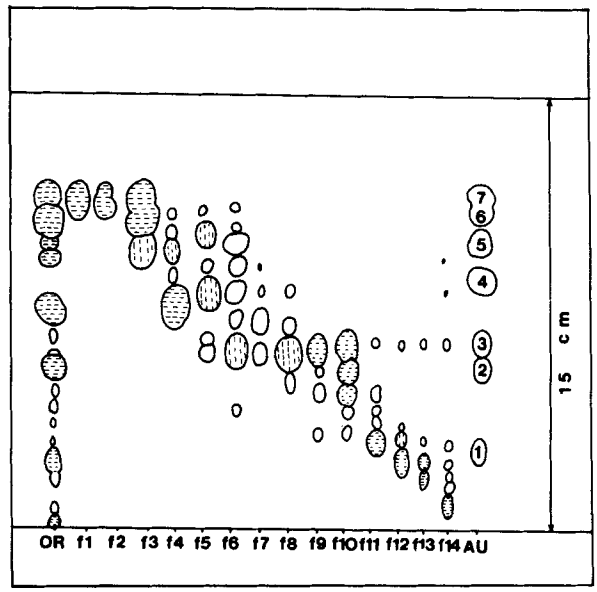

Figure 1—*TLC of the fractions obtained by column chromatographic separation of the dansyl derivatives from the urine of a patient with hepatoma. Solutions tested were: OR, solution of the dansyl derivatives obtained from urine before application to the column; f1–f14, fractions 1–14 obtained after column separation; and AU, mixture of the authentic samples of the dansyl derivatives of IV (1), VI (2), VII (3), ammonia (4), I (5), II (6), and III (7).*

isomeric didansylmonoacetylspermidines (1.48 mg, 22.61% yield), and elution with chloroform–ethanol (90:10) provided a mixture of the dansyldiacetylspermidines (2.18 g, 47.1% yield). Finally, elution with chloroform–ethanol (80:20) provided an unknown fluorescent substance (0.88 g). The fraction containing the didansylmonoacetylspermidines was chromatographed on a column of neutral alumina[3] (28 × 3.0 cm i.d.). Elution with chloroform–0.75% ethanol provided a mixture of XV and XIX (0.76 g) in approximately a 1:6 ratio. Elution with chloroform–ethanol (97:3) gave XX (0.52 g, 40% of total didansylmonoacetylspermidines).

Preparation of Dansyl Derivatives of *N*-[3-[[4-(3-Aminopropyl)aminobutyl]amino]propyl]acetamide (XXI) and *N*-[4-[(3-Aminopropyl)amino]butyl]-*N*-(4-aminobutyl)acetamide (XXII)—A solution of III (0.25 g, 1.21 mmoles) and triethylamine (0.12 g, 1.21 mmoles) in chloroform (15 ml) at 0° was treated dropwise with a solution of acetic anhydride (0.123 g, 1.21 mmoles) in chloroform (10 ml) and then allowed to stand at room temperature for 2 hr. The reaction mixture was treated dropwise with a solution of triethylamine (0.366 g, 3.6 mmoles) and dansyl chloride (1.03 g, 3.82 mmoles) in chloroform (5 ml), allowed to stand overnight, treated with aqueous sodium carbonate, and stirred for 1 hr.

The reaction mixture was extracted with water, dried over anhydrous sodium sulfate, and evaporated to dryness. The residue was chromatographed on a silica gel column and eluted with chloroform containing increasing amounts of ethanol. Elution with chloroform alone provided the unreacted dansyl chloride (0.12 g) followed by a fluorescent uncharacterized compound (0.135 g). Elution with chloroform–ethanol (99:1) provided tetradansylspermine (0.05 g), and elution with chloroform–ethanol (98:2) provided the tridansylmonoacetylspermines (0.132 g, 11.7% yield). Elution with chloroform–ethanol (95:5) provided the didansyldiacetylspermines (0.285 g, 31.3%).

The fraction containing the tridansylmonoacetylspermines was chromatographed on a neutral alumina column. Elution with chloroform–petroleum ether (8:2) provided XXI (one part), and elution with chloroform provided XXII (0.65 part).

Extraction and Dansylation of IV, VI, and VII from Human Urine—A 24-hr urine (1680 ml) was collected from one patient with diagnosed hepatoma who had not received therapy. The urine was collected over toluene, refrigerated during collection, and stored at −20° until analysis. An aliquot of urine (1580 ml) was adjusted to pH 10–11 with 2 *N* NaOH (about 50 ml) and extracted with 3-methyl-1-butanol (4 × 300 ml). Nitrogen was bubbled through the organic solvent extract

[2] Baker analyzed reagent, silica gel powder, 60–200 mesh.

[3] Woelm neutral alumina oxide, Activity IV.

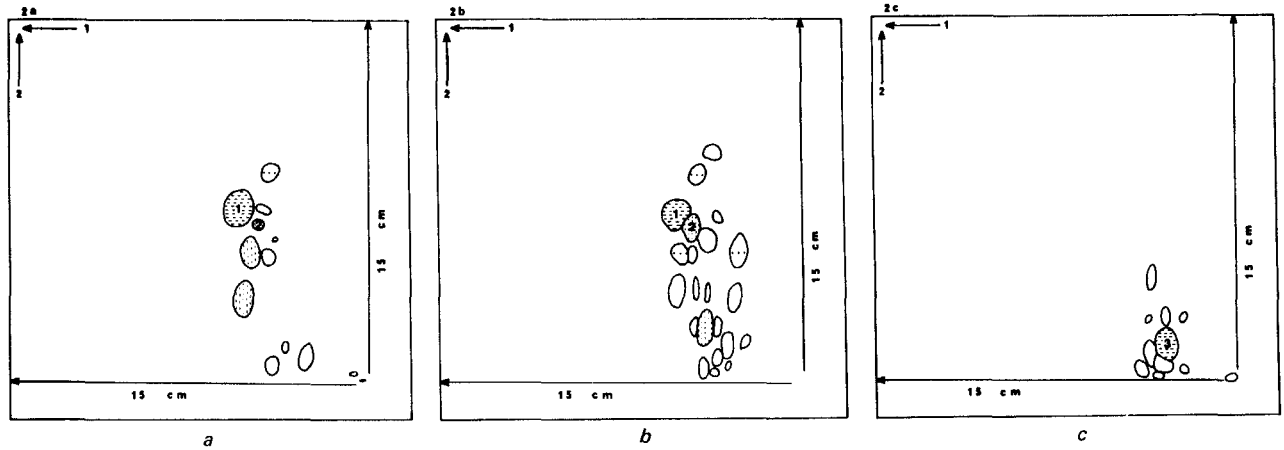

Figure 2—*Two-dimensional TLC of selected fractions obtained by column chromatographic separation of the dansyl derivatives from the urine of a patient with hepatoma. Fractions 9 (2a), 10 (2b), and 11 (2c) were examined. Key: spot 1, XV; spot 2, XIX; and spot 3, X.*

to remove ammonia. Concentrated hydrochloric acid (30 ml) was added to the extract, and the mixture was concentrated to dryness *in vacuo* at 45°.

The residue was dissolved in 5% HCl (10 ml), and the flask was rinsed with additional water (25 ml) and acetone (20 ml). Then the solution was adjusted to pH 8.5–9 with anhydrous sodium carbonate and treated with a solution of dansyl chloride (0.538 g, 2 mmoles) in acetone (20 ml). The mixture was stirred at room temperature for about 12 hr in a covered flask and was concentrated to remove the acetone. Water (70 ml) was added to dissolve the precipitated solids, and the reaction mixture was extracted with chloroform (3 × 100 ml). The combined chloroform extract was washed with saturated sodium bicarbonate solution (80 ml) and water (50 ml) and dried over anhydrous sodium sulfate, and the solvent was evaporated to dryness *in vacuo* to give a dark-brown oil.

Isolation and Purification of X, XV, and XIX—*Column Chromatography*—The residue obtained from the dansylation reaction was dissolved in chloroform, applied on a column (30 × 2.4 cm i.d.) of silica gel[4], and eluted with chloroform–ethanol. The elution on the column was monitored with a long wavelength UV lamp, and 15 fluorescent fractions were collected. The solvent composition and volumes (milliliters) of the fractions were: chloroform (containing 0.75% ethanol), 200, 300, 300, 400, and 500; chloroform–ethanol (98:2), 150, 100, 300, and 200; chloroform–ethanol (95:5), 500, 300, 300, 400, and 200; and chloroform–ethanol (8:2), 300.

A sample of each fraction was applied to a TLC silica gel GF plate (250 μm, 20 × 20 cm). A sample of the crude dansylation reaction prior to the column separation and a mixture of the authentic samples of the dansyldiamines, dansyl polyamines, and *N*-(monoaminoalkyl)- and *N*-(polyaminoalkyl)acetamides were also applied to the same plate. The plate was developed in chloroform–2-propanol (10:1) and examined under a long wavelength UV lamp (Fig. 1).

Fraction 9 contained primarily XV and a small amount of XIX together with other fluorescent impurities. Fraction 10 contained a mixture of XV and XIX together with some fluorescent impurities. The dansyl derivative of IV was eluted in fraction 11. Each fraction was examined by two-dimensional TLC (Fig. 2).

Analytical TLC—Silica gel GF plates[5] (250 μm, 20 × 20 cm) were used in one- or two-dimensional analysis. The solvent systems used were: Solvent 1, chloroform–2-propanol (10:1); and Solvent 2, chloroform–triethylamine (10:2). The developed plates were examined under a long wavelength UV lamp. Samples from selected fractions after column separation were applied to the corner of a TLC plate, and the plate was developed in one dimension for 15 cm with Solvent 1. The plate then was dried at room temperature and developed in a second dimension with Solvent 2.

The desired spots were scraped from the plates and immediately extracted with a mixture of equal volumes of triethylamine and 2-propanol (8 ml). The extracts were evaporated to dryness in a nitrogen stream at 40°, and the residues were stored at 4° until analysis by one-dimensional TLC and high-pressure liquid chromatography (HPLC). Immediately before analysis, the residues were dissolved in chloroform, and aliquots were spotted on a TLC plate or injected in the HPLC system. The TLC plates were developed in Solvents 1 and 2 in one dimension.

HPLC[6]—The separation of the dansyl derivatives was achieved, using a modification of a published method (22), on a silica[7] column (120 cm × 2.2 mm i.d.) with chloroform (containing 0.75% ethanol)–triethylamine (100:3).

Preparative TLC—Selected fractions after column separation were concentrated to dryness, and the residue was dissolved in an aliquot of chloroform. The solution was streaked on silica gel GF plates[5] (250 μm, 20 × 20 cm), and the plates were developed in either Solvent 1 or 2. The fluorescent bands corresponding to the desired compounds were scraped off and immediately extracted with a mixture of equal volumes of triethylamine and 2-propanol. The extract was evaporated to dryness in a nitrogen stream at 40°, and the residue was stored at 4°.

Compound XV was obtained in the preparative scale from fraction 9 using Solvent 2. The residue obtained from the fluorescent band corresponding in position to XV was examined by HPLC (22) to confirm its purity and was submitted for mass spectroscopic analysis. The mass spectrum of the residue, together with that of an authentic sample of XV, is shown in Fig. 3.

Compound XIX was obtained from fraction 10 using Solvent 1, which was especially good for the separation of XV and XIV (22). The developed chromatograms contained two intense fluorescent bands. The upper band had the same R_f as XV, and the lower band had the same R_f as XIX. The extract from the lower band (crude XIX) was concentrated and streaked on TLC plates, and the plates were developed in Solvent 2. The residue obtained from the fluorescent band that corresponded in position to XIX was identified as XIX by comparison of its mass spectrum with that of an authentic sample and by its chromatographic mobility on TLC and HPLC. Since it contained some low molecular weight impurities, the residue was purified on a small silica gel column. After evaporation of the solvent, the residue was submitted for mass spectroscopic analysis. This mass spectrum, together with that of an authentic sample of XIX, is shown in Fig. 4.

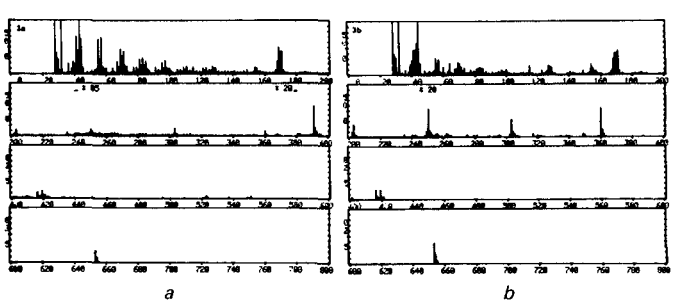

Figure 3—*Mass spectra of the dansyl derivative of VI obtained from the urine of a hepatoma patient (3a) and of the authentic sample of XV (3b).*

[4] E. Merck, Gel-60, 230–400 mesh.
[5] Analtech, Newark, Del.
[6] Model 6000 solvent delivery system, Waters Associates, Milford, Mass., and LDC model 1209 fluoromonitor, Laboratory Data Control, Riviera Beach, Fla.
[7] Corasil II, Waters Associates, Milford, Mass.

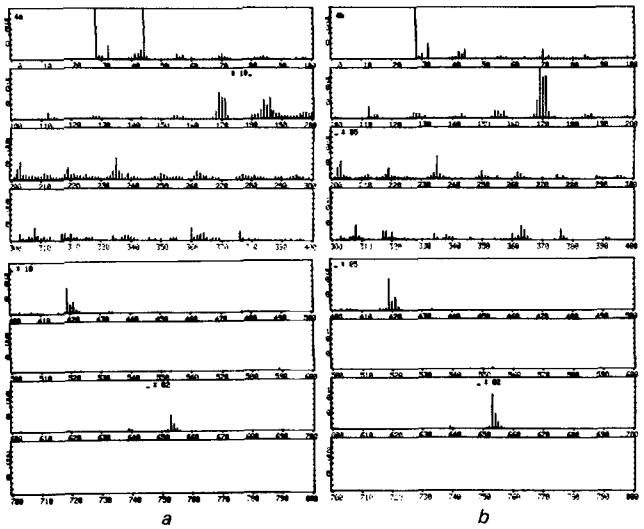

Figure 4—*Mass spectra of the dansyl derivative of VII obtained from the urine of a hepatoma patient (4a) and of the authentic sample of XIX (4b).*

Compound X was purified from fraction 11 using Solvent 1. The concentrated extract from the fluorescent band corresponding to X was rechromatographed on silica gel plates with Solvent 2. The residue obtained from the fluorescent band corresponding to X was submitted for mass spectroscopic analysis. Figure 5 represents the mass spectrum of X obtained from urine (5*a*) and that of an authentic sample of X (5*b*).

Column Chromatographic Purification of XIX—The residue obtained after preparative TLC was dissolved in chloroform, applied to a column (12 × 1.5 cm i.d.) of silica gel[4], and eluted with chloroform–2-propanol (97:3). The central fraction was collected and concentrated to dryness, and the residue was stored at 4°.

RESULTS AND DISCUSSION

All target compounds were verified by their elemental analysis (Table I) and spectral properties. IR, PMR, and electron-impact mass spectra of these compounds were in accord with the proposed structures. IR and PMR spectra of XV and XIX were identical. However, these compounds showed different chromatographic mobilities on TLC and HPLC and different electron-impact mass spectra. IR spectra of the monosubstituted amides (VIII–XI, XV, XIX, and XXI) showed the characteristic band near 1550 cm^{-1} (amide II), which was absent in the spectra of the disubstituted amides (XX and XXII).

The electron-impact mass spectra of the dansyl derivatives (Figs. 3–5) showed relatively intense molecular ions at *m/e* 653 for XV and XIX and at *m/e* 363 for X. These spectra also showed the expected fragments at *m/e* 170 and 234 due to the dimethylaminonaphthyl and dansyl ions, respectively. The fragment corresponding to $(M - C_{12}H_{12}NO_2S)^+$ appeared at *m/e* 419 for XV and XIX and at *m/e* 126 for X.

CONCLUSIONS

TLC and HPLC examination of the dansyl derivatives from the urine of a cancer patient (hepatoma) indicated the presence of VI, VII, and IV

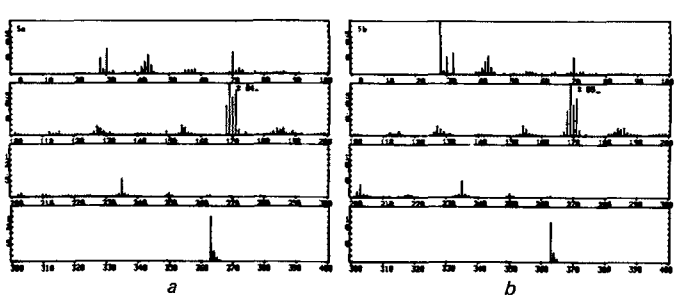

Figure 5—*Mass spectra of the dansyl derivative of IV obtained from the urine of a hepatoma patient (5a) and of the authentic sample of X (5b).*

Table I—Elemental Analyses of the Dansyl Derivatives of *N*-(Monoaminoalkyl)- and *N*-(Polyaminoalkyl)acetamides

Compound	Molecular Formula		Analysis, % Calc.	Found	Melting Point
VIII	$C_{16}H_{21}N_3O_3S$	C	57.29	57.17	102–103°
		H	6.31	6.22	
		N	12.53	12.61	
IX	$C_{17}H_{23}N_3O_3S$	C	58.43	58.60	97°
		H	6.63	6.59	
		N	12.02	11.93	
X	$C_{18}H_{25}N_3O_3S$	C	59.48	59.26	100–101°
		H	6.93	6.74	
		N	11.56	11.41	
XI	$C_{19}H_{27}N_3O_3S$	C	60.45	60.23	Oil
		H	7.21	7.48	
		N	11.13	10.89	
XV	$C_{33}H_{43}N_5O_5S_2$	C	60.62	60.46	Oil
		H	6.63	6.51	
		N	10.71	10.60	
XIX	$C_{33}H_{43}N_5O_5S_2$	C	60.62	60.44	Oil
		H	6.63	6.77	
		N	10.71	10.45	
XX	$C_{33}H_{43}N_5O_5S_2$	C	60.62	60.72	Oil
		H	6.63	6.57	
		N	10.71	10.48	
XXI	$C_{48}H_{61}N_7O_7S_3$	C	61.06	60.80	Oil
		H	6.51	6.52	
		N	10.38	10.19	
XXII	$C_{48}H_{61}N_7O_7S_3$	C	61.06	61.00	Oil
		H	6.51	6.63	
		N	10.38	10.14	

in appreciable amounts. The dansyl derivatives of VI, VII, and IV were isolated and purified using a variety of chromatographic methods. The mass spectra of these compounds were similar to those of authentic samples (Figs. 2, 4, and 5). These data confirmed the identity of these compounds and established the presence of VII as well as VI and IV in human urine.

After the completion of the work described, a report appeared describing the identification of both VI and VII in the urine of normal subjects and cancer patients (23). In that study, the authors isolated these compounds from the urine and established their identity on the basis of IR spectra, elemental analysis, and the analysis of products obtained by acid hydrolysis. The findings reported in the present paper corroborate those of Tsuji *et al.* (23) and provide an unambiguous identification of IV in human urine.

REFERENCES

(1) T. A. Smith, *Endeavour*, **31**, 22 (1972).

(2) D. H. Russell, C. C. Levy, S. C. Schimpff, and I. A. Hawk, *Cancer Res.*, **31**, 1555 (1971).

(3) M. D. Denton, H. S. Glazer, D. C. Zellner, and F. G. Smith, *Clin. Chem.*, **19**, 904 (1973).

(4) L. J. Marton, D. H. Russell, and C. C. Levy, *ibid.*, **19**, 923 (1973).

(5) C. W. Gehrke, K. C. Kuo, R. W. Zumwalt, and T. P. Waalkes, *J. Chromatogr.*, **89**, 231 (1974).

(6) H. Veening, W. W. Pitt, Jr., and G. Jones, Jr., *ibid.*, **90**, 129 (1974).

(7) G. Dreyfuss, R. Doir, A. Harell, and R. Chayen, *Clin. Chim. Acta*, **49**, 65 (1973).

(8) D. H. Russell and S. D. Russell, *Clin. Chem.*, **21**, 860 (1975).

(9) A. Lipton, L. M. Sheehan, and G. F. Kessler, Jr., *Cancer*, **35**, 464 (1975).

(10) D. C. Tormey, T. P. Waalkes, D. Ahmann, C. W. Gehrke, R. W. Zumwalt, J. Snyder, and H. Hansen, *ibid.*, **35**, 1095 (1975).

(11) T. L. Perry, S. Hansen, and L. MacDougal, *J. Neurochem.*, **14**, 775 (1967).

(12) T. L. Perry, S. Hansen, and L. MacDougal, *Nature*, **214**, 484 (1967).

(13) T. Nakajima, J. F. Zack, Jr., and F. Wolfgram, *Biochim. Biophys. Acta*, **184**, 651 (1969).

(14) T. Walle, in "Polyamines in Normal and Neoplastic Growth," D. H. Russell, Ed., Raven, New York, N.Y., 1973, pp. 355, 365.

(15) C. W. Tabor and L. G. Dobbs, *J. Biol. Chem.*, **245**, 2086 (1970).

(16) J. L. G. Nilsson, P. Stenberg, C. Ljunggren, O. Eriksson, and R.

Lunden, *Acta Pharm. Suec.*, **8**, 497 (1971).
(17) M. Israel, J. S. Rosenfield, and E. J. Modest, *J. Med. Chem.*, **7**, 710 (1964).
(18) H. C. Brown, P. Heim, and N. M. Yoon, *J. Am. Chem. Soc.*, **92**, 1637 (1970).
(19) H. Tabor, C. W. Tabor, and L. DeMeis, in "Methods in Enzymology," vol. 17B, H. Tabor and C. W. Tabor, Eds., Academic, New York, N.Y., 1971, p. 829.
(20) E. L. Jackson, *J. Org. Chem.*, **21**, 1374 (1956).
(21) M. Freifelder, *J. Am. Chem. Soc.*, **82**, 2386 (1960).
(22) M. M. Abdel-Monem and K. Ohno, *J. Chromatogr.*, **107**, 416 (1975).
(23) M. Tsuji, T. Nakajima, and I. Sano, *Clin. Chim. Acta*, **59**, 161 (1975).

ACKNOWLEDGMENTS AND ADDRESSES

Received February 26, 1976, from the *College of Pharmacy, University of Minnesota, Minneapolis, MN 55455.*
Accepted for publication September 23, 1976.
Supported by U.S. Public Health Service Grant CA 14239.
The authors thank I. Fortuny, M.D., for assistance in providing the urine samples from the cancer patients.
[x] To whom inquiries should be directed.

Dissolution Kinetics of Cholesterol in Simulated Bile I: Influence of Bile Acid Type and Concentration, Bile Acid–Lecithin Ratio, and Added Electrolyte

K. H. KWAN [*], W. I. HIGUCHI [*x], A. M. MOLOKHIA [*], and A. F. HOFMANN [‡]

Abstract □ A physical model approach was utilized to investigate cholesterol monohydrate dissolution kinetics in simulated bile. The static pellet method and the Berthoud theory were employed to assess the contributions of the diffusion–convection mass transfer resistance and those of the interfacial resistance to the overall kinetics. For almost all situations studied, the interfacial resistance was the dominant rate-determining factor. The effects of four bile acids and their concentrations, the bile acid–lecithin ratio, and the added electrolytes and their concentrations on the interfacial resistance were examined. The results were correlated with those obtained with human bile samples, and the indications were that the kinetics of cholesterol dissolution in bile may be explainable on the basis of the principal bile acids, lecithin, and the electrolytes in the bile.

Keyphrases □ Cholesterol monohydrate—pellets, dissolution kinetics in simulated bile, effect of bile acid type and concentration, ratio to lecithin, and added electrolytes □ Dissolution kinetics—cholesterol monohydrate pellets in simulated bile, effect of bile acid type and concentration, ratio to lecithin, and added electrolytes □ Bile acids—effect of type and concentration on dissolution of cholesterol monohydrate pellets in simulated bile □ Lecithin—ratio to bile acid concentration, effect on dissolution kinetics of cholesterol monohydrate pellets in simulated bile □ Electrolytes—effect on dissolution kinetics of cholesterol monohydrate pellets in simulated bile □ Gallstones, model—cholesterol monohydrate pellets, dissolution kinetics in simulated bile, effect of bile acid type and concentration, ratio to lecithin, and added electrolytes □ Steroids—cholesterol monohydrate pellets, dissolution kinetics in simulated bile, effect of bile acid type and concentration, ratio to lecithin, and added electrolytes

During the past decade, major advances have been made in understanding the cholesterol gallstone problem. But, until recently, the only treatment for cholesterol gallstones was surgery. Recent studies (1–4) demonstrated that oral administration of chenodeoxycholic acid, a naturally occurring bile acid, to patients with cholesterol gallstones decreased the relative concentration of cholesterol in bile and induced dissolution of stones in 6–36 months.

While much is known (5–8) about the thermodynamic factors governing cholesterol gallstone formation and dissolution *in vivo*, there is relatively little information on the kinetics of gallstone dissolution. Such studies could be important, since a relatively slow rate of dissolution of cholesterol gallstones was observed in several clinical studies. A theoretical treatment by Higuchi *et al.* (9) led to the proposal that *in vivo* dissolution of cholesterol gallstones occurred at rates much slower than anticipated when dissolution was solubility–diffusion controlled; therefore, the anomalously slow rates for gallstone dissolution observed previously (1) indicated that interfacial factors might be important *in vivo*.

Indeed, experimental studies (10, 11) showed that *in vitro* dissolution of cholesterol gallstones in simulated bile was dominated by an interfacial barrier at the crystal–solution interface. Subsequent dissolution rate experiments with model gallstones (compressed pellets of cholesterol monohydrate crystals) yielded comparable results and suggested that cholesterol monohydrate pellets were valid model gallstones in studies of cholesterol gallstone dissolution kinetics.

Analyses of biliary lipids in patients showing gallstone dissolution during chenodeoxycholic acid treatment (3) confirmed that desaturation of bile occurs in most instances. Preliminary experiments on the *in vitro* dissolution of cholesterol gallstones, as well as cholesterol monohydrate pellets in micellar bile acid solutions, showed (10, 11) that added lecithin significantly decreased the dissolution rate, even though its addition enhanced equilibrium cholesterol solubility. A review of the chemical composition of human gallbladder bile (12) along with these observations suggested that the major determinants of the dissolution rate process would be the bile acid type and its concentration, the bile acid–lecithin molar ratio, and the electrolytes and their concentrations. This paper reports a systematic study of the effects of these factors on

Lunden, *Acta Pharm. Suec.*, **8**, 497 (1971).
(17) M. Israel, J. S. Rosenfield, and E. J. Modest, *J. Med. Chem.*, **7**, 710 (1964).
(18) H. C. Brown, P. Heim, and N. M. Yoon, *J. Am. Chem. Soc.*, **92**, 1637 (1970).
(19) H. Tabor, C. W. Tabor, and L. DeMeis, in "Methods in Enzymology," vol. 17B, H. Tabor and C. W. Tabor, Eds., Academic, New York, N.Y., 1971, p. 829.
(20) E. L. Jackson, *J. Org. Chem.*, **21**, 1374 (1956).
(21) M. Freifelder, *J. Am. Chem. Soc.*, **82**, 2386 (1960).
(22) M. M. Abdel-Monem and K. Ohno, *J. Chromatogr.*, **107**, 416 (1975).
(23) M. Tsuji, T. Nakajima, and I. Sano, *Clin. Chim. Acta*, **59**, 161 (1975).

ACKNOWLEDGMENTS AND ADDRESSES

Received February 26, 1976, from the *College of Pharmacy, University of Minnesota, Minneapolis, MN 55455.*
Accepted for publication September 23, 1976.
Supported by U.S. Public Health Service Grant CA 14239.
The authors thank I. Fortuny, M.D., for assistance in providing the urine samples from the cancer patients.
[x] To whom inquiries should be directed.

Dissolution Kinetics of Cholesterol in Simulated Bile I: Influence of Bile Acid Type and Concentration, Bile Acid–Lecithin Ratio, and Added Electrolyte

K. H. KWAN [*], W. I. HIGUCHI [*x], A. M. MOLOKHIA [*], and A. F. HOFMANN [‡]

Abstract □ A physical model approach was utilized to investigate cholesterol monohydrate dissolution kinetics in simulated bile. The static pellet method and the Berthoud theory were employed to assess the contributions of the diffusion–convection mass transfer resistance and those of the interfacial resistance to the overall kinetics. For almost all situations studied, the interfacial resistance was the dominant rate-determining factor. The effects of four bile acids and their concentrations, the bile acid–lecithin ratio, and the added electrolytes and their concentrations on the interfacial resistance were examined. The results were correlated with those obtained with human bile samples, and the indications were that the kinetics of cholesterol dissolution in bile may be explainable on the basis of the principal bile acids, lecithin, and the electrolytes in the bile.

Keyphrases □ Cholesterol monohydrate—pellets, dissolution kinetics in simulated bile, effect of bile acid type and concentration, ratio to lecithin, and added electrolytes □ Dissolution kinetics—cholesterol monohydrate pellets in simulated bile, effect of bile acid type and concentration, ratio to lecithin, and added electrolytes □ Bile acids—effect of type and concentration on dissolution of cholesterol monohydrate pellets in simulated bile □ Lecithin—ratio to bile acid concentration, effect on dissolution kinetics of cholesterol monohydrate pellets in simulated bile □ Electrolytes—effect on dissolution kinetics of cholesterol monohydrate pellets in simulated bile □ Gallstones, model—cholesterol monohydrate pellets, dissolution kinetics in simulated bile, effect of bile acid type and concentration, ratio to lecithin, and added electrolytes □ Steroids—cholesterol monohydrate pellets, dissolution kinetics in simulated bile, effect of bile acid type and concentration, ratio to lecithin, and added electrolytes

During the past decade, major advances have been made in understanding the cholesterol gallstone problem. But, until recently, the only treatment for cholesterol gallstones was surgery. Recent studies (1–4) demonstrated that oral administration of chenodeoxycholic acid, a naturally occurring bile acid, to patients with cholesterol gallstones decreased the relative concentration of cholesterol in bile and induced dissolution of stones in 6–36 months.

While much is known (5–8) about the thermodynamic factors governing cholesterol gallstone formation and dissolution *in vivo*, there is relatively little information on the kinetics of gallstone dissolution. Such studies could be important, since a relatively slow rate of dissolution of cholesterol gallstones was observed in several clinical studies. A theoretical treatment by Higuchi *et al.* (9) led to the proposal that *in vivo* dissolution of cholesterol gallstones occurred at rates much slower than anticipated when dissolution was solubility–diffusion controlled; therefore, the anomalously slow rates for gallstone dissolution observed previously (1) indicated that interfacial factors might be important *in vivo*.

Indeed, experimental studies (10, 11) showed that *in vitro* dissolution of cholesterol gallstones in simulated bile was dominated by an interfacial barrier at the crystal–solution interface. Subsequent dissolution rate experiments with model gallstones (compressed pellets of cholesterol monohydrate crystals) yielded comparable results and suggested that cholesterol monohydrate pellets were valid model gallstones in studies of cholesterol gallstone dissolution kinetics.

Analyses of biliary lipids in patients showing gallstone dissolution during chenodeoxycholic acid treatment (3) confirmed that desaturation of bile occurs in most instances. Preliminary experiments on the *in vitro* dissolution of cholesterol gallstones, as well as cholesterol monohydrate pellets in micellar bile acid solutions, showed (10, 11) that added lecithin significantly decreased the dissolution rate, even though its addition enhanced equilibrium cholesterol solubility. A review of the chemical composition of human gallbladder bile (12) along with these observations suggested that the major determinants of the dissolution rate process would be the bile acid type and its concentration, the bile acid–lecithin molar ratio, and the electrolytes and their concentrations. This paper reports a systematic study of the effects of these factors on

the kinetics of cholesterol monohydrate dissolution *in vitro* in simulated bile.

THEORETICAL

A physical model approach was utilized (9). The physical model provides a semiquantitative treatment of the kinetic data that should help identify possible rate-limiting situations and establish reasonable correlations between clinical and *in vitro* results.

Dissolution of a nonionic, inert solid involves (*a*) the contact of the solvent with the solid surface where (*b*) an interaction occurs, followed by (*c*) the disengagement of the solute molecule and its transport away from the interface into the bulk solution. Usually step *a* occurs instantaneously, and steps *b* and/or *c* are generally considered to be rate determining. The following equation was derived by Berthoud (13) to account for both the interfacial resistance and the diffusional resistance across the Nernst diffusion layer in a dissolution process:

$$J = \frac{A(C_s - C_b)}{R} = \frac{A(C_s - C_b)}{(h/D + 1/P)} \qquad \text{(Eq. 1)}$$

where:

J = dissolution rate
A = surface area of dissolving solid exposed to solution
C_s = concentration of solute in solution at saturation
C_b = concentration of solute in the bulk (under sink conditions, $C_b = 0$)
R = total resistance to dissolution
D = diffusion coefficient of solute in solution
h = Nernst diffusion layer thickness
P = effective permeability coefficient of the interfacial barrier

When interactions at the surface occur rapidly, $1/P$ becomes negligible, Eq. 1 reduces to the Nernst equation (14):

$$J = \frac{AD(C_s - C_b)}{h} \qquad \text{(Eq. 2)}$$

and the dissolution process becomes diffusion controlled. If surface interactions take place slowly, $1/P$ becomes much greater than h/D, in which case:

$$J = AP(C_s - C_b) \qquad \text{(Eq. 3)}$$

and the dissolution process becomes interfacial barrier controlled.

Both the Berthoud and the Nernst theories represent only semiempirical treatments of the dissolution process and assume a purely diffusional resistance, h/D, for the transfer of solid across the diffusion layer. However, in most dissolution situations, both convection and diffusion are expected to be important. Thus, for example, in the rotating-disk dissolution situation (15), it can be shown by the Levich treatment (16) that there may be a substantial contribution to mass transfer by convection, and the dissolution rate is given by:

$$J = \frac{A(C_s - C_b)}{(1.612D^{-2/3}\upsilon^{1/6}\omega^{-1/2}) + 1/P} \qquad \text{(Eq. 4)}$$

where υ is the kinematic viscosity of the solvent, and ω is the angular velocity of rotation. The corresponding effective diffusion layer thickness may be written as:

$$h = 1.612D^{1/3}\upsilon^{1/6}\omega^{-1/2} \qquad \text{(Eq. 5)}$$

In previous studies (17, 18), both Eqs. 1 and 4 were employed to analyze the experimental data on cholesterol monohydrate pellet dissolution in bile acid–lecithin solutions. With the rotating-disk technique, the rotation speed dependence predicted by Eq. 4 and the experimental results generally agreed well for a wide range of P values. This study established a general method for quantitatively determining the interfacial barrier transport coefficient, P, even when $1/P$ was comparable to the diffusional resistance term.

EXPERIMENTAL

Design and Considerations—The semiquantitative static pellet dissolution method (11) was chosen over the more quantitative rotating-disk method (15) since only one rotation speed is required with the static-pellet method. [With the rotating-disk method, dissolution rates must be determined at several rotation speeds to utilize the Levich (16) treatment.] The static-disk method required one-tenth the volume of the solvent system that would have been required with the rotating-disk method. Use of this more rapid method resulted in a great saving of chemicals and permitted the rapid, semiquantitative assessment of a large number of variables. Despite its semiempirical nature and its limitations, the static-pellet method accompanied by the Berthoud treatment is more than adequate for the present purposes.

Table I—Influence of Sodium Chloride Concentration on Solubility (C_s), Dissolution Rate (J/A), Total Resistance (R), and $1/P$ of Cholesterol Monohydrate in 116 mM Bile Acid–32 mM Lecithin Solutions Containing 0.01 M Phosphate Buffer at pH 7.4

Sodium Chloride, M	Parameter	I	II	III	IV
0	C_s[a]	3.37	3.36	2.95	3.15
	(J/A)[b] $\times 10^4$	0.0584	0.0314	0.168	0.022
	R[c] $\times 10^{-3}$	577	1070	176	1419
	$(1/P)$[c] $\times 10^{-3}$	574.7	1067.7	173.7	1416.7
0.10	C_s	4.07	3.96	3.00	3.34
	$(J/A) \times 10^4$	0.466	0.384	0.274	0.121
	$R \times 10^{-3}$	87.3	103	110	276
	$(1/P) \times 10^{-3}$	85.0	100.7	107.7	273.7
0.25	C_s	4.17	4.32	3.07	3.45
	$(J/A) \times 10^4$	1.64	1.10	0.685	0.200
	$R \times 10^{-3}$	25.4	39.3	44.8	173
	$(1/P) \times 10^{-3}$	23.1	37.0	42.5	170.7
0.50	C_s	—	—	3.20	3.69
	$(J/A) \times 10^4$	—	—	1.61	0.632
	$R \times 10^{-3}$	—	—	19.9	58.4
	$(1/P) \times 10^{-3}$	—	—	17.6	56.1

[a] In mg cm^{-3}. [b] In mg cm^{-2} sec^{-1}. [c] In sec cm^{-1}.

It was decided to utilize Eq. 1 in the following way with the static-pellet method. The parameters J and C_s were to be measured in all cases so that R could be calculated. To determine P, an h/D value for the static-pellet system was estimated that was expected to be applicable to all situations involving micellar cholesterol in the bile acid–lecithin solutions to within about a factor of two. It was based upon representative diffusivity measurements in various cholesterol–bile acid–lecithin solutions, an h determination using a benzoic acid pellet (19), and the assumption that h is proportional to $D^{1/3}$ (18). For most situations in this study, $1/P \gg h/D$ or $R \cong 1/P$. Therefore, even though the uncertainty in h/D is large, rather accurate P values could be obtained for the cases of interest.

With regard to the solvent compositions to be used, a review of the chemical composition of human gallbladder bile (12) suggested the following:

1. The conjugated bile acids, cholyltaurine, cholylglycine, chenodeoxycholyltaurine, and chenodeoxycholylglycine, constitute over 80% of the major bile acids in bile, and dissolution kinetics for each bile acid should be defined. Since sodium is the major cation in bile, solutions should be prepared with the sodium salt.
2. The bile acid to lecithin molar ratio in bile samples from normal subjects and gallstone patients varies over a wide range. Ratios of 2.72, 3.63, and 5.44 should be adequate for defining the influence of this variable over the physiological range.
3. The major inorganic ions in bile are Na^+, Ca^{2+}, and Cl^-. Sodium chloride is a 1:1 electrolyte with a monovalent cation, and calcium chloride represents a typical 2:1 electrolyte providing a divalent cation. For sodium chloride, concentrations from 0.1 to 0.5 M should adequately cover the range; for calcium chloride, 0.025–0.10 M appears reasonable on the basis of published data.
4. The bile acid–lecithin concentration level should be important since earlier studies (20) indicated that dissolution in the more dilute duodenal bile was much slower than in gallbladder bile. While 116 mM bile acid–32 mM lecithin represents a reasonable level of bile acid–lecithin concentration in gallbladder bile, a wider range is assumed for the often diluted duodenal bile, namely from 23.2 mM bile acid–6.4 mM lecithin to 46.4 mM bile acid–12.8 mM lecithin (21).
5. The pH of the solutions should be maintained at 7.40 using 0.01 M sodium phosphate buffer to simulate physiological pH as well as to ensure that all bile acids in solution are fully ionized species. The pKa's of all bile acids studied are less than 5.0 (22). Exploratory studies already showed that at pH $\geq$ 7.0, both J and C_s are constant for each of the four bile acids studied.

Materials—Commercial cholesterol[1] was recrystallized three times

[1] Eastman Kodak Co., Rochester, N.Y.

Table II—Influence of Sodium Chloride Concentration on Solubility (C_s), Dissolution Rate (J/A), Total Resistance (R), and $1/P$ of Cholesterol Monohydrate in 46.4 m*M* Bile Acid–12.8 m*M* Lecithin Solutions Containing 0.01 *M* Phosphate Buffer at pH 7.40

Sodium Chloride, *M*	Parameter	I	II	III	IV
0	C_s[a]	1.10	1.50	0.784	1.05
	(J/A)[b] $\times 10^4$	0.00752	0.00859	0.0360	0.00657
	R[c] $\times 10^{-3}$	1463	1746	218	1600
	$(1/P)$[c] $\times 10^{-3}$	1460.7	1743.7	215.7	1597.7
0.10	C_s	1.27	1.63	0.802	1.12
	$(J/A) \times 10^4$	0.077	0.0286	0.0382	0.0192
	$R \times 10^{-3}$	165	570	210	584
	$(1/P) \times 10^{-3}$	162.7	567.7	207.7	581.7
0.25	C_s	1.39	2.01	0.832	1.19
	$(J/A) \times 10^4$	0.243	0.322	0.105	0.0491
	$R \times 10^{-3}$	57.2	50.2	79.2	242
	$(1/P) \times 10^{-3}$	54.9	47.9	76.9	239.7
0.50	C_s	1.56	—	1.19	1.30
	$(J/A) \times 10^4$	0.996	—	0.274	0.0844
	$R \times 10^{-3}$	15.7	—	43.4	154
	$(1/P) \times 10^{-3}$	13.4	—	41.1	151.7

[a] In mg cm^{-3}. [b] In mg cm^{-2} sec^{-1}. [c] In sec cm^{-1}.

from 95% ethanol. Radioactive cholesterol monohydrate was prepared by mixing 5 g of the recrystallized cholesterol with 100 μCi of a benzene solution of 4-^{14}C-cholesterol[2] in 400 ml of 95% ethanol at 60°. This solution was filtered while hot, and the filtrate was allowed to stand for 48 hr at room temperature. Then the cholesterol monohydrate crystals were filtered and dried *in vacuo* for 24 hr. The crystals obtained were stored in the dark in a desiccator saturated with water vapor at room temperature.

NMR studies quantitatively confirmed the monohydrate nature of the crystals. TLC studies indicated the absence of any impurities (23). X-ray crystallography[3] studies indicated that they were indeed cholesterol monohydrate crystals and that they had a lattice system similar to that of cholesterol found in human biliary calculi (24). The monohydrate crystals will lose their water content readily on exposure to low humidity and light.

The sodium salts of chenodeoxycholyltaurine (I) and chenodeoxycholylglycine (II) were prepared by the method of Norman (25) with certain modifications (26). The sodium salts of cholyltaurine (III) and cholylglycine (IV) were prepared using the method of Norman (25) with certain modifications[4] (27). The purity of these compounds was checked and confirmed by TLC using a destructive detection method (28).

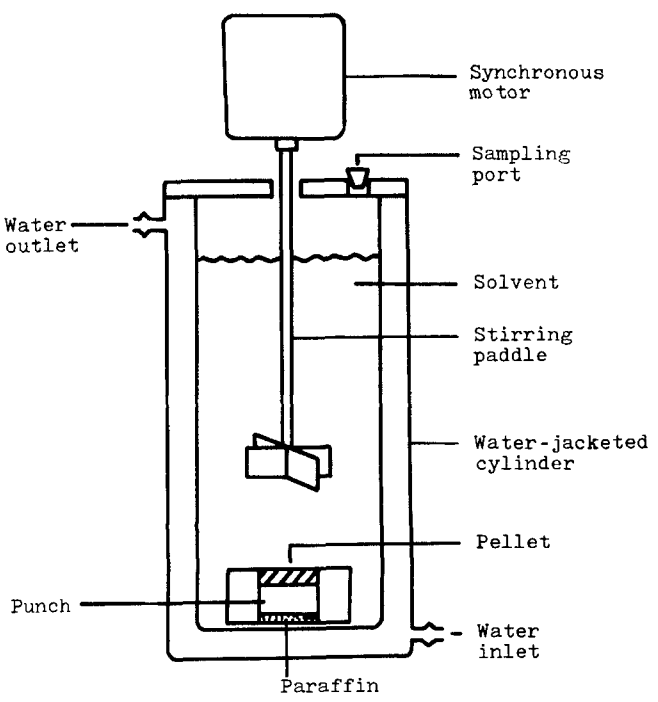

Figure 1—*Diagrammatic representation of the static-pellet dissolution apparatus.*

Egg lecithin was prepared from fresh egg yolks and subsequently stored according to the method of Singleton *et al.* (29). Chromatographically homogeneous lecithin, mol. wt. 771, was obtained. Monobasic sodium phosphate, dibasic sodium phosphate, sodium chloride, and calcium chloride[5] were analytical grade and were used as received.

Preparation of Solutions—All bile acid–lecithin solutions were prepared as follows. The sodium salt of the bile acid was dissolved in sufficient distilled water. The desired electrolyte, sodium chloride or calcium chloride, was added to the bile acid solution. For solutions containing no calcium chloride, 0.01 *M* sodium phosphate buffer at pH 7.40 was also added. Lecithin was dissolved separately in sufficient distilled water until a homogeneous colloidal suspension was obtained.

The lecithin suspension was then added to the bile acid–electrolyte solution and was diluted to the desired value with distilled water. The mixture was then shaken and allowed to stand overnight at 5° so that complete solubilization of lecithin was obtained. With sodium glycocholate, complete lecithin solubilization took more than 24 hr. The resulting clear solutions were then used for both dissolution rate and solubility determinations.

Dissolution Rate Determination—Pellets of ^{14}C-cholesterol monohydrate were prepared by directly compressing 100 mg of the material in a die, 1.27 cm (0.50 in.) i.d., under a force of 1362 kg (3000 lb) using a laboratory press[6]. The exposed surface area of the resulting pellets was 1.267 cm^2. The pellet was held firmly in a die by covering the bottom with melted paraffin. This die was then placed on the bottom of a water-jacketed cylinder, with the pellet facing a stirring paddle inserted at the top of the cylinder (Fig. 1). The stirring speed was maintained at 150 rpm during dissolution by a constant-speed motor[7].

Exactly 10 ml of the dissolution medium preequilibrated at 37° was added into the cylinder. Immediately, the first 0.50-ml sample was withdrawn using a pipet. Four other samples were taken at suitable time intervals. The ^{14}C-labeled samples were subsequently counted using a liquid scintillation counter[8], and the amount of cholesterol dissolved in the solvent was plotted against time.

Solubility Determination—The solubilities of cholesterol monohydrate in various solvent media were determined by introducing an excess of ^{14}C-cholesterol monohydrate, about 20 mg, into 2 ml of a solvent in a test tube. The tube was flushed with nitrogen, capped, and then shaken by a wrist-action shaker[9] in a water bath at 37°. After 4 days, a sample was taken and quickly filtered through a glass wool-wrapped, long tipped pipet preequilibrated at 37°. Exactly 0.2 ml of the filtrate was then assayed for cholesterol using a liquid scintillation counter[8].

More samples were taken every 2 days and assayed for cholesterol. The

[2] New England Nuclear Corp., Boston, Mass.
[3] Performed by Dr. C. Nordman, Department of Chemistry, University of Michigan, Ann Arbor, Mich.
[4] By A. F. Hofmann.
[5] Matheson, Coleman and Bell, Norwood, Ohio.
[6] Model B, Fred Carver Inc., Summit, N.J.
[7] Model CA, Hurst, Princeton, Ind.
[8] Model LS 200, Beckman Instruments, Fullerton, Calif.
[9] Burrell Corp., Pittsburgh, Pa.

Table III—Influence of Sodium Chloride Concentration on Solubility (C_s), Dissolution Rate (J/A), Total Resistance (R), and $1/P$ of Cholesterol Monohydrate in 23.2 mM Bile Acid–6.4 mM Lecithin Solutions Containing 0.01 M Phosphate Buffer at pH 7.40

Sodium Chloride, M	Parameter	I	II	III	IV
0.25	C_s[a]	0.952	0.864	0.664	0.814
	(J/A)[b] $\times 10^4$	0.0769	0.082	0.0342	0.0130
	R[c] $\times 10^{-3}$	123.8	105.2	194	626
	$(1/P)$[c] $\times 10^{-3}$	121.5	102.9	191.7	623.7
0.50	C_s	1.03	0.993	0.872	0.976
	$(J/A) \times 10^4$	0.343	0.411	0.0872	0.0565
	$R \times 10^{-3}$	30.0	24.2	100	173
	$(1/P) \times 10^{-3}$	27.7	21.9	97.7	170.7

[a] In mg cm^{-3}. [b] In mg cm^{-2} sec^{-1}. [c] In sec cm^{-1}.

solubility of cholesterol monohydrate in the medium was obtained when the concentration reached a constant level.

RESULTS

Figure 2 shows typical raw data obtained for the dissolution of cholesterol monohydrate in two solvent media. The dissolution rates were obtained by taking the slopes of the dissolution curves. The duplicate sets of data indicate the typical degree of reproducibility obtainable. For one solution, a standard deviation of 5% was obtained; for the other solution, a deviation close to 10% was obtained when the rates were much slower.

Figure 3 shows plots of amounts of cholesterol monohydrate solubilized in the same two solvent media (Fig. 2) as a function of time. Multiple samples were taken until a constant value for the equilibrium solubility was obtained for each solvent. Again, excellent reproducibility was obtained, with standard deviations of the equilibrium values lying within the range of 3–5%. Based on these solubility values, it may be estimated that at the end of the dissolution experiments (Fig. 2), the solvents become, at the most, around 15% saturated in cholesterol. Thus, sink conditions are maintained during dissolution, which justifies the use of the initial linear portions of plots of the type presented in Fig. 2 to calculate the dissolution rate for sink conditions, *i.e.*, $C_s \gg C_b$.

Figures 4–11 and Tables I–V summarize all results. The tabulated C_s and J/A values represent the average of at least two determinations. The value of R was calculated using Eq. 1 and assuming sink conditions, so that $C_b = 0$. The R values shown in the tables were calculated from the average C_s and J/A values.

As can be seen in Figs. 4–6 and Tables I–III, an increase in sodium chloride concentration resulted in a decrease in R for all four bile acids at all three bile acid concentrations. Studies at higher concentrations of sodium chloride were not possible for chenodeoxycholyltaurine (I) and chenodeoxycholylglycine (II) due to the salting out of the bile acids. For all three concentrations of bile acids, the R values of the chenodeoxycholate conjugates were generally lower than those of their cholate counterparts at all sodium chloride concentrations, except in the absence of sodium chloride. In general, differences among individual bile acids were significant.

A similar, but by far more remarkable, effect was observed with calcium chloride (Table IV). These systems were not buffered with 0.01 M phosphate, because calcium would precipitate as phosphates. However, the pH of the solutions remained at around 7.7 ± 0.15 during the dissolution rate and solubility determinations. No data were obtained for II, because this conjugate salted out in the presence of only a trace amount of calcium chloride. For the other three bile acids, an increase in calcium chloride concentration resulted in large reductions in R. At the same electrolyte concentrations, the effects of calcium chloride on R were greater than those of sodium chloride (Table I), the difference being eightfold for cholyltaurine (III) and 35-fold for cholylglycine (IV) on a concentration basis. Compound I precipitated out at higher calcium chloride concentrations.

In Figs. 7–10, R was plotted as a function of the bile acid–lecithin concentration at various sodium chloride concentrations for the four bile acids. In all cases, a smaller R was obtained at a higher bile acid–lecithin

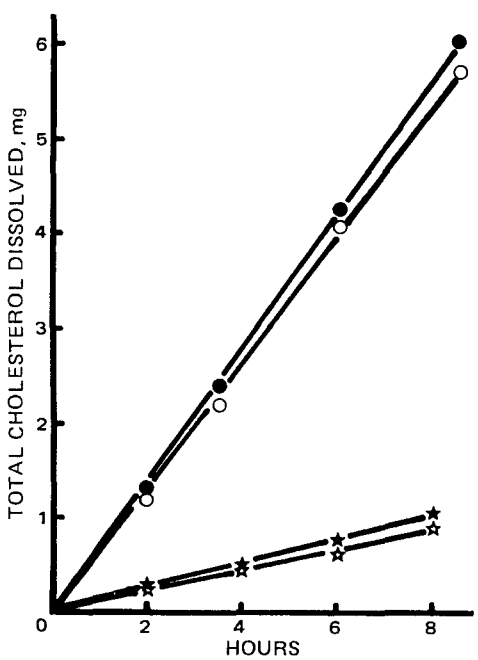

Figure 2—*Dissolution of cholesterol monohydrate at 37° in two solvent media. Key:* ●, ○, *in 116 m*M *cholyltaurine, 32 m*M *lecithin, 0.50* M *sodium chloride, and 0.01* M *phosphate buffer, pH 7.4; and* ★, ☆, *in 46.4 m*M *cholyltaurine, 12.8 m*M *lecithin, 0.50* M *sodium chloride, and 0.01* M *phosphate buffer, pH 7.4.*

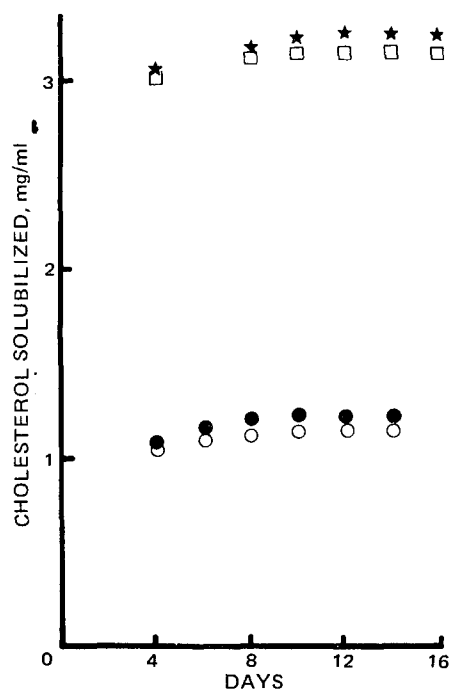

Figure 3—*Solubility of cholesterol monohydrate at 37° in two solvent media. Key:* ★, □, *in 116 m*M *cholyltaurine, 32 m*M *lecithin, 0.50* M *sodium chloride, and 0.01* M *phosphate buffer, pH 7.4; and* ●, ○, *in 46.4 m*M *cholyltaurine, 12.8 m*M *lecithin, 0.50* M *sodium chloride, and 0.01* M *phosphate buffer, pH 7.4.*

Table IV—Influence of Calcium Chloride Concentration on Solubility (C_s), Dissolution Rate (J/A), Total Resistance (R), and $1/P$ of Cholesterol Monohydrate in 116 mM Bile Acid–32 mM Lecithin Solutions

Bile Acid	Calcium Chloride, M	C_s, mg/cm^3	$(J/A) \times 10^4$, mg/cm^2 sec	$R \times 10^{-3}$, sec/cm	$(1/P) \times 10^{-3}$, sec/cm
I	0.0250	4.04	2.56	15.8	13.5
	0.050	4.35	5.37	8.10	5.80
III	0.050	3.34	1.64	20.4	18.1
	0.10	3.78	2.76	13.7	11.4
IV	0.050	3.69	3.27	11.3	9.0
	0.10	4.14	5.30	7.81	5.51

concentration. Again, the differences among bile acids were pronounced.

Figure 11 indicates that as the bile acid–lecithin molar ratio was increased from 2.72 to 5.44 with the lecithin concentration kept constant at 32 mM, a gradual reduction of R was obtained. Striking differences were again observed among bile acids. Extremely large R values were observed for III and IV at 0.25 M sodium chloride at the lowest bile acid–lecithin ratio of 2.72.

DISCUSSION

Surface-Controlled *versus* Diffusion-Controlled Kinetics—An evaluation of the magnitude of h/D (Eq. 1) permits the assessment of the relative importance of the two resistances involved in cholesterol dissolution kinetics. Representative cholesterol diffusivity determinations were carried out (18) over the range of conditions reported in the present study, and the D values were generally in the range of $1.0–1.5 \times 10^{-6}$ cm^2/sec. These values were in good agreement with those recently reported by Sehlin *et al.* (30) for similar situations. An h value of 62 μm was determined for the present system with benzoic acid as a reference compound (19). Then, by assuming the relationship of:

$$\frac{h_1}{h_2} = \left(\frac{D_1}{D_2}\right)^{1/3} \qquad \text{(Eq. 6)}$$

and using an average D value of 1.25×10^{-6} cm^2/sec for micellar cholesterol and $D = 14.0 \times 10^{-6}$ cm^2/sec for benzoic acid (11), the effective h for the cholesterol–micelle system was found to be 28.2 μm. Hence, an h/D value for the cholesterol–bile acid–lecithin system of 2.3×10^3 sec/cm may be estimated.

Thus, for most conditions (Tables I–V), $h/D \ll 1/P$. This finding underscores the earlier suggestion (9–11) that the interfacial barrier may indeed be the dominant rate-determining factor in cholesterol gallstone and cholesterol monohydrate dissolution.

The results of this study and similar investigations using human gallbladder bile (20) have great bearing on the issue of whether cholesterol gallstone dissolution rate accelerators have a place *in vivo*. Recent clinical studies (1–4) showed that cholesterol gallstones may be dissolved by the oral administration of chenodeoxycholic acid. In most instances, however, the treatment times were long, often extending beyond 12 months and sometimes to 36 months.

It was suggested earlier (9–11), on the basis of limited studies, that the dissolution of cholesterol gallstones may be controlled by an interfacial barrier rather than by a diffusion–convection barrier and, therefore, offers a very attractive "handle" in seeking out potential agents that may act as dissolution rate accelerators. It had been apparent for some time (31) that, if stone dissolution was primarily diffusion–convection controlled, a purely medical approach involving the use of an agent coadministered with chenodeoxycholic acid would not be promising. Since bile itself is such an efficient solubilizing agent, increases in dissolution rates based upon a solubility-enhancing principle were expected to offer at best around 50% increases under the most favorable conditions.

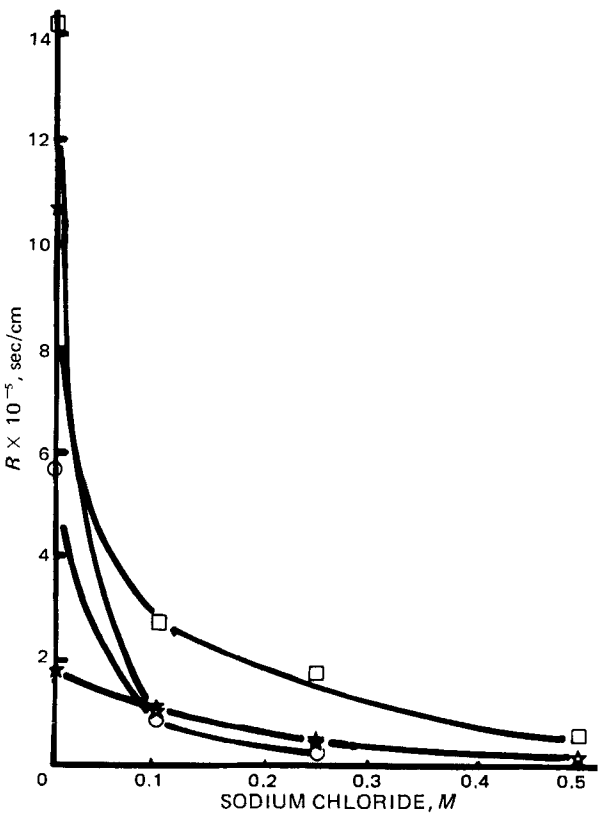

Figure 4—*Effect of sodium chloride on* R *in 116 m*M *bile acid, 32 m*M *lecithin, and 0.01* M *phosphate buffer, pH 7.4, at 37°. Key:* ○, *I;* ★, *II;* ☆, *III; and* □, *IV.*

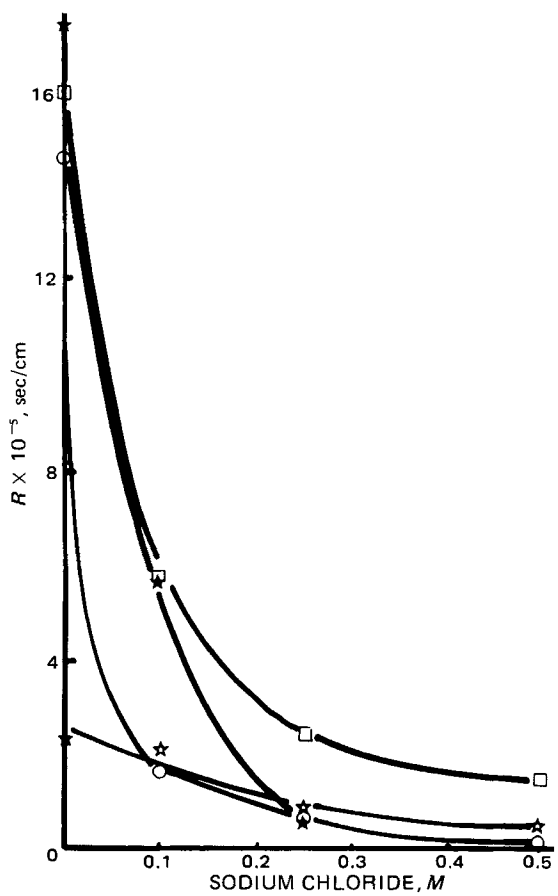

Figure 5—*Effect of sodium chloride on* R *in 46.4 m*M *bile acid, 12.8 m*M *lecithin, and 0.01* M *phosphate buffer, pH 7.4, at 37°. Key:* ○, *I;* ★, *II;* ☆, *III; and* □, *IV.*

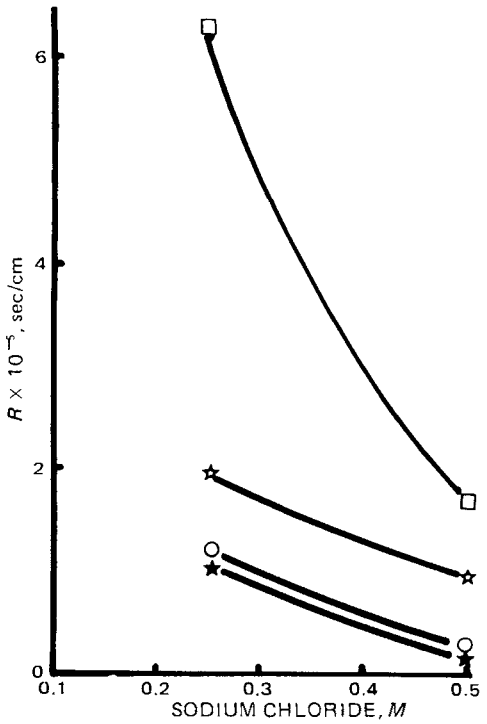

Figure 6—*Effect of sodium chloride on* R *in 23.2 m*M *bile acid, 6.4 m*M *lecithin, and 0.01* M *phosphate buffer, pH 7.4, at 37°. Key:* ○, *I;* ★, *II;* ☆, *III; and* □, *IV.*

The interfacial barrier and dissolution rate acceleration concepts based upon this premise were subsequently tested in a series of limited *in vitro* studies (10, 11) in which sodium cholate–lecithin and sodium taurocholate–lecithin were employed as synthetic biles. Under the prevailing *in vitro* hydrodynamic conditions, interfacial resistances up to around 20–50 times larger than diffusion–convection mass transfer resistances were present. Furthermore, a large number of compounds (32) were found to be effective dissolution accelerators and, in some cases, yielded dissolution rate increases up to 20–50 times the control rates.

Table V—Influence of Bile Acid Concentration on Solubility (C_s), Dissolution Rate (J/A), Total Resistance (R), and $1/P$ of Cholesterol Monohydrate in Solutions Containing 32 m*M* Lecithin, 0.25 *M* Sodium Chloride, and 0.01 *M* Phosphate Buffer at pH 7.40

Bile Acid	Parameter	Bile Acid–Lecithin Molar Ratio 2.72	3.63	5.44
I	C_s [a]	3.68	4.17	4.51
	(J/A) [b] $\times 10^4$	0.99	1.64	3.13
	R [c] $\times 10^{-3}$	37.2	25.4	14.4
	$(1/P)$ [c] $\times 10^{-3}$	34.9	23.1	12.1
II	C_s	3.71	4.32	4.80
	$(J/A) \times 10^4$	0.548	1.10	2.74
	$R \times 10^{-3}$	67.7	39.3	17.5
	$(1/P) \times 10^{-3}$	65.4	37.0	15.2
III	C_s	2.82	3.07	3.90
	$(J/A) \times 10^4$	0.182	0.685	1.93
	$R \times 10^{-3}$	155	44.8	20.2
	$(1/P) \times 10^{-3}$	152.7	42.5	17.9
IV	C_s	3.32	3.45	3.84
	$(J/A) \times 10^4$	0.0520	0.200	0.730
	$R \times 10^{-3}$	638	173	52.6
	$(1/P) \times 10^{-3}$	635.7	170.7	50.3

[a] In mg cm^{-3}. [b] In mg cm^{-2} sec^{-1}. [c] In sec cm^{-1}.

The major unsolved problem is the lack of understanding of the nature of the flow of bile in the human gallbladder. To relate past and present studies meaningfully to the question of whether the interfacial barrier can be *clinically* important requires an estimate of the time average value for *h, in vivo,* or an alternative estimate of the time average diffusion–

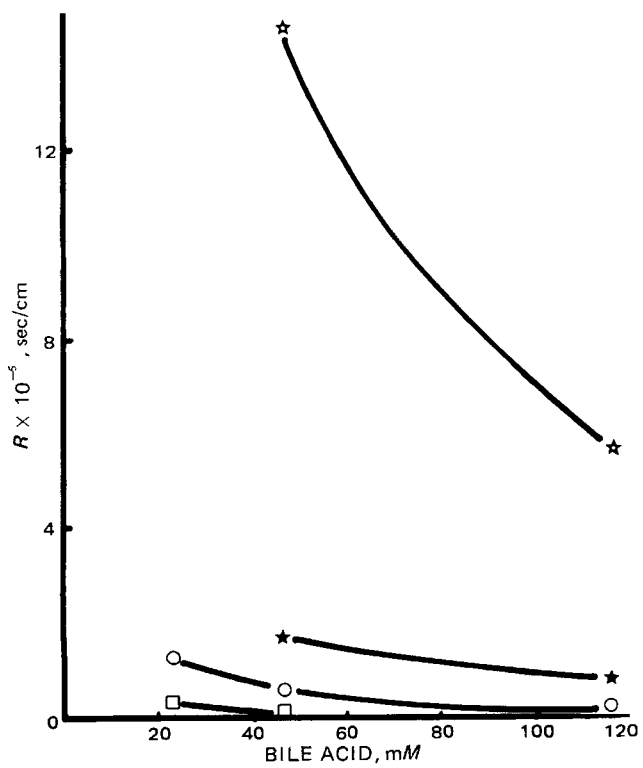

Figure 7—*Effect of I concentration on* R *at various sodium chloride concentrations with the bile acid–lecithin molar ratio kept constant at 3.63. Key:* ☆, *no sodium chloride;* ★, *0.10* M *sodium chloride;* ○, *0.25* M *sodium chloride; and* □, *0.50* M *sodium chloride.*

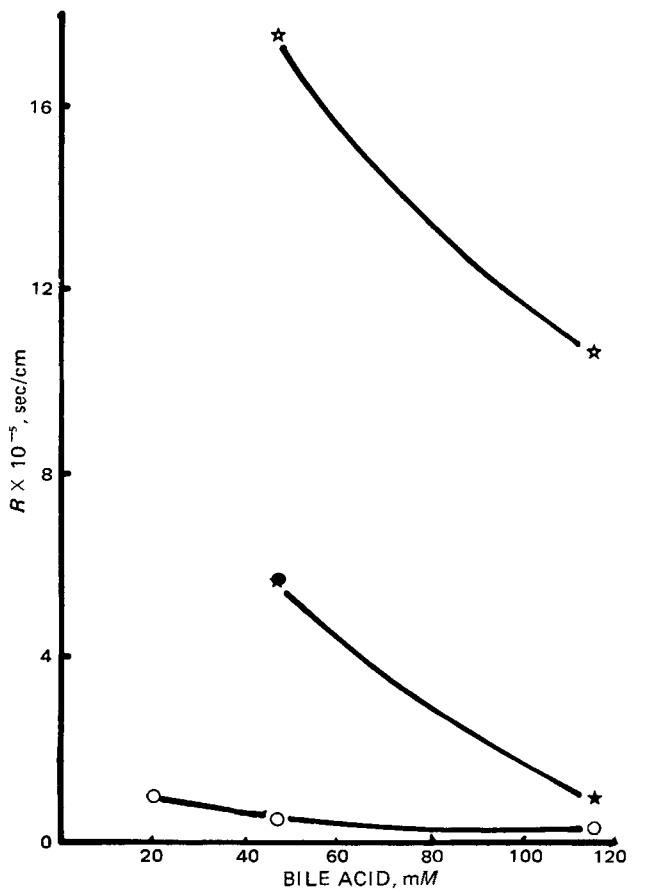

Figure 8—*Effect of II concentration on* R *at various sodium chloride concentrations with the bile acid–lecithin molar ratio kept constant at 3.63. Key:* ☆, *no sodium chloride;* ★, *0.10* M *sodium chloride; and* ○, *0.25* M *sodium chloride.*

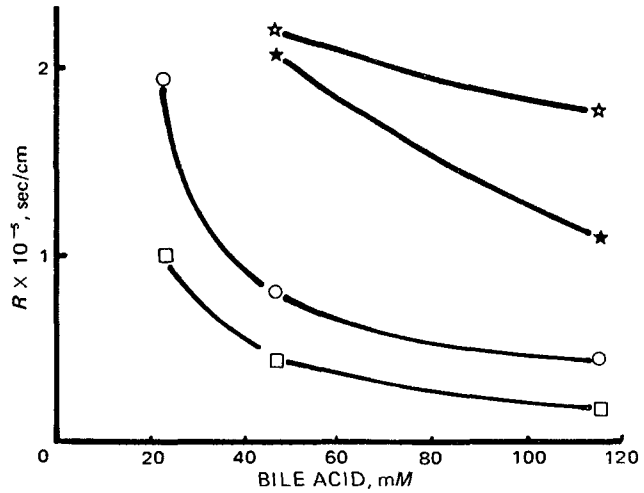

Figure 9—*Effect of III concentration on* R *at various sodium chloride concentrations with the bile acid–lecithin molar ratio kept constant at 3.63. Key:* ☆, *no sodium chloride;* ★, *0.10* M *sodium chloride;* ○, *0.25* M *sodium chloride; and* □, *0.50* M *sodium chloride.*

convection mass transfer coefficient as suggested, for example, by Tao *et al.* (31). The problem is difficult because of the irregularity of bile flow rates and general gallbladder dynamics.

Based upon what is generally considered to be the range of h values for natural (free) convection and/or slow bile flow, however, an estimate for the time average h may be proposed (9, 18, 33, 34). Previously (9, 18), an h value of around 200 μm was suggested as a reasonable upper limit, *i.e.*, for slow bile flow and/or free convection. Subsequently, Tao *et al.* (31), arguing that slow bile flow should result primarily from free convection, gave an estimate of the range for the mass transfer coefficient, K, for cholesterol stone dissolution in bile. Figure 3 of Ref. 31 shows that this range is $0 \leq K \cong 1.5 \times 10^{-4}$ cm/sec. Since:

$$K = \frac{D}{h} \qquad \text{(Eq. 7)}$$

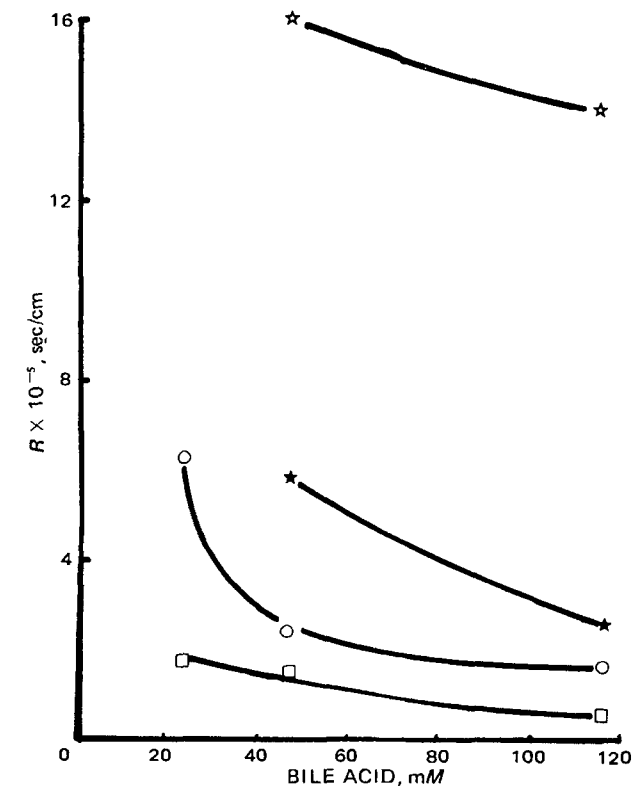

Figure 10—*Effect of IV concentration on* R *at various sodium chloride concentrations with the bile acid–lecithin ratio kept constant at 3.63. Key:* ☆, *no sodium chloride;* ★, *0.10* M *sodium chloride;* ○, *0.25* M *sodium chloride; and* □, *0.50* M *sodium chloride.*

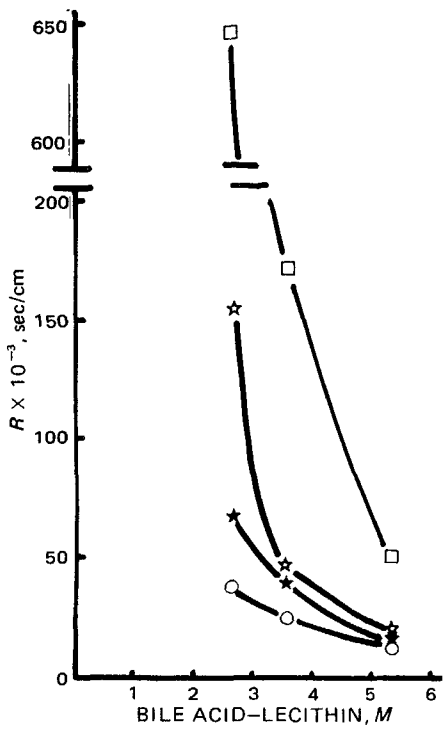

Figure 11—*Effect of bile acid–lecithin molar ratio on* R *for various bile acids in the presence of 0.25* M *sodium chloride and 0.01* M *phosphate buffer at pH 7.4 with the lecithin concentration kept constant at 32 m*M. *Key:* □, *IV;* ☆, *III;* ★, *II; and* ○, *I.*

when Eq. 2 is considered, with $D = 1.8 \times 10^{-6}$ cm²/sec, $\infty \gtrsim h \cong 120$ μm, therefore giving an independent assessment of what might be a reasonable range for h *in vivo*. Thus, an h value of around 200 μm should be a reasonable (or, at least, a reasonably liberal) estimate of the effective diffusion–convection barrier. This value would approximately correspond to the midpoint of the range for slow flow suggested by Tao *et al.* (31).

At this point, it is instructive to compare the proposed $(h/D)_{in\ vivo} = 1.6 \times 10^4$ sec/cm value (for $h = 200$ μm and $D = 1.25 \times 10^{-6}$ cm²/sec) with the $1/P$ values given in Tables I–V. While in some cases the values are comparable, $1/P \gg (h/D)_{in\ vivo}$ in many instances. Several aspects in this connection are noteworthy.

First, even at 0.10–0.25 *M* NaCl levels, which may be considered to be physiological, the $1/P$ values for the bile acid–lecithin ratio of 3.63 are two to 40 times larger than the diffusion–convection resistance estimate of 1.6×10^4 sec/cm (Tables I–III). This indicates the probable dominance of the interfacial resistance over the diffusion–convection resistance *in vivo* in certain situations.

The second noteworthy aspect is the situation involving the bile acid–lecithin ratio. At the high bile acid–lecithin ratio of 5.44, the interfacial resistance may only be comparable to the diffusion–convection resistance in the case of I and II and moderately larger for III and IV. However, at the bile acid–lecithin ratio of 2.72, the results indicate that the interfacial resistance may become the strongly dominating resistance in bile with $1/P$ values as high as 6×10^5 sec/cm. Apropos to this point are the recent experiments (20) employing human gallbladder bile taken from patients during surgery, where values for $1/P$ of around 3×10^5 sec/cm were found with bile from two patients having bile acid–lecithin ratios of 2.3 and 2.9. This result corresponds to a dominance of the interfacial resistance over the diffusion–convection resistance by a factor of 20. These very large $1/P$ values, which are believed to be clinically significant, may be contrasted with the smaller values ($2.5–5 \times 10^4$) found (20) with several specimens for which the bile acid–lecithin ratios were high—*viz.*, $\gtrsim 3.6$. When it is noted that about 30% of the 20 human bile samples investigated thus far in these laboratories showed bile acid–lecithin ratios $\cong 2.7$, one may infer that the interfacial resistance may be a substantial rate-determining factor in cholesterol stone dissolution in a large fraction of the population undergoing chenodeoxycholic acid treatment[10].

[10] Data on bile acid–lecithin ratios taken from published reports (35–37) were also considered. Analyses made of 66 human bile samples revealed that about 19 had bile acid–lecithin ratios $\gtrsim 2.7$, in good agreement with the present results.

REFERENCES

(1) R. G. Danzinger, A. F. Hofmann, L. J. Schoenfield, and J. L. Thistle, *N. Engl. J. Med.*, **286**, 1 (1972).

(2) J. L. Thistle and A. F. Hofmann, *ibid.*, **289**, 655 (1973).

(3) R. G. Danzinger, A. F. Hofmann, J. L. Thistle, and L. J. Schoenfield, *J. Clin. Invest.*, **52**, 2809 (1973).

(4) G. D. Bell, B. Whitney, and R. H. Dowling, *Lancet*, **2**, 1213 (1972).

(5) W. H. Admirand and D. M. Small, *J. Clin. Invest.*, **47**, 1043 (1968).

(6) D. M. Small, *Adv. Intern. Med.*, **16**, 243 (1970).

(7) H. Dam and F. G. Hegardt, *Z. Ernaehrungswiss.*, **10**, 239 (1971).

(8) D. H. Gregory, Z. R. Vlahcevic, and L. Swell, *Am. J. Dig. Dis.*, **19**, 268 (1974).

(9) W. I. Higuchi, F. Sjuib, D. Mufson, A. P. Simonelli, and A. F. Hofmann, *J. Pharm. Sci.*, **62**, 942 (1973).

(10) W. I. Higuchi, S. Prakongpan, V. Surpuriya, and F. Young, *Science*, **178**, 633 (1972).

(11) W. I. Higuchi, S. Prakongpan, and F. Young, *J. Pharm. Sci.*, **62**, 945 (1973).

(12) "Geigy Scientific Tables," 7th ed., Geigy Pharmaceuticals, Ardsley, N.Y., 1973, pp. 653–656.

(13) A. Berthoud, *J. Chim. Phys.*, **10**, 624 (1912).

(14) W. Nernst and E. Brunner, *Z. Phys. Chem.*, **47**, 52 (1904).

(15) D. P. Gregory and A. C. Riddiford, *J. Chem. Soc.*, **1956**, 3756.

(16) V. G. Levich, "Physicochemical Hydrodynamics," Prentice-Hall, Englewood Cliffs, N.J., 1962.

(17) S. Prakongpan, W. I. Higuchi, K. H. Kwan, and A. M. Molokhia, *J. Pharm. Sci.*, **65**, 685 (1976).

(18) S. Prakongpan, Ph.D. thesis, University of Michigan, Ann Arbor, Mich., 1974.

(19) C. V. King and S. S. Brodie, *J. Am. Chem. Soc.*, **59**, 1375 (1957).

(20) A. M. Molokhia, A. F. Hofmann, W. I. Higuchi, M. Tuchinda, K. Feld, S. Prakongpan, and R. G. Danzinger, *J. Pharm. Sci.*, **66**, 1101 (1977).

(21) H. Dam, I. Kruse, I. Prange, H. E. Kallehauge, H. J. Fenger, and M. K. Jensen, *Z. Ernaehrungswiss.*, **10**, 160 (1971).

(22) P. P. Nair and D. Kritchevsky, "The Bile Acids," vol. 1, Plenum, New York, N.Y., 1971.

(23) A. T. James and L. J. Morris, "New Biochemical Separations," Van Nostrand, London, England, 1964, chap. 10.

(24) H. Bogren and K. Larsson, *Biochim. Biophys. Acta*, **75**, 65 (1963).

(25) A. Norman, *Ark. Kemi*, **8**, 331 (1955).

(26) A. F. Hofmann, *Acta Chem. Scand.*, **17**, 173 (1963).

(27) J. L. Pope, *J. Lipid Res.*, **8**, 146 (1967).

(28) A. F. Hofmann, *ibid.*, **3**, 127 (1962).

(29) W. S. Singleton, M. S. Gray, M. L. Brown, and J. L. White, *J. Am. Oil Chem. Soc.*, **42**, 53 (1965).

(30) R. C. Sehlin, E. L. Cussler, and D. F. Evans, *Biochim. Biophys. Acta*, **388**, 385 (1975).

(31) J. C. Tao, E. L. Cussler, and D. F. Evans, *Proc. Natl. Acad. Sci. USA*, **71**, 3917 (1974).

(32) W. I. Higuchi, S. Prakongpan, and F. Young, *J. Pharm. Sci.*, **62**, 1207 (1973).

(33) W. E. Ranz and W. R. Marshall, *Chem. Eng. Progr.*, **48**, 146 (1952).

(34) A. P. Simonelli, D. R. Flanagan, and W. I. Higuchi, *J. Pharm. Sci.*, **57**, 1629 (1968).

(35) H. Dam, I. Kruse, H. E. Kallehauge, O. E. Hartkopp, and M. K. Jensen, *Scand. J. Clin. Lab. Invest.*, **18**, 385 (1966).

(36) Z. R. Vlahcevic, C. C. Bell, and L. Swell, *Gastroenterology*, **59**, 62 (1970).

(37) D. M. Small and S. Rapo, *N. Engl. J. Med.*, **283**, 53 (1970).

ACKNOWLEDGMENTS AND ADDRESSES

Received July 1, 1976, from the *College of Pharmacy, University of Michigan, Ann Arbor, MI 48109, and the ‡Gastroenterology Unit, Division of Gastroenterology, Department of Internal Medicine, Mayo Clinic and Mayo Foundation, Rochester, MN 55901.

Accepted for publication September 28, 1976.

Supported by Grant AM 16694 from the National Institute of Arthritis, Metabolism, and Digestive Diseases and in part by National Institutes of Health Research Grant AM 16770.

ˣ To whom inquiries should be directed.

Dissolution Rates of Model Gallstones in Human and Animal Biles and Importance of Interfacial Resistance

A. M. MOLOKHIA *, A. F. HOFMANN ‡, W. I. HIGUCHI *ˣ, M. TUCHINDA *, K. FELD *, S. PRAKONGPAN *, and R. G. DANZINGER §

Abstract □ Cholesterol monohydrate dissolution kinetics in human gallbladder bile were studied to determine the magnitudes of the *in vitro* dissolution rates, the rate resistances in human gallbladder bile, and the extent that the interfacial resistance is the rate-determining factor. Dissolution rate studies also were conducted using human duodenal bile and animal bile for comparison. The dissolution rate resistance, R, ranged from 10^4 sec/cm for chicken bile to 10^4–10^6 sec/cm for human bile. Interfacial resistance was the rate-determining factor for essentially all results. Where chemical composition data were obtained, the R values for the human bile samples were consistent with predictions made from the simulated bile studies. In two human gallbladder specimens having low bile acid–lecithin molar ratios (*i.e.*, 2.9 and 2.3), very high R values of 1.9×10^5 and 4.1×10^5 sec/cm were found. These values were in good agreement with the findings in the simulated bile studies and suggest that stone dissolution in patients with low bile acid–lecithin ratios may proceed very slowly, even when the bile is highly undersaturated with respect to cholesterol.

Keyphrases □ Cholesterol monohydrate—pellets, dissolution kinetics in human, animal, and simulated bile, effect of interfacial resistance □ Dissolution—kinetics, cholesterol monohydrate pellets in human, animal, and simulated bile, effect of interfacial resistance □ Gallstones, model—cholesterol monohydrate pellets, dissolution kinetics in human, animal, and simulated bile, effect of interfacial resistance □ Biles, various—dissolution kinetics of cholesterol monohydrate pellets in human, animal, and simulated bile, effect of interfacial resistance □ Steroids—cholesterol monohydrate pellets, dissolution kinetics in human, animal, and simulated bile, effect of interfacial resistance

Chenodeoxycholic acid is an effective agent for cholesterol gallstone dissolution in humans (1), but relatively lengthy treatment times are necessary. In a recent evaluation of 243 patients (1), treatment times of 8–24 months were required to obtain complete gallstone dissolution. Consequently, recent investigations (2–8) have been di-

REFERENCES

(1) R. G. Danzinger, A. F. Hofmann, L. J. Schoenfield, and J. L. Thistle, *N. Engl. J. Med.*, **286**, 1 (1972).

(2) J. L. Thistle and A. F. Hofmann, *ibid.*, **289**, 655 (1973).

(3) R. G. Danzinger, A. F. Hofmann, J. L. Thistle, and L. J. Schoenfield, *J. Clin. Invest.*, **52**, 2809 (1973).

(4) G. D. Bell, B. Whitney, and R. H. Dowling, *Lancet*, **2**, 1213 (1972).

(5) W. H. Admirand and D. M. Small, *J. Clin. Invest.*, **47**, 1043 (1968).

(6) D. M. Small, *Adv. Intern. Med.*, **16**, 243 (1970).

(7) H. Dam and F. G. Hegardt, *Z. Ernaehrungswiss.*, **10**, 239 (1971).

(8) D. H. Gregory, Z. R. Vlahcevic, and L. Swell, *Am. J. Dig. Dis.*, **19**, 268 (1974).

(9) W. I. Higuchi, F. Sjuib, D. Mufson, A. P. Simonelli, and A. F. Hofmann, *J. Pharm. Sci.*, **62**, 942 (1973).

(10) W. I. Higuchi, S. Prakongpan, V. Surpuriya, and F. Young, *Science*, **178**, 633 (1972).

(11) W. I. Higuchi, S. Prakongpan, and F. Young, *J. Pharm. Sci.*, **62**, 945 (1973).

(12) "Geigy Scientific Tables," 7th ed., Geigy Pharmaceuticals, Ardsley, N.Y., 1973, pp. 653–656.

(13) A. Berthoud, *J. Chim. Phys.*, **10**, 624 (1912).

(14) W. Nernst and E. Brunner, *Z. Phys. Chem.*, **47**, 52 (1904).

(15) D. P. Gregory and A. C. Riddiford, *J. Chem. Soc.*, **1956**, 3756.

(16) V. G. Levich, "Physicochemical Hydrodynamics," Prentice-Hall, Englewood Cliffs, N.J., 1962.

(17) S. Prakongpan, W. I. Higuchi, K. H. Kwan, and A. M. Molokhia, *J. Pharm. Sci.*, **65**, 685 (1976).

(18) S. Prakongpan, Ph.D. thesis, University of Michigan, Ann Arbor, Mich., 1974.

(19) C. V. King and S. S. Brodie, *J. Am. Chem. Soc.*, **59**, 1375 (1957).

(20) A. M. Molokhia, A. F. Hofmann, W. I. Higuchi, M. Tuchinda, K. Feld, S. Prakongpan, and R. G. Danzinger, *J. Pharm. Sci.*, **66**, 1101 (1977).

(21) H. Dam, I. Kruse, I. Prange, H. E. Kallehauge, H. J. Fenger, and M. K. Jensen, *Z. Ernaehrungswiss.*, **10**, 160 (1971).

(22) P. P. Nair and D. Kritchevsky, "The Bile Acids," vol. 1, Plenum, New York, N.Y., 1971.

(23) A. T. James and L. J. Morris, "New Biochemical Separations," Van Nostrand, London, England, 1964, chap. 10.

(24) H. Bogren and K. Larsson, *Biochim. Biophys. Acta*, **75**, 65 (1963).

(25) A. Norman, *Ark. Kemi*, **8**, 331 (1955).

(26) A. F. Hofmann, *Acta Chem. Scand.*, **17**, 173 (1963).

(27) J. L. Pope, *J. Lipid Res.*, **8**, 146 (1967).

(28) A. F. Hofmann, *ibid.*, **3**, 127 (1962).

(29) W. S. Singleton, M. S. Gray, M. L. Brown, and J. L. White, *J. Am. Oil Chem. Soc.*, **42**, 53 (1965).

(30) R. C. Sehlin, E. L. Cussler, and D. F. Evans, *Biochim. Biophys. Acta*, **388**, 385 (1975).

(31) J. C. Tao, E. L. Cussler, and D. F. Evans, *Proc. Natl. Acad. Sci. USA*, **71**, 3917 (1974).

(32) W. I. Higuchi, S. Prakongpan, and F. Young, *J. Pharm. Sci.*, **62**, 1207 (1973).

(33) W. E. Ranz and W. R. Marshall, *Chem. Eng. Progr.*, **48**, 146 (1952).

(34) A. P. Simonelli, D. R. Flanagan, and W. I. Higuchi, *J. Pharm. Sci.*, **57**, 1629 (1968).

(35) H. Dam, I. Kruse, H. E. Kallehauge, O. E. Hartkopp, and M. K. Jensen, *Scand. J. Clin. Lab. Invest.*, **18**, 385 (1966).

(36) Z. R. Vlahcevic, C. C. Bell, and L. Swell, *Gastroenterology*, **59**, 62 (1970).

(37) D. M. Small and S. Rapo, *N. Engl. J. Med.*, **283**, 53 (1970).

ACKNOWLEDGMENTS AND ADDRESSES

Received July 1, 1976, from the *College of Pharmacy, University of Michigan, Ann Arbor, MI 48109, and the ‡Gastroenterology Unit, Division of Gastroenterology, Department of Internal Medicine, Mayo Clinic and Mayo Foundation, Rochester, MN 55901.

Accepted for publication September 28, 1976.

Supported by Grant AM 16694 from the National Institute of Arthritis, Metabolism, and Digestive Diseases and in part by National Institutes of Health Research Grant AM 16770.

ˣ To whom inquiries should be directed.

Dissolution Rates of Model Gallstones in Human and Animal Biles and Importance of Interfacial Resistance

A. M. MOLOKHIA *, A. F. HOFMANN ‡, W. I. HIGUCHI *ˣ, M. TUCHINDA *, K. FELD *, S. PRAKONGPAN *, and R. G. DANZINGER §

Abstract □ Cholesterol monohydrate dissolution kinetics in human gallbladder bile were studied to determine the magnitudes of the *in vitro* dissolution rates, the rate resistances in human gallbladder bile, and the extent that the interfacial resistance is the rate-determining factor. Dissolution rate studies also were conducted using human duodenal bile and animal bile for comparison. The dissolution rate resistance, R, ranged from 10^4 sec/cm for chicken bile to 10^4–10^6 sec/cm for human bile. Interfacial resistance was the rate-determining factor for essentially all results. Where chemical composition data were obtained, the R values for the human bile samples were consistent with predictions made from the simulated bile studies. In two human gallbladder specimens having low bile acid–lecithin molar ratios (*i.e.*, 2.9 and 2.3), very high R values of 1.9×10^5 and 4.1×10^5 sec/cm were found. These values were in good agreement with the findings in the simulated bile studies and suggest that stone dissolution in patients with low bile acid–lecithin ratios may proceed very slowly, even when the bile is highly undersaturated with respect to cholesterol.

Keyphrases □ Cholesterol monohydrate—pellets, dissolution kinetics in human, animal, and simulated bile, effect of interfacial resistance □ Dissolution—kinetics, cholesterol monohydrate pellets in human, animal, and simulated bile, effect of interfacial resistance □ Gallstones, model—cholesterol monohydrate pellets, dissolution kinetics in human, animal, and simulated bile, effect of interfacial resistance □ Biles, various—dissolution kinetics of cholesterol monohydrate pellets in human, animal, and simulated bile, effect of interfacial resistance □ Steroids—cholesterol monohydrate pellets, dissolution kinetics in human, animal, and simulated bile, effect of interfacial resistance

Chenodeoxycholic acid is an effective agent for cholesterol gallstone dissolution in humans (1), but relatively lengthy treatment times are necessary. In a recent evaluation of 243 patients (1), treatment times of 8–24 months were required to obtain complete gallstone dissolution. Consequently, recent investigations (2–8) have been di-

Table I—Effect of Centrifugation on Human Gallbladder Bile Lipids

Bile Sample	Before Centrifugation: Bile Acids, μmoles/ml	Lecithin, μmoles/ml	Bile Acid/ Lecithin Ratio	Cholesterol, μmoles/ml	After Centrifugation: Bile Acids, μmoles/ml	Lecithin, μmoles/ml	Bile Acid/ Lecithin Ratio	Cholesterol, μmoles/ml
1	195.0	57.1	3.4	9.6	194.1	41.3	4.7	6.1
2	95.4	36.8	2.6	13.4	77.2	34.4	2.3	6.4
3	232.4	80.9	2.9	35.5	219.0	82.9	2.6	13.8

rected toward a better understanding of the kinetics of cholesterol gallstone dissolution and of methods for accelerating stone dissolution in patients under chenodeoxycholic acid therapy and in other situations, *e.g.*, the dissolution of retained common duct stones.

The physical model approach by Higuchi *et al.* (2) suggested that the dissolution of cholesterol gallstones *in vivo* may be rate limited by surface resistance to micellar solubilization rather than by the conventional diffusion–convection mass transfer of cholesterol molecules from the stone surface into the bile media. Further investigations (3–7) showed that *in vitro* cholesterol dissolution in simulated bile solutions was 20–100 times slower than predicted by the diffusion–convection-controlled mechanism. That the rate-limiting step for dissolution could be a surface reaction also was supported by the finding (6, 7) that the addition of a small amount of a dissolution rate accelerator for cholesterol, such as benzalkonium chloride, dramatically enhanced the dissolution process to a point where the rates were almost identical to those predicted by the physical model for "diffusion-controlled" kinetics.

The primary purpose of this study was to examine the cholesterol monohydrate dissolution kinetics in human gallbladder bile to determine the magnitudes of the *in vitro* dissolution rates and the rate resistances for cholesterol monohydrate pellets in human gallbladder bile compared to simulated bile. Dissolution rate experiments also were conducted using human bile samples obtained by duodenal drainage as well as gallbladder bile from several animals.

EXPERIMENTAL

Materials—*Bile*—Human gallbladder bile was collected by aspiration from patients undergoing cholecystectomy and was frozen. Before the experiments, the human gallbladder bile samples were thawed and centrifuged[1] for 30 min at 100,000×*g*, and the supernates were used. One sample was taken from a patient receiving chenodeoxycholic acid therapy; the others were from regular patients. Human duodenal bile was collected by duodenal aspiration after cholecystokinin injection from patients who were receiving chenodeoxycholic acid for about 1 year. The bile was then filtered through a 0.22-μm filter[2] and frozen prior to use.

Baboon gallbladder bile[3] from control animals and from animals fed with chenodeoxycholic acid, dog gallbladder bile[4], and chicken gallbladder bile[5] were filtered through 0.22-μm filters[2] and frozen prior to use.

Cholesterol—4-^{14}C-Cholesterol monohydrate was recrystallized from 95% ethanol (3). For the dissolution experiments, about 100 mg of cholesterol monohydrate crystals was compressed[6] in a 1.27-cm diameter die under a pressure of 1362 kg (3000 lb).

General Design Considerations—To achieve the primary goals of this study, it would have been ideal to experiment with freshly collected human gallbladder bile. However, for two important reasons, fresh bile was not used.

First, most specimens of human gallbladder bile under normal conditions are nearly saturated or supersaturated with cholesterol. Therefore, dissolution rate experiments would be either impossible or practically unsuitable unless the cholesterol levels were lowered significantly by some means without seriously altering the other bile constituents.

Second, the bile specimens had to be shipped several hundred miles by air and some means for preservation was needed. Freezing of the bile, thawing, and then centrifuging prior to the experiments solved both of these problems. Invariably, the cholesterol levels of the supernates were significantly lowered while the phospholipid and bile acid levels were altered little or none at all by this procedure. Also, the transporting of the bile was convenient and routine. Bile samples were received frozen and were transferred immediately to a freezer for storage until the experiment.

Because of the relatively small amounts (~15 ml) of human gallbladder bile available from each patient and because future plans include evaluating patient-to-patient variations in the cholesterol dissolution rate properties of bile, a smaller dissolution apparatus than used previously (3) was designed. It consisted of similar components, *i.e.*, a stirrer attached to a constant-speed motor (150 rpm), a water-jacketed beaker, and a die holding the compressed cholesterol monohydrate pellet. The hydrodynamic conditions were assessed from the dissolution rate of a benzoic acid pellet in 0.01 *N* hydrochloric acid solution, which is known to be a diffusion–convection-controlled process (9).

Effect of Centrifugation on Human Gallbladder Bile Lipids—Three human gallbladder bile samples were thawed for 1 hr at 37°, and then each was divided into two portions. One was immediately centrifuged[1] for 30 min at 100,000×*g*, and then 1.0 ml of the supernate was pipetted into 9 ml of 2-propanol for lipid analysis. The second portion was agitated on a wrist-action shaker[7] at 37° for 24 hr to disperse any insoluble matter. Then 1.0 ml of the mixture was pipetted into 9 ml of 2-propanol for analysis.

Solubility Determination—About 30 mg of ^{14}C-cholesterol monohydrate crystals was added to 2 ml of bile in a 15-ml firmly stoppered test tube, and the suspension was continuously agitated in a wrist-action shaker[7]. Samples of 0.1 ml were taken after 3 days and every other day thereafter until the cholesterol analysis indicated a constant solubility. Each sample was filtered through glass wool before analysis in a liquid scintillation counter[8]. These data represented the differences between the actual solubility, C_s, and the initial concentration of cholesterol, C_b. In addition, both C_b and C_s for cholesterol were determined for a number of samples by the colorimetric method of Sperry and Webb (10).

Dissolution Rate Determination—Exactly 10 ml[9] of bile was used for each run, and the cholesterol dissolution experiments were carried out as described previously (3), except that 0.2-ml samples were taken for determining the total amount dissolved at each time interval by means of liquid scintillation counting.

Diffusivity Measurements—The small diaphragm cell employed previously (3, 7) was used for the determination of cholesterol diffusivity in human duodenal and dog gallbladder bile samples.

Analysis of Biliary Lipids—Total bile acids were determined using an automated steroid dehydrogenase procedure (11). Phospholipids were determined colorimetrically (12) using an ethanol–ether solution of bile. Total cholesterol was determined colorimetrically after saponification and extraction into hexane using the method of Abell *et al.* (13). The solubilities of cholesterol in several bile samples were calculated based on their bile acid and lecithin contents (14) using the polynomial equations derived by Thomas and Hofmann (15).

[1] Model L3-40 ultracentrifuge, Beckman Instruments, Fullerton, Calif.
[2] Millipore Filter Corp., Bedford, Mass.
[3] Dr. C. K. McScherry, New York Hospital, Cornell Medical Center, New York, N.Y.
[4] Pel Freez Biologicals Inc., Rogers, Ark.
[5] Eastern Poultry Co., Detroit, Mich.
[6] Model B lab press, Fred Carver Inc., Summit, N.J.
[7] Burrel Corp., Pittsburgh, Pa.
[8] Beckman Instruments, Fullerton, Calif.
[9] The volume was 5 ml for baboon bile and the human gallbladder bile of the chenodeoxycholic acid-treated patient.

Table II—Comparison of the Cholesterol Solubility Determined Experimentally and the Value Calculated from the Polynomial Equation of Thomas and Hofmann (15)

Bile Sample	Bile Acids, μmoles/ml	Lecithin, μmoles/ml	Bile Acid/ Lecithin Ratio	Cholesterol C_s, μmoles/ml (Colorimetry)	Cholesterol Equivalent C_s, μmoles/ml (Calculated)
1	194.1	41.3	4.7	12.9	13.2
2	133.7	24.9	5.4	9.7	8.2
3	237.2	64.9	3.7	18.1	19.8
4	85.4	21.3	4.0	5.2	6.6

THEORETICAL

According to the Nernst diffusion theory (16), the dissolution rate of a solid solute into a liquid solvent is given by:

$$J/A = \frac{D}{h}(C_s - C_b) \quad \text{(Eq. 1)}$$

where J is the rate of dissolution, A is the area of solid–liquid contact, D is the diffusion coefficient, h is the effective diffusion layer thickness, and C_s and C_b are as previously defined.

While the factor h/D is a purely diffusional resistance in the Nernst theory, it is generally recognized (7) that, when applied to dissolution rate situations such as in this work, this factor actually represents contributions from both diffusion and convection.

For the case where the resistance to the dissolution process is associated with interactions at the crystal surface, the dissolution rate can be expressed as (2):

$$J/A = P(C_s - C_b) \quad \text{(Eq. 2)}$$

with $1/P$ representing the interfacial resistance, and P is the effective permeability coefficient across the interfacial barrier.

When both resistances—the diffusion–convection resistance and the interfacial resistance—are important, the overall dissolution rate can be given as (17):

$$J/A = \frac{C_s - C_b}{\frac{h}{D} + \frac{1}{P}} \quad \text{(Eq. 3)}$$

or:

$$J/A = \frac{C_s - C_b}{R} \quad \text{(Eq. 4)}$$

and:

$$R = \frac{h}{D} + \frac{1}{P} \quad \text{(Eq. 5)}$$

where R is the total resistance to dissolution.

When $1/P$ is negligible, Eq. 3 reduces to Eq. 1. On the other hand, when the dissolution rate is controlled by the interfacial barrier, $1/P$ is large compared to h/D and Eq. 3 reduces to Eq. 2.

In a given dissolution apparatus in which the hydrodynamics remain constant, the effective diffusion–convection resistance, h/D, for a compressed pellet dissolving in a solvent can be estimated independently. The diffusion coefficient, D, can be measured directly using a diffusion cell. The effective diffusion layer thickness, h, may be determined for a benzoic acid pellet dissolving in 0.01 N hydrochloric acid, and the corresponding h value for the particular system under investigation can then be deduced from $h \propto D^n$, where n varies from zero to one-third[10]. As will be seen in this study, the choice of the n value does not make much difference because the resistance for cholesterol dissolution in human and animal bile is always on the high side where the h/D contribution to R is relatively small.

Thus, for each dissolution experiment, if the resistance, R, calculated from the experimental results of J/A, C_s, and C_b with Eq. 4 approaches the estimated h/D value, the dissolution process is said to be fast and controlled by diffusion across the diffusion layer. If, on the other hand, the R value is significantly larger than h/D, the interfacial resistance may be important and the dissolution process is said to be slower than a diffusion-controlled process by a factor $R/(h/D)$.

[10] According to the Levich theory (18) and recent investigations with the rotating-disk dissolution apparatus (7), an h dependency on $D^{1/3}$ is obeyed. Also, for a static disk dissolution apparatus similar to the one used in this study, Prakongpan (19) recently showed that $h \propto D^{1/3}$ is a better approximation than $h \propto D^0$.

RESULTS

Effect of Centrifugation on Bile Lipids—Table I shows the effect of centrifugation on the total bile acids, lecithin, and cholesterol contents of three human gallbladder bile samples after freezing and thawing. While the changes in the bile acids and lecithin contents were relatively small, if any, the cholesterol contents were reduced significantly. The bile acid–lecithin ratios after centrifugation (Table I) remained within the physiological range.

Hydrodynamics and h/D Value for Micellar Cholesterol in Dissolution Apparatus—The baseline dissolution experiments with benzoic acid showed a linear relationship between the amount dissolved and time with a slope, J, equal to 1.23×10^{-2} mg/sec. By using Eq. 1 and substituting for the experimentally determined values of $J/A = 9.7 \times 10^{-3}$ mg/cm^2/sec, $C_s = 4.7$ mg/cm^3, and $D = 1.4 \times 10^{-5}$ cm^2/sec, an h value of 6.8×10^{-3} cm was obtained.

Because of the availability of only relatively small amounts of the human gallbladder bile and because the h/D term generally contributed little to the total resistance, R, for most situations, the diffusivity experiments with micellar cholesterol were carried out with only a few representative samples. A diffusivity value of $(1.0 \pm 0.3) \times 10^{-6}$ cm^2/sec was found with several human duodenal and dog bile specimens. This value was used to estimate the diffusion–convection resistance, h/D, for all bile samples tested. When using Eq. 6 with $n = 1/3$ and the benzoic acid dissolution data, an effective diffusion layer thickness of 2.82×10^{-3} cm was obtained for the cholesterol–bile micellar system. This value corresponds to an h/D value of 2.82×10^3 sec/cm.

Cholesterol Monohydrate Dissolution in Human Gallbladder Bile—Table II compares the cholesterol solubilities, C_s, determined colorimetrically for some bile samples with the values calculated as described previously (15) from the Hegardt and Dam (14) relationship based on the bile acid and lecithin contents of these bile specimens. The experimental and calculated values were in good agreement.

Table III summarizes the dissolution rates, solubilities, and resistances to dissolution of cholesterol monohydrate in 10 human gallbladder bile samples. For the three samples in which the cholesterol monohydrate values of $(C_s - C_b)$ were determined both colorimetrically and by the ^{14}C-analysis, good agreement between the two techniques was obtained. The R values, calculated using Eq. 4, ranged from 10×10^3 to 400×10^3 sec/cm. Bile Sample 8, obtained from a patient receiving chenodeoxycholic acid therapy, showed an R value of 40.3×10^3 sec/cm, which was in the range for the normals studied in this investigation.

As discussed, the h/D value was 2.82×10^3 sec/cm for these experiments. Thus, $(h/D) \ll (1/P)$ for essentially all R values given in Table III. Therefore, the interfacial resistance factor dominated the dissolution kinetics with all tested samples.

Cholesterol Monohydrate Dissolution in Human Duodenal Bile—Table IV shows the results of cholesterol monohydrate dissolution in two human duodenal bile samples. The dissolution rates were much lower and the R values were much larger with the duodenal bile than with the gallbladder bile. Experiments with other human duodenal bile samples gave R values that were always at least as large as those shown in Table IV. The addition of 1.25% benzalkonium chloride to the two samples increased the $(C_s - C_b)$ value up to sixfold and decreased R by about 100-fold.

Cholesterol Monohydrate Dissolution in Animal Bile—The data presented in Table V show that the resistance to cholesterol monohydrate dissolution was the highest in baboon bile and the lowest in chicken bile. The bile collected from chenodeoxycholic acid-fed baboons showed about the same resistance as that of the bile collected from normal baboons.

The two dog gallbladder bile samples examined gave almost the same resistance values. While the addition of 1.25% benzalkonium chloride to Sample I showed no effect on cholesterol solubility, a threefold decrease in the resistance was observed. The effect of dilution on cholesterol dissolution was studied by diluting an aliquot of Sample I with an equal

Table III—Dissolution Rates, Solubilities, and Transport Resistances of Cholesterol Monohydrate in Human Gallbladder Bile

Sample	Bile Acid/ Lecithin Ratio	$(J/A) \times 10^4$, mg/cm²/sec	Cholesterol after Centrifuging, C_b, μmoles/ml (Colorimetry)	Solubility, C_s, μmoles/ml (Colorimetry)	$C_s - C_b$, μmoles/ml (Radiometry)	$C_s - C_b$, μmoles/ml (Colorimetry)	$R^a \times 10^{-3}$, sec/cm
1	4.70	1.23	3.88	12.9	8.5	9.02	26.63
2	—	0.05	—	—	0.623	—	48.2
3	—	0.38	3.88	—	5.2	—	52.84
4	5.38	0.44	4.20	9.7	3.45	5.5	30.59
5	3.65	1.13	7.95	18.1	11.75	10.15	40.13
6	4.00	0.391	—	5.2	1.00	—	9.87
7	4.46	1.42	7.75	—	9.02	—	24.50
8[b]	3.71	0.27	—	—	2.84	—	40.30
9	2.29	0.3125	—	—	14.53	—	187.8
10	2.93	0.0684	—	—	6.98	—	412.3

[a] Calculated from Eq. 4 and using $(C_s - C_b)$ values determined by radiolabeling. [b] Patient was receiving chenodeoxycholic acid.

volume of double-distilled water and by using the resulting mixture for cholesterol dissolution and solubility determinations. The dissolution rate in the diluted sample was about 11 times slower than that in the original sample due to a decrease in the cholesterol solubility and an increase in the resistance to dissolution.

Chicken gallbladder bile offered only a modest resistance to cholesterol dissolution of 11.5×10^3 sec/cm.

DISCUSSION

These results, the first of their kind, provide the first insights regarding the possible importance of the interfacial resistance in cholesterol gallstone dissolution in real bile. These data, together with results obtained for chemically defined "synthetic bile," should permit the assessment of whether the kinetics of gallstone dissolution may be explained and predicted on the basis of the bile acids, lecithin, and the electrolytes in the bile.

Correlation with Studies in Synthetic Bile—The ranges of the R values found in this study with human and animal bile samples were consistent with those found by Kwan *et al.* (20) with the synthetic systems. The R values for the human gallbladder biles were in the range of $25\text{–}400 \times 10^3$ sec/cm. These values were within about a factor of two of predictions (20) based upon the R values for cholesterol monohydrate dissolution in lecithin solutions of taurocholate, glycocholate, taurochenodeoxycholate, and glycochenodeoxycholate at various electrolyte concentrations. Thus, while more experiments under a wider range of conditions are required, the indications so far are that the kinetics of cholesterol gallstone dissolution may be explainable on the basis of the principal bile acids, lecithin, and the electrolytes in any particular bile.

The unusually high R values found with human gallbladder bile Samples 9 and 10 are particularly noteworthy. The significant difference between these samples and the others was the bile acid–lecithin ratio. Both samples had rather low ratios—*viz.*, 2.3 and 2.9. Although other factors, such as the electrolytes and the bile acid concentration, must be considered, the much higher R values were consistent with the trends found by Kwan *et al.* (20) with the chemically defined synthetic systems.

The human duodenally aspirated biles (Table IV) gave R values much larger than those of most gallbladder bile samples in Table III. The bile acid and lecithin concentrations and the bile acid–lecithin ratios were not determined for these samples. According to the results of Kwan *et al.* (20) for chemically defined media, however, both of these variables may significantly influence the R values. Other evidence (21) confirms that the duodenally aspirated bile is indeed more dilute (two to four times) than gallbladder bile, and the difference in R values could well be explained by the bile acid and lecithin levels as seen with the synthetic systems (20). As shown in Table V, a twofold dilution with dog bile yielded a fourfold increase in R. Clearly, however, more studies are needed to answer this question.

The results with the animal biles were also consistent with the ranges of R values observed (20) for the synthetic systems. Again, in the absence of chemical analysis data, more cannot be said at this time since several variables may be at work simultaneously.

Possible *In Vivo* Implications—The R values of $25\text{–}400 \times 10^3$ sec/cm given in Table III correspond to 10–200 times the diffusion–convection resistance for cholesterol monohydrate dissolution in the present *in vitro* experiments. Therefore, it can be said that the rates are 90–99% "surface reaction controlled" for this situation. A clinically important question is what the effect of diffusion–convection resistance might be *in vivo*. Recent assessments (20) of this problem suggest that the order of magnitude of the time average $(h/D)_{in\ vivo}$ may be 16×10^3 sec/cm. This would mean that R values of $25\text{–}400 \times 10^3$ sec/cm represent 2–25 times the diffusion–convection resistance factor. Thus, gallstone dissolution acceleration of two- to 25-fold might be maximally achievable for these cases *in vivo*.

The effectiveness of the cholesterol gallstone accelerator benzalkonium chloride is demonstrated in Table IV. The addition of 1.25% of this compound in human duodenal bile taken from patients receiving chenodeoxycholic acid treatment showed a 500-fold acceleration in rate and about a 100-fold decrease in R. The observed R value of around 4×10^3 sec/cm was within a factor of two of purely diffusion–convection-controlled kinetics for these *in vitro* experiments.

Table IV—Dissolution Rates, Solubilities, and Transport Resistances of Cholesterol Monohydrate in Human Duodenal Biles

Bile Sample[a]	$(J/A) \times 10^4$, mg/cm²/sec	$\Delta C(C_s - C_b)$, mg/ml	$R \times 10^{-3}$, sec/cm
I	0.0191	0.91	483
II	0.0124	0.46	330
I plus 1.25% benzalkonium chloride	9.7	4.20	4.3
II plus 1.25% benzalkonium chloride	7.9	2.85	3.6

[a] Bile pooled from patients after about 1 year of chenodeoxycholic acid therapy.

Table V—Dissolution Rates, Solubilities, and Transport Resistances of Cholesterol Monohydrate in Animal Bile

Animal Bile	$(J/A) \times 10^4$, mg/cm²/sec	$\Delta C(C_s - C_b)$, mg/ml	$R \times 10^{-3}$, sec/cm
Control baboon	0.072	0.74	102.8
Chenodeoxycholic acid-treated baboon	0.248	2.24	90.3
Dog I	2.71	7.60	28
Dog II	1.15	3.09	27
Dog I plus 1.25% benzalkonium chloride	9.20	7.80	8.5
Dog I, 2× dilution	0.24	2.80	120
Chicken	2.88	3.30	11.5

REFERENCES

(1) A. F. Hofmann and G. Paumgartner, "Chenodeoxycholic Acid Therapy of Gallstones," Progress Report 1975, Schattauer Verlag, Stuttgart, West Germany, 1975.

(2) W. I. Higuchi, F. Sjuib, D. Mufson, A. P. Simonelli, and A. F. Hofmann, *J. Pharm. Sci.*, **62**, 942 (1973).

(3) W. I. Higuchi, S. Prakongpan, and F. Young, *ibid.*, **62**, 945 (1973).

(4) W. I. Higuchi, S. Prakongpan, V. Surpuriya, and F. Young,

Science, **178**, 633 (1972).
(5) W. I. Higuchi, V. Surpuriya, S. Prakongpan, and F. Young, *J. Pharm. Sci.*, **62**, 695 (1973).
(6) W. I. Higuchi, S. Prakongpan, and F. Young, *ibid.*, **62**, 1207 (1973).
(7) S. Prakongpan, W. I. Higuchi, K. H. Kwan, and A. M. Molokhia, *ibid.*, **65**, 685 (1976).
(8) A. M. Molokhia, W. I. Higuchi, and A. F. Hofmann, *ibid.*, **64**, 2029 (1975).
(9) C. V. King and S. S. Brodie, *J. Am. Chem. Soc.*, **59**, 1375 (1937).
(10) W. M. Sperry and M. Webb, *J. Biol. Chem.*, **187**, 97 (1950).
(11) R. H. Palmer, in "Methods in Enzymology," vol. 15, S. P. Colowick and N. O. Kaplan, Eds., Academic, New York, N.Y., 1969, p. 280.
(12) C. H. Fiske and Y. Subbarow, *J. Biol. Chem.*, **66**, 375 (1925).
(13) L. L. Abell, B. B. Levy, B. B. Brodie, and F. E. Kendall, *ibid.*, **195**, 357 (1952).
(14) F. Hegardt and H. Dam, *Z. Ernaehrungswiss.*, **10**, 223 (1971).
(15) P. J. Thomas and A. F. Hofmann, *Gastroenterology*, **65**, 698 (1973).
(16) W. Nernst and E. Brunner, *Z. Phys. Chem.*, **47**, 52 (1904).
(17) A. Berthoud, *J. Chim. Phys.*, **10**, 624 (1912).
(18) V. G. Levich, "Physicochemical Hydrodynamics," Prentice-Hall, Englewood Cliffs, N.J., 1962.
(19) S. Prakongpan, Ph.D. dissertation, University of Michigan, Ann Arbor, Mich., 1974.
(20) K. H. Kwan, W. I. Higuchi, A. M. Molokhia, and A. F. Hofmann, *J. Pharm. Sci.*, **66**, 1094 (1977).
(21) H. Dam, I. Kruse, I. Prange, H. E. Kallehauge, H. J. Fenger, and M. K. Jensen, *Z. Ernaehrungswiss.*, **10**, 160 (1971).

ACKNOWLEDGMENTS AND ADDRESSES

Received July 1, 1976, from the *College of Pharmacy, University of Michigan, Ann Arbor, MI 48109, the ‡Gastroenterology Unit, Division of Gastroenterology, Department of Medicine, Mayo Clinic and Mayo Foundation, Rochester, MN 55901, and the §Department of Surgery, University of Manitoba, Winnipeg, Canada.

Accepted for publication September 27, 1976.

Supported by Grant AM 16694 from the National Institute of Arthritis, Metabolism, and Digestive Diseases, Grant AM 16770 from the National Institutes of Health, and a grant from the Canadian Medical Research Council.

* To whom inquiries should be directed.

Cholesterol Gallstone Dissolution Rate Accelerators I: Exploratory Investigations

K. H. KWAN *, W. I. HIGUCHI *x, A. M. MOLOKHIA *, and A. F. HOFMANN ‡

Abstract □ Various compounds that might function as cholesterol gallstone dissolution accelerators were studied. The dissolution rates of cholesterol monohydrate pellets in synthetic bile (116 m*M* sodium cholate–32 m*M* lecithin) containing the agent at various concentration levels were determined. In the absence of any dissolution rate accelerator, the dissolution kinetics for cholesterol previously were found to be interfacial resistance controlled, and the rates were around 20 times less than the diffusion-controlled rates in the present experiments. Primary, secondary, and tertiary amines and quaternary ammonium compounds were effective accelerators. When the alkyl chain lengths were long enough and/or when the agent concentrations were high enough, the dissolution rates generally approached diffusion-controlled rates. Steroidal amines generally had good activity. Anionic and nonionic surfactants had little or negative activity.

Keyphrases □ Cholesterol monohydrate—pellets, dissolution rate in synthetic bile, effect of various nitrogen-containing compounds and surfactants □ Dissolution rate—cholesterol monohydrate pellets, effect of various nitrogen-containing compounds and surfactants □ Gallstones, model—cholesterol monohydrate pellets, dissolution rate in synthetic bile, effect of various nitrogen-containing compounds and surfactants □ Bile, synthetic—dissolution rate of cholesterol monohydrate pellets, effect of various nitrogen-containing compounds and surfactants □ Amines and ammonium salts, various—effect on dissolution rate of cholesterol monohydrate pellets in synthetic bile □ Surfactants, various—effect on dissolution rate of cholesterol monohydrate pellets in synthetic bile □ Steroids—cholesterol monohydrate pellets, dissolution rate in synthetic bile, effect of various nitrogen-containing compounds and surfactants

Recent investigations (1–7) showed that a substantial interfacial resistance (or interfacial barrier) is associated with the *in vitro* dissolution of cholesterol gallstones and cholesterol monohydrate pellets in human and simulated bile (bile acid–lecithin solutions). The magnitudes of these transport resistances may be large enough (6, 7) to affect significantly the rate of cholesterol stone dissolution *in vivo*. Accordingly, rate accelerators might have therapeutic value in decreasing the time required for total gallstone dissolution in patients receiving chenodeoxycholic acid.

The purposes of this study were to explore the kinds of compounds that might function as cholesterol gallstone dissolution accelerators and to begin to define structure–activity relationships.

EXPERIMENTAL

Materials—Commercial cholesterol[1] was recrystallized three times from 95% ethanol. Radioactive cholesterol monohydrate was prepared by mixing 5 g of the recrystallized cholesterol with 100 μCi of a benzene solution of 4-^{14}C-cholesterol[2] in 400 ml of 95% ethanol at 60°. This solution was filtered while hot, and the filtrate was allowed to stand for 48 hr at room temperature. Then the cholesterol monohydrate crystals were filtered and dried *in vacuo* for 24 hr. The crystals obtained were stored in the dark in a desiccator saturated with water vapor at room temperature.

NMR studies quantitatively confirmed the monohydrate nature of the crystals. TLC studies indicated the absence of any impurities (8). X-ray crystallography[3] studies indicated that the crystals were indeed cholesterol monohydrate crystals and that they had a lattice system similar to that of cholesterol found in human biliary calculi (9). If exposed to low humidity and light, these crystals lose their water content readily.

Sodium cholate[4] and the amines[1,4,5,6] were analytical grade and were

[1] Eastman Kodak Co., Rochester, N.Y.
[2] New England Nuclear Corp., Boston, Mass.
[3] Performed by Dr. C. Nordman, Department of Chemistry, University of Michigan, Ann Arbor, Mich.
[4] Schwarz Mann, Orangeburg, N.Y.
[5] J. T. Baker Chemical Co., Phillipsburg, N.J.
[6] Lonza Inc., Fair Lawn, N.J.

Science, **178**, 633 (1972).
(5) W. I. Higuchi, V. Surpuriya, S. Prakongpan, and F. Young, *J. Pharm. Sci.*, **62**, 695 (1973).
(6) W. I. Higuchi, S. Prakongpan, and F. Young, *ibid.*, **62**, 1207 (1973).
(7) S. Prakongpan, W. I. Higuchi, K. H. Kwan, and A. M. Molokhia, *ibid.*, **65**, 685 (1976).
(8) A. M. Molokhia, W. I. Higuchi, and A. F. Hofmann, *ibid.*, **64**, 2029 (1975).
(9) C. V. King and S. S. Brodie, *J. Am. Chem. Soc.*, **59**, 1375 (1937).
(10) W. M. Sperry and M. Webb, *J. Biol. Chem.*, **187**, 97 (1950).
(11) R. H. Palmer, in "Methods in Enzymology," vol. 15, S. P. Colowick and N. O. Kaplan, Eds., Academic, New York, N.Y., 1969, p. 280.
(12) C. H. Fiske and Y. Subbarow, *J. Biol. Chem.*, **66**, 375 (1925).
(13) L. L. Abell, B. B. Levy, B. B. Brodie, and F. E. Kendall, *ibid.*, **195**, 357 (1952).
(14) F. Hegardt and H. Dam, *Z. Ernaehrungswiss.*, **10**, 223 (1971).
(15) P. J. Thomas and A. F. Hofmann, *Gastroenterology*, **65**, 698 (1973).
(16) W. Nernst and E. Brunner, *Z. Phys. Chem.*, **47**, 52 (1904).
(17) A. Berthoud, *J. Chim. Phys.*, **10**, 624 (1912).
(18) V. G. Levich, "Physicochemical Hydrodynamics," Prentice-Hall, Englewood Cliffs, N.J., 1962.
(19) S. Prakongpan, Ph.D. dissertation, University of Michigan, Ann Arbor, Mich., 1974.
(20) K. H. Kwan, W. I. Higuchi, A. M. Molokhia, and A. F. Hofmann, *J. Pharm. Sci.*, **66**, 1094 (1977).
(21) H. Dam, I. Kruse, I. Prange, H. E. Kallehauge, H. J. Fenger, and M. K. Jensen, *Z. Ernaehrungswiss.*, **10**, 160 (1971).

ACKNOWLEDGMENTS AND ADDRESSES

Received July 1, 1976, from the *College of Pharmacy, University of Michigan, Ann Arbor, MI 48109, the ‡Gastroenterology Unit, Division of Gastroenterology, Department of Medicine, Mayo Clinic and Mayo Foundation, Rochester, MN 55901, and the §Department of Surgery, University of Manitoba, Winnipeg, Canada.

Accepted for publication September 27, 1976.

Supported by Grant AM 16694 from the National Institute of Arthritis, Metabolism, and Digestive Diseases, Grant AM 16770 from the National Institutes of Health, and a grant from the Canadian Medical Research Council.

* To whom inquiries should be directed.

Cholesterol Gallstone Dissolution Rate Accelerators I: Exploratory Investigations

K. H. KWAN *, W. I. HIGUCHI *x, A. M. MOLOKHIA *, and A. F. HOFMANN ‡

Abstract □ Various compounds that might function as cholesterol gallstone dissolution accelerators were studied. The dissolution rates of cholesterol monohydrate pellets in synthetic bile (116 m*M* sodium cholate–32 m*M* lecithin) containing the agent at various concentration levels were determined. In the absence of any dissolution rate accelerator, the dissolution kinetics for cholesterol previously were found to be interfacial resistance controlled, and the rates were around 20 times less than the diffusion-controlled rates in the present experiments. Primary, secondary, and tertiary amines and quaternary ammonium compounds were effective accelerators. When the alkyl chain lengths were long enough and/or when the agent concentrations were high enough, the dissolution rates generally approached diffusion-controlled rates. Steroidal amines generally had good activity. Anionic and nonionic surfactants had little or negative activity.

Keyphrases □ Cholesterol monohydrate—pellets, dissolution rate in synthetic bile, effect of various nitrogen-containing compounds and surfactants □ Dissolution rate—cholesterol monohydrate pellets, effect of various nitrogen-containing compounds and surfactants □ Gallstones, model—cholesterol monohydrate pellets, dissolution rate in synthetic bile, effect of various nitrogen-containing compounds and surfactants □ Bile, synthetic—dissolution rate of cholesterol monohydrate pellets, effect of various nitrogen-containing compounds and surfactants □ Amines and ammonium salts, various—effect on dissolution rate of cholesterol monohydrate pellets in synthetic bile □ Surfactants, various—effect on dissolution rate of cholesterol monohydrate pellets in synthetic bile □ Steroids—cholesterol monohydrate pellets, dissolution rate in synthetic bile, effect of various nitrogen-containing compounds and surfactants

Recent investigations (1–7) showed that a substantial interfacial resistance (or interfacial barrier) is associated with the *in vitro* dissolution of cholesterol gallstones and cholesterol monohydrate pellets in human and simulated bile (bile acid–lecithin solutions). The magnitudes of these transport resistances may be large enough (6, 7) to affect significantly the rate of cholesterol stone dissolution *in vivo*. Accordingly, rate accelerators might have therapeutic value in decreasing the time required for total gallstone dissolution in patients receiving chenodeoxycholic acid.

The purposes of this study were to explore the kinds of compounds that might function as cholesterol gallstone dissolution accelerators and to begin to define structure–activity relationships.

EXPERIMENTAL

Materials—Commercial cholesterol[1] was recrystallized three times from 95% ethanol. Radioactive cholesterol monohydrate was prepared by mixing 5 g of the recrystallized cholesterol with 100 μCi of a benzene solution of 4-^{14}C-cholesterol[2] in 400 ml of 95% ethanol at 60°. This solution was filtered while hot, and the filtrate was allowed to stand for 48 hr at room temperature. Then the cholesterol monohydrate crystals were filtered and dried *in vacuo* for 24 hr. The crystals obtained were stored in the dark in a desiccator saturated with water vapor at room temperature.

NMR studies quantitatively confirmed the monohydrate nature of the crystals. TLC studies indicated the absence of any impurities (8). X-ray crystallography[3] studies indicated that the crystals were indeed cholesterol monohydrate crystals and that they had a lattice system similar to that of cholesterol found in human biliary calculi (9). If exposed to low humidity and light, these crystals lose their water content readily.

Sodium cholate[4] and the amines[1,4,5,6] were analytical grade and were

[1] Eastman Kodak Co., Rochester, N.Y.
[2] New England Nuclear Corp., Boston, Mass.
[3] Performed by Dr. C. Nordman, Department of Chemistry, University of Michigan, Ann Arbor, Mich.
[4] Schwarz Mann, Orangeburg, N.Y.
[5] J. T. Baker Chemical Co., Phillipsburg, N.J.
[6] Lonza Inc., Fair Lawn, N.J.

Table I—Effect of Primary Amines (34 m*M*) on Dissolution Rate of Cholesterol Monohydrate in 116 m*M* Sodium Cholate–32 m*M* Lecithin Solution Buffered with 0.10 *M* Phosphate at pH 7.40 and 37°

Compound	$(J/A) \times 10^4$, mg/cm² sec	C_s, mg/ml	$D \times 10^6$, cm²/sec	$R = \left(\frac{h^a}{D} + \frac{1}{P}\right) \times 10^{-3}$, sec/cm	$(h/D) \times 10^{-3}$, sec/cm	$(1/P) \times 10^{-3}$, sec/cm
—	0.96	3.00	1.50	31.5	1.84	29.66
Ia	4.77	3.20	1.50	6.71	1.84	4.87
Ib	5.98	3.70	1.44	6.19	1.92	4.27
Ic	5.35	3.52	1.41	6.58	1.96	4.62
Id	7.40	4.25	1.35	5.74	2.04	3.70
Ie	12.75	4.93	1.29	3.87	2.14	1.73

[a] h = 27.6μm for the prevailing hydrodynamic conditions.

used as received. Egg lecithin was prepared by the method of Small *et al.* (10), except that commercial egg lecithin of purified grade[4] was used as the starting material. The cholylamine[7], 20,25-diazacholesterol hydrochloride[7], and 3-amino-7α,12α-dihydroxy-5β-cholanoic acid[8] (12) were used as received.

Cholylcholamine was synthesized[9] as described by Lack and Weiner (11). 6-Aminohexanoic acid[1], sodium *N*-lauroyl sarcosinate[10], polysorbate 80[11], sodium lauryl sulfate[5], and sodium laurate[5] were analytical grade and were used as received.

Methods—The procedures adopted for the determination of the cholesterol monohydrate solubility, dissolution rate, and diffusivity in the solvent media were described previously (1). In this study, a synthetic bile system of 116 m*M* sodium cholate and 32 m*M* lecithin in 100 m*M* phosphate buffer, pH 7.4, was used. This system is believed to simulate the average human gallbladder bile concentrations of total bile acids and lecithin as well as the pH.

The experimental data are presented as J/A, the dissolution rate per unit surface area; C_s, the equilibrium solubility; and R, the total resistance to cholesterol dissolution calculated from the following equation:

$$\frac{J}{A} \approx \frac{C_s - C_b}{R} \qquad \text{(Eq. 1)}$$

with C_b, the initial cholesterol concentration in the bulk, equal to zero.

Equation 1 was derived by Berthoud (13), and R was given as:

$$R = \frac{h}{D} + \frac{1}{P} \qquad \text{(Eq. 2)}$$

where h is the effective diffusion layer thickness, D is the diffusivity, and P is the effective permeability coefficient of the interfacial barrier. The terms h/D and $1/P$ represent the contribution to the total resistance from the diffusion–convection and the interfacial barriers, respectively.

RESULTS

Straight-chain aliphatic primary (Ia–Ie), secondary (IIa and IIb), and tertiary (IIIa–IIIc) amines; quaternary ammonium salts (IVa–IVd, Va, and Vb); steroidal amines (VIa–VId); long chain nitrogen-containing compounds [6-aminohexanoic acid (VIIa) and sodium *N*-lauroyl sarcosinate (VIIb)]; one nonionic surfactant (polysorbate 80); and two anionic surfactants (sodium lauryl sulfate and sodium laurate) were screened for acceleration activity. Table I shows the effects on cholesterol dissolution rate, solubility, and dissolution resistance when primary alkylamines were added to the synthetic bile system. The addition of 34 m*M* *n*-hexylamine (Ia) to the sodium cholate–lecithin solution lowered the total resistance, R, by a factor of about 5. Increasing the number of carbon atoms of the amine and keeping the concentration constant decreased R and $1/P$. However, from C_6 to C_9 (Ia–Ic), these decreases with increasing chain length were rather modest—*viz.*, 10–20% in R per carbon atom. A much larger effect upon R was observed for the C_{10} (Id) and C_{12} (Ie) amines.

With the addition of 34 m*M* of the amine, only moderate increases in the solubility were observed in all cases. The addition of the amines to the synthetic bile system had little or no effect on the diffusivity of cholesterol. Thus, the reduction in the total resistance to cholesterol dissolution in the presence of these amines could be attributed primarily to the reduction in the interfacial resistance ($1/P$), with the diffusion–convection resistance remaining almost constant.

Tables II and III show the concentration effect of *n*-octylamine (Ib) and *n*-dodecylamine (Ie), respectively, on cholesterol dissolution. The R values decreased with increasing amine concentration. The effect on $1/P$ began to level off at concentrations above 30 m*M*.

Table IV shows the effect of the presence of 34 m*M* of some secondary and tertiary amines and quaternary ammonium salts. The resistance to

$C_nH_{2n+1}NH_2$

Ia: n = 6
Ib: n = 8
Ic: n = 9
Id: n = 10
Ie: n = 12

$C_nH_{2n+1}NH(CH_3)$

IIa: n = 8
IIb: n = 12

$C_nH_{2n+1}N(CH_3)_2$

IIIa: n = 8
IIIb: n = 10
IIIc: n = 12

$C_nH_{2n+1}N^+(CH_3)_3$ X^-

IVa: n = 12, X = Br
IVb: n = 12, X = Cl
IVc: n = 16, X = Br
IVd: n = 16, X = Cl

$(C_nH_{2n+1})_2N^+(CH_3)_2$ Cl^-

Va: n = 8
Vb: n = 10

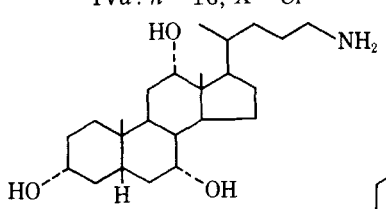

VIa

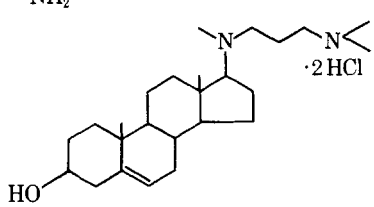

VIb

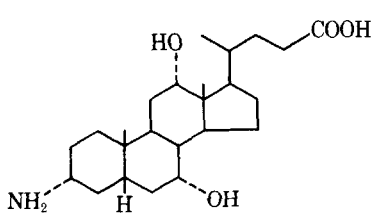

VIc

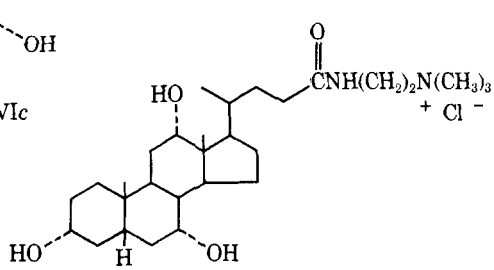

VId

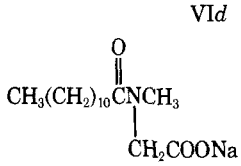

VIIb

[7] Supplied by Dr. R. Counsell, Department of Medicinal Chemistry, College of Pharmacy, University of Michigan, Ann Arbor, Mich.
[8] Supplied by Dr. A. S. Jones, Sheffield University.
[9] D. T. E. Belobaba, Mayo Clinic.
[10] Proctor and Gamble Co., Cincinnati, Ohio.
[11] Tween 80, Sargent-Welch Scientific Co., Detroit, Mich.

Table II—Effect of Concentration of I*b* on Cholesterol Monohydrate Dissolution in 116 m*M* Sodium Cholate–32 m*M* Lecithin Solution Buffered with 0.10 *M* Phosphate at pH 7.40 and 37°

Concentration, m*M*	$(J/A) \times 10^4$, mg/cm² sec	C_s, mg/ml	$D \times 10^6$, cm²/sec	$R = \left(\frac{h}{D} + \frac{1}{P}\right) \times 10^{-3}$, sec/cm	$(h/D) \times 10^{-3}$, sec/cm	$(1/P) \times 10^{-3}$, sec/cm
—	0.96	3.00	1.50	31.5	1.84	29.66
3.61	1.22	3.10	1.30	25.4	2.12	23.28
13.23	3.05	3.23	1.40	10.6	1.97	8.63
21.64	5.48	3.60	1.40	6.60	1.97	4.63
34.0	5.98	3.70	1.44	6.19	1.92	4.27

Table III—Effect of Concentration of I*e* on Cholesterol Monohydrate Dissolution in 116 m*M* Sodium Cholate–32 m*M* Lecithin Solution Buffered with 0.10 *M* Phosphate at pH 7.40 and 37°

Concentration, m*M*	$(J/A) \times 10^4$, mg/cm² sec	C_s, mg/ml	$D \times 10^6$, cm²/sec	$R = \left(\frac{h}{D} + \frac{1}{P}\right) \times 10^{-3}$, sec/cm	$(h/D) \times 10^{-3}$, sec/cm	$(1/P) \times 10^{-3}$, sec/cm
—	0.96	3.00	1.50	31.5	1.84	29.66
2.88	0.92	3.08	1.30	33.5	2.12	31.38
9.38	2.49	3.11	1.30	12.50	2.12	10.38
34.0	12.75	4.93	1.29	3.87	2.14	1.73
84.31	19.90	6.33	1.25	3.18	2.21	0.97

Table IV—Effect of 34 m*M* of Secondary and Tertiary Amines and Quaternary Ammonium Salts on Dissolution

Compound	$(J/A) \times 10^4$, mg/cm² sec	C_s, mg/ml	$D \times 10^6$, cm²/sec	$R = \left(\frac{h}{D} + \frac{1}{P}\right) \times 10^{-3}$, sec/cm	$(h/D) \times 10^{-3}$, sec/cm	$(1/P) \times 10^{-3}$, sec/cm
—	0.96	3.00	1.50	31.5	1.84	29.66
II*a*	5.26	3.25	1.42	6.18	1.94	4.24
II*b*	7.13	3.85	1.37	5.40	2.01	3.39
III*a*	3.39	3.43	1.42	10.12	1.94	8.18
III*b*	4.12	3.98	1.38	9.65	2.00	7.65
III*c*	4.98	4.47	1.32	8.98	2.09	6.89
IV*a*	5.48	4.87	1.54	8.89	1.79	7.10
IV*b*	3.32	4.50	1.52	13.55	1.82	11.73
IV*c*	5.41	5.15	1.50	9.52	1.84	7.68
IV*d*	5.42	5.15	1.50	9.50	1.84	7.66
V*a*	19.34	6.45	1.50	3.33	1.84	1.49
V*b*	22.00	7.23	1.50	3.30	1.84	1.46

cholesterol dissolution changed with the number of methyl groups as well as with the number of carbon atoms in the long side chains. For the *n*-alkylamines, increasing the number of methyl groups on the amine nitrogen increased the resistance; *i.e.*, for cholesterol dissolution acceleration, the following order of effectiveness was observed: primary > secondary > tertiary > quaternary. However, V*a* was a more effective accelerator than IV*d*. Thus, the number of side chains may be more important than the number of carbon atoms in determining the effectiveness of these accelerators.

Other nitrogen-containing compounds as well as several anionic and nonionic surfactants (Table V) were ineffective as cholesterol dissolution rate accelerators. With the anionic surfactants, a retardation effect was actually observed.

The steroid derivatives were effective even at relatively low concentrations (Table VI). Compounds VI*a* and VI*b* reduced the total resistance by almost a factor of 5 at around 10 m*M*. Due to the limited availability of these compounds, studies at higher concentrations were not possible.

Table V—Effect of Some Nitrogen-Containing Compounds and Nonionic and Anionic Surfactants on Dissolution

Compound and Concentration	$(J/A) \times 10^4$, mg/cm² sec	C_s, mg/ml	$R = \left(\frac{h}{D} + \frac{1}{P}\right) \times 10^{-3}$, sec/cm
—	0.96	3.00	31.5
VII*a*, 32 m*M*	0.61	2.10	35.4
VII*b*, 34 m*M*	1.24	3.50	28.2
Polysorbate 80, 1.25%	0.27	1.35	50.0
Sodium lauryl sulfate, 34 m*M*	0.066	1.65	250
Sodium laurate, 34 m*M*	0.044	2.84	645

DISCUSSION

Together with the limited earlier results (4, 5) for benzalkonium chloride and cetylpyridinium chloride, these results represent the first assessment of the nature of compounds that may act as cholesterol gallstone dissolution accelerators. The primary, secondary, and tertiary amines and the quaternary ammonium salts all appear to be effective. Chain length and/or the degree of hydrophobicity also seem to be important, as do steric or structural features other than pure hydrophobicity as evidenced by the fact that the dioctyl quaternary (V*a*) was more effective than the monohexadecyl quaternary (IV*d*).

Surface activity *per se* does not appear to be important, since the nonionic and the anionic surfactants showed little or negative accelerator activity in these tests. Indirectly, however, surface activity may be important.

The data presented in Tables I–VI are complicated by the fact that

Table VI—Effect of Steroidal Amines on Cholesterol Monohydrate Dissolution in 116 m*M* Sodium Cholate–32 m*M* Lecithin Solution Buffered with 0.10 *M* Phosphate at pH 7.40 and 37°

Compound	Concentration, m*M*	C_s, mg/ml	$(J/A) \times 10^4$, mg/cm²/sec	$R \times 10^{-3}$, sec/cm
VI*a*	0	3.00	0.96	31.5
	5.29	3.00	2.31	13.0
	9.86	3.26	5.08	6.42
VI*b*	2.69	3.00	1.37	21.9
	5.29	3.06	2.19	14.0
	8.05	3.19	3.29	9.70
VI*c*	8.24	3.05	1.83	16.67
VI*d*	10.0	3.56	1.84	19.35

the accelerator in question may be bound to varying degrees to the micelles and other components of the synthetic bile. Thus, meaningful structure–activity relationships can only be considered when the "free" concentration, or the thermodynamic activity, of the accelerator is known. Further progress in this area depends on conducting studies in which the "intrinsic" activities of these agents can be determined.

A method based on the dialysis rate principle for determining the free accelerator concentration in simulated bile is being developed and appears feasible (14). It appears, for example, that the actual (or the intrinsic) difference between *n*-hexylamine and *n*-octylamine in the cholic acid–lecithin media is closer to a factor of 10 or 15 than to the marginal difference seen in Table I. As such data become available, one may begin to understand the action of these accelerators at the molecular level.

Of course, the search for suitable adjuvants for gallstone dissolution in humans *via* the oral route will require additional studies on the absorption, biliary excretion, metabolism, and toxicity of these compounds. While this fact may appear to make this approach impractical or very difficult, one needs only to note that VI*b*, 20,25-diazacholesterol, an established hypocholesterolemic agent, is orally absorbed in humans (15, 16) and in other animal species. Studies also showed (17) that significant percentages of high molecular weight quaternary ammonium cations such as dibenzyldimethylammonium, tribenzylmethylammonium, and benzomethamine are excreted in quantity in rat, rabbit, and human bile when given intravenously. Therefore, compounds such as the steroidal amines and the bile acid derivatives containing the amine nitrogen or the quaternary nitrogen functional groups may offer promise for this approach.

REFERENCES

(1) W. I. Higuchi, S. Prakongpan, V. Surpuriya, and F. Young, *Science*, **178**, 633 (1972).

(2) W. I. Higuchi, F. Sjuib, D. Mufson, A. P. Simonelli, and A. F. Hofmann, *J. Pharm. Sci.*, **62**, 942 (1973).

(3) W. I. Higuchi, S. Prakongpan, and F. Young, *ibid.*, **62**, 945 (1973).

(4) *Ibid.*, **62**, 1207 (1973).

(5) S. Prakongpan, W. I. Higuchi, K. H. Kwan, and A. M. Molokhia, *J. Pharm. Sci.*, **65**, 685 (1976).

(6) K. H. Kwan, W. I. Higuchi, A. M. Molokhia, and A. F. Hofmann, *ibid.*, **66**, 1094 (1977).

(7) A. M. Molokhia, A. F. Hofmann, W. I. Higuchi, M. Tuchinda, K. Feld, S. Prakongpan, and R. G. Danzinger, *ibid.*, **66**, 1101 (1977).

(8) A. T. James and L. J. Morris, "New Biochemical Separations," Van Nostrand, London, England, 1964, chap. 10.

(9) H. Bogren and K. Larsson, *Biochim. Biophys. Acta*, **75**, 65 (1963).

(10) D. M. Small, M. C. Bourges, and D. G. Dervichian, *ibid.*, **125**, 563 (1966).

(11) L. Lack and I. M. Weiner, *Am. J. Physiol.*, **210**, 1142 (1966).

(12) A. S. Jones, *J. Chem. Soc.*, **1949**, 2164.

(13) A. Berthoud, *J. Chim. Phys.*, **10**, 624 (1912).

(14) D. Patel, W. I. Higuchi, and A. M. Molokhia, presented at the APhA Academy of Pharmaceutical Sciences, Orlando meeting, Nov. 1976.

(15) R. E. Counsell, P. D. Klimstra, L. N. Nysted, and R. E. Ranney, *J. Med. Chem.*, **8**, 45 (1965).

(16) B. A. Sachs and L. Wolfman, *Arch. Intern. Med.*, **116**, 366 (1965).

(17) R. L. Smith, "The Excretory Function of Bile," Chapman and Hall, London, England, 1973, pp. 84–88.

ACKNOWLEDGMENTS AND ADDRESSES

Received July 1, 1976, from the *College of Pharmacy, University of Michigan, Ann Arbor, MI 48109, and the ‡Gastroenterology Unit, Mayo Clinic and Mayo Foundation, Rochester, MN 55901.

Accepted for publication September 27, 1976.

Supported by Grant AM 16694 from the National Institute of Arthritis, Metabolism, and Digestive Diseases and in part by National Institutes of Health Research Grant AM 16770.

ˣ To whom inquiries should be directed.

Spectrophotometric Determination of Cephapirin, a Cephalosporin Antibacterial

J. E. BODNAR, W. G. EVANS, and D. L. MAYS ˣ

Abstract □ A simple and specific method for the quantitative determination of cephapirin, a cephalosporin antibacterial, in finished bulk and dosage forms is reported. The method is based on reproducible degradation under controlled conditions to an unidentified species, which is measured spectrophotometrically at 375 nm. The procedure can be performed manually on a short series of samples in about 15 min or can be automated for large runs. Precursors and related substances show minimal interference. The coefficient of variation of the automated system is about 1% within days and 1.3% among days.

Keyphrases □ Cephapirin—spectrophotometric analysis, bulk drug and pharmaceutical formulations □ Spectrophotometry—analysis, cephapirin, bulk drug and pharmaceutical formulations □ Antibacterials—cephapirin, spectrophotometric analysis, bulk drug and pharmaceutical formulations

Cephapirin sodium (I), a new cephalosporin antibacterial for parenteral use, has the advantage of being less painful and better tolerated than cephalothin (1). The two methods of analysis officially approved for certification are the microbiological agar-plate diffusion method and the colorimetric hydroxylamine method (2). However, this paper reports a more rapid and selective spectrophotometric method for convenient and accurate product control of finished bulk and dosage forms. The method has been automated to accommodate large numbers of stability samples. Products arising through hydrolysis of the acetyl function show little or no interference. The method is selective for only a few cephalosporins.

Manual and automated procedures, the effects of several operating conditions, and validation of the method are presented.

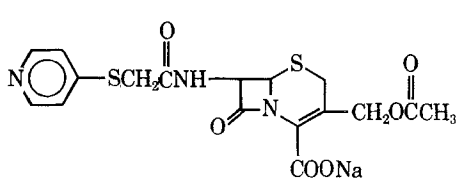

I

the accelerator in question may be bound to varying degrees to the micelles and other components of the synthetic bile. Thus, meaningful structure–activity relationships can only be considered when the "free" concentration, or the thermodynamic activity, of the accelerator is known. Further progress in this area depends on conducting studies in which the "intrinsic" activities of these agents can be determined.

A method based on the dialysis rate principle for determining the free accelerator concentration in simulated bile is being developed and appears feasible (14). It appears, for example, that the actual (or the intrinsic) difference between *n*-hexylamine and *n*-octylamine in the cholic acid–lecithin media is closer to a factor of 10 or 15 than to the marginal difference seen in Table I. As such data become available, one may begin to understand the action of these accelerators at the molecular level.

Of course, the search for suitable adjuvants for gallstone dissolution in humans *via* the oral route will require additional studies on the absorption, biliary excretion, metabolism, and toxicity of these compounds. While this fact may appear to make this approach impractical or very difficult, one needs only to note that VI*b*, 20,25-diazacholesterol, an established hypocholesterolemic agent, is orally absorbed in humans (15, 16) and in other animal species. Studies also showed (17) that significant percentages of high molecular weight quaternary ammonium cations such as dibenzyldimethylammonium, tribenzylmethylammonium, and benzomethamine are excreted in quantity in rat, rabbit, and human bile when given intravenously. Therefore, compounds such as the steroidal amines and the bile acid derivatives containing the amine nitrogen or the quaternary nitrogen functional groups may offer promise for this approach.

REFERENCES

(1) W. I. Higuchi, S. Prakongpan, V. Surpuriya, and F. Young, *Science*, **178**, 633 (1972).

(2) W. I. Higuchi, F. Sjuib, D. Mufson, A. P. Simonelli, and A. F. Hofmann, *J. Pharm. Sci.*, **62**, 942 (1973).

(3) W. I. Higuchi, S. Prakongpan, and F. Young, *ibid.*, **62**, 945 (1973).

(4) *Ibid.*, **62**, 1207 (1973).

(5) S. Prakongpan, W. I. Higuchi, K. H. Kwan, and A. M. Molokhia, *J. Pharm. Sci.*, **65**, 685 (1976).

(6) K. H. Kwan, W. I. Higuchi, A. M. Molokhia, and A. F. Hofmann, *ibid.*, **66**, 1094 (1977).

(7) A. M. Molokhia, A. F. Hofmann, W. I. Higuchi, M. Tuchinda, K. Feld, S. Prakongpan, and R. G. Danzinger, *ibid.*, **66**, 1101 (1977).

(8) A. T. James and L. J. Morris, "New Biochemical Separations," Van Nostrand, London, England, 1964, chap. 10.

(9) H. Bogren and K. Larsson, *Biochim. Biophys. Acta*, **75**, 65 (1963).

(10) D. M. Small, M. C. Bourges, and D. G. Dervichian, *ibid.*, **125**, 563 (1966).

(11) L. Lack and I. M. Weiner, *Am. J. Physiol.*, **210**, 1142 (1966).

(12) A. S. Jones, *J. Chem. Soc.*, **1949**, 2164.

(13) A. Berthoud, *J. Chim. Phys.*, **10**, 624 (1912).

(14) D. Patel, W. I. Higuchi, and A. M. Molokhia, presented at the APhA Academy of Pharmaceutical Sciences, Orlando meeting, Nov. 1976.

(15) R. E. Counsell, P. D. Klimstra, L. N. Nysted, and R. E. Ranney, *J. Med. Chem.*, **8**, 45 (1965).

(16) B. A. Sachs and L. Wolfman, *Arch. Intern. Med.*, **116**, 366 (1965).

(17) R. L. Smith, "The Excretory Function of Bile," Chapman and Hall, London, England, 1973, pp. 84–88.

ACKNOWLEDGMENTS AND ADDRESSES

Received July 1, 1976, from the *College of Pharmacy, University of Michigan, Ann Arbor, MI 48109, and the ‡Gastroenterology Unit, Mayo Clinic and Mayo Foundation, Rochester, MN 55901.

Accepted for publication September 27, 1976.

Supported by Grant AM 16694 from the National Institute of Arthritis, Metabolism, and Digestive Diseases and in part by National Institutes of Health Research Grant AM 16770.

ˣ To whom inquiries should be directed.

Spectrophotometric Determination of Cephapirin, a Cephalosporin Antibacterial

J. E. BODNAR, W. G. EVANS, and D. L. MAYS ˣ

Abstract □ A simple and specific method for the quantitative determination of cephapirin, a cephalosporin antibacterial, in finished bulk and dosage forms is reported. The method is based on reproducible degradation under controlled conditions to an unidentified species, which is measured spectrophotometrically at 375 nm. The procedure can be performed manually on a short series of samples in about 15 min or can be automated for large runs. Precursors and related substances show minimal interference. The coefficient of variation of the automated system is about 1% within days and 1.3% among days.

Keyphrases □ Cephapirin—spectrophotometric analysis, bulk drug and pharmaceutical formulations □ Spectrophotometry—analysis, cephapirin, bulk drug and pharmaceutical formulations □ Antibacterials—cephapirin, spectrophotometric analysis, bulk drug and pharmaceutical formulations

Cephapirin sodium (I), a new cephalosporin antibacterial for parenteral use, has the advantage of being less painful and better tolerated than cephalothin (1). The two methods of analysis officially approved for certification are the microbiological agar-plate diffusion method and the colorimetric hydroxylamine method (2). However, this paper reports a more rapid and selective spectrophotometric method for convenient and accurate product control of finished bulk and dosage forms. The method has been automated to accommodate large numbers of stability samples. Products arising through hydrolysis of the acetyl function show little or no interference. The method is selective for only a few cephalosporins.

Manual and automated procedures, the effects of several operating conditions, and validation of the method are presented.

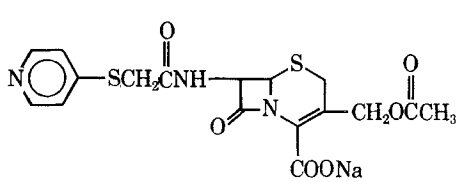

I

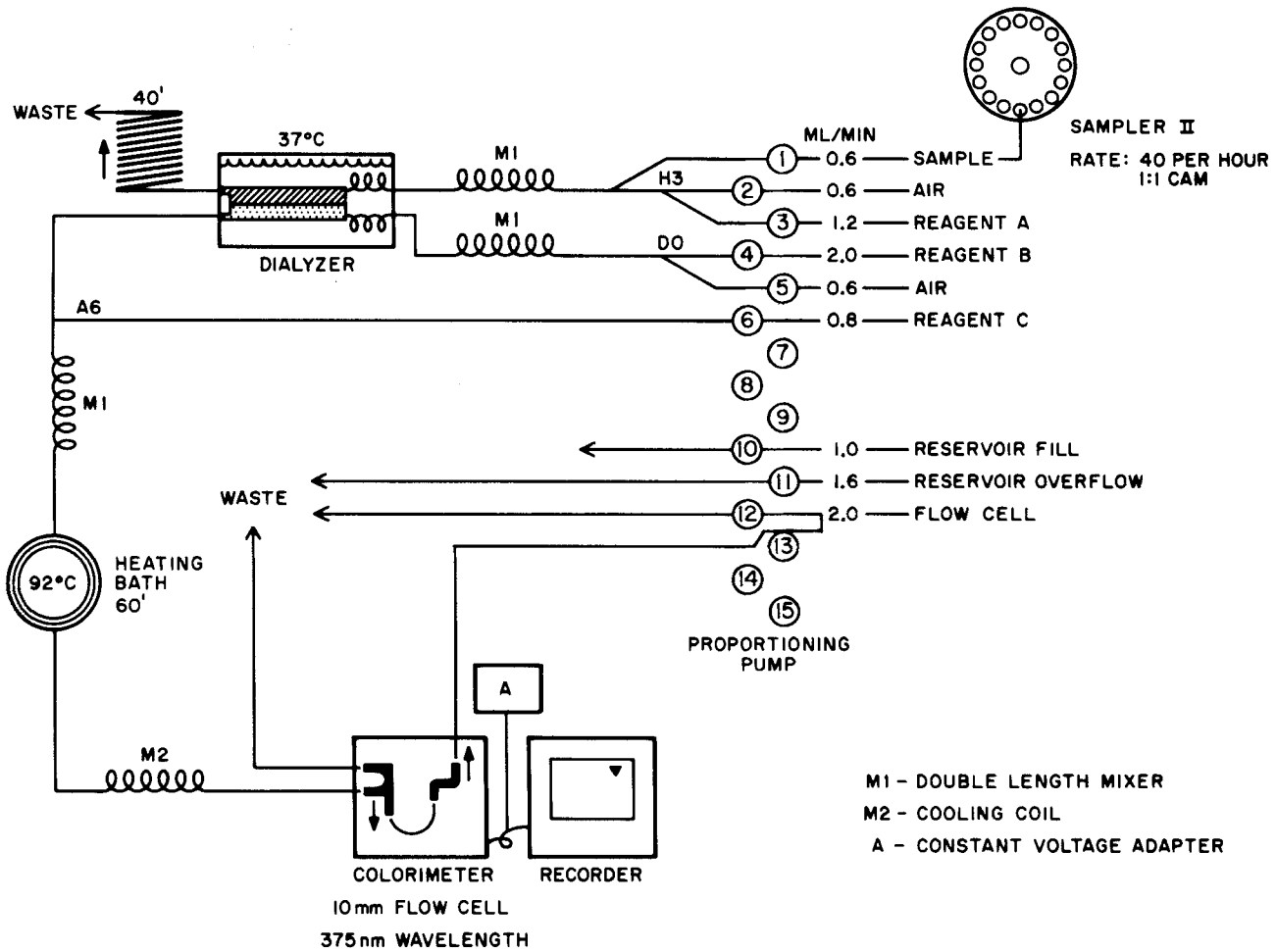

Figure 1—*Flow diagram of automated spectrophotometric assay for cephapirin.*

EXPERIMENTAL

Instrumentation—A standard pH meter[1] and two spectrophotometers[2] were used for developing the manual method. The automated system consisted of a continuous-flow analyzer[3] assembled as shown in Fig. 1. The spectrophotometer[4] output was fed into the recorder[3] *via* a special adaptor for single-voltage input (3). A proportional temperature controller[5] was used to maintain the heating bath temperature.

Reagents—*Manual Method*—The sample diluent was prepared by dissolving 51 g of potassium biphthalate[6] and 0.9 g of imidazole[7] in 800 ml of water, adjusting the pH to 6.50 ± 0.02 with 10 *N* NaOH, and diluting to 1 liter with water.

Automated Method—The sample diluent was prepared as for the manual method but without the imidazole. This reagent, with the addition of 5 drops/liter of polysorbate 20[8], was also used for the continuous-flow analyzer (Reagent A). The dialyzer recipient (Reagent B) was 0.2 *M* NaCl with 5 drops/liter of polysorbate 20. Reagent C was prepared by dissolving 23 g of potassium biphthalate and 1.0 g of imidazole in 450 ml of water, adjusting the pH to 6.50 ± 0.02 with 10 *N* NaOH, and diluting to 500 ml with water.

Procedure—*Manual Determination*—Dissolve 50 mg of cephapirin sodium reference standard in 100 ml of sample diluent. Dilute 5-, 10-, 15-, 20-, and 25-ml aliquots to 50 ml with the diluent. Dissolve samples in diluent to contain 0.1–0.2 mg of cephapirin/ml. Transfer 4 ml of each dilution to separate 25-ml volumetric flasks. Stopper the flasks and heat

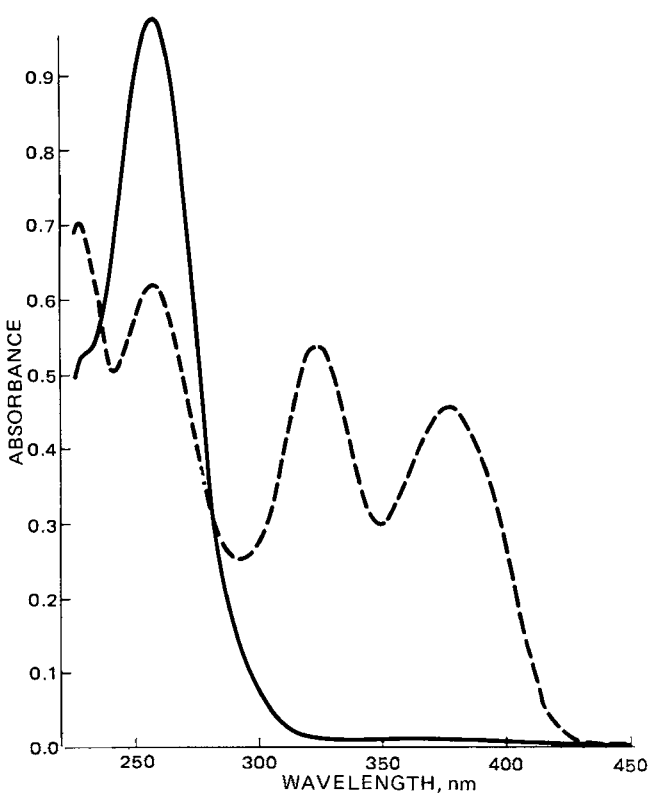

Figure 2—*Absorption spectra of cephapirin in pH 6.5 phosphate buffer unheated (—) and heated for 9 min at 100° (- -).*

[1] Radiometer model 26.
[2] Beckman DU and Cary model 14.
[3] Technicon Autoanalyzer modules as follows: Sampler II with a 40/hr 1:1 cam, Pump II, a dialyzer (37°), a heating bath (92°) containing 6.1- and 12.2-m (20- and 40-ft) glass holding coils, and a single-pen recorder.
[4] Turner model 350.
[5] RFL Industries model 7-115 with Sensor 27686-3.
[6] Matheson, Coleman & Bell.
[7] Eastman Chemical Co.
[8] Tween 20, Atlas Products.

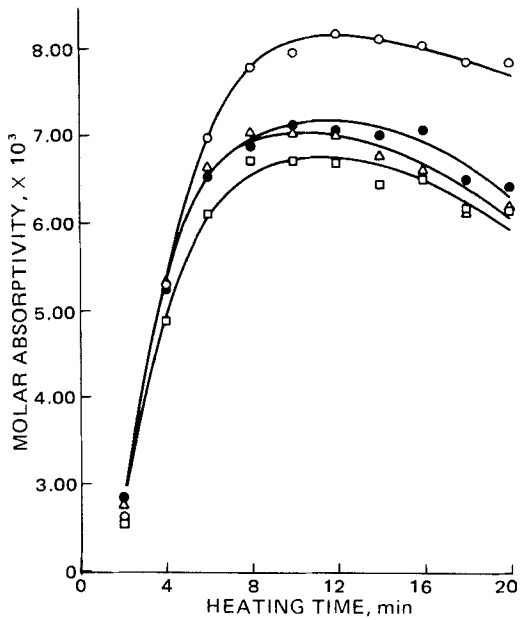

Figure 3—*Rate of formation of 375-nm chromophore as a function of heating time (100°) in several buffers. Key:* □, *0.25* M *pH 6.5 phthalate;* △, *0.1* M *pH 6.5 phosphate;* ●, *0.1* M *pH 6.5 acetate; and* ○, *0.25* M *pH 6.5 phthalate plus 0.013* M *imidazole.*

in a boiling water bath for exactly 9 min.

Immediately after heating, cool the flasks in an ice water bath for about 1 min. Then allow the flasks to equilibrate to room temperature, and dilute them to volume with diluent. Prepare the blanks similarly, but do not heat or cool. Determine the absorbance of each standard at 375 nm *versus* the respective blank. Prepare a standard curve of absorbance *versus* concentration. Calculate the cephapirin content of the samples from the standard curve.

Automated Determination—Dissolve 100 mg of cephapirin sodium reference standard in 100 ml of sample diluent. Dilute 5-, 10-, 15-, 20-, and 25-ml aliquots to 25 ml with sample diluent. Prepare samples to contain about 0.5 mg of drug/ml of sample diluent. Fill the sample cups with standard and sample solutions, applying a set of standards at both the beginning and end of each series of samples. Sample blanks are not required but could be obtained by lowering the heating bath temperature to 25°. Obtain the absorbance from the peak maxima of standards and samples. Prepare a working curve of absorbance *versus* concentration, and calculate the cephapirin content of samples from the working curve.

RESULTS AND DISCUSSION

Optimum Conditions—The UV absorption spectra of heated and unheated cephapirin in pH 6.5 phosphate buffer are shown in Fig. 2. The

Table I—Within-Day Reproducibility of an Automated Spectrophotometric Determination of Cephapirin

Sample	Percent Cephapirin in Cephapirin Sodium				Coefficient of Variation, %
	Run 1	Run 2	Run 3	Mean	
			Day 1		
A	93.4	94.3		93.8	0.66
B	82.8	83.6		83.2	0.68
C	85.2	83.0		84.1	1.85
D	89.5	88.0		88.8	1.20
E	88.4	86.5		87.4	1.53
F	91.1	90.5		90.8	0.46
Pooled standard error = 1.28%					
			Day 2		
A	94.3	93.7	95.7	94.6	1.59
B	84.1	83.2	84.2	83.8	0.65
C	80.8	81.4	81.2	81.1	0.38
D	91.1	89.2	91.1	90.5	1.21
E	90.7	91.1	90.2	90.7	0.50
F	91.9	92.1	91.3	91.8	0.46
Pooled standard error = 0.92%					

Table II—Across-Day Reproducibility of an Automated Spectrophotometric Determination of Cephapirin

Sample	Percent Cephapirin in Cephapirin Sodium						Coefficient of Variation, %
	Day 1	Day 2	Day 3	Day 4	Day 5	Mean	
G	94.1	95.2	94.3	93.1	94.2	94.2	0.8
H	94.1	94.7	95.5	93.3	94.9	94.5	0.9
I	93.8	94.8	95.1	92.7	92.7	93.8	1.2
Pooled standard error = 0.98%							

treated samples showed partial loss of the main peak at 258 nm and generation of new peaks at 320 and 375 nm. The peak at 375 nm was chosen for analytical purposes, since interferences generally occurred less frequently toward the visible region. The unheated sample made a suitable blank. When heated at 100°, the chromophore increased rapidly, reaching a maximum in about 9 min, and then decreased slowly (Fig. 3). The absorbance remained constant for at least 1 hr after cooling.

A plot of absorbance at 375 nm *versus* concentration was linear and passed through the origin, obeying Beer's law over a fivefold concentration range (8–40 μg/ml in the final dilution for the manual method and 200–1000 μg/ml in the sample cup for the automated method). The limit of detection was about 2 μg/ml for the manual method and about 50 μg/ml for the automated procedure.

The chromophore intensity was pH dependent, with the maximum response observed at pH 6.5 (Fig. 4). Phosphate, acetate, or phthalate buffers can be used (Fig. 3). Other buffers (borate, citrate, glycine, and tromethamine), especially those containing chloride ion, are not suitable. Sample absorbance was increased in the presence of imidazole but was relatively independent of imidazole concentration over a broad range (Figs. 3 and 5).

Reproducibility and Accuracy—The pooled standard error among automated runs within 1 day on an assortment of crude samples was calculated from replicate runs made on 2 separate days (Table I). In both cases, the within-day standard error was less than 1.5%. The reproducibility of results across days is shown in Table II. A comparison of results obtained between days on good quality samples yielded a pooled standard error of less than 1%.

Results of a series of samples analyzed by both the automated spectrophotometric and the biological turbidimetric methods are shown in Table III. Results of the proposed procedure agreed within 1% overall with those of the standard biological method. The average absolute error was 1.7%.

Specificity—There appeared to be little or no interference from 7-aminocephalosporanic acid or the desacetyl derivative of cephapirin and only slight interference from the lactone of the desacetyl derivative, all potential impurities in cephapirin (Table IV). Cephapirin treated for 15 min with cephalosporinase[9] yielded no measurable 375-nm chromophore upon heating, demonstrating that cephapirin degradation products arising *via* β-lactam cleavage did not interfere.

Several commercial cephalosporins and intermediates in cephapirin production were screened for applicability of the method. In addition

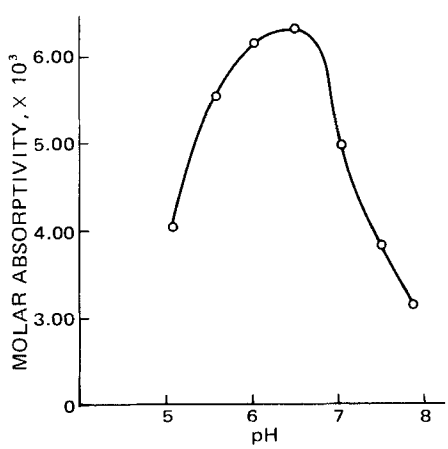

Figure 4—*Extent of formation of 375-nm chromophore as a function of pH in 0.25* M *phthalate buffer without imidazole (heated for 9 min at 100°).*

[9] Obtained from *Enterobacter cloacae*, P 99.

Table III—Comparison of Automated Spectrophotometric and Biological Turbidimetric Methods of Determination of Cephapirin (Percent) in Cephapirin Sodium

Sample	Chemical Method[a]	Biological Method[b]
1	94.0	90.5
2	92.8	91.5
3	90.5	92.5
4	92.5	93.5
5	90.3	93.5
6	93.6	93.5
7	92.7	90.3
8	93.9	92.7
9	91.9	93.0
10	94.2	91.0
11	94.3	92.0
12	94.2	92.0
13	94.2	91.5
14	94.5	92.0
15	93.8	93.5
16	94.2	94.0
17	94.2	95.0
18	93.2	93.5
19	92.6	94.0
Average	93.2	92.5
Average absolute deviation = 1.7%		
Overall deviation = 0.7%		

[a] Each result is the mean of four determinations. [b] Each result is the mean of individual determinations made on 2 or 3 separate days.

to cephapirin, cephalothin sodium and cephalosporin D sodium[10] can be determined by this method. Cephalosporins that do not respond to the test include cephaloridine, cefazolin sodium, cephalexin, and cephalosporin C sodium.

Mechanism of Reaction—Consideration of the structures of the cephalosporins that respond to the test indicates that an easily displaced 3-methyl substituent is required for chromophore formation and that a primary amine in the 7-position substituent inhibits the conversion. The heated solution appeared to contain a mixture of products, since some of the 258-nm absorption band remained. The species absorbing at 375 nm has not been isolated. When using TLC or column chromatography, the concentration of the test solution was insufficient. At a substantially greater concentration, the conversion was very poor and essentially cephapirin was recovered. Upon lyophilization, the 375-nm absorption was lost, indicating either further degradation or loss by volatility.

Upon heating under controlled conditions, penicillins rearrange to penicillenic acids which have UV absorption around 320 nm. These penicillenic acids are stabilized by copper or mercury salts and catalyzed by imidazole to give much higher conversion yields (4, 5). Addition of copper sulfate or mercuric chloride to the cephapirin test solution drastically diminished the 375-nm absorbance, indicating that a penicillenic acid type of rearrangement was not involved.

If external or internal nucleophilic displacement of the acetoxy group is involved, then addition of reagents known to displace this group might

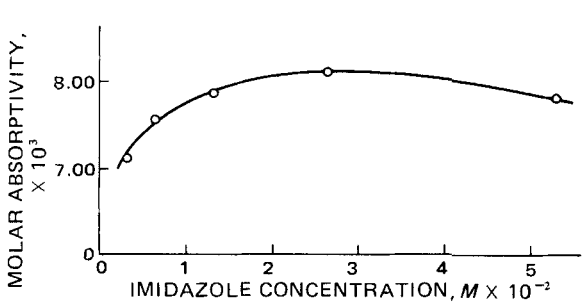

Figure 5—*Molar absorptivity at 375 nm in 0.25 M phthalate buffer as a function of imidazole concentration (heated for 9 min at 100°).*

[10] Cephalosporin D, the *N*-isobutyloxycarbonyl derivative of cephalosporin C, is an intermediate in the production of 7-aminocephalosporanic acid.

Table IV—Percent Recovery of Assayed Cephapirin Content of Cephapirin Sodium after Spiking with Potential Impurities

Impurity Added	Run	Proportion of Impurity Added 1%	5%	10%	Grand Mean, %
7-Aminocephalosporanic acid	1	98.8	99.6	100.4	
	2	99.6	100.4	100.4	
	3	100.9	100.9	101.7	
	Mean	99.8	100.3	100.8	100.3
Desacetyl derivative of cephapirin	1	99.6	98.0	99.6	
	2	98.1	98.1	98.1	
	3	100.9	100.9	102.4	
	Mean	99.5	99.0	100.0	99.5
Lactone of desacetyl derivative	1	100.4	101.2	102.7	
	2	100.4	101.2	103.5	
	Mean	100.4	101.2	103.1	101.6

be expected to increase or decrease the reaction yield. Various heterocyclic tertiary amines (6, 7) including niacinamide (8) displace the acetoxy group. Addition of niacinamide had no effect on chromophore development, which may suggest that any displacement of the acetoxy group must occur from internal expulsion of that group as a result of an internal rearrangement.

Imidazole is known to catalyze hydroxylaminolysis of the β-lactam of penicillins (9). The addition of imidazole to this reaction showed some increase in yield of the 375-nm absorbing species, and the amount of yield increase was only slightly dependent on imidazole concentration over a broad range. This finding might suggest that the reaction is initiated through the β-lactam of cephapirin and is catalyzed by imidazole. Some molecular rearrangement occurs, giving perhaps a number of products, one or more of which absorb at 375 nm. The apparent necessity of the acetoxy group in the molecule may simply correlate with those cephalosporins having less stable β-lactams. An optimum pH of near neutral is consistent, since simple lactam hydrolysis with further rapid degradation may compete with the observed rearrangement at higher pH values.

These suggestions, however, are quite speculative; definite conclusions must await more evidence.

REFERENCES

(1) *Med. Actual.*, **9**, 55 (1973).

(2) Code of Federal Regulations, Title 21, Paragraph 442.29a (1975).

(3) A. F. Krieg and B. A. Hutchinson, *Clin. Chem.*, **16**, 443 (1970).

(4) J. W. G. Smith, G. E. DeGrey, and V. J. Patel, *Analyst*, **92**, 247 (1967).

(5) H. Bundgaard and K. Ilver, *J. Pharm. Pharmacol.*, **24**, 790 (1972).

(6) R. B. Morin and B. G. Jackson, *Fortschr. Chem. Org. Naturst.*, **28**, 343 (1970).

(7) C. W. Hale, G. G. F. Newton, and E. P. Abraham, *Biochem. J.*, **79**, 403 (1961).

(8) M. O. Redstone, presented at the Eleventh Interscience Conference on Antimicrobial Agents and Chemotherapy, Atlantic City, N.J., Oct. 1971.

(9) T. Yamana, A. Tsuji, E. Miyamoto, and E. Kiya, *J. Pharm. Pharmacol.*, **27**, 283 (1975).

ACKNOWLEDGMENTS AND ADDRESSES

Received July 26, 1976, from the *Analytical Research and Development Department, Bristol Laboratories Division, Bristol-Myers Company, Syracuse, NY 13201*

Accepted for publication September 29, 1976.

The authors are grateful to Dr. Felix Leitner, Microbiological Research Department, and Dr. Bernard Heinemann and Miss Gloria Harty, Fermentation Development Department, for preparing and providing the cephalosporinase. They also thank Mr. Naseem Muhammad for advice and efforts to characterize the cephapirin reaction product and for preparation of the desacetyl and the lactone of the desacetyl derivatives of cephapirin.

[x] To whom inquiries should be directed.

Chromatographic Assays for Folic Acid

VAN D. REIF ˣ, JEANNE T. REAMER, and LEE T. GRADY

Abstract □ TLC and high-pressure liquid chromatographic (HPLC) assays for folic acid were developed. In the TLC procedure, the folic acid band was extracted from the silica gel after development and determined spectrophotometrically by an oxidation and Bratton–Marshall sequence. A column packed with octadecylsilane chemically bonded to microparticulate silica gel was used for the HPLC assay. Potentiometric determination of water in folic acid samples was necessary to obtain accurate purity values. In a comparison of four assay methods, a direct colorimetric method gave precise, but unspecific, results, while the USP XIX colorimetric method lacked both precision and specificity. The two chromatographic methods were both precise and specific and gave the same assay results. Both methods separated *p*-aminobenzoic acid, *N*-(*p*-aminobenzoyl)-L-glutamic acid, 2-amino-1,4-dihydro-4-oxo-6-pteridinecarboxylic acid, 2-amino-4(1*H*)-pteridinone, and several unidentified impurities from folic acid.

Keyphrases □ Folic acid—TLC and high-pressure liquid chromatographic analyses, bulk drug □ TLC—analysis, folic acid bulk drug □ High-pressure liquid chromatography—analysis, folic acid bulk drug □ Vitamins—folic acid, TLC and high-pressure liquid chromatographic analyses, bulk drug

Folic acid has been analyzed by direct UV spectroscopy (1), fluorometry after oxidation to 2-amino-1,4-dihydro-4-oxo-6-pteridinecarboxylic acid (1–3), polarography (4, 5), and colorimetry (6–9). The USP XIX colorimetric method (6) involves permanganate oxidation of folic acid to *p*-aminobenzoic acid, which is diazotized and coupled with the Bratton–Marshall reagent [*N*-(1-naphthyl)ethylenediamine dihydrochloride] for determination by spectrophotometry. In this standard addition method, assay values are corrected for diazotizable impurities by performing the colorimetric reaction on unoxidized material. Other colorimetric methods involve reduction of folic acid with zinc instead of oxidation (7, 9) and conversion of diazotizable impurities to phenols before permanganate oxidation (8). Experiments in this laboratory showed that commercial folic acid contains fluorescent pteridines, diazotizable amines, and compounds other than folic acid that cleave to give the functional groups measured in the colorimetric assays. Therefore, these methods are unspecific, and separation of folic acid from its impurities prior to quantitation is necessary.

A TLC method with colorimetric quantitation (10) and a similar method with UV quantitation (11) were reported, but less mobile impurities were *not* separated in the solvent systems used since folic acid did not move from the origin. Williams *et al.* (12) and, separately, investigators in this laboratory used high-pressure anion-exchange chromatography, but these systems require a solvent gradient which makes quantitation unreliable. Also, the separation of impurities from folic acid was not fully demonstrated. This paper reports the development of improved TLC and high-pressure liquid chromatographic (HPLC) assays.

EXPERIMENTAL

Materials—Reference compounds for *p*-aminobenzoic acid, 2-amino-1,4-dihydro-4-oxo-6-pteridinecarboxylic acid, 2-amino-4(1*H*)-pteridinone, *N*-(*p*-aminobenzoyl)-L-glutamic acid, dihydrofolic acid, and tetrahydrofolic acid were used as received[1]. Leucovorin calcium was also used as obtained[2]. Except for commercial folic acid samples, other reagents were USP, NF, or ACS grade. Two lots of USP reference standard folic acid[3], designated A and B, were used for assay evaluations.

Moisture Determination—The water content of folic acid samples was determined by direct potentiometric titration[4] according to USP XIX Method I (Karl Fischer determination) (13) except that chloroform–methanol (4:1) was used as the solvent in place of methanol[5]. Sample sizes of 10–15 mg and 100 ml of solvent were used. Since folic acid is hygroscopic, the water content was determined at the time the samples were weighed.

Chromatographic Assays—*Standard Preparation*—Transfer 40-, 50-, and 60-mg samples of USP folic acid reference standard, accurately weighed and corrected for moisture, to individual 5-ml volumetric flasks. Then dissolve and dilute to volume with 0.3 *N* ammonium hydroxide. These solutions should be made fresh daily.

Assay Preparation—Prepare as directed under *Standard Preparation*, using the 50-mg sample size.

TLC Assay—On suitable TLC plates coated with a 250-μm layer of fluorescent silica gel[6], predeveloped with ethyl acetate and air dried, make a 2-cm streak with 10 μl of the assay preparation. Apply a 2-cm, 10-μl streak of spotting solvent to serve as a blank. Similarly streak 10-μl portions of the standard preparations. Develop the chromatograms about 13 cm in 1.48 *N* ammonium hydroxide–1-propanol (1:3). Remove the plate from the developing chamber, dry it under a nitrogen stream for 5–10 min, and view it under long and short wavelength UV light.

Mark the folic acid main band, taking care to exclude adjacent impurity bands. Quantitatively and separately remove the silica gel mixture containing each of the main spots of the standard and assay preparations. Remove a corresponding area of silica gel from the blank, spotting at the same R_f as the folic acid main spot. Transfer the material to separate 25-ml test tubes with polytef-lined screw caps, add exactly 15 ml of 0.17 *M* dibasic potassium phosphate to each, and shake mechanically for 15 min. Centrifuge the tubes for 10 min at 1000 rpm (10-cm radius) or until clear.

Pipet a 10.0-ml aliquot of each preparation into separate 25-ml conical flasks, add 1.0 ml of 0.4% (w/v) aqueous potassium permanganate solution (freshly prepared and filtered), and allow to stand for 2–3 min. Add 1.0 ml of 2% (w/v) sodium nitrite solution and 1.0 ml of 5 *N* hydrochloric acid, mix, and allow to stand for 2 min. Add 1.0 ml of 5% (w/v) ammonium sulfamate solution, and mix with swirling until the nitrogen dioxide has been dispelled. Then add 1.0 ml of 0.1% (w/v) *N*-(1-naphthyl)ethylenediamine dihydrochloride solution (freshly prepared and filtered), mix, and allow to stand for 10 min.

Determine the absorbance of each solution at the maximum at about 550 nm, with a suitable spectrophotometer[7], using 0.17 *M* dibasic potassium phosphate as the blank. Calculate the quantity, in milligrams, of folic acid in each milliliter of the assay preparation by the formula $C(A_U - A_B/A_S - A_B)$, in which C is the concentration, in milligrams per milliliter, of folic acid in the standard preparations; A_U and A_S are the absorbances of the solutions from the assay and standard preparations, respectively; and A_B is the absorbance from the blank.

HPLC Assay—*Chromatographic System*—The chromatograph[8] was equipped with a fixed wavelength (254 nm) UV detector and a 30-cm × 4-mm i.d. stainless steel column packed with siliceous microbeads, 5–10 μm in diameter, to which octadecylsilane[9] was chemically bonded.

[1] Sigma Chemical Co.
[2] Lederle Laboratories.
[3] USP Reference Standards, Rockville, MD 20852.
[4] Radiometer, Copenhagen, Denmark.
[5] M. M. Tuckerman, Temple University School of Pharmacy, Philadelphia, Pa., personal communication.
[6] Merck silica gel F-254 precoated glass plates.
[7] Cary model 14.
[8] DuPont model 820.
[9] The method was developed using μBondapak C_{18}, Waters Associates. In this or in other laboratories, comparable separations were obtained with the following columns: Spherisorb 10 μm ODS, Spectra-Physics; Zorbax ODS, du Pont; and Partisil-10 ODS-2, Whatman.

Table I—Assay Results

Day[a]	USP Colorimetric Assay Lot B/A, %	Lot A/B, %	Lot A/A, %	Direct Colorimetric, Lot B/A, %
1	108.8	103.2	101.9, 105.2	101.6
2	103.3	105.0	108.0, 108.0	103.3

TLC Assay

Day[a]	Lot	Mean, $\frac{\text{Absorbance}}{\mu g \text{ Spotted}} \times 100$	n	*RSD*, %	B/A + 95% C.I.[b]
1	B	0.476	3	1.63	101.9 ± 1.6
1	A	0.467	3	0.98	
2	B	0.468	3	0.47	102.2 ± 0.5
2	A	0.458	3	0.40	

HPLC Assay

Day[a,c]	Lot[d]	n	*RSD*[e], %	% A + 95% C.I.[b]
1	B	5	1.56	101.7 ± 1.2
1	A	4	0.93	
2	B	5	1.20	101.6 ± 1.2
2	A	8	1.47	
3	B	5	1.18	101.2 ± 0.7
3	A	5	0.67	
4	B	5	0.87	101.0 ± 0.9
4	A	3	0.36	
3	C	4	1.18	93.8 ± 0.8
4	C	3	0.83	95.3 ± 0.7
4	D	3	0.60	96.5 ± 0.6
5	D	4	1.78	96.7 ± 1.4
5	A	4	1.46	
4	E	3	0.87	96.7 ± 0.7
5	E	3	1.17	97.5 ± 1.7

[a] Values for Days 1 and 2 are based on the same moisture determinations for each USP lot, A and B. [b] TLC and HPLC values for Days 1 and 2 are based on sampling from the same solutions. [c] Values for Days 3–5 are based on the same moisture determinations for each lot. Lot A and B material used for Days 3 and 4 was drawn from different sublots (A_2 and B_2 in Table III) than those used for Days 1 and 2 (A_1 and B_1 in Table III) and had different moisture levels. [d] Commercial lots of folic acid are designated by C, D, and E. [e] Precision of multiple, n, injections of the same sample preparation.

Prepare the mobile phase by adding 35.1 g of sodium perchlorate monohydrate, 1.36 g of monobasic potassium phosphate, 6.94 ml of 1 *N* potassium hydroxide, and 40 ml of methanol to a 1-liter volumetric flask and diluting to volume with water. If necessary, adjust the pH to 7.2 with 1 *N* potassium hydroxide. The amount of methanol may be varied by several percent to give a suitable retention time for folic acid as long as system suitability requirements are met. Degas and membrane filter[10] the mobile phase. During chromatography, maintain a pressure of about 76 atm and ambient temperature so that the flow is about 1.0–1.5 ml/min.

System Suitability Preparation—Prepare a solution containing about 5 mg/ml each of folic acid and leucovorin calcium in 0.3 *N* ammonium hydroxide. Filter before use.

System Suitability Test—Chromatograph six to 10 injections of the 50-mg standard preparation, and measure the peak response[11] as directed under *Procedure*. The relative standard deviation, 100 × (standard deviation/mean response), for the peak response does not exceed 2%. When 5 μl of the system suitability preparation is injected, the resolution factor (14) between leucovorin calcium and folic acid is not less than 3.6.

Procedure—Introduce equal volumes (about 3 μl) of the assay preparation and of the 50-mg standard preparation into the high-pressure liquid chromatograph by means of a suitable sampling valve or microsyringe. Measure the response of the peaks, at identical retention times, obtained with the assay and standard preparations. Then calculate the quantity, in milligrams, of folic acid in each milliliter of the assay preparation by the formula $C(A_U/A_S)$, in which C is the concentration in milligrams per milliliter of folic acid in the standard preparation, and A_U and A_S are the peak responses of the solutions from the assay and standard preparations, respectively.

Direct Colorimetric Assay—*Standard Preparation*—Dissolve about 50 mg of USP folic acid reference standard, accurately weighed, in a mixture of 50 ml of water and 2 ml of 6 *N* ammonium hydroxide in a 100-ml volumetric flask. When solution is complete, dilute with water to volume; mix. Dilute a measured portion of this stock solution with 0.17 *M* dibasic potassium phosphate to give a concentration of about 10 μg of folic acid/ml, calculated on the anhydrous basis.

Assay Preparation—Prepare as directed under *Standard Preparation*.

Procedure—Add 5 ml of the standard and assay preparations to separate 25-ml conical flasks. Continue as directed under *TLC Assay*, beginning with "add 1.0 ml of 0.4% (w/v) aqueous potassium permanganate solution . . . ." Calculate the quantity, in micrograms, of folic acid in each milliliter of the assay preparation by the formula $C(A_U/A_S)$, in which C is the concentration in micrograms per milliliter of folic acid in the standard preparation, and A_U and A_S are the absorbances of the solutions from the assay and standard preparations, respectively.

Correlation of Impurity Separations—Commercial folic acid (300 μg) was analyzed by HPLC, using 0.1% (w/v) ammonium carbonate as the elution solvent. Fractions containing individual impurities were collected and reduced under a nitrogen stream to approximately 20 μl. Ten microliters was examined by TLC using the assay system, and 10 μl was subjected to HPLC using the perchlorate–phosphate–methanol system.

RESULTS AND DISCUSSION

TLC—Chromatographic systems for folic acid and related compounds were evaluated. In many of these systems, folic acid remained at the origin and/or the impurities did not separate. None of the published systems separated impurities as well as the system described in this report (Fig. 1).

When the sample was extracted from the silica gel with 0.3 *N* ammonium hydroxide, silicon dioxide interfered with the UV quantitation of folic acid at 255, 283, and 365 nm. However, no interference was observed using the colorimetric determination at 550 nm; precise results (Table I) were obtained. Three brands of commercial silica gel plates[12] yielded the same results.

A plot of absorbance *versus* weights of folic acid spotted gave a linear regression coefficient of 0.999 for amounts between 50 and 200 μg. Upon extrapolation below 50 μg, the line did not pass through the origin; however, a blank determination gave a zero absorbance reading. Although the curve was not linear below the 50-μg level, the assay was made well within the linear region of the curve.

[10] Millipore HA, 0.45 μm.

[11] Infotronics CRS digital integrator, Columbia Scientific.

[12] E. Merck, Brinkmann; Analtech; and Quantum.

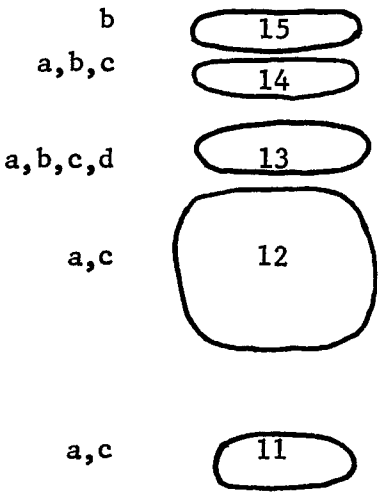

Figure 1—*Thin-layer chromatogram of folic acid (100 μg). Visualization was by shortwave UV light (a), longwave UV light (b), potassium permanganate followed by diazotization and Bratton–Marshall reagents (c), and diazotization and Bratton–Marshall reagents only (d). The indicated bands cochromatographed with the following compounds: 12, folic acid; 13, 2-amino-1,4-dihydro -4-oxo-6- pteridinecarboxylic acid and N-(p-aminobenzoyl) -L- glutamic acid; and 15, 2-amino-4(1H)-pteridinone.*

Duplicates of the standards, blank, and two samples can be determined in 1 day, allowing 2.5 hr for plate development. The use of autopipets is recommended for the colorimetric sequence. It may not be necessary to have all standard preparations for each testing, preparing only the 50-mg/5-ml standards and performing the standard curve only at set intervals. The standard curve procedure given here is designed to ensure accurate assay values for samples that may be considerably different from the standard.

HPLC—Based on reported use in the assay of methotrexate (15) and other acidic compounds (16), columns packed with octadecylsilane bonded to 5–10-μm microparticulate silica gel were investigated. Water–methanol solvent systems resulted in poor retention and tailing of folic acid. A 0.1% ammonium carbonate mobile phase gave resolution of several impurities, but the reproducibility of this system was poor. Phosphate buffers, pH 6–8, were tried; a pH near 7.2 gave optimum results.

The perchlorate–phosphate–methanol system described under *Chromatographic System* gave the best balance between resolution of impurities and retention times (Fig. 2). The system gave reproducible separations on columns from several different manufacturers[9], except that occasionally an individual column did not adequately resolve unidentified component 4 (Fig. 2). Anticipated variations in column retentiveness were overcome by altering the methanol concentration by several percent. After several months of use, no column degradation peculiar to this mobile phase was noted. However, after several months of general use, some commercial columns showed signs of degradation, resulting in unsymmetrical peaks with two maxima. This phenomenon may be due to compression of the column packing, which leads to dead space at the column inlet.

Numerous compounds were investigated as potential internal standards, but due to the number of impurities normally present in folic acid, it was difficult to find a suitable internal standard. To compensate for syringe sample size errors, either multiple syringe injections of folic acid sample and standard preparations or a more precise valve loop system were used. Leucovorin is not well resolved from several minor unidentified folic acid impurities, but its resolution from folic acid enables it to be used in a system suitability test (Fig. 3). This test specifies a minimum resolution between folic acid and leucovorin which, consequently, defines a system capable of separating impurities from folic acid. Systems with a resolution less than 3.6 gave an inadequate separation of impurities. Systems with resolution greater than 3.6 gave adequate separation of impurities, except that occasionally a column did not adequately separate component 4 (Fig. 2).

A comparison of chromatographic parameters at two temperatures is given in Table II. A 35–40° temperature may be used to reduce retention times of folic acid; however, component 4 (Fig. 2) was not completely resolved under these conditions. Resolution between leucovorin and folic acid was also reduced from approximately 4.0 to 3.0, and there was a decrease in the number of theoretical plates. This decrease indicated that absorption rather than true partition chromatography was being observed and that folic acid was chromatographing as a surfactant rather than partitioning as a solute. This finding was also consistent in part with the TLC results, where adsorption chromatography was observed. Impurities with thin-layer mobilities greater than folic acid also exhibited lower HPLC retention times, while an unidentified impurity [HPLC component 6 (Fig. 2), TLC band 11 (Fig. 1)] was more retentive than folic acid in both systems.

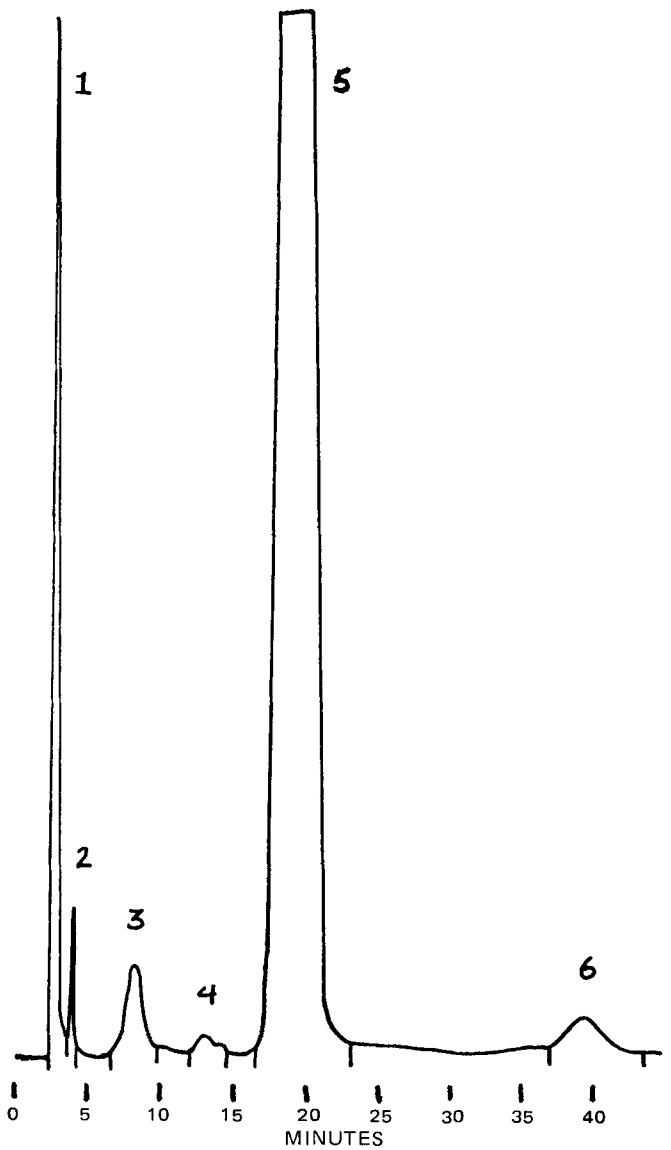

Figure 2—*High-pressure liquid chromatogram of folic acid (30 μg) using the assay system and a 254-nm photometer at 0.08 aufs. The indicated peaks cochromatographed with the following compounds: 1, p-aminobenzoic acid and N-(p-aminobenzoyl)-L-glutamic acid; 2, 2-amino-1,4-dihydro-4-oxo-6-pteridinecarboxylic acid; 3, 2-amino-4(1H)-pteridinone; and 5, folic acid.*

Plots of both peak heights and integrator counts *versus* amount injected by microsyringe gave a linear regression coefficient of 0.999 for amounts between 15 and 60 μg. Injections in amounts up to 140 μg were made. Electronic measurements remained linear, but a saturation phenomenon was indicated above 60 μg by a gradual leveling in the slope of the peak height *versus* amount curve. A standard and four samples with at least triplicate injections of each can be determined in 1 day.

Folic Acid Injection—The HPLC system probably can be adapted for assay of folic acid injection. The product examined[13] contained 5 mg of folic acid/ml in pH 9 sodium hydroxide with edetate sodium[14] and benzyl alcohol added. A 6-μl aliquot was injected directly into the instrument without prior sample preparation. In addition to the benzyl alcohol, $k' = 4.4$, two unidentified components ($k' = 0.75$ and 10.1) were separated that were not observed in the lots of folic acid examined.

Identity of Impurities—Where authentic samples of reported impurities could be obtained, direct chromatography of them in both TLC

[13] Folvite, Lederle.
[14] Sequestrene Sodium, Lederle.

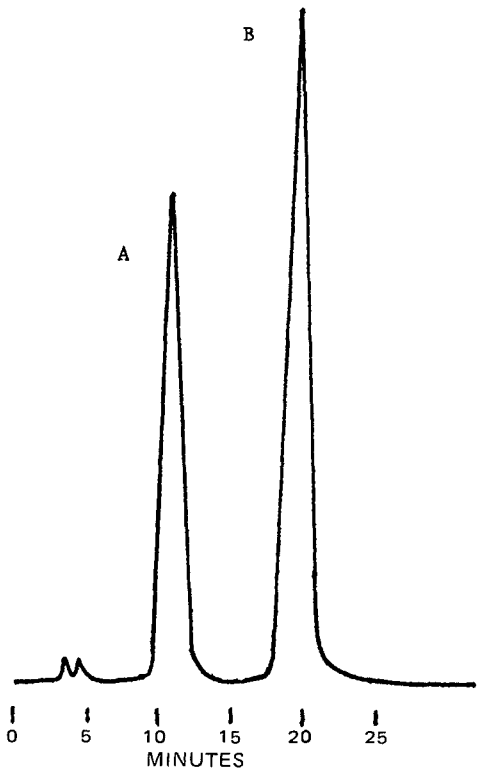

Figure 3—*High-pressure liquid chromatogram of leucovorin calcium (A) and folic acid (B) using the assay system.*

and HPLC systems demonstrated that all were separated by both methods. There was no rank-order correlation between R_f and k' values.

Figure 1 shows a typical chromatogram of folic acid, R_f 0.50, well separated from its impurities at R_f 0.28, 0.66, 0.74, and 0.80. Plates were sprayed with colorimetric reagents as directed under *TLC Assay*. The unidentified impurities in bands 11 and 14 reacted with colorimetric reagents only after potassium permanganate treatment, indicating that these impurities are measured along with folic acid in the USP XIX and similar colorimetric methods.

The presence of *N*-(*p*-aminobenzoyl)-L-glutamic acid in band 13 was indicated by R_f comparison with reference material and by its reaction to the colorimetric reagent sprays both before and after the potassium permanganate spray. The R_f and fluorescent character of band 13 indicated that it also contained 2-amino-1,4-dihydro-4-oxo-6-pteridinecarboxylic acid.

The R_f and fluorescent character of band 15 indicated the presence of 2-amino-4(1*H*)-pteridinone. Although the R_f of band 15 also corresponded to *p*-aminobenzoic acid, it did not give the characteristic color reaction. Thus, *p*-aminobenzoic acid was not an impurity in the folic acid lots examined.

Extraction of thin-layer bands and subsequent HPLC was not entirely satisfactory in correlating TLC and HPLC separations. The HPLC analysis of the 0.3 *N* ammonia extract of the TLC folic acid band demonstrated the presence of several impurities known to be separated by TLC, indicating folic acid decomposition during isolation. Likewise, the high phosphate–perchlorate concentrations in fractions collected from HPLC interfered with subsequent TLC analysis. When 0.1% ammonium carbonate was employed as an HPLC mobile phase, collected fractions could be analyzed by TLC.

Figure 2 shows a typical HPLC separation of folic acid (k' = 6.5) from its impurities at k' = 0.12, 0.35, 2.2, 4.4, and 14.3. HPLC component 1 cochromatographed with *N*-(*p*-aminobenzoyl)-L-glutamic acid and *p*-aminobenzoic acid. HPLC component 2 cochromatographed with 2-amino-1,4-dihydro-4-oxo-6-pteridinecarboxylic acid. Components 1 and 2 collected from the ammonium carbonate HPLC system gave an R_f value comparable to band 13.

HPLC component 3 (k' = 2.2) cochromatographed with 2-amino-4(1*H*)-pteridinone. After collection of component 3 (HPLC ammonium carbonate system) and subsequent TLC, bands 14 and 15 were detected by longwave UV light. TLC band 15 cochromatographed with 2-amino-4(1*H*)-pteridinone, while TLC band 14 has not yet been identified.

Table II—HPLC Parameters

Peak	Retention Time, min		Capacity Factor, k'[a]	
	Ambient[b]	35°	Ambient[b]	35°
1	2.9	2.7	0.12	~0
2	3.5	2.7	0.35	~0
3	8.2	5.7	2.2	1.1
4	13.9	—[c]	4.4	—[c]
Folic acid[d]	19.4	12.1	6.5	3.5
6	39.8	23.2	14.3	7.6

[a] $k' = (T_r - T_0)/T_0$, where T_r = folic acid retention time, and T_0 = retention time of unretained component. [b] Approximate room temperature, 25°. [c] Peak not resolved. [d] The number of theoretical plates, $N = 5.54\ (T_r/W_{1/2})^2$, where T_r = retention time and $W_{1/2}$ = peak width at half height, was 1950 at ambient temperature and 670 at 35°.

The correspondence of HPLC component 4 and TLC band 14 has not been confirmed. Both appeared to be a composite of at least two impurities. HPLC component 4 (k' = 4.4) was not separated in the ammonium carbonate system where it may have chromatographed with component 3 or with folic acid (component 5). When component 3 was collected (HPLC ammonium carbonate system) and rechromatographed in the perchlorate–phosphate–methanol system, component 4 as well as component 3, 2-amino-4(1*H*)-pteridinone, was detected.

The folic acid peak was collected from the ammonium carbonate system in two portions. Chromatography of both the first half and the second half of the collected folic acid peak in the perchlorate–phosphate–methanol system yielded detectable amounts of components 1, 2, 3, and 4 (k' = 0.12, 0.35, 2.2, and 4.4, respectively) as well as folic acid itself. TLC of both portions of the collected folic acid gave bands 14 and 15 as well as folic acid. These results indicate some decomposition of folic acid during collection and preparation for rechromatography, making it difficult to substantiate the purity of the folic acid peak.

TLC band 11 corresponded to HPLC component 6 (k' = 14.3). Both were present in the present USP reference standard (designated A) and commercial lots but were absent in a previous USP reference standard (designated B).

An unidentified trace impurity (0.05%, k' = 2.5) eluting between components 3 and 4 was detected in 1-day-old solutions of folic acid but not in fresh solutions. When a standard preparation (10 mg/ml) was heated with aeration at 80° for 2 hr, this decomposition product increased along with HPLC components 1–4. Decomposition of aerated and heated solutions was also shown by TLC; an additional fluorescent band above band 15 (R_f 0.87) was detected.

Tetrahydrofolic acid and dihydrofolic acid were chromatographed to aid in impurity identification. Both gave a k' = 7.6 and were resolved from folic acid (k' = 6.5) when present at the 30% level. In addition to the dihydrofolic acid and tetrahydrofolic acid main peaks, numerous peaks, including one cochromatographing with folic acid, were present, indicating sample impurity and/or rapid decomposition. Likewise, numerous thin-layer bands were detected by shortwave and longwave light as well as a shortwave absorbing band cochromatographing with the folic acid main band. TLC results indicated ongoing sample decomposition. With either compound, the number of bands present made it difficult to determine which were attributable to dihydrofolic or tetrahydrofolic acid.

Moisture Determination—Determination of folic acid moisture content is nearly as important in determination of purity as the assay procedure. Commercial folic acid samples usually contain 7–9.5% moisture, but they readily equilibrate with atmospheric humidity. Because the moisture content of a sample so quickly changes, it is necessary to determine the moisture content at the same time that the sample is weighed for the assay determination.

The British Pharmacopoeia (9) specifies drying at 100° in vacuum to constant weight. Samples that had lost 6–7% in weight at these conditions still contained sufficient moisture by Karl Fischer titration to indicate predominance of the monohydrate (3.9% moisture) after drying. The dried material rapidly picked up moisture to return to the 7–9% range. Since the drying conditions do not remove all moisture and the dried material is hygroscopic, this procedure is not satisfactory.

Attempts at moisture determination using the USP XIX direct titrimetric procedure (13) resulted in unreliable moisture values, which varied by several percent. The poor results were due to the low solubility of folic acid in the methanolic media usually used. Even if the medium was stirred during folic acid addition, large clumps formed with entrapped moisture. Similar difficulties were reported[5] with the direct determination in

Table III—Moisture Determination[a]

Lot[b]	Moisture, % ± *SD*[c]
A_1	7.68 ± 0.18
B_1	9.05 ± 0.20
A_2	8.46 ± 0.15
B_2	8.55 ± 0.19
C	7.75 ± 0.15
D	8.48 ± 0.14
E	8.48 ± 0.03

[a] Values were determined potentiometrically (Karl Fischer determination) using chloroform–methanol (4:1) as the solvent. [b] Subscripts denote different sublots of the USP reference standard Lots A and B. Commercial lots are denoted by C, D, and E. [c] Values are the means of at least three determinations.

methanol, and a back-titration procedure (13) was complex and tedious, but a mixture of chloroform–methanol (4:1) dispersed the folic acid particles and allowed the release of water for titration. In this laboratory, use of chloroform–methanol (4:1) eliminated the problem of particle aggregation and led to reproducible values for the lots of folic acid tested (Table III). Increasing the chloroform beyond the specified amount led to poor electrode response.

Assay Comparison—Results for direct colorimetric, USP XIX colorimetric, TLC, and HPLC methods are given in Table I. Confidence limits at 95% were calculated by the range method (17). The values in Table I are all corrected for moisture by the same titrimetric determinations for each lot made at the time samples were weighed. This correction allowed a comparison of results without concern about significant variations in moisture content and its determination. Furthermore, TLC and HPLC assays were conducted using subsampling from the same solutions.

The USP XIX colorimetric assay gave anomalous results. For example, assay of Lots B *versus* A, Lots A *versus* B, and Lots A *versus* A all gave >100% (101–109%). This result may have been due to the fact that sample and standard were not treated similarly. Also, the calculation procedure concentrates measurement uncertainties, making achievement of precision and accuracy most difficult. For example, a realistic 0.5% difference in true absorbance for "tube 1" (6) leads to a difference of 1.8% in the final assay value. Also, values for "tubes 3 and 4" (used to subtract amounts of *p*-aminobenzoic acid and other diazotizable impurities) are sufficiently low to make accurate determination difficult, yet they have a considerable effect on the final purity value when taken through the calculation. Another problem is that the method is unspecific for folic acid in the presence of any impurities that oxidize to diazotizable compounds.

In contrast, the direct colorimetric determination results for relatively pure reference standard material are more consistent with the chromatographic assays. However, direct colorimetry lacks the control of specific impurities offered by the chromatographic assays and could give misleading purity values for commercial folic acid. This method would be suitable for tablet content uniformity determination.

The two chromatographic assays gave comparable results on separate days for reference standard (B *versus* A) evaluation. This result was not unexpected, since the precision, linearity, and specificity of both methods were demonstrated. The choice of one procedure over the other depends on the resources of a particular laboratory. Unlike the HPLC method, the TLC method does not require a substantial investment in equipment or the availability of reproducible and dependable columns. Since fewer manipulative steps are required with HPLC, precision is less chemist dependent, the method is less work intensive, and less elapsed time is required for completion of an assay.

REFERENCES

(1) M. Hashmi, "Assay of Vitamins in Pharmaceutical Preparations," Wiley, New York, N.Y., 1973, p. 215.

(2) Y. A. Popova and E. Kovacheva, *Nauchni. Tr. Vissh Inst. Khranit. Vkusova Promst., Plovdiv,* **17,** 351 (1970); through *Chem. Abstr.,* **77,** 52391n (1972).

(3) *Ibid.,* **16,** (1969); through *Chem. Abstr.,* **77,** 168685r (1972).

(4) M. Hashmi, "Assay of Vitamins in Pharmaceutical Preparations," Wiley, New York, N.Y., 1973, p. 222.

(5) W. J. Mader and H. A. Frediani, *Anal. Chem.,* **20,** 1199 (1948).

(6) "The United States Pharmacopeia," 19th rev., Mack Publishing Co., Easton, Pa., 1974, pp. 211, 624.

(7) B. L. Hutchings, E. L. R. Stokstad, J. H. Boothe, J. H. Mowat, C. W. Waller, R. B. Angier, J. Semb, and Y. Subbarow, *J. Biol. Chem.,* **168,** 705 (1947).

(8) W. D. Hubbard, M. E. Hintz, and D. A. Libby, *J. Assoc. Offic. Anal. Chem.,* **49,** 804 (1966).

(9) "British Pharmacopoeia 1973," Her Majesty's Stationery Office, London, England, 1973, p. 210.

(10) H. S. R. Iyer and B. K. Apte, *Indian J. Pharm.,* **31,** 58 (1969); M. Hashmi, "Assay of Vitamins in Pharmaceutical Preparations," Wiley, New York, N.Y., 1973, p. 221.

(11) F. Y. Tripet and U. W. Kesselring, *Pharm. Acta Helv.,* **50,** 312 (1975).

(12) R. C. Williams, D. R. Baker, and J. A. Schmit, *J. Chromatogr. Sci.,* **11,** 618 (1973).

(13) "The United States Pharmacopeia," 19th rev., Mack Publishing Co., Easton, Pa., 1975, pp. 668, 669.

(14) *Ibid.,* p. 640.

(15) W. P. Tong, J. Rosenberg, and D. B. Ludlum, *Lancet,* **2,** 719 (1975).

(16) P. J. Twitchett and H. C. Moffat, *J. Chromatogr.,* **111,** 149 (1975).

(17) E. L. Bauer, "A Statistical Manual for Chemists," Academic, New York, N.Y., 1971, p. 152.

ACKNOWLEDGMENTS AND ADDRESSES

Received May 21, 1976, from the *Drug Research and Testing Laboratory, United States Pharmacopeia, Rockville, MD 20852.*

Accepted for publication September 23, 1976.

Presented in part at the Pharmaceutical Analysis and Control Section, APhA Academy of Pharmaceutical Sciences, New Orleans meeting, April 1976.

The authors thank Dr. George Kurtz, Sherer Corp., for the folic acid samples.

[x] To whom inquiries should be directed.

High-Performance Liquid Chromatographic Determination of Perphenazine and Amitriptyline Hydrochloride in Two-Component Tablet Formulations

A. G. BUTTERFIELD ˣ and R. W. SEARS

Abstract □ A rapid, precise, and accurate high-performance liquid chromatographic procedure is presented for the simultaneous determination of perphenazine and amitriptyline hydrochloride in two-component tablet formulations. An aliquot of a methanolic extract of the tablet, containing trifluoperazine hydrochloride as an internal standard, is chromatographed on a nitrile bonded phase microparticulate column using a 0.005 *M* ammonium acetate–methanol (20:80) mobile phase. Quantitation is by peak area. The relative standard deviations for the procedure are 0.34 and 0.54% for the simultaneous determination of perphenazine and amitriptyline, respectively. Eight commercial tablet formulations were analyzed and found to contain 96.5–101.5 and 96.5–103.3% of the labeled amounts of perphenazine and amitriptyline hydrochloride, respectively.

Keyphrases □ Perphenazine—high-performance liquid chromatographic analysis, pharmaceutical formulations containing amitriptyline hydrochloride □ Amitriptyline hydrochloride—high-performance liquid chromatographic analysis, pharmaceutical formulations containing perphenazine □ High-performance liquid chromatography—analyses, perphenazine and amitriptyline hydrochloride, two-component pharmaceutical formulations □ Tranquilizers—perphenazine, high-performance liquid chromatographic analysis, pharmaceutical formulations containing amitriptyline hydrochloride □ Antidepressants—amitriptyline hydrochloride, high-performance liquid chromatographic analysis, pharmaceutical formulations containing perphenazine

Perphenazine–amitriptyline hydrochloride two-component tablet formulations are produced by several manufacturers (1). To monitor the quality of these preparations, a rapid, accurate procedure, applicable to all formulations, was required for the simultaneous determination of both drugs. Conventional methods of analysis (2–6), such as the pharmacopeial procedures for the individual drugs (5, 6) are not suitable because of interference from the other components.

High-performance liquid chromatography (HPLC), however, is ideally suited to the analysis of mixtures (7–9) and has been employed extensively for the analysis of both phenothiazine (10–13) and dibenzcycloheptadiene (14, 15) drugs, including the quantitative determination of amitriptyline hydrochloride (15). This report describes an HPLC procedure for the simultaneous determination of perphenazine and amitriptyline hydrochloride in two-component tablet formulations.

EXPERIMENTAL

Materials—Amitriptyline hydrochloride USP[1] and perphenazine NF[2] were used as received. Both drug substances were compared chromatographically (HPLC) for retention time, impurities, and response factor to appropriate reference standards (NF and USP) and were assayed by nonaqueous titration procedures (5, 6). Both drug substances were essentially identical to their respective reference standards.

Trifluoperazine hydrochloride[3] was used as received. Solvents and reagents were commercial analytical reagent grade. Water was double distilled in an all-glass still and filtered through a 0.2-μm filter[4] with the aid of suction.

Apparatus—A liquid chromatograph[5], fitted with a septumless injection port[5], a fixed wavelength UV detector[5] (254 nm), and a computing integrator[6], was used. The detector was attenuated to 0.08 absorbance unit full scale (aufs), and the integrator output was attenuated ×4 throughout.

Column—A 25 × 0.216-cm i.d. column containing a nitrile bonded phase packing[7] was used at ambient temperature and at a mobile phase flow rate of 80 ml/hr (150 bar).

Mobile Phase—Methanol–0.005 *M* ammonium acetate in double-distilled water (80:20) was prepared as required, degassed (refluxed for 5 min), and then stored in the solvent reservoir of the instrument.

Internal Standard Solution—A solution of trifluoperazine hydrochloride in methanol (0.25 mg/ml) was used.

Standard Curves—Methanolic stock solutions of perphenazine (1.0 mg/ml), amitriptyline hydrochloride (5.0 mg/ml), and trifluoperazine hydrochloride (1.25 mg/ml) were prepared. Standard solutions were prepared by pipetting 5.0 ml of trifluoperazine stock solution into each of seven 25-ml volumetric flasks along with 10.0, 8.0, 6.0, 5.0, 4.0, 2.0, or 1.0 ml of both perphenazine and amitriptyline stock solutions. Each solution was diluted to volume with methanol, if necessary, and duplicate 5-μl aliquots of each standard solution were chromatographed.

Calibration Standard Solutions—Approximately 3 mg of perphenazine and 15 mg of amitriptyline hydrochloride, accurately weighed, were transferred to a 20 × 150-mm screw-capped culture tube[8] and dissolved in 25.0 ml of internal standard solution. Duplicate 5-μl aliquots of the resulting solution were chromatographed periodically to check the slopes of the calibration curves.

Analysis of Pharmaceuticals—*Single-Tablet Assay*—A tablet was placed in a 20 × 150-mm screw-capped culture tube and crushed to a fine powder with a glass rod. Internal standard solution, 25.0 ml, was added to the tube, which was then closed, tumbled on a rotator[9] at 30 rpm for 15 min, and centrifuged[10] at 2000 rpm for 5 min. Duplicate 5-μl aliquots of the supernate were chromatographed.

Tablet Composite Assay—A tablet composite was prepared by grinding 20 tablets in a mechanical mill[11]. A quantity of powdered tablet material equivalent to one tablet was transferred to a 20 × 150-mm screw-capped culture tube. The sample was treated as described previously.

Quantitation—Quantitation was by peak area ratio of the sample to the internal standard.

RESULTS AND DISCUSSION

Evaluation of Chromatographic Systems—Table I lists retention times (R_T), column efficiency (N), capacity factors (k'), selectivity (α), and resolution (R) data for perphenazine and amitriptyline hydrochloride on three bonded phase columns. Perphenazine eluted behind amitriptyline on the octadecylsilane bonded phase column[12] and ahead on the fluoroether bonded phase column[13]. The early elution of perphenazine is desirable, since it is the minor component in perphenazine–amitriptyline formulations. The fluoroether column was not as efficient and did not provide as high resolution as the nitrile bonded phase

[1] Merck Sharp and Dohme, Kirkland, Quebec, Canada.
[2] Schering, Pointe-Claire, Quebec, Canada.
[3] Smith Kline and French, Montreal, Canada.
[4] FGLP04700, Millipore Ltd., Mississauga, Ontario, Canada.
[5] Model 4100, Varian Aerograph, Palo Alto, Calif.
[6] Autolab System I, Spectra-Physics, Santa Clara, Calif.
[7] Micropak-CN, Varian Aerograph, Palo Alto, Calif.
[8] Canadian Laboratory Supplies, Montreal, Canada.
[9] Multi-Purpose rotator, Scientific Industries, Springfield, Mass.
[10] Model K, International Equipment Co., Needham Heights, Mass.
[11] Micro Mill, Chemical Rubber Co., Cleveland, Ohio.
[12] Prepared by bonding octadecyltrichlorosilane (Aldrich) to dried LiChrosorb SI-60 (Merck) under anhydrous conditions.
[13] FE Sil-X-I, Perkin-Elmer Corp., Norwalk, Conn.

Table I—Comparison of Chromatographic Parameters for Perphenazine and Amitriptyline Hydrochloride on Three Columns

Column	Retention Time, R_T, min	Capacity Factor, k'	Number of Theoretical Plates, N	Selectivity, α	Resolution, R	Compound
A[a]	4.2	3.2	560	—	—	Perphenazine
	3.0	2.0	800	1.6	2.2	Amitriptyline
B[b]	3.5	3.7	175	—	—	Perphenazine
	4.9	5.5	340	1.5	1.5	Amitriptyline
C[c]	1.3	1.5	490	—	—	Perphenazine
	4.2	8.0	820	5.3	6.0	Amitriptyline

[a] Octadecyltrichlorosilane reacted with dry 10-μm silica under anhydrous conditions. The mobile phase was 2 drops of acetic acid–30% 0.1 *M* ammonium acetate–70% acetonitrile. The column was 250 × 2.2 mm i.d., and the flow rate was 60 ml/hr. [b] Commercial fluoroether bonded phase. The column was 250 × 2.2 mm i.d., and the flow rate was 60 ml/hr. The mobile phase was the same as for Column A, except that 50% acetonitrile was used. [c] Commercial nitrile bonded phase. The column was 250 × 2.2 mm i.d., and the flow rate was 80 ml/hr. The mobile phase was 20% 0.005 *M* ammonium acetate–80% methanol.

column[7], which also allowed perphenazine to elute first; accordingly, the nitrile column was chosen.

While searching for a suitable internal standard, various related phenothiazines, dibenzcycloheptadienes, and several dibenzazepines were chromatographed on the nitrile column (Table II). Trifluoperazine hydrochloride eluted between the two compounds of interest and was chosen.

Figure 1 shows a chromatogram obtained when a representative tablet formulation was analyzed by the described procedure. The internal standard and the two compounds of interest were well resolved in less than 6 min.

Linearity and Standard Curves—A plot of peak area *versus* the amount of trifluoperazine hydrochloride injected was linear below about 3 μg/injection (0.6 mg/ml). A level of 0.25 mg/ml was used in the analytical procedure.

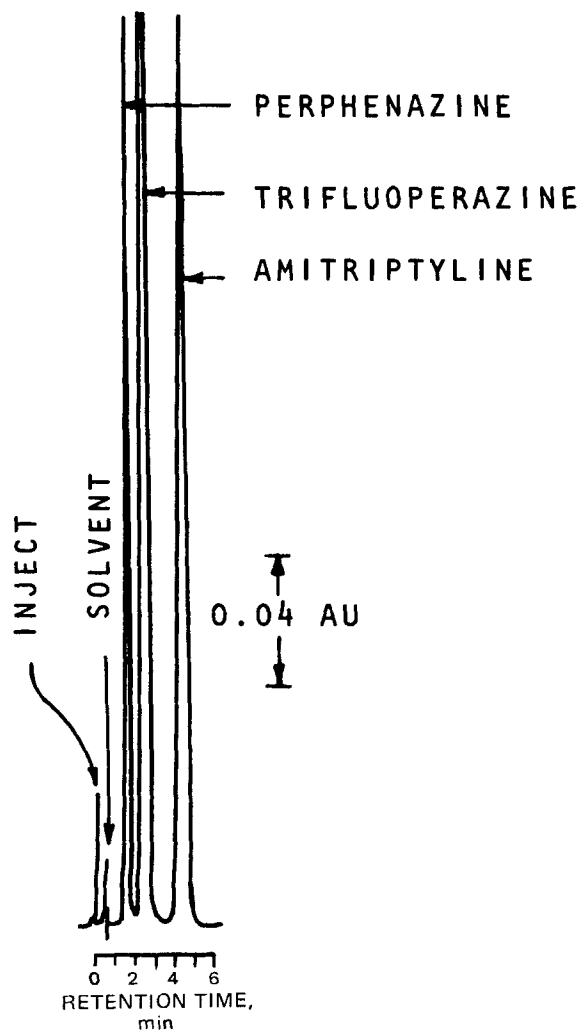

Figure 1—*High-performance liquid chromatogram of an extract of a perphenazine–amitriptyline hydrochloride tablet (4 and 25 mg, respectively).*

Standard curves for perphenazine and amitriptyline hydrochloride were constructed by plotting sample to internal standard peak area ratios *versus* sample to internal standard weight ratios.

The standard curve for perphenazine was linear with a negligible intercept to >1.25 μg/injection when examined over the range of 0.2–2.0 μg/injection (40–400 μg/ml). The mean slope of the linear portion of the line was 1.37 with a relative standard deviation of 1.4%. Similarly, the standard curve for amitriptyline hydrochloride was linear with a negligible intercept to >8 μg/injection when examined over the range of 1.0–10.0 μg/injection (0.2–2.0 mg/ml). The mean slope of the linear portion of the line was 0.42 with a relative standard deviation of 1.8%. Therefore, the standard curves are applicable to tablets containing from 1 to 6 mg of perphenazine and from 5 to 40 mg of amitriptyline hydrochloride using the described procedure.

Duplicate injections of replicate calibration standard solutions were chromatographed periodically to determine the slopes of the standard curves. When using a single calibration standard, stored at 4° between uses, the relative standard deviations for the slopes of the perphenazine and amitriptyline hydrochloride standard curves over 4 weeks were ±1.1 and ±0.7%, respectively.

Sample Preparation—Various extraction solvents and conditions were tried. When water, water–methanol, or water–acetonitrile was used as the extraction solvent, all tablets disintegrated rapidly, but a fine suspension did not completely settle when centrifuged for 10 min at 2000 rpm. The use of methanol as the extraction solvent did not result in a suspension but also would not disintegrate coated tablets. Crushing the tablets before extraction allowed rapid extraction of both drugs with methanol.

The time for constant extraction of perphenazine and amitriptyline hydrochloride from the tablet mass was determined by tumbling crushed

Table II—Retention Times of Various Phenothiazine, Dibenzcycloheptadiene, and Dibenzazepine Drugs

Compound	Retention Time[a], min
Phenothiazines	
Perphenazine	1.4
Trifluoperazine hydrochloride	2.2
Phenothiazine	0.5[b]
2-(Trifluoromethyl)phenothiazine	0.5[b]
10-(3-Chloropropyl)-2-(trifluoromethyl)-phenothiazine	0.5[b]
Isopromethazine hydrochloride	2.6
Promethazine hydrochloride	3.2
Promazine hydrochloride	5.4
Chlorpromazine hydrochloride	4.0
Trifluopromazine hydrochloride	3.3
Methotrimeprazine hydrochloride	3.7
Thioproperazine	3.0
Prochlorperazine maleate	2.9
Dibenzcycloheptadienes	
Amitriptyline hydrochloride	4.0
Nortriptyline hydrochloride	4.1
Protriptyline hydrochloride	4.3
Dibenzocycloheptanone	0.5[b]
Dibenzazepines	
Trimipramine maleate	3.7
Imipramine hydrochloride	5.0
Desipramine hydrochloride	4.6

[a] The column was 250 × 2.2-mm i.d. Micropak-CN, the flow rate was 80 ml/hr, and the mobile phase was 0.005 *M* ammonium acetate–methanol (20:80). [b] Solvent front (t_0).

Table III—Analysis of Synthetic Solutions

Sample	Amitriptyline Hydrochloride			Perphenazine		
	Calculated, mg/ml	Found, mg/ml	Recovery, %	Calculated, mg/ml	Found, mg/ml	Recovery, %
1	1.013	1.033	102.0	0.0962	0.0966	100.4
2	0.648	0.655	101.0	0.144	0.143	99.3
3	0.432	0.430	99.4	0.192	0.190	99.0
4	1.048	1.035	98.8	0.195	0.195	100.0
5	0.311	0.311	100.0	0.0962	0.0956	99.4
Mean recovery, %			100.2			99.6
RSD, %			1.2			0.6

single tablets of a representative formulation for 5, 10, and 15 min in 25 ml of the internal standard solution. In each case, the sample was centrifuged briefly after each 5-min period and a 5-μl aliquot was chromatographed. The peak area ratios were identical at all three times, indicating constant extraction of both compounds in less than 5 min. Extraction was approximately complete based on response factor data and the label claims for the formulation used; however, a dilution procedure was used to prove this finding. When tablet composite samples equivalent to the weights of one-half, one, and one and one-half tablets were analyzed by the described procedure, using a 15-min tumbling time, the concentrations of perphenazine and amitriptyline hydrochloride were in the ratio 1:2:3. These data showed that constant and complete extraction of the compounds of interest was effected in less than 15 min under the conditions described.

Quantitation—Quantitation was by peak area. The reproducibility of the chromatographic system was shown by chromatographing 12 5-μl aliquots of a calibration standard solution containing 1.04 mg of amitriptyline hydrochloride/ml, 0.096 mg of perphenazine/ml, and 0.55 mg of trifluoperazine hydrochloride/ml. The relative standard deviations of the peak area ratios were ±0.29 and ±0.74% for perphenazine and amitriptyline hydrochloride, respectively.

Five solutions containing perphenazine and amitriptyline hydrochloride, prepared in the same manner as the calibration standard solutions, were analyzed using the described procedure. Table III shows that the mean recoveries for the two compounds were 99.6 and 100.2%, respectively.

Table IV—Analysis of Perphenazine–Amitriptyline Hydrochloride Tablet Formulations [a] by HPLC

Formulation	Perphenazine		Amitriptyline Hydrochloride	
	Label, mg	Found[b], %	Label, mg	Found, %
A	3	97.9	15	96.9
B	4	96.8	25	99.5
C	2	96.5	25	98.9
D	2	101.5	25	103.3
E	4	96.8	25	96.5
F	2	99.9	25	102.0
G	4	100.0	10	102.2
H	2	98.9	25	100.4

[a] Tablet composite assay. [b] Percent of label claim.

Seven replicate samples of a formulation composite, prepared from tablets labeled to contain 4 mg of perphenazine and 25 mg of amitriptyline hydrochloride, were also assayed. The relative standard deviations of the peak ratios were 0.34% for perphenazine and 0.54% for amitriptyline hydrochloride.

Eight commercial formulations of perphenazine–amitriptyline hydrochloride tablets were analyzed in duplicate. Table IV shows that the levels of both drugs varied between 96.5 and 103.3% of the label claim amount.

REFERENCES

(1) "Compendium of Pharmaceuticals and Specialties," 11th ed., Canadian Pharmaceutical Association, Toronto, Canada, 1976.

(2) H. Hoshino and A. Tsuji, *Jpn. Anal.*, **22**, 163 (1973); through *Anal. Abstr.*, **27**, 1621 (1974).

(3) J. Dobrecky and A. M. Z. deSuffrite, *Proanalisis*, 2(3), 10 (1969); through *Anal. Abstr.*, **18**, 4311 (1970).

(4) H. Basinska, H. Puzanowska-Tarasiewicx, and M. Tarascewicz, *Chem. Anal.*, **15**, 405 (1970); through *Anal. Abstr.*, **20**, 265 (1971).

(5) "The National Formulary," 14th ed., Mack Publishing Co., Easton, Pa., 1975.

(6) "The United States Pharmacopeia," 19th rev., Mack Publishing Co., Easton, Pa., 1975.

(7) A. Menyharth, F. P. Mahn, and J. E. Heveran, *J. Pharm. Sci.*, **63**, 430 (1974).

(8) J. S. Mayell, C. F. Hiskey, and L. Lachman, *Anal. Chem.*, **46**, 449 (1974).

(9) T. L. Sprieck, *J. Pharm. Sci.*, **63**, 591 (1974).

(10) W. Lindner, R. W. Frei, and W. Santi, *J. Chromatogr.*, **108**, 299 (1975).

(11) D. H. Rodgers, *J. Chromatogr. Sci.*, **12**, 742 (1974).

(12) M. Caude, L. X. Phan, B. Terlain, and J. P. Thomas, *ibid.*, **13**, 390 (1975).

(13) N. J. Pound and R. W. Sears, *Can. J. Pharm. Sci.*, **8**(3), 84 (1973).

(14) J. H. Knox and J. Jurand, *J. Chromatogr.*, **103**, 311 (1975).

(15) I. D. Watson and M. J. Stewart, *ibid.*, **110**, 389 (1975).

ACKNOWLEDGMENTS AND ADDRESSES

Received August 20, 1976, from the *Drug Research Laboratories, Health Protection Branch, Ottawa, Canada, K1A 0L2.*

Accepted for publication September 27, 1976.

[x] To whom inquiries should be directed.

Synthesis of Various Geometric and Enantiomeric Oxime *O*-(α- and β-Methylcholinyl) Ethers as Potential Anticholinergic Agents

PEDRO L. HUERTA *, EUGENE I. ISAACSON ‡, ROBERT G. BROWN, and JAIME N. DELGADO ˣ

Abstract □ Various enantiomeric and geometric oxime *O*-(α- and β-methylcholinyl) ethers were synthesized as potential anticholinergic agents. The synthesis, separation, resolution, and structural characterization of these compounds are reported. The first step of the synthetic pathway involved an oxime formation, with subsequent *O*-alkylation of the respective oxime with 2-chloro-*N*,*N*-dimethylpropylamine hydrochloride. The separation of the α- and β-structural isomers utilized vacuum fractional distillation and/or column chromatography, and the resolution of the enantiomers was accomplished *via* the formation of tartrate diastereoisomers. A preliminary pharmacological evaluation for anticholinergic activity was conducted using a rat ileum assay. Structure–activity relationships, including some stereochemical properties and antimuscarinic activity, are discussed.

Keyphrases □ Oxime *O*-(α- and β-methylcholinyl) ethers—synthesized, enantiomeric and geometric isomers separated, anticholinergic activity evaluated □ *O*-(α- and β-Methylcholinyl) ether derivatives of oximes—synthesized, enantiomeric and geometric isomers separated, anticholinergic activity evaluated □ Anticholinergic activity—evaluated in series of oxime *O*-(α- and β-methylcholinyl) ethers □ Structure–activity relationships—various oxime *O*-(α- and β-methylcholinyl) ethers, anticholinergic activity evaluated

The premise that a compound must possess optimal stereochemical properties for significant antimuscarinic activity has been well established by structure–activity relationship studies of atropine (1, 2), hyoscine (2–4), β-methylcholine esters of α-methyltropic acid and cyclohexylphenylglycolic acid (5, 6), and 2-substituted 4-dimethylaminomethyl-1,3-dioxolanes (7, 8).

Furthermore, the work dealing with β-methylcholine esters of α-methyltropic acid and cyclohexylphenylglycolic acid (5, 6) concluded that the stereochemistry of the amino alcohol moiety was not important for antimuscarinic activity, since the enantiomeric potency ratios were not very large when the absolute configuration of the β-methylcholine moiety was varied. However, in the same reports (5, 6) and in earlier work (9), the data indicated that β-methyl substitution reduced anticholinergic activity but that the converse was true for α-methyl substitution. Therefore, α-methylcholine derivatives should be studied as potential anticholinergic agents.

In view of this earlier work and of the fact that oxime *O*-ethers exhibited high antimuscarinic activity (10–12) and served as good models for studying geometric isomerism (12), a series of geometric and enantiomeric oxime *O*-(α- and β-methylcholinyl) ethers was synthesized. A preliminary pharmacological evaluation was also conducted, since these data could lead to postulated receptor interactions if certain limitations are considered, such as comparing data of analogous compounds (13) and ensuring relative stereochemical purity (14).

DISCUSSION

Synthesis—The major steps in the synthesis of the racemic *O*-(α- and β-methylcholinyl) ethers of 1-methyl-4-piperidone oxime (Iα and Iβ), benzophenone oxime (IIα and IIβ), (*E*)-phenyl 2-pyridyl oxime (IIIα and IIIβ), and (*Z*)-phenyl 2-pyridyl oxime (IVα and IVβ) (Table I) are depicted in Scheme I.

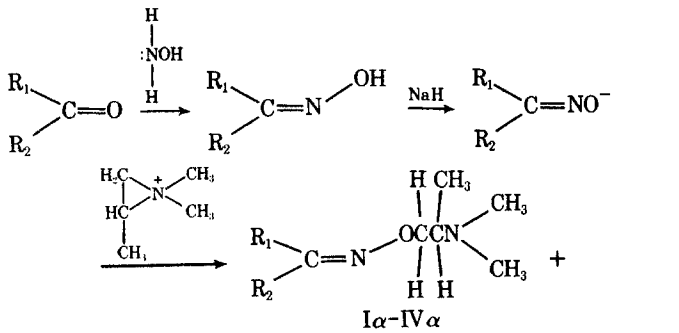

Scheme I

Oxime formation was the first step (Scheme I). The oxime from 1-methyl-4-piperidone was produced with a method adapted from Kochhar *et al.* (10). Benzophenone, (*E*)-phenyl 2-pyridyl, and (*Z*)-phenyl 2-pyridyl oximes were obtained by utilizing the Wylie *et al.* (15) base-catalyzed procedure. However, the synthetic procedure employing phenyl 2-pyridyl ketone formed a mixture of the (*E*)- and (*Z*)-geometric isomers.

Separation of the geometric isomers was accomplished by selective crystallization of the oximes when the pH of the acidic solution containing the oxime hydrochloride salts was adjusted to 2.5 with an aqueous 10% sodium hydroxide solution. Each of two consecutive adjustments to a pH value less than 2.5 with the sodium hydroxide solution yielded the (*Z*)-isomer, while a third adjustment to a pH of 2.5 produced a mixture of both isomers. Subsequent adjustments to a pH value greater than 2.5 caused the precipitation of the (*E*)-isomer. The (*Z*)-isomer was precipitated first, since it existed primarily in the monoprotonated form (*X*) and was the stronger conjugate acid. The (*E*)-isomer remained in solution until a higher pH value was reached, because the protonated pyridyl nitrogen (*Y*) was the weaker conjugate acid.

The difference in the degree of availability of the electrons of the pyridyl nitrogen in the formation of the hydrochloride salts was accounted for by variations in intramolecular hydrogen bonding. The IR spectrum for the (*E*)-isomer in chloroform demonstrated a free hydroxyl group at 3550 cm^{-1}, but a similar one was absent in the spectrum of the (*Z*)-isomer. The NMR data also substantiated the intramolecular hydrogen bonding in the (*Z*)-isomer when the chemical shifts of the hydrogen atoms (a) on the carbon atoms adjacent to the nitrogens of the 2-pyridyl substituents

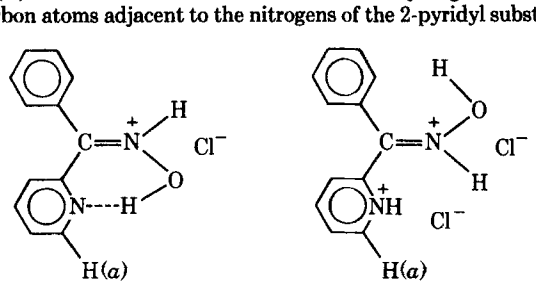

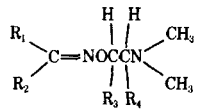

Table I—Oxime *O*-(α- and β-Methylcholinyl) Ethers

Compound	R_1	R_2	R_3, NMR Chemical Shift (τ)	R_4, NMR Chemical Shift (τ)	Boiling Point	Yield, g, %	Oxime, g, mole	Sodium Hydride, g, mole	Alkyl Halide, g, mole
(±)-Iα	$CH_3NC_5H_8$		H (6.11)	CH_3 (9.06)	92–94° (1.15 mm Hg)	32, 79	25.6, 0.2	18.8, 0.4	31.6, 0.2
(±)-Iβ	$CH_3NC_5H_8$		CH_3 (8.82)	H (7.60)	88–90° (2 mm Hg)	30, 71	29.55, 0.15	14.4, 0.309	23.7, 0.15
(±)-IIα	C_6H_5	C_6H_5	H (5.88)	CH_3 (9.06)	133–137° (0.15 mm Hg)	28, 89	22, 0.112	10.4, 0.224	17.6, 0.112
(±)-IIβ	C_6H_5	C_6H_5	CH_3 (8.73)	H (7.62)	106–109° (0.1 mm Hg)	15, 95	11, 0.056	5.2, 0.112	8.8, 0.056
(±)-IIIα	C_5H_4N	C_6H_5	H (5.88)	CH_3 (9.06)	—	—	—	—	—
(±)-IIIβ	C_5H_4N	C_6H_5	CH_3 (8.73)	H (7.60)	—	—	—	—	—
(±)-IVα	C_5H_4N	C_6H_5	H (5.88)	CH_3 (9.06)	—	—	—	—	—
(±)-IVβ	C_5H_4N	C_6H_5	CH_3 (8.73)	H (7.62)	—	—	—	—	—

were studied. The NMR spectrum of Form *X* did not demonstrate a significant variation in the chemical shifts of the analogous (*a*) protons when compared to the NMR spectrum of the free oxime, because protonation did not take place on the pyridyl nitrogen since its electrons were already involved in intramolecular hydrogen bonding. However, the analogous (*a*) proton in Form *Y* was shifted downfield (0.80 τ) relative to the (*a*) proton (1.40 τ) of the (*E*)-isomer, since it was deshielded when the pyridyl nitrogen was protonated.

The next step of the synthetic pathway (Scheme I) consisted of the generation of the anionic oxime derivatives when sodium hydride was added. The etherification mechanism generally encompasses a nucleophilic attack by the anionic oxime derivative on the alkyl halide, resulting in the displacement of the halide ion. However, in this investigation the interaction between the nucleophiles and 2-chloro-*N*,*N*-dimethylpropylamine did not proceed exactly as in the other *O*-alkylation reactions, since α- and β-methyl structural isomers were obtained from the same reaction mixtures.

The formation of Iα–IVα and Iβ–IVβ may be rationalized *via* the etherification procedures involving a cyclic aziridinium-ion intermediate, which was formed when the neighboring amino group anchimerically assisted the displacement of the halide ion and became internally bonded to two different positions in the molecule (16, 17). The reactions proceeded *via* a nucleophilic attack on the cyclic immonium ion, producing Iα–IVα when the attack took place on the secondary carbon atom but Iβ–IVβ when the reactive site was the tertiary carbon atom. The α/β isomeric ratios demonstrated that the nucleophilic attack was more predominant at the least substituted carbon atom.

The α- and β-structural isomers were separated and purified with two techniques. Compounds Iα, Iβ, IIα, and IIβ were isolated *via* vacuum fractional distillation. Compounds IIα and IIβ were also separated with adsorption column chromatography, which proved successful in the separation of IIIα, IIIβ, IVα, and IVβ. The distillations and chromatographic separations were monitored using GLC, comparison of refractive indexes, TLC, and NMR and IR spectra.

Resolution—The two most commonly used methods for the resolution of racemic modifications (18, 19) are stereospecific synthesis and diastereoisomer formation. The stereospecific synthesis of the optically pure

Table II—Oxime *O*-(α- and β-Methyltrimethylaminoethyl) Ether Bromides

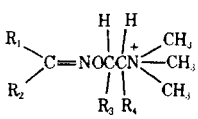

Compound	Melting Point	Empirical Formula	Analysis, % Calc.	Found
(±)-Iα CH_3Br	218–222°	$C_{13}H_{29}Br_2N_3O$	C 38.72	38.51
			H 7.19	7.16
			N 10.42	10.65
(±)-Iβ CH_3Br	209–211°	$C_{13}H_{29}Br_2N_3O$	C 38.72	38.06
			H 7.19	7.37
			N 10.42	9.70
(±)-IIα CH_3Br	189–190°	$C_{19}H_{25}BrN_2O$	C 60.49	60.76
			H 6.63	6.87
			N 7.43	7.38
(±)-IIβ CH_3Br	165–166°	$C_{19}H_{25}BrN_2O$	C 60.49	60.46
			H 6.63	6.75
			N 7.43	7.89

enantiomers was not considered because: (*a*) the synthetic pathway (Scheme I) was designed to take advantage of the formation of both structural isomers since the research proposal involved α- and β-isomeric derivatives, and (*b*) it has not been established that *O*-alkylation of oximes with 2-chloro-*N*,*N*-dimethylpropylamine proceeds exclusively *via* an S_N2 mechanism and any products formed by an S_N1 mechanism would lead to racemization.

The decision was made to resolve these racemates by the formation of diastereoisomeric derivatives and subsequent separation of the two different components *via* fractional crystallization. The first resolving agent, *d*-10-camphorsulfonic acid, did not prove satisfactory. The diastereoisomeric salts did not precipitate from the reaction mixture, and the mixture resisted separation with column chromatography when silica gel was used as the adsorbent material. However, (+)-tartaric acid formed stable diastereoisomeric derivatives. Subsequent treatment of the tartrates with triethylamine regenerated the free enantiomers, which were converted to the methylbromide derivatives (Tables II and III).

The relative purity of the diastereoisomers and corresponding methylbromide derivatives of the enantiomers from IIα and IIIα was determined by repeated recrystallizations until constant melting points and optical rotations were achieved (Table III). The methylbromide derivatives exhibited opposite optical rotations for the *dextro*- and *levo*-enantiomers (Table III), which also verified their relative purity. These physical properties have been employed previously (18) to substantiate the relative purity of diastereoisomers and crystalline enantiomeric derivatives.

Both types of derivatives, diastereoisomers and methylbromides, were subjected to elemental analyses (Table III) to substantiate their characterizations. An NMR spectral analysis of the diastereoisomers did not supply unambiguous data, even though some diastereoisomers exhibit significant differences when the appropriate solvent system is utilized (20).

Table III—Oxime *O*-(α-Methylcholinyl) Ether Tartrates and Methylbromides

Compound	Melting Point	$[\alpha]_D^{26}$	Empirical Formula	Analysis, % Calc.	Found
IIα Tartrate	128–130°	+8.38°	$C_{22}H_{28}N_2O_7$	C 61.11	60.91
				H 6.48	6.58
				N 6.48	6.52
(+)-IIα CH_3Br	177–179.5°	+17.28°	$C_{19}H_{25}BrN_2O$	C 60.49	60.36
				H 6.63	6.61
				N 7.43	7.33
IIα Tartrate	155–156°	+19.33°	$C_{22}H_{28}N_2O_7$	C 61.11	60.65
				H 6.48	6.58
				N 6.48	6.36
(−)-IIα CH_3Br	188–190°	−17.26°	$C_{19}H_{25}BrN_2O$	C 60.49	60.76
				H 6.63	6.88
				N 7.43	7.40
IIIα Tartrate	136–139°	+8.42°	$C_{21}H_{27}N_3O_7$	C 58.19	58.31
				H 6.23	6.15
				N 9.70	9.87
(+)-IIIα CH_3Br	176–178°	+20.4°	$C_{18}H_{24}BrN_3O$	C 57.16	57.07
				H 6.35	6.51
				N 11.11	11.31
IIIα Tartrate	156–158°	+19.4°	$C_{21}H_{27}N_3O_7$	C 58.19	58.13
				H 6.23	6.54
				N 9.70	9.80
(−)-IIIα CH_3Br	185–187°	−23.46°	$C_{18}H_{24}BrN_3O$	C 57.16	57.03
				H 6.35	6.28
				N 11.11	11.16

Table IV—Summary of Pharmacological Data of Oxime *O*-(α-Methyltrimethylaminoethyl) Ether Bromides

Compound (as Methylbromide Salt)	Dose[a], m*M*/70 ml	ED_{50}[b], m*M*	Potency[c] Ratio	Determinations[d]
(±)-IIα	1.33×10^{-5}	4.14×10^{-3} [e]	2.11	4
(±)-IIβ	1.33×10^{-5}	1.96×10^{-3} [e]		
(+)-IIα	7.96×10^{-6}	1.89×10^{-3} [e]	1.18	4
(−)-IIα	7.96×10^{-6}	1.60×10^{-3} [e]		
(+)-IIα	7.96×10^{-6}	10.3×10^{-5} [f]	1.05	4
(−)-IIα	7.96×10^{-6}	9.82×10^{-5} [f]		
(+)-IIIα	1.19×10^{-5}	1.37×10^{-3} [e]	1.61	4
(−)-IIIα	1.19×10^{-5}	2.21×10^{-3} [e]		
(+)-IIIα	1.19×10^{-5}	3.70×10^{-5} [f]	1.69	4
(−)-IIIα	1.19×10^{-5}	6.24×10^{-5} [f]		
(+)-IIIα	9.92×10^{-6}	4.43×10^{-5} [f]	1.79	6
(−)-IIIα	9.92×10^{-6}	7.93×10^{-5} [f]		

[a] Dose of spasmolytic agent introduced prior to the addition of the spasmogen dose increments. [b] Spasmogen doses necessary to elicit a 50% response after pretreatment with the spasmolytic agent. [c] Comparison of the spasmolytic activities based on the respective ED_{50}. [d] Number of consecutive determinations using the same muscle strip. [e] Urecholine as spasmogen. [f] Carbachol as spasmogen.

Compounds IIβ and IVα resisted resolution, and only one diastereoisomer was obtained in each case. The isolation of the enantiomers of IIβ was not pursued, since preliminary pharmacological data substantiated that (±)-IIα possessed greater anticholinergic activity than (±)-IIβ (Table IV). Resolution of IIIβ and IVβ was not attempted for the same reason.

Since it was confirmed previously (12) that dimethylaminoethyl *O*-ether derivatives of (*E*)- and (*Z*)-phenyl 2-pyridyl oximes were equipotent, the recovery of the corresponding diastereoisomer of IVα was discontinued. Elemental analyses of Iα and Iβ indicated that diquaternization occurred, which complicated the resolution procedure; therefore, the synthesis of these compounds as antimuscarinic agents was not pursued.

EXPERIMENTAL[1]

Oximes—*1-Methyl-4-piperidone*—A modified method of Kochhar *et al.* (10) was used. Sodium bicarbonate (79.2 g, 0.84 mole) was added, with constant stirring, to a 600-ml aqueous solution containing hydroxylamine hydrochloride (66 g, 0.84 mole). The reagent, 1-methyl-4-piperidone (67.2 g, 0.6 mole), was added next, and the reaction mixture was stirred at room temperature for 5 hr with a magnetic stirrer. The mixture was then saturated with sodium carbonate and extracted with five 50-ml portions of chloroform. The combined chloroform extracts were evaporated under reduced pressure. The crude product, after recrystallization from anhydrous benzene–petroleum ether (7:1), yielded a crystalline material (56 g, 75%) that melted at 128–129°. The IR spectrum demonstrated characteristic bands for C=N (1630 cm^{-1}) and NOH (920–970 cm^{-1}).

Benzophenone—The method described by Wylie *et al.* (15) was followed by combining benzophenone (100 g, 0.53 mole), previously dissolved in 200 ml of warm ethanol (95%), with hydroxylamine hydrochloride (50 g, 0.89 mole), which was previously dissolved in 40 ml of distilled water. Sodium hydroxide pellets (110 g, 2.75 moles) were added to the mixture with constant stirring and cooling when necessary. The reaction mixture was allowed to cool to room temperature prior to its combination with 2 liters of distilled water containing 300 ml of 36% hydrochloric acid. The precipitate was recrystallized from 95% ethanol, and the pure oxime (88 g, 81%) melted at 143–144°. Its IR spectrum indicated the presence of the characteristic bands for the C=N (1580 cm^{-1}) and aromatic (2920 and 1900 cm^{-1}) moieties.

Phenyl 2-Pyridyl Ketone—A modified method of Wylie *et al.* (15) was employed by adding a 50-ml aqueous hydroxylamine hydrochloride (50 g, 0.89 mole) solution to a solution of phenyl 2-pyridyl ketone (100 g, 0.53 mole) in 350 ml of warm 95% ethanol. Sodium hydroxide (110 g, 2.75 moles) was added in small portions to the mixture with stirring and cooling when the heat of reaction became excessive. After allowing the reaction mixture to cool to room temperature, an aqueous hydrochloric acid solution (300 ml of 37% HCl in 2 liters of distilled water) was added to the mixture. A mixture of the (*E*)- and (*Z*)-geometric isomers precipitated but dissolved upon continued addition of the acidic solution and subsequent heating. A precipitate (2.8 g) formed after the solution cooled to room temperature. This precipitate was recrystallized from 95% ethanol, and its melting point (166–168°) coincided with the one reported by Haney (12) for the (*Z*)-isomer.

The pH (1.8) of the acidic solution containing the soluble hydrochloride salts was adjusted to 2.1 with an aqueous sodium hydroxide solution (10%). Precipitation occurred, and the solution was heated to allow the solid material to dissolve. The precipitate that formed upon subsequent cooling to room temperature was recrystallized from ethanol (95%) and melted at 165–168° (9 g). A second adjustment was made to pH 2.3, and the solution was heated to dissolve the precipitate that had formed. The solid material that formed when this last solution cooled to room temperature was recrystallized from ethanol (95%), mp 164–166° (7 g).

The melting point and NMR data demonstrated that each product obtained from the first and second pH adjustments was the (*Z*)-geometric isomer. However, a third pH adjustment to 2.5 afforded a mixture (13.4 g) of the (*Z*)- and (*E*)-geometric isomers. A fourth adjustment to pH 6 produced the (*E*)-isomer (32.3 g), mp 151–153°, after recrystallization from ethanol (95%). The NMR spectra demonstrated characteristic chemical shifts for the protons adjacent to the pyridyl nitrogen in the (*Z*)-(1.25 τ) and (*E*)- (1.40 τ) isomers.

Oxime *O*-Ethers—Pertinent preparative data and physical constants for each synthesized compound are given in Tables I–III.

Synthesis—The respective oxime was dissolved in warm absolute ethanol and placed in a three-necked round-bottom flask equipped with an electric stirrer, a water condenser, and a dropping funnel. Sodium hydride as a 51.6% mineral oil dispersion was added to this solution in small portions with constant stirring and cooling. The alkyl halide, 2-chloro-*N,N*-dimethylpropylamine hydrochloride, was dissolved in hot absolute ethanol and placed in a dropping funnel. The solution in the funnel was heated with a heating tape when precipitation of the alkyl halide occurred while it was being added dropwise to the refluxing reaction mixture. The hot reaction mixture was filtered, and the solvent was evaporated under reduced pressure. The resultant oily material containing the α- and β-structural isomers was extracted with anhydrous petroleum ether for I and II, but isopropyl ether was used for III and IV. The mixture was filtered, and the solvent was evaporated under reduced pressure.

Separation—The α- and β-structural isomers of I were separated *via* vacuum fractional distillation utilizing a microdistillation apparatus with a heated 14-cm fractionating column. The isomers of II were separated by both vacuum fractional distillation, using an 18-cm vacuum-jacketed fractionating column, and column chromatography. In addition, the structural isomers of III and IV were separated by column chromatography.

An isomeric mixture (19.7 g) of II was chromatographed on silica gel (200 g). The eluting solvents, benzene, benzene–ether (95:5), benzene–ether (4:1), and ether, successfully separated IIα and IIβ. Another chromatographic separation also proved successful when 45.5 g of the reaction mixture (II) was introduced on a column packed with 355 g of silica gel and eluted with cyclohexane, cyclohexane–benzene (3:1), cyclohexane–benzene (1:1), cyclohexane–benzene (1:3), benzene, benzene–ether (4:1), and benzene–ether (1:1).

A mixture (24.4 g) of α- and β-isomers from III was incorporated on a chromatography column packed with 200 g of silica gel. Separation was accomplished when the column was eluted with successive portions of benzene, benzene–ether (9:1, 85:15, 4:1, 3:1, and 1:1), ether, ether–ethanol (1:1), and ethanol. An isomeric mixture (14.2 g) of IV was also successfully separated using 200 g of silica gel and a similar eluting system.

The IR spectra of the α-isomers displayed a characteristic carbonyl stretching band at 1040 cm^{-1}, while the β-isomers' corresponding bands were at 1060 or 1075 cm^{-1}. The separations also were monitored with TLC, GLC, and NMR spectroscopy. Correct elemental analyses of the methylbromide derivatives also were used to characterize the structural isomers of I and II. These derivatives were obtained by recrystallization of the precipitates that developed when the respective isomers, while in isopropyl ether, were treated with excess bromomethane and placed in the freezer for 24 hr.

Resolution—The diastereoisomers from IIα were prepared with (+)-tartaric acid. The oxime *O*-ether (12.51 g, 0.044 mole) was dissolved

[1] The melting points are uncorrected; a Thomas-Hoover Uni-Melt apparatus was used. Elemental analyses were conducted by Schwarzkopf Microanalytical Laboratory, Woodside, N.Y. IR spectra of all final products were measured on a Beckman IR-8 spectrophotometer. NMR spectra were obtained with a Varian A-60 spectrometer (tetramethylsilane and dimethyl sulfoxide as the internal standards). Optical rotations were obtained with a Perkin-Elmer 141 polarimeter. Pharmacological determinations were made on a Marco physiograph desk model DMP-4A.

in absolute ethanol (200 ml), and this mixture was combined with 200 ml of absolute ethanol containing an isomolar amount of (+)-tartaric acid (6.66 g, 0.044 mole). The reaction mixture was refluxed for 1 hr, but heavy precipitation necessitated the addition of 80 ml more of absolute ethanol. The precipitate resulting after the mixture stood at room temperature for 1 hr was purified by recrystallizing it twice from absolute ethanol [6.9 g, mp 155–156°, $[\alpha]_D^{26}$ +19.33° (c 1.5%, absolute methanol)]. Anhydrous isopropyl ether (150 ml) was added to the original filtrate to promote precipitation of the other diastereoisomer. The precipitate (6 g, mp 125–130°) was collected and recrystallized four times from isopropyl alcohol [2 g, mp 128°–130°, $[\alpha]_D^{26}$ +8.38° (c 5%, absolute methanol)].

The methylbromide derivative of (−)-IIα from the higher melting diastereoisomer was prepared following the regeneration of the free base. The diastereoisomeric salt (3 g) was dissolved in 16 ml of distilled water, and this mixture was combined with triethylamine (10 ml) and stirred for 30 min at room temperature. Anhydrous isopropyl ether (30 ml) was added, and the reaction mixture was stirred for an additional 15 min. The isopropyl ether layer was isolated, and the solvent was evaporated under reduced pressure. The residue was dissolved in anhydrous isopropyl ether, and this mixture was treated with excess bromomethane. Then the mixture was placed in the freezer for 12 hr, and the resulting precipitate was recrystallized three times from isopropyl alcohol. The analytically pure sample melted at 188–190° (0.4 g) and possessed an optical rotation of $[\alpha]_D^{26}$ −17.26° (c 5%, chloroform).

The methylbromide derivative of (+)-IIα from the lower melting diastereoisomer was prepared following the regeneration of the free base. The diastereoisomeric salt (2 g) was dissolved in 12 ml of distilled water, and this mixture was combined with 7 ml of triethylamine. The reaction mixture was stirred for 30 min at room temperature. Anhydrous isopropyl ether (20 ml) was then added, and the reaction mixture was stirred for an additional 15 min. The isopropyl ether layer was separated from the aqueous layer, and the solvent was evaporated under reduced pressure. The residue was dissolved in anhydrous isopropyl ether, and this mixture was treated with excess bromomethane.

The reaction mixture was stored in the freezer for 12 hr. The precipitate (0.9 g, mp 182–185°) was recrystallized three times from a mixture of anhydrous isopropyl ether (2%) and isopropyl alcohol, but a significant optical rotation was not achieved. The filtrates from these recrystallizations were combined and placed in the freezer. The solid material (mp 178–183°) was recrystallized four times from a solvent system composed of anhydrous isopropyl ether (5%) and isopropyl alcohol. An analytically pure sample (0.2 g) was obtained [mp 177–179.5°, $[\alpha]_D^{26}$ +17.28° (c 5%, chloroform)].

The diastereoisomers from IIIα were formed with (+)-tartaric acid. The oxime *O*-ether (3.74 g, 0.0132 mole) was dissolved in 200 ml of absolute ethanol, and this mixture was combined with 200 ml of absolute ethanol containing an isomolar quantity of (+)-tartaric acid (1.98 g, 0.0132 mole). The reaction mixture was refluxed for 1 hr and stirred for 12 hr at room temperature. Then the mixture was heated to dissolve the solid material and allowed to stand at room temperature for 12 hr. The precipitate [2.1 g, mp 143–150°, $[\alpha]_D^{26}$ +13.88° (c 2.5%, absolute methanol)] was recrystallized three times from absolute ethanol.

The analytically pure sample (1 g) melted at 156–158° with an optical rotation of $[\alpha]_D^{26}$ +19.4° (c 2.5%, absolute methanol). Anhydrous isopropyl ether (450 ml) was added to the original filtrate while heating and stirring, and the mixture was allowed to stand at room temperature until precipitation occurred. The precipitate [1.7 g, mp 132–136°, $[\alpha]_D^{26}$ +9.52° (c 5%, absolute methanol)] was recrystallized three times from a mixture of anhydrous isopropyl ether and absolute methanol. An analytically pure sample (0.8 g) was obtained [mp 136–139°, $[\alpha]_D^{26}$ +8.42° (c 5%, absolute methanol)].

The methylbromide derivative of (−)-IIIα from the higher melting diastereoisomer was prepared after the regeneration of the free base. Excess triethylamine was added to the diastereoisomer (1 g), and the mixture was stirred for 15 min. Distilled water (20 ml) was then added, and the reaction mixture was stirred until all gummy material dissolved. Anhydrous isopropyl ether (20 ml) was combined with the mixture, and the resultant mixture was stirred for an additional 15 min. The isopropyl ether layer was segregated and evaporated under reduced pressure.

The residual oil (0.7 g) was dissolved in anhydrous isopropyl ether, and this mixture was treated with excess bromomethane. The reaction mixture was stored in the freezer for 12 hr. The precipitate was recrystallized three times from a mixture of anhydrous isopropyl ether and isopropyl alcohol. The analytically pure derivative (0.3 g) melted at 185–187°, $[\alpha]_D^{26}$ −23.46° (c 5%, chloroform).

The methylbromide derivative of (+)-IIIα from the lower melting diastereoisomer was prepared after the regeneration of the free base. Excess triethylamine was added to the diastereoisomer (0.8 g), and the mixture was stirred for 15 min. Distilled water (20 ml) was added, and the reaction mixture was stirred until all gummy material dissolved. Anhydrous isopropyl ether (20 ml) was combined with the mixture, and this final mixture was stirred for an additional 15 min. The isopropyl ether layer was separated and evaporated under reduced pressure.

The residual oil was dissolved in anhydrous isopropyl ether, and this mixture was treated with excess bromomethane. The reaction mixture was stored in the freezer for 12 hr. The precipitate was recrystallized six times from a mixture of anhydrous isopropyl ether and isopropyl alcohol. The analytically pure derivative (0.1 g) melted at 176–178°, $[\alpha]_D^{26}$ +20.4° (c 5%, chloroform).

PHARMACOLOGY

A preliminary pharmacological evaluation was conducted to determine the antimuscarinic activity of the methylbromide derivatives of (±)-IIα, (±)-IIβ, (+)-IIα, (−)-IIα, (+)-IIIα, and (−)-IIIα. Antimuscarinic activity was determined relative to atropine sulfate (3.60×10^{-7} mmole/ml) when urecholine and/or carbachol were utilized as spasmogens. The concentrations of the spasmogen solutions were determined so that 5.1×10^{-4} mmole of urecholine and 1.23×10^{-5} or 1.64×10^{-5} mmole of carbachol were added per increment.

Method—The general method (6) consisted of the inhibition of spasmogen-induced contractions by a spasmolytic agent on excised strips of rat ileum. The ileum strip was kept at constant temperature (37 ± 0.5°) in an aerated 80-ml glass chamber that was filled to 70 ml with a Tyrode bathing solution and was attached to a myograph transducer connected to a physiograph.

Results—A summary of the experimental data is found in Table IV. The synthesized compounds were tested as the methylbromide salts. The pharmacological data demonstrated that the racemic IIα structural isomer was more active than the corresponding (±)-IIβ isomer, which was in accord with previous results (9).

The data pertinent to (+)-IIα, (−)-IIα, (+)-IIIα, and (−)-IIIα indicated that, relative to atropine sulfate, the first two compounds possessed higher antimuscarinic potency than the latter two and that (−)-IIα and (+)-IIα were equipotent. On the other hand, (−)-IIIα was more active than (+)-IIIα, demonstrating enantiomeric potency ratios of 1.61 and 1.79 when urecholine and carbachol were used, respectively, as spasmogens. However, these data were not consistent with Pfeiffer's rule (21), which states that the more active compounds should possess a higher degree of stereospecificity.

Recent reports (13, 14, 22) elaborated on the fact that minor structural changes in a compound produce unusually large differences in affinity which cannot be ascribed simply to the binding or failure to bind of one group. These studies illustrated the need to consider the effect of a new group on the binding of the rest of the molecule with the receptor since it may force a realignment of other important functional groups. This concept can account for the difference in activity between (±)-IIα and (±)-IIβ. The α-methyl group in (±)-IIα demonstrated an overall positive contribution regardless of whether it produced the preferred conformation or supplied an additional site for a greater interaction with the receptor.

The activities of the enantiomers, (+)-IIα, (−)-IIα, (+)-IIIα, and (−)-IIIα, may be discussed similarly, since it has been reported (14) that differences in stereospecificity arise from greater disturbances in the binding of one enantiomer than in the other corresponding one.

Compounds (−)-IIIα and (+)-IIIα possess an unsymmetrical flat umbrella-like moiety at one end of the molecule while (−)-IIα and (+)-IIα possess a symmetrical one. If the theory that the receptor demonstrates selective affinity for the phenyl and 2-pyridyl functions is invoked as in the study where the effect of a cyclohexyl group was compared with a phenyl group (22), a change in the overall conformation of (+)-IIα and (−)-IIα would not affect the binding with the receptor, but this would not be the case with (+)-IIIα and (−)-IIIα.

Therefore, the absence and presence, respectively, of enantiomeric potency ratios in (−)-IIα, (+)-IIα, (−)-IIIα, and (+)-IIIα may be rationalized on the basis that the α-methyl group alters the overall binding of the molecule with the receptor. In (+)-IIα and (−)-IIα, the alteration did not demonstrate a significant enantiomeric potency ratio, since the opposite end of the molecule consisted of a symmetrical umbrella-like moiety. On the other hand, a significant one was observed in (−)-IIIα and (+)-IIIα, since they possess an unsymmetrical umbrella-like moiety. This observation, however, is not in complete agreement with the study concluding that an α-methyl group contributed considerably to antiacetylcholine potency but that the contribution was not dependent on stereochemistry (23).

In view of existing evidence, it appears that a methyl group alpha to the alkylamino function influences anticholinergic activity. Furthermore, the postulated ability of this group to alter the orientation between the molecule and the receptor should further substantiate the premise that the binding of an important moiety of an antagonist may be affected considerably by modifying other parts of the same molecule.

REFERENCES

(1) R. B. Barlow, "Introduction to Chemical Pharmacology," Methuen, London, England, 1964, p. 198.

(2) H. R. Ing, "The Alkaloids," vol. 5, R. H. F. Manske and H. L. Holmes, Eds., Academic, New York, N.Y., 1955, p. 243.

(3) W. R. Buckett and C. G. Haining, *Br. J. Pharmacol.*, **24**, 138 (1965).

(4) A. Bebbington and R. W. Brimblecombe, *Adv. Drug Res.*, **2**, 154 (1965).

(5) E. J. Ariens, in "Advances in Drug Research," vol. 3, N. J. Harper and A. B. Simmonds, Eds., Academic, London, England, 1966, p. 260.

(6) B. W. J. Ellenbroek, R. J. F. Nivard, J. M. Van Rossum, and E. J. Ariens, *J. Pharm. Pharmacol.*, **17**, 393 (1965).

(7) M. May, H. F. Ridley, and D. J. Triggle, *J. Med. Chem.*, **12**, 320 (1969).

(8) R. W. Brimblecombe and T. D. Inch, *J. Pharm. Pharmacol.*, **22**, 881 (1970).

(9) A. M. Lands, E. Ananenko, G. Jones, J. O. Hoppe, and T. J. Becker, *J. Pharmacol. Exp. Ther.*, **96**, 1 (1949).

(10) M. M. Kochhar, R. G. Brown, and J. N. Delgado, *J. Pharm. Sci.*, **54**, 393 (1965).

(11) S. K. Gomer, E. I. Isaacson, R. G. Brown, and J. N. Delgado, *ibid.*, **57**, 1586 (1968).

(12) W. G. Haney, Jr., Ph.D. dissertation, University of Texas, Austin, Tex., 1970. W. G. Haney, R. G. Brown, J. N. Delgado, and E. I. Isaacson, *J. Pharm. Sci.*, in press.

(13) R. B. Barlow, *J. Pharm. Pharmacol.*, **23**, 90 (1971).

(14) R. B. Barlow, F. M. Frank, and J. D. M. Pearson, *J. Med. Chem.*, **16**, 439 (1973).

(15) B. B. Wylie, E. I. Isaacson, and J. N. Delgado, *J. Pharm. Sci.*, **54**, 1373 (1965).

(16) A. Liberles, "Introduction to Theoretical Organic Chemistry," Macmillan, New York, N.Y., 1968, p. 591.

(17) E. S. Gould, "Mechanism and Structure in Organic Chemistry," Holt, Rinehart and Winston, New York, N.Y., 1959, p. 570, and references cited therein.

(18) E. L. Eliel, "Stereochemistry of Carbon Compounds," McGraw-Hill, New York, N.Y., 1962, p. 47, and references cited therein.

(19) R. Bentley, "Molecular Asymmetry in Biology," vol. 1, Academic, New York, N.Y., 1969, p. 69, and references cited therein.

(20) F. A. Bovey, "Nuclear Magnetic Resonance Spectroscopy," Academic, New York, N.Y., 1969, pp. 161, 164, and references cited therein.

(21) C. C. Pfeiffer, *Science*, **124**, 29 (1956).

(22) F. B. Abramson, R. B. Barlow, M. G. Mustafa, and R. P. Stephenson, *Br. J. Pharmacol.*, **37**, 207 (1969).

(23) R. W. Brimblecombe, D. M. Green, T. D. Inch, and P. B. J. Thompson, *J. Pharm. Pharmacol.*, **23**, 745 (1971).

ACKNOWLEDGMENTS AND ADDRESSES

Received April 5, 1976, from the *College of Pharmacy, University of Texas at Austin, Austin, TX 78712.*

Accepted for publication September 30, 1976.

* Present address: School of Pharmacy, Southwestern Oklahoma State University, Weatherford, OK 73096.

‡ Present address: College of Pharmacy, Idaho State University, Pocatello, ID 83201.

ˣ To whom inquiries should be directed.

Chelates of Dicumarol I: Preparation and Structure Identification of Magnesium Chelate

LYLE D. BIGHLEY ˣ and R. J. SPIVEY *

Abstract □ A magnesium chelate of dicumarol was prepared by reacting a suspension of dicumarol and magnesium oxide in 50% water–methanol. GLC, thermogravimetric, and elemental analyses showed that this compound has a 2:1 ligand–metal stoichiometry with 2 moles of water associated with the complex. Although the chelate does not melt, two endothermic peaks at 205 and 274° were observed in the thermogram, in contrast to a single endothermic peak corresponding to a melting point of 288° for dicumarol. IR spectroscopy indicated that the magnesium is bonded between the carbonyl at C-2 and the oxygen at C-4′ (or vice versa).

Keyphrases □ Dicumarol—chelate with magnesium prepared, structure elucidated □ Chelates—dicumarol–magnesium, prepared, structure elucidated □ Magnesium—chelate with dicumarol prepared, structure elucidated □ Metals—magnesium, chelate with dicumarol prepared, structure elucidated □ Anticoagulants—dicumarol, chelate with magnesium prepared, structure elucidated

Dicumarol [3,3′-methylenebis(4-hydroxycoumarin)] (I) is an oral anticoagulant utilized for the prevention and therapy of thromboembolic vascular disease. However, many problems are associated with its use: concomitant administration with certain drugs can inhibit or potentiate its anticoagulant effect (1), it is slowly and erratically absorbed from tablet dosage forms (2), and its bioavailability from tablets depends on the type and amount of excipients in the formulation (3).

Reported bioavailability differences from various tablet formulations provided the stimulus for a study of potential solid–solid interactions between I and various metal-containing excipients (4). Chemisorption of I occurred with several excipients, but the interaction with the magnesium-containing excipients was postulated to be chelation.

In subsequent studies (5, 6) in dogs and humans, concomitant administration of I with magnesium-containing adjuvants resulted in faster and more complete drug absorption. These investigators postulated that the enhanced bioavailability may be due to chelate formation within the GI tract.

This investigation was undertaken to prepare, isolate, and study the physicochemical properties and bioavailability of the magnesium chelate of dicumarol. This report details the preparation, stoichiometry, and structure

In view of existing evidence, it appears that a methyl group alpha to the alkylamino function influences anticholinergic activity. Furthermore, the postulated ability of this group to alter the orientation between the molecule and the receptor should further substantiate the premise that the binding of an important moiety of an antagonist may be affected considerably by modifying other parts of the same molecule.

REFERENCES

(1) R. B. Barlow, "Introduction to Chemical Pharmacology," Methuen, London, England, 1964, p. 198.

(2) H. R. Ing, "The Alkaloids," vol. 5, R. H. F. Manske and H. L. Holmes, Eds., Academic, New York, N.Y., 1955, p. 243.

(3) W. R. Buckett and C. G. Haining, *Br. J. Pharmacol.*, **24**, 138 (1965).

(4) A. Bebbington and R. W. Brimblecombe, *Adv. Drug Res.*, **2**, 154 (1965).

(5) E. J. Ariens, in "Advances in Drug Research," vol. 3, N. J. Harper and A. B. Simmonds, Eds., Academic, London, England, 1966, p. 260.

(6) B. W. J. Ellenbroek, R. J. F. Nivard, J. M. Van Rossum, and E. J. Ariens, *J. Pharm. Pharmacol.*, **17**, 393 (1965).

(7) M. May, H. F. Ridley, and D. J. Triggle, *J. Med. Chem.*, **12**, 320 (1969).

(8) R. W. Brimblecombe and T. D. Inch, *J. Pharm. Pharmacol.*, **22**, 881 (1970).

(9) A. M. Lands, E. Ananenko, G. Jones, J. O. Hoppe, and T. J. Becker, *J. Pharmacol. Exp. Ther.*, **96**, 1 (1949).

(10) M. M. Kochhar, R. G. Brown, and J. N. Delgado, *J. Pharm. Sci.*, **54**, 393 (1965).

(11) S. K. Gomer, E. I. Isaacson, R. G. Brown, and J. N. Delgado, *ibid.*, **57**, 1586 (1968).

(12) W. G. Haney, Jr., Ph.D. dissertation, University of Texas, Austin, Tex., 1970. W. G. Haney, R. G. Brown, J. N. Delgado, and E. I. Isaacson, *J. Pharm. Sci.*, in press.

(13) R. B. Barlow, *J. Pharm. Pharmacol.*, **23**, 90 (1971).

(14) R. B. Barlow, F. M. Frank, and J. D. M. Pearson, *J. Med. Chem.*, **16**, 439 (1973).

(15) B. B. Wylie, E. I. Isaacson, and J. N. Delgado, *J. Pharm. Sci.*, **54**, 1373 (1965).

(16) A. Liberles, "Introduction to Theoretical Organic Chemistry," Macmillan, New York, N.Y., 1968, p. 591.

(17) E. S. Gould, "Mechanism and Structure in Organic Chemistry," Holt, Rinehart and Winston, New York, N.Y., 1959, p. 570, and references cited therein.

(18) E. L. Eliel, "Stereochemistry of Carbon Compounds," McGraw-Hill, New York, N.Y., 1962, p. 47, and references cited therein.

(19) R. Bentley, "Molecular Asymmetry in Biology," vol. 1, Academic, New York, N.Y., 1969, p. 69, and references cited therein.

(20) F. A. Bovey, "Nuclear Magnetic Resonance Spectroscopy," Academic, New York, N.Y., 1969, pp. 161, 164, and references cited therein.

(21) C. C. Pfeiffer, *Science*, **124**, 29 (1956).

(22) F. B. Abramson, R. B. Barlow, M. G. Mustafa, and R. P. Stephenson, *Br. J. Pharmacol.*, **37**, 207 (1969).

(23) R. W. Brimblecombe, D. M. Green, T. D. Inch, and P. B. J. Thompson, *J. Pharm. Pharmacol.*, **23**, 745 (1971).

ACKNOWLEDGMENTS AND ADDRESSES

Received April 5, 1976, from the *College of Pharmacy, University of Texas at Austin, Austin, TX 78712.*

Accepted for publication September 30, 1976.

* Present address: School of Pharmacy, Southwestern Oklahoma State University, Weatherford, OK 73096.

‡ Present address: College of Pharmacy, Idaho State University, Pocatello, ID 83201.

ˣ To whom inquiries should be directed.

Chelates of Dicumarol I: Preparation and Structure Identification of Magnesium Chelate

LYLE D. BIGHLEY ˣ and R. J. SPIVEY *

Abstract □ A magnesium chelate of dicumarol was prepared by reacting a suspension of dicumarol and magnesium oxide in 50% water–methanol. GLC, thermogravimetric, and elemental analyses showed that this compound has a 2:1 ligand–metal stoichiometry with 2 moles of water associated with the complex. Although the chelate does not melt, two endothermic peaks at 205 and 274° were observed in the thermogram, in contrast to a single endothermic peak corresponding to a melting point of 288° for dicumarol. IR spectroscopy indicated that the magnesium is bonded between the carbonyl at C-2 and the oxygen at C-4′ (or vice versa).

Keyphrases □ Dicumarol—chelate with magnesium prepared, structure elucidated □ Chelates—dicumarol–magnesium, prepared, structure elucidated □ Magnesium—chelate with dicumarol prepared, structure elucidated □ Metals—magnesium, chelate with dicumarol prepared, structure elucidated □ Anticoagulants—dicumarol, chelate with magnesium prepared, structure elucidated

Dicumarol [3,3′-methylenebis(4-hydroxycoumarin)] (I) is an oral anticoagulant utilized for the prevention and therapy of thromboembolic vascular disease. However, many problems are associated with its use: concomitant administration with certain drugs can inhibit or potentiate its anticoagulant effect (1), it is slowly and erratically absorbed from tablet dosage forms (2), and its bioavailability from tablets depends on the type and amount of excipients in the formulation (3).

Reported bioavailability differences from various tablet formulations provided the stimulus for a study of potential solid–solid interactions between I and various metal-containing excipients (4). Chemisorption of I occurred with several excipients, but the interaction with the magnesium-containing excipients was postulated to be chelation.

In subsequent studies (5, 6) in dogs and humans, concomitant administration of I with magnesium-containing adjuvants resulted in faster and more complete drug absorption. These investigators postulated that the enhanced bioavailability may be due to chelate formation within the GI tract.

This investigation was undertaken to prepare, isolate, and study the physicochemical properties and bioavailability of the magnesium chelate of dicumarol. This report details the preparation, stoichiometry, and structure

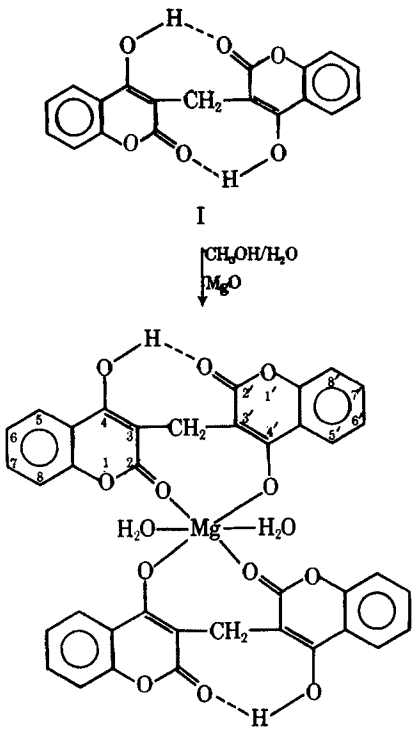

Scheme I

identification of the dicumarol–magnesium chelate (II). The physicochemical properties and bioavailability will be the subject of a later report.

EXPERIMENTAL

Materials—Dicumarol[1], methanol[2], ethylenediaminetetraacetic acid disodium salt[2], eriochrome black T[2], 2-propanol[2], heavy magnesium oxide[3], dimethylformamide[4], methanolic tetrabutylammonium hydroxide solution[4] (25%), atomic absorption magnesium standard[5], zinc metal[5], dimethyl sulfoxide[5], benzoic acid[5], pyridine[6], 4A molecular sieves[6], ammonium chloride[7], hydrochloric acid[8], tetrabutylammonium chloride[9], ammonium hydroxide[10] (58%), benzene[10], sodium hydroxide[10], and ethanol[11] were used without further purification, except that I was recrystallized from benzene. The melting point of I was verified using a differential thermal analyzer.

Ammonium chloride–ammonium hydroxide buffer (pH 10) was prepared by dissolving 14 g of ammonium chloride in 114 ml of ammonium hydroxide and diluting to 200 ml with distilled water (7).

A 0.5% (w/v) eriochrome black T solution was prepared by dissolving 0.125 g in sufficient ethanol to make 25 ml.

Ethylenediaminetetraacetic acid disodium salt solution (0.025 *M*) was prepared by dissolving 9.306 g in enough water to make 1000 ml. Standardization was accomplished by titrating with a solution of zinc chloride, prepared by dissolving an accurately weighed amount of zinc metal in dilute hydrochloric acid USP (7).

Tetrabutylammonium hydroxide solution was standardized by potentiometrically titrating a 0.0106 *M* methanolic benzoic acid solution using a modified procedure described by Connors (8).

Preparation of II—Three grams (0.0089 mole) of I, recrystallized from benzene, and 0.324 g (0.008 mole) of heavy magnesium oxide were suspended in 600 ml of methanol (Scheme I). When the reactants were wetted, 600 ml of distilled water was added, and the mixture was stirred in a covered, light-protected beaker for 24 hr. Undissolved material was removed by filtration; the filtrate was collected in a 1000-ml round-bottom flask, covered, and placed in a refrigerator (5°) until crystallization was complete. The crystals were collected on a Büchner funnel, washed thoroughly with distilled water, and dried *in vacuo* at room temperature for 24 hr. Approximately 1.5 g of white crystalline material was obtained.

Atomic Absorption—An atomic absorption spectrophotometer[12], equipped with a single-slot burner head (10-cm pathlength) and a magnesium hollow cathode lamp, was used to determine the magnesium content of II. Instrumental parameters were: wavelength, 285.2 nm; hollow cathode lamp current, 5 mamp; fuel, acetylene (flowmeter 4, 10 psig); oxidizer, air (flowmeter 20, 35 psig); monochromator entrance slit width, 50 μm; monochromator exit slit width, 75 μm; gain, 1; and pathlength, 10 cm.

Commercially available magnesium reference standard (10,000 ppm) was diluted with dimethylformamide to prepare standard solutions equivalent to 0.1–1.0 ppm of magnesium. After optimizing the wavelength and zeroing the instrument while aspirating dimethylformamide, a standard curve was prepared from the standard solutions by plotting absorbance *versus* concentration. Standard solutions of magnesium spiked with I showed no enhancement or depression of absorption.

Solutions of II were prepared by dissolving approximately 25 mg in 100 ml of dimethylformamide and diluting an aliquot 20-fold with dimethylformamide to give a magnesium concentration of approximately 0.4 ppm. The actual magnesium content of II was obtained by reference to the standard curve.

Complexometric Titration—The magnesium content of II also was determined by a modified complexometric titration procedure (9). To release the magnesium, the chelate was reacted with base prior to titration by dissolving accurately weighed samples of II (approximately 125 mg) in 10 ml of 1 *N* sodium hydroxide, adding 10 ml of distilled water, and stirring for 15 min. The magnesium was solubilized by adding 10 ml of dilute hydrochloric acid USP and stirring the solution an additional 15 min.

The acidic solution was filtered to remove the precipitated I, and the precipitate was washed with distilled water until the washings were neutral to litmus paper. After neutralizing the filtrate with 1 *N* sodium hydroxide, 5 ml of ammonium chloride–ammonium hydroxide buffer and 0.5 ml of 0.5% (w/v) ethanolic eriochrome black T indicator solution were added. Then the filtrate was titrated with 0.025 *M* ethylenediaminetetraacetic acid disodium salt solution until the wine-red color changed to blue.

GLC—A gas chromatograph[13], equipped with a thermal conductivity detector and two commercially prepared 3-mm × 1.83-m (6-ft) stainless steel columns packed with 10% Carbowax 20M on 80–100-mesh Chromosorb W AW[14], was used to confirm the presence of water in II. Operating conditions were: injection port, 240°; column, 180°; detector, 260°; carrier gas (helium), 40 ml/min (50 psig); attenuation, 2; and bridge current, 175 mamp.

Dimethyl sulfoxide, dried over 4A molecular sieves, was spiked with known amounts of water, and 5-μl samples containing 5–20 μg of water were injected[15]. The retention times, from injection to peak maximum, were 0.4 min for water and 2.2 min for dimethyl sulfoxide. Confirmation of water in II was obtained by dissolving samples, which had been dried at 85°, in dried dimethyl sulfoxide, injecting 5 μl, and comparing retention times to those of the water-spiked dimethyl sulfoxide samples.

Thermogravimetric Analysis—The water content of II also was determined by mass loss on a thermobalance[16]. A heating rate of 20°/min, a *y*-axis sensitivity of 0.4 mg/2.54 cm, and a dynamic nitrogen atmosphere (40 ml/min, 5 psig) were used for all analyses. Sample sizes ranged from 14 to 17 mg.

Differential Thermal Analysis—Endothermic or exothermic transitions were determined by thermal analysis[17] using 2–3-mg samples. A heating rate of 20°/min and a dynamic nitrogen atmosphere (flowmeter 3, 5 psig) were used for all analyses. The differential temperature sensitivities used were 1°/2.54 cm for I and 0.2°/2.54 cm for II. Temperatures were corrected for the nonlinear response of the chromel–alumel thermocouple.

[1] Sigma Chemical Co.
[2] Reagent, J. T. Baker.
[3] Technical, Matheson, Coleman & Bell.
[4] Reagent, Matheson, Coleman & Bell.
[5] Certified, Fisher Scientific Co.
[6] Technical, Fisher Scientific Co.
[7] Laboratory, Fisher Scientific Co.
[8] Reagent, Fisher Scientific Co.
[9] Eastman Organic Chemicals.
[10] Reagent, Mallinckrodt Chemical Works.
[11] U.S. Industrial Chemicals Co.
[12] Model 82-270, Jarrel-Ash.
[13] Model 5750B, Hewlett-Packard.
[14] Supelco.
[15] 701SN, Hamilton Co.
[16] Model 950, DuPont.
[17] Model 900, DuPont.

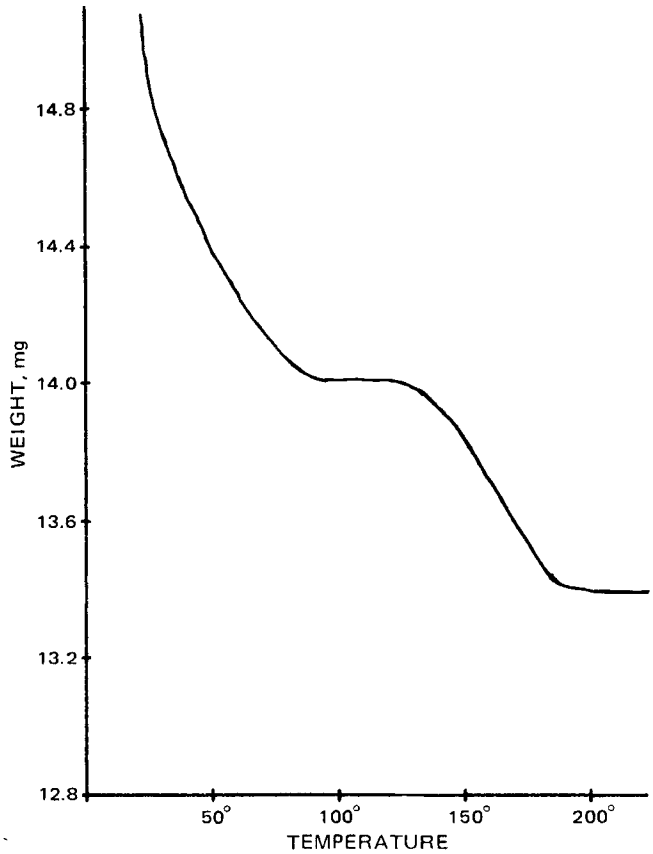

Figure 1—*Thermogravimetric analysis of dicumarol–magnesium chelate.*

IR Spectroscopy—IR spectra were obtained[18] from approximately a 0.33% dispersion in potassium bromide using a 5-min scan period.

NMR Spectroscopy—Proton spectra were obtained[19] in deuterated chloroform. Chemical shifts were reported in parts per million relative to tetramethylsilane as an internal standard.

Nonaqueous Titration—A nonaqueous titration was performed on II to quantitate the enolic protons. An accurately weighed sample (40–80 mg), dissolved in 50 ml of pyridine, was titrated with 1.027 *M* methanolic tetrabutylammonium hydroxide solution delivered from a micrometer syringe[20]. Potential measurements were recorded using a digital pH meter[21] equipped with a combination electrode. End-point drift was minimized by using a saturated solution of tetrabutylammonium chloride in 2-propanol as the internal electrolyte.

Carbon and Hydrogen Analyses—Carbon and hydrogen analyses were performed[22] on II, and calculated percentages were based on a molecular formula of $C_{38}H_{26}MgO_{14}$.

RESULTS AND DISCUSSION

Initial attempts to prepare the magnesium chelate of I centered around the preparation of the disodium salt of I, which could subsequently be reacted with a water-soluble magnesium salt. Preparation of the disodium salt was attempted by four different procedures: (*a*) reacting I suspended in 2-propanol with sodium hydroxide, (*b*) reacting I suspended in ether with sodium hydride, (*c*) adding I to a pH 8.9 phosphate buffer, and (*d*) dissolving I in an equivalent amount of 1.0 *N* sodium hydroxide and adjusting to a known volume with distilled water (10). None of these methods was successful; the isolated product was yellow or became yellow upon standing, suggesting that degradation had occurred.

Subsequently, direct preparation of II was accomplished by reacting a suspension of I and magnesium oxide in a 50% water–methanol mixture (Scheme I). As the reaction progressed, the solution became less turbid.

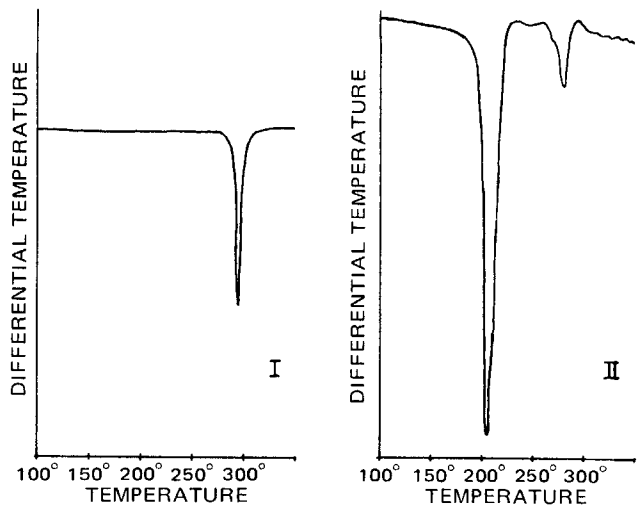

Figure 2—*Differential thermal analysis of I and II.*

The isolated reaction product, later identified as II, was a white, crystalline material. Methanol was used in the reaction medium because water alone would not wet I; however, the volume was chosen empirically. Subsequently, the solubility of II was found to be greater in methanol–water mixtures, preventing precipitation of II and aiding its separation from unreacted materials after preparation.

The optimum reaction time was determined by spectrophotometrically analyzing samples of the supernate for total ligand (I). After 24 hr, no further increase in absorbance was observed. Although water-soluble magnesium salts were tried in an attempt to prepare the chelate by this procedure, only magnesium oxide was useful. The pH increase in the microenvironment produced by the magnesium hydroxide may be sufficiently high to remove an enolic proton from the ligand, enabling the chelate to form.

Before a reliable estimate of the stoichiometry of II could be obtained, it was necessary to determine the number of water molecules associated with the complex. The presumption of the presence of water subsequently was confirmed by thermogravimetric analysis and GLC. Thermograms of II (Fig. 1) showed a loss of loosely bound water between 30 and 100°, followed by constant weight to 140°. Between 140 and 190°, sigmoidal curves representing a mass loss of 4.81–4.98% were obtained. The theoretical percentage of water in a 2:1 chelate, based on two water molecules, is 4.93%. Identical treatment of I resulted in no mass loss; consequently, two molecules of water were associated with each chelate molecule.

However, since thermogravimetric analysis represents only mass loss, GLC was used qualitatively to confirm that the weight loss was due to water. Chromatograms of samples of II, dried *in vacuo* at 85° to remove surface water, showed a peak with the same retention time as water-spiked dimethyl sulfoxide samples. Under the chromatographic conditions used, II was not eluted from the column. These results substantiated that the mass loss observed between 140 and 190° was attributable to water associated with the chelate.

After quantitation of the water of coordination or, possibly, water of crystallization occupying lattice sites (11) and after carbon, hydrogen, and magnesium analyses, the analytical data clearly indicate a 2:1 ligand–metal stoichiometry.

Anal.—Calc.: C, 62.45; H, 3.59; Mg, 3.33; water, 4.93. Found (standard error of the mean of three determinations): C, 62.66; H, 3.67; Mg, 3.29 (0.012) (complexometric titration) and 3.33 (0.026) (atomic absorption); water, 4.91 (0.050) (thermogravimetry).

Differential thermal analysis of I and II showed substantial differences (Fig. 2). Thermograms of I exhibited a single, sharp endothermic peak at a corrected temperature of 288°, which was within the reported melting point range of 287–293° (12). The thermogram of II showed two broad endothermic peaks: a large peak at 205° and a small peak at 274°. Visual observation in a melting-point apparatus suggested that both peaks may have been due to degradation. A color change from white to yellow was observed at approximately 200° and a brown carmelized mass resulted at 280°, but no melt was observed at any temperature.

NMR spectra obtained in deuterated chloroform showed identical chemical shifts for I and II. The spectra had a single signal of 3.7 ppm arising from the methylene protons, a complex multiplet between 7 and 8 ppm corresponding to the aromatic protons, and a single signal at 11.3

[18] Model 267, Perkin-Elmer.
[19] Bruker Hx 90 equipped with an sxp RF pulse amplifier and an R-NC 12 data system.
[20] Burroughs Wellcome & Co.
[21] Model 76008, Beckman.
[22] Galbraith Laboratories, Knoxville, Tenn.

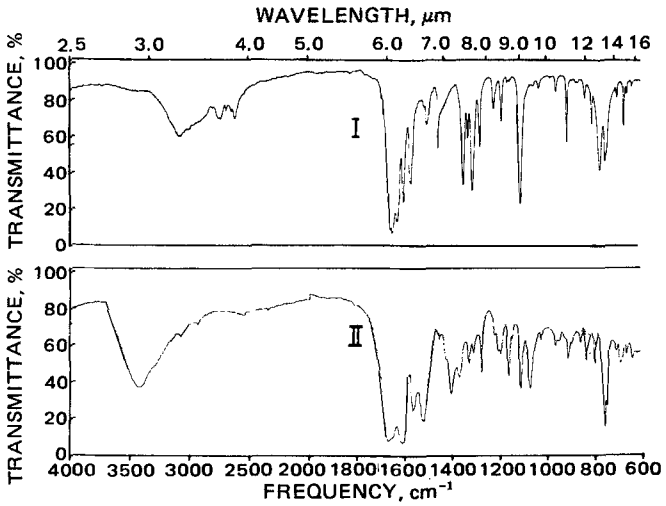

Figure 3—*IR spectra of I and II.*

ppm due to the hydrogen-bonded (enolic) protons at C-4 and/or C-4′ (13).

The poor solubility of II in deuterated chloroform necessitated the use of an NMR spectrometer equipped with a Fourier transform data system. The sample was analyzed overnight; all peaks were identifiable and appeared at their expected chemical shifts, but the spectrum could not be quantitated. Therefore, nonaqueous titration was used to quantitate the enolic protons. As expected, titration curves of II yielded two sharp breaks corresponding to two protons. One proton is believed to be at C-4 or C-4′ on each ligand molecule.

The IR spectra of I and II are shown in Fig. 3. Due to intramolecular hydrogen bonding, the carbonyl stretching frequency of I appeared at 1660 cm^{-1} (13). When I was *O*-methylated and no intramolecular hydrogen bonding could occur, the carbonyl peak was shifted to 1725 cm^{-1} (13). Since there was no shift to longer wave numbers in the carbonyl stretching frequency of II, both carbonyl groups in each ligand probably were bonded. Based on the presence of two titratable protons on II, it seems reasonable that one carbonyl group in each ligand was still intramolecularly hydrogen bonded and that the other carbonyl was bonded with magnesium.

Intramolecular hydrogen bonding also affected the position of the hydroxyl peak in the IR region. This peak appeared at 3100 cm^{-1} for I; however, II exhibited a large, broad water band between 3700 and 2800 cm^{-1}. Since II is believed to retain one intramolecular hydrogen bond on each ligand, the hydroxyl band at 3100 cm^{-1} was probably concealed beneath the water band.

In summary, elemental analyses conclusively established a 2:1 ligand–metal stoichiometry for II and the IR and other analytical data are consistent with Structure II in Scheme I. X-ray studies on the chelate are currently underway to substantiate further the structure.

REFERENCES

(1) D. Bernstein, *Drug Intel. Clin. Pharm.*, **5**, 276 (1971).

(2) R. A. O'Reilly, P. M. Aggeler, and L. S. Leong, *Thromb. Diath. Haemorrh.*, **11**, 1 (1964).

(3) E. Losinski, *Can. Med. Assoc. J.*, **83**, 177 (1960).

(4) J. L. Lach and L. D. Bighley, *J. Pharm. Sci.*, **59**, 1261 (1970).

(5) M. J. Akers, J. L. Lach, and L. J. Fischer, *ibid.*, **62**, 391 (1973).

(6) J. J. Ambre and L. J. Fischer, *Clin. Pharmacol. Ther.*, **14**, 231 (1973).

(7) K. A. Connors, "A Textbook of Pharmaceutical Analysis," Wiley, New York, N.Y., 1967, pp. 68, 69.

(8) K. A. Connors, "A Textbook of Pharmaceutical Analysis," Wiley–Interscience, New York, N.Y., 1974, p. 61.

(9) J. P. Leyda, in "Pharmaceutical Chemistry," vol. 1, L. G. Chatten, Ed.; Dekker, New York, N.Y., 1966, p. 277.

(10) J. D. McCallister, T. F. Chin, and J. L. Lach, *J. Pharm. Sci.*, **59**, 1286 (1970).

(11) R. H. Gore and W. W. Wendlandt, *Anal. Chem. Acta*, **52**, 83 (1970).

(12) "The Merck Index," 7th ed., Merck & Co., Rahway, N.J., 1960, p. 153.

(13) D. W. Hutchinson and J. A. Tomlinson, *Tetrahedron*, **25**, 2531 (1969).

ACKNOWLEDGMENTS AND ADDRESSES

Received July 2, 1976, from the *Division of Pharmaceutics, College of Pharmacy, University of Iowa, Iowa City, IA 52242.*

Accepted for publication September 27, 1976.

Presented in part at the Basic Pharmaceutics Section, APhA Academy of Pharmaceutical Sciences, San Diego meeting, November 1973.

Abstracted in part from a dissertation presented by R. J. Spivey to the University of Iowa in partial fulfillment of Doctor of Philosophy degree requirements.

The authors thank Dr. William Bennett, Department of Chemistry, University of Iowa, for useful discussions.

* Present address: Warner–Lambert Research Institute, Morris Plains, NJ 07950.

ˣ To whom inquiries should be directed.

X-Ray Analysis of Sulfur-Containing Colchicine Derivatives

CATHERINE KOERNTGEN and T. N. MARGULIS ˣ

Abstract □ The crystal and molecular structures of deacetylthiocolchicine hydrochloride dihydrate and thiocolchicine hexahydrate were determined by X-ray diffraction. The replacement of oxygen by sulfur on the C ring methoxy group causes greater puckering of the troponoid ring. The conformation of one A ring methoxy group differs from that of colchicine derivatives that do not contain sulfur.

Keyphrases □ Colchicine derivatives—X-ray diffraction determination of crystal and molecular structures □ Thiocolchicines, various—X-ray diffraction determination of crystal and molecular structures □ X-ray diffraction—determination of crystal and molecular structures of various thiocolchicines □ Crystal and molecular structures—various thiocolchicines, X-ray diffraction determination

Colchicine (I), an ancient drug, is used primarily in the treatment of gout. Attempts to use this powerful mitotic inhibitor in the treatment of human malignancies have been largely unsuccessful. Other mitotic poisons, however, are being used successfully with human tumors. In particular, vinblastine and vincristine are used for the treat-

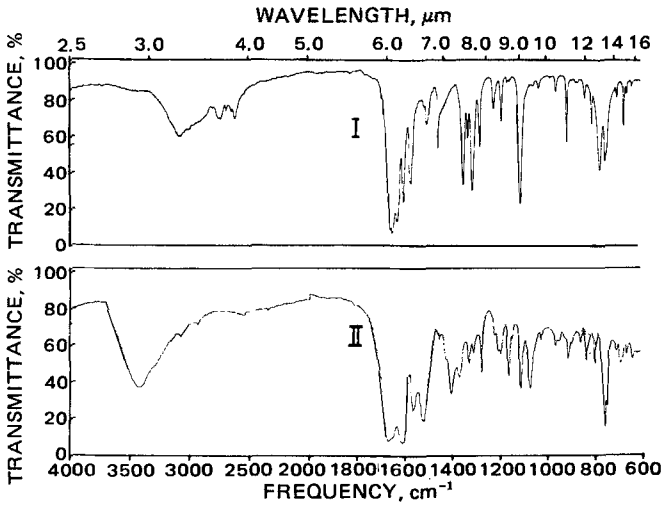

Figure 3—*IR spectra of I and II.*

ppm due to the hydrogen-bonded (enolic) protons at C-4 and/or C-4′ (13).

The poor solubility of II in deuterated chloroform necessitated the use of an NMR spectrometer equipped with a Fourier transform data system. The sample was analyzed overnight; all peaks were identifiable and appeared at their expected chemical shifts, but the spectrum could not be quantitated. Therefore, nonaqueous titration was used to quantitate the enolic protons. As expected, titration curves of II yielded two sharp breaks corresponding to two protons. One proton is believed to be at C-4 or C-4′ on each ligand molecule.

The IR spectra of I and II are shown in Fig. 3. Due to intramolecular hydrogen bonding, the carbonyl stretching frequency of I appeared at 1660 cm^{-1} (13). When I was *O*-methylated and no intramolecular hydrogen bonding could occur, the carbonyl peak was shifted to 1725 cm^{-1} (13). Since there was no shift to longer wave numbers in the carbonyl stretching frequency of II, both carbonyl groups in each ligand probably were bonded. Based on the presence of two titratable protons on II, it seems reasonable that one carbonyl group in each ligand was still intramolecularly hydrogen bonded and that the other carbonyl was bonded with magnesium.

Intramolecular hydrogen bonding also affected the position of the hydroxyl peak in the IR region. This peak appeared at 3100 cm^{-1} for I; however, II exhibited a large, broad water band between 3700 and 2800 cm^{-1}. Since II is believed to retain one intramolecular hydrogen bond on each ligand, the hydroxyl band at 3100 cm^{-1} was probably concealed beneath the water band.

In summary, elemental analyses conclusively established a 2:1 ligand–metal stoichiometry for II and the IR and other analytical data are consistent with Structure II in Scheme I. X-ray studies on the chelate are currently underway to substantiate further the structure.

REFERENCES

(1) D. Bernstein, *Drug Intel. Clin. Pharm.*, **5**, 276 (1971).

(2) R. A. O'Reilly, P. M. Aggeler, and L. S. Leong, *Thromb. Diath. Haemorrh.*, **11**, 1 (1964).

(3) E. Losinski, *Can. Med. Assoc. J.*, **83**, 177 (1960).

(4) J. L. Lach and L. D. Bighley, *J. Pharm. Sci.*, **59**, 1261 (1970).

(5) M. J. Akers, J. L. Lach, and L. J. Fischer, *ibid.*, **62**, 391 (1973).

(6) J. J. Ambre and L. J. Fischer, *Clin. Pharmacol. Ther.*, **14**, 231 (1973).

(7) K. A. Connors, "A Textbook of Pharmaceutical Analysis," Wiley, New York, N.Y., 1967, pp. 68, 69.

(8) K. A. Connors, "A Textbook of Pharmaceutical Analysis," Wiley–Interscience, New York, N.Y., 1974, p. 61.

(9) J. P. Leyda, in "Pharmaceutical Chemistry," vol. 1, L. G. Chatten, Ed.; Dekker, New York, N.Y., 1966, p. 277.

(10) J. D. McCallister, T. F. Chin, and J. L. Lach, *J. Pharm. Sci.*, **59**, 1286 (1970).

(11) R. H. Gore and W. W. Wendlandt, *Anal. Chem. Acta*, **52**, 83 (1970).

(12) "The Merck Index," 7th ed., Merck & Co., Rahway, N.J., 1960, p. 153.

(13) D. W. Hutchinson and J. A. Tomlinson, *Tetrahedron*, **25**, 2531 (1969).

ACKNOWLEDGMENTS AND ADDRESSES

Received July 2, 1976, from the *Division of Pharmaceutics, College of Pharmacy, University of Iowa, Iowa City, IA 52242.*

Accepted for publication September 27, 1976.

Presented in part at the Basic Pharmaceutics Section, APhA Academy of Pharmaceutical Sciences, San Diego meeting, November 1973.

Abstracted in part from a dissertation presented by R. J. Spivey to the University of Iowa in partial fulfillment of Doctor of Philosophy degree requirements.

The authors thank Dr. William Bennett, Department of Chemistry, University of Iowa, for useful discussions.

* Present address: Warner–Lambert Research Institute, Morris Plains, NJ 07950.

ˣ To whom inquiries should be directed.

X-Ray Analysis of Sulfur-Containing Colchicine Derivatives

CATHERINE KOERNTGEN and T. N. MARGULIS ˣ

Abstract □ The crystal and molecular structures of deacetylthiocolchicine hydrochloride dihydrate and thiocolchicine hexahydrate were determined by X-ray diffraction. The replacement of oxygen by sulfur on the C ring methoxy group causes greater puckering of the troponoid ring. The conformation of one A ring methoxy group differs from that of colchicine derivatives that do not contain sulfur.

Keyphrases □ Colchicine derivatives—X-ray diffraction determination of crystal and molecular structures □ Thiocolchicines, various—X-ray diffraction determination of crystal and molecular structures □ X-ray diffraction—determination of crystal and molecular structures of various thiocolchicines □ Crystal and molecular structures—various thiocolchicines, X-ray diffraction determination

Colchicine (I), an ancient drug, is used primarily in the treatment of gout. Attempts to use this powerful mitotic inhibitor in the treatment of human malignancies have been largely unsuccessful. Other mitotic poisons, however, are being used successfully with human tumors. In particular, vinblastine and vincristine are used for the treat-

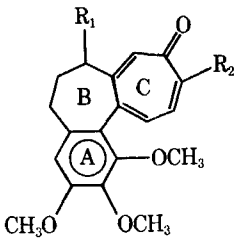

I: R_1 = $NHCOCH_3$, R_2 = OCH_3
II: R_1 = NH_3^+, R_2 = SCH_3
III: R_1 = $NHCOCH_3$, R_2 = SCH_3
IV: R_1 = $NHCOCH_3$, R_2 = SC_2H_5
V: R_1 = $NHCOCH_3$, R_2 = S-*n*-C_4H_9
VI: R_1 = $NHCH_3$, R_2 = OCH_3

ment of Hodgkin's disease, leukemia, and some solid cancers (1).

Thiocolchicines, in which sulfur replaces oxygen in the troponoid methoxy group of a colchicine derivative, were first prepared in 1954 (2–5). Recently, a series of new thiocolchicines was prepared (6) with groups larger than methyl on the sulfur atom. In general, substitution of sulfur for oxygen in itself does not inhibit, and in some cases may increase, colchicine activity.

Deacetylthiocolchicine hydrochloride (II) inhibited the binding of colchicine to microtubule protein and had nearly equivalent antimitotic and anti-inflammatory activities (7). Compound II also had about the same activity against mouse leukemia as colchicine (6). In the *allium* test, II and thiocolchicine (III) were somewhat more active than colchicine in their ability to arrest mitosis (8). With groups larger than methyl attached to the sulfur atom, activity was diminished; ethylthiocolchicine (IV) was slightly active and *n*-butylthiocolchicine (V) was inactive (6).

Colchicine is believed to bind to tubulin, preventing assembly into microtubules. Microtubules are involved in several important biological processes including chromosome movement, development of asymmetric cell shape, cell motility, and, possibly, nerve transmission. To gain a detailed understanding of the colchicine–tubulin interaction, X-ray diffraction studies of inactive, as well as active, colchicine derivatives and other antimitotic drugs are being performed. This report describes the crystal and molecular structures of II and III.

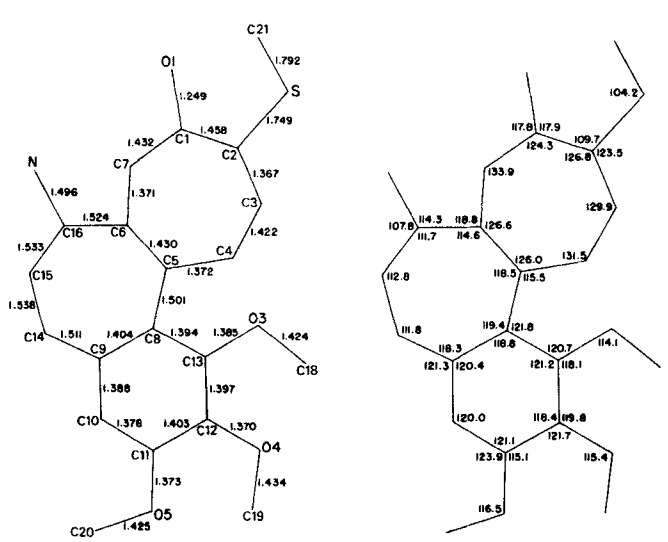

Figure 1—*Bond lengths (Å) and bond angles (°) for atoms other than hydrogen in II. Standard deviations are approximately 0.005 Å and 0.4°, respectively.*

Table I—Coordinates of Atoms Other than Hydrogen in II [a]

Atom	x	y	z
S	0.75908 (14)	−0.34348 (9)	0.39608 (4)
Cl	−0.03668 (15)	0.38244 (10)	0.44701 (6)
N	0.1248 (4)	0.0095 (2)	0.4998 (1)
O-1	0.5744 (4)	−0.2684 (2)	0.47997 (9)
O-3	0.5451 (3)	0.1921 (2)	0.33360 (9)
O-4	0.3745 (4)	0.3709 (2)	0.2862 (1)
O-5	0.0204 (3)	0.3636 (2)	0.2689 (2)
Water O-1	−0.2595 (6)	−0.0944 (4)	0.5601 (1)
Water O-2	−0.1420 (4)	0.1675 (3)	0.5137 (1)
C-1	0.5251 (5)	−0.2092 (3)	0.4417 (1)
C-2	0.6118 (5)	−0.2281 (3)	0.3910 (1)
C-3	0.5887 (5)	−0.1655 (3)	0.3460 (1)
C-4	0.4834 (5)	−0.0664 (3)	0.3369 (1)
C-5	0.3597 (4)	−0.0120 (3)	0.3677 (1)
C-6	0.3073 (4)	−0.0454 (3)	0.4197 (1)
C-7	0.3846 (5)	−0.1285 (3)	0.4502 (1)
C-8	0.2691 (4)	0.0889 (3)	0.3428 (1)
C-9	0.0848 (4)	0.0858 (3)	0.3348 (1)
C-10	−0.0011 (5)	0.1763 (3)	0.3101 (1)
C-11	0.0940 (5)	0.2711 (3)	0.2942 (1)
C-12	0.2777 (5)	0.2781 (3)	0.3026 (1)
C-13	0.3633 (4)	0.1854 (3)	0.3264 (1)
C-14	−0.0166 (5)	−0.0172 (3)	0.3548 (1)
C-15	−0.0256 (5)	−0.0196 (3)	0.4153 (1)
C-16	0.1477 (4)	0.0194 (3)	0.4414 (1)
C-18	0.5971 (6)	0.2217 (5)	0.3858 (2)
C-19	0.3480 (8)	0.4740 (4)	0.3161 (2)
C-20	−0.1682 (6)	0.3653 (4)	0.2651 (2)
C-21	0.8542 (7)	−0.3551 (4)	0.3316 (2)

[a] Estimated standard deviations are given in parentheses as deviations in the last figure. The numbering system omits O-2 and C-17 to make it compatible with the numbering used in demecolcine (10).

EXPERIMENTAL

All X-ray data for cell dimensions and intensities were collected on an automatic diffractometer with monochromatized CuKα (λ = 1.54178 Å) radiation. Cell dimensions were calculated by least-squares fitting of the diffractometer angles for 15 reflections. Intensities were measured with $2\theta - \theta$ scans and converted to structure factors without correction for absorption. Densities were measured by flotation. Refinement of each structure was accomplished by full-matrix least squares with atomic scattering factors from the literature (9).

The structure of II was solved by the conventional heavy atom method. The crystal[1], obtained by slow evaporation from aqueous solution, had approximate dimensions of 0.2 × 0.2 × 0.4 mm. The final value of $R = \Sigma||F_{obs}| - |F_{cal}||/\Sigma|F_{obs}|$ was 0.035 for 1911 observed reflections[2]. In

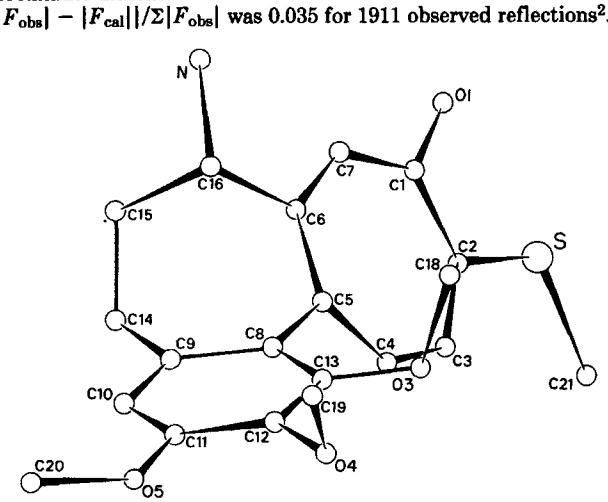

Figure 2—*One molecule of II, with hydrogen atoms omitted.*

[1] Obtained from Roussel-Uclaf.

[2] Observed and calculated structure factors and thermal parameters are available from the authors.

Table II—Hydrogen Atom Coordinates and Bond Lengths for II [a]

Hydrogen Atom Bonded to	x	y	z	D[b], Å
Water O-1	0.648	−0.033	0.564	1.0
Water O-1′	0.676	−0.143	0.543	0.9
Water O-2	−0.178	0.227	0.485	1.0
Water O-2′	−0.249	0.155	0.523	0.9
N	0.022	0.067	0.509	1.1
N′	0.094	−0.055	0.510	0.8
N″	0.248	0.044	0.519	1.1
C-3	0.658	−0.189	0.311	1.1
C-4	0.514	−0.039	0.299	1.0
C-7	0.345	−0.141	0.487	1.0
C-10	−0.132	0.166	0.302	1.0
C-14	−0.137	−0.011	0.340	1.0
C-14′	0.043	−0.104	0.342	1.2
C-15	−0.063	−0.097	0.428	1.0
C-15′	−0.129	0.038	0.428	1.1
C-16	0.152	0.103	0.435	1.0
C-18	0.726	0.233	0.386	1.0
C-18′	0.559	0.290	0.396	0.9
C-18″	0.557	0.168	0.415	1.0
C-19	0.395	0.469	0.348	0.9
C-19′	0.450	0.533	0.298	1.1
C-19″	0.217	0.471	0.341	1.2
C-20	0.782	0.298	0.246	1.0
C-20′	0.801	0.431	0.247	0.9
C-20″	0.770	0.366	0.300	1.0
C-21	0.944	−0.267	0.333	1.2
C-21′	0.912	−0.425	0.327	0.9
C-21″	0.760	−0.356	0.307	1.0

[a] Estimated standard deviations are approximately 0.005, 0.003, and 0.001 for x, y, and z, respectively, and 0.1 Å for bond lengths. [b] CH, OH, or NH bond length.

the final cycles, hydrogen atoms, located in a difference map, were refined with isotropic temperature factors while all other atoms were refined anisotropically.

Thiocolchicine[1] yields crystals easily from aqueous solution, but they lose water rapidly. Therefore, data were collected with a crystal, approximately 0.3-mm cube, in a capillary surrounded by mother liquor[3]. A trial structure was obtained by direct methods using the computer program MULTAN. A difference map gave the location of one full water and two partially occupied water sites but showed evidence of considerable disorder in the water structure. This map also revealed about half of the hydrogen atoms, but they were not included in the refinement. The final R factor, with all atoms anisotropic, with one ordered and two half water oxygen atoms, was 0.12 for 1613 nonzero reflections[2].

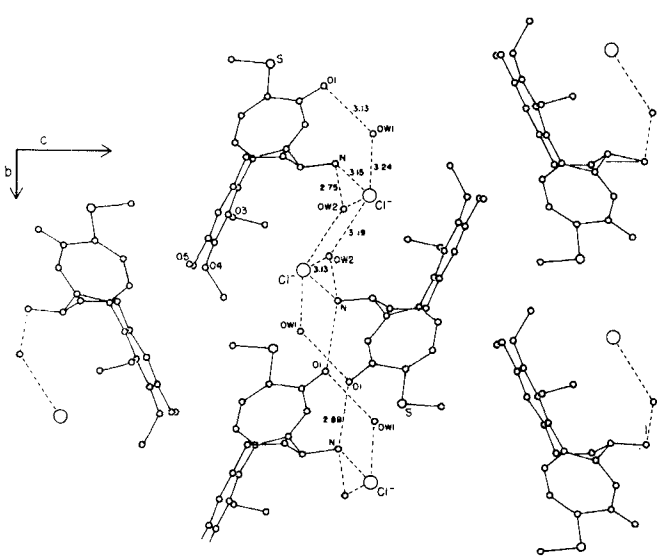

Figure 3—*Crystal structure of II. Dashed lines are hydrogen bonds. Hydrogen atoms are omitted.*

[3] Thiocolchicine also forms crystals from ethyl acetate. These are monoclinic, space group $P2_1$ with a = 21.23 ± 0.03, b = 7.188 ± 0.004, and c = 18.59 ± 0.05 Å, and β = 110.9 ± 0.2°, Z = 4.

Table III—Selected Torsion Angles, τ, in Biologically Active Colchicine Derivatives

Atom	τ°, VI[a]	τ°, II[b]	τ°, III[b]
Troponoid Ring			
C-7–C-1–C-2–C-3	−3.0	7.7	3
C-1–C-2–C-3–C-4	0.9	2.5	1
C-2–C-3–C-4–C-5	−0.8	−8.6	−2
C-3–C-4–C-5–C-6	3.1	0.6	3
C-4–C-5–C-6–C-7	−3.7	8.2	−7
C-5–C-6–C-7–C-1	0.0	−3.8	10
C-6–C-7–C-1–C-2	3.1	−7.1	−8
B Ring			
C-8–C-5–C-6–C-16	−4.5	6.5	−3
C-5–C-6–C-16–C-15	80.8	73.8	82
C-6–C-16–C-15–C-14	−48.3	−51.7	−50
C-16–C-15–C-14–C-9	−41.3	−38.9	−39
C-15–C-14–C-9–C-8	71.1	70.3	68
C-14–C-9–C-8–C-5	4.2	3.5	7
C-9–C-8–C-5–C-6	−53.9	−60.1	−55
OCH_3 and SCH_3			
C-12–C-13–O-3–C-18	82	101	104
C-11–C-12–O-4–C-19	−82	72	78
C-10–C-11–O-5–C-20	8	8	1
C-3–C-2–(S or O-2)–C-21	0	0	−2

[a] See Ref. 10. [b] This work.

RESULTS AND DISCUSSION

Compound II dihydrate, $C_{20}H_{24}NO_4S^+Cl^-\cdot 2\,H_2O$, forms orthorhombic crystals, space group $P2_12_12_1$, with a = 7.538, b = 11.663, and c = 25.375 Å and four molecules per unit cell. All atoms are in general positions given by x, y, and z: ½ −x, −y, and ½ +z; ½ +x, ½ −y, and −z; and −x, ½ +y, and ½ −z. Atomic parameters are listed in Tables I and II. These parameters are used to calculate the bond lengths and angles given in Fig. 1. A picture of a single molecule is given in Fig. 2.

The crystal structure of II is illustrated in Fig. 3. The dashed lines show hydrogen bonds that link the molecules in sheets running perpendicular to the c axis. The ions are linked directly by an NH···O hydrogen bond in the same manner as is found in the crystal structure (10) of demecolcine (VI). In addition, there are hydrogen bonds from N to Cl^- and to water, from O-1 to water, from water to water, and from water to Cl^-. There are no intramolecular hydrogen bonds and no hydrogen bonding between sheets.

The substitution of sulfur for oxygen causes small, but significant, changes in the troponoid ring. While tropolone had been considered to be aromatic, recent results indicate that there is not complete delocalization of the π-electrons. The best diffraction work shows a clear alternation in bond lengths about the ring, whereas an aromatic ring ought to have equal lengths. Hamor and Derry (11) found that the tropolone ring is not planar but may be described as a boat with angles of about 2° between its planes.

In II, some of these effects are exaggerated because the sulfur provides less opportunity for electron delocalization than oxygen. The bond length alternation is apparent with the formally double bonds averaging 1.370

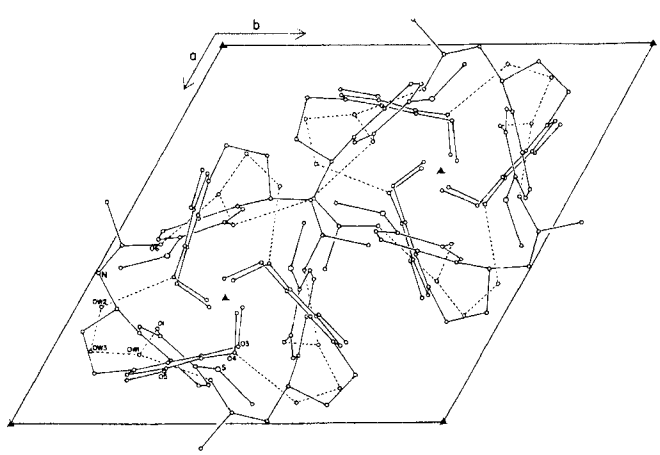

Figure 4—*Crystal structure of hydrated III. Dashed lines are hydrogen bonds. The region around the origin and corners of the unit cell contain disordered water of hydration. Some atoms in the C ring, the troponoid ring, are displaced for clarity.*

Table IV—Positional Parameters in III [a]

Atom	x	y	z
S	0.5907 (5)	0.4963 (5)	0.7583 (2)
O-1	0.799 (1)	0.561 (1)	0.7407 (5)
O-3	0.574 (1)	0.372 (1)	0.4847 (5)
O-4	0.574 (1)	0.388 (1)	0.3684 (5)
O-5	0.712 (1)	0.571 (1)	0.3168 (5)
O-6	0.883 (1)	0.405 (1)	0.5748 (5)
N	0.994 (2)	0.589 (1)	0.5739 (7)
Water O-1	0.816 (2)	0.209 (1)	0.5273 (7)
Water O-2	0.314 (4)	0.368 (4)	0.601 (2)
Water O-3	0.283 (4)	0.192 (4)	0.303 (2)
C-1	0.763 (2)	0.553 (2)	0.6932 (7)
C-2	0.650 (2)	0.518 (2)	0.6901 (7)
C-3	0.589 (2)	0.502 (2)	0.6427 (7)
C-4	0.615 (2)	0.510 (2)	0.5836 (7)
C-5	0.714 (2)	0.543 (2)	0.5601 (7)
C-6	0.811 (2)	0.570 (1)	0.5887 (7)
C-7	0.836 (2)	0.582 (2)	0.6464 (7)
C-8	0.714 (2)	0.548 (2)	0.4948 (7)
C-9	0.786 (2)	0.641 (2)	0.4711 (8)
C-10	0.796 (2)	0.664 (2)	0.4079 (8)
C-11	0.714 (2)	0.565 (2)	0.3759 (8)
C-12	0.645 (2)	0.471 (2)	0.4011 (9)
C-13	0.646 (2)	0.465 (2)	0.4622 (7)
C-14	0.872 (2)	0.734 (2)	0.5061 (8)
C-15	0.955 (2)	0.709 (2)	0.5298 (8)
C-16	0.907 (2)	0.596 (2)	0.5492 (7)
C-17	0.976 (2)	0.499 (2)	0.5809 (8)
C-18	0.619 (2)	0.306 (2)	0.5041 (9)
C-19	0.620 (2)	0.329 (2)	0.3364 (9)
C-20	0.788 (2)	0.671 (2)	0.2891 (8)
C-21	0.456 (2)	0.458 (2)	0.7469 (8)
C-22	1.066 (2)	0.474 (2)	0.598 (1)

[a] See footnote *a*, Table I.

Å and the formally single bonds[4] averaging 1.428 Å. The ring may be described as a boat consisting of three planes: (C-3–C-4–C-5–C-6), (C-2–C-3–C-6–C-7), and (C-1–C-2–C-7–O-1). The dihedral angle is 6.7° between the first and second of these planes and 5.1° between the second and third, larger angles than are seen in other tropolones.

Table III lists the torsion angles around some selected bonds for II and VI. The larger torsion angles of the troponoid ring in II are a measure of the lack of planarity, since a planar ring would have all torsion angles zero. This buckling of the troponoid ring leads to some changes in distances between atoms on the A and C rings. In particular, the O-1–O-3 distance is 6.79 Å in VI and 6.53 Å in II. Torsion angles for the B ring (Table III) are similar to those in VI, the difference being due to differences in the troponoid ring buckling.

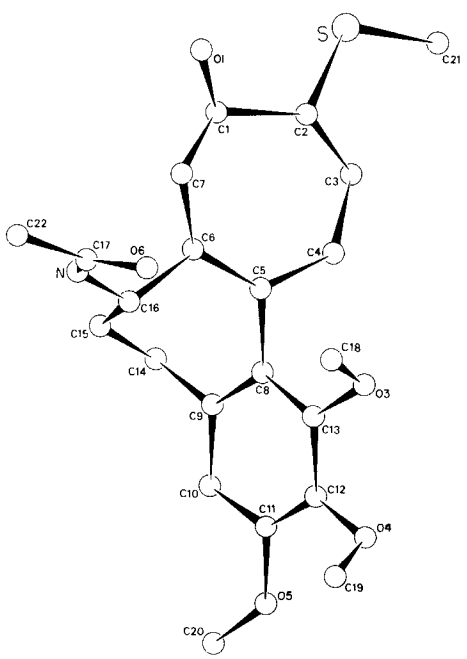

Figure 5—*One molecule of III.*

Compound III forms trigonal crystals, space group $P3_121$, with a = b = 14.532 ± 0.02 and c = 23.453 ± 0.03 Å. The observed density is 1.23 g/cm³. With six water molecules per molecule, the calculated density is 1.22 g/cm³. The compound is thus formulated as $C_{22}H_{25}NO_5S{\cdot}6H_2O$ with six formula weights per unit cell. All atoms are in general positions given by x, y, and z: −y, x − y, and ⅓ +z; y − x, −x, and ⅔ +z; y, x, and −z; −x, y − x, and ⅓ −z; and x − y, −y, and ⅔ −z. The thiocolchicine molecules are arranged around the 3_1 axis, leaving a large opening containing water of crystallization (Fig. 4). The methoxy groups point in, toward another 3_1 axis, giving a hydrophobic area in the crystal.

As in II and VI, there is an NH···O hydrogen bond to O-1. Most of the water is disordered. The oxygen of the one ordered water forms hydrogen bonds to carboxyls O-1 on one molecule and O-6 on another; two disordered waters, refined as half atoms, are hydrogen bonded to O-4 (a methoxy oxygen) and to water. A difference map shows numerous other small peaks due to disordered water in the hole at the origin. The disorder in the water structure accounts for the rather high *R* factor and leads to large standard deviations in bond lengths. For this reason, bond lengths and angles are not listed in detail. The molecule has the same structure as II within the limits of this analysis. Atomic parameters are listed in Table IV, and one molecule is shown in Fig. 5.

The conformation of the methoxy group is different in these two sulfur derivatives from that in VI. In general, methoxy groups on benzenoid rings adopt either a planar conformation (torsion angle $\tau = 0°$) with the methyl carbon in the plane of the benzenoid ring or a perpendicular conformation ($\tau = 90°$) with the methyl group sticking out as far as possible from this plane[5]. If the methyl group is on the opposite side of the ring from that of $\tau = 90°$, it would be described as $\tau = -90°$.

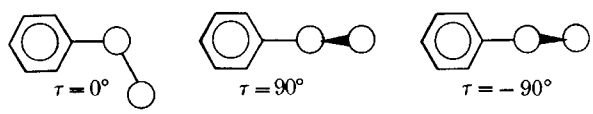

While the conformation of all three compounds is the same at O-3, O-5, and SCH_3 or OCH_3 on the troponoid ring, the O-4 methoxy is on the opposite side of the benzenoid ring in the sulfur-containing compounds (Table III).

Except for the large conformational changes possible in the methoxy groups, the colchicine molecule is rigid. All derivatives may be described as containing two nearly planar moieties twisted by about 54–60° from each other. Indeed, even inactive molecules such as colchicoside and isocolchicine (12) fit this basic description. The methoxy groups in such a wide variety of natural products are probably crucial to the interaction with tubulin (10, 12, 13). The structure of thiocolchicine serves as a reminder that an OCH_3 group may participate in hydrogen bonding and is not necessarily associated with hydrophobic interactions. In addition, methoxy can rather easily change conformation, which may play a role in the specificity of these molecules. For example, a change in the methoxy conformation may take place just before binding, with the methoxy group protecting the ring until the binding site is reached.

REFERENCES

(1) S. K. Carter and L. M. Kershner, *Pharm. Times*, **Aug. 1975,** 56.

(2) L. Velluz and G. Muller, *Bull. Soc. Chim.*, **1954,** 755.

(3) *Ibid.*, **1954,** 1072.

(4) *Ibid.*, **1955,** 194.

(5) *Ibid.*, **1955,** 198.

(6) G. T. Shiau, K. K. De, and R. E. Harmon, *J. Pharm. Sci.*, **64,** 646 (1975).

(7) M. H. Zwieg and C. F. Chignell, *Biochem. Pharmacol.*, **22,** 2141 (1973).

(8) G. Deysson, in "International Review of Cytology," vol. 24, G. H. Bourne and J. F. Danielli, Eds., Academic, New York, N.Y., 1968, p. 99.

(9) "International Tables for X-ray Crystallography," vol. III, Kynoch Press, Birmingham, England, 1962, p. 201.

(10) T. N. Margulis, *J. Am. Chem. Soc.*, **96,** 899 (1974).

(11) T. A. Hamor and J. E. Derry, *Acta Crystallogr.*, **B29,** 2649 (1973).

[4] Excluding C-1–C-2, which is probably less involved in the π-electron delocalization (11).

[5] For colchicine derivatives, $\tau = 90°$ is defined as the methyl group on O-3, O-4, or O-5, pointing in the direction of C-16 and N (Fig. 5).

(12) T. N. Margulis, in "Microtubules and Microtubule Inhibitors," M. Borgers and M. de Brabander, Eds., North-Holland, Amsterdam, The Netherlands, 1975, p. 67.

(13) F. Cortese, B. Bhattacharyya, and J. Wolff, *Fed. Proc.*, **35**, 1482 (1976).

ACKNOWLEDGMENTS AND ADDRESSES

Received August 27, 1976, from the *Department of Chemistry, University of Massachusetts–Boston, Harbor Campus, Boston, MA 02125.*

Accepted for publication October 5, 1976.

Supported by Public Health Service Research Grant CA17436-01 from the National Cancer Institute.

The authors thank Dr. Andre Courtin and Dr. G. Muller for gifts of chemicals, Dr. John Clark for assistance in crystal growing, and the staff of the Research Computer Center for help.

[x] To whom inquiries should be directed.

Simultaneous Automated Determination of Spironolactone Metabolites in Serum

PETER NEUBERT [x] **and KLAUS KOCH**

Abstract □ An automated two-phase method for the simultaneous fluorometric determination of the spironolactone metabolites canrenone (II) and canrenoic acid (III) in serum is described. The determination is performed by two dichloroethane extractions of the same serum sample at different pH values. The fluorescence developed in 65% (v/v) sulfuric acid is measured in two separate fluorometers (one each for canrenone and canrenoic acid). Comparable specificity and sensitivity to the manual procedure are obtained, with sensitivity limits of 20 ng of II/ml and of 30 ng of III/ml in serum. This method is applicable to the automated determination of drugs and metabolites in biological material when several extraction steps are involved.

Keyphrases ◻ Canrenone and canrenoic acid—automated simultaneous fluorometric analyses, serum □ Fluorometry—automated simultaneous analyses, canrenone and canrenoic acid, serum □ Automated analyses—simultaneous fluorometric analyses of canrenone and canrenoic acid, serum □ Spironolactone metabolites—canrenone and canrenoic acid, automated simultaneous fluorometric analyses, serum ◻ Aldosterone antagonists—canrenone and canrenoic acid, automated simultaneous fluorometric analyses, serum

Spironolactone[1] (I) inhibits the aldosterone-initiated reabsorption of sodium ions from the distal portion of the renal tubule. The increased excretion of sodium ions is the underlying principle of the diuretic action in the treatment of edema.

Compound I is rapidly metabolized in the body after oral administration (1, 2). The elimination of the thioacetyl group on C-7 gives rise to canrenone[2] (II). Canrenone, as a γ-lactone, is in a pH-dependent equilibrium with the corresponding γ-hydroxycarbonic acid, canrenoic acid[2] (III) (Scheme I).

Compounds II and III are relatively stable in the physiological pH range of 5–9, but greater pH changes and enzymatic processes change the ratio of the two metabolites (3). For this reason, knowledge of the blood level curves for both metabolites is important for assessing the absorption, distribution, and excretion of spironolactone.

Gochmann and Gantt (4) first described the procedure for the fluorometric determination of canrenone by measurement of the fluorescence in 65% sulfuric acid. The structure of the fluorophore (IV) produced by the reaction of sulfuric acid with canrenone and canrenoic acid was elucidated (5).

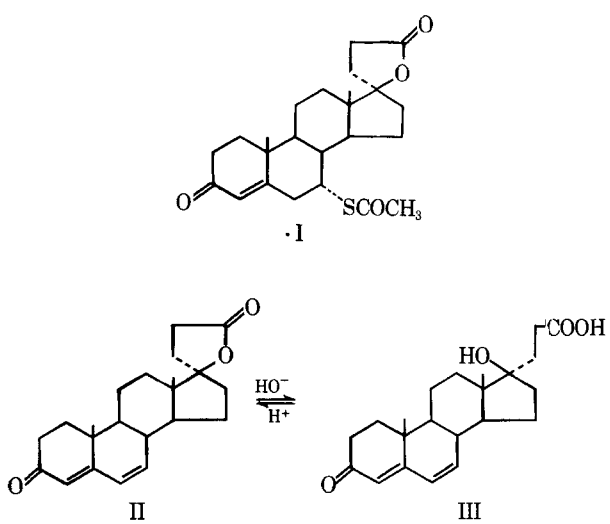

Scheme I

The high intensity of the fluorescence of the trienone (IV) in 65% sulfuric acid permits the sensitive determination of the metabolites in both manual (6) and automated procedures. The manual procedure is time consuming since four extractions are necessary. The analysis is complicated further by the caustic nature of the reagents dichloroethane and 65% sulfuric acid. The automation of the analytical procedure was therefore desirable and is the subject of this report.

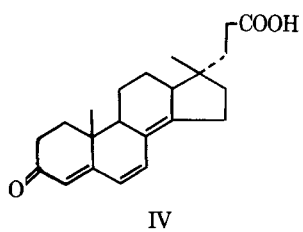

[1] Aldactone, Boehringer Mannheim GmbH.

[2] Compound II was formerly referred to as aldadiene, and III was referred to as aldadienic acid (1, 2).

(12) T. N. Margulis, in "Microtubules and Microtubule Inhibitors," M. Borgers and M. de Brabander, Eds., North-Holland, Amsterdam, The Netherlands, 1975, p. 67.

(13) F. Cortese, B. Bhattacharyya, and J. Wolff, *Fed. Proc.*, **35**, 1482 (1976).

ACKNOWLEDGMENTS AND ADDRESSES

Received August 27, 1976, from the *Department of Chemistry, University of Massachusetts–Boston, Harbor Campus, Boston, MA 02125.*

Accepted for publication October 5, 1976.

Supported by Public Health Service Research Grant CA17436-01 from the National Cancer Institute.

The authors thank Dr. Andre Courtin and Dr. G. Muller for gifts of chemicals, Dr. John Clark for assistance in crystal growing, and the staff of the Research Computer Center for help.

[x] To whom inquiries should be directed.

Simultaneous Automated Determination of Spironolactone Metabolites in Serum

PETER NEUBERT [x] **and KLAUS KOCH**

Abstract □ An automated two-phase method for the simultaneous fluorometric determination of the spironolactone metabolites canrenone (II) and canrenoic acid (III) in serum is described. The determination is performed by two dichloroethane extractions of the same serum sample at different pH values. The fluorescence developed in 65% (v/v) sulfuric acid is measured in two separate fluorometers (one each for canrenone and canrenoic acid). Comparable specificity and sensitivity to the manual procedure are obtained, with sensitivity limits of 20 ng of II/ml and of 30 ng of III/ml in serum. This method is applicable to the automated determination of drugs and metabolites in biological material when several extraction steps are involved.

Keyphrases ◻ Canrenone and canrenoic acid—automated simultaneous fluorometric analyses, serum □ Fluorometry—automated simultaneous analyses, canrenone and canrenoic acid, serum □ Automated analyses—simultaneous fluorometric analyses of canrenone and canrenoic acid, serum □ Spironolactone metabolites—canrenone and canrenoic acid, automated simultaneous fluorometric analyses, serum ◻ Aldosterone antagonists—canrenone and canrenoic acid, automated simultaneous fluorometric analyses, serum

Spironolactone[1] (I) inhibits the aldosterone-initiated reabsorption of sodium ions from the distal portion of the renal tubule. The increased excretion of sodium ions is the underlying principle of the diuretic action in the treatment of edema.

Compound I is rapidly metabolized in the body after oral administration (1, 2). The elimination of the thioacetyl group on C-7 gives rise to canrenone[2] (II). Canrenone, as a γ-lactone, is in a pH-dependent equilibrium with the corresponding γ-hydroxycarbonic acid, canrenoic acid[2] (III) (Scheme I).

Compounds II and III are relatively stable in the physiological pH range of 5–9, but greater pH changes and enzymatic processes change the ratio of the two metabolites (3). For this reason, knowledge of the blood level curves for both metabolites is important for assessing the absorption, distribution, and excretion of spironolactone.

Gochmann and Gantt (4) first described the procedure for the fluorometric determination of canrenone by measurement of the fluorescence in 65% sulfuric acid. The structure of the fluorophore (IV) produced by the reaction of sulfuric acid with canrenone and canrenoic acid was elucidated (5).

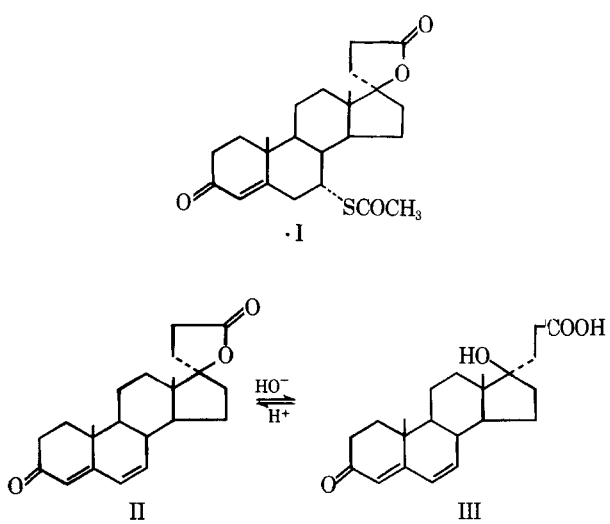

Scheme I

The high intensity of the fluorescence of the trienone (IV) in 65% sulfuric acid permits the sensitive determination of the metabolites in both manual (6) and automated procedures. The manual procedure is time consuming since four extractions are necessary. The analysis is complicated further by the caustic nature of the reagents dichloroethane and 65% sulfuric acid. The automation of the analytical procedure was therefore desirable and is the subject of this report.

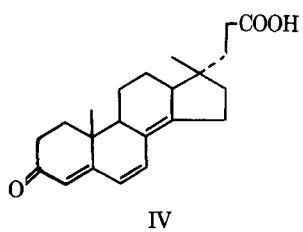

[1] Aldactone, Boehringer Mannheim GmbH.

[2] Compound II was formerly referred to as aldadiene, and III was referred to as aldadienic acid (1, 2).

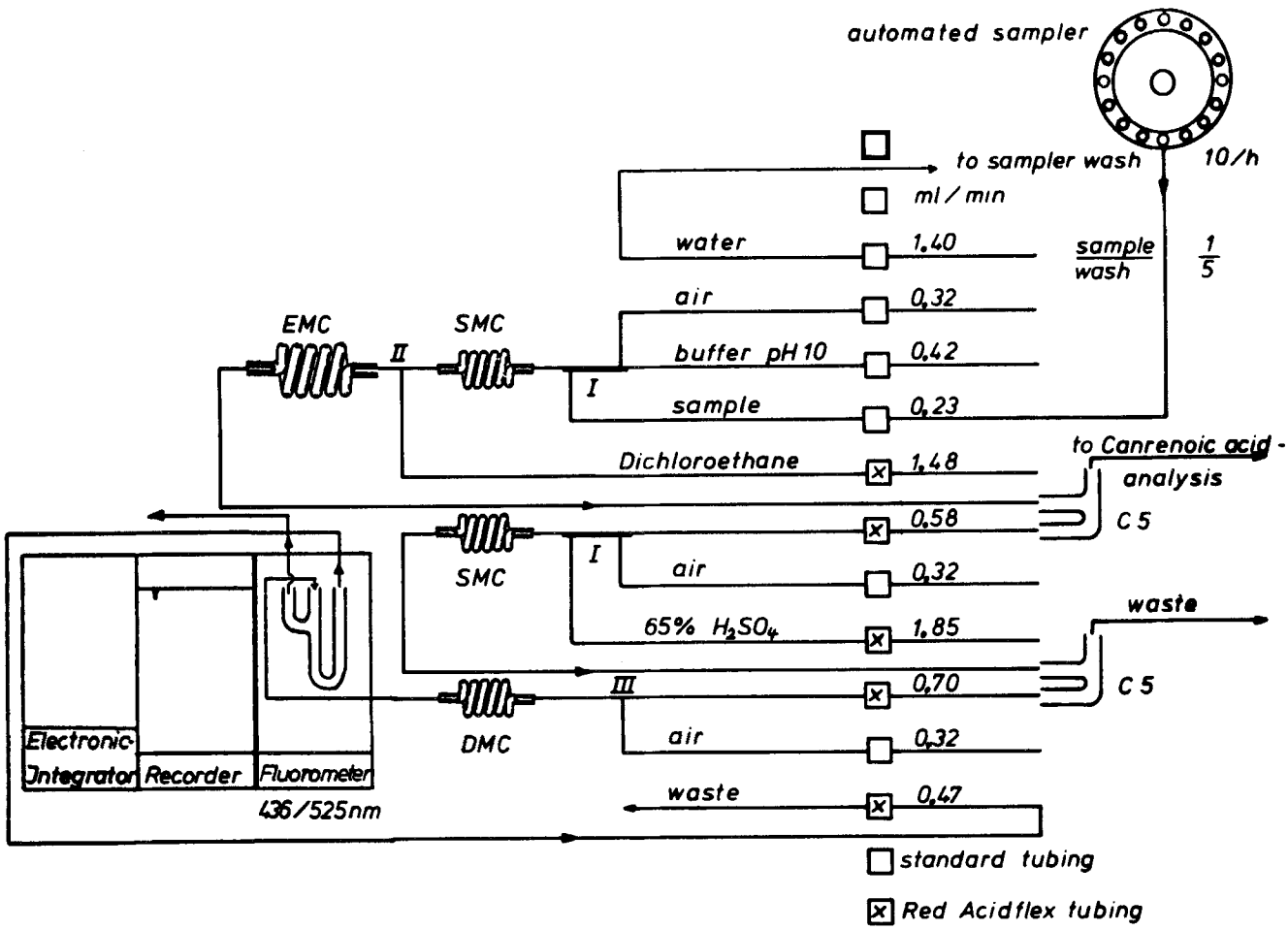

Figure 1—*Flow diagram for automated determination of canrenone. Key: SMS, single mixing coil; DMC, double mixing coil; EMC, extracting mixing coil; C5, phase separators; and I, II, and III, glass connectors.*

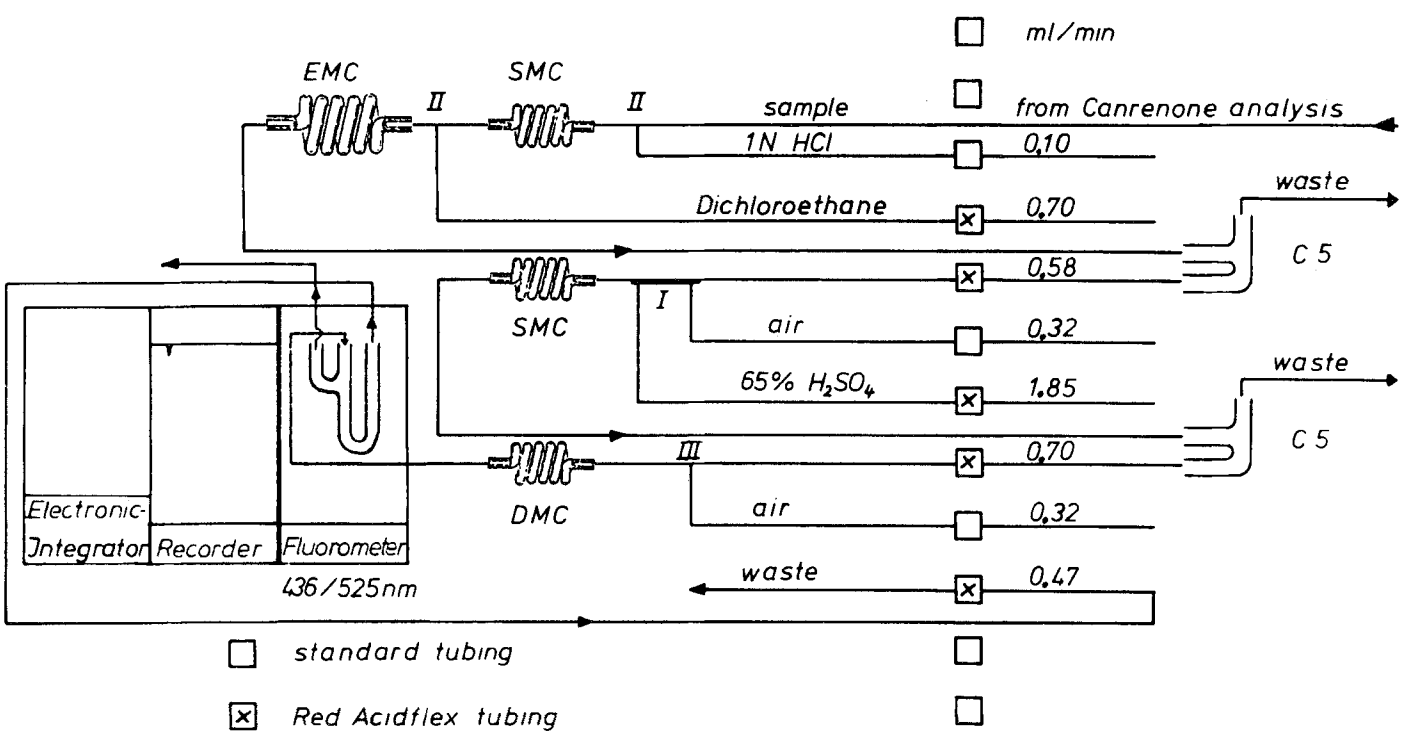

Figure 2—*Flow diagram for automated determination of canrenoic acid. Key: same as Fig. 1.*

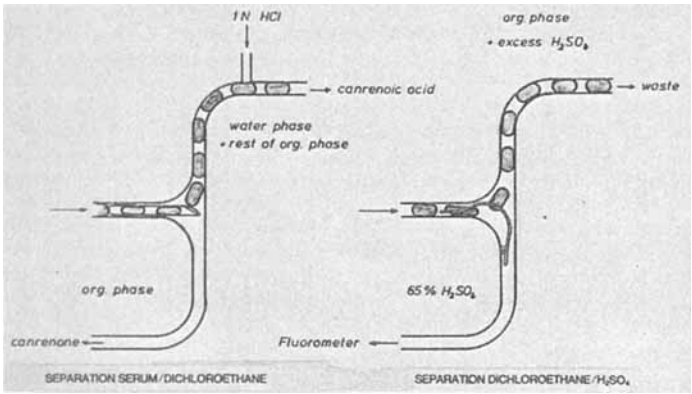

Figure 3—*Phase separation.*

EXPERIMENTAL

Apparatus—An automatic sampler and proportioning pump[3], two fluorescence spectrophotometers[4] with flowcells and a special cell holder designed to measure the fluorescence of 65% sulfuric acid in a continuous flow, a recorder[5], an electronic integrator[6], and a computer[7] were used.

Materials—The 0.04 *M* Britton–Robinson universal buffer (pH 10), 1 *N* hydrochloric acid containing 0.1 ml of wetting agent[8]/liter, dichloroethane containing 1.0 ml of wetting agent[8]/liter, and 65% (v/v) sulfuric acid (68 ml of 96% sulfuric acid plus 32 ml of water) were analytical reagent grade.

Standards—Separate stock solutions of canrenone and canrenoic acid, 500 mg/liter, were prepared in methanol. Working solutions were obtained by appropriate dilution with water. Suitable aliquots of the solutions were added to blank serum as standards.

Automated Analysis—The flow diagrams of the automated system for the determination of canrenone and canrenoic acid are shown in Figs. 1 and 2, respectively. The 19 pump tubes, however, only require one pump.

Canrenone—The sample was mixed in the predetermined volume ratio with previously air-segmented buffer to obtain a pH of 9. Dichloroethane was added as a solvent to give a two-phase system. The sample passed through an extracting mixing coil (EMC) followed by phase separation. The upper aqueous phase was led to the determination of canrenoic acid (Fig. 2). An aliquot of the organic phase was taken from below and reacted with 65% sulfuric acid. The organic phase was discarded, and an aliquot of the sulfuric acid phase was fed into the fluorometer. A delaying mixing coil (DMC) ensured an adequate reaction time.

The intensity of the fluorescence measured in the fluorometer was recorded. The corresponding peak height was determined with an electronic integrator[6], which could be used to print either peak areas or peak heights. The data were transferred to a punch tape and processed by means of an off-line programmed computer[7].

Canrenoic Acid—The simultaneous determination of canrenoic acid in the same serum sample ran in parallel but with a slight time delay. The serum sample was acidified with 1 *N* hydrochloric acid after removal of canrenone. This acid pH caused the lactonization of canrenoic acid to canrenone. The other steps were the same as those described for canrenone.

RESULTS AND DISCUSSION

The simultaneous determination of canrenone and canrenoic acid in the same serum sample with retention of the two-phase system requires four extraction steps and, correspondingly, four phase separations.

The separation of the phases takes place in small separators (Fig. 3) on the basis of the differing solvent densities and the differing wettability of the polytef tongue. Phase separation usually was facilitated with a small polytef rod. This technique also was used for the separation of dichloroethane and sulfuric acid. The separation of serum and dichloroethane, however, is more critical. In this case, optimal results were obtained by using a piece of polytef tubing (0.8 mm i.d.).

The best solvent for separation and extraction was dichloroethane because of the marked difference in density with regard to serum and sulfuric acid and because of the lower tendency to form emulsions in comparison with chloroform.

Tubings[9] made of material resistant to acid and solvents were used in the pump region for the transport of the solvents and sulfuric acid. All connecting pieces within the analytical unit were glass.

Phase separation and transport with low carryover were greatly facil-

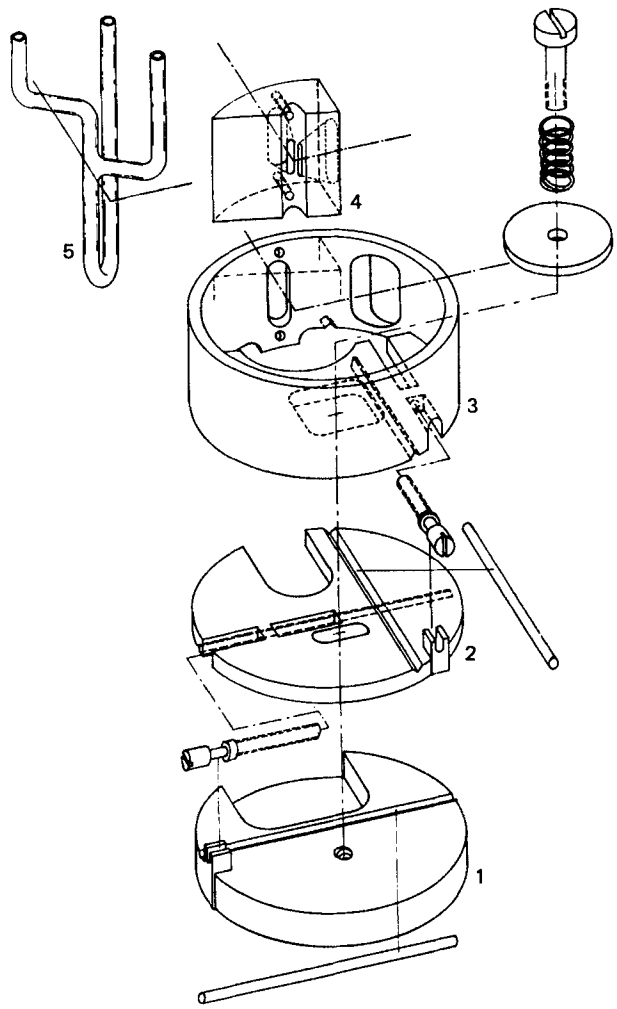

Figure 4—*Cell holder consisting of three brass plates. The ground plate (1) is made fitting to the base of the fluorometer cell compartment. The next plate (2) is adjustable by means of a screw in the direction of the excitation source. The other parts are the upper plate (3), the carrying slit (4), and the flowcell (5) which fits to plate 2 in an angle of 90°.*

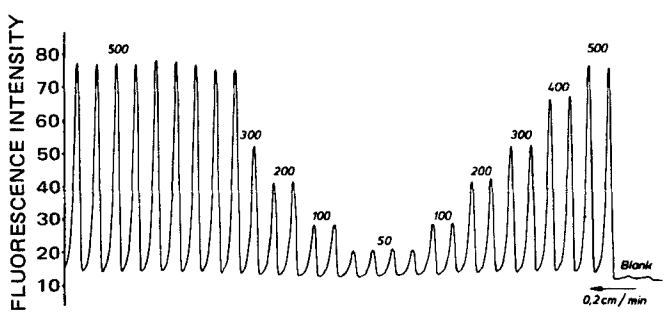

Figure 5—*Chart recordings of the determination of canrenone in serum (50–500 μg/liter).*

[3] Sampler IV and proportioning pump III of AutoAnalyzer II, Technicon GmbH, Bad Vilbel, Germany.
[4] Model 203, Perkin-Elmer GmbH, Ueberlingen, Germany.
[5] Kompensograph III, Siemens AG, Karlsruhe, Germany.
[6] Autolab Minigrator, Spectra Physics GmbH, Darmstadt, Germany.
[7] Model 9830, Hewlett-Packard, Frankfurt, Germany.
[8] Triton X-100.
[9] Acidflex, Technicon GmbH.

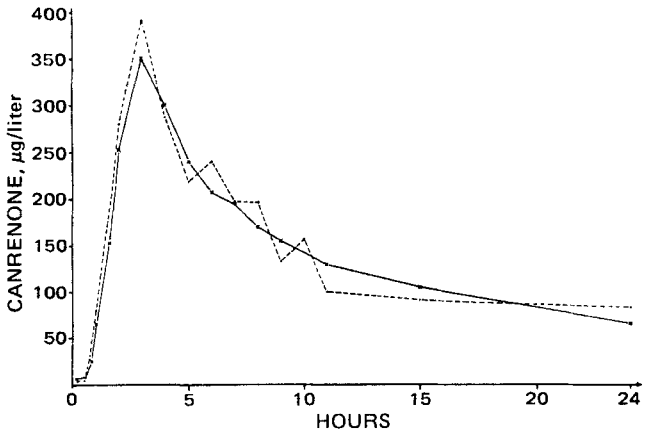

Figure 6—*Blood canrenone level after oral administration of 100 mg of spironolactone. Data determined by the manual (- - -) and automated (—) procedures are compared.*

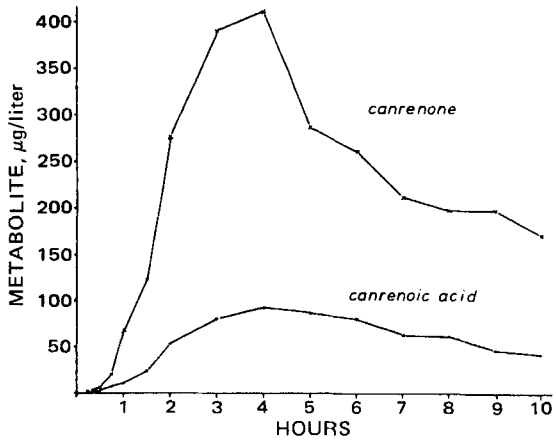

Figure 7—*Blood canrenone and canrenoic acid levels after oral administration of spironolactone determined with automated procedure.*

itated by the addition of wetting agents[8]. Carryover, a particular susceptibility of two-phase systems, was avoided by setting the number of samples relatively low, 10/hr. Furthermore, the ratio of sample volume to wash solution volume was set at 1:5. Thus, with proper functioning, the effect on the analytical results by carryover from sample to sample was very small and correction was not necessary.

A very high sensitivity of fluorescence measurement was achieved by optimally mounting the flowcell in the light path of the fluorometer. This was accomplished by having a cell holder that was adjustable in two axes (Fig. 4).

The fluorescence measured in the two fluorometers was recorded on two separate recorders. The records obtained (Fig. 5) showed that washing with water between individual samples was virtually complete so that the initial baseline was reached between sample peaks. With the aid of an integrating device[6], the peak heights were calculated from the intensity of the fluorescence and were printed out.

A good correlation existed between canrenone concentration and peak height. The curve was linear from 50 to 5000 μg of canrenone or canrenoic acid/liter. The lowest limits of detection were 20 μg/liter for canrenone and 30 μg/liter for canrenoic acid; *i.e.*, when using a 0.23-ml sample, less than 10 ng of the metabolite could be detected quantitatively.

Figure 6 shows the blood level curve for canrenone up to 24 hr after oral administration of 100 mg of spironolactone. The manually determined canrenone concentrations were compared with those obtained with the automated procedure. Control analyses of serum samples with known canrenone concentrations were included at regular intervals (*e.g.*, every 15 samples) to allow detection of time delays and to check the precision and accuracy of the analyses. From 50 analyses of control serum with 500 μg of canrenone/liter, a coefficient of variation from day to day of 5.2% was determined. Determination of canrenoic acid gave a somewhat higher value of 6.3%. From multiple analyses of one specimen with the same concentration (Fig. 5, 500 μg of canrenone/liter), a coefficient of variation in series of 1.8% was calculated.

Figure 7 shows the canrenone and canrenoic acid blood levels obtained after oral administration of 100 mg of spironolactone determined with the automated procedure.

Partition of canrenone between the aqueous and organic phases was not quantitative and reached a certain equilibrium only, in contrast to the manual procedure where phase distribution was almost complete. Consequently, a certain proportion of canrenone remained in the aqueous phase and was determined together with canrenoic acid. The value for canrenoic acid, therefore, had to be corrected for the amount of previously unextracted canrenone as follows:

$$C_{CS} = C_{C/CS} - FC_C \qquad \text{(Eq. 1)}$$

where:

C_{CS} = corrected value of canrenoic acid concentration
$C_{C/CS}$ = uncorrected value of canrenoic acid concentration containing canrenone determined as canrenoic acid with canrenoic acid standard
C_C = canrenone concentration of same sample determined with canrenone standard
$F = C_T/T$ where T is the concentration of canrenone standard, and C_T is that part of the canrenone standard T that is determined as canrenoic acid with a canrenoic acid standard

In spite of the comparatively low number of analyses of 20 determinations/hr, the time saved by automation is considerable in comparison with the manual procedure. Canrenone and canrenoic acid analyses to determine the blood level curves, which previously took 2 days, can now be carried out in 2–3 hr. The sensitivity was adequate in spite of the one-third lower serum requirement, and the precision was considerably increased.

REFERENCES

(1) A. Karim, R. E. Ranney, and H. I. Maibach, *J. Pharm. Sci.*, **60**, 708 (1971).

(2) W. Sadée, M. Dagjioglu, and R. Schröder, *J. Pharmacol. Exp. Ther.*, **185**, 686 (1973).

(3) E. R. Garrett and C. M. Won, *J. Pharm. Sci.*, **60**, 1801 (1971).

(4) N. Gochman and C. L. Gantt, *J. Pharmacol. Exp. Ther.*, **135**, 312 (1962).

(5) W. Sadée, S. Riegelman, and L. F. Johnson, *Steroids*, **17**, 595 (1971).

(6) W. Sadée, M. Dagjioglu, and S. Riegelman, *J. Pharm. Sci.*, **61**, 1126 (1972).

ACKNOWLEDGMENTS AND ADDRESSES

Received April 2, 1976, from the *Department "Bioanalytik" of Chemical and Pharmaceutical Research, Boehringer Mannheim GmbH, 6800 Mannheim, West Germany.*

Accepted for publication September 24, 1976.

Presented in part at the Annual Meeting of the Federation of German Chemical Society, Cologne, West Germany, September 1975.

The authors thank Mr. K. E. Wallach for designing the cell holder and Mr. G. Kilian for technical assistance.

ˣ To whom inquiries should be directed.

Plant Anticancer Agents III: Isolation of Indole and Bisindole Alkaloids from *Tabernaemontana holstii* Roots

DAVID G. I. KINGSTON ˣ, BERNARD T. LI, and FLORIN IONESCU

Abstract □ Certain active antileukemic and cytotoxic fractions prepared from *Tabernaemontana holstii* roots were investigated, resulting in the isolation of the known indole alkaloids conoduramine, conodurine, coronaridine, gabunine, 19-oxocoronaridine, pericyclivine, perivine, and vobasine. Two new alkaloids were assigned the structures 19-oxoconodurine and 19-(2-oxopropyl)conodurine. Both gabunine and 19-(2-oxopropyl)conodurine showed significant inhibitory activity against P-388 cell culture. All of the alkaloids are reported for the first time from *T. holstii;* conodurine, conoduramine, gabunine, perivine, and pericyclivine are reported for the first time from any *Tabernaemontana* species.

Keyphrases □ Alkaloids, indole—isolated from *Tabernaemontana holstii* roots, cytotoxic activity evaluated □ *Tabernaemontana holstii*—root extract, various indole alkaloids isolated, cytotoxic activity evaluated □ Cytotoxic activity—evaluated in various indole alkaloids isolated from *Tabernaemontana holstii* roots

A random screening of botanical sources for anticancer activity showed that the aqueous alcoholic extract of the roots of *Tabernaemontana holstii* K. Schum (family Apocynaceae) gave reproducible activity against the cell culture (KB) of a human carcinoma of the nasopharynx and also against P-388 lymphocytic leukemia in the mouse. Systematic fractionation of the extract led to the isolation of the known indole alkaloids conoduramine (I), conodurine (II), gabunine (III), coronaridine (VI), 19-oxocoronaridine (VII), perivine (VIII), vobasine (IX), and pericyclivine (X). In addition, two new alkaloids were isolated, and their structures were determined as 19-oxoconodurine (IV) and 19-(2-oxopropyl)conodurine (V). Both of these compounds, as well as VII, are probably artifacts formed during extraction and purification. Significant cytotoxicity in the P-388 cell culture system was shown by gabunine and 19-(2-oxopropyl)conodurine. No previous work on this plant species has been reported, although several other *Tabernaemontana* species have been investigated and contain many different indole alkaloids (1).

EXPERIMENTAL[1]

Plant Material—The air-dried roots[2] of *T. holstii* K. Schum (Apocynaceae) were collected in Kenya during 1971.

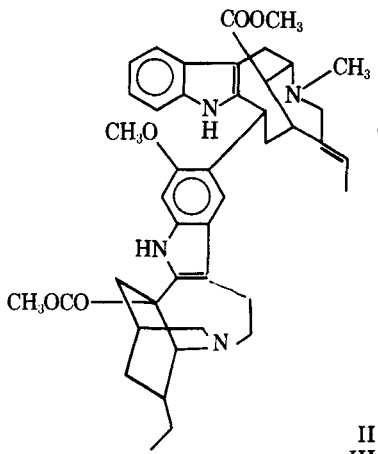

I

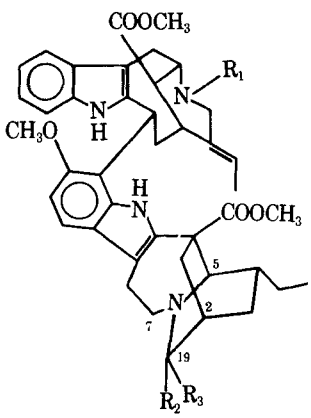

II: $R_1 = CH_3$, $R_2 = H$, $R_3 = H$
III: $R_1 = H$, $R_2 = H$, $R_3 = H$
IV: $R_1 = CH_3$, $R_2R_3 = O$
V: $R_1 = CH_3$, $R_2 = H$, $R_3 = CH_2COCH_3$

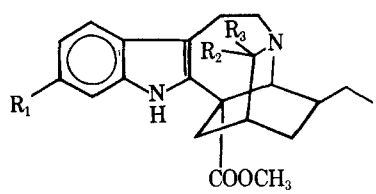

VI: $R_1 = H$, $R_2 = H$, $R_3 = H$
VII: $R_1 = H$, $R_2R_3 = O$
XIV: $R_1 = OCH_3$, $R_2 = H$, $R_3 = CH_2COCH_3$

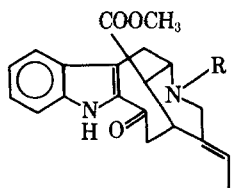

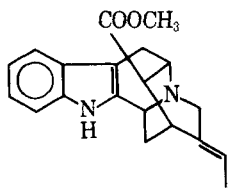

VIII: R = H
IX: R = CH_3

X

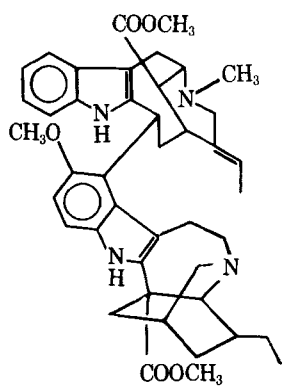

XIII

[1] Melting points were determined in open capillary tubes or on microscope slides and are uncorrected. UV spectra were taken in ethanol on a Cary model 14 spectrophotometer. IR spectra were measured in chloroform solution or as potassium bromide pellets *versus* air with a Beckman model IR-20 spectrophotometer. Mass spectra were recorded at 70 ev using a Hitachi Perkin-Elmer RMU-7 mass spectrometer, operated in the direct probe mode. NMR spectra were determined in deuterochloroform, containing tetramethylsilane as the internal standard, using a Jeol PS-100 spectrometer. All concentrations and evaporations were carried out with water pump vacuum at less than 40°.

Column chromatography was carried out on silica gel 60, 0.063–0.200 mm (E. Merck), silica gel, 60–200 mesh (Baker), or Woelm alumina as indicated. Routine TLC was carried out using silica gel GF (Merck) plates, and visualization was by means of UV absorption and by the ceric ammonium sulfate reagent (2). The solvent systems used were: A, chloroform–methanol (95.5); and B, ethanol–ethyl acetate (1:4). Preparative thick-layer chromatography was carried out on silica gel PF_{254} (Merck) 1-mm layers, resolved components being detected by quenching under 254-nm UV light. Appropriate zones were scraped from the plates; pure components were recovered from the removed zones by elution with methanol–chloroform, followed by filtration and removal of the solvent. High-performance liquid chromatography (HPLC) was carried out on the apparatus previously described (3), using as packing materials Porasil C, Porasil E, or Bondapak C_{18}/Porasil B, referred to in the text as C, E, and B, respectively.

[2] Voucher specimens are on deposit with Dr. R. E. Perdue, Jr., U. S. Department of Agriculture, Beltsville, Md.

Extraction of Alkaloids—Plant material (4 kg) was extracted twice with 95% ethanol by stirring at room temperature for 24 hr, followed by one extraction with ammoniacal ethanol at 50° for 4 hr. The combined ethanol extract (A) (24 liters) was evaporated to 0.4 liter and treated with

0.5 liter of water, and this brown extract was extracted exhaustively with ethyl acetate in a separator and finally in a liquid–liquid extractor until an aliquot of the aqueous phase gave only a faint positive reaction with Mayer's reagent.

A small quantity of material that formed a suspension in the ethyl acetate was filtered off and put aside, and the ethyl acetate was concentrated to a volume of 1 liter. The concentrated ethyl acetate solution was then extracted six times with 50-ml portions of 5% sulfuric acid, followed by washing of the combined acid extracts with ethyl acetate. Neutralization of the acid with ammonia, followed by extraction with chloroform, yielded 17.6 g (0.44%) of crude tertiary bases after solvent evaporation (Extract B). The residual ethyl acetate after acid extraction was evaporated to yield a nonbasic extract (C).

Chromatographic Separation of Crude Alkaloids on Alumina—The crude alkaloid mixture from two extractions (30 g) was transferred to 300 g of alumina (neutral, activity III), and this material was added to the top of a 5-cm glass column containing 600 g of the same adsorbent. Elution with benzene (4.5 liters) yielded Fraction D (8.1 g), elution with chloroform (1.5 and 2.2 liters) yielded Fractions E (6.2) and F (8.1 g), and elution with methanol (1.2 and 7.3 liters) gave Fractions G (4.8 g) and H (4.0 g).

Separation of Fraction D—Fraction D (7 g) was chromatographed in a 2.5-cm column on 250 g of silica gel, with elution by methanol–chloroform (2:98) and collection of 150-ml fractions. The material eluted in fractions 2–5 (3.5 g) was combined and rechromatographed on a similar column with elution by methanol–dichloromethane (1:99) (33 fractions of 30 ml) and methanol–dichloromethane (2:98) (33 fractions of 30 ml). Fractions 9–16 were combined to yield Fraction I (1.1 g), and fractions 23–42 were combined to yield Fraction J (1.6 g).

Isolation of Coronaridine (VI)—Fraction I was chromatographed in a 2.5-cm column on 100 g of silica gel, with elution by methanol–dichloromethane (1:99) and collection of 30-ml fractions. Fractions 4 and 5 were combined (390 mg) and treated with methanolic hydrogen chloride to yield 100 mg of colorless crystals, mp 221–224° [lit. (4) mp 232–233°]; $[\alpha]_D^{24}$ −8.7° (c 0.32 in methanol). The isolate was homogeneous by TLC and gave a blue color with the ceric ammonium sulfate reagent; it had an R_f value of 0.95 in Solvent System A. The UV absorption spectrum showed λ_{max} (ethanol) 225 (log ϵ 4.29), 286 (3.73), and 293 (3.67) nm. The IR, UV, and mass spectral data for the compound were identical with those published for coronaridine hydrochloride (5, 6), and the NMR spectrum was consistent with this structure assignment.

Isolation of 19-Oxocoronaridine (VII)—Fraction J was combined with similar material from another batch of Fraction D to yield 3.4 g of material, which was chromatographed on a 2.5-cm column packed with 240 g of silica gel. Elution with dichloromethane (3.8 liters), followed by methanol–dichloromethane (0.5:99.5) (1 liter) and methanol–dichloromethane (1:99) (3 liters), yielded a new component in the fraction eluted with from 2–2.5 liters of the last solvent (390 mg).

Purification of this material by HPLC on Packing E [four 0.61 m × 0.94 cm (four 2 ft × 0.37 in.)] with elution with methanol–dichloromethane (0.25:99.75) yielded homogeneous material as the second peak eluted (100 mg). The material did not crystallize but was homogeneous on HPLC and TLC. It gave a yellow color with ceric ammonium sulfate and had an R_f value of 0.9 in Solvent System A. Its UV absorption spectrum showed λ_{max} 227 (log ϵ 4.52), 285 (3.81), and 295 (3.86) nm; its IR spectrum showed strong bands at 1730 and 1660 cm^{-1}. Its mass spectrum had major peaks at *m/e* 352 (54), 214 (10), 195 (20), 154 (30), 143 (10), 138 (10), and 124 (100). Comparison of its IR, NMR, and mass spectra with those obtained for 19-oxocoronaridine, recently isolated from *T. heyneana* (7), showed them to be identical, and the compound was identified as 19-oxocoronaridine.

Separation of Fractions E and F—Alkaloid material corresponding to Fractions E and F (12 g) was chromatographed on a 5-cm column on 600 g of silica gel with elution by methanol–chloroform (5:95). The material eluting between 1000 and 1860 ml was combined to yield Fraction K (3.7 g), and that eluting between 2900 and 3840 ml yielded Fraction L (2.2 g).

Isolation of Conodurine (II)—Fraction K was chromatographed on a 2.5-cm column on 170 g of silica gel with elution by ethyl acetate–carbon tetrachloride–ethanol (50:40:10). The resulting fractions were combined into five major fractions on the basis of TLC similarities. The most polar fraction (1.2 g) was chromatographed on a 5 × 75-cm column of silica gel and eluted with methanol–chloroform (3:97); 90-ml fractions were collected. The second fraction yielded crystalline material (40 mg) on evaporation of the solvent but was shown by TLC to consist of two components. Preparative TLC [methanol–chloroform (5:95), multiple development] gave pure material after crystallization from methanol, mp 210° dec. [lit. (8) mp 222–225°]. It had the same R_f values in Solvent Systems A (0.50) and B (0.56) as an authentic sample of conodurine (9) and gave the same yellow-green color with the ceric ammonium sulfate reagent. Its IR, UV, and mass spectra were identical with those of authentic conodurine.

Isolation of Perivine (VIII)—Fraction L was chromatographed on a 2.5-cm column on 200 g of silica gel. Elution with ethyl acetate–carbon tetrachloride–ethanol (50:40:10) and collection of 30-ml fractions gave a major fluorescent product in fractions 16–28 (1.5 g). Combination of this material with similar material from another batch of extract, chromatography of the combined material (2.4 g) on a 2.5-cm column on 200 g of silica gel, elution with methanol–dichloromethane (8:92), and collection of 30-ml fractions gave homogeneous material in fractions 14–17. Crystallization of this material from methanol yielded off-white crystals (150 mg), mp 179–180°, undepressed in admixture with an authentic sample of perivine (10). The IR and UV spectra of the isolate also were identical with those determined for the authentic sample.

Separation of Fraction E—Fraction E (6 g) from a second batch of crude alkaloid was chromatographed on a 5-cm column on 240 g of silica gel 60. After elution with chloroform (10.7 liters), Fraction M (2.0 g) was eluted with methanol–chloroform (1:99) (2 liters) and Fraction N (1.3 g) was eluted with a further 2.5 liters of the same solvent. A portion of Fraction M (1.75 g) was further chromatographed on a silica gel 60 column, 4 × 25 cm, with elution by methanol–chloroform (1:199) (2.1 liters), methanol–chloroform (1:99) (1.5 liters), methanol–chloroform (2:98) (1.7 liters), and methanol–chloroform (5:95) (2.2 liters). Evaporation of the first 600 ml of the methanol–chloroform (2:98) eluate yielded Fraction O (0.22 g), and evaporation of the final 1200 ml yielded Fraction P (0.45 g).

Isolation of Vobasine (IX)—Fraction O was purified by HPLC on Packing C, 1.8 cm × 1.83 m (0.75 in. × 6 ft), with elution by methanol–chloroform (1:99). The material giving rise to the second major UV absorbing peak in this chromatogram was collected to yield 35 mg of homogeneous alkaloid. This material did not crystallize but was shown to be homogeneous by analytical HPLC and TLC in Solvent Systems A and B. It gave a blue color with the ceric ammonium sulfate reagent, had an R_f value of 0.85 in Solvent System A, and cochromatographed with a sample of vobasine prepared from perivine (11) in Solvent Systems A and B. Its mass spectrum showed peaks at *m/e* 352 (30), 293 (14), 194 (5), 180 (100), and 122 (9); its UV spectrum showed peaks corresponding to those published (5) for vobasine. Its IR spectrum was identical with that published (5) for vobasine.

Isolation of Ketonic Alkaloid V—Fraction P was subjected to HPLC on Packing C, 1.27 cm × 1.22 m (0.5 in. × 4 ft), with elution by methanol–chloroform (1:99) containing 0.1% ammonia. The major fraction was rechromatographed on Packing B, using methanol–water–concentrated ammonia (90:5:5). Evaporation of the fourth fraction yielded a homogeneous material, which was recrystallized from methanol to yield a new alkaloid (20 mg), mp 203–204°. The compound was homogeneous by TLC, having an R_f value of 0.85 in System A, and gave a yellow-green color with the ceric ammonium sulfate reagent.

The UV spectrum of the isolate showed λ_{max} (ethanol) 225 (log ϵ 4.68), 285 (4.08), and 295 (4.08) nm. An IR spectrum showed a strong absorption band at ν_{max} 1730 cm^{-1}. The mass spectrum showed principal ions at *m/e* 774 (2), 760 (M^+, 4), 704 (2), 703 (2), 702 (2), 682 (4), 565 (5), 509 (4), 194 (23), 192 (6), 182 (50), 181 (74), 180 (100), 178 (8), 136 (32), 122 (96), and 58 (100).

The NMR spectrum showed a triplet at δ 0.90 ppm (3H) and a doublet at δ 1.82 ppm (3H). Five three-proton singlets were observed at δ 2.16, 2.66, 2.84, 3.84, and 4.12 ppm, while signals in the aromatic region showed the presence of eight protons between δ 6.8 and 8.0 ppm. These signals could be assigned to six protons on the indole ring and two protons attached to nitrogen; one of the aromatic protons was clearly visible as a doublet at δ 7.02 ppm. A two-proton multiplet was evident at δ 5.5 ppm, and additional signals were apparent in the δ 4.5–1.5-ppm range.

Isolation of Pericyclivine (X)—Fraction N[3] was purified by HPLC on Packing C to yield a pure fraction as described. On crystallization from methanol, the material had a melting point of 226–228° [lit. (11) mp 226–228° or (12) 232–233°], $[\alpha]_D^{24}$ +2.0° (c 0.40 in chloroform), and an R_f value of 0.60 in Solvent System A; it gave a gray-purple color with the ceric ammonium sulfate reagent. Its UV absorption spectrum showed λ_{max} 226 (log ϵ 4.29), 284 (3.65), and 292 (3.59) nm; its mass spectrum showed peaks at *m/e* 322 (20), 249 (20), 169 (100), and 168 (100). Finally, a comparison of the material with a sample of pericyclivine prepared from perivine (IR) showed that the two were identical.

[3] Previously designated F 176 (3).

Isolation of Conoduramine (I) and a New Amide (IV)—Material giving rise to the first major peak given by Fraction N on HPLC on Packing C (Fig. 1 of Ref. 3) (518 mg) was rechromatographed on Packing B [0.94 cm × 2.44 m (0.37 in. × 8 ft)] with elution by methanol–water–concentrated ammonia (90:5:5). Collection of the two major fractions and rechromatography under the same conditions yielded homogeneous material from both fractions.

The material from the first fraction (10 mg after crystallization from methanol) was identified as a new bisindole amide. It had a melting point of 217–218° and an R_f value of 0.70 in System A; it gave a yellow-blue color with ceric ammonium sulfate reagent.

The UV spectrum of the isolate showed λ_{max} 224 (log ϵ 4.60), 286 (4.16), and 295 (4.15) nm. An IR spectrum showed strong bands at ν_{max} 1730 and 1670 cm^{-1}. The mass spectrum showed principal ions at *m/e* 732 (5), 718 (M^+, 100), 687 (10), 659 (10), 523 (77), 492 (69), 194 (17), 182 (57), 181 (76), 180 (60), 150 (10), 136 (12), and 122 (43). The NMR spectrum (in acetone-d_6) showed a triplet at δ 0.90 ppm (3H), a doublet at 1.68 ppm (3H), and four three-proton singlets at δ 2.60, 2.68, 3.66, and 3.99 ppm. Signals for two NH protons at δ 7.6 ppm and for six aromatic protons from δ 6.8 to 7.4 ppm were visible, with a clear indication of an *AB* pattern at 6.90 and 7.24 ppm (2H). A broadened two-proton peak at δ 4.30 ppm was clearly visible in addition to a multiplet at δ 5.30 ppm (2H) and other peaks in the 4.0–1.5-ppm range.

The second fraction was identified as conoduramine on the basis of the following evidence. The material was crystallized from methanol to give 20 mg of white crystals, mp 220° dec. [lit. (13) mp 215–218°]. The material had identical TLC behavior in Solvent Systems A and B (R_f 0.75 and 0.44) as an authentic sample of conoduramine (9) and gave a blue color with the ceric ammonium sulfate reagent. Its UV spectrum showed λ_{max} 229 (log ϵ 4.71), 286 (4.22), and 295 (4.20) nm; its IR spectrum was superimposable on that of authentic conoduramine (9).

Isolation of Gabunine (III)—Material corresponding to Fractions E and F from a third extraction of plant material (13.8 g) was chromatographed on a 7-cm column on 740 g of silica gel 60. Elution with benzene–dichloromethane–ether (5:4:3) containing 1.5% methanol and collection of 30-ml fractions yielded 13 major combined fractions. Fraction 8 (0.56 g), a combination of tubes 741–1040, was subjected to preparative thick-layer chromatography in benzene–dichloromethane–ether (5:4:3) containing 10% methanol to yield two alkaloids. The slower moving compound (75 mg) was identified as perivine, identical with the sample isolated previously. The faster moving compound (50 mg) was purified by preparative HPLC on a 10-μm octadecylsilyl silica gel packing with elution by methanol–0.1% ammonium carbonate (70:30).

The compound was homogeneous by TLC and had an R_f value of 0.4 in Solvent System A. Its NMR spectrum showed a triplet at δ 0.85 ppm (3H), three methyl singlets at δ 2.54, 3.70, and 3.98 ppm, and a three-proton doublet at δ 1.65 ppm. An aromatic proton signal at δ 6.8 ppm was visible as a doublet (J = 8.5 Hz), corresponding to the similar absorption in conodurine and its derivatives. The mass spectrum showed ions at *m/e* 690 (M^+, 6), 672 (28), 660 (30), 646 (29), 630 (10), 614 (80), 226 (32), 208 (9), 194 (30), 183 (70), 182 (26), 180 (27), 166 (21), 136 (100), 122 (65), and 108 (21). The IR spectrum and TLC behavior of the material were identical with those of an authentic sample of gabunine (9).

Cytotoxic Activities—All isolated compounds were examined for activity against Eagles 9KB carcinoma of the nasopharynx or the P-388 leukemia in cell culture[4]. 19-(2-Oxopropyl)conodurine and gabunine were active in the P-388 system (ED_{50} 2.4 and 3.2 μg/ml, respectively).

DISCUSSION

19-Oxoconodurine (IV)—The mass spectrum of IV indicated clearly that the compound was a bisindole alkaloid consisting of a vobasan unit linked to a modified voacangine or isovoacangine moiety. Peaks at *m/e* 122 and 136 are characteristic of the iboga portion of such an alkaloid, while peaks at *m/e* 122, 180, 181, and 194 indicate the presence of a vobasan moiety (6). The molecular ion of the compound at *m/e* 718 [together with the usual $(M + 14)^{+\cdot}$ ion at *m/e* 732] was 14 mass units higher than that of conodurine and similar bisindole alkaloids, suggesting the presence of an additional oxygen atom in the molecule. Placement of this atom as the carbonyl oxygen of an amide group was demanded by the IR spectrum of IV, which showed a strong amide absorption at 1670 cm^{-1}. In view of the known (14, 15) ready oxidation at the 19-position of the iboga skeleton, it seemed most likely that the new carbonyl group should

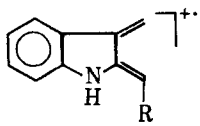

XI: R = voacangine or isovoacangine
XII: R = oxovoacangine or oxoisovoacangine

be located at this position, leading to the assignment of Structure IV (or an isomer thereof) to the new alkaloid.

Support for the placement of the additional oxygen atom on the iboga portion of the molecule came from further analysis of its mass spectrum. In bisindole alkaloids of the voacamine type, an abundant ion at *m/e* 509 was assigned Structure XI by Thomas and Biemann (16). In the spectrum of IV, this ion was replaced by an abundant ion at *m/e* 523, which is only explicable if this ion has Structure XII where the additional oxygen atom is retained in the isovoacangine or voacangine moiety.

Finally, the NMR spectrum of the compound offered confirmation that its structure was indeed 19-oxoconodurine (IV). The spectrum showed all peaks characteristic of a molecule of the conodurine type, including signals for the six methyl groups (four singlets, one doublet, and one triplet) and signals for an aromatic *AB* system at 6.90 and 7.24 ppm. The presence of a conodurine system rather than the isomeric voacamidine system (XIII) was indicated by the fact that the downfield methoxycarbonyl group absorbed at 3.66 ppm (3.62 ppm in deuterochloroform), similar to the 3.68 ppm observed for II and quite different from the 3.08 ppm seen for XIII. Since it was unlikely that the presence of a carbonyl group in the 19-position could influence the chemical shift of the methoxycarbonyl group to this extent (VI and VII have nearly identical shifts for their methoxycarbonyl groups), this evidence indicated that the new alkaloid was related to II rather than XIII. The placement of the carbonyl group at C-19 was indicated by the signal at 4.30 ppm, which appeared to be a one-proton singlet superimposed on a broader one-proton signal. This pattern was noted in the spectrum of 19-oxovoacangine and assigned to the protons at C-5 and C-2 (15).

The ready oxidation of the iboga alkaloids at C-19 suggested that IV might well be an artifact of the isolation process.

19-(2-Oxopropyl)conodurine (V)—The mass spectrum of the isolated compound indicated that it had a molecular weight 56 mass units higher than that of II. Apart from the presence of peaks at *m/e* 703 (M − 57), 702 (M − 58), and 58, the remainder of the mass spectrum was very similar to that of II and its isomeric bisindole alkaloids. Thus, peaks at *m/e* 122 and 136 could be identified as deriving from an isovoacangine or modified isovoacangine moiety, while peaks at *m/e* 122, 180, 181, and 194 indicated the presence of a vobasan moiety (6). The peaks at *m/e* 702 and 58 most reasonably arise by a McLafferty rearrangement involving a 2-oxopropyl group attached to the alkaloid at some position (17).

Confirmation of a 2-oxopropyl group in the compound was obtained from its NMR spectrum, which showed a sharp three-proton singlet at δ 2.16 ppm, characteristic of a methyl group bonded to a carbonyl function. In addition, a two-proton doublet at δ 3.04 ppm could be assigned to the group $CHCH_2COCH_3$; the downfield shift of the signal was in accord with similar shifts observed for protons alpha to carbonyl groups in other indole alkaloids (15). The remainder of the NMR spectrum was in accord with the assignment of a modified II structure to the compound. The methyl resonances in particular were characteristic for this structure, while the upfield portion of an *AB* quartet visible at δ 7.02 ppm was evidence for a II rather than a I type of structure. The II structure was favored over the isomeric XIII structure on the same grounds as discussed for VII; the downfield methoxycarbonyl group absorbed at δ 3.84 ppm in V.

The remaining question in the assignment of a structure to the compound concerned position of attachment of the 2-oxopropyl group to the molecule. The observation of two weak peaks in the mass spectrum of the compound at *m/e* 178 (122 + 56) and 192 (136 + 56) suggested that the 2-oxopropyl unit was linked to the isovoacangine portion of the molecule, since ions with *m/e* 122 and 136 are characteristic of the iboga skeleton represented by isovoacangine. The chemical shift of the methylene protons of the 2-oxopropyl unit is only consistent with a linkage of this unit to the isovoacangine moiety at position 7 or 19, and the latter position is favored on the grounds that oxidation of the iboga system occurs much more readily at position 19 than at position 7.

In confirmation of the proposed structure, a recent paper[5] described the properties of 19-(2-oxopropyl)isovoacangine (XIV) (18). This compound was isolated from a crude alkaloid mixture which also contained

[4] Bioassays were performed by the A. D. Little Co., Cambridge, Mass., using established protocols.

[5] Published after the conclusions above were reached independently.

19-hydroxyisovoacangine, and it probably was formed by reaction between acetone and the latter alkaloid. The spectral properties of XIV were consistent with those of V. In particular, XIV showed peaks at *m/e* 192, 136, and 122 in its mass spectrum, as did V, and both compounds also showed strong peaks in their IR spectra at about 1720 cm^{-1} for the ester and ketonic carbonyl absorptions. It is concluded, therefore, that the new ketonic alkaloid possesses Structure V, in which the stereochemistry at C-19 is unknown. It is likely that this alkaloid also was formed as an artifact by reaction of 19-hydroxyconodurine with traces of acetone present in the methanol during extraction or chromatography.

REFERENCES

(1) M. Hesse, "Indolalkaloide in Tabellen," Springer-Verlag, Berlin, West Germany, 1964 and 1968.

(2) I. M. Jakovljevic, L. D. Seay, and R. W. Shaffer, *J. Pharm. Sci.*, **53**, 553 (1964).

(3) D. G. I. Kingston and B. T. Li, *J. Chromatogr.*, **104**, 431 (1975).

(4) T. R. Govindachari, B. S. Joshi, A. K. Saksena, S. S. Sathe, and N. Viswanathan, *Chem. Commun.*, **1966**, 97.

(5) N. Neuss, "Physical Data of Indole and Dihydroindole Alkaloids," Eli Lilly, Indianapolis, Ind., 1964.

(6) M. Hesse, in "Progress in Mass Spectrometry," vol. 1, H. Budzikiewicz, Ed., Verlag Chemie, Weinheim, West Germany, 1974.

(7) W. E. Meyer, J. A. Coppola, and L. Goldman, *J. Pharm. Sci.*, **62**, 1199 (1973).

(8) U. Renner and H. Fritz, *Tetrahedron Lett.*, **1964**, 283.

(9) M. P. Cava, S. K. Talapatra, J. A. Weisbach, B. Douglas, R. F. Raffauf, and J. L. Beal, *ibid.*, **1965**, 931.

(10) G. H. Svoboda, N. Neuss, and M. Gorman, *J. Am. Pharm. Assoc., Sci. Ed.*, **48**, 659 (1959).

(11) M. Gorman and J. Sweeny, *Tetrahedron Lett.*, **1964**, 3105.

(12) N. R. Farnsworth, W. D. Loub, R. N. Blomster, and M. Gorman, *J. Pharm. Sci.*, **53**, 1558 (1964).

(13) U. Renner, D. A. Prins, and W. G. Stoll, *Helv. Chim. Acta*, **42**, 1572 (1959).

(14) G. Büchi, R. E. Manning, and S. A. Monti, *J. Am. Chem. Soc.*, **86**, 4631 (1964).

(15) G. B. Guise, E. Ritchie, and W. C. Taylor, *Aust. J. Chem.*, **18**, 1279 (1965).

(16) D. W. Thomas and K. Biemann, *J. Am. Chem. Soc.*, **87**, 5447 (1965).

(17) D. G. I. Kingston, J. T. Bursey, and M. M. Bursey, *Chem. Rev.*, **74**, 215 (1974).

(18) V. C. Agwada, Y. Morita, U. Renner, M. Hesse, and H. Schmid, *Helv. Chim. Acta*, **58**, 1001 (1975).

ACKNOWLEDGMENTS AND ADDRESSES

Received January 2, 1976, from the *Department of Chemistry, Virginia Polytechnic Institute and State University, Blacksburg, VA 24061.*

Accepted for publication September 27, 1976.

Supported by Research Grant CA-12831 from the National Cancer Institute, U.S. Department of Health, Education, and Welfare, Bethesda, MD 20014.

The authors thank Dr. M. P. Cava for samples of conodurine, conoduramine, and gabunine, Dr. G. H. Svoboda and the Eli Lilly Co. for a sample of perivine, Dr. U. Renner for a sample of voacamidine, Dr. L. Goldman for spectral data of 19-oxocoronaridine, Dr. N. R. Farnsworth and Dr. H. H. S. Fong for the IR spectrum of pericyclivine, and Dr. R. E. Perdue, Jr., for plant material.

Previous paper in this series: D. G. I. Kingston, B. B. Gerhart, and F. Ionescu, *Tetrahedron Lett.*, **1976**, 649.

[x] To whom inquiries should be directed.

Physiologically Based Pharmacokinetic Model for Digoxin Distribution and Elimination in the Rat

LESTER I. HARRISON [x] and MILO GIBALDI [x]

Abstract □ A plasma flow rate-limited pharmacokinetic model was developed to describe the distribution of digoxin to the heart, liver, kidneys, skeletal muscle, and GI tract in the rat. The model also provides for renal, hepatic (metabolic and biliary), and GI clearance as well as for biliary and GI secretion and GI reabsorption of digoxin. Predicted concentrations of digoxin in the heart, liver, skeletal muscle, and plasma were consistent with experimental observations in conscious rats after an intravenous dose. The model was extended to describe digoxin concentrations in the plasma of bile duct-ligated rats and ureter-ligated rats, simply by modifying appropriate clearance parameters. Excellent agreement was obtained between predicted and observed urinary excretion rates of digoxin for 12 hr after an intravenous dose to normal and bile duct-ligated rats.

Keyphrases □ Digoxin—pharmacokinetic model for distribution and elimination, effect of ligation of bile duct or ureter, rats □ Pharmacokinetics—digoxin, model for distribution and elimination, effect of ligation of bile duct or ureter, rats □ Distribution, tissue—digoxin, pharmacokinetic model, effect of ligation of bile duct or ureter, rats □ Elimination—digoxin, pharmacokinetic model, effect of ligation of bile duct or ureter, rats □ Cardiotonic agents—digoxin, pharmacokinetic model for distribution and elimination, effect of ligation of bile duct or ureter, rats

Compartment models to describe the pharmacokinetics of drug disposition are usually developed by curve fitting plasma concentration data with multiexponential equations. Due to the limitations of this approach, usually no representation more complex than a two-compartment open model is justified to describe the time course of drug concentrations in plasma. In almost all instances, compartment volumes and transfer constants have no anatomical or physiological reality. Moreover, these models are very species dependent. Although classical pharmacokinetic models have many clinical applications, the amount of basic information they provide is intrinsically limited.

In recent years, there has been considerable interest in the development of anatomically and physiologically realistic pharmacokinetic models for drug disposition based on organ blood or plasma flows and volumes (1). In principle, these models permit the prediction of drug concentrations in any target tissue at any time and may provide considerable insight to drug dynamics. Furthermore, drug distribution in certain pathophysiologic conditions may be simulated by altering estimates of organ blood flow (2, 3). Perhaps most important, physiologically based models can be scaled to apply to several species (4). Thus, the large data base required to develop a physiological pharmacokinetic model may be collected in a laboratory animal

19-hydroxyisovoacangine, and it probably was formed by reaction between acetone and the latter alkaloid. The spectral properties of XIV were consistent with those of V. In particular, XIV showed peaks at *m/e* 192, 136, and 122 in its mass spectrum, as did V, and both compounds also showed strong peaks in their IR spectra at about 1720 cm^{-1} for the ester and ketonic carbonyl absorptions. It is concluded, therefore, that the new ketonic alkaloid possesses Structure V, in which the stereochemistry at C-19 is unknown. It is likely that this alkaloid also was formed as an artifact by reaction of 19-hydroxyconodurine with traces of acetone present in the methanol during extraction or chromatography.

REFERENCES

(1) M. Hesse, "Indolalkaloide in Tabellen," Springer-Verlag, Berlin, West Germany, 1964 and 1968.

(2) I. M. Jakovljevic, L. D. Seay, and R. W. Shaffer, *J. Pharm. Sci.*, **53**, 553 (1964).

(3) D. G. I. Kingston and B. T. Li, *J. Chromatogr.*, **104**, 431 (1975).

(4) T. R. Govindachari, B. S. Joshi, A. K. Saksena, S. S. Sathe, and N. Viswanathan, *Chem. Commun.*, **1966**, 97.

(5) N. Neuss, "Physical Data of Indole and Dihydroindole Alkaloids," Eli Lilly, Indianapolis, Ind., 1964.

(6) M. Hesse, in "Progress in Mass Spectrometry," vol. 1, H. Budzikiewicz, Ed., Verlag Chemie, Weinheim, West Germany, 1974.

(7) W. E. Meyer, J. A. Coppola, and L. Goldman, *J. Pharm. Sci.*, **62**, 1199 (1973).

(8) U. Renner and H. Fritz, *Tetrahedron Lett.*, **1964**, 283.

(9) M. P. Cava, S. K. Talapatra, J. A. Weisbach, B. Douglas, R. F. Raffauf, and J. L. Beal, *ibid.*, **1965**, 931.

(10) G. H. Svoboda, N. Neuss, and M. Gorman, *J. Am. Pharm. Assoc., Sci. Ed.*, **48**, 659 (1959).

(11) M. Gorman and J. Sweeny, *Tetrahedron Lett.*, **1964**, 3105.

(12) N. R. Farnsworth, W. D. Loub, R. N. Blomster, and M. Gorman, *J. Pharm. Sci.*, **53**, 1558 (1964).

(13) U. Renner, D. A. Prins, and W. G. Stoll, *Helv. Chim. Acta*, **42**, 1572 (1959).

(14) G. Büchi, R. E. Manning, and S. A. Monti, *J. Am. Chem. Soc.*, **86**, 4631 (1964).

(15) G. B. Guise, E. Ritchie, and W. C. Taylor, *Aust. J. Chem.*, **18**, 1279 (1965).

(16) D. W. Thomas and K. Biemann, *J. Am. Chem. Soc.*, **87**, 5447 (1965).

(17) D. G. I. Kingston, J. T. Bursey, and M. M. Bursey, *Chem. Rev.*, **74**, 215 (1974).

(18) V. C. Agwada, Y. Morita, U. Renner, M. Hesse, and H. Schmid, *Helv. Chim. Acta*, **58**, 1001 (1975).

ACKNOWLEDGMENTS AND ADDRESSES

Received January 2, 1976, from the *Department of Chemistry, Virginia Polytechnic Institute and State University, Blacksburg, VA 24061.*

Accepted for publication September 27, 1976.

Supported by Research Grant CA-12831 from the National Cancer Institute, U.S. Department of Health, Education, and Welfare, Bethesda, MD 20014.

The authors thank Dr. M. P. Cava for samples of conodurine, conoduramine, and gabunine, Dr. G. H. Svoboda and the Eli Lilly Co. for a sample of perivine, Dr. U. Renner for a sample of voacamidine, Dr. L. Goldman for spectral data of 19-oxocoronaridine, Dr. N. R. Farnsworth and Dr. H. H. S. Fong for the IR spectrum of pericyclivine, and Dr. R. E. Perdue, Jr., for plant material.

Previous paper in this series: D. G. I. Kingston, B. B. Gerhart, and F. Ionescu, *Tetrahedron Lett.*, **1976**, 649.

[x] To whom inquiries should be directed.

Physiologically Based Pharmacokinetic Model for Digoxin Distribution and Elimination in the Rat

LESTER I. HARRISON [x] and MILO GIBALDI [x]

Abstract □ A plasma flow rate-limited pharmacokinetic model was developed to describe the distribution of digoxin to the heart, liver, kidneys, skeletal muscle, and GI tract in the rat. The model also provides for renal, hepatic (metabolic and biliary), and GI clearance as well as for biliary and GI secretion and GI reabsorption of digoxin. Predicted concentrations of digoxin in the heart, liver, skeletal muscle, and plasma were consistent with experimental observations in conscious rats after an intravenous dose. The model was extended to describe digoxin concentrations in the plasma of bile duct-ligated rats and ureter-ligated rats, simply by modifying appropriate clearance parameters. Excellent agreement was obtained between predicted and observed urinary excretion rates of digoxin for 12 hr after an intravenous dose to normal and bile duct-ligated rats.

Keyphrases □ Digoxin—pharmacokinetic model for distribution and elimination, effect of ligation of bile duct or ureter, rats □ Pharmacokinetics—digoxin, model for distribution and elimination, effect of ligation of bile duct or ureter, rats □ Distribution, tissue—digoxin, pharmacokinetic model, effect of ligation of bile duct or ureter, rats □ Elimination—digoxin, pharmacokinetic model, effect of ligation of bile duct or ureter, rats □ Cardiotonic agents—digoxin, pharmacokinetic model for distribution and elimination, effect of ligation of bile duct or ureter, rats

Compartment models to describe the pharmacokinetics of drug disposition are usually developed by curve fitting plasma concentration data with multiexponential equations. Due to the limitations of this approach, usually no representation more complex than a two-compartment open model is justified to describe the time course of drug concentrations in plasma. In almost all instances, compartment volumes and transfer constants have no anatomical or physiological reality. Moreover, these models are very species dependent. Although classical pharmacokinetic models have many clinical applications, the amount of basic information they provide is intrinsically limited.

In recent years, there has been considerable interest in the development of anatomically and physiologically realistic pharmacokinetic models for drug disposition based on organ blood or plasma flows and volumes (1). In principle, these models permit the prediction of drug concentrations in any target tissue at any time and may provide considerable insight to drug dynamics. Furthermore, drug distribution in certain pathophysiologic conditions may be simulated by altering estimates of organ blood flow (2, 3). Perhaps most important, physiologically based models can be scaled to apply to several species (4). Thus, the large data base required to develop a physiological pharmacokinetic model may be collected in a laboratory animal

and scaled to apply to humans. This approach has been investigated with thiopental (5), methotrexate (6), cytarabine (7), lidocaine (2), and sulfobromophthalein (8).

The present report describes the development of a physiologically based pharmacokinetic model for digoxin distribution and elimination in normal rats and the application of suitably modified forms of this model to describe the time course of digoxin concentrations in the plasma of rats with total obstruction of the common bile duct or ureters.

EXPERIMENTAL

The drugs, chemicals, and surgical procedures used were described previously (9). Briefly, male Sprague–Dawley rats, 300–400 g, were cannulated *via* the jugular vein. The common bile duct in one group and the ureters in a second group of rats were ligated. The bile duct and ureters of control animals also were isolated and traumatized, but no ligations were made. All animals were allowed to recover overnight with food and water available and were conscious during all experiments.

For the intravenous bolus studies, the rats were injected through the cannula with a 1-mg/kg dose of digoxin containing 3 μg of ^{3}H-digoxin[1], specific activity 6.19 Ci/mmole. Blood samples were withdrawn through the cannula at various times after dosing and collected in heparinized centrifuge tubes. Urine was collected at timed intervals. Control animals were sacrificed at 5, 11, 22, 40, 60, and 94 min after digoxin administration by an injection of air into the jugular vein. The heart, liver, and a portion of skeletal muscle (right anterior thigh) were excised, rinsed well with ice-cold saline, blotted, weighed, and frozen until analyzed for drug content.

For the infusion studies, a loading dose of 0.12 mg, followed by a constant-rate infusion of 0.036 mg of digoxin in 1.1 ml of saline/hr, was administered to control rats and to bile duct-ligated rats. All injection solutions contained ^{3}H-digoxin at the same specific activity. Based on the data collected after the intravenous bolus injection of digoxin, this infusion rate was expected to yield steady-state plasma digoxin concentrations of about 100 ng/ml.

The infusion was interrupted briefly at 10 hr to obtain a blood sample and terminated at 12 hr after removal of a second blood sample. The similarity of digoxin concentrations in these samples indicated that steady state with respect to plasma digoxin levels was attained within 10 hr. Urine and feces were collected continuously during infusion. The animals were sacrificed right after the infusion was terminated. The heart, liver, kidneys, skeletal muscle, and GI tract were excised, rinsed, and weighed. These tissues, as well as the carcass, were frozen until analyzed for drug content.

Plasma and urine samples were extracted and chromatographed to separate digoxin from its metabolites as described previously (9). Tissue samples were homogenized with a five- to 10-fold excess of 40% ethanol in an all-glass tissue grinder. The carcass was skinned and homogenized in a small meat grinder.

Five milliliters of each homogenate was extracted first with a two- to threefold excess of chloroform and then twice with chloroform–methanol (1:1). The extracts were reduced under vacuum and chromatographed. In addition, 200–400 mg of each homogenate was combusted in a tissue oxidizer[2] to determine radioactivity. The efficiency of combustion based on ^{3}H-spiked samples was 98%.

The chromatography system consisted of chloroform–acetic acid–ethyl acetate (5:5:90). Spots were identified by comparison to standards, scraped into vials, and counted in a dioxane-based scintillator as described previously (9). Recovery of radioactivity from ^{3}H-spiked tissues and urine was better than 90% in all cases.

RESULTS AND DISCUSSION

Intravenous Bolus Studies—The time course of digoxin concentrations in the plasma was biexponential in all cases. Figures 1, 2, and 3 show typical results in a control, bile duct-ligated, and ureter-ligated rat, respectively. Plasma digoxin concentration–time curves were quite similar in control rats and in rats with ligated bile ducts. The data from rats with ligated ureters indicated a longer half-life and a reduced total clearance of digoxin compared to those observed in control rats.

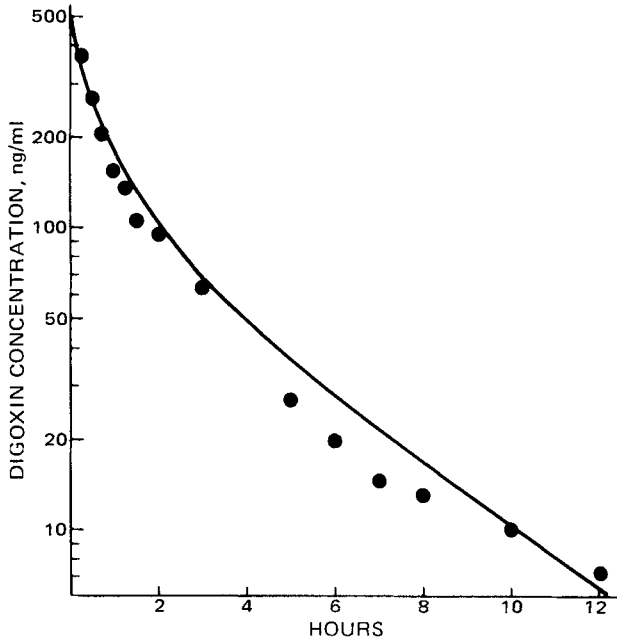

Figure 1—*Predicted* (—) *and observed* (●) *plasma digoxin concentrations after a 1-mg/kg iv injection to a control rat.*

Digoxin concentrations in heart, skeletal muscle, and liver of control rats are shown in Fig. 4. The drug levels in the heart and muscle were comparable to plasma digoxin levels. Digoxin concentrations in the liver were much greater than those in the plasma, suggesting considerable binding of the drug in this tissue.

Infusion Studies—Steady-state digoxin concentrations in various tissues after a 12-hr constant-rate infusion in normal rats are shown in Table I. This table also includes the tissue-to-plasma partition coefficients observed in each animal.

Digoxin was taken up efficiently by the GI tract and the liver. About 80% of the digoxin in the GI tract was found in the small intestine and cecum; less than 1% was in the stomach. High digoxin concentrations in these organs also were found in the dog (10). In humans, digoxin is poorly concentrated by the GI tissues (11).

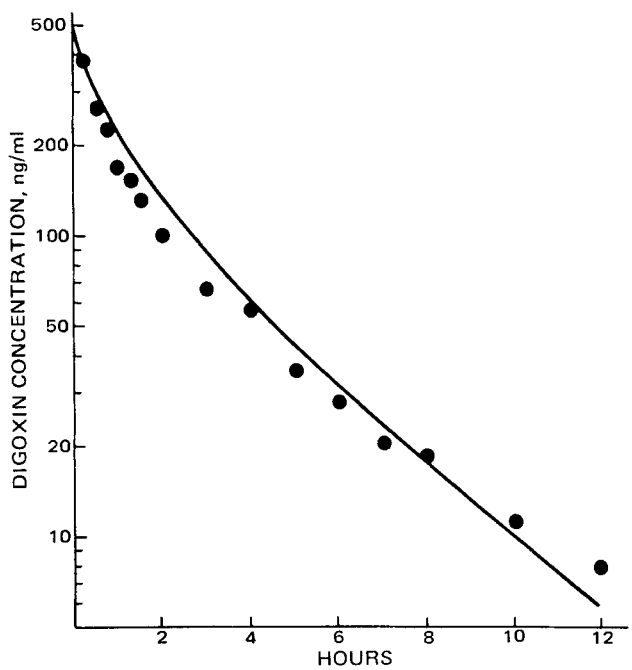

Figure 2—*Predicted* (—) *and observed* (●) *plasma digoxin concentrations after a 1-mg/kg iv injection to a bile duct-ligated rat.*

[1] New England Nuclear Corp., Boston, Mass.
[2] Packard Instruments, Downers Grove, Ill.

Table I—Steady-State Digoxin Concentrations after a 12-hr Constant-Rate Infusion in Two Rats [a]

Tissue	Experiment	Digoxin Concentration			Total Radioactivity	
		μg/g	μg/Tissue	R_i [b]	μg/Tissue	% of Dose
Plasma	1	0.125	—	—	—	—
	2	0.126	—	—	—	—
Liver	1	0.987	12	7.9	13	2.4
	2	0.807	8.3	6.4	9.8	1.8
Skeletal muscle	1	0.171	34 [c]	1.4	—	—
	2	0.178	34 [c]	1.4	—	—
Heart	1	0.138	0.14	1.1	0.20	<0.1
	2	0.204	0.21	1.6	0.17	<0.1
Kidneys	1	0.213	0.64	1.7	0.98	0.2
	2	0.237	0.67	1.9	0.91	0.2
GI tract	1	9.51	160	76	240	43
	2	6.69	98	53	230	42
Skin	1	—	—	—	12	2.2
	2	—	—	—	9.2	1.7
Carcass	1	—	—	—	50	9.1
	2	—	—	—	57	10
Urine	1	—	89	—	130	23
	2	—	86	—	160	29
Feces	1	—	14	—	15	2.7
	2	—	8	—	17	3.1

[a] Digoxin concentrations were determined by TLC; concentrations of total radioactivity were determined by combustion. [b] Tissue-to-plasma partition coefficients, R_i, were calculated from the ratio of micrograms of digoxin per gram of tissue to micrograms of digoxin per milliliter of plasma at 12 hr. [c] Estimated by assuming that skeletal muscle represents 50% of body weight.

The kidneys and heart showed little ability to concentrate digoxin. These findings in the rat contrast sharply with data from dogs (12) and humans (13), which show kidney-to-plasma and heart-to-plasma ratios of digoxin concentration to be 30 or more. Distribution ratios of digoxin in the heart and skeletal muscle were slightly greater than one. These results are consistent with earlier studies in rats (14, 15).

The mass balance of total radioactivity (Table I) showed that about 83% of the dose was recovered in one rat and about 88% in the other. Digoxin metabolites accounted for about one-half of the total radioactivity. In agreement with previous results in rats (16), almost all radioactivity remaining in the body after the 12-hr infusion was localized in the GI tract. Also, more than 70% of the intact digoxin in the body at 12 hr was found in the GI tract. These results support the notion that biliary and/or GI secretion and enterohepatic cycling play an important role in the distribution of digoxin in the rat (17, 18).

The steady-state distribution of digoxin between the GI tissues and contents in control and bile duct-ligated rats is shown in Table II. The average contents to tissue digoxin concentration ratio was about three in control animals and about two in rats with biliary obstruction. In control animals, this ratio varied from site to site in the GI tract, generally increasing in a distal direction. Ratios of about one in the stomach and small intestine, about three in the cecum, and about eight in the large intestine were found. A similar pattern was not apparent in bile duct-ligated rats. Digoxin concentrations in both the GI tissues and contents were considerably lower in rats with biliary obstruction than in normal rats. Nevertheless, substantial amounts were found in the intestinal contents in the absence of biliary secretion, indicating that GI secretion is a factor in the disposition of the drug in rats.

Pharmacokinetic Model—The experimental observations suggested that the physiologically based model shown in Scheme I could describe the distribution and elimination of digoxin in the rat. This model assumes that: (*a*) each tissue acts as a well-stirred compartment, (*b*) drug distribution is plasma flow limited, and (*c*) all processes are linear, *i.e.*, renal, hepatic, and GI clearances, and tissue-to-plasma partition coefficients are drug concentration independent.

In a single rat, digoxin concentrations in the heart and plasma 12 hr after a 4-mg/kg iv bolus dose of digoxin were four times higher than the concentrations in control rats 12 hr after a 1-mg/kg dose; this finding supports the last assumption. All experimentally observed modes of digoxin elimination in the rat were included in the model, as were GI secretion and enterohepatic circulation of digoxin.

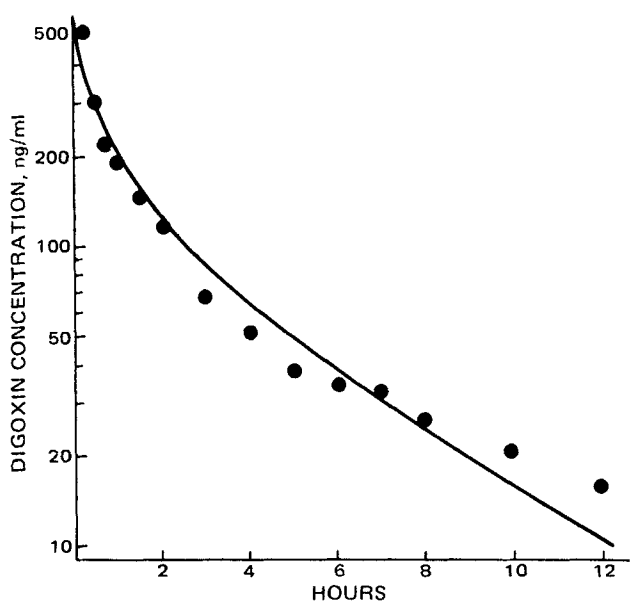

Figure 3—*Predicted* (—) *and observed* (●) *plasma digoxin concentrations after a 1-mg/kg iv injection to a ureter-ligated rat.*

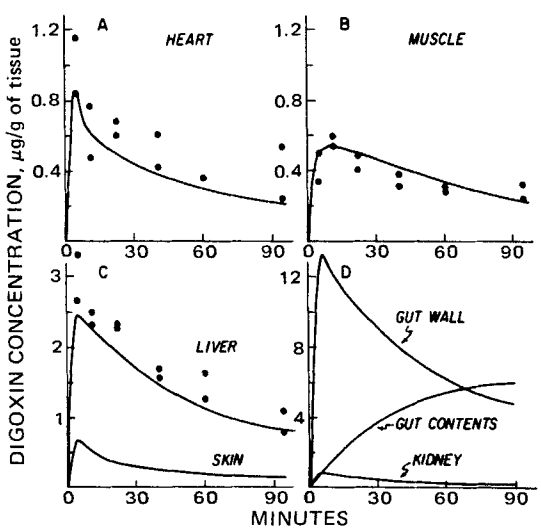

Figure 4—*Predicted* (—) *and observed* (●) (n = 2) *tissue digoxin concentrations after a 1-mg/kg iv injection to control rats.*

Table II—Distribution of Digoxin between GI Tissues and Contents and Corresponding Plasma Concentrations after a 12-hr Infusion in Two Control and Two Bile Duct-Ligated Rats [a]

Tissue	Experiment	Digoxin Concentration μg/g	Digoxin Concentration μg/Tissue	R_i [b]
	Control Rats			
Plasma	1	0.17	—	—
	2	0.12	—	—
GI tissues	1	3.46	25	20
	2	4.11	35	34
GI contents	1	8.58	75	—
	2	11.4	120	—
	Bile Duct-Ligated Rats			
Plasma	1	0.16	—	—
	2	0.14	—	—
GI tissues	1	0.70	5.8	4.4
	2	1.07	4.9	7.6
GI contents	1	1.49	25	—
	2	1.99	24	—

[a] The GI tract was sliced lengthwise, homogenized, and extracted as described for the tissue. [b] Tissue-to-plasma partition coefficient.

A mathematical description of the model is given in the *Appendix*. Organ volumes and plasma flows for a 360-g rat are listed in Table III. Table III also contains the tissue-to-plasma partition coefficients used in testing the model.

Estimates of the various clearance parameters and rate constants are listed in Table IV. Renal clearance was estimated directly in four rats by simultaneous measurement of digoxin concentrations in plasma and urine. A total body clearance of 5.75 ml/min was estimated by dividing the intravenous bolus dose by the area under the plasma digoxin concentration *versus* time curve (9). Since total body clearance was virtually identical in normal and bile duct-ligated rats, it was assumed that this value essentially reflected the sum of renal and hepatic clearances. Therefore, hepatic clearance was estimated by difference. Biliary secretion was calculated from literature data (19).

An initial estimate of GI or fecal clearance of 0.02 ml/min was made by assuming a 12-hr half-life for gut transit (20) and a 20-ml volume for GI contents. Simulations based on this value resulted in an overestimate of digoxin concentrations in the plasma after an intravenous dose to normal rats compared to observed results. After testing several estimates, a value of 0.05 ml/min was selected. The requirement for a higher estimate of GI clearance may indicate that digoxin transit from the absorption site is faster than the average transit of fluid through the gut or that other processes such as gut or bacterial metabolism contribute to the elimination of digoxin from the GI tract.

The first-order absorption rate constant, k_a (Table IV), was obtained by assuming that the absorption half-life of digoxin in the rat is 2 hr (17). The steady-state distribution of digoxin between gut tissues and contents in bile duct-ligated rats (Table II) indicates a ratio of rate constants for gut secretion to gut absorption of about two.

The differential equations listed in the *Appendix* and the constants shown in Tables III and IV served as input for a digital computer analog simulation program (21) to calculate digoxin concentrations in the various model compartments. Modification of these equations to incorporate a zero-order input function yielded predicted steady-state concentrations

Table III—Physiological Constants for the Distribution of Digoxin in the Rat

Tissue	Volume, ml [a]	Plasma Flow, ml/min [b]	R_i [c]
Plasma	10.6	—	—
Heart	2	4.1	1.6
Skeletal muscle	180	8.7	1.4
Skin, fat, *etc.* [d]	90	8.7	1.0 [e]
Kidneys	3.4	14.5	1.9
Liver	13.4	17.4	7.9
GI tissues	10	13.9	30.0
GI contents	17.6	—	—

[a] Based on 360-g rat (20, 22, 23). [b] Total plasma flow = 53.4 ml/min (23–26). [c] Tissue-to-plasma partition coefficient. [d] Miscellaneous compartment for all other body regions. [e] Estimated from total radioactivity data.

Table IV—Clearance and Rate Constants for Digoxin Distribution and Elimination in the Rat

Parameter	Estimate
Renal clearance, K_k	1.25 ml/min
Metabolic clearance, K_l	4.5 ml/min
Biliary clearance, K_b	4.0 ml/min
GI clearance, K_g	0.05 ml/min
Absorption rate constant, k_a	0.006 min^{-1}
Secretion rate constant, k_s	0.012 min^{-1}

of 0.125, 0.2, 0.175, 0.23, 0.98, and 3.75 μg/g for plasma, heart, skeletal muscle, kidney, liver, and GI tissues, respectively. The values are in agreement with the data in Table I and indicate that the model is internally consistent.

Predicted and observed digoxin concentrations in plasma and in liver, heart, and skeletal muscle after a 1-mg/kg iv bolus dose to normal rats are shown in Figs. 1 and 4, respectively. Most model predictions agreed reasonably well with observed values. The predicted and observed plasma digoxin concentrations were compared in three additional control rats, with fits similar to those seen in Fig. 1. For the first 8 hr, observed plasma concentrations (13 time points/animal) were within 40% of the predicted values.

Excellent agreement was obtained between predicted and observed urinary excretion rates of digoxin for 12 hr after an intravenous bolus dose (Table V).

An attempt was made to extend the pharmacokinetic model developed in normal rats to describe digoxin disposition in rats with cholestasis or with renal failure. The mass balance equations in the *Appendix* were solved simultaneously using all constants in Tables III and IV, except biliary secretion or renal clearance which was set equal to zero. These results were then compared with digoxin concentrations in the plasma of a rat with a ligated bile duct or ligated ureters (Figs. 2 and 3, respectively). Apparently, the same pharmacokinetic model can be used to describe plasma digoxin concentrations in normal rats and in bile duct-ligated or ureter-ligated rats, simply by modifying the appropriate parameters.

The fit of the model was tested in four additional rats: two bile duct ligated and two ureter ligated. In the bile duct-ligated animals, predicted and observed plasma digoxin concentrations were in good agreement, with fits similar to those seen in Fig. 2. For the first 8 hr, the observed plasma concentrations (13 time points/animal) were always within 40% of the predicted plasma concentrations. For the ureter-ligated rats, however, the variability in plasma digoxin levels between animals was too great to allow any correlation of observed and predicted plasma concentrations after 2 hr.

In general, the simulation of cholestasis caused only minor changes in the predicted tissue distribution of digoxin compared to that predicted in normal rats (Fig. 4). Concentrations of digoxin, however, were significantly lower in the GI tissues and contents in the model for cholestasis than in the model for normal rats, in agreement with the distribution data in Table II.

Urinary excretion rates of digoxin for 12 hr after an intravenous bolus dose, predicted by the pharmacokinetic model (modified by assuming a biliary secretion of zero) and observed in bile duct-ligated rats, were compared (Table V). There was good agreement between these data sets.

An important goal in the development of physiologically based pharmacokinetic models in laboratory animals is the potential application to humans simply by scaling blood flows and tissue volumes. This goal was not attainable in these studies, because there are substantial differences in tissue-to-plasma partition coefficients of digoxin between rats

Table V—Comparison of Observed and Predicted Urinary Excretion of Digoxin, Expressed as Percent of Dose, in Control and Bile Duct-Ligated Rats after a 1-mg/kg iv Dose

Hours	Control Rats Observed [a]	Control Rats Predicted	Bile Duct-Ligated Rats Observed [b]	Bile Duct-Ligated Rats Predicted
0–4	13.5 ± 4.4	14.2	17.7 ± 8.6	16.5
4–8	2.8 ± 0.6	2.3	4.2 ± 0.9	2.8
8–12	1.1 ± 0.4	0.9	2.0 ± 0.5	0.9
0–12	17.4 ± 4.7	17.4	23.9 ± 8.9	20.2

[a] Mean ± 1 *SD*; $n = 5$. [b] Mean ± 1 *SD*; $n = 6$.

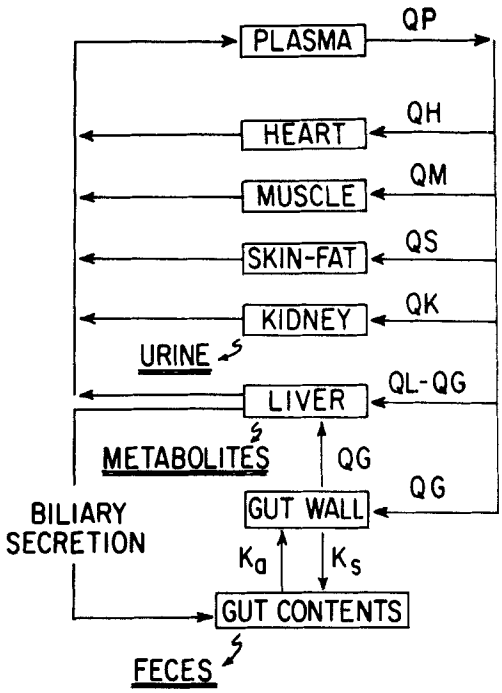

Scheme I—Pharmacokinetic model for digoxin disposition in the rat; QH, QL, QK, etc., denote plasma flow rates to the various organs; QP denotes total plasma flow rate.

and humans (11). The possible application of the present pharmacokinetic model for digoxin to humans using tissue-to-plasma partition coefficients determined in the dog is under investigation.

APPENDIX

The following mass balance–plasma flow equations describe the concentrations in each compartment of the pharmacokinetic model shown in Scheme I:

$$V_p(dC_p/dt) = (Q_hC_h/R_h) + (Q_mC_m/R_m) + (Q_sC_s/R_s) + (Q_kC_k/R_k) + (Q_lC_l/R_l) - Q_pC_p \quad \text{(Eq. A1)}$$

$$V_h(dC_h/dt) = Q_h[C_p - (C_h/R_h)] \quad \text{(Eq. A2)}$$

$$V_m(dC_m/dt) = Q_m[C_p - (C_m/R_m)] \quad \text{(Eq. A3)}$$

$$V_s(dC_s/dt) = Q_s[C_p - (C_s/R_s)] \quad \text{(Eq. A4)}$$

$$V_k(dC_k/dt) = Q_k[C_p - (C_k/R_k)] - (K_kC_k/R_k) \quad \text{(Eq. A5)}$$

$$V_l(dC_l/dt) = (Q_l - Q_g)C_p + (Q_gC_g/R_g) - (Q_lC_l/R_l) - (K_lC_l/R_l) - (K_bC_l/R_l) \quad \text{(Eq. A6)}$$

$$V_g(dC_g/dt) = Q_g[C_p - (C_g/R_g)] + k_aV_cC_c - k_sV_gC_g \quad \text{(Eq. A7)}$$

$$V_c(dC_c/dt) = k_sV_gC_g + (K_bC_l/R_l) - k_aV_cC_c - K_gC_c \quad \text{(Eq. A8)}$$

where K_k, K_l, K_b, and K_g represent renal, metabolic, biliary, and GI clearances, respectively; and k_a and k_s represent first-order rate constants for GI absorption and secretion, respectively. The terms V_i, C_i, Q_i, and R_i represent tissue volumes, drug concentrations, plasma flow rates, and tissue-to-plasma partition coefficients, respectively. The subscripts of these terms are as follows: p = plasma; h = heart; m = skeletal muscle, s = skin, fat, *etc.*; k = kidney; l = liver; g = GI tissues; and c = GI contents.

REFERENCES

(1) K. B. Bischoff and R. G. Brown, *Chem. Eng. Prog. Symp. Ser. No. 66.*, **62**, 33 (1966).

(2) N. Benowitz, R. P. Forsyth, K. L. Melmon, and M. Rowland, *Clin. Pharmacol. Ther.*, **16**, 87 (1974).

(3) *Ibid.*, **16**, 99 (1974).

(4) R. L. Dedrick, *J. Pharmacokinet. Biopharm.*, **1**, 435 (1973).

(5) K. B. Bischoff and R. L. Dedrick, *J. Pharm. Sci.*, **57**, 1346 (1968).

(6) K. B. Bischoff, R. L. Dedrick, D. S. Zaharko, and J. A. Longstreth, *ibid.*, **60**, 1128 (1971).

(7) R. L. Dedrick, D. D. Forrester, J. N. Cannon, S. M. El Dareer, and L. M. Mellett, *Biochem. Pharmacol.*, **22**, 2405 (1973).

(8) B. Montandon, R. J. Roberts, and L. J. Fisher, *J. Pharmacokinet. Biopharm.*, **3**, 277 (1975).

(9) L. I. Harrison and M. Gibaldi, *Drug Metab. Dispos.*, **4**, 88 (1976).

(10) F. I. Marcus, A. Peterson, A. Salel, J. Scully, and G. G. Kapadia, *J. Pharmacol. Exp. Ther.*, **152**, 372 (1966).

(11) J. E. Doherty, W. H. Perkins, and W. J. Flanigan, *Ann. Intern. Med.*, **66**, 116 (1967).

(12) J. E. Doherty and W. H. Perkins, *Am. J. Cardiol.*, **17**, 47 (1966).

(13) K. E. Anderson, Å. Bertler, and G. Wettrell, *Acta Paediatr. Scand.*, **64**, 497 (1975).

(14) S. Dutta and H. Marks, *Life Sci.*, **5**, 915 (1966).

(15) V. K. Buchetala, H. Hackel, M. Königstein, and J. Schläger, *Wien. Med. Wochenschr.*, **118**, 86 (1968).

(16) G. T. Okita, *Fed. Proc.*, **26**, 1125 (1967).

(17) N. Rietbrock, U. Abshagen, K. v. Bergmann, and H. Kewitz, *Naunyn Schmiedebergs Arch. Pharmacol.*, **274**, 171 (1972).

(18) U. Abshagen, K. v. Bergmann, and N. Rietbrock, *ibid.*, **275**, 1 (1972).

(19) J. Q. Russell and C. D. Klaassen, *J. Pharmacol. Exp. Ther.*, **186**, 455 (1973).

(20) R. C. Thompson and O. L. Hollis, *Am. J. Physiol.*, **194**, 308 (1958).

(21) "MIMED, State University of New York at Buffalo Computer Center Adaptation of MIMIC," Publication 44610400, Control Data Corp., St. Paul, Minn., 1968.

(22) E. F. Adolph, *Science*, **109**, 579 (1949).

(23) L. Jansky and J. S. Hart, *Can. J. Physiol. Pharmacol.*, **46**, 653 (1968).

(24) Y. Sasaki and H. N. Wagner, *J. Appl. Physiol.*, **30**, 879 (1971).

(25) L. A. Sapirstein, E. H. Sapirstein, and A. Bredemyer, *Circ. Res.*, **8**, 135 (1960).

(26) L. Takács, K. Kállay, and V. Vajda, *Acta Physiol. Acad. Sci. Hung.*, **21**, 87 (1962).

ACKNOWLEDGMENTS AND ADDRESSES

Received April 15, 1976, from the *Department of Pharmaceutics, School of Pharmacy, State University of New York at Buffalo, Amherst, NY 14260.*

Accepted for publication September 29, 1976.

Supported in part by Grant GM-20852 from the National Institute of General Medical Sciences, National Institutes of Health.

* Present address: Drug Metabolism, Riker Laboratories, 3M Center, St. Paul, MN 55101.

ˣ To whom inquiries should be directed.

Quantitative Determination of Isosorbide Dinitrate and Two Metabolites in Plasma

DAVID A. CHIN *, DAVID G. PRUE, JOHN MICHELUCCI, B. T. KHO ˣ, and CHARLES R. WARNER ‡

Abstract □ A GLC method for the determination of plasma isosorbide dinitrate and two metabolites, isosorbide 2-mononitrate and isosorbide 5-mononitrate, is described. The three substances are extracted from alkalinized plasma with ether. Quantitation is effected by electron-capture detection after GLC separation with a 30% SE-30 column. The unusually heavy liquid phase loading is necessary to eliminate irreversible adsorption on the solid support. The electron-capture detector provides excellent sensitivity and specificity because of the electronegative nature of the nitric ester. The method was used to study the blood levels of isosorbide dinitrate and two metabolites in four beagle dogs after single oral doses of 40 mg of isosorbide dinitrate and in two human volunteers after a sublingual dose of 10 mg of isosorbide dinitrate.

Keyphrases □ Isosorbide dinitrate—and metabolites, electron-capture GLC analysis, plasma □ GLC, electron capture—analysis, isosorbide dinitrate and metabolites, plasma □ Vasodilators, coronary—isosorbide dinitrate and metabolites, electron-capture GLC analysis, plasma

Nitric esters of various polyols are used in the treatment of angina pectoris (1). Isosorbide dinitrate (1,4:3,6-dianhydro-D-glucitol 2,5-dinitrate) (I) is widely used as a coronary vasodilator. The purpose of this work was to develop a method that would yield quantitative data for I and two metabolites, isosorbide 2-mononitrate (II) and isosorbide 5-mononitrate (III).

TLC was used to study levels of I–III in biological fluids (2, 3), and ^{14}C-labeled I was utilized to study its metabolism in dogs (4, 5). A GLC method using a flame-ionization detector was developed to determine I in plasma (6), and it was found that the previously reported TLC procedures (5) did not give the required sensitivity. GLC with electron-capture detection appeared to be the best methodology available for analysis of plasma samples.

An electron-capture GLC method (7) detected I–III within the same chromatogram; subsequently, this method was applied to plasma samples (8). Unfortunately, even with an elaborate cleanup, extracts of blank plasma sometimes yielded high background responses that interfered with the assay of II and III.

The goal of this work was to develop a more sensitive and convenient method that would lend itself to the analysis of a large number of plasma samples. A very simple and rapid extraction without further purification of the extract was feasible if the electron-capture GLC system was capable of detecting 150 pg each of I, II, and III. None of the previously described electron-capture GLC procedures had the necessary sensitivity for all three substances, apparently because of the irreversible interaction of these substances with the partially exposed solid support. The desired sensitivity was obtained when the active sites on the solid support were reduced through the use of a packing with 30% SE-30, an unusually high percentage of liquid phase. The result was an order of magnitude increase in sensitivity over previously described procedures for II and III (7, 8).

This methodology was used for the analysis of dog and human plasma after administration of I. Plasma I–III concentrations were determined after single oral doses of 40 mg of I. Plasma I–III levels also were measured in two human volunteers after a sublingual dose of 10 mg of I.

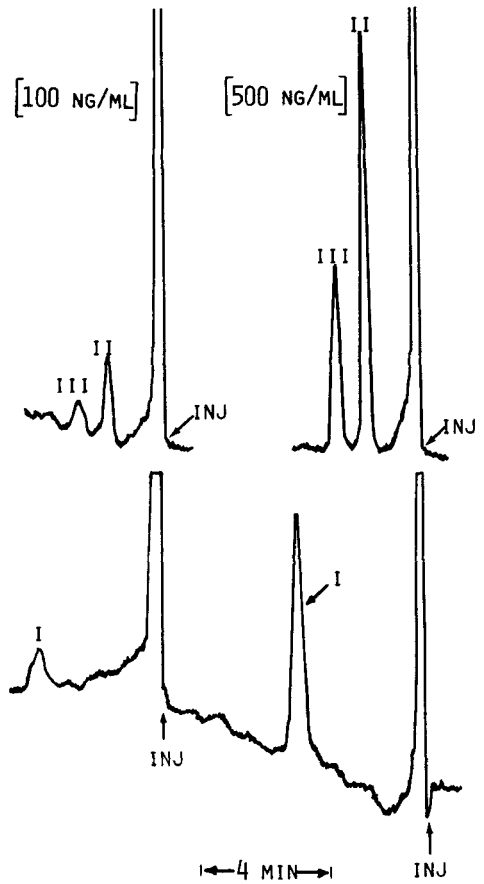

Figure 1—*Typical gas chromatographic results derived for I–III. Injections of 3 μl were used. The figures in brackets correspond to the concentrations of the stock solution.*

EXPERIMENTAL

Apparatus—A gas chromatograph[1] equipped with a ^{63}Ni-electron-capture detector was used. The carrier gas had a flow rate of ~60 ml/min. A silanized glass column, 2 mm i.d. × 1.83 m, was packed with 30% SE-30 on 60–80-mesh Gas Chrom Q[2]. Injection port, column, and detector temperatures were maintained at 190, 165, and 250°, respectively. Injections of 2–3 μl were made with a 10-μl syringe[3]. The preparation of the column packing must be done carefully to ensure good chromatographic results.

Reagents and Chemicals—Authentic samples of II and III were synthesized[4]. Compound I was purified by recrystallization from ethanol.

[1] Microtek MT-220 or Varian model 2100-20.
[2] Applied Science Labs, State College, Pa.
[3] Hamilton Co., Reno, Nev.
[4] By Dr. B. Palameta, Ayerst Research Laboratories, Montreal, Quebec, Canada.

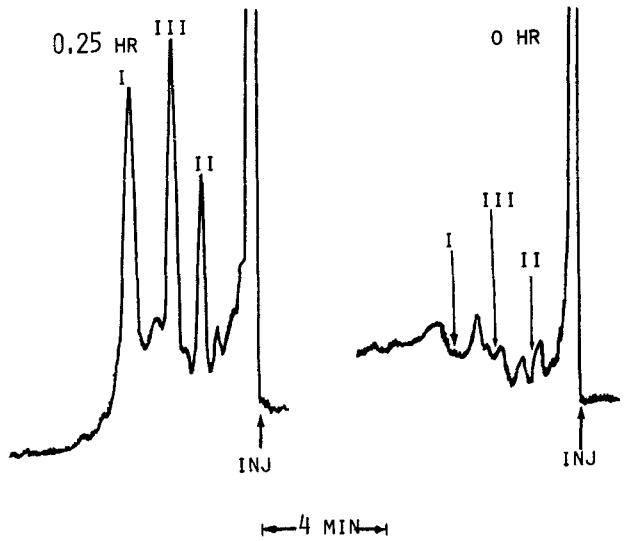

Figure 2—*Results obtained after oral administration of 40 mg of I to a dog. The 0.25-hr levels correspond to I, II, and III levels of 80, 41, and 120 ng/ml, respectively.*

The purity was 99.9% by differential scanning calorimetry. All other reagents were reagent grade except ethyl acetate, which was pesticide quality[5].

Determination of I–III in Plasma—To a 3-ml sample of dog plasma or to 4 ml of human plasma in a 50-ml centrifuge tube, equipped with a polypropylene stopper, was added 2 ml of 1 *N* NaOH or 1 ml of 2 *N* NaOH, respectively. Then 30 ml of ether was added, and the tube was stoppered and shaken mechanically[6] at low speed for 20 min. It was centrifuged at 1500 rpm for 5 min, and the aqueous layer was discarded. Then 0.5 g of anhydrous magnesium sulfate was added, and the mixture was shaken and centrifuged.

A 25-ml aliquot of the ether layer was transferred to a 30-ml centrifuge tube and evaporated to dryness under a gentle stream of nitrogen with the water bath held below 30°. The residue was redissolved in 1.0 ml of ethyl acetate. An aliquot (1–3 μl) of this solution was injected and compared with the calibration curve.

Calibration Curve—Calibration was done with the external standard procedure. Separate solutions of I–III were prepared in ethyl acetate at three different concentrations ranging from 100 to 500 ng/ml. The response as a percentage of the total standing current for each substance was plotted as a function of concentration.

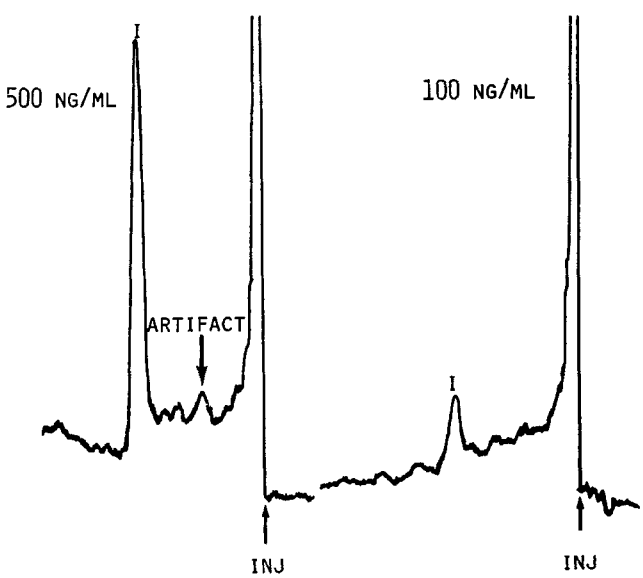

Figure 3—*Chromatograms illustrating artifact formation with exhausted column.*

[5] Fisher.
[6] Eberbach Corp.

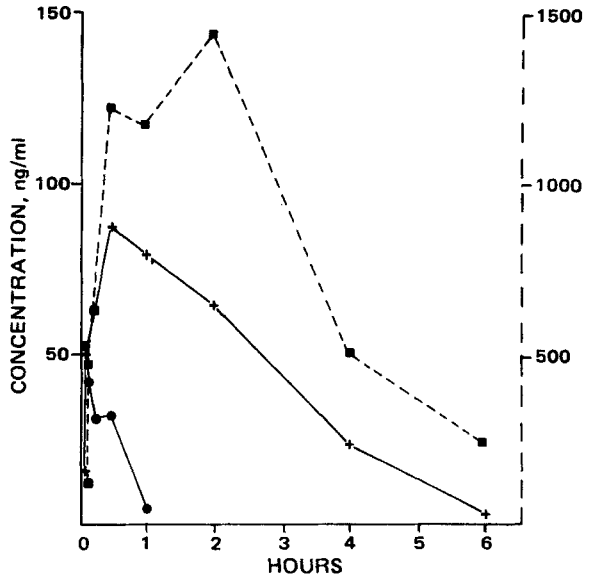

Figure 4—*Average plasma levels of I (●), II (+), and III (■, right-hand scale) in four beagle dogs after an oral administration of 40 mg of I.*

***In Vivo* Studies**—Beagle dogs, 10–12 kg, were given a single oral dose of 40 mg of I (eight 5-mg tablets[7]) after an overnight fast. Water was allowed *ad libitum*, and food was withheld until completion of sampling. Blood samples (7 ml) were collected in tubes[8] with edetate disodium at premedication and at 0, 5, 10, 15, 30, 60, 120, 240, and 360 min postmedication. Samples were centrifuged, and the plasma was separated and stored in a freezer until analysis.

In a second study, two human volunteers were given two 5-mg sublingual tablets[9]. Blood samples were taken using tubes[8] with edetate disodium at 0, 10, 20, 30, 60, 120, and 240 min postmedication. Plasma was separated and frozen until assayed.

RESULTS AND DISCUSSION

Typical gas chromatograms for I–III are shown in Fig. 1. The false positive levels were determined for 16 different samples of dog plasma and were equivalent to less than 2 ng/ml for I and II. A peak often interfered with III, but the magnitude never exceeded 5 ng/ml, far below the peak levels ordinarily observed for medicated dogs.

The chromatograms illustrated in Fig. 2 are typical of the results obtained after oral administration of I. The response of the electron-capture detector to I–III was linear with concentration over the 50–1000-ng/ml

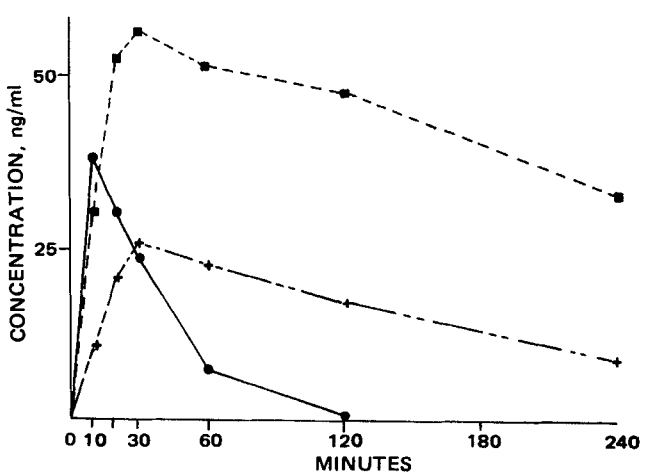

Figure 5—*Average plasma levels of I (●), II (+), and III (■) in two human volunteers after sublingual administration of 10 mg of I.*

[7] Isordil, Laboratories Ayerst LTDA, Sao Paulo, Brazil.
[8] Vacutainers.
[9] Isordil, Ives Laboratories, New York, N.Y.

Table I—Recoveries of I–III from Plasma

Compound	Dog Plasma			Human Plasma		
	n	Recovery, %	*CV*	*n*	Recovery, %	*CV*
I	7	83	7	16	67	10
II	8	59	9	16	65	8
III	8	71	12	16	59	16

range, having a standing current of 4.7×10^{-9} amp in the pulse mode with a width of 5 μsec at 44 v and a pulse interval of 220 μsec.

The partition ratios for I, II, and III between ether and physiological saline proved to be ~6, 0.5, and 0.35, respectively. The recovery from spiked samples for each substance is given in Table I.

After considerable usage, a column that otherwise appeared to be performing satisfactorily gave rise to an artifact upon injection of I. This artifact had the same retention time as II (Fig. 3). For this reason, the I standard was chromatographed at the beginning, middle, and end of the day without the two isosorbide mononitrates. The column was discarded as soon as the artifact peak was detected; however, additional useful column life was obtained by removing the top 5 cm of packing from the inlet end of the column and replacing with new conditioned packing. Under continuous use, a column lasted for approximately 1 month.

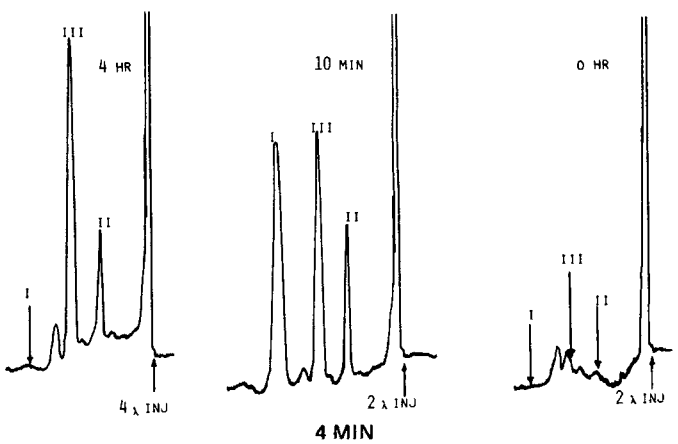

Figure 6—*Chromatograms illustrating the determinations of I–III in human plasma after sublingual administration of 10 mg of I.*

The average plasma I–III levels in four dogs are shown in Fig. 4. The results are in qualitative agreement with the data obtained in a ^{14}C-labeled study (4). There were very low and erratic blood levels of I, consistently higher levels of II, and much higher and prevalent levels of III. Very rapid absorption of I took place, since I levels were detected at 5 min postadministration.

The average plasma levels of I–III in two human volunteers are depicted in Fig. 5. Significant I levels were detected at 10, 20, and 30 min and up to 1 hr postadministration. The two metabolites reached a maximum at 30 min, and the III levels were approximately twice the II levels. Typical chromatograms are presented in Fig. 6.

REFERENCES

(1) M. H. Litchfield, *Drug Metab. Rev.*, **2**, 239 (1973).

(2) P. Needleman and F. E. Hunter, Jr., *Mol. Pharmacol.*, **1**, 77 (1965).

(3) A. J. Dietz, Jr., *Biochem. Pharmacol.*, **16**, 2447 (1967).

(4) S. F. Sisenwine and H. W. Ruelius, *J. Pharmacol. Exp. Ther.*, **176**, 296 (1971).

(5) D. E. Reed, J. F. May, L. G. Hart, and D. H. McCurdy, *Arch. Int. Pharmcodyn. Ther.*, **191**, 318 (1971).

(6) D. A. Sherber, M. Marcus, and S. Kleinberg, *Biochem. Pharmacol.*, **19**, 607 (1970).

(7) M. T. Rosseel and M. G. Bogaert, *J. Chromatogr.*, **64**, 364 (1972).

(8) M. T. Rosseel and M. G. Bogaert, *J. Pharm. Sci.*, **62**, 754 (1973).

ACKNOWLEDGMENTS AND ADDRESSES

Received July 14, 1976, from *Ayerst Laboratories, Rouses Point, NY 12979.*

Accepted for publication October 8, 1976.

Presented at the Pharmaceutical Analysis and Control Section, APhA Academy of Pharmaceutical Sciences, New Orleans meeting, November 1974.

The authors are grateful to Dr. Bruce Downey for performing the animal work, to Dr. R. O. Davies for directing the human study, and to J. Brisson, J. Robinson, and B. Pakrasi for analytical assistance.

* Present address: Smith Kline and French Canada Ltd., Montreal, Quebec, Canada.

‡ Present address: Division of Chemistry and Physics, Food and Drug Administration, Washington, DC 20204.

ˣ To whom inquiries should be directed.

Selective Photometric Determination of Betamethasone Benzoate and Other 21-Hydroxycorticosteroids

LESTER CHAFETZ ˣ and DIMITRI C. TSILIFONIS

Abstract □ Condensation of the glyoxal obtained by cupric acetate oxidation of 21-hydroxycorticosteroids with acetous phenylhydrazine reagent affords a near UV chromophore. All of the tested corticosteroids, including triamcinolone acetonide, which gives low color yields in the Porter–Silber reaction and its Lewbart–Mattox modification, gave similar absorption maxima (362–370 nm) and molar absorptivities (ϵ = 17,000–20,500). Since corticosteroid 21-esters and oxidation products do not undergo the reaction, the assay method based on it is stability indicating for betamethasone benzoate and the other test compounds. Procedures are described for the assay of two topical betamethasone benzoate preparations and hydrocortisone and prednisolone tablets; recovery and precision data are given.

Keyphrases □ Betamethasone benzoate—UV photometric analysis, bulk drug and pharmaceutical formulations □ UV photometry—analysis, betamethasone benzoate and other 21-hydroxycorticosteroids, bulk drug and pharmaceutical formulations □ 21-Hydroxycorticosteroids, various—UV photometric analysis, bulk drug and pharmaceutical formulations □ Glucocorticoids, various—UV photometric analysis, bulk drug and pharmaceutical formulations

The Porter–Silber reaction (1) for the colorimetric determination of corticosteroids is applicable only to steroids with a 17-dihydroxyacetone side chain ($COHCOCH_2OH$) or their derivatives that are readily hydrolyzed in the strongly acid reaction medium. Its mechanism (2, 3) was elucidated as a two-stage reaction: acid-catalyzed rearrangement of the side chain to a 17-deoxy-20-one-21-al ($CHCOCHO$), followed by condensation of this glyoxal

Table I—Recoveries of I–III from Plasma

Compound	Dog Plasma			Human Plasma		
	n	Recovery, %	*CV*	*n*	Recovery, %	*CV*
I	7	83	7	16	67	10
II	8	59	9	16	65	8
III	8	71	12	16	59	16

range, having a standing current of 4.7×10^{-9} amp in the pulse mode with a width of 5 μsec at 44 v and a pulse interval of 220 μsec.

The partition ratios for I, II, and III between ether and physiological saline proved to be ~6, 0.5, and 0.35, respectively. The recovery from spiked samples for each substance is given in Table I.

After considerable usage, a column that otherwise appeared to be performing satisfactorily gave rise to an artifact upon injection of I. This artifact had the same retention time as II (Fig. 3). For this reason, the I standard was chromatographed at the beginning, middle, and end of the day without the two isosorbide mononitrates. The column was discarded as soon as the artifact peak was detected; however, additional useful column life was obtained by removing the top 5 cm of packing from the inlet end of the column and replacing with new conditioned packing. Under continuous use, a column lasted for approximately 1 month.

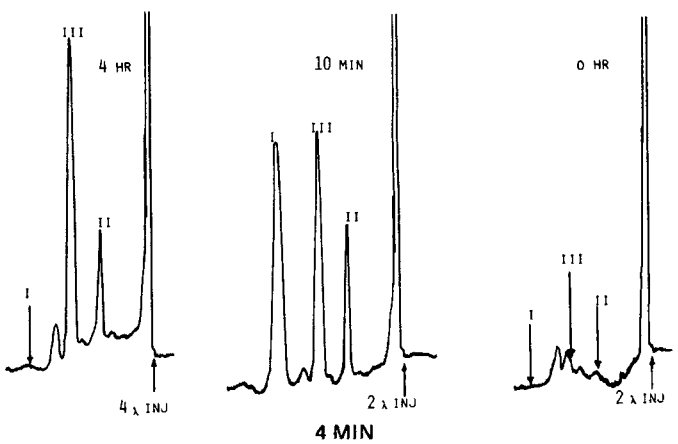

Figure 6—*Chromatograms illustrating the determinations of I–III in human plasma after sublingual administration of 10 mg of I.*

The average plasma I–III levels in four dogs are shown in Fig. 4. The results are in qualitative agreement with the data obtained in a ^{14}C-labeled study (4). There were very low and erratic blood levels of I, consistently higher levels of II, and much higher and prevalent levels of III. Very rapid absorption of I took place, since I levels were detected at 5 min postadministration.

The average plasma levels of I–III in two human volunteers are depicted in Fig. 5. Significant I levels were detected at 10, 20, and 30 min and up to 1 hr postadministration. The two metabolites reached a maximum at 30 min, and the III levels were approximately twice the II levels. Typical chromatograms are presented in Fig. 6.

REFERENCES

(1) M. H. Litchfield, *Drug Metab. Rev.*, **2**, 239 (1973).

(2) P. Needleman and F. E. Hunter, Jr., *Mol. Pharmacol.*, **1**, 77 (1965).

(3) A. J. Dietz, Jr., *Biochem. Pharmacol.*, **16**, 2447 (1967).

(4) S. F. Sisenwine and H. W. Ruelius, *J. Pharmacol. Exp. Ther.*, **176**, 296 (1971).

(5) D. E. Reed, J. F. May, L. G. Hart, and D. H. McCurdy, *Arch. Int. Pharmcodyn. Ther.*, **191**, 318 (1971).

(6) D. A. Sherber, M. Marcus, and S. Kleinberg, *Biochem. Pharmacol.*, **19**, 607 (1970).

(7) M. T. Rosseel and M. G. Bogaert, *J. Chromatogr.*, **64**, 364 (1972).

(8) M. T. Rosseel and M. G. Bogaert, *J. Pharm. Sci.*, **62**, 754 (1973).

ACKNOWLEDGMENTS AND ADDRESSES

Received July 14, 1976, from *Ayerst Laboratories, Rouses Point, NY 12979.*

Accepted for publication October 8, 1976.

Presented at the Pharmaceutical Analysis and Control Section, APhA Academy of Pharmaceutical Sciences, New Orleans meeting, November 1974.

The authors are grateful to Dr. Bruce Downey for performing the animal work, to Dr. R. O. Davies for directing the human study, and to J. Brisson, J. Robinson, and B. Pakrasi for analytical assistance.

* Present address: Smith Kline and French Canada Ltd., Montreal, Quebec, Canada.

‡ Present address: Division of Chemistry and Physics, Food and Drug Administration, Washington, DC 20204.

ˣ To whom inquiries should be directed.

Selective Photometric Determination of Betamethasone Benzoate and Other 21-Hydroxycorticosteroids

LESTER CHAFETZ ˣ and DIMITRI C. TSILIFONIS

Abstract □ Condensation of the glyoxal obtained by cupric acetate oxidation of 21-hydroxycorticosteroids with acetous phenylhydrazine reagent affords a near UV chromophore. All of the tested corticosteroids, including triamcinolone acetonide, which gives low color yields in the Porter–Silber reaction and its Lewbart–Mattox modification, gave similar absorption maxima (362–370 nm) and molar absorptivities (ϵ = 17,000–20,500). Since corticosteroid 21-esters and oxidation products do not undergo the reaction, the assay method based on it is stability indicating for betamethasone benzoate and the other test compounds. Procedures are described for the assay of two topical betamethasone benzoate preparations and hydrocortisone and prednisolone tablets; recovery and precision data are given.

Keyphrases □ Betamethasone benzoate—UV photometric analysis, bulk drug and pharmaceutical formulations □ UV photometry—analysis, betamethasone benzoate and other 21-hydroxycorticosteroids, bulk drug and pharmaceutical formulations □ 21-Hydroxycorticosteroids, various—UV photometric analysis, bulk drug and pharmaceutical formulations □ Glucocorticoids, various—UV photometric analysis, bulk drug and pharmaceutical formulations

The Porter–Silber reaction (1) for the colorimetric determination of corticosteroids is applicable only to steroids with a 17-dihydroxyacetone side chain ($COHCOCH_2OH$) or their derivatives that are readily hydrolyzed in the strongly acid reaction medium. Its mechanism (2, 3) was elucidated as a two-stage reaction: acid-catalyzed rearrangement of the side chain to a 17-deoxy-20-one-21-al ($CHCOCHO$), followed by condensation of this glyoxal

Table I—Structures and Absorptivity Data for 21-Hydroxycorticosteroids

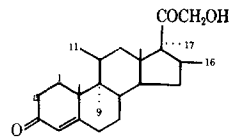

Steroid	Position 1–2	9	11	16	17	Absorptivity Data[a] λ_{max}, nm	α, liters/g cm	ϵ, liters/mole cm
Betamethasone	Unsaturated	α-F	β-OH	β-CH_3	α-OH	362	52.1	20,500
Betamethasone benzoate	Unsaturated	α-F	β-OH	β-CH_3	α-$OCOC_6H_5$	364	40.8	20,300
Corticosterone	Saturated	α-H	β-OH	H	H	352	56.0	19,400
Dexamethasone	Unsaturated	α-F	β-OH	α-CH_3	α-OH	362	47.5	19,700
Hydrocortisone	Saturated	α-H	β-OH	H	α-OH	364	51.9	19,000
Prednisolone	Unsaturated	α-H	β-OH	H	α-OH	366	47.0	17,000
Prednisone	Unsaturated	α-H	=O	H	α-OH	366	49.3	17,600
Triamcinolone acetonide	Unsaturated	α-F	β-OH	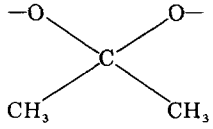		370	44.4	19,800

[a] Obtained using the proposed method.

with phenylhydrazine to form the protonated 21-monophenylhydrazone, the characteristic chromophore.

Lewbart and Mattox (4) extended the Porter–Silber reaction to the microdetermination of 17-deoxy-α-ketolic steroids, using oxidation with methanolic cupric acetate to produce the requisite glyoxal intermediate. This procedure was shown to be selective for betamethasone benzoate[1] (I), the 17-substituted ester, in the presence of its acyl migration product, betamethasone 21-benzoate (II) (Scheme I) (5).

The chromogenic reaction proceeded much more sluggishly with betamethasone benzoate than with other corticosteroids tested, necessitating heating at 60° for 15 min. Although the method proved useful in the assay of pharmaceutical preparations of the steroid, the exothermic reaction of the strongly acid reagent with the methanolic cupric acetate solution and the subsequent heating step were difficult to reproduce and reduced precision when many replicate determinations were performed.

Further study of reaction conditions revealed that phenylhydrazone formation could be accomplished facilely by adding an acetous solution of phenylhydrazine hydrochloride to the dried residue obtained by evaporating a mixture of cupric acetate and the steroid in methanol. Simple dilution of the reaction mixture with alcohol provides a means for the UV spectrophotometric determination of 21-hydroxycorticosteroids at about 360 nm as the (unprotonated) 21-phenylhydrazone. Details of the procedure and examples of its scope and applications are presented.

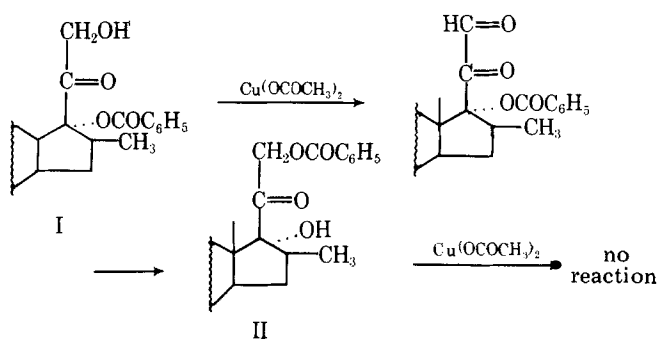

Scheme I

EXPERIMENTAL

Materials[2]—Betamethasone benzoate and betamethasone 21-benzoate were used as received[3]. Betamethasone, dexamethasone, hydrocortisone, prednisolone, prednisone, and triamcinolone acetonide were USP or NF grades. Corticosterone was obtained commercially[4].

Cupric Acetate Solution—Dissolve 100 mg of cupric acetate monohydrate in methanol and dilute to 100.0 ml.

Phenylhydrazine Reagent—Dissolve 100 mg of phenylhydrazine hydrochloride in 1.5 ml of water, add 8.5 ml of acetic acid, and mix.

General Procedure for Test Compounds—Accurately weigh a suitable amount of 21-hydroxycorticosteroid, dissolve it in methanol, and dilute quantitatively and stepwise to obtain a solution containing about 50 μg/ml. Add 0.1 ml of cupric acetate solution to 1.0 ml of the test solution in a test tube, mix, let stand 10 min, and evaporate to dryness in a nitrogen stream at about 45°. Dissolve the residue in 0.2 ml of phenylhydrazine reagent with the aid of a vibrating mixer[5]. Let stand at room temperature for 5 min, then add 5.0 ml of alcohol by pipet, and mix. Determine the absorbance of the solution at the wavelength of maximum absorbance (Table I) against a reagent blank.

Procedure for Betamethasone Benzoate Gel or Viscous Solution, 0.025%—Accurately weigh about 2 g of the product, transfer it to a 125-ml separator with about 20 ml of water, and add 1 ml of saturated sodium acetate solution. Extract the mixture with three 25-ml portions of chloroform, shaking about 2 min with each portion. Combine the extracts in a second separator, wash with 10 ml of water, and filter the chloroform through paper into a conical flask with the aid of several small portions of chloroform. Evaporate the chloroform nearly to dryness on the steam bath with the aid of a nitrogen stream, removing the last traces of solvent without heating. Dissolve the residue in exactly 10.0 ml of methanol.

Transfer 1.0 ml of the solution under test, 1.0 ml of a standard preparation containing 50 μg/ml of betamethasone benzoate reference standard in methanol, and 1.0 ml of methanol (as the blank) to separate test tubes. Add 0.1 ml of cupric acetate solution to each, mix, and let stand 10 min. Evaporate the contents of each tube to dryness in a nitrogen stream at about 45°. Then dissolve the residue in 0.2 ml of phenylhydrazine reagent with a vibrating mixing device. Let stand at room temperature for 5 min, then add 5.0 ml of alcohol by pipet, and mix.

[1] USAN name for 9-fluoro-11β,17,21-trihydroxy-16β-methylpregna-1,4-diene-3,20-dione 17-benzoate.

[2] The pharmaceutical preparations tested were formulated at Warner–Lambert Research Institute.

[3] Warner–Lambert Research Institute.

[4] Mann Research Laboratories.

[5] Vortex Genie.

Table II—Relationship of Absorbance and Concentration of Three 21-Hydroxycorticosteroids

Hydrocortisone		Prednisone		Triamcinolone Acetonide	
Concentration, μg/ml	Absorbance at 364 nm	Concentration, μg/ml	Absorbance at 365 nm	Concentration, μg/ml	Absorbance at 370 nm
10.16	0.100	10.8	0.103	9.6	0.095
20.32	0.200	32.4	0.292	28.8	0.272
30.48	0.295	54.0	0.497	48.0	0.453
40.64	0.422	—	—	—	—
50.80	0.515	—	—	—	—

Determine the absorbance of the solution from the test preparation and from the standard in 1-cm cells at the wavelength of maximum absorbance at about 364 nm, using the reagent blank in the reference cell. Calculate the quantity, in milligrams, of betamethasone benzoate in the portion of the product taken for assay by the formula $0.01C(A_U/A_S)$, where C is the exact concentration, in micrograms per milliliter, of the standard solution, and A_U and A_S are the absorbances of the solutions from the product and the standard, respectively.

Procedure for Tablets—Weigh and finely powder not less than 20 tablets. Transfer an amount of powdered tablet equivalent to about 5 mg of steroid to a separator containing 20 ml of water. Extract the mixture with three 25-ml volumes of chloroform and one 20-ml volume, filtering the extract through cotton into a 100-ml volumetric flask. Then dilute the solution to volume with chloroform and mix.

Transfer 2.0-ml portions of the solution under test and of a solution of the appropriate USP reference standard in chloroform, containing a known concentration of about 50 μg/ml, to test tubes. Evaporate the solutions to dryness with a nitrogen stream, and dissolve the residues with 1.0 ml of methanol. Follow the *General Procedure*, beginning with: "Add 0.1 ml of cupric acetate . . . ," except add 10.0 ml of alcohol.

Determine the absorbance of the solutions, *versus* a reagent blank, in 1-cm cells in a suitable spectrophotometer at the wavelength of maximum absorbance (Table I). Calculate the quantity, in milligrams, of 21-hydroxycorticosteroid in the sample taken by the formula $0.1C(A_U/A_S)$, where C is the exact concentration, in micrograms per milliliter, of the solution of the reference standard, and A_U and A_S are the absorbances of the solutions from the tablet and the standard, respectively.

RESULTS AND DISCUSSION

Scope and Selectivity—The structures, wavelength maxima, and absorptivity data of the steroids tested are presented in Table I. The molar absorptivities varied considerably less with structure than was observed previously (5).

Because the cupric acetate oxidation proceeds only with free 21-hydroxy compounds, 21-esters are not chromogenic in the reaction. This condition was verified in trials with betamethasone 21-benzoate, hydrocortisone 21-acetate, and prednisolone 21-phosphate, none of which provided a near-UV chromophore in the proposed method. The chromophore obtained in the reaction is the 21-monophenylhydrazone of the steroids.

Absence of a chromophore with the corticosteroid 21-esters tested shows that the 1,4-dien-3-one and 4-en-3-one conjugated ketone systems are not chromogenic with phenylhydrazine. Androsten-3,11,17-trione also gave no color under the reaction conditions of the proposed method, showing no interference from 11- and 17-keto functions and confirming the absence of interference from the 4-en-3-one system. Moreover, addition of 5 ml of a mixture of two volumes of 80% sulfuric acid and one volume of methanol to the reaction mixture in place of 5 ml of alcohol provided a chromophore with maximum absorbance at 425 nm for all steroids in Table I, the wavelength at which the protonated 21-monophenylhydrazone of the Lewbart–Mattox method (4) is maximum. This color, however, was unstable.

Table III—Results of Intralaboratory Collaborative Study on Betamethasone Benzoate

Betamethasone Benzoate, μg/ml	Absorbance Obtained by Chemist				
	A	B	C	D	E
4.81	0.186	0.188	0.196	0.196	0.190
9.62	0.368	0.376	0.399	0.398	0.390
14.42	0.554	0.564	0.569	0.575	0.588
19.23	0.749	0.758	0.754	0.772	0.770
24.04	0.949	0.951	0.881	0.949	0.955

Table IV—Recovery and Precision on 21-Hydroxycorticosteroid Products

Trial	Betamethasone Benzoate			Prednisolone Tablets, 5 mg
	Viscous Solution, 0.025%		Gel, 0.025%	
1	99.8	98.6	99.0	101.6
2	98.9	98.3	99.0	99.8
3	98.5	99.3	97.2	100.8
4	98.5	99.1	97.4	100.0
5	100.7	99.3	100.0	99.2
6	99.3	100.0	99.6	99.4
Average recovery	99.3	99.1	98.7	100.1
RSD, %	0.89	0.68	1.13	0.96

Görög and Szepesi (6) used a similar scheme for the photometric determination of 21-hydroxycorticosteroids: oxidation with cupric acetate in methanol, followed by condensation with *o*-phenylenediamine or 4,5-dimethyl-*o*-phenylenediamine to form quinoxalines with maxima at 318 or 331 nm, respectively, in methanol and at 331 or 351 nm, respectively, in 1 *N* hydrochloric acid. Molar absorptivities were higher in the acid medium but were about half those obtained in the procedure described here. Their method is inapplicable to betamethasone benzoate, possibly because of the steric hindrance of the 16- and 17-substituents to quinoxaline ring closure.

Stability of Chromophore—The absorbance of the colors obtained with betamethasone benzoate, hydrocortisone, and triamcinolone acetonide was constant for at least 1 hr by scanning their spectra on a recording spectrophotometer. Spectrograms after 1 hr or more were superimposable on those determined immediately after color development.

Linearity and Precision—Solutions of hydrocortisone, prednisone, and triamcinolone acetonide, containing 10–50 μg/ml in methanol, were analyzed by the proposed method. The results (Table II) indicate that the chromophore follows Beer's law. To determine the effect of interanalyst variation, one chemist prepared a stock solution of betamethasone benzoate in methanol and five different chemists determined the absorbance of scalar concentrations at five levels by the proposed method (Table III). Each obtained rectilinear results.

Precision and Recovery on 21-Hydroxycorticosteroid Products—Experiments with placebo formulations of the gel and viscous solution and of steroid tablets showed no interference. Recovery studies were run by adding a weighed amount of the reference standard to formulation excipients or a placebo formulation and performing the assay six times to obtain the average recovery and an estimate of precision as the relative standard deviation (*RSD*), calculated by the method of Dean and Dixon (7). Two separate experiments were run with the viscous solution (Table IV). Precision data were obtained similarly with formulated products. The betamethasone benzoate gel assay had a relative standard deviation of 1.40%; for 10-mg hydrocortisone tablets, a relative standard deviation of 1.65% was found on six assays of a composite sample.

Limitations of Method—Attempts to extend the method to the assay of betamethasone benzoate creams and lotion have so far been unsuccessful owing to coextraction of materials that complex with or precipitate cupric acetate. Formulation excipient materials that form near-UV chromophores with the phenylhydrazine reagent could interfere, but none of these has been encountered in these studies.

Further Applications—The proposed procedure could easily be adapted to estimation of steroidal 21-alcohol as a synthesis precursor or hydrolysis product in corticosteroid 21-esters such as acetates, hemisuccinates, and phosphates.

REFERENCES

(1) C. C. Porter and R. H. Silber, *J. Biol. Chem.*, **185**, 201 (1950).

(2) D. H. R. Barton, T. C. McMorris, and R. Segovia, *J. Chem. Soc.*, **1961**, 2027.

(3) M. L. Lewbart and V. R. Mattox, *J. Org. Chem.*, **29**, 513 (1961).

(4) M. L. Lewbart and V. R. Mattox, *Anal. Chem.*, **33**, 559 (1961).

(5) L. Chafetz, D. C. Tsilifonis, and C. Moran, *J. Pharm. Sci.*, **63**, 1771 (1974).

(6) S. Görög and G. Szepesi, *Anal. Chem.*, **44**, 1079 (1972).
(7) R. B. Dean and W. B. Dixon, *ibid.*, **23**, 636 (1951).

ACKNOWLEDGMENTS AND ADDRESSES

Received June 11, 1976, from the *Pharmaceutical Research and Development Laboratories, Warner-Lambert Research Institute, Morris Plains, NJ 07950.*

Accepted for publication September 22, 1976.

The authors thank Mr. T.-M. Chem, Dr. R. E. Daly, and Mrs. C. Moran for technical assistance.

[x] To whom inquiries should be directed.

High-Pressure Liquid Chromatographic Analysis of Cimetidine, a Histamine H_2-Receptor Antagonist, in Blood and Urine

W. C. RANDOLPH [x], V. L. OSBORNE, S. S. WALKENSTEIN, and A. P. INTOCCIA

Abstract □ A method is described for extraction of cimetidine, a histamine H_2-receptor antagonist, from whole blood and urine with subsequent analysis by high-pressure liquid chromatography (HPLC). The drug is extracted from biological fluids with 1-octanol and back-extracted into dilute acid and then into a small volume of ethanol by saturation with potassium carbonate. HPLC analysis is performed on a column of 5-μm silica with a mixed mobile phase consisting primarily of acetonitrile. The method measures concentrations of cimetidine as low as 0.05 μg/ml and is reproducible. Blood levels and urinary excretion data obtained with the analytical procedure are given for a group of human subjects who received 200-mg oral doses of cimetidine.

Keyphrases □ Cimetidine—high-pressure liquid chromatographic analysis, blood and urine □ High-pressure liquid chromatography—analysis, cimetidine, blood and urine □ Histamine H_2-receptor antagonists—cimetidine, high-pressure liquid chromatographic analysis, blood and urine

The two types of pharmacological receptors in the mediation of histamine-induced responses are referred to as H_1 and H_2 (1, 2). The classical antihistaminic compounds are effective through antagonism of the action of histamine H_1-receptor sites. Several new compounds, defined as H_2-receptor antagonists, have been effective in reducing histamine-induced gastric acid secretion. Cimetidine[1], *N″*-cyano-*N*-methyl-*N′*-[2-[[(5-methyl-1*H*-imidazol-4-yl)methyl]thio]ethyl]guanidine (I), is currently undergoing trials to assess its effectiveness in the treatment of gastric and duodenal ulcer patients. The chemistry and pharmacology of this drug were discussed previously (3).

This paper describes methodology for extraction and concentration of cimetidine from whole blood and urine with subsequent analysis by high-pressure liquid chromatography (HPLC). Numerous samples from various clinical studies were analyzed by this method, which proved highly satisfactory in providing necessary bioavailability information.

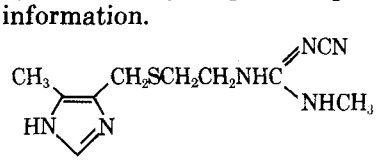

I

[1] Tagamet, Smith Kline & French Laboratories, Philadelphia, Pa.

EXPERIMENTAL

Instrumentation—A constant flow liquid chromatograph[2] was used in conjunction with a variable wavelength UV detector[3] set at 228 nm. The stainless steel column, 3.2 mm i.d. × 25 cm long, was obtained prepacked with 5-μm silica[4]. A rotary injection valve[5] was used for introducing samples at the column inlet.

Reagents—Certified grade 1-octanol[6] was used for extraction of cimetidine from biological fluids. The HPLC mobile phase consisted of UV grade acetonitrile[7], glass-distilled methanol[7], glass-distilled water, and concentrated ammonium hydroxide (1000:60:20:5).

Standard Solutions (Blood)—Dissolve 10 mg of cimetidine in 10 ml of methanol. Add 0.05 ml of this drug solution to 25 ml of heparinized whole human blood and mix thoroughly. From this blood stock, containing 2.0 μg of cimetidine/ml, make appropriate dilutions with heparinized whole blood to provide a concentration range of 0.1–2.0 μg/ml. Weigh 30 mg of metiamide, *N*-methyl-*N′*-[2-[[(5-methyl-1*H*-imidazol-4-yl)methyl]thio]ethyl]thiourea (internal standard), into a 100-ml volumetric flask. Dissolve and bring the contents to volume with methanol.

Standard Solutions (Urine)—Dissolve 50 mg of cimetidine in 10 ml of methanol. Pipet 1 ml of the drug solution into a 25-ml volumetric flask, and bring to volume with control human urine. Make dilutions of the urine stock (containing 200 μg of cimetidine/ml) with control urine to provide a concentration range of 10–150 μg/ml. Dissolve 30 mg of metiamide in 10 ml of methanol for use as the internal standard.

Extraction (Blood)—Heparinize and freeze whole blood samples as quickly as possible after collection. Prior to extraction, thaw the samples and pipet 5-ml aliquots of the lysed blood into 40-ml centrifuge tubes. Add 10 μl of the internal standard solution (containing 3 μg of metiamide) to each sample and adjust to pH 9 with 1 *N* NaOH. Add 10 ml of 1-octanol to each tube, place horizontally on a reciprocating shaker, and shake 15 min at low speed (about 60 oscillations/min).

After shaking, centrifuge the tubes briefly to obtain a sharp separation of layers. With a pipet, remove 9.5 ml of the octanol layer to a second 40-ml centrifuge tube, add 5 ml of 0.03 *N* HCl, and shake horizontally on a reciprocating shaker at high speed (about 120 oscillations/min). Again, centrifuge to achieve phase separation and aspirate and discard the octanol layer. Transfer 4.5 ml of the aqueous phase to a 12-ml centrifuge tube, add 0.3 ml of absolute ethanol, and vortex briefly to mix. Add sufficient granular potassium carbonate to saturate the solution (about 5.5 g), and vortex vigorously for 30 sec. Centrifuge the tubes at 1300×*g* for 5 min, thereby separating the ethanol as a layer over the aqueous phase. Remove 0.2 ml of the ethanol fraction to a small vial for HPLC analysis.

[2] Perkin-Elmer 1220.
[3] Perkin-Elmer LC-55.
[4] Altex Scientific Inc., Berkeley, Calif.
[5] Valco Instruments Co., Houston, Tex.
[6] Fisher Scientific Co.
[7] Burdick and Jackson.

(6) S. Görög and G. Szepesi, *Anal. Chem.*, **44**, 1079 (1972).
(7) R. B. Dean and W. B. Dixon, *ibid.*, **23**, 636 (1951).

ACKNOWLEDGMENTS AND ADDRESSES

Received June 11, 1976, from the *Pharmaceutical Research and Development Laboratories, Warner-Lambert Research Institute, Morris Plains, NJ 07950.*

Accepted for publication September 22, 1976.

The authors thank Mr. T.-M. Chem, Dr. R. E. Daly, and Mrs. C. Moran for technical assistance.

[x] To whom inquiries should be directed.

High-Pressure Liquid Chromatographic Analysis of Cimetidine, a Histamine H_2-Receptor Antagonist, in Blood and Urine

W. C. RANDOLPH [x], V. L. OSBORNE, S. S. WALKENSTEIN, and A. P. INTOCCIA

Abstract □ A method is described for extraction of cimetidine, a histamine H_2-receptor antagonist, from whole blood and urine with subsequent analysis by high-pressure liquid chromatography (HPLC). The drug is extracted from biological fluids with 1-octanol and back-extracted into dilute acid and then into a small volume of ethanol by saturation with potassium carbonate. HPLC analysis is performed on a column of 5-μm silica with a mixed mobile phase consisting primarily of acetonitrile. The method measures concentrations of cimetidine as low as 0.05 μg/ml and is reproducible. Blood levels and urinary excretion data obtained with the analytical procedure are given for a group of human subjects who received 200-mg oral doses of cimetidine.

Keyphrases □ Cimetidine—high-pressure liquid chromatographic analysis, blood and urine □ High-pressure liquid chromatography—analysis, cimetidine, blood and urine □ Histamine H_2-receptor antagonists—cimetidine, high-pressure liquid chromatographic analysis, blood and urine

The two types of pharmacological receptors in the mediation of histamine-induced responses are referred to as H_1 and H_2 (1, 2). The classical antihistaminic compounds are effective through antagonism of the action of histamine H_1-receptor sites. Several new compounds, defined as H_2-receptor antagonists, have been effective in reducing histamine-induced gastric acid secretion. Cimetidine[1], *N″*-cyano-*N*-methyl-*N′*-[2-[[(5-methyl-1*H*-imidazol-4-yl)methyl]thio]ethyl]guanidine (I), is currently undergoing trials to assess its effectiveness in the treatment of gastric and duodenal ulcer patients. The chemistry and pharmacology of this drug were discussed previously (3).

This paper describes methodology for extraction and concentration of cimetidine from whole blood and urine with subsequent analysis by high-pressure liquid chromatography (HPLC). Numerous samples from various clinical studies were analyzed by this method, which proved highly satisfactory in providing necessary bioavailability information.

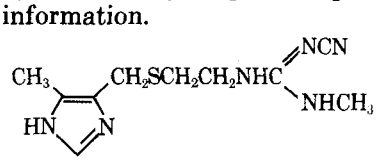

I

[1] Tagamet, Smith Kline & French Laboratories, Philadelphia, Pa.

EXPERIMENTAL

Instrumentation—A constant flow liquid chromatograph[2] was used in conjunction with a variable wavelength UV detector[3] set at 228 nm. The stainless steel column, 3.2 mm i.d. × 25 cm long, was obtained prepacked with 5-μm silica[4]. A rotary injection valve[5] was used for introducing samples at the column inlet.

Reagents—Certified grade 1-octanol[6] was used for extraction of cimetidine from biological fluids. The HPLC mobile phase consisted of UV grade acetonitrile[7], glass-distilled methanol[7], glass-distilled water, and concentrated ammonium hydroxide (1000:60:20:5).

Standard Solutions (Blood)—Dissolve 10 mg of cimetidine in 10 ml of methanol. Add 0.05 ml of this drug solution to 25 ml of heparinized whole human blood and mix thoroughly. From this blood stock, containing 2.0 μg of cimetidine/ml, make appropriate dilutions with heparinized whole blood to provide a concentration range of 0.1–2.0 μg/ml. Weigh 30 mg of metiamide, *N*-methyl-*N′*-[2-[[(5-methyl-1*H*-imidazol-4-yl)methyl]thio]ethyl]thiourea (internal standard), into a 100-ml volumetric flask. Dissolve and bring the contents to volume with methanol.

Standard Solutions (Urine)—Dissolve 50 mg of cimetidine in 10 ml of methanol. Pipet 1 ml of the drug solution into a 25-ml volumetric flask, and bring to volume with control human urine. Make dilutions of the urine stock (containing 200 μg of cimetidine/ml) with control urine to provide a concentration range of 10–150 μg/ml. Dissolve 30 mg of metiamide in 10 ml of methanol for use as the internal standard.

Extraction (Blood)—Heparinize and freeze whole blood samples as quickly as possible after collection. Prior to extraction, thaw the samples and pipet 5-ml aliquots of the lysed blood into 40-ml centrifuge tubes. Add 10 μl of the internal standard solution (containing 3 μg of metiamide) to each sample and adjust to pH 9 with 1 *N* NaOH. Add 10 ml of 1-octanol to each tube, place horizontally on a reciprocating shaker, and shake 15 min at low speed (about 60 oscillations/min).

After shaking, centrifuge the tubes briefly to obtain a sharp separation of layers. With a pipet, remove 9.5 ml of the octanol layer to a second 40-ml centrifuge tube, add 5 ml of 0.03 *N* HCl, and shake horizontally on a reciprocating shaker at high speed (about 120 oscillations/min). Again, centrifuge to achieve phase separation and aspirate and discard the octanol layer. Transfer 4.5 ml of the aqueous phase to a 12-ml centrifuge tube, add 0.3 ml of absolute ethanol, and vortex briefly to mix. Add sufficient granular potassium carbonate to saturate the solution (about 5.5 g), and vortex vigorously for 30 sec. Centrifuge the tubes at 1300×*g* for 5 min, thereby separating the ethanol as a layer over the aqueous phase. Remove 0.2 ml of the ethanol fraction to a small vial for HPLC analysis.

[2] Perkin-Elmer 1220.
[3] Perkin-Elmer LC-55.
[4] Altex Scientific Inc., Berkeley, Calif.
[5] Valco Instruments Co., Houston, Tex.
[6] Fisher Scientific Co.
[7] Burdick and Jackson.

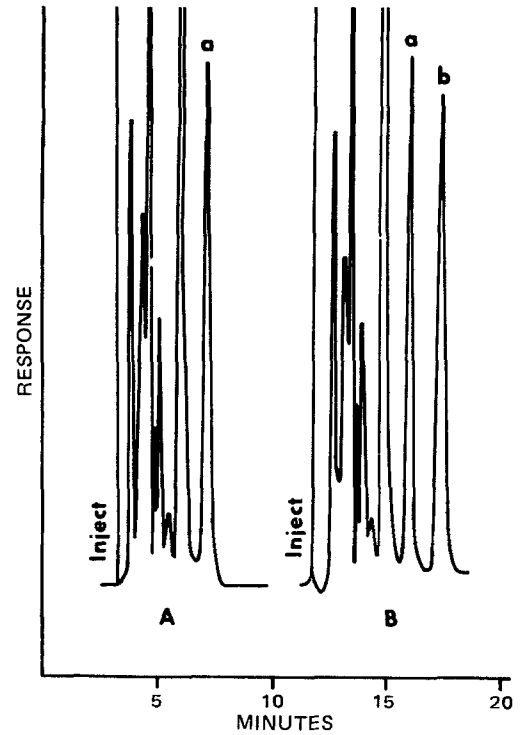

Figure 1—*Chromatograms of extracts from control human blood (A) and blood containing 0.5 μg of cimetidine/ml (B). Key: a, metiamide (internal standard); and b, cimetidine.*

Extraction (Urine)—Dilute 1-ml aliquots of each urine sample with 4 ml of distilled water in 40-ml centrifuge tubes. Add 10 μl of the appropriate internal standard solution (containing 30 μg of metiamide), and adjust the tube contents to pH 9 with 0.1 *N* NaOH. Proceed with the extraction as described for blood.

Chromatography—Condition new columns by flushing for 8 hr with methanol–water (98:2) at 0.5 ml/min followed by the analytical mobile phase, 1 ml/min for 2 hr. Perform all analyses at a flow rate of 1 ml/min with the pressure variable between 1000 and 2000 psi, depending on column characteristics. (If pressures rise above 2000 psi, replacement of both inlet and outlet frits will usually reduce the back-pressure significantly.)

Inject 15-μl aliquots of the ethanol extracts. Monitor the column effluent with a variable wavelength UV detector at 228 nm, and record detector response with a strip-chart recorder. For blood extracts, use attenuations of 0.02 and 0.04 absorbance unit full scale (aufs). For urine samples, use attenuations from 0.10 to 1.00 aufs. Retention times with this system are about 5.5 min for cimetidine and 4 min for metiamide.

Quantitation—Calculate the ratio of cimetidine peak height to metiamide peak height for standards, and plot ratio *versus* concentration of cimetidine. Use the resulting curve to convert peak height ratios of unknown samples to cimetidine concentration.

Clinical Study—A clinical study was performed in which 12 normal human subjects each received two identical oral doses of 200 mg of cimetidine in aqueous solution; 7 days separated the doses. Whole blood samples were collected by venipuncture at designated time intervals, immediately heparinized, and frozen for analysis. Total urine output was collected in the intervals of 0–3, 3–12, and 12–24 hr. Urine volumes were measured, and aliquots were kept frozen prior to analysis.

RESULTS AND DISCUSSION

The development of an analytical method for measuring cimetidine in biological fluids was complicated by the difficulty in extracting the drug from aqueous media. Of various solvents tested, 1-octanol provided the most efficient extraction. The low volatility of octanol, combined with characteristics of the drug itself, made GLC analysis impractical. Certain other analytical techniques, such as spectrophotometry, were ruled out by the small amount of drug present in blood and the large number of interfering substances extracted from biological fluids by octanol. Two relatively new advances in HPLC, variable wavelength UV detectors and microparticulate column packings, made possible the HPLC analysis of cimetidine following extraction from blood and urine.

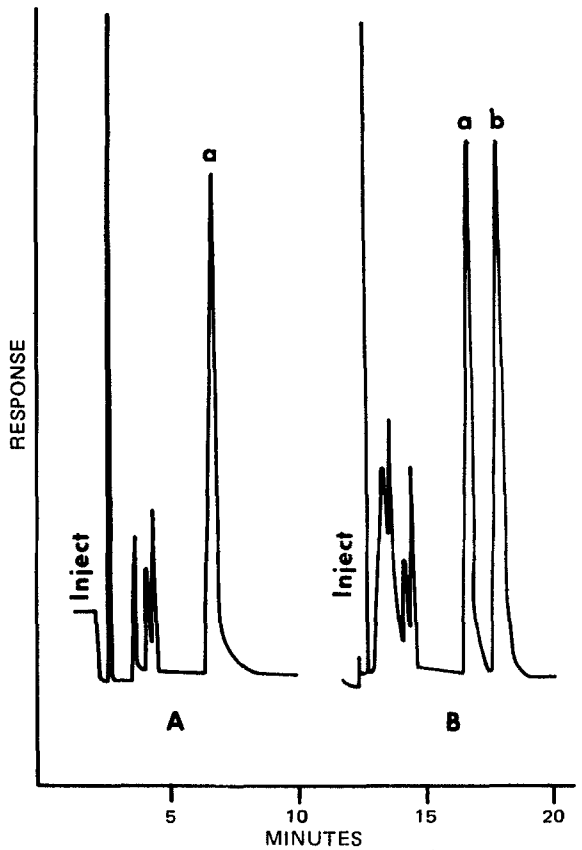

Figure 2—*Chromatograms of extracts from control human urine (A) and urine containing 25 μg of cimetidine/ml (B). Key: a, metiamide (internal standard); and b, cimetidine.*

The recovery of cimetidine from whole blood was determined by addition of the drug, labeled with carbon-14, to control blood and extraction as described under *Experimental*. The radioactive content of the final 0.3-ml ethanol fraction, measured by liquid scintillation counting, contained 63% of the initial blood radioactivity (absolute recovery).

Typical chromatograms obtained from control human blood and blood containing 0.5 μg of cimetidine/ml are shown in Fig. 1. Of the several hundred control blood samples analyzed, none contained any material that interfered with the analysis of cimetidine. The major metabolite of cimetidine, the sulfoxide, was tested in the chromatographic system and eluted much later than the parent compound. The internal standard peak (metiamide) was completely resolved from the drug peak and eluted prior to cimetidine, thus not adding to analysis time.

The efficiency of the column used to obtain the chromatogram in Fig. 1 was about 7000 plates/25 cm. Efficiency varies somewhat between columns but may often be improved by reconditioning and paying particular attention to elimination of all possible deadspace. Column life has been very good, especially when considering the alkaline nature of the mobile phase. Approximately 1000 samples were analyzed on one column before a significant loss of efficiency was noted.

The relationship between peak height ratios and concentration of cimetidine in whole blood from 0.05 to 2.00 μg/ml was linear. Two groups of replicate blood samples, eight each containing 0.50 and 1.00 μg of drug/ml, were prepared to test the accuracy of the method. The groups were divided into halves, and one-half was extracted and analyzed on each successive day. Of all 16 samples, an average of 102 ± 4% of the actual cimetidine content was measured by HPLC analysis. Although peaks were obtained at lower concentrations, 0.05 μg/ml represented the lowest level of cimetidine that could be measured accurately in blood.

Figure 2 shows typical chromatograms obtained with control human urine and urine containing 25 μg of cimetidine/ml. The relationship between drug concentration in urine and peak height ratio was linear with drug concentrations between 10 and 150 μg/ml. The accuracy of the urinary analysis was tested by adding known amounts of drug to eight urine samples at two concentrations, 25 and 100 μg/ml. One-half of each group was analyzed on each successive day. The average recovery of added

Table I—Urinary Excretion and Whole Blood Concentrations of Cimetidine with Related Parameters in 12 Human Subjects following Administration of Two Identical Single Oral Doses of 200 mg of Cimetidine

Parameter	Dose I	Dose II	Δ Dose II[a]
Average whole blood concentration and average intrasubject change, Dose I → Dose II, μg/ml, at:			
0.5 hr	0.65	0.71	0.19
1.0 hr	1.02	0.98	0.16
1.5 hr	0.86	0.85	0.12
2.0 hr	0.72	0.71	0.13
3.0 hr	0.59	0.58	0.15
4.0 hr	0.37	0.40	0.09
6.0 hr	0.16	0.17	0.04
8.0 hr	0.09	0.08	0.03
Average of individual peak whole blood concentrations, μg/ml	1.07	1.01	
Average peak time, hr	1.13	1.25	
Average area under whole blood concentration curves, 0 → 8 hr, μg/ml × hr	3.52	3.59	
Mean elimination half-life, hr	1.90	1.72	
Mean urinary excretion of cimetidine and mean intrasubject change, Dose I → Dose II, as % of dose, in intervals of:			
0–3 hr	32.4	33.0	5.6
3–12 hr	23.4	23.2	7.7
12–24 hr	1.9	1.6	1.1

[a] Δ Dose II is the absolute difference, regardless of the direction of change.

drug from the 16 spiked samples was 99.2 ± 1.1%. None of the control urines tested contained material that interfered with the analysis of cimetidine.

Mean blood levels and urinary excretion of drug for the 12 human subjects in the clinical study are shown in Table I. Also presented are parameters related to blood concentration data. Elimination half-lives of the drug in blood were obtained by fitting concentration data from the 4-, 6-, and 8-hr blood samples, using the method of least squares. Areas under blood level curves were computed with a trapezoidal program. No statistically significant differences were found in mean blood levels or urinary excretion of cimetidine, or in any related parameters, when Doses I and II were compared.

Metiamide, also an H_2-receptor antagonist, was employed in earlier studies of the effects of this class of compounds on gastric acid secretion. Obviously, since the method employs metiamide as the internal standard in the analysis of cimetidine, the reverse situation may be applied to analyze for metiamide. This analysis was successful on a number of samples. The only changes were that a detector wavelength of 235 nm was used and that concentrations of cimetidine in internal standard solutions were 0.5 (blood) and 5 (urine) mg/ml.

The described method is satisfactory for analysis of cimetidine and metiamide, both in its reproducibility and sensitivity. By application of the analytical procedure, it was determined that cimetidine is well absorbed following an oral dose, as indicated by the urinary excretion and blood levels of the drug. In clinical trials, the blood levels of cimetidine were measured and correlated with the inhibition of gastric acid secretion (4–6). These correlations, obtained with different doses of cimetidine, have been helpful in assessing the effect of circulating drug on gastric acid secretion.

REFERENCES

(1) A. S. F. Ash and H. O. Schild, *Br. J. Pharmacol. Chemother.*, **49**, 427 (1966).

(2) J. W. Black, W. A. M. Duncan, G. J. Durant, C. R. Ganellin, and M. E. Parsons, *Nature*, **236**, 385 (1972).

(3) R. W. Brimblecombe, W. A. M. Duncan, G. J. Durant, J. C. Emmett, C. R. Ganellin, and M. E. Parsons, *J. Int. Med. Res.*, **3**, 86 (1975).

(4) R. M. Henn, J. I. Isenberg, N. Maxwell, and R. A. L. Sturdevant, *N. Engl. J. Med.*, **293**, 371 (1975).

(5) R. E. Pounder, J. G. Williams, J. J. Misiewicz, and G. J. Milton-Thompson, *Proc. Br. Soc. Gastroenterol.*, **1975**, 32 (Abstract).

(6) G. F. Longstreth, J. R. Malagelada, and V. L. W. Go, *Gastroenterology*, **68**, A-85/942 (Abstract) (1975).

ACKNOWLEDGMENTS AND ADDRESSES

Received February 18, 1976, from *Smith Kline & French Laboratories, Philadelphia, PA 19101.*

Accepted for publication September 20, 1976.

The authors thank R. Stote, M.D., and the staff of the Clinical Research Group of Presbyterian-University of Pennsylvania Medical Center for conducting the bioavailability study described. The authors also gratefully acknowledge the contributions of the biochemistry staff of The Research Institute, Welwyn Garden City, United Kingdom, and the technical assistance of Mr. Albert Bernstein and Mr. Gerald Joseph.

[x] To whom inquiries should be directed.

Anthelmintic 2-Arylhydrazino- and 2-Arylazo-2-thiazolines

M. T. WU, F. S. WAKSMUNSKI, D. R. HOFF, M. H. FISHER[x], J. R. EGERTON, and A. A. PATCHETT

Abstract □ Some 2-arylhydrazino- and 2-arylazo-2-thiazolines were synthesized for anthelmintic testing. The most potent compound, 2-(*o*-tolylazo)-2-thiazoline, was orally effective in sheep against a broad range of helminths.

Keyphrases □ Thiazolines, substituted—synthesized, evaluated for anthelmintic activity in sheep □ Anthelmintic activity—evaluated in various substituted thiazolines in sheep □ Structure–activity relationships—various substituted thiazolines evaluated for anthelmintic activity in sheep

In a search for anthelmintic activity in novel structures, the known neuromuscular blocking agent 2-amino-2-thiazoline (I) (1) had a paralytic effect on third-stage larvae of *Haemonchus contortus in vitro*, similar to that of the anthelmintic drugs tetramisole and pyrantel. No activity could be demonstrated in *in vivo* assays. However, with this *in vitro* activity as a starting point, a series of related compounds was synthesized and tested for *in vivo* anthelmintic activity.

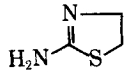

I

Table I—Urinary Excretion and Whole Blood Concentrations of Cimetidine with Related Parameters in 12 Human Subjects following Administration of Two Identical Single Oral Doses of 200 mg of Cimetidine

Parameter	Dose I	Dose II	Δ Dose II[a]
Average whole blood concentration and average intrasubject change, Dose I → Dose II, μg/ml, at:			
0.5 hr	0.65	0.71	0.19
1.0 hr	1.02	0.98	0.16
1.5 hr	0.86	0.85	0.12
2.0 hr	0.72	0.71	0.13
3.0 hr	0.59	0.58	0.15
4.0 hr	0.37	0.40	0.09
6.0 hr	0.16	0.17	0.04
8.0 hr	0.09	0.08	0.03
Average of individual peak whole blood concentrations, μg/ml	1.07	1.01	
Average peak time, hr	1.13	1.25	
Average area under whole blood concentration curves, 0 → 8 hr, μg/ml × hr	3.52	3.59	
Mean elimination half-life, hr	1.90	1.72	
Mean urinary excretion of cimetidine and mean intrasubject change, Dose I → Dose II, as % of dose, in intervals of:			
0–3 hr	32.4	33.0	5.6
3–12 hr	23.4	23.2	7.7
12–24 hr	1.9	1.6	1.1

[a] Δ Dose II is the absolute difference, regardless of the direction of change.

drug from the 16 spiked samples was 99.2 ± 1.1%. None of the control urines tested contained material that interfered with the analysis of cimetidine.

Mean blood levels and urinary excretion of drug for the 12 human subjects in the clinical study are shown in Table I. Also presented are parameters related to blood concentration data. Elimination half-lives of the drug in blood were obtained by fitting concentration data from the 4-, 6-, and 8-hr blood samples, using the method of least squares. Areas under blood level curves were computed with a trapezoidal program. No statistically significant differences were found in mean blood levels or urinary excretion of cimetidine, or in any related parameters, when Doses I and II were compared.

Metiamide, also an H_2-receptor antagonist, was employed in earlier studies of the effects of this class of compounds on gastric acid secretion. Obviously, since the method employs metiamide as the internal standard in the analysis of cimetidine, the reverse situation may be applied to analyze for metiamide. This analysis was successful on a number of samples. The only changes were that a detector wavelength of 235 nm was used and that concentrations of cimetidine in internal standard solutions were 0.5 (blood) and 5 (urine) mg/ml.

The described method is satisfactory for analysis of cimetidine and metiamide, both in its reproducibility and sensitivity. By application of the analytical procedure, it was determined that cimetidine is well absorbed following an oral dose, as indicated by the urinary excretion and blood levels of the drug. In clinical trials, the blood levels of cimetidine were measured and correlated with the inhibition of gastric acid secretion (4–6). These correlations, obtained with different doses of cimetidine, have been helpful in assessing the effect of circulating drug on gastric acid secretion.

REFERENCES

(1) A. S. F. Ash and H. O. Schild, *Br. J. Pharmacol. Chemother.*, **49**, 427 (1966).

(2) J. W. Black, W. A. M. Duncan, G. J. Durant, C. R. Ganellin, and M. E. Parsons, *Nature*, **236**, 385 (1972).

(3) R. W. Brimblecombe, W. A. M. Duncan, G. J. Durant, J. C. Emmett, C. R. Ganellin, and M. E. Parsons, *J. Int. Med. Res.*, **3**, 86 (1975).

(4) R. M. Henn, J. I. Isenberg, N. Maxwell, and R. A. L. Sturdevant, *N. Engl. J. Med.*, **293**, 371 (1975).

(5) R. E. Pounder, J. G. Williams, J. J. Misiewicz, and G. J. Milton-Thompson, *Proc. Br. Soc. Gastroenterol.*, **1975**, 32 (Abstract).

(6) G. F. Longstreth, J. R. Malagelada, and V. L. W. Go, *Gastroenterology*, **68**, A-85/942 (Abstract) (1975).

ACKNOWLEDGMENTS AND ADDRESSES

Received February 18, 1976, from *Smith Kline & French Laboratories, Philadelphia, PA 19101.*

Accepted for publication September 20, 1976.

The authors thank R. Stote, M.D., and the staff of the Clinical Research Group of Presbyterian-University of Pennsylvania Medical Center for conducting the bioavailability study described. The authors also gratefully acknowledge the contributions of the biochemistry staff of The Research Institute, Welwyn Garden City, United Kingdom, and the technical assistance of Mr. Albert Bernstein and Mr. Gerald Joseph.

[x] To whom inquiries should be directed.

Anthelmintic 2-Arylhydrazino- and 2-Arylazo-2-thiazolines

M. T. WU, F. S. WAKSMUNSKI, D. R. HOFF, M. H. FISHER[x], J. R. EGERTON, and A. A. PATCHETT

Abstract □ Some 2-arylhydrazino- and 2-arylazo-2-thiazolines were synthesized for anthelmintic testing. The most potent compound, 2-(*o*-tolylazo)-2-thiazoline, was orally effective in sheep against a broad range of helminths.

Keyphrases □ Thiazolines, substituted—synthesized, evaluated for anthelmintic activity in sheep □ Anthelmintic activity—evaluated in various substituted thiazolines in sheep □ Structure–activity relationships—various substituted thiazolines evaluated for anthelmintic activity in sheep

In a search for anthelmintic activity in novel structures, the known neuromuscular blocking agent 2-amino-2-thiazoline (I) (1) had a paralytic effect on third-stage larvae of *Haemonchus contortus in vitro*, similar to that of the anthelmintic drugs tetramisole and pyrantel. No activity could be demonstrated in *in vivo* assays. However, with this *in vitro* activity as a starting point, a series of related compounds was synthesized and tested for *in vivo* anthelmintic activity.

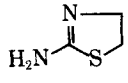

I

Table I—Physical Properties of 1-Substituted 3-Thiosemicarbazides[a]

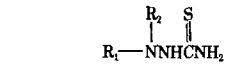

Compound	R_1	R_2	Yield, %	Crystallization Solvent	Melting Point	Molecular Formula	Analysis, %	Calc.	Found
II	2-$CH_3C_6H_4$	H	85	Ethanol	158–160°	$C_8H_{11}N_3S$	C	53.03	52.89
							H	6.12	6.26
							N	23.19	23.47
III	3-$CH_3C_6H_4$	H	54	Ethanol–water	146–147°	$C_8H_{11}N_3S$	C	53.03	52.98
							H	6.12	6.04
							N	23.19	23.16
IV	4-$CH_3C_6H_4$	H	58	Ethanol	176–177.5°	$C_8H_{11}N_3S$	C	53.03	52.67
							H	6.12	6.05
							N	23.19	23.10
V	2-$C_2H_5C_6H_4$	H	69	Ethanol	182–183°	$C_9H_{13}N_3S$	C	55.36	55.55
							H	6.71	6.68
							N	21.52	21.56
VI	2-$CH_3OC_6H_4$	H	42	Ethanol	190–191°	$C_8H_{11}N_3OS$	C	48.73	49.10
							H	5.62	5.47
							N	21.31	21.29
VII[b]	4-$CH_3OC_6H_4$	H	22	Ethanol	212–213°	$C_8H_{11}N_3OS$	C	48.73	49.02
							H	5.62	5.71
							N	21.31	20.98
VIII[c]	2-ClC_6H_4	H	46	Ethanol	187–188°	$C_7H_8ClN_3S$	C	41.69	41.77
							H	4.00	4.17
							N	20.84	20.56
IX[d]	4-ClC_6H_4	H	11	Ethanol	200–201°	$C_7H_8ClN_3S$	C	41.69	41.67
							H	4.00	4.06
							N	20.84	20.80
X	4-$NO_2C_6H_4$	H	90	Ethanol–water	187–189°	$C_7H_8N_4O_2S$	C	39.63	39.77
							H	3.80	3.64
							N	26.41	26.27
XI	2,6-$(CH_3)_2C_6H_3$	H	46	Ethanol	204–205°	$C_9H_{13}N_3S$	C	55.35	55.26
							H	6.71	6.92
							N	21.52	21.34
XII	2,6-$(Cl)_2C_6H_3$	H	99	Ethanol–water	232–233.5°	$C_7H_7Cl_2N_3S$	C	35.60	35.61
							H	2.97	3.02
							N	17.77	17.83
XIII	C_6H_5	CH_3	46	Ethanol	191–192°	$C_8H_{11}N_3S$	C	53.03	52.69
							H	6.12	6.12
							N	23.19	22.81
XIV	C_6H_5	C_6H_5	53	Ethanol	213–215°	$C_{13}H_{13}N_3S$	C	64.19	64.32
							H	5.39	5.15
							N	17.27	17.36

[a] Method A was used; see *Experimental.* [b] T. Pyl, K. H. Scheel, and H. Beyer, *J. Prakt. Chem.*, 20 (5–6), 255 (1963). [c] P. M. Parish and C. V. Delwali, *Indian J. Chem.*, 3, 45 (1965). [d] J. V. Mandlik and V. A. J. Patwardhan, *Univ. Poona Sci. Technol., No. 1*, 20, 45 (1961); through *Chem. Abstr.*, 55, 27274e (1961).

RESULTS AND DISCUSSION

Chemistry—The compounds prepared are listed in Tables I–IV. Synthetic procedures, generalized where possible, are described under *Experimental.*

1-Aryl-3-thiosemicarbazides (Table I, II–XIV) were prepared from the corresponding arylhydrazine hydrochlorides by treatment with ammonium thiocyanate. Arylhydrazine hydrochlorides not commercially available were prepared by a described procedure (2). 2-Arylhydrazino-2-thiazolines (Table II, XV–XXVI, XXVIII, and XXIX) were synthesized by reaction of 1-aryl-3-thiosemicarbazides with 2-bromoethylamine hydrobromide in refluxing 2-propanol (3). 2-Arylazo-2-thiazolines (Table III, XXX–XXXIV) were prepared by oxidation of the corresponding 2-arylhydrazino-2-thiazolines with silver oxide in ethyl acetate (Scheme I). 2-(2-Pyridylhydrazino)-2-thiazoline (XXVII) was synthesized by direct reaction of 2-hydrazinopyridine with 2-methylmercapto-2-thiazoline (4) (Scheme II).

Air oxidation of 2-(*o*-tolylhydrazino)-2-thiazoline (XVI) mixed with sodium carbonate in refluxing ethanol gave 2-(*o*-tolylazo)thiazole (XXXV) in good yield (Scheme I). The dihydrothiazine (XXXVI) was obtained from the reaction of *o*-tolylhydrazine hydrochloride with 3-chloropropyl isothiocyanate (5) in the presence of triethylamine. Oxidation to the azo derivative (XXXVII) was achieved with silver oxide (Scheme III).

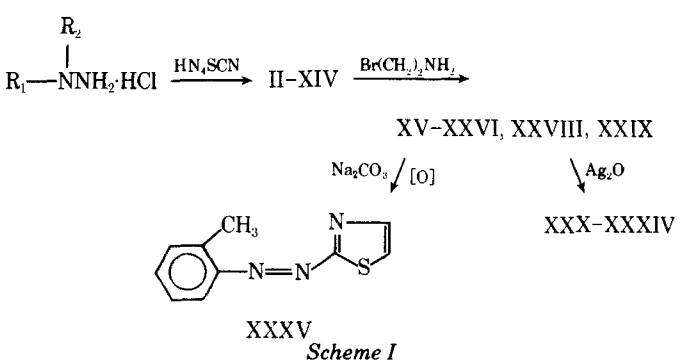

Scheme I

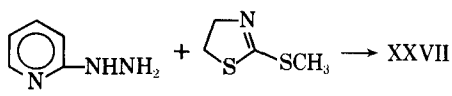

Scheme II

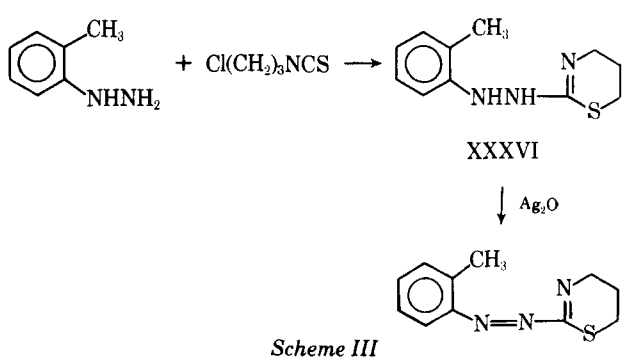

Scheme III

Table II—Physical Properties of 2-Arylhydrazino-2-thiazolines[a]

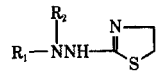

Compound	R_1	R_2	Yield, %	Crystallization Solvent	Melting Point	Molecular Formula	Analysis, %	Calc.	Found
XV	C_6H_5	H	24	Ethanol–water	135–136°	$C_9H_{11}N_3S$	C	55.95	55.87
							H	5.74	5.63
							N	21.75	21.37
XVI	2-$CH_3C_6H_4$	H	43	Methanol–water	126–127°	$C_{10}H_{13}N_3S$	C	57.96	57.62
							H	6.32	6.35
							N	20.28	20.34
XVII	3-$CH_3C_6H_4$	H	75	Ethyl acetate–hexane	95–97°	$C_{10}H_{13}N_3S$	C	57.96	57.72
							H	6.32	6.17
							N	20.28	20.15
XVIII	4-$CH_3C_6H_4$	H	70	Ethanol–water	136–138°	$C_{10}H_{13}N_3S$	C	57.96	57.70
							H	6.32	6.33
							N	20.28	20.23
XIX	2-$C_2H_5C_6H_4$	H	86	Ether	101–103°	$C_{11}H_{15}N_3S$	C	59.70	59.94
							H	6.83	6.77
							N	18.99	18.90
XX	2-$CH_3OC_6H_4$	H	48	Ethanol	141–142°	$C_{10}H_{13}N_3OS$	C	53.81	53.73
							H	5.87	5.82
							N	18.82	18.68
XXI	4-$CH_3OC_6H_4$	H	51	Methanol	124–126°	$C_{10}H_{13}N_3OS$	C	53.81	53.91
							H	5.87	5.76
							N	18.82	18.90
XXII	2-ClC_6H_4	H	71	Ethanol	98–100°	$C_9H_{10}ClN_3S$	C	47.50	47.68
							H	4.42	4.61
							N	18.45	17.94
XXIII	4-ClC_6H_4	H	85	Ethanol–water	146–149°	$C_9H_{10}ClN_3S$	C	47.50	47.37
							H	4.42	4.09
							N	18.45	18.44
XXIV	4-$NO_2C_6H_4$	H	37	Ethanol	203–205°	$C_9H_{10}N_4O_2S$	C	45.38	45.46
							H	4.23	4.36
							N	23.52	23.26
XXV	2,6-$(CH_3)_2C_6H_3$	H	63	Ethanol	159–161°	$C_{11}H_{15}N_3S$	C	59.70	59.30
							H	6.83	7.09
							N	18.99	18.83
XXVI	2,6-$(Cl)_2C_6H_3$	H	8	Ethanol–water	140–142°	$C_9H_9Cl_2N_3S$	C	41.20	41.01
							H	3.43	3.53
							N	16.04	16.30
XXVII	2-Pyridyl	H	40	Ethanol	248–250°	$C_8H_{10}N_4S$	C	49.46	49.75
							H	5.19	4.96
							N	28.84	29.14
XXVIII	C_6H_5	CH_3	25	Ethanol	113–114°	$C_{10}H_{13}N_3S$	C	57.96	58.07
							H	6.32	6.36
							N	20.28	20.15
XXIX	C_6H_5	C_6H_5	29	Ethanol	183–184°	$C_{15}H_{15}N_3S$	C	66.90	66.83
							H	5.61	5.40
							N	15.60	15.61

[a] Method B was used except for XXVII; see *Experimental.*

Biology—Biological results are shown in Table V. Anthelmintic activity was determined by a modification of the assay of Lynch and Nelson (6).

None of the intermediate thiosemicarbazides in Table I had anthelmintic activity. Of the compounds in Table V, the highest activity was found with the 2-arylhydrazino-2-thiazolines and their oxidized derivatives. Within these groups, structural requirements for activity were quite narrow. 2-Phenylhydrazino-2-thiazoline (XV) was slightly active

Table III—Physical Properties of 2-Arylazo-2-thiazolines[a]

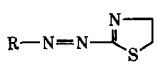

Compound	R	Yield, %	Crystallization Solvent	Melting Point	Molecular Formula	Analysis, %	Calc.	Found
XXX	C_6H_5	79	Ethanol–water	73–75°	$C_9H_9N_3S$	C	56.54	56.74
						H	4.74	4.46
						N	21.98	22.04
XXXI	2-$CH_3C_6H_4$	85	Ethanol–water	79–80°	$C_{10}H_{11}N_3S$	C	58.53	58.61
						H	5.40	5.60
						N	20.48	20.18
XXXII	2-$CH_3C_6H_4$	25	Ethanol	88–90°	$C_{10}H_{11}N_3S$	C	58.53	58.50
						H	5.40	5.34
						N	20.48	20.50
XXXIII	2-$C_2H_5C_6H_4$·HCl	92	Methanol–ether	133° dec.	$C_{11}H_{13}N_3S$·HCl	C	51.66	51.28
						H	5.52	5.56
						N	16.43	16.22
XXXIV	2-$CH_3OC_6H_4$	63	Ethyl acetate–hexane	67–68°	$C_{10}H_{11}N_3OS$	C	54.30	54.18
						H	5.01	4.99
						N	18.99	18.84

[a] Method C was used; see *Experimental.*

Table IV—Physical Properties of Several Miscellaneous Analogs [a]

Compound	Yield, %	Crystallization Solvent	Melting Point	Molecular Formula	Analysis, % Calc.	Found
XXXV	66	Ethanol–water	48–49°	$C_{10}H_9N_3S$	C 59.11	58.98
					H 4.46	4.57
					N 20.68	20.63
XXXVI	44	Ethanol	116–117°	$C_{11}H_{15}N_3S$	C 59.71	60.05
					H 6.83	6.93
					N 18.99	19.03
XXXVII	73	Methanol–ether	160–161°	$C_{11}H_{13}N_3S \cdot HCl$	C 51.65	51.41
					H 5.52	5.24
					N 16.44	16.29

[a] For XXXVII, Method C was used; see *Experimental.*

at 200 mg/kg; insertion of a 2-methyl substituent gave XVI, which was fully active at 25 mg/kg. Analogs containing chloro, methoxy, and ethyl substituents in the *ortho*-position were not active at 200 mg/kg, nor did movement of the methyl group to the 3- or 4-position yield active compounds.

Surprisingly, the 2,6-dimethyl analog (XXV) was completely inactive. Oxidation of the hydrazine (XVI) to the azo derivative (XXXI) gave the most potent compound in the series, active at 12.5 mg/kg. Replacement of the thiazoline ring by thiazole (XXXV) substantially reduced activity, whereas expansion of the ring to the thiazines (XXXVI and XXXVII) abolished activity at the screening level.

It was considered that perhaps all activity could be accounted for by reductive cleavage to 2-amino-2-thiazoline *in situ.* Such conversion would constitute a delivery system for the established neuromuscular blocking agent. *In vitro* evaluation of I, XVI, and XXXI against third-stage larvae of *H. contortus* showed all three compounds to have a similar paralytic effect, but XXXI was the most potent. Furthermore, examination of the urine of sheep dosed orally with XVI or XXXI revealed only the presence of the azo compound, XXXI. These data suggest that although all three compounds have intrinsic activity *in vitro*, XXXI is mainly responsible for the *in vivo* activity.

2-(*o*-Tolylazo)-2-thiazoline (XXXI) was tested in sheep at a single oral dose of 76 mg/kg and was effective against *Haemonchus, Ostertagia, Trichostrongylus, Cooperia, Nematodirus, Oesophagostomum,* and *Dictyocaulus* species.

EXPERIMENTAL[1]

Method A: 1-(*o*-Tolyl)-3-thiosemicarbazide (II)—A mixture of *o*-tolylhydrazine hydrochloride (15.9 g, 0.1 mole), ammonium thiocyanate (15.2 g, 0.2 mole), 30 ml of water, and 300 ml of ethanol was heated under reflux for 24 hr. The solvent was evaporated, and water was added. The solid residue was crystallized from aqueous ethanol to obtain 15 g (85%) of II, mp 158–160°.

Method B: 2-(*o*-Tolylhydrazino)-2-thiazoline (XVI)—A stirred mixture of II (27.2 g, 0.15 mole), 2-bromoethylamine hydrobromide (30.8 g, 0.15 mole), and 2-propanol (800 ml) was heated under reflux for 16 hr. The resulting mixture was filtered hot to remove ammonium bromide, and the filtrate was allowed to cool slowly. The precipitated solid (XVI hydrobromide) was collected, dissolved in hot water, and neutralized with dilute sodium bicarbonate solution. The precipitated title compound was filtered, washed well with water, and recrystallized from methanol to yield 13.2 g (43%) of product, mp 126–127°.

Method C: 2-(*o*-Tolylazo)-2-thiazoline (XXXI)—To a stirred solution of XVI (8 g, 0.0386 mole) in 400 ml of ethyl acetate was added 4 g of silver oxide. After stirring for 18 hr at room temperature, silver oxide was filtered off. The residue obtained upon evaporation was crystallized from aqueous ethanol to give 6.7 g (85%) of XXXI as orange needles, mp 79–80°.

2-(*o*-Tolylazo)thiazole (XXXVII)—A mixture of XVI (0.5 g, 0.0024 mole), sodium carbonate (1 g), and ethanol (50 ml) was refluxed for 3 days. The sodium carbonate was filtered, the solvent was removed *in vacuo*, and the residue was crystallized from aqueous ethanol to give 0.32 g (66%) of orange prisms, mp 48–49°.

5,6-Dihydro-2-(*o*-tolylhydrazino)-1,3(4*H*)-thiazine Hydrochloride (XXXVI)—To a stirred solution of 3-chloropropyl isothiocyanate (5) (15.6 g, 0.115 mole) and *o*-tolylhydrazine hydrochloride (18.3 g, 0.115 mole) in 200 ml of ethanol, triethylamine (11.7 g, 0.115 mole) was added. The reaction mixture was refluxed for 16 hr. The separated solids were filtered hot, washed with cold ethanol, and dried, yielding 8.9 g (30%), mp 255–256°.

A solution of XXXVI hydrochloride in water was neutralized with sodium bicarbonate. The solid residue was recrystallized twice from ethanol to give its free base as white platelets, mp 116–117°.

2-(2-Pyridylhydrazino)-2-thiazoline (XXVII)—2-Methylmercapto-2-thiazoline hydroiodide (4) (26.1 g, 0.1 mole) and 2-hydrazinopyridine (10.9 g, 0.1 mole) in methanol (100 ml) were heated together under reflux for 5 hr. The reaction mixture was diluted with methanol (1.5 liters) and passed through a resin[2] column (500 ml) in the hydroxyl form with methanol. The column was eluted with methanol, and the eluate was evaporated *in vacuo.* The residue was triturated with 2-propanol and recrystallized from ethanol, yielding 7.8 g (40%), mp 248–250°.

Table V—Anthelmintic Activity of 2-Arylhydrazino- and 2-Arylazo-2-thiazolines and Analogs

Compound	Activity[a]
XV	SA 200
XVI	A 25
XVII	I 200
XVIII	I 200
XIX	I 200
XX	I 200
XXI	I 200
XXII	SA 200
XXIII	I 200
XXIV	I 200
XXV	I 200
XXVI	I 200
XXVII	I 200
XXVIII	SA 200
XXIX	I 200
XXX	SA 100
XXXI	A 12.5
XXXII	I 200
XXXIII	SA 100
XXXIV	I 200
XXXV	SA 200
XXXVI	I 200
XXXVII	I 200
Thiabendazole	A 50

[a] Activity expressed as A (active), SA (slightly active), or I (inactive) at the test level shown in milligrams per kilogram given orally.

REFERENCES

(1) H. Ozawa and K. Kubota, *Yakugaku Zasshi,* **89,** 1 (1969).

(2) G. H. Coleman, *Org. Synth.,* I, 442 (1941).

(3) T. P. Johnson, C. R. Stringfellow, Jr., and A. Gallagher, *J. Org. Chem.,* **30,** 2073 (1965).

(4) A. F. McKay, D. J. Whittingham, and M. E. Kreling, *J. Am. Chem. Soc.,* **80,** 3339 (1958).

(5) P. Friis, *Acta Chem. Scand.,* **19,** 766 (1965).

(6) J. E. Lynch and B. Nelson, *J. Parasitol.,* **45,** 659 (1959).

ACKNOWLEDGMENTS AND ADDRESSES

Received July 28, 1976, from the *Merck Sharp & Dohme Research Laboratories, Division of Merck & Co., Inc., Rahway, NJ 07065.*

Accepted for publication October 26, 1976.

Microanalyses were determined by Mr. R. N. Boos and Mr. J. P. Gilbert and their associates.

[x] To whom inquiries should be directed.

[1] Melting points were determined on a Thomas-Hoover Unimelt apparatus and are uncorrected. All intermediates and final products were checked by IR and NMR spectroscopy, and their spectra were in accord with the structures assigned. IR spectra were obtained as mineral oil mulls using a Perkin-Elmer model 137 Infracord spectrophotometer. NMR spectra were obtained in deuterochloroform using a Varian T-60A spectrometer and tetramethylsilane as an internal standard.

[2] IRA-401.

Time-Dependent Kinetics III: Diurnal Oscillations in Steady-State Plasma Valproic Acid Levels in Rhesus Monkeys

R. H. LEVY ˣ, J. S. LOCKARD, I. H. PATEL, and W. C. CONGDON

Abstract □ Valproic acid was administered by constant rate intravenous infusion to catheterized chaired rhesus monkeys for 8–10 weeks under controlled environmental conditions. Steady-state plasma levels were monitored at 2-hr intervals for 26 hr (10 am–12 noon on the following day), 1 day/week for 6 weeks. Individual steady-state plasma concentration–time plots exhibited the following characteristics. During Period A (10 am–6 pm), plasma levels remained stable or decreased. During Period B (6 pm–6 am), plasma levels increased, reached a maximum, and remained markedly higher than during Period A. The maximum concentrations were 40–140% higher than the observed minimum concentrations. During Period C (6 am–noon), plasma levels tended to decline from the maximum concentrations achieved in Period B. In most cases, plasma concentrations at 10 am and 12 noon of the 2nd experimental day fell within 10% of their respective values on the previous day. The mean (±*SD*) periods obtained by cross-correlation analysis of individual plasma concentration–time plots were 30.7 (±3.7) and 22.8 (±3.6) hr for Animals 903 and 923, respectively. The corresponding mean (±*SD*) amplitudes were 27.3 (±12.6) and 17.4 (±2.3)%. A circadian rhythm in total body clearance was hypothesized, and its pharmacokinetic implications are discussed.

Keyphrases □ Valproic acid—steady-state plasma levels, time-dependent kinetics, monkeys □ Kinetics, time dependent—valproic acid, steady-state plasma levels, monkeys □ Pharmacokinetics, time dependent—valproic acid, steady-state plasma levels, monkeys □ Anticonvulsants—valproic acid, steady-state plasma levels, time-dependent kinetics, monkeys □ Circadian rhythm—valproic acid, steady-state plasma levels, time-dependent kinetics, monkeys

Preliminary studies dealt with the pharmacokinetic properties of valproic acid (dipropylacetic acid) following single-dose administration at several dose levels to six male rhesus monkeys (1). These studies were undertaken to determine appropriate dosage regimens of the drug in view of its efficacy testing in an epileptic monkey model (2, 3). Analysis of single-dose data revealed that: (*a*) the pharmacokinetic behavior of valproic acid could be described adequately by a one-compartment open model, (*b*) the total body clearance was 0.19 liter/hr/kg and dose independent, and (*c*) the elimination half-life was 0.7 hr.

The short biological half-life of valproic acid suggested that a discontinuous mode of administration such as multiple oral dosing would be inappropriate since the frequency of administration required to obtain less than 50% oscillations in plasma levels would not be practical. A continuous mode of administration such as constant rate chronic intravenous infusion was then considered.

Monitoring of steady-state plasma levels during constant rate zero-order infusion of the drug to monkeys revealed noticeable fluctuations in plasma levels. Diurnal oscillations in steady-state plasma ethosuximide levels were previously observed under comparable experimental conditions (4, 5). A similar phenomenon was suspected for valproic acid, and it was investigated further under controlled experimental conditions.

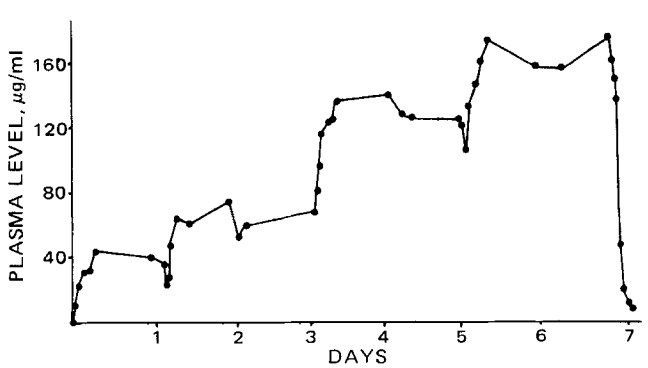

Figure 1—*Four-stage infusion of valproic acid to Animal 913.*

EXPERIMENTAL

Three chronically catheterized male rhesus monkeys (733, 903, and 923) with implanted electrodes in the skull were used. Animals 903 and 923 had been used previously to investigate the diurnal variations in steady-state plasma ethosuximide levels (5). The animals received continuous zero-order infusions of valproic acid over 8–10 weeks (sterile valproic acid solutions in normal saline; infusion rates of 30–40 mg/hr yielding steady-state plasma levels of 30–55 μg/ml).

Plasma samples of 0.5 ml were collected 1 day/week at 2-hr intervals over 26 hr for 6 consecutive weeks. Plasma fractions, 0.2 ml, were assayed for valproic acid in duplicate using a previously described GLC procedure (6). Electroencephalogram (EEG) data were collected by continuous EEG monitoring (10 am–10 am or 10 pm–6 am) with or without blood sampling. Only 1 week of data could be obtained for Animal 733 because of technical difficulties with catheters.

The other experimental conditions used in the present study were similar to those described previously (5). These included: housing of animals in an isolated room with diurnal lighting (light during day, 6 am–6 pm; and dark during night, 6 pm–6 am); strict feeding protocol (6 am, monkey chow; and 5:30 pm, monkey chow and fresh fruits) and noise schedule (moderately high volume, 6 am–6 pm; and low volume, 6 pm–6 am); infusion of drug solutions; blood sampling; and EEG monitoring from an adjacent room.

Periodic analysis of the data was performed using the cross-correlation technique (7) as reported earlier (5).

RESULTS

Preliminary Observations—Previous studies[1] in these laboratories involved single-stage and multistage constant rate infusions of valproic acid to four monkeys to achieve steady-state plasma levels between 20 and 150 μg/ml. An example of the data collected is shown in Fig. 1. Because of its short elimination half-life, steady-state levels of valproic acid were achieved within a few hours. However, appreciable variations in steady-state plasma levels were apparent in each stage. The difference between maximum and minimum steady-state plasma concentrations ranged from 10 to 50%. Similar variations in steady-state plasma levels were also noticed in other animals.

Fluctuations in steady-state plasma levels could be related to variations in experimental factors such as drug assay and/or infusion pump. The GLC assay precision was 6% or better and could not totally explain the observed fluctuations (6). Previously (5), the delivery rate of infusion

[1] Unpublished data.

Table I—Oscillations in Steady-State Plasma Levels of Valproic Acid during Six Sampling Periods

Animal	Week	C_{max}, μg/ml	C_{min}, μg/ml
733	5	50.1	28.2
903	1	44.8	30.1
	2	48.0	23.9
	3	44.0	31.2
	4	56.2	31.2
	5	53.5	35.3
	6	59.5	28.6
923	1	44.1	18.5
	2	35.3	21.1
	3[a]	—	—
	4	37.4	25.4
	5	42.6	26.3
	6	41.3	25.7

[a] Plasma samples were not collected because of technical difficulties with the infusion catheter.

pumps was shown to be relatively constant over several 24-hr periods. These considerations suggested that the observed fluctuations in steady-state plasma valproic acid levels represent a real phenomenon. This phenomenon could possibly be related to diurnal variations in total body clearance, as was observed for ethosuximide (5). To investigate this hypothesis further, additional studies were carried out under controlled conditions.

EEG and Plasma Concentration–Time Data—The sleeping behavior of animals was established by EEG monitoring. Animals were awake during most of the day periods and were in various stages of sleep during the night periods. These data are consistent with those obtained previously (5).

Figures 2A and 3A show typical diurnal fluctuations in steady-state plasma levels observed over a given sampling period (Week 2) for Animals 903 and 923, respectively, and Figs. 2B and 3B represent the corresponding average diurnal oscillations over six sampling periods. Plasma levels were not constant but fluctuated appreciably over the sampling period. The following characteristics were present in individual steady-state plasma concentration–time plots:

Period A (10 am–6 pm)—Plasma levels remained stable (Animal 903, Weeks 1, 3, and 5; and Animal 923, Weeks 1, 2, and 6) or decreased (Animal 733, Week 5; Animal 903, Week 4; and Animal 923, Week 4).

Period B (6 pm–6 am)—In all cases, plasma levels increased and remained markedly higher than those observed during Period A. The C_{max} (highest concentration during the 26-hr observation period) was always reached during this period: between 2 am and 6 am for Animal 903 and between midnight and 6 am for Animal 923. The C_{max} values were generally 40–140% higher than the corresponding C_{min} values (lowest concentration during the 26-hr observation period) (Table I).

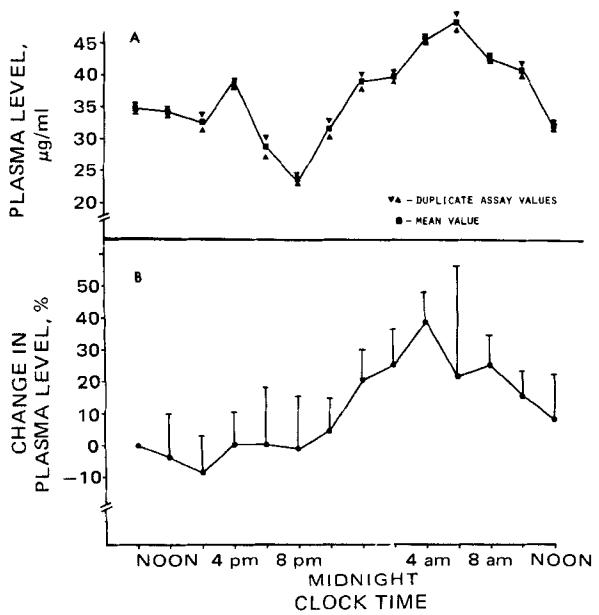

Figure 2—*Plots of typical diurnal changes in steady-state plasma levels during a given sampling period (A) and mean (±SD) percent changes in plasma levels* versus *time (B) for Animal 903.*

Table II—Cross-Correlation Analysis of Experimental Data

Animal	Week	Period, hr	Amplitude, %
733	5	21.0	17.24
903	1	26.0	16.69
	2	33.0	46.77
	3[a]	—	—
	4	34.5	29.51
	5	27.5	15.75
	6	32.5	27.78
	Mean ± *SD*	30.7 ± 3.7	27.30 ± 12.55
	Mean profile	31.5	17.92
923	1	22.0	20.07
	2	17.0	17.48
	3[b]	—	—
	4	25.0	15.96
	5	24.0	19.09
	6	26.0	14.34
	Mean ± *SD*	22.8 ± 3.6	17.39 ± 2.31
	Mean profile	25.5	14.41

[a] The cross-correlation analysis failed to give meaningful estimates of period and amplitude. [b] Plasma samples were not collected because of technical difficulties with the infusion catheter.

Period C (6 am–Noon)—As in Period B, the behavior of plasma levels was quite consistent within and between animals. Plasma levels tended to decline from the C_{max} achieved during Period B. In most cases, plasma concentrations at 10 am and 12 noon of the 2nd experimental day fell within 10% of their respective values on the previous day.

In a previous study (5), application of the cross-correlation analysis (7) to experimental data obtained using a similar protocol was evaluated and was satisfactory. In the present study, sets of individual plasma concentration–time data as well as the mean set of data for each animal were analyzed with that technique to obtain estimates of period and amplitude (Table II). The mean (±*SD*) periods were 30.7 (±3.7) and 22.8 (±3.6) hr for Animals 903 and 923, respectively. The corresponding periods obtained from mean profiles (Figs. 2B and 3B) were 31.5 and 25.5 hr. These values suggest the possibility of a circadian rhythm in steady-state plasma levels. The estimated mean (±*SD*) amplitudes were relatively large, 27.3 (±12.6) and 17.7 (±2.3)% for Animals 903 and 923, respectively.

DISCUSSION

Variations in experimental factors such as GLC assay and/or infusion pump could not explain the diurnal oscillations in steady-state plasma levels observed in the present study. The latter could be related to a circadian rhythm in total body clearance (volume of distribution, renal

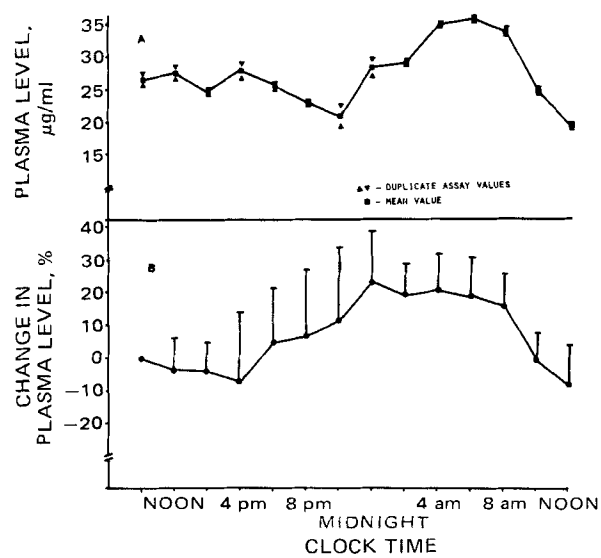

Figure 3—*Plots of typical diurnal changes in steady-state plasma levels during a given sampling period (A) and mean (±SD) percent changes in plasma levels* versus *time (B) for Animal 923.*

excretion, and/or metabolism), as was suggested for another acidic anticonvulsant, ethosuximide (5).

Valproic acid is highly bound to plasma proteins in monkeys ($\beta = 0.9$ at 100 μg/ml). Free fatty acids in plasma are highly protein bound, and they have been reported to displace clofibrate, a highly protein-bound hypolipidemic agent, from albumin binding sites (8). Crouthamel (9) suggested that these observations may have widespread significance, particularly since free fatty acid concentrations fluctuate widely. Concentrations of blood free fatty acids are markedly influenced by such stimuli as exercise, fasting, emotional stress, insulin, and glucose and by such clinical conditions as diabetes, infection, hypothyroidism, hemodialysis, and adrenergic stimulation (9, 10), Thus, the observed oscillations in plasma levels of valproic acid may possibly be related to fluctuations in free fatty acid levels and competitive displacement from protein binding sites.

An appreciable fraction of valproic acid (5–30%) is excreted unchanged in urine in monkeys (1). Diurnal variations in excretion rate, possibly related to a diurnal urinary pH rhythm, were reported in humans for sulfasymazine (11), salicylate (12), and amphetamine (13). It is not known whether a circadian rhythm in uninary pH exists in monkeys. However, a rhythm in the excretion rate of valproic acid would require urinary pH values around 4.5 [pKa of valproic acid = 4.5 (14)].

Circadian variations in the rates of *in vitro* metabolism of drugs undergoing oxidative metabolic transformations (hexobarbital, aminopyrine, *p*-nitroanisole, and 4-dimethylaminoazobenzene) were reported (15–19). Valproic acid is metabolized to a significant extent (70–95%) in monkeys (1), and some metabolic pathways in rats involve oxidative processes (20, 21). Thus, circadian variations in the activities of hepatic drug-metabolizing enzymes, if present in monkeys, could contribute to the observed oscillations in steady-state plasma levels.

Diurnal variations in steady-state plasma ethosuximide levels in monkeys were observed previously under similar experimental conditions (5). Although ethosuximide and valproic acid are both weak acids, they differ from each other both structurally and pharmacokinetically. The total body clearance of valproic acid is 10 times larger than that of ethosuximide [195 *versus* 19.2 ml/hr/kg (1, 22)], and the elimination half-life of the former is one-fortieth that of the latter [0.7 *versus* 28.5 hr (1, 22)]. Moreover, valproic acid is highly protein bound whereas ethosuximide is only negligibly bound to plasma proteins (23, 24). The fact that diurnal oscillations are present for both drugs in spite of these differences leads one to speculate whether other drugs would also exhibit diurnal variations in steady-state plasma levels under similar conditions.

In linear pharmacokinetics (dose and time independent), zero-order intravenous infusion represents the most reliable method of maintaining stable steady-state drug levels. The present study shows that in the presence of time dependency, stable steady-state levels could not be maintained with a zero-order infusion approach. These and other experimental findings (5) clearly indicate the need for pharmacokinetic models with oscillatory disposition functions. Such models are not yet available. The need for new approaches to drug administration is also apparent.

REFERENCES

(1) R. H. Levy and L. Martis, presented at the Basic Pharmaceutics Section, APhA Academy of Pharmaceutical Sciences, New Orleans meeting, Nov. 1974, Abstract 26.

(2) J. S. Lockard and R. I. Barensten, *Electroencephalogr. Clin. Neurophysiol.*, **22,** 482 (1967).

(3) J. S. Lockard, V. Uhlir, L. L. DuCharme, J. A. Farquhar, and B. J. Huntsman, *Epilepsia,* **16,** 301 (1975).

(4) I. H. Patel and R. H. Levy, *ibid.*, **16,** 717 (1975).

(5) I. H. Patel, R. H. Levy, and J. S. Lockard, *J. Pharm. Sci.*, **66,** 650 (1977).

(6) L. Martis and R. H. Levy, presented at the Pharmaceutical Analysis and Control Section, APhA Academy of Pharmaceutical Sciences, Chicago meeting, Aug. 1974, Abstract 2.

(7) F. Koehler, F. K. Okano, L. R. Elveback, F. Halberg, and J. Bittner, *Exp. Med. Surg.*, **14,** 5 (1956).

(8) W. G. Crouthamel and R. J. Cenedella, presented at the Basic Pharmaceutics Section, APhA Academy of Pharmaceutical Sciences, Atlanta meeting, Nov. 1975, Abstract 47.

(9) W. G. Crouthamel, presented at the Basic Pharmaceutics Section, APhA Academy of Pharmaceutical Sciences, New Orleans meeting, Apr. 1976, p. 12.

(10) J. M. Court, M. E. Dunlop, and R. F. Leonard, *J. Appl. Physiol.*, **31,** 345 (1971).

(11) L. Dettli and P. Spring, *Helv. Med. Acta,* **33,** 291 (1967).

(12) A. Reinberg, Z. W. Zagula-Mally, J. Ghata, and F. Halberg, *Proc. Soc. Exp. Biol. Med.*, **124,** 826 (1967).

(13) A. H. Beckett and M. Rowland, *Nature (London),* **204,** 1203 (1964).

(14) F. Sirokman and L. Otvos, *Acta Phys. Chem.*, **2,** 127 (1956).

(15) F. M. Radzialowski and W. F. Bousquet, *Life Sci.*, **6,** 2545 (1967).

(16) F. M. Radzialowski and W. F. Bousquet, *J. Pharmacol. Exp. Ther.*, **163,** 229 (1968).

(17) P. Roberts, M. J. Turnbull, and A. Winterburn, *Eur. J. Pharmacol.*, **12,** 375 (1970).

(18) A. Jori, E. DiSalle, and V. Santini, *Biochem. Pharmacol.*, **20,** 2965 (1971).

(19) E. S. Vesell, *Ann. N.Y. Acad. Sci.*, **151,** 900 (1968).

(20) T. Kuhara and I. Matsumoto, *Int. Res. Commun. Syst.*, **2,** 1382 (1974).

(21) T. Kuhara and I. Matsumoto, *Biomed. Mass Spectrom.*, **1,** 291 (1974).

(22) I. H. Patel, R. H. Levy, and T. Bauer, *Epilepsia,* **16,** 705 (1975).

(23) A. L. Sherwin and P. Robb, in "Antiepileptic Drugs," D. M. Woodbury, J. K. Penry, and R. P. Schmidt, Eds., Raven, New York, N.Y., 1972, pp. 443–448.

(24) T. Chang, W. A. Dill, and A. J. Glazko, in *ibid.*, pp. 417–423.

ACKNOWLEDGMENTS AND ADDRESSES

Received May 26, 1976, from the *Department of Pharmaceutical Sciences, School of Pharmacy, and the Department of Neurological Surgery, School of Medicine, University of Washington, Seattle, WA 98195.*

Accepted for publication October 8, 1976.

Presented at the Basic Pharmaceutics Section, APhA Academy of Pharmaceutical Sciences, New Orleans meeting, April 1976.

Supported by National Institutes of Health Research Contract N01-NS-1-2282 and Research Grant NS-04053, National Institute of Neurological and Communicative Disorders and Strokes, U.S. Public Health Service.

The authors thank Abbott Laboratories for valproate sodium powder. They are also grateful to Mr. L. DuCharme, Ms. J. McNeill, Ms. C. Hurlburt, and Ms. B. Oyloe for technical assistance and Ms. K. Beard for secretarial help.

[x] To whom inquiries should be directed.

Fluorescent Probe Study of Sulfonamide Binding to Povidone

C. H. HSIAO, H. J. RHODES †, and M. I. BLAKE ×

Abstract □ The possibility of using a fluorescent probe technique for the study of drug–povidone (I) interactions was investigated. 1-Anilino-8-naphthalenesulfonate (II) was used as the probe. Sulfanilamide, sulfacetamide, and sulfabenzamide were used as the binding competitors. Both sulfacetamide and sulfabenzamide decreased the fluorescence intensity of the I–II complex, while sulfanilamide increased the intensity. The fluorescence depression was greater with sulfabenzamide than with sulfacetamide, indicating that the former is more strongly bound to povidone. Since sulfabenzamide has a greater hydrophobic group (phenyl) than sulfacetamide (methyl), the binding of these sulfonamides to povidone is probably at least partially hydrophobic in nature. The enhanced fluorescence intensity of the I–II complex in the presence of sulfanilamide is believed to involve hydrogen bonding in which the sulfanilamide acts as an intermediary between I and II. Double reciprocal plots for the I–II and sulfonamide–I interactions were employed to obtain a binding constant of $3.2 \times 10^4\ M^{-1}$ for the I–II interaction. The association constants for sulfacetamide and sulfabenzamide were calculated by means of the Klotz equation to be 13.4 and 56.8 M^{-1}, respectively. The povidone molecules appear to have 1.28 binding sites for these compounds under the experimental conditions.

Keyphrases □ Sulfonamides, various—binding to povidone, fluorescent probe study □ Povidone—binding to various sulfonamides, fluorescent probe study □ Fluorescent probes—study of binding of various sulfonamides to povidone □ Binding—various sulfonamides to povidone, fluorescent probe study □ Antibacterials—various sulfonamides, binding to povidone, fluorescent probe study

The interaction of povidone (I) with drugs is of theoretical interest and some practical importance inasmuch as it may influence their availability, efficacy, and transport. The fluorescence probe technique is used widely to study the interaction between drugs and macromolecules. The concept of a fluorescent probe was first introduced in 1952 (1). Fluorescent probes are defined (2) as compounds whose spectral behavior (such as fluorescence, excitation, emission, and quantum yield) is influenced by their physical and chemical environment.

In some cases, the fluorescence properties of both ligand molecules and polymers may be changed by interactions (3–5). Some fluorescent compounds become quenched whereas others are only fluorescent when bound (6). Certain dyes, referred to as fluorescent probes, fluoresce weakly in aqueous solutions but fluoresce strongly when bound to proteins (1) or other polymers (7). They have been used for the indirect determination of the protein binding parameters of other drugs by competitive binding (8–12). The large increase in fluorescence emission and hypsochromic shift in the presence of protein has been attributed to the binding of the probe at hydrophobic sites (13, 14).

The fluorescent probe 1-anilino-8-naphthalenesulfonate (II) also fluoresces strongly when bound to I (7). The basis of this investigation was to explore the possibility of using this fluorescent probe technique to study the interaction of I with the sulfonamide drugs sulfanilamide, sulfacetamide, and sulfabenzamide.

EXPERIMENTAL

Materials—Povidone[1] (I), pharmaceutical grade, average molecular weight 40,000, was purified by passing its aqueous solution (5%) through a mixed-bed ion-exchange resin[2], then dialyzed against distilled water in dialysis tubing[3], and finally lyophilized. The fluorescent probe 1-anilino-8-naphthalenesulfonate (II) was recrystallized twice from distilled water.

Sulfanilamide[1], sulfacetamide[4], and sulfabenzamide[5] were used without further purification. Phosphate buffer, pH 7.4, was prepared according to a literature method (15). Other chemicals and solvents were reagent grade and were used without further purification.

Apparatus—All fluorescence measurements were made on a spectrophotofluorometer[6].

Methods—The binding of the probe, II, to I was determined by measuring the increase in fluorescence following the titration of the I solution with the probe. The fluorescence intensity was measured on the fluorescence spectrophotometer with excitation at 365 nm and emission at 480 nm. Solutions of I were prepared in pH 7.4 phosphate buffer. Aliquots, 3 ml of low ($2.5 \times 10^{-5}\ M$) and high (6.25×10^{-4} and $12.5 \times 10^{-4}\ M$) concentrations in a 1-cm cell, were titrated by successive additions of 2 μl of $6 \times 10^{-3}\ M$ II, delivered from a microsyringe[7]. Experiments were carried out at room temperature (21 ± 2°).

Titrations of the low concentration I solution were repeated in the presence of $2 \times 10^{-2}\ M$ sulfanilamide, sulfacetamide, and sulfabenzamide, individually. The drugs were added to the solution prior to titration. All titrations were run in triplicate.

RESULTS AND DISCUSSION

The fluorometric titration results are shown in Fig. 1. In the absence of I, the fluorescence of II was not significant (curve a); but when I was added, the intensity was greatly enhanced (curves b and c). At the two high I concentrations (6.25×10^{-4} and $12.5 \times 10^{-4}\ M$), the titration gave essentially identical fluorescence intensity (curve c), indicating that all II added was fully bound under these conditions. At low I concentrations, II was only partially bound (curve b).

The fraction of II bound (X) is usually determined according to:

$$X = \frac{F_p - F_0}{F_b - F_0} \qquad \text{(Eq. 1)}$$

where F_p and F_0 are the fluorescence intensities of a given concentration of II in a solution of low I concentration and in a solution without I, respectively; and F_b is the fluorescence intensity of the same concentration of II fully bound to a high concentration of I. Such treatment yields true values of X, provided the fluorescence intensity of the bound species, I–II, is a linear function of the concentration. However, the linearity of F_b with the concentration of the I–II complex can only be realized when the absorbance of I–II at the exciting wavelength is low (<0.02) (16). This can be seen from the fluorescence–absorbance relationship equation (17):

$$F_b - F_0 = \phi I_0 \left[2.3A - \frac{(2.3A)^2}{2!} + \frac{(2.3A)^3}{3!} - \frac{(2.3A)^4}{4!} + \ldots \right] \qquad \text{(Eq. 2)}$$

where ϕ is the quantum yield of the emitting species, I_0 is the intensity of the exciting radiation, and A is the absorbance. When the absorbance is low, the higher power terms in the equation become negligible. When

[1] Sigma Chemical Co., St. Louis, Mo.
[2] Fisher Scientific Co., Pittsburgh, Pa.
[3] Scientific Products Co., McGraw Park, Ill.
[4] K & K Laboratories, Plainview, N.Y.
[5] Matheson, Coleman and Bell, Norwood, Ohio.
[6] Perkin-Elmer fluorescence spectrophotometer model 203, Perkin-Elmer Corp., Norwalk, Conn.
[7] Hamilton.

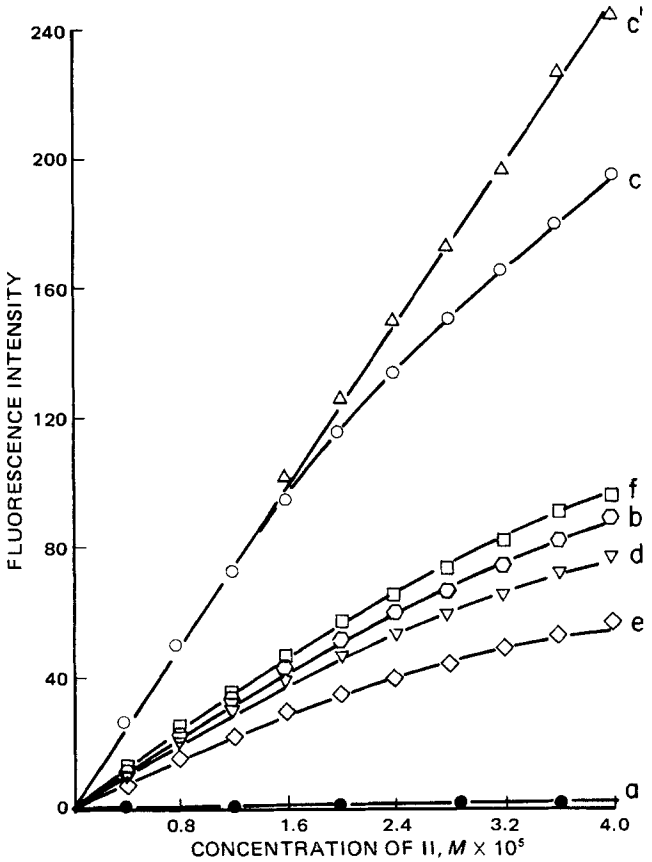

Figure 1—*Fluorescence titration curves of I with II in the absence of I (a), at high I concentrations (6.25×10^{-4} and 12.5×10^{-4} M) uncorrected and corrected for absorbance effect (c and c'), and at low I concentration (2.5×10^{-5} M) alone (b) and in the presence of 2×10^{-2} M sulfacetamide (d), 2×10^{-2} M sulfabenzamide (e), and 2×10^{-2} M sulfanilamide (f), individually.*

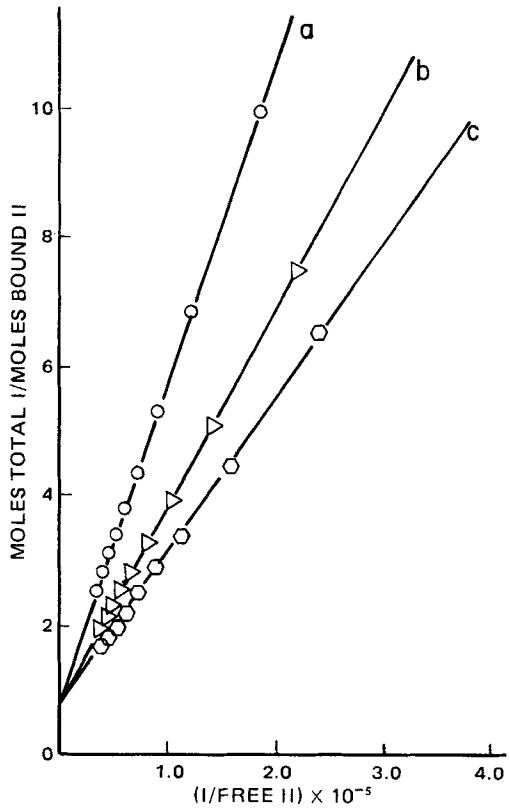

Figure 2—*Double reciprocal plot of the binding of II alone (a) or in the presence of 2×10^{-2} M sulfacetamide (b) or sulfabenzamide (c) to 0.1% I in pH 7.4 phosphate buffer at room temperature.*

the absorbance is high, the second or even the third term must be considered.

At the excitation wavelength, 365 nm, the molar absorptivity for the I–II complex was 5.9×10^3 liters/mole (II) cm. Therefore, at a II concentration greater than 3.4×10^{-5} M ($A = 0.02$), the deviation from linearity will be greater than 2%. It is then necessary to take into account the second term, $(1.63A)^2$, for the titration with the I concentration. Curve c in Fig. 1 was plotted using the observed values of $F_b - F_0$. After the correction to the observed fluorescence intensities was applied, a straight-line plot (line c' in Fig. 1) was obtained, verifying that the deviation from linearity of curve c was indeed due to the absorbance effect.

When the titrations are carried out at low I concentration (curve b), II is only partially bound, and the fluorescence intensity of bound II is approximately a linear function of its concentration. In other words, the absorbance, A, is so small that the second term in Eq. 2 is negligible. Thus, the readings from curve b can be compared directly to the corresponding readings on curve c to obtain the fraction of II bound using Eq. 1. The fluorescence intensity at any point on curve b can be considered as arising from the bound ligand concentration giving the same observed intensity on curve c. From these values, one can also calculate the fraction of II bound as:

$$X = \frac{[\text{II}]_c}{[\text{II}]_b} \qquad \text{(Eq. 3)}$$

where $[\text{II}]_b$ is the concentration of II corresponding to curve b, and $[\text{II}]_c$ is the concentration of II giving the same observed fluorescence intensity in curve c.

Figure 1 shows the titration results of the fluorescence intensity of the I–II complex in the presence of sulfacetamide (curve d) and sulfabenzamide (curve e). Since no change of the pH or the emission maxima was observed, the decrease in fluorescence intensity of the I–II complex could only be attributed to the competition between II and the sulfonamides for the binding sites. The difference in fluorescence intensities with and without sulfonamides is related to the binding of drug and is used to calculate the binding constant for the sulfonamide–I complex.

The fluorescence depression was greater with sulfabenzamide than with sulfacetamide, indicating that the former was more strongly bound to I. Since sulfabenzamide has a greater hydrophobic group (phenyl) than sulfacetamide (methyl), the binding of sulfonamides to I is probably at least partially hydrophobic in nature.

In contrast, the fluorescence intensity of the I–II complex was enhanced in the presence of sulfanilamide (curve f, Fig. 1). One possible explanation for this unexpected phenomenon is that sulfanilamide enhances the I–II binding through some mechanism since I–sulfanilamide or II–sulfanilamide did not show any significant amount of fluorescence at the wavelength employed. Dollery *et al.* (18) observed that chlorothiazide could increase fourfold the binding of the ganglionic blocking agent pempidine (1,2,2,6,6-pentamethylpiperidine) to albumin. It seems likely that the anionic chlorothiazide acts as an intermediary between the albumin and the cationic pempidine. Similarly, sulfanilamide may act, through hydrogen bonding, as an intermediary between I and II.

The binding parameters of the I–II interaction can be obtained by a double reciprocal plot constructed according to:

$$\frac{1}{r} = \left(\frac{1}{N} + \frac{1}{NK}\right)\frac{1}{A} \qquad \text{(Eq. 4)}$$

where r is the average number of moles of II bound per mole of I = X ($[\text{II}]/[\text{I}]$), N is the number of binding sites, K is the binding association constant, and A is the concentration of free II = $(1 - X)[\text{II}]$.

Figure 2 shows the results of the double reciprocal plot for the I–II interaction (curve a) and for sulfonamides–I interactions (curves b and c). The straight line with a common ordinate intercept indicates the competitive nature of the binding interaction (13). Based on the graphs, the binding constant for the I–II interaction was 3.2×10^4 M^{-1}.

The association constants for sulfacetamide and sulfabenzamide can be calculated according to the Klotz equation (19):

$$K_b = \left(\frac{N[P_0]KA - K[A][PA] - [PA]}{CK[A] - [P_0]K[A] + K[A][PA] + [PA]}\right)\frac{K[A]}{[PA]} \qquad \text{(Eq. 5)}$$

where K_b is the association constant for the competitor, K is the association constant for the probe, A is the concentration of free probe, PA is the concentration of bound probe, N is the number of binding sites, P_0 is the total polymer concentration, and C is the total competitor concentration. By means of this equation, the association constants for sul-

facetamide and sulfabenzamide were estimated to be 13.4 and 56.8 M^{-1}, respectively. The I molecules appear to have 1.28 binding sites for these compounds under the described conditions.

In conclusion, the fluorescent probe technique can provide a simple, sensitive, and rapid determination of the extent and nature of binding between sulfonamides and I. The technique, however, may not be applicable for some drugs such as sulfanilamide.

REFERENCES

(1) G. Weber, *Biochem. J.*, **51**, 155 (1952).

(2) R. F. Chen, in "Fluorescent Theory, Instrumentation and Practice," G. C. Guilblaut, Ed., Dekker, New York, N.Y., 1967, p. 443.

(3) H. F. Fischer, *Proc. Natl. Acad. Sci. USA*, **51**, 1285 (1964).

(4) S. F. Velick, *J. Biol. Chem.*, **223**, 1455 (1958).

(5) S. F. Velick, S. W. Parker, and H. N. Eisen, *Proc. Natl. Acad. Sci. USA*, **46**, 1470 (1960).

(6) D. J. R. Laurence, *Biochem. J.*, **51**, 168 (1952).

(7) K. Kono, T. Nagai, and H. Nogami, *Chem. Pharm. Bull.*, **21**, 366 (1973).

(8) T. Kinoshita, F. Linumd, I. Moriguchi, and A. Tsuji, *ibid.*, **19**, 861 (1971).

(9) H. W. Jun, R. T. Mayer, C. M. Himel, and L. A. Luzzi, *J. Pharm. Sci.*, **60**, 1821 (1971).

(10) H. W. Jun, L. A. Luzzi, and P. L. Hsu, *ibid.*, **61**, 1835 (1972).

(11) P. L. Hsu, J. K. H. Ma, H. W. Jun, and L. A. Luzzi, *ibid.*, **63**, 27 (1974).

(12) H. W. Jun, L. A. Luzzi, and J. K. H. Ma, *ibid.*, **64**, 493 (1975).

(13) L. Stryer, *J. Mol. Biol.*, **13**, 482 (1965).

(14) G. M. Edelman and W. O. McClure, *Acc. Chem. Res.*, **1**, 65 (1968).

(15) "Scientific Tables," K. Diem and C. Lenter, Eds., 7th ed., Ciba-Geigy, Basle, Switzerland, 1971, p. 281.

(16) D. V. Naik, W. L. Paul, R. M. Threatte, and S. G. Schulman, *Anal. Chem.*, **47**, 267 (1975).

(17) G. Weber and L. B. Young, *J. Biol. Chem.*, **239**, 1415 (1964).

(18) C. T. Dollery, D. Emslie-Smith, and D. F. Muggleton, *Br. J. Pharmacol. Chemother.*, **17**, 488 (1941).

(19) I. M. Klotz, H. Triwush, and F. M. Walker, *J. Am. Chem. Soc.*, **70**, 2935 (1948).

ACKNOWLEDGMENTS AND ADDRESSES

Received April 15, 1976, from the *Department of Pharmacy, College of Pharmacy, University of Illinois at the Medical Center, Chicago, IL 60612.*

Accepted for publication September 17, 1976.

† Deceased.

* To whom inquiries should be directed.

Rate and Proposed Mechanism of Anhydrotetracycline Epimerization in Acid Solution

T. D. SOKOLOSKI *, L. A. MITSCHER *, P. H. YUEN, J. V. JUVARKAR, and B. HOENER ‡

Abstract □ The pathway through which the toxic tetracycline degradation product epianhydrotetracycline forms in solution was studied using high-performance liquid chromatography and circular dichroism, taking advantage of the large difference in ellipticity between the reactant and the product at 285 nm. The epimerization of anhydrotetracycline followed a reversible first-order process, and both analytical methods yielded the same rate constants. The rate constants indicate that anhydrotetracycline epimerization is faster than tetracycline epimerization. The equilibrium favored anhydrotetracycline, and the activation energies for the forward and reverse rates were almost the same as those for tetracycline epimerization. The epimerization was catalyzed by phosphate. Activation energies in 0.1 and 1 *M* phosphate were essentially the same. The equilibrium constants for both anhydrotetracycline and tetracycline favored the natural configuration rather than the epi series. Possible rationalization based on conformational and hydrogen bonding effects is presented.

Keyphrases □ Anhydrotetracycline—epimerization, kinetics and mechanism in acid solution, high-performance liquid chromatographic and circular dichroism study □ Tetracycline degradation—kinetics and mechanism of anhydrotetracycline epimerization in acid solution, high-performance liquid chromatographic and circular dichroism study □ Epimerization—anhydrotetracycline in acid solution, kinetics and mechanism, high-performance liquid chromatographic and circular dichroism study □ High-performance liquid chromatography—study of epimerization of anhydrotetracycline in acid solution □ Circular dichroism—study of epimerization of anhydrotetracycline in acid solution □ Antibacterials—tetracycline degradation, epimerization of anhydrotetracycline in acid solution

Among the degradative pathways of the tetracyclines, those leading to the toxic epianhydrotetracycline by epimerization and dehydration are of special concern. Formation of epianhydrotetracycline (I) from tetracycline (IV) occurs along two routes (Scheme I). Epimerization of tetracycline occurs *via* a reversible first-order process between pH 3 and 5 (1–4). Dehydration of tetracycline to anhydrotetracycline (II) and of epitetracycline (III) to epianhydrotetracycline occurs *via* a pseudo-first-order process at low pH (5–7).

The epimerization of anhydrotetracycline is the only reaction of Scheme I whose kinetics have not yet been reported, probably because of a lack of a suitable method of

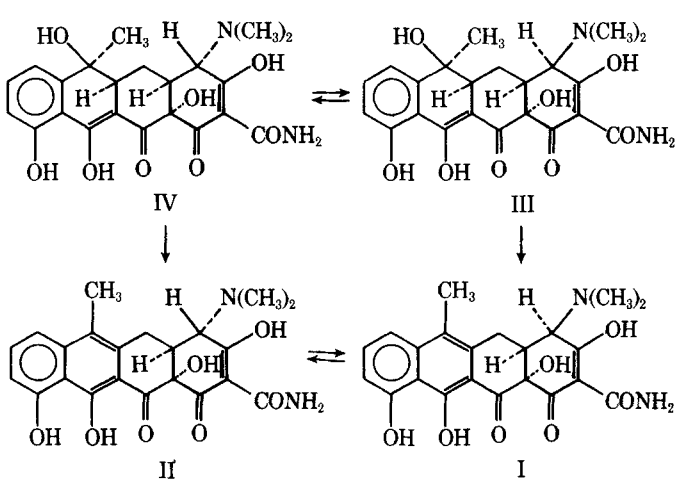

Scheme I

facetamide and sulfabenzamide were estimated to be 13.4 and 56.8 M^{-1}, respectively. The I molecules appear to have 1.28 binding sites for these compounds under the described conditions.

In conclusion, the fluorescent probe technique can provide a simple, sensitive, and rapid determination of the extent and nature of binding between sulfonamides and I. The technique, however, may not be applicable for some drugs such as sulfanilamide.

REFERENCES

(1) G. Weber, *Biochem. J.*, **51**, 155 (1952).

(2) R. F. Chen, in "Fluorescent Theory, Instrumentation and Practice," G. C. Guilblaut, Ed., Dekker, New York, N.Y., 1967, p. 443.

(3) H. F. Fischer, *Proc. Natl. Acad. Sci. USA*, **51**, 1285 (1964).

(4) S. F. Velick, *J. Biol. Chem.*, **223**, 1455 (1958).

(5) S. F. Velick, S. W. Parker, and H. N. Eisen, *Proc. Natl. Acad. Sci. USA*, **46**, 1470 (1960).

(6) D. J. R. Laurence, *Biochem. J.*, **51**, 168 (1952).

(7) K. Kono, T. Nagai, and H. Nogami, *Chem. Pharm. Bull.*, **21**, 366 (1973).

(8) T. Kinoshita, F. Linumd, I. Moriguchi, and A. Tsuji, *ibid.*, **19**, 861 (1971).

(9) H. W. Jun, R. T. Mayer, C. M. Himel, and L. A. Luzzi, *J. Pharm. Sci.*, **60**, 1821 (1971).

(10) H. W. Jun, L. A. Luzzi, and P. L. Hsu, *ibid.*, **61**, 1835 (1972).

(11) P. L. Hsu, J. K. H. Ma, H. W. Jun, and L. A. Luzzi, *ibid.*, **63**, 27 (1974).

(12) H. W. Jun, L. A. Luzzi, and J. K. H. Ma, *ibid.*, **64**, 493 (1975).

(13) L. Stryer, *J. Mol. Biol.*, **13**, 482 (1965).

(14) G. M. Edelman and W. O. McClure, *Acc. Chem. Res.*, **1**, 65 (1968).

(15) "Scientific Tables," K. Diem and C. Lenter, Eds., 7th ed., Ciba-Geigy, Basle, Switzerland, 1971, p. 281.

(16) D. V. Naik, W. L. Paul, R. M. Threatte, and S. G. Schulman, *Anal. Chem.*, **47**, 267 (1975).

(17) G. Weber and L. B. Young, *J. Biol. Chem.*, **239**, 1415 (1964).

(18) C. T. Dollery, D. Emslie-Smith, and D. F. Muggleton, *Br. J. Pharmacol. Chemother.*, **17**, 488 (1941).

(19) I. M. Klotz, H. Triwush, and F. M. Walker, *J. Am. Chem. Soc.*, **70**, 2935 (1948).

ACKNOWLEDGMENTS AND ADDRESSES

Received April 15, 1976, from the *Department of Pharmacy, College of Pharmacy, University of Illinois at the Medical Center, Chicago, IL 60612.*

Accepted for publication September 17, 1976.

† Deceased.

* To whom inquiries should be directed.

Rate and Proposed Mechanism of Anhydrotetracycline Epimerization in Acid Solution

T. D. SOKOLOSKI *, L. A. MITSCHER *, P. H. YUEN, J. V. JUVARKAR, and B. HOENER ‡

Abstract □ The pathway through which the toxic tetracycline degradation product epianhydrotetracycline forms in solution was studied using high-performance liquid chromatography and circular dichroism, taking advantage of the large difference in ellipticity between the reactant and the product at 285 nm. The epimerization of anhydrotetracycline followed a reversible first-order process, and both analytical methods yielded the same rate constants. The rate constants indicate that anhydrotetracycline epimerization is faster than tetracycline epimerization. The equilibrium favored anhydrotetracycline, and the activation energies for the forward and reverse rates were almost the same as those for tetracycline epimerization. The epimerization was catalyzed by phosphate. Activation energies in 0.1 and 1 *M* phosphate were essentially the same. The equilibrium constants for both anhydrotetracycline and tetracycline favored the natural configuration rather than the epi series. Possible rationalization based on conformational and hydrogen bonding effects is presented.

Keyphrases □ Anhydrotetracycline—epimerization, kinetics and mechanism in acid solution, high-performance liquid chromatographic and circular dichroism study □ Tetracycline degradation—kinetics and mechanism of anhydrotetracycline epimerization in acid solution, high-performance liquid chromatographic and circular dichroism study □ Epimerization—anhydrotetracycline in acid solution, kinetics and mechanism, high-performance liquid chromatographic and circular dichroism study □ High-performance liquid chromatography—study of epimerization of anhydrotetracycline in acid solution □ Circular dichroism—study of epimerization of anhydrotetracycline in acid solution □ Antibacterials—tetracycline degradation, epimerization of anhydrotetracycline in acid solution

Among the degradative pathways of the tetracyclines, those leading to the toxic epianhydrotetracycline by epimerization and dehydration are of special concern. Formation of epianhydrotetracycline (I) from tetracycline (IV) occurs along two routes (Scheme I). Epimerization of tetracycline occurs *via* a reversible first-order process between pH 3 and 5 (1–4). Dehydration of tetracycline to anhydrotetracycline (II) and of epitetracycline (III) to epianhydrotetracycline occurs *via* a pseudo-first-order process at low pH (5–7).

The epimerization of anhydrotetracycline is the only reaction of Scheme I whose kinetics have not yet been reported, probably because of a lack of a suitable method of

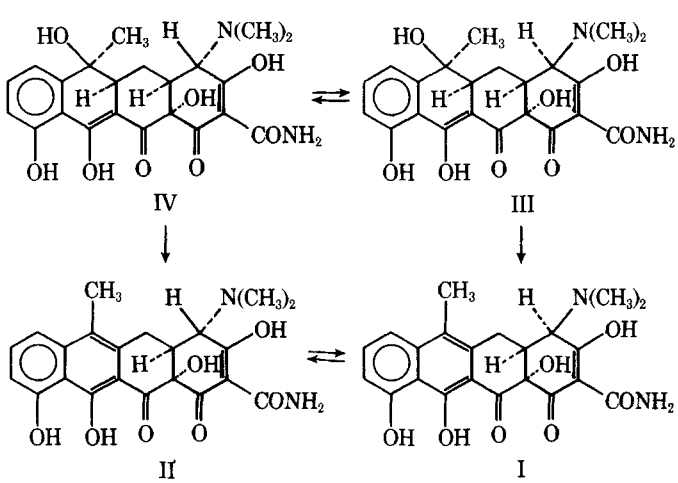

Scheme I

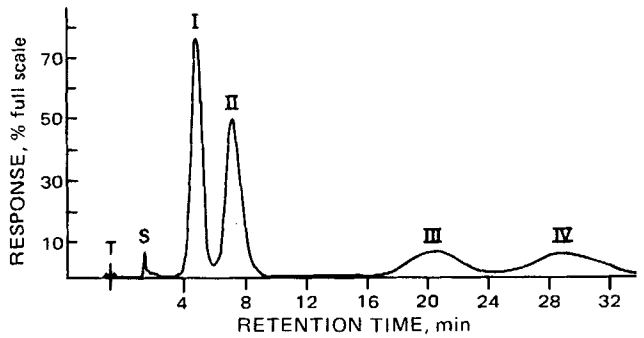

Figure 1—*High-performance liquid chromatogram for a mixture of tetracycline (IV), epitetracycline (III), anhydrotetracycline (II), and epianhydrotetracycline (I). The T is the time of injection, and S is the solvent peak. Four microliters of a solution containing 0.466 mg/ml of IV, 0.346 mg/ml of III, 0.436 mg/ml of II, and 0.512 mg/ml of I was injected with instrument attenuation at 0.08 absorbance unit. Flow rate was 1.08 ml/min (2000 psi).*

analysis for the reactant and the product. However, separation of tetracycline from its degradation products and from rolitetracycline by liquid chromatography recently was described (8–11). The present study utilized a different liquid chromatographic system, as suggested previously[1]. The other potential method to study the reaction is circular dichroism, as suggested by previous results which showed large differences in the ellipticity of anhydrotetracycline and epianhydrotetracycline at 285 nm in 0.03 *N* HCl (12). It thus seems feasible to follow the rate of epimerization by following the rate of change in ellipticity at this wavelength.

EXPERIMENTAL

Materials—Tetracycline hydrochloride[2], 4-epitetracycline ammonium salt[3], anhydrotetracycline hydrochloride[4], and 4-epianhydrotetracycline[5] were used as obtained. All other chemicals were reagent grade.

Apparatus—High-performance liquid chromatographic[6] (HPLC) studies were made using a UV detector at 254 nm with a 1-m × 2.1-mm i.d. column[7]. Circular dichroism measurements[8] were made using a jacketed 1-cm pathlength cell at constant temperature[9]. Visible and UV light[10] absorption measurements were made using a thermostated 1-cm cell.

Chromatographic Methods—For the separation and quantification of anhydrotetracycline and epianhydrotetracycline, the following method was used. The mobile phase consisted of 0.07 *M* sodium phosphate and 0.008 *M* ethylenediaminetetraacetic acid adjusted to pH 7. The degassed solvent was stored in the solvent reservoir of the instrument[6]. The instrument, with a 1-m cation-exchange column[7], was operated at a flow rate of 1 ml/min (1800 psi) at ambient temperature. Known amounts of anhydrotetracycline and epianhydrotetracycline dissolved in 0.03 *N* HCl were placed in an ice bath, and known volumes (2–5 μl) were withdrawn and injected into the chromatographic column using a 5-μl high-pressure syringe. The resulting areas under the chromatograms were measured using a planimeter.

The procedure used in the kinetic studies was as follows. Monobasic potassium phosphate solution at a given concentration was adjusted to pH 4.2 with concentrated hydrochloric acid. The solution was equilibrated at the desired temperature. Appropriate amounts of anhydrotetracycline were weighed into flasks and brought to volume with the phosphate solution. Final concentrations ranged from 7.7 to 13 × 10^{-4} *M*. The flask was immediately placed in a water bath, and a fixed volume (3.5–5 μl) was injected onto the chromatographic column at about 10-min intervals for the first 2 hr and at 30-min intervals thereafter until equilibrium was established. The area under the response (0.08 absorbance unit full scale) *versus* time chromatograms for anhydrotetracycline (and epianhydrotetracycline) were measured and equated to the concentration through a standard curve.

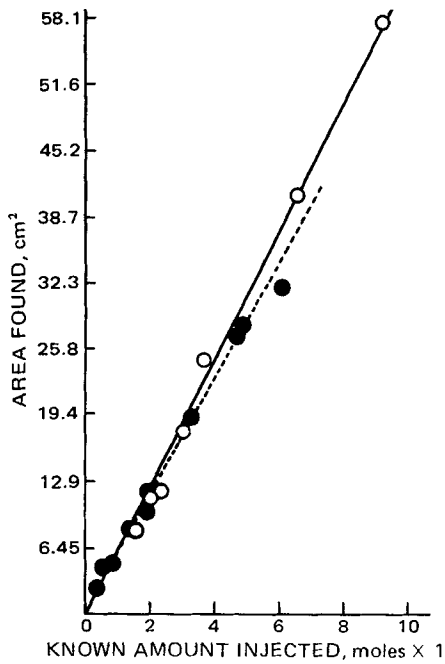

Figure 2—*Relation between the area under the HPLC peak and the amount injected for anhydrotetracycline (●, - - -) and epianhydrotetracycline (○, —).*

Spectropolarimetric Methods—In the rate studies, stock solutions of anhydrotetracycline or epianhydrotetracycline were prepared by weighing each into separate 10-ml volumetric flasks. The materials were dissolved and brought to volume with 0.03 *N* HCl at room temperature, and the solutions were immediately refrigerated. One or 2 ml of the stock solution was diluted to 50 ml with phosphate solution (pH 4.2). The ellipticity of the various concentrations of pure anhydrotetracycline or epianhydrotetracycline was then measured at 285 nm.

Phosphate solution was prepared by adding concentrated hydrochloric acid to several different concentrations of monobasic potassium phosphate to give pH 4.2. Salt effects were studied by adjusting ionic strength with potassium chloride. The phosphate solution was equilibrated at the temperature to be used before mixing with a known volume of stock solution of anhydrotetracycline, resulting in solutions having a concentration of approximately 3 × 10^{-5} *M*. The solution was immediately transferred to a thermostated circular dichroism cell, and the change in ellipticity was measured continuously for about 5–6 hr at 285 nm. An equilibrium ellipticity was determined about 15 hr later.

This same procedure was repeated using tetracycline or epitetracycline as the starting material. The ellipticity of the solutions was measured as a function of time at 270 nm, and standard curves for pure materials were also determined at this wavelength. At a wavelength of 270 nm and pH

Table I—Rate Constants for the C-4 Epimerization of Anhydrotetracycline in 0.1 *M* Phosphate at pH 4.2 and Several Temperatures Studied Using HPLC

Temperature ±2.0°	Forward Reaction Rate Constant, $k_1 \times 10$ hr^{-1}	Reverse Reaction Rate Constant, $k_{-1} \times 10$ hr	Equilibrium Constant
45°	0.89 (0.07)[a]	1.82 (0.13)	0.489
50°	1.35 (0.10)	2.67 (0.21)	0.506
55°	2.38 (0.66)	4.85 (1.38)	0.491
60°	3.55 (0.23)	7.27 (0.50)	0.488

[a] Parentheses contain root mean square error of two determinations.

[1] G. Manning, Alza Corp., Palo Alto, CA 94304, July 1972, personal communication.
[2] Lot 420433, Parke, Davis and Co.
[3] Batch 430, British Pharmacopoeia Commission.
[4] Batch 428, British Pharmacopoeia Commission.
[5] GS-6659, Lot 3339-99-1, Pfizer Inc., and Batch 429, British Pharmacopoeia Commission.
[6] DuPont model 830 high-performance liquid chromatograph.
[7] DuPont SCX column.
[8] Durrum Jasco ORD/UV-5 spectropolarimeter with the Sprowl Scientific SS-20-2 modification.
[9] MGM Lauda K2 water bath.
[10] Cary model 16 spectrophotometer.

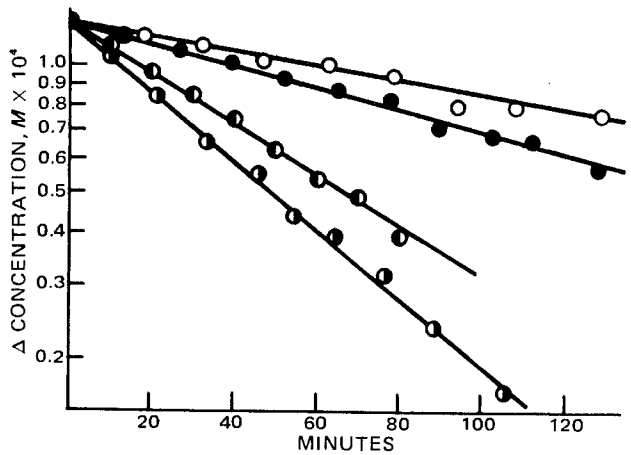

Figure 3—*Relation between the logarithm of the difference in concentration of anhydrotetracycline at time* t *and its equilibrium concentration and the time for anhydrotetracycline epimerization at pH 4.2 in 0.1* M *phosphate. Anhydrotetracycline and its epimer were separated by HPLC and detected using UV spectrophotometry at 45° (○), 50° (●), 55° (◐), and 60° (◑).*

4.2, there was a large difference in the circular dichroism spectra of tetracycline and epitetracycline, similar to those found in 0.03 *N* HCl (12). Visible and UV absorbances at 427 and 269 nm for epianhydrotetracycline and anhydrotetracycline in 0.1 *M* phosphate at 60° were measured as a function of time by withdrawing samples from solutions at 30-min intervals.

Circular dichroism studies of the anhydrotetracycline epimers at several pH values were conducted by making stock solutions at 0.003% in 0.03 *N* HCl. The materials were dissolved in approximately 2 ml of methanol and diluted to 100 ml with 0.03 *N* HCl. To 5.0 ml of stock solution was added 5.0 ml of 0.001 *N* HCl, and the pH was adjusted to its final value (1.00, 3.25, 7.25, and 9.25) with a few drops of strong hydrochloric acid or sodium hydroxide. The circular dichroism spectrum of each sample was determined immediately. A solvent blank was made in the same manner but without drug.

RESULTS

The HPLC procedure provided adequate separation of anhydrotetracycline and epianhydrotetracycline within 10 min and also of tetracycline and epitetracycline after 30 min (Fig. 1). When the area under the chromatograms for anhydrotetracycline and its epimer was measured for known amounts of material injected, it accurately represented the amount present (Fig. 2). The sensitivity achievable at 0.08 absorbance unit full scale permits analysis of compounds in concentrations of 10^{-5}–10^{-4} *M*.

With the HPLC procedure, solutions of anhydrotetracycline kept at various temperatures and phosphate concentrations were analyzed for anhydrotetracycline (and epianhydrotetracycline) content by the measurement of areas under the chromatograms. It was assumed that, like tetracycline, the epimerization followed a reversible first-order process where:

$$\ln\left(\frac{C_0 - C_\infty}{C_t - C_\infty}\right) = (k_1 + k_{-1})t \qquad \text{(Eq. 1)}$$

Table II—Activation Energies for the C-4 Epimerization of Anhydrotetracycline at pH 4.2 in Phosphate

Buffer Concentration, *M*	Reaction	Activation Energy[a], kcal/mole: HPLC Results	Activation Energy[a], kcal/mole: Circular Dichroism Results
0.1	Forward	19.9 (15.8–24.1)	18.6 (15.7–21.5)
0.1	Reverse	20.0 (14.6–25.4)	18.6 (15.7–21.6)
1	Forward		17.9 (17.3–18.6)
1	Reverse		17.5 (17.1–17.9)

[a] Parentheses contain the upper and lower 95% confidence limits obtained from linear regression analysis.

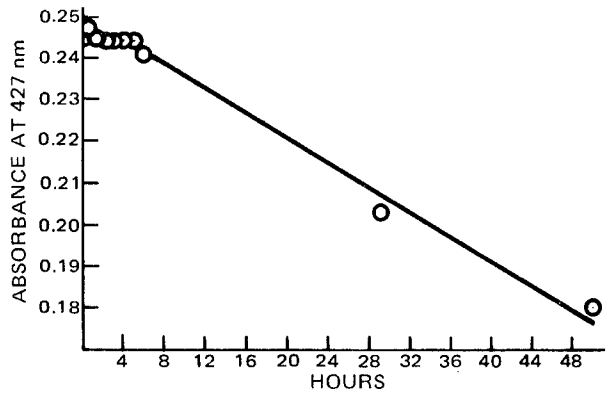

Figure 4—*Absorbance of a solution of anhydrotetracycline at 427 nm as a function of time at 60° in 0.1* M *phosphate.*

describes the kinetic reaction where C_0, C_t, and C_∞ are the concentrations of anhydrotetracycline at times 0, t, and equilibrium, respectively; k_1 and k_{-1} are the forward and reverse rate constants, respectively; and t is time. Based on Eq. 1, a semilogarithmic plot of the difference in concentration ($C_t - C_\infty$) *versus* time should be linear with a slope of ($k_1 + k_{-1}$).

Figure 3 plots the results of such studies at four temperatures. The sum of the rate constants together with the equilibrium constants obtained after about 10 half-lives permitted the calculation of the forward and reverse rate constants (Table I). Based on the data of Table I, the activation energies for the reaction were calculated (Table II). A precipitate formed in the solutions upon storage after epimerization, particularly at higher temperatures after standing for a few days. A study of the absorbance of anhydrotetracycline at 427 nm at 60° in 0.1 *M* phosphate showed that the content of anhydrotetracyclines decreased after a lag phase of about 6 hr (Fig. 4). The wavelength chosen should reflect total anhydro solution content (12).

Although the HPLC procedure is acceptable for following epimerization kinetics, the reaction was also studied utilizing the large difference in ellipticity of anhydrotetracycline and epianhydrotetracycline at around 285 nm (Fig. 5). The results obtained when ellipticity at 285 nm was measured as a function of time at various temperatures and phosphate

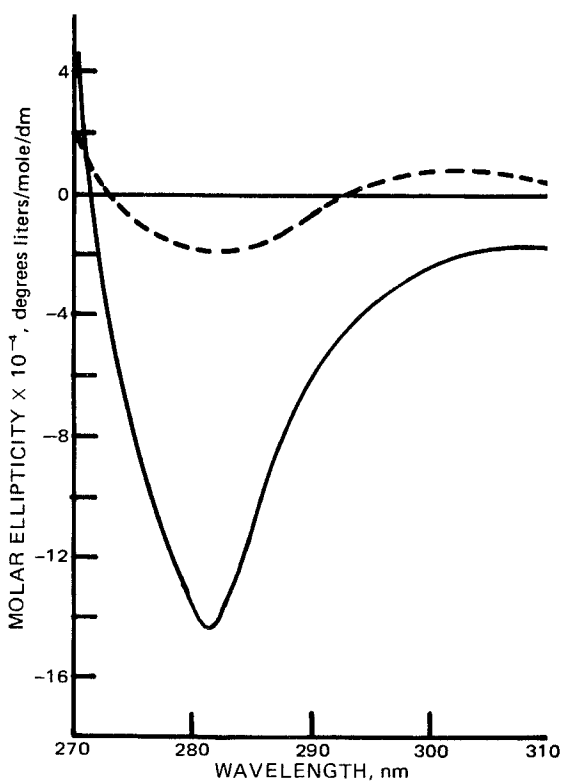

Figure 5—*Molar ellipticity of epianhydrotetracycline (—) and anhydrotetracycline (- - -) as a function of wavelength at pH 4.2 in 0.1* M *phosphate at ambient temperature (29°).*

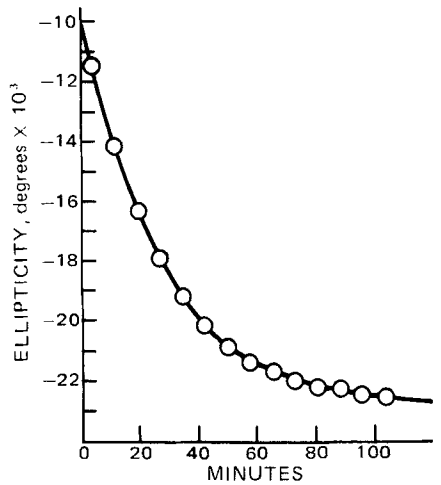

Figure 6—*Relation between ellipticity at 285 nm and time for anhydrotetracycline epimerization at pH 4.2 in 1* M *phosphate at 50°.*

concentrations are typified by those given in Fig. 6. When such data are treated assuming a reversible first-order process following the relationship:

$$\ln \frac{\psi_0 - \psi_\infty}{\psi_t - \psi_\infty} = (k_1 + k_{-1})t \qquad \text{(Eq. 2)}$$

for the reaction anhydrotetracycline ⇄ epianhydrotetracycline, where the ψ values are the ellipticities in degrees with subscripts 0, t, and ∞ referring to initial, time t, and equilibrium values, respectively, and k_1, k_{-1}, and t are as defined for Eq. 1, a linear relationship should be obtained when $\ln (\psi_t - \psi_\infty)$ is plotted as a function of time. The ψ_∞ is obtained after about 10 half-lives. A linear relationship was found for studies made at five different temperatures in 1 *M* phosphate solution (Fig. 7). The slopes of these lines provide the sum of the rate constants. The equilibrium constant, K, can be obtained from:

$$K = \frac{k_1}{k_{-1}} = \frac{\psi_0 - \psi_\infty}{\psi_\infty - bC_0} \qquad \text{(Eq. 3)}$$

where b relates the concentration of epianhydrotetracycline to its ellipticity, C_0 is the initial concentration of anhydrotetracycline, and the other terms are as defined previously. By using Eqs. 2 and 3, it is possible to get the forward and reverse rate constants. The constant b was obtained from a linear relationship found for ellipticity as a function of epianhydrotetracycline concentration; b has a value of $-975°/M$. The similar constant for anhydrotetracycline is $-186°/M$. The forward and reverse rate constants for studies made in 1 *M* phosphate using Eqs. 2 and 3 are given in Table III, and the activation energy values calculated using these data are found in Table II.

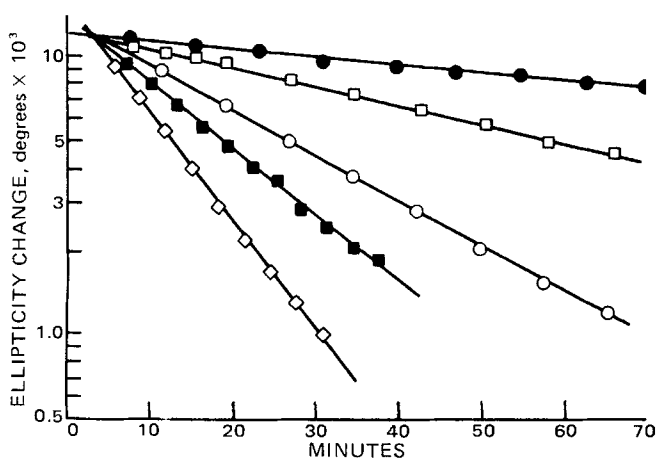

Figure 7—*Semilogarithmic relation between the change in ellipticity (time* t *minus equilibrium value) and the time for anhydrotetracycline epimerization at 30° (●), 40° (□), 50° (○), 55° (■), and 60° (◇). Ellipticity is measured at 285 nm in solutions at pH 4.2 (1* M *phosphate).*

Table III—Rate Constants for the C-4 Epimerization of Anhydrotetracycline in 1 *M* Phosphate at pH 4.2 Studied Using Circular Dichroism at Several Temperatures

Temperature ±2°	Forward Reaction Rate Constant, hr^{-1}	Reverse Reaction Rate Constant, hr^{-1}	Equilibrium Constant
30°	0.118 (0.111–0.125)[a]	0.244 (0.226–0.255)	0.484
40°	0.303 (0.301–0.311)	0.616 (0.605–0.625)	0.492
50°	0.754 (0.735–0.760)	1.50 (1.48–1.52)	0.503
55°	1.10 (1.09–1.12)	2.18 (2.15–2.21)	0.505
60°	1.76 (1.74–1.80)	3.57 (3.49–3.63)	0.493

[a] Parentheses contain the upper and lower 95% confidence limits obtained from linear regression analysis.

Studies made at lower phosphate concentrations, where the reaction was slower, gave ellipticity *versus* time plots for which it was difficult to estimate an infinity ellipticity, probably because of interference from the secondary reaction resulting in precipitation, as observed in the HPLC studies. As a consequence, the epimerization reactions occurring in 0.1 *M* phosphate were analyzed differently than those previously presented. In these cases, an equilibrium ellipticity was calculated from the equilibrium constant found in Tables I and III. The equilibrium constant did not change with temperature, and values obtained in lower temperature studies were considered reliable since the precipitation reaction was minimal. By using such calculated values and only ellipticities at times shorter than 2 hr, semilogarithmic plots of $\psi_t - \psi_\infty$ *versus* time were constructed (Fig. 8). The plots showed curvature at longer times, but rate constants calculated from the slopes of the linear portion of such lines together with the equilibrium constant (*via* Eq. 3) were in excellent agreement with the rate constants calculated from initial rate data. Initial rates were obtained from plots of ellipticity *versus* time data (Table IV). Activation energies calculated from the data of Table IV are given in Table II.

In addition to the rate studies made at 0.1 and 1.0 *M* phosphate at pH 4.2, studies using circular dichroism were made at 50° and at a constant

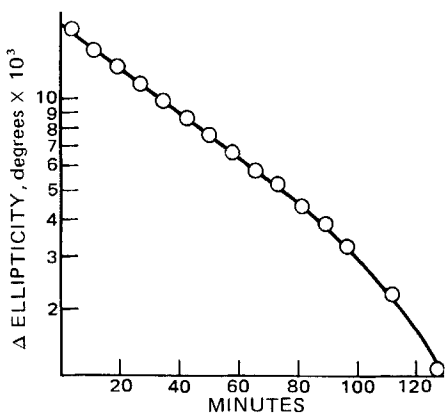

Figure 8—*Relation between the logarithm of the change in ellipticity for solutions of anhydrotetracycline at time* t *and that estimated for equilibrium and the time at 60°, pH 4.2 (0.1* M *phosphate).*

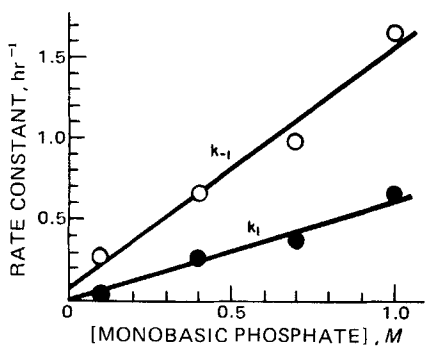

Figure 9—*Forward (●) and reverse (○) rate constants for anhydrotetracycline epimerization as a function of phosphate concentration at pH 4.2 at 50° and constant ionic strength (1* M*).*

Table IV—Rate Constants for the C-4 Epimerization of Anhydrotetracycline in 0.1 *M* Phosphate at pH 4.2 Studied Using Circular Dichroism at Several Temperatures

Temperature ±2°	Forward Reaction Rate Constant, $k_1 \times 10\ hr^{-1}$ ± Average Error[a]		Reverse Reaction Rate Constant, $k_{-1} \times 10\ hr^{-1}$ ± Average Error[a]	
	From Semilog Data	From Initial Rates	From Semilog Data	From Initial Rates
43.5°	0.945 ± 0.001[b]	0.91 ± 0.02[b]	1.93 ± 0.001[b]	1.89 ± 0.03[b]
48.5°	1.59	1.56	3.25	3.18
53°	2.40 ± 0.008[b]	2.44 ± 0.03[b]	4.89 ± 0.018[b]	4.98 ± 0.08[b]
58°	3.58 ± 0.022[c]	3.66 ± 0.25[c]	7.32 ± 0.050[c]	7.47 ± 0.98[c]

[a] Calculated as the root mean square. [b] Average of two values. [c] Average of three values.

ionic strength (1 *M*) at various total phosphate concentrations (0.1–1 *M*). A plot of the rate constants obtained as a function of monobasic phosphate concentration (essentially the total phosphate) gave the results shown in Fig. 9.

For comparative purposes, the epimerization of tetracycline was studied making use of the difference in spectra between tetracycline and epitetracycline at 270 nm. This difference was previously reported in 0.03 *N* HCl and substantiated at pH 4.2 (12). When starting with either tetracycline or epitetracycline, the change in ellipticity was treated as a reversible first-order process as reported in several studies (1–4). With Eqs. 2 and 3, modified for the reaction tetracycline $\rightleftarrows$ epitetracycline, where b for tetracycline and for epitetracycline is -521.6 and $376.6°/M$, respectively, excellent conformance with the reversible first-order process was obtained (Fig. 10), giving the rate constants listed in Table V.

The relations between molar ellipticity and wavelength found for anhydrotetracycline and epianhydrotetracycline at four pH values (1.0, 3.25, 7.25, and 9.25) are presented in Figs. 11 and 12.

DISCUSSION

The HPLC method used to separate tetracycline and its degradation products is different from that reported previously (8, 9, 11). The separation achievable for anhydrotetracycline and epianhydrotetracycline allows a valid and convenient study of the epimerization, since peaks are sharp and retention times are small. The procedure used may not be as convenient in a study of tetracycline epimerization, since bandwidths are broad and retention times are longer for tetracycline and its epimer.

With HPLC, epimerization of anhydrotetracycline complies with a reversible first-order process just as does the epimerization of tetracycline (2–4, Fig. 10). A reaction other than epimerization occurs for anhydrotetracycline at pH 4.2 and results in precipitation. Such a reaction occurs slowly at high temperatures but occurs even at lower temperatures at apparently slower rates. Identification of this product(s) is being undertaken.

Circular dichroism provides an especially convenient way to study the epimerization reaction. It is only necessary to place a solution of either anhydrotetracycline or its epimer in the instrument cell and to follow the change of ellipticity as a function of time at a fixed temperature. The results obtained for the rate constants using circular dichroism were in very close agreement with those obtained using HPLC (Tables I and IV), showing that the circular dichroism method is perfectly valid. The difference between the methods averaged 7% (2–12% range), which was the expected error limit with either method.

The secondary reaction especially observable at high temperatures complicated analysis of circular dichroism data for slower reactions (lower phosphate concentrations). However, this reaction is sufficiently slow and has an induction period (Fig. 4) that permits analysis of ellipticity changes at early times (40–60 min) as an uncomplicated reversible first-order process. It is valid to use early data points because it is possible to calculate expected infinity ellipticity values. The reason for this approach is that the equilibrium constant for this reaction was found to be independent of temperature (Table I), and reliable equilibrium constants can be obtained at lower temperatures where the precipitation reaction is slow.

In comparison with tetracycline epimerization, anhydrotetracycline is apparently faster by an average of 28% (Tables I, III, and V), and the energy of activation is perhaps 2 kcal/mole less than that of tetracycline when compared with reported values (2–4). Whether significant differences are present, however, is questionable because of the uncertainties in estimating energies of activation (Table II).

Just like tetracycline, phosphate catalyzes the epimerization of anhydrotetracycline (2, Fig. 9). Neither intercept obtained was significantly different from zero. These results support the hypotheses that anhydrotetracycline epimerization may be general base catalyzed and that, in the case of phosphate, the monobasic form is a likely candidate for the catalytic species.

The special role phosphate plays in these reactions is possibly a consequence of its interesting ability to act as a molecular proton conductor (Scheme II).

One interesting result of these studies and those of others (1–4) involving tetracycline is that the equilibrium favors the solution species (tetracycline or anhydrotetracycline) that would not be conformationally favored at acid pH, providing hydrogen bond formation is ignored. The results can be rationalized using the following argument.

Because of the flexible *cis*-A/B ring juncture, anhydrotetracyclines may adopt two opposite solution conformations in which both the A-ring

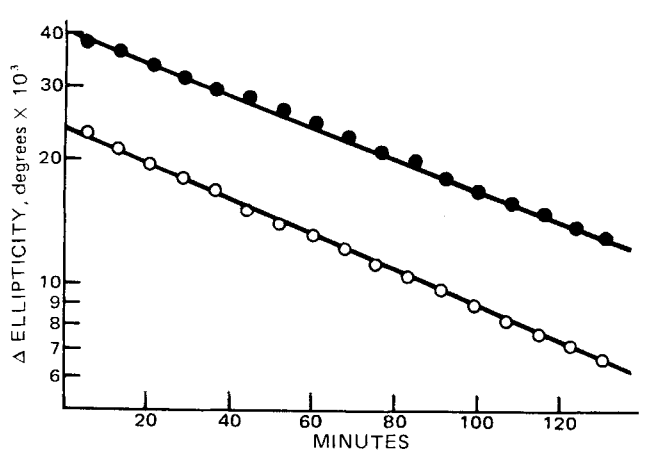

Figure 10—*Semilogarithmic plot of the difference in ellipticity (at time t and equilibrium) at 270 nm and the time using tetracycline (○) and epitetracycline (●) as the starting material. Study made at 40°, pH 4.2, and 1 M phosphate.*

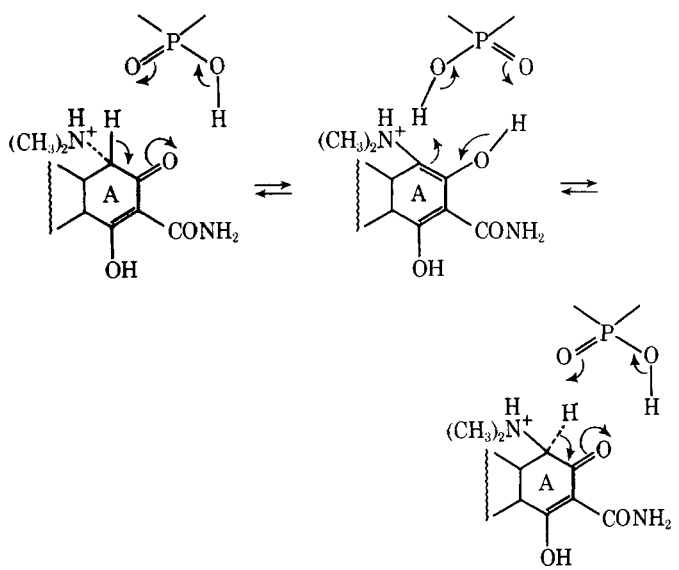

Scheme II

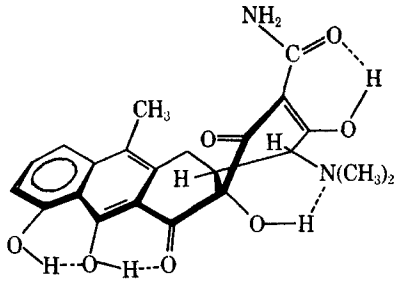

IIa

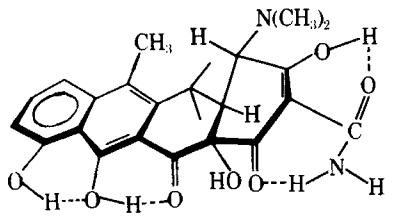

IIb

and the BCD-ring chromophores are planar and in which there is no readily apparent bond angle strain (IIa and IIb). Conformation IIa is the same as that previously assigned to the parent antibiotic, tetracycline, as fitting best the bulk of the available data collected in neutral to moderately acidic solutions (12–14). Conformation IIb is that attributed to 5,12a-diacetyloxytetracycline in the crystal (15) and to 5-hydroxytetracyclines in alkaline solutions (12–14).

Neither conformation is the same as that adopted by various tetracycline antibiotic salts, as shown by X-ray studies (16–21) and circular dichroism studies in strongly acidic solutions (12–14). Under these conditions, a twisted form of conformation IIa is favored in which the $N(CH_3)_2$ group rotates slightly away from its interaction with the 12a-OH group and toward ring B. It does not, however, go all the way to conformation IIb. The only corresponding X-ray study of an anhydrotetracycline salt showed essentially conformation IIa (22). The reason why this conformation should be favored in the crystal of anhydrotetracycline hydrobromide is not readily apparent, because it is the only member of this family that clearly has conformation IIa.

In fact, conformation IIb would appear to be intuitively more satisfactory based on relief of the C-4–C-12a interaction and the resulting equatorial orientation of the dimethylamino group. Other independent evidence, however, rules this out. Dimethyl sulfoxide-d_6 solutions of various anhydrotetracyclines show a small H-4–H-4a coupling constant (5 Hz), which is consistent with conformation IIa or the twisted tetracycline conformation but not with conformation IIb. The circular dichroism spectra of anhydrotetracycline in aqueous methanol solutions at various pH's (Fig. 11) show that there is no dramatic conformational change below pH 7 and can be rationalized best by invoking either conformation IIa or, better, the twist form (16–21). The situation differs somewhat with 4-epianhydrotetracycline. The PMR spectrum of chelocardin (23), for example, shows a small (4.5 Hz) coupling constant.

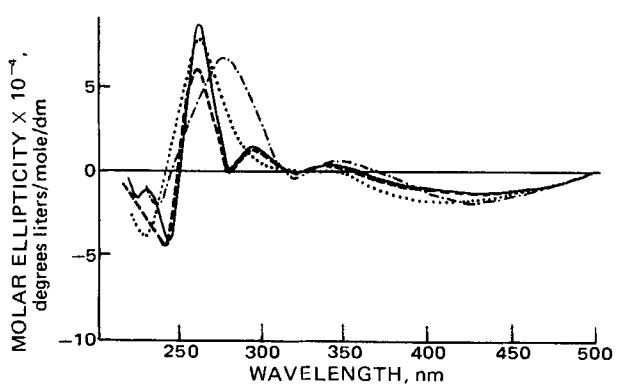

Figure 11—*Molar ellipticity of anhydrotetracycline as a function of wavelength at various pH values. Key: —, 1.0; - - -, 3.25; . . . . , 7.25; and . - . - ., 9.25.*

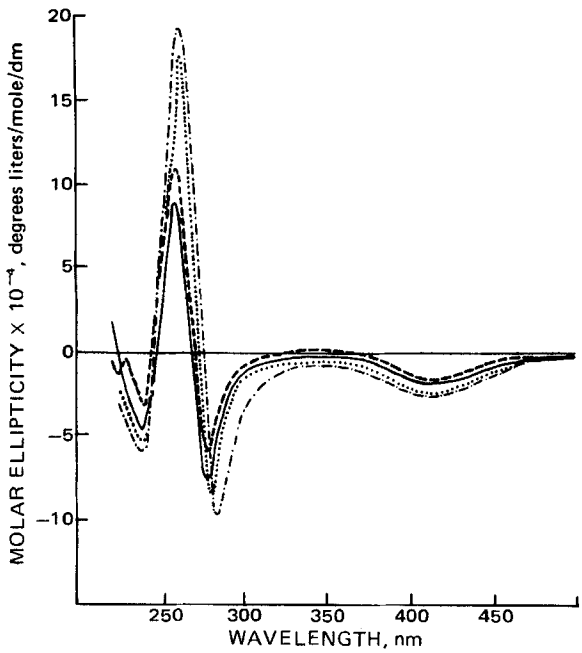

Figure 12—*Molar ellipticity of epianhydrotetracycline as a function of wavelength at various pH values. Key: —, 1.0; - - -, 3.25, ... , 7.25; and . - . - ., 9.25.*

However, either conformation IIa or IIb gives an intermediate sized J value, so PMR measurements of this type do not help.

The circular dichroism spectra of 4-epianhydrotetracycline do not change significantly with rising pH (Fig. 12), indicating a stable conformation, but differ significantly from that of anhydrotetracycline itself under the same conditions. In particular, at all pH levels measured, strong exciton coupling is evident (24, 25). This finding would be expected with conformation IIa, in which the A-ring chromophore is very close in space to the BCD chromophore so that such coupling is possible. Furthermore, the A-ring peak (λ_{max} 275 nm) is of the correct energy content to couple with the middle BCD-ring transition occurring at about the same wavelength. Such circular dichroism bands characteristically are biphasic and bilaterally symmetrical about the zero ellipticity line and have their amplitude median at approximately the same wavelength as the UV transition from which they are derived. Deviation from ideality is expected when they are superimposed on a noncoupled band.

Inspection of Fig. 12 shows that these relationships are obeyed and that the peaks in question are those at approximately 255 and 285 nm. Lack of such coupling with anhydrotetracycline is strong evidence for different conformations for the two series. Conformation IIb would be expected to allow exciton coupling also but with opposite signs. This lack, along with the other data described, suggests that anhydrotetracyclines possess the twist tetracycline conformation (16–21) in which the chromophores are fixed farther apart in space.

With anhydrotetracycline and 4-epianhydrotetracycline apparently possessing different ground-state conformations, the kinetic expression should ultimately contain contributions from conformational as well as configurational components. This situation involves a balance of subtle factors of presently indeterminable magnitude.

These two conformations allow an acceptable rationale for the long known, but unexplained, observation that the 4-epi series are stronger bases than the naturally occurring series (26). Intramolecular hydrogen bonding in the natural series would reduce the external availability of

Table V—Rate Constants for the C-4 Epimerization of Tetracycline in Phosphate at pH 4.2

Buffer Concentration, M	Temperature	Forward Rate Constant, hr^{-1} ± Average Error[a]	Reverse Rate Constant, hr^{-1} ± Average Error[a]
0.1	60°	0.311 ± 0.008[b]	0.508 ± 0.013[b]
1	40°	0.216 ± 0.012[c]	0.352 ± 0.019[c]

[a] Calculated as the root mean square. [b] Average of two values. [c] Average of three values.

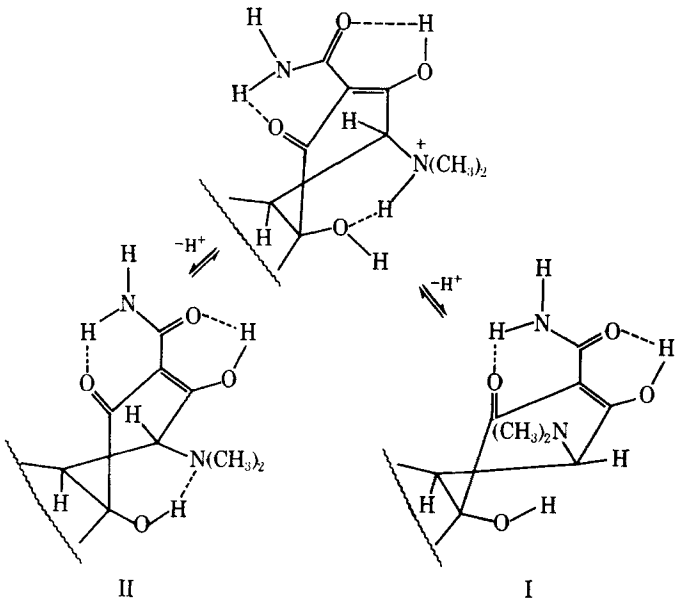

Scheme III

the lone-pair electrons of the $N(CH_3)_2$ group to acids. It may be presumed that the molecule gains sufficient stabilization from this effect to overcome in part the destabilization induced by 1,3-diaxial steric bulk interactions, and this stabilization explains the small but definite preference for the natural configuration when at equilibrium (Scheme III). The picture is, however, somewhat further complicated by the superposition of a conformational equilibrium, since the two epimers do not have the same ground-state conformation.

REFERENCES

(1) J. R. D. McCormick, S. M. Fox, L. L. Smith, B. A. Bitler, J. Reichenthal, V. E. Origoni, W. H. Muller, R. Winterbottom, and A. P. Doerschuk, *J. Am. Chem. Soc.*, **79,** 2849 (1957).

(2) E. G. Remmers, G. M. Sieger, and A. P. Doerschuk, *J. Pharm. Sci.*, **52,** 752 (1963).

(3) D. A. Hussar, P. J. Niebergall, E. T. Sugita, and J. T. Doluisio, *J. Pharm. Pharmacol.*, **20,** 239 (1968).

(4) K. D. Schlecht and C. W. Frank, *J. Pharm. Sci.*, **62,** 258 (1973).

(5) H. J. Pryves, M.S. thesis, Columbia University, New York, N.Y., 1957.

(6) B. Hoener, T. D. Sokoloski, L. A. Mitscher, and L. Malspeis, *J. Pharm. Sci.*, **63,** 1901 (1974).

(7) K. D. Schlecht and C. W. Frank, *ibid.*, **64,** 352 (1975).

(8) A. G. Butterfield, D. W. Hughes, N. J. Pound, and W. L. Wilson, *Antimicrob. Ag. Chemother.*, **4,** 11 (1973).

(9) K. T. Tsuji, J. H. Robertson, and W. F. Beyer, *Anal. Chem.*, **46,** 593 (1974).

(10) A. G. Butterfield, D. W. Hughes, W. L. Wilson, and N. J. Pound, *J. Pharm. Sci.*, **64,** 316 (1975).

(11) K. Tsuji and J. H. Robertson, *ibid.*, **65,** 400 (1976).

(12) R. F. Miller, T. D. Sokoloski, L. A. Mitscher, A. C. Bonacci, and B. Hoener, *ibid.*, **62,** 1143 (1973).

(13) L. A. Mitscher, A. C. Bonacci, B. Slater-Eng, A. K. Hacker, and T. D. Sokoloski, *Antimicrob. Ag. Chemother.*, **1969,** 111.

(14) L. A. Mitscher, B. Slater-Eng, and T. D. Sokoloski, *ibid.*, **2,** 66 (1972).

(15) R. B. VonDreele and R. E. Hughes, *J. Am. Chem. Soc.*, **93,** 7290 (1971).

(16) J. Donahue, J. D. Dunitz, K. N. Trueblood, and M. S. Webster, *ibid.*, **85,** 851 (1963).

(17) Y. Takeuchi and M. J. Buerger, *Proc. Natl. Acad. Sci. USA*, **46,** 1366 (1960).

(18) S. Hirokawa, Y. Okaya, F. M. Lovell, and R. Pepinsky, *Acta Crystallogr.*, **12,** 811 (1959).

(19) S. Hirokawa, Y. Okaya, F. M. Lovell, and R. Pepinsky, *Z. Kristallogr.*, **112,** 439 (1959).

(20) H. Cid-Dresdner, *ibid.*, **121,** 170 (1965).

(21) K. Kamiya, M. Asai, Y. Wada, and M. Nishikawa, *Experientia*, **27,** 363 (1971).

(22) R. Restivo and G. J. Palantik, *Biochem. Biophys. Res. Commun.*, **36,** 621 (1969).

(23) L. A. Mitscher, J. V. Juvarkar, W. Rosenbrook, Jr., W. W. Andres, J. Schenck, and R. S. Egan, *J. Am. Chem. Soc.*, **92,** 6070 (1970).

(24) A. D. Buckingham and P. J. Stiles, *Acc. Chem. Res.*, **7,** 258 (1974).

(25) N. Harada and K. Nakanishi, *ibid.*, **5,** 257 (1972).

(26) N. E. Rigler, S. P. Bag, D. E. Leyden, J. L. Sudmeier, and C. N. Reilley, *Anal. Chem.*, **37,** 872 (1975).

ACKNOWLEDGMENTS AND ADDRESSES

Received May 28, 1976, from the *College of Pharmacy, Ohio State University, Columbus, OH 43210.*

Accepted for publication September 21, 1976.

Supported by Research Grant 5R01-FD-00689-02 from the Food and Drug Administration, U.S. Department of Health, Education, and Welfare, Rockville, MD 20852, and by Pfizer Inc., Groton, CT 06340.

* Present address: Department of Medicinal Chemistry, University of Kansas, Lawrence, KS 66044.

‡ Present address: School of Pharmacy, University of California, San Francisco, CA 94143.

ˣ To whom inquiries should be directed.

GLC Determination of Free and Conjugated Triclosan in Human Plasma and Urine

ANTOINE SIOUFI ˣ, FRANÇOISE CAUDAL, and DANIELLE GRIMAULT

Abstract □ A method for the determination of free and conjugated triclosan at concentrations as low as 2 ng/ml in human plasma or urine is described. Conjugated metabolites are split by enzyme hydrolysis. After addition of an internal standard, triclosan is extracted at acid pH into petroleum ether, transferred to an alkaline aqueous solution, and back-extracted into petroleum ether after acidification. Both compounds are acetylated with acetic anhydride in the presence of pyridine. The acetyl derivatives are determined by GLC using a ^{63}Ni-electron-capture detector.

Keyphrases □ Triclosan—GLC analysis, free and conjugated, human plasma and urine □ GLC—analysis, free and conjugated triclosan, human plasma and urine □ Disinfectants—triclosan, free and conjugated, GLC analysis, human plasma and urine

Triclosan[1] [5-chloro-2-(2,4-dichlorophenoxy)phenol] (I) is a bacteriostatic agent. Radiolabeled triclosan was used to study its percutaneous absorption and metabolic fate in humans and animals (1). A GLC technique quantitatively determined free and conjugated triclosan in whole blood without an internal standard (2).

This paper describes an improved procedure for the GLC determination of free and conjugated triclosan in plasma and urine, at concentrations as low as 2 ng/ml, using 5-bromo-2-(2,4-dichlorophenoxy)phenol (II) as an internal standard. β-Glucuronidase is used for the specific determination of the glucuronide; enzymatic hydrolysis with a mixture of β-glucuronidase and sulfatase is preferred to acid hydrolysis for the determination of total (free plus conjugated) triclosan.

EXPERIMENTAL

Reagents—The acetate buffer was prepared by adding 4.8 ml of 0.2 *M* acetic acid to 35.2 ml of 0.2 *M* sodium acetate. Acetic anhydride was purified before use by adding 20 g of sodium acetate to 100 ml of acetic anhydride and boiling under reflux for 15 min. Then acetic anhydride was distilled and collected between 135 and 140°.

Pyridine was distilled at 115–116° with potassium hydroxide pellets and stored over potassium hydroxide pellets. β-Glucuronidase was bacterial β-glucuronidase[2] containing about 47,000 units/g. The mixture of β-glucuronidase and aryl sulfatase[3] contained about 5 and 8 units/ml, respectively. All other reagents were analytical grade[4,5].

Test solutions of acetyl derivatives of both triclosan and internal standard were prepared according to the procedure described under *Acetylation and GLC*. The petroleum ether solution, containing 200 μg of each derivative, was applied as a stripe on a TLC plate (silica gel with fluorescent indicator) to separate and eliminate underivatized triclosan and the internal standard from their acetyl derivatives. The plate was developed with benzene–toluene–formic acid–methanol (50:50:5:10 v/v).

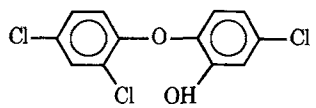

I

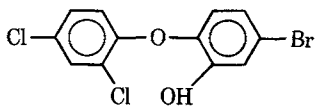

II

[1] Irgasan DP 300, Ciba-Geigy.
[2] Sigma Type 2.
[3] Calbiochem.
[4] Mallinckrodt.
[5] Merck A.G.

Table I—Precision and Accuracy of the Assay Applied to Spiked Human Plasma Samples

Amount Added, ng/ml	Amount Found, Average of Five Assays, ng/ml	95% Confidence Interval	*SE*, %
2	2.6	2.3–3.0	4.9
5	4.7	3.7–5.6	6.5
20	19	16–22	5.0
50	50	48–52	1.4
200	200[a]	194–205	1.0
500	500	488–512	0.8
1000	998	970–1026	1.0
3000	3087	2870–3303	2.5
6000	5961	5729–6192	1.4

[a] Four assays only.

Table II—Free Triclosan in Urine (Percent of Administered Dose)

Hours	Isotope Dilution Analysis	GLC
0–8	0.08	0.05
8–24	0.60	0.56
24–48	0.09	0.10
48–72	0.03	0.02

After the addition of 2 *N* HCl, the derivative was eluted into petroleum ether.

The 1 *N* sodium hydroxide internal standard solution contained 500 ng of II/ml.

Materials—The glassware was dried at 100° and immersed for 0.5 hr in an ultrasonic bath, first in water and then in methanol.

The gas chromatograph[6] was equipped with a linear 15-mCi ^{63}Ni-electron-capture detector[7]. The peak areas were given by an electronic integrator[8]. The operating temperatures were: column, 200°; injector, 230°; and detector, 290°. The argon–methane (90:10) flow rate was 60 ml/min.

Glass columns were washed with 1 *N* hydrochloric acid, distilled water, acetone, and benzene and then silanized with a 1% (v/v) solution of hexamethyldisilazane in benzene. After this treatment, the columns were washed again with benzene and dried at 100°.

The column packing was 2% OV 1[9]–2% QF 1[9] on 80–100-mesh Chromosorb W HP[9]. The filled column was flushed with the carrier gas at 50° for 30 min, then gradually heated to 240° at a rate of 1°/min with a flow rate of 30 ml/min, and kept at 245° for 3 days.

Triclosan Glucuronide Enzyme Hydrolysis—Aliquots of 1 ml of plasma or urine, 1 ml of pH 5.5 acetate buffer, and 10 mg of β-glucuronidase were incubated for 1 hr at 38°. Distilled water, 1 ml, was then added, and extraction was performed as described under *Extraction*.

Triclosan Glucuronide and Sulfate Enzyme Hydrolysis in Plasma—A 1-ml aliquot of plasma, 1 ml of distilled water, and 0.5 ml of β-glucuronidase–sulfatase mixture, diluted with pH 5.5 acetate buffer (1:10 v/v), were incubated for 15 hr at 38°. Distilled water, 0.5 ml, was then added, and extraction was performed as described under *Extraction*.

Triclosan Conjugates Acid Hydrolysis—Aliquots of 1 ml of plasma or urine and 3 ml of concentrated hydrochloric acid were heated for 1 hr at 100°. Then extraction was performed as described under *Extraction*.

Extraction—A 1-ml aliquot of the internal standard solution was

[6] Hewlett-Packard 5710 A.
[7] Hewlett-Packard 18713 A.
[8] Infotronics.
[9] Applied Science Laboratories.

Table III—Free and Conjugated Triclosan in Urine (Percent of Administered Dose)

Hours	Total Radioactivity	Hydrolysis with β-Glucuronidase: Isotope Dilution Analysis	Hydrolysis with β-Glucuronidase: GLC	Hydrolysis with Hydrochloric Acid: Isotope Dilution Analysis	Hydrolysis with Hydrochloric Acid: GLC
0–8	23.78	23.75	29.80	24.02	24.92
8–24	15.82	14.18	12.82	14.30	12.96
24–48	11.24	9.67	9.66	9.92	9.68
48–72	3.57	2.69	2.78	2.35	3.03

measured into a stoppered glass tube. Then 1 ml of the sample, 2 ml of distilled water, 500 mg of anhydrous sodium sulfate, and 1 ml of concentrated formic acid were added. This solution was mixed thoroughly[10], and the pH was checked (it must be 1–2).

Petroleum ether, 3 ml, was added, and the tube was shaken mechanically for 5 min and centrifuged at 5000 rpm for 5 min.

An aliquot volume of the petroleum ether extract was transferred to another 10-ml tube, and 3 ml of 1 *N* sodium hydroxide was added. The tube was shaken for 5 min and centrifuged for 3 min at 4000 rpm. The petroleum ether phase was separated and discarded. In the same tube, 2 ml of 2 *N* hydrochloric acid and 3 ml of petroleum ether were added to the sodium hydroxide phase. The tube was shaken for 5 min and centrifuged for 3 min at 4000 rpm.

An aliquot volume of the petroleum ether phase was transferred to another tube and taken to dryness under a nitrogen stream in a water bath at 37°.

Acetylation and GLC—To the dry residue were added 100 μl of acetic anhydride and 10 μl of pyridine. After mixing, the tube was allowed to stand for 15 min at room temperature. Then excess reagent was removed by evaporation to dryness at 37° under a gentle nitrogen stream; 500 μl of petroleum ether was added, and the tube was shaken on a mixer.

A 3-μl portion of the petroleum ether solution was injected into the gas chromatograph using the solvent-flush technique. The triclosan content was calculated from the peak area ratio by reference to a calibration curve, prepared from a series of 1 *N* sodium hydroxide–triclosan solutions added to plasma to yield concentrations between 2 and 50, 50 and 500, or 500 and 6000 ng/ml, depending on the concentration range studied.

Human Experiments—*Experiment 1*—One healthy volunteer was given a single oral dose of 203.57 mg of ^{14}C-triclosan (100.15 μCi) in a gelatin capsule. Heparinized blood samples were drawn 2, 4, 8, and 24 hr after treatment and centrifuged immediately. Plasma was collected and stored at −20° until analysis. Urine was collected after treatment as follows: 0–8, 8–24, 24–48, and 48–72 hr.

Experiment 2—Two healthy volunteers were each given a single oral dose of 25 mg of triclosan in a cachet. Blood was collected 2, 4, 6, and 8 hr after administration.

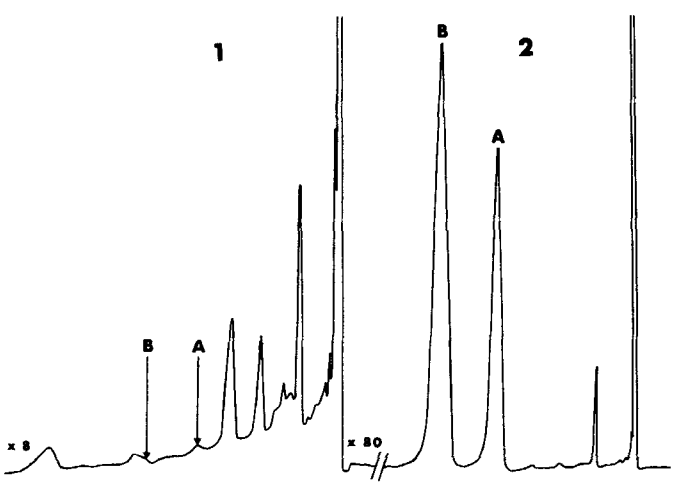

Figure 1—*Examples of chromatograms of human plasma blank (1) and 500 ng/ml of triclosan (A) and internal standard (B) in human plasma (2).*

[10] Vortex mixer.

RESULTS AND DISCUSSION

Analytical Yield—The duration of the acetylation reaction was varied from 5 to 30 min. A maximum was reached after 15 min.

The overall analytical yield was determined by comparing samples spiked with known amounts of triclosan and internal standard with corresponding extracts to which known amounts of the two acetyl derivatives had been added just before injection. The average yields (±*SE*) of five assays were 59.6 ± 6.0% for triclosan and 77.0 ± 4.5% for the internal standard in plasma and 65.2 ± 4.0% for triclosan and 77.2 ± 4.7% for the internal standard in urine.

Sensitivity and Accuracy—Table I gives the results obtained with spiked plasma samples in the concentration range of 2–6000 ng/ml. The 95% confidence intervals were calculated for five replicate analyses on each sample. The lower concentration may be taken as the sensitivity limit of the assay, although even lower concentrations could be detected.

Plasma or Urine Interference—Figure 1 shows the chromatograms of a blank human plasma extract and of plasma spiked with 500 ng of both triclosan and internal standard. No interference of the normal plasma components was recorded. Urine contained fewer detectable substances. Enzyme or acid hydrolysis did not change the chromatograms.

Specificity—Since the metabolism of triclosan has not been fully elucidated, the specificity of the assay was tested by comparing GLC with isotope dilution analysis after administration of the ^{14}C-labeled drug.

In urine, there was a satisfactory agreement between the two techniques for free (Table II) and free plus conjugated triclosan (Table III). The conjugate present in urine was entirely a glucuronide, as shown by the similar results obtained by acid and β-glucuronidase hydrolysis.

In plasma, a first experiment (Table IV) showed a large difference between these two types of hydrolysis. After β-glucuronidase hydrolysis,

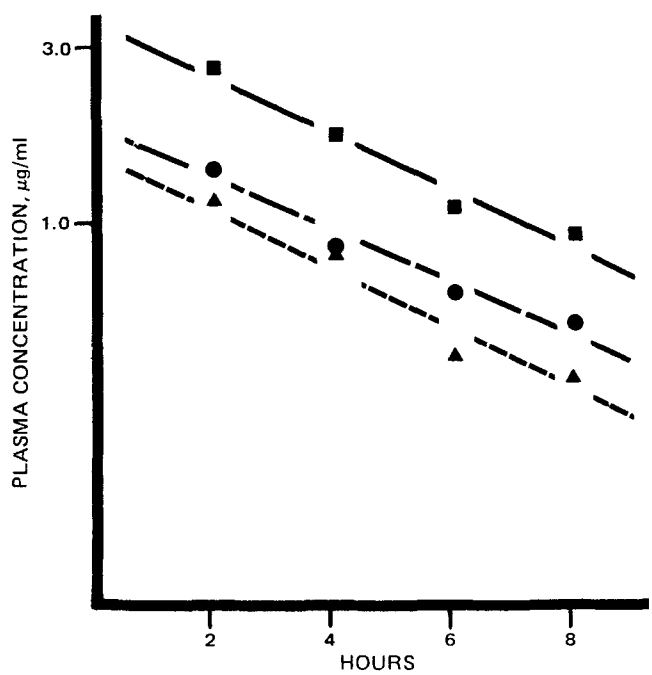

Figure 2—*Plasma concentrations of triclosan conjugated metabolites after oral administration of 25 mg of triclosan. Key: ▲, glucuronide; ■, glucuronide plus sulfate; and ●, sulfate (by difference).*

Table IV—Free and Conjugated Triclosan (Micrograms per Milliliter) in Plasma after Human Experiment 1

Hours	Total Radioactivity	Hydrolysis with β-Glucuronidase: Isotope Dilution Analysis	Hydrolysis with β-Glucuronidase: GLC	Hydrolysis with Hydrochloric Acid, Isotope Dilution Analysis
2	1.11	0.56	0.56	1.00
4	10.54	4.70	6.02	8.32
8	8.28	2.73	3.85	7.05
24	2.45	1.13	1.32	1.97

however, GLC and isotope dilution analysis gave comparable results. The conjugate present in plasma was only partly a glucuronide.

A second experiment (Table V) demonstrated that the same results were obtained by acid hydrolysis and by treatment with β-glucuronidase and sulfatase. The second conjugate thus appeared to be a sulfate.

Table V—Free and Conjugated Triclosan (Micrograms per Milliliter) in Plasma after Human Experiment 2

Volunteer	Hours	Hydrolysis by β-Glucuronidase: Alone	Hydrolysis by β-Glucuronidase: With Added Sulfatase	Hydrolysis by Hydrochloric Acid
1	2	1.10	2.72	2.56
	6	0.36	1.36	1.34
	8	0.28	1.14	1.12
2	2	1.18	2.62	2.46
	4	0.86	1.74	1.60
	6	0.46	1.15	1.08
	8	0.41	0.98	0.96

Hydrolysis Reproducibility—Glucuronidase-sulfatase enzyme hydrolysis gives reproducible results. Acid hydrolysis may create problems, which seem to be due to partial degradation of triclosan and the internal standard, to differing extents, during acid treatment. Therefore, enzyme hydrolysis is preferable.

Application—The technique was applied to a study of the elimination of triclosan after oral administration to human subjects (Experiment 2). The concentrations of free triclosan were extremely low. The two conjugated metabolites were eliminated at the same rate, corresponding to a half-life of about 4 hr (Fig. 2).

Conclusion—The proposed technique permits the quantitative assay of triclosan and its conjugated metabolites in human plasma and urine. It is specific, reproducible, and sufficiently sensitive for the determination of the absorption of triclosan in humans.

REFERENCES

(1) J. G. Black, D. Howes, and T. Rutherford, *Toxicology*, **3**, 33 (1975).

(2) J. Schulze, F. H. Marcquardt, F. Lyman, and C. Spitzer, *J. Am. Oil Chem. Soc.*, **52**, 215 (1975).

ACKNOWLEDGMENTS AND ADDRESSES

Received August 13, 1976, from *Ciba-Geigy Biopharmaceutical Research Center, B.P. 130, 92505 Rueil-Malmaison, France.*

Accepted for publication September 29, 1976.

The authors thank Dr. H. Stierlin and Dr. J. W. Faigle (Pharmacological Chemistry Department, Ciba-Geigy, Basel, Switzerland) for performing the isotope dilution analysis and for helpful discussions about the metabolism of triclosan. The authors are also grateful to Dr. W. Theobald (Medical Department, Ciba-Geigy, Basel, Switzerland) for the clinical trials.

[x] To whom inquiries should be directed.

Fluorometric Determination of Nadolol in Human Serum and Urine

EUGENE IVASHKIV

Abstract □ To determine nadolol, a new β-adrenergic blocking agent, in serum and urine, the drug is extracted into *n*-butyl acetate or ether from alkaline potassium chloride saturated samples. After back-extraction into 0.1 *N* HCl, the drug is oxidized with periodic acid; the resulting aldehyde is coupled with *o*-phenylenediamine to produce a fluorescent compound. The method can measure as little as 0.01 μg of nadolol/sample.

Keyphrases □ Nadolol—fluorometric analysis, human serum and urine □ Fluorometry—analysis, nadolol in human serum and urine □ Antiadrenergics—nadolol, fluorometric analysis in human serum and urine

Nadolol (I), a new β-adrenergic blocking agent, is designated chemically as *cis*-5-[3-[(1,1-dimethylethyl)-amino]-2-hydroxypropoxy] - 1,2,3,4-tetrahydro-2,3-naphthalenediol. Its pharmacology (1–4), antiarrhythmic action (5–8), and specificity of action (9) were discussed previously.

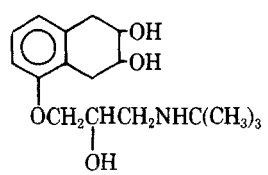

I

For measuring microgram or nanogram levels of nadolol in human urine or serum, a sensitive method is needed. This paper describes a fluorometric method based on the oxidation of the drug with periodic acid and coupling of the resulting aldehyde with *o*-phenylenediamine.

EXPERIMENTAL

Apparatus—Fluorometric measurements were made in a spectrofluorometer[1] equipped with a colored filter[2] and round microcells. Samples were shaken on a heavy-duty shaker[3]. Screw-capped, 150-mm test tubes and plastic caps with polypropylene linings[4] were washed by shaking with 20 ml of 1 *N* HCl for 1 hr, rinsed three times with tap water and three times with distilled water, and then dried.

[1] Perkin-Elmer model 204.
[2] Corning No. 3-73.
[3] Fisher Scientific.
[4] Polyseal Corp.

Table IV—Free and Conjugated Triclosan (Micrograms per Milliliter) in Plasma after Human Experiment 1

Hours	Total Radioactivity	Hydrolysis with β-Glucuronidase: Isotope Dilution Analysis	Hydrolysis with β-Glucuronidase: GLC	Hydrolysis with Hydrochloric Acid, Isotope Dilution Analysis
2	1.11	0.56	0.56	1.00
4	10.54	4.70	6.02	8.32
8	8.28	2.73	3.85	7.05
24	2.45	1.13	1.32	1.97

however, GLC and isotope dilution analysis gave comparable results. The conjugate present in plasma was only partly a glucuronide.

A second experiment (Table V) demonstrated that the same results were obtained by acid hydrolysis and by treatment with β-glucuronidase and sulfatase. The second conjugate thus appeared to be a sulfate.

Table V—Free and Conjugated Triclosan (Micrograms per Milliliter) in Plasma after Human Experiment 2

Volunteer	Hours	Hydrolysis by β-Glucuronidase: Alone	Hydrolysis by β-Glucuronidase: With Added Sulfatase	Hydrolysis by Hydrochloric Acid
1	2	1.10	2.72	2.56
	6	0.36	1.36	1.34
	8	0.28	1.14	1.12
2	2	1.18	2.62	2.46
	4	0.86	1.74	1.60
	6	0.46	1.15	1.08
	8	0.41	0.98	0.96

Hydrolysis Reproducibility—Glucuronidase-sulfatase enzyme hydrolysis gives reproducible results. Acid hydrolysis may create problems, which seem to be due to partial degradation of triclosan and the internal standard, to differing extents, during acid treatment. Therefore, enzyme hydrolysis is preferable.

Application—The technique was applied to a study of the elimination of triclosan after oral administration to human subjects (Experiment 2). The concentrations of free triclosan were extremely low. The two conjugated metabolites were eliminated at the same rate, corresponding to a half-life of about 4 hr (Fig. 2).

Conclusion—The proposed technique permits the quantitative assay of triclosan and its conjugated metabolites in human plasma and urine. It is specific, reproducible, and sufficiently sensitive for the determination of the absorption of triclosan in humans.

REFERENCES

(1) J. G. Black, D. Howes, and T. Rutherford, *Toxicology*, **3**, 33 (1975).

(2) J. Schulze, F. H. Marcquardt, F. Lyman, and C. Spitzer, *J. Am. Oil Chem. Soc.*, **52**, 215 (1975).

ACKNOWLEDGMENTS AND ADDRESSES

Received August 13, 1976, from *Ciba-Geigy Biopharmaceutical Research Center, B.P. 130, 92505 Rueil-Malmaison, France.*

Accepted for publication September 29, 1976.

The authors thank Dr. H. Stierlin and Dr. J. W. Faigle (Pharmacological Chemistry Department, Ciba-Geigy, Basel, Switzerland) for performing the isotope dilution analysis and for helpful discussions about the metabolism of triclosan. The authors are also grateful to Dr. W. Theobald (Medical Department, Ciba-Geigy, Basel, Switzerland) for the clinical trials.

[x] To whom inquiries should be directed.

Fluorometric Determination of Nadolol in Human Serum and Urine

EUGENE IVASHKIV

Abstract □ To determine nadolol, a new β-adrenergic blocking agent, in serum and urine, the drug is extracted into *n*-butyl acetate or ether from alkaline potassium chloride saturated samples. After back-extraction into 0.1 *N* HCl, the drug is oxidized with periodic acid; the resulting aldehyde is coupled with *o*-phenylenediamine to produce a fluorescent compound. The method can measure as little as 0.01 μg of nadolol/sample.

Keyphrases □ Nadolol—fluorometric analysis, human serum and urine □ Fluorometry—analysis, nadolol in human serum and urine □ Antiadrenergics—nadolol, fluorometric analysis in human serum and urine

Nadolol (I), a new β-adrenergic blocking agent, is designated chemically as *cis*-5-[3-[(1,1-dimethylethyl)-amino]-2-hydroxypropoxy] - 1,2,3,4-tetrahydro-2,3-naphthalenediol. Its pharmacology (1–4), antiarrhythmic action (5–8), and specificity of action (9) were discussed previously.

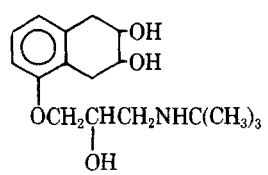

I

For measuring microgram or nanogram levels of nadolol in human urine or serum, a sensitive method is needed. This paper describes a fluorometric method based on the oxidation of the drug with periodic acid and coupling of the resulting aldehyde with *o*-phenylenediamine.

EXPERIMENTAL

Apparatus—Fluorometric measurements were made in a spectrofluorometer[1] equipped with a colored filter[2] and round microcells. Samples were shaken on a heavy-duty shaker[3]. Screw-capped, 150-mm test tubes and plastic caps with polypropylene linings[4] were washed by shaking with 20 ml of 1 *N* HCl for 1 hr, rinsed three times with tap water and three times with distilled water, and then dried.

[1] Perkin-Elmer model 204.
[2] Corning No. 3-73.
[3] Fisher Scientific.
[4] Polyseal Corp.

All pipets and volumetric flasks were soaked in 3 *N* HCl overnight and rinsed with tap and distilled water. A centrifuge[5] with stainless steel adapters was used. Reagents were added with automatic pipets[6].

Reagents—Specially purified sodium hydroxide[7] and potassium chloride[3] were used. One liter of *n*-butyl acetate[8] was shaken with 100 ml of pure 5 *N* NaOH, washed with distilled water, and distilled from glass. One liter of petroleum ether, bp 30–60°, was shaken with 100-ml portions of concentrated sulfuric acid until the acid layer was colorless. The petroleum ether layer was washed with distilled water and distilled from glass. Anhydrous ether[3] suitable for electronic use and microanalysis was used without purification. Two liters of acetic acid was refluxed with 10 g of 2,4-dinitrophenylhydrazine for 1 hr and distilled from glass.

o-Phenylenediamine dihydrochloride[8], 20 mg, was dissolved in 1 ml of 0.1 *N* HCl, and 0.3 ml was immediately diluted to 30 ml with redistilled acetic acid. This reagent was used within 30 min. A 10-ml aliquot of 1% sodium metaperiodate[3] was prepared in 0.1 *N* HCl. Sodium arsenite[3] was prepared by dissolving 0.4 g in 9 ml of 0.1 *N* HCl and adding 1 ml of concentrated hydrochloric acid. All three reagents were prepared daily.

A nadolol stock standard solution at 500 μg/ml was prepared in 0.1 *N* HCl and kept in a refrigerator no longer than 3 months. Working standards were prepared daily by the dilution of the stock standard solution with 0.1 *N* HCl to 0.02, 0.1, 0.150, and 1.0 μg/ml.

Extraction—*Urine*—Thaw urine samples at temperatures below 25°. Mix the thawed urine samples well and then centrifuge at about 3000 rpm for 5 min. Transfer 1.0 ml of the urine sample to a 150-mm screw-capped test tube containing 4 ml of 0.1 *N* HCl. Pipet 5.0 ml of 0.1 *N* HCl (reagent blank) and 5.0 ml of diluted standards at 0.150 and 1.0 μg/ml into 150-mm screw-capped test tubes.

To each tube, add 3 g of potassium chloride and 2 ml of pure 5 *N* NaOH. Cover the tubes with clean plastic caps and shake mechanically for 5 min[9]. Then pipet 10.0 ml of absolute ether into each tube. Cover the tubes with plastic caps, shake for 5 min, and centrifuge at about 3000 rpm for 5 min.

Serum—Thaw serum samples at temperatures below 25°. Pipet 5.0 ml of 0.1 *N* HCl (reagent blank), 5.0 ml of the diluted standards at 0.02 and 0.1 μg/ml, and 5 ml of mixed serum samples into clean 150-mm screw-capped test tubes. To each tube, add 3 g of potassium chloride and 2 ml of pure 5 *N* NaOH. Cover the tubes with clean plastic caps and shake for 5 min[9]. Then pipet 10.0 ml of purified redistilled *n*-butyl acetate into each tube. Without mixing, cover the tubes with plastic caps. Shake the tubes for 5 min and immediately centrifuge at about 3000 rpm for 5 min[10].

Back-Extraction and Purification—By means of a pipet filler[11], transfer 8.0 ml of the top *n*-butyl acetate or ether layer to a clean 150-mm screw-capped test tube containing 1.50 ml of 0.1 *N* HCl and 20 ml of redistilled petroleum ether. Shake the tubes for 5 min and centrifuge at about 3000 rpm for 5 min.

Hold the tubes against a white background and aspirate and discard the top solvent layer. Add 10 ml of purified petroleum ether and shake the tubes for 2 min. Centrifuge the tubes at about 3000 rpm for 2 min. Aspirate completely and discard the top petroleum ether layer[12].

Reaction—With an automatic syringe, add 0.10 ml of sodium periodate to each tube and mix well on a vortex mixer. Centrifuge the tubes at about 3000 rpm for 2 min. Fifteen minutes after the last tube was mixed, add 0.20 ml of sodium arsenite with an automatic syringe and mix well on the vortex mixer. Centrifuge the tubes at about 3000 rpm for 2 min. Five minutes after the last tube was mixed, add 1.0 ml of *o*-phenylenediamine solution with an automatic syringe and mix well on the vortex mixer. Centrifuge the tubes at about 3000 rpm for 2 min. Keep the tubes in the dark. Thirty minutes after the last tube was mixed, measure the fluorescence of samples and standards.

Fluorescence Measurement—Set the excitation wavelength at 305 nm and the fluorescence wavelength at 445 nm. Insert the filter[2] in the fluorescence optical path between the cell compartment and the detector[13].

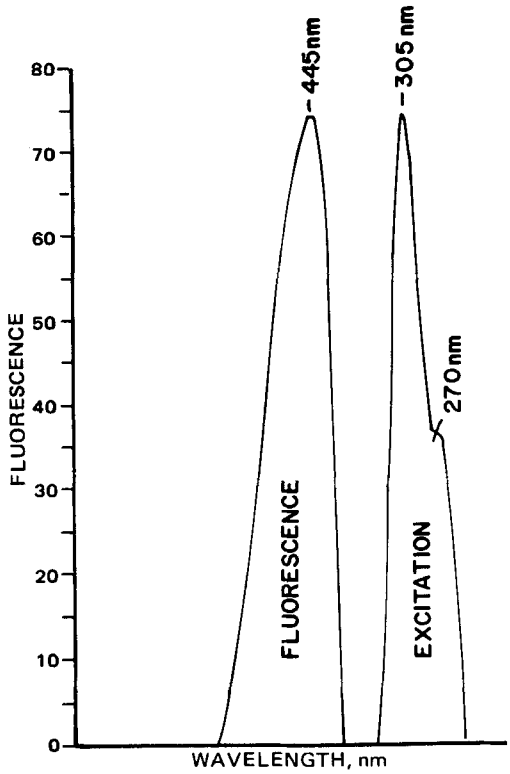

Figure 1—*Excitation and fluorescence spectra of 200 ng of oxidized nadolol.*

The concentration of nadolol per milliliter of urine or serum is calculated from the concentration and fluorescence of a nadolol standard with the same instrument settings used for the sample and standard measurements.

RESULTS AND DISCUSSION

Nadolol has no native fluorescence and has a very low absorption in the UV region. Fluorescence of nadolol at 400 nm and excitation at 260 nm can be induced by heating samples at 100° in concentrated sulfuric acid. Because of interferences and variations in fluorescence, the method cannot be used for serum and urine level assays of nadolol.

Since nadolol has adjacent hydroxyl groups in the saturated ring and hydroxyl and amino groups in the side chain, oxidation of the molecule with periodate appeared to be a convenient analytical approach. Malaprade (10) introduced periodic acid as a reagent for the oxidation of 1,2-glycols. Its use in structure determinations and as a selective analytical reagent was reviewed (11–13).

Apparently, only the saturated ring with two adjacent hydroxyl groups is oxidized with periodate. If the side chain of the drug is oxidized, formaldehyde and *tert*-butylamine would form. Neither of these compounds was detected by qualitative color testing of a nadolol solution after periodate oxidation. The chromotropic acid test for formaldehyde was negative, as was a succinaldehyde test for *tert*-butylamine. Propranolol, which differs in the side chain from nadolol only by a methyl group, does not produce a secondary amine and aldehyde after oxidation.

To prove that the saturated ring of nadolol was oxidized with periodate, *cis*-5,6,7,8-tetrahydro-1,6,7-naphthalenetriol (II) was treated with the reagent. Both nadolol and II gave a red color with phenylhydrazine and potassium ferricyanide after periodate oxidation. The oxidized II did not fluoresce when coupled with *o*-phenylenediamine, indicating that the side chain of nadolol is a prerequisite for the compound to fluoresce.

On the basis of these experiments, one can postulate that the side chain of nadolol is not oxidized with periodate. Chafetz (14) stated that compounds having the bulky *tert*-butyl substituent on the amine function are not affected by periodate even under vigorous reaction conditions.

[5] International IEP 2741, Scientific Products Co.
[6] Finnpipettes, Markson Science Co.
[7] Aristar, BDH Chemicals Ltd.
[8] Eastman.
[9] After sodium hydroxide is added, the samples must be extracted immediately to prevent any decomposition in the strong alkaline medium at room temperature.
[10] If the tubes are not centrifuged immediately after shaking, an emulsion forms which is difficult to break. Therefore, two centrifuges are needed when 21 serum samples are analyzed at one time. If an emulsion is formed, mix the top *n*-butyl acetate layer and the middle interface layer with a spatula and centrifuge the tubes again for 10 min.
[11] Spectronics Corp.
[12] The capillary pipet of the aspirator must always be kept above the aqueous layer to prevent aspiration of that layer.
[13] The maximum excitation or fluorescence wavelengths can vary. Therefore, it is recommended to check the maximum wavelengths by using a standard.

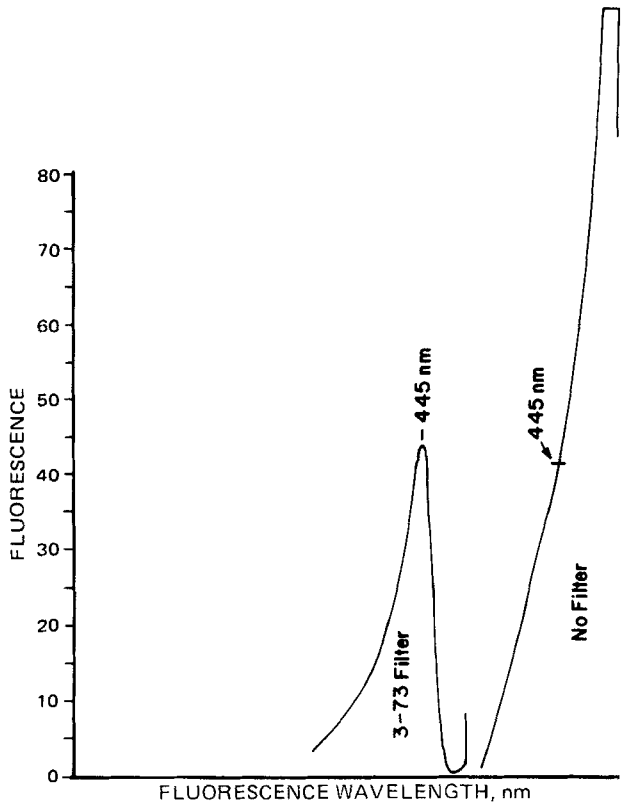

Figure 2—*Resolution of the fluorescence spectrum with a filter at a low concentration of nadolol.*

Excess periodate is used for effective and complete cleavage of the carbon–carbon bond between the two hydroxyl groups on the nadolol ring. For example, 0.1 mg of sodium periodate produced only 70% of the product when 0.5 μg of nadolol was oxidized. The maximum oxidation product was obtained when 0.3–2 mg of sodium periodate/0.50 μg of nadolol was used. Amounts of sodium periodate larger than 2 mg/tube produced lower fluorescence. At least 3 min was needed for a complete reaction. Oxidation of nadolol with periodate at 50° was faster than at room temperature, but the same amount of a product was obtained at both temperatures. The oxidized nadolol is stable in the solution for at least 4 hr.

Nadolol was oxidized in solutions ranging in pH from 0.1 to 10 (in increments of 1 pH unit or less) and in 0.1 *N* NaOH. The same oxidation rate and the same amount of product were obtained in all solutions, except sodium hydroxide. The oxidation rate in 0.1 *N* NaOH was rapid, and the oxidation product decomposed. After 1 hr of oxidation, about 10% of the expected fluorescence was obtained.

Excess periodate and iodate formed in the oxidation interfere in the coupling of the aldehyde with *o*-phenylenediamine. On the addition of *o*-phenylenediamine to the reaction mixture, a red color develops since *o*-phenylenediamine reacts with periodate and iodate. This color formation can be overcome by the addition of sodium arsenite before the addition of *o*-phenylenediamine. At least 0.05 ml of 4% sodium arsenite is needed per 0.1 ml of 1% sodium metaperiodate. The amount of hydrochloric acid present in the reaction mixture is important for successful elimination of the periodate, iodate, and iodine. At low concentrations of hydrochloric acid, the reactions are slow and sometimes do not go to completion. It takes about 3 min to destroy the excess periodate. The oxidation product in such solutions is stable at room temperature for at least 4 hr.

Fluorometric methods customarily used for quantitation of aliphatic aldehydes involve several reagents such as acetylacetone (15), ammonia (15), 6-amino-1-naphthol-3-sulfonic acid (16), dimedone (17), 4,4′-sulfonyldianiline (18), 4-aminobenzoic acid or its ethyl ester (18), 4-aminoacetophenone (18), *o*-phenylenediamine (19), and 3,5-diaminobenzoic acid (20). Synthesis of fluorescent compounds of numerous substituted quinoxalines was originally reported by Hinsberg (21), who used both 3,4-diaminotoluene and *o*-phenylenediamine as reagents. The condensation reactions of *o*-phenylenediamine with carbonyl compounds and the analytical use of these reactions were reviewed (22). Fluorometric methods for aldehydes were reviewed by Pesez and Bartos (23).

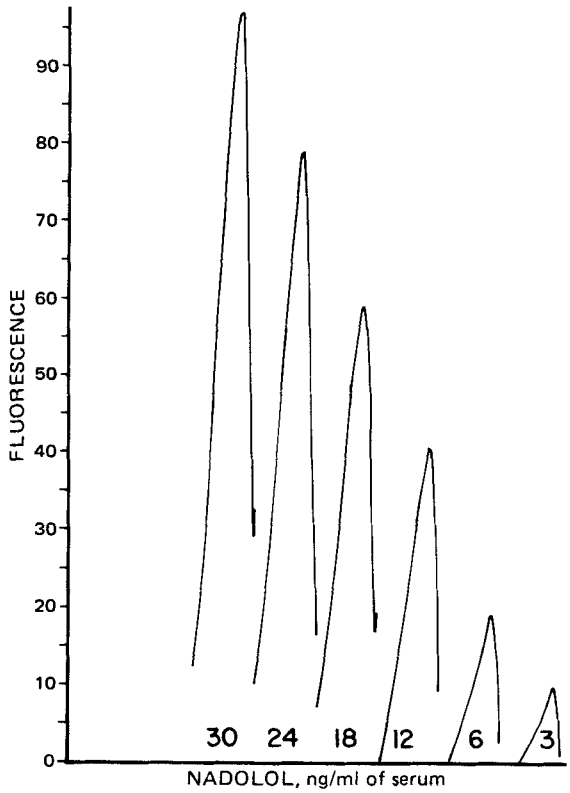

Figure 3—*Fluorescence spectrum at different concentrations of nadolol.*

Condensation of oxidized nadolol (I*a*) with *o*-phenylenediamine (III) in an acid medium probably takes place according to Scheme I. Excess III is needed for successful coupling with oxidized nadolol, but a large excess of the reagent has a slight quenching effect on fluorescence. The contribution of III to the reagent blank at the concentration used is negligible.

Addition of ethanol or acetic acid increases the fluorescence. This increase is a function of the amount of the diluent added. About 35% or more of ethanol or acetic acid is needed in the reaction mixture to give the highest fluorescence. When formic acid was substituted for acetic acid, only 38% of the fluorescence was obtained; propionic acid produced 90% of the fluorescence compared to acetic acid. Although ethanol is a good diluent, acetic acid is used because some batches of ethanol produce high reagent blanks even after purification.

It takes about 30 min for maximum fluorescence development at room temperature. Fluorescence of a solution is stable in the dark at least 6 hr. When samples are exposed to laboratory light for more than 1 hr, fluo-

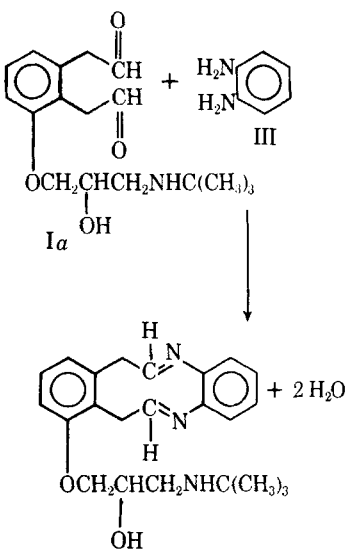

Scheme I

Table I—Recovery of Nadolol from 5 ml of Pooled Human Serum

Nadolol, ng/ml		
Added	Found[a]	Recovery, %
200	200.0	100.0
160	161.9	101.2
120	119.0	99.2
80	80.4	100.5
40	40.8	101.9
30	30.4	101.3
24	23.8	99.2
18	18.3	101.7
12	11.8	98.3
6	6.2	103.3
3	3.0	100.0
1.5	1.4	93.3
0	0.7	—

[a] Reading of serum blank was subtracted from sample readings, and the nadolol concentration was calculated.

rescence decreases slightly probably due to a quenching effect of an excess of III, which produces a brownish color on exposure to light for a longer time.

As shown in Fig. 1, the excitation spectrum has a maximum at 305 nm; the fluorescence spectrum has a maximum at 445 nm. At low concentrations of nadolol, high sensitivity settings of the fluorometer must be used. At high sensitivity settings, there is an interference from reagents and no resolution of the fluorescence spectrum is obtained. Fluorescence readings must be taken on a slope, and this procedure leads to variable results.

Various filters were tried to eliminate the interfering fluorescence. The colored filters[14] 5-57, 5-61, 4-69, 3-71, 3-74, and 3-75 did not eliminate the interference. Only colored filter 3-73[2] facilitated the fluorescence spectrum resolution (Fig. 2). Filter 3-72[14] shifted the fluorescence spectrum to 475 nm and decreased the sensitivity. No improvement was observed when filters were used to eliminate some interference at the excitation wavelength. Glass filters 7-30[14], 7-54[14], 9-54[14], SN 1.25[15], 2ND 0.15-2[15], and 2ND 0.3-2[15] were tried. Filters 4-69[14], SS 2900-2[15], SS 3000-2[15], and SS 3100-2[15] and filters from the 2780 polarized set[16] eliminated fluorescence completely.

Various solvents such as 1-butanol, 1-methyl-1-propanol, 3-methyl-1-butanol, 1-pentanol, ether, ethyl acetate, and *n*-butyl acetate were tried for extracting nadolol from serum and urine. 1-Butanol is an excellent solvent for the extraction of nadolol from serum samples, but high blanks were obtained. Low recoveries of nadolol were obtained when 1-butanol was used for extracting the drug from urine samples. This result could have been due to the quenching effect of extraneous materials extracted from urine with 1-butanol. Ether is an excellent extractant for nadolol from urine samples; about 80% of the drug was extracted from serum with ether. *n*-Butyl acetate is the solvent of choice for the extraction of nadolol from serum. Complete extraction of the drug and negligible blanks were obtained. Other solvents produced low nadolol recoveries from serum and urine samples.

Nadolol can be extracted only from highly alkaline solutions of pH above 13. When potassium carbonate was used to saturate the samples and raise the pH to the desired value, low recoveries of nadolol from

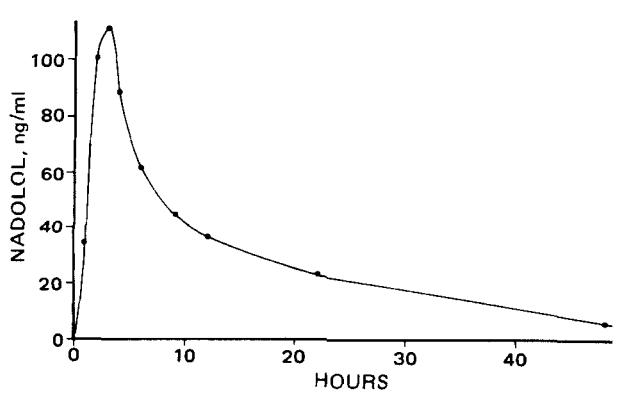

Figure 4—*Serum nadolol levels.*

[14] Corning.
[15] Corion.
[16] Oriel.

Table II—Recovery of Nadolol from 1 ml of Human Urine

Nadolol, μg/ml		
Added	Found[a]	Recovery, %
20	20.16	100.8
10	10.03	100.3
5	4.98	99.6
2.5	2.52	100.8
1.25	1.27	101.6
0.50	0.505	101.0
0.125	0.126	100.8
0.025	0.026	104.0
0	0.005	—

[a] Reading of urine blank was subtracted from sample readings, and the nadolol concentration was calculated.

serum samples were obtained. Recoveries varied from sample to sample and sometimes were below 25%. In biochemical experiments, chloride ions are often used for the breakage of weak interactions of compounds. It can be assumed that chloride ions perform the same function in the extraction of nadolol from urine and serum samples. Sodium chloride and potassium chloride can be used successfully in the extraction of nadolol. For some unknown reasons, no fluorescence in serum, urine, and standards was found when ammonium sulfate and potassium bromide were used in the extraction. Magnesium chloride produced a yellow color after the addition of all reagents to the extracts.

For concentration and purification of the nadolol extracts, the drug is back-extracted into an acid aqueous solution. A 0.1 *N* phosphate buffer (pH 2.5), aqueous solutions of pH up to 8.5, and 0.1 *N* HCl extracted nadolol from organic solvents completely. The volume of acid for the back-extraction of nadolol from solvents is not critical. A smaller volume is better because of the concentration of nadolol.

Petroleum ether is added to the solvent extracts to decrease the solubility of the aqueous layer. Petroleum ether also removes traces of solvents used for extraction and some interferences carried with the extraction.

It is important that test tubes, plastic caps, pipets, and other glassware be absolutely clean and unscratched. As recommended in the procedure, acid washing of glassware with hydrochloric acid is sufficient to remove possible interferences. Solvents also must be purified as recommended because unpurified solvents produce very high reagent blanks and sometimes cause quenching of fluorescence.

Standards and reagent blanks must be run with each set of samples because of a small volume change in the back-extraction and some contribution from solvents and chemicals used in the extraction. It is also important that the organic solvent is aspirated completely before oxidation. This aspiration is accomplished easily by the technique given in the procedure. Samples have to be centrifuged after each addition of a reagent and mixing because aqueous droplets adhere to the walls of the tubes. This can lead to a red color development when III reagent is added and can cause a variation of results.

Recovery of nadolol as a function of serum or urine volume was studied. Serum and urine samples from 1 to 5 ml gave the same extraction efficiency. There was a small blank in almost every serum and urine sample, which varied from individual to individual. Blanks as high as 0.005 μg of nadolol/ml of serum and 0.05 μg/ml of urine were observed in some individuals. Some commercial serum samples may have a blank as high as 0.01 μg/ml.

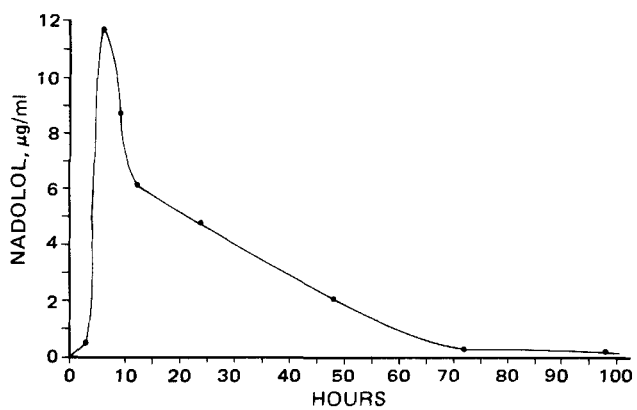

Figure 5—*Urine nadolol levels.*

Table III—Reproducibility of Results

Nadolol	*RSD*, %
Serum, ng/ml	
10	2.22
80	1.00
200	1.41
Urine, μg/ml	
0.04	1.39
20.00	0.73

Standard curves were prepared in the ranges between 0 and 0.03, 0 and 0.2, 0 and 2, and 0 and 20 μg/ml. Fluorescence was proportional to nadolol concentration. Concentrations in all ranges tested produced straight lines that passed through the origin. The fluorescence spectrum of nadolol at different concentrations was recorded (Fig. 3).

The recovery study was carried out by the addition of nadolol in 0.1 *N* HCl to 5-ml serum blanks or 1-ml urine blanks. Recovery from serum varied from 93.3% for a low concentration of nadolol to 103.3% (Table I); from urine, recovery varied from 99.6 to 104% (Table II).

The reproducibility of results was checked by analyzing spiked samples 10 times (Table III).

Standard nadolol acid solutions are stable at room temperature at least 1 week and at 5° at least 3 months.

The method has performed reliably in a number of clinical studies[17]. For example, serum and urine nadolol levels after oral administration of a single 80-mg dose to a male patient are shown in Figs. 4 and 5. It is believed that only unchanged drug produces fluorescence when oxidized and coupled with III. 4-Hydroxynadolol does not fluoresce.

REFERENCES

(1) K. K. Wong, J. Dreyfuss, J. M. Shaw, J. J. Ross, and E. C. Schreiber, *Pharmacologist*, **15**, 245 (1973).

(2) R. J. Lee, D. B. Evans, S. H. Baky, and R. J. Laffan, *Eur. J. Pharmacol.*, **33**, 371 (1975).

(3) J. K. Gibson, H. Gelband, and A. L. Bassett, *Pharmacologist*, **16**, 201 (1974).

(4) J. M. Shaw and J. Dreyfuss, *Fed. Proc.*, **35**, 365 (1976).

(5) M. Peschka, D. B. Evans, and R. J. Laffan, *ibid.*, **32**, 780 (1973).

(6) R. A. Vukovich, A. Sasahara, P. Zombrano, J. Belko, P. Goldin, and L. Brannick, *Am. Soc. Clin. Pharm. Ther.*, **19**, 118 (1976).

(7) D. B. Evans, M. T. Peschka, R. J. Lee, and R. J. Laffan, *Eur. J. Pharmacol.*, **35**, 17 (1976).

(8) J. K. Gibson, H. Gelband, and A. L. Bassett, *Am. J. Cardiol.*, **37**, 138 (1976).

(9) A. Morales-Aquilera, "First Chemical Congress of North American Continent" (Mexico City, Nov.–Dec. 1975), Port City Press, Baltimore, Md., Abstr. 141.

(10) L. Malaprade, *C. R.*, **186**, 382 (1928). L. Malaprade, *Bull. Soc. Chim. Fr.*, **43**, 683 (1928).

(11) E. L. Jackson, in "Organic Reactions," vol. II, R. Adams, Ed., Wiley, New York, N.Y., 1944, p. 341.

(12) J. R. Dyer, in "Methods in Biochemical Analysis," vol. III, D. Glick, Ed., Interscience, New York, N.Y., 1956, p. 111.

(13) C. A. Bunton, in "Oxidation in Organic Chemistry—Part A," K. B. Wiberg, Ed., Academic, New York, N.Y., 1965, p. 367.

(14) L. Chafetz, *J. Pharm. Sci.*, **60**, 291 (1971).

(15) S. Belman, *Anal. Chim. Acta*, **29**, 120 (1963).

(16) E. Sawicki, T. W. Stanley, and J. D. Ptaff, *ibid.*, **28**, 156 (1963).

(17) E. Sawicki and R. A. Carnes, *Microchim. Acta*, **1968**, 148.

(18) E. Sawicki, J. W. Stanley, and H. Johnson, *Anal. Chem.*, **35**, 199 (1963).

(19) E. Sawicki, J. D. Ptaff, and R. A. Taft, *Chem.-Anal.*, **55**, 6 (1966).

(20) R. A. Salvador and R. W. Albers, *J. Biol. Chem.*, **234**, 922 (1959).

(21) O. Hinsberg, *Ann. Chem.*, **237**, 327 (1887).

(22) J. Velisel and J. Davidek, *Chem. Listy*, **67**, 513 (1973).

(23) M. Pesez and J. Bartos, "Colorimetric and Fluorometric Analysis of Organic Compounds and Drugs," Dekker, New York, N.Y., 1974.

[17] To be published.

ACKNOWLEDGMENTS AND ADDRESSES

Received August 3, 1976, from the *Squibb Institute for Medical Research, New Brunswick, NJ 08903.*

Accepted for publication October 29, 1976.

The author thanks Dr. John M. Dunham for valuable suggestions and discussions.

Influence of Crystal Form on Tensile Strength of Compacts of Pharmaceutical Materials

M. P. SUMMERS *, R. P. ENEVER *x, and J. E. CARLESS

Abstract □ The tensile strengths of compacts of different crystal forms of aspirin, sulfathiazole, and barbital were determined with a modified tablet hardness tester. For each material, the tensile strength could be correlated with the amount of plastic flow and/or crushing undergone by each crystal form during compression.

Keyphrases □ Crystal form—effect on tensile strength of compacts of aspirin, sulfathiazole, and barbital □ Tensile strength—compacts of aspirin, sulfathiazole, and barbital, effect of crystal form □ Aspirin—compacts, effect of crystal form on tensile strength □ Sulfathiazole—compacts, effect of crystal form on tensile strength □ Barbital—compacts, effect of crystal form on tensile strength □ Tablets—aspirin, sulfathiazole, and barbital, effect of crystal form on tensile strength □ Dosage forms—tablets, aspirin, sulfathiazole, and barbital, effect of crystal form on tensile strength

Previously, the use of a physical testing instrument[1] for measurement of the tensile strengths of compacts of pharmaceutical materials was reported (1). A subsequent study (2) indicated that the test could be used to predict the tensile strength of lactose compacts, and another report (3) indicated that this parameter was a fundamental material property independent of the compact dimensions.

The present paper describes the use of a modified tablet hardness tester[2] for measuring the tensile strength of

[1] Instron Engineering Corp., Park Ridge, Ill.

[2] Erweka type TBT tester, Erweka Apparatebau GmbH, Main, West Germany.

Table III—Reproducibility of Results

Nadolol	*RSD*, %
Serum, ng/ml	
10	2.22
80	1.00
200	1.41
Urine, μg/ml	
0.04	1.39
20.00	0.73

Standard curves were prepared in the ranges between 0 and 0.03, 0 and 0.2, 0 and 2, and 0 and 20 μg/ml. Fluorescence was proportional to nadolol concentration. Concentrations in all ranges tested produced straight lines that passed through the origin. The fluorescence spectrum of nadolol at different concentrations was recorded (Fig. 3).

The recovery study was carried out by the addition of nadolol in 0.1 *N* HCl to 5-ml serum blanks or 1-ml urine blanks. Recovery from serum varied from 93.3% for a low concentration of nadolol to 103.3% (Table I); from urine, recovery varied from 99.6 to 104% (Table II).

The reproducibility of results was checked by analyzing spiked samples 10 times (Table III).

Standard nadolol acid solutions are stable at room temperature at least 1 week and at 5° at least 3 months.

The method has performed reliably in a number of clinical studies[17]. For example, serum and urine nadolol levels after oral administration of a single 80-mg dose to a male patient are shown in Figs. 4 and 5. It is believed that only unchanged drug produces fluorescence when oxidized and coupled with III. 4-Hydroxynadolol does not fluoresce.

REFERENCES

(1) K. K. Wong, J. Dreyfuss, J. M. Shaw, J. J. Ross, and E. C. Schreiber, *Pharmacologist*, **15**, 245 (1973).

(2) R. J. Lee, D. B. Evans, S. H. Baky, and R. J. Laffan, *Eur. J. Pharmacol.*, **33**, 371 (1975).

(3) J. K. Gibson, H. Gelband, and A. L. Bassett, *Pharmacologist*, **16**, 201 (1974).

(4) J. M. Shaw and J. Dreyfuss, *Fed. Proc.*, **35**, 365 (1976).

(5) M. Peschka, D. B. Evans, and R. J. Laffan, *ibid.*, **32**, 780 (1973).

(6) R. A. Vukovich, A. Sasahara, P. Zombrano, J. Belko, P. Goldin, and L. Brannick, *Am. Soc. Clin. Pharm. Ther.*, **19**, 118 (1976).

(7) D. B. Evans, M. T. Peschka, R. J. Lee, and R. J. Laffan, *Eur. J. Pharmacol.*, **35**, 17 (1976).

(8) J. K. Gibson, H. Gelband, and A. L. Bassett, *Am. J. Cardiol.*, **37**, 138 (1976).

(9) A. Morales-Aquilera, "First Chemical Congress of North American Continent" (Mexico City, Nov.–Dec. 1975), Port City Press, Baltimore, Md., Abstr. 141.

(10) L. Malaprade, *C. R.*, **186**, 382 (1928). L. Malaprade, *Bull. Soc. Chim. Fr.*, **43**, 683 (1928).

(11) E. L. Jackson, in "Organic Reactions," vol. II, R. Adams, Ed., Wiley, New York, N.Y., 1944, p. 341.

(12) J. R. Dyer, in "Methods in Biochemical Analysis," vol. III, D. Glick, Ed., Interscience, New York, N.Y., 1956, p. 111.

(13) C. A. Bunton, in "Oxidation in Organic Chemistry—Part A," K. B. Wiberg, Ed., Academic, New York, N.Y., 1965, p. 367.

(14) L. Chafetz, *J. Pharm. Sci.*, **60**, 291 (1971).

(15) S. Belman, *Anal. Chim. Acta*, **29**, 120 (1963).

(16) E. Sawicki, T. W. Stanley, and J. D. Ptaff, *ibid.*, **28**, 156 (1963).

(17) E. Sawicki and R. A. Carnes, *Microchim. Acta*, **1968**, 148.

(18) E. Sawicki, J. W. Stanley, and H. Johnson, *Anal. Chem.*, **35**, 199 (1963).

(19) E. Sawicki, J. D. Ptaff, and R. A. Taft, *Chem.-Anal.*, **55**, 6 (1966).

(20) R. A. Salvador and R. W. Albers, *J. Biol. Chem.*, **234**, 922 (1959).

(21) O. Hinsberg, *Ann. Chem.*, **237**, 327 (1887).

(22) J. Velisel and J. Davidek, *Chem. Listy*, **67**, 513 (1973).

(23) M. Pesez and J. Bartos, "Colorimetric and Fluorometric Analysis of Organic Compounds and Drugs," Dekker, New York, N.Y., 1974.

[17] To be published.

ACKNOWLEDGMENTS AND ADDRESSES

Received August 3, 1976, from the *Squibb Institute for Medical Research, New Brunswick, NJ 08903.*

Accepted for publication October 29, 1976.

The author thanks Dr. John M. Dunham for valuable suggestions and discussions.

Influence of Crystal Form on Tensile Strength of Compacts of Pharmaceutical Materials

M. P. SUMMERS *, R. P. ENEVER *x, and J. E. CARLESS

Abstract □ The tensile strengths of compacts of different crystal forms of aspirin, sulfathiazole, and barbital were determined with a modified tablet hardness tester. For each material, the tensile strength could be correlated with the amount of plastic flow and/or crushing undergone by each crystal form during compression.

Keyphrases □ Crystal form—effect on tensile strength of compacts of aspirin, sulfathiazole, and barbital □ Tensile strength—compacts of aspirin, sulfathiazole, and barbital, effect of crystal form □ Aspirin—compacts, effect of crystal form on tensile strength □ Sulfathiazole—compacts, effect of crystal form on tensile strength □ Barbital—compacts, effect of crystal form on tensile strength □ Tablets—aspirin, sulfathiazole, and barbital, effect of crystal form on tensile strength □ Dosage forms—tablets, aspirin, sulfathiazole, and barbital, effect of crystal form on tensile strength

Previously, the use of a physical testing instrument[1] for measurement of the tensile strengths of compacts of pharmaceutical materials was reported (1). A subsequent study (2) indicated that the test could be used to predict the tensile strength of lactose compacts, and another report (3) indicated that this parameter was a fundamental material property independent of the compact dimensions.

The present paper describes the use of a modified tablet hardness tester[2] for measuring the tensile strength of

[1] Instron Engineering Corp., Park Ridge, Ill.

[2] Erweka type TBT tester, Erweka Apparatebau GmbH, Main, West Germany.

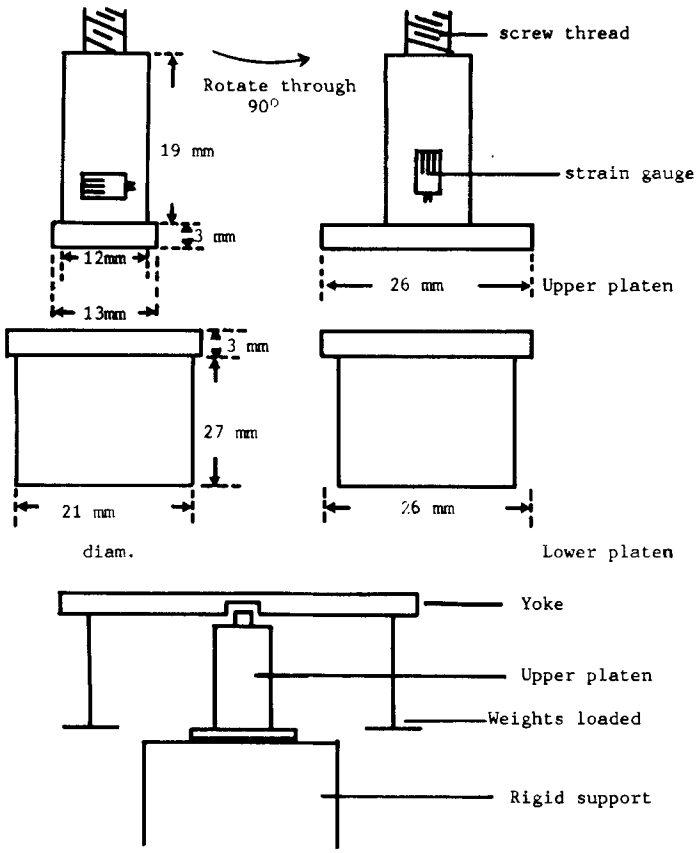

Figure 1—*Diagram of modified platens and calibration of upper platen.*

compacts of various crystal forms of drugs. Such an instrument is of more general use in the pharmaceutical industry than the much more elaborate physical testing instrument. The relationship between the tensile strengths of compacts of different crystal forms of aspirin, sulfathiazole, and barbital and the degree of plastic flow and/or crushing occurring during compact formation also is reported.

EXPERIMENTAL

Modification and Calibration of Tablet Hardness Tester[2]—The platen assembly of the tester (4) was replaced by smooth, flat-faced, platens of 3-mm thick mild steel. The upper platen was 13 × 26 mm, and the lower platen was 26 mm square. To determine the compact breaking load, four foil strain gauges[3] were bonded onto the 12-mm diameter shank of the upper platen (Fig. 1). The gauges were placed diametrically opposite one another in a Poisson arrangement (5) and connected so that each was an active arm of a Wheatstone bridge circuit. They were protected from damage by a coating of a silicone rubber compound[4].

A carrier amplifier[5] (oscillator frequency 5 kHz, input voltage 1 v) was used to energize the bridge network. The output from the network was displayed on a UV galvanometer recorder[6].

The strain-gauge assembly on the upper platen was calibrated by placing a yoke on the shank and loading 1-kg weights onto the yoke to apply compressive forces of up to 12 kg (Fig. 1). The relationship between galvanometer deflection and applied force was recorded and was linear over this range.

Compacts for Tensile Strength Measurements—To evaluate the modified tester, spray-dried lactose[7] (104–152-μm) compacts of 600 and 700 mg were prepared using an instrumented tablet machine[8] to apply axial forces of 1080, 1390, 1720, 2015, 2380, and 3000 kg (6). The compacts were aged for 24 hr before determining their tensile strength. The need to standardize compact age was advised previously (7).

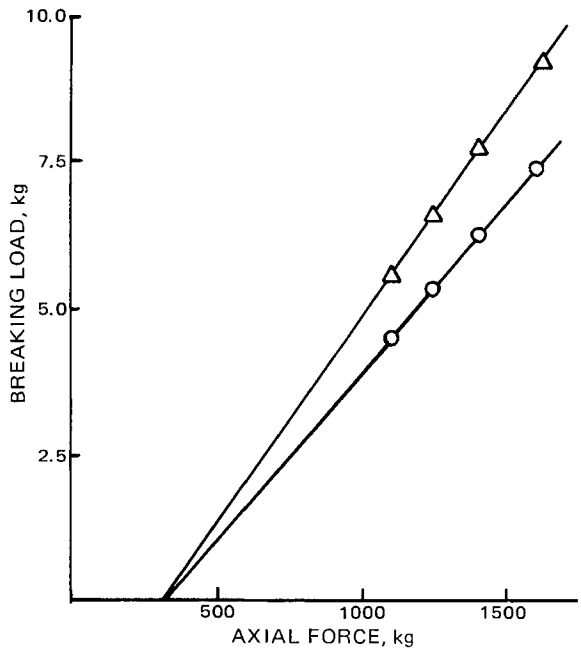

Figure 2—*Breaking load of spray-dried lactose compacts at a range of axial compaction forces. Key: ○, 600-mg compacts; and △, 700-mg compacts.*

Compacts also were produced from various crystal forms of barbital, sulfathiazole, and aspirin. Forms II and III of barbital were obtained by recrystallization of a commercial sample[9] from water and a dilute ammoniacal aqueous solution, respectively; Form I was prepared by heating Form II at 160° until transformation was complete (10–20 min).

Sulfathiazole Forms I and II were produced by recrystallization of sulfathiazole[10] from water and 1-propanol, respectively. Both 190–251- and 104–152-μm fractions of these various crystal forms were used for the compacts. Aspirin Forms I, II, and IV were produced by recrystallization of a commercial sample[11] from 96% ethanol at 20°, *n*-hexane at 0°, and *n*-octane at 20°, respectively. The 250–253-μm sieve fraction was collected in all cases.

With each crystal form, the die of the tablet machine was filled with a weight of material that produced a compact 4.0 ± 0.2 mm in thickness at each force level. These force levels were chosen so that the data could be correlated with the radial stress transmission characteristics of the crystal forms (6). The compacts also were stored for 24 hr before testing.

To characterize the various crystal forms and to ensure that transformation did not occur during the compaction process, crystals and compacts were subjected to differential scanning calorimetry[12] and, where appropriate, IR spectrophotometry[13] as described elsewhere (6).

Measurement of Tensile Strength—The dimensions of each compact were measured with vernier calipers (±0.01 mm) prior to the test. Strips of paper (1.3 mm wide × 0.1 mm thick) were placed between the platens and the compact as padding material throughout the test. The machine was operated in the normal manner to apply an increasing force to the compact *via* the top platen at a rate of 0.4 kg/sec.

When the compact failed, the tester stopped automatically and the galvanometer deflection of the UV recorder rapidly returned to zero. The failure load was calculated from the maximum galvanometer deflection. Only data for those compacts that appeared to have failed in tension were

[3] Micro Measurements type EA-06-125-BT-120, 120 ± 0.15% Ω resistance, Welwyn Strain Measurements Ltd., Basingstoke, England.
[4] R.S. Components, London, England.
[5] Honeywell type 2506 carrier amplifier, Honeywell Controls Ltd., Hemel Hempstead, England.
[6] Honeywell 1706 Visicorder equipped with type BB250A mirror galvanometer, Honeywell Controls Ltd., Hemel Hempstead, England.
[7] α-Monohydrate form, McKesson and Robbins Ltd., Kent, England.
[8] Manesty E2 tablet machine, Manesty, Speke, Liverpool, England.
[9] British Drug Houses Ltd., Poole, Dorset, England.
[10] Evans Medical Ltd., Liverpool, England.
[11] Aspro-Nicholas Ltd., London, England.
[12] DSC 1, Perkin-Elmer, Beaconsfield, Bucks., England.
[13] Unicam SP200 recording spectrophotometer, Pye-Unicam, Cambridge, England.

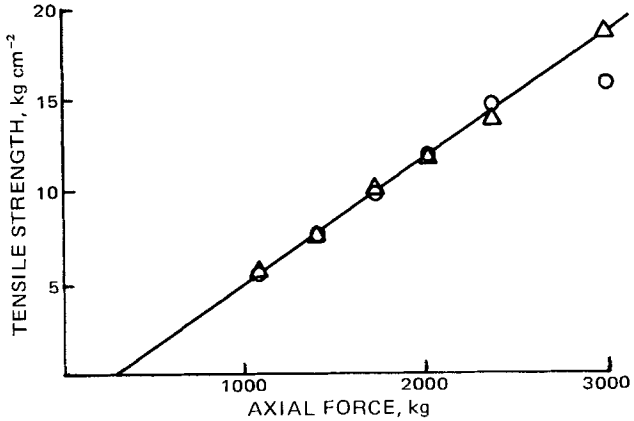

Figure 3—*Variation of tensile strength of lactose compacts with applied axial force. Key: O, 600-mg compacts; and Δ, 700-mg compacts.*

used. Tensile failure was checked by visual observation of the fractured compacts. The tensile strength, σ, of each compact was calculated using:

$$\sigma = \frac{2P}{\pi Dt} \qquad \text{(Eq. 1)}$$

where P is the breaking load, D is the compact diameter, and t is the compact thickness. An average value was determined from the failure of five compacts prepared at each compression level.

RESULTS AND DISCUSSION

Evaluation of Tensile Tester Using Lactose Compacts—Figure 2 shows the relationship between breaking load, P, and the axial force of compaction for 600- and 700-mg lactose compacts; differing linear relationships were obtained. If, however, the data are plotted as tensile strength against axial force (Fig. 3), then all points fall on a single straight line. Repeated determinations gave results that fell on this line. If only the compacts failing in tension are used to calculate results, the reproducibility of the measurements is good and the modified tester affords a method of tensile strength measurement. Furthermore, since tensile strength is independent of compact dimensions, it is a fundamental material property.

The rejection rate of compacts not showing tensile failure varied considerably. At the lowest compression forces used, and with materials prone to lamination and capping, the rejection rate was 50–60%. For materials possessing good bonding characteristics, the rejection rate could be as low as 5%. This variability in rejection rate may be due to the fact that the loading rate of 0.4 kg/sec may be excessive and not ensure uniform stress distribution in the compact on each occasion. This problem is aggravated by unequal distribution of density (8) and hardness (9) in the compact. Another factor is that, at the low compression forces where there may be little appreciable bonding between the particles, the elastic rebound of the unbonded particles may adversely affect the stress distribution throughout the compact because of flaw formation.

Figure 3 also shows that deviation of mean tensile strength from the linear relation occurred with the 600-mg compacts at the highest compression force used. The relatively low value of tensile strength under these conditions is attributed to the fact that no significant additional particle–particle bonds are formed at these higher pressures and the tensile strength tends to a constant value. Rees and Shotton (10) noticed a similar effect when investigating the effect of compact dimensions on the crushing strength of sodium chloride tablets.

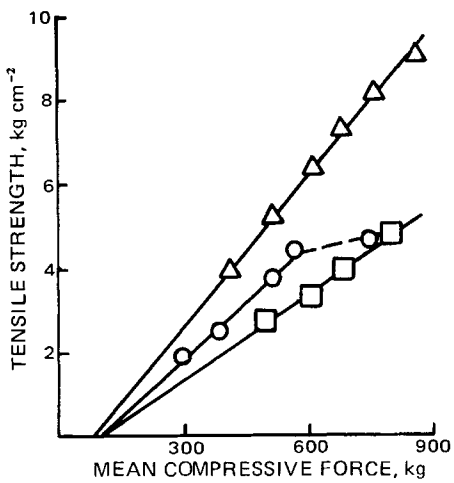

Figure 5—*Tensile strength of compacts of barbital polymorphic forms (104–152 μm). Key: O, Form I; □, Form II; and Δ, Form III.*

Influence of Crystal Form on Tensile Strength of Pharmaceutical Compacts—The relationships between tensile strength and mean compression force (mean of axial and radially transmitted forces) for the various crystal forms of sulfathiazole, barbital (104–152 μm), and aspirin (253–353-μm size) are shown in Figs. 4, 5, and 6, respectively. For any given mean compressive force, the tensile strength of sulfathiazole compacts was Form II > Form I (Fig. 4); for barbital, it was Form III > Form I > Form II (Fig. 5).

The tensile strength of a compact of any material is a function of the area of contact between the particles and the strength of the bond produced between them. Since the less stable polymorphic form of a material is considered to possess higher potential energy and weaker bonding (11), the strength of the particle–particle bond should be less than that of the stable form. However, the area of contact between particles depends on the degree of plastic flow or crushing of particles during compression, and this is likely to be greater for an unstable polymorphic form that will have lower resistance to plastic flow and crushing.

The degree of plastic flow and/or crushing during compression was evaluated by Leigh (12), who measured the change in the relative density of a compact, ϕ, during this stage of compaction. Summers (13) determined the ϕ values for the various crystal forms of sulfathiazole and barbital (104–152 μm) used in this study. These data are shown in Table I together with the tensile strength value of the compacts at an arbitrary mean compression force of 400 kg; a correlation between ϕ and tensile strength existed. Since barbital Form II and sulfathiazole Form I are the stable polymorphic forms of the two materials and compacts of these forms have the lower tensile strengths, the findings suggest that the overriding influence on compact strength is the area of contact developed

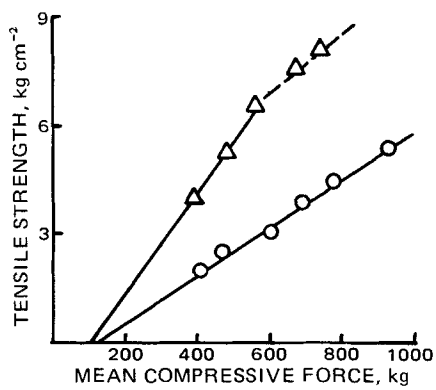

Figure 4—*Tensile strength of compacts of sulfathiazole polymorphic forms (104–152 μm). Key: O, Form I; and Δ, Form II.*

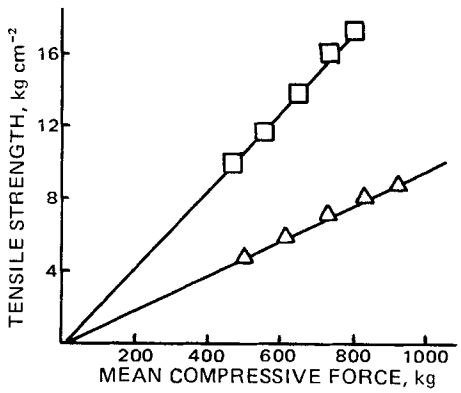

Figure 6—*Tensile strength of compacts of aspirin crystal forms (250–353 μm). Key: Δ, Form I; and □, Form IV.*

Table I—Comparison of Tensile Strength of Compacts Compressed at a Mean Force of 400 kg and the Relative Density Change Occurring during Plastic Flow and/or Crushing, ϕ

Crystal Form	Tensile Strength, kg/cm^2	ϕ
Barbital (104–152 μm)		
Form I	2.8 ± 0.1	0.21 ± 0.008
Form II	2.0 ± 0.2	0.21 ± 0.008
Form III	3.8 ± 0.1	0.23 ± 0.007
Sulfathiazole (104–152 μm)		
Form I	1.9 ± 0.1	0.22 ± 0.008
Form II	4.2 ± 0.2	0.24 ± 0.008
Aspirin (250–353 μm)		
Form I	3.8 ± 0.1	0.14 ± 0.008
Form IV	8.4 ± 0.2	0.23 ± 0.007

between particles in the powder bed rather than the bond strength between particles. Support for this hypothesis is obtained from the data relating particle size to tensile strength of barbital Form II and sulfathiazole Form I compacts (Table II). At any mean compression force, the smaller particle-size fraction of both drugs produced the stronger compact. There will be a greater number of point contacts within compacts made from the smaller fraction and, hence, a greater area of contact between particles.

Compacts of the aspirin crystal forms also showed differences in tensile strength at a given mean compression force (Fig. 6). Tensile strength values could not be obtained for compacts of aspirin Form II because of the layering tendency of the needle-shaped crystals (6). When Form II compacts were subjected to diametral crushing, the compacts laminated.

Table II—Influence of Particle Size on the Tensile Strength of Barbital and Sulfathiazole Compacts over a Range of Mean Compression Forces

Mean Compressive Force, kg	Tensile Strength, kg/cm^2 ± 0.1			
	Barbital Form II		Sulfathiazole Form I	
	104–152 μm	190–251 μm	104–152 μm	190–251 μm
610	3.4	2.9	3.3	2.5
713	4.1	3.3	4.0	2.7
815	4.8	3.7	4.7	2.9
917	5.5	4.3	5.3	3.1

As with the polymorphic forms of sulfathiazole and barbital, there was a correlation between ϕ and the tensile strength of the compacts for aspirin Forms I and IV. The lower melting-point Form IV had the higher tensile strength at any given mean compression force, again indicating that the area of contact between particles is the overriding influence on compact strength for materials existing in different crystal forms.

REFERENCES

(1) J. T. Fell and J. M. Newton, *J. Pharm. Pharmacol.*, **20**, 657 (1968).

(2) J. T. Fell and J. M. Newton, *J. Pharm. Sci.*, **59**, 688 (1970).

(3) J. M. Newton, G. Rowley, J. T. Fell, D. G. Peacock, and K. Ridgway, *J. Pharm. Pharmacol.*, **23**, 195S (1971).

(4) D. P. Brook and K. Marshall, *J. Pharm. Sci.*, **57**, 481 (1968).

(5) C. C. Perry and H. R. Lisner, "The Strain Gauge Primer," McGraw-Hill, London, England, 1962, p. 64.

(6) M. P. Summers, R. P. Enever, and J. E. Carless, *J. Pharm. Pharmacol.*, **28**, 89 (1976).

(7) J. E. Rees and E. Shotton, *ibid.*, **22**, 17S (1970).

(8) D. Train, *ibid.*, **8**, 745 (1956).

(9) K. Ridgway, M. Aulton, and P. H. Rosser, *ibid.*, **22**, 70S (1970).

(10) J. E. Rees and E. Shotton, *ibid.*, **21**, 731 (1969).

(11) M. J. Buerger, in "Phase Transformations in Solids," R. Smoluchowski, J. E. Mayer, and W. A. Weyl, Eds., Wiley, New York, N.Y., 1951, p. 183.

(12) S. Leigh, Ph.D. thesis, London University, London, England, 1969.

(13) M. P. Summers, Ph.D. thesis, London University, London, England, 1972.

ACKNOWLEDGMENTS AND ADDRESSES

Received June 21, 1976, from the *Department of Pharmacy, Chelsea College, University of London, London, SW3 6LX, England.*

Accepted for publication October 4, 1976.

M. P. Summers thanks the Science Research Council for a research studentship to allow this work to be undertaken.

* Present address: School of Pharmacy, University of London, 29/39 Brunswick Square, London, WC1N 1AX, England.

ˣ To whom inquiries should be directed.

Degradation Kinetics of a Substituted Carbinolamine in Aqueous Media

H. V. MAULDING ˣ and M. A. ZOGLIO *

Abstract □ The apparent first-order breakdown of the medicinally active agent 3-(*p*-chlorophenyl)-2-ethyl-2,3,5,6-tetrahydroimidazo[2,1-*b*]thiazol-3-ol was studied in aqueous solutions where dehydration gave the unsaturated compound 3-(*p*-chlorophenyl)-5,6-dihydro-2-ethylimidazo[2,1-*b*]thiazole. This thiazole was the primary solvolytic product produced in approximately quantitative yields for the temperature range studied and ostensibly underwent no further reaction in acidic media even on prolonged heating. Investigations were carried out at various pH values in standard buffers at constant ionic strength. The ionization constants of the compounds are reported as well as the apparent activation energies for the degradation in acid and acetate buffers. The influence of ionic strength on the velocity constant was determined.

Keyphrases □ Thiazol-3-ol, substituted—kinetics of degradation in aqueous media, effect of temperature, pH, and ionic strength □ Degradation kinetics—substituted thiazol-3-ol, in aqueous media, effect of temperature, pH, and ionic strength □ Kinetics, degradation—substituted thiazol-3-ol, in aqueous media, effect of temperature, pH, and ionic strength □ Anorexic agents, potential—3-(*p*-chlorophenyl)-2-ethyl-2,3,5,6-tetrahydroimidazo[2,1-*b*]thiazol-3-ol, kinetics of degradation in aqueous media, effect of temperature, pH, and ionic strength

The degradation kinetics of 3-(*p*-chlorophenyl)-2-ethyl-2,3,5,6-tetrahydroimidazo[2,1-*b*]thiazol-3-ol[1] (I) were investigated in aqueous solution at varying hydrogen-ion concentrations.

Compound I exhibits anorexic activity, and its breakdown in aqueous media is important in the formulation of

[1] No. 43976, Sandoz Pharmaceuticals, Hanover, NJ 07936.

Table I—Comparison of Tensile Strength of Compacts Compressed at a Mean Force of 400 kg and the Relative Density Change Occurring during Plastic Flow and/or Crushing, ϕ

Crystal Form	Tensile Strength, kg/cm^2	ϕ
Barbital (104–152 μm)		
Form I	2.8 ± 0.1	0.21 ± 0.008
Form II	2.0 ± 0.2	0.21 ± 0.008
Form III	3.8 ± 0.1	0.23 ± 0.007
Sulfathiazole (104–152 μm)		
Form I	1.9 ± 0.1	0.22 ± 0.008
Form II	4.2 ± 0.2	0.24 ± 0.008
Aspirin (250–353 μm)		
Form I	3.8 ± 0.1	0.14 ± 0.008
Form IV	8.4 ± 0.2	0.23 ± 0.007

between particles in the powder bed rather than the bond strength between particles. Support for this hypothesis is obtained from the data relating particle size to tensile strength of barbital Form II and sulfathiazole Form I compacts (Table II). At any mean compression force, the smaller particle-size fraction of both drugs produced the stronger compact. There will be a greater number of point contacts within compacts made from the smaller fraction and, hence, a greater area of contact between particles.

Compacts of the aspirin crystal forms also showed differences in tensile strength at a given mean compression force (Fig. 6). Tensile strength values could not be obtained for compacts of aspirin Form II because of the layering tendency of the needle-shaped crystals (6). When Form II compacts were subjected to diametral crushing, the compacts laminated.

Table II—Influence of Particle Size on the Tensile Strength of Barbital and Sulfathiazole Compacts over a Range of Mean Compression Forces

Mean Compressive Force, kg	Tensile Strength, kg/cm^2 ± 0.1			
	Barbital Form II		Sulfathiazole Form I	
	104–152 μm	190–251 μm	104–152 μm	190–251 μm
610	3.4	2.9	3.3	2.5
713	4.1	3.3	4.0	2.7
815	4.8	3.7	4.7	2.9
917	5.5	4.3	5.3	3.1

As with the polymorphic forms of sulfathiazole and barbital, there was a correlation between ϕ and the tensile strength of the compacts for aspirin Forms I and IV. The lower melting-point Form IV had the higher tensile strength at any given mean compression force, again indicating that the area of contact between particles is the overriding influence on compact strength for materials existing in different crystal forms.

REFERENCES

(1) J. T. Fell and J. M. Newton, *J. Pharm. Pharmacol.*, **20**, 657 (1968).

(2) J. T. Fell and J. M. Newton, *J. Pharm. Sci.*, **59**, 688 (1970).

(3) J. M. Newton, G. Rowley, J. T. Fell, D. G. Peacock, and K. Ridgway, *J. Pharm. Pharmacol.*, **23**, 195S (1971).

(4) D. P. Brook and K. Marshall, *J. Pharm. Sci.*, **57**, 481 (1968).

(5) C. C. Perry and H. R. Lisner, "The Strain Gauge Primer," McGraw-Hill, London, England, 1962, p. 64.

(6) M. P. Summers, R. P. Enever, and J. E. Carless, *J. Pharm. Pharmacol.*, **28**, 89 (1976).

(7) J. E. Rees and E. Shotton, *ibid.*, **22**, 17S (1970).

(8) D. Train, *ibid.*, **8**, 745 (1956).

(9) K. Ridgway, M. Aulton, and P. H. Rosser, *ibid.*, **22**, 70S (1970).

(10) J. E. Rees and E. Shotton, *ibid.*, **21**, 731 (1969).

(11) M. J. Buerger, in "Phase Transformations in Solids," R. Smoluchowski, J. E. Mayer, and W. A. Weyl, Eds., Wiley, New York, N.Y., 1951, p. 183.

(12) S. Leigh, Ph.D. thesis, London University, London, England, 1969.

(13) M. P. Summers, Ph.D. thesis, London University, London, England, 1972.

ACKNOWLEDGMENTS AND ADDRESSES

Received June 21, 1976, from the *Department of Pharmacy, Chelsea College, University of London, London, SW3 6LX, England.*

Accepted for publication October 4, 1976.

M. P. Summers thanks the Science Research Council for a research studentship to allow this work to be undertaken.

* Present address: School of Pharmacy, University of London, 29/39 Brunswick Square, London, WC1N 1AX, England.

ˣ To whom inquiries should be directed.

Degradation Kinetics of a Substituted Carbinolamine in Aqueous Media

H. V. MAULDING ˣ and M. A. ZOGLIO *

Abstract □ The apparent first-order breakdown of the medicinally active agent 3-(*p*-chlorophenyl)-2-ethyl-2,3,5,6-tetrahydroimidazo[2,1-*b*]thiazol-3-ol was studied in aqueous solutions where dehydration gave the unsaturated compound 3-(*p*-chlorophenyl)-5,6-dihydro-2-ethylimidazo[2,1-*b*]thiazole. This thiazole was the primary solvolytic product produced in approximately quantitative yields for the temperature range studied and ostensibly underwent no further reaction in acidic media even on prolonged heating. Investigations were carried out at various pH values in standard buffers at constant ionic strength. The ionization constants of the compounds are reported as well as the apparent activation energies for the degradation in acid and acetate buffers. The influence of ionic strength on the velocity constant was determined.

Keyphrases □ Thiazol-3-ol, substituted—kinetics of degradation in aqueous media, effect of temperature, pH, and ionic strength □ Degradation kinetics—substituted thiazol-3-ol, in aqueous media, effect of temperature, pH, and ionic strength □ Kinetics, degradation—substituted thiazol-3-ol, in aqueous media, effect of temperature, pH, and ionic strength □ Anorexic agents, potential—3-(*p*-chlorophenyl)-2-ethyl-2,3,5,6-tetrahydroimidazo[2,1-*b*]thiazol-3-ol, kinetics of degradation in aqueous media, effect of temperature, pH, and ionic strength

The degradation kinetics of 3-(*p*-chlorophenyl)-2-ethyl-2,3,5,6-tetrahydroimidazo[2,1-*b*]thiazol-3-ol[1] (I) were investigated in aqueous solution at varying hydrogen-ion concentrations.

Compound I exhibits anorexic activity, and its breakdown in aqueous media is important in the formulation of

[1] No. 43976, Sandoz Pharmaceuticals, Hanover, NJ 07936.

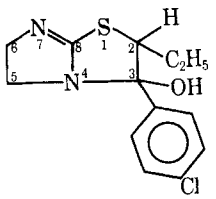

I

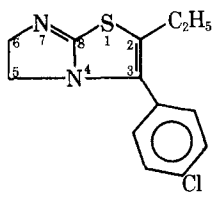

II

solid and liquid dosages as well as in stability prediction of these dosage forms.

It is a somewhat unusual structural prototype in the tertiary[2] hydroxyl group on C-3 adjacent to N-4. These two features comprise a relatively stable carbinolamine not frequently encountered, and the structure is similar to the "pseudobases" characteristically formed from the reaction of certain quaternary heterocyclics with OH^- (1).

The possible existence of several isomers of I is obvious; however, X-ray crystallographic data reveal no diastereoisomerism and one conformation consisting of a *trans*-relationship between the *p*-chlorophenyl and ethyl substituents[3]. Kinetic evidence also rules out diastereoisomerism barring equal reaction rate constants. This finding is illustrated by the lack of deviation from a first-order plot present in parallel first-order reactions producing a common product (2).

The conversion of I to its dehydration product, 3-(*p*-chlorophenyl)-5,6-dihydro -2- ethylimidazo[2,1-*b*]thiazole[4] (II), was the primary route of aqueous transformation of I under the conditions employed. The present work was concerned principally with this reaction.

EXPERIMENTAL

Spectrophotometric Studies in Acidic Solution—Aliquots of 10 ml of an aqueous stock solution of I hydrobromide, 2.83×10^{-3} *M*, were mixed with 190 ml of hydrochloric acid of the appropriate strength, previously equilibrated in a constant-temperature bath. The final concentration was 1.42×10^{-4} *M* with A_∞ of 1.760. Samples, 10 ml, were removed at various times and diluted to 20 ml with distilled water. The spectra were determined[5] at 272 nm against blanks having the same composition but lacking I hydrobromide, $A_\infty = 1.760/2 = 0.880$.

Spectrophotometric Studies in Buffer Solution—Standard buffer solutions were prepared and adjusted to constant ionic strength using sodium chloride. These solutions were equilibrated in constant-temperature baths, and the same procedure was carried out as described for acidic solutions. UV spectra were determined at 272 nm using the appropriate buffers as blanks.

Determination of Ionization Constants—The hydrobromide salt of I (0.005 mole in 100 ml of water) was titrated potentiometrically with 10 equal increments of 0.1 *N* KOH following the method outlined by Albert and Sergeant (3). Precipitation of the base occurred before complete neutralization, but enough points were evaluated to give a pKa of 7.60 (±0.04).

A stock solution of II (4.12×10^{-3} *M*) was prepared. The maximum difference in the absorption spectrum, at 310 nm, was obtained using 0.01 *N* HCl and 0.01 *N* NaOH solutions for the ionized and nonionized species, respectively. Aliquots of 4 ml of this solution were diluted to 200 ml with seven borate buffers, pH 8.6–9.8 and an ionic strength of less than 0.005 (4). The pKa′ value was 9.38 (±0.04) and was verified by titration with 0.1 *N* KOH.

RESULTS AND DISCUSSION

With the conditions investigated, it was convenient to assay for the dehydration product, II, rather than the parent compound, I. Compound II exhibited a UV absorption maximum at 272 nm which was absent in I. The molar absorptivity, a_M, was evaluated at 1.238×10^4 liters/cm mole (272 nm). Compound I exhibited an absorption maximum at 222–223 nm, $a_M = 2.55 \times 10^4$ liters/cm mole. The principal degradation route was the conversion of I to II under the conditions listed.

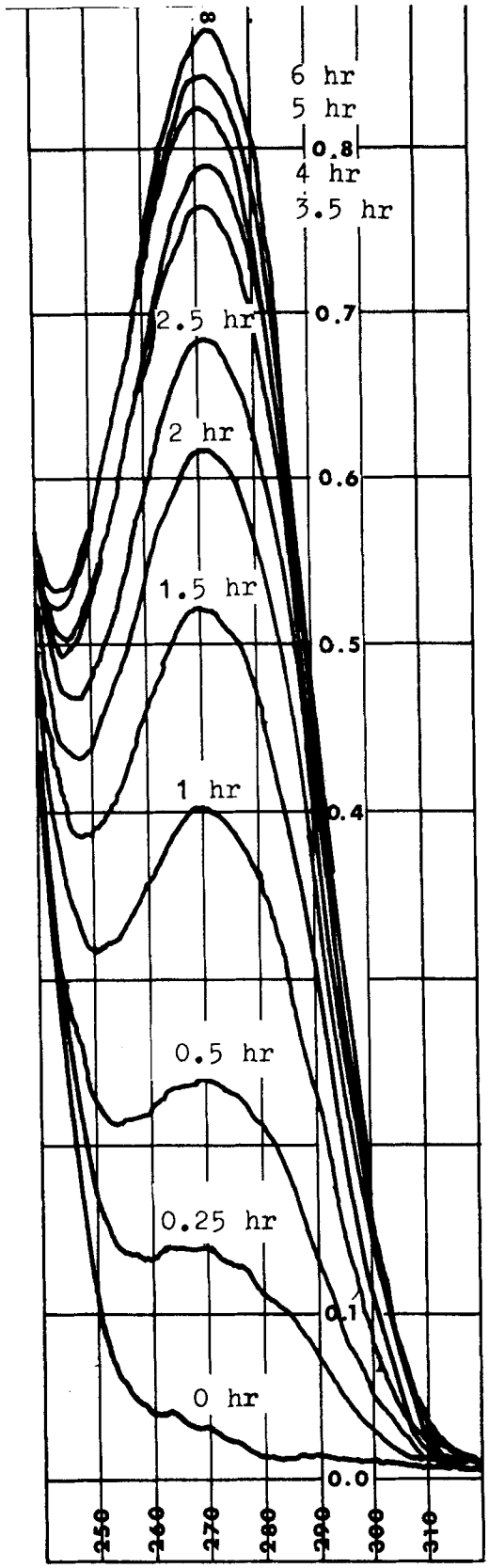

Figure 1—*UV spectra for the appearance of II from I (7.07×10^{-5} M acetate buffer, pH 4.9, 70°, ionic strength 0.1) at various times.*

[2] It is not a tertiary carbon atom in the true sense because it is attached to two other carbons and one nitrogen.

[3] Unpublished results.

[4] No. 43978, Sandoz Pharmaceuticals, Hanover, NJ 07936.

[5] Cary model 14 spectrophotometer.

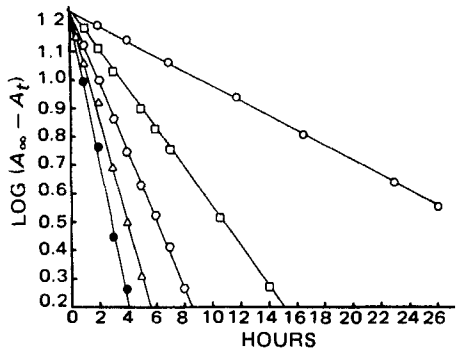

Figure 2—*First-order plot for the dehydration of 7.07 × 10⁻⁵ M I as a function of the increase in absorbance (272 nm) in hydrochloric acid at 49°. Key (hydrochloric acid concentration): ○, 0.1 N; □, 0.25 N; ○, 0.5 N; △, 0.75 N; and ●, 1.0 N.*

The transformation of I to II is somewhat similar to the reported solvolysis of several cycloheximide antibiotics (5–7). However, with the cycloheximides, an equilibrium is attained between the starting material and the anhydro product.

The apparent first-order rate constants for conversion of I to II were determined using:

$$\ln (A_\infty - A_t) = -kt + \ln (A_\infty - A_0) \qquad \text{(Eq. 1)}$$

by which the concentration of a product of a first-order process is governed. In Eq. 1, A_∞ is the maximum absorbance, A_t is the absorbance at time t, and k is the velocity constant for the reaction.

Figure 1 illustrates the UV assay of II, with the chromophore appearing as a function of time at 272 nm. These spectra are characteristic of those obtained from pH 7 down to 2.0 *N* HCl and are typical of the protonated form of II, pKa = 9.38 (±0.04). The positive charge, when present in both I and II, is probably located on N-7 of the amidino grouping[3]. The parent carbinolamine, I, showed no absorbance at 272 nm, and the previously stated analytical procedure had applicability for the interval from pH 7 to highly acid regions.

The transformation of I to II is an almost quantitative reaction. Equimolar amounts (7.07×10^{-5} *M*) of I and I hydrobromide on protracted heating at several different temperatures and the previously mentioned pH's led to spectra identical to the initial spectra of II under these circumstances. Figure 1 shows a typical example where the final absorbance is 0.880 for a 7.07×10^{-5} *M* solution. No further spectral change was noted on long heating at 95°.

Acid-Catalyzed Dehydration—The hydrogen-ion-catalyzed breakdown of I was carried out in 0.01–2.0 *N* HCl. A typical plot of these data is shown in Fig. 2 where Eq. 1 is utilized.

Figure 3 demonstrates the linear relationship of the apparent first-order velocity constants to the actual hydrogen-ion activity at several temperatures according to:

$$k = k_{H^+}[H^+] + k_0 \qquad \text{(Eq. 2)}$$

where $[H^+]$ was calculated from the experimental concentrations and the literature values for activity coefficients (8). The bimolecular rate constants, k_{H^+} in liters per mole hours, computed from the slopes of the lines in Fig. 3 (9–11) were: 0.24, 40°; 0.78, 49°; 3.20, 60°; and 8.50, 70°. The heat of activation, ΔH_a, for the dehydration reaction was calculated by an Arrhenius plot of log k_{H^+} *versus* $1/T^0$ (absolute) for these k_{H^+} values and was 25.5 kcal/mole.

The *y* intercepts in Fig. 3 are equivalent to k_0 (Eq. 2) in the acidic region where $[OH^-] \sim 0$, making $k_{OH^-}[OH^-]$ approximately equal to zero (10). The extrapolated values for k_{H_2O} were: 0.25, 40°; 0.74, 49°; 2.2, 60°; and 5.8, 70°; with a resultant heat of activation of 22.5 kcal/mole.

Ionic Strength Influence—In the dehydration of a molecule containing a positive center such as I, primary kinetic salt effects may be anticipated. Perturbation of the reaction rate constant on addition of neutral salts is to be expected from the Bronsted–Bjerrum equation (12):

$$\log k = \log k_0 + 1.02 Z_A Z_B \sqrt{\mu} \qquad \text{(Eq. 3)}$$

Equation 3 may be applied to reactions between ionic species where k_0 is the rate constant in an infinitely dilute solution, Z_A and Z_B are the charges on reactants *A* and *B*, and μ is the ionic strength. From this expression, a positive salt effect should occur in a hydronium-ion-catalyzed

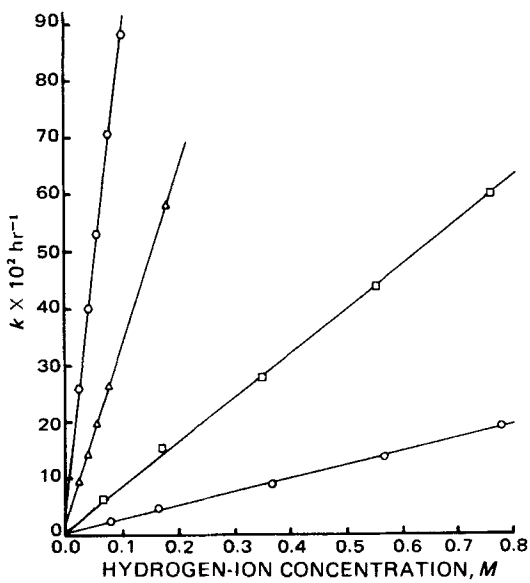

Figure 3—*Rate constants, k, in hr⁻¹ for the apparent first-order degradation of I as a function of the hydrogen-ion activity, [H⁺], at 70° (○), 60° (△), 49° (□), and 40° (○).*

dehydration of I and a negative effect should occur where the reaction is catalyzed by negative ions, *i.e.*, hydroxide and acetate. These salt effects should be evident at pH values below 5.5 [pKa of I = 7.60 (±0.04)] where I is 99+% in the cationic form.

Unfortunately, the equation only holds for extremely dilute solutions, μ = 0.01 or less, of 1:1 electrolytes. Although the relationship has no theoretical justification at higher ionic strengths (13), qualitative agreement may be seen in many cases with both positive and negative deviations as predicted (14–16).

Breakdown of I with a loss of water to give II was carried out in 0.05 *N* HCl made to final ionic strengths with sodium chloride. The temperature was 70°; UV analysis was performed at 272 nm. Figure 4 illustrates the linear relationship obtained when the log apparent first-order velocity constants were plotted *versus* the square root of the ionic strength. The same straight-line relationship is shown in Fig. 5 describing the dehydration of I at 40° in pH 4.48 acetate buffer (0.1 *M* CH_3COONa) with sodium chloride added to increase the ionic strength.

The equation predicts a slope of 1.02 under proper conditions, but Figs. 4 and 5 show that a slope of considerably less than one was obtained in both cases. These results give information concerning the primary salt effects. A linear dependence of log *k* *versus* $\sqrt{\mu}$ was seen throughout the ranges of ionic strength studied, with the expected slope signs positive for hydronium-ion-catalyzed breakdown (Fig. 4) and negative for hydroxide- and acetate-catalyzed degradation (Fig. 5). The positive slope of Fig. 4 indicates two positive ions in the transition state, while the negative slope of Fig. 5 indicates a positive and a negative charge according to the Bronsted equation.

pKa Determinations—Compound II offered no significant difficulties in the evaluation of its ionization constant because the ionized and nonionized species exhibited considerable differences in absorbance at 310 nm. The pKa of 9.38 (±0.04) was determined spectrophotometrically

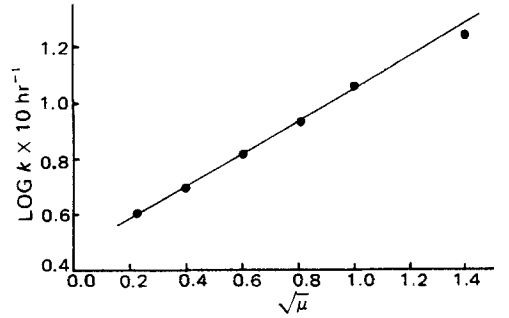

Figure 4—*Effect of ionic strength on the rate of hydronium-ion-catalyzed degradation of I at 70° in 0.05 N HCl. Sodium chloride was added as the neutral salt to increase ionic strength.*

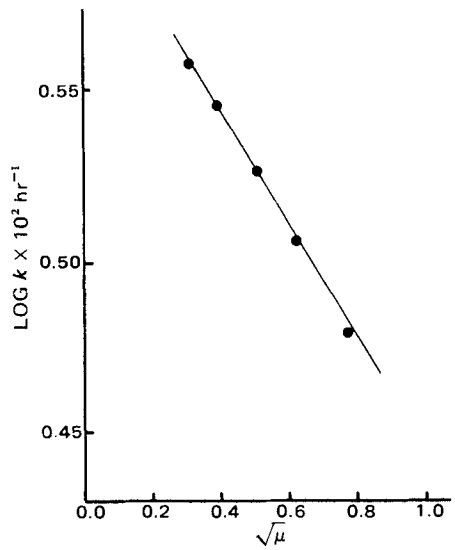

Figure 5—*Effect of ionic strength on the rate of dehydration of I at 40°, pH 4.48, and 0.1* M *sodium acetate. Sodium chloride was added to increase ionic strength.*

in the usual manner (4) by UV readings in a series of borate buffers and was corroborated by titration.

Compound I posed a problem in the absence of an easily usable UV spectrum and precipitation of the free base on attempted titration of the hydrobromide salt by potassium hydroxide (3). The more difficult solubility procedure (4) could not be easily applied in this situation due to complications arising from the conversion of I to II in the buffers needed for the studies.

A modification of the titration method was adapted using:

$$\text{pKa} = \text{pH} + \log \frac{\text{BH}^+}{\text{B}} \qquad \text{(Eq. 4)}$$

where BH^+ = I hydrobromide and B = I (free base), both in concentration terms. Previously, good results were attained by partial titration, even in instances of free base precipitation (17). The pKa values were calculated for the interval log (BH^+/B) = 49/1 to 9/1. No precipitation of base was noted in this range, and the pKa value obtained was 7.60 (±0.04).

Degradation in Buffers—Tables I and II list the observed first-order rate constants obtained in formate and acetate buffers, pH 3–5, under the experimental conditions. Figure 6 shows the observed rate constants (Tables I and II) for formate buffer, pH 4.1, 70°, and acetate buffer, pH 4.1, 60 and 70°, plotted against acetate- and formate-ion concentrations. This plot constitutes the usual test for general base catalysis (10). The data points are not aligned in the predicted linear manner but curve rather sharply downward at low buffer concentrations. The same situation is noted in Fig. 8, where acetate concentration ranged between 0.003 and 0.200 *M*.

This somewhat unusual phenomenon was encountered (18) in the sulfur to nitrogen acetyl transfer reaction of *S*-acetyl-β-mercaptoethylamine and was described as a two-step mechanism with a rate-limiting buffer-catalyzed step. The reaction rate rises sharply at low acetate- and formate-ion concentrations followed by an uncatalyzed rate-limiting step at high buffer concentrations. This nonlinear dependence of the rate constants on acetate and formate concentration is characterized by a considerable decrease in slope at relatively high buffer concentrations.

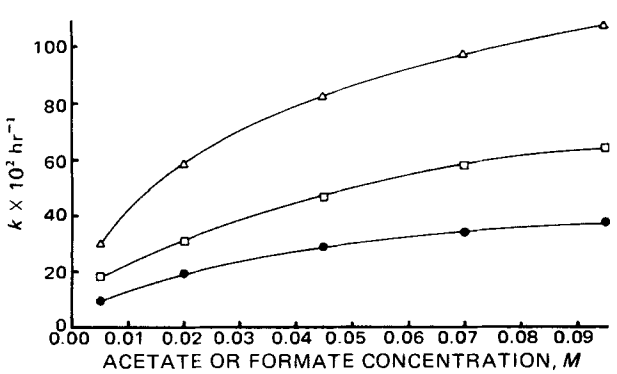

Figure 6—*Plot of the observed first-order rate constants for dehydration of I in* k × 10^2 hr^{-1} *as a function of acetate or formate concentration. Ionic strength was constant at 0.10, and the pH was 4.1. Key:* △, *acetate at 70°;* ●, *acetate at 60°; and* □, *formate at 70°.*

Table I—Observed First-Order Rate Constants[a] (k, hr^{-1}) for Dehydration of 7.07 × 10^{-5} *M* I in Formate Buffer at 70°[b]

pH	Formate Ion, *M*	k, hr^{-1}
3.0	0.005	0.20
	0.020	0.32
	0.070	0.59
3.5	0.005	0.20
	0.020	0.31
	0.048	0.49
	0.070	0.56
	0.095	0.69
4.1	0.005	0.18
	0.020	0.31
	0.045	0.46
	0.070	0.58
	0.095	0.64

[a] Based on UV absorbance data for formation of unsaturated product (Eq. 1). [b] The pH values were read at the indicated temperature on a pH meter standardized at the temperature. Ionic strength was made up to 0.1 with sodium chloride in all solutions.

In the I → II transformation, a similar two-step process occurs with a relatively large catalytic constant at low acetate or formate concentrations and a smaller constant at higher acetate or formate concentrations. Barnett and Jencks (19) further clarified this mechanism by dissecting the data into appropriate rate constants through computerization and standard techniques.

Tables I and II show the rate constants to be relatively independent of pH for the acetate (pH 4–5) and formate (pH 3–4) systems, which is in agreement with previous work (18, 19).

Arrhenius plots for the decomposition of I in pH 4.1 acetate buffer (Table II) are shown in Fig. 7. The apparent energies of activation ranged between 24 and 25.5 kcal/mole for the various acetate concentrations.

Table II—Observed First-Order Rate Constants[a] (k, hr^{-1}) and Experimental Conditions for Dehydration of 7.07 × 10^{-5} *M* I in Acetate Buffer Solution

pH[b]	Acetate Ion, *M*	Ionic[c] Strength	k, hr^{-1} 40°	60°	70°
4.1	0.005	0.10	0.0075	0.0962	0.29
	0.020		0.0181	0.1994	0.58
	0.045		0.0265	0.2887	0.82
	0.070		0.0327	0.3408	0.96
	0.095		0.0359	0.3794	1.08
4.5	0.005	0.10	—	0.0984	0.30
	0.020		—	0.2101	0.61
	0.045		—	0.2986	0.86
	0.070		—	0.3569	1.00
	0.095		—	0.3658	1.09
5.0	0.005	0.10	0.0112	0.1006	0.31
	0.020		0.0209	0.2094	0.60
	0.045		0.0166	0.2951	0.89
	0.070		0.0310	0.3583	1.00
	0.095		0.0351	0.3755	1.07
4.1	0.015	0.20	—	—	0.48
	0.045		—	—	0.82
4.5	0.015	0.20	—	0.1598	0.50
	0.045		—	0.2725	0.81
	0.095		—	0.3522	—
	0.145		—	0.3906	—
	0.195		—	0.4120	—
5.0	0.015	0.20	—	0.2071	0.51
	0.045		—	0.2910	0.85
	0.095		—	0.4173	—
	0.145		—	0.4407	—
	0.195		—	0.4998	—

[a] See Table I. [b] See Table I. [c] Sodium chloride was added to produce proper ionic strength.

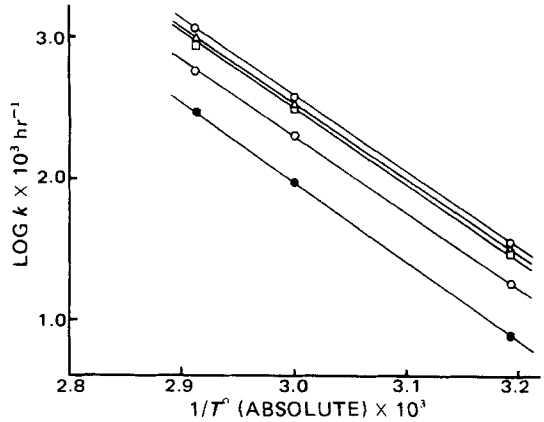

Figure 7—*Typical Arrhenius plots for degradation of I in pH 4.1 acetate buffer (Table II) at various acetate-ion concentrations. Key (acetate concentration):* ●, *0.005* M; ○, *0.020* M; □, *0.045* M; △, *0.070* M; *and* ○, *0.095* M.

Concentrations of acetate below 3×10^{-3} *M* (Fig. 8) could not be employed with the pH maintained constant, thus preventing studies at lower acetate-ion concentrations. The results in Fig. 8 should theoretically extrapolate at zero buffer concentration to the k_0 value (Eq. 2). Examination of k_0 for the acetate system in Fig. 8 shows that of its three components, k_{H_2O}, $k_{H^+}[H^+]$, and $k_{OH^-}[OH^-]$, the first has a predominant importance, $k_{H_2O} = 2.2$, 60°. The reasoning is that the $[H^+]$ of 3×10^{-5} *M*, pH 4.5, multiplied by $k_{H^+} = 3.2$, 60°, provides a negligible contribution, while k_{OH^-} seems to play a relatively unimportant role due to the small effect noted on the rate constants in the pH 4–5 range.

The values in Table II for the various pH values at a given temperature are almost within the limits of experimental error. Thus, it appears that the value for k_0 (Fig. 8) should be somewhat above the value of 2.2 hr^{-1} for k_{H_2O} at 60°. Figure 6 shows that the *y* intercept for formate and acetate ions at 70° also might be extrapolated to approximately the k_{H_2O} value at that temperature. This nonlinear dependency of the data upon anionic concentrations may be noted in all results listed in Tables I and II.

Notari *et al.* (20) reported a similar phenomenon taking place in a deamination reaction, except that the acidic buffer component exerted the principal catalytic effect.

These results are indicative of a reaction rate constant plateau in the pH range of 3–5 with little OH^- or H^+ effect. The primary route of breakdown is water attack on the protonated form of I. In this pH 3–5 region, general bases catalyze in what may be a two-step sequence (18–20).

Preliminary investigations with phosphate buffers demonstrate this nonlinear dependency at pH 5.7 as was found with the acetate systems. However, at higher pH values (6.0 and 6.7), typical linear data were encountered (Table III). Studies were not carried out above pH 6.7 due to the insolubility of the basic form of I, pKa 7.6.

Table III—Observed First-Order Rate Constants[a] (k, hr^{-1}) for Dehydration of 7.07×10^{-5} *M* I in Phosphate Buffer at 60°[b]

	Buffer Composition, *M*[d]		
pH[c]	Monobasic Sodium Phosphate Monohydrate	Dibasic Sodium Phosphate Heptahydrate	k, hr^{-1}
5.70 ± 0.04	0.150	0.015	0.42
	0.110	0.011	0.39
	0.070	0.007	0.33
	0.030	0.003	0.26
6.00 ± 0.05	0.115	0.0283	0.54
	0.0805	0.0198	0.50
	0.0575	0.0142	0.47
	0.046	0.0113	0.45
	0.023	0.0057	0.42
6.70 ± 0.04	0.050	0.050	0.64
	0.035	0.035	0.60
	0.030	0.030	0.57
	0.020	0.020	0.52
	0.005	0.005	0.44

[a] See Table I. [b] See Table I. [c] The pH values were read at the indicated temperatures before, during, and after a run. [d] Stock solutions were diluted to give indicated strengths followed by addition of sodium chloride to obtain an ionic strength of 0.2.

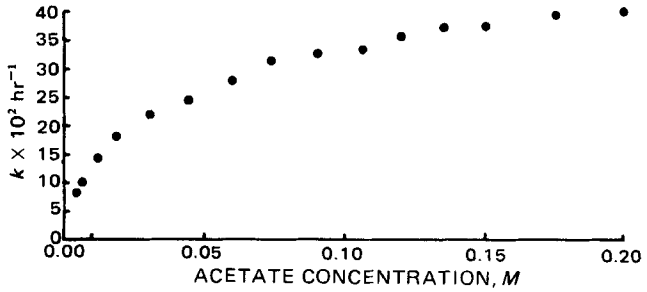

Figure 8—*Plot of the observed first-order rate constant for dehydration of I* versus *acetate concentration at 60°, pH 4.5, with ionic strength maintained with sodium chloride. The pH values were measured at 60° on a pH meter standardized at that temperature and were within 0.04 of the stated value of 4.5. Rate constants were reproducible within 5%. Ionic strength was constant at 0.20. These data are not listed in Table II.*

SUMMARY

Compound I undergoes apparent first-order degradation under the conditions examined, producing the dehydration product II in almost quantitative yields.

Elimination of the C-2 hydrogen and the C-3 hydroxyl substituents of I takes place in aqueous solution since their *trans*-conformational relationship tends to facilitate this reaction.

The mechanism of acid-catalyzed dehydration probably involves protonation of the hydroxyl group followed by formation of a carbonium ion and elimination of a proton to produce the dehydro product. Conversely, base catalysis is initiated by removal of a proton followed by elimination of an OH^-. These well-known processes were discussed for streptovitacin A dehydration (7).

Observed rate constants did not show the usual linear dependency in acetic acid–acetate buffers. Curves were obtained with negative deviation from linearity. This result was probably due to a change in the rate-determining step.

The observed rate constant for this transformation in the absence of other species (*e.g.*, buffers and salts) may be written to pH 5 as $k = k_{H^+}[H^+] + k_{H_2O}$ with actual data closely following calculated values. Water attack on the protonated substrate occurred and seemed to be the principal cause of degradation in the pH 3–5 range. The molecule exhibited greatest stability in this region, but degradation was accelerated considerably by addition of general bases.

The compound shows rather pronounced salt effects, both positive and negative, depending on the reaction conditions.

REFERENCES

(1) D. Magrath and J. Phillips, *J. Chem. Soc.*, **1949**, 1940.

(2) H. C. Brown and R. S. Fletcher, *J. Am. Chem. Soc.*, **71**, 1845 (1949).

(3) A. Albert and E. P. Sergeant, "Ionization Constants of Acids and Bases," Wiley, New York, N.Y., 1962, pp. 16–42.

(4) *Ibid.*, pp. 69–91.

(5) E. R. Garrett and R. E. Notari, *J. Org. Chem.*, **31**, 425 (1966).

(6) E. R. Garrett and R. E. Notari, *J. Pharm. Sci.*, **54**, 209 (1965).

(7) R. E. Notari and S. M. Caiola, *ibid.*, **58**, 1203 (1969).

(8) H. S. Harned and R. B. Owen, "The Physical Chemistry of Electrolytic Solutions," 3rd ed., Reinhold, New York, N.Y., 1958.

(9) E. R. Garrett, *J. Am. Chem. Soc.*, **82**, 827 (1960).

(10) E. R. Garrett, *J. Pharm. Sci.*, **51**, 811 (1962).

(11) E. R. Garrett, "Advances in Pharmaceutical Sciences," vol. 2, Academic, New York, N.Y., 1967, p. 1.

(12) S. Glasstone, K. J. Laidler, and H. Eyring, "The Theory of Rate Processes," McGraw-Hill, New York, N.Y., 1941, p. 427.

(13) A. G. Frost and R. G. Pearson, "Kinetics and Mechanism," 2nd ed., Wiley, New York, N.Y., 1965, p. 151.

(14) S. Siegel, L. Lachman, and L. Malspeis, *J. Am. Pharm. Assoc.*,

Sci. Ed., **48**, 431 (1959).
(15) R. B. Bell and F. J. Lindlars, *J. Chem. Soc.*, **1954**, 4601.
(16) E. R. Garrett, *J. Am. Chem. Soc.*, **79**, 5206 (1957).
(17) H. V. Maulding and M. A. Zoglio, *J. Pharm. Sci.*, **59**, 700 (1970).
(18) R. B. Martin, R. I. Heddrick, and A. Parcell, *J. Org. Chem.*, **29**, 3197 (1964).
(19) R. E. Barnett and W. P. Jencks, *J. Am. Chem. Soc.*, **91**, 2358 (1969).
(20) R. E. Notari, M. L. Chin, and A. Cardoni, *J. Pharm. Sci.*, **59**, 28 (1970).

ACKNOWLEDGMENTS AND ADDRESSES

Received February 9, 1970, from the *Pharmacy Research and Development Department, Sandoz Pharmaceuticals, Hanover, NJ 07936.*

Accepted for publication April 8, 1970. (Publication delayed at request of authors.)

The authors acknowledge the technical assistance of Miss Virginia Nieman.

* Present address: Merrell-National Laboratories, Cincinnati, OH 45215.

[x] To whom inquiries should be directed.

Quantification of Lidocaine and Several Metabolites Utilizing Chemical-Ionization Mass Spectrometry and Stable Isotope Labeling

S. D. NELSON, W. A. GARLAND, G. D. BRECK, and W. F. TRAGER [x]

Abstract □ Quantification of the suspected metabolites of lidocaine in humans was carried out using the direct insertion probe and chemical-ionization mass spectrometry. Deuterated analogs of the metabolites of lidocaine were added to serial human plasma and urine samples and were used as internal standards following oral administration of 250 mg of lidocaine hydrochloride monohydrate to two male subjects and 202 mg of lidocaine free base to one male subject. The average results after analysis of the 0–24-hr urine samples, before β-glucuronidase–sulfatase treatment, indicated the presence of seven of the possible metabolites in the following amounts (percent of administered dose based on the free base): lidocaine, 1.95; ω-ethylamino-2,6-dimethylacetanilide, 4.90; ω-amino-2,6-dimethylacetanilide, 0.88; *m*- and/or *p*-hydroxylidocaine, 0.73; *m*- and/or *p*-hydroxy-ω-ethylamino-2,6-dimethylacetanilide, 0.56; 2,6-dimethylaniline, 0.97; and 4-hydroxy-2,6-dimethylaniline, 63.5. Both *N*-ethyl- and *N,N*-diethylglycine were detected in human and Rhesus monkey urine, although quantification was not achieved.

Keyphrases □ Lidocaine and various metabolites—chemical-ionization mass spectrometric and stable isotope labeling analyses, human plasma and urine □ Chemical-ionization mass spectrometry—analyses, lidocaine and various metabolites, human plasma and urine □ Stable isotope labeling—analyses, lidocaine and various metabolites, human plasma and urine □ Anesthetics, local—lidocaine and various metabolites, chemical-ionization mass spectrometric and stable isotope labeling analyses, human plasma and urine

Lidocaine (I*a*) is a widely used local anesthetic and antiarrhythmic agent. At present, it is generally considered the most useful drug in suppressing ventricular arrhythmias, which occur in approximately 80% of all myocardial infarction cases (1–3). Based on the structure of the drug, three sites are susceptible to metabolic attack: the tertiary amino group, the amide linkage, and the aromatic ring. The tertiary amino group is susceptible to *N*-oxidation and oxidative *N*-dealkylation (4). The amide linkage is susceptible to hydrolysis by microsomal amidases (5) and to oxidation by liver microsomes to an *N*-hydroxyamide (4). The aromatic ring and the aryl methyl groups are also susceptible to hydroxylation (4). Many of these reactions were detected using nonspecific colorimetric assays and paper chromatography (6–9) and, more recently, more specific GC methods (10–12).

Using electron-impact mass spectrometry, Breck and Trager (13) confirmed the presence of lidocaine, ω-ethylamino-2,6-dimethylacetanilide (I*b*), and 2,6-dimethylaniline (II*a*) in human urine following an oral dose or an intravenous infusion of lidocaine. They also detected small amounts of a new cyclic metabolite of lidocaine, N^1-ethyl-2-methyl-N^3-(2,6-dimethylphenyl)-4-imidazolidinone (III). GC–mass spectrometry was used to detect and quantify lidocaine and its two *N*-deethylated metabolites, I*b* and ω-amino-2,6-dimethylacetanilide (I*c*), in the plasma and urine of patients receiving intravenous infusions of the drug for the treatment of cardiac arrhythmias (14, 15). Under these conditions, lidocaine levels ranged from 1.2 to 15 μg/ml, I*b* levels ranged from 0.2 to 2.4 μg/ml, and I*c* levels ranged from <1.0 to 2.7 μg/ml, with

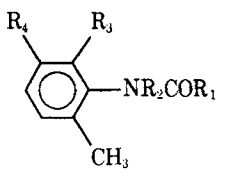

I*a*: $R_1 = CH_2N(CH_2CH_3)_2$, $R_2 = H$, $R_3 = CH_3$, $R_4 = H$
I*a*-d_4: $R_1 = CH_2N(CD_2CH_3)_2$
I*b*: $R_1 = CH_2NHCH_2CH_3$, $R_2 = H$, $R_3 = CH_3$, $R_4 = H$
I*b*-d_3: $R_1 = CH_2NHCH_2CD_3$
I*c*: $R_1 = CH_2NH_2$, $R_2 = H$, $R_3 = CH_3$, $R_4 = H$
I*c*-d_2: $R_1 = CD_2NH_2$
I*d*: $R_1 = CH_2N(CH_2CH_3)_2$, $R_2 = H$, $R_3 = CH_3$, $R_4 = OH$
I*d*-d_4: $R_1 = CH_2N(CD_2CH_3)_2$
I*e*: $R_1 = CH_2NHCH_2CH_3$, $R_2 = H$, $R_3 = CH_3$, $R_4 = OH$
I*e*-d_3: $R_1 = CH_2NHCH_2CD_3$
I*f*: $R_1 = CH_2N(CH_2CH_3)_2$, $R_2 = H$, $R_3 = CH_2OH$, $R_4 = H$
I*g*: $R_1 = CH_2NHCH_2CH_3$, $R_2 = H$, $R_3 = CH_2OH$, $R_4 = H$
I*g*-d_2: $R_3 = CD_2OH$
I*h*: $R_1 = CH_2N(CH_2CH_3)_2$, $R_2 = OH$, $R_3 = CH_3$, $R_4 = H$
I*h*-d_4: $R_1 = CH_2N(CD_2CH_3)_2$
I*i*: $R_1 = CH_2NHCH_2CH_3$, $R_2 = OH$, $R_3 = CH_3$, $R_4 = H$
I*i*-d_3: $R_1 = CH_2NHCH_2CD_3$
I*j*: $R_1 = CH_2N(CH_2CH_3)_2$, $R_2 = H$, $R_3 = CH_3$, $R_4 = H$

Sci. Ed., **48**, 431 (1959).
(15) R. B. Bell and F. J. Lindlars, *J. Chem. Soc.*, **1954**, 4601.
(16) E. R. Garrett, *J. Am. Chem. Soc.*, **79**, 5206 (1957).
(17) H. V. Maulding and M. A. Zoglio, *J. Pharm. Sci.*, **59**, 700 (1970).
(18) R. B. Martin, R. I. Heddrick, and A. Parcell, *J. Org. Chem.*, **29**, 3197 (1964).
(19) R. E. Barnett and W. P. Jencks, *J. Am. Chem. Soc.*, **91**, 2358 (1969).
(20) R. E. Notari, M. L. Chin, and A. Cardoni, *J. Pharm. Sci.*, **59**, 28 (1970).

ACKNOWLEDGMENTS AND ADDRESSES

Received February 9, 1970, from the *Pharmacy Research and Development Department, Sandoz Pharmaceuticals, Hanover, NJ 07936.*

Accepted for publication April 8, 1970. (Publication delayed at request of authors.)

The authors acknowledge the technical assistance of Miss Virginia Nieman.

* Present address: Merrell-National Laboratories, Cincinnati, OH 45215.

[x] To whom inquiries should be directed.

Quantification of Lidocaine and Several Metabolites Utilizing Chemical-Ionization Mass Spectrometry and Stable Isotope Labeling

S. D. NELSON, W. A. GARLAND, G. D. BRECK, and W. F. TRAGER [x]

Abstract □ Quantification of the suspected metabolites of lidocaine in humans was carried out using the direct insertion probe and chemical-ionization mass spectrometry. Deuterated analogs of the metabolites of lidocaine were added to serial human plasma and urine samples and were used as internal standards following oral administration of 250 mg of lidocaine hydrochloride monohydrate to two male subjects and 202 mg of lidocaine free base to one male subject. The average results after analysis of the 0–24-hr urine samples, before β-glucuronidase–sulfatase treatment, indicated the presence of seven of the possible metabolites in the following amounts (percent of administered dose based on the free base): lidocaine, 1.95; ω-ethylamino-2,6-dimethylacetanilide, 4.90; ω-amino-2,6-dimethylacetanilide, 0.88; *m*- and/or *p*-hydroxylidocaine, 0.73; *m*- and/or *p*-hydroxy-ω-ethylamino-2,6-dimethylacetanilide, 0.56; 2,6-dimethylaniline, 0.97; and 4-hydroxy-2,6-dimethylaniline, 63.5. Both *N*-ethyl- and *N,N*-diethylglycine were detected in human and Rhesus monkey urine, although quantification was not achieved.

Keyphrases □ Lidocaine and various metabolites—chemical-ionization mass spectrometric and stable isotope labeling analyses, human plasma and urine □ Chemical-ionization mass spectrometry—analyses, lidocaine and various metabolites, human plasma and urine □ Stable isotope labeling—analyses, lidocaine and various metabolites, human plasma and urine □ Anesthetics, local—lidocaine and various metabolites, chemical-ionization mass spectrometric and stable isotope labeling analyses, human plasma and urine

Lidocaine (I*a*) is a widely used local anesthetic and antiarrhythmic agent. At present, it is generally considered the most useful drug in suppressing ventricular arrhythmias, which occur in approximately 80% of all myocardial infarction cases (1–3). Based on the structure of the drug, three sites are susceptible to metabolic attack: the tertiary amino group, the amide linkage, and the aromatic ring. The tertiary amino group is susceptible to *N*-oxidation and oxidative *N*-dealkylation (4). The amide linkage is susceptible to hydrolysis by microsomal amidases (5) and to oxidation by liver microsomes to an *N*-hydroxyamide (4). The aromatic ring and the aryl methyl groups are also susceptible to hydroxylation (4). Many of these reactions were detected using nonspecific colorimetric assays and paper chromatography (6–9) and, more recently, more specific GC methods (10–12).

Using electron-impact mass spectrometry, Breck and Trager (13) confirmed the presence of lidocaine, ω-ethylamino-2,6-dimethylacetanilide (I*b*), and 2,6-dimethylaniline (II*a*) in human urine following an oral dose or an intravenous infusion of lidocaine. They also detected small amounts of a new cyclic metabolite of lidocaine, N^1-ethyl-2-methyl-N^3-(2,6-dimethylphenyl)-4-imidazolidinone (III). GC–mass spectrometry was used to detect and quantify lidocaine and its two *N*-deethylated metabolites, I*b* and ω-amino-2,6-dimethylacetanilide (I*c*), in the plasma and urine of patients receiving intravenous infusions of the drug for the treatment of cardiac arrhythmias (14, 15). Under these conditions, lidocaine levels ranged from 1.2 to 15 μg/ml, I*b* levels ranged from 0.2 to 2.4 μg/ml, and I*c* levels ranged from <1.0 to 2.7 μg/ml, with

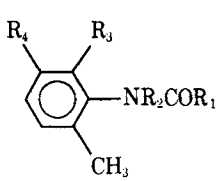

I*a*: $R_1 = CH_2N(CH_2CH_3)_2$, $R_2 = H$, $R_3 = CH_3$, $R_4 = H$
I*a*-d_4: $R_1 = CH_2N(CD_2CH_3)_2$
I*b*: $R_1 = CH_2NHCH_2CH_3$, $R_2 = H$, $R_3 = CH_3$, $R_4 = H$
I*b*-d_3: $R_1 = CH_2NHCH_2CD_3$
I*c*: $R_1 = CH_2NH_2$, $R_2 = H$, $R_3 = CH_3$, $R_4 = H$
I*c*-d_2: $R_1 = CD_2NH_2$
I*d*: $R_1 = CH_2N(CH_2CH_3)_2$, $R_2 = H$, $R_3 = CH_3$, $R_4 = OH$
I*d*-d_4: $R_1 = CH_2N(CD_2CH_3)_2$
I*e*: $R_1 = CH_2NHCH_2CH_3$, $R_2 = H$, $R_3 = CH_3$, $R_4 = OH$
I*e*-d_3: $R_1 = CH_2NHCH_2CD_3$
I*f*: $R_1 = CH_2N(CH_2CH_3)_2$, $R_2 = H$, $R_3 = CH_2OH$, $R_4 = H$
I*g*: $R_1 = CH_2NHCH_2CH_3$, $R_2 = H$, $R_3 = CH_2OH$, $R_4 = H$
I*g*-d_2: $R_3 = CD_2OH$
I*h*: $R_1 = CH_2N(CH_2CH_3)_2$, $R_2 = OH$, $R_3 = CH_3$, $R_4 = H$
I*h*-d_4: $R_1 = CH_2N(CD_2CH_3)_2$
I*i*: $R_1 = CH_2NHCH_2CH_3$, $R_2 = OH$, $R_3 = CH_3$, $R_4 = H$
I*i*-d_3: $R_1 = CH_2NHCH_2CD_3$
I*j*: $R_1 = CH_2N(CH_2CH_3)_2$, $R_2 = H$, $R_3 = CH_3$, $R_4 = H$

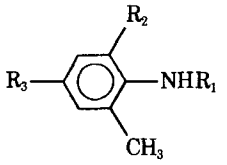

IIa: R_1 = H, R_2 = CH_3, R_3 = H IIa-d_2: R_2 = CHD_2
IIb: R_1 = H, R_2 = CH_2OH, R_3 = H IIb-d_2: R_2 = CD_2OH
IIc: R_1 = OH, R_2 = CH_3, R_3 = H
IId: R_1 = H, R_2 = CH_3, R_3 = OH IId-d_2: R_2 = CHD_2

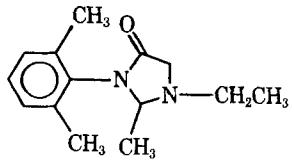

III

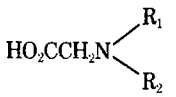

IVa: R_1 = CH_2CH_3, R_2 = CH_2CH_3
IVa-d_4: R_1 = CD_2CH_3, R_2 = CD_2CH_3
IVb: R_1 = CH_2CH_3, R_2 = H
IVb-d_3: R_1 = CH_2CD_3, R_2 = H

Ic levels <1.0 μg/ml not measurable. A rapid, specific, analytical technique for monitoring these metabolites might be useful, since one or more of these biotransformation products may be responsible for some of the central nervous system toxicity associated with lidocaine therapy.

A more direct quantification of quinidine, lidocaine, and their metabolites in human plasma, utilizing a combination of stable isotope labeling and chemical-ionization mass spectrometry, was described previously (16). This technique is now applied to the quantification of lidocaine and several of its metabolites in human plasma and urine.

The chemical-ionization mass spectrometry–stable isotope technique, combined with some more classical techniques, confirmed (at least under the *in vivo* conditions of dosage and analysis used in this study) the presence of many suspected lidocaine metabolites and showed the absence of others. To carry out this analysis, the 17 suspected metabolites (Ia–Ij, IIa–IId, III, IVa, and IVb) and the deuterated analogs were synthesized.

EXPERIMENTAL[1]

Equipment—Melting points[2] are uncorrected. When obtaining chemical-ionization mass spectra, the electron gun voltage was set at 510 v and the ion repeller was set between 0.0 and 1.0 v. The source and analyzer ion gauges read 1.8×10^{-4} and 7.6×10^{-6} torr, respectively. The source chamber pressure was 0.5 torr as read from a calibrated McLeod gauge some distance from the ion chamber. Both sample and reagent gas were introduced *via* a specially designed direct insertion probe (17, 18).

All mass spectra were run at an accelerating voltage of 8 kv and a mass resolution of $m/\Delta = 3500$ (5% valley definition). All samples were dissolved in either ethanol[3] or methanolic hydrogen chloride, the solution was applied to the ceramic probe tip, and the solvent was evaporated with a gentle stream of nitrogen. Elemental analyses[4] were obtained where appropriate.

Lidocaine (Ia)—Compound Ia[5] was recrystallized from purified petroleum ether (bp 30–60°) to obtain colorless needles, mp 67–68° (19). The chemical-ionization mass spectrum showed that the MH^+ ion at *m/e* 235 and its ^{13}C-satellite represented 84.8% of the total ion current; *m/e* 164 represented 15.2% of the total ion current from *m/e* 100 to 300.

Lidocaine-d_4 (Ia-d_4)—A mixture of freshly distilled acetonitrile (4.10 g, 0.1 mole) and 200 mg of Adam's catalyst in freshly distilled acetic anhydride (30 ml) was hydrogenated (30 psi, deuterium gas) for 4 hr. An additional 100 mg of catalyst was added, and the hydrogenation was continued an additional 2 hr. After removal of reduced platinum by suction filtration, the filtrate was distilled through a short-path fractionating column to yield *N*-ethylacetamide-d_2, bp 204–207° (7.1 g, 80%).

To an ice bath-cooled solution of aluminum trideuteride (~46 mmoles generated from lithium aluminum deuteride and sulfuric acid) in tetrahydrofuran was added dropwise a tetrahydrofuran solution of *N*-ethylacetamide-d_2 (1.90 g, 23 mmoles) over 60 min. The solution was slowly allowed to come to room temperature and was stirred an additional 18 hr under nitrogen. Excess aluminum trideuteride was destroyed with 4 ml of tetrahydrofuran–water (1:1), followed by hydrolysis of aluminate complexes with 8 ml of 15% NaOH. The liberated diethylamine-d_4 was codistilled with tetrahydrofuran at 59–60°.

To the tetrahydrofuran solution, 60 ml, containing diethylamine-d_4 was added ω-chloro-2,6-dimethylacetanilide (19) (1.97 g, 10 mmoles), and the solution was stirred at reflux for 3 hr. To the solution was added 450 mg of sodium hydroxide in 2 ml of water, and the reaction was refluxed an additional 2 hr. Rotary evaporation of solvent yielded a pale-yellow liquid, which was taken up in ether, washed with water, and extracted into 10% HCl. The acid extract was made basic with 5 *N* NaOH and back-extracted into ether. The ether back-extract was washed with water, filtered through anhydrous sodium sulfate, and dried over calcium sulfate[6]. Removal of solvent and three recrystallizations from petroleum ether yielded 1.4 g (59%), mp 65–67°; NMR: δ^T 1.13 [broad s, $N(CD_2CH_3)_2$], 2.23 (s, aryl methyls), 3.20 (s, $O{=}CCH_2N$), 7.07 (s, aromatics), and 8.90 (broad s, $HNC{=}O$) ppm; high-resolution mass measurement: calc. for $C_{14}H_{18}{}^2H_4N_2O$, 238.1983; found, 238.1979.

A chemical-ionization mass spectral analysis showed the following isotopic abundances: lidocaine-d_4, 71.5% (*m/e* 239); lidocaine-d_3, 19.0% (*m/e* 238); lidocaine-d_2, 4.4% (*m/e* 237); lidocaine-d_1, 5.1% (*m/e* 236); and lidocaine, 0% (*m/e* 235).

ω-(β-^{2}H-Ethylamino)-2,6-dimethylacetanilide (Ib-d_3)—Ethylamine-d_3 hydrochloride was synthesized, according to the procedure of Ross *et al.* (20), by lithium aluminum hydride reduction of acetonitrile-d_3.

To a magnetically stirred mixture of ω-chloro-2,6-dimethylacetanilide (295 mg, 2 mmoles) and ethylamine-d_3 hydrochloride (254 mg, 3 mmoles) in dioxane (20 ml) and water (5 ml) was added anhydrous potassium carbonate (420 mg, 3 mmoles) in 20-mg portions over 2 hr while the reaction was heated at 60° in an oil bath. After the addition was complete, the reaction was stirred an additional 3 hr. Rotary evaporation of the solvent yielded a white crystalline mass, which was worked up as described for Ib. Removal of solvent gave a pale-yellow liquid, which was taken up in 20 ml of purified hexane and recrystallized to yield 350 mg (80%) of small needles, mp 49–51°. The hydrochloride was made by dissolving the free base in absolute ethanol and bubbling through anhydrous hydrogen chloride. Light needles formed and were collected by suction filtration, mp 285–288° dec.

A chemical-ionization mass spectral analysis showed the following isotopic abundances: Ib-d_3, 66.0% (*m/e* 210); Ib-d_2, 22.4% (*m/e* 209); Ib-d_1, 8.0% (*m/e* 208); and Ib, 3.6% (*m/e* 207).

ω-Amino-2,6-dimethylacetanilide (Ic)—To a magnetically stirred solution of freshly distilled 2,6-dimethylaniline (1.21 g, 0.01 mole) and *N*-benzyloxycarbonylglycine[7] (2.10 g, 0.01 mole) in dichloromethane (50 ml) was added dicyclohexylcarbodiimide[7] (25 ml) over 20 min. During the addition, a heavy white precipitate formed. Additional dichloromethane (75 ml) was added, and the slurry was stirred for 2 hr at room temperature.

The white precipitate, containing both dicyclohexylurea and ω-benzyloxycarbonylamino-2,6-dimethylacetanilide, was collected by suction

[1] IR spectra were recorded on either a Perkin-Elmer 337 or Varian IR-5A spectrophotometer. NMR spectra in chloroform-d_3, unless otherwise indicated, were recorded on a Varian A-60 (δ) or T-60 (δ^T); all chemical shift values are reported as δ values with tetramethylsilane as internal standard. Electron-impact mass spectra were obtained on an AEI MS 902 (direct inlet; 70 ev); chemical-ionization mass spectra were obtained on an AEI MS-9 double-focusing mass spectrometer modified for chemical ionization, using isobutane as the reagent gas (17).

[2] Fischer-Johns.

[3] Gold shield.

[4] Huffman Laboratories, Wheatbridge, Colo.

[5] Astra Pharmaceutical Products, Worcester, Mass.

[6] Drierite.

[7] Aldrich Chemicals, San Leandro, Calif.

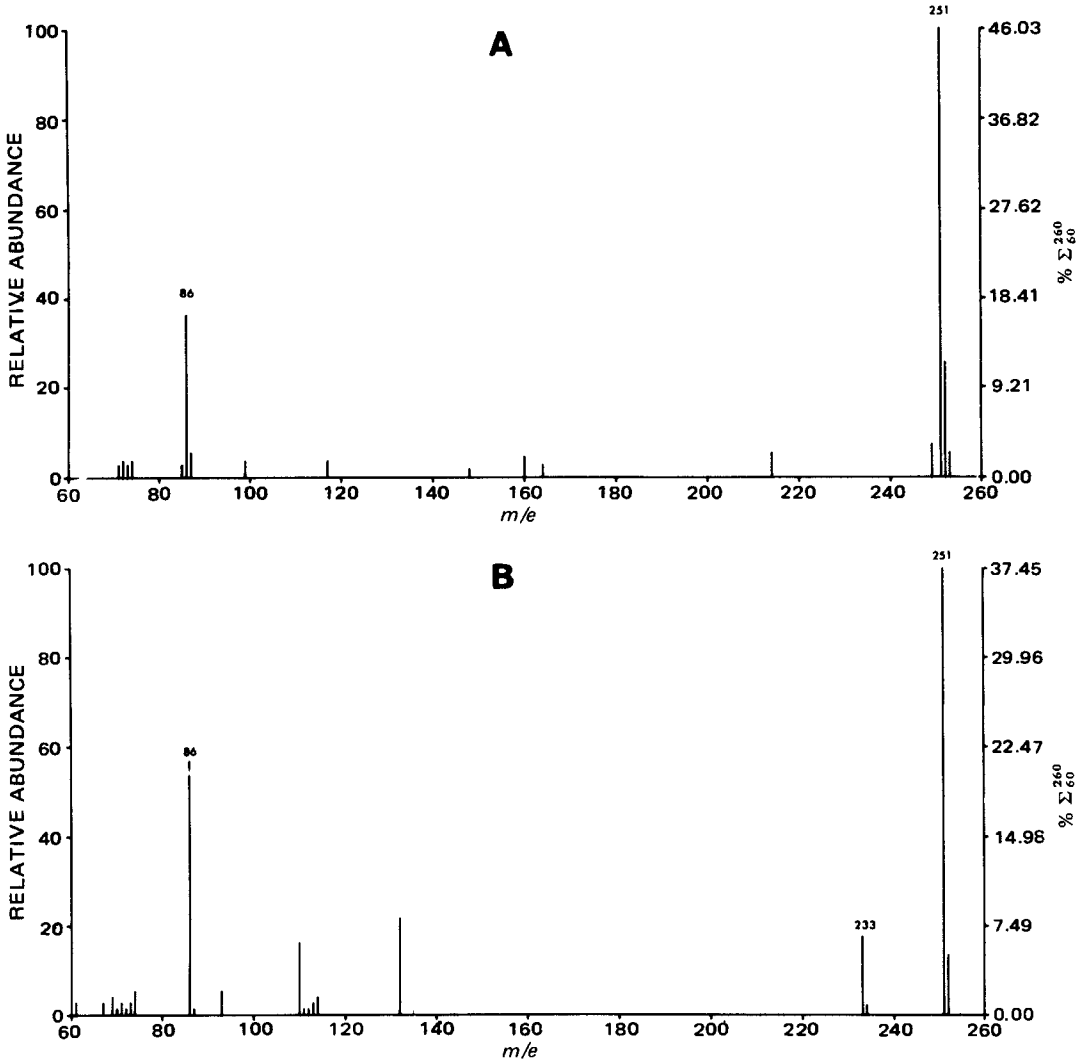

Figure 1—*Comparative chemical-ionization mass spectra of Id (A) and If (B).*

filtration and dissolved in aldehyde-free ethanol (75 ml) (21). The mixture was hydrogenated (25 psi hydrogen) on a Paar shaker over 300 mg of 10% palladium-on-carbon for 15 hr at room temperature. Rotary evaporation of ethanol gave a pale-yellow liquid, which was dissolved in purified chloroform (50 ml) (22) and extracted with two portions of 10% HCl (25 ml). Combined acid extracts were made basic with 5 *N* NaOH and back-extracted into ether.

The ethereal solution was washed with water, dried over anhydrous sodium sulfate, and evaporated to yield a semisolid mass. Recrystallization from purified hexane–2-propanol gave 750 mg (42%) of white needles, mp 80–88° [lit. (15) mp 79–80°]; IR (KBr): 3400 (NH_2), 3300 (amide NH), and 1660 (amide C=O) cm^{-1}; NMR: δ^T 1.55 (broad m, NH_2), 2.20 (s, aryl methyls), 3.50 (t, J = 7 Hz, O=CCH_2NH_2), 7.05 (s, aromatics), and 8.80 (broad s, HNC=O) ppm. Addition of deuterium oxide showed loss of the broad multiplet at 1.65 ppm and collapse of the triplet at 3.50 ppm to a singlet.

The isobutane chemical-ionization mass spectrum of Ic showed that the MH^+ ion at *m/e* 179 and its ^{13}C-satellite represented 96.8% and *m/e* 164 was 3.2% of the total ion current. The electron-impact spectrum of Ic was published previously (15).

α-^{2}H-ω-Amino-2,6-dimethylacetanilide (Ic-d_2)—To a solution of ω-amino-2,6-dimethylacetanilide (750 mg) in 99.7% deuterium oxide (20 ml) and freshly distilled tetrahydrofuran (5 ml) was added 0.5 g of anhydrous potassium carbonate. The solution was heated at 90° for 24 hr, cooled, and lyophilized; this procedure was repeated three times. After the final lyophilization, the white crystalline residue was taken up in purified chloroform (50 ml) and water (30 ml) and shaken vigorously. The chloroform extract was washed with two additional portions of water (10 ml) and dried over anhydrous sodium sulfate. Rotary evaporation yielded a pale-yellow crystalline solid, which was recrystallized from purified hexane–2-propanol to give 510 mg (68%) of white needles, mp 79–80.5°; NMR: δ^T 1.55 (broad s, NH_2), 2.20 (s, aryl methyls), and 8.80 (broad s, HNC=O) ppm.

The chemical-ionization mass spectrum showed the following isotopic abundances: Ic-d_2, 99.0% (*m/e* 181); Ic-d_1, 1.0% (*m/e* 180); and Ic, 0% (*m/e* 179).

3-Hydroxy-ω-diethylamino-2,6-dimethylacetanilide (Id)—Compound Id was synthesized in 52% overall yield, according to the method of Keenaghan and Boyes (12), by nitration of lidocaine, reduction to the aromatic amino compound, diazotization, and hydrolysis to yield the phenol as white hexagonal plates from benzene–ethyl acetate, mp 203–204°. The chemical-ionization mass spectrum is shown in Fig. 1.

3-Hydroxy-ω-(α,α-^{2}H-diethylamino) -2,6-dimethylacetanilide (Id-d_4)—Compound Id-d_4 was synthesized in 57% overall yield, according to the method of Keenaghan and Boyes (12), starting with lidocaine-d_4, mp 202–204°, after sublimation (140°, 0.3 mm Hg); NMR: δ 1.13 [broad s, $N(CD_2CH_3)_2$], 2.05 and 2.17 (s, aryl methyls), 3.30 (s, O=CCH_2N), 6.75 (*AB* m, J = 9 Hz, aromatics), and 8.90 (broad s, HNC=O) ppm.

The chemical-ionization mass spectrum showed the following isotopic abundances: Id-d_4, 71.0% (*m/e* 255); Id-d_3, 22.9% (*m/e* 254); Id-d_2, 4.0% (*m/e* 253); Id-d_1, 2.0% (*m/e* 252); and Id, 0% (*m/e* 251).

3-Hydroxy-ω-ethylamino-2,6-dimethylacetanilide (Ie)—Compound Ie was synthesized in 38% overall yield, according to the method of Keenaghan and Boyes (12), using the same reaction sequence as described for Id but starting with Ib, to yield off-white small plates from purified chloroform, mp 147–149°; NMR: δ^T 1.18 (t, J = 7 Hz, NCH_2CH_3), 2.05 and 2.17 (s, aryl methyls), 2.80 (q, J = 7 Hz, NCH_2CH_3), 3.40 (s, O=CCH_2N), 4.60 (broad s, OH and NH), 6.75 (*AB* m, J = 9 Hz, aromatics), and 8.90 (broad s, HNC=O) ppm.

3-Hydroxy-ω-(β-^{2}H-ethylamino)-2,6-dimethylacetanilide (Ie-d_3)—Compound Ie-d_3 was synthesized in 28% overall yield, according to the method of Keenaghan and Boyes (12), starting with Ib-d_3, mp 147–149°; NMR: δ^T 2.05 and 2.17 (s, aryl methyls), 2.80 (broad s, NCH_2CD_3), 3.40 (s, O=CCH_2N), 4.60 (broad s, OH and NH), 6.75 (*AB* m, J = 9 Hz, aromatics), and 8.90 (broad s, HNC=O) ppm.

The chemical-ionization mass spectrum showed the following isotopic abundances: Ie-d_3, 64.8% (*m/e* 226); Ie-d_2, 22.5% (*m/e* 225); Ie-d_1, 9.0% (*m/e* 224); and Ie, 3.7% (*m/e* 223).

2-Amino-3-methylbenzyl Alcohol (IIb)—A solution of 2-amino-3-methylbenzoic acid[7] (151 mg, 1 mmole) in tetrahydrofuran (10 ml, freshly distilled from lithium aluminum hydride) was added dropwise to a magnetically stirred slurry of lithium aluminum hydride (60 mg, 1.7 mmoles) in tetrahydrofuran (10 ml) over 20 min. The reaction was stirred 1 additional hr at room temperature. To the slurry, water (0.06 ml), 15% NaOH (0.06 ml), and water (0.18 ml) were added in succession. After stirring for 15 min, the granular white precipitate was removed by suction filtration. Rotary evaporation of the filtrate yielded 120 mg (89%) of off-white crystalline solid, which was recrystallized from chloroform–hexane (3:2) to give white prisms, mp 69–70° [lit. (23) mp 71°]; IR (KBr): 3450 (OH) and 3300 (NH_2) cm^{-1}; NMR: δ 2.05 (s, aryl methyls), 3.58 (broad s, NH_2 and OH), 4.41 (s, benzyl CH_2), and 6.80 (A_2B m, aromatics) ppm.

Chemical-ionization mass spectrometry showed that the MH^+ ion at *m/e* 138 and its ^{13}C-satellite represented 46.6% while ($MH^+ - 18$) at *m/e* 120 was 53.4% of the total ion current.

2-Amino-3-methyl-α-^{2}H-benzyl Alcohol (IIb-d_2)—Compound IIb-d_2 was synthesized in 92% yield, using the same procedure outlined for the nondeuterated analog with lithium aluminum deuteride, mp 69–70°; NMR (δ) showed the same peaks as the nondeuterated compound except for the loss of resonance at 4.41 ppm for the methylene hydrogens of the benzyl carbon.

Chemical-ionization mass spectrometry showed the following isotopic abundances: IIb-d_2, 91.8% (*m/e* 140); IIb-d_1, 8.2% (*m/e* 139); and IIb, 0% (*m/e* 138).

(^{2}H-2-Methyl)-2,6-dimethylaniline (IIa-d_2)—A solution of IIb-d_2 (1.37 g, 10 mmoles) in 95% ethanol (50 ml) containing concentrated hydrochloric acid (1 ml) was hydrogenated (30 psi hydrogen) over 10% palladium-on-carbon (150 mg) for 4 hr on a Paar hydrogenator at room temperature. The catalyst was removed by suction filtration, and the filtrate was rotary evaporated to yield a semisolid residue. This residue was taken up in water (20 ml) and made basic with 10% Na_2CO_3, and the free amine was extracted into ether. The extract was washed with water and dried over calcium sulfate. The solvent was removed, and the product was vacuum distilled to give 950 mg (79%) of a clear liquid (bp 37–41°/0.3 mm Hg); NMR: δ 2.07 (s, aryl methyls), 3.42 (broad s, NH_2), and 6.8 (A_2B complex m, aromatics) ppm; integration ratio 4:2:3, respectively.

Chemical-ionization mass spectrometry showed the following isotopic abundances: IIa-d_2, 77.2% (*m/e* 124); and IIa-d_1, 22.8% (*m/e* 122).

ω-Diethylamino-2-hydroxymethyl-6-methylacetanilide (If)—To an ice bath-cooled, magnetically stirred solution of IIb (2.6 g, 20 mmoles) in tetrahydrofuran (30 ml) and benzene (20 ml) was added dropwise a solution of chloroacetic anhydride (3.4 g, 20 mmoles) in tetrahydrofuran (30 ml). After 30 min, a white crystalline precipitate formed and continued to form over the entire addition period. The slurry was warmed to room temperature and stirred an additional 2 hr. After cooling again in ice, the slurry was suction filtered, and the filter pad was washed with three portions of water (30 ml). After air drying, the white crystals were recrystallized from chloroform (40 ml) to yield 3.7 g (94%) of ω-chloro-2-hydroxymethyl-6-methylacetanilide, mp 130–132°; IR (KBr): 3400 (OH), 3300 (amide NH), and 1665 (amide C=O) cm^{-1}; NMR: δ 2.17 (s, aryl methyl), 2.77 (broad s, OH), 4.20 (s, O=CCH_2Cl), 4.58 (s, CH_2OH), 7.20 (s, aromatics), and 8.38 (broad s, HNC=O) ppm.

Anal.—Calc. for $C_{10}H_{12}ClNO_2$: C, 56.20; H, 5.66; N, 6.56. Found: C, 56.15; H, 5.61; N, 6.52.

A solution of ω-chloro-2-hydroxymethyl-6-methylacetanilide (641 mg, 3 mmoles) and 0.78 ml of diethylamine (550 mg, 7.5 mmoles) in dry dioxane (20 ml) was heated at 70–75° for 3 hr, during which a white precipitate of diethylamine hydrochloride formed. The mixture was cooled to 15°, suction filtered to remove the amine salt, and rotary evaporated to yield a pale-yellow liquid. The liquid was recrystallized from 30 ml of benzene–petroleum ether (80:20) to give cubic white crystals, mp 113–115°; IR (KBr): 3400 (OH), 3300 (amide NH), and 1660 (amide C=O) cm^{-1}; NMR: δ 1.17 [t, J = 7 Hz, $N(CH_2CH_3)_2$], 2.15 (s, aryl methyl), 2.85 [q, J = 7 Hz, $N(CH_2CH_3)_2$], 3.38 (s, O=CCH_2N), 3.71 (broad s, OH), 4.57 (s, CH_2OH), 7.21 (s, aromatics), and 8.60 (broad s, HNC=O) ppm.

Chemical-ionization mass spectrometry showed that the MH^+ ion at *m/e* 251 and its ^{13}C-satellite represented 64.0%, ($MH^+ - 18$) at *m/e* 233 represented 11.5%, *m/e* 132 was 13.0%, and from *m/e* 100 to 300 was 11.5% of the total ion current.

Anal.—Calc. for $C_{14}H_{22}N_2O_2$: C, 67.17; H, 8.86; N, 11.19. Found: C, 67.41; H, 8.90; N, 11.41.

ω-Ethylamino-(α-^{2}H-2-hydroxymethyl)-6-methylacetanilide (Ig-d_2)—Compound Ig-d_2 was synthesized in 79% yield, using the same procedure as described for the diethylamino derivative with a threefold excess of ethylamine and IIb-d_2, mp 81–83° from chloroform; IR (KBr): 3400 (OH and NH), 3300 (amide NH), and 1660 (amide C=O) cm^{-1}; NMR: δ 1.13 (t, J = 7 Hz, NCH_2CH_3), 2.21 (s, aryl methyl), 2.68 (q, NCH_2CH_3), 3.38 (s, O=CCH_2N), 3.68 (broad s, OH), 7.20 (s, aromatics), and 8.60 (broad s, HNC=O) ppm; high-resolution electron-impact mass spectrometry: calc. for $C_{12}H_{16}{}^2H_2N_2O_2$, 224.1494; found, 224.1492.

Chemical-ionization mass spectrometry showed that the MH^+ ion at *m/e* 225 and its ^{13}C-satellite represented 52.8%, ($MH^+ - 18$) at *m/e* 207 was 38.1%, *m/e* 122 was 5.2%, and *m/e* 104 was 3.9% of the total ion current.

2,6-Dimethylphenylhydroxylamine (IIc)—To a vigorously stirred solution of 2,6-dimethylnitrobenzene[7] (15.1 g, 0.1 mole) in absolute ethanol (30 ml) was added in one portion a solution of ammonium chloride (1 g) in water (15 ml) followed by small portions of zinc dust (94%, 15.0 g). The temperature of the reaction mixture was maintained between 65 and 70° by the portionwise addition of zinc dust until all had been added. The grayish-white slurry was then allowed to cool slowly to 55° with continued vigorous stirring. The warm mixture was suction filtered, and the filter pad was washed with anhydrous ether (30 ml). Rotary evaporation of the filtrate gave a pale-yellow precipitate, which was recrystallized twice from purified petroleum ether–benzene (1:1) to yield 12.2 g (88%) of white needles, mp 103–104° [lit. (24) mp 99°]; IR (KBr): 3300 (NH stretch), 3200 (OH), and 860 (NO stretch) cm^{-1}; NMR: δ 2.35 (s, aryl methyls), 6.50 (broad s, NH and OH), and 7.05 (s, aromatics) ppm.

Chemical-ionization mass spectrometry showed that the MH^+ ion at *m/e* 138 and its ^{13}C-satellite represented 23.0%, ($MH^+ - 16$) at *m/e* 122 was 56.0%, *m/e* 243 was 18.0%, and *m/e* 259 was 3% of the total ion current. The ions at *m/e* 243 and 259 probably resulted from reaction to yield dimerized products in the gas phase.

Anal.—Calc. for $C_8H_{11}NO$: C, 70.04; H, 8.08; N, 10.21. Found: C, 69.95; H, 8.11; N, 10.04.

ω-Chloro-*N*-hydroxy-2,6-dimethylacetanilide—To a magnetically stirred two-phase mixture of IIc (4.12 g, 0.03 mole) in ether (100 ml) and sodium bicarbonate (2.80 g, 0.034 mole) in water (12 ml), cooled to −5° in an ice–salt bath, was added dropwise chloroacetyl chloride[7] (3.39 g, 0.03 mole) in ether (20 ml) over 30 min. The reaction was stirred an additional 20 min at −5° and then poured into a separator and washed with two portions of water (50 ml). The pale-yellow ether layer was filtered through anhydrous magnesium sulfate and evaporated to a volume of 50 ml, and the product was crystallized in the cold to yield 3.52 g (63%) of white rhombic crystals, mp 138.5–140°; IR (KBr): 3200 (OH) and 1650 (CO) cm^{-1}; NMR: δ 2.1 and 2.32 (s, aryl methyls), 3.76 and 4.41 (s, O=CCH_2Cl), 7.05 and 7.25 (m, aromatics), and 1.15 (broad s, deuterium oxide exchangeable OH) ppm. Integration indicated two isomers existing in a 1:2 ratio, presumably imino–enol to *N*-hydroxyamide.

Anal.—Calc. for $C_{10}H_{12}ClNO_2$: C, 56.21; H, 5.66; N, 6.56. Found: C, 56.33; H, 5.60; N, 6.51.

ω-Diethylamino-*N*-hydroxy-2,6-dimethylacetanilide (Ih)—A solution of ω-chloro-*N*-hydroxy-2,6-dimethylacetanilide (2.13 g, 0.01 mole) and diethylamine (2.8 ml = 2.2 g, 0.03 mole) in benzene (30 ml) was magnetically stirred for 4 hr at 65–70°. The orange-colored solution was cooled in ice, suction filtered to remove precipitated diethylamine hydrochloride, and then extracted with three portions of 10% HCl (5 ml). The acid extracts were combined and carefully adjusted to pH 8.5 with 5 *N* NaOH. The opaque mixture was back-extracted with three portions (20 ml) of purified chloroform, which were combined and washed with water (10 ml) and dried over anhydrous sodium sulfate.

Rotary evaporation of the solvent at room temperature yielded a pale-yellow liquid, which was recrystallized three times from purified hexane to yield 1.6 g (64%) of small white needles, mp 81–82°; IR (CCl_4): 3250 (OH) and 1650 (CO) cm^{-1}; NMR: δ 0.85 and 1.15 [t, J = 7 Hz, $N(CH_2CH_3)_2$], 2.30 and 2.35 (s, aryl methyls), 2.50–3.00 [overlapped q, J = 7 Hz, $N(CH_2CH_3)_2$], 3.55 and 4.60 (s, $OCCH_2N$), and 7.10–7.20 (m, aromatics plus OH exchangeable with deuterium oxide) ppm. Integration indicated two isomers in a ratio of 1:1; high-resolution electron-impact mass spectrometry: calc. for $C_{14}H_{22}N_2O_2$, 250.16812; found, 250.16873.

Chemical-ionization mass spectrometry showed that the MH^+ ion at *m/e* 251 and its ^{13}C-satellite represented 65.1%, ($MH^+ - 16$) at *m/e* 235

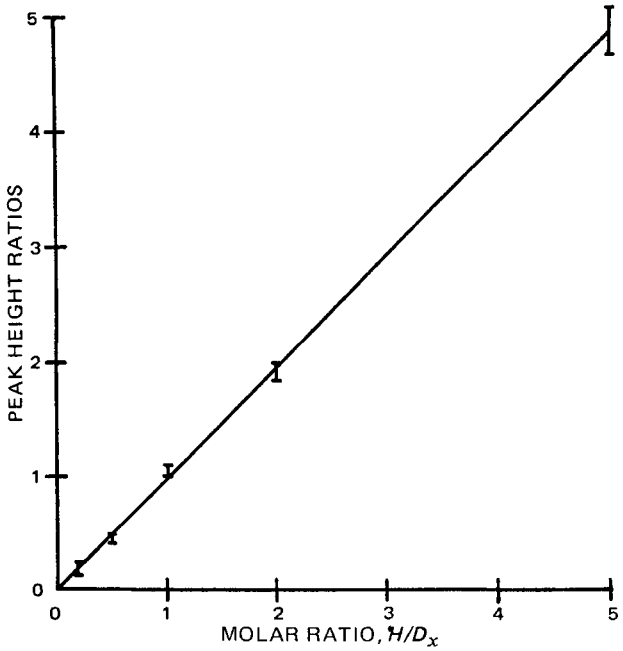

Figure 2—*Standard curve of lidocaine and six of its metabolites plus their deuterated standards extracted from urine. The bars* (I) *represent the range of peak height ratios observed in chemical-ionization mass spectral analysis for various amounts of lidocaine and the six metabolites added to 10-ml blank urine samples containing the following amounts of deuterated standards: 100 μg of lidocaine-*d_4, *150 μg of I*b-d_3, *100 μg of I*c-d_2, *50 μg of I*d-d_4, *50 μg of I*e-d_3, *50 μg of II*a-d_2, *and 200 μg of II*d-d_2. *The variances observed for all compounds and their deuterated analogs were from 1 to 5%, except for samples of I*c versus *I*c-d_2 *where variances as much as ±10% were found due to interfering ions observed in the chemical-ionization mass spectra of control urine at* m/e *179, 180, and 181.*

was 19.9%, *m/e* 233 was 11.7%, and *m/e* 103 from *m/e* 100 to 300 was 3.3% of the total ion current.

Anal.—Calc. for $C_{14}H_{22}N_2O_2$: C, 67.17; H, 8.86; N, 11.19. Found: C, 67.40; H, 8.70; N, 11.30.

The hydrochloride was made by adding the calculated amount of concentrated hydrochloric acid to a solution of I*h* in 2-propanol and cooling the solution in a freezer to give small white crystals, mp 182–184°; IR (KBr): 3450 (OH), 2700 (N^+H), and 1665 (C=O) cm^{-1}; NMR: δ (acetone-d_6, tetramethylsilane) 1.45 [t, J = 7 Hz, $N(CH_2CH_3)_2$], 2.30 (s, aryl methyls), 3.55 [q, J = 7 Hz, $N(CH_2CH_3)_2$], 4.09 (broad s, N^+H and OH), 4.72 (s, $O{=}CCH_2N$), and 7.23 (s, aromatics) ppm.

ω-(α,α-^{2}H-Diethylamino)-*N*-hydroxy-2,6-dimethylacetanilide (I*h*-d_4)—Compound I*h*-d_4 was synthesized by the same procedure as the nondeuterated compound, using diethylamine-d_4, mp (hydrochloride) 182–184°.

Chemical-ionization mass spectrometry showed the following isotopic abundances: I*h*-d_4, 72.0% (*m/e* 255); I*h*-d_3, 20.6% (*m/e* 254); I*h*-d_2, 5.9% (*m/e* 253); I*h*-d_1, 1.5% (*m/e* 252); and I*h*, 0% (*m/e* 251).

ω-Ethylamino-*N*-hydroxy-2,6-dimethylacetanilide (I*i*)—A solution of ω-chloro-*N*-hydroxy-2,6-dimethylacetanilide (2.13 g, 0.01 mole) and anhydrous ethylamine (1.95 ml = 1.35 g, 0.03 mole) in purified dioxane (30 ml) was stirred for 4.5 hr at 50–55°. As the reaction proceeded, a large amount of fine white precipitate formed. The slurry was cooled in ice and suction filtered to give a mixture of product and ethylamine hydrochloride (2.3 g, mp 70–102°). The precipitate was taken up in chloroform–petroleum ether (2:1) and suction filtered to remove the ethylamine hydrochloride. The filtrate was then evaporated, and the residue was recrystallized twice from benzene to yield 1.4 g (63%), mp 103–105°; IR (CCl_4): 3250 (OH) and 1650 (C=O) cm^{-1}; NMR: δ 1.05 and 1.17 (t, J = 7 Hz, NCH_2CH_3), 2.15 and 2.20 (s, aryl methyls), 2.57 and 2.64 (q, J = 7 Hz, NCH_2CH_3), 3.00 and 3.85 (s, $O{=}CCH_2N$), 5.95 (s, OH and NH exchangeable with deuterium oxide), and 7.10 and 7.20 (s, aromatics) ppm. Integration indicated two isomers in an approximate ratio of 1:2, with the presumed *N*-hydroxy form predominant; high-resolution electron-impact mass spectrometry: calc. for $C_{12}H_{18}N_2O_2$, 222.13726; found, 222.13682.

Chemical-ionization mass spectrometry showed that the MH^+ ion at *m/e* 233 and its ^{13}C-satellite represented 70.4%, ($MH^+ - 16$) at *m/e* 207 was 20.8%, and ($MH^+ - H_2O$) at *m/e* 205 from *m/e* 100 to 300 was 8.8% of the total ion current.

Anal.—Calc. for $C_{12}H_{18}N_2O_2$: C, 64.84; H, 8.16; N, 12.60. Found: C, 64.75; H, 8.41; N, 12.62.

The hydrochloride was made by adding the calculated amount of concentrated hydrochloric acid to a solution of I*i* in 2-propanol and cooling the solution in a freezer to give small white crystals, mp 186–188°; IR (KBr): 3450 (OH), 2700–2900 (N^+H), and 1665 (C=O) cm^{-1}; NMR: δ (acetone-d_6, tetramethylsilane) 1.40 (t, J = 7 Hz, NCH_2CH_3), 2.35 (s, aryl methyls), 3.35 (q, J = 7 Hz, NCH_2CH_3), 4.25 (broad s, N^+H and OH), 4.50 (s, $O{=}CCH_2N$), and 7.20 (s, aromatics) ppm.

ω-(β-^{2}H-Ethylamino)-*N*-hydroxy-2,6-dimethylacetanilide (I*i*-d_3)—Compound I*i*-d_3 was synthesized by the same procedure as the nondeuterated compound using ethylamine-d_3, mp (hydrochloride) 185–187°.

Chemical-ionization mass spectrometry showed the following isotopic abundances: I*i*-d_3, 66.7% (*m/e* 226); I*i*-d_2, 19.3% (*m/e* 225); I*i*-d_1, 10.7% (*m/e* 224); and I*i*, 3.3% (*m/e* 223).

N^1-Ethyl-2-methyl-N^3-(2,6-dimethylphenyl)-4-imidazolidinone (III)—Compound III was synthesized as previously described (25).

Lidocaine *N*-Oxide (I*j*)—To an ice bath-cooled, magnetically stirred solution of lidocaine (2.34 g, 0.01 mole) in dichloromethane (20 ml) was added a cold solution of *m*-chloroperoxybenzoic acid[7] (85%, 2.23 g, 0.011 mole) in dichloromethane (30 ml). After a dropwise addition over 30 min, the reaction mixture was allowed to come to room temperature and was stirred overnight. The reaction mixture was then poured through a basic alumina column (150 g). Unreacted lidocaine was eluted with chloroform (100 ml), followed by 200 ml of chloroform–methanol (95:5), which yielded a pale-yellow liquid after rotary evaporation of the solvent. Recrystallization from ether–dichloromethane (70:30) in the cold gave 1.8 g (72%) of a white hygroscopic crystalline solid, mp 105–107°; IR (KBr): 3100–3400 (OH of hydrate and amide NH) and 1690 (amide C=O) cm^{-1}; NMR: δ 1.37 [t, J = 7 Hz, $N(CH_2CH_3)_2$], 2.25 (s, aryl methyls), 2.92 (broad s, HNC=O and H_2O), 3.45 [q, J = 7 Hz, $N(CH_2CH_3)_2$], 3.90 (s, $O{=}CCH_2N$), and 7.06 (s, aromatics) ppm.

Chemical-ionization mass spectrometry showed that the MH^+ ion at *m/e* 251 and its ^{13}C-satellite represented 3.2%, ($MH^+ - 16$) at *m/e* 235 was 11.4%, ($MH^+ - H_2O$) at *m/e* 233 was 16.9%, *m/e* 223 was 19.4%, *m/e* 221 was 4.7%, *m/e* 207 was 8.4%, *m/e* 205 was 17.9%, and *m/e* 178 from *m/e* 100 to 300 was 11.9% of the total ion current.

Anal.—Calc. for $C_{14}H_{22}N_2O_2{\cdot}H_2O$: C, 62.66; H, 9.01; N, 10.44. Found: C, 62.37; H, 8.81; N, 10.43.

4-Hydroxy-2,6-dimethylaniline (II*d*)—Compound II*d* was synthesized according to known procedures (26), mp 179–181°.

4-Hydroxy-(^{2}H-2-methyl)-2,6-dimethylaniline (II*d*-d_2)—Compound II*d*-d_2 was synthesized by the method outlined by Wepster (27). The method involved formation of the *p*-toluenesulfonamide of II*a*-d_2, followed by nitration and reduction to yield the *p*-amino-*p*-toluenesulfonamide. This material was diazotized, treated with water to yield the phenol, and finally hydrolyzed to yield crude II*d*-d_2. The crude material was sublimed (80–90°, 3 mm Hg) to give 60% very pure white powder crystals, mp 179–181°, and 40% slightly impure light-purple crystals, mp 175–180°; NMR: δ 2.06 (s, aryl methyls), 4.22 (broad s, NH_2), 6.47 (s, OH), and 6.59 (s, aromatics) ppm; integration ratio 4:2:1:2, respectively; high-resolution electron-impact mass spectrometry: calc. for $C_8H_9{}^2H_2NO$, 139.0966; found, 139.0932.

Chemical-ionization mass spectrometry showed that MH^+ ions represented 100% of the total ion current with the following isotopic abundances: II*d*-d_2, 60.2% (*m/e* 140); II*d*-d_1, 22.4% (*m/e* 139); and II*d*, 17.4% (*m/e* 138).

***N*,*N*-Diethylglycine (IV*a*)**—Compound IV*a* was prepared by the method of Bowman and Stroud (28), using reductive alkylation of glycine with excess acetaldehyde and hydrogen, mp 133–135°.

***N*,*N*-α,α,α′,α′-^{2}H-Diethylglycine (IV*a*-d_4)**—A mixture of glycine (3.8 g, 0.05 mole) and freshly distilled acetaldehyde (9.0 g, 0.2 mole) in 70% ethanol-d_1–deuterium oxide was hydrogenated (20 psi, deuterium) over 1.5 g of 10% palladium-on-carbon for 14 hr at room temperature. The catalyst was removed by suction filtration, and the filtrate was rotary evaporated to yield a viscous pale-yellow liquid, which was recrystallized as the hydrochloride from 75 ml of methanol–acetone (1:4) to give 5.7 g (67%) of a white crystalline solid, mp 124–126° [lit. (29) mp 126–127°].

Chemical-ionization mass spectrometry showed that deuterium scrambling had occurred during the reductive alkylation, with incorporation ranging from zero to eight deuteriums into the *N*-alkyl side chains. The resultant deuterium envelope showed the greatest deuterium incorporation for IV*a*-d_3, 21.0% (*m/e* 135). Parent $MH(D)^+{}_x$ ions repre-

Table I—Serial Plasma Levels of Lidocaine, Ib, and III

Minutes[a]	Subject	Lidocaine m/e 235[b] / m/e 239	Lidocaine μg/ml	Ib m/e 207[b] / m/e 210	Ib μg/ml	III m/e 233 / m/e 235	III μg/ml
30	A	84.2/29.6	2.03	22.3/90.0.	0.13	0.049	0.10
	B	93.5/83.3	0.81	10.2/38.7	0.13	0.043	0.03
	C	18.1/90.6[c]	0.002	Not measurable		Not measurable	
60	A	90.6/44.0	1.47	45.2/41.0	0.55	0.075	0.11
	B	60.3/64.8	0.67	17.4/34.5	0.25	0.079	0.05
	C	5.3/64.2	0.05	5.8/50.3	0.06	0.093	0.04
90	A	60.5/34.9	1.22	11.9/26.6	0.23	0.048	0.06
	B	50.7/77.8	0.47	21.6/34.5	0.21	0.054	0.02
	C	40.7/68.8	0.42	7.3/57.7	0.06	0.076	0.04
180	A	49.0/37.0	0.95	8.7/19.7	0.22	0.066	0.06
	B	38.7/121	0.23	10.1/26.6	0.16	0.063	0.01
	C	58.7/102	0.41	7.9/60.8	0.06	0.112	0.04

[a] Refers to the time the blood sample was taken after subject received an oral dose of lidocaine hydrochloride monohydrate (A and B) or lidocaine as the free base (C). [b] The peak heights as measured from the chemical-ionization mass spectrum after correcting for ^{13}C-abundances and deuterium incorporation. [c] Based on ^{13}C-satellite peak of lidocaine-d_4 internal standard.

sented 70.1% and ($MH^+ - C_2H_2O_2$) ions were 22.4% of the total ion current.

***N*-Ethylglycine (IV*b*)**—Compound IV*b* was prepared by the method of Hanke (30), which involves hydrolysis of *N*-ethylaminoacetonitrile generated from the condensation of ethylamine, formaldehyde, and potassium cyanide.

β-^{2}H-*N*-Ethylglycine (IV*b*-d_3)—Compound IV*b*-d_3 was synthesized by the method of Hanke (30), using ethylamine-d_3 hydrochloride, mp 180–182° dec.

Chemical-ionization mass spectrometry showed the following isotopic abundances: IV*b*-d_3, 57.9% (*m/e* 107); IV*b*-d_2, 20.8% (*m/e* 106); IV*b*-d_1, 13.2% (*m/e* 105); and IV*b*, 8.1% (*m/e* 104).

Mass Spectral Studies—Chemical-ionization mass spectrometry was performed on all suspected lidocaine metabolites and their deuterated analogs. All of the benzyl alcohols (I*f*, I*g*, and II*b*) produced major ($MH^+ - 18$) ions as a result of a loss of water from the MH^+ ion. Because of this characteristic water loss, any benzyl alcohol metabolites should be easily differentiated from the isomeric phenolic metabolites (I*d*, I*e*, and II*d*). Figure 1 shows comparative chemical-ionization mass spectra of I*f* and I*d*.

Unfortunately, the *N*-hydroxyamides (I*h* and I*i*), II*c*, and I*j* lost oxygen under all temperature and chemical-ionization mass spectrometry conditions employed to give ($MH^+ - 16$) ions, which interfered with quantification of lidocaine, I*b*, and 2,6-dimethylaniline. Therefore, these possible oxygenated metabolites were quantified by a combination of the chemical-ionization mass spectrometry–stable isotope technique and other methods as previously described (31). This facile loss of oxygen is probably the result of a thermal homolytic cleavage of the weak nitrogen–oxygen bond and was observed previously (32, 33).

Preliminary Experiment—To determine the spectrum of lidocaine metabolites detectable by chemical-ionization mass spectrometry in plasma and urine samples, a healthy 75-kg male subject received orally an encapsulated dose of 202 mg of lidocaine free base. Prior to the dose, a 24-hr urine control sample was collected and stored in a freezer. Immediately prior to dosing, a 15-ml "zero-time" blood sample was collected in a heparinized tube, and the plasma was separated by spinning the sample at 800×*g* for 15 min. Similar samples were collected at 30, 60, 90, and 180 min after dosing and stored in a freezer at −15° until further workup. Serial urine samples were collected at the following intervals; 0–2, 2–4, 4–8, and 8–24 hr, and stored in glass bottles in a freezer.

Plasma and urine samples were extracted at pH 8.5 with two volumes of dichloromethane. The residue, after evaporation of the solvent, was subjected to chemical-ionization mass spectrometry. Compared to the zero-time plasma sample, only MH^+ ions corresponding to lidocaine, I*b*, and possibly Ic could be seen in the plasma extracts. In the urine extracts, MH^+ ions corresponding to II*a*, II*d*, Ic, I*b*, hydroxylated I*b*, I*a*, and hydroxylated I*a* could readily be detected. No major peaks corresponding to the ($MH^+ - 18$) loss of water from possible benzyl alcohol metabolites could be found, even though these compounds were readily extractable from urine and plasma.

Isolation and Assay Procedures—Collection bottles for urine and Pyrex culture tubes for plasma were thoroughly washed with steaming water and detergent, rinsed three times with hot water, and finally rinsed five times with distilled water. A stock solution (200 ml) containing 1.60 mg of I*d*-d_4, 8.00 mg of I*a*-d_4, 1.60 mg of I*e*-d_3, 20.00 mg of I*b*-d_3, 4.00 mg of Ic-d_2, and 2.06 mg of II*a*-d_2 was made the morning of the *in vivo* experiment. All weighings were performed on an electrobalance[8]. All solvents used for extractions were purified (23) and distilled prior to use. Conjugates were hydrolyzed enzymatically[9].

Two healthy male volunteers (A = 80 kg, B = 70 kg) received a 250-mg oral dose of encapsulated lidocaine hydrochloride monohydrate[10]; a third subject (C = 75 kg) received a molar equivalent (202 mg) of lidocaine free base[11]. All doses were given in the morning with no restriction on diet or smoking. Prior to the experiment, 24-hr urine controls were collected from each subject and stored in a freezer (−15°). Immediately prior to dosing, a 15-ml zero-time blood sample was drawn into a heparinized tube. Successive 15-ml blood samples were taken 30, 60, 90, and 180 min following drug administration; the plasma was immediately separated by centrifugation at 800×*g* for 15 min. To 2-ml samples of each plasma fraction were added 2 ml of 1.01 μg of I*a*-d_4/ml, 1 ml of 1.00 μg of I*b*-d_3/ml, and 0.5 ml of 1.00 μg of Ic-d_2/ml. Samples were then stored frozen until further workup.

Serial urine samples were collected 0–2, 2–4, 4–8, and 8–24 hr following drug administration. One-third of each sample was transferred at the collection time to a glass bottle containing 10 ml of the stock solution of deuterated standards. To two-tenths of this sample containing the deuterated standards (times one-third) was added 1.0 mg of II*d*-d_2, and the samples were stored in a freezer (−15°) until further workup. To one-twentieth of the 0–24-hr urine aliquots from each subject were added 1.0 mg each of the deuterated amino acids, IV*a*-d_2 and IV*b*-d_3.

Plasma—All plasma samples were extracted the day following collection. To the 5.5 ml of sample containing 2 ml of plasma and 3.5 ml of deuterated standards solution was added 0.5 ml of 5 *N* NaOH, and the basified mixture was extracted with 10 ml of benzene in 30-ml Pyrex culture tubes fitted with polytef caps. The sample was then centrifuged at 800×*g* for 5 min, and the benzene layer was removed and rotary evaporated at 20°. The residue was dissolved in 0.05 ml of ethanol and placed on the ceramic tip of the direct insertion probe. The probe was inserted into the mass spectrometer, and the chemical-ionization mass spectrum was determined at 120°.

Urine—Urine samples, including urine controls, were extracted within 2 days following collection. One-half of each urine sample, containing all deuterated standards (*i.e.*, $\frac{1}{2} \times \frac{2}{10} \times \frac{1}{3} = \frac{1}{30}$ of each serial urine sample), was basified to pH 8.5 ± 0.2 with 5 *N* NaOH and extracted with two volumes of purified dichloromethane. The extract was filtered through anhydrous sodium sulfate and rotary evaporated at 20°. The residue was transferred to a 1-dram vial with 1 ml of purified dichloromethane. The solvent was evaporated under a gentle stream of nitrogen, and samples were stored in a desiccator in a freezer until chemical-ionization mass spectrometry was performed.

The other half of each urine sample was diluted with an equal volume of pH 5.0 Walpole acetate buffer and hydrolyzed for 24 hr on a shaker-incubator set at 37.0° and 100 oscillations/min. β-Glucuronidase–sulfatase was added in two 0.5-ml portions, once at the beginning of the incubation and again 12 hr after the incubation was started. Extraction of each β-glucuronidase-treated sample was carried out in the same manner as for untreated urine. All of these samples, however, required a primary

[8] Model M-10, Cahn electrobalance.
[9] Sigma Type II β-glucuronidase–sulfatase from *Helix pomatia*.
[10] Xylocaine, Astra Pharmaceutical Products, Worcester, Mass.
[11] Prepared in this laboratory.

Table II—Quantification of Lidocaine and Its Metabolites in Human Urine

Compound	Percentage of Administered Dose Recovered in 0–24-hr Urine[a]					
	Subject A		Subject B		Subject C	
	Before Enzyme, %	After[b] Enzyme, %	Before Enzyme, %	After[b] Enzyme, %	Before Enzyme, %	After Enzyme, %
Lidocaine	1.78	1.51	3.33	2.90	0.74	0.74
Ib	4.17	4.02	8.80	8.36	1.74	1.73
Ic	0.23	—[c]	1.32	—[c]	1.08	—[c]
m- and/or *p*-Hydroxylidocaine	0.06	0.80	0.10	0.43	0.06	0.97
m- and/or *p*-Hydroxy Ib	0	0.62	0.20	0.80	0.03	0.25
IIa	1.41	—[c]	0.27	—[c]	1.22	—[c]
IId	1.37	68.2	0.70	61.7	0.	60.5
Total	9.02	75.2	14.7	74.2	4.87	64.2

[a] Quantified as molar concentrations of free bases in Subjects A and B after an oral dose of 250 mg of lidocaine hydrochloride monohydrate and in Subject C after an oral dose of lidocaine free base. [b] After treatment with β-glucuronidase–sulfatase for 24 hr, some of the metabolite levels decreased inexplicably. [c] The β-glucuronidase–sulfatase treatment somehow affected both the metabolite and internal standard so that they were inextractable.

suction filtration through glass wool to break difficult emulsions before filtration through anhydrous sodium sulfate. All residues of the hydrolyzed urine were dark, foul smelling, and tarry.

Chemical-ionization mass spectrometric analysis was accomplished by dissolving each residue in 0.05 ml of methanolic hydrogen chloride, evaporating the sample on the probe tip with a gentle stream of nitrogen, and temperature programming each sample from 90 to 220°; spectra were taken approximately every 20°. Temperature programming was necessary to determine the more volatile IIa (90–110°) and IId (120–150°) and also to rid the spectrum of some interfering peaks near *m/e* 180 so that Ic could be determined above 170°. The methanolic hydrogen chloride treatment served two purposes. It converted the metabolites to their less volatile amine hydrochlorides and, combined with temperature programming, it destroyed any *N*-hydroxyamides that might have been present by causing Bamberger-type reactions (34) so that these compounds would not interfere with quantification of lidocaine and Ib.

Calculations—Peak heights were measured using a caliper. A standard procedure (35) was followed in subtracting isotope contributions from the preceding two peaks. The contributions of nondeuterated or unreacted ionic species present in the reference solution (internal standard) were then subtracted. A comparison of the corrected peak heights of labeled and unlabeled compound was made, and the concentration of drug or metabolite initially present in the plasma or urine sample was determined.

Standardization Experiments—*Plasma*—Previous work showed that extraction and mass spectral response to a compound and a deuterated analog of that compound are equivalent (36, 37). To test this finding under the chemical-ionization mass spectrometry conditions used, Ia and Ia-d_4 (1 μg/ml), Ib and Ib-d_3 (0.5 μg/ml), and Ic and Ic-d_2 (0.25 μg/ml) were added to 2-ml blank plasma samples and extracted according to the procedures outlined previously. Chemical-ionization mass spectrometric analysis was performed on duplicate samples and the corrected peak height ratios of nondeuterated *versus* deuterated standards showed good agreement between known and calculated concentrations, the largest variance being 2.2% for Ia *versus* Ia-d_4.

Urine—To 10 10-ml blank urine samples in 50-ml Pyrex culture tubes was added 1.0 mg of IId-d_2 plus 1 ml of the deuterated standards stock solution. To these samples was added 1 ml of stock solutions containing the same nondeuterated compounds to obtain five sets of duplicate samples with concentrations of nondeuterated–deuterated analogs ranging from 1:5 to 5:1. The 12 ml of solution was basified to pH 8.5 with 5 *N* NaOH and extracted with 20 ml of purified dichloromethane. Chemical-ionization mass spectrometric analysis with temperature programming was performed as described previously. Calculations showed that the response was linear over the range analyzed and that the lidocaine-derived compounds and their deuterated analogs behaved identically (Fig. 2).

Quantification of Amino Acid Metabolites—All radioactive determinations (*MSE* = 1.5%) were made using scintillation counting[12]. The samples were dissolved in 10 ml of scintillation fluid[13] and corrected for quenching using internal standardization with either ^{3}H-toluene standard[13] or ^{14}C-toluene standard[13]. GLC was performed[14] using flame-ionization detectors with a nitrogen carrier gas flow rate at 40 ml/min. Separation was obtained at 55° on 3% OV-17 on 100–120-mesh Chromosorb W in a 1.67-m × 0.63-cm (5.5-ft × 0.25-in.) × 2-mm i.d. glass U column equipped with a 10:1 effluent splitter.

Urease[15] was used to hydrolyze urea. TLC separation was accomplished on 20 × 20-cm plates[16] with silica gel or cellulose adsorbent.

Using Radioactivity Measurements—Two human subjects received an oral dose of 500 mg of randomly tritiated lidocaine hydrochloride monohydrate (13). An aliquot of the urine (0–72 hr) was treated with urease and, after filtration, was lyophilized. The lyophilate was extracted (soxhlet) with successive portions of dichloromethane, 2-propanol, and methanol to constant activity. The 2-propanol extract, accounting for 70% of the activity in the lyophilate, was evaporated under reduced pressure, taken up in 10 ml of water, and placed on a 250-ml (20 × 4-cm) cation-exchange column[17], which was then washed with 1.5 liters of water, 2 liters of 8 *N* acetic acid, and 4 liters of water. Very small amounts of activity were eluted in these fractions. Finally, a linear gradient from water to 2 *N* HCl was run (2 liters total volume), and 10-ml fractions were collected.

Eighty percent of the activity applied to the column was found between fractions 105 and 130. The fractions were combined and lyophilized repeatedly to remove excess hydrochloric acid, and the white residue was washed repeatedly with 2-propanol. Combined extracts were evaporated to a small volume and streaked on two 20 × 20-cm silica gel plates[18]. The plates were developed twice in butanol–acetic acid–water (4:1:1). Radiochromatogram scanning showed only one radioactive band, R_f 0.3, which was scraped from the plates and eluted with ethanol. Evaporation of ethanol yielded a residue, which was treated with diazomethane in ether and gas chromatographed. One peak was found (retention time of 6.2 min), collected, and determined to be radioactive by scintillation counting.

Electron-impact mass spectrometry of the trifluoroacetic acid salt of the methylated amino acid showed peaks at *m/e* 145, 86, 69, and 58. *N,N*-Diethylglycine, prepared by the method of Bowman and Stroud (28) and methylated with thionyl chloride in methanol, showed identical GLC and mass spectral characteristics. Isotopic dilution of samples of the isolated amino acid in the synthetic amino acid, with continuous recrystallization to constant specific activity, confirmed the identification of the metabolite.

Aliquots (100 ml) of urine from two subjects receiving 500 mg of randomly tritiated lidocaine hydrochloride monohydrate (13) were incubated with urease and filtered, and 50 ml of the filtrate was lyophilized with 362 mg of nonradioactive synthetic *N,N*-diethylglycine. The material was lyophilized twice to ensure removal of any exchangeable tritium. The lyophilate was triturated with three 50-ml portions of boiling benzene and filtered, and the benzene was evaporated carefully under nitrogen at room temperature. The residue was recrystallized repeatedly from boiling benzene to constant specific activity.

Using Chemical-Ionization Mass Spectrometry–Stable Isotope Dilution Technique—The one-twentieth aliquots of urine from each subject, containing 1.0 mg each of the deuterated amino acids, were

[12] Tri-Carb model 3375 scintillation counter.
[13] Aquasol, New England Nuclear, Boston, Mass.
[14] Model 1100, Varian Aerograph.
[15] Sigma Type M.
[16] Eastman Chemical.
[17] Dowex AG-50 WX4, hydrogen form.
[18] Analtech, silica gel HR, 2504.

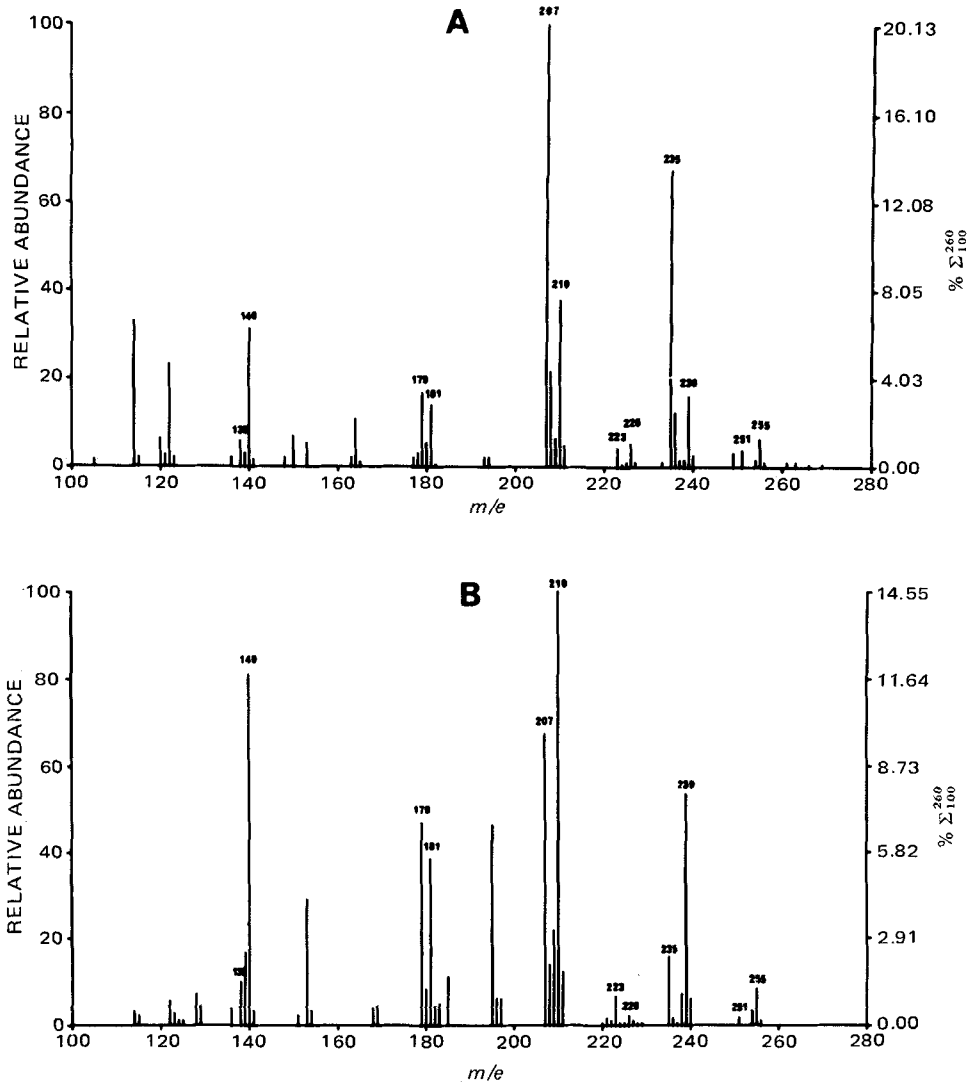

Figure 3—*Comparative chemical-ionization mass spectra of the methylene chloride extracts from basified (pH 8.5) Subject B 0–2-hr (A) and 8–24-hr (B) urine samples. The labeled peaks represent the following metabolites and their deuterated standards:* m/e *138, II*d; m/e *140, II*-d_2; m/e *179, Ic;* m/e *181, Ic*-d_2; m/e *207, Ib;* m/e *210, Ib*-d_3; m/e *223,* m- *and/or* p-*Ie;* m/e *226, Ie*-d_3; m/e *235, Ia;* m/e *239, Ia*-d_4; m/e *251,* m- *or* p-*Id; and* m/e *255, Id*-d_4.

treated with urease (100 mg) at 30° with shaking for 72 hr in an equal volume of pH 7.0 sodium phosphate buffer. Each sample was then lyophilized to yield approximately 600 mg of light-brown powder, which was extracted with 10 ml of hot methanol. The methanol extract was rotary evaporated, and the residue was sublimed (130°/0.3 mm Hg) for 3 hr. The sublimate was taken up in a few drops of methanol and chromatographed on silica gel plates, using 1-butanol–water–acetic acid (8:3:2) as the developing solvent. The appropriate area (R_f 0.2–0.4), as determined by cochromatography with standards, was scraped off and eluted with methanol, followed by rechromatography in the same system. TLC on silica gel of a sample of the final extract showed a ninhydrin-sensitive area corresponding to the R_f region for both *N,N*-diethylglycine and monoethylglycine. TLC on cellulose, using 95% ethanol–2-propanol–water (6:3:1), also indicated ninhydrin-sensitive areas for *N,N*-diethylglycine (R_f 0.51, very pale-pink spot) and monoethylglycine (R_f 0.27, purple-pink spot).

Chemical-ionization mass spectrometry of each extract showed small peaks at both *m/e* 104 and 132 corresponding to the amino acids, along with envelopes of peaks attributable to their deuterated internal standards. However, due to the large number of peaks in the same mass range, meaningful quantification was virtually impossible.

RESULTS

Plasma—The results of the quantification are presented in Table I and were partially given in a previous publication (16). In all samples with measurable levels of I*b*, small but measurable amounts of what appeared to be Metabolite III could be detected. Based on the peak height ratio of the MH^+ of the cyclic metabolite at *m/e* 233 *versus* the MH^+ ion of lidocaine at *m/e* 235, the concentration of the cyclic metabolite in plasma followed approximately the same time course as I*b*[19]. The peak concentration appeared at 60 min and reached a concentration level of approximately one-fifth that of the I*b* level in Subjects A and B (Table I). These concentrations of cyclic metabolite must be considered as rather crude estimates. However, the presence of this metabolite as a real *in vivo* generated product is strongly suggested, since there was no concomitant increase in *m/e* 236 compared to control values. This finding would be expected if the substance was arising from the condensation of exogenous acetaldehyde with I*b* (25), since the acetaldehyde should also condense with the deuterated analog to generate *m/e* 236. The problem of the cyclic metabolite will be considered in a future publication.

Urine—Lidocaine and six of its metabolites were quantified simultaneously using the chemical-ionization mass spectrometry–stable isotope dilution procedure. Basically, this procedure involved collection of serial urine samples with immediate addition of a stock solution containing known amounts of the deuterated standards to urine aliquots. The urine

[19] Although the MH^+ ion for the cyclic metabolite was found in all plasma samples, the deuterium standard of the cyclic metabolite was not added to the plasma because of its facile hydrolysis to I*b* plus acetaldehyde. Due to the almost identical extraction characteristics of the cyclic metabolite and lidocaine, deuterated lidocaine was used as the reference standard.

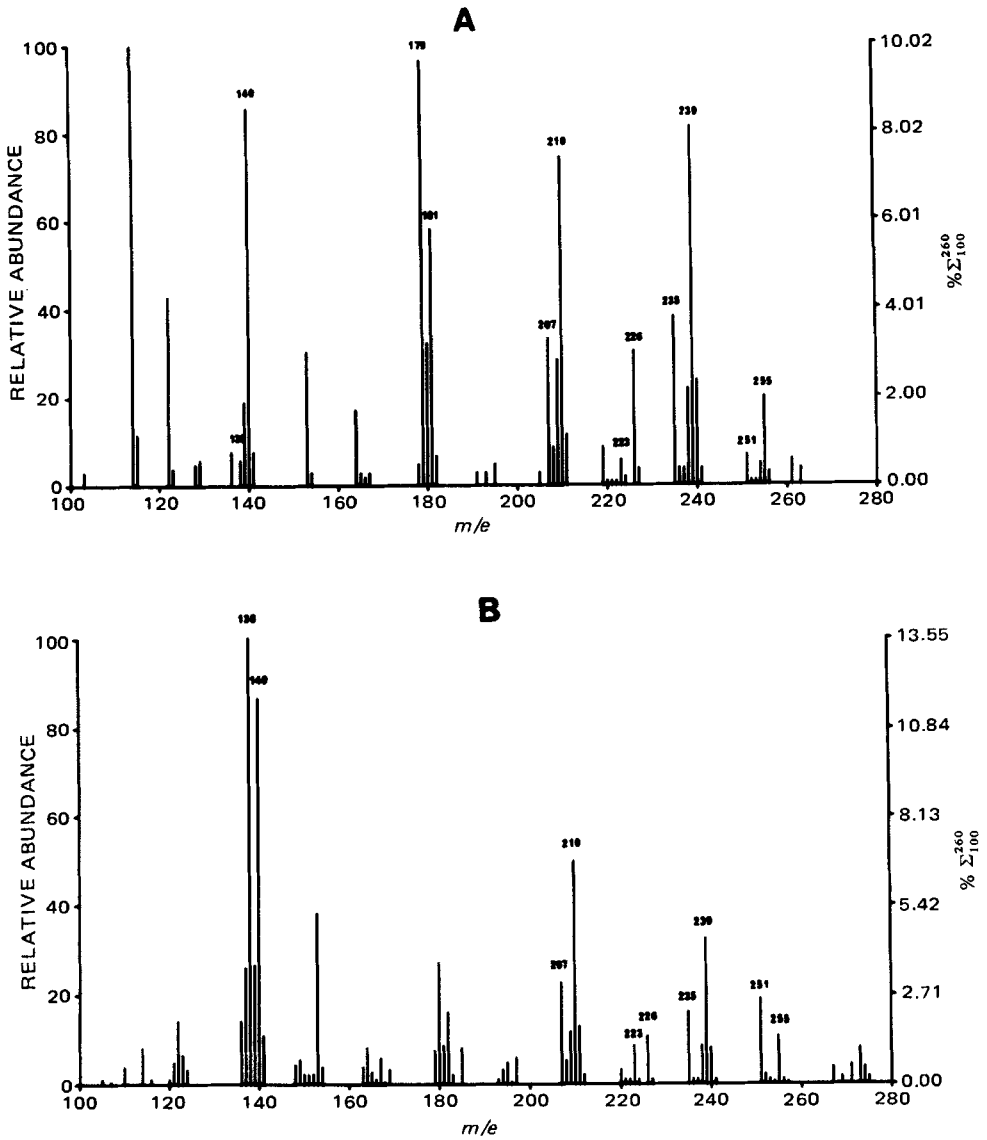

Figure 4—*Comparative chemical-ionization mass spectra of the methylene chloride extracts from basified (pH 8.5) 4–8-hr urine samples from Subject C before (A) and after (B) β-glucuronidase–sulfatase treatment. The labeled peaks represent the following metabolites and their deuterated standards:* m/e *138, II*d; m/e *140, II*d-d_2; m/e *179, I*c; m/e *181, I*c-d_2; m/e *207, I*b; m/e *210, I*b-d_3; m/e *223,* m- *and/or* p-*Ic;* m/e *226, I*c-d_3; m/e *235, I*a; m/e *239, I*a-d_4; m/e *251,* m- *and/or* p-*Id; and* m/e *255, I*d-d_4.

was then stored in a freezer (−15°) until further workup. By using this procedure, any structural change occurring in these metabolites was reflected in identical changes in the added standards. Quantification was carried out before and after β-glucuronidase–sulfatase treatment (Table II). Comparative chemical-ionization mass spectra of the 0–2- and 8–24-hr urine extracts of Subject B are shown in Fig. 3, and comparative spectra of the 4–8-hr urine extracts of Subject C before and after β-glucuronidase–sulfatase treatment are shown in Fig. 4.

Amino Acid Metabolites—The standard isotope dilution methods reported under *Experimental* revealed that minimally *N,N*-diethylglycine represented 35% of the excreted dose in two human subjects. Although some inexact TLC and chemical-ionization mass spectrometry data indicated that monoethylglycine was also present, this amino acid eluded quantification. However, in a Rhesus monkey, both amino acids were quantified *via* ion-exchange chromatography coupled with GLC and chemical-ionization mass spectrometry analysis[20]. After receiving 100 mg iv of radiolabeled lidocaine, this monkey excreted a minimum of 15% of IV*a* and 19% of IV*b* of the total administered dose.

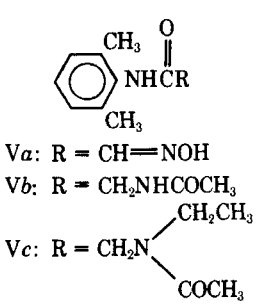

V*a*: R = CH=NOH

V*b*: R = $CH_2NHCOCH_3$

V*c*: R = $CH_2N(CH_2CH_3)(COCH_3)$

DISCUSSION

The results of this work show the extreme usefulness of the chemical-ionization mass spectrometry technique in both clinical analysis and drug metabolism studies. By using this procedure in a study of human lidocaine metabolism, several metabolites and their deuterated internal standards could be simultaneously monitored and quantified in a single temperature-programmed analysis. The technique combines speed, accuracy, and specificity in determining and quantifying metabolites; it also offers safety for the investigator. Drawbacks of the method include cost and upkeep of the instrument, time and expense required to synthesize the necessary deuterated standards, and inability to provide in-

[20] Unpublished results, this laboratory.

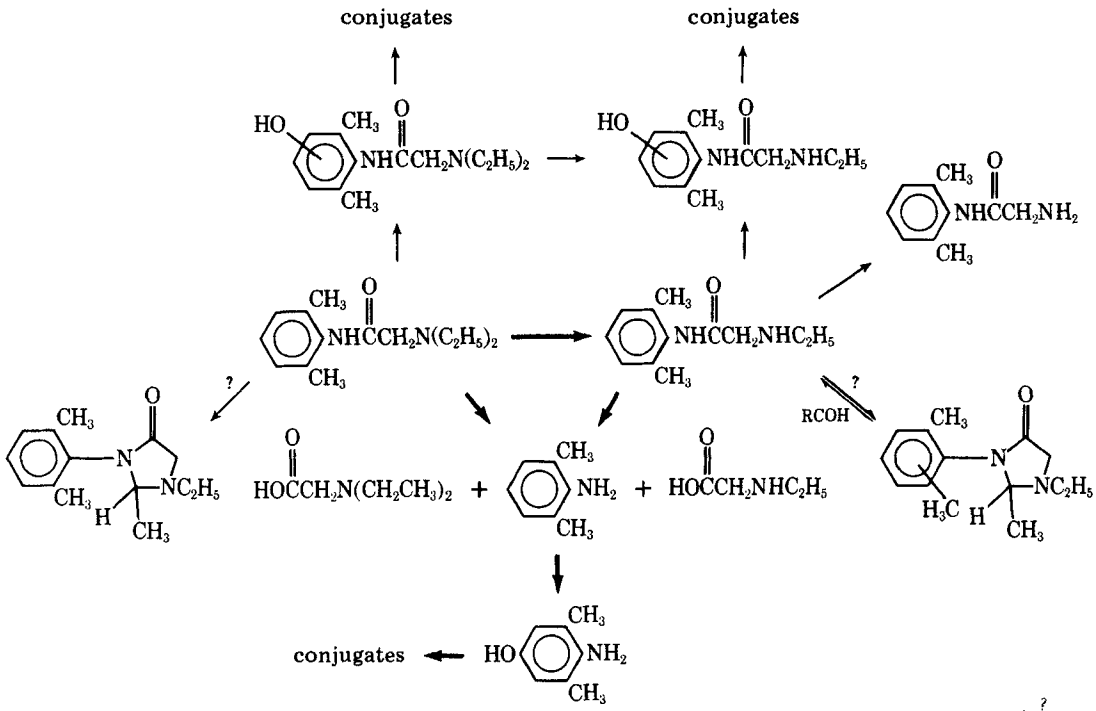

Scheme I—Basic pathways of lidocaine metabolism. Key: ⟹, *major metabolic pathway;* →, *minor metabolic pathway; and* $\xrightarrow{?}$, *probable metabolic pathway extent unknown.*

formation necessary to differentiate similar structural isomers of a metabolite such as *m*- and *p*-hydroxylidocaines.

Certain ions not present in control urine were detected in small amounts including ions at *m/e* 177, 221, and 249, which might represent V*a*, V*b*, and V*c*, respectively. Compound V*a* is an oxime, which could arise from oxidation and reduction of I*c*; V*b* might come from acetylation of I*c*, and V*c* might come from acetylation of I*b*. All of these pathways are known to be operative in humans. Computer acquisition of chemical-ionization data at moderate resolution to determine exact masses might support or refute the presence of such minor metabolites.

By using the chemical-ionization mass spectrometry–stable isotope dilution technique, 70–80% of lidocaine metabolism in humans can be accounted for. The results support the metabolic sequence outlined by Keenaghan and Boyes (12) with some modifications (Scheme I). As in most species studied, the major primary pathway of lidocaine biotransformation in humans appears to be *N*-dealkylation followed by secondary oxidations, conjugations, and hydrolysis. Any major contributions to lidocaine metabolism by oxidation of the aromatic methyl groups or *N*-hydroxyamide formation (31) were ruled out. However, whereas Keenaghan and Boyes (12) suggested only hydrolysis of the amide linkage after deethylation, the present results indicate that a substantial amount of direct hydrolysis of lidocaine takes place to yield both *N*,*N*-diethyl- and *N*-monoethylglycine plus 2,6-dimethylaniline, which is further oxidized to *p*-hydroxy-2,6-dimethylaniline, the major urinary metabolites of lidocaine in humans.

REFERENCES

(1) R. P. Lasser, *N.Y. State J. Med.*, **1973**, 1775.

(2) J. I. Grossman, L. A. Lublow, J. Frieden, and I. L. Rubin, *Arch. Intern. Med.*, **121**, 396 (1968).

(3) L. Lemberg, A. Castellanos, Jr., A. G. Arecebal, and R. N. V. Iyengar, *Med. Clin. N. Am.*, **55**, 273 (1971).

(4) J. R. Gillette, in "Microsomes and Drug Oxidation," J. R. Gillette, Ed., Academic, New York, N.Y., 1969.

(5) K. Krisch, *Biochem. Z.*, **55**, 273 (1963).

(6) R. G. McMahon and L. A. Woods, *J. Pharmacol. Exp. Ther.*, **103**, 354 (1951).

(7) C. Y. Sung and A. P. Truant, *ibid.*, **112**, 432 (1954).

(8) I. C. Geddes, *Anesth. Analg. Reanim.*, **15**, 908 (1958).

(9) G. Hollunger, *Acta Pharmacol. Toxicol.*, **17**, 356 (1960).

(10) A. H. Beckett, R. N. Boyes, and P. J. Appleton, *J. Pharm. Pharmacol.*, **7**, 755 (1965).

(11) C. A. DiPazio and R. E. Brown, *Anesthesiology*, **36**, 239 (1972).

(12) J. B. Keenaghan and R. N. Boyes, *J. Pharmacol. Exp. Ther.*, **180**, 454 (1972).

(13) G. D. Breck and W. F. Trager, *Science*, **173**, 544 (1971).

(14) J. M. Strong and A. J. Atkinson, Jr., *Anal. Chem.*, **44**, 2287 (1972).

(15) J. M. Strong, M. Parker, and A. J. Atkinson, Jr., *Clin. Pharmacol. Ther.*, **14**, 67 (1973).

(16) W. A. Garland, W. F. Trager, and S. D. Nelson, *Biomed. Mass Spectrom.*, **1**, 124 (1974).

(17) W. A. Garland, Ph.D. thesis, University of Washington, Seattle, Wash., 1974.

(18) W. A. Garland, R. J. Weinkam, and W. F. Trager, *Chem. Instrum.*, **5**, 271 (1974).

(19) N. Lofgren and B. Lundqvist, *Sven. Kem. Tidskr.*, **58**, 206 (1946).

(20) A. E. Ross, L. Keefer, and W. Lijinsky, *J. Natl. Cancer Inst.*, **47**, 789 (1971).

(21) D. D. Perrin, W. L. F. Armarego, and D. R. Perrin, "Purification of Laboratory Chemicals," Pergamon, Oxford, England, 1966, p. 158.

(22) D. P. Schwartz and D. W. Parks, *Anal. Chem.*, **33**, 1396 (1961).

(23) F. Mayer, W. Schafer, and J. Rosenbach, *Arch. Pharm.*, **1929**, 581.

(24) E. Bamberger, *Ber.*, **59**, 426 (1926).

(25) S. D. Nelson, G. D. Breck, and W. F. Trager, *J. Med. Chem.*, **16**, 1106 (1973).

(26) "Organic Synthesis," vol. II., A. H. Blatt, Ed., Wiley, New York, N.Y., 1943, p. 35.

(27) B. M. Wepster, *Rec. Trav.*, **73**, 814 (1954).

(28) R. E. Bowman and H. H. Stroud, *J. Chem. Soc.*, **1950**, 1342.

(29) A. L. Remizov, *Zh. Obshch. Khim.*, **34**, 3187 (1964).

(30) H. Hanke, *Pharm. Zentral.*, **99**, 318 (1960).

(31) S. D. Nelson, W. A. Garland, and W. F. Trager, *Res. Commun. Chem. Pathol. Pharmacol.*, **8**, 45 (1974).

(32) A. I. Cohen, J. Dreyfuss, and H. M. Fales, *J. Med. Chem.*, **15**, 542 (1972).

(33) H. Bartsch, M. Traut, and H. Hecker, *Biochim. Biophys. Acta*, **237**, 556 (1971).

(34) E. Bamberger, *Ann.*, **424**, 233 (1921).

(35) K. Bieman, "Mass Spectrometry: Organic Chemical Applications," McGraw-Hill, New York, N.Y., 1962, p. 223.

(36) R. W. Kelly, *Anal. Chem.*, **45**, 2079 (1973).

(37) A. K. Cho, B. Lindeke, B. Hodsdon, and D. J. Jenden, *ibid.*, 45, 570 (1973).

ACKNOWLEDGMENTS AND ADDRESSES

Received April 19, 1976, from the *Department of Pharmaceutical Chemistry, University of California, San Francisco, CA 94143,* and the *University of Washington, Seattle, WA 98195.*

Accepted for publication September 21, 1976.

Supported by grants from the Seattle Foundation (W. A. Garland and W. F. Trager), the Rubenstein Fund of the School of Pharmacy, University of Washington (W. A. Garland), and National Institutes of Health Training Grant 5-T01-GM00728 (S. D. Nelson) and in part by National Institutes of Health Grant GM-16496. The authors also thank J. Einch, Arizona State University, for making available his MASS PLOT computer program.

[x] To whom inquiries should be directed (at the University of Washington).

Application of Ion-Pair Methods to Extraction of Fluorouracil from Aqueous Fluids

ANDRÉ P. De LEENHEER,*[x], MARIE-CLAIRE COSYNS-DUYCK *, and P. MAURICE VAN VAERENBERGH [‡]

Abstract □ The polar molecule, fluorouracil, is a monoanion at pH 10 and may be quantitatively extracted from aqueous solutions with quaternary alkylammonium ions into an organic solvent such as dichloromethane as the ion-pair. Extraction constants of fluorouracil with the tetrapentylammonium ion in dichloromethane or dichloromethane–1-butanol (9:1) and with the tetrahexylammonium ion in dichloromethane were determined. Slope analysis demonstrated that association of the ion components in the aqueous phase occurred as the side reaction. A column ion-pair extraction technique, using tetrapentylammonium as the counterion and dichloromethane as the eluting phase, was developed and allowed quantitative transfer of fluorouracil to the organic solvent. The applicability of this method was shown by determining plasma levels of fluorouracil in cancer patients to whom 1 g of active substance was administered intravenously.

Keyphrases □ Fluorouracil—ion-pair extraction from aqueous solutions with quaternary alkylammonium ions into organic solvents □ Ion-pair extraction—fluorouracil from aqueous solutions with quaternary alkylammonium ions into organic solvents □ Antineoplastic agents—fluorouracil, ion-pair extraction from aqueous solutions with quaternary alkylammonium ions into organic solvents

Few methods have been published on the determination of fluorouracil in biological materials. A microbiological assay and a direct spectrophotometric method were used to determine plasma fluorouracil levels in cancer patients (1). Neither of these methods is sufficiently specific. Procedures using GLC were reported (2, 3), and a sensitive and highly specific mass fragmentographic method was recently described (4). However, in all of these techniques, the isolation of fluorouracil from aqueous biological materials into an organic solvent remains a weak point.

Dialysis and subsequent evaporation to dryness (2) and double-phase extraction with 2-propanol–ether (3, 4) were utilized. However, the first method is cumbersome and time consuming, and the two-phase extraction suffers from low specificity. A more polar system is required for extraction of the highly polar fluorouracil, a pyrimidine derivative.

The purpose of the present investigation was to study ion-pair systems, using quaternary alkylammonium counterions, for the extraction of fluorouracil from an aqueous matrix to an organic phase.

EXPERIMENTAL

Apparatus—A pH meter[1] equipped with a combination electrode[2], a magnetic stirrer[3], and a mechanical shaking apparatus[4] were used. Spectrophotometric measurements were performed with an automatic UV–visible double-beam instrument[5] using 10-mm quartz cells.

Chemicals and Reagents—Fluorouracil[6] was used as received. Dichloromethane[7], tetrapentylammonium iodide[8], and tetrahexylammonium bromide[8] were analytical grade. Tetrapentylammonium and tetrahexylammonium hydrogen phosphate solutions, about 0.15 and 0.01 *M*, respectively, were prepared as follows. To the 0.2 *M* aqueous solutions of the halides was added an equivalent amount of silver oxide, and the mixtures were continuously stirred for 24 hr. After filtration, concentrated phosphoric acid was added to pH 10. The solutions were extracted three times with small volumes of dichloromethane (phase ratio, aqueous–organic, 10:1) to remove the unreacted iodide and bromide salts (5). The true concentrations of the tetraalkylammonium ions were determined by an ion-pair extraction method with picric acid (6).

Cellulose[7] for column chromatography was purified in a column by washing with ethanol and dichloromethane until the absorbance of the eluate at 269 nm was constant at 0.010. Carbonate buffer, pH 10 and ionic strength 0.1, was prepared for back-extraction experiments by mixing 25.0 ml of 1 *M* $NaHCO_3$ with 50.0 ml of 0.5 *M* Na_2CO_3 and diluting to 1000 ml. A concentrated carbonate buffer for plasma determinations was made by dissolving 2.1 g of sodium hydrogen carbonate and 2.6 g of sodium carbonate in 40 ml of water.

All other substances were analytical grade and were used without purification. Mutually saturated solvents were used throughout the experiments.

Extraction Constants—Constants for ion-pair extraction and ion-pair association in the aqueous phase were determined by a partition technique. The partition experiments were performed in centrifuge tubes using 20-ml volumes of aqueous and organic solutions. These solutions were mechanically shaken at room temperature for 30 min to establish equilibrium. After centrifugation, the phases were separated and the absorbance of the aqueous phase, A_1, was measured at 269 nm.

A 10.0-ml aliquot of the organic phase was subsequently reequilibrated with 10.0 ml of 0.01 *M* $NaClO_4$ in carbonate buffer, pH 10, by shaking for 15 min at room temperature. (A shorter time for establishing the equilibrium was used because of the much higher extraction constant of

[1] Radiometer Titrator TTT 1c, Copenhagen, Denmark.
[2] Radiometer GK 2321 C, Copenhagen, Denmark.
[3] Cenco Instruments N.V. 16632 B, Breda, The Netherlands.
[4] Wilten and Co., Berchem, Belgium.
[5] Pye Unicam SP 1800, Cambridge, England.
[6] Donated by N.V. Produits Roche, Brussels, Belgium.
[7] E. Merck AG, Darmstadt, West Germany.
[8] Eastman Kodak, Rochester, N.Y.

(37) A. K. Cho, B. Lindeke, B. Hodsdon, and D. J. Jenden, *ibid.*, 45, 570 (1973).

ACKNOWLEDGMENTS AND ADDRESSES

Received April 19, 1976, from the *Department of Pharmaceutical Chemistry, University of California, San Francisco, CA 94143,* and the *University of Washington, Seattle, WA 98195.*

Accepted for publication September 21, 1976.

Supported by grants from the Seattle Foundation (W. A. Garland and W. F. Trager), the Rubenstein Fund of the School of Pharmacy, University of Washington (W. A. Garland), and National Institutes of Health Training Grant 5-T01-GM00728 (S. D. Nelson) and in part by National Institutes of Health Grant GM-16496. The authors also thank J. Einch, Arizona State University, for making available his MASS PLOT computer program.

[x] To whom inquiries should be directed (at the University of Washington).

Application of Ion-Pair Methods to Extraction of Fluorouracil from Aqueous Fluids

ANDRÉ P. De LEENHEER,*[x], MARIE-CLAIRE COSYNS-DUYCK *, and P. MAURICE VAN VAERENBERGH [‡]

Abstract □ The polar molecule, fluorouracil, is a monoanion at pH 10 and may be quantitatively extracted from aqueous solutions with quaternary alkylammonium ions into an organic solvent such as dichloromethane as the ion-pair. Extraction constants of fluorouracil with the tetrapentylammonium ion in dichloromethane or dichloromethane–1-butanol (9:1) and with the tetrahexylammonium ion in dichloromethane were determined. Slope analysis demonstrated that association of the ion components in the aqueous phase occurred as the side reaction. A column ion-pair extraction technique, using tetrapentylammonium as the counterion and dichloromethane as the eluting phase, was developed and allowed quantitative transfer of fluorouracil to the organic solvent. The applicability of this method was shown by determining plasma levels of fluorouracil in cancer patients to whom 1 g of active substance was administered intravenously.

Keyphrases □ Fluorouracil—ion-pair extraction from aqueous solutions with quaternary alkylammonium ions into organic solvents □ Ion-pair extraction—fluorouracil from aqueous solutions with quaternary alkylammonium ions into organic solvents □ Antineoplastic agents—fluorouracil, ion-pair extraction from aqueous solutions with quaternary alkylammonium ions into organic solvents

Few methods have been published on the determination of fluorouracil in biological materials. A microbiological assay and a direct spectrophotometric method were used to determine plasma fluorouracil levels in cancer patients (1). Neither of these methods is sufficiently specific. Procedures using GLC were reported (2, 3), and a sensitive and highly specific mass fragmentographic method was recently described (4). However, in all of these techniques, the isolation of fluorouracil from aqueous biological materials into an organic solvent remains a weak point.

Dialysis and subsequent evaporation to dryness (2) and double-phase extraction with 2-propanol–ether (3, 4) were utilized. However, the first method is cumbersome and time consuming, and the two-phase extraction suffers from low specificity. A more polar system is required for extraction of the highly polar fluorouracil, a pyrimidine derivative.

The purpose of the present investigation was to study ion-pair systems, using quaternary alkylammonium counterions, for the extraction of fluorouracil from an aqueous matrix to an organic phase.

EXPERIMENTAL

Apparatus—A pH meter[1] equipped with a combination electrode[2], a magnetic stirrer[3], and a mechanical shaking apparatus[4] were used. Spectrophotometric measurements were performed with an automatic UV–visible double-beam instrument[5] using 10-mm quartz cells.

Chemicals and Reagents—Fluorouracil[6] was used as received. Dichloromethane[7], tetrapentylammonium iodide[8], and tetrahexylammonium bromide[8] were analytical grade. Tetrapentylammonium and tetrahexylammonium hydrogen phosphate solutions, about 0.15 and 0.01 *M*, respectively, were prepared as follows. To the 0.2 *M* aqueous solutions of the halides was added an equivalent amount of silver oxide, and the mixtures were continuously stirred for 24 hr. After filtration, concentrated phosphoric acid was added to pH 10. The solutions were extracted three times with small volumes of dichloromethane (phase ratio, aqueous–organic, 10:1) to remove the unreacted iodide and bromide salts (5). The true concentrations of the tetraalkylammonium ions were determined by an ion-pair extraction method with picric acid (6).

Cellulose[7] for column chromatography was purified in a column by washing with ethanol and dichloromethane until the absorbance of the eluate at 269 nm was constant at 0.010. Carbonate buffer, pH 10 and ionic strength 0.1, was prepared for back-extraction experiments by mixing 25.0 ml of 1 *M* $NaHCO_3$ with 50.0 ml of 0.5 *M* Na_2CO_3 and diluting to 1000 ml. A concentrated carbonate buffer for plasma determinations was made by dissolving 2.1 g of sodium hydrogen carbonate and 2.6 g of sodium carbonate in 40 ml of water.

All other substances were analytical grade and were used without purification. Mutually saturated solvents were used throughout the experiments.

Extraction Constants—Constants for ion-pair extraction and ion-pair association in the aqueous phase were determined by a partition technique. The partition experiments were performed in centrifuge tubes using 20-ml volumes of aqueous and organic solutions. These solutions were mechanically shaken at room temperature for 30 min to establish equilibrium. After centrifugation, the phases were separated and the absorbance of the aqueous phase, A_1, was measured at 269 nm.

A 10.0-ml aliquot of the organic phase was subsequently reequilibrated with 10.0 ml of 0.01 *M* $NaClO_4$ in carbonate buffer, pH 10, by shaking for 15 min at room temperature. (A shorter time for establishing the equilibrium was used because of the much higher extraction constant of

[1] Radiometer Titrator TTT 1c, Copenhagen, Denmark.
[2] Radiometer GK 2321 C, Copenhagen, Denmark.
[3] Cenco Instruments N.V. 16632 B, Breda, The Netherlands.
[4] Wilten and Co., Berchem, Belgium.
[5] Pye Unicam SP 1800, Cambridge, England.
[6] Donated by N.V. Produits Roche, Brussels, Belgium.
[7] E. Merck AG, Darmstadt, West Germany.
[8] Eastman Kodak, Rochester, N.Y.

the perchlorate ion-pair in the organic phase.) After centrifugation to separate the two layers, the absorbance at 269 nm of this aqueous phase, A_2, was determined. Distilled water (20 ml) was treated identically to the fluorouracil solutions, and the resulting phases were used as the blank in the reference cell for both spectrophotometric measurements.

According to the described method, three complete series of experiments were performed:

1. To 10 ml of 0.004 *M* fluorouracil (previously adjusted to pH 10 with 1 *M* NaOH) was added 10.0 ml of tetrapentylammonium hydrogen phosphate solution of known concentration (aliquots of the stock solution of 0.138 *M* tetrapentylammonium hydrogen phosphate were diluted with appropriate volumes of 0.075 *M* NaH_2PO_4), and the aqueous phase was equilibrated with 20.0 ml of dichloromethane as the organic phase. Counterion stock and phosphate solution had the same ionic strength of 0.225, which remained constant throughout the experiments.
2. Same as Series 1, but dichloromethane–1-butanol (9:1) was used as the organic phase.
3. Same as Series 1, but a 2.06×10^{-4} *M* fluorouracil solution, a 5×10^{-3} *M* tetrahexylammonium hydrogen phosphate stock solution, and dichloromethane as the organic phase were used.

Plasma Samples—Ten cancer patients received 1 g of fluorouracil by intravenous injection in the right arm. Blood samples were drawn into heparinized syringes from the left arm by venous puncture at various intervals for 30 min after administration. Plasma was separated from the red blood cells by centrifugation and frozen until assayed.

Determination of Fluorouracil in Plasma—Volumes of 1.0 ml of plasma, 1.0 ml of 0.15 *M* tetrapentylammonium counterion, and 200 μl of pH 10 carbonate buffer were mixed thoroughly with 4 g of cellulose in a 100-ml beaker until dry. The adsorbent was packed in a glass column (1×50 cm) and eluted with 10 ml of dichloromethane. The first 5 ml of eluate was collected in 10-ml screw-capped centrifuge tubes.

To the organic phase, 3 ml of 0.2 *M* $NaClO_4$ in pH 10 carbonate buffer was added, and the phases were allowed to equilibrate by shaking for 15 min at room temperature. After centrifugation, the aqueous phase was measured spectrophotometrically at 269 nm against 0.2 *M* $NaClO_4$ in pH 10 carbonate buffer. For each patient, a plasma sample collected just before the fluorouracil administration was used as a blank.

RESULTS AND DISCUSSION

As indicated by its high water solubility [11.78 g/liter (2)], fluorouracil is a highly polar compound. Its extraction from an aqueous medium with usual double-phase techniques requires the use of polar systems [ether–lipophilic alcohols (8:2)] (3, 4). However, such systems possess a rather low selectivity. Because fluorouracil is an ionizable substance [*i.e.*, a weak diprotic acid (H_2FU) having a $pKa_1 = 8.0$ and a $pKa_2 = 13$ (7)], the possible application of an ion-pair extraction method was investigated. In aqueous solutions buffered at pH 10, 99.0% of fluorouracil exists as the monoanionic species HFU^-. Experiments were carried out to investigate the feasibility of extracting fluorouracil as a 1:1 ion-pair into a dichloromethane phase with tetrapentyl- or tetrahexylammonium as monocationic counterions.

The extraction of fluorouracil as an ion-pair from an aqueous phase buffered at pH 10 into an organic phase may be represented by Scheme I:

$$HFU^-_{aq} + Q^+_{aq} \rightleftharpoons HFU^-Q^+_{org}$$

Scheme I

where HFU^-_{aq} represents the monoanionic species of fluorouracil in the aqueous phase; Q^+_{aq} is the counterion, *i.e.*, the tetraalkyl (pentyl or hexyl) ammonium ion in the aqueous phase; and $HFU^-Q^+_{org}$ is the ion-pair in the organic phase.

The ion-pair extraction constant, E, is defined by:

$$E = \frac{[HFU^-Q^+]_{org}}{[HFU^-]_{aq}\,[Q^+]_{aq}} \qquad \text{(Eq. 1)}$$

where $[\,]_{aq}$ and $[\,]_{org}$ are the concentrations of the species indicated in the aqueous and organic phases, respectively.

However, to examine the influence of side reactions on the extraction, a conditional extraction constant, E^*, is used:

$$E^* = \frac{C_{HFU^-Q^+_{org}}}{C_{HFU^-_{aq}}\,C_{Q^+_{aq}}} = E\,\frac{\alpha_{HFU^-Q^+_{org}}}{\alpha_{HFU^-_{aq}}\,\alpha_{Q^+_{aq}}} \qquad \text{(Eq. 2)}$$

where C is the actual concentration, and α is the activity coefficient that compensates for side reaction(s) of the species indicated.

The concentration of the monoanionic species of fluorouracil in the aqueous phase, $C_{HFU^-_{aq}}$, is measured by spectrophotometry at 269 nm (A_1), using the molar absorption coefficient $\epsilon = 4.12 \times 10^3$ liters/mole cm. The concentration of the ion-pair in the organic phase, $C_{HFU^-Q^+_{org}}$, is estimated by an indirect procedure. Because the spectral properties of the ion-pair $HFU^-Q^+_{org}$ in the organic phase were not known accurately, a back-extraction was performed with 0.01 *M* $NaClO_4$ in pH 10 carbonate buffer. However, the perchlorate anion is a much stronger ion-pair former than the monoanion of fluorouracil [*i.e.*, $E_{ClO_4^-Q^+}$ is much larger than $E_{HFU^-Q^+}$ (8)], and the equilibrium will be displaced far to the right as shown by Scheme II.

$$HFU^-Q^+_{org} + ClO^-_{4aq} \rightleftharpoons ClO^-_4Q^+_{org} + HFU^-_{aq}$$

Scheme II

Therefore, all fluorouracil originally present as an ion-pair in the organic phase will be quantitatively transferred to the aqueous phase, HFU^-_{aq}. Spectrophotometry at 269 nm of the latter yields A_2, which allows calculation of $C_{HFU^-Q^+_{org}}$ (using the molar absorptivity $\epsilon = 4.12 \times 10^3$ liters/mole cm) for substitution in Eq. 2. Finally, the concentration of the counterion in the aqueous phase, $C_{Q^+_{aq}}$, is obtained from Eq. 3 by difference between the initial concentration of counterion, $C_Q{}^0$, and the measured ion-pair concentration, $C_{HFU^-Q^+_{org}}$:

$$C_{Q^+_{aq}} = C_Q{}^0 - C_{HFU^-Q^+_{org}} \qquad \text{(Eq. 3)}$$

Substitution of the concentration terms in Eq. 2 by absorbance values (Lambert–Beer $C = A/\epsilon$ for 1.0-cm pathlength) and expansion with Eq. 3 give:

$$E^* = \frac{A_2/\epsilon}{A_1/\epsilon\,(C_Q{}^0 - A_2/\epsilon)} \qquad \text{(Eq. 4)}$$

which may also be written:

$$E^* = \frac{A_2\epsilon}{A_1(C_Q{}^0\epsilon - A_2)} \qquad \text{(Eq. 5)}$$

and which is used experimentally for calculation of the conditional extraction constants E^*.

Data for fluorouracil ion-pairs, as determined using three sets of experimental conditions, are given in Table I. Within each experimental series, the value found for E^* increases with the decreasing initial concentration of counterion $C_Q{}^0$. This effect strongly suggests the existence of a side reaction, specifically the association of the ion-pair components in the aqueous phase (9–11), which is defined in Scheme III.

$$HFU^-_{aq} + Q^+_{aq} \rightleftharpoons HFU^-Q^+_{aq}$$

Scheme III

For this equilibrium, the apparent association constant, K_a, is given by:

$$K_a = \frac{[HFU^-Q^+]_{aq}}{[HFU^-]_{aq}\,[Q^+]_{aq}} \qquad \text{(Eq. 6)}$$

where $[HFU^-Q^+]_{aq}$ is the concentration of the fluorouracil ion-pair in the aqueous phase.

Furthermore, if association of the ion-pair components in the aqueous phase occurs as the only side reaction, the following values for the activity coefficients α ($\alpha = C/[\,]$, where C is the actual concentration and $[\,]$ is the theoretical concentration of the species subscribed) should be assigned and substituted in Eq. 2. Then $\alpha_{HFU^-Q^+_{org}} = 1$, since the actual and theoretical concentrations of the ion-pair in the organic phase are equal; *i.e.*, $C_{HFU^-Q^+_{org}} = [HFU^-Q^+]_{org}$ (assuming no side reaction occurs in the organic phase); $\alpha_{Q^+_{aq}} = 1$ because there is always an excess of tetraalkylammonium counterion, Q^+, present in the aqueous phase or its actual and theoretical concentrations are practically equal, *i.e.*, $C_{Q^+_{aq}} \approx [Q^+]_{aq}$; and $\alpha_{HFU^-_{aq}}$ or the activity coefficient of the fluorouracil monoanion in the aqueous phase is then given by Eq. 7:

$$\alpha_{HFU^-_{aq}} = \frac{C_{HFU^-_{aq}}}{[HFU^-]_{aq}} = \frac{[HFU^-]_{aq} + [HFU^-Q^+]_{aq}}{[HFU^-]_{aq}} \qquad \text{(Eq. 7)}$$

which can be rearranged by use of Eq. 6 to the following form:

$$\alpha_{HFU^-_{aq}} = 1 + K_a[Q^+]_{aq} \qquad \text{(Eq. 8)}$$

Substituting the values for α in Eq. 2 yields the expression for E^*, which is valid when association of the ion-pair components in the aqueous phase occurs as the only side reaction:

$$E^* = \frac{E}{\alpha_{HFU^-_{aq}}} = \frac{E}{1 + K_a[Q^+]_{aq}} \qquad \text{(Eq. 9)}$$

Table I—Determination of Extraction Constants of Fluorouracil Ion-Pairs [a]

C_Q^0, $M \times 10^{-3}$	$C_{HFU^-_{aq}}$, $M \times 10^{-3}$	$C_{HFU\text{-}Q^+_{org}}$, $M \times 10^{-3}$	$C_{Q^+_{aq}}$, $M \times 10^{-3}$	E^*, M^{-1}	$1/E^*$, $M \times 10^{-3}$	$D = E^* C_{Q^+_{aq}}$
First Series: Tetrapentylammonium and Dichloromethane; $C^0_{fluorouracil} = 2.048 \times 10^{-3}\ M$						
69.0	0.34	1.89	67.11	82.8	12.1	5.58
34.5	0.54	1.68	32.82	94.8	10.6	3.11
17.25	0.86	1.36	15.89	99.5	10.1	1.58
8.63	1.22	1.00	7.63	107.4	9.3	0.82
Second Series: Tetrapentylammonium and Dichloromethane–1-Butanol (9:1); $C^0_{fluorouracil} = 2.011 \times 10^{-3}\ M$						
75.0	0.0455	1.97	73.03	593	1.69	—
37.5	0.0600	1.95	35.55	914	1.09	—
18.75	0.0941	1.90	16.85	1,198	0.83	—
9.38	0.158	1.86	7.52	1,565	0.64	—
Third Series: Tetrahexylammonium and Dichloromethane; $C^0_{fluorouracil} = 0.103 \times 10^{-3}\ M$						
2.85	0.00300	0.100	2.75	12,120	0.0825	—
1.43	0.00494	0.0982	1.33	14,950	0.0669	—
0.71	0.00833	0.0947	0.62	18,340	0.0545	—
0.36	0.0156	0.0874	0.27	20,750	0.0481	—

[a] C^0 is the initial concentration of the compound indicated and taken through the experiment; C is the actual concentration of the species indicated after reaching equilibrium.

By taking the reciprocals, Eq. 9 is linearized to:

$$\frac{1}{E^*} = \frac{1}{E} + \frac{K_a}{E}[Q^+]_{aq} \qquad \text{(Eq. 10)}$$

Thus, if the assumption of association of the ion-pair components in the aqueous phase is correct, slope analysis of the experimental data according to Eq. 10, namely the reciprocal of the conditional extraction constant, $1/E^*$, *versus* the concentration of the counterion in the aqueous phase, $[Q^+]_{aq}$ (which is approximated by the actual concentration $C_{Q^+_{aq}}$), should yield straight lines. The experimental data points of the three systems considered all fit Eq. 10, supporting the validity of the hypothesis. By using the same relationship, the theoretical extraction constant E and the association constant K_a of each series were derived: 109 and 5 M^{-1}, tetrapentylammonium and dichloromethane; 1855 and 30 M^{-1}, tetrapentylammonium and dichloromethane–1-butanol (9:1); and 21,761 and 298 M^{-1}, tetrahexylammonium and dichloromethane. Although the two latter systems afforded a high extraction efficiency of 97–98%, they were less selective and their applicability was limited to fluorouracil extracts that had undergone a preliminary cleanup.

The tetrapentylammonium and dichloromethane system yielded values for E^* that approached $E = 109\ M^{-1}$ as the concentration of the counterion, $C_{Q^+_{aq}}$, decreased. Thus, under appropriate experimental conditions, the effect of the side reaction identified would be negligible. For example, when the activity coefficient of the fluorouracil monoanion in the aqueous phase, $\alpha_{HFU^-_{aq}}$, equals 1.01, E^* approximates $E = 109\ M^{-1}$ (see Eq. 9, first term). When solving Eq. 8 for the activity coefficient $\alpha_{HFU^-_{aq}} = 1.01$ (chosen) and the association constant $K_a = 5\ M^{-1}$ (found), the highest concentration of tetrapentylammonium counterion in the aqueous phase that might be used would be 0.002 M.

However, under such conditions, the presence of higher concentrations of competitive anions, comparable to much higher extraction constants (*e.g.*, the chloride ion), would probably exhaust the tetrapentylammonium counterion and prevent the extraction of fluorouracil, even at rather low concentrations. Therefore, the feasibility of the ion-pair extraction of fluorouracil with the tetrapentylammonium and dichloromethane system under circumstances where the influence of the association phenomenon should be minor will not be investigated further. As mentioned previously, a low numerical value for the theoretical extraction constant E (= 109 M^{-1}) was obtained for the tetrapentylammonium and dichloromethane system. Evidently, this value entirely governs the quantitative aspect of the ion-pair extraction.

In general, the percentage of the ion-pair extraction, P, is given by:

$$P = \frac{100}{1 + \frac{1}{D}\frac{V_{aq}}{V_{org}}} \qquad \text{(Eq. 11)}$$

and:

$$D = \frac{C_{HFU\text{-}Q^+_{org}}}{C_{HFU^-_{aq}}} \qquad \text{(Eq. 12)}$$

or by combining Eqs. 12 and 2:

$$D = E^* C_{Q^+_{aq}} \qquad \text{(Eq. 13)}$$

where D is the partition ratio of the fluorouracil monoanion between the organic and aqueous phases, and V_{aq}/V_{org} is the ratio of the volumes of the aqueous phase to the organic phase.

The extraction is considered quantitative when P numerically equals 99%. Thus, in the present study where the ratio $V_{aq}/V_{org} = 1.00$, D should be 100. By using Eq. 13 (rearranged for the conditional extraction constant E^*) and simplifying for approximating actual and theoretical counterion concentrations in the aqueous phase ($C_{Q^+_{aq}} = [Q^+]_{aq}$), Eq. 10 (which takes into account the only side reaction observed) can be written:

$$\frac{1}{D} = \frac{K_a}{E} + \frac{1}{E} C_{Q^+_{aq}} \qquad \text{(Eq. 14)}$$

where $C_{Q^+_{aq}}$ is the actual concentration of the tetrapentylammonium counterion in the aqueous phase. Plotting the experimental points for the first series (Table I) according to Eq. 14 (the reciprocal of the partition

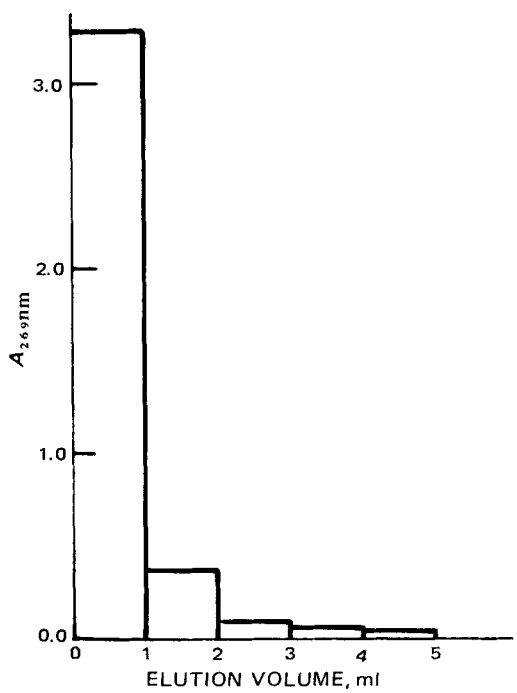

Figure 1—*Elution pattern of fluorouracil with column ion-pair extraction.*

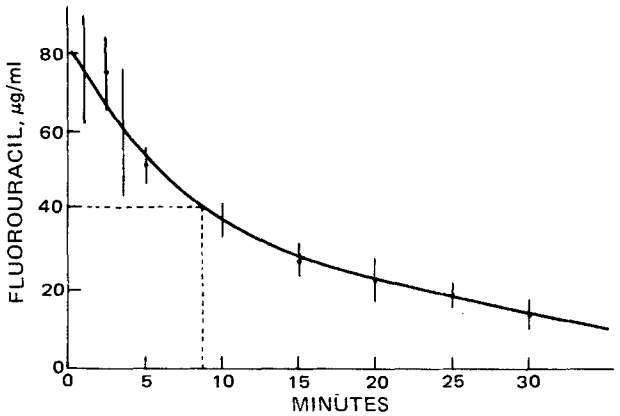

Figure 2—*Plasma fluorouracil concentration (1 g iv total amount) in 10 cancer patients.*

ratio $1/D$ as a function of the concentration of the tetrapentylammonium counterion in the aqueous phase ($C_{Q^+_{aq}}$) afforded a straight line, establishing that, for $D = 100$, $C_{Q^+_{aq}}$ should be about 1 M. However, the highest counterion concentration that could be prepared was about 0.15 M. Thus, the water solubility of tetrapentylammonium hydrogen phosphate is insufficient to meet the necessary 1 M calculated value. Therefore, as follows from Eq. 11, the unique solution of this problem was to increase the ratio of volumes employed, V_{org}/V_{aq}.

This solution was realized by adsorbing an aliquot of aqueous sample, buffered at pH 10 and containing the fluorouracil monoanion, with an excess of the tetrapentylammonium counterion onto an adsorbent such as cellulose. The mixture was packed in a glass column, and the ion-pair HFU^-Q^+ eluted with the necessary volume of dichloromethane. Figure 1 shows the elution pattern of fluorouracil at an initial concentration of 100 μg/ml; all fluorouracil was recovered in the first 5 ml of dichloromethane.

Recovery studies were performed by preparing a blank plasma pool to which fluorouracil was added, covering the range of 0–100 μg/ml. Each sample, *i.e.*, 0, 10, 20, 30, 40, 50, 60, 80, and 100 μg/ml, was taken through the complete procedure three times. The recovery as calculated from all results was 99.6 ± 0.6%, but appreciable absorbance values (up to 0.500) were measured for the blank sample. These values were due to unidentified interferences from cellulose (that could not be removed entirely prior to analysis) or from compounds coextracted from plasma. This result, together with the low molecular absorptivity of fluorouracil, set the detection limit of the ion-pair column extraction method at about 10 μg/ml of plasma.

To demonstrate the applicability of the ion-pair column extraction to blood samples, 1 g of fluorouracil was administered intravenously to 10 cancer patients. At 1, 2.5, 3.5, 5, 10, 15, 20, and 30 min after injection, blood samples were collected. Results of the analysis of each plasma sample are presented as a mean plasma level curve in Fig. 2. The fluorouracil concentration leveled off rapidly, from more than 100 μg/ml (at 1 min) to about 10 μg/ml (at 30 min) with a biological half-life of 9 min. These data correspond to those reported earlier (3, 4). The determination of plasma fluorouracil levels below 10 μg/ml is an analytical problem currently being investigated.

Although the quantitative ion-pair extraction of fluorouracil in the concentration range of 0.1–10 μg/ml was feasible, combining the ion-pair extraction with GLC was not successful. In fact, extractive methylation, *i.e.*, simultaneous extraction and methylation of the fluorouracil monoanion in the ion-pair form, produced chromatograms wherein the *N,N'*-dimethyl derivative of fluorouracil was overlapped by multiple interfering peaks originating from irreproducible thermal degradation reaction(s) of the residual counterion (tetrapentylammonium or tetrahexylammonium cation) in the organic phase. An attempt was made to solve this problem by purification of the *N,N'*-dimethyl derivative through selective extraction with ether (12) and by column chromatography on magnesium silicate[9] (13), alumina[10], or a cation-exchange resin[11]. None of these approaches gave satisfactory results. This fundamental problem has been recognized (14, 15), and it may be the major reason that the combination of ion-pair extraction with GLC has not been utilized.

REFERENCES

(1) B. Clarkson, A. O'Connor, L. Winston, and D. Hutchison, *Clin. Pharmacol. Ther.*, **5**, 581 (1964).

(2) J. J. Windheuser, J. L. Sutter, and E. Auen, *J. Pharm. Sci.*, **61**, 301 (1972).

(3) J. L. Cohen and P. B. Brennan, *ibid.*, **62**, 572 (1973).

(4) C. Finn and W. Sadée, *Cancer Chemother.*, **59**, 279 (1975).

(5) K. Gustavii and G. Schill, *Acta Pharm. Suec.*, **3**, 259 (1966).

(6) *Ibid.*, **3**, 241 (1966).

(7) I. Shugar and J. J. Fox, *Biochim. Biophys. Acta*, **9**, 199, 369 (1952).

(8) K. Gustavii, *Acta Pharm. Suec.*, **4**, 233 (1967).

(9) G. Schill, *ibid.*, **2**, 13 (1965).

(10) B. A. Person and G. Schill, *ibid.*, **3**, 281 (1966).

(11) R. Modin and G. Schill, *ibid.*, **4**, 301 (1967).

(12) J. A. F. de Silva, I. Bekersky, C. V. Puglisi, M. A. Brooks, and R. E. Weinfeld, *Anal. Chem.*, **48**, 1 (1976).

(13) J. M. Rosenfeld and V. Y. Taguchi, *ibid.*, **48**, 4 (1976).

(14) M. Ervik and K. Gustavii, *ibid.*, **46**, 39 (1974).

(15) E. Ehrsson, *ibid.*, **46**, 922 (1974).

ACKNOWLEDGMENTS AND ADDRESSES

Received July 6, 1976, from the **Laboratoria voor Medische Biochemie en voor Klinische Analyse, Faculteit van de Farmaceutische Wetenschappen, and the ‡Kliniek voor Radiotherapie en Kerngeneeskunde, Faculteit van de Geneeskunde, Rijksuniversiteit, Academisch Ziekenhuis, 135 De Pintelaan, 9000-Gent, Belgium.*

Accepted for publication October 8, 1976.

Supported by Grant 20 452 from the National Foundation for Medical Research (F.G.W.O.).

The authors thank Professor G. Schill, University of Uppsala, Uppsala, Sweden, for training in his laboratories and S. Eksborg and P. O. Lagerström for helpful discussions.

ˣ To whom inquiries should be directed.

[9] Florisil 60-100 U.S. mesh, BDH Chemical Co., Poole, England.
[10] Neutral alumina AG 7, Bio-Rad, Richmond, Va.
[11] Cation-exchange resin AG 50W-X8, Bio-Rad, Richmond, Va.

Antitumor Agents XXIII: Helenalin, an Antitumor Principle from *Anaphalis morrisonicola* HAY.

KUO-HSIUNG LEE *x, MITSUMASA HARUNA *, HUAN-CHANG HUANG ‡, BI-SHIA WU *, and IRIS H. HALL *

Abstract □ A chloroform extract of the whole plant of *Anaphalis morrisonicola* HAY. showed significant antitumor activity against Ehrlich ascites carcinoma, Walker 256 carcinosarcoma, and P-388 lymphocytic leukemia. Systematic fractionation of the extract led to isolation and characterization of helenalin, a pseudoguaianolide, as the major active principle.

Keyphrases □ Helenalin—isolated from whole plant chloroform extract of *Anaphalis morrisonicola* □ *Anaphalis morrisonicola*—whole plant chloroform extract, antitumor activity evaluated, helenalin isolated □ Antitumor activity—whole plant chloroform extract of *Anaphalis morrisonicola* evaluated

In the continuing search among Formosan plants for new potential antitumor agents (1), the chloroform extract of the whole plant of *Anaphalis morrisonicola* HAY. (2) (Compositae), a hitherto uninvestigated species, showed significant inhibitory activity. This paper reports the isolation and characterization of the major active constituent of this extract, which was identified as helenalin (I). *In vivo* antitumor activity was assayed by using literature methods (3, 4). Previously, helenalin at 33.3 mg/kg/day caused 99% inhibition of Ehrlich ascites cell growth[1]; at 2.5 mg/kg/day, it produced significant (T/C ≥ 125%) inhibitory activity against the growth of Walker 256 ascites carcinosarcoma in rats (T/C = 316%); and at 25 mg/kg/day, it inhibited P-388 lymphocytic leukemia[1] (T/C = 127%).

DISCUSSION

The extraction of the active principles was carried out according to the procedure described previously (5). The final chloroform extract of the active crude preparation was separated further by silica gel column chromatography. Each fraction (C–H) was subsequently tested *in vivo* for antitumor activity (Ehrlich ascites carcinoma) and led to the isolation of the active principle, I, in 0.00032% yield. Compound I was obtained as colorless needles by preparative TLC followed by recrystallization from benzene (mp 170–173° and empirical formula $C_{15}H_{18}O_4$).

Compound I exhibited IR bands at 3450 (OH), 1765 (γ-lactone), and 1710 (cyclopentenone) cm^{-1} and NMR signals at δ 0.98 (3H, s, C_5-CH_3), 1.28 (3H, d, J = 6, C_{10}-CH_3), 4.45 (1H, d, J = 4.5, H_6), 5.00 (1H, t, J = 6, H_8), 5.85 (1H, d, J = 3, H_{13}), 6.09 (1H, dd, J = 6, 3, H_3), and 7.77 (1H, dd, J = 6, 1.5, H_2) ppm. The correspondence of the properties of this compound with those described in the literature (6) and its mixed melting-point and TLC determinations, as well as superimposable IR and NMR spectra, established its identity as helenalin, a pseudoguaianolide isolated previously from *Helium autumnale* (7), *H. microcephalum* (8), and *Balduina angustifolia* (6).

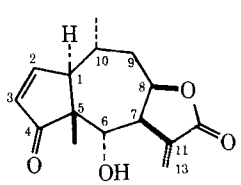

I

Table I—Effects of Fractions from *A. morrisonicola* on Inhibition of Ehrlich Ascites Tumor Growth

Fraction	Survival at Day 7	Volume, ml	Ascitocrit	Inhibition, %
0.05% Polysorbate control	6/6	2.33[a]	37.0[a]	—
A	5/6	1.54	12.8	77.0
B	6/6	1.92	37.0	18.0
C	6/6	1.18	39.0	47.0
D	6/6	1.67	45.0	13.0
E	6/6	1.00	26.0	70.0
F	5/6	0.04	10.0	99.5
G	6/6	1.82	36.0	24.0
H	6/6	2.51	36.0	0.0

[a] Standard deviation on the control ascitocrit was 7.8; on the volume, it was 1.2.

The structural requirement for the significant antitumor activity of helenalin (I) is the presence of an O=CC=CH_2 system as part of a ketone, such as a β-unsubstituted cyclopentenone, or as part of a lactone, such as an α-methylene-γ-lactone, as previously postulated by extensive structure–activity relationship studies (9–11). Further studies on the mechanisms of action of helenalin are in progress[1].

EXPERIMENTAL[2]

Extraction of *A. morrisonicola* HAY.—The *A. morrisonicola* was collected in Mt. Ho-Fan, Nan-Tau Shen, Taiwan[3], during September 1975. The ground, air-dried, whole plant material (2.5 kg) was extracted with chloroform at room temperature, yielding, after removal of the solvent, a thick green-black tar (Fraction A). This fraction showed 77% inhibition of Ehrlich ascites tumor growth and T/C = 193% inhibition against Walker 256 ascites (survival system) carcinosarcoma.

Fraction A was shaken with a mixture of methanol (1.5 liters), hexane (1.5 liters), and water (0.5 liter). The hexane layer was not investigated further since it caused only 18% inhibition of Ehrlich ascites tumor growth. The aqueous layer was concentrated *in vacuo* and extracted with chloroform. The chloroform extract, upon evaporation, yielded 14.7 g of a dark-brown syrup.

Isolation of Helenalin (I)—The syrup was chromatographed on silica gel (6 × 70 cm) with elution with 1 liter of hexane–benzene (1:1) (Fractions C and D, 500 ml each), 500 ml of chloroform (Fraction E), and 3.5 liters of 0.5% methanol–chloroform (Fractions F–H). As seen in Table I, the active principles were concentrated in Fraction F (99.5% inhibition),

[1] See I. H. Hall, K. H. Lee, E. C. Mar, C. O. Starnes, and T. G. Waddell, *J. Med. Chem.*, **20**, 333 (1977).

[2] Unless otherwise specified, melting points were determined on a Thomas-Hoover melting-point apparatus and are corrected. IR spectra were determined in chloroform with a Perkin-Elmer 257 grating IR spectrophotometer. NMR spectra were measured in $CDCl_3$ with a Jeolco C 60 HL NMR spectrometer, using tetramethylsilane as an internal standard. Silica gel for column chromatography refers to EM silica gel 60; silica gel for TLC and preparative TLC refers to Merck silica gel G and EM silica gel GF-254, respectively. The plates were developed with chloroform–acetone (3:1) and visualized by spraying with concentrated sulfuric acid and heating.

[3] Collected and identified by H.-C. Huang. A voucher specimen was deposited at the Herbarium of the Department of Botany, School of Pharmacy, Kaohsiung Medical College, Taiwan, Republic of China.

which gave a major single fluorescent spot on TLC under UV light together with traces of five nonfluorescent components. Subsequent isolation of this single fluorescent spot by preparative TLC led to a crystalline residue, which was recrystallized from benzene to yield colorless needles (8 mg), mp 170–173°. The identity of this compound with an authentic sample of helenalin (I) was established by TLC, IR, and NMR spectroscopic comparisons and by mixed melting-point determination.

REFERENCES

(1) K. H. Lee, T. Ibuka, H. C. Huang, and D. L. Harris, *J. Pharm. Sci.*, **64**, 1077 (1975), and references cited therein.

(2) A. T. Hsieh and T. I. Yang, "Nomenclature of Plants in Taiwan," National Taiwan University, Taiwan, Republic of China, 1969, p. 910.

(3) C. Piantadosi, C. S. Kim, and J. L. Irvin, *J. Pharm. Sci.*, **58**, 821 (1969).

(4) R. I. Geran, N. H. Greenberg, M. M. MacDonald, A. M. Schumacher, and B. J. Abbott, *Cancer Chemother. Rep. (Part 3)*, **3**, 1 (1972).

(5) K. H. Lee, H. C. Huang, E. S. Huang, and H. Furukawa, *J. Pharm. Sci.*, **61**, 629 (1972).

(6) K. H. Lee, D. C. Anuforo, E. S. Huang, and C. Piantadosi, *ibid.*, **61**, 626 (1972), and references cited therein.

(7) K. H. Lee, T. Ibuka, M. Kozuka, A. T. McPhail, and K. D. Onan, *Tetrahedron Lett.*, **1974**, 2287, and references cited therein.

(8) K. H. Lee, Y. Imakura, D. Sims, A. T. McPhail, and K. D. Onan, *Chem. Commun.*, **1976**, 341, and references cited therein.

(9) K. H. Lee, E. S. Huang, C. Piantadosi, J. S. Pagano, and T. A. Geissman, *Cancer Res.*, **31**, 1649 (1971).

(10) K. H. Lee, H. Furukawa, and E. S. Huang, *J. Med. Chem.*, **15**, 609 (1972).

(11) K. H. Lee, T. Ibuka, and R. Y. Wu, *Chem. Pharm. Bull.*, **22**, 2206 (1974).

ACKNOWLEDGMENTS AND ADDRESSES

Received July 15, 1976, from the *Department of Medicinal Chemistry, School of Pharmacy, University of North Carolina, Chapel Hill, NC 27514, and the ‡School of Pharmacy, Kaohsiung Medical College, Kaohsiung, Taiwan, Republic of China.

Accepted for publication September 1, 1976.

Supported by U.S. Public Health Service Research Grant CA 17625 from the National Cancer Institute and American Cancer Society Grant CH-19.

ˣ To whom inquiries should be directed.

Polyamine Metabolism II: *N*-(Monoaminoalkyl)- and *N*-(Polyaminoalkyl)acetamides in Human Urine

MAHMOUD M. ABDEL-MONEM ˣ and KOSEI OHNO

Abstract □ TLC and high-pressure liquid chromatographic examination of the dansyl derivatives obtained from human urine indicated the presence of *N*-[3-[(4-aminobutyl)amino]propyl]acetamide (N^1-acetylspermidine), *N*-[4-[(3-aminopropyl)amino]butyl]acetamide (N^8-acetylspermidine), *N*-(4-aminobutyl)acetamide (*N*-acetylputrescine), and *N*-(5-aminopentyl)acetamide (*N*-acetylcadaverine). The ratio of N^1- to N^8-acetylspermidine ranged from 10.3 in the urine of a patient with hepatoma to 1.1 in the urine of a normal subject. The three cancer patients had a considerably higher ratio of N^1- to N^8-acetylspermidine than did the three normal subjects. These findings indicate that the ratio of N^1- to N^8-acetylspermidine in the 24-hr urine may serve as a biochemical marker for cancer.

Keyphrases □ Polyamines—*N*-(monoaminoalkyl)- and *N*-(polyaminoalkyl)acetamides, dansyl derivatives, TLC and high-pressure liquid chromatographic analysis, human urine □ *N*-(Aminoalkyl)acetamides—dansyl derivatives, TLC and high-pressure liquid chromatographic analysis, human urine □ Dansyl derivatives—*N*-(monoaminoalkyl)- and *N*-(polyaminoalkyl)acetamides, TLC and high-pressure liquid chromatographic analysis, human urine □ TLC—analysis, dansyl derivatives of *N*-(monoaminoalkyl)- and *N*-(polyaminoalkyl)acetamides, human urine □ High-pressure liquid chromatography—analysis, dansyl derivatives of *N*-(monoaminoalkyl)- and *N*-(polyaminoalkyl)acetamides, human urine

The diamine 1,4-butanediamine (putrescine) (I) and the polyamines *N*-(3-aminopropyl)-1,4-butanediamine (spermidine) (II) and *N,N'*-bis(3-aminopropyl)-1,4-butanediamine (spermine) (III) are excreted in human urine mainly in the form of conjugates which produce the free amines after hydrolysis (1). *N*-(4-Aminobutyl)acetamide (*N*-acetylputrescine) (IV) was identified in the urine of normal subjects (2), and *N*-(5-aminopentyl)acetamide (*N*-acetylcadaverine) (V) was identified in the urine of

$RHN(CH_2)_nNH_2$ $\qquad$ $RHN(CH_2)_3NH(CH_2)_4NH_2$

I: R = H, $n = 4$ $\qquad$ II: R = H

IV: R = CH_3CO, $n = 4$ $\qquad$ VI: R = CH_3CO

V: R = CH_3CO, $n = 5$

$H_2N(CH_2)_3NH(CH_2)_4NH(CH_2)_3NH_2$

III

$CH_3COHN(CH_2)_4NH(CH_2)_3NH_2$

VII

schizophrenic patients (3). *N*-[3-[(4-Aminobutyl)amino]propyl]acetamide (N^1-acetylspermidine) (VI), but not *N*-[4-[(3-aminopropyl)amino]butyl]acetamide (N^8-acetylspermidine) (VII), also was detected in urine of healthy children (4) and a patient with acute myelocytic leukemia (5). Recently, both VI and VII were identified in urine of normal subjects and cancer patients (6, 7).

The present paper reports the determination of the ratio of VI to VII in the urine of normal subjects and cancer patients who had not received therapy.

EXPERIMENTAL

Extraction of Polyamines and Conjugated Polyamines from Urine—Twenty-four hour urine samples were collected from three adults and one child as normal subjects and from three patients with diagnosed cancer (hepatoma, melanoma, and thyroid cancer) who had not received therapy. The urine was collected over toluene, kept refrigerated during collection, and stored at −20° until analysis.

An aliquot of urine (100 ml) was adjusted to pH 10–11 with 2 *N* NaOH (5 ml) and extracted with 2-methyl-1-butanol (4 × 50 ml). Nitrogen was bubbled through the organic solvent extract to remove ammonia. Concentrated hydrochloric acid (5 ml) was added to the extract, and the mixture was evaporated to dryness *in vacuo* at 45°.

which gave a major single fluorescent spot on TLC under UV light together with traces of five nonfluorescent components. Subsequent isolation of this single fluorescent spot by preparative TLC led to a crystalline residue, which was recrystallized from benzene to yield colorless needles (8 mg), mp 170–173°. The identity of this compound with an authentic sample of helenalin (I) was established by TLC, IR, and NMR spectroscopic comparisons and by mixed melting-point determination.

REFERENCES

(1) K. H. Lee, T. Ibuka, H. C. Huang, and D. L. Harris, *J. Pharm. Sci.*, **64**, 1077 (1975), and references cited therein.

(2) A. T. Hsieh and T. I. Yang, "Nomenclature of Plants in Taiwan," National Taiwan University, Taiwan, Republic of China, 1969, p. 910.

(3) C. Piantadosi, C. S. Kim, and J. L. Irvin, *J. Pharm. Sci.*, **58**, 821 (1969).

(4) R. I. Geran, N. H. Greenberg, M. M. MacDonald, A. M. Schumacher, and B. J. Abbott, *Cancer Chemother. Rep. (Part 3)*, **3**, 1 (1972).

(5) K. H. Lee, H. C. Huang, E. S. Huang, and H. Furukawa, *J. Pharm. Sci.*, **61**, 629 (1972).

(6) K. H. Lee, D. C. Anuforo, E. S. Huang, and C. Piantadosi, *ibid.*, **61**, 626 (1972), and references cited therein.

(7) K. H. Lee, T. Ibuka, M. Kozuka, A. T. McPhail, and K. D. Onan, *Tetrahedron Lett.*, **1974**, 2287, and references cited therein.

(8) K. H. Lee, Y. Imakura, D. Sims, A. T. McPhail, and K. D. Onan, *Chem. Commun.*, **1976**, 341, and references cited therein.

(9) K. H. Lee, E. S. Huang, C. Piantadosi, J. S. Pagano, and T. A. Geissman, *Cancer Res.*, **31**, 1649 (1971).

(10) K. H. Lee, H. Furukawa, and E. S. Huang, *J. Med. Chem.*, **15**, 609 (1972).

(11) K. H. Lee, T. Ibuka, and R. Y. Wu, *Chem. Pharm. Bull.*, **22**, 2206 (1974).

ACKNOWLEDGMENTS AND ADDRESSES

Received July 15, 1976, from the *Department of Medicinal Chemistry, School of Pharmacy, University of North Carolina, Chapel Hill, NC 27514, and the ‡School of Pharmacy, Kaohsiung Medical College, Kaohsiung, Taiwan, Republic of China.

Accepted for publication September 1, 1976.

Supported by U.S. Public Health Service Research Grant CA 17625 from the National Cancer Institute and American Cancer Society Grant CH-19.

ˣ To whom inquiries should be directed.

Polyamine Metabolism II: *N*-(Monoaminoalkyl)- and *N*-(Polyaminoalkyl)acetamides in Human Urine

MAHMOUD M. ABDEL-MONEM ˣ and KOSEI OHNO

Abstract □ TLC and high-pressure liquid chromatographic examination of the dansyl derivatives obtained from human urine indicated the presence of *N*-[3-[(4-aminobutyl)amino]propyl]acetamide (N^1-acetylspermidine), *N*-[4-[(3-aminopropyl)amino]butyl]acetamide (N^8-acetylspermidine), *N*-(4-aminobutyl)acetamide (*N*-acetylputrescine), and *N*-(5-aminopentyl)acetamide (*N*-acetylcadaverine). The ratio of N^1- to N^8-acetylspermidine ranged from 10.3 in the urine of a patient with hepatoma to 1.1 in the urine of a normal subject. The three cancer patients had a considerably higher ratio of N^1- to N^8-acetylspermidine than did the three normal subjects. These findings indicate that the ratio of N^1- to N^8-acetylspermidine in the 24-hr urine may serve as a biochemical marker for cancer.

Keyphrases □ Polyamines—*N*-(monoaminoalkyl)- and *N*-(polyaminoalkyl)acetamides, dansyl derivatives, TLC and high-pressure liquid chromatographic analysis, human urine □ *N*-(Aminoalkyl)acetamides—dansyl derivatives, TLC and high-pressure liquid chromatographic analysis, human urine □ Dansyl derivatives—*N*-(monoaminoalkyl)- and *N*-(polyaminoalkyl)acetamides, TLC and high-pressure liquid chromatographic analysis, human urine □ TLC—analysis, dansyl derivatives of *N*-(monoaminoalkyl)- and *N*-(polyaminoalkyl)acetamides, human urine □ High-pressure liquid chromatography—analysis, dansyl derivatives of *N*-(monoaminoalkyl)- and *N*-(polyaminoalkyl)acetamides, human urine

The diamine 1,4-butanediamine (putrescine) (I) and the polyamines *N*-(3-aminopropyl)-1,4-butanediamine (spermidine) (II) and *N,N'*-bis(3-aminopropyl)-1,4-butanediamine (spermine) (III) are excreted in human urine mainly in the form of conjugates which produce the free amines after hydrolysis (1). *N*-(4-Aminobutyl)acetamide (*N*-acetylputrescine) (IV) was identified in the urine of normal subjects (2), and *N*-(5-aminopentyl)acetamide (*N*-acetylcadaverine) (V) was identified in the urine of

$RHN(CH_2)_nNH_2$ $\qquad$ $RHN(CH_2)_3NH(CH_2)_4NH_2$

I: R = H, $n = 4$ $\qquad$ II: R = H

IV: R = CH_3CO, $n = 4$ $\qquad$ VI: R = CH_3CO

V: R = CH_3CO, $n = 5$

$H_2N(CH_2)_3NH(CH_2)_4NH(CH_2)_3NH_2$

III

$CH_3COHN(CH_2)_4NH(CH_2)_3NH_2$

VII

schizophrenic patients (3). *N*-[3-[(4-Aminobutyl)amino]propyl]acetamide (N^1-acetylspermidine) (VI), but not *N*-[4-[(3-aminopropyl)amino]butyl]acetamide (N^8-acetylspermidine) (VII), also was detected in urine of healthy children (4) and a patient with acute myelocytic leukemia (5). Recently, both VI and VII were identified in urine of normal subjects and cancer patients (6, 7).

The present paper reports the determination of the ratio of VI to VII in the urine of normal subjects and cancer patients who had not received therapy.

EXPERIMENTAL

Extraction of Polyamines and Conjugated Polyamines from Urine—Twenty-four hour urine samples were collected from three adults and one child as normal subjects and from three patients with diagnosed cancer (hepatoma, melanoma, and thyroid cancer) who had not received therapy. The urine was collected over toluene, kept refrigerated during collection, and stored at −20° until analysis.

An aliquot of urine (100 ml) was adjusted to pH 10–11 with 2 *N* NaOH (5 ml) and extracted with 2-methyl-1-butanol (4 × 50 ml). Nitrogen was bubbled through the organic solvent extract to remove ammonia. Concentrated hydrochloric acid (5 ml) was added to the extract, and the mixture was evaporated to dryness *in vacuo* at 45°.

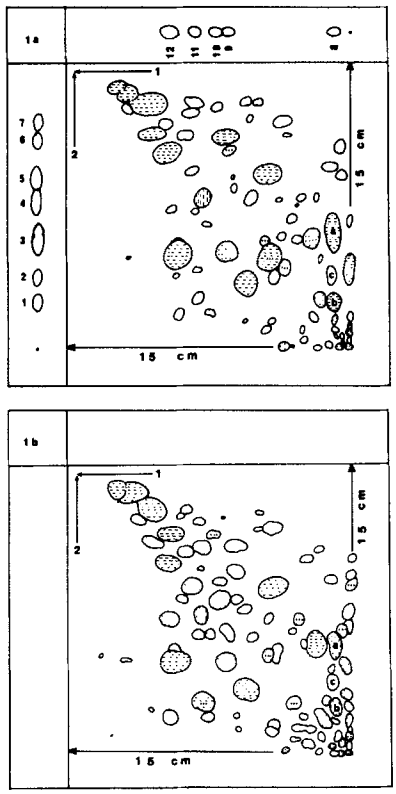

Figure 1—*Two-dimensional TLC of the dansyl derivatives obtained from the urine of a patient with hepatoma* (a) *and a normal subject* (b). *Compounds tested were the dansyl derivatives of: IV (1); V (2); VI, VII, N^4-acetylspermidine, and ammonia (3); I, 1,3-propanediamine, and N^4-acetylspermine (4); N^1-acetylspermine (5); II (6); III (7); IV, V, acetylspermidines, and acetylspermines (8); III (9); II (10); 1,3-propanediamine and I (11); ammonia (12); VI and VII (spot a); IV (spot b); and V (spot c).*

Formation of 5-(Dimethylamino)-1-naphthalenesulfonyl (Dansyl) Derivatives of Urine Extracts—The residue obtained after evaporation of the solvent was dissolved in 2% HCl (5 ml), and then the flask was rinsed with water (5 ml) and acetone (15 ml). The solution was adjusted to pH 8.5–9 with anhydrous sodium carbonate (about 2.0 g) and then treated with dansyl chloride (26.9 mg, 0.1 mmole) in acetone (10 ml).

The mixture was stirred at room temperature for 12 hr in a covered flask and concentrated to remove the acetone. Water (30 ml) was added to dissolve the precipitated solids, and the reaction mixture was extracted with chloroform (4 × 25 ml). The combined chloroform extract was washed with water (10 ml) and dried over anhydrous sodium sulfate. The extract was evaporated to dryness *in vacuo*.

Isolation and Purification of Dansyl Derivatives of *N*-(Monoaminoalkyl)- and *N*-(Polyaminoalkyl)acetamides—The residue obtained from the dansylation reaction was dissolved in 1.0 ml of chloroform, and 10 μl of this solution was applied to a TLC silica gel GF plate[1] (250 μm, 20 × 20 cm). A mixture of the authentic samples of the dansyl derivatives of the *N*-(monoaminoalkyl)- and *N*-(polyaminoalkyl)acetamides also was spotted on some plates for comparison. Each plate was developed using cyclohexane–ether (1:9) for an elution distance of 14 cm and then in a second dimension using chloroform–triethylamine (10:1). The plates were examined under a long wavelength UV lamp.

The desired spots were scraped separately from the plates and immediately extracted with a mixture of equal volumes of triethylamine and 2-propanol (10 ml). The extract was evaporated to dryness in a nitrogen stream at 40°, and the residue was stored in a refrigerator until analysis by high-pressure liquid chromatography (HPLC). Immediately before HPLC analysis, the residue was dissolved in 50 or 25 μl of chloroform, and a 5- or 10-μl aliquot was injected.

Determination of Dansyl Derivatives Using HPLC[2]—The separation of the dansyl derivatives was achieved, using a modification of a published method (8), on a silica column[3] (120 cm × 2.2 mm i.d.) with chloroform (distilled over anhydrous calcium chloride)–2-propanol (100:6).

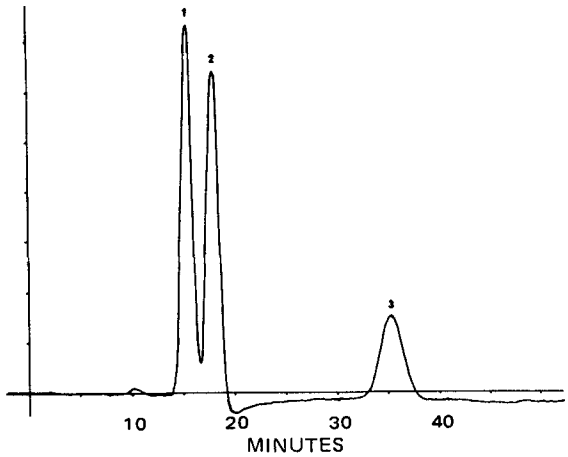

Figure 2—*HPLC separation of a standard solution containing 100 pmoles of each dansyl derivative of: VI (1), VII (2), and IV (3).*

RESULTS

Typical chromatograms of the TLC separation of the dansyl derivatives from the urine of a patient with hepatoma and a normal subject are shown in Figs. 1*a* and 1*b*, respectively. Cochromatography of a mixture of authentic samples of IV–VII permitted the identification of the position of each compound on the chromatogram of the derivatives from urine.

A typical HPLC separation of a mixture of IV, VI, and VII (100 pmoles of each) is shown in Fig. 2. Different amounts of each dansyl derivative of *N*-(monoaminoalkyl)- and *N*-(polyaminoalkyl)acetamides were injected, and a linear correlation was observed between the peak height and the amount injected for each compound.

Figures 3 and 4 represent the chromatograms obtained by HPLC examination of extracts from the spots corresponding to a mixture of VI and VII (spot a) and IV (spot b), respectively, on the thin-layer chromatogram of the dansyl derivatives from urine of a hepatoma patient (*a*) and a normal subject (*b*).

The concentration of each dansyl derivative was calculated by comparison of its peak height with that obtained from known concentrations of an authentic sample. Table I presents the quantitative results obtained for three normal subjects, one child, and three cancer patients. The values were not corrected for losses during the analytical procedure and may be underestimates of the actual values.

DISCUSSION

TLC and HPLC examination of the dansyl derivatives of the amines

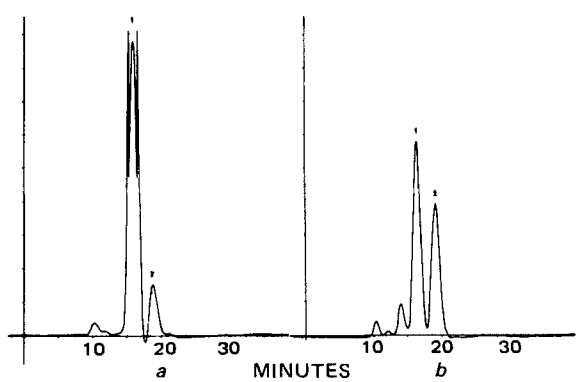

Figure 3—*HPLC separation of the dansyl derivatives of the monoacetylspermidines obtained from the urine of a patient with hepatoma* (a) *and a normal subject* (b). *Key: 1, VI; and 2, VII. Peak intensity for VI in a was reduced to one-half its size for comparison. The amount injected in a was one-half the amount injected in* b.

[1] Analtech, Newark, Del.

[2] Model 6000 solvent delivery system, Waters Associates, Milford, Mass., and LDC model 1209 fluoroMonitor, Laboratory Data Control, Riviera Beach, Fla.

[3] Corasil II, Waters Associates, Milford, Mass.

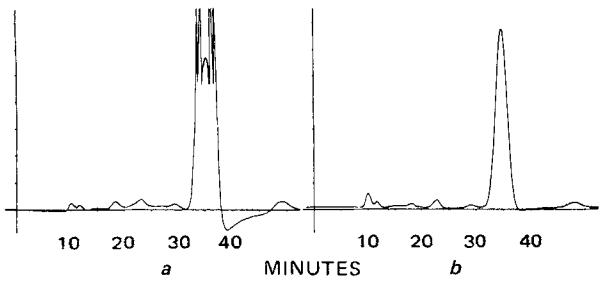

Figure 4—*HPLC separation of the dansyl derivatives of IV obtained from the urine of a patient with hepatoma* (a) *and a normal subject* (b). *The peak intensity for IV in* a *was reduced to one-fourth its actual size for comparison.*

in human urine indicated the presence of IV–VII in appreciable amounts in all samples examined. *N*-(4-Aminobutyl)-*N*-(3-aminopropyl)acetamide (N^4-acetylspermidine) and the two isomeric N^1- and N^4-monoacetyl derivatives of III were not present in detectable amounts. The identity of IV, VI, and VII obtained from human urine was confirmed by mass spectral analysis (7). Compound V was present in low concentrations and was not quantified.

In the seven samples examined, the ratio of VI to VII was greater than 1. The highest ratio was observed in the urine of a patient with hepatoma (10.3); the lowest ratio was observed in the urine of a normal subject (1.1). The considerably higher levels of VI in the urine of the hepatoma patient is noteworthy. The three cancer patients had a considerably higher ratio of VI to VII than did the three normal subjects. These findings indicate that normal subjects and cancer patients not only differ in their levels of urinary polyamines (1) but also in the nature of the polyamine conjugates. Moreover, the ratio of VI to VII in the 24-hr urine may serve as a biochemical marker for cancer and is being further studied in this laboratory.

A ratio of concentration of VI to VII greater than 1 indicates a higher rate of formation and/or a lower rate of degradation of VI relative to VII. Unfortunately, little is known about the enzymes responsible for the formation of these acetylated aliphatic amines and their fate in mammalian tissues. Recently, Seiler and Al-Therib (9) described the *in vitro* acetylation of I to IV catalyzed by acetyl coenzyme A putrescine *N*-acetyltransferase from rat tissues. This enzyme was specific for the acetylation of I; the highest activity was observed in the brain, especially in the nuclei.

Spermidine and spermine did not inhibit the enzymatic acetylation of putrescine, indicating that these compounds did not act as substrates for this enzyme and that the enzymes responsible for acetylation of the diamines and polyamines possess a high degree of substrate specificity. Therefore, mammalian tissues may conceivably contain separate enzymes that acetylate spermidine to form either VI or VII and cancer tissue may have higher activity of the N^1-spermidine *N*-acetyltransferase. On the other hand, Seiler and Al-Therib (10) showed that IV was oxidatively deaminated both *in vitro* and *in vivo* by monoamine oxidase. It is possible, therefore, that the acetylspermidines also are oxidatively deaminated by amine oxidases and that the higher ratio of VI to VII in cancer tissues reflects a higher rate of degradation of VII in these tissues.

Table I—Concentrations of *N*-(Monoaminoalkyl)- and *N*-(Polyaminoalkyl)acetamides in Urine of Normal Subjects and Cancer Patients

Subject	Micromoles per 24 hr[a]			
	VI	VII	VI/VII	IV
Normal adult	0.277	0.237	1.17	1.503
Normal adult	0.135	0.118	1.14	1.181
Normal adult	0.735	0.562	1.31	3.613
Child[b]	0.115	0.070	1.64	0.569
Thyroid cancer patient	0.403	0.229	1.76	2.587
Melanoma patient	1.075	0.610	1.76	5.800
Hepatoma patient	4.413	0.428	10.31	12.810

[a] Values are not corrected for losses during the analytical procedure. [b] Micromoles per 100 ml for the urine sample voided in the morning (110 ml).

The concentration of IV was 2.6–4.7 times greater than the total amount of the isomeric acetylspermidines. There was an apparent linear correlation (r = 0.970) between the levels of IV and those of the acetylspermidine in urine.

REFERENCES

(1) D. H. Russell, C. C. Levy, S. C. Schimpff, and I. A. Hawk, *Cancer Res.*, **31**, 1555 (1971).

(2) T. L. Perry, S. Hansen, and L. MacDougal, *J. Neurochem.*, **14**, 775 (1967).

(3) T. L. Perry, S. Hansen, and L. MacDougal, *Nature*, **214**, 484 (1967).

(4) T. Nakajima, J. F. Zack, Jr., and F. Wolfgram, *Biochim. Biophys. Acta*, **184**, 651 (1969).

(5) T. Walle, in "Polyamines in Normal and Neoplastic Growth," D. H. Russell, Ed., Raven, New York, N.Y., 1973, pp. 355–365.

(6) M. Tsuji, T. Nakajima, and I. Sano, *Clin. Chim. Acta*, **59**, 161 (1975).

(7) M. M. Abdel-Monem and K. Ohno, *J. Pharm. Sci.*, **66**, 1089 (1977).

(8) M. M. Abdel-Monem and K. Ohno, *J. Chromatogr.*, **107**, 416 (1975).

(9) N. Seiler and M. J. Al-Therib, *Biochim. Biophys. Acta*, **354**, 206 (1974).

(10) N. Seiler and M. J. Al-Therib, *Biochem. J.*, **144**, 29 (1974).

ACKNOWLEDGMENTS AND ADDRESSES

Received February 26, 1976, from the *College of Pharmacy, University of Minnesota, Minneapolis, MN 55455.*

Accepted for publication July 6, 1976.

Supported by U.S. Public Health Service Grant CA 14239.

The authors thank I. Fortuny, M.D., for assistance in providing the urine samples from the cancer patients.

[x] To whom inquiries should be directed.

Factors Affecting Serum Oxytetracycline Levels in Beef Calves

H. DWIGHT MERCER *x, LARRY D. ROLLINS *, GORDON G. CARTER ‡, RICHARD P. GURAL §, DAVID W. A. BOURNE §, and LEWIS W. DITTERT §

Abstract □ Fifteen Aberdeen Angus steers, 295–364 kg, were dosed with either 4.4 or 11 mg of oxytetracycline hydrochloride/kg im. The antimicrobial activity of the serum was determined periodically, and the resulting data were treated statistically to determine the sources of variation. Variance in serum levels of oxytetracycline activity was attributed to dose, time of bleeding, order of dosing, animal, and assay. The total variance component was proportionately greater for the 11-mg/kg dose than for the 4.4-mg/kg dose. Animal variance increased with the higher dose level of oxytetracycline. The influence of dose on serum level was tested by applying a t test to the mean serum levels and their standard deviations at each bleeding time. The 4.4- and 11-mg/kg serum levels were significantly different ($p < 0.01$) at all bleeding times. The 4.4-mg/kg serum levels multiplied by 2.5 were not significantly different ($p < 0.05$) from the 11-mg/kg serum levels at all bleeding times.

Keyphrases □ Oxytetracycline—factors affecting serum levels, calves □ Drug levels, serum—oxytetracycline, factors causing variance, calves □ Antibacterials—oxytetracycline, factors affecting serum levels, calves

Blood or serum drug levels are often utilized to determine the absorption, availability, or excretion rates of certain drugs and chemical compounds. These levels have also been used to assess the bioavailability or bioequivalency of similar drug products. Previous reports (1–5) found undesirable variability in the drug level data from both human and animal studies. To compensate for these variables, large numbers of animals or humans may be required.

Certain parameters, such as route of administration and drug formulation, obviously can influence variability. Other factors, such as animal, dose period, dose, and assay variance, have been less well defined as sources of variation. More insidious factors, such as ion chelation and protein binding, also may contribute to the animal variance factor and, therefore, to the overall variance component. The physical preparation of analytical samples may introduce additional variations in results.

Since it is not feasible to control all potential variables in a given blood level study, it was deemed advisable to determine, directly or indirectly, the extent that these factors contribute to the overall variance component in a study of serum levels of an antibiotic (oxytetracycline) in animals (calves). Five critical factors, comprising a major portion of the variance component, were studied. These factors were animal, dose, order of dosing, time of bleeding, and assay.

EXPERIMENTAL

Dosing and Animal Handling—Fifteen purebred Aberdeen Angus steers, 295–364 kg, were divided into two groups of seven and eight calves each. Each group was further subdivided into two treatment levels. One group was given 4.4 mg, and the other was given 11 mg of oxytetracycline hydrochloride[1]/kg im. Treatments were administered one time to each animal for each sampling period. The dose was adjusted according to individual weights at each treatment interval.

One group of animals was dosed and bled on Day 1, and the other group was dosed and bled 1 week later. This sequence of events was defined as Period 1. Seven weeks later, the groups were reversed according to a double-crossover design, and the study was repeated. These events were defined as Period 2.

The animals were maintained in a drylot paddock area with free access to feed and water. They were observed daily for any deviation from normal health. No clinical illness was observed during the trials.

Blood Sampling—Blood samples were collected from the jugular vein immediately prior to treatment and at intervals of 0.5, 1, 2, 4, 6, 8, 12, 15, and 18 hr after Period 1 dosing. After Period 2 dosing, samples were taken at 2, 4, 6, 8, and 15 hr. Blood samples were protected from direct sunlight and refrigerated immediately after collection. Serum was harvested from the samples as rapidly as clot retraction occurred or generally within the hour. The serum samples were then frozen and protected from light until assayed, which generally occurred within 48 hr to 1 week. Quadruplicate assays were performed on each serum sample.

Assay—Concentrations of oxytetracycline in serum were determined by using the microbiological cylinder plate assay method (6) with *Bacillus cereus* var. *mycoides* (ATCC 11778) as the test organism.

Statistical Analysis—The data were treated statistically using a computer[2] with a statistical analysis system (7). The following adjustments and assumptions were made:

1. Only bleeding times common to both periods of the experiment (*i.e.*, 2, 4, 6, 8, and 15 hr following drug administration) were treated.
2. From pharmacokinetic considerations, it was assumed that time of bleeding would influence the serum levels following drug administration in a definable way (8); this parameter was not included in the statistical analyses. It was anticipated that the influence of time could be depicted as plots of the mean serum levels ± *SD versus* time. These plots for the 4.4- and 11-mg/kg doses are shown in Fig. 1.
3. It was assumed, *a priori*, that dose would influence the serum levels; this parameter was not included in the analysis of variance. It was anticipated that the influence of dose could be examined by applying the Student t test to the mean serum levels for the two doses at each time point.
4. It was assumed that the order of dosing (*i.e.*, 4.4 followed by 11 mg/kg or vice versa) might influence the results but that the division of the animals into four groups and the handling of the groups on different days would not have an influence.
5. It was assumed that the serum assays were carried out in a perfectly random manner.

The data were divided into units consisting of the assay results for all animals at a single bleeding time following a single dose, and the variance components due to order of dosing, animal, and assay were determined. The "animal" parameter was "nested" within the "order of dosing" parameter. The variance component of each parameter and the total variance component are defined by the following equations (9):

$$\text{variance component}_{\text{assay}} = \sigma^2 = \text{mean square}_{\text{assay}} \quad \text{(Eq. 1)}$$

$$\text{variance component}_{\text{animal}} = \sigma^2 \text{ animal} = \frac{\text{mean square}_{\text{animal}} - \text{mean square}_{\text{assay}}}{\text{number of replicates per animal}} \quad \text{(Eq. 2)}$$

$$\text{variance component}_{\text{order}} = \sigma^2 \text{ order} = \frac{\text{mean square}_{\text{order}} - \text{mean square}_{\text{animal}}}{\text{number of replicates per order}} \quad \text{(Eq. 3)}$$

$$\text{total variance component} = \sigma^2 + \sigma^2 \text{ animal} + \sigma^2 \text{ order} \quad \text{(Eq. 4)}$$

[1] Liquamycin injectable (50 mg/ml), Pfizer Inc., New York, N.Y.

[2] IBM 360/50.

Table I—Effect of Assay, Animal, and Order of Dosing on Mean Serum Oxytetracycline Levels in Calves [a]

Bleeding Time, hr	Mean Serum Level, μg/ml	Total Variance Component	Variance Component (V.C.) and Percent of Total Variance Component Due to: Assay V.C.	Assay %	Animal V.C.	Animal %	Order of Dosing V.C.	Order of Dosing %
			Dose = 4.4 mg/kg im					
2	1.85	0.36	0.05	14.7	0.31	84.2	0.004	1.2
4	2.33	0.51	0.19	38.2	0.24	47.1	0.07	14.6
6	2.68	1.76	1.00	56.8	0.38	21.8	0.38	21.4
8	2.49	0.97	0.43	44.6	0.43	44.5	0.11	10.9
15	2.03	1.21	0.80	65.8	0.00	0.0	0.42	34.2
Average		0.96	0.49		0.27		0.19	
Average, %		100.0	51.5		28.2		20.3	
			Dose = 11 mg/kg im					
2	4.15	2.67	0.22	8.4	1.21	45.4	1.23	46.2
4	5.62	3.16	1.38	43.8	0.52	16.5	1.26	39.7
6	6.23	9.41	3.80	40.4	2.74	29.1	2.87	30.5
8	5.47	2.92	1.08	37.0	1.38	47.2	0.46	15.9
15	4.78	6.73	2.69	40.0	1.19	17.7	2.85	42.3
Average		4.98	1.84		1.41		1.73	
Average, %		100.0	36.9		28.3		34.8	

[a] All fractions were calculated using six decimal places and rounded to two or three figures.

RESULTS AND DISCUSSION

The results are given in Table I in terms of mean serum levels for individual bleeding times following a given dose with variance components due to assay, animal, and order of dosing. Only results common to both periods (*i.e.*, 0, 2, 4, 6, 8, and 15 hr) are included. The influences of dose and time of bleeding were not included in the statistical analyses.

The results showed that the absolute value of the total variance component was proportionately greater for the 11-mg/kg dose than for the 4.4-mg/kg dose. The percent contribution of the animal component was the same in each case, indicating that the animal groups were well matched. As expected, the fraction of the variance component attributable to the assay was greater for the 4.4-mg/kg dose, since this dose resulted in lower serum levels, which presumably would produce more variable assays. The percent contribution of the order of dosing was greater after the higher dose.

Unfortunately, the bleeding schedule was insufficient to define the entire serum level–time curves. If this had been possible, the influence of dose on the serum levels could have been expressed in terms of the areas under the curves, which would have revealed any differences in the absorption efficiencies of the two doses. If both doses were equally well absorbed, the area under the 11-mg/kg curve would be exactly 2.5 times the area under the 4.4-mg/kg curve (10). Definition of the entire serum level–time curves would also have revealed any differences in absorption or elimination kinetics of the two doses.

In the absence of complete serum level–time curves, the influence of

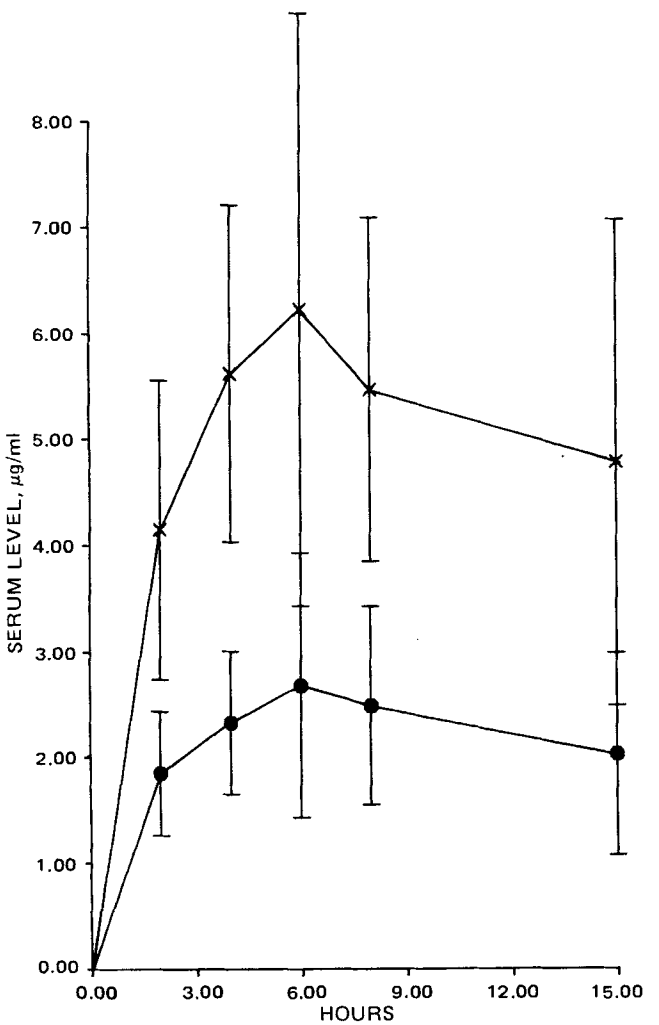

Figure 1—*Mean serum levels (micrograms per milliliter ± SD) of oxytetracycline in 15 Aberdeen Angus calves following intramuscular administration of 4.4- (●) and 11-(×) mg/kg doses. Each point contains results from quadruplicate assays from 15 serum samples, except that 14 samples were run for the 15-hr point of the 4.4-mg/kg dose.*

Table II—*t* Test of Difference in Mean Serum Oxytetracycline Levels in Calves (4.4 *versus* 11 mg/kg)

Bleeding Time, hr	4.4 mg/kg Mean Serum Level, μg/ml	4.4 mg/kg *SD*	11 mg/kg Mean Serum Level, μg/ml	11 mg/kg *SD*	t [a]
2	1.85	0.59	4.15	1.41	11.66
4	2.33	0.68	5.62	1.59	14.74
6	2.68	1.25	6.23	2.80	8.97
8	2.49	0.94	5.47	1.62	12.32
15	2.03	0.96	4.78	2.29	8.58

[a] All serum levels were significantly different at $p < 0.01$.

Table III—*t* Test of Difference in 2.5 × Mean Serum Oxytetracycline Levels in Calves (4.4 *versus* 11 mg/kg)

Bleeding Time, hr	2.5 × 4.4 mg/kg Mean Serum Level, μg/ml	$SD \times (2.5)^{1/2}$	11 mg/kg Mean Serum Level, μg/ml	11 mg/kg *SD*	t
2	4.63	0.93	4.15	1.41	2.20[a]
4	5.83	1.08	5.62	1.59	0.85[b]
6	6.70	1.98	6.23	2.80	1.06[b]
8	6.23	1.49	5.47	1.62	2.67[a]
15	5.08	1.52	4.78	2.29	0.86[b]

[a] Serum levels were not significantly different at $p < 0.05$. [b] Serum levels were not significantly different at $p < 0.01$.

dose on serum level can be defined by comparing the mean serum levels for the two doses at each bleeding time (10). A t test was applied to the mean serum levels and their standard deviations, and the results (Table II) showed that the mean serum levels were significantly different ($p < 0.01$) at each bleeding time.

A t test was also performed between the serum levels following the 11-mg/kg dose and 2.5 times the serum levels following the 4.4-mg/kg dose. There was no significant difference ($p < 0.05$) between the serum levels following the 11-mg/kg dose and 2.5 times the serum levels following the 4.4-mg/kg dose (Table III). These results suggest that serum levels are directly proportional to dose levels.

REFERENCES

(1) D. C. Blair, R. W. Barnes, E. L. Wildner, and W. J. Murray, *J. Am. Med. Assoc.*, **215** 251 (1971).

(2) L. E. Davis, C. A. Neff, J. D. Baggot, and T. E. Powers, *Am. J. Vet. Res.*, **33**, 2259 (1972).

(3) H. D. Mercer, J. N. Geleta, J. Kramer, and G. Carter, *J. Am. Vet. Med. Assoc.*, **158**, 47 (1971).

(4) L. D. Rollins, R. H. Teske, R. J. Condon, and G. G. Carter, *ibid.*, **161**, 490 (1972).

(5) R. H. Teske, L. D. Rollins, R. J. Condon, and G. G. Carter, *ibid.*, **162**, 119 (1973).

(6) J. Kramer, G. G. Carter, B. Arret, J. Wilner, W. W. Wright, and A. Kirshbaum, "Antibiotic Residues in Milk, Dairy Products, and Animal Tissues: Methods, Reports, and Protocols," National Center for Antibiotic Analysis, Food and Drug Administration, Washington, D.C., 1968.

(7) "A User's Guide to the Statistical Analysis System," Service J.: Student Supply Stores, North Carolina State University, Raleigh, N.C., 1972.

(8) R. E. Notari, "Biopharmaceutics and Pharmacokinetics: An Introduction," 2nd ed., Dekker, New York, N.Y., 1975, p. 81.

(9) G. W. Snedecor and W. G. Cochran, "Statistical Methods," 6th ed., Iowa State University Press, Ames, Iowa, 1971, pp. 286–288.

(10) W. J. Westlake, in "Current Concepts in the Pharmaceutical Sciences," vol. 2, J. Swarbrick, Ed., Lea & Febiger, Philadelphia, Pa., 1973, chap. 5.

ACKNOWLEDGMENTS AND ADDRESSES

Received September 12, 1975, from the *Division of Veterinary Medical Research, Bureau of Veterinary Medicine, Food and Drug Administration, Beltsville, MD 20705, †The National Center for Antibiotic Analysis, Bureau of Drugs, Food and Drug Administration, Washington, DC 20204, and the §College of Pharmacy, University of Kentucky, Lexington, KY 40506.

Accepted for publication September 22, 1976.

The authors thank Dr. D. Kratzer of the Department of Statistics, University of Kentucky, for helpful discussions and suggestions concerning the statistical analysis system.

ˣ To whom inquiries should be directed.

Anomalous Chemical Shifts of Methyl Groups of 2,4-Dimethylbenzo[g]quinoline

JERRY L. BORN ˣ and C. E. HARSIN

Abstract □ The chemical shifts of the methyl groups of 2,4-dimethylbenzo[g]quinoline are defined with respect to concentration, showing that the methyl resonances are reversed from their expected positions in concentrations normally used in NMR spectroscopy. The phenomenon is explained in terms of the probable "fixation" of bonds in the hetero ring.

Keyphrases □ 2,4-Dimethylbenzo[g]quinoline—NMR spectrum, chemical shifts of methyl groups defined, effect of concentration □ NMR—spectrum, 2,4-dimethylbenzo[g]quinoline, chemical shifts of methyl groups defined, effect of concentration □ Quinoline, substituted—2,4-dimethylbenzo[g]quinoline, NMR spectrum, chemical shifts of methyl groups defined, effect of concentration

During a study of the possibility of converting 2,4-dimethylbenzo[g]quinoline (I) to benzo[g]cinchoninic acid, large concentration chemical shifts for the methyl groups of I were observed. At low concentrations (3.4×10^{-2} M), the absorptions for the methyl groups appeared as a doublet at δ 2.76 (J = 1.2 Hz) and as a singlet at δ 2.69. As the concentration of I was increased, the expected upfield shifts of the methyl groups occurred, but the downfield methyl resonance showed a larger upfield shift than the methyl resonance at δ 2.69. Therefore, at a concentration of 2.74×10^{-1} M, the two methyl signals had overlapped to produce a single resonance at δ 2.64. When the concentration was increased to 6.4×10^{-1} M, a singlet at δ 2.57 and a doublet at δ 2.5 (J = 1 Hz) were observed.

The classical assignment of the downfield resonance to the 2-methyl of I cannot be accommodated by this information. The chemical shift of the 2-methyl group would be expected to remain relatively constant as the concentration of I is increased while the 4-methyl group would be expected to have the greatest shift due to solute–solute interactions (1). This observation led to assignment of the resonance at δ 2.76 (J = 1.2 Hz) (3.4×10^{-2} M) to the 4-methyl group and at δ 2.69 to the 2-methyl group of I.

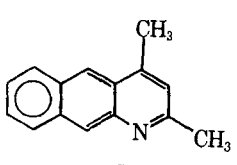

I

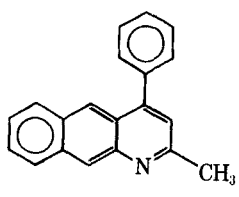

II

EXPERIMENTAL

Samples were weighed on a microbalance[1] and then diluted to volume with benzene-d_6 or spectrograde carbon tetrachloride containing 1% tetramethylsilane as an internal standard. The NMR spectra were obtained using a 60-MHz spectrometer[2] equipped with a double-resonance accessory.

2,4-Dimethylbenzo[g]quinoline (I) was prepared as reported previously

[1] Cahn RTL.
[2] Perkin-Elmer R12-A.

dose on serum level can be defined by comparing the mean serum levels for the two doses at each bleeding time (10). A t test was applied to the mean serum levels and their standard deviations, and the results (Table II) showed that the mean serum levels were significantly different ($p < 0.01$) at each bleeding time.

A t test was also performed between the serum levels following the 11-mg/kg dose and 2.5 times the serum levels following the 4.4-mg/kg dose. There was no significant difference ($p < 0.05$) between the serum levels following the 11-mg/kg dose and 2.5 times the serum levels following the 4.4-mg/kg dose (Table III). These results suggest that serum levels are directly proportional to dose levels.

REFERENCES

(1) D. C. Blair, R. W. Barnes, E. L. Wildner, and W. J. Murray, *J. Am. Med. Assoc.*, **215** 251 (1971).

(2) L. E. Davis, C. A. Neff, J. D. Baggot, and T. E. Powers, *Am. J. Vet. Res.*, **33**, 2259 (1972).

(3) H. D. Mercer, J. N. Geleta, J. Kramer, and G. Carter, *J. Am. Vet. Med. Assoc.*, **158**, 47 (1971).

(4) L. D. Rollins, R. H. Teske, R. J. Condon, and G. G. Carter, *ibid.*, **161**, 490 (1972).

(5) R. H. Teske, L. D. Rollins, R. J. Condon, and G. G. Carter, *ibid.*, **162**, 119 (1973).

(6) J. Kramer, G. G. Carter, B. Arret, J. Wilner, W. W. Wright, and A. Kirshbaum, "Antibiotic Residues in Milk, Dairy Products, and Animal Tissues: Methods, Reports, and Protocols," National Center for Antibiotic Analysis, Food and Drug Administration, Washington, D.C., 1968.

(7) "A User's Guide to the Statistical Analysis System," Service J.: Student Supply Stores, North Carolina State University, Raleigh, N.C., 1972.

(8) R. E. Notari, "Biopharmaceutics and Pharmacokinetics: An Introduction," 2nd ed., Dekker, New York, N.Y., 1975, p. 81.

(9) G. W. Snedecor and W. G. Cochran, "Statistical Methods," 6th ed., Iowa State University Press, Ames, Iowa, 1971, pp. 286–288.

(10) W. J. Westlake, in "Current Concepts in the Pharmaceutical Sciences," vol. 2, J. Swarbrick, Ed., Lea & Febiger, Philadelphia, Pa., 1973, chap. 5.

ACKNOWLEDGMENTS AND ADDRESSES

Received September 12, 1975, from the *Division of Veterinary Medical Research, Bureau of Veterinary Medicine, Food and Drug Administration, Beltsville, MD 20705, †The National Center for Antibiotic Analysis, Bureau of Drugs, Food and Drug Administration, Washington, DC 20204, and the §College of Pharmacy, University of Kentucky, Lexington, KY 40506.

Accepted for publication September 22, 1976.

The authors thank Dr. D. Kratzer of the Department of Statistics, University of Kentucky, for helpful discussions and suggestions concerning the statistical analysis system.

ˣ To whom inquiries should be directed.

Anomalous Chemical Shifts of Methyl Groups of 2,4-Dimethylbenzo[g]quinoline

JERRY L. BORN ˣ and C. E. HARSIN

Abstract □ The chemical shifts of the methyl groups of 2,4-dimethylbenzo[g]quinoline are defined with respect to concentration, showing that the methyl resonances are reversed from their expected positions in concentrations normally used in NMR spectroscopy. The phenomenon is explained in terms of the probable "fixation" of bonds in the hetero ring.

Keyphrases □ 2,4-Dimethylbenzo[g]quinoline—NMR spectrum, chemical shifts of methyl groups defined, effect of concentration □ NMR—spectrum, 2,4-dimethylbenzo[g]quinoline, chemical shifts of methyl groups defined, effect of concentration □ Quinoline, substituted—2,4-dimethylbenzo[g]quinoline, NMR spectrum, chemical shifts of methyl groups defined, effect of concentration

During a study of the possibility of converting 2,4-dimethylbenzo[g]quinoline (I) to benzo[g]cinchoninic acid, large concentration chemical shifts for the methyl groups of I were observed. At low concentrations (3.4×10^{-2} M), the absorptions for the methyl groups appeared as a doublet at δ 2.76 (J = 1.2 Hz) and as a singlet at δ 2.69. As the concentration of I was increased, the expected upfield shifts of the methyl groups occurred, but the downfield methyl resonance showed a larger upfield shift than the methyl resonance at δ 2.69. Therefore, at a concentration of 2.74×10^{-1} M, the two methyl signals had overlapped to produce a single resonance at δ 2.64. When the concentration was increased to 6.4×10^{-1} M, a singlet at δ 2.57 and a doublet at δ 2.5 (J = 1 Hz) were observed.

The classical assignment of the downfield resonance to the 2-methyl of I cannot be accommodated by this information. The chemical shift of the 2-methyl group would be expected to remain relatively constant as the concentration of I is increased while the 4-methyl group would be expected to have the greatest shift due to solute–solute interactions (1). This observation led to assignment of the resonance at δ 2.76 (J = 1.2 Hz) (3.4×10^{-2} M) to the 4-methyl group and at δ 2.69 to the 2-methyl group of I.

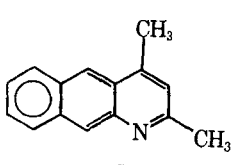

I

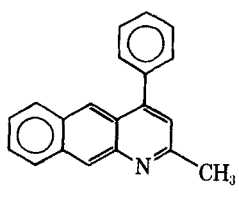

II

EXPERIMENTAL

Samples were weighed on a microbalance[1] and then diluted to volume with benzene-d_6 or spectrograde carbon tetrachloride containing 1% tetramethylsilane as an internal standard. The NMR spectra were obtained using a 60-MHz spectrometer[2] equipped with a double-resonance accessory.

2,4-Dimethylbenzo[g]quinoline (I) was prepared as reported previously

[1] Cahn RTL.
[2] Perkin-Elmer R12-A.

Table I—Chemical Shifts (δ) of the Protons of I at Various Concentrations [a]

Concentration, M	H_3	H_5	H_{10}	2-CH_3	4-CH_3	$H_{6,7,8,9}$
3.4×10^{-2}	7.02	8.38	8.53	2.69	d, 2.76, J = 1.2 Hz	m, 7.44 and 7.98
2.74×10^{-1}	6.9	8.24	8.48	2.64	2.64	m, 7.42 and 7.98
6.4×10^{-1}	6.77	8.14	8.43	2.57	d, 2.50, J = 1 Hz	m, 7.36 and 7.86
Benzene-d_6	5.8	8.20	8.89	2.58	d, 2.27, J = 0.66 Hz	m, 7.25 and 7.8

[a] Except as noted, spectra were run in carbon tetrachloride; 1% tetramethylsilane was utilized as the internal standard (δ = 0.0) in all samples.

(2). The chemical shifts for the protons of I at various concentrations are shown in Table I.

Compound I, 150 mg, was refluxed for 15 min in 4 ml of methyl alcohol-d_1, to which had been added 200 mg of metallic sodium. The reaction was then treated with 25 ml of water, the mixture was extracted with ether, and this extract was dried with magnesium sulfate. The residue remaining after evaporation under vacuum was recrystallized from petroleum ether, mp 92–93° [lit. (2) mp 92–93°], and the NMR spectrum was determined in benzene-d_6. The downfield methyl resonance contained 26% less protons than the upfield 4-methyl group.

2-Methyl-4-phenylbenzo[g]quinoline (II) was prepared as described by Huisgen (3). The product melted at 110° [lit. (3) mp 110°]; NMR: δ 8.58 (s, 1H), 8.27 (s, 1H), 8.14 (m, 9H), 7.09 (s, 1H), and 2.76 (s, 3H). No appreciable change in the spectrum was found when the concentration of II was changed.

DISCUSSION

The lack of coupling between proton H_3 and the methyl group of 2-methylquinoline and the fact that the methyl protons of 4-methylquinoline were observed as a doublet (J = 0.95 Hz) (4) supported the discussed assignment of the methyl resonances of I. In addition, the methyl resonance of II was a singlet. To show that the doublet of I was the result of coupling to proton H_3 rather than to a long-range interaction, proton H_3 was irradiated to produce a singlet for the 4-methyl resonance of I. The ability of benzene to produce larger upfield chemical shifts for methyl groups on the 4-position of quinoline or pyridine is well documented (1), and the same physical phenomenon should result in an upfield shift for the 4-methyl of I.

When the spectrum of I was run in benzene-d_6, the methyls appeared as expected as a singlet at δ 2.58 and as a doublet at δ 2.27 (J = 0.66 Hz). When I was treated with sodium methoxide–methyl alcohol-d_1, the downfield resonance as observed in benzene-d_6 exchanged more rapidly than the upfield resonance, showing that the downfield resonance in benzene-d_6 was due to the more acidic 2-methyl group (5).

The finding of Clar and MacKay (6) that the splitting between methyl-substituted anthracenes and aromatic protons was directly related to the extent of double bond fixation has application to the benzo[g]quinoline system. Since the resonance energy of benzo[g]quinoline is 21.2 kcal/mole less than anthracene, the possibility of even greater bond localization exists with I than with anthracene. The lack of coupling between proton H_3 and the 2-methyls of I and II substantiated the localization of bonds in the hetero ring of benzo[g]quinolines as shown in Structures I and II.

The localization of the bonds in the hetero ring results in less paramagnetic shielding for the 2-methyl group because it is removed from the aromatic naphthalene ring. The 4-methyl group is affected by the paramagnetic shielding of the naphthalene section of the molecule, resulting in its downfield position with respect to the 2-methyl in dilute solutions where solute–solute interactions are minimized. In more concentrated solutions, increased shielding of the 4-methyl group due to solute–solute interactions produces a spectrum that conforms to the classical absorption pattern.

REFERENCES

(1) J. Ronayne and D. H. Williams, in "Annual Review of NMR Spectroscopy," vol. 2, E. F. Mooney, Ed., Academic, New York, N.Y., 1969, chap. 3.

(2) W. S. Johnson and F. O. Mathews, *J. Am. Chem. Soc.*, **66**, 210 (1944).

(3) R. Huisgen, *Ann. Chem.*, **564**, 16 (1949).

(4) H. Rottendorf and Sternhell, *Aust. J. Chem.*, **17**, 1315 (1964).

(5) N. Singh and A. B. Lal, *J. Indian Chem. Soc.*, **41**, 352 (1964).

(6) E. Clar and C. C. MacKay, *Tetrahedron Lett.*, **1970**, 871.

ACKNOWLEDGMENTS AND ADDRESSES

Received August 11, 1976, from the *Department of Medicinal Chemistry, College of Pharmacy, Butler University, Indianapolis, IN 46208.*

Accepted for publication September 29, 1976.

[x] To whom inquiries should be directed. Present address: College of Pharmacy, University of New Mexico, Albuquerque, NM 87131.

Quantitative Determination of Phenol by High-Pressure Liquid Chromatography

JOSEPH D. MUSTO, JAYANT N. SANE, and VICTOR D. WARNER [x]

Abstract □ High-pressure liquid chromatography was used with a 5-μm silica gel column to quantitate the phenol in phenolated calamine lotion USP and a commercial antiseptic solution. This method requires less than 10 min/assay, and other compounds present in the products analyzed did not interfere.

Keyphrases □ Phenol—high-pressure liquid chromatographic analysis, pharmaceutical preparations □ High-pressure liquid chromatography—analysis, phenol in pharmaceutical preparations □ Antipruritics—phenol, high-pressure liquid chromatographic analysis in pharmaceutical preparations

Methods for the quantitative analysis of phenol include a bromometric analysis (1), a colorimetric analysis based on the reaction of phenol with copper sulfate (2), and, most recently, a colorimetric analysis based on the reaction of phenol with ferric chloride (3). This report describes a rapid quantitative method for the analysis of the phenol

Table I—Chemical Shifts (δ) of the Protons of I at Various Concentrations [a]

Concentration, M	H_3	H_5	H_{10}	2-CH_3	4-CH_3	$H_{6,7,8,9}$
3.4×10^{-2}	7.02	8.38	8.53	2.69	d, 2.76, J = 1.2 Hz	m, 7.44 and 7.98
2.74×10^{-1}	6.9	8.24	8.48	2.64	2.64	m, 7.42 and 7.98
6.4×10^{-1}	6.77	8.14	8.43	2.57	d, 2.50, J = 1 Hz	m, 7.36 and 7.86
Benzene-d_6	5.8	8.20	8.89	2.58	d, 2.27, J = 0.66 Hz	m, 7.25 and 7.8

[a] Except as noted, spectra were run in carbon tetrachloride; 1% tetramethylsilane was utilized as the internal standard (δ = 0.0) in all samples.

(2). The chemical shifts for the protons of I at various concentrations are shown in Table I.

Compound I, 150 mg, was refluxed for 15 min in 4 ml of methyl alcohol-d_1, to which had been added 200 mg of metallic sodium. The reaction was then treated with 25 ml of water, the mixture was extracted with ether, and this extract was dried with magnesium sulfate. The residue remaining after evaporation under vacuum was recrystallized from petroleum ether, mp 92–93° [lit. (2) mp 92–93°], and the NMR spectrum was determined in benzene-d_6. The downfield methyl resonance contained 26% less protons than the upfield 4-methyl group.

2-Methyl-4-phenylbenzo[g]quinoline (II) was prepared as described by Huisgen (3). The product melted at 110° [lit. (3) mp 110°]; NMR: δ 8.58 (s, 1H), 8.27 (s, 1H), 8.14 (m, 9H), 7.09 (s, 1H), and 2.76 (s, 3H). No appreciable change in the spectrum was found when the concentration of II was changed.

DISCUSSION

The lack of coupling between proton H_3 and the methyl group of 2-methylquinoline and the fact that the methyl protons of 4-methylquinoline were observed as a doublet (J = 0.95 Hz) (4) supported the discussed assignment of the methyl resonances of I. In addition, the methyl resonance of II was a singlet. To show that the doublet of I was the result of coupling to proton H_3 rather than to a long-range interaction, proton H_3 was irradiated to produce a singlet for the 4-methyl resonance of I. The ability of benzene to produce larger upfield chemical shifts for methyl groups on the 4-position of quinoline or pyridine is well documented (1), and the same physical phenomenon should result in an upfield shift for the 4-methyl of I.

When the spectrum of I was run in benzene-d_6, the methyls appeared as expected as a singlet at δ 2.58 and as a doublet at δ 2.27 (J = 0.66 Hz). When I was treated with sodium methoxide–methyl alcohol-d_1, the downfield resonance as observed in benzene-d_6 exchanged more rapidly than the upfield resonance, showing that the downfield resonance in benzene-d_6 was due to the more acidic 2-methyl group (5).

The finding of Clar and MacKay (6) that the splitting between methyl-substituted anthracenes and aromatic protons was directly related to the extent of double bond fixation has application to the benzo[g]quinoline system. Since the resonance energy of benzo[g]quinoline is 21.2 kcal/mole less than anthracene, the possibility of even greater bond localization exists with I than with anthracene. The lack of coupling between proton H_3 and the 2-methyls of I and II substantiated the localization of bonds in the hetero ring of benzo[g]quinolines as shown in Structures I and II.

The localization of the bonds in the hetero ring results in less paramagnetic shielding for the 2-methyl group because it is removed from the aromatic naphthalene ring. The 4-methyl group is affected by the paramagnetic shielding of the naphthalene section of the molecule, resulting in its downfield position with respect to the 2-methyl in dilute solutions where solute–solute interactions are minimized. In more concentrated solutions, increased shielding of the 4-methyl group due to solute–solute interactions produces a spectrum that conforms to the classical absorption pattern.

REFERENCES

(1) J. Ronayne and D. H. Williams, in "Annual Review of NMR Spectroscopy," vol. 2, E. F. Mooney, Ed., Academic, New York, N.Y., 1969, chap. 3.

(2) W. S. Johnson and F. O. Mathews, *J. Am. Chem. Soc.*, **66**, 210 (1944).

(3) R. Huisgen, *Ann. Chem.*, **564**, 16 (1949).

(4) H. Rottendorf and Sternhell, *Aust. J. Chem.*, **17**, 1315 (1964).

(5) N. Singh and A. B. Lal, *J. Indian Chem. Soc.*, **41**, 352 (1964).

(6) E. Clar and C. C. MacKay, *Tetrahedron Lett.*, **1970**, 871.

ACKNOWLEDGMENTS AND ADDRESSES

Received August 11, 1976, from the *Department of Medicinal Chemistry, College of Pharmacy, Butler University, Indianapolis, IN 46208.*

Accepted for publication September 29, 1976.

[x] To whom inquiries should be directed. Present address: College of Pharmacy, University of New Mexico, Albuquerque, NM 87131.

Quantitative Determination of Phenol by High-Pressure Liquid Chromatography

JOSEPH D. MUSTO, JAYANT N. SANE, and VICTOR D. WARNER [x]

Abstract □ High-pressure liquid chromatography was used with a 5-μm silica gel column to quantitate the phenol in phenolated calamine lotion USP and a commercial antiseptic solution. This method requires less than 10 min/assay, and other compounds present in the products analyzed did not interfere.

Keyphrases □ Phenol—high-pressure liquid chromatographic analysis, pharmaceutical preparations □ High-pressure liquid chromatography—analysis, phenol in pharmaceutical preparations □ Antipruritics—phenol, high-pressure liquid chromatographic analysis in pharmaceutical preparations

Methods for the quantitative analysis of phenol include a bromometric analysis (1), a colorimetric analysis based on the reaction of phenol with copper sulfate (2), and, most recently, a colorimetric analysis based on the reaction of phenol with ferric chloride (3). This report describes a rapid quantitative method for the analysis of the phenol

Table I—Assay Results (Percent Concentration of Phenol) on Phenolated Calamine Lotion and a Commercial Antiseptic Solution

Assay	Phenolated Calamine Lotion		Commercial Antiseptic Solution	
	Assay	USP	Assay	Reported[a]
1	1.01	1.00	1.36	1.4
2	1.02	1.00	1.34	1.4
3	0.96	1.00	1.35	1.4
4	1.02	1.00	1.35	1.4
SD	0.03		0.008	
CV	3.0%		0.59%	
Average deviation	0.02		0.005	

[a] Data from "Handbook of Non-Prescription Drugs," G. B. Griffenhagen and L. L. Hawkins, Eds., American Pharmaceutical Association, Washington, D.C., 1973, p. 130.

present in commercial products using high-pressure liquid chromatography (HPLC).

EXPERIMENTAL

Reagents and Chemicals—All chemicals and reagents were USP, NF, ACS, or chromatographic grade. Phenolated calamine lotion USP (1% phenol) and a commercial antiseptic solution (1.4% phenol) were purchased locally.

Preparation of Solutions—Solutions of 1.00% (w/v) phenol and 1.00% (w/v) hexylresorcinol were prepared in methylene chloride. Five standard solutions were prepared by placing 2 ml of the 1.00% hexylresorcinol in each of five 10-ml volumetric flasks, adding varying amounts of 1.00% phenol (0.5–2.0 ml) to each flask, and diluting to 10 ml with methylene chloride. These dilutions yielded five standard solutions of phenol ranging from 0.050 to 0.200% with the internal standard (0.200% hexylresorcinol). These solutions were used to establish the accuracy and linearity of the chromatographic response. An aqueous standard containing 0.110% (w/v) phenol was used as the primary standard for analysis of the unknown samples.

Establishment of Linearity—The five standard phenol–hexylresorcinol solutions (0.050–0.200%) in methylene chloride served to establish the linearity of response. Ten microliters of each solution was injected into the chromatograph, and the peak height ratio of the phenol to the internal standard (0.200% hexylresorcinol) was calculated and plotted *versus* the phenol concentration. The data indicated that the chromatographic response was linear up to the highest phenol concentration (0.200%) tested.

Assay Procedure—The phenolated calamine lotion was thoroughly mixed. A 10-ml aliquot of the emulsion was diluted to 100 ml with distilled water, and 10 ml of this diluted sample was centrifuged. An aliquot of 5 ml of the supernate was extracted by adding 1.0 ml of 1 *N* HCl, 4 ml of methylene chloride, and 1 ml of the internal standard (1.00% hexylresorcinol in methylene chloride). The mixture was centrifuged, and the aqueous layer was discarded. Ten microliters of the methylene chloride extracts was injected into the chromatograph.

The commercial antiseptic solution, 10 ml, was diluted to 100 ml with distilled water. A 5-ml aliquot of the diluted solution was extracted by adding 1.0 ml of 1 *N* HCl, 4 ml of methylene chloride, and 1 ml of the internal standard (1.00% hexylresorcinol in methylene chloride). The mixture was centrifuged, and the aqueous layer was discarded. Ten microliters of the methylene chloride extract was injected.

The aqueous phenol standard containing 0.110% phenol was extracted by adding 1.0 ml of 1 *N* HCl, 4 ml of methylene chloride, and 1 ml of the internal standard (1.00% hexylresorcinol in methylene chloride). The mixture was centrifuged, and the aqueous layer was discarded. Ten microliters of the methylene chloride extract was injected. The final concentration of the internal standard in the aqueous phenol standard extract and sample extracts was 0.200%.

The 0.100% phenol standard solution containing 0.200% internal standard (hexylresorcinol in methylene chloride) was always injected during the analysis to monitor instrument response.

The percent phenol in the analyzed sample (% *S*) was calculated according to:

$$\% S = \frac{R_s}{R_{std}} \% \text{ std } D \qquad \text{(Eq. 1)}$$

where % std is the percent phenol in the aqueous phenol standard solution, R_s is the ratio of the peak height of phenol and hexylresorcinol in the extracted sample, R_{std} is the ratio of the peak height of phenol and hexylresorcinol in the extracted aqueous phenol standard solution, and *D* is the dilution factor (= 10).

Interference from Other Components—In the analysis of phenolated calamine, no interference was observed in the chromatogram. The commercial antiseptic solution contained thymol and menthol in addition to phenol, but neither agent interfered with the assay. Thymol eluted at 1.97 min; menthol, as expected, was not observed by the UV detector.

Instrument Parameters—A high-pressure liquid chromatograph[1] with a UV detector (254 nm) was used with a solvent system containing 63% heptane, 34% chloroform, and 3% methanol. The column[2] was 0.63 cm (¼ in.) o.d., 15 cm long, and packed with 5-μm silica gel[3]. The temperature was ambient, and the solvent flow was 3 ml/min (at an inlet pressure of 1000 psi). Samples and standards of 10 μl were injected, giving an elution order of phenol (2.75 min) and hexylresorcinol (4.73 min).

DISCUSSION

The results (Table I) show that phenol can be readily assayed in phenolated calamine lotion USP and a commercial antiseptic solution using a simple HPLC method. The extraction and HPLC analyses gave a linear response with phenol concentrations between 0.050 and 0.200%. An aqueous phenol standard containing 0.110% phenol was assayed with each batch of samples, and the concentrations of the samples were calculated based upon this standard. This aqueous phenol standard very closely simulated the unknown samples and was carried through the identical extraction procedure.

A control was also run with each batch to monitor instrument conditions. This procedure minimized assay errors due to technique. Total analysis time per sample was less than 10 min.

REFERENCES

(1) R. J. Kiposki and B. F. Allen, *Drug Stand.*, **25**, 17 (1957).

(2) G. L. Stanko and H. G. DeKay, *Am. J. Pharm.*, **124**, 328 (1952).

(3) V. D. Gupta and K. A. Bomer, *J. Pharm. Sci.*, **64**, 1199 (1975).

ACKNOWLEDGMENTS AND ADDRESSES

Received July 15, 1976, from the *Department of Medicinal Chemistry and Pharmacology, College of Pharmacy and Allied Health Professions, Northeastern University, Boston, MA 02115.*

Accepted for publication November 4, 1976.

Supported in part by National Institutes of Health Grant RR07143.

ˣ To whom inquiries should be directed.

[1] Waters Associates model ALC 202.

[2] Hi-Eff Micropart.

[3] Applied Sciences Laboratories.

Spironolactone: Relationship between Concentrations of Dethioacetylated Metabolite in Human Serum and Milk

DALE L. PHELPS * and AZIZ KARIM ‡x

Abstract □ The concentration of canrenone, a principal metabolite of spironolactone, was determined in human serum and milk. The milk to serum concentration ratios of this metabolite were 0.72 at 2 hr and 0.51 at 14.5 hr after ingestion of spironolactone. It was estimated that the maximum quantity of canrenone ingested daily by a human infant *via* its mother's milk would be approximately 0.2% of the daily dose of spironolactone given to the mother.

Keyphrases □ Spironolactone metabolite—canrenone, human milk to serum concentration ratio □ Canrenone—human milk to serum concentration ratio □ Aldosterone antagonists—canrenone, human milk to serum concentration ratio

Excretion of drugs and/or their biologically active metabolites in human milk in amounts sufficient to elicit pharmacological responses in the nursing infant is a potential risk associated with numerous drugs (1). High lipid solubility, nonionization at blood pH, and low binding to plasma proteins are some factors that favor drug transfer from blood to milk. Several reviews (2–4) documented excretion of various classes of drug molecules in human milk; however, for spironolactone[1], no information is available regarding milk excretion of either the unchanged drug or its metabolites.

Previous studies showed that spironolactone is rapidly and extensively metabolized in humans. The unchanged drug has not been detected in the urine (5–8). The principal metabolite in the blood is the dethioacetylated derivative, canrenone[2], which is extensively (98%) bound to plasma proteins and has a log-linear phase half-life of about 17 hr (8). Recently, the single oral dose of canrenone was reported to have about one-third the activity of spironolactone in inhibiting the action of fludrocortisone on electrolyte elimination in humans (9). This paper reports findings on the relationship between the concentration of canrenone in human serum and milk.

EXPERIMENTAL

A 28-year-old primagravida Caucasian patient with documented primary hyperaldosteronism took 25 mg of spironolactone twice a day until the spontaneous onset of labor at 37 weeks gestation, resulting in the normal delivery of a healthy female infant (2.69 kg). Breast feeding was permitted, and the infant's serum electrolytes were monitored. Seventeen days after birth, the mother's blood and expressed breast milk specimens were taken in the morning, 14.5 hr after her last 25-mg dose. (The dosage by that time had been increased to 25 mg four times a day.) The mother took her first dose of the day, and 2 hr later (after nursing) the maternal blood and expressed milk specimens were again obtained. Serum was separated within 30 min of collection, and biological specimens were stored at −20° until analysis.

Canrenone levels were assayed by the spectrofluorometric method of Gochman and Gantt (5). Since this method does not describe canrenone measurement in milk, initial recovery studies were performed after known amounts of canrenone were added to the control milk of a healthy mother. In the concentration range of 50–400 ng/ml, the recovery was between 95 and 115% and the coefficient of variation ($n = 3$) was less than 14%. For a 1-ml sample, the lowest limit of detection was 25 ng/ml.

RESULTS

At 2 hr after ingestion of spironolactone (25 mg), the serum and milk concentrations of canrenone (average ± *SD* of three determinations) were 144 ± 8 and 104 ± 4 ng/ml, respectively. At 14.5 hr, the corresponding values were 92 ± 4 and 47 ± 3 ng/ml. The milk to serum concentration ratios at early and late periods were 0.72 and 0.51, respectively, indicating that the canrenone concentration in the milk declined at a rate similar to that in the serum.

DISCUSSION

Canrenone is a lipid-soluble steroid and exists in the unionized form in the blood. These factors tend to favor its transfer from blood to milk. The low milk concentration of canrenone in the present study can be attributed to its extensive binding to the plasma proteins (8). Karim *et al.* (10) found that the maximum and minimum steady-state plasma levels of canrenone in healthy males who received twice the usual recommended doses of spironolactone (200 mg once a day) were approximately 500 and 100 ng/ml, respectively.

If it is assumed that the milk to serum (or plasma) concentration ratio of canrenone is 0.8 and that the infant's breast milk intake per day is 1000 ml, then the maximum quantity of canrenone that could be ingested by the infant per day would be about 0.2% of the mother's daily dose of spironolactone. In the present study, serum levels of sodium and potassium were monitored in the infant and were in the normal range. In this case, the amount of canrenone excreted in milk while the mother was receiving therapeutic doses of spironolactone was not clinically significant. However, nursing infants of treated mothers should have their electrolyte balance monitored (serum and urine) until additional data can be collected to allow for possible biological variation.

REFERENCES

(1) C. S. Catz and G. P. Giacoia, *Ped. Clin. N. Am.*, **19**, 151 (1972).
(2) B. E. Takyi, *J. Hosp. Pharm.*, **28**, 317 (1970).
(3) J. A. Knowles, *Clin. Toxicol.*, **7**, 69 (1974).
(4) T. E. O'Brien, *Am. J. Hosp. Pharm.*, **31**, 844 (1974).
(5) N. Gochman and C. L. Gantt, *J. Pharmacol. Exp. Ther.*, **135**, 312 (1962).
(6) A. Karim and E. A. Brown, *Steroids*, **20**, 41 (1972).
(7) W. Sadee, M. Dagcioglu, and R. Schroder, *J. Pharmacol. Exp. Ther.*, **185**, 686 (1973).
(8) A. Karim, J. Zagarella, J. Hribar, and M. Dooley, *Clin. Pharmacol. Ther.*, **19**, 158 (1976).
(9) G. J. Huston, P. Turner, and M. Leighton, *Br. J. Clin. Pharmacol.*, **3**, 201 (1976).
(10) A. Karim, J. Zagarella, T. C. Hutsell, and M. Dooley, *Clin. Pharmacol. Ther.*, **19**, 177 (1976).

ACKNOWLEDGMENTS AND ADDRESSES

Received August 11, 1976, from the *Department of Pediatrics, School of Medicine, Center of the Health Sciences, Los Angeles, CA 90024, and the ‡Department of Drug Metabolism and Radiochemistry, Searle Laboratories, Chicago, IL 60680.

Accepted for publication October 8, 1976.

The authors are indebted to Dr. T. Hutsell, Bioanalytical Department, Searle Laboratories, for the determination of canrenone in serum and milk.

x To whom inquiries should be directed.

[1] Aldactone, G. D. Searle & Co., is 17β-hydroxy-7α-acetylthio-3-oxopregn-4-ene-21-carboxylic acid γ-lactone.

[2] Also known as Aldadiene, Phanurane, and SC-9376 and is 17β-hydroxy-3-oxopregna-4,6-diene-21-carboxylic acid γ-lactone.

Imidazo[4,5-*f*]quinolines III: Antibacterial 7-Methyl-9-(substituted Arylamino)imidazo[4,5-*f*]quinolines

HARRY R. SNYDER, Jr.[x], CLAUDE F. SPENCER, and RAYMOND FREEDMAN

Abstract □ A series of 7-methyl-9-(substituted arylamino)imidazo-[4,5-*f*]quinolines was prepared and screened against four varieties of bacteria. The compounds possessed antibacterial activity against both Gram-positive and Gram-negative organisms.

Keyphrases □ Imidazo[4,5-*f*]quinolines, substituted—synthesized, screened for antibacterial activity □ Antibacterial activity—various substituted imidazo[4,5-*f*]quinolines screened □ Structure–activity relationships—various substituted imidazo[4,5-*f*]quinolines screened for antibacterial activity

Synthesis and biological evaluation of a series of 9-(substituted amino)imidazo[4,5-*f*]quinolines (1, 2) as anthelmintic agents against the tapeworm *Hymenolepis nana* led to the screening of these compounds for antibacterial properties. Several 7-methyl-9-(substituted arylamino)imidazo[4,5-*f*]quinolines (2) were particularly effective against *Haemophilis vaginalis*. Accordingly, a series of these compounds was prepared to explore this activity further.

DISCUSSION

Chemistry—All but two of the compounds listed in Table I were prepared by treating 9-chloro-7-methylimidazo[4,5-*f*]quinoline (II) (3) with the appropriate anilines as previously described (2) (Scheme I). Most prerequisite anilines were purchased. However, the anilines for VI, XII–XIV, and XX were obtained by the catalytic reduction of the corresponding nitro compounds. Compounds VIII and X were obtained by the acid hydrolysis of VII and IX, respectively. With the exception of VI, all products were obtained as the hydrochloride salts.

Biological Screening and Results—Compounds III–XXIII were screened *in vitro* against *Staphylococcus aureus* (Mi-12)[1], *Escherichia coli* (Es-2)[1], *Corynebacterium liquefaciens* (Co-11)[1], and *Haemophilis vaginalis* (He-127)[1].

Screening data for the compounds are listed in Table I, along with data for nitrofurazone[2] for comparison. These compounds possess activity against Gram-positive and Gram-negative organisms.

EXPERIMENTAL

Synthesis—The anilines for VI and XX were prepared by catalytic reduction of 9-nitroanthracene and 2-chloro-4-nitrophenol, respectively, which were purchased. The prerequisite amines for XII, XIII, and XIV were obtained from 4-pyrrolidinonitrobenzene (4), 4-morpholinonitrobenzene (4), and 3-chloro-4-morpholinonitrobenzene (5), respectively, which were synthesized by literature procedures.

Melting points[3] were taken in open capillary tubes and are uncorrected. IR spectra (mineral oil mull) and NMR spectra)dimethyl sulfoxide-d_6) were consistent with the assigned structures. The physical constants of all final products are listed in Table I, and analytical data are listed in Table II.

3-Chloro-4-morpholinoaniline—A 500-ml reduction bottle was charged with 3-chloro-4-morpholinonitrobenzene (5) (19.5 g, 0.08 mole) and absolute ethanol. Raney active nickel catalyst (2.5 ml in water) was added, and the mixture was shaken under hydrogen at 40 psi until absorption was complete. The catalyst was removed by filtration, and the filtrate was concentrated to 80 ml under reduced pressure. The residue was chilled and filtered to yield 10.8 g, mp 93–97°. The filtrate was concentrated to 10 ml, chilled, and filtered to yield 3.2 g, mp 92–93°. The total yield was 14.0 g (82%). A small sample (1.0 g) was recrystallized from absolute ethanol to yield 0.5 g, mp 97–100°.

Anal.—Calc. for $C_{10}H_{13}ClN_2O$: C, 56.47; H, 6.16; N, 13.17. Found: C, 56.43; H, 6.05; N, 13.19.

7-Methyl-9-(substituted Arylamino)imidazo[4,5-*f*]quinolines (III–XXIII)—All of these compounds, except VIII and X, were prepared by the procedure of Spencer *et al.* (2).

9-(4-Aminoanilino)-7-methylimidazo[4,5-*f*]quinoline Hydrochloride (VIII)—A solution of VII (20.0 g, 0.05 mole) in concentrated hydrochloric acid was heated under reflux for 30 min. A clear yellow solution formed after about 15 min; in another 5 min, crystals began to separate. After cooling, the product was filtered, washed with hydrochloric acid and then with methanol, and air dried to give 20 g of yellow crystals. These crystals contained a variable amount of hydrogen chloride even after drying *in vacuo*.

The product was converted to the monohydrochloride by the following procedure. A solution of the material in water (200 ml) was made alkaline with ammonium hydroxide. The yellow precipitate was filtered, washed with water, and suspended in water (300 ml). One equivalent (4.2 ml) of concentrated hydrochloric acid was added, and the mixture was heated on the steam bath (solution incomplete) and then kept overnight at room temperature. The product was filtered, washed with absolute ethanol, and air dried to give 12 g of VIII. Drying at 100° *in vacuo* removes the water, but it is rapidly reabsorbed on exposure to the atmosphere.

Compound XI was hydrolyzed in a similar manner to give X directly with no additional workup required.

Biological Testing—Compounds III–XXIII were screened *in vitro* against three varieties of bacteria, *S. aureus*, *E. coli*, and *C. liquefaciens*, according to procedures previously described (6). In addition, the compounds were tested against *H. vaginalis* by the following method. The inoculum of *H. vaginalis* was prepared by growing the organism for 18–20 hr at 37° in brain–heart infusion broth[4] with 0.1% agar and 10% calf serum added. The culture was adjusted in fresh medium to an optical density of 0.4 in a spectrometer[5] set at 440 nm. Cotton-plugged tubes containing 2 ml of the growth medium, 5% calf serum, and diluted test compound were inoculated with 0.2 ml of the adjusted culture. After the inoculum was added, the tubes were incubated without being shaken for 24 hr at 37° and then observed for turbidity.

REFERENCES

(1) C. F. Spencer and H. R. Snyder, Jr., U.S. pat. 3,878,206 (Apr. 15, 1975).

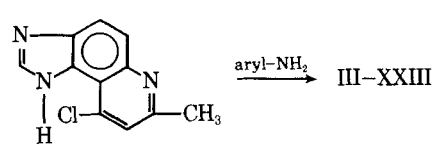

II

Scheme I

[1] The Norwich Pharmacal Co. strain number.
[2] Furacin, Eaton Laboratories Division, Morton-Norwich Products.
[3] Mel-Temp melting-point apparatus.
[4] Difco.
[5] Bausch and Lomb Spectronic 20.

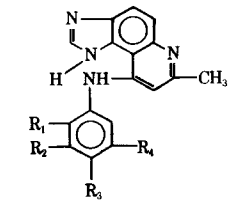

Table I—7-Methyl-9-(substituted Arylamino)imidazo[4,5-*f*]quinolines

Compound	R_1	R_2	R_3	R_4	Melting Point	Yield, %	Recrystallization Solvent	MIC[a], μg/ml *H. vaginalis*	*S. aureus*	*E. coli*	*C. liquefaciens*
III	H	H	C_2H_5	H	327–332°	100	2-Propanol	6.25	3.1	6.25	3.1
IV	H	H	CH_2CH_2OH	H	302–308°	81	Water	25.0	100	50	100
V	H	H	$C_{12}H_{25}$-*n*	H	216–220°	80	Dimethylformamide	25.0	>50	>50	50
VI	2,3-benzo		H	5,6-benzo	192–198°	74	Methanol	50.0	25	50	25
VII	H	H	$NHCOCH_3$	H	381–383°	81	Methanol	12.5	>50	50	>50
VIII	H	H	NH_2	H	>350°	65	Water	12.5	100	25	100
IX	H	H	$N(CH_3)COCH_3$	H	315–317°	48	Methanol	62.5	500	125	125
X	H	H	$NHCH_3$	H	<330° dec.	86	Methanol	6.25	50	50	25
XI	H	H	$N(CH_3)CH_2CH_2OH$	H	299–303°	100	Methanol–ether	25	100	100	50
XII	H	H		H	364–372°	93	Methanol–ether	12.5	3.1	6.25	1.5
XIII	H	H		H	351–353°	99	Methanol–ether	25.0	50	100	100
XIV	H	Cl		H	322–327°	100	Methanol–ether	12.5	12.5	12.5	50
XV	H	H	Cl	H	Gradual decomposition	29	Methanol	6.25	6.25	3.1	1.5
XVI	H	Cl	H	H	351–353°	88	Methanol	12.5	6.25	3.1	6.25
XVII	H	H	F	H	341–345°	57	Absolute ethanol	3.1	25	12.5	25
XVIII	H	H	OH	H	393–395°	48	Methanol	6.25	50	50	25
XIX	H	OH	H	H	396–398°	89	Absolute ethanol	1.5	25	25	25
XX	H	Cl	OH	H	387° dec.	97	Methanol–ether	6.25	>50	25	3.1
XXI	OCH_3	H	H	$COCH_3$	>400°	69	Methanol	15.5	500	250	>1000
XXII	H	H	COC_6H_5	H	348–350°	90	Methanol	50	12.5	100	50
XXIII	H	H	$COOC_2H_5$	H	275–280°	60	Absolute ethanol	25	12.5	12.5	12.5
Nitrofurazone								0.75	12.5	3.1	25

[a] MIC = minimal inhibitory concentration, which is the lowest concentration of a compound that prevents visible growth after 24-hr incubation at 37°.

Table II—Elemental Analysis Data for III–XXIII

Compound	Formula	Calc./Found, % C	H	N
III	$C_{19}H_{18}N_4 \cdot HCl$	67.34/66.94	5.65/5.56	16.54/16.48
IV	$C_{19}H_{18}N_4O \cdot HCl$	64.31/64.12	5.40/5.23	15.79/15.80
V	$C_{29}H_{38}N_4 \cdot HCl \cdot 0.25\ H_2O$	72.02/72.05	8.23/8.32	11.59/11.70
VI	$C_{25}H_{18}N_4 \cdot 0.5\ H_2O$	78.30/78.53	4.99/4.71	14.61/14.73
VII	$C_{19}H_{17}N_5O \cdot HCl$	62.04/61.66	4.93/4.69	19.04/19.06
VIII	$C_{17}H_{15}N_5 \cdot HCl \cdot 0.5\ H_2O$	60.98/60.99	5.12/5.04	20.92/20.99
IX	$C_{20}H_{19}N_5O \cdot HCl \cdot 1.5\ H_2O$	58.75/58.97	5.67/5.32	17.13/17.33
X	$C_{18}H_{17}N_5 \cdot 2\ HCl \cdot H_2O$	54.83/55.17	5.37/5.25	17.76/17.71
XI	$C_{20}H_{21}N_5O \cdot HCl \cdot 0.5\ H_2O$	61.13/61.48	5.90/5.92	17.83/17.81
XII	$C_{21}H_{21}N_5 \cdot HCl$	66.39/65.99	5.84/5.85	18.44/18.17
XIII	$C_{21}H_{21}N_5O \cdot HCl$	63.71/63.59	5.60/5.70	17.69/17.43
XIV	$C_{21}H_{20}ClN_5O \cdot HCl \cdot 3\ H_2O$	52.07/52.19	5.62/5.39	14.46/14.42
XV	$C_{17}H_{13}ClN_4 \cdot HCl \cdot 1.25\ H_2O$	55.67/55.83	4.26/4.31	15.28/15.20
XVI	$C_{17}H_{13}ClN_4 \cdot HCl$	59.14/59.32	4.09/4.08	16.23/16.04
XVII	$C_{17}H_{13}FN_4 \cdot HCl$	62.10/62.50	4.29/4.32	17.04/17.15
XVIII	$C_{17}H_{14}N_4O \cdot HCl \cdot 0.5\ H_2O$	60.81/60.55	4.80/5.11	16.69/16.71
XIX	$C_{17}H_{14}N_4O \cdot HCl$	62.48/62.18	4.63/4.65	17.15/16.87
XX	$C_{17}H_{13}ClN_4O \cdot HCl$	56.52/56.25	3.91/3.91	15.51/15.29
XXI	$C_{20}H_{18}N_4O_2 \cdot HCl \cdot 0.5\ H_2O$	61.30/61.26	5.14/5.02	14.64/14.26
XXII	$C_{24}H_{18}N_4O \cdot HCl$	69.48/69.08	4.62/4.68	13.51/13.58
XXIII	$C_{20}H_{18}N_4O_2 \cdot HCl$	62.74/62.56	5.00/4.88	14.64/14.75

(2) C. F. Spencer, H. R. Snyder, Jr., H. A. Burch, and C. J. Hatton, *J. Med. Chem.*, **20**, 829 (1977).

(3) C. F. Spencer, H. R. Snyder, Jr., and R. J. Alaimo, *J. Heterocycl. Chem.*, **12**, 1319 (1975).

(4) J. E. LuValle, D. B. Glass, and A. Weissberger, *J. Am. Chem. Soc.*, **70**, 2226 (1948).

(5) R. H. Harrandence and F. Lions, *J. Proc. Roy. Soc. N.S. Wales*, **70**, 406 (1937); through *Chem. Abstr.*, **31**, 6662 (1937).

(6) R. Freedman and R. E. Chamberlain, *Antimicrob. Ag. Chemother.*, **1967**, 502.

ACKNOWLEDGMENTS AND ADDRESSES

Received September 29, 1976, from the *Research and Development Department, Norwich Pharmacal Company, a Division of Morton-Norwich Products, Inc., Norwich, NY 13815.*

Accepted for publication October 28, 1976.

The authors are indebted to Mr. Patrick Moynihan, Mr. Raymond C. Finch, Mr. Edwin Woodrick, Mr. Ronald Storrin, Mr. Frederick Abbott, Mr. Warren Smith, and Mr. D. Richard Anthony for technical assistance and to Mr. Grant Gustin and his staff for the analytical data.

[x] To whom inquiries should be directed.

New Compounds: Synthesis of D-Arabinofuranosylurea Derivatives

ALBERT M. FLEISCHNER [*], JOHN M. CROSS [*], ALVIN B. SEGELMAN [*], and THEODORUS van ES [‡x]

Abstract □ Procedures are described for the preparation of a series of D-arabinofuranosylurea derivatives.

Keyphrases □ D-Arabinofuranosylurea derivatives—synthesis described □ Ureas, D-arabinofuranosyl—synthesis described

The structural resemblance of D-arabinofuranosylurea derivatives to nucleosides possessing cytotoxic activity such as cytarabine (1) suggested the synthesis of a series of these urea derivatives.

Oxidation of the pyrimidine base in 2′,3′,5′-tri-(*O*-acetyl)uridine or its N^3-methyl derivative (2) with permanganate, ozone, or osmium tetroxide gave, apart from unchanged starting material, urea or methylurea and poor yields of compounds whose structures were not established unambiguously.

Ureidoglycosides have been formed by an acid-catalyzed reaction between monosaccharides and urea (3). Normally, this reaction would result in the formation of ureidopyranosides. For the preparation of ureidofuranosides, protected furanose derivatives are required so that pyranosides are not formed under acidic reaction conditions. 2′,3′,5′-Tri-(*O*-benzyl)-D-arabinofuranose and a variety of ureas (Table I) were used. This particular derivative offered the advantage that the benzyl groups could be removed by catalytic hydrogenolysis (4) to give the required D-arabinofuranosylureas. The urea derivatives were obtained by heating the benzylated sugar, appropriate urea, and acetone (or acetone–water) with sulfuric acid or perchloric acid as a catalyst (5).

EXPERIMENTAL

Chemical-ionization mass spectra[1], with isobutane as the reagent gas, and NMR spectra were obtained[2]. Chemical shift data were measured relative to tetramethylsilane as an internal standard and are given in parts per million. Evaporations were conducted under diminished pressure at a bath temperature below 50°. Column chromatography was carried out on silica gel (60–200 mesh).

N^3-Methyl -2′,3′,5′-tri- (*O*-acetyl)uridine—2′,3′,5′-Tri-(*O*-ace-

[1] DuPont 21-490F mass spectrograph.

[2] Varian T-60 instrument.

Table II—Elemental Analysis Data for III–XXIII

Compound	Formula	Calc./Found, % C	H	N
III	$C_{19}H_{18}N_4 \cdot HCl$	67.34/66.94	5.65/5.56	16.54/16.48
IV	$C_{19}H_{18}N_4O \cdot HCl$	64.31/64.12	5.40/5.23	15.79/15.80
V	$C_{29}H_{38}N_4 \cdot HCl \cdot 0.25\ H_2O$	72.02/72.05	8.23/8.32	11.59/11.70
VI	$C_{25}H_{18}N_4 \cdot 0.5\ H_2O$	78.30/78.53	4.99/4.71	14.61/14.73
VII	$C_{19}H_{17}N_5O \cdot HCl$	62.04/61.66	4.93/4.69	19.04/19.06
VIII	$C_{17}H_{15}N_5 \cdot HCl \cdot 0.5\ H_2O$	60.98/60.99	5.12/5.04	20.92/20.99
IX	$C_{20}H_{19}N_5O \cdot HCl \cdot 1.5\ H_2O$	58.75/58.97	5.67/5.32	17.13/17.33
X	$C_{18}H_{17}N_5 \cdot 2\ HCl \cdot H_2O$	54.83/55.17	5.37/5.25	17.76/17.71
XI	$C_{20}H_{21}N_5O \cdot HCl \cdot 0.5\ H_2O$	61.13/61.48	5.90/5.92	17.83/17.81
XII	$C_{21}H_{21}N_5 \cdot HCl$	66.39/65.99	5.84/5.85	18.44/18.17
XIII	$C_{21}H_{21}N_5O \cdot HCl$	63.71/63.59	5.60/5.70	17.69/17.43
XIV	$C_{21}H_{20}ClN_5O \cdot HCl \cdot 3\ H_2O$	52.07/52.19	5.62/5.39	14.46/14.42
XV	$C_{17}H_{13}ClN_4 \cdot HCl \cdot 1.25\ H_2O$	55.67/55.83	4.26/4.31	15.28/15.20
XVI	$C_{17}H_{13}ClN_4 \cdot HCl$	59.14/59.32	4.09/4.08	16.23/16.04
XVII	$C_{17}H_{13}FN_4 \cdot HCl$	62.10/62.50	4.29/4.32	17.04/17.15
XVIII	$C_{17}H_{14}N_4O \cdot HCl \cdot 0.5\ H_2O$	60.81/60.55	4.80/5.11	16.69/16.71
XIX	$C_{17}H_{14}N_4O \cdot HCl$	62.48/62.18	4.63/4.65	17.15/16.87
XX	$C_{17}H_{13}ClN_4O \cdot HCl$	56.52/56.25	3.91/3.91	15.51/15.29
XXI	$C_{20}H_{18}N_4O_2 \cdot HCl \cdot 0.5\ H_2O$	61.30/61.26	5.14/5.02	14.64/14.26
XXII	$C_{24}H_{18}N_4O \cdot HCl$	69.48/69.08	4.62/4.68	13.51/13.58
XXIII	$C_{20}H_{18}N_4O_2 \cdot HCl$	62.74/62.56	5.00/4.88	14.64/14.75

(2) C. F. Spencer, H. R. Snyder, Jr., H. A. Burch, and C. J. Hatton, *J. Med. Chem.*, **20**, 829 (1977).

(3) C. F. Spencer, H. R. Snyder, Jr., and R. J. Alaimo, *J. Heterocycl. Chem.*, **12**, 1319 (1975).

(4) J. E. LuValle, D. B. Glass, and A. Weissberger, *J. Am. Chem. Soc.*, **70**, 2226 (1948).

(5) R. H. Harrandence and F. Lions, *J. Proc. Roy. Soc. N.S. Wales*, **70**, 406 (1937); through *Chem. Abstr.*, **31**, 6662 (1937).

(6) R. Freedman and R. E. Chamberlain, *Antimicrob. Ag. Chemother.*, **1967**, 502.

ACKNOWLEDGMENTS AND ADDRESSES

Received September 29, 1976, from the *Research and Development Department, Norwich Pharmacal Company, a Division of Morton-Norwich Products, Inc., Norwich, NY 13815.*

Accepted for publication October 28, 1976.

The authors are indebted to Mr. Patrick Moynihan, Mr. Raymond C. Finch, Mr. Edwin Woodrick, Mr. Ronald Storrin, Mr. Frederick Abbott, Mr. Warren Smith, and Mr. D. Richard Anthony for technical assistance and to Mr. Grant Gustin and his staff for the analytical data.

[x] To whom inquiries should be directed.

New Compounds: Synthesis of D-Arabinofuranosylurea Derivatives

ALBERT M. FLEISCHNER [*], JOHN M. CROSS [*], ALVIN B. SEGELMAN [*], and THEODORUS van ES [‡x]

Abstract □ Procedures are described for the preparation of a series of D-arabinofuranosylurea derivatives.

Keyphrases □ D-Arabinofuranosylurea derivatives—synthesis described □ Ureas, D-arabinofuranosyl—synthesis described

The structural resemblance of D-arabinofuranosylurea derivatives to nucleosides possessing cytotoxic activity such as cytarabine (1) suggested the synthesis of a series of these urea derivatives.

Oxidation of the pyrimidine base in 2′,3′,5′-tri-(*O*-acetyl)uridine or its N^3-methyl derivative (2) with permanganate, ozone, or osmium tetroxide gave, apart from unchanged starting material, urea or methylurea and poor yields of compounds whose structures were not established unambiguously.

Ureidoglycosides have been formed by an acid-catalyzed reaction between monosaccharides and urea (3). Normally, this reaction would result in the formation of ureidopyranosides. For the preparation of ureidofuranosides, protected furanose derivatives are required so that pyranosides are not formed under acidic reaction conditions. 2′,3′,5′-Tri-(*O*-benzyl)-D-arabinofuranose and a variety of ureas (Table I) were used. This particular derivative offered the advantage that the benzyl groups could be removed by catalytic hydrogenolysis (4) to give the required D-arabinofuranosylureas. The urea derivatives were obtained by heating the benzylated sugar, appropriate urea, and acetone (or acetone–water) with sulfuric acid or perchloric acid as a catalyst (5).

EXPERIMENTAL

Chemical-ionization mass spectra[1], with isobutane as the reagent gas, and NMR spectra were obtained[2]. Chemical shift data were measured relative to tetramethylsilane as an internal standard and are given in parts per million. Evaporations were conducted under diminished pressure at a bath temperature below 50°. Column chromatography was carried out on silica gel (60–200 mesh).

N^3-Methyl -2′,3′,5′-tri- (*O*-acetyl)uridine—2′,3′,5′-Tri-(*O*-ace-

[1] DuPont 21-490F mass spectrograph.

[2] Varian T-60 instrument.

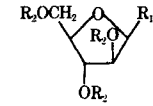

Table I—Urea Derivatives of β-D-Arabinofuranoside

Compound	R_1	R_2	Melting Point	Yield, %	Molecular Formula	Analysis, %		Molecular Weight[a]		NMR Data[b]		
						Calc.	Found	Calc.	Found	N—CH_3	N′—CH_3	NH_2
I (Procedure A)	$NHCONH_2$	$C_6H_5CH_2$	95–98°	12	$C_{27}H_{30}N_2O_5$	C 70.13 H 6.54 N 6.06	70.28 6.47 6.20	462	—	—	—	5.3 (br s)
I (Procedure B)	$NHCONH_2$	$C_6H_5CH_2$	Oil	25	$C_{27}H_{30}N_2O_5$							
I (Procedure C)	$NHCONH_2$	$C_6H_5CH_2$	95–98°	19	$C_{27}H_{30}N_2O_5$							
I (Procedure D)	$NHCONH_2$	$C_6H_5CH_2$	Oil	21	$C_{27}H_{30}N_2O_5$							
II	$NHCONHCH_3$	$C_6H_5CH_2$	83–85°	50	$C_{28}H_{32}N_2O_5$	C 70.59 H 6.72 N 5.88	70.62 6.68 5.90	476	—	—	2.6 (d)	—
III	$NCONHCH_3$ (N-CH_3)	$C_6H_5CH_2$	Oil	36	$C_{29}H_{34}N_2O_5$	C 71.02 H 6.93 N —	70.37 6.97 —	490	491 (M + 1)	2.8 (m)	2.8 (m)	—
IV	$NHCONHCONH_2$	$C_6H_5CH_2$	142–146°	14	$C_{28}H_{31}N_3O_6$	C 66.53 H 6.14 N 8.32	66.14 6.15 8.38	505	—	—	—	5.8 (br s)
V	$NHCSNH_2$	$C_6H_5CH_2$	200°[c]	51	$C_{27}H_{30}N_2O_4S$	C 67.78 H 6.33 N 5.86	67.90 6.28 5.61	478	—	—	—	5.4 (s)
VI	$NHCSNHCH_3$	$C_6H_5CH_2$	Oil	54	$C_{28}H_{32}N_2O_4S$	C 68.29 H 6.50 N 5.69	68.21 6.52 5.74	492	493 (M + 1)	—	3.0 (d)	—
VII	$NCSNHCH_3$ (N-CH_3)	$C_6H_5CH_2$	Oil	11	$C_{29}H_{34}N_2O_4S$	C 72.80 H 7.11 N —	72.21 7.19 —	506	—	2.4 (d) or 2.7 (d)	2.7 (d) or 2.4 (d)	—
VIII	$NHCONHCH_3$	H	150°	26	$C_7H_{14}N_2O_5$	C 40.78 H 6.80 N —	40.83 6.81 —	206	—	—	2.8 (d)	—
IX	$NCONHCH_3$ (N-CH_3)	H	Oil	96	$C_8H_{16}N_2O_5$	C 43.64 H 7.27 N 12.73	43.59 7.29 12.71	220	—	3.39 (s)	2.8 (s)	—

[a] By mass spectrometer. [b] Compounds VIII and IX in deuterium oxide; all others in deuterochloroform. [c] Compounds charred at the indicated temperature.

tyl)uridine (3.0 g) was dissolved in hot ethylene dichloride (10 ml). To the cooled solution was added a solution of diazomethane in ether (100 ml) prepared from nitrosomethylurea (10 g). The solution was allowed to stand at room temperature until no further nitrogen was evolved, and then the solution was evaporated to an oil (3.0 g). The oil was applied to a silica gel column with methanol–benzene (1:10) to give the title compound.

Anal.—Calc. for $C_{16}H_{20}N_2O_9$: C, 50.00; H, 5.46. Found: C, 49.72; H, 5.31.

2′,3′,5′-Tri-(*O*-benzyl)-β-D-arabinofuranosylurea (I)—*Procedure A*—Urea (1.0 g, 0.017 mole), 2′,3′,5′-tri-(*O*-benzyl)-β-D-arabinofuranose (1.0 g, 0.0025 mole), acetone (30 ml), water (10 ml), and concentrated sulfuric acid (0.34 g, 0.9% w/w) were heated for 48 hr at 70° under reflux with stirring. The solution was cooled and neutralized with lead carbonate. The suspension was filtered, and the filtrate was evaporated. The residue was extracted with chloroform and water, and the chloroform extracts were evaporated to yield a syrup (1.2 g). Chromatography of the syrup on silica gel with benzene–ethyl acetate (7:3) yielded I as a syrup, which was crystallized from ether (0.13 g).

Procedure B—The steps were as described under *Procedure A*, except that no water was used in the reaction mixture. The yield of I was 0.28 g (oil).

Procedure C—The steps were as described under *Procedure A*, except that 0.9% (w/w) perchloric acid was used as a catalyst instead of sulfuric acid. The yield of I was 0.21 g (crystals from ether).

Procedure D—The steps were as described under *Procedure C*, except that no water was used in the reaction mixture. The yield of I was 0.15 g (oil). This procedure was used for the preparation of II–VII. The products from Procedures A–D showed identical NMR spectra.

***N*-β-D-Arabinofuranosyl-*N*′-methylurea (VIII)**—To a solution of II (1.94 g) in methanol (500 ml) was added 5% palladium-on-charcoal (100 mg). The reaction mixture was hydrogenated at 320 psi for 120 hr and then filtered through diatomaceous earth[3], and the filtrate was evaporated to an oil. The oil was crystallized from methanol to give VIII (0.24 g), mp 150°. Compound IX was prepared by the same procedure.

REFERENCES

(1) G. A. Fischer and M. Y. Chu, *Biochem. Pharmacol.*, **11**, 423 (1962).

(2) D. W. Visser, G. Baran, and R. Beltz, *J. Am. Chem. Soc.*, **75**, 2017 (1953).

(3) M. H. Benn and A. S. Jones, *J. Chem. Soc.*, **1960**, 3837.

(4) R. Barker and H. G. Fletcher, Jr., *J. Org. Chem.*, **26**, 4605 (1961).

(5) N. G. Shkantova, M. S. Dudkin, and S. I. Grinshpun, *Zh. Prik. Khim.*, **40**, 164 (1970).

ACKNOWLEDGMENTS AND ADDRESSES

Received June 30, 1976, from the *Department of Pharmaceutical Chemistry, College of Pharmacy, and the ‡Department of Biochemistry, Rutgers College, Rutgers—The State University, New Brunswick, NJ 08903.

Accepted for publication September 2, 1976.

[x] To whom inquiries should be directed.

[3] Celite.

New Compounds: Total Synthesis of *dl*-3a,4,6a-*cis*-4-(4-Carboxybutyl)-hexahydropyrrolo[3,4-*d*]imidazol-2-one Hydrochloride (*dl*-Azabiotin Hydrochloride)

HENRY C. WORMSER and HANLEY N. ABRAMSON [x]

Abstract □ The total synthesis of *dl*-3a,4,6a-*cis*-4-(4-carboxybutyl)-hexahydropyrrolo[3,4-*d*]imidazol-2-one hydrochloride (*dl*-azabiotin hydrochloride) was accomplished in a seven-step sequence from 2-ethoxycarbonylazepin-7-one.

Keyphrases □ Pyrroloimidazolone, substituted—synthesized in seven-step sequence □ Azabiotin—synthesized in seven-step sequence □ Biotin analog—substituted pyrroloimidazolone synthesized in seven-step sequence

Biotin (I), a coenzyme, functions in several significant carbon dioxide fixation reactions in the cell. It is involved in carboxylation reactions catalyzed by propionyl coenzyme A carboxylase, acetyl coenzyme A carboxylase, pyruvate carboxylase, and β-methylcrotonyl coenzyme A carboxylase among others. Numerous aspects of the biochemical role of biotin were reviewed recently (1, 2).

BACKGROUND

Several analogs of biotin were synthesized, but few of these compounds substituted for biotin as a coenzyme. While biotin methyl ester and desthiobiotin show growth-promoting activity equivalent to that of biotin in many microorganisms, oxybiotin, biocytin, and biotin sulfoxide exhibit only limited activity. Many analogs possess substantial antibiotin activity.

The fact that carbobiotin (3) and oxybiotin have growth-promoting activity qualitatively, although not quantitatively, equivalent to that of biotin indicates that the sulfur atom of biotin is not essential for activity. The actual role of this sulfur atom has been a matter for debate. Glasel (4), on the basis of NMR data, postulated that the sulfur may act as a hydrogen acceptor in interactions with the protein component of biotin enzymes. This interpretation was challenged by Caplow (5), who pointed out that Glasel's observation could also be accounted for by assuming protonation of the ureide moiety.

However, Olah and White (6), employing conditions that hardly simulated biological media, presented unequivocal evidence that the sulfur is indeed protonated in magic acid (FSO_3H-SbF_5-SO_2). They suggested that the sulfur protonation occurs on the side *trans* to the carboxyl-

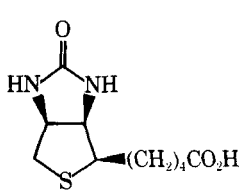

I

tyl)uridine (3.0 g) was dissolved in hot ethylene dichloride (10 ml). To the cooled solution was added a solution of diazomethane in ether (100 ml) prepared from nitrosomethylurea (10 g). The solution was allowed to stand at room temperature until no further nitrogen was evolved, and then the solution was evaporated to an oil (3.0 g). The oil was applied to a silica gel column with methanol–benzene (1:10) to give the title compound.

Anal.—Calc. for $C_{16}H_{20}N_2O_9$: C, 50.00; H, 5.46. Found: C, 49.72; H, 5.31.

2′,3′,5′-Tri-(*O*-benzyl)-β-D-arabinofuranosylurea (I)—*Procedure A*—Urea (1.0 g, 0.017 mole), 2′,3′,5′-tri-(*O*-benzyl)-β-D-arabinofuranose (1.0 g, 0.0025 mole), acetone (30 ml), water (10 ml), and concentrated sulfuric acid (0.34 g, 0.9% w/w) were heated for 48 hr at 70° under reflux with stirring. The solution was cooled and neutralized with lead carbonate. The suspension was filtered, and the filtrate was evaporated. The residue was extracted with chloroform and water, and the chloroform extracts were evaporated to yield a syrup (1.2 g). Chromatography of the syrup on silica gel with benzene–ethyl acetate (7:3) yielded I as a syrup, which was crystallized from ether (0.13 g).

Procedure B—The steps were as described under *Procedure A*, except that no water was used in the reaction mixture. The yield of I was 0.28 g (oil).

Procedure C—The steps were as described under *Procedure A*, except that 0.9% (w/w) perchloric acid was used as a catalyst instead of sulfuric acid. The yield of I was 0.21 g (crystals from ether).

Procedure D—The steps were as described under *Procedure C*, except that no water was used in the reaction mixture. The yield of I was 0.15 g (oil). This procedure was used for the preparation of II–VII. The products from Procedures A–D showed identical NMR spectra.

***N*-β-D-Arabinofuranosyl-*N*′-methylurea (VIII)**—To a solution of II (1.94 g) in methanol (500 ml) was added 5% palladium-on-charcoal (100 mg). The reaction mixture was hydrogenated at 320 psi for 120 hr and then filtered through diatomaceous earth[3], and the filtrate was evaporated to an oil. The oil was crystallized from methanol to give VIII (0.24 g), mp 150°. Compound IX was prepared by the same procedure.

REFERENCES

(1) G. A. Fischer and M. Y. Chu, *Biochem. Pharmacol.*, **11**, 423 (1962).

(2) D. W. Visser, G. Baran, and R. Beltz, *J. Am. Chem. Soc.*, **75**, 2017 (1953).

(3) M. H. Benn and A. S. Jones, *J. Chem. Soc.*, **1960**, 3837.

(4) R. Barker and H. G. Fletcher, Jr., *J. Org. Chem.*, **26**, 4605 (1961).

(5) N. G. Shkantova, M. S. Dudkin, and S. I. Grinshpun, *Zh. Prik. Khim.*, **40**, 164 (1970).

ACKNOWLEDGMENTS AND ADDRESSES

Received June 30, 1976, from the *Department of Pharmaceutical Chemistry, College of Pharmacy, and the ‡Department of Biochemistry, Rutgers College, Rutgers—The State University, New Brunswick, NJ 08903.

Accepted for publication September 2, 1976.

[x] To whom inquiries should be directed.

[3] Celite.

New Compounds: Total Synthesis of *dl*-3a,4,6a-*cis*-4-(4-Carboxybutyl)-hexahydropyrrolo[3,4-*d*]imidazol-2-one Hydrochloride (*dl*-Azabiotin Hydrochloride)

HENRY C. WORMSER and HANLEY N. ABRAMSON [x]

Abstract □ The total synthesis of *dl*-3a,4,6a-*cis*-4-(4-carboxybutyl)-hexahydropyrrolo[3,4-*d*]imidazol-2-one hydrochloride (*dl*-azabiotin hydrochloride) was accomplished in a seven-step sequence from 2-ethoxycarbonylazepin-7-one.

Keyphrases □ Pyrroloimidazolone, substituted—synthesized in seven-step sequence □ Azabiotin—synthesized in seven-step sequence □ Biotin analog—substituted pyrroloimidazolone synthesized in seven-step sequence

Biotin (I), a coenzyme, functions in several significant carbon dioxide fixation reactions in the cell. It is involved in carboxylation reactions catalyzed by propionyl coenzyme A carboxylase, acetyl coenzyme A carboxylase, pyruvate carboxylase, and β-methylcrotonyl coenzyme A carboxylase among others. Numerous aspects of the biochemical role of biotin were reviewed recently (1, 2).

BACKGROUND

Several analogs of biotin were synthesized, but few of these compounds substituted for biotin as a coenzyme. While biotin methyl ester and desthiobiotin show growth-promoting activity equivalent to that of biotin in many microorganisms, oxybiotin, biocytin, and biotin sulfoxide exhibit only limited activity. Many analogs possess substantial antibiotin activity.

The fact that carbobiotin (3) and oxybiotin have growth-promoting activity qualitatively, although not quantitatively, equivalent to that of biotin indicates that the sulfur atom of biotin is not essential for activity. The actual role of this sulfur atom has been a matter for debate. Glasel (4), on the basis of NMR data, postulated that the sulfur may act as a hydrogen acceptor in interactions with the protein component of biotin enzymes. This interpretation was challenged by Caplow (5), who pointed out that Glasel's observation could also be accounted for by assuming protonation of the ureide moiety.

However, Olah and White (6), employing conditions that hardly simulated biological media, presented unequivocal evidence that the sulfur is indeed protonated in magic acid (FSO_3H-SbF_5-SO_2). They suggested that the sulfur protonation occurs on the side *trans* to the carboxyl-

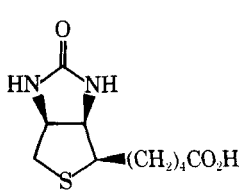

I

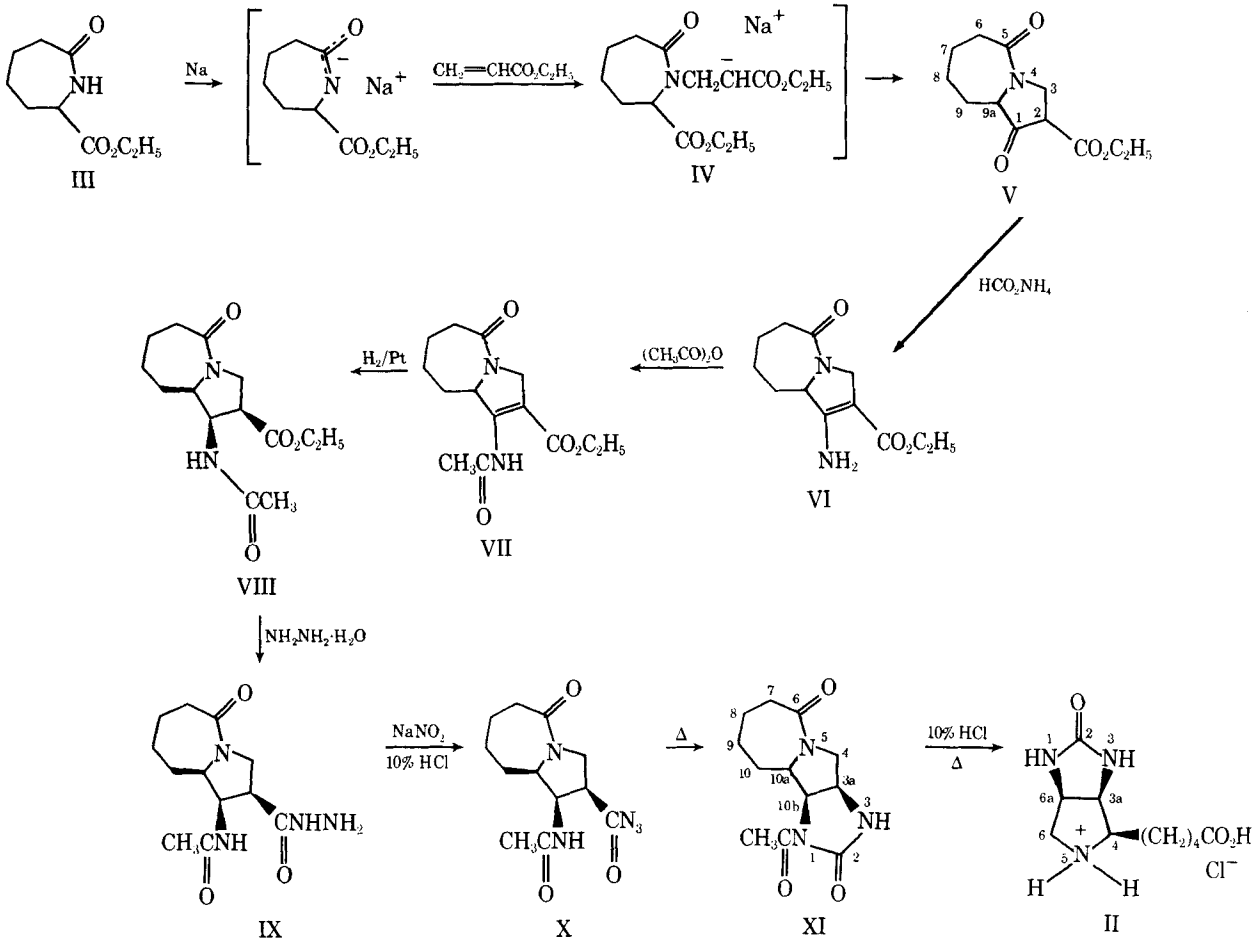

Scheme I

containing side chain, although it was subsequently demonstrated (7) that this protonation occurs *cis* to the side chain. Other studies (8) revealed that Mn^{2+} and Cu^{2+} are capable of weakly coordinating with sulfur orbitals of biotin on the side *trans* to the side chain, which might also serve to explain interaction with the protein of the holoenzyme.

Earlier reports (3, 9–12) were directed at the synthesis of biotin analogs containing either nitrogen or carbon in place of the sulfur atom. These efforts have now culminated in the development of a facile, totally synthetic route to the nitrogen analog of biotin, referred to as azabiotin (II).

DISCUSSION

The starting material in this synthesis (Scheme I) was 2-ethoxycarbonylazepin-7-one (III), prepared by the method of Shechter and Kirk (13). Treatment of III in dry benzene with sodium sand gave the sodio derivative, which was added to ethyl acrylate to give the intermediate IV. Compound IV underwent Dieckmann cyclization under the reaction conditions to yield the β-keto ester (V) as an impure oil. When this oil was refluxed with ammonium formate in 2-propanol, the crystalline enamine (VI) was isolated in 25% overall yield from III.

The enamine (VI) was acetylated by refluxing in acetic anhydride, and the crystalline enamine acetate (VII) was smoothly hydrogenated over platinum in ethanol to yield VIII. The acetamido ester (VIII) yielded the hydrazide (IX) when warmed with hydrazine hydrate in ethanol. Treatment of IX with nitrous acid gave the intermediate acyl azide (X), which underwent cyclization to the ureide (XI) when refluxed in ethyl acetate solution. The title compound (II) was prepared by acid-catalyzed hydrolysis of XI.

The stereochemistry of II was demonstrated by X-ray crystallography[1] to be all *cis* with respect to the substituents at C-4, C-3a, and C-6a. This arrangement is the same as that found in biotin (I). The stereochemical control apparent in this synthesis was not unexpected, since the reduction of VII was presumed to proceed by *cis*-addition of the two incoming hydrogen atoms from the less hindered face of the molecule.

EXPERIMENTAL[2]

1,5-Dioxo-2-ethoxycarbonyloctahydro-1*H*-pyrrolo[1,2-*a*]azepine (V)—A suspension of 1.35 g (58.5 mmoles) of sodium sand in 30 ml of dry benzene was heated to reflux with vigorous stirring under nitrogen and treated dropwise with a solution of 7.73 g (42.0 mmoles) of 2-ethoxycarbonylazepin-7-one (III) (13) in 40 ml of dry benzene. The reaction mixture was refluxed for 1 hr after the addition was completed, cooled to room temperature, and then treated dropwise with 10 ml of ethyl acrylate. The mixture was again refluxed for 1 hr, cooled, and poured with stirring onto a mixture of ice and 50 ml of 10% hydrochloric acid. The product was extracted with chloroform.

The organic layer was washed twice with water, dried over anhydrous sodium sulfate, and concentrated to a thick oil, 10.1 g. TLC of the oil (5% methanol in chloroform) revealed one major spot at R_f 0.4 and one minor spot at R_f 0.6; both spots gave a deep-purple color with ferric chloride; IR: ν_{max} (chloroform) 3700, 3020, 2960, 2880, 1775, 1735, 1680, and 1460 cm^{-1}; UV: λ_{max} 250 nm, shifting to 279 nm with increased absorbance upon addition of base[3]. This oil decomposed upon standing in air or upon attempted distillation under high vacuum but was suitable for the subsequent amination procedure.

1-Amino-2-ethoxycarbonyl -5- oxo-5,6,7,8,9,9a-hexahydro-3*H*-pyrrolo[1,2-*a*]azepine (VI)—A solution of 10.1 g of crude V was re-

[1] Details of this study will be published elsewhere (14).

[2] Melting points were taken on a Fisher-Johns melting-point stage and are corrected. UV absorption spectra were determined in 95% ethanol on a Beckman model DK2A recording spectrophotometer. IR spectra were recorded on Beckman models 8 and 33 recording spectrophotometers. NMR spectra were determined on a Varian EM 360 spectrometer. Microanalyses were performed by Spang Microanalytical Laboratory, Ann Arbor, Mich. TLC was performed with silica gel GF_{254}.

[3] The absorptivity was not calculated because the product was not homogeneous.

fluxed with 5.20 g (82.0 mmoles) of ammonium formate and 50 ml of 2-propanol for 6 hr. The reaction mixture was concentrated to dryness, and the residue was partitioned between chloroform and water. The chloroform layer was washed with water, dried over anhydrous sodium sulfate, and concentrated to a thick oil (9.02 g).

When the oil was scratched under isopropyl ether, VI precipitated out as fine needles, 2.50 g, mp 210–214°. Recrystallization from ethanol–water gave the analytical sample, mp 226–227°; IR: ν_{max} (chloroform) 3520, 3460, 3380, 3010, 2950, 2880, 1730, 1685, and 1639 cm^{-1}; UV: λ_{max} 276 nm (ϵ 20,400); NMR[4] ($CDCl_3$): δ 6.11 (s, 2H, NH_2), 4.60 (m, 1H, NCHC=C), 4.33 (s, 2H, NCH_2C=C), 4.19 (q, 2H, J = 7 Hz, OCH_2CH_3), 2.55 [m, 2H, CH_2C(=O)N], 1.60–2.33 [m, 6H, $(CH_2)_3$], and 1.28 (t, 3H, J = 7 Hz, OCH_2CH_3) ppm.

Anal.—Calc. for $C_{12}H_{18}N_2O_3$: C, 60.49; H, 7.61; N, 11.76. Found: C, 60.48; H, 7.67; N, 11.70.

1-Acetamido-2-ethoxycarbonyl -5- oxo-5,6,7,8,9,9a-hexahydro-3*H*-pyrrolo[1,2-*a*]azepine (VII)—A solution of 3.68 g (15.4 mmoles) of VI in 50 ml of acetic anhydride was refluxed for 2 hr. The solvent was removed *in vacuo*, and the residual oil was scratched under isopropyl ether. The resulting solid was removed by filtration and washed with isopropyl ether to give 3.01 g (70% yield) of light-brown powder, mp 112–113°. Recrystallization from isopropyl ether gave the analytical sample, mp 116–116.5°; IR: ν_{max} (chloroform) 3320, 3010, 2950, 2880, 1715, 1680, and 1640 cm^{-1}; UV: λ_{max} 274 nm (ϵ 20,500); NMR[4] ($CDCl_3$): δ 10.16 (s, 1H, NH), 5.48 (m, 1H, NCHC=C), 4.35 (s, 2H, NCH_2C=C), 4.28 (q, 2H, J = 7 Hz, OCH_2CH_3), 2.50–2.80 [m, 2H, CH_2C(=O)N], 2.25 [s, 3H, NC(=O)CH_3], 1.80–2.20 [m, 6H, $(CH_2)_3$], and 1.33 (t, 3H, J = 7 Hz, OCH_2CH_3) ppm.

Anal.—Calc. for $C_{14}H_{20}N_2O_4$: C, 59.99; H, 7.19; N, 9.99. Found: C, 60.03; H, 7.13; N, 10.02.

1-Acetamido-2-ethoxycarbonyl -5- oxooctahydro-1,2,9a-*cis*-1*H*-pyrrolo[1,2-*a*]azepine (VIII)—A solution of 1.73 g (6.30 mmoles) of VII in 50 ml of absolute alcohol was treated with 1.0 g of platinum oxide and hydrogenated at 45 psi for 21 hr. The catalyst was removed by filtration and washed thoroughly with absolute alcohol. The ethanolic solution was concentrated to dryness to give 1.72 g (97% yield) of crystals, mp 209–210°. Recrystallization from methanol gave the analytical sample, mp 209–210°; IR: ν_{max} (chloroform) 3440, 3300, 3000, 2940, 2870, 1730, 1676, and 1625 cm^{-1}; NMR[4] ($CDCl_3$): δ 7.40 (d, 1H, J = 10 Hz, NH), 4.19 (q, 2H, J = 7 Hz, OCH_2CH_3), 3.64–4.00 (m, 2H, C-1 and C-9a H's), 3.10–3.25 [m, 2H, CH_2NC(=O)], 2.70–3.00 (m, 1H, $CHCO_2C_2H_5$), 2.33–2.70 [m, 2H, CH_2C(=O)], 2.05 [s, 3H, CH_3C(=O)N], 1.48–1.90 [m, 6H, $(CH_2)_3$], and 1.26 (t, 3H, J = 7 Hz, OCH_2CH_3) ppm.

Anal.—Calc. for $C_{14}H_{22}N_2O_4$: C, 59.56; H, 7.85; N, 9.92. Found: C, 59.65; H, 7.53; N, 9.91.

1-Acetamido-2-hydrazinocarbonyl -5- oxooctahydro-1,2,9a-*cis*-1*H*-pyrrolo[1,2-*a*]azepine (IX)—A solution of 500 mg (1.91 mmoles) of VIII in 10 ml of absolute ethanol was treated with 2 ml of hydrazine hydrate and stirred at 40–50° for 7 hr. The reaction mixture was cooled in the refrigerator overnight and filtered to give 260 mg of colorless crystals, mp 278–279°. An additional 75 mg of this solid, mp 276–278°, was obtained when the mother liquor was concentrated to about half of the original volume, giving a total yield of 335 mg (65%) of pure IX. Recrystallization from aqueous methanol gave the analytical sample, mp 280–281°; IR: ν_{max} (mineral oil) 3280, 1670, and 1600 cm^{-1}; NMR[5] (D_2O): δ 3.38–3.83 (m, 2H, C-1 and C-9a H's), 3.02–3.35 [m, 2H, CH_2NC(=O)], 2.65–2.98 (m, 1H, $CHCO_2C_2H_5$), 2.10–2.48 [m, 2H, CH_2C(=O)N], 2.03 [s, 3H, NC(=O)CH_3], and 1.20–1.67 [m, 6H, $(CH_2)_3$] ppm.

Anal.—Calc. for $C_{12}H_{20}N_4O_3$: C, 53.72; H, 7.51; N, 20.88. Found: C, 53.62; H, 7.41; N, 20.80.

1-Acetyl-2,6-dioxododecahydro- 10a,10b,3a- *cis*-imidazo[4,5-*c*]pyrrolo[1,2-*a*]azepine (XI)—A solution of 143 mg (0.53 mmole) of IX in 5 ml of 10% hydrochloric acid was cooled to 0° and treated dropwise with a solution of 130 mg of sodium nitrite in 3 ml of water. The solution was stirred at 0° for 30 min and then extracted with six 50-ml portions of ethyl acetate. The organic extract was dried over anhydrous magnesium sulfate and concentrated *in vacuo* to give 120 mg of the crude azide (X) as a yellow oil; IR: ν_{max} (neat) 3300, 2920, 2850, 2160, 1710, 1660, and 1610 cm^{-1}.

The azide was redissolved in 25 ml of ethyl acetate and refluxed for 2 hr. Then the reaction mixture was concentrated to dryness to give an oil, which solidified when scratched under ether. The solid was removed by filtration and washed with ether to give 103 mg (77% yield from IX), mp 233–235°. Recrystallization from ethyl acetate–acetone gave the analytical sample, mp 237–238°; IR: ν_{max} (mineral oil) 3280, 1750, 1740, and 1640 cm^{-1}; NMR[5] (CD_3SOCD_3): δ 8.00 (s, 1H, NH), 4.98 (t, 1H, C-10b H, $J_{10a-10b}$ = 8 Hz, J_{10b-3a} = 8 Hz), 4.01–4.37 (m, 2H, C-3a and C-10a H's), 3.10–3.35 (m, 2H, C-4 H), 2.43–2.60 [m, 2H, CH_2C(=O)N], 2.40 [s, 3H, NC(=O)CH_3], and 1.20–2.08 [m, 6H, $(CH_2)_3$] ppm.

Anal.—Calc. for $C_{12}H_{17}N_3O_3$: C, 57.36; H, 6.82; N, 16.72. Found: C, 57.36; H, 6.78; N, 16.68.

***dl*-3a,4,6a-*cis*-4-(4-Carboxybutyl)octahydropyrrolo[3,4-*d*]imidazol-2-one Hydrochloride (II)**—A solution of 100 mg (0.40 mmole) of XI in 0.4 ml of 10% hydrochloric acid was heated in a sealed tube at 120° for 16 hr. The reaction mixture was cooled and concentrated to dryness *in vacuo*. The residue was scratched with ether to give a light-brown solid, which was filtered off and washed with ether. The crude product weighed 65 mg (62% yield) and was homogeneous on TLC [1-propanol–water (7:3) or 1-propanol–water–concentrated ammonium hydroxide (8:1:1)].

The analytical sample was prepared by recrystallization from ethanol; this solid melted at 132°, slowly resolidified at 140–150°, and melted again at 163–164°; IR: ν_{max} (mineral oil) 3450, 3300, 3230, 1690, and 1600 cm^{-1}; NMR[5] (D_2O): δ 4.50–4.72 (m, 2H, C-3a and C-6a H's), 3.50–3.68 (m, 1H, C-4 H), 3.28–3.46 (m, 2H, C-6 H), 2.42 (t, 2H, J = 6 Hz, CH_2CO_2H), and 1.32–1.80 [m, 6H, $(CH_2)_3$] ppm.

Anal.—Calc. for $C_{10}H_{18}ClN_3O_3$: C, 45.53; H, 6.87; N, 15.93. Found: C, 45.53; H, 7.01; N, 15.77.

[4] Tetramethylsilane as the internal standard.

[5] Sodium 2,2-dimethyl-2-silapentanesulfonate as the internal standard.

REFERENCES

(1) J. Knappe, *Ann. Rev. Biochem.*, **39,** 757 (1970).

(2) J. Moss and M. D. Lane, *Adv. Enzymol.*, **35,** 321 (1971).

(3) H. C. Wormser, S. Israsena, M. S. Meiling, C. Williams, and D. Perlman, *J. Pharm. Sci.*, **61,** 1168 (1972).

(4) J. A. Glasel, *Biochemistry*, **5,** 1851 (1966).

(5) M. Caplow, *ibid.*, **8,** 2656 (1969).

(6) G. A. Olah and A. M. White, *J. Am. Chem. Soc.*, **90,** 6087 (1968).

(7) R. Griessler and D. B. McCormick, *Arch. Biochem. Biophys.*, **160,** 667 (1974).

(8) H. Sigel, D. B. McCormick, R. Griessler, B. Prijs, and L. D. Wright, *Biochemistry*, **8,** 2687 (1969).

(9) H. C. Wormser, *J. Pharm. Sci.*, **58,** 1038 (1969).

(10) *Ibid.*, **59,** 1732 (1970).

(11) H. C. Wormser and H. N. Abramson, *J. Pharm. Sci.*, **64,** 1882 (1975).

(12) *Ibid.*, **64,** 1514 (1975).

(13) H. Shechter and J. C. Kirk, *J. Am. Chem. Soc.*, **73,** 3087 (1951).

(14) M. D. Glick, H. C. Wormser, and H. N. Abramson, *Acta Crystallogr.*, **B33,** 1095 (1977).

ACKNOWLEDGMENTS AND ADDRESSES

Received May 24, 1976, from the *College of Pharmacy and Allied Health Professions, Wayne State University, Detroit, MI 48202.*

Accepted for publication September 17, 1976.

[x] To whom inquiries should be directed.

Quantitative IR Spectrophotometric Calculations

Keyphrases □ IR spectrophotometry—analysis, carbachol, absorbance calculation, error reported □ Absorbance calculations—IR spectrophotometric analysis of carbachol, error reported □ Carbachol—IR spectrophotometric analysis, absorbance calculation, error reported □ Cholinergics, ophthalmic—carbachol, IR spectrophotometric analysis, absorbance calculation, error reported

To the Editor:

In a recent paper (1), the authors made a common technical error in the calculation of absorbance from the observed values of percent transmittance as read off the recorder chart paper. According to the instructions by Frank and Chafetz (1), the length of the line read off the chart is a linear displacement of the absorption maximum along the chart ordinate from 100% transmission, in other words, a $1 - T$ absorption value.

It is fundamental that the concentration of an active absorbing species is not proportional to $1 - T$ but to log $1/T$. This is an error of a type, but a related error also was made by taking the log of $1/1 - T$ and equating this term to log $1/T$.

This point has been treated in the reference text literature (2). The correct procedure is to measure the log I_0/I values from the experimental values, using the experimental technique otherwise correctly described. This approach is well illustrated in the ASTM Recommended Practices (3).

As pointed out by Potts (2), log $1/T$ (correctly determined) is essentially directly proportional to $1 - T$ at high transmission values, and it is reasonable to assume from the excellent results reported by Frank and Chafetz (1) that this also holds for log $1/1 - T$ values. Since reflection and scatter effects are small and reproducible in transmission measurements of solutions and the baseline falls at high transmission values relative to the initial 100% T set-point, the practical effects in this work were small, with little detectable bias error in the final result.

However, since this paper is one of the few in dosage form analysis utilizing IR quantitation, clearly demonstrating the value of the specificity imparted by this technique, it is important to point out this academic procedural point.

(1) J. Frank and L. Chafetz, *J. Pharm. Sci.*, **66**, 439 (1977).

(2) W. J. Potts, Jr., "Chemical Infrared Spectroscopy," vol. I, Wiley, New York, N.Y., 1963, chap. 6.

(3) "Manual on Recommended Practices in Spectrophotometry, ASTM Committee E-13, Recommended Practices for General Techniques of Infrared Quantitative Analysis," 3rd ed., American Society for Testing and Materials, Philadelphia Pa., 1969.

Mario J. Cardone
Pharmaceutical Research Division
Norwich Pharmacal Company
Norwich, NY 13815

Received May 9, 1977.
Accepted for publication June 1, 1977.

Tissue Binding of Drugs

Keyphrases □ Phenytoin—tissue binding, normal, nephrotic, and uremic humans compared □ Warfarin—tissue binding, rats with intrinsic high and low plasma binding ability compared □ Tissue binding—phenytoin compared in normal, nephrotic, and uremic humans, warfarin in rats with intrinsic high and low plasma binding ability □ Binding, tissue—phenytoin compared in normal, nephrotic, and uremic humans, warfarin in rats with intrinsic high and low plasma binding ability □ Anticonvulsants—phenytoin, tissue binding, normal, nephrotic, and uremic humans compared □ Anticoagulants—warfarin, tissue binding, rats with intrinsic high and low plasma binding ability compared

To the Editor:

Intersubject variability in plasma protein binding of drugs because of genetic or disease-related factors is widely recognized (1–5). The degree of variability in tissue binding of drugs, however, is essentially unknown. An important exception is the work of Jusko and Weintraub (6), who found a positive correlation between postmortem myocardial-to-serum concentration ratios and antemortem creatinine clearances in 15 patients. Based on these observations, they suggested that reduced tissue binding may explain the relatively small apparent volume of distribution of digoxin found in patients with impaired renal function (7).

A more general approach to gaining insight to variability in tissue binding was recently suggested (8, 9) based on the physiological approach to distribution developed by Gillette (10). It can be shown that:

$$V_{ss} = V_B + V_T \frac{f_B}{f_T} \qquad \text{(Eq. 1)}$$

where V_{ss} is the apparent volume of distribution at steady state, V_B is blood volume, V_T is the volume of other tissues in the body, and f_B and f_T are the fractions of unbound drug in blood and tissue, respectively. For most lipid-soluble drugs, the sum of V_B and V_T is equivalent to total body water; for drugs that do not penetrate cells, the sum of V_B and V_T is equivalent to the extracellular space. The term f_T may be viewed as the average fraction of unbound drug in the extravascular space weighted for tissue mass.

We used a modification of this equation to determine differences in the tissue binding of phenytoin between normal healthy volunteers and nephrotic (3) or uremic (4) patients and in the tissue binding of warfarin in rats who were intrinsically high or low plasma binders of the drug (5). This approach represents a new application of this equation. Assuming that V_β (11) is about equivalent to V_{ss} and incorporating the red blood cell volume into the "tissue" space give:

$$f_T = \frac{V_T(f_p)}{V_\beta - V_p} \qquad \text{(Eq. 2)}$$

where f_p is the fraction of drug unbound in plasma, V_p is plasma water, and V_T is the volume of total body water minus plasma volume. The term f_T incorporates binding to red blood cells. Apparent volumes of distribution and

Quantitative IR Spectrophotometric Calculations

Keyphrases □ IR spectrophotometry—analysis, carbachol, absorbance calculation, error reported □ Absorbance calculations—IR spectrophotometric analysis of carbachol, error reported □ Carbachol—IR spectrophotometric analysis, absorbance calculation, error reported □ Cholinergics, ophthalmic—carbachol, IR spectrophotometric analysis, absorbance calculation, error reported

To the Editor:

In a recent paper (1), the authors made a common technical error in the calculation of absorbance from the observed values of percent transmittance as read off the recorder chart paper. According to the instructions by Frank and Chafetz (1), the length of the line read off the chart is a linear displacement of the absorption maximum along the chart ordinate from 100% transmission, in other words, a $1 - T$ absorption value.

It is fundamental that the concentration of an active absorbing species is not proportional to $1 - T$ but to log $1/T$. This is an error of a type, but a related error also was made by taking the log of $1/1 - T$ and equating this term to log $1/T$.

This point has been treated in the reference text literature (2). The correct procedure is to measure the log I_0/I values from the experimental values, using the experimental technique otherwise correctly described. This approach is well illustrated in the ASTM Recommended Practices (3).

As pointed out by Potts (2), log $1/T$ (correctly determined) is essentially directly proportional to $1 - T$ at high transmission values, and it is reasonable to assume from the excellent results reported by Frank and Chafetz (1) that this also holds for log $1/1 - T$ values. Since reflection and scatter effects are small and reproducible in transmission measurements of solutions and the baseline falls at high transmission values relative to the initial 100% T set-point, the practical effects in this work were small, with little detectable bias error in the final result.

However, since this paper is one of the few in dosage form analysis utilizing IR quantitation, clearly demonstrating the value of the specificity imparted by this technique, it is important to point out this academic procedural point.

(1) J. Frank and L. Chafetz, *J. Pharm. Sci.*, **66**, 439 (1977).

(2) W. J. Potts, Jr., "Chemical Infrared Spectroscopy," vol. I, Wiley, New York, N.Y., 1963, chap. 6.

(3) "Manual on Recommended Practices in Spectrophotometry, ASTM Committee E-13, Recommended Practices for General Techniques of Infrared Quantitative Analysis," 3rd ed., American Society for Testing and Materials, Philadelphia Pa., 1969.

Mario J. Cardone
Pharmaceutical Research Division
Norwich Pharmacal Company
Norwich, NY 13815

Received May 9, 1977.
Accepted for publication June 1, 1977.

Tissue Binding of Drugs

Keyphrases □ Phenytoin—tissue binding, normal, nephrotic, and uremic humans compared □ Warfarin—tissue binding, rats with intrinsic high and low plasma binding ability compared □ Tissue binding—phenytoin compared in normal, nephrotic, and uremic humans, warfarin in rats with intrinsic high and low plasma binding ability □ Binding, tissue—phenytoin compared in normal, nephrotic, and uremic humans, warfarin in rats with intrinsic high and low plasma binding ability □ Anticonvulsants—phenytoin, tissue binding, normal, nephrotic, and uremic humans compared □ Anticoagulants—warfarin, tissue binding, rats with intrinsic high and low plasma binding ability compared

To the Editor:

Intersubject variability in plasma protein binding of drugs because of genetic or disease-related factors is widely recognized (1–5). The degree of variability in tissue binding of drugs, however, is essentially unknown. An important exception is the work of Jusko and Weintraub (6), who found a positive correlation between postmortem myocardial-to-serum concentration ratios and antemortem creatinine clearances in 15 patients. Based on these observations, they suggested that reduced tissue binding may explain the relatively small apparent volume of distribution of digoxin found in patients with impaired renal function (7).

A more general approach to gaining insight to variability in tissue binding was recently suggested (8, 9) based on the physiological approach to distribution developed by Gillette (10). It can be shown that:

$$V_{ss} = V_B + V_T \frac{f_B}{f_T} \qquad \text{(Eq. 1)}$$

where V_{ss} is the apparent volume of distribution at steady state, V_B is blood volume, V_T is the volume of other tissues in the body, and f_B and f_T are the fractions of unbound drug in blood and tissue, respectively. For most lipid-soluble drugs, the sum of V_B and V_T is equivalent to total body water; for drugs that do not penetrate cells, the sum of V_B and V_T is equivalent to the extracellular space. The term f_T may be viewed as the average fraction of unbound drug in the extravascular space weighted for tissue mass.

We used a modification of this equation to determine differences in the tissue binding of phenytoin between normal healthy volunteers and nephrotic (3) or uremic (4) patients and in the tissue binding of warfarin in rats who were intrinsically high or low plasma binders of the drug (5). This approach represents a new application of this equation. Assuming that V_β (11) is about equivalent to V_{ss} and incorporating the red blood cell volume into the "tissue" space give:

$$f_T = \frac{V_T(f_p)}{V_\beta - V_p} \qquad \text{(Eq. 2)}$$

where f_p is the fraction of drug unbound in plasma, V_p is plasma water, and V_T is the volume of total body water minus plasma volume. The term f_T incorporates binding to red blood cells. Apparent volumes of distribution and

Table I—Apparent Volumes of Distribution and Binding Parameters for Phenytoin in Healthy Volunteers, Nephrotic Patients, and Uremic Patients

Clinical Condition	V_β, liters/kg	f_p	f_T
Healthy volunteers (n = 6)[a]	0.3	0.10	0.22
Nephrotic patients (n = 6)[a]	0.6	0.19	0.19
Healthy volunteers (n = 4)[b]	0.64	0.12	0.11
Uremic patients (n = 4)[b]	1.40	0.26	0.11

[a] Apparent volumes of distribution and plasma binding data reported in Ref. 3. [b] Apparent volumes of distribution and plasma binding data reported in Ref. 4.

Table II—Apparent Volumes of Distribution and Binding Parameters for Warfarin in Rats

	V_β, liters/kg[a]	f_p[a]	f_T
High plasma binders (n = 6)	0.14	0.004	0.025
Low plasma binders (n = 7)	0.19	0.014	0.058

[a] Values were reported in Ref. 5.

plasma binding data were obtained from the literature (3–5). Total body water was assumed to be 599 ml/kg in humans and 660 ml/kg in rats. Plasma volume was assumed to be 46 ml/kg in humans and 42 ml/kg in rats.

The findings with phenytoin are summarized in Table I. Both types of renal disease resulted in a twofold increase in both the fraction of free drug in the plasma and the apparent volume of distribution compared to those observed in healthy volunteers. Consequently, in neither case was the apparent tissue binding affected. The reduced plasma binding observed in nephrotic patients was essentially secondary to hypoalbuminemia (3), whereas that observed in uremic patients was presumably due to changes in the molecular structure of albumin or to the accumulation of an avidly bound endogenous inhibitor that acts like a displacing agent (12).

In view of the unaltered tissue binding of phenytoin in nephrotic patients, either hypoalbuminemia in the extravascular space is less pronounced than that observed in the vascular space or molecules other than albumin are principally responsible for binding phenytoin in the tissues. In uremic patients, phenytoin binding sites in the tissue are less susceptible to disease-related changes than phenytoin binding sites in the plasma.

As shown in Table II, differences in plasma protein binding of warfarin in rats were paralleled by qualitatively similar differences in tissue binding. Rats that showed relatively high plasma binding of warfarin also showed relatively high tissue binding of the drug. Consistent with this finding is the observation that the fraction of warfarin unbound to liver homogenates correlated strongly with the fraction of warfarin unbound to serum in the same animals (5). Perhaps a similar factor is responsible for the intersubject variability of warfarin binding in both plasma and tissue of rats.

The examples presented illustrate the utility, at least in a conceptual sense, of considering drug distribution in a physiological framework (10). Estimations of apparent tissue binding can provide guidelines for more extensive distribution studies.

(1) B. Alexanderson, *Eur. J. Clin. Pharmacol.*, **6**, 44 (1973).

(2) M. M. Ghoneim and H. Pandya, *Anesthesiology*, **42**, 545 (1975).

(3) R. Gugler, D. W. Shoeman, D. H. Huffman, J. B. Cohlmia, and D. L. Azarnoff, *J. Clin. Invest.*, **55**, 1182 (1975).

(4) I. Odar-Cederlöf and O. Borga, *Eur. J. Clin. Pharmacol.*, **7**, 31 (1974).

(5) A. Yacobi and G. Levy, *J. Pharm. Sci.*, **64**, 1660 (1975).

(6) W. J. Jusko and M. Weintraub, *Clin. Pharmacol. Ther.*, **16**, 449 (1974).

(7) R. H. Reuning, R. A. Sams, and R. E. Notari, *J. Clin. Pharmacol.*, **13**, 127 (1973).

(8) G. R. Wilkinson and D. G. Shand, *Clin. Pharmacol. Ther.*, **18**, 377 (1975).

(9) G. R. Wilkinson and S. Schenker, *Biochem. Pharmacol.*, **25**, 2675 (1976).

(10) J. R. Gillette, *Ann. N.Y. Acad. Sci.*, **179**, 43 (1971).

(11) M. Gibaldi, R. Nagashima, and G. Levy, *J. Pharm. Sci.*, **58**, 193 (1969).

(12) D. S. Campion, *Toxicol. Appl. Pharmacol.*, **25**, 391 (1973).

Milo Gibaldi [x]
Patrick J. McNamara

Department of Pharmaceutics
School of Pharmacy
State University of New York at Buffalo
Buffalo, NY 14260

Received March 28, 1977.

Accepted for publication May 5, 1977.

Supported in part by Grant GM-20852 from the National Institutes of Health.

[x] To whom inquiries should be directed.

Characterization of Biotin Trimethylsilyl Derivative

Keyphrases □ Biotin trimethylsilyl derivative—structure determined □ Trimethylsilyl derivative of biotin—structure determined □ GLC–mass spectrometry—analysis, trimethylsilyl derivatives of biotin, structure determined □ Vitamins—biotin, structure of trimethylsilyl derivative determined

To the Editor:

Analytical methods are available for the determination of biotin (1, 2). In view of the need for a stability-indicating assay procedure, the GLC method (2) was investigated. The purpose of this communication is to report that the silyl derivative actually prepared according to this procedure is not the silyl ester reported (I) but the trisilyl de-

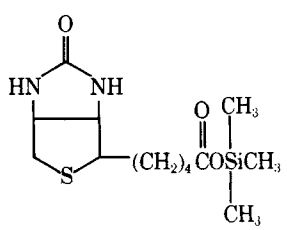

I

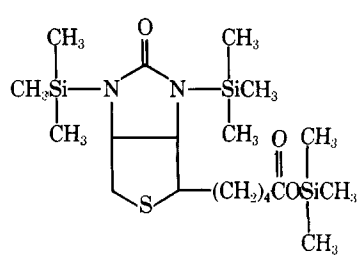

II

Table I—Apparent Volumes of Distribution and Binding Parameters for Phenytoin in Healthy Volunteers, Nephrotic Patients, and Uremic Patients

Clinical Condition	V_β, liters/kg	f_p	f_T
Healthy volunteers (n = 6)[a]	0.3	0.10	0.22
Nephrotic patients (n = 6)[a]	0.6	0.19	0.19
Healthy volunteers (n = 4)[b]	0.64	0.12	0.11
Uremic patients (n = 4)[b]	1.40	0.26	0.11

[a] Apparent volumes of distribution and plasma binding data reported in Ref. 3. [b] Apparent volumes of distribution and plasma binding data reported in Ref. 4.

Table II—Apparent Volumes of Distribution and Binding Parameters for Warfarin in Rats

	V_β, liters/kg[a]	f_p[a]	f_T
High plasma binders (n = 6)	0.14	0.004	0.025
Low plasma binders (n = 7)	0.19	0.014	0.058

[a] Values were reported in Ref. 5.

plasma binding data were obtained from the literature (3–5). Total body water was assumed to be 599 ml/kg in humans and 660 ml/kg in rats. Plasma volume was assumed to be 46 ml/kg in humans and 42 ml/kg in rats.

The findings with phenytoin are summarized in Table I. Both types of renal disease resulted in a twofold increase in both the fraction of free drug in the plasma and the apparent volume of distribution compared to those observed in healthy volunteers. Consequently, in neither case was the apparent tissue binding affected. The reduced plasma binding observed in nephrotic patients was essentially secondary to hypoalbuminemia (3), whereas that observed in uremic patients was presumably due to changes in the molecular structure of albumin or to the accumulation of an avidly bound endogenous inhibitor that acts like a displacing agent (12).

In view of the unaltered tissue binding of phenytoin in nephrotic patients, either hypoalbuminemia in the extravascular space is less pronounced than that observed in the vascular space or molecules other than albumin are principally responsible for binding phenytoin in the tissues. In uremic patients, phenytoin binding sites in the tissue are less susceptible to disease-related changes than phenytoin binding sites in the plasma.

As shown in Table II, differences in plasma protein binding of warfarin in rats were paralleled by qualitatively similar differences in tissue binding. Rats that showed relatively high plasma binding of warfarin also showed relatively high tissue binding of the drug. Consistent with this finding is the observation that the fraction of warfarin unbound to liver homogenates correlated strongly with the fraction of warfarin unbound to serum in the same animals (5). Perhaps a similar factor is responsible for the intersubject variability of warfarin binding in both plasma and tissue of rats.

The examples presented illustrate the utility, at least in a conceptual sense, of considering drug distribution in a physiological framework (10). Estimations of apparent tissue binding can provide guidelines for more extensive distribution studies.

(1) B. Alexanderson, *Eur. J. Clin. Pharmacol.*, **6**, 44 (1973).

(2) M. M. Ghoneim and H. Pandya, *Anesthesiology*, **42**, 545 (1975).

(3) R. Gugler, D. W. Shoeman, D. H. Huffman, J. B. Cohlmia, and D. L. Azarnoff, *J. Clin. Invest.*, **55**, 1182 (1975).

(4) I. Odar-Cederlöf and O. Borga, *Eur. J. Clin. Pharmacol.*, **7**, 31 (1974).

(5) A. Yacobi and G. Levy, *J. Pharm. Sci.*, **64**, 1660 (1975).

(6) W. J. Jusko and M. Weintraub, *Clin. Pharmacol. Ther.*, **16**, 449 (1974).

(7) R. H. Reuning, R. A. Sams, and R. E. Notari, *J. Clin. Pharmacol.*, **13**, 127 (1973).

(8) G. R. Wilkinson and D. G. Shand, *Clin. Pharmacol. Ther.*, **18**, 377 (1975).

(9) G. R. Wilkinson and S. Schenker, *Biochem. Pharmacol.*, **25**, 2675 (1976).

(10) J. R. Gillette, *Ann. N.Y. Acad. Sci.*, **179**, 43 (1971).

(11) M. Gibaldi, R. Nagashima, and G. Levy, *J. Pharm. Sci.*, **58**, 193 (1969).

(12) D. S. Campion, *Toxicol. Appl. Pharmacol.*, **25**, 391 (1973).

Milo Gibaldi [x]
Patrick J. McNamara

Department of Pharmaceutics
School of Pharmacy
State University of New York at Buffalo
Buffalo, NY 14260

Received March 28, 1977.

Accepted for publication May 5, 1977.

Supported in part by Grant GM-20852 from the National Institutes of Health.

[x] To whom inquiries should be directed.

Characterization of Biotin Trimethylsilyl Derivative

Keyphrases □ Biotin trimethylsilyl derivative—structure determined □ Trimethylsilyl derivative of biotin—structure determined □ GLC–mass spectrometry—analysis, trimethylsilyl derivatives of biotin, structure determined □ Vitamins—biotin, structure of trimethylsilyl derivative determined

To the Editor:

Analytical methods are available for the determination of biotin (1, 2). In view of the need for a stability-indicating assay procedure, the GLC method (2) was investigated. The purpose of this communication is to report that the silyl derivative actually prepared according to this procedure is not the silyl ester reported (I) but the trisilyl de-

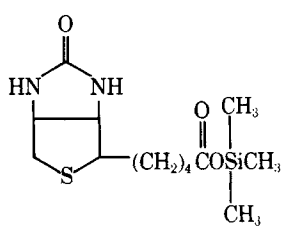

I

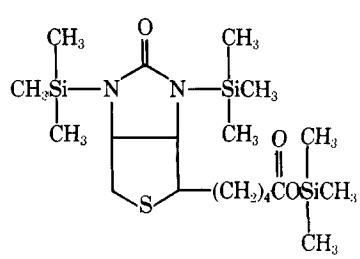

II

rivative (II) with the proposed structure indicated. It seems appropriate to correct the record now since I was again proposed as the structure for silylated biotin in a recent review (3).

The possibility that the proposed structure for the silyl ester (I) might be incomplete appeared when we prepared the methyl ester of biotin using diazomethane. Although this methyl ester could be chromatographed, the compound had a much longer retention time compared with the silylated compound and produced a peak that tailed badly. This large difference in chromatographic behavior is not expected for two compounds that are supposed to be simple esters. It also was observed that when the silylating agent [bis(trimethylsilyl)trifluoroacetamide] (III) was added to the previously formed methyl ester, the late eluting broad peak disappeared and a sharp, early eluting peak was obtained. These observations led to a more definitive study of the derivatives formed.

The fully silylated derivatives can be formed by reacting 5 mg of biotin with 1 ml of a 1:1 (v/v) solution of III and pyridine. After heating at 60° for 15 min, the sample is ready for analysis. The partially silylated derivative can be formed by first reacting 5 mg of biotin in ether with excess diazomethane until the yellow color persists. After 10 min, the methyl ester solution is evaporated to dryness and then silylated as described.

These samples were then analyzed[1] on a gas chromatograph–mass spectrometer[2] using a 1.9-m 3% OV-17 on 100–120-mesh Gas Chrom Q[3] column. The mass spectrum of the fully silylated derivative produced molecular ion 460 together with a base peak at *m/e* 73, supporting Structure II. The mass spectrum of the methylated biotin trimethylsilyl derivative gave *m/e* 402, again with a base peak at *m/e* 73, supporting the biotin methyl ester *N,N*-trimethylsilyl structure.

(1) C. Plinton, F. P. Mahn, M. Hawrylyshyn, V. S. Venturella, and B. Z. Senkowski, *J. Pharm. Sci.*, **58**, 875 (1969).
(2) V. Viswanathan, F. P. Mahn, V. S. Venturella, and B. Z. Senkowski, *ibid.*, **59**, 400 (1970).
(3) S. Ahuja, *ibid.*, **65**, 163 (1976).

Raymond N. Johnson [x]
George R. Boyden
Analytical Research and Development Laboratory
Ayerst Laboratories, Inc.
Rouses Point, NY 12979

Received February 24, 1977.
Accepted for publication May 24, 1977.
[x] To whom inquiries should be directed.

[1] Courtesy of Dr. G. Schilling, Analytical Research, Ayerst Laboratories, Montreal, Quebec, Canada.
[2] LKB 9000.
[3] Applied Science Laboratories, State College, Pa.

BOOKS

REVIEWS

Annual Reports in Medicinal Chemistry. Vol. 11. Edited by FRANK H. CLARKE *et al.* Academic, 111 5th Ave., New York, NY 10003, 1976. 339 pp. 17 × 25.5 cm. Price $16.50.

The new editor-in-chief of this series, Dr. Frank Clarke, is to be congratulated on maintaining the quality of content, presentation, and timeliness found in earlier volumes. The 32 chapters of this volume are grouped into six principal sections. Six section editors (three of them new) have the responsibility for the contributions in their areas.

Most chapters survey the literature of 1975 on new compounds reported to have pharmacologic activity. A few chapters cover the years since a report last appeared in this series. Some of the most interesting chapters present a mini-review of some biological process or disease state and point the way to potential new approaches for drug therapy. A third type of chapter deals with general methods of possible utility in the synthesis, design, or testing of drugs.

The section on CNS Agents has three chapters that update previous coverage of antidepressants, antipsychotic agents, antianxiety agents, anticonvulsants, sedative–hypnotics, analgesics (including endogenous peptides), and narcotic antagonists. In addition, there are two excellent chapters on the currently "hot" areas of opiate receptors and biological factors in psychiatric disorders. The Pharmacodynamic Agents section covers pulmonary and antiallergy drugs, antihypertensives, diuretics, and the structure–activity relationships of prostaglandins. The Chemotherapeutic Agents section has chapters on antibiotics and antifungal, antiviral, antiparasitic, and antineoplastic agents.

The section on Metabolic Diseases and Endocrine Function has chapters devoted to immunosuppressive and immunostimulatory agents, steroids, peptide hormones, diabetes, disorders of lipid metabolism, drug metabolism, and antiobesity agents. The Topics in Biology section features particularly pertinent chapters on membrane regulators, active transport across membranes, the antimetabolite concept, comparative toxicology, and chronopharmacology. The last section on Topics in Chemistry has the usual chapter on synthetic reactions of interest plus chapters concerning the synthesis of β-lactam antibiotics, synthesis of cyclic adenosine monophosphate and cyclic guanidine monophosphate derivatives, syntheses employing polymeric reagents, quantitative drug design, and use of NMR for drug binding studies.

As expected with any work by 46 different authors, the writing style is far from uniform. However, the readability of this volume is generally quite good. Every medicinal chemist and most pharmacologists would surely find several chapters of interest.

Reviewed by James F. Stubbins
Virginia Commonwealth University
Richmond, VA 23298

Chinese Herbs: Their Botany, Chemistry, and Pharmacodynamics. By JOHN D. KEYS. Tuttle, Rutland, VT 05701, 1976. 338 pp. 15 × 22 cm. Price $15.00.

This book is a compendium of monographs of Chinese medicinal plants arranged by botanical classification. Each monograph includes an illustration and Chinese characters as well as a botanical, chemical, and pharmacological description. There are also supplementary sections on mineral- and animal-derived drugs, a collection of Chinese prescriptions, and a table of toxic herbs.

This book is a good compilation of the medicinal plants of China, done mainly through translation of Chinese works, some as old as the 6th century. The botanical description seems quite complete, while the chemical and pharmacodynamic sections appear too outdated and su-

rivative (II) with the proposed structure indicated. It seems appropriate to correct the record now since I was again proposed as the structure for silylated biotin in a recent review (3).

The possibility that the proposed structure for the silyl ester (I) might be incomplete appeared when we prepared the methyl ester of biotin using diazomethane. Although this methyl ester could be chromatographed, the compound had a much longer retention time compared with the silylated compound and produced a peak that tailed badly. This large difference in chromatographic behavior is not expected for two compounds that are supposed to be simple esters. It also was observed that when the silylating agent [bis(trimethylsilyl)trifluoroacetamide] (III) was added to the previously formed methyl ester, the late eluting broad peak disappeared and a sharp, early eluting peak was obtained. These observations led to a more definitive study of the derivatives formed.

The fully silylated derivatives can be formed by reacting 5 mg of biotin with 1 ml of a 1:1 (v/v) solution of III and pyridine. After heating at 60° for 15 min, the sample is ready for analysis. The partially silylated derivative can be formed by first reacting 5 mg of biotin in ether with excess diazomethane until the yellow color persists. After 10 min, the methyl ester solution is evaporated to dryness and then silylated as described.

These samples were then analyzed[1] on a gas chromatograph–mass spectrometer[2] using a 1.9-m 3% OV-17 on 100–120-mesh Gas Chrom Q[3] column. The mass spectrum of the fully silylated derivative produced molecular ion 460 together with a base peak at *m/e* 73, supporting Structure II. The mass spectrum of the methylated biotin trimethylsilyl derivative gave *m/e* 402, again with a base peak at *m/e* 73, supporting the biotin methyl ester *N,N*-trimethylsilyl structure.

(1) C. Plinton, F. P. Mahn, M. Hawrylyshyn, V. S. Venturella, and B. Z. Senkowski, *J. Pharm. Sci.*, **58**, 875 (1969).
(2) V. Viswanathan, F. P. Mahn, V. S. Venturella, and B. Z. Senkowski, *ibid.*, **59**, 400 (1970).
(3) S. Ahuja, *ibid.*, **65**, 163 (1976).

Raymond N. Johnson [x]
George R. Boyden
Analytical Research and Development Laboratory
Ayerst Laboratories, Inc.
Rouses Point, NY 12979

Received February 24, 1977.
Accepted for publication May 24, 1977.
[x] To whom inquiries should be directed.

[1] Courtesy of Dr. G. Schilling, Analytical Research, Ayerst Laboratories, Montreal, Quebec, Canada.
[2] LKB 9000.
[3] Applied Science Laboratories, State College, Pa.

BOOKS

REVIEWS

Annual Reports in Medicinal Chemistry. Vol. 11. Edited by FRANK H. CLARKE *et al.* Academic, 111 5th Ave., New York, NY 10003, 1976. 339 pp. 17 × 25.5 cm. Price $16.50.

The new editor-in-chief of this series, Dr. Frank Clarke, is to be congratulated on maintaining the quality of content, presentation, and timeliness found in earlier volumes. The 32 chapters of this volume are grouped into six principal sections. Six section editors (three of them new) have the responsibility for the contributions in their areas.

Most chapters survey the literature of 1975 on new compounds reported to have pharmacologic activity. A few chapters cover the years since a report last appeared in this series. Some of the most interesting chapters present a mini-review of some biological process or disease state and point the way to potential new approaches for drug therapy. A third type of chapter deals with general methods of possible utility in the synthesis, design, or testing of drugs.

The section on CNS Agents has three chapters that update previous coverage of antidepressants, antipsychotic agents, antianxiety agents, anticonvulsants, sedative–hypnotics, analgesics (including endogenous peptides), and narcotic antagonists. In addition, there are two excellent chapters on the currently "hot" areas of opiate receptors and biological factors in psychiatric disorders. The Pharmacodynamic Agents section covers pulmonary and antiallergy drugs, antihypertensives, diuretics, and the structure–activity relationships of prostaglandins. The Chemotherapeutic Agents section has chapters on antibiotics and antifungal, antiviral, antiparasitic, and antineoplastic agents.

The section on Metabolic Diseases and Endocrine Function has chapters devoted to immunosuppressive and immunostimulatory agents, steroids, peptide hormones, diabetes, disorders of lipid metabolism, drug metabolism, and antiobesity agents. The Topics in Biology section features particularly pertinent chapters on membrane regulators, active transport across membranes, the antimetabolite concept, comparative toxicology, and chronopharmacology. The last section on Topics in Chemistry has the usual chapter on synthetic reactions of interest plus chapters concerning the synthesis of β-lactam antibiotics, synthesis of cyclic adenosine monophosphate and cyclic guanidine monophosphate derivatives, syntheses employing polymeric reagents, quantitative drug design, and use of NMR for drug binding studies.

As expected with any work by 46 different authors, the writing style is far from uniform. However, the readability of this volume is generally quite good. Every medicinal chemist and most pharmacologists would surely find several chapters of interest.

Reviewed by James F. Stubbins
Virginia Commonwealth University
Richmond, VA 23298

Chinese Herbs: Their Botany, Chemistry, and Pharmacodynamics. By JOHN D. KEYS. Tuttle, Rutland, VT 05701, 1976. 338 pp. 15 × 22 cm. Price $15.00.

This book is a compendium of monographs of Chinese medicinal plants arranged by botanical classification. Each monograph includes an illustration and Chinese characters as well as a botanical, chemical, and pharmacological description. There are also supplementary sections on mineral- and animal-derived drugs, a collection of Chinese prescriptions, and a table of toxic herbs.

This book is a good compilation of the medicinal plants of China, done mainly through translation of Chinese works, some as old as the 6th century. The botanical description seems quite complete, while the chemical and pharmacodynamic sections appear too outdated and su-

perficial for the pharmaceutical scientist. However, this book should be of interest to the lay reader or scientist specifically interested in Chinese herbs and herbal medicine.

Reviewed by David J. Slatkin
University of Pittsburgh
School of Pharmacy
Pittsburgh, PA 15261

Advances in Modern Toxicology, Vol. 1, Part 1: New Concepts in Safety Evaluation. Edited by MYRON A. MEHLMAN, RAYMOND E. SHAPIRO, and HERBERT BLUMENTHAL. Halsted, 605 Third Ave., New York, NY 10016, 1976. 455 pp. 16 × 25 cm.

Today there is increased governmental and industrial concern regarding the toxicity of chemicals, with emphasis on development of test procedures designed to reveal adverse effects before a particular substance becomes available for direct or indirect human ingestion. A text such as this one can assist scientists in fulfilling this objective.

Three of the 13 chapters focus on teratogenicity. Chapter 6, Current Methodology in Teratology Research, provides useful information regarding selection of the animal model and time of administration. Chapter 12, Distribution, Metabolism and Perinatal Toxicity of Pesticides with References to Food Safety Evaluation: A Review of Selected Literature, is a compilation of previously reported data on various pesticides, *e.g.*, DDT, aldrin, and dieldrin. Chapter 13, Transplacental Toxicity of Diethylstilbestrol: A Special Problem in Safety Evaluation, includes detailed descriptions of the pharmacology and toxicology of diethylstilbestrol in both animals and humans.

Two interesting sections devoted to methodology are Chapter 3, Potential Contribution of Inbred Syrian Hamsters to Future Toxicology, and Chapter 9, Radioautographic Methods for Physiologic Disposition and Toxicology Studies.

Chapter 8 is especially timely since it describes fundamental pharmacokinetic principles and their application to toxicological investigations.

Nonlethal Parameters as Indices of Acute Toxicity: Inadequacy of the Acute LD50 is the title of Chapter 7, which stresses the need to look beyond the LD50 value itself, *e.g.*, careful observation of all animals in the postadministration period, and pathological examination of survivors to detect latent toxicity.

Portions of the book suffer from inadequate editorial supervision. Numerous tables (*e.g.*, Chapter 4, Table 13, and associated Appendix; and Chapter 11, Tables 1 and 20) contain facts that are not organized on any basis. Individual chemicals could have been listed alphabetically within each table but instead appear in semirandom fashion. It is unfortunate that these defects, which could have easily been corrected, were overlooked.

On the positive side, background data are accompanied by extensive reference sections, and potential sources of error in development and interpretation of toxicity studies are emphasized. This text is a good comprehensive source of information for those conducting toxicological research.

Reviewed by Frederick J. Goldstein
Philadelphia College of Pharmacy and Science
Philadelphia, PA 19104

International Nonproprietary Names (INN) for Pharmaceutical Substances. Cumulative List No. 4. World Health Organization, Health and Biomedical Information Programme, 1211 Geneva 27, Switzerland, 1976. 314 pp. 17.5 × 24 cm. Price $19.20.

This book is a computer printout of international nonproprietary names (INN) of pharmaceutical substances in alphabetical order of the Latin names. Each entry includes the INN in English, French, Russian, and Spanish; indicates the national compendia in which the names appear; and lists national compendial names that differ from the INN. The Chemical Abstracts Service (CAS) registry number and molecular formula are also given. The book includes all INN published in the *WHO Chronicle* through March 1976. In addition, there is an appendix of national names that differ from INN, a molecular formula index, and a CAS registry number index. All of the text appears in both English and French.

Staff review

Molecular Connectivity in Chemistry and Drug Research. By LEMONT B. KIER and LOWELL H. HALL. Academic, 111 Fifth Ave., New York, NY 10003, 1976. 257 pp. 15 × 24 cm. Price $27.00.

This book represents the results of recent research into the utility of the connectivity index as a parameter for correlating physical, chemical, and biological properties. The 10 chapters in the book may be divided into roughly three sections.

The first section contains Chapters 1–3 on Structure and Properties, Elements of Graph Theory and Topological Indices, and Molecular Connectivity, respectively. These provide a general introduction to their topics. Both Chapters 2 and 3 may appear to be more abstract and formal than necessary on first reading. However, the equations and algorithms provided for the calculation of the various connectivity indices are very general. Computational facility may be gained through working the many examples provided in the numerous tables and in Appendix A.

The second part of the book, Chapter 4 on Molecular Properties and Chapter 5 on Molar (Bulk) Properties and Molecular Connectivity, provide examples of the correlation between the various connectivity indices and such properties as heat of formation and atomization, molar polarizibility, diamagnetic susceptibility, heat of vaporization, boiling point, aqueous solubility, and partition coefficient. In general, for each physical property the discussion is organized and correlations are presented by functional group.

The third part of the book focuses on biological activity correlations. Chapter 6 considers nonspecific biological activity (anesthetic and narcotic activity), while Chapter 7 considers more specific responses such as enzyme inhibition and microbial inhibition. Chapter 8 considers the use of multiple chi (connectivity) and chi-squared terms in correlating biological activities, while Chapter 9 considers the use of chi terms plus other physical property terms, primarily the Hammett sigma values, in correlation analyses. Finally, Chapter 10 concludes the book with reflections on the nature and future of connectivity. In this chapter, the authors ask such questions as: "Is the particular choice of chi important?" and "How is one to interpret the chi terms?", note problem areas such as *cis–trans*-isomerism, conformation, and high structural complexity, and suggest some possible future uses of chi.

While much of the content is available in the literature, the book pulls everything together, plus offers more of an introduction to graph theory and the development of the various connectivity indices. As the authors clearly state, much remains to be investigated. In the reviewer's opinion, it is too early to assess the value of molecular connectivity relative to other parameters. However, the index is no more difficult to compute than other commonly employed parameters, and the technique is easily generalized to the computation of number of indices. The method certainly merits the attention of researchers in structure–activity work as another (more fundamental?) parameter to aid in drug design. Although the book is more introductory and preliminary than one might like (it represents, for the most part, the results of investigations by one research group over the past 2–3 years), it can be recommended, particularly to investigators interested in structure–activity methodology, as a new and potentially useful technique.

Finally, some simple calculations reveal a cost of over 10 cents per page. This seems particularly steep since approximately one-third of the text is occupied by tables.

Reviewed by Gordon L. Amidon
School of Pharmacy
University of Wisconsin
Madison, WI 53706

rivative (II) with the proposed structure indicated. It seems appropriate to correct the record now since I was again proposed as the structure for silylated biotin in a recent review (3).

The possibility that the proposed structure for the silyl ester (I) might be incomplete appeared when we prepared the methyl ester of biotin using diazomethane. Although this methyl ester could be chromatographed, the compound had a much longer retention time compared with the silylated compound and produced a peak that tailed badly. This large difference in chromatographic behavior is not expected for two compounds that are supposed to be simple esters. It also was observed that when the silylating agent [bis(trimethylsilyl)trifluoroacetamide] (III) was added to the previously formed methyl ester, the late eluting broad peak disappeared and a sharp, early eluting peak was obtained. These observations led to a more definitive study of the derivatives formed.

The fully silylated derivatives can be formed by reacting 5 mg of biotin with 1 ml of a 1:1 (v/v) solution of III and pyridine. After heating at 60° for 15 min, the sample is ready for analysis. The partially silylated derivative can be formed by first reacting 5 mg of biotin in ether with excess diazomethane until the yellow color persists. After 10 min, the methyl ester solution is evaporated to dryness and then silylated as described.

These samples were then analyzed[1] on a gas chromatograph–mass spectrometer[2] using a 1.9-m 3% OV-17 on 100–120-mesh Gas Chrom Q[3] column. The mass spectrum of the fully silylated derivative produced molecular ion 460 together with a base peak at *m/e* 73, supporting Structure II. The mass spectrum of the methylated biotin trimethylsilyl derivative gave *m/e* 402, again with a base peak at *m/e* 73, supporting the biotin methyl ester *N,N*-trimethylsilyl structure.

(1) C. Plinton, F. P. Mahn, M. Hawrylyshyn, V. S. Venturella, and B. Z. Senkowski, *J. Pharm. Sci.*, **58**, 875 (1969).
(2) V. Viswanathan, F. P. Mahn, V. S. Venturella, and B. Z. Senkowski, *ibid.*, **59**, 400 (1970).
(3) S. Ahuja, *ibid.*, **65**, 163 (1976).

Raymond N. Johnson [x]
George R. Boyden
Analytical Research and Development Laboratory
Ayerst Laboratories, Inc.
Rouses Point, NY 12979

Received February 24, 1977.
Accepted for publication May 24, 1977.
[x] To whom inquiries should be directed.

[1] Courtesy of Dr. G. Schilling, Analytical Research, Ayerst Laboratories, Montreal, Quebec, Canada.
[2] LKB 9000.
[3] Applied Science Laboratories, State College, Pa.

BOOKS

REVIEWS

Annual Reports in Medicinal Chemistry. Vol. 11. Edited by FRANK H. CLARKE *et al.* Academic, 111 5th Ave., New York, NY 10003, 1976. 339 pp. 17 × 25.5 cm. Price $16.50.

The new editor-in-chief of this series, Dr. Frank Clarke, is to be congratulated on maintaining the quality of content, presentation, and timeliness found in earlier volumes. The 32 chapters of this volume are grouped into six principal sections. Six section editors (three of them new) have the responsibility for the contributions in their areas.

Most chapters survey the literature of 1975 on new compounds reported to have pharmacologic activity. A few chapters cover the years since a report last appeared in this series. Some of the most interesting chapters present a mini-review of some biological process or disease state and point the way to potential new approaches for drug therapy. A third type of chapter deals with general methods of possible utility in the synthesis, design, or testing of drugs.

The section on CNS Agents has three chapters that update previous coverage of antidepressants, antipsychotic agents, antianxiety agents, anticonvulsants, sedative–hypnotics, analgesics (including endogenous peptides), and narcotic antagonists. In addition, there are two excellent chapters on the currently "hot" areas of opiate receptors and biological factors in psychiatric disorders. The Pharmacodynamic Agents section covers pulmonary and antiallergy drugs, antihypertensives, diuretics, and the structure–activity relationships of prostaglandins. The Chemotherapeutic Agents section has chapters on antibiotics and antifungal, antiviral, antiparasitic, and antineoplastic agents.

The section on Metabolic Diseases and Endocrine Function has chapters devoted to immunosuppressive and immunostimulatory agents, steroids, peptide hormones, diabetes, disorders of lipid metabolism, drug metabolism, and antiobesity agents. The Topics in Biology section features particularly pertinent chapters on membrane regulators, active transport across membranes, the antimetabolite concept, comparative toxicology, and chronopharmacology. The last section on Topics in Chemistry has the usual chapter on synthetic reactions of interest plus chapters concerning the synthesis of β-lactam antibiotics, synthesis of cyclic adenosine monophosphate and cyclic guanidine monophosphate derivatives, syntheses employing polymeric reagents, quantitative drug design, and use of NMR for drug binding studies.

As expected with any work by 46 different authors, the writing style is far from uniform. However, the readability of this volume is generally quite good. Every medicinal chemist and most pharmacologists would surely find several chapters of interest.

Reviewed by James F. Stubbins
Virginia Commonwealth University
Richmond, VA 23298

Chinese Herbs: Their Botany, Chemistry, and Pharmacodynamics. By JOHN D. KEYS. Tuttle, Rutland, VT 05701, 1976. 338 pp. 15 × 22 cm. Price $15.00.

This book is a compendium of monographs of Chinese medicinal plants arranged by botanical classification. Each monograph includes an illustration and Chinese characters as well as a botanical, chemical, and pharmacological description. There are also supplementary sections on mineral- and animal-derived drugs, a collection of Chinese prescriptions, and a table of toxic herbs.

This book is a good compilation of the medicinal plants of China, done mainly through translation of Chinese works, some as old as the 6th century. The botanical description seems quite complete, while the chemical and pharmacodynamic sections appear too outdated and su-

perficial for the pharmaceutical scientist. However, this book should be of interest to the lay reader or scientist specifically interested in Chinese herbs and herbal medicine.

Reviewed by David J. Slatkin
University of Pittsburgh
School of Pharmacy
Pittsburgh, PA 15261

Advances in Modern Toxicology, Vol. 1, Part 1: New Concepts in Safety Evaluation. Edited by MYRON A. MEHLMAN, RAYMOND E. SHAPIRO, and HERBERT BLUMENTHAL. Halsted, 605 Third Ave., New York, NY 10016, 1976. 455 pp. 16 × 25 cm.

Today there is increased governmental and industrial concern regarding the toxicity of chemicals, with emphasis on development of test procedures designed to reveal adverse effects before a particular substance becomes available for direct or indirect human ingestion. A text such as this one can assist scientists in fulfilling this objective.

Three of the 13 chapters focus on teratogenicity. Chapter 6, Current Methodology in Teratology Research, provides useful information regarding selection of the animal model and time of administration. Chapter 12, Distribution, Metabolism and Perinatal Toxicity of Pesticides with References to Food Safety Evaluation: A Review of Selected Literature, is a compilation of previously reported data on various pesticides, *e.g.*, DDT, aldrin, and dieldrin. Chapter 13, Transplacental Toxicity of Diethylstilbestrol: A Special Problem in Safety Evaluation, includes detailed descriptions of the pharmacology and toxicology of diethylstilbestrol in both animals and humans.

Two interesting sections devoted to methodology are Chapter 3, Potential Contribution of Inbred Syrian Hamsters to Future Toxicology, and Chapter 9, Radioautographic Methods for Physiologic Disposition and Toxicology Studies.

Chapter 8 is especially timely since it describes fundamental pharmacokinetic principles and their application to toxicological investigations.

Nonlethal Parameters as Indices of Acute Toxicity: Inadequacy of the Acute LD50 is the title of Chapter 7, which stresses the need to look beyond the LD50 value itself, *e.g.*, careful observation of all animals in the postadministration period, and pathological examination of survivors to detect latent toxicity.

Portions of the book suffer from inadequate editorial supervision. Numerous tables (*e.g.*, Chapter 4, Table 13, and associated Appendix; and Chapter 11, Tables 1 and 20) contain facts that are not organized on any basis. Individual chemicals could have been listed alphabetically within each table but instead appear in semirandom fashion. It is unfortunate that these defects, which could have easily been corrected, were overlooked.

On the positive side, background data are accompanied by extensive reference sections, and potential sources of error in development and interpretation of toxicity studies are emphasized. This text is a good comprehensive source of information for those conducting toxicological research.

Reviewed by Frederick J. Goldstein
Philadelphia College of Pharmacy and Science
Philadelphia, PA 19104

International Nonproprietary Names (INN) for Pharmaceutical Substances. Cumulative List No. 4. World Health Organization, Health and Biomedical Information Programme, 1211 Geneva 27, Switzerland, 1976. 314 pp. 17.5 × 24 cm. Price $19.20.

This book is a computer printout of international nonproprietary names (INN) of pharmaceutical substances in alphabetical order of the Latin names. Each entry includes the INN in English, French, Russian, and Spanish; indicates the national compendia in which the names appear; and lists national compendial names that differ from the INN. The Chemical Abstracts Service (CAS) registry number and molecular formula are also given. The book includes all INN published in the *WHO Chronicle* through March 1976. In addition, there is an appendix of national names that differ from INN, a molecular formula index, and a CAS registry number index. All of the text appears in both English and French.

Staff review

Molecular Connectivity in Chemistry and Drug Research. By LEMONT B. KIER and LOWELL H. HALL. Academic, 111 Fifth Ave., New York, NY 10003, 1976. 257 pp. 15 × 24 cm. Price $27.00.

This book represents the results of recent research into the utility of the connectivity index as a parameter for correlating physical, chemical, and biological properties. The 10 chapters in the book may be divided into roughly three sections.

The first section contains Chapters 1–3 on Structure and Properties, Elements of Graph Theory and Topological Indices, and Molecular Connectivity, respectively. These provide a general introduction to their topics. Both Chapters 2 and 3 may appear to be more abstract and formal than necessary on first reading. However, the equations and algorithms provided for the calculation of the various connectivity indices are very general. Computational facility may be gained through working the many examples provided in the numerous tables and in Appendix A.

The second part of the book, Chapter 4 on Molecular Properties and Chapter 5 on Molar (Bulk) Properties and Molecular Connectivity, provide examples of the correlation between the various connectivity indices and such properties as heat of formation and atomization, molar polarizibility, diamagnetic susceptibility, heat of vaporization, boiling point, aqueous solubility, and partition coefficient. In general, for each physical property the discussion is organized and correlations are presented by functional group.

The third part of the book focuses on biological activity correlations. Chapter 6 considers nonspecific biological activity (anesthetic and narcotic activity), while Chapter 7 considers more specific responses such as enzyme inhibition and microbial inhibition. Chapter 8 considers the use of multiple chi (connectivity) and chi-squared terms in correlating biological activities, while Chapter 9 considers the use of chi terms plus other physical property terms, primarily the Hammett sigma values, in correlation analyses. Finally, Chapter 10 concludes the book with reflections on the nature and future of connectivity. In this chapter, the authors ask such questions as: "Is the particular choice of chi important?" and "How is one to interpret the chi terms?", note problem areas such as *cis–trans*-isomerism, conformation, and high structural complexity, and suggest some possible future uses of chi.

While much of the content is available in the literature, the book pulls everything together, plus offers more of an introduction to graph theory and the development of the various connectivity indices. As the authors clearly state, much remains to be investigated. In the reviewer's opinion, it is too early to assess the value of molecular connectivity relative to other parameters. However, the index is no more difficult to compute than other commonly employed parameters, and the technique is easily generalized to the computation of number of indices. The method certainly merits the attention of researchers in structure–activity work as another (more fundamental?) parameter to aid in drug design. Although the book is more introductory and preliminary than one might like (it represents, for the most part, the results of investigations by one research group over the past 2–3 years), it can be recommended, particularly to investigators interested in structure–activity methodology, as a new and potentially useful technique.

Finally, some simple calculations reveal a cost of over 10 cents per page. This seems particularly steep since approximately one-third of the text is occupied by tables.

Reviewed by Gordon L. Amidon
School of Pharmacy
University of Wisconsin
Madison, WI 53706

perficial for the pharmaceutical scientist. However, this book should be of interest to the lay reader or scientist specifically interested in Chinese herbs and herbal medicine.

Reviewed by David J. Slatkin
University of Pittsburgh
School of Pharmacy
Pittsburgh, PA 15261

Advances in Modern Toxicology, Vol. 1, Part 1: New Concepts in Safety Evaluation. Edited by MYRON A. MEHLMAN, RAYMOND E. SHAPIRO, and HERBERT BLUMENTHAL. Halsted, 605 Third Ave., New York, NY 10016, 1976. 455 pp. 16 × 25 cm.

Today there is increased governmental and industrial concern regarding the toxicity of chemicals, with emphasis on development of test procedures designed to reveal adverse effects before a particular substance becomes available for direct or indirect human ingestion. A text such as this one can assist scientists in fulfilling this objective.

Three of the 13 chapters focus on teratogenicity. Chapter 6, Current Methodology in Teratology Research, provides useful information regarding selection of the animal model and time of administration. Chapter 12, Distribution, Metabolism and Perinatal Toxicity of Pesticides with References to Food Safety Evaluation: A Review of Selected Literature, is a compilation of previously reported data on various pesticides, *e.g.*, DDT, aldrin, and dieldrin. Chapter 13, Transplacental Toxicity of Diethylstilbestrol: A Special Problem in Safety Evaluation, includes detailed descriptions of the pharmacology and toxicology of diethylstilbestrol in both animals and humans.

Two interesting sections devoted to methodology are Chapter 3, Potential Contribution of Inbred Syrian Hamsters to Future Toxicology, and Chapter 9, Radioautographic Methods for Physiologic Disposition and Toxicology Studies.

Chapter 8 is especially timely since it describes fundamental pharmacokinetic principles and their application to toxicological investigations.

Nonlethal Parameters as Indices of Acute Toxicity: Inadequacy of the Acute LD50 is the title of Chapter 7, which stresses the need to look beyond the LD50 value itself, *e.g.*, careful observation of all animals in the postadministration period, and pathological examination of survivors to detect latent toxicity.

Portions of the book suffer from inadequate editorial supervision. Numerous tables (*e.g.*, Chapter 4, Table 13, and associated Appendix; and Chapter 11, Tables 1 and 20) contain facts that are not organized on any basis. Individual chemicals could have been listed alphabetically within each table but instead appear in semirandom fashion. It is unfortunate that these defects, which could have easily been corrected, were overlooked.

On the positive side, background data are accompanied by extensive reference sections, and potential sources of error in development and interpretation of toxicity studies are emphasized. This text is a good comprehensive source of information for those conducting toxicological research.

Reviewed by Frederick J. Goldstein
Philadelphia College of Pharmacy and Science
Philadelphia, PA 19104

International Nonproprietary Names (INN) for Pharmaceutical Substances. Cumulative List No. 4. World Health Organization, Health and Biomedical Information Programme, 1211 Geneva 27, Switzerland, 1976. 314 pp. 17.5 × 24 cm. Price $19.20.

This book is a computer printout of international nonproprietary names (INN) of pharmaceutical substances in alphabetical order of the Latin names. Each entry includes the INN in English, French, Russian, and Spanish; indicates the national compendia in which the names appear; and lists national compendial names that differ from the INN. The Chemical Abstracts Service (CAS) registry number and molecular formula are also given. The book includes all INN published in the *WHO Chronicle* through March 1976. In addition, there is an appendix of national names that differ from INN, a molecular formula index, and a CAS registry number index. All of the text appears in both English and French.

Staff review

Molecular Connectivity in Chemistry and Drug Research. By LEMONT B. KIER and LOWELL H. HALL. Academic, 111 Fifth Ave., New York, NY 10003, 1976. 257 pp. 15 × 24 cm. Price $27.00.

This book represents the results of recent research into the utility of the connectivity index as a parameter for correlating physical, chemical, and biological properties. The 10 chapters in the book may be divided into roughly three sections.

The first section contains Chapters 1–3 on Structure and Properties, Elements of Graph Theory and Topological Indices, and Molecular Connectivity, respectively. These provide a general introduction to their topics. Both Chapters 2 and 3 may appear to be more abstract and formal than necessary on first reading. However, the equations and algorithms provided for the calculation of the various connectivity indices are very general. Computational facility may be gained through working the many examples provided in the numerous tables and in Appendix A.

The second part of the book, Chapter 4 on Molecular Properties and Chapter 5 on Molar (Bulk) Properties and Molecular Connectivity, provide examples of the correlation between the various connectivity indices and such properties as heat of formation and atomization, molar polarizibility, diamagnetic susceptibility, heat of vaporization, boiling point, aqueous solubility, and partition coefficient. In general, for each physical property the discussion is organized and correlations are presented by functional group.

The third part of the book focuses on biological activity correlations. Chapter 6 considers nonspecific biological activity (anesthetic and narcotic activity), while Chapter 7 considers more specific responses such as enzyme inhibition and microbial inhibition. Chapter 8 considers the use of multiple chi (connectivity) and chi-squared terms in correlating biological activities, while Chapter 9 considers the use of chi terms plus other physical property terms, primarily the Hammett sigma values, in correlation analyses. Finally, Chapter 10 concludes the book with reflections on the nature and future of connectivity. In this chapter, the authors ask such questions as: "Is the particular choice of chi important?" and "How is one to interpret the chi terms?", note problem areas such as *cis–trans*-isomerism, conformation, and high structural complexity, and suggest some possible future uses of chi.

While much of the content is available in the literature, the book pulls everything together, plus offers more of an introduction to graph theory and the development of the various connectivity indices. As the authors clearly state, much remains to be investigated. In the reviewer's opinion, it is too early to assess the value of molecular connectivity relative to other parameters. However, the index is no more difficult to compute than other commonly employed parameters, and the technique is easily generalized to the computation of number of indices. The method certainly merits the attention of researchers in structure–activity work as another (more fundamental?) parameter to aid in drug design. Although the book is more introductory and preliminary than one might like (it represents, for the most part, the results of investigations by one research group over the past 2–3 years), it can be recommended, particularly to investigators interested in structure–activity methodology, as a new and potentially useful technique.

Finally, some simple calculations reveal a cost of over 10 cents per page. This seems particularly steep since approximately one-third of the text is occupied by tables.

Reviewed by Gordon L. Amidon
School of Pharmacy
University of Wisconsin
Madison, WI 53706

perficial for the pharmaceutical scientist. However, this book should be of interest to the lay reader or scientist specifically interested in Chinese herbs and herbal medicine.

Reviewed by David J. Slatkin
University of Pittsburgh
School of Pharmacy
Pittsburgh, PA 15261

Advances in Modern Toxicology, Vol. 1, Part 1: New Concepts in Safety Evaluation. Edited by MYRON A. MEHLMAN, RAYMOND E. SHAPIRO, and HERBERT BLUMENTHAL. Halsted, 605 Third Ave., New York, NY 10016, 1976. 455 pp. 16 × 25 cm.

Today there is increased governmental and industrial concern regarding the toxicity of chemicals, with emphasis on development of test procedures designed to reveal adverse effects before a particular substance becomes available for direct or indirect human ingestion. A text such as this one can assist scientists in fulfilling this objective.

Three of the 13 chapters focus on teratogenicity. Chapter 6, Current Methodology in Teratology Research, provides useful information regarding selection of the animal model and time of administration. Chapter 12, Distribution, Metabolism and Perinatal Toxicity of Pesticides with References to Food Safety Evaluation: A Review of Selected Literature, is a compilation of previously reported data on various pesticides, *e.g.*, DDT, aldrin, and dieldrin. Chapter 13, Transplacental Toxicity of Diethylstilbestrol: A Special Problem in Safety Evaluation, includes detailed descriptions of the pharmacology and toxicology of diethylstilbestrol in both animals and humans.

Two interesting sections devoted to methodology are Chapter 3, Potential Contribution of Inbred Syrian Hamsters to Future Toxicology, and Chapter 9, Radioautographic Methods for Physiologic Disposition and Toxicology Studies.

Chapter 8 is especially timely since it describes fundamental pharmacokinetic principles and their application to toxicological investigations.

Nonlethal Parameters as Indices of Acute Toxicity: Inadequacy of the Acute LD50 is the title of Chapter 7, which stresses the need to look beyond the LD50 value itself, *e.g.*, careful observation of all animals in the postadministration period, and pathological examination of survivors to detect latent toxicity.

Portions of the book suffer from inadequate editorial supervision. Numerous tables (*e.g.*, Chapter 4, Table 13, and associated Appendix; and Chapter 11, Tables 1 and 20) contain facts that are not organized on any basis. Individual chemicals could have been listed alphabetically within each table but instead appear in semirandom fashion. It is unfortunate that these defects, which could have easily been corrected, were overlooked.

On the positive side, background data are accompanied by extensive reference sections, and potential sources of error in development and interpretation of toxicity studies are emphasized. This text is a good comprehensive source of information for those conducting toxicological research.

Reviewed by Frederick J. Goldstein
Philadelphia College of Pharmacy and Science
Philadelphia, PA 19104

International Nonproprietary Names (INN) for Pharmaceutical Substances. Cumulative List No. 4. World Health Organization, Health and Biomedical Information Programme, 1211 Geneva 27, Switzerland, 1976. 314 pp. 17.5 × 24 cm. Price $19.20.

This book is a computer printout of international nonproprietary names (INN) of pharmaceutical substances in alphabetical order of the Latin names. Each entry includes the INN in English, French, Russian, and Spanish; indicates the national compendia in which the names appear; and lists national compendial names that differ from the INN. The Chemical Abstracts Service (CAS) registry number and molecular formula are also given. The book includes all INN published in the *WHO Chronicle* through March 1976. In addition, there is an appendix of national names that differ from INN, a molecular formula index, and a CAS registry number index. All of the text appears in both English and French.

Staff review

Molecular Connectivity in Chemistry and Drug Research. By LEMONT B. KIER and LOWELL H. HALL. Academic, 111 Fifth Ave., New York, NY 10003, 1976. 257 pp. 15 × 24 cm. Price $27.00.

This book represents the results of recent research into the utility of the connectivity index as a parameter for correlating physical, chemical, and biological properties. The 10 chapters in the book may be divided into roughly three sections.

The first section contains Chapters 1–3 on Structure and Properties, Elements of Graph Theory and Topological Indices, and Molecular Connectivity, respectively. These provide a general introduction to their topics. Both Chapters 2 and 3 may appear to be more abstract and formal than necessary on first reading. However, the equations and algorithms provided for the calculation of the various connectivity indices are very general. Computational facility may be gained through working the many examples provided in the numerous tables and in Appendix A.

The second part of the book, Chapter 4 on Molecular Properties and Chapter 5 on Molar (Bulk) Properties and Molecular Connectivity, provide examples of the correlation between the various connectivity indices and such properties as heat of formation and atomization, molar polarizibility, diamagnetic susceptibility, heat of vaporization, boiling point, aqueous solubility, and partition coefficient. In general, for each physical property the discussion is organized and correlations are presented by functional group.

The third part of the book focuses on biological activity correlations. Chapter 6 considers nonspecific biological activity (anesthetic and narcotic activity), while Chapter 7 considers more specific responses such as enzyme inhibition and microbial inhibition. Chapter 8 considers the use of multiple chi (connectivity) and chi-squared terms in correlating biological activities, while Chapter 9 considers the use of chi terms plus other physical property terms, primarily the Hammett sigma values, in correlation analyses. Finally, Chapter 10 concludes the book with reflections on the nature and future of connectivity. In this chapter, the authors ask such questions as: "Is the particular choice of chi important?" and "How is one to interpret the chi terms?", note problem areas such as *cis–trans*-isomerism, conformation, and high structural complexity, and suggest some possible future uses of chi.

While much of the content is available in the literature, the book pulls everything together, plus offers more of an introduction to graph theory and the development of the various connectivity indices. As the authors clearly state, much remains to be investigated. In the reviewer's opinion, it is too early to assess the value of molecular connectivity relative to other parameters. However, the index is no more difficult to compute than other commonly employed parameters, and the technique is easily generalized to the computation of number of indices. The method certainly merits the attention of researchers in structure–activity work as another (more fundamental?) parameter to aid in drug design. Although the book is more introductory and preliminary than one might like (it represents, for the most part, the results of investigations by one research group over the past 2–3 years), it can be recommended, particularly to investigators interested in structure–activity methodology, as a new and potentially useful technique.

Finally, some simple calculations reveal a cost of over 10 cents per page. This seems particularly steep since approximately one-third of the text is occupied by tables.

Reviewed by Gordon L. Amidon
School of Pharmacy
University of Wisconsin
Madison, WI 53706

perficial for the pharmaceutical scientist. However, this book should be of interest to the lay reader or scientist specifically interested in Chinese herbs and herbal medicine.

Reviewed by David J. Slatkin
University of Pittsburgh
School of Pharmacy
Pittsburgh, PA 15261

Advances in Modern Toxicology, Vol. 1, Part 1: New Concepts in Safety Evaluation. Edited by MYRON A. MEHLMAN, RAYMOND E. SHAPIRO, and HERBERT BLUMENTHAL. Halsted, 605 Third Ave., New York, NY 10016, 1976. 455 pp. 16 × 25 cm.

Today there is increased governmental and industrial concern regarding the toxicity of chemicals, with emphasis on development of test procedures designed to reveal adverse effects before a particular substance becomes available for direct or indirect human ingestion. A text such as this one can assist scientists in fulfilling this objective.

Three of the 13 chapters focus on teratogenicity. Chapter 6, Current Methodology in Teratology Research, provides useful information regarding selection of the animal model and time of administration. Chapter 12, Distribution, Metabolism and Perinatal Toxicity of Pesticides with References to Food Safety Evaluation: A Review of Selected Literature, is a compilation of previously reported data on various pesticides, *e.g.*, DDT, aldrin, and dieldrin. Chapter 13, Transplacental Toxicity of Diethylstilbestrol: A Special Problem in Safety Evaluation, includes detailed descriptions of the pharmacology and toxicology of diethylstilbestrol in both animals and humans.

Two interesting sections devoted to methodology are Chapter 3, Potential Contribution of Inbred Syrian Hamsters to Future Toxicology, and Chapter 9, Radioautographic Methods for Physiologic Disposition and Toxicology Studies.

Chapter 8 is especially timely since it describes fundamental pharmacokinetic principles and their application to toxicological investigations.

Nonlethal Parameters as Indices of Acute Toxicity: Inadequacy of the Acute LD50 is the title of Chapter 7, which stresses the need to look beyond the LD50 value itself, *e.g.*, careful observation of all animals in the postadministration period, and pathological examination of survivors to detect latent toxicity.

Portions of the book suffer from inadequate editorial supervision. Numerous tables (*e.g.*, Chapter 4, Table 13, and associated Appendix; and Chapter 11, Tables 1 and 20) contain facts that are not organized on any basis. Individual chemicals could have been listed alphabetically within each table but instead appear in semirandom fashion. It is unfortunate that these defects, which could have easily been corrected, were overlooked.

On the positive side, background data are accompanied by extensive reference sections, and potential sources of error in development and interpretation of toxicity studies are emphasized. This text is a good comprehensive source of information for those conducting toxicological research.

Reviewed by Frederick J. Goldstein
Philadelphia College of Pharmacy and Science
Philadelphia, PA 19104

International Nonproprietary Names (INN) for Pharmaceutical Substances. Cumulative List No. 4. World Health Organization, Health and Biomedical Information Programme, 1211 Geneva 27, Switzerland, 1976. 314 pp. 17.5 × 24 cm. Price $19.20.

This book is a computer printout of international nonproprietary names (INN) of pharmaceutical substances in alphabetical order of the Latin names. Each entry includes the INN in English, French, Russian, and Spanish; indicates the national compendia in which the names appear; and lists national compendial names that differ from the INN. The Chemical Abstracts Service (CAS) registry number and molecular formula are also given. The book includes all INN published in the *WHO Chronicle* through March 1976. In addition, there is an appendix of national names that differ from INN, a molecular formula index, and a CAS registry number index. All of the text appears in both English and French.

Staff review

Molecular Connectivity in Chemistry and Drug Research. By LEMONT B. KIER and LOWELL H. HALL. Academic, 111 Fifth Ave., New York, NY 10003, 1976. 257 pp. 15 × 24 cm. Price $27.00.

This book represents the results of recent research into the utility of the connectivity index as a parameter for correlating physical, chemical, and biological properties. The 10 chapters in the book may be divided into roughly three sections.

The first section contains Chapters 1–3 on Structure and Properties, Elements of Graph Theory and Topological Indices, and Molecular Connectivity, respectively. These provide a general introduction to their topics. Both Chapters 2 and 3 may appear to be more abstract and formal than necessary on first reading. However, the equations and algorithms provided for the calculation of the various connectivity indices are very general. Computational facility may be gained through working the many examples provided in the numerous tables and in Appendix A.

The second part of the book, Chapter 4 on Molecular Properties and Chapter 5 on Molar (Bulk) Properties and Molecular Connectivity, provide examples of the correlation between the various connectivity indices and such properties as heat of formation and atomization, molar polarizibility, diamagnetic susceptibility, heat of vaporization, boiling point, aqueous solubility, and partition coefficient. In general, for each physical property the discussion is organized and correlations are presented by functional group.

The third part of the book focuses on biological activity correlations. Chapter 6 considers nonspecific biological activity (anesthetic and narcotic activity), while Chapter 7 considers more specific responses such as enzyme inhibition and microbial inhibition. Chapter 8 considers the use of multiple chi (connectivity) and chi-squared terms in correlating biological activities, while Chapter 9 considers the use of chi terms plus other physical property terms, primarily the Hammett sigma values, in correlation analyses. Finally, Chapter 10 concludes the book with reflections on the nature and future of connectivity. In this chapter, the authors ask such questions as: "Is the particular choice of chi important?" and "How is one to interpret the chi terms?", note problem areas such as *cis–trans*-isomerism, conformation, and high structural complexity, and suggest some possible future uses of chi.

While much of the content is available in the literature, the book pulls everything together, plus offers more of an introduction to graph theory and the development of the various connectivity indices. As the authors clearly state, much remains to be investigated. In the reviewer's opinion, it is too early to assess the value of molecular connectivity relative to other parameters. However, the index is no more difficult to compute than other commonly employed parameters, and the technique is easily generalized to the computation of number of indices. The method certainly merits the attention of researchers in structure–activity work as another (more fundamental?) parameter to aid in drug design. Although the book is more introductory and preliminary than one might like (it represents, for the most part, the results of investigations by one research group over the past 2–3 years), it can be recommended, particularly to investigators interested in structure–activity methodology, as a new and potentially useful technique.

Finally, some simple calculations reveal a cost of over 10 cents per page. This seems particularly steep since approximately one-third of the text is occupied by tables.

Reviewed by Gordon L. Amidon
School of Pharmacy
University of Wisconsin
Madison, WI 53706

Journal of Pharmaceutical Sciences

SEPTEMBER 1977

VOLUME 66 NUMBER 9

MARY H. FERGUSON
Editor

SHELLY ELLIOTT
Production Editor

JANET D. SHOFF
Copy Editor

EDWARD G. FELDMANN
Contributing Editor

SAMUEL W. GOLDSTEIN
Contributing Editor

DAVID BOHARDT
Acting Director of Publications

L. LUAN CORRIGAN
Assistant Director of Publications

EDITORIAL ADVISORY BOARD

JOHN AUTIAN
NORMAN R. FARNSWORTH
WILLIAM O. FOYE
WILLIAM J. JUSKO
HARRY B. KOSTENBAUDER
HERBERT A. LIEBERMAN
DAVID E. MANN, JR.
GERALD J. PAPARIELLO

The *Journal of Pharmaceutical Sciences* is published monthly by the American Pharmaceutical Association at 2215 Constitution Ave., N.W., Washington, DC 20037. Second-class postage paid at Washington, D.C., and at additional mailing office.

All expressions of opinion and statements of supposed fact appearing in articles or editorials carried in this journal are published on the authority of the writer over whose name they appear and are not to be regarded as necessarily expressing the policies or views of the American Pharmaceutical Association.

Offices—Editorial, Advertising, and Subscription Offices: 2215 Constitution Ave., N.W., Washington, DC 20037. Printing Offices: 20th & Northampton Streets, Easton, PA 18042.

Annual Subscriptions—United States and foreign, industrial and government institutions $50, educational institutions $50, individuals *for personal use only* $30; single copies $5. All foreign subscriptions add $5 for postage. Subscription rates are subject to change without notice. Members of the American Pharmaceutical Association may elect to receive the *Journal of Pharmaceutical Sciences* as a part of their annual $60 (foreign $65) APhA membership dues.

Claims—Missing numbers will not be supplied if dues or subscriptions are in arrears for more than 60 days or if claims are received more than 60 days after the date of the issue, or if loss was due to failure to give notice of change of address. The Association cannot accept responsibility for foreign delivery when its records indicate shipment has been made.

Change of Address—Members and subscribers should notify at once both the Post Office and the American Pharmaceutical Association, 2215 Constitution Ave., N.W., Washington, DC 20037, of any change of address.

Microfilm—Microfilm volumes are available from University Microfilms International, 300 N. Zeeb Road, Ann Arbor, MI 48106.

© Copyright 1977, American Pharmaceutical Association, 2215 Constitution Ave., N.W., Washington, DC 20037; all rights reserved.

KEEPING "BASICS" IN BALANCE

As this column is being written, the Washington metropolitan area is experiencing a severe short-term water shortage attributable to malfunctioning equipment. Other water shortages ominously face the area due to a combination of decreased precipitation and increased demand. The prospect of long-term water shortages may well have been avoided had various plans been implemented a decade or two earlier which called for a comprehensive series of dams and other water-related projects on the upper Potomac River which provides the city's major source of water.

However, the timing was off in the sense that this comprehensive proposal was advanced at the tail end of the nationwide dam-building era of the postdepression years. Delays resulted during which the pendulum of public sentiment swung so far in the other direction that not only was the comprehensive plan abandoned, but the opponents were successful in blocking approval for even a scaled-down version.

Since the oil embargo of the winter of 1973–74, the entire country has been going through alternate periods of "feast or famine" with respect to energy use and conservation as well as legislative proposals and tax incentives to modify or affect use of our energy resources.

Approximately 15 years ago, the Washington suburbs were in the midst of a tremendous building boom which threatened to pave over the entire metropolitan area with real estate and other development. Conservationists successfully brought an abrupt halt to this activity about 7 to 8 years ago through the implementation of various sewer and water-line restrictions as well as other zoning controls which virtually put a complete brake on development in the local area. The supply of new housing then did not keep pace with demand and the prices for comparable property more than tripled during this period.

The common element in all of the examples cited above—as well as others which could be mentioned—is that Americans have a characteristic tendency to go overboard in one direction or the other in various programs, policies, projects, and activities. The result is a type of "overkill" which, while rectifying the original concern, frequently creates a greater problem in its place.

We see a similar tendency in our approach to education. On taking office during the Annual Meeting in New York City in late May, Academy of Pharmaceutical Sciences President George Zografi laid out some of his concerns about the future of pharmaceutical research and the training and education of future pharmacy students.

President Zografi traced the recent history of pharmacy education in the United States and the marked improvement in the quality of scientific knowledge developed and taught in pharmacy following World War II. He went on to say:

"This led to a marked increase in graduate education and, in turn, to an influx of many well-educated pharmacists into scientific research and development. At the same time, we were producing well-educated pharmacists who became practitioners, but we were deficient in not providing the type of professional education and training which allowed large numbers of these individuals to utilize their education in their practice to the fullest extent. More recently, the directions pharmacy practice must take have become clearer and the schools of pharmacy have responded with greater emphasis on such areas as therapeutics, biopharmaceutics, and clinical education."

But Dr. Zografi went on to caution his listeners:

"However, I now detect a general climate which is tending to downgrade the importance of basic science knowledge for professional practitioners—knowledge which must serve as a basis for the uncertainties of our future professional practice. It often appears that all of pharmacy's problems are being blamed on our so-called over-emphasis of the basic scientific portion of our educational program."

There is a good deal of merit in Dr. Zografi's concern. Pharmacy education, as in the case of the subjects discussed in the opening paragraphs of this column, has been subject to sharp swings in attitude depending upon what may be of current primary interest and concern. In our efforts to remedy past omissions and deficiencies, it would be indeed regrettable if the basics are neglected or fall from favor.

We need only look at our national experience at the grade school level of education. As our educators eagerly embraced the so-called modern methods, they were quick to discard and even reject the basic elements. The result has led to a hue and cry among high school and college educators with respect to the students who are now reaching those levels. Repeatedly, we hear complaints that "Johnny can't read" and "Mary can't add."

It appears to us that if pharmacy education in its effort to meet the need for therapeutics, biopharmaceutics, and clinical education displaces the basic sciences—rather than supplements them—we run the risk that a parallel situation will develop with respect to our pharmacy graduates. In conclusion, both of these elements are necessary for competent practitioners, and they must be kept in proper proportion by those responsible for pharmacy education. —EGF

Journal of Pharmaceutical Sciences

SEPTEMBER 1977

VOLUME 66 NUMBER 9

MARY H. FERGUSON
Editor

SHELLY ELLIOTT
Production Editor

JANET D. SHOFF
Copy Editor

EDWARD G. FELDMANN
Contributing Editor

SAMUEL W. GOLDSTEIN
Contributing Editor

DAVID BOHARDT
Acting Director of Publications

L. LUAN CORRIGAN
Assistant Director of Publications

EDITORIAL ADVISORY BOARD

JOHN AUTIAN
NORMAN R. FARNSWORTH
WILLIAM O. FOYE
WILLIAM J. JUSKO
HARRY B. KOSTENBAUDER
HERBERT A. LIEBERMAN
DAVID E. MANN, JR.
GERALD J. PAPARIELLO

The *Journal of Pharmaceutical Sciences* is published monthly by the American Pharmaceutical Association at 2215 Constitution Ave., N.W., Washington, DC 20037. Second-class postage paid at Washington, D.C., and at additional mailing office.

All expressions of opinion and statements of supposed fact appearing in articles or editorials carried in this journal are published on the authority of the writer over whose name they appear and are not to be regarded as necessarily expressing the policies or views of the American Pharmaceutical Association.

Offices—Editorial, Advertising, and Subscription Offices: 2215 Constitution Ave., N.W., Washington, DC 20037. Printing Offices: 20th & Northampton Streets, Easton, PA 18042.

Annual Subscriptions—United States and foreign, industrial and government institutions $50, educational institutions $50, individuals *for personal use only* $30; single copies $5. All foreign subscriptions add $5 for postage. Subscription rates are subject to change without notice. Members of the American Pharmaceutical Association may elect to receive the *Journal of Pharmaceutical Sciences* as a part of their annual $60 (foreign $65) APhA membership dues.

Claims—Missing numbers will not be supplied if dues or subscriptions are in arrears for more than 60 days or if claims are received more than 60 days after the date of the issue, or if loss was due to failure to give notice of change of address. The Association cannot accept responsibility for foreign delivery when its records indicate shipment has been made.

Change of Address—Members and subscribers should notify at once both the Post Office and the American Pharmaceutical Association, 2215 Constitution Ave., N.W., Washington, DC 20037, of any change of address.

Microfilm—Microfilm volumes are available from University Microfilms International, 300 N. Zeeb Road, Ann Arbor, MI 48106.

© Copyright 1977, American Pharmaceutical Association, 2215 Constitution Ave., N.W., Washington, DC 20037; all rights reserved.

KEEPING "BASICS" IN BALANCE

As this column is being written, the Washington metropolitan area is experiencing a severe short-term water shortage attributable to malfunctioning equipment. Other water shortages ominously face the area due to a combination of decreased precipitation and increased demand. The prospect of long-term water shortages may well have been avoided had various plans been implemented a decade or two earlier which called for a comprehensive series of dams and other water-related projects on the upper Potomac River which provides the city's major source of water.

However, the timing was off in the sense that this comprehensive proposal was advanced at the tail end of the nationwide dam-building era of the postdepression years. Delays resulted during which the pendulum of public sentiment swung so far in the other direction that not only was the comprehensive plan abandoned, but the opponents were successful in blocking approval for even a scaled-down version.

Since the oil embargo of the winter of 1973–74, the entire country has been going through alternate periods of "feast or famine" with respect to energy use and conservation as well as legislative proposals and tax incentives to modify or affect use of our energy resources.

Approximately 15 years ago, the Washington suburbs were in the midst of a tremendous building boom which threatened to pave over the entire metropolitan area with real estate and other development. Conservationists successfully brought an abrupt halt to this activity about 7 to 8 years ago through the implementation of various sewer and water-line restrictions as well as other zoning controls which virtually put a complete brake on development in the local area. The supply of new housing then did not keep pace with demand and the prices for comparable property more than tripled during this period.

The common element in all of the examples cited above—as well as others which could be mentioned—is that Americans have a characteristic tendency to go overboard in one direction or the other in various programs, policies, projects, and activities. The result is a type of "overkill" which, while rectifying the original concern, frequently creates a greater problem in its place.

We see a similar tendency in our approach to education. On taking office during the Annual Meeting in New York City in late May, Academy of Pharmaceutical Sciences President George Zografi laid out some of his concerns about the future of pharmaceutical research and the training and education of future pharmacy students.

President Zografi traced the recent history of pharmacy education in the United States and the marked improvement in the quality of scientific knowledge developed and taught in pharmacy following World War II. He went on to say:

"This led to a marked increase in graduate education and, in turn, to an influx of many well-educated pharmacists into scientific research and development. At the same time, we were producing well-educated pharmacists who became practitioners, but we were deficient in not providing the type of professional education and training which allowed large numbers of these individuals to utilize their education in their practice to the fullest extent. More recently, the directions pharmacy practice must take have become clearer and the schools of pharmacy have responded with greater emphasis on such areas as therapeutics, biopharmaceutics, and clinical education."

But Dr. Zografi went on to caution his listeners:

"However, I now detect a general climate which is tending to downgrade the importance of basic science knowledge for professional practitioners—knowledge which must serve as a basis for the uncertainties of our future professional practice. It often appears that all of pharmacy's problems are being blamed on our so-called over-emphasis of the basic scientific portion of our educational program."

There is a good deal of merit in Dr. Zografi's concern. Pharmacy education, as in the case of the subjects discussed in the opening paragraphs of this column, has been subject to sharp swings in attitude depending upon what may be of current primary interest and concern. In our efforts to remedy past omissions and deficiencies, it would be indeed regrettable if the basics are neglected or fall from favor.

We need only look at our national experience at the grade school level of education. As our educators eagerly embraced the so-called modern methods, they were quick to discard and even reject the basic elements. The result has led to a hue and cry among high school and college educators with respect to the students who are now reaching those levels. Repeatedly, we hear complaints that "Johnny can't read" and "Mary can't add."

It appears to us that if pharmacy education in its effort to meet the need for therapeutics, biopharmaceutics, and clinical education displaces the basic sciences—rather than supplements them—we run the risk that a parallel situation will develop with respect to our pharmacy graduates. In conclusion, both of these elements are necessary for competent practitioners, and they must be kept in proper proportion by those responsible for pharmacy education. —EGF

Journal of Pharmaceutical Sciences

SEPTEMBER 1977

VOLUME 66 NUMBER 9

RESEARCH ARTICLES

Effect of Shear Mixing on *In Vitro* Drug Release of Capsule Formulations Containing Lubricants

K. S. MURTHY [x] and J. C. SAMYN

Abstract □ The influence of shear mixing on the *in vitro* dissolution properties of several experimental capsule formulations containing lubricants was investigated. The studies were carried out in a 2.8-liter laboratory V-blender equipped with a high-speed intensifier bar, using nitrofurantoin and procainamide hydrochloride as active drugs, powdered lactose and starch as excipients, and magnesium stearate and magnesium lauryl sulfate as lubricants. These studies revealed a pronounced inhibitory effect on drug dissolution due to shear in powder mixtures containing magnesium stearate; even at the maximum lubricant level of only 2%, high shear mixing markedly altered the *in vitro* dissolution rate. In systems with magnesium lauryl sulfate, the shear effect was less pronounced (nitrofurantoin blends) or absent (procainamide hydrochloride blends). The poor dissolution characteristics noted with magnesium stearate–shear combinations seem to result from the formation of a hydrophobic film around the powder mass, preventing wetting and deaggregation.

Keyphrases □ Capsules—containing lubricants, effect of shear mixing on *in vitro* dissolution □ Dissolution, *in vitro*—capsules containing lubricants, effect of shear mixing □ Shear mixing—effect on *in vitro* dissolution of capsules containing lubricants □ Dosage forms—capsules containing lubricants, effect of shear mixing on *in vitro* dissolution

Magnesium stearate is a widely used lubricant in tablet and capsule formulations. In tableting, it is believed to reduce interparticle friction during compression and friction between the tablet and die wall during ejection (1, 2). In encapsulation with automatic capsule-filling equipment, magnesium stearate altered the force–time curves of the material being filled by reducing or eliminating the ejection forces (3).

BACKGROUND

One problem associated with magnesium stearate in solid dose formulations (4, 5) is its tendency to waterproof the dosage form and to retard *in vitro* drug release. Levy and Gumtow (5), based on their studies with nondisintegrating disks of salicylic acid, concluded that hydrophobic lubricants such as magnesium stearate decrease the effective drug–solvent interfacial area and thereby reduce the dissolution rate. Conversely, the dissolution rate enhancing effect of a hydrophilic lubricant, *e.g.*, sodium lauryl sulfate, was viewed as due to better penetration of the solvent into the tablets and component granules, resulting in greater availability of drug surface.

Samyn and Jung (6) studied the *in vitro* disintegration and dissolution rates of several experimental capsule formulations consisting of drug, lactose, or dibasic calcium phosphate, with magnesium stearate as the lubricant. The poor disintegration and dissolution properties noted were attributed to the limited area of contact between the powder mass and the solvent because of poor or incomplete wetting of the solid. They reasoned that this reduced erosion and drug dissolution.

Recently, a new water-soluble compound, magnesium lauryl sulfate, was investigated as a tablet lubricant (7). The evidence indicated that this material may possess lubricating properties comparable to magnesium stearate in the systems studied without its water-repellent effect (8).

In laboratory and industrial blending operations, the mixer is usually equipped with a mechanical device such as an agitator bar, deflector, or baffle to facilitate breakup of aggregates and to ensure good mixing. High speed attrition or shearing devices are often necessary for homogeneous distribution of the active component in high potency, low dose drug mixtures (9). Only a few studies are available concerning the effect of high speed shear mixing on *in vitro* drug release characteristics of powder mixtures containing lubricants. Ganderton (10) investigated the effect of the distribution of magnesium stearate on the penetration of tablets by water. His data suggested that the inhibition of liquid penetration in the presence of magnesium stearate is approximately proportional to the concentration of the lubricant in the system and is susceptible to the mixing method: the more intimate the dispersion of the lubricant, the greater the inhibition of liquid penetration.

The effects of magnesium stearate and the degree of mixing on the physical properties of amylose and sodium chloride tablets also were reported (11). Blending was carried out in a Turbula mixer at a loading level of 20% capacity. When the concentration of magnesium stearate or the mixing time was increased, the intrinsic dissolution rate of sodium chloride was reduced. Furthermore, the effects due to the degree of mixing were pronounced at low lubricant levels. Based on photomicro-

Table I—Composition of Powder Mixtures

Component, mg/capsule	Series I (Nitrofurantoin Blends) Formulations							Series II (Procainamide Hydrochloride Blends) Formulations						
	A	B	C	D	E	F	G	H	I	J	K	L	M	N
Drug	100	100	100	100	100	100	100	100	100	100	100	100	100	100
Lactose powder	250	250	250	—	—	—	250	250	250	250	—	—	—	250
Starch powder	—	—	—	250	250	250	—	—	—	—	250	250	250	—
Magnesium stearate	—	1.75	7.0	—	1.75	7.0	—	—	1.75	7	—	1.75	7.0	—
Magnesium lauryl sulfate	—	—	—	—	—	—	7	—	—	—	—	—	—	7

graphic evidence, a mechanism was suggested involving the formation of a lubricant film around the solid particle during the mixing stage.

The aim of the current investigations was to evaluate the influence of shear mixing on the *in vitro* drug release of powder mixtures containing magnesium stearate as a lubricant in capsule blends of a relatively water-insoluble drug and a water-soluble drug. Nitrofurantoin was selected as the prototype of a low water-soluble drug, and procainamide hydrochloride served as the high water-soluble drug substance. Powdered lactose and starch were the diluents since they are common fillers, both soluble and insoluble, in capsule formulations. Although most investigations employed magnesium stearate as the lubricant, magnesium lauryl sulfate also was included.

EXPERIMENTAL

Magnesium stearate[1], nitrofurantoin[2], procainamide hydrochloride[3], lactose powder[4], and starch powder[5] were USP grade. These chemicals and magnesium lauryl sulfate[6] were purchased commercially and used as received.

The compositions of the various blends prepared and tested are shown in Table I. Series I (Formulations A–G) contains mixtures of nitrofurantoin, while Series II (Formulations H–N) is procainamide hydrochloride blends. Two levels of lubricant were studied, 0.5 and 2%. Both concentrations are relatively low and represent levels used or exceeded in marketed products.

The drug substances were prescreened through a No. 30 sieve to minimize any aggregates that might be present. The materials were introduced into a stainless steel 2.8-liter capacity V-blender[7] with the diluent at the bottom and the drug and the lubricant over it. The blender was loaded to about half its capacity when the total charge of 1.4 kg was present. Shear was applied through the action of the intensifier bar. The blending sequence adopted in these experiments was 15 min of tumble blending without the intensifier bar action followed by tumble blending with shear for 30 min. The powder was sampled immediately before the intensifier bar was turned on ("0"-min sample) and after applying 5, 15, and 30 min of shear.

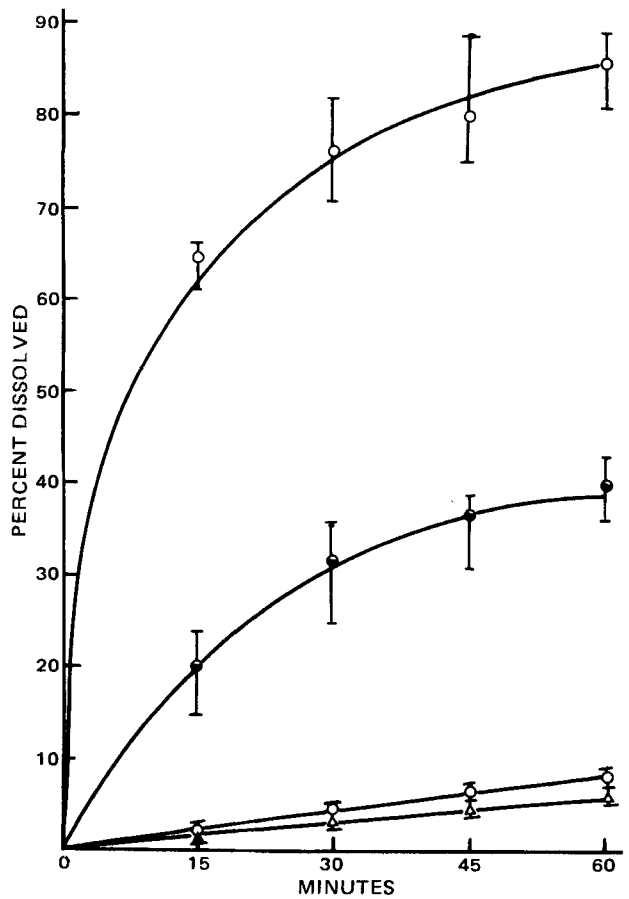

Figure 1—*Effect of shear on the drug dissolution in the nitrofurantoin–lactose mixture (Formulation C). Key: ○, 0 min; ◒, 5 min; ●, 15 min; △, 30 min of mixing with intensifier bar; and ⊖, intercapsule variation.*

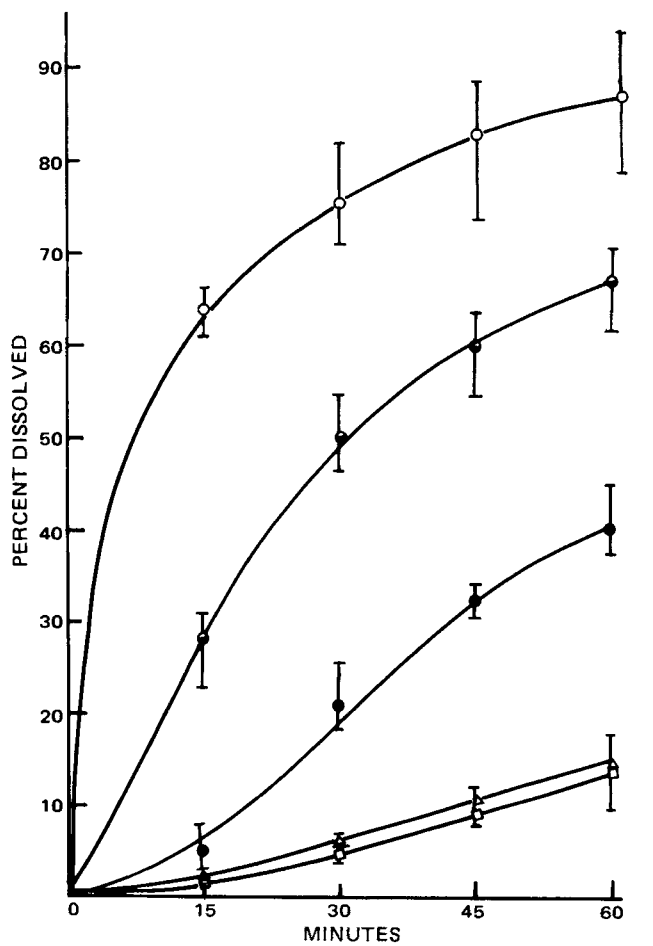

Figure 2—*Effect of shear on the drug dissolution in the nitrofurantoin–starch mixture (Formulation F). Key: ○, 0 min; ◒, 5 min; ●, 15 min; △, 30 min; and □, 45 min of mixing with the intensifier bar.*

[1] Mallinckrodt, St. Louis, Mo.
[2] H. Reisman Corp., Orange, N.J.
[3] Parke, Davis & Co., Holland, Mich.
[4] Humko Sheffield Chemical, Lyndhurst, N.J.
[5] A. E. Staley Manufacturing Co., Decatur, Ill.
[6] Alcolac Corp., Baltimore, Md.
[7] Porta-Shell lab blender equipped with disperser bar assembly, Patterson Industries, East Liverpool, Ohio.

Table II—Dissolution Values (Minutes) for Procainamide Hydrochloride–Lactose Mixtures in 0.1 *N* HCl at 100 rpm and 37°

Amount of Shear, min of Blending with Intensifier Bar	Formulation H			Formulation I			Formulation J			Formulation N		
	T_{20}	T_{50}	T_{80}	T_{20}	T_{50}	T_{80}	T_{20}	T_{50}	T_{80}	T_{20}	T_{50}	T_{80}
0	1.3	2.8	4.7	1.7	4.3	8.1	3.7	6.9	9.5	1.0	2.6	4.2
5	—	—	—	2.8	6.9	13.3	8.0	17.4	45.3	—	—	—
15	1.3	3.0	4.8	7.1	15.6	24.5	13.4	73.0	>180	1.1	2.8	4.5
30	1.2	2.9	4.6	8.1	19.8	27.2	14.0	75.0	>180	1.1	2.9	4.6

In testing nitrofurantoin powder mixtures for *in vitro* drug release, the dissolution apparatus[8] and the general conditions described in USP XIX were followed (12). The temperature was maintained at 37 ± 0.5°, the basket was rotated at 100 rpm, and 900 ml of pH 7.2 phosphate buffer served as the solvent medium. The powder mixture, 353 ± 7 mg, was hand filled into a No. 0 size natural capsule[9], which served as the dosage unit for the test. This fill weight corresponds to a low powder density and was chosen to avoid the effect on the drug release of the tightness of the powder bed packing within the capsule.

At periodic intervals, 5 ml of filtered samples was withdrawn and diluted 10-fold with distilled water. The absorbance of each sample was measured at 367 nm in a UV spectrophotometer[10]. The nitrofurantoin concentration in solution was determined from the standard Beer's law plot prepared with the pure drug material. Preliminary experiments showed that the error involved in not replacing the withdrawn volume of fluid was insignificant.

For procainamide hydrochloride mixtures, the test procedure used was identical to that described, except that the solvent medium and the diluting fluid were 0.1 *N* HCl and the sample absorption was read at 224 nm.

Except where the drug dissolution was very rapid, the release rates were followed through 60 min. Each dissolution profile is the average of three to five individual determinations. The ranges are indicated in the various graphs.

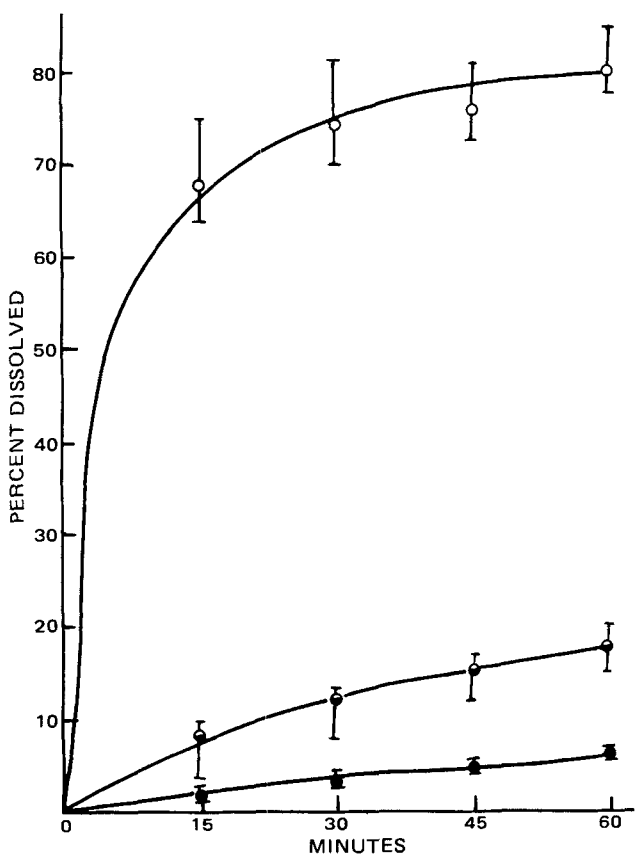

Figure 3—*Dissolution profiles of nitrofurantoin–lactose mixtures subjected to 30 min of shear as a function of lubricant concentration. Key:* ○, *Formulation A (0%);* ◒, *Formulation B (0.5%); and* ●, *Formulation C (2% magnesium stearate).*

[8] Multiple spindle dissolution drive, model 72B, Hanson Research Corp., Northridge, Calif.

[9] Parke, Davis & Co., Detroit, Mich.

[10] Model 25, Beckman Instruments, Fullerton, Calif.

RESULTS AND DISCUSSION

In each test series, two formulations (A and D in Series I and H and K in Series II) did not contain a lubricant and served as controls. Also, two different base materials, powdered lactose and powdered starch, were used. In addition to the controls, the blends studied contained lubricant concentrations of 0.5 or 2% of the drug–diluent mixtures. Formulations G and N contained 2% magnesium lauryl sulfate as the lubricant.

The effect of shear on the dissolution profiles of nitrofurantoin powder mixtures containing 2% magnesium stearate is shown in Fig. 1 (lactose as filler) and Fig. 2 (starch as filler). At this level of lubricant, shear mixing had a pronounced inhibitory effect on drug dissolution. In Fig. 1 (Formulation C), the amount of drug in solution at 1 hr declined from about 86% in the absence of shear to 8% after 15 min of blending with the intensifier bar. The shear effect appears to be greater with lactose as the base material compared to starch. This finding is somewhat unexpected in that water-soluble lactose should have aided in bringing about more rapid drug dissolution.

With both filler materials, after the capsule shells dissolved, the powders that displayed poor dissolution characteristics typically yielded an intact plug of solid with a central dry core at the end of the dissolution test run. This result occurred in spite of the intentionally low packing of the powder. Furthermore, the amount of drug released approached an equilibrium state with the application of shear. With the lactose blends, this state was attained after 15 min of blending time; with ni-

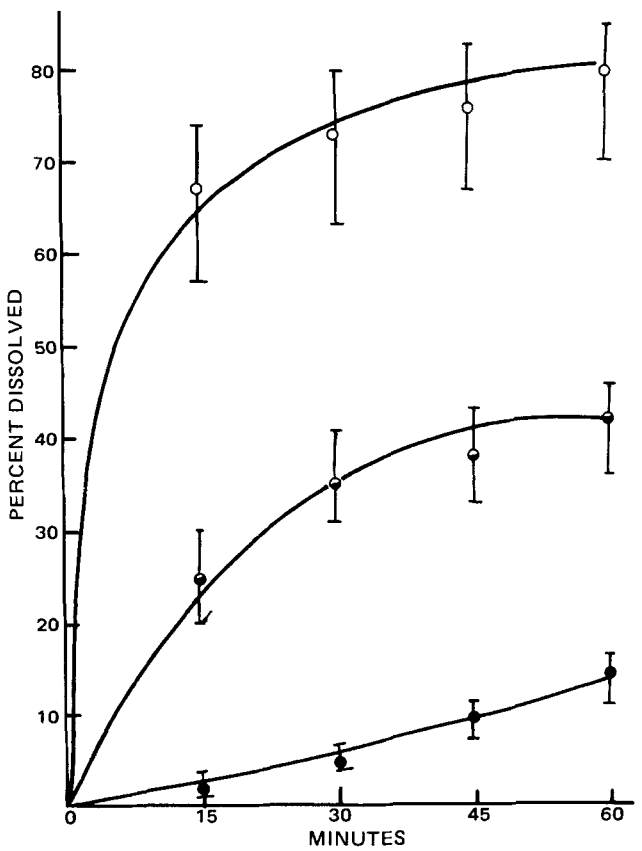

Figure 4—*Dissolution profiles of nitrofurantoin–starch mixtures subjected to 30 min of shear as a function of lubricant concentration. Key:* ○, *Formulation D (0%);* ◒, *Formulation E (0.5%); and* ●, *Formulation F (2% magnesium stearate).*

Table III—Dissolution Values (Minutes) for Procainamide Hydrochloride–Starch Mixtures in 0.1 *N* HCl at 100 rpm and 37°

Amount of Shear, min of Blending with Intensifier Bar	Formulation K			Formulation L			Formulation M		
	T_{20}	T_{50}	T_{80}	T_{20}	T_{50}	T_{80}	T_{20}	T_{50}	T_{80}
0	1.3	3.2	5.3	1.4	3.6	6.8	5.6	10.3	13.6
5	—	—	—	4.0	7.5	10.9	9.4	18.9	30.6
15	1.2	3.1	5.0	5.3	11.6	16.1	10.9	25.8	40.1
30	1.2	3.0	4.7	8.5	15.9	25.3	22.2	52.0	91.0

trofurantoin–starch–magnesium stearate mixtures (Formulations E and F), equilibrium was not reached until 30 min or longer of blending. Shorter high shear mixing times (5 min) resulted in a significant drop in the *in vitro* drug availability (Figs. 1 and 2). In the current investigations, rapid dissolution occurred at a level of 2% magnesium stearate when high shear was not applied.

Figures 3 and 4 summarize data on the *in vitro* release of nitrofurantoin in phosphate buffer at 100 rpm from formulations containing different concentrations of magnesium stearate. In these instances, 30 min of shear was applied to all powder mixtures. The retarding effect of shear on the dissolution rate was dependent on the level of magnesium stearate in the formulation; the larger the concentration of the lubricant, the slower was the drug release after the application of shear.

As shown previously, with any given concentration of magnesium stearate in the mixture, the inhibitory effect on drug dissolution is related to the degree of shear applied to the system. Thus, the greatest impairment of dissolution is likely to result in systems containing high levels of magnesium stearate subjected to long periods of shear. Among the blends investigated, formulations containing 2% magnesium stearate (C and F) experienced the largest reduction in dissolution rate after 30 min of mixing with the intensifier bar. There was no effect of shear in formulations devoid of lubricant (A and D).

Figure 5 illustrates the findings of shear studies carried out on Formulation G, which contained a water-soluble lubricant, 2% magnesium lauryl sulfate. The effect here was minimal. After 5 min of shear, the amount of drug in solution in 1 hr was reduced from 78 to 54%. Additional blending with the intensifier bar for up to 30 min resulted in no further reduction in the drug dissolution.

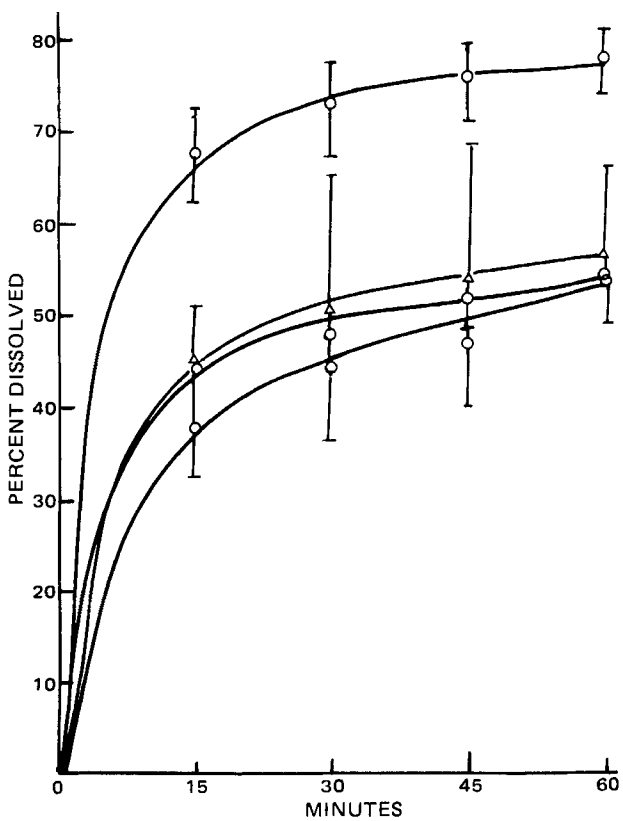

Figure 5—*Effect of shear on the drug dissolution in the nitrofurantoin–lactose–magnesium lauryl sulfate mixture (Formulation G). Key: ○, 0 min; ◒, 5 min; ●, 15 min; and △, 30 min of mixing with the intensifier bar.*

In Figs. 6 and 7, the dissolution rates of procainamide hydrochloride mixtures are shown at various mixing times with the intensifier bar. Figure 6 deals with Formulation J where lactose was used as the excipient, while Fig. 7 displays data for Formulation M where starch served as the base material. The lubricant was at the 2% level in both formulations. There was a marked reduction in dissolution due to shear in both blends, despite the high solubility of the drug substance. In Formulation J, the release rate reached an equilibrium state within 15 min of blending, in contrast to Formulation M where the system still showed a decreased dissolution rate even after 30 min of shear. Formulation J appeared to be particularly susceptible to the shear effect, since mixing for 5 min with the bar resulted in T_{80} (time for 80% of the drug to be in solution) values increasing from 9.5 to 45.3 min.

Tables II and III list the various T_{20} (time for 20% of the drug to be in solution), T_{50}, and T_{80} values of the procainamide hydrochloride formulations (H–M). The findings recorded with this water-soluble drug are similar to those for the nitrofurantoin powder mixtures in that the inhibitory effect on drug dissolution is related to the level of magnesium stearate in the formula and the duration of shear mixing. However, in contrast to the slight reduction in the dissolution rate noted for the nitrofurantoin mixture containing 2% magnesium lauryl sulfate (Fig. 5), no shear effect was apparent with Formulation N (Table II).

In addition to altering the dissolution properties, shear influenced both

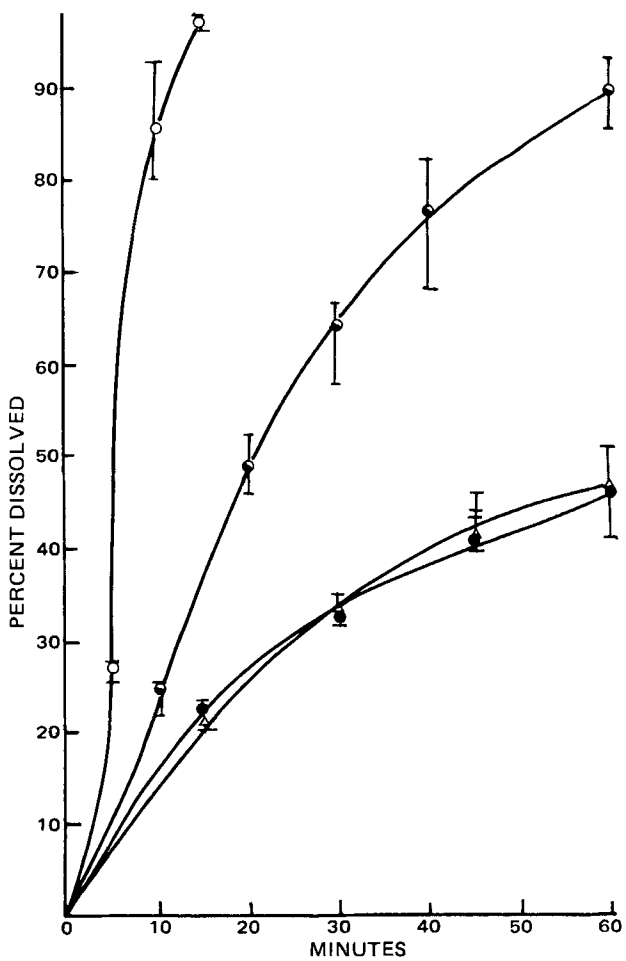

Figure 6—*Effect of shear on the drug dissolution in the procainamide hydrochloride–lactose mixture (Formulation J). Key: ○, 0 min; ◒, 5 min; ●, 15 min; and △, 30 min of mixing with the intensifier bar.*

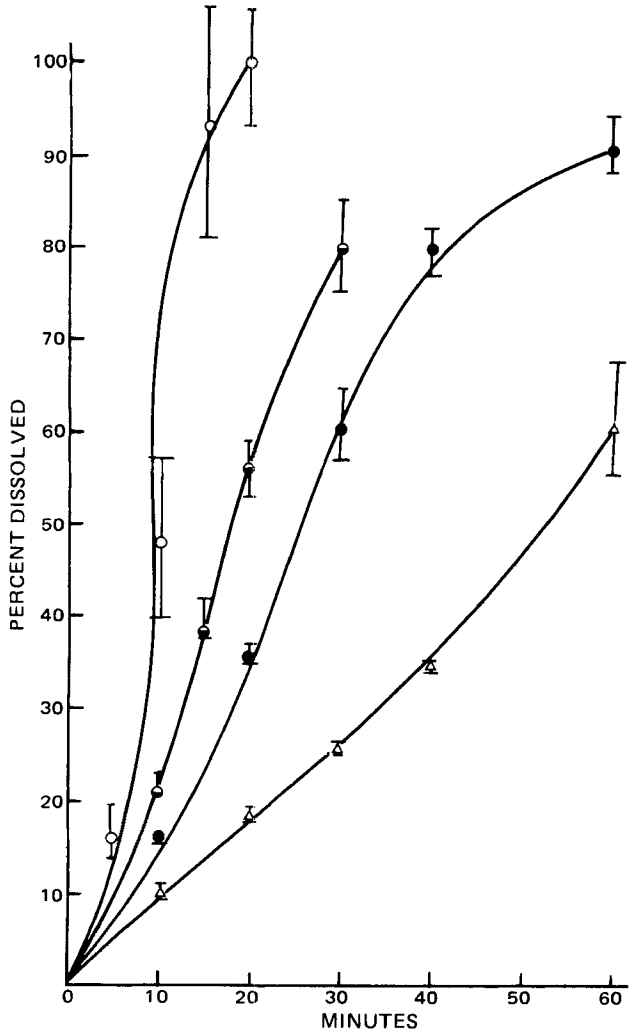

Figure 7—*Effect of shear on the drug dissolution in the procainamide hydrochloride–starch mixture (Formulation M). Key: ○, 0 min; ◒, 5 min; ●, 15 min; and △, 30 min of mixing with the intensifier bar.*

loose and packing densities of powder blends containing magnesium stearate. The powder densities increased with blending time up to maximum limiting values. These changes in the density characteristics of powders with shear are presumably related to improved flow properties and are frequently reflected in their subsequent processing, *e.g.*, in the fill weight and weight control during encapsulation.

The evidence presented in this paper illustrates the potential liabilities stemming from the indiscriminate use of shearing or mixing devices to break up aggregates in the blending operations where magnesium stearate and other hydrophobic lubricants are in the formula. The intensity of mixing is an important processing variable, capable of altering the *in vitro* availability characteristics of pharmaceutical formulations. This result, in turn, potentially may influence the bioavailability of the dosage form. A knowledge of the shear effect on drug dissolution should be an integral part of formula development and scale-up studies of drug preparations.

REFERENCES

(1) R. E. King, in "Remington's Pharmaceutical Sciences," 15th ed., J. E. Hoover, Ed., Mack Publishing Co., Easton, Pa., 1975, p. 1579.

(2) E. Shotton and J. A. Hersey, in "The Theory and Practice of Industrial Pharmacy," L. Lachman, H. A. Lieberman, and J. L. Kanig, Eds., Lea & Febiger, Philadelphia, Pa., 1970, p. 192.

(3) G. C. Cole and G. May, *J. Pharm. Pharmacol.*, **27**, 353 (1975).

(4) W. A. Strickland, Jr., E. Nelson, L. W. Busse, and T. Higuchi, *J. Am. Pharm. Assoc., Sci. Ed.*, **45**, 51 (1956).

(5) G. Levy and R. H. Gumtow, *J. Pharm. Sci.*, **52**, 1139 (1963).

(6) J. C. Samyn and W. Y. Jung, *ibid.*, **59**, 169 (1970).

(7) A. M. Salpekar and L. L. Augsburger, *ibid.*, **63**, 289 (1974).

(8) H. C. Caldwell and W. J. Westlake, *ibid.*, **61**, 985 (1972).

(9) J. C. Samyn and K. S. Murthy, *ibid.*, **63**, 370 (1974).

(10) D. Ganderton, *J. Pharm. Pharmacol.*, **21**, 95 (1969).

(11) G. K. Bolhuis, C. F. Lerk, H. T. Zijlstra, and A. H. De Boer, *Pharm. Weekbl.*, **110**, 317 (1975).

(12) "The United States Pharmacopeia," 19th rev., Mack Publishing Co., Easton, Pa., 1975, p. 651.

ACKNOWLEDGMENTS AND ADDRESSES

Received September 10, 1976, from the *Department of Pharmaceutical Research and Development, Parke, Davis & Co., Detroit, MI 48232.*

Accepted for publication November 3, 1976.

The authors thank Mr. S. A. Patel for his initial observations on the subject.

ˣ To whom inquiries should be directed.

High-Pressure Liquid Chromatographic Analysis of Methotrexate in Presence of Its Degradation Products

DULAL C. CHATTERJI and JOSEPH F. GALLELLI ˣ

Abstract □ Two high-pressure liquid chromatographic methods are described for the quantitative determination of methotrexate in the presence of its contaminants and degradation products. Method 1 takes less than 15 min and is recommended for routine assays of methotrexate in commercial products. Method 2 takes about 35 min and is the method of choice to detect and quantitate large amounts of degradation products. Quantitation to a level of 1 μg of methotrexate/ml is feasible by these methods and thus provides potential applicability for the analysis of methotrexate in biological fluids.

Keyphrases □ Methotrexate—high-pressure liquid chromatographic analysis, commercial preparations □ High-pressure liquid chromatography—analysis, methotrexate in commercial preparations □ Antineoplastic agents—methotrexate, high-pressure liquid chromatographic analysis in commercial preparations

Methotrexate is a folic acid antagonist widely used in cancer chemotherapy. However, methotrexate is contaminated with its degradation products and other closely related folic acid analogs. Quantitation of the contami-

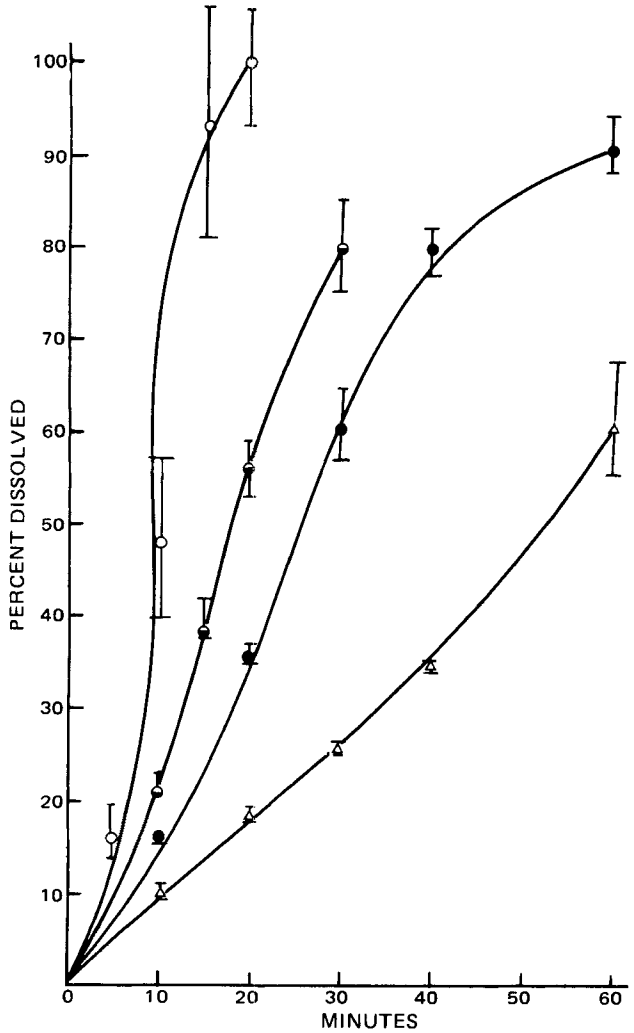

Figure 7—*Effect of shear on the drug dissolution in the procainamide hydrochloride–starch mixture (Formulation M). Key: ○, 0 min; ◒, 5 min; ●, 15 min; and △, 30 min of mixing with the intensifier bar.*

loose and packing densities of powder blends containing magnesium stearate. The powder densities increased with blending time up to maximum limiting values. These changes in the density characteristics of powders with shear are presumably related to improved flow properties and are frequently reflected in their subsequent processing, *e.g.*, in the fill weight and weight control during encapsulation.

The evidence presented in this paper illustrates the potential liabilities stemming from the indiscriminate use of shearing or mixing devices to break up aggregates in the blending operations where magnesium stearate and other hydrophobic lubricants are in the formula. The intensity of mixing is an important processing variable, capable of altering the *in vitro* availability characteristics of pharmaceutical formulations. This result, in turn, potentially may influence the bioavailability of the dosage form. A knowledge of the shear effect on drug dissolution should be an integral part of formula development and scale-up studies of drug preparations.

REFERENCES

(1) R. E. King, in "Remington's Pharmaceutical Sciences," 15th ed., J. E. Hoover, Ed., Mack Publishing Co., Easton, Pa., 1975, p. 1579.

(2) E. Shotton and J. A. Hersey, in "The Theory and Practice of Industrial Pharmacy," L. Lachman, H. A. Lieberman, and J. L. Kanig, Eds., Lea & Febiger, Philadelphia, Pa., 1970, p. 192.

(3) G. C. Cole and G. May, *J. Pharm. Pharmacol.*, **27**, 353 (1975).

(4) W. A. Strickland, Jr., E. Nelson, L. W. Busse, and T. Higuchi, *J. Am. Pharm. Assoc., Sci. Ed.*, **45**, 51 (1956).

(5) G. Levy and R. H. Gumtow, *J. Pharm. Sci.*, **52**, 1139 (1963).

(6) J. C. Samyn and W. Y. Jung, *ibid.*, **59**, 169 (1970).

(7) A. M. Salpekar and L. L. Augsburger, *ibid.*, **63**, 289 (1974).

(8) H. C. Caldwell and W. J. Westlake, *ibid.*, **61**, 985 (1972).

(9) J. C. Samyn and K. S. Murthy, *ibid.*, **63**, 370 (1974).

(10) D. Ganderton, *J. Pharm. Pharmacol.*, **21**, 95 (1969).

(11) G. K. Bolhuis, C. F. Lerk, H. T. Zijlstra, and A. H. De Boer, *Pharm. Weekbl.*, **110**, 317 (1975).

(12) "The United States Pharmacopeia," 19th rev., Mack Publishing Co., Easton, Pa., 1975, p. 651.

ACKNOWLEDGMENTS AND ADDRESSES

Received September 10, 1976, from the *Department of Pharmaceutical Research and Development, Parke, Davis & Co., Detroit, MI 48232.*

Accepted for publication November 3, 1976.

The authors thank Mr. S. A. Patel for his initial observations on the subject.

ˣ To whom inquiries should be directed.

High-Pressure Liquid Chromatographic Analysis of Methotrexate in Presence of Its Degradation Products

DULAL C. CHATTERJI and JOSEPH F. GALLELLI ˣ

Abstract □ Two high-pressure liquid chromatographic methods are described for the quantitative determination of methotrexate in the presence of its contaminants and degradation products. Method 1 takes less than 15 min and is recommended for routine assays of methotrexate in commercial products. Method 2 takes about 35 min and is the method of choice to detect and quantitate large amounts of degradation products. Quantitation to a level of 1 μg of methotrexate/ml is feasible by these methods and thus provides potential applicability for the analysis of methotrexate in biological fluids.

Keyphrases □ Methotrexate—high-pressure liquid chromatographic analysis, commercial preparations □ High-pressure liquid chromatography—analysis, methotrexate in commercial preparations □ Antineoplastic agents—methotrexate, high-pressure liquid chromatographic analysis in commercial preparations

Methotrexate is a folic acid antagonist widely used in cancer chemotherapy. However, methotrexate is contaminated with its degradation products and other closely related folic acid analogs. Quantitation of the contami-

nants in commercial methotrexate preparations is important because of the recent use of large doses (10–15 g) in humans.

Most methods (1, 2) for the assay of intact methotrexate in the presence of its contaminants and/or degradation products are time consuming. The USP (1) quantitative TLC method is subject to limitations of accuracy without an internal standard. Other methods such as competitive protein binding (3), although sensitive, are only suitable for biological samples because of their large coefficient of variation. A high-pressure liquid chromatographic (HPLC) method was reported for the separation of impurities in methotrexate (4). However, the quantitation of methotrexate in the presence of its degradation products was not demonstrated.

This report presents a sensitive and rapid HPLC method for the quantitative determination of methotrexate in the presence of its contaminants and degradation products.

EXPERIMENTAL

Apparatus—A liquid chromatograph[1] equipped with an injection valve[2] capable of withstanding 7000 psig was used. The valve was such that any volume less than the loop volume could be loaded directly into the loop and subsequently injected into the column without stopping the flow. The liquid chromatograph also was equipped with a fixed wavelength UV detector for monitoring the column effluent at 254 nm[3], a chart recorder[4], and an electronic integrator[5]. The columns used were 50-cm × 2.1-mm (i.d.) stainless steel tubing prepacked with anion-exchange resin[6] (30–44 μm) and 30-cm × 4-mm (i.d.) stainless steel tubing prepacked with bonded amine[7].

Reagents—USP methotrexate reference standard[8], mp 182–189°, was used.

Commercial preparations of methotrexate sodium for injection, 25 mg/ml[9], and 2.5-mg methotrexate tablets[10] also were used. Acetonitrile was a glass-distilled spectrophotometric grade[11], and all other reagents were analytical grade.

Two mobile phase solvents were used. Each liter of Solvent 1 contained 0.3 mole of sodium perchlorate, 0.15 mole of monobasic sodium phosphate, 0.15 mole of dibasic sodium phosphate, and 15 ml of acetonitrile. Each liter of Solvent 2 contained 0.075 mole of sodium perchlorate, 0.0375 mole of monobasic sodium phosphate, 0.0375 mole of dibasic sodium phosphate, and 20 ml of acetonitrile.

Unless otherwise noted, all solutions to be assayed were brought to volume with 0.1 *M* ammonia–ammonium bicarbonate buffer (pH 8.3).

Reference Solution—A reference solution of methotrexate USP was prepared by accurately weighing approximately 10 mg of methotrexate USP in a 100-ml volumetric flask and bringing to volume with 0.1 *M* ammonia–ammonium bicarbonate buffer (pH 8.3). The reference solution was freshly prepared every 2 weeks, wrapped in aluminum foil, and stored in the refrigerator (2–4°). To generate a standard curve for calculations, this reference solution was appropriately diluted.

Sample Solutions—All sample solutions were diluted to approximately 10 mg of methotrexate/100 ml and assayed.

Tablets—To minimize tablet weight variation, 10 tablets were triturated in a glass mortar and the total powder was accurately weighed. A portion of the powder equivalent to one-tenth of the total weight was then accurately weighed, placed in a 25-ml volumetric flask, and diluted to volume with 0.1 *M* ammonia–ammonium bicarbonate buffer (pH 8.3). After shaking for 10 min, the solution was filtered and assayed.

Injections—The contents of each vial were further diluted to an appropriate volume with ammonia buffer and assayed.

[1] Model 3500B, Spectra-Physics, Santa Clara, Calif.
[2] Velco type valve, Spectra-Physics, Santa Clara, Calif.
[3] Model 225, Spectra-Physics, Santa Clara, Calif.
[4] Varian A-25, Varian Associates, Palo Alto, CA 94303.
[5] Autolab System I, Spectra-Physics, Santa Clara, Calif.
[6] Vydac, E. Merck, Germany, marketed by Spectra-Physics, No. AX-107.
[7] μBondapak NH_2, marketed by Waters Associates, Milford, Mass.
[8] Lot 1260X8105, Lederle Laboratories, Pearl River, N.Y.
[9] Lot 467-164, 50 mg in 2-ml vials, Lederle Laboratories, Pearl River, N.Y.
[10] Lot 422-109, Lederle Laboratories, Pearl River, N.Y.
[11] Aldrich Chemical Co., Milwaukee, WI 53233.

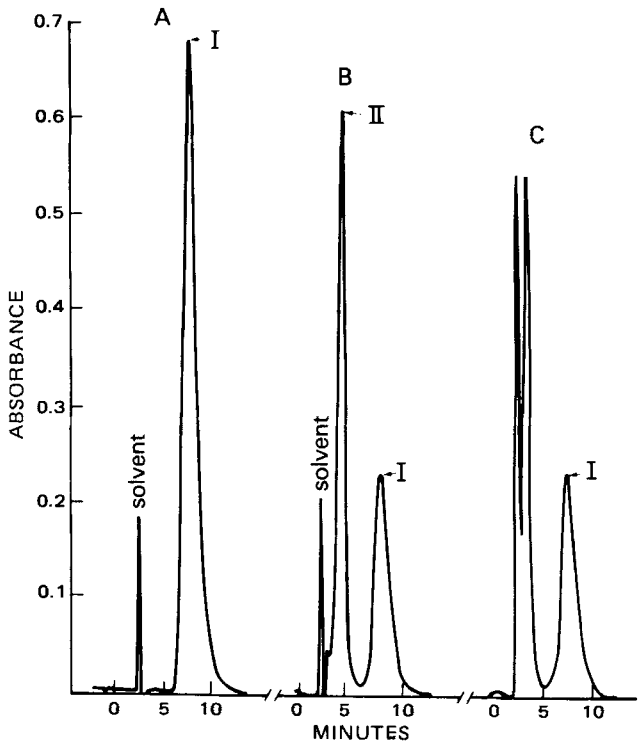

Figure 1—*High-pressure liquid chromatograms of USP methotrexate reference standard solution by Method 1. Key: A, initial; B, heat degraded, approximately 60%; C, light degraded, approximately 60%; I, methotrexate; and II,* N^{10}*-methylfolic acid.*

Heat-Degraded Solution—Approximately 10 mg of USP methotrexate reference standard was accurately weighed, placed in a 100-ml volumetric flask, and brought to volume with ammonia buffer. The solution was then packaged into ampuls, heated in an oven at 85° for 10 days, and assayed.

Light-Degraded Solution—Approximately 10 mg of USP methotrexate reference standard was accurately weighed, placed in a 100-ml flask, and brought to volume with ammonia buffer. The solution was then placed under a fluorescent light at room temperature for 6 days and assayed.

Various degradation mixtures were then made up by accurately mixing known amounts of reference solutions and heat- and light-degraded solutions.

Chromatographic Methods—*HPLC Method 1*—A 50-cm anion-exchange column[6] with the mobile phase (Solvent 1) at a flow rate of 0.6 ml/min and pressure of about 500 psi was used. A 10-μl full loop sample volume was injected quantitatively into the column with the recorder set at 0.04 full scale. After methotrexate was eluted, appearing as the last peak on the chromatogram, the column was ready for another run.

The areas obtained under the peak heights were used for the calculations. Total run time was 12–15 min. No internal standard was used, because a full loop volume was always quantitatively injected and the precision was calculated to be about 1%. Each sample run was immediately followed by a run with the reference solution.

A standard curve was prepared by determining the area ratios of different concentrations of the reference solution and plotting them against their respective known concentration ratios:

$$\text{area ratio} = \frac{\text{area of peak 1 of various dilutions of reference solution}}{\text{area of peak 1 of reference solution}} \quad \text{(Eq. 1)}$$

$$\text{concentration ratio} = \frac{\text{concentration of various dilutions of reference solution}}{\text{concentration of reference solution}} \quad \text{(Eq. 2)}$$

HPLC Method 2—Two columns, a bonded amine column[7] nearer the injection site and an anion-exchange resin column[6] in series, with the mobile phase (Solvent 2) at a flow rate of 0.8 ml/min and pressure of about 1300 psig were used. The procedure was otherwise the same as Method

Table I—Comparison of Assay Results for Intact Methotrexate in Various Samples by HPLC Method 1 and the Cellulose Column Method

Sample	Description	Methotrexate, % Expected Value	By HPLC Method 1[a]	By Cellulose Column Method
1	25.0 ml[b]	100	100	100
2	20.0 ml[b] + 5.0 ml[c]	88.4	88.34 ± 1.01	89.0
3	15.0 ml[b] + 10.0 ml[c]	76.8	76.93 ± 0.79	
4	10.0 ml[b] + 15.0 ml[c]	65.2	65.58 ± 0.94	66.7
5	5.0 ml[b] + 20.0 ml[c]	53.6	54.20 ± 0.32	
6	25.0 ml[c]	42.0	42.00 ± 0.47	42.6

[a] Average of three runs. [b] A USP methotrexate reference standard solution assigned a value of 100%. [c] A heat-degraded solution of methotrexate calculated to contain 42% methotrexate based on Sample 1 as calculated by Method 1.

1. A standard curve was prepared the same way as described for Method 1.

Cellulose Column Method—Assay on a diethylaminoethylcellulose column was performed by the method of Gallelli and Yokoyama (2), but the resin was not discarded after each run. At the end of an assay, when the last peak was eluted, the column was washed with 100 ml of 0.1 *M* ammonia–ammonium bicarbonate buffer (pH 8.3); the column was then ready for another assay. Aliquots of 10 ml of sample or reference solution were used in each run.

RESULTS AND DISCUSSION

N^{10}-Methylfolic acid is a heat-degraded product, while 2,4-diamino-6-pteridine carboxylic acid and its aldehyde are light-degraded products of methotrexate. Figure 1 shows typical chromatograms of methotrexate, light-degraded methotrexate, and heat-degraded methotrexate, using Method 1. In all three chromatograms, methotrexate was very strongly bound to the column's resin and eluted last. The light-degraded products of methotrexate eluted with the solvent front (Fig. 1C). Excellent separation between methotrexate and the major heat degradation product, N^{10}-methylfolic acid, is shown in Fig. 1B. Since the light-degraded products of methotrexate eluted with the solvent front and in no way interfered in the assay of intact methotrexate, a series of mixtures of methotrexate and heat-degraded methotrexate solutions was prepared and assayed by Method 1 and the cellulose column method. The values obtained by Method 1 were in excellent agreement with the expected values (Table I). Also, there was reasonably good agreement with the values obtained by Method 1 and the cellulose column method, although the latter values were consistently higher by about 1%.

During the analysis of various heat-degraded methotrexate solutions by Method 1, a shoulder peak (r_t = 10 min, Fig. 2*b*) appeared immediately preceding the methotrexate peak. This shoulder was especially evident when a more dilute buffer was used as the eluent (Fig. 2). Although the area of the shoulder peak was initially less than 1% of the area of the methotrexate peak, its relative percentage became increasingly important when the drug was degraded more than 70%; the shoulder peak was then 10–15% of the small methotrexate peak.

Repeated attempts using Method 1 with various buffer strengths and flow rates were unsuccessful in reproducibly separating the shoulder peak from the methotrexate peak. Success was finally achieved with a bonded amine column[7] in series with the anion-exchange resin column[6] and Solvent 2. Method 2 not only separated the shoulder peak (r_t = 13.5 min, Fig. 2*a*) from the methotrexate peak but also separated other heat degradation products more effectively, allowing for their possible quantitation.

To calculate methotrexate levels, a standard curve was prepared by plotting area ratios against concentration ratios (see *Experimental*). Although the area ratios were slightly lower than a 1:1 ratio at a concentration below 4 mg/100 ml and slightly higher than a 1:1 ratio at a concentration above 12 mg/100 ml, an excellent linear fit was obtained over a 15-fold concentration range (r = 0.9996, n = 7).

The area ratios of the various samples assayed were calculated, and their corresponding concentration ratios were determined from the standard curve. The explicit quantity of intact methotrexate in various samples was calculated as follows:

$$\text{concentration of intact methotrexate in sample} = (\text{concentration ratio})\,(R) \quad \text{(Eq. 3)}$$

$$\text{concentration of intact methotrexate in injections} = (\text{concentration ratio})\,(R)\,(2.5) \quad \text{(Eq. 4)}$$

$$\text{amount of intact methotrexate per tablet} = \frac{W_{av}}{W} \times (\text{concentration ratio})\,(R)\,(0.25) \quad \text{(Eq. 5)}$$

Table II—Results Obtained for the Assay of Methotrexate Tablets, Injectables, and Heat-Degraded and Light-Degraded Samples

Sample	Methotrexate[a], % By HPLC Method 1	By HPLC Method 2	By Cellulose Column Method
Heat degraded, approximately 60%	42.0	41.2	42.6
Heat degraded, approximately 80%	24.2	21.0	21.7
Light degraded, approximately 70%	30.4	29.4	30.2
Tablet	121.2[b] (105.1)	121.6[b] (105.4)	123.1 (106.7)
Injection	123.6[b] (107.2)	123.2[b] (107.8)	125.2 (108.5)

[a] Relative to reference solution containing 10.05 mg of methotrexate/100 ml. [b] Both tablet and injection samples contained more than 120% of the labeled amount when compared to USP methotrexate reference standard and as such violated the USP limits (90–110%). However, USP methotrexate reference standard was analyzed and found to contain 86.3% pure methotrexate (on anhydrous basis, as calculated by the method in Ref. 2). Explicit values of methotrexate present in tablets and injectables (calculated relative to USP methotrexate reference standard by the method described in this paper) should, therefore, be multiplied by 0.863 to give the true value of methotrexate content. These corrected values, represented as percent of labeled amount, are reported in parentheses.

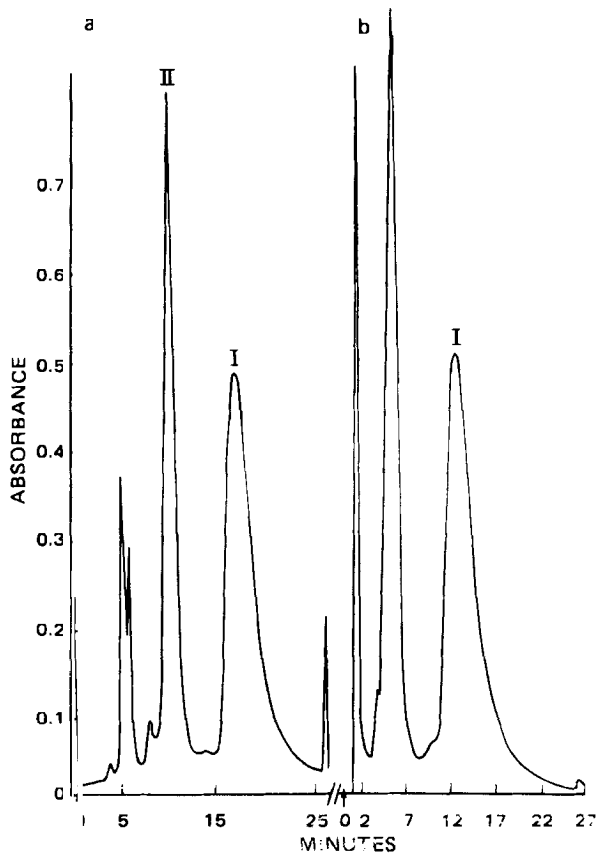

Figure 2—*High-pressure liquid chromatograms of a heat-degraded solution of methotrexate. Key:* a, *using Method 2;* b, *using Method 1 with a dilute buffer (mobile phase 2); I, methotrexate; and II,* N^{10}*-methylfolic acid.*

where R is the concentration of USP methotrexate reference solution in milligrams per 100 ml, W_{av} is the average weight of one tablet in milligrams, and W is the weight of an aliquot of the tablet triturate taken for assay.

Table II summarizes the values of various samples obtained by Methods 1 and 2 and the cellulose column method. All three methods gave essentially similar values with light-degraded methotrexate samples and less than 70% heat-degraded methotrexate samples. Therefore, considering the relative quickness of the assay procedure by Method 1 (less than 15 min), this method is recommended for routine assays of methotrexate in commercial products. Method 2 is more important in studying the kinetics of methotrexate and for quantitating its degradation products. Also, it is essential to use Method 2 in methotrexate samples that are more than 70% heat degraded.

The sensitivity of Method 1 was determined using a 100-μl sample size to detect a concentration of 0.25 μg of methotrexate/ml of solution. An aqueous solution containing 1 μg of methotrexate/ml of solution, when analyzed by Method 1, gave a recovery of 93.1 ± 4.7% of methotrexate (average of three runs). Thus, Method 1 could be potentially useful in quantitating to a level of 1 μg of methotrexate/ml in biological fluids.

The tablet excipient dye did not interfere with the assay, as seen by the close agreement between the values obtained by Methods 1 and 2 and the cellulose column method. In the latter method, the dye could be seen as a yellow band remaining at the top of the cellulose column. The benzyl alcohol preservative present in the injectables is nonionic and eluted almost with the solvent front. Other preservatives such as methylparaben and propylparaben eluted immediately following the solvent front and did not interfere with the assay of intact methotrexate.

In all of the described assays, the amount of intact methotrexate in the unknown is calculated as a percentage of the reference solution. The explicit quantities are then calculated from the known concentration of methotrexate USP in the reference solution. However, methotrexate USP has been reported (2) to be only 85–90% pure. Therefore, explicit quantities in the assays, which are calculated by assuming methotrexate USP as 100% pure, must be interpreted accordingly. However, in the determination of relative amounts in various preparations or in the determination of percentage degradation, this consideration is obviated.

REFERENCES

(1) "The United States Pharmacopeia," 19th rev., Mack Publishing Co., Easton, Pa., 1975, p. 315.

(2) J. F. Gallelli and G. Yokoyama, *J. Pharm. Sci.*, **56**, 387 (1967).

(3) C. E. Myers, M. E. Lippman, M. E. Helen, and A. Bruce, *Proc. Natl. Acad. Sci. USA*, **72**, 3863 (1976).

(4) W. P. Tong, J. Rosenberg, and D. B. Ludlum, *Lancet*, **2**, 719 (1975).

ACKNOWLEDGMENTS AND ADDRESSES

Received July 15, 1976, from the *Pharmacy Department, The Clinical Center, Public Health Service, National Institutes of Health, Bethesda, MD 20014.*

Accepted for publication November 3, 1976.

[x] To whom inquiries should be directed.

Vehicle Effects on Ocular Drug Bioavailability II: Evaluation of Pilocarpine

JAMES W. SIEG and JOSEPH R. ROBINSON [x]

Abstract □ The influence of vehicle composition on ocular penetration of pilocarpine was studied in the albino rabbit. Increasing the pH of a vehicle promoted increased corneal penetration for pilocarpine, in accordance with the pH–partition hypothesis, but a similar series of experiments with a nonionizable drug, glycerin, gave similar results. The extent of pH-induced lacrimation by the vehicle and its effect on precorneal drug concentration also was determined. Increased pilocarpine absorption at neutral to slightly alkaline pH was due primarily to its peculiar solubility characteristics coupled with less irritation and lacrimation rather than a direct pH effect on the molecule. Incorporation of pilocarpine into a petrolatum-based ointment vehicle resulted in increased aqueous humor pilocarpine levels above those provided by an equivalent dose of aqueous solution. The mechanism of this increase was determined to be a higher effective concentration of pilocarpine in the ointment vehicle coupled with an increase in contact time of the dose. The ointment system also exerted an unusual form of vehicle control in that it promoted the corneal penetration of pilocarpine while impeding uniform mixing of the dose with tears and thereby imposed a restriction on the amount of pilocarpine available to the ocular tissues.

Keyphrases □ Pilocarpine—effect of vehicle composition and pH on ocular bioavailability, rabbits □ Vehicles—effect of composition and pH on ocular bioavailability of pilocarpine, rabbits □ Bioavailability, ocular—pilocarpine, effect of vehicle composition and pH, rabbits □ Ocular bioavailability—pilocarpine, effect of vehicle composition and pH, rabbits □ Ophthalmic cholinergic agents—pilocarpine, effect of vehicle composition and pH on ocular bioavailability, rabbits

The first report in this series dealt with vehicle influence on the ocular bioavailability of the relatively water-insoluble steroid fluorometholone (1). In that study, mechanisms of vehicle effects on ocular bioavailability were based on the interplay of the steroid and vehicle properties with the physiological and physicochemical nature of the drug administration site, *i.e.*, the precorneal portion of the eye. The present study extended this work to include the important water-soluble antiglaucoma drug pilocarpine. Thus, this examination of a water-soluble drug, along with earlier work on the relatively water-insoluble steroid, provides considerable perspective on factors that should be considered when formulating an ophthalmic drug for topical delivery to the eye to obtain maximum drug benefit.

BACKGROUND

During the past 30 years, numerous vehicles have been screened for various drugs to improve the overall intraocular penetration of topically applied drugs. Because of an inadequate understanding of the interplay between drug–vehicle–precorneal area properties, the primary thrust of much research has been directed toward prolonging the presence of the instilled dose in the precorneal area, usually referred to as increasing the contact time. Most often, these formulations rely mainly upon the viscosity character of the vehicle and its subsequent rheological effect on drainage loss of the dose *via* the nasolacrimal duct. Thus, most topically applied ocular vehicles have included viscous polymers such as hydroxypropylcellulose (2–4), methylcellulose (5–12), and polyvinyl alcohol (2–4, 6–8, 13–15).

Detailed studies of the drainage loss rate of these vehicles also have been performed (3, 5, 13, 16, 17) to permit selection of vehicles exhibiting

where R is the concentration of USP methotrexate reference solution in milligrams per 100 ml, W_{av} is the average weight of one tablet in milligrams, and W is the weight of an aliquot of the tablet triturate taken for assay.

Table II summarizes the values of various samples obtained by Methods 1 and 2 and the cellulose column method. All three methods gave essentially similar values with light-degraded methotrexate samples and less than 70% heat-degraded methotrexate samples. Therefore, considering the relative quickness of the assay procedure by Method 1 (less than 15 min), this method is recommended for routine assays of methotrexate in commercial products. Method 2 is more important in studying the kinetics of methotrexate and for quantitating its degradation products. Also, it is essential to use Method 2 in methotrexate samples that are more than 70% heat degraded.

The sensitivity of Method 1 was determined using a 100-μl sample size to detect a concentration of 0.25 μg of methotrexate/ml of solution. An aqueous solution containing 1 μg of methotrexate/ml of solution, when analyzed by Method 1, gave a recovery of 93.1 ± 4.7% of methotrexate (average of three runs). Thus, Method 1 could be potentially useful in quantitating to a level of 1 μg of methotrexate/ml in biological fluids.

The tablet excipient dye did not interfere with the assay, as seen by the close agreement between the values obtained by Methods 1 and 2 and the cellulose column method. In the latter method, the dye could be seen as a yellow band remaining at the top of the cellulose column. The benzyl alcohol preservative present in the injectables is nonionic and eluted almost with the solvent front. Other preservatives such as methylparaben and propylparaben eluted immediately following the solvent front and did not interfere with the assay of intact methotrexate.

In all of the described assays, the amount of intact methotrexate in the unknown is calculated as a percentage of the reference solution. The explicit quantities are then calculated from the known concentration of methotrexate USP in the reference solution. However, methotrexate USP has been reported (2) to be only 85–90% pure. Therefore, explicit quantities in the assays, which are calculated by assuming methotrexate USP as 100% pure, must be interpreted accordingly. However, in the determination of relative amounts in various preparations or in the determination of percentage degradation, this consideration is obviated.

REFERENCES

(1) "The United States Pharmacopeia," 19th rev., Mack Publishing Co., Easton, Pa., 1975, p. 315.

(2) J. F. Gallelli and G. Yokoyama, *J. Pharm. Sci.*, **56**, 387 (1967).

(3) C. E. Myers, M. E. Lippman, M. E. Helen, and A. Bruce, *Proc. Natl. Acad. Sci. USA*, **72**, 3863 (1976).

(4) W. P. Tong, J. Rosenberg, and D. B. Ludlum, *Lancet*, **2**, 719 (1975).

ACKNOWLEDGMENTS AND ADDRESSES

Received July 15, 1976, from the *Pharmacy Department, The Clinical Center, Public Health Service, National Institutes of Health, Bethesda, MD 20014.*

Accepted for publication November 3, 1976.

[x] To whom inquiries should be directed.

Vehicle Effects on Ocular Drug Bioavailability II: Evaluation of Pilocarpine

JAMES W. SIEG and JOSEPH R. ROBINSON [x]

Abstract □ The influence of vehicle composition on ocular penetration of pilocarpine was studied in the albino rabbit. Increasing the pH of a vehicle promoted increased corneal penetration for pilocarpine, in accordance with the pH–partition hypothesis, but a similar series of experiments with a nonionizable drug, glycerin, gave similar results. The extent of pH-induced lacrimation by the vehicle and its effect on precorneal drug concentration also was determined. Increased pilocarpine absorption at neutral to slightly alkaline pH was due primarily to its peculiar solubility characteristics coupled with less irritation and lacrimation rather than a direct pH effect on the molecule. Incorporation of pilocarpine into a petrolatum-based ointment vehicle resulted in increased aqueous humor pilocarpine levels above those provided by an equivalent dose of aqueous solution. The mechanism of this increase was determined to be a higher effective concentration of pilocarpine in the ointment vehicle coupled with an increase in contact time of the dose. The ointment system also exerted an unusual form of vehicle control in that it promoted the corneal penetration of pilocarpine while impeding uniform mixing of the dose with tears and thereby imposed a restriction on the amount of pilocarpine available to the ocular tissues.

Keyphrases □ Pilocarpine—effect of vehicle composition and pH on ocular bioavailability, rabbits □ Vehicles—effect of composition and pH on ocular bioavailability of pilocarpine, rabbits □ Bioavailability, ocular—pilocarpine, effect of vehicle composition and pH, rabbits □ Ocular bioavailability—pilocarpine, effect of vehicle composition and pH, rabbits □ Ophthalmic cholinergic agents—pilocarpine, effect of vehicle composition and pH on ocular bioavailability, rabbits

The first report in this series dealt with vehicle influence on the ocular bioavailability of the relatively water-insoluble steroid fluorometholone (1). In that study, mechanisms of vehicle effects on ocular bioavailability were based on the interplay of the steroid and vehicle properties with the physiological and physicochemical nature of the drug administration site, *i.e.*, the precorneal portion of the eye. The present study extended this work to include the important water-soluble antiglaucoma drug pilocarpine. Thus, this examination of a water-soluble drug, along with earlier work on the relatively water-insoluble steroid, provides considerable perspective on factors that should be considered when formulating an ophthalmic drug for topical delivery to the eye to obtain maximum drug benefit.

BACKGROUND

During the past 30 years, numerous vehicles have been screened for various drugs to improve the overall intraocular penetration of topically applied drugs. Because of an inadequate understanding of the interplay between drug–vehicle–precorneal area properties, the primary thrust of much research has been directed toward prolonging the presence of the instilled dose in the precorneal area, usually referred to as increasing the contact time. Most often, these formulations rely mainly upon the viscosity character of the vehicle and its subsequent rheological effect on drainage loss of the dose *via* the nasolacrimal duct. Thus, most topically applied ocular vehicles have included viscous polymers such as hydroxypropylcellulose (2–4), methylcellulose (5–12), and polyvinyl alcohol (2–4, 6–8, 13–15).

Detailed studies of the drainage loss rate of these vehicles also have been performed (3, 5, 13, 16, 17) to permit selection of vehicles exhibiting

the best retention characteristics. In addition, the chemical nature of the vehicle, such as buffer composition and pH (18–22), has been modified in hopes of presenting the most favorable form of the drug to the eye for optimum corneal uptake and permeation.

While most studies provided some qualitative and semiquantitative information concerning corneal drug penetration, the primary drawback has been a consistent lack of correlation between the physicochemical characteristics of the drug and the properties of the chosen vehicle. The contact time of the vehicle is all too often assigned primary importance, whereas release of the drug from the vehicle and its subsequent corneal permeation mechanism are rarely considered.

For an ophthalmic dosing system to provide optimum ocular drug penetration, a balance must be achieved between the requirements of both the drug and the vehicle, given the constraints of the corneal pocket. The only suitable means to attain this goal is to determine the mechanism(s) of vehicle effects and to relate them quantitatively to the mechanism of ocular penetration of the drug. The effect of vehicles on the transcorneal permeation of pilocarpine was examined in this study, and a mechanistic interpretation of the interactions among the drug, the vehicle, ocular fluids, and transport dynamics is given.

EXPERIMENTAL

Materials—Tritiated pilocarpine alkaloid (specific activity of 4.1 Ci/mmole) in ethanol and ^{14}C-glycerin (specific activity of 10 mCi/mmole) in sterile aqueous solution were obtained commercially[1]. The pilocarpine was purified by vacuum distillation immediately prior to each series of experiments to prevent errors due to tritium exchange (23). The ointment vehicle was a commercially available, sterile, petrolatum-based product[2]. All other chemicals were either reagent or analytical grade and were used as received.

Male albino rabbits[3], 1.8–2.4 kg, were fed a regular diet with no restrictions on the amounts of food or water consumed.

Pilocarpine and Glycerin Solutions—The pilocarpine solutions were prepared fresh before each experiment by adding a solution of 10^{-2} *M* pilocarpine alkaloid in the desired buffer to the purified labeled material. It was determined that 0.25 mCi of tritiated pilocarpine alkaloid/ml of final solution was sufficient to ensure good counting efficiency, *i.e.*, 150,000–175,000 counts/min/μl. The glycerin solutions were prepared by adding an aqueous aliquot of the isotopic species to a 0.14 *M* solution of glycerin in the appropriate buffer. The final solution had an activity of 20,000 counts/min/μl.

The small amount of labeled material added to the drug solutions did not alter the molarity of the final solutions. Unless otherwise specified, all solutions were isoosmotic with 0.9% sodium chloride.

Pilocarpine Ointment—A small quantity of distilled water, *i.e.*, 0.05 ml/g of ointment, containing 2.08 mg of pilocarpine alkaloid/0.05 ml of solution was added to a sufficient amount of the purified tritiated material so that the final activity was 0.25 mCi/g of ointment. This solution then was mixed carefully with the ointment vehicle, yielding a 10^{-2} *M* pilocarpine ointment containing 5% water. Final counts in the ointment were 160,000 counts/min/mg.

For the experiment in which the percent water was increased, the ointment was prepared by simply adding more water in the first step. Homogeneity of the final product was verified by the reproducibility of measured radioactivity among weighed samples of ointment. Ointments were prepared fresh prior to each experimental run.

Removal of Corneal Epithelium—Two drops of 0.5% tetracaine hydrochloride solution were instilled into the eyes of the animals, and the epithelial layer was removed *in toto* by scraping with a scalpel. The eye was then blotted with moist tissue to remove any loose epithelium fragments from the precorneal area. Dosing was initiated after 1 hr to allow the effect of the local anesthetic to diminish.

Aqueous Humor Drug Concentration–Time Profiles—*Pilocarpine and Glycerin Solutions*—The basic experimental techniques used for monitoring aqueous humor drug levels after topical dosing with solutions in both intact and abraded eyes were described previously (1, 24). Unanesthetized animals were used, and a standard 25-μl dose was instilled in all experiments. Standard liquid scintillation counting techniques were used for analysis of the aqueous humor samples.

Pilocarpine Ointment—Individual doses of ointment were weighed on an analytical balance. The weighed dose was transferred carefully to a microspatula and then placed inside the center of the lower cul-de-sac, with care being taken not to irritate the eye or to touch the corneal surface. The lower lid was gently moved across the cornea to spread the dose evenly and was then released. No further mechanical action was performed, and the remainder of the run was carried out using the technique previously mentioned.

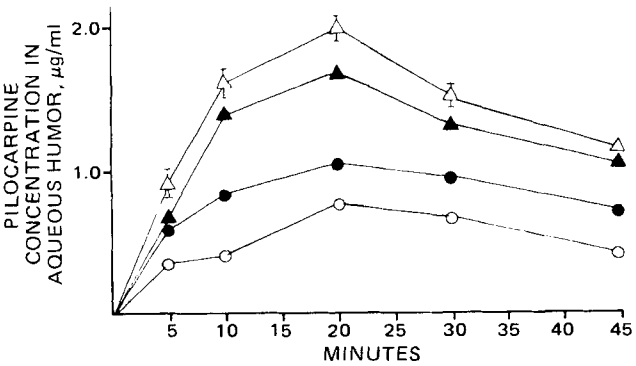

Figure 1—*Aqueous humor drug concentration–time profiles after topical dosing with 10^{-2} M pilocarpine solutions. Key: ○, pH 5.0; ●, pH 6.24; ▲, pH 7.0; and △, pH 8.0. All points represent an average of at least six eyes, and error bars represent the standard error of the mean. Where no error bar is indicated, the standard error of the mean is smaller than the size of the symbol used.*

Measurement of Glycerin Concentration in Tears *versus* Time as a Function of Instilled Solution pH—Unanesthetized rabbits were placed into wooden restraining boxes in a normal upright posture. Isotonic 0.14 *M* ^{14}C-glycerin solutions were prepared using Sorenserts buffer at pH 5 and 8, and 25-μl doses were topically instilled as in the aqueous humor studies. Tear samples were removed at 0, 1, 2, 3, 4, and 5 min postinstillation using 1-μl disposable capillary pipets[4]. The zero-time sample was removed from the eye within 10 sec after the dose was instilled. Eyes were used only once, and both buffers were used for each animal. Left and right eyes were alternated for the two buffers, and extreme care was exercised not to irritate the eye during sample removal.

Only the tip of the capillary tube was placed into the tear pool in contact with the cornea along the lid margin, and the filled pipets were transferred to sample vials for liquid scintillation counting. The raw counts per minute data were converted to a microgram per microliter basis using a standard 1-μl sample withdrawn from the solution prior to dosing. Errors due to the loss of volume and drug from sample removal were neglected on the basis of the small sample size and number and the relatively greater volume of the precorneal pool during the sampling interval.

RESULTS

Effect of Vehicle pH on Aqueous Humor Pilocarpine Levels—Previous studies with pilocarpine suggested that raising the dosing solution pH enhances its corneal penetration (25). Although such increases were reported (18–22), the data have not been sufficient to allow a precise mechanistic interpretation. The current studies were performed to provide a more complete analysis of this effect.

The aqueous humor concentration *versus* time profiles for pilocarpine at four vehicle pH values, using isotonic Sorensen's phosphate buffer, are presented in Fig. 1. As the pH was raised from 5 to 8, there was a two- to threefold increase in the amount of pilocarpine reaching the anterior chamber. The peak aqueous humor drug concentration occurred at 20 min after dosing, and subsequent drug elimination from the aqueous humor followed first-order kinetics with an associated rate constant of 0.017–0.024 min^{-1}.

Since the peak time in the aqueous humor did not appear to change for the four initial pH experiments, additional pH data were obtained at 20 min postinstillation using other buffer combinations. In this way, a broad range of pH values was examined to estimate the overall pH influence. Data at pH 4 and 5 were obtained using a phthalate buffer; data at pH 9, 10, and 11 were obtained with the Atkins–Pantin buffer.

Both buffers were moderately hypertonic. However, as a precaution against tonicity effects, an overlapping pH experiment was performed

[1] New England Nuclear, Boston, Mass, and ICN, Isotope and Nuclear Division, Cleveland, Ohio.
[2] Lacri-Lube, Allergan Pharmaceuticals, Irvine, Calif.
[3] Klubertanz, Edgerton, Wis.
[4] Drummond Microcap, Scientific Glass Apparatus Co., Bloomfield, N.J.

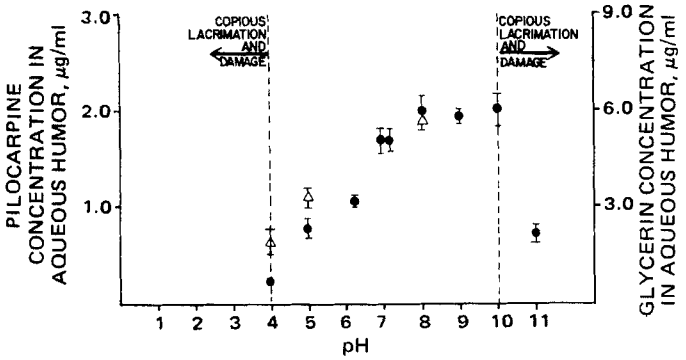

Figure 2—*Influence of vehicle pH on the aqueous humor concentration of pilocarpine and glycerin. Key:* ●, 10^{-2} M *pilocarpine solutions; and* △, *0.14* M *glycerin solutions. All samples were obtained at 20 min postinstillation and represent a minimum of six eyes.*

in both the acidic and alkaline regions. For example, both the Sorensen phosphate buffer and the phthalate buffer were used for pH 5, and the Sorensen and Atkins–Pantin buffers were used at pH 8. Since no differences in aqueous humor drug levels were detectable for the buffer pairs, tonicity effects were assumed negligible for the pH range studied. Further support for this assumption comes from the results of corneal perfusion studies (26) in which the epithelial permeability did not change over the tonicity range of 0.9–10% sodium chloride.

The results obtained at 20 min postinstillation for all pH values are summarized in Fig. 2. The extent of corneal penetration by pilocarpine gradually increased as the vehicle pH was raised. The exception to this behavior occurred at pH 11. However, excessive lacrimation and reddening of the eyes were evident at both extremes of the pH range. Maurice (26) also found ocular damage outside the range of pH 4–10 (indicated as vertical dotted lines in Fig. 2), and this finding appears to be consistent with the visual appearance of ocular irritation in the present studies.

Effect of Vehicle pH on Aqueous Humor Glycerin Levels—Glycerin is a nonionizable drug. According to the pH–partition hypothesis, the direct influence of pH on the extent of absorption of such a molecule should be negligible. An examination of the effect of vehicle pH on the corneal penetration of glycerin would make possible a separation of the direct and indirect effects of pH on an ionizable molecule such as pilocarpine.

The results of the glycerin experiments are shown in Fig. 2. All values were obtained at 20 min after dosing. The effect of pH on glycerin penetration was nearly identical to that observed for pilocarpine. Increasing the vehicle pH from 5 to 8 produced a twofold increase in the amount of glycerin penetrating to the anterior chamber. Also, as in the pilocarpine experiments, lowering the pH to 4 caused obvious irritation to the eye and a corresponding decrease in aqueous humor drug levels. The implications of this behavior relative to the mechanism of the pH effect observed with pilocarpine will be discussed subsequently.

Effect of Vehicle pH on Lacrimation and Precorneal Glycerin Concentration—The precorneal dynamics of a topically instilled dose of pilocarpine were extensively discussed previously (27–29). Drainage of the dose *via* the nasolacrimal duct removes only an amount of drug from the precorneal pocket and has no direct effect upon the drug concentration. The precorneal drug concentration can only be reduced by the loss of drug without an attendant loss of solution volume or by addition of tears to the precorneal pool *via* the lacrimal apparatus. Accordingly, the instilled drug concentration is decreased by initial mixing of the dose with the normal resident precorneal tear volume, by drug loss *via* absorption into the ocular tissues or systemic circulation, and by dose-induced lacrimation as well as normal tear turnover.

The data presented in Fig. 3 show the effect of vehicle pH on the precorneal concentration of glycerin as a function of time. The pH 5 solution induced a greater degree of lacrimation than the pH 8 solution. The first-order decline of precorneal glycerin concentration was twice as fast for the acidic solution, being 0.87 min^{-1} for pH 5 and 0.40 min^{-1} for pH 8. Of course, concentration changes can also arise due to drug absorption into ocular tissues, but this influence was presumed to be small since only a small percentage of the total dose was absorbed. Thus, lacrimation is the predominant factor responsible for the fall in precorneal drug concentration.

Table I presents the percent reduction of precorneal glycerin concentration *versus* time for the two pH values. The fall in tear concentration was markedly accelerated with the acidic solution. The percent reduction

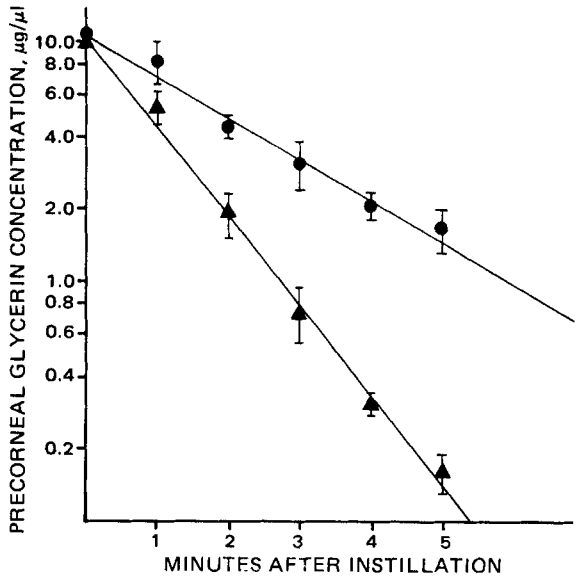

Figure 3—*Precorneal concentration of glycerin in tears* versus *time as a function of vehicle pH. Key:* ●, *pH 8.0; and* ▲, *pH 5.0. All points represent a minimum of six determinations.*

for the zero-time samples, taken within 10 sec after instillation, was 20% for both pH values. This value corresponds very well to the calculated 23% reduction in initial concentration when the 25-μl dose is mixed with the 7.5-μl resident tear volume. Therefore, aqueous solutions with viscosities similar to water equilibrate very rapidly with tears in the precorneal area.

Another important observation of the lacrimation study is that the fall in precorneal glycerin levels for the pH 8 solution could be accelerated to a rate as great or greater than the pH 5 solution by simply irritating the eye with the capillary tube during sample removal. A precipitous fall in precorneal concentration could be suddenly induced at any time after dosing as a result of reflux tearing in response to the mechanical stimulus.

Mishima *et al.* (30) showed that tear flow can increase suddenly due to a variety of factors, and even very subtle stimuli produce a dramatically increased tear turnover rate in a matter of seconds. In studies with humans, it was noted that the turnover rate could increase by a factor of 8–10 without being noticed by the subject; such variations in turnover did not cause an overflow of tears from the cul-de-sac.

Aqueous Humor Levels of Pilocarpine after Dosing with 10^{-2} *M* Ointment—*Intact* versus *Abraded Eyes*—The results obtained after instilling 25-mg doses of pilocarpine ointment into intact and abraded eyes are shown in Fig. 4. In the intact eye, pilocarpine reached a peak concentration in the aqueous humor in 20 min. This peak time corresponded to that obtained for an equivalent dose of solution in intact eyes, but the peak concentration obtained with the ointment was approximately three to four times higher than that with the solution. When the same ointment was applied to abraded eyes, the drug reached peak levels in the anterior chamber within 5 min, consistent with the abraded solution data.

However, in contrast to results with intact eyes, the aqueous humor drug levels in an abraded eye with the ointment were substantially less than the abraded eye solution data. In fact, with the exception of the shift in peak time, the amount of pilocarpine penetrating to the aqueous humor from the ointment was nearly the same for both intact and abraded eyes. This behavior is markedly different from that seen with the solution. Elimination of the drug from the anterior chamber remained unchanged in each case, with an attendant first-order rate constant of approximately 0.02 min^{-1}.

Table I—Percent Reduction of Precorneal Glycerin Concentration *versus* Time as a Function of Instilled Solution pH

pH	Minutes after Instillation					
	0	1	2	3	4	5
5	20	59	85	94	98	99
8	20	35	66	76	84	87

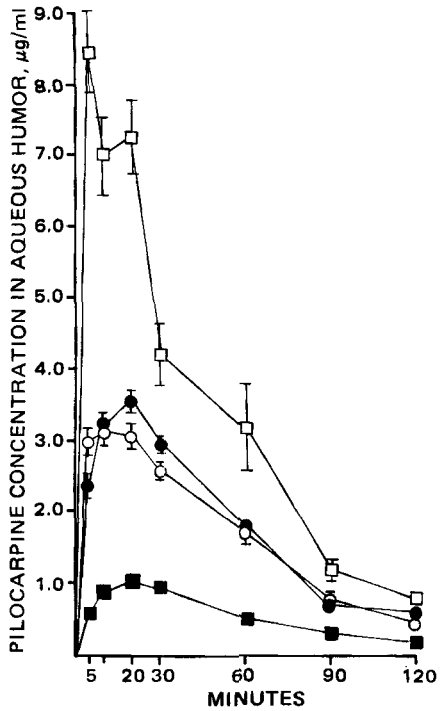

Figure 4—*Aqueous humor levels of pilocarpine after dosing with 10^{-2} M ointment and solution in intact and abraded eyes. Key: ●, 25 mg of ointment, intact eyes; ○, 25 mg of ointment, abraded eyes; ■, 25 μl of solution, intact eyes; and □, 25 μl of solution, abraded eyes. All points represent an average of eight to 16 eyes.*

Variation of Dose—Since incorporation of pilocarpine into a viscous oleaginous vehicle may increase the contact time of a dose with the precorneal area, the effect of increasing the dose was investigated. In this way, it was anticipated that any beneficial effects associated with increased contact time could be magnified.

Figure 5 presents the data obtained with various doses of ointment. The amount of pilocarpine reaching the anterior chamber increased as the dose was increased. In addition, the peak time shifted to later times for the larger doses, occurring at 20 min for the 25-mg dose and at 30 min for the 50-mg dose. No definitive statement regarding the peak time for the 10-mg dose can be made since the 10- and 20-min points were not statistically different. The areas under the curve for the 25- and 50-mg studies were consistent with the doses, showing a twofold increase for the higher dose. The 10-mg dose also was reasonably consistent with the area, being one-half that of the 25-mg dose. The first-order rate constants for elimination for all cases were 0.017–0.022 min^{-1}.

Variation of Percent Water—To determine if the amount of water incorporated into the ointment had any effect on the availability of pilocarpine from the vehicle, an ointment was prepared using 10% water rather than 5%. There was no statistically significant difference between the profiles for 5 and 10% water (Fig. 4). Higher percentages of water were attempted, but serious problems with bleeding of the water from the oleaginous vehicle occurred and a satisfactory ointment could not be prepared.

DISCUSSION

Effect of Vehicle pH on Corneal Penetration of Pilocarpine—The vehicle pH has long been considered to be an important parameter for the passive diffusion of ionizable compounds into and through the cornea (31). The pH–partition hypothesis predicts that maximum penetration will occur when an alkaloidal drug is presented to a membrane as the uncharged free base. This form is generally more lipid soluble than the ionized species and will readily penetrate a lipophilic tissue such as the corneal epithelium. Since the epithelium is the primary barrier to corneal drug uptake, such compounds should show marked increases in corneal penetration as the vehicle pH is raised, reaching a maximum at pH's above values corresponding to their pK's.

The pK_1 for pilocarpine is 7.15, and previous studies (18–22) indicated that corneal penetration does increase as the pH of the dosing solution is increased. For example, Ramer and Gasset (18) observed an approximate doubling of corneal penetration when the vehicle pH was raised

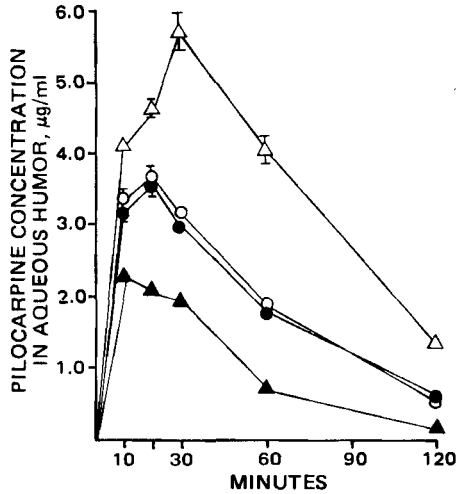

Figure 5—*Aqueous humor levels of pilocarpine after topical dosing with 10^{-2} M ointment in intact eyes. Key: ●, 25 mg of ointment, 5% water; ○, 25 mg of ointment, 10% water; ▲, 10 mg of ointment, 5% water; and △, 50 mg of ointment, 5% water.*

from 5 to 8 and attributed this increase to a predominance of the free base form at the higher pH. However, while such results are certainly consistent with the pH-related event, they are not conclusive.

The results of the current studies (Fig. 2) also show a two- to threefold increase in corneal penetration between pH 5 and 8, as well as the expected sigmoidal shape, but an important aspect of pilocarpine's physical character must be considered before a mechanistic judgment is made. Pilocarpine is somewhat unique in the sense that the free base form of the drug is more soluble in water than are any of the salts. Pilocarpine is freely soluble in water, whereas the solubilities of the hydrochloride and the nitrate are 1 g/0.3 ml and 1 g/4 ml, respectively (32). The preferential aqueous solubility of the free alkaloid is responsible for the diminished absorption sensitivity of pilocarpine to changes in vehicle pH. However, the true impact of this solubility effect only becomes apparent when the results of the glycerin study (Fig. 2) are considered.

Glycerin is a nonionizable compound that should not derive any direct benefit from pH manipulation for its corneal penetration. Nevertheless, the results of the glycerin study show that a twofold increase is also apparent when the pH is varied between 5 and 8. Such behavior strongly suggests that some mechanism other than a direct pH effect on the drug molecule is operating to produce this increase and that this same mechanism must also be responsible for the increase observed for pilocarpine. The existence of another mechanism is also implied by the data for pilocarpine since the inflection point for the pilocarpine data in Fig. 2, corresponding to the pK_1 for pilocarpine, occurs nearly 1 full pH unit lower than expected.

The results obtained from the lacrimation study (Fig. 3 and Table I) show that pH-induced lacrimation is responsible. The magnitude of the difference in aqueous humor levels at pH 5 and 8 corresponds to the observed changes in precorneal glycerin concentration for the two solutions. The greater amount of drug reaching the anterior chamber when the pH 8 vehicle is used is simply the result of a smaller pH-induced lacrimation response in the precorneal area. These results are consistent with previous work that indicated that the eye is better able to tolerate a basic pH than an acidic pH (33).

The data in Fig. 2 for the pH 11 solution provide further support for pH-induced lacrimation. As the pH of the vehicle became sufficiently alkaline to irritate the eye, the level of pilocarpine in the anterior chamber fell to a value similar to the pH 5 solution. During these experiments, both the pH 5 and 11 solutions caused eye irritation and copious lacrimation, as indicated by an abnormally high blink rate and eye wetness after instillation of the dose.

The curves presented in Fig. 1 also are remarkably similar to previous data when the pilocarpine dose was rinsed away from the precorneal area with saline at various times after instillation (24). This rinsing process, which essentially accelerates the drainage process to a maximum and thereby represents the upper limit of lacrimation, creates an identical variation in the magnitude of the levels of pilocarpine in the anterior chamber. An extensive discussion of the effects of normal and accelerated loss of drug from the precorneal area was presented previously (24, 34).

The current results indicate that the highest pH influence on corneal

penetration will be observed for a drug with a pKa greater than 6 or 7, since above neutrality the extent of pH-induced lacrimation, which opposes a direct pH effect on the drug molecule, is diminished. However, while this should be the case with pilocarpine since its pK_1 is 7.15, it does not occur because of the preferential aqueous solubility of this molecule throughout the pH spectrum.

A major point of concern in any discussion of vehicle pH in the eye is how fast the eye is able to return to a normal physiological pH. Although the precise buffer capacity of the ocular fluids has not been determined, a few general considerations support the contention that an instilled buffer is not readily altered by the eye. Since the normal resident tear volume in the rabbit is about 7.5 μl (30), instillation of 25 μl of a moderately strong buffer would be expected to overwhelm momentarily the ocular fluids and to establish the buffer pH in the eye. Although tear turnover in the rabbit occurs at the rate of 0.66 μl/min, it does not become significant until drainage has removed the bulk of instilled solution *via* the nasolacrimal duct (27). However, by the time the drainage process is completed, permeation of drug into the cornea is also nearly at an end (24), so the instilled solution pH can be expected to remain constant for at least as long as the majority of the absorption process. Therefore, the possibility of an altered solution pH after instillation can be neglected. Further support for this approach comes from recent work in which the precorneal pH remained equal to the buffer pH for a considerable time after dosing[5].

The effect of pH on the corneal penetration of pilocarpine is substantially different than previously believed. While pH partitioning or some other mechanism (35) may contribute to some small extent, the primary overriding influence is pH-induced lacrimation. Thus, the observed effect of pH is, in reality, largely an indirect one, influencing both ionizable and nonionizable drugs to a similar extent and by similar means. The magnitude of this effect must be considered when evaluating the effect of vehicle pH on the ocular penetration of any drug from an instilled solution.

Effect of Vehicle on Corneal Penetration of Pilocarpine—One primary disadvantage of a topically applied ophthalmic solution is the rapid drainage loss that occurs in the precorneal area. Attempts to increase the corneal drug penetration often begin by increasing the viscosity of the vehicle to delay this loss. Previous work with pilocarpine showed that viscous polymer solutions (5, 9, 13) are only moderately successful in enhancing its corneal penetration. The intent of the present series of experiments was to formulate an explanation for these observations within the context of the mechanism of pilocarpine's transcorneal permeation as detailed previously (24).

The data in Fig. 4 show that the ointment vehicle used in the present study was superior to an aqueous solution. Equivalent doses of each vehicle, containing the same amount of pilocarpine, were delivered into intact eyes, and the ointment gave three to four times higher aqueous humor drug levels. Before a precise discussion of this observed effect, it will be beneficial to consider some important general aspects of the corneal penetration of a drug from its vehicle.

Figure 6 depicts some theoretical profiles of corneal drug penetration as a function of time. This figure illustrates two primary absorption parameters associated with transcorneal dynamics: increased concentration of the dosing system and extended contact time of the instilled dose.

In Fig. 6, profiles A, B, and C represent successively higher concentrations of a drug in a given vehicle (*e.g.*, a solution). As the concentration is increased, the amount of drug reaching the aqueous humor increases also so that higher levels are evident throughout the profile. However, the peak time does not change since the absorption mechanism remains unchanged.

Profiles D and E illustrate the case in which the contact time of the dose is extended (*e.g.*, the use of a viscous polymer solution rather than a simple aqueous solution). Increasing the contact time allows for an extension of the time permitted for the absorption process. As a result, the aqueous humor levels continue to increase beyond those obtained for the simple solution, the peak time is shifted to a later time, and the magnitude of the peak shift is determined by the degree to which drainage loss is delayed. The most important aspect of this case is that the early portion of the profile remains essentially unchanged; that is, increasing the contact time simply extends the profile obtained for the original dosing solution.

The reason for this behavior is that the peak time obtained for a topically applied drug solution is determined by the rapid parallel first-order drainage process occurring in the precorneal area (34). Rapid loss of drug

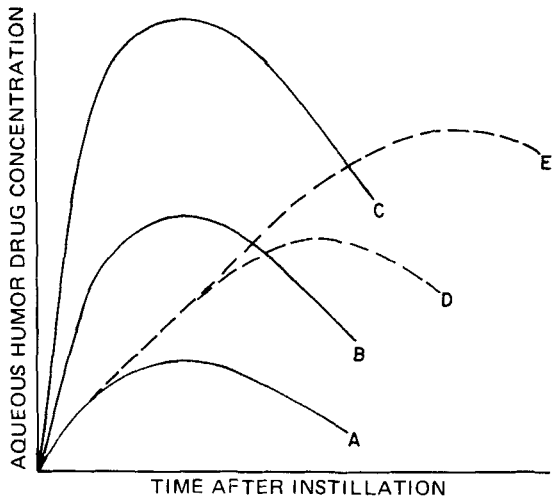

Figure 6—*Graphical representation of aqueous humor drug concentration, showing the influence of increasing concentration and extended contact time of the dosing system. Key: curves A, B, and C, effect of increasing concentration; and curves A, D, and E, effect of extended contact time.*

from the absorption depot creates an artificial peak in ocular tissues and results in subsequent overestimation of the absorption rate constant. Thus, any process that prolongs the presence of the drug at the absorption site extends the absorption process and shifts the apparent peak time to the right. The limit of this effect is, of course, the true peak time of the drug, beyond which a plateau is observed and only the times at which elimination of drug from the aqueous humor parallels those of a simple solution are shifted. This effect can be readily recognized in recent work with pilocarpine where the drainage ducts of rabbits were plugged prior to dosing with a solution (29).

In light of this discussion, it is easy to recognize why past attempts to increase the corneal penetration of pilocarpine through the use of viscous solutions met with only limited success. The maximum benefit that can be derived from such endeavors is the provision of more pilocarpine to the anterior chamber at later times after dosing. However, even this aspect has realized only limited potential, even in the extreme case where the drainage apparatus has been totally blocked (29). Increasing the aqueous humor pilocarpine levels at early times above those provided by a simple aqueous solution can only be achieved by increasing the concentration of the instilled solution or by altering the absorption mechanism.

It can now be recognized from the data in Fig. 4 that the ointment vehicle exhibits characteristics similar to those obtained when the applied pilocarpine concentration is increased. The peak time in the aqueous humor is the same as for the solution. Also, the pilocarpine level in the anterior chamber is raised, but the elimination rate is unchanged. This behavior is characteristic of a "pulsed-dose" mechanism (36), in which the cornea is simply presented with a greater amount of drug for a brief time, rather than any type of sustaining mechanism.

What must now be considered is the question of how a dose of ointment containing the same total amount of pilocarpine as an equivalent dose of solution could behave as though a higher drug concentration was being applied to the eye. The explanation lies in the physical composition of the ointment.

When pilocarpine is placed into an oleaginous vehicle, it is introduced into a medium unfavorable to its solubility. In the current studies, the alkaloid did not possess sufficient oil solubility to prepare a true solution of the drug in the ointment vehicle alone. To demonstrate this point, a 25-ml sample of 10^{-2} *M* tritiated pilocarpine alkaloid solution was shaken with an equal volume of light liquid petrolatum, and the two phases were analyzed by liquid scintillation techniques for pilocarpine content. The results showed that the water–oil ratio of pilocarpine was approximately 1500:1.

To achieve solution of the alkaloid, it was decided to dissolve the drug in a minimum amount of water (5%) and to incorporate it into the hydrophilic vehicle. The pilocarpine would be expected to remain in the water when mixed with the vehicle. Therefore, the ointment consisted of two phases: the bulk oleaginous phase containing little or no pilocarpine and the aqueous phase containing essentially all of the drug. A 25-mg dose of ointment would have all of its pilocarpine dissolved in only 1.25 μl of

[5] N. Keller, Alza Research Corp., Palo Alto, Calif., personal communication.

water, in contrast to the same amount of pilocarpine dissolved in a 25-μl dose of solution. As a result, the effective concentration of pilocarpine in the ointment was 20 times more than the solution. For this reason, the ointment behaved as though a higher concentration of drug was applied to the eye and gave corresponding increases in the aqueous humor drug levels at all times in the profile.

It might also be expected that the 20-fold difference in effective concentration should have produced even higher levels of pilocarpine than were actually observed, since previously corneal penetration of pilocarpine was linear over a wide concentration range (23). However, the results can be easily rationalized on the basis of the mixing problems existing between the oleaginous ointment and the aqueous tears.

To test the effective concentration mechanism, a 10% water vehicle was prepared and applied to intact eyes. However, the results were inconclusive. Although doubling the water content reduced the effective concentration by 50%, the amount of water in the ointment film in contact with the cornea was doubled; the differences were apparently offsetting at such a low percentage of water. Unfortunately, higher percentages of water could not be satisfactorily tested to prove the proposed mechanism.

Another important aspect of the ointment system can be seen by referring to Fig. 5. While the 25-mg dose apparently obeyed an increased concentration type of mechanism, the overall behavior when the dose was varied between 10 and 50 mg was somewhat different. The peak time shifted to a later time, and there were increased levels of pilocarpine at all times throughout the profile. Therefore, the ointment vehicle also extended the contact time of the dose. This effect becomes recognizable as the dose is increased, and the greater volume of the larger doses undoubtedly plays a role in prolonging the contact time.

The overall behavior of the ointment can be discussed in relation to three hypothetical mechanisms: (*a*) the ointment system is well behaved and exhibits classical vehicle control characteristics, (*b*) the ointment forms an occlusive nonrenewable film over the corneal surface, and (*c*) the ointment exhibits surface mixing only, and drug within the bulk is unavailable to the ocular fluids.

Each alternative can now be discussed in terms of supportive and nonsupportive data from the present experiments.

Figure 4 depicts a rather interesting result in that the ointment produced similar aqueous humor levels in both intact and abraded eyes. The area under the curve (*AUC*) was the same for each case, so it must be concluded that this *AUC* represents some limiting amount of pilocarpine available from the ointment vehicle.

It might be tempting to attribute this behavior to vehicle control in the ointment system. This is not possible, however in a classical sense, since the peak time is essentially unchanged from that obtained when using a solution and the aqueous humor levels are increased at times immediately following dosing rather than decreased. Therefore, the ointment mechanism is not true vehicle control in the sense of delayed release or partitioning of drug from the vehicle.

The behavior of the pilocarpine ointment is in direct contrast to results from a similarly conducted study with the steroid fluorometholone (1). In that study, the steroid in the same oleaginous vehicle exhibited true classical vehicle control. Aqueous humor drug levels were decreased for the first 60 min, and the peak time was not achieved until 3 hr after dosing, as compared to 30 min for a suspension or a solution. In addition, increasing the dose of fluorometholone ointment from 25 to 50 mg did not increase aqueous humor drug levels, which further demonstrates the effect of vehicle control. A comparison of the results from the two studies can be made by referring to Fig. 7. The behavior of the steroid was not unexpected, since the relatively water-insoluble steroid had preference for its oleaginous vehicle; in the present study, the solubility character of pilocarpine makes its solubilization or retention in the vehicle thermodynamically unfavorable.

The results of the steroid study also prove that the ointment vehicle is indeed retained in the eye for a considerable time, since aqueous humor steroid levels were maintained for up to 7 hr after dosing as compared with 2 hr for a solution. This evidence, coupled with the previously described similar behavior of pilocarpine ointment in both intact and abraded eyes, gives strong support to mechanism (*b*). In this case, a stagnant ointment film is postulated to exist at the corneal surface. The film is not renewed, even under a mechanical influence such as blinking. As a result, permeation of pilocarpine into the cornea would stop as soon as pilocarpine is depleted from the water in the film. This mechanism would adequately account for the observed similarity with intact and abraded eyes; in each case, the film is rapidly depleted of drug and further penetration is inhibited by the occlusive film. However, this film would not present itself as an absolute barrier to the penetration of a drug such as

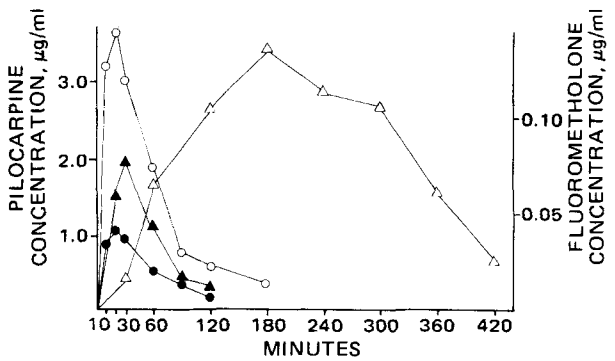

Figure 7—*Aqueous humor levels after dosing with pilocarpine and fluorometholone in ointment and aqueous solution (1, 24). Key:* ●, 10^{-2} M *pilocarpine solution, 25 μl;* ○, 10^{-2} M *pilocarpine ointment, 25 mg;* ▲, *saturated fluorometholone solution, 50 μl; and* △, *0.1% fluorometholone ointment, 50 mg.*

fluorometholone, since the steroid's lipid solubility permits slow diffusion through the vehicle to replenish the concentration of drug in the film adjacent to the corneal surface.

To determine if this mechanism is reasonable, a calculation was performed to determine the amount of pilocarpine present in a film of ointment covering the corneal surface. By assuming an average corneal diameter of 15 mm (37), it can be easily shown that a layer of ointment 10 μm thick contains 3.3 μg of pilocarpine. From analysis of the *AUC* for the ointment, it can be determined that the amount of drug penetrating the cornea to the aqueous humor is 3.2 μg. If 10 μm is accepted as a reasonable thickness for the film, the amount of drug reaching the aqueous humor would be the same as that present in the initial film. This assumption does not appear to be unreasonable, since the original tear film covering the cornea is also about 10 μm thick (38).

Although these calculations appear to confirm the existence of a nonrenewable ointment film at the corneal surface, two major contradictions reject this mechanism. The first, and most obvious, is the observation that larger doses of ointment give increased corneal penetration of pilocarpine. It should be clear that a stagnant film at the corneal surface would not be influenced by the remainder of the dose in the cul-de-sac. If such a mechanism is operative, increasing the size of the dose should have no effect. Second, an additional study showed that predosing the cornea with drug-free ointment vehicle had no effect upon subsequent doses of 10^{-2} *M* pilocarpine ointment or solution. If an occlusive barrier is formed by the vehicle, little or no drug penetration would be possible under such conditions. However, the observed unimpeded penetration of pilocarpine from both dosing systems clearly demonstrates that the ointment film *per se* is not a barrier.

At this point, it is clear that mechanism (*c*) is the only postulate consistent with all data. In this mechanism, pilocarpine is only available from the water present at the ointment surface. This amount of drug, fixed by the size of the dose, mixes with the tears and creates the precorneal drug concentration that is the driving force for corneal drug uptake. This approach easily explains why the same amount of drug penetrates both intact and abraded eyes. A homogeneous dose of ointment of a given size will present the same limited amount of drug, *via* surface mixing, without regard to the condition of the corneal surface. Once this amount has been absorbed or lost *via* the parallel elimination pathways (34), penetration into the cornea ceases, since drug entrapped within the bulk of the ointment is unavailable to the ocular fluids which cannot penetrate the oleaginous vehicle. Increasing the dose will have a positive effect, since the larger surface area allows more drug to mix with the fixed resident tear volume. This creates a higher precorneal drug concentration and subsequent increased corneal penetration.

The overall mechanism of the ointment can thus be described as being composed of combined influences, wherein an increased effective concentration is operating in conjunction with a limited extension of contact time. The ointment exerts a somewhat unusual form of vehicle control inasmuch as it impedes uniform mixing of the entrapped pilocarpine with the ocular fluids. At the same time, it serves to prolong the contact time, particularly with larger doses. The end result is a complex sum of positive and negative effects, with the ointment ultimately achieving superiority over the solution at all times after dosing. However, many characteristics of the solution are retained by virtue of the water contained within the ointment.

Whenever pilocarpine is presented to the cornea in an immediately

available form (*i.e.*, in aqueous solution), it will penetrate to the anterior chamber. The implication of this behavior is that sustained release of pilocarpine to the ocular tissues is only possible if the release of the drug from its vehicle is rate limiting. Simply increasing the contact time (viscosity) of the vehicle is not sufficient, since this process merely results in pulse-dose behavior rather than sustained release. However, the release characteristics must also be such that the dosing system can overcome the constraints of the precorneal pocket in terms of fluid dynamics and nonproductive absorption.

SUMMARY

Several important findings emerged from the present study relative to behavior of pilocarpine in ocular vehicles and subsequent corneal absorption characteristics. The corneal absorption of pilocarpine is increased in neutral to alkaline solutions as compared to acid solutions, in keeping with observations of others. However, the mechanism of this improved absorption does not appear due to the specific pH–partition behavior usually attributed to this phenomenon but rather to the nonspecific lacrimation that occurs at acid pH. Thus, all drugs will show an improved absorption pattern, irrespective of whether they are ionized or not, in the neutral to alkaline range simply because there is less lacrimation in this region and, hence, less drug loss. This observation is important; before a claim of significant pH effect can be made with other drugs, the baseline of lacrimation effect must be considered.

Earlier studies established that polymer solutions would provide only a moderate improvement in the corneal absorption of pilocarpine at the low levels of viscosity generally used for ocular solutions. An ointment system for pilocarpine, based on improved contact time, was also expected to show an improved fraction of dose absorbed and a sustaining effect. However, when using essentially a lipophilic ointment vehicle, no sustaining effect for pilocarpine was observed and only a moderate improvement in the fraction of dose absorbed across the cornea occurred. These observations were contrary to what was observed when the identical ointment was employed with the relatively water-insoluble steroid fluorometholone. This difference was ascribed to the difference in the solubility of the two drugs in the ointment.

Since pilocarpine was insoluble in the vehicle, it was first dissolved in a small amount of water and then incorporated into the ointment to generate a dilute water-in-oil emulsion. This system was unable to provide drug uniformly from the ointment, and only that drug in immediate contact with the tear film became available to eye tissues. The conclusion from the ointment study is that the drug solubility in the ointment dictates the success or failure of this drug delivery system in terms of improved bioavailability and sustaining effect. Extension of the pilocarpine ointment study suggests that an appropriate ointment vehicle for this drug should be water soluble or perhaps an oil-in-water emulsion.

Although definitive guidelines for the formulation of topical ocular drug systems are not complete, we do have considerable quantitative data and theories on two drugs with extremes in water solubility, namely, pilocarpine and fluorometholone. Merely placing a drug in a stable favorite vehicle is inappropriate for ocular drug delivery systems. One must consider the properties of the drug and the vehicle in combination with the unusual characteristics of the precorneal pocket to formulate a drug delivery system with optimum delivery properties. A comprehensive picture of the interplay among drug, dosage form, and site of ocular delivery is emerging.

REFERENCES

(1) J. W. Sieg and J. R. Robinson, *J. Pharm. Sci.*, **64,** 931 (1975).

(2) K. Green and S. J. Downs, *Arch. Ophthalmol.*, **93,** 1165 (1975).

(3) F. C. Bach, J. B. Adam, H. C. McWhirter, and J. E. Johnson, *Ann. Ophthalmol.*, **4,** 116 (1972).

(4) S. R. Waltman and T. C. Patrowicz, *Invest. Ophthalmol.*, **9,** 966 (1970).

(5) S. S. Chrai and J. R. Robinson, *J. Pharm. Sci.*, **63,** 1218 (1974).

(6) R. E. Hardberger, C. Hanna, and R. Goodart, *Am. J. Ophthalmol.*, **80,** 133 (1975).

(7) C. A. Adler, D. M. Maurice, and M. E. Paterson, *Exp. Eye. Res.*, **11,** 34 (1971).

(8) A. A. Swanson, D. J. Jeter, and C. R. Cregor, *Ophthalmologica*, **156,** 425 (1968).

(9) J. S. Haas and D. L. Merrill, *Am. J. Ophthalmol.*, **54,** 21 (1962).

(10) J. L. Mims, *Arch. Ophthalmol.*, **46,** 664 (1951).

(11) W. H. Mueller and D. L. Deardorff, *J. Am. Pharm. Assoc., Sci. Ed.*, **45,** 334 (1956).

(12) K. C. Swan, *Arch. Ophthalmol.*, **33,** 378 (1945).

(13) T. F. Patton and J. R. Robinson, *J. Pharm. Sci.*, **64,** 1312 (1975).

(14) A. A. Swanson, D. J. Jeter, and P. Tucker, *Ophthalmologica*, **160,** 265 (1970).

(15) N. Krishna and F. Brow, *Am. J. Ophthalmol.*, **57,** 99 (1964).

(16) R. Hardberger, C. Hanna, and M. Boyd, *Arch. Ophthalmol.*, **93,** 42 (1975).

(17) M. L. Linn and L. T. Jones, *Am. J. Ophthalmol.*, **65,** 76 (1968).

(18) R. M. Ramer and A. R. Gasset, *Ann. Ophthalmol.*, **7,** 293 (1975).

(19) R. A. Anderson and J. B. Cowle, *Br. J. Ophthalmol.*, **52,** 607 (1968).

(20) J. Boberg-Ans, K. V. Grove-Rasmussen, and E. R. Hammerlund, *ibid.*, **43,** 670 (1959).

(21) S. Riegelman and D. G. Vaughn, *J. Am. Pharm. Assoc., Pract. Pharm. Ed.*, **19,** 474 (1958).

(22) G. Floyd, P. C. Kronfeld, and J. E. McDonald, *J. Am. Pharm. Assoc., Sci. Ed.*, **42,** 333 (1953).

(23) S. S. Chrai and J. R. Robinson, *Am. J. Ophthalmol.*, **77,** 735 (1974).

(24) J. W. Sieg and J. R. Robinson, *J. Pharm. Sci.*, **65,** 1816 (1976).

(25) D. G. Cogan and E. O. Hirsch, *Arch. Ophthalmol.*, **32,** 276 (1944).

(26) D. M. Maurice, *Br. J. Ophthalmol.*, **39,** 463 (1955).

(27) S. S. Chrai, T. F. Patton, A. Mehta, and J. R. Robinson, *J. Pharm. Sci.*, **62,** 1112 (1973).

(28) T. F. Patton and J. R. Robinson, *ibid.*, **64,** 1312 (1975).

(29) *Ibid.*, **65,** 1295 (1976).

(30) S. Mishima, A. Gasset, S. D. Klyce, and J. L. Baum, *Invest. Ophthalmol.*, **5,** 264 (1966).

(31) K. C. Swan and N. G. White, *Am. J. Ophthalmol.*, **25,** 1043 (1942).

(32) "The Merck Index," 8th ed., Merck and Co., Rahway, N.J., 1968.

(33) C. Trolle-Lassen, *Pharm. Weekbl.*, **93,** 148 (1958).

(34) M. C. Makoid, J. W. Sieg, and J. R. Robinson, *J. Pharm. Sci.*, **65,** 150 (1976).

(35) V. F. Smolen and F. P. Siegel, *ibid.*, **57,** 378 (1968).

(36) D. M. Maurice, *Sight-saving Rev.*, **42,** 42 (1972).

(37) J. H. Prince, in "The Rabbit in Eye Research," J. H. Prince, Ed., Charles C Thomas, Springfield, Ill., 1964, p. 86.

(38) S. Mishima, *Arch. Ophthalmol.*, **73,** 233 (1965).

ACKNOWLEDGMENTS AND ADDRESSES

Received June 22, 1976, from the *School of Pharmacy, University of Wisconsin, Madison, WI 53706.*

Accepted for publication October 6, 1976.

Supported by Allergan Pharmaceuticals, Irvine, CA 92664, and Grant EY-01332 from the National Institutes of Health.

[x] To whom inquiries should be directed.

Kinetics and Mechanisms of Monolayer Interactions IV: Surface Activity of Alkanols and Energies of Their Interaction with Dipalmitoyllecithin and Dipalmitoylphosphatidylethanolamine

FEDERICO A. VILALLONGA ˣ, EDWARD R. GARRETT, and JOHANNA S. HUNT

Abstract □ The free energies of adsorption of the C_1 to C_{14} alkanols at the air–water interface, estimated from plots of the surface pressure ($\pi \leq 5$ dynes/cm) against the bulk concentration, were a linear function of the chain length for 1-alkanols. From C_3 to C_8, the 2- and 3-isomers showed lower values than the 1-isomers. The energies of interaction of the C_1 to C_{14} alkanols with dipalmitoylphosphatidylethanolamine and dipalmitoyllecithin monolayers, previously spread at the air–water interface, were estimated from the increase of the surface pressure with increasing concentrations of the injected alkanol. The energies of interaction of the C_1 to C_5 1-alkanols were linear functions of the chain length. The energy of interaction per methylene group of the alkyl chain suggests that the phospholipid monolayers behaved as ultrathin "oil" phases. The 2- and 3-isomers presented marked departures from linearity. The literature data for reflection coefficients in biomembranes and for partition coefficients between olive oil and water, red cell membranes and water, and phospholipid liposomes and water for the C_1 to C_5 alkanols show similar linearities with the chain length for the 1-isomers and comparable departures for the 2- and 3-isomers.

Keyphrases □ Monolayer interactions—various aliphatic alcohols, free energies of adsorption and energies of interaction with phospholipids at air–water interface □ Alcohols, various aliphatic—free energies of adsorption and energies of interaction with phospholipid monolayers at air–water interface □ Phospholipid monolayers—energies of interaction with various aliphatic alcohols at air–water interface □ Surface activity—various aliphatic alcohols, energies of interaction with phospholipid monolayers at air–water interface

The process of permeation of a solute across the lipid regions of biomembranes can be separated (1) into three successive events that contribute to the total permeation rate: (*a*) adsorption of the hydrated solute at the lipid–water interface, (*b*) dehydration, and (*c*) diffusion of the solute through the lipid region. Monolayers of phospholipids spread at the air–water interface are considered to be suitable models for the study of the adsorption of solutes to ordered arrays of lipid molecules (2, 3).

The effect of chain length and the nature of the polar group of homologous series of *n*-alkyl sulfates and *n*-alkylammonium ions on the energy of their interaction with dipalmitoylglycerol, dipalmitoyllecithin, and dipalmitoylphosphatidylethanolamine monolayers were estimated recently (2, 3) from the variation of the equilibrium surface pressure with varying concentrations of subphase-injected *n*-alkyl derivatives on the premise of a collision model and a constant entropy factor.

The present work compares the energies of adsorption of alkanols at a "clean" air–aqueous interface with the energies of their interaction with dipalmitoyllecithin (I) and dipalmitoylphosphatidylethanolamine (II) monolayers. The implications of these relations on the permeability of alkanols through biomembranes are discussed. A clean interface is defined here as an air–aqueous interface without any previously spread monolayer.

EXPERIMENTAL

Reagents—Dipalmitoyllecithin[1] and dipalmitoylphosphatidylethanolamine[1] were chromatographically homogeneous by TLC (4, 5). The purity of the reagent grade alcohols used, methanol[2], ethanol[3], 1-propanol[2], 2-propanol[4], 1-butanol[5], 2-butanol[6], 1-pentanol[6], 2-pentanol[6], 3-pentanol[6], 1-hexanol[7], 2-hexanol[6], 3-hexanol[6], 1-octanol[4], 2-octanol[7], 1-decanol[8], 1-dodecanol[9], and 1-tetradecanol[10], was better than 99.5% as tested by GLC. The hexane[10], used to prepare the spreading solutions and the distilled water used to prepare the alkanol solutions and as a subphase for the monolayers fulfilled the requirements described previously (2, 3).

Instruments—A 9-cm diameter polytef dish, provided with two identical microburets[11] and a polytef-coated stirring bar (1.25 × 0.8 cm), was used as a trough in a closed system described previously (2, 3). Surface tension was measured with a Wilhelmy platinum plate (2.5 × 1.25 × 0.01 cm) attached to an electrobalance[12], and the output was fed into a dual-pen recorder[13].

Surface Tensions of Alkanol Solutions—The aqueous alkanol solution was slowly added to the polytef dish so that it just contacted the lower end of the positioned platinum plate (6). The surface tension, γ, was continuously recorded after 1 min, and the equilibrium values, γ_{eq}, reported here were determined from values that remained constant for 30 min. The time necessary to reach equilibrium varied with the alcohol concentration. The reproducibility of the surface tension measurements was within ±0.2 dyne/cm. All experiments were performed at 21 ± 1°.

The surface pressure, π, of the alcohol solutions is the difference between the previously determined surface tension of the pure water, γ_0, and the equilibrium surface tension, γ_{eq}. The surface pressure was fitted to a function of the concentration, C (moles per liter), of the alkanol by digital computerized nonlinear regression to exponential equations of the form:

$$\pi = \gamma_0 - \gamma_{eq} = B_1 e^{[B_2(\log C)^2 + B_3 \log C]} \qquad \text{(Eq. 1)}$$

where the B_i values were adjustable parameters. This equation was chosen because the computer fittings of π to polynomial functions of concentration were significantly aberrant for experimental points at low surface pressures.

At constant temperature and pressure, the Gibbs adsorption equation may be written (7):

$$d\pi = \sum_i \Gamma_i \, d\mu_i = \sum_i \Gamma_{i \neq 1}^1 \, d\mu_i \qquad \text{(Eq. 2)}$$

where π is the surface pressure, and Γ_i, μ_i, and Γ_i^1 are the number of moles per unit area, the chemical potential, and the surface excess of the ith species, respectively. The surface excess, Γ_i^1, of an ith species is defined by (8):

$$\Gamma_i^1 = \Gamma_i - \frac{X_i}{X_1}\Gamma_1 \qquad \text{(Eq. 3)}$$

[1] Mann Research Laboratories, Orangeburg, N.Y.
[2] Mallinckrodt Chemical Works, St. Louis, Mo.
[3] W. A. Industrial Chemicals, New York, N.Y.
[4] Fisher Scientific Co., Fair Lawn, N.J.
[5] J. T. Baker Chemical Co., Phillipsburg, N.J.
[6] Aldrich Chemical Co., Milwaukee, Wis.
[7] Eastman Kodak Co., Rochester, N.Y.
[8] Chemical Samples, Columbus, Ohio.
[9] Supelco, Supelco Park, Bellefonte, Pa.
[10] Matheson, Coleman and Bell, East Rutherford, N.J.
[11] Manostat, New York, N.Y.
[12] Cahn Division, Ventron Instruments Corp., Paramount, Calif.
[13] Leeds and Northrup, North Wales, Pa.

Table I—Surface Tensions, γ, Energies of Adsorption, ΔG, and Areas per Molecule, A_0, at the Air–Water Interface

Alkanol	γ(Alkanol/Air), dynes/cm	From Plot of π *versus* X_2			From Plot of Reciprocal π *versus* A	
		r	Slope π/X_2	ΔG, kcal/mole	r	A_0, Å^2/molecule
Methanol	23.5	0.9972	4.65×10^2	3.59	0.9995	9.7
Ethanol	22.4	0.9983	1.27×10^3	4.18	0.9961	18.5
1-Propanol	23.8	0.9993	3.96×10^3	4.84	0.9992	19.6
2-Propanol	20.7	0.9986	3.41×10^3	4.75	0.9999	18.5
1-Butanol	24.5	0.9994	1.09×10^4	5.43	0.9999	16.1
2-Butanol	23.0	0.9986	1.00×10^4	5.38	0.9989	26.1
1,1-Dimethyl-1-ethanol	—	0.9985	7.33×10^3	5.20	0.9999	20.2
2-Methyl-1-propanol	22.1	0.9999	1.14×10^4	5.46	0.9999	17.7
1-Pentanol	24.9	0.9998	3.98×10^4	6.19	0.9996	18.7
2-Pentanol	23.8	0.9977	3.39×10^4	6.10	0.9992	21.9
3-Pentanol	24.4	0.9981	2.34×10^4	5.88	0.9996	21.3
1-Hexanol	25.8	0.9922	1.13×10^5	6.80	0.9999	15.7
2-Hexanol	24.7	0.9984	9.45×10^4	6.70	0.9999	19.2
3-Hexanol	24.0	0.9997	9.00×10^4	6.60	0.9999	9.5
1-Octanol	27.0	0.9917	1.23×10^6	8.20	0.9998	9.5
2-Octanol	25.5	0.9997	9.51×10^5	8.05	0.9999	14.8
1-Decanol	—	0.9882	1.12×10^7	9.49	—	—
1-Dodecanol	—	0.9837	1.32×10^8	10.93	—	—

where X_i is the mole fraction of the ith component, and the solvent is denoted by $i = 1$. Thus, for a two-component mixture:

$$\Gamma_2^1 = \Gamma_2 - \frac{X_2}{X_1}\Gamma_1 \qquad \text{(Eq. 4)}$$

where X_2 is the mole fraction of the solute.

For a dilute aqueous solution with a single solute ($X_2/X_1 \leq 0.01$), it can be reasonably assumed that $\Gamma_2^1 \approx \Gamma_2$.

Since the chemical potential is defined as:

$$d\mu_2 = RT\, d \ln a_2 \approx RT\, d \ln C_2 \qquad \text{(Eq. 5)}$$

where a_2 is the activity and C_2 is the solute concentration, substitution into Eq. 2 gives:

$$\Gamma_2 = \frac{d\pi}{d \ln C_2}\frac{1}{kT} \qquad \text{(Eq. 6)}$$

where Γ_2 is the surface concentration (molecules per square centimeter) of the solute, k is the Boltzmann constant (ergs per molecule degree), T is the absolute temperature (°K), π is the surface pressure (dynes per centimeter), and C_2 is the solute concentration (moles per liter) in the bulk solution.

The derivative ($d\pi/d \ln C_2$) of the exponential equation (Eq. 1) that characterized the dependence of the surface pressure on concentration was computed with respect to the logarithm of the solute concentration. Substitution of these values into Eq. 5 permitted calculation of the surface concentration, Γ_2, at any bulk concentration, C_2. The reciprocal $1/\Gamma_2 = A$ is the apparent area occupied by a molecule in square Angstroms per molecule and is the area within which one molecule of solute can be found at the interface.

Densities of the alcohol solutions for the calculation of mole fractions were determined, using 10-ml specific gravity bottles previously calibrated with water. The precision of the weighing was ±0.1 mg. Densities of methanol, ethanol, 1-propanol, 1-butanol, and 1-pentanol solutions were obtained from the literature (9).

Injection beneath Phospholipid Monolayer—With the platinum plate and the microburets in position in the previously described apparatus (2), water was added slowly just to make contact with the lower edge of the platinum plate. After recording the surface tension for 1 min, the volume was adjusted to 45 cm^3. The hexane spreading solution of I or II was delivered dropwise at the air–water interface with a microsyringe[14] with simultaneous stirring and rapid nitrogen flow to facilitate rapid hexane elimination until the desired surface pressure was achieved. In all reported experiments, the initial surface pressure of the monolayer was 5 ± 0.1 dynes/cm.

A given volume of water, equal to the volume of alcohol solution to be injected, was withdrawn from the dish by the appropriate microburet. The alcohol solution was injected within 30 sec from the other microburet, with simultaneous magnetic stirring, into the bulk phase below the surface. Since no significant differences were observed in the changes in surface pressure after stirring 1, 3, 5, or 10 min for a given final alcohol concentration, the stirring was halted after 1 min and the surface tension was continuously recorded. The criterion of equilibrium was the constancy (±0.1 dyne/cm) of the surface pressure increment, $\Delta\pi$, during 30 min. The experiments were performed at 21 ± 1°.

[14] Hamilton.

RESULTS

Adsorption of Alkanols at a Clean Air–Aqueous Interface—The surface tensions of the alkanols (Table I) in the pure state against air agreed with the literature (10–14).

Typical plots of the surface pressure, π, against the logarithm of the concentration, C (moles per liter), for some studied alkanols are given in Fig. 1.

The apparent linear slope of the plot of the surface tension, γ, against concentration for very dilute solutions increased by a factor of three for each additional methylene group in the alkyl chain of a homologous series of aliphatic compounds (15). A simple expression for the free energy change was derived (7) from thermodynamic and molecular kinetic considerations:

$$\Delta G_{\delta s} = -RT \ln \frac{\pi}{X^*_2} \qquad \text{(Eq. 7)}$$

where $\Delta G_{\delta s}$ is the change in standard free energy associated with the adsorption process at a clean air–aqueous solution interface, π is the surface pressure, and X^*_2 is the activity of the solute. Thus, the numerical

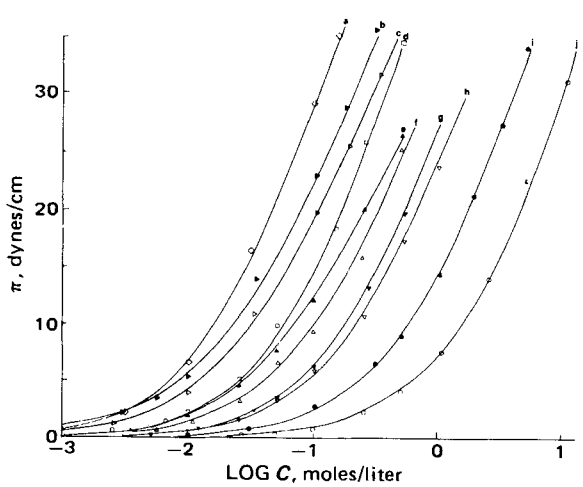

Figure 1—*Plots of the surface pressure, π, against the logarithm of the bulk concentration, C, for alkanols from C_1 to C_5. Key:* a, *1-pentanol;* b, *2-pentanol;* c, *3-pentanol;* d, *1-butanol;* e, *2-butanol;* f, *1,1-dimethyl-1-ethanol;* g, *1-propanol;* h, *2-propanol,* i, *ethanol; and* j, *methanol. The lines drawn through the experimental points were the best fit to Eq. 1 obtained from the computer.*

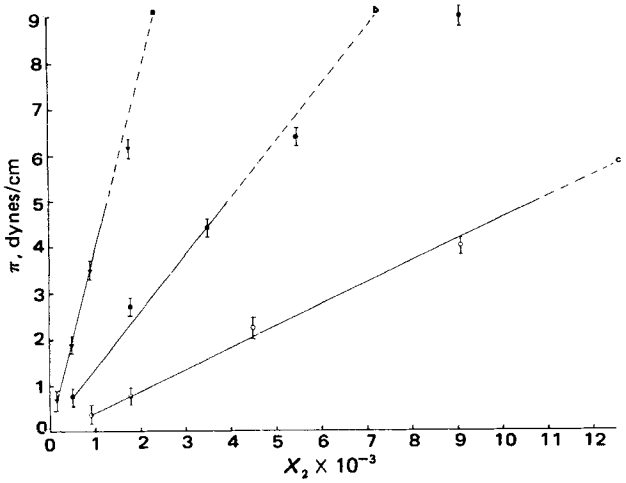

Figure 2—*Plots of the surface pressure, π (≤5 dynes/cm), against the mole fraction, X_2, for methanol (a), ethanol (b), and 1-propanol (c). The lines drawn through the experimental points were the best fit to Eq. 1 obtained from the computer.*

value of $\Delta G_{\delta s}$ can be calculated from the slope (π/X^*_2) of a *linear* plot of the surface pressure against the mole fraction, X_2, of the solute in bulk solution when $X_2 \rightarrow 0$ and $X_2 \rightarrow X^*_2$ at low mole fractions.

For all alkanols, plots of the surface pressure against the concentration of the alcohol in the bulk solution were reasonably linear in the region $\pi \leq 5$ dynes/cm under the experimental conditions. Typical plots for some alkanols are given in Figs. 2 and 3. The correlation coefficients, r, the slopes, and the estimated values of ΔG obtained from such plots are given in Table I. The plot was also linear in this range for 1-hexanol in contrast to a previous report (7).

Plots of the calculated free energies of adsorption, $\Delta G_{\delta s}$ (Eq. 7), against the number of carbon atoms in the alkyl chain, C_n, are given in Fig. 4. The experimental points that corresponded to the primary or 1-alkanols determined a straight line within the limits of the experimental error (±0.2 kcal/mole). The numerical values of $\Delta G_{\delta s}$ (Table I) for the 1-alkanols, C_1 to C_5, were in excellent agreement with the literature (7). The change of the position of the hydroxyl group along the hydrocarbon chain produced a small, but significant, decrease in the ΔG value.

The slope of the plot ΔG *versus* C_n for the 1-alkanols from C_1 to C_{12} was −0.66 kcal/mole and agreed with the literature values of from −0.600 to −0.625 kcal/mole reported for the free energy of adsorption per methylene group of a hydrocarbon chain that adsorbs at the air–aqueous solution interface (16–20). The free energy of adsorption of the hydroxyl group can be estimated from the intercept on the assumption that the extrapolation of the straight line to $C_n = 0$ gives a numerical value related to the free energy of adsorption of the polar moiety of the alcohol molecule and is −2.87 kcal/mole.

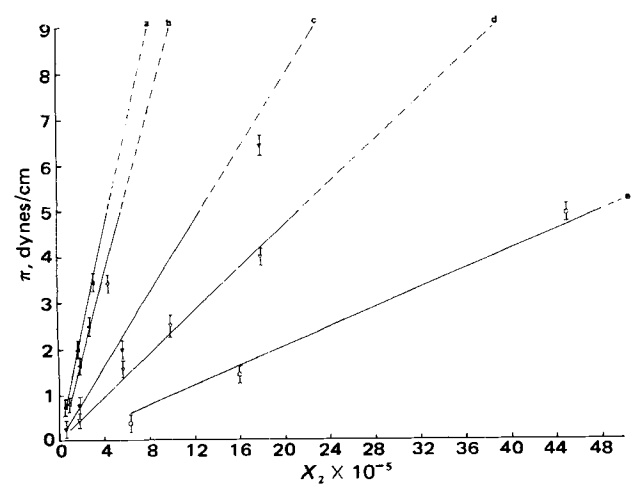

Figure 3—*Plots of the surface pressure, π (≤5 dynes/cm), against the mole fraction, X_2, for: 1-hexanol (a); 3-hexanol (b); 1-pentanol (c); 3-pentanol (d); and 1-butanol (e). The lines drawn through the experimental points were the best fit to Eq. 1 obtained from the computer.*

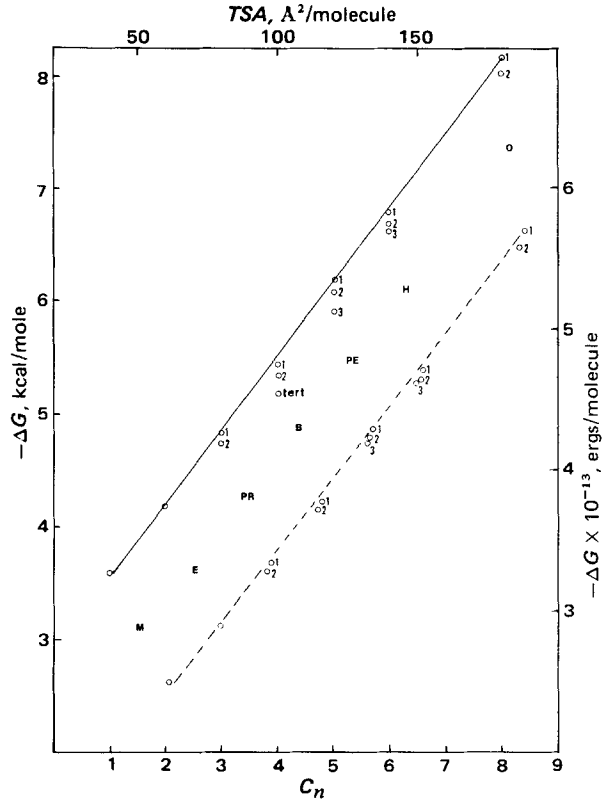

Figure 4—*Left and lower coordinates: plot of the free energy of adsorption at the air–aqueous solution interface, ΔG (kcal/mole), against the number of carbon atoms, C_n, of alkanols from C_1 to C_8. Right and upper coordinates: plot of the free energy of adsorption at the air–water interface, ΔG (ergs per molecule), against the total molecular surface area, TSA (square Angstroms per molecule). Key: M, methanol; E, ethanol; PR, propanols; B, butanols; PE, pentanols; H, hexanols; O, octanols; and tert, 1,1-dimethyl-1-ethanol. Numbers represent the position of the hydroxyl group.*

Interaction of 1-Alkanols with Phospholipid Monolayers—The energies of interactions, Ψ, can be estimated from the slopes of the reciprocals of the equilibrium surface pressures, $\Delta\pi_{eq}$, after injection against the reciprocals of the final concentrations, n (molecules per cubic centimeter), of the subphase injected alcohol (2, 3). Such energies are plotted in Fig. 5 against the number of carbon atoms, C_n, of the 1-alkanol chain.

The plot was linear from C_1 to C_5 for both I and II. Departures from linearity were observed for the energy of interaction of 1-hexanol with the two phospholipids and for 1-octanol with II. In the C_{10} to C_{14} region, the experimental points obtained for both phospholipids were again on the straight line determined by the five first members of the 1-alkanol series.

The energies of interaction per methylene group of the injected 1-alkanol with the molecules that form the monolayer were calculated from the regression coefficient of the best straight line through the experimental points from C_1 to C_5. They were 0.81 and 0.83 kcal/mole/methylene for II and I monolayers, respectively. The energy of interaction of the hydroxyl group was calculated from the intercepts of the straight lines based on the previously stated assumption. The values were 0.73 and 0.42 kcal/mole/methylene for II and I, respectively.

DISCUSSION

Adsorption of Alkanols at Clean Air–Water Interface—The surface activity of alkanols arises from the presence in the same molecule of a soluble hydroxyl group and an insoluble hydrocarbon chain (21). The ratios of the instantaneous slopes of π against ln C_2 at a given C_2 and temperature for different alkanols are the ratios of the adsorptions, Γ_2, of the solutes at the liquid interface (Eq. 5).

The relatively parallel slopes for higher concentrations of alkanols (Fig. 1) indicate that the same number of molecules of any of the alkanols is adsorbed per unit area of the interface. The relative linearity of the curves in this region indicates that the interfacial concentration is not signifi-

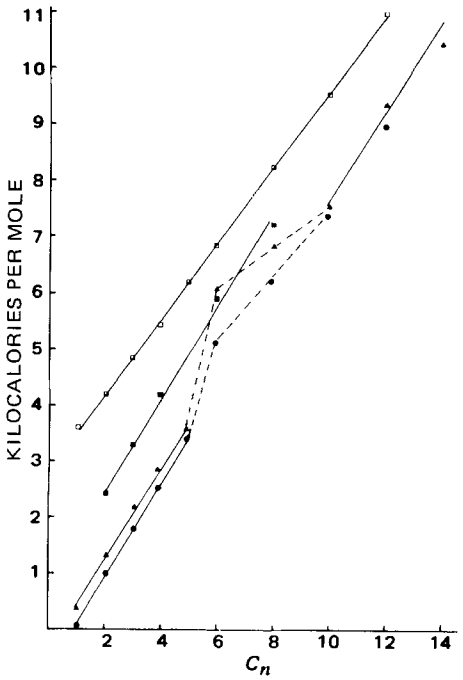

Figure 5—*Plots of energies of adsorption and energies of interactions against the number of carbon atoms of 1-alkanols from C_1 to C_{14}. Key: □, free energy of adsorption at the air–aqueous solution interface; ■, free energy of adsorption at the petroleum ether–aqueous solution interface (33); ▲, energy of interaction with II monolayers; and ●, energy of interaction with I monolayers.*

cantly increased when the solution concentration is increased and that the adsorbed molecules are too closely packed on the interface to admit others after a certain bulk concentration.

The equation of state (22, 23):

$$\pi = \frac{kT}{(A - A_0)} \qquad \text{(Eq. 8)}$$

where π is the surface pressure (dynes per centimeter or ergs per square centimeter), k is the Boltzmann constant (1.3805×10^{-16} erg/molecule), T is the absolute temperature (°K), A is the area per molecule (square Angstroms per molecule) at π, and A_0 is the limiting area (square Angstroms per molecule), was tested for all alkanols studied. Table I lists the values of the limiting areas, A_0, and the correlation coefficients estimated from plots of $1/\pi$ against A from 30 to 100 Å^2/molecule, where $A = 1/\Gamma_2$ was calculated from Eq. 6. With the exception of methanol, 3-hexanol, and 1-octanol, the values of A_0 were between 15 and 25 Å^2/molecule. Values of 18.5 Å^2/molecule were reported previously for ethanol at the air–water interface (24, 25) and for ethanol, 1-propanol, and 1-butanol at the petroleum ether–water interface (22).

These values roughly correspond to the cross-sectional area of an aliphatic hydrocarbon chain. This fact can be taken to mean that, under conditions of quasisaturation of the interface, the adsorbed molecules are arranged parallel to one another and at a steep angle to the interface.

The values of A_0 found for methanol, 3-hexanol, and 1-octanol were roughly one-half of the average A_0 values of the other alkanols and may suggest an association of those molecules that takes place at the air–water interface (7).

On the assumptions that the alkanol molecules are oriented quasi-perpendicular to the plane of the interface and that the stretched hydrocarbon chains are immersed completely in the aqueous phase, the volume, V_s, of this interfacial region containing the number of molecules per square centimeter that corresponds to the surface concentration, Γ_2 (Eq. 5), can be approximately estimated from the length of the alkanol molecule.

The plots of the concentration of such a thin interfacial region [$\Gamma_2' = (\Gamma_2/V_s)$ in moles per liter] estimated from these volumes and from the surface concentration (Γ_2 in molecules per square centimeter) against the bulk concentration (C in moles per liter) are given in Fig. 6 for some 1-alkanols and indicate that the concentration of the adsorbed alkanols in the thin interfacial region (<30 Å) could be up to 10^3 times greater than that of the bulk solutions when equilibrium is attained.

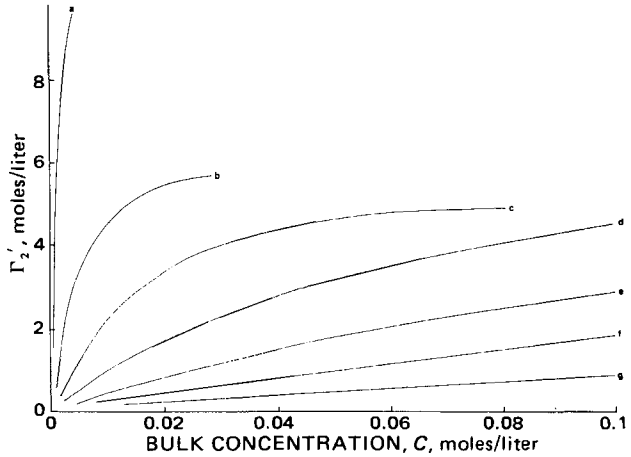

Figure 6—*Plots of the concentration at the interfacial region, Γ_2' (moles per liter), against the bulk concentration, C (moles per liter), of 1-alkanols from C_1 to C_8. Key: a, octanol; b, hexanol; c, pentanol; d, butanol; e, propanol; f, ethanol; and g, methanol.*

The surface activity of alkanols is the result of the hydrophilic–hydrophobic balance between the hydroxyl and the methylene groups, and the free energy of adsorption is linearly related to the number of carbon atoms, C_n, in their hydrocarbon chain (Fig. 4). However, the values for 2- and 3-alkanols deviate from the linearity of their corresponding 1-alkanols and indicate that free energy is also affected by the position of the hydroxyl group along the hydrocarbon chain.

Recent studies (26, 27) showed a striking correlation between the solubility of alkanols in water and their molecular surface areas, *i.e.*, the surface area of the alkanol molecule in the bulk solution around which the water molecules can be packed. The group surface area corresponding to the hydroxyl group decreased from an average value of 20.2 Å^2 in the 1-position to 17.3 Å^2 for the 3-position of the alkanols (27).

The plot of the free energy of adsorption (ergs per molecule) against the total molecular surface area (square Angstroms per molecule) of some 1-alkanols and their 2- and 3-isomers is compared in Fig. 4 (right and upper coordinates) with that of the free energy of adsorption (kilocalories per mole) as a function of the number of carbon atoms in the hydrocarbon chain. The excellent linearity for all alkanols independent of the hydroxyl position indicates that the simultaneous effect of chain length and of position of the hydroxyl group on the surface activity of alkanols is best described by the total molecular surface area of the alkanol molecule.

Interaction of Alkanols with Phospholipid Monolayers—Compound II forms a condensed liquid monolayer at the air–water interface. The surface area that corresponds to each molecule that forms the monolayer was 40 ± 2 Å^2 at 5 ± 0.1 dynes/cm and 22 ± 1° (3). On the assumption that the stretched molecules were submerged completely in the water phase with the phosphatidylethanolamine group parallel to the interface, the concentration in this thin (~30 Å) crust of water was estimated to be 1.4 moles/liter (3). The percentage of water in this interfacial region estimated from its volume and the volume occupied by the phospholipid molecules was 1.9%. It follows that this interfacial region

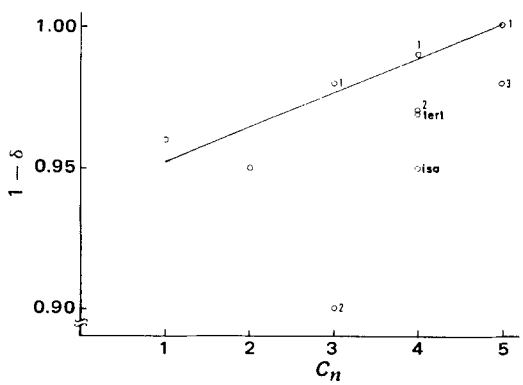

Figure 7—*Plot of $1 - \delta$ obtained from Ref. 29 against the number of carbon atoms of alkanols from C_1 to C_5. Numbers represent the position of the hydroxyl group. Key: tert, 1,1-dimethyl-1-ethanol; and iso, 2-methyl-1-propanol.*

may be considered to be a predominantly hydrocarbon phase approximately 30 Å thick.

Compound I forms a relatively less condensed liquid monolayer at the air–water interface. The surface area that corresponds to each molecule at 5 dynes/cm and 22° was 55 ± 2 Å^2. On the same assumptions, its concentration in the 30-Å crust of water was estimated to be 1.0 mole/liter and the percentage of water at the interfacial region was estimated to be 29.4% (3).

Plots of the energies of interaction of the injected 1-alkanols with each phospholipidic monolayer against the chain length are compared in Fig. 5 with those of the free energies of adsorption at the clean air–water interface obtained in the present work and at the clean petroleum ether–water interface obtained from the literature (23).

Up to pentanol, the energy of interaction per methylene group with the phospholipid monolayers compares with the free energy of adsorption per methylene group at the clean petroleum ether–water interface (0.82 kcal/mole/methylene) within the limits of the experimental error; *i.e.*, the slopes in Fig. 5 are parallel up to $C_n = 5$. This finding seems to indicate that the phospholipid monolayers behave as ultrathin simple hydrocarbon phases in their interaction with the injected 1-alkanol and also that the polar moiety of the phospholipid does not have a major influence on the adsorption of the hydrocarbon chain of the 1-alkanols. The energies of interaction per hydroxyl group of the 1-alkanols, on the other hand, seem to be influenced by the nature of the nonaqueous phase, as indicated by the numerical values of the corresponding intercepts: air, 2.84; petroleum ether, 0.84; II, 0.73; and I, 0.42.

The origin of the sudden discontinuity observed for the values of the energies of interactions of 1-hexanol and 1-octanol with II and of 1-hexanol with I is as yet unexplained. It was suggested (3) that entropic factors associated with the configuration of the molecules at the interfacial region *do* contribute to the energy of interaction. Thus, the simplified assumption of a common entropy factor (2, 3) for such interactions on which the calculations of energies were based may be an oversimplification of a more complex process. The difference between the experimental value of the energy of interaction of 1-hexanol with II and the value expected from the extrapolation of the straight line through the first five terms was 1.65 kcal/mole. If this difference were totally an entropic contribution, it would correspond to 5.5 entropic units, which is not an unreasonable value for entropic changes associated with adsorption and desorption processes at oil–water interfaces (28).

The experimental points corresponding to the interaction of 1-decanol, 1-dodecanol, and 1-tetradecanol with the phospholipid monolayers were again on the extrapolation of the straight line determined by the first five numbers of the 1-alkanol series. Perhaps the increased chain length of the C_{10} to C_{14} 1-alkanols permits the adoption of configurations to compensate for the entropic deviation of the C_6 to C_8 alkanols. The latter's lengths are optimum for cyclization.

Correlations with Permeability Processes—"The permeability of biological membranes to nonelectrolytes depends intimately upon molecular structure, so that a small change in the structure of a solute often causes a profound change in its permeating power" (29). Reflection coefficients, δ, of alkanols for epithelial cells of rabbit gallbladder were measured (29). The reflection coefficient is 1 for an impermeant solute and 0 for a solute as permeant as the solvent itself. In general, it decreases from 1.0 to 0 with increasing lipid–water partition coefficients, which seems to indicate that the intermolecular forces governing the permeability of nonelectrolytes are similar to those governing partition between a bulk lipid phase and water. For most solutes, the values of $(1 - \delta)$ give the same permeability sequences as the solute permeability coefficient in Nitella (30) and rabbit gallbladder (31) and the partition coefficients and reflection coefficients in goldfish bladder, bullfrog gallbladder, bullfrog intestine, and guinea pig intestine (32) are well correlated, indicating that the $(1 - \delta)$ parameter is a good measure of permeability for nonelectrolyte solutes permeating *via* membrane lipids.

The values of $(1 - \delta)$ obtained from Ref. 29 are linearly related to the chain length of the primary alkanols from C_1 to C_5 (Fig. 7). The position of the hydroxyl group does affect the permeability of these alkanols. The deviation of methanol has been explained by the premise that small polar solutes, which should interact the least with the hydrocarbon moiety of membrane lipids, must have an alternative route of permeation through the localized concentration of membrane polar groups associated with "frozen" water molecules (29). The deviation of ethanol, if experimentally significant, is difficult to explain on the premise of the linear relation assumed for Fig. 5.

Plots of the energies of interaction of these alkanols with I and II monolayers are represented in Fig. 8. No deviation was observed for the lowest members of the series as compared with the plots of $(1 - \delta)$ against

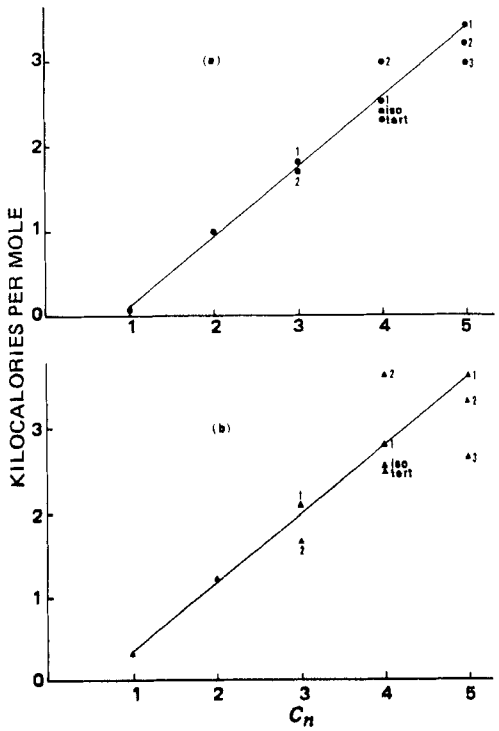

Figure 8—*Plot of the energy of interaction of alkanols from C_1 to C_5 with I(a) and II(b) monolayers. Numbers represent the position of the hydroxyl group. Key: tert, 1,1-dimethyl-1-ethanol; and iso, 2-methyl-1-propanol.*

the chain length. The nonexistence of "localized" concentrations of polar groups associated with frozen water molecules for the phospholipid monolayers may explain the absence of anomalies in these plots for methanol. Thus, for the 1-alkanols, plots of their energies of interaction with the lipid monolayer against the chain length show an acceptable correlation with the permeation of these substances across biological membranes.

The different permeation behavior of the 1- and 2-propanols is not reflected, within the limits of experimental error, in their energies of interaction with the I monolayers. However, with II, a small significant difference between the energies of interaction can be observed.

2-Butanol and 1,1-dimethyl-1-ethanol have less permeability than 1-butanol (Fig. 7), and both have higher permeability (*i.e.*, $1 - \delta$) than 2-methyl-1-propanol. The directions of the deviations of these alkanols from the energy of interaction of 2-butanol with the phospholipid monolayers (Fig. 8) do not correlate with the direction of these permeability differences.

3-Pentanol has a lower permeability than 1-pentanol (Fig. 7), consistent with the fact that the energies of interaction of the pentanols with I and II monolayers decreased in the sequence 1 → 2 → 3 for the three isomers (Fig. 8).

Presently accepted membrane models (33) postulate the existence of lipid regions, formed mainly by phospholipids with a bilayer configuration, in cell membranes. The experimental model used in the present work could represent an external monolayer of the lipid regions of cell membranes. Thus, it seems plausible that correlations exist between the energies of interaction of the 1-alkanols with the phospholipid monolayers and their permeability across cell membranes. The fact that even the effect of the hydroxyl group position of the isomers is reflected in their energies of interaction indicates that this experimental model may present interesting perspectives for future work with more complex molecules.

Partition coefficients were measured previously between olive oil–aqueous solution (30), erythrocyte membrane–aqueous solution (34), and dimyristoyllecithin liposomes–aqueous solution (35) for some of the C_1 to C_5 alkanols. For dimyristoyllecithin liposomes, the equation:

$$\Delta F = -RT \ln K \qquad \text{(Eq. 9)}$$

in which R is the universal gas constant, T is the absolute temperature, and K is the experimentally measured partition coefficient, was used to estimate a ΔF with the physical meaning (35) of the change in free energy

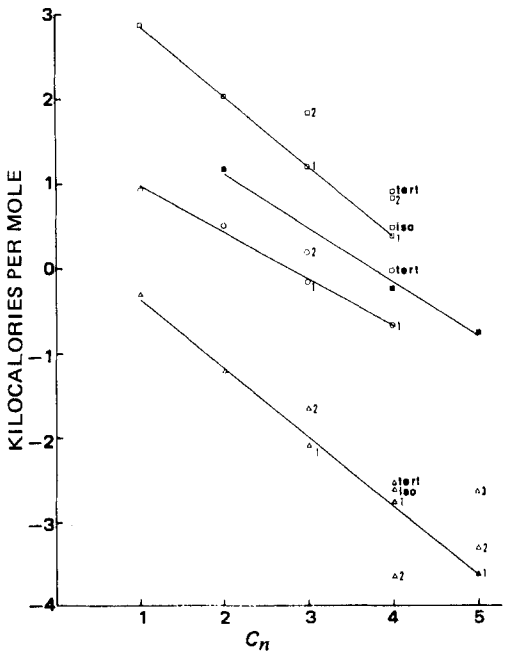

Figure 9—*Plot of the free energy of transfer from an aqueous phase to a nonaqueous phase against the number of carbon atoms of alkanols from C_1 to C_5. Key: □, olive oil–aqueous solution, calculated from Ref. 30; ■, red blood cell membrane–aqueous solution, calculated from Ref. 34; ○, dimyristoyllecithin liposomes–aqueous solution (35); ▲, II monolayer–aqueous solution; tert, 1,1-dimethyl-1-ethanol; and iso, 2-methyl-1-propanol. Numbers represent the position of the hydroxyl group.*

of the transfer of 1 mole of solute from a hypothetical aqueous solution to a hypothetical lipid solution.

On the assumptions that the given numerical values of the energies of interaction of the C_1 to C_5 alkanols with the phospholipid monolayer were valid (*i.e.*, entropies were invariant among the alkanols) and that the same energies were operative under the conditions of the studied partition coefficients, the changes in free energies corresponding to the partition coefficients of Refs. 30, 34, and 35 were calculated (Eq. 9).

Acceptable correlations were observed between the free energy values that correspond to these four different "lipidic phases" and the number of carbon atoms of alkanols from C_1 to C_5 (Fig. 9). The slopes that correspond to the olive oil–aqueous solution and II monolayer–aqueous solution interfaces were the same (0.83 and 0.81 kcal/mole/methylene, respectively) within the limits of experimental error. The slope for the red blood cell membrane–aqueous solution interface was lower (0.65 kcal/mole/methylene) and may be due to the nonhomogeneous distribution of the lipids of the cell membrane which permits alternative routes of permeation. The slope for the dimyristoyllecithin liposome–aqueous solution interface (0.55 kcal/mole/methylene) may be due to the lax structure of the phospholipid monolayer of the liposome.

These results and correlations may give further insight into the interaction of biomembranes with approaching molecules. They indicate that the energies of interaction of alkanols from C_1 to C_5 with phospholipid monolayers spread at the air–water interface may be taken as a criterion to predict their relative behavior in the permeation process across cell membranes.

REFERENCES

(1) B. E. Cohen, *J. Membrane Biol.*, **20,** 205 (1975).

(2) F. A. Vilallonga, E. R. Garrett, and M. Cereijido, *J. Pharm. Sci.*, **61,** 1720 (1972).

(3) F. A. Vilallonga and E. R. Garrett, *ibid.*, **62,** 1605 (1973).

(4) D. O. Shah and J. H. Schulman, *J. Colloid Interface Sci.*, **25,** 107 (1967).

(5) G. M. Adams and T. L. Sallee, *J. Chromatogr.*, **49,** 552 (1970).

(6) R. Ruyssen, *Rec. Trav. Chim.*, **65,** 580 (1946).

(7) J. H. Clint, J. M. Corkill, J. F. Goodman, and J. R. Tate, *J. Colloid Interface Sci.*, **28,** 522 (1968).

(8) J. J. Kipling, "Adsorption from Solutions of Non-Electrolytes," Academic, New York, N.Y., 1965, p. 193.

(9) M. E. Friedman and H. A. Scheraga, *J. Phys. Chem.*, **69,** 2795 (1965).

(10) "Handbook of Chemistry and Physics," 56th ed., CRC Press, Cleveland, Ohio, 1975.

(11) K. Nakanishi, T. Matsumoto, and M. Hayatso, *J. Chem. Eng. Data*, **16,** 44 (1971).

(12) F. M. Fowkes, *Ind. Eng. Chem.*, **56,** 40 (1964).

(13) J. R. Dann, *J. Colloid Interface Sci.*, **32,** 302 (1970).

(14) G. Zografi and S. H. Yalkowsky, *J. Pharm. Sci.*, **63,** 1533 (1974).

(15) J. Traube, *Ann.*, **265,** 27 (1891).

(16) I. Langmuir, *J. Am. Chem. Soc.*, **39,** 1883 (1917).

(17) D. A. Haydon and F. H. Taylor, *Phil. Trans. Roy. Soc.*, **A252,** 255 (1960).

(18) J. Llopis and P. Artalejo, *An. Fis. Quim. (Madrid)*, **58,** 367 (1962).

(19) H. Kimizuka, L. G. Abood, T. Tahara, and K. Kaibara, *J. Colloid Interface Sci.*, **40,** 27 (1972).

(20) M. Nakagaki and T. Handa, *Bull. Chem. Soc. Jpn.*, **48,** 630 (1975).

(21) R. Defay and I. Prigogine, "Surface Tension and Adsorption," Longsmans Green, New York, N.Y., 1957, p. 94.

(22) J. J. Kipling, "Adsorption from Solutions of Non-Electrolytes," Academic, New York, N.Y., 1965, p. 198.

(23) D. A. Haydon and F. R. Taylor, *Phil. Trans. Roy. Soc.*, **A252,** 225 (1960).

(24) E. A. Guggenheim and N. K. Adam, *Proc. Roy. Soc.*, **A139,** 218 (1933).

(25) D. V. Cornford, J. J. Kipling, and E. R. M. Wright, *Trans. Faraday Soc.*, **58,** 74 (1962).

(26) G. L. Amidon, S. H. Yalkowsky, and S. Leung, *J. Pharm. Sci.*, **63,** 1858 (1974).

(27) S. C. Valvani, S. H. Yalkowsky, and G. L. Amidon, *J. Phys. Chem.*, in press.

(28) J. T. Davies and E. K. Rideal, "Interfacial Phenomena," Academic, New York, N.Y., 1961, pp. 161–163. J. L. Kavanau, "Structure and Functions in Cell Membranes," vol. I, Holden-Day, San Francisco, Calif., 1965, pp. 80–83.

(29) J. M. Diamond and E. M. Wright, *Proc. Roy. Soc.*, **B172,** 273 (1969).

(30) R. Collander, *Physiol. Plant.*, **7,** 420 (1954).

(31) A. P. Smulders and E. M. Wright, *J. Membrane Biol.*, **5,** 297 (1971).

(32) J. M Diamond and Y. Katz, *ibid.*, **17,** 121 (1974).

(33) S. J. Singer and G. L. Nicolson, *Science*, **175,** 720 (1972).

(34) S. Roth and P. Seeman, *Biochim. Biophys. Acta*, **255,** 207 (1972).

(35) Y. Katz and J. M. Diamond, *J. Membrane Biol.*, **17,** 101 (1974).

ACKNOWLEDGMENTS AND ADDRESSES

Received August 27, 1976, from the *College of Pharmacy, University of Florida, Gainesville, FL 32610.*

Accepted for publication October 26, 1976.

* To whom inquiries should be directed.

Flow Rates and Repose Angles of Wet-Processed Granulations

J. T. CARSTENSEN ˣ **and PING CHING CHAN**

Abstract □ The equation of McDougall and Evans was found not to apply to granulations. The functional relationships among volumetric powder flow rates, angles of repose, and particle size were demonstrated to exhibit maxima (rather than minima) in five common pharmaceutical granulations produced by wet processing. The angular behavior of granules (such as the experienced range of angles) is explained *via* supported stacking geometries, and the shallow maxima in the angle of repose *versus* granule diameter was derived from this model.

Keyphrases □ Granulations, wet processed—relationships among volumetric powder flow rates, angles of repose, and particle size □ Flow rates, powder—relationship to angles of repose and particle size in wet-processed granulations □ Repose angles—relationship to volumetric powder flow rates and particle size in wet-processed granulations □ Particle size—relationship to volumetric powder flow rates and angles of repose in wet-processed granulations □ Dosage forms—wet-processed granulations, relationships among volumetric powder flow rates, angles of repose, and particle size

Many publications have dealt with flow rates and repose angles (1–11). Attempts to relate these two properties failed to generate firm conclusions or equations of general validity (12, 13) for powders. Flow properties are of particular interest to the pharmaceutical researcher and technologist because of the effect of flow properties on the quality of the resulting solid dosage forms (2).

BACKGROUND

Repose angle measurements for powders have been viewed with the purpose of obtaining information on the cohesion of a powder. There is a theoretical correlation between the cohesion and the repose angle of a smooth slant heap (14), but such factors as the bulk density of the sample, *i.e.*, the extent of its consolidation prior to measurement, affect the repose angle (15, 16). Therefore, it is not possible to draw quantitative conclusions regarding the cohesion from repose angles. For materials above 100 μm, this approach is still followed since such powders cannot be tested in shear cells due to crushing during consolidation and low cohesion and tensile strength. The repose angle, α, relates to the diameter, d, of a fine *powder* (17) *via* the inverse relationship $\alpha = (q/d) + s$, where q and s are constants for a particular powder. For a coarse powder or granulation, experimental evidence (16) indicates that α, when measured *via* flow from a funnel, gives rise to a shallow maximum at a particular particle diameter. Hence, $\alpha = h(d)$, where h denotes "function of."

Flow rates, W, are a function of particle diameter (18), so $W = g(d)$, where g denotes "function of." This function has a maximum at a particular diameter (18). Since $W = g(d)$ and $\alpha = h(d)$, it follows that $d = h^{-1}(\alpha)$ and $W = g[h^{-1}(\alpha)]$ in the regions where $h(d)$ is a monotonically increasing or decreasing function; *i.e.*, there must be a relationship between W and α, *i.e.*, $W = f(\alpha)$, where f denotes "function of." The functionalities h and g are not universal but depend on experimental parameters such as orifice diameter.

McDougall and Evans (1) derived such a relationship on theoretical grounds:

$$W = \frac{\pi}{4}\left[\frac{g}{2\mu}(1 + 3\mu^2)\right]^{0.5}\rho D^{2.5} = j[(1 + 3\mu^2)/\mu]^{0.5} \qquad \text{(Eq. 1)}$$

where W is the flow rate, g is the gravitational acceleration, μ is the coefficient of internal friction, ρ is apparent density, and D is the diameter of the efflux tube.

One purpose of this study was to examine whether extrema in $\alpha = h(d)$ and $W = g(d)$ can logically produce extrema in $W = f(\alpha)$.

It is a general rule (9) in solid dosage form technology that a repose angle of 25–40° is a good working range. Therefore, for theory to fall in line with practice, Eq. 2 should yield a maximum in this repose angle range. Theoretical Eq. 2 is depicted in Fig. 1, and it is seen that the flow rate has a minimum (not a maximum) at $\mu = 0.6$. For a cohesionless powder:

$$\mu = \tan\alpha \qquad \text{(Eq. 2)}$$

so $\mu = 0.6$ corresponds to $\alpha = 30°$. Kaneniwa *et al.* (17) classified powders of particle size below 50 μm as being cohesive, and Pilpel (16) classified powders in the 50–150-μm range as mildly cohesive; larger fractions are essentially noncohesive. These ranges are, of course, general rules and do not apply to all powders [carboxymethylcellulose and pyrogenic silica being notable exceptions (16)].

This study dealt with granulations of particle diameters above 150 μm. The intent was to show that repose angles of granulations essentially depend on the stacking characteristics, which explain the shallow maxima in α *versus* d curves.

Table I—Formulas for Granulations Used in the Repose Angle Studies

Ingredient	Granulation I	II	III	IV	V
FD&C Yellow No. 5, g	6	—	—	—	—
Starch USP (dry), g	180	440	100	—	—
Lactose USP, g	1515	1755	1375	1000	1000
Starch USP (paste), g	45	15	—	—	—
Water, g	450	300	—	90	117
Sucrose USP, g	—	1110	—	—	—
Povidone, g	—	—	40	—	—
Alcohol USP (95%), g	—	—	360	—	—
Acacia, g	—	—	—	10	—
Gelatin, g	—	—	—	—	13

EXPERIMENTAL

Five different formulations (Table I) were prepared. The dried granulations were screened through a nest of U.S. Standard sieves, and the various mesh fractions were subjected to angle of repose measurements in the following fashion. Bulk volume of material, 250 cc, was added to an aluminum funnel with the following dimensions: diameter at top, 10 cm; height from base of cone to apex, 7.5 cm; diameter of efflux tube, 0.95 cm; and height of efflux tube, 2.5 cm. The funnel was closed at the bottom of the efflux tube by fitting it flush with a piece of fiberboard, and the assembly was placed 10.2 cm (measured from the bottom of the efflux tube) above a piece of paper on a flat surface. The fiberboard was removed; the height, h, of the resulting heap was measured with a cathetometer; and the area of the base of the heap, A, was determined by cutting out the paper trace of the cone and weighing it (3). The repose

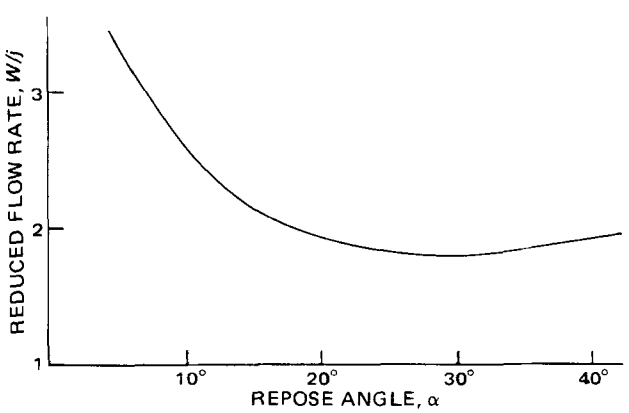

Figure 1—W/j *as a function of* α $(= \tan^{-1}\mu)$ *according to Eq. 1.*

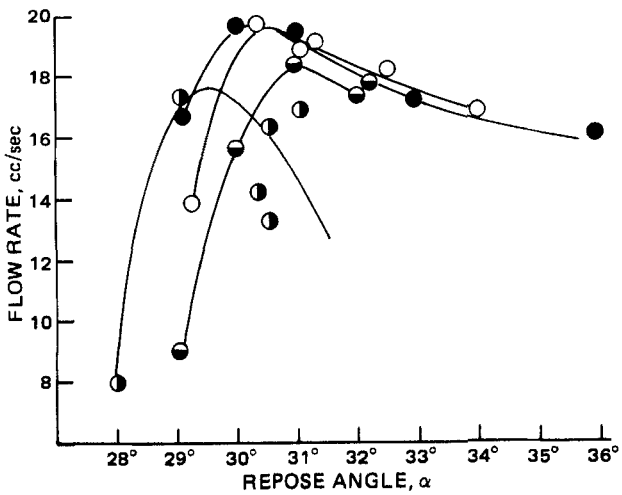

Figure 2—*Flow rates as a function of repose angle based on a 100-g powder charge. Granulation V had relatively close α values (30.6–31.6) and could not be graphed in the scaling shown. Key: ○, Granulation I; ◑, Granulation II; ◒, Granulation III; and ●, Granulation IV.*

angle, α, is then given by $\tan^{-1}[h/(\sqrt{A/\pi})]$. The flow rate was recorded by an electric timer.

Granulations I–III were tested again in a similar fashion using 100 g of each rather than 250 cc.

The porosities of the powder heaps were determined by determining the apparent densities of the heap and the particle density (not true density) of the granules. Since the height and the base area of the heap are known, the volume, v, can be calculated. The apparent density, ρ', can then be calculated from the weight, L, as $\rho' = L/v$.

The particle densities were determined as follows. The procedure for determining true density pycnometrically using organic solvents was followed. The figure thus obtained was the volume of liquid displaced, V_1, per sample weight, q_1, of granules. Since some (but not total) solvent penetration can be expected, the particles were removed from the solvent and subjected to a drying curve. The point where the falling rate started was noted; the volume of solvent at this point corresponds to the volume of voids, V_2, penetrated by the liquid. Hence, the particle density, ρ_p, is $q_1/(V_1 + V_2)$, and the bed porosity, ϵ_b, is then given by $\epsilon_b = 1 - (\rho'/\rho_p)$.

Povidone granulations could not be included in the part of the study dealing with α *versus* ϵ relationships, because of the solubility of povidone in organic solvents.

RESULTS AND DISCUSSION

Figure 1 shows that the flow of a particular granulation through a particular orifice should have a minimum for a granulation with an angle of repose of about 30°. Equation 1 predicts this finding because the derivative with respect to μ of Eq. 1:

$$\frac{\partial W}{\partial \mu} = -0.5j[(1 + 3\mu^2)/\mu]^{-0.5}[3 - (1/\mu^2)] \qquad \text{(Eq. 3)}$$

equals zero when $\mu = \tan \alpha = 1/\sqrt{3}$ or when $\alpha = 30°$. The second derivative of Eq. 3 is:

$$\frac{\partial^2 W}{\partial \mu^2} = -0.25j[(1 + 3\mu^2)/\mu]^{-1.5}[3 - (1/\mu^2)]^2 + 0.5j[(1 + 3\mu^2)/\mu]^{-0.5}(2/\mu^3) \qquad \text{(Eq. 4)}$$

This equation, when $\mu = 1/\sqrt{3}$ is inserted, gives the following value of the second derivative:

$$\frac{\partial^2 W}{\partial \mu^2} = -0 + 0.5j[(1 + 1)/\sqrt{3}]^{-0.5}2.3\sqrt{3} \qquad \text{(Eq. 5)}$$

which is larger than zero. Therefore, Eq. 1 does predict a *minimum* at a repose angle of 30° for a cohesionless powder. In contrast, the granulations reported here showed a *maximum* in flow rate at about 30–33° (Fig. 2 and Table II).

Table II—Repose Angles at which Flow Was Maximum

Granulation	Amount	Repose Angle at Maximum Flow	
		cc/sec	g/sec
I	250 cc	29.6°	29.6°
II	250 cc	29.4°	29.4°
III	250 cc	31.6°	29.8°
IV	220 cc	30.4°	29.2°
V	200 cc	30.8°	30.8°
I	100 g	30.7°	30.7°
II	100 g	29.3°	29.3°
III	100 g	31°	31°
IV	100 g	31°	30°
V	100 g	31.6°	30.6°

The different repose angles in this study were obtained by separating different mesh cuts of the granulations. Flow, of course, is a function of the mean diameter of the powder sample (10). The flow of the granulations is shown as a function of granule size in Fig. 3, and the flow exhibited the same dependence as reported elsewhere in the literature for powders (10) and granulations (19).

The repose angle, α, is plotted as a function of d, the mean mesh fraction diameter, in Fig. 4. A maximum occurred; this finding is somewhat different, functionally, from what has been reported in the literature for fine powders (4, 11) but is in accordance with some findings regarding coarse materials (16).

The behavior of granules is shown in Figs. 2–4; there are, of course, only two independent relations out of the three. The functional relations from Figs. 2, 3, and 4, respectively, are:

$$W = f(\alpha) \qquad \text{(Eq. 6)}$$

$$W = g(d) \qquad \text{(Eq. 7)}$$

and:

$$\alpha = h(d) \qquad \text{(Eq. 8)}$$

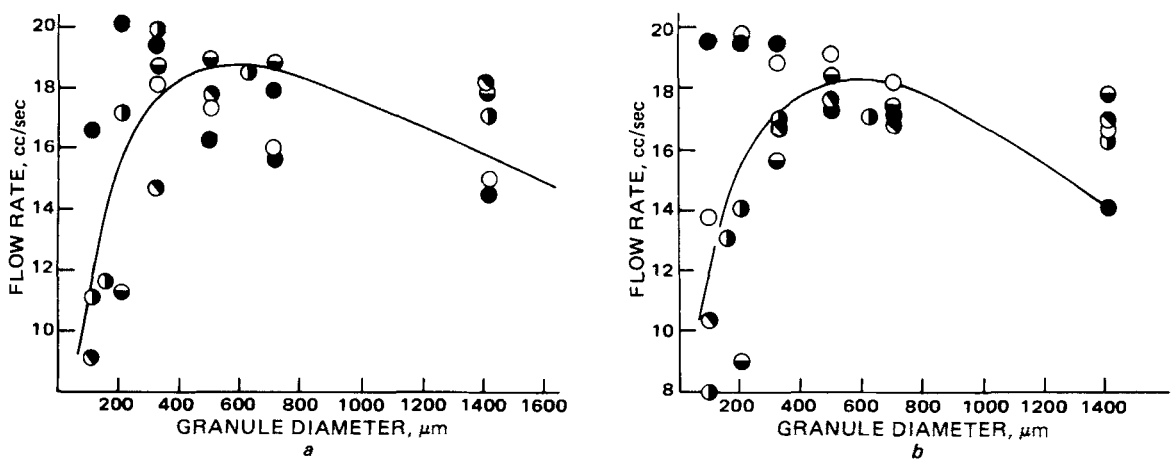

Figure 3—*Flow rates as a function of granule diameter. Figure 3a is based on a 250-cc powder charge; Fig. 3b is based on a 100-g charge. Key: ○, Granulation I; ◑, Granulation II; ◒, Granulation III; ●, Granulation IV; and ◔, Granulation V.*

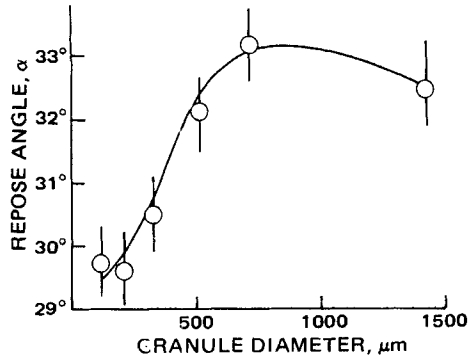

Figure 4—*Repose angles as a function of particle diameter. Each point represents the average of the five granulations, and the bars indicate the 90% confidence limits on the average.*

That a maximum can exist in *all* of the functional relationships is best demonstrated by approximating the curves in Figs. 2 and 4 by parabolas, *i.e.*:

$$W - W_{max} = -k_1(\alpha - \alpha_{max})^2 \qquad \text{(Eq. 9)}$$

and:

$$(\alpha - \alpha_{max}) = -k_2(d - d_{max})^2 \qquad \text{(Eq. 10)}$$

where the subscript max denotes the maximum value of the dependent variable or the value of the independent variable at which the dependent variable attains its maximum. The curves in Figs. 2 and 4 imply that extrema *may* occur but that they need not necessarily occur. One restriction in the argument given is that it assumes coinciding maxima in α and W.

If Eq. 10 is inserted in Eq. 9, then:

$$W - W_{max} = -k_1k_2^2(d - d_{max})^4 \qquad \text{(Eq. 11)}$$

which describes a curve with a maximum, *i.e.*, of the shape shown in Fig. 3.

A closely packed heap of spheres is shown in Fig. 5, and one (of many possible) metastable heap of loose packing is shown in Fig. 6. The porosity of a heap, as opposed to solid populations in confining vessels, has not been covered to any extent in the literature (18, 19). The apparent density of spheres in cylinders was discussed by Scott (20), who overcame difficulties stemming from wall effects (21) by plotting the packing density $(1 - \epsilon)$ *versus* the reciprocal of the vessel diameter $(1/D_0)$. He found a linear relationship, which, when extrapolated to $1/D_0 \rightarrow 0$ (*i.e.*, to $D_0 \rightarrow \infty$), gave a porosity of 0.36. This value compares favorably with the findings of Berg *et al.* (22) that one-dimensional vertical shaking of steel

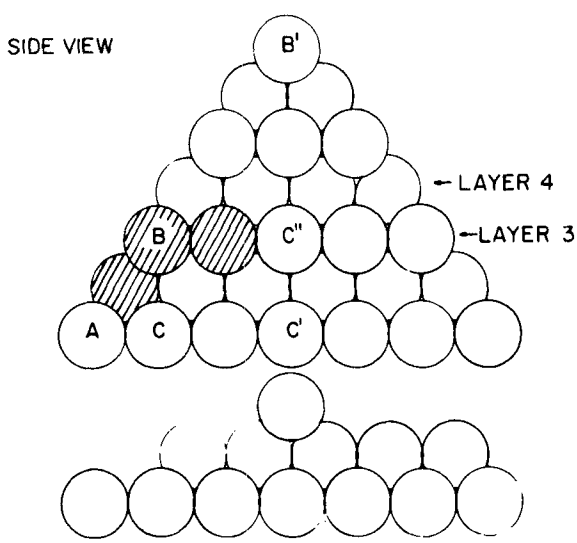

Figure 5—*A closely packed heap of spheres. Key: top* (AC'B'), *unsupported by extra unloaded spheres; and left part of bottom* (AC'C''), *supported by an extra unloaded sphere* (e.g., A) *in each layer* [i.e., *cross-hatched* (B) *spheres disappear*].

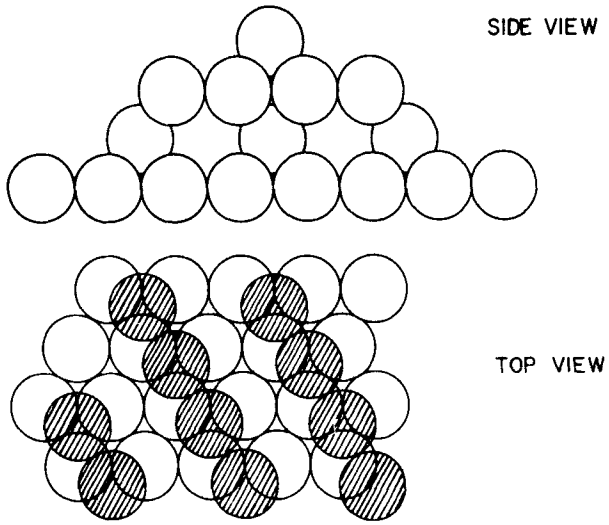

Figure 6—*Loose packing resulting from removing every second sphere from every second layer in the supported structure shown in Fig. 5. The partially depleted layer is shown by cross-hatched spheres in an arbitrary layer.*

spheres gave a porosity of 39% and that three-dimensional shaking gave 26% porosity and with the findings of Newitt and Conway-Jones (23) of a porosity of 38% for closely packed (wet) sand.

In each of these cases, the populations of steel balls or particles were confined by a vessel which, of course, makes them different from a heap. If a heap of spheres were cohesive, then loosely and closely packed heaps would have repose angles of the order of 60° as shown in Fig. 5. Indeed, Berg *et al.* (24) found a 60° angle of the powder remaining in a cubical container (where there is wall support). However, the 60° figure does *not* correlate with the finding here that the angles are in a range of 28–36°.

To evaluate the porosity of a conical heap, as shown in Fig. 5, circles were drawn as shown in Fig. 7 with radii $1.5\,d, 2.5\,d, \ldots, q\,d/2$ about an arbitrarily chosen central sphere (S) in every second layer. For instance, as shown in Fig. 7, in layer 3 a circle with radius $2.5\,d$ is drawn around the central sphere and there are $q = 5$ spheres in the diagnoal layer. In alternate layers, circles of radii $d, 2\,d, \ldots, q\,d/2$ were drawn around the center of the diagonal which now is at the point (P) where two spheres touch. The number of spheres in a circle (layer) was counted with the arbitrary rule that if the center of a sphere were inside the circle, then the sphere was also "inside" the circle, *i.e.*, part of the layer.

For instance in Fig. 7, N and M are part of layer 4 but not part of layer 3. In this fashion it is possible to calculate the number of spheres in the top layer, the next highest layer, and so on; *i.e.*, the number of spheres can be calculated for successive values of q. The distance between each

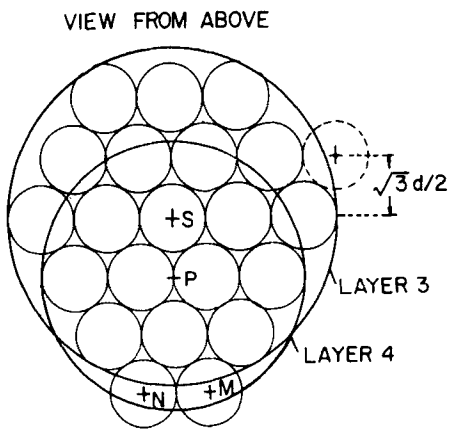

Figure 7—*Spheres in two-dimensional close packing. In one layer, the center will be in the center of a sphere* (S); *in the layer above and below it, the center of the layer will be between two spheres* (P). *Spheres are counted as being inside the circle* (*part of the layer*) *if the center of a sphere is inside the circle. For instance,* N *and* M *are part of layer 4. The dotted sphere is not part of layer 3.*

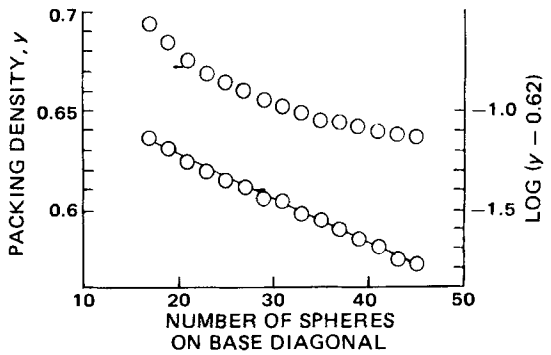

Figure 8—*Packing densities of heaps as a function of the number of spheres on the diagonal of the base (number of layers in the heap) (upper curve). By assuming various asymptote values, subtracting these from the packing densities, and plotting them semilogarithmically* versus q, *the best straight line,* i.e., *the one with the smallest residual of squares (lower curve), occurred with an asymptote value of 0.62.*

layer is $(\sqrt{2}/2)d$, so that the height of the cone is $[(q-1)(\sqrt{2}/2)+1]d$, which approaches $q\sqrt{2}/2$ for large values of q. The area of the base is $\pi(dq)^2/4$; *i.e.,* the cone volume can be calculated. Dividing the volume of all spheres by the cone volume then gives the packing density and, hence (by subtracting the latter from one), the porosity. Figure 8 shows that the packing density approaches 0.62 (*i.e.,* $\epsilon = 0.38$). The bed porosities found in this study ranged from 0.28 to 0.54.

Making reference to Fig. 5 and noting that there are q spheres on the base diagonal, one sees that $AC' \to qd/2$ and $B'C' \to q\sqrt{2}\,d/2$ as $q \to \infty$. The repose angle hence approaches:

$$\alpha = \tan^{-1}[qd\sqrt{2}/(qd)] = 54.7° \qquad \text{(Eq. 12)}$$

This value is obviously much higher than is generally encountered for cohesionless powders and granulations.

A conical heap (Fig. 5) is only stable if: (*a*) the friction between the plane support and the lower (outside) spheres is sufficiently high, and (*b*) the friction between spheres is sufficiently high to support the outside spheres. If this is not the case, the spheres "slip" out until there are sufficient spheres in the horizontal plane without spheres over them that can serve as retainers of the first sphere in the plane that carries spheres above it. If the cross-hatched spheres are removed, the shallower cone results, which has two supporting spheres on each diagonal. The diagonal of the base still contains q spheres, but the first layer above contains $q-3$ and the ith layer above the base contains $q-3i$ spheres on the diagonal. There would be $q/3$ layers in the center and the repose angle for large values of q would equal:

$$\alpha = \tan^{-1}[(q/3)(\sqrt{2}/2)/(q/2)] = \tan^{-1}(\sqrt{2}/3) = 25.2° \qquad \text{(Eq. 13)}$$

With these assumptions and restrictions, it can be assessed that a closely packed conical heap has a repose angle of $\alpha_c = 25.2°$ and a porosity of $\epsilon_c = 0.38$.

Loosely packed structures can be visualized in many ways. Figure 6 shows an example of a loose structure constructed by removing every second sphere in every second layer of the supported structure shown in Fig. 5. Therefore, the packing density would be $0.75 \times 0.62 = 0.46$; *i.e.,* the porosity would be 0.54. The repose angle is obtained by noting that there are q (four) spheres to the right (and to the left) of the base center and that there are also q (four) layers (which are $d\sqrt{2}/2$ cm apart). Hence, the repose angle for large values of q approaches:

$$\alpha = \tan^{-1}[(qd\sqrt{2}/2)/(qd)] = \tan^{-1}(\sqrt{2}/2) = 35.3° \qquad \text{(Eq. 14)}$$

The experimentally determined bed porosities ranged from 0.28 to 0.54, in agreement with the calculations, as is the fact that the repose angles ranged from 28.1 to 35.8°.

SUMMARY

1. For *monodisperse granulations,* experimental flow rates maximize (not minimize) at a particular repose angle around 30°.

2. Based on packing geometries and support layers, the expected repose angles should be 25.2–35.3°, which correlates well with experimental data ranging from 28.1 to 35.8°.

3. Based on packing geometries and support layers, the expected porosities should be 0.38–0.54; the experimentally determined bed porosities were in a range of 0.28–0.54.

REFERENCES

(1) I. R. McDougall and A. C. Evans, *Rheol. Acta,* **4,** 218 (1965).

(2) J. Gillard, L. Delattre, F. Jaminet, and M. Roland, *J. Pharm. Belg.,* **27,** 713 (1972).

(3) D. Train, *J. Pharm. Pharmacol.,* **10,** 127T (1958).

(4) N. Pilpel, *ibid.,* **16,** 705 (1964).

(5) H. G. Kristensen and V. G. Jensen, *Dansk. Tidsskr. Farm.,* **43,** 104 (1969).

(6) L. Delattre, J. Gillard, M. Roland, and F. Jaminet, *J. Pharm. Belg.,* **28,** 575 (1973).

(7) F. A. Rocke, *Powder Technol.,* **4,** 180 (1970).

(8) J. T. Carstensen, "Theory of Pharmaceutical Systems," vol. II, Academic, New York, N.Y., 1973, p. 187.

(9) J. T. Carstensen, *ibid.,* p. 242.

(10) R. Carr, *Chem. Eng.,* **67**(4), 121 (1960).

(11) N. Kaneniwa, *Chem. Pharm. Bull.,* **15,** 1441 (1965).

(12) G. Gold, R. N. Duvall, and B. T. Palermo, *J. Pharm. Sci.,* **55,** 1133 (1966).

(13) G. Gold, R. N. Duvall, B. T. Palermo, and J. G. Slater, *ibid.,* **55,** 1291 (1966).

(14) E. Hiestand, *ibid.,* **55,** 1325 (1966).

(15) T. M. Jones and N. Pilpel, *J. Pharm. Pharmacol.,* **18,** 182S (1966).

(16) N. Pilpel, "Advances in Pharmaceutical Science," vol. 3, Academic, New York, N.Y., 1971, p. 174.

(17) N. Kaneniwa, A. Ikekawa, T. Ozaki, C. Shinya, N. Sugimoto, and Y. Hoxumi, *Yakugaku Zasshi,* **88,** 1642 (1968).

(18) W. A. Gray, "The Packing of Solid Particles," Chapman & Hall, London, England, 1968, p. 125.

(19) J. T. Carstensen, "Pharmaceutics of Solids," Badger Freund, Fond du Lac, Wis., 1974, p. 94.

(20) G. D. Scott, *Nature,* **194,** 956 (1962).

(21) *Ibid.,* **188,** 909 (1960).

(22) T. G. O. Berg, R. L. McDonald, and R. J. Trainor, Jr., *Powder Technol.,* **3,** 183 (1969).

(23) D. M. Newitt and J. M. Conway-Jones, *Trans. Inst. Chem. Eng.,* **36,** 422 (1958).

(24) T. G. O. Berg, R. L. McDonald, and R. J. Trainor, Jr., *Powder Technol.,* **3,** 56 (1969).

ACKNOWLEDGMENTS AND ADDRESSES

Received June 20, 1975, from the *School of Pharmacy, University of Wisconsin, Madison, WI 53706.*

Accepted for publication October 28, 1976.

[x] To whom inquiries should be directed.

Smooth Muscle Relaxant Properties and Vasomotor Actions of 2-Amino-1-*p*-nitrophenylpropane-1,3-diol

SACHCHIDANANDA BANERJEE [x], CHANDAN MITRA, and ARUN KUMAR MUKHERJEE

Abstract □ Experiments with the guinea pig ileum, trachea, and vas deferens, the rat fundal strip, the rabbit jejunum and aortic strip, and the toad heart indicated that 2-amino-1-*p*-nitrophenylpropane-1,3-diol, the hydrolytic product of chloramphenicol, inhibited smooth muscles. Its action was direct and not through any mediators. After intravenous administration, the compound produced vasodepression followed by an overshooting rise of blood pressure. Vasodepression was not mediated by adrenergic, cholinergic, or histaminergic mechanisms. Hypertension was a sympathomimetic effect. Muscle relaxant and cardiovascular effects of the compound were similar to those of chloramphenicol, although it had no antibacterial effect.

Keyphrases □ 2-Amino-1-*p*-nitrophenylpropane-1,3-diol—evaluated for smooth muscle relaxant and vasomotor activities, various guinea pig, rat, rabbit, and toad muscles □ Chloramphenicol and hydrolytic product—evaluated for smooth muscle relaxant and vasomotor activities, various guinea pig, rat, rabbit, and toad muscles □ Relaxants, smooth muscle—chloramphenicol and its hydrolytic product evaluated, various guinea pig, rat, rabbit, and toad muscles □ Vasomotor activity—chloramphenicol and its hydrolytic product evaluated, various guinea pig, rat, rabbit, and toad muscles

In an earlier study (1), chloramphenicol inhibited smooth muscles, decreasing both the height and frequency of spontaneous contractions; the induced relaxation was not mediated through adrenergic, cholinergic, or histaminergic mechanisms. Chloramphenicol is hydrolyzed to 2-amino-1-*p*-nitrophenylpropane-1,3-diol (I), which has no antibacterial properties (2). Therefore, it was of interest to determine if I has muscle relaxant properties like chloramphenicol (II) to associate or dissociate the antibacterial and muscle relaxant properties of II. Cardiovascular effects of these two compounds also were investigated.

EXPERIMENTAL

The experimental procedures with smooth muscles of various animal species were the same as described earlier for II (1). Compound I was used in place of II.

Adult cats of either sex, 2.5–4 kg, were anesthetized with phenobarbital sodium, 150 mg/kg im. Standard pharmacological methods (3) were used for the cat spinal preparation and blood pressure recording.

RESULTS

Effect of I—*On Isolated Guinea Pig Ileum*—The agonist was acetylcholine. A significant alteration in the height of contraction of the guinea pig ileum was observed with a relatively higher dose of I, 80 μg/ml of bath. Incremental increases in concentrations from 80 to 1280 μg/ml of bath progressively inhibited the height of contraction (Table I).

On Isolated Rat Fundal Strip, Isolated Guinea Pig Trachea, Isolated Guinea Pig Vas Deferens, and Isolated Rabbit Aortic Strip—The agonists used were 5-hydroxytryptamine, histamine, epinephrine, and epinephrine for the fundal strip, trachea, vas deferens, and aortic strip, respectively. The height of contraction (relaxation in the guinea pig trachea) was significantly altered at a relatively high concentration of I, 250 μg/ml of bath. Incremental increases in I concentration from 250 μg to 2 mg/ml of bath progressively reduced the height of contraction (Table I).

On Perfused Toad Heart—Reductions in the rate and height of contraction of the spontaneously beating toad heart could be observed when the minimum dose of I was 250 μg. Incremental increases in the concentration of I from 250 μg to 2 mg progressively reduced the amplitude of contraction, but the frequency of the beat changed significantly only when the I dose was 2 mg, which produced a state of heart contracture (Table II). Although the action of the compound was similar to that of chloramphenicol, a much higher dose of the latter was needed to change significantly the frequency of the heart beat and to inhibit contraction totally (1).

Table I—Compound I-Induced Inhibition of Smooth Muscles Using Various Agonists

Tissue Preparation	Agonist, μg/ml of Bath	Compound I, μg/ml of Bath	Inhibition Compared to Agonist-Induced Contraction[a], %
Guinea pig ileum	Acetylcholine, 0.66	80	23 ± 4
		160	40 ± 4
		320	52 ± 15
		640	66 ± 15
		1280	88 ± 3
Rat fundus strip	5-Hydroxytryptamine, 0.23	250	20 ± 2
		500	32 ± 3
		1000	63 ± 7
		2000	79 ± 1
Guinea pig trachea	Histamine, 6.0	250	11 ± 2
		500	29 ± 1
		1000	54 ± 6
		2000	80 ± 4
Guinea pig vas deferens	Epinephrine, 1.4	250	6 ± 0.5
		500	19 ± 1
		1000	45 ± 1
		2000	92 ± 3
Rabbit aortic strip	Epinephrine, 15	250	20 ± 2
		500	51 ± 5
		1000	83 ± 6
		2000	90 ± 3

[a] Values are means of seven observations ± *SE*.

Epinephrine and histamine were used, and Compound I reduced the force and rate of contraction of the heart stimulated by these agonists. The protocol and pattern of experiments were similar to those for chloramphenicol (1).

To ascertain that the action of I was direct and not mediated through inhibition or release of mediators, the effects of several blocking agents were studied. The experiments were similar to those described for chloramphenicol (1). The action of I was direct and not influenced by mediators (Table III).

On Isolated Rabbit Ileum—Epinephrine, 0.133 μg/ml of bath, produced maximal relaxation. An increase in the concentration of epinephrine to 0.267 μg/ml of bath diminished the relaxation response. Phentolamine hydrochloride, 2.5 μg/ml, was added to the bath. After 0.5 hr, epinephrine, 0.133 μg/ml of bath, was added. The dose of phentolamine was sufficient to block the maximum epinephrine-induced relaxation, indicating the total block of adrenergic α-receptors. Compound

Table II—Compound I-Induced Inhibition of Rate (Frequency) and Height (Amplitude) of Contraction of Toad Heart

Dose of I, mg	Inhibition[a], %	
	Frequency/min	Amplitude, mm
0.25	16 ± 3	20 ± 3
0.50	18 ± 6	30 ± 4
1.00	22 ± 4	68 ± 2
2.00	78 ± 4	100 (total)

[a] Values are means of seven observations ± *SE*.

Table III—Effect of I on the Perfused Toad Heart with Various Agonists and Blocking Agents [a]

Control	Effect of I	Agonist or Blocker Used	Effect of Agonist or Blocker	Combined Effect of Agonist or Blocker plus I
		Heart Beats per Minute		
44 ± 2	33 + 2 (3 mg)	Epinephrine (0.2 μg)	57 ± 1, $p < 0.005$	40 ± 4
41 ± 0.5	20 + 5 (3 mg)	Histamine (10 μg)	53 ± 1, $p < 0.005$	13 ± 4
55 ± 2	22 ± 5 (3 mg)	Propranolol (0.2 μg/ml)	50 ± 3	17 ± 6
69 ± 2	35 + 2 (4 mg)	Atropine (0.25 μg/ml)	68 ± 4	31 ± 3
44 ± 1	29 ± 1 (4 mg)	Physostigmine (5 μg/ml)	39 ± 1	23 ± 4
		Height of Contraction, mm		
24 ± 0.5	Complete inhibition (3 mg)	Epinephrine (0.2 μg)	69 ± 1, $p < 0.005$	Complete inhibition
25 ± 1	Complete inhibition (3 mg)	Histamine (10 μg)	32 ± 5	Complete inhibition
25 ± 2	Complete inhibition (3 mg)	Propranolol (0.2 μg/ml)	20 ± 3	Complete inhibition
64 ± 3	Complete inhibition (4 mg)	Atropine (0.25 μg/ml)	64 ± 7	Complete inhibition
29 ± 1	Complete inhibition (4 mg)	Physostigmine (5 μg/ml)	25 ± 2	Complete inhibition

[a] Values are means of seven observations ± *SE*. Figures in parentheses are the doses of the drug. Total doses of I and agonists are per milliliter of perfused fluid. Differences in the values in columns 1 and 4 and in columns 2 and 5 are not statistically significant except where *p* values are given.

I, 2 mg/ml of bath, when added to the combined presence of blocker (phentolamine) and challenger (epinephrine), produced almost the same degree of relaxation as the control response of I.

On Isolated Rabbit Jejunum—The dose, pattern, and protocol of experiments were similar to those used with II (1). The minimum concentration of I to produce alteration in the frequency and amplitude of spontaneously occurring rhythmic pendular contraction was 250 μg/ml of bath. Higher concentrations produced a dose-dependent reduction in the frequency of spontaneous contractions. At concentrations above 2 mg/ml of bath, the jejunum was paralyzed. The normal control rhythm, however, could be restored by washing (Table IV).

When the jejunum was stimulated with 0.01 μg of acetylcholine/ml of bath, the frequency of pendular contractions, 15/min, did not change. The addition of 1 mg of I/ml of bath in the presence of the same amount of acetylcholine reduced the frequency of contractions to four/min (Table IV). When barium chloride was added as a nonspecific stimulant, 25 μg/ml of bath, the frequency of jejunal contractions did not change significantly. Addition of I, 2 mg/ml, reduced the frequency of contractions from 12 to five/min. The reduction could be reversed by washing (Table IV).

On Isolated Guinea Pig Trachea—The protocol and pattern of experiments were similar to those used with II (1). Addition of 6 μg of histamine/ml of bath produced a sustained contraction of the trachea, which could be antagonized minimally by 0.25 mg of I/ml and maximally by 2 mg/ml. When I was added before histamine to the bath, the histamine response diminished. The reduction in the height of contraction was dose dependent (Table V).

Diphenhydramine hydrochloride, 2.5 μg/ml, inhibited the histamine response by approximately 76%. The addition of I in the bath, 1 mg/ml, further reduced the height of contraction; the total inhibition was 86%. Propranolol hydrochloride, 2.5 μg/ml, also reduced the histamine response by 10%, but the addition of I to propranolol reduced the histamine response to 82% (Table V).

On Calcium Release in Bath Fluid—Experiments were performed with the isolated rabbit jejunum and rabbit aortic strip as described previously for II (1). The presence of I did not influence the concentration of calcium in the bath, indicating no change in the availability of calcium in the tissues.

Cardiovascular Response to I and II—In experiments with cats, intravenous injections of both I and II, 2.5–50 mg/kg, progressively decreased blood pressure. The vasodepressor responses at higher dose levels were prompt and longer in duration (5–10 min). Repeated intravenous administration, 2.5 mg/kg, at 5-min intervals over 30 min, showed no evidence of tachyphylaxis or anaphylaxis; *i.e.*, the vascular response neither decreased nor increased. Regardless of the dose–response relationship, blood pressure did not promptly return to the preinjection control levels. The responses of I were similar to those of II.

Vasodepressive Response to I and II—*With Antihistaminic*—To determine if the vasodepressor response to I and II was due to the release of endogenous histamine, I and II were administered 30 min before and after producing histamine block in cats. An intravenous test dose of histamine acid phosphate, 0.5 μg/kg, was injected 20 min before and after the intravenous injection of antazoline methanesulfate, 4 mg/kg, to examine the efficiency of the histamine block. After a satisfactory, but varying, degree of histamine block was established in each animal, the intravenous injection of I and II, 20 mg/kg, produced a vasodepressor response in all animals that was identical in pattern and degree to the preblock control response (Table VI).

With β-Adrenergic Blockade—To determine if I and II produced the vasodepressor response through direct stimulation of β-adrenergic receptors, they were injected intravenously, 20 mg/kg, to cats before and after complete β-receptor block by propranolol hydrochloride, 0.3 mg/kg. To appraise the adequacy of the block, a challenging dose of isoproterenol sulfate, 0.01 mg/kg, was administered intravenously after the propranolol injection. No significant alteration in the vasodepressor responses of I and II was observed between the pre- and postblocked conditions (Table VI).

With Atropine—To determine if I and II produced the vasodepressor response by elaboration of mediator acetylcholine, they were administered before and after producing acetylcholine block in cats. An intravenous test dose of acetylcholine, 1 μg/kg, was administered 15 min before and 45 min after atropine sulfate, 1 mg/kg iv, to examine the efficacy of the block. The marked vasodepressor responses to acetylcholine were blocked adequately by atropine sulfate in all experiments. After the block was established, the intravenous injection of both I and II, 20 mg/kg, produced a vasodepressor response in all animals that was identical in pattern and degree to the preblock control response (Table VI).

With α-Adrenergic Blockade—Compounds I and II were injected

Table IV—Effect of I on Pendular Contractions of the Isolated Rabbit Jejunum

Drugs Used per Milliliter of Bath	Pendular Contractions per Minute [a]
Control	12 ± 0.44
I, 0.25 mg	11 ± 0.40
I, 0.50 mg	10 ± 0.40
I, 1.00 mg	7 ± 1.00
I, 2.00 mg	2 ± 0.50
Acetylcholine, 0.01 μg	15 ± 0.45
plus I, 1 mg	4 ± 1.00
Barium chloride, 25 μg	12 ± 0.45
plus I, 2 mg	5 ± 1.00

[a] Values are means of six observations ± *SE*.

Table V—Effect of I on the Height of Contraction of Guinea Pig Trachea with Agonist and Blocking Agents

Drugs Used per Milliliter of Bath	Height of Contraction [a], mm
Histamine, 6 μg	13.0 ± 0.47
plus I, 0.25 mg	11.5 ± 0.47
plus I, 0.50 mg	9.0 ± 0.57
plus I, 1 mg	6.0 ± 1.00
plus I, 2 mg	2.5 ± 0.70
Histamine, 7 μg	22.0 ± 3.40
Diphenhydramine, 2.5 μg, plus histamine, 7 μg	5.3 ± 0.40
Diphenhydramine, 2.5 μg, plus histamine, 7 μg, plus I, 1 mg	3.0 ± 0.57
Propranolol, 2.5 μg, plus histamine, 7 μg	20.0 ± 2.20
Propranolol, 2.5 μg, plus histamine, 7 μg, plus I, 2 mg	4.0 ± 1.00

[a] Values are means of six observations ± *SE*.

Table VI—Effect of Pretreatment with Blocking Agents on the Vasodepressor Action of I and II in Anesthetized Cats [a]

Reduction with I or II, %	Blocker Used	Reduction in Blood Pressure Using Blockers followed by I or II, %
	II, 20 mg/kg	
56 ± 6	Antazoline methanesulfate, 4 mg/kg	56 ± 8
42 ± 5	Atropine sulfate, 1 mg/kg	41 ± 5
45 ± 5	Propranolol hydrochloride, 0.3 mg/kg	41 ± 5
43 ± 4	Phentolamine hydrochloride, 5 mg/kg	44 ± 4
38 ± 5	Physostigmine salicylate, 0.3 mg/kg	48 ± 3
	I, 20 mg/kg	
38 ± 6	Antazoline methanesulfate, 4 mg/kg	35 ± 4
47 ± 6	Atropine sulfate, 1 mg/kg	45 ± 5
33 ± 4	Propranolol hydrochloride, 0.3 mg/kg	39 ± 4
33 ± 6	Phentolamine hydrochloride, 5 mg/kg	43 ± 6
40 ± 13	Physostigmine salicylate, 0.3 mg/kg	49 ± 14

[a] Values are means of five observations ± *SE*. The mean control blood pressure was 90 ± 7 mm Hg.

intravenously, 20 mg/kg, to cats before and after complete α-receptor blockade with phentolamine hydrochloride, 5 mg/kg. The adequacy of the block was tested by intravenous injection of a challenging dose of epinephrine, 1 μg/kg, after the injection of phentolamine. The vasodepression observed was similar in all respects to the pretreated control response of I and II in all animals (Table VI).

With Physostigmine—To determine if the vasodepressor action of I and II was potentiated or prolonged by acetylcholinesterase inhibition, they were injected, 20 mg/kg, before and after the intravenous administration of physostigmine salicylate, 0.3 mg/kg. One hour after physostigmine injection, there was no significant change in the vasodepressor response to either I or II (Table VI). Atropine block of the muscarine effects of the elevated acetylcholine level induced by physostigmine also failed to modify the characteristic vasodepressor response to both I and II.

Effect of Spinal Transection or Vagotomy on Vasodepressor Action of I and II—Elimination of effects of higher centers by spinal transection or of vagal stimulation by bilateral vagotomy could not modify the vasodepressive effect of either I or II.

Table VII—Vasopressor Response of I and II in Anesthetized Cats

Drug Used	Rise in Blood Pressure[a], %
II, 20 mg/kg	39 ± 9
plus pretreatment for 1 hr with phentolamine, 5 mg/kg	21 ± 7
plus pretreatment for 1 hr with propranolol, 0.3 mg/kg	10 ± 5
I, 20 mg/kg	31 ± 5
plus pretreatment for 1 hr with phentolamine, 5 mg/kg	39 ± 4
plus pretreatment for 1 hr with propranolol, 0.3 mg/kg	0
Epinephrine, 1 μg/kg	27 ± 5
plus pretreatment for 1 hr with II	76 ± 7
Epinephrine, 2 μg/kg	44 ± 8
plus pretreatment for 1 hr with II	82 ± 9
Epinephrine, 4 μg/kg	50 ± 15
plus pretreatment for 1 hr with II	94 ± 12
plus pretreatment for 1 hr with I	93 ± 5

[a] Values are means of five observations ± *SE*. The mean control blood pressure was 88 ± 3 mm Hg.

Response to I and II with β-Adrenergic, Acetylcholinergic, or Histaminergic Blockades in Isolated Rabbit Aortic Strip Preparation—Both I and II produced significant dose-dependent relaxation in the aortic strip after a contraction was produced by the agonist epinephrine. After a satisfactory epinephrine-induced contraction for 4 min, either I or II, 4 mg/ml of bath, was added at the peak height of contraction. The muscle relaxation effect immediately ensued, continued for the next 6 min, and was not inhibited by propranolol (β-adrenergic blocker), atropine (cholinergic blocker), or antazoline (histaminergic blocker) in concentrations of 40 μg/ml of bath added to the bath 10–15 min prior to the addition of I or II.

Vasopressor Response of I and II in Cats—The vasodepression produced by I and II was followed by a compensatory overshooting rise of blood pressure much higher than the basal blood pressure. The response persisted after spinal transection. After α-receptor block with phentolamine, 5 mg/kg, for 1 hr, I and II behaved differently. The after rise of blood pressure was enhanced by I and did not change significantly with II. After β-receptor block with propranolol, 0.3 mg/kg for 20–30 min, the vasopressor effects of I and II were checked. Epinephrine injected intravenously in cats pretreated with I and II produced a potentiated vasopressor response in all animals in comparison with the control epinephrine-induced vasopressor response (Table VII). The response was present in spinal transected preparations also.

DISCUSSION

Experiments with I clearly indicated a close correlation of results obtained with II (1). Like II, I not only inhibited the autogenous contractile drive but also was active when the contractile mechanism was magnified by agonists. Compound I inhibited smooth muscles, nonspecifically acting as a nonspecific spasmolytic substance, and the muscle relaxation seemed due to a direct action like that of II.

The most significant cardiovascular response to both I and II was the persistent hypotensive action on rapid intravenous injection, which could not be inhibited by any of the mediator blocking agents (Table VI). Both I and II had relaxation effects on rabbit aortic strips not influenced by propranolol, atropine, and antazoline. Therefore, I and II possibly acted directly on vascular smooth muscle, leading to vasodepression in intact animals.

Vasodepressive action of I and II was followed by an overshooting rise of blood pressure, which could be prevented by β-receptor block. Epinephrine-induced vasopressor response was potentiated after intravenous administration of I and II (Table VII). These observations indicated that the rise in blood pressure after intravenous administration of I and II was possibly due to a sympathomimetic effect.

On hydrolysis, II loses dichloroacetic acid and I is formed, which has no bactericidal property (2). The smooth muscle relaxation properties of II seem to be due to the I moiety.

REFERENCES

(1) S. Banerjee and C. Mitra, *J. Pharm. Sci.*, **65**, 704 (1976).

(2) A. J. Glazko, W. A. Dill, and M. C. Rebstock, *J. Biol. Chem.*, **183**, 679 (1950).

(3) M. N. Ghosh, "Fundamentals of Experimental Pharmacology," Scientific Book Agency, Calcutta-1, India, 1971, p. 70.

ACKNOWLEDGMENTS AND ADDRESSES

Received August 23, 1976, from the *Research and Development Division, Dey's Medical Stores Manufacturing Ltd., Calcutta-19, India.*

Accepted for publication November 3, 1976.

The authors thank Sri B. N. Dey for laboratory facilities.

[x] To whom inquiries should be directed.

Constituents of West African Medicinal Plants XIX: Funiferine *N*-Oxide, a New Alkaloid from *Tiliacora funifera* (Menispermaceae)

D. DWUMA-BADU *, T. U. OKARTER, A. N. TACKIE ‡, J. A. LOPEZ, D. J. SLATKIN, J. E. KNAPP, and P. L. SCHIFF, Jr. ˣ

Abstract □ A phytochemical investigation of the roots of *Tiliacora funifera* (Menispermaceae) resulted in the isolation and identification of funiferine *N*-oxide, a new bis(benzylisoquinoline) alkaloid.

Keyphrases □ Funiferine *N*-oxide—isolated from extract of roots of *Tiliacora funifera*, structure elucidated □ *Tiliacora funifera*—extract of roots, funiferine *N*-oxide isolated and identified □ Alkaloids—funiferine *N*-oxide, isolated from extract of roots of *Tiliacora funifera*, structure elucidated

Tiliacora funifera (*T. warneckei*) Engl. ex Diels (Menispermaceae) is a stout spreading undershrub or woody climber found in the grassy regions and thickets along coastal areas of Ghana (1). The plant is used natively as a medicinal for the treatment of gastric fevers, strangulated hernia, and menstrual irregularities (2).

A number of alkaloids have been isolated from several *Tiliacora* species. Tiliacorine, a biphenyldibenzodioxin bis(benzylisoquinoline) alkaloid, was isolated from *T. acuminata* (3), *T. racemosa* (4, 5), and *T. funifera* (6); its diastereoisomer, tiliacorinine, was found in *T. racemosa* (5) and *T. dinklagei* (7). Several secondary amine derivatives of tiliacorine and tiliacorinine were isolated, including nortiliacorinine A from *T. racemosa* (5), *T. funifera* (8), and *T. dinklagei* (7); nortiliacorinine B from *T. racemosa* (5); and nortiliacorine A from *T. funifera* (8). Funiferine (I), a nondibenzodioxin bis(benzylisoquinoline) biphenyl alkaloid, was found in *T. funifera* (6, 9, 10) and *T. dinklagei* (7); tiliageine (II), a closely related base, was isolated from *T. dinklagei* (7, 11). Furthermore, several incompletely characterized alkaloids were isolated from *T. triandra* (12) and *T. racemosa* (13, 14).

This paper reports the isolation and identification of funiferine *N*-oxide (III), a new alkaloid from the roots of *T. funifera*. This base, previously isolated from *T. funifera* (15), was designated TB-2. This study was undertaken to reisolate and subsequently identify this alkaloid to the exclusion of the other known alkaloids (6, 8–10) of this species.

DISCUSSION

Dried, powdered roots were extracted by percolation with ethanol, and the ethanolic extract was concentrated (40°, *in vacuo*) to a syrupy residue. The residue was partitioned between dilute hydrochloric acid and chloroform, and the acidic fraction was made basic with ammonium hydroxide and extracted with chloroform. The chloroform extract was chromatographed over silicic acid in chloroform and chloroform–methanol mixtures. Elution with chloroform–methanol (95:5) afforded a fraction that was twice rechromatographed over silicic acid in chloroform–methanol mixtures to afford a mixture of I and III. These bases were subsequently separated by preparative TLC.

Compound III was obtained as a white powder, mp 207–209° dec.; $[\alpha]_D^{25}$ +44.0° (c 0.1, methanol); λ_{max} (methanol): 216 (log ϵ 4.75) and 288 (3.95) nm; ν_{max} (KBr): 1500 cm^{-1}. The NMR spectrum showed signals at δ 2.62 (s, 3H) and 3.16 (s, 3H) ppm, corresponding to two *N*-methyl groups, the latter at a lower field than expected (16); 3.27 (s, 3H), 3.51 (s, 3H), 3.81 (s, 3H), and 3.91 (s, 3H) ppm, corresponding to four *O*-methyl groups; and 6.30–7.55 (m, 9H) ppm, corresponding to nine aromatic protons. The mass spectrum showed the molecular ion at *m/e* 638 (32) and other significant fragment ions at *m/e* 622 (100), 621 (75), 607 (18), 515 (1), 431 (1), 430 (1), 396 (25), 395 (83), 381 (30), 198 (72), 175 (25), and 174 (32).

These spectral data were indicative of a bis(benzylisoquinoline) alkaloid with a molecular ion 16 mass units higher than that of I and a prominent M − 16 ion characteristic of *N*-oxides (17, 18). Furthermore, the NMR spectrum showed that one *N*-methyl signal was shifted downfield (δ 3.16 ppm), which is also characteristic of *N*-oxides (19, 20). Therefore, it was considered likely that III was an *N*-oxide of I or a closely related base. To prove this assumption, it was decided to reduce III with sulfurous acid (21) to the parent base.

Treatment of III with sulfurous acid overnight afforded I, identical by a direct comparison (UV, IR, NMR, and mass spectra; TLC; and melting point and mixed melting point) with an authentic reference sample (10). Thus, III corresponded to a funiferine *N*-oxide, and it remained to be established with which nitrogen atom in funiferine the oxide was associated. A comparison of the NMR chemical shift values of III and I showed that the methoxy signals (I, δ 3.39, 3.48, 3.79, and 3.87 ppm; and III, δ 3.27, 3.51, 3.80, and 3.89 ppm) and the aromatic signals [I, δ 6.33–7.25 (9H) ppm; and III, δ 6.30–7.55 (9H) ppm] were similar. Furthermore, one of the two *N*-methyl signals of each was quite similar (I, δ 2.36 and 2.64 ppm; and III, δ 2.62 and 3.16 ppm).

The NMR spectral signals for the *N*-methyl groups of I can be postulated as δ 2.36 for N-2 (ring A) and δ 2.64 for N-2′ (ring D). This postulation is valid since a controlled oxidation of bis(benzylisoquinoline) alkaloids with potassium permanganate in acetone is reported to cleave the benzylic bond of the isoquinoline moiety, which is unsubstituted at C-8 (or C-8″), to afford a tertiary lactone and an aromatic aldehyde (22). Oxidation of *O*-methylfuniferine (IV) gave a product (V) with *N*-methyl signals at δ 2.32 and 3.05 ppm, assigned to the N-2 (ring A) and N-2′ (ring

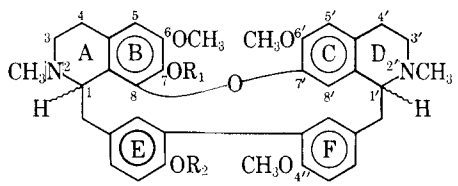

I: $R_1 = CH_3$, $R_2 = H$
II: $R_1 = R_2 = H$
IV: $R_1 = R_2 = CH_3$

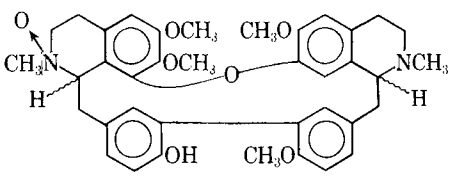

III

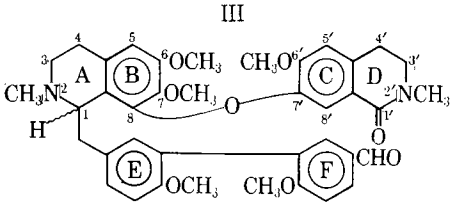

V

D) positions, respectively. Therefore, the NMR spectral signals for the *N*-methyl groups of I can be unequivocally established as δ 2.36 ppm for the ring A group and δ 2.64 ppm for the ring D group. Since the signal at δ 2.36 ppm in I is shifted downfield to δ 3.16 ppm in III and the signal at δ 2.64 ppm in I is virtually in the same position (δ 2.62 ppm) in III, the structure of III as a funiferine *N*-oxide may be assigned as shown.

Finally, III was prepared by oxidation of I according to established procedures (21) for the preparation of *N*-oxides. Treatment of I in ethanol with hydrogen peroxide (15%) for 30 min at room temperature gave at least four compounds (TLC) in addition to unreacted starting material. Repeated chromatography of this mixture over silica gel G afforded a compound that was identical with III by a direct comparison (UV, IR, NMR, and mass spectra; melting point and mixed melting point; and TLC).

It is unlikely that III is an artifact formed during the isolation procedure, since it can be detected by TLC in fresh extracts of *T. funifera* roots. In addition, I subjected to the same isolation procedure as described earlier does not produce detectable amounts of III.

This paper is the first reported isolation of an *N*-oxide from a *Tiliacora* species and of an *N*-oxide of the bis(benzylisoquinoline) group. Alkaloid *N*-oxides previously were reviewed, and it was suggested that many alkaloids might occur naturally in the form of their *N*-oxides (23). Numerous plant families contain alkaloid *N*-oxides, including the Apocynaceae (24), Leguminosae (25), Gramineae (26), Polygonaceae (27), Rubiaceae (28), Solanaceae (20), Monimiaceae (29), Ranunculaceae (30), Boraginaceae (31), Compositae (32), and Orchidaceae (33). *N*-Oxides have been reported for many differing alkaloidal classes such as monomeric indole (26), dimeric indole (24), pyrrolizidine (32), quinolizidine (25), aporphine (29), tropane (34), pyridine–pyrrolidine (20), and piperidine (33).

EXPERIMENTAL[1]

Plant Material—The plant material[2] was collected in Ghana in 1975. The roots were separated from the aboveground material, dried, and ground to a coarse powder.

Extraction and Fractionation—*T. funifera* roots (6 kg) were extracted with 95% ethanol (40 liters) in a glass percolator to yield a syrupy residue (57 g), which was partitioned between 5% hydrochloric acid (700 ml) and chloroform (700 ml) three times. The aqueous layer was made basic with ammonium hydroxide and extracted with chloroform (700 ml) four times. These chloroform extracts were pooled, dried over anhydrous sodium sulfate, and evaporated *in vacuo* to yield a nonquaternary alkaloid fraction (10 g).

Chromatography and Isolation of III—The nonquaternary alkaloid fraction was dissolved in chloroform (50 ml) and chromatographed over a silicic acid[3] (100 mesh) (600 g) column prepared by slurry in chloroform. Elution was begun with chloroform, and the polarity was increased gradually by the addition of methanol. Fractions, 500 ml, were collected and monitored by TLC. Eventual elution with chloroform–methanol (4:1) afforded a fraction (1.2 g) that was dissolved in chloroform–methanol (95:5) and chromatographed over a column of silica gel G[4] (80 mesh) (180 g) prepared by slurry[5] in chloroform–methanol (95:5).

Elution was begun with chloroform–methanol (95:5), and the polarity was gradually increased by the addition of methanol. Fractions of 50 ml were collected and monitored by TLC. Eventual elution with chloroform–methanol (9:1) gave a fraction (180 mg) (R_f 0.37, 0.42, and 0.60) that was subsequently rechromatographed over a column of silica gel G (80 mesh)[4] (180 g) prepared in the same manner[5] as before. Elution was begun in chloroform–methanol (95:5), and the polarity was increased gradually to chloroform–methanol (9:1). Fractions of 25 ml were collected and monitored by TLC.

Elution with chloroform–methanol (9:1) afforded fractions that were combined on the basis of TLC (R_f 0.37 and 0.42) to yield a residue (36 mg). Finally, this residue was subjected to preparative TLC over silica gel G [chloroform–methanol–concentrated ammonium hydroxide (10:2:0.1)] (four plates) to afford III (26 mg), mp 207–209°, R_f 0.37; $[\alpha]_D^{25}$ +44.0° (c 0.1, methanol); λ_{max} (methanol): 261 (log ε 4.75) and 288 (3.95) nm; ν_{max} (KBr): 1500 cm^{-1}; NMR: δ 2.62 (s, 3H, N-2′ NCH_3), 3.16 (s, 3H, N-2 NCH_3), 3.27 (s, 3H, C-7 OCH_3), 3.51 (s, 3H, C-6′ OCH_3), 3.81 (s, 3H, C-6 OCH_3), 3.91 (s, 3H, C-4″ OCH_3), and 6.30–7.55 (m, 9H, ArH) ppm; mass spectrum: M^+ *m/e* 638 (32) for $C_{38}H_{42}N_2O_7$, 622 (100), 621 (75), 607 (18), 515 (1), 431 (1), 430 (1), 396 (25), 395 (83), 381 (30), 364 (3), 349 (2), 198 (72), 175 (24), and 174 (32).

Reduction of III—To III (22 mg) was added sulfurous acid (6%) (5.0 ml), and the solution was allowed to stand overnight. Then the solution was diluted with water (50 ml), made basic with concentrated ammonium hydroxide, and extracted four times with chloroform (50 ml). The chloroform extracts were combined, dried (anhydrous sodium sulfate), filtered, and evaporated *in vacuo* to afford I as a white amorphous powder (20 mg), mp 178–180°; R_f 0.65 in chloroform–methanol–concentrated ammonium hydroxide (10:0.5:0.1); λ_{max} (methanol): 212 (log ε 4.63) and 288 (3.80) nm; ν_{max} (KBr): 3400, 2930, 2840, 2790, 1600, 1580, 1500, 1450, 1410, 1350, 1312, 1270, 1235, 1115, 1065, 1020, and 875 cm^{-1}; NMR: δ 2.35 (s, 3H, NCH_3), 2.63 (s, 3H, NCH_3), 3.39 (s, 3H, OCH_3), 3.47 (s, 3H, OCH_3), 3.78 (s, 3H, OCH_3), 3.86 (s, 3H, OCH_3), and 6.32–7.25 (m, 9H, ArH) ppm; mass spectrum: M^+ *m/e* 622 (65), 515 (1), 396 (20), 395 (67), 381 (23), 364 (6), 349 (4), 198 (100), 175 (32), and 174 (30). The identity of the reduction product as I was established by direct comparison (UV, IR, NMR, and mass spectra and mixed melting point) with an authentic sample.

Preparation of III from I—Compound I (400 mg) was dissolved in ethanol (15 ml) and stirred with 15% hydrogen peroxide[6] (15 ml) at room temperature for 30 min. The reaction mixture was diluted with water (150 ml) and extracted four times with chloroform (150 ml). The combined chloroform extracts were evaporated *in vacuo* and examined by TLC [chloroform–methanol–concentrated ammonium hydroxide (10:1.5:0.1)]. The product was a mixture of at least four compounds (R_f 0.42, 0.37, 0.25, and 0.14), besides some unreacted starting material (R_f 0.85). These compounds were separated by column chromatography on silica gel G. A column (2.0 × 25 cm) was prepared with silica gel G[5] (30 g) by slurry in chloroform–methanol–concentrated ammonium hydroxide solution (10:1:0.1).

The sample was dissolved and eluted with the same solvent system in which the column was packed, with small fractions (6 ml) being collected. Attention was focused on fractions 42 and 43, a mixture of two compounds, one of which (R_f 0.37) showed the same R_f as III. Fractions 42 and 43 subsequently were subjected to column chromatography over silica gel G[5] (20 g) (column 1.5 × 25 cm), using chloroform–methanol–concentrated ammonium hydroxide (10:1:0.1) as the eluent.

Small fractions were collected (4 ml), and the compound at R_f 0.37 was obtained in pure form from fractions 53–59. This compound was a white crystalline substance, mp 206–207° dec.; $[\alpha]_D^{25}$ +40.0° (c 0.1, methanol); λ_{max} (methanol): 216 (log ε 4.80) and 288 (3.94) nm; ν_{max} (KBr): 3400 (br), 2930, 2830, 2790, 1600, 1580, 1500, 1450, 1420, 1360, 1320, 1270, 1240, 1125, 1060, 1015, 875, and 815 cm^{-1}; NMR: δ 2.60 (s, 3H, NCH_3), 3.15 (s, 3H, NCH_3), 3.26 (s, 3H, OCH_3), 3.51 (s, 3H, OCH_3), 3.80 (s, 3H, OCH_3), 3.89 (s, 3H, OCH_3), and 6.30–7.55 (m, 9H, ArH) ppm; mass spectrum: M^+ *m/e* 638 (17), 622 (83), 621 (58), 607 (13), 515 (1), 431 (1), 430 (1), 396 (27), 395 (82), 381 (35), 364 (6), 349 (4), 198 (100), 175 (38), and 174 (37).

Compound III and this synthetic product (R_f 0.37) were shown to be identical by a direct comparison (IR, UV, and NMR spectra; melting point and mixed melting point; and TLC).

Oxidation of IV—To IV (150 mg) [prepared from I by methylation with ethereal diazomethane (35)] dissolved in acetone (150 ml) was added potassium permanganate (75 mg) in acetone (100 ml) dropwise over 1 hr. The reaction was allowed to stand for 6 more hr at room temperature with constant stirring and was then filtered and evaporated. TLC analysis showed two spots [chloroform–methanol (9:1)], the lower one (R_f 0.40) corresponding to the original material and the higher one (R_f 0.65) corresponding to the oxidation product (V). The mixture was separated over a column (1.5 × 25 cm) on silica gel G[5] (25 g) in chloroform–methanol (95:5). Small fractions (8 ml) were collected using the same solvent system in which the column was packed.

---

[1] Melting points were taken on a Thomas-Hoover apparatus or a Fisher-Johns apparatus and are uncorrected. UV spectra were obtained on a Perkin-Elmer model 202 recording spectrophotometer, and IR spectra were determined on a Perkin-Elmer model 257 recording spectrophotometer in potassium bromide pellets. NMR spectra were recorded in deuterated chloroform on a Hitachi Perkin-Elmer model R-24 high-resolution spectrometer, with tetramethylsilane as the internal standard and chemical shifts reported in δ (parts per million) units. Mass spectra were taken with a LKB-9000 mass spectrometer. The optical rotations were measured on a Perkin-Elmer model 241 polarimeter. TLC was done on silica gel G (Merck) plates coated with 0.25 mm of adsorbent and activated at 110° for 1 hr. The solvent system of chloroform–methanol–concentrated ammonium hydroxide (10:1.5:0.1) was used unless otherwise noted. The alkaloids were visualized by spraying with Dragendorff reagent (Munier). All reagents were analytical grade unless otherwise noted.

[2] The plant material was collected and identified by Mr. K. Obeng-Darko, Faculty of Agriculture, University of Science and Technology, Kumasi, Ghana. Voucher specimens are on deposit at the Faculty of Pharmacy, University of Science and Technology, Kumasi, Ghana.

[3] Mallinckrodt, St. Louis, Mo.

[4] E. Merck, Darmstadt, Germany.

[5] A slurry of silica gel G in distilled water (1:2) was prepared, stirred for 5 min, dried overnight at 110°, and passed through an 80-mesh sieve.

[6] J. T. Baker Co.

Fractions 21–25 afforded a slightly yellowish compound (35 mg), mp 123–125°; $[\alpha]_D^{25}$ +27° (c 0.15, methanol); λ_{max} (methanol): 231 (log ϵ 4.60), 275 (4.14), 285 (4.13), and 295 (sh) (4.10) nm; ν_{max} (KBr): 2940, 2840, 1690, 1650, 1600, 1500, 1450, 1415, 1340, 1280, 1270, 1200, 1190, 1120, 1070, 1025, and 820 cm^{-1}; NMR: δ 2.32 (s, 3H, N-2 NCH_3), 3.05 (s, 3H, N-2' NCH_3), 3.68 (s, 3H, OCH_3), 3.75 (s, 6H, 2-OCH_3), 3.83 (s, 3H, OCH_3), 3.86 (s, 3H, OCH_3), 7.10–8.00 (m, 9H, ArH), and 10.00 (s, 1H, ArCHO) ppm; mass spectrum: M^+ *m/e* 666 (1), 411 (100), 256 (26), 241 (1), 206 (4), and 204 (3).

REFERENCES

(1) F. R. Irvine, "Woody Plants of Ghana," Oxford University Press, London, England, 1961, p. 36.

(2) A. N. Tackie, D. Dwuma-Badu, J. E. Knapp, and P. L. Schiff, Jr., *Lloydia*, **35**, 474 (1972).

(3) L. VanItallie and A. J. Steenhauer, *Pharm. Weekbl.*, **59**, 1381 (1922).

(4) K. V. J. Rao and L. R. Row, *J. Sci. Ind. Res., Sect. B*, **16**, 156 (1957).

(5) B. Anjaneyulu, T. R. Govindachari, S. S. Sathe, N. Viswanathan, K. W. Gopinath, and B. R. Pai, *Tetrahedron*, **25**, 3091 (1969).

(6) A. N. Tackie and A. Thomas, *Planta Med.*, **16**, 158 (1968).

(7) A. N. Tackie, D. Dwuma-Badu, J. S. K. Ayim, T. T. Dabra, J. E. Knapp, D. J. Slatkin, and P. L. Schiff, Jr., *Lloydia*, **38**, 210 (1975).

(8) A. N. Tackie, D. Dwuma-Badu, J. E. Knapp, and P. L. Schiff, Jr., *Phytochemistry*, **12**, 203 (1973).

(9) A. N. Tackie and A. Thomas, *Ghana J. Sci.*, **5**, 11 (1965).

(10) A. N. Tackie, D. Dwuma-Badu, J. E. Knapp, and P. L. Schiff, Jr., *Lloydia*, **36**, 66 (1973).

(11) A. N. Tackie, D. Dwuma-Badu, T. T. Dabra, J. E. Knapp, D. J. Slatkin, and P. L. Schiff, Jr., *Experientia*, **30**, 847 (1974).

(12) R. R. Paris and S. K. Sasorith, *Ann. Pharm. Fr.*, **25**, 627 (1967).

(13) T. K. Palit and M. P. Khare, *Phytochemistry*, **8**, 1559 (1969).

(14) A. K. Baru, P. Chakrabarti, and A. S. Dutta Gupta, *J. Indian Chem. Soc.*, **47**, 920 (1970).

(15) T. U. Okarter, M. Pharm. thesis, University of Science and Technology, Kumasi, Ghana, 1971.

(16) J. R. Dyer, "Applications of Absorption Spectroscopy of Organic Compounds," Prentice-Hall, Englewood Cliffs, N.J., 1965, p. 84.

(17) N. Bild and M. Hesse, *Helv. Chim. Acta*, **50**, 1887 (1967).

(18) T. A. Bryce and J. R. Maxwell, *J. Chem. Soc., Chem. Commun.*, **1965**, 206.

(19) E. Weiss, K. Bernauer, and A. Girardet, *Helv. Chim. Acta*, **54**, 1342 (1971).

(20) J. D. Phillipson and S. S. Handa, *Phytochemistry*, **14**, 2683 (1975).

(21) E. J. Shellard, J. D. Phillipson, and K. Sarpong, *Xenobiotica*, **1**, 455 (1971).

(22) M. Shamma and J. E. Foy, *Tetrahedron Lett.*, **1975**, 2249.

(23) J. D. Phillipson, *Xenobiotica*, **1**, 419 (1971).

(24) F. Puisieux, J.-P. Devissaguet, C. Miet, and J. Poisson, *Bull. Soc. Chim. Fr.*, **1967**, 251.

(25) A. Kh. Aslanov, A. S. Sadykov, V. N. Zainutdinov, and Yu. K. Kushmaradov, *Nauch. Tr. Goszapov*, **286**, 63 (1966); through *Chem. Abstr.*, **67**, 71108.

(26) S. K. Dutta and S. Ghosal, *Chem. Ind.*, **1967**, 2046.

(27) B. A. Abdusalamov, A. S. Sadykov, and K. A. Aslanov, *Nauch. Tr. Tash. Gas. Univ.*, **263**, 3 (1964); through *Chem. Abstr.*, **63**, 3314.

(28) E. J. Shellard, J. D. Phillipson, and K. Sarpong, *Phytochemistry*, **10**, 2505 (1971).

(29) E. Weiss, K. Bernauer, and A. Giraret, *Helv. Chim. Acta*, **54**, 1342 (1971).

(30) V. G. Khozhdaev, S. K. Maekh, and S. Y. Yunusov, *Khim. Prirodn. Soed.*, **1972**, 631.

(31) Z. Jerzmanowska and Z. Sykulska, *Dissnes. Pharm. Warsz.*, **16**, 71 (1964).

(32) R. Schoental, *J. Chem. Soc.*, **1960**, 2375.

(33) S. Brandänge and B. Lüning, *Acta Chem. Scand.*, **24**, 353 (1970).

(34) J. D. Phillipson and S. S. Handa, *Phytochemistry*, **14**, 999 (1976).

(35) A. I. Vogel, "Practical Organic Chemistry," 3rd ed., Wiley, New York, N.Y., 1956, p. 971.

ACKNOWLEDGMENTS AND ADDRESSES

Received May 25, 1976, from the *Department of Pharmacognosy, School of Pharmacy, University of Pittsburgh, Pittsburgh, PA 15261.*

Accepted for publication October 18, 1976.

Supported in part by Research Grant R-15 from the Health Research and Services Foundation, Pittsburgh, Pa. The mass spectrometry facility was supported by Research Grant RR-00273 to the University of Pittsburgh from the National Institutes of Health.

* Present address: Faculty of Pharmacy, University of Science and Technology, Kumasi, Ghana, West Africa.

‡ Present address: Council for Scientific and Industrial Research, Accra, Ghana, West Africa. This author gratefully acknowledges the Council for International Exchange of Scholars for a Fulbright–Hays Visiting Research Scientist Fellowship.

ˣ To whom inquiries should be directed.

Cardiovascular Actions of Three Harmala Alkaloids: Harmine, Harmaline, and Harmalol

DARRYL H. AARONS, G. VICTOR ROSSI, and RAYMOND F. ORZECHOWSKI ˣ

Abstract □ Each of three harmala alkaloids, harmine, harmaline, and harmalol, decreased heart rate and increased pulse pressure, peak aortic flow, and myocardial contractile force in intact normotensive anesthetized dogs. Harmine reduced systemic arterial blood pressure and total peripheral vascular resistance; harmaline-evoked decreases were frequently followed by a secondary increase; and the effects of harmalol on these two parameters were inconsistent. A direct negative chronotropic effect of harmala alkaloids was suggested by observations of bradycardia in the isolated perfused rat heart and in the intact dog; neither vagotomy nor atropinization affected harmala alkaloid-induced bradycardia in the dog. Reduction in femoral vascular resistance by the alkaloids was not apparently due to activation of cholinergic, β-adrenergic, or histaminic (H_1) receptors.

Keyphrases □ Alkaloids, harmala—cardiovascular activity in dogs □ Harmine—cardiovascular activity in dogs □ Harmaline—cardiovascular activity in dogs □ Harmalol—cardiovascular activity in dogs □ Cardiovascular activity—three harmala alkaloids in dogs

Although the seeds of *Peganum harmala* have been used for centuries as a folk medicine, the harmala alkaloids continue to be of interest because of the effects they elicit on the central nervous system (CNS) and the cardiovas-

Fractions 21–25 afforded a slightly yellowish compound (35 mg), mp 123–125°; $[\alpha]_D^{25}$ +27° (c 0.15, methanol); λ_{max} (methanol): 231 (log ϵ 4.60), 275 (4.14), 285 (4.13), and 295 (sh) (4.10) nm; ν_{max} (KBr): 2940, 2840, 1690, 1650, 1600, 1500, 1450, 1415, 1340, 1280, 1270, 1200, 1190, 1120, 1070, 1025, and 820 cm^{-1}; NMR: δ 2.32 (s, 3H, N-2 NCH_3), 3.05 (s, 3H, N-2' NCH_3), 3.68 (s, 3H, OCH_3), 3.75 (s, 6H, 2-OCH_3), 3.83 (s, 3H, OCH_3), 3.86 (s, 3H, OCH_3), 7.10–8.00 (m, 9H, ArH), and 10.00 (s, 1H, ArCHO) ppm; mass spectrum: M^+ *m/e* 666 (1), 411 (100), 256 (26), 241 (1), 206 (4), and 204 (3).

REFERENCES

(1) F. R. Irvine, "Woody Plants of Ghana," Oxford University Press, London, England, 1961, p. 36.

(2) A. N. Tackie, D. Dwuma-Badu, J. E. Knapp, and P. L. Schiff, Jr., *Lloydia*, **35**, 474 (1972).

(3) L. VanItallie and A. J. Steenhauer, *Pharm. Weekbl.*, **59**, 1381 (1922).

(4) K. V. J. Rao and L. R. Row, *J. Sci. Ind. Res., Sect. B*, **16**, 156 (1957).

(5) B. Anjaneyulu, T. R. Govindachari, S. S. Sathe, N. Viswanathan, K. W. Gopinath, and B. R. Pai, *Tetrahedron*, **25**, 3091 (1969).

(6) A. N. Tackie and A. Thomas, *Planta Med.*, **16**, 158 (1968).

(7) A. N. Tackie, D. Dwuma-Badu, J. S. K. Ayim, T. T. Dabra, J. E. Knapp, D. J. Slatkin, and P. L. Schiff, Jr., *Lloydia*, **38**, 210 (1975).

(8) A. N. Tackie, D. Dwuma-Badu, J. E. Knapp, and P. L. Schiff, Jr., *Phytochemistry*, **12**, 203 (1973).

(9) A. N. Tackie and A. Thomas, *Ghana J. Sci.*, **5**, 11 (1965).

(10) A. N. Tackie, D. Dwuma-Badu, J. E. Knapp, and P. L. Schiff, Jr., *Lloydia*, **36**, 66 (1973).

(11) A. N. Tackie, D. Dwuma-Badu, T. T. Dabra, J. E. Knapp, D. J. Slatkin, and P. L. Schiff, Jr., *Experientia*, **30**, 847 (1974).

(12) R. R. Paris and S. K. Sasorith, *Ann. Pharm. Fr.*, **25**, 627 (1967).

(13) T. K. Palit and M. P. Khare, *Phytochemistry*, **8**, 1559 (1969).

(14) A. K. Baru, P. Chakrabarti, and A. S. Dutta Gupta, *J. Indian Chem. Soc.*, **47**, 920 (1970).

(15) T. U. Okarter, M. Pharm. thesis, University of Science and Technology, Kumasi, Ghana, 1971.

(16) J. R. Dyer, "Applications of Absorption Spectroscopy of Organic Compounds," Prentice-Hall, Englewood Cliffs, N.J., 1965, p. 84.

(17) N. Bild and M. Hesse, *Helv. Chim. Acta*, **50**, 1887 (1967).

(18) T. A. Bryce and J. R. Maxwell, *J. Chem. Soc., Chem. Commun.*, **1965**, 206.

(19) E. Weiss, K. Bernauer, and A. Girardet, *Helv. Chim. Acta*, **54**, 1342 (1971).

(20) J. D. Phillipson and S. S. Handa, *Phytochemistry*, **14**, 2683 (1975).

(21) E. J. Shellard, J. D. Phillipson, and K. Sarpong, *Xenobiotica*, **1**, 455 (1971).

(22) M. Shamma and J. E. Foy, *Tetrahedron Lett.*, **1975**, 2249.

(23) J. D. Phillipson, *Xenobiotica*, **1**, 419 (1971).

(24) F. Puisieux, J.-P. Devissaguet, C. Miet, and J. Poisson, *Bull. Soc. Chim. Fr.*, **1967**, 251.

(25) A. Kh. Aslanov, A. S. Sadykov, V. N. Zainutdinov, and Yu. K. Kushmaradov, *Nauch. Tr. Goszapov*, **286**, 63 (1966); through *Chem. Abstr.*, **67**, 71108.

(26) S. K. Dutta and S. Ghosal, *Chem. Ind.*, **1967**, 2046.

(27) B. A. Abdusalamov, A. S. Sadykov, and K. A. Aslanov, *Nauch. Tr. Tash. Gas. Univ.*, **263**, 3 (1964); through *Chem. Abstr.*, **63**, 3314.

(28) E. J. Shellard, J. D. Phillipson, and K. Sarpong, *Phytochemistry*, **10**, 2505 (1971).

(29) E. Weiss, K. Bernauer, and A. Giraret, *Helv. Chim. Acta*, **54**, 1342 (1971).

(30) V. G. Khozhdaev, S. K. Maekh, and S. Y. Yunusov, *Khim. Prirodn. Soed.*, **1972**, 631.

(31) Z. Jerzmanowska and Z. Sykulska, *Dissnes. Pharm. Warsz.*, **16**, 71 (1964).

(32) R. Schoental, *J. Chem. Soc.*, **1960**, 2375.

(33) S. Brandänge and B. Lüning, *Acta Chem. Scand.*, **24**, 353 (1970).

(34) J. D. Phillipson and S. S. Handa, *Phytochemistry*, **14**, 999 (1976).

(35) A. I. Vogel, "Practical Organic Chemistry," 3rd ed., Wiley, New York, N.Y., 1956, p. 971.

ACKNOWLEDGMENTS AND ADDRESSES

Received May 25, 1976, from the *Department of Pharmacognosy, School of Pharmacy, University of Pittsburgh, Pittsburgh, PA 15261.*

Accepted for publication October 18, 1976.

Supported in part by Research Grant R-15 from the Health Research and Services Foundation, Pittsburgh, Pa. The mass spectrometry facility was supported by Research Grant RR-00273 to the University of Pittsburgh from the National Institutes of Health.

* Present address: Faculty of Pharmacy, University of Science and Technology, Kumasi, Ghana, West Africa.

‡ Present address: Council for Scientific and Industrial Research, Accra, Ghana, West Africa. This author gratefully acknowledges the Council for International Exchange of Scholars for a Fulbright–Hays Visiting Research Scientist Fellowship.

ˣ To whom inquiries should be directed.

Cardiovascular Actions of Three Harmala Alkaloids: Harmine, Harmaline, and Harmalol

DARRYL H. AARONS, G. VICTOR ROSSI, and RAYMOND F. ORZECHOWSKI ˣ

Abstract □ Each of three harmala alkaloids, harmine, harmaline, and harmalol, decreased heart rate and increased pulse pressure, peak aortic flow, and myocardial contractile force in intact normotensive anesthetized dogs. Harmine reduced systemic arterial blood pressure and total peripheral vascular resistance; harmaline-evoked decreases were frequently followed by a secondary increase; and the effects of harmalol on these two parameters were inconsistent. A direct negative chronotropic effect of harmala alkaloids was suggested by observations of bradycardia in the isolated perfused rat heart and in the intact dog; neither vagotomy nor atropinization affected harmala alkaloid-induced bradycardia in the dog. Reduction in femoral vascular resistance by the alkaloids was not apparently due to activation of cholinergic, β-adrenergic, or histaminic (H_1) receptors.

Keyphrases □ Alkaloids, harmala—cardiovascular activity in dogs □ Harmine—cardiovascular activity in dogs □ Harmaline—cardiovascular activity in dogs □ Harmalol—cardiovascular activity in dogs □ Cardiovascular activity—three harmala alkaloids in dogs

Although the seeds of *Peganum harmala* have been used for centuries as a folk medicine, the harmala alkaloids continue to be of interest because of the effects they elicit on the central nervous system (CNS) and the cardiovas-

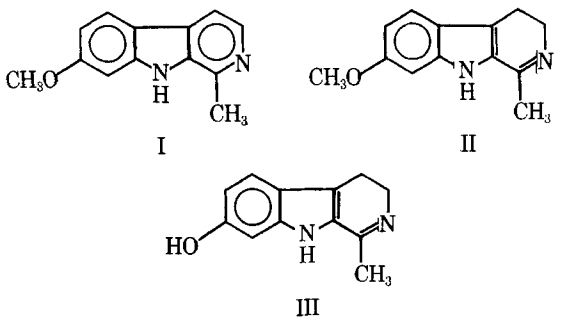

I II III

cular system. Among their pharmacological actions are a central tremorigenic action (1, 2), behavioral effects including hallucinogenesis (3), hypothermia (4), monoamine oxidase inhibition (5), and cardiovascular alterations, notably hypotension, bradycardia, and cardiac arrhythmias (6–8).

Studies of the harmala alkaloids have largely focused on their CNS effects; relatively little information exists on their cardiovascular actions. This investigation compared the cardiovascular pharmacodynamics of three major harmala alkaloids, *i.e.*, harmine (I), harmaline (II), and harmalol (III).

EXPERIMENTAL

Cardiovascular Actions in Intact Anesthetized Dogs—Mongrel dogs, 5.5–12 kg, of either sex were anesthetized with a barbiturate–urethan combination[1] (0.6 ml/kg iv). Arterial blood pressure was measured from a cannulated femoral artery[2]. Mean arterial blood pressure was derived as diastolic pressure plus one-third of pulse pressure. Heart rate was obtained from lead II electrocardiogram (ECG) tracings.

Animals were respired artificially *via* a tracheal cannula with a respirator[3]. Myocardial contractile force was recorded with a strain-gauge arch[4] sutured directly to the surface of the right ventricle (9). Aortic blood flow was measured with an electromagnetic flow probe positioned around the root of the aorta and connected to a flowmeter[5]. Total peripheral vascular resistance was calculated as the ratio of mean arterial blood pressure (millimeters mercury) to cardiac output (milliliters per minute). Recordings were made on a polygraph[6].

Each alkaloid was administered intravenously *via* a cannulated femoral vein to separate groups of dogs at increasing doses of 1, 2, 4, and, in some cases, 8 mg/kg; 60 min separated successive doses. Alkaloids were dissolved in 0.9% saline; each dose, contained in a 2-ml volume, was infused slowly over 2 min. Control dogs received 2 ml of 0.9% saline at equivalent time intervals.

Femoral Vascular Resistance Studies in Dogs—Blood from the right carotid artery of anesthetized dogs was shunted *via* polyethylene tubing[7] into the right femoral artery. The rate of blood flow into the leg was regulated by a constant-flow pump[8]. Femoral perfusion pressure was measured from a "T" connection in the tubing on the outflow side of the pump. Blood flow was adjusted so that perfusion pressure was approximately equal to systemic blood pressure recorded directly from the left femoral artery. Drugs were injected intraarterially into the perfusion circuit *via* a small section of rubber tubing interposed between two portions of the polyethylene shunt. Heparin, 5 mg/kg iv, was administered as the anticoagulant.

In one series of experiments, the alkaloids were administered directly into the blood entering the femoral artery in doses of 0.016–4.0 mg. Each dose was injected twice, consecutively, in 0.1–0.2 ml of 0.9% saline. The order of administration of the three alkaloids, as well as the order of the various doses, was randomized. Histamine and levarterenol were injected intraarterially to test the responsiveness of the experimental system. Equivalent volumes of 0.9% saline were injected for control purposes.

In a second group of experiments, the harmala alkaloids were injected twice before and at least once after administration of a pharmacological antagonist: atropine (0.5–1.0 mg/kg), propranolol (0.2–0.6 mg/kg), or brompheniramine (5.0 mg/kg) in 2 ml of 0.9% saline given by intraarterial injection over 1 min. To confirm that the antagonist produced effective blockade, a corresponding agonist (*i.e.*, acetylcholine, 2.5–5.0 μg; isoproterenol, 0.4–5.0 μg; or histamine, 5.0–10.0 μg) was injected before and after administration of the blocking agent.

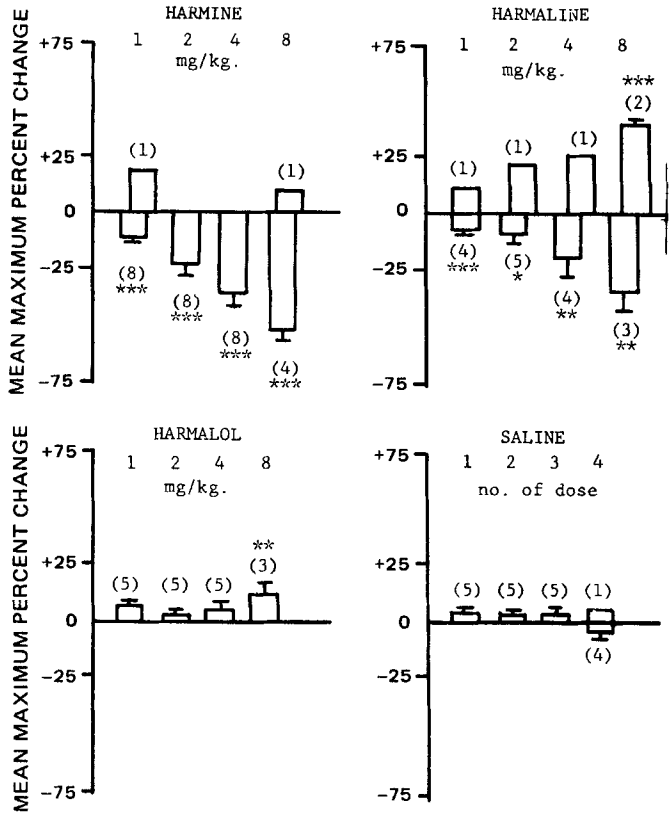

Figure 1—*Effects of intravenously administered harmala alkaloids on mean arterial blood pressure in anesthetized dogs. Key: The bars directly above and below each other indicate that opposing responses were observed in different animals receiving the same dose. Bars that overlap at the zero axis indicate that biphasic responses were observed in some animals. The sequence of the overlap indicates the order of the drug response. Numbers in parentheses refer to the number of responses comprising each mean value. Vertical lines indicate standard errors, and the level of significance is shown by the asterisks as follows:* *, $p \leq 0.05$; **, $p \leq 0.01$; *and* ***, $p \leq 0.001$.

The dose of each harmala alkaloid varied among experiments but was constant in a given animal; the dose selected was sufficient to cause a moderate (15–48%) change in femoral perfusion pressure without affecting systemic arterial pressure. Dose ranges were: harmine, 0.25–1.0 mg; harmaline, 0.25–1.0 mg; and harmalol, 1.0–4.0 mg.

Isolated Perfused Rat Hearts—The heart isolated from an adult rat was attached to a coronary perfusion apparatus[9] and perfused with Krebs–Henseleit solution aerated with 5% CO_2–95% O_2 and warmed to 38° (10). Force of contraction and heart rate were recorded with a myograph transducer[10] attached to a clamp at the apex of the heart. Initial resting tension was adjusted to 5 g. The harmala alkaloids, 0.031, 0.063, 0.125, and 0.25 mg in 0.1 ml of 0.9% saline, were introduced into the perfusate as it entered the heart. Each heart received only one alkaloid; each compound was tested in four isolated hearts. A separate group of five hearts received a series of 0.9% saline doses.

The drugs used were harmine hydrochloride hydrate, harmaline hydrochloride dihydrate, harmalol hydrochloride[11], acetylcholine chloride, atropine sulfate, brompheniramine maleate[12], histamine diphosphate, isoproterenol hydrochloride, levarterenol hydrochloride, and propranolol hydrochloride[13]. Doses of all drugs are expressed as their respective salts.

[1] Dial-Urethane, Ciba-Geigy Laboratories.
[2] Statham pressure transducer model P23AC.
[3] Harvard Apparatus.
[4] Walton-Brodie.
[5] Biotronix model T-BL 610.
[6] Grass Instrument model 5.
[7] PE240.
[8] Sigmamotor model T-8.
[9] Anderson, Metro Scientific.
[10] Narco Biosystems Linear Core F-50.
[11] Aldrich.
[12] A. H. Robins.
[13] Ayerst Laboratories.

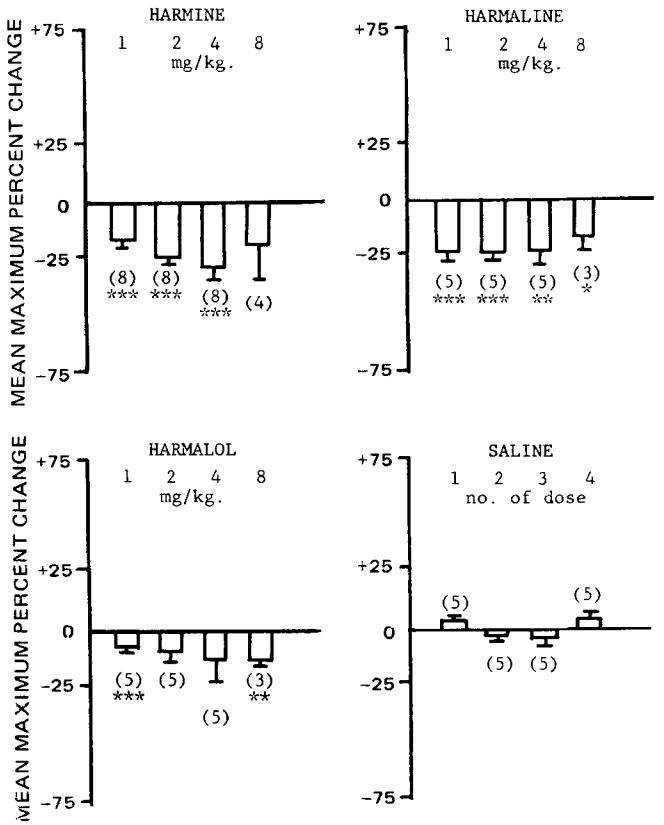

Figure 2—*Effects of intravenously administered harmala alkaloids on heart rate in anesthetized dogs. Key: see Fig. 1.*

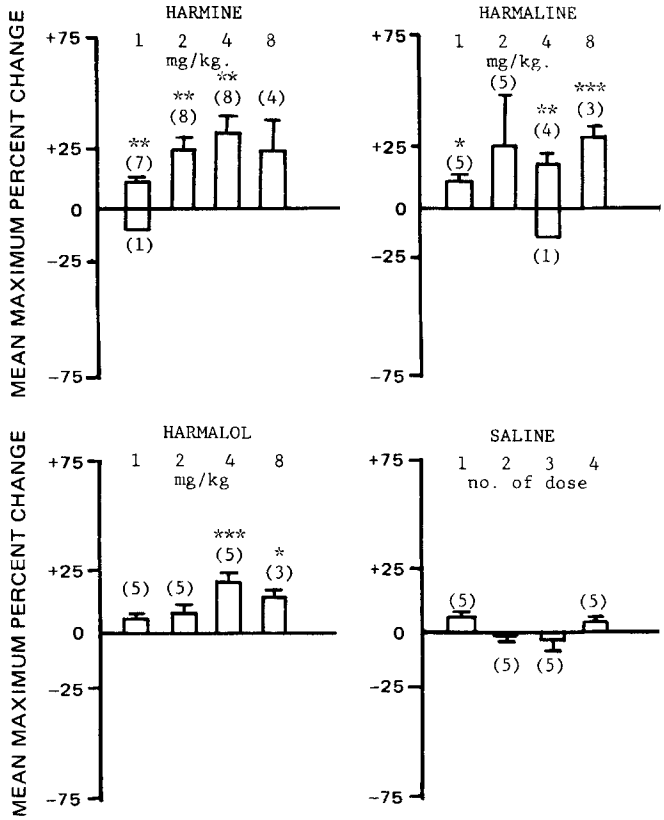

Figure 3—*Effects of intravenously administered harmala alkaloids on peak aortic flow in anesthetized dogs. Key: see Fig. 1.*

The purity of the harmala alkaloids, as assessed by TLC and NMR spectra, indicated that no significant contaminants were present.

RESULTS

Cardiovascular Effects in Intact Dogs—Harmine produced a consistent dose-related reduction in mean systemic arterial pressure in doses of 1–8 mg/kg iv; harmaline evoked similar hypotension, although less consistently and with a tendency for a secondary hypertensive response; harmalol produced variable and insignificant effects on arterial pressure at these doses (Fig. 1). Since diastolic pressure was reduced to a greater extent than systolic pressure, pulse pressure was usually increased. These effects occurred immediately after alkaloid administration and persisted from 2 to 20 min.

Bradycardia was produced by each harmala alkaloid (Fig. 2). Harmine and harmaline exhibited similar potencies, whereas harmalol was less active. The onset of heart rate reduction was immediate, and the duration was generally longer than the blood pressure changes.

Peak aortic flow was increased by all three alkaloids (Fig. 3). The smallest increase was obtained with harmalol; harmine and harmaline produced approximately equal responses. Mean aortic flow was elevated only by harmine; variable responses were elicited by harmaline and harmalol.

All three alkaloids produced significant dose-related increases in myocardial contractile force (Fig. 4). Maximum increases in contractile force usually occurred after the peak change in blood pressure.

Harmine produced a consistent and dose-related reduction of total peripheral vascular resistance. A biphasic response pattern occurred with harmaline, and harmalol produced inconsistent effects.

Cardiac arrhythmias were detected in four of seven dogs receiving harmaline and harmalol but not harmine. The dysrhythmias identified included atrial fibrillation and flutter, premature ventricular contractions, and heart block in addition to unidentified bizarre alterations. Arrhythmias were observed at various dosage levels and lasted for up to 1 hr. Elevation of the T wave of the ECG was observed with harmine (five of eight dogs), harmaline (five of seven dogs), and harmalol (one of seven dogs).

Vagotomized or Atropinized Dogs—Neither bilateral cervical vagotomy nor pretreatment with atropine antagonized the effects of harmine on heart rate and arterial blood pressure in anesthetized dogs (n = 4) (Fig. 5). The responses to harmine were essentially identical before and after doses of atropine that effectively blocked the cardiac and blood pressure changes induced by test doses of acetylcholine.

Femoral Vascular Resistance in Dog Hindlimbs—Harmine, harmaline, and harmalol, in doses of 1×10^{-4}–1×10^{-2} mmole, each reduced femoral vascular resistance (Fig. 6). The potencies of harmine and harmaline were similar, whereas harmalol was four to eight times less potent. Prior administration of atropine, propranolol, and brompheniramine did not inhibit significantly the reduction in perfusion pressure induced by harmine, harmaline, or harmalol (n = 4 in each antagonist–alkaloid series).

Isolated Perfused Rat Hearts—Each harmala alkaloid produced a dose-related slowing of the isolated rat heart (Fig. 7). The decreases observed with harmine and harmaline were approximately equal; harmalol produced a lesser reduction. A dose-related reduction in the force of contraction of isolated hearts was observed with harmine at doses of 0.031 mg and greater; variable responses were produced by harmaline and harmalol (Fig. 8).

DISCUSSION

Certain similarities, as well as distinct differences, in the cardiovascular responses to the three structurally related harmala alkaloids were observed in anesthetized dogs (Table I). Qualitatively similar responses were produced by each alkaloid on heart rate, myocardial contractile force, peak aortic flow, and pulse pressure. The most striking similarities were seen with respect to their effect on the heart. Each alkaloid reduced cardiac rate and increased myocardial force; harmine and harmaline were essentially equivalent while harmalol was less active. This finding agrees with the previous finding (11, 12) that a methoxy group on the indole nucleus (harmine and harmaline but not harmalol) enhanced the ability to reduce heart rate. Because of the rapidity of onset and relatively brief duration of the cardiovascular effects, these actions apparently are unrelated to the monoamine oxidase inhibiting properties of the harmala alkaloids. A similar conclusion was drawn by Goldberg and Sjoerdsma (7) in their report of the cardiovascular properties of several monoamine oxidase inhibitors.

Significant increases in myocardial contractile force were produced by the three alkaloids. In contrast, harmine and harmaline were reported to exert a negative inotropic effect in the anesthetized dog (7). The reason for this discrepancy is not apparent.

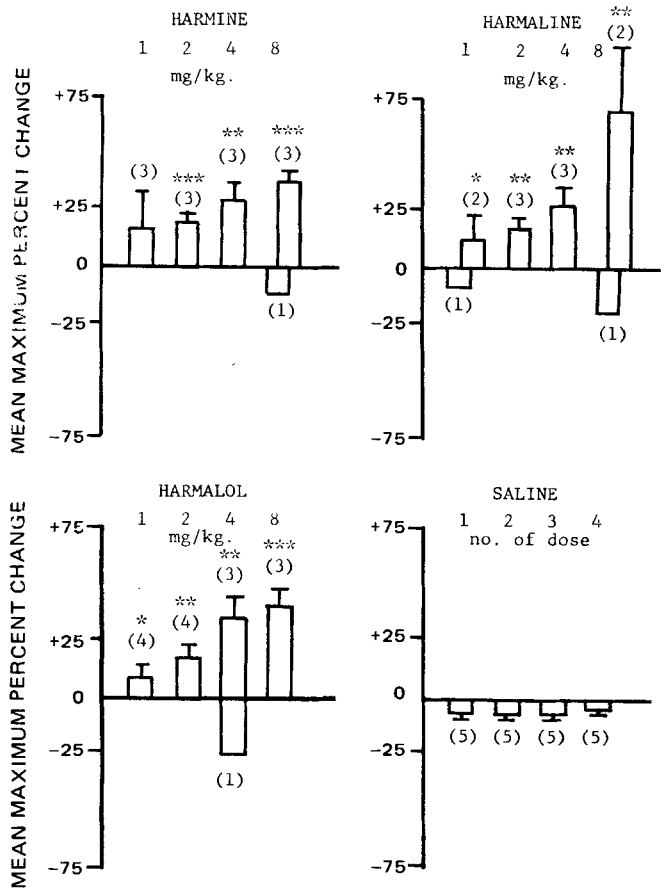

Figure 4—*Effects of intravenously administered harmala alkaloids on myocardial contractile force in anesthetized dogs. Key: see Fig. 1.*

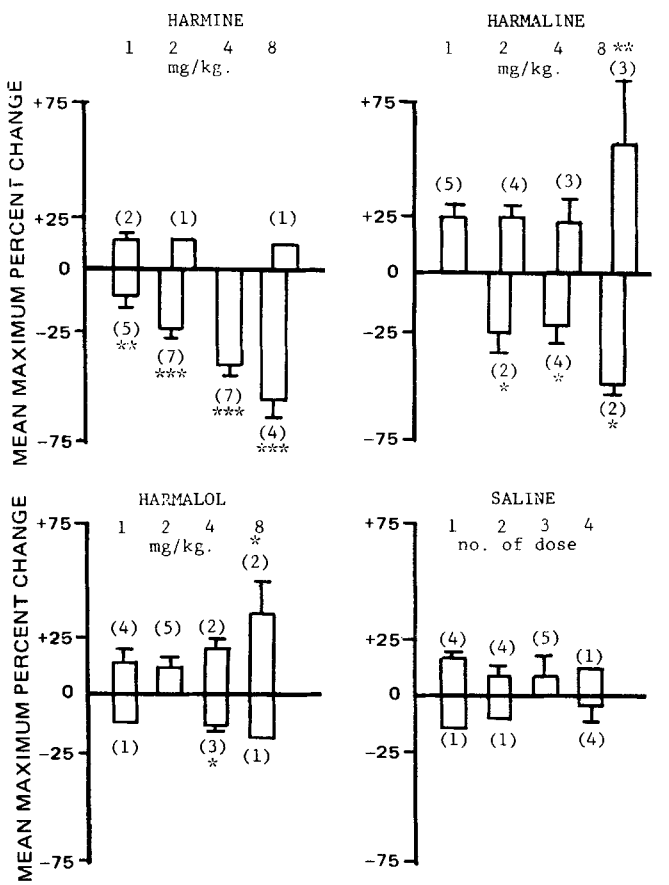

Figure 5—*Effects of intravenously administered harmala alkaloids on total peripheral vascular resistance in anesthetized dogs. Key: see Fig. 1.*

Differences among the harmala alkaloids were noted in their effects on blood pressure and total peripheral vascular resistance. The hypotensive response to intravenous administration of harmine and harmaline is in agreement with previous studies conducted in anesthetized animals and nonanesthetized humans (6–8, 11, 13). Reduction in diastolic blood pressure was primarily responsible for the hypotensive action of harmine and harmaline. Schmitt *et al.* (13) reported a similar finding in dogs receiving harmaline.

Although peak aortic flow and myocardial contractile force were increased by harmine and harmaline, minimal elevations in systolic blood pressure were occasionally observed after low doses (1 and 2 mg/kg) of these alkaloids. Higher doses predominantly reduced systolic pressure. Since the reduction in diastolic pressure was greater than that of systolic pressure, an increase in pulse pressure was obtained. Harmaline-induced reductions in mean arterial, systolic, and diastolic pressures were frequently followed by a secondary increase. This biphasic response did not occur with harmine. Harmalol had no effect on, or produced only a slight increase in, blood pressure.

Calculated values of total peripheral vascular resistance reflect changes produced by harmine and harmaline that were directionally similar to changes in systemic arterial pressure. A dose-related decrease in total peripheral resistance was produced by harmine. A biphasic response, consisting of an initial decrease frequently followed by a secondary increase, was noted with harmaline. Variable changes were produced by harmalol.

These studies demonstrated that structural variations among the harmala alkaloids result in differences in cardiovascular activity. Reduction of harmine to harmaline (dihydroharmine) had little or no effect on primary cardiovascular responses. With the exception of mean aortic flow, each parameter was initially affected similarly by the two alkaloids. This structural change, however, appeared related to secondary responses in total peripheral resistance and systemic blood pressure observed frequently with harmaline. With harmalol, in which a 7-hydroxy group replaces the 7-methoxy group of harmine, quantitative differences were seen in the effects on heart rate and peak aortic flow, while total peripheral resistance and mean systemic blood pressure differed qualitatively.

Harmaline and harmalol frequently produced cardiac arrhythmias. Although harmine did not evoke dysrhythmias in this study, it was reported previously (8) to induce ventricular arrhythmias in the cat, which were not eliminated by bilateral vagotomy or atropinization.

The negative chronotropic effect of the harmala alkaloids suggested the possibility of a parasympathomimetic mechanism. Slotkin and DiStefano (8) reported that bradycardia produced by harmaline in cats was eliminated by vagotomy. In the present study, neither bilateral vagotomy nor atropinization significantly influenced the chronotropic effect of the harmala alkaloids in dogs. Furthermore, a negative chronotropic effect was evident in the isolated rat heart, a preparation devoid of neurally mediated influences. These data do not support the possibility of a cholinergic mechanism in the cardiac slowing effect of the harmala alkaloids.

Zetler *et al.* (11) reported similar findings with harmine and harmane

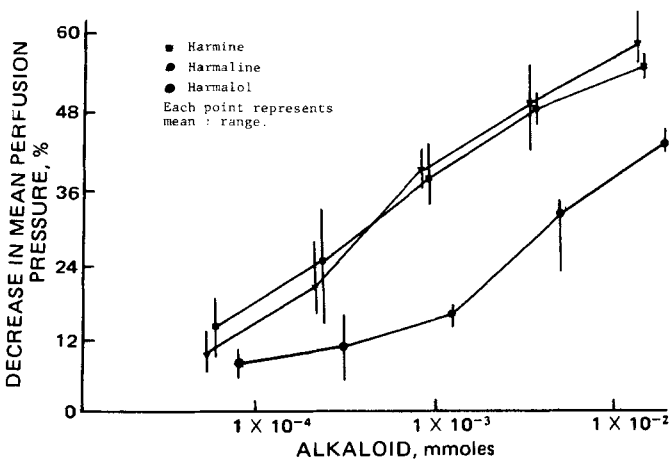

Figure 6—*Effects of three harmala alkaloids on perfusion pressure in the perfused hindlimb of dogs.*

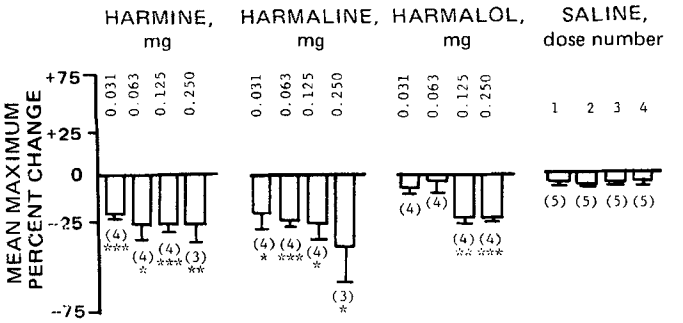

Figure 7—*Effects of three harmala alkaloids on heart rate in perfused isolated rat hearts. Key: see Fig. 1.*

in intact guinea pigs and on isolated guinea pig atria. Harmine has been reported to increase the functional refractory period of isolated guinea pig atria, but it was without effect on papillary muscle (14). Thus, cardiac slowing may result from a prolongation of the atrial refractory period.

The consistent dose-related increase in myocardial contractile force elicited in intact dogs by the three harmala alkaloids was not observed in the isolated rat heart preparation. Harmine induced a dose-dependent reduction in the force of the isolated heart, and variable responses were produced by harmaline and harmalol. Maximal increases in cardiac contractile force occurred in the intact dog after the peak effects on systemic blood pressure. Although the effects on blood pressure varied, the direction and magnitude of the responses produced by each alkaloid on myocardial contractile force were similar. This result suggests that a reflex mechanism secondary to changes in systemic blood pressure may not be responsible for the increase in contractile force. Harmine was reported to reduce myocardial contractility in the isolated guinea pig atrium driven electrically at 3/sec but to elicit a positive inotropic effect in the atria driven at a lower frequency, *i.e.*, 1/sec (15, 16). It was concluded that the positive inotropic effect of harmine, characterized by tachyphylaxis and antagonized by reserpine and propranolol, was mediated by release of endogenous norepinephrine (15, 16).

In the perfused hindlimb preparation in dogs, harmine, harmaline, and harmalol each decreased femoral vascular resistance at intraarterial doses insufficient to alter systemic arterial pressure. The nature of the vascular response to the harmala alkaloids suggested possible activation of cholinergic, β-adrenergic, or histaminergic (H_1) receptors. However, failure of specific pharmacological antagonists (atropine, propranolol, and brompheniramine) to inhibit the effect of the alkaloids on femoral vasculature eliminated involvement of the corresponding receptors. Additional evidence against a parasympathomimetic mechanism was failure of atropine or bilateral vagotomy to block the hypotensive response to harmine in intact dogs. Slotkin and DiStefano (8) reported similar results in studies with cats. Thus, vasodilation may be due to direct relaxation of vascular smooth muscle or activation of other receptor types [*e.g.*, serotonergic and histaminergic (H_2)] by harmine.

Harmaline-induced hypotension and reduction in total peripheral resistance were occasionally followed by a secondary elevation. This biphasic pattern was not observed with either harmine or harmalol. These secondary effects may result from a reflex vasoconstriction triggered in response to the fall in systemic blood pressure produced by harmaline. Support is offered by the fact that only monophasic responses were seen in the localized femoral artery preparation, in which systemic pressure was not altered. However, this finding fails to explain why harmine-induced decreases in systemic pressure did not initiate a secondary increase.

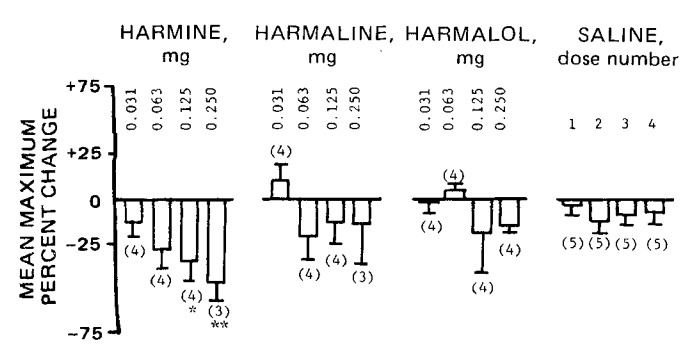

Figure 8—*Effects of three harmala alkaloids on myocardial contractile force in perfused isolated rat hearts. Key: see Fig. 1.*

Table I—Results of the Cardiovascular Analysis in Intact Anesthetized Dogs [a]

Parameter	Harmine	Harmaline	Harmalol
Mean blood pressure	− −	−−/(++)	+
Pulse pressure	++	++	++
Heart rate	− −	− −	−
Peak aortic flow	++	++	+
Mean aortic flow	++	±	±
Myocardial contractile force	++	++	++
Total peripheral vascular resistance	− −	−−/(++)	±

[a] + or − = average response less than 20%, ++ or −− = average response greater than 20%, ± = variable response, ( ) = inconsistent response, and / = biphasic response.

It is conceivable that, in addition to a relaxant effect, harmaline may activate "receptors" that produce a more prolonged vasoconstrictive response. Experimental results suggest that the vasoconstrictor component had a lower threshold of activation than did the vasodilator action. An increase in total peripheral resistance was observed in all animals receiving 1 mg of harmaline/kg.

At higher doses, both receptor types would be activated. In situations where the relaxant effect terminated before the constrictive action, a biphasic response would result. The possibility of opposing dual actions is strengthened by the fact that the effects of harmaline on mean, systolic, and diastolic pressures were less than those produced by harmine. Summation of the two opposing actions would result in a net response that was less intense than would be observed if either was unopposed.

Since anesthetics may alter neural cardioregulatory mechanisms, interpretation of the cardiovascular effects of the harmala alkaloids may have been confounded by the anesthetic agent. Cardiovascular responses in nonanesthetized animals and humans may, at least in part, be the result of a CNS action of the harmala alkaloids (17). Pressor effects of harmine in unanesthetized dogs and sheep were not blocked by atropine, suggesting that this activity is not due to cholinergic activation of the ascending reticular formation (17). Further studies are needed to delineate possible central mechanisms of the harmala alkaloids in the conscious subject.

REFERENCES

(1) B. Cox and D. Potkaniak, *Eur. J. Pharmacol.*, **16,** 39 (1971).

(2) Y. Lamarre and L. A. Mercier, *Can. J. Physiol. Pharmacol.*, **49,** 1049 (1971).

(3) H. H. Pennes and P. H. Hoch, *Am. J. Psychiat.*, **113,** 887 (1957).

(4) J. Bruinvel, *Arch. Int. Pharmacodyn. Ther.*, **182,** 403 (1969).

(5) S. Udenfriend, B. Witkop, B. C. Redfield, and H. Weissbach, *Biochem. Pharmacol.*, **1,** 160 (1958).

(6) J. A. Gunn, *Arch. Int. Pharmacodyn. Ther.*, **50,** 379 (1935).

(7) L. I. Goldberg and A. Sjoerdsma, *J. Pharmacol. Exp. Ther.*, **127,** 212 (1959).

(8) T. A. Slotkin and V. DiStefano, *Proc. Soc. Exp. Biol. Med.*, **133,** 662 (1970).

(9) K. J. Boniface, O. J. Brodie, and R. P. Walton, *ibid.*, **84,** 263 (1953).

(10) F. F. Anderson and B. N. Craver, *J. Pharmacol. Exp. Ther.*, **93,** 135 (1948).

(11) G. Zetler, E. Lenschow, and W. Prenger-Berninghoff, *Naunyn-Schmiedeberg's Arch. Pharmacol.*, **260,** 26 (1968).

(12) G. Zetler and G. Singbartl, *Pharmacology*, **4,** 129 (1970).

(13) H. Schmitt, H. Schmitt, and M. Laubie, *Therapie*, **20,** 311 (1965).

(14) H. Iven and G. Zetler, *Naunyn-Schmiedeberg's Arch. Pharmacol., Suppl. R*, **282,** 38 (1974).

(15) H. Iven and G. Zetler, *ibid.*, **283,** 181 (1974).

(16) G. Zetler, *ibid.*, **283,** 165 (1974).

(17) S. Gershon and W. J. Lang, *Arch. Int. Pharmacodyn. Ther.*, **135,** 31 (1962).

ACKNOWLEDGMENTS AND ADDRESSES

Received September 3, 1976, from the *Department of Biological Sciences, Philadelphia College of Pharmacy and Science, Philadelphia, PA 19104.*

Accepted for publication November 9, 1976.

[x] To whom inquiries should be directed.

Everted Rat Intestinal Sacs as an *In Vitro* Model for Assessing Absorptivity of New Drugs

Z. T. CHOWHAN ˣ and A. A. AMARO

Abstract □ An *in vitro* model that utilizes everted rat intestinal sacs was evaluated for assessing the absorptivity of several analogs of potential drug substances prior to formulation work and clinical trials. This model not only is a useful qualitative tool for assessing absorptivity of structurally related compounds but also yields some insight into the process involved in drug absorption. Notwithstanding the complexities involved in the absorption processes, the data support the hypothesis that the absorption of organic electrolytes mainly takes place by the partitioning of the unionized species into the lipoidal membranes and then diffusion.

Keyphrases □ Absorptivity, GI—assessed for analogs of potential drug substances using everted rat intestinal sacs □ GI absorptivity—assessed for analogs of potential drug substances using everted rat intestinal sacs □ Models, absorption—everted rat intestinal sacs, GI absorptivity assessed for analogs of potential drug substances

In the development of dosage forms and dosage regimens for new drug entities prior to formulation work and clinical trials, it is important to evaluate the absorptivity of several analogs of the potential drug substances. For this assessment, several simple, relatively rapid, inexpensive, and reproducible screening methods have been used. Since the drug must dissolve and then permeate through GI membranes, both these parameters should be evaluated.

BACKGROUND

For permeability studies, an *in vitro* procedure (1) utilizing everted rat intestinal sacs was valuable (2) in predicting the permeability characteristics of various drug classes. An interesting application of this technique was the study of dosage form variables and the effects of excipients and additives on drug permeation (3–5). This model was used to study the effect of complex formation on drug absorption (6). The effects of physiological (7) and nonphysiological (8) surfactants on drug transport also were investigated using this *in vitro* model. With this same method, the existence of several drug metabolizing enzyme systems in the intestine, which play an important role in drug absorption, was established (9–12). The transfer of salicylic acid across everted rat intestinal sacs was decreased by the presence of potassium and several electrolytes and sugars, such as glucose (13, 14).

The everted rat intestinal sac method has been used for the mechanistic understanding of absorption. The introduction of the pH–partition hypothesis (15–19) stimulated interest in the mechanism of drug absorption. Several studies considered the question of active and passive transport (6, 20–22). The interrelationships among the drug absorption rate, the dissociation constant (pKa), and the absorption site pH is known as the pH–partition hypothesis (15). This hypothesis states that the passage of drugs across the GI barrier is restricted to the undissociated drug form; therefore, the absorption rate depends on the proportion of drug present in this form. In other words, the absorption rate depends not only on the lipid solubility of the drug but on its degree of ionization; the latter, in turn, is a function of the pKa and pH of the absorbing surface.

The validity of the pH–partition hypothesis was tested using the everted rat intestinal sac method. The absorption of flufenamic acid through the everted rat intestine (21) was in agreement with the pH–partition hypothesis. Partial agreement with the pH–partition hypothesis was reported in studies using barbituric acid derivatives and the *in situ* rat small intestine (23). With the pH higher than the pKa, absorption was decreased according to the fraction of unionized form computed from the pKa, indicating that the unionized form was preferentially absorbed. But, at the acidic range, where no significant difference is considered in the fraction of the unionized moiety, the absorption rate of all derivatives studied decreased gradually with the decrease in the perfusion fluid pH.

In vitro and *in situ* absorption experiments using nalidixic acid (24) supported the pH–partition hypothesis; nalidixic acid was absorbed more slowly at a pH yielding a low partition coefficient where the drug was ionized considerably. Phenylbutazone permeation through the everted rat intestine did not obey the pH–partition hypothesis. The noncompliance with the pH–partition theory was described in terms of the general theory of pH effects (25).

This investigation analyzed the usefulness and limitations of the everted rat intestinal sac method as a model for the assessment of absorptivity of new drug analogs. Several complicating factors such as metabolism before and during absorption, accumulation in the intestinal membranes, and the influence of the pH of the perfusing solution on drug permeation, metabolism, and accumulation were considered. The results indicate that this model is a useful qualitative tool for the assessment of absorptivity across GI membranes during early phases of the drug development program.

EXPERIMENTAL

Materials—The following compounds were used as tracers containing tritium: sodium 7-methylsulfinyl-2-xanthonecarboxylate (I), sodium 7-methylthio-2-xanthonecarboxylate (II), sodium 7-isopropoxy-2-xanthonecarboxylate (III), 5-isopropoxy-7-methylthio-2-xanthonecarboxylic acid (IV), methyl 5-isopropoxy-7-methylthio-2-xanthonecarboxylate (V), and *d*-2-(6′-methoxy-2′-naphthyl)propionic acid (VI). The radiochemical purity of these compounds was at least 95% and the chemical purity was 99%.

Sodium chloride[1], potassium chloride[1], calcium chloride[2], anhydrous dextrose[1], anhydrous dibasic sodium phosphate[3], monobasic sodium phosphate[3], citric acid[3], acetic acid[4], and sodium acetate[1] were analytical reagent grade. 1,4-Bis[2-(4-methyl-5-phenyloxazolyl)]benzene[5], 2,5-diphenyloxazole[5], naphthalene[1], 2,6-bis(*tert*-butyl)-4-methylphenol[6], reagent grade methanol, spectrograde dioxane[3], and scintillation grade toluene[2] were used in the scintillation cocktail.

Everted Intestinal Sac Preparation—Young male Sprague–Dawley rats[7], 200 ± 35 g, were used. Food was removed 18 hr prior to use, but water was allowed *ad libitum*. When the rats were sacrificed, the large and small intestines were immediately removed *via* a midline incision of the abdomen and placed in a normal saline solution. Any one of the four intestinal sections was examined from each rat.

For each section, 9-cm segments were cut, sleeved onto a glass rod, everted, and washed in normal saline. The segment was attached at the proximal end of the hose adapter with a silk thread (000), trimmed to 7.5 cm, and ligated at the distal end so that 6.5 cm of the everted sac would be exposed to the mucosal solution. An 8-g stainless steel weight was attached to the ligated end of the sac to maintain it in a vertical position during the experiment.

Permeation Studies—The permeation apparatus (Fig. 1) was a modification of an apparatus described previously (2). It consisted of a 50-ml culture tube with a plastic cap. The tube, containing 40 ml of the buffer solution with the drug, was maintained at 37 ± 1° in a constant-temperature water bath. A mixture of oxygen–carbon dioxide (95:5) was bubbled continuously through an 18-gauge blunt needle. At zero time, the everted sac and assembly were placed in the culture tube.

The serosal side of the sac was filled with the same buffer solution (approximately 2 ml) without the drug, with a fluid level always visible in the vinyl polymer tubing[8]. At 10-min intervals, the solution from the

[1] J. T. Baker Chemical Co., Phillipsburg, NJ 08865.
[2] Mallinckrodt Chemical Works, St. Louis, MO 63147.
[3] Matheson, Coleman & Bell, Norwood, OH 45212.
[4] E. I. du Pont de Nemours & Co., Wilmington, Del.
[5] Arapahoe Chemical, Boulder, Colo.
[6] Aldrich Chemical Co., Milwaukee, WI 53210.
[7] Simonsen Laboratories, Gilroy, CA 95020.
[8] Tygon.

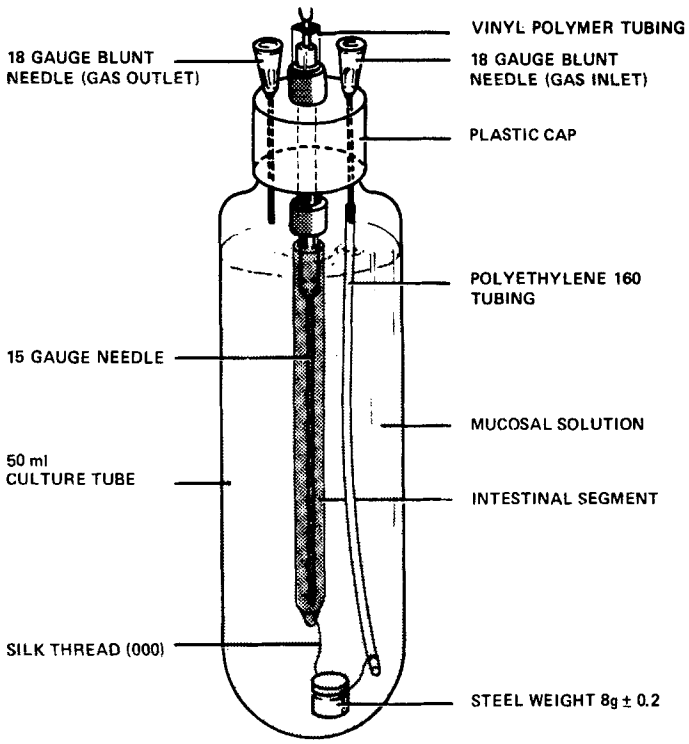

Figure 1—*Schematic representation of the permeation apparatus used in everted rat intestinal sac studies.*

intestinal sac was withdrawn using a hypodermic syringe attached to a long 15-gauge needle. The serosal side of the sac was rinsed by adding 1 ml of fresh buffer solution.

The sample from the serosal side and the rinse were combined. The mucosal side was sampled using a 50-μl disposable pipet. The samples were assayed for radioactivity using a liquid scintillation counter[9]. The composition of the scintillation cocktail was 1 liter of toluene, 1 liter of dioxane, 600 ml of methanol, 208 g of naphthalene, 13 g of 2,5-diphenyloxazole, 260 mg of 1,4-bis[2-(4-methyl-5-phenyloxazolyl)]benzene, and 250 mg of 2,6-bis(*tert*-butyl)-4-methylphenol.

Drug Solutions—The drug solutions were made in 0.008 *M* phosphate (pH 8, 7, and 6), citrate–phosphate (pH 5), or acetate (pH 3) buffer. The buffer solution also contained 0.134 *M* NaCl, 0.011 *M* KCl, 0.0001 *M* $CaCl_2$, and 0.02 *M* glucose. The concentration of drug varied depending on the experiment.

TLC—Precoated silica gel F-254 plates[10] were utilized with a developing solvent system of 80 ml of ethyl acetate[2], 80 ml of hexane[2], 20 ml of methanol[3], and 4 ml of acetic acid[1]. This system allowed distinct separation of I (R_f 0.302) from II (R_f 0.671). Aliquots of 50 μl of both the serosal and mucosal solutions were spotted along with the standards of I and II. Following development, the plates were scraped and the samples were assayed for radioactivity.

RESULTS AND DISCUSSION

Plots of the cumulative amount of I transported from the mucosal to the serosal side of the everted rat intestinal sacs prepared from duodenum and jejunum *versus* time are given in Fig. 2. After the initial lag time, these plots were linear, indicating that the transport of drug to the serosal side followed zero-order kinetics. This plotting procedure has been widely used (2–7, 13, 26, 27). The rate of drug transport or drug clearance is calculated from the slope of the linear portion. The lag time is determined by extrapolation of the linear segment to the abscissa.

The flux at steady state and the lag time for I obtained in this fashion are summarized in Table I. These data indicate that in spite of the anatomical and physiological differences in various parts of intestine, the flux is similar. However, the lag time showed a decrease in the order duodenum > jejunum > ileum > colon. A similar flux of I through various parts of the everted rat intestine is in agreement with the absorption of salicylic acid and aniline in the upper, middle, and lower one-third of the *in situ* rat small intestine (17).

[9] Nuclear Chicago, Des Plaines, IL 60018.
[10] Brinkmann.

Table I—Steady-State Flux and Lag Time Determined from the *In Vitro* Transport of I across Everted Rat Gut Segments

Segment	Flux, μg/min	Mean Flux, μg/min	Lag Time, min	Mean Lag Time, min
Duodenum	0.075	0.074	13	12.7
	0.073		12.5	
	0.073		12.5	
Jejunum	0.076	0.079	14	10.5
	0.072		9	
	0.079		8	
	0.090		11	
Ileum	0.082	0.078	3	5.7
	0.080		7	
	0.071		7	
Colon	0.103	0.088	1	5
	0.082		5	
	0.079		9	

To determine if the xanthone analogs might be absorbed by specific processes, the transport of I and II was measured at various concentrations. The flux *versus* initial concentration plots were linear over a wide concentration range (Fig. 3). This failure to find evidence of saturation suggests that the xanthone analogs are absorbed by a passive process.

The comparison of the flux data for five analogs of xanthone (I–V) is given in Table II. Because of the low solubility of V in buffer, the flux was extrapolated to the same initial concentration (10 mg/ml) for comparison. In view of the linear relationship between the flux of I and II and the initial concentration on the mucosal side, the extrapolation appeared reasonable. From the flux data given in Table II, qualitative judgment about the absorptivity of these compounds could be made. In agreement with these qualitative observations, the absorption studies in animals and humans showed that II and III were well absorbed from the GI tract while I was not well absorbed orally. Large variations were seen in the average lag time (Table II), and no relationship between lag time and flux was observed.

The results of the effect of buffer pH on the total flux of I were interesting (Fig. 4). The flux at a pH below the pKa (3.8) was higher; at pH values above the pKa, it was lower. Although these results are consistent with the pH–partition theory, the transport data cannot be explained solely on the basis of the unionized species partitioning into the lipoidal membrane and then permeating.

The effects of lightly shaking the intestinal sacs by means of a wrist-action shaker are also shown in Fig. 4. At lower pH's, the flux increased as a result of shaking. However, at pH 8 the flux was essentially the same,

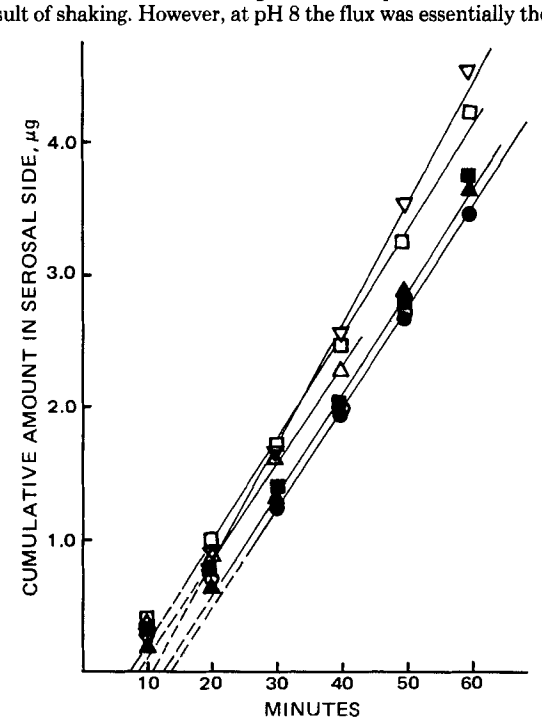

Figure 2—In vitro *transport of I from the mucosal side to the serosal side of everted rat intestinal sacs. Open symbols represent sacs made from jejunum; solid symbols represent sacs made from duodenum. Different symbols represent data points from different rats.*

Table II—Steady-State Flux and Lag Time of Xanthone Analogs at pH 7 and 8 across Everted Rat Intestinal Sacs [a]

Compound	pH 8				pH 7			
	Flux, μg/min	Mean Flux, μg/min	Lag Time, min	Mean Lag Time, min	Flux, μg/min	Mean Flux, μg/min	Lag Time, min	Mean Lag Time, min
I	0.090	0.085	12.5	8.3	0.076	0.079	14	10.5
	0.110		10.5		0.072		9	
	0.055		2.0		0.079		8	
					0.090		11	
II	0.257	0.240	30.0	24.3	0.245	0.233	14.8	14.4
	0.230		23.0		0.230		16.8	
	0.234		20.0		0.225		26.5	
III	0.300	0.290	32.0	25.5	0.300	0.263	24.0	24.3
	0.325		18.5		0.235		28.5	
	0.245		26.0		0.255		30.4	
IV	0.174	0.168	31.5	30.0	0.150	0.131	27.5	31.0
	0.175		25.5		0.135		30.5	
	0.155		33.0		0.108		35.0	
V	—	—	—	—	0.0164	0.020	26.0	22.0
					0.0180		25.0	
					0.0208		20.0	
					0.0256		17.0	

[a] The initial drug concentration was 10 μg/ml.

with or without shaking, suggesting that at this pH there is no effect of shaking on the integrity of the rate-limiting barrier. Since most drug is in the ionized form, there is little effect on diffusion either. This result would at least suggest that the integrity of the rate-limiting barrier is also not being affected at other pH values by the shaking.

The effects of buffer solution pH on the total flux of II and III are illustrated in Fig. 5. These compounds were transported at a faster rate at pH's above the pKa and at a slower rate at pH's close to the pKa. The pKa of the free acid of II, determined by the solubility method at 37° and at 0.1 ionic strength, was 4.4. Shaking the intestinal sacs increased the flux of III but did not alter the general profile. These results are in disagreement with the pH–partition hypothesis.

In view of these results, the flux of another organic acid (VI, pKa = 4.45) with known absorption characteristics (28) at different pH's was investigated (Fig. 6). At pH values higher than the pKa, absorption was not decreased according to the fraction of unionized form computed from the pKa, indicating that the unionized form was not preferentially absorbed. These results disagree with the pH–partition hypothesis. As observed earlier for III, the effect of shaking the intestinal sacs was an overall increase in the flux of VI. This increase in flux caused by diffusion layer effects did not change the overall shape of the pH profile.

The results showing the effect of buffer solution pH on the flux of II, III, and VI were similar to the recent observations of the effect of pH on the permeation of phenylbutazone across the everted rat intestine (5). Lovering and Black (5) attributed the disagreement of their data with the pH–partition hypothesis to diffusion layer effects. They claimed that this discrepancy could be best explained by using a modification of Higuchi's general equation relating pH and the permeation rate (25). The shaking and nonshaking results of this study indicate that, although the diffusion layer plays an important role in permeation studies, the major disagreement with the pH–partition hypothesis cannot be explained only on the basis of diffusion layer effects.

The rates of the transport of flufenamic acid (21) and phenylbutazone (5) at different pH's were obtained under the assumption that the drug transport followed zero-order kinetics. The same procedure was used to obtain the pH profiles given in Figs. 4–6. In treating the data, an assumption was made that the drug concentration on the mucosal side of the everted rat intestinal sacs remained constant during the experimental run. Because of differences in the effective partition coefficient values

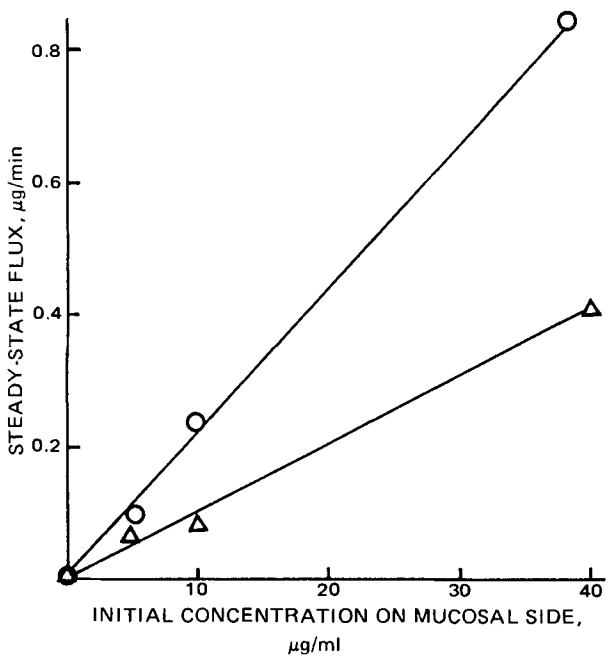

Figure 3—*Steady-state flux across everted rat intestinal sacs as a function of initial concentration. Key: △, I; and ○, II. Each data point represents the mean of at least three rats.*

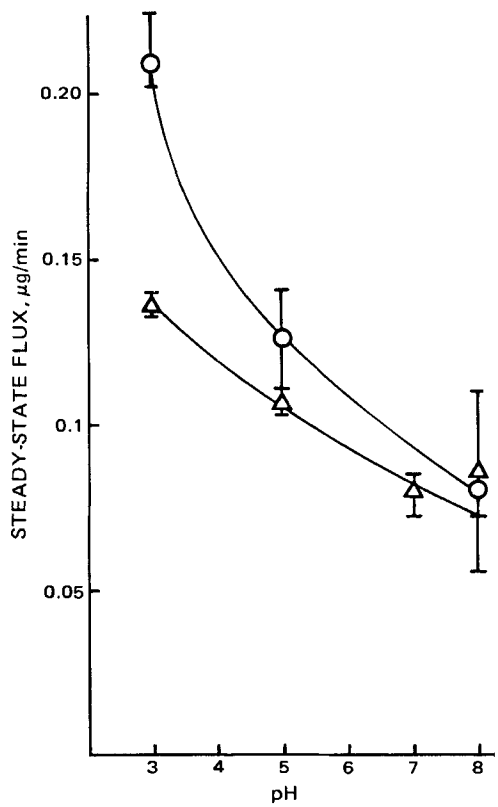

Figure 4—*Effect of pH and shaking on the steady-state flux of I across everted rat intestinal sacs. Each data point represents the mean of at least three rats. Vertical bars represent the range. Key: ○, with shaking, and △, without shaking.*

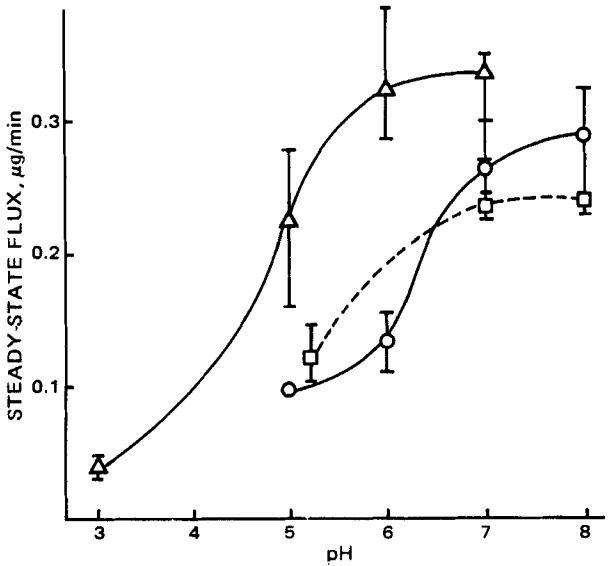

Figure 5—*Effect of pH on the steady-state flux of II and III. Key: △, III with shaking; ○, III without shaking; and □, II without shaking. Each data point represents the mean of at least three rats. Vertical bars represent the range.*

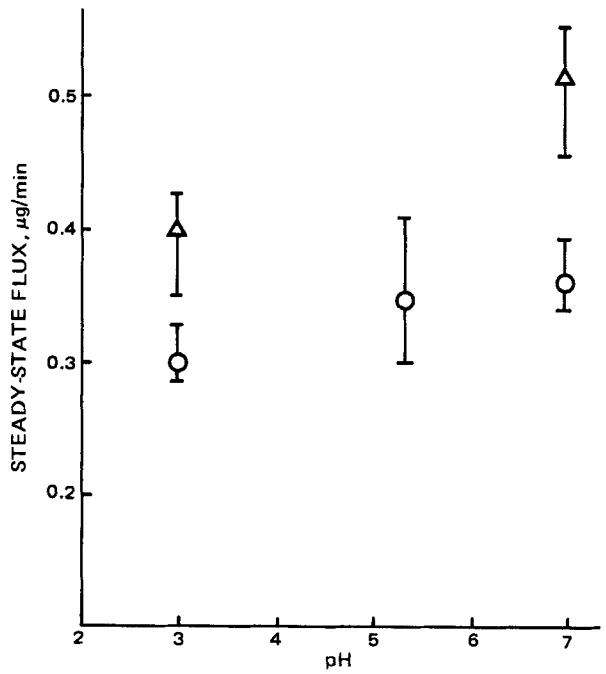

Figure 6—*Effect of pH on the steady-state flux of VI. Key: △, with shaking; and ○, without shaking. Each data point represents the mean of at least three rats. Vertical bars represent the range.*

between the lipoidal membrane and the buffer solutions resulting from the intrinsic partition coefficient difference of structurally related compounds and different degrees of ionization as a result of different pH's of the buffer solutions, drug saturation levels in the membranes could vary from compound to compound and from pH to pH. Under these circumstances, it is conceivable that the drug concentration on the mucosal side may constantly decrease or remain constant after the apparent lag time.

An examination of the amount of I and III accumulated in the everted rat intestinal sac *versus* time at different pH's confirmed that the drug accumulation in the membranes was a function of the effective partition coefficient of the drug, which, in turn, was determined by the degree of ionization. The results in Fig. 7 were obtained by subtracting the mucosal plus serosal amounts in solution from the total drug added. The accumulation of I at pH 8 in the intestinal sacs was very small. The result of decreasing the buffer solution pH was a severalfold increase in the drug accumulation (Fig. 7). At pH 3, approximately 5% drug was accumulated in the membrane during the first 20 min. An additional 4% drug accumulation resulted between 20 and 80 min. The total accumulation of drug at pH 8 was only about 2.5% at the end of 80 min.

The flux data obtained from the cumulative amount *versus* time plots may be quite valid at high pH's. However, no definite conclusion about the validity of the pH–partition hypothesis is possible because of the complications resulting from the degrees of drug saturation in the intestinal membranes and the time to reach a plateau level in the membranes. For III, there was a remarkable difference in the rates and amount of drug accumulation resulting from a relatively small change in pH (Fig. 7). For example, the accumulated amount in the intestinal sacs at the end of 80 min at pH 7 was approximately 16% of the total amount, as compared to 25% accumulation at pH 6. No plateau effect was seen at either pH. At lower pH's, the rate and amount of drug accumulation in the intestinal sacs would be larger because of the higher concentration of unionized species in solution. It should be obvious that the plots of flux *versus* pH given in Figs. 4–6 have very little meaning, and this treatment of the data cannot be explained on the basis of diffusion layer effects as reported previously for phenylbutazone (5).

These data suggest that the cumulative amount of drug transported to the serosal side *versus* time plots only provide qualitative information on the absorptivity of several analogs of potential drug compounds. At constant pH, the rate and amount of drug accumulation in the membranes for several analogs may be completely different because of differences in the effective partition coefficient. Different degrees of drug accumulation in the intestinal sac membranes could also result from differences in the solution concentration of unionized species resulting from changes in the pH.

The experimental design generally used for studying the absorptivity of drugs across the everted rat intestinal sac model is optimally suitable for monitoring the drug transport by sampling the serosal side. The results of this study indicate that, although the transport data obtained by sampling the serosal side appears to follow zero-order kinetics, the concentration in the mucosal solution may vary depending upon the drug and the mucosal solution pH. The data given in Fig. 7 suggest that a nonsteady-state situation in the membranes may exist during the entire experimental run. In view of these findings, it may be important to examine the concentration changes in the mucosal solution.

Figure 8 gives the log of the drug remaining in the mucosal solution *versus* time plots for compounds (II, III, and VI) showing higher drug accumulation in the membrane. These curves suggest that the uptake of drug from the mucosal solution follows a biexponential function. These

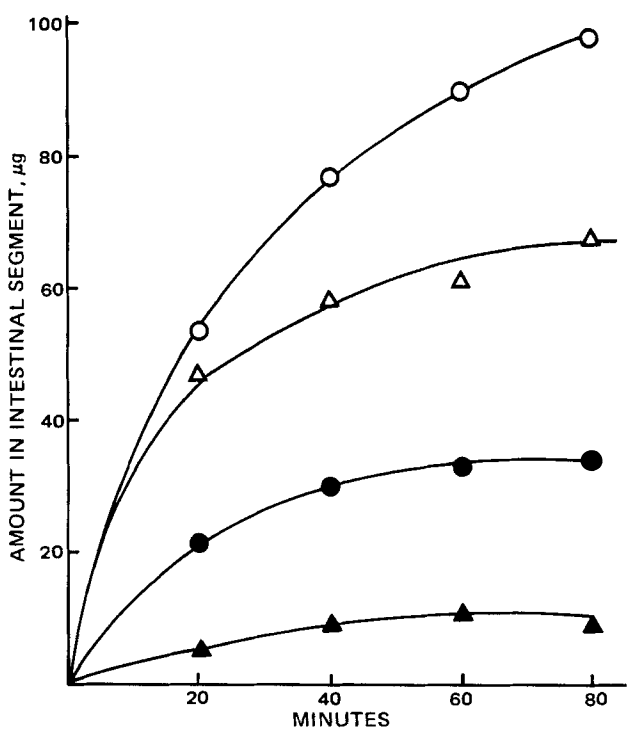

Figure 7—*Accumulation of I and III in the everted intestinal sacs as a function of time at different pH's. Key: ▲, I, pH 8; ●, I, pH 3; △, III, pH 7; and ○, III, pH 6.*

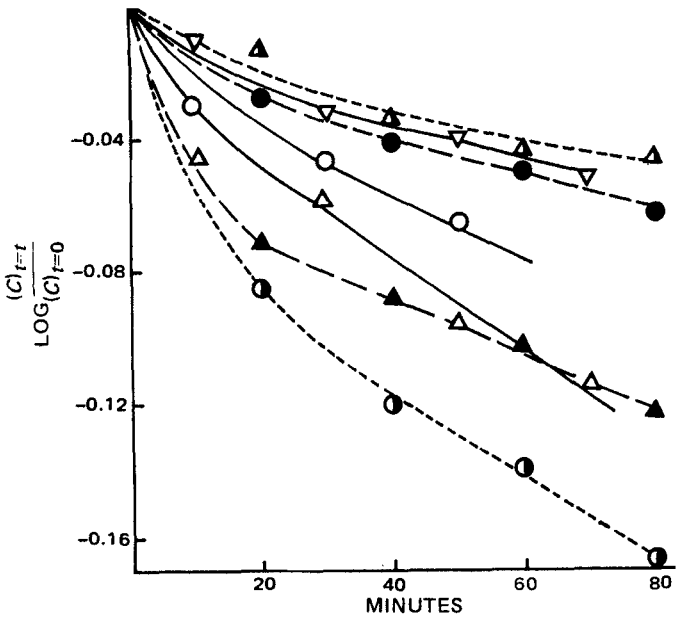

Figure 8—*Semilogarithmic plots of the drug remaining* [$(C)_{t=t}$ = *total drug concentration in the mucosal solution at time* t, *and* $(C)_{t=0}$ = *total drug concentration in the mucosal solution at time zero*] *in the mucosal solution* versus *time at different bulk mucosal solution pH's. Key:* ▽, *III, pH 7;* ○, *III, pH 6;* △, *III, pH 5;* ●, *II, pH 8;* ▲, *II, pH 5.25;* ◭, *VI, pH 7; and* ◑, *VI, pH 3.*

data also indicate higher uptake rates by the intestinal membranes from the mucosal solutions containing a higher concentration of the unionized drug, which is consistent with the pH–partition theory. Since these results cannot be explained solely on the basis of the unionized species partitioning into the lipoidal region of the membranes and diffusing, these compounds may also be transported through the aqueous-filled pores.

The differences seen in the drug transport on the mucosal and serosal sides of the everted sacs cannot be explained on the basis of drug binding to the intestinal tissue. The data given in Fig. 3 suggest that the absorption of these compounds takes place by nonsaturable processes such as passive diffusion. Also, the drug binding in the intestinal tissues would not automatically lead to a zero-order transport on the serosal side. It is possible that the barrier to drug transport in these *in vitro* studies is located in the muscle tissue or in the serosa rather than in the mucosal epithelium.

This idea may not be too surprising if one considers the changes in the functional and structural integrity of the everted intestine. On the basis of histological studies of the everted rat gut preparations, Levine *et al.* (29) reported that, although the intestinal sacs were morphologically intact after eversion, they began to lose structural integrity rapidly after 10–15 min of incubation under conditions normally employed even in the absence of drug. The apparent lack of effect of loss of the structural integrity on everted intestine transfer rates of nonpolar, lipid-soluble compounds was pointed out earlier (13, 30). This suggestion led to the observation (13, 30) that the epithelial border may not be the rate-limiting barrier to transport across the everted rat intestinal sac.

In spite of these complications from the absorption mechanism viewpoint, the everted rat intestinal sac model provides a useful quick screening procedure for assessing the absorptivity of several analogs of potential drugs. It may also provide information related to the rate of drug disappearance from the intestinal lumen, drug accumulation in the intestinal membranes, and metabolism before and during the absorption process. Preliminary studies indicated that I in pH 7 buffer solution, on incubation at 37° for 24 hr with the everted rat intestinal sacs, was completely transformed to II. In light of this observation, it seemed important to investigate the degree of transformation during a permeability run.

When the serosal side samples were analyzed by separating the components by TLC, 82, 81, and 84% of the total drug transported between 0 and 10, 20 and 30, and 50 and 60 min, respectively, was I. A similar analysis of the mucosal side solution at the end of 70 min indicated that 96.8% of the total drug was I. These data indicated that the transformation of I to II was taking place either by the gut microflora or by the intestinal enzymes. Incubation of the everted rat intestinal sacs for 24 hr at 37° with I dissolved in pH 5 buffer solution resulted in no transformation of I to II. A similar TLC analysis of the serosal side solution (pH 7) during the transport of II indicated significant transformation to I by the intestinal lumen. No transformation of III–VI by the everted rat intestine was seen during the *in vitro* transport runs.

In summary, the everted rat intestinal sac model is useful for assessing absorptivity of several analogs of potential new drugs prior to formulation work and clinical trials. This model also provides qualitative information related to the absorption processes including biotransformation before and during absorption through the intestinal membranes. The model does not lend itself to definite conclusions about the mechanism of drug absorption, mainly because of the complicated nature of the processes involved. In spite of the complications involved in treating the transport data, the results of this study suggest that the major species involved in the absorption of organic electrolytes are the unionized species.

REFERENCES

(1) R. K. Crane and T. H. Wilson, *J. Appl. Physiol.*, **12,** 145 (1958).

(2) S. A. Kaplan and S. Cotler, *J. Pharm. Sci.*, **61,** 1361 (1972).

(3) A. Aguiar, *Drug Inform. Bull.*, **3,** 17 (1969).

(4) P. Singh, J. K. Guillory, T. D. Sokoloski, L. Z. Benet, and V. N. Bhatia, *J. Pharm. Sci.*, **55,** 63 (1966).

(5) E. G. Lovering and D. B. Black, *ibid.*, **63,** 671 (1974).

(6) R. Reuning and G. Levy, *ibid.*, **57,** 1342 (1968).

(7) S. Feldman and M. Gibaldi, *ibid.*, **58,** 425 (1969).

(8) W. Saski, *ibid.*, **57,** 836 (1968).

(9) G. Levy and M. J. Angelino, *ibid.*, **57,** 1449 (1968).

(10) N. R. Strahl and W. H. Barr, *ibid.*, **60,** 278 (1971).

(11) W. H. Barr and S. Riegelman, *ibid.*, **59,** 154 (1970).

(12) *Ibid.*, **59,** 164 (1970).

(13) L. Z. Benet, J. M. Orr, R. H. Turner, and H. S. Webb, *J. Pharm. Sci.*, **60,** 234 (1971).

(14) M. Mayersohn and M. Gibaldi, *ibid.*, **60,** 225 (1971).

(15) P. A. Shore, B. B. Brodie, and C. A. M. Hogben, *J. Pharmacol. Exp. Ther.*, **119,** 361 (1957).

(16) C. A. M. Hogben, D. J. Tocco, B. B. Brodie, and L. S. Schanker, *ibid.*, **125,** 275 (1959).

(17) L. S. Schanker, D. J. Tocco, B. B. Brodie, and C. A. M. Hogben, *ibid.*, **123,** 81 (1958).

(18) L. S. Schanker, *J. Med. Chem.*, **2,** 343 (1960).

(19) L. S. Schanker, *Ann. Rev. Pharmacol.*, **1,** 29 (1961).

(20) L. S. Schanker and D. J. Tocco, *J. Pharmacol. Exp. Ther.*, **128,** 115 (1960).

(21) A. J. Aguiar and R. J. Fifelski, *J. Pharm. Sci.*, **55,** 1387 (1966).

(22) M. J. Taraszka, *ibid.*, **60,** 946 (1971).

(23) K. Kakemi, T. Arita, R. Hori, and R. Komishi, *Chem. Pharm. Bull.*, **15,** 1883 (1967).

(24) N. Takasugi, K. Nakamura, T. Hayashi, N. Tsunakawa, and Y. Takeya, *ibid.*, **16,** 13 (1968).

(25) A. Suzuki, W. I. Higuchi, and N. F. H. Ho, *J. Pharm. Sci.*, **59,** 644 (1970).

(26) G. Levy and T. Matsuzawa, *ibid.*, **54,** 1003 (1965).

(27) R. H. Turner, C. S. Mehta, and L. Z. Benet, *ibid.*, **59,** 590 (1970).

(28) R. A. Runkel, K. Kraft, G. Boost, H. Sevelius, E. Forchielli, R. Hill, R. Magoun, J. B. Szakacs, and E. Segre, *Chem. Pharm. Bull.*, **20,** 1457 (1972).

(29) R. R. Levine, W. F. McNary, P. J. Kornguth, and R. LeBlanc, *Eur. J. Pharmacol.*, **9,** 211 (1970).

(30) M. Gibaldi and B. Grundhofer, *J. Pharm. Sci.*, **61,** 116 (1972).

ACKNOWLEDGMENTS AND ADDRESSES

Received October 6, 1975, from *Syntex Research, Palo Alto, CA 94304.*

Accepted for publication October 4, 1976.

[x] To whom inquiries should be directed.

Powder Inhalation Aerosol Studies I: Selection of a Suitable Drug Entity for Bronchial Delivery of New Drugs

Z. T. CHOWHAN [x] and A. A. AMARO

Abstract □ Micronized powders of 7-methylsulfinyl-2-xanthone carboxylic acid and its sodium salt with similar particle-size distributions were used in formulating powder inhalation aerosol dosage forms. Large differences between the two micronized powders were observed in the distribution on plates of the air sampler. The micronized powders were highly cohesive, the sodium salt being slightly more cohesive than the carboxylic acid. The absorption and desorption isotherms obtained at 23 and 37° indicated considerable moisture uptake following equilibration under different relative humidities and the occurrence of hysteresis of moisture content for the sodium salt–lactose blend and the empty gelatin capsules. The carboxylic acid–lactose blend gained only a small amount of moisture. The drug distribution to the lower plates of the air sampler from the sodium salt blend was reduced to a negligible amount after equilibration at high relative humidities during the moisture absorption experiment. There was no significant change in the drug distribution to the lower plates of the air sampler for the carboxylic acid–lactose blend equilibrated up to 93% relative humidity at 23° and up to 100% relative humidity at 37° during the moisture absorption experiment. During the moisture desorption experiment, essentially no change in the drug distribution to the lower plates of the air sampler was observed for the sodium salt blend at 23 and 37° and the carboxylic acid blend at 23°. At 37°, the drug delivery from the carboxylic acid blend appeared to improve during the desorption experiment. These data suggest that studies of this nature may be useful in the selection of appropriate drug species for designing powder aerosol dosage forms during early phases of the drug development program.

Keyphrases □ Aerosols, powder inhalation—micronized powders of substituted 2-xanthonecarboxylic acid and sodium salt, effect of lactose concentration, humidity, and temperature □ 2-Xanthonecarboxylic acid, substituted—and sodium salt, micronized powders used in formulating powder inhalation aerosols, effect of lactose concentration, humidity, and temperature □ Dosage forms—powder inhalation aerosols, micronized powders of substituted 2-xanthonecarboxylic acid and sodium salt, effect of lactose concentration, humidity, and temperature □ Powders, micronized—substituted 2-xanthonecarboxylic acid and sodium salt used in formulating powder inhalation aerosols, effect of lactose concentration, humidity, and temperature

Inhalation aerosols offer a unique drug delivery system for the administration of pharmacologically active substances in the treatment of bronchial obstructive disorders. By delivering drugs directly to the affected organs, relatively small amounts of very potent medicinal compounds may be employed with minimal side effects. The most popular dosage forms in this category are pressurized inhalation aerosol solutions and suspensions, inhalation aerosol solutions, and powder inhalation aerosols.

BACKGROUND

The use of fluorocarbon propellants in the preparation of pressurized inhalation aerosols has suffered adverse publicity. The major limitation of this delivery system, however, lies in the amount of drug that can be delivered per actuation. The total drug concentration in solution- and suspension-type pressurized systems is limited by the drug solubility in the fluorocarbon propellants and by the physical stability of the suspension. Most fluorocarbon-propelled canisters intended for bronchial drug delivery require synchronization of the inhalation and the generation of the aerosol cloud during the breathing cycle. In a recent clinical study (1), in spite of careful instructions, 14% of the patients used the pressurized device inefficiently. When patients who were unable to inhale correctly from a pressurized canister used a breath-actuated powder inhalation device, 95.5% had no difficulty (1).

Continuous liquid aerosol therapy is used widely in the treatment and control of obstructive respiratory diseases, particularly cystic fibrosis. The output of the liquid aerosol from inhalation aerosol solutions is limited by the physicochemical characteristics of drug solubility and solution viscosity (2). The evaporation of solvent continually increases the concentration of solute in the liquid remaining in the nebulizer. This increase, in turn, increases the concentration of airborne solute in the useful aerosol and shifts the size distribution of the residual aerosol to a larger volume.

One important factor that determines the site and extent of drug delivery to the respiratory tract is the particle-size distribution of the aerosol cloud. For formulating an aerosol suspension in pressurized canisters and for designing a powder aerosol dosage form, the drug particles should be in a finely divided state. Micronization is generally used to ensure that the drug particles are in the desirable particle-size range. The formulation of the powder inhalation aerosols of new drug substances requires some knowledge of the solid-state properties of the drug. Micronized powders of complex organic medicinals are generally cohesive and adhesive.

The generation of an aerosol cloud comprised of singly dispersed solid particles from micronized powders is impossible. In some cases, the powder aerosol efficiency is improved by adding diluents. Unfortunately, only lactose has been studied and has gained general acceptance. Thus, the solid-state properties of the micronized drug substance generally control the characteristics of the generated aerosol. If the drug is hygroscopic, it may present additional problems of moisture transfer from the atmosphere to the hard gelatin capsule and to the drug in the capsule, acting as a sink (3). Unless careful controls are maintained during manufacturing, packaging, and storage, the net result may be a serious loss in the aerosolization efficiency.

Because of the nature of the powder inhalation aerosol dosage form, solid-state properties of the potential drugs may be important in determining the site and extent of drug delivery to the tracheobronchial tree. A proper choice between an organic acid and a salt, for example, may significantly affect the drug delivery characteristics. This investigation compared the aerosolization efficiency of 7-methylsulfinyl-2-xanthone carboxylic acid (I) and its sodium salt (II) from powder aerosol blends containing different ratios of lactose. Relative changes in the aerosolization efficiency of drug–lactose blends were monitored following equilibration of the powders under various humidity conditions at 23 and 37°. Comparative information on the aerosolization efficiency and changes in the aerosol characteristics as a function of the storage conditions was obtained. These data, in addition to the comparative absorption rates from the alveolar–capillary membranes (4), can be employed to select the most appropriate drug entity for designing a powder inhalation aerosol dosage form early in the drug development program.

EXPERIMENTAL

Materials—Phosphorus pentoxide[1] (solid), lithium chloride[1], potassium acetate[1], hydrated magnesium chloride[2], hydrated potassium carbonate[1], hydrated magnesium nitrate[2], sodium nitrite[1], sodium chloride[1], potassium chloride[1], monobasic ammonium phosphate[1], lead nitrate[2], and hydrochloric acid[1] were all analytical reagent grade. Potassium hydroxide[3] and hydrous lactose[4] were USP grade. The hard gelatin capsules[5] were size 2, with a brown cap and opaque brown body. The purity of I and II[6], as determined by high-pressure liquid chromatography, was 98.4 and 98.8%, respectively. The loss on drying at 60° under vacuum at equilibrium was 0.07% for I and 2.2% for II.

Methods—Similar conditions were used to micronize[7] I and II. The

[1] Mallinckrodt Chemical Works, St. Louis, MO 63160.
[2] J. T. Baker Chemical Co., Phillipsburg, NJ 08865.
[3] Matheson, Coleman & Bell, Norwood, OH 45212.
[4] Foremost Food Co., Foremost-McKesson, San Francisco, CA 94140.
[5] Elanco Products Co., Indianapolis, IN 46206.
[6] Institute of Organic Chemistry, Syntex Research, Palo Alto, Calif.
[7] Production micronizer, 10.1 cm (4 in.), Jet Pulverizer Co., Palmyra, N.J.

grind and feed pressures were 30–35 and 35–40 psi, respectively, throughout the micronization procedure. Regular grade lactose was screened[8] through a 200-mesh screen to remove particles smaller than 75-μm diameter. Samples of the drug–lactose blends were prepared by mixing the micronized drug and sieved lactose with a spatula. For the air sampler[9] particle-size distribution studies, blends of drug and lactose at different ratios were prepared. Hard gelatin capsules containing 10 mg of the active compound were made and used in the Andersen impactor studies.

Powder blends containing one part of micronized drug and two parts of sieved lactose were used in the relative humidity studies. The powder blends were evenly spread and accurately weighed (approximately 1.5 g) in 6-cm diameter glass petri dishes (bottoms only). Approximately 1.5 g of empty hard gelatin capsules, separated into caps and bodies, also was weighed accurately in 10-cm diameter petri dishes. The accurately weighed powder blend samples and empty capsule samples were used to monitor the weight changes as a function of the relative humidity. Additional samples of the powder blends also were prepared (approximately 3 g) in 10-cm diameter petri dishes. Approximately 200 mg of the powder blends was sampled following equilibration at each specific humidity condition, and capsules containing 10 mg of active compounds were immediately prepared and used in the air sampler test.

For maintaining constant relative humidity conditions at room temperature and 37°, desiccators containing saturated salt solutions were employed. The salt solution selections were similar to those used by Bell *et al.* (3) (Table I). For the water absorption curve, the samples were prepared by drying in desiccators containing phosphorus pentoxide at 45° until there was no weight loss. The samples were transferred to higher humidity conditions after each equilibration. The samples for the water desorption curves were prepared by equilibration above water or a salt solution at 23 or 37°. These samples were then transferred to lower humidity conditions after each equilibration.

The particle-size distribution of the micronized I and II was determined[10]. The electrolyte for the acid was 0.6% HCl, which was equilibrated with the micronized powder at room temperature. 2-Propanol containing 5% ammonium thiocyanate equilibrated with the micronized powder at room temperature was used as an electrolyte for the sodium salt. The electrolytes were filtered using a 0.45-μm average pore size filter[11]. Approximately 2 mg of the micronized powder was suspended in 50 ml of electrolyte solution using an ultrasonic bath[12], and the suspension was suitably diluted and used in the particle-size determination. A 50-μm aperture tube and a sample volume of 50-μl were used. The instrument was calibrated using 2.02-μm diameter latex particles[10], and the mean of three counts was taken.

Cohesiveness of the micronized powders was measured by a modification of the method introduced by Carr (5). A sonic sifter[13] was used in the determination of cohesiveness of micronized powders. For the test, 2 g of the micronized powder was placed on top of a nest of 60-, 120-, and 200-mesh screens. The sieve assembly was vibrated for 29 sec at a pulse and sift setting of 6. The amount of powder left on each sieve was weighed, and the results are expressed by scoring on a scale that allocated cohesiveness points for each 0.1 g as follows: on 60 mesh, 5 points; on 120 mesh, 2 points; and on 200 mesh, 1 point.

Figure 1 shows a diagram of the apparatus used for determining the particle-size distribution using an air sampling technique. It consisted of an air sampler[9], a throat assembly[14], an air pump[15], and a developmental inhalation device. The air pump was adjusted to draw 29 ± 1 liters/min of air through the air sampler using a flowmeter[16].

The cap of the hard gelatin capsule containing the powder blend was removed, and the body was inserted into the inhalation device. The inhalation device was then attached to the throat adaptor. The whole system was inspected for a tight fit. The pump was operated for 3 sec. Then the capsule body was removed and set aside, along with the top, for rinsing. Five capsules were emptied in the air sampler one after the other using the described procedure.

The inhalation device, the adaptor, and the capsules were washed with 0.1% potassium hydroxide solution into a 140-mm glass petri dish bottom. The throat and the first two aluminum pieces of the air sampler were rinsed into the next petri dish. Each of the seven glass plates was rinsed with 0.1% potassium hydroxide into separate glass petri dish bottoms. The aluminum piece below each plate was tapped to collect any adhering powder into the corresponding petri dish. The contents of each petri dish were transferred to volumetric flasks of appropriate sizes and diluted to volume with water. The absorbance of each sample was determined at 342 μm. The total amount of active compound recovered from each stage was calculated and used to determine the fraction of the total on each stage.

Table I—Saturated Salt Solutions Used for the Maintenance of a Constant Relative Humidity

Salt	Relative Humidity, % 23°	37°
Lithium chloride	13	11
Potassium acetate	20	20
Magnesium chloride hexahydrate	33	32
Potassium carbonate·1.5H_2O	44	40
Magnesium nitrate hexahydrate	54	50
Sodium nitrite	65	62
Sodium chloride	76	75
Potassium chloride	85	82
Monobasic ammonium phosphate	93	91
Lead nitrate	97	96
Water	100	100

RESULTS AND DISCUSSION

The results of the particle-size distribution of I and II micronized powders are given as log–probability plots in Fig. 2. Although the particle-size distributions were similar, 89% of the mass of the sodium salt was smaller than 5-μm diameter compared to the 82% of the mass of the carboxylic acid. These differences were also reflected in the mass median diameter, 2.5 μm for II compared to the 2.9 μm for I.

The cohesiveness of micronized I equilibrated at 23° with 0, 28, and 93% relative humidities was 75.9, 79.6, and 77.9, respectively. The cohesiveness of II equilibrated at 23° with 0, 28, and 93% relative humidities was 83.2, 84.1, and 86.7, respectively. The cohesiveness of these powders was measured by sifting the powders through the specified screens and allocating points on a scale of zero to 100. If all material remained on the 60-mesh screen, the score would have been 100; it would have been zero

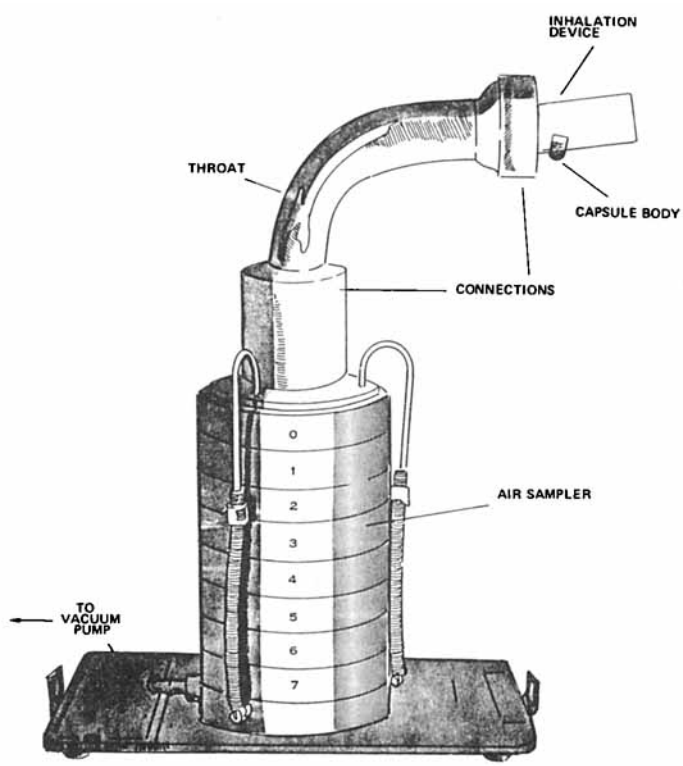

Figure 1—*Schematic representation of the apparatus used in testing the delivery of drugs to various stages of the air sampler.*

[8] Ro-Tap testing sieve shaker, W. S. Tyler Co., Cleveland, Ohio.
[9] Model 21-000, Andersen 2000, Salt Lake City, UT 84107.
[10] Coulter counter model TA, Coulter Electronics, Hialeah, FL 33010.
[11] Metricel GA-6, Gelman Instrument Co., Ann Arbor, Mich.
[12] Model 8845-6, Cole-Parmer Instrument Co., Chicago, IL 60648.
[13] Model L3P, Allen Bradley Co., Milwaukee, Wis.
[14] Syntex Research Shop, Palo Alto, Calif.
[15] Model 1531-109-G288, Gast Manufacturing Corp., Benton Harbor, Mich.
[16] Size 5, Roger Gilmont Instruments, Great Neck, NY 11021.

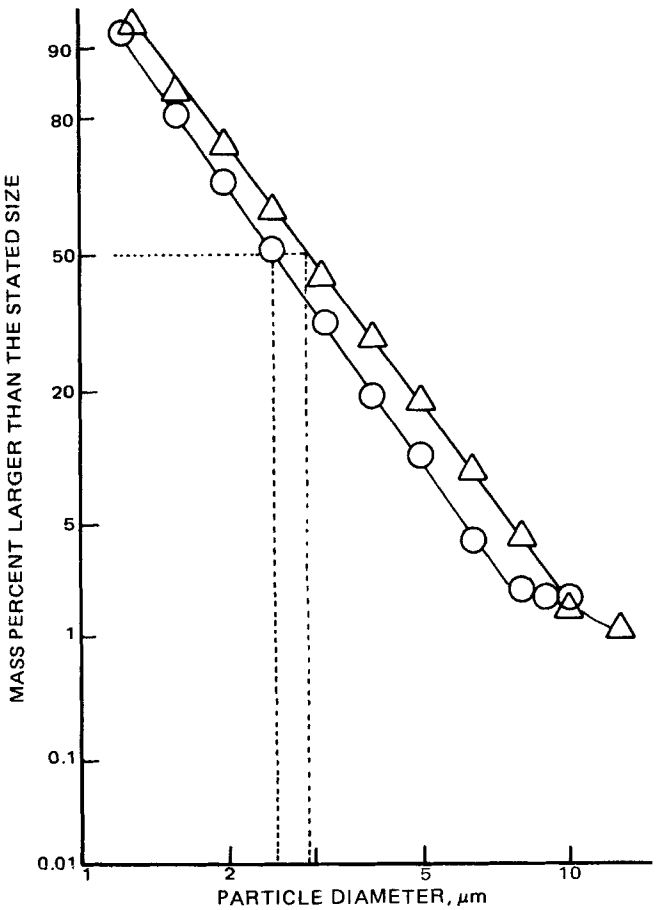

Figure 2—*Particle-size distributions of the micronized powders. Key: △, I; and ○, II.*

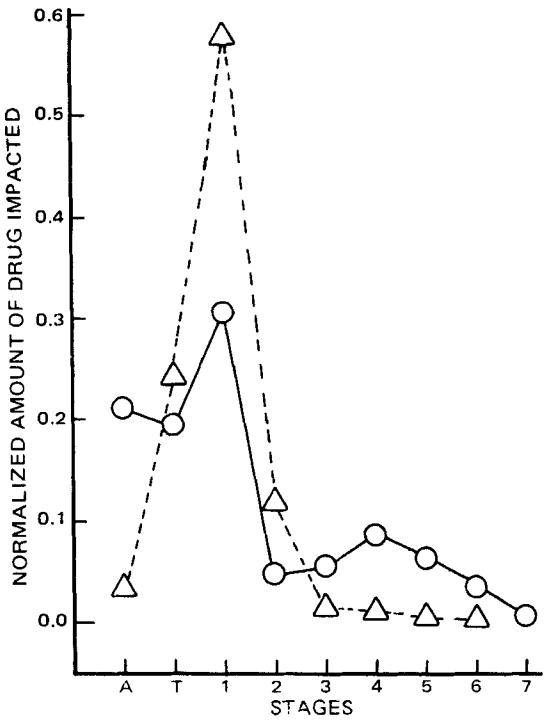

Figure 3—*Distribution of drug to stages of the air sampler under ambient conditions. Stage A represents the amount remaining in the capsule plus the amount impacted in the inhalation device. Stage T represents the amount impacted on the throat plus the amount impacted on stage zero. Key: △, II; and ○, I.*

if all powder passed through a 200-mesh screen. The intermediate results provide a suitable measure of the cohesiveness by relating it to the amount of energy spent in pulling apart the aggregates in a specified time.

These results are means of three experiments and indicate that both powders are highly cohesive, II being more cohesive than I at all relative humidities. The cohesiveness of the powders did not increase significantly as a function of the relative humidity, perhaps because both powders gave a relatively high score for cohesiveness after equilibration at 0% relative humidity.

Lactose was added to the micronized drugs to improve aerosolization properties by breaking up the cohesive bonds of the drug particles. Preliminary studies suggested that the lactose particles retained on a 200-mesh screen resulted in optimized aerosol properties. Microscopic examination of the lactose particles retained on a 200-mesh screen indicated no cohesion of lactose particles. It was not possible to test the cohesiveness of the mixture of micronized drug and coarse lactose particles. For testing cohesiveness by the described method, the particles of the powder mixtures must be smaller than the smallest screen size (200 mesh) used.

Figure 3 shows the delivery of I and II to the inhalation device, throat, and stages 1–7 of the air sampler from a mixture of 10 mg of drug and 20 mg of lactose. Indirect means of particle-size measurements such as impaction should be used for simulating powder inhalation aerosols, because the deposition of aerosol particles in the respiratory tract involves mechanisms such as inertial impaction, gravitational sedimentation, and Brownian diffusion. Impaction devices provide one simple method of determining activity distribution in terms of the aerodynamic diameter. The aerodynamic diameter is the diameter of a sphere of unit density having the same settling velocity as the particles in question, regardless of their shape and density. Thus, a small particle of high density has the same aerodynamic diameter as a large particle of lower density.

The impaction devices[9], like other similar devices, provide an *in vitro* model for the human lungs and have obvious similarities in its ability to separate particles of different sizes. At each stage of the impactor, air impinges upon a glass-collecting surface and is deflected through 90°. Particles with sufficient inertia are thrown out of the air stream onto a collecting surface. By decreasing the jet width, the air velocity through the jet becomes progressively larger so that each stage collects smaller particles than the preceding stage. The calibration of the instrument was carried out using spherical particles of carnauba wax.

The particles retained on each stage corresponded to a narrow size distribution. Stages 4–7 corresponded to particles smaller than 5.5-μm aerodynamic diameter. According to the air sampler model[9], these particles are deposited in the trachea, bronchi, and alveoli, depending upon the size. In the treatment of bronchial obstructive disorders, the powder aerosol should deliver particles to the tracheobronchial tree. The efficiency of delivering drug particles to stages 4–7 of the air sampler would be expected to serve as a good index of what is expected *in vivo*.

The data in Fig. 3 indicate that the delivery of the drug to stages 4–7 from the II–lactose blend was considerably lower than from the I–lactose blend (1.4% from II compared to 18.8% from I). This result could not be predicted based on the particle-size distribution data (Fig. 2), but it is not surprising since the particle-size distribution represents the size distribution of singly dispersed particles. The micronized powders of organic medicinals, however, do not generate aerosol clouds of singly dispersed particles because of the cohesive nature of the powders. The test used for measuring cohesiveness did not distinctly separate the large differences between the two powders seen in the air sampler study. Although micronized II appeared to be more cohesive than micronized I, the differences were small.

The results of the effect of various drug to lactose ratios on the percent drug impacted on stages 4–7 are given in Fig. 4. The drug delivery from the II blend was only improved when the powder mixture contained 10 mg of drug and 40 mg of lactose. A considerable increase in the percent drug delivery from the I blend was produced by adding lactose to the formulation. Although some differences in the cohesiveness of the I and II powders were observed, the test measuring cohesiveness was not sensitive enough to explain fully the large differences in the particle-size distribution.

These results clearly suggest that II would deliver a small fraction of the dose to the tracheobronchial tree compared to I and thus would not provide a suitable drug entity for a powder inhalation aerosol drug delivery system. However, I would be an appropriate drug entity for such a system and should deliver around 10% of the dose to the tracheobronchial tree.

Another aspect that should be thoroughly investigated during the initial stages of the development of a powder inhalation aerosol dosage

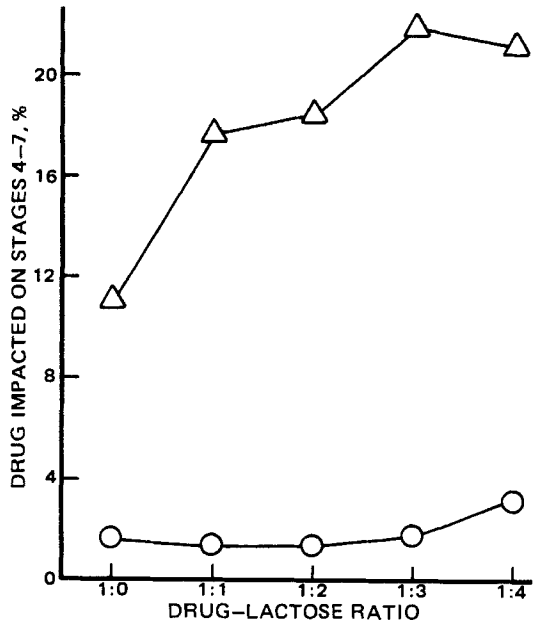

Figure 4—*Effect of drug–lactose ratio on the percent drug impacted on stages 4–7. Key: △, I; and ○, II.*

form relates to the physical stability of the powder with regard to the generation of an aerosol cloud. If the dosage form utilizes hard gelatin capsules, moisture exchange characteristics between the gelatin capsules and the powder should be evaluated carefully. Moisture could be gained or lost by pharmaceutical powders in contact with hard gelatin capsules (6). Bell *et al.* (3) reported that moisture transfer occurred from hard gelatin capsules to cromolyn sodium–lactose blends at elevated temperature during shelf tests, even if the materials were equilibrated previously at the same relative humidity.

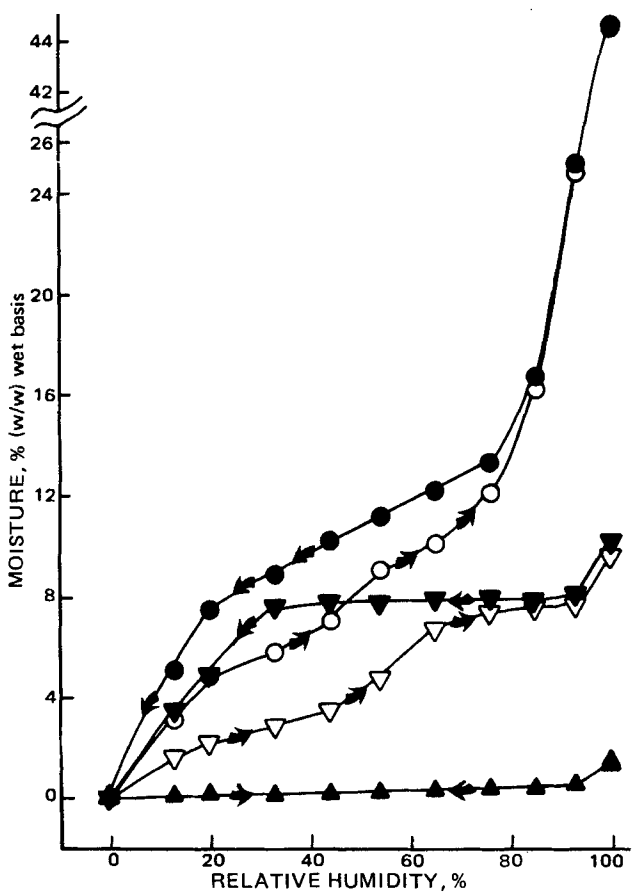

Figure 5—*Absorption and desorption isotherms at 23°. Key: ○ and ●, empty hard gelatin capsules; ▽ and ▼, II; and △ and ▲, I. Open symbols represent absorption isotherms; closed symbols represent desorption isotherms.*

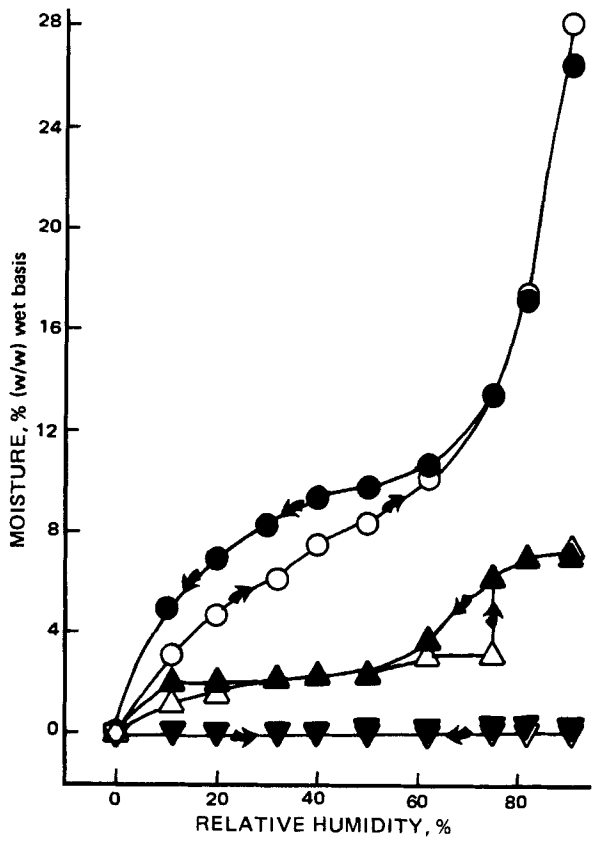

Figure 6—*Absorption and desorption isotherms at 37°. Key: ○ and ●, empty hard gelatin capsules; △ and ▲, II; and ▽ and ▼, I. Open symbols represent absorption isotherms; closed symbols represent desorption isotherms.*

Figure 5 gives the results of the absorption and desorption isotherms for hard gelatin capsules and for the blends of I and II (one part drug and two parts lactose) at 23°. These data indicate that the I blend absorbed only a small amount of moisture up to almost 93% relative humidity. At 100% relative humidity, the total amount of water absorbed was 1.5%. The absorption and desorption isotherms were essentially the same. However, the empty gelatin capsules absorbed a considerable amount of water, depending upon the relative humidity. Since the powder blend of I did not absorb significant moisture, the moisture transfer effects from the capsule wall to the powder blend would be minimal, even at high humidities. The II blend however, absorbed a considerable amount of water, depending on the relative humidity.

The absorption and desorption isotherms of the II blend and the empty gelatin capsules suggest the occurrence of hysteresis of the moisture content. The existence of a hysteresis loop for the capsules confirms earlier work (3). Hysteresis loops have been reported for other pharmaceuticals including cromolyn sodium (3), pentobarbital sodium, bacitracin, casein, corn starch, and aluminum magnesium silicate (7). Based on previous observations (3), one might predict that moisture transfer would occur from the hard gelatin capsule to the II blend even if the materials were equilibrated previously. These results suggest that the aerosolization efficiency of the II blend would decrease considerably as a result of the moisture transfer effects.

Figure 6 gives the results of the absorption and desorption isotherms for hard gelatin capsules and for the powder blends of I and II at 37°. No noticeable differences at 37° were seen in the absorption and desorption isotherms of the I blend. The percent moisture absorbed by the II blend was lower at 37°, and the absorption and desorption isotherms showed only a small hysteresis of moisture.

The results of the percent drug impacted on stages 4–7 of the air sampler as a function of the relative humidity during the moisture absorption experiment from the powder blends of I and II at 23 and 37° are given in Fig. 7. Drug delivery from the I powder blend equilibrated under various relative humidities at 23 and 37° remained essentially similar.

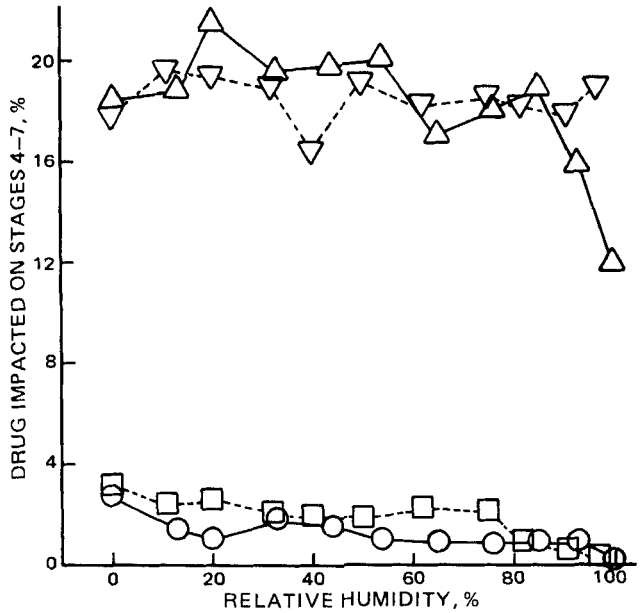

Figure 7—*Percent drug delivery to stages 4–7 as a function of the relative humidity during the moisture absorption experiment. Key: △, I at 23°; ▽, I at 37°; ○, II at 23°; and □, II at 37°.*

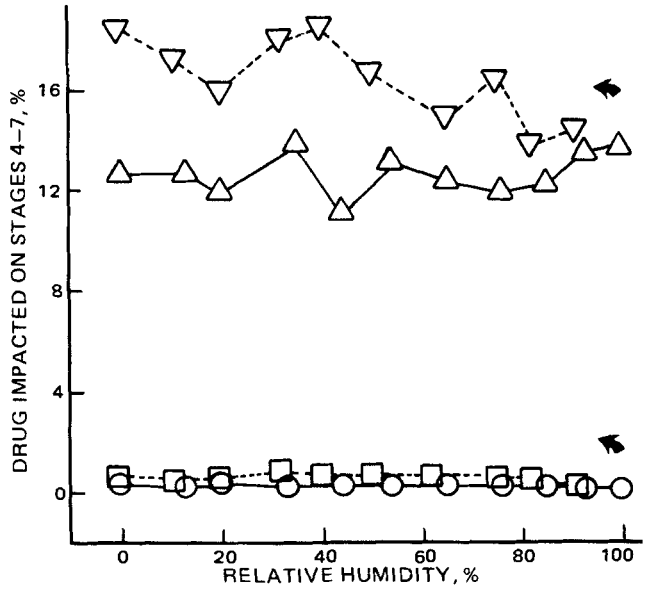

Figure 8—*Percent drug delivery to stages 4–7 as a function of the relative humidity during the moisture desorption experiment. Key: △, I at 23°; ▽, I at 37°; ○, II at 23°; and □, II at 37°.*

Some decrease in drug delivery was observed from the powder blends equilibrated at 23° under 100% relative humidity. The already low delivery of the II blend showed a considerable decrease after equilibration at higher humidities.

Similar data were obtained during the moisture desorption experiment for I and II blends (Fig. 8). Drug delivery remained essentially zero when the II blends, which were equilibrated under 100 or 91% relative humidity at 23 and 37°, were gradually equilibrated at lower humidities. At 23°, the drug delivery from the I blend initially equilibrated at 100% relative humidity did not improve during the moisture desorption experiment. Samples of the I blend initially equilibrated under 91% relative humidity at 37° showed some improvement in the air sampler delivery at lower humidities during the moisture desorption experiment. These results suggest that the reduction of the drug delivery from the I blend caused by moisture uptake at 91% relative humidity can be reversed by storing the powder blend at slightly elevated temperature.

Each data point in Figs. 3, 4, 7, and 8 represents the mean of five capsules emptied one after the other in the air sampler. The variability from test to test was small due to our interest in the sum of the drug impacted on stages 4–7 of the air sampler. The data in Figs. 7 and 8 showing the effect of two temperatures and various relative humidities on aerosol properties of the drug–lactose mixtures illustrate the good reproducibility of the test method.

In summary, the results demonstrate the importance of the selection of the proper drug entity in designing powder inhalation aerosol dosage forms. The usefulness of such studies at an early stage of the drug development program cannot be overemphasized.

REFERENCES

(1) I. C. Paterson and G. K. Crompton, *Br. Med. J.*, **1**, 76 (1976).

(2) J. H. Bell, P. S. Hartley, and J. S. G. Cox, *J. Pharm. Sci.*, **60**, 1559 (1971).

(3) J. H. Bell, N. A. Stevenson, and J. E. Taylor, *J. Pharm. Pharmacol. Suppl.*, **25**, 96P (1973).

(4) Z. T. Chowhan and A. A. Amaro, *J. Pharm. Sci.*, **65**, 1669 (1976).

(5) R. L. Carr, Jr., *Chem. Eng.*, **Jan. 8, 1965**, 163.

(6) W. A. Strickland, Jr., and M. Moss, *J. Pharm. Sci.*, **51**, 1002 (1962).

(7) W. A. Strickland, Jr., *ibid.*, **51**, 310 (1962).

ACKNOWLEDGMENTS AND ADDRESSES

Received August 16, 1976, from *Syntex Research, Palo Alto, CA 94304.*

Accepted for publication November 17, 1976.

[x] To whom inquiries should be directed.

Kinetics of Indomethacin Degradation II: Presence of Alkali plus Surfactant

J. E. DAWSON, B. R. HAJRATWALA ˣ, and H. TAYLOR

Abstract □ The kinetics of indomethacin were studied in the presence of the surfactants ethoxylated lanolin, polysorbate 80, and cetrimonium bromide under alkaline conditions at 30.3°. The degradation followed apparent first-order kinetics. Plots of k_{obs} *versus* surfactant concentrations were curved with negative slopes for nonionic surfactants; but with the ionic surfactant, the plots showed a marked positive change in k_{obs} as the surfactant concentration passed through the critical micelle concentration. Literature model systems adequately explained the data for nonionic surfactants but not for the ionic surfactant. A new set of equations was derived for each case using electrochemical potentials. The experimental data for all three surfactants fit the derived equations quite well.

Keyphrases □ Indomethacin—degradation kinetics in presence of ionic and nonionic surfactants in alkaline solutions □ Degradation kinetics—indomethacin in presence of ionic and nonionic surfactants in alkaline solutions □ Kinetics, degradation—indomethacin in presence of ionic and nonionic surfactants in alkaline solutions □ Surfactants, ionic and nonionic—effect on degradation kinetics of indomethacin in alkaline solutions □ Anti-inflammatory agents—indomethacin, degradation kinetics in presence of ionic and nonionic surfactants in alkaline solutions

In Part I of this series (1), indomethacin degradation in the presence of alkali was studied over a temperature range of 20.1–40.7°. The rate constant–hydroxyl-ion concentration profile was linear with a positive slope. Activation energies and other related parameters were calculated from Arrhenius-type plots. This report describes the effect of some added surfactants on the kinetics of degradation at one temperature.

EXPERIMENTAL

Materials—All materials were analytical grade, including indomethacin[1], sodium hydroxide, and sodium chloride. In addition, three surfactants were used: ethoxylated lanolin[2], polysorbate 80[3], and cetrimonium bromide[4]. The ethoxylated lanolin was obtained from lanolin containing 25 ethylene oxide units. Double-distilled water from an all-glass still was used throughout the study.

Kinetic Studies—Stock solutions of 2 mg of indomethacin/ml, 0.1 *M* sodium hydroxide, and 1% (w/v) surfactant were prepared. In all runs, 2 ml of stock indomethacin was used plus a fixed volume of sodium hydroxide (2, 3, or 5 ml) in an increasing concentration of surfactant up to 1%. All runs were made at 30.3° as described previously (1).

RESULTS AND DISCUSSION

Results for indomethacin degradation in the presence of the nonionic surfactants, ethoxylated lanolin and polysorbate 80, and in the presence of the ionic surfactant, cetrimonium bromide, are shown in Figs. 1 and 2, respectively.

Plots of k_{obs} *versus* surfactant concentration were usually curved, as with the nonionic surfactants (Fig. 1). However, with cetrimonium bromide (Fig. 2), there was a marked change in k_{obs} as the surfactant concentration passed through the critical micelle concentration (CMC). The CMC's of ethoxylated lanolin, polysorbate 80, and cetrimonium bromide are 7.15×10^{-5}, 8.20×10^{-4} (2), and 2.09×10^{-3} (% w/w), respectively, at 37°.

[1] Lot L-590, 229-00A108, Merck Sharp & Dohme, Rahway, N.J.
[2] Solulan 25, lot 108F, 4251, American Cholesterol Products Inc.
[3] Lot 1026-1740, Sigma Chemical Co.
[4] Imperial Chemical Industries Ltd.

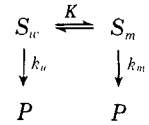

Scheme I

Model systems explaining chemical changes in the presence of micelle-forming surfactants usually have postulated that micelles formed in aqueous systems form a second phase into which reactants partition so that the ratio of concentrations in the micelle and water phases is a constant and that this equilibrium is maintained during chemical change. Rates of change are considered to be first order, as is usually observed in practice (Scheme I).

In this scheme, S_w and S_m represent the substrate in water and the micelle, respectively; C_w and C_m are corresponding concentrations of the substrate, which decomposes to product P both in water and in the micelle; k_w and k_m are rate constants for degradation of the substrate in water and the micelle, respectively; and the partition coefficient, K, is a ratio of C_m and C_w. Scheme I has led to several equations relating observed rates to postulated contributing rates (3–5). The following equation is essentially that of Winterborn *et al.* (4):

$$k_{obs} = \frac{k_w - k_w V + k_m K V}{1 - V + KV} \qquad \text{(Eq. 1)}$$

where k_{obs} is the observed rate constant related to the total amount of the substrate in the total volume; and V is the volume fraction of the micellar phase, which is given by the ratio of the volume of the micellar phase in milliliters, V_m, to the total volume in milliliters, V_T.

By rearrangement of Eq. 1:

$$k_{obs} = k_m + \frac{(1 - V)}{K}\frac{(k_w - k_{obs})}{V} \qquad \text{(Eq. 2)}$$

Since the highest concentration of surfactant used was 1%, the largest value of V is approximately 0.01. Thus, Eq. 2 simplifies to:

$$k_{obs} = k_m + \frac{1}{K}\frac{(k_w - k_{obs})}{V} \qquad \text{(Eq. 3)}$$

From Eq. 3, plots of k_{obs} *versus* $(k_w - k_{obs})/V$ should be linear with the intercept at zero surfactant concentration equal to k_m and the slope equal to $1/K$ (Figs. 3 and 4). Surfactant solutions (C_s) were prepared on a weight per volume basis. Conversion of C_s to V requires a knowledge of micelle phase density. Since it was not known, the density was arbitrarily taken as 1 g/cm³. Any error should not affect graph linearity.

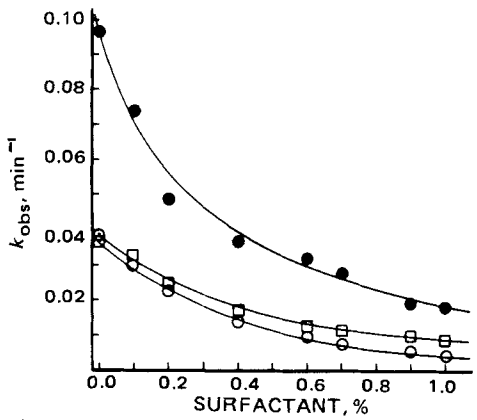

Figure 1—*Observed rate constant,* k_{obs}, versus *varying concentrations of surfactants in alkaline aqueous solutions at 30.3°. Key:* ○, *ethoxylated lanolin in 0.002* M *hydroxide-ion concentration;* ●, *ethoxylated lanolin in 0.005* M *hydroxide-ion concentration; and* □, *polysorbate 80 in 0.002* M *hydroxide-ion concentration.*

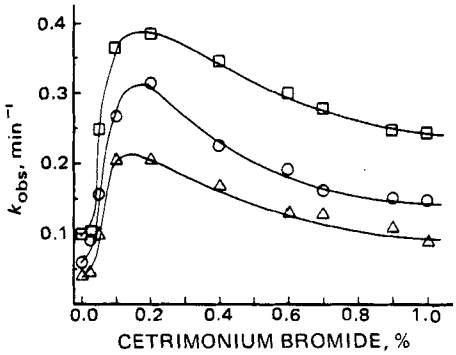

Figure 2—*Observed rate constant,* k_{obs}, versus *varying concentrations of cetrimonium bromide in alkaline aqueous solutions at 30.3°. Key (hydroxide-ion concentration):* △, *0.002* M; ○, *0.003* M; *and* □, *0.005* M.

Figure 3 shows that plots based on Eq. 4 were satisfactorily linear for the nonionic surfactants, but the plots show gross curvature for cetrimonium bromide (Fig. 4). Correcting for the fraction of surfactant not micellized (by subtracting the CMC from the total concentration) made no appreciable difference.

Values of k_m and K derived from the intercepts and slopes of Figs. 3 and 4 are given in Table I. Values of K, which depend upon the value used for micelle density, are unlikely to be grossly in error through use of the value 1 g/cm^3, and the choice permits comparisons to be made. The values of k_m and K derived for cetrimonium bromide are of low reliability, being obtained from the first portion of the curves, but are included for comparison. Some Eq. 3 values of k_m in Table I are negative, which is physically impossible. Such values may reflect experimental error or a model that does not account for all factors.

Divergence from model behavior may arise from false assumptions in model development or from neglect of some relevant factor. One assumption that should be questioned is the maintenance of an equilibrium between the substrate in the water phase and in the micelle. Studies of transfer rates in such cases (6) show that equilibria are rapidly established and that this factor is not likely to be relevant. The effects of micellar and substrate charges on the phase equilibrium are neglected in the model used. Even with the nonionic surfactants, indomethacin in the presence of sodium hydroxide is ionized, so solubilized molecules will confer a charge on the micelle.

For solubilized ions and charged micelles, an equilibrium between the phases depends on electrochemical potentials, not simply on chemical potentials. Thus, at equilibrium:

$$\bar{\mu}_{iw} = \bar{\mu}_{im} \qquad \text{(Eq. 4)}$$

where $\bar{\mu}_{iw}$ and $\bar{\mu}_{im}$ are electrochemical potentials of ion i in water and the micelle, respectively. The bulk of the water phase is arbitrarily assigned a zero potential, while the micelle has potential ϕ_m. When using molar concentrations, C_i, as approximations for activities and Z_i for ion valency, the following equation can be written (7):

$$\mu^\circ_{iw} + RT \ln C_{iw} = \mu^\circ_{im} + RT \ln C_{im} + Z_i F \phi_m \qquad \text{(Eq. 5)}$$

where F is the Faraday constant, R is the gas constant, and the μ°_i terms refer to standard ordinary chemical potentials. Upon rearrangement, Eq. 5 yields:

$$\frac{C_{im}}{C_{iw}} = \exp\left[-\left(\frac{1}{RT}\right)(\Delta\mu^\circ_i + Z_i F \phi_m)\right] \qquad \text{(Eq. 6)}$$

$$\frac{C_{im}}{C_{iw}} = K' \exp\left(-Z_i F \phi_m / RT\right) \qquad \text{(Eq. 7)}$$

The effect of charge and surfactant concentration on the right-hand side of Eq. 7 may be approximated on the basis of simplified colloid theory. Such a treatment (see *Appendix*) leads to expressions for $Z_i F \phi_m$ as follows.

For nonionic surfactants:

$$Z_i F \phi_m = \frac{K_1 K_2 n C_m}{A_m \sqrt{\Sigma C_{iw}}} \qquad \text{(Eq. 8)}$$

For the ionic surfactants:

$$Z_i F \phi_m = -\frac{K_1 n (1 - K_2 C_m)}{A_m \sqrt{(\Sigma C_{iw} + C_{is})}} \qquad \text{(Eq. 9)}$$

where n is the micelle aggregation number, A_m is the surface area of the micelle, ΣC_{iw} is the counterion concentration not derived from surfactant ions, C_{is} is the counterion concentration derived from the surfactant, and K_1 and K_2 (see *Appendix*) are constants.

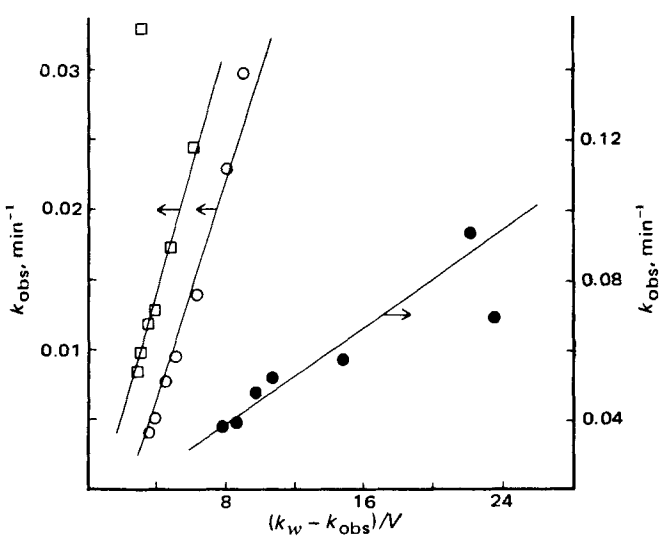

Figure 3—*Relationship between observed rate constants and function of the volume fraction of micelles. Key:* ○, *ethoxylated lanolin in 0.002* M *hydroxide-ion concentration;* ●, *ethoxylated lanolin in 0.005* M *hydroxide-ion concentration; and* □, *polysorbate 80 in 0.002* M *hydroxide-ion concentration.*

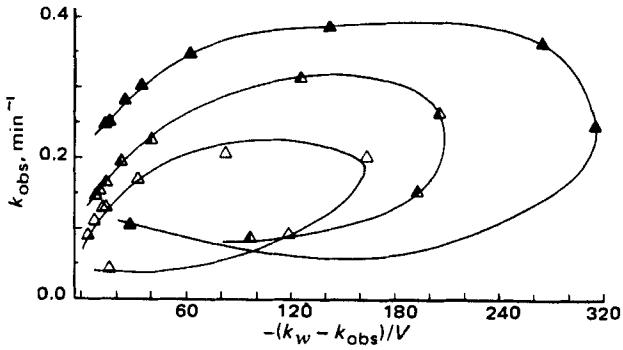

Figure 4—*Relationship between observed rate constants and function of volume fraction of cetrimonium bromide micelles. Key (hydroxide-ion concentration):* △, *0.002* M; ▲, *0.003* M; *and* ▲, *0.005* M.

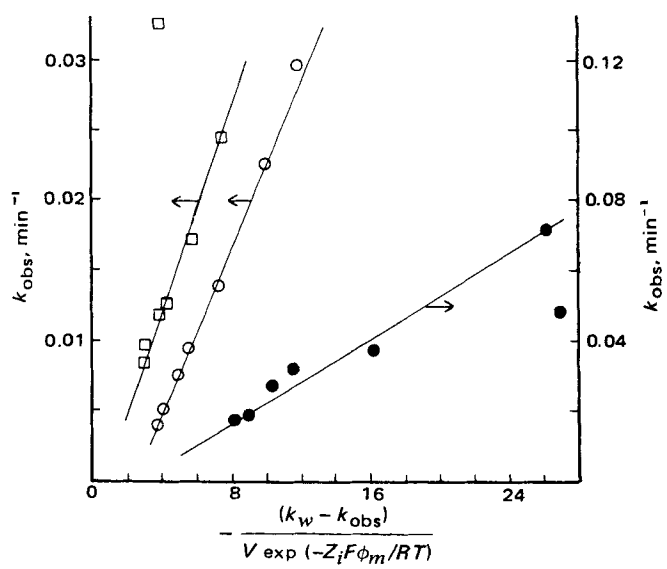

Figure 5—*Relationship between observed rate constants and the function of the micellar potential. Key:* ○, *ethoxylated lanolin in 0.002* M *hydroxide-ion concentration;* ●, *ethoxylated lanolin in 0.005* M *hydroxide-ion concentration; and* □, *polysorbate 80 in 0.002* M *hydroxide-ion concentration.*

Table I—Rate Constants (Minutes^{-1}) for Scheme I based on Eqs. 3 and 11 for Various Surfactants in Varying Concentrations of Hydroxide Ion

Surfactant	Hydroxide Ion, M	k_w	From Eq. 3 k_m	From Eq. 3 K (10^{-2})	From Eq. 11 k_m	From Eq. 11 K' (10^{-2})
Ethoxylated lanolin	0.002	0.039	−0.013	2.2	−0.007	2.9
	0.005	0.096	−0.012	2.7	−0.008	3.2
Polysorbate 80	0.002	0.036	−0.004	2.2	−0.001	3.0
Cetrimonium bromide	0.002	0.040	0.080	3.6	0.044	0.2
	0.003	0.061	0.120	3.5	0.071	0.2
	0.005	0.100	0.205	3.5	0.160	0.3

Table II—Observed First-Order Rate Constants for the Degradation of Indomethacin in Alkaline Solutions in the Presence of Varying Concentrations of Ethoxylated Lanolin at 30.3°

Surfactant Concentration, % (w/v)	Volume Fraction[a] of Micellar Phase (V)	Concentration[b] of Indomethacin in Micelles (C_m), M	$\frac{\exp(-Z_iF\phi_m)}{RT}$	k_{obs}, min^{-1}
	In Presence of 0.002 M NaOH			
0	0	0	—	3.85×10^{-2} [c]
0.1	0.001	0.027	0.77	2.96×10^{-2}
0.2	0.002	0.022	0.81	2.27×10^{-2}
0.4	0.004	0.016	0.86	1.39×10^{-2}
0.6	0.006	0.012	0.98	9.50×10^{-3}
0.7	0.007	0.011	0.90	7.64×10^{-3}
0.9	0.009	0.009	0.92	5.13×10^{-3}
1.0	0.010	0.008	0.92	4.06×10^{-3}
	In Presence of 0.005 M NaOH			
0	0	0	—	9.63×10^{-2} [c]
0.1	0.001	0.029	0.84	7.37×10^{-2}
0.2	0.002	0.023	0.87	4.88×10^{-2}
0.4	0.004	0.016	0.91	3.65×10^{-2}
0.6	0.006	0.012	0.93	3.21×10^{-2}
0.7	0.007	0.011	0.94	2.77×10^{-2}
0.9	0.009	0.009	0.95	1.90×10^{-2}
1.0	0.010	0.008	0.95	1.82×10^{-2}

[a] Assuming micellar density = 1. [b] From Eq. 10. [c] k_w.

The "uncharged" partition coefficient, K of Eq. 7, is equivalent to exp $(-\Delta\mu°/RT)$ and is a constant, so it does not change. The value of C_{im}/C_{iw} of Eq. 7 will be decreased with nonionic surfactants because of the sign of $Z_iF\phi_m$ and will be increased with the ionic surfactant because C_m in Eq. 8 depends on C_s (see *Appendix*) and is given by:

$$C_m = \frac{K'C_T \exp(-Z_iF\phi_m/RT)}{1 - V + KV \exp(-Z_iF\phi_m/RT)} \qquad \text{(Eq. 10)}$$

where the value of $Z_iF\phi_m$ is obtained from either Eq. 8 or 9, depending upon whether the surfactant is nonionic or ionic. Because ϕ_m contains C_m, an iterative calculator program was used for evaluation of C_m from Eq. 10. It is also necessary to assume a value for K to solve Eq. 10. Tables II–IV show values for $\exp(-Z_iF\phi_m/RT)$.

The "charged" partition coefficient, K' exp $(-Z_iF\phi_m/RT)$ of Eq. 7, corresponds to partition coefficient K of Eqs. 1–3 and should replace it.

Table III—Observed First-Order Rate Constants for the Degradation of Indomethacin in 0.002M NaOH in the Presence of Varying Concentrations of Polysorbate 80 at 30.3°

Surfactant Concentration, % (w/v)	Volume Fraction[a] of Micellar Phase (V)	Concentration[b] of Indomethacin in Micelles (C_m), M	$\frac{\exp(-Z_iF\phi_m)}{RT}$	k_{obs}, min^{-1}
0	0	0	—	3.56×10^{-2} [c]
0.1	0.001	0.027	0.77	3.29×10^{-2}
0.2	0.002	0.022	0.81	2.44×10^{-2}
0.4	0.004	0.016	0.86	1.71×10^{-2}
0.6	0.006	0.012	0.89	1.26×10^{-2}
0.7	0.007	0.011	0.90	1.18×10^{-2}
0.9	0.009	0.009	0.92	9.74×10^{-3}
1.0	0.010	0.008	0.92	8.38×10^{-3}

[a] Assuming micellar density = 1. [b] From Eq. 10. [c] k_w.

Table IV—Observed First-Order Rate Constants for the Degradation of Indomethacin in Alkaline Solutions in the Presence of Varying Concentrations of Cetrimonium Bromide at 30.3°

Surfactant Concentration, % (w/v)	Volume Fraction[a] of Micellar Phase (V)	Concentration[b] of Indomethacin in Micelles (C_m), M	$\frac{\exp(-Z_iF\phi_m)}{RT}$	k_{obs}, min^{-1}
	In Presence of 0.002 M NaOH			
0	0	0		4.01×10^{-2} [c]
0.025	0.00025	0.21	210	4.39×10^{-2}
0.05	0.0005	0.12	140	9.90×10^{-2}
0.1	0.001	0.058	69	2.04×10^{-1}
0.2	0.002	0.027	30	2.04×10^{-1}
0.4	0.004	0.013	13	1.69×10^{-1}
0.6	0.006	0.0096	8.8	1.28×10^{-1}
0.7	0.007	0.007	7.6	1.28×10^{-1}
0.9	0.009	0.006	6.1	1.08×10^{-1}
1.0	0.01	0.005	5.6	8.89×10^{-2}
	In Presence of 0.003 M NaOH			
0	0	0		6.13×10^{-2}
0.025	0.00025	0.14	110	8.45×10^{-2} [c]
0.05	0.0005	0.088	79	1.58×10^{-1}
0.1	0.001	0.049	47	2.67×10^{-1}
0.2	0.002	0.025	24	3.15×10^{-1}
0.4	0.004	0.012	12	2.24×10^{-1}
0.6	0.006	0.008	8.3	1.93×10^{-1}
0.7	0.007	0.007	7.2	1.62×10^{-1}
0.9	0.009	0.006	5.9	1.51×10^{-1}
1.0	0.01	0.005	5.4	1.48×10^{-1}
	In Presence of 0.005 M NaOH			
0	0	0		1.00×10^{-1}
0.025	0.00025	0.075	46	1.07×10^{-1} [c]
0.05	0.0005	0.056	38	2.48×10^{-1}
0.1	0.001	0.036	28	3.65×10^{-1}
0.2	0.002	0.021	18	3.85×10^{-1}
0.4	0.004	0.011	10	3.47×10^{-1}
0.6	0.006	0.008	7.5	3.01×10^{-1}
0.7	0.007	0.007	6.7	2.77×10^{-1}
0.9	0.009	0.006	5.5	2.48×10^{-1}
1.0	0.01	0.005	5.2	2.48×10^{-1}

[a] Assuming micellar density = 1. [b] From Eq. 10. [c] k_w.

Equation 3 can now be rewritten (combining Eqs. 7 and 3) as:

$$k_{obs} = k_m + \frac{1}{K'} \frac{(k_w - k_{obs})}{V \exp(-Z_iF\phi_m/RT)} \qquad \text{(Eq. 11)}$$

Plots of k_{obs} *versus* $(k_w - k_{obs})/V \exp(-Z_iF\phi_m/RT)$ were satisfactorily linear and much improved (Figs. 5 and 6) over plots of k_{obs} *versus* $(k_w - k_{obs})/V$ for cetrimonium bromide results (compare Figs. 4 and 6). The

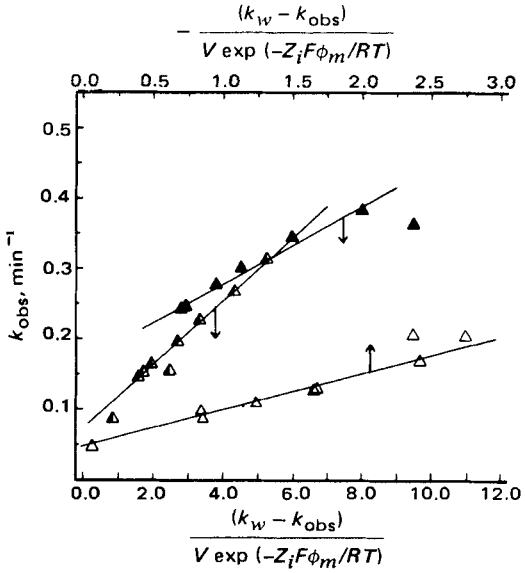

Figure 6—*Relationship between observed rate constants and function of cetrimonium bromide micellar potential. Key (hydroxide-ion concentration):* △, *0.002* M; ▲, *0.003* M; *and* ▲, *0.005* M.

intercept gave the value of k_m, and the slope was equal to $1/K'$. A repeat of the calculation process using the K' values obtained from these plots only slightly altered the values of the constants (Table I).

Values of k_m obtained in this way are near zero for nonionic surfactants, consistent with the absence of a rate increase in the presence of surfactants for indomethacin decomposition. Values of k_m obtained for the ionic surfactant are larger than k_u values but not greatly so.

Negligibly low micellar rates for nonionic surfactants are a result of the near zero k_m values. The rate constant k_m is a composite quantity, containing $k_m{}^0[OH^-]$, $k_m{}^0$ being the value at unit hydroxide-ion concentration. The micellar concentration of hydroxide ion must be near zero through repulsion of this ion by the negative charge conferred on the nonionic surfactant micelles through solubilization of ionized indomethacin.

Values of the partition coefficient K obtained for nonionic surfactants are considerably larger than those obtained for the ionic surfactant. This unexpected result may be due to the simplifications and assumptions made in the derivation. For C_m and k_m also, the simplifications and assumptions mean that no great reliance can be placed on their numerical values. Nevertheless, the improvements in plot linearity, especially for the ionic surfactant, support the general approach and stimulate further work to evaluate unknown quantities and to test the hypothesis more rigorously.

APPENDIX

Assumptions—Several assumptions were made to permit calculation:

1. The micelle phase density was 1 g/ml in all cases.
2. The surfactant molecular weights were: ethoxylated lanolin, 1500; polysorbate 80, 1300; and cetrimonium bromide, 360 (on the basis of the approximate composition).
3. The initial K' values chosen were 300 for nonionic surfactants and 200 for cetrimonium bromide [literature values vary from 20 to 5000 (4, 8, 9)].
4. The CMC value of a surfactant was a negligible proportion of the total surfactant concentration.
5. Indomethacin was completely ionized.
6. Micelles are spherical. The volume of a micelle, V_{m1}, is given by:

$$V_{m1} = \frac{4\pi r^3}{3} \qquad \text{(Eq. A1)}$$

where r is the radius of the micelle. The volume of a micelle also can be obtained as:

$$V_{m1} = \frac{Mn}{N\rho_m} \qquad \text{(Eq. A2)}$$

where M is the molecular weight of the surfactant, n is the aggregation number, N is Avogadro's number, and ρ_m is the density of a micelle. Equations A1 and A2 yield:

$$r = \left(\frac{3nM}{4\pi N\rho_m}\right)^{1/3} \qquad \text{(Eq. A3)}$$

Since the surface area of a sphere is given by $4\pi r^2$, the surface area of a micelle, A_m, is then given by:

$$A_m = 4\pi\left[\frac{3nM}{4\pi N\rho_m}\right]^{2/3} \qquad \text{(Eq. A4)}$$

7. The micelle aggregation numbers are 100 for nonionic surfactants and 50 for cetrimide (9).
8. Hydroxide ions are not specifically adsorbed.
9. As a result of counterion adsorption into the stern layer, the effective value of $Z_iF\phi_m$ is reduced to one-fifth of the value given by Eq. A13 for nonionic surfacts and to one-tenth of the value given by Eq. A14 for the more highly charged cetrimonium bromide micelles (10).

Derivation of Eqs. 8 and 9—The surface charge density, σ, of the double layer around a spherical particle is given by (11):

$$\sigma = \frac{\chi\epsilon}{4\pi}\psi_\alpha \qquad \text{(Eq. A5)}$$

where ψ_α is the electrical potential, ϵ is the dielectric potential, and the quantity $1/\chi$ is a rough measure of the thickness of the double layer, δ (12). Treating a micelle as a charged spherical colloidal particle and applying and rearranging Eq. A5 give micelle potential ϕ_m (in place of ψ_α) as:

$$\phi_m = \frac{4\pi\delta\sigma_m}{\epsilon} \qquad \text{(Eq. A6)}$$

where σ_m is the surface charge density and ϵ is the dielectric constant for water. Double layer thickness, δ, is given by (13):

$$\delta = \frac{K_3}{(|Z|\sqrt{\Sigma C_{iw} + C_{is}})} \qquad \text{(Eq. A7)}$$

where K_3 is a combination of fundamental constants and temperature [$K_1 = 4\pi K_3 eF/\epsilon = 1.44 \times 10^6$; $K_2 = 0.1VM/C_s = 10^{-3}\,M/\rho_m = 1.5$ for ethoxylated lanolin, 1.3 for polysorbate 80, and 0.36 for cetrimonium bromide; and $K_3 = \{\epsilon kT/[(8\pi e^2)(6.02 \times 10^{20})]\}^{1/2} = 4.97 \times 10^{-9}$], Z is the counterion valency, and C_{iw} and C_{is} are molar concentrations of counterions in water and the surfactant, respectively.

The surface charge density of the micelle, σ_m, can be obtained from the ratio of the total charge on all ions in the micelle surface to the micellar surface area, A_m. If Z_s is the charge on the surfactant ions (n in the micelle) and if Z_i is the charge on the number of counterions, then:

$$\sigma_m = \frac{ne}{A_m}\left(Z_s + \frac{0.001\Sigma Z_i V_m C_{im} N}{n\nu}\right) \qquad \text{(Eq. A8)}$$

where n is the micelle aggregation number, e is the electronic charge, V_m is the volume of micellar phase, ν is the number of micelles, N is Avogadro's number, and C_{im} is the molar concentration of counterions in micelles.

The number of micelles, ν, in the total volume, V_T, is given by:

$$\nu = \frac{NC_sV_T}{100Mn} \qquad \text{(Eq. A9)}$$

where M is the molecular weight of the surfactant, and C_s is the surfactant concentration. Substitution of Eq. A9 into Eq. A8 gives:

$$\sigma_m = \frac{ne}{A_m}\left(Z_s + \frac{0.1MV}{C_s}\Sigma Z_i C_{im}\right) \qquad \text{(Eq. A10)}$$

Since all ions are univalent in this work, Eq. A10 reduces to:

$$\sigma_m = \frac{ne}{A_m}(Z_s + K_2\Sigma C_{im}) \qquad \text{(Eq. A11)}$$

Combining Eqs. A6, A7, and A11 yields:

$$\phi_m = \frac{4\pi K_3 ne}{\epsilon A_m}\left(\frac{Z_s + K_2\Sigma C_{im}}{\sqrt{\Sigma C_{iw} + C_{is}}}\right) \qquad \text{(Eq. A12)}$$

Multiplying each side by Z_iF and combining constant terms yield:

$$Z_iF\phi_m = \frac{K_1 n}{A_m}\left(\frac{Z_s + K_2 C_{im}}{\sqrt{\Sigma C_{iw} + C_{is}}}\right) \qquad \text{(Eq. A13)}$$

The sign of $Z_iF\phi_m$ will be a combination of the signs of Z_i and ϕ_m. Since the solubilization of indomethacin ions is considered here, Z_i is negative. For the nonionic micelles, incorporation of indomethacin ions makes ϕ_m negative so that $Z_iF\phi_m$ is positive. For positively charged surfactant ions, solubilization alters the total charge but is unlikely to alter its sign. Therefore, for cetrimonium bromide micelles, $Z_iF\phi_m$ is negative.

Equation A13 can be put into a more useful form if the values for Z_s, C_{is}, ΣC_{im}, and ΣC_{iw} can be obtained for nonionic and ionic surfactants.

Values for Z_s—For nonionic surfactants, $Z_s = 0$. For ionic surfactants, $Z_s = +1$.

Values for C_{is}—For nonionic surfactants, $C_{is} = 0$. For ionic surfactants, $C_{is} = C_s$.

Value for ΣC_{im}—Since the only ion likely to be solubilized is that of indomethacin, $\Sigma C_{im} = C_m$.

Value for ΣC_{iw}—For nonionic or ionic surfactants, the value of C_{iw} could be found using:

$$C_T = VC_m + (1 - V)C_w \qquad \text{(Eq. A14)}$$

where C_m, C_w, and C_T are the concentrations of indomethacin in the micelle, water, and the total volume, respectively.

Solving for C_w yields:

$$C_w = \frac{(C_T - VC_m)}{1 - V} \qquad \text{(Eq. A15)}$$

Since the highest value of V in this study is 0.01, then:

$$C_w = C_T - VC_m \qquad \text{(Eq. A16)}$$

Since:

$$\Sigma C_{iw} = C_{NaOH} + C_w \qquad \text{(Eq. A17)}$$

for ionic surfactants and:

$$\Sigma C_{iw} = C_w \qquad \text{(Eq. A18)}$$

for nonionic surfactants, substituting Eq. A16 in Eqs. A17 and A18 yields:

$$\Sigma C_{iw} = C_{NaOH} + C_T - VC_m \quad \text{(Eq. A19)}$$

for ionic surfactants and:

$$\Sigma C_{iw} = C_T - VC_m \quad \text{(Eq. A20)}$$

for nonionic surfactants.

By substituting values for Z_s, C_{is}, ΣC_{im}, and ΣC_{iw}, Eq. A13 is reduced to:

$$Z_i F\phi_m = \frac{K_1 K_2 n C_m}{A_m\sqrt{C_T - VC_m}} \quad \text{(Eq. A21)}$$

for nonionic surfactants and:

$$Z_i F\phi_m = -\frac{K_1 n(1 + K_2 C_m)}{A_m\sqrt{C_{NaOH} + C_T - VC_m + C_s}} \quad \text{(Eq. A22)}$$

for the ionic surfactant. Equations A21 and A22 are equivalent to Eqs. 8 and 9.

Evaluation of C_m (Derivation of Eq. 10)—The value for C_m can be obtained as follows. Since the only ion likely to be solubilized is that of indomethacin, then $C_{im} = C_m$ and $C_{iw} = C_w$. When solving Eq. 7 for C_w:

$$C_w = \frac{C_m}{K' \exp(-Z_i F\phi_m/RT)} \quad \text{(Eq. A23)}$$

Equation A23 is equal to Eq. A15. Solving for C_m yields Eq. 10.

REFERENCES

(1) B. R. Hajratwala and J. E. Dawson, *J. Pharm. Sci.*, **66**, 27 (1977).

(2) B. R. Hajratwala and H. Taylor, *J. Pharm. Pharmacol.*, in press.

(3) E. J. Fendler and H. J. Fendler, in "Advances in Physical Organic Chemistry," vol. 8, 5th ed., V. Gold, Ed., Academic, New York, N.Y., 1970, pp. 271–406.

(4) I. K. Winterborn, B. J. Meakin, and D. J. G. Davies, *J. Pharm. Sci.*, **63**, 64 (1974).

(5) G. D. Smith, D. R. Kennedy, and J. G. Nairn, *ibid.*, **63**, 712 (1974).

(6) M. Gibaldi, S. Feldman, and N. D. Weiner, *ibid.*, **58**, 132 (1969).

(7) J. T. Davies and E. K. Rideal, "Interfacial Phenomena," Academic, New York, N.Y., 1961, p. 60.

(8) A. G. Mitchell and J. F. Broadhead, *J. Pharm. Sci.*, **56**, 1261 (1967).

(9) K. Shinoda, T. Nakagawa, B. Tamamushi, and T. Isemur, "Colloidal Surfactants," Academic, New York, N.Y., 1963, pp. 20, 120.

(10) *Ibid.*, p. 22.

(11) E. J. W. Verwey and J. T. G. Overbeek, "Theory of the Stability of Lyophobic Colloids," Elsevier, New York, N.Y., 1948, p. 38.

(12) *Ibid.*, p. 30.

(13) K. J. Mysels, "Introduction to Colloid Chemistry," Interscience, New York, N.Y., 1959, p. 328.

ACKNOWLEDGMENTS AND ADDRESSES

Received November 18, 1975, from the *Department of Pharmacy, University of Otago, Dunedin, New Zealand.*

Accepted for publication November 9, 1976.

Grateful acknowledgment is made to the New Zealand Medical Research Council for providing a Summer Student Scholarship to Mrs. J. E. Dawson.

[x] To whom inquiries should be directed.

High-Pressure Liquid Chromatographic–Mass Spectrometric Determination of Δ^9-Tetrahydrocannabinol in Human Plasma following Marijuana Smoking

J. L. VALENTINE [x], PAUL J. BRYANT, PAUL L. GUTSHALL, OWEN H. M. GAN, PATRICIA D. LOVEGREEN, EVERETT D. THOMPSON, and HSIEN CHI NIU

Abstract □ A method was developed for analyzing Δ^9-tetrahydrocannabinol (I), a psychotomimetic constituent found in marijuana smoke. The developed method utilizes a high-pressure liquid chromatographic (HPLC) gradient elution program to separate I from the other major cannabinoids in marijuana smoke. To achieve the sensitivity required to detect I in human plasma following marijuana smoking, a mass spectrometric quantification method was developed to analyze the HPLC eluant. To 1 ml of human plasma was added a known amount of internal standard, trideuterated I. This stable isotope provided a check on extraction efficiency, a marker for UV monitoring of the HPLC effluent and subsequent collection, and a convenient mass for mass spectrometric quantification. An ion-counting techique was used in conjunction with the peak matching accessory of the mass spectrometer to provide for a rapid comparison between molecular ions of I and the internal standard. The method was linear, accurate, and reproducible over the concentration range expected for I in plasma following marijuana smoking; 2.5 ng/ml was the lower practical limit of detection. Plasma from 11 male subjects was analyzed by the method at appropriate intervals up to 24 hr after the smoking of a marijuana cigarette containing 10.8 mg of I. Results demonstrated that levels of I could be determined accurately in the plasma of marijuana smokers in the 1-hr period following smoking.

Keyphrases □ Δ^9-Tetrahydrocannabinol—high-pressure liquid chromatographic–mass spectrometric analysis, human plasma after smoking marijuana □ High-pressure liquid chromatography–mass spectrometry—analysis, Δ^9-tetrahydrocannabinol, human plasma after smoking marijuana □ Marijuana constituents—Δ^9-tetrahydrocannabinol, high-pressure liquid chromatographic–mass spectrometric analysis, human plasma after smoking marijuana □ Psychotomimetic agents—Δ^9-tetrahydrocannabinol, high-pressure liquid chromatographic–mass spectrometric analysis, human plasma after smoking marijuana

Marijuana smoking is quite prevalent in certain segments of the populace in the United States (1). Most marijuana contains four principal constituents (2): Δ^9-tetrahydrocannabinol (I), cannabidiol (II), cannabinol (III), and cannabichromene (IV). Compound I is believed to be responsible for the psychotomimetic properties of marijuana (3). Some of the physiological responses in humans were shown to change following smoking of cigarettes

for nonionic surfactants, substituting Eq. A16 in Eqs. A17 and A18 yields:

$$\Sigma C_{iw} = C_{NaOH} + C_T - VC_m \quad \text{(Eq. A19)}$$

for ionic surfactants and:

$$\Sigma C_{iw} = C_T - VC_m \quad \text{(Eq. A20)}$$

for nonionic surfactants.

By substituting values for Z_s, C_{is}, ΣC_{im}, and ΣC_{iw}, Eq. A13 is reduced to:

$$Z_i F\phi_m = \frac{K_1 K_2 n C_m}{A_m\sqrt{C_T - VC_m}} \quad \text{(Eq. A21)}$$

for nonionic surfactants and:

$$Z_i F\phi_m = -\frac{K_1 n(1 + K_2 C_m)}{A_m\sqrt{C_{NaOH} + C_T - VC_m + C_s}} \quad \text{(Eq. A22)}$$

for the ionic surfactant. Equations A21 and A22 are equivalent to Eqs. 8 and 9.

Evaluation of C_m (Derivation of Eq. 10)—The value for C_m can be obtained as follows. Since the only ion likely to be solubilized is that of indomethacin, then $C_{im} = C_m$ and $C_{iw} = C_w$. When solving Eq. 7 for C_w:

$$C_w = \frac{C_m}{K' \exp(-Z_i F\phi_m/RT)} \quad \text{(Eq. A23)}$$

Equation A23 is equal to Eq. A15. Solving for C_m yields Eq. 10.

REFERENCES

(1) B. R. Hajratwala and J. E. Dawson, *J. Pharm. Sci.*, **66**, 27 (1977).

(2) B. R. Hajratwala and H. Taylor, *J. Pharm. Pharmacol.*, in press.

(3) E. J. Fendler and H. J. Fendler, in "Advances in Physical Organic Chemistry," vol. 8, 5th ed., V. Gold, Ed., Academic, New York, N.Y., 1970, pp. 271–406.

(4) I. K. Winterborn, B. J. Meakin, and D. J. G. Davies, *J. Pharm. Sci.*, **63**, 64 (1974).

(5) G. D. Smith, D. R. Kennedy, and J. G. Nairn, *ibid.*, **63**, 712 (1974).

(6) M. Gibaldi, S. Feldman, and N. D. Weiner, *ibid.*, **58**, 132 (1969).

(7) J. T. Davies and E. K. Rideal, "Interfacial Phenomena," Academic, New York, N.Y., 1961, p. 60.

(8) A. G. Mitchell and J. F. Broadhead, *J. Pharm. Sci.*, **56**, 1261 (1967).

(9) K. Shinoda, T. Nakagawa, B. Tamamushi, and T. Isemur, "Colloidal Surfactants," Academic, New York, N.Y., 1963, pp. 20, 120.

(10) *Ibid.*, p. 22.

(11) E. J. W. Verwey and J. T. G. Overbeek, "Theory of the Stability of Lyophobic Colloids," Elsevier, New York, N.Y., 1948, p. 38.

(12) *Ibid.*, p. 30.

(13) K. J. Mysels, "Introduction to Colloid Chemistry," Interscience, New York, N.Y., 1959, p. 328.

ACKNOWLEDGMENTS AND ADDRESSES

Received November 18, 1975, from the *Department of Pharmacy, University of Otago, Dunedin, New Zealand.*

Accepted for publication November 9, 1976.

Grateful acknowledgment is made to the New Zealand Medical Research Council for providing a Summer Student Scholarship to Mrs. J. E. Dawson.

[x] To whom inquiries should be directed.

High-Pressure Liquid Chromatographic–Mass Spectrometric Determination of Δ^9-Tetrahydrocannabinol in Human Plasma following Marijuana Smoking

J. L. VALENTINE [x], PAUL J. BRYANT, PAUL L. GUTSHALL, OWEN H. M. GAN, PATRICIA D. LOVEGREEN, EVERETT D. THOMPSON, and HSIEN CHI NIU

Abstract □ A method was developed for analyzing Δ^9-tetrahydrocannabinol (I), a psychotomimetic constituent found in marijuana smoke. The developed method utilizes a high-pressure liquid chromatographic (HPLC) gradient elution program to separate I from the other major cannabinoids in marijuana smoke. To achieve the sensitivity required to detect I in human plasma following marijuana smoking, a mass spectrometric quantification method was developed to analyze the HPLC eluant. To 1 ml of human plasma was added a known amount of internal standard, trideuterated I. This stable isotope provided a check on extraction efficiency, a marker for UV monitoring of the HPLC effluent and subsequent collection, and a convenient mass for mass spectrometric quantification. An ion-counting techique was used in conjunction with the peak matching accessory of the mass spectrometer to provide for a rapid comparison between molecular ions of I and the internal standard. The method was linear, accurate, and reproducible over the concentration range expected for I in plasma following marijuana smoking; 2.5 ng/ml was the lower practical limit of detection. Plasma from 11 male subjects was analyzed by the method at appropriate intervals up to 24 hr after the smoking of a marijuana cigarette containing 10.8 mg of I. Results demonstrated that levels of I could be determined accurately in the plasma of marijuana smokers in the 1-hr period following smoking.

Keyphrases □ Δ^9-Tetrahydrocannabinol—high-pressure liquid chromatographic–mass spectrometric analysis, human plasma after smoking marijuana □ High-pressure liquid chromatography–mass spectrometry—analysis, Δ^9-tetrahydrocannabinol, human plasma after smoking marijuana □ Marijuana constituents—Δ^9-tetrahydrocannabinol, high-pressure liquid chromatographic–mass spectrometric analysis, human plasma after smoking marijuana □ Psychotomimetic agents—Δ^9-tetrahydrocannabinol, high-pressure liquid chromatographic–mass spectrometric analysis, human plasma after smoking marijuana

Marijuana smoking is quite prevalent in certain segments of the populace in the United States (1). Most marijuana contains four principal constituents (2): Δ^9-tetrahydrocannabinol (I), cannabidiol (II), cannabinol (III), and cannabichromene (IV). Compound I is believed to be responsible for the psychotomimetic properties of marijuana (3). Some of the physiological responses in humans were shown to change following smoking of cigarettes

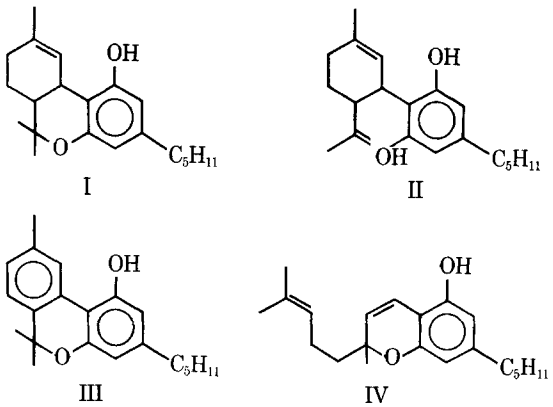

containing I, and these changes correlated with plasma levels of I and its metabolites (4). However, such studies were performed using radiolabeled I since no methods were available for plasma assays. More recently, methods such as GLC (5, 6), GLC–mass spectrometry (7, 8), and radioimmunoassay (9, 10) were proposed for the analysis of I in plasma.

The present method utilizes a high-pressure liquid chromatographic (HPLC)–mass spectrometric technique for determining nanogram per milliliter quantities of I in human plasma. Problems associated with direct coupling of the liquid chromatograph to the mass spectrometer (10) are circumvented. Fractions of the mobile phase emanating from the liquid chromatograph are collected and subsequently analyzed *via* the direct insertion probe of the mass spectrometer.

Inherent in this method is the use of a stable deuterated isotope of I for controlling extraction efficiency, as a marker for collection of the HPLC effluent, and as an internal standard for mass spectrometric quantification. Thus, the plasma has enough internal standard added to allow its detection by a UV spectrophotometer connected to the output of the liquid chromatograph. Once the internal standard is detected, fractions of the mobile phase eluant are collected and introduced *via* the direct insertion probe of the mass spectrometer for quantification.

This method was validated for I over a concentration range of 1–100 ng/ml in human plasma. Prior studies (4, 7–9) indicated that this range was expected for plasma levels of I following the smoking of cigarettes containing I. The new assay method was then used to determine plasma I levels in 11 male volunteers during 24 hr following the smoking of a marijuana cigarette.

EXPERIMENTAL

HPLC—All HPLC analyses were conducted on a gradient elution instrument[1] utilizing a recording spectrophotometer[2] set at 273.7 nm and a 10-μm silica gel, 25-cm × 2-mm (i.d.) column[3]. A gradient elution program was developed using heptane and methylene chloride. To separate the cannabinoids satisfactorily as well as to assure accurate mass spectrometric quantitation, it was necessary to record routinely the UV spectrum of each lot of heptane and methylene chloride prior to its use. Only lots that gave minimum absorbance in the 260–280-nm region were used.

A gradient elution program was used starting from 95:5% and proceeding to 5:95% heptane–methylene chloride over 9 min. The program was reversed, *i.e.*, from 5:95% to the initial 95:5% heptane–methylene chloride mixture, thereby regenerating the column. A solvent flow rate of 120 ml/hr was used for all determinations. Using these conditions, both I and its stable isotope, trideuterated I, had a retention time of 4.8 min or appeared at a gradient elution mixture of 53:48% methylene chloride–heptane. The other major constituents of marijuana, II, III, and IV, had retention times of 4.3, 4.5, and 5.6 min, respectively (Fig. 1).

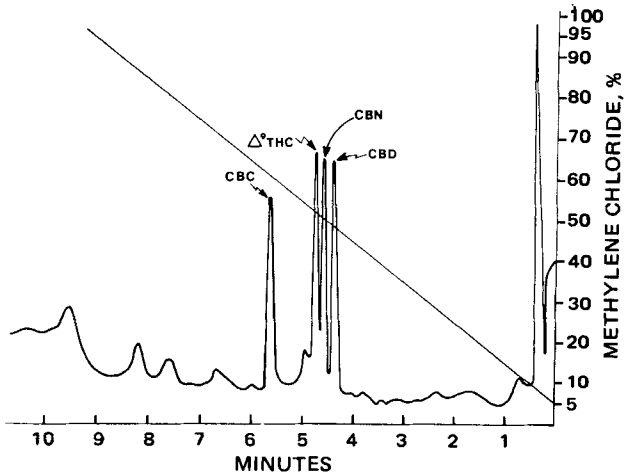

Figure 1—*HPLC analysis of pooled human plasma from nonsmokers to which 1.0 μg of II (CBD), 0.25 μg of III (CBN), 1.0 μg of I (Δ⁹-THC), and 0.25 μg of IV (CBC) were added.*

The amount of I-d_3 added to the plasma was sufficient to allow UV detection of total I (labeled plus unlabeled) as it eluted from the column. A 10-cm "zero dead volume" stainless steel tube was attached to the flowcell of the spectrophotometer to facilitate collection of the effluent droplets almost instantaneously after detection in the flowcell.

Mass Spectrometric Quantification—All mass spectrometric analyses were accomplished using a high-resolution, double-focusing mass spectrometer[4]. A new ion-counting technique was developed in conjunction with the peak matching accessory of the mass spectrometer, which provided for a rapid comparison between data from the molecular ion of the internal standard (*m/e* 317) and the assayed compound (*m/e* 314). Each sample coming from the liquid chromatograph was introduced into the mass spectrometer *via* the direct insertion probe, and the instrument initially was focused on *m/e* 317. Then, through the action of the peak matching unit and with a resolution of 2500, it was alternately focused to *m/e* 314.

As this alternation from *m/e* 317 to 314 occurred, the number of ion counts for each compound was recorded and stored in two registers of a dedicated computer[5]. This unit summed the number of ion events occurring in both *m/e* 314 and 317 and stored them in two registers (A and B). Thus, a running total of ions detected from the *m/e* 317 internal standard and the unknown amount of *m/e* 314 were stored separately by the counter. The peak matching accessory was set to dwell for 67 msec on each mass before alternating to the other mass. A time of 67 msec was required to sweep each mass peak across the electron multiplier.

A total counting time of 67 sec combined with a probe temperature of 65° gave optimum results. The probe temperature was programmed from ambient to 65° within 2 sec. Thus, in 67 sec, the alternating cycle was repeated 500 times, yielding 1000 bits of data for comparison and quantification. With time, the sample was depleted, but the ratio based on the internal standard remained linear and provided dependable quantification.

Linear plots were obtained from a computer-plotter[6] by using the data from Register B (*m/e* 314) for the ordinate and from Register A (*m/e* 317) for the abscissa and determining the least-squares best straight line. The slope of the line gives the *m/e* 314–317 ratio, which can be multiplied by the amount of internal standard added to get the concentration of I. In actual practice, the stable isotope compound used[7] contained a small amount of I. A mass spectrometric determination of the amount of *m/e* 314 in the internal standard was made by analyzing 10 samples of 1.6 μg of I-d_3 that had been added to 1 ml of plasma (Table I). This value for

[1] Varian 8520 liquid chromatograph.
[2] Varian 635M UV-visible spectrophotometer.
[3] Varian Si-10.
[4] Varian MAT model SM1-B.
[5] Princeton Applied Research, model SSR 1110.
[6] Hewlett-Packard model 9820A.
[7] Obtained from Research Triangle Institute through the National Institute on Drug Abuse. The trideuterated label was in the 11-position.

Table I—Precision and Accuracy in Recovery of I Added to Human Plasma

Added, ng/ml	Found[a], ng/ml	*n*	±*RSD*	*RE*
0	11.3 (9.35–13.6)[b]	10	11.15	—
1	1.2 (0.6–1.5)	3	43.3	20.0
5	4.5 (4.0–4.7)	3	9.0	−11.12
10	10.5 (9.5–12.4)	10	10.0	5.0
20	20.0 (19.1–21.1)	3	5.14	0.0
40	41.2 (39.6–42.5)	3	3.58	3.0
60	62.1 (61.3–62.8)	3	1.26	3.5
80	82.8 (74.9–90.7)	3	9.55	3.5
100	103.7 (99.3–106.0)	3	3.65	3.7
	Average percent recovered = 103.8			

[a] Average (range) of *n* determinations. [b] This value represents the amount of I found in 1.6 μg of the internal standard. Other values are corrected for this amount.

I in the internal standard was subtracted from the amount of I found in the assayed samples to give the actual found value.

Methods of Plasma Analysis—All glassware was silylated using a reported method (11). Whole blood was centrifuged at 2600 rpm for 20 min to obtain plasma. To 1 ml of plasma was added 1.6 μg of I-d_3 (0.5 ml of a 3.2-μg/ml solution in methanol) followed by extraction three times, using 2 ml of petroleum ether for each extraction. The extracts were combined and evaporated to dryness under nitrogen at room temperature. The resultant residue was reconstituted in 300 μl of heptane, and the entire solution was injected into the liquid chromatograph.

A 100-μl wash of heptane was used on the vessel containing the extracts; it was also injected into the chromatograph, and the gradient elution program previously described was used for separation. When the peak for combined I and I-d_3 was observed on the recorder, the eluant was collected in a silanized screw-capped vial[8]. Collection of the eluant was correlated with the recorder tracing so that equal amounts of the top one-half were obtained from both sides of the symmetrical peak. In general, approximately 0.5 ml of eluant was collected for each I-I-d_3 peak.

Samples thus collected from the chromatograph were stored at −5° until mass spectrometric analysis. Prior to analysis, each sample was evaporated under nitrogen at room temperature to approximately 25 μl. A microsyringe was used to transfer this solution in successive portions to a 5-μl gold cup. The solution was allowed to air evaporate, and the gold cup was placed into the direct insertion probe of the mass spectrometer. Quantification was accomplished as described.

Validity of Plasma Assay—Control blood samples from 10 laboratory workers known to be nonusers of marijuana were drawn and analyzed as described. Each sample contained some I, since the 1.6 μg of I-d_3 added to each plasma sample contained an average of 11.3 ng of I (Table I). To demonstrate the reproducibility and accuracy of the developed method, pooled human plasma samples were analyzed to which known amounts of I had been added (Table I). A plot of these data gave a linear curve whose intercept passed not through the origin but rather through a point corresponding to the 11.3 ng of I contained in the internal standard.

Marijuana Smoking Studies[9]—Eleven healthy male volunteers, 21–26 years old, were used. Each subject was within 10% of ideal body weight and received both medical and psychological examinations prior to the experiment. Values for the following tests were determined prior to the study, and each subject was required to be within the normal range: ECG, chest X-ray, creatinine, blood urea nitrogen, lactic dehydrogenase, serum glutamic–oxaloacetic transaminase, alkaline phosphatase, blood sugar, calcium, phosphorus, bilirubin, total protein, albumin, cholesterol, uric acid, hematocrit, hemoglobin, platelet count, and prothrombin time.

All subjects were moderate marijuana smokers. Each was requested not to smoke marijuana for 2 days prior to reporting for the study. The subjects were brought into the hospital ward 12 hr prior to smoking, and they were not allowed food or drink after 12:00 am of the study day. At approximately 8:00 am of the test day, each subject had a heparin-lock placed in a forearm vein and 5 ml of blood was withdrawn and placed in a silanized heparinized vacuum tube. Each blood sample was handled so that the blood did not come in contact with the rubber stopper.

All blood samples were immediately centrifuged at 2600 rpm, and the plasma was removed, placed in another silanized tube, and frozen for later analysis. This initial 5 ml of blood drawn prior to smoking constituted the 0-hr sample. Each subject smoked one marijuana cigarette[10], which contained 10.8 mg of I, 2.16 mg of III, 0.9 mg of IV, and 0.63 mg of II. Upon completion of smoking, timing was begun. Blood samples (5 ml) were withdrawn at 0.25, 0.5, 1, 2, 3, 4, 12, and 24 hr. Each blood sample was handled as described. Table II gives the blood I levels found for each subject.

Table II—Amount of I (Nanograms per Milliliter) Found in Human Plasma following Marijuana Smoking

	Hours								
Subject	0	0.25	0.5	1	2	3	4	12	24
D.L.	3.6	23.0	10.1	12.2	7.1	0.9	3.5	2.7	0
B.N.	1.2	39.0	11.7	3.8	0.9	0	0.7	0	1.7
B.B.	1.6	34.1	23.3	16.8	1.4	1.1	0	2.0	0.9
D.J.	0	66.7	19.7	11.8	3.0	3.8	4.3	0	3.1
F.R.	4.2	38.4	20.1	6.8	8.4	2.8	6.3	0.6	0.9
B.W.	0.4	57.9	24.8	14.8	10.7	2.4	6.2	5.8	2.5
W.Z.	1.2	39.7	19.7	6.8	5.3	4.9	2.0	0	0
R.B.	5.7	43.7	18.9	27.6	6.7	4.4	2.5	0.1	3.4
L.G.	7.6	15.3	39.9	8.1	2.1	11.1	7.5	9.7	2.5
T.V.	11.3	34.6	16.5	10.1	5.1	4.2	2.3	1.6	2.8
K.C.	4.7	20.6	22.4	14.5	8.4	7.7	4.7	5.0	2.5
Mean	3.8	37.5	20.7	12.1	5.2	3.9	3.6	2.5	1.9

RESULTS AND DISCUSSION

Analysis of trace substances in a biological system is often limited by the sensitivity and accuracy of the method employed. This was precisely the case with I, since prior literature reports documented the rather low levels of I occurring in blood following marijuana smoking. Therefore, in the present work, a technique was developed that took advantage of the resolving ability of HPLC and the sensitivity of mass spectrometry to quantitate very low levels of I in human plasma.

To achieve the needed accuracy and reproducibility, a stable isotopic form of I was added to the plasma to control extraction efficiency, to prevent losses during the chromatographic elution, as a marker for eluant collection, and as a convenient mass for mass spectrometric quantification. The HPLC program used permits a selective quantification of I, since the other cannabinoids with *m/e* 314 (II and IV) in marijuana are adequately resolved from I. In addition, the moderate resolution used in the mass spectrometric quantification prevents analysis of other satellite masses present due to constituents in the plasma also having an *m/e* close to 314.

Plasma was extracted three times to introduce to the mass spectrometer sufficient stable isotope for accurate quantification while not using excessive amounts of the isotope as the internal standard. The other important use of I-d_3 was to permit the total amount of I (both labeled and unlabeled) to be detectable by the UV spectrophotometer attached to the output of the liquid chromatograph. When using the described HPLC program and UV wavelength monitoring, a minimum of 100 ng/ml of I in plasma could be detected. This finding was in agreement with the reported (12) low absorptivity of I. However, as already discussed, the levels of I following marijuana smoking were known to be significantly lower than the 100-ng/ml levels detectable by HPLC–UV spectrophotometry. Thus, by using 1.6 μg of I-d_3 as the internal standard, a clearly detectable peak was observed on the resultant chromatogram.

The observed range for the determinations on control plasma with added I-d_3 was 9.35–13.6 ng/ml, with an average value of 11.3 ng/ml (Table I). Applying the Student distribution or *t* values to these data gave ±2.29 ng/ml for a 99% confidence limit. The other data given in Table I were obtained by adding a known amount of I as well as 1.6 μg of I-d_3 as the internal standard to pooled human plasma from nonsmokers of marijuana. Each value obtained from the known I addition experiments was corrected for the contribution from unlabeled material present in the internal standard—*viz.*, 11.3 ng/ml.

The reproducibility and accuracy were good for all levels of I added to plasma except the 1-ng/ml level. The lack of accuracy at this level was due to the overlap of confidence limits between the internal standard and this low level of added I. Although a precise determination of the lower limits of sensitivity was not made, 2.5 ng/ml apparently would be the lower limit of detection for the assay. Such a value would be above the

[8] Reacti-Vial, Pierce Chemical Co.

[9] All smoking studies were performed at the Marijuana Research Institute, School of Medicine, University of California–Los Angeles.

[10] Supplied by National Institute on Drug Abuse.

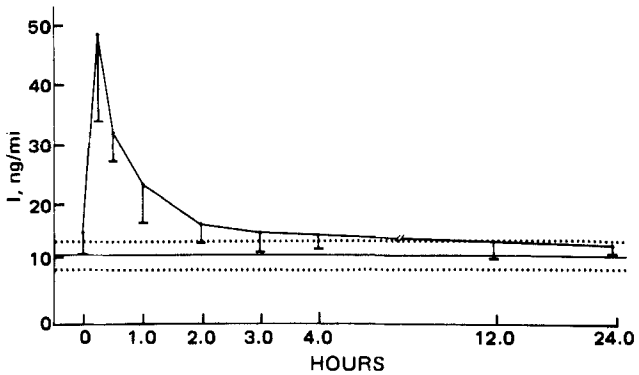

Figure 2—*Average plasma levels of I (Δ^9-THC) for 11 marijuana smokers (not corrected for contribution of I-d_3) and 10 nonsmokers. The solid horizontal line represents the average plasma level of I found in nonusers and is due to the impurity present in the internal standard, whereas the 99% confidence limits for this value are represented by the horizontal dotted lines. The vertical lines at each data point represent the lower half of the confidence limits for those 11 determinations made in the marijuana smokers at the appropriate time interval.*

99% confidence limits of I found as a contaminant in the internal standard.

Figure 2 is a plot of the average uncorrected plasma I levels of 11 male volunteers who smoked one marijuana cigarette of known I content. The maximum blood I level occurred at 0.25 hr. Also the I level in the control or 0-hr sample was positive. This fact can be explained on the basis of the type of subject used in the marijuana smoking studies. All subjects were moderate marijuana users. Each was confined 12 hr prior to smoking and was asked not to smoke marijuana for 2 days prior to the study. The analytical data obtained on the plasma of each subject indicated that only five individuals conformed to the established protocol.

The 99% confidence levels, as determined by the Student distribution (t-value) method, are shown by the vertical bars at each data point. The horizontal lines represent the average value (dark line) for 10 nonsmokers of marijuana as well as the 99% confidence limits (dotted lines). Wherever the confidence limits for data from both marijuana smokers and nonsmokers coalesce, a time period exists where marijuana use could not be assigned with 99% confidence. Thus, for up to 1 hr after marijuana smoking, the levels of I are clearly determinable and marijuana use can be assigned with 99% confidence using the present assay method.

The HPLC–mass spectrometric methodology described would be applicable to the study of other drug entities in biological fluids where very low detection levels are required along with precise specificity. However, for such determinations, the stable isotopic form of the drug is needed.

REFERENCES

(1) "Marijuana and Health," Fifth Annual Report to the U.S. Congress, 1975, p. 2.

(2) N. J. Doorenbos, P. S. Fetterman, M. W. Quimby, and C. E. Turner, *Ann. N.Y. Acad. Sci.*, **191**, 3 (1971).

(3) H. Y. Edery, F. Grunfeld, F. Ben-Zvi, and R. Mechoulam, *ibid.*, **191**, 40 (1971).

(4) M. Galanter, R. J. Wyatt, L. Lemberger, H. Weingartner, T. B. Vaughn, and W. T. Roth, *Science*, **176**, 934 (1972).

(5) D. C. Fenimore, R. R. Freeman, and P. R. Loy, *Anal. Chem.*, **45**, 2331 (1973).

(6) E. R. Garrett and C. A. Hunt, *J. Pharm. Sci.*, **62**, 1211 (1973).

(7) S. Agurell, B. Gustafsson, B. Holmsteadt, K. Leander, J. Lindgren, I. Nilsson, F. Sandberg, and M. Saberg, *J. Pharm. Pharmacol.*, **25**, 554 (1973).

(8) J. J. Rosenfeld, B. Bowins, J. Roberts, J. Perkins, and A. S. Macpherson, *Anal. Chem.*, **46**, 2232 (1974).

(9) J. D. Teale, L. J. King, E. J. Forman, and V. Marks, *Lancet*, **2**, 553 (1974).

(10) S. J. Gross, J. R. Soares, S. L. R. Wong, and R. E. Schuster, *Nature*, **252**, 581 (1974).

(11) R. E. Lovins, S. R. Ellis, G. D. Tolbert, and C. R. McKinney, *Anal. Chem.*, **45**, 1553 (1973).

(12) E. R. Garrett and C. A. Hunt, *J. Pharm. Sci.*, **63**, 1056 (1974).

ACKNOWLEDGMENTS AND ADDRESSES

Received June 1, 1976, from the *Bio-Analytics Laboratory, School of Pharmacy and Department of Physics, University of Missouri–Kansas City, Kansas City, MO 64108.*

Accepted for publication November 4, 1976.

Supported by Contract DOT HS 4 00968 from the Department of Transportation and the National Institute on Drug Abuse and in part by a Faculty Research Grant from the University of Missouri.

The authors are grateful for the assistance provided by Ms. Phyllis Lessin and Mr. Robert Nowlan of the Marijuana Research Institute, School of Medicine, University of California–Los Angeles. The authors also thank the School of Medicine, University of Missouri–Kansas City, for providing facilities for this work.

[x] To whom inquiries should be directed.

Radioimmunoassay of Minoxidil in Human Serum

MAX E. ROYER [x], HOWARD KO, TERRY J. GILBERTSON, JOHN M. McCALL, KAREN T. JOHNSTON, and RONALD STRYD

Abstract □ A simple, sensitive, and specific radioimmunoassay for determining minoxidil was developed. Antiserums to two minoxidil haptens were compared for cross-reactivity and assay levels on human serums. One antiserum had little cross-reactivity with minoxidil metabolites. The radioimmunoassay is specific for determining minoxidil directly in serum without extraction. Human serum minoxidil levels were determined from a single oral dose.

Keyphrases □ Minoxidil—radioimmunoassay, human serum □ Radioimmunoassay—minoxidil in human serum □ Antihypertensives—minoxidil, radioimmunoassay in human serum

Minoxidil (2,4-diamino-6-piperidinopyrimidine 3-oxide) (I) is a potent hypotensive agent useful in the treatment of severe hypertension (1, 2). A sensitive assay was needed for determining serum I levels. Attempts with a GLC procedure indicated that sizable amounts of the several derivatives tried were lost on the column. High-pressure liquid chromatography (HPLC) would have adequate sensitivity for only the higher serum concentrations encountered at normal dosage levels of I. Chromatographic methods for I in serum also require extraction and a preliminary chromatographic cleanup step. Such procedures are tedious and time consuming. Radioimmunoassay, however, permits analysis of many samples without extraction and with adequate sensitivity.

Antiserums were developed in rabbits against two bovine serum albumin conjugates of the N-4-glutaryl (II) and

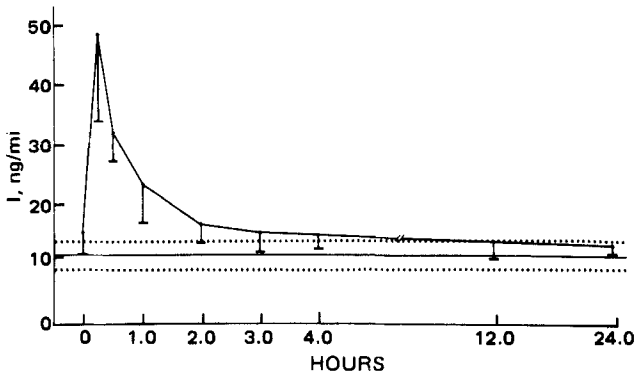

Figure 2—*Average plasma levels of I (Δ^9-THC) for 11 marijuana smokers (not corrected for contribution of I-d_3) and 10 nonsmokers. The solid horizontal line represents the average plasma level of I found in nonusers and is due to the impurity present in the internal standard, whereas the 99% confidence limits for this value are represented by the horizontal dotted lines. The vertical lines at each data point represent the lower half of the confidence limits for those 11 determinations made in the marijuana smokers at the appropriate time interval.*

99% confidence limits of I found as a contaminant in the internal standard.

Figure 2 is a plot of the average uncorrected plasma I levels of 11 male volunteers who smoked one marijuana cigarette of known I content. The maximum blood I level occurred at 0.25 hr. Also the I level in the control or 0-hr sample was positive. This fact can be explained on the basis of the type of subject used in the marijuana smoking studies. All subjects were moderate marijuana users. Each was confined 12 hr prior to smoking and was asked not to smoke marijuana for 2 days prior to the study. The analytical data obtained on the plasma of each subject indicated that only five individuals conformed to the established protocol.

The 99% confidence levels, as determined by the Student distribution (t-value) method, are shown by the vertical bars at each data point. The horizontal lines represent the average value (dark line) for 10 nonsmokers of marijuana as well as the 99% confidence limits (dotted lines). Wherever the confidence limits for data from both marijuana smokers and nonsmokers coalesce, a time period exists where marijuana use could not be assigned with 99% confidence. Thus, for up to 1 hr after marijuana smoking, the levels of I are clearly determinable and marijuana use can be assigned with 99% confidence using the present assay method.

The HPLC–mass spectrometric methodology described would be applicable to the study of other drug entities in biological fluids where very low detection levels are required along with precise specificity. However, for such determinations, the stable isotopic form of the drug is needed.

REFERENCES

(1) "Marijuana and Health," Fifth Annual Report to the U.S. Congress, 1975, p. 2.

(2) N. J. Doorenbos, P. S. Fetterman, M. W. Quimby, and C. E. Turner, *Ann. N.Y. Acad. Sci.*, **191**, 3 (1971).

(3) H. Y. Edery, F. Grunfeld, F. Ben-Zvi, and R. Mechoulam, *ibid.*, **191**, 40 (1971).

(4) M. Galanter, R. J. Wyatt, L. Lemberger, H. Weingartner, T. B. Vaughn, and W. T. Roth, *Science*, **176**, 934 (1972).

(5) D. C. Fenimore, R. R. Freeman, and P. R. Loy, *Anal. Chem.*, **45**, 2331 (1973).

(6) E. R. Garrett and C. A. Hunt, *J. Pharm. Sci.*, **62**, 1211 (1973).

(7) S. Agurell, B. Gustafsson, B. Holmsteadt, K. Leander, J. Lindgren, I. Nilsson, F. Sandberg, and M. Saberg, *J. Pharm. Pharmacol.*, **25**, 554 (1973).

(8) J. J. Rosenfeld, B. Bowins, J. Roberts, J. Perkins, and A. S. Macpherson, *Anal. Chem.*, **46**, 2232 (1974).

(9) J. D. Teale, L. J. King, E. J. Forman, and V. Marks, *Lancet*, **2**, 553 (1974).

(10) S. J. Gross, J. R. Soares, S. L. R. Wong, and R. E. Schuster, *Nature*, **252**, 581 (1974).

(11) R. E. Lovins, S. R. Ellis, G. D. Tolbert, and C. R. McKinney, *Anal. Chem.*, **45**, 1553 (1973).

(12) E. R. Garrett and C. A. Hunt, *J. Pharm. Sci.*, **63**, 1056 (1974).

ACKNOWLEDGMENTS AND ADDRESSES

Received June 1, 1976, from the *Bio-Analytics Laboratory, School of Pharmacy and Department of Physics, University of Missouri–Kansas City, Kansas City, MO 64108.*

Accepted for publication November 4, 1976.

Supported by Contract DOT HS 4 00968 from the Department of Transportation and the National Institute on Drug Abuse and in part by a Faculty Research Grant from the University of Missouri.

The authors are grateful for the assistance provided by Ms. Phyllis Lessin and Mr. Robert Nowlan of the Marijuana Research Institute, School of Medicine, University of California–Los Angeles. The authors also thank the School of Medicine, University of Missouri–Kansas City, for providing facilities for this work.

[x] To whom inquiries should be directed.

Radioimmunoassay of Minoxidil in Human Serum

MAX E. ROYER [x], HOWARD KO, TERRY J. GILBERTSON, JOHN M. McCALL, KAREN T. JOHNSTON, and RONALD STRYD

Abstract □ A simple, sensitive, and specific radioimmunoassay for determining minoxidil was developed. Antiserums to two minoxidil haptens were compared for cross-reactivity and assay levels on human serums. One antiserum had little cross-reactivity with minoxidil metabolites. The radioimmunoassay is specific for determining minoxidil directly in serum without extraction. Human serum minoxidil levels were determined from a single oral dose.

Keyphrases □ Minoxidil—radioimmunoassay, human serum □ Radioimmunoassay—minoxidil in human serum □ Antihypertensives—minoxidil, radioimmunoassay in human serum

Minoxidil (2,4-diamino-6-piperidinopyrimidine 3-oxide) (I) is a potent hypotensive agent useful in the treatment of severe hypertension (1, 2). A sensitive assay was needed for determining serum I levels. Attempts with a GLC procedure indicated that sizable amounts of the several derivatives tried were lost on the column. High-pressure liquid chromatography (HPLC) would have adequate sensitivity for only the higher serum concentrations encountered at normal dosage levels of I. Chromatographic methods for I in serum also require extraction and a preliminary chromatographic cleanup step. Such procedures are tedious and time consuming. Radioimmunoassay, however, permits analysis of many samples without extraction and with adequate sensitivity.

Antiserums were developed in rabbits against two bovine serum albumin conjugates of the N-4-glutaryl (II) and

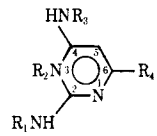

Table I—Specificity of Antiseruns to Bovine Serum Albumin Conjugates of Compounds II and III

Compound	R_1	R_2	R_3	R_4	Cross-Reactivity[a], % Anti-II	Anti-III
I	H	O	H		100	100
II	H	O	$C(CH_2)_3COH$		144	2.3
III	H	O	H	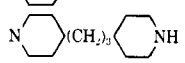	<0.1	760
IV	H	O	H	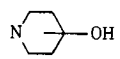	0.7	28
V	$CH_3C(=O)$	O	CH_3C—		5.1	<0.1
VI	H	—	H		<0.1	<0.1
VII	—[b]	—[b]	—[b]		1.4	1.3
VIII	H	O	H	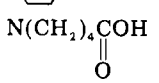	<0.1	0.4

[a] Defined as: (100 × concentration of I at 50% binding)/concentration of compound tested at 50% binding. [b] Position of the glucuronic acid attachment not established.

dipiperidine (III) derivatives of minoxidil (Table I). These antiserums were compared for specificity, and one was chosen for further development of the radioimmunoassay.

EXPERIMENTAL

Synthesis of II and Conjugation to Bovine Serum Albumin—Two grams of ^{14}C-minoxidil and 1.09 g of glutaric anhydride were refluxed for 2 hr in 150 ml of dry acetone. The residue was filtered and washed to give 2.8 g of II. TLC in methanol–benzene–ammonium hydroxide (100:100:1) indicated one component. The NMR shift of the proton at the 5-position and X-ray crystallography of the methyl ester of II indicated a single substitution on the amino group at the 4-position.

Anal.—Calc. for $C_{14}H_{21}N_5O_4$: C, 53.40; H, 6.87; N, 20.76. Found: C, 53.51; H, 6.96; N, 21.07.

Compound II, 165 mg, and 300 mg of bovine serum albumin were dissolved in 10 ml of 50% pyridine (3). Over 15 min, 193 mg of 1-ethyl-3-(3-dimethylaminopropyl)carbodiimide hydrochloride was added slowly; the mixture was then stirred for 16 hr. After dialysis and freeze drying, 383 mg of material was recovered.

A portion of the conjugate was washed exhaustively with acetone followed by chloroform to remove any undialyzed II. The amount of ^{14}C-II remaining on bovine serum albumin indicated that approximately 29 moles of II/mole of bovine serum albumin was covalently linked.

Preparation of III and Conjugation of Bovine Serum Albumin and III to Agarose Gel Support—A solution of 3.0 g of 2,4-diamino-6-chloropyrimidine 3-oxide in 11.15 g of 4,4′-trimethylenedipiperidine was heated at 80° and then stirred with aqueous sodium bicarbonate. The product (III) was dissolved in methanol and precipitated by addition of acetonitrile.

Compound III was attached to a modified agarose gel[1] which, in turn, was conjugated to bovine serum albumin analogous to the preparation of solid phase immunogens described by Trump (4). A slurry of 430 mg of modified agarose gel and 360 mg of bovine serum albumin in 20 ml of water was stirred for 3 hr. A solution of 430 mg of III in 20 ml of dimethylformamide was added. After 3 hr, 50 mg of sodium bicarbonate was added. After 12 hr, the conjugate was filtered and washed. The material was stored as a wet slurry.

Immunization and Antiserum Production—The conjugate of II (8 mg), 4 ml of 0.9% saline, and 4 ml of Freund's complete adjuvant[2] were emulsified in a blender[3]. A total of 1 ml was injected intradermally at multiple sites in the back and flanks of each of six New Zealand White rabbits. The rabbits were challenged again at 4 months with a similar injection except that Freund's incomplete adjuvant was used[2]. Only one rabbit gave significant antibody titer. Of the eight bleedings during 289 days after the first injection, the bleeding at Day 129 had the highest titer and was used for the radioimmunoassay.

Blood was collected by cutting the ear vein and applying gentle suction. The blood was allowed to clot 1–2 hr at room temperature and then was centrifuged. The serum was divided into aliquots and stored at −70°.

The immunization and bleeding schedules were carried out in a similar manner for the antiserum to the conjugate of III.

Assay Reagents—*Buffer A*—One hundred and ninety-two grams of tris(hydroxymethyl)aminomethane, 1 g of thimerosal[4], and 1 liter of 1.0 *N* HCl were diluted to make 10 liters of pH 7.8 (0.1 μ) buffer.

Buffer B—Human serum albumin[4] (0.1%) was added to Buffer A.

Counting Solution—Five hundred milliliters of nonionic detergent[5], 170 ml of scintillator fluid[6], and 3.79 liters of toluene (analytical reagent) were mixed.

Primary Antibody—Rabbit antiserum was diluted 1:100.

Secondary Antibody—Goat antirabbit antibody was diluted to give maximal precipitation of the primary antibody (1:8).

Label—3′,4′,5′(*n*)-^3H-Minoxidil, 25.6 Ci/mmole (5), approximately 13,000 dpm/ml in Buffer B, was the label.

Standards—Minoxidil was diluted in Buffer B.

Assay Procedure—Buffer B (for unknown samples) and pretreatment serum (for standards) were added to separate 12 × 75-mm glass culture tubes[7] with a 50-μl pipet[8]. The unknown sample or standard, 50 μl, and label, 500 μl, were added with an automatic pipet[9], and the tubes were incubated 1–2 hr at 25°. A normal standard curve consisted of duplicate standards with concentrations of 1, 2, 4, 8, 16, 32, 64, and 128 ng/ml. Four blanks (B_0) with no unlabeled drug and two infinity samples (>30,000 ng/ml) were also run. Approximately 75% of the label was bound at B_0. When the expected concentration of I was high, only 10 μl of the unknown was sampled and 40 μl of pretreatment serum was added to give a fivefold

[1] Affi-Gel 10, Bio-Rad Laboratories, Richmond, Calif.

[2] Difco Laboratories, Detroit, Mich.
[3] Sorvall, Ivan Sorvall, Inc., Newton, Conn.
[4] Sigma Chemical Co., St. Louis, Mo.
[5] BioSolv, Beckman Instruments, Fullerton, Calif.
[6] Liquifluor, New England Nuclear, Boston, Mass.
[7] Dispo, Scientific Products, McGaw Park, Ill.
[8] Eppendorf, Brinkmann Instrument Co., Westbury, N.Y.
[9] Model 25004, Micromedic Systems Inc., Philadelphia, Pa.

Table II—Recovery and Within-Day and Between-Day Coefficients of Variation (*CV*) (*n* = 66)

Actual Amount, ng/ml	Amount Found, ng/ml	Recovery (*SEM*), %	*CV*, % Within Day	*CV*, % Between Day
8	7.12	89.0 ± 0.8	5.4	5.7
64	64.76	101.2 ± 1.1	6.5	6.5
256	253.68	99.1 ± 0.9	7.0	3.4

dilution. Primary antibody, 200 μl, was added to each tube, and the tubes were incubated 16–24 hr at 25°; then 200 μl of secondary antibody was added, and the tubes were incubated 40–72 hr at 5°.

The tubes were centrifuged at 1000×*g* for 30 min at 5°, and the supernate was immediately poured into counting vials[10]. The tubes were left to drain at an angle in the counting vials for about 30 min and then were discarded (6). Counting solution (15 ml) was added, and the samples were counted on a liquid scintillation counter[11] for 10,000 counts or 10 min. The counts of samples that may have contained quenching materials (*e.g.*, hemoglobin) and that had changes in counting efficiencies greater than ±0.5% from the median efficiency were corrected for counting efficiency by the external standard method.

The results were calculated by computer[12] using the Rodbard and Lewald (7) program. Six control samples also were run as unknowns at 8, 64, and 256 ng/ml. Since 256 ng/ml is outside the normal standard curve range, 40 μl of Buffer B was added to the tubes and only 10 μl was sampled (5× dilution).

The cross-reactivity of the antiserums was determined from plots of the standard curves measured for each compound tested. Serum, 50 μl, was added to each standard tube to approximate the conditions normally found in the assay.

RESULTS AND DISCUSSION

The following general considerations were followed in the radioimmunoassay development: (*a*) the antibodies should not cross-react significantly with known metabolites; (*b*) the assay should require a minimum of sample preparation; (*c*) where possible, precision and accuracy should be emphasized rather than sensitivity and speed; and (*d*) the assay should be generally applicable to measuring I in serum at many dosage levels.

Specificity—The major urinary metabolites of I are the glucuronide (VII) in humans and the 4′-hydroxy metabolite (IV) in dogs (8–10). The reduced analog (VI) and carboxy derivative (VIII) are also known metabolites of I. The cross-reactivities of these metabolites and several other I derivatives with antiserums to both II and III are shown in Table I. Both antiserums had the same titer and had adequate specificity against all known metabolites, with the exception of the 28% cross-reactivity of IV using the antiserum against III.

Since this might be a source of error in assaying for I in dog serum, the antiserum against II was selected for further assay development. At time points (2–4 hr after oral administration) at which metabolites in human serum would likely be observed, the apparent concentrations of I measured by the two antiserums (II and III) were not significantly different ($p > 0.05$). Either antiserum should have adequate specificity to determine I in human serum.

Factors Affecting Accuracy—If 50 μl of buffer were substituted for serum in the standards, a positive bias of about 2–11% would result. Because little was known about the subject-to-subject variation in protein binding and its effect on the radioimmunoassay, 50 μl of a subject's own pretreatment serum was added to each standard tube. A separate standard curve was run before and after each set of unknowns. This procedure ensured that the standards and samples contained as nearly as possible the same constituents and that systematic errors in pipetting or equilibrating during an assay averaged out.

The long equilibration times at each step ensured equilibrium conditions at each stage of the assay (11). Although shorter equilibration times may be permissible, the long equilibration times do not seriously affect the number of samples that can be run over a long period.

No binding loss of I to glass was observed after 10 sequential transfers from tube to tube. To ensure that I remained in solution, 0.1% human serum albumin was used as diluent for the label and standard solutions (11). Serum that contained significant amounts of hemoglobin gave low counts due to quenching. Corrections were made only if the counting efficiency was changed by more than ±0.5% from the median value of the subject's samples.

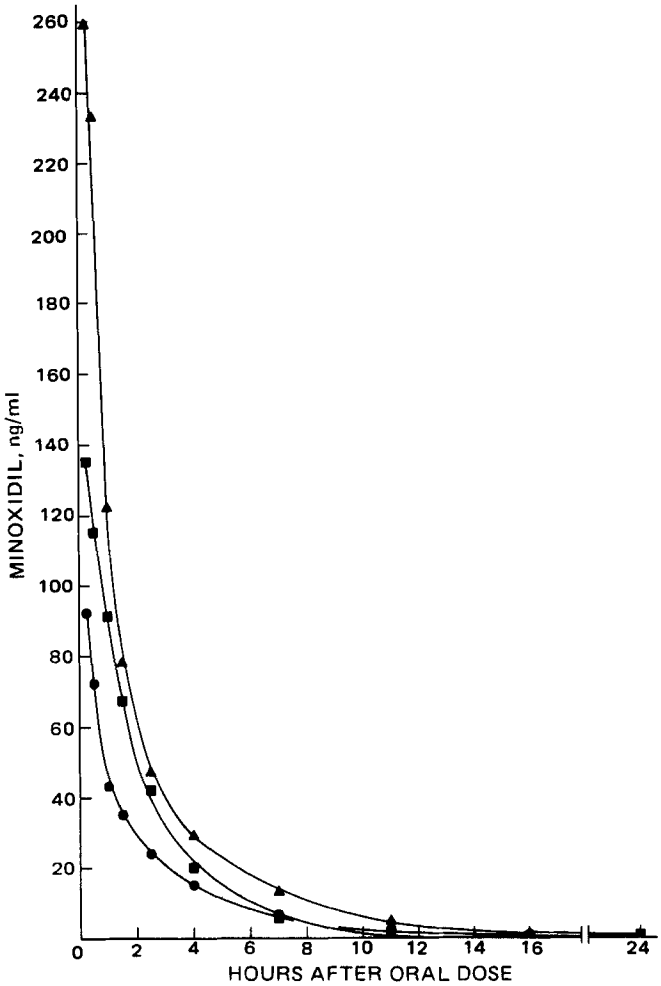

Figure 1—*Serum minoxidil levels after a single oral dose. Key:* ●, *Patient A, 10 mg;* ■, *Patient P, 20 mg; and* ▲, *Patient J, 30 mg.*

Assay Statistics—The mean limit of detection, as determined by the Rodbard and Lewald (7) program, for 18 standard curves was 3.02 ± 1.52 ng/ml (*SD*). With a primary antibody dilution of only 1:100, the assay as run was not set up for maximal sensitivity. The detection limit would be much lower if the primary antibody was further diluted and/or larger sample volumes were taken.

The recovery and the within-day and between-day coefficients of variation are shown in Table II. At 8 and 64 ng/ml, the percentage of label bound relative to that for B_0 was approximately 80 and 20%, respectively.

Human Serum Minoxidil Levels—Levels of ^{14}C-minoxidil and its metabolites previously were determined in human, dog, and monkey serum (8, 9). The radioimmunoassay offers a convenient means of determining I in human serum without administering radioactive I to the patient and without requiring subsequent chromatography of the metabolites.

Three volunteer patients with hypertension that was not controlled by other drugs were given single oral doses of I. Their serum levels of I are shown in Fig. 1. For 20 patients receiving a single dose of 5–100 mg, the peak serum levels were reached at 0.6 ± 0.5 hr (mean ± *SD*) and the mean (±*SD*) half-life was 1.4 ± 0.9 hr as determined by the radioimmunoassay.

Therefore, the radioimmunoassay for I has (*a*) adequate specificity for measuring serum I levels in the presence of other metabolites, (*b*) no requirement for extraction or extensive sample preparation (some dilution may be necessary at high levels), (*c*) adequate precision and accuracy for comparing serum levels and determining serum half-life, and (*d*) sufficient sensitivity and applicability to large numbers of samples.

[10] Packard Instrument Co., Downers Grove, Ill.
[11] Packard Tri-Carb model 3375.
[12] IBM 370/155 computer.

REFERENCES

(1) E. Gilmore, J. Weil, and C. A. Chidsey, *N. Engl. J. Med.*, **282**, 521 (1970).

(2) T. B. Gottleib, F. H. Katz, and C. A. Chidsey, *Circulation*, **45**, 571 (1972).

(3) G. E. Abraham and P. K. Grover, "Principles of Competitive Protein-Binding Analysis," W. D. O'Dell and W. H. Daughaday, Eds., Lippincott, Philadelphia, Pa., 1972, pp. 140–152.

(4) G. N. Trump, *Biochem. Biophys. Res. Commun.*, **54**, 544 (1973).

(5) T. J. Gilbertson, *J. Labeled Compd. Radiopharm.*, **12**, 463 (1976).

(6) M. E. Royer, H. Ko, J. A. Campbell, H. C. Murray, J. S. Evans, and D. G. Kaiser, *Steroids*, **23**, 713 (1974).

(7) D. Rodbard and J. E. Lewald, *Karolinska Symp. Res. Methods Reprod. Endocrinol., 2nd Symp.*, **1970**, 79.

(8) T. B. Gottleib, R. C. Thomas, and C. A. Chidsey, *Clin. Pharmacol. Ther.*, **13**, 436 (1972).

(9) R. C. Thomas, R. S. P. Hsi, H. Harpootlian, and R. W. Judy, *J. Pharm. Sci.*, **64**, 1360 (1975).

(10) R. C. Thomas and H. Harpootlian, *ibid.*, **64**, 1366 (1975).

(11) M. E. Royer, H. Ko, J. S. Evans, and K. T. Johnston, *Anal. Lett.*, **9**, 629 (1976).

ACKNOWLEDGMENTS AND ADDRESSES

Received September 3, 1976, from the *Drug Metabolism Research Section, The Upjohn Company, Kalamazoo, MI 49001.*

Accepted for publication November 10, 1976.

The authors thank Dr. Richard C. Thomas for the minoxidil glucuronide, Murray M. Cooper for adaption of the Rodbard and Lewald computer program, C. G. Wickrema Sinha for the X-ray crystallographic structure proof, and Dr. G. R. Lang, Dr. D. T. Lowenthal, and Dr. G. Bailey for the serum samples from volunteer patients.

[x] To whom inquiries should be directed.

Evaluation and Optimal Combination of TLC Systems for Qualitative Identification I: Sulfonamides

H. De CLERCQ, D. L. MASSART [x], and L. DRYON

Abstract □ A mathematical criterion for the evaluation of chromatographic analysis procedures is given by the information content as derived from Shannon's equation. This information content yields a numerical value representative of the merits of each chromatographic separation and thus allows selection of the optimal systems. In most cases, however, one analysis is not sufficient to allow the qualitative identification of the sample. Therefore, several chromatographic systems are combined. Two approaches allow the desired combination; one either calculates the information content of several procedures as one mathematical value or classifies the systems according to mutual resemblance by numerical taxonomy techniques. From the resulting groups of dissimilar systems, one optimal system can be chosen per group according to the information content. The results obtained by these mathematical procedures are illustrated with a practical example: the selection and evaluation of systems for the TLC analysis of sulfonamides.

Keyphrases □ TLC—systems, evaluation and optimal combination for qualitative determination of sulfonamides □ Sulfonamides, various—TLC systems for qualitative determination, evaluation and optimal combination

TLC is one major method in pharmaceutical analysis for the identification of organic compounds, and there is an enormous literature on the subject. It is not always easy to select the best TLC systems from the many that have been published, and it is more difficult to select the optimal combination of two or more systems. The reasons for this difficulty are:

1. The systems (any combination of stationary phase and solvent) are developed by many different workers, who use slightly different development procedures, saturation conditions, *etc.*

2. Most investigators do not use objective value judgments but rather state that their separation procedures yield either "good" or "excellent" or "poor" results for a group of substances. Furthermore, while it is rather easy to characterize a separation of two substances, it is often more difficult to characterize a separation of 10 substances.

3. Even if the selection of the individually best systems is possible, it is often nearly impossible to obtain, on sight, the optimal combination, since the best combination of n systems does not necessarily contain the n individually best systems.

It is necessary to create some order out of this chaotic literature. One way to do this is to compile the literature available for restricted application domains (1). Another approach consists of a comparison under standardized conditions of reported systems (and, in the present case, of some new systems). Formal methods are then used for the evaluation and optimal combination of the TLC systems.

EXPERIMENTAL

Reagents and Chemicals—All solvents were reagent grade, and reference sulfonamides were used as 0.2% (w/v) solutions in acetone. Sulfanilamide was always used as an internal standard.

Adsorbent—Precoated TLC silica gel 60 F-245 plates[1] and precoated TLC aluminum oxide 60 F-254 plates[1] (type E) were used.

Detection was by UV light (254 nm).

Apparatus—The plates were developed in carefully controlled saturation conditions[2] and standardized at 40% relative humidity.

RESULTS

The separation systems proposed in the literature and a few others were investigated (Tables I and II). Table I contains those systems for which a preliminary screening with seven sulfonamides yielded unpromising results (bad streaking of the spots, all hR_f values near 0 or 100, *etc.*).

Table II lists the systems that passed the screening stage. The sul-

[1] Merck, Darmstadt, Germany.

[2] Vario-KS-Chamber, Camag, Muttenz, Switzerland.

REFERENCES

(1) E. Gilmore, J. Weil, and C. A. Chidsey, *N. Engl. J. Med.*, **282**, 521 (1970).

(2) T. B. Gottleib, F. H. Katz, and C. A. Chidsey, *Circulation*, **45**, 571 (1972).

(3) G. E. Abraham and P. K. Grover, "Principles of Competitive Protein-Binding Analysis," W. D. O'Dell and W. H. Daughaday, Eds., Lippincott, Philadelphia, Pa., 1972, pp. 140–152.

(4) G. N. Trump, *Biochem. Biophys. Res. Commun.*, **54**, 544 (1973).

(5) T. J. Gilbertson, *J. Labeled Compd. Radiopharm.*, **12**, 463 (1976).

(6) M. E. Royer, H. Ko, J. A. Campbell, H. C. Murray, J. S. Evans, and D. G. Kaiser, *Steroids*, **23**, 713 (1974).

(7) D. Rodbard and J. E. Lewald, *Karolinska Symp. Res. Methods Reprod. Endocrinol., 2nd Symp.*, **1970**, 79.

(8) T. B. Gottleib, R. C. Thomas, and C. A. Chidsey, *Clin. Pharmacol. Ther.*, **13**, 436 (1972).

(9) R. C. Thomas, R. S. P. Hsi, H. Harpootlian, and R. W. Judy, *J. Pharm. Sci.*, **64**, 1360 (1975).

(10) R. C. Thomas and H. Harpootlian, *ibid.*, **64**, 1366 (1975).

(11) M. E. Royer, H. Ko, J. S. Evans, and K. T. Johnston, *Anal. Lett.*, **9**, 629 (1976).

ACKNOWLEDGMENTS AND ADDRESSES

Received September 3, 1976, from the *Drug Metabolism Research Section, The Upjohn Company, Kalamazoo, MI 49001.*

Accepted for publication November 10, 1976.

The authors thank Dr. Richard C. Thomas for the minoxidil glucuronide, Murray M. Cooper for adaption of the Rodbard and Lewald computer program, C. G. Wickrema Sinha for the X-ray crystallographic structure proof, and Dr. G. R. Lang, Dr. D. T. Lowenthal, and Dr. G. Bailey for the serum samples from volunteer patients.

[x] To whom inquiries should be directed.

Evaluation and Optimal Combination of TLC Systems for Qualitative Identification I: Sulfonamides

H. De CLERCQ, D. L. MASSART [x], and L. DRYON

Abstract □ A mathematical criterion for the evaluation of chromatographic analysis procedures is given by the information content as derived from Shannon's equation. This information content yields a numerical value representative of the merits of each chromatographic separation and thus allows selection of the optimal systems. In most cases, however, one analysis is not sufficient to allow the qualitative identification of the sample. Therefore, several chromatographic systems are combined. Two approaches allow the desired combination; one either calculates the information content of several procedures as one mathematical value or classifies the systems according to mutual resemblance by numerical taxonomy techniques. From the resulting groups of dissimilar systems, one optimal system can be chosen per group according to the information content. The results obtained by these mathematical procedures are illustrated with a practical example: the selection and evaluation of systems for the TLC analysis of sulfonamides.

Keyphrases □ TLC—systems, evaluation and optimal combination for qualitative determination of sulfonamides □ Sulfonamides, various—TLC systems for qualitative determination, evaluation and optimal combination

TLC is one major method in pharmaceutical analysis for the identification of organic compounds, and there is an enormous literature on the subject. It is not always easy to select the best TLC systems from the many that have been published, and it is more difficult to select the optimal combination of two or more systems. The reasons for this difficulty are:

1. The systems (any combination of stationary phase and solvent) are developed by many different workers, who use slightly different development procedures, saturation conditions, *etc.*

2. Most investigators do not use objective value judgments but rather state that their separation procedures yield either "good" or "excellent" or "poor" results for a group of substances. Furthermore, while it is rather easy to characterize a separation of two substances, it is often more difficult to characterize a separation of 10 substances.

3. Even if the selection of the individually best systems is possible, it is often nearly impossible to obtain, on sight, the optimal combination, since the best combination of n systems does not necessarily contain the n individually best systems.

It is necessary to create some order out of this chaotic literature. One way to do this is to compile the literature available for restricted application domains (1). Another approach consists of a comparison under standardized conditions of reported systems (and, in the present case, of some new systems). Formal methods are then used for the evaluation and optimal combination of the TLC systems.

EXPERIMENTAL

Reagents and Chemicals—All solvents were reagent grade, and reference sulfonamides were used as 0.2% (w/v) solutions in acetone. Sulfanilamide was always used as an internal standard.

Adsorbent—Precoated TLC silica gel 60 F-245 plates[1] and precoated TLC aluminum oxide 60 F-254 plates[1] (type E) were used.

Detection was by UV light (254 nm).

Apparatus—The plates were developed in carefully controlled saturation conditions[2] and standardized at 40% relative humidity.

RESULTS

The separation systems proposed in the literature and a few others were investigated (Tables I and II). Table I contains those systems for which a preliminary screening with seven sulfonamides yielded unpromising results (bad streaking of the spots, all hR_f values near 0 or 100, *etc.*).

Table II lists the systems that passed the screening stage. The sul-

[1] Merck, Darmstadt, Germany.

[2] Vario-KS-Chamber, Camag, Muttenz, Switzerland.

Table I—Systems Investigated but Rejected after the Screening Test

Solvent	Stationary Phase	Reference
Chloroform–ethanol (80:15)	Aluminum oxide	2
Chloroform–2-propanol (80:15)	Aluminum oxide	2
Chloroform–1-butanol (80:15)	Aluminum oxide	2
Chloroform–propanol (80:15)	Aluminum oxide	2
Chloroform–1-pentanol (80:15)	Aluminum oxide	2
Chloroform–acetone (50:50)	Aluminum oxide	2
Chloroform–acetic acid (95:5)	Aluminum oxide	2
Chloroform–acetic acid (90:10)	Aluminum oxide	2
Ether–methanol (90:10)	Aluminum oxide	2
Ether–ethanol (90:10)	Aluminum oxide	2
Benzene–ethanol (80:20)	Aluminum oxide	2
Ethyl acetate saturated with water	Aluminum oxide	—
Chloroform–methanol (80:15)	Aluminum oxide	—
Methanol–1-pentanol–benzene (31:15:45)	Aluminum oxide	—
Acetone–methanol–25% ammonia (85:15:15)	Aluminum oxide	—
Acetone–methanol–25% ammonia (75:10:5)	Aluminum oxide	—
Acetone	Aluminum oxide	—
Ethyl acetate	Aluminum oxide	—
Ethanol	Aluminum oxide	—
Chloroform	Silica gel	—
Chloroform–methanol (95:5)	Silica gel	3, 4
Chloroform–methanol (90:10)	Silica gel	5
Chloroform–methanol (80:20)	Silica gel	6
Chloroform–methanol (70:30)	Silica gel	—
Chloroform–dioxane (95:5)	Silica gel	3
Chloroform–ethanol (80:10)	Silica gel	7
Chloroform–acetic acid (95:5)	Silica gel	—
Benzene–ethanol (90:10)	Silica gel	—
1-Butanol–water (90:9)	Silica gel	—
5% (v/v) Ammonia–1-butanol (50:50)	Silica gel	7
Methanol–water (96:8)	Silica gel	—
Methyl ethyl ketone–pyridine (75:5)	Silica gel	7, 8
Acetone–methanol–diethylamine (90:10:10)	Silica gel	7, 8
Diethylamine (absolute)–2-propanol–water (10:50:40)	Silica gel	9
Chloroform–methanol–butylamine (85:10:5)	Silica gel	3
Dioxane–ammonia–water (100:3:10)	Silica gel	10
Chloroform–methanol–acetic acid (94:5:1)	Silica gel	3
Cyclohexane–acetone–acetic acid (40:50:10)	Silica gel	7, 8
1-Butanol–acetic acid–water (30:30:30)	Silica gel	11
Methanol–1-pentanol–benzene (31:15:45)	Silica gel	12
Methanol–1-pentanol–benzene–water (31:15:45:7)	Silica gel	12
Acetone–butanol–water (20:50:30)	Silica gel	10
Acetone–benzene–water (65:30:5)	Silica gel	10
Benzene–1-butanol–pyridine (30:5:5)	Silica gel	13
1-Butanol–methanol–acetone–diethylamine (90:10:10:10)	Silica gel	14
Butyl acetate–1-butanol–acetone–10% ammonia (30:30:40:10)	Silica gel	15

fonamides in Table III were chromatographed with each system in Table II.

DISCUSSION

Evaluation of Individual Systems—To evaluate the systems objectively, it is necessary to assign a figure of merit to each of the 56 systems remaining after the screening test. This assignment is done by calculating I, the information content, using a procedure analogous to the one introduced by Massart (31). The R_f range is divided into m R_f groups of given class width (*e.g.*, 0.05 R_f unit); for each m group, there is a distinct probability, p_k, that the unknown sulfonamide will have an R_f value within the limits of this class. If there is an equal probability of occurrence for each sulfonamide in the set, the probability, p_k, of finding an R_f value from an R_f class containing r_k members of the n that comprise the complete set equals r_k/n.

The information content, expressed in bit, can then be described by Shannon's (32) equation:

$$I = -\sum_{i=1}^{m} \frac{r_k}{n} \log_2 \left(\frac{r_k}{n}\right) \qquad \text{(Eq. 1)}$$

For example, in System 1 (Table III), four R_f values are found in the first R_f class (0–0.04), one R_f value is found in the next class (0.05–0.09), *etc.* Therefore, the information content of the first R_f class equals $-(4/22) \log_2 (4/22) = 0.45$.

By addition of the information content calculated for each class, a global information content value is obtained, characteristic of the merit of the chromatographic system under investigation. The information content (expressed in bit) of each one of the 56 systems remaining after the screening test is given in Table III.

Selection of an Optimal Combination of Two or More Systems—For the selection of an optimal combination of two or more chromatographic systems, *i.e.*, a set of systems containing as much information as possible, two approaches have been proposed. A combination of the individually best systems is not necessarily appropriate, since often a number of those systems give the same information (correlated and, therefore, redundant information).

The first approach is to consider every possible combination of two or more systems and to calculate the quantity of information obtained. Such a procedure was introduced to calculate the information content of combinations of stationary phases in GLC (33) and to compute "the discriminating power" for individual systems and for each combination of two, three, or four systems in chromatographic and spectroscopic procedures (34).

The second approach is used here; it has the advantage of versatility. Comparisons of this method with the first approach (33, 34) were published elsewhere (35, 36). This second approach is based on the classification or clustering of chromatographic systems according to their resemblance, *i.e.*, according to similarities in their chromatographic behavior. Similar systems are grouped into one class; from each resulting group (with dissimilar chromatographic characteristics), the individually best system can be chosen according to an evaluation criterion such as the information content.

One such classification procedure is numerical taxonomy (NT). Its application was introduced recently to the choice of optimal sets of solvents in TLC (37). In classification by numerical taxonomy, an $n \times n$ similarity matrix is constructed, using, for instance, taxonomic distance (37, 38) or correlation coefficients to measure the resemblance between each pair of systems. The reduction of this matrix can be carried out by various grouping techniques, *e.g.*, by weighted (37) or unweighted (39) pair group methods using the arithmetic average.

In a first reduction step, the most similar systems, i and j, are selected,

Table II—Systems Selected after the Screening Test

Number	Solvent	Stationary Phase	Reference
1	Ether	Silica gel	16
2	1-Pentanol	Silica gel	—
3	1-Butanol	Silica gel	—
4	1-Hexanol	Silica gel	—
5	Chloroform–methanol (60:30)	Silica gel	—
6	Chloroform–methanol (100:30)	Silica gel	—
7	Chloroform–methanol (80:15)	Silica gel	7, 8
8	Chloroform–methanol (100:10)	Silica gel	16, 17
9	Chloroform–ethanol (80:15)	Silica gel	—
10	Chloroform–2-propanol (80:15)	Silica gel	—
11	Chloroform–1-butanol (80:15)	Silica gel	—
12	Chloroform–1-propanol (80:15)	Silica gel	—
13	Chloroform–1-pentanol (80:15)	Silica gel	—
14	Chloroform–acetone (50:50)	Silica gel	—
15	Chloroform–dioxane (80:20)	Silica gel	3
16	Chloroform–acetonitrile (50:50)	Silica gel	7
17	Chloroform–acetic acid (90:10)	Silica gel	—
18	Chloroform–hexanol (80:15)	Silica gel	—
19	Benzene–ethanol (80:20)	Silica gel	—
20	Benzene–ethanol (70:30)	Silica gel	—
21	Ether–methanol (90:10)	Silica gel	—
22	Ether–ethanol (90:10)	Silica gel	—
23	Ethyl acetate saturated with water	Silica gel	12
24	Ethyl acetate–methanol (90:10)	Silica gel	6, 18
25	1-Butanol saturated with water	Silica gel	10
26	1-Butanol–chloroform–diethylamine (70:70:10)	Silica gel	19
27	Chloroform–methanol–dimethylformamide (100:10:5)	Silica gel	20
28	1-Butanol–formamide–water (50:10:50) upper phase	Silica gel	10
29	Methyl isobutyl ketone–acetone–25% ammonia (25:100:25)	Silica gel	21
30	Chloroform–methanol–25% ammonia (90:15:2.4)	Silica gel	22
31	Chloroform–acetone–methanol–6 *N* ammonia (60:10:25:0.5)	Silica gel	23
32	25% Ammonia–1-methylpropanol–2-propanol–water (15:40:40:5)	Silica gel	9
33	25% Ammonia–1-methylpropanol–2-propanol (15:35:40)	Silica gel	9
34	Ethyl acetate–methanol–25% ammonia (85:15:15)	Silica gel	—
35	Ethyl acetate–methanol–25% ammonia (85:30:25)	Silica gel	—
36	Diethylamine–1-methylpropanol–2-propanol–water (15:40:40:5)	Silica gel	9
37	1-Butanol–chloroform–methanol–25% ammonia (40:15:15:15)	Silica gel	24
38	1-Butanol–chloroform–acetone–diethylamine (90:10:10:10)	Silica gel	24
39	Chloroform–methanol–acetic acid (90:5:5)	Silica gel	3
40	Chloroform–1-butanol–petroleum ether (30:30:30)	Silica gel	25
41	Chloroform–1-butanol–ether (10:10:10)	Silica gel	26
42	Chloroform–ethanol–pentane (35:30:25)	Silica gel	7
43	Chloroform–ethanol–heptane (10:10:10) plus 1.5% water	Silica gel	27
44	Chloroform–ethanol–heptane (10:10:10)	Silica gel	28, 23
45	Chloroform–1-butanol–acetone–formic acid (40:10:10:10)	Silica gel	15, 17
46	Cyclohexane–acetone–chloroform–ethyl acetate–ethanol (5:10:20:5:5)	Silica gel	5
A1	1-Butanol–water (1:1)	Aluminum oxide	29
A2	Chloroform–methanol (70:30)	Aluminum oxide	30
A3	Methanol–water (96:8)	Aluminum oxide	29
A4	1-Butanol saturated with water	Aluminum oxide	—
A5	Chloroform–acetone (30:70)	Aluminum oxide	—
A6	Acetone–25% ammonia (75:25)	Aluminum oxide	—
A7	Acetone–25% ammonia (80:15)	Aluminum oxide	—
A8	Ethyl acetate–methanol–25% ammonia (85:15:15)	Aluminum oxide	21
A9	Methanol–1-pentanol–benzene–water (31:15:45:7)	Aluminum oxide	—
A10	Acetone–methanol–25% ammonia (85:15:10)	Aluminum oxide	—

i.e., the systems showing the smallest taxonomic distance, Δ_{ij}, or the highest correlation coefficient, ρ_{ij}. These systems are considered to form one group, i'. The similarity between group i' and all other systems (*e.g.*, 1) is then calculated as follows (for instance for weighted pair grouping of distances):

$$\Delta_{i'1} = \Delta_{(i,j)1} = \tfrac{1}{2}(\Delta_{i1} + \Delta_{j1}) \qquad \text{(Eq. 2)}$$

A new $(n-1) \times (n-1)$ similarity matrix is constructed by reduction with one column and one row of the original matrix. This reduction is completed when all systems are linked to another system or group of systems in one nonoverlapping hierarchic system of groups and subgroups, eventually depicted in what is called a dendrogram.

Figure 1 represents the dendrogram resulting from a numerical taxonomic classification of the chromatographic systems in function of the taxonomic distance. Figure 2 shows the dendrogram in function of the correlation between the systems.

Systems 34–38 (Table III) are not taken into account for the numerical taxonomy classifications, because too many sulfonamides dissociate in two or more spots when developed with these solvent combinations.

Successive breaking of the links on the lowest three levels of the dendrogram yields, consecutively, two, three, and four groups of systems. In Fig. 1, the individually best systems (*i.e.*, with the highest information content) in each group are Systems 4 and A7, successively joined by Systems 29 and A9. A combination of these four systems allows identification of 20 out of 22 sulfonamides. System 29, however, was selected out of a group consisting of only one element. Therefore, the possibility exists that the chosen system indeed shows a peculiar chromatographic behavior but, nevertheless, has a poor separating capability.

To prevent this situation, Systems 29 and A9 are replaced by System A9 and one of the best systems out of the group formed by breaking off the link immediately following, or else by System A9 and a system that allows separation of both sulfonamides that could not be separated by the foregoing combination. Some of these systems are A4, 32, 33, and 45. A combination of Systems 4, A7, A9, and 45 (or 33, 32, or A4) yields an optimal separation pattern in which all sulfonamides under investigation can be identified by their R_f values.

The dendrogram in Fig. 2 yields a similar conclusion. The classification followed by selection of systems with the described procedure leads to a combination of System 4 with A7, successively followed by Systems 29 and A2 (two sulfonamides cannot be separated). Since System 29 is again selected out of a group containing only one element, the combination of 29 and A2 is replaced by A2 and the most informative system out of the group on the level immediately following, *i.e.*, System 45. The combi-

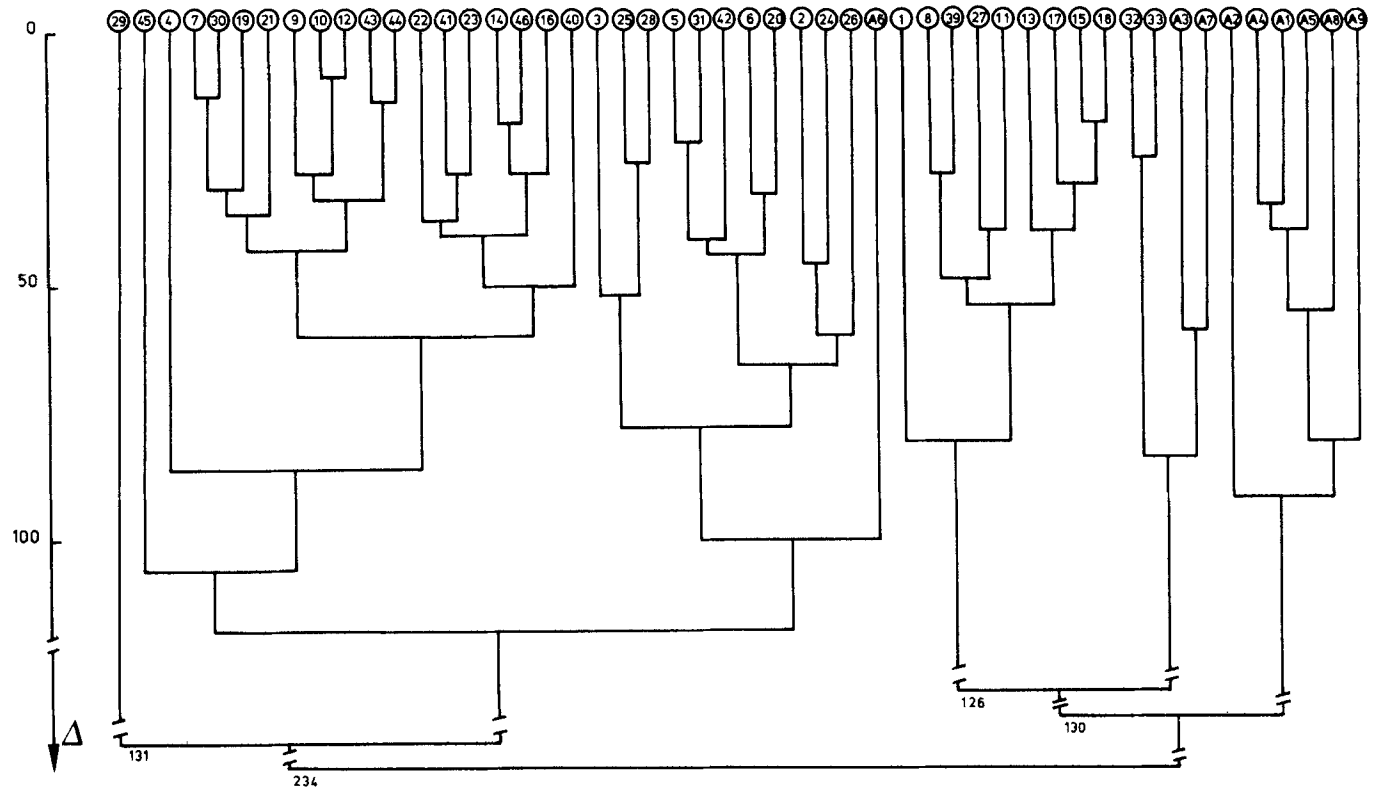

Figure 1—*Classification obtained by weighted pair arithmetic average linkage numerical taxonomy with the taxonomic distance, Δ, as the similarity parameter.*

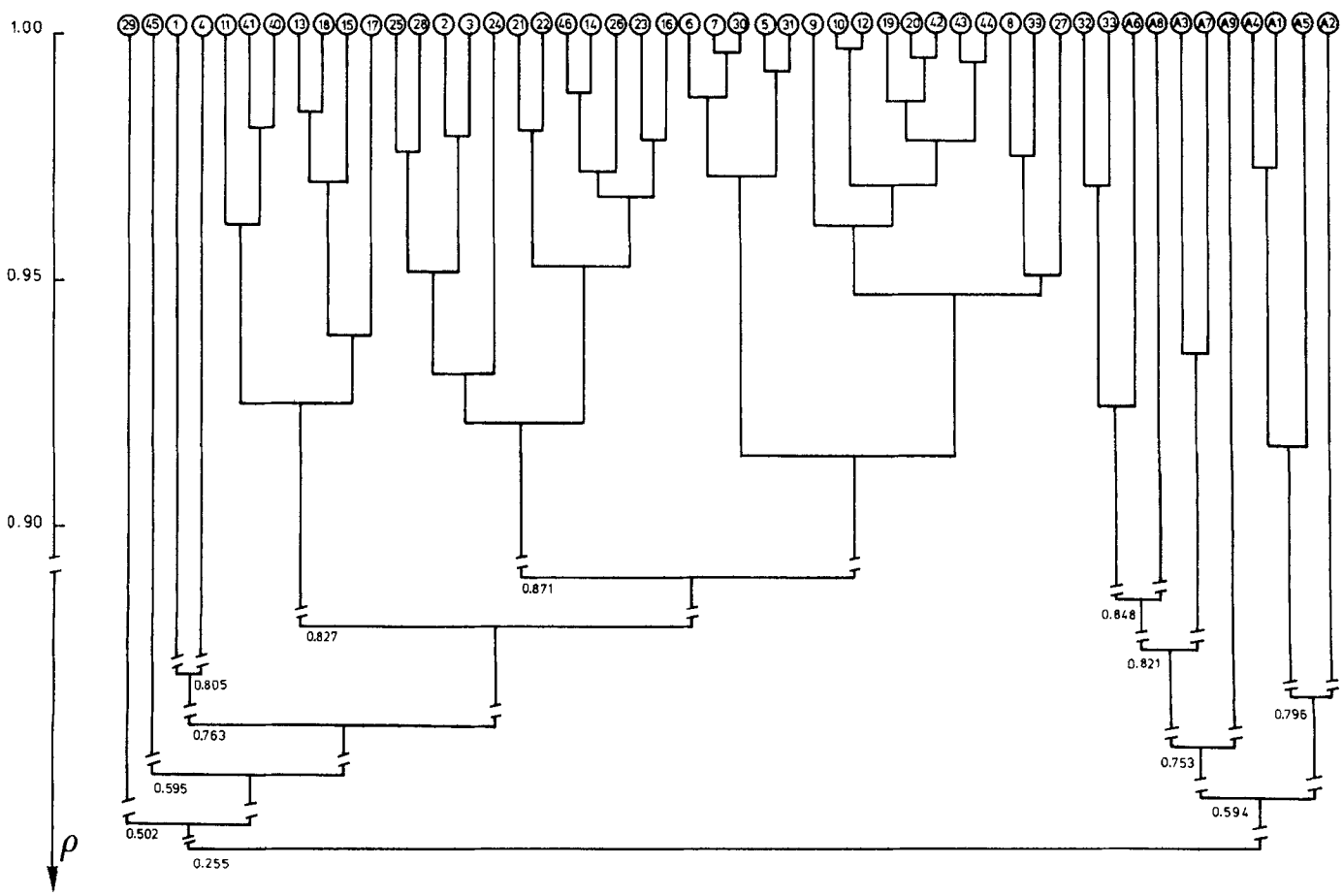

Figure 2—*Classification obtained by weighted pair arithmetic average linkage numerical taxonomy with the correlation coefficient, ρ, as the similarity parameter.*

Table III—R_f Values × 100 of the Sulfonamides in the Systems Selected after the Screening Test and Information Content of the Individual Systems (Expressed in Bit) (t = tailing)

Compound		1	2	3	4	5	6	7	8	9	10	11	12	13	14	15	16	17	18	19
Sulfanilamide	1	29	75	85	61	67	54	35	18	35	31	23	30	18	55	16	59	9	16	37
Sulfacetamide	2	18	72	84	53	74	63	44	26	49	42	29	42	22	59	19	58	16	19	40
Sulfaguanidine	3	1	48	70	21	53	39	18	6	15	9	5	8	3	20	2	19	2	2	15
Sulfapyridine	4	24	69	79	47	79	73	57	38	61	53	38	52	29	63	24	60	36	25	50
Sulfadiazine	5	20[t]	63[t]	78[t]	24[t]	79	72	57	44	65	59	45	58	38	61	30	63	35	33	47
Sulfamerazine	6	26	66	80	33	79	73	60	42	66	66	51	63	40	66	34	67	37	36	53
Sulfathiazole	7	3	70	80	53	77	66	52	31	48	42	29	41	21	43	7	47	19	16	38
Isosulfamerazine	8	25[t]	68	79[t]	25[t]	79	71	57	43	66	67	54	67	42	67	34	70	38	39	56
Sulfamethazine	9	30	68	80	50	79	71	60	44	66	68	53	67	40	69	37	68	40	36	57
Sulfisomidine	10	8	26	52	11	78	72	55	34	46	34	20	32	12	37	12	25	13	10	32
Sulfaphenazole	11	36	95	97	89	79	73	60	43	66	69	63	72	54	68	42	80	36	47	59
Sulfisoxazole	12	35	84	93	74	76	66	55	32	62	61	48	58	38	70	31	72	27	29	53
Sulfamethizole	13	10	67	79	46	72	73	53	28	55	52	37	48	26	45	14	40	26	18	44
Sulfamethoxypyridazine	14	18	74	84	53	79	73	60	39	65	66	52	64	41	63	27	61	37	35	60
Sulfameter	15	18	73	84	55	79	72	60	39	66	66	38	66	46	67	33	70	37	37	58
Sulfadimethoxine	16	40	90	94	85	78	73	60	40	67	69	69	71	64	77	44	82	53	50	62
Phthalylsulfathiazole	17	1	0	18	2	29	16	5	2	3	3	2	2	1	2	0	0	4	0	0
Butylsulfanilureum	18	28	97	98	90	79	73	57	40	66	68	57	66	47	68	35	73	42	37	60
Tolbutamide	19	55	100	98	98	79	73	58	44	67	72	69	72	70	87	74	82	56	70	57
Chlorpropamide	20	26	91	98	84	78	73	58	43	57	71	71	73	70	73	57	80	56	56	61
Sulfamethoxazole	21	48	95	97	88	79	71	60	41	66	69	61	66	51	71	37	77	38	40	61
Succinylsulfathiazole	22	0	0	8	2	21	14	5	1	3	1	0	1	2	2	0	1	3	1	0
Information content		3.17	3.17	2.77	3.60	1.46	1.61	2.29	2.33	2.24	2.71	3.33	3.11	3.33	3.14	3.22	3.24	2.79	3.08	2.91

Compound		20	21	22	23	24	25	26	27	28	29	30	31	32	33	34	35	36	37	38
Sulfanilamide	1	54	61	73	73	74	84	68	27	85	91	34	69	83	80	77	82	86	80	84
Sulfacetamide	2	60	54	67	66	71	85	75	38	85	25	44	72	38	32	9	39/79	39/86	41/84	86
Sulfaguanidine	3	31	19	15	16	50	49	15	11	69	73	18[t]	49	60	56	48	76	24/75	49	73/86
Sulfapyridine	4	68	58	70	72	72	81	75	45	81	92	57	74	52	46	76	80	45/80	82	85
Sulfadiazine	5	66	57	66	63	67	73	78	46	73	24	57	73	35	27	12	38/79	39/78	40	30/81
Sulfamerazine	6	70	57	66	68	70	80	85	48	81	90	57	75	38	31	77	81	51/82	44/86	85
Sulfathiazole	7	56	43	44	42	62	81	73	37	82	35	49	72	47	41	70	77	43/82	46/82	25/83
Isosulfamerazine	8	73	55	68	67	70	82	83	50	84	91	56	74	30	29	19	80	52	41/86	87
Sulfamethazine	9	72	57	74	73	74	80	81	49	81	91	57	74	43	35	75	81	58/82	45/87	87
Sulfisomidine	10	51	44	45	30	57	61	48	42	65	30	51	75	40	43	17	76	58	51	48/68
Sulfaphenazole	11	74	65	85	84	83	98	97	52	99	94	57	74	58	55	18	84	58/95	52	97
Sulfisoxazole	12	69	63	84	82	82	91	88	45	92	94	51	74	46	46	82/14	84	51/91	58/86	92
Sulfamethizole	13	60	45	63	53	65	79	75	38	78	87	50[tt]	69	44	42	69/13	43/78	45/80	48	30/82
Sulfamethoxypyridazine	14	72	55	65	66	57	83	85	49	84	94	57	75	43	39	73/23	80	57/87	89	88
Sulfameter	15	72	63	70	68	71	83	83	48	83	94	57	75	34	30	75/20	81	48/83	50/88	86
Sulfadimethoxine	16	73	62	85	83	84	95	97	53	94	95	57	75	44	47	78/24	85	57/91	53/95	95
Phthalylsulfathiazole	17	9	0	0	1	0	43	0	1	55	49	0	17	32	20	4/69	23	26/40, 86	37	8/84
Butylsulfanilureum	18	74	64	76	82	81	99	96	48	98	93	56	76	47	41	85	83	59/96	79/88	98
Tolbutamide	19	76	59	73	96	93	99	100	66	99	49	57	76	55	56	92	82	99	90	6
Chlorpropamide	20	75	60	76	84	80	98	100	66	99	92	57	75	60	60	79	82	96	79	97
Sulfamethoxazole	21	75	60	75	86	87	97	95	48	97	94	56	39	44	39	90	87	94	88	97
Succinylsulfathiazole	22	7	0	0	1	0	40	0	0	49	47	0	13	20	13	1	17	18	39	3
Information content		2.46	2.49	3.00	3.10	2.76	2.37	2.87	2.55	2.76	2.29	1.96	2.19	2.92	3.14	—	—	—	—	—

(continued)

Table III—(*Continued*)

Compound	39	40	41	42	43	44	45	46	A1	A2	A3	A4	A5	A6	A7	A8	A9	A10
Sulfanilamide	1 17	42	59	61	46	42	40	55	71	66	92	73	71	97	96	69	64	100
Sulfacetamide	2 26	47	64	67	50	50	62	61	2	4	40	6	2	58	37	3	12	9
Sulfaguanidine	3 6	16	25	41	29	26	22	24	38	48	74	52	31	92	90	48	49	92
Sulfapyridine	4 45	49	61	73	55	53	58	65	28	73	25	46	50	67	43	15	55	13
Sulfadiazine	5 45	52	64	74	55[t]	52	67	64	5	3	6	6	2	52	22	3	3	4
Sulfamerazine	6 48	58	69	82	61	60	72	66	4	7	11	9	5	57	18	5	17	7
Sulfathiazole	7 31	42	52	62	47	45	48	47	7	5	16	14	4	73	40	9	16	13
Isosulfamerazine	8 48	61[t]	70	84	65	63	74	68	5	4	10	8	10	55	18	4	14	4
Sulfamethazine	9 50	65	72	85	68	67	74	69	13	62	28	19	33	62	27	8	8	8
Sulfisomidine	10 38	26	38	63	45	45	27	45	10	20	51	12	7	69	49	8	25	18, 92
Sulfaphenazole	11 48	80	87	86	69	70	82	71	16	13	66	23	25	85	70	17	40	64, 97
Sulfisoxazole	12 38	64	80	78	58	59	72	71	4	4	52	8	2	76	48	12	17	30, 87
Sulfamethizole	13 39	47	59	71	47	50	64	54	2	2	10	4	1	69	36	8	7	14
Sulfamethoxypyridazine	14 45	60	69	82	68	64	70	67	10	50	12	20	3	61	26	10	38	12
Sulfameter	15 45	60	68	81	64	61	72	69	6	15	8	13	3	52	17	6	19	11
Sulfadimethoxine	16 52	83	85	85	75	73	83	72	10	34	35	18	4	77	52	18	36	33
Phthalylsulfathiazole	17 8	2	4	11	1	7	51	1	4	4	2	13	0	40	4	1	1	2
Butylsulfanilureum	18 45	84	87	87	73	70	80	69	5	7	17	12	4	70	27	13	21	11
Tolbutamide	19 50	94	94	89	79	77	44	80	5	4	28	11	2	90	35	22	48	16
Chlorpropamide	20 52	93	93	88	79	67	84	75	4	3	34	9	1	87	43	33	51	18
Sulfamethoxazole	21 44	81	86	86	69	7	80	68	3	2	13	6	3	74	33	8	14	14
Succinylsulfathiazole	22 8	2	5	12	0		42	2	0	1	2	1	0	44	1	0	2	0
Information content	2.57	3.24	3.39	2.68	2.95	3.15	2.92	2.88	2.31	2.73	3.35	2.59	1.85	3.26	3.41	2.60	3.39	—

nation of Systems 4, A7, A2, and 45 allows unambiguous identification of all 22 sulfonamides.

CONCLUSION

A practical conclusion is that, for the identification of sulfonamides by TLC, the following systems should be used in the order given: Systems 4, A7, A9 or A2, and 45 or 33, 32, or A4.

The best of all systems investigated is a very simple one (only one solvent). This practical conclusion confirms the experience of many practicing TLC or paper chromatography specialists that there is often no need for complex, multicomponent solvent systems and that good or, as in this case, even the best results are obtained with simple, easy-to-handle systems.

Our more general conclusion is that the use of formal methods for the evaluation and combination of TLC systems based on classification with numerical taxonomy, followed by selection of the individually best systems, leads to an optimal set of silica gel and aluminum oxide systems. This set allows the complete qualitative identification of commonly used sulfonamides.

REFERENCES

(1) G. H. Wagman and M. J. Weinstein, "Chromatography of Antibiotics," Elsevier, New York, N.Y., 1973.

(2) M. Sarsunova, V. Schwarz, E. Feketeova, and J. Protiva, *Pharmazie*, **21**, 219 (1966).

(3) M. Gajdos, *Cesk. Farm.*, **14**, 71 (1965).

(4) H. R. Klein and W. J. Mader, *J. Pharm. Sci.*, **60**, 448 (1971).

(5) K. C. Guven and O. Pekin, *Eczacilik Bul.*, **8**, 146 (1966); through *Chem. Abstr.*, **65**, 19928b (1966).

(6) E. G. C. Clarke and D. J. Humphreys, *J. Pharm. Pharmacol.*, **22**, 845 (1970).

(7) H. G. Gänshirt, in "Thin-Layer Chromatography," E. Stahl, Ed., Springer-Verlag, New York, N.Y., 1969, p. 544.

(8) W. Kamp, *Pharm. Weekbl.*, **99**, 1309 (1964).

(9) G. Ritschel-Beurlin, *Arzneim.-Forsch.*, **15**, 1247 (1965).

(10) R. D. Strickland, *J. Chromatogr.*, **24**, 455 (1966).

(11) K. C. Guven, S. Geçgil, and O. Pekin, *Eczacilik Bul.*, 8 158 (1966); through *Chem. Abstr.*, **65**, 18427d (1966).

(12) G. Wagner and J. Wandel, *Pharmazie*, **21**, 105 (1965).

(13) J. Pastor and R. Raimondi, *Trav. Soc. Pharm. Montpellier*, **23**, 220 (1963); through *Chem. Abstr.*, **62**, 11634 (1965).

(14) J. Reisch, H. Bornfleth, and J. Rheinbay, *Pharm. Ztg. (Frankfurt)*, **107**, 920 (1962).

(15) J. Zarnack and S. Pfeiffer, *Pharmazie*, **19**, 216 (1964).

(16) T. Bičan-Fister and V. Kajganovič, *J. Chromatogr.*, **11**, 492 (1963).

(17) J. L. Kiger and J. G. Kiger, *Ann. Pharm. Fr.*, **24**, 593 (1966).

(18) M. I. Walash and S. P. Agarwal, *J. Pharm. Sci.*, **61**, 277 (1972).

(19) J. Reisch, H. Bornfleth, and G. L. Tittle, *Pharm. Ztg. (Frankfurt)*, **109**, 74 (1964); through *Chem. Abstr.*, **63**, 16129g (1965).

(20) J. Pastor and R. Raimondi, *Bull. Soc. Pharm. Marseille*, **13**, 193 (1964); through *Chem. Abstr.*, **63**, 16133d (1965).

(21) M. T. Van der Venne and J. B. T'Siobbel, *J. Pharm. Belg.*, **18**, 557 (1963).

(22) T. Bičan-Fister and V. Kajganovič, *J. Chromatogr.*, **16**, 503 (1964).

(23) W. Kamp, *Pharm. Weekbl.*, **101**, 181 (1966).

(24) R. Neidlein, G. Klügel, and U. Lebert, *Pharm. Ztg.*, **20**, 651 (1965).

(25) N. Karpitschka, *Mikrochim. Ichnoanalyt. Acta*, **1**, 157 (1963).

(26) C. H. Pao, *Yao Hseuh Hseush Pao*, **13**, 67 (1966); through *Anal. Abstr.*, **14**, 3540 (1967).

(27) S. Klein and B. T. Kho, *J. Pharm. Sci.*, **51**, 966 (1962).

(28) E. G. Wollish, M. Schmall, and M. Hawrylyshyn, *Anal. Chem.*, **33**, 1138 (1961).

(29) J. Wandel, in "Thin-Layer Chromatography," E. Stahl, Ed., Springer-Verlag, New York, N.Y., 1969.

(30) L. R. Alexander and E. R. Stanley, *J. Assoc. Offic. Agr. Chem.*, **48**, 278 (1965).

(31) D. L. Massart, *J. Chromatogr.*, **79**, 157 (1973).

(32) C. E. Shannon, "A Mathematical Theory of Communication," *Bell Syst. Tech. J.* (1948).

(33) P. F. Dupuis and A. Dijkstra, *Anal. Chem.*, **47**, 379 (1975).

(34) A. C. Moffat and K. W. Smalldon, *J. Chromatogr.*, **90**, 9 (1974).

(35) A. Eskes, P. F. Dupuis, A. Dijkstra, H. De Clercq, and D. L. Massart, *Anal. Chem.*, **47**, 2168 (1975).
(36) H. De Clercq and D. L. Massart, *J. Chromatogr.*, **115**, 1 (1975).
(37) D. L. Massart and H. De Clercq, *Anal. Chem.*, **46**, 1988 (1974).
(38) P. H. A. Sneath and R. R. Sokal, "Numerical Taxonomy," Freeman, San Francisco, Calif., 1973, p. 124.
(39) H. De Clercq, D. Van Oudheusden, and D. L. Massart, *Analysis*, **3**, 527 (1975).

ACKNOWLEDGMENTS AND ADDRESSES

Received July 15, 1976, from the *Farmaceutisch Instituut, Vrije Universiteit Brussel, Paardenstraat 67, B-1640 Sint-Genesius-Rode, Belgium.*

Accepted for publication September 16, 1976.

Presented in part at the 27th Pittsburgh Conference on Analytical Chemistry and Applied Spectroscopy, Cleveland, Ohio, March 1976.

The authors thank the Fonds voor Geneeskundig Wetenschappelijk Onderzoek for financial support. They also thank the following manufacturers for supplying pure drug samples: Bayer Belgium N.V., Ciba-Geigy N.V., Hoechst Belgium N.V., Janssen Pharmaceutica Beerse, Labaz N.V., Merck Darmstadt, Parke-Davis N.V., Pfizer; Roche N.V., Schering, Substantia N.V., and Wellcome N.V.

[x] To whom inquiries should be directed.

Comparative Pharmacokinetics of Coumarin Anticoagulants XXIX: Elimination Kinetics and Anticoagulant Activity of (*S*)-(−)-Warfarin in Rats before and after Chronic Administration

AVRAHAM YACOBI and GERHARD LEVY [x]

Abstract □ The kinetics of elimination and the anticoagulant effect of (*S*)-(−)-warfarin were determined in adult male rats before and after daily drug administration for 13 days. There was a small but statistically significant ($p < 0.05$) decrease in the body clearance of (*S*)-(−)-warfarin (from 4.84 to 4.37 ml/hr/kg) and an increase in the serum free fraction of racemic warfarin (added to serum *in vitro*) from 0.00850 to 0.0107 ($p < 0.05$). The concentration of (*S*)-(−)-warfarin in serum at which the synthesis rate of prothrombin complex activity is one-half of the prewarfarin rate increased from 0.532 to 0.655 μg/ml on the average ($p < 0.05$).

Keyphrases □ Warfarin—elimination kinetics and anticoagulant activity, effect of chronic administration, rats □ Elimination kinetics—warfarin, effect of chronic administration, rats □ Anticoagulants—warfarin, elimination kinetics and activity, effect of chronic administration, rats □ Coumarins—warfarin, elimination kinetics and anticoagulant activity, effect of chronic administration, rats

The coumarin anticoagulants act by inhibiting the synthesis of the vitamin K-dependent clotting factors II (prothrombin), VII, IX, and X. This inhibitory effect is accompanied by the formation of so-called abnormal prothrombin in humans (1–4), oxen and cows (5–8), and rats (9–12). In humans treated with a coumarin anticoagulant, abnormal prothrombin can be detected within 8–12 hr after drug administration and becomes the predominant form of prothrombin in plasma after 24–84 hr (3). The earlier investigations suggested that abnormal prothrombin has no coagulant activity; more recently, it has become apparent that there are several abnormal prothrombins and that some do have activity, but considerably less than that of normal prothrombin (4, 8). Apparently, abnormal prothrombin is a precursor of normal prothrombin and accumulates during treatment with coumarin anticoagulants, because these vitamin K antagonists interfere with the conversion of the precursor to its fully biologically active form (9, 11, 12).

The clinical implications of the accumulation of abnormal forms of prothrombin during chronic treatment with dicumarol or warfarin are not known. In view of the potential hazards of conducting such studies in humans, an investigation was carried out in rats to determine the relationship between the anticoagulant effect and the warfarin concentration in plasma before and after chronic drug administration. While the results may differ quantitatively from those in humans, it is considered likely that they will reflect in principle the events that may be encountered clinically.

EXPERIMENTAL

This investigation was carried out in five phases: (*a*) screening of rats for serum protein binding of warfarin, (*b*) administration of a single large dose of warfarin to rats whose serum free fraction of warfarin varied widely and determination of the time courses of drug concentration and anticoagulant activity in plasma, (*c*) daily administration of a maintenance dose of warfarin to these rats for 13 days, (*d*) administration of a second large dose of warfarin and determination of the time courses of drug concentration and anticoagulant activity in plasma, and (*e*) determination of serum protein binding of warfarin.

A 3-ml blood sample was taken from the tail artery of 26 adult male Sprague–Dawley rats, and the serum was separated. The serum was spiked with racemic ^{14}C-warfarin, about 1 μg/ml, and the free fraction was determined by equilibrium dialysis (13).

Based on the results of the screening study, 12 rats with widely differing serum free fraction values for warfarin were selected. Their body weights ranged from 350 to 440 g during all phases of the investigation. They received a 0.6-mg/kg iv injection of ^{3}H-(*S*)-(−)-warfarin (specific activity, 1.43 mCi/mg).

Blood samples (0.45 ml) were taken serially from the tail artery until prothrombin complex activity had returned to between 60 and 80% of the prewarfarin level. Plasma warfarin concentrations were determined by scintillation counting after extraction and TLC using a slight modification of a previously described method (14). To 0.2-ml samples of plasma was added 5 μl of unlabeled (*S*)-(−)-warfarin, 1 mg/ml, in acetone solution. The samples were then acidified and extracted with 2.5 ml of ethylene dichloride from which 2 ml was evaporated under nitrogen for chromatography (14). Recovery of ^{3}H-(*S*)-(−)-warfarin from spiked samples was 88.3 ± 2.4% (mean ± *SD*, $n = 16$) in the 0.013–6.33-μg/ml concentration range and was independent of concentration. Determinations of prothrombin complex activity and pharmacokinetic calculations were carried out as previously described (14).

After completion of the single-dose warfarin study, the rats received daily injections of ^{3}H-(*S*)-(−)-warfarin, 83–98 μg/kg ip, for 13 days to maintain prothrombin complex activity synthesis rate (R_{syn}) at about 30% of normal.

Two days after the last maintenance dose, the rats received another

(35) A. Eskes, P. F. Dupuis, A. Dijkstra, H. De Clercq, and D. L. Massart, *Anal. Chem.*, **47**, 2168 (1975).
(36) H. De Clercq and D. L. Massart, *J. Chromatogr.*, **115**, 1 (1975).
(37) D. L. Massart and H. De Clercq, *Anal. Chem.*, **46**, 1988 (1974).
(38) P. H. A. Sneath and R. R. Sokal, "Numerical Taxonomy," Freeman, San Francisco, Calif., 1973, p. 124.
(39) H. De Clercq, D. Van Oudheusden, and D. L. Massart, *Analysis*, **3**, 527 (1975).

ACKNOWLEDGMENTS AND ADDRESSES

Received July 15, 1976, from the *Farmaceutisch Instituut, Vrije Universiteit Brussel, Paardenstraat 67, B-1640 Sint-Genesius-Rode, Belgium.*

Accepted for publication September 16, 1976.

Presented in part at the 27th Pittsburgh Conference on Analytical Chemistry and Applied Spectroscopy, Cleveland, Ohio, March 1976.

The authors thank the Fonds voor Geneeskundig Wetenschappelijk Onderzoek for financial support. They also thank the following manufacturers for supplying pure drug samples: Bayer Belgium N.V., Ciba-Geigy N.V., Hoechst Belgium N.V., Janssen Pharmaceutica Beerse, Labaz N.V., Merck Darmstadt, Parke-Davis N.V., Pfizer; Roche N.V., Schering, Substantia N.V., and Wellcome N.V.

[x] To whom inquiries should be directed.

Comparative Pharmacokinetics of Coumarin Anticoagulants XXIX: Elimination Kinetics and Anticoagulant Activity of (*S*)-(−)-Warfarin in Rats before and after Chronic Administration

AVRAHAM YACOBI and GERHARD LEVY [x]

Abstract □ The kinetics of elimination and the anticoagulant effect of (*S*)-(−)-warfarin were determined in adult male rats before and after daily drug administration for 13 days. There was a small but statistically significant ($p < 0.05$) decrease in the body clearance of (*S*)-(−)-warfarin (from 4.84 to 4.37 ml/hr/kg) and an increase in the serum free fraction of racemic warfarin (added to serum *in vitro*) from 0.00850 to 0.0107 ($p < 0.05$). The concentration of (*S*)-(−)-warfarin in serum at which the synthesis rate of prothrombin complex activity is one-half of the prewarfarin rate increased from 0.532 to 0.655 μg/ml on the average ($p < 0.05$).

Keyphrases □ Warfarin—elimination kinetics and anticoagulant activity, effect of chronic administration, rats □ Elimination kinetics—warfarin, effect of chronic administration, rats □ Anticoagulants—warfarin, elimination kinetics and activity, effect of chronic administration, rats □ Coumarins—warfarin, elimination kinetics and anticoagulant activity, effect of chronic administration, rats

The coumarin anticoagulants act by inhibiting the synthesis of the vitamin K-dependent clotting factors II (prothrombin), VII, IX, and X. This inhibitory effect is accompanied by the formation of so-called abnormal prothrombin in humans (1–4), oxen and cows (5–8), and rats (9–12). In humans treated with a coumarin anticoagulant, abnormal prothrombin can be detected within 8–12 hr after drug administration and becomes the predominant form of prothrombin in plasma after 24–84 hr (3). The earlier investigations suggested that abnormal prothrombin has no coagulant activity; more recently, it has become apparent that there are several abnormal prothrombins and that some do have activity, but considerably less than that of normal prothrombin (4, 8). Apparently, abnormal prothrombin is a precursor of normal prothrombin and accumulates during treatment with coumarin anticoagulants, because these vitamin K antagonists interfere with the conversion of the precursor to its fully biologically active form (9, 11, 12).

The clinical implications of the accumulation of abnormal forms of prothrombin during chronic treatment with dicumarol or warfarin are not known. In view of the potential hazards of conducting such studies in humans, an investigation was carried out in rats to determine the relationship between the anticoagulant effect and the warfarin concentration in plasma before and after chronic drug administration. While the results may differ quantitatively from those in humans, it is considered likely that they will reflect in principle the events that may be encountered clinically.

EXPERIMENTAL

This investigation was carried out in five phases: (*a*) screening of rats for serum protein binding of warfarin, (*b*) administration of a single large dose of warfarin to rats whose serum free fraction of warfarin varied widely and determination of the time courses of drug concentration and anticoagulant activity in plasma, (*c*) daily administration of a maintenance dose of warfarin to these rats for 13 days, (*d*) administration of a second large dose of warfarin and determination of the time courses of drug concentration and anticoagulant activity in plasma, and (*e*) determination of serum protein binding of warfarin.

A 3-ml blood sample was taken from the tail artery of 26 adult male Sprague–Dawley rats, and the serum was separated. The serum was spiked with racemic ^{14}C-warfarin, about 1 μg/ml, and the free fraction was determined by equilibrium dialysis (13).

Based on the results of the screening study, 12 rats with widely differing serum free fraction values for warfarin were selected. Their body weights ranged from 350 to 440 g during all phases of the investigation. They received a 0.6-mg/kg iv injection of ^{3}H-(*S*)-(−)-warfarin (specific activity, 1.43 mCi/mg).

Blood samples (0.45 ml) were taken serially from the tail artery until prothrombin complex activity had returned to between 60 and 80% of the prewarfarin level. Plasma warfarin concentrations were determined by scintillation counting after extraction and TLC using a slight modification of a previously described method (14). To 0.2-ml samples of plasma was added 5 μl of unlabeled (*S*)-(−)-warfarin, 1 mg/ml, in acetone solution. The samples were then acidified and extracted with 2.5 ml of ethylene dichloride from which 2 ml was evaporated under nitrogen for chromatography (14). Recovery of ^{3}H-(*S*)-(−)-warfarin from spiked samples was 88.3 ± 2.4% (mean ± *SD*, $n = 16$) in the 0.013–6.33-μg/ml concentration range and was independent of concentration. Determinations of prothrombin complex activity and pharmacokinetic calculations were carried out as previously described (14).

After completion of the single-dose warfarin study, the rats received daily injections of ^{3}H-(*S*)-(−)-warfarin, 83–98 μg/kg ip, for 13 days to maintain prothrombin complex activity synthesis rate (R_{syn}) at about 30% of normal.

Two days after the last maintenance dose, the rats received another

Table I—Pharmacokinetic Constants of (*S*)-(−)-Warfarin before and after Chronic Drug Administration to Selected Rats

Constant	Range		Mean		Ratio[a], Before/After
	Before	After	Before	After	
Half-life, hr	10.4–46.7	10.3–47.8	22.4	24.1[b]	0.938 ± 0.114
Volume of distribution[c], ml/kg	88.2–145	86.7–145	117	113[b]	1.05 ± 0.089
Total clearance, ml/hr/kg	1.68–9.58	1.47–8.13	4.84	4.37[d]	1.14 ± 0.180
Serum free fraction of racemic warfarin, × 100	0.247–1.74	0.238–2.31	0.850	1.07[d]	0.819 ± 0.121

[a] Mean ± *SD*, $n = 11$. [b] Not statistically significantly different from the Before value. [c] The apparent volume of distribution after chronic administration was determined by dividing the intravenous dose by the extrapolated zero-time drug concentration minus the concentration immediately before injection. [d] Statistically significantly different ($p < 0.05$) from the Before value by paired t test.

0.6-mg/kg iv dose and serial blood samples were again obtained for the determination of warfarin concentration and prothrombin complex activity.

Ten days after the second large intravenous dose, the rats were sacrificed by removing blood from the aorta under ether anesthesia. Serum was separated and used for the determination of the serum free fraction values of racemic and (*S*)-(−)-warfarin.

The pharmacokinetic studies were preceded by an experiment to rule out artifacts due to possible tritium exchange. Two rats received a very large dose of (*S*)-(−)-warfarin (12 mg/kg iv) together with ^{3}H-(*S*)-(−)-warfarin, 0.6 mg/kg iv. Blood samples were obtained repeatedly over 29 hr and assayed by scintillation counting as previously described as well as by spectrophotometry (15). The ratio of warfarin concentrations determined by the two methods was 1.01 ± 0.05 (mean ± *SD*, $n = 7$) and was independent of time after injection.

RESULTS

The rats selected had serum free fraction values for racemic warfarin ranging from 0.00247 to 0.0174 (representing from 98.26 to 99.75% protein binding). Since one of the 12 rats died during the study, data from only 11 animals are reported. Figure 1 shows the time course of warfarin concentrations in the plasma of two animals, the most rapid and the slowest eliminator of the drug, before and after chronic warfarin administration. The results of all pharmacokinetic studies are summarized in Table I. As intended by selection of rats with widely varying serum warfarin free fraction values, the pharmacokinetic constants differed appreciably between animals. These constants changed only slightly after chronic drug administration, but the increases in total clearance and in serum free fraction were statistically significant.

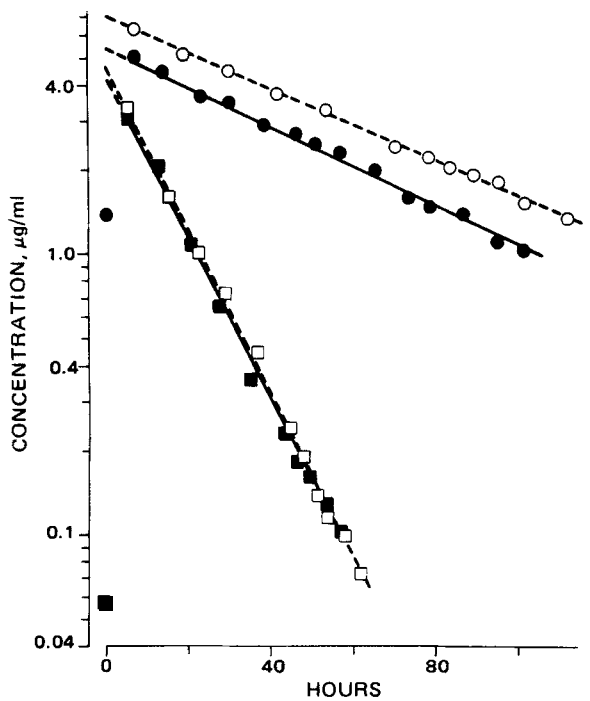

Figure 1—*Concentration of warfarin in serum of the rat with the highest clearance (squares) and the rat with the lowest clearance (circles) after intravenous injection of* (S)-(−)-*warfarin, 0.6 mg/kg, before (solid symbols) and after (open symbols) daily administration of the drug for 13 days. The symbols at zero time are the warfarin concentrations immediately before injection of the final dose.*

Strong and highly statistically significant ($p < 0.001$) correlations were observed between the pre- and postchronic administration values for the following pharmacokinetic constants in individual animals: serum free fraction of racemic warfarin ($r = 0.976$), biological half-life ($r = 0.957$), apparent volume of distribution ($r = 0.876$), and total clearance of (*S*)-(−)-warfarin ($r = 0.910$). The ratio of serum free fraction values, racemic/(*S*)-(−)-warfarin, was 1.28 ± 0.175 (mean ± *SD*) after chronic administration. Consistent with previously developed theory and experimental data on racemic warfarin (16), the total clearance of (*S*)-(−)-warfarin was proportional to the serum free fraction value of the drug in individual animals (Fig. 2).

The prothrombin complex activity of the animals before administration of the first warfarin dose was 105 ± 2% of the normal standard. Forty-eight hours after the last chronic (maintenance) dose, the prothrombin complex activity ranged from 30.5 to 91.7% (mean, 68.6%) of the standard. Animals with the highest total clearance of warfarin showed the most rapid recovery from the anticoagulant effect of the drug.

As in previous studies, the relationship between anticoagulant effect (inhibition of synthesis rate of prothrombin complex activity) and the logarithm of plasma warfarin concentration was essentially linear and could be characterized by a slope value (m) and a point. The latter is reported here as the concentration of (*S*)-(−)-warfarin at which the synthesis rate of prothrombin complex activity (R_{syn}) is one-half of normal (R^0_{syn}). The results obtained before and after chronic warfarin administration are presented in Table II. There was no significant change in slope, but there was a significant lateral shift of the effect–log concentration curve toward a higher concentration range, as reflected by the statistically significant increase in concentration at 0.5 R^0_{syn} after chronic warfarin treatment.

DISCUSSION

The two enantiomers of warfarin differ from one another with respect to elimination kinetics and anticoagulant potency (15). The ratio of plasma concentrations of the enantiomers changes, therefore, as a function of time (17). To circumvent possible interpretive problems in data analysis due to changing enantiomer concentration ratios, (*S*)-(−)-warfarin rather than the racemic mixture of (*S*)-(−)- and (*R*)-(+)-warfarin was used. As a further precaution, labeled drug was used not only for the single-dose experiments before and after chronic drug administration but also for the administration of maintenance doses. The use of unlabeled warfarin for maintenance dosing could introduce problems if a "deep" compartment exists for the drug that is not apparent upon administration of single doses.

Because of the pronounced interindividual differences in the serum protein binding of warfarin and of the consequent differences in the total clearance of the drug in rats (13), the serum free fraction of warfarin was determined in a relatively large group of rats and a smaller group with a relatively even and wide distribution of free fraction values was selected. It was possible, therefore, to examine the effect of chronic drug administration on rapid as well as on slow eliminators of warfarin.

There were only small and statistically not significant differences in the biological half-life and apparent volume of distribution of (*S*)-(−)-warfarin before and after chronic drug administration. However, the approximately 14% decrease in total clearance (based on individual clearance ratios) was statistically significant. Since the serum protein binding of racemic warfarin decreased by about 18% (based on individual free fraction ratios), the *intrinsic* clearance of warfarin (total clearance/free fraction) decreased even more than the total clearance. This conclusion is justified since there is a strong and linear correlation between the serum free fraction values of (*S*)-(−)- and racemic warfarin (18).

Essentially linear correlations were observed between the serum free fraction and total clearance values before and after chronic drug administration. These observations indicate that the changes in pharmacokinetic parameter values were of the same *relative* magnitude in

Table II—Relationship between Anticoagulant Effect and Serum Warfarin Concentration before and after Chronic Administration of (*S*)-(−)-Warfarin to Selected Rats

Rat	− Slope (− *m*)		Ratio of *m* Values, Before/After	Plasma Concentration at 0.5 R^0_{syn}, μg/ml		Ratio of Concentrations, Before/After
	Before	After		Before	After	
1	1.13	0.966	1.17	0.163	0.129	1.26
2	1.63	1.22	1.34	0.178	0.166	1.07
3	1.16	1.49	0.778	0.191	0.223	0.856
4	1.53	1.25	1.22	0.232	0.315	0.736
5	0.962	1.00	0.962	0.155	0.158	0.981
6	1.07	1.53	0.699	0.266	0.255	1.04
7	1.89	1.88	1.00	0.898	1.15	0.781
8	1.50	—[a]	—	0.529	—[a]	—
9	1.86	1.84	1.01	0.843	0.998	0.845
10	1.52	1.79	0.849	1.11	1.42	0.782
11	1.26	2.33	0.541	1.28	1.74	0.736
Mean[b]	1.40	1.53[c]	0.957	0.532	0.655[d]	0.909
SD			0.247			0.173

[a] This rat was given vitamin K to prevent bleeding. [b] All means without Rat 8. [c] Not statistically significantly different from the Before value. [d] Statistically significantly different ($p < 0.05$) from the Before value.

rapid and slow eliminators of warfarin. The reasons for these changes are not evident. They could be age dependent, but this possibility is unlikely since the time interval between experiments was well within the middle age phase of the animals. Another possibility, also entirely speculative, is that accumulation of drug metabolites caused product inhibition of warfarin biotransformation.

The anticoagulant effect–log plasma warfarin concentration curves were significantly shifted to the higher concentration range after chronic drug administration. The magnitude of this shift was even greater in terms of unbound drug concentration, since plasma protein binding of warfarin decreased somewhat after chronic drug administration. It would have been desirable to monitor steady-state drug concentrations and prothrombin complex activity during chronic administration, but this could not be done because the number of blood withdrawals from the tail artery of the rat is limited by scarification of the tail at the site of puncture.

The shift of the anticoagulant effect–log drug concentration curve toward higher concentrations could be due to changes in the normal rates of synthesis or degradation of vitamin K-dependent clotting factors or in the interaction between warfarin and its site of action. Accumulation of warfarin metabolities with anticoagulant activity would have had the opposite effect. On an entirely hypothetical basis, warfarin metabolites with no anticoagulant activity might, in fact, compete with warfarin at the latter's site of action and thereby act as inhibitors of the anticoagulant effect of warfarin. Finally, the observed effect can be a consequence of the accumulation, during warfarin treatment, of abnormal forms of prothrombin with some coagulant activity (4, 8). This possibility is most attractive, since it is based on experimental evidence rather than on inferences.

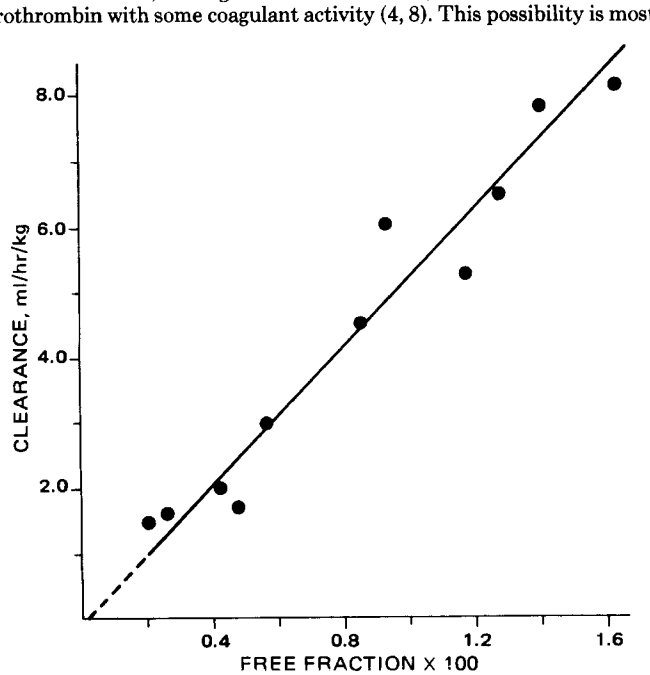

Figure 2—*Relationship between the total clearance and the serum free fraction of* (S)-(−)-*warfarin in 11 rats after chronic dosing* (r = *0.972*, p < *0.001*).

The changes in anticoagulant activity and total clearance of warfarin after chronic administration, as observed in this study, are relatively small and tend to cancel out. After chronic warfarin administration, higher drug concentrations are required to produce a given degree of anticoagulation, but the same dosing rate causes higher warfarin concentrations since drug clearance is decreased. The magnitude of these opposing effects in humans remains to be determined. It is possible that they occur in the initial "loading" or presteady-state phase of warfarin therapy and, therefore, may have little or no effect on the therapeutic management of patients receiving anticoagulant therapy.

REFERENCES

(1) P. O. Ganrot and J.-E. Nilêhn, *Scand. J. Clin. Lab. Invest.*, **22**, 23 (1968).

(2) F. Josso, J. M. Lavergne, M. Gouault, O. Prou-Wartelle, and J. P. Soulier, *Thromb. Diath. Haemorrh.*, **20**, 88 (1968).

(3) M. Brozović and L. Gurd, *Br. Haematol.*, **24**, 579 (1973).

(4) S. A. Morrison and M. P. Esnouf, *Nature New Biol.*, **242**, 92 (1973).

(5) G. L. Nelsestuen and J. W. Suttie, *J. Biol. Chem.*, **247**, 8176 (1972).

(6) J. Stenflo and P.-O. Ganrot, *ibid.*, **247**, 8160 (1972).

(7) J. Stenflo, *ibid.*, **247**, 8167 (1972).

(8) C. W. Prowse, P. Mattack, M. P. Esnouf, and A. M. Russell, *Biochim. Biophys. Acta*, **434**, 265 (1976).

(9) H. V. Johnson, C. Boyd, J. Martinovic, G. Valkovich, and B. C. Johnson, *Arch. Biochem. Biophys.*, **148**, 431 (1972).

(10) M. Pereira and D. Couri, *Biochim. Biophys. Acta*, **230**, 373 (1971).

(11) J. W. Suttie, D. V. Shah, and G. A. Grant, *Thromb. Diath. Haemorrh., Suppl.*, **57**, 13 (1974).

(12) C. T. Esmon, G. A. Grant, and J. W. Suttie, *Biochemistry*, **14**, 1595 (1975).

(13) A. Yacobi and G. Levy, *J. Pharm. Sci.*, **64**, 1660 (1975).

(14) A. Yacobi, L. B. Wingard, Jr., and G. Levy, *ibid.*, **63**, 868 (1974).

(15) A. Yacobi and G. Levy, *J. Pharmacokinet. Biopharm.*, **2**, 239 (1974).

(16) G. Levy and A. Yacobi, *J. Pharm. Sci.*, **63**, 805 (1974).

(17) G. Levy, R. A. O'Reilly, and L. B. Wingard, Jr., *Res. Commun. Chem. Pathol. Pharmacol.*, **7**, 359 (1974).

(18) A. Yacobi and G. Levy, *J. Pharmacokinet. Biopharm.*, **5**, 123 (1977).

ACKNOWLEDGMENTS AND ADDRESSES

Received November 8, 1976, from the *Department of Pharmaceutics, School of Pharmacy, State University of New York at Buffalo, Amherst, NY 14260.*

Accepted for publication December 13, 1976.

Supported in part by Grant GM 20852 from the National Institute of General Medical Sciences, National Institutes of Health.

Previous paper in this series: A. Yacobi and G. Levy, *J. Pharm. Sci.*, **66**, 145 (1977).

ˣ To whom inquiries should be directed.

Influence of Training and Pharmacological Treatment on Muscular Enzymatic Activities

G. BENZI ˣ, R. F. VILLA, A. MONTANI, O. PASTORIS, E. ARCELLI, P. STRADA, and E. ARRIGONI

Abstract □ The adaptation of some enzymatic activities of glycogenolysis (adenyl cyclase and phosphorylase), glycolysis (phosphofructokinase, pyruvate kinase, and lactate dehydrogenase), the tricarboxylic acid cycle (citrate synthase, isocitrate dehydrogenase, 2-ketoglutarate dehydrogenase, and malate dehydrogenase), and subsidiary pathways of pyruvate metabolism (glutamate pyruvate transaminase) was studied in the rat as a function of training time (25, 50, 100, 125, and 150 days). The workload was set at 25 m/min for 150 min/day. Some groups of animals were treated daily with vasodilators such as papaverine, caffeine, nicergoline, or bamethan. With a steady daily workload, at least three different periods can be recognized as a function of training time: (*a*) noncompensated mitochondrial adaptation, where an increase is observed both in the Krebs cycle enzymatic activities and in the enzymatic activities related to glycogenolysis and glycolysis; (*b*) compensated mitochondrial adaptation, where mitochondrial enzymatic activities further increase while activities of glycogenolysis and glycolysis return to base values; and (*c*) overcompensated mitochondrial adaptation, where mitochondrial enzymatic activities are in a steady state while pyruvate is largely transaminated to 2-ketoglutarate and somewhat reduced to lactate. The phase of mitochondrial adaptation is compensated for by the actual workload performed. As a consequence, a variation in the intensity factor causes the biological system to go back to the stage of mitochondrial noncompensation. Drugs play a role during the phase of noncompensated mitochondrial adaptation by modifying the aerobic mechanism (*e.g.*, nicergoline), the anaerobic mechanism (*e.g.*, caffeine), or both (*e.g.*, bamethan). These actions do not seem to be ascribable to the vasodilating properties of these drugs, since papaverine is always inactive. The administration of the drugs is totally ineffective when the adaptation of enzymatic activities to the endurance workload has been reached.

Keyphrases □ Enzyme activity—effect of training time and treatment with various vasodilators, rats □ Vasodilators—papaverine, caffeine, nicergoline, and bamethan, effect on muscular enzyme activity, rats □ Training time—effect on muscular enzyme activity, rats □ Papaverine—effect on muscular enzyme activity, rats □ Caffeine—effect on muscular enzyme activity, rats □ Nicergoline—effect on muscular enzyme activity, rats □ Bamethan—effect on muscular enzyme activity, rats

Blood and muscular concentrations of lactate and pyruvate during a submaximal exercise are lower in trained subjects than in untrained ones (1–4), the pyruvate being metabolized through the potentiation of various metabolic pathways as a function of training. Indeed, adequate endurance training causes an increase in mitochondrial oxidative power (5–7). Therefore, one might assume that the increased oxidation of pyruvate represents a decisive limiting factor, at least at the mitochondrial level.

In the Krebs cycle, the metabolic fate of acetyl coenzyme A is closely related to the condensation reaction with oxaloacetate. Consequently, the availability of oxaloacetate in the muscle becomes a limiting factor, both because of the condensation reaction and because of the catalytic reaction caused by the oxaloacetate dependence of the citrate synthase. In this case, the shunt of pyruvate to 2-ketoglutarate, malate, or oxaloacetate might represent an important subsidiary metabolic pathway (8–10).

Pharmacological treatment may influence enzymatic adaptation to endurance training, but virtually no data are available except for results showing that some vasodilating drugs can anticipate the time increase of some mitochondrial enzymatic activities induced in muscle by training. However, these drugs do not modify the plateau of these enzymatic activities, nor do they contribute to maintaining the level attained against the spontaneous decrease as a response to reduced muscular work (5).

In this investigation, the effect of training on the activity of the enzymes of glycogenolysis, glycolysis, the tricarboxylic acid cycle, and possible subsidiary pathways of pyruvate metabolism in the gastrocnemius muscle of rats was studied. In addition, the effect of some vasodilating drugs (papaverine, caffeine, nicergoline, and bamethan) on enzymatic adaptation was evaluated.

EXPERIMENTAL

Male Wistar rats (n = 151), 120–140 g, were chosen from a group of 400 animals raised under standard conditions (temperature, 23 ± 1°; and relative humidity, 55–60%) and fed a pellet diet[1] and water *ad libitum*.

During the first stage, 400 rats were submitted to psychomotor adaptation for 6 days/week for 2 consecutive weeks on a rotarod apparatus[2] in which the performance time could be recorded automatically. During this stage, the animals increased their motor activity from 2.5 to 10 m/min. For the second stage, 200 rats were chosen whose average performance time at the rate of 10 m/min, after the training period, was close to the mean of the sample examined.

In the exercising animals, the continuous run was progressively increased from 20 m/min for 60 min/day to 25 m/min for 150 min/day within a maximum of 50 days. The animals that were not able to attain this working capacity within this time were discarded. Consequently, the enzymatic recordings on the 25th day were carried out on the assumption that the animals examined would execute their performance within the established time. At any rate, the recordings on the 25th day were carried out in rats with a working capacity of 25 m/min for at least 120 min/day. Progressing from this workload to that of the 50th day (25 m/min for 150 min/day) caused the discarding of approximately 20% of the animals.

In addition to the training activity, 103 animals were treated daily with 0.5 ml/kg ip of a 1.6, 4, or 10×10^{-3} M solution of papaverine, caffeine, nicergoline, or bamethan. The rats were submitted to the test 30 min after treatment. For these drugs, these dosages fall in the range commonly used experimentally.

The 151 rats finally examined were taken from the following lots: (*a*) sedentary rats (n = 8); (*b*) rats trained for 25 days (n = 8); (*c*) rats trained for 25 days and treated with the three dose levels (0.5 ml/kg ip of 1.6, 4, or 10×10^{-3} M solutions) of one of the four drugs (n = 63); (*d*) rats trained for 50 days (n = 8); (*e*) rats trained for 100 days (n = 8); (*f*) rats trained for 100 days and treated with 0.5 ml/kg ip of a 4×10^{-3} M solution of one of the drugs tested (n = 20); (*g*) rats trained for 125 days (n = 8); (*h*) rats trained for 150 days (n = 8); and (*i*) rats trained for 150 days and treated with 0.5 ml/kg ip of a 4×10^{-3} M solution of one of the drugs tested (n = 20).

The biochemical observations were carried out after 25, 50, 100, 125, and 150 days of training. Training was discontinued 72 hr prior to sacrifice. The rats were then beheaded, and their gastrocnemius muscles were isolated from the surrounding tissue and rapidly weighed. The muscle homogenates were prepared according to standard procedures (11) using 250 mM sucrose as the homogenization medium. The operative procedure was performed in a precooled refrigerator with a Potter–Elvehjem apparatus at 0–5°. The homogenates were diluted to 10% (w/v) before

[1] Rieper.
[2] Basile Research Instruments, Comerio, Italy.

Table I—Activities of Gastrocnemius Muscle Enzymes of Sedentary Rats and of Rats Trained to Run Continuously for 150 min/day at 25 m/min [a]

Exercise Group	Adenyl Cyclase $\times 10^{-6}$	Phospho-rylase	Phospho-fructo-kinase	Pyruvate Kinase	Lactate Dehydro-genase	Citrate Synthase	Isocitrate Dehydro-genase	2-Keto-glutarate Dehydro-genase	Succinate Dehydro-genase	Malate Dehydro-genase	Glutamate Pyruvate Trans-aminase
Seden-tary	28.6 ± 1.7	19.6 ± 1.3	31.2 ± 2.5	248 ± 12	516 ± 11	22.7 ± 1.9	2.65 ± 0.16	1.24 ± 0.11	3.84 ± 0.19	278 ± 27	21.4 ± 1.2
25 Days	52.4[b] ± 3.9	29.6[b] ± 1.1	45.6[b] ± 3.4	338[b] ± 23	759[b] ± 74	32.5[b] ± 1.8	3.92[b] ± 0.29	1.66 ± 0.10	5.33[b] ± 0.29	366 ± 26	20.3 ± 1.5
50 Days	32.5 ± 2.1	21.2 ± 1.7	35.3 ± 2.5	287 ± 8	592 ± 21	36.6[b] ± 1.7	4.45[b] ± 0.23	1.74 ± 0.10	6.33[b] ± 0.26	411[b] ± 42	24.3 ± 2.3
100 Days	26.5 ± 1.7	18.6 ± 1.1	26.8 ± 2.6	204 ± 20	485 ± 17	41.6[b] ± 3.2	5.12[b] ± 0.34	1.92[b] ± 0.09	6.97[b] ± 0.27	444[b] ± 38	33.3[b] ± 1.4
150 Days	30.6 ± 1.5	22.2 ± 0.6	33.8 ± 1.2	271 ± 9	366[b] ± 29	44.5[b] ± 1.8	5.16[b] ± 0.22	1.85[b] ± 0.11	7.17[b] ± 0.32	464[b] ± 14	51.3[b] ± 3.1

[a] The activities are expressed as micromoles of substrate utilized per minute per gram wet weight of tissue. Values are means ± *SEM* of eight rats. [b] Significantly different from controls, $p < 0.01$ (Student t test).

fractionation and then centrifuged[3] at 700×*g* for 10 min.

The supernate was decanted and centrifuged again at 700×*g* for 10 min. The supernate was then centrifuged at 14,000×*g* for 15 min, and the pellet was suspended in 250 m*M* sucrose (11). The following enzymatic activities were evaluated: adenyl cyclase (12, 13), phosphorylase (14), phosphofructokinase (15), pyruvate kinase (15), lactate dehydrogenase (16), citrate synthase (17, 18), isocitrate dehydrogenase (19), 2-ketoglutarate dehydrogenase (20), succinate dehydrogenase (21), malate dehydrogenase (15, 22), and glutamate pyruvate transaminase (10). Protein concentration was determined according to Lowry *et al.* (23).

Spectrophotometric assays were performed in a double-beam spectrophotometer[4] with a thermostated cell compartment, in 3-ml cells of 1-cm light path, at 25°. Initial reaction rates were determined from a segment of the linear portion of the change in absorbance and corrected for the rates of any nonspecific activity. The assays were performed only under conditions where the reaction rate was proportional to enzyme concentration. The enzymatic activities are referred to as micromoles of substrate utilized per minute per gram of fresh tissue.

RESULTS

In the rat gastrocnemius muscle, the enzymatic adaptation to intensive endurance training (25 m/min for 150 min/day) occurred in both the hyaloplasm and the mitochondria. On the 25th day of training, several mitochondrial enzymatic activities were significantly increased (citrate synthase, isocitrate dehydrogenase, and succinate dehydrogenase), while others were not significantly modified (2-ketoglutarate dehydrogenase and malate dehydrogenase) (Table I). At the same time, a significant increase in the enzymatic activities of both glycogenolysis (adenyl cyclase and phosphorylase) and glycolysis (phosphofructokinase, pyruvate kinase, and lactate dehydrogenase) was observed.

The findings relative to the 50th and 100th days of training demonstrated a progressive increase in mitochondrial enzymatic activities, whereas by that time hyaloplasmic activities had returned to base values (Table I). This result proves that mitochondrial activity tended to reach steady state with the endurance muscular work to which the animals were submitted.

Following this steady-state phase, while training was regularly being carried on at the rate and intensity described, a marked increase in the activity of glutamate pyruvate transaminase and a decrease in the lactate dehydrogenase activity were found on the 150th day of training (Table I). This finding indicates that the former enzyme was increasingly capable of competing for pyruvate with the latter one, thus making pyruvate exceeding the Krebs cycle available more for transamination to 2-ketoglutarate than for reduction to lactate.

All these enzymatic adaptations were directly related with the endurance workload. Table II shows the results obtained in animals trained for 100 days at 25 m/min for 150 min/day and then submitted to a workload of 30 m/min for 150 min/day during the following 25 days. In these animals, which were already in a steady state between endurance work intensity and mitochondrial enzymatic adaptation, the daily work intensity was only moderately increased. Nevertheless, the rate change (from 25 to 30 m/min) was more than sufficient to modify the steady state and to increase significantly both glycogenolysis and glycolysis enzymatic activities. Therefore, this situation was analogous to the initial one observed when sedentary rats were submitted to the endurance work.

In some animals, the training (25 m/min for 150 min/day) was associated with the intraperitoneal administration of three doses of drugs exerting a peripheral vasodilating action. On the 25th day of training, papaverine was not inducing any significant change in the enzymatic activities examined (Table III). Caffeine caused an increase in several glycogenolysis and glycolysis activities but no significant modifications in mitochondrial enzymatic activities. With nicergoline, succinate dehydrogenase and malate dehydrogenase activities were increased, while lactate dehydrogenase was significantly decreased. Finally, the admin-

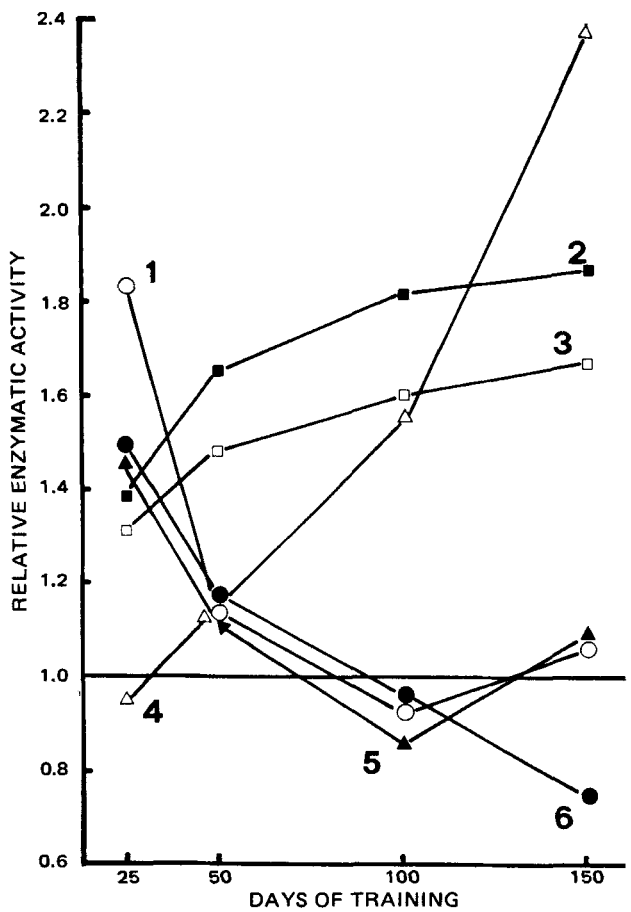

Figure 1—*Relative enzymatic activities of gastrocnemius muscle of rats trained to run continuously for 150 min/day at 25 m/min, expressed as a function of training time. Enzymatic activity was expressed by assuming the activity of sedentary controls (at time 0) was equal to 1. Each point represents the mean of eight rats. Key: 1, adenyl cyclase; 2, succinate dehydrogenase; 3, malate dehydrogenase; 4, glutamate pyruvate transaminase; 5, phosphofructokinase; and 6, lactate dehydrogenase.*

[3] Sorvall RC-5 supercentrifuge.
[4] Perkin-Elmer 124/56.

Table II—Activities of Gastrocnemius Muscle Enzymes of Rats Trained to Run Continuously for 150 min/day for 100 Days at 25 m/min with or without Subsequent Training for 25 Days at 30 m/min [a]

Exercise Group	Adenyl Cyclase $\times 10^{-6}$	Phospho-rylase	Phospho-fructo-kinase	Pyruvate Kinase	Lactate Dehydro-genase	Citrate Synthase	Isocitrate Dehydro-genase	2-Keto-glutarate Dehydro-genase	Succinate Dehydro-genase	Malate Dehydro-genase	Glutamate Pyruvate Trans-aminase
100 Days at 25 m/min	26.5 ± 1.7	18.6 ± 1.1	26.8 ± 2.6	204 ± 20	485 ± 17	41.6 ± 3.2	5.12 ± 0.34	1.92 ± 0.09	6.97 ± 0.27	444 ± 38	33.3 ± 1.4
100 Days at 25 m/min + 25 days at 30 m/min	44.7[b] ± 4.0	26.8[b] ± 2.0	38.8[b] ± 1.6	285 ± 14	687[b] ± 34	43.2 ± 2.6	5.26 ± 0.18	2.15 ± 0.13	7.23 ± 0.23	470 ± 36	40.3 ± 3.4

[a] The activities are expressed as micromoles of substrate utilized per minute per gram wet weight of tissue. Values are means ± *SEM* of eight rats. [b] Significant difference, $p < 0.01$ (Student t test).

istration of bamethan significantly increased both adenyl cyclase and succinate dehydrogenase activities.

However, these pharmacological actions were no longer observable in animals trained and treated for 100 or 150 days (Table IV). This finding suggests that drugs act only during the first stage of noncompensated physiological adaptation to endurance training. Indeed, after physiological adaptation had taken place, the drugs tested were totally inactive.

DISCUSSION

For the same endurance workload, the evaluated muscular enzymatic activities varied in a nonhomogeneous way as a function of the training time. Changes in the hyaloplasmic enzymatic activities were different from those observed in the mitochondrial ones. Among mitochondrial activities themselves, those of the tricarboxylic acid cycle showed quantitatively different modifications. However, these discrepancies in behavior can be partially regarded as merely apparent ones. With an effective workload (5), at least three successive phases (as a function of the training time) can be hypothesized.

Noncompensated Mitochondrial Adaptation—The initial increase (Fig. 1) in the mitochondrial enzymatic activities of the Krebs cycle was accompanied by a significant increase in the hyaloplasmic ones. In particular, the increased activity of adenyl cyclase and phosphorylase and of phosphofructokinase and pyruvate kinase demonstrates the activation of glycogenolysis and glycolysis, respectively. The increase in the lactate dehydrogenase activity suggests that a certain amount of pyruvate is reduced to lactate instead of being utilized as acetyl coenzyme A in the tricarboxylic acid cycle. If this were the case, the adaptation of mitochondrial activities would not be able to meet the actual energy requirements consequent to training and the lactacid anaerobic compensative mechanism would then activate.

This hypothesis is further supported by the role of the drugs tested. Nicergoline is an α-blocking agent that activates the mitochondrial oxidative processes (5, 24–26) and, in part, the adenyl cyclase system (27). As compared to trained untreated animals, during this first stage nicergoline (Fig. 2) caused both an increase of several mitochondrial enzymatic activities and a lower training-induced increase in the lactate dehydrogenase activity.

Caffeine is a xanthine drug, known to activate the adenyl cyclase system through phosphodiesterase inhibition (28). As compared to trained untreated animals, during this first stage caffeine did not significantly increase mitochondrial activities, but it increased the activity of adenyl cyclase (activation of glycogenolysis), phosphofructokinase (activation of glycolysis), and lactate dehydrogenase (activation of the reduction of pyruvate to lactate). Bamethan is a catecholamine-like agent, stimulating the adenyl cyclase system (29) and partially the oxidative processes (24, 25). As compared to trained untreated animals, bamethan induced an increase in a few mitochondrial activities and in the hyaloplasmic enzymatic activity adenyl cyclase.

The behavior of enzymatic systems, examined also with regard to the effect of varying exogenous stimuli (such as those caused by the drugs tested), confirmed the existence of a "see-saw" mechanism between mitochondrial oxidative adaptation and the lactacid anaerobic mechanism to meet the energy requirements consequent to training.

Finally, it should be stressed that chronic administration of papaverine at the doses capable of exerting an effective peripheral vasodilating action did not change any glycolytic and mitochondrial enzymatic activities.

Compensated Mitochondrial Adaptation—With training continuing at the set constant level, the progressive increase in the Krebs cycle mitochondrial enzymatic activities became more evident during the second phase. However, the enzymatic activities connected with glycogenolysis and glycolysis showed a constant decrease, down to values close to the initial pretraining ones (Fig. 1). During this phase, the increase in mitochondrial activities would appear to be able to meet the energy requirements brought about by training, with no need for any hyaloplasmic compensation. During this phase, the chronic treatment with the drugs tested did not modify the overall pattern of mitochondrial adaptation phenomena.

Overcompensated Mitochondrial Adaptation—With training continuing at the set intensity level, mitochondrial enzymatic activities were practically in a steady state. However, a concomitant increase was noted in some enzymatic activities connected with pyruvate metabolic pathways (*e.g.*, pyruvate + glutamate $\rightleftharpoons$ alanine + 2-ketoglutarate, catalyzed by glutamate pyruvate transaminase) (Fig. 1). Lactate dehydrogenase was, on the other hand, decreased to values lower than pretraining ones. Therefore, during this phase, even though mitochondrial enzymatic activities were adequate to the daily workload, a "third way"

Table III—Activities of Gastrocnemius Muscle Enzymes of Rats Trained to Run Continuously for 150 min/day at 25 m/min for 25 Days with or without Drug Treatment (0.5 ml/kg ip Daily of a 1.6, 4, or 10 $\times 10^{-3}$ *M* Solution) [a]

Trained Group	Concen-tration, $M \times 10^{-3}$	n	Adenyl Cyclase $\times 10^{-6}$	Phospho-rylase	Phospho-fructo-kinase	Lactate Dehydro-genase	Citrate Synthase	Succinate Dehydro-genase	Malate Dehydro-genase	Glutamate Pyruvate Trans-aminase
Untreated	—	8	52.4 ± 3.9	29.6 ± 1.1	45.6 ± 3.4	759 ± 74	32.5 ± 1.8	5.33 ± 0.29	366 ± 26	20.3 ± 1.5
Treated with caffeine	1.6	5	66.3[b] ± 3.7	35.2 ± 3.9	52.4 ± 4.4	850 ± 21	29.2 ± 1.7	5.04 ± 0.36	321 ± 17	24.6 ± 2.7
	4.0	5	68.9[b] ± 5.4	34.8 ± 3.0	56.3[b] ± 2.3	905[b] ± 23	35.2 ± 1.4	5.40 ± 0.46	375 ± 10	21.6 ± 1.5
	10.0	5	70.2[b] ± 4.6	33.3 ± 2.8	58.4[b] ± 3.1	876[b] ± 32	31.4 ± 2.3	4.92 ± 0.61	354 ± 16	17.6 ± 3.8
Treated with papaverine	1.6	5	52.6 ± 3.3	25.6 ± 3.1	40.6 ± 2.6	730 ± 64	27.7 ± 3.6	5.52 ± 0.46	348 ± 21	19.9 ± 2.2
	4.0	5	49.2 ± 4.1	26.6 ± 2.4	47.1 ± 2.6	782 ± 35	30.2 ± 2.2	5.20 ± 0.21	324 ± 23	22.1 ± 1.6
	10.0	5	47.7 ± 3.2	24.7 ± 2.5	39.2 ± 1.8	765 ± 71	29.3 ± 1.8	5.28 ± 0.17	402 ± 61	24.3 ± 1.9
Treated with bamethan	1.6	5	60.2 ± 4.8	29.9 ± 2.1	43.6 ± 2.2	858 ± 70	32.4 ± 2.7	5.96 ± 0.31	336 ± 26	19.1 ± 2.0
	4.0	5	69.5[b] ± 5.0	33.5 ± 3.3	52.6 ± 3.1	842 ± 53	37.3 ± 1.7	6.37[b] ± 0.19	404 ± 28	23.0 ± 1.6
	10.0	5	71.8[b] ± 6.3	37.4[b] ± 1.7	47.4 ± 3.6	836 ± 50	37.6 ± 2.0	6.23[b] ± 0.24	473[b] ± 28	25.6 ± 3.7
Treated with nicergoline	1.6	6	49.4 ± 4.6	27.2 ± 1.3	39.4 ± 4.2	613[b] ± 48	36.6 ± 2.9	6.18[b] ± 0.37	394 ± 17	20.6 ± 1.9
	4.0	6	57.6 ± 1.9	31.2 ± 1.5	47.7 ± 1.8	642[b] ± 14	40.4 ± 3.5	6.74[b] ± 0.41	438[b] ± 25	22.5 ± 1.8
	10.0	6	58.4 ± 2.6	29.2 ± 1.4	41.3 ± 3.3	600[b] ± 36	40.2 ± 4.1	6.82[b] ± 0.51	444[b] ± 36	21.4 ± 1.7

[a] The activities are expressed as micromoles of substrate utilized per minute per gram wet weight of tissue. Values are means ± *SEM* of n rats. [b] Significantly different from trained untreated rats, $p < 0.01$ (Student t test).

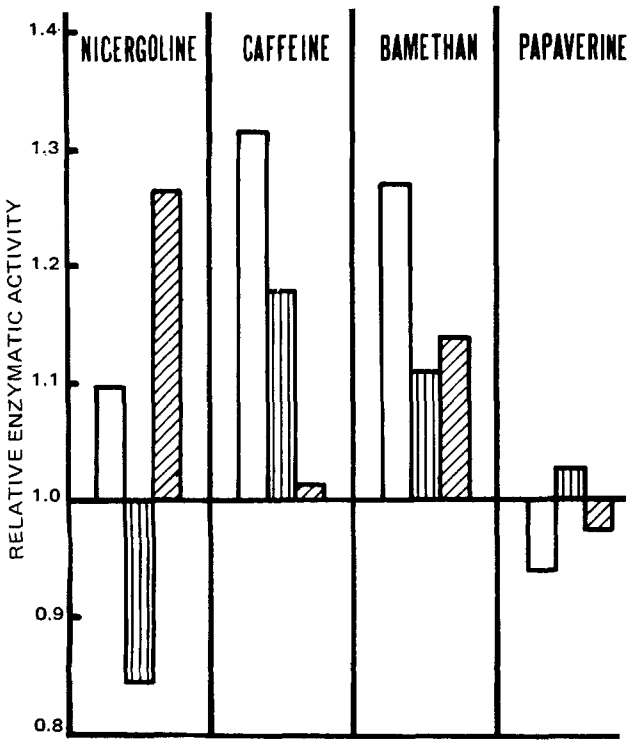

Figure 2—*Relative enzymatic activities of gastrocnemius muscle of rats trained to run continuously for 150 min/day at 25 m/min for 25 days and treated daily with drugs (0.5 ml/kg ip of a 4 × 10^{-3} M solution) expressed as a function of the activity of trained untreated rats. Key:* □, *adenyl cyclase;* ▩, *lactate dehydrogenase; and* ▨, *succinate dehydrogenase.*

of pyruvate metabolism became evident. This side pathway (8, 10) would permit the utilization of pyruvate instead of its reduction to lactate.

Under those experimental conditions (*i.e.*, constant intensity and duration of work), this further specialization of a metabolic shunt with the Krebs cycle, at a time when the values of the enzymatic activities of the Krebs cycle itself have reached a high plateau, seems rather strange. Moreover, it is not totally clear why, for example, after 100 days of training some enzymatic activities of the Krebs cycle had increased by 80–90% (*e.g.*, isocitrate dehydrogenase and succinate dehydrogenase) while others had increased by only 50–60% (*e.g.*, 2-ketoglutarate dehydrogenase and malate dehydrogenase).

The methods used to determine enzymatic activities completely upset the autoregulative interactions that maintain the cell as a functionally integrated system (5). A thorough and reliable picture of enzymatic functions can be provided only by an extensive investigation of biochemical relationships at the subcellular level. Indeed, an evaluation of the activity of an enzyme cannot yield any information about the concentration of the enzyme itself. Nor can an overall evaluation of mitochondrial proteins give reliable information on the concentration of a single mitochondrial enzyme. Nevertheless, even knowing the amount of the purified enzyme provides little satisfactory information when the characteristic more effectively modulated by training or by drug is, for example, the affinity between the enzyme and the substrate. Absolute conclusions are not drawn from experimental data which, even though numerous and sophisticated, might be only relatively related to each other.

The phases of mitochondrial adaptation are relative to the actual workload. Thus, after the phase of compensated mitochondrial adaptation, an increase in the workload causes biological substrates to go back to the state of noncompensated mitochondrial adaptation. Significant increases in the enzymes of glycogenolysis (adenyl cyclase and phosphorylase), glycolysis (phosphofructokinase), and pyruvate reduction (lactate dehydrogenase) are again induced.

Only the phase of noncompensated mitochondrial adaptation seems to be affected by drugs, with the extent depending more on the drug's specific characteristics than on its vasodilating action. Some drugs act mainly on oxidative processes (nicergoline), others act on glycolysis

Table IV—Activities of Gastrocnemius Muscle Enzymes of Rats Trained to Run Continuously for 150 min/day at 25 m/min for 100 Days with or without Treatment by Some Drugs (0.5 ml/kg ip Daily of a 4 × 10^{-3} *M* Solution)

Trained Group	*n*	Adenyl Cyclase × 10^{-6}	Lactate Dehydrogenase	Succinate Dehydrogenase
Untreated	8	26.5 ± 1.7	485 ± 17	6.97 ± 0.27
Treated with caffeine	5	30.2 ± 2.6	510 ± 22	7.10 ± 0.37
Treated with papaverine	5	24.3 ± 2.4	510 ± 25	6.65 ± 0.20
Treated with bamethan	5	31.2 ± 3.6	503 ± 33	6.72 ± 0.27
Treated with nicergoline	5	27.6 ± 1.8	468 ± 24	7.20 ± 0.35

[a] The activities are expressed as micromoles of substrate utilized per minute per gram wet weight of tissue. Values are means ± *SEM* of *n* rats.

(caffeine), while still others exhibit intermediate characteristics (bamethan). With regard to the phases of compensated mitochondrial adaptation, the drugs tested proved totally inactive.

REFERENCES

(1) L. A. Cobb and W. P. Johnson, *J. Clin. Invest.*, **42**, 800 (1963).
(2) S. Robinson and P. M. Harmon, *Am. J. Physiol.*, **132**, 757 (1941).
(3) B. Saltin and J. Karlsson, in "Muscle Metabolism during Exercise," B. Pernow and B. Saltin Eds., Plenum, New York, N.Y., 1971, p. 289.
(4) *Ibid.*, p. 395.
(5) G. Benzi, P. Panceri, M. De Bernardi, R. F. Villa, E. Arcelli, L. D'angelo, E. Arrigoni, and F. Berté, *J. Appl. Physiol.*, **38**, 565 (1975).
(6) J. O. Holloszy, *J. Biol. Chem.*, **242**, 2278 (1967).
(7) J. O. Holloszy, L. B. Oscai, I. J. Don, and P. A. Molè, *Biochem. Biophys. Res. Commun.*, **40**, 1368 (1970).
(8) G. Benzi and R. F. Villa, *Farmaco, Ed. Sci.*, **30**, 311 (1975).
(9) P. Felig and J. Wahren, *J. Clin. Invest.*, **50**, 2703 (1971).
(10) P. A. Molè, K. M. Baldwin, R. L. Terjung, and J. O. Holloszy, *Am. J. Physiol.*, **224**, 50 (1973).
(11) L. B. Oscai and J. O. Holloszy, *J. Biol. Chem.*, **246**, 6968 (1971).
(12) R. W. Butcher, R. J. Ho, H. C. Meng, and E. W. Sutherland, *J. Biol. Chem.*, **240**, 4515 (1965).
(13) E. De Robertis, G. Rodriguez De Lores Arnaiz, and M. Alberici, *ibid.*, **242**, 3487 (1967).
(14) A. Bass, D. Brdiczka, P. Eyer, S. Hofer, and D. Pette, *Eur. J. Biochem.*, **10**, 198 (1969).
(15) C. E. Shonk and G. E. Boxer, *Cancer Res.*, **24**, 709 (1964).
(16) A. R. Pesce, R. H. McKay, F. Stolzenbach, R. D. Cahn, and N. O. Kaplan, *J. Biol. Chem.*, **239**, 1753 (1964).
(17) S. Ochoa, *Methods Enzymol.*, **1**, 685 (1955).
(18) P. A. Srere, *ibid.*, **13**, 3 (1969).
(19) G. W. E. Plaut, *ibid.*, **13**, 34 (1969).
(20) L. J. Reed and B. B. Mukherjee, *ibid.*, **13**, 55 (1969).
(21) W. D. Bonner, *ibid.*, **1**, 722 (1955).
(22) S. Ochoa, *ibid.*, **1**, 735 (1955).
(23) O. H. Lowry, N. J. Rosebrough, A. L. Farr, and R. J. Randall, *J. Biol. Chem.*, **193**, 265 (1951).
(24) G. Benzi, E. Arrigoni, L. Manzo, M. De Bernardi, A. Ferrara, P. Panceri, and F. Berté, *J. Pharm. Sci.*, **62**, 758 (1973).
(25) G. Benzi, *Jpn. J. Pharmacol.*, **25**, 251 (1975).
(26) A. Moretti and G. Arcari, *Farmaco, Ed. Sci.*, **27**, 800 (1972).
(27) R. F. Villa, *ibid.*, **30**, 561 (1975).
(28) E. W. Sutherland and T. W. Rall, *Pharmacol. Rev.*, **12**, 265 (1960).
(29) G. Benzi and R. F. Villa, *J. Neurol. Neurosurg. Psychol.*, **39**, 77 (1976).

ACKNOWLEDGMENTS AND ADDRESSES

Received April 16, 1976, from the *Departments of Pharmacology and Biological Chemistry, University of Pavia, 27100 Pavia, Italy.*
Accepted for publication November 10, 1976.
The authors thank Mrs. G. Garlaschi for technical assistance.
[x] To whom inquiries should be directed.

Photosensitization by Drugs

DOUGLAS E. MOORE

Abstract □ UV irradiation (365 nm) of air-saturated methanol solutions of 20 drugs absorbing in the 300–400-nm region gave rise to oxygen uptake, as determined with a polarographic oxygen electrode. The drugs were tested for photosensitizing capability by either a Type I (free radical) or a Type II (singlet molecular oxygen) mechanism. This testing was done by the inclusion of either acrylamide or 2,5-dimethylfuran in the irradiated drug solution, with observation of the subsequent polymerization or oxidation, respectively. Phenothiazine and thiazide derivatives appear capable of photosensitization by both mechanisms; promethazine, trifluoperazine, and furosemide show relatively high reactivity. Diazepam (weak), hexachlorophene, aminacrine, pyrilamine, tetracycline, demeclocycline, quinine, and anthracene (strong) react only by a Type II mechanism, with a photosensitizing efficiency increasing in the order given. A correlation appears to exist with reports of *in vivo* photosensitivity.

Keyphrases □ Photosensitization—various drugs irradiated, polymerization of acrylamide determined by dilatometry or oxidation of 2,5-dimethylfuran determined using polarographic oxygen electrode □ UV irradiation—effect on various drugs, polymerization of acrylamide determined by dilatometry or oxidation of 2,5-dimethylfuran determined by polarographic oxygen electrode □ Polarography—oxygen electrode used to determine oxidation of 2,5-dimethylfuran by various drugs after UV irradiation □ Oxygen uptake—various drugs after UV irradiation, oxidation of 2,5-dimethylfuran determined using polarographic oxygen electrode

Certain drugs and chemicals increase the sensitivity of the skin to solar radiation (1, 2). While it is possible to avoid such side effects with the appropriate topical sunscreens or even by systemic treatment (3), a photochemical basis is needed from which to classify a drug as a potential photosensitizer.

The mechanism of the adverse reaction is believed to be initiated by the photosensitized oxidation of skin components, with the drug functioning as the photosensitizing agent. Implicated in this process are drugs with significant light absorption in that portion of the solar spectrum reaching the earth's surface (280–800 nm). Window glass, opaque to radiation below about 310 nm, is said to afford protection from the photosensitizing effects of several drugs (2).

The mechanisms by which photooxidation may occur were classified as follows (4). Type I is a free radical chain process generally termed autoxidation. Type II involves excited singlet molecular oxygen and is termed oxygenation. Recently, the tetracyclines, with absorption maxima around 370 nm, were shown (5) to act as photosensitizers by a Type II mechanism. Chlorpromazine, however, on irradiation (6), produced free radicals as well as singlet molecular oxygen, thereby implying both Type I and II mechanisms of photooxidation. The Type I and II mechanisms may relate to the photoallergic and phototoxic effects of a photosensitizing drug, respectively (6).

The present investigation examined the effects of UV irradiation on compounds with light absorption in the 300–400-nm region. Included were some phenothiazine and thiazide derivatives reported to have photosensitizing effects in humans. All irradiations were performed using a glass filter to restrict the incident light to wavelengths above 310 nm. Two substrates were employed to enable classification of the mechanism of a drug's participation, if any, in photooxidations. The substrates were 2,5-dimethylfuran, an efficient acceptor for singlet oxygen (7), and acrylamide, an effective free radical scavenger thereby undergoing polymerization (8).

EXPERIMENTAL

Apparatus—The experimental design was based on the polarographic oxygen electrode and irradiation apparatus used successfully to measure oxygen uptake in both the Type I photooxidation of benzaldehyde (9) and the Type II photooxidation of the tetracyclines (5). The cylindrical reaction vessel (30-ml volume) was constructed[1] of spectroscopic grade silica with plane parallel faces 38 mm in diameter and 20 mm apart. Two standard taper joints carried the oxygen electrode[2] and a belt-driven stirrer for oxygen uptake measurements.

For free radical polymerization measurements, the reaction vessel was converted into a dilatometer by fitting a glass stopper and a 100-mm length of 0.4-mm bore capillary glass tubing to the standard taper joints.

A glass filter[3] with 28% transmittance at 365 nm and an overall transmission range of 310–420 nm and a screen with a 35-mm diameter aperture were positioned between the reaction vessel and the irradiation source[4]. The whole apparatus was immersed in a thermostat at 30.0 ± 0.05°.

Materials—2,5-Dimethylfuran[5] was purified immediately before solution preparation by twice distilling at room temperature at a pressure of 10^{-4} mm Hg on an all-glass high vacuum line. Acrylamide[6] was twice recrystallized from distilled chloroform and dried under vacuum (mp 85°). Only when these purification procedures were adopted did the control irradiations of solutions not containing potential sensitizers show negligible reaction.

The drugs tested for photosensitizing ability (Tables I–III) were the purest grades available commercially. All irradiations were performed in solution in analytical reagent grade methanol[7]. In this solvent, the photochemistry is simpler than in aqueous solution.

Procedures—Three situations were studied for each drug.

Irradiation of Drug Alone—In this procedure, 1 ml of freshly prepared drug solution (2–8 m*M* in methanol) was added to 50 ml of air-saturated methanol at 30°. The mixture was quickly transferred to the reaction vessel, and the oxygen uptake was measured after irradiation as previously described (9). The absorption spectrum of the reaction mixture was recorded[8] both before and after irradiation.

Irradiation of Drug plus 2,5-Dimethylfuran—This procedure was identical with that for drug alone except that 50 ml of 2,5-dimethylfuran solution (0.0936 *M*) in methanol was used.

Irradiation of Drug plus Acrylamide—A weighed quantity (10–20 mg) of drug was dissolved in 50 ml of methanol in a 250-ml round-bottom flask, modified by addition of a sidearm to the neck. Solid acrylamide (0.300 g) was weighed into the dry reaction vessel, which was then connected to the sidearm. The flask was then connected to a high-vacuum line, and the contents were deaerated by three freeze–pump–thaw cycles. After deaeration, the flask was tilted so that the drug solution flowed into the reaction vessel, dissolving the acrylamide. The reaction vessel was removed from the sidearm, and the dilatometer capillary was quickly inserted. The reaction vessel was then placed in its irradiation position in the thermostat, and the movement of the liquid level in the capillary was observed with a cathetometer.

[1] Thermal Syndicate Ltd., Wallsend, England.
[2] Type E5046, Radiometer, Copenhagen, Denmark.
[3] Corning CS 7-37.
[4] Engelhard Hanovia 125-w medium pressure mercury lamp.
[5] Fluka AG, Switzerland.
[6] Eastman Kodak, Rochester, N.Y.
[7] Ajax Chemicals, Sydney, Australia.
[8] Varian Techtron model 635 UV–visible spectrophotometer.

Table I—Photooxidation of Phenothiazine Derivatives

Compound	λ_{max}, nm	Absorbance at 365 nm	Rate of Oxygen Uptake, μmoles/liter/min: Compound Alone (1.28×10^{-4} M)	Rate of Oxygen Uptake, μmoles/liter/min: Compound (1.28×10^{-4} M) plus Dimethylfuran (0.0936 M)
Promethazine hydrochloride	303	0.008	2.7	16.2
Promazine hydrochloride	304	0.010	2.4	13.4
Chlorpromazine hydrochloride	308	0.015	3.4	13.7
Prochlorperazine maleate	312	0.030	3.0	25.1
Trifluoperazine hydrochloride	313	0.072	5.9	44.7
Thioridazine hydrochloride	315	0.018	4.3	16.9
Chlorpromazine sulfoxide hydrochloride	342	0.012	2.5	8.4

RESULTS AND DISCUSSION

Photooxidation—The oxygen uptake rates measured for the UV-irradiated drug solutions in the absence and presence of dimethylfuran are recorded in Table I for phenothiazine derivatives, in Table II for thiazides and related compounds, and in Table III for miscellaneous compounds with absorption in the 300–400-nm region. Each value is the mean of at least three determinations with a maximum standard deviation of 5%. There was no dark reaction, and the oxygen uptake was linear with time, *i.e.*, zero order, indicating that the absorption of light was the rate-limiting factor in all cases except furosemide.

To assess relative photosensitizing ability, the drug concentration was selected to give an absorbance of approximately 0.5 at its wavelength of maximum absorption, λ_{max}, in the 300–400-nm region. For most drugs, the λ_{max} corresponds to the least intense absorption and in some cases is only a shoulder (sh) on the principal absorption peak. Comparisons are perhaps more realistically based on the absorbance of the drug solution at 365 nm, corresponding to the major irradiating wavelength.

The output of the medium pressure mercury lamp is discontinuous, the relevant lines being at 303, 313, 334, 365, and 405 nm with relative intensities of 23.9, 50, 9.3, 100, and 42, respectively (10). The presence of the glass filter means that the relative intensities incident on the reaction vessel are 0, 4.8, 5.3, 100, and 10.2, respectively. Therefore, most drugs listed in Tables I–III experience only a relatively small amount of light of a wavelength near to their λ_{max}. However, for most, the absorption band is broad, meaning that the 313- and 334-nm light is absorbed and that there is some residual absorbance at 365 nm (Tables I–III).

Phenothiazines—The phenothiazine derivatives react approximately in accordance with their absorbance at 365 nm (Table I). The UV absorption characteristics of these compounds are determined principally by the phenothiazine nucleus, with only minor effects due to the substituents (11). Therefore, the mechanism of energy transfer through the excited singlet and triplet states is expected to be similar within the phenothiazine series. Close similarities were found in the transient species formed on flash photolysis of chlorpromazine and promazine (6).

Chlorpromazine sulfoxide was identified as an oxidation product of chlorpromazine (12), yet it appears to be oxidized in proportion to its absorbance at 365 nm. In aqueous solution, chlorpromazine and its sulfoxide degrade in the presence of oxygen and UV light below 365 nm to give apparently similar products (12). Furthermore, with extended periods of irradiation of aqueous chlorpromazine solutions, numerous products are found (13). While some of these may be secondary in nature, the sulfoxide clearly is an intermediate rather than the final product.

Changes in the absorption spectrum of the irradiated phenothiazine were most marked with promethazine and prochlorperazine. Promethazine was the most reactive compound studied since the oxygen uptake rate (Table I) exceeded what might be expected from the absorbance at 365 nm. After 1 hr of irradiation of promethazine alone, the absorbance increased by 20% at the λ_{max} and from 0.01 to 0.18 at 342 nm, which could be indicative of sulfoxide formation. Furthermore, the solution developed a pink color, with a broad absorption centered on 506 nm, a phenomenon not seen with the other phenothiazines.

Prochlorperazine, on irradiation, showed the development of a broad shoulder at 330 nm and the narrowing of the original peak at 312 nm. Pending more study, including the analysis of transient species, no conclusions can be made. Spectral changes occurred for promazine, chlorpromazine, thioridazine, and trifluoperazine but were minor in comparison. The reaction of chlorpromazine sulfoxide could be followed by the decrease in absorbance at 342 nm.

Thiazides—Chlorothiazide and hydrochlorothiazide are reported to be potent photosensitizers, yet in the system studied here they showed less reactivity than the phenothiazines. This result may have been due in part to lower absorbances at 365 nm, although the results for cyclopenthiazide do not support that suggestion.

Hydrochlorothiazide and cyclopenthiazide had clearly defined absorption peaks at 318 nm. Upon irradiation, the peak structure gradually submerged to become a shoulder on the major absorption centered on about 270 nm, thereby resembling the chlorothiazide spectrum.

Chlorthalidone and furosemide, while not thiazides, were included because of similarities in their properties. Chlorthalidone had essentially zero absorbance above 300 nm, yet a very slight reactivity was observed. This substance was strongly susceptible to the shorter wavelength UV light, so this result may represent a very small amount transmitted through the filter.

Furosemide had a relatively high absorbance at 365 nm and a corresponding high photosensitizing capability. One unusual feature of the irradiation of furosemide alone was an initial rapid oxygen uptake, gradually decreasing to the steady value recorded in Table II. The initial reaction may have been due to formation of free radicals which were rapidly scavenged by oxygen molecules. The steady rate may, in fact, correspond to a secondary reaction. The overall reaction also could be

Table II—Photooxidation of Thiazides and Related Compounds

Compound	λ_{max}, nm	Concentration $\times 10^4$ M	Absorbance at 365 nm	Rate of Oxygen Uptake, μmoles/liter/min: Compound Alone	Rate of Oxygen Uptake, μmoles/liter/min: Compound plus Dimethylfuran (0.0936 M)
Chlorthalidone	284	1.5	<0.002	0.4	1.4
Hydrochlorothiazide	318	1.32	0.006	0.9	5.0
Chlorothiazide	280, 320 (sh)	1.30	0.006	1.4	3.4
Cyclopenthiazide	318	1.44	0.002	1.4	10.5
Furosemide	340	0.95	0.185	5.5	81.2

Table III—Photooxidation of Selected Compounds with UV Absorption in the 300–400-nm Region

Compound	λ_{max}, nm	Concentration $\times 10^4$ M	Absorbance at 365 nm	Rate of Oxygen Uptake, μmoles/liter/min: Compound Alone	Rate of Oxygen Uptake, μmoles/liter/min: Compound plus Dimethylfuran (0.0936 M)
Diazepam	316	1.93	0.005	0	3.9
Chlordiazepoxide	350 (sh)	1.90	0.335	1.8	2.0
Pyrilamine maleate	308	1.03	<0.002	1.1	4.8
Hexachlorophene	300, 317 (sh)	1.30	0.006	0.6	2.7
Quinine hydrochloride	335	0.84	0.003	7.8	38.8
Tetracycline hydrochloride	362	0.40	0.528	0.5	10.9
Demeclocycline hydrochloride	368	0.40	0.510	0.6	12.5
Anthracene	340, 357, 377	0.43	0.18	1.4	112.0
Aminacrine hydrochloride	382	0.68	0.210	0.8	4.1

Table IV—Photoinitiated Polymerization of Acrylamide Solutions Containing Phenothiazine and Thiazide Derivatives

Drug	Dilatometer Contraction Rate, mm/hr
Promethazine hydrochloride	60
Promazine hydrochloride	40
Chlorpromazine hydrochloride	26
Prochlorperazine maleate	38
Trifluoperazine hydrochloride	48
Thioridazine hydrochloride	19
Hydrochlorothiazide	10
Chlorothiazide	9
Cyclopenthiazide	11
Furosemide	28

followed by the decrease in absorbance of the peak at 340 nm.

Other Compounds—Of the substances listed in Table III, only quinine and anthracene showed a high photosensitizing ability. These compounds fluoresced strongly and also were able to transfer a considerable amount of energy to molecular oxygen. Aminacrine, also a strong fluorescer, was relatively inefficient as a photosensitizer.

Diazepam was a very weak sensitizer in neutral methanol solution, while chlordiazepoxide did not appear to sensitize the photooxygenation of dimethylfuran. In acidified methanol solution, the absorption spectra of both diazepam and chlordiazepoxide changed dramatically and photosensitization occurred, although it was complicated by acid-catalyzed hydrolysis.

Results for the tetracyclines reported previously (5) were obtained with a different reaction vessel. The values in Table III for tetracycline and demeclocycline were redetermined so that these compounds could be compared more readily as photosensitizers.

Other compounds tested in this system and found to have zero reactivity were warfarin sodium, dicumarol, and sodium aminosalicylate. Many more substances with absorption in the near UV region could be examined. One difficulty to overcome is the low solubility in the reaction system, although some heterogeneous techniques have been developed for such a situation (14).

The conclusion to be drawn from the results in Tables I–III is that every compound listed except chlordiazepoxide appears capable to a greater or lesser extent of photosensitizing oxygenation of dimethylfuran by the Type II mechanism involving singlet molecular oxygen. This finding does not necessarily preclude the possibility of direct energy transfer between the sensitizer and dimethylfuran, a process that can occur at these higher concentrations of the acceptor (15).

Photopolymerization—The observation that many compounds absorbed oxygen when irradiated in the absence of substrate is indicative of one or both of the following possibilities. Either (*a*) the drugs act as photosensitizers for their own oxygenation *via* a singlet oxygen mechanism, the rate being small because of the relatively low concentration of drug in solution, or (*b*) the drugs, on irradiation, yield free radicals that are scavenged by oxygen molecules with a 1:1 stoichiometry.

The generation of free radicals is well known in the phenothiazine derivatives (11), so these compounds served as references for comparison of other series. The measurement of oxygen uptake using an autoxidizable substrate such as benzyl alcohol or benzaldehyde is conveniently done in the apparatus but does not give an unambiguous indication of free radical formation because of the possible simultaneous occurrence of mechanism *a* or *b*.

For these reasons, the monomeric substrate acrylamide was used in deaerated conditions as a detector of free radicals. All compounds (Tables I–III) were tested with acrylamide, and Table IV lists those that photosensitized the polymerization. The polymerization reaction was evident in two ways: by the appearance of turbidity in the reaction mixture due to the insolubility of polyacrylamide and by the contraction in volume of the reaction mixture observed in the dilatometer capillary. The turbidity meant that only initial rates could be measured from the initial linear portion of the contraction–time plot. No reaction was observed when the acrylamide solution was irradiated by itself.

The fact that molecules such as anthracene show a very high photosensitizing capability with dimethylfuran but are unreactive with acrylamide indicates that the photopolymerization system is a reasonable test of radical formation and not just energy transfer.

The phenothiazines and thiazides are the only groups of drugs tested for which free radical formation appears to occur on irradiation. Within the phenothiazine series, promethazine and promazine displayed a reactivity out of proportion to their absorbance at 365 nm. Davies *et al.* (6) suggested that irradiation of chlorpromazine promotes carbon–chlorine bond fission, as shown by titration of the free chloride ion formed in the solution. The high reactivity of promethazine and promazine, which do not contain chlorine in the 2-position, suggests that other mechanisms of radical formation are possible. Further work, including an electron spin resonance study of the radicals, is required for clarification of the reaction mechanisms.

CONCLUSIONS

Phenothiazine and thiazide derivatives are capable of photosensitization by both Type I (free radical) and Type II (singlet oxygen) mechanisms. Reports of *in vivo* photosensitivity (2) indicate that both photoallergic and phototoxic reactions have been seen with these groups of drugs. Anthracene and the tetracyclines, which have been shown to participate only in a Type II mechanism, are reported to have the more direct phototoxic effect only. Some adverse reactions to quinine are optical in nature (16) but have not been specifically defined as photosensitivity.

Of particular interest is the thiazide-like substance furosemide, which shows a photosensitizing capability similar to the phenothiazines. Perhaps the reported skin rash reaction among patients taking furosemide (17) has a photosensitivity component. The spectral properties of the substances involved in this study are likely to vary depending on the polarity of the system in which they are incorporated. Nevertheless, it is unlikely that window glass will afford complete protection from photosensitivity reactions due to the compounds listed in Tables I–III.

REFERENCES

(1) R. L. Baer and L. C. Harber, *J. Am. Med. Assoc.*, **192,** 147 (1965).

(2) E. Stempel and R. Stempel, *J. Am. Pharm. Assoc.*, **NS13,** 200 (1973).

(3) M. M. Mathews-Roth, *Photochem. Photobiol.*, **22,** 302 (1975).

(4) J. G. Calvert and J. N. Pitts, Jr., "Photochemistry," Wiley, New York, N.Y., 1966, p. 548.

(5) J. A. Wiebe and D. E. Moore, *J. Pharm. Sci.*, **66,** 186 (1977).

(6) A. K. Davies, S. Navaratnam, and G. O. Phillips, *J. Chem. Soc. Perkin II*, **1976,** 25.

(7) C. S. Foote, *Acc. Chem. Res:*, **1,** 104 (1968).

(8) F. S. Dainton, "Chain Reactions," 2nd ed., Methuen, London, England, 1966, chap. 7, p. 171.

(9) D. E. Moore, *J. Pharm. Sci.*, **65,** 1447 (1976).

(10) J. G. Calvert and J. N. Pitts, Jr., "Photochemistry," Wiley, New York, N.Y., 1966, p. 696.

(11) C. Bodea and I. Silberg, "Advances in Heterocyclic Chemistry," vol. 9, Academic, New York, N.Y., 1968, p. 321.

(12) A. Felmeister and C. A. Discher, *J. Pharm. Sci.*, **53,** 756 (1964).

(13) C. L. Huang and F. L. Sands, *J. Chromatogr.*, **13,** 246 (1964).

(14) R. Nilsson and D. R. Kearns, *Photochem. Photobiol.*, **19,** 181 (1974).

(15) Y. Usui and K. Kamagawa, *ibid.*, **19,** 245 (1974).

(16) I. M. Rollo, in "Meyler's Side Effects of Drugs," vol. 8, M. N. G. Dukes, Ed., Excerpta Medica, Amsterdam, The Netherlands, 1975, p. 664.

(17) H. J. Dargie and C. T. Dollery, in *ibid.*, p. 484.

ACKNOWLEDGMENTS AND ADDRESSES

Received August 16, 1976, from the *Department of Pharmacy, University of Sydney, Sydney, NSW 2006, Australia.*

Accepted for publication November 9, 1976.

The author acknowledges the following pharmaceutical companies for providing samples of compounds: Ciba-Geigy Australia Ltd.; May & Baker Australia Ltd.; Sandoz Australia Ltd.; Merck Sharp & Dohme (Australia) Pty. Ltd.; Hoechst Australia Ltd.; Roche Products Pty. Ltd., Sydney; Pfizer Laboratories, Sydney; and Lederle Laboratories, Cyanamid Australia Ltd.

Intraindividual Relationships between Serum Protein Binding of Drugs in Normal Human Subjects, Patients with Impaired Renal Function, and Rats

AVRAHAM YACOBI and GERHARD LEVY ˣ

Abstract □ The serum protein binding of phenytoin, salicylic acid, sulfisoxazole, and warfarin was determined in normal human adults, in patients with impaired renal function (kidney donor and recipient), and in adult male Sprague–Dawley rats. The free fraction values for salicylate and sulfisoxazole were significantly correlated in all three groups. The other correlations were statistically significant in only one or two of these groups. There was a statistically significant negative correlation between albumin concentration and the free fraction values of salicylic acid and sulfisoxazole (but not of phenytoin and only under special circumstances with warfarin) in normal human subjects and of phenytoin, salicylic acid, and sulfisoxazole (but not warfarin) in rats. No such correlation was observed for any of the drugs in patients with impaired renal function. These observations show that no single weakly acidic drug can serve as an index for quantitatively determining the effect of disease or species differences on the serum protein binding of other weakly acidic drugs.

Keyphrases □ Protein binding, serum—phenytoin, salicylic acid, sulfisoxazole, and warfarin compared, normal and renally impaired humans, rats □ Binding, serum protein—phenytoin, salicylic acid, sulfisoxazole, and warfarin compared, normal and renally impaired humans, rats □ Phenytoin—serum protein binding compared to salicylic acid, sulfisoxazole, and warfarin, normal and renally impaired humans, rats □ Salicylic acid—serum protein binding compared to phenytoin, sulfisoxazole, and warfarin, normal and renally impaired humans, rats □ Sulfisoxazole—serum protein binding compared to phenytoin, salicylic acid, and warfarin, normal and renally impaired humans, rats □ Warfarin—serum protein binding compared to phenytoin, salicylic acid, and sulfisoxazole, normal and renally impaired humans, rats

The serum protein binding of drugs is affected by age and disease and differs among species (1–4). There are pronounced interindividual differences in the protein binding of some drugs even among relatively homogeneous groups of healthy humans (5) or animals (6). Since serum protein binding can significantly affect the pharmacokinetic characteristics of drugs (7, 8), considerable effort has been directed to the study of different variables that affect the binding of drugs to serum protein. It would be convenient if one or two acidic, neutral, and basic drugs could serve as representative index compounds in such studies. Therefore, the intrasubject relationships between the serum protein binding of several weakly acidic drugs (phenytoin, salicylic acid, sulfisoxazole, and warfarin) in normal human adults, patients with impaired renal function, and normal adult rats were studied.

EXPERIMENTAL

A single venous blood sample was obtained from 39 normal adults[1], consisting of 19 males (age 31.6 ± 8.5 years, range 21–54) and 20 females (age 27.1 ± 7.8 years, range 18–52). Periodic venous blood samples were obtained from a 9-year-old white male recipient of a renal transplant and from the donor, his 29-year-old mother. Blood sampling began before the transplant, while the recipient was bilaterally anephric, and continued for almost 3 months, during which the recipient experienced a rejection episode which was overcome in about 18 days. Further details of this case have been published elsewhere (9). Single blood samples were obtained from adult male Sprague–Dawley rats, 300–460 g, maintained on a standard diet[2].

Serum was separated, and phenytoin (15 μg/ml, including ^{14}C-phenytoin), salicylic acid (300 μg/ml), sulfisoxazole (100 μg/ml), and ^{14}C-warfarin (0.8 μg/ml) were added to different portions of each serum sample or to the buffer phase of the dialysis system. The serum samples were dialyzed to equilibrium against an equal volume of pH 7.4 phosphate buffer at 37°. Details of the dialysis procedures and analytical methods were described elsewhere (5, 9, 10).

The binding data are expressed as free fraction values, *i.e.*, the ratio of concentrations of unbound to total (free and bound) drug. Total serum protein concentration was determined by the method of Gornall *et al.* (11), and the fraction of albumin was measured with a commercial[3] electrophoresis system. Crystalline human and rat albumins were used as standards.

Table I—Relationship between Serum Free Fraction (*f*) Values of Various Drugs in Normal Human Adults

Drug Pair	*f* Range[a]	*r*	*n*	*p*
Phenytoin–salicylic acid	0.111–0.151 (I) 0.181–0.296 (II)	0.122	30	>0.6
Phenytoin–sulfisoxazole	0.111–0.151 (I) 0.0819–0.125 (III)	0.398	22	>0.1
Salicylic acid–sulfisoxazole	0.182–0.296 (II) 0.0819–0.125 (III)	0.736	22	<0.001
Warfarin–phenytoin	0.00503–0.0186 (IV) 0.111–0.155 (I)	0.032	39	>0.8
Warfarin–salicylic acid	0.00503–0.0172 (IV) 0.181–0.296 (II)	−0.292	30	>0.1
Warfarin–sulfisoxazole	0.00503–0.0172 (IV) 0.0819–0.125 (III)	0.007	22	>0.9

[a] Ranges of *f* are listed for phenytoin (I), salicylic acid (II), sulfisoxazole (III), and warfarin (IV) for the stated number of subjects (*n*).

RESULTS

The results of all protein binding correlation studies are summarized in Tables I–III. These tables include the results of previously published

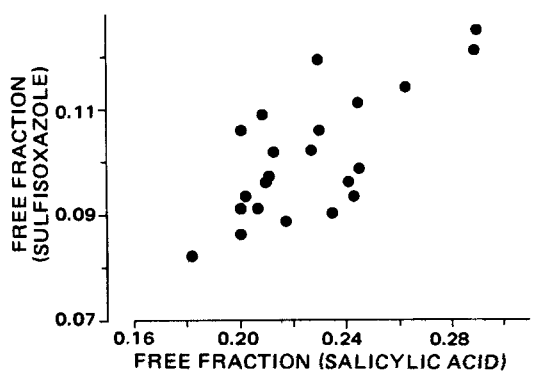

Figure 1—*Relationship between free fraction values of salicylic acid and sulfisoxazole in serum of 22 normal human adults;* r = *0.736,* p < *0.001.*

[1] Thirty-seven were Caucasian, one was Oriental, and one was of Peruvian ancestry. Most of the subjects were faculty, graduate students, and research personnel.

[2] Charles River Formula 4RF.

[3] Gelman Sepratek.

Table II—Relationship between Serum Free Fraction (f) Values of Various Drugs in Patients with Impaired Renal Function[a]

Drug Pair	f Range	r	n	p
Phenytoin–salicylic acid	0.143–0.233 (I) 0.192–0.374 (II)	0.867	17	<0.001
Phenytoin–sulfisoxazole	0.143–0.233 (I) 0.080–0.261 (III)	0.789	17	<0.001
Salicylic acid–sulfisoxazole	0.190–0.374 (II) 0.075–0.261 (III)	0.822	24	<0.001
Warfarin–phenytoin	0.00686–0.0162 (IV) 0.143–0.233 (I)	0.768	8	<0.05
Warfarin–salicylic acid	0.00686–0.0162 (IV) 0.190–0.374 (II)	0.837	13	<0.001
Warfarin–sulfisoxazole	0.00686–0.0162 (IV) 0.075–0.261 (III)	0.798	13	<0.005

[a] Designations as in Table I, except that n indicates the number of blood samples obtained from a kidney donor and recipient over a period of time.

Table III—Relationship between Free Fraction (f) Values of Various Drugs in Normal Adult Rats[a]

Drug Pair	f Range	r	n	p
Phenytoin–salicylic acid	0.179–0.280 (I) 0.390–0.690 (II)	0.866	18	<0.001
Phenytoin–sulfisoxazole	0.179–0.280 (I) 0.0685–0.196 (III)	0.785	18	<0.001
Salicylic acid–sulfisoxazole	0.390–0.690 (II) 0.0685–0.196 (III)	0.817	20	<0.001
Warfarin–phenytoin	0.00405–0.0296 (IV) 0.179–0.280 (I)	0.079	18	>0.7
Warfarin–salicylic acid	0.00405–0.0386 (IV) 0.390–0.690 (II)	0.323	20	>0.1
Warfarin–sulfisoxazole	0.00405–0.0386 (IV) 0.0685–0.196 (III)	0.289	20	>0.2

[a] Designations as in Table I.

investigations of protein binding correlations of warfarin–phenytoin in normal human adults (5) and of salicylic acid–sulfisoxazole in patients with impaired renal function (9) and in rats (12). The additional protein binding data reported here were obtained from the same serum samples, except that not all binding determinations could be done on all samples because of the limited volume of serum. The results of the determinations of the relationship between serum albumin concentration and the free fraction values of the different drugs are summarized in Tables IV–VI.

Studies in Normal Human Subjects—There was a statistically significant correlation between the free fraction values of salicylic acid and sulfisoxazole (Fig. 1) but not between any of the other combinations. The relatively widest range of serum free fraction values was found for warfarin (approximately 3.5-fold); the other three drugs had a considerably smaller intersubject variation (approximately 1.5-fold). There was a

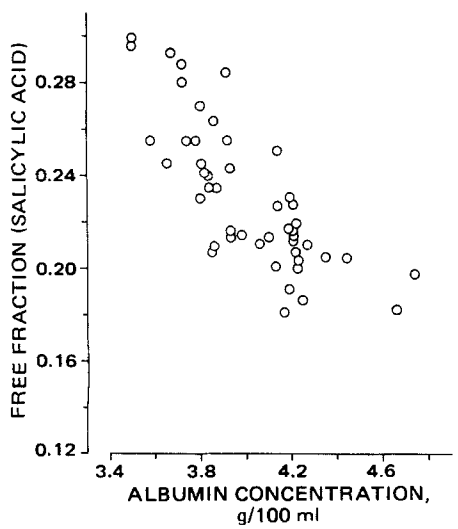

Figure 2—*Relationship between free fraction values of salicylic acid and albumin concentration in serum of 48 normal human adults; r = −0.772, p < 0.001. Eighteen subjects were from a previous study.*

Table IV—Relationship between Albumin Concentration and Free Fraction (f) Values of Various Drugs in Serum of Normal Human Adults

Drug	Range of f and A[a]	r	n	p
Phenytoin	0.111–0.155 3.50–4.72	−0.188	39	>0.2
Salicylic acid	0.181–0.299 3.50–4.74	−0.772	48	<0.001
Sulfisoxazole	0.0819–0.125 3.50–4.66	−0.699	22	<0.001
Warfarin	0.00503–0.0172 3.50–4.66	(See *Discussion*)		

[a] Range of f is on upper line; range of albumin concentration (A) is on lower line.

Table V—Relationship between Albumin Concentration and Free Fraction (f) Values of Various Drugs in Serum of Patients with Impaired Renal Function

Drug	Range of f and A[a]	r	n	p
Phenytoin	0.143–0.233 3.55–5.00	−0.259	17	>0.3
Salicylic acid	0.190–0.374 3.55–5.25	−0.126	24	>0.5
Sulfisoxazole	0.075–0.261 3.55–5.25	0.034	24	>0.8
Warfarin	0.00686–0.0162 3.95–5.12	−0.093	13	>0.7

[a] Range of f is on upper line; range of albumin concentration (A) is on lower line.

statistically significant negative correlation between the serum albumin concentration and the serum free fraction values of salicylic acid (Fig. 2) and sulfisoxazole. No such correlation was found for phenytoin and warfarin.

Studies on Patients with Impaired Renal Function—Figure 3 shows the change in free fraction values of phenytoin in the donor and recipient of a renal transplant over ~3 months. The serum free fraction in the donor increased shortly after removal of the kidney and eventually returned to normal. The free fraction in the serum of the recipient was substantially elevated while he was anephric, decreased to near normal shortly after the transplant, increased again during the rejection episode, and then decreased to normal some time after the rejection episode had been overcome. Similar patterns were observed with respect to the serum protein binding of salicylic acid and sulfisoxazole (9) and warfarin.

Statistically highly significant correlations were found between the free fraction values of all combinations of the four drugs (Table II). Since there was no significant difference between donor and recipient with respect to the correlation slopes (Figs. 4 and 5 and Ref. 9), the data were combined for the statistical analysis. There was no apparent correlation between the serum albumin concentration and the free fraction values of any of the drugs (Table V).

Studies on Normal Adult Rats—Highly statistically significant correlations between serum free fraction values were found for the drug pairs phenytoin–salicylic acid, phenytoin–sulfisoxazole, and salicylic acid–sulfisoxazole, while no significant correlation was apparent for warfarin–phenytoin, warfarin–salicylic acid, or warfarin–sulfisoxazole (Table III). The free fraction values for phenytoin, salicylic acid, and sulfisoxazole showed a significant negative correlation with the albumin concentration in serum; no such correlation was found with respect to warfarin (Table VI).

Table VI—Relationship between Albumin Concentration and Free Fraction (f) Values of Various Drugs in Serum of Normal Adult Rats

Drug	Range of f and A[a]	r	n	p
Phenytoin	0.179–0.280 3.00–3.79	−0.646	18	<0.005
Salicylic acid	0.390–0.690 3.00–3.79	−0.565	20	<0.01
Sulfisoxazole	0.0685–0.196 3.00–3.79	−0.543	20	<0.02
Warfarin	0.00405–0.0386 3.00–3.79	−0.0277	20	>0.9

[a] Range of f is on upper line; range of albumin concentration (A) is on lower line.

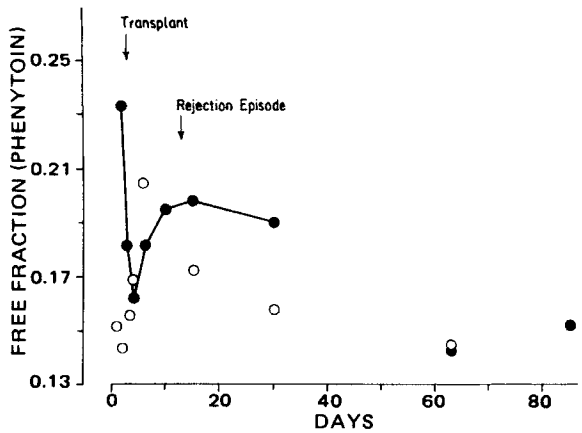

Figure 3—*Free fraction of phenytoin in serum of donor (○) and recipient (●) of a kidney transplant as a function of time.*

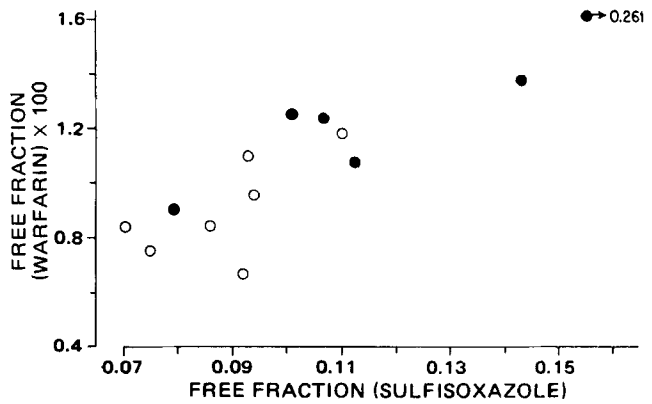

Figure 5—*Relationship between the serum free fraction values of sulfisoxazole and warfarin in serum samples from a kidney donor (○) and recipient (●) obtained over ~3 months;* r = *0.798,* p < *0.005.*

DISCUSSION

There are several possible approaches to the study of correlations between the serum protein binding of different drugs under various conditions. A relatively fundamental approach is the determination of the classic binding parameters of the drugs in solutions of pure albumin. This investigation focused more directly on the clinically relevant aspects of the problem by use of undiluted serum and widely used drugs at concentrations in the therapeutic range.

In comparing the results obtained with serum from normal humans, normal rats, and humans with impaired renal function, it should be recognized that data from the latter group essentially reflect intra- rather than interindividual differences because only two patients were studied and serum was obtained repeatedly during periods of changing renal function. It was considered desirable to use this study design rather than to make one-point-in-time determinations of protein binding in serum from a larger group of patients since it is important to determine, from a clinical pharmacokinetic point of view, the time course of events in patients with impaired renal function.

The serum free fraction values of all drugs studied in this investigation varied appreciably between subjects in the normal humans and rats. The most pronounced variation was found with respect to warfarin, particularly in rats. Such variation may be due to differences in albumin concentration or structure or be caused by endogenous inhibitors of protein binding (13) that may differ among subjects in concentration or kind. Albumin concentration is an important determinant of the serum protein binding of salicylic acid and sulfisoxazole in normal humans and rats and of phenytoin in rats (Table II). A statistically significant negative correlation was demonstrated between the albumin concentration and the warfarin free fraction in the serum of fasted normal humans (14) but not of subjects whose food intake was not restricted or controlled (5), as in this study (Table IV). Apparently, variations in the concentration of fatty acids or other food-derived substances obscure the effect of interindividual differences in the serum albumin concentration on the serum protein binding of warfarin. The very pronounced interindividual variation in the serum protein binding of warfarin in rats may be due to genetic influences, since the free fraction values show a trimodal frequency distribution in these animals (6) but are unimodal in humans (5).

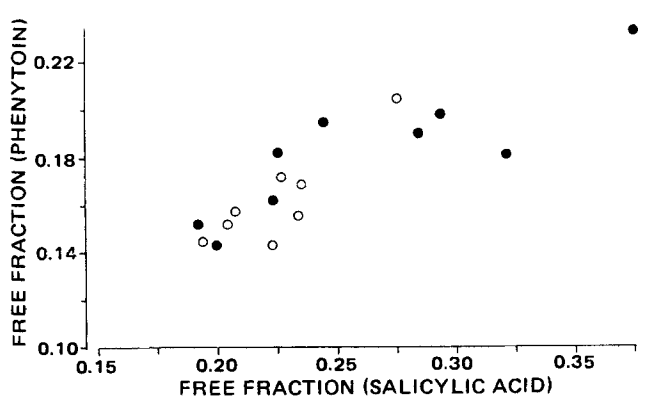

Figure 4—*Relationship between the free fraction values of phenytoin and salicylic acid in serum samples from a kidney donor (○) and recipient (●) obtained over ~3 months;* r = *0.867,* p < *0.001.*

The only statistically significant correlation of free fraction values in all three groups was found for salicylic acid–sulfisoxazole. Data suggesting competitive inhibition between salicylate and a sulfonamide for binding sites on albumin were reported previously (15). All possible pairs of drugs showed statistically significant correlations of free fraction values in the patients with impaired renal function. There is indirect evidence that this pathological condition is associated with pronounced elevation of endogenous inhibitors of serum protein binding (13), and this variable apparently affects all drugs used in this investigation. It also apparently obscures the effect of variations in albumin concentration, since there was no statistically significant relationship between free fraction values for any of the drugs and the serum albumin concentration in the serum of the two patients. However, if these relationships are examined separately for donor and recipient, a statistically significant negative correlation is found between the albumin concentration and the free fraction of salicylate in the serum of the donor ($r = -0.718$, $p < 0.01$).

The observations on the change in the free fraction values of phenytoin and warfarin after renal transplantation are in agreement with results obtained by Odar-Cederlöf (16), but this investigator studied the patients for a shorter period, did not encounter a rejection episode, and did not examine the serum binding characteristics of kidney donors.

There can be several reasons for the lack of correlation between the serum free fraction values of different drugs. They may have different binding sites, their association constant with albumin may differ significantly so that an endogenous inhibitor may effectively displace one but not the other drug, and the molar concentration ratio of drug to albumin in the therapeutic drug concentration range may differ appreciably. The latter two variables can influence the sensitivity of the free fraction value to changes in albumin concentration. These same factors, as well as qualitative and quantitative differences in albumin and/or endogenous inhibitors, may be responsible for species differences and differences between healthy subjects and patients with renal or other diseases (7). Consequently, it appears that no single drug can serve as an index compound for a group of other drugs. The investigation described in this report demonstrates this fact with respect to a group of weakly acidic drugs.

REFERENCES

(1) W. J. Jusko and M. Gretch, *Drug Metab. Rev.*, **5**, 43 (1976).

(2) M. M. Reidenberg, *Clin. Pharmacokinet.*, **1**, 121 (1976).

(3) M. Ehrnebo, S. Agurell, B. Jalling, and L. O. Borèus, *Eur. J. Clin. Pharmacol.*, **3**, 189 (1971).

(4) J. A. Sturman and M. J. H. Smith, *J. Pharm. Pharmacol.*, **19**, 621 (1967).

(5) A. Yacobi, T. Lampman, and G. Levy, *Clin. Pharmacol. Ther.*, **21**, 283 (1977).

(6) J. T. Slattery, A. Yacobi, and G. Levy, *Life Sci.*, **19**, 447 (1976).

(7) G. Levy, in "The Effect of Disease States on Drug Pharmacokinetics," L. Z. Benet, Ed., APhA Academy of Pharmaceutical Sciences, Washington, D.C., 1976.

(8) G. Levy, *J. Pharm. Sci.*, **65**, 1264 (1976).

(9) G. Levy, T. Baliah, and J. A. Procknal, *Clin. Pharmacol. Ther.*, **20**, 512 (1976).
(10) A. Yacobi and G. Levy, *J. Pharm. Sci.*, **64**, 1660 (1975).
(11) A. C. Gornall, C. J. Bardawill, and M. M. Davis, *J. Biol. Chem.*, **177**, 751 (1949).
(12) A. Yacobi, S. Øie, and G. Levy, *J. Pharm. Sci.*, **66**, 1025 (1977).
(13) I. Sjöholm, A. Kober, I. Odar-Cederlöf, and O. Borgå, *Biochem. Pharmacol.*, **25**, 1205 (1976).
(14) A. Yacobi, R. G. Stoll, A. R. DiSanto, and G. Levy, *Res. Commun. Chem. Pathol. Pharmacol.*, **14**, 743 (1976).
(15) A. H. Anton and W. T. Corey, *Acta Pharmacol. Toxicol., Suppl. 3*, **29**, 134 (1971).
(16) I. Odar-Cederlöf, Ph.D. thesis, Karolinska Institutet, Stockholm, Sweden, 1975.

ACKNOWLEDGMENTS AND ADDRESSES

Received October 26, 1976, from the *Department of Pharmaceutics, School of Pharmacy, State University of New York at Buffalo, Amherst, NY 14260.*

Accepted for publication December 3, 1976.

Supported in part by Grants GM 19568 and 20852 from the National Institute of General Medical Sciences, National Institutes of Health.

[x] To whom inquiries should be directed.

Isolation and Identification of Morphine 3- and 6-Glucuronides, Morphine 3,6-Diglucuronide, Morphine 3-Ethereal Sulfate, Normorphine, and Normorphine 6-Glucuronide as Morphine Metabolites in Humans

S. Y. YEH [x], C. W. GORODETZKY, and H. A. KREBS

Abstract □ Morphine metabolites were isolated with column chromatography on a resin and neutral aluminum oxide and TLC from the urine of morphine-dependent subjects maintained on morphine sulfate at a dose of 240 mg/day. These metabolites were characterized as morphine 3-glucuronide, morphine 6-glucuronide, morphine 3,6-diglucuronide, morphine 3-ethereal sulfate, normorphine, normorphine 6-glucuronide, and, possibly, normorphine 3-glucuronide by free phenol and glucuronide tests, enzymatic hydrolysis, GLC, TLC, UV spectroscopy, and GLC–mass spectrometry.

Keyphrases □ Morphine metabolites, various—column chromatographic and TLC isolation from human urine □ Chromatography, column—isolation of various morphine metabolites from human urine □ TLC—isolation of various morphine metabolites from human urine □ Narcotic analgesics—various morphine metabolites, column chromatographic and TLC isolation from human urine

Studies with animals and humans have shown metabolism of morphine by the following pathways: (*a*) conjugation to give morphine 3-glucuronide, morphine 6-glucuronide, and morphine 3-ethereal sulfate (1–8); (*b*) *N*-demethylation to yield normorphine, which was then conjugated (9–15); (*c*) *O*-methylation to form codeine (16, 17); and (*d*) oxidation to form dihydromorphinone (18). Recently, a minor metabolite, tentatively identified as morphine 2,3-quinone, was reported in the urine of rats given morphine and after incubation of morphine with rat brain homogenates (19). Also, one study was unable to confirm the conversion of morphine to codeine (20).

Only morphine 3-glucuronide has been isolated as a morphine metabolite in humans (2), and a small amount of morphine 6-glucuronide was detected by TLC (5). The present paper reports the isolation and identification of morphine 3- and 6-glucuronides, morphine 3,6-diglucuronide, morphine 3-ethereal sulfate, normorphine, normorphine 6-glucuronide, and, possibly, normorphine 3-glucuronide from the urine of morphine-dependent human subjects.

EXPERIMENTAL

Materials and Subjects—The morphine sulfate USP used was a commercial product; normorphine hydrochloride was used as received[1]. Pseudomorphine and morphine *N*-oxide were synthesized according to the procedures of Fulton (21) and Freund and Speyer (22), respectively. Morphine 3-glucuronide, codeine 6-glucuronide, and morphine 3-ethereal sulfate were isolated from the urine of dogs and cats given morphine and codeine, respectively (3, 9, 23).

Four adult postaddict males[2] were judged to be in good health from recent history and physical and laboratory examinations, including tests of hematological, renal, hepatic, and cardiac functions. The subjects had an average age of 33 years (range of 27–41) and an average weight of 66 kg (range of 61–71). All subjects were given morphine sulfate injections in gradually increasing doses from 10 to 60 mg sc four times daily. Urine was collected from subjects during maintenance on morphine sulfate at 60 mg after several months and stored in a refrigerator.

Extraction of Morphine and Its Metabolites—Morphine, normorphine, and other possible metabolites were extracted from samples according to the procedure described previously (14). Samples were adjusted to about pH 10, buffered at pH 10.4 with 2 ml of 40% phosphate buffer (37% K_2HPO_4 and 3% K_3PO_4), salted, and extracted with 1,2-dichloroethane (glass distilled) containing 30% (v/v) 2-propanol.

The organic phase was shaken with 1 *N* HCl; then the acidic aqueous phase was separated and adjusted to pH 10.4, buffered, salted, and extracted again with the organic solvent. The residue obtained upon evaporation of the organic phase to dryness was used for TLC and GLC identification of morphine metabolites. For GLC identification, a derivative was prepared using 25% trimethylsilylimidazole in pyridine[3].

TLC—TLC was performed with either 250-μm silica gel plates with a preadsorbent area[4] or instant TLC sheets impregnated with silica gel[5].

[1] Courtesy of Dr. E. L. May, National Institutes of Health.
[2] Federal prisoner volunteers, incarcerated at the National Institute on Drug Abuse Research Center. Informed consent was obtained in writing in the presence of a witness.
[3] Pierce Chemical Co., Rockford, Ill.
[4] Quantum Industries, Fairfield, N.J.
[5] Gelman Instrument Co., Ann Arbor, Mich.

(9) G. Levy, T. Baliah, and J. A. Procknal, *Clin. Pharmacol. Ther.*, **20**, 512 (1976).
(10) A. Yacobi and G. Levy, *J. Pharm. Sci.*, **64**, 1660 (1975).
(11) A. C. Gornall, C. J. Bardawill, and M. M. Davis, *J. Biol. Chem.*, **177**, 751 (1949).
(12) A. Yacobi, S. Øie, and G. Levy, *J. Pharm. Sci.*, **66**, 1025 (1977).
(13) I. Sjöholm, A. Kober, I. Odar-Cederlöf, and O. Borgå, *Biochem. Pharmacol.*, **25**, 1205 (1976).
(14) A. Yacobi, R. G. Stoll, A. R. DiSanto, and G. Levy, *Res. Commun. Chem. Pathol. Pharmacol.*, **14**, 743 (1976).
(15) A. H. Anton and W. T. Corey, *Acta Pharmacol. Toxicol., Suppl. 3*, **29**, 134 (1971).
(16) I. Odar-Cederlöf, Ph.D. thesis, Karolinska Institutet, Stockholm, Sweden, 1975.

ACKNOWLEDGMENTS AND ADDRESSES

Received October 26, 1976, from the *Department of Pharmaceutics, School of Pharmacy, State University of New York at Buffalo, Amherst, NY 14260.*

Accepted for publication December 3, 1976.

Supported in part by Grants GM 19568 and 20852 from the National Institute of General Medical Sciences, National Institutes of Health.

[x] To whom inquiries should be directed.

Isolation and Identification of Morphine 3- and 6-Glucuronides, Morphine 3,6-Diglucuronide, Morphine 3-Ethereal Sulfate, Normorphine, and Normorphine 6-Glucuronide as Morphine Metabolites in Humans

S. Y. YEH [x], C. W. GORODETZKY, and H. A. KREBS

Abstract □ Morphine metabolites were isolated with column chromatography on a resin and neutral aluminum oxide and TLC from the urine of morphine-dependent subjects maintained on morphine sulfate at a dose of 240 mg/day. These metabolites were characterized as morphine 3-glucuronide, morphine 6-glucuronide, morphine 3,6-diglucuronide, morphine 3-ethereal sulfate, normorphine, normorphine 6-glucuronide, and, possibly, normorphine 3-glucuronide by free phenol and glucuronide tests, enzymatic hydrolysis, GLC, TLC, UV spectroscopy, and GLC–mass spectrometry.

Keyphrases □ Morphine metabolites, various—column chromatographic and TLC isolation from human urine □ Chromatography, column—isolation of various morphine metabolites from human urine □ TLC—isolation of various morphine metabolites from human urine □ Narcotic analgesics—various morphine metabolites, column chromatographic and TLC isolation from human urine

Studies with animals and humans have shown metabolism of morphine by the following pathways: (*a*) conjugation to give morphine 3-glucuronide, morphine 6-glucuronide, and morphine 3-ethereal sulfate (1–8); (*b*) *N*-demethylation to yield normorphine, which was then conjugated (9–15); (*c*) *O*-methylation to form codeine (16, 17); and (*d*) oxidation to form dihydromorphinone (18). Recently, a minor metabolite, tentatively identified as morphine 2,3-quinone, was reported in the urine of rats given morphine and after incubation of morphine with rat brain homogenates (19). Also, one study was unable to confirm the conversion of morphine to codeine (20).

Only morphine 3-glucuronide has been isolated as a morphine metabolite in humans (2), and a small amount of morphine 6-glucuronide was detected by TLC (5). The present paper reports the isolation and identification of morphine 3- and 6-glucuronides, morphine 3,6-diglucuronide, morphine 3-ethereal sulfate, normorphine, normorphine 6-glucuronide, and, possibly, normorphine 3-glucuronide from the urine of morphine-dependent human subjects.

EXPERIMENTAL

Materials and Subjects—The morphine sulfate USP used was a commercial product; normorphine hydrochloride was used as received[1]. Pseudomorphine and morphine *N*-oxide were synthesized according to the procedures of Fulton (21) and Freund and Speyer (22), respectively. Morphine 3-glucuronide, codeine 6-glucuronide, and morphine 3-ethereal sulfate were isolated from the urine of dogs and cats given morphine and codeine, respectively (3, 9, 23).

Four adult postaddict males[2] were judged to be in good health from recent history and physical and laboratory examinations, including tests of hematological, renal, hepatic, and cardiac functions. The subjects had an average age of 33 years (range of 27–41) and an average weight of 66 kg (range of 61–71). All subjects were given morphine sulfate injections in gradually increasing doses from 10 to 60 mg sc four times daily. Urine was collected from subjects during maintenance on morphine sulfate at 60 mg after several months and stored in a refrigerator.

Extraction of Morphine and Its Metabolites—Morphine, normorphine, and other possible metabolites were extracted from samples according to the procedure described previously (14). Samples were adjusted to about pH 10, buffered at pH 10.4 with 2 ml of 40% phosphate buffer (37% K_2HPO_4 and 3% K_3PO_4), salted, and extracted with 1,2-dichloroethane (glass distilled) containing 30% (v/v) 2-propanol.

The organic phase was shaken with 1 *N* HCl; then the acidic aqueous phase was separated and adjusted to pH 10.4, buffered, salted, and extracted again with the organic solvent. The residue obtained upon evaporation of the organic phase to dryness was used for TLC and GLC identification of morphine metabolites. For GLC identification, a derivative was prepared using 25% trimethylsilylimidazole in pyridine[3].

TLC—TLC was performed with either 250-μm silica gel plates with a preadsorbent area[4] or instant TLC sheets impregnated with silica gel[5].

[1] Courtesy of Dr. E. L. May, National Institutes of Health.
[2] Federal prisoner volunteers, incarcerated at the National Institute on Drug Abuse Research Center. Informed consent was obtained in writing in the presence of a witness.
[3] Pierce Chemical Co., Rockford, Ill.
[4] Quantum Industries, Fairfield, N.J.
[5] Gelman Instrument Co., Ann Arbor, Mich.

When silica gel plates with a preadsorbent area were used, samples were spotted on the preadsorbent area. The R_f value was calculated using the beginning of the silica gel section as the origin. Two solvent systems were used for development of the chromatograms: A, 1-butanol–acetic acid–water (35:3:10); and B, ethyl acetate–methanol–ammonium hydroxide (17:2:1). Chromatograms were visualized by spraying with iodoplatinate reagent.

GLC—A gas chromatograph[6] equipped with dual columns and dual flame-ionization detectors was used. A 0.9-m × 2-mm glass column was packed with 3% OV-17 coated on 60–80-mesh Gas Chrom Q. A 1.5-m × 2-mm stainless steel column was packed with 3% SE-30 coated on 100–120-mesh Varaport. The temperatures of the injector, column, and detector were 255, 220, and 295°, respectively; gas flow rates were 30 ml/min for nitrogen and hydrogen and 300–400 ml/min for dried compressed air.

GLC–Mass Spectrometry—Chemical-ionization mass spectral data were obtained on a gas chromatograph–mass spectrometer[7] equipped with an interactive data system[8] and a glass column (1.5 m × 2 mm) packed with 3% OV-17 coated on Gas Chrom Q. The gas chromatograph was coupled to the mass spectrometer by a 0.31-cm (0.125-in.) glass-lined stainless steel tube and a venting valve. The electron energy was 80 ev, and the ion repeller voltage was 3 v.

Methane with a flow rate giving an ion chamber pressure of about 1000 μm was used as the carrier gas as well as the chemical-ionization reagent gas in the ion source. The temperatures of the injector, column, and ion source were 230, 210, and 100°, respectively. Aliquots of 3–5 μl of the silylated sample were injected. After injection, the venting valve was opened for the first 30 sec, allowing excess derivatizing reagent and solvent to escape without entering the ionization chamber.

Hydrolysis of Conjugated Metabolites—Conjugated morphine metabolites were hydrolyzed to free base alkaloids by acid hydrolysis, incubation with β-glucuronidase (type II, bacterial powder)[9], or incubation with β-glucuronidase–sulfatase[10] according to a procedure described previously (14). After hydrolysis, the samples were adjusted to about pH 10, buffered, and extracted according to the described procedure.

Glucuronic Acid Determination—The content of glucuronic acid in the conjugated morphine metabolites was determined according to the procedure of Dische (24).

Free Phenol Test—Free phenol was determined by a modified procedure of Volterra (25) using the reagent of Folin and Ciocalteu (using one-tenth of the volume of samples and reagents stated).

Purification of Morphine Metabolites with Column Chromatography—Aliquots (200 ml) of urine from each subject were centrifuged to remove the insoluble material and passed at a flow rate of 2–4 ml/min through a resin[11] column (2.1 × 40 cm) previously washed with methanol and water. The column was washed with 150 ml of distilled water and eluted with 300 ml of methanol. The first 100 ml of washing was discarded. The remaining washing and methanol eluate were collected separately and concentrated separately to about 2 ml under reduced pressure in an evaporator[12] in a water bath at about 50°. (All evaporations in these studies were done in this manner.) A total of 6 liters of urine was thus chromatographed through the resin.

An aliquot of the methanol eluate was chromatographed on an instant TLC sheet, and the eluate was diluted with 15 ml of 5% NH_4OH. Each 5-ml aliquot of eluate was extracted three times with 15 ml of 1,2-dichloroethane containing 30% 2-propanol. The organic and aqueous phases were separately evaporated to dryness, and the residue of the organic phase was dissolved in methanol.

Organic Phase—An aliquot of the organic phase was chromatographed on an instant TLC sheet impregnated with silica gel, and the chromatogram was developed with System B. The region with R_f 0.4 (0.3–0.5), corresponding to morphine 3-ethereal sulfate and morphine *N*-oxide, was eluted with methanol and water (Fraction I). The region with R_f 0.85 (0.7–1.0), corresponding to morphine and normorphine, was eluted with methanol (Fraction II).

Another aliquot was concentrated, adsorbed on 10 g of neutral alumina, and added on a neutral alumina (50 g) column (2.1 × 150 cm). The column was sequentially eluted with 100 ml each of benzene, chloroform, acetone, acetone–methanol (50:50), and 500 ml of methanol, and the eluate was collected in 20-ml fractions. Morphine and its metabolites in each fraction were monitored by chromatographing an aliquot (100 μl) on TLC silica gel plates with System B. Spots with R_f 0.4, corresponding to morphine, were observed in fractions 21–35. In addition to morphine, spots with R_f ~0.2, corresponding to normorphine, were observed in fractions 26–30. Other spots whose R_f values did not correspond to any hypothesized morphine metabolites, probably due to nicotine and caffeine and their metabolites, were observed in fractions 15–19.

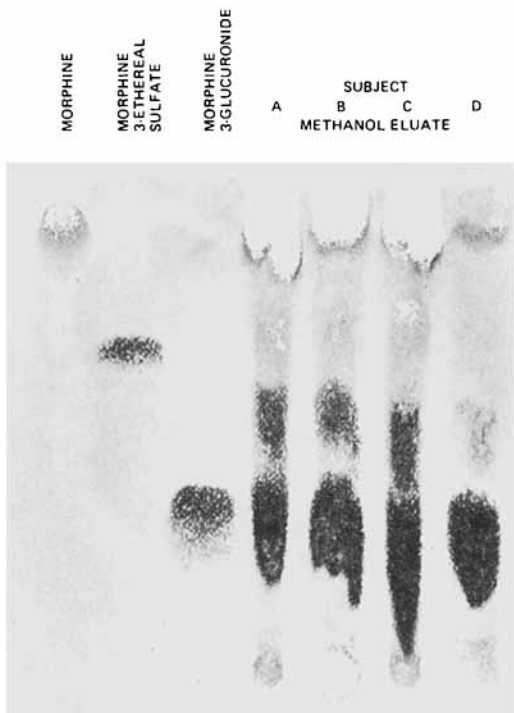

Figure 1—*Chromatogram of the methanol eluate obtained from a resin column on an instant TLC sheet impregnated with silica gel and developed with 1-butanol–acetic acid–water (35:3:10).*

The eluates collected in fractions 21–25, 26–30, and 31–35 were streaked on TLC silica gel plates, and the chromatograms were developed with System B. The regions with R_f 0.2 and 0.4 were separately eluted with methanol to yield Fractions III and IV, respectively.

Aqueous Phase—The residue of the aqueous phase was triturated with methanol to yield methanol-soluble and methanol-insoluble portions. The methanol-insoluble material was recrystallized in aqueous methanol to yield Fraction V and a mother liquid, which was combined with the methanol-soluble portion. This portion was again evaporated to a syrupy residue and triturated with methanol to yield new methanol-soluble and methanol-insoluble portions. These processes were repeated several times to separate the maximum of the methanol-insoluble material from the methanol-soluble portion.

The methanol-soluble portion was adsorbed on neutral alumina and placed on a 50-g neutral alumina column (2.1 × 150 cm). The column was sequentially eluted with 100 ml each of methanol and methanol–water (in proportions of 75:25, 50:50, and 25:75) and, finally, with 500 ml of water. The eluate was collected in 20-ml fractions, and morphine and its metabolites were monitored by chromatographing 100-μl aliquots of each fraction on instant TLC sheets impregnated with silica gel. The chromatograms developed with System A showed that fractions 5–9 contained one spot with R_f 0.85, corresponding to morphine; fractions 11–14 showed two spots with R_f 0.4 and 0.65; and fractions 17–35 showed four spots with R_f 0.1, 0.3, 0.5, and 0.6.

The eluates collected in fractions 17–35 were evaporated to syrupy residues and triturated with methanol to yield methanol-soluble and methanol-insoluble fractions. The methanol-insoluble fractions were combined with Fraction V. The methanol-soluble fractions were chromatographed on instant TLC sheets impregnated with silica gel (20 × 20 cm), and the chromatogram was developed with System A. The zones corresponding to the spots with R_f 0.1, 0.3, 0.5, and 0.6 were horizontally cut off and eluted with aqueous methanol. The eluates were evaporated to dryness and crystallized from aqueous methanol to yield Fractions VI,

[6] Varian model 2700.
[7] Finnigan model 3300.
[8] Finnigan model 6000.
[9] Sigma Chemical Co., St. Louis, Mo.
[10] Glusulase, Endo Laboratories, Garden City, N.Y.
[11] Amberlite XAD-2, Rohm & Haas Chemical Co., Philadelphia, Pa.
[12] Buchler Instruments, Fort Lee, N.J.

Table I—TLC, GLC, and Chemical-Ionization GLC–Mass Spectrometric Characteristics of Morphine Metabolites Isolated from Human Urine

Sample	Instant TLC, R_f Solvent A	Instant TLC, R_f Solvent B	TLC, Solvent B, R_f	Phenol Test	Glucuronide Test	As Trimethylsilyl Derivative: GLC R_t, min	Chemical-Ionization GLC–Mass Spectrometry, m/e: M − 15	M + 1	M + 29
Authentic:									
Morphine	0.85	0.9	0.4	+	−	6.0	414	430	458
Normorphine	0.85	0.85	0.2	+	−	7.2	400	416	444
Morphine 3-glucuronide	0.3	0	0	−	+				
Morphine 3-ethereal sulfate	0.6	0.4	0	−	−	6.0	414	430	458
Codeine 6-glucuronide	0.5	0	0	−	+				
Isolated:									
Fraction I	0.6	0.4	0	−	−	6.0	414	430	458
Hydrolyzed I	0.85	0.9	0.4	+	−	6.0	414	430	458
Fraction II	0.85	0.9	0.2[a]	+	−				
			0.4[b]	+	−	6.0	414	430	458
Fraction III	0.85	0.8	0.2	+	−	7.2	400	416	444
Fraction IV	0.85	0.9	0.4	+	−	6.0	414	430	458
Fraction V	0.3	0	0	−	+				
Hydrolyzed V	0.85	0.9	0.2[a]	+	−	7.2	400	416	444
			0.4[b]	+	−	6.0	414	430	458
Fraction VI	0.1	0	0	−	+				
Hydrolyzed VI	0.85	0.9	0.4	+	−	6.0	414	430	458
Fraction VII	0.3	0	0	−	+				
Hydrolyzed VII	0.85	0.9	0.2[a]	+	−	7.2	400	416	444
			0.4[b]	+	−	6.0	414	430	458
Fraction VIII	0.5	0	0	+	+				
Hydrolyzed VIII	0.85	0.8	0.4	+	−	6.0[b]	414	430	458
						7.2[a]	400	416	444
Fraction IX	0.6	0	0	+	+				
Hydrolyzed IX	0.85	0.85	0.2	+	−	6.0[a]	414	430	458
						7.2[b]	400	416	444
Fraction X	0.4			−	−				
Fraction XI	0.6	0.4	0	−	−	6.0	414	430	458
Hydrolyzed XI	0.85	0.9	0.4	+	−	6.0	414	430	458

[a] Minor. [b] Major.

VII, VIII, and IX, respectively. The metabolite with R_f 0.1, Fraction VI, could not be crystallized from methanol. After evaporation to dryness, this residue was triturated with ether and dried under vacuum to yield about 10 mg of hygroscopic material.

The eluates collected in fractions 11–14 were concentrated and streaked on instant TLC sheets impregnated with silica gel and the chromatogram was developed with System A. The zones corresponding to R_f 0.4 and 0.65 were horizontally cut off and eluted with aqueous methanol. The eluates were separately evaporated to dryness, and the residues were dissolved in water to yield Fractions X and XI, respectively.

RESULTS

The chromatogram of the methanol eluate from a resin column developed with System A showed five iodoplatinate positive spots with R_f values equal to 0.1 (unknown), 0.3 (corresponds to morphine 3-glucuronide), 0.5 (unknown), 0.6 (corresponds to morphine 3-ethereal sulfate), and 0.85 (corresponds to morphine) (Fig. 1). Results of TLC, GLC, GLC–mass spectrometry, and phenolic and glucuronide tests for all fractions are shown in Table I.

Identification of Morphine 3-Glucuronide—A major morphine metabolite, located in Fractions V and VII, was isolated in crystalline form in a yield of 600 mg. The metabolite on TLC had the same R_f values as authentic morphine 3-glucuronide and was negative in the free phenol test. Its UV spectrum in an alkaline medium did not show a bathochromic shift. This metabolite was positive in the glucuronide test and hydrolyzed with β-glucuronidase to yield morphine, identified by TLC, GLC, and GLC–mass spectrometry. The ratio of glucuronic acid to morphine was about 1:1. Based on these data, the identity of this metabolite was established as morphine 3-glucuronide.

Identification of Morphine 6-Glucuronide—The metabolite located in Fraction VIII was isolated in crystalline form in a yield of 40 mg. This metabolite was positive in both the free phenol and glucuronide tests. Its UV spectrum in an alkaline medium showed a bathochromic shift (Fig. 2). After hydrolysis with acid or β-glucuronidase, it yielded morphine and a small amount of normorphine (3–5%), identified by TLC, GLC, and GLC–mass spectrometry (Fig. 3). The ratio of morphine to glucuronic acid was about 1:1. The identity of this metabolite was thus established as morphine 6-glucuronide.

Identification of Morphine 3,6-Diglucuronide—The metabolite located in Fraction VI was positive in the glucuronide test and negative in the free phenol test. After hydrolysis with acid or β-glucuronidase, it yielded morphine, identified by GLC and GLC–mass spectrometry (Fig. 4). The ratio of morphine to glucuronic acid was about 1:2. The metabolite was thus identified as morphine 3,6-diglucuronide.

Identification of Morphine 3-Ethereal Sulfate—The metabolite located in Fraction XI on TLC had the same R_f value as authentic morphine 3-ethereal sulfate, was negative in the free phenol and glucuronide tests, and was not hydrolyzed with β-glucuronidase, but it was hydrolyzed with arylsulfatase to yield morphine, identified by TLC. The metabolite prior to or after hydrolysis and derivatization with 25% trimethylsilylimidazole in pyridine showed a peak having the same retention time and

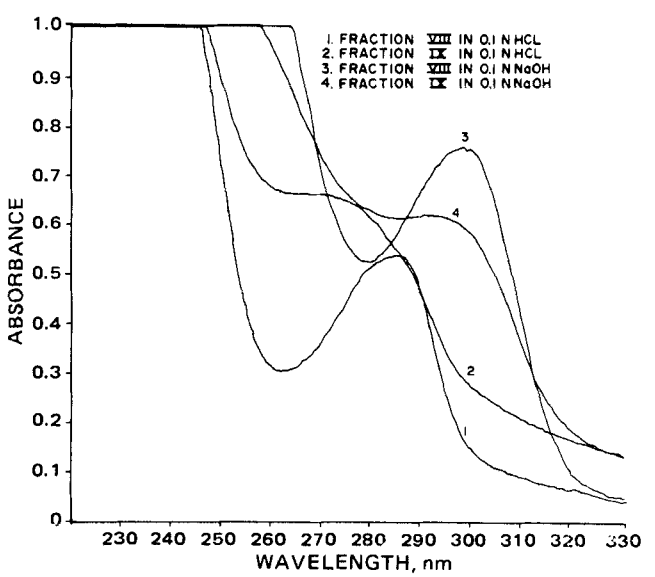

Figure 2—*UV spectrum of Fractions VIII and IX in 0.1 N HCl and 0.1 N NaOH.*

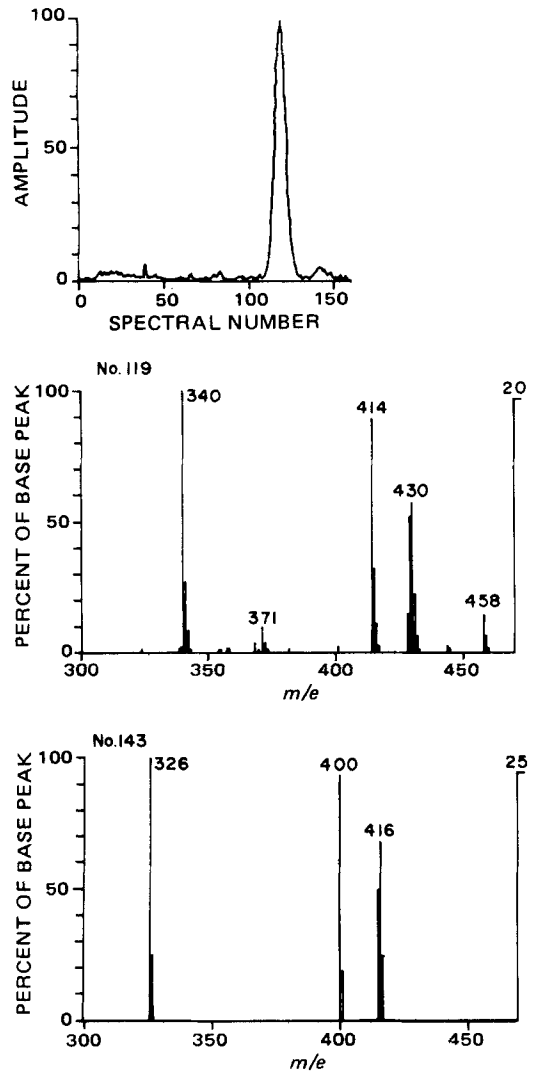

Figure 3—*Integrated total ion current chromatogram (top) of an extract of hydrolyzed Fraction VIII as the trimethylsilyl derivative and mass spectra No. 119, identified as morphine, and No. 143, identified as normorphine.*

mass fragmentation pattern as morphine. Authentic morphine 3-ethereal sulfate, derivatized with 25% trimethylsilylimidazole in pyridine, also showed a peak with the same retention time as morphine. The result indicated that morphine 3-ethereal sulfate was probably hydrolyzed to morphine during the derivatization.

The metabolite located in Fraction I on TLC had the same R_f value as morphine 3-ethereal sulfate as well as morphine *N*-oxide, was not reduced with sodium bisulfite, was negative in the free phenol and glucuronide tests, and was tentatively identified as morphine 3-ethereal sulfate.

Identification of Normorphine—The metabolite located in Fraction III on TLC had the same R_f value as authentic normorphine (Fig. 5). After derivatization with 25% trimethylsilylimidazole in pyridine or acetic anhydride, it showed a peak on GLC with the retention time and mass fragmentation pattern of normorphine (Fig. 6, lower panel).

Identification of Normorphine 6-Glucuronide—The metabolite located in Fraction IX was positive in the free phenol and glucuronide tests. Its UV spectrum in an alkaline medium showed a bathochromic shift (Fig. 2). After hydrolysis with acid or β-glucuronidase, it yielded mainly normorphine and a small amount of morphine (5%), identified by GLC and GLC–mass spectrometry (Fig. 7). The ratio of normorphine to glucuronic acid was about 1:1. The R_f value of the metabolite (0.6) on instant TLC sheets, impregnated with silica gel and developed with System A, was close to that of morphine 3-ethereal sulfate (0.65). However, when these two metabolites were cochromatographed, the chromatogram showed two definite spots. The metabolite was identified as normorphine 6-glucuronide.

Identification of Normorphine 3-Glucuronide—Fractions V and VII were hydrolyzed and extracted. The extract was chromatographed on TLC and developed with System B. The chromatogram showed a major spot of morphine and a minor spot of normorphine (Fig. 5). The normorphine conjugate, crystallized together with morphine 3-glucuronide, had a different R_f value than that of normorphine 6-glucuronide and was enzymatically hydrolyzed with β-glucuronidase. It was tentatively identified as normorphine 3-glucuronide.

Analysis of Fraction X did not reveal any hypothesized morphine metabolites.

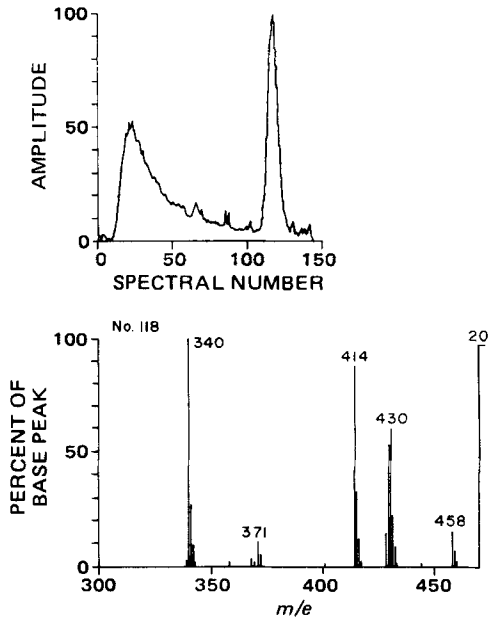

Figure 4—*Integrated total ion current chromatogram (top) of an extract of hydrolyzed Fraction VI as the trimethylsilyl derivative and mass spectrum No. 118, identified as morphine.*

DISCUSSION

The finding of morphine 3- and 6-glucuronides in the urine of morphine-dependent subjects confirmed previous observations (2, 5). In addition to morphine 3- and 6-glucuronides, morphine 3,6-diglucuronide was isolated. In an earlier study on the metabolism of morphine in the dog (1), one morphine conjugate was crystallized from aqueous methanol and was identified as morphine 3-glucuronide dihydrate, but another conjugate was more polar and could not be obtained in crystalline form. It was postulated to be morphine 3-ethereal sulfate 6-glucuronide. The amount of morphine conjugates was reported to account for 55–64% of the administered dose (14).

Morphine 6-glucuronide could result from enzymatic conjugation *in vivo* or hydrolysis of morphine 3,6-diglucuronide either *in vivo* or during analysis, since the glucuronide conjugate at the 3-position hydrolyzes easier than that at the 6-position (26). Although the R_f value of isolated morphine 6-glucuronide on instant TLC sheets, impregnated with silica gel and developed with System A, was close to that of codeine 6-glucuronide, after hydrolysis of the isolated material followed by extraction and derivatization, analysis by GLC and GLC–mass spectrometry indicated only morphine and a small amount of normorphine but no codeine.

A previous study demonstrated that the administered morphine sulfate sample contained about 0.04% codeine (20), which could be biotransformed to morphine and norcodeine, which could then be conjugated (27). However, no codeine or norcodeine was found in the present study. The amount of these conjugates was probably too small to be detectable. The amount of morphine 6-glucuronide and morphine 3,6-diglucuronide was estimated to be about 1% that of morphine 3-glucuronide.

Morphine 3-ethereal sulfate was isolated from the urine of humans and located in Fractions I and XI. The R_f value of the spot of Fraction I corresponded to the values of both morphine *N*-oxide and morphine 3-ethereal sulfate. However, it was not reduced with sodium bisulfite, ruling out morphine *N*-oxide. Use of an authentic standard confirmed that morphine 3-ethereal sulfate could be extracted into the organic phase under the experimental conditions. The ethereal sulfate group of morphine 3-ethereal sulfate, like dopamine 3- and 4-ethereal sulfates (28),

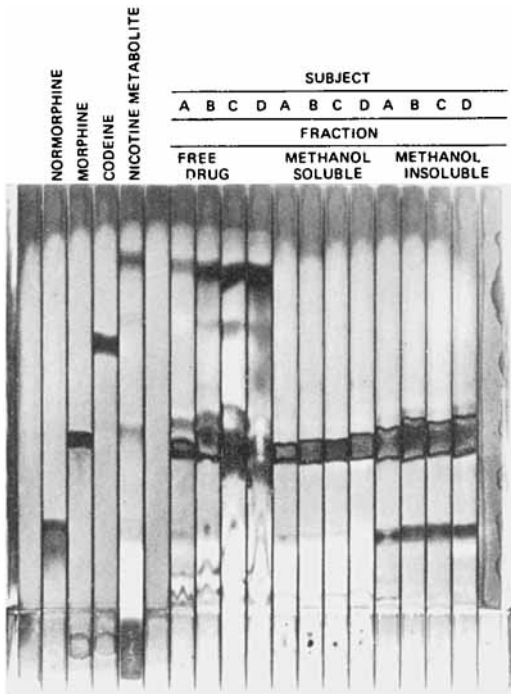

Figure 5—*Thin-layer chromatogram of the organic phase, the methanol-soluble and the acid-hydrolyzed methanol-insoluble fractions on TLC silica gel plates developed with System B. The methanol eluate of nicotine metabolites was obtained by chromatographing 200 ml of drug-free cigarette smoker's urine through a resin column and treating it as for the isolation of morphine metabolites.*

can be hydrolyzed during derivatization with 25% trimethylsilylimidazole in pyridine. The amount of morphine 3-ethereal sulfate was estimated to be about 1% that of morphine 3-glucuronide.

Although *N*-demethylation of morphine in humans was reported using radioisotopes (9, 15) and GLC (14), no report on the isolation of free and conjugated normorphine appears in the literature. The amount of free and conjugated normorphine was reported to account for about 1 and 4%, respectively, of the administered dose (14). Normorphine conjugates, like morphine glucuronides, could exist in two forms: one conjugated as glucuronide at the 3-position and the other conjugated at the 6-position.

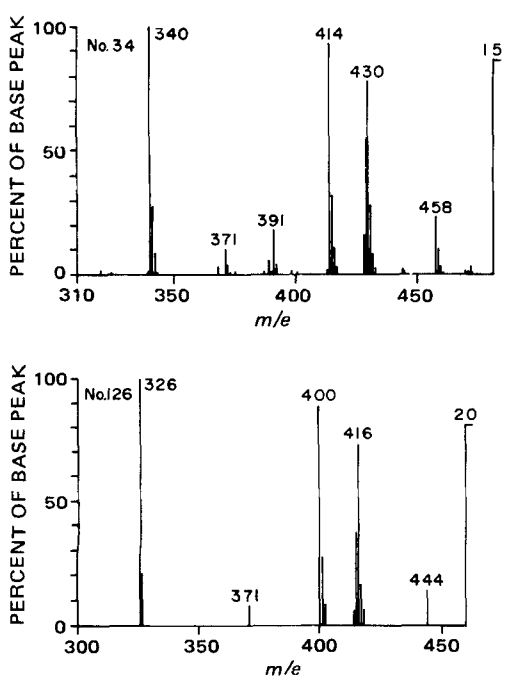

Figure 6—*Upper panel: mass spectrum (No. 34) of GLC peak for Fraction IV, identified as morphine. Lower panel: mass spectrum (No. 126) of GLC peak for Fraction III, identified as normorphine.*

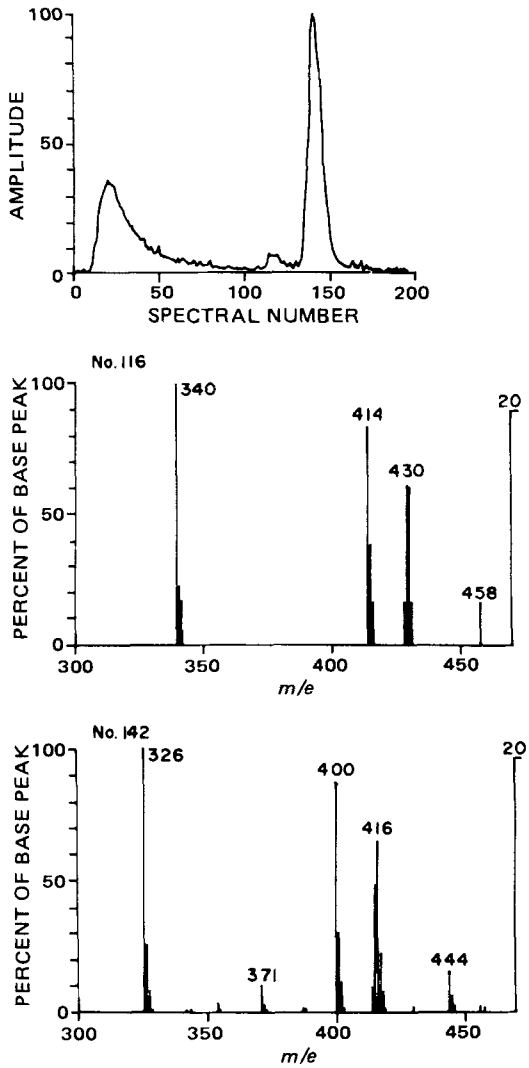

Figure 7—*Integrated total ion current chromatogram (top) of an extract of hydrolyzed Fraction IX as the trimethylsilyl derivative and mass spectra No. 116, identified as morphine, and No. 142, identified as normorphine.*

Normorphine 3-glucuronide was probably less soluble in methanol and crystallized together with morphine 3-glucuronide in aqueous methanol; normorphine 6-glucuronide, like morphine 6-glucuronide, was more soluble in methanol and was isolated from the methanol-soluble fraction. The present study was performed in morphine-dependent subjects. The extent of *N*-demethylation of morphine after acute administration in nondependent humans needs further study.

Although dihydromorphinone was detected in the urine of various animal species given morphine (18, 29), dihydromorphinone was not detected in the urine of morphine-dependent subjects in the present study.

The existence of morphine 2,3-quinone or 2-hydroxymorphine in the urine of humans is inconclusive. Samples were derivatized with 25% trimethylsilylimidazole in pyridine and scanned for morphine 2,3-quinone or 2-hydroxymorphine by GLC–mass spectrometry, and no evidence of their presence was found. In the organic phase, an iodoplatinate positive spot with R_f 0.1 was observed on instant TLC sheets impregnated with silica gel and developed with both Systems A and B. This spot was difficult to elute with methanol or water but could be eluted with 2.5% acetic acid in methanol. After derivatization with trifluoroacetic anhydride or 25% trimethylsilylimidazole in pyridine, it did not show any peak on GLC at a high column temperature (275° for 30 min). No peak was observed with the solid probe of the mass spectrometer at 300°. The chromatographic characteristics of this spot were similar to those of an authentic morphine 2,3-quinone sample[13] (19).

[13] Obtained from Dr. Misra, New York State Office of Drug Abuse Services Testing and Research Laboratory, Brooklyn, N.Y.

REFERENCES

(1) L. A. Woods, *J. Pharmacol. Exp. Ther.*, **112**, 158 (1954).
(2) J. M. Fujimoto and E. L. Way, *ibid.*, **121**, 340 (1957).
(3) S. Y. Yeh and L. A. Woods, *ibid.*, **175**, 69 (1970).
(4) A. L. Misra, S. Y. Yeh, and L. A. Woods, *Biochem. Pharmacol.*, **19**, 1536 (1970).
(5) K. Oguri, S. Ida, H. Yoshimura, and H. Tsukamoto, *Chem. Pharm. Bull.*, **18**, 2414 (1970).
(6) L. A. Woods and H. I. Chernov, *Pharmacologist*, **8**, 206 (1966).
(7) J. M. Fujimoto and V. B. Haarstad, *J. Pharmacol. Exp. Ther.*, **165**, 45 (1969).
(8) S. Y. Yeh, H. I. Chernov, and L. A. Woods, *J. Pharm. Sci.*, **60**, 469 (1971).
(9) H. W. Elliott, B. M. Tolbert, T. K. Adler, and H. H. Anderson, *Proc. Soc. Exp. Biol. Med.*, **85**, 77 (1954).
(10) J. Axelrod, *J. Pharmacol. Exp. Ther.*, **117**, 322 (1956).
(11) A. L. Misra, S. J. Mulé, and L. A. Woods, *ibid.*, **132**, 317 (1961).
(12) K. Milther, *Acta Pharmacol. Toxicol.*, **19**, 149 (1962).
(13) L. Tampier and A. Panna-Herreros, *Arch. Biol. Med. Exp.*, **3**, 146 (1966).
(14) S. Y. Yeh, *J. Pharmacol. Exp. Ther.*, **192**, 201 (1975).
(15) S. F. Frunk and M. Delle, *Clin. Pharmacol. Ther.*, **16**, 51 (1974).
(16) C. Ellison and H. W. Elliott, *J. Pharmacol. Exp. Ther.*, **144**, 265 (1964).
(17) U. Borner and S. Abbott, *Experientia*, **29**, 180 (1973).
(18) K. Klutch, *Drug Metab. Disp.*, **2**, 23 (1973).
(19) A. L. Misra, N. L. Vadlamani, R. B. Pontani, and S. J. Mulé, *Biochem. Pharmacol.*, **22**, 2129 (1973).
(20) S. Y. Yeh, *Experientia*, **30**, 265 (1974).
(21) C. C. Fulton, *Am. J. Pharm.*, **105**, 103 (1933).
(22) M. Freund and E. Speyer, *Ber.*, **48**, 499 (1915).
(23) S. Y. Yeh and L. A. Woods, *J. Pharmacol. Exp. Ther.*, **173**, 21 (1970).
(24) D. Dische, *J. Biol. Chem.*, **167**, 189 (1947).
(25) M. Volterra, *Am. J. Clin. Pathol.*, **12**, 525 (1942). P. B. Hawk, B. L. Oser, and W. H. Summerson, "Practical Physiological Chemistry," 13th ed., Blakiston, New York, N.Y., 1954, p. 939.
(26) S. Y. Yeh and L. A. Woods, *J. Pharm. Sci.*, **59**, 380 (1970).
(27) T. K. Adler, J. M. Fujimoto, E. L. Way, and E. M. Baker, *J. Pharmacol. Exp. Ther.*, **114**, 251 (1955).
(28) R. L. Bronaugh, S. E. Hattox, M. M. Hoehn, R. C. Murphy, and C. O. Rutledge, *ibid.*, **195**, 441 (1975).
(29) S. Y. Yeh, *Fed. Proc.*, **35**, 469 (1976).

ACKNOWLEDGMENTS AND ADDRESSES

Received October 12, 1976, from the *National Institute on Drug Abuse, Division of Research, Addiction Research Center, Lexington, KY 40511.*

Accepted for publication December 1, 1976.

Presented at the Federation of American Societies for Experimental Biology, Atlantic City meeting, April 1973.

The authors thank Dr. E. J. Cone for helping to obtain some of the mass spectra.

[x] To whom inquiries should be directed.

Polymer Sorption of Nitroglycerin and Stability of Molded Nitroglycerin Tablets in Unit-Dose Packaging

M. J. PIKAL [x], D. A. BIBLER, and B. RUTHERFORD

Abstract □ The sorption of nitroglycerin by thermoplastic polymers and the stability of molded nitroglycerin tablets in strip packaging were studied. The polymers investigated varied greatly in their affinity for nitroglycerin, the order of decreasing affinity being: vinyls ≫ low density polyethylene > ionomers > high density polyethylene. With the proper choice of packaging, molded nitroglycerin tablets stabilized with povidone maintained acceptable potency for up to 2 years at 26° when strip packaged in unit doses. Chemical decomposition (hydrolysis) of nitroglycerin also was investigated. Povidone accelerated the decomposition of nitroglycerin; at high temperature, decomposition was a significant factor in tablet stability for tablets containing povidone.

Keyphrases □ Nitroglycerin—sorption by thermoplastic polymers and stability of molded tablets in various strip packages, effect of povidone □ Sorption—nitroglycerin by thermoplastic polymers in various packaging materials □ Stability—molded nitroglycerin tablets in various strip packages, effect of povidone □ Packaging materials, various—sorption by thermoplastic polymers and stability of molded nitroglycerin tablets, effect of povidone □ Povidone—effect on stability of molded nitroglycerin tablets in various strip packages □ Tablets, molded—nitroglycerin, sorption by thermoplastic polymers and stability in various strip packages □ Dosage forms—molded nitroglycerin tablets, sorption by thermoplastic polymers and stability in various strip packages □ Vasodilators, coronary—nitroglycerin, sorption by thermoplastic polymers and stability of molded tablets in various strip packages, effect of povidone

Recently, the stability of nitroglycerin tablets has been studied extensively (1–4). Nitroglycerin tablets potentially can lose potency in four ways: chemical decomposition, loss to the atmosphere by vaporization, intertablet migration, and sorption by packaging materials. Nitroglycerin undergoes thermal decomposition at elevated temperature (5) and may undergo basic hydrolysis (6). However, nitroglycerin decomposition in tablets has not been demonstrated.

At 25°, the air space above nitroglycerin tablets contains 1–7 μg of nitroglycerin/liter (4), the exact figure depending on the formulation. Thus, when nitroglycerin tablets are exposed to adequate circulation of room air, measurable losses in potency occur within a few days *via* vaporization (1, 2). Intertablet migration of nitroglycerin, resulting in decreased content uniformity upon aging, is a serious problem with conventional molded tablets (1, 4). Because of the migration problem, stabilizing additives have been incorporated into tablets (1, 4). The stabilizing additive lowers the vapor pressure of nitroglycerin sufficiently to prevent most of the migration that would otherwise occur (4).

Sorption of nitroglycerin by packaging materials may also have serious consequences for tablet stability (2–5, 7, 8). Conventional tablets strip packaged in an aluminum foil–low density polyethylene laminate lost 90% of their nitroglycerin to the package (7). Sorption losses were less for stabilized tablets (2). However, none of the strip

REFERENCES

(1) L. A. Woods, *J. Pharmacol. Exp. Ther.*, **112**, 158 (1954).
(2) J. M. Fujimoto and E. L. Way, *ibid.*, **121**, 340 (1957).
(3) S. Y. Yeh and L. A. Woods, *ibid.*, **175**, 69 (1970).
(4) A. L. Misra, S. Y. Yeh, and L. A. Woods, *Biochem. Pharmacol.*, **19**, 1536 (1970).
(5) K. Oguri, S. Ida, H. Yoshimura, and H. Tsukamoto, *Chem. Pharm. Bull.*, **18**, 2414 (1970).
(6) L. A. Woods and H. I. Chernov, *Pharmacologist*, **8**, 206 (1966).
(7) J. M. Fujimoto and V. B. Haarstad, *J. Pharmacol. Exp. Ther.*, **165**, 45 (1969).
(8) S. Y. Yeh, H. I. Chernov, and L. A. Woods, *J. Pharm. Sci.*, **60**, 469 (1971).
(9) H. W. Elliott, B. M. Tolbert, T. K. Adler, and H. H. Anderson, *Proc. Soc. Exp. Biol. Med.*, **85**, 77 (1954).
(10) J. Axelrod, *J. Pharmacol. Exp. Ther.*, **117**, 322 (1956).
(11) A. L. Misra, S. J. Mulé, and L. A. Woods, *ibid.*, **132**, 317 (1961).
(12) K. Milther, *Acta Pharmacol. Toxicol.*, **19**, 149 (1962).
(13) L. Tampier and A. Panna-Herreros, *Arch. Biol. Med. Exp.*, **3**, 146 (1966).
(14) S. Y. Yeh, *J. Pharmacol. Exp. Ther.*, **192**, 201 (1975).
(15) S. F. Frunk and M. Delle, *Clin. Pharmacol. Ther.*, **16**, 51 (1974).
(16) C. Ellison and H. W. Elliott, *J. Pharmacol. Exp. Ther.*, **144**, 265 (1964).
(17) U. Borner and S. Abbott, *Experientia*, **29**, 180 (1973).
(18) K. Klutch, *Drug Metab. Disp.*, **2**, 23 (1973).
(19) A. L. Misra, N. L. Vadlamani, R. B. Pontani, and S. J. Mulé, *Biochem. Pharmacol.*, **22**, 2129 (1973).
(20) S. Y. Yeh, *Experientia*, **30**, 265 (1974).
(21) C. C. Fulton, *Am. J. Pharm.*, **105**, 103 (1933).
(22) M. Freund and E. Speyer, *Ber.*, **48**, 499 (1915).
(23) S. Y. Yeh and L. A. Woods, *J. Pharmacol. Exp. Ther.*, **173**, 21 (1970).
(24) D. Dische, *J. Biol. Chem.*, **167**, 189 (1947).
(25) M. Volterra, *Am. J. Clin. Pathol.*, **12**, 525 (1942). P. B. Hawk, B. L. Oser, and W. H. Summerson, "Practical Physiological Chemistry," 13th ed., Blakiston, New York, N.Y., 1954, p. 939.
(26) S. Y. Yeh and L. A. Woods, *J. Pharm. Sci.*, **59**, 380 (1970).
(27) T. K. Adler, J. M. Fujimoto, E. L. Way, and E. M. Baker, *J. Pharmacol. Exp. Ther.*, **114**, 251 (1955).
(28) R. L. Bronaugh, S. E. Hattox, M. M. Hoehn, R. C. Murphy, and C. O. Rutledge, *ibid.*, **195**, 441 (1975).
(29) S. Y. Yeh, *Fed. Proc.*, **35**, 469 (1976).

ACKNOWLEDGMENTS AND ADDRESSES

Received October 12, 1976, from the *National Institute on Drug Abuse, Division of Research, Addiction Research Center, Lexington, KY 40511.*

Accepted for publication December 1, 1976.

Presented at the Federation of American Societies for Experimental Biology, Atlantic City meeting, April 1973.

The authors thank Dr. E. J. Cone for helping to obtain some of the mass spectra.

[x] To whom inquiries should be directed.

Polymer Sorption of Nitroglycerin and Stability of Molded Nitroglycerin Tablets in Unit-Dose Packaging

M. J. PIKAL [x], D. A. BIBLER, and B. RUTHERFORD

Abstract □ The sorption of nitroglycerin by thermoplastic polymers and the stability of molded nitroglycerin tablets in strip packaging were studied. The polymers investigated varied greatly in their affinity for nitroglycerin, the order of decreasing affinity being: vinyls ≫ low density polyethylene > ionomers > high density polyethylene. With the proper choice of packaging, molded nitroglycerin tablets stabilized with povidone maintained acceptable potency for up to 2 years at 26° when strip packaged in unit doses. Chemical decomposition (hydrolysis) of nitroglycerin also was investigated. Povidone accelerated the decomposition of nitroglycerin; at high temperature, decomposition was a significant factor in tablet stability for tablets containing povidone.

Keyphrases □ Nitroglycerin—sorption by thermoplastic polymers and stability of molded tablets in various strip packages, effect of povidone □ Sorption—nitroglycerin by thermoplastic polymers in various packaging materials □ Stability—molded nitroglycerin tablets in various strip packages, effect of povidone □ Packaging materials, various—sorption by thermoplastic polymers and stability of molded nitroglycerin tablets, effect of povidone □ Povidone—effect on stability of molded nitroglycerin tablets in various strip packages □ Tablets, molded—nitroglycerin, sorption by thermoplastic polymers and stability in various strip packages □ Dosage forms—molded nitroglycerin tablets, sorption by thermoplastic polymers and stability in various strip packages □ Vasodilators, coronary—nitroglycerin, sorption by thermoplastic polymers and stability of molded tablets in various strip packages, effect of povidone

Recently, the stability of nitroglycerin tablets has been studied extensively (1–4). Nitroglycerin tablets potentially can lose potency in four ways: chemical decomposition, loss to the atmosphere by vaporization, intertablet migration, and sorption by packaging materials. Nitroglycerin undergoes thermal decomposition at elevated temperature (5) and may undergo basic hydrolysis (6). However, nitroglycerin decomposition in tablets has not been demonstrated.

At 25°, the air space above nitroglycerin tablets contains 1–7 μg of nitroglycerin/liter (4), the exact figure depending on the formulation. Thus, when nitroglycerin tablets are exposed to adequate circulation of room air, measurable losses in potency occur within a few days *via* vaporization (1, 2). Intertablet migration of nitroglycerin, resulting in decreased content uniformity upon aging, is a serious problem with conventional molded tablets (1, 4). Because of the migration problem, stabilizing additives have been incorporated into tablets (1, 4). The stabilizing additive lowers the vapor pressure of nitroglycerin sufficiently to prevent most of the migration that would otherwise occur (4).

Sorption of nitroglycerin by packaging materials may also have serious consequences for tablet stability (2–5, 7, 8). Conventional tablets strip packaged in an aluminum foil–low density polyethylene laminate lost 90% of their nitroglycerin to the package (7). Sorption losses were less for stabilized tablets (2). However, none of the strip

packaging studied maintained adequate tablet potency for the stabilized molded tablets (2).

This study concerned the sorption of nitroglycerin by packaging materials and the corresponding stability of nitroglycerin tablets in strip packaging. Previous studies considered only packaging with low density polyethylene as the thermoplastic component (*i.e.*, the thermoplastic material directly exposed to the tablet that is needed to seal the package). Vinyls, ionomers, and high density polyethylene may also be used as the thermoplastic component or heat-seal film. It will be demonstrated that with proper selection of packaging, stabilized molded nitroglycerin tablets maintain acceptable potency for up to 2 years at 26° when packaged in unit doses.

EXPERIMENTAL

Materials—The nontablet nitroglycerin samples were the same as previously described (4). Except when specifically noted otherwise, the tablets were commercial lots[1] stabilized with povidone, present as 1% of the total tablet weight. Packages I–IX were obtained commercially[2].

Procedures—*Assay Methods*—Tablets were assayed by one of two methods: Method A, an adaptation of Bell's method (9), which is essentially the same as that described by Fusari (3); and Method B, whereby nitroglycerin is extracted from an aqueous solution of the tablets into isooctane and then analyzed by the method of Wells *et al.* (10). Method B has been automated for unit-dose analysis of the tablets.

Nitroglycerin was extracted from the packaging by shaking the packaging with ethanol until the concentration of nitroglycerin in ethanol did not change (1–2 days). The nitroglycerin–ethanol solution was assayed according to Method B, omitting the isooctane extraction step. In several cases, a second extraction of the packaging was made to verify that no nitroglycerin remained. Except for Package IX, blank experiments with packaging devoid of nitroglycerin demonstrated that assay interference from the package was negligible. A large blank was obtained with Package IX. When extracted with isooctane instead of ethanol, this problem was eliminated. Therefore, package assays on Package IX were performed by extraction with isooctane.

Dinitroglycerin was determined by semiquantitative TLC following the procedure of Page *et al.* (11).

Packaging Procedures—Tablets packaged in strip packaging, 30 tablets/pouch, were heat sealed using a laboratory packaging apparatus[3]. Tablets strip packaged in unit dose, one tablet/pouch, were packaged using production machinery[4].

Film Thickness Measurement—The thickness of a heat-seal polymer was determined by weighing a known area of polymer film of known density (12). The heat seal was separated from the packaging either by soaking in aqueous hydrochloric acid (foil-containing packages) or by soaking in butyl acetate (Packages VI and VIII).

X-Ray Scattering Measurements—X-ray scattering data were obtained using an X-ray diffractometer[5] with copper radiation and a nickel filter.

Solubility Measurements—Saturation concentrations of nitroglycerin in the heat-seal polymer for a given package were determined by exposing only the heat-seal film to nitroglycerin vapor from 10% nitroglycerin on lactose. Sample holders were constructed from the cutoff top of a high density polyethylene bottle and the corresponding screw cap. A disk of packaging was placed in the cap with the heat-seal film exposed, and the bottle top was screwed down tightly. This procedure effectively eliminated vapor phase contact between nitroglycerin and the side of packaging not covered with the heat-seal film under investigation. Thus, the nitroglycerin sorbed by the packaging was sorbed only by the heat-seal film, assuming that permeation of the aluminum foil was negligible.

The samples (in the holders) were then placed in a glass desiccator containing a large excess of nitroglycerin, a moderate vacuum was applied (~10 Torr), and the desiccator was sealed. The nitroglycerin content of the packaging was assayed after several equilibration times, and the saturation value was taken as the nitroglycerin content after equilibrium was achieved (1–2 months).

[1] Eli Lilly and Co., Indianapolis, Ind.

[2] Package I: aluminum foil–vinyl; Anaconda Aluminum Co., Louisville, KY 40203. Package II: paper, polyethylene, aluminum foil–vinyl; Aluminum Co. of America, Pittsburgh, PA 15219. Package III: aluminum foil–vinyl; F-200, Aluminum Co. of America, Pittsburgh, PA 15219. Package IV: high density polyethylene film; B-74, American Can Co., Greenwich, CT 06830. Package V: cellophane, polyethylene, aluminum foil–low density polyethylene; Ivers Lee, Division of Becton-Dickinson, West Caldwell, NJ 07006. Package VI: nylon, Saran–low density polyethylene. Package VII: Surlyn 1707 film; du Pont, Wilmington, Del. Package VIII: nylon, Saran–Surlyn 1601, du Pont, Wilmington, Del. Package IX: paper, polyethylene, aluminum foil–Surlyn 1604; FL 1674, Rexham Corp., Hemington, NJ 08822. The foil had been treated with an adhesion promotor identified as Rexham REP01.

[3] Sentinel impulse heat sealer, model 125C, Packaging Industries, Hyannis, Mass.

[4] Model VPH4, Wrap-Ade, Clifton, N.J.

[5] Norelco, Mt. Vernon, N.Y.

Table I—Hydrolysis of Nitroglycerin in Nitroglycerin–Povidone Systems [a]

Weight Ratio, Povidone to Nitroglycerin	Nitroglycerin Loss, %[b]		Dinitroglycerin Content, %[c]	
	1.5 years, 25°	1.5 years, 25° plus 1 month, 50°	1.5 years, 25°	1.5 years, 25° plus 1 month, 50°
0.22	2	11	1	2
0.65	7	22	4	7
1.04	12	22	3	9
1.56	—	—	4	8
2.13	—	—	5	8

[a] Samples were prepared by dry blending povidone and 10% nitroglycerin trituration on β-lactose. [b] Determined from nitroglycerin assay on initial and aged samples. [c] Expressed as weight percent of total nitroglycerin compounds (*i.e.*, dinitroglycerin and trinitroglycerin); determined by semiquantitative TLC procedure.

RESULTS

The chemical decomposition of nitroglycerin *via* hydrolysis was studied for nitroglycerin–povidone–lactose systems (Table I). Both 1,2-dinitroglycerin and 1,3-dinitroglycerin were present in the aged samples in roughly equal amounts. Dinitroglycerin content is expressed as weight percent of the total nitroglycerin compounds. Within the uncertainty of the data, both the nitroglycerin loss and dinitroglycerin content were independent of the povidone concentration above a weight ratio of 0.6. Although the TLC assay is only semiquantitative, the data demonstrate that a significant fraction of the nitroglycerin loss was due to hydrolysis of the trinitro ester to dinitroglycerin species.

High temperature stability of tablets containing povidone are compared with other formulations in Table II. Potency loss at high temperature was significantly greater with the povidone-containing formulation. TLC analysis showed significant amounts of the 1,2- and 1,3-dinitroglycerin moieties in the aged povidone formulation but only trace amounts in other formulations.

X-ray diffraction patterns were obtained from the heat-seal films investigated (Fig. 1). Diffraction patterns from the ionomers of Packages VII and VIII were similar to the one shown in Fig. 1 for the ionomer of Package IX. The vinyls were completely amorphous and gave no peaks in the diffraction pattern. The peaks at $2\theta = 21°$ and $2\theta = 24°$ are characteristic of polyethylene crystallinity. The peak at $2\theta = 4°$ from the ionomer is characteristic of ionomers and may be caused by clustering of cations (13). Taking the intensity and sharpness of the diffraction peaks as an index of crystallinity, the crystallinity of the heat-seal films decreased in the order: high density polyethylene ≫ low density polyethylene (VI) > low density polyethylene (V) > ionomers > vinyls.

Saturation levels of nitroglycerin in the heat-seal films of various packages are summarized in Table III.

Potency losses of 0.4-mg stabilized tablets stored in various pouch-type packages are summarized in Table IV. The corresponding package assays are also listed. If it is assumed that chemical decomposition in the pouch package is identical to that in the control package (~300 tablets in glass with tin-lined screw cap), the package assay, in micrograms per square

Table II—Potency Loss of 0.3-mg Tablets at High Temperature: Comparison of Formulations [a]

Formulation	Potency Loss, %	
	6 months, 37°	6 months, 45°
Conventional tablet, no stabilizer	9	7
Stabilized tablet, 1% povidone	17	36
Stabilized tablet[b], polyethylene glycol	—	8

[a] Tablets were stored in screw-capped glass bottles with rayon stuffing, 100 tablets/bottle. [b] Nitrostat, Parke-Davis and Co.

Table III—Heat-Seal Film Sorption of Nitroglycerin at Saturation (Nitroglycerin Source Was 10% Nitroglycerin on Lactose) [a]

Package[b] (Heat-Seal Thickness)	Sorption of Nitroglycerin 25°, μg/cm²	37° μg/cm²	37° wt. %
I (4.2 μm)	210	180	24.8
II (3.8 μm)	160	130	20.8
III (3.2 μm)	160	130	24.0
IV (53 μm)	1.5	1.4	0.028
V (19 μm)	52	40	2.3
VII (69 μm)	20	25	0.39
IX (26 μm)	20	22	0.89

[a] Nitroglycerin vapor pressure, in Torr, is (4) 5.5×10^{-4} at 25° and 22×10^{-4} at 37°. [b] See Footnote 2 in the text.

centimeter, will be identical (within experimental error) to the corresponding potency loss when no nitroglycerin leaves the package through diffusion. With Packages VII and IV, and perhaps with Package II, the potency loss was significantly greater than the package sorption, suggesting diffusion of nitroglycerin through the package.

Data regarding the rate of nitroglycerin removal from the heat-seal films of packages are summarized in Table V. The experimental data are compared with values calculated from the appropriate solution of Fick's law (14):

$$F(t) = 1 - \sum_{n=0}^{\infty} \frac{8}{(2n+1)^2\pi^2} \exp\left[-\frac{D(n+\frac{1}{2})^2\pi^2 t}{l^2}\right] \quad \text{(Eq. 1)}$$

where $F(t)$ is the fractional attainment of equilibrium, *i.e.*, $F(t) = 1$ at infinite time when all nitroglycerin is removed from the packaging; D is the diffusion coefficient of nitroglycerin in the film; l is the thickness of the film for Package V and is one-half the film thickness for Package VII (*i.e.*, diffusion occurs from both sides of the film); and t is time.

The assumption in Eq. 1 is that the distribution of nitroglycerin in the heat-seal film is initially homogeneous. The values of D were chosen to give the best fit of Eq. 1 to the data. With Package VII, agreement between diffusion theory and experimental data was excellent. For Package V, agreement was good only at times greater than about 10 hr. At small times, nitroglycerin release by the package was slower than predicted by *simple* diffusion theory (Eq. 1).

Table VI and Fig. 2 compare the stability of nitroglycerin tablets in unit-dose strip packages of Package IX with the stability in both conventional packaging and the control package (~300 tablets in glass with tin-lined screw cap). In Table VI, the third and fourth columns give the parameters evaluated by a least-squares fit of the data to the equation:

$$\ln N = \ln N_0 - k_1 t \qquad t \geq 1 \text{ month} \qquad \text{(Eq. 2)}$$

where k_1 is the first-order rate constant reflecting chemical decomposition of nitroglycerin, N is the tablet potency at time t, and N_0 is the tablet potency extrapolated to zero time. The difference between the N_0 values for the control package and the unit-dose package represents the quantity of nitroglycerin absorbed by the heat-seal film of the unit-dose package. The uncertainty given for k_1 is the standard deviation of this parameter. The last column of Table VI summarizes the mean content uniformities for a number of package–tablet–temperature combinations. The measure of content uniformity used here is the relative standard deviation for the assay of 30 tablets when the assay results are expressed in weight of nitroglycerin per unit tablet weight.

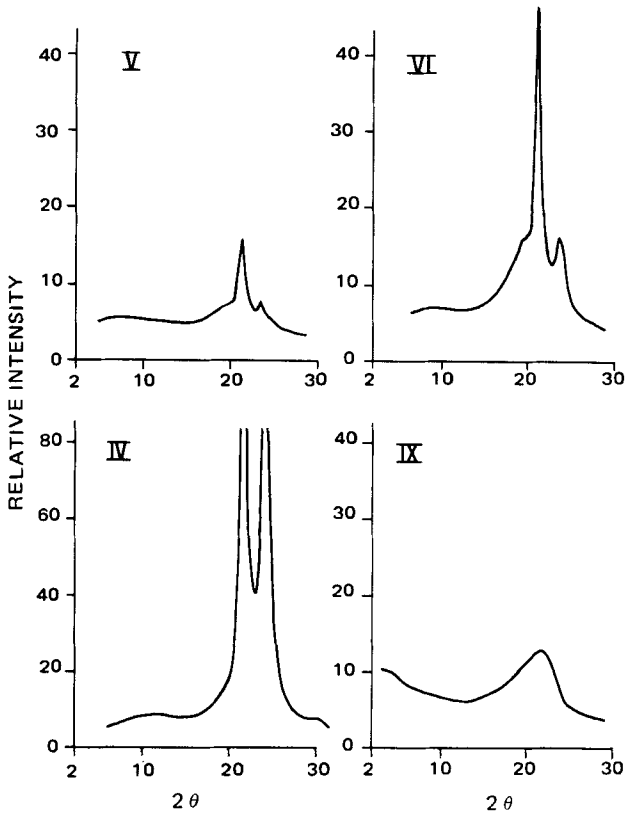

Figure 1—*X-ray diffraction patterns from the heat-seal polymers of packaging materials. Key: V, low density polyethylene; VI, low density polyethylene; IV, high density polyethylene; and IX, ionomer.*

DISCUSSION

Decomposition—In previous studies (1–4, 7–9), it was assumed that chemical decomposition does not contribute significantly to the potency loss of nitroglycerin tablets. The present data demonstrate that potency loss through decomposition may be significant, at least when povidone is present. Povidone apparently functions as a catalyst for nitroglycerin hydrolysis. Although the decomposition rate (Table VI) was slow at 26°, ~0.4%/month, the decomposition rate increased sharply with increasing temperature. Clearly, one may not assume that the addition of a nominally inert additive, such as povidone, has no effect on the chemical stability of nitroglycerin.

Package Sorption of Nitroglycerin—It is not immediately obvious whether nitroglycerin is adsorbed on the heat-seal film's surface or whether nitroglycerin is dissolved in the polymer. The slow rate of nitroglycerin removal from the packaging (Table V) suggests that most nitroglycerin is dissolved in the polymer. The data for Package VII are completely consistent with the diffusion theory based on assumption of a homogeneous solution of nitroglycerin in the polymer.

The diffusion theory is less satisfactory for Package V. However, the experimental rate is slower than the rate calculated from diffusion theory at small times. Thus, the data are not consistent with a surface adsorption model but rather suggest a diffusion model where, in Package V, the

Table IV—Potency Loss of Tablets and Package Sorption of Nitroglycerin at 37° [a]

Package[b] (Heat-Seal Thickness)	Package Assay[c] 1 month, μg/cm²	2 months μg/cm²	2 months wt. %	Potency Loss[d] 1 month, μg/cm²	Potency Loss[d] 2 months, μg/cm²
II (3.8 μm)	13	14	2.8	19	25
III (3.2 μm)	14	19	4.6	14	21
V (19 μm)	16	16	0.92	11	14
VI (76 μm)	16	16	0.23	22	22
VII (69 μm)	3.0	3.2	0.049	16	29
VIII	17	18	—	17	19
IX (26 μm)	3.8	4.3	0.17	7	7
IV (53 μm) 26°		(4 months) 0.3	0.005		(4 months) 5

[a] Thirty tablets were sealed in a package with 141 cm² package area exposed to the tablets (4.7 cm²/tablet). All tablets were 0.4 mg initial potency and contained 0.36 mg of povidone as a stabilizer. Initial vapor pressure of nitroglycerin (37°) was 12.3×10^{-4} Torr (4). [b] See Footnote 2 in the text. [c] Estimated uncertainty, ±10% relative error in micrograms per square centimeter data. [d] Estimated uncertainty, ±2 μg/cm². Calculated from the difference between tablet assays on strip-packaged tablets and on tablets in the control package (~300 tablets in glass with tin-lined screw cap).

Table V—Rate of Nitroglycerin Removal from Packaging in a Well-Stirred Infinite Water Medium at 25°

Hours	Nitroglycerin Content of Package, % of Initial: Experimental	Diffusion Theory, Eq. 1
	Package VII, $D = 2.02 \times 10^{-10}$ cm²/sec	
0.50	78.7	80.2
1.66	64.9	63.7
3.67	51.4	46.0
5.75	31.8	34.0
21.7	3.2	3.0
	Package V, $D = 2.54 \times 10^{-11}$ cm²/sec	
3.64	81.4	65.1
5.05	77.4	58.5
7.30	66.3	50.0
22.5	19.4	18.6
27.0	12.5	13.8
31.4	9.6	10.4
46.7	3.9	3.8
55.2	2.8	2.2

diffusion constant of nitroglycerin increases with time at small times due to water absorption by the polymer. Presumably, equilibration with water is so rapid with the more hydrophilic ionomer (Package VII) that the polymer is water saturated throughout the period of nitroglycerin diffusion.

With the assumption that nitroglycerin is dissolved in the polymer, nitroglycerin sorption by various films is best compared in terms of weight percent nitroglycerin in the film. The data in Tables III and IV demonstrate that the heat-seal films studied varied greatly in their affinity for nitroglycerin. The sorption of nitroglycerin was less when the nitroglycerin source was a stabilized tablet (Table IV) than when pure nitroglycerin was exposed to the polymer (Table III). This observation is consistent with the significantly lower vapor pressure of nitroglycerin in the stabilized tablets (4). However, even for stabilized tablets, loss of nitroglycerin to the packaging was excessively high for some types of packaging.

The order of decreasing affinity for nitroglycerin was: vinyls ≫ low density polyethylene > ionomers > high density polyethylene. The low solubility of nitroglycerin in high density polyethylene is undoubtedly due to the high crystallinity of this polymer film (Fig. 1). The solubilities of nitroglycerin in Packages V and VI, both low density polyethylene, were not identical. The lower solubility in Package VI may have resulted from the higher degree of crystallinity of the polyethylene in this package (Fig. 1).

Crystallinity is not the only important factor affecting the sorption of nitroglycerin by a polymer film. Chemical structure of the polymer is also important. For example, the ionomers have very low crystallinities, but nitroglycerin solubility in these films is low. The chemical structure of an ionomer differs from polyethylene in that the ionomer contains

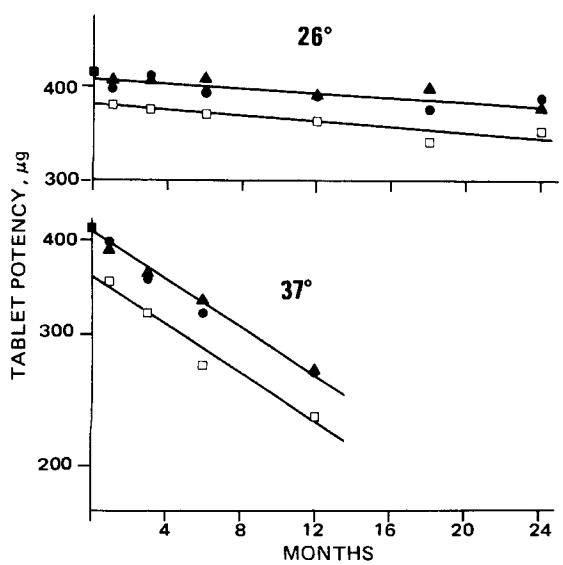

Figure 2—*Stability of nitroglycerin tablets in various packages. Key:* ■, *initial assay;* ▲, *control package;* ●, *conventional package; and* □, *unit-dose package, foil–ionomer (IX).*

Table VI—Stability of Nitroglycerin Tablets in Unit-Dose Packages: Comparison of Unit-Dose Package IX with Conventional Packaging[a]

Nominal Tablet Potency, µg/Storage Temperature	Package	N_0[b], µg/35.6 mg Tablet	k_1 ($\pm\sigma$)[b], month^{-1}	Mean Content Uniformity, σ, mg/mg
300/26°	Control	323	0.004 ± 0.002	—
	Conventional	318	0.005 ± 0.002	5.3
	IX	297	0.005 ± 0.002	3.3
400/26°	Control	411	0.003 ± 0.001	—
	Conventional	402	0.002 ± 0.001	6.3
	IX	376	0.004 ± 0.002	4.2
600/26°	Control	610	0.004 ± 0.002	—
	Conventional	590	0.001 ± 0.001	6.8
	IX	554	0.003 ± 0.002	4.0
300/37°	Control	324	0.030 ± 0.002	—
	Conventional	313	0.041 ± 0.013	7.7
	IX	284	0.040 ± 0.008	5.2
400/37°	Control	408	0.036 ± 0.002	—
	Conventional	407	0.037 ± 0.003	5.9
	IX	356	0.037 ± 0.005	5.0
600/37°	Control	617	0.020 ± 0.003	—
	Conventional	616	0.039 ± 0.005	8.2
	IX	511	0.022 ± 0.007	5.3

[a] 4.7 cm² of the unit-dose package was exposed to each tablet. The conventional package was 100 tablets in a glass bottle with rayon stuffing and a low density polyethylene-lined screw top closure. The control package was ~300 tablets in a glass bottle without stuffing and a tin foil-lined screw top closure. [b] The parameters N_0 and k_1 are defined by $\ln N = \ln N_0 - k_1 t$, where N is the mean tablet potency at time t, $t \geq 1$ month.

structurally bound anions and their corresponding counterions. Perhaps the electrostatic field of the ions is sufficient to salt out nitroglycerin in much the same way that electrolytes decrease the aqueous solubility of many nonpolar solutes.

Package Permeability—Diffusion of nitroglycerin through the package is not a source of potency loss whenever the barrier component of the package is essentially impermeable to nitroglycerin. For packages containing aluminum foil, one would not expect significant permeability to nitroglycerin. Thus, the potency loss should not exceed the nitroglycerin content of the package. With the possible exception of Package II, the data in Table IV support this conclusion. Even for films where the nitroglycerin solubility is very low, permeation of the film apparently can be significant. Permeability was quite high for ionomer (VII) film, while high density polyethylene film exhibited small, but probably significant, permeability to nitroglycerin even at 26°.

Unit-Dose Nitroglycerin—To achieve stability in a unit-dose package comparable to the stability in conventional packaging, the heat-seal film employed must have a low affinity for nitroglycerin and the barrier should be impermeable to nitroglycerin. The data in Tables III and IV indicate that, of the packaging studied, Package IX would be the best choice for unit-dose nitroglycerin. Although having a low affinity for nitroglycerin, Package IV (high density polyethylene) would probably not be suitable for a shelflife of several years. Permeability of the magnitude suggested by the data would lead to a potency loss of ~30% over 2 years at 26°.

Figure 2 and Table V summarize the results of a 2-year stability study with unit-dose nitroglycerin in Package IX. The control package was ~300 tablets (full bottle) in a glass bottle closed with a tin-lined screw cap. Because of the large number of tablets, the impermeability of the container, and the lack of package material that could absorb nitroglycerin, tablets in the control package could lose potency only through chemical decomposition. Potency losses in the unit-dose or conventional

packages in excess of that for the control package would indicate sorption by the packaging and/or permeation of the package by nitroglycerin.

The potency–time curves for the control package and the conventional package are not significantly different. Except for a drop in potency shortly after packaging due to absorption (8% at 26°), the potency–time curves for the unit-dose package are indistinguishable from those for the control package. Therefore, permeation of the package by nitroglycerin is not significant.

The mean content uniformity (Table VI) appears to be slightly better for the unit-dose package than for the conventional package. Although the tablets studied were stabilized, a small amount of intertablet migration (~2% increase in standard deviation) apparently occurred as the tablets were aged in conventional containers. Since intertablet migration was prevented in the unit-dose package, the content uniformity remained essentially unchanged upon aging.

In summary, acceptable stability for up to 2 years[6] at 26° was demonstrated for unit-dose nitroglycerin in Package IX. The tablets employed in this research were stabilized tablets; conventional tablets would probably lose excessive nitroglycerin through absorption.

REFERENCES

(1) S. A. Fusari, *J. Pharm. Sci.*, **62**, 2012 (1973).

(2) B. Dorsch and R. Shangraw, *Am. J. Hosp. Pharm.*, **32**, 795 (1975).

(3) S. A. Fusari, *J. Pharm. Sci.*, **62**, 122 (1973).

(4) M. J. Pikal, A. L. Lukes, and L. F. Ellis, *ibid.*, **65**, 1278 (1976).

(5) J. B. Segur, in "Glycerol," C. S. Miner and N. N. Dalton, Eds., American Chemical Society Monograph Series, Reinhold Publishing Corp., New York, N.Y., 1953.

(6) R. T. M. Fraser, *Chem. Ind. (London)*, **1968**, 1117.

(7) D. Banes, *J. Pharm. Sci.*, **57**, 893 (1968).

(8) B. Edelman, A. M. Contractor, and R. Shangraw, *J. Am. Pharm. Assoc.*, **NS11**, 30 (1971).

(9) F. K. Bell, *J. Pharm. Sci.*, **53**, 752 (1964).

(10) C. E. Wells, H. M. Miller, and Y. H. Pfabe, *J. Assoc. Offic. Anal. Chem.*, **53**, 579 (1970).

(11) D. P. Page, N. A. Carson, C. A. Buhr, P. E. Flinn, C. E. Wells, and M. T. Randall, *J. Pharm. Sci.*, **64**, 140 (1975).

(12) *Mod. Packag. Encycl.*, **44**, 144 (1971).

(13) J. Kao, R. S. Stein, W. J. MacKnight, W. P. Taggart, and G. S. Cargill, III, *Macromolecules*, **7**, 95 (1974).

(14) J. Crank, "The Mathematics of Diffusion," Oxford University Press, London, England, 1956.

ACKNOWLEDGMENTS AND ADDRESSES

Received September 8, 1976, from the *Lilly Research Laboratories, Eli Lilly and Co., Indianapolis, IN 46206.*

Accepted for publication November 11, 1976.

The authors thank Mr. Herbert W. Smith and Mr. Dale A. Spurgeon for performing the X-ray diffractometer measurements.

[x] To whom inquiries should be directed.

[6] Since the potency does decrease slightly with time due to decomposition, the exact time period during which the tablets will meet USP standards will depend upon the tablet potency before packaging. The excess over label claim was generally small for the tablets studied. More recent lots of Lilly nitroglycerin tablets are formulated to provide a larger excess over label claim at the time of manufacture.

Disposition of Sulfonamides in Food-Producing Animals V: Disposition of Sulfathiazole in Tissue, Urine, and Plasma of Sheep following Intravenous Administration

RICHARD F. BEVILL *x, GARY D. KORITZ *, LEWIS W. DITTERT ‡, and DAVID W. A. BOURNE ‡

Abstract □ The plasma, urine, and tissue sulfathiazole concentrations were determined at various times following intravenous administration to 12 sheep. The plasma and urine data were consistent with a one-compartment pharmacokinetic model, with an elimination half-life of 1.1 hr and a volume of distribution of 0.39 liter/kg. Sulfathiazole was eliminated by excretion of unchanged drug in urine (67%) and by formation of two metabolites. The data obtained from eight tissue sites were consistent with the one-compartment pharmacokinetic model presented and confirmed that tissue residues of sulfathiazole can be calculated from serum and urine drug concentrations.

Keyphrases □ Sulfonamides—disposition of sulfathiazole in tissue, urine, and plasma of sheep following intravenous administration □ Sulfathiazole—disposition in tissue, urine, and plasma of sheep following intravenous administration, pharmacokinetic model □ Pharmacokinetics—sulfathiazole in sheep following intravenous administration□ Disposition, biological—sulfathiazole in tissue, urine, and plasma of sheep following intravenous administration, pharmacokinetic model □ Antibacterials—sulfathiazole, disposition in tissue, urine, and plasma of sheep following intravenous administration, pharmacokinetic model

When food-producing animals are treated with antibacterial drugs, significant drug concentrations may remain for some time in food tissues. Human consumption of meat containing drug residues may subsequently cause the development of hypersensitivity to drugs used therapeutically or the preferential selection of bacterial strains resistant to those drugs (1).

BACKGROUND

Normally, drug residues in the food tissues of animals are controlled by cessation of treatment at some minimum specified time, *i.e.*, the withdrawal time, before slaughter, allowing the drug to "washout" from the food tissues. However, field surveys reporting the number of carcasses with illegal concentrations of antibacterial drugs suggest that a sufficient withdrawal time often is not allowed (2).

The current method for controlling the appearance of drug-contaminated meat on the market consists of randomly checking carcasses at the slaughterhouse. This method is inefficient because drug assays of tissue are generally expensive and time consuming and the detection of contaminated carcasses may cause the condemnation of complete carcass lots. If a method could be developed to detect animals whose meat contained more than the tolerance limit of a drug before slaughter, it would be possible to delay slaughtering until the drug is below tolerated levels, thereby saving the carcass from needless destruction. Furthermore, if the detection method analyzed blood or urine instead of tissue specimens, it should be possible to reduce the cost and time involved in assay and thereby increase the efficiency of surveillance.

packages in excess of that for the control package would indicate sorption by the packaging and/or permeation of the package by nitroglycerin.

The potency–time curves for the control package and the conventional package are not significantly different. Except for a drop in potency shortly after packaging due to absorption (8% at 26°), the potency–time curves for the unit-dose package are indistinguishable from those for the control package. Therefore, permeation of the package by nitroglycerin is not significant.

The mean content uniformity (Table VI) appears to be slightly better for the unit-dose package than for the conventional package. Although the tablets studied were stabilized, a small amount of intertablet migration (~2% increase in standard deviation) apparently occurred as the tablets were aged in conventional containers. Since intertablet migration was prevented in the unit-dose package, the content uniformity remained essentially unchanged upon aging.

In summary, acceptable stability for up to 2 years[6] at 26° was demonstrated for unit-dose nitroglycerin in Package IX. The tablets employed in this research were stabilized tablets; conventional tablets would probably lose excessive nitroglycerin through absorption.

REFERENCES

(1) S. A. Fusari, *J. Pharm. Sci.*, **62**, 2012 (1973).

(2) B. Dorsch and R. Shangraw, *Am. J. Hosp. Pharm.*, **32**, 795 (1975).

(3) S. A. Fusari, *J. Pharm. Sci.*, **62**, 122 (1973).

(4) M. J. Pikal, A. L. Lukes, and L. F. Ellis, *ibid.*, **65**, 1278 (1976).

(5) J. B. Segur, in "Glycerol," C. S. Miner and N. N. Dalton, Eds., American Chemical Society Monograph Series, Reinhold Publishing Corp., New York, N.Y., 1953.

(6) R. T. M. Fraser, *Chem. Ind. (London)*, **1968**, 1117.

(7) D. Banes, *J. Pharm. Sci.*, **57**, 893 (1968).

(8) B. Edelman, A. M. Contractor, and R. Shangraw, *J. Am. Pharm. Assoc.*, **NS11**, 30 (1971).

(9) F. K. Bell, *J. Pharm. Sci.*, **53**, 752 (1964).

(10) C. E. Wells, H. M. Miller, and Y. H. Pfabe, *J. Assoc. Offic. Anal. Chem.*, **53**, 579 (1970).

(11) D. P. Page, N. A. Carson, C. A. Buhr, P. E. Flinn, C. E. Wells, and M. T. Randall, *J. Pharm. Sci.*, **64**, 140 (1975).

(12) *Mod. Packag. Encycl.*, **44**, 144 (1971).

(13) J. Kao, R. S. Stein, W. J. MacKnight, W. P. Taggart, and G. S. Cargill, III, *Macromolecules*, **7**, 95 (1974).

(14) J. Crank, "The Mathematics of Diffusion," Oxford University Press, London, England, 1956.

ACKNOWLEDGMENTS AND ADDRESSES

Received September 8, 1976, from the *Lilly Research Laboratories, Eli Lilly and Co., Indianapolis, IN 46206.*

Accepted for publication November 11, 1976.

The authors thank Mr. Herbert W. Smith and Mr. Dale A. Spurgeon for performing the X-ray diffractometer measurements.

[x] To whom inquiries should be directed.

[6] Since the potency does decrease slightly with time due to decomposition, the exact time period during which the tablets will meet USP standards will depend upon the tablet potency before packaging. The excess over label claim was generally small for the tablets studied. More recent lots of Lilly nitroglycerin tablets are formulated to provide a larger excess over label claim at the time of manufacture.

Disposition of Sulfonamides in Food-Producing Animals V: Disposition of Sulfathiazole in Tissue, Urine, and Plasma of Sheep following Intravenous Administration

RICHARD F. BEVILL *x, GARY D. KORITZ *, LEWIS W. DITTERT ‡, and DAVID W. A. BOURNE ‡

Abstract □ The plasma, urine, and tissue sulfathiazole concentrations were determined at various times following intravenous administration to 12 sheep. The plasma and urine data were consistent with a one-compartment pharmacokinetic model, with an elimination half-life of 1.1 hr and a volume of distribution of 0.39 liter/kg. Sulfathiazole was eliminated by excretion of unchanged drug in urine (67%) and by formation of two metabolites. The data obtained from eight tissue sites were consistent with the one-compartment pharmacokinetic model presented and confirmed that tissue residues of sulfathiazole can be calculated from serum and urine drug concentrations.

Keyphrases □ Sulfonamides—disposition of sulfathiazole in tissue, urine, and plasma of sheep following intravenous administration □ Sulfathiazole—disposition in tissue, urine, and plasma of sheep following intravenous administration, pharmacokinetic model □ Pharmacokinetics—sulfathiazole in sheep following intravenous administration□ Disposition, biological—sulfathiazole in tissue, urine, and plasma of sheep following intravenous administration, pharmacokinetic model □ Antibacterials—sulfathiazole, disposition in tissue, urine, and plasma of sheep following intravenous administration, pharmacokinetic model

When food-producing animals are treated with antibacterial drugs, significant drug concentrations may remain for some time in food tissues. Human consumption of meat containing drug residues may subsequently cause the development of hypersensitivity to drugs used therapeutically or the preferential selection of bacterial strains resistant to those drugs (1).

BACKGROUND

Normally, drug residues in the food tissues of animals are controlled by cessation of treatment at some minimum specified time, *i.e.*, the withdrawal time, before slaughter, allowing the drug to "washout" from the food tissues. However, field surveys reporting the number of carcasses with illegal concentrations of antibacterial drugs suggest that a sufficient withdrawal time often is not allowed (2).

The current method for controlling the appearance of drug-contaminated meat on the market consists of randomly checking carcasses at the slaughterhouse. This method is inefficient because drug assays of tissue are generally expensive and time consuming and the detection of contaminated carcasses may cause the condemnation of complete carcass lots. If a method could be developed to detect animals whose meat contained more than the tolerance limit of a drug before slaughter, it would be possible to delay slaughtering until the drug is below tolerated levels, thereby saving the carcass from needless destruction. Furthermore, if the detection method analyzed blood or urine instead of tissue specimens, it should be possible to reduce the cost and time involved in assay and thereby increase the efficiency of surveillance.

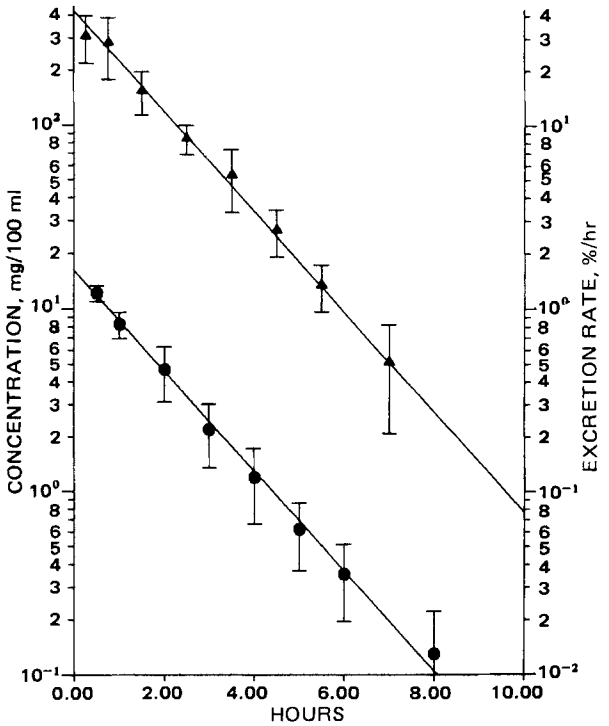

Figure 1—*Semilogarithmic plot of average plasma sulfathiazole concentration (●) and average rate of urinary excretion of unchanged sulfathiazole (▲) versus time following intravenous administration to sheep. The points were experimentally determined (±1 SD), and the lines were calculated using the pharmacokinetic model (Scheme II) and the values of the parameters presented in Table II.*

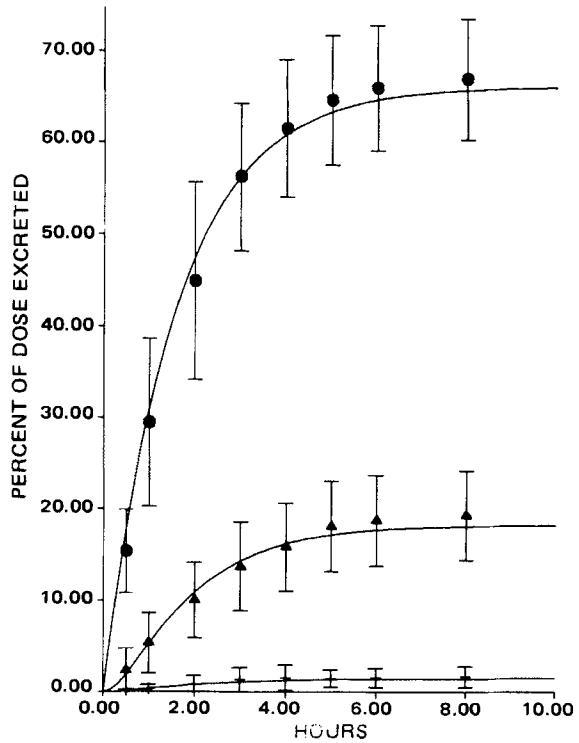

Figure 2—*Plot of cumulative amount of sulfathiazole (●), acetyl metabolite (▲), and polar metabolite (+) excreted in urine versus time following intravenous administration to sheep. The points were experimentally determined (±1 SD), and the lines were calculated using the pharmacokinetic model (Scheme II) and the values of the parameters presented in Table II.*

If a relationship could be established between tissue concentrations and plasma and/or urine concentrations of the drug and if the pharmacokinetics of the drug were known, it would be possible to predict when the tissue concentrations in an animal reach the tolerance limits. Also, by judicious use of pharmacokinetic relationships, the effects of changes in drug products, route of administration, or dosing regimens on withdrawal times could be investigated without the need for expensive slaughter studies.

The preliminary pharmacokinetics of sulfathiazole in sheep following intravenous and oral administrations were presented previously (3). Sulfathiazole disposition was described in terms of a one-compartment pharmacokinetic model (3). In this study, the pharmacokinetic model previously developed was confirmed, and correlations between the drug concentration in various tissues and drug concentrations in plasma and urine following intravenous administration were investigated.

EXPERIMENTAL

Animals—Fifteen mixed-breed female lambs[1] were randomly assigned to groups of three and placed in individual metabolism cages 72 hr prior to drug administration. Twenty-four hours prior to dosing, each animal was weighed and fitted with a Foley retention catheter[2], and the area over each jugular vein was clipped. Hay and water were provided *ad libitum*, but grain was limit fed throughout the acclimation and treatment periods.

Drug Administration and Specimen Collection—A 12.5% solution of sulfathiazole sodium[3] (72 mg/kg) was injected rapidly into the right jugular vein of each animal. Plasma specimens were collected *via* the left jugular vein at 0, 0.5, 1, 2, 3, 4, 5, 6, 8, 12, 16, and 24 hr after administration. The total voided urine volume was measured, and urine specimens were collected at 0, 0.5, 1, 2, 3, 4, 5, 6, 8, 12, 16, and 24 hr following administration.

Groups of three animals were sacrificed at 2, 4, 8, 16, and 24 hr after drug administration. Three untreated control animals[1] were slaughtered after the other treatments were completed. Portions of liver, heart, kidney, shoulder muscle, loin muscle, hindlimb muscle, body fat, and omental fat tissues were obtained from each slaughtered animal.

Plasma and urine specimens were stored at −5° until assayed. Tissue specimens were frozen in liquid nitrogen, blended to a powder, and stored at −10° until assayed (4).

Assay Methods—Plasma was analyzed for sulfathiazole by the modified Bratton–Marshall method of Annino (5).

Urine was analyzed for unchanged sulfathiazole and its acetyl and polar metabolites by the method of Bevill *et al.* (4), except that ethyl acetate was used to develop the TLC plates instead of chloroform–acetone as used previously.

Tissues were analyzed for sulfathiazole by the method of Bevill *et al.* (4), except that three 25-ml volumes of hexane were used to remove the eluates from the round-bottom flasks after the flash evaporation step, and the flasks were washed with 5 ml of acetone after each hexane wash. Standard curves were prepared as described previously (4). Tissue samples containing 0.1–20 ppm of sulfathiazole were employed.

RESULTS AND DISCUSSION

Analytical Results—The average plasma sulfathiazole concentrations at various times following intravenous administration are shown in Fig. 1. The plasma concentrations decreased rapidly with time, reaching 0.1 mg % (approximate limit of detection) in about 10 hr. The average plasma concentration was below 5 mg % (a therapeutically effective concentration) within 2 hr.

The results of analysis of urine collected at various times following intravenous administration are presented in Fig. 2 as the average cumulative percent of dose excreted as unchanged sulfathiazole and as the acetyl and polar metabolites. Approximately 67% of the dose was excreted as unchanged sulfathiazole, 19% as the acetyl metabolite, and less than 2% as the polar metabolite.

The results of residue analysis of various tissues of lambs slaughtered at various times following drug administration are shown in Table I.

Selection of a Pharmacokinetic Model—Semilogarithmic plots of the average plasma concentration *versus* time and the average rate of excretion of unchanged sulfathiazole in urine *versus* time are presented in Fig. 1. Both these plots were linear with constant and similar slopes,

[1] From the University of Illinois Agricultural Experiment Station, Dixon Springs, Ill.

[2] Bardex, 16 Fr, C. R. Bard Inc., Murray Hill, N.J.

[3] Holmes Serum Co., Springfield, Ill.

Table I—Average Sulfathiazole Concentrations in Tissues of Lambs at Various Times after Administration of Sulfathiazole, 72 mg/kg iv

Hours after Dosing	Average Tissue Concentration, ppm ± *SD*							
	Kidney	Heart	Leg Muscle	Shoulder Muscle	Loin Muscle	Liver	Body Fat	Omental Fat
2.0	308 ±145	34 ±11	22 ±7.5	23 ±8.1	22 ±5.7	40 ±13	11 ±5.2	6.7 ±2.9
4.0	55 ±24	9.3 ±5.9	5.0 ±2.6	4.7 ±2.5	4.9 ±2.8	9.4 ±4.9	3.5 ±1.9	1.4 ±0.54
8.0	2.3 ±1.3	0.32 ±0.12	0.26 ±0.11	0.27 ±0.12	0.23 ±0.11	0.70 ±0.29	0.26 ±0.13	0.12 ±0.04
16.0	0.36 ±0.13	0.08 ±0.03	n.s.[a]	n.s.	0.05 ±0.02	0.30 ±0.14	n.s.	n.s.
24.0	0.11 ±0.06	0.07 ±0.03	n.s.	n.s.	n.s.	0.12 ±0.05	n.s.	n.s.

[a] n.s. = not significant ($p < 0.01$).

Table II—Values of the Parameters of the Pharmacokinetic Model Describing Sulfathiazole Disposition in Lambs (Scheme II)

	V_d[a]	k_{el}[b]	$k_{sulfathiazole}$[b]	$k_{miscellaneous}$[b]	k_{AB}[b]	k_{PB}[b]	k_{AU}[b]	k_{PU}[b]
$\bar{x}$[c]	0.389	0.625	0.424	0.071	0.116	0.013	2.53	1.88
SD[c]	0.044	0.144	0.120	0.046	0.047	0.015	2.4	2.70
Averaged[d]	0.373	0.629	0.417	0.088	0.115	0.009	2.03	1.32

[a] Volume of distribution, liter per kilogram. [b] Rate constants, hour^{-1}. [c] Average and standard deviation of values from individual animals 4–15. [d] Results from fitting Scheme II to averaged plasma and urine data.

suggesting that the overall elimination of sulfathiazole in lambs follows first-order kinetics:

$$\text{rate of elimination} = k_{el}C_p \qquad \text{(Eq. 1)}$$

where C_p is the concentration of unchanged sulfathiazole in plasma.

The biological half-life of sulfathiazole in lambs (Fig. 1) is approximately 1.1 hr; therefore, k_{el}, the overall elimination rate constant, is approximately 0.63 hr^{-1}. Since there was no apparent distribution phase in Fig. 1, it was concluded that sulfathiazole pharmacokinetics in lambs could be described by a one-compartment model such as that shown in Scheme I.

sulfathiazole in plasma $\xrightarrow[0.63\ hr^{-1}]{k_{el}=}$ sulfathiazole eliminated from plasma

Scheme I

Urinary excretion data also were collected for unchanged sulfathiazole and its acetyl and polar metabolites, so the pharmacokinetic model could be expanded to include these features. Moreover, since the entire dose was not recovered in the urine, the amount not recovered was represented by a "miscellaneous" process. It was assumed that unchanged sulfathiazole entered the urine directly from the plasma compartment whereas the metabolites were first formed in the plasma (or body) compartment and then cleared into the urine. Based on these assumptions, the model in Scheme II was selected.

Fitting Model to Data—Scheme II was fitted to the data for unchanged sulfathiazole in plasma and urine and for the metabolites of sulfathiazole in urine by obtaining values for each rate constant. First, initial estimates of the rate constants were obtained by the method described previously (6). Then the averaged plasma concentrations of sulfathiazole and averaged urine outputs of sulfathiazole and its metabolites *versus* time were fitted to the model in Scheme II by iterative least-squares computation, using the SAAM 23 program (7) and a digital computer[4].

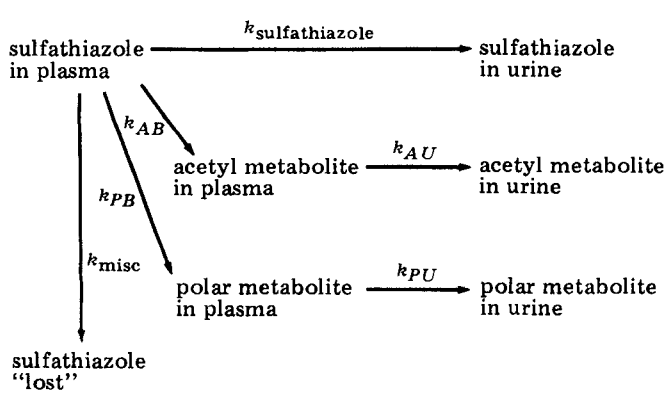

Scheme II

The calculated values of the parameters of Scheme II for averaged plasma and urine data are presented in Table II. The overall elimination rate constant, k_{el}, was 0.63 hr^{-1} (biological half-life of 1.1 hr), and the volume of distribution was 0.37 liter/kg.

The close agreement between the model and the averaged experimental data is illustrated in Figs. 1 and 2. The lines in these figures were generated by the pharmacokinetic model shown in Scheme II with the "best

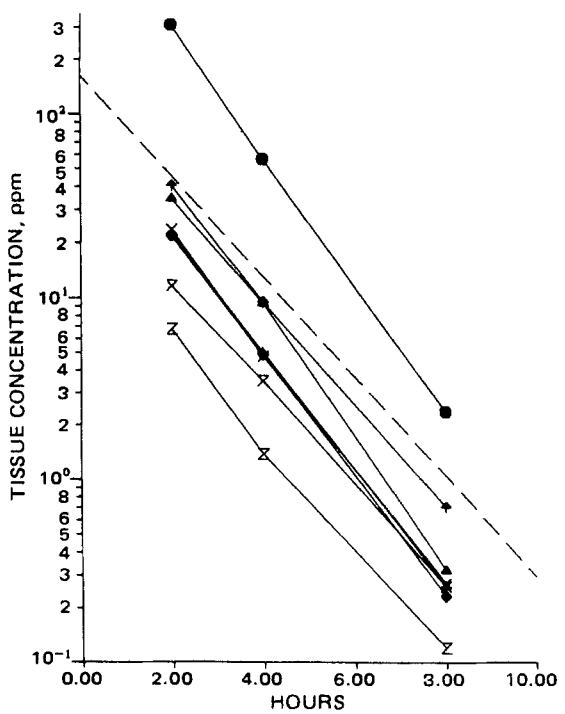

Figure 3—*Semilogarithmic plot of sulfathiazole concentration in various tissues* versus *time following intravenous administration to sheep. The points (with solid connecting lines) were experimentally determined in kidney (●), heart (▲), liver (↑), loin muscle (♦), leg muscle (+), shoulder muscle (×), body fat (⊠), and omental fat (Z) tissue. The dashed line represents the plasma concentration calculated using the pharmacokinetic model (Scheme II) and the values of the parameters presented in Table II.*

[4] IBM 370/165.

Table III—Linear Regression Analysis of Average Plasma Sulfathiazole Concentration and Excretion Rate of Unchanged Sulfathiazole *versus* the Sulfathiazole Concentration in Various Tissues following Administration of Sulfathiazole, 72 mg/kg iv

Hours	Average Plasma Concentration, mg/100 ml	Average Excretion Rate, % dose/hr	Concentration in Tissues, ppm					
			Kidney	Liver	Heart	Muscle	Body Fat	Omental Fat
2.0	4.7	13.4	308	40	34	22	11	6.7
4.0	1.2	4.3	55	9.4	9.3	4.9	3.5	1.4
8.0	0.1	0.7	2.3	0.7	0.3	0.3	0.3	0.1
			r (between plasma and tissue concentrations)					
			1.000	1.000	1.000	0.999	0.998	0.998
			r (between excretion rate and tissue concentration)					
			0.990	0.996	0.998	0.995	1.000	0.992

fit" constants for averaged data shown in Table II. In each figure, the points are the averaged values from the remaining lambs at each sampling time, with 1 *SD* indicated by error bars.

Variations in the values of the rate constants due to variations within the lamb populations were estimated by fitting the data from each animal individually to the model in Scheme II. The results obtained from the averaged data were used as initial estimates. The values obtained for the parameters of Scheme II following iterative least-squares fitting to the individual animal data are presented in Table II. The average overall elimination rate constant was 0.62 ± 0.14 hr^{-1} (biological half-life of 1.1 ± 0.2 hr) and the average volume of distribution was 0.39 ± 0.04 liter/kg. These figures compare favorably with the results obtained by fitting averaged plasma and urine data and with the results obtained previously in sheep (3).

The observed one-compartment pharmacokinetics in lambs imply that the extravascular tissues into which sulfathiazole penetrates are in rapid equilibrium with plasma throughout the entire time that the drug is in the body. In the present study, the one-compartment nature of sulfathiazole pharmacokinetics beyond 2 hr can be observed in the experimentally determined drug concentrations in representative tissue specimens. This result is illustrated in Fig. 3, which shows plasma concentrations of unchanged sulfathiazole calculated using the pharmacokinetic model and concentrations of unchanged sulfathiazole in eight tissues obtained from the animals at slaughter.

According to the proposed model, the drug concentration in each tissue should be directly proportional to the plasma concentration and to the urinary excretion rate of unchanged sulfathiazole determined at the same time. The correlation coefficients obtained by linear regression of the plasma and urine data with the residual concentrations in various tissues are shown in Table III. These excellent correlations demonstrate that the plasma concentrations and the urine outputs of sulfathiazole accurately reflect tissue residues of sulfathiazole in the lamb. Thus, the time required for sulfathiazole to reach negligible levels in various tissues that might be used as food can be determined by plasma and/or urine analysis without slaughtering the animals.

REFERENCES

(1) H. D. Mercer, *Vet. Clin. N. Am.*, **5**, 3 (1975).

(2) W. G. Huber, *Pure Appl. Chem.*, **35**, 377 (1972).

(3) G. D. Koritz, D. W. A. Bourne, L. W. Dittert, and R. F. Bevill, *Am. J. Vet. Res.*, **38**, 979 (1977).

(4) R. F. Bevill, R. M. Sharma, S. H. Meachum, S. C. Wozniak, D. W. A. Bourne, and L. W. Dittert, *ibid.*, **38**, 973 (1977).

(5) J. S. Annino, in "Standard Methods of Clinical Chemistry," vol. 3, Academic, New York, N.Y., 1961, pp. 200–206.

(6) D. W. A. Bourne, R. F. Bevill, R. M. Sharma, R. P. Gural, and L. W. Dittert, *Am. J. Vet. Res.*, **38**, 967 (1977).

(7) M. Berman and M. F. Weiss, "Users Manual for SAAM," National Institute for Arthritis and Metabolic Diseases, Bethesda, Md., 1968.

ACKNOWLEDGMENTS AND ADDRESSES

Received March 8, 1976, from the *Department of Veterinary Physiology and Pharmacology, College of Veterinary Medicine, University of Illinois, Urbana, IL 61801, and the ‡College of Pharmacy, University of Kentucky, Lexington, KY 40506.

Accepted for publication December 2, 1976.

Supported by FDA Grant 74-178.

ˣ To whom inquiries should be directed.

Cascarosides A and B

J. W. FAIRBAIRN ˣ, F. J. EVANS, and J. D. PHILLIPSON

Abstract □ Electron-impact and field desorption mass spectrometry, together with NMR and circular dichroism spectroscopy, were used to confirm that cascarosides A and B are C-10 isomers of 8-*O*-(β-D-glucopyranosyl)barbaloin. Several batches of cascarosides A and B were prepared and oxidatively hydrolyzed to aloe-emodin. The results are discussed in relation to the assay for cascara given in the European Pharmacopoeia, 1971.

Keyphrases □ Cascarosides A and B—electron-impact and field desorption mass spectrometric and NMR and circular dichroism spectroscopic structural identification □ Barbaloin derivatives—cascarosides A and B, electron-impact and field desorption mass spectrometric and NMR and circular dichroism spectroscopic structural identification □ Mass spectrometry, electron impact and field desorption—structural identification of cascarosides A and B □ NMR spectroscopy—structural identification of cascarosides A and B □ Circular dichroism spectroscopy—structural identification of cascarosides A and B

Cascarosides A and B previously were isolated from *Rhamnus purshiana* DC. bark and shown to contain glucose and barbaloin (1). Later work proved that cascarosides A and B were glucosides of (+)- and (−)-barbaloin, respectively, although it was suggested that the molecules contained additional carbon fragments (2). This suggestion was partly based on the fact that the yield of barbaloin and aloe-emodin after hydrolysis was significantly less than theory for a glucoside of barbaloin. Molecular weight determinations, mass spectrometry, NMR spectroscopy, and

Table III—Linear Regression Analysis of Average Plasma Sulfathiazole Concentration and Excretion Rate of Unchanged Sulfathiazole *versus* the Sulfathiazole Concentration in Various Tissues following Administration of Sulfathiazole, 72 mg/kg iv

Hours	Average Plasma Concentration, mg/100 ml	Average Excretion Rate, % dose/hr	Concentration in Tissues, ppm					
			Kidney	Liver	Heart	Muscle	Body Fat	Omental Fat
2.0	4.7	13.4	308	40	34	22	11	6.7
4.0	1.2	4.3	55	9.4	9.3	4.9	3.5	1.4
8.0	0.1	0.7	2.3	0.7	0.3	0.3	0.3	0.1
			r (between plasma and tissue concentrations)					
			1.000	1.000	1.000	0.999	0.998	0.998
			r (between excretion rate and tissue concentration)					
			0.990	0.996	0.998	0.995	1.000	0.992

fit" constants for averaged data shown in Table II. In each figure, the points are the averaged values from the remaining lambs at each sampling time, with 1 *SD* indicated by error bars.

Variations in the values of the rate constants due to variations within the lamb populations were estimated by fitting the data from each animal individually to the model in Scheme II. The results obtained from the averaged data were used as initial estimates. The values obtained for the parameters of Scheme II following iterative least-squares fitting to the individual animal data are presented in Table II. The average overall elimination rate constant was 0.62 ± 0.14 hr^{-1} (biological half-life of 1.1 ± 0.2 hr) and the average volume of distribution was 0.39 ± 0.04 liter/kg. These figures compare favorably with the results obtained by fitting averaged plasma and urine data and with the results obtained previously in sheep (3).

The observed one-compartment pharmacokinetics in lambs imply that the extravascular tissues into which sulfathiazole penetrates are in rapid equilibrium with plasma throughout the entire time that the drug is in the body. In the present study, the one-compartment nature of sulfathiazole pharmacokinetics beyond 2 hr can be observed in the experimentally determined drug concentrations in representative tissue specimens. This result is illustrated in Fig. 3, which shows plasma concentrations of unchanged sulfathiazole calculated using the pharmacokinetic model and concentrations of unchanged sulfathiazole in eight tissues obtained from the animals at slaughter.

According to the proposed model, the drug concentration in each tissue should be directly proportional to the plasma concentration and to the urinary excretion rate of unchanged sulfathiazole determined at the same time. The correlation coefficients obtained by linear regression of the plasma and urine data with the residual concentrations in various tissues are shown in Table III. These excellent correlations demonstrate that the plasma concentrations and the urine outputs of sulfathiazole accurately reflect tissue residues of sulfathiazole in the lamb. Thus, the time required for sulfathiazole to reach negligible levels in various tissues that might be used as food can be determined by plasma and/or urine analysis without slaughtering the animals.

REFERENCES

(1) H. D. Mercer, *Vet. Clin. N. Am.*, **5**, 3 (1975).

(2) W. G. Huber, *Pure Appl. Chem.*, **35**, 377 (1972).

(3) G. D. Koritz, D. W. A. Bourne, L. W. Dittert, and R. F. Bevill, *Am. J. Vet. Res.*, **38**, 979 (1977).

(4) R. F. Bevill, R. M. Sharma, S. H. Meachum, S. C. Wozniak, D. W. A. Bourne, and L. W. Dittert, *ibid.*, **38**, 973 (1977).

(5) J. S. Annino, in "Standard Methods of Clinical Chemistry," vol. 3, Academic, New York, N.Y., 1961, pp. 200–206.

(6) D. W. A. Bourne, R. F. Bevill, R. M. Sharma, R. P. Gural, and L. W. Dittert, *Am. J. Vet. Res.*, **38**, 967 (1977).

(7) M. Berman and M. F. Weiss, "Users Manual for SAAM," National Institute for Arthritis and Metabolic Diseases, Bethesda, Md., 1968.

ACKNOWLEDGMENTS AND ADDRESSES

Received March 8, 1976, from the *Department of Veterinary Physiology and Pharmacology, College of Veterinary Medicine, University of Illinois, Urbana, IL 61801, and the ‡College of Pharmacy, University of Kentucky, Lexington, KY 40506.

Accepted for publication December 2, 1976.

Supported by FDA Grant 74-178.

ˣ To whom inquiries should be directed.

Cascarosides A and B

J. W. FAIRBAIRN ˣ, F. J. EVANS, and J. D. PHILLIPSON

Abstract □ Electron-impact and field desorption mass spectrometry, together with NMR and circular dichroism spectroscopy, were used to confirm that cascarosides A and B are C-10 isomers of 8-*O*-(β-D-glucopyranosyl)barbaloin. Several batches of cascarosides A and B were prepared and oxidatively hydrolyzed to aloe-emodin. The results are discussed in relation to the assay for cascara given in the European Pharmacopoeia, 1971.

Keyphrases □ Cascarosides A and B—electron-impact and field desorption mass spectrometric and NMR and circular dichroism spectroscopic structural identification □ Barbaloin derivatives—cascarosides A and B, electron-impact and field desorption mass spectrometric and NMR and circular dichroism spectroscopic structural identification □ Mass spectrometry, electron impact and field desorption—structural identification of cascarosides A and B □ NMR spectroscopy—structural identification of cascarosides A and B □ Circular dichroism spectroscopy—structural identification of cascarosides A and B

Cascarosides A and B previously were isolated from *Rhamnus purshiana* DC. bark and shown to contain glucose and barbaloin (1). Later work proved that cascarosides A and B were glucosides of (+)- and (−)-barbaloin, respectively, although it was suggested that the molecules contained additional carbon fragments (2). This suggestion was partly based on the fact that the yield of barbaloin and aloe-emodin after hydrolysis was significantly less than theory for a glucoside of barbaloin. Molecular weight determinations, mass spectrometry, NMR spectroscopy, and

Table I—Results of Oxidative Hydrolysis of Several Independently Prepared Samples of Cascarosides

Sample Date	$E^{1\%}_{1\,cm}$ in Water at λ_{max} 267–269 nm	294–295 nm	323–325 nm	Aloe-emodin, %	Corresponding $E^{1\%}_{1\,cm}$ for Cascaroside
		Cascaroside A			
1965	119	164	140	39.8	127
1975	115	176	151	38.5	124
1976	111	173	150	40.7	131
1976	112	173	151	41.5	133
		Cascaroside B			
1961	114	161	143	40.6	130
1967	116	169	146	39.3	126
1975	118	173	149	37.2	119
1976	107	166	146	39.8	127

synthesis of glucosides of barbaloin were investigated, but it was not possible to confirm the presence of an additional component[1].

It was proposed (3, 4) that cascarosides A and B are 8-monoglucosides of barbaloin and that no further component is present. However, accurate molecular weight determinations were not obtained because of thermal decomposition in electron-impact mass spectrometry and because conventional methods gave values of 561 and 533 for cascarosides A and B, respectively (theoretical for dihydrate, 616). It was reported (5) that field desorption mass spectrometry clearly indicated that cascarosides A and B have a molecular weight of 580. On the basis of mass spectral and NMR studies, cascaroside A was confirmed to be the 8-*O*-β-D-glucoside of (+)-barbaloin and cascaroside B was reported to be the corresponding diastereoisomer of (−)-barbaloin (5). Independently, Wagner and Demuth (6) reached the same conclusion on the basis of partial hydrolyses, sugar analyses, and spectral data.

The present report gives details of spectral data that confirm and amplify those already published. In addition, several new batches of cascarosides were prepared to confirm whether the yield of aloe-emodin previously reported is correct. This value has been used as the basis of an officially recommended colorimetric method for the assay of cascara bark and extract (7) and is now incorporated in the European Pharmacopoeia, 1971.

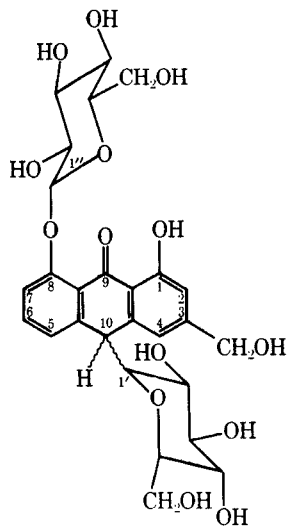

I

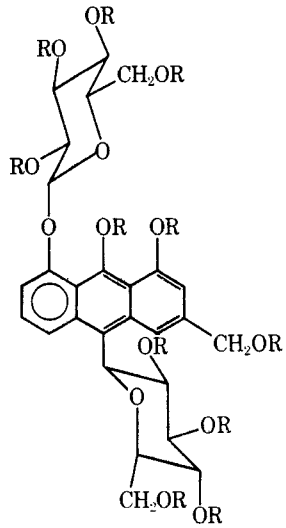

IIa: R = CH_3CO
IIb: R = $SiH(CH_3)_3$

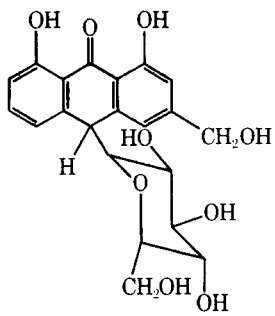

III

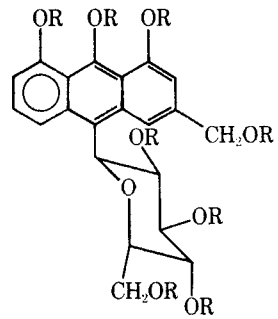

IVa: R = CH_3CO
IVb: R = $SiH(CH_3)_3$

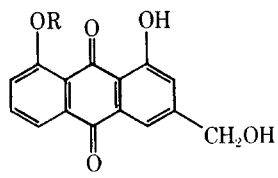

Va: R = glucose
Vb: R = H

EXPERIMENTAL[2]

Isolation of Cascarosides A and B—The method used was previously described (1), except that separation of cascarosides A and B was effected by paper chromatography rather than by countercurrent methods. The bands corresponding to cascarosides A and B on 3-mm paper[3], after development with ethyl acetate–methanol–water (100:17:13) (8), were eluted with methanol, and the eluates were evaporated to dryness. The residues were extracted with hot 2-propanol and filtered, and the filtrates were allowed to stand in the dark at room temperature overnight. The microcrystalline precipitates that formed were collected and dried.

Further yields were obtained by evaporating the supernate and dissolving the residue in 10 volumes of anhydrous methanol (filtering off insoluble matter if necessary). Ethyl methyl ketone was added slowly with vigorous stirring until the solution became cloudy. After centrifuging, a reddish-yellow precipitate formed, which was discarded.

The process was repeated until the precipitate that formed was bright yellow. At this stage, ethyl methyl ketone–methanol (10:1) was added. The bright-yellow precipitate was allowed to settle and was then filtered off. Before becoming dry, it was washed with methanol–petroleum ether (bp 40–60°) (1:1) and then petroleum ether and dried *in vacuo*.

Cascaroside A (I)—UV data are presented in Table I. Paper chromatography R_f values were as previously reported (1). Electron-impact mass spectrum: no $M^{+\cdot}$, *m/e* (relative intensity) 256 (100%), further fragmentation similar to that of barbaloin. Field desorption mass spectrum, 17 mamp and 80°, from methanol: *m/e* 603 ($M^{+\cdot}$ + [Na^+], 100%), 620 ($M^{+\cdot}$ + [K^+], 5), 605 ($M^{+\cdot}$ + [Na^+ + 2], 8), 604 ($M^{+\cdot}$ + [Na^+ + 1], 18), 602 (M^+ + [Na^+ − 1], 40), and 580 ($M^{+\cdot}$, 12); from water: *m/e* 674 ($M^{+\cdot}$ + [(Na^+ × 4) + 2], 12%), 620 (40), 606 (M^+ + [Na^+ + 3], 14), 605 (12), 604 (8), 603 (100), 602 (9), and 580 (10). Fragment ions consistently present in spectra obtained from methanol or from water: *m/e* 442 ($M^{+\cdot}$ + [Na^+ − 161], 50%), 418 ($M^{+\cdot}$ − [162], 12), 280 (100), and 256 (20). NMR (dimethyl sulfoxide-d_6): δ 3.0–3.50 (glucosyl hydrogens), 4.68 (3H, s, aryl CH_2O and aryl-CH–aryl), 5.10 (1H, m, H-1′), 6.84 (1H, broad s, H-2), 7.0 (1H, broad s, H-4), 7.1–7.80 (3H, m, H-5, H-6, and H-7), and 11.89 (1H, s, aryl OH) ppm. Circular dichroism spectrum (methanol): 4.39 mg/5 ml, Δε +4.6 (355 nm), −8.8 (316), −2.8 sh (282), +1.4 sh (258), +4.4 sh (240), +5.0 (234), and −13.2 (211).

Cascaroside B (I)—UV data are presented in Table I. Paper chromatography R_f values were as previously reported (1). Electron-impact mass spectrum: no $M^{+\cdot}$, *m/e* (relative intensity) 256 (100%), further fragmentation similar to that of barbaloin. Field desorption mass spec-

[1] Unpublished observations.

[2] Mass spectra were obtained on an AEI MS 902 mass spectrometer at 70 ev by direct insertion at 180°. NMR spectra were obtained using a Perkin-Elmer 12A 60-MHz spectrometer with trimethylsilane = 0.00 ppm. Cascara bark of European Pharmacopoeia (1971) standard was obtained from W. Ransom and Son Ltd., Hitchin, England.

[3] Whatman.

trum, 17 mamp and 80°, from methanol: *m/e* 604 (18%), 603 (70), 581 (23), 580 (M^{+}·, 44), 280 (100), and 256 (100); from water: *m/e* 605 (8%), 604 (8), 603 (100), 580 (18), 442 (80), 280 (75), and 256 (68). NMR (dimethyl sulfoxide-d_6): δ 3.0–3.8 (glucosyl hydrogens), 4.54 (3H, s, aryl CH_2O and aryl–CH–aryl), 4.90 (1H, m, H-1′), 6.64–7.6 (5H, m, H-2, H-4, H-5, H-6, and H-7), and 12.1 (1H, s, aryl OH) ppm. Circular dichroism spectrum (methanol): 2.63 mg/ml, $\Delta\epsilon$ −1.8 (368 nm), +1.0 (324), −1.2 (290), −0.8 (263), +0.3 (251), −7.0 (230), and +9.2 (210).

Cascaroside Acetate (IIa)—Cascarosides A and B (20 mg of each) were dissolved separately in 4 ml of anhydrous pyridine–acetic anhydride (2:1) and allowed to stand in the dark and under nitrogen for 2 days. Excess water was added, and the resulting suspension was centrifuged. The residues were washed with water, recentrifuged until free from pyridine, and dried *in vacuo* at 60° for 24 hr. TLC [silica gel GF, 1-propanol–ethyl acetate–water (40:30:40)] indicated that the products from cascarosides A and B were identical.

Electron-impact mass spectrum: no M^{+}·, *m/e* (relative intensity) 653 (M^{+}· − [acetylglucose], 17%), 494 (2), 452 (7), 410 (14), 368 (21), and 331 (100). Field desorption mass spectrum, 14 mamp, from chloroform: *m/e* 1042 (M^{+}·, 100%) and 1043 (M^{+}· + [1], 40). NMR (deuterochloroform): δ 1.82–2.53 (11 × 3H, s, 11 × CH_3CO), 5.33 (2H, s, aryl CH_2O), 5.95 (1H, broad s, H-1′), and 7.0–8.93 (5H, m, H-2, H-4, H-5, H-6, and H-7) ppm.

Cascaroside Trimethylsilyl Ether (IIb, R = Trimethylsilyl)—Cascarosides A and B (20 mg of each) were dissolved separately in 2 ml of anhydrous pyridine. To each solution were added 0.5 ml of hexamethyldisilazane and 0.5 ml of trimethylchlorosilane. After standing for 5 min at room temperature, the solvents were removed by vacuum distillation. The dry residue was extracted with carbon tetrachloride and filtered, and the solutions were evaporated to 0.5 ml for NMR spectroscopy.

The NMR spectra obtained from the trimethylsilyl ethers of cascarosides A and B were identical: δ 3.50 (12H, m, glucosyl hydrogens), 4.35 (1H, m, H-1′), 5.15 (1H, m, H-1″), 4.66 (2H, s, aryl CH_2O), and 6.9–7.5 (5H, m, H-2, H-4, H-5, H-6, and H-7) ppm.

Barbaloin (III)—This compound was prepared from commercial aloin (9). Electron-impact mass spectrum: *m/e* (relative intensity) 418 (M^{+}·, 0.5%), 256 (M^{+}· − [162], 100), 238 (M^{+}· − [162 + 18], 5), 228 (M^{+}· − [162 + 28], 7), 210 (M^{+}· − [162 + 28 + 18], 4), 197 (M^{+}· − [162 + 28 + 31], 3), 181 (5), and 165 (3). Field desorption mass spectrum, 14 mamp, from methanol: *m/e* 418 (M^{+}·, 100%) and 256 (M^{+}· − [162], 11). NMR (dimethyl sulfoxide-d_6): δ 2.78–3.50 (6H, m, glucosyl hydrogens), 4.58 (3H, 3, aryl CH_2O and aryl–CH–aryl), 5.1 (1H, m, H-1′), 7.60 (1H, t, H-6), 7.05 (1H, d, H-5), 6.90 (1H, d, H-7), 7.05 (1H, s, H-4), 6.88 (1H, s, H-2), and 11.3 and 11.4 (2 × 1H, s, aryl OH) ppm.

Barbaloin Acetate (IVa)—Aloin (5 mg) was converted into the acetate by the method described under *Cascaroside Acetate*. TLC [silica gel G, 1-propanol–ethyl acetate–water (40:30:40)] showed the presence of a single compound. Electron-impact mass spectrum: *m/e* (relative intensity) 754 (M^{+}·, 5%), 713 (<5), 694 (<5), 676 (30), 652 (40), 628 (30), 611 (10), 568 (12), 550 (6), 508 (11), 448 (25), and 331 (100). Field desorption mass spectrum, 17 mamp, from methanol: *m/e* 754 (M^{+}·, 100%), 755 (50), 756 (20), 714 (10), and 715 (10). NMR (carbon tetrachloride): δ 1.91–2.40 (8 × 3H, s, 8 × CH_3CO), 5.40 (2H, s, aryl CH_2O), 6.00 (1H, broad s, H-1′), and 7.0–8.95 (5H, m, H-2, H-4, H-5, H-6, and H-7) ppm.

Barbaloin Trimethylsilyl Ether (IVb)—Aloin (20 mg) was converted into its trimethylsilyl ether by the method described for IIb. NMR (carbon tetrachloride): δ 3.23 (6H, m, glucosyl protons), 4.18 (1H, m, H-1′), 4.43 (2H, s, aryl CH_2O), 6.60 (4H, m, H-2, H-4, H-5, and H-7), and 7.05 (1H, m, H-6) ppm.

Aloe-emodin 8-Monoglucoside[4] (Va)—Electron-impact mass spectrum: no M^{+}·, *m/e* (relative intensity) 270 (M^{+}· − [glucose], 100%), 253 (M^{+}· − [17], 6), 241 (M^{+}· − [29], 58), 225 (M^{+}· − [17 + 28], 12), 213 (M^{+}· − [29 + 28], 17), 197 (M^{+}· − [17 + 56], 7), 185 (M^{+}· − [29 + 56], 5), 139 (24), and 121 (33). Field desorption mass spectrum, 17 mamp, from methanol: *m/e* 432 (M^{+}·, 100%), 433 (M^{+}· + [1], 65), 455 (M^{+}· + [Na^{+}], 100), 269 (90), 271 (70), and 270 (75). NMR (dimethyl sulfoxide-d_6): δ 3.40 (6H, m, glucosyl hydrogens), 4.55 (2H, s, aryl CH_2O), 7.25–7.90 (5H, m, H-2, H-4, H-5, H-6, and H-7), and 10.91 (1H, s, aryl OH) ppm.

Aloe-emodin (Vb)—This compound was prepared from barbaloin by oxidative hydrolysis using the method described previously (9). Electron-impact mass spectrum (280°): *m/e* (relative intensity) 270 (M^{+}·, 100%), 253 (M^{+}· − [17], 4), 242 (M^{+}· − [28], 4), 225 (M^{+}· − [17 + 28], 5), 224 (M^{+}· − [18 + 28], 6), 213 (M^{+}· − [29 + 28], 8), 197 (M^{+}· − [17 + 56], 3), 185 (2), 139 (8), and 121 (12). Metastable peaks corresponding to the following transitions were observed, $270 \xrightarrow{237.1} 253$, $270 \xrightarrow{216.9} 242$, $242 \xrightarrow{187.5} 213$, and $242 \xrightarrow{207.3} 224$. NMR (dimethyl sulfoxide-d_6): δ 4.62 (2H, s, aryl CH_2O), 7.33 (2H, m, H-2 and H-7), and 7.73 (3H, m, H-4, H-5, and H-6) ppm.

Oxidative Hydrolysis of Cascarosides A and B to Aloe-emodin—Four separate batches of cascaroside A and four of cascaroside B were prepared as described. Their purity was checked by paper chromatography, UV spectrum, melting point, and, mainly, the $E^{1\%}_{1\,cm}$ values at the UV_{max} (these varied less than the melting point) (1).

Quantities of 10–20 mg were dried *in vacuo* over magnesium chlorate at 90–100° for 1 hr to remove moisture and water of crystallization. The anhydrous material was dissolved in 50 ml of water, and 10 ml was subjected to ferric chloride–hydrochloric acid treatment (10). The aloe-emodin produced was measured colorimetrically in 1 *N* NaOH at 500 nm, and the quantity was calculated using the $E^{1\%}_{1\,cm}$ value of 320. The corresponding $E^{1\%}_{1\,cm}$ value for the cascarosides was also calculated (Table I).

DISCUSSION

Spectrometry—Electron-impact mass spectrometry can be used for the characterization of the aglycone aloe-emodin (Vb) since the M^{+}· ion was observed as the base peak at *m/e* 270 and further fragmentation was observed by ion peaks at *m/e* 253, 242, 225, 224, and 213. However, electron-impact mass spectrometry of the *O*-glycoside aloe-emodin 8-glucoside (Va) resulted in the absence of an M^{+}· ion and a spectrum that was similar to that of the aglycone. Electron-impact mass spectrometry of the C-glycoside barbaloin (III) showed only a small M^{+}· ion at *m/e* 418 (0.5%), and the base peak was observed at *m/e* 256. Further fragmentation occurred by loss of 16, 28, or 29 mass units progressively from the M^{+}· ion, similarly to that of aloe-emodin and other anthraquinones.

Furthermore, electron-impact mass spectrometry did not result in the presence of an M^{+}· ion for either cascaroside A or B, the highest mass ion fragment again occurring at *m/e* 256 due to the loss of both sugar units from the molecule. Electron-impact mass spectrometry of the acetate, which is common to cascarosides A and B, also failed to produce an M^{+}· ion, the highest mass fragment ion being observed as a peak at *m/e* 653, corresponding to the loss of acetylglucose.

Ever since the cascarosides were first isolated (1), attempts at characterization have failed largely because of the difficulty in obtaining accurate molecular weights (2, 4). A solution to this problem is field desorption mass spectrometry (5, 6). Spectra of cascarosides A and B were obtained from aqueous and methanolic solutions, and the presence of quasimolecular ions such as M^{+}· + [Na^{+}], M^{+}· + [K^{+}], and M^{+}· + [H^{+}] were of use in establishing that the M^{+}· ion occurs at *m/e* 580. Peaks corresponding to the presence of such ions in the spectra of glycosides from polar solvents also were reported for flavonoids (11), and their significance to molecular weight determination was discussed (12). To eliminate the formation of quasimolecular ions, the acetates of both cascarosides were prepared (IIa). The M^{+}· ion occurred at *m/e* 1042 (100%), thus confirming the molecular weight of the cascarosides as 580. This result is also in agreement with the suggestions (2) that three acetyl moieties are present in the aglycone position and that the tetrahedral arrangement at C-10 is lost on acetylation.

Field desorption mass spectrometry was superior to electron-impact mass spectrometry for the molecular weight determination of other anthraquinone glycosides since the spectra of barbaloin (III) and of its acetate (IVa) had base peaks at *m/e* 418 and 754, respectively, corresponding to the M^{+}· ions. The spectrum of aloe-emodin 8-glucoside (Va) also showed the presence of an M^{+}· ion peak, which occurred at *m/e* 432 (100%); quasimolecular ions were formed as illustrated by the presence of a peak at *m/e* 455, corresponding to M^{+}· + [Na^{+}].

The NMR spectra of cascarosides A and B and of the related compounds were also important in confirming the structure of cascarosides A and B. Signals for the five aromatic hydrogens between δ 7.33 and 7.73 ppm and for the aromatic methylenehydroxy at δ 4.62 ppm were readily observed in the NMR spectrum of the aglycone aloe-emodin. For Va, a six-proton glucosyl envelope was observed at δ 3.4 ppm in addition to the signals of the five aromatic hydrogens, the aromatic methylenehydroxy, and the phenolic hydrogen, which appeared at δ 10.91 ppm.

In the NMR spectrum of barbaloin (III), a six-proton glucosyl envelope at δ 2.78–3.50 ppm was also evident, and the presence of a three-proton singlet at δ 4.58 ppm was attributed to the aromatic methylenehydroxy and H-10 protons. The H-1′ signal appeared at δ 5.1 ppm, and the five aromatic protons showed as a multiplet between δ 6.88 and 7.60 ppm; two

[4] Supplied by Professor H. Wagner.

downfield singlets at δ 11.3 and 11.4 ppm were due to the hydrogen-bonded phenolic hydrogens. Signals for eight acetyl groups were observed in the spectrum of IV*a* between δ 1.90 and 2.40 ppm, and the signal for the hydrogen at C-10 disappeared. A similar result was also obtained for the NMR spectrum of IV*b*.

In the NMR spectrum of cascaroside A, the H-1′ glucosyl proton appeared as a singlet at δ 5.10 ppm, and the methylenehydroxy and H-10 proton appeared together as a 3H singlet at δ 4.68 ppm. Signals for five aromatic protons between δ 6.84 and 7.80 ppm and a single hydrogen-bonded phenolic proton signal at δ 11.89 ppm were also evident. However, because of the difficulty in removing traces of moisture from the cascaroside, it was not possible to assess the number of protons in the glucosyl envelope between δ 3.0 and 3.50 ppm. A similar NMR spectrum was obtained for cascaroside B.

Therefore, derivatives of cascarosides A and B were produced to ascertain the number of glucosyl protons. The acetate (II*a*) common to cascarosides A and B showed the presence of 11 acetyl group signals at δ 1.82–2.53 ppm and the absence of the H-10 signal in an analogous way to the spectrum of barbaloin acetate. NMR of II*b* showed a 12H multiplet at δ 3.50 ppm, representing the proton envelope of the two glucose residues. The other two glucosyl protons at H-1′ and H-1″ produced signals at δ 4.35 and 5.15 ppm, respectively.

Hence, the application of field desorption mass and NMR spectral techniques to cascarosides A and B, the aglycone-aloe-emodin, and its monoglucosides barbaloin and aloe-emodin 8-glucoside confirms that the cascarosides are *O*-glucosides of barbaloin and that, despite previous hydrolysis results (2), no additional moieties are present. Partial hydrolysis of cascarosides A and B indicated that the *O*-glucose is situated at C-8 and enzyme hydrolysis confirmed that this linkage is beta (6). Partial hydrolysis of cascarosides A and B resulting in (+)- and (−)-aloins, respectively (2), confirmed that cascaroside A is 8-*O*-β-D-glucopyranosyl-(+)-barbaloin and that cascaroside B is 8-*O*-β-D-glucopyranosyl-(−)-barbaloin, in agreement with the proposals of Wagner and Demuth (6). The circular dichroism spectra (see *Experimental*) of cascarosides A and B clearly showed that the two compounds are diastereoisomers that can be represented as I.

Oxidative Hydrolysis—The results in Table I confirm earlier findings (10) that anhydrous cascarosides A and B only yield about 40% aloe-emodin (theoretical 46.6%). Since the molecular weight of these cascarosides is now established to be 580, if they are quantitatively converted into aloe-emodin (molecular weight 270, $E^{1\%}_{1\,cm}$ = 500 nm in 1 *N* NaOH gives 320), they should have a corresponding $E^{1\%}_{1\,cm}$ value of 149. The average value in Table I is 127, which is very close to the value of 125 based on earlier samples and used in the recommended method (7). Therefore, the equivalent amount of dihydroxyanthraquinone used in the European Pharmacopoeia, 1971, should stand.

The comparatively low yield of aloe-emodin (86% of theory) is in marked contrast to results with barbaloin in identical oxidative hydrolysis conditions when almost quantitative conversion to aloe-emodin takes place (63.6% found, 64.6% theory) (9). Although Wagner and Demuth (6) obtained almost theoretical yields from samples of cascarosides A and B, this result was based on comparative oxidative hydrolysis of cascarosides and aloin. In absolute terms, their experimental results indicated that their cascaroside A yielded 21.3% aloe-emodin, their cascaroside B yielded 21.5% aloe-emodin, and their barbaloin yielded 31% aloe-emodin (theoretical 64.6%). Clearly, their oxidative hydrolysis conditions did not completely convert to aloe-emodin. Furthermore, their extinctions of the final red solution were not read at the maximum of about 500 nm ($E^{1\%}_{1\,cm}$ = 320) but at 546 nm. From our own curves of aloe-emodin in 1 *N* NaOH, the $E^{1\%}_{1\,cm}$ value at this wavelength is 194; this latter value was used in making our calculations.

REFERENCES

(1) J. W. Fairbairn and S. Simic, *J. Pharm. Pharmacol., Suppl.*, **12,** 45T (1960).

(2) J. W. Fairbairn, C. A. Friedmann, and S. Simic, *ibid.*, **15,** 292T (1963).

(3) G. Demuth, Inaugural Dissertation, L.-Maximil. Universität, München, West Germany, 1972.

(4) H. Wagner and G. Demuth, *Z. Naturforsch.*, **29c,** 204 (1974).

(5) F. J. Evans, J. W. Fairbairn, and J. D. Phillipson, *J. Pharm. Pharmacol., Suppl.*, **27,** 91P (1975).

(6) H. Wagner and G. Demuth, *Z. Naturforsch.*, **31b,** 267 (1976).

(7) *Analyst*, **98,** 830 (1973).

(8) L. Hörhammer, H. Wagner, and G. Bittner, *Pharm. Ztg.*, **108,** 259 (1963).

(9) J. W. Fairbairn and S. Simic, *J. Pharm. Pharmacol.*, **15,** 325 (1963).

(10) *Ibid.*, **16,** 450 (1964).

(11) H. R. Schulten and H. D. Beckey, *Org. Mass Spectrom.*, **7,** 1103 (1973).

(12) H. D. Beckey and H. R. Schulten, *Angew. Chem. Int. Ed.*, 14 (6), 403 (1975).

ACKNOWLEDGMENTS AND ADDRESSES

Received August 2, 1976, from the *Department of Pharmacognosy, School of Pharmacy, University of London, London WC1N 1AX, England.*

Accepted for publication December 1, 1976.

The authors are indebted to Dr. D. E. Games, Department of Chemistry, University of Wales, Cardiff, for determining the field desorption mass spectra, to Dr. P. M. Scopes, Department of Chemistry, Westfield College, University of London, for determining the circular dichroism spectra, and to Mr. D. Carter and Mr. W. Baldeo, Department of Pharmaceutical Chemistry, School of Pharmacy, University of London, for determining the mass and NMR spectra, respectively. They also thank Professor H. Wagner, University of Munich, West Germany, for a sample of aloe-emodin 8-glucoside. They are grateful to Mr. M. Bragg for technical assistance.

[x] To whom inquiries should be directed.

Evaluation of Immunosuppressive Potential of Cryogenine Using Developing and Established Adjuvant Arthritis in Rats

WILLIAM C. WATSON * and MARVIN H. MALONE ˣ

Abstract □ Both developing (Days −1–+12 relative to inoculation) and established (Days +18–+29) stages of *Mycobacterium butyricum* adjuvant-induced polyarthritis in rats were treated orally with cryogenine (100 mg/kg/day), a prototype anti-inflammatory (phenylbutazone, 100 mg/kg/day), or a prototype immunosuppressive (cyclophosphamide, 6 mg/kg/day). During developing adjuvant arthritis, cryogenine and phenylbutazone significantly reduced the nonimmune-mediated inflammation in the inoculated hindpaw. Neither cryogenine nor phenylbutazone provided protection against the development of the delayed-onset, immune-mediated inflammation and the reduction in growth rate seen after Day +12 in unmedicated rats. Cyclophosphamide failed to reduce the nonimmune-mediated inflammation, but it provided significant protection against both the delayed-onset, immune-mediated inflammation and the reduced growth rate. During established adjuvant arthritis, cryogenine and phenylbutazone were effective against the established inflammation, while cyclophosphamide was ineffective. These results confirm the known anti-inflammatory and immunosuppressive activities of phenylbutazone and cyclophosphamide, respectively, and indicate that cryogenine lacks immunosuppressive capability at the effective anti-inflammatory dosage level used.

Keyphrases □ Cryogenine—immunosuppressive activity evaluated in developing and established adjuvant arthritis, rats □ Immunosuppressive activity—cryogenine evaluated in developing and established adjuvant arthritis, rats □ Anti-inflammatory activity—cryogenine evaluated in developing and established adjuvant arthritis, rats

Cryogenine[1] (I), an isoquinolizidine lactone, mol. wt. 435.53, has been shown to be effective against adjuvant-induced polyarthritis in the rat (1). Protection was provided against the disseminated lesions during therapy, and a continued anti-inflammatory effect was noted after discontinuance of therapy. Because the disseminated lesions are thought to be immune mediated (2), it was considered possible that part of the pharmacological activity of I might be attributable to immunosuppression. Earlier investigations documented the anti-inflammatory effectiveness of I in experimental models of nonimmune-mediated inflammation: yeast-induced foot edema (3), cotton-pellet granuloma (4), carrageenan-induced foot edema (4–6), and UV-induced erythema (7).

The immune basis of various animal and human inflammatory conditions and the efficacy of immunotherapy in such conditions have been established (8). Perper *et al.* (9) were able to discriminate between clinically effective immunosuppressive agents and anti-inflammatory drugs by selectively treating animals during either the developing (Days 0–+12 relative to inoculation) or established (Days +18–+29) stages of adjuvant-induced arthritis. The present investigation attempted to determine the immunosuppressive capability of I in the intact rat using the experimental design employed by Perper *et al.* (9).

[1] For structure, see *Tetrahedron Lett.*, **30**, 3641 (1966). This drug is not to be confused with the trade name product Cryogénine (phenylsemicarbazide, mol. wt. 151.2) distributed by Laboratoires Sarbach, Châtillon, France.

EXPERIMENTAL

Animals—Approximately 7-week-old, male, Sprague–Dawley albino rats, 120–170 g, were allowed to acclimate for at least 6 days prior to experimentation. Body weights were checked for normal growth patterns. The animals were supplied with block lab chow[2] and water *ad libitum*.

Adjuvant Preparation and Inoculation—Heat-killed, desiccated *Mycobacterium butyricum*[3] was triturated initially with light mineral oil and then homogenized in a tissue homogenizer equipped with an electrically driven pestle (about 10 complete strokes with the pestle spinning at approximately 1500 rpm). The finely divided suspension was autoclaved at 49° at 20 psi for 20 min. The final adjuvant preparation represented 5 mg of *M. butyricum*/ml of oil (10).

On Day 0, animals were lightly anesthetized with pentobarbital sodium (30 mg/5 ml/kg ip), and adjuvant then was injected intradermally (0.05 ml) under the subplantar surface of the right hindpaw in the metatarsal region. Positive controls and drug-treated animals received the adjuvant inoculation, while negative controls received only a subplantar injection of light mineral oil.

Drugs—The following drugs were used: I base[4] (100 mg/kg/day), phenylbutazone[5] (100 mg/kg/day), and cyclophosphamide[6] (6 mg/kg/day). Each was suspended or dissolved in aqueous 0.25% agar[7] and orally administered in a dosage volume of 10 ml/kg. Negative and positive controls received 10 ml/kg of the agar vehicle only.

Developing Adjuvant Arthritis—Animals were randomly divided into the various treatment groups, 10 animals/group (except the negative control group which consisted of 12 animals). On Day −1, rats were dosed with either the agar vehicle or one drug treatment. Dosing continued once daily through Day +12.

Established Adjuvant Arthritis—Ten animals were randomly selected and designated as negative controls. The remaining animal population was inoculated with adjuvant. On Day +18, animals with left hindpaw volumes between 2.09 and 4.35 ml were randomly assigned (block randomization) to a treatment group, 10 animals/group. Animals were dosed with either the agar vehicle or a test drug, beginning on Day +18 and continuing daily through Day +29.

Evaluation of Adjuvant Arthritis—Experimental measurements began just prior to the inoculation and were repeated every 3rd day thereafter. Drug effects were assessed according to changes in body weight, generalized inflammatory symptoms, and hindpaw volume. Generalized inflammatory symptoms were evaluated according to a subjective scoring system similar to systems used previously (1, 11–13). Each of the three anatomical regions of both the forepaws (carpal, metacarpal, and phalanx) and the hindpaws (tarsal, metatarsal, and phalanx) was graded with respect to the severity of swelling (range 0–2); each forepaw or hindpaw was separately graded with respect to the severity of erythema (range 0–2); the tibiotarsal joints of both hindpaws were individually graded with respect to the degree of dorsiflexion (0 = 150° of movement, 1 = >60–<150°, 2 = 30–60°, and 3 = <30°); the tail was graded with respect to both the severity of swelling (range 0–2) and the number of nodules (range 0–2); and the auricles of both ears were separately graded with respect to both the severity of erythema (range 0–2) and the number of nodules (range 0–2).

With this scoring system, an animal on a given day could develop an inflammogram score ranging from 0 to 50. Volumes for both the inoculated and the contralateral hindpaws were determined to the top edge of the lateral malleolus using a mercury-displacement technique similar

[2] Purina Laboratory Chow.
[3] No. 0640-33, Difco Laboratories, Detroit, Mich.
[4] Isolated from the Mexican plant, *Heimia salicifolia* Link & Otto, in this laboratory.
[5] Ciba Pharmaceutical Co., Summit, N.J.
[6] Mead Johnson Laboratories, Evansville, Ind.
[7] No. 0140-01, Difco Laboratories, Detroit, Mich.

Table I—Drug Effects on Inflammogram Scores in Developing Adjuvant Arthritis [a]

Day	Positive Control, Mean Score ± *SE*	Cryogenine, 100 mg/kg		Phenylbutazone, 100 mg/kg		Cyclophosphamide, 6 mg/kg	
		Mean Score ± *SE*	Inhibition, %	Mean Score ± *SE*	Inhibition, %	Mean Score ± *SE*	Inhibition, %
+3	5.2 ± 0.3	4.6 ± 0.3	−12	4.2 ± 0.2	−19[b]	6.1 ± 0.3	—
+6	6.1 ± 0.6	4.8 ± 0.4	−21	3.7 ± 0.4	−39[c]	6.6 ± 0.4	—
+9	6.3 ± 0.6	4.5 ± 0.4	−28[b]	4.1 ± 0.5	−35[b]	6.7 ± 0.4	—
+12	10.2 ± 2.0	8.3 ± 1.7	−19	6.5 ± 1.1	−36	6.1 ± 0.4	−40
+15	14.8 ± 2.7	13.2 ± 2.7	−11	15.3 ± 1.9	—	6.4 ± 0.5	−57[b]
+18	17.6 ± 3.0	16.7 ± 2.7	−5	17.6 ± 2.4	—	9.0 ± 2.0	−49[b]
+21	18.0 ± 2.4	18.0 ± 2.4	—	15.6 ± 2.1	−13	10.4 ± 2.4	−42[b]
+24	16.4 ± 3.0	17.1 ± 2.8	—	14.2 ± 1.9	−13	4.8 ± 0.7	−71[c]
+27	15.3 ± 2.9	14.9 ± 2.0	−3	13.0 ± 1.8	−15	5.0 ± 0.7	−67[c]
+30	14.6 ± 3.3	14.3 ± 2.2	−2	12.1 ± 2.1	−17	6.4 ± 1.8	−56[b]

[a] Drugs administered orally daily from Day −1 through and including Day +12. The negative control mean score was zero at all times. [b] Significantly different from positive control values at $p = 0.05$. [c] Very significantly different from positive controls at $p = 0.01$.

to the one described by Winter and Nuss (14). A dynograph[8] connected to a strain-gauge pressure transducer[9] was employed for recording hindpaw volumes. Drug effects were translated in terms of percentage change of increased hindpaw volume as described by Newbould (15):

$$\text{percentage change} = 100\{1 - [(a - x)/(b - y)]\} \qquad \text{(Eq. 1)}$$

where y is the mean hindpaw volume of positive control rats immediately prior to adjuvant inoculation, b is the mean hindpaw volume of positive control rats on a particular day, x is the mean hindpaw volume of drug-treated rats immediately prior to adjuvant inoculation, and a is the mean hindpaw volume of drug-treated rats on a particular day. Statistical analyses were generated using the Student t test.

RESULTS AND DISCUSSION

Treatment of Developing Adjuvant Arthritis—The inoculation of the rat hindpaw with adjuvant initially produces a nonimmune-mediated acute inflammatory reaction (16, 17). This reaction, characterized by swelling and erythema of the inoculated hindpaw, usually reaches maximum intensity between 6 and 9 days after injection. The course of this acute reaction in the positive control animals can be seen in Fig. 1 (inoculated hindpaw volume) and Table I (inflammogram). Because the swelling and erythema represent symptoms of nonimmune-mediated inflammation, any drug reducing these symptoms may be considered to have anti-inflammatory activity (9).

Phenylbutazone significantly reduced inoculated hindpaw volume on Days +3 (53% inhibition), +6 (46%), and +9 (38%), and a significant reduction of the inflammogram score was noted on these days. Cyclophosphamide, a clinically effective immunosuppressive agent, was inactive against the nonimmune-mediated inflammatory symptoms. Compound I was significantly effective against inoculated hindpaw swelling on Days +3 (26% inhibition), +6 (32%), +9 (36%), and +12 (31%) and significantly reduced the inflammogram score on Day +9.

The secondary increase in hindpaw volume seen beginning on Day +15 (Fig. 1, positive controls) represents the development of immune-mediated inflammation. The increases in both the contralateral hindpaw volume (Fig. 2, positive controls) and the inflammogram score (Table I, positive controls) beginning around Day +12 represent the dissemination of the immune response (18, 19). Collectively, these delayed-onset symptoms in the rat represent the adjuvant arthritis syndrome (20). This syndrome has been linked to a delayed hypersensitivity reaction specifically triggered by sensitized lymph node cells released into the circulation between Days +8 and +14 (19).

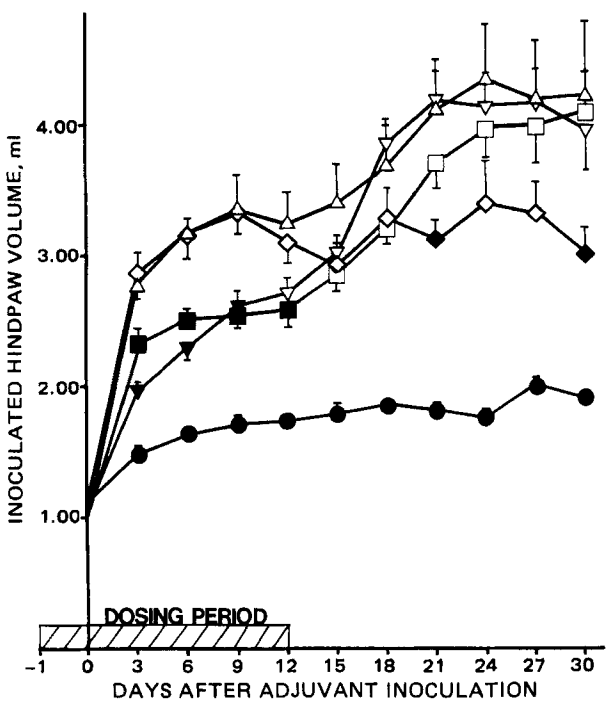

Figure 1—*Drug effects on inoculated hindpaw volume during developing adjuvant arthritis. Key:* ○, *negative control (10 ml/kg/day agar vehicle);* △, *positive control (10 ml/kg/day agar vehicle);* □, *cryogenine (100 mg/kg/day);* ▽, *phenylbutazone (100 mg/kg/day); and* ◇, *cyclophosphamide (6 mg/kg/day). Vertical bars indicate* ±SE. *Solid symbols indicate values significantly different from positive control values at* $p \leq 0.05$.

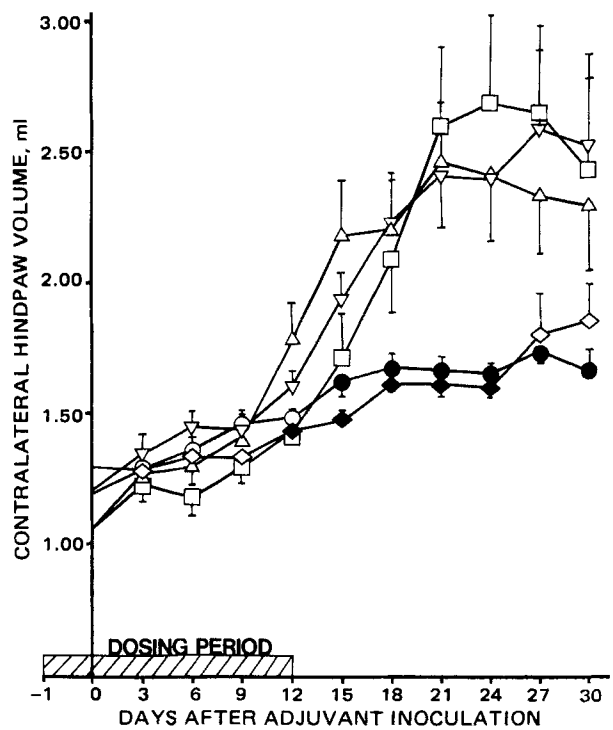

Figure 2—*Drug effects on contralateral hindpaw volume during developing adjuvant arthritis. Key:* ○, *negative control (10 ml/kg/day agar vehicle);* △, *positive control (10 ml/kg/day agar vehicle);* □, *cryogenine (100 mg/kg/day);* ▽, *phenylbutazone (100 mg/kg/day); and* ◇, *cyclophosphamide (6 mg/kg/day). Vertical bars indicate* ±SE. *Solid symbols indicate values significantly different from positive control values at* $p \leq 0.05$.

[8] Beckman RS.
[9] Statham.

Table II—Drug Effects on Body Weight in Developing Adjuvant Arthritis [a]

Day	Mean Body Weight, g ± *SE*				
	Negative Control	Positive Control	Cryogenine, 100 mg/kg	Phenylbutazone, 100 mg/kg	Cyclophosphamide, 6 mg/kg
0	152 ± 3	142 ± 4	140 ± 5	148 ± 5	155 ± 2
+3	166 ± 4[b]	148 ± 4	140 ± 5	153 ± 5	154 ± 4
+6	189 ± 5[b]	163 ± 5	158 ± 4	174 ± 6	171 ± 4
+9	213 ± 6[c]	179 ± 5	175 ± 5	194 ± 7	187 ± 5
+12	235 ± 7[c]	188 ± 7	182 ± 5	210 ± 8	203 ± 6
+15	256 ± 8[c]	198 ± 9	191 ± 5	220 ± 8	219 ± 6
+18	280 ± 7[c]	199 ± 11	195 ± 8	218 ± 9	229 ± 8[d]
+21	291 ± 10[c]	204 ± 14	200 ± 11	225 ± 11	243 ± 9[d]
+24	308 ± 11[c]	207 ± 17	194 ± 12	236 ± 10	256 ± 10[d]
+27	331 ± 10[c]	214 ± 18	204 ± 14	247 ± 11	272 ± 12[d]
+30	344 ± 10[c]	236 ± 19	217 ± 18	260 ± 12	295 ± 13[d]

[a] Drugs administered orally daily from Day −1 through and including Day +12. [b] Very significantly different from positive control values at $p = 0.01$. [c] Very highly significantly different from positive control values at $p = 0.001$. [d] Significantly different from positive control values at $p = 0.05$.

A drug that prevents the development of this syndrome when administered just up to the expected appearance of the associated inflammatory symptoms may be considered to have immunosuppressive activity (9). In the present study, cyclophosphamide was significantly effective in preventing the development of the delayed-onset, immune-mediated inflammatory syndrome. With respect to inoculated hindpaw volume (Fig. 1), cyclophosphamide pretreatment prevented the secondary increase. This reduction reached statistical significance on Day +21 (37% inhibition).

The total volume increase for the inoculated hindpaw seen after Day +12 (Fig. 1, positive controls) represents the sum of the residual nonimmune inflammatory effects resulting from the trauma of inoculation plus the immune-mediated inflammatory effects resulting from the delayed hypersensitivity reaction. In contrast, the increased volume of the contralateral hindpaw seen after Day +12 (Fig. 2, positive controls) can only represent immune-mediated inflammation (9). Cyclophosphamide significantly prevented the development of contralateral hindpaw edema (Fig. 2) on Days +12 (80% inhibition), +15 (85%), +18 (73%), +21 (77%), and +24 (78%). In addition, dissemination of immune-mediated inflammatory lesions to the forepaws, ears, and tail was significantly reduced beginning on Day +15 (Table I, inflammogram).

Body weights for animals during developing adjuvant arthritis are recorded in Table II. Growth rates for positive controls were significantly less than those for uninoculated negative control animals. These results are similar to those reported by others (1, 20). An observable reduction in growth rate is consistent with an ongoing, chronic, inflammatory disease. A drug treatment that prevents the development of the immune-mediated inflammatory syndrome, therefore, should prevent this reduced growth rate. Cyclophosphamide-pretreated animals grew at a significantly greater rate relative to the positive controls beginning on Day +18 (Table II). This effect on growth rate remained statistically significant through Day +30.

Phenylbutazone and I were ineffective in preventing the development of the immune-mediated inflammatory syndrome (Fig. 1, inoculated hindpaw volume; Fig. 2, contralateral hindpaw volume; and Table I, inflammogram) and in preventing the reduced growth rate (Table II).

Phenylbutazone treatment reduced the nonimmune-mediated acute inflammatory reaction in the inoculated hindpaw but failed to prevent the development of the immune-mediated inflammatory syndrome. Cyclophosphamide treatment failed to reduce the nonimmune-mediated

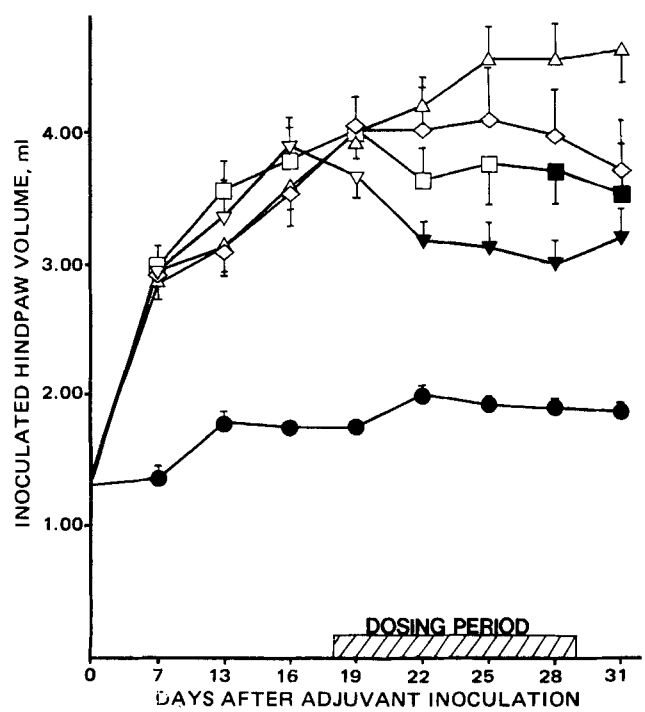

Figure 3—*Drug effects on inoculated hindpaw volume during established adjuvant arthritis. Key:* ○, *negative control (10 ml/kg/day agar vehicle);* △, *positive control (10 ml/kg/day agar vehicle);* □, *cryogenine (100 mg/kg/day);* ▽, *phenylbutazone (100 mg/kg/day); and* ◇, *cyclophosphamide (6 mg/kg/day). Vertical bars indicate* ±SE. *Solid symbols indicate values significantly different from positive control values at* $p \leq 0.05$.

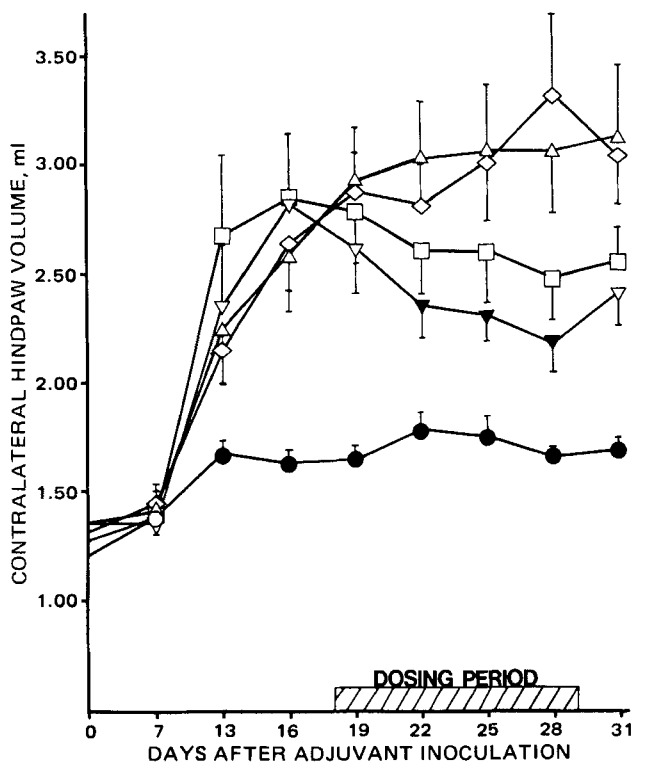

Figure 4—*Drug effects on contralateral hindpaw volume during established adjuvant arthritis. Key:* ○, *negative control (10 ml/kg/day agar vehicle);* △, *positive control (10 ml/kg/day agar vehicle);* □, *cryogenine (100 mg/kg/day);* ▽, *phenylbutazone (100 mg/kg/day); and* ◇, *cyclophosphamide (6 mg/kg/day). Vertical bars indicate* ±SE. *Solid symbols indicate values significantly different from positive control values at* $p \leq 0.05$.

Table III—Drug Effects on Inflammogram Scores in Established Adjuvant Arthritis [a]

Day	Positive Control, Mean Score ± *SE*	Cryogenine, 100 mg/kg		Phenylbutazone, 100 mg/kg		Cyclophosphamide, 6 mg/kg	
		Mean Score ± *SE*	Inhibition, %	Mean Score ± *SE*	Inhibition, %	Mean Score ± *SE*	Inhibition, %
+7	4.1 ± 0.4	5.7 ± 0.4[a]	—	4.6 ± 0.7	—	4.7 ± 0.8	—
+13	11.1 ± 2.2	16.8 ± 2.4	—	13.6 ± 2.2	—	13.3 ± 1.9	—
+16	18.3 ± 2.6	21.9 ± 2.7	—	20.7 ± 3.0	—	18.1 ± 2.3	—
+19	20.3 ± 2.0	21.9 ± 2.7	—	19.6 ± 2.5	−3	19.4 ± 2.0	−4
+22	19.4 ± 1.5	20.1 ± 2.3	—	18.4 ± 2.0	−5	19.3 ± 1.9	—
+25	20.1 ± 1.5	18.3 ± 2.5	−9	16.6 ± 2.0	−17	16.5 ± 2.6	−18
+28	19.9 ± 1.6	18.5 ± 2.7	−7	14.4 ± 2.2	−28	18.0 ± 2.9	−10
+31	20.1 ± 1.7	16.1 ± 3.0	−20	13.6 ± 1.8	−32[b]	16.8 ± 3.0	−16

[a] Drugs administered orally daily from Day +18 through and including Day +29. The negative control mean score was zero at all times. [b] Significantly different from positive control values at $p = 0.05$.

Table IV—Drug Effects on Body Weight in Established Adjuvant Arthritis [a]

Day	Mean Body Weight, g ± *SE*				
	Negative Control	Positive Control	Cryogenine, 100 mg/kg	Phenylbutazone, 100 mg/kg	Cyclophosphamide, 6 mg/kg
0	137 ± 4	143 ± 3	143 ± 4	145 ± 4	143 ± 5
+7	191 ± 7	180 ± 5	173 ± 4	175 ± 5	177 ± 5
+13	237 ± 9	205 ± 6	183 ± 5[b]	189 ± 6	194 ± 6
+16	261 ± 10[c]	203 ± 6	177 ± 7[b]	196 ± 10	186 ± 6
+19	281 ± 10[c]	198 ± 6	171 ± 8[b]	187 ± 9	180 ± 7
+22	298 ± 11[c]	194 ± 7	164 ± 9[b]	192 ± 12	178 ± 9
+25	310 ± 12[c]	200 ± 8	169 ± 10[b]	208 ± 12	181 ± 11
+28	323 ± 11[c]	208 ± 10	174 ± 13[b]	209 ± 14	184 ± 13
+31	329 ± 12[c]	212 ± 12	174 ± 16	231 ± 15	204 ± 14

[a] Drugs administered orally daily from Day +18 through and including Day +29. [b] Significantly different from positive control values at $p = 0.05$. [c] Very highly significantly different from positive control values at $p = 0.001$.

acute inflammatory reaction but prevented the development of the secondary immune-mediated syndrome. These results are in agreement with those observed previously (9). Results for I tended to parallel those of phenylbutazone. The activity observed against the nonimmune-mediated inflammatory reaction is consistent with the results recorded by Kosersky *et al.* (1).

Treatment of Established Adjuvant Arthritis—Sensitized lymph node cells are released into the circulation up to Day +14 (19). Pharmacological treatment during Days +18–+30 (*i.e.*, after the immunologically related induction period) should then detect only drugs having anti-inflammatory activity (9). However, this interpretation should be made cautiously, since (*a*) established adjuvant arthritis may be partially sustained by an autoimmune mechanism similar to the one proposed for rheumatoid arthritis (21–23), and (*b*) the hepatic microsomal mixed-function oxidase system is impaired in adjuvant arthritic rats during the established period of the disease (24).

In the present study, phenylbutazone treatment during Days +18 through +29 was significantly effective in reducing the already established chronic inflammation. Inoculated hindpaw volume (Fig. 3) was significantly reduced on Days +22 (37% inhibition), +25 (46%), +28 (50%), and +31 (45%). Contralateral hindpaw volume (Fig. 4) was significantly reduced on Days +22 (40% inhibition), +25 (44%), and +28 (52%). In addition, the inflammogram score (Table III) was significantly reduced on Day +31 (32% inhibition). Cyclophosphamide was ineffective against all of these experimental parameters. These results are in essential agreement with those of Perper *et al.* (9).

Treatment with I significantly reduced inoculated hindpaw volume (Fig. 3) on Days +28 (25% inhibition) and +31 (33%), but the apparent effects on contralateral hindpaw swelling (Fig. 4) and on the inflammogram score (Table III) were statistically not significant. Animals designated for treatment with I weighed significantly less than positive controls prior to the dosing period (Days +13 and +16) (Table IV). These animals continued to weigh significantly less through Day +28. The inflammogram score (Table III) was significantly greater prior to the dosing period (Day +7) for this same group of animals. On Day +18, the population of positive controls was randomly divided into the various drug treatment groups on the basis of an equivalent range of contralateral hindpaw swelling (*i.e.*, 2.09–4.35 ml). By chance, animals designated for I treatment may have been stronger reactors to the adjuvant inoculation. This possibility seems to explain the weight loss observed during drug treatment and accounts for why the drug's anti-inflammatory activity was less than expected. Previous investigators documented a weight gain for adjuvant-arthritic animals treated daily for 20 days with 100 mg/kg po of I (1). Moreover, in a preliminary study using a small group of rats with established adjuvant arthritis, I at 100 mg/kg po daily for 1 week appeared to reduce the already established inflammation (25).

The overall results using both developing and established treatment models tend to substantiate the known anti-inflammatory and immunosuppressive roles of phenylbutazone and cyclophosphamide, respectively. Assessment of the overall activity of I during both developing and established treatment periods suggests the lack of an immunosuppressive-type capability and supports previous investigations that indicated a nonimmune-type anti-inflammatory action mechanism for I (3–7).

REFERENCES

(1) D. S. Kosersky, J. K. Brown, and M. H. Malone, *J. Pharm. Sci.*, **62**, 1965 (1973).

(2) H. L. F. Currey and M. Ziff, *J. Exp. Med.*, **127**, 185 (1968).

(3) J. Jiu, *Lloydia*, **29**, 250 (1966).

(4) L. DeCato, Jr., J. K. Brown, and M. H. Malone, *Eur. J. Pharmacol.*, **26**, 22 (1974).

(5) Y.-C. Chang and M. H. Malone, *J. Pharm. Sci.*, **60**, 416 (1971).

(6) A. B. Kocialski, F. J. Marozzi, and M. H. Malone, *ibid.*, **61**, 1202 (1972).

(7) D. S. Kosersky, W. C. Watson, and M. H. Malone, *Proc. West. Pharmacol. Soc.*, **16**, 249 (1973).

(8) H. E. Paulus and M. W. Whitehouse, *Ann. Rev. Pharmacol.*, **13**, 107 (1973).

(9) R. J. Perper, B. Alvarez, C. Colombo, and H. Schroder, *Proc. Soc. Exp. Biol. Med.*, **137**, 506 (1971).

(10) M. W. Whitehouse, *Agents Actions*, **3**(4), 221 (1973).

(11) M. L. Graeme, E. Fabry, and E. B. Sigg, *J. Pharmacol. Exp. Ther.*, **153**, 373 (1966).

(12) K. F. Swingle, L. W. Jaques, and D. C. Kyam, *Proc. Soc. Exp. Biol. Med.*, **132**, 608 (1969).

(13) M. E. Rosenthale, *Arch. Int. Pharmacodyn. Ther.*, **188**, 14 (1970).

(14) C. A. Winter and G. W. Nuss, *Arthritis Rheum.*, **9**, 394 (1966).

(15) B. B. Newbould, *Br. J. Pharmacol.*, **21**, 127 (1963).

(16) B. B. Newbould, *Ann. Rheum. Dis.*, **23**, 392 (1964).

(17) L. Sokoloff, in "Mechanisms of Hypersensitivity," J. H. Schaffer, G. A. LoGrippo, and M. W. Chase, Eds., Little, Brown, Boston, Mass., 1959, p. 692.

(18) B. H. Waksman and C. Wennersten, *Int. Arch. Allergy*, **23**, 129 (1963).

(19) C. M. Pearson and F. D. Wood, *J. Exp. Med.*, **120**, 547 (1964).

(20) C. M. Pearson, *Proc. Soc. Exp. Biol. Med.*, **91**, 95 (1956).

(21) S. J. Piliero and C. Colombo, *J. Pharmacol. Exp. Ther.*, **165**, 294 (1969).
(22) G. Weissmann, *Lancet*, **2**, 1373 (1964).
(23) L. H. Katz, *Diss. Abstr.*, **28(B)**, 3937B (1968).
(24) M. W. Whitehouse and F. J. Beck, *Drug Metab. Disp.*, **1**, 251 (1973).
(25) D. S. Kosersky, Ph.D. dissertation, University of the Pacific, Stockton, Calif., 1971.

ACKNOWLEDGMENTS AND ADDRESSES

Received August 9, 1976, from the *Section of Physiology–Pharmacology, School of Pharmacy, University of the Pacific, Stockton, CA 95211.*

Accepted for publication December 1, 1976.

Presented at the Immunopharmacology/Anti-Inflammatory Section, American Society of Pharmacology and Experimental Therapeutics, Montreal meeting, August 1974, and at the Pharmacology and Toxicology Section, APhA Academy of Pharmaceutical Sciences, Chicago meeting, July 1974.

Supported in part by Research Grant AM-14066 from the National Institute of Arthritis and Metabolic Diseases, U.S. Public Health Service.

The authors acknowledge the technical assistance of Deborah Asrican Bailey and Nekati Aksoy.

* Present address: Flavor and Extract Manufacturers' Association of the United States, Washington, DC 20006.

[x] To whom inquiries should be directed.

Calcium–Prostaglandin Aggregation and Its Effect on Prostaglandin Uptake by Isolated Rabbit Intestine

ANWAR B. BIKHAZI *[x], NABIL S. NADIR *, and JEAN-JACQUES HAJJAR [‡]

Abstract □ A quantitative estimate of the role of calcium ions on the lipid–water partition coefficients of prostaglandin E_1 and dinoprost suggested the possibility of prostaglandin molecules and calcium ions aggregating in a 14:1 ratio to produce a lipid-soluble aggregate. The aggregation is postulated to be a characteristic of prostaglandin molecules as compared to simple fatty acids, *e.g.*, 1-octanoic acid, which, in the presence of calcium, behave differently than the prostaglandins. The uptake of prostaglandins by the mucosal surface of the rabbit intestine increased in the presence of calcium. For example, at 25 m*M* calcium, prostaglandin E_1 was transported at approximately twice the rate as in the system containing no calcium. The uptake rate of dinoprost was estimated to be three times faster with 10 m*M* calcium than in the absence of calcium. Therefore, it is proposed that a carrier-mediated diffusion process, for both the prostaglandin molecules and calcium ions, takes place in the uptake mechanism. Diffusion coefficients ranging from 0.48×10^{-5} to 7.19×10^{-5} cm²/sec and permeability coefficients ranging from 1.04×10^{-2} to 15.6×10^{-2} cm/sec were estimated for all systems studied.

Keyphrases □ Prostaglandin E_1—aggregation with calcium ions, effect on lipid–water partition coefficients and uptake by isolated rabbit intestine □ Dinoprost—aggregation with calcium ions, effect on lipid–water partition coefficients and uptake by isolated rabbit intestine □ Calcium ions—aggregation with prostaglandin E_1 and dinoprost, effect on lipid–water partition coefficients and uptake by isolated rabbit intestine □ Partition coefficients, lipid–water—prostaglandin E_1 and dinoprost, effect of aggregation with calcium ions □ Intestinal uptake, isolated—prostaglandin E_1 and dinoprost, effect of aggregation with calcium ions

Recent studies on the physical, physiological, and biochemical relationships between prostaglandin and calcium dealt with the cellular distribution of prostaglandins (1), the prostaglandin and cellular calcium interaction (2–5), and the effect of prostaglandin on the GI tract, including its influence on glucose, water, and electrolyte absorption (6–8). Very few studies attempted to explain the physical interaction between calcium and prostaglandins (9, 10).

The present study attempts to explain the nature of this interaction and to correlate the data to prostaglandin uptake by the intestinal mucosa of the rabbit.

EXPERIMENTAL

Partition Coefficient—The *n*-octane[1]–water, 1-octanol[2]–water, and 1-octanoic acid[3]–water partition coefficients of 5,6(n)-^{3}H-prostaglandin E_1[4] (I) and 5,6,8,11,12,14,15(n)-^{3}H-dinoprost (II) were measured as follows. In 10-ml screw-capped test tubes, 2.0 ml of the oil phase and 2.0 ml of a pH 5 aqueous phase containing the desired amount of I (24.4×10^{-9} m*M*), II (2.88×10^{-9} m*M*), and calcium ions (2.5, 5.0, 10.0, 25.0, 40.0, 50.0, 75.0, 100.0, 150.0, or 200.0 m*M*) were added. Prior to equilibration, nitrogen gas was cautiously bubbled into each test tube to ensure the displacement of air from the upper void spaces. The test tubes were then tightly capped and attached with rubber bands to the shaft of a rotating-bottle disintegration apparatus[5].

The apparatus with the test tubes was put in a stainless steel tank filled with water thermostatically controlled at 25°. The motor was allowed to rotate, mixing the two phases in the test tubes for 30 min. After equilibration, each test tube was detached from the apparatus and allowed to stand for 15 min at 25° for complete phase separation. Then 1.0 ml of each oil and aqueous phase was individually pipetted and assayed for I and II in a three-channel liquid scintillation spectrometer[6]. The calculated partition coefficients were the averages of four samples for each oil–water system.

The same procedure was followed for the estimation of the partition coefficient while varying the concentration of I and II and keeping the concentration of calcium ions constant (5 or 50 m*M*).

Partition Coefficient of 1-Octanoic Acid—Since prostaglandins are considered to be fatty acids, it was essential to compare their partition behavior with that of a fatty acid such as 1-octanoic acid in the presence of calcium ions. A potentiometric method was used for the quantitative analysis of 1-octanoic acid in the aqueous phase. A standard aqueous 1-octanoic acid solution (32.0 m*M*) was prepared and potentiometrically[7] titrated with 0.01 *N* sodium hydroxide. The standard solution was employed as the aqueous phase in the partition experiments after the addition of the desired amount of calcium ions (0, 100, or 200 m*M*). The oil phase chosen was 1-octanol.

Thus, for a single calcium-ion concentration system, two sets of 250-ml separators were prepared. For the 0 m*M* calcium system (A and A′),

[1] Eastman Kodak Co., Rochester, N.Y.
[2] Riedel-De Haen AG, Seelze-Hannover, West Germany.
[3] Hopkin and Williams Ltd., Chadwell Heath, Essex, England.
[4] Radiochemical Center, Amersham, Buckinghamshire, England.
[5] Ernest D. Menold, Lester, Pa.
[6] Packard Tri-Carb model 3320, Packard Instrument Co., Downers Grove, Ill.
[7] Radiometer, pH meter model 22, Copenhagen, Denmark.

(21) S. J. Piliero and C. Colombo, *J. Pharmacol. Exp. Ther.*, **165**, 294 (1969).
(22) G. Weissmann, *Lancet*, **2**, 1373 (1964).
(23) L. H. Katz, *Diss. Abstr.*, **28(B)**, 3937B (1968).
(24) M. W. Whitehouse and F. J. Beck, *Drug Metab. Disp.*, **1**, 251 (1973).
(25) D. S. Kosersky, Ph.D. dissertation, University of the Pacific, Stockton, Calif., 1971.

ACKNOWLEDGMENTS AND ADDRESSES

Received August 9, 1976, from the *Section of Physiology–Pharmacology, School of Pharmacy, University of the Pacific, Stockton, CA 95211.*

Accepted for publication December 1, 1976.

Presented at the Immunopharmacology/Anti-Inflammatory Section, American Society of Pharmacology and Experimental Therapeutics, Montreal meeting, August 1974, and at the Pharmacology and Toxicology Section, APhA Academy of Pharmaceutical Sciences, Chicago meeting, July 1974.

Supported in part by Research Grant AM-14066 from the National Institute of Arthritis and Metabolic Diseases, U.S. Public Health Service.

The authors acknowledge the technical assistance of Deborah Asrican Bailey and Nekati Aksoy.

* Present address: Flavor and Extract Manufacturers' Association of the United States, Washington, DC 20006.

[x] To whom inquiries should be directed.

Calcium–Prostaglandin Aggregation and Its Effect on Prostaglandin Uptake by Isolated Rabbit Intestine

ANWAR B. BIKHAZI *[x], NABIL S. NADIR *, and JEAN-JACQUES HAJJAR [‡]

Abstract □ A quantitative estimate of the role of calcium ions on the lipid–water partition coefficients of prostaglandin E_1 and dinoprost suggested the possibility of prostaglandin molecules and calcium ions aggregating in a 14:1 ratio to produce a lipid-soluble aggregate. The aggregation is postulated to be a characteristic of prostaglandin molecules as compared to simple fatty acids, *e.g.*, 1-octanoic acid, which, in the presence of calcium, behave differently than the prostaglandins. The uptake of prostaglandins by the mucosal surface of the rabbit intestine increased in the presence of calcium. For example, at 25 m*M* calcium, prostaglandin E_1 was transported at approximately twice the rate as in the system containing no calcium. The uptake rate of dinoprost was estimated to be three times faster with 10 m*M* calcium than in the absence of calcium. Therefore, it is proposed that a carrier-mediated diffusion process, for both the prostaglandin molecules and calcium ions, takes place in the uptake mechanism. Diffusion coefficients ranging from 0.48×10^{-5} to 7.19×10^{-5} cm²/sec and permeability coefficients ranging from 1.04×10^{-2} to 15.6×10^{-2} cm/sec were estimated for all systems studied.

Keyphrases □ Prostaglandin E_1—aggregation with calcium ions, effect on lipid–water partition coefficients and uptake by isolated rabbit intestine □ Dinoprost—aggregation with calcium ions, effect on lipid–water partition coefficients and uptake by isolated rabbit intestine □ Calcium ions—aggregation with prostaglandin E_1 and dinoprost, effect on lipid–water partition coefficients and uptake by isolated rabbit intestine □ Partition coefficients, lipid–water—prostaglandin E_1 and dinoprost, effect of aggregation with calcium ions □ Intestinal uptake, isolated—prostaglandin E_1 and dinoprost, effect of aggregation with calcium ions

Recent studies on the physical, physiological, and biochemical relationships between prostaglandin and calcium dealt with the cellular distribution of prostaglandins (1), the prostaglandin and cellular calcium interaction (2–5), and the effect of prostaglandin on the GI tract, including its influence on glucose, water, and electrolyte absorption (6–8). Very few studies attempted to explain the physical interaction between calcium and prostaglandins (9, 10).

The present study attempts to explain the nature of this interaction and to correlate the data to prostaglandin uptake by the intestinal mucosa of the rabbit.

EXPERIMENTAL

Partition Coefficient—The *n*-octane[1]–water, 1-octanol[2]–water, and 1-octanoic acid[3]–water partition coefficients of 5,6(n)-^{3}H-prostaglandin E_1[4] (I) and 5,6,8,11,12,14,15(n)-^{3}H-dinoprost (II) were measured as follows. In 10-ml screw-capped test tubes, 2.0 ml of the oil phase and 2.0 ml of a pH 5 aqueous phase containing the desired amount of I (24.4×10^{-9} m*M*), II (2.88×10^{-9} m*M*), and calcium ions (2.5, 5.0, 10.0, 25.0, 40.0, 50.0, 75.0, 100.0, 150.0, or 200.0 m*M*) were added. Prior to equilibration, nitrogen gas was cautiously bubbled into each test tube to ensure the displacement of air from the upper void spaces. The test tubes were then tightly capped and attached with rubber bands to the shaft of a rotating-bottle disintegration apparatus[5].

The apparatus with the test tubes was put in a stainless steel tank filled with water thermostatically controlled at 25°. The motor was allowed to rotate, mixing the two phases in the test tubes for 30 min. After equilibration, each test tube was detached from the apparatus and allowed to stand for 15 min at 25° for complete phase separation. Then 1.0 ml of each oil and aqueous phase was individually pipetted and assayed for I and II in a three-channel liquid scintillation spectrometer[6]. The calculated partition coefficients were the averages of four samples for each oil–water system.

The same procedure was followed for the estimation of the partition coefficient while varying the concentration of I and II and keeping the concentration of calcium ions constant (5 or 50 m*M*).

Partition Coefficient of 1-Octanoic Acid—Since prostaglandins are considered to be fatty acids, it was essential to compare their partition behavior with that of a fatty acid such as 1-octanoic acid in the presence of calcium ions. A potentiometric method was used for the quantitative analysis of 1-octanoic acid in the aqueous phase. A standard aqueous 1-octanoic acid solution (32.0 m*M*) was prepared and potentiometrically[7] titrated with 0.01 *N* sodium hydroxide. The standard solution was employed as the aqueous phase in the partition experiments after the addition of the desired amount of calcium ions (0, 100, or 200 m*M*). The oil phase chosen was 1-octanol.

Thus, for a single calcium-ion concentration system, two sets of 250-ml separators were prepared. For the 0 m*M* calcium system (A and A′),

[1] Eastman Kodak Co., Rochester, N.Y.
[2] Riedel-De Haen AG, Seelze-Hannover, West Germany.
[3] Hopkin and Williams Ltd., Chadwell Heath, Essex, England.
[4] Radiochemical Center, Amersham, Buckinghamshire, England.
[5] Ernest D. Menold, Lester, Pa.
[6] Packard Tri-Carb model 3320, Packard Instrument Co., Downers Grove, Ill.
[7] Radiometer, pH meter model 22, Copenhagen, Denmark.

Table I—Effect of Varying Calcium Concentration on the Apparent Partition Coefficient[a] (k') of I in *n*-Octane–Water, 1-Octanol–Water, and 1-Octanoic Acid–Water Systems

Calcium-Ion Concentration, mM[b]	$k' \times 10^{-2}$, *n*-Octane–Water	k', 1-Octanol–Water	k', 1-Octanoic Acid–Water
0	3.20[c]	59.68[c]	17.67[c]
2.5	3.04	66.12	17.50
10.0	3.07	69.34	19.70
25.0	3.20	74.25	19.29
40.0	3.39	80.14	21.38
50.0	3.48	86.53	20.75
75.0	3.75	85.92	22.39
100.0	3.96	88.97	23.92
150.0	—	91.85	24.70
200.0	4.05	98.61	26.40

[a] The k' values are averages of at least four samples. [b] At pH 5. [c] The k' values at 0 mM calcium are values for k, the true partition coefficient.

separator A contained 200 ml of 32 mM 1-octanoic acid as the aqueous phase, while separator A′ contained 200 ml of double-distilled water as the aqueous phase. To sets A and A′, 0.5 ml of 1-octanol as the oil phase was added. For the 100 mM calcium system (B and B′), separator B contained 200 ml of 32 mM 1-octanoic acid with 100 mM calcium ions in the aqueous phase, while B′ contained only 200 ml of 100 mM calcium ions as the aqueous phase. A 0.5-ml aliquot of 1-octanol was added to sets B and B′ as the oil phase. For the 200 mM calcium system (C and C′), separator C contained 200 ml of 32 mM 1-octanoic acid with 200 mM calcium ions in the aqueous phase, while C′ contained only 200 ml of 200 mM calcium as the aqueous phase. A 0.5-ml aliquot of 1-octanol was added to sets C and C′ as the oil phase.

The aqueous phases in all sets were adjusted to pH 5 before equilibration. The separators were shaken after attachment to the rotating-bottle disintegration apparatus for 30 min at 25°. After equilibration was completed, 100 ml of the aqueous phase was filtered through analytical filter paper. The filtrate was potentiometrically assayed for 1-octanoic acid left in the aqueous phase. The volume of 0.01 N sodium hydroxide consumed by sets A′, B′, and C′ was subtracted as controls from the volume consumed by sets A, B, and C, respectively. If the difference in volume of base consumed was not altered, calcium ions had no effect on the partition behavior of 1-octanoic acid between the 1-octanol and the water phase.

Uptake of I and II by Isolated Rabbit Intestine—The treatment of animals, apparatus, and sampling and assay of samples were described previously (11). Ringer's solution was not employed in the present study. Instead, four calcium chloride solutions (0, 10, 25, and 50 mM) were prepared and made isotonic with sodium chloride. The pH of all solutions was adjusted to 5. Into these isotonic solutions, the desired amount of I (24.4×10^{-9} mM) or II (2.88×10^{-9} mM) was added.

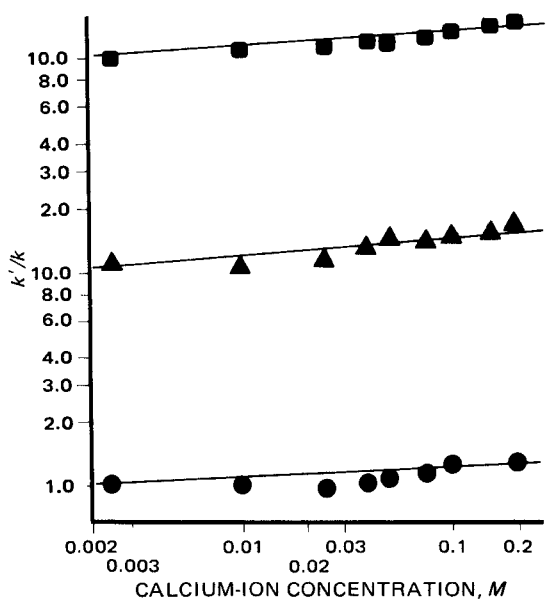

Figure 1—*Least-squares line plot of log* k′/k versus *log calcium concentration as applied to Eq. 8 for I. Key:* ●, n-*octane–water;* ▲, *1-octanol–water; and* ■, *1-octanoic acid–water.*

Table II—Effect of Varying Calcium Concentration on the Apparent Partition Coefficient[a] (k') of II in *n*-Octane–Water, 1-Octanol–Water, and 1-Octanoic Acid–Water Systems

Calcium-Ion Concentration, mM[b]	$k' \times 10^{-2}$, *n*-Octane–Water	k', 1-Octanol–Water	k', 1-Octanoic Acid–Water
0	1.86[c]	125.25[c]	37.40[c]
2.5	2.02	130.00	36.70
10.0	2.08	134.50	39.40
25.0	2.05	138.50	45.90
40.0	2.22	136.00	45.00
50.0	2.37	146.75	47.60
75.0	2.52	161.75	51.30
100.0	3.12	169.00	53.40
150.0	3.43	178.50	57.00
200.0	3.63	189.25	60.20

[a] The k' values are averages of at least four samples. [b] At pH 5. [c] The k' values at 0 mM calcium are values of k, the true partition coefficient.

Calculations—*Partition Coefficient Studies*—The true partition coefficient, k, is defined as:

$$k = \frac{[PG]_{TO}}{[PG]_{TW}} \qquad \text{(Eq. 1)}$$

where $[PG]_{TO}$ represents the total concentration of prostaglandin in the oil phase, and $[PG]_{TW}$ is the total concentration of prostaglandin in the water phase at equilibrium. At pH 5 [the pKa of prostaglandins is ~6.3 (12)] and at 0 mM calcium-ion concentration, Eq. 1 completely applies. But in the presence of calcium ions in the aqueous phase and at pH 5, it is assumed that the total prostaglandin concentration in the aqueous phase is:

$$[PG]_{TW} = [PG]_{FW} + [PG(Ca^{2+})_n]_W \qquad \text{(Eq. 2)}$$

where $[PG]_{FW}$ is the concentration of the free prostaglandin in equilibrium with the prostaglandin–calcium complex, $[PG(Ca^{2+})_n]_W$, in the aqueous phase. Therefore, the apparent partition coefficient, k', can be defined as:

$$k' = \frac{[PG]_{TO}}{[PG]_{FW} + [PG(Ca^{2+})_n]_W} \qquad \text{(Eq. 3)}$$

If it is assumed that the reaction mechanism of the formation of the complex, $[PG(Ca^{2+})_n]_W$, is:

$$PG + nCa^{2+} \rightleftharpoons PG(Ca^{2+})_n$$

then:

$$K_d = \frac{[PG]_{FW}[Ca^{2+}]_W{}^n}{[PG(Ca^{2+})_n]_W} \qquad \text{(Eq. 4)}$$

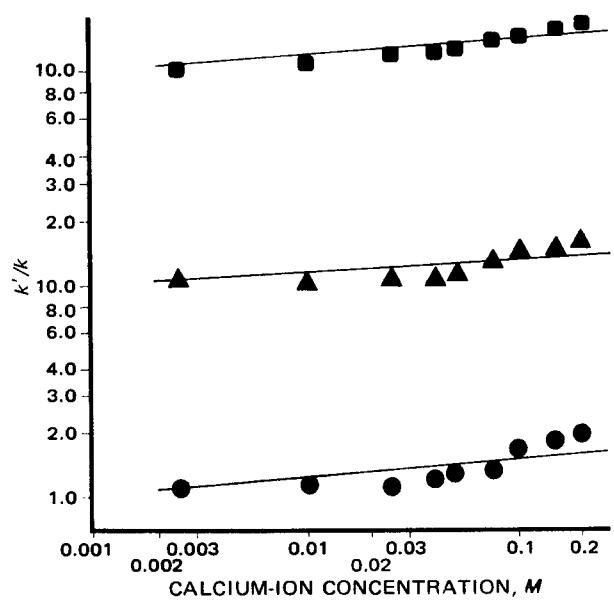

Figure 2—*Least-squares line plot of log* k′/k versus *log calcium concentration as applied to Eq. 8 for II. Key:* ●, n-*octane–water;* ▲, *1-octanol–water; and* ■, *1-octanoic acid–water.*

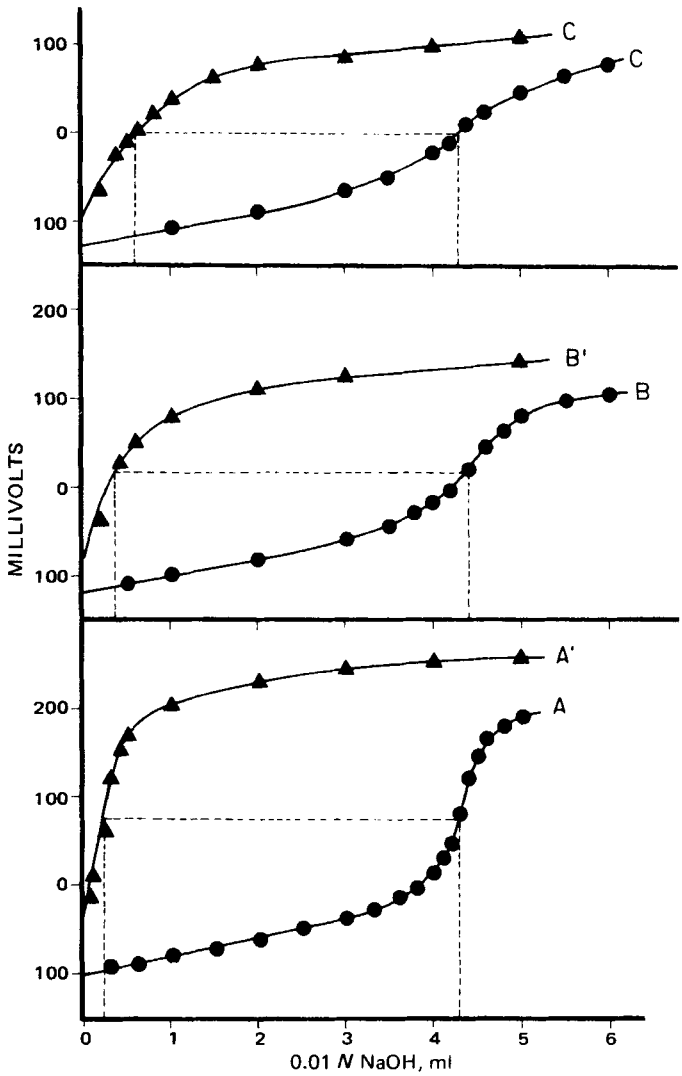

Figure 3—*Potentiometric titration plot of millivolts* versus *milliliters of 0.01* N *sodium hydroxide for 1-octanoic acid in the aqueous phase left after partitioning. Key: A and A' represent the 0 m*M *calcium system, and the volume of base consumed was 4.10 ml; B and B' represent the 100 m*M *calcium system, and the volume of base consumed was 4.05 ml; and C and C' represent the 200 m*M *calcium system, and the volume of base consumed was 3.70 ml.*

where K_d is the dissociation constant of the complex. Rearranging Eq. 4 and substituting for $[PG]_{FW}$ into Eq. 3 would result in:

$$k' = \frac{[PG]_{TO}[Ca^{2+}]_W{}^n}{([PG(Ca^{2+})_n]_W)(K_d + [Ca^{2+}]_W{}^n)} \quad \text{(Eq. 5)}$$

Eagling *et al.* (10) reported K_d values in the range of 24 ± 8; since $[Ca^{2+}]$ is in millimoles per liter, one can assume that $K_d > [Ca^{2+}]_W{}^n$. Therefore, Eq. 5 is reduced to:

$$k' = \frac{[PG]_{TO}[Ca^{2+}]_W{}^n}{([PG(Ca^{2+})_n]_W)(K_d)} \quad \text{(Eq. 6)}$$

Dividing the numerator and the denominator of Eq. 6 by $[PG]_{TW}$, substituting with Eq. 1, and rearranging yield:

$$\frac{k'}{k} = \frac{[Ca^{2+}]_W{}^n}{\frac{[PG(Ca^{2+})_n]_W}{[PG]_{TW}} K_d} \quad \text{(Eq. 7)}$$

Taking the logarithm of both sides of Eq. 7, one gets:

$$\log \frac{k'}{k} = n \log[Ca^{2+}]_W - \log \frac{[PG(Ca^{2+})_n]_W}{[PG]_{TW}} K_d \quad \text{(Eq. 8)}$$

From Eq. 8, the plot of $\log k'/k$ *versus* $\log [Ca^{2+}]_W$ should be linear with a slope equal to n.

Intestinal Uptake Studies—The apparatus and the mathematical model utilized were as reported previously (11). The following relationships describe the situation for the uptake rate:

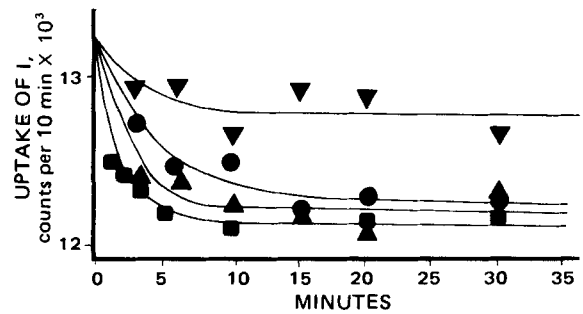

Figure 4—*Plot of* ^{3}*H-labeled I in counts per 10 min left in solution* versus *time in minutes. Key:* ●, *0 m*M *calcium;* ■, *10 m*M *calcium;* ▲, *25 m*M *calcium; and* ▼, *50 m*M *calcium.*

$$\frac{d[PG]_{TW}}{dt} = -\frac{D_W A}{h V_W}[PG]_{TW} \quad \text{(Eq. 9)}$$

Separating variables and integrating yield:

$$\ln [PG]_{TW} = -\frac{D_W A}{h V_W} t + \text{constant} \quad \text{(Eq. 10)}$$

where D_W represents the aqueous solute diffusion coefficient, A is the total surface area of exposed mucosal surface, h is the diffusion layer thickness, V_W is the aqueous bulk volume, and t is time. Therefore, when the partition coefficient, k', of the solute is relatively large, the data are expected to deviate from linearity at large t. Consequently, a semilogarithmic plot of $[PG]_{TW}$ *versus* t yields a straight line at the initial data points whose slope $[-(D_W A/hV_W)]$ is the initial uptake rate constant. Values of h, V_W, and A were experimentally measured and reported (11). The value of D_W can be calculated from measurement of the initial rate. The permeability coefficient, $P = D_W/h$, is also calculated.

RESULTS

Partition Coefficient of I in Oil–Water Systems—Table I shows the true (k at 0 mM calcium ions) and the apparent (k') partition coefficients calculated for I in n-octane–water, 1-octanol–water, and 1-octanoic acid–water systems. When Eq. 8 was applied to the data of Table I, Fig. 1 was obtained. The best straight lines through all points were drawn utilizing the method of least squares. The best least-squares line fits shown in Fig. 1 gave average slopes of approximately 0.07. Thus, the value of n in Eq. 8 is 0.07. Therefore, for every 14 molecules of I, one ion of calcium is needed to produce the complex.

Partition Coefficient of II in Oil–Water Systems—The true (k at 0 mM calcium ions) and apparent (k') partition coefficients of II are reported in Table II. Figure 2 represents a plot of $\log k'/k$ *versus* $\log [Ca^{2+}]$ of the data in Table II. The average slope of the least-squares lines in Fig. 2 was calculated to be around 0.07 and, therefore, is equal to n in Eq. 8. Thus, 14 molecules of II interact with one ion of calcium to produce the complex.

Effect of Calcium Ions on Partitioning of 1-Octanoic Acid in 1-Octanol–Water System—Figure 3 represents the data of the potentiometric titration of 1-octanoic acid with 0.01 N sodium hydroxide. For the 0 mM calcium system, 4.10 ml of 0.01 N sodium hydroxide was consumed for titrating the 1-octanoic acid remaining in the aqueous phase

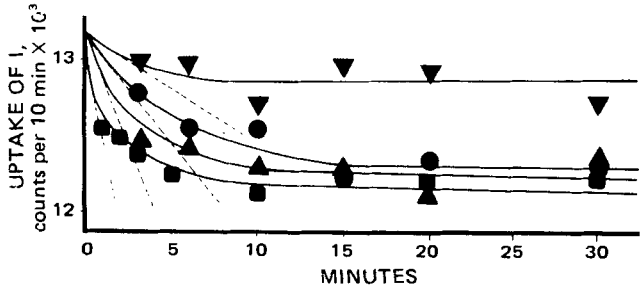

Figure 5—*Semilogarithmic plot of* ^{3}*H-labeled I in counts per 10 min left in solution* versus *time in minutes. Key:* ●, *0 m*M *calcium;* ■, *10 m*M *calcium;* ▲, *25 m*M *calcium; and* ▼, *50 m*M *calcium. The dotted lines join the early experimental data points. Their slopes were employed in the treatment of the data.*

Table III—Estimated Initial Rates and Relative Initial Rates of I and II into Rabbit Intestine as a Function of Calcium-Ion Concentration

Calcium-Ion Concentration, mM[a]	Initial Rate Constant[b], min^{-1}	Relative Initial Rate Constant[c]
	Compound I	
0	0.0163	1.00
10.0	0.0492	3.00
25.0	0.0242	1.48
50.0	0.0064	0.40
	Compound II	
0	0.0395	1.00
10.0	0.0552	1.40
25.0	0.0948	2.40
50.0	0.0208	0.525

[a] At pH 5. [b] Calculated from the first few experimental points of the semilogarithmic plot. [c] Calculated by dividing the initial rate in the presence of calcium ions by the initial rate at 0 mM calcium.

after equilibration. The volumes of base consumed for the 100 and 200 mM calcium systems were 4.05 and 3.70 ml of 0.01 N sodium hydroxide, respectively. It was concluded, therefore, that the distribution of 1-octanoic acid between 1-octanol and water was not drastically influenced by calcium ions. For example, 4.10 and 4.05 ml of 0.01 N sodium hydroxide were needed to titrate the remaining 1-octanoic acid in the aqueous phase, after equilibration, for the 0 and 100 mM calcium-ion systems, respectively.

Effect on Partition Coefficient of Varying Prostaglandin Concentration while Keeping Calcium Concentration Constant—There was no observable effect on the apparent partition coefficient when varying the I and II concentrations while keeping the calcium concentration constant.

Uptake of I by Isolated Rabbit Intestine—Figure 4 is a rectangular coordinate plot of I (in counts per 10 min) remaining in solution *versus* time in minutes. Each point on the graph represents at least four experimental runs. Figure 5 represents the corresponding semilogarithmic plot of I concentration in counts per 10 min *versus* time. The dotted lines are extensions of the slopes to the curves through the initial data points.

The calculated initial rate constants from the slopes are reported in Table III. The data indicated an increase in the initial rates at 10 and 25 mM calcium ions as compared to the 0 mM calcium concentration. At 50 mM calcium, the rate decreased to a value smaller than the rate at the 0 mM calcium-ion concentration.

Uptake of II by Isolated Rabbit Intestine—Figures 6 and 7 represent the rectangular and semilogarithmic plots, respectively, of II in counts per 10 min left *versus* time in minutes. The data for II showed an increase in the initial rate constant and relative initial rates at 10 and 25 mM calcium as compared to the 0 mM calcium-ion concentration system (Table III). At 50 mM calcium, the rate decreased to a lower value than in the absence of calcium ions.

DISCUSSION

The results of the partition coefficient studies revealed that I and II interacted with calcium to produce a lipid-soluble complex. As compared with ordinary fatty acids, I and II showed an increase in the oil–water partition coefficient in the presence of calcium ions. The partition coefficient of 1-octanoic acid between oil and water was not altered in the presence of calcium ions. Therefore, the acid (pKa ~6.3) at pH 5 apparently did not favor coordination with the ionic species, thus resulting in

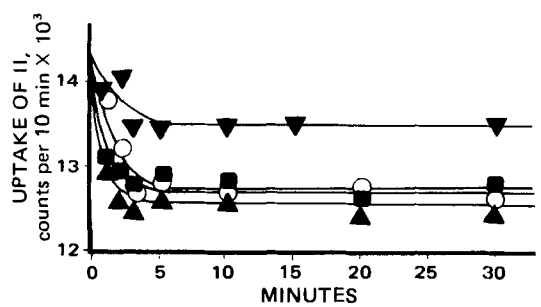

Figure 6—*Plot of ^3H-labeled II in counts per 10 min left in solution* versus *time in minutes. Key:* ○, *0 m*M *calcium;* ■, *10 m*M *calcium;* ▲, *25 m*M *calcium; and* ▼, *50 m*M *calcium.*

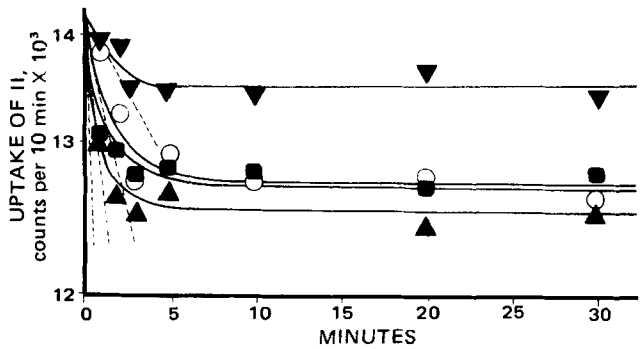

Figure 7—*Semilogarithmic plot of ^3H-labeled II in counts per 10 min left in solution* versus *time in minutes. Key:* ○, *0 m*M *calcium;* ■, *10 m*M *calcium;* ▲, *25 m*M *calcium; and* ▼, *50 m*M *calcium. The dotted lines join the early experimental data points. Their slopes were employed in the treatment of the data.*

an unsubstantial increase in the oil–water partition coefficient. If conditions were identical with I and II, their oil–water partition coefficients would remain unchanged in the presence of calcium. However, there was a substantial increase in the partition coefficients. Therefore, although I and II may not have favored coordination with calcium at pH 5, they were intermolecularly aggregating (9) to produce aggregates in a ratio of 14 prostaglandin molecules to one calcium ion. The formation of the lipid-soluble aggregate could be explained on the basis of intermolecular hydrophilic and/or hydrophobic bonding, probably similar to surfactant aggregation in micelle formation.

Tables I and II show that the partition coefficients of I (which is less polar than II) were higher in the less polar oil–water systems, namely, the *n*-octane–water and 1-octanoic acid–water systems. Even though the presence of calcium ions increased the lipid solubility of I and II, the inherent polarity of the prostaglandin molecules in the aggregated state showed the same effect on the k' values.

The transport studies of I and II through the mucosal surface of the isolated rabbit intestine revealed a direct influence of calcium ions on prostaglandin uptake. The apparatus and techniques employed (11) assured constant hydrodynamics at the mucosal surface and, therefore, allowed the quantitative estimation of initial rates, diffusion coefficients, and permeability coefficients.

Table III reports the estimated initial uptake rates for I and II by the rabbit intestine in the absence and presence of calcium. At 10 and 25 mM calcium, the relative initial uptake rates increased but were followed by a decrease at 50 mM calcium. The decrease at 50 mM calcium may be attributed to the toxic effect of calcium on the mucosal membrane at such a relatively high concentration. The increase in the relative initial uptake rates at 10 and 25 mM calcium may result from an increase in the mucosal–water partition tendency of prostaglandins in the prostaglandin–calcium aggregated form; *i.e.*, the calcium ions and/or the prostaglandin molecules could be acting as carrier species (9) in the uptake process.

Table IV includes the estimated diffusion and permeability coefficients of I and II utilizing the data in Table III. The estimated diffusion coefficient values of I and II in the absence of calcium should theoretically be equal when calculated by the Stokes–Einstein approximation (D_W = 2–4 × 10^{-5} cm^2/sec). Table IV revealed the D_W value of I to be almost twice as large as that of II at 0 mM calcium, which is in the order of magnitude of the ratio of their partition coefficients. The estimated

Table IV—Estimated Diffusion and Permeability Coefficients of I and II Uptake into Rabbit Intestine as a Function of Calcium-Ion Concentration

Calcium-Ion Concentration, mM[a]	Diffusion Coefficient, $cm^2/sec \times 10^{-5}$	Permeability Coefficient, $cm/sec \times 10^{-2}$
	Compound I	
0	2.92	6.34
10.0	4.26	9.26
25.0	7.19	15.60
50.0	1.57	3.41
	Compound II	
0	1.23	2.70
10.0	3.73	8.10
25.0	1.83	4.00
50.0	0.48	1.04

[a] At pH 5.

diffusion coefficients for I and II increased as the calcium concentration increased and then decreased at the 50 m*M* level. The corresponding permeability coefficients agreed fairly well with the sequence of the results. At 0 m*M* calcium, the estimated permeability coefficient of I is almost double that of II, which is also in the order of magnitude of the ratios of their partition coefficients. The permeability coefficients increased with an increase in the calcium-ion concentration, followed by a decrease at the 50 m*M* calcium level.

It is, therefore, proposed that both the prostaglandin molecules and the calcium ions constituting the aggregates crossed intact the diffusion barrier into the mucosal surface. Both species were self-carried in a fashion similar to a carrier-mediated process through the intestinal membrane.

These results may be important in understanding prostaglandin movement through biological fluids and membranes.

REFERENCES

(1) S. M. M. Karim, K. Hillier, and J. Devlin, *J. Pharm. Pharmacol.*, **20**, 749 (1968).

(2) T. M. Parkinson, J. C. Schneider, Jr., J. J. Krake, and W. L. Miller, *Life Sci.*, **7**, 883 (1968).

(3) E. Carafoli and F. Crovetti, *Arch. Biochem. Biophys.*, **154**, 40 (1973).

(4) M. E. Carsten, *Am. J. Obstet. Gynecol.*, **117**, 824 (1973).

(5) P. Hedqvist, *Acta Physiol. Scand.*, **90**, 153 (1974).

(6) C. Matuchansky and J. J. Bernier, *Gastroenterology*, **64**, 1111 (1973).

(7) S. L. Waller, *Gut*, **14**, 402 (1973).

(8) Y. Graziani and A. Livne, *Biochim. Biophys. Acta*, **291**, 612 (1973).

(9) S. J. Kirtland and H. Baum, *Nature New Biol.*, **236**, 47 (1972).

(10) E. M. Eagling, H. G. Lovell, and V. R. Pickles, *Br. J. Pharmacol.*, **44**, 510 (1972).

(11) A. B. Bikhazi and J. J. Hajjar, *J. Pharm. Sci.*, **63**, 1703 (1974).

(12) P. W. Ramwell, J. E. Shaw, G. B. Clarke, M. F. Grostic, D. G. Kaiser, and J. E. Pike, "Prostaglandins in Progress in the Chemistry of Fats and Other Lipids," vol. IX, Part 2, Pergamon, New York, N.Y., 1968.

ACKNOWLEDGMENTS AND ADDRESSES

Received November 24, 1975, from the **School of Pharmacy and the ‡Physiology Department, American University of Beirut, Beirut, Lebanon.*

Accepted for publication December 2, 1976.

Presented at the Basic Pharmaceutics Section, APhA Academy of Pharmaceutical Sciences, Atlanta meeting, November 1975.

Supported in part by a grant from the University Medical Research Fund, American University of Beirut, Beirut, Lebanon.

[x] To whom inquiries should be directed.

Thermal Decomposition of Amorphous β-Lactam Antibacterials

M. J. PIKAL [x], A. L. LUKES, and J. E. LANG

Abstract □ Thermal decomposition rates for amorphous samples of penicillin G potassium, cephalothin sodium, cefamandole sodium, and cefamandole nafate were determined as a function of water content and temperature. Even when rigorously dry, amorphous cephalosporins were at least one order of magnitude less stable than the corresponding unsolvated crystalline form. Absorbed water generally increased both the number of decomposition products and the net decomposition rate. Reaction kinetics were usually apparent first order, but an anomalously high effective reaction order was observed in several systems. Nonlinear Arrhenius plots were observed, and a qualitative model based on molecular relaxation in glasses is proposed. Although decomposition rates at 25° were small for dry samples, even slight decomposition produced visually detectable changes. Thus, the unsolvated crystalline form was noticeably more stable, even at 25°.

Keyphrases □ Decomposition, thermal—amorphous samples of various antibacterials, effect of water content and temperature □ Cephalosporins, various—thermal decomposition of amorphous samples, effect of water content and temperature □ Penicillin G potassium—thermal decomposition of amorphous samples, effect of water content and temperature □ Antibacterials, various—thermal decomposition of amorphous samples, effect of water content and temperature

Cephalosporins are often difficult to obtain in crystalline form and, even when crystallized, the products may be partially amorphous (1). Thus, information on the stability of amorphous forms is necessary. Several organic reactions were studied in crystalline solids (2–4), but amorphous solids have received little attention. The intuitive notion that an amorphous solid is more reactive than the corresponding crystalline form has some experimental support (5–11) and is probably a useful generalization. However, crystalline reactions are often only slightly slower than the corresponding reactions in the liquid state (2) and some crystalline reactions are considerably faster (12, 13). While the decomposition of cephalosporins and penicillins in aqueous solution has been studied (14–22), data regarding thermal decomposition in the amorphous solid state are limited to several brief reports where the water content of the sample was either high or unspecified (8–11).

This study investigated the thermal decomposition rates of several β-lactam antibacterials in their amorphous and unsolvated crystalline forms as a function of temperature and water content. The amorphous samples studied were amorphous to X-rays and were nonbirefringent when examined microscopically under polarized light. The compounds chosen were penicillin G potassium and three cephalosporins: cephalothin sodium, cefamandole sodium, and cefamandole nafate.

EXPERIMENTAL

Materials—Crystalline cephalothin sodium and crystalline penicillin G potassium were commercial samples[1]. The corresponding amorphous samples were prepared by freeze drying from a 20% aqueous solution. To avoid partial crystallization, the solutions were frozen and partially dried at low temperature (−20°) before allowing the temperature to increase

[1] Eli Lilly and Co., Indianapolis, Ind.

diffusion coefficients for I and II increased as the calcium concentration increased and then decreased at the 50 m*M* level. The corresponding permeability coefficients agreed fairly well with the sequence of the results. At 0 m*M* calcium, the estimated permeability coefficient of I is almost double that of II, which is also in the order of magnitude of the ratios of their partition coefficients. The permeability coefficients increased with an increase in the calcium-ion concentration, followed by a decrease at the 50 m*M* calcium level.

It is, therefore, proposed that both the prostaglandin molecules and the calcium ions constituting the aggregates crossed intact the diffusion barrier into the mucosal surface. Both species were self-carried in a fashion similar to a carrier-mediated process through the intestinal membrane.

These results may be important in understanding prostaglandin movement through biological fluids and membranes.

REFERENCES

(1) S. M. M. Karim, K. Hillier, and J. Devlin, *J. Pharm. Pharmacol.*, **20**, 749 (1968).

(2) T. M. Parkinson, J. C. Schneider, Jr., J. J. Krake, and W. L. Miller, *Life Sci.*, **7**, 883 (1968).

(3) E. Carafoli and F. Crovetti, *Arch. Biochem. Biophys.*, **154**, 40 (1973).

(4) M. E. Carsten, *Am. J. Obstet. Gynecol.*, **117**, 824 (1973).

(5) P. Hedqvist, *Acta Physiol. Scand.*, **90**, 153 (1974).

(6) C. Matuchansky and J. J. Bernier, *Gastroenterology*, **64**, 1111 (1973).

(7) S. L. Waller, *Gut*, **14**, 402 (1973).

(8) Y. Graziani and A. Livne, *Biochim. Biophys. Acta*, **291**, 612 (1973).

(9) S. J. Kirtland and H. Baum, *Nature New Biol.*, **236**, 47 (1972).

(10) E. M. Eagling, H. G. Lovell, and V. R. Pickles, *Br. J. Pharmacol.*, **44**, 510 (1972).

(11) A. B. Bikhazi and J. J. Hajjar, *J. Pharm. Sci.*, **63**, 1703 (1974).

(12) P. W. Ramwell, J. E. Shaw, G. B. Clarke, M. F. Grostic, D. G. Kaiser, and J. E. Pike, "Prostaglandins in Progress in the Chemistry of Fats and Other Lipids," vol. IX, Part 2, Pergamon, New York, N.Y., 1968.

ACKNOWLEDGMENTS AND ADDRESSES

Received November 24, 1975, from the **School of Pharmacy and the ‡Physiology Department, American University of Beirut, Beirut, Lebanon.*

Accepted for publication December 2, 1976.

Presented at the Basic Pharmaceutics Section, APhA Academy of Pharmaceutical Sciences, Atlanta meeting, November 1975.

Supported in part by a grant from the University Medical Research Fund, American University of Beirut, Beirut, Lebanon.

[x] To whom inquiries should be directed.

Thermal Decomposition of Amorphous β-Lactam Antibacterials

M. J. PIKAL [x], A. L. LUKES, and J. E. LANG

Abstract □ Thermal decomposition rates for amorphous samples of penicillin G potassium, cephalothin sodium, cefamandole sodium, and cefamandole nafate were determined as a function of water content and temperature. Even when rigorously dry, amorphous cephalosporins were at least one order of magnitude less stable than the corresponding unsolvated crystalline form. Absorbed water generally increased both the number of decomposition products and the net decomposition rate. Reaction kinetics were usually apparent first order, but an anomalously high effective reaction order was observed in several systems. Nonlinear Arrhenius plots were observed, and a qualitative model based on molecular relaxation in glasses is proposed. Although decomposition rates at 25° were small for dry samples, even slight decomposition produced visually detectable changes. Thus, the unsolvated crystalline form was noticeably more stable, even at 25°.

Keyphrases □ Decomposition, thermal—amorphous samples of various antibacterials, effect of water content and temperature □ Cephalosporins, various—thermal decomposition of amorphous samples, effect of water content and temperature □ Penicillin G potassium—thermal decomposition of amorphous samples, effect of water content and temperature □ Antibacterials, various—thermal decomposition of amorphous samples, effect of water content and temperature

Cephalosporins are often difficult to obtain in crystalline form and, even when crystallized, the products may be partially amorphous (1). Thus, information on the stability of amorphous forms is necessary. Several organic reactions were studied in crystalline solids (2–4), but amorphous solids have received little attention. The intuitive notion that an amorphous solid is more reactive than the corresponding crystalline form has some experimental support (5–11) and is probably a useful generalization. However, crystalline reactions are often only slightly slower than the corresponding reactions in the liquid state (2) and some crystalline reactions are considerably faster (12, 13). While the decomposition of cephalosporins and penicillins in aqueous solution has been studied (14–22), data regarding thermal decomposition in the amorphous solid state are limited to several brief reports where the water content of the sample was either high or unspecified (8–11).

This study investigated the thermal decomposition rates of several β-lactam antibacterials in their amorphous and unsolvated crystalline forms as a function of temperature and water content. The amorphous samples studied were amorphous to X-rays and were nonbirefringent when examined microscopically under polarized light. The compounds chosen were penicillin G potassium and three cephalosporins: cephalothin sodium, cefamandole sodium, and cefamandole nafate.

EXPERIMENTAL

Materials—Crystalline cephalothin sodium and crystalline penicillin G potassium were commercial samples[1]. The corresponding amorphous samples were prepared by freeze drying from a 20% aqueous solution. To avoid partial crystallization, the solutions were frozen and partially dried at low temperature (−20°) before allowing the temperature to increase

[1] Eli Lilly and Co., Indianapolis, Ind.

gradually to 25°. The resulting amorphous plugs were then lightly mortar ground and vacuum dried[2]. Water contents were then determined by Karl Fischer assay.

Cefamandole nafate was recrystallized from methanol by addition of 2-propanol, yielding nonsolvated crystalline material. The "wet" crystals were first air dried and then vacuum dried (1). The amorphous sample was prepared as described for cephalothin sodium.

Since no unsolvated crystalline forms of cefamandole sodium have been prepared, only amorphous forms were studied. To optimize purity, crystalline solids (solvates) were used. The dioxane solvate of cefamandole sodium was obtained by adding dioxane to a concentrated aqueous solution. The resulting crystals were repeatedly dissolved in water, freeze dried to remove dioxane, and finally spray dried (1) from an aqueous solution to yield amorphous cefamandole sodium. The sample was dried at reduced pressure[2]. Residual dioxane was less than 0.1% (w/w) (NMR). The freeze-dried cefamandole sodium sample used in the decomposition studies was prepared from the methanol solvate of cefamandole sodium using the procedure described for cephalothin sodium. Crystalline methanol solvate was obtained by adding sodium acetate to a methanol solution of purified cefamandole acid.

Samples containing water were prepared by allowing the dried samples to absorb water from saturated aqueous salt solutions of fixed water vapor pressure. The amount of water absorbed was determined gravimetrically.

Procedures—All samples were protected from light during storage. Cephalothin sodium, cefamandole nafate, and penicillin G potassium were stored in glass sealed ampuls; ~300 mg of sample was sealed with about 10 ml of dry air. Cefamandole sodium was stored in 15-ml ampuls sealed with butyl rubber closures. To ensure that the dry sample did not absorb water during ampul filling, filling was carried out at near zero relative humidity[3]. Karl Fischer assay indicated that no measurable water (<0.1%) was absorbed during the filling and sealing operations. In general, each sample for a given time–temperature aging condition was prepared in duplicate.

Some amorphous cephalothin sodium samples were subjected to high vacuum drying conditions. The sample, dried as previously discussed, was pumped on at 10^{-6} Torr and 25° for 24 hr and was then sealed in vacuum.

Assay Methods—Cephalothin sodium and penicillin G potassium were assayed by an automated iodometric titration procedure (23). This assay measures intact β-lactam[4]. The mean difference between assays on the duplicate samples was 1.8%. To check accuracy, a number of decomposed cephalothin sodium samples were assayed both by the iodometric procedure and by a microbiological automated assay[5] using *Staphylococcus aureus* (ATCC 9144) (23). The extents of decomposition measured by the two techniques differed by less than 2%.

Cefamandole nafate and cefamandole sodium were assayed by a polarographic technique (24) that determines intact cefamandole and cefamandole nafate. The method does not distinguish between cefamandole nafate and cefamandole sodium. The difference between assays on duplicate samples averaged 1.4%. All cefamandole nafate and cefamandole sodium samples were assayed for the decomposition product, 1-methyl-5-mercapto-1,2,3,4-tetrazole (X), by polarography (25, 26).

Thin-layer chromatograms were obtained by loading a 250-μg sample on a precoated 0.25-mm silica gel 60 F-254 TLC plate[6]. The developing solvent was ethyl acetate–acetone–acetic acid–water (5:2:1:1). Chromatographic zones were examined by shortwave UV light (254 nm).

RESULTS

Decomposition Products—Decomposition products of aqueous and amorphous cephalosporins, as revealed by TLC, are compared in Fig. 1. The extent of decomposition was in the 10–50% range for all samples. The degree of shading used to indicate a zone is a rough indication of the intensity of that zone as observed on the TLC plate. A broken line indicates streaking. The R_f values for the cephalosporins and their hydroxymethyl

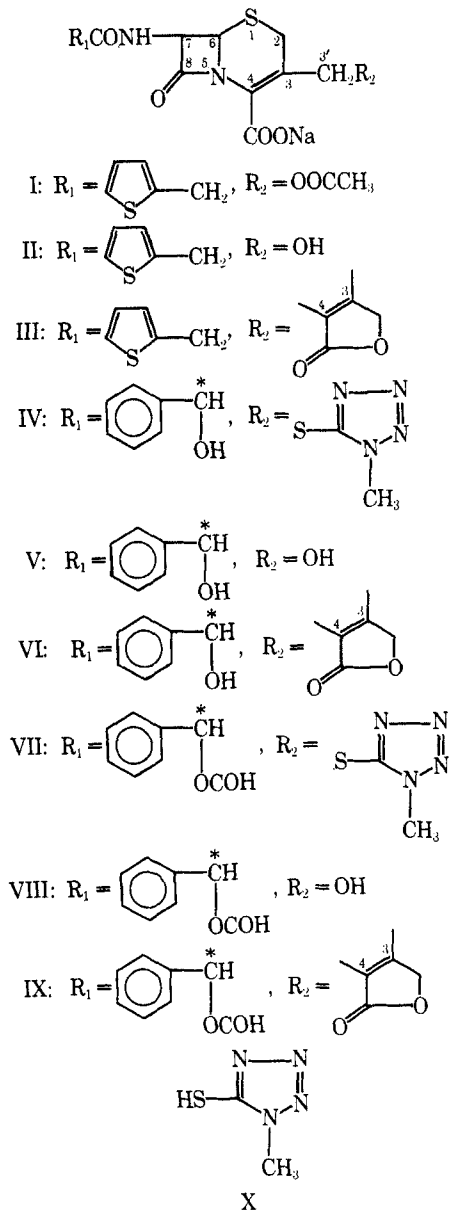

X

and lactone derivatives were: cephalothin sodium (I), 0.65; deacetylcephalothin (II), 0.46; deacetylcephalothin lactone (III), 0.88; cefamandole sodium (IV), 0.50; V, 0.34 (25); cefamandole lactone (VI), 0.82 (25); cefamandole nafate (VII), 0.59; cefamandole nafate lactone (IX), 0.92; and X, 0.92.

The decomposition products present (Fig. 1) depended strongly on the water content of the decomposition medium. For cephalothin sodium, the leading component had the same R_f value as the lactone analog (III). Although little lactone was found in decomposed, dry (≤0.1% H_2O) cephalothin sodium, lactone was a major decomposition product for the wet solid (4.4% H_2O)[7]. The 3-hydroxymethyl analog (II) of cephalothin, R_f 0.46, was not present in either solid sample but appeared to be a major product for the aged aqueous sample (Fig. 1). Similarly, the 3-hydroxymethyl analogs of cefamandole and cefamandole nafate[8] were present *only* in the aged aqueous solutions.

Decomposition to form the 3-hydroxymethyl or lactone analogs is accompanied by formation of an equal molar quantity of the free 3′-side chain (X, R_f 0.92). Rupture of the β-lactam bond should be accompanied by release of the 3′-side chain, provided the 3′-group is a good leaving group (17, 22). Thus, the usual decomposition reactions would be expected to yield 1 mole of X for each mole decomposed. However, for decomposed amorphous cefamandole nafate and cefamandole sodium, the

[2] Dried at reduced pressure (≃ 15 Torr) with a dry air bleed (100 ml/min) for ~16 hr at 25° and ~20 hr at 40°.

[3] The glove bag (Instruments for Research and Industry, Cheltenham, Pa.) was continuously purged with air at equilibrium with anhydrous calcium sulfate.

[4] The cephalothin decomposition product, deacetylcephalothin lactone, contains an intact β-lactam and, therefore, should not be distinguished from cephalothin by the iodometric assay. However, samples of pure lactone gave essentially zero β-lactam content by the iodometric method, presumably due to the insolubility of the lactone in the aqueous systems used in the assay.

[5] Autoturb.

[6] Merck.

[7] The wet solid (4.4% H_2O) contained ~10% (w/w) crystalline III (identified by X-ray diffraction).

[8] Presumably, the components at R_f 0.36 and 0.43 were the 3-hydroxymethyl analogs of cefamandole and cefamandole nafate, respectively.

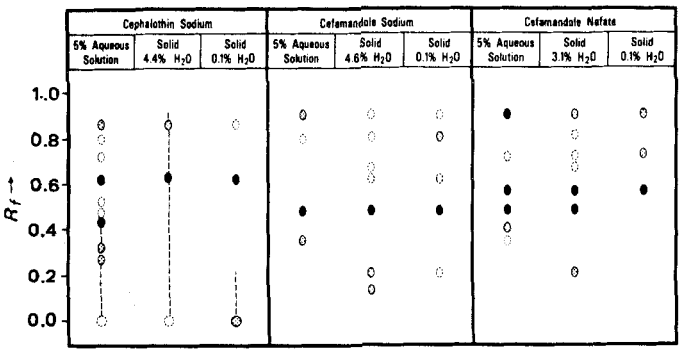

Figure 1—*TLC of decomposed cephalosporins; a comparison between aqueous solution and amorphous solids. Cephalothin sodium 5% aqueous solution was aged 1 hr at 75° and solids were aged 1 week at 75°; cefamandole sodium 5% aqueous solution was aged 2 hr at 50° and solids were aged 1 month at 50°; and cefamandole nafate 5% aqueous solution was aged 2 hr at 50° and solids were aged 2 months at 50° (0.1% H_2O) and 3 weeks at 50° (3.1% H_2O).*

mole percent of X (by assay) was less than the mole percent decomposition. Either one of the decomposition products contains an intact 3′-side chain or X is unstable.

Amorphous cephalothin sodium rapidly developed an amber color upon aging. Even samples that showed no evidence of decomposition by iodometric assay or TLC were highly colored both in the solid form and when dissolved in water. Although column chromatography[9] suggested that the colored products were polymeric, details of the structures are unknown. For amorphous cefamandole and cefamandole nafate, the extent of color formation was *much* less than that noted for cephalothin sodium aged under similar conditions[10].

Decomposition Rates—*Amorphous Cephalothin Sodium*—In general, samples were assayed over a period corresponding to at least 10% decomposition. Periodic microscopic examination verified that the samples remained amorphous during the stability study. Typical data are shown in Fig. 2. Assay data are expressed relative to the initial assays as percent of initial, *P*. Thus, the percentage decomposition is $100 - P$. Although in most cases insufficient decomposition had occurred to establish the reaction order unambiguously, all data were consistent with first-order kinetics.

First-order rate constants were evaluated by least-squares analysis. *No differences* in decomposition or extent of color formation between dry samples (≤0.1% H_2O) stored in air and those stored in vacuum were observed. Thus, these data were combined for the rate constant calculations (Table I). For the dry samples stored at 25°, no decomposition could be demonstrated over 600 days. However, the powder did develop an amber color, indicating that some decomposition occurred.

Amorphous Penicillin G Potassium—Microscopic examination of aged

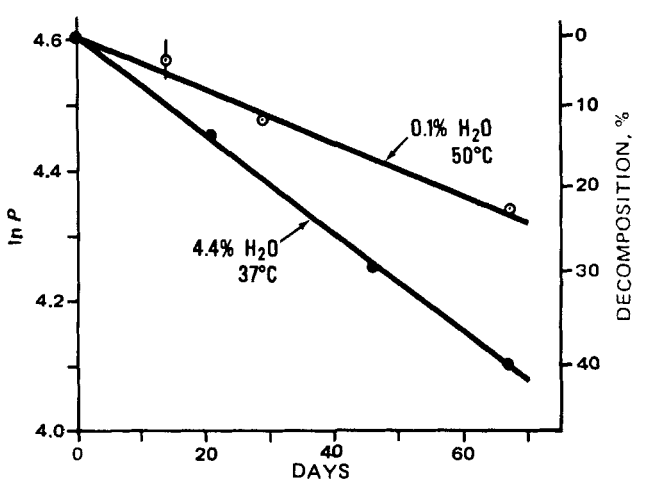

Figure 2—*Kinetics of thermal decomposition of amorphous cephalothin sodium. P is the iodometric assay in percent of initial.*

[9] Sephadex.

[10] Exposure of cefamandole nafate to laboratory light significantly increased the color formation rate.

Table I—First-Order Rate Constants for the Thermal Decomposition of Amorphous Freeze-Dried Cephalothin Sodium

	100 × First-Order Rate Constant, $10^2 k_1$, day^{-1}			
Water, %	25°	37°	50°	75°
0.1	0.000 ± 0.002[a]	0.022 ± 0.005	0.40 ± 0.1	4.9 ± 0.4
0.9	—	0.051 ± 0.016	0.55 ± 0.04	—
1.8	—	0.18 ± 0.02	0.70 ± 0.07	—
4.4	0.084 ± 0.008	0.76 ± 0.02	0.9 ± 0.1	4.2 ± 0.9

[a] The uncertainties given are the standard deviations of the parameters.

samples indicate that, while the dry sample (0.5% H_2O) at 50° remained essentially amorphous[11], the wet samples (5.7% H_2O) partially crystallized early during the stability study (Fig. 3). The dry samples showed no decomposition either by iodometric assay or by visual examination. By contrast, the wet samples decomposed rapidly at both 25 and 50°, with the decomposition rate decreasing much faster with time than would be consistent with first-order kinetics.

Amorphous Cefamandole Nafate and Cefamandole Sodium (Figs. 4 and 5)—Microscopic examination of aged samples showed no evidence of crystallization. Dry (0.1% H_2O) cefamandole nafate at 25° decomposed slightly (3.6%) within 3 months, but the assays remained essentially constant between 3 and 12 months. The line drawn in Fig. 4 reflects the apparent invariance of the assay with respect to time after 3 months. If this plateau effect is rejected as an artifact and all data are fitted to a first-order decay model, $10^2 k_1 = 0.005$ day^{-1}.

Since the stability study for cefamandole sodium was terminated after 3 months, no information regarding a plateau effect for this compound was obtained. The solid line and the value of $10^2 k_1$ in Fig. 4 for dry cefamandole sodium at 25° assume first-order decomposition. Clear deviations from first-order decomposition were observed for wet (3.1% H_2O) cefamandole nafate at 50° and for wet (4.6% H_2O) cefamandole sodium at 40 and 50°. For these samples, therefore, the solid lines and values of $10^2 k_1$ shown in Figs. 4 and 5 are intended only as crude approximations for the initial decomposition rates.

Spray-dried and freeze-dried cefamandole sodium, although both amorphous, are not identical forms. Spray-dried material appears to be an annealed form of the freeze-dried material (1), having an energy about 2 kcal/mole less than the freeze-dried form. Thus, in principle, the reactivity of spray-dried cefamandole sodium may be different from the reactivity of freeze-dried material (1). Decomposition data for freeze-dried and spray-dried cefamandole sodium are compared in Fig. 5. Although the data are insufficient to reveal small differences in reactivity, reactivities of freeze-dried and spray-dried samples are clearly of the same order of magnitude.

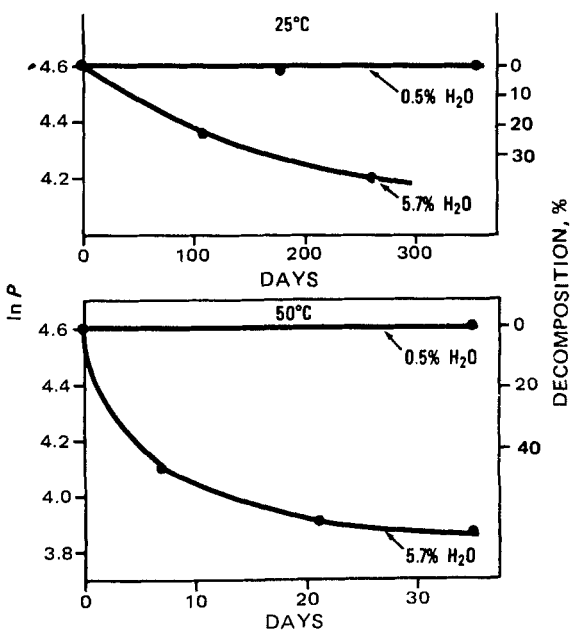

Figure 3—*Kinetics of thermal decomposition of penicillin G potassium. P is the iodometric assay in percent of initial.*

[11] After 12 months at 25°, the dry sample had crystallized.

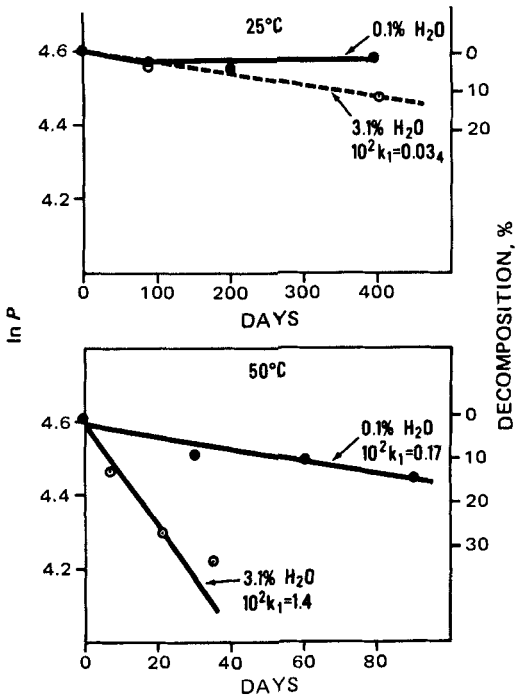

Figure 4—*Kinetics of thermal decomposition of cefamandole nafate. P is the polarographic assay in percent of initial.*

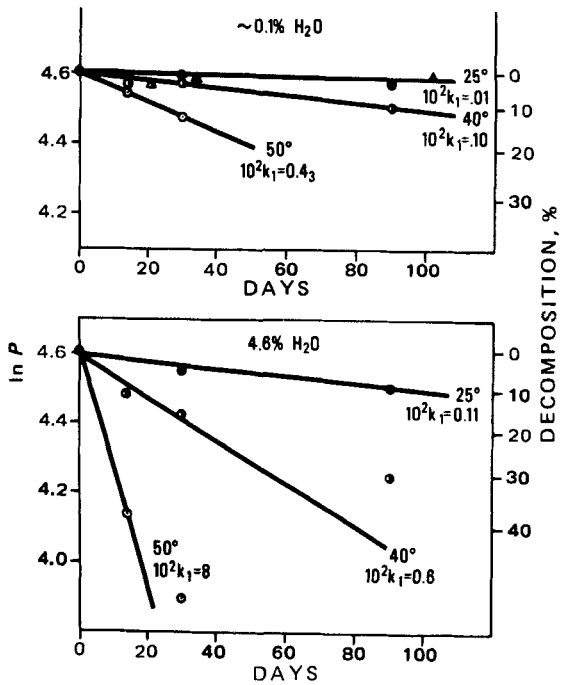

Figure 5—*Kinetics of thermal decomposition of cefamandole sodium. P is the polarographic assay in percent of initial. The circles are spray-dried samples; the triangles are freeze-dried samples.*

Crystalline Forms—The unsolvated crystalline forms of cephalothin sodium, penicillin G potassium, and cefamandole nafate were subjected to aging conditions at least as severe as those used for the corresponding amorphous samples. Assay data did not reveal decomposition under any test condition. From the precision of the assay data and the duration of the stability studies, the decomposition rates, k_1 (day^{-1}), for the crystalline materials studied are estimated to be less than 10^{-4} day^{-1} at 50°. Thus, at least for the cephalosporins studied, the effect of crystallinity is to increase the thermal stability by *at least* one order of magnitude.

DISCUSSION

Kinetics—The amorphous materials studied did not exhibit the sigmoid or "S"-shaped decomposition curves frequently observed with crystalline solids (3). In general, the data are consistent with first-order kinetics, although clear deviations from first-order behavior occurred in several cases. With wet (5.7% H_2O) penicillin G potassium, the sharp decrease in decomposition rate with increasing time was probably due to sample crystallization. The interpretation of the high temperature kinetic data for wet cefamandole sodium and wet cefamandole nafate is less obvious. Here, no crystallization was observed. Similar kinetics for amorphous ampicillin led to the speculation (8) that, upon aging, the amorphous form initially present underwent a transition to a less reactive amorphous form.

While amorphous freeze-dried cefamandole nafate and cefamandole sodium apparently undergo a structural change (annealing) upon aging, amorphous spray-dried cefamandole sodium *is* an annealed form (1). Since similar kinetics are observed for both freeze-dried and spray-dried (*i.e.*, annealed) samples, the deviations from first-order decomposition apparently are not the result of an annealing phenomenon.

If a major decomposition pathway involves attack on the β-lactam by water, the reaction rate would depend on the concentration of water in the system. If a solution model were used for the amorphous solids studied, second-order kinetics are predicted[12]. However, the effective reaction order for the data under discussion is ~5. Therefore, the observed deviations from first-order behavior constitute an anomaly for which no convincing explanation can be offered.

Effect of Water—In general, the decomposition rate was increased significantly by the presence of water. This effect was particularly striking for penicillin G potassium (Fig. 3). At low water content (0.5%), decomposition was not measurable; but at high water content (5.7%), decomposition was faster than for any other solid studied. Although the effect of moisture on the decomposition of amorphous cephalothin sodium was quite significant at low temperatures, the decomposition rate at 75° was essentially independent of water content (Table I).

Effect of Temperature/Mechanisms—Arrhenius plots for the cephalothin sodium data (Table I) are given in Fig. 6. The measured rate constant for dry cephalothin sodium at 25° was zero. Although this point could not be included in Fig. 6, the smooth curve was drawn to reflect a very low decomposition rate at 25°. Significant curvature exists in the Arrhenius plots, particularly for dry material where the effective activation energy decreased from ~40 kcal/mole at low temperature to ~20 kcal/mole at high temperature. At least at low temperature, the effective activation energy for the wet (4.4% H_2O) solid was significantly less than the corresponding activation energy for the dry solid.

If amorphous cephalothin sodium decomposed *via* two degradation pathways with significantly different activation energies, nonlinear Ar-

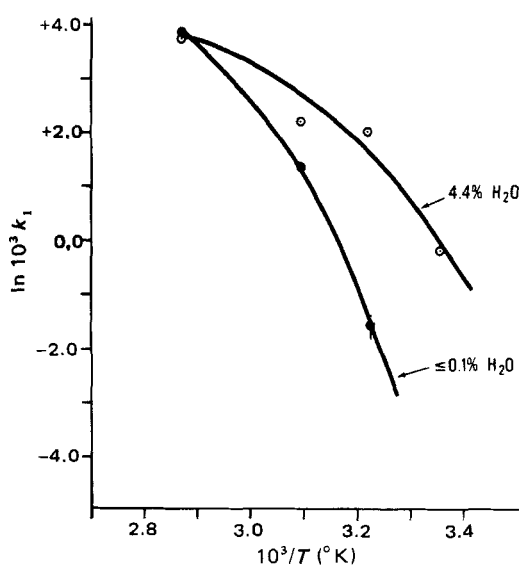

Figure 6—*Arrhenius plots of first-order rate constants for the thermal decomposition of amorphous cephalothin sodium.*

[12] For a solution model, the rate is proportional to the product of the cephalosporin concentration and the water concentration. In the moisture-containing amorphous systems studied, the initial mole ratio of cephalosporin to water was about unity. Thus, for a 1:1 reaction stoichiometry, the cephalosporin and water concentrations would be roughly equal at all times, leading to second-order kinetics.

rhenius plots would result. However, in such a case the effective activation energy, defined by the slope of the Arrhenius plot, would *increase* with increasing temperature. This intuitive conclusion is supported by the following mathematical argument. The observed rate constant, k, is:

$$k = \sum_{i=1}^{n} k_i = \sum_{i=1}^{n} A_i \exp(-E_i/RT) \qquad \text{(Eq. 1)}$$

where A_i, E_i, and k_i represent the preexponential factor, activation energy, and rate constant, respectively, for the ith decomposition pathway. The effective activation energy, E^*, is defined by:

$$E^* = -R \frac{d \ln k}{d(1/T)} \qquad \text{(Eq. 2)}$$

Performing the indicated differentiation yields:

$$E^* = \sum_{i=1}^{n} \frac{k_i}{k} E_i \qquad \text{(Eq. 3)}$$

Differentiation of Eq. 3 and algebraic manipulation then yield:

$$RT^2 \frac{dE^*}{dT} = \sum_{i=1}^{n} \frac{k_i}{k} [E_i - E^*]^2 \geq 0 \qquad \text{(Eq. 4)}$$

Thus, provided two or more degradation pathways exist ($E_i \neq E^*$), dE^*/dT is always positive; *e.g.*, an increase in temperature increases E^*. Experimentally, however, the effective activation energy *decreases* as the temperature increases.

The observed temperature dependence (Fig. 6) is consistent with the following qualitative model. For decomposition to occur, the reacting molecule and its immediate neighbors must undergo considerable reorientation. For example, if attack on the β-lactam by a nucleophilic group from a neighboring molecule is involved, reorientation must occur to provide the geometry needed for the reaction to proceed. This model assumes that molecular reorientation is the rate-determining step for thermal decomposition. Thus, the reaction rate is proportional to a molecular relaxation rate.

For liquids at low temperature (24) and glassy polymers (27), molecular relaxation rates may show pronounced non-Arrhenius behavior near the glass transition temperature; the activation energy for molecular relaxation decreases as the temperature increases. Similar behavior might be expected for amorphous cephalosporins near 25°, provided the glass transition temperature is near 25°. The glass transition temperature, T_g, for dry cephalothin sodium may be estimated[13] as $T_g \approx 300$ °K. Thus, according to the described model, the non-Arrhenius behavior demonstrated in Fig. 6 is a consequence of the decreasing activation energy for molecular relaxation as the temperature increases from T_g.

CONCLUSIONS

Even when rigorously dry, the amorphous cephalosporins studied are much less stable than their crystalline forms. In general, absorbed water increases the number of decomposition products and greatly increases the net decomposition rate. The activation energy is high and, at least for cephalothin sodium, the effective activation energy increases with decreasing temperature.

Provided the solid is dry, decomposition rates at 25° are small[14]. If potency were the only consideration, the amorphous compounds studied would be viable product forms in the dry state. Loss of product elegance is the more serious problem. Amorphous cephalothin sodium develops excessive amber color well before a potency loss is measurable. With amorphous cefamandole sodium and cefamandole nafate, even slight decomposition lowers the pH of a reconstituted solution to the point where the cephalosporin acid precipitates.

[13] As a rough rule, $T_g/T_m \approx 0.6$ (28, 29), where T_m is the melting point (°K) of the crystalline solid. Crystalline cephalothin sodium melts (with decomposition) at ~470 °K.

[14] Amorphous dry cephalothin sodium stored at 25° maintains initial potency for 2 years. However, upon equilibration of the solid with 30% relative humidity (4.4% H_2O), the projected shelflife (less than 10% potency loss) at 25° is only 4 months.

REFERENCES

(1) M. J. Pikal, A. L. Lukes, J. E. Lang, and K. Gaines, *J. Pharm. Sci.*, in press.

(2) I. C. Paul and D. Y. Curtin, *Acc. Chem. Res.*, **6**, 217 (1973).

(3) J. T. Carstensen, *J. Pharm. Sci.*, **63**, 1 (1974).

(4) S. R. Byrn, *ibid.*, **65**, 1 (1976).

(5) E. O. Hornig and J. E. Willard, *J. Am. Chem. Soc.*, **79**, 2429 (1957).

(6) Y. S. Lipatov, L. I. Bezruk, and Y. P. Gomza, *Vysokomol. Soedin., Ser. B*, **16**, 328 (1974); through *Chem. Abstr.*, **81**, 78396a (1974).

(7) C. N. Patel, *J. Polym. Sci., Polym. Phys. Ed.*, **13**, 361 (1975).

(8) A. L. Lo and E. Shefter, "Abstracts, 19th National Meeting of the APhA Academy of Pharmaceutical Sciences," vol. 5, American Pharmaceutical Association, Washington, D.C., 1975.

(9) A. G. Mathews, C. J. Schram, and D. Minty, *Nature*, **211**, 959 (1966).

(10) K. Kariyone, H. Harada, M. Kurita, and T. Takano, *J. Antibiot.*, **23**, 131 (1970).

(11) R. R. Pfeiffer, G. L. Engel, and D. Coleman, *Antimicrob. Agents Chemother.*, **9**, 848 (1976).

(12) F. W. Stacey, J. C. Sauer, and B. C. McKusick, *J. Am. Chem. Soc.*, **81**, 987 (1959).

(13) C. N. Sukenik, J. A. P. Bonapace, N. S. Mandel, R. G. Bergman, P. Lau, and G. Wood, *ibid.*, **97**, 5290 (1975).

(14) H. Smith and A. C. Marshall, *Nature*, **232**, 45 (1971).

(15) W. E. Walsh, H. Markowitz, J. D. Jones, and G. J. Gleich, *Allergy*, **47**, 159 (1971).

(16) H. Bundgaard, *J. Pharm. Sci.*, **60**, 1273 (1971).

(17) C. H. O'Callaghan, S. M. Kirby, A. Morris, R. E. Waller, and R. E. Duncombe, *J. Bacteriol.*, **110**, 988 (1972).

(18) J. Konecny, E. Felber, and J. Gruner, *J. Antibiot.*, **26**, 135 (1973).

(19) T. Yamana, A. Tsuji, K. Kanayama, and O. Nakano, *ibid.*, **27**, 1000 (1974).

(20) J. M. Indelicato and W. L. Wilham, *J. Med. Chem.*, **17**, 528 (1974).

(21) J. M. Indelicato, T. T. Norvilas, R. R. Pfeiffer, W. J. Wheeler, and W. L. Wilham, *ibid.*, **17**, 523 (1974).

(22) H. Bundgaard, *Arch. Pharm. Chem. Sci. Ed.*, **3**, 94 (1975).

(23) L. P. Marrelli, in "Cephalosporins and Penicillins," Academic, New York, N.Y., 1972, chap. 14.

(24) C. A. Angell, *J. Phys. Chem.*, **70**, 2793 (1966).

(25) E. C. Rickard and G. G. Cooke, *J. Pharm. Sci.*, **66**, 379 (1977).

(26) D. A. Hall, *ibid.*, **62**, 980 (1973).

(27) G. Allen, in "Amorphous Materials," R. W. Douglas and B. Ellis, Eds., Wiley–Interscience, New York, N.Y., 1972, p. 361.

(28) W. Kauzmann, *Chem. Rev.*, **43**, 219 (1948).

(29) C. A. Angell and K. J. Rao, *J. Chem. Phys.*, **57**, 470 (1972).

ACKNOWLEDGMENTS AND ADDRESSES

Received October 29, 1976, from the *Pharmaceutical Research Department, Lilly Research Laboratories, Indianapolis, IN 46206.*

Accepted for publication December 14, 1976.

The authors thank the members of the Analytical Chemistry Groups at Eli Lilly and Co. for performing the assay work. They also thank Mr. K. S. Yang, Dr. S. Schildcrout, and Dr. L. Tensmeyer for providing samples of cephalosporins.

[x] To whom inquiries should be directed.

Colorimetric Assay of Quinine and Quinidine in Raw Materials, Formulations, and Biological Fluids

MOHAMED S. KARAWYA ˣ and ALY M. DIAB

Abstract □ The two characteristic erythroquinine and thalleioquin tests for quinine and quinidine were studied to optimize the experimental conditions for quantitative analysis. Both methods were quantitatively sensitive for either quinine or quinidine in a concentration range of 0.1–10 μg/ml with the erythroquinine method and of 3–50 μg/ml with the thalleioquin method. A TLC–colorimetric method also is described for the assay of quinine and quinidine in the presence of cinchonine, cinchonidine, and other cinchona alkaloids. The results were compared with those obtained with a spectrophotometric method.

Keyphrases □ Quinine—colorimetric analysis, pharmaceutical formulations and biological fluids □ Quinidine—colorimetric analysis, pharmaceutical formulations and biological fluids □ Colorimetry—analyses, quinine and quinidine, pharmaceutical formulations and biological fluids □ Alkaloids, cinchona—quinine and quinidine, colorimetric analyses, pharmaceutical formulations and biological fluids □ Antimalarials—quinine, colorimetric analysis, pharmaceutical formulations and biological fluids □ Cardiac depressants—quinidine, colorimetric analysis, pharmaceutical formulations and biological fluids

The separation and estimation of the major cinchona alkaloids, especially quinine (I) and quinidine (II), are complicated and difficult due to their many common properties; only a few methods are analytically useful. Several spectrometric assays for quinine and quinidine, either alone or in mixtures, were reported; the most important and widely used are UV spectrophotometry (1–3) and fluorometry (4–6).

Numerous colorimetric methods were adopted for estimating quinine and quinidine involving potassium-chromic thiocyanate (7, 8), cobalt thiocyanate (9), picric acid (10), reineckate salt (11), tropaeolin 00 (12), titanium trichloride (13), and bromthymol blue (14). TLC separation followed by UV spectrophotometry (15) or colorimetry (16), as well as other techniques such as paper (17), triple-column (18), and ion-exchange (19) chromatography, also were described.

Although the two characteristic erythroquinine (20) and thalleioquin (21) tests are most selective and specific for the detection of quinine, their quantitative application was not fully studied. Allport and Friend (22) found that the erythroquinine test suggested by Monnet (23) was very difficult to apply quantitatively due to certain uncontrollable factors; the bromine water was a critical factor and the reaction was time, temperature, and light dependent.

The purposes of this work were to: (*a*) quantify the erythroquinine and thalleioquin color tests, (*b*) develop a selective colorimetric method to assay quinine and quinidine in the presence of other cinchona alkaloids, and (*c*) apply these methods to bulk drug, dosage forms, and biological fluids.

EXPERIMENTAL

Materials—*Pharmaceuticals*—Liquid extract and tincture of cinchona[1] were used. The following also were studied: quinine ampuls containing 300 mg of quinine dihydrochloride; quinine tablets containing 150 mg of quinine sulfate; quinidine tablets containing 200 mg of quinidine sulfate; compound quinine tablets containing 20 mg of quinine hydrobromide, 15 mg of papaverine, 20 mg of phenobarbital, and 50 mg of crataegus extract; and dipyrone–quinine tablets containing 150 mg of dipyrone calcium salt and 100 mg of quinine.

Biological Fluids—Blood samples were collected from five male adult volunteers; each volunteer swallowed a single capsule containing 0.2 g of quinine sulfate and 0.2 g of quinidine sulfate 3 hr before blood was drawn. Urine samples were collected for 6 hr after drug administration.

Bromate–Bromide Solution—Prepare 0.5 *N* potassium bromate by dissolving 13.92 g of potassium bromate in distilled water. Add 60 g of potassium bromide and mix. After the salts have dissolved, adjust the volume to 1 liter with distilled water.

Potassium Ferricyanide Reagent—Prepare a 10% solution of potassium ferricyanide in distilled water.

Standard Quinine and Quinidine Solution—Dissolve a 5-mg sample of either quinine sulfate reference material[2] or quinidine sulfate reference material[3] in 10 ml of 2 *N* sulfuric acid.

Standard Solution of Mixed Cinchona Alkaloids—Dissolve 5 mg each of quinine, quinidine, cinchonine, and cinchonidine in 10 ml of 2 *N* sulfuric acid.

Apparatus—Glass plates (20 × 20 cm) coated with a slurry consisting of 30 g of silica gel G in 60 ml of distilled water to give a layer 0.25 mm thick were dried at 100° for 1 hr. A UV–visible colorimeter[4] was used.

Erythroquinine Reaction—Dilute 1 ml of either quinine or quinidine standard solutions to 10 ml with distilled water. Pipet 0.02, 0.1, 0.2, 1.0, 1.5, 2.0, and 2.5 ml of the dilute solutions in separate test tubes, dilute to ~3 ml with distilled water, and add 2 drops of hydrochloric acid. Add, dropwise, the bromate–bromide solution, shaking after each addition until a faint-yellow color appears; then shake for 20 sec, and add 10 drops of the potassium ferricyanide solution.

Make the solution just alkaline with dilute ammonium hydroxide. Extract the erythroquinine formed with chloroform (5 × 3 ml), transferring the chloroform extracts to a 10-ml volumetric flask, and dilute to volume with chloroform. Pipet 1 ml of chloroform solution, and measure the absorbance at 510 nm against a reagent blank.

A calibration curve of 0.1–10 μg of quinine or quinidine/ml *versus* color intensity obeyed Beer's law with a standard deviation of ±0.38%.

Thalleioquin Reaction—Pipet 0.04, 0.06, 0.1, 0.2, 0.4, 0.8, 1, and 1.1 ml of either quinine or quinidine standard solution into separate 10-ml volumetric flasks, dilute to ~2 ml with distilled water, and add 2 drops of hydrochloric acid. Add, dropwise, the bromate–bromide solution (~10 drops), shaking after each addition until a faint-yellow color appears. Continue shaking for 20 sec, add 10 drops of ammonium hydroxide (25%), and shake again for 15 sec. Dilute to volume with absolute methanol, and directly measure the absorbance at 450 nm against a reagent blank.

A calibration curve of 3–50 μg of quinine or quinidine/ml *versus* color intensity obeyed Beer's law with a standard deviation of ±1.2%.

TLC–Colorimetric Estimation of Quinine and Quinidine—To avoid interferences caused by cinchonine, cinchonidine, and other minor cinchona alkaloids, a TLC method for separating quinine and quinidine prior to their estimation is performed as follows. Submit 0.1 and 0.15 ml of the standard solution of mixed alkaloids and 0.01, 0.05, 0.1, 0.15, and 0.2 ml of each standard quinine and quinidine solution to chromatography on silica gel G plates, using benzene–ethyl acetate–diethylamine (2:2:1) as the solvent system (development ~2 hr). Locate the quinine and quinidine spots on the dried plate with UV light, and remove the respective spots quantitatively to separate test tubes. Add 5 ml of 0.1 *N* hydrochloric acid, heat for 10 min at 60° on a water bath, shake thoroughly for 5 min while hot, and then cool. Centrifuge or filter the contents of test tubes, and apply the proposed erythroquinine or thalleioquin

[1] Porter & Clark Ltd., London, England.

[2] N. V. Amsterdamache Chininefabriek, Amsterdam, The Netherlands.
[3] WPP, Wallace Pharmaceutical Products, Ltd., London, England.
[4] Spekol, Carl Zeiss, Jena, East Germany.

Table I—Assay of Quinine (I) and Quinidine (II) in Cinchona Preparations by the Proposed Methods

Preparation	Amount Declared, mg/ml		Amount Found[a], mg/ml: Thalleioquin Method		Amount Found[a], mg/ml: Erythroquinine Method		Amount Added, mg		Amount Found[a], mg/ml: Thalleioquin Method		Amount Found[a], mg/ml: Erythroquinine Method		Recovery, %: Thalleioquin Method	Recovery, %: Erythroquinine Method
	I	II	I	II	I	II	I	II	I	II	I	II		
Liquid extract of cinchona	40	2.0	46	1.95	45	1.92	40	2	85.8	3.92	84.8	3.9	99.5	99.2
Tincture	0.95	0.2	0.97	0.21	0.95	0.19	1	0.2	1.93	0.41	1.93	0.39	99.5	99

[a] Results are averages of five experiments.

Table II—Assay of I and II in Formulations by Proposed and AOAC Methods

Preparation, Label I or II Claim	Amount Found[a], mg: Thalleioquin Method	Amount Found[a], mg: Erythroquinine Method	Amount Found[a], mg: AOAC Method	Amount Added, mg	Amount Found[a], mg: Thalleioquin Method	Amount Found[a], mg: Erythroquinine Method	Amount Found[a], mg: AOAC Method	Recovery, %: Thalleioquin Method	Recovery, %: Erythroquinine Method	Recovery, %: AOAC Method
Quinine tablets, 150 mg	152	150.5	155	50	202	200	204.8	100	99	99.6
Quinidine tablets, 200 mg	201	200	202	50	250	249	253	98	98	102
Quinine ampul, 300 mg	299	298	302	50	348	347	352	98	98	100
Compound quinine tablets, 20 mg	19.5	19.2	21	10	29.4	29	31	99	98	101
Dipyrone–quinine tablets, 52 mg	51.9	51.2	—	50	101.6	100.4	—	99.4	98.4	—
SD								±0.38	±1.2	±0.85

[a] Results are averages of five experiments.

method to the filtrates against a reagent blank. Construct calibration curves for both quinine and quinidine.

Estimation of Quinine and Quinidine in Raw Materials—*Cinchona Extract*—The application of the proposed procedures to cinchona extract or tincture involves the extraction of alkaloids prior to the TLC–colorimetric estimation.

Extraction—Transfer 1.0 ml of liquid extract of cinchona into a 50-ml volumetric flask, add 6 ml of 10% formic acid, heat on a water bath for 30 min, and cool. Add 40 ml of tetrahydrofuran, shake the mixture vigorously for 10 min, filter, and dilute to 50 ml with tetrahydrofuran.

Carry out the TLC–colorimetric estimation of quinine and quinidine using 0.1 and 0.2 ml of tetrahydrofuran extract. Calculate the amount of quinine and quinidine from their respective calibration curves.

Estimation of Quinine and Quinidine in Formulations—*Quinine Ampuls*—Dilute 0.1 ml of injectable solution with distilled water to 5 ml, make alkaline with ammonium hydroxide, and extract with chloroform (3 × 10 ml). Evaporate the chloroform extracts to dryness on a water bath, dissolve the residue in 100 ml of 1% H_2SO_4, transfer to a 1-liter volumetric flask, and adjust to volume with distilled water. Perform any of the proposed colorimetric assay methods on 1 ml of this solution.

Simple and Compound Quinine Tablets—Weigh accurately a quantity of finely powdered tablets equivalent to 5 mg of quinine, and extract exhaustively with 1% H_2SO_4 (3 × 10 ml). Filter the acid extract, make alkaline with ammonia, and extract with chloroform (3 × 10 ml). Evaporate the chloroform extract to dryness on a water bath, and dissolve in 100 ml of 1% H_2SO_4 in a volumetric flask. Perform any of the proposed procedures on 1 ml of this solution.

Dipyrone–Quinine Tablets—Weigh accurately a quantity of the finely powdered tablets (10 mg of dipyrone–quinine salt), extract with 1% H_2SO_4 (3 × 10 ml), filter the acid extract, make distinctly alkaline to litmus with sodium hydroxide solution, and extract with chloroform (3 × 10 ml). Evaporate the chloroform on a water bath, and dissolve the residue in 100 ml of 1% H_2SO_4 in a volumetric flask. Carry out the erythroquinine or thalleioquin assay procedures on 1 ml.

Estimation of Quinine and Quinidine in Biological Fluids—*Blood*—Mix 5 ml of blood with an equal volume of hydrochloric acid, and heat on a boiling water bath for 1 hr. Cool, dilute with 5 ml of distilled water, and filter. Wash the residue with distilled water (3 × 5 ml). Combine the filtrate and washings, make the solution alkaline with ammonium hydroxide, and extract with chloroform (2 × 30 ml). Dry the combined chloroform extracts with anhydrous sodium sulfate, filter, and dilute to 100 ml with chloroform. Evaporate an aliquot of the chloroform extract to dryness, dissolve in the least amount of 2 *N* sulfuric acid, and estimate quinine and quinidine by the TLC–colorimetric method using the erythroquinine reaction.

Urine—Prepare the 6-hr sample exactly as described for blood, omitting the dilution with water. Estimate quinine and quinidine by the TLC–colorimetric method using either the erythroquinine or thalleioquin method.

RESULTS AND DISCUSSION

The modifications proposed for the thalleioquin and erythroquinine reactions proved to be simple and specific in comparison with the AOAC (1970) method (24). The latter method depends upon measuring the UV absorption of the 0.1 *N* hydrochloric acid extract of the alkaloid at 347.5 nm and is liable to interferences caused by any substance absorbing at 347.5 nm, *e.g.*, aloin, podophyllin, anthraquinones and their derivatives, other cinchona alkaloids, and yellow dyes (24). The color reactions, however, seem very selective. During this work, these reactions could be

Table III—Assay of I and II in Blood and Urine Sample by the Proposed Methods

Sample	Volunteer	Amount Found, mg: Thalleioquin Method		Amount Found, mg: Erythroquinine Method		Amount Added, mg		Amount Found, mg: Thalleioquin Method		Amount Found, mg: Erythroquinine Method		Recovery, %: Thalleioquin Method	Recovery, %: Erythroquinine Method
		I	II	I	II	I	II	I	II	I	II		
Blood	1			0.04	0.04	0.1	0.1	—	—	0.14	0.140	—	100
	2			0.04	0.04	0.2	0.1	—	—	0.239	0.138	—	98.78
	3			0.044	0.44	0.15	0.15	—	—	0.194	0.194	—	100
	4			0.04	0.04	0.1	0.2	—	—	0.138	0.238	—	98.5
	5			0.38	0.035	0.1	0.1	—	—	0.138	0.138	—	100
Urine	1	10	10	10	9.5	5	5	14.9	15.05	14.7	14.6	99.5	98
	2	10.5	10	10.2	9.2	7.5	7.5	17.7	17.75	17.1	17.1	99.6	98.5
	3	9.5	9	9	9	1	1	10.26	10.22	10.0	9.97	99.0	98.5
	4	11	8.5	10	8	2.5	2.5	12.23	12.23	11.3	11.5	99.2	99
	5	8.8	9	8.5	8.5	5	5	13.72	13.73	15	15	99.5	98.9

safely carried out in the presence of crataegus extract and other alkaloids such as papaverine, strychnine, morphine, and atropine.

Although the proposed reactions are specific for quinine and quinidine, a TLC procedure is necessary for cinchona preparations to separate quinine and quinidine and to eliminate other interfering constituents. The four main cinchona alkaloids showed good separation; the R_f values of quinine, quinidine, cinchonine, and cinchonidine were 0.18, 0.44, 0.55, and 0.41, respectively.

Ammonium hydroxide was not capable of releasing quinine base from the dipyrone–quinine salt, while sodium hydroxide solution was satisfactory.

The proposed methods also were applied successfully to the recovery of quinine and quinidine from blood and urine with reproducible results. With blood, because of the small concentration of the alkaloids present, only the more sensitive erythroquinine method was adopted.

Good recoveries at different concentrations and spiking and reasonable standard deviations were obtained with dosage forms and biological fluids by the erythroquinine and thalleioquin methods (Tables I–III).

To obtain protein-free aqueous filtrates from blood and urine, the samples were digested with hydrochloric acid to liberate strongly conjugated alkaloids. Hydrochloric acid digestion was preferable to other procedures.

REFERENCES

(1) J. D. Endiz, *J. Assoc. Offic. Anal. Chem.*, **46**, 637 (1963).

(2) R. N. Bhattacharya and G. K. Ganguly, *J. Pharm. Pharmacol.*, **6**, 191 (1954).

(3) S. Bruno, *Farmaco, Ed. Sci.*, **10**, 922 (1955).

(4) P. Brockman, V. R. Severen, and L. Moeseke, *Pharm. Tijdschr. Belg.*, **40**, 113 (1963).

(5) J. Eisenbrand, *Z. Anal. Chem.*, **179**, 170 (1961).

(6) B. B. Brodie and S. Udenfriend, *J. Pharmacol.*, **78**, 154 (1943).

(7) P. Spacu and C. Ianu, *Z. Anal. Chem.*, **174**, 87 (1960).

(8) R. Dorr, *ibid.*, **226**, 417 (1967).

(9) J. Bosly, *Farmaco, Ed. Prat.*, **19**, 448 (1964).

(10) N. M. Chuev and P. A. Arzamastsev, *Apotechn. Delo*, **8**, 45 (1959).

(11) O. Adam, *Acta Pol. Pharm.*, **27**, 249 (1970); through *Chem. Abstr.*, **74**, 91219 V (1971).

(12) S. Smith and W. Manges, *Dtsch. Apoth. Ztg.*, **97**, 747 (1957).

(13) I. A. Volkova and E. T. Man, *Get. Ukr. Khim. Zn.*, **31**, 1320 (1965).

(14) A. Suszko-Purzycka and W. Trzebny, *Chem. Anal. (Warsaw)*, **9**, 1103 (1964).

(15) B. Horst and R. Bitsch, *Arch. Pharm.*, **303**, 418 (1960).

(16) A. Suszko-Purzycka and W. Trzebny, *J. Chromatogr.*, **19**, 239 (1964).

(17) H. Steger and A. A. Storz, *Pharmazie*, **16**, 126 (1961).

(18) J. Leving, *J. Assoc. Offic. Anal. Chem.*, **145**, 595 (1962).

(19) E. Haberli and E. Beguin, *Pharm. Acta Helv.*, **34**, 65 (1959).

(20) Abensour, *J. Pharm.*, **26**, 25 (1907); through C. H. Thienes and T. J. Haley, "Clinical Toxicology," 4th ed., Lea & Febiger, Philadelphia, Pa., 1964, p. 543.

(21) Andre, *Ann. Chim. Phys.*, **1835**, 195; through C. H. Thienes and T. J. Haley, "Clinical Toxicology," 4th ed., Lea & Febiger, Philadelphia, Pa., 1964, p. 543.

(22) L. N. Allport and D. Friend, *Q. J. Pharm. Pharmacol.*, **11**, 450 (1938).

(23) R. Monnet, *J. Pharm. Chim.*, **18**, 59 (1933).

(24) "Official Methods of Analysis," 10th ed., Association of Official Analytical Chemists, Washington, DC 20044, 1970, secs. 36.147.

ACKNOWLEDGMENTS AND ADDRESSES

Received February 23, 1976, from the *Department of Pharmacognosy, Faculty of Pharmacy, Cairo University, Cairo, Egypt.*

Accepted for publication September 23, 1976.

[x] To whom inquiries should be directed.

High-Pressure Liquid Chromatographic Determination of Tetracyclines in Urine

J. P. SHARMA [*], G. D. KORITZ [*], E. G. PERKINS [‡], and R. F. BEVILL [*x]

Abstract □ The quantitation of oxytetracycline, tetracycline, and chlortetracycline was accomplished by high-pressure liquid chromatography using an anion-exchange column. The tetracyclines were extracted from urine as their calcium complexes. Concentrations as low as 12 μg of oxytetracycline/ml and 4 μg of tetracycline and chlortetracycline/ml were quantitated accurately. The relative standard deviation of the method varied from 0 to 5%.

Keyphrases □ Oxytetracycline—high-pressure liquid chromatographic analysis, urine □ Tetracycline—high-pressure liquid chromatographic analysis, urine □ Chlortetracycline—high-pressure liquid chromatographic analysis, urine □ High-pressure liquid chromatography—analyses, oxytetracycline, tetracycline, and chlortetracycline in urine □ Antibacterials—oxytetracycline, tetracycline, and chlortetracycline, high-pressure liquid chromatographic analyses, urine

To establish the urinary excretion rate of tetracyclines in the urine of cattle, sheep, and swine following intravenous drug administration, an accurate method for the quantitation of oxytetracycline, tetracycline, and chlortetracycline was required. TLC (1–5) and paper chromatographic (6–9) methods were laborious and lacked sufficient sensitivity and accuracy. One GLC method (10) required the formation of trimethylsilyl derivatives and sometimes resulted in the formation of tetracycline degradation products. None of the previously reported fluorometric methods (11–14) could be used due to large and variable amounts of fluorescent material in urine obtained from untreated control animals.

Several high-pressure liquid chromatographic (HPLC) methods for the separation and determination of tetracyclines have been reported. A low efficiency column packing was used for the separation of tetracyclines, but the method lacked the sensitivity required for analysis of biological samples (15). The experimental conditions required for the qualitative separation of several tetracyclines were discussed (16), but the quantitative utility of this method was not reported. Several reports (17, 18) did not include oxytetracycline. The purpose of this study was

safely carried out in the presence of crataegus extract and other alkaloids such as papaverine, strychnine, morphine, and atropine.

Although the proposed reactions are specific for quinine and quinidine, a TLC procedure is necessary for cinchona preparations to separate quinine and quinidine and to eliminate other interfering constituents. The four main cinchona alkaloids showed good separation; the R_f values of quinine, quinidine, cinchonine, and cinchonidine were 0.18, 0.44, 0.55, and 0.41, respectively.

Ammonium hydroxide was not capable of releasing quinine base from the dipyrone–quinine salt, while sodium hydroxide solution was satisfactory.

The proposed methods also were applied successfully to the recovery of quinine and quinidine from blood and urine with reproducible results. With blood, because of the small concentration of the alkaloids present, only the more sensitive erythroquinine method was adopted.

Good recoveries at different concentrations and spiking and reasonable standard deviations were obtained with dosage forms and biological fluids by the erythroquinine and thalleioquin methods (Tables I–III).

To obtain protein-free aqueous filtrates from blood and urine, the samples were digested with hydrochloric acid to liberate strongly conjugated alkaloids. Hydrochloric acid digestion was preferable to other procedures.

REFERENCES

(1) J. D. Endiz, *J. Assoc. Offic. Anal. Chem.*, **46**, 637 (1963).

(2) R. N. Bhattacharya and G. K. Ganguly, *J. Pharm. Pharmacol.*, **6**, 191 (1954).

(3) S. Bruno, *Farmaco, Ed. Sci.*, **10**, 922 (1955).

(4) P. Brockman, V. R. Severen, and L. Moeseke, *Pharm. Tijdschr. Belg.*, **40**, 113 (1963).

(5) J. Eisenbrand, *Z. Anal. Chem.*, **179**, 170 (1961).

(6) B. B. Brodie and S. Udenfriend, *J. Pharmacol.*, **78**, 154 (1943).

(7) P. Spacu and C. Ianu, *Z. Anal. Chem.*, **174**, 87 (1960).

(8) R. Dorr, *ibid.*, **226**, 417 (1967).

(9) J. Bosly, *Farmaco, Ed. Prat.*, **19**, 448 (1964).

(10) N. M. Chuev and P. A. Arzamastsev, *Apotechn. Delo*, **8**, 45 (1959).

(11) O. Adam, *Acta Pol. Pharm.*, **27**, 249 (1970); through *Chem. Abstr.*, **74**, 91219 V (1971).

(12) S. Smith and W. Manges, *Dtsch. Apoth. Ztg.*, **97**, 747 (1957).

(13) I. A. Volkova and E. T. Man, *Get. Ukr. Khim. Zn.*, **31**, 1320 (1965).

(14) A. Suszko-Purzycka and W. Trzebny, *Chem. Anal. (Warsaw)*, **9**, 1103 (1964).

(15) B. Horst and R. Bitsch, *Arch. Pharm.*, **303**, 418 (1960).

(16) A. Suszko-Purzycka and W. Trzebny, *J. Chromatogr.*, **19**, 239 (1964).

(17) H. Steger and A. A. Storz, *Pharmazie*, **16**, 126 (1961).

(18) J. Leving, *J. Assoc. Offic. Anal. Chem.*, **145**, 595 (1962).

(19) E. Haberli and E. Beguin, *Pharm. Acta Helv.*, **34**, 65 (1959).

(20) Abensour, *J. Pharm.*, **26**, 25 (1907); through C. H. Thienes and T. J. Haley, "Clinical Toxicology," 4th ed., Lea & Febiger, Philadelphia, Pa., 1964, p. 543.

(21) Andre, *Ann. Chim. Phys.*, **1835**, 195; through C. H. Thienes and T. J. Haley, "Clinical Toxicology," 4th ed., Lea & Febiger, Philadelphia, Pa., 1964, p. 543.

(22) L. N. Allport and D. Friend, *Q. J. Pharm. Pharmacol.*, **11**, 450 (1938).

(23) R. Monnet, *J. Pharm. Chim.*, **18**, 59 (1933).

(24) "Official Methods of Analysis," 10th ed., Association of Official Analytical Chemists, Washington, DC 20044, 1970, secs. 36.147.

ACKNOWLEDGMENTS AND ADDRESSES

Received February 23, 1976, from the *Department of Pharmacognosy, Faculty of Pharmacy, Cairo University, Cairo, Egypt.*

Accepted for publication September 23, 1976.

[x] To whom inquiries should be directed.

High-Pressure Liquid Chromatographic Determination of Tetracyclines in Urine

J. P. SHARMA [*], G. D. KORITZ [*], E. G. PERKINS [‡], and R. F. BEVILL [*x]

Abstract □ The quantitation of oxytetracycline, tetracycline, and chlortetracycline was accomplished by high-pressure liquid chromatography using an anion-exchange column. The tetracyclines were extracted from urine as their calcium complexes. Concentrations as low as 12 μg of oxytetracycline/ml and 4 μg of tetracycline and chlortetracycline/ml were quantitated accurately. The relative standard deviation of the method varied from 0 to 5%.

Keyphrases □ Oxytetracycline—high-pressure liquid chromatographic analysis, urine □ Tetracycline—high-pressure liquid chromatographic analysis, urine □ Chlortetracycline—high-pressure liquid chromatographic analysis, urine □ High-pressure liquid chromatography—analyses, oxytetracycline, tetracycline, and chlortetracycline in urine □ Antibacterials—oxytetracycline, tetracycline, and chlortetracycline, high-pressure liquid chromatographic analyses, urine

To establish the urinary excretion rate of tetracyclines in the urine of cattle, sheep, and swine following intravenous drug administration, an accurate method for the quantitation of oxytetracycline, tetracycline, and chlortetracycline was required. TLC (1–5) and paper chromatographic (6–9) methods were laborious and lacked sufficient sensitivity and accuracy. One GLC method (10) required the formation of trimethylsilyl derivatives and sometimes resulted in the formation of tetracycline degradation products. None of the previously reported fluorometric methods (11–14) could be used due to large and variable amounts of fluorescent material in urine obtained from untreated control animals.

Several high-pressure liquid chromatographic (HPLC) methods for the separation and determination of tetracyclines have been reported. A low efficiency column packing was used for the separation of tetracyclines, but the method lacked the sensitivity required for analysis of biological samples (15). The experimental conditions required for the qualitative separation of several tetracyclines were discussed (16), but the quantitative utility of this method was not reported. Several reports (17, 18) did not include oxytetracycline. The purpose of this study was

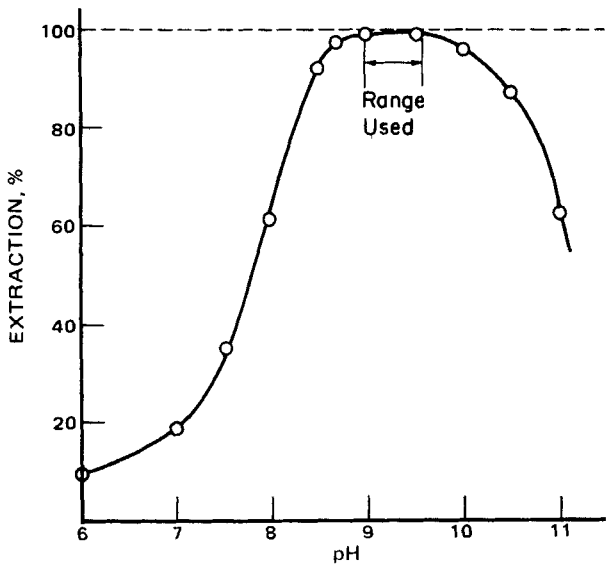

Figure 1—*Effect of pH on the extraction of tetracycline–calcium complexes from cattle urine.*

to develop an HPLC method for the quantitation of tetracyclines in urine.

EXPERIMENTAL

Apparatus—An HPLC unit[1] equipped with a variable wavelength UV detector[2] was used. The UV spectra of the tetracyclines were recorded with a double-beam spectrophotometer[3].

Reagents and Materials—Mobile Phase A was 0.005 *M* ethylenediaminetetraacetic acid[4] (disodium salt) (I), 0.05 *M* NaCl[5], and 5% methanol[6] in distilled water; Phase B was 0.005 *M* I, 0.05 *M* NaCl, and 30% methanol in distilled water. The distilled water was degassed prior to use, and the pH of each mobile phase was adjusted to 9.9 with ammonium hydroxide[7] solution.

A 1.0 *N* solution of hydrochloric acid[7] was used for back-extraction of tetracyclines. A trichloroacetic acid[8]–calcium chloride[8] reagent was prepared by dissolving 40.0 g of trichloroacetic acid and 4.0 g of calcium chloride dihydrate in 100 ml of distilled water. The sodium hydroxide solution[8] contained 9 g of sodium hydroxide/100 ml of water. Barbital sodium[8] contained 10.3 g/100 ml of distilled water. Fresh solutions were prepared every 2 weeks. Pure standards of oxytetracycline[9], tetracycline[10], and chlortetracycline[10] as the hydrochlorides were dried *in vacuo* prior to use.

Columns were dry packed with anion-exchange material[11] after conditioning in a 0.02 *M* solution of ethylenediaminetetraacetic acid.

Chromatographic Procedures—Isocratic solvent elutions with Mobile Phase A (oxytetracycline) or B (tetracycline and chlortetracycline) were used for tetracycline quantitation. Stock standards were prepared by adding 50 mg of the tetracycline to be quantitated (sample drug) and an internal standard (a second tetracycline) to separate 100-ml volumetric flasks containing distilled water and 0.5 ml of 1.0 *N* hydrochloric acid. Working standards were prepared by combining aliquots of each stock standard in a 25-ml flask and diluting with distilled water.

Duplicate 3-ml aliquots of urine were placed in 20-ml screw-capped tubes and spiked with 1 ml of the working standard. The trichloroacetic acid–calcium chloride reagent (1 ml) was added to each tube, which was then agitated (2 min) and centrifuged (2000 rpm for 10 min). The supernates (4.5 ml) were transferred to tubes containing 1.0 ml of both sodium hydroxide and barbital sodium solutions.

The contents of the tubes were partitioned with 5.0 ml of ethyl acetate and centrifuged, and aliquots (8 μl) of the upper layer were injected on the column. An average response factor was calculated from the ratio of the peak heights produced by the sample drug and the internal standard as follows:

$$\text{response factor } (f) = \frac{H_s}{H_{std}} \times \frac{W_{std}}{W_s} \qquad \text{(Eq. 1)}$$

where H_s/H_{std} is the ratio of the peak heights of the sample drug to the internal standard, and W_{std}/W_s is the weight ratio of the internal standard to the sample drug.

Urine samples containing variable amounts of the sample drug were spiked with known amounts of the internal standard and prepared for injection as previously described. Following injection of the urine extracts, the amount of sample drug was calculated using:

$$\text{amount} = \frac{R \times W'_{std}}{f} \qquad \text{(Eq. 2)}$$

where R is the ratio of peak heights of the unknown amount of sample drug to the known amount of internal standard (W'_{std}).

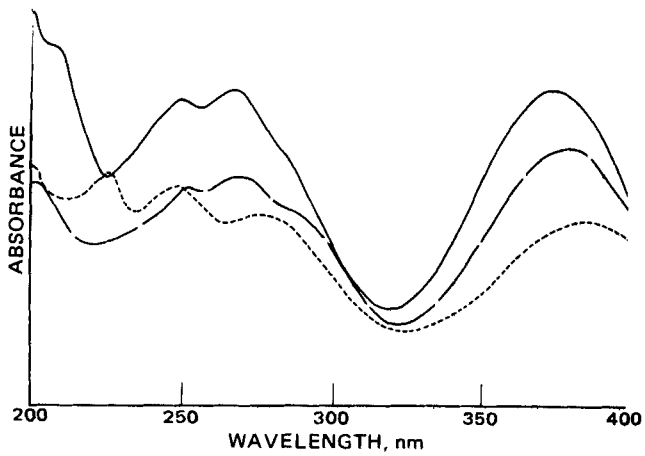

Figure 2—*UV absorption spectrum of tetracycline (– –), oxytetracycline (—), and chlortetracycline (- - -) in Mobile Phase A.*

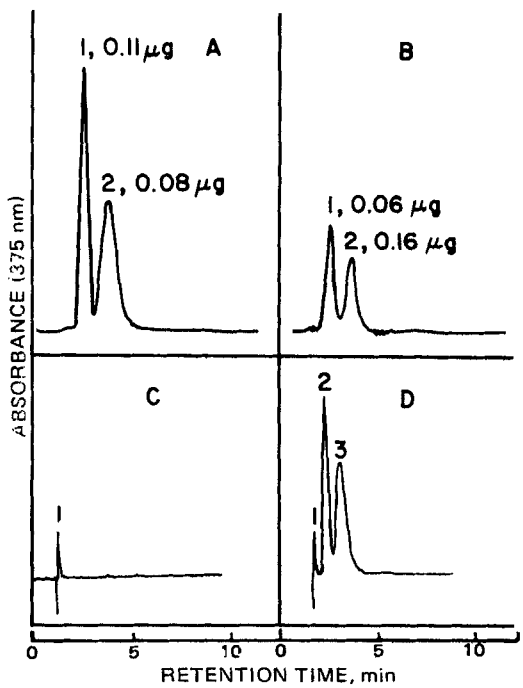

Figure 3—*(A) Elution of oxytetracycline (1) and tetracycline (2) standards with Mobile Phase A. (B) Elution of tetracycline (1) and chlortetracycline (2) standards with Mobile Phase B. (C) Chromatogram of swine urine extract blank with Mobile Phase A showing only the solvent peak (1). (D) Chromatogram of the extract of swine urine spiked with 50 μg of oxytetracycline/ml (2) and 50 μg of tetracycline/ml (3) with Mobile Phase A. Peak 1 is the solvent peak.*

[1] Model 1220, Perkin-Elmer Corp., Norwalk, Conn.
[2] Model LC-55, Perkin-Elmer Corp., Norwalk, Conn.
[3] Model 25, Beckman Instruments, Fullerton, Calif.
[4] Reagent grade, Hach Chemical Co., Ames, Iowa.
[5] Certified ACS, Fisher Scientific Co.
[6] Spectroscopic grade, Burdick and Jackson, Muskegan, Mich.
[7] Analytical reagent, du Pont, Wilmington, Del.
[8] Analytical reagent, Mallinckrodt, St. Louis, Mo.
[9] Sigma Chemical Co., St. Louis, Mo.
[10] Lederle Laboratories, Division of American Cyanamid, Pearl River, N.Y.
[11] Ion-X-SA, Perkin-Elmer Corp., Norwalk, Conn.

Table I—Determination of Tetracyclines in Swine, Sheep, and Cattle Urine

Tetracycline	Average Response Factor	Amount Spiked, μg/ml	Amount Recovered, μg/ml	Recovery, % (Average Recovery, %)	± RSD[a], %
			Swine		
Oxytetracycline	1.305 (±0.007)	12.8	12.7	99.2	2.3
		30.0	30.5	107.6	2.2
		50.0	51.5	103.0	1.3
		70.0	68.5	97.8	1.0
				(101.9)	
Tetracycline	0.964 (±0.006)	4.3	4.4	102.3	0.5
		37.0	36.5	98.6	1.9
		62.0	60.0	96.7	0.0
		87.0	89.5	102.8	0.8
				(100.1)	
Chlortetracycline	0.263 (±0.019)	7.0	7.3	104.2	2.3
		44.0	49.0	111.3	2.8
		73.0	73.0	100.0	1.9
		103.0	104.0	100.9	2.7
				(104.1)	
			Sheep		
Oxytetracycline	0.999 (±0.015)	17.0	17.2	101.1	2.2
		66.0	61.0	92.4	5.0
		93.0	91.0	97.8	2.3
				(97.1)	
Tetracycline	0.997 (±0.017)	5.7	5.8	101.7	5.4
		35.0	36.5	104.2	4.5
		77.0	77.5	100.6	3.8
		101.0	102.0	100.9	2.0
				(101.8)	
Chlortetracycline	0.249 (±0.015)	9.0	8.6	95.5	0.3
		49.0	51.0	104.0	2.7
		59.0	64.0	108.4	5.4
		74.0	71.0	95.9	1.9
				(100.9)	
			Cattle		
Oxytetracycline	1.315 (±0.007)	20.0	19.4	97.0	0.5
		66.0	65.5	99.2	1.0
		133.0	134.5	101.1	0.5
				(99.1)	
Tetracycline	0.856 (±0.003)	7.5	7.8	104.0	1.2
		39.0	40.0	102.5	2.0
		72.0	72.5	100.6	0.9
				(102.3)	
Chlortetracycline	0.298 (±0.014)	10.0	9.3	93.0	0.3
		49.0	46.5	94.8	1.5
		59.0	63.0	106.7	4.4
		74.0	74.0	100.0	2.8
				(98.6)	

[a] Duplicate samples were analyzed at each concentration.

RESULTS AND DISCUSSION

Tetracyclines form extractable complexes with Ca^{2+} when combined in a weakly basic medium (11, 19). A series of aqueous samples containing 30 μg of tetracycline/ml were adjusted to different pH values, from 6 to 11, with hydrochloric acid or sodium hydroxide and extracted with equal volumes of ethyl acetate. The extraction efficiency was determined by comparing the peak heights obtained after equal volumes of the aqueous and organic phases from each sample were injected. The extraction profile is presented in Fig. 1. Optimum extraction of tetracycline was obtained at pH 8.5–10 and was the same for other tetracyclines.

Extraction of urine samples was preceded by a deproteinization step using 40% trichloroacetic acid. During this process, 10–20% of the tetracyclines present in the urine sample was lost. Greater losses occurred during the deproteinization of cattle urine, whereas the losses associated with the deproteinization of swine urine were lower. Following deproteinization, the urine was adjusted to pH 9.0–9.5 with sodium hydroxide and 0.5 *M* barbital sodium. The extraction of oxytetracycline from the urine of cattle, sheep, and swine varied from 65 to 72%, but greater extraction efficiencies (98–99%) were realized with tetracycline and chlortetracycline. The extraction of all three drugs was reproducible, and no deterioration of the extracted calcium complexes was noted during the first 10 hr following their partition into ethyl acetate.

UV spectroscopy at 254 and 280 nm was used previously for the detection of tetracyclines (15–17). In the present study, ethyl acetate (UV cutoff 260 nm) produced a pronounced solvent peak at 254 nm which interfered with the determination of oxytetracycline. Similar complications were encountered when monitoring was performed at 280 nm as a result of the extraction of UV-absorbing components in urine simultaneously eluting with the tetracyclines. To circumvent these problems, 375 nm was selected on the basis of the UV spectra presented in Fig. 2.

Two solvent systems were required to reduce the elution time of each tetracycline and to provide for separation of the sample drug and the internal standard. Oxytetracycline, tetracycline, and chlortetracycline were separated with Mobile Phase A, but the retention of chlortetracycline was prolonged. Chlortetracycline and tetracycline were separated and the chlortetracycline retention time was greatly reduced with Mobile Phase B, but oxytetracycline eluted with the solvent front.

On the basis of these findings, oxytetracycline was quantitated in Mobile Phase A using tetracycline as an internal standard (Fig. 3A). Mobile Phase B was used for the quantitation of tetracycline and chlortetracycline with either of the two drugs serving as an internal standard (Fig. 3B). The solvent peak, which appeared when urine extracts were injected (Fig. 3C), was well separated from sample peaks (Fig. 3D) irrespective of the use of Mobile Phase A or B. The results of the determination of the three tetracyclines in swine, sheep, and cattle urine are presented in Table I. The relative standard deviation of the method ranged from 0 to 5%.

REFERENCES

(1) D. Sonanini and L. Anker, *Pharm. Acta Helv.*, **39**, 518 (1964).

(2) P. P. Ascione, J. B. Zagar, and G. P. Chrekian, *J. Pharm. Sci.*, **56**, 1393 (1967).

(3) N. D. Ghyanchandani, I. J. McGilveray, and D. W. Hughes, *ibid.*, **59**, 224 (1970).
(4) A. A. Fernandez, V. T. Noceda, and E. S. Carrera, *ibid.*, **58**, 443 (1969).
(5) C. Radecka and W. L. Wilson, *J. Chromatogr.*, **57**, 297 (1971).
(6) E. Addison and R. G. Clark, *J. Pharm. Pharmacol.*, **15**, 286 (1963).
(7) R. G. Kelly, *J. Pharm. Sci.*, **53**, 1551 (1964).
(8) F. Bailey, *J. Pharm. Pharmacol.*, **21**, 41A (1969).
(9) B. W. Griffith, R. Brunet, and L. Greenburg, *Can. J. Pharm. Sci.*, **5**, 10 (1970).
(10) K. Tsuji and J. H. Robertson, *Anal. Chem.*, **45**, 2136 (1973).
(11) K. W. Kohn, *ibid.*, **33**, 862 (1961).
(12) M. Lever, *Biochem. Med.*, **6**, 216 (1972).
(13) R. G. Kelly, L. M. Peets, and K. D. Hoyt, *Anal. Biochem.*, **28**, 222 (1969).
(14) K. H. Ibsen, R. L. Saunders, and M. R. Urist, *ibid.*, **5**, 505 (1963).
(15) E. R. White, M. A. Corroll, J. E. Zarembo, and A. D. Bender, *J. Antibiot.*, **28**, 205 (1975).
(16) A. G. Butterfield, D. W. Hughes, N. J. Pound, and W. L. Wilson, *Antimicrob. Agents Chemother.*, **4**, 11 (1973).
(17) J. H. Knox and J. Jurand, *J. Chromatogr.*, **110**, 103 (1975).
(18) K. Tsuji, J. H. Robertson, and W. F. Beyer, *Anal. Chem.* **46**, 539 (1974).
(19) M. Ishidate and T. Sakaguchi, *Pharm. Bull. (Tokyo)*, **3**, 147 (1955).

ACKNOWLEDGMENTS AND ADDRESSES

Received May 3, 1976, from the *Department of Veterinary Physiology and Pharmacology and the ‡Department of Food Science, University of Illinois at Urbana–Champaign, Urbana, IL 61801.

Accepted for publication November 9, 1976.

Supported by Food and Drug Administration Contract 223-74-7178 and the Illinois Agricultural Experiment Station.

ˣ To whom inquiries should be directed.

Drug Interactions with Isoniazid Metabolism in Rats

BARRY H. THOMAS ˣ and GNANAPRAKASAM SOLOMONRAJ

Abstract □ ^{14}C-Isoniazid (20 mg/kg po or iv) was administered alone or in combination with aspirin (100 mg/kg po), rifampin (30 mg/kg po), ethambutol (100 mg/kg po), or ethanol (3 g/kg po) to rats. In another experiment, phenobarbital sodium (40 mg/kg/day ip) was administered for 3 days prior to isoniazid. Aspirin and ethanol retarded the rate of isoniazid absorption from the GI tract. None of the drugs significantly altered the ^{14}C-elimination rate from the blood over the first 4 hr. A tissue distribution study showed that changes in the blood levels produced by ethanol were reflected in the other tissues. When isoniazid was given intravenously, ethanol increased the amount of carbon-14 excreted in urine up to 24 hr after dosing; no other changes were observed in the total carbon-14 recovered in urine. Aspirin inhibited the conjugation of isonicotinic acid with glycine. Ethanol increased *N*-acetylisoniazid excretion and decreased isonicotinic acid excretion. None of the other treatments had more than a slight effect on isoniazid metabolism. Acute doses of isoniazid failed to produce any signs of hepatotoxicity, as judged by measurement of serum transaminase levels. The data do not suggest that any of the drugs studied are likely to potentiate the hepatotoxicity of isoniazid when administered acutely. Isoniazid metabolism in rats differed quantitatively from that reported for humans.

Keyphrases □ Isoniazid—absorption, tissue distribution, excretion, and metabolism, effect of aspirin, rifampin, ethambutol, ethanol, and phenobarbital, radiochemical analysis, rats □ Absorption—isoniazid, effect of various drugs, radiochemical analysis, rats □ Distribution, tissue—isoniazid, effect of various drugs, radiochemical analysis, rats □ Excretion—isoniazid, effect of various drugs, radiochemical analysis, rats □ Metabolism—isoniazid, effect of various drugs, radiochemical analysis, rats □ Radiochemistry—analysis, isoniazid, effect of various drugs on absorption, tissue distribution, excretion, and metabolism, rats □ Interactions, drug—isoniazid, absorption, tissue distribution, excretion, and metabolism, effect of aspirin, rifampin, ethambutol, ethanol, and phenobarbital, radiochemical analysis, rats □ Antibacterials, tuberculostatic—isoniazid, absorption, tissue distribution, excretion, and metabolism, effect of various drugs, rats

Interest in the metabolism and toxicity of isoniazid was aroused by the death of two patients and the development of clinical hepatotoxicity in 17 others in 1970 following an isoniazid chemoprophylactic program (1). Furthermore, the antituberculous drug rifampin increased the incidence of hepatotoxicity in humans when given with isoniazid (2). This same association was observed in rats (3).

Recently, it was shown that metabolism by the microsomal mixed function oxidase system is responsible for isoniazid hepatotoxicity (4). It was suggested that it is necessary to acetylate isoniazid before it can be a substrate for the toxication pathway. The purposes of this study were to screen drugs likely to be taken by tuberculous patients and to observe their influence on isoniazid metabolism as a clue to possible toxic drug interactions.

EXPERIMENTAL

[^{14}C-Carboxyl]-isoniazid[1] had a specific activity of 11.3 mCi/mmole and a radiochemical purity of 96–97%, as determined in two paper chromatography and two TLC systems. Aspirin[2], ethambutol[3], rifampin[4], phenobarbital sodium[5], and absolute ethanol[6] were obtained commercially.

Male Wistar rats[7], 170–200 g, were deprived of food but not water for 16 hr prior to dosing and were housed in metabolism cages[8] that separated urine and feces. In most experiments, ^{14}C-isoniazid was given orally at a dose of 20 mg/kg in 10 ml of water/kg. In one experiment, ^{14}C-isoniazid was given intravenously into the saphenous vein at a dose of 20 mg/kg in 1.0 ml/kg. The dose of carbon-14 in all experiments was 25 μCi/kg.

Aspirin (100 mg/kg) in 0.25% gum tragacanth, ethambutol (100 mg/kg), rifampin (30 mg/kg), and ethanol (3 g/kg) were given orally immediately prior to the dose of isoniazid in 10 ml of water/kg. Phenobarbital sodium, 40 mg/kg/day ip, was administered for 3 days prior to isoniazid. Control animals were dosed similarly with saline for 3 days.

Duplicate 10-μl blood samples were collected from the tail at 0.25, 0.5, 1.0, 2.0, 3.0, 4.0, 6.0, and 12 hr after dosing using calibrated capillary tubes. The total carbon-14 in the samples was determined by digestion and

[1] Amersham/Searle, Oakville, Ontario, Canada.
[2] J. T. Baker Chemical Co., Phillipsburg, N.J.
[3] Myambutol, Cyanamid of Canada, Montreal, Quebec, Canada.
[4] Rimactane, Ciba-Geigy Canada Ltd., Dorval, Quebec, Canada.
[5] B.D.H. Canada Ltd., Toronto, Ontario, Canada.
[6] Consolidated Alcohols Ltd., Toronto, Ontario, Canada.
[7] Woodlyn Farms, Guelph, Ontario, Canada.
[8] Model 4-640-000, Acme Research Products, Cincinnati, Ohio.

(3) N. D. Ghyanchandani, I. J. McGilveray, and D. W. Hughes, *ibid.*, **59**, 224 (1970).
(4) A. A. Fernandez, V. T. Noceda, and E. S. Carrera, *ibid.*, **58**, 443 (1969).
(5) C. Radecka and W. L. Wilson, *J. Chromatogr.*, **57**, 297 (1971).
(6) E. Addison and R. G. Clark, *J. Pharm. Pharmacol.*, **15**, 286 (1963).
(7) R. G. Kelly, *J. Pharm. Sci.*, **53**, 1551 (1964).
(8) F. Bailey, *J. Pharm. Pharmacol.*, **21**, 41A (1969).
(9) B. W. Griffith, R. Brunet, and L. Greenburg, *Can. J. Pharm. Sci.*, **5**, 10 (1970).
(10) K. Tsuji and J. H. Robertson, *Anal. Chem.*, **45**, 2136 (1973).
(11) K. W. Kohn, *ibid.*, **33**, 862 (1961).
(12) M. Lever, *Biochem. Med.*, **6**, 216 (1972).
(13) R. G. Kelly, L. M. Peets, and K. D. Hoyt, *Anal. Biochem.*, **28**, 222 (1969).
(14) K. H. Ibsen, R. L. Saunders, and M. R. Urist, *ibid.*, **5**, 505 (1963).
(15) E. R. White, M. A. Corroll, J. E. Zarembo, and A. D. Bender, *J. Antibiot.*, **28**, 205 (1975).
(16) A. G. Butterfield, D. W. Hughes, N. J. Pound, and W. L. Wilson, *Antimicrob. Agents Chemother.*, **4**, 11 (1973).
(17) J. H. Knox and J. Jurand, *J. Chromatogr.*, **110**, 103 (1975).
(18) K. Tsuji, J. H. Robertson, and W. F. Beyer, *Anal. Chem.* **46**, 539 (1974).
(19) M. Ishidate and T. Sakaguchi, *Pharm. Bull. (Tokyo)*, **3**, 147 (1955).

ACKNOWLEDGMENTS AND ADDRESSES

Received May 3, 1976, from the *Department of Veterinary Physiology and Pharmacology and the ‡Department of Food Science, University of Illinois at Urbana–Champaign, Urbana, IL 61801.

Accepted for publication November 9, 1976.

Supported by Food and Drug Administration Contract 223-74-7178 and the Illinois Agricultural Experiment Station.

ˣ To whom inquiries should be directed.

Drug Interactions with Isoniazid Metabolism in Rats

BARRY H. THOMAS ˣ and GNANAPRAKASAM SOLOMONRAJ

Abstract □ ^{14}C-Isoniazid (20 mg/kg po or iv) was administered alone or in combination with aspirin (100 mg/kg po), rifampin (30 mg/kg po), ethambutol (100 mg/kg po), or ethanol (3 g/kg po) to rats. In another experiment, phenobarbital sodium (40 mg/kg/day ip) was administered for 3 days prior to isoniazid. Aspirin and ethanol retarded the rate of isoniazid absorption from the GI tract. None of the drugs significantly altered the ^{14}C-elimination rate from the blood over the first 4 hr. A tissue distribution study showed that changes in the blood levels produced by ethanol were reflected in the other tissues. When isoniazid was given intravenously, ethanol increased the amount of carbon-14 excreted in urine up to 24 hr after dosing; no other changes were observed in the total carbon-14 recovered in urine. Aspirin inhibited the conjugation of isonicotinic acid with glycine. Ethanol increased *N*-acetylisoniazid excretion and decreased isonicotinic acid excretion. None of the other treatments had more than a slight effect on isoniazid metabolism. Acute doses of isoniazid failed to produce any signs of hepatotoxicity, as judged by measurement of serum transaminase levels. The data do not suggest that any of the drugs studied are likely to potentiate the hepatotoxicity of isoniazid when administered acutely. Isoniazid metabolism in rats differed quantitatively from that reported for humans.

Keyphrases □ Isoniazid—absorption, tissue distribution, excretion, and metabolism, effect of aspirin, rifampin, ethambutol, ethanol, and phenobarbital, radiochemical analysis, rats □ Absorption—isoniazid, effect of various drugs, radiochemical analysis, rats □ Distribution, tissue—isoniazid, effect of various drugs, radiochemical analysis, rats □ Excretion—isoniazid, effect of various drugs, radiochemical analysis, rats □ Metabolism—isoniazid, effect of various drugs, radiochemical analysis, rats □ Radiochemistry—analysis, isoniazid, effect of various drugs on absorption, tissue distribution, excretion, and metabolism, rats □ Interactions, drug—isoniazid, absorption, tissue distribution, excretion, and metabolism, effect of aspirin, rifampin, ethambutol, ethanol, and phenobarbital, radiochemical analysis, rats □ Antibacterials, tuberculostatic—isoniazid, absorption, tissue distribution, excretion, and metabolism, effect of various drugs, rats

Interest in the metabolism and toxicity of isoniazid was aroused by the death of two patients and the development of clinical hepatotoxicity in 17 others in 1970 following an isoniazid chemoprophylactic program (1). Furthermore, the antituberculous drug rifampin increased the incidence of hepatotoxicity in humans when given with isoniazid (2). This same association was observed in rats (3).

Recently, it was shown that metabolism by the microsomal mixed function oxidase system is responsible for isoniazid hepatotoxicity (4). It was suggested that it is necessary to acetylate isoniazid before it can be a substrate for the toxication pathway. The purposes of this study were to screen drugs likely to be taken by tuberculous patients and to observe their influence on isoniazid metabolism as a clue to possible toxic drug interactions.

EXPERIMENTAL

[^{14}C-Carboxyl]-isoniazid[1] had a specific activity of 11.3 mCi/mmole and a radiochemical purity of 96–97%, as determined in two paper chromatography and two TLC systems. Aspirin[2], ethambutol[3], rifampin[4], phenobarbital sodium[5], and absolute ethanol[6] were obtained commercially.

Male Wistar rats[7], 170–200 g, were deprived of food but not water for 16 hr prior to dosing and were housed in metabolism cages[8] that separated urine and feces. In most experiments, ^{14}C-isoniazid was given orally at a dose of 20 mg/kg in 10 ml of water/kg. In one experiment, ^{14}C-isoniazid was given intravenously into the saphenous vein at a dose of 20 mg/kg in 1.0 ml/kg. The dose of carbon-14 in all experiments was 25 μCi/kg.

Aspirin (100 mg/kg) in 0.25% gum tragacanth, ethambutol (100 mg/kg), rifampin (30 mg/kg), and ethanol (3 g/kg) were given orally immediately prior to the dose of isoniazid in 10 ml of water/kg. Phenobarbital sodium, 40 mg/kg/day ip, was administered for 3 days prior to isoniazid. Control animals were dosed similarly with saline for 3 days.

Duplicate 10-μl blood samples were collected from the tail at 0.25, 0.5, 1.0, 2.0, 3.0, 4.0, 6.0, and 12 hr after dosing using calibrated capillary tubes. The total carbon-14 in the samples was determined by digestion and

[1] Amersham/Searle, Oakville, Ontario, Canada.
[2] J. T. Baker Chemical Co., Phillipsburg, N.J.
[3] Myambutol, Cyanamid of Canada, Montreal, Quebec, Canada.
[4] Rimactane, Ciba-Geigy Canada Ltd., Dorval, Quebec, Canada.
[5] B.D.H. Canada Ltd., Toronto, Ontario, Canada.
[6] Consolidated Alcohols Ltd., Toronto, Ontario, Canada.
[7] Woodlyn Farms, Guelph, Ontario, Canada.
[8] Model 4-640-000, Acme Research Products, Cincinnati, Ohio.

Table I—Urinary Excretion of Isoniazid Metabolites in Groups of Five Rats Dosed Orally with ^{14}C-Isoniazid (20 mg/kg) and Either Saline (Control) or Aspirin (100 mg/kg) [a]

Metabolite	Hours	Treatment	
		Control	Aspirin
I	0–6	5.08 ± 0.49	6.26 ± 0.79
	0–12	5.19 ± 0.51	6.49 ± 1.96
	0–24	5.22 ± 0.52	6.76 ± 0.64
II	0–6	3.99 ± 0.68	0[b]
	0–12	4.51 ± 0.69	0.16 ± 0.17[b]
	0–24	4.90 ± 0.70	0.16 ± 0.17[b]
III	0–6	14.55 ± 1.05	14.52 ± 2.79
	0–12	17.21 ± 1.22	19.74 ± 1.85
	0–24	17.72 ± 1.27	21.14 ± 1.81
IV	0–6	32.75 ± 2.58	29.64 ± 6.43
	0–12	40.11 ± 2.10	42.33 ± 4.06
	0–24	42.02 ± 1.71	44.98 ± 3.80

[a] The proportion of each metabolite is expressed as a percentage of the isoniazid dose. Values are means ± *SE*. [b] $p < 0.001$ (compared to control).

liquid scintillation counting as previously described (5). Urine was collected at 6, 12, and 24 hr after dosing, and the total carbon-14 was determined (5). The metabolites of isoniazid were separated by paper[9] chromatography using 2-propanol–water (85:15) as the solvent as described previously (6, 7). The location and quantity of each metabolite were determined by serially sectioning the chromatograms into 1-cm strips and counting in a liquid scintillation counter.

The tissue distribution of carbon-14 was studied in groups of rats killed by decapitation at either 0.5 or 3 hr after dosing. The liver, kidneys, lungs, brain, skeletal muscle (sample from the hindleg), and blood were collected. The concentration of carbon-14 was estimated in these tissues as previously described (5).

In a small-scale study of acute hepatotoxicity, isoniazid (50, 200, and 500 mg/kg) was administered orally to groups of three rats. Blood samples (0.2 ml) were withdrawn from the tail at 6, 12, and 18 hr after dosing for estimation of serum glutamic–oxaloacetic transaminase and serum glutamic–pyruvic transaminase. The transaminases were analyzed by a spectrophotometric method (8) using an automatic enzyme analyzer[10].

Differences between treatment groups were analyzed by the unpaired Student *t* test. When there were several treatments and only one control, the significance of the *t* values was evaluated using Dunnett's method (9). The half-lives ($T_{1/2}$) of elimination of carbon-14 from blood were determined using the regression analysis equations from the literature (18G) (10) on a minicomputer[11]. These same equations were used to test for a change in $T_{1/2}$ between control and treatment groups.

RESULTS

Blood Profiles and Urine—Analysis of the blood data indicated the presence of two compartments, but it was not possible to define the later phase because of insufficient data points. Estimation of carbon-14 in this later phase was difficult due to the low counts. Since the urine data showed that over 50% of the drug had been excreted in the first 6 hr, this period is the most important phase of elimination.

Paper chromatography of the urine separated the radioactivity into three major peaks, one small peak, and several variable minor peaks. All corresponded in terms of R_f with reported values (6). On the basis of the published R_f and concurrently run authentic specimens, one major peak was identified as isonicotinic acid (III). On the basis of R_f values, the other two major peaks were tentatively identified as *N*-acetylisoniazid (IV) and isonicotinoylglycine (II) and the small peak was tentatively identified as α-ketoglutaric isonicotinoylhydrazone (I) (Table I). Isoniazid itself was present in only trace quantities, as were the two spots due to pyruvic acid isonicotinoylhydrazone.

Aspirin—The blood profile shown in Fig. 1 indicates little effect of aspirin on the elimination of carbon-14 from blood. Analysis of the regression lines between 1 and 4 hr showed no significant differences between the two groups, and the calculated $T_{1/2}$ values[12] over this period were 1.09 (0.96–1.25) hr for the control group and 1.28 (1.12–1.50) hr for the aspirin-treated group.

Elimination of carbon-14 in urine was rapid and constituted the major excretion route (control: 0–6 hr, 57.25 ± 4.09%; 0–12 hr, 67.97 ± 8.69%; 0–24 hr, 70.93 ± 3.00%; and aspirin: 0–6 hr, 50.56 ± 8.69%; 0–12 hr, 66.92 ± 5.64%; 0–24 hr, 73.24 ± 5.08%). No significant treatment effects were observed. Only one of the four metabolites estimated was affected; II was markedly inhibited by aspirin.

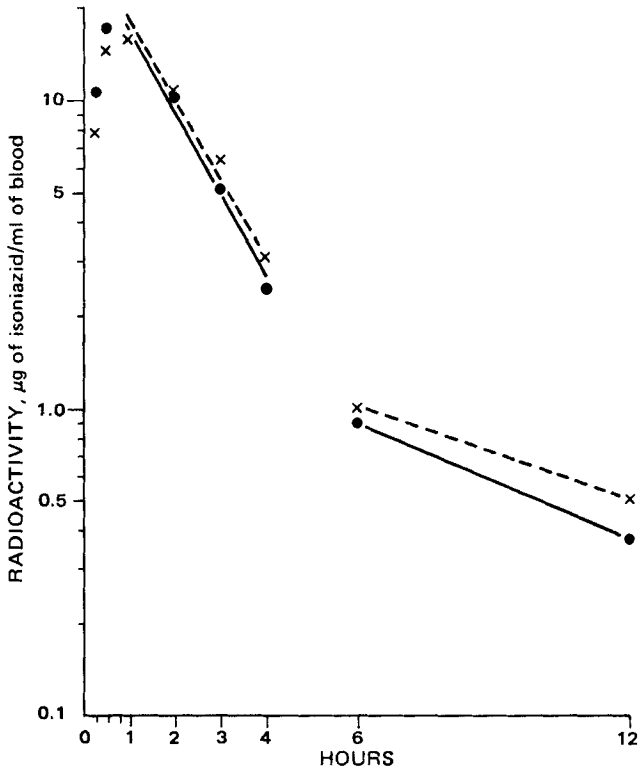

Figure 1—*Effect of aspirin on the blood carbon-14 concentration, expressed as micrograms of isoniazid per milliliter of blood. Values are means from groups of five rats dosed orally with ^{14}C-isoniazid (20 mg/kg). Key: ●, isoniazid alone; and ×, isoniazid and aspirin (100 mg/kg).*

Rifampin and Ethambutol—These two antitubercular drugs are considered together because they were studied on the same day against one control group. The blood profiles (Fig. 2) were all similar, with the calculated $T_{1/2}$ values between 1 and 4 hr being 1.23 (1.14–1.33) hr for the control group, 1.31 (1.22–1.44) hr for the rifampin group, and 1.40 (1.28–1.54) hr for the ethambutol group. Neither treatment had a significant effect on the $T_{1/2}$.

Elimination of carbon-14 was not affected at any of the times studied, and the excretion of isoniazid metabolites (Table II) was only slightly changed by one treatment. Ethambutol reduced the excretion of III at 6, 12, and 24 hr.

Ethanol and Oral Isoniazid—The linear portion of the blood profile shown in Fig. 3 is shorter than in the other interactions studied, probably

Table II—Urinary Excretion of Isoniazid Metabolites in Groups of Three Rats Dosed Orally with ^{14}C-Isoniazid (20 mg/kg) and Saline (Control), Rifampin (30 mg/kg), or Ethambutol (100 mg/kg) [a]

Metabolite	Hours	Treatment		
		Control	Rifampin	Ethambutol
I	0–6	1.45 ± 0.30	2.27 ± 0.51	1.38 ± 0.07
	0–12	1.72 ± 0.24	2.41 ± 0.55	1.48 ± 0.05
	0–24	1.88 ± 0.34	2.46 ± 0.50	1.56 ± 0.05
II	0–6	6.68 ± 0.82	6.14 ± 0.33	9.14 ± 0.92
	0–12	6.99 ± 0.76	7.92 ± 0.87	9.15 ± 0.93
	0–24	7.64 ± 0.80	8.61 ± 0.94	9.15 ± 0.93
III	0–6	12.52 ± 0.94	10.53 ± 0.94	9.20 ± 0.68[b]
	0–12	14.51 ± 0.95	11.28 ± 1.02	11.01 ± 0.22[b]
	0–24	16.18 ± 0.76	12.22 ± 1.39	11.56 ± 0.28[b]
IV	0–6	27.54 ± 3.02	27.72 ± 2.51	29.38 ± 3.82
	0–12	33.30 ± 4.16	32.73 ± 3.18	37.23 ± 4.13
	0–24	37.67 ± 3.71	34.83 ± 3.47	38.54 ± 3.87

[a] The proportion of each metabolite is expressed as a percentage of the isoniazid dose. Values are means ± *SE*. [b] $p < 0.05$ (compared to control).

[9] Whatman No. 1.
[10] Abbott bichromatic analyzer, ABA-100.
[11] Datagen Nova 800.
[12] The 95% confidence limits are given in parentheses.

Table III—Urinary Excretion of Isoniazid Metabolites in Groups of Five Rats Dosed Orally with ^{14}C-Isoniazid (20 mg/kg) and Either Saline (Control) or Ethanol (3 g/kg) [a]

Metabolite	Hours	Treatment	
		Control	Ethanol
I	0–6	0.97 ± 0.17	2.13 ± 0.52
	0–12	0.98 ± 0.14	2.33 ± 0.50[b]
	0–24	1.05 ± 0.13	2.35 ± 0.50[b]
II	0–6	9.00 ± 1.09	3.52 ± 0.80[b]
	0–12	10.44 ± 1.07	5.64 ± 0.60[b]
	0–24	11.97 ± 1.04	6.21 ± 0.61[b]
III	0–6	14.19 ± 0.79	6.98 ± 0.57[b]
	0–12	15.70 ± 0.80	9.99 ± 0.81[b]
	0–24	17.02 ± 0.73	11.22 ± 0.83[b]
IV	0–6	35.58 ± 3.05	40.35 ± 4.34
	0–12	38.85 ± 3.21	56.37 ± 3.53[b]
	0–24	42.20 ± 2.40	59.27 ± 3.78[b]

[a] The proportion of each metabolite is expressed as a percentage of the isoniazid dose. Values are means ± *SE*. [b] $p < 0.05$ (compared to control).

Table IV—Urinary Excretion of Isoniazid Metabolites in Groups of Four Rats Dosed Intravenously with ^{14}C-Isoniazid (20 mg/kg) and Orally with Either Saline (Control) or Ethanol (3 g/kg) [a]

Metabolite	Hours	Treatment	
		Control	Ethanol
I	0–6	1.01 ± 0.12	1.62 ± 0.41
	0–12	1.16 ± 0.15	1.71 ± 0.39
	0–24	1.26 ± 0.15	1.72 ± 0.39
II	0–6	3.38 ± 1.59	4.82 ± 0.60
	0–12	5.06 ± 1.87	5.67 ± 0.65
	0–24	5.88 ± 1.94	6.24 ± 0.66
III	0–6	14.75 ± 2.01	10.87 ± 0.34
	0–12	17.18 ± 1.81	12.09 ± 0.36[b]
	0–24	18.31 ± 1.91	12.94 ± 0.40[b]
IV	0–6	34.04 ± 1.23	47.27 ± 1.37[b]
	0–12	42.55 ± 2.50	53.20 ± 1.05[b]
	0–24	44.87 ± 2.29	55.59 ± 1.00[b]

[a] The proportion of each metabolite is expressed as a percentage of the isoniazid dose. Values are means ± *SE*. [b] $p < 0.02$ (compared to control).

because of a marked effect during the absorption phase. The concentration of carbon-14 was significantly lower in the ethanol-treated group at 0.25, 0.5, and 1 hr, suggesting that ethanol reduced the isoniazid absorption rate. Over the linear 2–4-hr period, the $T_{1/2}$ values were 1.26 (1.09–1.48) hr for the control group and 1.22 (1.05–1.44) hr for the ethanol-treated group. The difference was not significant. At 12 hr, the blood concentration of carbon-14 was significantly higher in the ethanol group.

Elimination of carbon-14 into urine was once more unaffected by the treatment, but changes were observed in the proportions of the isoniazid metabolites (Table III). Both II and III were inhibited by ethanol treatment, but I and IV were increased. These opposing shifts in metabolism canceled each other out, resulting in no overall change in renal elimination.

The tissue distribution of carbon-14 at 0.5 and 3 hr after dosing is shown in Fig. 4. At 0.5 hr, the highest concentration was observed in the kidneys followed by the lungs. The liver and muscle were close to the blood level, and the brain was less than the blood level. In all tissues except the lungs, ethanol reduced the concentration significantly. At 3 hr, the effect of ethanol was essentially the same, but the reduction was then significant in the lung and not in the kidney tissues. All tissue concentrations were substantially lower at 3 than 0.5 hr, except for the brain where the decline was not as great.

Ethanol and Intravenous Isoniazid—Since some significant changes were observed with ethanol, most likely including an effect on absorption, it was decided to give isoniazid intravenously. The blood profile (Fig. 5) shows little indication of any effect of ethanol on elimination. The $T_{1/2}$ values over 1–4 hr were 1.19 (1.07–1.33) hr for the controls and 1.18 (1.08–1.29) hr for the ethanol group. At 2 hr, the carbon-14 concentration was significantly higher in the ethanol group than in the controls, but this effect was the only significant one.

Urinary elimination was similar in magnitude to that observed after oral dosing (controls: 0–6 hr, 51.45 ± 9.02%; 0–12 hr, 71.42 ± 2.26%; 0–24 hr, 75.92 ± 2.11%; and ethanol treated: 0–6 hr, 64.17 ± 6.70%; 0–12 hr, 79.79 ± 2.11%; 0–24 hr, 83.68 ± 2.68%), but in this case ethanol significantly ($p < 0.05$) increased the amount excreted at 12 and 24 hr. This effect may be related to a significant increase in urine volume in the ethanol-treated group during 0–6 hr (controls: 1.78 ± 0.17 ml; and ethanol treated: 3.64 ± 0.27 ml; $p < 0.001$). However, by 12 hr, the difference was

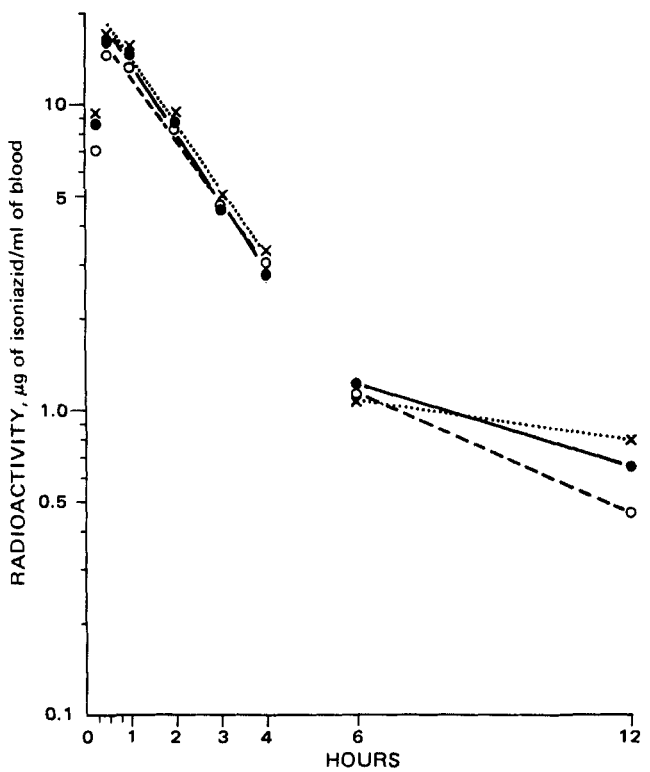

Figure 2—*Effect of rifampin and ethambutol on the blood carbon-14 concentration, expressed as micrograms of isoniazid per milliliter of blood. Values are means from groups of five rats dosed orally with ^{14}C-isoniazid (20 mg/kg). Key: ●, isoniazid alone; ×, isoniazid and rifampin (30 mg/kg); and ○, isoniazid and ethambutol (100 mg/kg).*

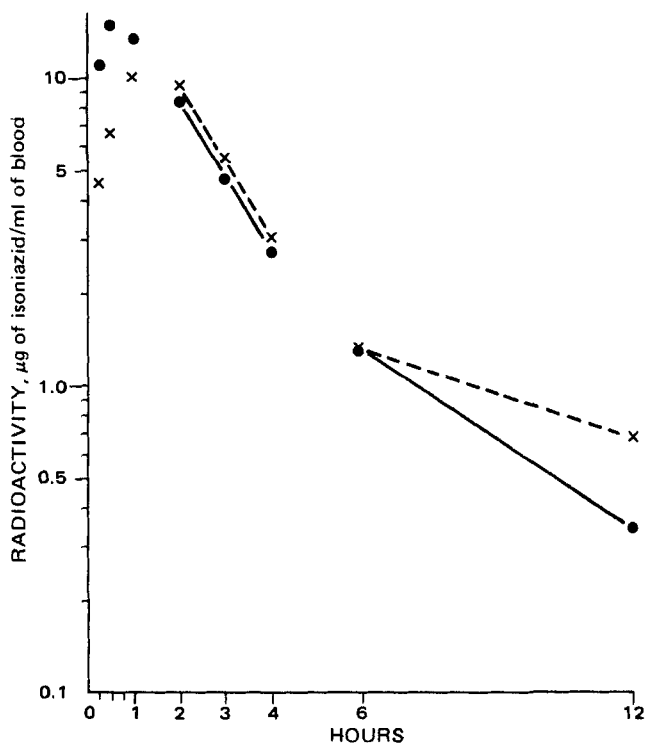

Figure 3—*Effect of ethanol on the blood carbon-14 concentration, expressed as micrograms of isoniazid per milliliter of blood. Values are means from groups of five rats dosed orally with ^{14}C-isoniazid (20 mg/kg). Key: ●, isoniazid alone; and ×, isoniazid and ethanol (3 g/kg).*

Table V—Urinary Excretion of Isoniazid Metabolites in Six Rats Dosed with Phenobarbital Sodium (40 mg/kg ip) for 3 Days and in Four Control Rats that Received Similar Doses of Saline; All Rats Were Dosed Orally with ^{14}C-Isoniazid (20 mg/kg) on the Following Day [a]

Metabolite	Hours	Treatment	
		Control	Phenobarbital
I	0–6	1.72 ± 0.71	1.01 ± 0.44
	0–12	2.00 ± 0.73	1.36 ± 0.50
	0–24	2.05 ± 0.71	1.38 ± 0.50
II	0–6	3.55 ± 1.12	2.61 ± 1.05
	0–12	7.20 ± 2.32	9.41 ± 0.92
	0–24	8.80 ± 2.45	10.97 ± 1.06
III	0–6	12.62 ± 1.92	5.16 ± 1.57[b]
	0–12	17.80 ± 2.65	13.19 ± 1.53
	0–24	19.84 ± 2.68	14.80 ± 1.62
IV	0–6	21.80 ± 2.56	15.09 ± 3.77
	0–12	31.54 ± 3.84	27.34 ± 1.41
	0–24	37.50 ± 2.60	33.68 ± 3.06

[a] The proportion of each metabolite is expressed as a percentage of the isoniazid dose. Values are means ± *SE*. [b] $p < 0.025$ (compared to control).

no longer significant. The metabolite data in Table IV confirm that ethanol inhibited III excretion and increased IV excretion, but in this case the increase in IV was sufficient to increase overall excretion.

Phenobarbital—Treatment with phenobarbital for 3 days to induce the microsomal enzyme system had no significant effect on the elimination of carbon-14 from blood (Fig. 6). The $T_{1/2}$ values over 1–6 hr were 1.41 (1.28–1.57) hr for the controls and 1.59 (1.47–1.73) hr for the phenobarbital-treated group, and the difference was not significant. None of the individual blood values was significantly different.

Renal excretion was unaffected by the pretreatment, and only at 6 hr was the excretion of isoniazid metabolites changed (Table V). At this one time, less III was excreted by the pretreated rats.

Serum Transaminases—Isoniazid was not hepatotoxic in the rat when given as single doses, even in large amounts (Table VI). In no case was there a significant increase in the transaminase levels.

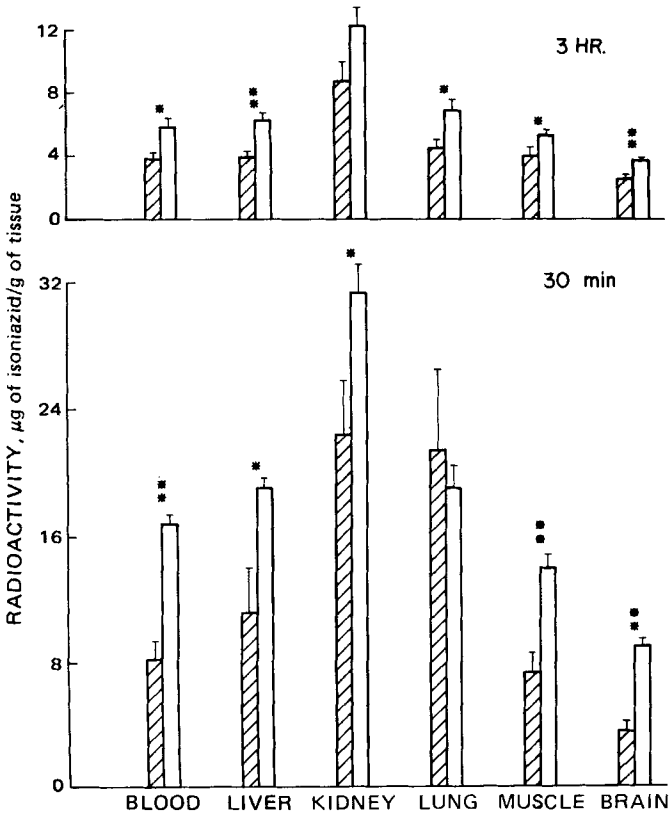

Figure 4—*Effect of ethanol on the tissue distribution of radioactivity, expressed as micrograms of isoniazid per milliliter of blood. Values are means and standard errors from groups of five rats dosed orally with ^{14}C-isoniazid (20 mg/kg) and killed at 0.5 or 3 hr. Key: □, isoniazid alone; ▨, isoniazid and ethanol (3 g/kg); *, p < 0.05; and **, p < 0.01.*

Table VI—Serum Glutamic-Oxaloacetic Transaminase (V) and Serum Glutamic-Pyruvic Transaminase (VI) Activities in Groups of Three Rats Administered Three Different Doses of Isoniazid [a]

Treatment, mg/kg	Hours after Dosing					
	6		12		18	
	V	VI	V	VI	V	VI
Control	106 ± 9	34 ± 1	136 ± 11	30 ± 1	97 ± 4	73 ± 3
Isoniazid						
50	100 ± 6	33 ± 4	112 ± 6	29 ± 5	96 ± 7	61 ± 6
200	75 ± 3	33 ± 1	90 ± 3	27 ± 1	84 ± 3	52 ± 2[b]
500	42 ± 1	34 ± 2	70 ± 10	24 ± 2	93 ± 6	44 ± 3[b]

[a] The activities of each enzyme are expressed as international units. Values are means ± *SE*. [b] $p < 0.05$ (compared to control).

DISCUSSION

Isoniazid was eliminated rapidly by rats. The $T_{1/2}$ of carbon-14 in the first phase of elimination, during which over half of the dose was excreted in the urine, had a mean value of about 1.2 hr in the control animals. Due to this extremely rapid elimination, it was not possible to define the second phase, which commenced at about 6 hr after dosing. None of the drugs significantly changed the calculated $T_{1/2}$. Grassi and Grassi (11) also observed that acute doses of ethanol in rats did not affect the serum isoniazid level but that chronic doses of 5 g of ethanol/kg/day did significantly increase serum isoniazid levels. Aspirin and ethanol probably retarded the isoniazid absorption rate, because the blood carbon-14 concentration was lower in the rats treated with these drugs during the first 0.5 hr after dosing.

The tissue distribution study showed that isoniazid and/or its metabolites can enter the brain; but since the level was less than that in the blood, it was inferred that there was some barrier to the passage from blood to brain. The highest concentration of carbon-14 at both 0.5 and 3 hr was observed in the kidneys, while in the control animals the other tissues resembled the blood level. The results are in accord with those reported for rats (12) when the smaller dose and different sampling times are taken into consideration.

The changes in blood level produced by ethanol, which are attributed

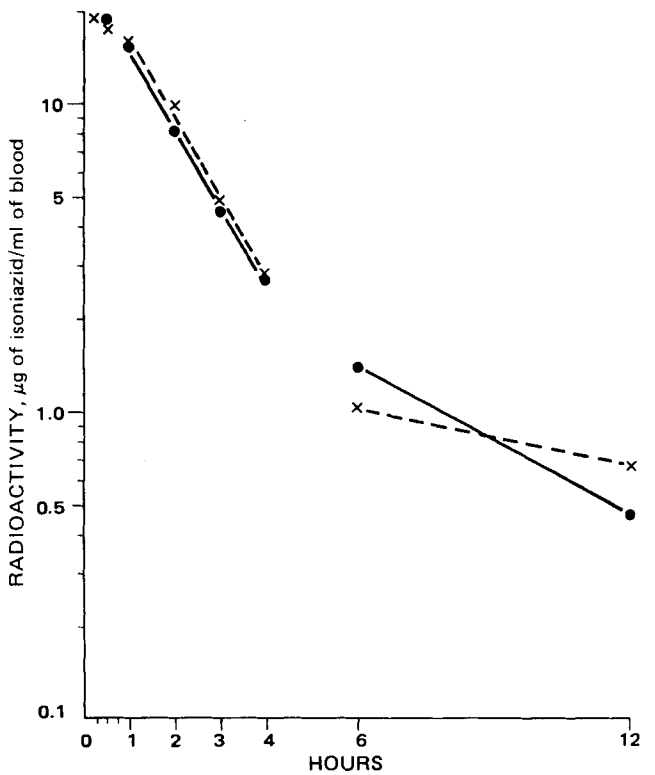

Figure 5—*Effect of ethanol on the blood carbon-14 concentration, expressed as micrograms of isoniazid per milliliter of blood. Values are means from groups of five rats dosed intravenously with ^{14}C-isoniazid (20 mg/kg). Key: ●, isoniazid alone; and ×, isoniazid and ethanol (3 g/kg).*

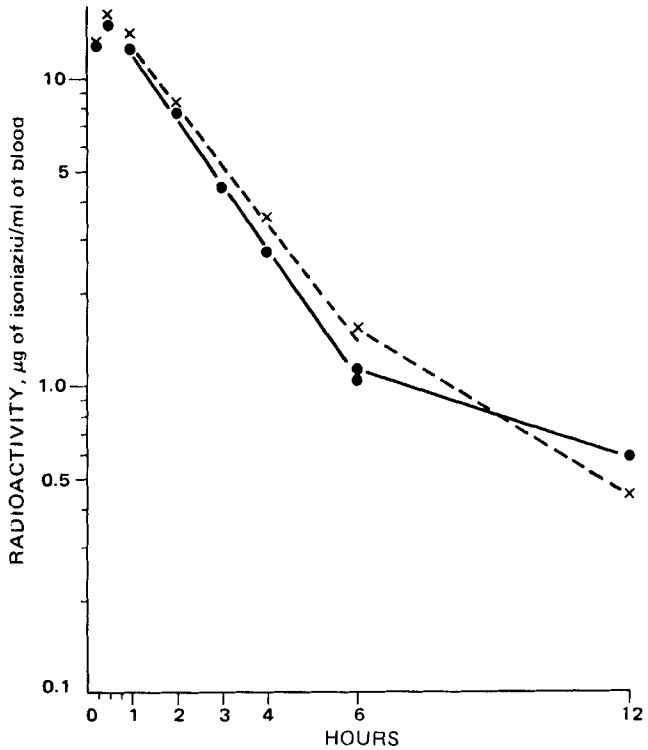

Figure 6—*Effect of phenobarbital pretreatment on the blood carbon-14 concentration, expressed as micrograms of isoniazid per milliliter of blood. Values are means from a group of six rats pretreated with phenobarbital sodium (40 g/kg/day ip) for 3 days and a group of four control rats that received saline. All rats were dosed orally with ^{14}C-isoniazid (20 mg/kg). Key: ●, saline-dosed controls; and ×, phenobarbital-pretreated rats.*

mostly to an effect on absorption, were generally reflected in the tissues. Hence, estimation of the blood carbon-14 level is a good indication of the situation in the whole body. One possible exception is that at 0.5 hr the lung level of carbon-14 was significantly ($p < 0.05$) higher than the blood in the ethanol-treated rats. This effect was not apparent at 3 hr, where the lung level reflected the blood level with a significantly lower level in the ethanol-treated rats.

Renal excretion was the major route of isoniazid elimination, with about 70–80% of the dose of carbon-14 being recovered in the urine in 24 hr. Only ethanol affected the amount of carbon-14 excreted and then only when isoniazid was administered intravenously. In this case, ethanol treatment significantly increased the amount of carbon-14 excreted, which could have been due to the diuretic effect of ethanol.

Most treatments produced some change in the proportions of the isoniazid metabolites excreted in urine. Aspirin almost completely inhibited II excretion, probably due to salicylate competing for the glycine pool since salicylglycine is an aspirin metabolite (13). Rifampin did not produce any significant changes, and ethambutol caused only a slight decrease in the amount of III excreted. Phenobarbital pretreatment produced a similar effect but only up to 6 hr after dosing.

Ethanol produced the most marked interaction. When isoniazid was given orally, all four metabolites estimated were affected: II and III were decreased and I and IV were increased. However, when isoniazid was administered intravenously, only III was decreased and IV was increased. If the theory of Peters *et al.* (14) that isoniazid is acetylated prior to being hydrolyzed to isonicotinic acid is true, then ethanol is blocking the cleavage of *N*-acetylhydrazine. Since it may be at this stage that hepatotoxicity is caused, there is reason to believe that acute doses of ethanol will not potentiate isoniazid-induced liver damage. Nevertheless, prolonged ethanol abuse will no doubt increase the danger of liver damage and isoniazid may potentiate this effect. At present, it is not possible to explain why ethanol has this effect on isoniazid metabolism, but it is similar to other cases where acute doses of ethanol block drug metabolism (5).

Measurement of serum transaminase levels in rats dosed with isoniazid showed that the rat is not susceptible to an acute hepatotoxic reaction to this drug. Mitchell and Jollow (4) also reported that hepatic necrosis could not be produced in the rat even after lethal isoniazid doses. However, their observation (4) that very little III is formed after isoniazid administration to rats is contrary to the present results, in which ~25% of the isoniazid dose was metabolized to II and III. Hence, the resistance of the rat to the hepatotoxicity of isoniazid remains unexplained.

One possibility is that the metabolic activation of *N*-acetylhydrazine (15) is poorly developed in the strain of rats used. Comparison of the total amounts of II, III, and IV with recent human data (16) shows that the amount of IV in the rat is about the same as in rapid acetylator humans but that the amount of III in the rat is less than in either slow or rapid acetylator humans. These results could indicate that the rat is not able to cleave acetylhydrazine from IV as rapidly as the human. This also could explain the low hepatic toxicity in the rat.

It is concluded that, of the drugs studied, only ethanol had a significant interaction with isoniazid metabolism. Nevertheless, this effect did not change the elimination rate from the blood. Based on current knowledge of the mechanism of isoniazid-induced hepatotoxicity, it is not likely that acute doses of ethanol potentiate isoniazid toxicity. The rat is not a good model for the study of isoniazid-induced hepatotoxicity and its metabolism of isoniazid does differ quantitatively from that observed in humans.

REFERENCES

(1) R. A. Garibaldi, R. E. Drusin, S. H. Ferebee, and M. Gregg, *Am. Rev. Resp. Dis.*, **106**, 357 (1972).

(2) A. W. Lees, G. W. Allan, J. Smith, W. F. Tyrrell, and R. J. Fallon, *Tubercle*, **52**, 182 (1971).

(3) F. C. Hughes, C. Marche, and J. Marche, *Thérapie*, **24**, 392 (1975).

(4) J. R. Mitchell and D. J. Jollow, *Gastroenterology*, **68**, 392 (1975).

(5) B. H. Thomas, B. B. Coldwell, G. Solomonraj, W. Zeitz, and H. L. Trenholm, *Biochem. Pharmacol.*, **21**, 2605 (1972).

(6) V. W. Diller, E. Kruger-Thiemer, and E. Wempe, *Arzneim.-Forsch.*, **9**, 432 (1959).

(7) V. Zamboni and A. Defranceschi, *Biochim. Biophys. Acta*, **14**, 430 (1959).

(8) R. J. Henry, N. Chiamori, O. J. Golub, and S. Berkman, *Am. J. Clin. Pathol.*, **34**, 381 (1960).

(9) C. W. Dunnett, *J. Am. Stat. Assoc.*, **50**, 1096 (1955).

(10) "Documenta Geigy Scientific Tables," 6th ed., K. Diem, Ed., Geigy Pharmaceuticals, Montreal, Quebec, Canada, 1972, p. 177.

(11) G. G. Grassi and C. Grassi, *Int. J. Clin. Pharmacol.*, **11**, 216 (1975).

(12) I. U. Boone, M. Magee, and D. F. Turney, *J. Biol. Chem.*, **221**, 781 (1956).

(13) B. B. Coldwell, G. Solomonraj, and B. H. Thomas, *Pharmacology*, **12**, 201 (1974).

(14) J. H. Peters, K. S. Miller, and P. Brown, *J. Pharmacol. Exp. Ther.*, **150**, 298 (1965).

(15) S. D. Nelson, J. R. Mitchell, J. A. Timbrell, W. R. Snodgrass, and G. B. Corcoran, *Science*, **193**, 901 (1976).

(16) G. A. Ellard and P. T. Gammon, *J. Pharmacokinet. Biopharm.*, **4**, 83 (1976).

ACKNOWLEDGMENTS AND ADDRESSES

Received May 17, 1976, from the *Drug Research Laboratories, Health Protection Branch, Health and Welfare Canada, Tunney's Pasture, Ottawa, Ontario, K1A 0L2, Canada.*

Accepted for publication December 14, 1976.

[x] To whom inquiries should be directed.

Characteristics of Medicated and Unmedicated Microglobules Recovered from Complex Coacervates of Gelatin–Acacia

DAVID W. NEWTON *, JEAN N. McMULLEN ‡, and CHARLES H. BECKER ˣ

Abstract □ Medicated and unmedicated microglobules prepared from complex coacervates of Type A gelatin and acacia were recovered as water-insoluble powders consisting of discrete units, which were spontaneously revertible to highly disperse systems when suspended in water or physiological electrolyte solutions. Spherical microglobules containing up to 15% (w/w) sulfamerazine had a nominal diameter of 30 μm in aqueous suspension. Larger but irregularly shaped products containing up to 45% (w/w) sulfamerazine were also recovered. The relationships of the weight of sulfamerazine added per coacervate batch to weight yield and percent (w/w) included sulfamerazine of the microglobules were both linear.

Keyphrases □ Microglobules—medicated and unmedicated, prepared from gelatin–acacia coacervates, physical parameters evaluated for use as dosage forms □ Coacervates—gelatin–acacia, medicated and unmedicated microglobules prepared, physical parameters evaluated for use as dosage forms □ Gelatin–acacia—coacervates, medicated and unmedicated microglobules prepared, physical parameters evaluated for use as dosage forms □ Dosage forms, potential—medicated and unmedicated microglobules prepared from gelatin–acacia coacervates, physical parameters evaluated

Incipient, fundamental studies of complex coacervation, specifically of the gelatin–acacia system, were reported previously (1, 2).

Several patents were cited in reviews on microencapsulation as evidence of the first commercially successful uses of the gelatin–acacia system (3–5). Various studies involving gelatin–acacia coacervates were predominantly directed toward drug microencapsulation (6–9). Pharmaceutical uses of microencapsulated products prepared by coacervation and other processes also were reported (3–5, 10–14).

This study was undertaken to evaluate certain parameters of the complex coacervate system of Type A gelatin and acacia (gum arabic) for producing medicated microglobules suitable in various pharmaceutical dosage forms. The products were to be recovered as powders consisting of water-insoluble, discrete, nonvacuolated spherical units that would spontaneously revert to highly dispersed suspensions upon reconstitution with aqueous vehicles.

EXPERIMENTAL

Materials—Type A gelatin[1] and acacia[2] were used as 3% (w/v) solutions containing 1% (v/v) benzyl alcohol[3] for preservation. Glycerin (99.6%)[3], formaldehyde solution (37%)[3], 2-propanol (99%)[3], pancreatin[4], pepsin[4], collagenase B[5], micronized sulfamerazine[6] (majority of particles 5 μm or less), and finely powdered chloramphenicol[7] were used as received. Other solvents and reagents were analytical reagent grade or purity.

Preparation and Recovery of Microglobules—The coacervation pH (3.9–4.0), dry gelatin–acacia ratio (0.8–1.0:1.0), and sol concentration (3% w/v) were initially determined as the criteria necessary to optimize the yield of microglobules.

Except where the effects of glycerin or formaldehyde were studied in particular, microglobules were prepared by mixing at 40° 40 ml each of 3% (w/v) gelatin sol (adjusted to pH 10) and 3% (w/v) acacia sol, stirring the mixture at 250–400 rpm, and either dispersing 1.5 g of the drug for 3 min in the batch at pH 5.5 and then adjusting the pH to 3.9–4.0 or adjusting to pH 3.9–4.0 and then dispersing the drug. Over 30 min, 40 ml of glycerin was added dropwise and the batch was cooled under ambient conditions to 24–26° and then rapidly chilled to 2–5° in an ice water bath.

Microscopic examination was made to assess encapsulation. After 15 min at 2–5°, the pH was raised to 5–6, 15 ml of formaldehyde was added, and stirring was continued for 30–45 min at 2–5°. The batch was then covered and allowed to stand at room temperature (22–25°) for approximately 20 hr. The clear supernate was then discarded, the white sediment layer (50–70 ml) was brought with stirring to 75% (v/v) of 2-propanol, and the batch was allowed to stand for 10 min. Then the supernate was decanted, the batch was brought to 90% (w/v) of 2-propanol, and the flocculated system was filtered using qualitative paper on a buchner funnel. The product was washed with 99% 2-propanol and dried at 36° for 12–16 hr, and the dried yield was vibrated gently on a No. 40 screen to obtain a powder.

All batches were prepared in 250-ml glass beakers and stirred by a mixer[8] equipped with a three-blade marine-type impeller 4 cm in diameter. Gelatin and acacia sols were prepared in distilled water and refrigerated at 2–5° for not more than 30 days prior to use. The gelatin sols were warmed to, and maintained at, 45° for not more than 3 hr and were discarded after two such uses on consecutive days. Acacia sols were initially heated to 85–90° for 1 hr to destroy the activity of any potentially interfering enzymes (15, 16).

Influence of Additives and Conditions—Batches of unmedicated microglobules were prepared using 0.5, 1.0, 2.0, 2.5, and 3.0% (w/v) sols of each gelatin and acacia. Gross yields were compared by measuring the apparent volumes of liquid coacervate layers at 40° and the dry weight yields of microglobules recovered as specified earlier.

Glycerin volumes of 5, 10, 20, 30, 40, 50, 60, 70, 80, and 100 ml were added dropwise to separate unmedicated batches. Likewise, a 40-ml portion of 1,2,6-hexanetriol[6], polyethylene glycol 200[9], polyethylene glycol 400[10], 70% (w/w) sorbitol[3], and syrup USP was added to separate batches.

Batches of unmedicated microglobules were treated with 5, 10, and 15 ml of formaldehyde. Batches to which 15 ml of formaldehyde had been added also were recovered at preselected times over 0.5–4 hr to determine the minimum treatment period required for the retrieval of readily dispersible products.

For unmedicated microglobules, batches were decanted to 100 ml (about 60 ml of sediment and 40 ml of clear supernate). From these batches, a 10-ml sample was mixed individually with 5, 8, 10, 15, 20, 30, 40, 60, and 90 ml each of acetone, methanol, ethanol, 1-propanol, and 2-propanol in 100-ml cylinders. The systems were kept at room temperature for 5 min after each addition of acetone or an alcohol. The percent (v/v) of the solvents at which flocculation occurred and the apparent degree of sedimentation were recorded.

Finally, the influence of stirring rate in the 250–400-rpm range and in excess of 450 rpm on the morphology of the microglobules was compared using standard and baffled 250-ml beakers.

Extraction and Digestion of Microglobules—About 100 mg of microglobules containing approximately 15% (w/w) sulfamerazine was placed in 20-ml Type I glass vials with 10-ml portions of the following media: collagenase B solution, 20 units/ml, at pH 7.0 in 0.05 *M* tris(hy-

[1] Isoelectric point 8.6, 275 bloom, Fisher Scientific Co., Fair Lawn, N.J.
[2] USP white powder, Fisher Scientific Co., Fair Lawn, N.J.
[3] Fisher Scientific Co., Fair Lawn, N.J.
[4] Wilson Labs., Chicago, Ill.
[5] Calbiochem, San Diego, Calif.
[6] Matheson, Coleman & Bell, Norwood, Ohio.
[7] Courtesy of Parke-Davis & Co.
[8] Lightin model F, Mixing Equipment Co., Rochester, N.Y.
[9] Dow Chemical Co., Midland, Mich.
[10] Union Carbide Corp., New York, N.Y.

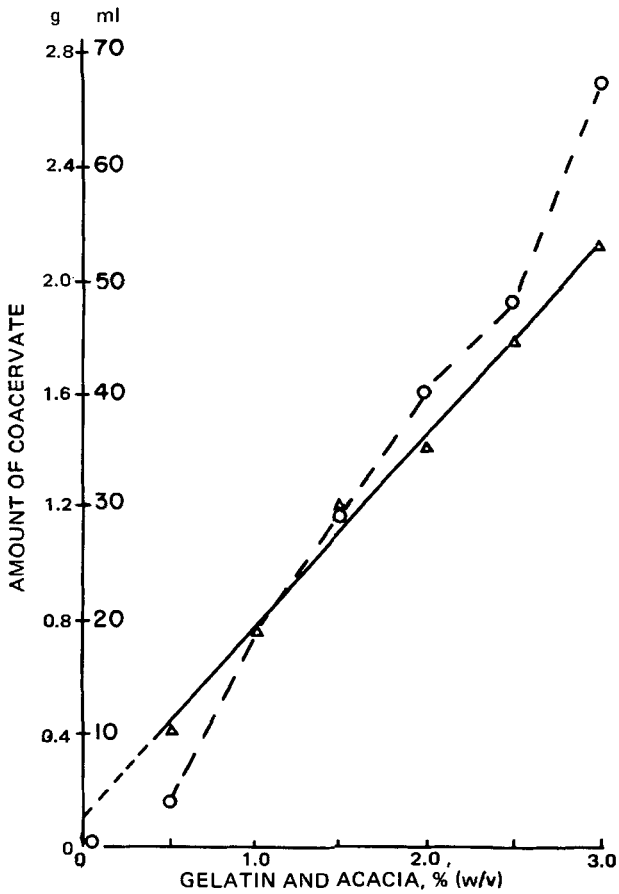

Figure 1—*Apparent volumes (○, ml) and dry weight (△, g) yields of coacervates produced at pH 3.9 from isovolumetric (40 ml) gelatin and acacia sols of selected percent (w/v) concentration.*

droxymethyl)aminomethane[11] and 0.005 *M* calcium chloride (17); 50% (v/v) ethanol; gastric fluid[12]; intestinal fluid[12]; and replacement electrolyte solution[13]. The vials were sealed with pretreated rubber closures and aluminum crimps and rotated at 25 ± 3 rpm at 37 ± 0.1° in an apparatus similar to that used by Souder and Ellenbogen (18).

The suspensions were observed visually and microscopically at 0.5, 1.0, 2.0, 3.0, 4.0, 8.0, and 20.0 hr to estimate the extent of digestion of the microglobules and/or extraction of sulfamerazine therefrom. Similarly, samples containing 12.7% (w/w) sulfamerazine were extracted for up to 12 hr in 10.0 ml of replacement electrolyte solution.

Assay of Sulfamerazine Content—The microglobules were washed in 2-propanol–acetone (1:2) by dispersing them in 150 ml of mixture per gram of sulfamerazine originally added and stirring for 5 min.

The spectrophotometric assay of sulfamerazine content was adapted from Clarke (19). An accurately weighed 100-mg sample of microglobules was digested with 15 ml of intestinal fluid for 3 hr at 37°, the mixture was adjusted to pH 3–4, and 20 ml of acetone was added. The sample was extracted with four 15-ml portions of ether, and the fractions were pooled and evaporated to dryness at room temperature.

The residue was quantitatively transferred to a 50-ml volumetric flask, first with 5 ml of distilled water and then with portions of absolute ethanol sufficient to achieve the final volume. The absorbance of the sample, appropriately diluted in 90% (v/v) ethanol, was determined at 270 nm[14], and the value was compared to a standard (Beer's) plot to calculate the percent (w/w) sulfamerazine within an aliquot of microglobules from the batch.

Sulfamerazine was isolated from the aqueous microglobule digest to preclude the error of additive UV absorbance by water-soluble residues of gelatin and pancreatin, in particular. Furthermore, the complete evaporation of acetone, which partitions into the ether phase, is necessitated because of its interfering absorbance at about 265 nm (20).

[11] THAM, Fisher Scientific Co., Fair Lawn, N.J.

[12] Simulated, TS, "The United States Pharmacopeia," 19th rev., Mack Publishing Co., Easton, Pa., 1975, p. 765.

[13] Normosol-R pH 7.4, Abbott Laboratories, North Chicago, Ill.

[14] Beckman DB-GT, Beckman Instruments, Fullerton, Calif.

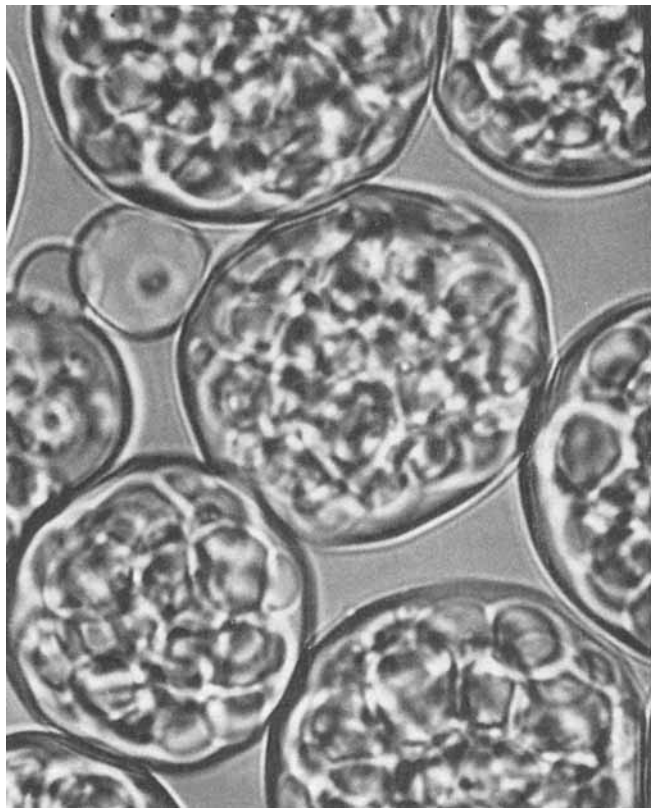

Figure 2—*Vacuolated, unmedicated gelatin–acacia microglobules (1000×).*

RESULTS AND DISCUSSION

Influence of Additives and Conditions—The advantage of measuring microglobule yields by dry weight after recovery rather than apparent coacervate volumes is evident from the plots in Fig. 1. The reliability of coacervate volume measurements is limited because the water content of gelatin–acacia coacervates increases as more concentrated sols are used (1).

The addition of glycerin and other polyols increased the viscosity and density of the coacervate systems, which appeared to inhibit deformation of the spherical droplets caused by the rotational velocity and turbulence of stirring. The spherical shape of the coacervate droplets also may be favored by an intensification of the complex ionic relations between gelatin and acacia in a system containing, for instance, 28.7% (v/v) glycerin and possessing, therefore, a dielectric constant nearer to 70 than to 80 as for water (21).

Upon cooling the coacervates to less than 28°, a glycerin concentration of 20–40% (v/v) in the system prevented vacuolation of the microglobules. Since glycerin lowers the gelation temperature and affects gelatin hydration (22), these effects may prevent vacuolation, which otherwise occurs when gelatin–acacia complex coacervate droplets are cooled to below about 28° (1). The polyols 1,2,6-hexanetriol, polyethylene glycol 200 and 400, 70% (w/w) sorbitol, and syrup USP did not prevent vacuolation of the microglobules in a concentration of 28.7% (v/v), a typical value at which glycerin was effective for this purpose.

Figure 2 shows the vacuolation caused by gelation of unmedicated microglobules from a coacervate system prepared in the absence of glycerin. In contrast, Fig. 3 shows nonvacuolated microglobules when the system contained 28.7% (v/v) glycerin.

To recover spherical microglobules, readily revertible to highly dispersed suspensions, from the coacervates, a formaldehyde concentration of 4.0% and a treatment time of at least 4 hr were required.

Flocculation and sedimentation efficiency of formaldehyde-treated microglobules as a function of concentration, percent (v/v), of the aliphatic solvents revealed the order: acetone (48.5%) > 2-propanol (52.6%) = 1-propanol (52.6%) > ethanol (71.4%) > methanol (85.1%). However, only 2-propanol and 1-propanol were capable of flocculating the micro-

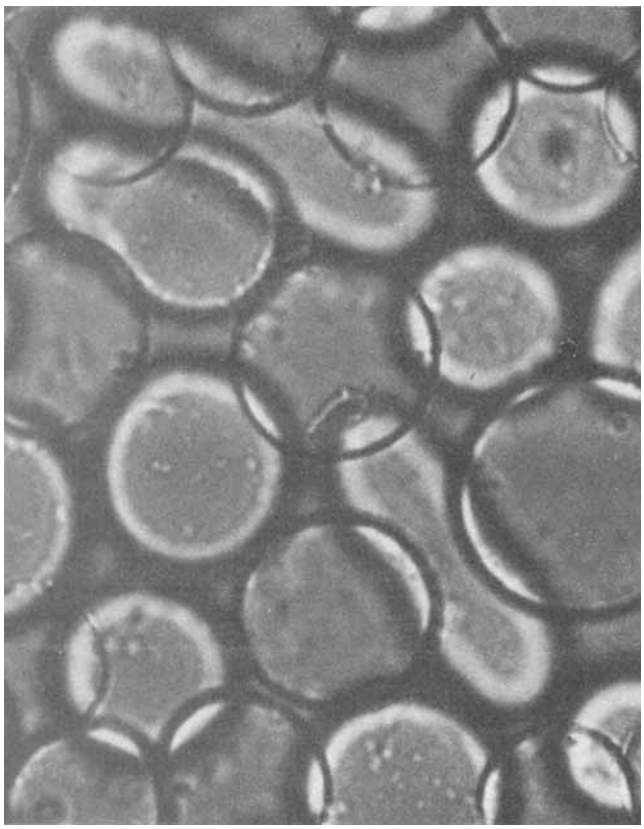

Figure 3—*Nonvacuolated, unmedicated gelatin–acacia microglobules (particulate matter unintended; 1000×).*

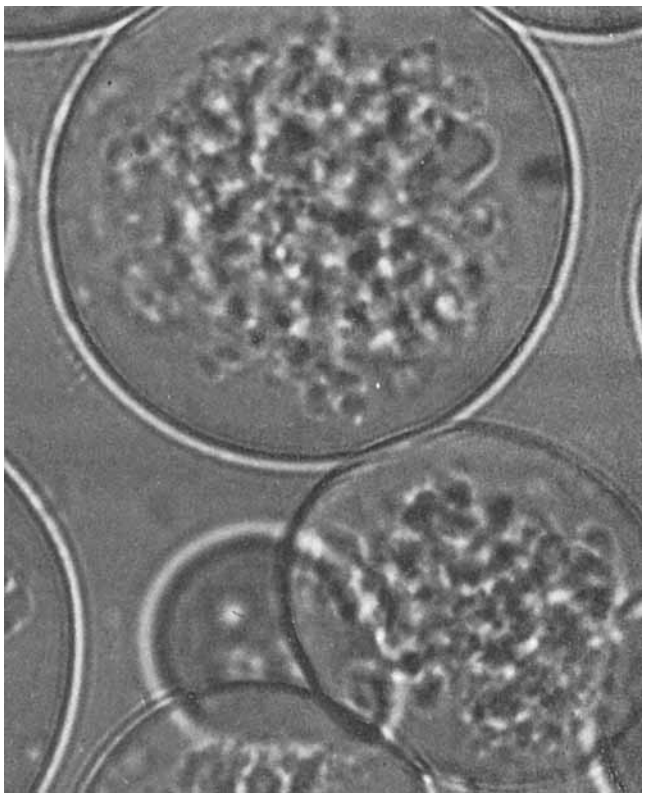

Figure 4—*Gelatin–acacia microglobules containing 12–15% (w/w) micronized sulfamerazine (1000×).*

globules to produce filter cakes, which, after drying, would spontaneously form highly dispersed suspensions in water. These results are in agreement with those of previous work (23).

When the 2-propanol concentration reached 40–45% (v/v), the microglobule suspensions changed from translucent to opaque in appearance, probably due to the precipitation of acacia within the microglobules. A 2-propanol concentration of 75% (v/v) or greater produced complete sedimentation within 10 min, and 90% (v/v) provided the greatest aqueous dispersibility of the recovered powders.

There was no difference in the morphology of the microglobules recovered for a given substance when powdered aluminum, barium sulfate, chloramphenicol, hydrocortisone acetate, phenobarbital, phenolphthalein, scarlet red, sulfamerazine, and sulfur were added to the coacervates either before or after the pH end-point. These observations and others, as well as previous evidence (1, 24), support the theory that drugs and other materials are included within gelatin–acacia coacervates exclusively by surface-active phenomena of wetting and spreading.

The nominal equilibrium size of unmedicated, spherical microglobules was 30 μm in aqueous suspension. The shape and diameter were also characteristic of microglobules recovered from batches to which not more than 1.0 g of micronized sulfamerazine had been added (Fig. 4). However, when a nonmicronized powder whose particles were larger than about 20 μm or more than 1 g of micronized sulfamerazine was added to the batches, the spherical shape was lost; irregular, larger microglobules resulted (Fig. 5).

Stirring is required to produce distinct microglobules from complex coacervates of gelatin–acacia. Stirring rates of 250–400 rpm resulted in the formation of spherical microglobules. However, rates at or exceeding about 450 rpm usually resulted in ellipsoidal or more irregularly distorted microglobules, as well as in the gross entrainment of air and vacuolation of the coavervate products. The use of a baffled beaker accounted for undesirable products at rates greater than 300 rpm, perhaps because of greatly increased turbulence and air entrainment.

Previous reports (9) recognized the spontaneous separation of complex coacervates of gelatin and acacia into two immiscible layers, but also discussed droplet size of the coacervates as a function of temperature. When batches at 40° or higher were rapidly sampled from a stirring system and observed microscopically, the coacervate droplets coalesced and spread over the glass slide almost instantly because of the affinity of gelatin–acacia coacervates for glass (1). Therefore, it may be unrealistic to discuss droplet size in these systems above about 35°, the approximate gelation temperature of most gelatins (25–29).

Extraction and Digestion of Microglobules—The results of extraction tests of spherical microglobules containing approximately 15% (w/w) sulfamerazine with five media are summarized in Table I. The most significant influence was demonstrated by intestinal fluid, which completely digested the formaldehyde-treated microglobules in only 30 min. Previously (23), extraction of sulfamerazine from formaldehyde-treated gelatin microcapsules was 100% complete after 2 hr with intestinal fluid but only 70% complete after 8 hr with gastric fluid.

Other studies (30, 31) found greater release of pentobarbital from formaldehyde-treated gelatin–acacia microcapsules with gastric than with intestinal fluid; the percent (w/w) pentobarbital in the products was not reported. These latter findings may have resulted because the spectrophotometric analyses of pentobarbital were conducted on filtered extracts of the aqueous media at pH 9.25. However, experimental validation from the present study showed significant absorbance below 300 nm by such digests of nonmedicated gelatin–acacia microglobules.

Although the medicated microglobules prepared in this study required 8 hr for digestion in gastric fluid, their included sulfamerazine dissolved completely after only 5 min of extraction. In the intestinal fluid, the

Table I—Effect of Extraction in Specified Media at 37° on Morphology and Contents of Microglobules Containing 15% (w/w) Sulfamerazine

Medium	Minimum Time for Complete Digestion, hr[a]	Microscopic Appearance of Suspension[b]
Collagenase B, 20 units/ml	8.0	d
Ethanol, 50% (v/v)	NS	*i*
Gastric fluid	8.0	s
Intestinal fluid	0.5	d
Replacement electrolyte solution, pH 7.4	NS	i

[a] NS = not sufficient time for digestion of microglobules through 20 hr of extraction. [b] At 100×: i = intact spheres containing sulfamerazine, d = microglobules completely digested but sulfamerazine crystals present, and s = completely digested microglobules and their sulfamerazine contents in solution.

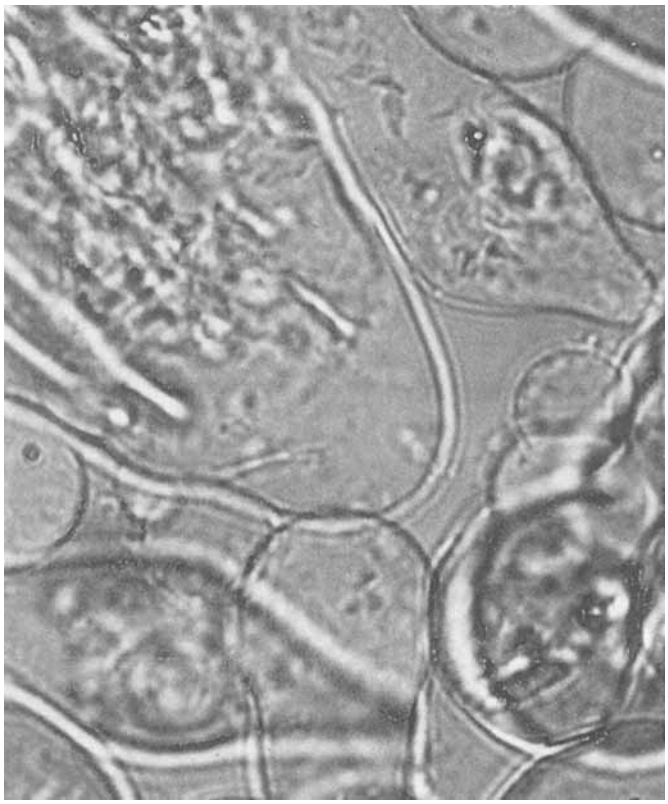

Figure 5—*Nonvacuolated gelatin–acacia microglobules containing an undetermined fraction of chloramphenicol (1000×).*

microglobules were completely digested within 30 min, but with incomplete dissolution of the included sulfamerazine. Other extractions of the microglobules showed less than 5% loss of included sulfamerazine when suspended and stirred for 5–10 min in pure acetone. Furthermore, extensive or complete loss of sulfamerazine from the intact microglobules in similar tests was observed in binary systems composed of 20–80% water and acetone, suggesting that the microglobules lack a system of "fixed pores or channels," thus requiring hydration before access to included sulfamerazine by a solvent such as acetone can be afforded *via* imbibition and a "wicking type of action."

The pKa value for the loss of a proton by the sulfonamido moiety of sulfamerazine to form a sodium salt is 7.06 (32). Therefore, at pH 7.4, such as in intestinal fluid[12], the drug would be 69% ionized. However, the pKa of the anilino group on sulfamerazine may be approximated at about 3.0 (33). Thus, at pH 1.2, such as in gastric fluid[12], sulfamerazine would be 98% protonated, thereby favoring greater drug solubility.

The extraction of spherical microglobules containing 12.7% (w/w) sulfamerazine with replacement electrolyte solution, pH 7.4, at 37° showed little variation in the fraction of sulfamerazine released. Only 26.8 ± 2.2% was extracted over periods of up to 12 hr. The results are in agreement with a previously published report (34).

REFERENCES

(1) "Colloid Science," vol. II, H. R. Kruyt, Ed., Elsevier, New York, N.Y., 1949, pp. 338–384, 433–450.

(2) "Industrial Gums," R. L. Whistler, Ed., Academic, New York, N.Y., 1959, pp. 256–263.

(3) L. A. Luzzi, *J. Pharm. Sci.*, **59,** 1367 (1970).

(4) "The Theory and Practice of Industrial Pharmacy," 2nd ed., L. Lachman, H. A. Lieberman, and J. L. Kanig, Eds., Lea & Febiger, Philadelphia, Pa., 1976, pp. 420–438.

(5) "Encyclopedia of Chemical Technology," vol. 13, A. Standen, Ed., Wiley, New York, N.Y., 1967, pp. 436–456.

(6) L. A. Luzzi and R. J. Gerraughty, *J. Pharm. Sci.*, **53,** 429 (1964).

(7) S. Javidan, R. U. Haque, and R. G. Mrtek, *ibid.*, **60,** 1825 (1971).

(8) P. L. Madan, L. A. Luzzi, and J. C. Price, *ibid.*, **61,** 1586 (1972).

(9) A. B. Dhruv, T. C. Needham, Jr., and L. A. Luzzi, *Can. J. Pharm. Sci.*, **10,** 33 (1975).

(10) J. Nack, *J. Soc. Cosmet. Chem.*, **21,** 85 (1970).

(11) J. A. Bakan and J. L. Anderson, *Drug Cosmet. Ind.*, **110,** 34 (1972).

(12) *Manuf. Chem.*, **33,** 16 (1962).

(13) P. A. Kramer, *J. Pharm. Sci.*, **63,** 1646 (1974).

(14) J. Whitmore, Ph.D. thesis, University of Florida, Gainesville, Fla., 1966.

(15) "Industrial Gums," R. L. Whistler, Ed., Academic, New York, N.Y., 1959, p. 266.

(16) C. L. Mantell, "The Water-Soluble Gums," Reinhold, New York, N.Y., 1947, pp. 35–39.

(17) "Methods in Enzymology," vol. V, S. P. Colowick and N. O. Kaplan, Eds., Academic, New York, N.Y., 1962, pp. 659–665.

(18) J. C. Souder and W. C. Ellenbogen, *Drug Stand.*, **26,** 77 (1958).

(19) "Isolation and Identification of Drugs," E. G. C. Clarke, Ed., Pharmaceutical Press, London, England, 1969, pp. 550, 551.

(20) K. A. Connors, "A Textbook of Pharmaceutical Analysis," Wiley, New York, N.Y., 1967, p. 179.

(21) D. L. Sorby, R. G. Bitter, and J. G. Webb, *J. Pharm. Sci.*, **52,** 1149 (1963).

(22) K. H. Gustavson, "The Chemistry and Reactivity of Collagen," Academic, New York, N.Y., 1956, pp. 204–207.

(23) J. R. Nixon, S. A. H. Khalil, and J. E. Carless, *J. Pharm. Pharmacol.*, **20,** 528 (1968).

(24) G. N. Paradisis and E. L. Parrott, *J. Clin. Pharmacol.*, **8,** 54 (1968).

(25) "Encyclopedia of Chemical Technology," vol. 10, A. Standen, Ed., Wiley, New York, N.Y., 1966, p. 501.

(26) A. Veis, "The Macromolecular Chemistry of Gelatin," Academic, New York, N.Y., 1964, pp. 255, 267.

(27) K. H. Gustavon, "The Chemistry and Reactivity of Collagen," Academic, New York, N.Y. 1956, pp. 288, 289.

(28) H. Boedtker and P. Doty, *J. Phys. Chem.*, **58,** 968 (1954).

(29) "Treatise on Collagen," vol. I, G. N. Ramachandran, Ed., Academic, New York, N.Y., 1967, p. 261.

(30) L. A. Luzzi and R. J. Gerraughty, *J. Pharm. Sci.*, **56,** 634 (1967).

(31) *Ibid.*, **56,** 1174 (1967).

(32) A. N. Martin, J. Swarbrick, and A. Cammarata, "Physical Pharmacy," 2nd ed., Lea & Febiger, Philadelphia, Pa., 1969, p. 194.

(33) A. Albert and E. P. Serjeant, "Ionization Constants of Acids and Bases," Wiley, New York, N.Y., 1962, p. 148.

(34) J. R. Nixon and S. E. Walker, *J. Pharm. Pharmacol.*, **23,** 147S (1971).

ACKNOWLEDGMENTS AND ADDRESSES

Received June 3, 1976, from the *College of Pharmacy, University of Florida, Gainesville, FL 32610.*

Accepted for publication December 15, 1976.

Abstracted in part from a dissertation presented by D. W. Newton to the University of Florida in partial fulfillment of the Doctor of Philosophy degree requirements.

The authors thank Mrs. Ruby Wilson for the preparation of the manuscript, Mr. George Perry for the construction of Fig. 1, and Mr. Louis Mallory for the photomicrographs in Figs. 2–5.

* Present address: Department of Pharmaceutics, Massachusetts College of Pharmacy, Boston, MA 02115.

‡ Present address: Glaxo Laboratories, Toronto, Ontario, M8Z 4W1, Canada.

ˣ To whom inquiries should be directed.

Selective Estimation of Aconitine in Presence of Aconine and Benzoylaconine

MOHAMED S. KARAWYA ˣ and ALY M. DIAB

Abstract □ A selective and simple colorimetric method is presented for the estimation of aconitine in drugs in the presence of aconine and benzoylaconine. The method is based on the formation of an iron hydroxamate complex through the acetate ester group to which the biological activity is due. The color is measured at 530 nm (5–250 μg/ml). Under the experimental conditions, neither the benzoyl group of benzoylaconine nor aconine is involved in the process of hydroxylaminolysis.

Keyphrases □ Aconitine—colorimetric analysis, pharmaceutical formulations in presence of aconine and benzoylaconine □ Colorimetry—analysis, aconitine, pharmaceutical formulations in presence of aconine and benzoylaconine □ Alkaloids—aconitine, colorimetric analysis, pharmaceutical formulations in presence of aconine and benzoylaconine □ Analgesics, topical—aconitine, colorimetric analysis, pharmaceutical formulations in presence of aconine and benzoylaconine

The effectiveness of tincture of aconite in the local relief of neuralgia, sciatica, acute rheumatism, and toothache is mainly attributed to aconitine (acetylbenzoylaconine). Since aconitine gives no specific color reaction, most analytical methods depend on the determination of its relative toxicity (1–3). Other assay methods are gravimetric (4), aqueous (5, 6) and nonaqueous (7) titrimetric, and spectrophotometric (8). Paper chromatography in combination with UV spectrophotometry (9) also was reported for the assay of different aconite alkaloids.

The aim of this work was to develop a rather simple colorimetric method for the selective determination of aconitine in the presence of other aconite alkaloids such as aconine and benzoylaconine. Since the acetyl group of aconitine is essential for its biological activity (10), it was necessary to seek an assay involving the reaction of this group. Therefore, the hydroxamic acid test (11) was optimized for the quantitative assay of aconitine.

EXPERIMENTAL

Materials and Reagents—Aconite extract[1] and aconite tincture, French Codex 1949, were used as received.

Aconitine Standard Solution—Dissolve 100 mg of aconitine[2] in 100 ml of absolute ethanol.

Acetate Buffer, pH 1.5—Adjust 0.1 *M* sodium acetate to pH 1.5 with 70% perchloric acid.

Alkaline Hydroxylamine Hydrochloride Reagent (11)—Prepare Solution 1, 12.5% (w/v) methanolic sodium hydroxide, by refluxing 12.5 g of sodium hydroxide in absolute methanol for 5 min. Prepare Solution 2, 12.5% (w/v) methanolic hydroxylamine hydrochloride, by refluxing 12.5 g of hydroxylamine hydrochloride in absolute methanol for 5 min. Mix equal volumes of Solutions 1 and 2 and filter.

Ammonium Ferric Sulfate Reagent—Dissolve 20 g of ammonium ferric sulfate dodecahydrate in 100 ml of 70% perchloric acid.

Determination of Aconitine in Standards—Transfer 0.1, 0.25, 0.5, 1, 2, 4, 5, and 6 ml of aconitine standard solution to separate 25-ml flasks, and dilute to about 8 ml with absolute ethanol. Add 3 ml of alkaline hydroxylamine reagent and place the flasks in a water bath at 40–45° for 30 min. Then remove the flasks from the water bath and cool to room temperature. Add gradually 5 ml of the ammonium ferric sulfate reagent with continuous stirring. Rapidly transfer the contents of the flasks into 25-ml volumetric flasks with acetate buffer, and adjust the volume to 25 ml with the same buffer. Directly read the absorbance at 530 nm against a reagent blank.

A calibration curve of 5–250 μg of aconitine/ml *versus* color intensity obeyed Beer's law with a standard deviation of ±0.8%.

Determination of Aconitine in Products—*Extract of Aconite*—Measure accurately 1 ml of extract, dilute to 5 ml with distilled water, render alkaline with dilute ammonia solution, and extract with 20-, 10-, 10-, and 10-ml portions of ether. Dry the combined ether extract with anhydrous sodium sulfate, distill the ether to dryness, and dissolve the residue in 5 ml of absolute ethanol. Complete the assay as described for standards, beginning with: "Add 3 ml of alkaline . . . ."

Tincture of Aconite—Measure 10 ml of tincture, concentrate to 1–2 ml, and complete the assay as under *Extract of Aconite*.

[1] Les Laboratoires Givaudan, Lavirotte & Cie, Lyon, France.
[2] E. Merck, Germany.

Table I—Assay of Aconitine by Proposed Method in Synthetic Mixtures of Aconitine and Benzoylaconine

Mixture		
Aconitine, mg	Benzoylaconine, mg	Aconitine Found, mg
3	1	2.98
2	2	2.00
1	3	0.99
2	1	1.98

RESULTS AND DISCUSSION

Aconitine and benzoylaconine cannot be separated from each other by any of the usual methods (6). However, the hydroxamic acid method proved to be selective for aconitine; benzoylaconine did not interfere under the specified conditions. Application of the hydroxamic acid method to benzoylaconine, prepared according to Majima *et al.* (12), showed that hydroxylaminolysis of benzoylaconine required a longer time and a higher temperature. Moreover, investigation of the visible spectrum of the iron hydroxamate of benzoylaconine showed λ_{max} 558 nm, which was sufficiently far from that of aconitine–iron hydroxamate (530 nm).

With synthetic mixtures of both aconitine and benzoylaconine, the hydroxamic acid method under the specified conditions gave only the expected amount of aconitine (Table I). Also, aconine, being an amino alcohol, is very soluble in water and, unlike aconitine, is unextractable with ether. Therefore, it does not interfere. Furthermore, aconine does

Table II—Assay of Aconitine in Aconite Preparations by Proposed Method

Preparation	Amount Declared, mg/ml	Amount Found, mg/ml	Amount Added, mg/ml	Amount Found, mg/ml	Recovery, %
Extract of aconite	3.00	3.60	2.00	5.580	99
Tincture of aconite	0.320	0.350	0.500	0.844	98.8
Average recovery					98.9
SD					0.1

not contain an ester group or any other group that may react with the hydroxylamine reagent.

Therefore, the method is rather specific and is preferably used in the analysis of aconitine in aconite preparations that generally contain benzoylaconine and aconine. The method showed good recovery (99.8%) and a reasonable standard deviation (±0.8%) (Table II).

REFERENCES

(1) C. C. Haskell, *Am. Drug.*, **4**, 596 (1916).

(2) R. Paris and J. Vavasseur, *Ann. Pharm. Fr.*, **9**, 718 (1951).

(3) "The United States Pharmacopeia," 10th rev., Lippincott, Philadelphia, Pa., 1926.

(4) M. Ribaut, *Bull. Sci. Pharmacol.*, **17**, 634 (1910).

(5) "The Egyptian Pharmacopoeia" (The English Text), Cairo University Press, Cairo, Egypt, 1963.

(6) G. Baker and C. B. Jordan, *J. Am. Pharm. Assoc., Sci. Ed.*, **25**, 291 (1936).

(7) L. G. Chatten, M. Pernarowski, and L. Levi, *ibid.*, **44**, 332 (1955).

(8) E. Berman and H. N. Wright, *Arch. Ind. Hyg. Occup. Med.*, **8**, 518 (1935).

(9) H. Yoshida, S. Kuwano, Y. Matsunaga, and S. Takagi, *J. Pharm. Soc. Jpn.*, **85**, 709 (1965).

(10) F. Bamford, "Poisons: Their Isolation and Identifications," 3rd ed., J. and A. Churchill Ltd., London, England, 1951, p. 41.

(11) R. F. Goddu, N. F. Le Blanc, and C. M. Wright, *Anal. Chem.*, **27**, 1251 (1955).

(12) R. Majima, H. Suginome, and S. Mario, *Ber.*, **57**, 1456 (1924).

ACKNOWLEDGMENTS AND ADDRESSES

Received June 11, 1976, from the *Pharmacology Section, Basic Medical Sciences Laboratory, National Research Center, Dokki, Cairo, Egypt.*

Accepted for publication September 23, 1976.

[x] To whom inquiries should be directed. Present address: Department of Pharmacognosy, Faculty of Pharmacy, Cairo University, Cairo, Egypt.

Synthesis and Antituberculosis Activity of Thiocarboxamide Derivatives of Schiff Bases

VICTOR ISRAEL COHEN *[x], NOEL RIST [‡], and CHRISTIANE DUPONCHEL [‡]

Abstract □ Synthesis of some *N*-(4-thiocarboxamidobenzylidene)arylamines and *N*-(substituted benzylidene)-*p*-thiocarboxamidoanilines from various arylaldehydes and arylamines is described. Fourteen representative compounds were tested *in vitro* on the ground $H_{37}RV$.

Keyphrases □ Thiocarboxamides, various—synthesized, screened for antituberculosis activity □ Antituberculosis activity—screened in various thiocarboxamide derivatives □ Structure–activity relationships—various thiocarboxamide derivatives screened for antituberculosis activity

In a search for antituberculosis agents (1–3), some thiocarboxamide derivatives of Schiff bases of series I and II were prepared from various arylaldehydes and arylamines and studied for biological activity.

EXPERIMENTAL[1]

An attempt was made to prepare Schiff bases of series I through the thiolysis of corresponding nitriles (III) in anhydrous medium, but the reaction took an unusual path, yielding disulfide IV (4) (Scheme I). Consequently, the following route was established to synthesize the compounds: preparation of the key intermediate, *p*-thiocarboxamidobenzaldehyde, from *p*-cyanobenzylidene acetate, followed by condensation of the key intermediate with amines.

Schiff bases of series II were obtained by heating *p*-thiocarboxamidoaniline with aromatic aldehydes.

Fourteen representative compounds were tested *in vitro* on the ground $H_{37}RV$. None showed significant antituberculosis activity against either 0.01 or 0.05 mg of the bacillus at 40 μg/ml.

***p*-Cyanobenzylidene Acetate (V)**—Compound V was obtained by the method of Lieberman and Connor (5). The crude product was crystallized from alcohol and obtained in 73% yield, mp 100°.

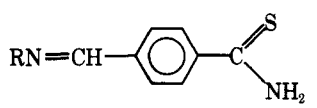

Ia: R = C_6H_5
Ib: R = *p*-IC_6H_4
Ic: R = *p*-ClC_6H_4
Id: R = $C_6H_5CH_2$
Ie: R = *p*-$CH_3C_6H_4$
If: R = *p*-$CH_3OC_6H_4$
Ig: R = *p*-$C_2H_5OC_6H_4$
Ih: R = *p*-$CONH_2C_6H_4$

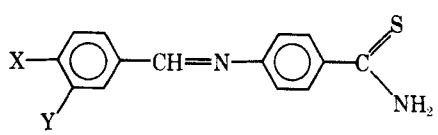

IIa: X = Y = H
IIb: X = CH_3, Y = H
IIc: X = Cl, Y = H
IId: X = CH_3O, Y = H
IIe: X = $(CH_3)_2N$, Y = H
IIf: X = H, Y = NO_2
IIg: X = S=CNH_2, Y = H

***p*-Thiocarboxamidobenzylidene Acetate (VI)**—Compound V (23.3 g, 0.1 mole) was dissolved in anhydrous pyridine (120 ml), and 20 ml of triethylamine was added. Dry hydrogen sulfide was passed through the solution for 4 hr. The reaction mixture was left at room temperature for 5 hr and was then poured into cold water and extracted with ether. The ether solution was treated with dilute hydrochloric acid, washed with water, dried over anhydrous sodium sulfate, and evaporated to dryness. The residue, which was either solid or oily, was suitable for the next step. Recrystallization from methyl ethyl ketone gave yellow crystals in 70% yield, mp 220°.

Anal.—Calc. for $C_{12}H_{13}NO_4S$: C, 53.94; H, 4.87; N, 5.24; S, 11.99. Found: C, 53.55; H, 4.90; N, 5.40; S, 12.34.

***p*-Thiocarboxamidobenzaldehyde (VII)**—Hydrolysis of VI was

[1] Melting points were measured on a Kofler hot-bench apparatus. A Beckman IR-20A spectrophotometer was used for IR spectra, which were run in potassium bromide. Microanalyses were performed by Service Central de Microanalyse, 94-Thias, France.

not contain an ester group or any other group that may react with the hydroxylamine reagent.

Therefore, the method is rather specific and is preferably used in the analysis of aconitine in aconite preparations that generally contain benzoylaconine and aconine. The method showed good recovery (99.8%) and a reasonable standard deviation (±0.8%) (Table II).

REFERENCES

(1) C. C. Haskell, *Am. Drug.*, **4**, 596 (1916).

(2) R. Paris and J. Vavasseur, *Ann. Pharm. Fr.*, **9**, 718 (1951).

(3) "The United States Pharmacopeia," 10th rev., Lippincott, Philadelphia, Pa., 1926.

(4) M. Ribaut, *Bull. Sci. Pharmacol.*, **17**, 634 (1910).

(5) "The Egyptian Pharmacopoeia" (The English Text), Cairo University Press, Cairo, Egypt, 1963.

(6) G. Baker and C. B. Jordan, *J. Am. Pharm. Assoc., Sci. Ed.*, **25**, 291 (1936).

(7) L. G. Chatten, M. Pernarowski, and L. Levi, *ibid.*, **44**, 332 (1955).

(8) E. Berman and H. N. Wright, *Arch. Ind. Hyg. Occup. Med.*, **8**, 518 (1935).

(9) H. Yoshida, S. Kuwano, Y. Matsunaga, and S. Takagi, *J. Pharm. Soc. Jpn.*, **85**, 709 (1965).

(10) F. Bamford, "Poisons: Their Isolation and Identifications," 3rd ed., J. and A. Churchill Ltd., London, England, 1951, p. 41.

(11) R. F. Goddu, N. F. Le Blanc, and C. M. Wright, *Anal. Chem.*, **27**, 1251 (1955).

(12) R. Majima, H. Suginome, and S. Mario, *Ber.*, **57**, 1456 (1924).

ACKNOWLEDGMENTS AND ADDRESSES

Received June 11, 1976, from the *Pharmacology Section, Basic Medical Sciences Laboratory, National Research Center, Dokki, Cairo, Egypt.*

Accepted for publication September 23, 1976.

[x] To whom inquiries should be directed. Present address: Department of Pharmacognosy, Faculty of Pharmacy, Cairo University, Cairo, Egypt.

Synthesis and Antituberculosis Activity of Thiocarboxamide Derivatives of Schiff Bases

VICTOR ISRAEL COHEN *[x], NOEL RIST [‡], and CHRISTIANE DUPONCHEL [‡]

Abstract □ Synthesis of some *N*-(4-thiocarboxamidobenzylidene)arylamines and *N*-(substituted benzylidene)-*p*-thiocarboxamidoanilines from various arylaldehydes and arylamines is described. Fourteen representative compounds were tested *in vitro* on the ground $H_{37}RV$.

Keyphrases □ Thiocarboxamides, various—synthesized, screened for antituberculosis activity □ Antituberculosis activity—screened in various thiocarboxamide derivatives □ Structure–activity relationships—various thiocarboxamide derivatives screened for antituberculosis activity

In a search for antituberculosis agents (1–3), some thiocarboxamide derivatives of Schiff bases of series I and II were prepared from various arylaldehydes and arylamines and studied for biological activity.

EXPERIMENTAL[1]

An attempt was made to prepare Schiff bases of series I through the thiolysis of corresponding nitriles (III) in anhydrous medium, but the reaction took an unusual path, yielding disulfide IV (4) (Scheme I). Consequently, the following route was established to synthesize the compounds: preparation of the key intermediate, *p*-thiocarboxamidobenzaldehyde, from *p*-cyanobenzylidene acetate, followed by condensation of the key intermediate with amines.

Schiff bases of series II were obtained by heating *p*-thiocarboxamidoaniline with aromatic aldehydes.

Fourteen representative compounds were tested *in vitro* on the ground $H_{37}RV$. None showed significant antituberculosis activity against either 0.01 or 0.05 mg of the bacillus at 40 μg/ml.

***p*-Cyanobenzylidene Acetate (V)**—Compound V was obtained by the method of Lieberman and Connor (5). The crude product was crystallized from alcohol and obtained in 73% yield, mp 100°.

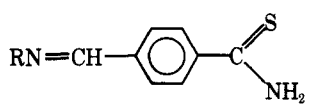

Ia: R = C_6H_5
Ib: R = *p*-IC_6H_4
Ic: R = *p*-ClC_6H_4
Id: R = $C_6H_5CH_2$
Ie: R = *p*-$CH_3C_6H_4$
If: R = *p*-$CH_3OC_6H_4$
Ig: R = *p*-$C_2H_5OC_6H_4$
Ih: R = *p*-$CONH_2C_6H_4$

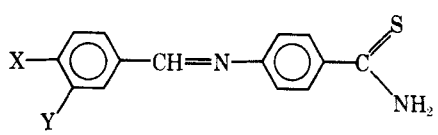

IIa: X = Y = H
IIb: X = CH_3, Y = H
IIc: X = Cl, Y = H
IId: X = CH_3O, Y = H
IIe: X = $(CH_3)_2N$, Y = H
IIf: X = H, Y = NO_2
IIg: X = S=CNH_2, Y = H

***p*-Thiocarboxamidobenzylidene Acetate (VI)**—Compound V (23.3 g, 0.1 mole) was dissolved in anhydrous pyridine (120 ml), and 20 ml of triethylamine was added. Dry hydrogen sulfide was passed through the solution for 4 hr. The reaction mixture was left at room temperature for 5 hr and was then poured into cold water and extracted with ether. The ether solution was treated with dilute hydrochloric acid, washed with water, dried over anhydrous sodium sulfate, and evaporated to dryness. The residue, which was either solid or oily, was suitable for the next step. Recrystallization from methyl ethyl ketone gave yellow crystals in 70% yield, mp 220°.

Anal.—Calc. for $C_{12}H_{13}NO_4S$: C, 53.94; H, 4.87; N, 5.24; S, 11.99. Found: C, 53.55; H, 4.90; N, 5.40; S, 12.34.

***p*-Thiocarboxamidobenzaldehyde (VII)**—Hydrolysis of VI was

[1] Melting points were measured on a Kofler hot-bench apparatus. A Beckman IR-20A spectrophotometer was used for IR spectra, which were run in potassium bromide. Microanalyses were performed by Service Central de Microanalyse, 94-Thias, France.

Table I—Physical Properties of *N*-(4-Thiocarboxamidobenzylidene)arylamines (I*a*–I*h*) and *N*-(Substituted Benzylidene)-*p*-thiocarboxamidoanilines (II*a*–II*g*)

Compound	Yield, %	Recrystallization Solvent	Melting Point	C=N, cm^{-1}	C—H, cm^{-1}	Formula	Analysis, %	Calc.	Found
I*a*	80	1-Butanol	205°	1620	3150	$C_{14}H_{12}N_2S$	C	70.00	69.86
							H	4.99	4.90
							N	11.65	11.40
							S	13.34	13.35
I*b*	75	Xylene	239°	1610	3120	$C_{14}H_{11}IN_2S$	C	45.92	46.02
							H	3.00	3.10
							N	7.64	7.53
							S	8.74	8.85
I*c*	80	Ethanol	210°	1622	3150	$C_{14}H_{11}ClN_2S$	C	61.44	61.35
							H	4.01	4.08
							N	10.23	10.28
							S	11.71	11.59
I*d*	85	Xylene	161°	1640	3150	$C_{15}H_{14}N_2S$	C	70.86	70.94
							H	5.50	5.60
							N	11.01	10.82
							S	12.61	12.81
I*e*	75	Xylene	210°	1620	3140	$C_{15}H_{14}N_2S$	C	70.86	70.98
							H	5.50	5.54
							N	11.01	10.98
							S	12.61	12.63
I*f*	80	Xylene	214°	1622	3150	$C_{15}H_{14}N_2OS$	C	66.67	66.48
							H	5.18	5.34
							N	10.36	10.08
							S	11.86	12.12
I*g*	75	Methyl phenyl ether	216°	1610	3110	$C_{16}H_{16}N_2OS$	C	67.61	67.32
							H	5.62	5.52
							N	9.85	9.66
							S	11.28	10.98
I*h*	80	Benzyl alcohol	299°	1605	3130	$C_{15}H_{13}N_3OS$	C	63.61	63.47
							H	4.59	4.66
							N	14.83	14.57
							S	11.32	11.15
II*a*	83	Ethanol	191°	1608	3110	$C_{14}H_{12}N_2S$	C	70.00	69.70
							H	4.99	5.23
							N	11.65	11.43
							S	13.34	13.30
II*b*	80	Xylene	205°	1618	3152	$C_{15}H_{14}N_2S$	C	70.86	70.94
							H	5.50	5.60
							N	11.01	11.18
							S	12.61	12.53
II*c*	75	Ethanol	217°	1624	3150	$C_{14}H_{11}ClN_2S$	C	61.44	61.16
							H	4.01	4.16
							N	10.23	10.10
							S	11.79	11.44
II*d*	85	Ethanol	202°	1623	3150	$C_{15}H_{14}N_2OS$	C	66.67	66.46
							H	5.18	5.27
							N	10.36	10.51
							S	11.86	11.92
II*e*	65	1-Butanol	276°	1615	3123	$C_{16}H_{17}N_3S$	C	67.84	67.61
							H	6.00	6.12
							N	14.52	14.57
							S	11.32	11.05
II*f*	80	Propanol	181°	1625	3185	$C_{14}H_{11}N_3O_2S$	C	58.55	58.99
							H	3.85	4.06
							N	14.72	14.62
							S	11.14	11.40
II*g*	85	Pyridine–ether	270°	1612	3130	$C_{15}H_{13}N_3S_2$	C	60.19	60.01
							H	4.34	4.35
							N	14.03	14.10
							S	21.42	21.50

accomplished according to a previous method (5). A mixture of 53.5 g (0.2 mole) of VI, 125 ml of ethanol, 125 ml of water, and 10 ml of concentrated sulfuric acid was heated to reflux for 30 min and then filtered. Water was added to the filtrate until the crystals of VII appeared. After 1 night, the solid was filtered off. The analytical sample was crystallized from xylene to yield 22.5 g (68%) of product, mp 158°.

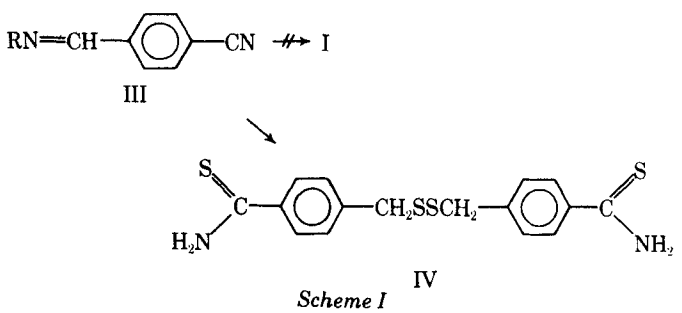

Scheme I

Anal.—Calc. for C_8H_7NOS: C, 58.18; H, 4.24; N, 8.48; S, 19.41. Found: C, 58.35; H, 4.28; N, 8.21; S, 19.68.

***p*-Thiocarboxamidoaniline (VIII)**—Hydrogen sulfide was passed through a solution of *p*-cyanoaniline in pyridine and triethylamine (6).

***N*-(4-Thiocarboxamidobenzylidene)-*p*-iodoaniline (I*b*)**—To a solution of 2.2 g (0.01 mole) of *p*-iodoaniline in 15 ml of ethanol were added 1.65 g (0.01 mole) of VII and 3 drops of acetic acid. The mixture was refluxed for 10 min. The precipitated crystals were collected by filtration and recrystallized from xylene to give 2.8 g (76%) of pure product.

Compounds I*a*, I*c*–I*h*, and II*a*–II*g* were prepared similarly (Table I).

REFERENCES

(1) V. I. Cohen, N. Rist, and S. Clavel, *Eur. J. Med. Chem.*, **10**, 134 (1975).

(2) *Ibid.*, **10**, 137 (1975).

(3) *Ibid.*, **10**, 140 (1975).

(4) V. I. Cohen, *Helv. Chim. Acta*, **59**, 840 (1976).

(5) S. V. Lieberman and R. Connor, *Org. Synth.*, **II**, 441 (1969).

(6) A. E. S. Fairfull, J. L. Lowe, and D. A. Peak, *J. Chem. Soc.*, **1952**, 742.

ACKNOWLEDGMENTS AND ADDRESSES

Received July 9, 1976, from the *Organic Chemistry Laboratory, Sciences Faculty, Ferdowsi University, Mashhad, Iran, and the ‡Service de la Tuberculose et des Mycobacteries de l'Institut Pasteur, Paris, France.

Accepted for publication October 18, 1976.

Supported by the Ministry of Sciences and Higher Education of Iran.

ˣ To whom inquiries should be directed.

TLC Determination of Iodochlorhydroxyquin and Its Conjugate in Plasma

P. DEL SOLDATO

Abstract □ A simple, specific, reliable, and sensitive method for the determination of iodochlorhydroxyquin and/or its conjugate in biological fluids is described. The method is based on a quantitative ether–acetone (1:1) extraction of plasma samples followed by TLC separation, visualization, elution, and determination at 267 nm. Iodochlorhydroxyquin released by hydrolysis of its conjugate was analyzed. Both compounds are detectable in amounts as low as 0.04 μg/ml. Application of the one-compartment open model to the data (assuming the biotransformation of the drug in conjugated form) provides a pharmacokinetic profile for the 50-mg/kg dose of iodochlorhydroxyquin in Wistar male rats.

Keyphrases □ Iodochlorhydroxyquin—and conjugate, TLC analysis, biological fluids □ TLC—analysis, iodochlorhydroxyquin and conjugate, biological fluids □ Antiamebic agents—iodochlorhydroxyquin, TLC analysis, biological fluids

Iodochlorhydroxyquin (I) has been widely used for over 30 years to treat various intestinal and vaginal infections. In view of debatable evidence of its neurotoxicity (1, 2), it is surprising that a method for the determination of I and/or its conjugate (II) in blood is not available. This paper describes a fast and simple TLC procedure for the detection of I and II in biological fluids and its use in pharmacokinetic studies.

EXPERIMENTAL

Reagents and Materials—Compound I was used as received[1]. All solvents were analytical reagent grade[2], and the developing solvent [1-butanol–acetone–diethylamine–water (30:20:4:30)] was prepared fresh daily. Silica gel plates, 250 μm thick, were activated at 105° for 1 hr[3].

Instrumentation—A 250-nm UV lamp[4], grating spectrophotometer[5], and 1-cm quartz microcells[6] were used.

Standard Preparation—Compound I was dissolved in acetone or 3 *N* HCl. Aliquots equivalent to 1, 2, 4, and 6 μg were placed in glass-stoppered centrifuge tubes and evaporated to dryness under a gentle stream of nitrogen. Plasma, 1 ml, from untreated rats was added to each tube and mixed well. These standards and the appropriate blanks were handled in the same manner as described for the plasma specimens.

Sample Preparation—One volume (1–5 ml) of plasma from treated animals and five volumes of 0.1 *N* NaOH were introduced into a 100-ml separator. Compound I was extracted with two 10-volume portions of ether–acetone (1:1 v/v).

Free I—The ether–acetone extracts were pooled, washed with five volumes of 0.1 *N* NaOH and five volumes of water, dried with sodium sulfate, and flash evaporated to about 5 ml. This final amount as well as the ether–acetone washes was transferred to a glass-stoppered centrifuge tube and evaporated to dryness under a gentle stream of nitrogen. The standards and the appropriate blanks were handled in a similar manner.

Compound II—The water phase was heated with one volume of 8 *N* HCl in a boiling water bath for 40 min, and three volumes of 3 *N* NaOH were added to the mixture. After the mixture was cooled at room temperature, I was released by hydrolysis and treated as described under *Free I*.

TLC—Each sample was taken up in 0.1 ml of acetone. Aliquots of 0.09 ml were spotted 2 cm from the edge of the chromatographic plate. Aliquots equivalent to 1.1, 2.2, 4.4, and 6.6 μg of I standard acetone solution were also spotted on the plate.

The chromatograms were developed in an ascending system of 1-butanol–acetone–diethylamine–water (30:20:4:30) in a saturated atmosphere. After 90 min, the solvent front was marked and the plates were dried at room temperature. Spots of I, visualized by exposure to UV light, were scraped into glass-stoppered centrifuge tubes, eluted with 0.6 ml of 3 *N* HCl, and shaken every 15 min for 45 min. A similar spotless area (blank) was scraped off and subjected to an identical procedure.

The test tubes were then centrifuged at 4000 rpm for 10 min, and the relative absorbance of the supernates was measured at 267 nm against a blank.

Calculations—Calibration curves were prepared by plotting absorbance at 267 nm against a known concentration of I in either plasma or 3 *N* HCl. Values for the unknown concentration of I in plasma specimens were calculated from the slope of the standard curve.

Drug Administration to Rats—Male albino Wistar rats, 200–250 g, were divided into eight groups of three animals each. Compound I was suspended in an aqueous vehicle consisting of 0.9% sodium chloride, 0.4% polysorbate 80, 0.5% carboxymethylcellulose sodium, and 0.9% benzyl alcohol and administered by gavage at a dose of 50 mg/kg in a constant volume of 5 ml/kg. Blood samples were obtained by cardiac puncture by means of a heparinized syringe at time intervals ranging from 30 min up to 24 hr after drug administration. Plasma samples were obtained by centrifugation at 2000 rpm for approximately 10 min.

Application to Pharmacokinetic Analysis—Experimental data were fitted by the method of least squares (3) applied to each exponential segment of the blood level–time curve. The extent of biotransformation of I to II was measured by employing a one-compartment open model with extravascular drug administration. The blood concentration–time curve of I after oral administration of 50 mg/kg in male rats is represented by the following biexponential equation:

$$I = I_0 \frac{K_a}{(K_a - K)} (e^{-Kt} - e^{-K_a t}) \qquad \text{(Eq. 1)}$$

[1] Gianni, Milan, Italy.
[2] Merck.
[3] Merck 60 F_{254}.
[4] Mineral Light UVS 11.
[5] Beckman DBG.
[6] Hellma 108/2 QS.

REFERENCES

(1) V. I. Cohen, N. Rist, and S. Clavel, *Eur. J. Med. Chem.*, **10**, 134 (1975).

(2) *Ibid.*, **10**, 137 (1975).

(3) *Ibid.*, **10**, 140 (1975).

(4) V. I. Cohen, *Helv. Chim. Acta*, **59**, 840 (1976).

(5) S. V. Lieberman and R. Connor, *Org. Synth.*, **II**, 441 (1969).

(6) A. E. S. Fairfull, J. L. Lowe, and D. A. Peak, *J. Chem. Soc.*, **1952**, 742.

ACKNOWLEDGMENTS AND ADDRESSES

Received July 9, 1976, from the *Organic Chemistry Laboratory, Sciences Faculty, Ferdowsi University, Mashhad, Iran, and the ‡Service de la Tuberculose et des Mycobacteries de l'Institut Pasteur, Paris, France.

Accepted for publication October 18, 1976.

Supported by the Ministry of Sciences and Higher Education of Iran.

ˣ To whom inquiries should be directed.

TLC Determination of Iodochlorhydroxyquin and Its Conjugate in Plasma

P. DEL SOLDATO

Abstract □ A simple, specific, reliable, and sensitive method for the determination of iodochlorhydroxyquin and/or its conjugate in biological fluids is described. The method is based on a quantitative ether–acetone (1:1) extraction of plasma samples followed by TLC separation, visualization, elution, and determination at 267 nm. Iodochlorhydroxyquin released by hydrolysis of its conjugate was analyzed. Both compounds are detectable in amounts as low as 0.04 μg/ml. Application of the one-compartment open model to the data (assuming the biotransformation of the drug in conjugated form) provides a pharmacokinetic profile for the 50-mg/kg dose of iodochlorhydroxyquin in Wistar male rats.

Keyphrases □ Iodochlorhydroxyquin—and conjugate, TLC analysis, biological fluids □ TLC—analysis, iodochlorhydroxyquin and conjugate, biological fluids □ Antiamebic agents—iodochlorhydroxyquin, TLC analysis, biological fluids

Iodochlorhydroxyquin (I) has been widely used for over 30 years to treat various intestinal and vaginal infections. In view of debatable evidence of its neurotoxicity (1, 2), it is surprising that a method for the determination of I and/or its conjugate (II) in blood is not available. This paper describes a fast and simple TLC procedure for the detection of I and II in biological fluids and its use in pharmacokinetic studies.

EXPERIMENTAL

Reagents and Materials—Compound I was used as received[1]. All solvents were analytical reagent grade[2], and the developing solvent [1-butanol–acetone–diethylamine–water (30:20:4:30)] was prepared fresh daily. Silica gel plates, 250 μm thick, were activated at 105° for 1 hr[3].

Instrumentation—A 250-nm UV lamp[4], grating spectrophotometer[5], and 1-cm quartz microcells[6] were used.

Standard Preparation—Compound I was dissolved in acetone or 3 *N* HCl. Aliquots equivalent to 1, 2, 4, and 6 μg were placed in glass-stoppered centrifuge tubes and evaporated to dryness under a gentle stream of nitrogen. Plasma, 1 ml, from untreated rats was added to each tube and mixed well. These standards and the appropriate blanks were handled in the same manner as described for the plasma specimens.

Sample Preparation—One volume (1–5 ml) of plasma from treated animals and five volumes of 0.1 *N* NaOH were introduced into a 100-ml separator. Compound I was extracted with two 10-volume portions of ether–acetone (1:1 v/v).

Free I—The ether–acetone extracts were pooled, washed with five volumes of 0.1 *N* NaOH and five volumes of water, dried with sodium sulfate, and flash evaporated to about 5 ml. This final amount as well as the ether–acetone washes was transferred to a glass-stoppered centrifuge tube and evaporated to dryness under a gentle stream of nitrogen. The standards and the appropriate blanks were handled in a similar manner.

Compound II—The water phase was heated with one volume of 8 *N* HCl in a boiling water bath for 40 min, and three volumes of 3 *N* NaOH were added to the mixture. After the mixture was cooled at room temperature, I was released by hydrolysis and treated as described under *Free I*.

TLC—Each sample was taken up in 0.1 ml of acetone. Aliquots of 0.09 ml were spotted 2 cm from the edge of the chromatographic plate. Aliquots equivalent to 1.1, 2.2, 4.4, and 6.6 μg of I standard acetone solution were also spotted on the plate.

The chromatograms were developed in an ascending system of 1-butanol–acetone–diethylamine–water (30:20:4:30) in a saturated atmosphere. After 90 min, the solvent front was marked and the plates were dried at room temperature. Spots of I, visualized by exposure to UV light, were scraped into glass-stoppered centrifuge tubes, eluted with 0.6 ml of 3 *N* HCl, and shaken every 15 min for 45 min. A similar spotless area (blank) was scraped off and subjected to an identical procedure.

The test tubes were then centrifuged at 4000 rpm for 10 min, and the relative absorbance of the supernates was measured at 267 nm against a blank.

Calculations—Calibration curves were prepared by plotting absorbance at 267 nm against a known concentration of I in either plasma or 3 *N* HCl. Values for the unknown concentration of I in plasma specimens were calculated from the slope of the standard curve.

Drug Administration to Rats—Male albino Wistar rats, 200–250 g, were divided into eight groups of three animals each. Compound I was suspended in an aqueous vehicle consisting of 0.9% sodium chloride, 0.4% polysorbate 80, 0.5% carboxymethylcellulose sodium, and 0.9% benzyl alcohol and administered by gavage at a dose of 50 mg/kg in a constant volume of 5 ml/kg. Blood samples were obtained by cardiac puncture by means of a heparinized syringe at time intervals ranging from 30 min up to 24 hr after drug administration. Plasma samples were obtained by centrifugation at 2000 rpm for approximately 10 min.

Application to Pharmacokinetic Analysis—Experimental data were fitted by the method of least squares (3) applied to each exponential segment of the blood level–time curve. The extent of biotransformation of I to II was measured by employing a one-compartment open model with extravascular drug administration. The blood concentration–time curve of I after oral administration of 50 mg/kg in male rats is represented by the following biexponential equation:

$$I = I_0 \frac{K_a}{(K_a - K)} (e^{-Kt} - e^{-K_a t}) \qquad \text{(Eq. 1)}$$

[1] Gianni, Milan, Italy.
[2] Merck.
[3] Merck 60 F_{254}.
[4] Mineral Light UVS 11.
[5] Beckman DBG.
[6] Hellma 108/2 QS.

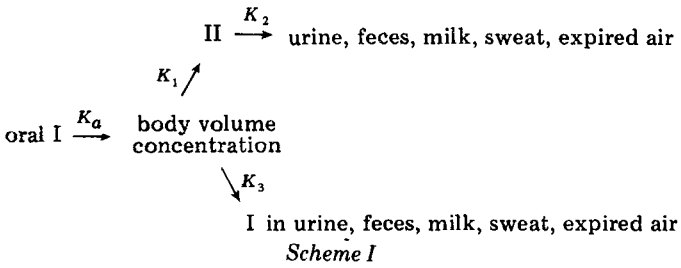

Scheme I

while that of the conjugate II is represented by the following triexponential equation:

$$II = I_0 K_a K_1 \left[\left[\frac{e^{-Kt}}{(K_a - K)(K_2 - K_a)} - \frac{e^{-K_a t}}{(K_a - K)(K_2 - K_a)} \right] + \frac{e^{-K_2 t}}{(K_2 - K_a)(K_2 - K)} \right] \quad \text{(Eq. 2)}$$

where I_0 is the intercept of the back-extrapolated monoexponential overall elimination line or monoexponential absorption line with the ordinate; t is the time intervals following I administration; and K_a, K, K_1, and K_2 represent rate constants of I absorption, I overall elimination, II formation, and II elimination, respectively, calculated from the appropriate relationship (4).

The one-compartment body model is illustrated in Scheme I, where K_a, K, K_1, and K_2 are as defined and K_3 is the rate constant of I excretion in urine, feces, milk, sweat, and expired air. It follows that $K = K_1 + K_3$.

The goodness of fit of the one-compartment model was tested by the paired t test between the observed mean data at each time interval and the calculated value.

RESULTS

Evaluation of Assay Method—Known amounts of I were added to plasma or acetone. The percentage recovery of I from plasma compared to that from acetone directly spotted on the plate provides an accuracy index of 96.3% (Table I). This method is adequately specific, since it is unaffected by the presence of endogenous substances.

Preliminary chromatograms of I added to plasma indicate that a recovery of 100 ± 2.2% can be obtained following an elution time of 45 min. Compound I has an R_f value of 0.58. Due to a sufficiently high molar absorptivity ($E^{1\%}_{1cm}$ in 3 N HCl at 267 nm is 852), I can be determined in amounts as low as 0.04–0.2 μg/ml.

Ten determinations to assess the precision of the procedure were carried out on unconjugated portions of two plasma samples obtained at 2 and 4 hr following I administration (Table II). Statistical evaluation of the data provided the following values: relative mean standard deviation (RSD) = 4.0% and reproducibility limits = $\overline{X} \pm RSDt_{18,0.05} = \overline{X}$ ± 8.4% of $\overline{X}$. The time required to determine I and II concentrations in plasma varies according to number of samples, *i.e.*, about 4 hr for one and 1 day for 10 samples.

Pharmacokinetic Analysis—Experimental data shown in Fig. 1 were analyzed by using the proposed one-compartment open model; the calculated pharmacokinetic parameters are: K_a = 0.26396 hr^{-1}, K = 0.08994 hr^{-1}, K_1 = 0.07902 hr^{-1}, K_2 = 0.14238 hr^{-1}, and K_3 = 0.01092 hr^{-1}, with half-lives of 2.6, 7.7, 8.8, 4.9, and 63.6 hr, respectively.

Table I—Recovery of I Added to Rat Plasma or Acetone

Amount of I Added, μg/ml	Amount[a], μg/ml, Recovered from Plasma	Acetone
1	0.93	0.99
2	1.85	1.93
4	3.92	4.06
6	5.88	5.94
Recovery (mean ± *SD*), %	95.41 ± 3.11	99.12 ± 3.74

[a] Mean of three replications.

Table II—Assay Precision Evaluation[a]

Sample	2 hr	4 hr
Mean	0.58	1.30
SD	0.02	0.06
RSD	0.34	4.61

[a] See text for discussion.

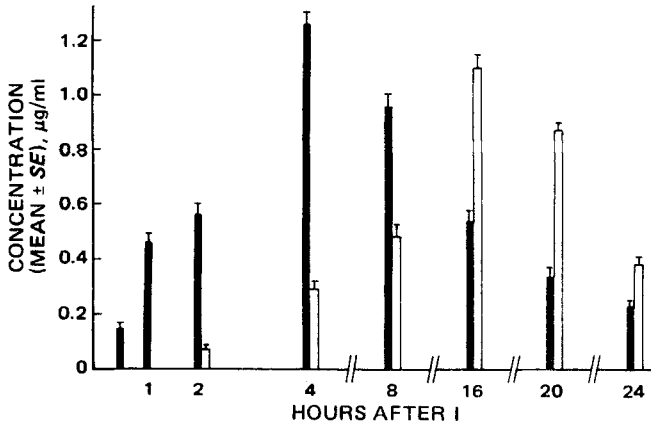

Figure 1—*Concentration of I in plasma of male rats at different time intervals after oral administration of 50 mg/kg. Key: ■, I; and □, II.*

The exponential functions representing the blood level–time curve of I and II are:

$$I = 3.11739\,(e^{-0.08994t} - e^{-0.26396t}) \quad \text{(Eq. 3)}$$

$$II = 4.63386\,e^{-0.08994t} + 1.99868\,e^{-0.26369t} - 6.63250\,e^{-0.142377t} \quad \text{(Eq. 4)}$$

The test for goodness of fit (t_{15}) = 0.63.

DISCUSSION

Because of insufficient sensitivity, previous methods (5–7) were limited to the determination of I and/or II in urine. The reported method is rapid, reliable, and sensitive enough for the determination of I and/or II in biological fluids of both experimental animals and humans. The usual therapeutic dosage of I ranges from 500 to 750 mg three times daily (8). Since intestinal absorption of labeled I amounts to 43.6% of the administered dose as calculated from urinary excretion during the 10–18-day observation period (9), plasma levels of I and/or II are well within the ranges of the sensitivity of this method.

The present method has two definite advantages: (*a*) its specificity, because I can be determined in amounts as low as those detectable by the radiochemical method (10); and (*b*) its usefulness, since I and II can be determined separately. This model provides a pharmacokinetic profile for this oral dose of I in rats; the K_a and K values indicate fairly rapid absorption and elimination rates.

The very small difference between K and K_1 suggests that biotransformation by the liver plays a major role in the process of irreversible drug elimination. Excretion of unaltered I in the urine, feces, expired air, milk, and sweat is insignificant.

Results of the goodness of fit test clearly indicate that the model is appropriate. It could be usefully employed clinically for: (*a*) estimation of drug absorption following oral administration or topical application and, therefore, indication of potential systemic toxicity (11); and (*b*) study of absorption and/or metabolic disposition of I as influenced by the presence of other substances (12).

REFERENCES

(1) R. Kono, *Jpn. J. Med. Sci.*, **24**, 195 (1971).

(2) R. Hess, W. P. Koella, G. Krinke, H. Petermann, P. Thomann, and F. Zak, *Arzneim.-Forsch.*, **23**, 1566 (1973).

(3) D. Colqhoun, "Lectures on Biostatistics," Clarendon, Oxford, England, 1971, pp. 239–243.

(4) W. A. Ritschel, "Handbook of Basic Pharmacokinetics," Drug Intelligence Publications, Hamilton, Ill., 1976, pp. 185, 186.

(5) W. T. Haskins and G. W. Luttermoser, *Anal. Chem.*, **23**, 456, (1951).

(6) D. J. Vadodaria, B. R. Desai, and S. P. Mukherji, *Indian J. Pharm.*, **27**, 257 (1965).

(7) L. Bergren and O. Hansonn, *Clin. Pharmacol. Ther.*, **9**, 67 (1968).

(8) "AMA Drug Evaluations," 2nd ed., Publishing Sciences Group, Acton, Mass., 1973, p. 620.
(9) K. Liewendahl and B. A. Lamberg, *Nucl. Med. Isotope Med. Biol.*, **6**, 20 (1967).
(10) K. Schmid, G. Krinke, F. Fruth, and H. Keberle, *Arzneim.-Forsch.*, **23**, 1560 (1973).
(11) D. R. Lawrence and A. L. Bachrach, "Evaluation of Drug Activities: Pharmacometrics," vol. I, Academic, London, England, 1964, p. 155.
(12) S. Riegelman, in "Principles and Techniques of Human Research and Therapeutics," vol. 3, F. G. Mc Mahon, Ed., Futura, Mount Kisco, N.Y., 1974, p. 29.

ACKNOWLEDGMENTS AND ADDRESSES

Received August 3, 1976, from the *Pharmacology Department, A. Menarini Pharmaceuticals Research Laboratories, Florence, Italy.*

Accepted for publication November 4, 1976.

The author is indebted to Professor A. Meli, Research Director, for his interest and advice.

Phytochemical Investigation of *Adenium obesum* Forskal (Apocynaceae): Isolation and Identification of Cytotoxic Agents

JOSEPH J. HOFFMANN * and JACK R. COLE ˣ

Abstract □ An ethanol extract of *Adenium obesum* exhibited cytotoxic activity against the human epidermoid carcinoma of the nasopharynx test system. Constituents in the active extract were identified as the cardenolides somalin, honghelioside A, 16-acetylstrospeside, and honghelin and the flavonol 3,3′-bis(*O*-methyl)quercetin. Their identities were proven by IR, UV, proton magnetic resonance, and mass spectrometry; elemental analyses; preparation of derivatives; and melting-point determinations. An inactive triterpene, dihydroifflaionic acid, and an inactive flavonol, 3-*O*-methylkaempferol, also were isolated and identified.

Keyphrases □ *Adenium obesum*—ethanol extract of aboveground parts, various cardenolides and flavonol isolated and identified, evaluated for cytotoxic activity □ Cardenolides, various—isolated from ethanol extract of aboveground parts of *Adenium obesum*, evaluated for cytotoxic activity □ Flavonols—3,3′-bis(*O*-methyl)quercetin isolated from ethanol extract of aboveground parts of *Adenium obesum*, evaluated for cytotoxic activity □ Cytotoxic activity—evaluated in various cardenolides and flavonol isolated from ethanol extract of aboveground parts of *Adenium obesum*

In the continuing search for plants having antitumor properties, an ethanol extract of the stems, leaves, and flowers of *Adenium obesum* Forskal (Apocynaceae)[1] exhibited cytotoxic activity against the human epidermoid carcinoma of the nasopharynx (KB) test system[2].

DISCUSSION

The chloroform fraction, obtained from an ethanol extract of the ground stems, leaves, and flowers of *A. obesum* by partitioning between chloroform and water, was systematically fractionated by solvent extractions. The highly active ether-soluble fraction, consisting of seven major constituents, was subjected to multiple column chromatography, preparative TLC, and fractional crystallizations.

The seven compounds were identified as the triterpene dihydroifflaionic acid, the flavonols 3,3′-bis(*O*-methyl)quercetin and 3-*O*-methylkaempferol, and the cardenolides somalin, honghelioside A, 16-acetylstrospeside, and honghelin by means of IR, UV, proton magnetic resonance (PMR), and mass spectrometry; elemental analyses; preparation of derivatives; and melting-point determinations. In addition, the structures of the flavonols were substantiated by microanalytical UV spectroscopy. Somalin and honghelioside A, previously isolated from other *Adenium* species (1–5), were hydrolyzed to their respective genins and carbohydrate moieties.

Somalin, honghelin, honghelioside A, 16-acetylstrospeside, and 3,3′-bis(*O*-methyl)quercetin exhibited cytotoxic activities at levels < 0.01, 0.02, 0.035, 0.035, and 3.08 μg/ml, respectively. Dihydroifflaionic acid and 3-*O*-methylkaempferol were inactive. Activity in the KB test system is defined as $ED_{50} \leq 20$ μg/ml (6).

EXPERIMENTAL[3]

Isolation Procedure—The stems, leaves, and flowers (15 kg) of *A. obesum* were ground to a powder and extracted exhaustively in a Lloyd-type extractor with petroleum ether and then with 95% ethanol. The air-dried ethanol extract (1.2 kg) was partitioned between chloroform (10 liters) and water (10 liters). The air-dried chloroform fraction (468 g) was stirred mechanically with petroleum ether three times, the residue (324 g) was stirred mechanically with acetone three times, and the air-dried filtrate was stirred mechanically with ether three times.

The ether-soluble fraction (100 g) was subjected to a silica gel G (1.5 kg) column (7 × 81 cm) eluted with petroleum ether–ether–chloroform (1:3:1). Fractions were collected with an automatic fraction collector (25 ml/tube) and combined according to their TLC profiles. The first fractions (A) contained dihydroifflaionic acid. The next set of fractions (B) consisted of a mixture of two flavonols. The third set (C) contained somalin. The fourth set (D) consisted mainly of honghelioside A.

The fifth fraction (E, 50 g) was rechromatographed on a silica gel 60 (1.2 kg) column (6 × 70 cm) eluted with chloroform–methanol–water (188:12:1). The first fractions consisted of mainly 16-acetylstrospeside, the middle fractions contained an overlap mixture, and the latter fractions contained honghelin.

Isolation of Dihydroifflaionic Acid—The air-dried residue of Fraction A was treated with petroleum ether. The resultant precipitate was filtered, washed with petroleum ether, dissolved in chloroform–petroleum ether (1:1), and stored at 5° overnight. The resultant powder was filtered and subsequently crystallized from methanol to yield stout white crystals of dihydroifflaionic acid, mp 259–260° [lit. (7) mp 260°]; mass spectrum: *m/e* 456 (M^+) and 248 (base); IR[4]: ν_{max} 3400–3500, 1700, 1450, 1390, 1280, 1020, and 990 cm^{-1}; PMR[4]: δ 4.50 (m, 1H), 3.42 (broad

[1] Identification was confirmed by Dr. Robert E. Perdue, Chief, Medicinal Plant Resources Laboratory, U.S. Department of Agriculture, Beltsville, Md., where a reference specimen (PR 26176) is maintained. The plant was collected in the Kilifi District of Kenya by R. W. Spjut and P. D. Ensor in November 1972.

[2] Data on the cytotoxic activity were provided through the courtesy of the Divison of Cancer Treatment, National Cancer Institute, National Institutes of Health, Bethesda, Md.

[3] Carbon and hydrogen analyses were performed by Chemalytics, Inc., Tempe, Ariz. PMR, IR, UV, and mass spectral data were determined using a Varian T-60 spectrophotometer, a Beckman IR-33, a Beckman DB-G spectrophotometer, and a Hitachi Perkin-Elmer double-focusing spectrometer (model RMU-6E), respectively. Melting points were determined on a Kofler hot-stage apparatus and are uncorrected.

[4] These data were not reported previously.

(8) "AMA Drug Evaluations," 2nd ed., Publishing Sciences Group, Acton, Mass., 1973, p. 620.
(9) K. Liewendahl and B. A. Lamberg, *Nucl. Med. Isotope Med. Biol.*, **6**, 20 (1967).
(10) K. Schmid, G. Krinke, F. Fruth, and H. Keberle, *Arzneim.-Forsch.*, **23**, 1560 (1973).
(11) D. R. Lawrence and A. L. Bachrach, "Evaluation of Drug Activities: Pharmacometrics," vol. I, Academic, London, England, 1964, p. 155.
(12) S. Riegelman, in "Principles and Techniques of Human Research and Therapeutics," vol. 3, F. G. Mc Mahon, Ed., Futura, Mount Kisco, N.Y., 1974, p. 29.

ACKNOWLEDGMENTS AND ADDRESSES

Received August 3, 1976, from the *Pharmacology Department, A. Menarini Pharmaceuticals Research Laboratories, Florence, Italy.*

Accepted for publication November 4, 1976.

The author is indebted to Professor A. Meli, Research Director, for his interest and advice.

Phytochemical Investigation of *Adenium obesum* Forskal (Apocynaceae): Isolation and Identification of Cytotoxic Agents

JOSEPH J. HOFFMANN * and JACK R. COLE ˣ

Abstract □ An ethanol extract of *Adenium obesum* exhibited cytotoxic activity against the human epidermoid carcinoma of the nasopharynx test system. Constituents in the active extract were identified as the cardenolides somalin, honghelioside A, 16-acetylstrospeside, and honghelin and the flavonol 3,3′-bis(*O*-methyl)quercetin. Their identities were proven by IR, UV, proton magnetic resonance, and mass spectrometry; elemental analyses; preparation of derivatives; and melting-point determinations. An inactive triterpene, dihydroifflaionic acid, and an inactive flavonol, 3-*O*-methylkaempferol, also were isolated and identified.

Keyphrases □ *Adenium obesum*—ethanol extract of aboveground parts, various cardenolides and flavonol isolated and identified, evaluated for cytotoxic activity □ Cardenolides, various—isolated from ethanol extract of aboveground parts of *Adenium obesum*, evaluated for cytotoxic activity □ Flavonols—3,3′-bis(*O*-methyl)quercetin isolated from ethanol extract of aboveground parts of *Adenium obesum*, evaluated for cytotoxic activity □ Cytotoxic activity—evaluated in various cardenolides and flavonol isolated from ethanol extract of aboveground parts of *Adenium obesum*

In the continuing search for plants having antitumor properties, an ethanol extract of the stems, leaves, and flowers of *Adenium obesum* Forskal (Apocynaceae)[1] exhibited cytotoxic activity against the human epidermoid carcinoma of the nasopharynx (KB) test system[2].

DISCUSSION

The chloroform fraction, obtained from an ethanol extract of the ground stems, leaves, and flowers of *A. obesum* by partitioning between chloroform and water, was systematically fractionated by solvent extractions. The highly active ether-soluble fraction, consisting of seven major constituents, was subjected to multiple column chromatography, preparative TLC, and fractional crystallizations.

The seven compounds were identified as the triterpene dihydroifflaionic acid, the flavonols 3,3′-bis(*O*-methyl)quercetin and 3-*O*-methylkaempferol, and the cardenolides somalin, honghelioside A, 16-acetylstrospeside, and honghelin by means of IR, UV, proton magnetic resonance (PMR), and mass spectrometry; elemental analyses; preparation of derivatives; and melting-point determinations. In addition, the structures of the flavonols were substantiated by microanalytical UV spectroscopy. Somalin and honghelioside A, previously isolated from other *Adenium* species (1–5), were hydrolyzed to their respective genins and carbohydrate moieties.

Somalin, honghelin, honghelioside A, 16-acetylstrospeside, and 3,3′-bis(*O*-methyl)quercetin exhibited cytotoxic activities at levels < 0.01, 0.02, 0.035, 0.035, and 3.08 μg/ml, respectively. Dihydroifflaionic acid and 3-*O*-methylkaempferol were inactive. Activity in the KB test system is defined as $ED_{50} \leq 20$ μg/ml (6).

EXPERIMENTAL[3]

Isolation Procedure—The stems, leaves, and flowers (15 kg) of *A. obesum* were ground to a powder and extracted exhaustively in a Lloyd-type extractor with petroleum ether and then with 95% ethanol. The air-dried ethanol extract (1.2 kg) was partitioned between chloroform (10 liters) and water (10 liters). The air-dried chloroform fraction (468 g) was stirred mechanically with petroleum ether three times, the residue (324 g) was stirred mechanically with acetone three times, and the air-dried filtrate was stirred mechanically with ether three times.

The ether-soluble fraction (100 g) was subjected to a silica gel G (1.5 kg) column (7 × 81 cm) eluted with petroleum ether–ether–chloroform (1:3:1). Fractions were collected with an automatic fraction collector (25 ml/tube) and combined according to their TLC profiles. The first fractions (A) contained dihydroifflaionic acid. The next set of fractions (B) consisted of a mixture of two flavonols. The third set (C) contained somalin. The fourth set (D) consisted mainly of honghelioside A.

The fifth fraction (E, 50 g) was rechromatographed on a silica gel 60 (1.2 kg) column (6 × 70 cm) eluted with chloroform–methanol–water (188:12:1). The first fractions consisted of mainly 16-acetylstrospeside, the middle fractions contained an overlap mixture, and the latter fractions contained honghelin.

Isolation of Dihydroifflaionic Acid—The air-dried residue of Fraction A was treated with petroleum ether. The resultant precipitate was filtered, washed with petroleum ether, dissolved in chloroform–petroleum ether (1:1), and stored at 5° overnight. The resultant powder was filtered and subsequently crystallized from methanol to yield stout white crystals of dihydroifflaionic acid, mp 259–260° [lit. (7) mp 260°]; mass spectrum: *m/e* 456 (M^+) and 248 (base); IR[4]: ν_{max} 3400–3500, 1700, 1450, 1390, 1280, 1020, and 990 cm^{-1}; PMR[4]: δ 4.50 (m, 1H), 3.42 (broad

[1] Identification was confirmed by Dr. Robert E. Perdue, Chief, Medicinal Plant Resources Laboratory, U.S. Department of Agriculture, Beltsville, Md., where a reference specimen (PR 26176) is maintained. The plant was collected in the Kilifi District of Kenya by R. W. Spjut and P. D. Ensor in November 1972.

[2] Data on the cytotoxic activity were provided through the courtesy of the Divison of Cancer Treatment, National Cancer Institute, National Institutes of Health, Bethesda, Md.

[3] Carbon and hydrogen analyses were performed by Chemalytics, Inc., Tempe, Ariz. PMR, IR, UV, and mass spectral data were determined using a Varian T-60 spectrophotometer, a Beckman IR-33, a Beckman DB-G spectrophotometer, and a Hitachi Perkin-Elmer double-focusing spectrometer (model RMU-6E), respectively. Melting points were determined on a Kofler hot-stage apparatus and are uncorrected.

[4] These data were not reported previously.

t, 16 Hz, 1H), 1.23 (s, 6H), 1.01 (s, 3H), 1.10 (s, 6H), 1.00 (d, J = 5 Hz, 3H), and 0.80 (s, 3H) ppm.

Anal.—Calc. for $C_{30}H_{48}O_3$: C, 78.89; H, 10.59; mol. wt. 456. Found: C, 78.65; H, 10.58; *m/e* 456 (M^+).

Acetate of Dihydroifflaionic Acid—Acetylation of dihydroifflaionic acid with acetic anhydride in pyridine at room temperature for 48 hr yielded the acetate, which crystallized directly from water, mp 189–191°; mass spectrum: *m/e* 498 (M^+) and 207 (base); IR: ν_{max} 1735 and 1245 cm^{-1}.

Methyl Ester of Dihydroifflaionic Acid—Esterification of dihydroifflaionic acid with diazomethane yielded crystals from methanol, mp 209–210° [lit. (8) mp 207–209°]; mass spectrum: *m/e* 470 (M^+) and 262 (base); IR: ν_{max} 1730 and 1130–1140 cm^{-1}.

Methyl Ester of Acetyldihydroifflaionic Acid—Esterification of acetyldihydroifflaionic acid with diazomethane yielded crystals from methanol, mp 228–230°; PMR: δ 3.60 (s, 3H), 2.03 (s, 3H), and 4.50 (broad t, 16 Hz, 1H) ppm.

Isolation of 3,3′-Bis(*O*-methyl)quercetin—A chloroform solution of Fraction B was treated with an equal volume of petroleum ether. The resultant precipitate was filtered and separated into two flavonols on preparative TLC plates developed in dichloromethane–methanol (96:4). The upper spot was recovered and purified on preparative TLC plates developed in chloroform–methanol–water (188:12:1). The recovered material was crystallized from 95% ethanol to yield yellow needles, mp 256–259° [lit. (9) mp 258–259°]; IR[4]: ν_{max} 3100–3190, 1650, 880, and 810 cm^{-1}; PMR[4]: δ 12.73 (s, 1H), 10.80 (broad s, 1H), 10.40 (broad s, 1H), 7.62 (d, J = 2 Hz, 1H), 7.56 (d, J = 7 Hz, 1H), 6.97 (dd, J = 7 and 1 Hz, 1H), 6.45 (d, J = 2 Hz, 1H), 6.20 (d, J = 2 Hz, 1H), 3.87 (s, 3H), and 3.80 (s, 3H) ppm. The UV data were consistent with the literature data (10).

Anal.—Calc. for $C_{17}H_{14}O_7$: C, 61.82; H, 4.28; mol. wt. 330. Found: C, 62.14; H, 4.61; *m/e* 330 (M^+).

3,3′-Bis(*O*-methyl)quercetin Triacetate—Acetylation of 3,3′-bis(*O*-methyl)quercetin with acetic anhydride in pyridine at room temperature for 24 hr yielded the triacetate. Crystallization from methanol yielded white needles, mp 195° [lit. (11) mp 195°]; IR: ν_{max} 1760 and 1200 cm^{-1}.

Isolation of 3-*O*-Methylkaempferol—The lower spot from the previous preparative TLC plates was purified in the same manner. The recovered material was crystallized from methanol to yield yellow platelets, mp 270–272° [lit. (12) mp 270–272°]; PMR: δ 12.73 (s, 1H), 10.80 (broad s, 1H), 10.40 (broad s, 1H), 7.95 (dd, 2H), 6.88 (dd, 2H), 6.45 (d, J = 2 Hz, 1H), 6.20 (d, J = 2 Hz, 1H), and 3.80 (s, 3H) ppm. The UV and IR data were identical to the literature data (13, 14).

Anal.—Calc. for $C_{16}H_{12}O_6$: C, 64.00; H, 4.03; mol. wt. 300. Found: C, 64.21; H, 4.61; *m/e* 300 (M^+).

3-*O*-Methylkaempferol Triacetate—Acetylation of 3-*O*-methylkaempferol with acetic anhydride in pyridine at room temperature for 24 hr yielded the triacetate. Recrystallization from petroleum ether and ethyl acetate yielded yellow needles, mp 163° [lit. (12) mp 161–163°].

Isolation of Somalin—Somalin crystallized directly from Fraction C when dissolved in 20% aqueous methanol. Recrystallization from absolute methanol yielded fine white needles, mp 197–198° [lit. (15) mp 197°]; UV: λ_{max} 220 nm (log ϵ = 4.18); IR[4]: ν_{max} 1790, 1740, and 1620 cm^{-1}; PMR[4]: δ 5.87 (1H), 4.90 (2H), 4.70 (1H), 4.00 (1H), 3.43 (3H), 1.25 (d, J = 6 Hz, 3H), 0.93 (s, 3H), and 0.87 (s, 3H) ppm.

Anal.—Calc. for $C_{30}H_{46}O_7$: C, 69.47; H, 8.94; mol. wt. 518. Found: C, 69.47; H, 9.11; *m/e* 518 (M^+).

Mild Acid Hydrolysis of Somalin—The acid hydrolysis procedure was reported previously (16). The products isolated were digitoxigenin, mp 247–250° [lit. (15) mp 250°], and D-cymarose, mp 92–94° [lit. (17) mp 93–94°].

Isolation of Honghelosides A—Fraction D (2.5 g) was purified on a silica gel G (250-g) column (4 × 42 cm) eluted with dichloromethane–methanol (9:1). Fractions containing honghelosides A were purified further on preparative TLC plates developed in benzene–methanol (9:1). Honghelosides A was then crystallized from methanol and water, mp 209–211° [lit. (18) mp 208–211°]; mass spectrum: *m/e* 576 (M^+) and 355 (base); UV: λ_{max} 220 nm (log ϵ = 4.12); IR[4]: ν_{max} 1785, 1750, 1625, and 1245 cm^{-1}; PMR[4]: δ 5.93 (1H), 5.45 (m, 18 Hz), 4.90 (2H), 4.70 (dd, J = 9 and 1.5 Hz, 1H), 4.00 (1H), 3.43 (s, 3H), 1.98 (s, 3H), 1.25 (d, J = 6 Hz, 3H), and 0.93 (s, 6H) ppm.

Anal.—Calc. for $C_{32}H_{48}O_9$: C, 66.64; H, 8.39; mol. wt. 576. Found: C, 66.63; H, 8.38; *m/e* 576 (M^+).

Mild Acid Hydrolysis Product—The deacetylated derivative of honghelosides A was hydrolyzed with the same procedure as somalin into D-cymarose, mp 92–94°, and gitoxigenin, mp 225–227° [lit. (16) mp 224°].

Isolation of 16-Acetylstrospeside—The fractions containing 16-acetylstrospeside were purified on preparative TLC plates developed in ether–chloroform (85:15). The recovered material was subsequently crystallized from aqueous methanol to yield colorless platelets, mp 208–210° (mp 189–190° after drying under vacuum); mass spectrum: base at *m/e* 355; UV: λ_{max} 220 nm (log ϵ = 4.31); IR[4]: ν_{max} 1785, 1745, 1620, and 1245 cm^{-1}; PMR[4]: δ 5.93 (1H), 4.95 (2H), 5.50 (m, 18 Hz), 4.00 (1H), 3.60 (s, 3H), 1.27 (d, J = 6 Hz, 3H), and 0.93 (s, 6H) ppm.

Anal.—Calc. for $C_{32}H_{48}O_{10}$: C, 64.84; H, 8.16. Found: C, 64.31; H, 8.21.

Strospeside—16-Acetylstrospeside (100 mg) was dissolved in methanol (20 ml). After the addition of 0.25 *M* $KHCO_3$ (4 ml), the reaction mixture was stirred at room temperature for 3 days. The air-dried residue was purified on preparative TLC plates developed in benzene–ethyl acetate–acetone–ethanol (4:3:2:1). The recovered material was crystallized from methanol and water, mp 252–253° [lit. (15) mp 252°].

16-Anhydrostrospeside—16-Acetylstrospeside (30 mg) was absorbed on basic aluminum oxide, introduced on top of a small alumina column (1.5 × 15 cm) and displaced with benzene–methanol (9:1), and the stopcock was closed. The column remained at room temperature for 1 week. Then the stopcock was opened, and the column was eluted with chloroform–methanol (1:1). The recovered material was crystallized from methanol and water, mp 240–243° [lit. (18) mp 242–246°]; UV: λ_{max} 270 nm (log ϵ = 4.25).

Isolation of Honghelin—The fractions containing honghelin were purified on preparative TLC plates developed in ether–chloroform (9:1). The recovered material formed hydrate crystals from methanol and water, mp 135–137° [lit. (18) mp 133–136°]; mass spectrum: *m/e* 534 (M^+), 357, 339, and 203; UV: λ_{max} 220 nm (log ϵ = 4.25); IR[4]: ν_{max} 1780, 1740, and 1620 cm^{-1}; PMR[4]: δ 5.83 (1H), 4.90 (2H), 4.00 (1H), 3.60 (s, 3H), 0.93 (s, 3H), and 0.87 (s, 3H) ppm.

Honghelin Diacetate—Acetylation of honghelin with acetic anhydride in pyridine at room temperature for 24 hr yielded the diacetate. It was crystallized from methanol and water, mp 218–220° [lit. (19) mp 217–220°]; PMR[4]: δ 2.07 (s, 3H), 2.10 (s, 3H), 4.90 (m, 28 Hz, 4H), and 4.40 (d, J = 8 Hz) ppm.

Anal.—Calc. for $C_{34}H_{50}O_{12}$: C, 66.00; H, 8.14. Found: C, 66.29, H, 8.20.

REFERENCES

(1) M. Hartmann and E. Schlittler, *Helv. Chim. Acta*, **23**, 548 (1940).

(2) A. Hunger and T. Reichstein, *ibid.*, **33**, 76 (1950).

(3) O. Schindler and T. Reichstein, *ibid.*, **34**, 18 (1951).

(4) J. C. Hess, A. Hunger, and T. Reichstein, *ibid.*, **35**, 2202 (1952).

(5) P. R. Striebel, C. Tamm, and T. Reichstein, *ibid.*, **38**, 1001 (1955).

(6) R. I. Geran, N. H. Greenberg, M. N. MacDonald, A. M. Schumacher, and B. J. Abbott, *Cancer Chemother. Rep.*, **3** (3), 17 (1972).

(7) A. A. Newman, "Chemistry of Terpenes and Terpenoids," Academic, New York, N.Y., 1972.

(8) J. A. Bosson, M. N. Gailbraith, E. Ritchie, and W. C. Taylor, *Aust. J. Chem.*, **16**, 491 (1963).

(9) N. K. Anand, S. R. Gupta, A. C. Jain, S. K. Mathur, K. S. Pankajamani, and T. R. Seshadri, *J. Sci. Ind. Res. (India)*, **21B**, 322 (1962); through *Chem. Abstr.*, **57**, 13713e (1962).

(10) T. A. Geisman, "Chemistry of Flavonoid Compounds," Macmillan, New York, N.Y., 1962.

(11) M. K. Shakhova, G. I. Samokhvalov, and N. A. Preobrazhenskii, *Zh. Obshsh. Khim.*, **32**, 390 (1962); through *Chem. Abstr.*, **58**, 1426e (1963).

(12) V. K. Rao and T. R. Seshadri, *J. Chem. Soc.*, **122**, 124 (1947).

(13) H. Pacheco and A. Grouiller, *Bull. Soc. Chim. Fr.*, **1965**, 779.

(14) L. H. Briggs and L. D. Colebrook, *Spectrochim. Acta*, **18**, 939 (1962).

(15) A. I. Scott and T. K. Devon, "Handbook of Naturally Occurring Compounds, Vol. II: Terpenes," Holden-Day, San Francisco, Calif., 1972.

(16) M. J. Frey and G. M. Jacobsohn, *Anal. Biochem.*, **36**, 78 (1970).

(17) "The Merck Index," 8th ed., Merck & Co., Rahway, N.J., 1968.

(18) W. Karrer, "Konstitution und Vorkommen der Organischen Pflanzenstoffe," Berkhauser Verlag, Basel, Switzerland, 1958.

(19) K. Reyle and T. Reichstein, *Helv. Chim. Acta*, **35**, 195 (1952).

ACKNOWLEDGMENTS AND ADDRESSES

Received June 1, 1976, from the *Division of Pharmaceutical Chemistry, College of Pharmacy, University of Arizona, Tucson, AZ 85721.*

Accepted for publication October 29, 1976.

Supported by Contract NOI-CM-33750 from the Division of Cancer Treatment, National Cancer Institute, National Institutes of Health, Department of Health, Education, and Welfare, Bethesda, MD 20014, and the Elsa U. Pardee Foundation, Midland, MI 48640.

* E. Mead Johnson Memorial Fellow of the American Foundation for Pharmaceutical Education.

[x] To whom inquiries should be directed.

Perfusion and Molecular Modification of Idoxuridine to Alter Its Cerebrospinal Fluid Metabolism

PHILIP H. GUTIN *, LEON D. PROCKOP [‡], K. F. YIP, JAMES D. WEINSTEIN, and K. C. TSOU [x]

Abstract □ Two methods to deter the rapid intrathecal degradation of idoxuridine were investigated: (*a*) rapid drug perfusion through the ventricular system, and (*b*) modification of the molecule to its uronic acid derivative, 2′-deoxy-5-iodo-5′-uridinecarboxylic acid, to make it less susceptible to enzymatic digestion. Perfusion of idoxuridine through the ventricular system (ventriculocisternal) of dogs at 0.97 ml/min saturated the metabolic pathway so that the outflow solution yielded a single spot (R_f 0.76) on TLC indicative of the intact molecule. The ^{125}I-labeled uronic acid was synthesized from the ^{125}I-labeled parent compound, and the labeled compounds were compared after their individual intracisternal injection in dogs. Since there was no difference in the disappearance rates, the stability of the uronic acid was, in fact, no greater than that of the parent compound *in vivo*. Ventricular perfusion of idoxuridine, however, seems a suitable means for increasing the amount of active drug delivered to central nervous system tumors and viral infections.

Keyphrases □ Idoxuridine—metabolism in cerebrospinal fluid, effect of rapid perfusion and molecular modification, dogs □ Metabolism—idoxuridine in cerebrospinal fluid, effect of rapid perfusion and molecular modification, dogs □ Perfusion, rapid—idoxuridine through ventricular system, effect on metabolism in cerebrospinal fluid, dogs □ Molecular modification—idoxuridine to uronic acid derivative, effect on metabolism in cerebrospinal fluid, dogs □ Antiviral agents—idoxuridine, metabolism in cerebrospinal fluid, effect of rapid perfusion and molecular modification, dogs

Idoxuridine (I), an antimetabolite, is a useful topical antiviral agent in the treatment of *Herpes simplex* infections of the cornea (1, 2). This agent has also been administered systemically in cases of disseminated *H. simplex* and *H. simplex* encephalitis, but its value in this respect remains largely unproved (3–5).

BACKGROUND

The development of the Ommaya reservoir made possible the direct intraventricular injection or even cerebrospinal fluid perfusion of chemotherapeutic agents for central nervous system (CNS) viral infection or malignant disease (6). This subcutaneously implanted reservoir, with a catheter extending to the lateral ventricle, facilitates the delivery of high concentrations of potentially useful drugs to the brain. This route of administration is safe for I administration to patients with brain tumors or encephalitis (7). However, reservoir-delivered intraventricular therapy with I for progressive multifocal leukoencephalopathy in one patient (8) and for malignant brain tumors in four patients treated on this neurosurgical service was of no value[1].

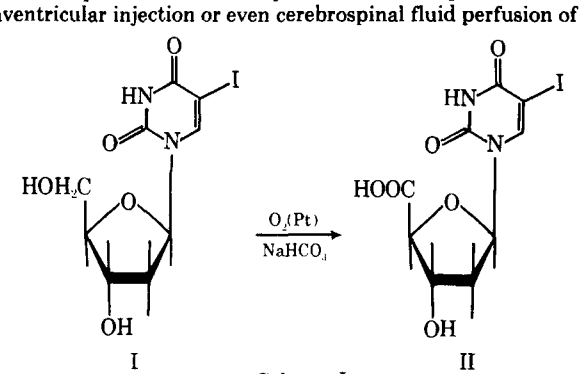

I II

Scheme I

The lack of efficacy of intraventricular I therapy may be related to the very rapid metabolism of the drug by enzymes believed to be associated with the glial, ependymal, neural, or choroid plexus cells in or near the cerebral ventricles, where the drug is degraded to iodouracil and then deiodinated by the rate-limiting step to iodide and uracil (9, 10). Therefore, two methods of minimizing such enzymatic degradation were investigated: (*a*) rapid ventriculocisternal perfusion of I to maintain high levels of drug in the ventricular cerebrospinal fluid and, consequently, saturate the metabolic pathways; and (*b*) modification of the parent compound to its uronic acid derivative, 2′-deoxy-5-iodo-5′-uridinecarboxylic acid, in the hope that it would retain its antiviral and antitumor activity but be less susceptible to enzymatic breakdown. The uronic acid of floxuridine was synthesized previously and showed dramatic resistance to hydrolysis by acid or phosphorylase while remaining moderately toxic to tumor cells *in vitro* (11).

EXPERIMENTAL

Ventriculocisternal Perfusion—Mongrel dogs, 7–20 kg, were anesthetized with pentobarbital, 60 mg/kg iv, with supplements given as needed. The dog was secured in a stereotactic head frame, and an endotracheal tube was placed to ensure adequate ventilatory exchange. A skin incision was made, and a bur hole was drilled in the skull so that its center lay 22–24 mm forward from the ear bar and 7–8 mm lateral to the midline. A No. 18 needle was placed percutaneously into the cisterna magna.

With continuous pressure monitoring, a No. 19 needle in a stereotactic holder was introduced slowly through the bur hole vertically to a depth of 16–18 mm until the pulsations of the choroid plexus transmitted to the cerebrospinal fluid were noted on the pressure recording to assure ventricular placement. Cerebrospinal fluid pressure was measured on a pressure transducer[2] and transmitted for reading on a polygraph[3].

Artificial cerebrospinal fluid was prepared as a modified Krebs–Ringer bicarbonate solution that closely resembled the ionic composition of normal spinal fluid (12). Compound I[4] was diluted to 0.1 mg/ml in artificial cerebrospinal fluid and infused through the ventricular needle first at 0.39 ml/min and then at 0.97 ml/min by means of a constant-infusion pump[5].

Samples were collected from the cisternal needle over timed periods after a 30-min perfusion to ensure homogeneity in the ventricular system,

[1] J. W. Weinstein, unpublished data.
[2] Stratham, Oxnard, Calif.
[3] Grass, Quincy, Mass.
[4] Schwarz/Mann, Orangeburg, N.Y.
[5] Harvard Apparatus, Millis, Mass.

ACKNOWLEDGMENTS AND ADDRESSES

Received June 1, 1976, from the *Division of Pharmaceutical Chemistry, College of Pharmacy, University of Arizona, Tucson, AZ 85721.*

Accepted for publication October 29, 1976.

Supported by Contract NOI-CM-33750 from the Division of Cancer Treatment, National Cancer Institute, National Institutes of Health, Department of Health, Education, and Welfare, Bethesda, MD 20014, and the Elsa U. Pardee Foundation, Midland, MI 48640.

* E. Mead Johnson Memorial Fellow of the American Foundation for Pharmaceutical Education.

[x] To whom inquiries should be directed.

Perfusion and Molecular Modification of Idoxuridine to Alter Its Cerebrospinal Fluid Metabolism

PHILIP H. GUTIN *, LEON D. PROCKOP [‡], K. F. YIP, JAMES D. WEINSTEIN, and K. C. TSOU [x]

Abstract □ Two methods to deter the rapid intrathecal degradation of idoxuridine were investigated: (*a*) rapid drug perfusion through the ventricular system, and (*b*) modification of the molecule to its uronic acid derivative, 2′-deoxy-5-iodo-5′-uridinecarboxylic acid, to make it less susceptible to enzymatic digestion. Perfusion of idoxuridine through the ventricular system (ventriculocisternal) of dogs at 0.97 ml/min saturated the metabolic pathway so that the outflow solution yielded a single spot (R_f 0.76) on TLC indicative of the intact molecule. The ^{125}I-labeled uronic acid was synthesized from the ^{125}I-labeled parent compound, and the labeled compounds were compared after their individual intracisternal injection in dogs. Since there was no difference in the disappearance rates, the stability of the uronic acid was, in fact, no greater than that of the parent compound *in vivo*. Ventricular perfusion of idoxuridine, however, seems a suitable means for increasing the amount of active drug delivered to central nervous system tumors and viral infections.

Keyphrases □ Idoxuridine—metabolism in cerebrospinal fluid, effect of rapid perfusion and molecular modification, dogs □ Metabolism—idoxuridine in cerebrospinal fluid, effect of rapid perfusion and molecular modification, dogs □ Perfusion, rapid—idoxuridine through ventricular system, effect on metabolism in cerebrospinal fluid, dogs □ Molecular modification—idoxuridine to uronic acid derivative, effect on metabolism in cerebrospinal fluid, dogs □ Antiviral agents—idoxuridine, metabolism in cerebrospinal fluid, effect of rapid perfusion and molecular modification, dogs

Idoxuridine (I), an antimetabolite, is a useful topical antiviral agent in the treatment of *Herpes simplex* infections of the cornea (1, 2). This agent has also been administered systemically in cases of disseminated *H. simplex* and *H. simplex* encephalitis, but its value in this respect remains largely unproved (3–5).

BACKGROUND

The development of the Ommaya reservoir made possible the direct intraventricular injection or even cerebrospinal fluid perfusion of chemotherapeutic agents for central nervous system (CNS) viral infection or malignant disease (6). This subcutaneously implanted reservoir, with a catheter extending to the lateral ventricle, facilitates the delivery of high concentrations of potentially useful drugs to the brain. This route of administration is safe for I administration to patients with brain tumors or encephalitis (7). However, reservoir-delivered intraventricular therapy with I for progressive multifocal leukoencephalopathy in one patient (8) and for malignant brain tumors in four patients treated on this neurosurgical service was of no value[1].

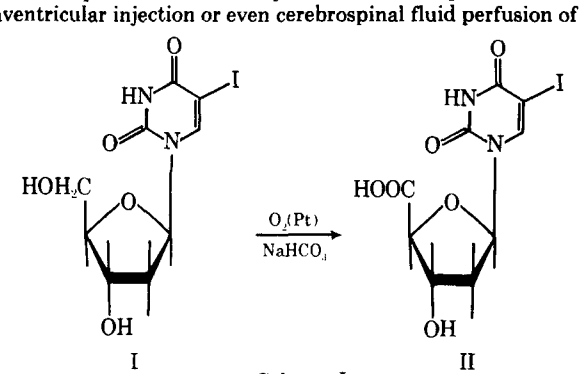

I II

Scheme I

The lack of efficacy of intraventricular I therapy may be related to the very rapid metabolism of the drug by enzymes believed to be associated with the glial, ependymal, neural, or choroid plexus cells in or near the cerebral ventricles, where the drug is degraded to iodouracil and then deiodinated by the rate-limiting step to iodide and uracil (9, 10). Therefore, two methods of minimizing such enzymatic degradation were investigated: (*a*) rapid ventriculocisternal perfusion of I to maintain high levels of drug in the ventricular cerebrospinal fluid and, consequently, saturate the metabolic pathways; and (*b*) modification of the parent compound to its uronic acid derivative, 2′-deoxy-5-iodo-5′-uridinecarboxylic acid, in the hope that it would retain its antiviral and antitumor activity but be less susceptible to enzymatic breakdown. The uronic acid of floxuridine was synthesized previously and showed dramatic resistance to hydrolysis by acid or phosphorylase while remaining moderately toxic to tumor cells *in vitro* (11).

EXPERIMENTAL

Ventriculocisternal Perfusion—Mongrel dogs, 7–20 kg, were anesthetized with pentobarbital, 60 mg/kg iv, with supplements given as needed. The dog was secured in a stereotactic head frame, and an endotracheal tube was placed to ensure adequate ventilatory exchange. A skin incision was made, and a bur hole was drilled in the skull so that its center lay 22–24 mm forward from the ear bar and 7–8 mm lateral to the midline. A No. 18 needle was placed percutaneously into the cisterna magna.

With continuous pressure monitoring, a No. 19 needle in a stereotactic holder was introduced slowly through the bur hole vertically to a depth of 16–18 mm until the pulsations of the choroid plexus transmitted to the cerebrospinal fluid were noted on the pressure recording to assure ventricular placement. Cerebrospinal fluid pressure was measured on a pressure transducer[2] and transmitted for reading on a polygraph[3].

Artificial cerebrospinal fluid was prepared as a modified Krebs–Ringer bicarbonate solution that closely resembled the ionic composition of normal spinal fluid (12). Compound I[4] was diluted to 0.1 mg/ml in artificial cerebrospinal fluid and infused through the ventricular needle first at 0.39 ml/min and then at 0.97 ml/min by means of a constant-infusion pump[5].

Samples were collected from the cisternal needle over timed periods after a 30-min perfusion to ensure homogeneity in the ventricular system,

[1] J. W. Weinstein, unpublished data.
[2] Stratham, Oxnard, Calif.
[3] Grass, Quincy, Mass.
[4] Schwarz/Mann, Orangeburg, N.Y.
[5] Harvard Apparatus, Millis, Mass.

Table I—TLC Characterization of I and II

Compound	Silica Gel Solvent 1[a]	Silica Gel Solvent 2[b]	Cellulose, Solvent 3[c]
I	0.50	0.60	0.76
II	0.36	0.10	0.64

[a] Propanol–ammonium hydroxide–water (7:1:2). [b] Chloroform–propanol (2:8). [c] 1 *M* ammonium acetate–ethanol (3:7).

and pressure was checked after each perfusion. Perfusion experiments used for compilation of the final data were considered technically satisfactory if the needles were placed successfully on the first pass, outflow solutions were free of blood cells, and the pressure remained less than 200 mm H_2O throughout the experiment. Outflow samples were analyzed by TLC for the integrity of the I molecule. The inflow solutions served as controls.

Synthesis of ^{125}I-Labeled 2′-Deoxy-5-iodo-5′-uridinecarboxylic Acid (II)—The synthesis of radiolabeled II from radiolabeled Compound I (Scheme I) was similar to that cited previously for 2′-deoxy-5-fluoro-5′-uridinecarboxylic acid (11). A solution of ^{125}I-labeled Compound I[6] (100 mg containing 100 μCi), sodium carbonate (4 mg), platinum black (100 mg), and 30 ml of water (pH of the mixture was 9.0) was oxidized with gaseous oxygen at 80° for 20 hr. After the solution was cooled to room temperature, the catalyst was removed by filtration.

The filtrate was evaporated to dryness, and the residue was dissolved in 100 ml of water and poured into a Sephadex A-25 (carbonate form) ion-exchange column (1.5 × 30 cm). Unreacted ^{125}I-labeled Compound I was eluted from the column by 0.02 *M* ammonium bicarbonate (500 ml). Compound II was removed by eluting the column with 0.2 *M* ammonium bicarbonate. The eluate was combined and lyophilized to give white solid II as the ammonium salt (29 mg, yield 28.5%, 28.5 μCi); IR (KBr): ν_{max} 3050 and 1700 cm^{-1}. The results of the TLC characterization of I and II are given in Table I.

Disappearance Studies—A No. 20 spinal needle was introduced into the cisterna magna of an anesthetized, intubated dog and was left there throughout the experiment. An aliquot of cerebrospinal fluid (1.5 ml) was removed and replaced by 1.0 ml of artificial cerebrospinal fluid containing 0.5 μCi of ^{125}I-labeled Compound I in one set of experiments and 0.5 μCi of II, prepared as described, in a second set of experiments. The second set occurred 6 months later and used the same animals. Injection of the compounds was followed by vigorous barbotage, and serial spinal fluid samples were taken at 30-min intervals. Gamma radiation in aliquots of the samples was measured in a gamma spectrometer[7].

RESULTS AND DISCUSSION

Ventriculocisternal Perfusion—Compound I (0.1 mg/ml), perfused through the dog ventricular system at 0.39 ml/min, yielded chromatographic spots on cellulose plates at R_f 0.41 and 0.55, indicating that the molecule was degraded. The unperfused inflow solution, serving as a control, yielded a single spot representative of the intact I molecule at R_f 0.76. An increase in the perfusion rate of the I solution to 0.97 ml/min saturated the degradative mechanisms, so the outflow solution contained only parent molecule (R_f 0.76).

Moderate perfusion rates protect against the degradation of I in the dog ventricular system. In humans, perfusions between a lateral ventricle and the spinal subarachnoid space, the lateral ventricle, and even the brain tumor bed have been accomplished (13). Compound I delivered by this method could be of therapeutic value in CNS viral or malignant disease and deserves further study.

Disappearance Studies—In a previous study (9), the intracisternal injection of I into dogs was followed by rapid disappearance of I and the concomitant appearance of iodouracil and iodide. Furthermore, after injection of ^{125}I-labeled Compound I, radioactivity disappeared with a half-time of about 45 min. The disappearance of the ^{125}I-label reflects in part the active transport of iodide (14, 15) cleaved from iodouracil. To some extent, however, the ^{125}I-label disappearance must also reflect the bulk flow of iodouracil from the cerebrospinal fluid since iodouracil → iodide + uracil is the rate-limiting step in the drug degradation (9). In any case, the disappearances of iodide and iodouracil as detected by serial cerebrospinal fluid ^{125}I-measurements represent the exit of the metabolites of inactivated drug and, therefore, provide a good index for following the degradation of ^{125}I-labeled I and II after intracisternal injection.

[6] Amersham/Searle, Arlington Heights, Ill.
[7] Baird-Atomic, Cambridge, Mass.

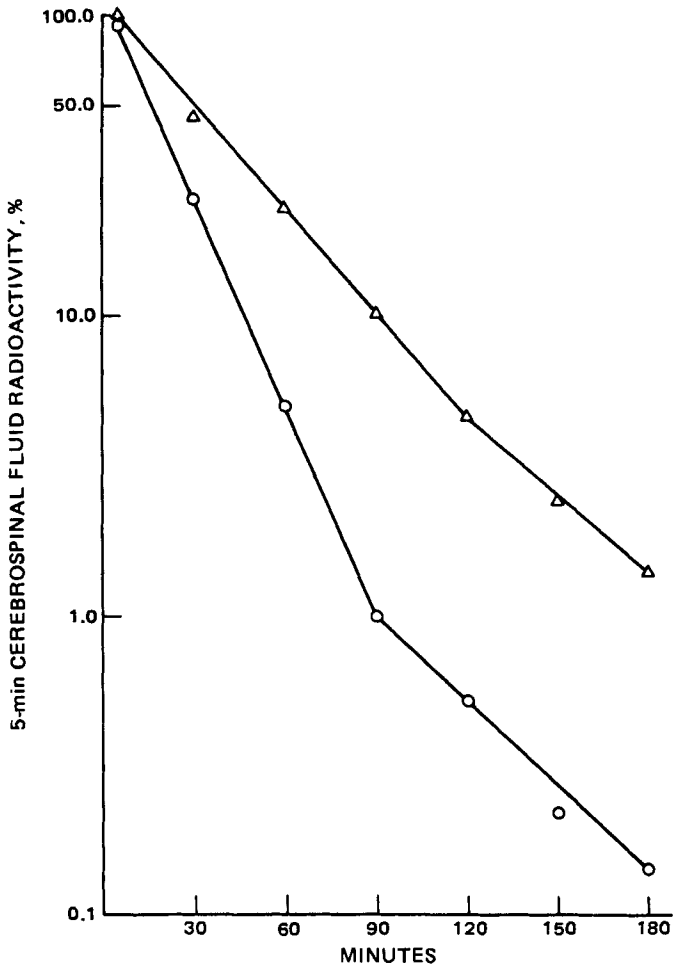

Figure 1—*Disappearance of radioactivity from cerebrospinal fluid of Dog 3 after injection of ^{125}I-labeled I (0.5 μCi) (○) or II (0.5 μCi) (△). Each curve is plotted as the percentage of the 5-min radioactivity. The initial rapid phase was due to mixing, and the slower late phase was due to drug clearance.*

Disappearance of radioactivity from cerebrospinal fluid after intracisternal injection of ^{125}I-labeled I or II was plotted on semilogarithmic paper. Half-times were determined by graphic analysis. There were two slopes to each curve: a more rapid initial phase, probably due to mixing within the cerebrospinal fluid compartment, and a slower, late phase, thought to represent primarily drug clearance (16). Data were expressed in terms of disappearance rates:

$$\text{disappearance rate (\%/min)} = \frac{\ln}{\text{half-time}} = \frac{0.693}{\text{half-time}} \quad \text{(Eq. 1)}$$

The mean of the disappearance rates of the ^{125}I-label from the cerebrospinal fluid of three dogs following ^{125}I-labeled Compound I injection was 0.024 ± 0.007 (*SD*). After II injection in the same animals, it was 0.021 ± 0.002. These numbers are not significantly different ($p > 0.40$). The disappearance plots from a typical animal are shown in Fig. 1.

The disappearances of the ^{125}I-label after injection of ^{125}I-labeled I and II were identical. This result indicates that the formation and clearance of the metabolites of these drugs occur at the same rate, so the chemical stability of uronic acids to hydrolysis by acid or phosphorylases seems to offer no advantage *in vivo*. Therefore, modification of the I molecule to its uronic acid holds little promise for discouraging the rapid intrathecal degradation of this agent.

REFERENCES

(1) H. E. Kaufman, *Proc. Soc. Exp. Biol. Med.*, **109**, 251 (1962).
(2) E. Maxwell, *Am. J. Ophthalmol.*, **56**, 571 (1963).
(3) L. W. Catalano, Jr., G. H. Safley, and M. Museles, *J. Pediatr.*, **79**, 393 (1971).
(4) C. J. Breeden, T. C. Hall, and M. R. Tyler, *Ann. Intern. Med.*, **65**, 1050 (1966).
(5) *N. Engl. J. Med.*, **292**, 599 (1975).

(6) A. K. Ommaya, R. C. Rubin, E. S. Henderson, D. P. Rall, F. G. Gieseke, E. A. Bering, and M. Bagan, *Med. Ann. D.C.*, **34**, 455 (1965).
(7) W. A. Creasey, S. Flanigan, R. W. McCollum, and P. Calabresi, *Proc. Am. Assoc. Cancer Res.*, **9**, 16 (1968).
(8) D. Tarsy, E. M. Holden, J. M. Segarra, P. Calabresi, and R. G. Feldman, *Cancer Chemother. Rep.*, **57**, 73 (1973).
(9) D. R. Clarkson, W. W. Oppelt, and P. Byvoet, *J. Pharmacol. Exp. Ther.*, **157**, 581 (1967).
(10) W. H. Prusoff, J. J. Jaffe, and H. Gunther, *Biochem. Pharmacol.*, **3**, 110 (1960).
(11) K. C. Tsou, N. J. Santora, and E. E. Miller, *J. Med. Chem.*, **12**, 173 (1969).
(12) W. W. Umbreit, R. H. Burris, and J. F. Stauffer, "Manometric Techniques," Burgess, Minneapolis, Minn., 1957, p. 149.
(13) R. C. Rubin, A. K. Ommaya, E. S. Henderson, E. A. Bering, and D. P. Rall, *Neurology*, **16**, 680 (1966).
(14) B. Becker, *Am. J. Physiol.*, **201**, 1149 (1961).
(15) D. J. Reed and D. M. Woodbury, *J. Physiol. (London)*, **169**, 816 (1963).
(16) L. D. Prockop, *Neurology*, **18**, 189 (1968).

ACKNOWLEDGMENTS AND ADDRESSES

Received July 28, 1976, from the *Departments of Neurology and Neurosurgery and the Harrison Department of Surgical Research, School of Medicine, University of Pennsylvania, and the Neurology Service, Philadelphia General Hospital, Philadelphia, PA 19104.*

Accepted for publication November 9, 1976.

Supported by U.S. Public Health Service Grant CA 07339 from the National Institutes of Health, Grant AT (30-1) 3784 (K. C. Tsou), and Grant NB 08029 (Philadelphia General Hospital).

* Present address: Department of Neurosurgery, University of California Medical Center, San Francisco, CA 94143.

‡ Present address: Neurology Section, Department of Internal Medicine, College of Medicine, University of South Florida, Tampa, FL 33612.

x To whom inquiries should be directed. Present address: Hospital of the University of Pennsylvania, Philadelphia, PA 19104.

Synthesis of 10α-Methoxy-Δ^{8,9}-lysergaldehyde from Elymoclavine

TUNG-CHUNG CHOONG, BRIAN L. THOMPSON *, and H. RICHARD SHOUGH x

Abstract □ A new synthesis is described for 10α-methoxy-Δ^{8,9}-lysergaldehyde involving the oxidation of elymoclavine with manganese dioxide in methanol. Lysergol and agroclavine provide no reaction under the same conditions.

Keyphrases □ 10α-Methoxy-Δ^{8,9}-lysergaldehyde—synthesized by oxidation of elymoclavine with manganese dioxide in methanol □ Alkaloids, ergot—10α-methoxy-Δ^{8,9}-lysergaldehyde, synthesized by oxidation of elymoclavine with manganese dioxide in methanol □ Elymoclavine—oxidized with manganese dioxide in methanol to 10α-methoxy-Δ^{8,9}-lysergaldehyde

Elymoclavine (I) is well established as an intermediate in the biosynthesis of the lysergic acid-type ergot alkaloids (1). The oxidation of elymoclavine at C-17 is of interest because Δ^{8,9}-lysergaldehyde (II) and/or Δ^{9,10}-lysergaldehyde are possible biosynthetic intermediates and because of the well-known pharmacological properties of the ergot alkaloids. Elymoclavine is easily oxidized to the 8-hydroxy-Δ^{9,10} derivatives penniclavine and isopenniclavine (2), and chanoclavine (6,7-*seco*-elymoclavine) is readily oxidized to chanoclavine aldehyde (3), but the hydroxymethyl group of elymoclavine has proven quite resistant to common oxidants (4, 5).

Lin *et al.* (4) obtained the enol acetate of Δ^{9,10}-lysergaldehyde (6-methyl-8-acetoxymethylene-9-ergolene) by dimethyl sulfoxide–acetic anhydride oxidation of elymoclavine. Mayer and Eich (5) obtained traces of lysergic acid by Oppenauer oxidation of elymoclavine and small yields of dihydrolysergic acid from dihydroelymoclavine. Dihydrolysergaldehyde has been prepared by reduction of lysergic acid derivatives (6).

The manganese dioxide oxidation of 10α-methoxyelymoclavine (III) to 10α-methoxy-Δ^{8,9}-lysergaldehyde (IV) was reported (7). Compound III was obtained by hydride reduction of the 10α-methoxy ester (V) prepared by mercuric acetate oxidation of methyl lysergate in methanol (8). This was the first successful attempt to obtain a lysergaldehyde by oxidation of an elymoclavine derivative.

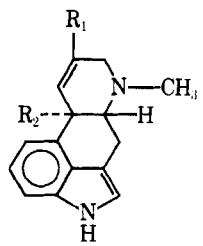

I: $R_1 = CH_2OH$, $R_2 = H$
II: $R_1 = CHO$, $R_2 = H$
III: $R_1 = CH_2OH$, $R_2 = OCH_3$
IV: $R_1 = CHO$, $R_2 = OCH_3$
V: $R_1 = COOCH_3$, $R_2 = OCH_3$
VI: $R_1 = CH_3$, $R_2 = H$

Previous attempts in this laboratory to prepare lysergaldehydes from elymoclavine also were unsuccessful. However, 10α-methoxy-Δ^{8,9}-lysergaldehyde (IV) can be prepared in good yield by the direct oxidation of elymoclavine with manganese dioxide in methanol.

EXPERIMENTAL[1]

For the preparation of 10α-methoxy-Δ^{8,9}-lysergaldehyde (IV), ely-

[1] Melting points were determined on a Thomas-Hoover Uni-Melt melting-point apparatus and are uncorrected. UV spectra were run on a Beckman model 24 spectrophotometer. IR spectra were run in potassium bromide using a Beckman IR-8 spectrophotometer. NMR spectra were obtained in deuterochloroform on a Jeol C-60H spectrometer with tetramethylsilane as the internal standard. Mass spectra were recorded on an LKB-9000S spectrometer.

(6) A. K. Ommaya, R. C. Rubin, E. S. Henderson, D. P. Rall, F. G. Gieseke, E. A. Bering, and M. Bagan, *Med. Ann. D.C.*, **34**, 455 (1965).
(7) W. A. Creasey, S. Flanigan, R. W. McCollum, and P. Calabresi, *Proc. Am. Assoc. Cancer Res.*, **9**, 16 (1968).
(8) D. Tarsy, E. M. Holden, J. M. Segarra, P. Calabresi, and R. G. Feldman, *Cancer Chemother. Rep.*, **57**, 73 (1973).
(9) D. R. Clarkson, W. W. Oppelt, and P. Byvoet, *J. Pharmacol. Exp. Ther.*, **157**, 581 (1967).
(10) W. H. Prusoff, J. J. Jaffe, and H. Gunther, *Biochem. Pharmacol.*, **3**, 110 (1960).
(11) K. C. Tsou, N. J. Santora, and E. E. Miller, *J. Med. Chem.*, **12**, 173 (1969).
(12) W. W. Umbreit, R. H. Burris, and J. F. Stauffer, "Manometric Techniques," Burgess, Minneapolis, Minn., 1957, p. 149.
(13) R. C. Rubin, A. K. Ommaya, E. S. Henderson, E. A. Bering, and D. P. Rall, *Neurology*, **16**, 680 (1966).
(14) B. Becker, *Am. J. Physiol.*, **201**, 1149 (1961).
(15) D. J. Reed and D. M. Woodbury, *J. Physiol. (London)*, **169**, 816 (1963).
(16) L. D. Prockop, *Neurology*, **18**, 189 (1968).

ACKNOWLEDGMENTS AND ADDRESSES

Received July 28, 1976, from the *Departments of Neurology and Neurosurgery and the Harrison Department of Surgical Research, School of Medicine, University of Pennsylvania, and the Neurology Service, Philadelphia General Hospital, Philadelphia, PA 19104.*

Accepted for publication November 9, 1976.

Supported by U.S. Public Health Service Grant CA 07339 from the National Institutes of Health, Grant AT (30-1) 3784 (K. C. Tsou), and Grant NB 08029 (Philadelphia General Hospital).

* Present address: Department of Neurosurgery, University of California Medical Center, San Francisco, CA 94143.

‡ Present address: Neurology Section, Department of Internal Medicine, College of Medicine, University of South Florida, Tampa, FL 33612.

x To whom inquiries should be directed. Present address: Hospital of the University of Pennsylvania, Philadelphia, PA 19104.

Synthesis of 10α-Methoxy-Δ^{8,9}-lysergaldehyde from Elymoclavine

TUNG-CHUNG CHOONG, BRIAN L. THOMPSON *, and H. RICHARD SHOUGH x

Abstract □ A new synthesis is described for 10α-methoxy-Δ^{8,9}-lysergaldehyde involving the oxidation of elymoclavine with manganese dioxide in methanol. Lysergol and agroclavine provide no reaction under the same conditions.

Keyphrases □ 10α-Methoxy-Δ^{8,9}-lysergaldehyde—synthesized by oxidation of elymoclavine with manganese dioxide in methanol □ Alkaloids, ergot—10α-methoxy-Δ^{8,9}-lysergaldehyde, synthesized by oxidation of elymoclavine with manganese dioxide in methanol □ Elymoclavine—oxidized with manganese dioxide in methanol to 10α-methoxy-Δ^{8,9}-lysergaldehyde

Elymoclavine (I) is well established as an intermediate in the biosynthesis of the lysergic acid-type ergot alkaloids (1). The oxidation of elymoclavine at C-17 is of interest because Δ^{8,9}-lysergaldehyde (II) and/or Δ^{9,10}-lysergaldehyde are possible biosynthetic intermediates and because of the well-known pharmacological properties of the ergot alkaloids. Elymoclavine is easily oxidized to the 8-hydroxy-Δ^{9,10} derivatives penniclavine and isopenniclavine (2), and chanoclavine (6,7-*seco*-elymoclavine) is readily oxidized to chanoclavine aldehyde (3), but the hydroxymethyl group of elymoclavine has proven quite resistant to common oxidants (4, 5).

Lin *et al.* (4) obtained the enol acetate of Δ^{9,10}-lysergaldehyde (6-methyl-8-acetoxymethylene-9-ergolene) by dimethyl sulfoxide–acetic anhydride oxidation of elymoclavine. Mayer and Eich (5) obtained traces of lysergic acid by Oppenauer oxidation of elymoclavine and small yields of dihydrolysergic acid from dihydroelymoclavine. Dihydrolysergaldehyde has been prepared by reduction of lysergic acid derivatives (6).

The manganese dioxide oxidation of 10α-methoxyelymoclavine (III) to 10α-methoxy-Δ^{8,9}-lysergaldehyde (IV) was reported (7). Compound III was obtained by hydride reduction of the 10α-methoxy ester (V) prepared by mercuric acetate oxidation of methyl lysergate in methanol (8). This was the first successful attempt to obtain a lysergaldehyde by oxidation of an elymoclavine derivative.

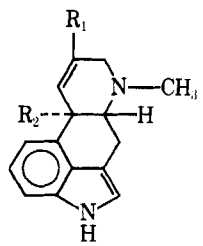

I: $R_1 = CH_2OH$, $R_2 = H$
II: $R_1 = CHO$, $R_2 = H$
III: $R_1 = CH_2OH$, $R_2 = OCH_3$
IV: $R_1 = CHO$, $R_2 = OCH_3$
V: $R_1 = COOCH_3$, $R_2 = OCH_3$
VI: $R_1 = CH_3$, $R_2 = H$

Previous attempts in this laboratory to prepare lysergaldehydes from elymoclavine also were unsuccessful. However, 10α-methoxy-Δ^{8,9}-lysergaldehyde (IV) can be prepared in good yield by the direct oxidation of elymoclavine with manganese dioxide in methanol.

EXPERIMENTAL[1]

For the preparation of 10α-methoxy-Δ^{8,9}-lysergaldehyde (IV), ely-

[1] Melting points were determined on a Thomas-Hoover Uni-Melt melting-point apparatus and are uncorrected. UV spectra were run on a Beckman model 24 spectrophotometer. IR spectra were run in potassium bromide using a Beckman IR-8 spectrophotometer. NMR spectra were obtained in deuterochloroform on a Jeol C-60H spectrometer with tetramethylsilane as the internal standard. Mass spectra were recorded on an LKB-9000S spectrometer.

moclavine[2] (2.0 g, 7.9 mmoles) in methanol (400 ml) was treated with 20 g of manganese dioxide (9), and the mixture was stirred at room temperature. After 12 hr, the mixture was filtered, the filtrate was evaporated to dryness, and the residue was dissolved in 10 ml of chloroform. TLC on silica gel G with an ethyl acetate–dimethylformamide–ethanol (13:1:1) solvent revealed a major product (R_f 0.77) that was nonfluorescent and gave a green color with Ehrlich's reagent, a small quantity of unreacted elymoclavine (R_f 0.23), and only traces of other Ehrlich-positive compounds.

Purification of the product was accomplished by chromatography on a silica gel (40 g) column with chloroform as the solvent. Recrystallization from chloroform–hexane provided 1.2 g (55% yield) of small white needles, mp 192–194° dec.; UV: λ_{max}(ethanol) 223 (log ϵ 4.58) and 297 (3.73) nm; IR: ν_{max} (KBr) 3170, 2930, 2800, 1680, 1400, 1180, 1070, 900, and 750 cm^{-1}; NMR: δ 2.56 (s, 3H, NCH_3), 3.13 (s, 3H, OCH_3), 6.94–7.44 (m, 4H, indole), 7.67 (s, 1H, 9=CH), 8.33 (s, 1H, NH), and 9.67 (s, 1H, CHO) ppm. The mass spectrum showed a molecular ion at *m/e* 282 (100) and a prominent ion at *m/e* 154 (48) characteristic of ergolines (10).

The product was compared with a reference sample[3] of IV and was identical in all respects (TLC; melting point; and UV, IR, NMR, and mass spectra).

DISCUSSION

Ergoline derivatives including ethers related to IV have been of interest recently as potential prolactin inhibitors (11) and α-adrenergic blocking agents (12). The manganese dioxide oxidation of elymoclavine in methanol provides a convenient one-step synthesis of IV from a readily available starting material.

It was also of interest to obtain some indication of whether manganese dioxide might be useful for the C-17 and/or C-10 oxidation of other ergolines. For this purpose, lysergol, the $\Delta^{9,10}$-isomer of elymoclavine (I), and agroclavine (VI) were treated under the same conditions used for the oxidation of elymoclavine. Lysergol was unchanged under these conditions, which was not surprising since manganese dioxide is most effective for the oxidation of allylic alcohols (13). However, it was interesting that agroclavine was also unreactive since C-10 oxidation of the $\Delta^{8,9}$-ergolenes can be accomplished with various oxidizing agents (1, 2). Additional studies are required to determine the precise utility of manganese dioxide for the C-17 and C-10 oxidation of ergolines.

[2] Isolated from ergot strain SD 58 provided by Dr. James E. Robbers, Department of Medicinal Chemistry and Pharmacognosy, Purdue University, West Lafayette, Ind.

[3] Provided by Dr. E. C. Kornfeld, Eli Lilly Co., Indianapolis, Ind.

REFERENCES

(1) E. Ramstad, *Lloydia*, **31**, 327 (1968).

(2) A. Hofmann, R. Brunner, H. Kobel, and A. Brack, *Helv. Chim. Acta*, **40**, 1358 (1957).

(3) B. Naidoo, J. M. Cassady, G. E. Blair, and H. G. Floss, *Chem. Commun.*, **1970**, 471.

(4) C.-C. Lin, G. E. Blair, J. M. Cassady, D. Groger, W. Maier, and H. G. Floss, *J. Org. Chem.*, **38**, 2249 (1973).

(5) K. Mayer and E. Eich, *Arch. Pharm.*, **308**, 819 (1975).

(6) F. Troxler, J. Rutschmann, and E. Schreier; through *Chem. Abstr.*, **70**, 58089x (1969).

(7) N. J. Bach and E. C. Kornfeld, *Tetrahedron Lett.*, **1974**, 3225.

(8) L. Bernardi, E. Gandini, and A. Temperilli, *Tetrahedron*, **30**, 3447 (1974).

(9) J. Attenburrow, A. F. B. Cameron, J. H. Chapman, R. M. Evans, B. A. Hems, A. B. A. Jansen, and T. Walker, *J. Chem. Soc.*, **1952**, 1104.

(10) M. Barber, J. A. Weisbach, B. Douglas, and G. O. Dudek, *Chem. Ind.*, **1965**, 1072.

(11) H. G. Floss, J. M. Cassady, and J. E. Robbers, *J. Pharm. Sci.*, **62**, 699 (1973).

(12) L. Bernardi, G. Bosisio, C. Elli, B. Patelli, A. Temperilli, G. Arcari, and H. A. Glaesser, *Farmaco, Ed. Sci.*, **30**, 789 (1975).

(13) J. S. Pizey, "Synthetic Reagents," vol. II, Wiley, New York, N.Y., 1974, pp. 143–174.

ACKNOWLEDGMENTS AND ADDRESSES

Received September 14, 1976, from the *Department of Biopharmaceutical Sciences, College of Pharmacy, University of Utah, Salt Lake City, UT 84112.*

Accepted for publication November 9, 1976.

Supported in part by a grant from the University of Utah Research Committee and by Grant IN-102 from the American Cancer Society.

* Graduate trainee supported by National Institutes of Health Grant CA05209-09.

ˣ To whom inquiries should be directed.

Direct Complexometric Titration of Calcium Phosphates

MURRAY M. TUCKERMAN ˣ and M. ELEANOR SANCHEZ de RAMOS

Abstract □ Calcium was determined in calcium phosphate samples by dissolving the sample in hydrochloric acid, adding hydroxynaphthol blue indicator and triethanolamine, adjusting the pH to 12.3–12.5 with potassium hydroxide solution, and titrating with standard disodium ethylenediaminetetraacetate solution. Time can be saved and the formation of a precipitate (which dissolves readily during the titration) can be avoided by adding at least 85% of the amount of complexing agent required for titration before adjusting the pH.

Keyphrases □ Calcium—complexometric analysis in dibasic and tribasic calcium phosphates, bulk drug and tablets □ Complexometry—analysis, calcium in dibasic and tribasic calcium phosphates, bulk drug and tablets

Previously, calcium was determined in the presence of phosphate complexometrically by the addition of excess complexing agent and determination of the excess, after separation from phosphate by ion exchange (1), and also after removal of phosphate by formation and extraction of phosphomolybdate (2). All of these efforts are based on the impossibility of a direct complexometric titration of calcium in the presence of equivalent amounts of phosphate. This paper reports a simple, rapid, direct complexometric titration of calcium in the presence of phosphate.

EXPERIMENTAL

All reagents and volumetric solutions were those specified in USP XIX. All experiments were done according to the following general directions, modified as indicated.

General Method—Dissolve a sample expected to contain about 225 mg of calcium, accurately weighed, in 15 ml of hydrochloric acid and 10 ml of water contained in a 100-ml volumetric flask, with the aid of gentle heat if necessary, and cool to room temperature. Dilute to volume with

moclavine[2] (2.0 g, 7.9 mmoles) in methanol (400 ml) was treated with 20 g of manganese dioxide (9), and the mixture was stirred at room temperature. After 12 hr, the mixture was filtered, the filtrate was evaporated to dryness, and the residue was dissolved in 10 ml of chloroform. TLC on silica gel G with an ethyl acetate–dimethylformamide–ethanol (13:1:1) solvent revealed a major product (R_f 0.77) that was nonfluorescent and gave a green color with Ehrlich's reagent, a small quantity of unreacted elymoclavine (R_f 0.23), and only traces of other Ehrlich-positive compounds.

Purification of the product was accomplished by chromatography on a silica gel (40 g) column with chloroform as the solvent. Recrystallization from chloroform–hexane provided 1.2 g (55% yield) of small white needles, mp 192–194° dec.; UV: λ_{max}(ethanol) 223 (log ϵ 4.58) and 297 (3.73) nm; IR: ν_{max} (KBr) 3170, 2930, 2800, 1680, 1400, 1180, 1070, 900, and 750 cm^{-1}; NMR: δ 2.56 (s, 3H, NCH_3), 3.13 (s, 3H, OCH_3), 6.94–7.44 (m, 4H, indole), 7.67 (s, 1H, 9=CH), 8.33 (s, 1H, NH), and 9.67 (s, 1H, CHO) ppm. The mass spectrum showed a molecular ion at *m/e* 282 (100) and a prominent ion at *m/e* 154 (48) characteristic of ergolines (10).

The product was compared with a reference sample[3] of IV and was identical in all respects (TLC; melting point; and UV, IR, NMR, and mass spectra).

DISCUSSION

Ergoline derivatives including ethers related to IV have been of interest recently as potential prolactin inhibitors (11) and α-adrenergic blocking agents (12). The manganese dioxide oxidation of elymoclavine in methanol provides a convenient one-step synthesis of IV from a readily available starting material.

It was also of interest to obtain some indication of whether manganese dioxide might be useful for the C-17 and/or C-10 oxidation of other ergolines. For this purpose, lysergol, the $\Delta^{9,10}$-isomer of elymoclavine (I), and agroclavine (VI) were treated under the same conditions used for the oxidation of elymoclavine. Lysergol was unchanged under these conditions, which was not surprising since manganese dioxide is most effective for the oxidation of allylic alcohols (13). However, it was interesting that agroclavine was also unreactive since C-10 oxidation of the $\Delta^{8,9}$-ergolenes can be accomplished with various oxidizing agents (1, 2). Additional studies are required to determine the precise utility of manganese dioxide for the C-17 and C-10 oxidation of ergolines.

[2] Isolated from ergot strain SD 58 provided by Dr. James E. Robbers, Department of Medicinal Chemistry and Pharmacognosy, Purdue University, West Lafayette, Ind.

[3] Provided by Dr. E. C. Kornfeld, Eli Lilly Co., Indianapolis, Ind.

REFERENCES

(1) E. Ramstad, *Lloydia*, **31**, 327 (1968).

(2) A. Hofmann, R. Brunner, H. Kobel, and A. Brack, *Helv. Chim. Acta*, **40**, 1358 (1957).

(3) B. Naidoo, J. M. Cassady, G. E. Blair, and H. G. Floss, *Chem. Commun.*, **1970**, 471.

(4) C.-C. Lin, G. E. Blair, J. M. Cassady, D. Groger, W. Maier, and H. G. Floss, *J. Org. Chem.*, **38**, 2249 (1973).

(5) K. Mayer and E. Eich, *Arch. Pharm.*, **308**, 819 (1975).

(6) F. Troxler, J. Rutschmann, and E. Schreier; through *Chem. Abstr.*, **70**, 58089x (1969).

(7) N. J. Bach and E. C. Kornfeld, *Tetrahedron Lett.*, **1974**, 3225.

(8) L. Bernardi, E. Gandini, and A. Temperilli, *Tetrahedron*, **30**, 3447 (1974).

(9) J. Attenburrow, A. F. B. Cameron, J. H. Chapman, R. M. Evans, B. A. Hems, A. B. A. Jansen, and T. Walker, *J. Chem. Soc.*, **1952**, 1104.

(10) M. Barber, J. A. Weisbach, B. Douglas, and G. O. Dudek, *Chem. Ind.*, **1965**, 1072.

(11) H. G. Floss, J. M. Cassady, and J. E. Robbers, *J. Pharm. Sci.*, **62**, 699 (1973).

(12) L. Bernardi, G. Bosisio, C. Elli, B. Patelli, A. Temperilli, G. Arcari, and H. A. Glaesser, *Farmaco, Ed. Sci.*, **30**, 789 (1975).

(13) J. S. Pizey, "Synthetic Reagents," vol. II, Wiley, New York, N.Y., 1974, pp. 143–174.

ACKNOWLEDGMENTS AND ADDRESSES

Received September 14, 1976, from the *Department of Biopharmaceutical Sciences, College of Pharmacy, University of Utah, Salt Lake City, UT 84112.*

Accepted for publication November 9, 1976.

Supported in part by a grant from the University of Utah Research Committee and by Grant IN-102 from the American Cancer Society.

* Graduate trainee supported by National Institutes of Health Grant CA05209-09.

ˣ To whom inquiries should be directed.

Direct Complexometric Titration of Calcium Phosphates

MURRAY M. TUCKERMAN ˣ and M. ELEANOR SANCHEZ de RAMOS

Abstract □ Calcium was determined in calcium phosphate samples by dissolving the sample in hydrochloric acid, adding hydroxynaphthol blue indicator and triethanolamine, adjusting the pH to 12.3–12.5 with potassium hydroxide solution, and titrating with standard disodium ethylenediaminetetraacetate solution. Time can be saved and the formation of a precipitate (which dissolves readily during the titration) can be avoided by adding at least 85% of the amount of complexing agent required for titration before adjusting the pH.

Keyphrases □ Calcium—complexometric analysis in dibasic and tribasic calcium phosphates, bulk drug and tablets □ Complexometry—analysis, calcium in dibasic and tribasic calcium phosphates, bulk drug and tablets

Previously, calcium was determined in the presence of phosphate complexometrically by the addition of excess complexing agent and determination of the excess, after separation from phosphate by ion exchange (1), and also after removal of phosphate by formation and extraction of phosphomolybdate (2). All of these efforts are based on the impossibility of a direct complexometric titration of calcium in the presence of equivalent amounts of phosphate. This paper reports a simple, rapid, direct complexometric titration of calcium in the presence of phosphate.

EXPERIMENTAL

All reagents and volumetric solutions were those specified in USP XIX. All experiments were done according to the following general directions, modified as indicated.

General Method—Dissolve a sample expected to contain about 225 mg of calcium, accurately weighed, in 15 ml of hydrochloric acid and 10 ml of water contained in a 100-ml volumetric flask, with the aid of gentle heat if necessary, and cool to room temperature. Dilute to volume with

Table I—Dibasic Calcium Phosphate [a] NF (Weighed Samples)

Sample	Weight, mg	0.0500 *M* Titrant, ml	Calcium, %
1	200.00	28.68	28.74
2	201.0	28.54	28.45
3	203.0	28.90	28.53
		Average	28.57
		SD	0.17
		RSD	0.6

[a] Medicinal, Mallinckrodt Chemical Works, St. Louis, Mo.

Table II—Aliquots (25 ml) of Dibasic Calcium Phosphate [a] Solution

Sample	0.0500 *M* Titrant, ml	Calcium, %
	800.0 mg in 100.0 ml	
1	28.80	28.86
2	28.50	28.56
3	28.38	28.44
	Average	28.62
	SD	0.25
	RSD	0.9
	720.0 mg in 100.0 ml	
1	25.85	28.78
2	25.90	28.83
3	25.80	28.72
	Average	28.78
	SD	0.005
	RSD	0.21
	880.0 mg in 100.0 ml	
1	31.50	28.69
2	31.46	28.66
3	31.48	28.68
	Average	28.68
	SD	0.018
	RSD	0.67

[a] Lot 761788, reagent grade, Fisher Scientific Co.

water and mix well. If the solution is not completely clear, filter through quantitative filter paper, discarding the first 10 ml of filtrate.

Transfer a 25-ml aliquot to a 250-ml vessel equipped with a magnetic stirrer and add water to make 125 ml. With constant stirring, add, in order, 0.5 ml of triethanolamine, 300 mg of hydroxynaphthol blue indicator, and, from a 50-ml buret, 97% of the calculated amount of standard 0.05 *M* disodium ethylenediaminetetraacetate solution. Add sodium hydroxide solution (45 in 100) until the initial red color changes to clear

Table III—Dibasic Calcium Phosphate [a] Solution

Initial 0.0500 *M* Titrant Added, ml	Total 0.0500 *M* Titrant Added, ml	Calcium, %
21	28.90	28.96
21	28.88	28.94
22	28.86	28.92
22	28.88	28.94
23	28.90	28.96
23	28.90	28.96
24	28.90	28.96
24	28.88	28.94
25	28.90	28.96
25	29.00	28.96
26	28.90	28.96
26	28.98	29.04
27	28.70	28.96
27	28.74	28.80
28	28.70	28.76
28	28.72	28.78
0	28.70	28.72
0	28.82	28.88
	Average	28.90
	SD	0.088
	RSD	0.3

[a] Lot 761788, reagent grade, Fisher Scientific Co.

Table IV—Tolerance for Added Phosphate

0.8% Na_2HPO_4 Solution Added, ml	Phosphorus to Calcium Molar Ratio	0.0500 *M* Titrant, ml	Calcium, %
5	1.07	28.84	28.90
5	1.07	28.82	28.88
10	1.15	28.82	28.88
10	1.15	28.80	28.86
25	1.38	28.80	28.86
25	1.38	28.80	28.86
50	1.77	28.80	28.86
50	1.77	28.78	28.84
100	2.53	28.70	28.76

blue, continue the addition dropwise until the color changes to violet, and then add an additional 0.5 ml (7–8 ml total is usually required). The pH should be between 12.3 and 12.5.

Under constant stirring, continue the titration of the solution dropwise with the standard 0.05 *M* disodium ethylenediaminetetraacetate solution (titrant) to a clear blue end-point that persists for at least 60 sec.

Dibasic Calcium Phosphate NF—Use a 200-mg sample of material as is (Table I).

Influence of Sample Size on Results—Use sample sizes of 180, 200, and 220 mg of dibasic calcium phosphate NF (Table II).

Influence of Volume of Standard 0.05 *M* Disodium Ethylenediaminetetraacetate—Use various volumes for initial addition to 25-ml aliquots of a solution containing 4.000 g of anhydrous dibasic calcium phosphate NF in 500 ml in place of the 97% of the calculated amount called for in the general directions (Table III).

Tolerance for Added Phosphate—Add various amounts of 0.8% Na_2HPO_4 to 25-ml aliquots of a solution containing 800.0 mg of anhydrous dibasic calcium phosphate NF in 100 ml (200.0 mg/sample) (Table IV).

Tribasic Calcium Phosphate NF—Use 135-, 150-, and 165-mg samples to show the influence of sample size (Table V).

Comparison with Extraction Method of Kleinman and Schriftman (2)—Use 5-ml aliquots of a solution containing 1.000 g of anhydrous dibasic calcium phosphate NF in 100 ml (50 mg/sample) (Tables VI and VII) or 5-ml aliquots of a solution containing 760.0 mg of tribasic calcium phosphate NF in 100 ml (38 mg/sample) (Table VIII).

Assay of Dibasic Calcium Phosphate Tablets—Weigh about 2.4 g of finely powdered tablets, dissolve in 30 ml of hydrochloric acid and 20 ml of water, and dilute to 200 ml. Take 25-ml aliquots for assay (Table IX).

Table V—Tribasic Calcium Phosphate [a] (25-ml Aliquots)

Sample	0.0500 *M* Titrant, ml	Calcium, %
	1.200 g in 200 ml	
1	27.78	37.11
2	27.80	37.14
3	27.76	27.09
4	27.78	37.11
5	28.00	37.41
6	28.00	37.41
7	27.72	37.03
	Average	37.19
	SD	0.14
	RSD	0.4
	540.0 mg in 100 ml	
1	25.20	37.41
2	25.22	37.44
3	25.00	37.11
	Average	37.32
	SD	0.22
	RSD	0.3
	660.0 mg in 100 ml	
1	30.20	36.68
2	30.24	36.72
3	30.22	36.70
	Average	36.70
	SD	0.029
	RSD	0.08

[a] Lot 25872, Baker Analyzed.

Table VI—Dibasic Calcium Phosphate [a] Solution (Extraction Method)

Sample	0.0500 *M* Titrant, ml	Calcium, %
1	7.10	28.46
2	7.08	28.38
3	7.10	28.46
4	7.10	28.46
	Average	28.44
	SD	0.039
	RSD	0.14

[a] Lot 761788, reagent grade, Fisher Scientific Co.

Table VII—Dibasic Calcium Phosphate [a] (Aliquots of Same Solution by Extraction and Direct Titration)

Sample	0.0500 *M* Titrant, ml	Calcium, %
	By Extraction	
1	7.04	28.22
2	7.04	28.22
3	7.04	28.22
	Average	28.22
	SD	0.00
	RSD	0
	By Direct Titration	
1	7.16	28.70
2	7.16	28.70
3	7.18	28.78
	Average	28.73
	SD	0.017
	RSD	0.2

[a] Lot 761788, reagent grade, Fisher Scientific Co.

RESULTS AND DISCUSSION

For the 30 direct titrations of a single sample of dibasic calcium phosphate NF[2] (Tables II, III, and VII), the average calcium content was 28.82%. The standard deviation was 0.16%, which gives a relative standard deviation of 0.6%. All standard deviations were calculated from range values using literature values of d_2 (3). When tested against the average for the 30 determinations of dibasic calcium phosphate, some subgroups of Table II, the duplicate groups of Table II, and the subgroup of Table VII did not meet the *F*-test for homogeneity of variance at the 95% confidence level. Therefore, it was not quite correct to test the significance of the difference between the individual subgroup average and the general average by the Student *t* test. However, when the test was applied, the differences between the subgroup average and the general average were not significant at the 95% confidence level. Therefore, neither a variation of up to 10% in the sample size nor the amount of complexing agent initially added in the titration affects the assay result, and the extraction method gives the same results as the general method.

Table VIII—Tribasic Calcium Phosphate [a] (Aliquots of Same Sample by Extraction and Direct Titration)

Sample	0.0500 *M* Titrant, ml	Calcium, %
	By Extraction	
1	6.92	36.49
2	6.92	36.49
3	6.92	36.49
	Average	36.49
	SD	0.00
	RSD	0
	By Direct Titration	
1[b]	6.98	
2	6.98	
3	6.96	
4[b]	6.92	
	Average	36.70
	SD	0.16
	RSD	0.4

[a] Lot 25872, Baker Analyzed. [b] Sample 1 had no ethylenediaminetetraacetate added initially; Sample 4 had 75% of the calculated amount of ethylenediaminetetraacetate added initially.

Table IX—Assay of Dibasic Calcium Phosphate Tablets

Aliquot	0.0500 *M* Titrant, ml	Dibasic Calcium Phosphate Dihydrate, mg per Average Tablet	Percent of Claim
		Lot A[a]	
1	28.16	476.08	97.96
2	28.12	475.40	97.82
3	28.08	474.72	97.68
4	28.10	475.06	97.75
		Average	97.80
		SD	0.14
		RSD	0.1
		Lot B[b]	
1	28.10	480.2	98.81
2	28.02	478.9	98.53
3	27.90	476.8	98.11
4	28.00	478.5	98.46
		Average	98.48
		SD	0.34
		RSD	0.3
		Lot C[c]	
1	28.20	479.7	98.70
2	28.54	485.5	99.89
3	28.38	482.7	99.33
4	28.52	485.1	99.82
		Average	99.44
		SD	0.58
		RSD	0.6

[a] For Lot A, the weight of 20 tablets was 11.7534 g, average tablet weight was 0.588 g, the label claim was 7.5 grains (486.0 mg)/tablet, sample weight was 2.3925 g, and a 25-ml aliquot contained 0.2991 g. [b] For Lot B, the weight of 20 tablets was 11.6618 g, average tablet weight was 0.583 g, the label claim was 7.5 grains (486.0 mg)/tablet, sample weight was 2.3483 g, and a 25-ml aliquot contained 0.2935 g. [c] For Lot C, the weight of 20 tablets was 12.0077 g, average tablet weight was 0.60039 g, the label claim was 7.5 grains (486.0 mg)/tablet, sample weight was 2.4278 g (in 200 ml), and a 25-ml aliquot contained 0.3035 g.

Comparison of the extraction method with the direct titration (Tables VII and VIII) shows that the difference is not significant at the 99% confidence level but is significant at the 95% confidence level. This result is attributed to the zero standard deviation of one set of determinations. The assumption of any reasonable standard deviation to replace the zero actually observed yields the result that the difference in averages is not significant at either confidence level.

The general method is applicable to solutions containing added phosphate until the molar ratio of phosphorus to calcium approaches 2:1 (Table IV). When this ratio was at 2.5:1, the precipitate formed dissolved so slowly that the end-point was unduly prolonged, even though the result was acceptable. These data indicate that the direct method for dibasic calcium phosphate (phosphorus to calcium ratio = 1:1) and tribasic calcium phosphate (phosphorus to calcium ratio = 2:3) should show no phosphate interference and that the general method should work in solutions containing a considerable molar excess of phosphate over calcium.

When three different lots of dibasic calcium phosphate tablets were analyzed, recoveries appeared to be acceptable and the standard deviations were in the range expected from the determinations of the parent compound (Table IX).

It was not possible to compare the proposed method with the currently official methods because the official methods determine the phosphate rather than the calcium content. However, the proposed method is much more rapid than the official methods for dibasic calcium phosphate NF and tribasic calcium phosphate NF, has acceptable reproducibility, and is comparable in results to the last published method for calcium phosphate (2). Moreover, it determines the physiologically active portion of the molecule (both official calcium phosphates are designated as "calcium supplement").

REFERENCES

(1) J. S. Kim and M. M. Tuckerman, *J. Pharm. Sci.*, **56**, 1309 (1967).

(2) L. M. Kleinman and H. Schriftman, *ibid.*, **56**, 516 (1967).
(3) E. L. Grant and R. S. Leavenworth, "Statistical Quality Control," 4th ed., McGraw-Hill, New York, N.Y., 1972.

ACKNOWLEDGMENTS AND ADDRESSES

Received September 20, 1976, from the *Department of Pharmaceutical Chemistry, School of Pharmacy, Temple University, Philadelphia, PA 19140.*

Accepted for publication November 11, 1976.

The authors thank Eli Lilly Co. for donations of calcium phosphate tablets and the suggestion that the direct complexometric titration was possible.

[x] To whom inquiries should be directed.

Mass Fragmentographic Determination of Plasma Etomidate Concentrations

MICHAEL J. VAN HAMME [*], JOHN J. AMBRE [‡x], and MOHAMED M. GHONEIM [*]

Abstract □ The intravenous anesthetic etomidate was measured in human plasma by mass fragmentography. The method is accurate, sensitive, and specific. Results of the analyses indicate that after a single 0.3-mg/kg iv dose of etomidate, there are at least three phases in its disappearance from human plasma. Detectable plasma concentrations exist for more than 6 hr after injection.

Keyphrases □ Etomidate—mass fragmentographic analysis, human plasma □ Mass fragmentography—analysis, etomidate in human plasma □ Hypnotics—etomidate, mass fragmentographic analysis, human plasma

Etomidate is a new imidazole hypnotic used intravenously for induction of anesthesia. Compared to thiopental, the standard intravenous anesthetic, etomidate produces less cardiovascular and respiratory depression (1, 2). Like thiopental, etomidate induces sleep rapidly (10–15 sec) and has a short duration of action (2). Unlike the short-acting barbiturates, however, it does not produce a "hangover" effect (3) due to its rapid disappearance from nervous tissue and plasma and the dependence of this process upon rapid metabolism rather than redistribution (4). However, etomidate disposition has not been studied extensively.

Because etomidate has promise as an anesthetic induction agent (5), a sensitive, specific assay for use in future clinical pharmacological studies was needed. The developed method is based on combined GLC–mass spectrometry and single ion monitoring, a technique called mass fragmentography.

EXPERIMENTAL

Reference Compounds—Authentic etomidate sulfate [(*R*)-(+)-ethyl 1-(1-phenylethyl)-1*H*-imidazole-5-carboxylate sulfate] and propoxate hydrochloride [(+)-propyl 1-(1-phenylethyl)-1*H*-imidazole-5-carboxylate hydrochloride] were used as received[1]. Aqueous solutions of propoxate, 1 and 2 μg/ml, were used as internal standards. All etomidate concentrations are expressed in terms of free base.

GLC–Mass Spectrometry—A quadrupole gas chromatograph was interfaced to a mass spectrometer[2] with a glass jet separator and glass transfer lines. A 1.5-m (5-ft) × 2-mm i.d. glass column was silanized and packed with 5% OV-225 on 100–120-mesh Supelcoport[3]. Helium was the carrier gas at a flow rate of 20 ml/min. The temperature of the injection port was 250°; the column, separator, and transfer line temperatures were 230, 260, and 230°, respectively. Operating conditions for the mass spectrometer were: electron energy, 70 ev; emission ion current, 200 amp; and power supply, 2.5 kv.

Complete mass spectra of authentic etomidate and propoxate were first obtained by using the solid probe inlet to the mass spectrometer. The identities of these compounds as they eluted from the chromatograph were confirmed by comparison of their complete mass spectra to those of the authentic compounds.

These operating conditions also were used for mass fragmentography. The intensity of the *m/e* 105 and 77 ions was monitored using a programmable multiple-ion monitor[4] (at a sensitivity of 10^{-9}) and a dual-pen strip-chart recorder. The *m/e* 105 ion was monitored for the detection and quantitation of both etomidate and propoxate since it was the most abundant. The mass marker was used to center the ion window with a window width of less than 1 amu. The mass marker was not in operation during sample analyses.

Procedure—Blood samples were obtained from patients who underwent anesthetic induction with etomidate for eye or ear surgery. All patients were otherwise healthy, had normal liver and kidney function, and were taking no other medication. Each received 10 mg of diazepam and 0.3 mg of scopolamine intramuscularly 30 min prior to etomidate injection.

An indwelling cannula was placed in an antecubital fossa vein, and a 10-ml control blood sample was withdrawn. Etomidate (0.3 mg/kg iv) was then administered over 30 sec into an antecubital fossa vein of the other arm. After induction with etomidate, anesthesia was maintained with nitrous oxide–oxygen and enflurane.

Blood samples of 10 ml were withdrawn through the cannula into heparinized glass syringes. Samples were taken at 1, 2, 4, 8, 15, and 30 min after injection and then hourly to 6 hr. The blood samples were immediately transferred to 15-ml glass-stoppered centrifuge tubes containing heparin and 10 μl of saturated potassium fluoride solution (to inhibit esterase activity) (6). The plasma was separated by centrifugation at 2000 rpm for 15 min and then frozen and stored at −15° until extracted.

Because of the wide range of etomidate concentrations, the 0–30-min samples were processed separately from later samples. Standard plasma samples containing etomidate concentrations ranging from 1.25 to 0.10 μg/ml were extracted with the 0–30-min patient plasma samples. Aliquots, 3 ml, of 0.05 *M* phosphate buffer, pH 7.4, and 1.0 ml of 1.0-μg/ml propoxate hydrochloride internal standard solution were first added to a 1.0-ml aliquot of each plasma sample. These samples were then subjected to the extraction procedure described below.

Patient plasma samples from later sampling times (1–6 hr) were analyzed with a separate set of standard plasma samples containing 0.25–0.001 μg of etomidate/ml. Aliquots, 1 ml, of a 0.2-μg/ml propoxate hydrochloride internal standard solution were added to 4.0-ml aliquots of these samples. These samples were then subjected to the following extraction procedure, which is a modification of that suggested by Wynants *et al.* (7):

[1] Courtesy of Janssen Pharmaceutica, Beerse, Belgium.
[2] Finnegan model 3200E.
[3] Supelco, Inc., Supelco Park, Bellefonte, Pa.
[4] Finnigan model 1015-80 PROMIM.

(2) L. M. Kleinman and H. Schriftman, *ibid.*, **56**, 516 (1967).
(3) E. L. Grant and R. S. Leavenworth, "Statistical Quality Control," 4th ed., McGraw-Hill, New York, N.Y., 1972.

ACKNOWLEDGMENTS AND ADDRESSES

Received September 20, 1976, from the *Department of Pharmaceutical Chemistry, School of Pharmacy, Temple University, Philadelphia, PA 19140.*

Accepted for publication November 11, 1976.

The authors thank Eli Lilly Co. for donations of calcium phosphate tablets and the suggestion that the direct complexometric titration was possible.

[x] To whom inquiries should be directed.

Mass Fragmentographic Determination of Plasma Etomidate Concentrations

MICHAEL J. VAN HAMME [*], JOHN J. AMBRE [‡x], and MOHAMED M. GHONEIM [*]

Abstract □ The intravenous anesthetic etomidate was measured in human plasma by mass fragmentography. The method is accurate, sensitive, and specific. Results of the analyses indicate that after a single 0.3-mg/kg iv dose of etomidate, there are at least three phases in its disappearance from human plasma. Detectable plasma concentrations exist for more than 6 hr after injection.

Keyphrases □ Etomidate—mass fragmentographic analysis, human plasma □ Mass fragmentography—analysis, etomidate in human plasma □ Hypnotics—etomidate, mass fragmentographic analysis, human plasma

Etomidate is a new imidazole hypnotic used intravenously for induction of anesthesia. Compared to thiopental, the standard intravenous anesthetic, etomidate produces less cardiovascular and respiratory depression (1, 2). Like thiopental, etomidate induces sleep rapidly (10–15 sec) and has a short duration of action (2). Unlike the short-acting barbiturates, however, it does not produce a "hangover" effect (3) due to its rapid disappearance from nervous tissue and plasma and the dependence of this process upon rapid metabolism rather than redistribution (4). However, etomidate disposition has not been studied extensively.

Because etomidate has promise as an anesthetic induction agent (5), a sensitive, specific assay for use in future clinical pharmacological studies was needed. The developed method is based on combined GLC–mass spectrometry and single ion monitoring, a technique called mass fragmentography.

EXPERIMENTAL

Reference Compounds—Authentic etomidate sulfate [(*R*)-(+)-ethyl 1-(1-phenylethyl)-1*H*-imidazole-5-carboxylate sulfate] and propoxate hydrochloride [(+)-propyl 1-(1-phenylethyl)-1*H*-imidazole-5-carboxylate hydrochloride] were used as received[1]. Aqueous solutions of propoxate, 1 and 2 μg/ml, were used as internal standards. All etomidate concentrations are expressed in terms of free base.

GLC–Mass Spectrometry—A quadrupole gas chromatograph was interfaced to a mass spectrometer[2] with a glass jet separator and glass transfer lines. A 1.5-m (5-ft) × 2-mm i.d. glass column was silanized and packed with 5% OV-225 on 100–120-mesh Supelcoport[3]. Helium was the carrier gas at a flow rate of 20 ml/min. The temperature of the injection port was 250°; the column, separator, and transfer line temperatures were 230, 260, and 230°, respectively. Operating conditions for the mass spectrometer were: electron energy, 70 ev; emission ion current, 200 amp; and power supply, 2.5 kv.

Complete mass spectra of authentic etomidate and propoxate were first obtained by using the solid probe inlet to the mass spectrometer. The identities of these compounds as they eluted from the chromatograph were confirmed by comparison of their complete mass spectra to those of the authentic compounds.

These operating conditions also were used for mass fragmentography. The intensity of the *m/e* 105 and 77 ions was monitored using a programmable multiple-ion monitor[4] (at a sensitivity of 10^{-9}) and a dual-pen strip-chart recorder. The *m/e* 105 ion was monitored for the detection and quantitation of both etomidate and propoxate since it was the most abundant. The mass marker was used to center the ion window with a window width of less than 1 amu. The mass marker was not in operation during sample analyses.

Procedure—Blood samples were obtained from patients who underwent anesthetic induction with etomidate for eye or ear surgery. All patients were otherwise healthy, had normal liver and kidney function, and were taking no other medication. Each received 10 mg of diazepam and 0.3 mg of scopolamine intramuscularly 30 min prior to etomidate injection.

An indwelling cannula was placed in an antecubital fossa vein, and a 10-ml control blood sample was withdrawn. Etomidate (0.3 mg/kg iv) was then administered over 30 sec into an antecubital fossa vein of the other arm. After induction with etomidate, anesthesia was maintained with nitrous oxide–oxygen and enflurane.

Blood samples of 10 ml were withdrawn through the cannula into heparinized glass syringes. Samples were taken at 1, 2, 4, 8, 15, and 30 min after injection and then hourly to 6 hr. The blood samples were immediately transferred to 15-ml glass-stoppered centrifuge tubes containing heparin and 10 μl of saturated potassium fluoride solution (to inhibit esterase activity) (6). The plasma was separated by centrifugation at 2000 rpm for 15 min and then frozen and stored at −15° until extracted.

Because of the wide range of etomidate concentrations, the 0–30-min samples were processed separately from later samples. Standard plasma samples containing etomidate concentrations ranging from 1.25 to 0.10 μg/ml were extracted with the 0–30-min patient plasma samples. Aliquots, 3 ml, of 0.05 *M* phosphate buffer, pH 7.4, and 1.0 ml of 1.0-μg/ml propoxate hydrochloride internal standard solution were first added to a 1.0-ml aliquot of each plasma sample. These samples were then subjected to the extraction procedure described below.

Patient plasma samples from later sampling times (1–6 hr) were analyzed with a separate set of standard plasma samples containing 0.25–0.001 μg of etomidate/ml. Aliquots, 1 ml, of a 0.2-μg/ml propoxate hydrochloride internal standard solution were added to 4.0-ml aliquots of these samples. These samples were then subjected to the following extraction procedure, which is a modification of that suggested by Wynants *et al.* (7):

[1] Courtesy of Janssen Pharmaceutica, Beerse, Belgium.
[2] Finnegan model 3200E.
[3] Supelco, Inc., Supelco Park, Bellefonte, Pa.
[4] Finnigan model 1015-80 PROMIM.

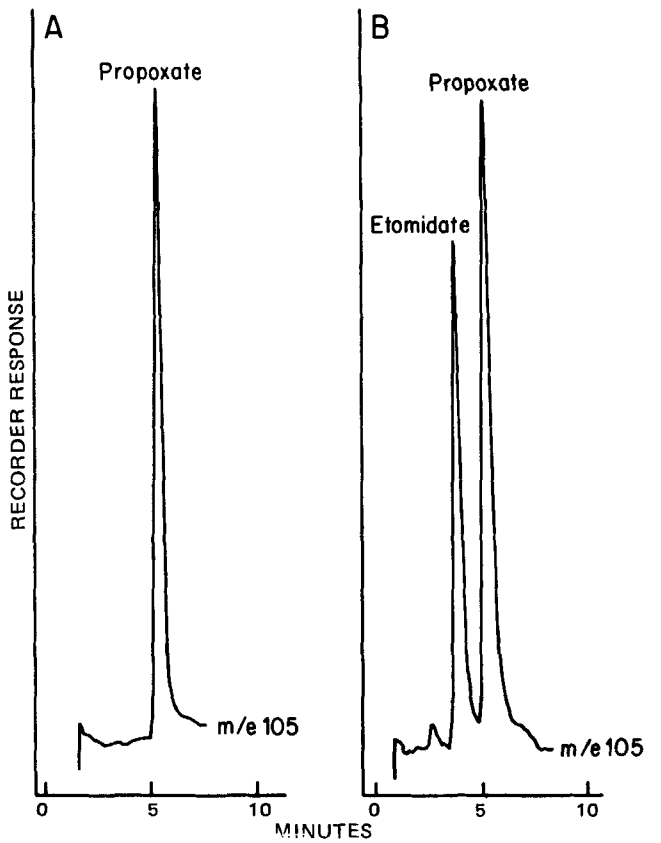

Figure 1—*Mass fragmentograms of plasma extracts from Patient 2, indicating elution position of etomidate and the internal standard propoxate. Key: A, control sample; and B, 3-hr sample containing 21.2 ng of etomidate/ml.*

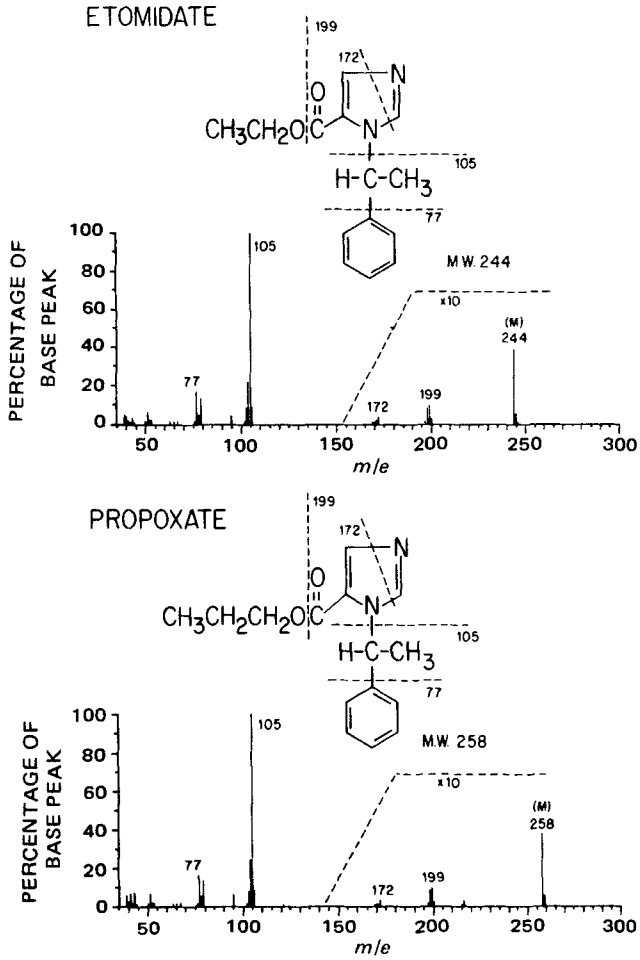

Figure 2—*Mass spectra of authentic etomidate and propoxate.*

1. Add 1.0 ml of 0.05 *M* borate buffer, pH 10, and mix on a vortex mixer.
2. Add 5.0 ml of ether, shake on a horizontal shaker for 10 min, centrifuge at 1500 rpm for 5 min, and quick freeze the plasma layer in a dry ice–acetone bath. Transfer as much of the organic phase as possible to another 15-ml screw-capped centrifuge tube and seal with a polytef-lined cap. (The quick-freeze step facilitates the recovery of the organic phase.)
3. Thaw frozen plasma samples in a 40° water bath and repeat Step 2. Centrifuge at 2000 rpm for 10 min, quick freeze, and combine the ether extracts.
4. Add 5.0 ml of 0.5 *M* H_2SO_4 to ether extracts, shake for 10 min, centrifuge at 1500 rpm for 5 min, and remove all ether by aspiration.
5. Add 3.0 ml of ether to the acidic aqueous extract; shake, centrifuge, and aspirate as in Step 4.
6. Add 1.0 ml of 3.0 *M* NH_4OH and mix on a vortex mixer.
7. Add 3.0 ml of methylene chloride; shake and centrifuge as in Step 4. Remove as much of the aqueous layer as possible by aspiration.
8. Carefully transfer the methylene chloride extract to an evaporating tube.
9. Evaporate to dryness.
10. Take up the residue in 10–50 μl of *n*-hexane and inject 1–5 μl on the chromatograph column.

A typical chromatogram is shown in Fig. 1. The magnitude of the detector response indicates the intensity of the *m/e* 105 ion.

Each standard curve was constructed by plotting the ratio of etomidate to propoxate peak heights against etomidate concentration. Standard curves were linear over the entire range of concentrations measured.

RESULTS AND DISCUSSION

Recovery of etomidate from extracted plasma was determined by comparing absolute peak height ratios of extracted standards to those obtained from unextracted primary standards. The actual recovery determined was 72 ± 3%.

The coefficient of variation obtained by extraction and analysis of five replicate standards at 100, 50, 10, 5, and 1 ng/ml of plasma was 2.4%. Reproducibility did not vary significantly from day to day.

As little as 100 pg of etomidate could be detected by injection on the chromatograph column. The practical limit of assay sensitivity is 1 ng/ml of plasma, which is at least 10-fold more sensitive than the method of Wynants *et al.* (7). The specificity of the mass fragmentography technique allows extraction of large volumes of plasma without interference from endogenous substances.

The conventional mass spectra of etomidate and propoxate are shown in Fig. 2. The base peak for each compound is at *m/e* 105. The proposed structures of the major fragments also are indicated. The *m/e* 105 ion is probably stabilized as the methyl tropylium structure (8). The *m/e* 199 ion arises from loss of the alkoxy side chain (9), while the *m/e* 172 ion may result from ring cleavage and loss of hydrogen cyanide, a pattern characteristic of imidazoles (10). Other possible origins for the *m/e* 199 and 172 ions are unlikely, since these ions have identical abundance in the mass spectra of both propoxate and etomidate. The *m/e* 77 ion probably represents the phenyl ring fragment.

During mass fragmentographic analysis, the *m/e* 77 ion also was monitored. The ratio of its intensity to that of the *m/e* 105 ion served as a check against the possibility that an endogenous component of plasma with the same retention time was contributing to the size of the *m/e* 105 peak (11).

Since the major metabolite of etomidate in humans is the corresponding carboxylic acid, it has been assumed that plasma pseudocholinesterase may hydrolyze the drug (6), although apparently this has not been studied. A 10-μl aliquot of a saturated solution of potassium fluoride was added to all blood samples to inhibit esterase activity. Etomidate concentrations in samples treated in this manner were unchanged for at least 2 hr at room temperature and for at least 1 month when frozen and stored at −15°.

Concentrations of etomidate in the plasma of patients given 0.3 mg/kg iv for induction of anesthesia are shown in Fig. 3. All values are the result of duplicate determinations. The large variation in concentrations in the 1–4-min samples probably reflects incomplete mixing of the drug within

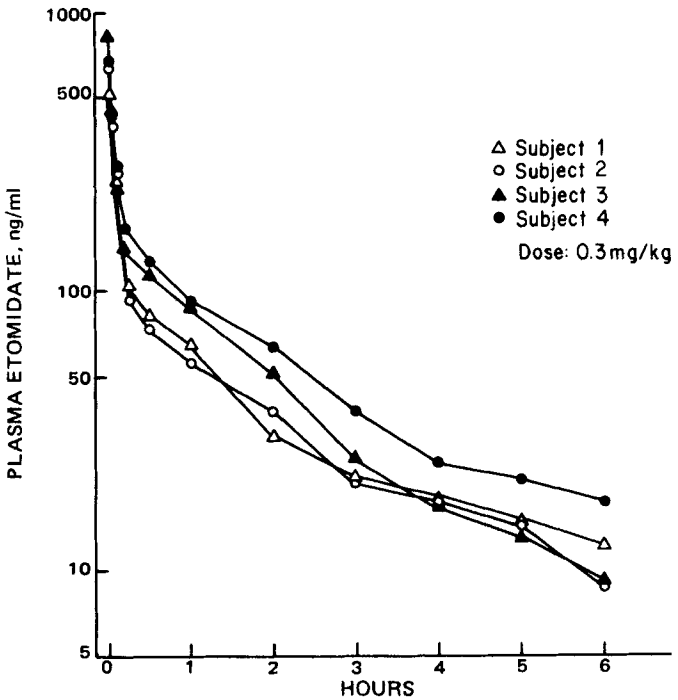

Figure 3—*Plasma concentrations following 0.3 mg of etomidate sulfate/kg iv. Concentrations in the 1-min samples from Patients 1 and 4 were 1170 and 1200 ng/ml, respectively.*

the vascular volume. Plasma etomidate concentrations in these patients at 6 hr after the injection were still well above the limits of assay sensitivity. Therefore, etomidate is detectable in plasma for several hours longer than previously indicated (7).

The semilogarithmic plot of these plasma level data (Fig. 3) indicates that there are at least three phases in the plasma disappearance of etomidate. This assay provides the sensitivity necessary to measure terminal phase plasma concentrations important in drug kinetic studies (12). A pharmacokinetic study involving a larger number of patients is currently in progress.

REFERENCES

(1) N. Morgan, J. Lumley, and J. Whitman, *Lancet*, **1**, 955 (1975).

(2) J. Gooding and G. Corssen, *Anesth. Analg.*, **55**, 286 (1976).

(3) B. Kay, *Br. J. Anaesth.*, **48**, 213 (1976).

(4) J. J. P. Heykants, W. E. G. Meuldermans, L. J. M. Michiels, P. J. Lewi, and P. A. J. Janssen, *Arch. Int. Pharmacodyn. Ther.*, **216**, 113 (1975).

(5) A. Doenicke, J. Kugler, G. Penzel, M. Lanb, L. Kalmar, I. Killian, and H. Bezecny, *Anaesthesist*, **22**, 357 (1973).

(6) W. E. G. Meuldermans and J. J. P. Heykants, *Arch. Int. Pharmacodyn. Ther.*, **221**, 150 (1976).

(7) J. Wynants, R. Woestenborghs, and J. Heykants, "A Gas Chromatographic Assay Method for Etomidate in Human Plasma," Biological Research Report R 26 490/13, Janssen Research Products Information Service, Janssen Pharmaceutica, B-2340 Beerse, Belgium, Dec. 1974.

(8) H. Budzikiewicz, C. Djerassi, and D. Williams, "Mass Spectrometry of Organic Compounds," Holden-Day, San Francisco, Calif., 1967, p. 599.

(9) Q. Porter and J. Baldis, "Mass Spectrometry of Heterocyclic Compounds," Wiley–Interscience, London, England, 1971, p. 454.

(10) J. Bowie, R. Cooks, S. Lawesson, and G. Schroll, *Aust. J. Chem.*, **20**, 1613 (1967).

(11) J. Strong and A. Atkinson, *Anal. Chem.*, **44**, 2287 (1972).

(12) T. Teorell, R. Dedrick, and P. Condliffe, "Pharmacology and Pharmacokinetics," Plenum, New York, N.Y., 1974, p. 62.

ACKNOWLEDGMENTS AND ADDRESSES

Received October 1, 1976, from the **Department of Anesthesiology and the ‡Department of Medicine and Pharmacology, College of Medicine, University of Iowa, Iowa City, IA 52242.*

Accepted for publication November 11, 1976.

ˣ To whom inquiries should be directed.

In Vitro Adsorption of Doxorubicin Hydrochloride on Insoluble Calcium Phosphate

ROY J. STURGEON, CYNTHIA FLANAGAN *, DATTA V. NAIK ‡, and STEPHEN G. SCHULMAN ˣ

Abstract □ The adsorption of doxorubicin hydrochloride, a potent antitumor agent, on solid tribasic calcium phosphate was studied *in vitro*. A Langmuir adsorption isotherm at pH 7.4 and the maximum adsorption capacity of tribasic calcium phosphate were established. Tribasic calcium phosphate was chosen as a model for solid bone samples, which are stained with doxorubicin in patients who have received long-term doxorubicin therapy.

Keyphrases □ Doxorubicin hydrochloride—adsorption on solid tribasic calcium phosphate *in vitro* □ Adsorption—doxorubicin hydrochloride on solid tribasic calcium phosphate *in vitro* □ Calcium phosphate, tribasic—adsorption of doxorubicin hydrochloride *in vitro*

Doxorubicin (I), an anthracycline antibiotic, has demonstrated antitumor activity against various solid tumors (1) as well as certain hematologic malignancies (2). Some serious complications encountered in the use of I are related to bone marrow depression, cardiac toxicity, stomatitis, and alopecia (3). Perhaps the most significant is bone marrow depression, primarily of leukocytes, which requires careful monitoring. In patients who have received extended I therapy, autopsies have shown that cross sections of bone tissue are stained with I (2, 4). Since solid bone samples are also stained, the process by which I is deposited in these areas is of interest.

The I molecule contains an anthraquinone moiety. Some mono- and dihydroxyanthraquinones are good chelating agents for several metal ions (5, 6). However, these compounds only form calcium chelates at pH 10–12, much greater than physiological pH. It was originally assumed that I would chelate a calcium ion in solution *in vivo* and be deposited in the outer layers of solid bone. Preliminary studies showed that I does not interact appreciably with calcium ions in solution at pH < 10 even when calcium ions are present in large excess.

To approximate bone samples, solid tribasic calcium

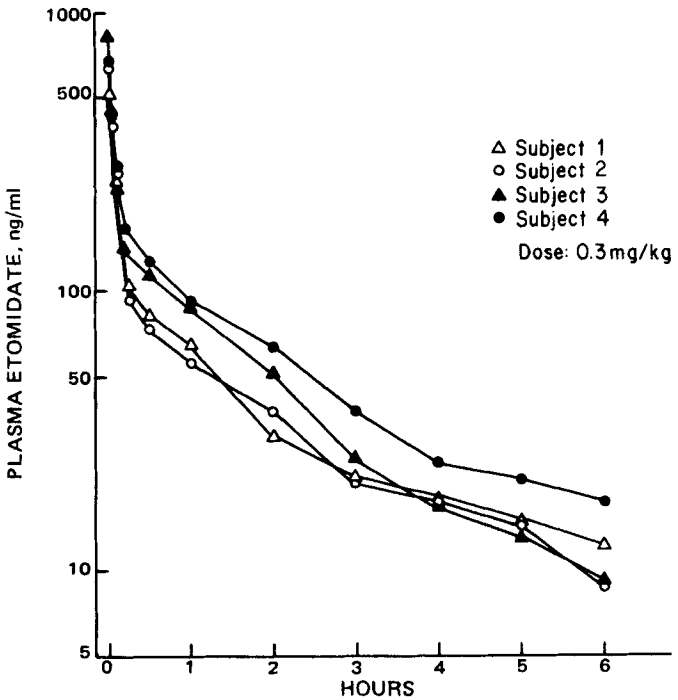

Figure 3—*Plasma concentrations following 0.3 mg of etomidate sulfate/kg iv. Concentrations in the 1-min samples from Patients 1 and 4 were 1170 and 1200 ng/ml, respectively.*

the vascular volume. Plasma etomidate concentrations in these patients at 6 hr after the injection were still well above the limits of assay sensitivity. Therefore, etomidate is detectable in plasma for several hours longer than previously indicated (7).

The semilogarithmic plot of these plasma level data (Fig. 3) indicates that there are at least three phases in the plasma disappearance of etomidate. This assay provides the sensitivity necessary to measure terminal phase plasma concentrations important in drug kinetic studies (12). A pharmacokinetic study involving a larger number of patients is currently in progress.

REFERENCES

(1) N. Morgan, J. Lumley, and J. Whitman, *Lancet*, **1**, 955 (1975).

(2) J. Gooding and G. Corssen, *Anesth. Analg.*, **55**, 286 (1976).

(3) B. Kay, *Br. J. Anaesth.*, **48**, 213 (1976).

(4) J. J. P. Heykants, W. E. G. Meuldermans, L. J. M. Michiels, P. J. Lewi, and P. A. J. Janssen, *Arch. Int. Pharmacodyn. Ther.*, **216**, 113 (1975).

(5) A. Doenicke, J. Kugler, G. Penzel, M. Lanb, L. Kalmar, I. Killian, and H. Bezecny, *Anaesthesist*, **22**, 357 (1973).

(6) W. E. G. Meuldermans and J. J. P. Heykants, *Arch. Int. Pharmacodyn. Ther.*, **221**, 150 (1976).

(7) J. Wynants, R. Woestenborghs, and J. Heykants, "A Gas Chromatographic Assay Method for Etomidate in Human Plasma," Biological Research Report R 26 490/13, Janssen Research Products Information Service, Janssen Pharmaceutica, B-2340 Beerse, Belgium, Dec. 1974.

(8) H. Budzikiewicz, C. Djerassi, and D. Williams, "Mass Spectrometry of Organic Compounds," Holden-Day, San Francisco, Calif., 1967, p. 599.

(9) Q. Porter and J. Baldis, "Mass Spectrometry of Heterocyclic Compounds," Wiley–Interscience, London, England, 1971, p. 454.

(10) J. Bowie, R. Cooks, S. Lawesson, and G. Schroll, *Aust. J. Chem.*, **20**, 1613 (1967).

(11) J. Strong and A. Atkinson, *Anal. Chem.*, **44**, 2287 (1972).

(12) T. Teorell, R. Dedrick, and P. Condliffe, "Pharmacology and Pharmacokinetics," Plenum, New York, N.Y., 1974, p. 62.

ACKNOWLEDGMENTS AND ADDRESSES

Received October 1, 1976, from the **Department of Anesthesiology and the ‡Department of Medicine and Pharmacology, College of Medicine, University of Iowa, Iowa City, IA 52242.*

Accepted for publication November 11, 1976.

ˣ To whom inquiries should be directed.

In Vitro Adsorption of Doxorubicin Hydrochloride on Insoluble Calcium Phosphate

ROY J. STURGEON, CYNTHIA FLANAGAN *, DATTA V. NAIK ‡, and STEPHEN G. SCHULMAN ˣ

Abstract □ The adsorption of doxorubicin hydrochloride, a potent antitumor agent, on solid tribasic calcium phosphate was studied *in vitro*. A Langmuir adsorption isotherm at pH 7.4 and the maximum adsorption capacity of tribasic calcium phosphate were established. Tribasic calcium phosphate was chosen as a model for solid bone samples, which are stained with doxorubicin in patients who have received long-term doxorubicin therapy.

Keyphrases □ Doxorubicin hydrochloride—adsorption on solid tribasic calcium phosphate *in vitro* □ Adsorption—doxorubicin hydrochloride on solid tribasic calcium phosphate *in vitro* □ Calcium phosphate, tribasic—adsorption of doxorubicin hydrochloride *in vitro*

Doxorubicin (I), an anthracycline antibiotic, has demonstrated antitumor activity against various solid tumors (1) as well as certain hematologic malignancies (2). Some serious complications encountered in the use of I are related to bone marrow depression, cardiac toxicity, stomatitis, and alopecia (3). Perhaps the most significant is bone marrow depression, primarily of leukocytes, which requires careful monitoring. In patients who have received extended I therapy, autopsies have shown that cross sections of bone tissue are stained with I (2, 4). Since solid bone samples are also stained, the process by which I is deposited in these areas is of interest.

The I molecule contains an anthraquinone moiety. Some mono- and dihydroxyanthraquinones are good chelating agents for several metal ions (5, 6). However, these compounds only form calcium chelates at pH 10–12, much greater than physiological pH. It was originally assumed that I would chelate a calcium ion in solution *in vivo* and be deposited in the outer layers of solid bone. Preliminary studies showed that I does not interact appreciably with calcium ions in solution at pH < 10 even when calcium ions are present in large excess.

To approximate bone samples, solid tribasic calcium

phosphate was added to solutions of varying concentrations of I buffered at pH 7.4. A substantial fraction of I was removed from solution. Compound I has a tendency to self-aggregate at concentrations greater than about 5×10^{-5} *M*; therefore, an adsorption isotherm (7) was established for only a very limited concentration range where only the monomer prevails. Comparisons of solutions of varying concentration and with varying amounts of adsorbent added are used to show that I can be deposited on bone by an adsorption mechanism.

EXPERIMENTAL

The pH measurements were made on a pH meter[1] employing a combination silver–silver chloride glass electrode[2]. Electronic absorption spectra were taken in 1-cm silica cells on a grating-type spectrophotometer[3]. Fluorescence measurements were taken on a fluorescence spectrophotometer[4] whose monochromators were calibrated against the line emission spectrum of xenon.

Doxorubicin hydrochloride[5] was used without further purification. Tribasic calcium phosphate[6] was triturated in a mortar until a relatively uniform particle size was obtained and then dried in an oven overnight. Phosphate buffers at pH 7.4 with a total buffer concentration of 0.05 *M* and the ionic strength adjusted to 0.16 with sodium chloride were used.

Bicarbonate buffers and sodium hydroxide solutions were used in studying the binding of calcium ions to I in the pH 7–12 range. Aliquots, 25 ml, of 1.00×10^{-1} *M* calcium perchlorate were added to 25 ml of 1.00×10^{-5} *M* I at varying pH's. The absorption and fluorescence spectra of these solutions were compared with those to which no calcium ions were added.

Accurately weighed amounts of tribasic calcium phosphate, 10–170 mg, were transferred to 25-ml test tubes with screw caps. After 25 ml of 1.00×10^{-5} *M* I was added to each test tube, the calcium phosphate suspensions were continuously mixed for 4 hr in a constant-temperature shaker at 37°. The suspensions were then centrifuged rapidly, and the clear supernate was assayed fluorometrically at 556 nm. Appropriate control solutions also were run and assayed to ensure control over experimental conditions.

The amount of I adsorbed on the calcium phosphate was determined on the basis of a previously established standard curve. The values used to construct the Langmuir isotherm were each the average of three separate measurements, and the standard deviation was no larger than ±0.05 unit in any set of measurements.

The solids from the centrifuged samples were collected by filtration and dried overnight. These solids were then reshaken in the phosphate buffer solutions, heated to 60°, and placed in an ultrasonic cleaning device for 5 min to desorb I partially. The absorption and fluorescence spectra of each solution after centrifugation were taken to ensure that I had not undergone any chemical reaction.

RESULTS AND DISCUSSION

Figure 1 illustrates the Langmuir adsorption isotherm for the uptake of I by tribasic calcium phosphate suspended in solution at pH 7.4. The reciprocal of the slope of the line gives the maximum binding capacity of tribasic calcium phosphate at pH 7.4. The wavelength absorption maxima of I at pH 7.0, 11.5, and 11.5 with 5.0×10^{-2} *M* Ca^{2+} were 495 (log ϵ = 3.97), 554 (3.76), and 556 (3.69) nm. For 1,8-dihydroxyanthraquinone, the wavelength absorption maxima at pH 7.0, 11.5, and 7.0 with 5.0×10^{-2} *M* Ca^{2+} were 415 (log ϵ = 3.74), 494 (3.91), and 500 (3.97) nm.

Since the absorption and fluorescence spectra of the monocation of I at pH 7 should show a dramatic red shift upon chelation of a metal ion such as Ca^{2+}, the lack of any perturbation of the spectra is indicative of no interaction. At physiological pH, the absorption and fluorescence spectra of I showed no changes in the presence of excess calcium ions. At pH 11.5 (where I is in the singly charged anionic form) in the presence of excess calcium ions, the absorption spectrum of I was slightly red shifted (1–2 nm) and showed a slight hypsochromic effect indicating that chelation took place at high pH. The hydroxyanthraquinones showed substantial shifts of their longest wavelength absorption bands upon binding to a metal ion. For example, the longest wavelength absorption band of 1,8-dihydroxyanthraquinone at pH 7.0 shifted from 410 to 500 nm upon the addition of excess calcium ions.

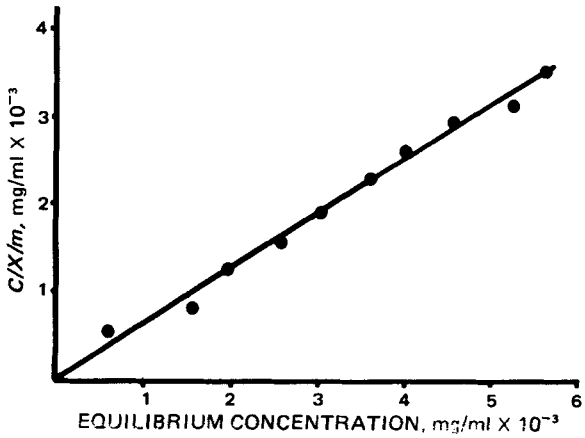

Figure 1—*Langmuir isotherm for the adsorption of I on tribasic calcium phosphate at pH 7.4; C is the equilibrium concentration in milligrams of doxorubicin per 100 ml of solution and* X/m *is the amount in milligrams of doxorubicin as the hydrochloride adsorbed per gram of calcium phosphate.*

The data indicate that the singly charged cation of I is adsorbed on the surface of the tribasic calcium phosphate. The ionic and lipophilic moieties of this drug probably promote drug adsorption through hydrophobic and electrostatic interactions with the surface of the calcium phosphate. The surface of the calcium phosphate crystal differs from the interior, and it is possible that the triply charged phosphates at the surface can contribute to the electrostatic part of the adsorption process. However, steric limitations on the chelation of calcium by I at the surface are imposed by the orbital structure of calcium. The forces of adsorption, whether they are electrostatic or hydrophobic, are certainly much weaker than the forces normally involved in coordinate–covalent bonding. The substantial dislodgement of I by gentle heating and sonication support these statements.

Under the given experimental conditions, the maximum adsorption capacity of calcium phosphate was estimated at 1.60 mg of I/g of calcium phosphate in suspension at pH 7.4. That the deposition of I on calcium phosphate is a physical adsorption process is further supported by the desorption of I from the tribasic calcium phosphate, which shows that no chemical alteration of I occurred. These results strongly suggest that the adsorption of I on solid bone does occur *in vivo*, resulting in the staining of bone samples upon extended treatment with this drug.

REFERENCES

(1) C. Tan, H. Tasaka, K. P. Yu, M. L. Murphy, and D. Karnovsky, *Cancer*, **20**, 333 (1967).

(2) D. H. Huffman, R. S. Benjamin, and N. R. Bachur, *Clin. Pharmacol. Ther.*, **13**, 895 (1972).

(3) N. R. Bachur, *Cancer Chemother. Rep., Part 3*, **4** (3), 74 (1973).

(4) R. K. Oldham and T. C. Pomeroy, *Cancer Chemother. Rep., Part 1*, **56** (5) (1972).

(5) M. H. Fletcher, C. E. White, and M. S. Sheffel, *Ind. Eng. Chem. Anal. Ed.*, **18**, 179 (1946).

(6) T. Po, *Khim. Khim. Tekhnol.*, **1**, 134 (1958).

(7) T. Tsuchiya and G. Levy, *J. Pharm. Sci.*, **61**, 586 (1972).

ACKNOWLEDGMENTS AND ADDRESSES

Received July 19, 1976, from the *College of Pharmacy, University of Florida, Gainesville, FL 32610.*

Accepted for publication November 17, 1976.

* Summer Research Assistant, Florida Foundation for Future Scientists, 1975. Present address: California Institute of Technology, Pasadena, Calif.

‡ Present address: Manhattanville College, Purchase, N.Y.

ˣ To whom inquiries should be directed.

[1] Markson Electromark.
[2] Markson 888.
[3] Beckman model 25.
[4] Perkin-Elmer MPF-2A.
[5] Adria Laboratories, Wilmington, Del.
[6] Merck & Co., Rahway, N.J.

Antitumor Agents from *Jatropha macrorhiza* (Euphorbiaceae) III: Acetylaleuritolic Acid

S. J. TORRANCE, R. M. WIEDHOPF, and J. R. COLE ˣ

Abstract □ The triterpene acetylaleuritolic acid was isolated from *Jatropha macrorhiza* (Euphorbiaceae) and showed tumor-inhibitory properties toward the P-388 lymphocytic leukemia test system. The compound was identified by means of IR, PMR, and mass spectrometry and by its transformation into the known methyl acetyloleanolate.

Keyphrases □ Acetylaleuritolic acid—isolated from ethanol extract of roots of *Jatropha macrorhiza*, antitumor activity evaluated □ *Jatropha macrorhiza*—ethanol extract of roots, acetylaleuritolic acid isolated and evaluated for antitumor activity □ Antitumor activity—evaluated in acetylaleuritolic acid isolated from ethanol extract of roots of *Jatropha macrorhiza*

In the continuing search for plants having tumor-inhibitory constituents[1], the ethanol extract of the roots of *Jatropha macrorhiza* Benth. (Euphorbiaceae)[2] was found to possess inhibitory activity toward the P-388 lymphocytic leukemia test system[3].

DISCUSSION

One constituent of the ethanol extract of *J. macrorhiza* Benth. roots is the triterpene acetylaleuritolic acid (I), $C_{32}H_{50}O_4$ (1). The IR spectrum of I indicated that this compound contained carboxylic acid (1695 cm^{-1}) and acetate (1730 and 1255 cm^{-1}) functional groups. The mass spectrum of I exhibited a fragmentation pattern consistent with that reported (1) for Δ^{14}-taraxerene derivatives and identical to the data for aleuritolic acetate (2). The physical data (2) for aleuritolic acid and its derivatives were also in agreement with those observed for I and its derivatives (II and III).

Because an authentic sample of I was unobtainable, its methyl ester (III) was converted *via* acid isomerization (2, 3) into IV, identical in all respects (TLC, IR and mass spectra, and mixed melting point) to an authentic specimen[4] of methyl acetyloleanolate (4).

Compound I demonstrated activities of 158 and 128% test/control (T/C) at dose levels of 1.0 and 1.4 mg/kg, respectively, in the P-388 system. Activity in the P-388 test system is defined as an increase in the survival of treated animals over that of controls resulting in a T/C ≥ 125% (5).

EXPERIMENTAL[5]

Extraction Procedure—The fresh ground roots (90.8 kg) of *J. macrorhiza* were extracted exhaustively in a Lloyd-type extractor with ethanol. The solvent from the ethanol extract was removed in air, and the residue was partitioned between chloroform and water (1:1). After the layers separated, the chloroform was removed in air, resulting in 130.3 g of residue.

Isolation of I—The residue from the chloroform phase (100 g) was stirred vigorously with ether (1.4 liters) and filtered. This process provided 7 g of ether-insoluble material and, after removal of the solvent *in vacuo*, 92 g of ether-soluble residue. The ether-soluble fraction (50 g) was then chromatographed over 850 g (55 × 840 mm) of silica gel 60[6]. Elution of the column was begun with benzene and continued with increasing amounts of chloroform in benzene. Elution with 80% chloroform produced a semicrystalline fraction (2 g), which was recrystallized from hexane, resulting in 375 mg of I as colorless needles, mp 298–300° (sublimes above 140°) [lit. (1) mp 278–281°], $[\alpha]_D^{25}$ −49° (c 0.2, $CHCl_3$). The IR [($CHCl_3$): 1730, 1695, and 1255 cm^{-1}], PMR [($CDCl_3$): δ 0.86 (s, 3H), 0.95 (s, 15H), 1.25 (s, 3H), 2.02 (s, 3H), 4.45 (m, 1H), and 5.51 (m, 1H) ppm], and mass [*m/e* 498 (M^+), 483, 438, 423, 377, 344, 329, 269, 248, 234 (base), 219, 203, 189, 135, and 119] spectra were in accord with Structure I.

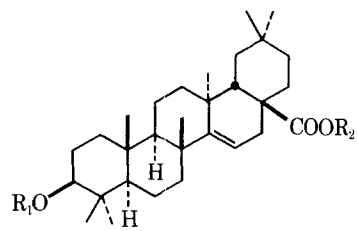

I: $R_1 = CH_3CO$, $R_2 = H$
II: $R_1 = R_2 = H$
III: $R_1 = CH_3CO$, $R_2 = CH_3$

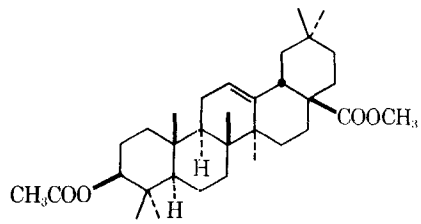

IV

Anal.—Calc. for $C_{32}H_{50}O_4 \cdot \frac{1}{2}H_2O$: C, 75.69; H, 10.12. Found: C, 75.31; H, 10.11.

The methyl ester (III) of I melted at 239–241° [lit. (1) mp 241–243°], and the desacetyl compound (aleuritolic acid, II) melted at 303–306° dec. (sublimes above 205°, turning into tiny needles) [lit. (1) mp 300–302° dec.].

Isomerization of Methyl Acetylaleuritolate (III) and Preparation of Methyl Acetyloleanolate (IV)—Compound III, 25 mg, in acetic acid (5 ml) was heated with concentrated hydrochloric acid (0.2 ml) on a steam bath for 30 min. The crystalline solid (22 mg) obtained after workup was recrystallized from ether–hexane, giving pure IV, mp 219–220°, $[\alpha]_D^{25}$ +58° (c 1.0, $CHCl_3$), identical (TLC, IR and mass spectra, and mixed melting point) with an authentic sample[4].

Anal.—Calc. for $C_{33}H_{52}O_4 \cdot \frac{1}{2}H_2O$: C, 75.96; H, 10.23. Found: C, 76.23; H, 10.36.

REFERENCES

(1) H. Budzikiewicz, J. M. Wilson, and C. Djerassi, *J. Am. Chem. Soc.*, **85**, 3688 (1963).

(2) D. R. Misra and H. N. Khastgir, *Tetrahedron*, **26**, 3017 (1970).

(3) J. M. Beaton and F. S. Spring, *J. Chem. Soc.*, **1955**, 2131.

(4) J. Simonsen and W. C. J. Ross, "The Terpenes," vol. V, Cambridge University Press, Cambridge, England, 1957, p. 201.

(5) R. I. Geran, N. H. Greenberg, M. M. MacDonald, A. M. Schumacher, and B. J. Abbott, *Cancer Chemother. Rep. Part 3*, **3**, 9 (1972).

[1] For Part I, see *J. Pharm. Sci.*, **62**, 1206 (1973). For Part II, see *J. Org. Chem.*, **41**, 1855 (1976).

[2] Identification was confirmed by R. M. Wiedhopf, College of Pharmacy, and Dr. Charles T. Mason, Botany Department, University of Arizona, Tucson, Ariz. A reference specimen was deposited in the University of Arizona Herbarium.

[3] Tested by the Drug Evaluation Branch, Drug Research and Development, Chemotherapy, National Cancer Institute.

[4] An authentic specimen of oleanolic acid was provided by Drug Research and Development, Chemotherapy, National Cancer Institute.

[5] Carbon and hydrogen analyses were performed by Chemalytics, Inc., Tempe, Ariz. Mass, PMR, and IR spectra were recorded using a Hewlett-Packard model 5930 spectrometer, a Varian T-60 spectrometer, and a Beckman IR-33, respectively. Optical rotations were obtained on a Rudolph model 70 polarimeter, and melting points were determined on a Kofler hot-stage apparatus and are uncorrected.

[6] E. Merck.

ACKNOWLEDGMENTS AND ADDRESSES

Received September 30, 1976, from the *Department of Pharmaceutical Sciences, College of Pharmacy, University of Arizona, Tucson, AZ 85721.*

Accepted for publication December 7, 1976.

Supported in part by Contract N01-CM33750 from the Division of Cancer Treatment, National Cancer Institute, National Institutes of Health, Department of Health, education, and Welfare, Bethesda, MD 20014, and by the Elsa U. Pardee Foundation, Midland, Mich.

[x] To whom inquiries should be directed.

Anthelmintic Dihydroquinoxalino[2,3-*b*]quinoxalines

MICHAEL H. FISHER [x], AINO LUSI, and JOHN R. EGERTON

Abstract □ A series of dihydroquinoxalino[2,3-*b*]quinoxalines was synthesized and tested for anthelmintic activity in a model assay. The most promising compound, 5,12-diacetyl-5,12-dihydroquinoxalino[2,3-*b*]quinoxaline, was orally effective in sheep at a dose of 200 mg/kg against a broad range of helminths.

Keyphrases □ Quinoxalines, substituted—synthesized, anthelmintic activity evaluated □ Dihydroquinoxalino[2,3-*b*]quinoxalines, substituted—synthesized, anthelmintic activity evaluated □ Anthelmintic activity—evaluated in series of substituted dihydroquinoxalino[2,3-*b*]quinoxalines □ Structure–activity relationships—series of substituted dihydroquinoxalino[2,3-*b*]quinoxalines evaluated for anthelmintic activity

In the continuing search for anthelmintic agents of novel structure, dihydroquinoxalino[2,3-*b*]quinoxaline showed erratic but definite anthelmintic activity in a preliminary assay. Therefore, several analogs were synthesized and tested for anthelmintic efficacy.

RESULTS AND DISCUSSION

Fluoflavin was first prepared by Hinsberg and Pollak (1), who formulated the structure as 5,12-dihydroquinoxalino[2,3-*b*]quinoxaline (I). Since then, there has been considerable speculation as to whether the compound is more accurately represented by the tautomeric 5,11-dihydro structure, II. A spectroscopic study (2) indicated that the 5,12-dihydro structure, I, is the most probable, and it is used for fluoflavin derivatives in this report. Derivatives having substituents in the benzo rings also may have ambiguous structures; no attempt was made to establish their exact structures.

The new compounds prepared are listed in Tables I and II together with some previously described compounds. Synthetic procedures, generalized where possible, are described under *Experimental*. All derivatives were synthesized by reacting appropriately substituted 1,2-phenylenediamines with 2,3-dichloroquinoxalines over sodium carbonate in refluxing dimethylformamide (3) (Scheme I). Acylation was generally accomplished by long heating in a large excess of the anhydride. Alternatively, conventional acylation with the acyl halide in pyridine was possible.

The diformyl derivative could only be prepared with 100% formic acid and *N,N'*-dicyclohexylcarbodiimide. Reduction of the nitro derivative (XXVIII) with hydrogen over palladium-on-carbon gave the amine (XXIX), which was acylated with methyl chloroformate to the carbamate (XXX). Oxidation of I with hydrogen peroxide in trifluoroacetic acid gave quinoxalino[2,3-*b*]quinoxaline 5,11-dioxide (XLIII), previously described by Kuhn and Skrabal (4) as the sole product isolated.

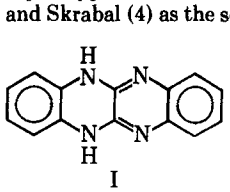

I

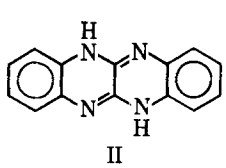

II

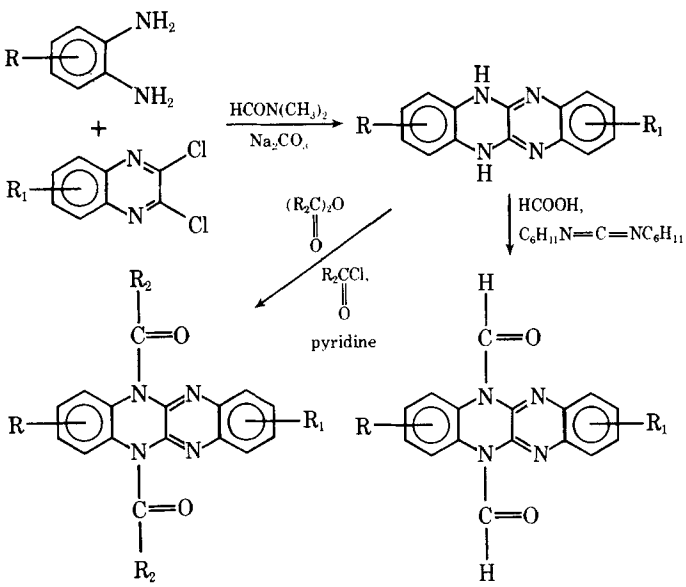

Scheme I

Biological results (the lowest oral doses demonstrating activity) are shown in Tables I and II. Compounds were tested for anthelmintic activity against *Trichostrongylus* in a standard laboratory animal model assay (5). The most potent compounds in the series, VIII–X, were lower acyl derivatives of the unsubstituted I.

The nonacylated compounds were all extremely insoluble; since I showed erratic but definite activity at 400 mg/kg, the main contribution of acylation was to achieve better absorption and distribution of the intrinsically active ring system. Acylation with groups larger than propionyl diminished activity, as did any of the ring substitutions tried. The aromatic analog (XLII) was inactive, but its bis(*N*-oxide) derivative (XLIII) was surprisingly among the most active compounds in the series. 5,12-Diacetyl-5,12-dihydroquinoxalino[2,3-*b*]quinoxaline (IX) was selected as the most promising and evaluated for anthelmintic efficacy in sheep. At an oral dose of 200 mg/kg, it was effective against *Haemonchus contortus, Ostertagia circumcincta, Trichostrongylus axei, Trichostrongylus colubriformis,* and *Cooperia* sp.

EXPERIMENTAL[1]

Method A: 2-Methoxy-5,12-dihydroquinoxalino[2,3-*b*]quinoxaline (XXIII)—A suspension of 20.0 g (0.144 mole) of 4-methoxy-1,2-phenylenediamine, 28.8 g (0.144 mole) of 2,3-dichloroquinoxaline, and 15.3 g (0.144 mole) of sodium carbonate in 100 ml of dimethylformamide was refluxed for 5 hr and then cooled to room temperature. The product was filtered off and crystallized from acetic acid, 23.1 g (60.3%), mp >340°.

[1] Melting points were taken on a Thomas-Hoover Unimelt apparatus and are uncorrected.

ACKNOWLEDGMENTS AND ADDRESSES

Received September 30, 1976, from the *Department of Pharmaceutical Sciences, College of Pharmacy, University of Arizona, Tucson, AZ 85721.*

Accepted for publication December 7, 1976.

Supported in part by Contract N01-CM33750 from the Division of Cancer Treatment, National Cancer Institute, National Institutes of Health, Department of Health, education, and Welfare, Bethesda, MD 20014, and by the Elsa U. Pardee Foundation, Midland, Mich.

[x] To whom inquiries should be directed.

Anthelmintic Dihydroquinoxalino[2,3-*b*]quinoxalines

MICHAEL H. FISHER [x], AINO LUSI, and JOHN R. EGERTON

Abstract □ A series of dihydroquinoxalino[2,3-*b*]quinoxalines was synthesized and tested for anthelmintic activity in a model assay. The most promising compound, 5,12-diacetyl-5,12-dihydroquinoxalino[2,3-*b*]quinoxaline, was orally effective in sheep at a dose of 200 mg/kg against a broad range of helminths.

Keyphrases □ Quinoxalines, substituted—synthesized, anthelmintic activity evaluated □ Dihydroquinoxalino[2,3-*b*]quinoxalines, substituted—synthesized, anthelmintic activity evaluated □ Anthelmintic activity—evaluated in series of substituted dihydroquinoxalino[2,3-*b*]quinoxalines □ Structure–activity relationships—series of substituted dihydroquinoxalino[2,3-*b*]quinoxalines evaluated for anthelmintic activity

In the continuing search for anthelmintic agents of novel structure, dihydroquinoxalino[2,3-*b*]quinoxaline showed erratic but definite anthelmintic activity in a preliminary assay. Therefore, several analogs were synthesized and tested for anthelmintic efficacy.

RESULTS AND DISCUSSION

Fluoflavin was first prepared by Hinsberg and Pollak (1), who formulated the structure as 5,12-dihydroquinoxalino[2,3-*b*]quinoxaline (I). Since then, there has been considerable speculation as to whether the compound is more accurately represented by the tautomeric 5,11-dihydro structure, II. A spectroscopic study (2) indicated that the 5,12-dihydro structure, I, is the most probable, and it is used for fluoflavin derivatives in this report. Derivatives having substituents in the benzo rings also may have ambiguous structures; no attempt was made to establish their exact structures.

The new compounds prepared are listed in Tables I and II together with some previously described compounds. Synthetic procedures, generalized where possible, are described under *Experimental*. All derivatives were synthesized by reacting appropriately substituted 1,2-phenylenediamines with 2,3-dichloroquinoxalines over sodium carbonate in refluxing dimethylformamide (3) (Scheme I). Acylation was generally accomplished by long heating in a large excess of the anhydride. Alternatively, conventional acylation with the acyl halide in pyridine was possible.

The diformyl derivative could only be prepared with 100% formic acid and *N,N'*-dicyclohexylcarbodiimide. Reduction of the nitro derivative (XXVIII) with hydrogen over palladium-on-carbon gave the amine (XXIX), which was acylated with methyl chloroformate to the carbamate (XXX). Oxidation of I with hydrogen peroxide in trifluoroacetic acid gave quinoxalino[2,3-*b*]quinoxaline 5,11-dioxide (XLIII), previously described by Kuhn and Skrabal (4) as the sole product isolated.

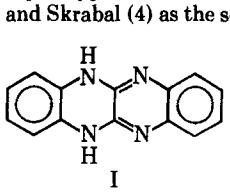

I

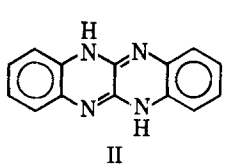

II

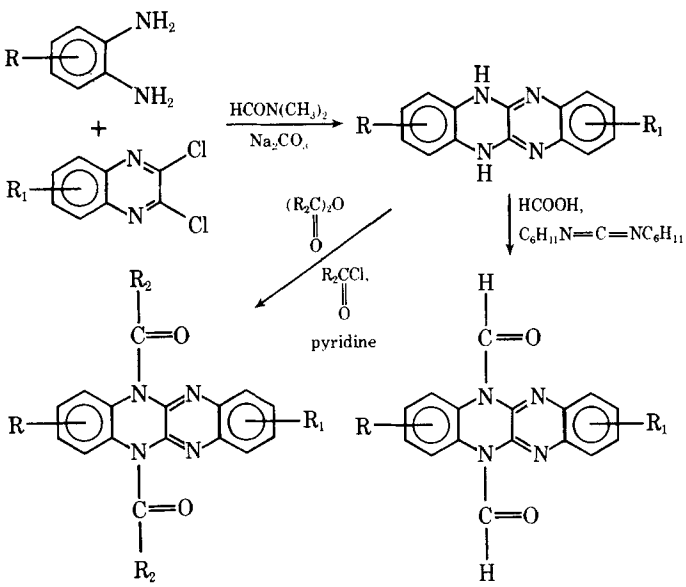

Scheme I

Biological results (the lowest oral doses demonstrating activity) are shown in Tables I and II. Compounds were tested for anthelmintic activity against *Trichostrongylus* in a standard laboratory animal model assay (5). The most potent compounds in the series, VIII–X, were lower acyl derivatives of the unsubstituted I.

The nonacylated compounds were all extremely insoluble; since I showed erratic but definite activity at 400 mg/kg, the main contribution of acylation was to achieve better absorption and distribution of the intrinsically active ring system. Acylation with groups larger than propionyl diminished activity, as did any of the ring substitutions tried. The aromatic analog (XLII) was inactive, but its bis(*N*-oxide) derivative (XLIII) was surprisingly among the most active compounds in the series. 5,12-Diacetyl-5,12-dihydroquinoxalino[2,3-*b*]quinoxaline (IX) was selected as the most promising and evaluated for anthelmintic efficacy in sheep. At an oral dose of 200 mg/kg, it was effective against *Haemonchus contortus, Ostertagia circumcincta, Trichostrongylus axei, Trichostrongylus colubriformis,* and *Cooperia* sp.

EXPERIMENTAL[1]

Method A: 2-Methoxy-5,12-dihydroquinoxalino[2,3-*b*]quinoxaline (XXIII)—A suspension of 20.0 g (0.144 mole) of 4-methoxy-1,2-phenylenediamine, 28.8 g (0.144 mole) of 2,3-dichloroquinoxaline, and 15.3 g (0.144 mole) of sodium carbonate in 100 ml of dimethylformamide was refluxed for 5 hr and then cooled to room temperature. The product was filtered off and crystallized from acetic acid, 23.1 g (60.3%), mp >340°.

[1] Melting points were taken on a Thomas-Hoover Unimelt apparatus and are uncorrected.

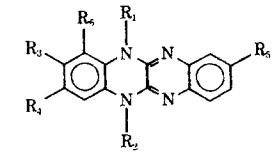

Table I—5,12-Dihydroquinoxalino[2,3-*b*]quinoxalines

Compound	R_1	R_2	R_3	R_4	R_5	R_6	Synthetic Method	Yield, %	Melting Point	Molecular Formula		Analysis, % Calc.	Analysis, % Found	Anthelmintic Activity[a], mg/kg
I	H	H	H	H	H	H	C[b]	—	>350°, >350° (1)	—	—	—	—	400
III	CH_3	H	H	H	H	H	D[c]	—	320°, 317–318° (2)	—	—	—	—	NA
IV	CH_3	CH_3	H	H	H	H	D	—	217°, 218–219° (2)	—	—	—	—	NA
V	C_6H_5	H	H	H	H	H	E[d]	—	323–327°	$C_{20}H_{14}N_4$	N	18.06	17.95	NA
VI	CH_3	$COCH_3$	H	H	H	H	D	—	190–191°, 190–191° (2)	—	—	—	—	NA
VII	C_6H_5	$COCH_3$	H	H	H	H	B	58	215–217°	$C_{22}H_{16}N_4O$	C H N	74.98 4.58 15.90	74.59 4.73 15.77	NA
VIII	CHO	CHO	H	H	H	H	—	37.9	225°	$C_{16}H_{10}N_4O_2$	C H N	66.21 3.45 19.31	66.15 3.27 19.14	100
IX	$COCH_3$	$COCH_3$	H	H	H	H	B	70	203–204°	$C_{18}H_{14}N_4O_2$	C H N	67.91 4.43 17.60	67.75 4.74 17.73	100
X	COC_2H_5	COC_2H_5	H	H	H	H	B	86	155°	$C_{20}H_{18}N_4O_2$	C H N	69.35 5.24 16.18	69.00 5.36 15.82	100
XI	CO-*n*-C_3H_7	CO-*n*-C_3H_7	H	H	H	H	B	55	144–145°	$C_{22}H_{22}N_4O_2$	C H N	70.57 5.92 14.96	70.30 6.04 15.08	400
XII	CO-iso-C_3H_7	CO-iso-C_3H_7	H	H	H	H	B	24	168–170°	$C_{22}H_{22}N_4O_2$	C H N	70.57 5.92 14.96	70.92 5.83 14.72	NA
XIII	COC_6H_5	COC_6H_5	H	H	H	H	—	12	219–220°	$C_{28}H_{18}N_4O_2$	C H N	76.01 4.10 12.66	75.81 4.36 12.57	400
XIV	$COOCH_3$	$COOCH_3$	H	H	H	H	B	20	151–152°	$C_{18}H_{14}N_4O_4$	C H N	61.71 4.03 16.00	61.44 4.10 15.88	200
XV	H	H	CH_3	H	H	H	A	56	350–360°	$C_{15}H_{12}N_4$	C H N	72.56 4.89 22.57	72.26 4.89 22.70	NA
XVI	$COCH_3$	$COCH_3$	CH_3	H	H	H	B	89	140–142°	$C_{19}H_{16}N_4O_2$	C H N	68.66 4.85 16.86	69.03 5.20 16.79	400
XVII	H	H	C_2H_5	H	H	H	A	30	340–345°	$C_{16}H_{14}N_4$	C H N	73.26 5.38 21.36	73.19 5.38 21.31	NA
XVIII	$COCH_3$	$COCH_3$	C_2H_5	H	H	H	B	66	160°	$C_{20}H_{18}N_4O_2$	C H N	69.35 5.24 16.18	69.53 5.39 16.22	NA
XIX	H	H	CF_3	H	H	H	A	76	300–307°	$C_{15}H_9F_3N_4$	C H N	59.61 3.00 18.57	59.47 3.18 18.53	NA
XX	$COCH_3$	$COCH_3$	CF_3	H	H	H	B	38	132–134°	$C_{19}H_{13}F_3N_4O_2$	C H N	59.23 3.14 14.74	59.64 3.17 14.79	NA

XXI	H	H	Cl	H	H	H	E	—	>350°, >350°(6)	—		—	—	NA
XXII	$COCH_3$	$COCH_3$	Cl	H	H	H	B	70	149–150°	$C_{18}H_{13}ClN_4O_2$	C	61.30	61.08	200
											H	3.72	4.03	
											N	15.88	15.64	
XXIII	H	H	OCH_3	H	H	H	A	60.3	>340°	$C_{15}H_{12}N_4O \cdot H_2O$	C	63.82	63.68	NA
											H	4.96	4.66	
											N	19.86	19.69	
XXIV	$COCH_3$	$COCH_3$	OCH_3	H	H	H	B	59	197–198°	$C_{19}H_{16}N_4O_3$	C	65.51	65.71	400
											H	4.63	4.73	
											N	16.08	16.01	
XXV	H	H	OC_2H_5	H	H	H	A	55	>350°	$C_{16}H_{14}N_4O$	C	69.05	69.21	NA
											H	5.07	4.89	
											N	20.13	20.01	
XXVI	$COCH_3$	$COCH_3$	OC_2H_5	H	H	H	B	85	148–151°	$C_{20}H_{18}N_4O_3$	C	66.28	66.14	NA
											H	5.01	5.15	
											N	15.46	15.56	
XXVII	H	H	NO_2	H	H	H	A	16	>350°	$C_{14}H_9N_5O_2$	C	60.20	59.83	NA
											H	3.25	3.31	
											N	25.08	25.33	
XXVIII	$COCH_3$	$COCH_3$	NO_2	H	H	H	B	57	139–141°	$C_{18}H_{13}N_5O_4$	C	59.50	59.43	NA
											H	3.61	3.94	
											N	19.28	19.49	
XXIX	$COCH_3$	$COCH_3$	NH_2	H	H	H	—	33	192–196°	$C_{18}H_{15}N_5O_2$	C	64.85	64.69	NA
											H	4.54	4.48	
											N	21.01	21.15	
XXX	$COCH_3$	$COCH_3$	$NHCOCH_3$	H	H	H	—	14	229–231°	$C_{20}H_{17}N_5O_4$	C	61.37	61.53	NA
											H	4.38	4.54	
											N	17.90	17.64	
XXXI	H	H	H	H	H	NO_2	A	77	>350°	$C_{14}H_9N_5O_2$	C	60.21	60.40	NA
											H	3.25	3.31	
											N	25.08	25.26	
XXXII	$COCH_3$	$COCH_3$	H	H	H	NO_2	B	30	165–168°	$C_{18}H_{13}N_5O_4$	C	59.30	59.35	NA
											H	3.58	3.20	
											N	19.28	19.89	
XXXIII	H	H	Cl	Cl	H	H	A	11	>350°	$C_{14}H_8Cl_2N_4$	C	55.46	55.15	NA
											H	2.66	2.60	
											N	18.48	18.20	
XXXIV	$COCH_3$	$COCH_3$	Cl	Cl	H	H	B	51	220–222°	$C_{18}H_{12}Cl_2N_4O_2$	C	55.83	55.47	NA
											H	3.12	3.15	
											Cl	18.31	18.66	
											N	14.47	14.29	
XXXV	H	H	CH_3	CH_3	H	H	A	68	350–355°	$C_{16}H_{14}N_4$	C	73.26	72.91	NA
											H	5.38	5.40	
											N	21.36	21.51	
XXXVI	$COCH_3$	$COCH_3$	CH_3	CH_3	H	H	B	89	199–203°	$C_{20}H_{18}N_4O_2$	C	69.35	69.43	NA
											H	5.24	5.25	
											N	16.18	16.24	
XXXVII	H	H	Cl	H	Cl	H	E	—	365°, >350° (6)	$C_{14}H_{18}Cl_2N_4$	C	55.46	55.26	NA
											H	2.66	2.60	
											Cl	23.39	23.39	
											N	18.48	18.61	
XXXVIII	$COCH_3$	$COCH_3$	Cl	H	Cl	H	B	55	150–153°	$C_{18}H_{12}Cl_2N_4O_2$	C	55.83	55.87	NA
											H	3.12	3.48	
											N	14.47	14.20	
XXXIX	H	H	NO_2	H	NO_2	H	A	71	>350°	$C_{14}H_8N_6O_4$	C	51.86	52.05	NA
											H	2.49	2.25	
											N	25.92	25.62	
XL	H	H	Cl	H	OCH_3	H	A	49	318–325°	$C_{15}H_{11}ClN_4O$	C	60.31	60.70	NA
											H	3.70	3.62	
											N	18.75	18.72	
XLI	$COCH_3$	$COCH_3$	Cl	H	OCH_3	H	B	95	165–170°	$C_{19}H_{15}ClN_4O_3$	C	59.61	59.93	400
											H	3.95	3.86	
											N	14.63	14.48	

[a] NA = not active at 400 mg/kg. [b] See Ref. 1. [c] See Ref. 2. [d] See Ref. 6. The melting point of V*a* was not given.

Table II—Quinoxalino[2,3-*b*]quinoxalines

Compound	Structure	Synthetic Method	Melting Point	Anthelmintic Activity[a], mg/kg
XLII	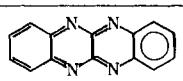	C[b]	>350°, >350° (1)	NA
XLIII[c]	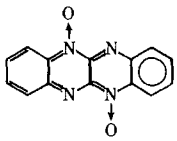	F[d]	>350°	100

[a] NA = not active at 400 mg/kg. [b] See Ref. 1. [c] *Anal.*—Calc. for $C_{18}H_{18}N_4O_2$: C, 63.63; H, 3.05; N, 21.20. Found: C, 63.46; H, 3.00; N, 21.09. [d] See Ref. 4. The melting point was not given.

Method B: 5,12-Diacetyl-5,12-dihydroquinoxalino[2,3-*b*]quinoxaline (IX)—A suspension of 1.0 g (0.004 mole) of I in 50 ml of acetic anhydride was refluxed for 20 hr until a clear solution was obtained. Excess acetic anhydride was evaporated, and the residue was crystallized from ethyl acetate, 0.95 g (70%), mp 203–204°.

5,12 - Diformyl -5,12- dihydroquinoxalino[2,3 - *b*]quinoxaline (VIII)—A mixture of 2.3 g (0.01 mole) of I, 0.94 g (0.02 mole) of 98–100% formic acid, and 4.12 g (0.020 mole) of *N,N'*-dicyclohexylcarbodiimide in 100 ml of dry dioxane was heated at 100° for 22 hr and then cooled. The dicyclohexylurea was filtered off, and the filtrate was evaporated. The residue was dissolved in benzene and filtered, and petroleum ether was added to the filtrate to crystallize the product, 1.1 g (37.9%), mp 225°.

5,12 - Dibenzoyl -5,12- dihydroquinoxalino[2,3 - *b*]quinoxaline (XIII)—A mixture of 1.0 g (0.004 mole) of I and 2 ml of benzoyl chloride in 10 ml of pyridine was allowed to stand at room temperature for 3 days. Addition of petroleum ether precipitated the product, which was crystallized from ethyl acetate, 0.23 g (12%), mp 219–220°.

8-Amino-5,12-diacetyl-5,12-dihydroquinoxalino[2,3-*b*]quinoxaline (XXIX)—A suspension of 1.09 g (0.0030 mole) of 5,12-diacetyl-8-nitro-5,12-dihydroquinoxalino[2,3-*b*]quinoxaline (XXVIII) and 0.11 g of palladium-on-carbon in 50 ml of dimethoxyethane was reduced with hydrogen at 25 psi. After filtration and evaporation of the solvent, the residue was crystallized from a mixture of ethyl acetate and ether, 300 mg (33%), mp 192–196°.

Methyl *N*-(5,12-Diacetyl-5,12-dihydroquinoxalino[2,3-*b*]-quinoxalin-8-yl)carbamate (XXX)—A solution of 0.74 g (0.0022 mole) of XXIX in 12.5 ml of pyridine was acylated by treatment with 2 g of methyl chloroformate at room temperature for 90 hr. The product was precipitated by addition of water and crystallized from methylene chloride, 0.125 g (14%), mp 229–231°.

REFERENCES

(1) O. Hinsberg and J. Pollak, *Chem. Ber.*, **29**, 784 (1896).
(2) G. M. Badger and P. J. Nelson, *Aust. J. Chem.*, **16**, 445 (1963).
(3) G. Riedel and W. Deutschel, British pat. 971,048 (1964); through *Chem. Abstr.*, **62**, 1774 (1965).
(4) R. Kuhn and P. Skrabal, *Chem. Ber.*, **101**, 3913 (1968).
(5) J. E. Lynch and B. Nelson, *J. Parasitol.*, **45**, 659 (1969).
(6) F. Kehrmann and C. Bener, *Helv. Chim. Acta*, **8**, 20 (1925).

ACKNOWLEDGMENTS AND ADDRESSES

Received October 12, 1976, from the *Merck Sharp & Dohme Research Laboratories, Division of Merck & Co., Inc., Rahway, NJ 07065.*

Accepted for publication December 1, 1976.

The authors thank Mr. R. N. Boos and associates for microanalyses.

[x] To whom inquiries should be directed.

Molecular Connectivity and Steric Parameters

WALLACE J. MURRAY

Abstract □ The possible relationship between molecular connectivity indexes, $^m\chi$, and E_s, a thermodynamically derived parameter used to estimate steric effects in organic reactions and sometimes used in biological structure–activity relationships, was investigated. The extended χ terms, $^2\chi$, $^3\chi$, and $^4\chi$, were correlated significantly to E_s (r = 0.961). Aralkyl esters deviated from the correlations, possibly due to intramolecular interactions.

Keyphrases □ Molecular connectivity indexes—relationship to E_s parameter used to estimate steric effects in organic reactions □ Steric parameters—E_s used to estimate steric effects in organic reactions correlated to molecular connectivity indexes □ Topological indexes—molecular connectivity indexes, relationship to E_s parameter used to estimate steric effects in organic reactions

The way atoms are connected to one another in a compound must ultimately influence the compound's physical and chemical properties. Changes in chemical structure most often lead to changes in biological activity. In correlating chemical structure and biological activity, statistical regression analyses, in which various physicochemical properties are used as surrogates for chemical structure, are used. These analyses have been called quantitative structure–activity relationships. The use of this term is unfortunate, since the properties of a molecule are not a description of the structure but rather are consequences of the structure. One is not relating structure to property but property to property. Norrington *et al.* (1) suggested the use of the term property–activity relationships to differentiate these methods from structure-based ones such as methods employing quantum mechanical calculations or the Free and Wilson approach (2).

Table II—Quinoxalino[2,3-*b*]quinoxalines

Compound	Structure	Synthetic Method	Melting Point	Anthelmintic Activity[a], mg/kg
XLII	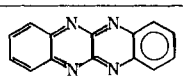	C[b]	>350°, >350° (1)	NA
XLIII[c]	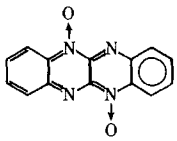	F[d]	>350°	100

[a] NA = not active at 400 mg/kg. [b] See Ref. 1. [c] *Anal.*—Calc. for $C_{18}H_{18}N_4O_2$: C, 63.63; H, 3.05; N, 21.20. Found: C, 63.46; H, 3.00; N, 21.09. [d] See Ref. 4. The melting point was not given.

Method B: 5,12-Diacetyl-5,12-dihydroquinoxalino[2,3-*b*]quinoxaline (IX)—A suspension of 1.0 g (0.004 mole) of I in 50 ml of acetic anhydride was refluxed for 20 hr until a clear solution was obtained. Excess acetic anhydride was evaporated, and the residue was crystallized from ethyl acetate, 0.95 g (70%), mp 203–204°.

5,12 - Diformyl -5,12- dihydroquinoxalino[2,3 - *b*]quinoxaline (VIII)—A mixture of 2.3 g (0.01 mole) of I, 0.94 g (0.02 mole) of 98–100% formic acid, and 4.12 g (0.020 mole) of *N,N'*-dicyclohexylcarbodiimide in 100 ml of dry dioxane was heated at 100° for 22 hr and then cooled. The dicyclohexylurea was filtered off, and the filtrate was evaporated. The residue was dissolved in benzene and filtered, and petroleum ether was added to the filtrate to crystallize the product, 1.1 g (37.9%), mp 225°.

5,12 - Dibenzoyl -5,12- dihydroquinoxalino[2,3 - *b*]quinoxaline (XIII)—A mixture of 1.0 g (0.004 mole) of I and 2 ml of benzoyl chloride in 10 ml of pyridine was allowed to stand at room temperature for 3 days. Addition of petroleum ether precipitated the product, which was crystallized from ethyl acetate, 0.23 g (12%), mp 219–220°.

8-Amino-5,12-diacetyl-5,12-dihydroquinoxalino[2,3-*b*]quinoxaline (XXIX)—A suspension of 1.09 g (0.0030 mole) of 5,12-diacetyl-8-nitro-5,12-dihydroquinoxalino[2,3-*b*]quinoxaline (XXVIII) and 0.11 g of palladium-on-carbon in 50 ml of dimethoxyethane was reduced with hydrogen at 25 psi. After filtration and evaporation of the solvent, the residue was crystallized from a mixture of ethyl acetate and ether, 300 mg (33%), mp 192–196°.

Methyl *N*-(5,12-Diacetyl-5,12-dihydroquinoxalino[2,3-*b*]-quinoxalin-8-yl)carbamate (XXX)—A solution of 0.74 g (0.0022 mole) of XXIX in 12.5 ml of pyridine was acylated by treatment with 2 g of methyl chloroformate at room temperature for 90 hr. The product was precipitated by addition of water and crystallized from methylene chloride, 0.125 g (14%), mp 229–231°.

REFERENCES

(1) O. Hinsberg and J. Pollak, *Chem. Ber.*, **29**, 784 (1896).
(2) G. M. Badger and P. J. Nelson, *Aust. J. Chem.*, **16**, 445 (1963).
(3) G. Riedel and W. Deutschel, British pat. 971,048 (1964); through *Chem. Abstr.*, **62**, 1774 (1965).
(4) R. Kuhn and P. Skrabal, *Chem. Ber.*, **101**, 3913 (1968).
(5) J. E. Lynch and B. Nelson, *J. Parasitol.*, **45**, 659 (1969).
(6) F. Kehrmann and C. Bener, *Helv. Chim. Acta*, **8**, 20 (1925).

ACKNOWLEDGMENTS AND ADDRESSES

Received October 12, 1976, from the *Merck Sharp & Dohme Research Laboratories, Division of Merck & Co., Inc., Rahway, NJ 07065.*

Accepted for publication December 1, 1976.

The authors thank Mr. R. N. Boos and associates for microanalyses.

[x] To whom inquiries should be directed.

Molecular Connectivity and Steric Parameters

WALLACE J. MURRAY

Abstract □ The possible relationship between molecular connectivity indexes, $^m\chi$, and E_s, a thermodynamically derived parameter used to estimate steric effects in organic reactions and sometimes used in biological structure–activity relationships, was investigated. The extended χ terms, $^2\chi$, $^3\chi$, and $^4\chi$, were correlated significantly to E_s (r = 0.961). Aralkyl esters deviated from the correlations, possibly due to intramolecular interactions.

Keyphrases □ Molecular connectivity indexes—relationship to E_s parameter used to estimate steric effects in organic reactions □ Steric parameters—E_s used to estimate steric effects in organic reactions correlated to molecular connectivity indexes □ Topological indexes—molecular connectivity indexes, relationship to E_s parameter used to estimate steric effects in organic reactions

The way atoms are connected to one another in a compound must ultimately influence the compound's physical and chemical properties. Changes in chemical structure most often lead to changes in biological activity. In correlating chemical structure and biological activity, statistical regression analyses, in which various physicochemical properties are used as surrogates for chemical structure, are used. These analyses have been called quantitative structure–activity relationships. The use of this term is unfortunate, since the properties of a molecule are not a description of the structure but rather are consequences of the structure. One is not relating structure to property but property to property. Norrington *et al.* (1) suggested the use of the term property–activity relationships to differentiate these methods from structure-based ones such as methods employing quantum mechanical calculations or the Free and Wilson approach (2).

Table I—Ester Hydrolysis Data [a] *versus* Molecular Connectivity Index

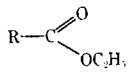

R	$^1\chi$	log k/k_0 (obs)	log k/k_0 (calc)
H	0.000	1.24	0.58
CH_3	0.707	0.00	0.38
C_2H_5	1.207	−0.07	−0.04
C_3H_7	1.707	−0.36	−0.58
n-C_4H_9	2.207	−0.39	−0.66
n-C_5H_{11}	2.707	−0.40	−0.71
$(CH_3)_2CHCH_2CH_2$	2.563	−0.35	−0.84
$C_6H_5CH_2$	2.264	−0.38	−0.93
$C_6H_5CH_2CH_2$	2.764	−0.43	−0.53
$C_6H_5CH_2CH_2CH_2$	3.264	−0.45	−1.22
$(CH_3)_2CH$	1.563	−0.47	−0.43
cyclo-C_6H_{11}	3.225	−0.79	−0.30
$(CH_3)_2CHCH_2$	2.063	−0.93	−1.23
cyclo-$C_6H_{11}CH_2$	3.725	−0.98	−1.27
$CH_3CH(CH_2CH_3)_2$	2.100	−1.13	−1.28
$C_6H_5CHCH_3$	3.185	−1.19	−1.58
$C_6H_5CHC_2H_5$	3.315	−1.50	−1.71
$(CH_3)_3C$	1.854	−1.54	−0.99
$(C_6H_5)_2CH$	4.808	−1.76	−1.73
$(CH_3CH_2)_2CH$	2.639	−1.98	−1.32
$C_6H_5CH{=}CH$	2.941	−1.99	−1.17
C_6H_5	2.265	−2.55	−0.93

[a] Data from Ref. 15.

BACKGROUND

Attempts have been made to develop a numerical description of a molecule derived not from experimental measurements of a property but from knowledge of the molecular structure itself (3–5). The molecular topological approach transcribes molecular structure into a topological graph from which is derived a number, the topological index. Attempts are then made to correlate these indexes to physicochemical properties. One such correlation, suggested by Randić (6) to describe the effects of branching, subsequently was developed into the molecular connectivity index, χ (7).

Molecular connectivity is a term used to describe molecular structure in terms of the attachments of constituent atoms in a molecule. Knowing the manner in which the atoms are attached permits calculation of χ, which seemingly encodes within it the additive and constitutive natures of a molecule. In a series of studies (7–10), χ was correlated significantly to several physicochemical properties.

One physicochemical property that correlated in a highly significant manner with χ ($r > 0.9990$) is molar refraction (5, 7). This property, often used in property–activity relationships (11), reflects the bulk or steric nature of a group (11, 12). Since χ shows such significant correlation to one steric parameter useful in property–activity relationships, its correlation with another parameter used to estimate steric effects, the E_s value of Taft (13), was investigated and is the subject of this report.

The parameter E_s has been particularly useful in reactions where the substituent is near the reaction center. It also was employed in property–activity relationship studies (14), but its usefulness is limited by the lack of experimental data. By showing a correlation between χ or extended terms of χ, it might be feasible to use these terms as estimators of steric hindrance terms in structure–activity relationships.

It seemed plausible that use of extended terms in χ ($^m\chi$) might be especially likely to yield good correlations, since these terms allow the inclusion of cluster subgraphs (5). Clusters of substituents around a reaction center would seem logically important in determining E_s values.

EXPERIMENTAL

Chi (χ) terms are computed from a hydrogen-suppressed formula or graph of the molecule. The simplest term, designated $^1\chi$ and called a connectivity χ, is computed by:

$$^1\chi = \sum(\delta_i\delta_j)^{-1/2} \qquad \text{(Eq. 1)}$$

where the sum is over all connections or edges in the hydrogen-suppressed graph, and δ_i and δ_j are numbers assigned to each atom reflecting the number of atoms adjacent or connected to atoms i and j, which are formally bonded. The nature of the atom is not considered in the calculation.

An extended term of χ of the order $^2\chi$ is computed from:

$$^2\chi = \sum(\delta_i\delta_j\delta_k)^{-1/2} \qquad \text{(Eq. 2)}$$

where i, j, and k are atoms bonded in sequence or in a path, and the sum is over all distinct sets of two-edge paths. In general, extended terms of χ, $^m\chi_p$, are computed for linear paths, p, of m bonds by:

$$^m\chi_p = \sum_{s=1}^{n_m} \prod_{i}^{m+1} (\delta_i)_s^{-1/2} \qquad \text{(Eq. 3)}$$

where n_m is the number of paths with m edges, and s identifies a particular subgraph.

Terms describing nonlinear arrangements of bonds such as clusters of three bonds, $^3\chi_C$, and circuits (or chains) of six atoms, $^6\chi_{CH}$, are computed in the same way. Examples of these extended term calculations are shown in Ref. 10.

Briefly, the nature of χ may be summarized by stating that it is a nonempirical, simply computed number (or numbers) that is a weighted count of bonds and connected sets of bonds. The weighting is based on the connectivity of each atom in a bond formula or graph of the molecule. The expectation is that χ or terms of χ encode within them structural information that is adequate to relate to numerous geometrical, physical, and even biological properties.

RESULTS AND DISCUSSION

To quantitate the steric effect of substituents on reactions rates, Taft (15) studied the esterification and hydrolysis rates of a series of aliphatic

Table II—Aliphatic E_s Values *versus* Molecular Connectivity Indexes [a]

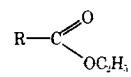

R	E_s(obs[b])	E_s(calc)	$^1\chi$	$^2\chi$	$^3\chi$	$^4\chi$
CH_3	0.00	0.27	0.707	0.000	0.000	0.000
CH_3CH_2	−0.07	0.04	1.207	0.500	0.000	0.000
$(CH_3)_2CH$	−0.47	−0.37	1.563	1.394	0.000	0.000
$(CH_3)_3C$	−1.54	−0.92	1.854	2.561	0.000	0.000
$CH_3(CH_2)_2$	−0.36	−0.60	1.707	0.854	0.354	0.000
$CH_3(CH_2)_3$	−0.39	−0.87	2.207	1.207	0.604	0.250
$(CH_3CH_2)_2CH$	−1.98	−1.81	2.639	1.683	0.866	0.289
$CH_3(CH_2)_4$	−0.40	−0.73	2.707	1.561	0.854	0.427
$(CH_3)_2CHCH_2CH_2$	−0.38	−1.36	2.563	2.036	0.781	0.408
$(CH_3)_3CCH_2$	−1.74	−2.06	2.354	2.811	0.750	0.000
$(CH_3CH_2CH_2)_2CH$	−2.11	−1.87	3.639	2.443	1.394	0.961
$(CH_3)_2CHCH_2CH(CH_3)$	−1.85	−1.88	3.247	3.462	0.961	1.045
$(CH_3)_2CHCH_2CHCH_2(CH_3)_2$	−2.47	−2.51	4.625	4.072	1.971	1.633
$(CH_3)_3CCH_2C(CH_3)_2$	−2.57	−1.78	3.561	5.109	1.362	1.436
$[(CH_3)_3CH_2]_2CH$	−3.18	−3.50	4.932	6.030	1.802	1.804
$(CH_3)_3CC(CH_3)_2$	−3.90	−3.28	3.104	4.134	2.030	0.000
$(CH_3CH_2)_3C$	−3.80	−4.22	3.536	2.561	2.250	0.750
$(CH_3)_3CH_2C(CH_3)C(CH_3)_3$	−4.00	−3.72	4.811	6.548	2.731	1.436

[a] Since the functional group $COOC_2H_5$ remains constant, a connection value, $\delta = 2$, was arbitrarily assigned to this group to facilitate calculations. [b] Data from Ref. 11.

and aryl esters. These studies led to the linear free energy-derived parameters, E_s, which are measures of the influence of steric factors associated with substituents in reaction rates.

Logically, groups clustering around a reaction center, *e.g.*, the C(=O)O$^-$ group of esters, will have the greatest influence on reaction rates dependent on steric effects. Extended χ terms, *e.g.*, $^2\chi$ and $^3\chi$, should reflect this clustering; therefore, a good correlation of E_s with these parameters should be expected.

The original hydrolysis data of a mixture of esters were examined first (Table I) (15). These data did not give a good correlation with any χ term. The best correlation was given when extended χ terms were utilized:

$$E_s = -0.566(\pm0.235)^2\chi - 1.22(\pm0.548)^3\chi + 2.14(\pm0.880)^4\chi + 0.387(\pm0.304) \quad \text{(Eq. 4)}$$
$$r = 0.738 \quad s = 0.610 \quad n = 22.0$$

This quality of correlation was not as high as expected and did not match previous correlations with other physicochemical properties (7–10). The problem is complex because combined with the purely topological aspect is a variable influence due to interactions across space. Since it was suspected that the aryl esters were leading to anomalous results, the aryl esters were deleted and the E_s values for 18 aliphatic esters were examined (13). Table II lists the data of E_s, their extended χ terms, and calculated E_s values using the equation giving the best fit.

The resulting correlation equations, correlation coefficients, and standard errors are:

$$E_s = -0.976(\pm0.135)^1\chi + 0.991(\pm0.397) \quad \text{(Eq. 5)}$$
$$r = 0.868 \quad s = 0.768 \quad n = 19$$

$$E_s = -1.161(\pm0.185)^3\chi - 0.056(\pm0.231) \quad \text{(Eq. 6)}$$
$$r = 0.904 \quad s = 0.662 \quad n = 19$$

$$E_s = -0.218(\pm0.018)^2\chi - 1.24(\pm0.261)^3\chi + 0.138(\pm0.241) \quad \text{(Eq. 7)}$$
$$r = 0.922 \quad s = 0.620 \quad n = 19$$

$$E_s = -0.544(\pm0.133)^2\chi - 1.40(\pm0.199)^3\chi + 1.09(\pm0.328)^4\chi + 0.403(\pm0.208) \quad \text{(Eq. 8)}$$
$$r = 0.961 \quad s = 0.460 \quad n = 19$$

The index $^1\chi$ does not give a good correlation with E_s ($r = 0.868$) and reflects primarily path length and, in general, steric bulk characteristics. It does not represent adequately steric influence around a reactive site. In terms of single χ parameters, $^3\chi$ gave the best correlation ($r = 0.904$, $s = 0.662$). A dual-parameter fit with $^2\chi$ and $^3\chi$ improved the correlation ($r = 0.922$, $s = 0.620$), and the three-parameter equation with $^2\chi$, $^3\chi$, and $^4\chi$ gave the best correlation ($r = 0.961$, $s = 0.460$).

These data suggest that extended χ terms are a good measure of intramolecular steric effects, especially when substituents are surrounding the reaction center and especially for aliphatic substituents. Previous high correlations with molar refraction (5, 7) indicate that $^1\chi$ terms give adequate representation of general bulk or steric bulk characteristics.

The poor correlation of χ terms with the aryl esters might be explained as follows. The aryl esters were of the form $C_6H_5(CH_2)_nCOOR$, where n varied from 1 to 3. With sufficient flexibility, there is a possibility for the ester group to fold over the aromatic ring, enabling the π-electrons of the phenyl ring to interact with the ester functional group (Structure I). This intramolecular interaction might be sufficient to affect hydrolysis of the ester moiety.

Several studies (16, 17) reported a similar problem when investigating the effects of the side chains of phenylpropyl derivatives on partition coefficients. The interaction of the side-chain substituent with the π-electrons of the phenyl ring was suggested to result in a folding together of these two portions of the molecule, leading to a more compact structure and a greater than expected water solubility (16).

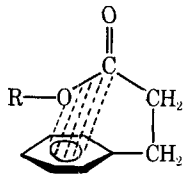

I

The use of extended χ terms as a measure of the effect of clustering about a reaction center or potential pharmacophoric group is a potentially powerful structure–activity relationship tool in drug analysis. For example, if a drug molecule possesses a site particularly susceptible to metabolic attack, *e.g.*, an ester group, calculation of χ cluster terms about that group should reflect the relative effect of steric hindrance of immediate neighbors on metabolic attack. Another possible application could be the determination of the effect of steric hindrance about a pharmacophoric group affecting the approach of drug to receptor features.

Structure–activity relationships in which $^1\chi$ terms are significantly correlated to biological activity might be viewed as reflecting a generalized dependence of activity on bulk, since $^1\chi$ was correlated significantly to molar refraction (7). It could also reflect a dependence on solubility or partitioning ability since $^1\chi$ also showed a significant correlation with these properties (8, 9). If, however, biological activity correlated significantly with extended χ terms, *e.g.*, $^3\chi$, then one should suspect the influence of steric hindrance effects about some pharmacophoric group.

REFERENCES

(1) F. E. Norrington, R. M. Hyde, S. G. Williams, and R. Wootton, *J. Med. Chem.*, **18**, 604 (1975).

(2) S. M. Free, Jr., and J. W. Wilson, *ibid.*, **7**, 395 (1964).

(3) D. H. Rouvray, *Am. Sci.*, **61**, 729 (1973).

(4) D. H. Rouvray, *J. Chem. Educ.*, **52**, 768 (1975).

(5) L. B. Kier and L. H. Hall, "Molecular Connectivity in Chemistry and Drug Research," Academic, New York, N.Y., 1976.

(6) M. Randić, *J. Am. Chem. Soc.*, **97**, 6609 (1975).

(7) L. B. Kier, L. H. Hall, W. J. Murray, and M. Randić, *J. Pharm. Sci.*, **64**, 1971 (1975).

(8) L. H. Hall, L. B. Kier, and W. J. Murray, *ibid.*, **64**, 1974 (1975).

(9) W. J. Murray, L. H. Hall, and L. B. Kier, *ibid.*, **64**, 1978 (1975).

(10) L. B. Kier, L. H. Hall, W. J. Murray, and M. Randić, *ibid.*, **65**, 1226 (1976).

(11) C. Silipo and C. Hansch, *J. Am. Chem. Soc.*, **97**, 6849 (1975).

(12) C. Hansch, A. Leo, S. H. Unger, K. H. Kim, D. Nikaitani, and E. J. Lien, *J. Med. Chem.*, **16**, 1207 (1973).

(13) R. W. Taft, in "Steric Effects in Organic Chemistry," M. S. Newman, Ed., Wiley, New York, N.Y., 1956, p. 556.

(14) E. Kutter and C. Hansch, *J. Med. Chem.*, **12**, 647 (1969).

(15) R. W. Taft, Jr., *J. Am. Chem. Soc.*, **74**, 3120 (1952).

(16) C. Hansch and S. M. Anderson, *J. Org. Chem.*, **32**, 2583 (1967).

(17) G. G. Nys and R. F. Rekker, *Eur. J. Med. Chem.*, **9**, 361 (1974).

ACKNOWLEDGMENTS AND ADDRESSES

Received April 28, 1976, from the *College of Pharmacy, University of Nebraska Medical Center, Omaha, NE 68105.*

Accepted for publication November 15, 1976.

Presented in part at the Medicinal Chemistry Section, APhA Academy of Pharmaceutical Sciences, New Orleans meeting, April 1976.

The author thanks Dr. L. B. Kier and Dr. L. H. Hall for their helpful suggestions and the Lederle Laboratories for a Pharmacy Faculty award.

Indolizine Derivatives with Biological Activity II: *N'*-Substituted Hydrazides of 2-Methyl-3-indolizinecarboxylic Acid

FRANCESCO CLAUDI ˣ, MARIO GRIFANTINI, UGO GULINI, SANTE MARTELLI, and PAOLO NATALINI *

Abstract □ Synthesis and study of the antimonoamine oxidase activity of some *N'*-substituted hydrazides of 2-methyl-3-indolizinecarboxylic acid are reported. The activities were generally of about the same order as those of the corresponding hydrazides of 2-indolizinecarboxylic acid.

Keyphrases □ Indolizine derivatives—various *N'*-substituted hydrazides of 2-methyl-3-indolizinecarboxylic acid synthesized, evaluated for effect on monoamine oxidase activity □ Hydrazides, *N'*-substituted—of 2-methyl-3-indolizinecarboxylic acid synthesized, evaluated for effect on monoamine oxidase activity □ Monoamine oxidase activity—effect of various *N'*-substituted hydrazides of 2-methyl-3-indolizinecarboxylic acid □ Structure–activity relationships—various *N'*-substituted hydrazides of 2-methyl-3-indolizinecarboxylic acid synthesized, evaluated for effect on monoamine oxidase activity

Previously (1), the synthesis and *in vitro* antimonoamine oxidase activity of a series of *N'*-substituted hydrazides of 2-indolizinecarboxylic acid, analogs of the well-known hydrazides of indolecarboxylic acids (2), were reported. The compounds were prepared for an investigation on analogs of biologically active indole derivatives in which indole was replaced by indolizine, which is related to it in structure and reactivity. To study structure–activity relationships in this new type of monoamine oxidase inhibitor, a series of *N'*-substituted hydrazides of 2-methyl-3-indolizinecarboxylic acid was prepared to determine the importance of the type of acyl radical.

In hydrazides of indolecarboxylic acids having the same alkyl radical on the *N'*-nitrogen, the activity is greater, at least within the limits in which such comparisons can be made, for derivatives in the 3-position (2).

EXPERIMENTAL

Chemistry—The *N'*-substituted hydrazides of 2-methyl-3-indolizinecarboxylic acid (XIV–XXII) were synthesized according to Scheme I. By reaction with aldehydes and ketones, 2-methyl-3-indolizinecarbohydrazide (I) provided the corresponding hydrazides (II–XIII) which were reduced with sodium borohydride.

It was not possible to reduce the *p*-methylbenzylidenehydrazide (X) by this method, and it was effected with lithium aluminum hydride. In spite of numerous attempts under various experimental conditions, it was not possible to reduce the benzylidenehydrazide (VIII), the 3,4-methylenedioxybenzylidenehydrazide (IX), and the α-methylbenzylidenehydrazide (XI) by the methods described. At the end of each reduction, the IR spectrum of the product obtained lacked the band characteristic of the C=N group of the initial hydrazides.

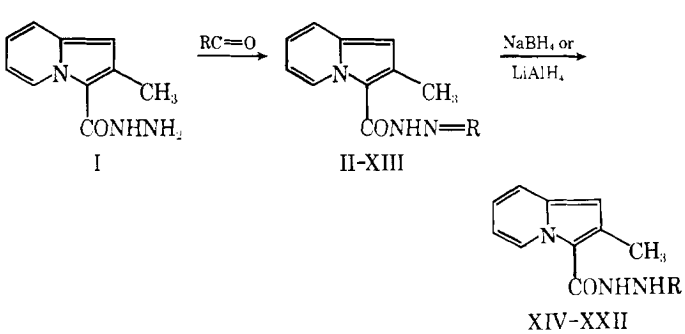

I II-XIII XIV-XXII

Scheme I

Synthesis[1]—*N'-Alkylidene- and N'-Arylalkylidenehydrazides (II–XIII)*—The appropriate aldehyde or ketone (0.006 mole) was added to a solution of 0.005 mole of I (3) in 65 ml of methanol. The mixture was stirred at room temperature or was heated for various times. With the 3,4-methylenedioxybenzaldehyde and ketones, the reaction was promoted by the addition of 0.005 mole of acetic acid. The products precipitated directly on cooling or by concentration of the solution and were crystallized from anhydrous ethanol (Table I).

N'-Alkyl- and N'-Arylalkyl-2-methyl-3-indolizinecarbohydrazides (XIV–XIX, XXI, and XXII)—Sodium borohydride (0.10–0.20 mole) was added slowly and with stirring to 0.021 mole of the appropriate hydrazide (II–VII, XII, or XIII) dissolved in the minimum amount of solvent. After the addition, stirring was continued for 5 hr. Then the solvent was driven off under vacuum, and the residue was treated with water and extracted with ether. The organic solution was dried over sodium sulfate, and the solvent was removed under reduced pressure. The residue was recrystallized from anhydrous ethanol (Table II).

N'-p-Methylbenzyl-2-methyl-3-indolizinecarbohydrazide (XX)—Compound X (0.0046 mole), in 50 ml of anhydrous tetrahydrofuran, was added to a suspension of 0.021 mole of lithium aluminum hydride in 20 ml of anhydrous tetrahydrofuran. The mixture was boiled under reflux for 5 hr and was stirred overnight at room temperature. Excess lithium aluminum hydride was destroyed with water-saturated ether. The mixture was filtered, the solvent was driven off from the filtrate under reduced pressure, and the residue was recrystallized from anhydrous ethanol, yielding 45%, mp 124–125°.

Antimonoamine Oxidase Activity *In Vitro*—The compounds (Table II) were tested *in vitro* as inhibitors of pig plasma monoamine oxidase at 37° and pH 6.98 using a spectrophotometer[2] at 253 nm. The enzyme preparation and the test procedure were described previously (1). The inhibitors were added as solutions in dioxane. The I_{50} values (I_{50} = molar concentration of the inhibitor producing 50% inhibition) were calculated graphically.

RESULTS AND DISCUSSION

All compounds tested were 3–7.5 times as active as iproniazid, used as a reference standard, in the inhibition of monoamine oxidase (Table II). In comparison to the corresponding hydrazides derived from 2-indolizinecarboxylic acid (1), I, XIV–XX, and XXII were less active, even if sometimes only slightly; the exception was XXI. The unsubstituted hydrazide (I) showed an activity one-tenth of that of the hydrazide of the preceding series (1). Apart from this last case, however, the position of the acyl radical in the indolizine system apparently did not have an excessively important role in the activity of the compound.

Concerning the type of substituent on the *N'*-nitrogen of the hydrazide chain, arylalkyl groups generally exercised a more favorable influence than simple alkyl groups. In the series having the alkyl group, the activity decreased with an increase in chain length (XIV–XVI); with the same number of carbons, branching appeared to have a positive effect (XVI and XVII).

[1] Melting points were determined with a Büchi apparatus and are not corrected. IR spectra were taken in mineral oil using a Perkin-Elmer 257 spectrophotometer.

[2] Cary 118.

Table I—*N'*-Alkylidene- and *N'*-Arylalkylidenehydrazides

Compound	R	Reaction Time, hr/ Reaction Temperature	Melting Point	Yield, %	Molecular Formula	Analysis, % Calc.	Found
II	$CHCH_3$	3/20°	177–179°	73	$C_{12}H_{13}N_3O$	C 66.95 H 6.09 N 19.52	67.11 6.03 19.41
III	$CHCH_2CH_3$	12/20°	148–150°	65	$C_{13}H_{15}N_3O$	C 68.10 H 6.59 N 18.33	68.21 6.54 18.11
IV	$CHCH_2CH_2CH_3$	12/20°	158–159°	76	$C_{14}H_{17}N_3O$	C 69.11 H 7.04 N 17.27	68.97 7.13 17.04
V	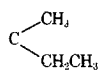	3/40°	101–102°	65	$C_{14}H_{17}N_3O$	C 69.11 H 7.04 N 17.27	69.21 6.94 17.15
VI		2/40°	158–160°	75	$C_{15}H_{17}N_3O$	C 70.56 H 6.71 N 16.46	70.42 6.88 16.31
VII		3/40°	130–131°	70	$C_{16}H_{19}N_3O$	C 71.34 H 7.11 N 15.60	71.62 7.14 15.48
VIII		12/20°	190–192°	86	$C_{17}H_{15}N_3O$	C 73.63 H 5.45 N 15.15	73.70 5.71 15.02
IX	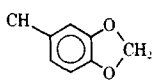	1/20°	202–204°	88	$C_{18}H_{15}N_3O_3$	C 67.28 H 4.71 N 13.08	67.12 4.72 13.20
X	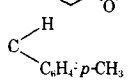	1/40°	185–187°	80	$C_{18}H_{17}N_3O$	C 74.20 H 5.88 N 14.42	74.02 5.80 14.35
XI		24/50°	167–169°	74	$C_{18}H_{17}N_3O$	C 74.20 H 5.88 N 14.42	74.29 5.91 14.59
XII	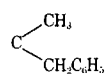	2/40°	130–131°	81	$C_{19}H_{19}N_3O$	C 74.73 H 6.27 N 13.76	74.87 6.12 13.54
XIII	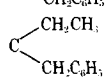	8/40°	118–119°	82	$C_{20}H_{21}N_3O$	C 75.21 H 6.63 N 13.16	75.37 6.71 13.40

Table II—*N'*-Alkyl- and *N'*-Arylalkyl-2-methyl-3-indolizinecarbohydrazides and Their Monoamine Oxidase Inhibitory Activity

Compound	R	Reaction Solvent[a]	Melting Point	Yield, %	I_{50}	X[b]	Molecular Formula	Analysis, % Calc.	Found
Iproniazid		—	—	—	9.42×10^{-4}	1	—	—	—
I	H	—	—	—	1.6×10^{-4}	5.89	—	—	—
XIV	CH_2CH_3	A	127–128°	75	2.15×10^{-4}	4.38	$C_{12}H_{15}N_3O$	C 66.34 H 6.96 N 19.34	66.50 7.01 19.52
XV	$CH_2CH_2CH_3$	A	113–114°	79	2.45×10^{-4}	3.84	$C_{13}H_{17}N_3O$	C 67.50 H 7.41 N 18.17	67.61 7.29 18.29
XVI	$CH_2CH_2CH_2CH_3$	A	95–97°	60	3.14×10^{-4}	3	$C_{14}H_{19}N_3O$	C 68.54 H 7.81 N 17.13	68.62 7.70 17.19
XVII		A	94–95°	72	2.08×10^{-4}	4.53	$C_{14}H_{19}N_3O$	C 68.54 H 7.81 N 17.13	68.71 7.92 16.97
XVIII		B	121–123°	63	2.25×10^{-4}	4.19	$C_{15}H_{19}N_3O$	C 70.00 H 7.44 N 16.33	70.13 7.35 16.22
XIX		B	121–122°	71	2.5×10^{-4}	3.77	$C_{16}H_{21}N_3O$	C 70.82 H 7.80 N 15.49	70.65 7.64 15.68
XX	$CH_2C_6H_4$-*p*-CH_3	—	124–125°	45	1.87×10^{-4}	5.04	$C_{18}H_{19}N_3O$	C 73.69 H 6.53 N 14.33	73.87 6.49 14.48
XXI		A	103–104°	83	1.26×10^{-4}	7.48	$C_{19}H_{21}N_3O$	C 74.24 H 6.89 N 13.67	74.45 6.81 13.72
XXII	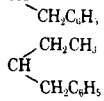	B	97–98°	79	2.29×10^{-4}	4.11	$C_{20}H_{23}N_3O$	C 74.74 H 7.21 N 13.07	74.53 7.27 13.20

[a] Solvent A = methanol; Solvent B = ethanol–methanol (1:1). [b] X = (I_{50} iproniazid/I_{50} compound).

Among the cycloalkyl substituents, the cyclopentyl group had a more favorable action than the cyclohexyl group.

REFERENCES

(1) M. Cardellini, F. Claudi, M. Grifantini, U. Gulini, and S. Martelli, *J. Pharm. Sci.*, **66**, 259 (1977).

(2) A. Alemany, M. Bernabe, C. Elorriaga, E. Fernandez Alvarez, M. Lora-Tamayo, and O. Nieto, *Bull. Soc. Chim. Fr.*, **1966**, 2486.

(3) D. O. Holland and J. H. C. Nayler, *J. Chem. Soc.*, **1955**, 1504.

ACKNOWLEDGMENTS AND ADDRESSES

Received August 4, 1976, from the *Istituto di Chimica Farmaceutica e di Chimica Organica, Università di Camerino, 62032 Camerino (MC), Italy.*

Accepted for publication December 15, 1976.

Supported by a contribution from the Consiglio Nazionale delle Ricerche (CNR), Rome, Italy.

The authors are indebted to Professor Mario Cardellini for advice.

* Laboratorio di Biochimica Applicata, Università di Camerino.

ˣ To whom inquiries should be directed.

COMMUNICATIONS

Correction to "Ionization Constants of Cephalosporin Zwitterionic Compounds"

Keyphrases □ Ionization constants—cephalosporin zwitterionic compounds, error in equations corrected □ Cephalosporin zwitterionic compounds—ionization constants, error in equations corrected □ Zwitterionic cephalosporin compounds—ionization constants, error in equations corrected

To the Editor:

In reviewing the derivation given in the paper "Ionization Constants of Cephalosporin Zwitterionic Compounds" (1), it was found that a factor was dropped in Eq. 12. This omission introduced an error into succeeding equations, and it is the purpose of this communication to correct this error.

The experimental results and calculations were made using the equations shown below rather than those in the paper and, therefore, do not need to be changed. In addition, the *Results and Discussion* section is correct in the paper.

The correct form of Eq. 12 is:

$$[A] = \left\{ \frac{[B] + [H^+] - [OH^-] - [A]}{K_3K_4 - \{H^+\}^2 \dfrac{Y_{NR^-}}{Y_{+HNRH}}} \right\} \left\{ K_3K_4 + K_3\{H^+\} \frac{Y_{NR^-}}{Y_{NRH}} \right\} + [Z]$$

The correct form of Eq. 13 is:

$$\{H^+\}^2 \frac{Y_{NR^-}}{Y_{+HNRH}} \{[Z] - [A]\} = K_3\{H^+\} \frac{Y_{NR^-}}{Y_{NRH}} \left\{ [B] + \frac{\{H^+\}}{Y_{H^+}} - \frac{K_\omega}{\{H^+\}Y_{OH^-}} - [A] \right\} + K_3K_4 \left\{ [B] + \frac{\{H^+\}}{Y_{H^+}} - \frac{K_\omega}{\{H^+\}Y_{OH^-}} - 2[A] + [Z] \right\}$$

The correct form of Eq. 14 is:

$$\delta = K_3\epsilon + K_3K_4\xi$$

A plot of δ/ξ *versus* ϵ/ξ will be linear with a slope of K_3 and δ/ξ will equal K_3K_4 at $\epsilon/\xi = 0$. Also, the value of ϵ/ξ at $\delta/\xi = 0$ will equal $-K_4$.

Equation 14 (as corrected here) may be solved using simultaneous equations by utilizing titrimetric and spectrophotometric data obtained at each of two pH values. By labeling the two sets of data as 1 and 2, K_3 and K_4 can be calculated according to:

$$K_3 = \frac{\dfrac{\delta_1}{\xi_1} - \dfrac{\delta_2}{\xi_2}}{\dfrac{\epsilon_1}{\xi_1} - \dfrac{\epsilon_2}{\xi_2}}$$

$$K_4 = \frac{\delta_1 - K_3\epsilon_1}{K_3\xi_1}$$

which are the corrected forms of Eqs. 15 and 16, respectively.

(1) W. H. Streng, H. E. Huber, J. L. DeYoung, and M. A. Zoglio, *J. Pharm. Sci.*, **65**, 1034 (1976).

William H. Streng

Merrell-National Laboratories
Division of Richardson-Merrell Inc.
Cincinnati, OH 45215

Received May 23, 1977.

Accepted for publication June 21, 1977.

Nitrofurantoin Solubility in Aqueous Pyridoxine Hydrochloride Solutions

Keyphrases □ Nitrofurantoin—aqueous solubility, effect of pyridoxine hydrochloride ■ Solubility—nitrofurantoin in aqueous solutions, effect of pyridoxine hydrochloride □ Pyridoxine hydrochloride—effect on aqueous solubility of nitrofurantoin ■ Antibacterials, urinary—nitrofurantoin, aqueous solubility, effect of pyridoxine hydrochloride □ Vitamins—pyridoxine hydrochloride, effect on aqueous solubility of nitrofurantoin

To the Editor:

Excess nitrofurantoin (approximately 50 mg) was added to 40 ml of an appropriate test solution (0–20.0% pyridoxine hydrochloride in aqueous pH 3 or 5 buffer[1]) in a 45-ml screw-capped bottle. The tightly closed container was wrapped in aluminum foil to keep out light, placed in a constant-temperature water bath at 37 ± 0.1°, and rotated[2] for at least 20 hr. Experiments indicated that equilibrium was established within 10–16 hr. The test so-

[1] Citric acid–dibasic sodium phosphate buffer; ionic strength of 0.7.

[2] Menhold rotating apparatus, Lester, Pa.

Among the cycloalkyl substituents, the cyclopentyl group had a more favorable action than the cyclohexyl group.

REFERENCES

(1) M. Cardellini, F. Claudi, M. Grifantini, U. Gulini, and S. Martelli, *J. Pharm. Sci.*, **66**, 259 (1977).

(2) A. Alemany, M. Bernabe, C. Elorriaga, E. Fernandez Alvarez, M. Lora-Tamayo, and O. Nieto, *Bull. Soc. Chim. Fr.*, **1966**, 2486.

(3) D. O. Holland and J. H. C. Nayler, *J. Chem. Soc.*, **1955**, 1504.

ACKNOWLEDGMENTS AND ADDRESSES

Received August 4, 1976, from the *Istituto di Chimica Farmaceutica e di Chimica Organica, Università di Camerino, 62032 Camerino (MC), Italy.*

Accepted for publication December 15, 1976.

Supported by a contribution from the Consiglio Nazionale delle Ricerche (CNR), Rome, Italy.

The authors are indebted to Professor Mario Cardellini for advice.

* Laboratorio di Biochimica Applicata, Università di Camerino.

ˣ To whom inquiries should be directed.

COMMUNICATIONS

Correction to "Ionization Constants of Cephalosporin Zwitterionic Compounds"

Keyphrases □ Ionization constants—cephalosporin zwitterionic compounds, error in equations corrected □ Cephalosporin zwitterionic compounds—ionization constants, error in equations corrected □ Zwitterionic cephalosporin compounds—ionization constants, error in equations corrected

To the Editor:

In reviewing the derivation given in the paper "Ionization Constants of Cephalosporin Zwitterionic Compounds" (1), it was found that a factor was dropped in Eq. 12. This omission introduced an error into succeeding equations, and it is the purpose of this communication to correct this error.

The experimental results and calculations were made using the equations shown below rather than those in the paper and, therefore, do not need to be changed. In addition, the *Results and Discussion* section is correct in the paper.

The correct form of Eq. 12 is:

$$[A] = \left\{ \frac{[B] + [H^+] - [OH^-] - [A]}{K_3K_4 - \{H^+\}^2 \dfrac{Y_{NR^-}}{Y_{+HNRH}}} \right\} \left\{ K_3K_4 + K_3\{H^+\} \frac{Y_{NR^-}}{Y_{NRH}} \right\} + [Z]$$

The correct form of Eq. 13 is:

$$\{H^+\}^2 \frac{Y_{NR^-}}{Y_{+HNRH}} \{[Z] - [A]\} = K_3\{H^+\} \frac{Y_{NR^-}}{Y_{NRH}} \left\{ [B] + \frac{\{H^+\}}{Y_{H^+}} - \frac{K_\omega}{\{H^+\}Y_{OH^-}} - [A] \right\} + K_3K_4 \left\{ [B] + \frac{\{H^+\}}{Y_{H^+}} - \frac{K_\omega}{\{H^+\}Y_{OH^-}} - 2[A] + [Z] \right\}$$

The correct form of Eq. 14 is:

$$\delta = K_3\epsilon + K_3K_4\xi$$

A plot of δ/ξ *versus* ϵ/ξ will be linear with a slope of K_3 and δ/ξ will equal K_3K_4 at $\epsilon/\xi = 0$. Also, the value of ϵ/ξ at $\delta/\xi = 0$ will equal $-K_4$.

Equation 14 (as corrected here) may be solved using simultaneous equations by utilizing titrimetric and spectrophotometric data obtained at each of two pH values. By labeling the two sets of data as 1 and 2, K_3 and K_4 can be calculated according to:

$$K_3 = \frac{\dfrac{\delta_1}{\xi_1} - \dfrac{\delta_2}{\xi_2}}{\dfrac{\epsilon_1}{\xi_1} - \dfrac{\epsilon_2}{\xi_2}}$$

$$K_4 = \frac{\delta_1 - K_3\epsilon_1}{K_3\xi_1}$$

which are the corrected forms of Eqs. 15 and 16, respectively.

(1) W. H. Streng, H. E. Huber, J. L. DeYoung, and M. A. Zoglio, *J. Pharm. Sci.*, **65**, 1034 (1976).

William H. Streng

Merrell-National Laboratories
Division of Richardson-Merrell Inc.
Cincinnati, OH 45215

Received May 23, 1977.

Accepted for publication June 21, 1977.

Nitrofurantoin Solubility in Aqueous Pyridoxine Hydrochloride Solutions

Keyphrases □ Nitrofurantoin—aqueous solubility, effect of pyridoxine hydrochloride ■ Solubility—nitrofurantoin in aqueous solutions, effect of pyridoxine hydrochloride □ Pyridoxine hydrochloride—effect on aqueous solubility of nitrofurantoin ■ Antibacterials, urinary—nitrofurantoin, aqueous solubility, effect of pyridoxine hydrochloride □ Vitamins—pyridoxine hydrochloride, effect on aqueous solubility of nitrofurantoin

To the Editor:

Excess nitrofurantoin (approximately 50 mg) was added to 40 ml of an appropriate test solution (0–20.0% pyridoxine hydrochloride in aqueous pH 3 or 5 buffer[1]) in a 45-ml screw-capped bottle. The tightly closed container was wrapped in aluminum foil to keep out light, placed in a constant-temperature water bath at 37 ± 0.1°, and rotated[2] for at least 20 hr. Experiments indicated that equilibrium was established within 10–16 hr. The test so-

[1] Citric acid–dibasic sodium phosphate buffer; ionic strength of 0.7.

[2] Menhold rotating apparatus, Lester, Pa.

Among the cycloalkyl substituents, the cyclopentyl group had a more favorable action than the cyclohexyl group.

REFERENCES

(1) M. Cardellini, F. Claudi, M. Grifantini, U. Gulini, and S. Martelli, *J. Pharm. Sci.*, **66**, 259 (1977).

(2) A. Alemany, M. Bernabe, C. Elorriaga, E. Fernandez Alvarez, M. Lora-Tamayo, and O. Nieto, *Bull. Soc. Chim. Fr.*, **1966**, 2486.

(3) D. O. Holland and J. H. C. Nayler, *J. Chem. Soc.*, **1955**, 1504.

ACKNOWLEDGMENTS AND ADDRESSES

Received August 4, 1976, from the *Istituto di Chimica Farmaceutica e di Chimica Organica, Università di Camerino, 62032 Camerino (MC), Italy.*

Accepted for publication December 15, 1976.

Supported by a contribution from the Consiglio Nazionale delle Ricerche (CNR), Rome, Italy.

The authors are indebted to Professor Mario Cardellini for advice.

* Laboratorio di Biochimica Applicata, Università di Camerino.

ˣ To whom inquiries should be directed.

COMMUNICATIONS

Correction to "Ionization Constants of Cephalosporin Zwitterionic Compounds"

Keyphrases □ Ionization constants—cephalosporin zwitterionic compounds, error in equations corrected □ Cephalosporin zwitterionic compounds—ionization constants, error in equations corrected □ Zwitterionic cephalosporin compounds—ionization constants, error in equations corrected

To the Editor:

In reviewing the derivation given in the paper "Ionization Constants of Cephalosporin Zwitterionic Compounds" (1), it was found that a factor was dropped in Eq. 12. This omission introduced an error into succeeding equations, and it is the purpose of this communication to correct this error.

The experimental results and calculations were made using the equations shown below rather than those in the paper and, therefore, do not need to be changed. In addition, the *Results and Discussion* section is correct in the paper.

The correct form of Eq. 12 is:

$$[A] = \left\{ \frac{[B] + [H^+] - [OH^-] - [A]}{K_3K_4 - \{H^+\}^2 \dfrac{Y_{NR^-}}{Y_{+HNRH}}} \right\} \left\{ K_3K_4 + K_3\{H^+\} \frac{Y_{NR^-}}{Y_{NRH}} \right\} + [Z]$$

The correct form of Eq. 13 is:

$$\{H^+\}^2 \frac{Y_{NR^-}}{Y_{+HNRH}} \{[Z] - [A]\} = K_3\{H^+\} \frac{Y_{NR^-}}{Y_{NRH}} \left\{ [B] + \frac{\{H^+\}}{Y_{H^+}} - \frac{K_\omega}{\{H^+\}Y_{OH^-}} - [A] \right\} + K_3K_4 \left\{ [B] + \frac{\{H^+\}}{Y_{H^+}} - \frac{K_\omega}{\{H^+\}Y_{OH^-}} - 2[A] + [Z] \right\}$$

The correct form of Eq. 14 is:

$$\delta = K_3\epsilon + K_3K_4\xi$$

A plot of δ/ξ *versus* ϵ/ξ will be linear with a slope of K_3 and δ/ξ will equal K_3K_4 at $\epsilon/\xi = 0$. Also, the value of ϵ/ξ at $\delta/\xi = 0$ will equal $-K_4$.

Equation 14 (as corrected here) may be solved using simultaneous equations by utilizing titrimetric and spectrophotometric data obtained at each of two pH values. By labeling the two sets of data as 1 and 2, K_3 and K_4 can be calculated according to:

$$K_3 = \frac{\dfrac{\delta_1}{\xi_1} - \dfrac{\delta_2}{\xi_2}}{\dfrac{\epsilon_1}{\xi_1} - \dfrac{\epsilon_2}{\xi_2}}$$

$$K_4 = \frac{\delta_1 - K_3\epsilon_1}{K_3\xi_1}$$

which are the corrected forms of Eqs. 15 and 16, respectively.

(1) W. H. Streng, H. E. Huber, J. L. DeYoung, and M. A. Zoglio, *J. Pharm. Sci.*, **65**, 1034 (1976).

William H. Streng

Merrell-National Laboratories
Division of Richardson-Merrell Inc.
Cincinnati, OH 45215

Received May 23, 1977.

Accepted for publication June 21, 1977.

Nitrofurantoin Solubility in Aqueous Pyridoxine Hydrochloride Solutions

Keyphrases □ Nitrofurantoin—aqueous solubility, effect of pyridoxine hydrochloride ■ Solubility—nitrofurantoin in aqueous solutions, effect of pyridoxine hydrochloride □ Pyridoxine hydrochloride—effect on aqueous solubility of nitrofurantoin ■ Antibacterials, urinary—nitrofurantoin, aqueous solubility, effect of pyridoxine hydrochloride □ Vitamins—pyridoxine hydrochloride, effect on aqueous solubility of nitrofurantoin

To the Editor:

Excess nitrofurantoin (approximately 50 mg) was added to 40 ml of an appropriate test solution (0–20.0% pyridoxine hydrochloride in aqueous pH 3 or 5 buffer[1]) in a 45-ml screw-capped bottle. The tightly closed container was wrapped in aluminum foil to keep out light, placed in a constant-temperature water bath at 37 ± 0.1°, and rotated[2] for at least 20 hr. Experiments indicated that equilibrium was established within 10–16 hr. The test so-

[1] Citric acid–dibasic sodium phosphate buffer; ionic strength of 0.7.

[2] Menhold rotating apparatus, Lester, Pa.

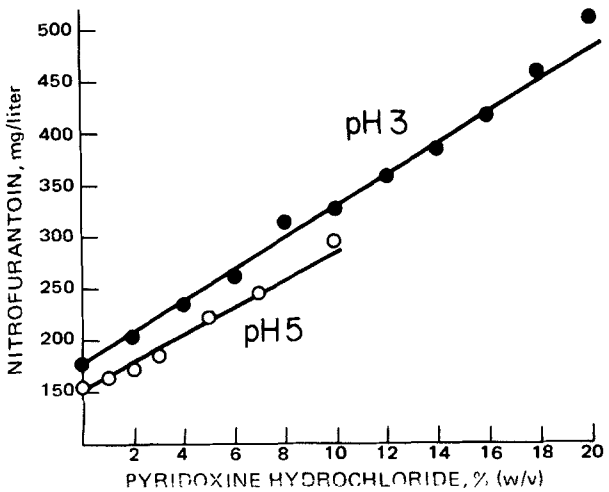

Figure 1—*Nitrofurantoin solubility in aqueous pyridoxine hydrochloride solutions at pH 3 and 5 at 37°.*

lutions were then filtered[3] (0.45-μm pore size), and the filtrate was diluted with deionized distilled water to a proper concentration (40–100 mg/liter) for spectrophotometric assay using the method of Conklin and Hollifield (1). At least three experimental runs were made for each test medium.

Figure 1 shows the effect of pyridoxine hydrochloride on nitrofurantoin solubility at two pH values. The addition of pyridoxine hydrochloride significantly increased nitrofurantoin solubility, and this increase was linearly dependent on the pyridoxine concentration. The higher initial solubility of nitrofurantoin in pH 3 solution than in pH 5 solution (no pyridoxine) agrees with earlier studies (2), and this trend of higher solubility was maintained for the experimental concentration range of pyridoxine hydrochloride.

Mattheus and Heise (3) reported that the nitrofurantoin concentration in urine during simultaneous administration in humans of pyridoxine (up to 100 mg) was increased on an average of 62%. They suggested that pyridoxine might increase nitrofurantoin absorption through the gut and also proposed possible effects on kidney filtration, plasma protein binding, and metabolic processes. Our data indicate that the relatively small amount of pyridoxine hydrochloride (100 mg) might increase slightly nitrofurantoin solubility in the gut if the two drugs are given simultaneously; however, this increased solubility could not account for the higher nitrofurantoin concentrations reported in the urine.

Any interaction between pyridoxine and nitrofurantoin molecules in solution could not be detected by spectral analysis including difference spectroscopy. Surface tension measurements indicated that pyridoxine hydrochloride had negligible surface activity.

Further investigations are being conducted in these laboratories to determine the effect of pyridoxine hydrochloride and pyridoxine derivatives on the solubility of other drugs and to elucidate the mechanism(s) of action of this solubilization phenomenon.

(1) J. D. Conklin and R. D. Hollifield, *Clin. Chem.*, **11**, 925 (1965).

(2) L. K. Chen, D. E. Cadwallader, and H. W. Jun, *J. Pharm. Sci.*, **65**, 868 (1976).

(3) A. Mattheus and H. Heise, *Dtsch. Ges. Wesen*, **28**, 716 (1973).

Donald E. Cadwallader [x]
Byung H. Lee
Howard C. Ansel
Department of Pharmacy
School of Pharmacy
University of Georgia
Athens, GA 30602

Received February 4, 1977.
Accepted for publication June 14, 1977.
[x] To whom inquiries should be directed.

[3] Millipore.

Cannabis sativa L. (Marijuana) IX: Lens Aldose Reductase Inhibitory Activity of Marijuana Flavone C-Glycosides

Keyphrases □ *Cannabis sativa*—three flavone C-glycosides isolated, effect on rat lens aldose reductase evaluated □ Flavone C-glycosides, various—isolated from *Cannabis sativa*, effect on rat lens aldose reductase □ Marijuana flavonoids—various flavone C-glycosides, effect on rat lens aldose reductase □ Aldose reductase, rat lens—effect of three flavone C-glycosides isolated from *Cannabis sativa*

To the Editor:

Pursuant to ongoing studies (1) dealing with the isolation and characterization of biologically active substances from *Cannabis sativa* L. (marijuana), we recently isolated and elucidated the structures of one known and two new flavone C-glycoside compounds from the aerial parts of a Mexican strain of marijuana[1]. The known compound was orientin (I) and the new compounds, named flavocannabiside (II) and flavosativaside (III), corresponded to orientin-2″-*O*-β-D-glucopyranoside and vitexin-2″-*O*-β-D-glucopyranoside, respectively[2].

A recent report (2) indicated that certain flavonoids were potent inhibitors of lens aldose reductase, an enzyme that has been implicated in the pathogenesis of cataracts in humans suffering from diabetes and galactosemia. In that report, eight flavonoids representing a limited number of flavonoid types were studied: one flavanone (hesperitin), two flavones (quercetin and morin), four flavonol glycosides [quercitrin (IV), myricitrin, rutin, and robinin], and one isoflavone (2-carbethoxy-5,7-dihdroxy-4′-methoxyisoflavone). Quercitrin, quercetin, and myricitrin were found to be more potent than two of the previously known aldose reductase inhibitors, tetramethyleneglutaric acid and 1,2-dioxo-1*H*-benz[*de*]isoquinoline-2(3*H*)-acetic acid. However, since no flavone C-glycosides were included in that study, it was considered worthwhile to evaluate the

[1] The plant material used was the air-dried flowering tops of female plants grown for 14 weeks and harvested at the University of Mississippi during the 1971 season. This material was identified as *Cannabis sativa* L. (Cannabaceae) by Dr. Maynard W. Quimby, Department of Pharmacognosy, University of Mississippi. A voucher specimen representing material (Batch 10-CMF-71-CT-72) collected for this investigation is available for inspection at the Herbarium, Department of Pharmacognosy, University of Mississippi.

[2] To be published.

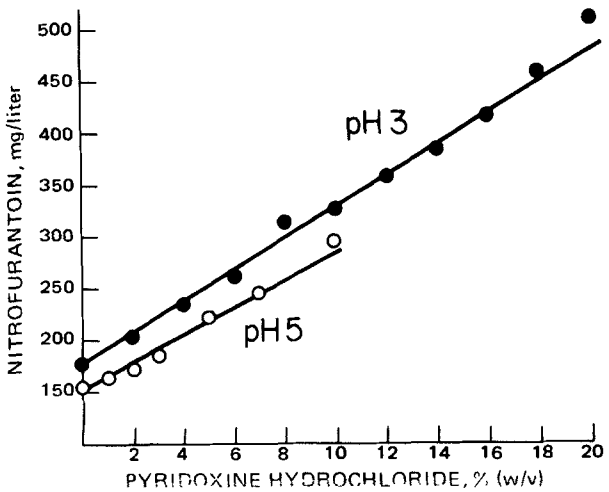

Figure 1—*Nitrofurantoin solubility in aqueous pyridoxine hydrochloride solutions at pH 3 and 5 at 37°.*

lutions were then filtered[3] (0.45-μm pore size), and the filtrate was diluted with deionized distilled water to a proper concentration (40–100 mg/liter) for spectrophotometric assay using the method of Conklin and Hollifield (1). At least three experimental runs were made for each test medium.

Figure 1 shows the effect of pyridoxine hydrochloride on nitrofurantoin solubility at two pH values. The addition of pyridoxine hydrochloride significantly increased nitrofurantoin solubility, and this increase was linearly dependent on the pyridoxine concentration. The higher initial solubility of nitrofurantoin in pH 3 solution than in pH 5 solution (no pyridoxine) agrees with earlier studies (2), and this trend of higher solubility was maintained for the experimental concentration range of pyridoxine hydrochloride.

Mattheus and Heise (3) reported that the nitrofurantoin concentration in urine during simultaneous administration in humans of pyridoxine (up to 100 mg) was increased on an average of 62%. They suggested that pyridoxine might increase nitrofurantoin absorption through the gut and also proposed possible effects on kidney filtration, plasma protein binding, and metabolic processes. Our data indicate that the relatively small amount of pyridoxine hydrochloride (100 mg) might increase slightly nitrofurantoin solubility in the gut if the two drugs are given simultaneously; however, this increased solubility could not account for the higher nitrofurantoin concentrations reported in the urine.

Any interaction between pyridoxine and nitrofurantoin molecules in solution could not be detected by spectral analysis including difference spectroscopy. Surface tension measurements indicated that pyridoxine hydrochloride had negligible surface activity.

Further investigations are being conducted in these laboratories to determine the effect of pyridoxine hydrochloride and pyridoxine derivatives on the solubility of other drugs and to elucidate the mechanism(s) of action of this solubilization phenomenon.

(1) J. D. Conklin and R. D. Hollifield, *Clin. Chem.*, **11**, 925 (1965).

(2) L. K. Chen, D. E. Cadwallader, and H. W. Jun, *J. Pharm. Sci.*, **65**, 868 (1976).

(3) A. Mattheus and H. Heise, *Dtsch. Ges. Wesen*, **28**, 716 (1973).

Donald E. Cadwallader [x]
Byung H. Lee
Howard C. Ansel
Department of Pharmacy
School of Pharmacy
University of Georgia
Athens, GA 30602

Received February 4, 1977.
Accepted for publication June 14, 1977.
[x] To whom inquiries should be directed.

[3] Millipore.

Cannabis sativa L. (Marijuana) IX: Lens Aldose Reductase Inhibitory Activity of Marijuana Flavone C-Glycosides

Keyphrases □ *Cannabis sativa*—three flavone C-glycosides isolated, effect on rat lens aldose reductase evaluated □ Flavone C-glycosides, various—isolated from *Cannabis sativa*, effect on rat lens aldose reductase □ Marijuana flavonoids—various flavone C-glycosides, effect on rat lens aldose reductase □ Aldose reductase, rat lens—effect of three flavone C-glycosides isolated from *Cannabis sativa*

To the Editor:

Pursuant to ongoing studies (1) dealing with the isolation and characterization of biologically active substances from *Cannabis sativa* L. (marijuana), we recently isolated and elucidated the structures of one known and two new flavone C-glycoside compounds from the aerial parts of a Mexican strain of marijuana[1]. The known compound was orientin (I) and the new compounds, named flavocannabiside (II) and flavosativaside (III), corresponded to orientin-2″-*O*-β-D-glucopyranoside and vitexin-2″-*O*-β-D-glucopyranoside, respectively[2].

A recent report (2) indicated that certain flavonoids were potent inhibitors of lens aldose reductase, an enzyme that has been implicated in the pathogenesis of cataracts in humans suffering from diabetes and galactosemia. In that report, eight flavonoids representing a limited number of flavonoid types were studied: one flavanone (hesperitin), two flavones (quercetin and morin), four flavonol glycosides [quercitrin (IV), myricitrin, rutin, and robinin], and one isoflavone (2-carbethoxy-5,7-dihdroxy-4′-methoxyisoflavone). Quercitrin, quercetin, and myricitrin were found to be more potent than two of the previously known aldose reductase inhibitors, tetramethyleneglutaric acid and 1,2-dioxo-1*H*-benz[*de*]isoquinoline-2(3*H*)-acetic acid. However, since no flavone C-glycosides were included in that study, it was considered worthwhile to evaluate the

[1] The plant material used was the air-dried flowering tops of female plants grown for 14 weeks and harvested at the University of Mississippi during the 1971 season. This material was identified as *Cannabis sativa* L. (Cannabaceae) by Dr. Maynard W. Quimby, Department of Pharmacognosy, University of Mississippi. A voucher specimen representing material (Batch 10-CMF-71-CT-72) collected for this investigation is available for inspection at the Herbarium, Department of Pharmacognosy, University of Mississippi.

[2] To be published.

Table I—*In Vitro* Inhibition of Rat Lens Aldose Reductase by Various Substances

Inhibitor	Inhibition[a], %			
	10^{-4} *M*	10^{-5} *M*	10^{-6} *M*	10^{-7} *M*
Total crude flavonoid fraction	74	37	0	0
Flavocannabiside	40	10	0	0
Flavosativaside	35	0	0	0
Orientin	90	82	45	0
Quercitrin	100	95	88	55

[a] Percentage of inhibition of the aldose reductase activity when compared with controls containing no inhibitors.

three isolated marijuana flavone C-glycosides as potential lens aldose reductase inhibitors.

In the present study, I–III as well as the total crude flavonoid fraction from which they were isolated were each tested for inhibitory activity against a partially purified rat lens aldose reductase enzyme according to previously reported methods (3). Each substance was tested four to six times; the results shown in Table I represent mean values. The standard deviation of the results was less than 5%.

The C-diglycosylflavones II and III were relatively weak inhibitors. The C-monoglycosylflavone I proved to be 45% inhibitory at 10^{-6} *M* and compared favorably with the flavonol glycoside IV, which caused a 55% inhibition at 10^{-7} *M*.

Work is underway to determine the inhibitory effect of I on aldose reductase in a rat lens organ culture assay (4),

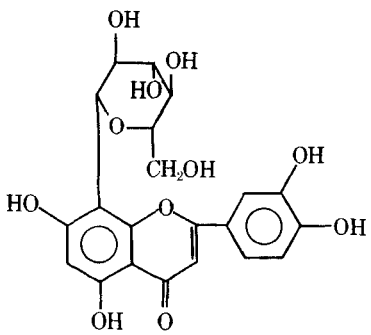

I

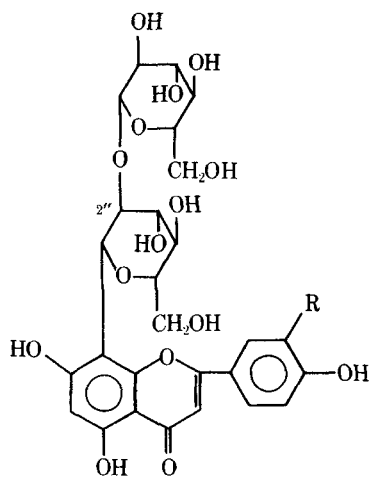

II: R = OH
III: R = H

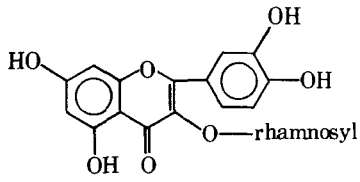

IV

and studies using additionally isolated marijuana flavonoids are anticipated[3].

(1) A. B. Segelman, R. D. Sofia, F. P. Segelman, J. J. Harakal, and L. C. Knobloch, *J. Pharm. Sci.*, **63**, 962 (1974).
(2) S. D. Varma, I. Mikuni, and J. H. Kinoshita, *Science*, **188**, 1215 (1975).
(3) S. Hayman and J. H. Kinoshita, *J. Biol. Chem.*, **240**, 877 (1965).
(4) S. D. Varma and J. H. Kinoshita, *Biochim. Biophys. Acta*, **338**, 632 (1974).

Alvin B. Segelman [x]
Florence P. Segelman
Department of Pharmacognosy
College of Pharmacy
Rutgers—The State University
New Brunswick, NJ 08903

S. D. Varma
Laboratory of Vision Research
National Eye Institute
National Institutes of Health
Bethesda, MD 20014

Hildebert Wagner
Otto Seligmann
Institut für Pharmazeutische
Arzneimittellehre der Universität
München
D-8000 München 2, West Germany

Received December 7, 1976.
Accepted for publication February 10, 1977.
Presented at the 17th Annual Meeting of the American Society of Pharmacognosy, Cable, Wis., July 14, 1976.
Supported by U.S. Public Health Service Grant DA-00328-03.
We thank Dr. J. H. Kinoshita, Chief, Laboratory of Vision Research, National Eye Institute, Bethesda, Md., for helpful discussions.
[x] To whom inquiries should be directed.

[3] *Added in proof:* The following recent reports describe further work dealing with diabetic cataracts and flavonoids: S. D. Varma and J. H. Kinoshita, *Biochem. Pharmacol.*, **25**, 2505 (1976); S. D. Varma, A. Mizuno, and J. H. Kinoshita, *Science*, **195**, 205 (1977).

Use of *In Vitro* Dissolution Data to Predict Plasma Drug Profiles

Keyphrases □ Plasma time profiles—predicted from *in vitro* dissolution data, validity evaluated □ Dissolution rates, *in vitro*—used to predict plasma time profiles, validity evaluated

To the Editor:

Recently, Vaughan and Leach (1) discussed a simple method for predicting plasma time profiles from *in vitro* dissolution data. Basically, their method is to relate the

Table I—*In Vitro* Inhibition of Rat Lens Aldose Reductase by Various Substances

Inhibitor	Inhibition[a], %			
	10^{-4} *M*	10^{-5} *M*	10^{-6} *M*	10^{-7} *M*
Total crude flavonoid fraction	74	37	0	0
Flavocannabiside	40	10	0	0
Flavosativaside	35	0	0	0
Orientin	90	82	45	0
Quercitrin	100	95	88	55

[a] Percentage of inhibition of the aldose reductase activity when compared with controls containing no inhibitors.

three isolated marijuana flavone C-glycosides as potential lens aldose reductase inhibitors.

In the present study, I–III as well as the total crude flavonoid fraction from which they were isolated were each tested for inhibitory activity against a partially purified rat lens aldose reductase enzyme according to previously reported methods (3). Each substance was tested four to six times; the results shown in Table I represent mean values. The standard deviation of the results was less than 5%.

The C-diglycosylflavones II and III were relatively weak inhibitors. The C-monoglycosylflavone I proved to be 45% inhibitory at 10^{-6} *M* and compared favorably with the flavonol glycoside IV, which caused a 55% inhibition at 10^{-7} *M*.

Work is underway to determine the inhibitory effect of I on aldose reductase in a rat lens organ culture assay (4),

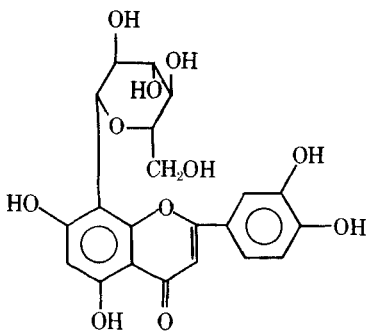

I

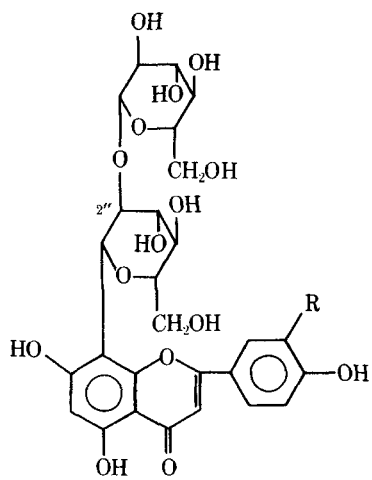

II: R = OH
III: R = H

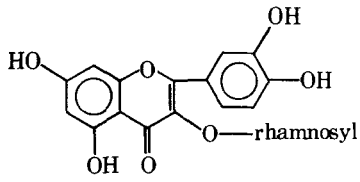

IV

and studies using additionally isolated marijuana flavonoids are anticipated[3].

(1) A. B. Segelman, R. D. Sofia, F. P. Segelman, J. J. Harakal, and L. C. Knobloch, *J. Pharm. Sci.*, **63**, 962 (1974).
(2) S. D. Varma, I. Mikuni, and J. H. Kinoshita, *Science*, **188**, 1215 (1975).
(3) S. Hayman and J. H. Kinoshita, *J. Biol. Chem.*, **240**, 877 (1965).
(4) S. D. Varma and J. H. Kinoshita, *Biochim. Biophys. Acta*, **338**, 632 (1974).

Alvin B. Segelman [x]
Florence P. Segelman
Department of Pharmacognosy
College of Pharmacy
Rutgers—The State University
New Brunswick, NJ 08903

S. D. Varma
Laboratory of Vision Research
National Eye Institute
National Institutes of Health
Bethesda, MD 20014

Hildebert Wagner
Otto Seligmann
Institut für Pharmazeutische
Arzneimittellehre der Universität
München
D-8000 München 2, West Germany

Received December 7, 1976.
Accepted for publication February 10, 1977.
Presented at the 17th Annual Meeting of the American Society of Pharmacognosy, Cable, Wis., July 14, 1976.
Supported by U.S. Public Health Service Grant DA-00328-03.
We thank Dr. J. H. Kinoshita, Chief, Laboratory of Vision Research, National Eye Institute, Bethesda, Md., for helpful discussions.
[x] To whom inquiries should be directed.

[3] *Added in proof:* The following recent reports describe further work dealing with diabetic cataracts and flavonoids: S. D. Varma and J. H. Kinoshita, *Biochem. Pharmacol.*, **25**, 2505 (1976); S. D. Varma, A. Mizuno, and J. H. Kinoshita, *Science*, **195**, 205 (1977).

Use of *In Vitro* Dissolution Data to Predict Plasma Drug Profiles

Keyphrases □ Plasma time profiles—predicted from *in vitro* dissolution data, validity evaluated □ Dissolution rates, *in vitro*—used to predict plasma time profiles, validity evaluated

To the Editor:

Recently, Vaughan and Leach (1) discussed a simple method for predicting plasma time profiles from *in vitro* dissolution data. Basically, their method is to relate the

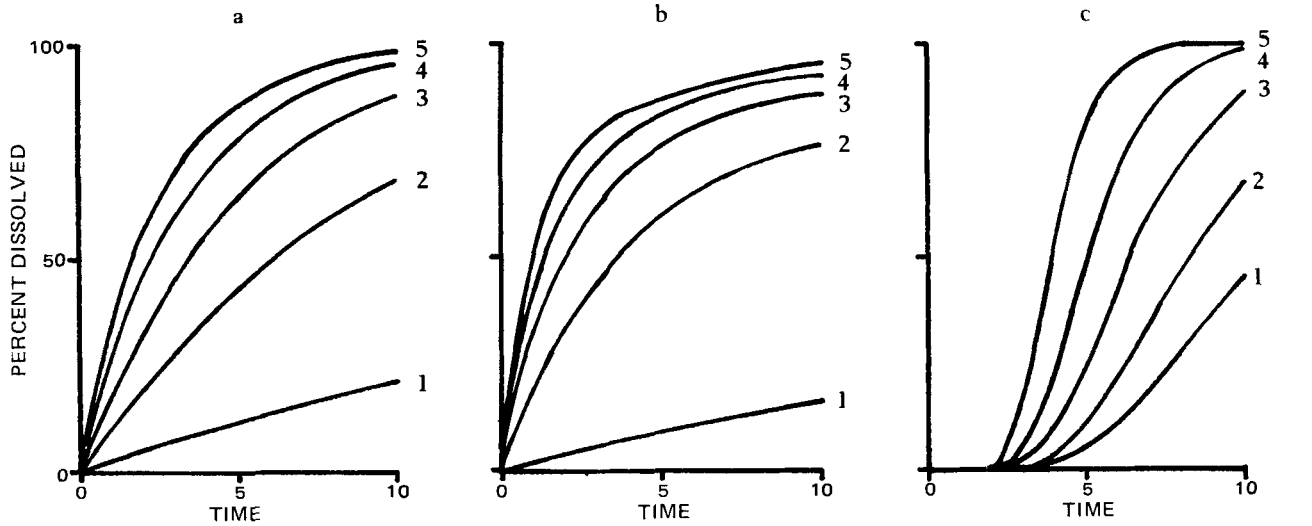

Figure 1—*Dissolution profiles from different formulations of a drug when dissolution is governed by linear (a), cube root (b), and log normal (c) dissolution laws. Parameters were adjusted so that the fastest dissolving formulation reached 90% dissolution at the same time for each law and the slowest dissolving formulation had reached 10% dissolution at this time.*

amount of drug dissolved at time t in an *in vitro* dissolution test, $dis_j(t)$, to the plasma drug concentration obtained following administration of an oral dose of the preparation, $Cp_j(t)$, *via:*

$$dis_j(t) = H(t)Cp_j(t) \qquad \text{(Eq. 1)}$$

where j refers to the jth formulation. Thus, if $H(t)$ is a specific function of t and is independent of the formulation, then the following relation exists between two different preparations, i and j:

$$\frac{dis_i(t)}{dis_j(t)} = \frac{Cp_i(t)}{Cp_j(t)} \qquad \text{(Eq. 2)}$$

Potentially, this method could be very useful in drug design or for predicting plasma profiles, avoiding many detailed pharmacokinetic analyses. However, $H(t)$ is not a formulation-independent function (even when dealing with linear pharmacokinetics as suggested by Vaughan and Leach), so the validity of Eq. 1 was investigated based on some simple pharmacokinetic models. Although it may be argued that these models are idealized, Eq. 1 was offered as a quite general relationship (although certain sensible restrictions were placed on its use by the authors which will be discussed later), and it must stand the test of abstracted models.

Table I—Calculated Values of $H(t)$ for Formulations with Drug Release Patterns Depicted in Fig. 1, Using Eq. 1, with $k_2 = 5$ and $k_3 = 0.5$

	Linear[a]					Cube Root					Log Normal				
Time	1	2	3	4	5	1	2	3	4	5	1	2	3	4	5
1.0	1.528	1.523	1.516	1.509	1.503	1.528	1.515	1.493	1.477	1.466	3.565	4.421	4.774	5.239	5.833
2.0	1.693	1.699	1.708	1.718	1.728	1.694	1.709	1.747	1.783	1.818	2.060	2.192	2.227	2.260	2.291
3.0	2.003	2.041	2.090	2.143	2.199	2.009	2.087	2.253	2.393	2.512	1.724	1.729	1.722	1.708	1.684
4.0	2.376	2.471	2.600	2.740	2.888	2.390	2.582	2.972	3.293	3.560	1.650	1.630	1.621	1.611	1.602
5.0	2.795	2.983	3.247	3.543	3.867	2.820	3.190	3.942	4.561	5.080	1.691	1.702	1.719	1.755	1.830
6.0	3.250	3.576	4.056	4.617	5.251	3.292	3.920	5.216	6.308	7.240	1.805	1.908	1.989	2.134	2.401
7.0	3.736	4.256	5.060	6.049	7.215	3.800	4.778	6.859	8.669	10.250	1.979	2.260	2.468	2.833	3.478
8.0	4.249	5.027	6.302	7.960	10.010	4.341	5.774	8.935	11.795	14.367	2.213	2.803	3.247	4.027	5.363
9.0	4.785	5.897	7.833	10.513	14.010	4.911	6.914	11.511	15.850	19.875	2.514	3.618	4.484	6.019	8.559
10.0	5.341	6.873	9.716	13.929	19.758	5.507	8.203	14.648	20.995	27.076	2.892	4.836	6.444	9.314	13.900

[a] The numbers refer to the dissolution profiles in Fig. 1.

Table II—Calculated Values of $H(t)$ for Formulations with Drug Release Patterns Depicted in Fig. 1, Using Eq. 1, with $k_2 = 5$ and $k_3 = 0.1$

	Linear					Cube Root					Log Normal				
Time	1	2	3	4	5	1	2	3	4	5	1	2	3	4	5
1.0	1.300	1.291	1.283	1.275	1.267	1.299	1.269	1.246	1.228	1.213	5.789	4.784	4.179	3.768	3.466
2.0	1.214	1.207	1.201	1.195	1.190	1.213	1.193	1.183	1.176	1.173	2.161	2.101	2.035	1.971	1.912
3.0	1.229	1.226	1.224	1.223	1.223	1.228	1.225	1.228	1.232	1.237	1.478	1.516	1.525	1.521	1.509
4.0	1.266	1.270	1.276	1.282	1.289	1.267	1.285	1.302	1.317	1.330	1.251	1.302	1.331	1.344	1.349
5.0	1.314	1.328	1.343	1.358	1.375	1.316	1.360	1.395	1.420	1.441	1.197	1.227	1.253	1.270	1.279
6.0	1.369	1.394	1.422	1.450	1.478	1.372	1.448	1.501	1.539	1.567	1.232	1.222	1.233	1.244	1.253
7.0	1.427	1.469	1.512	1.556	1.599	1.432	1.548	1.621	1.671	1.709	1.320	1.263	1.248	1.248	1.251
8.0	1.489	1.551	1.615	1.678	1.737	1.496	1.657	1.754	1.819	1.866	1.441	1.337	1.290	1.273	1.268
9.0	1.555	1.640	1.729	1.815	1.894	1.564	1.778	1.901	1.982	2.040	1.586	1.440	1.353	1.314	1.297
10.0	1.623	1.738	1.857	1.970	2.071	1.635	1.910	2.063	2.163	2.233	1.750	1.566	1.438	1.370	1.338

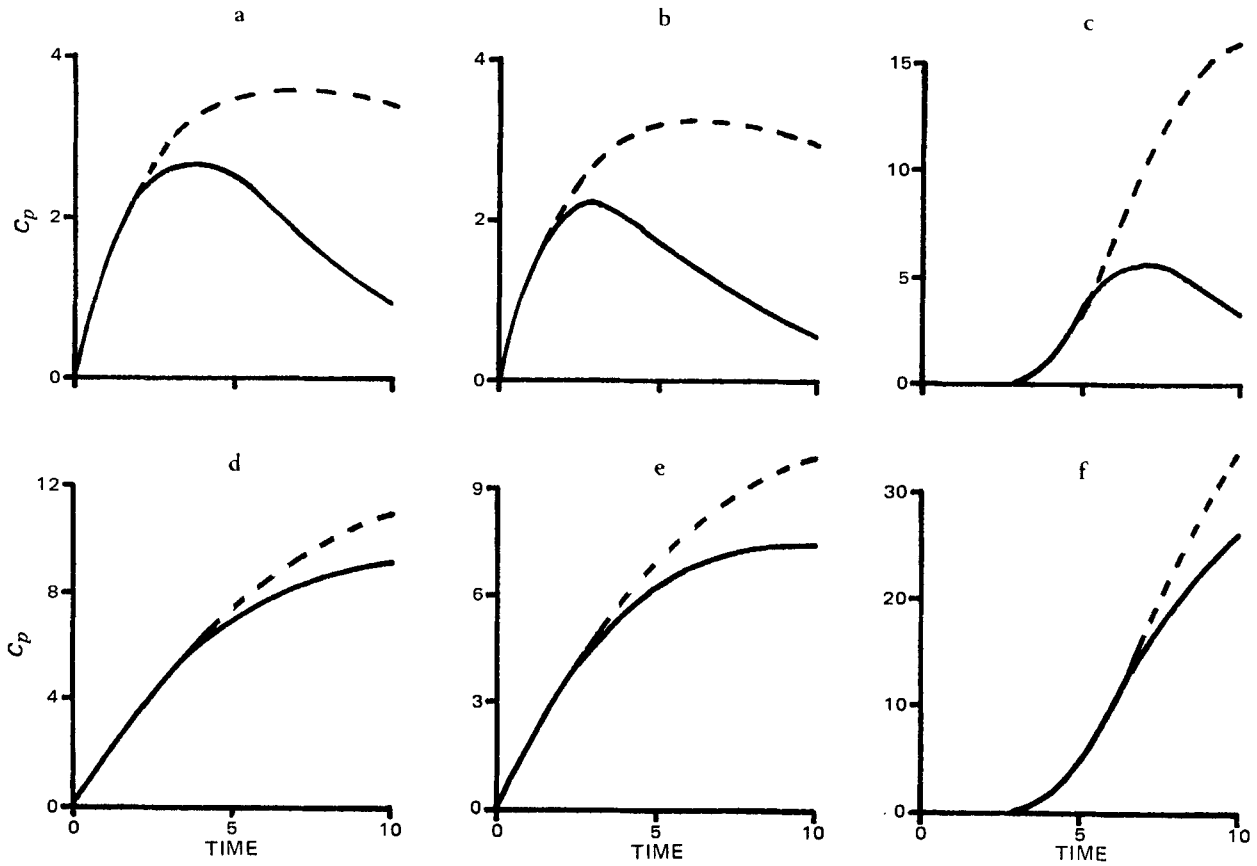

Figure 2—*Predicted (—) and correct (- - -) plasma profiles. Key: a, b, and c, linear, cube root, and log normal dissolution laws, respectively, with* $k_2 = 5$ *and* $k_3 = 0.5$*; and d, e, and f, linear, cube root, and log normal dissolution laws, respectively, with* $k_2 = 5$ *and* $k_3 = 0.1$.

One-Compartment Model—In the linear dissolution model shown in Scheme I, A, B, and C represent the

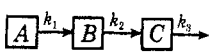

Scheme I

amounts of drug in the dosage form, in solution at the absorption site, and in the body, respectively; k_1, k_2, and k_3 are the corresponding first-order rate constants for the respective processes. The *in vitro* and *in vivo* dissolution profiles are assumed to be the same and are given by:

$$\text{dis}(t) = 100(1 - e^{-k_1 t}) \qquad \text{(Eq. 3)}$$

expressed as a percentage. In the same units, the time course of the drug in the body is:

$$Cp(t) = \frac{100k_1k_2[(k_2 - k_3)e^{-k_1 t} - (k_1 - k_3)e^{-k_2 t} + (k_1 - k_2)e^{-k_3 t}]}{(k_1 - k_2)(k_2 - k_3)(k_1 - k_3)} \qquad \text{(Eq. 4)}$$

such that:

$$H(t) = \frac{(k_1 - k_2)(k_2 - k_3)(k_1 - k_3)(1 - e^{-k_1 t})}{k_1k_2[(k_2 - k_3)e^{-k_1 t} - (k_1 - k_3)e^{-k_2 t} + (k_1 - k_2)e^{-k_3 t}]} \qquad \text{(Eq. 5)}$$

Differences in formulation are embodied in the parameter k_1; the larger k_1 is, the faster the drug dissolves.

It can be seen that $H(t)$ is a function of k_1 and is not formulation independent, as suggested in the introduction. It is instructive to look at several limiting forms of this function. In Case 1, $k_1 \gg k_2, k_3$. The drug dissolves so rapidly that it is effectively instantaneously available for absorption. By neglecting k_2 and k_3 with respect to k_1 and $e^{-k_1 t}$ with respect to $e^{-k_2 t}$ and $e^{-k_3 t}$, $H(t)$ becomes:

$$H(t) \sim \frac{(k_3 - k_2)}{k_2[e^{-k_2 t} - e^{-k_3 t}]} \qquad \text{(Eq. 6)}$$

Although $H(t)$ is now independent of k_1, it is useless for predictive purposes because it just relates a step function input to the plasma profile.

In Case 2, $k_2, k_3 \gg k_1$. Dissolution is rate limiting, and the limiting form of $H(t)$ approaches:

$$H(t) \sim \frac{k_3(1 - e^{-k_1 t})}{k_1 e^{-k_1 t}} \qquad \text{(Eq. 7)}$$

Here we find the most valid application of the method in that the plasma profile directly parallels the dissolution profile in the early phase ($k_1 t < 1$).

In Case 3, $k_1, k_2 \gg k_3$. The example of alprenolol discussed by Vaughan and Leach (1) approximately fits this category, and $H(t)$ reduces to $e^{k_3 t}$. Thus, as expected, after rapid dissolution and absorption, the plasma profile shows a simple exponential decline, reflecting elimination of drug from the body.

Simulations—The various limiting forms of $H(t)$ do not allow an assessment of how well or how badly this method works over an extended time scale. Therefore, it was necessary to resort to numerical integration. The studies were further extended to include two other kinds of dissolution,

cube root law (2) and log normal[1] (3). So that a meaningful comparison could be made between the three dissolution laws, it was arranged that $dis_j(t)$ for the fastest dissolving formulation reached 90% at the same time for each law and that the slowest dissolving formulation had reached 10% at this time. The rate constants k_2 and k_3 were fixed at 5 and 0.5 in one trial and at 5 and 0.1 in another. The time units are arbitrary.

The dissolution profiles for the three laws are shown in Fig. 1, and the values of $H(t)$ calculated using Eq. 1 are listed in Tables I and II. To obtain a better appreciation for the numbers, the plasma profile appropriate to the slowest dissolving formulation was calculated using the $H(t)$ appropriate to the fastest dissolving formulation and compared to the correct profile for each dissolution law. These values are displayed in Fig. 2.

Discussion—Although extensive parameter searches were not carried out, general trends revealed themselves. First, it is surprising how well the method works in these simulations at early times, *i.e.*, when dissolution is not complete. Vaughan and Leach (1) stressed this finding, and it is only reasonable that the method must break down when the drug in the fastest dissolving formulation has completely dissolved. As mentioned earlier, the method will be of most use when the dissolution rate limits input to the body. This condition was ensured in these simulations by having the drug pass rapidly through compartment B such that the ratio of $A/(A + B)$ was nearly 1 (0.98 for the linear case). Reducing k_3 increased the time over which there was close agreement between the predicted and correct values, but this agreement still only occurs on the rising phase of the plasma profile.

However, two important parameters are badly predicted by this method: the peak plasma concentration and the time required to reach it. The peak plasma concentration averages 30–40% in error, while the time required to reach it is over 100% out. The results for the log normal dissolution are particularly bad, but this function is probably "too nonlinear." To be of use to the pharmaceutical industry or the clinician, both parameters would need to be predicted better. Thus, we warn against noncritical use of the method, but the method can be very useful in certain instances. To obtain reliable prediction, the mechanism of dissolution between formulations should be the same both *in vitro* and *in vivo* (as emphasized by Vaughan and Leach). Since the time over which the predictions are reliable is limited by the fastest dissolving formulation to be of use, the dissolution profiles of the formulations to be compared must be similar.

In the present analysis, we took the optimal situation in which the *in vitro* dissolution profile has been assumed to be exactly the same as occurs *in vivo*. If the time scales, however, are different—and this cannot be predicted *a priori*—the difficulties that are created may invalidate the method.

[1] The dissolution profile for the log normal law was calculated using Wagner's (3) method:

$$\frac{dA}{dt} = \frac{e^{-x^2/2}}{\sqrt{2\pi}\sigma t \log_{10} e}$$

and:

$$x = \frac{\log_{10} t - x \text{ mean}}{\sigma}$$

where x mean and σ are the mean and standard deviation of the distribution, respectively. However, rather than fixing x mean and letting σ vary as Wagner did, we fixed the ratio of x mean/σ (= 5), thus giving a more realistic spread of dissolution profiles.

(1) D. P. Vaughan and R. H. Leach, *J. Pharm. Sci.*, **65**, 601 (1976).

(2) J. G. Wagner, "Biopharmaceutics and Relevant Pharmacokinetics," Drug Intelligence Publications, Hamilton, Ill., 1971, chap. 16.

(3) J. G. Wagner, *J. Pharm. Sci.*, **58**, 1253 (1969).

Leon J. Aarons
Malcolm Rowland [x]
Department of Pharmacy
University of Manchester
Manchester, M13 9PL
England

Received October 29, 1976.
Accepted for publication January 3, 1977.

[x] To whom inquiries should be directed.

Screening Procedure for Phorbol Esters Using Brine Shrimp (*Artemia salina*) Larvae

Keyphrases □ Phorbol esters, various—toxicity to brine shrimp larvae related to cocarcinogenic potency □ Brine shrimp larvae—toxicity of various phorbol esters related to cocarcinogenic potency □ Toxicity—various phorbol esters to brine shrimp larvae, related to cocarcinogenic potency □ Cocarcinogenic potency—various phorbol esters, related to toxicity to brine shrimp larvae

To the Editor:

In the continuing search for anticancer agents of natural origin, the recently discovered antileukemic property of phorbol 12-tigliate 13-decanoate (1), from *Croton tiglium* (Euphorbiaceae), is interesting since phorbol esters are better known as irritant cocarcinogens (2). Unlike other naturally occurring anticancer compounds, intensive work has been performed on the activity of phorbol esters in two-stage carcinogenesis experiments, including their interactions with nucleic acids and their effect on the uptake of precursors of these and other macromolecules by the mammalian cell (3). Isolation of further phorbol and related esters from the plant kingdom could, in addition to providing possible new antileukemic agents, yield unique structure–activity information on the complex relationships between irritancy, cocarcinogenicity, and antileukemic activity at the cellular level.

During the fractionation of anticancer compounds from plant sources, there is often a considerable delay between isolation and receipt of biological data. Several screening

Table I—ED_{50}'s of Phorbol Esters and Two Piscicides to *A. salina* Larvae (Brine Shrimp)

Compound	ED_{50}, μg/ml	$f_{ED_{50}}$	95–100% Confidence Limits, μg/ml
Phorbol 12-tetradecanoate 13-acetate	3.8	1.96	1.9–7.4
Phorbol 12,13-didecanoate	6.8	1.96	3.5–13.3
Phorbol 12,13-dibenzoate	11.8	1.96	6.0–23.1
Phorbol	>1000	—	—
4α-Phorbol 12,13-didecanoate	>1000	—	—
Rotenone	0.5	1.71	0.3–0.9
Picrotoxin	2510	1.75	1430–4400

cube root law (2) and log normal[1] (3). So that a meaningful comparison could be made between the three dissolution laws, it was arranged that $dis_j(t)$ for the fastest dissolving formulation reached 90% at the same time for each law and that the slowest dissolving formulation had reached 10% at this time. The rate constants k_2 and k_3 were fixed at 5 and 0.5 in one trial and at 5 and 0.1 in another. The time units are arbitrary.

The dissolution profiles for the three laws are shown in Fig. 1, and the values of $H(t)$ calculated using Eq. 1 are listed in Tables I and II. To obtain a better appreciation for the numbers, the plasma profile appropriate to the slowest dissolving formulation was calculated using the $H(t)$ appropriate to the fastest dissolving formulation and compared to the correct profile for each dissolution law. These values are displayed in Fig. 2.

Discussion—Although extensive parameter searches were not carried out, general trends revealed themselves. First, it is surprising how well the method works in these simulations at early times, *i.e.*, when dissolution is not complete. Vaughan and Leach (1) stressed this finding, and it is only reasonable that the method must break down when the drug in the fastest dissolving formulation has completely dissolved. As mentioned earlier, the method will be of most use when the dissolution rate limits input to the body. This condition was ensured in these simulations by having the drug pass rapidly through compartment B such that the ratio of $A/(A + B)$ was nearly 1 (0.98 for the linear case). Reducing k_3 increased the time over which there was close agreement between the predicted and correct values, but this agreement still only occurs on the rising phase of the plasma profile.

However, two important parameters are badly predicted by this method: the peak plasma concentration and the time required to reach it. The peak plasma concentration averages 30–40% in error, while the time required to reach it is over 100% out. The results for the log normal dissolution are particularly bad, but this function is probably "too nonlinear." To be of use to the pharmaceutical industry or the clinician, both parameters would need to be predicted better. Thus, we warn against noncritical use of the method, but the method can be very useful in certain instances. To obtain reliable prediction, the mechanism of dissolution between formulations should be the same both *in vitro* and *in vivo* (as emphasized by Vaughan and Leach). Since the time over which the predictions are reliable is limited by the fastest dissolving formulation to be of use, the dissolution profiles of the formulations to be compared must be similar.

In the present analysis, we took the optimal situation in which the *in vitro* dissolution profile has been assumed to be exactly the same as occurs *in vivo*. If the time scales, however, are different—and this cannot be predicted *a priori*—the difficulties that are created may invalidate the method.

[1] The dissolution profile for the log normal law was calculated using Wagner's (3) method:

$$\frac{dA}{dt} = \frac{e^{-x^2/2}}{\sqrt{2\pi}\sigma t \log_{10} e}$$

and:

$$x = \frac{\log_{10} t - x \text{ mean}}{\sigma}$$

where x mean and σ are the mean and standard deviation of the distribution, respectively. However, rather than fixing x mean and letting σ vary as Wagner did, we fixed the ratio of x mean/σ (= 5), thus giving a more realistic spread of dissolution profiles.

(1) D. P. Vaughan and R. H. Leach, *J. Pharm. Sci.*, **65**, 601 (1976).

(2) J. G. Wagner, "Biopharmaceutics and Relevant Pharmacokinetics," Drug Intelligence Publications, Hamilton, Ill., 1971, chap. 16.

(3) J. G. Wagner, *J. Pharm. Sci.*, **58**, 1253 (1969).

Leon J. Aarons
Malcolm Rowland [x]
Department of Pharmacy
University of Manchester
Manchester, M13 9PL
England

Received October 29, 1976.
Accepted for publication January 3, 1977.

[x] To whom inquiries should be directed.

Screening Procedure for Phorbol Esters Using Brine Shrimp (*Artemia salina*) Larvae

Keyphrases □ Phorbol esters, various—toxicity to brine shrimp larvae related to cocarcinogenic potency □ Brine shrimp larvae—toxicity of various phorbol esters related to cocarcinogenic potency □ Toxicity—various phorbol esters to brine shrimp larvae, related to cocarcinogenic potency □ Cocarcinogenic potency—various phorbol esters, related to toxicity to brine shrimp larvae

To the Editor:

In the continuing search for anticancer agents of natural origin, the recently discovered antileukemic property of phorbol 12-tigliate 13-decanoate (1), from *Croton tiglium* (Euphorbiaceae), is interesting since phorbol esters are better known as irritant cocarcinogens (2). Unlike other naturally occurring anticancer compounds, intensive work has been performed on the activity of phorbol esters in two-stage carcinogenesis experiments, including their interactions with nucleic acids and their effect on the uptake of precursors of these and other macromolecules by the mammalian cell (3). Isolation of further phorbol and related esters from the plant kingdom could, in addition to providing possible new antileukemic agents, yield unique structure–activity information on the complex relationships between irritancy, cocarcinogenicity, and antileukemic activity at the cellular level.

During the fractionation of anticancer compounds from plant sources, there is often a considerable delay between isolation and receipt of biological data. Several screening

Table I—ED_{50}'s of Phorbol Esters and Two Piscicides to *A. salina* Larvae (Brine Shrimp)

Compound	ED_{50}, μg/ml	$f_{ED_{50}}$	95–100% Confidence Limits, μg/ml
Phorbol 12-tetradecanoate 13-acetate	3.8	1.96	1.9–7.4
Phorbol 12,13-didecanoate	6.8	1.96	3.5–13.3
Phorbol 12,13-dibenzoate	11.8	1.96	6.0–23.1
Phorbol	>1000	—	—
4α-Phorbol 12,13-didecanoate	>1000	—	—
Rotenone	0.5	1.71	0.3–0.9
Picrotoxin	2510	1.75	1430–4400

procedures to hasten this time period previously were employed, including the use of goldfish (1) and killifish (4), acute toxicity to frogs (2), and irritant activity on the mouse ear (2). All of these methods require some cost in the provision of specialized laboratory personnel and in animal housing and maintenance. We have found the toxicity to brine shrimp (*Artemia salina*) larvae to be selective between phorbol esters of different cocarcinogenic potencies (1) and also to be sensitive when compared with the piscicides rotenone (4) and picrotoxin (5). This method not only allows the recovery of samples and requires little capital outlay of laboratory space but is capable of being performed by persons with little formal training in biology.

In the laboratory procedure, brine shrimp nauplii were hatched in artificial sea water and separated from unhatched eggs 2 days after seeding. Since phorbol esters are unstable even in the solid form (6), their purity was affirmed in several TLC systems (7). Solutions prepared in methanol were pipetted into numbered 30-ml beakers, with each dilution varying from the last by a factor of log 2. The solvent was removed, the residue in each beaker was dissolved in 0.2 ml of 1% polysorbate 60, and 2.8 ml of a brine shrimp suspension was added so that 30–50 *A. salina* were contained in 3.0 ml.

Forty-eight hours after setting up the experiment, counts were made of dead shrimp. The total population count was determined after sacrifice of survivors with 37.5% formaldehyde solution. Spontaneous mortality in polysorbate controls was <1% and was not considered in subsequent statistical evaluation. Mean values of percent dead animals were plotted on probability paper against log doses, and 95–100% confidence limits of the effective mortality dose (ED_{50}) were obtained in micrograms per milliliter by the method of Litchfield and Wilcoxon (8). Satisfactory statistical limits were obtained when eight replicates per compound were employed.

The potentiality of *A. salina* as an organism for monitoring phorbol esters is clearly shown in Table I. The highly cocarcinogenic compounds phorbol 12-tetradecanoate 13-acetate and phorbol 12,13-didecanoate and the weaker cocarcinogen phorbol 12,13-dibenzoate approached the high lethality of rotenone, approximately in proportion to their tumorigenic potencies (3). The low toxicity of picrotoxin demonstrated that the test system was not generally sensitive to potent phytotoxins. Phorbol, an inactive irritant cocarcinogen, did not affect the brine shrimp. The differential response of this Crustacean branchiopod to phorbol 12,13-didecanoate and its 4α-isomer, which is not cocarcinogenic, shows for the first time structural specificity about the C-4 hydroxyl of the tigliane skeleton in an invertebrate system.

(1) S. M. Kupchan, I. Uchida, A. R. Branfman, R. G. Kailey, and B. Yu Fei, *Science*, **191**, 572 (1976).
(2) E. Hecker and R. Schmidt, "Progress in the Chemistry of Organic Natural Products," vol. 31, Springer-Verlag, Vienna, Austria, 1974, pp. 377–467.
(3) R. K. Boutwell, "Critical Reviews in Toxicology," vol. 2, CRC Press, Cleveland, Ohio, 1974, pp. 419–443.
(4) K. Sakata, K. Kawazu, and T. Mitsui, *Agr. Biol. Chem.*, **35**, 1084 (1971).
(5) L. A. Porter, *Chem. Rev.*, **67**, 441 (1967).
(6) R. Schmidt and E. Hecker, *Cancer Res.*, **35**, 1375 (1975).
(7) F. J. Evans and A. D. Kinghorn, *J. Chromatogr.*, **87**, 443 (1973).
(8) H. T. Litchfield, Jr., and F. Wilcoxon, *J. Pharmacol. Exp. Ther.*, **96**, 99 (1949).

A. Douglas Kinghorn
Karla K. Harjes
Norman J. Doorenbos [x]
Department of Pharmacognosy
School of Pharmacy
University of Mississippi
University, MS 38677

Received January 28, 1977.
Accepted for publication June 15, 1977.
[x] To whom inquiries should be directed.

REVIEWS

Amino-Acids, Peptides, and Proteins, Vol. 8. A Specialist Periodical Report. Edited by R. C. SHEPPARD. The Chemical Society, Burlington House, London W1V OBN, England, 1976. 504 pp. 16 × 24 cm. Price $56.00. Available from Special Issue Sales, American Chemical Society, 1155 Sixteenth St., N.W., Washington, DC 20036.

This eighth volume of the continuing series on amino acids, peptides, and proteins covers the literature published in 1975. Like the previous volumes, it is of great help to all of us whose interests lie in peptide and protein chemistry.

The areas reviewed are: amino acids, including their synthesis and resolution; structural investigations of peptides and proteins, which covers protein isolation, characterization, chemical modification, sequence methodologies, and X-ray studies; peptide synthesis; peptides with structural features not typical of proteins; and a very welcome chapter on chemical structure and biological activity of hormones and related compounds. Included in the pertinent chapters are tabulations of primary structures published during 1975 as well as lists of syntheses achieved and of useful amino acid derivatives for peptide synthesis.

Overall, this volume maintains the very high standards we have been accustomed to in this series of Specialist Reports.

Reviewed by Brian J. Johnson
Department of Microbiology
University of Alabama Medical School
Birmingham, AL 35294

Contemporary Liquid Chromatography. By R. P. W. SCOTT. Wiley, 605 Third Ave., New York, NY 10016, 1976. 326 pp. 16 × 24 cm. Price $21.50.

The outstanding feature of this new book on liquid chromatography is the inordinate number of typographical errors. Errors in syntax and awkward terminology also abound. It is apparent that an editorial vacancy occurred during the production of this latest volume in the *Techniques in Chemistry* series. Hopefully this lapse can be avoided in future volumes.

There is definitely a need for a comprehensive book on modern chromatographic (gas as well as liquid) techniques. The present volume, which purports to cover liquid chromatography, falls far short of what is needed, primarily due to errors of omission and emphasis. There is, by intention, no coverage of thin layer chromatography, size exclusion chromatography, or affinity chromatography, thus abrogating coverage of at least 50% of "contemporary liquid chromatography." The author avoids meaningful discussion of applications to prevent the book from becoming dated. Unfortunately, this tactical maneuver leaves little to offer the practicing chromatographer. It would have clearly been better to discuss theoretical developments and instrumentation in the context of practical problem solving. Although a major portion of the book is devoted to theory, the theory presented is not adequately developed from first principles to interest the serious student, nor is it adequately explained to afford benefit to the casual applications-minded reader.

Approximately one-third of the book is devoted to instrumentation, and in these sections Scott is far more successful. The difficulty here is that the material is either out of date or has been adequately covered (at this survey level) in other recent texts. The author often fails to make value judgements about equipment options, but when an opinion is ventured, I find myself in disagreement. The statement that "it has obviously been established that LC/MS will be a common technique in the future" is typical of a number of shortsighted comments which cannot be substantiated.

The chapter devoted to Stationary and Mobile Phases for Liquid Chromatography suffers in the same manner as the rest of the volume. There is nothing new, there are unbelievable errors of omission (ion exchange is "not within the scope of this book"), and important recent developments have been given short shift (*e.g.*, the application of chemically bonded microparticle stationary phase materials).

As a whole, this book does not do justice to the excellent reputation of its author. Nevertheless, I am pleased to own a copy because there are many good individual sections and it is always useful to get a different perspective. I cannot recommend this volume for the beginner.

Reviewed by Peter T. Kissinger
Department of Chemistry
Purdue University
West Lafayette, IN 47907

Colorimetric and Fluorimetric Analysis of Steroids. By J. BARTOS and M. PESEZ. Academic (London), 24–28 Oval Rd., London, NW1 7DX, England, 1976. vii + 274 pp. 15.5 × 23.5 cm. Price $21.50.

Analytical methodology for steroids is important since these compounds are usually found at low concentrations not only in dosage forms but also in biological samples. There is an extensive literature regarding spectrophotometric analysis of steroids, while literature involving fluorometric methods is scant and many of the procedures are nonspecific. The authors of this book have successfully compiled a volume detailing many colorimetric and fluorometric procedures for those natural or synthetic steroids of physiological interest.

The methods reported are quantitative rather than qualitative, and only those based on chemical reactions that yield a color or fluorescence in solution are discussed. Many of the procedures were tested in the authors' laboratory and even modified when an improvement could be made. This testing provided a selection procedure for inclusion in the book, where several methods based on the reaction and reagents were found in the literature.

After general chapters on steroid nomenclature, functional group analysis of steroids, and halochromism and halofluorism reactions, there are specific sections dealing with sterols and vitamin D, bile acids, estrogens, gestogens, androgens, corticosteroids, contraceptive progestogens, cardiac glycosides, steroid saponins and sapogenins, and steroid alkaloids. Included in each chapter are general colorimetric and fluorometric procedures for the particular class of steroid. These are usually followed by specific methodology for the more important compounds in that class.

The book is well written and undoubtedly will be useful to pharmaceutical scientists involved in steroid research. It should be purchased for inclusion in a university science library collection. It is not recommended for use as a pharmacy course textbook since it is a compilation of analytical methodology. Whether or not it is included in a school of pharmacy library will depend upon the research interests of the staff since most undergraduates will not benefit from the volume.

Reviewed by James T. Stewart
School of Pharmacy
University of Georgia
Athens, GA 30602

Progress in Drug Metabolism. Vol. 1. Edited by J. W. BRIDGES and L. F. CHASSEAUD. Wiley, 605 Third Ave., New York, NY 10016, 1976. 286 pp. 15 × 25 cm.

This first volume of a new review series contains five chapters: Newer Developments in the Mass Spectrometry of Drugs and Metabolites by B. J. Millard, Bioactivation and Cytotoxicity by T. A. Connors, The Role of Epoxides in Bioactivation and Carcinogenesis by R. C. Garner, Clinical Aspects of Microsomal Enzyme Induction by J. O. Hunter and L. F.

REVIEWS

Amino-Acids, Peptides, and Proteins, Vol. 8. A Specialist Periodical Report. Edited by R. C. SHEPPARD. The Chemical Society, Burlington House, London W1V OBN, England, 1976. 504 pp. 16 × 24 cm. Price $56.00. Available from Special Issue Sales, American Chemical Society, 1155 Sixteenth St., N.W., Washington, DC 20036.

This eighth volume of the continuing series on amino acids, peptides, and proteins covers the literature published in 1975. Like the previous volumes, it is of great help to all of us whose interests lie in peptide and protein chemistry.

The areas reviewed are: amino acids, including their synthesis and resolution; structural investigations of peptides and proteins, which covers protein isolation, characterization, chemical modification, sequence methodologies, and X-ray studies; peptide synthesis; peptides with structural features not typical of proteins; and a very welcome chapter on chemical structure and biological activity of hormones and related compounds. Included in the pertinent chapters are tabulations of primary structures published during 1975 as well as lists of syntheses achieved and of useful amino acid derivatives for peptide synthesis.

Overall, this volume maintains the very high standards we have been accustomed to in this series of Specialist Reports.

Reviewed by Brian J. Johnson
Department of Microbiology
University of Alabama Medical School
Birmingham, AL 35294

Contemporary Liquid Chromatography. By R. P. W. SCOTT. Wiley, 605 Third Ave., New York, NY 10016, 1976. 326 pp. 16 × 24 cm. Price $21.50.

The outstanding feature of this new book on liquid chromatography is the inordinate number of typographical errors. Errors in syntax and awkward terminology also abound. It is apparent that an editorial vacancy occurred during the production of this latest volume in the *Techniques in Chemistry* series. Hopefully this lapse can be avoided in future volumes.

There is definitely a need for a comprehensive book on modern chromatographic (gas as well as liquid) techniques. The present volume, which purports to cover liquid chromatography, falls far short of what is needed, primarily due to errors of omission and emphasis. There is, by intention, no coverage of thin layer chromatography, size exclusion chromatography, or affinity chromatography, thus abrogating coverage of at least 50% of "contemporary liquid chromatography." The author avoids meaningful discussion of applications to prevent the book from becoming dated. Unfortunately, this tactical maneuver leaves little to offer the practicing chromatographer. It would have clearly been better to discuss theoretical developments and instrumentation in the context of practical problem solving. Although a major portion of the book is devoted to theory, the theory presented is not adequately developed from first principles to interest the serious student, nor is it adequately explained to afford benefit to the casual applications-minded reader.

Approximately one-third of the book is devoted to instrumentation, and in these sections Scott is far more successful. The difficulty here is that the material is either out of date or has been adequately covered (at this survey level) in other recent texts. The author often fails to make value judgements about equipment options, but when an opinion is ventured, I find myself in disagreement. The statement that "it has obviously been established that LC/MS will be a common technique in the future" is typical of a number of shortsighted comments which cannot be substantiated.

The chapter devoted to Stationary and Mobile Phases for Liquid Chromatography suffers in the same manner as the rest of the volume. There is nothing new, there are unbelievable errors of omission (ion exchange is "not within the scope of this book"), and important recent developments have been given short shift (*e.g.*, the application of chemically bonded microparticle stationary phase materials).

As a whole, this book does not do justice to the excellent reputation of its author. Nevertheless, I am pleased to own a copy because there are many good individual sections and it is always useful to get a different perspective. I cannot recommend this volume for the beginner.

Reviewed by Peter T. Kissinger
Department of Chemistry
Purdue University
West Lafayette, IN 47907

Colorimetric and Fluorimetric Analysis of Steroids. By J. BARTOS and M. PESEZ. Academic (London), 24–28 Oval Rd., London, NW1 7DX, England, 1976. vii + 274 pp. 15.5 × 23.5 cm. Price $21.50.

Analytical methodology for steroids is important since these compounds are usually found at low concentrations not only in dosage forms but also in biological samples. There is an extensive literature regarding spectrophotometric analysis of steroids, while literature involving fluorometric methods is scant and many of the procedures are nonspecific. The authors of this book have successfully compiled a volume detailing many colorimetric and fluorometric procedures for those natural or synthetic steroids of physiological interest.

The methods reported are quantitative rather than qualitative, and only those based on chemical reactions that yield a color or fluorescence in solution are discussed. Many of the procedures were tested in the authors' laboratory and even modified when an improvement could be made. This testing provided a selection procedure for inclusion in the book, where several methods based on the reaction and reagents were found in the literature.

After general chapters on steroid nomenclature, functional group analysis of steroids, and halochromism and halofluorism reactions, there are specific sections dealing with sterols and vitamin D, bile acids, estrogens, gestogens, androgens, corticosteroids, contraceptive progestogens, cardiac glycosides, steroid saponins and sapogenins, and steroid alkaloids. Included in each chapter are general colorimetric and fluorometric procedures for the particular class of steroid. These are usually followed by specific methodology for the more important compounds in that class.

The book is well written and undoubtedly will be useful to pharmaceutical scientists involved in steroid research. It should be purchased for inclusion in a university science library collection. It is not recommended for use as a pharmacy course textbook since it is a compilation of analytical methodology. Whether or not it is included in a school of pharmacy library will depend upon the research interests of the staff since most undergraduates will not benefit from the volume.

Reviewed by James T. Stewart
School of Pharmacy
University of Georgia
Athens, GA 30602

Progress in Drug Metabolism. Vol. 1. Edited by J. W. BRIDGES and L. F. CHASSEAUD. Wiley, 605 Third Ave., New York, NY 10016, 1976. 286 pp. 15 × 25 cm.

This first volume of a new review series contains five chapters: Newer Developments in the Mass Spectrometry of Drugs and Metabolites by B. J. Millard, Bioactivation and Cytotoxicity by T. A. Connors, The Role of Epoxides in Bioactivation and Carcinogenesis by R. C. Garner, Clinical Aspects of Microsomal Enzyme Induction by J. O. Hunter and L. F.

REVIEWS

Amino-Acids, Peptides, and Proteins, Vol. 8. A Specialist Periodical Report. Edited by R. C. SHEPPARD. The Chemical Society, Burlington House, London W1V OBN, England, 1976. 504 pp. 16 × 24 cm. Price $56.00. Available from Special Issue Sales, American Chemical Society, 1155 Sixteenth St., N.W., Washington, DC 20036.

This eighth volume of the continuing series on amino acids, peptides, and proteins covers the literature published in 1975. Like the previous volumes, it is of great help to all of us whose interests lie in peptide and protein chemistry.

The areas reviewed are: amino acids, including their synthesis and resolution; structural investigations of peptides and proteins, which covers protein isolation, characterization, chemical modification, sequence methodologies, and X-ray studies; peptide synthesis; peptides with structural features not typical of proteins; and a very welcome chapter on chemical structure and biological activity of hormones and related compounds. Included in the pertinent chapters are tabulations of primary structures published during 1975 as well as lists of syntheses achieved and of useful amino acid derivatives for peptide synthesis.

Overall, this volume maintains the very high standards we have been accustomed to in this series of Specialist Reports.

Reviewed by Brian J. Johnson
Department of Microbiology
University of Alabama Medical School
Birmingham, AL 35294

Contemporary Liquid Chromatography. By R. P. W. SCOTT. Wiley, 605 Third Ave., New York, NY 10016, 1976. 326 pp. 16 × 24 cm. Price $21.50.

The outstanding feature of this new book on liquid chromatography is the inordinate number of typographical errors. Errors in syntax and awkward terminology also abound. It is apparent that an editorial vacancy occurred during the production of this latest volume in the *Techniques in Chemistry* series. Hopefully this lapse can be avoided in future volumes.

There is definitely a need for a comprehensive book on modern chromatographic (gas as well as liquid) techniques. The present volume, which purports to cover liquid chromatography, falls far short of what is needed, primarily due to errors of omission and emphasis. There is, by intention, no coverage of thin layer chromatography, size exclusion chromatography, or affinity chromatography, thus abrogating coverage of at least 50% of "contemporary liquid chromatography." The author avoids meaningful discussion of applications to prevent the book from becoming dated. Unfortunately, this tactical maneuver leaves little to offer the practicing chromatographer. It would have clearly been better to discuss theoretical developments and instrumentation in the context of practical problem solving. Although a major portion of the book is devoted to theory, the theory presented is not adequately developed from first principles to interest the serious student, nor is it adequately explained to afford benefit to the casual applications-minded reader.

Approximately one-third of the book is devoted to instrumentation, and in these sections Scott is far more successful. The difficulty here is that the material is either out of date or has been adequately covered (at this survey level) in other recent texts. The author often fails to make value judgements about equipment options, but when an opinion is ventured, I find myself in disagreement. The statement that "it has obviously been established that LC/MS will be a common technique in the future" is typical of a number of shortsighted comments which cannot be substantiated.

The chapter devoted to Stationary and Mobile Phases for Liquid Chromatography suffers in the same manner as the rest of the volume. There is nothing new, there are unbelievable errors of omission (ion exchange is "not within the scope of this book"), and important recent developments have been given short shift (*e.g.*, the application of chemically bonded microparticle stationary phase materials).

As a whole, this book does not do justice to the excellent reputation of its author. Nevertheless, I am pleased to own a copy because there are many good individual sections and it is always useful to get a different perspective. I cannot recommend this volume for the beginner.

Reviewed by Peter T. Kissinger
Department of Chemistry
Purdue University
West Lafayette, IN 47907

Colorimetric and Fluorimetric Analysis of Steroids. By J. BARTOS and M. PESEZ. Academic (London), 24–28 Oval Rd., London, NW1 7DX, England, 1976. vii + 274 pp. 15.5 × 23.5 cm. Price $21.50.

Analytical methodology for steroids is important since these compounds are usually found at low concentrations not only in dosage forms but also in biological samples. There is an extensive literature regarding spectrophotometric analysis of steroids, while literature involving fluorometric methods is scant and many of the procedures are nonspecific. The authors of this book have successfully compiled a volume detailing many colorimetric and fluorometric procedures for those natural or synthetic steroids of physiological interest.

The methods reported are quantitative rather than qualitative, and only those based on chemical reactions that yield a color or fluorescence in solution are discussed. Many of the procedures were tested in the authors' laboratory and even modified when an improvement could be made. This testing provided a selection procedure for inclusion in the book, where several methods based on the reaction and reagents were found in the literature.

After general chapters on steroid nomenclature, functional group analysis of steroids, and halochromism and halofluorism reactions, there are specific sections dealing with sterols and vitamin D, bile acids, estrogens, gestogens, androgens, corticosteroids, contraceptive progestogens, cardiac glycosides, steroid saponins and sapogenins, and steroid alkaloids. Included in each chapter are general colorimetric and fluorometric procedures for the particular class of steroid. These are usually followed by specific methodology for the more important compounds in that class.

The book is well written and undoubtedly will be useful to pharmaceutical scientists involved in steroid research. It should be purchased for inclusion in a university science library collection. It is not recommended for use as a pharmacy course textbook since it is a compilation of analytical methodology. Whether or not it is included in a school of pharmacy library will depend upon the research interests of the staff since most undergraduates will not benefit from the volume.

Reviewed by James T. Stewart
School of Pharmacy
University of Georgia
Athens, GA 30602

Progress in Drug Metabolism. Vol. 1. Edited by J. W. BRIDGES and L. F. CHASSEAUD. Wiley, 605 Third Ave., New York, NY 10016, 1976. 286 pp. 15 × 25 cm.

This first volume of a new review series contains five chapters: Newer Developments in the Mass Spectrometry of Drugs and Metabolites by B. J. Millard, Bioactivation and Cytotoxicity by T. A. Connors, The Role of Epoxides in Bioactivation and Carcinogenesis by R. C. Garner, Clinical Aspects of Microsomal Enzyme Induction by J. O. Hunter and L. F.

Chasseaud, and Drug-Serum Protein Interactions and Their Biological Significance by J. W. Bridges and A. G. E. Wilson.

This volume is English in origin and evidently was planned to serve in conjunction with the Chemical Society's series "Foreign Compound Metabolism in Mammals." According to D. V. Parke's foreword, "Progress in Drug Metabolism" will review advances in the general fundamentals of drug metabolism, reactions, phenomena, techniques, *etc.*, while "Foreign Compound Metabolism in Mammals" will deal with the metabolic fate of individual chemicals. Presumably, this philosophy will continue to be observed in future volumes of this series.

Four of these five reviews are on topics that have been extensively and repeatedly reviewed in the past several years (Bioactivation and Cytotoxicity is the exception). Mass spectrometry, epoxidation, enzyme induction, and serum protein binding are all, of course, topics of continuing and intense interest in the area of drug metabolism, but progress is never sufficiently rapid to permit completely original reviews every 2 years or so. Most of the content of these reviews, therefore, has been covered recently. Three of the reviews, as originally written, had 1974 as their last reference dates, although one of these contained 1975 references in a note added in proof. The other two reviews, which have the editors of the volume among their authors, have 1975 references (and one reference to a 1976 paper of the authors in press). This first volume of "Progress in Drug Metabolism" was evidently a long time a-borning.

The reviews are uniformly well written, quite readable, and contain some interesting insights. Those who are relatively unfamiliar with the subject matter would do well to read these reviews in preference to other almost as recent reviews of the same topics. The rest of us could profit by rereading for fresh insight on these subjects. I'm glad I did. Libraries will certainly need to collect this series. Perhaps what's really needed is a series of short monographs which provide an annual drug metabolism-centered update.

The content of the review on plasma protein binding of drugs is especially interesting when it indicates that there is still a dearth of fundamental understanding of this area. Bridges and Wilson find it necessary to correct many of the same misconceptions that Goldstein was correcting in 1949. Perhaps there can't be too many reviews on topics of central importance to drug metabolism and pharmacokinetics.

Reviewed by Morris Pfeffer
Bristol Laboratories
Syracuse, NY 13201

Lehrbuch der Pharmazeutischen Chemie, 8th Ed. By HARRY AUTERHOFF and JOACHIM KNABE. Wissenschaftliche Verlagsgesellschaft m.b.H., 7 Stuttgart 1, Postfach 40, W. Germany, 1976. 591 pp. 17 × 25 cm. Price $25.00 (62 DM).

This review was undertaken on the assumption that my colleagues might find it of interest to know what is available to teachers of medicinal chemistry/pharmaceutical chemistry in German-speaking countries.

This book by Auterhoff (who is a professor at Tübingen University) and Knabe is in its eighth edition since 1962 and thus has had ample opportunity for frequent updating. However, despite occasional lapses into modernity, such as a brief discussion of prostaglandins (p. 177) and a mention of cyclic AMP (p. 487), it is basically an old-fashioned textbook.

There are several positive points. The first 99 pages, the so-called inorganic part, is a good review for the student. Beginning with nomenclature and going through the seven groups of the periodic system (each as a chapter), a mini subtext of inorganic pharmaceutical chemistry is presented. This section is not truly inorganic because organometallic drugs are discussed (*e.g.*, bismuth subgallate and tartar emetic), as are organic analytical reagents such as rhodamine B because of its use for the analysis of antimony compounds.

The second part of the book (the remainder) is much more organic than current American texts because it mixes more organic with the medicinal chemistry. Not only syntheses (which are certainly not excessive) but also some refresher material such as nomenclature, ring systems, fundamentals of physical methods (spectroscopy), and organic reactions, including aromatic substitution rules, are given. A little biochemistry is also reviewed, *e.g.*, the stereochemistry of amino and fatty acids and coenzyme A. The division of this section is very reminiscent of the older editions of Olsen's and Gisvold's "Textbook of Organic Medicinal and Pharmaceutical Chemistry" in that it contains chapters on olefins, alcohols, ketones, *etc.*, followed by chapters based on therapeutics. There is a separate chapter on hormones, vitamins, and enzymes and one on ADME, which curiously is at the end of the book rather than with the introductory chapters. There are some references, and the index appears adequate. The American reader will encounter unfamiliar trade names (*e.g.*, Endoxan for cyclophosphamide) and unfamiliar variants of familiar drugs [*e.g.*, flucloxacillin (floxacillin), where fluorine replaces one chlorine in dicloxacillin].

The grave shortcoming of the book, however, is the almost total absence of discussions of drug action mechanisms. A newcomer to the field, say one conversant with organic and some biochemistry, after studying the text, would still not really know what drugs are—in the modern sense. There are occasional brief, almost meaningless statements such as: "polymixin raises the permeability of the cell membrane," or, regarding penicillin, "it is the building of cell wall construction material, murein, which is inhibited," with no further explanation or discussion. Rather than discovering that asparagus contains 1.2 mg of folic acid/100 g, I would have preferred to see a discussion devoted to dihydrofolic acid reductase inhibition mechanisms of antimalarials, methotrexate, or sulfonamide action. In the chapter on sympathomimetics, there is a statement on receptors but no real explanation—not a word on structure–activity relationships. Because of this glaring shortcoming, I feel this book is not suitable for the modern pharmaceutical curriculum.

Reviewed by Alex Gringauz
Arnold and Marie Schwartz College of Pharmacy and Health Sciences
Long Island University
Brooklyn, NY 11201

Interactions of Drugs of Abuse. Annals of the New York Academy of Sciences, Vol. 281. Edited by ELLIOT S. VESELL and MONIQUE C. BRAUDE. The New York Academy of Sciences, 2 East 63rd St., New York, NY 10021, 1976. 489 pp. 15 × 23 cm.

This book contains the proceedings of the first Conference on Interactions of Drugs of Abuse held in New York, March 9–11, 1976, at the New York Academy of Sciences. This conference was rather timely since there is an ever-increasing polydrug use throughout the United States and the world.

The subject matter of the conference was divided into two parts: (*a*) general information concerning the molecular, cellular, and clinical aspects of drug interaction; and (*b*) the major thrust of the conference, determination of the interaction of specific drugs and drug classes including marijuana, narcotics and narcotic antagonists, CNS depressants, CNS stimulants, and hallucinogens. Although extensive effort was made to define all the potential ramifications of drug interactions, it is quite obvious that only the surface has been scratched. In discussing molecular, cellular, and clinical aspects of drug interaction, one could devote several volumes to describing results of experiments designed to study such interactions. Likewise, specific drug interactions could be the subject of a tremendous amount of research effort. In general, this book is well written and the data are presented in an organized fashion.

This conference has opened up a new area of research which will be explored vigorously in the next several years. Because our society is prone to polydrug use, the importance of drug interaction research becomes paramount not only for drugs of abuse but for all drugs in general.

Reviewed by R. Duane Sofia
Wallace Laboratories
Cranbury, NJ 08512

NOTICES

Venous Thromboembolism. Prevention and Treatment. Edited by JOHN L. MADDEN and MICHAEL HUME. Appleton-Century-Crofts, 292 Madison Ave., New York, NY 10017, 1976. 240 pp. 15 × 23 cm.

REVIEWS

Amino-Acids, Peptides, and Proteins, Vol. 8. A Specialist Periodical Report. Edited by R. C. SHEPPARD. The Chemical Society, Burlington House, London W1V OBN, England, 1976. 504 pp. 16 × 24 cm. Price $56.00. Available from Special Issue Sales, American Chemical Society, 1155 Sixteenth St., N.W., Washington, DC 20036.

This eighth volume of the continuing series on amino acids, peptides, and proteins covers the literature published in 1975. Like the previous volumes, it is of great help to all of us whose interests lie in peptide and protein chemistry.

The areas reviewed are: amino acids, including their synthesis and resolution; structural investigations of peptides and proteins, which covers protein isolation, characterization, chemical modification, sequence methodologies, and X-ray studies; peptide synthesis; peptides with structural features not typical of proteins; and a very welcome chapter on chemical structure and biological activity of hormones and related compounds. Included in the pertinent chapters are tabulations of primary structures published during 1975 as well as lists of syntheses achieved and of useful amino acid derivatives for peptide synthesis.

Overall, this volume maintains the very high standards we have been accustomed to in this series of Specialist Reports.

Reviewed by Brian J. Johnson
Department of Microbiology
University of Alabama Medical School
Birmingham, AL 35294

Contemporary Liquid Chromatography. By R. P. W. SCOTT. Wiley, 605 Third Ave., New York, NY 10016, 1976. 326 pp. 16 × 24 cm. Price $21.50.

The outstanding feature of this new book on liquid chromatography is the inordinate number of typographical errors. Errors in syntax and awkward terminology also abound. It is apparent that an editorial vacancy occurred during the production of this latest volume in the *Techniques in Chemistry* series. Hopefully this lapse can be avoided in future volumes.

There is definitely a need for a comprehensive book on modern chromatographic (gas as well as liquid) techniques. The present volume, which purports to cover liquid chromatography, falls far short of what is needed, primarily due to errors of omission and emphasis. There is, by intention, no coverage of thin layer chromatography, size exclusion chromatography, or affinity chromatography, thus abrogating coverage of at least 50% of "contemporary liquid chromatography." The author avoids meaningful discussion of applications to prevent the book from becoming dated. Unfortunately, this tactical maneuver leaves little to offer the practicing chromatographer. It would have clearly been better to discuss theoretical developments and instrumentation in the context of practical problem solving. Although a major portion of the book is devoted to theory, the theory presented is not adequately developed from first principles to interest the serious student, nor is it adequately explained to afford benefit to the casual applications-minded reader.

Approximately one-third of the book is devoted to instrumentation, and in these sections Scott is far more successful. The difficulty here is that the material is either out of date or has been adequately covered (at this survey level) in other recent texts. The author often fails to make value judgements about equipment options, but when an opinion is ventured, I find myself in disagreement. The statement that "it has obviously been established that LC/MS will be a common technique in the future" is typical of a number of shortsighted comments which cannot be substantiated.

The chapter devoted to Stationary and Mobile Phases for Liquid Chromatography suffers in the same manner as the rest of the volume. There is nothing new, there are unbelievable errors of omission (ion exchange is "not within the scope of this book"), and important recent developments have been given short shift (*e.g.*, the application of chemically bonded microparticle stationary phase materials).

As a whole, this book does not do justice to the excellent reputation of its author. Nevertheless, I am pleased to own a copy because there are many good individual sections and it is always useful to get a different perspective. I cannot recommend this volume for the beginner.

Reviewed by Peter T. Kissinger
Department of Chemistry
Purdue University
West Lafayette, IN 47907

Colorimetric and Fluorimetric Analysis of Steroids. By J. BARTOS and M. PESEZ. Academic (London), 24–28 Oval Rd., London, NW1 7DX, England, 1976. vii + 274 pp. 15.5 × 23.5 cm. Price $21.50.

Analytical methodology for steroids is important since these compounds are usually found at low concentrations not only in dosage forms but also in biological samples. There is an extensive literature regarding spectrophotometric analysis of steroids, while literature involving fluorometric methods is scant and many of the procedures are nonspecific. The authors of this book have successfully compiled a volume detailing many colorimetric and fluorometric procedures for those natural or synthetic steroids of physiological interest.

The methods reported are quantitative rather than qualitative, and only those based on chemical reactions that yield a color or fluorescence in solution are discussed. Many of the procedures were tested in the authors' laboratory and even modified when an improvement could be made. This testing provided a selection procedure for inclusion in the book, where several methods based on the reaction and reagents were found in the literature.

After general chapters on steroid nomenclature, functional group analysis of steroids, and halochromism and halofluorism reactions, there are specific sections dealing with sterols and vitamin D, bile acids, estrogens, gestogens, androgens, corticosteroids, contraceptive progestogens, cardiac glycosides, steroid saponins and sapogenins, and steroid alkaloids. Included in each chapter are general colorimetric and fluorometric procedures for the particular class of steroid. These are usually followed by specific methodology for the more important compounds in that class.

The book is well written and undoubtedly will be useful to pharmaceutical scientists involved in steroid research. It should be purchased for inclusion in a university science library collection. It is not recommended for use as a pharmacy course textbook since it is a compilation of analytical methodology. Whether or not it is included in a school of pharmacy library will depend upon the research interests of the staff since most undergraduates will not benefit from the volume.

Reviewed by James T. Stewart
School of Pharmacy
University of Georgia
Athens, GA 30602

Progress in Drug Metabolism. Vol. 1. Edited by J. W. BRIDGES and L. F. CHASSEAUD. Wiley, 605 Third Ave., New York, NY 10016, 1976. 286 pp. 15 × 25 cm.

This first volume of a new review series contains five chapters: Newer Developments in the Mass Spectrometry of Drugs and Metabolites by B. J. Millard, Bioactivation and Cytotoxicity by T. A. Connors, The Role of Epoxides in Bioactivation and Carcinogenesis by R. C. Garner, Clinical Aspects of Microsomal Enzyme Induction by J. O. Hunter and L. F.

Chasseaud, and Drug-Serum Protein Interactions and Their Biological Significance by J. W. Bridges and A. G. E. Wilson.

This volume is English in origin and evidently was planned to serve in conjunction with the Chemical Society's series "Foreign Compound Metabolism in Mammals." According to D. V. Parke's foreword, "Progress in Drug Metabolism" will review advances in the general fundamentals of drug metabolism, reactions, phenomena, techniques, *etc.*, while "Foreign Compound Metabolism in Mammals" will deal with the metabolic fate of individual chemicals. Presumably, this philosophy will continue to be observed in future volumes of this series.

Four of these five reviews are on topics that have been extensively and repeatedly reviewed in the past several years (Bioactivation and Cytotoxicity is the exception). Mass spectrometry, epoxidation, enzyme induction, and serum protein binding are all, of course, topics of continuing and intense interest in the area of drug metabolism, but progress is never sufficiently rapid to permit completely original reviews every 2 years or so. Most of the content of these reviews, therefore, has been covered recently. Three of the reviews, as originally written, had 1974 as their last reference dates, although one of these contained 1975 references in a note added in proof. The other two reviews, which have the editors of the volume among their authors, have 1975 references (and one reference to a 1976 paper of the authors in press). This first volume of "Progress in Drug Metabolism" was evidently a long time a-borning.

The reviews are uniformly well written, quite readable, and contain some interesting insights. Those who are relatively unfamiliar with the subject matter would do well to read these reviews in preference to other almost as recent reviews of the same topics. The rest of us could profit by rereading for fresh insight on these subjects. I'm glad I did. Libraries will certainly need to collect this series. Perhaps what's really needed is a series of short monographs which provide an annual drug metabolism-centered update.

The content of the review on plasma protein binding of drugs is especially interesting when it indicates that there is still a dearth of fundamental understanding of this area. Bridges and Wilson find it necessary to correct many of the same misconceptions that Goldstein was correcting in 1949. Perhaps there can't be too many reviews on topics of central importance to drug metabolism and pharmacokinetics.

Reviewed by Morris Pfeffer
Bristol Laboratories
Syracuse, NY 13201

Lehrbuch der Pharmazeutischen Chemie, 8th Ed. By HARRY AUTERHOFF and JOACHIM KNABE. Wissenschaftliche Verlagsgesellschaft m.b.H., 7 Stuttgart 1, Postfach 40, W. Germany, 1976. 591 pp. 17 × 25 cm. Price $25.00 (62 DM).

This review was undertaken on the assumption that my colleagues might find it of interest to know what is available to teachers of medicinal chemistry/pharmaceutical chemistry in German-speaking countries.

This book by Auterhoff (who is a professor at Tübingen University) and Knabe is in its eighth edition since 1962 and thus has had ample opportunity for frequent updating. However, despite occasional lapses into modernity, such as a brief discussion of prostaglandins (p. 177) and a mention of cyclic AMP (p. 487), it is basically an old-fashioned textbook.

There are several positive points. The first 99 pages, the so-called inorganic part, is a good review for the student. Beginning with nomenclature and going through the seven groups of the periodic system (each as a chapter), a mini subtext of inorganic pharmaceutical chemistry is presented. This section is not truly inorganic because organometallic drugs are discussed (*e.g.*, bismuth subgallate and tartar emetic), as are organic analytical reagents such as rhodamine B because of its use for the analysis of antimony compounds.

The second part of the book (the remainder) is much more organic than current American texts because it mixes more organic with the medicinal chemistry. Not only syntheses (which are certainly not excessive) but also some refresher material such as nomenclature, ring systems, fundamentals of physical methods (spectroscopy), and organic reactions, including aromatic substitution rules, are given. A little biochemistry is also reviewed, *e.g.*, the stereochemistry of amino and fatty acids and coenzyme A. The division of this section is very reminiscent of the older editions of Olsen's and Gisvold's "Textbook of Organic Medicinal and Pharmaceutical Chemistry" in that it contains chapters on olefins, alcohols, ketones, *etc.*, followed by chapters based on therapeutics. There is a separate chapter on hormones, vitamins, and enzymes and one on ADME, which curiously is at the end of the book rather than with the introductory chapters. There are some references, and the index appears adequate. The American reader will encounter unfamiliar trade names (*e.g.*, Endoxan for cyclophosphamide) and unfamiliar variants of familiar drugs [*e.g.*, flucloxacillin (floxacillin), where fluorine replaces one chlorine in dicloxacillin].

The grave shortcoming of the book, however, is the almost total absence of discussions of drug action mechanisms. A newcomer to the field, say one conversant with organic and some biochemistry, after studying the text, would still not really know what drugs are—in the modern sense. There are occasional brief, almost meaningless statements such as: "polymixin raises the permeability of the cell membrane," or, regarding penicillin, "it is the building of cell wall construction material, murein, which is inhibited," with no further explanation or discussion. Rather than discovering that asparagus contains 1.2 mg of folic acid/100 g, I would have preferred to see a discussion devoted to dihydrofolic acid reductase inhibition mechanisms of antimalarials, methotrexate, or sulfonamide action. In the chapter on sympathomimetics, there is a statement on receptors but no real explanation—not a word on structure–activity relationships. Because of this glaring shortcoming, I feel this book is not suitable for the modern pharmaceutical curriculum.

Reviewed by Alex Gringauz
Arnold and Marie Schwartz College of Pharmacy and Health Sciences
Long Island University
Brooklyn, NY 11201

Interactions of Drugs of Abuse. Annals of the New York Academy of Sciences, Vol. 281. Edited by ELLIOT S. VESELL and MONIQUE C. BRAUDE. The New York Academy of Sciences, 2 East 63rd St., New York, NY 10021, 1976. 489 pp. 15 × 23 cm.

This book contains the proceedings of the first Conference on Interactions of Drugs of Abuse held in New York, March 9–11, 1976, at the New York Academy of Sciences. This conference was rather timely since there is an ever-increasing polydrug use throughout the United States and the world.

The subject matter of the conference was divided into two parts: (*a*) general information concerning the molecular, cellular, and clinical aspects of drug interaction; and (*b*) the major thrust of the conference, determination of the interaction of specific drugs and drug classes including marijuana, narcotics and narcotic antagonists, CNS depressants, CNS stimulants, and hallucinogens. Although extensive effort was made to define all the potential ramifications of drug interactions, it is quite obvious that only the surface has been scratched. In discussing molecular, cellular, and clinical aspects of drug interaction, one could devote several volumes to describing results of experiments designed to study such interactions. Likewise, specific drug interactions could be the subject of a tremendous amount of research effort. In general, this book is well written and the data are presented in an organized fashion.

This conference has opened up a new area of research which will be explored vigorously in the next several years. Because our society is prone to polydrug use, the importance of drug interaction research becomes paramount not only for drugs of abuse but for all drugs in general.

Reviewed by R. Duane Sofia
Wallace Laboratories
Cranbury, NJ 08512

NOTICES

Venous Thromboembolism. Prevention and Treatment. Edited by JOHN L. MADDEN and MICHAEL HUME. Appleton-Century-Crofts, 292 Madison Ave., New York, NY 10017, 1976. 240 pp. 15 × 23 cm.

Chasseaud, and Drug-Serum Protein Interactions and Their Biological Significance by J. W. Bridges and A. G. E. Wilson.

This volume is English in origin and evidently was planned to serve in conjunction with the Chemical Society's series "Foreign Compound Metabolism in Mammals." According to D. V. Parke's foreword, "Progress in Drug Metabolism" will review advances in the general fundamentals of drug metabolism, reactions, phenomena, techniques, *etc.*, while "Foreign Compound Metabolism in Mammals" will deal with the metabolic fate of individual chemicals. Presumably, this philosophy will continue to be observed in future volumes of this series.

Four of these five reviews are on topics that have been extensively and repeatedly reviewed in the past several years (Bioactivation and Cytotoxicity is the exception). Mass spectrometry, epoxidation, enzyme induction, and serum protein binding are all, of course, topics of continuing and intense interest in the area of drug metabolism, but progress is never sufficiently rapid to permit completely original reviews every 2 years or so. Most of the content of these reviews, therefore, has been covered recently. Three of the reviews, as originally written, had 1974 as their last reference dates, although one of these contained 1975 references in a note added in proof. The other two reviews, which have the editors of the volume among their authors, have 1975 references (and one reference to a 1976 paper of the authors in press). This first volume of "Progress in Drug Metabolism" was evidently a long time a-borning.

The reviews are uniformly well written, quite readable, and contain some interesting insights. Those who are relatively unfamiliar with the subject matter would do well to read these reviews in preference to other almost as recent reviews of the same topics. The rest of us could profit by rereading for fresh insight on these subjects. I'm glad I did. Libraries will certainly need to collect this series. Perhaps what's really needed is a series of short monographs which provide an annual drug metabolism-centered update.

The content of the review on plasma protein binding of drugs is especially interesting when it indicates that there is still a dearth of fundamental understanding of this area. Bridges and Wilson find it necessary to correct many of the same misconceptions that Goldstein was correcting in 1949. Perhaps there can't be too many reviews on topics of central importance to drug metabolism and pharmacokinetics.

Reviewed by Morris Pfeffer
Bristol Laboratories
Syracuse, NY 13201

Lehrbuch der Pharmazeutischen Chemie, 8th Ed. By HARRY AUTERHOFF and JOACHIM KNABE. Wissenschaftliche Verlagsgesellschaft m.b.H., 7 Stuttgart 1, Postfach 40, W. Germany, 1976. 591 pp. 17 × 25 cm. Price $25.00 (62 DM).

This review was undertaken on the assumption that my colleagues might find it of interest to know what is available to teachers of medicinal chemistry/pharmaceutical chemistry in German-speaking countries.

This book by Auterhoff (who is a professor at Tübingen University) and Knabe is in its eighth edition since 1962 and thus has had ample opportunity for frequent updating. However, despite occasional lapses into modernity, such as a brief discussion of prostaglandins (p. 177) and a mention of cyclic AMP (p. 487), it is basically an old-fashioned textbook.

There are several positive points. The first 99 pages, the so-called inorganic part, is a good review for the student. Beginning with nomenclature and going through the seven groups of the periodic system (each as a chapter), a mini subtext of inorganic pharmaceutical chemistry is presented. This section is not truly inorganic because organometallic drugs are discussed (*e.g.*, bismuth subgallate and tartar emetic), as are organic analytical reagents such as rhodamine B because of its use for the analysis of antimony compounds.

The second part of the book (the remainder) is much more organic than current American texts because it mixes more organic with the medicinal chemistry. Not only syntheses (which are certainly not excessive) but also some refresher material such as nomenclature, ring systems, fundamentals of physical methods (spectroscopy), and organic reactions, including aromatic substitution rules, are given. A little biochemistry is also reviewed, *e.g.*, the stereochemistry of amino and fatty acids and coenzyme A. The division of this section is very reminiscent of the older editions of Olsen's and Gisvold's "Textbook of Organic Medicinal and Pharmaceutical Chemistry" in that it contains chapters on olefins, alcohols, ketones, *etc.*, followed by chapters based on therapeutics. There is a separate chapter on hormones, vitamins, and enzymes and one on ADME, which curiously is at the end of the book rather than with the introductory chapters. There are some references, and the index appears adequate. The American reader will encounter unfamiliar trade names (*e.g.*, Endoxan for cyclophosphamide) and unfamiliar variants of familiar drugs [*e.g.*, flucloxacillin (floxacillin), where fluorine replaces one chlorine in dicloxacillin].

The grave shortcoming of the book, however, is the almost total absence of discussions of drug action mechanisms. A newcomer to the field, say one conversant with organic and some biochemistry, after studying the text, would still not really know what drugs are—in the modern sense. There are occasional brief, almost meaningless statements such as: "polymixin raises the permeability of the cell membrane," or, regarding penicillin, "it is the building of cell wall construction material, murein, which is inhibited," with no further explanation or discussion. Rather than discovering that asparagus contains 1.2 mg of folic acid/100 g, I would have preferred to see a discussion devoted to dihydrofolic acid reductase inhibition mechanisms of antimalarials, methotrexate, or sulfonamide action. In the chapter on sympathomimetics, there is a statement on receptors but no real explanation—not a word on structure–activity relationships. Because of this glaring shortcoming, I feel this book is not suitable for the modern pharmaceutical curriculum.

Reviewed by Alex Gringauz
Arnold and Marie Schwartz College of Pharmacy and Health Sciences
Long Island University
Brooklyn, NY 11201

Interactions of Drugs of Abuse. Annals of the New York Academy of Sciences, Vol. 281. Edited by ELLIOT S. VESELL and MONIQUE C. BRAUDE. The New York Academy of Sciences, 2 East 63rd St., New York, NY 10021, 1976. 489 pp. 15 × 23 cm.

This book contains the proceedings of the first Conference on Interactions of Drugs of Abuse held in New York, March 9–11, 1976, at the New York Academy of Sciences. This conference was rather timely since there is an ever-increasing polydrug use throughout the United States and the world.

The subject matter of the conference was divided into two parts: (*a*) general information concerning the molecular, cellular, and clinical aspects of drug interaction; and (*b*) the major thrust of the conference, determination of the interaction of specific drugs and drug classes including marijuana, narcotics and narcotic antagonists, CNS depressants, CNS stimulants, and hallucinogens. Although extensive effort was made to define all the potential ramifications of drug interactions, it is quite obvious that only the surface has been scratched. In discussing molecular, cellular, and clinical aspects of drug interaction, one could devote several volumes to describing results of experiments designed to study such interactions. Likewise, specific drug interactions could be the subject of a tremendous amount of research effort. In general, this book is well written and the data are presented in an organized fashion.

This conference has opened up a new area of research which will be explored vigorously in the next several years. Because our society is prone to polydrug use, the importance of drug interaction research becomes paramount not only for drugs of abuse but for all drugs in general.

Reviewed by R. Duane Sofia
Wallace Laboratories
Cranbury, NJ 08512

NOTICES

Venous Thromboembolism. Prevention and Treatment. Edited by JOHN L. MADDEN and MICHAEL HUME. Appleton-Century-Crofts, 292 Madison Ave., New York, NY 10017, 1976. 240 pp. 15 × 23 cm.

Chasseaud, and Drug-Serum Protein Interactions and Their Biological Significance by J. W. Bridges and A. G. E. Wilson.

This volume is English in origin and evidently was planned to serve in conjunction with the Chemical Society's series "Foreign Compound Metabolism in Mammals." According to D. V. Parke's foreword, "Progress in Drug Metabolism" will review advances in the general fundamentals of drug metabolism, reactions, phenomena, techniques, *etc.*, while "Foreign Compound Metabolism in Mammals" will deal with the metabolic fate of individual chemicals. Presumably, this philosophy will continue to be observed in future volumes of this series.

Four of these five reviews are on topics that have been extensively and repeatedly reviewed in the past several years (Bioactivation and Cytotoxicity is the exception). Mass spectrometry, epoxidation, enzyme induction, and serum protein binding are all, of course, topics of continuing and intense interest in the area of drug metabolism, but progress is never sufficiently rapid to permit completely original reviews every 2 years or so. Most of the content of these reviews, therefore, has been covered recently. Three of the reviews, as originally written, had 1974 as their last reference dates, although one of these contained 1975 references in a note added in proof. The other two reviews, which have the editors of the volume among their authors, have 1975 references (and one reference to a 1976 paper of the authors in press). This first volume of "Progress in Drug Metabolism" was evidently a long time a-borning.

The reviews are uniformly well written, quite readable, and contain some interesting insights. Those who are relatively unfamiliar with the subject matter would do well to read these reviews in preference to other almost as recent reviews of the same topics. The rest of us could profit by rereading for fresh insight on these subjects. I'm glad I did. Libraries will certainly need to collect this series. Perhaps what's really needed is a series of short monographs which provide an annual drug metabolism-centered update.

The content of the review on plasma protein binding of drugs is especially interesting when it indicates that there is still a dearth of fundamental understanding of this area. Bridges and Wilson find it necessary to correct many of the same misconceptions that Goldstein was correcting in 1949. Perhaps there can't be too many reviews on topics of central importance to drug metabolism and pharmacokinetics.

Reviewed by Morris Pfeffer
Bristol Laboratories
Syracuse, NY 13201

Lehrbuch der Pharmazeutischen Chemie, 8th Ed. By HARRY AUTERHOFF and JOACHIM KNABE. Wissenschaftliche Verlagsgesellschaft m.b.H., 7 Stuttgart 1, Postfach 40, W. Germany, 1976. 591 pp. 17 × 25 cm. Price $25.00 (62 DM).

This review was undertaken on the assumption that my colleagues might find it of interest to know what is available to teachers of medicinal chemistry/pharmaceutical chemistry in German-speaking countries.

This book by Auterhoff (who is a professor at Tübingen University) and Knabe is in its eighth edition since 1962 and thus has had ample opportunity for frequent updating. However, despite occasional lapses into modernity, such as a brief discussion of prostaglandins (p. 177) and a mention of cyclic AMP (p. 487), it is basically an old-fashioned textbook.

There are several positive points. The first 99 pages, the so-called inorganic part, is a good review for the student. Beginning with nomenclature and going through the seven groups of the periodic system (each as a chapter), a mini subtext of inorganic pharmaceutical chemistry is presented. This section is not truly inorganic because organometallic drugs are discussed (*e.g.*, bismuth subgallate and tartar emetic), as are organic analytical reagents such as rhodamine B because of its use for the analysis of antimony compounds.

The second part of the book (the remainder) is much more organic than current American texts because it mixes more organic with the medicinal chemistry. Not only syntheses (which are certainly not excessive) but also some refresher material such as nomenclature, ring systems, fundamentals of physical methods (spectroscopy), and organic reactions, including aromatic substitution rules, are given. A little biochemistry is also reviewed, *e.g.*, the stereochemistry of amino and fatty acids and coenzyme A. The division of this section is very reminiscent of the older editions of Olsen's and Gisvold's "Textbook of Organic Medicinal and Pharmaceutical Chemistry" in that it contains chapters on olefins, alcohols, ketones, *etc.*, followed by chapters based on therapeutics. There is a separate chapter on hormones, vitamins, and enzymes and one on ADME, which curiously is at the end of the book rather than with the introductory chapters. There are some references, and the index appears adequate. The American reader will encounter unfamiliar trade names (*e.g.*, Endoxan for cyclophosphamide) and unfamiliar variants of familiar drugs [*e.g.*, flucloxacillin (floxacillin), where fluorine replaces one chlorine in dicloxacillin].

The grave shortcoming of the book, however, is the almost total absence of discussions of drug action mechanisms. A newcomer to the field, say one conversant with organic and some biochemistry, after studying the text, would still not really know what drugs are—in the modern sense. There are occasional brief, almost meaningless statements such as: "polymixin raises the permeability of the cell membrane," or, regarding penicillin, "it is the building of cell wall construction material, murein, which is inhibited," with no further explanation or discussion. Rather than discovering that asparagus contains 1.2 mg of folic acid/100 g, I would have preferred to see a discussion devoted to dihydrofolic acid reductase inhibition mechanisms of antimalarials, methotrexate, or sulfonamide action. In the chapter on sympathomimetics, there is a statement on receptors but no real explanation—not a word on structure–activity relationships. Because of this glaring shortcoming, I feel this book is not suitable for the modern pharmaceutical curriculum.

Reviewed by Alex Gringauz
Arnold and Marie Schwartz College of Pharmacy and Health Sciences
Long Island University
Brooklyn, NY 11201

Interactions of Drugs of Abuse. Annals of the New York Academy of Sciences, Vol. 281. Edited by ELLIOT S. VESELL and MONIQUE C. BRAUDE. The New York Academy of Sciences, 2 East 63rd St., New York, NY 10021, 1976. 489 pp. 15 × 23 cm.

This book contains the proceedings of the first Conference on Interactions of Drugs of Abuse held in New York, March 9–11, 1976, at the New York Academy of Sciences. This conference was rather timely since there is an ever-increasing polydrug use throughout the United States and the world.

The subject matter of the conference was divided into two parts: (*a*) general information concerning the molecular, cellular, and clinical aspects of drug interaction; and (*b*) the major thrust of the conference, determination of the interaction of specific drugs and drug classes including marijuana, narcotics and narcotic antagonists, CNS depressants, CNS stimulants, and hallucinogens. Although extensive effort was made to define all the potential ramifications of drug interactions, it is quite obvious that only the surface has been scratched. In discussing molecular, cellular, and clinical aspects of drug interaction, one could devote several volumes to describing results of experiments designed to study such interactions. Likewise, specific drug interactions could be the subject of a tremendous amount of research effort. In general, this book is well written and the data are presented in an organized fashion.

This conference has opened up a new area of research which will be explored vigorously in the next several years. Because our society is prone to polydrug use, the importance of drug interaction research becomes paramount not only for drugs of abuse but for all drugs in general.

Reviewed by R. Duane Sofia
Wallace Laboratories
Cranbury, NJ 08512

NOTICES

Venous Thromboembolism. Prevention and Treatment. Edited by JOHN L. MADDEN and MICHAEL HUME. Appleton-Century-Crofts, 292 Madison Ave., New York, NY 10017, 1976. 240 pp. 15 × 23 cm.

Chasseaud, and Drug-Serum Protein Interactions and Their Biological Significance by J. W. Bridges and A. G. E. Wilson.

This volume is English in origin and evidently was planned to serve in conjunction with the Chemical Society's series "Foreign Compound Metabolism in Mammals." According to D. V. Parke's foreword, "Progress in Drug Metabolism" will review advances in the general fundamentals of drug metabolism, reactions, phenomena, techniques, *etc.*, while "Foreign Compound Metabolism in Mammals" will deal with the metabolic fate of individual chemicals. Presumably, this philosophy will continue to be observed in future volumes of this series.

Four of these five reviews are on topics that have been extensively and repeatedly reviewed in the past several years (Bioactivation and Cytotoxicity is the exception). Mass spectrometry, epoxidation, enzyme induction, and serum protein binding are all, of course, topics of continuing and intense interest in the area of drug metabolism, but progress is never sufficiently rapid to permit completely original reviews every 2 years or so. Most of the content of these reviews, therefore, has been covered recently. Three of the reviews, as originally written, had 1974 as their last reference dates, although one of these contained 1975 references in a note added in proof. The other two reviews, which have the editors of the volume among their authors, have 1975 references (and one reference to a 1976 paper of the authors in press). This first volume of "Progress in Drug Metabolism" was evidently a long time a-borning.

The reviews are uniformly well written, quite readable, and contain some interesting insights. Those who are relatively unfamiliar with the subject matter would do well to read these reviews in preference to other almost as recent reviews of the same topics. The rest of us could profit by rereading for fresh insight on these subjects. I'm glad I did. Libraries will certainly need to collect this series. Perhaps what's really needed is a series of short monographs which provide an annual drug metabolism-centered update.

The content of the review on plasma protein binding of drugs is especially interesting when it indicates that there is still a dearth of fundamental understanding of this area. Bridges and Wilson find it necessary to correct many of the same misconceptions that Goldstein was correcting in 1949. Perhaps there can't be too many reviews on topics of central importance to drug metabolism and pharmacokinetics.

Reviewed by Morris Pfeffer
Bristol Laboratories
Syracuse, NY 13201

Lehrbuch der Pharmazeutischen Chemie, 8th Ed. By HARRY AUTERHOFF and JOACHIM KNABE. Wissenschaftliche Verlagsgesellschaft m.b.H., 7 Stuttgart 1, Postfach 40, W. Germany, 1976. 591 pp. 17 × 25 cm. Price $25.00 (62 DM).

This review was undertaken on the assumption that my colleagues might find it of interest to know what is available to teachers of medicinal chemistry/pharmaceutical chemistry in German-speaking countries.

This book by Auterhoff (who is a professor at Tübingen University) and Knabe is in its eighth edition since 1962 and thus has had ample opportunity for frequent updating. However, despite occasional lapses into modernity, such as a brief discussion of prostaglandins (p. 177) and a mention of cyclic AMP (p. 487), it is basically an old-fashioned textbook.

There are several positive points. The first 99 pages, the so-called inorganic part, is a good review for the student. Beginning with nomenclature and going through the seven groups of the periodic system (each as a chapter), a mini subtext of inorganic pharmaceutical chemistry is presented. This section is not truly inorganic because organometallic drugs are discussed (*e.g.*, bismuth subgallate and tartar emetic), as are organic analytical reagents such as rhodamine B because of its use for the analysis of antimony compounds.

The second part of the book (the remainder) is much more organic than current American texts because it mixes more organic with the medicinal chemistry. Not only syntheses (which are certainly not excessive) but also some refresher material such as nomenclature, ring systems, fundamentals of physical methods (spectroscopy), and organic reactions, including aromatic substitution rules, are given. A little biochemistry is also reviewed, *e.g.*, the stereochemistry of amino and fatty acids and coenzyme A. The division of this section is very reminiscent of the older editions of Olsen's and Gisvold's "Textbook of Organic Medicinal and Pharmaceutical Chemistry" in that it contains chapters on olefins, alcohols, ketones, *etc.*, followed by chapters based on therapeutics. There is a separate chapter on hormones, vitamins, and enzymes and one on ADME, which curiously is at the end of the book rather than with the introductory chapters. There are some references, and the index appears adequate. The American reader will encounter unfamiliar trade names (*e.g.*, Endoxan for cyclophosphamide) and unfamiliar variants of familiar drugs [*e.g.*, flucloxacillin (floxacillin), where fluorine replaces one chlorine in dicloxacillin].

The grave shortcoming of the book, however, is the almost total absence of discussions of drug action mechanisms. A newcomer to the field, say one conversant with organic and some biochemistry, after studying the text, would still not really know what drugs are—in the modern sense. There are occasional brief, almost meaningless statements such as: "polymixin raises the permeability of the cell membrane," or, regarding penicillin, "it is the building of cell wall construction material, murein, which is inhibited," with no further explanation or discussion. Rather than discovering that asparagus contains 1.2 mg of folic acid/100 g, I would have preferred to see a discussion devoted to dihydrofolic acid reductase inhibition mechanisms of antimalarials, methotrexate, or sulfonamide action. In the chapter on sympathomimetics, there is a statement on receptors but no real explanation—not a word on structure–activity relationships. Because of this glaring shortcoming, I feel this book is not suitable for the modern pharmaceutical curriculum.

Reviewed by Alex Gringauz
Arnold and Marie Schwartz College of Pharmacy and Health Sciences
Long Island University
Brooklyn, NY 11201

Interactions of Drugs of Abuse. Annals of the New York Academy of Sciences, Vol. 281. Edited by ELLIOT S. VESELL and MONIQUE C. BRAUDE. The New York Academy of Sciences, 2 East 63rd St., New York, NY 10021, 1976. 489 pp. 15 × 23 cm.

This book contains the proceedings of the first Conference on Interactions of Drugs of Abuse held in New York, March 9–11, 1976, at the New York Academy of Sciences. This conference was rather timely since there is an ever-increasing polydrug use throughout the United States and the world.

The subject matter of the conference was divided into two parts: (*a*) general information concerning the molecular, cellular, and clinical aspects of drug interaction; and (*b*) the major thrust of the conference, determination of the interaction of specific drugs and drug classes including marijuana, narcotics and narcotic antagonists, CNS depressants, CNS stimulants, and hallucinogens. Although extensive effort was made to define all the potential ramifications of drug interactions, it is quite obvious that only the surface has been scratched. In discussing molecular, cellular, and clinical aspects of drug interaction, one could devote several volumes to describing results of experiments designed to study such interactions. Likewise, specific drug interactions could be the subject of a tremendous amount of research effort. In general, this book is well written and the data are presented in an organized fashion.

This conference has opened up a new area of research which will be explored vigorously in the next several years. Because our society is prone to polydrug use, the importance of drug interaction research becomes paramount not only for drugs of abuse but for all drugs in general.

Reviewed by R. Duane Sofia
Wallace Laboratories
Cranbury, NJ 08512

NOTICES

Venous Thromboembolism. Prevention and Treatment. Edited by JOHN L. MADDEN and MICHAEL HUME. Appleton-Century-Crofts, 292 Madison Ave., New York, NY 10017, 1976. 240 pp. 15 × 23 cm.

Synthetic Peptides. Vol. 4. By GEORGE R. PETTIT. Elsevier/North-Holland, 52 Vanderbilt Ave., New York, NY 10017, 1976. 477 pp. 16 × 23 cm. Price $59.95.

An Introduction to Veterinary Pharmacology. By FRANK ALEXANDER. Churchill Livingstone, 19 W. 44th St., New York, NY 10036, 1976. 382 pp. 14 × 21 cm. Price $17.50.

Drug Therapy Reviews. Vol. 1. Edited by RUSSELL R. MILLER and DAVID J. GREENBLATT. Masson, 14 E. 60th St., New York, NY 10022, 1977. 260 pp. 16 × 24 cm. Price $26.00.

Tissue Responses to Addictive Drugs. Edited by DONALD H. FORD and DORIS H. CLOUET. Halsted, 605 Third Ave., New York, NY 10016, 1976. 704 pp. 16 × 24 cm. Price $50.00.

Progress in Drug Research. Vol. 20. Edited by ERNST JUCKER. Birkhäuser Verlag, P. O. Box 34, CH-4010 Basel, Switzerland, 1976. 632 pp. 17 × 25 cm. Price sFr 232.

The Anesthesiologist's Handbook. By DONALD G. CATRON. University Park Press, Chamber of Commerce Bldg., Baltimore, MD 21202, 1976. 201 pp. 12 × 17 cm. Price $8.95.

Encyclopaedia of Antibiotics. By JOHN S. GLASBY. Wiley, 605 Third Ave., New York, NY 10016, 1977. 369 pp. 19 × 26 cm. Price $42.50.

Current Developments in Psychopharmacology. Vol. 3. Edited by WALTER B. ESSMAN and L. VALZELLI. Halsted, 605 Third Ave., New York, NY 10016, 1976. 303 pp. 16 × 23 cm. Price $25.00.

Health Care in a Changing Setting: the UK Experience. Ciba Foundation Symposium 43 (new series). American Elsevier, 52 Vanderbilt Ave., New York, NY 10017, 1976. 188 pp. 17 × 24 cm.

Research and Medical Practice: Their Interaction. Ciba Foundation Symposium 44 (new series). American Elsevier, 52 Vanderbilt Ave., New York, NY 10017, 1976. 188 pp. 17 × 24 cm.

Polypeptide Hormones: Molecular and Cellular Aspects. Ciba Foundation Symposium 41 (new series). American Elsevier, 52 Vanderbilt Ave., New York, NY 10017, 1976. 388 pp. 17 × 24.5 cm.

The Biochemistry of the Tissues. By P. BANKS, W. BARTLEY, and L. M. BIRT. Wiley, 605 Third Ave., New York, NY 10016, 1976. 493 pp. 15.5 × 23.5 cm. Price $32.00.

Quantum Mechanics of Molecular Conformations. Edited by BERNARD PULLMAN. Wiley, 605 Third Ave., New York, NY 10016, 1976. 412 pp. 15.5 × 23.5 cm. Price $32.50.

Embryogenesis in Mammals. Ciba Foundation Symposium 40 (new series). CIBA Pharmaceutical Co., Division of CIBA-GEIGY Corp., Summit, NJ 07901, 1976. 308 pp. 17 × 24.5 cm.

Trace Amines and the Brain. Edited by EARL USDIN and MERTON SANDLER. Dekker, 270 Madison Ave., New York, NY 10016, 1976. 301 pp. 16 × 23.5 cm. Price $29.75.

Acute Diarrhoea in Childhood. Ciba Foundation Symposium 42 (new series). American Elsevier, 52 Vanderbilt Ave., New York, NY 10017, 1976. 375 pp. 17 × 25 cm.

Hormone-Receptor Interaction: Molecular Aspects. Edited by GERALD S. LEVEY. Dekker, 270 Madison Ave., New York, NY 10016, 1976. 488 pp. 15 × 23 cm. Price $45.75.

Receptors and Mechanism of Action of Steroid Hormones. Part I. Edited by JORGE R. PASQUALINI. Dekker, 270 Madison Ave., New York, NY 10016, 1976. 328 pp. 15 × 23 cm. Price $29.75.

Methods in Receptor Research. Part II. Edited by MELVIN BLECHER. Dekker, 270 Madison Ave., New York, NY 10016, 1976. 400 pp. 15 × 23 cm. Price $36.50.

Drug Design. Vol. VII. Edited by E. J. ARIENS. Academic, 111 Fifth Ave., New York, NY 10003, 1976. 295 pp. 16 × 24 cm. Price $30.00.

A Handbook of Treatment. Edited by H. W. PROCTOR and P. S. BYRNE. University Park Press, Chamber of Commerce Bldg., Baltimore, MD 21202, 1976. 434 pp. 18 × 26 cm. Price $19.50.

A Guide to the Vitamins. Their Role in Health and Disease. By JOHN MARKS. University Park Press, Chamber of Commerce Bldg., Baltimore, MD 21202, 1975. 207 pp. 16 × 25 cm. Price $19.50.

Encyclopedia of Electrochemistry of the Elements. Vol. V. Edited by ALLEN J. BARD. Dekker, 270 Madison Ave., New York, NY 10016, 1976. 407 pp. 18.5 × 26 cm. Price $69.50 single volume, $59.00 subscription.

Biology of Cholinergic Function. Edited by ALAN M. GOLDBERG and ISRAEL HANIN. Raven Press, 1140 Avenue of the Americas, New York, NY 10036, 1976. 716 pp. 16.5 × 24.5 cm. Price $35.00.

Advances in the Drug Therapy of Mental Illness. World Health Organization, Geneva, Switzerland, 1976. 170 pp. 16 × 24 cm. Price $12.00. Available from Q Corp., 49 Sheridan Ave., Albany NY 12210.

Reviews of Physiology, Biochemistry and Pharmacology. Vol. 75. Edited by R. H. ADRIAN, *et al.* Springer-Verlag New York, 44 Hartz Way, Secaucus, NJ 07094, 1976. 197 pp. 17 × 25 cm. Price $48.40.

Psychotherapeutic Drugs. Part 1—Principles. Edited by EARL USDIN and IRENE S. FORREST. Dekker, 270 Madison Ave., New York, NY 10016, 1976. 698 pp. 16 × 23.5 cm. Price $39.50.

Breast-Feeding and the Mother. Ciba Foundation Symposium 45 (new series). Elsevier North-Holland, 52 Vanderbilt Ave., New York, NY 10017, 1976. 280 pp. 16 × 24 cm.

Conservation of Resources. A Symposium Held at The University of Glasgow. The Chemical Society, Burlington House, London WIV OBN, England, 1976. 245 pp. 14 × 21 cm. Price $12.00.

Drug Assessment in Ferment: Multinational Comparisons, Vol. 6. Edited by CRAIG D. BURRELL. Interdisciplinary Communication Associates, 1717 Massachusetts Ave., N. W., Suite 101, Washington, DC 20036, 1976. 295 pp. 15 × 23 cm. Price $12.00.

Receptors and Recognition, Series A, Vol. 2. Edited by P. CUATRECASAS and M. F. GREAVES. Halsted, 605 Third Ave., New York, NY 10016, 1976. 229 pp. 15 × 24 cm. Price $24.50.

Microbiological Hazards of Infusion Therapy. Edited by I. PHILLIPS, P. D. MEERS, and P. F. D'ARCY. Publishing Sciences Group, 545 Great Rd., Littleton, MA 01460, 1976. 186 pp. 15 × 23 cm. Price $19.50.

Platelets in Biology and Pathology. Edited by J. L. GORDON. Elsevier North-Holland, 52 Vanderbilt Ave., New York, NY 10017, 1976. 389 pp. 16 × 24 cm. Price $53.95.

Index of Reviews in Organic Chemistry, Second Cumulative Volume. Compiled by D. A. LEWIS and P. CHARNOCK. The Chemical Society, Burlington House, London, W1V OBN, England, 1976. 308 pp. 20 × 29 cm. Price $13.00.

Advances in Chromatography, Vol. 15. Edited by J. CALVIN GIDDINGS, ELI GRUSHKA, JACK CAZES, and PHYLLIS R. BROWN. Dekker, 270 Madison Ave., New York, NY 10016, 1977. 352 pp. 15 × 23 cm. Price $29.75.

Birth Defects and Drugs in Pregnancy. By OLLI P. HEINONEN, DENNIS SLONE, and SAMUEL SHAPIRO. Publishing Sciences Group, 545 Great Rd., Littleton, MA 01460, 1977. 516 pp. 17 × 25 cm. Price $75.00.

Introduction to the Spectroscopy of Biological Polymers. Edited by D. W. JONES. Academic (London), 24–28 Oval Rd., London, NW1 7DX, England, 1977. 328 pp. 23 × 15 cm. Price $25.50.

The Fate of Drugs in the Organism: A Bibliographic Survey, Vol. 4. Edited by J. HIRTZ. Dekker, 270 Madison Ave., New York, NY 10016, 1977. 640 pp. 15 × 23 cm. Price $75.00.

Clinical Pharmacy and Clinical Pharmacology. Edited by WILLIAM A. GOUVEIA, GIANNI TOGNONI, and EPPO van der KLEIJN. Elsevier North-Holland, 52 Vanderbilt Ave., New York, NY 10017, 1977. 470 pp. 16 × 24 cm. Price $55.50.

Pesticides in the Environment, Vol. 3. Edited by ROBERT WHITE-STEVENS. Dekker, 270 Madison Ave., New York, NY, 10016, 1977. 384 pp. 15 × 23 cm. Price $38.50.

Essays in Neurochemistry and Neuropharmacology, Vol. 1. Edited by M. B. H. YOUDIM, W. LOVENBERG, D. F. SHARMAN, and J. R. LAGNADO. Wiley, 605 Third Ave., New York, NY, 10016, 1977. 195 pp. 15 × 23 cm. Price $21.50.

Abrégé de Pharmacie Galénique. Excipients, Opérations et Formes Pharmaceutiques, Second Ed. By A. LE HIR. Mason, 14 East 60th St., New York, NY, 1977. 346 pp. 13 × 21 cm.

Basic Medical Microbiology. By ROBERT F. BOYD and BRYAN G. HOERL. Little, Brown, 34 Beacon St., Boston, MA 02106, 1977. 578 pp. 20 × 24 cm.

Journal of Pharmaceutical Sciences

OCTOBER 1977

VOLUME 66 NUMBER 10

MARY H. FERGUSON
Editor

SHELLY ELLIOTT
Production Editor

JANET D. SHOFF
Copy Editor

EDWARD G. FELDMANN
Contributing Editor

SAMUEL W. GOLDSTEIN
Contributing Editor

DAVID BOHARDT
Director of Publications

L. LUAN CORRIGAN
Assistant Director of Publications

EDITORIAL ADVISORY BOARD

JOHN AUTIAN
NORMAN R. FARNSWORTH
WILLIAM O. FOYE
WILLIAM J. JUSKO
HARRY B. KOSTENBAUDER
HERBERT A. LIEBERMAN
DAVID E. MANN, JR.
GERALD J. PAPARIELLO

The *Journal of Pharmaceutical Sciences* is published monthly by the American Pharmaceutical Association at 2215 Constitution Ave., N.W., Washington, DC 20037. Second-class postage paid at Washington, D.C., and at additional mailing office.

All expressions of opinion and statements of supposed fact appearing in articles or editorials carried in this journal are published on the authority of the writer over whose name they appear and are not to be regarded as necessarily expressing the policies or views of the American Pharmaceutical Association.

Offices—Editorial, Advertising, and Subscription Offices: 2215 Constitution Ave., N.W., Washington, DC 20037. Printing Offices: 20th & Northampton Streets, Easton, PA 18042.

Annual Subscriptions—United States and foreign, industrial and government institutions $50, educational institutions $50, individuals *for personal use only* $30; single copies $5. All foreign subscriptions add $5 for postage. Subscription rates are subject to change without notice. Members of the American Pharmaceutical Association may elect to receive the *Journal of Pharmaceutical Sciences* as a part of their annual $60 (foreign $65) APhA membership dues.

Claims—Missing numbers will not be supplied if dues or subscriptions are in arrears for more than 60 days or if claims are received more than 60 days after the date of the issue, or if loss was due to failure to give notice of change of address. The Association cannot accept responsibility for foreign delivery when its records indicate shipment has been made.

Change of Address—Members and subscribers should notify at once both the Post Office and the American Pharmaceutical Association, 2215 Constitution Ave., N.W., Washington, DC 20037, of any change of address.

Microfilm—Microfilm volumes are available from University Microfilms International, 300 N. Zeeb Road, Ann Arbor, MI 48106.

© Copyright 1977, American Pharmaceutical Association, 2215 Constitution Ave., N.W., Washington, DC 20037; all rights reserved.

GETTING TO KNOW THE FDA

If the average pharmacist is asked what he or she thinks about the federal Food and Drug Administration, the answer is apt to be anything from a blank stare to a stream of profanity.

And why not? This shouldn't be very surprising because there is very little that health care practitioners—pharmacists, physicians, dentists, nurses, and others—really know about the agency, its workings, and its operations. There is a rather vague understanding that this is an all-powerful governmental arm that decides, among other things, what we shall have available to eat as well as what will be made available to us as medication.

Although this perception is partially accurate, there is little knowledge of how the agency operates, how much it initiates actions, how broad is its scope of responsibility, and the like.

As a result, there often is public furor over some FDA action; health care professionals may have a foggy understanding of the scientific reason for the action, but even they rarely have any concept of the legal aspects of the action. Whatever their merits on scientific grounds, FDA initiatives regarding saccharin, laetrile, phenformin, cyclamates, combination antibiotic products, and the many other rhubarbs that have been in the news over the past 20 years have been based upon FDA implementation of some law which was not of its own doing. Rather, these actions are the result of the agency attempting to do its assigned job as it interprets various statutes that Congress has enacted. We shall freely grant that, in the process, FDA has had some rather strained and unusual interpretations of what it believes Congress has said, but the courts are available to bring challenges when someone feels that the agency is overstepping its bounds. And the halls of justice have sustained the FDA in a high proportion of such cases.

At any rate, even today recent graduates of our pharmacy, medical, and other professional schools rarely have been given more than the most superficial exposure to the role of FDA as it relates to professional practice.

Well, we were pleased to read recently that this is an information gap that someone is doing something to correct. Specifically, in the last issue of the *American Journal of Pharmaceutical Education*, R. W. Jacobs and J. C. King of the School of Pharmacy at the University of the Pacific published a report entitled "Development of a Course of Study in FDA Drug Regulatory Procedures."

What they set about to do can be neatly summed up in a quote from their article:

> *"If one acknowledges the fact that the agency works to control the quality but cannot assure the absolute quality of drugs, then the pharmacist must share some responsibility for drug quality with the FDA. The need for a comprehensive understanding of the drug regulatory procedures of the FDA can be met by providing a course as a component of the curriculum in pharmacy school.*
>
> *"There exists an apparent lack of understanding of the functions and responsibilities of the Food and Drug Administration, the drug regulator, by the pharmacist, the drug dispenser. Since the common goal of both is to assure that only safe, effective, and good quality medications reach the patient, an interface between the FDA and the pharmacy profession needs to be created. While the FDA law is slighted in most pharmacy jurisprudence courses, there is need to expand course scope to include the implementation of the regulations associated with the various FDA programs."*

The Jacobs and King article describes the development of a residency program as a cooperative experience between the FDA and the school of pharmacy, from which evolved a syllabus for future residencies as well as textual material for a didactic course in FDA regulatory procedures. As an addendum to their report, the authors provide an outline of the residency program and the various units within the FDA operation which were studied for a minimum of one to two weeks each. These included the Bureau of Drugs, Pharmaceutical Research and Testing, Biometrics and Epidemiology, Compliance, Regional Operations, New Drug Evaluation, and Drug Monographs.

It was the conclusion of the authors that the insight gained from such a program and course serves to broaden the scope of cooperation between pharmacy and the FDA. Specifically identified in this regard are: drug recalls, the drug product defect reporting system, current good manufacturing practices, drug efficacy study implementation, over-the-counter drug evaluation, antibiotic and insulin certification, methadone monitoring, drug product packaging and stability, maximum allowable cost and bioequivalence regulations, and selected aspects of the IND/NDA new drug procedures.

As the form of pharmacy practice changes and as the role and responsibility of the pharmacist evolves, there appears to be increasing need for the pharmacist to be informed in these matters as part of the formal education process. Consequently, we hope that other schools will review the experience of this group and consider such a course for current students as well as a pragmatic subject for continuing education.

It may not result in pharmacists growing to love the FDA, but at least they will be able to deal with issues involving the FDA in a knowledgable rather than emotional way. And, as an added bonus, it will certainly help pharmacists to understand—and perhaps even to appreciate—the basis for many of the actions taken by their national professional society on various FDA matters. —EGF

Journal of Pharmaceutical Sciences

OCTOBER 1977

VOLUME 66 NUMBER 10

MARY H. FERGUSON
Editor

SHELLY ELLIOTT
Production Editor

JANET D. SHOFF
Copy Editor

EDWARD G. FELDMANN
Contributing Editor

SAMUEL W. GOLDSTEIN
Contributing Editor

DAVID BOHARDT
Director of Publications

L. LUAN CORRIGAN
Assistant Director of Publications

EDITORIAL ADVISORY BOARD

JOHN AUTIAN
NORMAN R. FARNSWORTH
WILLIAM O. FOYE
WILLIAM J. JUSKO
HARRY B. KOSTENBAUDER
HERBERT A. LIEBERMAN
DAVID E. MANN, JR.
GERALD J. PAPARIELLO

The *Journal of Pharmaceutical Sciences* is published monthly by the American Pharmaceutical Association at 2215 Constitution Ave., N.W., Washington, DC 20037. Second-class postage paid at Washington, D.C., and at additional mailing office.

All expressions of opinion and statements of supposed fact appearing in articles or editorials carried in this journal are published on the authority of the writer over whose name they appear and are not to be regarded as necessarily expressing the policies or views of the American Pharmaceutical Association.

Offices—Editorial, Advertising, and Subscription Offices: 2215 Constitution Ave., N.W., Washington, DC 20037. Printing Offices: 20th & Northampton Streets, Easton, PA 18042.

Annual Subscriptions—United States and foreign, industrial and government institutions $50, educational institutions $50, individuals *for personal use only* $30; single copies $5. All foreign subscriptions add $5 for postage. Subscription rates are subject to change without notice. Members of the American Pharmaceutical Association may elect to receive the *Journal of Pharmaceutical Sciences* as a part of their annual $60 (foreign $65) APhA membership dues.

Claims—Missing numbers will not be supplied if dues or subscriptions are in arrears for more than 60 days or if claims are received more than 60 days after the date of the issue, or if loss was due to failure to give notice of change of address. The Association cannot accept responsibility for foreign delivery when its records indicate shipment has been made.

Change of Address—Members and subscribers should notify at once both the Post Office and the American Pharmaceutical Association, 2215 Constitution Ave., N.W., Washington, DC 20037, of any change of address.

Microfilm—Microfilm volumes are available from University Microfilms International, 300 N. Zeeb Road, Ann Arbor, MI 48106.

© Copyright 1977, American Pharmaceutical Association, 2215 Constitution Ave., N.W., Washington, DC 20037; all rights reserved.

GETTING TO KNOW THE FDA

If the average pharmacist is asked what he or she thinks about the federal Food and Drug Administration, the answer is apt to be anything from a blank stare to a stream of profanity.

And why not? This shouldn't be very surprising because there is very little that health care practitioners—pharmacists, physicians, dentists, nurses, and others—really know about the agency, its workings, and its operations. There is a rather vague understanding that this is an all-powerful governmental arm that decides, among other things, what we shall have available to eat as well as what will be made available to us as medication.

Although this perception is partially accurate, there is little knowledge of how the agency operates, how much it initiates actions, how broad is its scope of responsibility, and the like.

As a result, there often is public furor over some FDA action; health care professionals may have a foggy understanding of the scientific reason for the action, but even they rarely have any concept of the legal aspects of the action. Whatever their merits on scientific grounds, FDA initiatives regarding saccharin, laetrile, phenformin, cyclamates, combination antibiotic products, and the many other rhubarbs that have been in the news over the past 20 years have been based upon FDA implementation of some law which was not of its own doing. Rather, these actions are the result of the agency attempting to do its assigned job as it interprets various statutes that Congress has enacted. We shall freely grant that, in the process, FDA has had some rather strained and unusual interpretations of what it believes Congress has said, but the courts are available to bring challenges when someone feels that the agency is overstepping its bounds. And the halls of justice have sustained the FDA in a high proportion of such cases.

At any rate, even today recent graduates of our pharmacy, medical, and other professional schools rarely have been given more than the most superficial exposure to the role of FDA as it relates to professional practice.

Well, we were pleased to read recently that this is an information gap that someone is doing something to correct. Specifically, in the last issue of the *American Journal of Pharmaceutical Education*, R. W. Jacobs and J. C. King of the School of Pharmacy at the University of the Pacific published a report entitled "Development of a Course of Study in FDA Drug Regulatory Procedures."

What they set about to do can be neatly summed up in a quote from their article:

> *"If one acknowledges the fact that the agency works to control the quality but cannot assure the absolute quality of drugs, then the pharmacist must share some responsibility for drug quality with the FDA. The need for a comprehensive understanding of the drug regulatory procedures of the FDA can be met by providing a course as a component of the curriculum in pharmacy school.*
>
> *"There exists an apparent lack of understanding of the functions and responsibilities of the Food and Drug Administration, the drug regulator, by the pharmacist, the drug dispenser. Since the common goal of both is to assure that only safe, effective, and good quality medications reach the patient, an interface between the FDA and the pharmacy profession needs to be created. While the FDA law is slighted in most pharmacy jurisprudence courses, there is need to expand course scope to include the implementation of the regulations associated with the various FDA programs."*

The Jacobs and King article describes the development of a residency program as a cooperative experience between the FDA and the school of pharmacy, from which evolved a syllabus for future residencies as well as textual material for a didactic course in FDA regulatory procedures. As an addendum to their report, the authors provide an outline of the residency program and the various units within the FDA operation which were studied for a minimum of one to two weeks each. These included the Bureau of Drugs, Pharmaceutical Research and Testing, Biometrics and Epidemiology, Compliance, Regional Operations, New Drug Evaluation, and Drug Monographs.

It was the conclusion of the authors that the insight gained from such a program and course serves to broaden the scope of cooperation between pharmacy and the FDA. Specifically identified in this regard are: drug recalls, the drug product defect reporting system, current good manufacturing practices, drug efficacy study implementation, over-the-counter drug evaluation, antibiotic and insulin certification, methadone monitoring, drug product packaging and stability, maximum allowable cost and bioequivalence regulations, and selected aspects of the IND/NDA new drug procedures.

As the form of pharmacy practice changes and as the role and responsibility of the pharmacist evolves, there appears to be increasing need for the pharmacist to be informed in these matters as part of the formal education process. Consequently, we hope that other schools will review the experience of this group and consider such a course for current students as well as a pragmatic subject for continuing education.

It may not result in pharmacists growing to love the FDA, but at least they will be able to deal with issues involving the FDA in a knowledgable rather than emotional way. And, as an added bonus, it will certainly help pharmacists to understand—and perhaps even to appreciate—the basis for many of the actions taken by their national professional society on various FDA matters. —EGF

GI Intolerance and Nitrofurantoin

Nitrofurantoin, 1-[(5-nitrofurfurylidene)amino]hydantoin, is an important agent in the arsenal of antibacterials used to fight urinary tract infections. Despite proven efficacy, the use of nitrofurantoin has been frequently associated with nausea and vomiting[1]. These effects have limited the use of the drug in some patients, thus denying them its therapeutic potential.

In a recent issue of this Journal, Parrott and Matheson[2] reported that nitrofurantoin can be absorbed when administered rectally in certain suppository formulations. Although absorption was poor, bacteriostatic concentrations (>1:100,000) were achieved in the urine and maintained for up to 4 hr after a 400-mg dose. The authors concluded that: "Persons who exhibit nausea and emesis after oral administration of nitrofurantoin possibly could receive nitrofurantoin therapy by the rectal route." This conclusion may not be justified.

Rectal administration itself will not always alleviate the problem of nausea associated with certain oral medications. If a drug is directly irritating to the GI mucosa, this approach is likely to succeed. However, if the nausea and emetic response caused by a drug are mediated predominantly through an effect on the central nervous system, then these side effects will not necessarily be avoided by using the rectal route.

Nitrofurantoin serves as an example of a drug that produces nausea and vomiting, at least in part, *via* a central mechanism. Support for this contention comes from data showing a relationship between blood levels of the drug and these side effects[3]. Decreased urinary excretion levels are also associated with the decreased incidence of nausea[4]. Furthermore, parenteral administration as an intravenous[5] or intramuscular[6–8] injection also produces nausea and vomiting.

Some success in reducing the frequency of these side effects has been achieved by decreasing the rate of nitrofurantoin absorption. Large crystals, in contrast to microcrystals, of the drug produce more gradual absorption and yet allow the achievement of therapeutic amounts in the urine[3]. This may be the reason macrocrystals of nitrofurantoin tend to produce less GI upset. Food, by delaying absorption[9], similarly seems to improve GI tolerance.

In the study by Parrott and Matheson[2], an oral dose (400 mg) of nitrofurantoin (fine, 320–325 mesh) produced gastric upset in four of their original eight subjects. The authors did not report whether nausea was produced in subjects who received the same dose rectally. The absence of nausea, if this were the case, could be the result of the relatively poor rectal absorption observed.

For nitrofurantoin, a reduced rate of bioavailability may uniquely diminish its side effects. These findings[2] should provide a stimulus for further pharmacokinetic and biopharmaceutical studies to improve therapeutics with drugs that may behave like nitrofurantoin.

T. S. Gaginella
Division of Pharmacology
College of Pharmacy
Ohio State University
Columbus, OH 43210

Received August 15, 1977.

[1] S. C. Harvey, in "The Pharmacological Basis of Therapeutics," 5th ed., L. S. Goodman and A. Gilman, Eds., Macmillan, New York, N.Y., 1975, p. 1009.
[2] E. L. Parrott and L. E. Matheson, Jr., *J. Pharm. Sci.*, **66**, 955 (1977).
[3] H. E. Paul, K. J. Hayes, M. F. Paul, and A. R. Borgmann, *J. Pharm. Sci.*, **56**, 882 (1967).
[4] I. M. Thompson and A. D. Amar, *J. Urol.*, **82**, 387 (1959).
[5] M. F. Vicchi, *Med. Pract.*, **22**, 3 (1967).
[6] C. E. Cox, F. J. O'Connor, and S. S. Lucy, *J. Urol.*, **105**, 113 (1971).
[7] M. F. Vicchi, H. Pierangeli, and O. Rodriguez, *Rev. Argent. Urol.*, **37**, 72 (1968).
[8] H. K. Reckendorf, R. G. Castringius, and H. K. Springler, *Antimicrob. Agents Chemother.*, **1962**, 531.
[9] T. R. Bates, J. A. Sequeira, and A. V. Tembo, *Clin. Pharmacol. Ther.*, **16**, 63 (1974).

Cancer Cell Aggregates: Temperature Elevation

Currently, there is controversy regarding the relationship of the quantity of blood present in cancerous tissue (*i.e.*, continuous uncontrolled growth in cell aggregates) to the temperature of such tissue. One group maintains that malignancies are characterized by high temperature because relatively large quantities of blood are present in the lesion. The opposing argument holds that elevated temperatures are present in cancerous tissue because the tissue contains a relatively lesser amount of blood. Proponents of this view believe that the lesser quantity of blood has a reduced coolant effect.

We wish to make the following contribution to the discussion. It is a basic fact that blood arrives at any given tumor site at roughly 37°. The temperature of the tumor is higher, approximately 38°. As is known, temperature is an intensive factor. Therefore, regardless of the amount of blood arriving at the lesion, heat can only flow from the higher temperature of the malignancy to the lower temperature of the blood. Given this fact, a greater quantity of blood might provide an increased coolant effect; it cannot be a source of temperature increase. Even if it may be assumed that there is an increased flow of blood to the tumor, in all cases the overall system still involves blood entering and leaving cancerous tissue at a temperature lower than that of the tumor. Thus, blood must act as a coolant.

To explain the temperature of any system, the rate of heat dissipation must be considered as well as heat input. One principal factor influencing the dissipation rate is the nature of the matrix through which heat conduction occurs. Aggregates of normal cells, *i.e.*, flocculated aggregates, contain an open network in which trapped bulk water acts as the coolant. Bulk water as it exists, for example, in blood plasma has excellent cooling properties. Ecanow and co-workers[1–5] proposed that cancer cells are aggregated in a structured matrix, *i.e.*, a coagulated system. In such systems, heat derived from metabolism is conserved because it is lost by conduction at a slower rate than the rate of loss through normal cell aggregates. Thus, because heat is conserved in malignant tissue, its temperature compared to normal surrounding tissue is elevated.

The conclusion to be drawn is that malignant tissue is warmer than normal tissue because: (*a*) there is more continuous metabolic heat production, (*b*) the structured intercellular coagulated matrix conserves heat, and (*c*) malignant tissue simply does not have sufficient blood circulating through it to be cooled to normal temperature.

B. Ecanow
B. H. Gold
J. W. McCreery
University of Illinois
(at the Medical Center)
Chicago, IL 60680

Received August 18, 1977.

[1] B. Ecanow and H. Klawans, in "Models of Human Neurological Disease," H. Klawans, Ed., Excerpta Medica, Amsterdam, The Netherlands, 1974.
[2] B. Ecanow, "Aggregation of Biological Suspension System," U.S. Copyright Registration A 825 763 Publ. Ecanow, Skokie, Ill., 1966.
[3] B. Ecanow, B. H. Gold, and R. Balagot, *Science*, **193**, 919 (1976).
[4] B. Ecanow, B. H. Gold, and M. Sadove, *Br. J. Cancer*, in press.
[5] B. Ecanow, B. H. Gold, and J. W. McCreery, *Clin. Oncol.*, in press.

GI Intolerance and Nitrofurantoin

Nitrofurantoin, 1-[(5-nitrofurfurylidene)amino]hydantoin, is an important agent in the arsenal of antibacterials used to fight urinary tract infections. Despite proven efficacy, the use of nitrofurantoin has been frequently associated with nausea and vomiting[1]. These effects have limited the use of the drug in some patients, thus denying them its therapeutic potential.

In a recent issue of this Journal, Parrott and Matheson[2] reported that nitrofurantoin can be absorbed when administered rectally in certain suppository formulations. Although absorption was poor, bacteriostatic concentrations (>1:100,000) were achieved in the urine and maintained for up to 4 hr after a 400-mg dose. The authors concluded that: "Persons who exhibit nausea and emesis after oral administration of nitrofurantoin possibly could receive nitrofurantoin therapy by the rectal route." This conclusion may not be justified.

Rectal administration itself will not always alleviate the problem of nausea associated with certain oral medications. If a drug is directly irritating to the GI mucosa, this approach is likely to succeed. However, if the nausea and emetic response caused by a drug are mediated predominantly through an effect on the central nervous system, then these side effects will not necessarily be avoided by using the rectal route.

Nitrofurantoin serves as an example of a drug that produces nausea and vomiting, at least in part, *via* a central mechanism. Support for this contention comes from data showing a relationship between blood levels of the drug and these side effects[3]. Decreased urinary excretion levels are also associated with the decreased incidence of nausea[4]. Furthermore, parenteral administration as an intravenous[5] or intramuscular[6–8] injection also produces nausea and vomiting.

Some success in reducing the frequency of these side effects has been achieved by decreasing the rate of nitrofurantoin absorption. Large crystals, in contrast to microcrystals, of the drug produce more gradual absorption and yet allow the achievement of therapeutic amounts in the urine[3]. This may be the reason macrocrystals of nitrofurantoin tend to produce less GI upset. Food, by delaying absorption[9], similarly seems to improve GI tolerance.

In the study by Parrott and Matheson[2], an oral dose (400 mg) of nitrofurantoin (fine, 320–325 mesh) produced gastric upset in four of their original eight subjects. The authors did not report whether nausea was produced in subjects who received the same dose rectally. The absence of nausea, if this were the case, could be the result of the relatively poor rectal absorption observed.

For nitrofurantoin, a reduced rate of bioavailability may uniquely diminish its side effects. These findings[2] should provide a stimulus for further pharmacokinetic and biopharmaceutical studies to improve therapeutics with drugs that may behave like nitrofurantoin.

T. S. Gaginella
Division of Pharmacology
College of Pharmacy
Ohio State University
Columbus, OH 43210

Received August 15, 1977.

[1] S. C. Harvey, in "The Pharmacological Basis of Therapeutics," 5th ed., L. S. Goodman and A. Gilman, Eds., Macmillan, New York, N.Y., 1975, p. 1009.
[2] E. L. Parrott and L. E. Matheson, Jr., *J. Pharm. Sci.*, **66**, 955 (1977).
[3] H. E. Paul, K. J. Hayes, M. F. Paul, and A. R. Borgmann, *J. Pharm. Sci.*, **56**, 882 (1967).
[4] I. M. Thompson and A. D. Amar, *J. Urol.*, **82**, 387 (1959).
[5] M. F. Vicchi, *Med. Pract.*, **22**, 3 (1967).
[6] C. E. Cox, F. J. O'Connor, and S. S. Lucy, *J. Urol.*, **105**, 113 (1971).
[7] M. F. Vicchi, H. Pierangeli, and O. Rodriguez, *Rev. Argent. Urol.*, **37**, 72 (1968).
[8] H. K. Reckendorf, R. G. Castringius, and H. K. Springler, *Antimicrob. Agents Chemother.*, **1962**, 531.
[9] T. R. Bates, J. A. Sequeira, and A. V. Tembo, *Clin. Pharmacol. Ther.*, **16**, 63 (1974).

Cancer Cell Aggregates: Temperature Elevation

Currently, there is controversy regarding the relationship of the quantity of blood present in cancerous tissue (*i.e.*, continuous uncontrolled growth in cell aggregates) to the temperature of such tissue. One group maintains that malignancies are characterized by high temperature because relatively large quantities of blood are present in the lesion. The opposing argument holds that elevated temperatures are present in cancerous tissue because the tissue contains a relatively lesser amount of blood. Proponents of this view believe that the lesser quantity of blood has a reduced coolant effect.

We wish to make the following contribution to the discussion. It is a basic fact that blood arrives at any given tumor site at roughly 37°. The temperature of the tumor is higher, approximately 38°. As is known, temperature is an intensive factor. Therefore, regardless of the amount of blood arriving at the lesion, heat can only flow from the higher temperature of the malignancy to the lower temperature of the blood. Given this fact, a greater quantity of blood might provide an increased coolant effect; it cannot be a source of temperature increase. Even if it may be assumed that there is an increased flow of blood to the tumor, in all cases the overall system still involves blood entering and leaving cancerous tissue at a temperature lower than that of the tumor. Thus, blood must act as a coolant.

To explain the temperature of any system, the rate of heat dissipation must be considered as well as heat input. One principal factor influencing the dissipation rate is the nature of the matrix through which heat conduction occurs. Aggregates of normal cells, *i.e.*, flocculated aggregates, contain an open network in which trapped bulk water acts as the coolant. Bulk water as it exists, for example, in blood plasma has excellent cooling properties. Ecanow and co-workers[1–5] proposed that cancer cells are aggregated in a structured matrix, *i.e.*, a coagulated system. In such systems, heat derived from metabolism is conserved because it is lost by conduction at a slower rate than the rate of loss through normal cell aggregates. Thus, because heat is conserved in malignant tissue, its temperature compared to normal surrounding tissue is elevated.

The conclusion to be drawn is that malignant tissue is warmer than normal tissue because: (*a*) there is more continuous metabolic heat production, (*b*) the structured intercellular coagulated matrix conserves heat, and (*c*) malignant tissue simply does not have sufficient blood circulating through it to be cooled to normal temperature.

B. Ecanow
B. H. Gold
J. W. McCreery
University of Illinois
(at the Medical Center)
Chicago, IL 60680

Received August 18, 1977.

[1] B. Ecanow and H. Klawans, in "Models of Human Neurological Disease," H. Klawans, Ed., Excerpta Medica, Amsterdam, The Netherlands, 1974.
[2] B. Ecanow, "Aggregation of Biological Suspension System," U.S. Copyright Registration A 825 763 Publ. Ecanow, Skokie, Ill., 1966.
[3] B. Ecanow, B. H. Gold, and R. Balagot, *Science*, **193**, 919 (1976).
[4] B. Ecanow, B. H. Gold, and M. Sadove, *Br. J. Cancer*, in press.
[5] B. Ecanow, B. H. Gold, and J. W. McCreery, *Clin. Oncol.*, in press.

Journal of Pharmaceutical Sciences

OCTOBER 1977
VOLUME 66 NUMBER 10

REVIEW ARTICLE

Complement: A Host Defense Mechanism Ready for Pharmacological Manipulation?

BRIAN J. JOHNSON

Keyphrases □ Complement—mechanism of activation, associated biological effects, role in human diseases, inhibitory drugs, review □ Immunological systems—complement, mechanism of activation, associated biological effects, role in human diseases, inhibitory drugs, review □ Anticomplement drugs—complement inhibitors, review

Complement is a group of 11 serum proteins that compose the nine different complement components. These components[1] are, in the order activated by the classical pathway, C1, C4, C2, C3, C5, C6, C7, C8, and C9. Complement is an important host defense mechanism against bacteria, viruses, and other injurious stimuli. Activation can be effected by antigen–antibody complexes, bacterial and plant polysaccharides, microbial and tissue enzymes, synthetic peptides and polypeptides, and cobra venom factor. Following activation, complement releases biologically active products that can effect increased vascular permeability, chemotaxis of polymorphonuclear leukocytes, enhancement of phagocytosis, and retention of leukocytes by immune adherence.

The past quarter of a century has seen great strides in the purification of the various complement components and their mechanistic role in the lysis of cellular material. All components of the classical pathway were obtained functionally pure from human serum (1). The purification of the components (C1q, C1r, and C1s) of the first complement protein C1 was described (2–4). The remaining components also were purified (5–11). Physicochemical characterization was achieved to varying extents (12). The serum concentrations of the various complement components range from traces of C8 and C9 to 1.3 mg/ml for C3. The molecular sizes of these components range from 100,000 to 200,000 daltons, with the exception of C1q (400,000 daltons) and C9 (79,000 daltons).

[1] This nomenclature follows the WHO recommendations: *Bull. WHO*, **39**, 939 (1968).

MECHANISM OF COMPLEMENT ACTIVATION

Activation of the complement system can follow two pathways. The first, the classical pathway, is probably the more studied of the two routes. This pathway (Scheme I) is activated by the binding of C1 through its C1q subunit to cell-bound antibody and consists of several steps resulting in the generation of the C1s subunit. The presence of Ca^{2+} ions is a prerequisite for C1 activation.

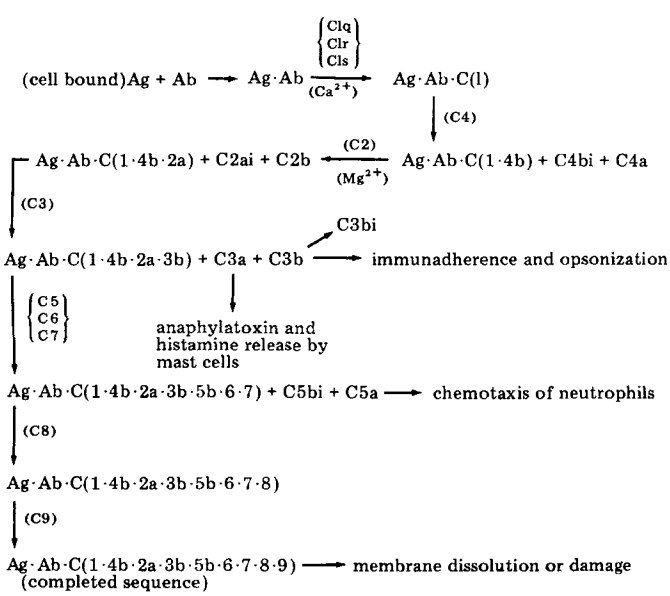

Scheme I

Usually, only the naturally occurring classes of immunoglobulins, IgG1, IgG2, IgG3, and IgM, are capable of binding C1q. Binding of C1 to monomeric IgG and IgM can be demonstrated *in vitro* under certain experimental conditions (13). However, a certain amount of aggregation of the immunoglobulins is necessary to bind C1q tightly. In fact, several studies showed no C1 binding until a critical number of IgG molecules had aggregated (14, 15). Specifically for immune hemolysis, at least two IgG molecules in close proximity are necessary for complement activation (16).

The next step consists of Ag·Ab·C(1)[2] enzymatically attacking and cleaving C4 into the large C4b fragment and a small C4a (15,500 daltons) fragment (17, 18). Failure of the C4b fragment to bind to the receptor site on the cell membrane results in the loss of the receptor site, and the C4b fragment becomes lytically inactive C4bi. The next occurrence is the absorption of C2 onto the cell-bound C4b. This reaction is reversible and requires Mg^{2+} (19). Component C2 is then cleaved into two fragments, C2a (81,000 daltons) and C2b (20, 21). Component C2b is released, and the C2a is bound to C4b to form Ag·Ab·C(1·4b·2a). Once formed, C(4b·2a) does not require the presence of Mg^{2+} or C(1) for its action.

The next sequence concerns the cleavage of C3 by C(4b·2a), generating two fragments, C3b and C3a (7200 daltons) (22, 23). Fragment C3a, which has anaphylatoxin and chemotactic factor activity, is released into the fluid phase. The C3b fragment can become attached to various parts of the cell membrane but most probably not to the C(4b·2a) site. Thus, the C(4b·2a) enzyme can produce a large number of C3b fragments, essentially by an amplification mechanism. Any C3b that does not become cell bound has a short half-life and becomes inactivated. When a C3b fragment binds to the immediate vicinity of the C(4b·2a) complex, a new enzyme C(4b·2a·3b) is created which can cleave C5. This cleavage produces two products, C5b and C5a (15,000 daltons) (24, 25). Product C5a has anaphylatoxin and chemotactic activities (26). The C5b fragment binds reversibly to the Ag·Ab·C(1·4b·2a·3b) to give Ag·Ab·C(1·4b·2a·3b·5b). This reaction is very inefficient, resulting in a large amount of C5bi (inactive).

The lytic activity of C5 is stabilized by the binding of C7 to form the trimolecular complex C(5b·6·7). Once bound, C(5b·6·7) forms a relatively stable site and lysis occurs upon reaction with C8 and C9 (27). The C8 component is physically absorbed onto the cell-bound C(5b·6·7) complex. The cell-bound C8 offers a binding site for C9, which completes the formation of a permanent membrane lesion on the cell membrane, leading to rapid lysis.

This discussion illustrated the activation of the complement system by a cellular antibody–antigen complex. However, immune complexes are not the only substances that can activate complement *via* the classical pathway. Other activating substances include protamine–heparin complexes (28), synthetic polynucleotides (29), single-stranded DNA–lysozyme complexes (30), and complexes of the acute phase C-reactive protein (CRP) with pneumococcal C-polysaccharide, lecithin, sphingomyelin, and protamine (31–33). Also, complexes of staphylococcal protein A or of reduced insulin with nonantibody IgG can activate the classical pathway (34–36). The evidence for the conclusions regarding the abilities of these substances to activate the classical pathway rests on their abilities to consume *in vitro* the total serum complement, including the early- as well as the late-acting components.

The second alternative pathway by which the complement system is activated was recognized in the study of the reaction of complement with naturally occurring materials. Only the late-acting components of complement, C3–C9, were consumed without the concomitant participation of C1, C4, and C2. The materials that accomplish this activation are bacterial and plant polysaccharides, bacterial lipopolysaccharides, cobra venom, and certain classes of immunoglobulins.

The mechanism of activation is through the generation of a C3 and a C5 cleaving enzyme rather than the respective classical pathway's C(4b·2a) and C(4b·2a·3b) enzymes. Once C5 is cleaved, activation of the remaining component, C6–C9, most probably proceeds *via* the classical pathway. The initiation of this alternative pathway apparently requires the participation of at least three proteins: properdin (P), factor B, and factor D. The presence of C3 is obviously needed. Not all of these factors may be required for activation by all substances. For example, properdin is thought to be necessary for activation of the complement system by polysaccharides but not by cobra venom factor (37).

A large amount of work was directed to understanding the mechanism of activation of complement *via* the alternative pathway. The activating mechanism initiated by zymosan was investigated (38, 39). Other bacterial polysaccharides and lipopolysaccharides from Gram-negative bacteria possess the property similar to that of zymosan of binding properdin and inactivating C3–C9 in whole serum (40). Properdin was obtained pure (41), factor B was identified as a C3 proactivator (42, 43), and factor A was identified as C3 (44, 45). Complement activation by bacterial lipopolysaccharides caused consumption of C3–C9 without consumption of C1, C4, and C2 (46, 47). Recently, the C3 and C5 cleaving enzymes on the surface of zymosan particles incubated with whole serum were studied (48–51).

Other mechanisms for activation of the alternative pathway can involve certain classes of immunoglobulins complexed to their homologous antigens. For example, guinea pig $\gamma 1$ immunoglobulin complexed with specific antigens consumed only the late-acting complement components C3–C9 without affecting C1, C4, and C2 (52). In contrast, guinea pig $\gamma 2$ consumed C1, C4, and C2 as well as C3–C9, indicating activation of the classical pathway (53, 54). Apparently, the site for the alternative pathway activation is in the $(Fab)_2$ portion of the immunoglobulin (55, 56), whereas the classical pathway activation locus is in the Fc portion (57, 58). IgA also appears capable of alternative pathway activation (59).

Another material that activates complement *via* the alternative pathway is cobra venom factor. The anticomplementary properties of cobra venom factor were first reported by Flexner and Noguchi (60). Cobra venom factor inactivates only the late-acting complement components without affecting C1, C4, and C2 (61, 62).

Cobra venom factor has been purified using ion-ex-

[2] In this review, a modification of the old nomenclature is used; the active complex is denoted by enclosure in parentheses rather than by a bar over the complex.

change and gel filtration chromatography and electrophoresis (63–65). It does not act on C3 directly but requires a normal serum cofactor. After incubation of cobra venom factor with whole serum, C3, C5, C6, C7, C8, and C9 were consumed with a concomitant generation of chemotactic activity (66). Cobra venom factor lysed unsensitized red blood cells, probably indicating the generation of hemolytically active C(5·6·7) complexes (64, 67). The generation of fluid phase C(5·6·7) complexes may contribute to the cobra venom factor-induced lysis of erythrocytes (68). Furthermore, the hemolytic potential of fluid phase C(5·6·7) generated during alternative pathway activation by cobra venom factor is regulated by C5·6·7 inhibitor (68).

In the first step, cobra venom factor forms a reversible complex with factor B (69). Factor B was described under various names including properdin factor B (70), β_2-glycoprotein type II (71), glycine-rich β-glycoprotein (GBG) (72), and C3-proactivator (C3PA) (73). The cobra venom factor complex with factor B is then cleaved in the presence of Mg^{2+} ions by the activated factor (D) into Ba (20,000 daltons) and Bb (60,000 daltons) (73). Fragment Bb remains bound to the cobra venom factor to form CVF·Bb (74). This complex has the ability to cleave C3 into C3a and C3b. The active site of this complex, CVF·Bb, resides on the Bb portion (75).

The activated (D) factor is a serine esterase (76). The precursor form of D can also be activated by trypsin. Other names for this activated (D) factor include C3PA convertase (44) and GBG-ase (77). A portion of factor D may exist in an active state in plasma (76). The generation of the C5 cleaving enzyme by cobra venom factor is not well understood (78). Obviously, cobra venom factor, unless administered to somebody, does not play a biological role *in vivo*. However, a cobra venom factor analog perhaps exists in human serum (79).

Component C3b, the larger fragment obtained upon cleavage of C3, might be considered as a cobra venom factor functional analog. Thus, incubation of C3b with factors B and D in the presence of Mg^{2+} ions results in the cleavage of B into Bb, with concomitant generation of C3 cleaving activity (44). Further evidence for this supposition was reported (80) when mixtures of highly purified cobra venom factor, factor B, and factor D in the presence of Mg^{2+} were chemotactic for human neutrophilic polymorphonuclear leukocytes. Thus, cleavage of C3 by either the classical or alternative pathway, *i.e.*, by C(1·4b·2a) or CVF·Bb, produces C3b. This C3b can then react with further quantities of factors B and D to form additional C3 convertase, probably C3b·Bb, leading to a further C3 cleavage. This reaction series is an amplification process. Furthermore, cell-bound C3b can react with factors B and D, giving rise to cell-bound C3-convertase which, upon reaction with C3, allows the cascade C3–C9 to occur, resulting in cell lysis (81). This cell-bound C3-convertase is very efficient in cleaving C3.

Evidence for the similarity between cobra venom factor and human C3 was reported (82). Rabbit anti-cobra venom factor cross reacts with human C3. However, as shown by electrophoresis, there was no change in the mobility of the cobra venom factor when incubated with human C3b inactivator. Also, there was no reduction in the ability of the cobra venom factor to inactivate C3 in normal human serum in the presence of this inactivator. However, incubation of cobra venom factor with cobra serum destroyed the ability of the cobra venom factor to induce C3 conversion in human serum. Possibly, cobra venom factor is altered cobra C3 that has the capacity, like human C3b, to activate the alternative pathway. The potent C3-inactivating activity of cobra venom factor probably derives from the fact that the cobra venom factor is not inactivated by mammalian C3b inactivator.

The complement system can also be activated by numerous enzymes. For example, plasmin activates C1s to the active form C(1s) (83). Lysosomal enzymes derived from human leukocytes activate C1s (84). Trypsin activates C1r to C(1r) (85), and this enzyme can replace C(1s) in the formation of C3-convertase from Ag·Ab·C(1·4b) and C2 (86). Trypsin can also replace factor (D) in the formation of CVF·Bb (74). The enzymes trypsin, plasmin, and pronase substitute for the factor (D) in the formation of C3-convertase by zymosan (51). Plasmin can directly cleave C3 to produce a fragment with chemotactic activity (87). Furthermore, trypsin, lysosomal enzymes from human leukocytes, and bacterial and tissue proteases can also cleave C3 and/or C5 directly to produce chemotactic factors and anaphylatoxins (88–91).

BIOLOGICAL ACTIVITIES ASSOCIATED WITH COMPLEMENT ACTIVATION

The biological activities generated by activation of the complement system are evident by acute inflammation and cell killing. These effects are manifest in increased vascular permeability, chemotaxis of leukocytes, enhanced phagocytosis, and membrane damage.

The release of a kinin and two anaphylatoxins results in increased vascular permeability. The kinin, which is released from C2 during its activation by C(1s) (92, 93), is distinguishable from bradykinin and, in contrast to the anaphylatoxins, has a direct effect on smooth muscle. It also is not histamine dependent and possibly plays a major role in the pathogenesis of hereditary angioedema (94).

Fragments C3a (7200 daltons) and C5a (15,000 daltons) are powerful anaphylatoxins (22, 26, 88, 92, 95, 96). Both of these materials induce *in vitro* contraction of guinea pig ileum and produce unresponsiveness after repeated applications. However, a smooth muscle made unresponsive to C3a is still reactive to C5a and vice versa (89). These anaphylatoxins also enhance vascular permeability and cause degranulation of mast cells. Unlike the kinin released from C2, these anaphylatoxins are mediated through release of histamine from the granules of mast cells (88, 89).

Both anaphylatoxins are chemotactic for leukocytes (97–101). The trimolecular complex C(5b·6·7) (27, 102) is also a potent chemotactic factor. Enhanced phagocytosis is another manifestation of the biological activity of complement. Phagocytosis is enhanced by the coating of cells with C3b, an opsonizing agent. Cells carrying C3b receptors include primate red cells, polymorphonuclear leukocytes, monocytes, and B-lymphocytes (103). This opsonizing effect probably is closely related to the capacity of the bound C3b to induce immune adherence (104, 105).

ROLE OF COMPLEMENT IN HUMAN DISEASES

From the discussion of the biological activities of the

complement system, it is seen that complement is an important *in vivo* effector system. Thus, *via* the anaphylatoxins, histamine may be released, causing smooth muscle contraction, peripheral vasodilation, increased vascular permeability, and edema. Through the action of its various chemotactic factors, polymorphonuclear leukocytes migrate into the area of complement activation. By providing immune adherence sites on surfaces such as the outer membranes of cells, the inner surface of blood vessels and capillaries, and deposits of immune precipitates, complement causes localization of chemotactically attracted or randomly moving leukocytes. In addition, through its opsonization function, it facilitates phagocytosis. Thus, complement is a very important host defense mechanism.

However, these advantageous biological activities of complement may become detrimental. For example, in acute glomerulonephritis, a deposition of an immune complex of γ-globulin and C3 along the glomerular capillary walls and in the mesangium (106–108) is seen. Serum complement component determinations indicate an acute reduction in circulating C1, C2, C3, C4, and C5 (109–113). The presence of bound complement in association with bound antibody in the kidneys strongly suggests that complement plays a role in the production of tissue damage in this disease.

In systemic lupus erythematosus, there is evidence that complement participates in the production of generalized tissue damage. There is usually a severe lowering of the serum level of multiple complement components (110, 112). The most probable cause of low serum hemolytic activity and increased complement catabolism is consumption of complement by circulating and localized immune complexes. The pattern of deposition of immunoglobulins and complement seen in blood vessels in numerous organs and the glomeruli is similar to that found in immune complex deposition diseases such as serum sickness (108, 114, 115). Bound complement has also been found in the skin in areas of the lupus rash but not in adjoining clinically normal skin (116).

Eluates of diseased kidneys reveal the presence of DNA (117) and anti-DNA (117, 118) in addition to antibody to various other antigens (117, 118). DNA–anti-DNA (119) and other complexes are complement fixing (116, 117). Lupus probably is caused by circulating complement-fixing immune complexes that become trapped and localized in various organs. Therefore, these complexes can trigger the complement system and cause tissue damage and inflammation.

Other diseases involving complement are the autoimmune hemolytic anemias. In many cases, the red cells are coated with complement proteins in the absence of detectable antibody (120). Possibly, the sensitivity of the detection systems used is too low for visualizing the antibody. Another possible explanation for this coating is a disease-related change in the red cell membrane that permits binding of complement without participation of antibody.

Rheumatoid arthritis is another disease that involves the complement system. Its cause is unknown, and the reason for joint predilection with the events leading to a generalized disease are poorly understood. However, there is no doubt that complement activation, with its potential for tissue damage, occurs within the joint space and probably explains the inflammatory symptoms. Thus, in the synovial joint fluid of patients with rheumatoid arthritis, whole complement (121, 122), C1 (123), C2 (121), and C4 (121, 123) are markedly depressed. Also γ-globulin, C3, and C4 are regularly deposited in the synovium of patients with active disease (124, 125). Rheumatoid joint fluids often contain leukocytes with inclusion bodies, and some of these inclusions contain γ-globulin. These findings indicate extensive activation of the complement system within the joint space.

Transplantation of tissue from genetically dissimilar patients obviously introduces new antigenic sites in the recipient. Even with extensive tissue typing of such histocompatibility antigens, the possible introduction of foreign immunogens always remains.

In studies on renal allograft rejection, two events appear to be necessary to sensitize the host. Immediately after transplantation, antigen from the donor organ is shed into the systemic circulation of the recipient by way of the renal vein. Processing of this antigen by macrophages may be necessary to transfer antigens to a form that causes sensitization of lymphocytes. Possibly, the RNA of the macrophage is linked to some part of the antigen that reaches a regional lymph node. This event initiates conversion of lymphocytes to lymphoblasts, which, in turn, divide to produce lymphocytes specifically sensitized to the graft.

Immune globulin produced by the sensitized lymphocyte (or plasma cells) may also be released as circulating antibody against the graft. Circulating lymphocytes are capable of being sensitized during their passage through the graft, perhaps by direct contact with antigens contained on the vascular endothelium of the graft. These sensitized lymphocytes homing to a lymph node may represent a population of sensitized lymphocytes that produce immune globulin specific for the graft. Both sensitized lymphoid cells (126) and humoral antibody from patients sensitized by previous kidney grafts (127) have been shown to be responsible for destruction of kidney cells cultured *in vitro* or utilized as a monolayer substrate. The destruction of the graft probably is mediated by both the immune cellular and humoral responses. This combination results in the release of macrophage migration inhibitory factor (MIF), which causes the clustering of monocytes at the vascular endothelium. Fixation of antibody activates the complement system with the release of chemotactic factor, leading to the accumulation of polymorphonuclear leukocytes.

Prolonged renal allograft rejection reactions in humans are characterized by reduced levels of C2 (128) and C3 (129), although in early rejection episodes the complement levels are variable and may be normal, elevated, or depressed (130). Three turnover studies with radiolabeled C3 and C4 were reported (131). Two of the C4 recipients and all of the C3 recipients showed increased rates of catabolism of the protein during rejection episodes. Furthermore, C1 and C3 were found in bound form in rejected renal allografts (132, 133). However, the role of complement in allograft rejection is far from clear. Thus, in dogs and mice, rejection episodes did not decrease complement levels, and complement suppression had no influence on rejection (134). C5-Deficient mice reject skin grafts normally (135), and studies with C6-deficient rabbits indi-

cated a significant prolongation of skin grafts in about half of the recipients (136). These data suggest that there may be two distinct pathways for rejection, only one of which is complement dependent.

The difference in tissue antigens between donor and recipient and the strength of these antigens may modify the histological and clinical phenomena accompanying the rejection. Thus, grafts between species are apt to be rejected violently, whereas those between identical twins undergo no rejection. However, this latter case is very uncommon in practice. Thus, the donor and recipient can be matched closely with such techniques as mixed lymphocyte culture and direct cross-matching using recipient serum and donor cells. However, even after these precautions, immunosuppressive drugs such as azathioprine, corticosteroids, and antilymphocyte globulin are still required.

These drugs can act at various levels of the immune response, including (*a*) interference with the initial sensitization or recognition of an antigen, (*b*) depression of the cellular proliferative response of either the cellular or humoral type, (*c*) interference with the function of the complement-sensitized cells, or (*d*) interference with the function of the secondary mediators that produce damage following interaction of antibody and tissue antigens. These drugs have serious side effects such as alopecia, anemia, leukopenia, hepatitis, bone marrow depression, nausea, vomiting, stomatitis, hyperglycemia, peptic ulceration, GI bleeding, and aseptic bond necrosis. The antilymphocyte globulin treatment has been reported to cause pain at the injection site, fever, and, in rare cases, anaphylaxis and thrombocytopenia.

SEARCH FOR ANTICOMPLEMENT DRUGS

One approach to immunosuppression would be to affect the complement system. Possibly by inhibiting or lowering the complement levels in the host by nontoxic anticomplement drugs, a useful therapeutic tool would become available. Such drugs would be useful not only for treating transplantation rejection but also for alleviating the distress caused by autoimmune diseases and those diseases where deposition of immune complexes can activate the complement system, *e.g.*, acute glomerulonephritis.

The idea of inhibiting or controlling the complement system is not new. Indeed, a natural control mechanism is built into the complement system itself, namely, the instability of the activated components such as C(4b·2a) and C(4b·2a·3b·5b). The rapid decay of these intermediates serves as a self-limiting mechanism. Moreover, there are naturally occurring inhibitors such as the C1 inhibitor (C1INH) and the C3b inactivator (C3bINA), also known as conglutinogen activating factor (KAF). The C1 inhibitor combines stoichiometrically with C(1s) to inhibit its hemolytic and esterolytic activities (137, 138). This inhibitor also inhibits the enzymatic activity of C(1r) (139), and it can block the action of other enzymes such as plasmin (140), kallikrein (141), and Hageman factor (142).

The inactivator C3bINA inhibits the hemolytic and immune adherence activities of bound and fluid phase C3b by cleaving it into two smaller fragments, C3d and C3c (143–147). The biological significance of these inhibitors of C1 and C3b is illustrated in patients deficient in them. Patients deficient in C1 inhibitor illustrate hereditary angioneurotic edema characterized by recurrent episodes of circumscribed edema of the skin, larynx, and intestinal mucosa (148). This edema is most probably due to uncontrolled activation of C1. The genetic deficiency of the C3b inhibitor increases the susceptibility of patients to pyogenic bacterial infections (149–151). Inactivators to C6 (143) and of C4b (152) also have been described. Recently, the C(5·6·7) inhibitor was discussed (153, 154); it acts upon C(5·6·7) reversibly in the fluid phase to prevent its attachment to bystanding erythrocytes during the short time the binding site of C(5·6·7) is active.

Synthetic inhibitors of the complement system have been used and reviewed (155). Ideally, it should be possible to obtain a series of inhibitors that inhibit specifically each complement component. However, this has not been achieved in practice. Indeed, one can argue that an inhibitor to be used as a therapeutic agent in humans need not have a stringent specificity of action for a particular complement component. As long as the action of the inhibitor on noncomplement systems does not lead to toxic effects, a certain degree of nonspecificity might even be desirable.

For example, if an inhibitor only affected C8 or C9, then the lytic properties of complement would be affected but not the production of the kinins, anaphylatoxins, and immune adherence fragments. Similarly, inhibition of the early-acting components might prevent activation of complement by the classical pathway, C1, C4, and C2, but not by the alternative pathway triggered at C3. Such a situation would be advantageous if a given immune complex only caused complement activation through the classical pathway. Thus, in designing an inhibitor, there are advantages in trying to obtain a material that inhibits either all of the complement components or just C3. This latter approach seems easier.

In the complement cascade, activation of one component then causes activation of the next in the sequence. Thus, an inhibitor, if it is to be effective, must be able to react with the active site of the particular complement enzyme in the short time interval between activation of the complement enzyme and reaction of the activated enzyme with the next component. An effective inhibitor must not only be very active in its action, but it should be present in high concentration. Many complement components not only have enzyme active sites but also have combining sites. Thus, inhibitors can be designed for blocking such binding sites, *e.g.*, C3b to the cell membrane. However, the requirements of high activity and high concentration of inhibitor are necessary.

Complement inhibitors have been used for a number of distinct purposes. One use has been to study the nature of the complement components and the mechanisms of their action, as in the studies with organophosphorus inhibitors such as isoflurophate (diisopropyl phosphorofluoridate) and phosphonate esters. Another use for complement inhibitors is to obtain evidence that a certain biological activity requires, or does not require, complement. Thus, for *in vivo* reactions, it is necessary to have an inhibitor that is highly active and highly specific. This latter requirement is difficult to obtain; cobra venom factor, a naturally occurring activator of complement, probably comes closest to the ideal. When inhibitors are used to determine com-

plement dependency, specificity is crucial. This inability to obtain synthetic materials possessing high specificity in their actions has led to the development of animals that are genetically deficient in a particular complement component.

Isoflurophate inhibits the activity of whole complement (156); it acts upon C(1) (157) by inhibiting C(1s) (158). This result is not surprising, since isoflurophate inactivates serine esterases. Baker and coworkers (159–161) synthesized a series of sulfonyl fluorides, many of which were irreversible inhibitors of C(1), and suggested that C(1) contained an anionic site in its active center. This conclusion was based on the ability of tosyl-L-arginine methyl ester to be a substrate for C(1). Indeed, this ester competitively interferes with the hemolytic activity of C(1) (162).

Bing and coworkers (163–165) showed that various aromatic compounds competitively inhibited the esterase activity of C(1s) and suggested that C(1s) possessed not only an anionic but also a hydrophobic site in its active center. ϵ-Aminocaproic acid in high concentrations prevents the activation of C1 to C(1) in its inhibition of the hemolytic activity of whole complement (166). Selective inhibition of C1 without effect on C4, C2, C3, and C9 levels in whole serum recently was reported (167). Furthermore, the effect was reversible by dialysis. In another study (168), high levels of ϵ-aminocaproic acid enhanced the cleavage of C3 with the accompanying appearance of the biologically active C3a. However, low levels of ϵ-aminocaproic acid inhibited, rather than enhanced, C3 cleavage in serum. The inhibitory activity of ϵ-aminocaproic acid was attributed to its interaction with the properdin factors. The enhancing effect of this ϵ-aminocaproic acid is thought to be due to its inhibitory effects on the C3b inactivator (168).

These inhibitors of C1 afford insights into the mechanism and nature of the active site of C(1). However, it is doubtful if these materials would be too useful for *in vivo* suppression of complement levels, since the biological activities of the complement fragments could still arise through activation of complement by the alternative pathway.

The aromatic amino acid derivatives or inhibitors of complement suggest that one component of complement might be a proteolytic enzyme with enhanced activity toward such moieties (169). The aromatic derivatives competitively inhibited the action of Ag·Ab·C(1·4b·2a·3b) in forming the heat-stable intermediate Ag·Ab·C(1·4b·2a·3b·5b·6·7) (170). This result then leads to the direct demonstration that C(1·4b·2a·3b) has peptidase activity for aromatic amino acid derivatives such as glycyl-L-tyrosine (171, 172).

Inhibitors of the binding sites of the various complement components have been investigated. Benzoxycarbonyl-L-glutamyl-L-tyrosine (173) and maleopimaric and maleofumaric acids presumably dissociate the activated C(5·6·7) complex (174, 175). Several diamines dissociate the activated C1, C(1), from the antigen–antibody complex, probably by chelating the Ca^{2+} ions necessary for the binding between C1q and the other C1 subcomponents (169).

Maleopimaric and maleofumaric acids are potent inhibitors of complement *in vitro*. Fumaropimaric acid given repeatedly over 3–4 days reduced complement levels (176), but its mode of action is not known.

Copper–chlorophyllin inhibited anaphylaxis (177), and this effect was related to inhibition of complement. This conclusion was confirmed (178); the inhibition of complement occurs at the reaction of Ag·Ab·C(1·4b·2a·3b) with C5.

Heparin has been long known to possess anticomplementary activity. Its major activity is reported to be with C1 (179). Interactions of heparin and protamine in fresh human serum, in amounts far below those required for complement depletion by either agent alone, induced virtually complete removal of total hemolytic complement activity (180). The predominant complement component depleted was C1. It has been suggested (180) that the reaction between heparin and protamine, like the interaction between antibody and antigen, markedly enhances the ability of heparin to interact with the first component of complement and that this activation goes through the classical pathway. It was also suggested (180) that interactions between certain polycations and polyanions, similar to those between antibodies and antigens, may have a role in the initiation of the inflammatory response.

However, in another study using multiple polyanions and polycations, a test for their ability to influence formation of E·C(5·6·7) from C(5·6), C7, and sheep erythrocytes (E) was performed (181). Six of the 11 polyanions tested, including polyanethol sulfonate, heparin, and dextran sulfate, inhibited this reaction. By contrast, five of seven polycations, including polybrene, protamine, and polyornithine, potentiated formation of E·C(5·6·7). This inhibition seemed to mimic the C(5·6·7)INH, while the potentiation seemed to involve the neutralization of this inhibitor (180).

Various polyanions alone react with the first component of complement (139, 182–187). The effect of eight different polyanions on the fluid phase and on bound C(1) as well as on purified C4 and C2 was tested (188). The polyanions were dextran sulfate, polyvinyl sulfate, polyanethol sulfonate, heparin, polyionsinic acid, chrondroitin sulfate, germinin, and pentosan-polysulfoester. These polyanions had no effect on purified C4 and C2, but they showed a strong inhibition of C(1) activity. Further investigation of the mode of interaction of some of these polyanions (189) indicated that they prevented the uptake of C2 by EA·C4b, where EA represents sensitized sheep erythrocytes. In contrast, treatment of the complex EA·C4b·2 with polyanions led to the dissociation into EA·C4b and C2.

Some synthetic polyanionic polypeptides were screened in this laboratory for their anticomplementary activities. The assay involved incubating the synthetic polypeptide with human serum and then, after dilution, performing a CH_{50} determination (190). Comparison of the number of CH_{50} units in the control with the number of CH_{50} units remaining in the test sample gave the amount of complement consumed (Table I).

Materials possessing aromatic moieties as well as the anionic groups consume complement. This criterion covers such diverse compounds as I and XXII (Table I). Compound I has a polypeptide backbone, and the aromatic, tyrosyl group is adjacent to the anionic glutamyl residue; XXII has a carbon backbone, and the aromatic and anionic moieties are randomly arrayed. This requirement of an

Table I—Complement-Consuming Abilities of Polyanions

Assigned Number	Compound[a]	Moles of Amino Acid Bound per Gram of Polymer	Percentage of CH_{50} Removed[b]	Number of CH_{50} Units Removed per Milligram of Material
—	Human IgG1	—	—	30.7
I	$(Tyr\text{-}Glu\text{-}Ala\text{-}Gly)_n Gly$	Equimolar	100	15.4
II	$(Phe\text{-}Glu\text{-}Ala\text{-}Gly)_n Gly$	Equimolar	0	—
III	$(Trp\text{-}Glu\text{-}Ala\text{-}Gly)_n Gly$	Equimolar	25	—
IV	$(Tyr\text{-}\gamma\text{-}Glu\text{-}Ala\text{-}Gly)_n Gly$	Equimolar	32	—
V	$(Tyr\text{-}Glu\text{-}Gly\text{-}Gly)_n Gly$	Equimolar	30	—
VI	$(Tyr\text{-}Glu\text{-}Ala\text{-}\beta\text{-}Ala)_n Gly$	Equimolar	100	—
VII	$(Ala\text{-}Glu\text{-}Ala\text{-}Gly)_n Gly$	Equimolar	0	—
VIII	$(Glu)_n$	Equimolar	0	—
IX	$(Glu\text{-}Ala)_n$	Equimolar	0	—
X	$(Glu\text{-}Ala\text{-}Tyr_4)_n$	$(3.6:6.7:0.25) \times 10^{-3}$	0	—
XI	$(Glu\text{-}Ala\text{-}Tyr_{10})_n$	$(3.4:6.3:0.61) \times 10^{-3}$	0	—
XII	(Maleic acid–vinyl methyl ether)$_n$	0	0	—
XIII	(Maleic acid–Tyr–methyl ether)$_n$	1.44×10^{-3}	100	58.9
XIV	(Maleic acid–Phe–vinyl methyl ether)$_n$	1.40×10^{-3}	100	43.5
XV	(Maleic acid–His–vinyl methyl ether)$_n$	1.10×10^{-3}	0	—
XVI	(Maleic acid–Leu–vinyl methyl ether)$_n$	1.20×10^{-3}	0	—
XVII	(Maleic acid–Pro–vinyl methyl ether)$_n$	1.77×10^{-3}	0	—
XVIII	(Maleic acid–Gly–vinyl methyl ether)$_n$	1.70×10^{-3}	0	—
XIX	(Maleic acid–Lys–vinyl methyl ether)$_n$	1.67×10^{-3}	0	—
XX	(Maleic acid–Trp–Gly–vinyl methyl ether)$_n$	1.35×10^{-3}	100	—
XXI	(Maleic acid–styrene)$_n$	0	100	87.0
XXII	(Maleic acid–styrene–Tyr)$_n$	0.75×10^{-3}	100	105.3

[a] Molecular weight greater than 30,000 daltons. [b] By 2000 μg.

aromatic moiety is illustrated by comparison of I and VII. Replacement of the tyrosyl residue in I by an alanyl moiety as in polymer VII produces a complete loss of complement-consuming ability.

Further evidence for the necessity of an aromatic residue is evident by comparison of XII, XIII, XIV, and XX. These materials are identical, except that polymers XIII, XIV, and XX have small amounts of aromatic residues attached to them. These residues are necessarily next to the anionic carboxyl residue, since these polymers were synthesized from the precursor polymer poly(maleic anhydride–vinyl methyl ether). Thus, XIII could be thought of as having repeating tyrosyl and carboxyl moieties along a carbon chain, somewhat analogous to I. Although II, X, and XI all have aromatic and anionic moieties, none consume complement. Compounds X and XI are random copolymers. It is possible that insufficient tyrosine is incorporated in them to satisfy the aromatic requirement or that the tyrosyl residues are not adjacent to the anionic carboxyl group of glutamic acid.

A weight basis comparison of the amounts of each polymer and the human immunoglobulin IgG1 to remove half of the available CH_{50} units per milliliter of human serum is given in Table I. Polymer I has half of the capability of the human immunoglobulin IgG1 to consume complement, whereas the other polymers are somewhat better. Comparison of the tyrosyl-substituted XXII with the unsubstituted XXI further indicates the role of the tyrosyl residue. The complement-consuming ability of the polymer is increased by 20% when this residue is incorporated. The potent anticomplementary activity of poly(maleic acid–styrene) indicates that the necessary structural requirement for anticomplementary activity in this series occurs when a carboxyl group is in close proximity to a side-chain carboxyl group. This requirement may possibly explain the lack of anticomplementary activity of the random copolymers X and XI, which possess small amounts of tyrosine. Since their sequences are random, there is the possibility that the tyrosyl residues are not situated in the correct sequence for anticomplementary activity.

Another area being pursued vigorously in this laboratory is the synthesis of peptides based on the knowledge of the complement-fixing sites of immunoglobulins. The modification of a few tryptophan residues in rabbit IgG and Fc with 2-hydroxy-5-nitrobenzyl bromide eliminated the anticomplementary activity of these protein molecules in the presence of whole guinea pig complement, but it did not significantly alter their C1q-binding capacity (191, 192). Furthermore, a particular tryptophan residue of V, a cleavage peptide of rabbit Fc, was most probably responsible for this change in anticomplementary activity. According to studies on the amino acid sequences of rabbit heavy chains (193), tryptophan residue No. 277 at the *N*-terminal side of the carbohydrate group and within the first intrachain disulfide bridge of the Fc appeared to be involved in complement fixation. Other reports (57, 58, 194–197) also indicated that the anticomplementary activity of IgG was associated with the Cγ2 domain of the immunoglobulin.

To define more closely the residues participating in the complement-binding and/or complement-fixing site of a human IgG1, human IgG1 was modified by dansylation (198–200), nitration (201), and alkylation with 2-hydroxy-5-nitrobenzyl bromide (191) and 2,3-butanedione reagent (202). The alkylation of human IgG1 with 2-hydroxy-5-nitrobenzyl bromide reduced its ability to consume complement. This result agrees with that already reported for rabbit IgG (191). Similarly, nitration, dansylation, and arginine modification with 2,3-butanedione each lowered the anticomplementary abilities of human IgG1. These results imply that the amino acid residues, tryptophan, lysine, arginine, and tyrosine (203), constitute part of the active site of the complement-fixing locus and/or part of the C1 binding site of the immunoglobulin.

Comparison of some amino acid sequences of the complement-fixing immunoglobulins of human IgG1 (204),

Table II—Sequence Comparisons of Various Immunoglobulins Possessing the Tryptophan Residue Implicated in Complement Fixation

Immunoglobulin C_H2 Domain	Amino Acid Residues	Sequence												
Human IgG1	271–283	Pro	Gln	Val	Lys	Phe	Asn	Trp	Tyr	Val	Asp	Gly	Val	Gln
Guinea pig IgG2	271–283	Pro	Glu	Val	Gln	Phe	Thr	Trp	Phe	Val	Asp	Asn	Lys	Pro
Rabbit IgG	271–283	Pro	Glu	Val	Glx	Phe	Thr	Trp	Tyr	Ile	Asx	Glu	Gln	Val
Murine IgG2a	271–283	Pro	Asp	Val	Gln	Ile	Ser	Trp	Phe	Val	Asp	Asn	Val	Glu
Human IgM[a]	482–494	Ala	Asp	Val	Phe	Val	Glu	Trp	Met	Gln	Arg	Gly	Glu	Pro
Human IgM	264–276	Phe	Ser	Pro	Arg	Gln	Val	Trp	Ser	Leu	Arg	Glu	Gly	Lys

[a] $C_\mu4$ domain.

guinea pig IgG2 (205), mouse IgG2 (197), rabbit IgG (206), and human IgM (207) is given in Table II. Several peptides based on these sequences were synthesized; those peptides that mimicked the sequences around the tryptophan residue at position 277 of human IgG1 fixed complement (208). These results confirm the hypothesis (183) that this tryptophan moiety is part of the complement-fixing site (209). These sequences surrounding this aromatic amino acid are hydrophobic and also contain anionic side-chain amino acid residues. These observations correlate quite well with previous work.

At the moment, neither *in vivo* studies nor the mechanisms of action of these materials have been investigated. However, due to their low molecular weights, these materials are not expected to be antigenic; should they lower complement levels *in vivo*, they should be capable of pharmacological manipulation.

CONCLUSIONS

Under normal circumstances, the complement system is a potent natural defense mechanism of the host. However, in certain situations, this mechanism can be disadvantageous, *i.e.*, in transplantation rejection, autoimmune diseases, and other diseases where deposition of immune complexes can activate the complement system such as acute glomerulonephritis. The time has come for the development of anticomplement drugs to alleviate this problem. Such drugs would ideally be specific for a particular complement component and also have a low toxicity and antigenicity.

The most promising area to exploit would be drugs that affect the third complement component, since activation of the complement system by either the classical or the alternative pathway involves this component. Indeed, lowering of the level of C3, or its temporary elimination, in the patient would reduce production of the anaphylatoxin C3a and its concomitant detrimental biological activity. At the moment, small peptides based on the sequences of known anticomplement materials such as the immunoglobulins appear promising. However, further investigations on the complement active sites of other anticomplement materials such as cobra venom factor are required. Such information will be of value in designing materials that specifically bind or activate particular complement components.

Another avenue of approach to this problem is the use of high molecular weight polyions. Even though some of these materials are antigenic (210), they may have therapeutic value if used in *in vitro* situations. For example, several investigators (211–213) suggested that complement plays an immunopathological role in the inflammatory periodontal disease process. The gingival crevicular fluid from normal patients possesses the complement components C3, C4, and C5; that from patients with inflamed gingiva contains properdin factor B and electrophoretically converted C3 (214). In addition, the functional nature of complement components in the crevicular fluid from periodontal patients was demonstrated (215).

If the levels of complement could be lowered in the gingival crevicular fluid, then tissue damage and inflammation due to complement activation could be controlled. Gingival crevicular fluid possesses some similarity to serum (216, 217); since some of the polyanionic polymers are good serum complement-removing materials, these polymers may find therapeutic use for patients with periodontal disease.

REFERENCES

(1) D. H. Vroon, D. R. Schutz, and R. M. Zarco, *Immunochemistry*, **7**, 43 (1970).

(2) K. Yonemasu and R. M. Stroud, *J. Immunol.*, **106**, 304 (1971).

(3) M. M. E. deBracco and R. M. Stroud, *J. Clin. Invest.*, **50**, 838 (1971).

(4) K. Nagaki and R. M. Stroud, *J. Immunol.*, **102**, 421 (1969).

(5) H. J. Müller-Eberhard and C. E. Biro, *J. Exp. Med.*, **118**, 447 (1963).

(6) M. J. Polley and H. J. Müller-Eberhard, *ibid.*, **128**, 533 (1968).

(7) U. R. Nillson and H. J. Müller-Eberhard, *ibid.*, **122**, 277 (1965).

(8) C. M. Arroyave and H. J. Müller-Eberhard, *Immunochemistry*, **8**, 995 (1971).

(9) C. M. Arroyave and H. J. Müller-Eberhard, *J. Immunol.*, **111**, 302 (1973).

(10) J. A. Manni and H. J. Müller-Eberhard, *J. Exp. Med.*, **130**, 1145 (1969).

(11) U. Hadding and H. J. Müller-Eberhard, *Immunology*, **16**, 719 (1969).

(12) J. E. Volanakis, *J. Oral Pathol.*, **4**, 3 (1975).

(13) W. Augener, H. W. Grey, N. R. Cooper, and H. J. Müller-Eberhard, *Immunochemistry*, **8**, 1011 (1971).

(14) K. Ishizaka, T. Ishizaka, and J. Banovitz, *J. Immunol.*, **95**, 824 (1965).

(15) N. E. Hyslop, R. R. Dourmashkin, N. M. Green, and R. R. Porter, *J. Exp. Med.*, **131**, 783 (1970).

(16) T. Borsos, H. J. Rapp, and U. L. Walz, *J. Immunol.*, **92**, 108 (1964).

(17) R. A. Patrick, S. B. Taubman, and I. H. Lepow, *Immunochemistry*, **7**, 217 (1970).

(18) D. B. Budzko and H. J. Müller-Eberhard, *ibid.*, **7**, 227 (1970).

(19) G. Sitomer, R. M. Stroud, and M. M. Mayer, *ibid.*, **3**, 59 (1966).

(20) R. M. Stroud, K. F. Austen, and M. M. Mayer, *ibid.*, **2**, 219 (1965).

(21) R. M. Stroud, M. M. Mayer, J. A. Miller, and A. T. McKenzie, *ibid.*, **3**, 163 (1966).

(22) D. B. Budzko, V. A. Bokisch, and H. J. Müller-Eberhard, *Biochemistry*, **10**, 1166 (1971).

(23) H. J. Müller-Eberhard, in "Progress in Immunology II," vol. 1, L. Brent and J. Holborow, Eds., North-Holland, New York, N.Y., 1974, pp. 173–182.

(24) H. S. Shin, R. J. Pickering, M. M. Mayer, and C. T. Cook, *J. Immunol.*, **101,** 813 (1968).
(25) U. Nillson and J. Mapes, *ibid.*, **111,** 293 (1973).
(26) J. A. Jensen, *Science,* **155,** 1122 (1967).
(27) P. J. Lachmann and R. A. Thompson, *J. Exp. Med.*, **131,** 643 (1970).
(28) R. Rent, N. Ertel, R. Eisenstein, and H. Gewurz, *Immunology,* **114,** 120 (1975).
(29) S. Yachnin, D. Rosenblum, and D. Chatman, *J. Immunol.*, **93,** 549 (1964).
(30) W. F. Willoughby, R. T. Ford, and H. S. Shin, *ibid.*, **111,** 296 (1973).
(31) M. H. Kaplan and J. E. Volanakis, *ibid.*, **112,** 2135 (1974).
(32) J. E. Volanakis and M. H. Kaplan, *ibid.*, **113,** 9 (1974).
(33) J. Siegel, R. Rent, and H. Gewurz, *J. Exp. Med.*, **140,** 631 (1974).
(34) J. Sjöquist and G. Stalenheim, *J. Immunol.*, **103,** 467 (1969).
(35) G. Kronvall and H. Gewurz, *Clin. Exp. Immunol.*, **7,** 211 (1970).
(36) J. W. Cantrell, R. M. Stroud, and K. M. Pruitt, *Diabetes,* **21,** 872 (1972).
(37) A. G. Osler and A. L. Sandberg, *Prog. Allergy,* **17,** 51 (1973).
(38) L. Pillemer, L. Blum, I. H. Lepow, O. A. Ross, E. W. Todd, and A. C. Wardlaw, *Science,* **120,** 279 (1954).
(39) L. Pillemer, L. Blum, I. H. Lepow, L. Wurz, and E. W. Todd, *J. Exp. Med.*, **103,** 1 (1956).
(40) L. Pillemer, M. D. Schoenberg, L. Blum, and L. Wurz, *Science,* **122,** 545 (1955).
(41) J. Pensky, C. F. Hinz, E. W. Todd, R. J. Wedgwood, J. T. Boyer, and I. H. Lepow, *J. Immunol.*, **100,** 42 (1968).
(42) I. Goodkofsky and I. H. Lepow, *ibid.*, **107,** 1200 (1971).
(43) C. A. Alper, I. Goodkofsky, and I. H. Lepow, *J. Exp. Med.*, **137,** 424 (1973).
(44) H. J. Müller-Eberhard and O. Götze, *ibid.*, **135,** 1003 (1972).
(45) I. Goodkofsky, A. H. Stewart, and I. H. Lepow, *J. Immunol.*, **111,** 287 (1973).
(46) H. A. Bladen, H. Gewurz, and S. E. Mergenhagen, *J. Exp. Med.*, **125,** 767 (1967).
(47) H. Gewurz, H. S. Shin, and S. E. Mergenhagen, *ibid.*, **128,** 1049 (1968).
(48) V. Brade, G. D. Lee, A. Nicholson, H. S. Shin, and M. M. Mayer, *J. Immunol.*, **111,** 1389 (1973).
(49) A. Nicholson, V. Brade, C. D. Lee, H. S. Shin, and M. M. Mayer, *ibid.*, **112,** 1115 (1974).
(50) V. Brade, A. Nicholson, G. D. Lee, and M. M. Mayer, *ibid.*, **112,** 1845 (1974).
(51) V. Brade, A. Nicholson, D. Bitter-Suermann, and U. Hadding, *ibid.*, **113,** 1735 (1974).
(52) A. G. Osler, B. Oliveira, H. S. Shin, and A. L. Sandberg, *ibid.*, **102,** 269 (1969).
(53) A. L. Sandberg, A. G. Osler, H. S. Shin, and B. Oliveira, *ibid.*, **104,** 329 (1970).
(54) A. L. Sandberg and A. G. Osler, *ibid.*, **107,** 1268 (1971).
(55) A. L. Sandberg, O. Götze, H. J. Müller-Eberhard, and A. G. Osler, *ibid.*, **107,** 920 (1971).
(56) K. B. M. Reid, *Immunology,* **20,** 649 (1971).
(57) J. M. Kehoe and M. Fougereau, *Nature,* **224,** 1212 (1969).
(58) J. R. Ellerson, D. Yasmeen, R. M. Painter, and K. J. Dorrington, *FEBS Lett.*, **24,** 318 (1972).
(59) H. L. Spiegelberg and O. Bötze, *Fed. Proc.*, **31,** 2478 (1972).
(60) S. Flexner and H. J. Noguchi, *J. Exp. Med.*, **6,** 277 (1903).
(61) H. Ritz, *Z. Immunol. Exp. Ther.*, **13,** 62 (1912).
(62) P. G. Klein and H. J. Wellensiek, *Immunology,* **8,** 590 (1965).
(63) R. A. Nelson, *Surv. Ophthalmol.*, **11,** 498 (1966).
(64) M. Ballow and C. G. Cochrane, *J. Immunol.*, **103,** 944 (1969).
(65) H. J. Müller-Eberhard and K. Fjellström, *ibid.*, **107,** 1666 (1971).
(66) H. S. Shin, H. Gewurz, and R. Snyderman, *Proc. Soc. Exp. Biol. Med.*, **131,** 203 (1969).
(67) R. J. Pickering, M. R. Wolfson, R. A. Good, and H. Gewurz, *Proc. Natl. Acad. Sci. USA,* **62,** 521 (1969).
(68) B. McLeod, R. F. Lint, P. Baker, C. Behrends, and H. Gewurz, *Immunology,* **28,** 741 (1975).
(69) N. R. Cooper, *J. Exp. Med.*, **137,** 451 (1973).
(70) L. Blum, L. Pillemer, and I. H. Lepow, *Z. Immunol. Exp. Ther.*, **118,** 349 (1959).
(71) H. Haupt and K. Heide, *Clin. Chim. Acta,* **12,** 419 (1965).
(72) T. Boenisch and C. A. Alper, *Biochim. Biophys. Acta,* **221,** 529 (1970).
(73) O. Götze and H. J. Müller-Eberhard, *J. Exp. Med.*, **134,** 905 (1971).
(74) W. Vogt, L. Dieminger, R. Lymen, and G. Schmidt, *Hoppe-Seyler's Z. Physiol. Chem.*, **355,** 171 (1974).
(75) N. R. Cooper, in "Contemporary Topics in Molecular Immunology," vol. 2, R. A. Reisfeld and W. J. Mandy, Eds., Plenum, New York, N.Y., 1973, p. 155.
(76) D. T. Fearon, K. F. Austen, and S. Ruddy, *J. Exp. Med.*, **139,** 355 (1974).
(77) C. A. Alper and F. S. Rosen, *Adv. Immunol.*, **14,** 251 (1971).
(78) L. G. Hunsicker, S. Ruddy, and K. F. Austen, *J. Immunol.*, **110,** 128 (1973).
(79) H. J. Müller-Eberhard, U. R. Nillson, A. P. Dalmasso, M. J. Polley, and M. A. Calcott, *Arch. Pathol.*, **82,** 205 (1966).
(80) S. Ruddy, K. F. Austen, and E. J. Goetzl, *J. Clin. Invest.*, **55,** 587 (1975).
(81) D. T. Fearon, K. F. Austen, and S. Ruddy, *J. Exp. Med.*, **138,** 1305 (1973).
(82) C. A. Alper and D. Balavitch, *Science,* **191,** 1275 (1976).
(83) O. D. Ratnoff and G. B. Naff, *J. Exp. Med.*, **125,** 377 (1967).
(84) S. B. Taubman, P. R. Goldschmidt, and I. H. Lepow, *Fed. Proc.*, **29,** 1065 (1970).
(85) G. Valet and N. R. Cooper, *J. Immunol.*, **112,** 1667 (1974).
(86) M. Loos, T. Borsos, and H. J. Rapp, *ibid.*, **109,** 434 (1972).
(87) P. A. Ward, *J. Exp. Med.*, **128,** 189 (1967).
(88) W. Dias da Silva and I. H. Lepow, *ibid.*, **125,** 921 (1967).
(89) C. G. Cochrane and H. J. Müller-Eberhard, *ibid.*, **127,** 371 (1968).
(90) J. H. Hill and P. A. Ward, *ibid.*, **130,** 505 (1969).
(91) I. H. Lepow, in "Progress in Immunology," vol. I, B. Amos, Ed., Academic, New York, N.Y., 1971, p. 567.
(92) M. R. Klemperer, F. S. Rosen, and V. H. Donaldson, *J. Clin. Invest.*, **48,** 44a (1969).
(93) I. H. Lepow, in "Biochemistry of the Acute Allergic Reactions," K. F. Austin and E. L. Becker, Eds., Blackwell, Oxford, England, 1971.
(94) V. H. Donaldson, D. D. Ratnoff, W. Dias da Silva, and F. S. Rosen, *J. Clin. Invest.*, **48,** 642 (1969).
(95) W. Dias da Silva, J. W. Eisle, and I. H. Lepow, *J. Exp. Med.*, **126,** 1027 (1967).
(96) H. S. Shin, R. Snyderman, E. Friedman, A. Mellors, and M. M. Mayer, *Science,* **162,** 361 (1968).
(97) R. Snyderman, H. Gewurz, and S. E. Mergenhagen, *J. Exp. Med.*, **128,** 259 (1968).
(98) V. A. Bokisch, H. J. Müller-Eberhard, and C. G. Cochrane, *ibid.*, **129,** 1109 (1969).
(99) P. A. Ward, in "Cellular and Humoral Mechanisms in Anaphylaxis and Allergy," H. Z. Movat, Ed., S. Karger, Basel, Switzerland, 1969, p. 279.
(100) J. A. Jensen, R. Snyderman, and S. E. Mergenhagen, in *ibid.*, p. 265.
(101) H. S. Shin, H. Gewurz, and R. Snyderman, *Proc. Soc. Exp. Biol. Med.*, **131,** 203 (1969).
(102) P. A. Ward, C. G. Cochrane, and H. J. Müller-Eberhard, *J. Exp. Med.*, **122,** 327 (1965).
(103) C. Bianco, R. Patrick, and V. Nussenzweig, *ibid.*, **132,** 702 (1970).
(104) I. Gigli and R. A. Nelson, *Exp. Cell. Res.*, **51,** 45 (1968).
(105) K. Nishioka and W. D. Linscott, *J. Exp. Med.*, **118,** 767 (1963).
(106) J. D. Feldman, M. R. Mardiney, and S. E. Shuler, *Lab. Invest.*, **15,** 283 (1966).
(107) D. Koffler and F. Paronetto, *J. Clin. Invest.*, **44,** 1665 (1965).
(108) P. J. Lachmann, H. J. Müller-Eberhard, H. G. Kunkel, and F. Paronetto, *J. Exp. Med.*, **115,** 63 (1962).
(109) C. A. Alper and F. S. Rosen, *J. Clin. Invest.*, **46,** 2021 (1967).
(110) H. Gewurz, R. J. Pickering, D. S. Clark, A. R. Page, J. Finstad, and R. A. Good, in "Immunologic Deficiency Diseases in Man," D. Bergsma, Ed., National Foundation, New York, N.Y., 1968.
(111) P. F. Kohler and H. J. Müller-Eberhard, *Clin. Res.*, **15,** 296 (1967).
(112) P. H. Schur and K. F. Austen, *Ann. Rev. Med.*, **19,** 1 (1968).
(113) C. D. West, J. D. Northway, and N. C. Davis, *J. Clin. Invest.*, **43,** 1507 (1964).
(114) F. Paronetto and D. Koffler, *ibid.*, **44,** 1657 (1965).

(115) K. H. Svec, J. D. Blair, and M. H. Kaplan, *ibid.*, **46,** 558 (1967).
(116) E. M. Tan and H. G. Kunkel, *Arthritis Rheum.*, **9,** 39 (1966).
(117) D. Koffler, P. Schur, and H. G. Kunkel, *J. Exp. Med.*, **126,** 607 (1967).
(118) C. Krishnam and M. H. Kaplan, *J. Clin. Invest.*, **46,** 569 (1967).
(119) E. Wasserman and L. Levine, *J. Immunol.*, **87,** 290 (1961).
(120) J. P. Leddy, *Semin. Hematol.*, **3,** 48 (1966).
(121) G. Fostiropoulos, K. F. Austen, and K. J. Block, *Arthritis Rheum.*, **8,** 219 (1965).
(122) H. Hedberg, *Acta Rheum. Scand.*, **9,** 165 (1963).
(123) N. J. Zvaifler and T. Pekin, *Clin. Res.*, **11,** 180 (1963).
(124) A. J. Fish, A. F. Michael, H. Gewurz, and R. A. Good, *Arthritis Rheum.*, **9,** 267 (1966).
(125) W. S. Rodman, R. C. Williams, R. J. Bilka, and H. J. Müller-Eberhard, *J. Lab. Clin. Med.*, **69,** 141 (1967).
(126) A. Covaerts, *J. Immunol.*, **129,** 724 (1960).
(127) F. Milgrom, B. I. Litvak, K. Kano, and E. Witebsky, *J. Am. Med. Assoc.*, **198,** 226 (1966).
(128) K. F. Austen and P. S. Russell, *Ann. N.Y. Acad. Sci.*, **129,** 657 (1966).
(129) C. B. Carpenter, T. J. McGill, J. P. Merrill, and G. S. Dammin, *Am. J. Med.*, **43,** 854 (1967).
(130) C. B. Carpenter, S. Ruddy, I. H. Shehadeh, J. P. Merrill, K. F. Austen, and H. J. Müller-Eberhard, *Transplant. Proc.*, **1,** 279 (1969).
(131) C. B. Carpenter, S. Ruddy, I. H. Shehadeh, H. J. Müller-Eberhard, J. P. Merrill, and K. F. Austen, *J. Clin. Invest.*, **48,** 1495 (1969).
(132) R. R. Linquist, R. P. Guttman, J. P. Merrill, and G. J. Dammin, *Am. J. Pathol.*, **53,** 851 (1968).
(133) K. A. Porter, G. A. Andres, M. W. Calder, J. B. Dossetor, K. C. Hsu, J. W. Rendall, B. C. Seegal, and T. E. Starzl, *Lab. Invest.*, **18,** 159 (1968).
(134) H. Gewurz, D. S. Clark, J. Finstad, W. D. Kelly, R. L. Varco, R. A. Good, and A. E. Gabrielson, *Ann. N.Y. Acad. Sci.*, **129,** 673 (1966).
(135) L. D. Caren and L. T. Rosenberg, *Immunology*, **9,** 359 (1965).
(136) U. Rother, D. L. Ballantyne, C. Cohen, and K. Rother, *J. Exp. Med.*, **126,** 565 (1967).
(137) O. D. Ratnoff and I. H. Lepow, *ibid.*, **106,** 327 (1957).
(138) L. R. Levy and I. H. Lepow, *Proc. Soc. Exp. Biol. Med.*, **101,** 608 (1959).
(139) G. B. Naff and O. D. Ratnoff, *J. Exp. Med.*, **128,** 571 (1968).
(140) O. D. Ratnoff, J. Pensky, D. Ogston, and G. B. Naff, *ibid.*, **129,** 315 (1969).
(141) I. Gigli, J. W. Mason, R. W. Coleman, and K. F. Austen, *J. Immunol.*, **104,** 574 (1970).
(142) A. D. Schreiber, A. P. Kaplan, and K. F. Austen, *J. Clin. Invest.*, **52,** 1402 (1973).
(143) N. Tamura and R. A. Nelson, *J. Immunol.*, **99,** 582 (1967).
(144) P. J. Lachmann and H. J. Müller-Eberhard, *ibid.*, **100,** 691 (1968).
(145) S. Ruddy and K. F. Austen, *ibid.*, **102,** 533 (1969).
(146) *Ibid.*, **107,** 742 (1971).
(147) J. D. Gitlin, F. S. Rosen, and P. J. Lachmann, *J. Exp. Med.*, **141,** 1221 (1975).
(148) V. H. Donaldson and R. R. Evans, *Am. J. Med.*, **35,** 37 (1963).
(149) C. A. Alper, N. Abramson, R. B. Johnston, J. H. Jandle, and F. S. Rosen, *N. Engl. J. Med.*, **282,** 349 (1970).
(150) N. Abramson, C. A. Alper, P. J. Lachmann, F. S. Rosen, and J. H. Jandle, *J. Immunol.*, **107,** 19 (1971).
(151) C. A. Alper and F. S. Rosen, *Adv. Immunol.*, **14,** 251 (1971).
(152) N. R. Cooper, *J. Exp. Med.*, **141,** 890 (1975).
(153) B. C. McLeod, P. Baker, and H. Gewurz, *Immunology*, **26,** 1145 (1974).
(154) B. C. McLeod, P. Baker, and H. Gewurz, *Int. Arch. Allergy Appl. Immunol.*, **47,** 623 (1974).
(155) E. L. Becker, in "Inflammation Mechanisms and Control," I. H. Lepow and P. A. Ward, Eds., Academic, new York, N.Y., 1972.
(156) L. Levine, *Biochim. Biophys. Acta*, **18,** 283 (1955).
(157) E. L. Becker, *J. Immunol.*, **77,** 462 (1956).
(158) A. L. Haines and I. H. Lepow, *ibid.*, **92,** 468 (1964).
(159) B. R. Baker and J. A. Hurlbut, *J. Med. Chem.*, **12,** 415 (1969).
(160) *Ibid.*, **12,** 902 (1969).
(161) B. R. Baker and M. Cory, *J. Med. Chem.*, **14,** 119 (1971).
(162) R. M. Stroud, K. F. Austen, and M. M. Mayer, *Immunochemistry*, **2,** 219 (1965).
(163) D. H. Bing, *Biochemistry*, **8,** 4503 (1969).
(164) D. H. Bing, J. L. Mernitz, and S. Spurlock, *ibid.*, **11,** 4263 (1972).
(165) D. H. Bing, M. Cory, and M. Doll, *J. Immunol.*, **113,** 584 (1974).
(166) F. B. Taylor and H. Fudenberg, *Immunology*, **7,** 319 (1964).
(167) N. A. Sorter, K. F. Austen, and I. Gigli, *J. Immunol.*, **114,** 928 (1975).
(168) W. Vogt, G. Schmidt, R. Lynen, and L. Dieminger, *ibid.*, **114,** 671 (1975).
(169) W. Cushman, E. L. Becker, and G. Wirtz, *ibid.*, **79,** 89 (1957).
(170) R. S. Basch, *ibid.*, **94,** 629 (1965).
(171) N. R. Cooper and E. L. Becker, *ibid.*, **98,** 119 (1967).
(172) N. R. Cooper and H. J. Müller-Eberhard, *Fed. Proc.*, **26,** 361 (1967).
(173) P. A. Ward, C. G. Cochrane, and H. J. Müller-Eberhard, *Immunology*, **11,** 141 (1966).
(174) M. M. Glovsky, E. L. Becker, and N. J. Halbrook, *J. Immunol.*, **100,** 979 (1968).
(175) M. M. Glovsky, P. A. Ward, E. L. Becker, and N. J. Halbrook, *ibid.*, **102,** 1 (1969).
(176) N. N. Azar and R. A. Good, *Proc. Soc. Exp. Biol. Med.*, **137,** 429 (1971).
(177) K. H. Busing, *Allerg. Asthma*, **3,** 15 (1957).
(178) D. Lorenz and H. Uebel, *Arzneim.-Forsch.*, **7,** 357 (1957).
(179) K. Lauenstein, H. G. Siedeutopf, and H. Fischer, *Z. Naturforsch.*, **206,** 575 (1965).
(180) R. Rent, N. Ertel, R. Eisenstein, and H. Gewurz, *J. Immunol.*, **114,** 120 (1975).
(181) P. J. Baker, T. F. Lint, B. C. McLeod, C. L. Behrends, and H. Gewurz, *ibid.*, **114,** 554 (1975).
(182) V. Agnello, R. I. Carr, D. Koffler, and H. G. Kunkel, *Fed. Proc.*, **28,** 2447 (1969).
(183) T. Borsos, H. J. Rapp, and C. Crisler, *J. Immunol.*, **94,** 662 (1965).
(184) G. E. Davies, *Immunology*, **6,** 561 (1963).
(185) M. Loos, T. Borsos, and H. J. Rapp, *J. Immunol.*, **108,** 683 (1972).
(186) S. Yachnin, *J. Clin. Invest.*, **42,** 1947 (1963).
(187) S. Yachnin, D. Rosenblum, and D. Chatman, *J. Immunol.*, **93,** 540 (1964).
(188) E. Raepple, H. U. Hill, and M. Loos, *Immunochemistry*, **13,** 251 (1976).
(189) M. Loos, J. E. Volanakis, and R. M. Stroud, *ibid.*, **13,** 257 (1976).
(190) E. A. Kabat and M. M. Mayer, in "Experimental Immunochemistry," 2nd ed., Charles C Thomas, Springfield, Ill., 1967, p. 133.
(191) R. Allan and H. Isliker, *Immunochemistry*, **11,** 175 (1974).
(192) *Ibid.*, **11,** 243 (1974).
(193) E. Appella, A. Chersi, R. G. Mage, and S. Dubiski, *Proc. Natl. Acad. Sci. USA*, **68,** 1341 (1971).
(194) S. Utsumi, *Biochem. J.*, **112,** 343 (1969).
(195) Z. Ovary, P. H. Saluk, L. Quijada, and M. E. Lamm, *J. Immunol.*, **116,** 1265 (1976).
(196) G. E. Connell and R. R. Porter, *Biochem. J.*, **124,** 53 (1971).
(197) J. M. Kehoe, J. A. Bourgois, J. D. Capra, and M. Forgereau, *Biochemistry*, **13,** 2499 (1974).
(198) G. Weber, *Biochem. J.*, **51,** 145 (1952).
(199) P. Wohl and G. Weber, *J. Mol. Biol.*, **30,** 371 (1967).
(200) J. K. Weltman and G. M. Edelman, *Biochemistry*, **6,** 1437 (1967).
(201) M. Z. Atassi and A. F. S. A. Habeeb, *ibid.*, **8,** 1385 (1969).
(202) A. L. Grossberg and D. Pressman, *ibid.*, **7,** 272 (1968).
(203) B. J. Johnson and K. E. Thames, *J. Pharm. Sci.*, **66,** 427 (1977).
(204) G. M. Edelman, B. A. Cunningham, W. E. Gall, P. D. Gottlieb, V. Rutishauer, and M. J. Waxdal, *Proc. Natl. Acad. Sci. USA*, **63,** 78 (1969).
(205) D. E. Tracey and J. J. Cebra, *Biochemistry*, **13,** 4796 (1974).
(206) R. L. Hill, H. E. Lebovitz, R. E. Fellows, and R. Delaney, in "Gamma Globulins, Proceedings of the 3rd Nobel Symposium," 1967, p. 109.
(207) F. W. Putman, G. Florent, C. Paul, T. Shinoda, and A. Shimizu, *Science*, **182,** 287 (1973).
(208) B. J. Johnson and K. E. Thames, *Fed. Proc.*, **35,** 494 (1976).
(209) B. J. Johnson and K. E. Thames, *J. Immunol.*, **117,** 1491 (1976).
(210) B. J. Johnson, *J. Pharm. Sci.*, **63,** 313 (1974).

(211) S. E. Mergenhagen, T. P. Tempel, and R. Snyderman, *J. Dent. Res.*, **49**, 256 (1970).
(212) R. Snyderman, *J. Am. Dent. Assoc.*, **87**, 1020 (1973).
(213) R. J. Genco, P. A Mashimo, G. Krygier, and S. A. Ellison, *J. Periodont.*, **45**, 330 (1974).
(214) R. Attström, A. Laurel, U. Lahsson, and A. Sjöholm, *J. Periodont. Res.*, **10**, 19 (1975).
(215) F. J. Courts, R. J. Boakle, H. H. Fudenberg, and M. S. Silverman, *J. Dent. Res.*, **56**, 327 (1977).
(216) P. Brandtzaeg, *Arch. Oral Biol.*, **10**, 795 (1965).
(217) E. J. Shillitoe and T. Lehner, *ibid.*, **17**, 241 (1972).

ACKNOWLEDGMENTS AND ADDRESSES

Received from the *Department of Microbiology, University of Alabama Medical School, Birmingham, AL 35294.*

Some work reported in this article was supported by Grant AI 11970 from the National Institutes of Health.

RESEARCH ARTICLES

Mechanism of Surface Lubrication: Influence of Duration of Lubricant–Excipient Mixing on Processing Characteristics of Powders and Properties of Compressed Tablets

A. C. SHAH ˣ and A. R. MLODOZENIEC

Abstract □ A mathematical expression for tablet hardness was related to lubricant mixing by considering increases in the surface coverage with prolonged mixing time. The duration of lubricant mixing significantly changed the apparent bulk volume of the mix, ejection force during tableting, hardness, and disintegration and dissolution properties of tablets. These findings may provide some rationale for the changes in processing characteristics and properties of finished drug products often encountered in the scale-up of solid dosage formulations. Several lubrication mechanisms are discussed in connection with the duration of mixing effects and scanning microscopy studies.

Keyphrases □ Tablets, compressed—effect of duration of lubricant–excipient mixing on physical properties □ Powders—effect of duration of lubricant–excipient mixing on processing characteristics □ Lubrication, surface—effect of duration of lubricant–excipient mixing on physical properties of tablets and processing characteristics of powders □ Dosage forms—tablets compressed, effect of duration of lubricant–excipient mixing on physical properties

The formulation of a solid dosage form often requires precise processing control of the powder mixture to ensure a volumetric delivery of a homogeneous aliquot. Thus, various adjuvants are gravimetrically added to form the bulk mix to achieve uniform mixing and flow of the powders as in capsule or tablet die filling.

In tablet formulation, a lubricant usually permits resolution of several production problems related to compression. As an essential unit operation in the production of a compressed tablet, lubrication facilitates glidancy of the powders during material flow, eliminates binding of the compact to the die, and minimizes sticking and picking by the punch face surfaces in contact with the compressed tablet. Lubrication, in general, involves adding small quantities of an antifriction agent to powders or granules and mixing them for a specified time.

BACKGROUND

Many studies evaluated different types of lubricants (1–5), the influence of lubricant concentration (6, 7), the relationship between lubricant effects and tablet properties (hardness and disintegration) (8, 9), and changes in physical properties of powder mixes as a function of lubrication (10–15). Few of these studies, however, concerned the influence of mixing time on the processing characteristics of the powder and, especially, the performance properties of the compressed tablet.

Properties of the compact critical to its performance include the ejection force, tablet hardness, disintegration, and dissolution. It is generally recognized that a lubricant modifies these properties. However, the duration of mixing in the lubricant component may not only affect the properties of the compact but also the properties of the blended mixture by altering the apparent bulk volume, the compression force required to make a prescribed compact, and the hydrophobic character of the mixture. The research studies described in this report concerned the interdependency of these physical properties for several model systems designed to test the effects of mixing time.

Previous mixing studies dealt with the homogeneity of the mixture (16–20), evaluations of mixing equipment (21–23), and segregation kinetics associated with model systems (24–27). This work emphasized the importance of solid–solid mixing related to drug distribution and homogeneity of the mix. Since content uniformity of the active ingredient is a primary control for accurately dosing a patient with a unit dosage form, emphasis is always given to the final composition of the assayed tablet or other dose form. Nonetheless, the release characteristics and performance criteria (such as physical integrity and stability) also rely on the nature and extent of distribution of inert excipients as well as the active ingredient. Of significance is the lubricant–excipient interaction and the manner in which these materials are affected by mixing. Possibly, mixing times can modify the intended role of these adjuvants, in some cases altering or diminishing their primary function.

The present work investigated the mixing of direct compaction excipients such as lactose and microcrystalline cellulose with various commonly used lubricants. Furthermore, the occasional nonpredicted increased disintegration time of a compressed tablet associated with a decreased hardness or crushing force requirement prompted an investigation of the effects of lubricants (*e.g.*, stearates) and mixing duration on the physical properties of a blended mixture and compact.

(211) S. E. Mergenhagen, T. P. Tempel, and R. Snyderman, *J. Dent. Res.*, **49**, 256 (1970).
(212) R. Snyderman, *J. Am. Dent. Assoc.*, **87**, 1020 (1973).
(213) R. J. Genco, P. A Mashimo, G. Krygier, and S. A. Ellison, *J. Periodont.*, **45**, 330 (1974).
(214) R. Attström, A. Laurel, U. Lahsson, and A. Sjöholm, *J. Periodont. Res.*, **10**, 19 (1975).
(215) F. J. Courts, R. J. Boakle, H. H. Fudenberg, and M. S. Silverman, *J. Dent. Res.*, **56**, 327 (1977).
(216) P. Brandtzaeg, *Arch. Oral Biol.*, **10**, 795 (1965).
(217) E. J. Shillitoe and T. Lehner, *ibid.*, **17**, 241 (1972).

ACKNOWLEDGMENTS AND ADDRESSES

Received from the *Department of Microbiology, University of Alabama Medical School, Birmingham, AL 35294.*

Some work reported in this article was supported by Grant AI 11970 from the National Institutes of Health.

RESEARCH ARTICLES

Mechanism of Surface Lubrication: Influence of Duration of Lubricant–Excipient Mixing on Processing Characteristics of Powders and Properties of Compressed Tablets

A. C. SHAH ˣ and A. R. MLODOZENIEC

Abstract □ A mathematical expression for tablet hardness was related to lubricant mixing by considering increases in the surface coverage with prolonged mixing time. The duration of lubricant mixing significantly changed the apparent bulk volume of the mix, ejection force during tableting, hardness, and disintegration and dissolution properties of tablets. These findings may provide some rationale for the changes in processing characteristics and properties of finished drug products often encountered in the scale-up of solid dosage formulations. Several lubrication mechanisms are discussed in connection with the duration of mixing effects and scanning microscopy studies.

Keyphrases □ Tablets, compressed—effect of duration of lubricant–excipient mixing on physical properties □ Powders—effect of duration of lubricant–excipient mixing on processing characteristics □ Lubrication, surface—effect of duration of lubricant–excipient mixing on physical properties of tablets and processing characteristics of powders □ Dosage forms—tablets compressed, effect of duration of lubricant–excipient mixing on physical properties

The formulation of a solid dosage form often requires precise processing control of the powder mixture to ensure a volumetric delivery of a homogeneous aliquot. Thus, various adjuvants are gravimetrically added to form the bulk mix to achieve uniform mixing and flow of the powders as in capsule or tablet die filling.

In tablet formulation, a lubricant usually permits resolution of several production problems related to compression. As an essential unit operation in the production of a compressed tablet, lubrication facilitates glidancy of the powders during material flow, eliminates binding of the compact to the die, and minimizes sticking and picking by the punch face surfaces in contact with the compressed tablet. Lubrication, in general, involves adding small quantities of an antifriction agent to powders or granules and mixing them for a specified time.

BACKGROUND

Many studies evaluated different types of lubricants (1–5), the influence of lubricant concentration (6, 7), the relationship between lubricant effects and tablet properties (hardness and disintegration) (8, 9), and changes in physical properties of powder mixes as a function of lubrication (10–15). Few of these studies, however, concerned the influence of mixing time on the processing characteristics of the powder and, especially, the performance properties of the compressed tablet.

Properties of the compact critical to its performance include the ejection force, tablet hardness, disintegration, and dissolution. It is generally recognized that a lubricant modifies these properties. However, the duration of mixing in the lubricant component may not only affect the properties of the compact but also the properties of the blended mixture by altering the apparent bulk volume, the compression force required to make a prescribed compact, and the hydrophobic character of the mixture. The research studies described in this report concerned the interdependency of these physical properties for several model systems designed to test the effects of mixing time.

Previous mixing studies dealt with the homogeneity of the mixture (16–20), evaluations of mixing equipment (21–23), and segregation kinetics associated with model systems (24–27). This work emphasized the importance of solid–solid mixing related to drug distribution and homogeneity of the mix. Since content uniformity of the active ingredient is a primary control for accurately dosing a patient with a unit dosage form, emphasis is always given to the final composition of the assayed tablet or other dose form. Nonetheless, the release characteristics and performance criteria (such as physical integrity and stability) also rely on the nature and extent of distribution of inert excipients as well as the active ingredient. Of significance is the lubricant–excipient interaction and the manner in which these materials are affected by mixing. Possibly, mixing times can modify the intended role of these adjuvants, in some cases altering or diminishing their primary function.

The present work investigated the mixing of direct compaction excipients such as lactose and microcrystalline cellulose with various commonly used lubricants. Furthermore, the occasional nonpredicted increased disintegration time of a compressed tablet associated with a decreased hardness or crushing force requirement prompted an investigation of the effects of lubricants (*e.g.*, stearates) and mixing duration on the physical properties of a blended mixture and compact.

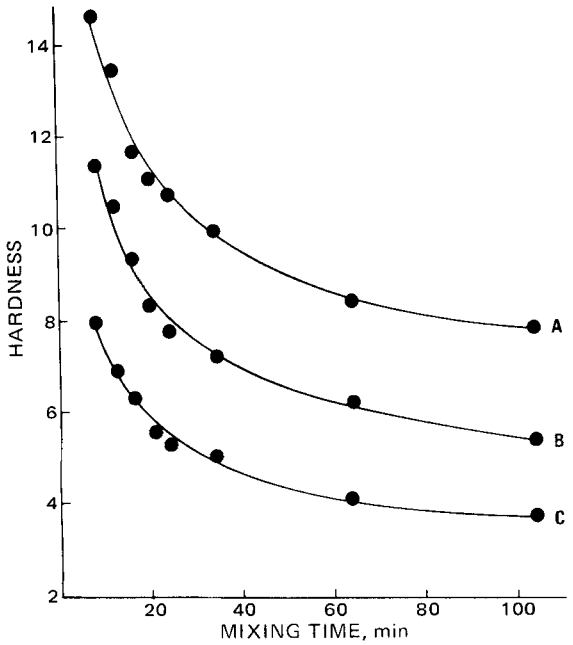

Figure 1—*Strong–Cobb hardness of lactose–1% magnesium stearate tablets (average of 10 tablets) plotted as a function of mixing time. Tablets were compressed at 1620 (A), 1300 (B), and 970 (C) kg.*

It has not been generally known that the mechanism of lubricant action can affect the bulk volume of the mix. Previous studies (10–15) showed that the bulk volume decreases by admixing the lubricant. The present studies demonstrate the effect of mixing time on processing characteristics and tablet performance properties. A mechanism for the role of lubricant materials as a function of mixing time was explored.

THEORY

The change of particle distribution with time caused by mixing has been described as three-dimensional shuffling (28). In such a case, the surface of separation (defined as the separation plane between dissimilar particles) can be used as a measure of the degree of mixing. Thus, for a pharmaceutical powder blend, the maximum surface of separation would correspond to a perfect mix. This qualitative variable can be employed to measure the effect of mixing time on the rate and extent of lubricity when the theory of lubrication assumes a surface coverage of lubricant adsorbed on a particle substrate. This model was applied to extend mixing theory to pharmaceutical powder lubrication. Several effects of different lubricating materials can be explained in this way.

Lubricancy in solid particles improves the fluidity and packing characteristics of a blended mix and permits a homogeneous mix to be transferred compositionally intact to a target volume such as a compressing die. Agents that reduce such interparticulate friction also alter the particle packing characteristics by modifying the particle size and shape factors and have been termed glidants. The degree and extent of surface coverage of a substrate particle by such agents can be described theoretically for pharmaceutical mixtures by invoking at least three different mechanisms: (*a*) adsorption or surface contact adhesions; (*b*) diffusion or solids penetration, which includes mechanical interlocking; and (*c*) delamination or deagglomeration of the lubricating agent to form a film coating (usually discontinuous) on the substrate particles. Whichever mechanisms may be involved, the effect of mixing time should modify both glidant and lubricant roles of the agent.

The true lubricant role of these antifriction agents in pharmaceutical mixes occurs during and after the primary compaction process in tablet manufacturing. While facilitating consolidation of particles in the die cavity, these agents prevent adhesion of the tablet surface to the dies and punches during compression. During ejection, the agents act as boundary lubricants by reducing the frictional force needed to overcome the shear strength at the die wall.

The nature and extent of surface coverage of the lubricant achieved by mixing often predetermine the strength or weakness of the consolidating forces. Ultimately, of course, the bonding forces must be designed to fail in cohesion and/or adhesion when the tablet performs, *i.e.*, disintegrates and dissolves. The duration of mixing exerts not only a statistical effect on randomizing the location of the lubricant within the compact but also affects surface characteristics of the powder and interparticular bond strength in the compact.

Hydrophobic surfaces are those granule or tablet surfaces on which water will not spread. Ganderton (9) described the effect of lubricant distribution on the penetration of a tablet by water. The degree of mixing, both in duration and shearing energy, may affect the porosity, air permeability, and liquid penetration rate of a tablet. Magnesium stearate is a widely used lubricant and is strongly hydrophobic. In general, it is not desirable to render a dosage form hydrophobic inasmuch as the poor wetting of a tablet or other solid dosage form can retard dissolution and drug release.

Thus, the hydrophobicity or water repellancy of a surface, when measured by contact angle (9), affects the capillary action involved in pore penetration. Even if the pores of a surface are hydrophobic, water vapor can pass through them if a sufficient hydrostatic pressure is imposed. The presence of hydrophilic sites, which are almost always present even on hydrophobic solids, also facilitates the interaction of water on a granule or tablet. Thus, it can be assumed that the nature of a hydrophobic surface coverage on a tablet or other solid dosage form enhances or retards the interaction rate but does not inhibit the primary intermolecular attractions at work during disintegration and dissolution.

The adsorption of a lubricant and its distribution on the substrate surface during mixing determines the hydrophobic matrix. The duration of mixing should be related to the clustering around specific sites on the solid surface, which will affect the polarity of the localized surface and create sufficient large or small areas of hydrophilic character; these areas can affect glidancy, consolidation, ejection, dissolution, and other tablet processing variables. The extent and effect on hydrophobicity due to lubricant coverage as modified by mixing are determined by the primary mechanism of action, which physically dominates at the granule or tablet surface. Each of the three general mechanisms previously described operates *via* different pathways in the various unit operations employed.

Mixing theory has generally been employed to help describe those operations in which some energy is applied to a given mass of material for the purpose of changing the initial particle arrangement into a more desirable one. By using kinetics and assuming that mixing is essentially a three-dimensional shuffling operation, Brothman *et al.* (28) derived an expression:

$$S_t = S_m(1 - e^{ct}) \qquad \text{(Eq. 1)}$$

where S_t is the instantaneous magnitude of a surface of separation, t is the time of mixing, S_m is the maximum theoretically possible surface of separation, and c is a constant depending on the substances to be mixed and the mixing equipment. Thus, the function of a V-shelled blender or other mixing device is to enlarge the initial plane of separation between ingredients such as excipients and lubricants. The degree of mixing can then be measured by the extent of the surface of separation at different mixing times. This approach allows the evaluation of the amount of surface enlargement that would occur in a given period of time as proportional to the difference between S_t, the instantaneous magnitude of the surface, and its greatest possible value, S_m.

According to the mechanisms of boundary lubrication put forward by Strickland *et al.* (3), solid lubricants such as magnesium stearate are adsorbed on the granule surface. These lubricants form a uniform surface-adsorbed film in a manner similar to a Langmuir-type adsorption. If it is assumed that during the mixing process lubricant particles first adsorb on the surface and then, upon continued mixing, distribute uniformly upon the granule surface, the breaking of these lubricant particles by delamination or deagglomeration may take place. Such processes would result in greater coverage of the granule surface by the lubricant, thereby producing a greater interfacial surface between the lubricant and the excipient granule, *i.e.*, surface of separation. The mixing process described by Eq. 1 should then relate an exponential relationship for mixing time and any surface coverage-oriented mixing parameter.

The extension of this mixing theory, based on the concept of the surface of separation, can be utilized to relate the interfacial strength of the boundaries of granules initiated through mixing and residing in a formed dosage unit such as a compressed tablet. Hardness, H, is related to the intergranular or interfacial bonds formed within a tablet. Shotton and Lewis (8) described the effect of a lubricant on tablet hardness. In this work, the surface of separation related by mixing time was interpreted to derive an expression for hardness as a function of mixing time:

$$H_t = H_m(1 - e^{-ct}) \qquad \text{(Eq. 2)}$$

where H_t and H_m represent instantaneous hardness at time t and theoretical maximum hardness, respectively. Predicting such an exponential

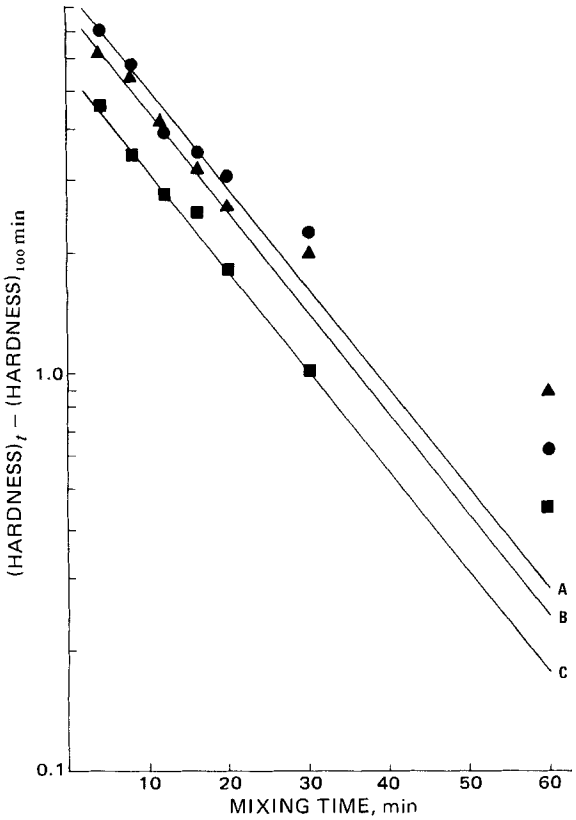

Figure 2—*Semilogarithmic relationship of tablet hardness data shown in Fig. 1.*

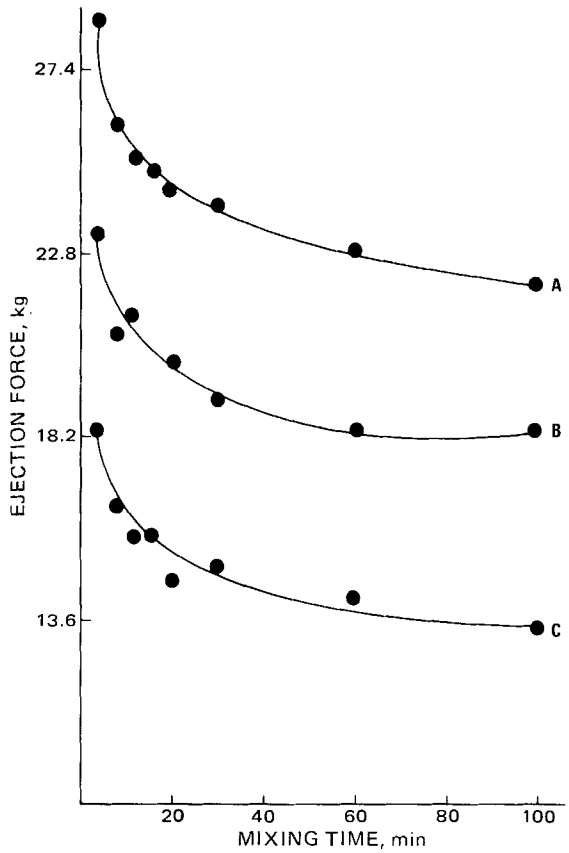

Figure 3—*Ejection force of lactose–1% magnesium stearate tablets as a function of mixing time. Tablets were compressed at 1620 (A), 1300 (B), and 970 (C) kg.*

relationship for hardness implies a direct mechanism whereby the surface of separation affected by mixing is controlling the lubricant–excipient interaction and, ultimately, the tablet crushing strength. The experimental results show that this approach provides some convenient guidelines for predicting lubricant action.

The systems involving magnesium stearate and excipients could be described by such a mechanism of time effects. However, it need not be the only explanation for lubricant action. Miyake *et al.* (15) postulated a diffusion mechanism for lubricant action. All such results seem to apply for magnesium stearate but not necessarily for all other pharmaceutical lubricants. Until more comparisons are made, one can only speculate on how lubricant action is altered by time effects. Nevertheless, there is ample evidence now that delamination is at least a primary mechanism for magnesium stearate.

The extension of mixing theory to lubricant–excipient interactions can be fully exploited if the surface of separation meets other criteria of physical models useful to pharmaceutical operations. Thus, glidancy, lubricancy, frictional flow, and compression (due to plastic deformation and flow) all can rely on the qualitative measure of degree of mixing described by three-dimensional shuffling and a surface of separation. Moreover, within the compact, the hydrophobicity (affecting disintegration and dissolution) as well as hardness (measured only as crushing strength) are equally extrapolatable to the time effects of mixing. Such concepts must be refined in controlled studies, however, since the c value, assumed to be a constant, could be a variant for the changing shear effects in a blender or the changes in particle character of materials.

EXPERIMENTAL

Materials used in the mixing study were spray-dried lactose USP, microcrystalline cellulose (medium powder) NF, magnesium stearate USP, talc (bolted) USP, stearic acid USP, colloidal silicon dioxide NF, calcium stearate NF, and salicylic acid USP. Throughout the study, a single lot of each material was used to eliminate the possibility of lot-to-lot variability.

Mixing operations were performed in a 3.8-liter stainless steel twin-shell V-shape mixer[1]. Unless specified otherwise, 1 kg of spray-dried lactose or 475 g of microcrystalline cellulose was employed in all studies. To prepare an excipient–lubricant mixture, a weighed amount of lubricant was screened through a 40-mesh screen over the bed of excipient; the mixture was then transferred into the mixer and allowed to blend at 22 rpm for a specified period. A series of mixtures blended for different time intervals was prepared similarly.

Tablets were compressed on an instrumented single-punch[2] machine, equipped with 1.9-cm diameter half-oval punches, at a machine speed

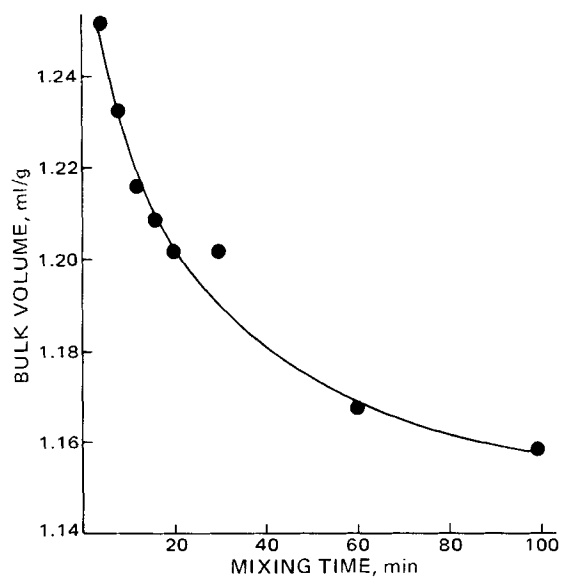

Figure 4—*Apparent bulk volume of lactose–1% magnesium stearate mixtures as a function of mixing time.*

[1] Patterson-Kelley Co., East Stroudsburg, Pa.

[2] Key Industries, Farmingdale, NJ 07727.

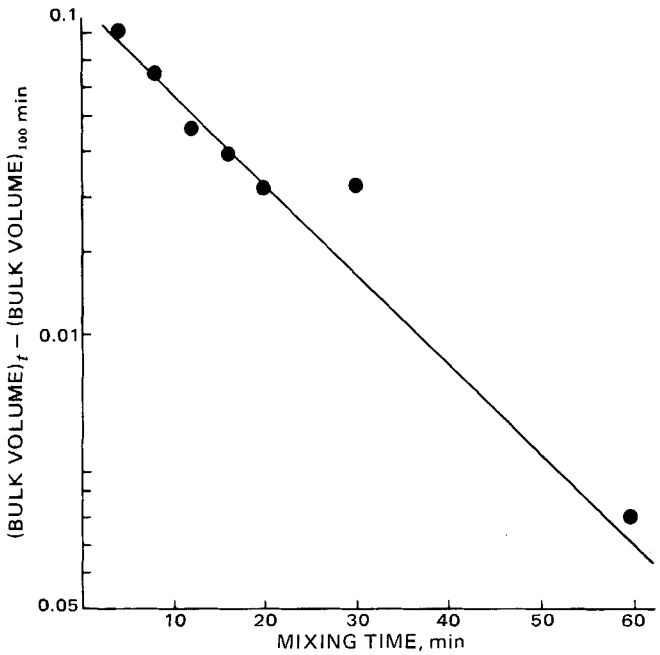

Figure 5—*Semilogarithmic relationship of apparent bulk volume data shown in Fig. 4.*

of 56 tablets/min. A tablet weight of 550 mg for the lactose tablets and of 372 mg for microcrystalline cellulose tablets was maintained. Compression and ejection forces were recorded by photographing the signals transmitted by strain gauges to an oscilloscope.

The apparent bulk volume of the powder mixture was determined by volumetric measurement of the mixture in a 500-ml conical flask. The mixture was transferred into the flask at a uniform rate of about 100 g/min by a mechanical conveyor. From the fill weight and volume of the flask, the apparent bulk volume of the mixture was calculated. During the filling operation, care was taken to avoid any vibration of the flask. Repeated measurements by this procedure showed less than 5% variation in the bulk volume values.

The dissolution rate of salicylic acid from an *in situ* constant-surface pellet was determined by the Levy and Hayes (29) beaker method with the pellet suspended 3 cm above the bottom of the beaker. The test conditions employed were 1000 ml of pH 7.5 phosphate buffer, 37°, and a 300-rpm stirring speed. The amount of salicylic acid dissolved was measured by automated spectrophotometric analysis of the dissolution medium.

RESULTS AND DISCUSSION

Spray-dried lactose and microcrystalline cellulose, typical direct compaction adjuvants, were selected as the major inert excipients.

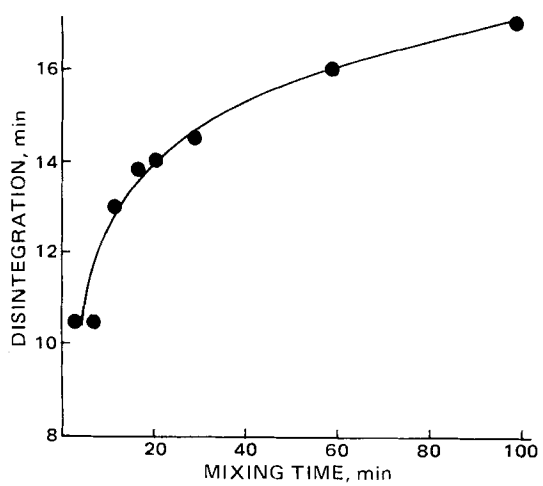

Figure 6—*Disintegration time (USP) of lactose–1% magnesium stearate tablets plotted as a function of mixing time. Tablets were compressed at 1300 kg.*

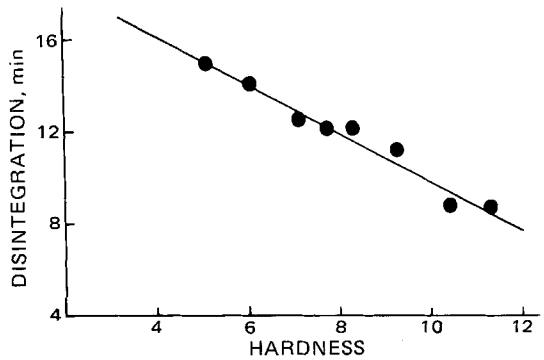

Figure 7—*Correlation between disintegration time and hardness of lactose–1% magnesium stearate tablets (r = 0.9544).*

Magnesium stearate was the common lubricating agent added. Among the properties of the excipient–lubricant mixtures evaluated as a function of mixing time were apparent bulk volume, surface morphology, ejection force during tablet compression, tablet hardness, and tablet disintegration.

Lactose–Magnesium Stearate Mixing Studies—Figure 1 shows the effect of mixing time upon tablet hardness for the lactose–1% magnesium stearate blends compressed at three different compression forces. The hardness continued to decrease and reached a constant value with the increased mixing time. A plot of log [(hardness at time t) − (hardness at 100 min)] *versus* mixing time (Fig. 2) suggests an apparent first-order rate of change in tablet hardness. These results correlate with Eq. 2, which predicts an exponential change in tablet hardness as a function of mixing time.

The effect of mixing time on the ejection force recorded during tablet compression is shown in Fig. 3. The decrease in the ejection force upon mixing would reflect increased lubrication efficiency of magnesium stearate as a result of greater surface coverage by the lubricant. The ratio of compression to ejection force at 100 min was about 31 kg for the three compression forces employed. This ratio may be considered as the optimum lubricant efficiency of magnesium stearate in this system. Similar results were also obtained with 0.5% magnesium stearate, but the lubrication efficiency ratio after 100 min of mixing was about half of that for the 1% magnesium stearate–lactose system.

During tablet compression, the die-fill weight tended to increase with a longer mixing time. To maintain constant weight, it was necessary to reduce the fill volume by adjusting the lower punch settings. This observation prompted a study of the effect of mixing time upon the apparent

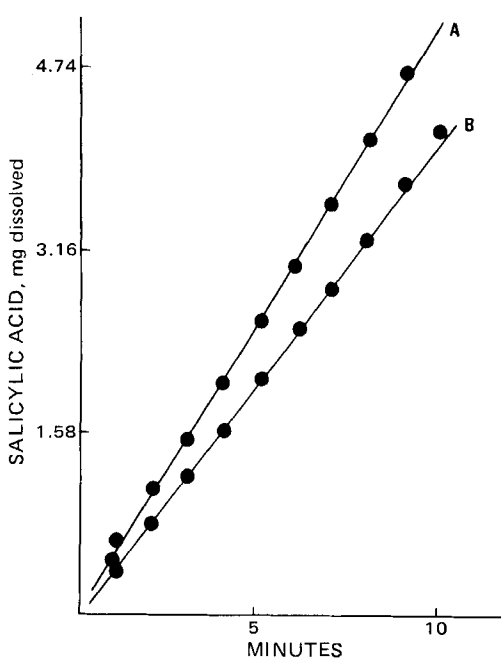

Figure 8—*Dissolution of salicylic acid from constant-surface pellets containing lactose and magnesium stearate. Lubricant mixing time was 10 (A) and 100 (B) min.*

Table I—Magnesium Stearate Concentration of Lactose Tablets Determined by Atomic Absorption Analysis

Mixing Time, min	Magnesium Stearate in Tablet, %						
	Tablet 1	Tablet 2	Tablet 3	Tablet 4	Tablet 5	Average	*SD*
4	102.9	86.1	104.8	106.6	102.9	100.7	8.23
100	104.8	111.3	106.6	97.3	107.6	105.5	5.17

bulk volume of the mixture samples. Figure 4 shows a decrease in the apparent bulk volume of lactose–1% magnesium stearate mixture with the longer mixing time. A log exponential relationship of [(bulk volume at time t) − (bulk volume at 100 min)] *versus* mixing time is shown in Fig. 5. These results suggest that, like tablet hardness, apparent bulk volume also changes by an apparent first-order rate with respect to mixing time. Furthermore, the first-order rate constant value of 4.33×10^{-2} min^{-1} for the tablet hardness estimated from Fig. 2 seems quite comparable with 5.54×10^{-2} min^{-1} for the apparent bulk volume, suggesting that the influence of mixing time upon both properties is probably a manifestation of the enlarged surface of separation or greater surface coverage by the lubricant upon mixing.

The duration of mixing had major effects upon the tablet disintegration. Figure 6 shows the USP disintegration time of lactose–1% magnesium stearate tablets plotted as a function of mixing time. The mixtures blended for a longer time yielded tablets with a slow disintegration. The observed effect upon tablet disintegration may be attributed to the formation of a hydrophobic surface by the lubricant upon mixing. A correlation of disintegration time with tablet hardness (Fig. 7) represents a unique case, where disintegration time is inversely proportional to tablet hardness (*i.e.*, the harder the tablet, the faster it disintegrates). This result is due to the decline in tablet hardness and prolongation of disintegration time as a result of the lubricant covering over the surface of lactose particles upon mixing.

In an effort to demonstrate the influence of mixing time upon drug dissolution, a well-mixed sample of lactose–1% salicylic acid was subjected to further mixing with 1% magnesium stearate for 10 and 100 min. Dissolution rates of salicylic acid were determined from constant-surface pellets of the two mixtures. The pellet prepared from the 10-min mixed sample dissolved at a relatively faster rate (0.53 mg/ml) compared to the 100-min mixed sample (0.40 mg/ml) (Fig. 8). This effect of lubricant upon the dissolution rate is attributed to the increased hydrophobicity of the compact with a prolonged mixing time.

The magnesium stearate content in the lactose tablets was examined to confirm the distribution of lubricant in each tablet during the continued mixing process. Atomic absorption analysis of tablet samples made at 4- and 100-min mixing intervals for the 1.0% magnesium stearate–lactose system is shown in Table I. The elemental analysis was reasonably uniform even after only 4 min of mixing.

Particle-size analysis of sieving also independently confirmed that the essential size distribution of each mixture was not altered during any of the lactose–stearate mixing studies.

Microcrystalline Cellulose–Lubricant Mixing Studies—These studies were performed similarly to the lactose studies. In these studies, 475 g of microcrystalline cellulose was used because the apparent bulk volume of this amount of microcrystalline cellulose is equivalent to 1.0 kg of spray-dried lactose. This amount kept the bulk volume essentially constant for mixing in a similar size mixer.

The effect of mixing time on tablet hardness is shown in Fig. 9 for microcrystalline cellulose–1% magnesium stearate tablets. These results show the same surface coverage-oriented mixing dependency of Eq. 2 as was found previously for lactose. This result again may be interpreted

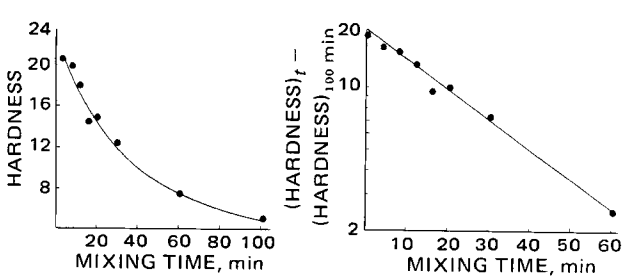

Figure 9—*Strong–Cobb tablet hardness of microcrystalline cellulose–1% magnesium stearate tablets plotted on a linear (left) and semilogarithmic (right) scale as a function of mixing time.*

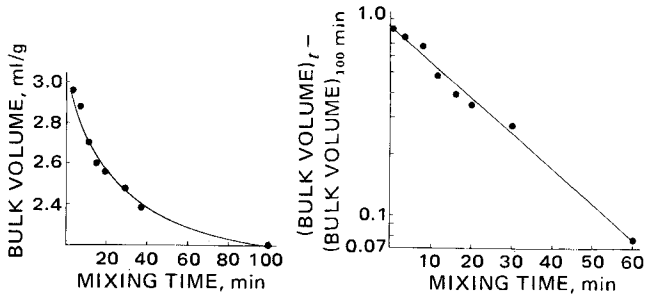

Figure 10—*Apparent bulk volume of a microcrystalline cellulose–1% magnesium stearate mix plotted on a linear (left) and semilogarithmic (right) scale as a function of mixing time.*

as the kinetics of a three-dimensional shuffling operation in which the surface of separation is enlarged upon mixing.

As in the lactose studies, the apparent bulk volume of the microcrystalline cellulose–1% magnesium stearate mixture decreased with mixing time (Fig. 10). The rate constant for the change in the bulk volume, $k = 4.07 \times 10^{-2}$ min^{-1}, is quite comparable to the $k = 3.46 \times 10^{-2}$ min^{-1} obtained for the hardness change (Fig. 9), suggesting that both properties are related to the extent of lubricant surface coverage.

The influence of mixing microcrystalline cellulose with various lubricants upon apparent bulk volume was examined. Mixing of microcrystalline cellulose alone, without lubricant, showed no apparent change in the bulk volume (Fig. 11). Stearic acid also produced no significant change. A rapid initial change observed with talc and colloidal silicon dioxide may be attributed to their action as glidants rather than as lubricants. Magnesium stearate and calcium stearate showed essentially a similar change in the bulk volume as a function of mixing time.

Scanning electron microscopy studies were performed on both lactose and microcrystalline cellulose systems lubricated with 1.0% magnesium stearate. The spray-dried lactose is relatively equidimensional in shape, characteristic of powders prepared in this manner. The morphology of microcrystalline cellulose is such that the powder can be assumed to be composed of microfibers with elongation ratios (length to width) typically in the 3.0–5.0 range. Magnesium stearate occurs as a lamellar solid, stacked in plate-like sheets resembling a deck of cards.

Magnesium stearate particles adhered to the surface of spray-dried lactose granules could be identified by scanning electron microscopic observations. However, they could not be identified on microcrystalline cellulose because of the similar morphology of the fine particle debris of microcrystalline cellulose itself. Figure 12 shows photomicrographs of lactose–magnesium stearate samples blended for 8 and 100 min. These photographs suggest that magnesium stearate adsorbs on the surface of lactose during the initial mixing time. As mixing proceeds at 100 min, the

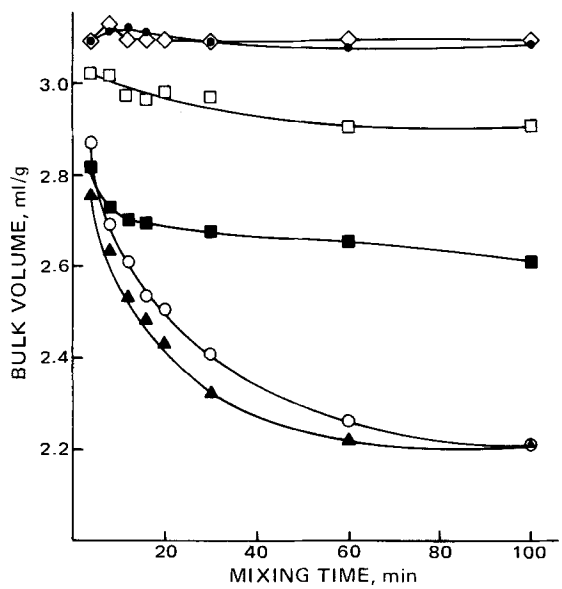

Figure 11—*Apparent bulk volume of microcrystalline cellulose–lubricant mixtures plotted as a function of mixing time. Key: ●, no lubricant; ◇, 1% stearic acid; □, 3% talc; ■, 0.3% colloidal silicon dioxide; ○, 1% magnesium stearate; and ▲, 1% calcium stearate.*

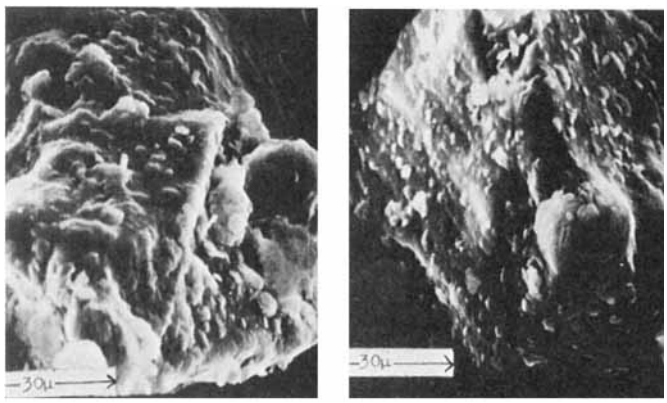

Figure 12—*Scanning electron microscopic photomicrographs of lactose–1% magnesium stearate 8- (left) and 100- (right) min mixes.*

population of individual magnesium particles increases by a delamination process, and a greater surface coverage of lactose particles by magnesium stearate results.

The mechanism of lubrication envisioned for magnesium stearate involves surface coverage due to adsorption upon initial mixing. As mixing continues, the shear effects induce delamination or deagglomeration of the lubricant to harness more stearate particles that slide or adhere on the excipient granule surface. The adhered particles, once they delaminate to individual "cards," no longer spread over the excipient surface during mixing. This process accounts for the leveling in the bulk volume and, perhaps, the hardness plots after long mixing times. This mechanism is called delamination or the "stack of cards" theory because the shear-induced effects of continued mixing are arrested at a given time in the mixing cycle.

Diffusion or solids penetration plays a minor role in the lubricant spreading, since mixing occurs as a function of time. Moreover, a continuous coating of lubricant does not completely occur during mixing, but surface contact adhesion (action of a boundary lubricant) may occur only after compression. Under compression, however, a mechanism of a lubricant may undergo diffusion adhesion or surface contact adhesion. This mixed mechanism of lubricant action may help to explain the changes in bulk specific volume and tablet hardness affected by mixing time.

The surface coverage-oriented parameters affected by mixing time include glidancy, frictional flow, hydrophobicity, and lubricancy as predicted by Eq. 1. The derived expression for hardness shown as Eq. 2 also appears to be related to a surface or separation phenomenon. This mixing effect would be expected to influence not only tablet hardness but tablet compression and hydrophobicity within the compact as well. Thus, it may help to explain the mixing time effects noted in the physical properties more important to drug release and bioavailability, such as disintegration and dissolution.

REFERENCES

(1) J. E. Wolff, H. G. DeKay, and G. L. Jenkins, *J. Am. Pharm. Assoc., Sci. Ed.*, **36**, 407 (1947).

(2) W. A. Strickland, Jr., T. Higuchi, and L. W. Busse, *ibid.*, **49**, 35 (1960).

(3) W. A. Strickland, Jr., E. Nelson, L. W. Busse, and T. Higuchi, *ibid.*, **45**, 51 (1956).

(4) C. J. Lewis and D. Train, *J. Pharm. Pharmacol.*, **17**, 577 (1965).

(5) C. J. Lewis and E. Shotton, *J. Pharm. Pharmacol. Suppl.*, **17**, 825 (1965).

(6) F. C. Hammerness and H. O. Thompson, *J. Am. Pharm. Assoc., Sci. Ed.*, **47**, 58 (1958).

(7) N. O. Lindberg, *Acta Pharm. Suec.*, **9**, 207 (1972).

(8) E. Shotton and C. J. Lewis, *J. Pharm. Pharmacol. Suppl.*, **16**, 11T (1964).

(9) D. Ganderton, *ibid.*, **21**, 9S (1969).

(10) M. Aoki, S. Ogawa, S. Hayashi, and M. Hirayama, *Yakuzaigaku*, **27**, 18 (1967).

(11) M. Aoki and S. Hayashi, *J. Pharm. Soc. Jpn.*, **87**, 1164 (1967).

(12) Y. Miyake, A. Shinoda, M. Furukawa, C. Sadakata, and S. Toyoshima, *ibid.*, **93**, 1112 (1973).

(13) D. J. Craik, *J. Pharm. Pharmacol.*, **10**, 73 (1958).

(14) Y. Miyake, C. Sadakata, and S. Toyoshima, *J. Pharm. Soc. Jpn.*, **92**, 1301 (1972).

(15) Y. Miyake, C. Sadakata, K. Tatsuishi, and S. Toyoshima, *ibid.*, **90**, 1107 (1970).

(16) D. Train, *Pharm. J.*, **1960**, 129.

(17) V. P. Speiser and R. Tawashi, *Pharm. Acta Helv.*, **37**, 529 (1962).

(18) T. Sakaino, *J. Ceram. Assoc.*, **65**, 171 (1956).

(19) J. Okada, Y. Matsuda, and Y. Matsuda, *Yakugaku Zasshi*, **89**, 1562 (1969).

(20) J. A. Hersey, *J. Pharm. Pharmacol. Suppl.*, **19**, 168S (1967).

(21) J. Okada, K. Hazumi, Y. Matsuda, and Y. Fukumori, *Yakagaku Zasshi*, **90**, 1532 (1970).

(22) H. W. Fowler, *Manuf. Chem.*, **4** (Jan. 1962).

(23) H. W. Cremer, "Chemical Engineering Practice," vol. 3, Academy Press, London, England, 1957, chap. 13.

(24) J. L. Olsen and E. G. Rippie, *J. Pharm. Sci.*, **53**, 147 (1964).

(25) E. G. Rippie, J. L. Olsen, and M. D. Faiman, *ibid.*, **53**, 1360 (1964).

(26) M. D. Faiman and E. G. Rippie, *ibid.*, **54**, 719 (1965).

(27) E. G. Rippie, M. D. Faiman, and M. K. Pramoda, *ibid.*, **56**, 1523 (1967).

(28) A. Brothman, G. N. Wollan, and S. M. Feldman, *Chem. Met. Eng.*, **52**, 102 (1945).

(29) G. Levy and B. A. Hayes, *N. Engl. J. Med.*, **262**, 1053 (1960).

ACKNOWLEDGMENTS AND ADDRESSES

Received November 23, 1976, from *Pharmacy Research, The Upjohn Co., Kalamazoo, MI 49001.*

Accepted for publication January 10, 1977.

Presented at the APhA Academy of Pharmaceutical Sciences, San Francisco meeting, March 1971.

[x] To whom inquiries should be directed.

GLC Determination of Lidocaine in Human Plasma

G. CAILLE *x, J. LELORIER *, Y. LATOUR ‡, and J. G. BESNER *

Abstract □ A specific, sensitive, rapid, and reproducible analytical GLC method for lidocaine in human plasma, including pharmacokinetic parameters, is described. Aminopyrine is the internal standard. The method was used to study pharmacokinetics in four healthy volunteers following the administration of a lidocaine bolus at a dose of 1 mg/kg iv and in one patient with cardiac arrhythmias who had been given a 50-mg bolus followed by a prolonged intravenous infusion for 30 hr.

Keyphrases □ Lidocaine—GLC analysis in human plasma, pharmacokinetics ■ GLC—analysis, lidocaine in human plasma ■ Pharmacokinetics—lidocaine in humans □ Anesthetics, local—lidocaine, GLC analysis in human plasma, pharmacokinetics

The administration of a lidocaine bolus (defined as a rapid intravenous injection) followed by a fairly long intravenous infusion has become a routine practice in the treatment of patients with myocardial infarcts. Yet, there is very little information concerning the pharmacokinetic behavior of lidocaine following a prolonged infusion, and this information is controversial. For example, some investigators (1, 2) observed a mean half-life of 90 min following an infusion of approximately 12 hr. However, after a prolonged infusion of more than 24 hr, half-lives of approximately 3.3 (3) and 10 (4) hr were found. The combined factors of this slower rate of elimination followed by hemodynamic changes in the patients and higher blood concentrations can increase the drug's toxicity.

To determine the pharmacokinetics of lidocaine following a prolonged infusion of more than 24 hr, a specific and reproducible analytical technique that provides an accurate picture of what occurs in the body is necessary. For this reason, the present paper emphasizes the analytical data, whereas subsequent studies will concentrate on the metabolism, pharmacokinetics, and distribution of lidocaine in humans and animals.

Several equally valid analytical methods (6–9) previously used GLC and an internal standard for quantitative determinations in biological media. However, none of these reports discussed possible interference from pharmacological agents given concomitantly with lidocaine, such as sedatives, opiates, diuretics, bronchodilators, and antispasmodics. Therefore, the aim of this study was to develop a simple and rapid analytical method for lidocaine that would remain specific in the presence of drugs routinely administered to patients with ventricular arrhythmias.

EXPERIMENTAL

Materials—Lidocaine[1] and aminopyrine[2] were not less than 98% pure. All reagents used for extraction were analytical grade[3]. Freshly drawn human blood[4], 300 ml, was centrifuged, and the plasma was analyzed initially to make certain that it contained no interfering substances.

Subjects—Four healthy volunteers whose body weight did not vary more than ±10 kg from the mean received a 1-mg/kg bolus of lidocaine. Heparinized blood samples were collected at 0.25, 0.50, 1, 2, 3, 4, and 6 hr following drug administration.

Apparatus—The determinations were performed by GLC using a flame-ionization detector[5]. A 1.8-m, 80–100-mesh, 3% OV-17 Gas Chrom Q column was used. The column, detector, and injection port temperatures were 210, 275, and 250°, respectively. The nitrogen gas flow rate was 56 ml/min.

Extraction Procedures—Distilled water, 2 ml, and 0.5 ml of 5 *N* NaOH were added to 2 ml of plasma containing 25 μg of aminopyrine internal standard in a 50-ml test tube. The mixture was shaken for 30 sec using a test tube mixer. Following the addition of 10 ml of methylene chloride, the sample was shaken for 5 min mechanically and centrifuged at 2000 rpm. After being extracted a second time, the organic phases were combined and dried over anhydrous sodium sulfate. The organic phase was then evaporated to dryness under nitrogen, and the residue was redissolved in 0.5 ml of chloroform and transferred into a 1-ml conical test tube. The solution was again evaporated to dryness under nitrogen, and the residue was dissolved in 50 μl of chloroform. Aliquots of 1.5 ± 0.2 μl were then analyzed.

The standard plasma samples were prepared by adding quantities equivalent to 0.5, 1.25, 2.5, 5, 12.5, and 25 μg of lidocaine to the internal standard of each tube. The retention times for lidocaine and the internal standard were 4.45 and 6.70 min, respectively.

The calibration curves were constructed using the ratio of the areas under the lidocaine and aminopyrine curves along the ordinate and the concentrations of lidocaine along the abscissa.

RESULTS AND DISCUSSION

The ratio of the areas under the lidocaine and aminopyrine curves was linear for concentrations from 0.10 to 12.5 μg/ml of plasma, concentrations normally found during treatment. The standard curves *in vitro* and following the lidocaine extraction from the plasma could be superimposed on each other; the slopes corresponded to an r^2 of 0.999, indicating that the extraction of lidocaine and aminopyrine was reproducible for the different concentrations studied.

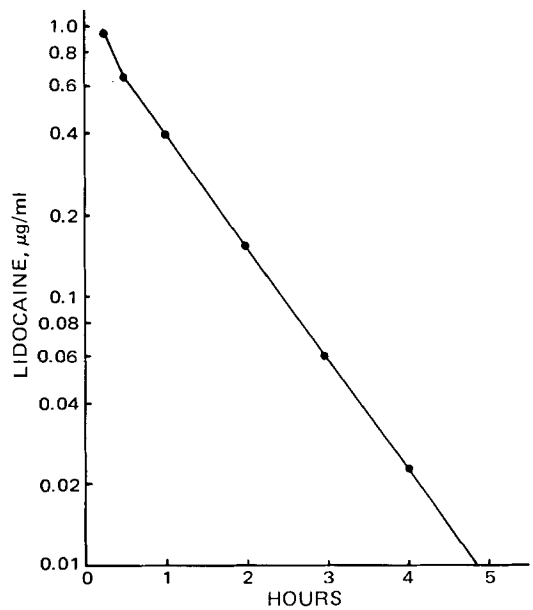

Figure 1—*Mean pharmacokinetic profile of lidocaine in a healthy volunteer after a rapid intravenous administration of a 1-mg/kg bolus.*

[1] Astra Pharmaceutical Products.
[2] British Drug House Chemicals.
[3] Fisher Scientific Co.
[4] American Red Cross.
[5] Model 5830-A, Hewlett-Packard, Montreal, Canada.

Table I—Plasma Lidocaine Concentrations (μg/ml) in Healthy Volunteers following Administration of a 1-mg/kg iv Bolus

Subject	Weight, kg	Hours[a] 0.25	0.50	1	2	3[b]	4[b]
A	52.16	1.15	0.60	0.40	0.15	0.06	0.02
B	68.04	0.85	0.69	0.50	0.22	0.10	0.04
C	62.00	0.82	0.59	0.28	0.11	0.04	0.01
D	54.34	1.01	0.71	0.41	0.14	0.05	0.01
Mean ± *SE*	59.14 ± 3.65	0.96 ± 0.08	0.65 ± 0.03	0.40 ± 0.03	0.16 ± 0.02	0.06 ± 0.01	0.02 ± 0.01

[a] At 6 hr postadministration, a 5-ml plasma sample was used and no lidocaine was detected. [b] A 5-ml plasma sample was used at these intervals.

Each point on the curves represents the mean of five different samples. Total recoveries of lidocaine and aminopyrine from the plasma were 99.04 ± 6.5 and 98.60 ± 4.2%, respectively.

This analytical method was specific, since none of the drugs administered concomitantly with lidocaine interfered. These drugs were propranolol, procainamide, furosemide, insulin, aspirin, methyprylon, cephalexin, digoxin, phenobarbital, quinidine, diazepam, meperidine, phenytoin, diphenhydramine, acepifylline, isosorbide, morphine, spironolactone, nitroglycerin, atropine, flurazepam, allopurinol, and hydrochlorothiazide. Several were eliminated during the extraction procedure in an alkaline medium; others, such as the benzodiazepines and narcotics, appeared on the chromatogram only with much higher column temperatures. The temperature of the column must be raised to 250° for 10 min after each determination to eliminate any interfering substances from the column.

The pharmacokinetic differences in the plasma clearance of lidocaine given as a rapid intravenous injection to healthy volunteers or as a rapid intravenous administration followed by a prolonged infusion of 24 hr or more to a patient suffering from ventricular arrhythmia were studied using the developed method. The pharmacokinetic behavior of lidocaine in both cases conformed to the two-compartment open model represented by the following equation (10):

$$C_{p(t)} = Ae^{-\alpha t} + Be^{-\beta t} \qquad \text{(Eq. 1)}$$

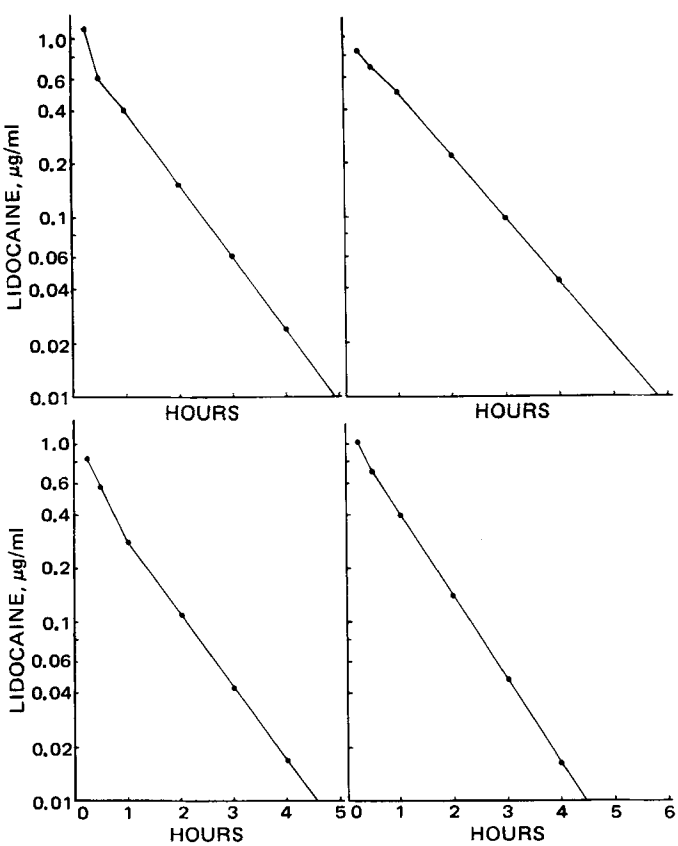

Figure 2—*Pharmacokinetic profile of lidocaine in four healthy volunteers after a rapid intravenous administration of a 1-mg/kg bolus. Key: top left, Subject A; top right, Subject B; bottom left, Subject C; and bottom right, Subject D.*

One can assume that all of the drug is in the central compartment, V_1, at the time of injection, so that:

$$V_1 = \frac{\text{dose}}{C_p{}^0} \qquad \text{(Eq. 2)}$$

Also it is assumed that its elimination is quantitative beginning with the central compartment and that an equilibrium is established between the central compartment and the peripheral tissue compartment, V_2:

$$V_1 + V_2 = V_{d_{ss}} = \frac{K_{12} + K_{21}}{K_{21}} V_1 \qquad \text{(Eq. 3)}$$

In Eq. 1, α and β are hybrid rate constants permitting the calculation of the plasma half-lives of phases α and β by the following equations:

$$T_{p1/2(\alpha)} = 0.693/\alpha \qquad \text{(Eq. 4)}$$

$$T_{p1/2(\beta)} = 0.693/\beta \qquad \text{(Eq. 5)}$$

where α is determined by the method of residuals, and β is determined by linear regression of a monoexponential equation.

The pharmacokinetics for the healthy volunteers were calculated using the mean results shown in Table I. The pharmacokinetic parameters in healthy volunteers following the administration of a bolus are fairly well known, and the results confirm the published data (11). However, since the α-phase is very short (less than 10 min) and the first sampling time was at the 15-min mark, a rather large error was introduced in its estimation. Experimentally, an α of $5.99^{h^{-1}}$, which gives a half-life of 7 min for this period, was obtained.

The β-phase was calculated to be $0.95^{h^{-1}}$, and the half-life for this phase of lidocaine clearance was 44 min. Figures 1 and 2 illustrate the individual and mean lidocaine elimination curves for the four healthy volunteers.

Figure 3 and Table II illustrate the response of a patient who received a 50-mg bolus of lidocaine by the intravenous route, followed by a prolonged infusion over 30 hr at 120 mg/hr. Two weeks after his first attack, the patient was readmitted to the hospital and given the same treatment but only for 24 hr.

The results presented in Fig. 3 demonstrate both the excellent repro-

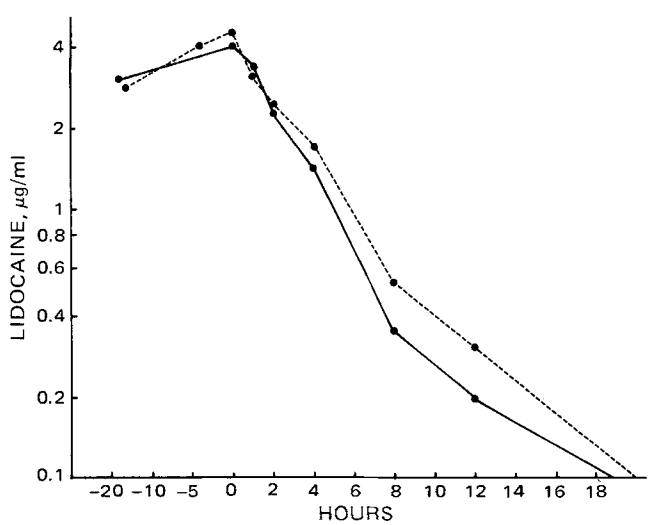

Figure 3—*Pharmacokinetic profile of a slow lidocaine infusion in a hospitalized patient. The two infusions, 120 mg/hr for 30 (—) and 24 (- - -) hr, respectively, were 2 weeks apart.*

Table II—Pharmacokinetics of Lidocaine in a Patient following a Prolonged Infusion[a]

Hours	First Infusion, μg/ml	Second Infusion, μg/ml
−29.45	0	0
−17.45	2.98	2.85
0	4.04	4.55
1	3.39	3.15
2	2.28	2.39
4	1.43	1.72
8	0.35	0.54
12	0.20	0.31
19	0.10	—
20	—	0.10
23	N.D.[b]	N.D.

[a] The first and second infusions were separated by 2 weeks. [b] N.D. = not detectable.

ducibility of this analytical method and the difference in the pharmacokinetic parameters of lidocaine following a prolonged infusion. The two phases, α and β, and their values were virtually identical for the two slow infusions. The first infusion resulted in a $T_{p1/2}(\alpha)$ of 2.08 hr and a $T_{p1/2}(\beta)$ of 6.18 hr; the second infusion resulted in a $T_{p1/2}(\alpha)$ of 2.14 hr and a $T_{p1/2}(\beta)$ of 4.93 hr.

Therefore, it can be concluded that the analytical method described confirms that the pharmacokinetic parameters of lidocaine are identical for any given subject on the same treatment. However, compared to the healthy volunteers, the pharmacokinetic parameters were quite different. A true equilibrium was not reached, since the drug concentrations increased continuously during the infusion. This phenomenon can be explained by the fact that lidocaine inhibits its own metabolism *via* its acetylated metabolite (5); moreover, its renal excretion is slower, due to a reduction in the cardiac inotropic form and rhythm which significantly reduce blood flow. The marked lengthening of the α- and β-phases indicates that considerable caution should be exercised when lidocaine is administered by slow infusion, because the toxic effects with lidocaine are greater when the blood levels are too high.

REFERENCES

(1) M. Rowland, P. D. Thomson, A. Guichard, and K. L. Melmon, *Ann. N.Y. Acad. Sci.*, **179**, 383 (1971).

(2) R. N. Boxes, D. B. Scott, P. J. Jebson, M. J. Goodman, and D. G. Julian, *Clin. Pharmacol. Ther.*, **12**, 105 (1971).

(3) L. F. Prescott and J. Nimmo, in "Lidocaine in the Treatment of Ventricular Arrhythmias," D. B. Scott and D. G. Julian, Eds., Livingston, Edinburg, Scotland, 1971, pp. 189–199.

(4) A. H. Hayes, in *ibid.*, pp. 168–177.

(5) J. Lelorier, Y. Latour, D. Grenon, G. Caillé, A. Brosseau, A. Solignac, and G. Dumont, *Clin. Res.*, **28**, 609-a (1975).

(6) J. B. Keenaghan and R. N. Boyes, *J. Pharmacol. Exp. Ther.*, **180**, 454 (1972).

(7) G. Svinhufvud, B. Ortengren, and S. E. Jacobsson, *Scand. J. Clin. Lab. Invest.*, **17**, 162 (1965).

(8) E. L. Pratt, H. P. Warrington, and J. Grego, *Anesthesiology*, **28**, 432 (1967).

(9) B. E. Ballard, *J. Pharm. Sci.*, **64**, 781 (1975).

(10) J. G. Wagner, "Biopharmaceutics and Relevant Pharmacokinetics," 1st ed., Drug Intelligence Publications, Hamilton, Ill., 1971, pp. 295–301.

(11) K. L. Melmon, M. Rowland, L. Sheiner, and W. Trager, "Biological Effects of Drugs in Relation to Their Plasma Concentrations," British Pharmacological Society Symposium, 1972, chap. 8, pp. 107–121.

ACKNOWLEDGMENTS AND ADDRESSES

Received May 17, 1976, from the *Department of Pharmacology, Faculty of Medicine, University of Montreal, Montreal, Quebec, Canada, and the ‡Department of Medicine, Hotel-Dieu Hospital, Montreal, Quebec, Canada.

Accepted for publication September 16, 1976.

Supported by a grant from the MacDonald Stewart Foundation.

The authors thank Mrs. M. Pharand for technical assistance and the nurses and residents of the Coronary Care Unit of the Hotel-Dieu Hospital, Montreal, for cooperation.

* To whom inquiries should be directed.

Kinetics and Mechanism of Blue Tetrazolium Reaction with Corticosteroids

RAUL M. OTEIZA *§, ROBERT S. WOOTEN *§, CHARLES T. KENNER*, ROBERT E. GRAHAM ‡, and EDWARD R. BIEHL *x

Abstract □ The kinetics of the reaction of blue tetrazolium with corticosteroids were investigated under pseudo-first-order conditions. The reaction rates for various corticosteroids were determined at various temperatures, and the enthalpy and entropy of activation for these compounds were determined. A mechanism is proposed in which an electron pair and a proton are transferred to blue tetrazolium from the anion formed by the action of tetramethylammonium hydroxide on the α-carbonyl moiety of the corticosteroid. The proposed mechanism is consistent with previous experimental results.

Keyphrases □ Blue tetrazolium—kinetics of reaction with various corticosteroids, effect of temperature, mechanism proposed □ Corticosteroids, various—kinetics of reaction with blue tetrazolium, effect of temperature, mechanism proposed □ Glucocorticoids, various—kinetics of reaction with blue tetrazolium, effect of temperature, mechanism proposed

Various forms of the blue tetrazolium reaction have been used for the quantitative determination of corticosteroids (1–4). The most widely used method is a slightly modified procedure of Mader and Buck (2), which is the official USP (5) and NF (6) method.

In strongly alkaline solution, blue tetrazolium [3,3′-[3,3′ - dimethoxy(1,1′-biphenyl)-4,4′-diyl]bis(2,5-diphenyl-2*H*-tetrazolium) dichloride] (I) oxidizes the α-carbonyl moiety of the C-17 side chain of the corticosteroid and is reduced quantitatively to a highly colored formazan whose concentration is measured spectrophotometrically. Extensive investigations (1, 3, 4, 7–16) of the reaction conditions established that the analytical procedure is subject to many variables, which are minimized by concurrently analyzing blank, standard, and sample.

Certain kinetic aspects of the blue tetrazolium reaction were reported, *e.g.*, the corticosteroid reaction is first order (17). Significant variations in the reaction rates of corticosteroids of closely related structures also were noted (1, 9, 14, 15, 18, 19). The reaction rate of corticosteroids with I was inversely related to the dielectric constant of the

Table II—Pharmacokinetics of Lidocaine in a Patient following a Prolonged Infusion[a]

Hours	First Infusion, μg/ml	Second Infusion, μg/ml
−29.45	0	0
−17.45	2.98	2.85
0	4.04	4.55
1	3.39	3.15
2	2.28	2.39
4	1.43	1.72
8	0.35	0.54
12	0.20	0.31
19	0.10	—
20	—	0.10
23	N.D.[b]	N.D.

[a] The first and second infusions were separated by 2 weeks. [b] N.D. = not detectable.

ducibility of this analytical method and the difference in the pharmacokinetic parameters of lidocaine following a prolonged infusion. The two phases, α and β, and their values were virtually identical for the two slow infusions. The first infusion resulted in a $T_{p1/2}(\alpha)$ of 2.08 hr and a $T_{p1/2}(\beta)$ of 6.18 hr; the second infusion resulted in a $T_{p1/2}(\alpha)$ of 2.14 hr and a $T_{p1/2}(\beta)$ of 4.93 hr.

Therefore, it can be concluded that the analytical method described confirms that the pharmacokinetic parameters of lidocaine are identical for any given subject on the same treatment. However, compared to the healthy volunteers, the pharmacokinetic parameters were quite different. A true equilibrium was not reached, since the drug concentrations increased continuously during the infusion. This phenomenon can be explained by the fact that lidocaine inhibits its own metabolism *via* its acetylated metabolite (5); moreover, its renal excretion is slower, due to a reduction in the cardiac inotropic form and rhythm which significantly reduce blood flow. The marked lengthening of the α- and β-phases indicates that considerable caution should be exercised when lidocaine is administered by slow infusion, because the toxic effects with lidocaine are greater when the blood levels are too high.

REFERENCES

(1) M. Rowland, P. D. Thomson, A. Guichard, and K. L. Melmon, *Ann. N.Y. Acad. Sci.*, **179**, 383 (1971).

(2) R. N. Boxes, D. B. Scott, P. J. Jebson, M. J. Goodman, and D. G. Julian, *Clin. Pharmacol. Ther.*, **12**, 105 (1971).

(3) L. F. Prescott and J. Nimmo, in "Lidocaine in the Treatment of Ventricular Arrhythmias," D. B. Scott and D. G. Julian, Eds., Livingston, Edinburg, Scotland, 1971, pp. 189–199.

(4) A. H. Hayes, in *ibid.*, pp. 168–177.

(5) J. Lelorier, Y. Latour, D. Grenon, G. Caillé, A. Brosseau, A. Solignac, and G. Dumont, *Clin. Res.*, **28**, 609-a (1975).

(6) J. B. Keenaghan and R. N. Boyes, *J. Pharmacol. Exp. Ther.*, **180**, 454 (1972).

(7) G. Svinhufvud, B. Ortengren, and S. E. Jacobsson, *Scand. J. Clin. Lab. Invest.*, **17**, 162 (1965).

(8) E. L. Pratt, H. P. Warrington, and J. Grego, *Anesthesiology*, **28**, 432 (1967).

(9) B. E. Ballard, *J. Pharm. Sci.*, **64**, 781 (1975).

(10) J. G. Wagner, "Biopharmaceutics and Relevant Pharmacokinetics," 1st ed., Drug Intelligence Publications, Hamilton, Ill., 1971, pp. 295–301.

(11) K. L. Melmon, M. Rowland, L. Sheiner, and W. Trager, "Biological Effects of Drugs in Relation to Their Plasma Concentrations," British Pharmacological Society Symposium, 1972, chap. 8, pp. 107–121.

ACKNOWLEDGMENTS AND ADDRESSES

Received May 17, 1976, from the *Department of Pharmacology, Faculty of Medicine, University of Montreal, Montreal, Quebec, Canada, and the ‡Department of Medicine, Hotel-Dieu Hospital, Montreal, Quebec, Canada.

Accepted for publication September 16, 1976.

Supported by a grant from the MacDonald Stewart Foundation.

The authors thank Mrs. M. Pharand for technical assistance and the nurses and residents of the Coronary Care Unit of the Hotel-Dieu Hospital, Montreal, for cooperation.

* To whom inquiries should be directed.

Kinetics and Mechanism of Blue Tetrazolium Reaction with Corticosteroids

RAUL M. OTEIZA *§, ROBERT S. WOOTEN *§, CHARLES T. KENNER*, ROBERT E. GRAHAM ‡, and EDWARD R. BIEHL *x

Abstract □ The kinetics of the reaction of blue tetrazolium with corticosteroids were investigated under pseudo-first-order conditions. The reaction rates for various corticosteroids were determined at various temperatures, and the enthalpy and entropy of activation for these compounds were determined. A mechanism is proposed in which an electron pair and a proton are transferred to blue tetrazolium from the anion formed by the action of tetramethylammonium hydroxide on the α-carbonyl moiety of the corticosteroid. The proposed mechanism is consistent with previous experimental results.

Keyphrases □ Blue tetrazolium—kinetics of reaction with various corticosteroids, effect of temperature, mechanism proposed □ Corticosteroids, various—kinetics of reaction with blue tetrazolium, effect of temperature, mechanism proposed □ Glucocorticoids, various—kinetics of reaction with blue tetrazolium, effect of temperature, mechanism proposed

Various forms of the blue tetrazolium reaction have been used for the quantitative determination of corticosteroids (1–4). The most widely used method is a slightly modified procedure of Mader and Buck (2), which is the official USP (5) and NF (6) method.

In strongly alkaline solution, blue tetrazolium [3,3′-[3,3′ - dimethoxy(1,1′-biphenyl)-4,4′-diyl]bis(2,5-diphenyl-2*H*-tetrazolium) dichloride] (I) oxidizes the α-carbonyl moiety of the C-17 side chain of the corticosteroid and is reduced quantitatively to a highly colored formazan whose concentration is measured spectrophotometrically. Extensive investigations (1, 3, 4, 7–16) of the reaction conditions established that the analytical procedure is subject to many variables, which are minimized by concurrently analyzing blank, standard, and sample.

Certain kinetic aspects of the blue tetrazolium reaction were reported, *e.g.*, the corticosteroid reaction is first order (17). Significant variations in the reaction rates of corticosteroids of closely related structures also were noted (1, 9, 14, 15, 18, 19). The reaction rate of corticosteroids with I was inversely related to the dielectric constant of the

solvating media in another study (20), and it was established that the α-carbonyl moiety of the corticosteroid reduces I (18).

Recently, a bimolecular scheme was proposed in which a "reduction unit" is transferred from the α-carbonyl moiety to I to produce a formazan (19); however, the reduction unit and the mode of transfer could not be ascertained. A free radical mechanism was proposed for the blue tetrazolium reaction (21), but this route has been disproven (19).

This paper reports the rate constants for selected corticosteroids at various temperatures and the obtained enthalpy and entropy of activation parameters. A mechanism consistent with the observed experimental data is proposed.

EXPERIMENTAL

Apparatus—A UV–visible recording spectrophotometer equipped with water-jacketed cell holders and 1-cm quartz cells[1], a microbalance[2], and a temperature-controlled circulating bath[3] were used.

Reagents—Alcohol USP and analytical grade absolute methanol were used as received. A 1% solution of tetramethylammonium hydroxide (II) was prepared. A 5.00-ml aliquot of II, 10% aqueous[4], was diluted to 50.0 ml with alcohol USP. Blue tetrazolium[5] (I), 5.0 mg/ml, was prepared in absolute methanol.

All corticosteroid standard solutions contained 0.010 mg/ml in alcohol USP.

General Procedure—The procedure, unless otherwise specified, is the official procedure given in the USP XIX (5), in which a 20.00-ml aliquot of standard or sample corticosteroid in alcohol USP is treated with 2.00 ml of I, 5.0 mg/ml, followed by 2.00 ml of 1% II. The absorbance is measured spectrophotometrically against a reagent blank 90 min after the II addition.

Rate Studies—A 20.00-ml aliquot of a standard corticosteroid and a 20.00-ml blank of alcohol USP were placed in jacketed cell holders and allowed to temperature equilibrate for 15 min. The aliquots were treated by the general procedure, with zero time taken as the time of addition of 1% II to the standard solution. Both solutions were transferred to cells as rapidly as possible and placed in the spectrophotometer, and absorbance readings were made each minute at 525 nm until the reaction reached essential completion. The procedure was repeated for five corticosteroids at five different temperatures.

RESULTS AND DISCUSSION

The results of the kinetics studies of the reaction of blue tetrazolium (I) with corticosteroids are shown in Table I. Pseudo-first-order rate constants were observed for all corticosteroids. The rate constants were obtained by performing a least-squares regression on the equation:

$$\ln (1 - A_i/A') = -k_r t_i + E \qquad \text{(Eq. 1)}$$

where A_i is the absorbance at time t_i, A' is the optimum absorbance, k_r is the observed rate constant, and E is the intercept. The correlation coefficient for all curves was greater than 0.99.

Figure 1 is a typical kinetic plot for prednisone. The value of A' was calculated from the average value of absorbance per micromole of formazan, 1.031 (19), and the initial micromolar concentration of the corticosteroid in the 20.00-ml aliquot. The estimation of A' was necessitated for two reasons. First, under the described reaction conditions, a mixture of two formazans of different geometrics and molar absorptivities is formed. The nature and properties of these formazans were investigated previously (20). Second, as the reaction time increases, base decomposition of the formazan begins, causing a decrease in the absorption maxima for the reaction.

To check the reliability of the results, the rate constants of certain corticosteroids were determined by the method developed by Guggenheim (22). The Guggenheim method was not applicable to all corticosteroid reactions because of the rapid completion and concurrent deviation from linearity of most of them at elevated temperatures. Some rates calculated from the Guggenheim method were within experimental accuracy of the previously obtained values (Table I).

Table I—Kinetic and Thermodynamic Parameters for the Reaction of Corticosteroids with Blue Tetrazolium

Corticosteroid	T, °K	k_r, min^{-1}
Dihydrocortisone[a]	303.77	2.809×10^{-1}
	303.76	2.708×10^{-1}
	303.39	3.116×10^{-1}
	300.38	2.030×10^{-1}
	296.41	1.333×10^{-1}
	292.48	1.103×10^{-1}
	287.49	5.775×10^{-2}
	285.80	4.552×10^{-2}
	284.13	3.450×10^{-2}
	283.95	3.608×10^{-2}
	283.87	3.421×10^{-2}
		1.146×10^{-1} [b]
		$\Delta H^{\ddagger} = 17.3$ kcal/mole
		$\Delta S^{\ddagger} = -12.2$ eu
Dexamethasone[c]	303.78	1.120×10^{-1}
	303.77	1.272×10^{-1}
	300.38	6.991×10^{-2}
	296.41	5.447×10^{-2}
	292.48	3.982×10^{-2}
	287.49	1.788×10^{-2}
	285.80	1.085×10^{-2}
	284.22	1.171×10^{-2}
	284.03	1.265×10^{-2}
		1.718×10^{-2}
		$\Delta H^{\ddagger} = 19.8$ kcal/mole
		$\Delta S^{\ddagger} = -5.7$ eu
Prednisone[d]	303.55	3.876×10^{-1}
	303.46	3.202×10^{-1}
	300.38	2.322×10^{-1}
	296.41	1.959×10^{-1}
	292.48	1.373×10^{-1}
	287.49	7.128×10^{-2}
	285.80	4.277×10^{-2}
	284.24	4.698×10^{-2}
	283.87	4.690×10^{-2}
	283.82	4.699×10^{-2}
		$\Delta H^{\ddagger} = 17.3$ kcal/mole
		$\Delta S^{\ddagger} = -11.7$ eu
Corticosterone[a]	303.72	1.320×10^{-1}
	303.71	1.211×10^{-1}
	300.38	7.025×10^{-2}
	296.41	6.324×10^{-2}
	292.48	3.880×10^{-2}
	287.49	2.115×10^{-2}
	285.80	1.096×10^{-2}
	283.74	1.286×10^{-2}
	283.70	1.236×10^{-2}
	283.68	1.314×10^{-2}
		2.207×10^{-2} [b]
		$\Delta H^{\ddagger} = 19.1$ kcal/mole
		$\Delta S^{\ddagger} = -8.1$ eu
5-Pregnene-3β,21-diol-20-one[a]	303.74	8.709×10^{-2}
	303.71	8.853×10^{-2}
	300.38	5.532×10^{-2}
	296.41	4.638×10^{-2}
	292.48	3.260×10^{-2}
	287.49	1.889×10^{-2}
	285.80	1.182×10^{-2}
	283.78	1.075×10^{-2}
	283.70	1.046×10^{-2}
	283.59	1.087×10^{-2}
		2.888×10^{-2} [b]

[a] Rates determined by method of Guggenheim (22). [b] Schwarz/Mann, Orangeburg, N.Y. [c] NF reference standard. [d] USP reference standard.

The enthalpy of activation and entropy of activation results are also shown in Table I. The values were obtained by performing a least-squares regression on the equation:

$$\ln (k_r h/kT) = -\Delta H^{\ddagger}/RT + \Delta S^{\ddagger}/R \qquad \text{(Eq. 2)}$$

where k_r is the observed rate constant, h is Planck's constant, k is Boltzman's constant, T is absolute temperature, R is the gas constant, and $\Delta H^{\ddagger}$ and $\Delta S^{\ddagger}$ are the enthalpy and entropy of activation, respectively. The correlation coefficient was greater than 0.95 in all cases.

[1] Cary model 118.
[2] Mettler model M.
[3] Neslab model RTE-3.
[4] Eastman Chemical Co.
[5] Dajae Laboratories.

IV + VI ⇌

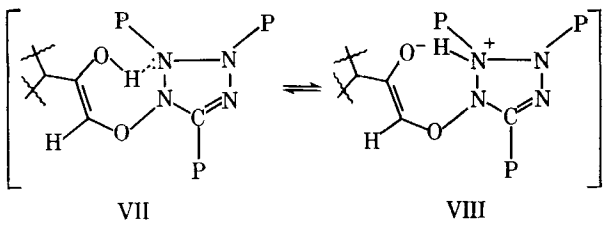

VII VIII

Scheme I

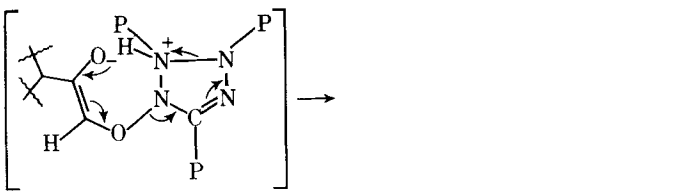

VIII

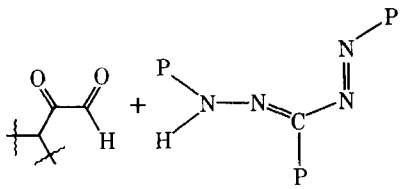

Scheme II

From these data and from previous observations (18, 19), the reactivity of the corticosteroids toward I appears to be, in part, a function of their molecular shape. Steroids with C-16 substitution in either the α- or β-position react the slowest, steroids that possess a planar A ring and have sp^3 C-11 substitution show intermediate reactivity, and steroids possessing a C-11 carbonyl react the fastest with I. These observations strongly imply that the approach of the I molecules occurs at the β-face of the steroid since the greatest rate retardation is observed for steroids having β-substitution near the carbonyl group.

The mechanism proposed for the reduction of I by corticosteroids is shown in Schemes I and II and involves the formation of a complex (VII ⇌ VIII) between the enolate ion, IV, of the corticosteroid molecule and I, followed by a transfer of an electron pair and a proton from the enolate portion of the complex to a positively charged nitrogen atom on the I portion to produce a glyoxal derivative and a formazan (IX). The glyoxal then decomposes to the various products characterized by Lewbart and Mattox (23, 24).

Compounds containing α-carbonyl groups undergo rearrangement in basic solution *via* an enediol intermediate (25–27); in some cases, the enediol itself is the more stable form (28). With regard to the enolate ion, a species such as IV would appear to be more stable than III because of its ability to exist in a cyclic five-membered species having intramolecular hydrogen bonding (Scheme III). In a basic solution, II exists as a resonance hybrid, in which V and VI (Scheme IV) are important contributing structures. The species VI would seem to contribute more to the hybrid

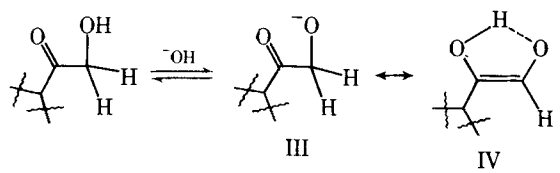

III IV

Scheme III

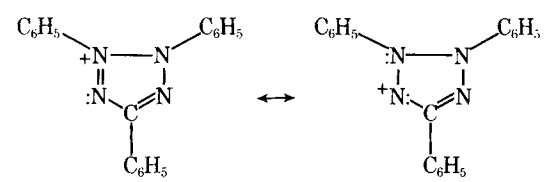

V VI

Scheme IV

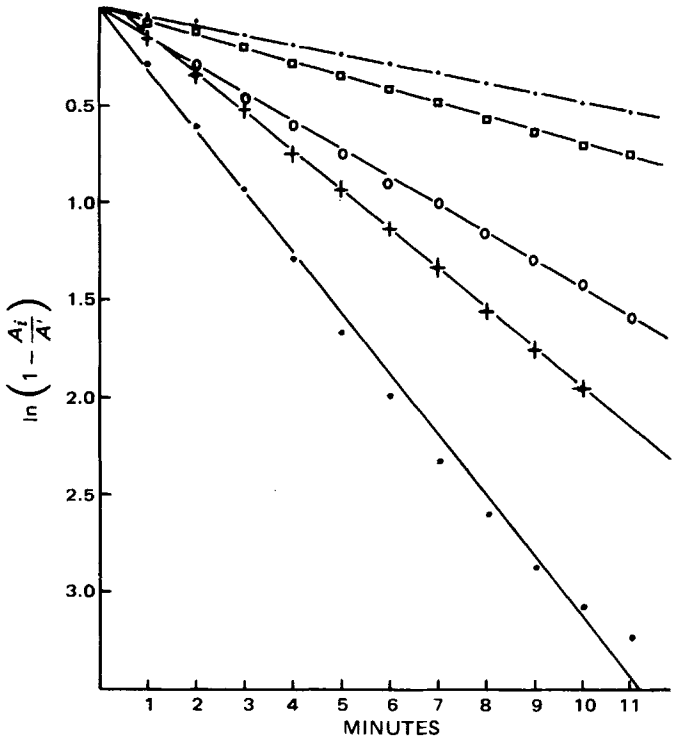

Figure 1—*Reaction rate of a typical corticosteroid at various temperatures. Key: ·, 10°; □, 15°; ○, 20°; +, 25°; and ●, 30°.*

than V since the lone pair of electrons of the nitrogen in VI can be further delocalized into the phenyl group.

The mechanism is in accordance with the observed experimental data. Bimolecular reactions involving a well-oriented cyclic transition complex generally have an entropy of activation value of from −5 to −15 eu simply as a result of the entropy requirement for bringing together two molecules to form a single complex (29). Thus, observed values of $\Delta S^{\ddagger}$ for the reaction of I with corticosteroids provide further evidence of the bimolecularity of the reaction path. The enthalpy of activation values are also consistent with results generally observed for bimolecular reactions in solution (30).

Furthermore, this mechanism predicts that an increase in the dielectric constant would decrease the intermediate complex because of the ionic nature of the reaction and, hence, decrease the reaction rate. This conclusion is in accordance with the observations of Graham *et al.* (20).

Construction of a Dreiding model of the intermediate complex exemplifies and supports the β-face attack and its subsequent decrease of rate. Also, if one follows the complex breakdown with the model, the geometry of the species formed is seen to be identical with that reported as the major formazan isomer (20).

REFERENCES

(1) C. Chen, J. Wheeler, and H. Tewell, *J. Lab. Clin. Med.*, **42**, 463 (1956).

(2) W. Mader and R. Buck, *Anal. Chem.*, **24**, 666 (1952).

(3) T. Weichselbaum and H. Margrof, *J. Clin. Endocrinol. Metab.*, **15**, 970 (1955).

(4) W. Nowaczynski, M. Goldner, and J. Genest, *J. Lab. Clin. Med.*, **45**, 818 (1955).

(5) "The United States Pharmacopeia," 19th rev., Mack Publishing Co., Easton, Pa., 1975, p. 622.

(6) "The National Formulary," 14th ed., Mack Publishing Co., Easton, Pa., 1975, p. 976.

(7) P. Ascione and C. Fogelin, *J. Pharm. Sci.*, **52**, 709 (1963).

(8) J. Callahan, F. Litterio, E. Brit, B. Rosen, and J. Owen, *ibid.*, **51**, 333 (1962).

(9) C. Johnson, R. King, and C. Vichers, *Analyst*, **85**, 714 (1960).

(10) F. Kunze and J. Davis, *J. Pharm. Sci.*, **53**, 1259 (1964).

(11) R. Kuhn and D. Jerchel, *Ber.*, **74**, 941 (1941).

(12) R. Graham, P. Williams, and C. Kenner, *J. Pharm. Sci.*, **59**, 1152 (1970).

(13) *Ibid.*, **59**, 1472 (1970).
(14) R. Rechnagel and M. Litteria, *J. Lab. Clin. Med.*, **48**, 463 (1956).
(15) A. Izzo, E. Keutmann, and R. Burton, *J. Clin. Endocrinol. Metab.*, **17**, 889 (1957).
(16) R. Graham and C. Kenner, *J. Pharm. Sci.*, **62**, 103 (1973).
(17) D. Guttman, *ibid.*, **55**, 919 (1966).
(18) A. Meyer and M. Lindberg, *Anal. Chem.*, **27**, 813 (1955).
(19) R. Graham, E. Biehl, C. Kenner, G. Luttrell, and D. Middleton, *J. Pharm. Sci.*, **64**, 226 (1975).
(20) R. Graham, C. Kenner, and E. Biehl, *ibid.*, **65**, 1048 (1976).
(21) J. Sinsheimer and E. Salim, *Anal. Chem.*, **37**, 566 (1965).
(22) E. Guggenheim, *Phil. Mag.*, **2**, 538 (1926).
(23) M. Lewbart and V. Mattox, *J. Org. Chem.*, **28**, 1773 (1963).
(24) *Ibid.*, **28**, 1779 (1963).
(25) S. Forsein and M. Nilsson, in "The Chemistry of the Carboxyl Group," vol. 1, J. Zabicky, Ed., Interscience, London, England, 1970, p. 228.
(26) C. Collins and J. Eastman, in "The Chemistry of the Carbonyl Group," vol. 1, S. Patai, Ed., Interscience, London, England, 1966, p. 778.
(27) E. Kohler and R. Thompson, *J. Am. Chem. Soc.*, **59**, 887 (1937).
(28) H. von Euler and H. Hasselquist, *Ark. Kemi*, **1**, 257 (1949).
(29) W. Jencks, "Catalysis in Chemistry and Enzymology," McGraw-Hill, New York, N.Y., 1969, p. 600 ff.
(30) A. Frost and R. Pearson, "Kinetics and Mechanism," Wiley, New York, N.Y., 1961, p. 99.

ACKNOWLEDGMENTS AND ADDRESSES

Received September 7, 1976, from **Southern Methodist University, Dallas, TX 75275,* and the *‡Dallas District, Food and Drug Administration, Dallas, TX 75204.*

Accepted for publication December 15, 1976.

Supported in part by Grant N-118 of the Robert A. Welch Foundation, Houston, Tex.

§ Robert A. Welch Undergraduate Scholar.

ˣ To whom inquiries should be directed.

Dosage Form Index: An Objective Criterion for Evaluation of Controlled-Release Drug Delivery Systems

F. THEEUWES ˣ and W. BAYNE

Abstract □ A dimensionless parameter, the dosage form index (DI_τ), is proposed for evaluating the performance of drug delivery systems. The index is defined as the ratio of the maximum to minimum concentrations of the drug in plasma within each interdose interval (in hours), τ, during repetitive administration of the dosage form in the quasisteady state. Dosage form indexes can be averaged among subjects or within subjects at successive time periods to arrive at a mean value. As an example, two GI therapeutic systems—the 15- and 20-mg/hr acetazolamide systems that deliver drug at constant rates for 6 and 12 hr and contain 125 and 250 mg, respectively—were compared in normal subjects with a commercial sustained-release product containing 500 mg of acetazolamide. The dosage form index, DI_{24}, was 4.9 for the sustained-release dosage form and 3.2 for the 20-mg/hr system; DI_{12} was 1.6 for the 15-mg/hr system.

Keyphrases □ Drug delivery systems—sustained-release product and 15- and 20-mg/hr GI acetazolamide systems compared in humans, dosage form index suggested as evaluating parameter □ Dosage form index—suggested as evaluating parameter for drug delivery systems, sustained-release product and 15- and 20-mg/hr GI acetazolamide systems compared in humans □ Acetazolamide—sustained-release product and 15- and 20-mg/hr GI drug delivery systems compared in humans, dosage form index suggested as evaluating parameter □ Carbonic anhydrase inhibitors—acetazolamide, sustained-release product and 15- and 20-mg/hr GI drug delivery systems compared, humans

Optimum therapy with repetitive administration of conventional dosage forms (*e.g.*, injectables, liquids, or tablets) can classically be pursued by dosage scheduling. The aim of this process is to maintain drug concentrations in a therapeutic range, above the minimum effective concentration and below the toxic concentration.

The time course of systemic drug concentrations following repetitive dosing of intravenous injections and tablets, based on different absorption and elimination rate constants, was described mathematically using one-compartment and multicompartment pharmacokinetic models (1–3).

BACKGROUND

To discuss optimum drug dosing, the therapeutic index (TI) should be defined in terms of plasma concentrations (4) rather than dose (5):

$$\mathrm{TI} = \frac{C^*_{max}}{C^*_{min}} \qquad \text{(Eq. 1)}$$

where C^*_{max} and C^*_{min} are the maximum and minimum desired plasma concentrations, respectively, and must be defined further for each specific drug in relation to pharmacological responses.

Dosage scheduling should be carried out at a frequency such that the ratio of maximum to minimum plasma concentrations is less than TI and at a dose of sufficient magnitude to yield effective levels.

For a linear, one-compartment system with repetitive intravenous injections at pseudo-steady state, the ratio of maximum to minimum plasma concentrations is given by:

$$\frac{C_{max}}{C_{min}} = e^{k\tau} \qquad \text{(Eq. 2)}$$

where k is the drug elimination rate constant, and τ is the dosing interval. The C_{max}/C_{min} ratio has been called (1) Q_{ext}, the ratio of asymptotic extreme concentrations within a dosing interval of the multiple-dose curve. When the therapeutic index (TI) is known, the proper dosage interval must then be dictated by:

$$e^{k\tau} \leq \mathrm{TI} \qquad \text{(Eq. 3)}$$

or:

$$\tau \leq t_{1/2}\frac{\ln \mathrm{TI}}{\ln 2} \qquad \text{(Eq. 4)}$$

For TI = 2, the dosing interval should maximally be equal to the biological half-life of the drug. For drugs with a half-life of less than 12 hr and a low therapeutic index, proper dosage schedules are inconveniently frequent. To alleviate these problems, therapeutic systems were developed (6–8).

Therapeutic systems are a class of dosage forms designed to improve drug therapy through controlled administration of drug substances, in time and space, to elicit the optimum sum total of pharmacological response. They are specified not by content, size, or shape but by function: the rate at which they deliver drug *in vivo* and the duration for which they do so.

(13) *Ibid.*, **59**, 1472 (1970).
(14) R. Rechnagel and M. Litteria, *J. Lab. Clin. Med.*, **48**, 463 (1956).
(15) A. Izzo, E. Keutmann, and R. Burton, *J. Clin. Endocrinol. Metab.*, **17**, 889 (1957).
(16) R. Graham and C. Kenner, *J. Pharm. Sci.*, **62**, 103 (1973).
(17) D. Guttman, *ibid.*, **55**, 919 (1966).
(18) A. Meyer and M. Lindberg, *Anal. Chem.*, **27**, 813 (1955).
(19) R. Graham, E. Biehl, C. Kenner, G. Luttrell, and D. Middleton, *J. Pharm. Sci.*, **64**, 226 (1975).
(20) R. Graham, C. Kenner, and E. Biehl, *ibid.*, **65**, 1048 (1976).
(21) J. Sinsheimer and E. Salim, *Anal. Chem.*, **37**, 566 (1965).
(22) E. Guggenheim, *Phil. Mag.*, **2**, 538 (1926).
(23) M. Lewbart and V. Mattox, *J. Org. Chem.*, **28**, 1773 (1963).
(24) *Ibid.*, **28**, 1779 (1963).
(25) S. Forsein and M. Nilsson, in "The Chemistry of the Carboxyl Group," vol. 1, J. Zabicky, Ed., Interscience, London, England, 1970, p. 228.
(26) C. Collins and J. Eastman, in "The Chemistry of the Carbonyl Group," vol. 1, S. Patai, Ed., Interscience, London, England, 1966, p. 778.
(27) E. Kohler and R. Thompson, *J. Am. Chem. Soc.*, **59**, 887 (1937).
(28) H. von Euler and H. Hasselquist, *Ark. Kemi*, **1**, 257 (1949).
(29) W. Jencks, "Catalysis in Chemistry and Enzymology," McGraw-Hill, New York, N.Y., 1969, p. 600 ff.
(30) A. Frost and R. Pearson, "Kinetics and Mechanism," Wiley, New York, N.Y., 1961, p. 99.

ACKNOWLEDGMENTS AND ADDRESSES

Received September 7, 1976, from **Southern Methodist University, Dallas, TX 75275,* and the *‡Dallas District, Food and Drug Administration, Dallas, TX 75204.*

Accepted for publication December 15, 1976.

Supported in part by Grant N-118 of the Robert A. Welch Foundation, Houston, Tex.

§ Robert A. Welch Undergraduate Scholar.

ˣ To whom inquiries should be directed.

Dosage Form Index: An Objective Criterion for Evaluation of Controlled-Release Drug Delivery Systems

F. THEEUWES ˣ and W. BAYNE

Abstract □ A dimensionless parameter, the dosage form index (DI_τ), is proposed for evaluating the performance of drug delivery systems. The index is defined as the ratio of the maximum to minimum concentrations of the drug in plasma within each interdose interval (in hours), τ, during repetitive administration of the dosage form in the quasisteady state. Dosage form indexes can be averaged among subjects or within subjects at successive time periods to arrive at a mean value. As an example, two GI therapeutic systems—the 15- and 20-mg/hr acetazolamide systems that deliver drug at constant rates for 6 and 12 hr and contain 125 and 250 mg, respectively—were compared in normal subjects with a commercial sustained-release product containing 500 mg of acetazolamide. The dosage form index, DI_{24}, was 4.9 for the sustained-release dosage form and 3.2 for the 20-mg/hr system; DI_{12} was 1.6 for the 15-mg/hr system.

Keyphrases □ Drug delivery systems—sustained-release product and 15- and 20-mg/hr GI acetazolamide systems compared in humans, dosage form index suggested as evaluating parameter □ Dosage form index—suggested as evaluating parameter for drug delivery systems, sustained-release product and 15- and 20-mg/hr GI acetazolamide systems compared in humans □ Acetazolamide—sustained-release product and 15- and 20-mg/hr GI drug delivery systems compared in humans, dosage form index suggested as evaluating parameter □ Carbonic anhydrase inhibitors—acetazolamide, sustained-release product and 15- and 20-mg/hr GI drug delivery systems compared, humans

Optimum therapy with repetitive administration of conventional dosage forms (*e.g.*, injectables, liquids, or tablets) can classically be pursued by dosage scheduling. The aim of this process is to maintain drug concentrations in a therapeutic range, above the minimum effective concentration and below the toxic concentration.

The time course of systemic drug concentrations following repetitive dosing of intravenous injections and tablets, based on different absorption and elimination rate constants, was described mathematically using one-compartment and multicompartment pharmacokinetic models (1–3).

BACKGROUND

To discuss optimum drug dosing, the therapeutic index (TI) should be defined in terms of plasma concentrations (4) rather than dose (5):

$$\mathrm{TI} = \frac{C^*_{max}}{C^*_{min}} \qquad \text{(Eq. 1)}$$

where C^*_{max} and C^*_{min} are the maximum and minimum desired plasma concentrations, respectively, and must be defined further for each specific drug in relation to pharmacological responses.

Dosage scheduling should be carried out at a frequency such that the ratio of maximum to minimum plasma concentrations is less than TI and at a dose of sufficient magnitude to yield effective levels.

For a linear, one-compartment system with repetitive intravenous injections at pseudo-steady state, the ratio of maximum to minimum plasma concentrations is given by:

$$\frac{C_{max}}{C_{min}} = e^{k\tau} \qquad \text{(Eq. 2)}$$

where k is the drug elimination rate constant, and τ is the dosing interval. The C_{max}/C_{min} ratio has been called (1) Q_{ext}, the ratio of asymptotic extreme concentrations within a dosing interval of the multiple-dose curve. When the therapeutic index (TI) is known, the proper dosage interval must then be dictated by:

$$e^{k\tau} \leq \mathrm{TI} \qquad \text{(Eq. 3)}$$

or:

$$\tau \leq t_{1/2}\frac{\ln \mathrm{TI}}{\ln 2} \qquad \text{(Eq. 4)}$$

For TI = 2, the dosing interval should maximally be equal to the biological half-life of the drug. For drugs with a half-life of less than 12 hr and a low therapeutic index, proper dosage schedules are inconveniently frequent. To alleviate these problems, therapeutic systems were developed (6–8).

Therapeutic systems are a class of dosage forms designed to improve drug therapy through controlled administration of drug substances, in time and space, to elicit the optimum sum total of pharmacological response. They are specified not by content, size, or shape but by function: the rate at which they deliver drug *in vivo* and the duration for which they do so.

The GI therapeutic system is a new oral dosage form designed to control plasma drug concentrations for one area of application. The system's delivery rate profile provides one extra degree of freedom in addition to scheduling to arrive at optimum therapy. The selection of the system's delivery rate characteristic allows the interval τ to be a convenient time period that is much less dependent on $t_{1/2}$ and TI, as was the case classically.

GI therapeutic systems are constructed according to elementary osmotic pump technology (9). This osmotic system was developed as an oral dosage form because of its desirable delivery rate characteristics (9). The rate is predictable, essentially constant during most of the drug release process, independent of pH and GI motility, and adjustable so that it can be of sufficient magnitude to be of interest as an oral dosage form.

The dosing interval for the GI therapeutic system must also permit the resulting ratio of the maximum to minimum plasma drug concentrations to be smaller or equal to TI. This ratio at pseudo-steady state on repetitive dosing of the system is different from Q_{ext} as defined for conventional dosage forms (1) and is now a function of the dosage form characteristics. Therefore, it is defined as the dosage form index, DI_τ. The dosage form index is a function of the intrinsic pharmacokinetic properties of the drug (*e.g.*, absorption, distribution, and elimination), the dosing interval, τ, and the dosage form delivery rate. At equal dosing intervals, two dosage forms can be compared. The system with the lowest DI may be superior therapeutically. The dosage form index can be used also as a criterion to select the optimum dosage form and dosing interval.

In a previous study of acetazolamide in humans (4), the therapeutic index, defined in terms of plasma concentrations, was given as:

$$TI = \frac{120\ \mu M}{45\ \mu M} = 2.7 \qquad \text{(Eq. 5)}$$

At a plasma acetazolamide concentration of 120 μM, noticeable impairment of carbon dioxide transport by the red cells is expected since 96% of their carbonic anhydrase activity is inhibited. However, 45 μM or 10 μg/ml was an adequate concentration for lowering intraocular pressure. In the same work (4), plasma concentration profiles were calculated as described by Dost (2) for a regimen of 250-mg acetazolamide tablets four times a day. This regimen was considered to produce an adequate therapeutic effect, and the dosage form index was 2.7, *i.e.*, equal to the therapeutic index.

More severe side effects may occur on administration of conventional acetazolamide tablets at twice the daily dose than with a sustained-release form of the drug[1] (10). The discontinuation rate was 47% on dosing 250-mg tablets four times a day *versus* 11% on dosing the sustained-release form (500 mg) once a day, while the efficacies were comparable.

Since the 500-mg sustained-release dosage form, once a day regimen was believed to be the optimum treatment, it was compared with two types of acetazolamide GI therapeutic systems on the basis of the dosage form index, plasma concentrations, and urinary excretion in normal human volunteers.

EXPERIMENTAL

The dosage forms investigated were a sustained-release dosage form containing 500 mg of acetazolamide, delivering the drug in quasiexponential declining fashion by *in vitro* tests, and 15- and 20-mg/hr acetazolamide GI therapeutic systems (9), delivering 70% of their total content at zero order by *in vitro* tests. The two GI systems contained a total of 125 and 250 mg of acetazolamide and delivered their contents over 6 and 12 hr, respectively.

The 6-hr system was administered twice a day. The 12-hr system and the sustained-release dosage form were given once a day, and both were studied in eight volunteers in a crossover study. Five of the eight volunteers also received the 6-hr system. Each dosage form was administered for up to 10 days to allow blood sampling during successive periods at steady state. Steady state was verified by sampling blood at frequent intervals during Days 1, 3, and 10.

The standard deviation is defined by:

$$SD = \left(\frac{\sum^{n} (X_i - \overline{X})^2}{(n-1)} \right)^{1/2} \qquad \text{(Eq. 6)}$$

where $\overline{X}$ is the arithmetic mean of the series of n observations X_i.

[1] Diamox Sequel, Lederle Laboratories, Division of American Cyanamid Co., Pearl River, NY 10965.

Plasma samples were analyzed according to a recently published high-speed liquid chromatographic method (11).

A specific liquid chromatographic method was developed for urine. To 1 ml of urine was added 200 μl of a stock solution (0.16 mg/ml) of sulfadiazine[2] in 0.1 M phosphate buffer (pH 7), followed by 1 ml of 2.0 M acetate buffer (pH 4.5). The aqueous solution was extracted twice with 10 ml of ether–methylene chloride–isopropyl alcohol (6:4:2) (12). The combined organic extract was then extracted with 2 ml of 1 M carbonate buffer (pH 11).

The organic phase was discarded, and 700 μl of acetic acid was added to the aqueous phase. The aqueous phase was extracted with 10 ml of the mixture of organic solvents described. The aqueous phase was discarded, and the organic phase was then evaporated to dryness in a nitrogen stream at 40°. The residue was reconstituted in 200 μl of 0.01 N NaOH.

The reconstituted extract was injected onto a high-pressure liquid chromatograph; the chromatographic column contained an octadecylsilane monolayer bonded to a microparticulate silica support[3], with 2% dimethylformamide in 0.05 M phosphate buffer (pH 6.2) as the mobile phase. The flow rate was maintained at 2 ml/min with a constant-flow reciprocating pump[4]. Acetazolamide and sulfadiazine were detected in the eluant using a high-pressure mercury source[5] at 254 nm. The retention times for sulfadiazine and acetazolamide were 10.5 and 13.5 min, respectively.

Standard curves were constructed with varying amounts of acetazolamide (1–62.5 μg) and a constant amount of sulfadiazine (32.5 μg) per milliliter of urine. To determine acetazolamide concentrations in urine, a known amount of sulfadiazine was added, and the measured response ratios were obtained and converted to concentrations based on the standard curve. Chromatograms from blank samples (before acetazolamide administration) showed no interfering peaks with the retention times of acetazolamide or the internal standard. The absolute extraction efficiency of the method was approximately 80% for both acetazolamide and sulfadiazine.

RESULTS

Plasma Concentrations of Acetazolamide—The average plasma concentrations obtained from eight human subjects following acetazolamide administration *via* the sustained-release dosage form and 12-hr system once a day are shown in Fig. 1. Also shown are the average plasma concentrations for five subjects following administration of a 6-hr system twice a day. A continuing increase in plasma concentrations on administering the 6-hr system on Day 1 was due to the twice a day administration schedule. No 6-hr system was administered on the second half of Day 10. The data in Fig. 1 show that the dosage form and regimen combination of the 6-hr system twice a day resulted in the least variable plasma concentration profiles at quasisteady state.

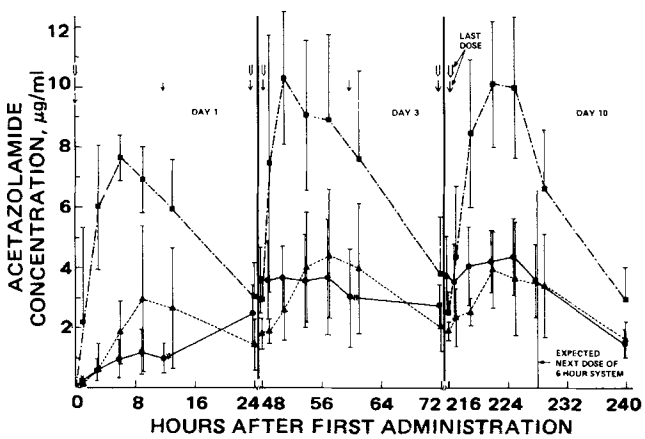

Figure 1—*Average plasma acetazolamide concentrations (±SD) in normal human subjects following administration of the sustained-release dosage form dosed once a day at ⇓, n = 8 (■); the 6-hr system dosed twice daily at ↓, offset 0.2 hr, n = 5 (●); and the 12-hr system dosed once a day at ⇓, n = 8 (▲).*

[2] K & K Laboratories, Plainview, N.Y.
[3] μBondapak C_{18}, Waters Associates, Milford, Mass.
[4] Model 6000, Waters Associates, Milford, Mass.
[5] Varian Instruments Division, Palo Alto, Calif.

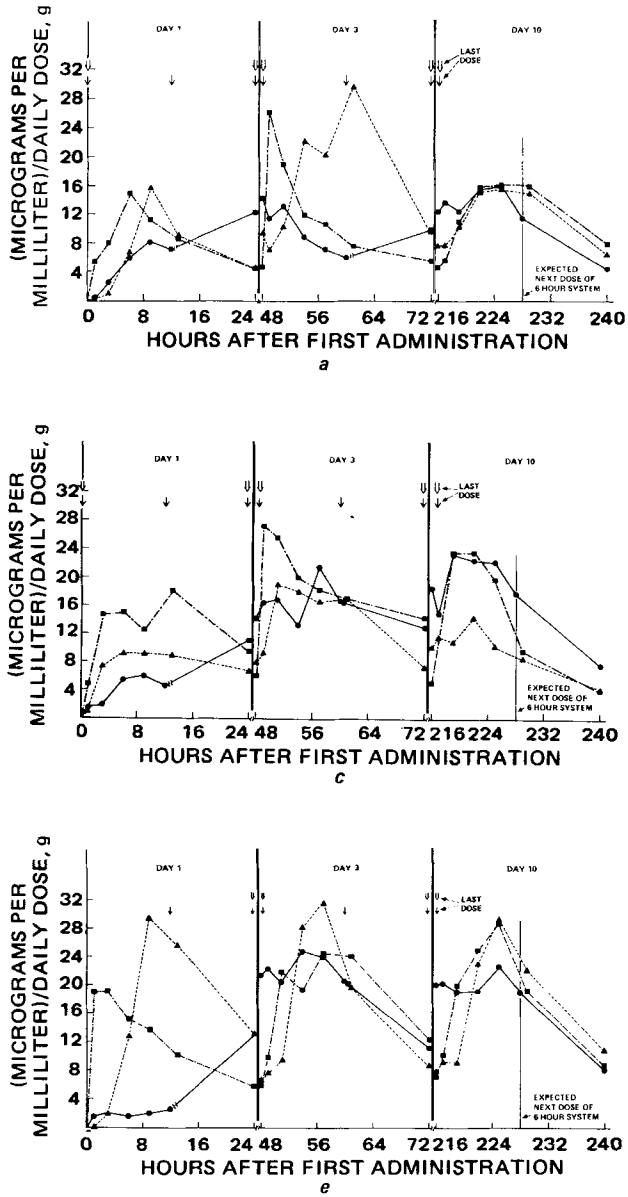

Figure 2—*Normalized plasma acetazolamide concentrations in normal human subjects following administration of three dosage forms. Key: a, Subject 287; b, Subject 337; c, Subject 263; d, Subject 297; and e, Subject 386. See Fig. 1 for definition of symbols.*

For each of the five subjects receiving each of the three dosage forms, the plasma concentrations were normalized to the daily dose (Fig. 2). Through normalization, plasma concentrations were calculated that would be obtained if 1 g of daily dose were administered from each of the dosage forms to the subjects, behaving as linear systems. The data were calculated by multiplying the actual plasma concentrations obtained following administration of the sustained-release dosage form once a day by two and by multiplying the plasma concentrations following administration of a 6-hr system twice a day and a 12-hr system once a day by four.

The average normalized plasma concentrations are shown in Fig. 3. The areas under the normalized plasma concentration–time curves (*AUC*) at steady state for each dosage form were calculated and averaged over all subjects for Days 3 and 10 (Fig. 4). The lack of significant difference in normalized areas under the plasma concentration–time curves indicates that the drug was absorbed from each dosage form to the same extent. This conclusion was supported by the urinary excretion data.

Urinary Excretion of Acetazolamide—Following administration of each dosage form, the urinary excretion of acetazolamide over 24 hr was determined for each subject. The 24-hr urinary recovery was averaged over all subjects for each dosage form as a percent of the daily dose and plotted as a function of time (Fig. 5).

The percent of the total dose administered over 10 days during each treatment recovered in the urine was averaged for all subjects and plotted in Fig. 6. On the average, 63% of the drug was excreted with each dosage form.

Dosage Form Indexes—Dosage form indexes were calculated for the sustained-release dosage form and the 12-hr system as the ratios of the maximum to minimum plasma concentrations encountered in a 24-hr dosing period during Days 3 and 10. For the 6-hr system, the index is the ratio of maximum to minimum plasma concentrations encountered in the 12-hr steady-state interval on Days 3 and 10, averaged over all

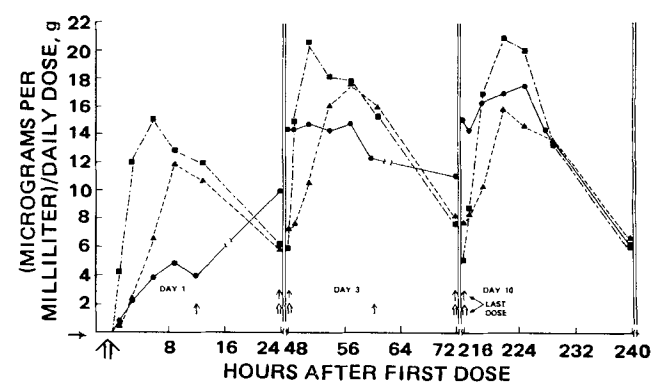

Figure 3—*Averaged normalized plasma acetazolamide concentrations in normal human subjects following administration of three dosage forms. Key: see Fig. 1.*

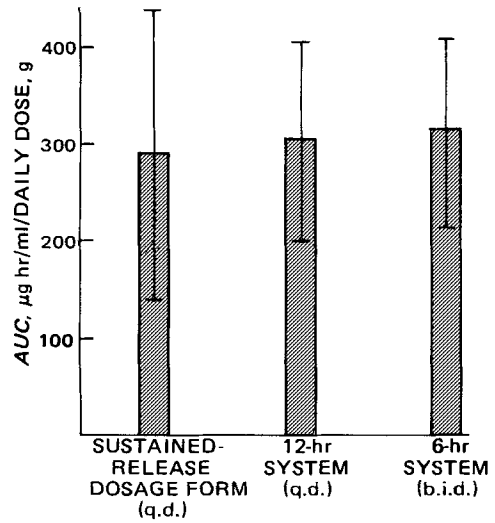

Figure 4—*Area under the normalized plasma concentration–time curves (±SD) averaged for all subjects on Days 3 and 10 (n = 10 for 6-hr system, n = 15 for 12-hr system, and n = 14 for sustained release).*

subjects. Since only one cycle of detailed plasma data was taken per day and per dosage form for all three dosage forms, one measure of the dosage form index was obtained per dosage form and per day. The averages of the dosage form indexes over all days and subjects are plotted in Fig. 7. The standard deviation indicates the variation from the mean over all subjects on Days 3 and 10.

The therapeutic value of a dosage form and schedule is expected to be greater when the dosage form index is small compared to the therapeutic index. By definition of the therapeutic index (Eq. 1), side effects are more likely to occur when DI_τ is large compared to TI, provided the minimum concentration, C_{min}, observed during treatment is larger or equal to C^*_{min}, the minimum effective concentration. The ratio:

$$SI = \left(\frac{DI_\tau}{TI}\right)_{C_{min}=C^*_{min}} \quad \text{(Eq. 7)}$$

can be defined as the side-effects index (SI), indicating the absence of side effects for SI < 1 and an increasing number and/or severity of side effects for SI > 1.

The dosage form indexes demonstrate that, relative to the sustained-release dosage form administered once daily, a decrease in the side-effects index was obtained by a factor of 1.5 for the 12-hr system dosed once a day and by 3.2 for the 6-hr system dosed twice a day. Figure 7 shows that an improvement was obtained by selecting the 12-hr system over the sustained-release dosage form. A further improvement was obtained by administering the 6-hr system twice a day. It is clear that the dosage form index decreases with more frequent dosing.

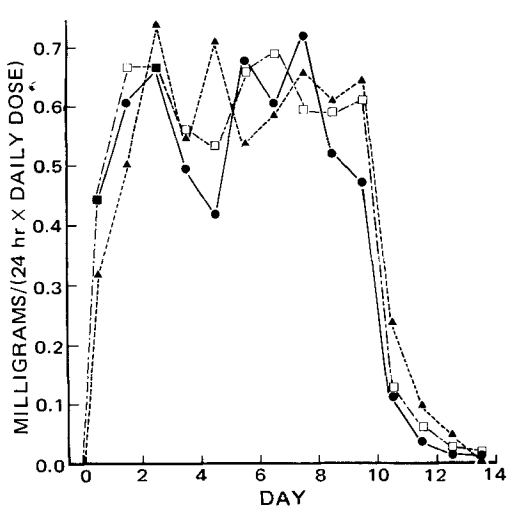

Figure 5—*Average fraction of 24-hr dose of acetazolamide excreted in the urine.*

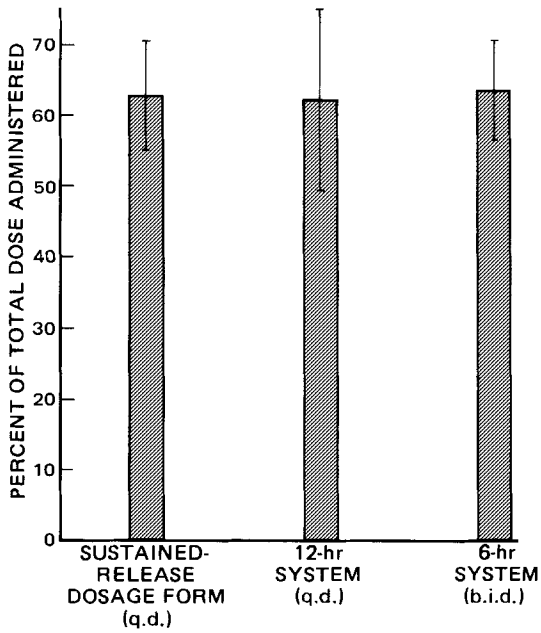

Figure 6—*Average percent of total acetazolamide dose (±SD), administered during 10 days, excreted in the urine.*

CONCLUSIONS

1. The average normalized areas under the plasma concentration–time curves are the same for the three dosage forms, about 300 (μg hr/ml)/g of daily dose.
2. The lack of significant difference in the normalized *AUC*'s indicates that all three dosage forms have essentially the same bioavailability.
3. The variability of the plasma acetazolamide concentration at the steady state is expressed as the dosage form index, DI_τ, during the dosing interval, τ, expressed in hours. The values of DI_τ, averaged within and among subjects, are: $DI_{24} = 4.9$ for the sustained-release dosage form, $DI_{24} = 3.2$ for the 12-hr system, and $DI_{12} = 1.6$ for the 6-hr system.

The 6-hr system twice a day is the only regimen with a dosage form index below 2.7, the therapeutic index for acetazolamide [Eq. 5 (4)]. This system is, therefore, expected to have a high efficacy and reduce side effects.

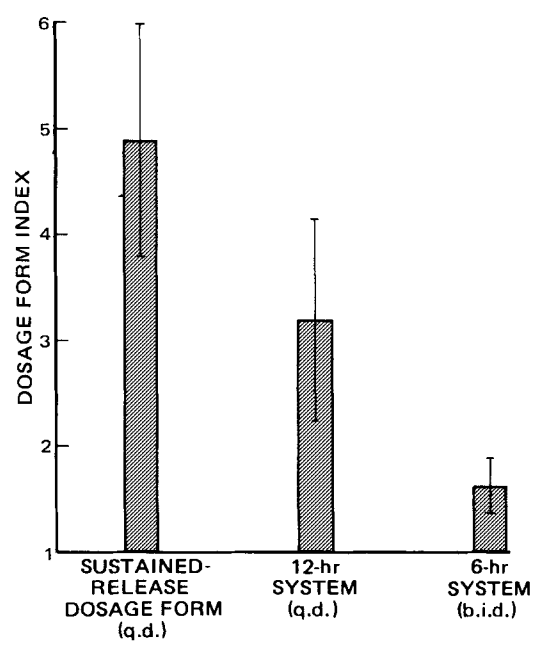

Figure 7—*Average of the maximum to minimum plasma acetazolamide concentration ratio on Days 3 and 10 (±SD).*

REFERENCES

(1) E. Kruger-Thiemer, in "Physico-Chemical Aspects of Drug Actions," vol. 7, Pergamon, New York, N.Y., 1965, pp. 63–113.

(2) F. H. Dost, "Grundlagen der Pharmakokinetik," 2nd ed., Georg Thieme Verlag, Stuttgart, West Germany, 1968.

(3) J. G. Wagner, "Fundamentals of Clinical Pharmacokinetics," 1st ed., Drug Intelligence Publications, Hamilton, Ill., 1975.

(4) B. Lehmann, E. Linner, and P. J. Wistrand, *Adv. Biosci.*, **5**, 197 (1969).

(5) J. G. Wagner, "Biopharmaceutics and Relevant Pharmacokinetics," 1st ed., Drug Intelligence Publications, Hamilton, Ill., 1971.

(6) A. Zaffaroni, *Pharm. J.*, **205**, 400 (1970).

(7) *Ibid.*, **207**, 414 (1971).

(8) A. Zaffaroni, presented at 31st International Congress of Pharmaceutical Sciences, Washington, D.C., 1971, Abstract, pp. 19, 20.

(9) F. Theeuwes, *J. Pharm. Sci.*, **64**, 1987 (1975).

(10) L. L. Garner, E. F. Carl, and J. R. Ferwerda, *Am. J. Ophthalmol.*, **55**, 323 (1963).

(11) W. Bayne, G. Rogers, and N. Crisologo, *J. Pharm. Sci.*, **64**, 402 (1975).

(12) S. M. Wallace, V. P. Shah, and S. Riegelman, in "Abstracts," APhA Academy of Pharmaceutical Sciences, American Pharmaceutical Association, Washington, D.C., 1975, p. 137.

ACKNOWLEDGMENTS AND ADDRESSES

Received September 15, 1976, from *Alza Research, Palo Alto, CA 94304.*

Accepted for publication December 7, 1976.

The authors thank Dr. John Urquhart and Dr. Gerhard Levy for their stimulating and constructive criticism of this work and Dr. R. C. Merrill and Ms. Carol Ferré for the execution of the clinical protocol.

[x] To whom inquiries should be directed.

Oxidation Kinetics of Phenothiazine and 10-Methylphenothiazine in Acidic Medium

H. ROSEBOOM [x] and J. H. PERRIN [x]

Abstract □ The rate of phenothiazine degradation in an acidic oxygen-saturated medium was studied. 3*H*-Phenothiazine-3-one and phenothiazine 5-oxide are produced by parallel reactions, and 7-(10′-phenothiazinyl)-3*H*-phenothiazine-3-one is produced in a more complex manner. The overall phenothiazine degradation rate appears to be pH independent up to pH 7.0. The degradation kinetics of 10-methylphenothiazine were studied after isolation and identification of its degradation products, 10-methylphenothiazine 5-oxide and 3*H*-phenothiazine-3-one. The main degradation product is 10-methylphenothiazine 5-oxide; but at low pH values and high temperatures, more 3*H*-phenothiazine-3-one is formed. The degradation rate of 10-methylphenothiazine is pH independent up to pH 7.

Keyphrases □ Phenothiazine and 10-methyl derivative—oxidative degradation in acidic oxygen-saturated medium, effect of pH □ Oxidation—degradation kinetics of phenothiazine and 10-methyl derivative in acidic oxygen-saturated medium, effect of pH □ Degradation kinetics—phenothiazine and 10-methyl derivative, oxidation in acidic oxygen-saturated medium, effect of pH

The oxidative degradation of phenothiazine has been the subject of many investigations (1–7), but little is known about the kinetics of this reaction. Previously, the isolation of some degradation products and their identification by TLC, melting point, and IR, UV, and mass spectral data were described (8). 7-(10′-Phenothiazinyl)-3*H*-phenothiazine-3-one was reported as a degradation product for the first time, and its structure has now been confirmed by NMR spectroscopy. The present paper reports the kinetics of the disappearance of phenothiazine (I) and the

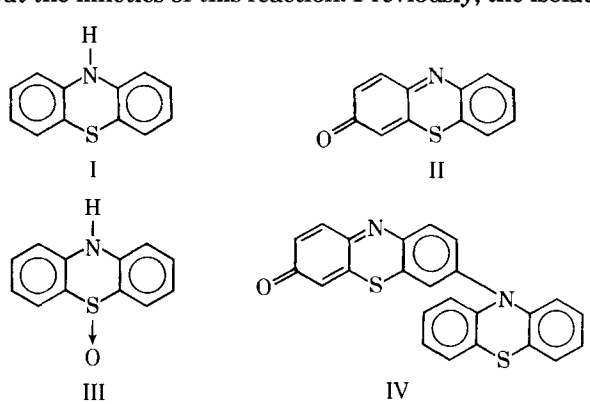

I II III IV

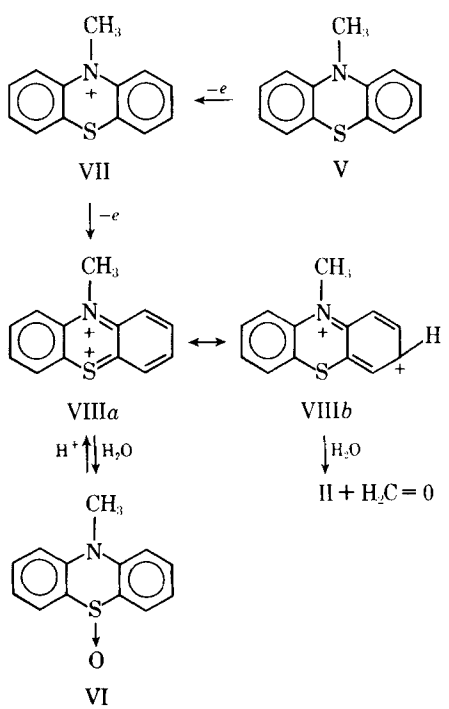

VII V VIIIa VIIIb VI

Scheme I

REFERENCES

(1) E. Kruger-Thiemer, in "Physico-Chemical Aspects of Drug Actions," vol. 7, Pergamon, New York, N.Y., 1965, pp. 63–113.

(2) F. H. Dost, "Grundlagen der Pharmakokinetik," 2nd ed., Georg Thieme Verlag, Stuttgart, West Germany, 1968.

(3) J. G. Wagner, "Fundamentals of Clinical Pharmacokinetics," 1st ed., Drug Intelligence Publications, Hamilton, Ill., 1975.

(4) B. Lehmann, E. Linner, and P. J. Wistrand, *Adv. Biosci.*, **5**, 197 (1969).

(5) J. G. Wagner, "Biopharmaceutics and Relevant Pharmacokinetics," 1st ed., Drug Intelligence Publications, Hamilton, Ill., 1971.

(6) A. Zaffaroni, *Pharm. J.*, **205**, 400 (1970).

(7) *Ibid.*, **207**, 414 (1971).

(8) A. Zaffaroni, presented at 31st International Congress of Pharmaceutical Sciences, Washington, D.C., 1971, Abstract, pp. 19, 20.

(9) F. Theeuwes, *J. Pharm. Sci.*, **64**, 1987 (1975).

(10) L. L. Garner, E. F. Carl, and J. R. Ferwerda, *Am. J. Ophthalmol.*, **55**, 323 (1963).

(11) W. Bayne, G. Rogers, and N. Crisologo, *J. Pharm. Sci.*, **64**, 402 (1975).

(12) S. M. Wallace, V. P. Shah, and S. Riegelman, in "Abstracts," APhA Academy of Pharmaceutical Sciences, American Pharmaceutical Association, Washington, D.C., 1975, p. 137.

ACKNOWLEDGMENTS AND ADDRESSES

Received September 15, 1976, from *Alza Research, Palo Alto, CA 94304.*

Accepted for publication December 7, 1976.

The authors thank Dr. John Urquhart and Dr. Gerhard Levy for their stimulating and constructive criticism of this work and Dr. R. C. Merrill and Ms. Carol Ferré for the execution of the clinical protocol.

[x] To whom inquiries should be directed.

Oxidation Kinetics of Phenothiazine and 10-Methylphenothiazine in Acidic Medium

H. ROSEBOOM [x] and J. H. PERRIN [x]

Abstract □ The rate of phenothiazine degradation in an acidic oxygen-saturated medium was studied. 3*H*-Phenothiazine-3-one and phenothiazine 5-oxide are produced by parallel reactions, and 7-(10′-phenothiazinyl)-3*H*-phenothiazine-3-one is produced in a more complex manner. The overall phenothiazine degradation rate appears to be pH independent up to pH 7.0. The degradation kinetics of 10-methylphenothiazine were studied after isolation and identification of its degradation products, 10-methylphenothiazine 5-oxide and 3*H*-phenothiazine-3-one. The main degradation product is 10-methylphenothiazine 5-oxide; but at low pH values and high temperatures, more 3*H*-phenothiazine-3-one is formed. The degradation rate of 10-methylphenothiazine is pH independent up to pH 7.

Keyphrases □ Phenothiazine and 10-methyl derivative—oxidative degradation in acidic oxygen-saturated medium, effect of pH □ Oxidation—degradation kinetics of phenothiazine and 10-methyl derivative in acidic oxygen-saturated medium, effect of pH □ Degradation kinetics—phenothiazine and 10-methyl derivative, oxidation in acidic oxygen-saturated medium, effect of pH

The oxidative degradation of phenothiazine has been the subject of many investigations (1–7), but little is known about the kinetics of this reaction. Previously, the isolation of some degradation products and their identification by TLC, melting point, and IR, UV, and mass spectral data were described (8). 7-(10′-Phenothiazinyl)-3*H*-phenothiazine-3-one was reported as a degradation product for the first time, and its structure has now been confirmed by NMR spectroscopy. The present paper reports the kinetics of the disappearance of phenothiazine (I) and the

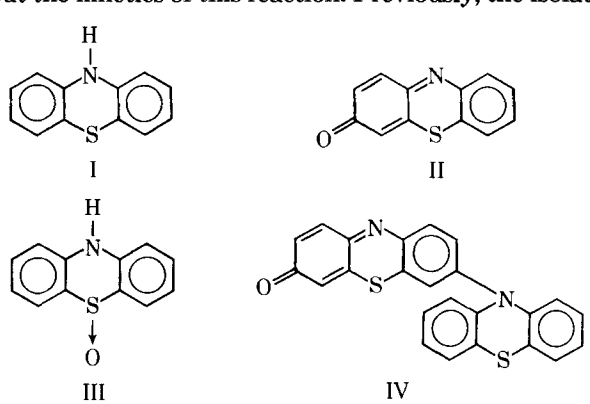

I II III IV

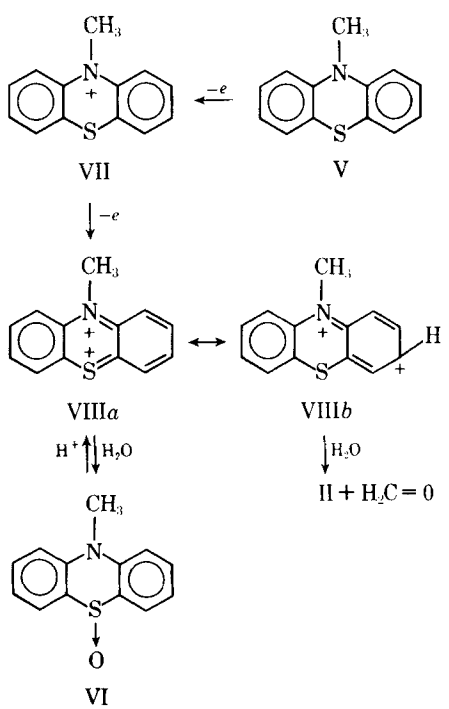

VII V VIIIa VIIIb VI

Scheme I

Table I—Apparent First-Order Rate Constants for the Degradation of I (k) and for the Appearance of II (k_3) and III (k_5) in 52.5% Ethanol at pH 2.8 at Various Temperatures

Temperature, °K	k, $hr^{-1} \times 10^3$	k_3, $hr^{-1} \times 10^4$	k_5, $hr^{-1} \times 10^3$
328	1.56	1.30	1.41
338	3.29	4.41	2.75
348	9.08	17.2	6.87
358	19.7	51.0	13.3

appearance of some degradation products (II–IV) in an oxygen-saturated acidic medium protected from light.

Since many commercial phenothiazines have side chains at the N-10 position, 10-methylphenothiazine (V, Scheme I) was synthesized and its degradation was investigated as a model compound. The oxidation potential of V was reported to be 150 mv higher than that of phenothiazine (2, 9), with 10-methylphenothiazine 5-oxide (VI) and 3*H*-phenothiazine-3-one (II) as the degradation products (10). The quantitative aspects of this degradation were not investigated.

In the current work, these products were synthesized and the influence of pH and temperature on the degradation rate was investigated after the degradation products were identified.

EXPERIMENTAL

Materials—Phenothiazine[1] gave a single spot using several TLC solvent systems and was used as supplied. Compound II, phenothiazine 5-oxide (III), and 7-(10′-phenothiazinyl)-3*H*-phenothiazine-3-one (IV) were prepared as previously described (8).

Compounds V (10, 11) and VI (10, 12) were synthesized as described in the literature. Compound V was recrystallized from ethanol, mp 100–101.5° [lit. (10, 11) mp 100.5–101.4°]. Compound VI was recrystallized from water, mp 194–196° [lit. (10, 12) mp 194–196°]. The structures were confirmed by IR and NMR spectroscopy.

All other materials were reagent grade, and deionized water was used throughout this study.

Isolation and Identification of Degradation Products—Compound V was dissolved in 52.5% ethanol, buffered to pH 4.7 (13), and stored in the dark at 85° for 5 days after saturation with oxygen. The products were extracted with carbon tetrachloride and isolated following TLC as described previously (8). Three zones, A, B, and C, were seen at R_f 0.80, 0.65, and 0.25, respectively.

Zone A was compared with V on the following TLC systems: silica gel GF_{254} and ether–petroleum ether (1:3), silica gel GF_{254} and acetone–6 *N* ammonia (50:1), and silica gel GF_{254} and chloroform. In all cases, V and Zone A behaved similarly; they had similar IR and NMR spectra, and the mixed melting point was 99–101°.

Zone B was compared with II in the same chromatographic systems. In all cases, Zone B and II behaved similarly; they had similar IR and NMR spectra, and the mixed melting point was 159–162°.

Zone C was compared with VI in the following TLC systems: silica gel GF_{254} and acetone–6 *N* ammonia (50:1), silica gel GF_{254} and ether–petroleum ether (1:3), silica gel GF_{254} and acetone–chloroform (3:2), and basic aluminum oxide and chloroform. In all cases, Zone C and VI behaved identically; they had similar IR and NMR spectra, and the mixed melting point was 193–196°. Compounds II and VI were the only degradation products of V found.

Methods—Phenothiazine was dissolved to a concentration of 500 μg/ml in a mixture of ethanol and a sodium acetate–hydrochloric acid buffer (13). The pH of this solution was measured[2] at 75°. The solution was placed in small screw-capped bottles, saturated with oxygen, and kept in an oxygen atmosphere in the dark at a fixed temperature.

Compounds I, II, and IV were determined spectrophotometrically after extraction from the reaction mixture with carbon tetrachloride and separation on a column of acidic alumina as previously described (14).

[1] Schuchardt, Munchen, Germany.

[2] The pH meter was calibrated at 75° with aqueous buffers of the National Bureau of Standards.

Table II—Rate Constants for the Disappearance of I (k) and the Appearance of II (k_3) and III (k_5) in 52.5% Ethanol at 75° at Various pH Values

pH	k, $hr^{-1} \times 10^3$	k_3, $hr^{-1} \times 10^4$	k_5, $hr^{-1} \times 10^3$
1.4	8.95	5.37	8.06
1.7	9.09	4.55	8.18
2.2	9.05	7.24	7.51
2.8	9.08	17.3	6.90
3.2	9.01	18.0	6.49
3.8	9.18	18.4	6.33
4.2	9.15	19.3	6.22
4.7	9.13	20.3	6.21
5.1	9.21	20.3	6.26
5.9	9.11	17.3	6.56
6.9	8.83	9.7	7.32

Compound III could be determined polarographically without isolation from the reaction mixture (14). The influence of temperature, pH, and ethanol concentration (weight per weight) on the degradation rate was followed in this manner.

The degradation kinetics of V were studied similarly. In this case, II was determined quantitatively as previously described (14) but without the chromatographic stage; V was determined by high-pressure liquid chromatography[3] using a silica[4] column and a UV detector. The solvent was a mixture of methanol and water (65:35) with a flow rate of 1 ml/min, and phenothiazine was the internal standard. The only other degradation product, VI, was determined by difference.

RESULTS AND DISCUSSION

Phenothiazine Degradation—*Temperature*—Under all circumstances, the degradation was always first order with respect to phenothiazine. Table I gives the observed rate constants at various temperatures for the oxidation in 52.5% ethanol at pH 2.8. The Arrhenius plot gives an E_a of 20.4 kcal/mole. This energy of activation includes a term for the variation of the oxygen solubility with temperature. The decreased solubility of oxygen with increasing temperature is partially compensated for by the increased solubility due to increased oxygen pressure above the solution as the temperature is raised.

If II–IV are formed by parallel reactions, then their appearance should satisfy the following equation (15):

$$A_i = A_0 + \frac{k_i}{k} P_0 (1 - e^{-kt}) \qquad \text{(Eq. 1)}$$

where A_i is the concentration of the degradation product at time t; P_0 and A_0 are the initial concentrations of phenothiazine and the degradation product, respectively; k is the first-order rate constant for phenothiazine degradation; and k_i is the first-order rate of appearance of A. A plot of A_i against $(1 - e^{-kt})$ should give a straight line if parallel re-

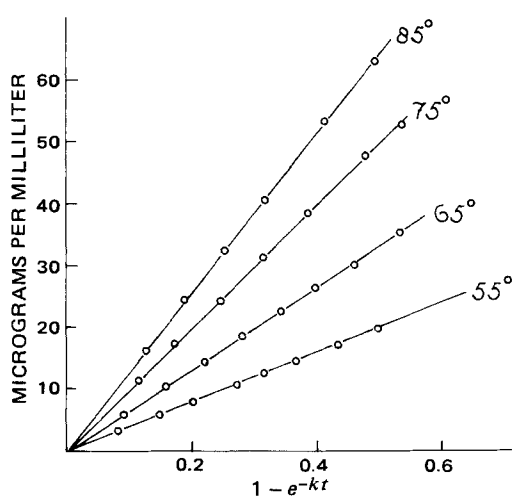

Figure 1—*Amount of II formed as a function of time at various temperatures in 52.5% ethanol at pH 2.8.*

[3] Model ALC/GPC 202/600, Waters Associates, Milford, Mass.

[4] Corasil C_{18}, Waters Associates, Milford, Mass.

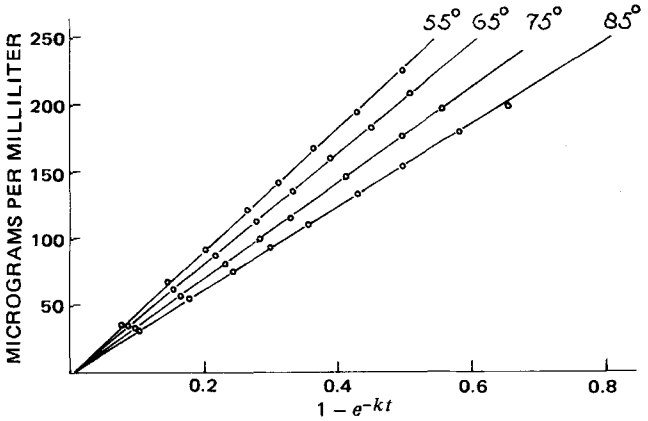

Figure 2—*Amount of III formed as a function of time at various temperatures in 52.5% ethanol at pH 2.8.*

action kinetics are obeyed, the value of the slope allowing k_i to be calculated.

Figures 1–3 show the plots for II, III, and IV, respectively, as a function of temperature. Compounds II and III seem to be formed *via* parallel reactions whereas IV does not; an intermediate product probably is involved in this latter case. The effects of temperature on the slopes in Figs. 1 and 2 are clearly very different, indicating that temperature greatly influences the amount of II and III formed.

The derived reaction rate constants for the appearance of II and III as a function of temperature are given in Table I. The Arrhenius plot gives an E_a of 17.9 kcal/mole for III and 29.2 kcal/mole for II. Table I also shows that III is the major degradation product.

Influence of pH—Table II lists the k, k_5, and k_3 values at different pH levels at a constant temperature of 75°. The values for k_3 at pH 1.4 and 1.7 are inaccurate because of the instability of II at these pH values; the values are calculated from the initial slope of the A_3 *versus* $(1 - e^{-kt})$ plot, because the plot is only a straight line in the early stages of the degradation at these pH values. Table II shows that phenothiazine degradation is pH independent, but at pH 4.7 there is a maximum in the formation of II and a minimum in the formation of III. This result could be due to the formation of II from III at this pH, so a solution of III in 52.5% ethanol at pH 4.7 was saturated with oxygen and assayed at 24, 48, 72, 96, and 120 hr. The recovery of III was 101, 101, 100, 100, and 99%, respectively, which clearly shows that the minimum in the formation of III is not due to its own instability.

The formation of IV was complex, and no rate constant for the formation could be measured; however, some idea of the influence of pH could be obtained by determining the amount formed during one half-life of phenothiazine as a function of pH. Figure 4 shows a maximum in the

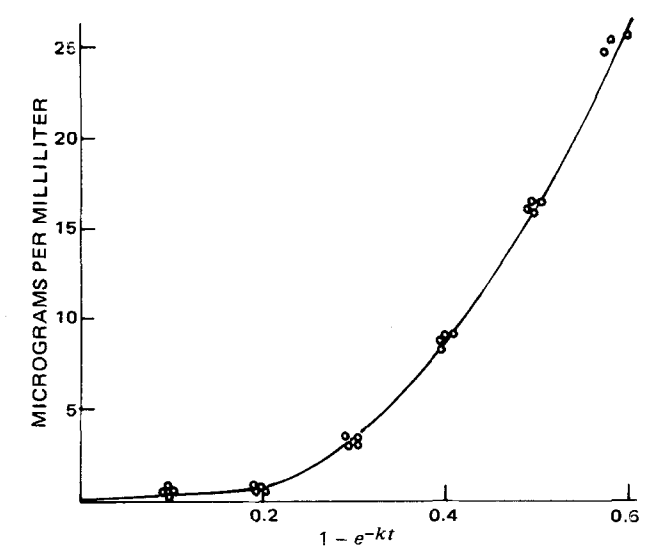

Figure 3—*Amount of IV formed as a function of time at various temperatures in 52.5% ethanol at pH 2.8.*

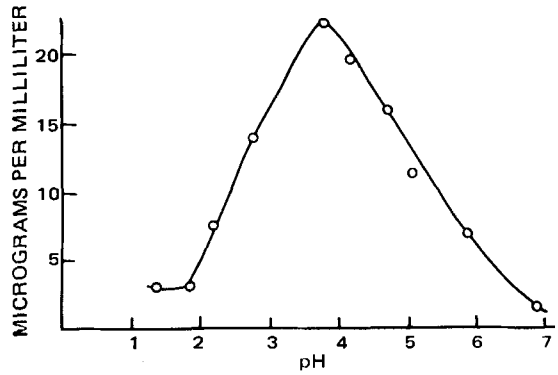

Figure 4—*Amount of IV formed during one half-life of I as a function of pH in 52.5% ethanol at 75°.*

formation at about pH 3.8.

Influence of Ethanol Concentration—Table III lists the k and k_3 values and the amounts of IV formed during one half-life of phenothiazine at pH 4.7 and 75° as a function of the ethanol concentration. The overall disappearance rate decreased with an increasing amount of ethanol in the solution, paralleling the decrease in oxygen solubility in the solvent. Both k_3 and the amount of IV produced increased with increasing ethanol concentrations. Above 62% ethanol, all changes were very small. Changes in ethanol concentration did not appear to alter significantly the amount of III, the major degradation product, formed.

These results show that II and III are formed from I by parallel reactions but do not elucidate the mechanism for the formation of the dimer. The dimer can be formed by at least two mechanisms: a coupling between I and II and a dimerization of I and its subsequent oxidation. An attempt to elucidate the total mechanism of degradation is reported in a companion paper (16).

Degradation of V—Under all conditions studied, V appears to degrade by a first-order process. Compounds II and VI, the only degradation products, seem to appear by parallel reactions. Treating the kinetic data as described for I gives the rate constants for the degradation of V (k) and for the formation of II (k_3) and VI (k_5) in 52.5% ethanol at pH 4.7 (Table IV). The pH has no influence on the degradation rate of V but does influence k_3 and k_5 and thus the relative amounts of degradation products formed (Table V).

Scheme I gives a probable mechanism for the degradation of V. It is oxidized in two steps to the phenazothionium ion that exists in two mesomeric forms, VIII*a* and VIII*b*, which hydrolyze to VI and II, respectively. No hydrogen ions are involved in the formation of VIII from V, so the degradation is pH independent (Table V) and there is probably no general acid–base catalysis. The hydrolysis of the ion VIII*a* to VI, however, is reversed by hydrogen ions. Therefore, at lower pH values, some II is formed; but at pH 6.9, this amount was negligible. Table V shows that at pH 1.7 less II is formed than at pH 3.8; however, II is unstable at the lower pH.

At the lower pH, a small amount of 7-hydroxy-3*H*-phenothiazine-3-one is formed. The energy of activation for the degradation of V is 16.9

Table III—Rate Constants for the Degradation of I (k) and the Appearance of II (k_3) and the Amounts of IV Formed during One Half-Life of I at 75° at pH 4.7 at Various Ethanol Concentrations

Ethanol, %	k, $hr^{-1} \times 10^3$	k_3, $hr^{-1} \times 10^3$	IV, μg/ml
47.5	17.4	3.31	11.3
52.5	9.08	2.00	16.2
62.0	6.40	1.60	34.5
72.7	6.19	1.55	32.5

Table IV—Rate Constants for the Degradation of V and the Appearance of II (k_3) and VI (k_5) in 52.5% Ethanol at pH 4.7

Temperature, °K	k, $hr^{-1} \times 10^4$	k_3, $hr^{-1} \times 10^4$	k_5, $hr^{-1} \times 10^4$
358	14.3	7.1	7.2
353	10.6	4.5	6.1
348	7.5	2.9	4.6
343	5.1	1.4	3.7

Table V—Rate Constants for the Degradation of V and the Appearance of II (k_3) and VI (k_5) in 52.5% Ethanol at 85°

pH	k, $hr^{-1} \times 10^3$	k_3, $hr^{-1} \times 10^3$	k_5, $hr^{-1} \times 10^3$
1.7	1.37	0.58	0.79
3.8	1.30	0.75	0.55
4.7	1.43	0.70	0.73
6.9	1.27	—	1.27

kcal/mole; for the formation of VI and II, it is 10.3 and 26.7 kcal/mole, respectively. This large difference results because VIII*b* is much less favored than VIII*a*, as in the degradation of I.

Comparison of the rate constants for the degradation of I and V under the same conditions shows that V is less easily oxidized. This finding is unexpected because the introduction of a methyl group should increase the electron density in the ring system and, therefore, favor the loss of an electron. This explanation can be a steric effect. Phenothiazines are bent around the nitrogen–sulfur axes (17), resulting in two possible conformations. In one conformation, the lone pair on the nitrogen can easily interact with π electrons of the ring system; in the other, the lone pair is forced outside the system. In I itself, the configuration is such that interaction is possible; however, in V, the lone pair is forced outside the system. The methyl group thus decreases the electron density in the aromatic system and increases the stability.

REFERENCES

(1) L. Michaelis and S. Granick, *J. Am. Chem. Soc.*, **64**, 1861 (1942).

(2) J. P. Billon, *Ann. Chim. Fr.*, **7**, 183 (1962).

(3) H. J. Shine and E. E. Mach, *J. Org. Chem.*, **30**, 2130 (1965).

(4) T. N. Tozer and L. D. Tuck, *J. Pharm. Sci.*, **54**, 1169 (1965).

(5) Y. Tsujino, *Tetrahedron Lett.*, **1968**, 2545, 4111.

(6) *Ibid.*, **1969**, 763.

(7) P. Hanson and R. O. C. Norman, *J. Chem. Soc. Perkin Trans. 2*, **1973**, 264.

(8) H. Roseboom and J. A. Fresen, *Pharm. Acta Helv.*, **50**, 55 (1975).

(9) J. C. Craig and M. E. Tate, in "Progress in Drug Research," vol. 3, E. Jucker, Ed., Birkhäuser, Basel, Switzerland, 1961, p. 75.

(10) C. D. M. ten Berge and C. H. P. Bruins, *Pharm. Weekbl.*, **104**, 1433 (1969).

(11) A. Burger and A. C. Schmalz, *J. Org. Chem.*, **19**, 1841 (1954).

(12) H. Gilman and R. O. Nelson, *J. Am. Chem. Soc.*, **75**, 5424 (1953).

(13) H. T. S. Britton, "Hydrogen Ions," vol. 1, 4th ed., Chapman and Hall Ltd., London, England, 1955, p. 357.

(14) H. Roseboom and J. A. Fresen, *Pharm. Acta Helv.*, **50**, 64 (1975).

(15) Z. G. Szabó, in "Comprehensive Chemical Kinetics," vol. 2, C. H. Bamford and C. F. H. Tipper, Eds., Elsevier, Amsterdam, The Netherlands, 1969, p. 14.

(16) H. Roseboom and J. H. Perrin, *J. Pharm. Sci.*, **66**, 1395 (1977).

(17) J. P. Malrieu and B. Pullman, *Theoret. Chim. Acta*, **3**, 293 (1964).

ACKNOWLEDGMENTS AND ADDRESSES

Received September 13, 1976, from the *Farmaceutisch Laboratorium Rijksuniversiteit Utrecht, Catharijnesingel 60, Utrecht, The Netherlands.*

Accepted for publication December 2, 1976.

* Present address: College of Pharmacy, University of Florida, J. H. Miller Health Center, Gainesville, FL 32610.

[x] To whom inquiries should be directed.

Mechanism for Phenothiazine Oxidation

H. ROSEBOOM [x] and J. H. PERRIN *

Abstract □ The mechanism of phenothiazine degradation was studied by following the degradation of 3,10′-diphenothiazine in ethanol–water mixtures as well as the electrochemical oxidation of phenothiazine. A mechanism, including the formation of an oxidized dimer and some polymers, is suggested.

Keyphrases □ Phenothiazine—electrochemical oxidation degradation in ethanol–water mixtures, mechanism suggested □ Oxidation—phenothiazine degradation in ethanol–water mixtures, mechanism suggested □ Degradation—phenothiazine in ethanol–water mixtures, mechanism suggested

The isolation and identification of some degradation products of phenothiazine were described previously (1), as were the kinetics of the oxidative degradation in an acidic medium (2). The degradation has been the subject of many investigations (3–9); however, no definite mechanism was established, particularly since 7-(10′-phenothiazinyl)-3*H*-phenothiazine-3-one was not recognized as a degradation product until recently (1, 2).

In this paper, further experiments to elucidate the mechanism of formation of 7-(10′-phenothiazinyl)-3*H*-phenothiazine-3-one (XIV) are described, and a mechanism for the overall oxidation is proposed (Scheme I).

EXPERIMENTAL

Materials—All materials were as previously described (2).

Phenothiazine (I) Oxidation in Presence of 3*H*-Phenothiazine-3-one (VII)—In a mixture of ethanol and water buffered with sodium acetate and hydrochloric acid, 500 μg of I/ml and 50 μg of VII/ml were dissolved. The solutions were saturated with oxygen, placed in screw-capped bottles, and stored in the dark at 75°. The solutions were assayed for I, VII, and XIV as described previously (10).

Oxidation of 3,10′-Diphenothiazine (IX*b*)—Solutions of 100 μg of IX*b*/ml were prepared and stored as described. The solution was extracted with carbon tetrachloride; the products were separated by TLC, using silica gel GF_{254} and developing with ether–petroleum ether (1:2). The products were assayed as described previously (10).

Electrochemical Oxidation of I—After dissolving 100 μg of I/ml in the buffered ethanol–water and flushing with nitrogen, a current–voltage curve[1] was recorded at various pH values, using a rotating platinum electrode and a silver–silver chloride reference electrode. Then I was oxidized at a constant potential[2], using a platinum working and auxiliary electrode and a silver–silver chloride reference electrode. The potential of the working electrode was 400 mv throughout this study.

The solution was stirred by bubbling nitrogen continuously through it. After completion of the reaction, the solution was allowed to stand in the dark in a nitrogen atmosphere until a permanent color was obtained.

[1] Polarograph E 44 S, Bruker, Brussels, Belgium.

[2] Potentiostat PRT 10-05, Tacussel, Villeurfanne, France.

Table V—Rate Constants for the Degradation of V and the Appearance of II (k_3) and VI (k_5) in 52.5% Ethanol at 85°

pH	k, $hr^{-1} \times 10^3$	k_3, $hr^{-1} \times 10^3$	k_5, $hr^{-1} \times 10^3$
1.7	1.37	0.58	0.79
3.8	1.30	0.75	0.55
4.7	1.43	0.70	0.73
6.9	1.27	—	1.27

kcal/mole; for the formation of VI and II, it is 10.3 and 26.7 kcal/mole, respectively. This large difference results because VIII*b* is much less favored than VIII*a*, as in the degradation of I.

Comparison of the rate constants for the degradation of I and V under the same conditions shows that V is less easily oxidized. This finding is unexpected because the introduction of a methyl group should increase the electron density in the ring system and, therefore, favor the loss of an electron. This explanation can be a steric effect. Phenothiazines are bent around the nitrogen–sulfur axes (17), resulting in two possible conformations. In one conformation, the lone pair on the nitrogen can easily interact with π electrons of the ring system; in the other, the lone pair is forced outside the system. In I itself, the configuration is such that interaction is possible; however, in V, the lone pair is forced outside the system. The methyl group thus decreases the electron density in the aromatic system and increases the stability.

REFERENCES

(1) L. Michaelis and S. Granick, *J. Am. Chem. Soc.*, **64**, 1861 (1942).

(2) J. P. Billon, *Ann. Chim. Fr.*, **7**, 183 (1962).

(3) H. J. Shine and E. E. Mach, *J. Org. Chem.*, **30**, 2130 (1965).

(4) T. N. Tozer and L. D. Tuck, *J. Pharm. Sci.*, **54**, 1169 (1965).

(5) Y. Tsujino, *Tetrahedron Lett.*, **1968**, 2545, 4111.

(6) *Ibid.*, **1969**, 763.

(7) P. Hanson and R. O. C. Norman, *J. Chem. Soc. Perkin Trans. 2*, **1973**, 264.

(8) H. Roseboom and J. A. Fresen, *Pharm. Acta Helv.*, **50**, 55 (1975).

(9) J. C. Craig and M. E. Tate, in "Progress in Drug Research," vol. 3, E. Jucker, Ed., Birkhäuser, Basel, Switzerland, 1961, p. 75.

(10) C. D. M. ten Berge and C. H. P. Bruins, *Pharm. Weekbl.*, **104**, 1433 (1969).

(11) A. Burger and A. C. Schmalz, *J. Org. Chem.*, **19**, 1841 (1954).

(12) H. Gilman and R. O. Nelson, *J. Am. Chem. Soc.*, **75**, 5424 (1953).

(13) H. T. S. Britton, "Hydrogen Ions," vol. 1, 4th ed., Chapman and Hall Ltd., London, England, 1955, p. 357.

(14) H. Roseboom and J. A. Fresen, *Pharm. Acta Helv.*, **50**, 64 (1975).

(15) Z. G. Szabó, in "Comprehensive Chemical Kinetics," vol. 2, C. H. Bamford and C. F. H. Tipper, Eds., Elsevier, Amsterdam, The Netherlands, 1969, p. 14.

(16) H. Roseboom and J. H. Perrin, *J. Pharm. Sci.*, **66**, 1395 (1977).

(17) J. P. Malrieu and B. Pullman, *Theoret. Chim. Acta*, **3**, 293 (1964).

ACKNOWLEDGMENTS AND ADDRESSES

Received September 13, 1976, from the *Farmaceutisch Laboratorium Rijksuniversiteit Utrecht, Catharijnesingel 60, Utrecht, The Netherlands.*

Accepted for publication December 2, 1976.

* Present address: College of Pharmacy, University of Florida, J. H. Miller Health Center, Gainesville, FL 32610.

[x] To whom inquiries should be directed.

Mechanism for Phenothiazine Oxidation

H. ROSEBOOM [x] and J. H. PERRIN *

Abstract □ The mechanism of phenothiazine degradation was studied by following the degradation of 3,10′-diphenothiazine in ethanol–water mixtures as well as the electrochemical oxidation of phenothiazine. A mechanism, including the formation of an oxidized dimer and some polymers, is suggested.

Keyphrases □ Phenothiazine—electrochemical oxidation degradation in ethanol–water mixtures, mechanism suggested □ Oxidation—phenothiazine degradation in ethanol–water mixtures, mechanism suggested □ Degradation—phenothiazine in ethanol–water mixtures, mechanism suggested

The isolation and identification of some degradation products of phenothiazine were described previously (1), as were the kinetics of the oxidative degradation in an acidic medium (2). The degradation has been the subject of many investigations (3–9); however, no definite mechanism was established, particularly since 7-(10′-phenothiazinyl)-3*H*-phenothiazine-3-one was not recognized as a degradation product until recently (1, 2).

In this paper, further experiments to elucidate the mechanism of formation of 7-(10′-phenothiazinyl)-3*H*-phenothiazine-3-one (XIV) are described, and a mechanism for the overall oxidation is proposed (Scheme I).

EXPERIMENTAL

Materials—All materials were as previously described (2).

Phenothiazine (I) Oxidation in Presence of 3*H*-Phenothiazine-3-one (VII)—In a mixture of ethanol and water buffered with sodium acetate and hydrochloric acid, 500 μg of I/ml and 50 μg of VII/ml were dissolved. The solutions were saturated with oxygen, placed in screw-capped bottles, and stored in the dark at 75°. The solutions were assayed for I, VII, and XIV as described previously (10).

Oxidation of 3,10′-Diphenothiazine (IX*b*)—Solutions of 100 μg of IX*b*/ml were prepared and stored as described. The solution was extracted with carbon tetrachloride; the products were separated by TLC, using silica gel GF_{254} and developing with ether–petroleum ether (1:2). The products were assayed as described previously (10).

Electrochemical Oxidation of I—After dissolving 100 μg of I/ml in the buffered ethanol–water and flushing with nitrogen, a current–voltage curve[1] was recorded at various pH values, using a rotating platinum electrode and a silver–silver chloride reference electrode. Then I was oxidized at a constant potential[2], using a platinum working and auxiliary electrode and a silver–silver chloride reference electrode. The potential of the working electrode was 400 mv throughout this study.

The solution was stirred by bubbling nitrogen continuously through it. After completion of the reaction, the solution was allowed to stand in the dark in a nitrogen atmosphere until a permanent color was obtained.

[1] Polarograph E 44 S, Bruker, Brussels, Belgium.

[2] Potentiostat PRT 10-05, Tacussel, Villeurfanne, France.

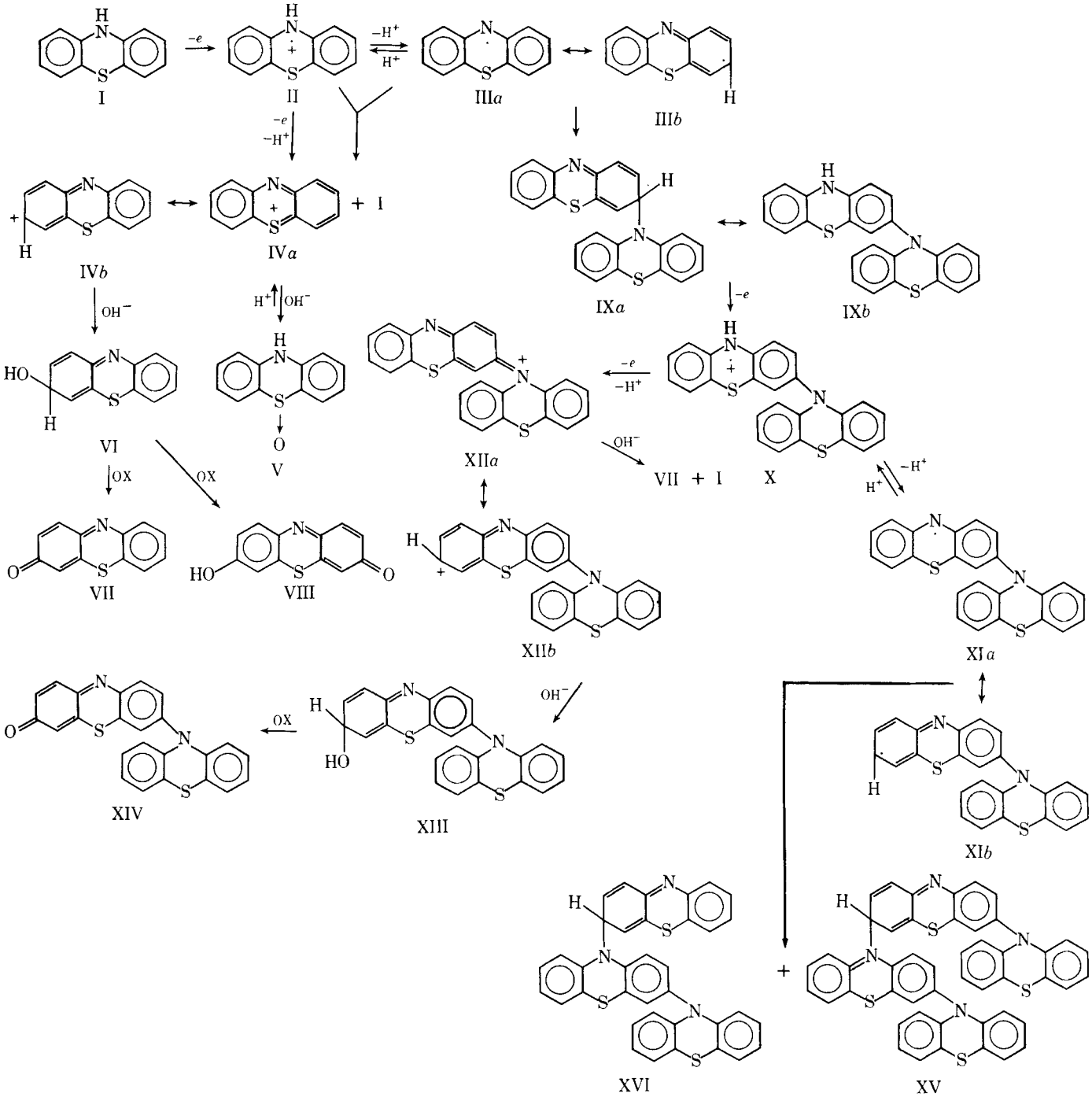

Scheme I

Then the solution was extracted, and the components were separated and analyzed for VII and XIV as described.

RESULTS

Oxidation of I in Presence of VII—The rate constants were determined as described previously (2) and were not significantly different from those obtained when no VII was added. The amount of XIV formed was not significantly different from the amount formed from I without the addition of VII. This result indicates that XIV is not formed from a coupling of I and VII.

Oxidation of IX*b*—The thin-layer chromatograms of partially oxidized IX*b* showed four spots, three of which were IX*b*, VII, and XIV. The fourth spot, with R_f 0.00, was colorless but turned green in daylight; the color was less intense after oxidation at low pH values. Figures 1 and 2 give the amounts of XIV and VII, respectively, formed as a function of time at different pH levels.

These figures show that IX*b* was completely oxidized in 80 hr. They also show the instability of VII and XIV at low pH values. Figure 3 shows the ultimate amount of VII and XIV formed from IX*b* as a function of pH. There was a maximum in the formation of XIV at pH 3.8 and of VII at pH 4.7. Table I shows the amounts of VII and XIV formed from IX*b*

Table I—Amounts of VII and XIV Formed on Oxidation of IX*b* at pH 4.7 and 75° at Various Ethanol Concentrations

Ethanol, % (w/w)	VII, μg/ml	XIV, μg/ml
47.5	24.2	25.5
52.5	22.1	24.4
62.0	24.5	25.5
72.5	25.5	23.6

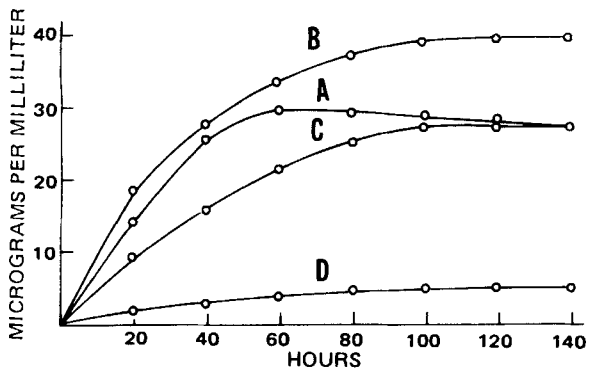

Figure 1—*Amount of XIV formed on oxidation of IX*b *in 52.5% ethanol at 75° at different pH levels as a function of time. Key: A, pH 1.7; B, pH 3.8; C, pH 4.7; and D, pH 6.9.*

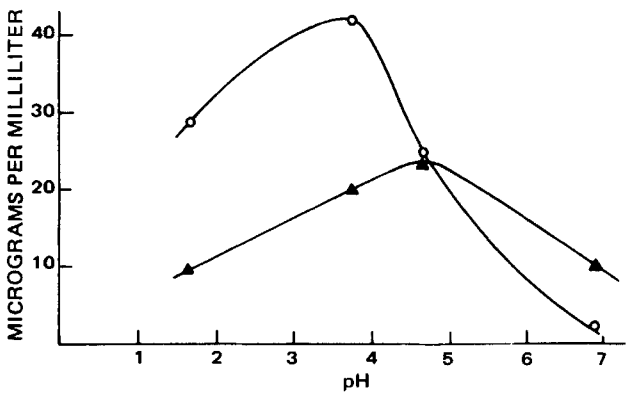

Figure 3—*Ultimate amount of XIV (○) and VII (△) formed from IX*b *in 52.5% ethanol at 75° as a function of pH.*

at different ethanol concentrations at pH 4.7 and 75°; ethanol had no significant influence on the amounts of products formed.

Electrochemical Oxidation of I—Figure 4 shows the current–voltage curves of I in 52.5% ethanol at various pH values. The half-wave potential of the first oxidation step was pH independent; the second half-wave potential was lowered at higher pH levels. Thin-layer chromatograms showed that, in all cases, V, VII, and XIV were formed. Two other spots were formed, both colorless but turning green in daylight; one had the chromatographic characteristics of IX*b* and the other had R_f 0.00.

Figure 5 shows the amounts of VII and XIV formed from the electrolysis of I as a function of pH, Fig. 6 gives the amounts as a function of the ethanol concentration in the solvent mixture, and Fig. 7 gives the amounts as a function of the working potential. The amount of VII produced increased with increasing pH, and there was a maximum in the formation of XIV at pH 4.7. The amounts of both products increased with increasing ethanol concentration, but this increase was less at higher concentrations. The amounts formed increased with increasing working potential but reached a plateau at 450 mv.

DISCUSSION

Scheme I represents the most probable mechanism for the oxidation of I. The first step is the loss of an electron from I to give the cationic free radical II. The radical can lose a proton to give the neutral radical III, lose a proton and an electron to give the phenazothionium ion IV*a*, and disproportionate together with III to give I and IV*a*, as shown by Hanson and Norman (8).

The phenazothionium ion exists in two mesomeric forms, IV*a* and IV*b*, which can hydrolyze to the 5-oxide (V) and to 3-hydroxyphenothiazine (VI). Compound VI is rapidly oxidized to 3*H*-phenothiazine-3-one (VII) and 7-hydroxy-3*H*-phenothiazine-3-one (VIII). The existence of the neutral radical III was first confirmed by Gilbert *et al.* (9), whose calculations of spin densities showed the largest densities to be located at the nitrogen atom and at C-3 and C-7. This situation is represented by the equilibrium between III*a* and III*b*.

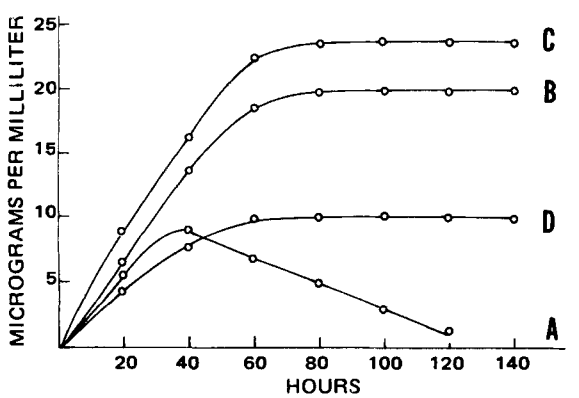

Figure 2—*Amount of VII formed on oxidation of IX*b *in 52.5% ethanol at 75° at different pH levels as a function of time. Key: A, pH 1.7; B, pH 3.8; C, pH 4.7; and D, pH 6.9.*

The formation of the dimer IX*b* has been reported to proceed *via* IX*a* (6, 8). This dimer can lose an electron to give the radical X, which can then behave like radical II, forming the ion XII*a* and the neutral radical XI*a*. The disproportionation of X and XI to give XII*a* and IX*b* is not shown for reasons of simplicity. The existence of XII*a* has been confirmed (8). Compound XII*a* hydrolyzes to I and VII; its mesomeric form XII*b* hydrolyzes to a 7-hydroxy dimer (XIII), which is rapidly oxidized to XIV.

The equilibrium between XI*a* and XI*b* is in principle the same as that between III*a* and III*b*. These radicals can give several products; two possibilities, shown in Scheme I, are the trimer XVI and the tetramer XV. Although these products were not isolated, their formation is analogous to that of the dimer IX; on oxidation of IX*b*, at least one product is formed that turns green in air, as do I and IX*b*. Also, the amounts of VII and XIV produced on oxidation of IX*b* do not account for all of the starting material, especially at higher pH values (Fig. 2). Raising the pH causes a shift in the equilibrium between X and XI, so that less of the ion XII*a* is formed and subsequently less VII and XIV. Compound VII is formed *via* two pathways, from the phenazothionium ion IV and from the ionic dimer XII. That the latter process occurs is proven by the appearance of VII from the oxidation of IX*b*.

The kinetic measurements of Ref. 2 support Scheme I. More VII and less V were formed at higher temperatures, and the relative amount of XIV formed was independent of temperature. The degradation of I was independent of pH, and there were a minimum in the formation of V at pH 4.7 and maxima in the formation of VII and XIV at pH's 4.7 and 3.8, respectively.

Increasing the percentage of ethanol in the solvent mixture decreases the degradation rate of I and increases the relative amounts of VII and XIV, up to a given ethanol concentration. The relative increase in the formation of VII at higher temperatures suggests that the mesomer IV*a* is energetically favored over mesomer IV*b*, so the formation of VII has a higher energy of activation than does the formation of V. The temperature independence of the amount of XIV formed is probably due to a shift of the acid–base equilibrium of II and III being compensated for by a comparable shift in the equilibria between X and XI, resulting in a temperature independence of the formation of the ion XII*a* and, therefore, of XIV.

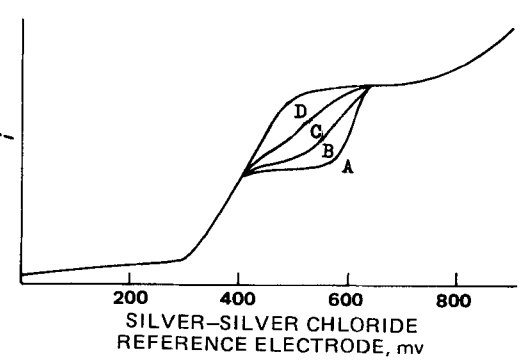

Figure 4—*Current* (i)*–voltage curves of I in 52.5% ethanol at various pH levels. Key: A, pH 1.7; B, pH 3.8; C, pH 4.7; and D, pH 6.9.*

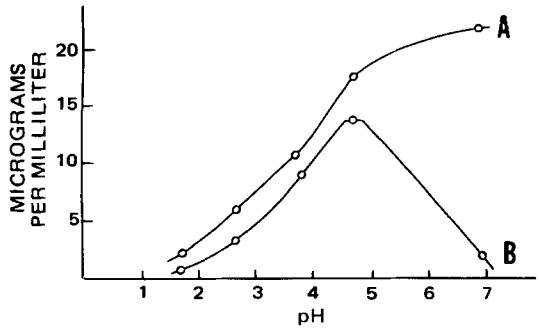

Figure 5—*Amounts of VII (A) and XIV (B) formed on electrolysis of I in 52.5% ethanol as a function of pH.*

The first step of the oxidation of I does not involve hydrogen ions, so the half-wave potential of the first step of the electrochemical oxidation (Fig. 4) and the degradation of I is pH independent. As a result of the acid–base equilibrium between II and III, there is more dimerization, so less IV and V are formed at higher pH values. At still higher pH values, the half-wave potential of the second oxidation step (II → IV) is lowered to such an extent that there are a large increase in the velocity of this step and a resultant increase in the formation of V. The net result is a minimum in the formation of V at pH 4.7 (2).

Because VII is produced *via* two mechanisms, the influence of pH is more difficult to predict; however, some estimate of the amounts produced by both pathways can be made from the data on the oxidation of IX*b*. The amount of VII produced *via* XII*a* is calculated from the ratio of the amounts of VII to XIV produced on the oxidation of IX*b*; this ratio is multiplied by the amount of XIV formed on oxidation of I. This value, subtracted from the total amount of VII, gives the amount produced *via* IV. The instability of the products at low pH values makes these calculations only approximate. Figure 8 shows the decrease in the amount of VII formed in one half-life of phenothiazine as the pH is raised, in spite of the fact that there is an increase in the formation of IV at pH levels above 4.7. This result is due to the pH dependence of the reaction IV → V (4, 5), favoring the formation of V at higher pH's.

At pH 4.7, there are a minimum in the formation of IV and a maximum in the formation of the dimer IX. On oxidation of the dimer, the cationic radical X is formed, which converts to the neutral radical XI and the ion XII*a*. At higher pH values, the formation of XII*a* is decreased, so the maximum in the formation of XII*a* from I is at a lower pH than the maximum in the formation of IX. From the oxidation of IX*b*, it is seen that at higher pH values the ratio of VII to XIV increases. Therefore, the maximum in the formation of XIV is at a lower pH than the maxima in the formation of XII and of VII. The maximum in the formation of XIV is at pH 3.8; for VII and IX*b*, it is at pH 4.7.

Increased ethanol concentration in the solvent mixture favors the formation of the nonionic III, resulting in more dimerization and more VII and XIV. However, at still higher ethanol concentrations, XI is favored over X, resulting in no further increase in the amounts of VII and XIV.

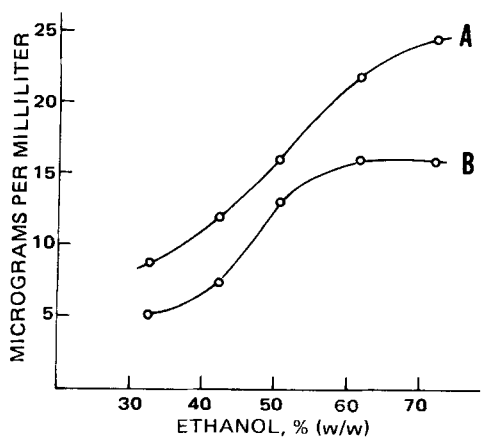

Figure 6—*Amounts of VII (A) and XIV (B) formed on electrolysis of I at pH 4.7 as a function of the ethanol concentration.*

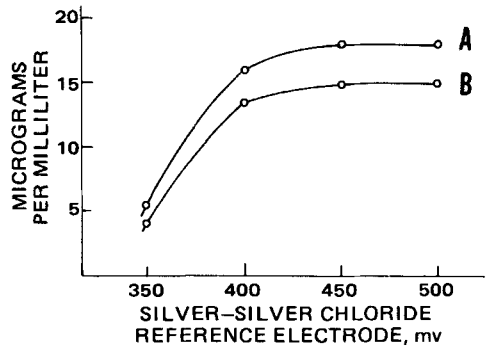

Figure 7—*Amounts of VII (A) and XIV (B) formed on electrolysis of I in 52.5% ethanol at pH 4.7 as a function of the potential of the working electrode.*

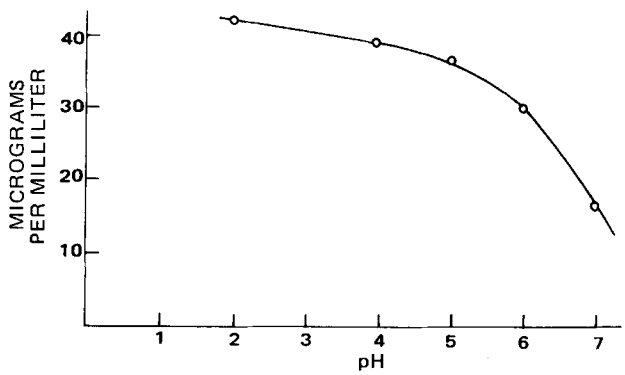

Figure 8—*Amount of VII formed* via *the ion IV in one half-life of I as a function of pH, calculated as described in the text.*

In the electrochemical oxidation of I, the rate-determining step is no longer the formation of the radical II. When the oxidation potential is high enough to oxidize I but not II, there is buildup of II. At high pH values, the radical is deprotonated, allowing considerable dimerization. The rapid oxidation of IX*b* suggests that it, as well as X, has a low oxidation potential and that the formation of XII*a* increases with pH. As the pH is raised, there is an increase of VII at the expense of XIV on electrochemical oxidation, resulting in a maximum in the formation of XIV (Fig. 5).

If it is assumed that increasing the oxidation potential increases the concentration of II, then dimerization and the formation of VII and XIV increase up to a maximum (Fig. 7).

REFERENCES

(1) H. Roseboom and J. A. Fresen, *Pharm. Acta Helv.*, **50,** 55 (1975).

(2) H. Roseboom and J. H. Perrin, *J. Pharm. Sci.*, **66,** 1392 (1977).

(3) J. P. Billon, *Ann. Chim. Fr.*, **7,** 183 (1962).

(4) H. J. Shine and E. E. Mach, *J. Org. Chem.*, **30,** 2130 (1965).

(5) T. N. Tozer and L. D. Tuck, *J. Pharm. Sci.*, **54,** 1169 (1965).

(6) Y. Tsujino, *Tetrahedron Lett.*, **1968,** 2545, 4111.

(7) *Ibid.*, **1969,** 763.

(8) P. Hanson and R. O. C. Norman, *J. Chem. Soc. Perkin Trans. 2,* **1973,** 264.

(9) B. C. Gilbert, P. Hanson, R. O. C. Norman, and B. T. Sutcliffe, *Chem. Commun.*, **1966,** 161.

(10) H. Roseboom and J. A. Fresen, *Pharm. Acta Helv.*, **50,** 64 (1975).

ACKNOWLEDGMENTS AND ADDRESSES

Received September 13, 1976, from the *Farmaceutisch Laboratorium Rijksuniversiteit Utrecht, Catharijnesingel 60, Utrecht, The Netherlands.*

Accepted for publication December 2, 1976.

* Present address: College of Pharmacy, University of Florida, J. H. Miller Health Center, Gainesville, FL 32610.

ˣ To whom inquiries should be directed.

Effect of Aspirin on a Subtoxic Dose of ^{14}C-Acetaminophen in Mice

L. W. WHITEHOUSE ˣ, C. J. PAUL, L. T. WONG, and B. H. THOMAS

Abstract □ The interaction of ^{14}C-acetaminophen, 150 mg/kg (20 μCi/kg), and aspirin, 200 mg/kg po, was studied in male mice. The radiolabel was rapidly absorbed from the GI tract, achieving maximum blood levels 0.25 hr after oral dosing. Radioactivity in the blood equilibrated rapidly with the tissues and was concentrated in the liver and kidney. At 14 hr, most of the dose was eliminated in urine as the glucuronide, cysteine, sulfate, free drug, and mercapturate. Pretreatment with aspirin tended to reduce the rate and extent of acetaminophen absorption and altered the percentage of the dose excreted in the urine as sulfate, mercapturate, glucuronide, and cysteine. Interpretation of these data toxicologically as an indication of the potentiation of either toxicity or protection was not possible.

Keyphrases □ Aspirin—effect on absorption, excretion, and metabolism of acetaminophen, radiochemical analysis, mice □ Acetaminophen—absorption, excretion, and metabolism, effect of aspirin, radiochemical analysis, mice □ Absorption—acetaminophen, effect of aspirin, radiochemical analysis, mice □ Excretion—acetaminophen, effect of aspirin, radiochemical analysis, mice □ Metabolism—acetaminophen, effect of aspirin, radiochemical analysis, mice □ Radiochemistry—analysis, effect of aspirin on absorption, excretion, and metabolism of acetaminophen, mice □ Analgesics—effect of aspirin on absorption, excretion, and metabolism of acetaminophen, radiochemical analysis, mice

Acetaminophen, a widely used nonnarcotic analgesic, is remarkably safe in therapeutic doses. Recently, it has been used in combination with aspirin in analgesic formulations. In view of a previous report of an aspirin–phenacetin metabolic interaction (1) and the fact that acetaminophen is the principal metabolite of phenacetin, a survey of some animal species was initiated to determine if aspirin affected the fate of ^{14}C-acetaminophen.

In the rat, absorption and metabolism were both markedly altered by aspirin (2); in the guinea pig, aspirin appeared to have its greatest inhibitory effect on biliary and urinary excretion (3). As a continuation of this survey, the fate of a subtoxic dose of ^{14}C-acetaminophen alone and in the presence of aspirin was examined in the mouse, a species markedly more susceptible to acetaminophen-induced hepatotoxicity than rats or guinea pigs (4).

EXPERIMENTAL

Materials—Carboxyl-labeled ^{14}C-aspirin[1], specific activity 122 μCi/mg, and uniformly ring-labeled ^{14}C-acetaminophen[2], specific activity 44.64 μCi/mg, were synthesized. Gum tragacanth[3] and unlabeled aspirin[4] and acetaminophen[5] were obtained commercially. Swiss Webster male mice, 28 ± 3 g, were purchased locally[6].

Methods—Animals were acclimatized for at least 1 week before each experiment; both food and water were supplied *ad libitum*. Sixteen hours prior to each experiment, food, but not water, was withdrawn.

Establishing Subtoxic Dose—In view of the much higher toxicity of acetaminophen in the mouse compared to the rat or guinea pig (4), it was essential to establish that 150 mg/kg was a subtoxic level of acetaminophen. As an index of toxicity, plasma levels of glutamic–oxalacetic transaminase (EC 2.6.1.1) and glutamic–pyruvic transaminase (EC 2.6.1.2) were monitored. Mice were pretreated with vehicle or aspirin (200 mg/kg po) and then treated with acetaminophen (150 or 250 mg/kg po) 30 min later as previously described (3).

Sixteen hours following acetaminophen administration, the mice were decapitated and blood was collected in heparinized Natelson blood-collecting tubes. Blood samples were centrifuged in a clinical centrifuge. The plasma was assayed for transaminases at 37° by the UV method of Henry *et al.* (5), using standard assay reagents[7] and a biochromatic analyzer[8]. Control transaminase levels were determined using plasma from mice not receiving treatment.

Blood Profiles—Radiolabeled aspirin, 200 mg/kg po, was administered as a 0.25% gum tragacanth suspension at 25 μCi/kg (10 ml/kg) to determine the profile of ^{14}C-aspirin-derived radioactivity in the blood. All subsequent experiments were performed with cold aspirin, which was administered at 200 mg/kg po 30 min prior to dosing with ^{14}C-acetaminophen. Radiolabeled acetaminophen was administered at 150 mg/kg po (20 μCi/kg) as described previously (3). Mice dosed intravenously (tail vein) received a solution of acetaminophen (150 mg/kg) at 7 ml/kg containing 10% ethanol. Duplicate blood samples were collected at various times and processed as reported previously (6).

Tissue Distribution and Urinary Excretion—The distribution of orally and intravenously administered ^{14}C-acetaminophen in blood (10 μl) and tissues (25–100 mg) from vehicle- and aspirin- (200 mg/kg) pretreated mice, collected at 0.25, 1, and 4 hr following ^{14}C-acetaminophen (150 mg/kg), was examined by reported methods (3, 6). Urine was collected from groups of eight orally dosed mice housed in metabolism cages. The volume of urine excreted per animal, the urinary concentration of total carbon-14 expressed as micrograms per milliliter, and the cumulative total carbon-14 excreted were determined by liquid scintillation counting (6).

Urinary Metabolites—Acetaminophen and its metabolites were separated using the alkaline paper chromatography system (System C) described by Shahidi (7) and modified by Thomas *et al.* (2). Some urine samples were also chromatographed on Sephadex gel G-10 as previously described (2). In addition to the chromatographic separation of neat (unadulterated) urine, aliquots of β-glucuronidase[9]-treated urine were chromatographed on paper (2).

The cysteine conjugate was identified in mouse urine, which had been desalted by passing it through an ion-exchange column[10]. Following the elution of salts and other highly water-soluble impurities with distilled water, radioactivity was eluted with methanol. The eluent was dried under a nitrogen stream, taken up in water, and separated by Sephadex gel G-10 column chromatography (2). The fractions collected were monitored for both a positive ninhydrin test and radioactivity.

The fractions giving a positive ninhydrin test and containing high concentrations of radioactivity were lyophilized and chromatographed in the alkaline system (2) and the 1-butanol–acetic acid–water (4:1:1) system (acidic system) reported previously (8). In addition, a mass spectrum of the lyophilized sample was obtained by the direct insert probe method using a low-resolution mass spectrometer[11] at an ionization energy of 80 ev and a source temperature of 210°.

Data Analysis—With the exception of the paper and Sephadex gel G-10 chromatography data, isotopic assays were performed in duplicate. Transaminase activities were also determined on duplicate plasma samples. Means and standard errors were computed from averaged data; statistical significance was determined by the unpaired Student t test, with $p < 0.05$ being considered significant. In cases where percentages were compared, arc–sin transformed data were used (9).

[1] Amersham/Searle Corp., Arlington Heights, IL 60005.
[2] Mallinckrodt, St. Louis, MO 63160.
[3] Fisher Scientific Co. Ltd., Toronto, Canada.
[4] B.D.H. Canada Ltd., Toronto, Canada.
[5] Eastman Kodak Co., Rochester, N.Y.
[6] Biobreeding Labs of Canada Ltd., Ottawa, Canada.
[7] Abbott Laboratories, Montreal, Canada, and Boehringer Mannheim Corp., New York, NY 10017.
[8] ABA-100, Abbott Scientific Products Division, South Pasadena, CA 91030.
[9] Ketodase, Warner-Chilcott, Morris Plains, NJ 07950.
[10] Amberlite XAD-2, Polystyrene Polymers, B.D.H. Canada Ltd., Toronto, Canada.
[11] Hitachi Perkin-Elmer RMS-4.

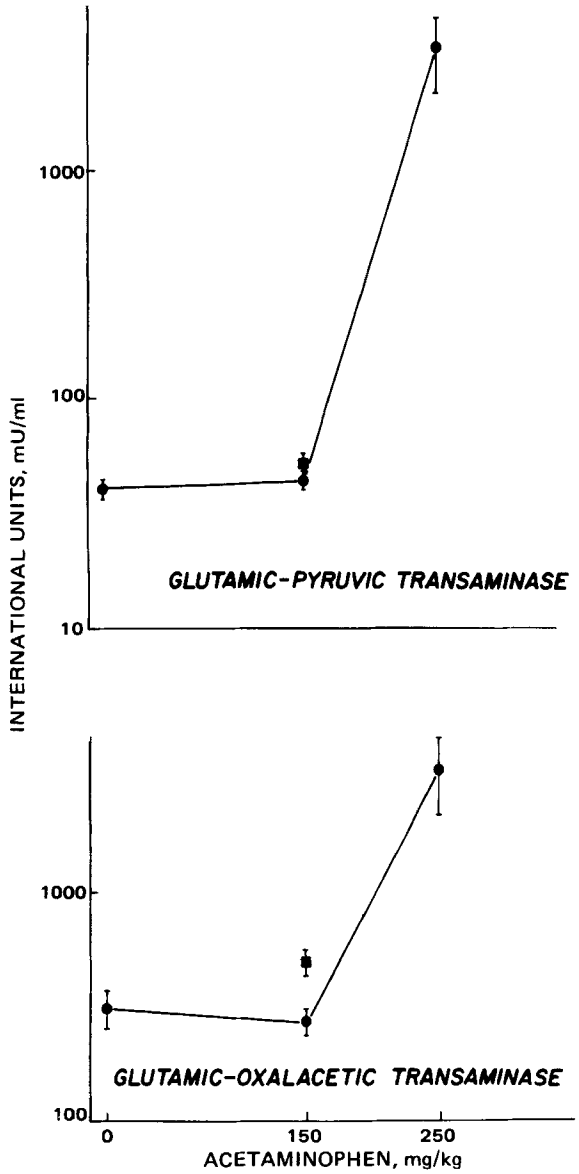

Figure 1—*Plasma transaminase dose–response curves in mice following administration of acetaminophen, 150 mg/kg po. Plasma glutamic–pyruvic transaminase and glutamic–oxalacetic transaminase levels were determined 16 hr following acetaminophen administration to mice orally pretreated with vehicle (●) or aspirin, 200 mg/kg (■), 0.5 hr prior to dosing with acetaminophen. Values are means ±SE from at least seven animals.*

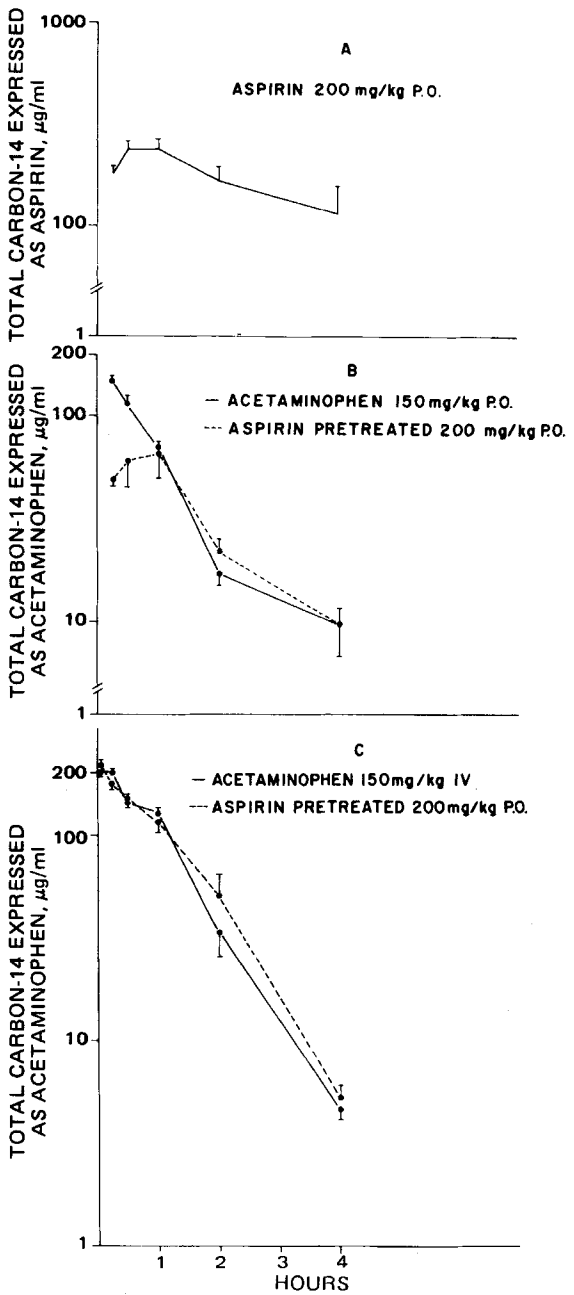

Figure 2—*Blood profiles of radioactivity following drug administration obtained from mice receiving: A, ^{14}C-aspirin, 200 mg/kg po; B, ^{14}C-acetaminophen, 150 mg/kg po; or C, ^{14}C-acetaminophen, 150 mg/kg iv. In both B and C, mice were orally pretreated with either vehicle (—) or cold aspirin, 200 mg/kg (- - -), 0.5 hr prior to receiving ^{14}C-acetaminophen. Values are means ±SE from three to five animals. In B, differences are significant at 0.25 and 0.5 hr at $p < 0.001$ and $p < 0.05$, respectively.*

RESULTS

As a criterion for establishing a subtoxic dose of acetaminophen, plasma transaminase activities were monitored and the dose–response was determined (Fig. 1). Vehicle-pretreated mice were dosed with different concentrations of acetaminophen to determine a "no effect level." At 150 mg/kg, vehicle-pretreated mice possessed plasma levels not significantly different from control animals; 250 mg/kg statistically elevated plasma transaminase levels, suggesting that this dose was hepatotoxic.

To ensure that 150 mg/kg remained a "no effect level" in the presence of aspirin, plasma transaminases were likewise monitored in aspirin-pretreated mice. Plasma glutamic–oxalacetic and glutamic–pyruvic transaminases were not significantly altered from control values (Fig. 1), establishing that acetaminophen, 150 mg/kg, alone or in combination with aspirin, 200 mg/kg, was a subtoxic dose.

Radioactivity in the blood of ^{14}C-aspirin-treated mice peaked 0.5–1 hr following administration (Fig. 2A). Consequently, all subsequent pretreatments with cold aspirin were administered 0.5 hr prior to ^{14}C-acetaminophen. Pretreatment with aspirin significantly reduced the blood levels of radioactivity at 0.25 ($p < 0.001$) and 0.5 ($p < 0.05$) hr following oral administration of ^{14}C-acetaminophen (Fig. 2B), whereas comparable blood levels were observed following intravenous administration (Fig. 2C).

The half-life and area under the blood profile curves following intravenous dosing ($t_{1/2}$ = 0.688 ± 0.023 hr; area = 238.8 ± 11.0 μg/ml × hr) were not altered by aspirin pretreatment ($t_{1/2}$ = 0.718 ± 0.072 hr; area = 240.6 ± 17.2 μg/ml × hr). This lack of statistical significance in the area under the blood profile curves between vehicle- and aspirin-pretreated mice was also seen in the oral study (vehicle pretreated = 182.5 ± 13.5 μg/ml × hr *versus* aspirin pretreated = 139.9 ± 11.0 μg/ml × hr), suggesting that aspirin pretreatment was not statistically altering the extent of absorption from the GI tract.

The distribution of radioactivity, expressed as micrograms of acetaminophen per milliliter or gram, in the blood, heart, liver, kidneys, and GI tract and contents at 0.25, 1.0, and 4.0 hr following oral or intravenous administration of 150 mg of ^{14}C-acetaminophen/kg is presented in Table

Table I—Effect of Aspirin on the Tissue Distribution of Radioactivity following ^{14}C-Acetaminophen[a]

Tissue	Hours	Oral		Intravenous	
		Vehicle Pretreated	Aspirin Pretreated	Vehicle Pretreated	Aspirin Pretreated
Blood	0.25	149.9 ± 7.3 (1.0)	49.4 ± 2.4 (1.0)**	202.2 ± 6.0 (1.0)	177.6 ± 5.0 (1.0)*
	1.0	70.2 ± 4.9 (1.0)	66.5 ± 16.5 (1.0)	128.4 ± 6.0 (1.0)	117.3 ± 15.8 (1.0)
	4.0	9.6 ± 2.9 (1.0)	9.6 ± 9.8 (1.0)	4.6 ± 0.5 (1.0)	5.3 ± 0.7 (1.0)
Heart	0.25	110.0 ± 6.9 (0.7)	39.2 ± 2.3 (0.8)**	148.3 ± 5.6 (0.7)	131.4 ± 3.8 (0.7)*
	1.0	40.2 ± 4.4 (0.5)	47.4 ± 12.0 (0.7)	82.3 ± 5.4 (0.6)	93.9 ± 10.2 (0.8)
	4.0	4.0 ± 1.0 (0.4)	6.8 ± 0.9 (0.7)*	3.6 ± 0.8 (0.8)	2.8 ± 0.2 (0.5)
Liver	0.25	516.2 ± 39.2 (3.4)	242.4 ± 23.4 (4.9)**	229.9 ± 9.5 (1.1)	207.1 ± 2.0 (1.2)
	1.0	310.6 ± 49.4 (4.4)	349.7 ± 72.2 (5.3)	165.1 ± 8.2 (1.3)	300.4 ± 127.5 (2.5)
	4.0	92.3 ± 39.1 (9.6)	97.9 ± 25.2 (10.2)	18.3 ± 2.2 (4.0)	20.0 ± 3.2 (3.8)
Kidney	0.25	310.3 ± 23.3 (2.1)	188.4 ± 40.4 (3.8)*	256.7 ± 3.4 (1.3)	237.1 ± 8.4 (1.3)
	1.0	233.5 ± 19.0 (3.3)	238.60 ± 55.8 (3.6)	229.5 ± 7.1 (1.8)	179.2 ± 33.9 (1.5)
	4.0	52.7 ± 10.0 (5.5)	79.6 ± 20.0 (8.3)	35.2 ± 3.5 (7.7)	27.7 ± 1.7 (5.2)
GI tract and contents	0.25	—	—	475.2 ± 20.5	450.2 ± 28.5
	1.0	—	—	557.6 ± 35.3	595.8 ± 163.2
	4.0	—	—	504.4 ± 61.4	588.8 ± 49.6

[a] Mice were orally pretreated with vehicle or aspirin (200 mg/kg) 0.5 hr prior to oral or intravenous administration of ^{14}C-acetaminophen (150 mg/kg). Radioactivity is expressed as grams per milliliter or grams of tissue. Statistical differences are indicated as $p < 0.05$ (*) and $p < 0.001$ (**). Values are means from three to five animals ± *SE*. Ratios of tissue to blood carbon-14 concentration are in parentheses.

Table II—Effect of Aspirin Pretreatment on Urinary Excretion of ^{14}C-Acetaminophen[a]

Hours	Pretreatment	Cumulative Volume of Urine per Animal, ml	Concentration, μg/ml	Cumulative Percentage of Dose Excreted
4	Vehicle	0.52 ± 0.12	2198.3 ± 328.8	25.3 ± 1.9
	Aspirin	0.62 ± 0.09	1950.5 ± 196.2	27.2 ± 2.4
12	Vehicle	1.31 ± 0.02	2008.7 ± 75.2	61.5 ± 3.3
	Aspirin	1.44 ± 0.17	1599.7 ± 207.0	57.8 ± 8.7
24	Vehicle	2.77 ± 0.05	532.0 ± 78.5	79.4 ± 2.2
	Aspirin	2.64 ± 0.21	737.7 ± 42.5	75.9 ± 6.5
48	Vehicle	5.19 ± 0.58	77.0 ± 27.1	83.3 ± 2.2
	Aspirin	4.67 ± 0.92	163.4 ± 35.2	83.8 ± 5.0

[a] Mice were divided into six groups of eight animals each and orally pretreated with vehicle or aspirin (200 mg/kg) 0.5 hr prior to receiving ^{14}C-acetaminophen (150 mg/kg po). Each value is the mean ± *SE* from three pools of eight mice.

I. In the oral study at 0.25 hr, blood, heart, liver, and kidney levels of carbon-14 from vehicle-pretreated mice were approximately two- to threefold higher than levels in corresponding tissues from aspirin-pretreated animals. At later time periods, the trend had reversed: tissues from aspirin-pretreated animals tended to possess higher levels of carbon-14 than tissues from control mice, although statistical significance could only be demonstrated in cardiac tissue at 4.0 hr.

With the exception of 0.25-hr blood and heart samples, vehicle- and aspirin-pretreated mice dosed intravenously with ^{14}C-acetaminophen gave comparable tissue carbon-14 levels. Blood and cardiac tissue collected at 0.25 hr from aspirin-pretreated mice possessed lower levels of radioactivity than the corresponding tissues from vehicle-pretreated mice.

Pretreatment with aspirin did not alter any of the urinary parameters examined (Table II) in mice dosed orally with ^{14}C-acetaminophen. Descending alkaline paper chromatography[12] of neat urine separated radioactivity into five distinct peaks (Fig. 3A), whereas urine samples treated with β-glucuronidase gave six peaks (Fig. 3B). Peaks 2, 3, 5, and 6 were previously identified in neat urine as the glucuronide, mercapturate, sulfate, and free acetaminophen, respectively (2). Peak 6 (Fig. 3B) increased following β-glucuronidase treatment and was attributed to acetaminophen derived from the hydrolysis of the acetaminophen–glucuronide conjugate. Peaks 1 and 4 were minor peaks and were not identified.

Preliminary TLC and GLC–mass spectrometry data suggested that peak 4 contained more than one ^{14}C-metabolite, at least one of which contained sulfur. Peak 2 (R_f 0.07–0.09) was tentatively identified as the acetaminophen–cysteine conjugate. Examination of the qualitative properties of the fraction isolated as the cysteine conjugate by Sephadex gel G-10 (Table III) confirmed the presence of the acetaminophen–cysteine conjugate in mouse urine, and a quantitative comparison of peak 2 and the acetaminophen–cysteine conjugate isolated by column chromatography gave comparable results.

The cumulative urinary excretion of free acetaminophen at 4, 8, and 14 hr following oral administration of ^{14}C-acetaminophen was not significantly altered by aspirin pretreatment (Table IV). During the first 8 hr, sulfate excretion was significantly reduced whereas mercapturate elimination was increased by aspirin pretreatment. By 14 hr, the effect of aspirin on cumulative urinary excretion of sulfate and mercapturate had disappeared and significant differences in the excretion of glucuronide and cysteine appeared. Glucuronide excretion was inhibited and the 14-hr cumulative excretion of the cysteine conjugate was increased by aspirin pretreatment.

[12] Whatman No. 1 filter paper.

DISCUSSION

The combination of orally administered aspirin and acetaminophen appeared to reduce the acetaminophen absorption rate during the absorptive phase (Fig. 2B), an observation previously reported for the rat (2) and guinea pig (3). Since urinary excretion (Table II) and the intravenous $t_{1/2}$ were comparable between vehicle- and aspirin-pretreated animals, elimination differences did not appear to be responsible for the altered blood profiles (Fig. 2B). In view of the fact that blood carbon-14 concentrations and areas under the blood concentration–time curves were comparable following intravenous administration to vehicle- and aspirin-pretreated animals, the reduced blood level of carbon-14 in aspirin-pretreated mice (Fig. 2B) was attributed to an inhibition of absorption.

The basis for this inhibitory effect of aspirin on absorption is not immediately apparent. Smith and Irving (10) reported that salicylate (100 mg) administered to rats reduced the gastric emptying rate. More recent reports indicated that acetaminophen absorption was dependent upon gastric emptying (11, 12). In view of these reports, retardation in absorption of radioactivity in aspirin-pretreated mice (Fig. 2B) was attributed to a reduction in the gastric emptying rate.

Tissue distribution of acetaminophen appeared to be dependent upon the route of administration. In the oral study, carbon-14 levels in the liver and kidneys during the 1st hr were 2.1–5.3-fold higher than blood concentrations (Table I); in the intravenous study, liver and kidney levels of radioactivity were only 1.1–2.5-fold higher than blood carbon-14 levels. Pretreatment with aspirin apparently had little effect on the distribution of intravenously administered acetaminophen. However, in the oral study, tissue-to-blood ratios of carbon-14 (Table I) tended to be higher in aspirin-pretreated mice than in vehicle-pretreated animals. These results suggested that ^{14}C-acetaminophen-derived radioactivity was more readily taken up following oral administration by tissues of aspirin-pretreated mice than by tissues from controls. This possibility prompted an examination of acetaminophen metabolism.

Table III—Properties of the Acetaminophen–Cysteine Conjugate[a]

Column chromatography	Cysteine conjugate/acetaminophen elution volume (ml), 38/85
Descending paper chromatography	R_f 0.28 in acidic system, R_f 0.07 in alkaline system
Color test	Ninhydrin, purple
Mass spectrometry	*m/e* ions 226, 209, 197, 183, 141, and 108

[a] The cysteine conjugate was isolated from Amberlite XAD-2 desalted mouse urine by Sephadex gel G-10 column chromatography. The acidic and alkaline paper chromatography systems were 1-butanol–acetic acid–water (4:1:1) and 2-propanol–water–ammonium hydroxide (20:2:1), respectively.

The major urinary metabolites of acetaminophen are glucuronide, mercapturate, sulfate, and free drug (2, 3, 13–16). In this study, chromatography of neat and β-glucuronidase-treated urine following 150 mg of ^{14}C-acetaminophen/kg separated radioactivity into six distinct peaks (Fig. 3). Four of these peaks were previously identified (2). Other peaks, with the exception of peak 2 (Fig. 3B), were minor and were not identified.

On the basis of migration in the descending alkaline paper chromatography system (Fig. 3B and Table III), peak 2 was tentatively identified as the acetaminophen–cysteine conjugate, previously reported (7, 17) to have R_f 0.10. To confirm the occurrence of the acetaminophen–cysteine conjugate in mouse urine, properties of the cysteine fraction were examined (Table III). It gave a positive ninhydrin test, which indicated a primary amine. Radioactivity in this fraction migrated in descending acidic and alkaline paper chromatography systems as single peaks with R_f values comparable to those previously reported (17). Mass spectrometry of the freeze-dried cysteine fraction (Table III) gave a fragmentation pattern identical to that reported for the acetaminophen–cysteine conjugate (16), unequivocally establishing the presence of the cysteine conjugate in mouse urine.

Glucuronide (27%) was the major urinary metabolite in 14-hr urine samples (Table IV), followed by cysteine (13.6%), sulfate (9.5%), free drug (3.9%), and mercapturate (1.9%). Jollow *et al.* (15) examined the 24-hr urine of mice dosed with ^{3}H-acetaminophen (100 mg/kg ip) and found radioactivity distributed as glucuronide (47.9%), sulfate (25.2%), free drug (13.4%), and mercapturate (12.4%) but failed to demonstrate the presence of the acetaminophen–cysteine conjugate. In view of their high glucuronide percentage and considering the fact that they eluted and then were treated with β-glucuronidase, the presence of the cysteine conjugate cannot be excluded as a possible contaminant of their glucuronide peak. On the other hand, a different strain of mouse (GP mice) from that used in this study (Swiss Webster mice) was utilized, which could account for the differences. A recent report (18) attested to mouse strain differences in inducibility of acetaminophen metabolism to produce hepatotoxicity, although acetaminophen metabolites were not examined *per se*.

The most significant metabolic effects of aspirin in this study were the reduction in sulfate and the increase in mercapturate at 4 and 8 hr (Table IV), effects previously reported in the rat (2). The biochemical basis for these effects was not established; however, Boström *et al.* (19) showed that salicylate inhibited the biosynthesis of mucopolysaccharide sulfates. These investigators suggested that the oxidative uncoupling action of salicylate reduced active sulfate (3′-phospho-5′-adenosine phosphosulfate) levels, thereby inhibiting sulfation. Since cysteine is a precursor for the synthesis of both the active sulfate and glutathione (15), it seems reasonable that reducing the active sulfate level would increase the pool of cysteine or precursors of cysteine (glutathione) available for conjugation with radioactivity derived from ^{14}C-acetaminophen. This result, in fact, was observed; aspirin-pretreated mice tended to excrete a larger percentage of the dose as cysteine and mercapturate than vehicle-pretreated animals (Table IV), but statistically significant differences could only be demonstrated in mercapturate excretion at 4 and 8 hr and cysteine excretion at 14 hr.

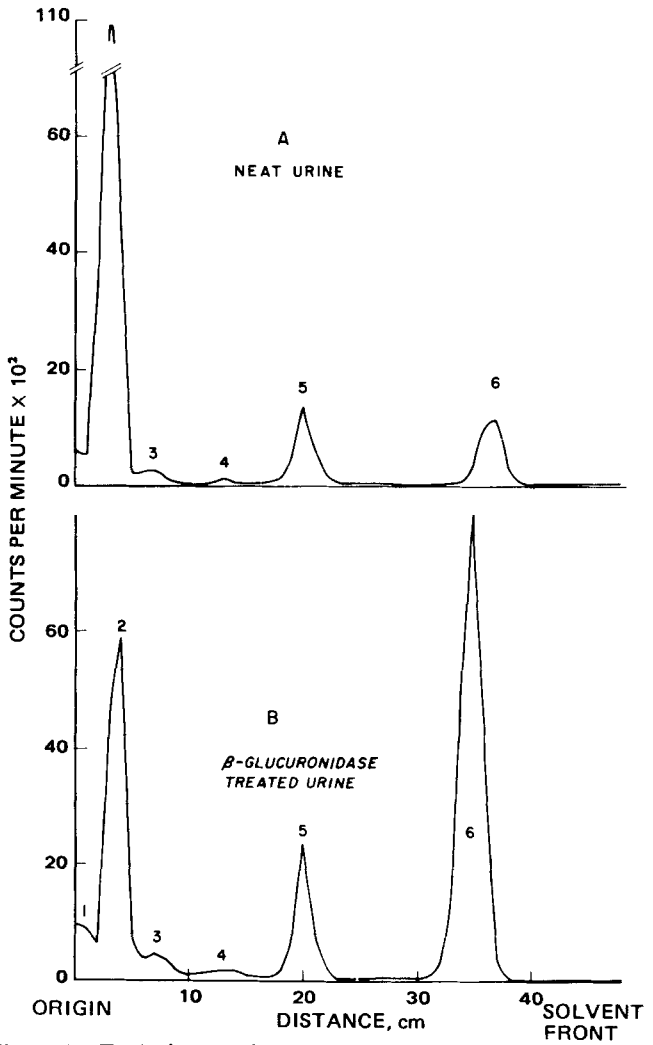

Figure 3—*Typical paper chromatographic separation of urinary metabolites of ^{14}C-acetaminophen in the mouse. Neat (A) and 16-hr β-glucuronidase-treated (B) urine, 10 and 20 μl, respectively, were applied as bands to filter paper and developed descendingly in 2-propanol–water–ammonium hydroxide (20:2:1). The paper was serially sectioned into 1-cm strips and assayed for carbon-14 by liquid scintillation counting. The separated peaks were: 1 and 4, unknown; 2, cysteine; 3, mercapturate; 5, sulfate; and 6, free acetaminophen. The increase in peak 6 following β-glucuronidase treatment was attributed to the glucuronide.*

Measurement of the acetaminophen–glutathione conjugate excreted in the urine as degradation products (mercapturate and cysteine conjugates) was suggested (20) as a suitable method for estimating the toxic pathway and the animal's susceptibility to acetaminophen. Since the susceptibility to acetaminophen-induced hepatotoxicity follows the order

Table IV—Effect of Aspirin on the Urinary Metabolites of ^{14}C-Acetaminophen in the Mouse[a]

Hours	Pretreatment	R_f 0.01–0.04, Metabolite 1	R_f 0.05–0.07, Glucuronide	R_f 0.07–0.09, Cysteine	R_f 0.14–0.18, Mercapturate	R_f 0.26–0.30, Metabolite 4	R_f 0.41–0.47, Sulfate	R_f 0.72–0.78, Acetaminophen
4.0	Vehicle	0.68 ± 0.15	11.18 ± 1.97	3.60 ± 0.67	0.40 ± 0.12	0.50 ± 0.06	3.16 ± 0.44	3.36 ± 0.90
	Aspirin	0.81 ± 0.06	8.25 ± 1.44	4.04 ± 0.22	1.41 ± 0.04*	0.43 ± 0.05	0.63 ± 0.02*	2.48 ± 0.24
8.0	Vehicle	0.95 ± 0.29	14.98 ± 1.47	5.89 ± 0.62	0.71 ± 0.11	0.73 ± 0.03	4.47 ± 0.16	3.70 ± 0.77
	Aspirin	1.23 ± 0.03	11.90 ± 1.03	6.44 ± 0.28	1.88 ± 0.10*	0.67 ± 0.10	0.99 ± 0.05**	2.78 ± 0.24
14.0	Vehicle	1.97 ± 0.59	27.00 ± 0.37	13.59 ± 0.10	1.87 ± 0.38	1.75 ± 0.18	9.51 ± 0.75	3.91 ± 0.72
	Aspirin	2.54 ± 0.30	21.16 ± 0.01*	17.63 ± 0.15*	3.88 ± 0.98	2.14 ± 0.54	7.33 ± 0.30	5.65 ± 0.55

[a] Mice were divided into six groups of eight animals each and orally pretreated with vehicle or aspirin (200 mg/kg) 0.5 hr prior to receiving ^{14}C-acetaminophen (150 mg/kg po). Metabolites were separated using a 2-propanol–water–ammonium hydroxide (20:2:1) descending paper chromatography system. Values are mean percentages of the dose ± *SE*. Statistical significance is indicated as $p < 0.001$ (**) and $p < 0.05$ (*) when compared to corresponding control group.

of mouse > rat > guinea pig (4), one would expect the excretion of glutathione degradation products in these three species to be mouse > rat > guinea pig. This pattern was observed; the mouse excreted 15.5% of the dose in 14 hr as glutathione degradation products (Table IV) compared to a 12-hr excretion of 5.1% in the rat (2) and 1% in the guinea pig (3). Excretion of glutathione degradation products in the mouse increased following aspirin pretreatment (Table IV). On the basis of the catabolite hypothesis (20), this result suggests that aspirin-pretreated mice are more susceptible to acetaminophen-induced hepatotoxicity than are vehicle-pretreated mice.

However, if aspirin increased the pool of cysteine or precursors of cysteine by reducing active sulfate levels, as already suggested, then the increased urinary excretion of glutathione degradation products could indicate an increase in the conjugative detoxication of the toxic metabolite or protection from acetaminophen-induced hepatotoxicity. In support of the latter hypothesis is a study where aspirin showed a protective effect against toxic doses of acetaminophen (21).

CONCLUSION

The metabolite profile of acetaminophen in the mouse was not exactly the same as that observed in humans (22, 23). However, the mouse biotransformed acetaminophen more like the human than either the rat (2) or the guinea pig (3). Since the mouse is more susceptible to acetaminophen hepatotoxicity than either the rat or the guinea pig (4) and biotransformation of acetaminophen in the mouse resembles that occurring in humans, the mouse is a better animal model than either the rat or guinea pig for toxicological studies involving acetaminophen.

REFERENCES

(1) B. H. Thomas, B. B. Coldwell, W. Zeitz, and G. Solomonraj, *Clin. Pharmacol. Ther.*, **13**, 906 (1972).

(2) B. H. Thomas, W. Zeitz, and B. Coldwell, *J. Pharm. Sci.*, **63**, 1367 (1974).

(3) L. W. Whitehouse, C. J. Paul, and B. H. Thomas, *ibid.*, **64**, 819 (1975).

(4) D. C. Davis, W. Z. Potter, D. J. Jollow, and J. R. Mitchell, *Life Sci.*, **14**, 2099 (1974).

(5) R. J. Henry, N. Chiamori, O. J. Golub, and S. Berkman, *Am. J. Clin. Pathol.*, **34**, 381 (1960).

(6) B. H. Thomas, B. B. Coldwell, G. Solomonraj, W. Zeitz, and H. L. Trenholm, *Biochem. Pharmacol.*, **21**, 2605 (1972).

(7) N. T. Shahidi, *Ann. N.Y. Acad. Sci.*, **151**, 822 (1968).

(8) O. R. Jagenburg and K. Toczko, *Biochem. J.*, **92**, 639 (1964).

(9) R. G. D. Steel and J. H. Torrie, "Principles and Procedures of Statistics," McGraw-Hill, Toronto, Canada, 1960, p. 158.

(10) M. J. T. Smith and J. D. Irving, *Br. J. Radiol.*, **28**, 39 (1955).

(11) R. C. Heading, J. Nimmo, L. F. Prescott, and P. Tothill, *Br. J. Pharmacol.*, **47**, 415 (1973).

(12) J. Nimmo, R. C. Heading, P. Tothill, and L. F. Prescott, *Br. Med. J.*, **1**, 587 (1973).

(13) A. J. Cummings, M. L. King, and B. K. Martin, *Br. J. Pharmacol. Chemother.*, **29**, 150 (1967).

(14) G. Levy and C.-G. Regårdh, *J. Pharm. Sci.*, **60**, 608 (1971).

(15) D. J. Jollow, S. S. Thorgeirsson, W. Z. Potter, M. Hashimoto, and J. R. Mitchell, *Pharmacology*, **12**, 251 (1974).

(16) J. E. Mrochek, S. Katz, W. H. Christie, and S. R. Dinsmore, *Clin. Chem.*, **20**, 1086 (1974).

(17) R. Jagenburg, A. Nagy, and S. Rodjer, *Scand. J. Clin. Lab. Invest.*, **22**, 11 (1968).

(18) S. S. Thorgeirsson, J. S. Felton, and D. W. Nebert, *Mol. Pharmacol.*, **11**, 159 (1975).

(19) H. Boström, K. Berntsen, and M. W. Whitehouse, *Biochem. Pharmacol.*, **13**, 413 (1964).

(20) J. R. Mitchell and D. J. Jollow, in "Drug Interactions," P. L. Morselli, S. Grattini, and S. N. Cohen, Eds., Raven, New York, N. Y., 1974, p. 65.

(21) L. W. Whitehouse, C. J. Paul, and B. H. Thomas, *Toxicol. Appl. Pharmacol.*, **38**, 571 (1976).

(22) J. R. Mitchell, S. S. Thorgeirsson, W. Z. Potter, D. J. Jollow, and H. Keiser, *Clin. Pharmacol. Ther.*, **16**, 676 (1974).

(23) M. Davis, C. J. Simmons, N. G. Harrison, and R. Williams, *Q. J. Med.*, **45**, 181 (1976).

ACKNOWLEDGMENTS AND ADDRESSES

Received August 23, 1976, from the *Health Protection Branch, Health and Welfare Canada, Tunney's Pasture, Ottawa, Ontario K1A OL2, Canada.*

Accepted for publication December 16, 1976.

[x] To whom inquiries should be directed.

Colorimetric Determination of Aliphatic Acids

JAMES W. MUNSON [x] and ROMAN BILOUS [*]

Abstract □ A colorimetric method for the determination of carboxylic acids based on the dicyclohexylcarbodiimide-coupled reaction of 2-nitrophenylhydrazine and carboxylic acids is described. The product of the reaction is extracted into aqueous sodium hydroxide to produce a blue color. This method is suitable for the analysis of aliphatic acids, but aromatic acids do not react under these conditions.

Keyphrases □ Aliphatic carboxylic acids—colorimetric analysis in solutions □ Carboxylic acids, aliphatic—colorimetric analysis in solutions □ Colorimetry—analysis, aliphatic carboxylic acids in solutions

The recent application of the coupling agent dicyclohexylcarbodiimide in the analysis of carboxylic acids *via* hydroxamic acid formation (1) prompted investigation of this reagent to couple carboxylic acids with 2-nitrophenylhydrazine. An earlier study (2) showed that the hydrazide resulting from the reaction of 2-nitrophenylhydrazine with activated carboxylic acid derivatives such as acid anhydrides and acid chlorides gives an intense blue color in aqueous hydroxide solutions. This color formation was useful for the colorimetric analysis of these substances.

The objective of this study was to adapt the dicyclohexylcarbodiimide-coupled reaction of carboxylic acids and 2-nitrophenylhydrazine to produce a colorimetric method for the determination of carboxylic acids.

EXPERIMENTAL

Materials—Unless otherwise stated, analytical reagent grade chemicals were used. Acetonitrile was distilled from phosphorus pentoxide, with the fraction boiling at 81.5° being collected. Dichloromethane was distilled directly, with the fraction boiling at 39.5° being collected. 2-Nitrophenylhydrazine was recrystallized from water–methanol (85:15), yielding yellow-orange needles, mp 92–92.5°.

of mouse > rat > guinea pig (4), one would expect the excretion of glutathione degradation products in these three species to be mouse > rat > guinea pig. This pattern was observed; the mouse excreted 15.5% of the dose in 14 hr as glutathione degradation products (Table IV) compared to a 12-hr excretion of 5.1% in the rat (2) and 1% in the guinea pig (3). Excretion of glutathione degradation products in the mouse increased following aspirin pretreatment (Table IV). On the basis of the catabolite hypothesis (20), this result suggests that aspirin-pretreated mice are more susceptible to acetaminophen-induced hepatotoxicity than are vehicle-pretreated mice.

However, if aspirin increased the pool of cysteine or precursors of cysteine by reducing active sulfate levels, as already suggested, then the increased urinary excretion of glutathione degradation products could indicate an increase in the conjugative detoxication of the toxic metabolite or protection from acetaminophen-induced hepatotoxicity. In support of the latter hypothesis is a study where aspirin showed a protective effect against toxic doses of acetaminophen (21).

CONCLUSION

The metabolite profile of acetaminophen in the mouse was not exactly the same as that observed in humans (22, 23). However, the mouse biotransformed acetaminophen more like the human than either the rat (2) or the guinea pig (3). Since the mouse is more susceptible to acetaminophen hepatotoxicity than either the rat or the guinea pig (4) and biotransformation of acetaminophen in the mouse resembles that occurring in humans, the mouse is a better animal model than either the rat or guinea pig for toxicological studies involving acetaminophen.

REFERENCES

(1) B. H. Thomas, B. B. Coldwell, W. Zeitz, and G. Solomonraj, *Clin. Pharmacol. Ther.*, **13**, 906 (1972).

(2) B. H. Thomas, W. Zeitz, and B. Coldwell, *J. Pharm. Sci.*, **63**, 1367 (1974).

(3) L. W. Whitehouse, C. J. Paul, and B. H. Thomas, *ibid.*, **64**, 819 (1975).

(4) D. C. Davis, W. Z. Potter, D. J. Jollow, and J. R. Mitchell, *Life Sci.*, **14**, 2099 (1974).

(5) R. J. Henry, N. Chiamori, O. J. Golub, and S. Berkman, *Am. J. Clin. Pathol.*, **34**, 381 (1960).

(6) B. H. Thomas, B. B. Coldwell, G. Solomonraj, W. Zeitz, and H. L. Trenholm, *Biochem. Pharmacol.*, **21**, 2605 (1972).

(7) N. T. Shahidi, *Ann. N.Y. Acad. Sci.*, **151**, 822 (1968).

(8) O. R. Jagenburg and K. Toczko, *Biochem. J.*, **92**, 639 (1964).

(9) R. G. D. Steel and J. H. Torrie, "Principles and Procedures of Statistics," McGraw-Hill, Toronto, Canada, 1960, p. 158.

(10) M. J. T. Smith and J. D. Irving, *Br. J. Radiol.*, **28**, 39 (1955).

(11) R. C. Heading, J. Nimmo, L. F. Prescott, and P. Tothill, *Br. J. Pharmacol.*, **47**, 415 (1973).

(12) J. Nimmo, R. C. Heading, P. Tothill, and L. F. Prescott, *Br. Med. J.*, **1**, 587 (1973).

(13) A. J. Cummings, M. L. King, and B. K. Martin, *Br. J. Pharmacol. Chemother.*, **29**, 150 (1967).

(14) G. Levy and C.-G. Regårdh, *J. Pharm. Sci.*, **60**, 608 (1971).

(15) D. J. Jollow, S. S. Thorgeirsson, W. Z. Potter, M. Hashimoto, and J. R. Mitchell, *Pharmacology*, **12**, 251 (1974).

(16) J. E. Mrochek, S. Katz, W. H. Christie, and S. R. Dinsmore, *Clin. Chem.*, **20**, 1086 (1974).

(17) R. Jagenburg, A. Nagy, and S. Rodjer, *Scand. J. Clin. Lab. Invest.*, **22**, 11 (1968).

(18) S. S. Thorgeirsson, J. S. Felton, and D. W. Nebert, *Mol. Pharmacol.*, **11**, 159 (1975).

(19) H. Boström, K. Berntsen, and M. W. Whitehouse, *Biochem. Pharmacol.*, **13**, 413 (1964).

(20) J. R. Mitchell and D. J. Jollow, in "Drug Interactions," P. L. Morselli, S. Grattini, and S. N. Cohen, Eds., Raven, New York, N. Y., 1974, p. 65.

(21) L. W. Whitehouse, C. J. Paul, and B. H. Thomas, *Toxicol. Appl. Pharmacol.*, **38**, 571 (1976).

(22) J. R. Mitchell, S. S. Thorgeirsson, W. Z. Potter, D. J. Jollow, and H. Keiser, *Clin. Pharmacol. Ther.*, **16**, 676 (1974).

(23) M. Davis, C. J. Simmons, N. G. Harrison, and R. Williams, *Q. J. Med.*, **45**, 181 (1976).

ACKNOWLEDGMENTS AND ADDRESSES

Received August 23, 1976, from the *Health Protection Branch, Health and Welfare Canada, Tunney's Pasture, Ottawa, Ontario K1A OL2, Canada.*

Accepted for publication December 16, 1976.

[x] To whom inquiries should be directed.

Colorimetric Determination of Aliphatic Acids

JAMES W. MUNSON [x] and ROMAN BILOUS [*]

Abstract □ A colorimetric method for the determination of carboxylic acids based on the dicyclohexylcarbodiimide-coupled reaction of 2-nitrophenylhydrazine and carboxylic acids is described. The product of the reaction is extracted into aqueous sodium hydroxide to produce a blue color. This method is suitable for the analysis of aliphatic acids, but aromatic acids do not react under these conditions.

Keyphrases □ Aliphatic carboxylic acids—colorimetric analysis in solutions □ Carboxylic acids, aliphatic—colorimetric analysis in solutions □ Colorimetry—analysis, aliphatic carboxylic acids in solutions

The recent application of the coupling agent dicyclohexylcarbodiimide in the analysis of carboxylic acids *via* hydroxamic acid formation (1) prompted investigation of this reagent to couple carboxylic acids with 2-nitrophenylhydrazine. An earlier study (2) showed that the hydrazide resulting from the reaction of 2-nitrophenylhydrazine with activated carboxylic acid derivatives such as acid anhydrides and acid chlorides gives an intense blue color in aqueous hydroxide solutions. This color formation was useful for the colorimetric analysis of these substances.

The objective of this study was to adapt the dicyclohexylcarbodiimide-coupled reaction of carboxylic acids and 2-nitrophenylhydrazine to produce a colorimetric method for the determination of carboxylic acids.

EXPERIMENTAL

Materials—Unless otherwise stated, analytical reagent grade chemicals were used. Acetonitrile was distilled from phosphorus pentoxide, with the fraction boiling at 81.5° being collected. Dichloromethane was distilled directly, with the fraction boiling at 39.5° being collected. 2-Nitrophenylhydrazine was recrystallized from water–methanol (85:15), yielding yellow-orange needles, mp 92–92.5°.

Carboxylic acid solutions were prepared by dilution of a stock solution of the acid in dichloromethane[1]. The exact concentrations of the stock solutions were determined by potentiometric titration with standard sodium hydroxide in methanol. Stock solutions of 2-nitrophenylhydrazine (in dichloromethane) and dicyclohexylcarbodiimide in acetonitrile were prepared fresh daily.

All reactions[2] were carried out at 60 ± 0.2° in 15-ml round-bottom centrifuge tubes with polytef-lined caps.

Effect of Pyridine on Color Formation—Appropriate volumes of acetic acid, dicyclohexylcarbodiimide, 2-nitrophenylhydrazine, and pyridine were added to a centrifuge tube. The amount of pyridine added was varied up to 40.5% (v/v), with dichloromethane being used to maintain a constant volume. The sealed tubes were heated for 15 min at 60° and cooled. Aliquots of 5 ml of 1 *N* NaOH were added to each tube. The tubes were then rocked for 15 min and centrifuged at 2000 rpm for 15 min.

The absorbance of the aqueous layer was measured at 535 nm in a 1-cm cell against an appropriate blank. The concentrations of the reagents in the reaction mixture were: acetic acid, 0.00014 *M*; dicyclohexylcarbodiimide, 0.0135 *M*; 2-nitrophenylhydrazine, 0.0132 *M*; and pyridine, 0–40.5% (v/v). The volume of the reaction mixture was 7.4 ml before heating and subsequent addition of 5 ml of 1 *N* NaOH.

Effect of 2-Nitrophenylhydrazine Concentration on Color Formation—Reaction mixtures were prepared as described, except that the 2-nitrophenylhydrazine concentration was varied while all other parameters were held constant. The samples were treated in the same way as described. The concentrations of reagents in the reaction mixture were: acetic acid, 0.00013 *M*; dicyclohexylcarbodiimide, 0.0119 *M*; pyridine, 16.67% (v/v)[3]; and 2-nitrophenylhydrazine, 0–0.0292 *M*. The volume of the reaction mixture was held constant at 8.4 ml before heating and subsequent addition of 5 ml of 1 *N* NaOH by addition of appropriate amounts of dichloromethane.

Effect of Dicyclohexylcarbodiimide Concentration on Color Formation—With the optimum concentrations of pyridine and 2-nitrophenylhydrazine as previously determined, reaction mixtures were prepared with varying amounts of dicyclohexylcarbodiimide (0–0.090 *M*) and a fixed acetic acid concentration. The samples were treated as before at 60°. The concentrations of reactants in the final reaction mixture were: acetic acid, 0.00018 *M*; 2-nitrophenylhydrazine, 0.0163 *M*; pyridine, 16.67% (v/v); and dicyclohexylcarbodiimide, 0–0.0417 *M*. The volume of the reaction mixture, before heating and subsequent addition of 5 ml of 1 *N* NaOH, was maintained at 8.0 ml by addition of acetonitrile and dichloromethane.

Determination of Reaction Time for Acetic Acid—Reaction mixtures were prepared containing acetic acid, 0.00017 *M*; dicyclohexylcarbodiimide, 0.042 *M*; pyridine, 16.67% (v/v); and 2-nitrophenylhydrazine, 0.0163 *M* (final volume 6.0 ml). The reaction mixture was heated at 60°, and samples were removed as a function of time. The samples were cooled, rocked for 15 min with 5.0 ml of 1 *N* NaOH, and centrifuged at 2000 rpm for 15 min. The absorbance of the aqueous layer was measured at 535 nm.

Suggested Analytical Procedure for Acetic Acid—Place 2.0 ml of an acetic acid solution in a 15-ml centrifuge tube. Add 1.0 ml of dicyclohexylcarbodiimide (0.250 *M*), 1.0 ml of pyridine, and 2.0 ml of 2-nitrophenylhydrazine (0.049 *M*). React at 60° for 30 min, cool, and add 5.0 ml of 1 *N* NaOH. Rock the tube, and centrifuge for 15 min at 2000 rpm. Measure the absorbance of the aqueous phase at 535 nm against an appropriately prepared blank.

Determination of Extent of Reaction of Other Carboxylic Acids—Reaction mixtures containing other carboxylic acids were prepared in the same manner as in the acetic acid studies. The reactions were carried out at 60°, with samples being withdrawn as a function of time and treated as previously described.

Determination of Extent of Reaction of Other Carboxylic Acid Derivatives—Reaction mixtures were prepared by using the suggested analytical procedure for acetic acid, with the samples being 10^{-3} and 10^{-2} *M* solutions of acetamide, butyrolactone, and ethyl acetate in dichloromethane. The reaction mixtures were then subjected to the suggested analytical procedure for acetic acid.

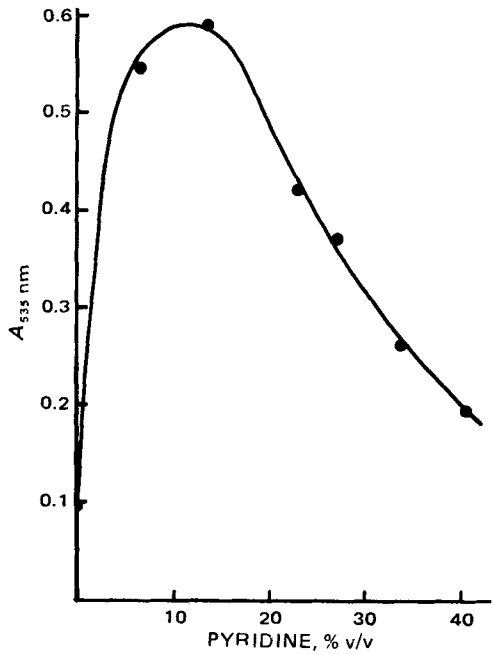

Figure 1—*Effect of pyridine concentration on color formation resulting from the reaction of acetic acid.*

RESULTS AND DISCUSSION

Preliminary experiments indicated that polar solvents facilitated the dicyclohexylcarbodiimide-coupled reaction of carboxylic acids and 2-nitrophenylhydrazine. Use of protic solvents such as methanol gave irreproducible results. This phenomenon was probably due to the condensation of the carboxylic acid and the solvent to form an unreactive ester. To find a suitable polar, aprotic solvent, a series of halogenated hydrocarbons was studied. Dichloromethane gave better results than chloroform or 1,2-dichloroethane. In an attempt to increase the polarity of the solvent by the addition of pyridine, the observation was made that pyridine catalyzed the reaction of interest. A systematic study was then undertaken to establish the optimum conditions for this reaction.

Figure 1 shows the effect of pyridine concentration on the color formation when acetic acid was used as the substrate. Absorbance measurements were made prior to the completion of the reaction. Consequently, differences in absorbances indicate differences in reaction rates. Pyridine apparently catalyzed the reaction at lower concentrations and inhibited the reaction at high concentrations. A more reasonable explanation is that the increasing pyridine concentration adversely affected the partitioning of the reaction product from the reaction mixture into the basic aqueous phase. Regardless of the cause of the observed behavior, addition of pyridine (16.7% v/v) produced an adequate increase in the reaction rate.

The effect of 2-nitrophenylhydrazine concentration was investigated under the same conditions with the optimum pyridine concentration. Color formation increased as a function of the 2-nitrophenylhydrazine concentration (Fig. 2). Since the blank absorbances were quite high at concentrations above 0.0175 *M*, a concentration of 0.0163 *M* was selected for future studies. This value gave sufficiently high yields with an acceptable blank level.

A similar study was conducted to find the optimum concentration of dicyclohexylcarbodiimide (Fig. 3). A maximum yield was obtained at a concentration of about 0.04 *M*. The decrease in absorbance at higher concentration is unexplained.

Under the conditions of optimum concentrations of pyridine, dicyclohexylcarbodiimide, and 2-nitrophenylhydrazine, acetic acid reacted completely within 30 min at 60°. Subsequently, multiple samples of acetic acid solutions of known concentration were subjected to the suggested analytical procedure. Three separate runs of seven concentrations each gave a linear regression line described by:

$$\text{absorbance} = 1527[\text{acetic acid } (M)] - 0.008 \qquad \text{(Eq. 1)}$$

The correlation coefficient for this equation was 0.994 with a standard

[1] In some instances, it was necessary to prepare stock solutions in a 50% (v/v) solution of dichloromethane and pyridine. The pyridine concentration was taken into account in later experiments.

[2] The rate of this reaction increases with temperature. However, the high volatility of the solvent (dichloromethane) prevents running these reactions at higher temperatures.

[3] Although the maximum yield was obtained at approximately 12% (v/v) pyridine, a concentration of 16.67% (v/v) was chosen for further studies to facilitate adding 1.0 ml into the samples. Very little sensitivity is sacrificed to obtain this experimental simplification.

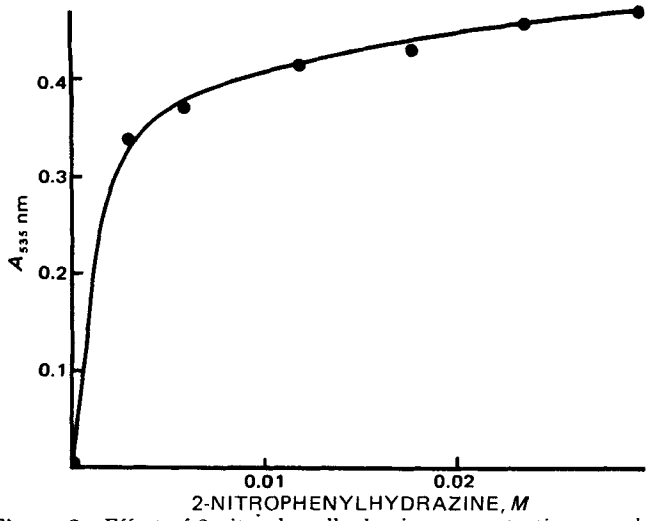

Figure 2—*Effect of 2-nitrophenylhydrazine concentration on color formation resulting from the reaction of acetic acid.*

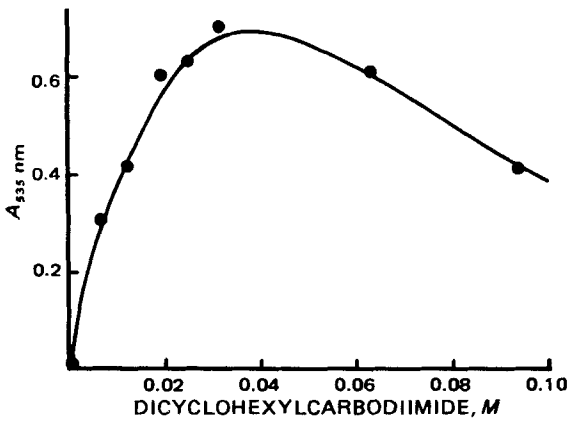

Figure 3—*Effect of dicyclohexylcarbodiimide concentration on color formation resulting from the reaction of acetic acid.*

error of the estimate (S_{xy}) of 0.049. Six separate determinations of 4.2×10^{-4} *M* acetic acid gave a standard deviation of 0.0092 (mean absorbance of 0.620). The concentration range for the linear regression analysis was $1\text{–}10 \times 10^{-4}$ *M*.

Several other carboxylic acids were studied under the optimum conditions as determined for acetic acid. At a reaction time of 45 min, butyric, succinic, and indoleacetic acids were detectable at concentrations of 10^{-4} *M* (absorbance greater than 0.1). Under the same conditions, phenylacetic, 2-methyl-2-hydroxypropanoic, and cinnamic acids were detectable at 10^{-3} *M*. Aromatic acids did not react under these conditions. Ethyl acetate, γ-butyrolactone, and acetamide at concentrations of 10^{-3} and 10^{-2} *M* gave no measurable absorbance.

The analysis of butyric acid extracted from aqueous solutions (five samples) produced a linear calibration curve described by:

$$\text{absorbance} = 333\ [\text{butyric acid } (M)] - 0.037 \qquad \text{(Eq. 2)}$$

The correlation coefficient for this equation was 0.991 with a standard error of the estimate (S_{xy}) of 0.054. The sensitivity was less than that expected from studies of butyric acid in nonaqueous solvents. This result was probably due to an incomplete recovery of butyric acid from the aqueous sample. The concentration range for this study was $1\text{–}5 \times 10^{-3}$ *M*. Nevertheless, these results demonstrate the feasibility of analyzing aliphatic acids in aqueous solution by this method.

Condition optimization is required for acids other than the simple aliphatic acids discussed here. This method does not appear to be suitable for the analysis of aromatic acids.

REFERENCES

(1) Y. Kasai, T. Tanimura, and Z. Tamura, *Anal. Chem.*, **47**, 34 (1975).

(2) J. W. Munson, *J. Pharm. Sci.*, **63**, 252 (1974).

ACKNOWLEDGMENTS AND ADDRESSES

Received August 23, 1976, from the *College of Pharmacy, University of Kentucky, Lexington, KY 40506.*

Accepted for publication December 17, 1976.

Presented at the Pharmaceutical Analysis and Control Section, APhA Academy of Pharmaceutical Sciences, New Orleans meeting, April 1976.

Supported in part by a grant from the Kentucky Tobacco and Health Research Institute.

The authors thank Kenneth Pearce and Larry Barnett for technical assistance.

* Present address: Faculty of Pharmacy, University of Manitoba, Winnipeg, Manitoba, Canada. Work was performed while on sabbatical leave at the University of Kentucky.

ˣ To whom inquiries should be directed.

Drug Migration during Drying of Tablet Granulations I: Effect of Particle Size of Major Diluent

J. W. WARREN, Jr. [x], and J. C. PRICE

Abstract □ Migration of a water-soluble drug, propoxyphene hydrochloride, during drying of tablet granulations was studied. Wet granulations of the drug were prepared using lactose as the major diluent and corn starch as a disintegrant. Particle-size fractions of lactose ranging from 53 to 177 μm in diameter were employed in different granulations to examine the effect of particle size of the major diluent on drug migration. Determination of drug concentration at various depths in a dried granulation bed was accomplished by using a drying cell consisting of four layers. A numerical coefficient of migration was developed to compare the extent of drug migration in the various lactose granulations. Migration increased with decreasing particle size of the major diluent, lactose. Two factors that may contribute to increased migration with smaller particles are increased entry suction due to decreased intragranular capillary size and increased intergranular contact area.

Keyphrases □ Tablets—effect of particle size of major diluent on drug migration during drying □ Particle size—of major diluent in tablet granulations, effect on drug migration during drying □ Migration, drug—during drying of tablet granulations, effect of particle size of major diluent □ Dosage forms—tablets, effect of particle size of major diluent on drug migration during drying

Drug migration during granulation drying is a relatively new area of investigation. Although migration of water-soluble dyes was studied as early as 1963 (1, 2), reports concerning migration of other granulation components have appeared only since 1971 (3–8).

In a study using 5% (w/w) of the tablet binder povidone in heavy magnesium carbonate, the extent of intragranular povidone migration increased with higher drying temperatures (3). When 2.7% (w/w) warfarin sodium in a wet granulation was studied, the addition of 5% acacia and 15% alginic acid to calcium phosphate reduced drug migration (6). The influence of the volume of solvent on aspirin migration was studied using absolute ethanol as the solvent and 1% (w/w) aspirin in a wet granulation (7). The influence of various drying methods on solute migration was studied with 2.5% (w/w) NaCl in heavy kaolin (8).

Although several factors common to all wet granulations may influence the migration of a soluble drug during drying, the effect of particle size of a major diluent on the extent of drug migration was investigated. Propoxyphene hydrochloride was chosen as a representative drug since it is freely soluble in water and its usual concentration in granulations is higher than other components examined previously.

EXPERIMENTAL

Materials—Propoxyphene hydrochloride, lactose, starch, and magnesium stearate were USP grade and were used without further purification. A single lot of each material was used for all experiments.

Wet Granulation Procedure—The wet granulation formulation (Formula I) used was as follows:

	per tablet, mg	per batch, g
propoxyphene hydrochloride USP	32	48.0
lactose USP	413	619.5
starch USP	50	75.0
magnesium stearate USP	5	7.5
total	500	750.0

Since the major diluent in Formula I was lactose, various particle-size fractions of lactose were collected as follows: Formula I-P1, 100% by weight of the lactose passed a No. 80 (177 μm) U.S. standard sieve but was retained on a No. 100 sieve; Formula I-P2, 100% by weight of the lactose passed a No. 100 (149 μm) U.S. standard sieve but was retained on a No. 140 sieve; Formula I-P3, 100% by weight of the lactose passed a No. 140 (105 μm) U.S. standard sieve but was retained on a No. 170 sieve; Formula I-P4, 100% by weight of the lactose passed a No. 200 (74 μm) U.S. standard sieve but was retained on a No. 270 sieve; and Formula I-P5, 100% by weight of the lactose passed a No. 270 (53 μm) U.S. standard sieve but was retained on a No. 325 sieve. The collected fractions of lactose were incorporated into five granulation batches.

For wet granulation of the five batches, the powders were first passed through a No. 12 U.S. standard sieve (1680 μm) to reduce large agglomerates. The powders were then blended for 15 min at low speed in a planetary mixer[1]. After blending, 150 ml of water was added in portions, approximately 50 ml/addition, to form the wet granulation mass, and the granulation was mixed for an additional 10–12 min.

Wet screening was accomplished by passing the wet granulated mass through a No. 12 (1680 μm) sieve. The wet mass was then placed in a drying cell and dried at 50° for 5 hr in a drying oven[2].

Drying Cell and Sampling Procedure—A drying cell made of acrylic plastic and consisting of four layers, 0.476 cm thick, was used to facilitate the determination of the concentration of propoxyphene hydrochloride at various depths in a granulation bed (Fig. 1). The total height of the cell was 1.90 cm. The cell was open on both ends of the cylinder formed by the layers; the opening was 10.16 cm in diameter. The layers of the cell were secured with screws during the drying process.

When used for migration studies, the drying cell was placed on a drying oven tray lined with porous paper. The granulation in the bottom layer was exposed to the paper during the drying process, which was similar to an actual industrial tray drying process. The wetted granulation, after being wet sieved, was filled into the drying cell with a spatula.

After drying, the top layer of the dried bed was sampled by removing portions of the top cell layer with a flat blade. Three samples were taken from each layer and designated as side 1, side 2, and center. The side 1 sample was taken from an area 3.2 cm from the beginning of air flow across the cell, and the side 2 sample was taken 3.2 cm from the side of the cell cylinder opposite side 1. At this point, the second layer was removed and the granulation was sampled in the same manner. This procedure was repeated for the third and fourth layers.

After mixing the granulation samples, 0.5 g of granulation from each of the 12 samples per cell, three from each layer, was then assayed for propoxyphene hydrochloride content. The average of the three assay results for each layer was used for further calculations and comparisons.

Drug Content Uniformity of Wet Granulations—Drug content uniformity in the wet granulation (Formula I-P1) was determined to establish whether the mixing and granulation wetting process resulted in a uniform mixture. Five random samples (approximately 2 g each) were taken from the wet mass immediately after granulation. After drying for 5 hr at 50°, the samples were assayed for drug.

Determination of Reproducibility of Cell Drying Procedure—To determine the reproducibility of the cell drying procedure, three batches of Formula I-P1 were wet granulated with 150 ml of water/batch; three drying cells from each batch were filled and dried. The top layer was then sampled and assayed, three samples per layer, from each of the nine cells.

To evaluate cell-to-cell differences within a batch and batch-to-batch differences relative to cells, a nested design analysis of variance was used (9).

Assay for Propoxyphene Hydrochloride—A colorimetric assay (10) was adapted for the determination of propoxyphene hydrochloride in the granulation samples. This method involves the formation of a color

[1] Readco mixer K-20, Read Standard, York, Pa.
[2] Power-O-Matic 60, Blue M Electric Co., Blue Island, Ill.

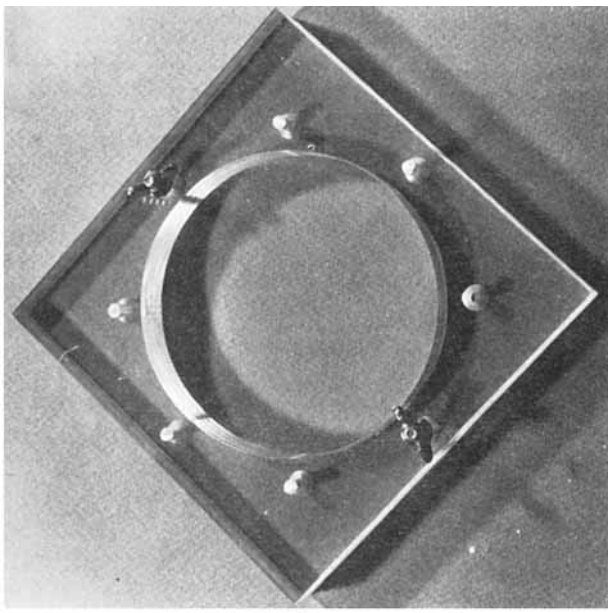

a

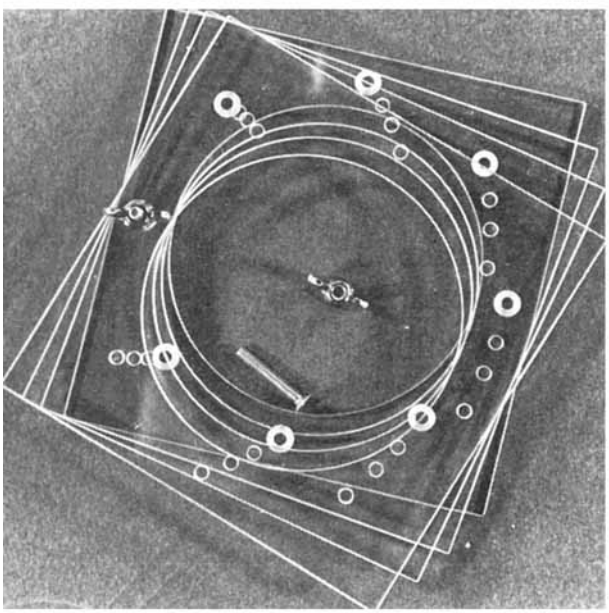

b

Figure 1—*Drying cell assembled* (a) *and partially disassembled to show construction* (b).

complex of bromcresol purple and propoxyphene hydrochloride. A granulation sample, equivalent to approximately 32 mg of propoxyphene hydrochloride, was extracted with 50 ml of methanol by shaking for 1 hr. After shaking, the sample was diluted to 100 ml with methanol. Five milliliters of this solution was diluted to 100 ml with water. Five milliliters of this final solution was then added to 20 ml of bromcresol purple reagent (50 mg of bromcresol purple/liter with 10 ml of acetic acid and sufficient 2 *N* NaOH to adjust the pH to 5.0) in a separator. Finally, 25 ml of chloroform was added.

After agitation for 3 min, a portion of the lower chloroform layer was collected. The absorbance of the collected solution was determined[3] at 405 nm using chloroform as a reference. A blank was prepared by adding 5.0 ml of water to 20 ml of the bromcresol purple solution and following the same analytical procedure. Five milliliters of a standard solution (32 mg of propoxyphene hydrochloride in a 100-ml volumetric flask diluted with methanol) was also carried through the procedure.

Physical Properties of Granulations—As a control measure, the weight of the drying cell contents, bulk density, moisture content, true volume, true density, apparent density, and intraparticle porosity of the granulation in each cell were determined.

The bulk density (grams per cubic centimeter) of the granulation in each cell was calculated using the weight of the drying cell contents and a cell volume of 153.98 cm^3. The moisture content of each granulation was determined using a moisture determination balance[4]. The true volume and the true density of the granulations were determined with an air comparison pycnometer[5].

By using a mercury pycnometer and procedures described by Strickland *et al.* (11), the granule density of each granulation was determined. From the true density and granule density values, the intraparticle porosity of each granulation was calculated.

Data Treatment—To specify the extent to which the drug migrated with a numerical value, the concept of a coefficient of migration was developed.

Since there are four layers in the drying cell, there can be six layer comparison classifications, *i.e.*, a comparative difference, sign ignored, of the average assay values of layer 1 to layer 2, layer 1 to layer 3, layer 1 to layer 4, layer 2 to layer 3, layer 2 to layer 4, and layer 3 to layer 4. These layer differences were determined relative to the amount of drug recovered and potentially present in any two layers. In general, then, the equation for calculating the comparative difference (D) between two layers (j and j') is:

$$D_{j-j'} = \frac{|L_j - L_{j'}|}{\frac{2\sum_{j=1}^{N} L_j}{N}} \qquad \text{(Eq. 1)}$$

where L_j represents the average of three assay values in a given layer, $L_{j'}$ is the average assay value in another layer, $\Sigma_{j=1}^{N}$ is the sum of the average assay values for N layers, and N is the number of layers in the drying cell.

The most divergent system using an open drying cell after drying can be represented as 64, 0, 0, and 64 mg/0.5 g for layers 1, 2, 3, and 4, respectively, where the drug has migrated from the inner layers to the two exposed evaporating surfaces. Again, using Eq. 1, the classification differences would be $D_{1-2} = (64 - 0)/64 = 1$, $D_{1-3} = (64 - 0)/64 = 1$, $D_{1-4} = (64 - 64)/64 = 0$, $D_{2-3} = (0 - 0)/64 = 0$, $D_{2-4} = (0 - 64)/64 = 1$, $D_{3-4} = (0 - 64)/64 = 1$, and total = 4. The coefficient of migration in this example is 4/4 = 1.

If 32 mg of drug/0.5 g of granulation is the theoretical average of the assay values per layer, then the most uniform system in a migration study using an open drying cell after drying can be represented as layer 1 = layer 2 = layer 3 = layer 4 = 32 mg/0.5 g.

With Eq. 1, the classification differences would be zero in all cases and the coefficient of migration would be 0/4 = 0. It follows that as the coefficient approaches one, the extent of migration is greater; as the coefficient approaches zero, the extent of migration is less.

By using the coefficient of migration as a measurement of the total upward or downward movement of drug in the granulation bed, Spearman's rank correlation method (12) was used to test for a significant correlation between the extent of drug migration and particle size of the major diluent.

RESULTS AND DISCUSSION

Drug Content Uniformity of Wet Granulation—The assay values for the five random samples taken from Formula I-P1 were 31.868, 30.800, 30.240, 31.506, and 30.439 mg/0.5 g for Samples 1, 2, 3, 4, and 5, respectively.

The theoretical amount of propoxyphene hydrochloride was 32 mg/0.5 g of granulation. The average value of the five samples was 30.971 mg of propoxyphene hydrochloride/0.5 g of granulation, and the standard deviation was 0.696 mg.

Reproducibility of Cell Drying Procedure—Top drying cell layer assay results of three lactose granulations used to determine the reproducibility of the cell drying procedure are given in Table I.

To evaluate cell-to-cell differences within a batch and batch-to-batch differences relative to cells, a nested design analysis of variance was used (9) (Table II). Since the calculated F value for batches was not significant at $p = 0.01$, there was no significant difference among the top layer assay values of the drying cells when the cells from batches 1, 2, and 3 were compared. Furthermore, because the calculated F value for cells was not

[3] Cary model 118 spectrophotometer, Varian Instrument Division, Palo Alto, Calif.

[4] Ohaus Scale Corp., Union, N.J.

[5] Model 930, Beckman Instruments, Fullerton, Calif.

Table I—Top Drying Cell Layer Assay Results[a] of Three Granulation Batches Used to Determine the Reproducibility of the Cell Drying Procedure

Batch	Sample	Cell 1	Cell 2	Cell 3
1	1	41.83	41.12	41.89
	2	39.12	39.34	38.88
	3	39.74	40.58	40.52
2	1	40.65	41.97	41.16
	2	39.96	39.60	39.11
	3	41.50	38.97	40.47
3	1	40.79	41.53	39.96
	2	39.55	41.28	38.38
	3	39.20	39.09	41.87

[a] Milligrams of propoxyphene hydrochloride/0.5 g of granulation.

Table II—Analysis of Variance to Determine the Reproducibility of the Cell Drying Procedure

Source	Degrees of Freedom	Sum of Squares	Mean Square	*F* Ratio	*F* (0.99)
Batch	2	0.1862	0.0931	0.3645	10.92
Cell (batch)	6	1.5326	0.2554	0.1546	4.01
Error	18	29.7456	1.6525		
	26	31.4644			

significant at $p = 0.01$, there was no significant difference among the three drying cells within a given batch.

Effect of Particle Size on Extent of Migration—A summary of the average assay values for Formulas I-P1–I-P5 is given in Table II. In general, the greatest amount of propoxyphene hydrochloride was found in layer 1 (top layer) in all formulations, and the least amount was found in layer 3. Formula I-P1, containing the largest particle-size lactose, showed the least drug migration.

The percent of the potential amount of propoxyphene hydrochloride depleted from the inner layers of the drying cell, layers 2 and 3, was calculated by dividing the amount of drug potentially present in the inner layers based on the total amount of drug recovered in the four layers (Table III) into the difference of the amount of drug potentially present in the inner layers of the drying cell and the actual amount recovered (Table IV). These data show rather dramatically that drug was transported toward the evaporating surfaces and was readily depleted from the inner layers of the granulation bed.

Water travels through a granulation material by capillary effect in the liquid state and then evaporates when it reaches the evaporating surface (13). It follows that propoxyphene hydrochloride would dissolve in the water and be transported toward the evaporating surfaces; thus, accumulation in layers 1 and 4 occurs when the water evaporates and deposits the drug in the granulation material.

To determine if there was a correlation between the extent of propoxyphene hydrochloride migration and the particle size of the major diluent, lactose, the coefficient of migration for Formulas I-P1–I-P5 was calculated from the results shown in Table III using Eq. 1. By using Spearman's rank correlation method (12), the formulas were ranked from 1 to 5 relative to the decreasing particle size of lactose. Then they were ranked from 1 to 5 relative to an increasing coefficient of migration (Table V).

Table III—Effect of Diluent Particle Size on Propoxyphene Hydrochloride Content[a] of Granulation Layers after Drying

Layer	Formula I-P1	Formula I-P2	Formula I-P3	Formula I-P4	Formula I-P5
1	39.38	37.35	41.35	48.40	48.55
2	29.12	22.74	23.96	22.33	23.06
3	24.12	19.62	17.72	19.76	20.48
4	35.83	35.85	39.02	38.17	39.46

[a] Each value represents an average of three assay determinations of milligrams of propoxyphene hydrochloride/0.5 g of granulation.

Table IV—Effect of Diluent Particle Size on Propoxyphene Hydrochloride Migration from the Inner Layers of the Drying Cell

Formula	Potential Amount in Inner Layers, mg	Amount Recovered from Inner Layers, mg	Amount Depleted from Inner Layers, %
I-P1	64.22	53.24	17.10
I-P2	57.78	42.36	26.69
I-P3	61.03	41.67	31.71
I-P4	64.33	42.09	34.57
I-P5	65.78	43.54	33.81

Table V—Spearman's Rank Correlation Determination for Effect of Particle Size on Extent of Migration

Formula	Particle Size Rank	Coefficient of Migration	Coefficient Rank	d_i	d_i^2
I-P1	1	0.204	1	0	0
I-P2	2	0.287	2	0	0
I-P3	3	0.352	3	0	0
I-P4	4	0.395	5	−1	1
I-P5	5	0.382	4	1	1
					2

$$r_s = 1 - \frac{(6)\sum_{i=1}^{n} d_i^2}{n^3 - n} = 1 - \frac{(6)(2)}{(5)^3 - 5} = 0.900$$

Table VI—Analysis of Variance to Determine the Limit of Migration in a Series of Lactose Granulations

Source	Degrees of Freedom	Sum of Squares	Mean Square	*F* Ratio	*F* (0.99)
Formula	1	3.1191	3.1191	0.4930	8.53
Layer	3	3268.0195	1089.3398	172.1644	5.29
Interaction	3	0.9702	0.3234	0.0511	5.29
Error	16	101.2372	6.3273		
	23	3373.3460			

Table VII—Bulk Density[a], Granule Density[a], and Porosity of Granulations

Formula	Bulk Density, g/cm³	Granule Density, g/cm³	Intraparticle Porosity, %	Moisture Content after Drying, %
I-P1	0.513	1.236	15.8	3.0
I-P2	0.510	1.206	16.3	3.2
I-P3	0.548	1.166	19.1	3.6
I-P4	0.530	1.154	20.3	3.0
I-P5	0.554	1.154	20.7	4.1

[a] Each value represents an average of three determinations.

The critical value for r_s at $n = 5$ is 0.900 at the 0.05 level of significance. The value computed in Table V, $r_s = 0.900$, is significant at the 0.05 level. Thus, a significant correlation existed between the extent of propoxyphene hydrochloride migration and the particle size of lactose. That is, as the particle size of lactose decreased, drug migration increased.

An entry suction tends to draw water from the interior of the granulation bed to the evaporating surfaces where subsequent evaporation occurs (14). It follows that as the radius of the particles is decreased, in this case lactose, the entry suction would increase because of the decreased capillary size. Thus, the resultant capillary forces tending to draw water from the interior of the granulation bed to the evaporating surface are increased as the particle size of lactose is decreased. As the entry suction increases, the movement of water through the bed toward the evaporating surfaces would be enhanced because the capillary state would be more readily maintained between individual granules; therefore, there would be greater potential for propoxyphene hydrochloride to be transported to the outer layers of the drying cell.

As the particle size of lactose is decreased, it is also feasible that an increased fine structure of smaller surface particles of individual granules occurs by increased granule surface contact. Thus, a capillary state would be achieved more easily and intergranular solvent flow would be sustained.

The results from Formulas I-P4 and I-P5 were very close. A two-factor analysis of variance comparing these results is given in Table VI. Since the calculated *F* value for the formulas was not significant at $p = 0.01$, there was apparently no difference in Formulas I-P4 and I-P5. The calculated *F* value for layers was significant, which denotes a layer difference. The interaction *F* value was not significant. It appears that increased migration due to increased capillary flow reached a limit. During the drying process, a point is reached when the capillary water no longer fills the capillary pores; water then evaporates within the granulation bed

and diffuses to the surface as a vapor (13). Thus, regardless of the potential entry suction (14) increasing with decreasing particle size, the amount of migration tends to reach a limit.

Physical Properties of Granulations—The bulk density, granule density, intraparticle porosity, and moisture content of the lactose granulations are given in Table VII. The average bulk density was 0.531 g/cm^3 with a range of 0.510–0.554 g/cm^3. The average moisture content was 3.4% with a range of 3.0–4.1%.

Although the intraparticle porosity increased with a decreased particle size of lactose, the changes in intraparticle porosity did not correlate well with the extent of propoxyphene hydrochloride migration in this series of granulations. Decreased capillary size and increased contact area with decreasing particle size probably are responsible for the observed results.

CONCLUSIONS

Variations in particle size of the major diluent in wet granulations may result in differences in drug content uniformity in different batches of granules. Control of particle size of the major diluent can minimize drug migration and improve product uniformity in some formulations.

REFERENCES

(1) G. Zografi and A. M. Mattocks, *J. Pharm. Sci.*, **52**, 1103 (1963).

(2) J. Jaffe and I. Lippman, *ibid.*, **53**, 441 (1964).

(3) K. Ridgway and M. H. Rubinstein, *J. Pharm. Pharmacol., Suppl.*, **26**, 24P (1974).

(4) *Ibid., Suppl.*, **23**, 11S (1971).

(5) *Ibid.*, **23**, 587 (1971).

(6) I. A. Chaudry and R. E. King, *J. Pharm. Sci.*, **61**, 1121 (1972).

(7) J. C. Samyn and K. S. Murthy, *ibid.*, **63**, 370 (1974).

(8) D. N. Travers, *J. Pharm. Pharmacol.*, **27**, 516 (1975).

(9) W. J. Dixon and F. J. Massey, Jr., in "Introduction to Statistical Analysis," McGraw-Hill, New York, N.Y., 1969, p. 289.

(10) N. R. Kuzel, in "Automation in Analytical Chemistry, Technicon Symposia 1966," vol. 1, Mediad, White Plains, N.Y., 1967, p. 218.

(11) W. A. Strickland, Jr., L. W. Busse, and T. Higuchi, *J. Am. Pharm. Assoc., Sci. Ed.*, **45**, 482 (1956).

(12) D. L. Harnett, in "Introduction to Statistical Methods," Addison-Wesley, Reading, Mass., 1970, p. 450.

(13) T. K. Sherwood, *Ind. Eng. Chem.*, **21**, 12, 976 (1929).

(14) J. F. Pearse, T. R. Oliver, and D. M. Newitt, *Trans. Inst. Chem. Eng.*, **27**, 1 (1949).

ACKNOWLEDGMENTS AND ADDRESSES

Received July 19, 1976, from the *School of Pharmacy, University of Georgia, Athens, GA 30602.*

Accepted for publication December 16, 1976.

Abstracted from a dissertation submitted by J. W. Warren, Jr., to the University of Georgia in partial fulfillment of the Doctor of Philosophy degree requirements.

The authors are grateful to Dr. R. L. Mikeal of the School of Pharmacy, University of Georgia, for help in developing the concept of a coefficient of migration.

[x] To whom inquiries should be directed. Present address: College of Pharmacy, Medical University of South Carolina, Charleston, SC 29401.

Drug Migration during Drying of Tablet Granulations II: Effect of Binder Solution Viscosity and Drying Temperature

J. W. WARREN, Jr.[x], and J. C. PRICE

Abstract □ The effect of binder solution viscosity and drying temperature on the intergranular migration of propoxyphene hydrochloride was studied. Wet granulations containing the drug were prepared using binder solutions with viscosities ranging from 1 to 1000 cps. Temperature studies were conducted using granulations prepared with a 3-cps binder solution and dried at 40, 50, 60, 70, and 80°. Drug migration decreased with increased binder solution viscosity, and insignificant migration occurred in granulations prepared with binder solutions having apparent viscosities above 90 cps. No significant effect on intergranular drug migration was observed within the drying temperature range studied. Tablets compressed from a granulation in which drug migration was high showed a greater tablet-to-tablet drug content variation than a granulation with lower migration, even though each dried granulation was thoroughly mixed before tableting.

Keyphrases □ Tablets—effect of binder solution viscosity and temperature on drug migration during drying □ Viscosity, binder solution—effect on drug migration during drying of tablet granulations □ Drying temperature—tablet granulations, effect on drug migration □ Migration, drug—during drying of tablet granulations, effect of binder solution viscosity and temperature □ Dosage forms—tablets, effect of binder solution viscosity and temperature on drug migration during drying

A study of warfarin sodium migration in wet granulations showed that the addition of 5% acacia and 15% alginic acid to a calcium phosphate granulation reduced drug migration (1). However, the extent of drug migration was not related to binder solution viscosity. Other reports dealt with the influence of solvent volume (2) and various granulation drying methods (3). The effect of drying temperature on intragranular migration of povidone was discussed (4), but apparently no investigations have been reported concerning the effect of drying temperature on intergranular migration. This study concerns the influence of binder solution viscosity and drying temperature on the extent of intergranular migration of a water-soluble drug, propoxyphene hydrochloride.

EXPERIMENTAL

The analytical method for the determination of propoxyphene hydrochloride, the drying cell and sampling procedure, the coefficient of migration, the uniformity of the granulations, and the reproducibility of the granulation and drying procedures were described previously (5).

Materials—Propoxyphene hydrochloride, corn starch, lactose, and magnesium stearate were USP grade. Dibasic calcium phosphate, povidone[1], and hydroxypropyl methylcellulose[2] were NF grade.

Formulations—Two formulations were used. Formula I contained (milligrams per 500-mg tablet): propoxyphene hydrochloride, 32; lactose,

[1] GAF Corp., New York, N.Y.

[2] Methocel E-15, Dow Chemical Co., Midland, Mich.

and diffuses to the surface as a vapor (13). Thus, regardless of the potential entry suction (14) increasing with decreasing particle size, the amount of migration tends to reach a limit.

Physical Properties of Granulations—The bulk density, granule density, intraparticle porosity, and moisture content of the lactose granulations are given in Table VII. The average bulk density was 0.531 g/cm^3 with a range of 0.510–0.554 g/cm^3. The average moisture content was 3.4% with a range of 3.0–4.1%.

Although the intraparticle porosity increased with a decreased particle size of lactose, the changes in intraparticle porosity did not correlate well with the extent of propoxyphene hydrochloride migration in this series of granulations. Decreased capillary size and increased contact area with decreasing particle size probably are responsible for the observed results.

CONCLUSIONS

Variations in particle size of the major diluent in wet granulations may result in differences in drug content uniformity in different batches of granules. Control of particle size of the major diluent can minimize drug migration and improve product uniformity in some formulations.

REFERENCES

(1) G. Zografi and A. M. Mattocks, *J. Pharm. Sci.*, **52**, 1103 (1963).

(2) J. Jaffe and I. Lippman, *ibid.*, **53**, 441 (1964).

(3) K. Ridgway and M. H. Rubinstein, *J. Pharm. Pharmacol., Suppl.*, **26**, 24P (1974).

(4) *Ibid., Suppl.*, **23**, 11S (1971).

(5) *Ibid.*, **23**, 587 (1971).

(6) I. A. Chaudry and R. E. King, *J. Pharm. Sci.*, **61**, 1121 (1972).

(7) J. C. Samyn and K. S. Murthy, *ibid.*, **63**, 370 (1974).

(8) D. N. Travers, *J. Pharm. Pharmacol.*, **27**, 516 (1975).

(9) W. J. Dixon and F. J. Massey, Jr., in "Introduction to Statistical Analysis," McGraw-Hill, New York, N.Y., 1969, p. 289.

(10) N. R. Kuzel, in "Automation in Analytical Chemistry, Technicon Symposia 1966," vol. 1, Mediad, White Plains, N.Y., 1967, p. 218.

(11) W. A. Strickland, Jr., L. W. Busse, and T. Higuchi, *J. Am. Pharm. Assoc., Sci. Ed.*, **45**, 482 (1956).

(12) D. L. Harnett, in "Introduction to Statistical Methods," Addison-Wesley, Reading, Mass., 1970, p. 450.

(13) T. K. Sherwood, *Ind. Eng. Chem.*, **21**, 12, 976 (1929).

(14) J. F. Pearse, T. R. Oliver, and D. M. Newitt, *Trans. Inst. Chem. Eng.*, **27**, 1 (1949).

ACKNOWLEDGMENTS AND ADDRESSES

Received July 19, 1976, from the *School of Pharmacy, University of Georgia, Athens, GA 30602.*

Accepted for publication December 16, 1976.

Abstracted from a dissertation submitted by J. W. Warren, Jr., to the University of Georgia in partial fulfillment of the Doctor of Philosophy degree requirements.

The authors are grateful to Dr. R. L. Mikeal of the School of Pharmacy, University of Georgia, for help in developing the concept of a coefficient of migration.

[x] To whom inquiries should be directed. Present address: College of Pharmacy, Medical University of South Carolina, Charleston, SC 29401.

Drug Migration during Drying of Tablet Granulations II: Effect of Binder Solution Viscosity and Drying Temperature

J. W. WARREN, Jr.[x], and J. C. PRICE

Abstract □ The effect of binder solution viscosity and drying temperature on the intergranular migration of propoxyphene hydrochloride was studied. Wet granulations containing the drug were prepared using binder solutions with viscosities ranging from 1 to 1000 cps. Temperature studies were conducted using granulations prepared with a 3-cps binder solution and dried at 40, 50, 60, 70, and 80°. Drug migration decreased with increased binder solution viscosity, and insignificant migration occurred in granulations prepared with binder solutions having apparent viscosities above 90 cps. No significant effect on intergranular drug migration was observed within the drying temperature range studied. Tablets compressed from a granulation in which drug migration was high showed a greater tablet-to-tablet drug content variation than a granulation with lower migration, even though each dried granulation was thoroughly mixed before tableting.

Keyphrases □ Tablets—effect of binder solution viscosity and temperature on drug migration during drying □ Viscosity, binder solution—effect on drug migration during drying of tablet granulations □ Drying temperature—tablet granulations, effect on drug migration □ Migration, drug—during drying of tablet granulations, effect of binder solution viscosity and temperature □ Dosage forms—tablets, effect of binder solution viscosity and temperature on drug migration during drying

A study of warfarin sodium migration in wet granulations showed that the addition of 5% acacia and 15% alginic acid to a calcium phosphate granulation reduced drug migration (1). However, the extent of drug migration was not related to binder solution viscosity. Other reports dealt with the influence of solvent volume (2) and various granulation drying methods (3). The effect of drying temperature on intragranular migration of povidone was discussed (4), but apparently no investigations have been reported concerning the effect of drying temperature on intergranular migration. This study concerns the influence of binder solution viscosity and drying temperature on the extent of intergranular migration of a water-soluble drug, propoxyphene hydrochloride.

EXPERIMENTAL

The analytical method for the determination of propoxyphene hydrochloride, the drying cell and sampling procedure, the coefficient of migration, the uniformity of the granulations, and the reproducibility of the granulation and drying procedures were described previously (5).

Materials—Propoxyphene hydrochloride, corn starch, lactose, and magnesium stearate were USP grade. Dibasic calcium phosphate, povidone[1], and hydroxypropyl methylcellulose[2] were NF grade.

Formulations—Two formulations were used. Formula I contained (milligrams per 500-mg tablet): propoxyphene hydrochloride, 32; lactose,

[1] GAF Corp., New York, N.Y.

[2] Methocel E-15, Dow Chemical Co., Midland, Mich.

Table I—Binder Solutions Employed to Granulate Formulas I and II[a]

Formula	Molecular Weight of Binder[b]	Total Amount of Aqueous Solution, ml	Apparent Viscosity, cps
I-BV1	—	150	1
I-BV2	10,000	150	3
I-BV3	40,000	150	10
I-BV4	160,000	150	100
I-BV5	360,000	150	1000
II-BV1	—	200	1
II-BV2	10,000	200	3
II-BV3	40,000	200	7
II-BV4	160,000	200	90
II-BV5	360,000	200	600

[a] The amount of binders used was 22.5 g except in Formulas I-BV1 and II-BV1 where none was added. [b] Molecular weights as given by the manufacturer of povidone. Manufacturer code numbers are k-15, k-30, k-60, and k-90 in order of increasing molecular weight.

413; corn starch, 50; and magnesium stearate, 5. Formula II contained (milligrams per 500-mg tablet): propoxyphene hydrochloride, 32; dibasic calcium phosphate, 413; corn starch, 50; and magnesium stearate, 5.

Wet Granulation—Each granulation batch weighed 750 g (1500 tablets). The powders were blended for 15 min at low speed in a planetary mixer[3], and water or binding solution then was added to form the wet granulation mass. Water or binder solution, 150 ml, was added to the lactose granulations (Formula I) and 200 ml was added to the dibasic calcium phosphate granulations (Formula II).

After addition of binder, the granulation was mixed for 10–12 min and wet screened through a No. 12 (1680 μm) U.S. standard sieve. The granulations were collected on porous paper and dried for 5 hr in a drying oven[4]. The drying temperature was 50° for the granulations in the binder solution viscosity studies.

Effect of Binder Solution Viscosity on Migration—Various binder solution viscosities of povidone were achieved by employing molecular weight grades of 10,000, 40,000, 160,000, and 360,000. Each was incorporated at a level of 3% (w/w) in both Formulas I and II. Viscosity measurements were made at 25° with a rotational viscometer[5]. Binder solution formulations and viscosities are given in Table I.

The formulations were wet granulated, placed in drying cells, and dried (5). The coefficient of migration (5) for each formulation was calculated and tested for a significant correlation between the extent of propoxyphene hydrochloride migration and increasing binder solution viscosity using Spearman's rank correlation method (6).

Effect of Temperature on Migration—Formula II, granulated with 22.5 g of povidone of 10,000 molecular weight in 200 ml of water (Formula II-BV2), was used for this study. The viscosity of the solution was 3 cps.

Five granulations, 750 g/batch, were prepared and dried in drying cells at 40, 50, 60, 70, and 80°, respectively. Samples were taken and assayed as described previously (5).

The coefficient of migration for each formulation was calculated and tested for a significant correlation (6) between the extent of propoxyphene hydrochloride migration and increased drying temperatures using Spearman's rank correlation method.

Effect of Extent of Migration on Tablet Content Uniformity—Formula II-BV2, granulated with binder solution having an apparent viscosity of 3 cps, and Formula II-BV5, granulated with binder solution having an apparent viscosity of 600 cps, were used to determine the effect of the extent of migration on the content uniformity of tablets. These formulas were selected because they had shown significant differences in drug migration in the dried granulations. The dried granulations were passed through a No. 20 sieve and mixed for 15 min in a twin-shell blender[6].

Five hundred tablets were compressed from each batch, using a single-station tablet compression machine equipped with 0.952-cm (0.38-in.) standard concave tooling.

The USP content uniformity test was run on tablets from each formulation; 30 tablets were randomly selected from each batch, and 10 individual tablets were assayed from the 30. The average drug content per tablet and the standard deviation were calculated for each batch of assayed tablets.

[3] Readco mixer K-20, Read Standard, York, Pa.
[4] Power-O-Matic 60, Blue M Electric Co., Blue Island, Ill.
[5] Model RVT, Brookfield Engineering Labs., Stoughton, Mass.
[6] Model LB201, Patterson-Kelley Co., East Stroudsberg, Pa.

Table II—Granulation Characteristics as a Function of Binder Viscosity

Formula	Granulation Weight in Cell, g	Bulk Density, g/cm^3	Moisture Content after Drying, %
I-BV1	79.0	0.513	3.0
I-BV2	73.0	0.474	2.7
I-BV3	75.0	0.487	3.0
I-BV4	88.0	0.572	3.8
I-BV5	80.0	0.520	3.4
II-BV1	79.5	0.517	4.0
II-BV2	80.1	0.520	4.0
II-BV3	79.0	0.513	2.5
II-BV4	87.0	0.565	3.0
II-BV5	78.4	0.509	2.5
II-BVE15[a]	83.0	0.539	3.0

[a] Binder viscosity was 600 cps.

Table III—Effect of Binder Solution Viscosity on Propoxyphene Hydrochloride Content[a] of Formula I

Layer	Formula I-BV1	Formula I-BV2	Formula I-BV3	Formula I-BV4	Formula I-BV5
1	39.38	40.61	37.67	33.05	31.02
2	29.12	32.50	31.27	31.83	31.25
3	24.12	24.35	24.70	31.85	31.92
4	35.83	37.40	34.63	31.81	32.12

[a] Each value represents an average of three assay determinations of milligrams of propoxyphene hydrochloride/0.5 g of granulation.

Table IV—Effect of Binder Solution Viscosity on Propoxyphene Hydrochloride Migrated from Inner Layers of Lactose Granulations

Formula	Potential Amount in Inner Layers, mg	Amount Recovered from Inner Layers, mg	Amount Depleted from Inner Layers, %
I-BV1	64.22	53.24	17.1
I-BV2	67.42	56.84	15.7
I-BV3	64.14	55.98	12.7
I-BV4	64.27	63.68	0.92
I-BV5	63.16	63.17	0.00

Characteristics of Granulations—The weight of the granulation contents in each drying cell and the moisture content for each granulation were determined (Table II). The average bulk density for the lactose granulations (Formulas I-BV1–I-BV5) was 0.513 g/cm^3 with a range of 0.474–0.572 g/cm^3. The dibasic calcium phosphate granulations (Formulas II-BV1–II-BV5 and II-BVE15) had an average bulk density of 0.527 g/cm^3 with a range of 0.509–0.565 g/cm^3. The average moisture content of the lactose granulations was 3.2% with a range of 2.7–3.8%; for the dibasic calcium phosphate granulations, the average was 3.2% with a range of 2.5–4.0%.

RESULTS AND DISCUSSION

Effect of Binder Solution Viscosity on Extent of Migration—The average assay values for propoxyphene hydrochloride in the four layers of the dried granulation for Formulas I-BV1–I-BV5 are summarized in Table III. From these data, the percent of the potential amount of propoxyphene hydrochloride depleted from the center section (layers 2 and 3) of each granulation in the drying cell was calculated as previously described (5) (Table IV). Increased binder solution viscosity retarded the depletion of drug from the center section of the granulation bed (Table IV). This result was particularly evident for Formulas I-BV4 (binder solution viscosity of 100 cps) and I-BV5 (binder solution viscosity of 1000 cps), where the percent depletion was virtually equal to zero and rather uniform layers were observed.

With Formulas I-BV1–I-BV3, the entry suction (5, 7) tended to draw water from the interior of the bed to the evaporating surfaces of the drying cell because the binder viscosities were relatively low. However, as the binder viscosities were increased (Formulas I-BV4 and I-BV5), the entry suction could not draw the binder solution to the surface at the rate at which evaporation took place. As the drying process continued, the binder solution was held in the capillaries or pores of the granulation bed and eventually the solvent evaporated from the interior of the bed and dif-

Table V—Effect of Binder Solution Viscosity on Propoxyphene Hydrochloride Content[a] of Formula II after Drying

Layer	Formula II-BV1	Formula II-BV2	Formula II-BV3	Formula II-BV4	Formula II-BV5
1	46.09	46.79	43.98	35.76	30.89
2	23.51	20.82	26.74	28.52	30.59
3	17.26	18.91	24.89	26.79	31.88
4	40.29	42.41	40.37	36.34	31.55

[a] Each value represents an average of three assay determinations of milligrams of propoxyphene hydrochloride/0.5 g of granulation.

Table VI—Propoxyphene Hydrochloride Depleted from Inner Layers of Dibasic Calcium Phosphate Granulations

Formula	Potential Amount in Inner Layers, mg	Amount Recovered from Inner Layers, mg	Amount Depleted from Inner Layers, %
II-BV1	63.57	40.77	35.9
II-BV2	64.47	39.73	38.4
II-BV3	67.99	51.63	24.0
II-BV4	63.71	55.31	13.2
II-BV5	62.46	62.47	0

fused through the bed as a vapor (6, 7). When vapor diffusion occurs from the interior of the bed, it follows that the drug will be deposited from the point of evaporation and more uniform layers will be seen in Formulas I-BV4 and I-BV5.

The average propoxyphene hydrochloride assay values for four layers of Formulas II-BV1–II-BV5 are summarized in Table V. From these data, the amount of propoxyphene hydrochloride depleted from the center section (layers 2 and 3) of each granulation was calculated (Table VI). Increased binder viscosity retarded the depletion of drug from the center section of the granulation bed with Formula II. Relatively uniform layers in Formula II-BV5 (with 600-cps binder solution) can also be attributed to the entry suction concept as explained for the lactose granulations (Formulas I-BV1–I-BV5).

With dibasic calcium phosphate (Formula II), more uniform layers did not occur until 600-cps binder solution was used; with lactose (Formula I), rather uniform layers were observed with 100-cps binder solution. There are three possible reasons for this result.

1. The particle size of the primary excipient, dibasic calcium phosphate (57% passes a No. 325 sieve), in Formula II was smaller than the particle size of the primary excipient, lactose (80% retained by a No. 325 sieve), in Formula I. Therefore, the resultant entry suction (1, 5) for Formula II was greater.

2. The amount of binder solution in Formula II was greater; thus, with more solution to evaporate, more drug was carried to the surface. Also, the larger amount of water (200 ml compared to 150 ml in the lactose formula) resulted in somewhat lower viscosities for the binder solutions.

3. Since the particle size of the dibasic calcium phosphate was smaller than the particle size of the lactose, increased granule surface contact in the dibasic calcium phosphate granulations may have facilitated intergranular solvent flow (5). Therefore, a higher binder solution viscosity would have been required to retard the flow of solvent from the interior of the bed.

To determine if a correlation existed between the extent of propoxyphene hydrochloride migration and increasing binder solution viscosity, the coefficient of migration for Formulas I-BV1–I-BV5 and Formulas II-BV1–II-BV5 was calculated as previously described (5) using Spearman's rank correlation method. The formulas were ranked from 1 to 5 relative to increasing binder solution viscosity and then ranked from 1 to 5 according to the calculated coefficient of migration, with rank 1 representing the smallest coefficient and rank 5 representing the largest (Tables VII and VIII).

The critical value for r_s at $n = 5$ is 0.900 at the 0.05 level of significance. Therefore, the values computed in Tables VII and VIII, $r_s = -0.900$, are significant at the 0.05 level. A significant negative correlation indicates that there was an inverse relationship between the extent of migration and increasing binder solution viscosity. That is, as the binder viscosity increased in both Formulas I and II, the extent of propoxyphene hydrochloride migration decreased.

The ability of a binder solution, other than povidone, to retard the migration of propoxyphene hydrochloride in the granulation bed was also investigated. Formula II was granulated with 8% (w/v) hydroxypropyl methylcellulose. This solution had an apparent viscosity of approximately 600 cps, which was comparable to the povidone apparent viscosity of 600 cps used to granulate Formula II-BV5. The methylcellulose granulation was designated as Formula II-BVE15. The average assay values for Formula II granulated with povidone and methylcellulose, respectively, are given in Table IX.

Table VII—Spearman's Rank Correlation Determination for Effect of Binder Solution Viscosity (Formula I) on Extent of Propoxyphene Hydrochloride Migration

Formula	Binder Viscosity Rank	Coefficient of Migration	Coefficient Rank	d_i	d_i^2
I-BV1	1	0.204	5	−4	16
I-BV2	2	0.199	4	−2	4
I-BV3	3	0.165	3	0	0
I-BV4	4	0.014	1	3	9
I-BV5	5	0.016	2	3	9
					38

$$r_s = 1 - \frac{6\sum_{i=1}^{n} d_i^2}{n^3 - n} = 1 - \frac{6(38)}{(5)^3 - 5} = -0.900$$

Table VIII—Spearman's Rank Correlation Determination for Effect of Binder Solution Viscosity (Formula II) on Extent of Propoxyphene Hydrochloride Migration

Formula	Binder Viscosity Rank	Coefficient of Migration	Coefficient Rank	d_i	d_i^2
II-BV1	1	0.406	4	−3	9
II-BV2	2	0.408	5	−3	9
II-BV3	3	0.260	3	0	0
II-BV4	4	0.141	2	2	4
II-BV5	5	0.018	1	4	16
					38

$$r_s = 1 - \frac{6\sum_{i=1}^{n} d_i^2}{n^3 - n} = 1 - \frac{6(38)}{(5)^3 - 5} = -0.900$$

Table IX—Comparison of Propoxyphene Content[a] of Layers of Dried Granulations Prepared from Different Binder Solutions of Equal Viscosity

Layer	Formula II-BV5, mg	Formula II-BVE15, mg
1	30.89	32.52
2	30.59	31.03
3	31.88	31.03
4	31.55	32.78

[a] Each value represents an average of three assay determinations of milligrams of propoxyphene hydrochloride/0.5 g of granulation.

Table X—Analysis of Variance Comparing Formula II-BV5 with Formula II-BVE15

Source	Degrees of Freedom	Sum of Squares	Mean Square	F Ratio	F (0.99)
Formula	1	2.5020	2.5020	4.7515	8.53
Layer	3	5.8911	1.9637	3.7293	5.29
Interaction	3	5.8082	1.9361	3.6768	5.29
Error	16	8.4250	0.5266		
	23	22.6263			

To compare Formula II-BVE15 with Formula II-BV5, a two-factor analysis of variance was used (Table X). Since the calculated F value for the formula factor is not significant at $p = 0.01$, there is apparently no difference between the extent of migration in Formulas II-BVE15 (with methylcellulose) and II-BV5 (with povidone). Also, since the calculated F value for layers is not significant, there is no apparent difference among the layer assay values within a formulation or when the layers of each formulation are compared. The interaction F value is not significant. Therefore, retardation of migration of propoxyphene hydrochloride appears to be a function of binder solution viscosity rather than a specific binding material.

Effect of Temperature on Migration—The average assay results

Table XI—Effect of Drying Temperature on Propoxyphene Hydrochloride Content[a] of Granulation Layers of Formula II-BV2

Layer	40°	50°	60°	70°	80°
1	45.15	46.09	48.02	48.65	43.18
2	21.01	23.51	24.46	21.99	26.23
3	19.65	17.26	19.47	19.35	21.40
4	40.70	40.29	38.92	39.66	38.03

[a] Each value represents an average of three assay determinations of milligrams of propoxyphene hydrochloride/0.5 g of granulation.

Table XII—Spearman's Rank Correlation Determination for Effect of Temperature on Extent of Propoxyphene Hydrochloride Migration in Formula II

Drying Temperature	Temperature Rank	Coefficient of Migration	Coefficient Rank	d_i	d_i^2
40°	1	0.380	2	−1	1
50°	2	0.408	5	−3	9
60°	3	0.382	3	0	0
70°	4	0.407	4	0	0
80°	5	0.299	1	4	16
					26

$$r_s = 1 - \frac{6\sum_{i=1}^{n} d_i^2}{n^3 - n} = 1 - \frac{6(26)}{(5)^3 - 5} = -0.300$$

for Formula II granulated with 3-cps povidone and dried at 40, 50, 60, 70, and 80° are summarized in Table XI.

To test for a significant correlation between the extent of migration and increased drying temperatures, the coefficient of migration for the granulation dried at each temperature was calculated. By using Spearman's rank correlation method, the results at each temperature were ranked from 1 to 5 relative to increased drying temperature, with rank 1 representing the smallest coefficient of migration and rank 5 representing the largest (Table XII).

The critical value for r_s at $n = 5$ is 0.900 at the 0.05 level of significance. The r_s value of −0.300 computed in Table XII is not significant. There apparently is not a significant correlation between the extent of intergranular migration of propoxyphene hydrochloride and increasing drying temperature.

Travers (3), investigating the intergranular migration of sodium chloride, explained that heat transfer by convection is slow and, therefore, evaporation is also slow enough to maintain a solvent flow to the evaporating surfaces. Since heat transfer, which occurs by surface absorption, is slow, the capillary state or film continuity is maintained between individual granules. As the capillary state is maintained and solvent flow continues toward the evaporating surfaces, the solute is transported with the solvent and the solute concentration reaches a maximum near the evaporating surfaces of the granulation bed. Between 40 and 80°, heat transfer and subsequent evaporation were apparently slow enough to maintain a solvent flow to the evaporating surfaces of the top and bottom layers. Consequently, migration of propoxyphene hydrochloride was not significantly different among the temperatures employed.

Effect of Extent of Migration on Tablet Content Uniformity—The final phase of this study was to determine the effect of migration on the content uniformity of tablets. Formula II-BV2, which exhibited considerable drug migration, and Formula II-BV5, which showed little migration, were used.

The assay values for the 10 tablets from Formula II-BV2 are given in Table XIII. The average assay value was 30.661 ± 1.458 (*SD*) mg of propoxyphene hydrochloride/tablet. The range was 88.1–102.6% of theory (32 mg of propoxyphene hydrochloride/tablet). The average tablet weight was 0.506 ± 0.05 (*SD*) g.

The assay values for the 10 tablets from Formula II-BV5 are given in Table XIV. The average assay value was 31.981 ± 0.626 (*SD*) mg of propoxyphene hydrochloride/tablet. The range was 96.1–102.4% of theory (32 mg of propoxyphene hydrochloride/tablet). The average tablet weight was 0.496 ± 0.04 (*SD*) g.

Both tablet batches conformed to the USP content uniformity test, and the data were not significantly different when tested statistically. However, the range of assay values was greater in the granulation exhibiting the greatest drug migration, in line with previous results (1). Content uniformity of tablets made from granulations showing a large amount of migration can be expected to be highly dependent on how well the granulation has been mixed after drying; less thoroughly mixed granulations should show greater variation.

Table XIII—Propoxyphene Hydrochloride Content of Tablets Made from Formula II-BV2 (Granulated with 3-cps Binder Solution)

Tablet Number	Tablet Weight, g	Theoretical Amount per Tablet, mg	Amount Recovered per Tablet, mg	Difference, mg
1	0.502	32.13	28.18	3.95
2	0.500	32.00	30.40	1.60
3	0.514	32.90	30.36	2.53
4	0.508	32.51	30.53	1.98
5	0.507	32.45	30.99	1.46
6	0.504	32.26	32.85	0.59
7	0.512	32.77	31.73	1.04
8	0.502	32.13	28.43	3.70
9	0.506	32.38	31.28	1.11
10	0.510	32.64	31.87	0.77

Table XIV—Propoxyphene Hydrochloride Content of Tablets Made from Formula II-BV5 (Granulated with 600-cps Binder Solution)

Tablet Number	Tablet Weight	Theoretical Amount per Tablet, mg	Amount Recovered per Tablet, mg	Difference, mg
1	0.500	32.00	30.75	1.25
2	0.498	31.87	32.78	0.91
3	0.493	31.55	31.51	0.04
4	0.504	32.26	32.43	0.17
5	0.499	31.94	31.95	0.01
6	0.493	31.55	31.58	0.03
7	0.491	31.42	32.19	0.77
8	0.493	31.55	31.58	0.03
9	0.495	31.63	32.57	0.89
10	0.501	32.06	32.47	0.41

CONCLUSIONS

Drug migration during drying of wet granulations was found to be a significant problem with a soluble drug, propoxyphene hydrochloride, formulated with at least two types of diluents (lactose and dibasic calcium phosphate). A drying temperature of 40–80° appears to have little effect, but an increase in binder solution viscosity can minimize migration with either diluent.

REFERENCES

(1) I. A. Chaudry and R. E. King, *J. Pharm. Sci.*, **61**, 1121 (1972).

(2) J. C. Samyn and K. S. Murthy, *ibid.*, **63**, 370 (1974).

(3) D. N. Travers, *J. Pharm. Pharmacol.*, **27**, 516 (1975).

(4) K. Ridgway and M. H. Rubinstein, *ibid.*, **26**, Suppl. 24P (1974).

(5) J. W. Warren, Jr., and J. C. Price, *J. Pharm. Sci.*, **66**, 1406 (1977).

(6) D. L. Harnett, in "Introduction to Statistical Methods," Addison-Wesley, Reading, Mass., 1970, p. 450.

(7) J. F. Pearse, T. R. Oliver, and D. M. Newitt, *Trans. Inst. Chem. Eng.*, **27**, 1 (1949).

ACKNOWLEDGMENTS AND ADDRESSES

Received July 19, 1976, from the *School of Pharmacy, University of Georgia, Athens, GA 30602.*

Accepted for publication December 16, 1976.

[x] To whom inquiries should be directed. Present address: College of Pharmacy, Medical University of South Carolina, Charleston, SC 29401.

Direct Spectrophotometric Determination of Sulfathiazole in Presence of Sulfadiazine and Sulfamerazine

LAWRENCE J. DOMBROWSKI ˣ, ROBERT S. BROWNING, and EDWARD L. PRATT

Abstract □ A direct spectrophotometric method for the quantitative determination of sulfathiazole and the total pyrimidyl sulfonamide content in a mixture containing sulfadiazine and sulfamerazine is reported. This three-component system was readily reduced to the problem of a simple two-component system analysis. Based on dual isoabsorptive wavelength spectroscopy, simultaneous equations were developed that required absorbance measurements at only two selected wavelengths, both isoabsorptive. The location of the isoabsorptive wavelengths was dependent on the pH of the solvent medium, and 0.1 *M* HCl gave the best results. The validity of the derived equations was demonstrated in a recovery study involving synthetic mixtures containing varying quantities of the three sulfonamides. The recovery was linear over a wide concentration range, and the precision of the method was about 1%.

Keyphrases □ Sulfathiazole—spectrophotometric analysis in mixtures with sulfadiazine and sulfamerazine □ Spectrophotometry—analysis, sulfathiazole in mixtures with sulfadiazine and sulfamerazine □ Sulfonamides—sulfathiazole, spectrophotometric analysis in mixtures with sulfadiazine and sulfamerazine □ Antibacterials—sulfathiazole, spectrophotometric analysis in mixtures with sulfadiazine and sulfamerazine

Previous quantitation methods for sulfonamides in mixtures include paper chromatography (1, 2), precipitation followed by UV absorbance measurement (3), complexometric titration (4), partition chromatography, TLC, and GLC (5–10). Most of these procedures require separation of the individual sulfonamides and are time consuming.

BACKGROUND

A direct spectrophotometric procedure was investigated to determine sulfonamides in combination more rapidly. Quantitative spectrophotometric analysis of two components in one system generally has been simplified by the use of simultaneous equations (11, 12). This process requires that absorbance measurements be made at two wavelengths, λ_1 and λ_2, chosen so that the absorptivity ratio, a_1/a_2, is a maximum at λ_1 and a minimum at λ_2. Knowledge of the four absorptivity values then permits the determination of both components in an unknown. Dual wavelength measurements were used to determine the relative concentration of two components by a graphical absorbance–ratio method (13). This method was greatly simplified when one selected wavelength was isoabsorptive, *i.e.*, a wavelength where numerical values of the individual absorptivities are equal. However, application of direct spectrophotometric analysis to three-component systems generally has not found much use because it requires absorbance measurements at wavelengths where the absorptivity ratios for the various components differ substantially. Therefore, this type of analysis is limited, in part, by the width of the individual absorption band. In addition, there is almost a complete lack of true three-component systems with isoabsorptive points.

Both sulfamerazine (I) and sulfadiazine (II) in 0.1 *M* HCl exhibit two isoabsorptive points at 239 and 279 nm, respectively. By using these analytical wavelengths, it was possible to determine the content of sulfathiazole (III) in a mixture containing all three sulfonamides without interference. Also, the sum total concentration of sulfamerazine and sulfadiazine was simultaneously obtained. Based on dual isoabsorptive wavelength spectroscopy, equations for the three-component system were readily reduced to equations for a two-component system, which greatly simplified the analysis. The method is illustrated by recoveries from a series of solution mixtures containing varying proportions of the three sulfonamides.

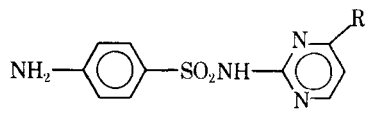

I: R = CH_3
II: R = H

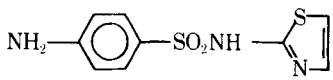

III

In certain cases where complete analyses are not required, the direct method based on dual isoabsorptive wavelength spectroscopy may be simple to use.

EXPERIMENTAL

Chemicals and Reagents—All sulfonamides were USP or NF grade. Acetate buffer was prepared by dissolving 27.3 g of sodium acetate trihydrate in 1000 ml of water and adjusting the pH to 6.0 with acetic acid.

Instrumentation—UV spectra of sulfamerazine[1], sulfadiazine[1], and sulfathiazole[2] were obtained using a recording spectrophotometer[3] with matched 1-cm cells.

Preparation of Solutions—Individual stock solutions of I, II, and III were prepared to contain 100.0 μg of drug/ml of 0.1 *M* HCl. Various aliquots of each stock solution ranging from 1.0 to 6.0 ml were transferred to 100-ml volumetric flasks, diluted to volume with 0.1 *M* HCl, and mixed (Table I). The total sulfonamide concentration in the final dilution was between 10.0 and 12.0 μg/ml, and the sulfathiazole concentration was between 1.0 and 5.0 μg/ml.

Analysis of Tablets—A quantity of the finely powdered tablet mixture, equivalent to 100 mg of total sulfonamides, was transferred to a 250-ml erlenmeyer flask. Exactly 100 ml of 0.1 *M* HCl was added, and the flask was shaken mechanically for 15 min to dissolve the sulfonamides. The solution was filtered, and 2.0 ml of the filtrate was transferred to a 100-ml volumetric flask and diluted to volume with 0.1 *M* HCl. Its absorbance was measured at 239 and 279 nm with 0.1 *M* HCl as a reference.

RESULTS AND DISCUSSION

Figure 1 shows the spectra of sulfadiazine (curve D) and sulfamerazine (curve M), which have two isoabsorptive points located at 239 and 279 nm, respectively. The spectrum for sulfathiazole is represented by curve T. At either one of these analytical wavelengths, Beer's law for a mixture containing the three sulfonamides may be written in general as:

$$A_{obs} = b(a_1c_1 + a_2c_2 + a_3c_3) \qquad \text{(Eq. 1)}$$

where c_1, c_2, and c_3 are the sulfamerazine, sulfadiazine, and sulfathiazole concentrations, respectively.

At both isoabsorptive wavelengths, the absorptivities are equal ($a_1 = a_2 = a_{iso}$) and the sum total concentration of the isoabsorptive species is $c_t = c_1 + c_2$. Consequently, the three-component system is reduced to a two-component system with:

$$A' = b(a'_{iso}c_t + a_3'c_3) \text{ at } 239 \text{ nm} \qquad \text{(Eq. 2)}$$

[1] Lederle Laboratories, Pearl River, N.Y.
[2] Eli Lilly, Indianapolis, Ind.
[3] Perkin-Elmer model 323.

Table I—Preparation of Sulfonamide Mixtures

Sample	Aliquots of Stock Solution, ml I	II	III	Total Sulfonamide Concentration in Final Dilution, μg/ml
1	3.0	3.0	4.0	10.0
2	3.0	4.0	3.0	10.0
3	4.0	3.0	3.0	10.0
4	3.0	3.0	4.0	10.0
5	2.0	4.0	4.0	10.0
6	4.0	2.0	4.0	10.0
7	4.0	4.0	2.0	10.0
8	5.0	4.0	1.0	10.0
9	5.0	3.0	3.0	11.0
10	3.0	5.0	3.0	11.0
11	3.0	3.0	5.0	11.0
12	4.0	4.0	3.0	11.0
13	5.0	5.0	1.0	11.0
14	4.0	4.0	4.0	12.0
15	5.0	5.0	2.0	12.0
16	5.0	2.0	5.0	12.0
17	2.0	5.0	5.0	12.0
18	3.0	4.0	5.0	12.0
19	5.0	6.0	1.0	12.0

and:

$$A'' = b(a''_{iso}\, c_t + a_3'' c_3) \text{ at } 279 \text{ nm} \qquad \text{(Eq. 3)}$$

Equations 2 and 3 can be used to determine the actual concentration of sulfathiazole and the total concentration of sulfadiazine and sulfamerazine. These simultaneous equations, when solved, yielded:

$$c_3 = -\frac{(a'_{iso}A'' - a''_{iso}A')}{(a''_{iso}a_3' - a_3''a'_{iso})} \qquad \text{(Eq. 4)}$$

and:

$$c_t = \frac{(a_3'A'' - a_3''A')}{(a''_{iso}a_3' - a_3''a'_{iso})} \qquad \text{(Eq. 5)}$$

To test the validity of Eqs. 4 and 5, the absorbance values at 239 and 279 nm were obtained for the series of mixed solutions listed in Table I. For the calculations, the experimentally derived absorptivity[4] values for each sulfonamide in 0.1 *M* HCl at λ_1 and λ_2 were employed. The λ_1 and λ_2 values were 57.1 and 12.6 for sulfadiazine, 57.1 and 12.6 for sulfamerazine, and 11.3 and 50.9 for sulfathiazole, respectively. The resulting recovery data for both sulfathiazole and the quantity c_t are shown in Table II. These results agree well with the known amounts of substances added.

The average recoveries found for sulfathiazole and the c_t were 100.2 ± 1.1 and 99.6 ± 0.6%, respectively. A 1.2–11.0-fold excess of the mixed pyrimidyl sulfonamides did not interfere with the sulfathiazole determination. Likewise, sulfathiazole did not interfere with the determination of the total pyrimidyl sulfonamide content. In addition, the sum of the

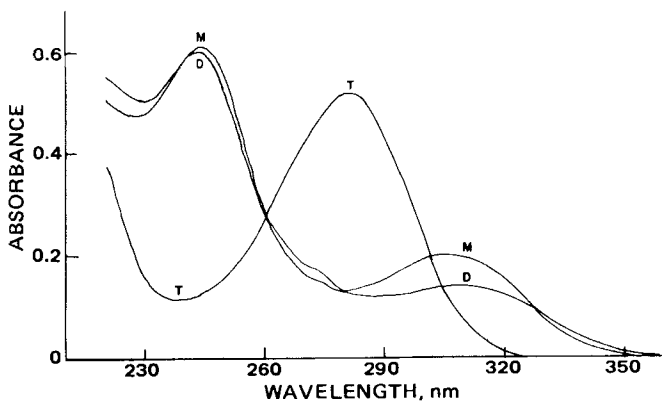

Figure 1—*UV spectra of sulfamerazine (curve M), sulfadiazine (curve D), and sulfathiazole (curve T) in 0.1* M *HCl. Concentration is 10.0 μg/ml.*

[4] Defined as the absorbance divided by the concentration expressed in grams per liter.

Table II—Recoveries from Synthetic Mixtures

Sample	Sulfathiazole μg/ml	Recovery, %	c_t[a] μg/ml	Recovery, %
1	3.94	98.5	5.93	98.8
2	2.98	99.3	6.94	99.2
3	2.99	99.7	6.96	99.4
4	4.02	100.5	6.03	100.5
5	4.02	100.5	6.03	100.5
6	4.00	100.0	6.03	100.5
7	2.01	100.5	8.02	100.3
8	1.00	100.0	8.84	98.2
9	2.97	99.0	7.98	99.8
10	2.99	99.7	7.96	99.5
11	5.01	100.2	5.96	99.3
12	3.06	102.0	8.00	100.0
13	1.00	100.0	9.94	99.4
14	4.07	101.8	7.98	99.8
15	2.03	101.5	9.97	99.7
16	4.98	99.6	6.94	99.2
17	4.98	99.6	6.94	99.2
18	4.96	99.2	6.95	99.3
19	1.03	103.0	10.90	99.1
Average		100.2 ± 1.1		99.6 ± 0.6

[a] c_t = sum of sulfamerazine and sulfadiazine concentration.

sulfathiazole content and the quantity c_t from Table II agreed well with the total sulfonamide concentrations given in Table I. The average recovery for the latter based on all 19 determinations was 99.7 ± 0.5%.

The effect of various excipients on the recovery from synthetic tablet mixtures also was investigated. The following excipients did not interfere when added individually or in combination to an equal weight of the mixed sulfonamides: starch, talc, magnesium stearate, microcrystalline cellulose, lactose, sodium lauryl sulfate, and dibasic calcium phosphate. The average recoveries for sulfathiazole and the c_t in the presence of these excipients were 99.8 ± 1.0 and 100.0 ± 0.8%, respectively.

Table III shows the results obtained from an analysis of an experimental triple sulfa tablet preparation. Five individual determinations were made from a single composite, and the resulting assays were in good agreement with the claimed levels.

The excellent recovery data reported with this procedure result from absorbance measurements taken at or near plateau regions in the spectrum. This fact is evident in Fig. 1 where the slope $\Delta A/\Delta\lambda$ is essentially constant at the wavelengths of interest. The first isoabsorptive wavelength (λ_1) is near the absorbance maximum of both pyrimidyl sulfonamides centered at 243 nm; the second isoabsorptive wavelength (λ_2) is located at the minimum between the first and second absorption bands of these same compounds. In addition, λ_1 and λ_2 occur at the minimum and maximum absorbances of sulfathiazole. Consequently, at these analytical wavelengths, the values of the absorptivity ratios a'_{iso}/a_3' and a''_{iso}/a_3'' are 5.05 (max) and 0.25 (min), respectively. These conditions are most favorable for the spectrophotometric determination of two components based on absorbance measurements at two selected wavelengths.

The location and intensity of the absorption bands in the UV absorbance spectra of I–III are both dependent on the solvent pH. Two additional pH's were examined to determine if the corresponding spectra were amenable to analysis by Eqs. 4 and 5. Figures 2 and 3 show the resulting spectra obtained in pH 6 acetate buffer and 0.1 *M* NaOH. Dual isoabsorptive points were found for the pyrimidyl compounds and showed a bathochromic displacement with increasing pH. For example, λ_1 shifted from 239 nm in acid to 249 nm in pH 6 buffer and to 266 nm in 0.1 *M*

Table III—Assay Results on an Experimental Triple Sulfa Tablet Composite[a]

Determination	Assay Results, % of Claim Sulfathiazole	Sulfamerazine plus Sulfadiazine
1	98.4	99.1
2	98.4	98.7
3	98.9	98.7
4	98.4	98.4
5	98.9	98.7
Average	98.6 ± 0.3	98.7 ± 0.3

[a] Claimed milligrams per tablet are: sulfathiazole, 186; and sulfamerazine plus sulfadiazine, 317.

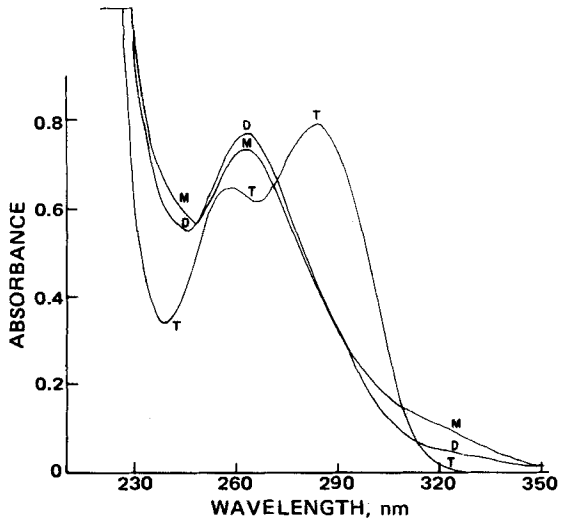

Figure 2—*UV spectra of sulfamerazine (curve M), sulfadiazine (curve D), and sulfathiazole (curve T) in pH 6 acetate buffer. Concentration is 10.0 μg/ml.*

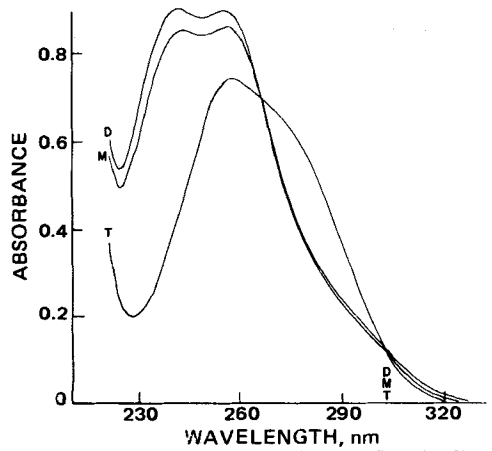

Figure 3—*UV spectra of sulfamerazine (curve M), sulfadiazine (curve D), and sulfathiazole (curve T) in 0.1 M NaOH. Concentration is 10.0 μg/ml.*

NaOH. Similarly, the shift observed for λ_2 was from 279 to 291 nm at the intermediate pH and finally to 303 nm in base.

Figures 2 and 3 show that the isoabsorptive points all occur on the steep slope of an absorption band. Also, the absorptivity ratios (a_{iso}/a_3), with one exception, are near unity. Consequently, absorbance measurements at these particular wavelengths in either solvent system are prone to considerable error and are not suitable for precise quantitative spectrophotometric analysis. This fact was demonstrated in a recovery study where both systems were applied to a synthetic tablet mixture. Based on six individual determinations, the best relative standard deviation obtained was only 6%. The use of 0.1 *M* HCl offers the obvious advantage of providing better precision.

The proposed method should be well suited for the routine analysis of a large number of samples. Both content uniformity testing and dissolution rate determinations of triple sulfa tablets would be practical examples.

REFERENCES

(1) "First Supplement to the United States Pharmacopeia," 18th rev., Mack Publishing Co., Easton, Pa., 1970, p. 29.

(2) "The National Formulary," 13th ed., Mack Publishing Co., Easton, Pa., 1970, p. 877.

(3) M. Matsuna and M. Mishimura, *Yakugaku Kenbyu*, **29**, 178 (1957).

(4) F. Said, M. Amer, and M. Walash, *Bull. Fac. Pharm. Cairo Univ.*, **6**, 199 (1967).

(5) H. M. Miller, *J. Assoc. Offic. Anal. Chem.*, **53**, 1100 (1970).

(6) B. Rader, *J. Pharm. Sci.*, **62**, 1148 (1973).

(7) T. Bican-Fister and V. Kajganovic, *J. Chromatogr.*, **16**, 503 (1964).

(8) C. A. Brunner, *J. Assoc. Offic. Anal. Chem.*, **55**, 194 (1972).

(9) S. N. Tewari and D. N. Tripalhi, *Z. Anal. Chem.*, **166**, 356 (1959).

(10) J. W. Turczan, *J. Pharm. Sci.*, **57**, 142 (1968).

(11) M. Ish-Shalom, J. D. Fitzpatrick, and M. Orchin, *J. Chem. Educ.*, **34**, 496 (1957).

(12) H. Jaffe and M. Orchin, "Theory and Application of Ultraviolet Spectroscopy," Wiley, New York, N.Y., 1965, p. 556.

(13) R. C. Hirt, F. T. King, and R. G. Schmitt, *Anal. Chem.*, **26**, 1270 (1954).

ACKNOWLEDGMENTS AND ADDRESSES

Received March 29, 1976, from *Sterling-Winthrop Research Institute, Rensselaer, NY 12144.*

Accepted for publication December 16, 1976.

[x] To whom inquiries should be directed.

Synthesis, Physicochemical Properties, and Antitumor Activities of Analogs of 1-Phenyl-3-benzyl-3-methyltriazenes

WILLIAM J. DUNN, III ˣ, and M. J. GREENBERG

Abstract □ To study the effect of substituents on the antitumor activities of analogs of 1-phenyl-3-benzyl-3-methyltriazenes, a series of compounds was designed and synthesized in which the substituent on the 1-phenyl was an electron-withdrawing group and the substituent on the 3-benzyl had a broad range of physicochemical properties. Of the 13 analogs prepared and tested against Sarcoma-180 in the mouse, five showed significant activity. The results were submitted to discriminant analysis to determine structure–activity relationships.

Keyphrases □ Triazenes, substituted—synthesized, antitumor activity evaluated, mice □ Antitumor activity—evaluated in various substituted triazenes, mice □ Structure–activity relationships—various substituted triazenes evaluated for antitumor activity

For 1-phenyl-3,3-dimethyltriazenes (I) (1), activity against Sarcoma-180 in the mouse recently was reported to be a function of the Hammett sigma constant for X, the phenyl group substituent. This relationship is given by:

$$pC_{130} = 3.41\ (\pm 0.03) - 0.69\ (\pm 0.09)\sigma \qquad \text{(Eq. 1)}$$

$$n = 13 \qquad r^2 = 0.85 \qquad s = 0.09$$

where pC_{130} is $-\log C_{130}$, and C is the molar concentration per kilogram of mouse required to increase the lifespan of the treated group 30% over the control. The derivatives on which the equation is based were designed using the cluster analysis scheme proposed by Hansch *et al.* (2).

The unusual aspect of this relationship is that activity is a function of the electronic nature of X. In a study of the structure–activity requirements of triazenes of Structure II, Hansch *et al.* (3) proposed that lipophilicity is significant in determining the level of activity against L-1210 in the mouse.

This report describes the synthesis and evaluation, as antitumor agents, of a series of triazenes of general Structure III.

EXPERIMENTAL

Synthesis—The triazenes were prepared by coupling the appropriate benzylamine with a diazonium cation using the procedure of Rondestvedt and Davis (4). The benzylamines were obtained commercially or were prepared using a reported procedure (5). The procedure is illustrated here for the synthesis of III*b*. The structures were verified by IR, PMR, and mass spectrometric methods (Table I).

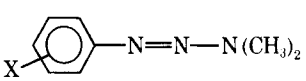

I

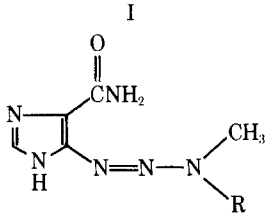

II

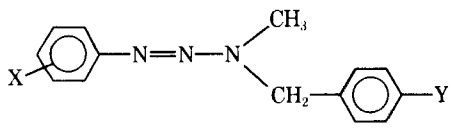

III

For III*b*, *p*-chlorobenzaldehyde (35.1 g) in dry benzene (75 ml) was placed in a three-necked flask equipped with a distilling trap. An aliquot of 200 ml of benzene saturated with methylamine was added, and the mixture was refluxed for 24 hr. Benzene was distilled at reduced pressure, and the imine that resulted was dissolved in absolute methanol. To this mixture was added sodium borohydride (14 g) in 70 ml of methanol.

After refluxing for 4 hr, the mixture was cooled to 0° and acetone was added to decompose the excess hydride. The mixture was extracted with 3 *N* HCl and ether to remove unreduced starting material. The amine was regenerated with 6 *N* sodium hydroxide and extracted with ether. The amine was dried, taken up in ether, and purified as the hydrochloride. The yield was 16.4 g (34%), mp 204° [lit. (5) mp 205°].

The amine (9.08 g) was reacted with the diazonium cation generated from *p*-aminobenzoic acid (5.48 g) and sodium nitrite (2.76 g) at −5°. The coupling reaction with the benzylamine at 0° yielded 6.20 g (51%) of triazene, mp 168° (methanol).

Anal.—Calc. for $C_{15}H_{14}ClN_3O_2$: C, 59.31; H, 4.99; N, 13.84. Found: C, 59.70; H, 4.76; N, 14.11.

Partition Coefficients—1-Octanol–water partition coefficients were determined according to a reported procedure (6). Those for the carboxylic acids were determined at pH 7.4 and corrected for ionization using the pKa = 4.20 determined for *p*-(3,3-dimethyl-1-triazeno)benzoic acid by the method of Bordwell and Cooper (7).

Hydrolysis—Each *p*-(3-benzyl-3-methyl-1-triazeno)benzoic acid was dissolved in methanol (10 ml). A 1-ml aliquot was taken from this solution and placed in a 100-ml volumetric flask. The volume was adjusted to 100 ml with pH 7.0, 0.01 *M* phosphate buffer, preheated to 37°. The disappearance of the maximum absorption for each triazene was followed spectrophotometrically.

Rate constants were calculated from the absorbance data using the technique of Guggenheim (8), and $t_{1/2}$ values are given in Table I. Rate constants also were determined as a function of pH for triazenes III*a* and III*c* (Fig. 1).

Biological Testing—The triazenes were tested for activity against Sarcoma-180 ascitic tumor in the mouse using a modification of the procedure of Sartorelli *et al.* (9). Donar mice were sacrificed by asphyxiation with chloroform, followed by removal of the top skin layer of the intraperitoneal cavity, and fluid was removed. A threefold dilution of this fluid was made with sterile saline, and 0.1 ml (approximately 2×10^6 cells) was injected into 15–18-g female albino Swiss mice. Each test group was composed of six mice; a control group of six mice was determined for each test.

The triazenes were suspended in sterile saline and administered on alternate sides of the intraperitoneal cavity 24 hr after implantation. This dosing was repeated daily for 3 days. Initial dosage levels were set at 0.25, 0.38, and 0.50 of the LD_{50} for that particular drug; other dosage levels were in this range. The mice were observed daily, and the day of death was recorded.

A dose–response curve was generated from which the log dose (milligrams per kilogram) required to give T/C = 130% was obtained. The error in such a determination can be as high as 25%. Compound III*d*, although active, did not give a suitable dose–response curve from which a standard response curve could be obtained.

The LD_{50} values were determined by the procedure of Turner (10) using suspensions prepared as previously described. The LD_{50} values reported were the moles per kilogram of animal lethal to 50% of a group of five mice in 1 week. Each LD_{50} was determined from a dose–response curve derived from at least four test groups. The activities are reported in Table I.

Discriminant Analysis—Analyses were carried out using a standard statistical package. The physicochemical constants were either deter-

Table I—Physical and Biological Properties of 1-Phenyl-3-benzyl-3-methyltriazenes

Compound	X	Y	Yield, %	Melting Point	Formula	Analysis, %		Chemical Shifts, ppm[a]			Biological Properties			
						Calc.	Found	3-Methyl	3-Benzyl	1-Phenyl	pC_{130}	pLD_{50}	Log P (Ion Corrected)	$t_{1/2}$, days
III*a*	*p*-CO_2H	H	53	149°	$C_{15}H_{15}N_3O_2$	C 66.88 H 5.63 N 15.61	66.76 5.57 15.69	3.15	4.93	7.25–8.10	Inactive	2.80	4.04	2.55
III*b*	*p*-CO_2H	Cl	51	168°	$C_{15}H_{15}ClN_3O_2$	C 59.31 H 4.99 N 13.84	59.70 4.76 14.11	3.15	4.98	7.28–7.93	3.19	2.65	4.85	3.05
III*c*	*p*-CO_2H	NO_2	51	156°	$C_{15}H_{14}N_4O_4$	C 57.31 H 4.50 N 17.83	57.23 4.54 18.07	3.30	5.20	7.47–8.30	Inactive	2.69	4.03	4.18
III*d*	*p*-CO_2H	CN	62	165°	$C_{16}H_{15}N_4O_2$	C 65.29 H 5.15 N 19.04	65.12 4.90 18.93	3.25	5.17	8.03–8.30	Active	2.62	3.60	3.96
III*e*	*p*-CO_2H	CH_3	72	166°	$C_{16}H_{17}N_3O_2$	C 67.82 H 6.06 N 14.83	67.86 6.03 15.07	3.20	5.02	7.23–8.02	3.25	2.75	4.75	2.65
III*f*	*p*-CO_2H	OCH_3	69	157°	$C_{16}H_{17}N_3O_3$	C 64.19 H 5.74 N 14.04	64.01 5.78 14.13	3.20	4.97	6.93–8.02	Inactive	2.77	4.43	2.64
III*g*	*p*-CO_2H	$NHCOCH_3$	49	193°	$C_{17}H_{18}N_4O_3$	C 62.55 H 5.57 N 17.17	62.40 5.60 17.23	3.22	5.02	7.23–8.02	Inactive	2.21	3.35	2.55
III*h*	*p*-CO_2H	$C(CH_3)_3$	37	146°	$C_{19}H_{23}N_3O_2$	C 70.12 H 7.14 N 12.91	70.15 7.18 12.99	3.20	4.98	7.34–7.96	3.20	2.75	6.09[b]	—
III*i*	*p*-CN	H	84	84°	$C_{15}H_{14}N_4$	C 71.97 H 5.65 N 22.39	71.89 5.73 22.28	3.12	4.93	7.27–7.47	Inactive	2.59	3.82	—
III*j*	*p*-CN	Cl	81	58°	$C_{15}H_{13}ClN_4$	C 63.21 H 4.61 N 19.68	63.39 4.74 19.96	3.31	4.90	7.18–7.48	Inactive	2.71	4.44[b]	—
III*k*	*m*-Cl	Cl	55	Dec.	$C_{14}H_{13}Cl_2N_3$	C 57.15 H 4.46 N 14.29	57.16 4.48 14.30	3.15	4.90	7.01–7.50	3.08	2.24	5.03[b]	—
III*l*	*p*-$CONH_2$	H	39	133°	$C_{15}H_{16}N_4O$	C 67.13 H 6.02 N 20.88	66.91 6.03 20.87	3.18	4.98	7.25–7.90	Inactive	2.98	2.76	—
III*m*	*p*- 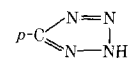	H	46	168°	$C_{15}H_{15}N_7$	C 61.41 H 5.16 N 33.43	61.05 5.23 33.20	3.19	5.06	7.62–8.10	Inactive	3.08	2.37[b]	—

[a] Relative to tetramethylsilane at 0 ppm. Solvents were deuterochloroform for III*a*, dimethyl sulfoxide-d_6 for III*b*–III*h*, III*l*, and III*m*; and carbon tetrachloride for III*i*–III*k*. [b] Estimated value.

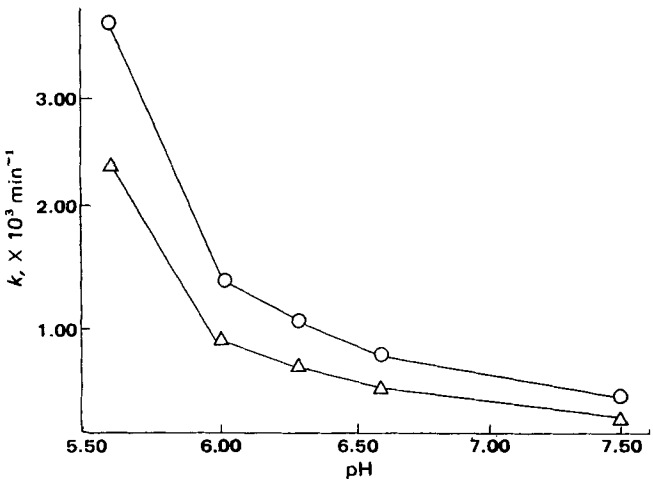

Figure 1—*The pH-rate profile for IIIa (○) and IIIc (△).*

mined or obtained from published compilations (11, 12) (Table II). In the analysis, prior probabilities for activity or inactivity were set as being equal.

RESULTS AND DISCUSSION

The synthetic procedures used to prepare this class of compounds generally gave good yields. The partition coefficients show that they were very lipophilic; the *tert*-butyl analog was too lipophilic to obtain a reliable measurement. At pH 7, the triazenes were relatively stable to hydrolysis, with $t_{1/2}$ in the range of 2.5–4.0 days. Hydrolysis is acid catalyzed, as can be seen from the pH-rate profile in Fig. 1.

The mass spectral fragmentation for the triazenes in this study produced fragments resulting mainly from cleavage of the 2–3-nitrogen bond of the triazene group. Thus, the fragmentation patterns were those of the diazonium cation and the benzylamine that resulted from such cleavage. For analogs in which X = COOH and Y varies, the fragmentation is given in Scheme I. When Y is electron withdrawing, the base peak is the benzoic acid cation; it is the substituted tropylium ion when Y is electron donating.

There was very little difference in the antitumor activities on a molar basis. The same was true for the toxicities; the analogs were essentially equitoxic. Since the compounds showed little variation in activity, they could not be used in a Hansch analysis.

The 13 analogs were classified as active and inactive and subjected to discriminant analysis. This technique was recently shown to be useful in classifying inhibitors of monoamine oxidase (10) on the basis of their

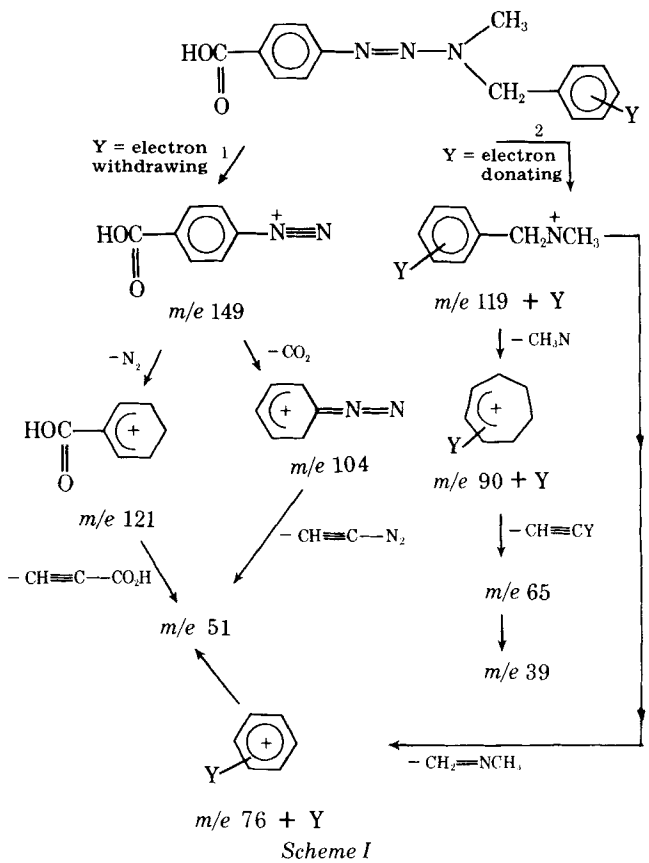

Scheme I

physicochemical properties. Ideally, the procedure results in a function that classifies the molecules into an active group and an inactive group. The results are given in Table III. The analysis classifies 11 of the 13 compounds correctly; one from each category is misclassified.

An examination of the discriminant functions shows that these results are consistent with a previous report (1) in that activity appears to be associated with electron-donating groups for the substituent X. Variation

Table II—Physicochemical Parameters

Compound	f_x	f_y	σ_x[a]	σ_y[a]
IIIa	−0.40[b]	0.19[b]	0.00	0.00
IIIb	−0.40[b]	0.81	0.00	0.23
IIIc	−0.40[b]	−0.01	0.00	0.78
IIId	−0.40[b]	−0.44	0.00	0.66
IIIe	−0.40[b]	0.71	0.00	−0.17
IIIf	−0.40[b]	0.39	0.00	−0.27
IIIg	−0.40[b]	−0.68	0.00	0.00
IIIh	−0.40[b]	2.24[b]	0.00	−0.20
IIIi	−0.22	0.19	0.66	0.00
IIIj	−0.22	0.81	0.66	0.23
IIIk	0.81	0.81	0.37	0.23
IIIl	−1.28	0.11	0.36	0.00
IIIm	−1.23[a]	0.19[b]	0.50	0.00

Correlation Matrix

	ACT	f_x	f_y	σ_x	σ_y
ACT	1.00	0.42	0.48	−0.37	0.09
f_x	0.42	1.00	0.22	0.01	0.18
f_y	0.48	0.22	1.00	0.02	0.38
σ_x	−0.37	−0.01	0.02	1.0	−0.05
σ_y	0.09	0.18	−0.38	−0.05	1.00

[a] Reference 12. [b] Reference 11.

Table III—Discriminant Analysis Results

Linearized Discriminant Function

	ACT 0	ACT 1
Constant	−0.59	−1.52
ACT	0.00	0.00
f_y	0.26	2.96
σ_x	3.79	−0.62
σ_y	1.19	4.32

Probability of Membership in ACT

Observed	From ACT	Classified into ACT	0	1
IIIa	0	0	0.60	0.40
IIIb	1	1	0.12	0.88
IIIc	0	1	0.19[a]	0.81
IIId	1	0	0.52[a]	0.48
IIIe	1	1	0.39	0.61
IIIf	0	0	0.67	0.33
IIIg	0	0	0.94	0.06
IIIh	1	1	0.01	0.99
IIIi	0	0	0.96	0.03
IIIj	0	0	0.72	0.28
IIIk	1	1	0.41	0.58
IIIl	0	0	0.90	0.10
IIIm	0	0	0.93	0.07

[a] Misclassified observation.

at Y does affect activity, with the more lipophilic and electron-withdrawing groups being classified as active.

The detection of the role of lipophilicity is consistent with the report of Hansch *et al.* (3), who found that the activity of analogs of II was a function of the lipophilicity of the substituents at the 3-nitrogen.

The interpretation of these results in terms of the mode of action of the triazenes can only be viewed as suggestive at this point. It was suggested previously that the triazenes must be demethylated to form an active metabolite (13). The compounds in this study are subject to such activation, but the physicochemical effect on metabolism of substituents removed from the site of *N*-demethylation has not been studied for triazenes. Therefore, further work is necessary before conclusions can be drawn.

REFERENCES

(1) W. J. Dunn, III, M. J. Greenberg, and S. Callejas, *J. Med. Chem.*, **19**, 1299 (1976).

(2) C. Hansch, S. H. Unger, and A. B. Forsythe, *ibid.*, **16**, 1217 (1973).

(3) C. Hansch, R. N. Smith, R. Engle, and H. Wood, *Cancer Chemother. Rep.*, **56**, 443 (1972).

(4) C. S. Rondestvedt and S. J. Davis, *J. Org. Chem.*, **22**, 200 (1957).

(5) V. V. Ranade, F. Kohen, and R. E. Counsell, *J. Med. Chem.*, **14**, 38 (1971).

(6) C. Hansch, T. Fujita, and J. Iwasa, *J. Am. Chem. Soc.*, **86**, 5175 (1964).

(7) F. Bordwell and G. D. Cooper, *ibid.*, **74**, 1058 (1972).

(8) E. A. Guggenheim, *Phil. Mag.*, **1**, 538 (1938).

(9) A. C. Sartorelli, B. A. Booth, and K. C. Agrawal, *J. Med. Chem.*, **11**, 700 (1968).

(10) Y. C. Martin, J. B. Holland, C. H. Jarboe, and N. Plotnikoff, *ibid.*, **17**, 409 (1974).

(11) G. G. Nys and R. F. Rekker, *Chim. Ther.*, **5**, 521 (1973).

(12) C. Hansch, A. Leo, S. H. Unger, K. H. Kim, D. Nikaitani, and E. J. Lien, *J. Med. Chem.*, **16**, 1207 (1973).

(13) T. A. Connors, P. M. Goddard, K. Merai, W. C. J. Ross, and D. E. V. Wilman, *Biochem. Pharmacol.*, **25**, 241 (1976).

ACKNOWLEDGMENTS AND ADDRESSES

Received August 18, 1976, from the *Department of Medicinal Chemistry, College of Pharmacy, University of Illinois at the Medical Center, Chicago, IL 60680.*

Accepted for publication December 9, 1976.

The authors acknowledge the American Cancer Society for financial support and Dr. Y. C. Martin, Abbott Laboratories, for helpful discussions of the discriminant analysis technique.

[x] To whom inquiries should be directed.

Rapid and Sensitive Direct TLC Fluorometric Method for Evaluation of Impurities in Oxytetracycline

GILBERT J. WILLEKENS

Abstract □ A rapid partition TLC method for the determination of oxytetracycline and its degradation products is described. Quantitative determination of the substances is performed by direct TLC fluorometry in 2 hr using plates prepared previously.

Keyphrases □ Oxytetracycline and impurities—TLC fluorometric analyses in prepared solutions □ TLC fluorometry—analyses, oxytetracycline and impurities in prepared solutions □ Fluorometry, TLC—analyses, oxytetracycline and impurities in prepared solutions □ Antibacterials—oxytetracycline and impurities, TLC fluorometric analyses in prepared solutions

Tetracyclines are sensitive to both acidic and alkaline degradation media (1). Storage under adverse moisture and temperature conditions gives rise to acidic degradation products. The first stage of acidic degradation is the formation of anhydro compounds, which have attracted a great deal of attention because of their potential toxicity (2, 3).

Although the most likely degradation products of oxytetracycline (I) are not toxic, an accurate and convenient analytical method is needed to investigate the purity of commercial I samples. Anhydrooxytetracycline (II), epioxytetracycline (III), α-apooxytetracycline (IV), and β-apooxytetracycline (V) occur as impurities in I, but little information has been published about their quantitative evaluation.

Compound I was determined by UV spectrophotometry (4) and fluorometry (5). Degradation products were separated from I by paper chromatography (6, 7). Some acidic degradation products of I were determined chromatographically using paper impregnated with 10% (w/v) urea in pH 5.0 McIlvaine's buffer (8). After elution, I was quantitated by spectrophotometry.

Compounds II, IV, V, and terrinolide (VI) were separated on a kieselguhr layer (9). Compound I also was separated from its impurities on a diatomaceous earth column, and I and V were evaluated by spectrophotometry (10).

The use of paper chromatography is undesirable (6–8) because the procedure is lengthy and not reproducible. A TLC separation of II, IV, and V from I on kieselguhr (9) could not be achieved in this laboratory.

The TLC procedure presented is rapid and allows the quantitation of traces of II–V in I by direct TLC fluorometry. The method is reproducible and is sensitive to 10^{-2} μg of II–V in a 1% (w/v) solution of I.

EXPERIMENTAL

Reagents—Disodium ethylenediaminetetraacetate (VII), ethylene glycol, acetone, ethyl formate, ethyl acetoacetate, and sodium hydroxide were analytical grade. Kieselguhr G[1] was used.

Preparation of Plates—A slurry of 20 g of kieselguhr and 47 ml of 5% (w/v) aqueous VII, previously adjusted to pH 9 with 20% NaOH, was prepared[2] and spread on glass plates at a thickness of 0.25–0.30 mm. The plates were dried in air for a minimum of 2 hr at room temperature (25°); a transverse channel of approximately 1-mm width was drawn in the layer

[1] Macherey, Nagel & Co, D-516 Düren, Germany.

[2] Desaga applicator, Heidelberg, Germany.

at Y does affect activity, with the more lipophilic and electron-withdrawing groups being classified as active.

The detection of the role of lipophilicity is consistent with the report of Hansch *et al.* (3), who found that the activity of analogs of II was a function of the lipophilicity of the substituents at the 3-nitrogen.

The interpretation of these results in terms of the mode of action of the triazenes can only be viewed as suggestive at this point. It was suggested previously that the triazenes must be demethylated to form an active metabolite (13). The compounds in this study are subject to such activation, but the physicochemical effect on metabolism of substituents removed from the site of *N*-demethylation has not been studied for triazenes. Therefore, further work is necessary before conclusions can be drawn.

REFERENCES

(1) W. J. Dunn, III, M. J. Greenberg, and S. Callejas, *J. Med. Chem.*, **19**, 1299 (1976).

(2) C. Hansch, S. H. Unger, and A. B. Forsythe, *ibid.*, **16**, 1217 (1973).

(3) C. Hansch, R. N. Smith, R. Engle, and H. Wood, *Cancer Chemother. Rep.*, **56**, 443 (1972).

(4) C. S. Rondestvedt and S. J. Davis, *J. Org. Chem.*, **22**, 200 (1957).

(5) V. V. Ranade, F. Kohen, and R. E. Counsell, *J. Med. Chem.*, **14**, 38 (1971).

(6) C. Hansch, T. Fujita, and J. Iwasa, *J. Am. Chem. Soc.*, **86**, 5175 (1964).

(7) F. Bordwell and G. D. Cooper, *ibid.*, **74**, 1058 (1972).

(8) E. A. Guggenheim, *Phil. Mag.*, **1**, 538 (1938).

(9) A. C. Sartorelli, B. A. Booth, and K. C. Agrawal, *J. Med. Chem.*, **11**, 700 (1968).

(10) Y. C. Martin, J. B. Holland, C. H. Jarboe, and N. Plotnikoff, *ibid.*, **17**, 409 (1974).

(11) G. G. Nys and R. F. Rekker, *Chim. Ther.*, **5**, 521 (1973).

(12) C. Hansch, A. Leo, S. H. Unger, K. H. Kim, D. Nikaitani, and E. J. Lien, *J. Med. Chem.*, **16**, 1207 (1973).

(13) T. A. Connors, P. M. Goddard, K. Merai, W. C. J. Ross, and D. E. V. Wilman, *Biochem. Pharmacol.*, **25**, 241 (1976).

ACKNOWLEDGMENTS AND ADDRESSES

Received August 18, 1976, from the *Department of Medicinal Chemistry, College of Pharmacy, University of Illinois at the Medical Center, Chicago, IL 60680.*

Accepted for publication December 9, 1976.

The authors acknowledge the American Cancer Society for financial support and Dr. Y. C. Martin, Abbott Laboratories, for helpful discussions of the discriminant analysis technique.

[x] To whom inquiries should be directed.

Rapid and Sensitive Direct TLC Fluorometric Method for Evaluation of Impurities in Oxytetracycline

GILBERT J. WILLEKENS

Abstract □ A rapid partition TLC method for the determination of oxytetracycline and its degradation products is described. Quantitative determination of the substances is performed by direct TLC fluorometry in 2 hr using plates prepared previously.

Keyphrases □ Oxytetracycline and impurities—TLC fluorometric analyses in prepared solutions □ TLC fluorometry—analyses, oxytetracycline and impurities in prepared solutions □ Fluorometry, TLC—analyses, oxytetracycline and impurities in prepared solutions □ Antibacterials—oxytetracycline and impurities, TLC fluorometric analyses in prepared solutions

Tetracyclines are sensitive to both acidic and alkaline degradation media (1). Storage under adverse moisture and temperature conditions gives rise to acidic degradation products. The first stage of acidic degradation is the formation of anhydro compounds, which have attracted a great deal of attention because of their potential toxicity (2, 3).

Although the most likely degradation products of oxytetracycline (I) are not toxic, an accurate and convenient analytical method is needed to investigate the purity of commercial I samples. Anhydrooxytetracycline (II), epioxytetracycline (III), α-apooxytetracycline (IV), and β-apooxytetracycline (V) occur as impurities in I, but little information has been published about their quantitative evaluation.

Compound I was determined by UV spectrophotometry (4) and fluorometry (5). Degradation products were separated from I by paper chromatography (6, 7). Some acidic degradation products of I were determined chromatographically using paper impregnated with 10% (w/v) urea in pH 5.0 McIlvaine's buffer (8). After elution, I was quantitated by spectrophotometry.

Compounds II, IV, V, and terrinolide (VI) were separated on a kieselguhr layer (9). Compound I also was separated from its impurities on a diatomaceous earth column, and I and V were evaluated by spectrophotometry (10).

The use of paper chromatography is undesirable (6–8) because the procedure is lengthy and not reproducible. A TLC separation of II, IV, and V from I on kieselguhr (9) could not be achieved in this laboratory.

The TLC procedure presented is rapid and allows the quantitation of traces of II–V in I by direct TLC fluorometry. The method is reproducible and is sensitive to 10^{-2} μg of II–V in a 1% (w/v) solution of I.

EXPERIMENTAL

Reagents—Disodium ethylenediaminetetraacetate (VII), ethylene glycol, acetone, ethyl formate, ethyl acetoacetate, and sodium hydroxide were analytical grade. Kieselguhr G[1] was used.

Preparation of Plates—A slurry of 20 g of kieselguhr and 47 ml of 5% (w/v) aqueous VII, previously adjusted to pH 9 with 20% NaOH, was prepared[2] and spread on glass plates at a thickness of 0.25–0.30 mm. The plates were dried in air for a minimum of 2 hr at room temperature (25°); a transverse channel of approximately 1-mm width was drawn in the layer

[1] Macherey, Nagel & Co, D-516 Düren, Germany.

[2] Desaga applicator, Heidelberg, Germany.

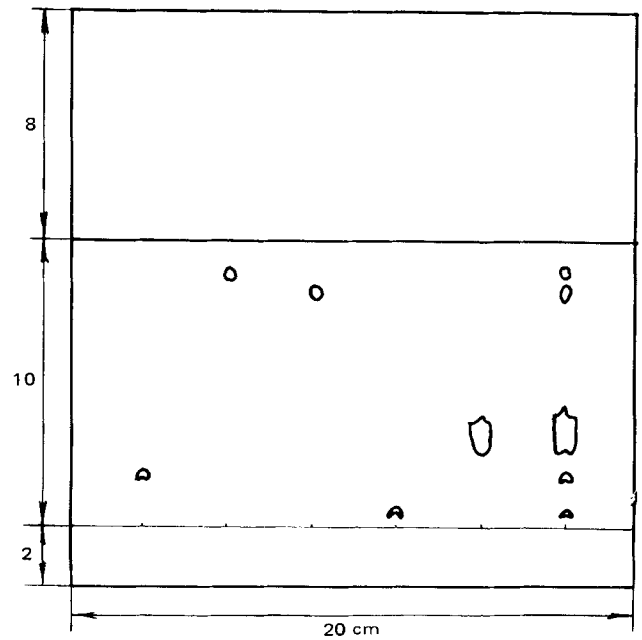

Figure 1—*Typical TLC separation of oxytetracycline impurities on kieselguhr with 5% VII at pH 9. Key (left to right): 0.1 μg of IV (greenish-blue), 0.1 μg of V (blue), 0.1 μg of II (brown), 0.1 μg of III (yellow), 5 μg of I (yellow), and a mixture of I–V.*

12 cm from the one edge of the plate to limit the movement of the solvent front.

The plates were stored in a drying chamber[3] at 30°. Prior to use, they were developed with the solvent system up to the transverse channel (20 min) and dried for 5 min in air and for another 15 min in the drying chamber at 30°. Unimpregnated plates could be stored for an unlimited time.

Solvent System—The system consisted of ethylene glycol–water–acetone–ethyl formate–ethyl acetoacetate (3:6:45:30:15 v/v).

Preparation of Solutions—Samples were dissolved in absolute methanol. For II–VI, a concentration of 0.1 μg/μl was used; I was used at 5 μg/μl. For quantitative TLC fluorometric evaluation, geometric dilutions of impurities were used to define the standardization curves.

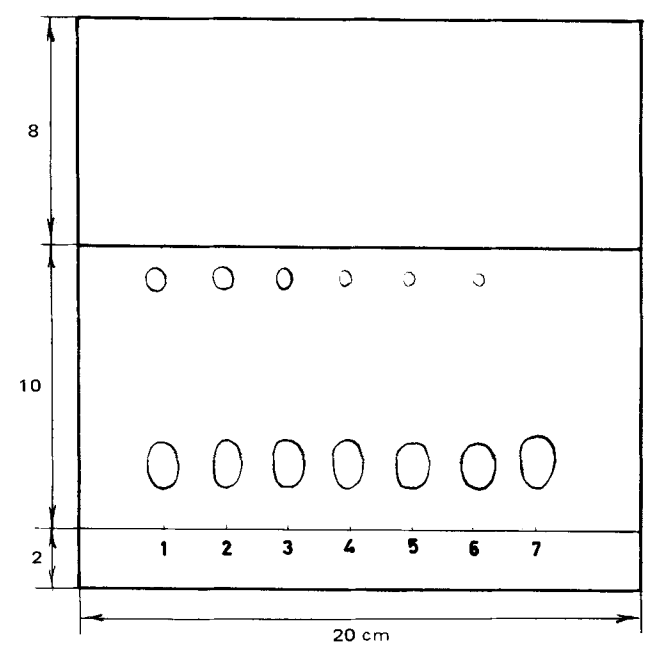

Figure 2—*TLC separation of V from I. Key: 1–7, 8.1 μg of I; 1 and 2, 0.154 μg of V; and 3–6, 0.077, 0.0385, 0.01925, and 0.00963 μg of V, respectively.*

[3] Bekso, Brussels, Belgium.

Table I—Conditions for TLC Fluorometric Determination of Each Impurity

Compound	Fluorescence Emission Wavelength, nm	Slit Width, mm	Slit Height, mm
II	516	0.5	6
III	526	0.3	3.5
IV	500	0.5	6
V	477	0.5	6

Apparatus—A TLC tank (20 × 20 × 8 cm) was lined with filter paper, and 100 ml of solvent was added. The tank was allowed to equilibrate for 1 hr before use. A TLC spectrophotometer[4], an electrobalance[5], and a recorder[6] also were used.

Application of Solutions—Volumes of 1 μl were spotted with disposable pipets[7].

Qualitative Chromatography—Immediately after a plate was removed from the drying chamber, all adsorbent above the origin was covered by a clean glass plate in close contact with the layer while 1-μl volumes were applied as spots on a line 2 cm above the lower edge of the plate. The loaded plate was returned to the drying chamber for 3 min and then placed in the tank and developed at room temperature (25°) in the dark until the solvent front traveled approximately 7 cm (7–10 min).

After development, the plate was dried in air. The spots were visualized under UV light (366 nm). The hR_f values observed for I–VI were 31, 83, 5, 18, 90, and 76, respectively. A typical TLC separation is shown in Fig. 1.

Quantitative Analysis—For each impurity, five reference solutions with concentrations in geometric progression were spotted (1 μl) on the baseline 2 cm above the lower edge of the plate and 2 cm apart, together with 1 μl of the test solution of I. The solution with the highest concentration was spotted twice, and 1 μl of the test solution of I also was applied separately. An example of this spotting procedure is shown in Fig. 2.

After development, the plate was dried in the air and inspected under UV light to remove dust particles in or near the spots under test. The TLC spectrophotometer was adjusted to the first spot with the highest concentration, and the transmission scale and recorder scale were adjusted to 100 units. A rectangular aperture was used for all measurements; the other conditions used for each impurity are listed in Table I.

The fluorescence was excited by the 365-nm mercury line and measured by scanning the accurately positioned spots in the x-axis direction with a scanning speed of 3 cm/min. The recorder speed was kept at 6 cm/min. The peak areas were cut out (11) and weighed to quantitate the spots (Table II).

RESULTS AND DISCUSSION

Separation of Oxytetracyclines—Several TLC systems were examined to find a separation method with sufficient resolution and sensitivity to determine the most likely degradation products of I by direct TLC fluorometry at the 10^{-2} μg level. The presented procedure separated V, II, VI, I, IV, and III quantitatively in that order. Figure 1 shows the arrangement of the spots.

The time required for a complete analysis of one oxytetracycline sample with two impurities was 2 hr using previously prepared plates. The solvent system could be used four times. Test and standard solutions, when kept at 0° in the dark, were stable for at least 3 weeks. However, solutions of II were not stable; II was exceptionally labile and was isomerized to a mixture of IV and V. Ambient atmospheric conditions such as temperature and relative humidity influenced impregnation and development markedly, and care was always taken to dry layers as described.

Optimization of Relative Humidity—The optimum water content in the support was determined by varying the drying conditions. All impurities were well separated on plates equilibrated at a relative humidity of less than 30%; at humidities above 50%, tailing of the spots resulted. For practical reasons, the use of a drying chamber was preferred to equilibration over appropriate saturated salt solutions or sulfuric acid dilutions.

Standard Curve—The relationship between fluorescence and quantity of a substance in a spot on the chromatogram is very complicated, and the shape of the standard curve was dependent upon many factors. Although a straight line passing through the origin might be

[4] Zeiss.
[5] Cahn.
[6] Varian A 25.
[7] Vitrex, Chr. Bardram Birkerod, Denmark.

Table II—Analysis of Known Mixtures of Oxytetracycline and Its Impurities by TLC and Direct Fluorometry

Compound	Spotted Quantity, μg	Recovery[a], μg	Confidence Limits		Recovery, %
			Maximum	Minimum	
I	2.066				
III	0.13630	0.13393	0.13561	0.13225	98.2
	0.06815	0.07273	0.07708	0.06838	106.7
	0.03408	0.03540	0.03802	0.03278	103.9
	0.01704	0.01657	0.01818	0.01496	97.3
	0.00852	0.00544	0.00716	0.00372	63.9
I	4.184				
III	0.13630	0.13527	0.13663	0.13391	99.2
	0.06815	0.07039	0.07323	0.06755	103.3
	0.03408	0.03375	0.03560	0.03190	99
	0.01704	0.01778	0.02048	0.01508	104.3
	0.00852	0.00689	0.00898	0.00480	80.9
I	9.668				
III	0.13630	0.13361	0.14081	0.12641	98
	0.06815	0.07499	0.09212	0.05786	110
	0.03408	0.03189	0.03498	0.02880	93.6
	0.01704	0.01613	0.02028	0.01198	94.6
	0.00852	0.00746	0.01136	0.00356	87.5
I	5.712				
IV	0.11930	0.12015	0.12184	0.11846	100.7
	0.05965	0.05766	0.06137	0.05395	96.6
	0.02983	0.03000	0.03283	0.02717	100.6
	0.01491	0.01569	0.01979	0.01159	105.2
	0.00746	0.00769	0.00991	0.00547	103.1
I	8.100				
IV	0.11930	0.11193	0.11495	0.10891	93.8
	0.05965	0.05994	0.06617	0.05371	100.5
	0.02983	0.02948	0.03426	0.02470	98.8
	0.01491	0.01410	0.01673	0.01147	94.6
	0.00746	0.00837	0.01210	0.00464	112.2
I	5.712				
V	0.15410	0.15320	0.16276	0.15188	99.4
	0.07704	0.07147	0.08239	0.06055	92.8
	0.03852	0.03507	0.03912	0.03102	91.0
	0.01926	0.02032	0.02456	0.01608	105.5
	0.00963	0.01437	0.01920	0.00954	149.2
I	8.100				
V	0.15410	0.15691	0.16309	0.15073	101.8
	0.07704	0.07229	0.08524	0.05934	93.8
	0.03852	0.03527	0.03912	0.03142	91.6
	0.01926	0.02016	0.02429	0.01603	104.7
	0.00963	0.01392	0.01935	0.00849	144.5
I	17.736				
V	0.15410	0.15470	0.15566	0.15374	100.4
	0.07704	0.07450	0.07785	0.07115	96.7
	0.03852	0.03670	0.04113	0.03227	95.3
	0.01926	0.01857	0.01929	0.01785	96.4
	0.00963	0.01308	0.01534	0.01082	135.8

[a] Mean of five determinations.

expected, the line was usually curved. The irregular distribution of a substance in the spot, the uneven thickness of a layer, the position of the origin, and the immersion depth of the plate were relatively unimportant, but the degree of curvature increased with increasing spot size, the amount of material spotted onto the plate, and the direction of scanning.

With a load not greater than 0.5 μg and with the origin spot area less than 5 mm^2, satisfactory results were obtained. Standard curves prepared using vertical scanning did not pass through the origin and were not reproducible. Horizontal scanning gave better results and was used. The movement of the solvent front was kept to a minimum to avoid unnecessary diffusion of spots.

Compounds II and V were sufficiently separated when the solvent front had moved 5–6 cm, and III and IV were separated with 8–9 cm of movement. The quantitation of IV was somewhat complicated by streaking of the I spot.

Reproducibility and Accuracy—The reproducibility was determined over a range of loads and proportions of impurities (Table II). Except for very low concentrations, the recovery was always better than 90%. The high percent recovery of V was due to demixing of the solvent at that part of the chromatogram. A part of the subfront became visible and fluorescent because of the irregular and insufficient drying of the plates. The V spot was accidentally hammered to this subfront. Despite the high recovery, the results conform to the 95% confidence limits, except for the last one. However, at the very low concentration levels (5–10 × 10^{-3} μg), a greater error of 30–40% is acceptable.

The individual regression lines calculated for each impurity when separated from 4-, 8-, and 16-mg/ml oxytetracycline solutions showed good linearity with a significant correlation coefficiënt (lowest value 0.9458). Also, the correlation between the impurity added (x_{th}) and the impurity recovered (x_{exp}) showed good linearity and was statistically significant (lowest value 0.9971). The confidence limits (95% confidence interval) of the means are given by $\bar{x} \pm (\sigma/\sqrt{n} \times t^*)$, where $\sigma/\sqrt{n}$ is the standard error and t^* is 2.78 (df 4 and $p = 0.05$). Each result is the mean of five determinations and illustrates the reproducibility and accuracy of the method.

REFERENCES

(1) F. A. Hochstein, C. R. Stephens, L. H. Conover, P. P. Regna, R. Pasternack, P. N. Gordon, F. J. Pilgrim, K. G. Brunings, and R. B. Woodward, *J. Am. Chem. Soc.*, **75**, 5455 (1953).

(2) G. W. Frimpter, A. E. Timpanelli, W. J. Eisenmenger, H. S. Stein, and L. I. Ehrlich, *J. Am. Med. Assoc.*, **184**, 111 (1963).

(3) B. Carey, *Paediatrics*, **31**, 697 (1963).

(4) F. Monastero, J. A. Means, T. C. Grenfell, and F. H. Hedger, *J. Am. Pharm. Assoc., Sci. Ed.*, **40**, 241 (1951).

(5) M. Serembe, *Boll. Soc. Ital. Biol. Sper.*, **27**, 1330 (1951).

(6) G. B. Selzer and W. W. Wright, *J. Antibiot. Chemother.*, **7**, 292 (1957).

(7) F. Sztaricskai, *Acta Pharm. Hung.*, **32**, 36 (1962).

(8) A. Sina, M. K. Youssef, A. A. Kassem, and I. A. Attia, *J. Pharm. Sci.*, **60**, 1544 (1971).

(9) J. Keiner, R. Hüttenrauch, and W. Poethke, *Pharm. Zentralh.*,

105, 705 (1966).
(10) F. Bailey, *J. Pharm. Pharmacol., Suppl.*, **21**, 40S (1969).
(11) G. J. Willekens, *J. Pharm. Sci.*, **64**, 1681 (1975).

ACKNOWLEDGMENTS AND ADDRESSES

Received August 2, 1976, from the *Instituut voor Hygiëne en Epidemiologie, Department of Farmatoxicologie, Afdeling Farmacopee en Standaarden, Juliette Wytsmanstraat 14, 1050 Brussels, Belgium.*

Accepted for publication December 23, 1976.

The author thanks Apr. A. van den Bulcke (I.H.E.-Brussel) and Dr. W. Van Gampelaere (Sidmar Gent) for valuable advice and Dr. J. W. Lightbown, Director, National Institute for Biological Standards and Control, Hampstead, London, England, for careful editing of this paper. The author also thanks Mr. Legrand (I.H.E.-Brussel) for the statistical analysis and Gist Brokades, Holland, for gifts of oxytetracyclines.

Kinetics and Mechanisms of Drug Action on Microorganisms XXIII: Microbial Kinetic Assay for Fluorouracil in Biological Fluids and Its Application to Human Pharmacokinetics

EDWARD R. GARRETT ˣ, GAIL H. HURST, and J. RUSSELL GREEN, Jr. *

Abstract □ The apparent first-order generation rate constant, k_{app}, of *Escherichia coli* is a function of fluorouracil concentration, C, *i.e.*, $1/(k_0 - k_{app}) = k_1(1/C) + k_2$, where k_0 is the constant in the absence of drug. A routine procedure, using only six counts to establish a daily calibration curve (at 125 and 225 min after medium inoculation and with 0, 15, and 30 ng of fluorouracil/ml), assayed unknown drug concentrations in plasma or urine diluted to 15–30 ng/ml with standard deviations of 12%. Uracil completely antagonized the inhibitory action of fluorouracil but not of 5-fluorouridine, 5-fluorodeoxyuridine, chloramphenicol, or tetracycline, so fluorouracil could be assayed in the presence of the latter compounds by kinetic studies with and without uracil. Fluorouracil degraded in generating cultures of *E. coli*, and the drug effects on filtered organisms persisted on their inoculation into drug-free medium. Potential products of fluorouracil solvolysis, barbituric and isobarbituric acids, had no significant effect on *E. coli* generation. Human plasma protein binding of fluorouracil averaged 10%. The pharmacokinetics of intravenously administered fluorouracil to cancer patients showed a dose-dependent two-compartment body model with a faster terminal phase of elimination at the lower dose. Total and metabolic plasma clearances increased with a decreasing intravenous dose and exceeded hepatic plasma flow to indicate extrahepatic metabolism. The initial distribution phase and the renal clearance did not appear dose dependent, and the terminal semilogarithmic plots of plasma levels against time were linear for both 0.5- and 1.0-g doses. A possible explanation is product- or metabolite-inhibited metabolism. Infusion studies of 1.0 g of fluorouracil showed increased metabolic clearances to confirm dose dependency and to be consistent with this postulate. The oral absorption of unchanged fluorouracil was highly variable between 1 and 15% of the administered dose, showing a large first-pass effect.

Keyphrases □ Fluorouracil—microbial kinetic analysis in biological fluids, pharmacokinetics in humans □ Microbial kinetics—analysis, fluorouracil in biological fluids □ Pharmacokinetics—fluorouracil in humans, studied using microbial kinetic analysis □ Antineoplastic agents—fluorouracil, microbial kinetic analysis in biological fluids, pharmacokinetics in humans

Facile, sensitive, and nontedious assays for fluorouracil in biological fluids are needed for the proper and routine evaluation of its pharmacokinetics and for the evaluation of proper dosage regimens. The bioavailability on oral administration also needs to be assessed. This paper reports the development of a microbial kinetic assay of fluorouracil in biological fluids and its application to human pharmacokinetics.

The GLC analysis of fluorouracil in biological fluids requires its separation and derivatization. Separation by 22-hr dialysis with subsequent trimethylsilylation permitted GLC analysis sensitive to drug concentrations down to 1 μg/ml (1). Separation for a similar GLC analysis was also effected by an 80% extraction from biological fluids buffered at pH 6 into 16% 1-propanol in ether (2). A sensitivity to drug concentrations down to 0.5 μg/ml was shown (2), and a reproducibility of ±5% was claimed. An ion-exchange recovery of the drug, with a subsequent GLC flash-methylation technique using trimethylanilinium hydroxide, also was reported; the apparent sensitivity was 1.0 μg/ml of urine (3). A recently published isotope dilution mass fragmentographic assay (4) claimed a standard deviation of ±6% for 10 ng/ml extracted from plasma.

A sensitive classical disk–agar plate microbiological assay based on the correlation of zones of inhibition of *Streptococcus faecalis* with fluorouracil was developed and applied to the time course of the drug in plasma and urine; the estimated error was ±25%/zonal measurement (5).

Fluorouracil lessens the generation rate of logarithmic phase microorganisms, and the degree of decrease can be related to the drug concentration (6). This ability provided the basis for a sensitive assay of fluorouracil in biological fluids below the drug levels necessary for complete inhibition of generation. The tedious and time-consuming separation procedures vital for GLC assays and the time lag necessary for organism incubation in the disk–agar plate studies were avoided. Also, since the inhibitory effect of fluorouracil on microbial generation can be reversed by the addition of excess uracil, fluorouracil can be specifically assayed in the presence of other antibacterial agents that do not show this reversibility. The assay was applied to the study of fluorouracil pharmacokinetics in humans.

EXPERIMENTAL

Organism—Replicate slants of *Escherichia coli* (ATCC 12407) were prepared from a single colony and stored at 4°.

105, 705 (1966).
(10) F. Bailey, *J. Pharm. Pharmacol., Suppl.*, **21**, 40S (1969).
(11) G. J. Willekens, *J. Pharm. Sci.*, **64**, 1681 (1975).

ACKNOWLEDGMENTS AND ADDRESSES

Received August 2, 1976, from the *Instituut voor Hygiëne en Epidemiologie, Department of Farmatoxicologie, Afdeling Farmacopee en Standaarden, Juliette Wytsmanstraat 14, 1050 Brussels, Belgium.*

Accepted for publication December 23, 1976.

The author thanks Apr. A. van den Bulcke (I.H.E.-Brussel) and Dr. W. Van Gampelaere (Sidmar Gent) for valuable advice and Dr. J. W. Lightbown, Director, National Institute for Biological Standards and Control, Hampstead, London, England, for careful editing of this paper. The author also thanks Mr. Legrand (I.H.E.-Brussel) for the statistical analysis and Gist Brokades, Holland, for gifts of oxytetracyclines.

Kinetics and Mechanisms of Drug Action on Microorganisms XXIII: Microbial Kinetic Assay for Fluorouracil in Biological Fluids and Its Application to Human Pharmacokinetics

EDWARD R. GARRETT ˣ, GAIL H. HURST, and J. RUSSELL GREEN, Jr. *

Abstract □ The apparent first-order generation rate constant, k_{app}, of *Escherichia coli* is a function of fluorouracil concentration, C, *i.e.*, $1/(k_0 - k_{app}) = k_1(1/C) + k_2$, where k_0 is the constant in the absence of drug. A routine procedure, using only six counts to establish a daily calibration curve (at 125 and 225 min after medium inoculation and with 0, 15, and 30 ng of fluorouracil/ml), assayed unknown drug concentrations in plasma or urine diluted to 15–30 ng/ml with standard deviations of 12%. Uracil completely antagonized the inhibitory action of fluorouracil but not of 5-fluorouridine, 5-fluorodeoxyuridine, chloramphenicol, or tetracycline, so fluorouracil could be assayed in the presence of the latter compounds by kinetic studies with and without uracil. Fluorouracil degraded in generating cultures of *E. coli*, and the drug effects on filtered organisms persisted on their inoculation into drug-free medium. Potential products of fluorouracil solvolysis, barbituric and isobarbituric acids, had no significant effect on *E. coli* generation. Human plasma protein binding of fluorouracil averaged 10%. The pharmacokinetics of intravenously administered fluorouracil to cancer patients showed a dose-dependent two-compartment body model with a faster terminal phase of elimination at the lower dose. Total and metabolic plasma clearances increased with a decreasing intravenous dose and exceeded hepatic plasma flow to indicate extrahepatic metabolism. The initial distribution phase and the renal clearance did not appear dose dependent, and the terminal semilogarithmic plots of plasma levels against time were linear for both 0.5- and 1.0-g doses. A possible explanation is product- or metabolite-inhibited metabolism. Infusion studies of 1.0 g of fluorouracil showed increased metabolic clearances to confirm dose dependency and to be consistent with this postulate. The oral absorption of unchanged fluorouracil was highly variable between 1 and 15% of the administered dose, showing a large first-pass effect.

Keyphrases □ Fluorouracil—microbial kinetic analysis in biological fluids, pharmacokinetics in humans □ Microbial kinetics—analysis, fluorouracil in biological fluids □ Pharmacokinetics—fluorouracil in humans, studied using microbial kinetic analysis □ Antineoplastic agents—fluorouracil, microbial kinetic analysis in biological fluids, pharmacokinetics in humans

Facile, sensitive, and nontedious assays for fluorouracil in biological fluids are needed for the proper and routine evaluation of its pharmacokinetics and for the evaluation of proper dosage regimens. The bioavailability on oral administration also needs to be assessed. This paper reports the development of a microbial kinetic assay of fluorouracil in biological fluids and its application to human pharmacokinetics.

The GLC analysis of fluorouracil in biological fluids requires its separation and derivatization. Separation by 22-hr dialysis with subsequent trimethylsilylation permitted GLC analysis sensitive to drug concentrations down to 1 μg/ml (1). Separation for a similar GLC analysis was also effected by an 80% extraction from biological fluids buffered at pH 6 into 16% 1-propanol in ether (2). A sensitivity to drug concentrations down to 0.5 μg/ml was shown (2), and a reproducibility of ±5% was claimed. An ion-exchange recovery of the drug, with a subsequent GLC flash-methylation technique using trimethylanilinium hydroxide, also was reported; the apparent sensitivity was 1.0 μg/ml of urine (3). A recently published isotope dilution mass fragmentographic assay (4) claimed a standard deviation of ±6% for 10 ng/ml extracted from plasma.

A sensitive classical disk–agar plate microbiological assay based on the correlation of zones of inhibition of *Streptococcus faecalis* with fluorouracil was developed and applied to the time course of the drug in plasma and urine; the estimated error was ±25%/zonal measurement (5).

Fluorouracil lessens the generation rate of logarithmic phase microorganisms, and the degree of decrease can be related to the drug concentration (6). This ability provided the basis for a sensitive assay of fluorouracil in biological fluids below the drug levels necessary for complete inhibition of generation. The tedious and time-consuming separation procedures vital for GLC assays and the time lag necessary for organism incubation in the disk–agar plate studies were avoided. Also, since the inhibitory effect of fluorouracil on microbial generation can be reversed by the addition of excess uracil, fluorouracil can be specifically assayed in the presence of other antibacterial agents that do not show this reversibility. The assay was applied to the study of fluorouracil pharmacokinetics in humans.

EXPERIMENTAL

Organism—Replicate slants of *Escherichia coli* (ATCC 12407) were prepared from a single colony and stored at 4°.

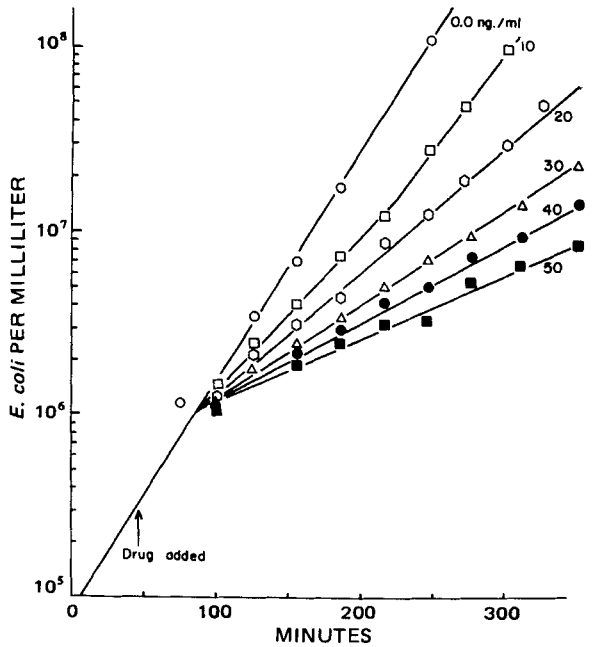

Figure 1—*Semilogarithmic plots of* E. coli *per milliliter against time in Anton's medium as affected by the stated fluorouracil concentrations at 37.5° and pH 7.*

Culture Medium and Materials—Anton's medium (7) was used with 3% casamino acids[1]. The media were passed through a 0.45-μm membrane filter[2] and autoclaved at 120° for 15 min. The final pH of the buffered medium was 7.0.

The stable (8) neutral aqueous solutions of fluorouracil[3], floxuridine[4], 5-fluorouridine[4], and uracil[5] were used in *in vitro* studies and could be stored indefinitely at room temperature after being autoclaved for 15 min. Chloramphenicol[6] was dissolved in sterile water and used without autoclaving.

Monitoring Generation Rates—The kinetics of bacterial generation in the logarithmic growth phase were monitored by counting[7] the numbers of cells with time (6, 9, 10). Predetermined volumes of a 37.5° balanced growth culture of *E. coli*, typically 9.9 ml of 3.5×10^5 cells/ml, were pipetted into 25-ml loosely capped conical flasks in a 37.5° constant-temperature bath equipped with a shaker. The biological fluids to be assayed were diluted with sterile water, medium, ultrafiltered plasma, or urine without drug; then 0.100 ml of fluorouracil was added by a micropipet to give final concentrations of 10–50 ng/ml in the cultures after 15 min of culture growth. The numbers of organisms at a specific time were obtained by micropipetting 0.50 or 1.0 ml into known volumes of a previously filtered[2] sterile solution of 0.85% sodium chloride and 1.0% formaldehyde to obtain counts in the range of 10,000–20,000/50 μl[7].

Construction of Calibration Curves—The apparent generation rate constants, k_{app}, of fluorouracil-affected cultures were obtained from the slopes of the linear plots (Fig. 1) of the natural logarithm of the number, N, of organisms per milliliter against time, t, in the 100–250-min interval after culture inoculation in accordance with (6, 9, 10):

$$\ln N = k_{app}t + \text{intercept} \qquad \text{(Eq. 1)}$$

Plots (Fig. 2) of these apparent generation rate constants, k_{app}, against fluorouracil concentration, FU, were nonlinear. Linear plots (Fig. 3) could be obtained (8) in accordance with:

$$y = 1/(k_0 - k_{app}) - 1/k_0 = k_1(1/[\text{FU}]) + k_2 \qquad \text{(Eq. 2)}$$

where k_0 is the first-order generation rate constant in the absence of drug, and $k_2 = 0$ for a simple saturable receptor site model (11).

Calibration curves were prepared for fluorouracil in plasma ultrafiltrate at various dilutions with sterile water, medium, or fluorouracil-free plasma ultrafiltrate. The plasma ultrafiltrate was prepared by ultrafiltration of plasma through a filter cone[8] in a centrifuge at 1600 rpm. Al-

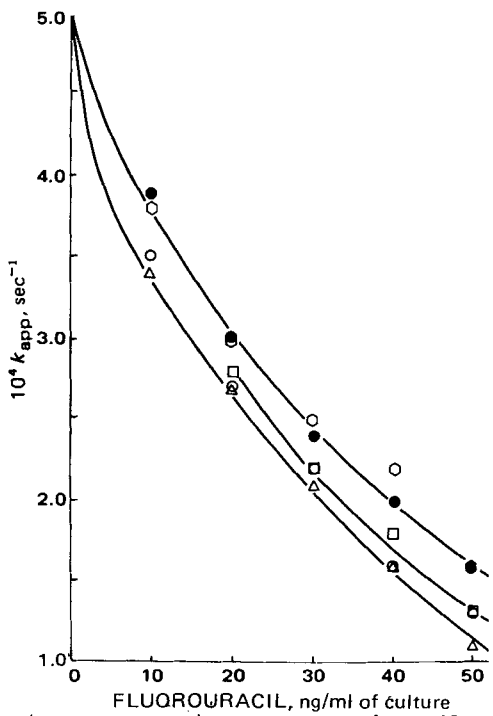

Figure 2—*Apparent generation rate constant,* k_{app}, *of* E. coli *in seconds*$^{-1}$ *at 37.5° and pH 7 as a function of fluorouracil concentration in Anton's medium and in the presence of diluted plasma ultrafiltrate. A 0.100-ml aliquot of plasma ultrafiltrate containing fluorouracil, diluted 1:2000 (○), 1:400 (△), 1:100 (□), 1:20 (●), and 1:5 (○) with sterile water or medium, was added to 9.9 ml of the generating culture.*

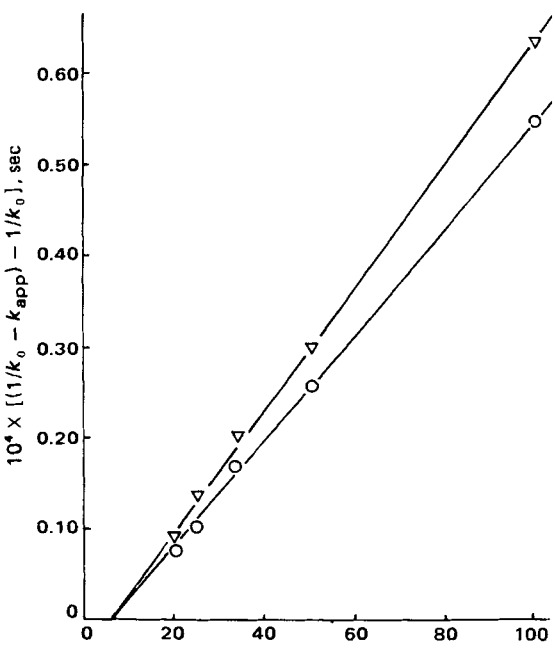

Figure 3—*Typical linear plots of a function,* $1/(k_{app} - 1/k_0) - 1/k_0$, *of the apparent generation rate constants at 37.5° and pH 7 in the presence,* k_{app}, *and absence,* k_0, *of fluorouracil against the reciprocal of the fluorouracil concentration in Anton's medium in the presence of diluted plasma ultrafiltrate. An aliquot (0.100 ml) of the plasma ultrafiltrates containing fluorouracil, diluted 1:2000 (○) and 1:5 (▽) with sterile water or medium, was added to 9.9 ml of the generating culture.*

[1] Difco Laboratories, Detroit, Mich.
[2] Millipore 0.45-μm HA filters.
[3] Hoffmann-La Roche Inc., Nutley, N.J.
[4] Courtesy of J. Fox, Sloan Kettering, Institute for Cancer Research, New York, N.Y.
[5] Sigma Chemical Co., St. Louis, Mo.
[6] Boehringer Mannheim, West Germany.
[7] Coulter counter models B and ZBI, Coulter Electronics Co., Hialeah, Fla.
[8] Ultrafiltration membrane cones 2100 CF 50, Amicon Corp., Lexington, Mass.

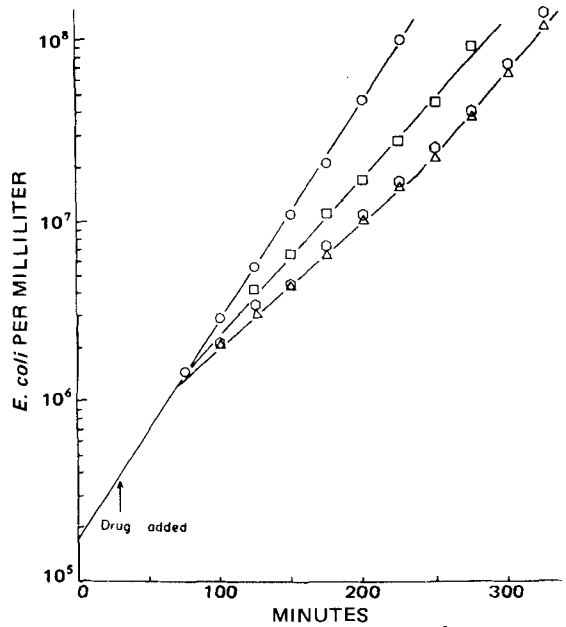

Figure 4—*Semilogarithmic plots of* E. coli *per milliliter against time in Anton's medium at 37.5° and pH 7 for 20 ng of fluorouracil/ml in the presence of diluted urines. An aliquot (0.100 ml) of the diluted urines containing fluorouracil, diluted 1:2000 (△), 1:400 (○), and 1:100 (□) with sterile water, was added at the time designated by the arrow to 9.9 ml of the generating culture. The other curve (○) is for the generation of a drug-free culture.*

though the generation rates of *E. coli* in the absence of fluorouracil were not significantly different in ultrafiltered plasma diluted 100- and 20-fold, the generation rates of fluorouracil-affected organisms were significantly modified by the content of plasma ultrafiltrate that had an antagonistic effect on fluorouracil inhibition of microbial generation rates (Figs. 2 and 3).

Therefore, all plasma samples to be assayed for fluorouracil were ultrafiltered and diluted to the proper range for assay with previously prepared ultrafiltered plasma without fluorouracil, preferably from the same individual. However, there were no significant differences among the generation rates of fluorouracil-affected cultures for the same amount of fluorouracil-free plasma ultrafiltrate from different individuals. The calibration curve constructed for aqueous solutions of fluorouracil could be employed when plasma samples were diluted 200-fold or more with sterile water.

The addition of urine to fluorouracil-affected generating cultures antagonized the generation rate inhibition of fluorouracil. If a urine sample could be diluted more than 1:400 (Fig. 4) with water to obtain 15–30 ng/ml, a calibration curve constructed from aqueous solutions of fluorouracil could be used. Dilution of urine containing fluorouracil with blank urine not containing any fluorouracil minimized this error, but there were significant differences in the antagonistic action of different blank urines from the same individual. A modified procedure was applicable to the assay of urine samples that could not be diluted more than 1:400. Fluorouracil itself was used as an internal standard.

A reasonable first approximation of k_2 in Eq. 2 is zero (11) (see also the intercepts in Fig. 3); if the total concentration of fluorouracil, $[FU]_T$, consists of the sum of the unknown concentration in the urine, $[FU]_U$, and that due to the added concentration of standard, $[FU]_S$, then, from Eq. 2:

$$y = \frac{1}{k_0 - k_{app}} - \frac{1}{k_0} \simeq \frac{k_{app}}{k_0(k_0 - k_{app})} = \frac{k_1}{[FU]_S + [FU]_U} \quad \text{(Eq. 3)}$$

which can be rearranged to:

$$\frac{1}{y} = k_0 \frac{(k_0 - k_{app})}{k_{app}} = \frac{1}{k_1}([FU]_S + [FU]_U) \quad \text{(Eq. 4)}$$

so that:

$$[FU]_S = k_1\left(\frac{1}{y}\right) - [FU]_U \quad \text{(Eq. 5)}$$

or:

$$[FU]_S = k_1 k_0\left(\frac{k_0 - k_{app}}{k_{app}}\right) - [FU]_U \quad \text{(Eq. 6)}$$

The value for the generation rate constant, k_0, in the absence of fluorouracil could be estimated from the slope of the logarithm of a generating culture against time when urine without drug was added to the culture. The values of y (Eq. 5) or $(k_0 - k_{app})/k_{app}$ (Eq. 6) were calculated from this k_0 and the values of the apparent generation rate constants, k_{app}, obtained at three different concentrations of $[FU]_S$ added to the sample urine and when $[FU]_S = 0$. Plots of the added concentrations of fluorouracil, $[FU]_S$, against $1/y$ (Eq. 5) or $(k_0 - k_{app})/k_{app}$ (Eq. 6) provided a straight line where the negative of the intercept was an estimate of the fluorouracil in the urine to be assayed, $[FU]_U$. This approximate procedure for dilute drug concentrations in urine had an average error of ±18% in four separate studies.

Procedures for Routine Assay of Fluorouracil in Biological Fluids—The consistent linearity of the plots of the natural logarithm of organisms against time from 100 to 250 min after drug addition to the generating culture (Fig. 1) permitted the routine estimation of slopes (or generation rate constants, k_{app}) from the counts of two samples obtained at 125 and 225 min after inoculation of 3×10^5 organisms.

The linearity of calibration curves in accordance with Eq. 2 (Fig. 3) permitted the daily estimation of k_1 and k_2 parameters from k_{app} values obtained at only two fluorouracil concentrations and from the k_0 value obtained from a drug-free generating culture where equivalent amounts of drug-free plasma ultrafiltrate or drug-free urine had been added. The two concentrations of drug, [FU], chosen were 15 and 30 ng/ml, straddling a concentration of 20 ng/ml that experimentally gave the minimum standard deviation of the calculated y parameter of Eq. 2. Three replicate assays were made at each concentration.

The slope, k_1, and intercept, k_2, of the line between these two points were obtained from the plot of the averaged y values against 1/[FU] in accordance with Eq. 2. The amount of fluorouracil in the diluted biological sample could be calculated from its observed k_{app} values (average of three replicates) and the derived y parameter from a rearranged Eq. 2:

$$[FU] = k_1/(y - k_2) \quad \text{(Eq. 7)}$$

All assayed samples were diluted into the response range given by the 15 and 30 ng/ml. The unknown original concentration was calculated from the necessary dilution.

This method of routine assay was challenged on each of 5 separate days, with a new calibration curve on each day. An aqueous solution of fluorouracil was diluted so that the drug concentration in the medium was 20 ng/ml. Three separate assays were performed on each day, and the averages ± *SD* for each day were: 20.3 ± 0.5, 22.1 ± 0.4, 20.8 ± 2.5, 19.5 ± 1.6, and 24.3 ± 0.9. The overall average was 21.4 ± 1.9, $n = 15$, with a standard deviation (in percent of the mean) of 7%. A similar study for plasma solutions of fluorouracil diluted 10-fold on addition to the culture had an average error for 20 ng/ml of 12%.

An analysis of variance of the calibration curves showed a significant variation among days. Thus, it was necessary to construct a daily calibration curve for the routine assay.

Antibacterial Effects of Derived Nucleosides and Potential Metabolites of Fluorouracil and Their Possible Inhibition by Uracil—The possible inhibition of the antibacterial effect of fluorouracil, 5-fluorouridine, and floxuridine on microbial generation by uracil was studied in similar systems, Anton's medium and 2.5×10^5/ml inocula. Similar studies were conducted with mixtures of fluorouracil, tetracycline, and/or chloramphenicol with and without uracil. The antimicrobial effects of potential products of fluorouracil solvolysis, barbituric and isobarbituric acids, were studied in the same system. The stability of fluorouracil in refrigerated whole blood, plasma, ultrafiltered plasma, and urine was monitored over 6 days.

Effect of Filtrates from Fluorouracil-Inhibited Microbial Cultures on Fresh Organisms and of Transference of Affected Organisms to Fresh Medium—A culture in logarithmic growth was divided into five portions. One served as the control, and the other four had 30 ng of fluorouracil/ml. Each of the four cultures was vacuum filtered through a sterile membrane filter (0.45 μm) at 123, 153, 254, and 279 min, respectively, after the parent culture was prepared. The filtrates were stored at 4° overnight.

The organisms were washed with sterile medium at 37.5°. The membrane filter was submerged in 50 ml of fresh medium, and the flask was shaken vigorously. Aliquots of the cultures prepared from the organisms filtered at the various times were monitored for generation rates. Aliquots (9.7 ml) of cultures also were added to 0.30 ml of uracil solution to give a uracil concentration of 32 μg/ml, and the generation rates were monitored. In some cases 1 ml of these cultures was diluted 10-fold into fresh medium at 37.5° and the generation rates were monitored.

Aliquots (8.0 ml) of the stored filtrates were warmed to 37.5° and added to 2.0 ml of culture for a population of 4×10^5 organisms/ml. In some cases, fluorouracil was added 15 min after the addition of filtrate to the culture to increase the drug concentration by 20 ng/ml. The generation rates of these cultures were monitored.

Human Plasma Protein Binding of Fluorouracil—Human plasma (3–4 ml), adjusted to pH 5.8, 7.2, and 9.0 with dropwise addition of 0.5 *N* HCl or 0.5 *N* NaOH and containing 2-^{14}C-fluorouracil[3] at 100, 1.0, and 0.1 μg/ml, was ultrafiltered at 1000 rpm through cone filters[8] in a centrifuge for 15 min to ultrafilter 20% of the volume. The cones, with a 50,000 molecular weight cutoff, were previously soaked in distilled water for 1 hr and centrifuged for 10 min at 1500 rpm. Aliquots (200 μl) of the ultrafiltrate and original plasma were assayed with 10 ml of a scintillation fluid[9] by liquid scintillation spectroscopy[10]. The possible plasma quenching of the counts was challenged by adding 25 μl of 0.520 μCi/ml of 2-^{14}C-fluorouracil to 200 μl of plasma and plasma ultrafiltrate and counting. The plasma counts were within 1% of the ultrafiltrate, indicating no significant quenching by plasma proteins.

Fluorouracil binding to the filter cones was determined by again filtering plasma ultrafiltrates, adjusted to various pH values and with added 2-^{14}C-fluorouracil at 1000 rpm for 3 min to effect 50% ultrafiltration. Aliquots (200 μl) of the original ultrafiltrate and the filtered ultrafiltrates were added to 10 ml of scintillation fluid and counted in a liquid scintillation spectrophotometer[10].

Pharmacokinetics of Fluorouracil Administered to Human Patients—Three patients who were receiving fluorouracil[11] for diagnosed metastatic carcinomas gave their informed consent for these studies[12].

Tests including alkaline phosphatase, serum glutamic-oxaloacetic transaminase, serum glutamic-pyruvic transaminase, prothrombin time, total proteins, and albumins were normal except for elevated levels of serum glutamic-oxaloacetic transaminase and serum glutamic-pyruvic transaminase in Patient RC. Urinalyses were all normal. Electrocardiograms, chest X-rays, and blood pressures were normal, as were blood tests that included hematocrit, hemoglobin, white blood cells, leucocytes, differential, erythrocytes, and platelets. In some studies, the patients were given morphine or thorazine concurrently, but other anticancer drugs were not administered.

The patients were supine during all experiments. An arm vein was catheterized 2 hr prior to drug administration for blood sampling during the intravenous bolus and oral studies. Veins in both arms were catheterized for the infusion studies. Isotonic saline was infused through the indwelling catheter at the rate of 50 ml/hr for 2 hr before drug administration until the end of each study. The patient was water loaded orally with 10 ml/kg in the hour before drug administration.

Intravenous bolus administration was effected over 1 min (20 ml × 50 mg/ml) or 10 sec (10 ml × 50 mg/ml) in the opposite arm from the catheter, except for Patient JC where venipuncture was difficult. The infusion of the dose (1000 mg) in isotonic saline was effected in the arm opposite that used for sampling. The drug was normally administered orally in 100 ml of orange juice, except for the 1-g study in Patient JC where distilled water was used. Patients were fasted for 12 hr before and 2 hr after oral administration. Patient RC had nausea and vomiting on oral administration and could not be studied by this route.

Blood samples were withdrawn from the catheter used for saline drip after a 2-ml blood withdrawal for flushing purposes. They were added to iced heparinized tubes until centrifugation and separation of plasma. The plasma ultrafiltrates were stored at 4°. The pH and volume of a urine collection were measured, and a portion was ultrafiltered and refrigerated. Urine pH values were ~7.5, except for Patient RC whose urine pH ranged between 8.0 and 8.7.

RESULTS AND DISCUSSION

Fluorouracil Assay by Microbial Generation—The described method is rapid and sensitive. It does not necessitate the tedious separative techniques from biological fluids required prior to GLC analysis (1–4), nor is it as time consuming as the classical disk-plate assay (5). Its accuracy is of the same order (±5%) as GLC for a complete calibration curve and is ±12% for the routine method proposed. Its sensitivity, however, is four to 20 times greater than that claimed for GLC. Twenty samples can be analyzed by one operator within an 8-hr working day.

[9] Scinti-Verse, Fisher Scientific Co., Fair Lawn, N.J.
[10] Beckman liquid scintillation, Beckman Instruments, Fullerton, CA 92634.
[11] Injectable solution, Hoffmann-La Roche Inc., Nutley, N.J.
[12] The protocol was approved by the Committee for the Protection of Human Subjects and the Clinical Research Center Advisory Board of the J. Hillis Miller Health Center, University of Florida.

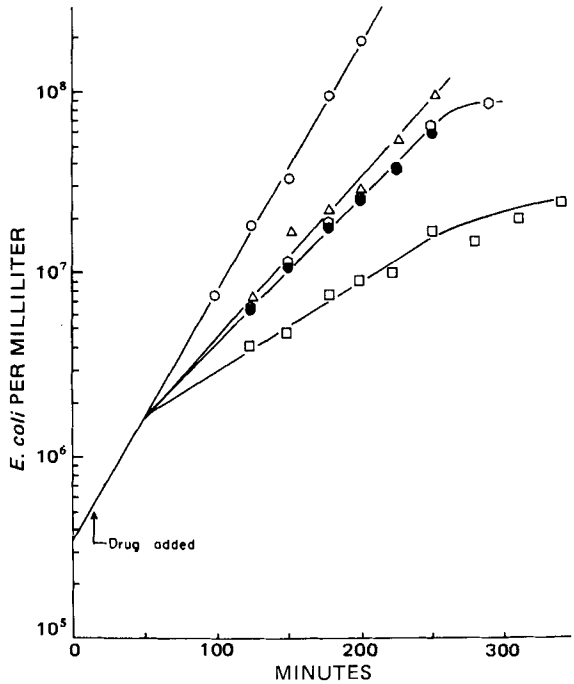

Figure 5—*Semilogarithmic generation curves of* E. coli *in Anton's medium at 37.5° and pH 7 without drug (○), with 20 ng of fluorouracil/ml (△), with 500 ng of chloramphenicol/ml (○), with the combination (□), and with the combination plus 10 μg of uracil/ml (●). These results are typical of assays in plasma and urine.*

Reversal of Fluorouracil Effect by Uracil in Presence of Tetracycline and Chloramphenicol—The inhibition of microbial generation effected by fluorouracil is reversed by uracil (6, 11). In Anton's medium, concentrations of uracil of 0.200 μg/ml completely reversed fluorouracil action at 0.020 and 0.030 μg/ml, where the generation rates in the 160 min after drug addition were 0.54 and 0.36, respectively, of the generation rate without fluorouracil.

Studies of microbial generation in the presence of no drug, 20 ng of fluorouracil/ml, 0.50 μg of chloramphenicol/ml, and the combination alone or with 10 μg of uracil/ml (Fig. 5) showed that the fluorouracil effect

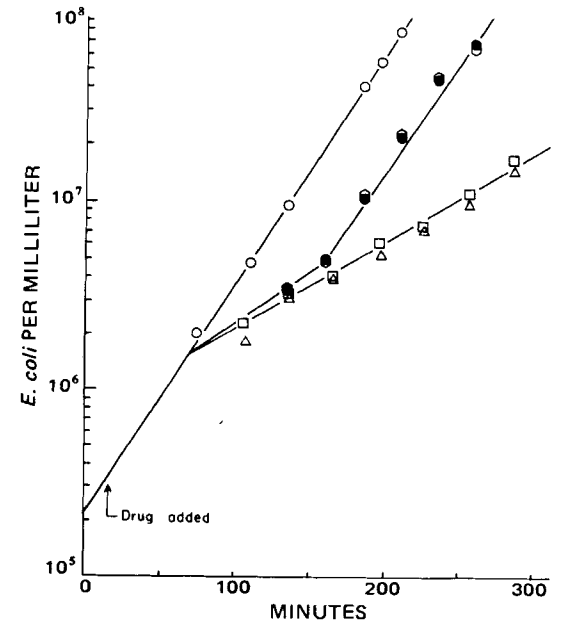

Figure 6—*Semilogarithmic generation curves of* E. coli *in Anton's medium at 37.5° and pH 7 without drug (○), with 9.5 ng of floxuridine/ml alone (○) and combined with 0.4 μg of uracil/ml (●), and with 60 ng of 5-fluorouridine/ml alone (□) and combined with 2.15 μg of uracil/ml (△).*

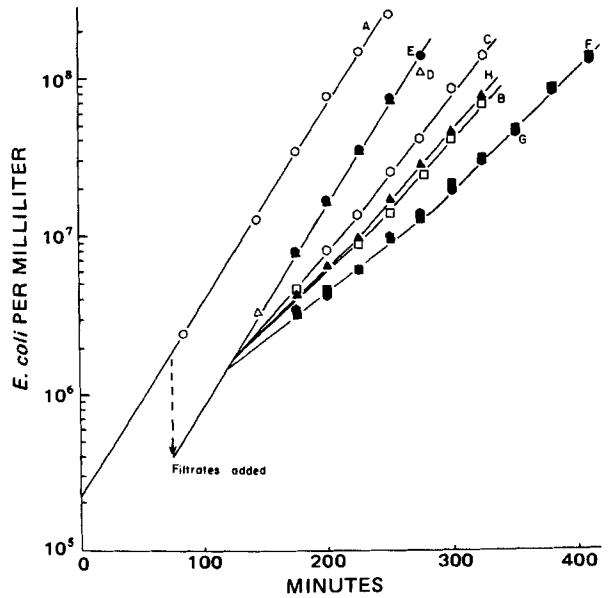

Figure 7—*Semilogarithmic plots of* E. coli *per milliliter against time at 37.5° and pH 7 when a fresh inoculum was introduced into the filtrates taken at various times from a fluorouracil-affected generating culture in Anton's medium. The curves and times after inoculation for the various filtrations were: B, 123 min (□); C, 153 min (○); D, 254 min (△); and E, 279 min (●). The generating culture of curve A (○) was diluted with the filtrates at the time indicated by the arrow to give the other generating curves. Curves F (■) and G (●) represent generating cultures with an additional 20 ng of fluorouracil/ml in media prepared from dilution of A with filtrates at 254 and 279 min, respectively. The drug was added at 90 min. Curve H (▲) represents a generating culture with 15 ng of fluorouracil/ml prepared from dilution of A with fresh Anton's medium.*

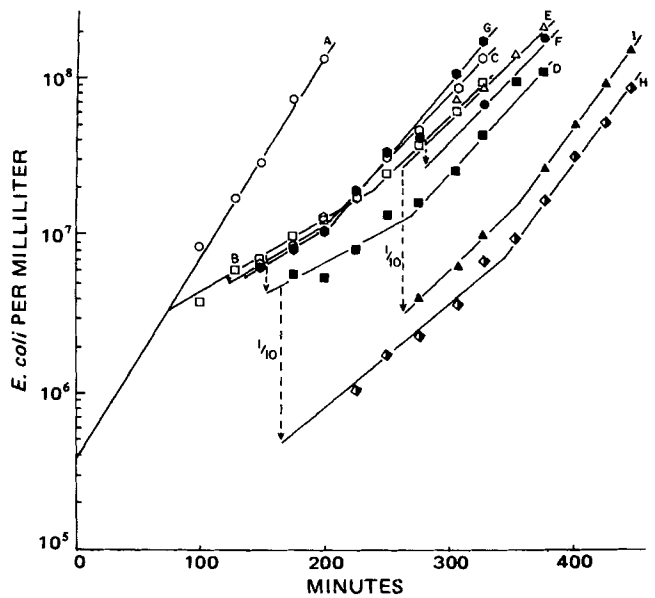

Figure 8—*Semilogarithmic plots of* E. coli *per milliliter against time at 37.5° and pH 7 in Anton's medium when inoculated with organisms filtered at various times from a previously fluorouracil-affected (30 ng/ml) generation curve B (□). The generation curves for the resuspended organisms in fresh media taken at the various times of filtration of curve B were: C, 123 min (○); D, 153 min (■); E, 254 min (△); and F, 279 min (●). Curve G (●) is for the 123-min filtered organisms generating in the presence of 3 μg of uracil/ml. Curves H (◆) and I (▲) are the generation curves after 1:10 dilution with fresh medium of the cultures of curves D and E, respectively, at the time indicated in the graph. Curve A (○) is for the generation of fresh inoculum in fresh medium without added drug.*

Table I—Apparent Total Binding of Fluorouracil to Human Plasma Protein and the Cones Used for Ultrafiltration

pH	Fluorouracil, μg/ml 100[a]	1.00[a]	0.10[b]	Average ± *SD*
5.7	3.1	6.0	7.4	5.5 ± 2.2
7.2	11.7	12.5	13.5	12.6 ± 0.9
9.0	7.8	8.4	6.6	7.6 ± 0.9
			Overall average	8.6

[a] Counts per minute were 8000. [b] Counts per minute were 1500.

in the presence of chloramphenicol was completely reversed by uracil. The generation rate of the triple mixture was the same as that of chloramphenicol alone. Similar results were obtained with a mixture of 0.49 μg of chloramphenicol/ml, 0.049 μg of tetracycline/ml, and 0.020 μg of fluorouracil/ml with and without added uracil, 2 μg/ml. The generation rate constant of 1.6×10^{-4} sec^{-1} of the combination was changed to 3.0×10^{-4} sec^{-1} on the addition of uracil, a rate constant that was the same for the mixture of chloramphenicol and tetracycline alone.

This phenomenon permits the assay of the fluorouracil content of biological fluids in the presence of other antibacterial agents. The microbial generation rates need to be studied in the presence and absence of added uracil, and the difference in the inhibitory rate constant can be assigned to fluorouracil action.

Action of Potential Nucleoside Derivatives and Solvolysis Products of Fluorouracil with and without Uracil Addition on Microbial Generation—Potential products of fluorouracil solvolysis (8), barbituric acid and isobarbituric acid at 1 μg/ml, had no significant effect on *E. coli* generation under the stated conditions. Solutions (2 μg/ml) of fluorouracil in whole blood, plasma, ultrafiltered plasma, and urine stored at 4° showed no significant loss in fluorouracil potency by this assay over 6 days and thus implied that no significant degradation occurred with these storage conditions.

Floxuridine and 5-fluorouridine have significant inhibitory effects on the generation of *E. coli* (6). Uracil did not reverse the action of 5-fluorouridine and had a negligible effect on floxuridine (Fig. 6), in contrast to the complete reversibility of the action of the precursor, fluorouracil (Fig. 5). Studies of floxuridine effects at 30, 400, and 500 ng/ml showed an initial phase of inhibition for 100 min and a subsequent increase in generation equivalent to a control without added drug. This result was in contrast to fluorouracil and 5-fluorouridine action, where the second phase of the higher generation rate was always significantly less than that of the control.

The accepted mechanism of fluorouracil antimicrobial or anticancer action is by its incorporation into 5-fluorouridine or floxuridine and their monophosphates, compounds that block DNA synthesis (6, 12). The lack of uracil reversal of the antibacterial action of these nucleosides implies that uracil interferes with the incorporation of fluorouracil into such nucleosides instead of antagonizing the nucleosidic or nucleic acid action *per se*.

Effect of Filtrates from Fluorouracil-Inhibited Microbial Cultures on Fresh Organisms and of Generation of Transferred Affected Organisms in Fresh Medium—Semilogarithmic plots of organisms against time over longer periods showed biphasic generation curves (6, 12). The initially inhibited generation rate in phase I (the portion used in the described assay) increased to a new steady state (phase II) after reasonable linearity for approximately 2 hr. The effect of dilution of the fluorouracil-affected organisms with fresh medium was studied (6) in peptone broth; the addition of the drug was not readily reversed by dilution. It took about 150 min for the generation rate on dilution in phase I to increase significantly. Diluted cultures were inhibited further to the expected extent by additional drug. These studies were repeated with 1:10 and 1:100 dilution with Anton's medium, and the results were the same.

It was suggested (6) that the slower phase II of fluorouracil-affected microbial generation, particularly observed in the nonbinding Anton's medium, was due to drug degradation in the presence of generating *E. coli*. Aliquots of a generating culture of *E. coli* in Anton's medium with 30 ng of fluorouracil/ml were filtered at various times and added to a fresh culture of organisms, 4:1 (Fig. 7). The fluorouracil contents of the diluted filtrates, presumably 24 ng/ml, were 17 ng/ml for the 123-min filtrate, 6 ng/ml for the 153-min filtrate, and 0 ng/ml for the 254- and 279-min filtrates as determined from a calibration curve constructed in fresh medium.

These results prove that fluorouracil is inactivated by the generating

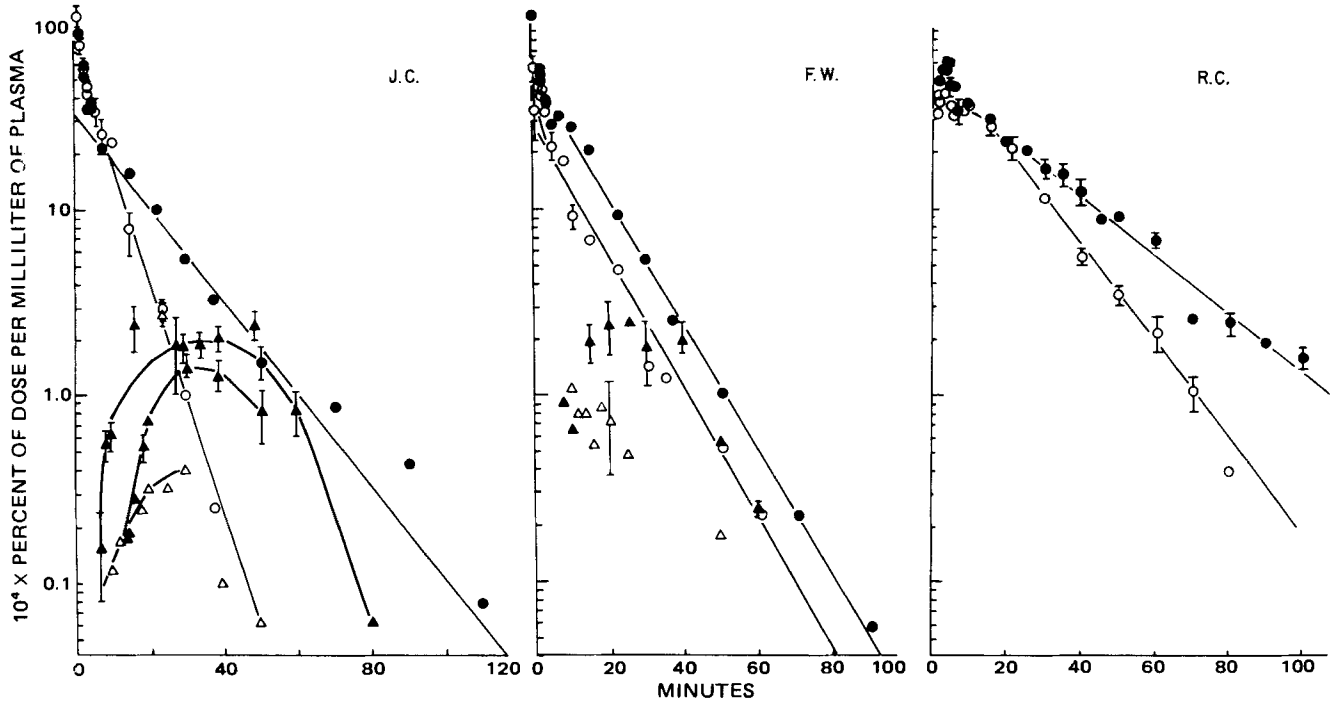

Figure 9—*Semilogarithmic plots for plasma fluorouracil levels in 10^4 μg/ml ÷ dose in micrograms against time on intravenous administration of 1000 (●) and 500 (○) mg and on oral administration of 1000 (▲) and 500 (△) mg. The vertical lines at several points designate the range of the average ± SD when three or more replicate assays were made.*

organism and/or an antagonist to this drug is produced by the generating organisms. However, when an additional 20 ng of drug/ml was added to the fresh culture-diluted filtrates, the resultant generation rate was equivalent to that expected from completely fresh medium. This finding denies the postulate of a produced antagonist and demonstrates the microbial inactivation of fluorouracil (Fig. 7). Studies of fluorouracil effects on microbial generation of *E. coli* at various inoculum sizes showed, after the initial inhibition, greater acceleration of generation rates with increased inocula, confirming the microbial inactivation of fluorouracil.

The filtered cells associated with these filtrates were resuspended in fresh medium without fluorouracil. Generation rates of these cultures and cultures with an added 1000-fold excess of uracil were monitored. The generation rates of the filtered organisms in fresh medium were similar to those observed prior to the removal of fluorouracil by filtration (Fig. 8). This result demonstrates the irreversibility of fluorouracil action. The drug is irreversibly incorporated into the organism, and the effects of these metabolites persist until the homeostatic processes compensate for the insult, which is consistent with the established mechanism where phosphorylated derived nucleosides would not readily be removed from the cell. Dilution of the generating drug-pretreated organism had no significant effect on this irreversibly affected generation rate (Fig. 8).

The addition of uracil to the resuspended organisms had no effect on the previously modified generation rate. This result further demonstrates that uracil antagonizes fluorouracil incorporation into active anabolites or catabolites and has no direct effect on deblocking DNA synthesis.

Human Plasma Protein Binding of Fluorouracil—The cone bindings for various concentrations of fluorouracil in percent of concentration ± *SD* were: 2.5 ± 0.4 at 0.1 μg/ml and 1850 cpm, 4.4 ± 1.8% at 0.4 μg/ml, 2.7 ± 2.8% at 1.0 μg/ml and 18,500 cpm, 3.6 ± 0.9% at 4.0 μg/ml and 1100 cpm, and 1.5 ± 0.5% at 100 μg/ml and 1100 cpm. The overall average was 3% with an averaged standard deviation of 1.5%. There was no significant difference between cone bindings at pH 7.9 and 7.1.

The total binding to plasma protein and the filter cones was not sig-

Table II—Pharmacokinetic Parameters for Intravenous Bolus Administration of Fluorouracil

Parameter	Patient RC[a] (F) Weight, kg 44.7	45.0	Patient FW[a] (M) Weight, kg 69.0	67.4	Patient JC (M) Weight, kg 98.6	—
Dose, D_0, mg	1000	500	1000	500	1000	500
α^b, min^{-1}	—	—	—	0.5	0.5	1.2
β^b, min^{-1}	0.036	0.059	0.081	0.082	0.058	0.137
$(t_{1/2})_\alpha$, min	—	—	(~10)	1.5	1.4	0.6
$(t_{1/2})_\beta$, min	19	12	8.6	8.4	12	5.1
A^b, μg/ml	—	—	—	27	94	—
B^b, μg/ml	50	35	60	15	33	32
$V_{extrap}{}^c$, liters	20	15	17	33	31	16
$V_C{}^d$, liters	—	—	—	12.1	10.6	—
AUC^e, μg/ml-min	1411	496	782	203	723	278
$V_{pss}{}^f$, liters	20	17	16	30	24	13
Total clearance, $Cl_{tot}{}^g$, ml/min	709	1008	1278	2469	1383	1801
Renal clearance, $Cl_{ren}{}^h$, ml/min	101	147	91	86	140[k]	157
Metabolic clearance[i], ml/min	608	861	1187	2383	1243	1644
Percent of dose excreted in urine [j]	14.2	14.6	7.1	3.5	10.1	8.7

[a] The creatinine clearances for Patients RC and FW were 83 and 74 and 65, 60, 70, and 50, respectively. [b] Parameters for time dependence, t in minutes, for plasma levels, b in micrograms of fluorouracil per milliliter of plasma: $b = (Ae^{-\alpha t} + Be^{-\beta t})$. [c] D_0/B. [d] Estimates of apparent volume of distribution of central compartment, $V_C = D_0/(A + B)$. [e] Area under plasma level–time curve by trapezoidal rule. Terminal area estimated from last plasma level, b_n, and observed β, *i.e.*, b_n/β. [f] Pseudo-steady-state overall apparent volume of distribution, $V_{pss} = Cl_{tot}/\beta$. [g] Total clearance, $Cl_{tot} = D_0/AUC$. [h] Renal clearance, $Cl_{ren} = (U_\infty/D_0)\ Cl_{tot}$, where U_∞ is total amount of drug excreted unchanged in urine. [i] $Cl_{tot} - Cl_{ren}$. [j] $10^2\ U_\infty/D_0$. [k] One infusion study gave a $Cl_{ren} = (\Delta U/\Delta t)/b_{avg}$ = (450 μg/min)/3.0 μg/ml = 150 ml/min at steady state.

nificantly concentration dependent (Table I), although the total binding at pH 7.2 did significantly exceed that at pH values of 5.7 and 9.0. Correction for cone binding implies a protein binding of fluorouracil of 10% at pH 7.2 and ~3% at the other pH values.

Pharmacokinetics of Fluorouracil on Bolus Intravenous Administration—The time courses of the plasma levels as percent of dose per milliliter of plasma on intravenous bolus injection are shown in Fig. 9, and the derived pharmacokinetic parameters are listed in Table II. A two-compartment body model is indicated by the biphasic semilogarithmic plots. The slow mixing for Patient RC did not permit observation of an α-phase when the drug was injected and taken from opposite arms. The half-lives for the preliminary distribution (α) phases for the other two subjects ranged from 0.6 to 1.5 min. The percent of dose–time plots of Fig. 9 for the initial data of both 1000- and 500-mg doses were reasonably superimposable when plotted in such a manner and do not deny the premise that the apparent 10–12-liter volume of distribution of the central compartment and the initial distribution rates are dose independent.

Various other pharmacokinetic parameters were calculated for the two studies where the data were adequate for estimation of α and A values. The first-order two-compartment body model where the intravenously administered drug distributes between the central compartment, C, and the peripheral compartment, P, and is eliminated or metabolized to E is shown in Scheme I.

$$E \xleftarrow{k_{CE}} C \underset{k_{PC}}{\overset{k_{CP}}{\rightleftarrows}} P$$

Scheme I

The estimated microscopic rate constants (13) in minutes^{-1} for Patients FW (500-mg dose) and JC (1000-mg dose) were, respectively: k_{PC}, 0.23, 0.17; k_{CP}, 0.17, 0.22; and k_{CE}, 0.18, 0.17. The apparent volumes of distribution of the central compartment, V_c = dose/(B + A), were 11.9 and 7.9 liters; of the peripheral compartment, $V_p = V_c k_{CP}/k_{PC}$, they were 8.9 and 9.9 liters. The total steady-state volumes of distribution, $V_{ss} = V_c + V_P$, were 21 and 18 liters, respectively. The areas (AUC) under the plasma level–time curves, calculated from the parameters given in Table II for the sum of exponentials fit of the plasma level, $b = Ae^{-\alpha t} + Be^{-\beta t}$, were 237 and 757 μg/ml-min from $AUC = A/\alpha + B/\beta$. Thus, the respective total clearances (dose/AUC) for these studies of Patients FW and JC were 2110 and 1321 ml/min, respectively, which were similar to those clearances determined from areas calculated by the trapezoidal rule (Table II).

There were lower plasma levels as percent of dose for the 500-mg bolus as opposed to the 1000-mg bolus in all three subjects (Fig. 9), thereby demonstrating a significant pharmacokinetic dose dependency. In two (JC and RC) out of the three studied subjects, the apparent first-order terminal rate constant of drug elimination was significantly higher at the lower dose, which could imply a saturable metabolism of fluorouracil. However, the continued linearity of the terminal semilogarithmic plots implies that it cannot be assigned to substrate-dependent metabolism alone since an increase in the terminal slope with time would be anticipated at the higher doses. A possible explanation could be product-inhibited metabolism, which would significantly decrease the slope of the terminal phase (Fig. 9) at the higher dose.

A possible alternative explanation may be based on the premise that fluorouracil is initially transformed reversibly to 5,6-dihydrofluorouracil. The subsequent irreversible process of ring opening of the latter may be a saturable process. Thus, higher plasma levels would promote the accumulation of the fluorouracil in equilibrium with the dihydrofluorouracil.

The dose-dependent metabolic clearances, Cl_{met} (Table II), exceeded the normal hepatic plasma flow of 812 ml/min (14). This result indicates that metabolism occurs at sites other than in the liver, and a high first-pass metabolism would be predicted on oral administration.

The renal clearances (Table II) in the three subjects did not appear to be dose dependent and averaged 124 (RC), 89 (FW), and 149 (JC) ml/min, in contrast to the two subjects studied by Clarkson *et al.* (5) on drug infusion with renal clearances of 159 and 180 ml/min. However, these subjects may have had normal renal clearances (one had an inulin clearance of 109 ml/min) whereas Patients RC and FW had significantly low creatinine clearances of 79 and 61 ml/min, respectively. The percent of drug previously reported (5) to be excreted unchanged in the urine on single intravenous injection was 16% (7.8% with impaired renal function) and was consistent with the present values (Table II).

Occasional microbial generation studies of plasma samples containing fluorouracil were made with added uracil. In all cases, the inhibitory action of the drug was completely reversed. This finding indicated no significant concentration of derived nucleoside in the plasma.

Table III—Pharmacokinetic Parameters on the Oral Administration of Fluorouracil Solutions

Parameter	Patient JC (M), 107.5 kg			Patient FW (M), 65.3 kg	
Dose, D_0, mg	1000	1000	500	1000	500
AUC_{po}[a], μg/ml-min	47	110	5.5	89	16
Percent of dose excreted in urine[b]	1.24	0.33	0.14	0.67	0.16
Percent apparent bioavailability					
From $10^2\ AUC_{po}/AUC_{iv}$[c]	12.4	3.3	1.6	9.4	4.6
From $10^2\ (U_\infty)_{po}/(U_\infty)_{iv}$[d]	15.1	6.4	0.8	11.3	8.0

[a] Area under plasma level–time curve by trapezoidal rule. Terminal area estimated from last plasma level, b_n, and observed β at 500-mg iv dose, *i.e.*, b_n/β. [b] $10^2(U_\infty)_{po}/D_0$, where U_∞ is total amount of drug excreted unchanged in urine. [c] From ratios of AUC for same doses, oral/intravenous. [d] From ratios of total amounts of drug excreted unchanged, U_∞, for same doses, oral/intravenous.

Pharmacokinetics of Fluorouracil on Constant-Rate Intravenous Infusion—Two studies, with Patients RC and FW, of constant-rate (k_0) intravenous infusion (6.67 mg/min) of 1000 mg (D_0) of fluorouracil were conducted with total areas under the plasma level–time curves of 336 and 197 μg/ml-min, respectively. Thus, the respective clearances, $Cl_{tot} = D_0/AUC$, were 2977 and 5085 ml/min. The average plasma levels on attainment of steady state (b_{ss}) were 2.65 μg/ml ± 0.46 (SD) for RC and 1.42 μg/ml ± 0.28 (SD) for FW. Thus, the respective estimated total clearances calculated from these values ($Cl_{tot} = k_0/b_{ss}$) were 2517 and 4697 ml/min, values consistent with the total clearances calculated from the AUC values. However, the averages of these total clearances, 2747 (RC) and 4891 (FW) ml/min, greatly exceeded, by more than twofold, the total clearances obtained on bolus intravenous injection of either 500 or 1000 mg of fluorouracil (Table II). When the total clearance was divided by the respective average pseudo-steady-state volume of distribution for each subject (Table II), the estimated elimination rate constants ($\beta = Cl_{tot}/V_{P_{ss}}$) were 0.15 (RC) and 0.20 (FW) min^{-1}. This finding confirms the indicated dose-dependent pharmacokinetics of fluorouracil. Slow infusion of the drug that increased the metabolic rates would give a lessened steady-state concentration of metabolites and would support the hypothesis of product-inhibited metabolism.

Patient RC excreted unchanged 7.1% of the dose in the urine, a value significantly less than the 14.4% observed on intravenous bolus administration. This decrease in the urinary excretion is normally expected with an increase in the rate of a parallel metabolism of a drug.

Pharmacokinetics of Fluorouracil on Oral Administration of Solutions—As previously reported (5, 15), the absorption of fluorouracil on oral administration was highly variable among and within subjects (Fig. 9). First approximations of the fraction of drug absorbed unchanged can be made from the ratios of drug excreted unchanged or from the ratios of the area under the curve, oral to intravenous for equivalent doses. These ratios ranged from 0.01 to 0.15 in the five studies conducted (Table III), where the ratios of the AUC values reasonably correlated with the ratios of the renal excretion of unchanged drug. These are not accurate quantitative values for bioavailability but are only coincident with true bioavailabilities if, and only if, elimination rates are dose independent.

These apparent bioavailabilities were much less than the 0.50 and 0.80 values reported for two subjects by Cohen *et al.* (15). However, their subjects had carcinomas of the colon metastatic to the liver. Other investigators (5, 16) indicated much lower amounts of drug available to the plasma on oral absorption.

The plasma fluorouracil levels of solutions (Fig. 9) peaked 10–15 min after oral administration; at the higher 1000-mg dose, they were prolonged, indicating a sustained zero-order absorption. The apparent bioavailabilities (Table III) at the 1000-mg oral dose always exceeded those at the lower 500-mg doses. This finding is consistent with a dose-dependent first-pass effect. Since hepatic clearances on intravenous administration (Table II) always exceeded hepatic plasma flow by more than twofold, there should have been negligible drug in the plasma by the oral route. The fact that significant drug was absorbed orally is indicative of highly saturable first-pass phenomena when high concentrations of drug enter the liver on oral administration and/or additional extrahepatic metabolic and elimination pathways that are not mediated by the absorption process.

REFERENCES

(1) J. J. Windheuser, J. L. Sutter, and E. Auen, *J. Pharm. Sci.*, **61**, 301 (1972).

(2) J. L. Cohen and P. B. Brennnan, *ibid.*, **62**, 572 (1973).

(3) K. V. Rao, K. Killion, and Y. Tanrikut, *ibid.*, **63**, 1328 (1974).

(4) C. Finn and W. Sadée, *Cancer Chemother. Rep.*, **59**, 279 (1975).

(5) B. Clarkson, A. O'Connor, L. Winston, and D. Hutchison, *Clin. Pharmacol. Ther.*, **5**, 581 (1964).

(6) E. R. Garrett and H. Nolte, *Chemotherapy*, **17**, 81 (1972).

(7) A. H. Anton, *J. Pharmacol. Exp. Ther.*, **129**, 282 (1960).

(8) E. R. Garrett, H. J. Nestler, and A. Somodi, *J. Org. Chem.*, **33**, 3460 (1968).

(9) E. R. Garrett and O. K. Wright, *J. Pharm. Sci.*, **56**, 1576 (1967).

(10) E. R. Garrett, S. M. Heman-Ackah, and G. L. Perry, *ibid.*, **59**, 1448 (1970).

(11) E. R. Garrett, in "Progress in Drug Research," E. Jucker, Ed., Birkhäuser Verlag, Basel, Switzerland, 1971, pp. 290, 301–303.

(12) S. Cohen, J. Flaks, H. D. Barner, M. R. Loeb, and J. Lichtenstein, *Proc. Natl. Acad. Sci. USA*, **44**, 1004 (1958).

(13) M. Gibaldi and D. Perrier, "Pharmacokinetics," Dekker, New York, N.Y., 1975.

(14) A. C. Guyton, "Textbook of Medical Physiology," 5th ed., Saunders, Philadelphia, Pa., 1968, p. 325.

(15) J. L. Cohen, L. E. Irwin, G. J. Marshall, H. Darvey, and J. R. Bateman, *Cancer Chemother. Rep.*, **58**, 723 (1974).

(16) H. O. Douglas, Jr., and A. Mittleman, *Proc. Am. Assoc. Cancer Res.*, **14**, 116 (1973).

ACKNOWLEDGMENTS AND ADDRESSES

Received October 18, 1976, from *The Beehive, College of Pharmacy, University of Florida, Gainesville, FL 32610.*

Accepted for publication December 16, 1976.

Supported in part by Grant NIH-RR-82 from the National Institutes of Health, Bethesda, MD 20014.

The technical assistance of George Perry and Kathleen L. Eberst is gratefully acknowledged. The authors thank the nursing staff of the Clinical Research Center, Shands Hospital, University of Florida, for assistance in performing the clinical studies.

* Present address: Department of Community Health and Family Medicine, University of Florida, Gainesville, FL 32610.

[x] To whom inquiries should be directed.

Factors Influencing Comparative Bioavailability of Spironolactone Tablets

J. M. CLARKE [x], L. E. RAMSAY *, J. R. SHELTON, M. J. TIDD [‡], S. MURRAY, and R. F. PALMER

Abstract □ The bioavailability of spironolactone from 10 tablet formulations, selected to provide a wide range of specifications and *in vitro* dissolution rates, was assessed from the plasma and urinary levels of its major unconjugated metabolite, canrenone, in a study of balanced incomplete block design using 11 healthy subjects. Significant but weak correlations existed between the amount of spironolactone in solution at 40 min *in vitro* and the area under the plasma concentration–time curve for canrenone and urinary canrenone excretion. The correlations between *in vitro* dissolution and bioavailability parameters appeared to be weakened by two tablet formulations, one with dibasic calcium phosphate as the principal excipient and the other formulated from micronized spironolactone bulk drug. Measurement of *in vitro* dissolution of spironolactone tablets is of value for quality control purposes, provided no major alteration is made in the formulation.

Keyphrases □ Spironolactone—bioavailability in humans related to *in vitro* dissolution, various tablet formulations compared □ Bioavailability—spironolactone in humans, related to *in vitro* dissolution, various tablet formulations compared □ Dissolution, *in vitro*—spironolactone, related to human bioavailability, various tablet formulations compared □ Diuretics—spironolactone, bioavailability in humans related to *in vitro* dissolution, various tablet formulations compared

Spironolactone[1], a synthetic steroid lactone having properties compatible with specific competitive antagonism of aldosterone and other mineralocorticoids (1–3), is of clinical value in the treatment of congestive heart failure, hepatic ascites, primary aldosteronism, and essential hypertension (4). The original tablet formulation of spironolactone had incomplete bioavailability, and reformulation yielded a tablet that proved to be fourfold superior with regard to plasma levels of the principal unconjugated metabolite (canrenone) (5–8), pharmacological activity (9, 10), and therapeutic efficacy (8).

It was suggested that the spironolactone absorption was limited by its dissolution rate, and some evidence indicated that the improved bioavailability of the new formulation could be related to more rapid *in vitro* dissolution (11). The new formulation of spironolactone (25-mg tablets) is still used, and little has been published on spironolactone bioavailability in recent years.

A new 100-mg spironolactone tablet was shown to be bioequivalent to four 25-mg tablets (12). Spironolactone was included in the long list of drugs for which more information on bioavailability is considered desirable (13, 14).

This paper presents the comparative bioavailability of 10 tablet formulations of spironolactone. The objective of the study was to determine whether dissolution *in vitro* is of value in predicting *in vivo* bioavailability and which factors in tablet specification may be important to bioavailability.

[1] Aldactone, G. D. Searle & Co.

EXPERIMENTAL

Formulations—Three experimental and seven production batch tablets were studied. All tablets were chemically equivalent inasmuch as they all complied with the BP monograph requirements for spironolactone. The tablets were selected specifically to provide the wide range

REFERENCES

(1) J. J. Windheuser, J. L. Sutter, and E. Auen, *J. Pharm. Sci.*, **61**, 301 (1972).

(2) J. L. Cohen and P. B. Brennnan, *ibid.*, **62**, 572 (1973).

(3) K. V. Rao, K. Killion, and Y. Tanrikut, *ibid.*, **63**, 1328 (1974).

(4) C. Finn and W. Sadée, *Cancer Chemother. Rep.*, **59**, 279 (1975).

(5) B. Clarkson, A. O'Connor, L. Winston, and D. Hutchison, *Clin. Pharmacol. Ther.*, **5**, 581 (1964).

(6) E. R. Garrett and H. Nolte, *Chemotherapy*, **17**, 81 (1972).

(7) A. H. Anton, *J. Pharmacol. Exp. Ther.*, **129**, 282 (1960).

(8) E. R. Garrett, H. J. Nestler, and A. Somodi, *J. Org. Chem.*, **33**, 3460 (1968).

(9) E. R. Garrett and O. K. Wright, *J. Pharm. Sci.*, **56**, 1576 (1967).

(10) E. R. Garrett, S. M. Heman-Ackah, and G. L. Perry, *ibid.*, **59**, 1448 (1970).

(11) E. R. Garrett, in "Progress in Drug Research," E. Jucker, Ed., Birkhäuser Verlag, Basel, Switzerland, 1971, pp. 290, 301–303.

(12) S. Cohen, J. Flaks, H. D. Barner, M. R. Loeb, and J. Lichtenstein, *Proc. Natl. Acad. Sci. USA*, **44**, 1004 (1958).

(13) M. Gibaldi and D. Perrier, "Pharmacokinetics," Dekker, New York, N.Y., 1975.

(14) A. C. Guyton, "Textbook of Medical Physiology," 5th ed., Saunders, Philadelphia, Pa., 1968, p. 325.

(15) J. L. Cohen, L. E. Irwin, G. J. Marshall, H. Darvey, and J. R. Bateman, *Cancer Chemother. Rep.*, **58**, 723 (1974).

(16) H. O. Douglas, Jr., and A. Mittleman, *Proc. Am. Assoc. Cancer Res.*, **14**, 116 (1973).

ACKNOWLEDGMENTS AND ADDRESSES

Received October 18, 1976, from *The Beehive, College of Pharmacy, University of Florida, Gainesville, FL 32610.*

Accepted for publication December 16, 1976.

Supported in part by Grant NIH-RR-82 from the National Institutes of Health, Bethesda, MD 20014.

The technical assistance of George Perry and Kathleen L. Eberst is gratefully acknowledged. The authors thank the nursing staff of the Clinical Research Center, Shands Hospital, University of Florida, for assistance in performing the clinical studies.

* Present address: Department of Community Health and Family Medicine, University of Florida, Gainesville, FL 32610.

[x] To whom inquiries should be directed.

Factors Influencing Comparative Bioavailability of Spironolactone Tablets

J. M. CLARKE [x], L. E. RAMSAY *, J. R. SHELTON, M. J. TIDD [‡], S. MURRAY, and R. F. PALMER

Abstract □ The bioavailability of spironolactone from 10 tablet formulations, selected to provide a wide range of specifications and *in vitro* dissolution rates, was assessed from the plasma and urinary levels of its major unconjugated metabolite, canrenone, in a study of balanced incomplete block design using 11 healthy subjects. Significant but weak correlations existed between the amount of spironolactone in solution at 40 min *in vitro* and the area under the plasma concentration–time curve for canrenone and urinary canrenone excretion. The correlations between *in vitro* dissolution and bioavailability parameters appeared to be weakened by two tablet formulations, one with dibasic calcium phosphate as the principal excipient and the other formulated from micronized spironolactone bulk drug. Measurement of *in vitro* dissolution of spironolactone tablets is of value for quality control purposes, provided no major alteration is made in the formulation.

Keyphrases □ Spironolactone—bioavailability in humans related to *in vitro* dissolution, various tablet formulations compared □ Bioavailability—spironolactone in humans, related to *in vitro* dissolution, various tablet formulations compared □ Dissolution, *in vitro*—spironolactone, related to human bioavailability, various tablet formulations compared □ Diuretics—spironolactone, bioavailability in humans related to *in vitro* dissolution, various tablet formulations compared

Spironolactone[1], a synthetic steroid lactone having properties compatible with specific competitive antagonism of aldosterone and other mineralocorticoids (1–3), is of clinical value in the treatment of congestive heart failure, hepatic ascites, primary aldosteronism, and essential hypertension (4). The original tablet formulation of spironolactone had incomplete bioavailability, and reformulation yielded a tablet that proved to be fourfold superior with regard to plasma levels of the principal unconjugated metabolite (canrenone) (5–8), pharmacological activity (9, 10), and therapeutic efficacy (8).

It was suggested that the spironolactone absorption was limited by its dissolution rate, and some evidence indicated that the improved bioavailability of the new formulation could be related to more rapid *in vitro* dissolution (11). The new formulation of spironolactone (25-mg tablets) is still used, and little has been published on spironolactone bioavailability in recent years.

A new 100-mg spironolactone tablet was shown to be bioequivalent to four 25-mg tablets (12). Spironolactone was included in the long list of drugs for which more information on bioavailability is considered desirable (13, 14).

This paper presents the comparative bioavailability of 10 tablet formulations of spironolactone. The objective of the study was to determine whether dissolution *in vitro* is of value in predicting *in vivo* bioavailability and which factors in tablet specification may be important to bioavailability.

[1] Aldactone, G. D. Searle & Co.

EXPERIMENTAL

Formulations—Three experimental and seven production batch tablets were studied. All tablets were chemically equivalent inasmuch as they all complied with the BP monograph requirements for spironolactone. The tablets were selected specifically to provide the wide range

Table I—Properties of the 10 Spironolactone Tablet Formulations Tested

Property	Tablet A	B	C	D	E	F	G	H	I	J
Weight of spironolactone per tablet, mg	25	25	25	100	100	100	100	25	50	100
Weight of tablet, mg	266	266	266	292	664	664	664	664	185	430
Source of spironolactone bulk drug	5	1	3	1	2	4	4	3	7	7
Site of manufacture of tablet	4	4	3	1	3	4	4	5	6	6
Principal excipient[a]	I	I	I	II	I	I	I	I	III	III
Chemical treatment[b]	U	U	U	U	U	U	U	U	M	U
In vitro dissolution, %, at:										
10 min	26	44	40	4	36	19	25	71	21	33
20 min	42	86	48	12	64	42	50	87	57	48
40 min	51	95	61	23	76	57	65	93	71	59

[a] Excipients were calcium sulfate dihydrate (I), dibasic calcium phosphate (II), and lactose (III). [b] M = micronized, and U = nonmicronized.

of specifications and *in vitro* dissolution properties shown in Table I. They were classified by weight of spironolactone per tablet (three categories), weight of tablet (five categories), sites of manufacture of chemical (six sites) and of tablets (five sites), principal excipient (three categories), and particle size (micronized or nonmicronized).

The bioavailability of Tablets B and D was tested in separate studies. Tablet D, a 100-mg tablet, had surprisingly high bioavailability considering its very slow *in vitro* dissolution (Table I) (15) and was included in the present study for this reason. The sparing solubility of the drug, which led to the original bioavailability problem (11), also precluded development of an intravenous formulation. In addition to the 10 tablet formulations, an oral spironolactone solution was included for between-study quality control purposes. Since the spironolactone dose in the solution was lower than that of the tablets, the results for the solution are not relevant to the main study and are not presented.

Dissolution Rate—The dissolution rates of the 10 tablet formulations were determined by a rotating-paddle method. Five liters of USP gastric juice without enzymes was equilibrated to 37° in a three-necked, round-bottom flask. The polytef paddle (132 × 24 mm) was immersed to 2 cm from the bottom of the flask and rotated at 100 rpm.

The amount of drug dissolved from tablets placed at the bottom of the flask was determined from samples removed at 10, 20, and 40 min. After removal, the solution was filtered and spironolactone was determined spectrophotometrically using a standard solution of spironolactone USP as the reference. The percentage dissolution of spironolactone from the 10 tablet formulations at the three sampling times is shown in Table I.

Subjects and Study Design—Eleven male subjects, 21–56 years old, were judged healthy after a medical history, physical examination, and biochemical and hematological screen; they gave informed consent to the study. The design was a balanced incomplete block termed a Youden square (16), with the 11 subjects each taking six of the 11 treatments (10 tablet treatments and one solution) on a single occasion. The six study phases were each separated by an interval of 1 week.

Procedure—The treatments were given with 250 ml of water at 9:00 am following an overnight fast, and the subjects continued fasting for 4 hr after treatment. The dose of the spironolactone tablets was 100 mg as one 100-mg tablet, two 50-mg tablets, or four 25-mg tablets. Venous blood was taken before treatment (for measurement of blank values), at nine timed sampling points in the 6 hr after treatment, and then at 12, 24, 36, 48, 72, and 96 hr. Urine was collected for 96 hr.

Blood samples were placed in heparin lithium anticoagulant and centrifuged within 1 hr, and the separated plasma was stored at −20° until assay. Aliquots of urine were also stored at −20°. The samples were stable over the analysis period as judged by quality control samples of plasma stored under similar conditions at known levels and assayed with each batch of clinical samples. The subjects abstained from alcohol during sampling periods, and all other medication was prohibited throughout the study. The subjects were ambulant and followed their normal diet apart from the periods of fasting.

Analytical—Spironolactone itself does not appear in plasma or urine in measurable quantities; bioavailability was assessed from the levels of its principal unconjugated metabolite, canrenone, in plasma and urine. Canrenone was measured by the fluorometric method of Gochman and Gantt (17). The mean recovery of canrenone from plasma was 75% (range of 62–81%); from urine, it was 98% (range of 93–100%).

From three quality control samples included with the plasma assays, the mean coefficient of variation between batches was 12%. For the urine assay, the between-batch coefficient of variation was 5% (mean for two

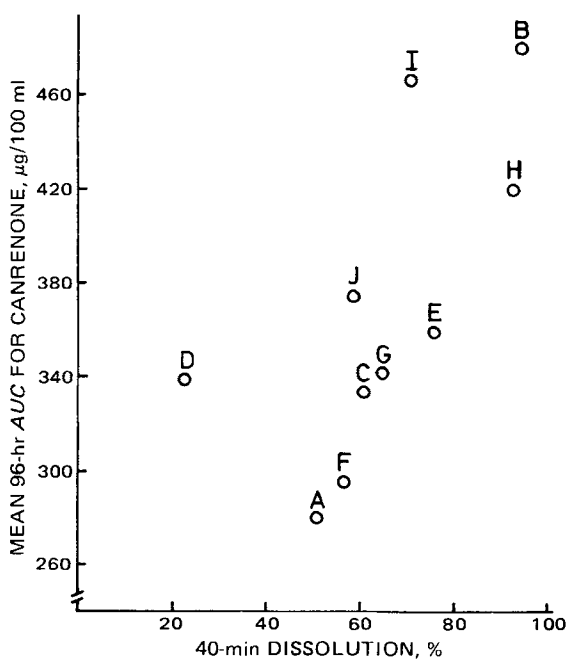

Figure 1—*Plot of AUC for canrenone* versus *40-min dissolution* in vitro.

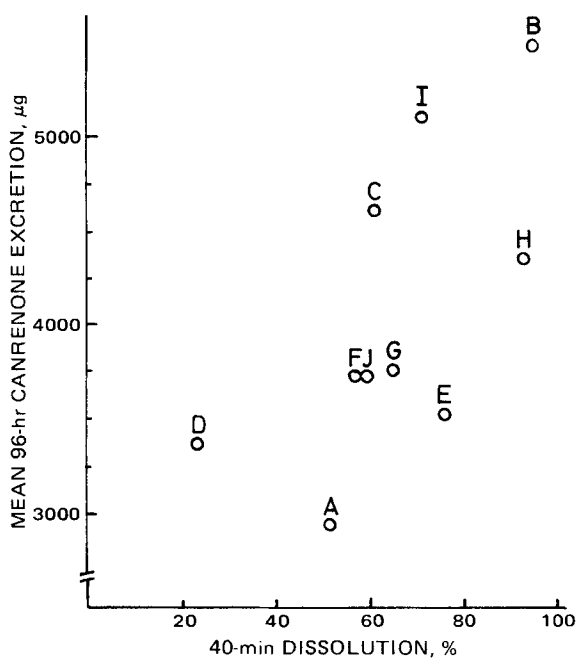

Figure 2—*Plot of mean 96-hr urinary canrenone excretion* versus *40-min dissolution* in vitro.

Table II—Adjusted Mean Results for the Bioavailability Parameters after Administration of 100 mg of Spironolactone in 10 Different Tablet Formulations

Parameter	Tablet A	B	C	D	E	F	G	H	I	J	p^a
Peak plasma canrenone, μg/100 ml	13.1 (2.2)[b]	24.9 (6.7)	16.7 (3.5)	20.0 (4.2)	23.7 (17.4)	17.5 (3.4)	20.2 (5.6)	27.1 (12.6)	29.0 (7.7)	16.6 (6.6)	<0.01
Time to peak canrenone level, hr	3.3 (0.8)	4.0 (1.4)	3.4 (1.2)	2.7 (1.0)	2.6 (0.8)	2.6 (0.8)	3.8 (1.1)	3.0 (1.0)	3.1 (1.2)	3.8 (1.3)	NS
96-hr *AUC* for canrenone, μg/100 ml × hr	267 (113)	478 (214)	332 (241)	338 (55)	349 (193)	296 (106)	341 (219)	420 (102)	465 (378)	373 (272)	<0.05
96-hr urinary canrenone excretion, μg	2960 (1031)	5484 (1279)	4608 (1417)	3385 (963)	3536 (1263)	3721 (1169)	3769 (1468)	4366 (1605)	5105 (1860)	3747 (1078)	<0.01
40-min dissolution, %	51	95	61	23	76	57	65	93	71	59	—

[a] The p values for significance of the differences between the 10 tablet formulations. [b] Figures in parentheses are unadjusted standard deviations with $n = 6$.

quality control samples). The mean ± *SD* of all plasma blank values was 0.63 ± 0.44 μg/100 ml. The plasma blank values did not differ significantly between the six study phases or between the 11 treatments, indicating that the 1-week interval between treatments was adequate and that the blank values had not biased the comparison of the treatments.

Statistical—The parameters of bioavailability analyzed were the peak plasma canrenone level, the time to peak, the area under the plasma concentration–time curve for canrenone from 0 to 96 hr (*AUC* for canrenone), and the total urinary excretion of canrenone over 96 hr. Since plasma canrenone levels often reached the lower limit of assay sensitivity before a terminal log-linear phase of the canrenone concentration–time curve was reached, the *AUC* values were not extrapolated to infinity. The *AUC* for canrenone, calculated by the trapezoidal method, therefore represents the average plasma canrenone level to the finite time of 96 hr.

The differences between the 10 tablet formulations were investigated by the analysis of variance appropriate to the Youden square design (16). Relationships between *in vivo* and *in vitro* measurements were examined by product-moment correlations, and the significance levels given are for two-tailed tests. The mean results of the parameters of bioavailability for each formulation were adjusted for differences between subjects (16).

RESULTS

The adjusted mean (and standard deviation) results of the parameters of bioavailability for the 10 tablet formulations are shown in Table II. The 10 formulations differed significantly regarding peak plasma levels of canrenone ($p < 0.01$), the *AUC* for canrenone ($p < 0.05$), and urinary canrenone excretion ($p < 0.01$) but not regarding the time to reach peak canrenone levels.

Bioavailability Parameters Related to *In Vitro* Dissolution—There were no significant correlations between the amount of spironolactone in solution at 10 min and the bioavailability parameters. The results for spironolactone dissolution at 20 and 40 min were very similar, and only the 40-min dissolution data will be presented (Table III).

The amount of spironolactone in solution at 40 min correlated significantly with the *AUC* for canrenone ($r = +0.66$, $p < 0.05$, Fig. 1) and with urinary canrenone excretion ($r = +0.65$, $p < 0.05$, Fig. 2). The correlation of 40-min dissolution with peak canrenone levels approached significance ($r = +0.61$, $p < 0.1$, Fig. 3), but that with the time to peak plasma canrenone ($r = +0.33$) was not significant ($p > 0.1$).

In Fig. 3 and, to a lesser extent, in Fig. 1, it can be seen that the correlations are improved if two of the 10 formulations, Tablets D and I, are excluded. There was a suggestion that these two formulations gave peak canrenone levels and *AUC* values for canrenone that are relatively high for a given dissolution. Examination of Table I shows that Tablets D and I were unique with regard to tablet weight, and Tablet I was also different with respect to the amount of spironolactone per tablet (50 mg). These variables did not appear to influence the relationship between *in vitro* dissolution and bioavailability for the other tablet formulations and are not considered to be the most probable causes of the findings. Tablet D was the only formulation with dibasic calcium phosphate as its principal excipient, and Tablet I was the only one formulated from micronized spironolactone bulk drug; these factors may be responsible for the different behavior of these formulations.

Table III—Correlations of the Amount of Spironolactone in Solution at 40 min with the Bioavailability Parameters for All 10 Spironolactone Tablets ($n = 10$) and Excluding the Results for Tablets D and I ($n = 8$)

40-min Dissolution *versus*	$n = 10$ r	p	$n = 8$ r	p
Peak plasma canrenone	+0.61	<0.1	+0.95	<0.001
Time to peak canrenone	+0.33	NS[a]	+0.13	NS
96-hr *AUC* for canrenone	+0.66	<0.05	+0.90	<0.005
96-hr urinary canrenone excretion	+0.65	<0.05	+0.72	<0.05

[a] NS = $p > 0.1$.

Recalculation of the correlation coefficients excluding the results for Tablets D and I (Table III) showed high correlations of the 40-min dissolution with the *AUC* for canrenone ($r = +0.90$) and peak canrenone level ($r = +0.95$) and a moderate correlation with urinary canrenone excretion ($r = +0.72$). There was still no correlation with the time to reach peak plasma canrenone concentration.

Variability between Subjects in Bioavailability Parameters—In Table IV the range of adjusted mean results observed between the 10 tablet formulations is compared to the range of adjusted mean results between the 11 subjects. The variability between subjects at least equaled that between formulations for each parameter. For the *AUC* for canrenone, the intersubject differences were considerably greater than the differences between formulations.

DISCUSSION

The marked and significant differences between the 10 tablets with regard to the *AUC* for canrenone in plasma and the urinary excretion of canrenone indicate that the total amount of spironolactone absorbed from different formulations may vary greatly. The adjusted mean 96-hr *AUC* for canrenone for the different formulations ranged from 267 to 478 μg/dl hr. Such a wide range was not observed among spironolactone tablets actually released for marketing; the formulations tested in this study were

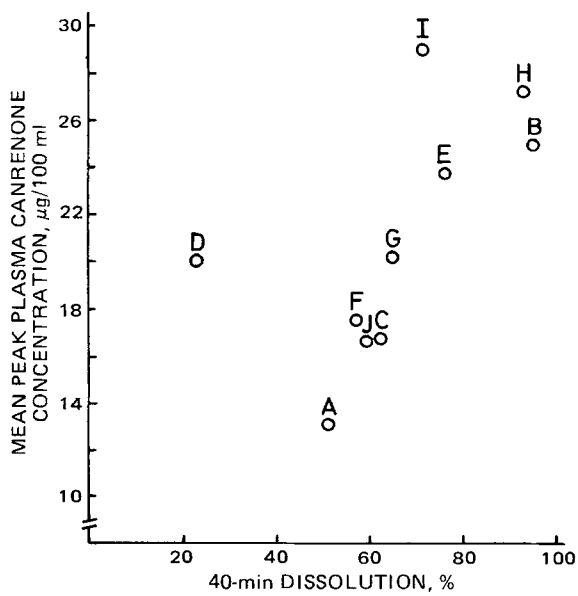

Figure 3—*Plot of mean peak plasma canrenone concentration* versus *40-min dissolution* in vitro.

Table IV—Range of Adjusted Mean Results Observed Comparing the Variability between 10 Spironolactone Formulations with the Variability between 11 Subjects

Parameter	Range of Observations	
	Between Formulations	Between Subjects
Peak plasma canrenone, μg/dl	13.1–29.0	14.7–31.7
Time to peak canrenone, hr	2.6–4.0	2.4–4.4
96-hr *AUC* for canrenone, μg/dl hr	267–478	231–878
96-hr urinary canrenone excretion, μg	2960–5484	2422–5119

selected specifically to provide variability and included three experimental preparations. In addition, the *in vitro* dissolution parameters of spironolactone tablets were already in use for quality control purposes prior to this study on a purely empirical basis. The present study shows that spironolactone bioavailability is potentially very variable, and as discussed below, gives some guidance as to how this variability can be controlled.

The present results confirm the suggestion of Levy (11) that the amount of spironolactone absorbed from tablet formulations is related to their dissolution characteristics. No such correlation was found in the earlier study of Tidd *et al.* (15), but this result is not surprising in view of the design of that study and the number and range of the formulations examined. In the present study, there were significant correlations of the amount of spironolactone in solution at 40 min *in vitro* with the *AUC* for canrenone and with urinary canrenone excretion and a similar trend with the peak plasma canrenone concentration. The range of times to reach peak canrenone levels was small, and the differences between the formulations were not significant. These results may account for the fact that the *in vitro* dissolution did not correlate with the time to reach peak canrenone levels, the parameter expected to relate most closely to the absorption rate of spironolactone.

The correlation between *in vitro* dissolution and the *AUC* for canrenone is important in confirming that spironolactone bioavailability is dissolution related (11), but it leaves a lot to be desired from the practical point of view. Ideally, such a correlation should be robust, so that the relationship holds despite even major alterations in tablet specification, and should have a coefficient high enough to allow reasonably accurate prediction of *in vivo* properties from the *in vitro* dissolution profile (18). With the results for all 10 formulations, the correlations observed fell short of these criteria. From the correlation coefficient for 40-min dissolution *versus* the *AUC* for canrenone ($r = +0.66$), it can be calculated that only 44% ($r^2 \times 100$) of the variability in the *AUC* for canrenone between formulations could be attributed to differences in 40-min dissolution. Although the observed correlation is probably an underestimate of the true correlation due to the experimental errors in the observed values of 40-min dissolution and particularly the mean *AUC*, part of the variability in the *AUC* values between formulations probably must be attributed to factors other than *in vitro* dissolution, as measured in the present study.

Inspection of the data gives some information suggesting the nature of these other factors and also suggests that the correlations between *in vitro* dissolution and *in vivo* parameters may be of value for quality control purposes. Certain factors in tablet specification had little or no influence on bioavailability independent of any effect on *in vitro* dissolution, including the weight of the tablet, the site of manufacture of spironolactone bulk drug, and the site of manufacture of the tablet. Similarly, the weight of spironolactone per tablet did not appear to influence bioavailability, supporting a previous report that four 25-mg tablets and one 100-mg tablet of spironolactone were bioequivalent (12).

However, two tablet formulations may have weakened what was otherwise a high correlation between *in vitro* dissolution and the *AUC* for canrenone. These findings may be attributed to a difference in the principal excipient for one tablet and to micronization of the spironolactone bulk drug in the other, although other factors in these formulations could equally be responsible. In any event, the results for these formulations indicate that the correlation between *in vitro* dissolution and bioavailability is not impervious to all changes in tablet specification. When the results for these formulations were excluded, the correlations of 40-min dissolution with the *AUC* for canrenone and the peak plasma canrenone concentration were considerably improved. Therefore, the *in vitro* dissolution of spironolactone tablets is likely to have value as a quality control procedure, particularly when there are no major changes in tablet specification. When the specifications are altered, for example by changing the particle size or a major excipient, reevaluation of the bioavailability by an *in vivo* study would be desirable.

The two tablets (D and I) that appeared to deviate from the relationship between *in vitro* dissolution and *in vivo* bioavailability are of interest. Formulation D was remarkable in having high bioavailability despite its extremely low *in vitro* dissolution (23% spironolactone in solution at 40 min). For some reason, the dissolution of this tablet in the GI tract may be more rapid than its *in vitro* dissolution. The high bioavailability of Tablet I may be attributed to micronization of the spironolactone bulk drug. Reduction in particle size has been shown to improve the bioavailability of other compounds with low water solubility, such as griseofulvin (19) and digoxin (20), and a similar effect from micronization previously was suggested for spironolactone (7). However, reduction in particle size would be expected to increase bioavailability through an increase in the dissolution rate of the drug (18), and it is not clear why the bioavailability of the micronized spironolactone tablet was higher than would be predicted from the *in vitro* dissolution rate.

REFERENCES

(1) C. M. Kagawa, J. A. Cella, and C. G. Van Arman, *Science*, **126**, 1015 (1957).

(2) C. M. Kagawa, *Endocrinology*, **67**, 125 (1960).

(3) V. A. Drill, *Jpn. J. Pharmacol.*, **11**, 77 (1962).

(4) A. Manitius and T. Suchecki, *Mater. Med. Pol.*, **4**, 83 (1972).

(5) C. L. Gantt, N. Gochman, and J. M. Dyniewicz, *Lancet*, **1**, 486 (1961).

(6) *Ibid.*, **1**, 1130 (1962).

(7) G. Bauer, P. Rieckmann, and W. Schaumann, *Arzneim.-Forsch.*, **12**, 487 (1962).

(8) S. Shaldon, J. A. Ryder, and M. Garsenstein, *Gut*, **4**, 16 (1963).

(9) P. R. Noel and J. S. Leahy, *Clin. Sci.*, **23**, 477 (1962).

(10) C. L. Gantt and J. M. Dyniewicz, *Metab. Clin. Exp.*, **12**, 1007 (1963).

(11) G. Levy, *Lancet*, **2**, 723 (1962).

(12) L. M. Hofmann, J. E. Dutt, L. G. Deysach, H. Loncin, and L. Tao, *J. Pharm. Sci.*, **63**, 1248 (1974).

(13) R. N. Smith, *Br. J. Clin. Pharmacol.*, **2**, 5 (1975).

(14) D. J. Chodos and A. R. Di Santo, "Basics of Bioavailability," The Upjohn Co., Kalamazoo, Mich., 1973.

(15) M. J. Tidd, W. T. Collins, and J. Chamberlain, *J. Int. Med. Res.*, **4**, 86 (1976).

(16) W. G. Cochran and G. M. Cox, "Experimental Designs," 2nd ed., Wiley, New York, N.Y., 1957, p. 507.

(17) N. Gochman and C. L. Gantt, *J. Pharmacol. Exp. Ther.*, **135**, 312 (1962).

(18) J. G. Wagner, "Biopharmaceutics and Relevant Pharmacokinetics," 1st ed., Drug Intelligence Publications, Hamilton, Ill., 1971, p. 121.

(19) S. Symchowicz and B. Katchen, *J. Pharm. Sci.*, **57**, 1383 (1968).

(20) A. J. Jounela, P. J. Pentikainen, and A. Sothmann, *Eur. J. Clin. Pharmacol.*, **8**, 365 (1975).

ACKNOWLEDGMENTS AND ADDRESSES

Received April 8, 1976, from the *Division of Scientific Affairs, G. D. Searle and Company Limited, Lane End Road, High Wycombe, Buckinghamshire, HP12 4HL, England.*

Accepted for publication December 21, 1976.

The authors are grateful to Mr. D. Edwards, Mrs. P. Hessian, Dr. B. Harlow, Mr. M. J. C. Howard, Mr. J. Linfoot, Mrs. M. Porteous, Mrs. M. Rogers, and Mr. J. Winslade for help in the design, conduct, and interpretation of the study and to Mr. I. Harrison and Mrs. R. S. Springell for help in the preparation of the manuscript. Canrenone assays were performed by the Hormone Assay Laboratory, Searle Scientific Services, G. D. Searle & Co., High Wycombe, England.

* Present address: Department of Medicine, Gardiner Institute, Western Infirmary, Glasgow, G11 6NT, Scotland.

‡ Present address: Syntex Research Centre, Research Park, Heriot-Watt University, Riccarton, Edinburgh, Scotland.

ˣ To whom inquiries should be directed.

Biopharmaceutic Factors that Influence Effects of Anticholinergic Drugs: Comparison of Propantheline, Hexocyclium, and Isopropamide

BARBARA GRUNDHOFER * and MILO GIBALDI ˣ

Abstract □ The antisecretory (determined from salivary flow rates) and antimotility (determined from riboflavin absorption) effects of usually recommended doses of propantheline, hexocyclium, and isopropamide were compared in four adult volunteers. Both propantheline and hexocyclium significantly decreased salivary flow and increased riboflavin absorption. Although the usual dose of propantheline was about twice as effective as the usual dose of hexocyclium in suppressing salivary flow, these doses produced comparable effects on riboflavin absorption. Isopropamide had little or no effect on either the salivary flow rate or riboflavin absorption. Propantheline and hexocyclium elicited little effect on salivary flow when administered after a meal. Prolonged-release dosage forms of these drugs produced effects comparable to those produced by much smaller doses in conventional tablets and gave no indication of providing prolonged anticholinergic effects.

Keyphrases □ Propantheline—antisecretory and antimotility effects compared to hexocyclium and isopropamide, humans □ Hexocyclium—antisecretory and antimotility effects compared to propantheline and isopropamide, humans □ Isopropamide—antisecretory and antimotility effects compared to propantheline and hexocyclium, humans □ Antisecretory effects—propantheline, hexocyclium, and isopropamide compared, humans □ Antimotility effects—propantheline, hexocyclium, and isopropamide compared, humans □ Anticholinergic agents—propantheline, hexocyclium, and isopropamide, antisecretory and antimotility effects compared, humans

Anticholinergic agents are among the most widely prescribed drugs for GI disorders (1). Their principal therapeutic effects are inhibition of gastric acid production and reduction of GI motility. Direct evaluation of the anticholinergic effects of a drug is difficult and causes discomfort to the patient, but relatively simple and noninvasive methods are available to evaluate such effects indirectly.

The antisecretory effect of anticholinergics is relatively nonspecific; suppression of gastric acid output is accompanied by a reduction in the secretion of pancreatic juice and saliva (1). Studies in which gastric acid and salivary secretions were measured simultaneously after administration of an anticholinergic drug indicated parallel decreases in flow rates (2). With the salivary flow rate as an index of anticholinergic response, the bioavailability of propantheline was reduced when the drug was given after a meal or in a sustained-release tablet compared to the bioavailability after administration of conventional tablets to fasted subjects (3).

Changes in GI motility can alter significantly the bioavailability of certain drugs. For example, propantheline increased the absorption of riboflavin in healthy volunteers (4) and of digoxin in patients (5), presumably by increasing the residence time of the drug at optimal absorption sites in the GI tract. Hence, changes in the absorption of such drugs may be a useful index of the antimotility effect of anticholinergic drugs.

The present study was undertaken to compare the effects of recommended doses of certain anticholinergic drugs on secretory activity, as reflected by the salivary flow rate, and GI motility, as reflected by riboflavin absorption in healthy volunteers, and to determine the influence of food and dosage form on these effects.

Table I—Suppression of Salivary Secretion (Milliliters)

Treatment	Subject M	B	W	A	Mean ± *SD*
Conventional Dosage Forms					
Propantheline, 15 mg	175	284	171	216	212 ± 52
Hexocyclium, 25 mg	104	184	102	60	112 ± 52
Isopropamide, 5 mg	0	58	58	3	30 ± 33
Conventional Dosage Forms with Food					
Propantheline, 15 mg	—	—	18	0	—
Hexocyclium, 25 mg	3	17	18	33	18 ± 12
Prolonged-Release Dosage Forms					
Propantheline, 30 mg	38	246	64	225	143 ± 107
Hexocyclium, 75 mg	100	149	88	174	128 ± 41

EXPERIMENTAL

Four male volunteers, 21–29 years of age and weighing 59–75 kg, were in apparent good health and gave informed consent.

The following drugs were studied: propantheline bromide[1], 15 mg; isopropamide iodide[2], 5 mg; and hexocyclium methylsulfate[3], 25 mg. Propantheline[4], 30 mg, and hexocyclium[5], 75 mg, prolonged-acting dosage forms also were studied. Riboflavin 5′-phosphate was obtained commercially[6].

Each subject received a single dose of each drug in the form of a conventional or prolonged-action tablet on the morning after an overnight fast. Food was withheld for an additional 3–4 hr after drug administration. All subjects were asked not to ingest any drugs or vitamins for at least 72 hr before and after each experiment.

The flow rate of mixed saliva was determined immediately before drug administration and at 30-min intervals thereafter for 6 hr in the manner described previously (3). During the study, on a nondrug day, normal salivary flow rates were determined in each fasting subject over the same time period.

Single doses of propantheline, 15 mg, or hexocyclium, 25 mg, were also taken immediately after a standard breakfast consisting of 60 g of cornflakes and 500 ml of milk, and salivary flow rates were determined. Normal salivary flow rates were determined on a nondrug day following the standard breakfast.

Each volunteer received an amount of riboflavin 5′-phosphate equivalent to 150 mg of riboflavin/m^2 of body surface area. The vitamin was dissolved in 200 ml of water and taken orally in the morning on an empty stomach. No food was permitted for 3 hr. This study was carried out on two occasions. In other experiments, the subjects received propantheline, 15 mg, isopropamide, 5 mg, or hexocyclium, 25 mg, 1 hr before ingestion of the vitamin solution. Urine was collected for 24 hr. Total riboflavin was determined fluorometrically (6); the data were corrected for normal

[1] Pro-Banthine, various lots, Searle.
[2] Darbid, lot 14D62, Smith Kline & French.
[3] Tral, lot 28-521-AF-22, Abbott.
[4] Pro-Bantheline P.A., lot 875-503, Searle.
[5] Tral Gradumet, lot 43-555-AF-26, Abbott.
[6] Roche Chemical Division.

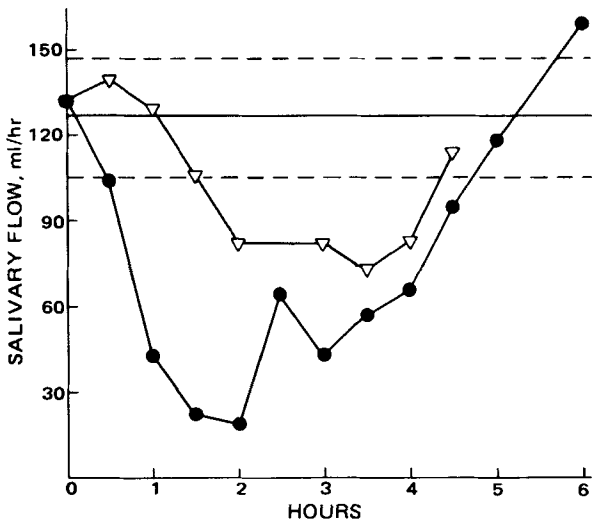

Figure 1—*Comparison of effects of propantheline, 15 mg (●), and hexocyclium, 25 mg (▽), on salivary flow in a healthy volunteer. The horizontal solid line indicates the mean normal salivary flow rate, and the broken lines denote the mean ± 1* SD.

physiological riboflavin excretion, which was determined from 24-hr blank collections of urine.

RESULTS AND DISCUSSION

The effect of various treatments on the salivary flow rate was estimated by determining the total area under the response (salivary flow) *versus* time curve over 6 hr as described previously (3) (Table I).

Administration of propantheline, 15 mg, in a conventional tablet under fasting conditions resulted in the most pronounced suppression of the salivary flow rate. Hexocyclium also reduced salivary flow but produced only about one-half the effect, on the average, of propantheline. Propantheline tended to evoke a more rapid and intense response after a single dose than did hexocyclium (Fig. 1).

Single 5-mg doses of isopropamide had little or no effect on the salivary flow rate (Table I). These findings are consistent with earlier reports indicating that doses of 10 mg (maximum recommended) or more are necessary to inhibit salivary flow and gastric acid secretion (1, 7).

Neither propantheline nor hexocyclium had much effect on salivary flow when administered after a standard breakfast (Table I). The fact that food decreases or abolishes the anticholinergic effect is a clinically relevant observation, since these drugs are usually prescribed to be taken

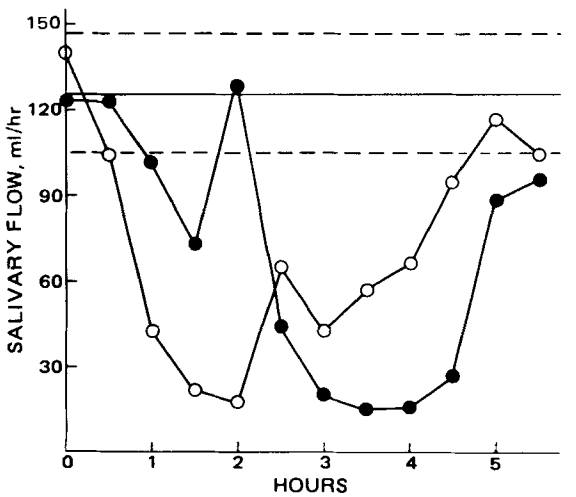

Figure 2—*Comparison of effects of different dosage forms of propantheline on salivary flow in a healthy volunteer. Key:* ○, *propantheline, 15 mg, in a conventional tablet; and* ●, *propantheline, 30 mg, in a prolonged-release dosage form. See Fig. 1 for additional details.*

Table II—Urinary Excretion of Riboflavin (Percent of Dose)

Treatment	Subject M	B	W	A	Mean ± *SD*
First control study	1.0	2.0	3.0	2.7	2.0 ± 0.6
Second control study	1.2	2.2	2.1	1.6	
Propantheline, 15 mg	4.2	3.4	3.8	3.2	3.6 ± 0.5[a]
Hexocyclium, 25 mg	3.7	3.8	5.4	3.2	4.0 ± 1.0[a]
Isopropamide, 5 mg	1.5	3.3	2.0	3.8	2.6 ± 1.1

[a] Significantly different from control value, $p < 0.05$, paired t test.

with meals. Maximal effects are likely to occur when the drug is given 1 to 2 hr before a meal. However, under these conditions, the degree of salivary suppression may be sufficient to interfere seriously with mastication and swallowing. If an anticholinergic is to be given immediately before or after a meal, larger doses than those currently recommended are required.

The present study continues to raise serious questions regarding the value of prolonged-release dosage forms of anticholinergic drugs. Previously, one lot of propantheline, 30 mg, failed to affect salivary flow (3). A newer lot, marketed after a major recall, was investigated during this study and was improved, but it was still less bioavailable than the conventional tablets. The prolonged-release form of propantheline produced effects comparable to the conventional dosage form in two subjects and less than the conventional form in the two others, even though the prolonged-release tablet contained twice as much drug (30 *versus* 15 mg) (Table I). In subjects showing comparable salivary suppression after either the conventional tablet or the prolonged-release tablet, the only difference in the effects produced by each was a delay in onset of salivary suppression after the prolonged-release form (Fig. 2). In no instance was there an indication of prolonged activity compared to that observed with the conventional tablet.

In general, the total salivary suppression and the time course of this effect resulting from 75 mg of hexocyclium in a prolonged-release dosage form were comparable to those observed after a 25-mg dose in a conventional tablet (Table I). The commercially available prolonged-release dosage forms of propantheline or hexocyclium appear to offer no advantage over considerably smaller doses in conventional dosage forms.

The effect of propantheline, hexocyclium, or isopropamide on riboflavin absorption is shown in Table II. Cumulative riboflavin excretion, corrected for excretion of endogenous and dietary riboflavin, was used as an index of the extent of absorption of the vitamin after the test dose. Excretion of apparent riboflavin in the absence of a test dose averaged 1.14 mg/24 hr in this panel of subjects. This result is in excellent agreement with a value of 1.0 mg/24 hr previously observed in five other subjects (4). A control study was carried out at the beginning of the investigation and a second one at the end of the investigation, several months later. Excretion of riboflavin ranged from 1 to 3% of the test dose. No significant differences were noted between the results of the first and second control studies.

Both propantheline and hexocyclium increased the extent of riboflavin absorption by about twofold. These statistically significant increases probably reflect the inhibitory effect of these drugs on gastric emptying and the intestinal transit rate. Although, at the usually recommended doses, propantheline was more effective than hexocyclium in reducing salivary flow, no difference in their effect on riboflavin absorption was noted. A 5-mg dose of isopropamide, which had little effect on salivary flow, failed to increase riboflavin absorption significantly.

The findings that propantheline and hexocyclium exert a quantitatively different effect on the salivary flow rate (probably reflective of changes in gastric acid output) but a quantitatively comparable effect on riboflavin absorption (probably reflective of changes in GI motility) suggest that a degree of selectivity in pharmacological response may be obtained through careful selection of anticholinergic drugs.

REFERENCES

(1) L. F. Fenster and E. Weser, in "Clinical Pharmacology," K. L. Melmon and H. F. Morelli, Eds., Macmillan, New York, N.Y., 1972, pp. 109–141.

(2) K. Ivey, *Gastroenterology*, **68**, 154 (1975).

(3) M. Gibaldi and B. Grundhofer, *Clin. Pharmacol. Ther.*, **18**, 457 (1975).

(4) G. Levy, M. Gibaldi, and J. Procknal, *J. Pharm. Sci.*, **61**, 798 (1972).

(5) V. Manninen, A. Apajalahti, J. Melin, and M. Karesoja, *Lancet*,

1, 398 (1973).
(6) G. Levy and W. J. Jusko, *J. Pharm. Sci.*, **55**, 285 (1966).
(7) M. I. Grossman, *Gastroenterology*, **35**, 312 (1958).

ACKNOWLEDGMENTS AND ADDRESSES

Received November 26, 1976, from the *Department of Pharmaceutics, School of Pharmacy, State University of New York at Buffalo, Amherst, NY 14260.*

Accepted for publication December 23, 1976.

Supported in part by Grant GM-20852 from the National Institutes of Health.

* Present address: Department of Clinical Pharmacology, University of Kansas Medical Center, Kansas City, KS 66103.

ˣ To whom inquiries should be directed.

General Class of Multiparticulate Dissolution Models

PETER VENG PEDERSEN ˣ and K. F. BROWN

Abstract □ The dissolution of multiparticulate systems under sink and nonsink conditions can be described rigorously according to a generally applicable formula on the basis of the single-particle dissolution model and the initial particle distribution. The kinetic model for log-normal systems dissolving under sink conditions is extended to nonsink conditions as a specific example. The equation presented describes a general class of multiparticulate models for various values of the dispersion parameter and the dissolution capacity coefficient.

Keyphrases □ Dissolution model—multiparticulate systems under sink and nonsink conditions, generally applicable equations derived □ Models, dissolution—multiparticulate systems under sink and nonsink conditions, generally applicable equations derived □ Multiparticulate systems—dissolution model under sink and nonsink conditions, generally applicable equations derived

Characterization of dissolution behavior is often facilitated by the use of an appropriate mathematical model that enables the process to be summarized in terms of one or more parameters such as the dissolution rate constant. Since most dissolution tests are performed under nonsink conditions, the kinetics under such conditions are of interest. Various nonsink dissolution equations for multiparticulate systems have been derived (1–4), but they are based on monodisperse systems which are rarely met in practice (5).

A proper characterization of dissolution behavior must account for the particle-size distribution. This paper provides a general and rigorous description of dissolution under nonsink conditions on the basis of a single-particle dissolution model and the initial particle distribution. Log-normal powders are considered as a specific example. The equation presented describes a large class of multiparticulate dissolution models for various values of the dispersion parameter and the dissolution capacity coefficient.

THEORY

A previous publication (6) showed how the dissolution kinetics of a multiparticulate system can be rigorously described theoretically when the single-particle dissolution equation is known together with the initial particle-size distribution. Although equations for the general case (Eqs. 12 and 13 in Ref. 6) were derived assuming sink conditions, they can also be applied to nonsink dissolution.

In the current context, sink condition is defined as interparticle independent dissolution[1]. This condition may be closely approximated in a noncumulating, open, flow-through system (7). A nonsink condition is defined as the condition in a solute-cumulating, closed system, where the particles are exposed to the same bulk concentration of solute. Dissolution according to the latter definition implies agitation that is intense enough to give a homogeneous bulk solute concentration and to suspend the dissolving particles freely in the vehicle.

The only difference between the mathematical description of the two systems is that, for nonsink conditions, dissolution is influenced by the bulk concentration of solute; therefore, the single-particle dissolution equation contains an additional time-dependent variable. Since this variable is a function of the total dissolution behavior of the system, mathematical analysis leads to an integral equation describing multiparticulate nonsink dissolution kinetics.

These principles can be illustrated on the basis of the well-known Noyes–Whitney kinetics (8) for log-normal powders and spherical particles without loss of generality. The choice of a log-normal distribution to approximate the initial particle distribution appears appropriate considering previous investigations (7, 9, 10).

Single-Particle Dissolution Equation—Consider a single spherical particle, in a polydisperse system, dissolving under nonsink conditions according to the Noyes–Whitney model:

$$dw/dt = -k_1 s(c_i - c) \doteq -k_2 w^{2/3}[c_s - (W_0 - W)/V] \quad \text{(Eq. 1)}$$

where w is the weight of the particle, s is its surface area, and c_i is the interfacial solute concentration which, in most cases, is close to the solubility concentration, c_s. Let it be assumed that k_1 and $k_2 = 4\pi(4/3\pi\rho)^{-2/3}k_1$ (ρ = density) are constants not dependent on the particle diameter. Such an assumption is reasonable, since it leads to the well-established cube root model (1) under sink conditions ($c = 0$). If the single-particle dissolution kinetics are different from the Noyes–Whitney kinetics (11) or if k (Eq. 1) is not constant, then the multiparticulate kinetics can still be treated similarly to the cases considered below. The bulk solute concentration, c (Eq. 1), is, according to the definition of nonsink conditions, equal to the ratio of the amount of powder dissolved, $(W_0 - W)$, to the vehicle volume, V.

It is useful to introduce the dissolution capacity coefficient defined by:

$$\alpha = [(c_s V - W_0)/W_0]^{1/3} \doteq [(c_i V - W_0)/W_0]^{1/3} \quad \text{(Eq. 2)}$$

Equation 1 then integrates to yield:

$$w = \left[w_0^{1/3} - \frac{3k_2 W_0 \alpha^3}{V} t - \frac{3k_2 W_0}{V} \int_0^t \frac{W}{W_0} dt \right]^3 \quad \text{(Eq. 3)}$$

For comparison with earlier derivations (6, 12), it is convenient also to

[1] This definition is different from the usual definition, which defines a sink condition as a condition where the solute bulk concentration does not increase beyond a small fraction (10–15%) of the solubility concentration.

1, 398 (1973).
(6) G. Levy and W. J. Jusko, *J. Pharm. Sci.*, **55**, 285 (1966).
(7) M. I. Grossman, *Gastroenterology*, **35**, 312 (1958).

ACKNOWLEDGMENTS AND ADDRESSES

Received November 26, 1976, from the *Department of Pharmaceutics, School of Pharmacy, State University of New York at Buffalo, Amherst, NY 14260.*

Accepted for publication December 23, 1976.

Supported in part by Grant GM-20852 from the National Institutes of Health.

* Present address: Department of Clinical Pharmacology, University of Kansas Medical Center, Kansas City, KS 66103.

ˣ To whom inquiries should be directed.

General Class of Multiparticulate Dissolution Models

PETER VENG PEDERSEN ˣ and K. F. BROWN

Abstract □ The dissolution of multiparticulate systems under sink and nonsink conditions can be described rigorously according to a generally applicable formula on the basis of the single-particle dissolution model and the initial particle distribution. The kinetic model for log-normal systems dissolving under sink conditions is extended to nonsink conditions as a specific example. The equation presented describes a general class of multiparticulate models for various values of the dispersion parameter and the dissolution capacity coefficient.

Keyphrases □ Dissolution model—multiparticulate systems under sink and nonsink conditions, generally applicable equations derived □ Models, dissolution—multiparticulate systems under sink and nonsink conditions, generally applicable equations derived □ Multiparticulate systems—dissolution model under sink and nonsink conditions, generally applicable equations derived

Characterization of dissolution behavior is often facilitated by the use of an appropriate mathematical model that enables the process to be summarized in terms of one or more parameters such as the dissolution rate constant. Since most dissolution tests are performed under nonsink conditions, the kinetics under such conditions are of interest. Various nonsink dissolution equations for multiparticulate systems have been derived (1–4), but they are based on monodisperse systems which are rarely met in practice (5).

A proper characterization of dissolution behavior must account for the particle-size distribution. This paper provides a general and rigorous description of dissolution under nonsink conditions on the basis of a single-particle dissolution model and the initial particle distribution. Log-normal powders are considered as a specific example. The equation presented describes a large class of multiparticulate dissolution models for various values of the dispersion parameter and the dissolution capacity coefficient.

THEORY

A previous publication (6) showed how the dissolution kinetics of a multiparticulate system can be rigorously described theoretically when the single-particle dissolution equation is known together with the initial particle-size distribution. Although equations for the general case (Eqs. 12 and 13 in Ref. 6) were derived assuming sink conditions, they can also be applied to nonsink dissolution.

In the current context, sink condition is defined as interparticle independent dissolution[1]. This condition may be closely approximated in a noncumulating, open, flow-through system (7). A nonsink condition is defined as the condition in a solute-cumulating, closed system, where the particles are exposed to the same bulk concentration of solute. Dissolution according to the latter definition implies agitation that is intense enough to give a homogeneous bulk solute concentration and to suspend the dissolving particles freely in the vehicle.

The only difference between the mathematical description of the two systems is that, for nonsink conditions, dissolution is influenced by the bulk concentration of solute; therefore, the single-particle dissolution equation contains an additional time-dependent variable. Since this variable is a function of the total dissolution behavior of the system, mathematical analysis leads to an integral equation describing multiparticulate nonsink dissolution kinetics.

These principles can be illustrated on the basis of the well-known Noyes–Whitney kinetics (8) for log-normal powders and spherical particles without loss of generality. The choice of a log-normal distribution to approximate the initial particle distribution appears appropriate considering previous investigations (7, 9, 10).

Single-Particle Dissolution Equation—Consider a single spherical particle, in a polydisperse system, dissolving under nonsink conditions according to the Noyes–Whitney model:

$$dw/dt = -k_1 s(c_i - c) \doteq -k_2 w^{2/3}[c_s - (W_0 - W)/V] \quad \text{(Eq. 1)}$$

where w is the weight of the particle, s is its surface area, and c_i is the interfacial solute concentration which, in most cases, is close to the solubility concentration, c_s. Let it be assumed that k_1 and $k_2 = 4\pi(4/3\pi\rho)^{-2/3}k_1$ (ρ = density) are constants not dependent on the particle diameter. Such an assumption is reasonable, since it leads to the well-established cube root model (1) under sink conditions ($c = 0$). If the single-particle dissolution kinetics are different from the Noyes–Whitney kinetics (11) or if k (Eq. 1) is not constant, then the multiparticulate kinetics can still be treated similarly to the cases considered below. The bulk solute concentration, c (Eq. 1), is, according to the definition of nonsink conditions, equal to the ratio of the amount of powder dissolved, $(W_0 - W)$, to the vehicle volume, V.

It is useful to introduce the dissolution capacity coefficient defined by:

$$\alpha = [(c_s V - W_0)/W_0]^{1/3} \doteq [(c_i V - W_0)/W_0]^{1/3} \quad \text{(Eq. 2)}$$

Equation 1 then integrates to yield:

$$w = \left[w_0^{1/3} - \frac{3k_2 W_0 \alpha^3}{V} t - \frac{3k_2 W_0}{V} \int_0^t \frac{W}{W_0} dt \right]^3 \quad \text{(Eq. 3)}$$

For comparison with earlier derivations (6, 12), it is convenient also to

[1] This definition is different from the usual definition, which defines a sink condition as a condition where the solute bulk concentration does not increase beyond a small fraction (10–15%) of the solubility concentration.

present the single-particle dissolution equation derived for sink conditions ($c = 0$, Eq.1):

$$w = (W_0^{1/3} - kt)^3 \qquad \text{(Eq. 4)}$$

where:

$$k = 3k_2c_s \qquad \text{(Eq. 5)}$$

According to Eqs. 2–5, Eq. 3 can be written in the following form:

$$w = (W_0^{1/3} - A)^3 \qquad \text{(Eq. 6)}$$

where:

$$A = \frac{\alpha^3 k}{1+\alpha^3} t + \frac{k}{1+\alpha^3} \int_0^t \frac{W}{W_0} dt \qquad \text{(Eq. 7)}$$

Multiparticulate Dissolution Equation—If log-normal powders are considered, the initial particle distribution is approximated by Eq. 15 from Ref. 6, which together with the single-particle dissolution model, Eq. 6, completely defines the multiparticulate dissolution according to Eq. 13 from Ref. 6. Equation 4 was used to derive the expression (Eq. 18 in Ref. 6) for dissolution of truncated log-normal powders under sink conditions. This equation was later presented in a more compact form (Eq. 15 in Ref. 12), which can be written using the notation defined previously (13):

$$\frac{W}{W_0} = \sum_{n=0}^{3} \binom{3}{n} (-K^*t)^{(3-n)} \times \frac{F(T_2 - n\sigma) - F(T_1 - n\sigma)}{F(j - 3\sigma) - F(-i - 3\sigma)} \exp[(n^2 - 9)\sigma^2/2] \qquad \text{(Eq. 8)}$$

where:

$$T_1 = \max(\ln K^*t, -i\sigma)/\sigma \qquad \text{(Eq. 9)}$$

$$T_2 = \max(\ln K^*t, j\sigma)/\sigma \qquad \text{(Eq. 10)}$$

$$F(x) = \frac{1}{\sqrt{2\pi}} \int_{-\infty}^{x} \exp(-x^2/2)\, dx \qquad \text{(Eq. 11)}$$

The use of the max relationship (Eqs. 9 and 10) in this expression is related to the fact that a rigorous definition of the single-particle dissolution equation is not given by Eq. 4 but by:

$$w = [\max(w_0^{1/3} - kt, 0)]^3 \qquad \text{(Eq. 12)}$$

since it is required that $w \to 0$ for $t \to \infty$, which is not the case in Eq. 4. The operator P introduced earlier (6) automatically accounts for this lack of generality. The "switch" in T_1 (Eq. 9) occurs at the so-called critical time (14–17) when the smallest particles start disappearing. The switch in T_2 denotes the completion of dissolution. At that time and thereafter, $T_1 = T_2\,[= \ln(K^*t)/\sigma]$, so $W/W_0 = 0$ as expected.

It is apparent from the the derivation of Eq. 8 (6, 13) that it can be readily extended to nonsink conditions. The only change in the derivation is that the single-particle dissolution equation (Eq. 6) is somewhat different from Eq. 4. However, this difference can be accounted for simply by substituting A for kt throughout. The following nonsink dissolution equation for log-normal powders results:

$$\frac{W}{W_0} = \sum_{n=0}^{3} \binom{3}{n} (-G)^{(3-n)} \times \frac{F(T_2 - n\sigma) - F(T_1 - n\sigma)}{F(j - 3\sigma) - F(-i - 3\sigma)} \exp[(n^2 - 9)\sigma^2/2] \qquad \text{(Eq. 13)}$$

where:

$$T_1 = \max(\ln G, -i\sigma)/\sigma \qquad \text{(Eq. 14)}$$

$$T_2 = \max(\ln G, j\sigma)/\sigma \qquad \text{(Eq. 15)}$$

$$G = \frac{\alpha^3 K^*}{1+\alpha^3} t + \frac{K^*}{1+\alpha^3} \int_0^t \frac{W}{W_0} dt \qquad \text{(Eq. 16)}$$

If the truncation parameters i and j are more than 3, then the particle distribution can be just as well approximated by an "ideal" distribution ($i = j = \infty$), which leads to (13):

$$\frac{W}{W_0} = \sum_{n=0}^{3} \binom{3}{n} (-G)^{(3-n)} \left[1 - F\left(\frac{1}{\sigma}\ln(G) - n\sigma\right)\right] \times \exp[(n^2 - 9)\sigma^2/2] \qquad \text{(Eq. 17)}$$

Equation 13 describes a general class of multiparticulate dissolution models for both mono- and polydisperse systems and nonsink and sink conditions (Table I). A monodisperse powder is described by letting $\sigma = 0$; the sink condition is described by letting $\alpha = \infty$. For closed systems (V = constant), α always is finite, so a sink condition can only be approached when $\alpha \to \infty$. Although α is not defined by Eq. 2 for open systems operating under sink conditions, it is meaningful and mathematically correct to define the dissolution capacity coefficient to be infinite ($\alpha = \infty$) for such systems. For example, according to Eq. 16, $G \to K^*t$ for $\alpha \to \infty$; *i.e.*, for $c_iV \gg W_0$, Eqs. 13 and 17 approach the equations valid for sink conditions as expected. A monodisperse system is described by letting $\sigma \to 0$, which leads to:

$$\frac{W}{W_0} = \sum_{n=0}^{3} \binom{3}{n} (-G)^{(3-n)} = (1 - G)^3 \qquad \text{(Eq. 18)}$$

or:

$$f = 1 - G \qquad \text{(Eq. 19)}$$

where $f = (W/W_0)^{1/3}$ is introduced for convenience. Differentiation and rearrangement of Eq. 19 give:

$$(\alpha^3 + 1)\frac{df}{\alpha^3 + f^3} = -K^*dt \qquad \text{(Eq. 20)}$$

which, for $\alpha \neq 0$, integrates to:

$$\phi(f) = \phi(1) - K^*t \qquad \max(-\alpha, 0) \le f \le 1 \qquad \text{(Eq. 21)}$$

where:

$$\phi(f) = \frac{\alpha^3 + 1}{\alpha^2}\left[\frac{1}{6}\ln\frac{(f+\alpha)^2}{f^2 - \alpha f + \alpha^2} + \frac{1}{\sqrt{3}}\tan^{-1}\frac{2f - \alpha}{\alpha\sqrt{3}}\right] \qquad \text{(Eq. 22)}$$

For $\alpha = 0$, Eq. 20 integrates to:

$$f^{-2} = 1 + 2K^*t \qquad 0 < f \le 1 \qquad \text{(Eq. 23)}$$

Furthermore, it can be seen (Eq. 19) that if a monodisperse system ($\sigma = 0$) is exposed to a large excess of solvent so that $c_iV \gg W_0$ ($\alpha \to \infty$), the dissolution kinetics approach the Hixson-Crowell cube root law:

$$f = (W/W_0)^{1/3} = 1 - K^*t \qquad \text{(Eq. 24)}$$

RESULTS AND DISCUSSION

Effective Particle Distribution—The description of the kinetics of polydisperse systems presented is based on a log-normal, spherical approximation to the initial particle distribution, the simplest approximation in most cases (7, 9, 10). Even if particle-size analysis reveals a significant deviation from log-normality and the particle shapes are considerably different from spherical, the effective size distribution may still be close to log-normal with respect to dissolution behavior. *The effective particle distribution is defined as the distribution of a hypothetical system of spherical particles where each individual spherical particle best approximates the real particle according to the single-particle dissolution equation expressed on a* w/w_0 *versus time basis.*

Most particle-size distributions are characterized by a pronounced skewness to the right (5, 9). The dispersion parameter, σ, takes into account not only how broad a distribution is but also such skewness. This single parameter, therefore, appears to be the simplest, general measure of the distribution effect. The value of K^* and σ in characterizing dissolution behavior was discussed previously (13). The equations summarized in Table I have considerable practical value, since they enable dissolution behavior to be characterized in terms of these parameters. Evaluation can be made under sink as well as nonsink conditions, thus making the approach generally applicable and feasible using almost any dissolution apparatus.

Numerical Treatment—The experimental determination of K^* and σ under sink conditions was described previously (13). A method for simultaneous determination of σ and K^* from nonsink dissolution data for polydisperse systems, employing Eq. 13 or 17, is described in the *Appendix*.

Effect of Dispersion Parameter—Theoretical dissolution profiles were calculated according to Eq. 17, with $\alpha^3 = 5$, using the numerical approach in the *Appendix*, to evaluate the effect of the dispersion parameter σ (Fig. 1). A cube root representation is used for a better comparison with the dissolution of monodisperse systems ($\sigma = 0$) dissolving under sink conditions (Eq. 24). Only a slight deviation from linearity is observed due to the nonsink conditions ($\alpha^3 = 5$) for the monodisperse systems (second curve from left). An increasing deviation from linearity is observed for increasing values of the dispersion parameter as expected.

Table I—A General Class of Multiparticulate Dissolution Models Based on Eq. 13

Dissolution Capacity Coefficient[a], α	Dispersion Parameter, σ	Truncation Parameters[b], i and j	Particle Distribution	Condition	Dissolution Model
$-1 < \alpha < \infty$	$\sigma > 0$	i and $j < \infty$	Truncated log-normal	Nonsink	Eq. 13
$-1 < \alpha < \infty$	$\sigma > 0$	$i = j = \infty$	Ideal log-normal	Nonsink	Eq. 17
$-1 < \alpha < \infty$	$\sigma = 0$	$i = j = 0$	Monodisperse	Nonsink	Eq. 21 ($\alpha \neq 0$), Eq. 23 ($\alpha = 0$)
$\alpha = \infty$	$\sigma > 0$	i and $j < \infty$	Truncated log-normal	Sink	Eq. 8
$\alpha = \infty$	$\sigma > 0$	$i = j = \infty$	Ideal log-normal	Sink	Eq. 17 with $G = K^*t$
$\alpha = \infty$	$\sigma = 0$	$i = j = 0$	Monodisperse	Sink	Eq. 24

[a] When $\alpha < 0$, dissolution will be incomplete: min $(W/W_0) = -\alpha^3$ [in general, min (W/W_0) = max $(-\alpha^3, 0)$]. [b] The cases for semiideal distributions; *i.e.*, $i = \infty, j < \infty$ or $i < \infty, j = \infty$ can similarly be described (13).

The numerical solution of Eq. 17 closely approached the numerical solution of Eq. 21 as $\sigma \to 0$, thus indicating satisfactory accuracy in the numerical technique used[2].

Deviations from Linearity in ϕ, (t) Plot for Polydisperse Systems—For monodisperse systems, Eq. 21 predicts a linear relationship between $\phi(f)$ and t, enabling K^* to be determined by linear regression. However, a deviation from linearity is expected in practice, since most systems are not monodisperse. The extent to which such deviations depend on σ is of interest. The exact theoretical curves in Fig. 1 for the nonsink dissolution of polydisperse systems were plotted according to Eq. 21, using K^*t instead of t as the independent variable for generality (Fig. 2)[3].

The deviation from linearity is not greatly affected by σ in the initial dissolution phases, but it becomes more pronounced toward the end for σ values greater than about 0.2. This result indicates the need to follow dissolution to completion or near completion to get a reliable estimate of the degree of dispersion of a multiparticulate system.

Dissolution of Dosage Forms—The given equations are derived for multiparticulate systems of pure compounds. Particle systems produced by fast disintegrating tablets and capsules are multiparticulate, although perhaps not as well defined as those considered. The equations presented should be valuable to characterize the dissolution behavior of such dosage forms.

If the disintegration time, τ, is significant compared to the dissolution time, the variable t in the equations presented should be redefined as:

$$t = \max(t - \tau, 0) \qquad \text{(Eq. 25)}$$

for a better description of the kinetics. In such cases, τ may be treated as an additional parameter that can be determined from the dissolution data.

Experimental analysis of dissolution kinetics of polydisperse systems under nonsink conditions considering those models is in progress.

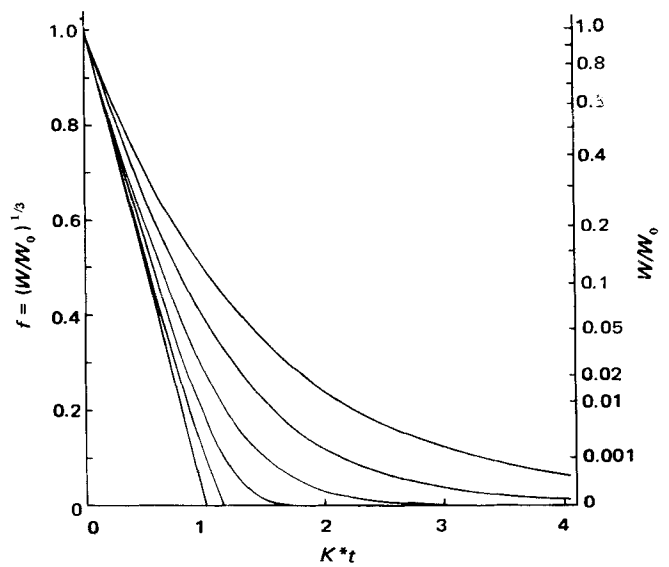

Figure 1—*Effect of the dispersion parameter, σ, on the intrinsic dissolution profile of log-normal powders dissolving (Eq. 17) under nonsink conditions with a dissolution capacity coefficient $\alpha^3 = 5$. The straight line at the far left (Eq. 24), representing a monodisperse system ($\sigma = 0$) dissolving under sink conditions ($\alpha = \infty$), is included for comparison. The other five curves represent, from left to right, $\sigma = 0, 0.1, 0.2, 0.3$, and 0.4, respectively.*

APPENDIX

Equations 13 and 17 appear somewhat complex to evaluate because the dependent variable, W/W_0, occurs in implicit, nonlinear, integral form. A general numerical approach for nonlinear integral equations (18) is too complex for practical purposes. Fortunately, however, the problem can be transformed into an initial value problem, which can be solved readily using established numerical techniques (19) as follows. Let:

$$y = \int_0^t \frac{W}{W_0} dt \qquad \text{(Eq. A1)}$$

$$y' = W/W_0 \qquad \text{(Eq. A2)}$$

Substitution of these equations into Eqs. 13 and 17 yields the initial value problem:

$$y' = h(t, y) \qquad y(0) = 0 \qquad \text{(Eq. A3)}$$

The function h is simply the right-hand side of Eq. 13 (or 17), where $\int_0^t W/W_0\, dt$ has been substituted by y. The $y(t)$ values obtained using a suitable integration algorithm will, when substituted into Eq. A3, give the required explicit functional relationship between the variables W/W_0 and t:

$$W/W_0 = y'(t) = h[t, y(t)] \qquad \text{(Eq. A4)}$$

Once this relationship is defined, the parameters σ and K^* (as well as i,

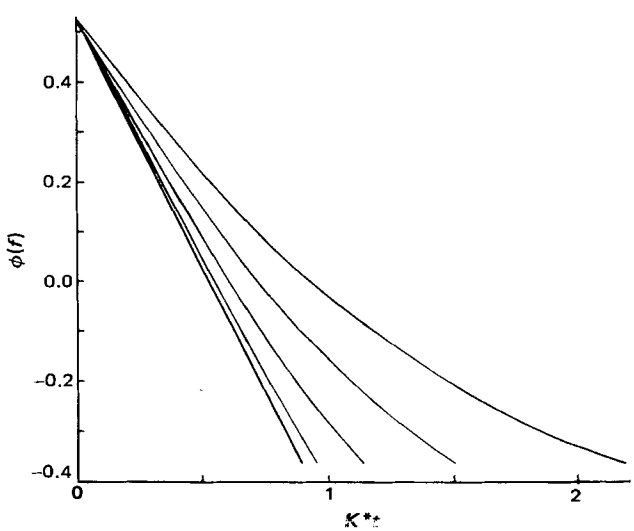

Figure 2—*Effect of the dispersion parameter, σ, on linearity when nonsink ($\alpha^3 = 5$) dissolution data from log-normal powders (Eq. 17 and Fig. 1) are plotted according to Eq. 21, which is based on monodisperse systems. From left to right, $\sigma = 0, 0.1, 0.2, 0.3$, and 0.4, respectively.*

[2] A fourth-order Rhunga–Kutta method was used to solve the initial value problem.

[3] Because Eq. 17 is based on an ideal distribution, the dissolution data are only plotted in Fig. 2 until 99% has dissolved to disregard approximation errors originating from the infinite tails of the untruncated distribution.

j, α, and τ) can then be determined directly from nonsink dissolution data (W/W_0 *versus* t) using a suitable nonlinear regression program.

REFERENCES

(1) A. W. Hixson and J. H. Crowell, *Ind. Eng. Chem.*, **23**, 923 (1931).

(2) M. P. Short, P. Sharkey, and C. T. Rhodes, *J. Pharm. Sci.*, **61**, 1732 (1972).

(3) P. Pothisiri and J. T. Carstensen, *ibid.*, **62**, 1468 (1973).

(4) M. Patel and J. T. Carstensen, *ibid.*, **64**, 1651 (1975).

(5) "Symposium on Particle Size Measurement," Special Technical Publication 234, American Society for Testing Materials, Philadelphia, Pa., 1958.

(6) P. Veng Pedersen and K. F. Brown, *J. Pharm. Sci.*, **64**, 1192 (1975).

(7) *Ibid.*, **65**, 1442 (1976).

(8) A. A. Noyes and W. R. Whitney, *J. Am. Chem. Soc.*, **19**, 930 (1897).

(9) T. Allen, "Particle Size Measurements," Chapman & Hall, London, England, 1974, chap. 4.

(10) "Advances in Pharmaceutical Sciences," vol. 2, H. S. Bean, A. H. Beckett, and J. E. Carless, Eds., Academic, New York, N.Y., 1967, p. 95.

(11) P. J. Niebergall, G. Milosovich, and J. E. Goyan, *J. Pharm. Sci.*, **52**, 236 (1963).

(12) P. Veng Pedersen and K. F. Brown, *ibid.*, **64**, 1981 (1975).

(13) P. Veng Pedersen, *ibid.*, **66**, 761 (1977).

(14) J. T. Carstensen and M. N. Musa, *ibid.*, **61**, 223 (1972).

(15) D. Brooke, *ibid.*, **62**, 795 (1973).

(16) *Ibid.*, **63**, 344 (1974).

(17) J. T. Carstensen and M. Patel, *J. Pharm. Sci.*, **64**, 1770 (1975).

(18) "Numerical Solution of Integral Equations," L. M. Delves and J. Walsh, Eds., Clarendon Press, Oxford, England, 1974, chap. 17.

(19) C. W. Gear, "Numerical Initial Value Problems in Ordinary Differential Equations," Prentice-Hall, Englewood Cliffs, N.J., 1971.

ACKNOWLEDGMENTS AND ADDRESSES

Received October 18, 1976, from the *Department of Pharmacy, University of Sydney, N.S.W. 2006, Australia.*

Accepted for publication December 16, 1976.

[x] To whom inquiries should be directed. Present address: Department of Pharmacy, University of California, San Francisco, CA 94143.

Bioavailability of Sulfadiazine in Rabbits Using Tablets Prepared by Direct Compression and Fluidized-Bed Granulation

W. A. RITSCHEL [x] and W. ERNI

Abstract □ Experimental sulfadiazine tablets prepared by direct compression, using a commercially available direct compression tablet mass, were compared with experimental sulfadiazine tablets prepared by fluidized-bed granulation and commercially available sulfadiazine tablets USP. The values for friability and the time required to release 10 and 50% of the direct compression tablets were between those of the fluidized-bed tablets and the commercial product. With the commercial tablet as a standard, the extent of bioavailability was determined in rabbits; it was slightly higher for both the direct compression and fluidized-bed tablets. A statistically significant difference was found between the direct compression tablets and the standard with respect to the extent of bioavailability and the time of the peak.

Keyphrases □ Sulfadiazine—bioavailability of tablets prepared by direct compression and fluidized-bed techniques compared to commercial product, rabbits □ Bioavailability—sulfadiazine, tablets prepared by direct compression and fluidized-bed techniques compared to commercial product, rabbits □ Tablets—sulfadiazine, prepared by direct compression and fluidized-bed techniques, bioavailability compared to commercial product, rabbits □ Antibacterials—sulfadiazine, bioavailability of tablets prepared by direct compression and fluidized-bed techniques compared to commercial product, rabbits

Sulfadiazine tablets are considered to present actual or potential bioequivalence problems (1). The use of a direct compression technique for their preparation seemed of particular interest, since numerous formulation factors influencing the *in vitro* dissolution rate and bioavailability previously were studied with sulfadiazine as a model substance. The compression pressure and binder concentration of acacia affected the dissolution rate of sulfadiazine tablets (2). The effects of disintegration agents, binders, fillers, and lubricants on the *in vitro* disintegration time and dissolution rate and the *in vivo* availability of various formulations were investigated (3). The highest blood levels in rabbits were found with formulations that did not contain magnesium stearate as the lubricant and lactose as the filler.

The influence of different lubricants in various concentrations on dissolution rate and bioavailability was studied (4). The highest bioavailability was obtained when the lubricant was kept at the minimum concentration with improved flow properties; a lubricant concentration resulting in optimum flow properties resulted in decreased bioavailability. Increasing amounts of starch paste, carboxymethylcellulose sodium, gelatin, or polyethylene glycol decreased *in vitro* drug release, whereas increasing amounts of povidone increased sulfadiazine release (5). Increasing amounts of carboxymethylcellulose sodium resulted in decreased bioavailability in rabbits (5).

The influence of the granulation method on the *in vitro* drug release and bioavailability of sulfadiazine tablets in rabbits was studied (6, 7). *In vitro* drug release decreased in the following order of granulation method: fluidized bed, nodulation, shaking, sieve pressure, and hole disk. *In vivo*

j, α, and τ) can then be determined directly from nonsink dissolution data (W/W_0 *versus* t) using a suitable nonlinear regression program.

REFERENCES

(1) A. W. Hixson and J. H. Crowell, *Ind. Eng. Chem.*, **23**, 923 (1931).

(2) M. P. Short, P. Sharkey, and C. T. Rhodes, *J. Pharm. Sci.*, **61**, 1732 (1972).

(3) P. Pothisiri and J. T. Carstensen, *ibid.*, **62**, 1468 (1973).

(4) M. Patel and J. T. Carstensen, *ibid.*, **64**, 1651 (1975).

(5) "Symposium on Particle Size Measurement," Special Technical Publication 234, American Society for Testing Materials, Philadelphia, Pa., 1958.

(6) P. Veng Pedersen and K. F. Brown, *J. Pharm. Sci.*, **64**, 1192 (1975).

(7) *Ibid.*, **65**, 1442 (1976).

(8) A. A. Noyes and W. R. Whitney, *J. Am. Chem. Soc.*, **19**, 930 (1897).

(9) T. Allen, "Particle Size Measurements," Chapman & Hall, London, England, 1974, chap. 4.

(10) "Advances in Pharmaceutical Sciences," vol. 2, H. S. Bean, A. H. Beckett, and J. E. Carless, Eds., Academic, New York, N.Y., 1967, p. 95.

(11) P. J. Niebergall, G. Milosovich, and J. E. Goyan, *J. Pharm. Sci.*, **52**, 236 (1963).

(12) P. Veng Pedersen and K. F. Brown, *ibid.*, **64**, 1981 (1975).

(13) P. Veng Pedersen, *ibid.*, **66**, 761 (1977).

(14) J. T. Carstensen and M. N. Musa, *ibid.*, **61**, 223 (1972).

(15) D. Brooke, *ibid.*, **62**, 795 (1973).

(16) *Ibid.*, **63**, 344 (1974).

(17) J. T. Carstensen and M. Patel, *J. Pharm. Sci.*, **64**, 1770 (1975).

(18) "Numerical Solution of Integral Equations," L. M. Delves and J. Walsh, Eds., Clarendon Press, Oxford, England, 1974, chap. 17.

(19) C. W. Gear, "Numerical Initial Value Problems in Ordinary Differential Equations," Prentice-Hall, Englewood Cliffs, N.J., 1971.

ACKNOWLEDGMENTS AND ADDRESSES

Received October 18, 1976, from the *Department of Pharmacy, University of Sydney, N.S.W. 2006, Australia.*

Accepted for publication December 16, 1976.

[x] To whom inquiries should be directed. Present address: Department of Pharmacy, University of California, San Francisco, CA 94143.

Bioavailability of Sulfadiazine in Rabbits Using Tablets Prepared by Direct Compression and Fluidized-Bed Granulation

W. A. RITSCHEL [x] and W. ERNI

Abstract □ Experimental sulfadiazine tablets prepared by direct compression, using a commercially available direct compression tablet mass, were compared with experimental sulfadiazine tablets prepared by fluidized-bed granulation and commercially available sulfadiazine tablets USP. The values for friability and the time required to release 10 and 50% of the direct compression tablets were between those of the fluidized-bed tablets and the commercial product. With the commercial tablet as a standard, the extent of bioavailability was determined in rabbits; it was slightly higher for both the direct compression and fluidized-bed tablets. A statistically significant difference was found between the direct compression tablets and the standard with respect to the extent of bioavailability and the time of the peak.

Keyphrases □ Sulfadiazine—bioavailability of tablets prepared by direct compression and fluidized-bed techniques compared to commercial product, rabbits □ Bioavailability—sulfadiazine, tablets prepared by direct compression and fluidized-bed techniques compared to commercial product, rabbits □ Tablets—sulfadiazine, prepared by direct compression and fluidized-bed techniques, bioavailability compared to commercial product, rabbits □ Antibacterials—sulfadiazine, bioavailability of tablets prepared by direct compression and fluidized-bed techniques compared to commercial product, rabbits

Sulfadiazine tablets are considered to present actual or potential bioequivalence problems (1). The use of a direct compression technique for their preparation seemed of particular interest, since numerous formulation factors influencing the *in vitro* dissolution rate and bioavailability previously were studied with sulfadiazine as a model substance. The compression pressure and binder concentration of acacia affected the dissolution rate of sulfadiazine tablets (2). The effects of disintegration agents, binders, fillers, and lubricants on the *in vitro* disintegration time and dissolution rate and the *in vivo* availability of various formulations were investigated (3). The highest blood levels in rabbits were found with formulations that did not contain magnesium stearate as the lubricant and lactose as the filler.

The influence of different lubricants in various concentrations on dissolution rate and bioavailability was studied (4). The highest bioavailability was obtained when the lubricant was kept at the minimum concentration with improved flow properties; a lubricant concentration resulting in optimum flow properties resulted in decreased bioavailability. Increasing amounts of starch paste, carboxymethylcellulose sodium, gelatin, or polyethylene glycol decreased *in vitro* drug release, whereas increasing amounts of povidone increased sulfadiazine release (5). Increasing amounts of carboxymethylcellulose sodium resulted in decreased bioavailability in rabbits (5).

The influence of the granulation method on the *in vitro* drug release and bioavailability of sulfadiazine tablets in rabbits was studied (6, 7). *In vitro* drug release decreased in the following order of granulation method: fluidized bed, nodulation, shaking, sieve pressure, and hole disk. *In vivo*

Table I—Composition of Experimental Tablets

Ingredients	Weight, mg/Tablet	
	Preparation I (Fluidized Bed)	Preparation II (Direct Compression)
Sulfadiazine[a]	250	250
Sorbitan monolaurate[b]	1.2	1.2
Lactose[c] USP	126.075	—
Direct compression mass[d]	—	193.575
Starch[e] USP	50[f]	5
Povidone[g]	22.5	—
Magnesium stearate[h]	0.225	0.225
2-Propanol[g]	q.s.	—

[a] USP, Lederle. [b] Atlas Chemical Ind. [c] Foremost. [d] Lot B 262-X, E. Mendell Co. [e] Merrell Co. [f] Ninety percent internal phase, 10% external phase. [g] Matheson, Coleman and Bell. [h] Witco Chemical.

tablets prepared by fluidized-bed granulation showed a statistically significant higher bioavailability than tablets prepared by hole disk granulation. Differences in bioavailability in humans of commercially available sulfadiazine tablets were reported (8, 9).

Literature reports on the use of direct compression tablet masses are limited and are concerned with physical properties of the tablets and *in vitro* release (10). The purpose of this study was to compare the extent of bioavailability of sulfadiazine tablets prepared by direct compression, using a commercially available direct tableting mass[1], with those prepared by fluidized-bed granulation; a commercial preparation served as the standard.

EXPERIMENTAL

The composition of Preparations I and II is given in Table I. Preparation III was a commercial[2] 500-mg sulfadiazine USP tablet.

For the fluidized-bed granulation, the powder mixture of the internal phase of the tablets was transferred into the fluidized-bed granulator[3], and 2-propanol was sprayed through a nozzle into the fluidized powder bed. The conditions were: drying temperature, 50°; fan capacity, position 10; and 2-propanol, 50 ml/min. The desired granule size range of 0.3–0.7 mm was screened out. After mixing with the external phase (lubricant plus 10% disintegrant), the granules were compressed on a single-punch machine[4] to biconvex tablets of 11 mm in diameter and a pressure resistance of 3.5 kg.

For the direct compression tablets, the ingredients were mixed in a cube mixer[5] for 30 min and compressed as described.

Powder and Granule Testing—The moisture content[6], pour and stamp volumes, flow time[7], flow factor, and angle of repose were determined for the direct compression powder, the mixture of the direct compression powder plus sulfadiazine, and the fluidized-bed granulation.

***In Vitro* Tablet Testing**—The following physical tablet tests were performed: weight uniformity, pressure resistance[8] (hardness), friability[9] at 20 rpm expressed in percent after 30 min, and dissolution time of six tablets using the USP dissolution rate tester and artificial gastric fluid without enzymes[10] at 37° and 100 rpm.

***In Vivo* Testing**—White male New Zealand rabbits kept under identical conditions were used for blood level studies. Rabbits were studied because this species metabolizes sulfadiazine qualitatively and quantitatively similarly to humans (11). Although a crossover design would have been desirable, it was not feasible due to the relatively large volume of blood taken for each study, prohibiting the reuse of the animal for at least 4 weeks.

Each tablet preparation was tested in three rabbits. Blood samples of 2.5 ml were obtained by heart puncture taken prior to the experiment and 1, 2, 3, 4, 5, 6, 8, 10, and 12 hr after dosing. The tablets were administered in the morning after overnight fasting using a self-made appli-

[1] Emcompress, E. Mendell Co.
[2] Lilly, Control 5HJ61A.
[3] Aeromatic labor model, Muttenz, CH-Switzerland.
[4] Korsch, type EKO-M.
[5] Erweka, type KB 15.
[6] Ohaus determination balance model 6010.
[7] Erweka flowmeter model 21920, type GDT.
[8] Heberlein model 2E/205.
[9] Roche friabilator.
[10] USP XIX.

Table II—Properties of Powders and Granules

Parameter	Direct Compression Powder	Direct Compression Powder plus Sulfadiazine	Fluidized-Bed Granulation
Moisture content, % ± *SD*	4.4 ± 0.2	2.4 ± 0.1	1.7 ± 0.1
Pour volume, ml/g ± *SD*	1.22 ± 0.04	1.93 ± 0.05	2.0 ± 0.04
Stamp volume, ml/g ± *SD*	1.04 ± 0.02	1.35 ± 0.02	1.75 ± 0.015
Flow time, sec ± *SD*	9.7 ± 1.0	24.38 ± 2.2	5.3 ± 0.7
Flow factor ± *SD*	—	0.975 ± 0.004	0.913 ± 0.003
Angle of repose, degrees ± *SD*	31.6 ± 1.75	40.2 ± 2.0	26.0 ± 1.5

Table III—Properties of Tablets Tested

Parameter	Preparation		
	I	II	III
Potency, mg	252	251	496
Weight uniformity, mg ± *SD*	454.5 ± 0.98	451.8 ± 1.75	654.81 ± 0.79
Pressure resistance (hardness), kg ± *SD*	3.52 ± 5.65	3.51 ± 7.6	5.845 ± 12.01
Friability, % within 30 min at 20 rpm	6.5	23.7	63.8
$T_{10\%}$, min	1	24	45
$T_{50\%}$, min	7	53	760

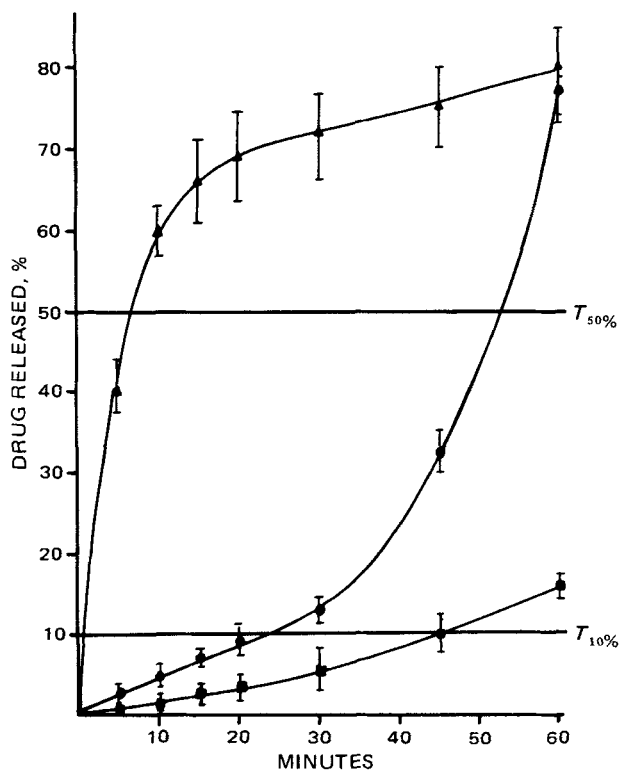

Figure 1—*Percent sulfadiazine released* versus *time of different tablet preparations. Key:* ■, *commercial product;* ▲, *tablets prepared by fluidized-bed granulation; and* ●, *tablets prepared by direct compression.*

Table IV—Average Blood Free Sulfadiazine Levels in Micrograms per Milliliter at Corrected Sampling Time

Preparation	Body Weight, g	Dose Size (Potency), mg	Rabbit	Hours 1	2	3	4	6	8	10	12
I	1780	252	1	7.26	25.40	32.24	33.24	29.16	23.04	17.68	13.30
	1900		2	2.93	22.67	29.74	30.67	25.81	19.44	114.11	10.10
	1800		3	8.76	25.44	31.77	32.74	28.24	21.87	16.28	11.92
			$\bar{x}$	6.315	24.50	31.25	33.27	27.74	21.45	16.02	11.77
			$\pm SD$	±3.0	±1.58	±1.32	±0.47	±1.73	±1.84	±1.79	±1.6
II	2300	251	1	4.65	24.78	31.18	31.075	24.35	16.93	11.25	7.34
	2150		2	11.39	26.23	30.67	29.99	23.31	16.12	10.62	6.83
	2450		3	6.44	22.24	27.13	26.86	21.15	14.89	10.07	6.69
			$\bar{x}$	7.49	24.42	29.66	29.31	22.94	15.98	10.64	6.95
			$\pm SD$	±3.40	±2.02	±2.20	±2.18	±1.63	±1.03	±0.59	±0.34
III	3380	496	1	13.42	30.11	35.40	35.01	28.14	20.32	14.08	9.57
	3550		2	13.28	30.00	35.31	34.94	28.09	20.30	14.07	9.57
	3480		3	15.34	32.88	38.69	38.45	31.1	22.47	15.48	10.43
			$\bar{x}$	14.01	31.0	36.43	36.13	29.11	21.03	14.54	9.85
			$\pm SD$	±1.15	±1.63	±1.87	±2.0	±1.72	±1.24	±0.82	±0.49

cator. Immediately after dosing, a stomach catheter was introduced and 5 ml of water was administered. Food was withheld for 6 hr after dosing; water was available *ad libitum*.

Assay of Sulfadiazine—A 2-ml aliquot of blood was mixed with 30 ml of water. After hemolysis, 8 ml of 15% (w/v) trichloroacetic acid was added. The precipitate was filtered off, and the filtrate was assayed by the Bratton–Marshall method (12).

Pharmacokinetic Analysis—The blood level–time data were computer[11] analyzed according to the one-compartment open model. Since it is difficult to keep the sampling time accurate to the minute, actual blood levels were corrected from the computer-fitted curves to the specified times.

RESULTS AND DISCUSSION

The physical properties of the powders and granules are listed in Table II. The smaller ratio of pour volume to stamp volume for the fluidized bed suggests that the weight uniformity should be higher than that of the direct compression mixture. The flow time and the angle of repose for the direct compression powder were much larger than for the fluidized-bed granulation, indicating that the latter is more suitable for compression for a high-speed tableting machine.

The tablet properties are listed in Table III. As suggested by the powder and granule testing, the tablets prepared by fluidized-bed granulation showed somewhat higher weight uniformity than those prepared by direct compression. However, all were within the general accepted limits. The pressure resistance (hardness) was maintained for both experimental preparations at 3.5 kg because any further increase in compression force resulted in capping of the direct compression preparation. The commercial preparation had a much higher pressure resistance. The friability of the tablets prepared by direct compression was between those prepared by fluidized-bed granulation and the commercial tablets.

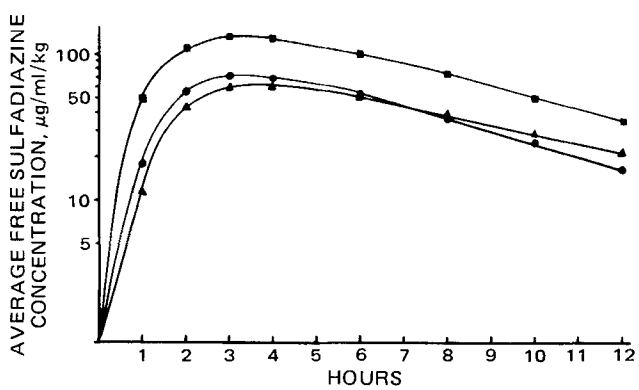

Figure 2—*Average blood free sulfadiazine concentrations* versus *time in micrograms per milliliter per kilogram. Key:* ■, *commercial product (500 mg);* ▲, *tablets prepared by fluidized-bed granulation (250 mg); and* ●, *tablets prepared by direct compression (250 mg).*

[11] Wang 700C, printer-plotter 702.

The *in vitro* drug release expressed in percent sulfadiazine released into artificial gastric fluid *versus* time (based on potency, not labeled amount) is shown in Fig. 1. Artificial gastric fluid was used as the test medium because sulfadiazine drug release is much higher in this medium than in water or artificial intestinal fluid (4–6, 9). Drug release was characterized by $T_{10\%}$ and $T_{50\%}$ and was highest for fluidized-bed tablets, followed by direct compression tablets and the commercial product.

The blood level data corrected for the specified sampling times are listed in Table IV. The average blood level–time curves, corrected for the body weight, are shown in Fig. 2. The standard deviations were omitted for clarity but are listed in Table IV.

Bioavailability is characterized by the area under the blood level–time curve, the time of the peak, and the concentration at the peak time (Table V). The areas under the curves were determined by the trapezoidal rule for the time from 0 to 12 hr, and the remaining areas were determined by dividing the last blood level point by the overall elimination rate constant, which was reported previously as 0.29 hr^{-1} after intravenous dosing (5, 7).

The extent of bioavailability, E, was determined using:

$$E = \frac{AUC_{\text{test}}^{0\to\infty} \dfrac{\text{dose}_{\text{standard}}}{\text{body weight}_{\text{standard}}}}{AUC_{\text{standard}}^{0\to\infty} \dfrac{\text{dose}_{\text{test}}}{\text{body weight}_{\text{test}}}} 100 \qquad \text{(Eq. 1)}$$

The 500-mg commercial preparation of sulfadiazine USP was considered as the standard. The highest extent of bioavailability was obtained with the tablets prepared by direct compression, followed by those prepared by fluidized-bed granulation. A statistically significant difference was found between the direct compression tablets and the standard with respect to the extent of bioavailability and the time of the peak.

Large differences were found in the *in vitro* dissolution studies, but only minimal differences existed *in vivo*. Part of the differences *in vitro* between the two experimental tablet preparations and the commercial preparation may be explained by the dose size differences of 250 and 500 mg, respectively. Saturation may be approached with the 500-mg dose. Since *in vivo* the peak times occurred in all three preparations in less than 3 hr, the drug is absorbed fast enough not to prevent dissolution due to saturation.

In conclusion, the direct compression tablet mass, when compared to a wet granulation (fluidized-bed) and a commercial tablet preparation,

Table V—Bioavailability Data

Preparation	Body Weight, g ± SD	Dose Size (Potency), mg	$AUC^{0\to\infty}$, (μg/ml) hr ± SD	t_p, hr ± SD	c_{tp}, μg/ml ± SD	Extent of Bioavailability, % ± SD
I	1826.6 ± 64.3	252	316.16 ± 26.16	2.97 ± 0.15	31.096 ± 1.85	106.14 ± 5.22
II	2300 ± 150.0	251	252.27 ± 17.82	2.63[a] ± 0.06	28.58 ± 2.15	106.98[a] ± 3.52
III	3470 ± 85.44	496	308.0 ± 17.14	2.83 ± 0.05	36.08 ± 2.0	100

[a] Statistically significant ($p < 0.05$) when compared to the standard.

resulted in an extent of bioavailability of at least that of the standard. The *in vitro* test revealed acceptable tablet properties with respect to weight uniformity, friability, and *in vitro* drug release. Considering the simple methodology employed in the manufacturing of direct compression tablets, this technique and the direct compression mass tested have a high potential for commercial use of a quality product.

REFERENCES

(1) Publication No. 76-3009, Department of Health, Education, and Welfare, Public Health Service, Rockville, Md., Jan. 1976.

(2) K. J. Randeri, *Diss. Abstr.*, **25**, 7212 (1965).

(3) P. D. Sheth and O. Nuessle, Ph.D. dissertation, University of Missouri, Kansas City, Mo., 1971.

(4) D. Schickling, M.S. thesis, University of Cincinnati, Cincinnati, Ohio, 1972.

(5) M. R. Scheffler and W. A. Ritschel, *Pharm. Ind.*, **37**, 511 (1975).

(6) W. Erni and W. A. Ritschel, *ibid.*, **39**, 284 (1977).

(7) *Ibid.*, in press.

(8) G. R. VanPetten, G. C. Becking, R. J. Withey, and H. F. Lettan, *J. Clin. Pharmacol.*, **11**, 27 (1971).

(9) W. A. Ritschel, G. Ritschel, C. R. Buncher, and J. Rotmensch, *Drug Intel. Clin. Pharm.*, **10**, 401 (1976).

(10) K. A. Khan and C. T. Rhodes, *Pharm. Acta Helv.*, **51**, 23 (1976).

(11) E. Reimerdes and J. H. Thumin, *Arzneim.-Forsch.*, **20**, 1176 (1970).

(12) A. C. Bratton and E. K. Marshall, Jr., *J. Biol. Chem.*, **128**, 537 (1939).

ACKNOWLEDGMENTS AND ADDRESSES

Received July 30, 1976, from the *College of Pharmacy, University of Cincinnati Medical Center, Cincinnati, OH 45267.*

Accepted for publication January 3, 1977.

[x] To whom inquiries should be directed.

Mathematical Model for Cyclocytidine Pharmacokinetics

K. J. HIMMELSTEIN [*x] and J. F. GROSS [‡]

Abstract □ The pharmacokinetics of the drug cyclocytidine in humans were modeled by using a physiological and anatomical approach. Each pertinent tissue is represented by a single compartment, and these compartments are linked together by the circulatory system. Each compartment is then represented by an ordinary differential equation that represents the rate of change in drug concentration as a function of convecting transport, metabolism, and urinary clearance. The models for cyclocytidine and cytarabine are linked together by a hydrolysis term in each equation set. The resulting equation sets are then solved numerically to predict the concentration of both drug species *in situ*. The models use physiological blood flows, tissue volumes, and clearance parameters. The results of the model show that cyclocytidine can act as a reservoir for cytarabine *in vivo* over the time studied. This effect is confined to relatively long times and relatively low plasma concentrations.

Keyphrases □ Cyclocytidine—pharmacokinetics in humans, mathematical model □ Pharmacokinetics—cyclocytidine in humans, mathematical model □ Models, mathematical—cyclocytidine pharmacokinetics in humans

Cytarabine (I) (NSC-63878), an effective antileukemic agent (1–3), has a very short half-life because of its rapid deamination to a biologically inactive compound. O^2,2′-Cyclocytidine (II) (NSC-145688), which is structurally similar to I, was more effective than I in several animal tumor systems (4, 5). The efficacy of II may be due to its hydrolysis to I (6). If so, its effects may be strongly related to the pharmacokinetics of both I and II *in vivo*.

The enhanced cytotoxic effect of II could possibly be due to its slower urinary clearance compared to the elimination of I by deamination and kidney clearance. Thus, II could act as a reservoir for the production of I *in vivo*. This paper presents a mathematical model to study the distribution and hydrolysis of II to I *in vivo*. This model demonstrates that the pharmacokinetic characteristics of II are important to its effective usage.

PHARMACOKINETIC MODEL

The model, an extension of the work by Dedrick *et al.* (7, 8), is based on the principle that anatomical and physiological parameters should be included to reflect biochemical interactions of the drug. The rationale for modeling on this basis as opposed to classical compartmental analysis was developed previously (9–15).

By using compartments to represent real organs, the actual blood flows and physiological volumes as well as terms to include metabolism, urinary clearance, and binding can be included. Thus, when the model is complete, it can provide predictive capability derived from a quantitative physiological and pharmacological basis. Since a model for the pharmacokinetics of I was described in detail (7, 8, 16), only key assumptions that deal directly with changes for the inclusion of II are discussed.

Scheme I represents the flow diagram of the various compartments used in the model. Each compartment represents a real organ, with the anatomical volume experimentally measured independently. The organs are contained in a network representing the systemic blood circulation. The blood flows are also measured independently for each compartment. A drug mass balance represents the rate of change of the mass of drug in the compartment as a function of the convective inflow and outflow rates, the metabolism rate, the elimination rate by urinary or other clearance, and the rate of drug introduction from external sources.

Dedrick *et al.* (7, 8) used the following assumptions to write differential equations describing the pharmacokinetics of I. Each organ is a volume of distribution for the drug, and deamination can be represented by a Michaelis–Menten expression. Urinary clearance is directly proportional to the concentration in the blood. For II, a similar compartmental network is considered. Since the chemical structures of II and I are closely related, it is assumed that they will act similarly, with no gross differences in distribution and urinary clearance from the body.

Compound II is not deaminated *in vivo* (17), and hydrolysis of II to I is assumed to take place in all tissues. Thus, a production term for I is included in each balance that is first order in II concentration (16). The balance equation on the blood compartment for I is:

$$V_B \frac{dC_B}{dt} = Q_H C_H + Q_{Li} C_{Li} + Q_M C_M + Q_K C_K + Q_{Le} C_{Le} - Q_B C_B - \frac{V_{max,B}\, C_B}{K_{m,B} + C_B} V_B + Mg(t) + K_h X_B \phi V_B \quad \text{(Eq. 1)}$$

resulted in an extent of bioavailability of at least that of the standard. The *in vitro* test revealed acceptable tablet properties with respect to weight uniformity, friability, and *in vitro* drug release. Considering the simple methodology employed in the manufacturing of direct compression tablets, this technique and the direct compression mass tested have a high potential for commercial use of a quality product.

REFERENCES

(1) Publication No. 76-3009, Department of Health, Education, and Welfare, Public Health Service, Rockville, Md., Jan. 1976.

(2) K. J. Randeri, *Diss. Abstr.*, **25**, 7212 (1965).

(3) P. D. Sheth and O. Nuessle, Ph.D. dissertation, University of Missouri, Kansas City, Mo., 1971.

(4) D. Schickling, M.S. thesis, University of Cincinnati, Cincinnati, Ohio, 1972.

(5) M. R. Scheffler and W. A. Ritschel, *Pharm. Ind.*, **37**, 511 (1975).

(6) W. Erni and W. A. Ritschel, *ibid.*, **39**, 284 (1977).

(7) *Ibid.*, in press.

(8) G. R. VanPetten, G. C. Becking, R. J. Withey, and H. F. Lettan, *J. Clin. Pharmacol.*, **11**, 27 (1971).

(9) W. A. Ritschel, G. Ritschel, C. R. Buncher, and J. Rotmensch, *Drug Intel. Clin. Pharm.*, **10**, 401 (1976).

(10) K. A. Khan and C. T. Rhodes, *Pharm. Acta Helv.*, **51**, 23 (1976).

(11) E. Reimerdes and J. H. Thumin, *Arzneim.-Forsch.*, **20**, 1176 (1970).

(12) A. C. Bratton and E. K. Marshall, Jr., *J. Biol. Chem.*, **128**, 537 (1939).

ACKNOWLEDGMENTS AND ADDRESSES

Received July 30, 1976, from the *College of Pharmacy, University of Cincinnati Medical Center, Cincinnati, OH 45267.*

Accepted for publication January 3, 1977.

[x] To whom inquiries should be directed.

Mathematical Model for Cyclocytidine Pharmacokinetics

K. J. HIMMELSTEIN [*x] and J. F. GROSS [‡]

Abstract □ The pharmacokinetics of the drug cyclocytidine in humans were modeled by using a physiological and anatomical approach. Each pertinent tissue is represented by a single compartment, and these compartments are linked together by the circulatory system. Each compartment is then represented by an ordinary differential equation that represents the rate of change in drug concentration as a function of convecting transport, metabolism, and urinary clearance. The models for cyclocytidine and cytarabine are linked together by a hydrolysis term in each equation set. The resulting equation sets are then solved numerically to predict the concentration of both drug species *in situ*. The models use physiological blood flows, tissue volumes, and clearance parameters. The results of the model show that cyclocytidine can act as a reservoir for cytarabine *in vivo* over the time studied. This effect is confined to relatively long times and relatively low plasma concentrations.

Keyphrases □ Cyclocytidine—pharmacokinetics in humans, mathematical model □ Pharmacokinetics—cyclocytidine in humans, mathematical model □ Models, mathematical—cyclocytidine pharmacokinetics in humans

Cytarabine (I) (NSC-63878), an effective antileukemic agent (1–3), has a very short half-life because of its rapid deamination to a biologically inactive compound. O^2,2′-Cyclocytidine (II) (NSC-145688), which is structurally similar to I, was more effective than I in several animal tumor systems (4, 5). The efficacy of II may be due to its hydrolysis to I (6). If so, its effects may be strongly related to the pharmacokinetics of both I and II *in vivo*.

The enhanced cytotoxic effect of II could possibly be due to its slower urinary clearance compared to the elimination of I by deamination and kidney clearance. Thus, II could act as a reservoir for the production of I *in vivo*. This paper presents a mathematical model to study the distribution and hydrolysis of II to I *in vivo*. This model demonstrates that the pharmacokinetic characteristics of II are important to its effective usage.

PHARMACOKINETIC MODEL

The model, an extension of the work by Dedrick *et al.* (7, 8), is based on the principle that anatomical and physiological parameters should be included to reflect biochemical interactions of the drug. The rationale for modeling on this basis as opposed to classical compartmental analysis was developed previously (9–15).

By using compartments to represent real organs, the actual blood flows and physiological volumes as well as terms to include metabolism, urinary clearance, and binding can be included. Thus, when the model is complete, it can provide predictive capability derived from a quantitative physiological and pharmacological basis. Since a model for the pharmacokinetics of I was described in detail (7, 8, 16), only key assumptions that deal directly with changes for the inclusion of II are discussed.

Scheme I represents the flow diagram of the various compartments used in the model. Each compartment represents a real organ, with the anatomical volume experimentally measured independently. The organs are contained in a network representing the systemic blood circulation. The blood flows are also measured independently for each compartment. A drug mass balance represents the rate of change of the mass of drug in the compartment as a function of the convective inflow and outflow rates, the metabolism rate, the elimination rate by urinary or other clearance, and the rate of drug introduction from external sources.

Dedrick *et al.* (7, 8) used the following assumptions to write differential equations describing the pharmacokinetics of I. Each organ is a volume of distribution for the drug, and deamination can be represented by a Michaelis–Menten expression. Urinary clearance is directly proportional to the concentration in the blood. For II, a similar compartmental network is considered. Since the chemical structures of II and I are closely related, it is assumed that they will act similarly, with no gross differences in distribution and urinary clearance from the body.

Compound II is not deaminated *in vivo* (17), and hydrolysis of II to I is assumed to take place in all tissues. Thus, a production term for I is included in each balance that is first order in II concentration (16). The balance equation on the blood compartment for I is:

$$V_B \frac{dC_B}{dt} = Q_H C_H + Q_{Li} C_{Li} + Q_M C_M + Q_K C_K + Q_{Le} C_{Le} - Q_B C_B - \frac{V_{max,B}\, C_B}{K_{m,B} + C_B} V_B + Mg(t) + K_h X_B \phi V_B \quad \text{(Eq. 1)}$$

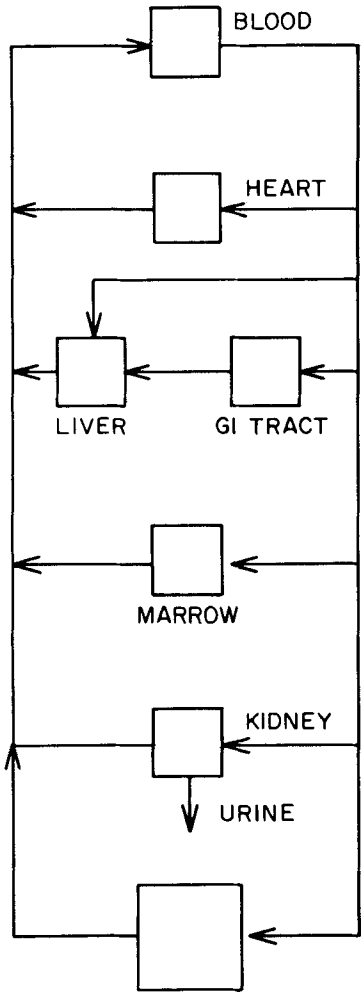

Scheme I

where V represents the compartment size in milliliters, C represents the concentration of I in milligrams per milliliter, Q is the blood flow rate in milliliters per minute, K_k is the I urinary clearance in milliliters per minute, V_{max} is the deamination activity at saturation in micrograms per minute, and K_m represents the Michaelis constant in micrograms per milliliter. The subscripts represent each compartment: H, heart; Li, liver; M, marrow; K, kidney; Le, lean; and B, blood. The term X represents the concentration of II in various compartments, M is the total dose of drug injected, $g(t)$ is the injection function, K_h is the hydrolysis rate constant, K_c is the kidney clearance of II, ϕ represents the ratio of the molecular weights of I to II, and t represents time. A sample equation for I for one compartment (the kidney) is given by:

$$V_K \frac{dC_K}{dt} = Q_K C_B - Q_K C_K - K_K C_B - \frac{V_{max,K}\, C_K}{K_{m,K} + C_K} V_K + K_h V_K \phi X_K \quad \text{(Eq. 2)}$$

Equation 3 represents the mass balance of II in the blood compartment:

$$V_B \frac{dX_B}{dt} = Q_H X_H + Q_{Li} X_{Li} + Q_M X_M + Q_K X_K + Q_{Le} X_{Le} + Mg(t) - K_h X_B V_B \quad \text{(Eq. 3)}$$

Equation 4 represents a typical compartment (the kidney) for II:

$$V_K \frac{dX_K}{dt} = Q_K X_B - Q_K X_K - K_C X_B - K_h X_K V_K \quad \text{(Eq. 4)}$$

A similar balance in each compartment for both II and I is made, resulting in a set of ordinary nonlinear differential equations to be solved simultaneously and numerically on a digital computer. When the equations are solved, the results are the time-dependent concentrations for each drug in each tissue compartment plus the blood compartment and the total urinary excretion, which is given for I by:

$$U_I = \int_0^t K_k C_B \, dt' \quad \text{(Eq. 5a)}$$

and for II by:

$$U_{II} = \int_0^t K_c X_B \, dt' \quad \text{(Eq. 5b)}$$

Table I—Model Parameters for Cyclocytidine Pharmacokinetic Model

Parameter	Value in Humans	Reference
Body weight, g	70,000	7
Volume, V, ml		
Blood	2,670	7
Liver	1,700	7
Gut	3,180	7
Heart	450	7
Kidneys	1,060	7
Lean	27,000	7
Marrow	2,000	7
Blood Flow, Q, ml/min		
Cardiac output (for model)	4,040	7
Liver	1,450	7
Gut	1,100	7
Heart	240	7
Kidneys	1,240	7
Lean	930	7
Marrow	180	7
Michaelis constant, K_m, μg/ml		
Heart	31	8
Liver	27	20
Kidneys	32	8
Deaminase activity, V_{max}, μg/g min		
Liver	119	19
Heart	6	20
Kidneys	20	20
Clearance, K_c, K_k, ml/min		
I	90	8
II	70	14
Hydrolysis rate, min^{-1} [a]	0.01(0.005)[a]	

[a] *In vitro* calculation from Ref. 16.

EXPERIMENTAL

In the current study, II was investigated in humans. The volumes in the compartments and the blood flows were estimated from the anatomical–physiological values for a 70-kg human. Since these values were not the weights of the selected subjects, these parameters were adjusted linearly for variations in the size of the patient. The volumes and blood flows were taken from Dedrick *et al.* (7), who found it necessary to adjust the volume of the lean compartment to explain adequately the pharmacokinetics of I. The lean compartment volume was so adjusted in the present model. The Michaelis constant, deaminase activity, and kidney clearance constant for I were also taken from Dedrick *et al.* (8).

Ho (16) presented *in vitro* hydrolysis data for II to I in human plasma, showing that the hydrolysis was first order in II concentration. Thus, it was assumed here that the hydrolysis *in vivo* is first order and that the *in vivo* hydrolysis rate can be estimated from the *in vitro* data, yielding a hydrolysis rate constant of 0.005 min^{-1}. When this constant was fitted into this model, it was too low to explain the appearance of I. Thus, the hydrolysis rate constant was adjusted to mirror accurately hydrolysis of II to I *in vivo*. Finally, the clearance of II was estimated from cumulative excretion data developed by Ho *et al.* (17, 18).

All parameters used in the models (Table I) were estimated from *in vivo* data, with the exception of the urinary clearances, which were estimated from *in vivo* cumulative excretion curves, and the hydrolysis rate constant, which was estimated from *in vitro* data and adjusted to reflect *in vivo* hydrolysis.

RESULTS AND DISCUSSION

The data modeled here are the data of Ho *et al.* (17, 18), where plasma concentration curves for II and I were represented as a function of time after mixed intravenous injections for several subjects. Only one subject is presented here. Several other subjects were modeled by altering the

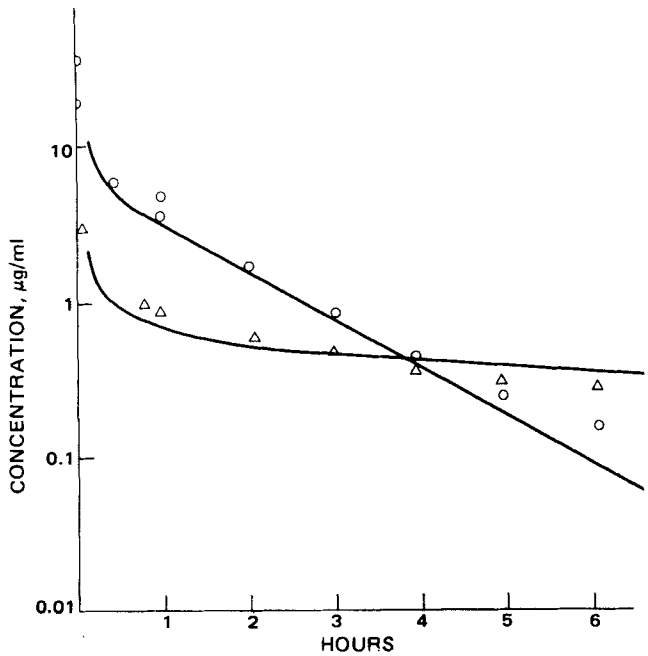

Figure 1—*Plasma concentration in 70-kg human after 2.84 × 10^5 μg iv of II and 9 × 10^4 μg iv of I. Hydrolysis rate = 0.01 min. Key: △, I; and ○, II.*

organ volumes and flow rates to reflect differences in subject sizes. Similar results to those discussed were obtained.

Figure 1 represents the plasma disappearance curve of II and I from blood in a human subject after an intravenous injection of II. Approximately 24% I is contained in the injection. The I impurity was considered a simultaneous injection with II and thus was included in the model. The solid lines represent the concentration of II and I as predicted by the model using a hydrolysis rate of 0.01 min^{-1}. There is reasonable agreement between the model and the experimental data. The model for I underpredicts the plasma concentration at times after 2 hr.

Figure 2 represents the same data, using the hydrolysis rate constant of 0.005 min^{-1}, the value calculated from *in vitro* data. The agreement in this case is not quite as good, indicating that hydrolysis *in vivo* occurs at a somewhat higher rate than *in vitro*. Figure 3 contains a hypothetical study whereby the concentration of I predicted by the model using an injection of II of the same size as that of Ho *et al.* (17, 18) is compared to a hypothetical injection of an equal mass of I only. Shortly after an injection of I only, the concentration was much higher than the I concentration due to both hydrolysis and impurity from an injection of II. However, at later times, the II injection provided for a higher concentration of I. This effect may be more apparent during times for which data were unavailable.

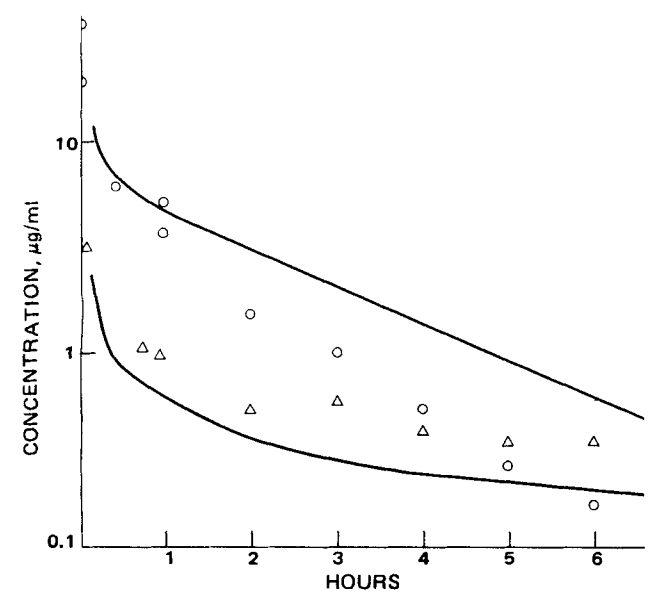

Figure 2—*Blood plasma concentration in 70-kg human after 2.84 × 10^5 μg iv of II and 9 × 10^4 μg iv of I. Hydrolysis rate = 0.005 min^{-1}. Key: △, I; and ○, II.*

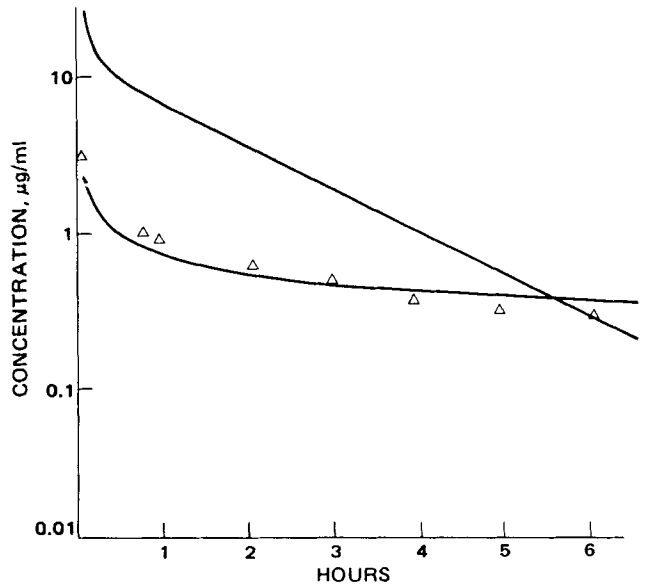

Figure 3—*Plasma I concentration in 70-kg human after simulated intravenous injection of equal masses of I and II. Key: upper curve, I alone; and lower curve, I from II.*

As previously stated by Ho (16), it is possible, based on pharmacokinetics, that the enhanced therapeutic effect of II is attributable to its action as a pool for I production, since the concentration of I is maintained at a somewhat higher level at longer periods when II is employed rather than I alone. The fact that a simple pharmacokinetic model agrees directly with the experimental results by the inclusion of a first-order hydrolysis term ascertained qualitatively *in vitro* supports this hypothesis. Since the main goal of therapy with either II or I is to maintain a concentration of I above the therapeutic level for as long as possible without toxic effects caused by high I concentrations, the model presented allows the manipulation and study of various dosage regimens prior to clinical application.

REFERENCES

(1) A. P. Bodey, E. J. Preireich, R. W. Monto, and J. S. Hewett, *Cancer Chemother. Rep.*, **53**, 59 (1969).

(2) R. R. Ellison, T. A. Silver, T. F. Holland, M. Weil, C. Jacquiliat, M. Boirow, J. Bernard, A. Sawitsky, F. Rosner, B. Gussoff, R. T. Silver, A. Karanas, F. Haurani, R. Kyle, J. L. Hutchison, R. J. Forcier, J. H. Moon, J. Cuttler, C. L. Spurr, D. M. Hayes, J. Blom, and L. A. Leone, *Blood*, **32**, 507 (1968).

(3) R. W. Talley and V. K. Vaitkevicius, *ibid.*, **21**, 352 (1963).

(4) A. Hoshi, R. Kanzaw, K. Kuretani, M. Saneyoshi, and Y. Arai, *Gann*, **62**, 145 (1971).

(5) J. M. Vanditti, M. C. Baratta, N. Greenberg, B. J. Abbott, and I. Kline, *Cancer Chemother. Rep.*, **56**, 483 (1972).

(6) J. P. Howard, N. Geuik, and M. L. Murphy, *ibid.*, **50**, 287 (1966).

(7) R. L. Dedrick, D. D. Forrester, J. N. Cannon, S. W. El Darrer, and L. B. Mellett, *Biochem. Pharmacol.*, **22**, 2405 (1973).

(8) R. L. Dedrick, D. D. Forrester, and D. H. W. Ho, *ibid.*, **21**, 1 (1972).

(9) K. B. Bischoff and R. L. Dedrick, *J. Pharm. Sci.*, **57**, 1346 (1968).

(10) K. B. Bischoff, R. L. Dedrick, and D. S. Zaharko, *ibid.*, **59**, 149 (1970).

(11) K. B. Bischoff and R. L. Dedrick, *J. Theoret. Biol.*, **29**, 63 (1970).

(12) K. B. Bischoff, R. L. Dedrick, D. S. Zaharko, and J. A. Longstreth, *J. Pharm. Sci.*, **60**, 1128 (1971).

(13) R. L. Dedrick and K. B. Bischoff, *Chem. Eng. Prog. Symp. Ser.*, **84**, 32 (1968).

(14) R. L. Gabelnick, R. L. Dedrick, and R. S. Bourke, *J. Appl. Physiol.*, **28**, 636 (1970).

(15) P. Harris and J. F. Gross, *Cancer Chemother. Rep., Part 1, No. 4*, **59**, 819 (1975).
(16) D. H. Ho, *Biochem. Pharmacol.*, **23**, 1235 (1974).
(17) D. H. W. Ho, V. Rodriquez, T. L. Loo, G. P. Bodgy, and E. J. Freireich, *Clin. Pharmacol. Ther.*, **17**, 66 (1975).
(18) D. H. W. Ho, C. J. K. Carter, T. L. Loo, R. L. Abbott, and C. M. McBride, *Drug Metab. Dispos.*, **3**, 309 (1976).
(19) G. W. Camiener, *Biochem. Pharmacol.*, **16**, 1981 (1967).
(20) G. W. Camiener and C. G. Smith, *ibid.*, **14**, 1405 (1965).

ACKNOWLEDGMENTS AND ADDRESSES

Received October 29, 1976, from the *Department of Chemical and Petroleum Engineering, University of Kansas, Lawrence, KS 66045, and the ‡Department of Chemical Engineering, University of Arizona, Tucson, AZ 85721.

Accepted for publication January 6, 1977.

Supported in part by HEW Grant HL 17421.

ˣ To whom inquiries should be directed.

Mass Spectrometry of Cannabinoids

T. B. VREE

Abstract □ The mechanism of fragmentation of cannabinoids to fragments *m/e* 314, 299, 271, 258, 246, 243, and 231 is given. Cannabidiol, cannabinodiol, cannabinol, Δ^6- and Δ^1-tetrahydrocannabinol, cannabichromene, cannabicyclol, derivatives with pentyl, propyl, and methyl side chains, their methyl ethers, and *cis–trans* and *ortho–para* isomers were analyzed by GLC–mass spectrometry using different energies for fragmentation during GLC elution. The following mechanism was distinguished: loss of a methyl radical, ring closure and rotation, McLafferty rearrangement, retro Diels–Alder, internal protonation, isomerization and internal bond formation, and one-step fragmentation to *m/e* 231.

Keyphrases □ Cannabinoids, various—mechanism of mass spectrometric fragmentation □ Mass spectrometry—mechanism of fragmentation of various cannabinoids

One rapid method of identification of cannabinoids is combined GLC–mass spectrometry. The mass spectra of cannabinoids can be distinguished from each other. The fragmentation process is relatively slow for most compounds, taking 40–50 ev before completion, after which the relative intensities of the fragments do not alter (Fig. 1). When the relative intensities of each particular mass fragment are plotted against the electron energy used, the fragmentation process can be characterized for each cannabinoid.

In the 10–20-ev range, the fragmentation just starts; differences in this process between the different structures are then relatively large. The technique of taking mass spectra at different electron voltages between 10 and 20 ev and plotting relative intensities against electron volts gives very characteristic electron voltage mass fragmentograms of the cannabinoids, which, for instance, led to the discovery of some propyl and methyl homologs of the known cannabinoids. This method is also useful in elucidating the various cannabinoid fragmentation pathways.

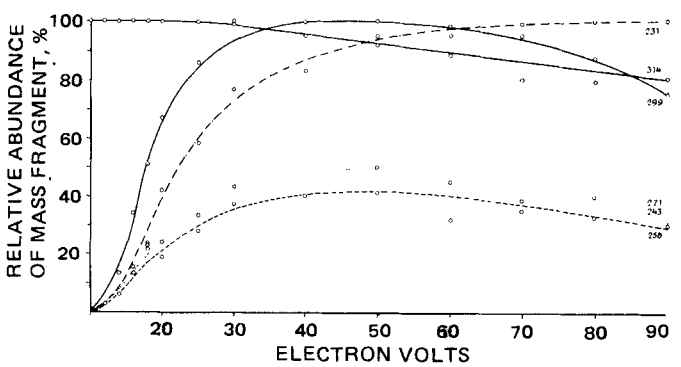

Figure 1—*Electron voltage mass fragmentogram of* trans-para-*Vb. Fragments are formed relatively slowly between 10 and 30 ev. In this particular interval, small structural differences of the cannabinoids may result in big differences in the formation rate of certain mass fragments.*

EXPERIMENTAL

Materials and Methods—A gas chromatograph–mass spectrometer[1] was used. Glass columns, 1.80 m × 4 mm i.d., were packed with 3% OV-17 on 60–80-mesh Gas Chrom Q. The temperatures were: oven, 200°; separator, 220°; and ion source, 250°. The helium flow was 20 ml/min. Repetitive mass spectra were taken at 20, 18, 16, 14, 12, and 10 ev during the elution of a GLC peak. The detector gain was increased in the 16–10-ev energy interval. The trap current was 60 μamp, and the accelerating voltage was 3.5 kv. The pressure in the analyzer tube was 2×10^{-6} Torr.

The gas chromatograms were recorded by a total-ion current monitor at 20 ev. Gas chromatograms of mixtures of natural and synthetic cannabinoids were published elsewhere (1). The mass spectra obtained were normalized, and the relative abundance of a particular mass fragment was plotted against the electron voltage.

Cannabinoids[2]—Lebanese, Nepalese, Moroccan, Columbian, Indonesian, and Congolese hashish samples and marijuana samples from Brazil and South Africa were powdered and extracted with ether or *n*-hexane by homogenizing for 10 min. After filtration of the extracts, most of the solvent was evaporated to give suitable concentrations for GLC–mass spectrometry. Synthetic samples were only dissolved in a small aliquot of ether.

RESULTS

Molecular Ion *m/e* 314—The aryl nucleus is the center of charge localization, and elimination of an electron from this nucleus gives the molecular ion *m/e* 314. At 10 ev, the molecular ion *m/e* 314 is the base peak. At 20 ev, large differences in the relative intensities between different cannabinoids can be observed (Table I).

Formation of Mass Fragment M − 15 (*m/e* 299 and 295)—The loss of the geminal methyl group, which nearly all structures have in common,

[1] LKB 9000.

[2] Natural Cannabis samples were obtained from and identified by Dr. A. H. Witte, Laboratory of Forensic Sciences, Ministry of Justice, The Hague, The Netherlands, and Dr. E. A. Carlini, Depto de Psicobiologia, Escola Paulista de Medicina, Sao Paulo, Brazil. Synthetic cannabinoids were a gift from Dr. T. Petrzilka, Eidgn. Hochschule Zurich, Department of Organic Chemistry, Zurich, Switzerland, where voucher specimens were deposited.

(15) P. Harris and J. F. Gross, *Cancer Chemother. Rep., Part 1, No. 4*, **59**, 819 (1975).
(16) D. H. Ho, *Biochem. Pharmacol.*, **23**, 1235 (1974).
(17) D. H. W. Ho, V. Rodriquez, T. L. Loo, G. P. Bodgy, and E. J. Freireich, *Clin. Pharmacol. Ther.*, **17**, 66 (1975).
(18) D. H. W. Ho, C. J. K. Carter, T. L. Loo, R. L. Abbott, and C. M. McBride, *Drug Metab. Dispos.*, **3**, 309 (1976).
(19) G. W. Camiener, *Biochem. Pharmacol.*, **16**, 1981 (1967).
(20) G. W. Camiener and C. G. Smith, *ibid.*, **14**, 1405 (1965).

ACKNOWLEDGMENTS AND ADDRESSES

Received October 29, 1976, from the *Department of Chemical and Petroleum Engineering, University of Kansas, Lawrence, KS 66045, and the ‡Department of Chemical Engineering, University of Arizona, Tucson, AZ 85721.

Accepted for publication January 6, 1977.

Supported in part by HEW Grant HL 17421.

ˣ To whom inquiries should be directed.

Mass Spectrometry of Cannabinoids

T. B. VREE

Abstract □ The mechanism of fragmentation of cannabinoids to fragments *m/e* 314, 299, 271, 258, 246, 243, and 231 is given. Cannabidiol, cannabinodiol, cannabinol, Δ^6- and Δ^1-tetrahydrocannabinol, cannabichromene, cannabicyclol, derivatives with pentyl, propyl, and methyl side chains, their methyl ethers, and *cis–trans* and *ortho–para* isomers were analyzed by GLC–mass spectrometry using different energies for fragmentation during GLC elution. The following mechanism was distinguished: loss of a methyl radical, ring closure and rotation, McLafferty rearrangement, retro Diels–Alder, internal protonation, isomerization and internal bond formation, and one-step fragmentation to *m/e* 231.

Keyphrases □ Cannabinoids, various—mechanism of mass spectrometric fragmentation □ Mass spectrometry—mechanism of fragmentation of various cannabinoids

One rapid method of identification of cannabinoids is combined GLC–mass spectrometry. The mass spectra of cannabinoids can be distinguished from each other. The fragmentation process is relatively slow for most compounds, taking 40–50 ev before completion, after which the relative intensities of the fragments do not alter (Fig. 1). When the relative intensities of each particular mass fragment are plotted against the electron energy used, the fragmentation process can be characterized for each cannabinoid.

In the 10–20-ev range, the fragmentation just starts; differences in this process between the different structures are then relatively large. The technique of taking mass spectra at different electron voltages between 10 and 20 ev and plotting relative intensities against electron volts gives very characteristic electron voltage mass fragmentograms of the cannabinoids, which, for instance, led to the discovery of some propyl and methyl homologs of the known cannabinoids. This method is also useful in elucidating the various cannabinoid fragmentation pathways.

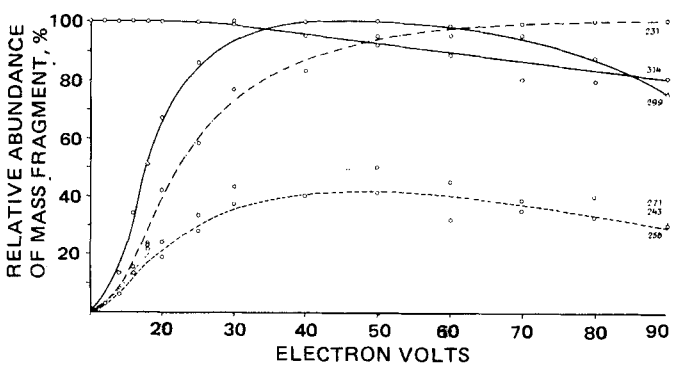

Figure 1—*Electron voltage mass fragmentogram of* trans-para-*Vb. Fragments are formed relatively slowly between 10 and 30 ev. In this particular interval, small structural differences of the cannabinoids may result in big differences in the formation rate of certain mass fragments.*

EXPERIMENTAL

Materials and Methods—A gas chromatograph–mass spectrometer[1] was used. Glass columns, 1.80 m × 4 mm i.d., were packed with 3% OV-17 on 60–80-mesh Gas Chrom Q. The temperatures were: oven, 200°; separator, 220°; and ion source, 250°. The helium flow was 20 ml/min. Repetitive mass spectra were taken at 20, 18, 16, 14, 12, and 10 ev during the elution of a GLC peak. The detector gain was increased in the 16–10-ev energy interval. The trap current was 60 μamp, and the accelerating voltage was 3.5 kv. The pressure in the analyzer tube was 2×10^{-6} Torr.

The gas chromatograms were recorded by a total-ion current monitor at 20 ev. Gas chromatograms of mixtures of natural and synthetic cannabinoids were published elsewhere (1). The mass spectra obtained were normalized, and the relative abundance of a particular mass fragment was plotted against the electron voltage.

Cannabinoids[2]—Lebanese, Nepalese, Moroccan, Columbian, Indonesian, and Congolese hashish samples and marijuana samples from Brazil and South Africa were powdered and extracted with ether or *n*-hexane by homogenizing for 10 min. After filtration of the extracts, most of the solvent was evaporated to give suitable concentrations for GLC–mass spectrometry. Synthetic samples were only dissolved in a small aliquot of ether.

RESULTS

Molecular Ion *m/e* 314—The aryl nucleus is the center of charge localization, and elimination of an electron from this nucleus gives the molecular ion *m/e* 314. At 10 ev, the molecular ion *m/e* 314 is the base peak. At 20 ev, large differences in the relative intensities between different cannabinoids can be observed (Table I).

Formation of Mass Fragment M − 15 (*m/e* 299 and 295)—The loss of the geminal methyl group, which nearly all structures have in common,

[1] LKB 9000.

[2] Natural Cannabis samples were obtained from and identified by Dr. A. H. Witte, Laboratory of Forensic Sciences, Ministry of Justice, The Hague, The Netherlands, and Dr. E. A. Carlini, Depto de Psicobiologia, Escola Paulista de Medicina, Sao Paulo, Brazil. Synthetic cannabinoids were a gift from Dr. T. Petrzilka, Eidgn. Hochschule Zurich, Department of Organic Chemistry, Zurich, Switzerland, where voucher specimens were deposited.

Table I—Relative Intensities of Molecular Ion *m/e* 314 of Different Cannabinoids Taken at 10 and 20 ev

Compound	10 ev	20 ev	Electron Volts of 50% Relative Abundance
Cannabicitran (I)	100	10	14
Cannabicyclol (II)	100	10	14
Cannabichromene (III)	100	10	11
Cannabidiol (IV)	100	25	16
Δ^6-*trans*-Tetrahydrocannabinol (V*a*)	100	100	—
Δ^1-*trans*-Tetrahydrocannabinol (V*b*)	100	100	—

depends strongly upon the structure of the compound. In cannabinol (VI), the main process is this particular fragmentation; other possible fragmentations are ruled out or contribute very little (2). The relative intensity of M − 15 increases when the double bond moves toward the aryl nucleus (Table II). When the double bond is in the 3–4-position as in synhexyl (IX), the only fragmentation of the alicyclic part is loss of a geminal methyl group (3) (Fig. 2). Substitution in the aryl nucleus has no influence on this fragmentation (Figs. 2 and 3).

The presence of the pyran ring is necessary for this kind of fragmentation. For IV, *m/e* 299 originates after ring closure (4), but this mechanism has strong competition with the retro Diels–Alder reaction and a one-step mechanism (5). This process is is also the most logical for the aromatic VII (3) (Schemes I and II).

With a series of derivatives of tetrahydrocannabinol [Δ^6 (V*a*), Δ^1 (V*b*),

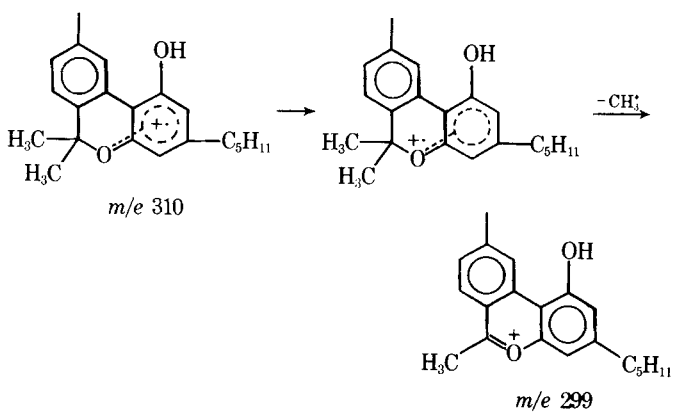

Scheme I

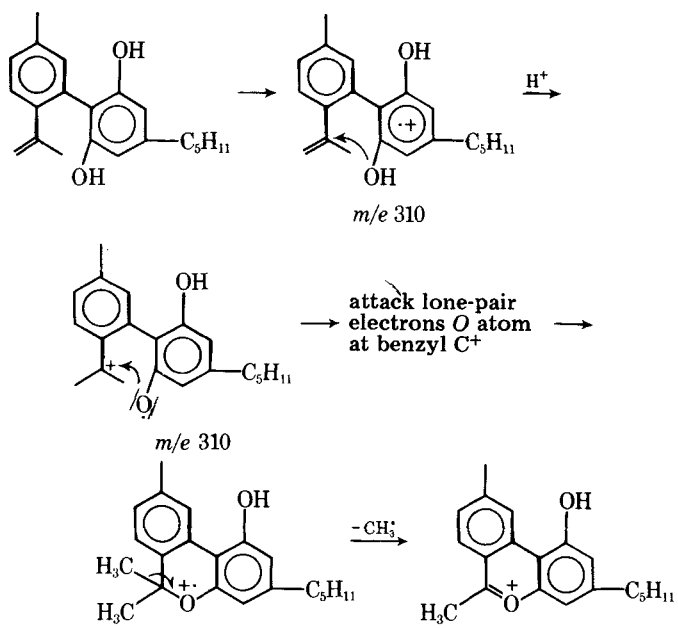

Scheme II

Table II—Relative Intensities of the M − 15 Fragment of Several Cannabinoids

Compound	Relative Abundance at 20 ev	Electron Volts of 50% Relative Abundance	Total Ion Current at 20 ev, %
II	5	—	3
III	5	—	3
IV	5	—	3
V*a*	10	—	5
V*b*	60	18	22
VI	100	12	83
Cannabinodiol (VII)	100	16	44

Δ^2 (V*c*), and Δ^3 (V*d*)], the loss of a geminal methyl group became the main process when all competing fragmentations were no longer possible (2). This influence of the double bond on the mass spectra might be used for the identification of tetrahydrocannabinol isomers because the ratios of relative intensities of M − 15 and M of the isomers were characteristic. The ratios were 0.13, 0.81, 2.8, 7.3, 5.5, 1.1, and 6.5 for V*a*, V*b*, V*c*, V*d*, VI, VII, and IX, respectively. The mechanism given in Scheme I is based on the concept of charge localization at the oxygen atom.

With 7,7,7-trideutero-V*a*, loss of a methyl radical resulted in equal relative abundances of *m/e* 299 and 302 (5). This observation leads to the conclusion that the methyl group at position 7 is lost and that the 1–6-double bond (Δ^6, V*a*) acts as a competitive center of charge localization. When the double bond moves toward the aryl nucleus, it becomes part of the main center of charge localization and the loss of the geminal methyl group becomes the main fragmentation process.

Formation of Mass Fragment M − 43 (*m/e* 271 and 285)—Mass fragment *m/e* 271 may be formed according to Scheme III (4). After ring opening, the possibility of hydrogen transfer or ring reclosure exists.

When the ring is open, rotation around 3–3′ axis may take place. If two hydroxyl groups are available for the reclosure, there is no difference in the position of the aromatic nucleus. If the alkyl side chain is in the *ortho*-position, the chance of ring reclosure statistically is only 0.5. The influence of the *ortho–para*-position of the side chain on the formation of *m/e* 271 is negligible, except in the case of Δ^6-tetrahydrocannabinol (Table III). Even methylation of the phenolic hydroxyl groups has no influence on the formation of *m/e* 271 (*m/e* 285). With 3-^{2}H-Δ^6-tetrahydrocannabinol, complete retention of the deuterium label was found (*m/e* 271 → *m/e* 272) (5). The finding that *m/e* 271 in Δ^1-*cis*-tetrahydrocannabinol is 100% for both *ortho*- and *para*-isomers may be explained by the relief of tension of the folded structure. Ring opening is, therefore, favored.

This energetically favored ring opening is not supported by the formation of *m/e* 271 in Δ^1-*cis*- or *trans*-tetrahydrocannabinol. If the concept of charge localization in the aromatic nucleus is maintained, then

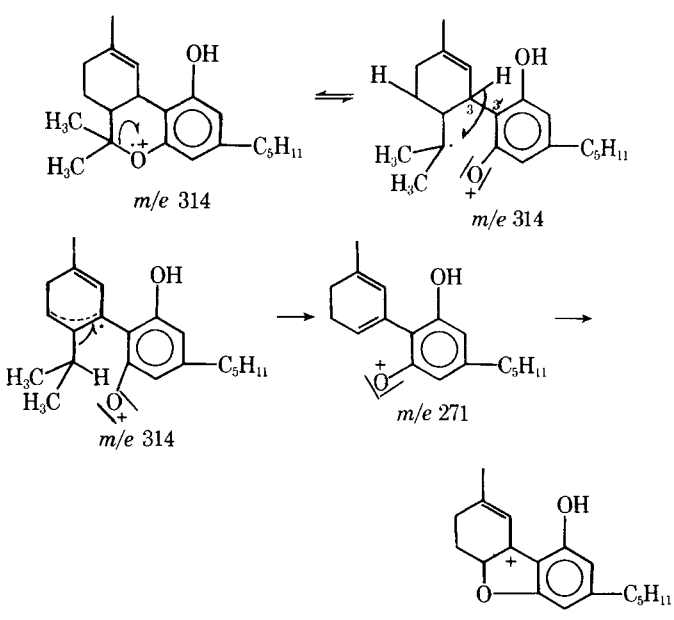

Scheme III

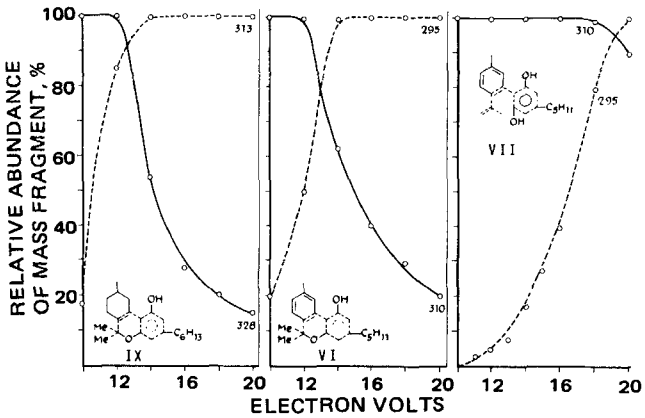

Figure 2—*Electron voltage mass fragmentograms of IX, VI, and VII.*

a shift of the hydrogen at C-5 can solve the problem of the formation of *m/e* 271. However, V*a* and V*b* isomers (*cis–trans–ortho–para*) deuterated at C-5 must be synthesized to give absolute proof of the mechanism.

Formation of Fragment M − 56 and Fragmentation of Side Chain (*m/e* 258)—The side chain is not fragmented carbon for carbon successively. Olivetol (X) itself shows the following mass spectra at 20 ev: *m/e* (relative abundance) 180 (M, 37), 165 (M − 15, 0.39), 151 (M − 29, 1.1), 138 (9.4), 137 (M − 43, 7.8), and 124 (M − 56, 100).

The butylene elimination is the main process (X*a*). If no other fragmentation reaction takes place in the cannabinoid molecule, this fragmentation should give the same formation rate and relative abundance of the M − 56 ion for all different kinds of cannabinoids.

McLafferty Rearrangement—This type of rearrangement is found for the derivatives of cannabinol (VI). Substituents in the aryl nucleus have no influence on the elimination of one of the geminal methyl groups (M − 15). The relative contribution of the fragmentation of the side chain in the total fragmentation process is strongly dependent upon the alicyclic structure of the cannabinoid. α-Carbon methyl substitution in the side chain favors the side-chain fragmentation, as evidenced by the relative abundances of the formation of M − 56 in various cannabinoids: I, 0; II, 5; III, 1; IV, 5; *trans-para*-V*a*, 45; *trans-para*-V*b*, 30; VI, 5; α-methyl-*trans-para*-V*a*, 80; α,α-dimethyl-*trans-para*-V*a*, 100; α-methylhexahydrocannabinol (VIII*b*), 100; and α,α-dimethylhexahydrocannabinol (VIII*c*), 100.

A fragmentation triggered only by the aryl nucleus also should rupture the substituted methyl group and, therefore, substantially increase the intensity of the M − 15 fragment (XI). This effect is not observed, so it must be concluded that the McLafferty rearrangement is favored. This proton transfer then is not sterically hindered by one or two substituted methyl groups. An increase in the fragmentation of the side chain can only be measured when the competing fragmentation reactions remain the same.

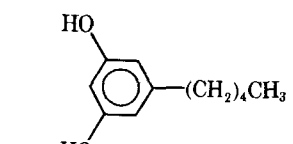

X

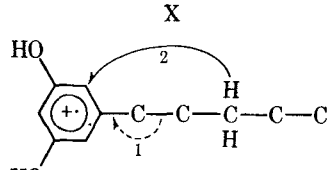

X*a*

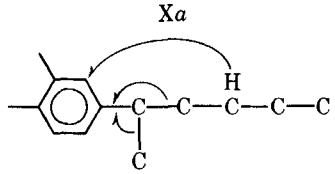

XI

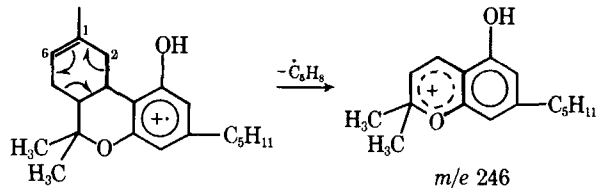

Scheme IV

Therefore, comparison of this fragmentation in all Δ⁶-tetrahydrocannabinol derivatives is possible (Table IV). The side chain of *tert*-butyl-Δ⁶-tetrahydrocannabinol is not fragmented at all, proving that the McLafferty rearrangement is the mechanism in the side-chain fragmentation. After the proton transfer, the carbon–carbon bond energy determines the fragmentation rate. There is no active participation of the alicyclic ring structure because saturation of the ring system does not alter the fragmentation pattern of the side chain (Table V).

Formation of Mass Fragment M − 68 (*m/e* 246)—Mass fragment *m/e* 246 is the result of a retro Diels–Alder reaction (Scheme IV). Loss of a geminal methyl group gives *m/e* 231, which has a pyran structure.

Is mass fragment *m/e* 246 a closed structure, as shown in Scheme IV, or an open structure resulting from the retro Diels–Alder reaction in, for instance, cannabidiol? With cannabidiol, the relative abundance of *m/e*

Table III—Formation of M − 43 in Different Isomers of Tetrahydrocannabinol (V) and Cannabidiol (IV) at 20 ev

Compound	Relative Intensity at 20 ev of *m/e* 271	*m/e* 285
Δ⁶-*cis-ortho*	6	
Δ⁶-*cis-para*	5	
Δ⁶-*trans-ortho*	60	
Δ⁶-*trans-para*	25	
Δ⁶-*trans-para-O*-methyl		25
Δ⁸-iso-*ortho*	12	
Δ⁸-iso-*para*	10	
Δ¹-*cis-ortho*	100	
Δ¹-*cis-para*	100	
Δ¹-*trans-ortho*	32	
Δ¹-*trans-para*	30	
Δ¹-*trans-para-O*-methyl		20
IV	1	

Table IV—Influence of Substitution of the Side Chain on the Formation of M − 56 in Δ⁶-*trans-para*-Tetrahydrocannabinol

Structure	C–C Bond	Relative Abundance of M − 56
–C–C–C–C–C	Secondary–secondary	45
–C(C)–C–C–C–C	Tertiary–secondary	80
–C(C)(C)–C–C–C–C	Quaternary–secondary	100
–C(C)–C	No McLafferty rearrangement	1

Table V—Influence of the Alicyclic Ring in Isomers of Tetrahydrocannabinol (V) and Hexahydrocannabinol (VIII*a*) on the Fragmentation of the Side Chain at 20 ev

Compound	Relative Abundance of M − 56
Δ⁶-*trans-para*-V	40
Δ⁶-*trans-para*-α-methyl-V	32
Δ¹-*trans-para*-V	28
Δ¹-*trans-para*-α-methyl-V	25
Δ⁶-*trans-ortho*-V	27
Δ⁶-*trans-ortho*-α-methyl-V	21
Δ¹-*trans-ortho*-V	40
Δ¹-*trans-ortho*-methyl-V	38
trans-ortho-VIII*a*	42
trans-ortho-VIII*b*	49
trans-para-VIII*a*	75
trans-para-VIII*b*	50

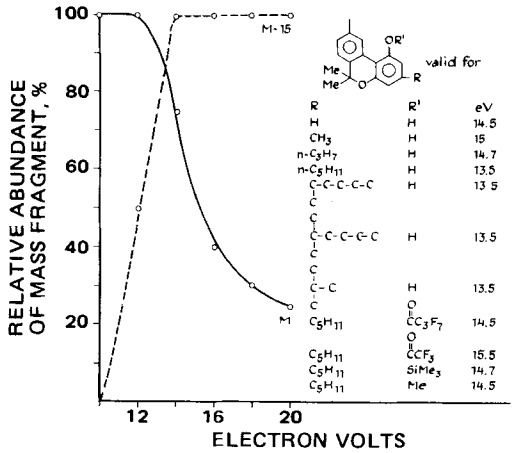

Figure 3—*Electron voltage mass fragmentograms of VI derivatives.*

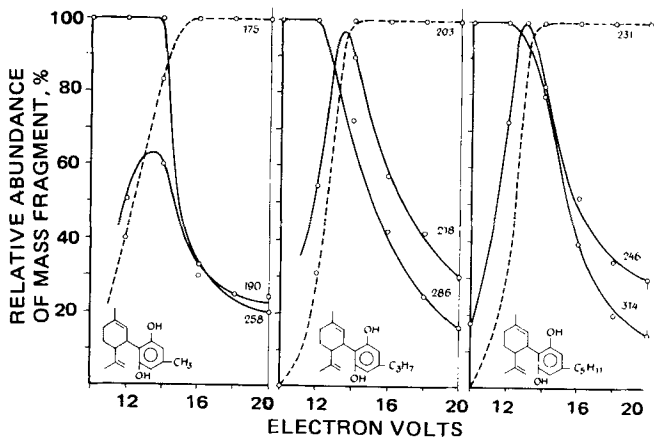

Figure 4—*Electron voltage mass fragmentograms of IV with different side chains occurring in natural hashish.*

246 shows a very characteristic rise and fall between 10 and 20 ev (Fig. 4), which is not seen in all other cannabinoids (6). The maximum relative abundance and, thus, the maximum concentration of the mass fragment occur at 14 ev. This finding may indicate that at the maximum the formation and fragmentation rates of *m/e* 246 are equal (Scheme V). In this case, ring closure must occur to make the loss of the geminal methyl group and the formation of *m/e* 231 possible.

This ring closure, prior to the loss of the methyl group, can be rationalized as follows. In cannabidiol, two aromatic hydroxyl groups are available for ring closure. If, due to methylation or to the *ortho*-position of the side chain, only one or no hydroxyl groups is available, there is no ring closure, followed by the loss of a geminal methyl group (Scheme VI). If two hydroxyl groups are available for ring closure, the maximum of *m/e* 246 is sharp at 14 ev when the relative abundance of *m/e* 246 is plotted against the electron energy used (Fig. 4 and Table VI).

If only one hydroxyl group is available such as in *o*-cannabidiol (Scheme VI) and *p*-methoxycannabidiol (Table VI), there is a broad maximum of *m/e* 246 or 260 of about 2–3 ev. It takes more energy for ring closure. When no hydroxyl groups are available for ring closure, then *m/e* 246 reaches its maximum at 14 ev and remains the base peak until at least 20 ev.

Thus, it may be concluded that about 4 ev is required for the retro Diels–Alder reaction only and that 2–3 ev is required for rotation of the aromatic moiety around axis 3–3′ and ring closure. A similar figure is obtained in the loss of a geminal methyl group from cannabinol and cannabinodiol (3). There is a difference of 5 between the electron volts in which the relative abundances of *m/e* 310 and 295 (M − 15) are equal (Fig. 3). As explained in the section on M − 15, this energy is required for ring closure of cannabinodiol.

When the two hydroxyl groups of cannabidiol are methylated, there is still a relatively high relative abundance of *m/e* 231. To form *m/e* 231, a methyl must first be lost from the methoxy group, followed by ring closure and loss of a geminal methyl group.

Besides the retro Diels–Alder mechanism, a one-step mechanism for the formation of *m/e* 231 was postulated (5). With cannabidiol, there is perfect competition between these two mechanisms, with the retro Diels–Alder being favored at low electron energy (14 ev). The retro Diels–Alder mechanism is preferred if the hydroxyl groups are methylated, thus preventing attack of the phenolic hydroxyl group at the double bond, and if the electron energy is too low for the one-step mechanism (5).

Formation of Mass Fragment *m/e* 243 (M − 15 − 56)—Mass fragment *m/e* 243 is formed from: (*a*) loss of a geminal methyl group (M − 15) followed by loss of the side chain (M − 56), or (*b*) loss of the side chain (M − 56) followed by loss of the geminal methyl group. From these two reaction sequences, it follows that fragments *m/e* 299, 258, and 243 are dependent upon each other. When the relative abundances of these three fragments are added together, they represent about 38% of the total ion intensity of V*b* and its isomers and 18% of the total ion current of V*a* derivatives. The difference in contribution of these two sequential mechanisms between V*a* and V*b* is mainly due to the loss of the geminal methyl group (10% in V*a* and 60% in V*b*) and hardly to side-chain fragmentation, which is substantiated by the ratios of the relative intensities of M − 15 to M and the relative abundances of the formation of M − 56. It must be kept in mind that M − 15 is partly originated from the loss of the C-7 methyl group in V*a* (5).

Formation of Mass Fragment *m/e* 231—Mass fragment *m/e* 231 appears to be important in the mass spectra of cannabinoids. Its relative intensity varies between 30 and 100%, depending upon the structure of the compound. There are several mechanisms for the formation of *m/e* 231, including a simple cleavage in cannabichromene (Scheme VII). The relative intensity of *m/e* 231 in cannabichromene becomes 100% at 12 ev. The intensity of the molecular ion *m/e* 314 decreases so rapidly that the formation of *m/e* 231 must be a relatively easy process (5). All other fragments have a relative abundance of below 5%. This rapid formation

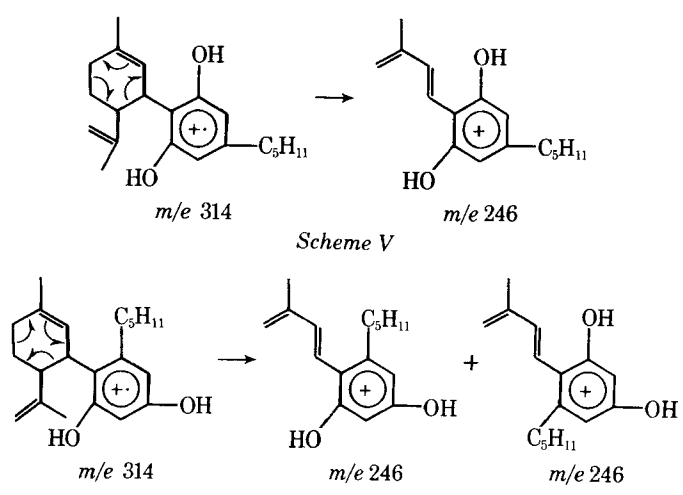

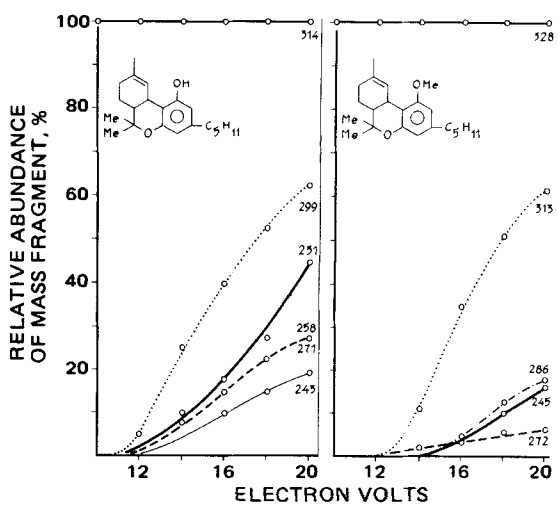

Figure 5—*Electron voltage mass fragmentograms of V*b *and its methyl ether. Note the difference in the formation rates of* m/e *231 and 245.*

Table VI—Mass Spectra of Cannabidiol Derivatives at 20 ev

Structure	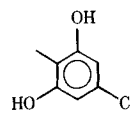	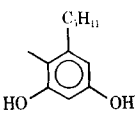	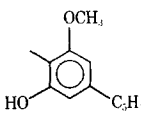	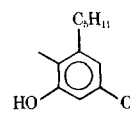	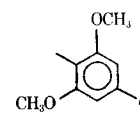	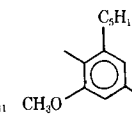	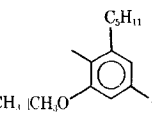
M	15	15	15	55	35	7	100
M − 15 (299)	1	1	1	15	5	5	75
M − 43 (271)	1	1	1	10	5	5	20
M − 56 (258)	5	5	5	15	5	5	7
(246)	30	60	85	100	100	100	10
(243)	1	1	1	35	5	5	25
(231)	100	100	100	45	25	20	30
Maximum of *m/e* 246 at	14 ev	14–16 ev	13–16 ev	14–20 ev	14–20 ev	14–20 ev	No ev
Ratio of *m/e* 246/231	0.30	0.60	0.85	2.22	4.0	5.0	0.33

of *m/e* 231 also occurs, in folded structures such as cannabicitran (I), cannabicyclol (II), and 7-hydroxycannabidiol (XII).

With increasing power of separation of the cannabinoids, more and more naturally occurring cannabinoids are discovered that show mass spectral behavior as described. The mechanism of the formation of *m/e* 231 in these complicated structures is not yet clear.

Compound V*a* is fragmented to *m/e* 231 by means of a retro Diels–Alder reaction (*m/e* 246), followed by the loss of a geminal methyl group (Scheme VIII). There is no influence from the free hydroxyl group itself nor from the side chain or the methylated hydroxyl group (Table VII) (7). There is also a one-step mechanism in the formation of *m/e* 231, and

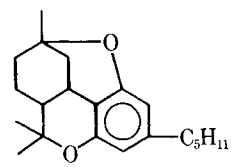

I

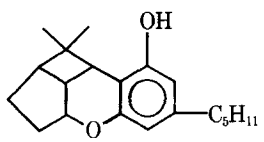

II

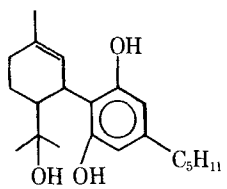

XII

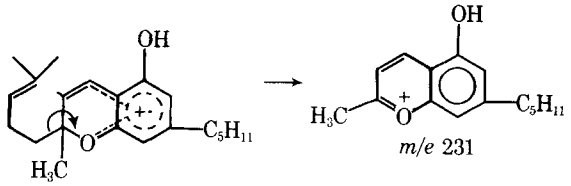

m/e 314 *m/e* 231

Scheme VII

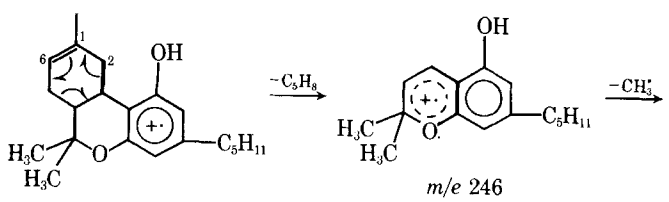

m/e 314 *m/e* 246

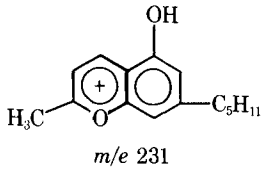

m/e 231

Scheme VIII

the two mechanisms are complementary (5).

In V*b*, a retro Diels–Alder reaction never results in the loss of fragment C_5H_8 and in *m/e* 246. Nevertheless, *m/e* 231 is found, so the delocalization of the 1–2-double bond (2, 4) must be possible, after which the one-step mechanism can take place.

The mass spectra of a series of derivatives and isomers of V*a* and V*b* reveal that more mechanisms are involved in the formation of *m/e* 231. Table VIII shows the mass spectra of *ortho*-V*b*, *para*-V*b*, and their methylated derivatives. Methylation of both *ortho*-V*b* and *para*-V*b* reveals that there is a sharp drop in the relative abundance of *m/e* 231 (*m/e* 245) in comparison with *ortho*- and *para*-V*b* (Fig. 5). This drop in intensity indicates that the phenolic proton is important for the generation of *m/e* 231 because it is not observed with V*a* and its methylated derivatives (7).

Strikingly, the mass spectrum of V*b*, deuterated at the phenolic hydroxyl group, shows complete retention of the deuterium label at the phenolic oxygen (5), in contradiction with the scheme given previously (7). This observation should mean that replacement of the phenolic hydrogen by a methyl group has no influence at the underlying mechanism of formation of mass fragment *m/e* 231. The mass spectra shown in Tables VII and VIII and those published elsewhere (5) are contradictory at first sight concerning the importance of the phenolic hydrogen. However, the retention of the phenolic proton observed in *m/e* 231 (5) and its influence on the formation of *m/e* 231 (7) can be rationalized satisfactorily by Scheme IX.

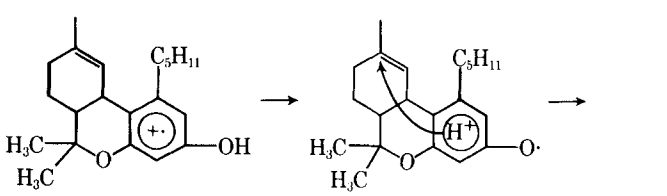

m/e 314

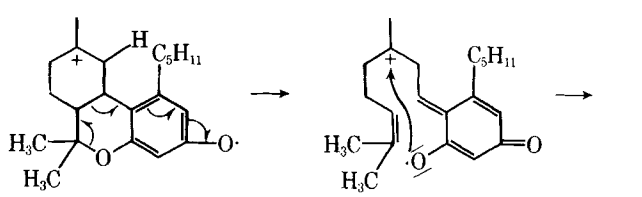

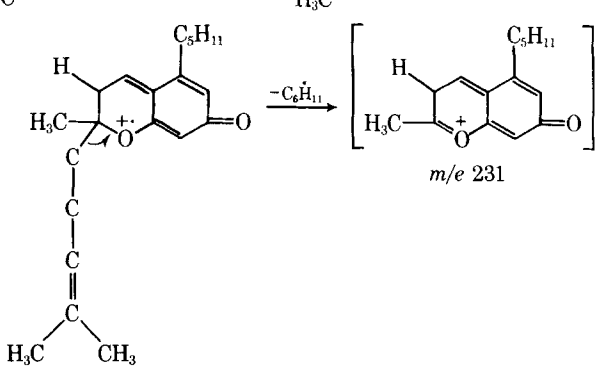

m/e 231

Scheme IX

Table VII—Partial Mass Spectra of *trans-ortho-* and *trans-para-*V*a* and Their Methyl Ethers at 20 ev

Fragment	*m/e*	*ortho-* V*a*	*ortho-* Methyl-V*a*	*para-* V*a*	*para-* Methyl-V*a*
M	314 (328)	100	100	100	100
M − 15	299 (313)	15	19	13	13
M − 43	271 (285)	60	70	25	22
M − 56	258 (272)	27	21	40	32
M − 68	246 (260)	10	5	17	22
	243 (257)	2	1	5	5
	231 (245)	65	60	60	75

Table VIII—Partial Mass Spectra of *trans-ortho-* and *trans-para-*V*b* and Their Methyl Ethers at 20 ev

Fragment	*m/e*	*ortho-* V*b*	*ortho-* Methyl-V*b*	*para-* V*b*	*para-* Methyl-V*b*
M	314 (328)	100	100	100	100
M − 15	299 (313)	55	77	63	62
M − 43	271 (285)	32	42	30	17
M − 56	258 (272)	25	31	27	26
M − 68	246 (260)	10	3	5	2
	243 (257)	10	5	20	5
	231 (245)	72	15	40	16

Table IX—Relative Abundance of *m/e* 231 (*m/e* 245) in the Mass Spectra of Several Tetrahydrocannabinol (V) Isomers Taken at 20 ev

Compound	Relative Abundance	Mechanism
*cis-ortho-*V*b*	11	Isomerization
*cis-para-*V*b*	12	Isomerization
*trans-ortho-O-*methyl-V*b*	15	Isomerization
*trans-para-O-*methyl-V*b*	16	Isomerization
*trans-ortho-*V*b*	72	Internal proton transfer plus isomerization
*trans-para-*V*b*	40	Internal proton transfer plus isomerization minus bond formation
*cis-ortho-*V*a*	100	Retro Diels–Alder
*cis-para-*V*a*	100	Retro Diels–Alder
*trans-ortho-*V*a*	65	Retro Diels–Alder
*trans-ortho-O-*methyl-V*a*	60	Retro Diels–Alder
*trans-para-*V*a*	60	Retro Diels–Alder
*trans-para-O-*methyl-V*a*	75	Retro Diels–Alder

The fragmentation of cannabinoids is strongly dependent upon ion source temperature (5) and electron voltage (6). Results obtained with, for instance, 10–20 (250°) and 70 (120°) ev may reveal a complete shift in the relative contribution of complementary mechanisms that are possible for the formation of *m/e* 231. Methylation of both *ortho-* and *para-*isomers of V*b* does not inhibit the formation of *m/e* 245 (*m/e* 231) completely. Since the relative abundance of *m/e* 245 is 15–16% in both isomers, the mechanism underlying this fragmentation must be the same: isomerization of the 1–2-double bond (Δ^1) to the 1–6-position (Δ^6) as suggested earlier (4) and visualized in Scheme X.

From the intensities of *m/e* 231 and 245, the spectra of *trans-ortho-*V*b* and its methyl ether (Table VIII), it can be calculated that about 80% of *m/e* 231 is generated by internal protonation at 20 ev and that the contribution of the isomerization of the double bond is 20%, assuming that

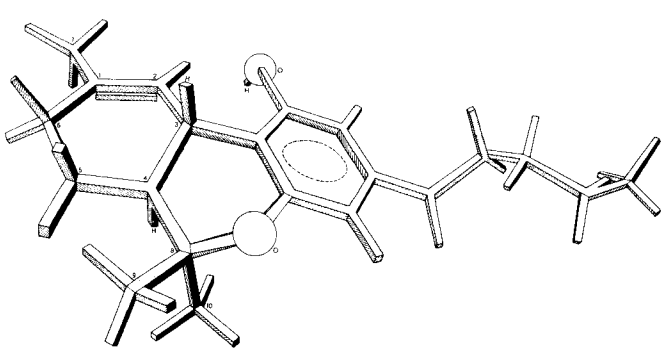

Figure 6—*Molecular structure of* trans-para-*V*b.

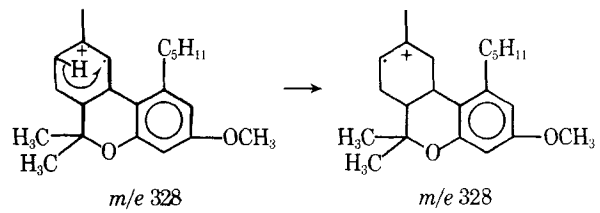

Scheme X

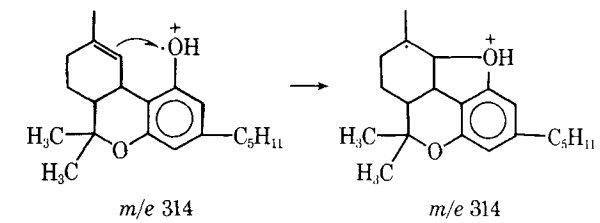

Scheme XI

the latter is not influenced by the methylation. After correction for the contribution of the isomerization (15%), the relative abundances of *m/e* 231 from *trans-ortho-* and *trans-para-*V*b* appear to be 57 and 25%, respectively. This difference is not observed for the relative intensities of *trans-ortho-* and *trans-para-*V*a* (Table VII).

This result implies that the internal protonation must be reduced, presumably due to the position of the phenolic hydroxyl group, because methylation does not influence the isomerization of the 1–2-double bond. A possible explanation is that the phenolic oxygen atom in *trans-para-*V*b* attacks the double bond, generating an ion with four fused rings. Whether this process occurs before or after phenolic proton transfer is not certain.

This bond destroys the 1–2-double bond, so that the phenolic proton can no longer be transferred to the alicyclic ring. This bond formation is impossible in *trans-ortho-*V*b* and *cis-para-* and *cis-ortho-*V*b* (11 and 12% of *m/e* 231, respectively) (Scheme XI). Therefore, in the formation of *m/e* 231 from *trans-para-*V*b*, three fragmentation pathways may be distinguished (at 20 ev): 35% internal protonation (plus a one-step mechanism), 20% isomerization of the 1–2-double bond (retro Diels–Alder plus a one-step mechanism), and 45% bond formation.

cis–trans*-Isomers of *ortho-* and *para-*V*b—In *cis-*V*a* and *cis-*V*b*, the alicyclic ring system is perpendicular to the aromatic system (Fig. 7, compare Fig. 6). Therefore, in the formation of *m/e* 231, there are no bond formation and internal shift. The relative abundances of *m/e* 231 derived from *cis-ortho-* and *cis-para-*V*b* are equal to those derived from the methyl ethers of *trans-ortho-* and *trans-para-*V*b* (Table IX).

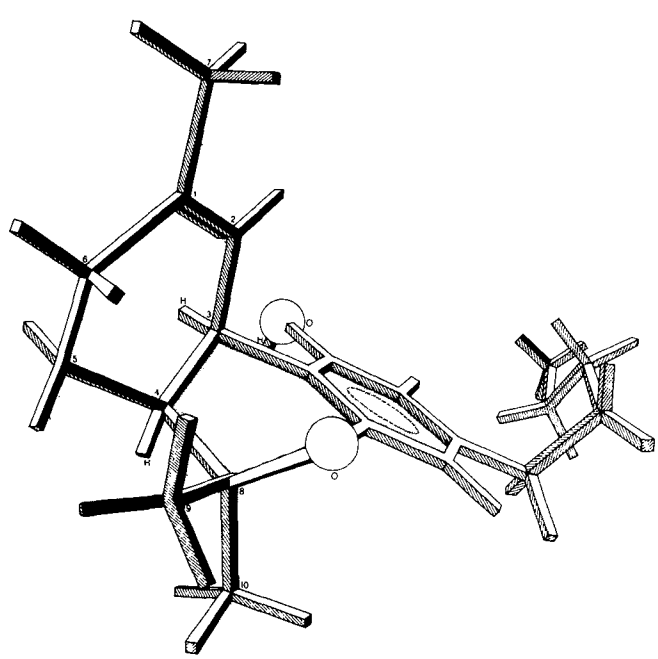

Figure 7—*Molecular structure of* cis-para-*V*b.

REFERENCES

(1) T. B. Vree, D. D. Breimer, C. A. M. van Ginneken, and J. M. van Rossum, *J. Chromatogr.*, **74**, 209 (1972).

(2) U. Claussen, H. W. Fehlhaber, and F. Korte, *Tetrahedron*, **22**, 3535 (1966).

(3) C. A. M. van Ginneken, T. B. Vree, D. D. Breimer, H. W. H. Thijssen, and J. M. van Rossum, in "Proceedings of the International Symposium on GC–MS, Isle of Elba, Italy, 1972," A. Frigerio, Ed., Tamburini, Milan, Italy, 1972, pp. 111–129.

(4) H. Budzikiewicz, R. T. Aplin, D. A. Lightner, C. Djerassi, R. Mechoulam, and Y. Gaoni, *Tetrahedron*, **21**, 1881 (1965).

(5) J. K. Terlouw, W. Heerma, P. C. Burgers, G. Dijkstra, A. Boon, H. F. Kramer, and C. A. Salemink, *ibid.*, **30**, 4243 (1974).

(6) T. B. Vree, D. D. Breimer, C. A. M. van Ginneken, and J. M. van Rossum, *J. Pharm. Pharmacol.*, **24**, 7 (1972).

(7) T. B. Vree and N. M. M. Nibbering, *Tetrahedron*, **29**, 3849 (1973).

ACKNOWLEDGMENTS AND ADDRESSES

Received March 8, 1976, from the *Department of Clinical Pharmacy, Radboudhospital, University of Nijmegen, Nijmegen, The Netherlands.*

Accepted for publication January 6, 1977.

The author thanks Dr. N. M. M. Nibbering, Laboratory for Organic Chemistry, University of Amsterdam, for discussing the fragmentation patterns.

Chronotropic and Cyclic Adenosine Monophosphate Response of Fetal Rat Heart in Organ Culture to Isoproterenol, Quinidine, and a Dysrhythmogenic Agent

CHARLES L. EYER ˣ and WILLIAM E. JOHNSON *

Abstract □ The fetal rat heart in organ culture was used to investigate rate changes by various cardioactive agents. Concomitantly, the effect of these pharmacologically induced rate changes on steady-state cyclic adenosine monophosphate levels was determined. Isoproterenol increased the fetal rat heart rate and cyclic adenosine monophosphate in a concentration-related fashion. Quinidine produced a concentration-related decrease in heart rate and no change in cyclic adenosine monophosphate level. The dysrhythmogenic agent produced concentration-related negative chronotropism in the fetal rat heart preparation and significant elevations in cyclic adenosine monophosphate at concentrations without chronotropic action. No correlation between chronotropic effect of a drug and cyclic adenosine monophosphate levels was observed.

Keyphrases □ Isoproterenol—effect on fetal rat heart rate related to levels of cyclic adenosine monophosphate, organ culture □ Quinidine—effect on fetal rat heart rate related to levels of cyclic adenosine monophosphate, organ culture □ Dysrhythmogenic agent—effect on fetal rat heart rate related to levels of cyclic adenosine monophosphate, organ culture □ Adenosine monophosphate, cyclic—levels in fetal rat heart in culture, related to rate changes caused by isoproterenol, quinidine, and dysrhythmogenic agent □ Cardioactive agents—isoproterenol, quinidine, and dysrhythmogenic agent, effect on fetal rat heart rate related to levels of cyclic adenosine monophosphate, organ culture □ Chronotropic effects—isoproterenol, quinidine, and dysrhythmogenic agent, fetal rat heart in culture, related to levels of cyclic adenosine monophosphate

Although the role of cyclic adenosine monophosphate (I) in cardiac inotropism has been investigated (1–3), there have been few attempts to study its role in cardiac chronotropism. The pacemaker region of the heart has been considered too small to be of use in determining adenyl cyclase activity, phosphodiesterase activity, or I levels (4). One study (5) demonstrated that chronotropic and inotropic cardiac responses to catecholamines were very similar with respect to dose dependence and sensitivity to β-blocking agents. This result might be considered as indirect evidence of a common mechanism for cardiac rate and force of contraction. Much evidence linking chronotropism and I comes from the study of cultured, beating heart cells isolated from the neonatal rat. The pulsation rate of these cells is accelerated by epinephrine, a known stimulator of adenyl cyclase (6). Dibutyryl I also imposes positive chronotropism in the same preparation (7).

Entire hearts from fetal mice can be cultured in such a manner as to beat consistently for a period of time (8). The cultured fetal mouse heart has been used as a pharmacological tool. Positive chronotropism was demonstrated using this preparation with liothyronine and levarterenol, and negative chronotropism was found with acetylcholine (9). The fetal mouse heart is capable of responding to these agents as early as the 12th day of gestation (10). The presence of the β-receptor was demonstrated in this same preparation (11).

In this study, the entire fetal rat heart was cultured and used to investigate the relationship between chronotropic effects and steady-state I levels in the myocardium. The fetal rat heart was chosen because it was larger than the mouse heart; this larger size facilitated tissue assay.

Three agents were chosen for pharmacological intervention. Isoproterenol was used for its positive chronotropic and β-adrenergic actions. Quinidine was employed for its negative chronotropic effect. Ethyl 3-ethoxycarbonyl-4-hydroxy-2*H*-1,2-benzothiazine-2-acetate 1,1-dioxide[1] (II), an experimental compound that produces ventricular fibrillation (12), was used to investigate the role of I in cardiac dysrhythmogenesis.

EXPERIMENTAL

Organ Culture—On their 19th day of gestation, pregnant Sprague–Dawley rats were sacrificed by cervical separation. The fetuses were quickly removed by Caesarean section.

The fetuses were decapitated, the chests were cut open, and the fetal hearts were removed as quickly and aseptically as possible. The hearts were trimmed of excessive connective tissue, rinsed in sterile saline, and

[1] McN-2165, McNeil Laboratories.

REFERENCES

(1) T. B. Vree, D. D. Breimer, C. A. M. van Ginneken, and J. M. van Rossum, *J. Chromatogr.*, **74**, 209 (1972).

(2) U. Claussen, H. W. Fehlhaber, and F. Korte, *Tetrahedron*, **22**, 3535 (1966).

(3) C. A. M. van Ginneken, T. B. Vree, D. D. Breimer, H. W. H. Thijssen, and J. M. van Rossum, in "Proceedings of the International Symposium on GC–MS, Isle of Elba, Italy, 1972," A. Frigerio, Ed., Tamburini, Milan, Italy, 1972, pp. 111–129.

(4) H. Budzikiewicz, R. T. Aplin, D. A. Lightner, C. Djerassi, R. Mechoulam, and Y. Gaoni, *Tetrahedron*, **21**, 1881 (1965).

(5) J. K. Terlouw, W. Heerma, P. C. Burgers, G. Dijkstra, A. Boon, H. F. Kramer, and C. A. Salemink, *ibid.*, **30**, 4243 (1974).

(6) T. B. Vree, D. D. Breimer, C. A. M. van Ginneken, and J. M. van Rossum, *J. Pharm. Pharmacol.*, **24**, 7 (1972).

(7) T. B. Vree and N. M. M. Nibbering, *Tetrahedron*, **29**, 3849 (1973).

ACKNOWLEDGMENTS AND ADDRESSES

Received March 8, 1976, from the *Department of Clinical Pharmacy, Radboudhospital, University of Nijmegen, Nijmegen, The Netherlands.*

Accepted for publication January 6, 1977.

The author thanks Dr. N. M. M. Nibbering, Laboratory for Organic Chemistry, University of Amsterdam, for discussing the fragmentation patterns.

Chronotropic and Cyclic Adenosine Monophosphate Response of Fetal Rat Heart in Organ Culture to Isoproterenol, Quinidine, and a Dysrhythmogenic Agent

CHARLES L. EYER ˣ and WILLIAM E. JOHNSON *

Abstract □ The fetal rat heart in organ culture was used to investigate rate changes by various cardioactive agents. Concomitantly, the effect of these pharmacologically induced rate changes on steady-state cyclic adenosine monophosphate levels was determined. Isoproterenol increased the fetal rat heart rate and cyclic adenosine monophosphate in a concentration-related fashion. Quinidine produced a concentration-related decrease in heart rate and no change in cyclic adenosine monophosphate level. The dysrhythmogenic agent produced concentration-related negative chronotropism in the fetal rat heart preparation and significant elevations in cyclic adenosine monophosphate at concentrations without chronotropic action. No correlation between chronotropic effect of a drug and cyclic adenosine monophosphate levels was observed.

Keyphrases □ Isoproterenol—effect on fetal rat heart rate related to levels of cyclic adenosine monophosphate, organ culture □ Quinidine—effect on fetal rat heart rate related to levels of cyclic adenosine monophosphate, organ culture □ Dysrhythmogenic agent—effect on fetal rat heart rate related to levels of cyclic adenosine monophosphate, organ culture □ Adenosine monophosphate, cyclic—levels in fetal rat heart in culture, related to rate changes caused by isoproterenol, quinidine, and dysrhythmogenic agent □ Cardioactive agents—isoproterenol, quinidine, and dysrhythmogenic agent, effect on fetal rat heart rate related to levels of cyclic adenosine monophosphate, organ culture □ Chronotropic effects—isoproterenol, quinidine, and dysrhythmogenic agent, fetal rat heart in culture, related to levels of cyclic adenosine monophosphate

Although the role of cyclic adenosine monophosphate (I) in cardiac inotropism has been investigated (1–3), there have been few attempts to study its role in cardiac chronotropism. The pacemaker region of the heart has been considered too small to be of use in determining adenyl cyclase activity, phosphodiesterase activity, or I levels (4). One study (5) demonstrated that chronotropic and inotropic cardiac responses to catecholamines were very similar with respect to dose dependence and sensitivity to β-blocking agents. This result might be considered as indirect evidence of a common mechanism for cardiac rate and force of contraction. Much evidence linking chronotropism and I comes from the study of cultured, beating heart cells isolated from the neonatal rat. The pulsation rate of these cells is accelerated by epinephrine, a known stimulator of adenyl cyclase (6). Dibutyryl I also imposes positive chronotropism in the same preparation (7).

Entire hearts from fetal mice can be cultured in such a manner as to beat consistently for a period of time (8). The cultured fetal mouse heart has been used as a pharmacological tool. Positive chronotropism was demonstrated using this preparation with liothyronine and levarterenol, and negative chronotropism was found with acetylcholine (9). The fetal mouse heart is capable of responding to these agents as early as the 12th day of gestation (10). The presence of the β-receptor was demonstrated in this same preparation (11).

In this study, the entire fetal rat heart was cultured and used to investigate the relationship between chronotropic effects and steady-state I levels in the myocardium. The fetal rat heart was chosen because it was larger than the mouse heart; this larger size facilitated tissue assay.

Three agents were chosen for pharmacological intervention. Isoproterenol was used for its positive chronotropic and β-adrenergic actions. Quinidine was employed for its negative chronotropic effect. Ethyl 3-ethoxycarbonyl-4-hydroxy-2*H*-1,2-benzothiazine-2-acetate 1,1-dioxide[1] (II), an experimental compound that produces ventricular fibrillation (12), was used to investigate the role of I in cardiac dysrhythmogenesis.

EXPERIMENTAL

Organ Culture—On their 19th day of gestation, pregnant Sprague–Dawley rats were sacrificed by cervical separation. The fetuses were quickly removed by Caesarean section.

The fetuses were decapitated, the chests were cut open, and the fetal hearts were removed as quickly and aseptically as possible. The hearts were trimmed of excessive connective tissue, rinsed in sterile saline, and

[1] McN-2165, McNeil Laboratories.

Table I—Formula of Medium Used to Culture Fetal Rat Hearts

Ingredient	Amount
Sodium chloride	116.40 mmoles
Potassium chloride	5.40 mmoles
Magnesium sulfate heptahydrate	0.80 mmole
Glucose	5.60 mmoles
Monobasic sodium phosphate monohydrate	1.00 mmole
Calcium chloride dihydrate	1.84 mmoles
Sodium bicarbonate	26.20 mmoles
Phenol red	20 mg
Human serum (not normally part of Earle's salts)	33 ml
Water	*q.s.* to 1000 ml
Penicillin G[a]	25 mg/200 ml
Streptomycin[a]	25 mg/200 ml
Hydrocortisone[a]	0.02 mg/200 ml
Insulin U-100 regular[a]	0.24 ml/200 ml

[a] Added just prior to use; the pH was adjusted to 7.40.

positioned carefully on stainless steel grids in 16 × 55-mm disposable petri dishes[2] as described by Wildenthal (13).

The culture medium was prepared from Earle's salts with various additives necessary to optimize survival of the organ culture (8) (Table I). Before being placed in the sterile petri dishes, the culture medium was sterilized by filtration through a 0.45-μm filter[3]. After removal, hearts were kept in their petri dishes in a laminar flow hood until transferred to an incubation chamber.

The organ cultures were placed in a humidified incubation chamber. The chamber was then filled with 95% O_2–5% CO_2, sealed, and incubated at 37° for 48 hr to allow the heart rhythm to stabilize.

After 48 hr of incubation, the culture medium was exchanged for freshly prepared medium. The hearts were equilibrated for at least 2 hr in the fresh medium, and each culture was then transferred to a constant-temperature chamber set at 37° (Fig. 1). The chamber was filled with 95% O_2–5% CO_2 and sealed. After 5 min for temperature equilibration, the hearts were observed with the aid of a dissecting microscope. The number of ventricular contractions was recorded for 1 min. The atrial rate and any anomalies of rhythm also were recorded. Hearts performing at a ventricular rate between 30 and 80 beats/min were retained for study, and the remainder was discarded.

After the predrug rate was recorded, the culture medium was exchanged for fresh medium containing a given drug concentration. The heart preparation was then returned to the incubation chamber for 90 min. (All drugs used in this study produced recognizable pharmacological effects within 45 min, and the effect was consistent for more than 120 min.) After this second incubation period, the petri dish was returned to the 37° incubation chamber and gassed with 95% O_2–5% CO_2. After equilibration for 5 min, the ventricular contractions were again counted for 1 min. Immediately after the second count, the heart was frozen in liquid nitrogen, weighed, and homogenized in 5 ml of ice-cold 6% trichloroacetic acid.

The homogenates were centrifuged at 2500×*g* in a clinical centrifuge for 20 min. The supernates were transferred to 50-ml screw-capped glass tubes and extracted four times with 20 ml of water-saturated ether. The samples were then placed in boiling water, the ether was boiled off, and the samples were stored at −20° until a I assay could be performed (14). The precipitated protein was saved and used to determine the total amount of protein in each heart.

Changes in heart rate were calculated as the ratio of the rate before incubation with the drug (predrug rate) to the rate after 90 min of drug incubation (postdrug rate). This value, R, would be greater than one if the heart rate increased after drug exposure and less than one if the heart rate decreased. Four to eight fetal hearts were generally used for each drug concentration.

Control hearts were randomly selected from various litters, and their heart rates were recorded in the same manner as the drug-treated hearts. Controls were incubated for 2 hr in fresh medium, counted for 1 min, incubated for 90 min, and again counted for 1 min to obtain an R value for each heart. The R values obtained for each concentration of a given drug were statistically compared with the control values and with each other.

Assay for I—Assay for I was performed by the saturation assay method of Brown *et al.* (15). The assay relies upon competition between tritium-labeled I and unlabeled I for binding sites in a protein fraction isolated from beef adrenals.

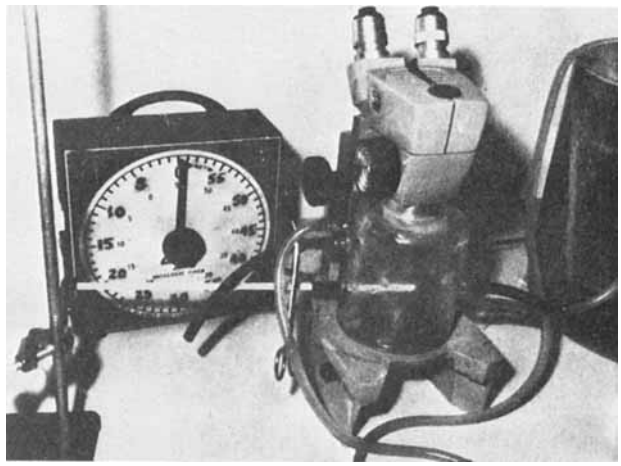

Figure 1—*Constant-temperature observation apparatus. Dark hoses are the gas inlet and outlet, and light hoses are the water jacket inlet and outlet. The thermometer lies across the face of the clock. The water bath is on the extreme right. A Spencer A/O binocular dissecting microscope is inserted through the top of the chamber.*

Assay tubes (50 × 10 mm) were prepared by the addition of 0.1 ml of tritiated I[4] (100,000 cpm/ml), 0.1 ml of sample or standard, and 0.3 ml of the appropriate dilution of binding protein. A standard curve was constructed using known concentrations of unlabeled I from 0.25 to 8 pmoles/tube. All standards and samples were determined in duplicate. Tubes were incubated at 4° for 12–16 hr in a shaker at low speed.

At the end of the incubation period, 0.5 ml of saturated ammonium sulfate was added to each tube to precipitate the binding protein (16). The tubes were immediately centrifuged at 60,000×*g* for 15 min in an ultracentrifuge. A 0.5-ml portion of supernate was transferred to a scintillation vial containing 10 ml of scintillation fluid[5]. All samples were counted to 50,000 counts in a liquid scintillation counter[6]. Since counting efficiency was essentially constant, ratios of counts per minute were used throughout. The ratio of counts per minute in each sample to the counts per minute in samples containing no unlabeled I was calculated and called the "fraction unbound."

A standard curve of the fraction unbound *versus* log picomoles per tube was constructed. Sample values were obtained by extrapolation from the standard curve.

The protein content of the fetal heart was determined by the method of Lowry *et al.* (17). Levels of I were expressed as picomoles per milligram of protein.

Statistical Procedures—Means and standard errors were calculated for each treatment group. The pooled Student t test was used to compare drug-treated values with their respective controls. Analysis of variance and Duncan's new multiple range test were employed to compare each value in an experiment with the other values in that experiment (18).

RESULTS AND DISCUSSION

Levels of I in the fetal hearts not treated with any drug were 25.88 ± 2.50 pmoles/mg of protein or 1.69 ± 0.31 nmoles/g of fresh weight. These values are about the same as reported values of 1.42 nmoles/g of fresh weight obtained (19) with the protein kinase assay in the adult rat ventricle. However, experimental values (20) with the bioluminescent assay were as high as 2.7 nmoles/g of fresh weight.

Quinidine sulfate decreased the heart rate significantly from the control value ($p < 0.05$) at concentrations of 1×10^{-4} M and greater (Table II). The response to the 5×10^{-6} M concentration was not significantly different from those of the 1×10^{-5} M concentration. At a concentration of 1×10^{-4} M, two hearts out of five stopped beating. The mean heart rate at this highest concentration was depressed to approximately 40% of the predrug level when the two hearts that stopped beating were included, and this value was significantly different from all other concen-

[2] Falcon 1007.
[3] Millipore type HA.
[4] New England Nuclear, 22.1 Ci/mM.
[5] PCS, Amersham/Searle.
[6] Packard Tri-Carb.

Table II—Effect of Quinidine Sulfate on Fetal Rat Heart Rate and I Level[a]

Concentration, M	n	R^b	R Mean Comparisons[c]	I, pmoles/mg of Protein	I Mean Comparisons[c]
Control	6	1.005 ± 0.044	α	25.88 ± 2.50	α, β
5×10^{-6}	5	0.939 ± 0.104	α, β	16.85 ± 4.09	β
1×10^{-6}	8	0.818 ± 0.053	β, γ	19.51 ± 4.26	β
5×10^{-5}	9	0.666 ± 0.067	γ	30.68 ± 3.52	α
1×10^{-4}	5[d]	0.405 ± 0.168	—	14.22 ± 1.80	β

[a] Values of R and I represent the mean ± SE. Sample size = n. [b] R = postdrug rate/predrug rate. [c] Treatment means that contain a common Greek letter were not significantly different from each other at the 5% level of significance. [d] Two hearts stopped beating after a concentration of 1×10^{-4} M quinidine sulfate.

trations. Levels of I were not significantly different from controls at any of these concentrations.

Although quinidine can prevent arrhythmias without altering heart rate, it produces negative chronotropism at less than toxic doses (21). At concentrations of 1–5 × 10^{-6} M, quinidine decreased the pulsation rate of cultured cells from the neonatal rat ventricle (22). In humans, blood levels greater than 2.5 × 10^{-5} M generally produced negative chronotropism (23). This result correlates well with the negative chronotropic response to quinidine observed in this study. A concentration of 5 × 10^{-5} M quinidine sulfate, equivalent to 1 × 10^{-5} M quinidine, was the lowest concentration of quinidine that produced significant negative chronotropism.

With use of analysis of variance, no I levels in the drug-treated group were significantly different from the control value. However, at the 1 × 10^{-4} M concentration, two hearts stopped beating at some time during the 90-min incubation. These two hearts had I levels of 19.30 and 17.61 pmoles/mg of protein as compared with 12.90, 10.95, and 10.33 pmoles/mg of protein for the three hearts still beating. Since it is not known when in this 90-min period the hearts stopped beating, the possibility that these two values were elevated after the hearts stopped beating must be considered.

Namm and Mayer (24) demonstrated that changes in I levels in dog and rat hearts were detectable only when the tissue could be frozen rapidly. The biopsy method could not detect changes in I levels because the tissue was not frozen quickly enough. Schmidt *et al.* (25) found that the I levels in brain tissue increased severalfold when rat brains were allowed to stand after decapitation before denaturation. From these studies, it seems reasonable that I levels could fluctuate considerably when the tissue is dying. However, Sutherland *et al.* (1) demonstrated that cardiac tissue retains its I responses to hormones and drugs even after it is no longer beating.

When the 1 × 10^{-4} M concentration of quinidine sulfate was compared with the control value for I by means of the Student t test, a significant difference was revealed ($p < 0.01$). The possibility that a high concentration of quinidine may lower I levels cannot be ignored. However, this concentration is lethal to about half of the hearts and probably this decrease in I levels is of no importance in the clinical usage of this drug.

Isoproterenol hydrochloride increased the heart rate significantly ($p < 0.05$) from the control value at concentrations of 5 × 10^{-6} and 1 × 10^{-5} M (Table III). At the highest concentration, the heart rate was approximately 1.7 times the predrug rate. The heart rate was gradually increased over the concentration range of 5 × 10^{-8}–1 × 10^{-5} M, but only the highest two concentrations caused significantly different rates from the control value at the 95% level of confidence. The rate at 5 × 10^{-8} M was significantly different from the rate at 1 × 10^{-5} M only, and rates at 1 × 10^{-7} and 5 × 10^{-7} M were not significantly different from any other rates at the 95% level of confidence.

Table III—Effect of Isoproterenol Hydrochloride on Fetal Rat Heart Rate and I Level[a]

Concentration, M	n	R^b	R Mean Comparisons[c]	I, pmoles/mg of Protein	I Mean Comparisons[c]
Control	6	1.005 ± 0.044	α	25.88 ± 2.50	α
5×10^{-8}	5	1.258 ± 0.126	α, β	36.93 ± 4.53	α
1×10^{-7}	4	1.306 ± 0.157	α, β, γ	36.94 ± 5.42	α
5×10^{-7}	6	1.342 ± 0.069	α, β, γ	34.28 ± 5.00	α
5×10^{-6}	6	1.698 ± 0.255	β, γ	41.65 ± 6.09	α
1×10^{-5}	8	1.741 ± 0.149	γ	66.35 ± 9.42	—

[a] Values of R and I represent the mean ± SE. Sample size = n. [b] R = postdrug rate/predrug rate. [c] Treatment means that contain a common Greek letter were not significantly different from each other at the 5% level of significance.

Table IV—Effect of II on Fetal Rat Heart Rate and I Level[a]

Concentration, M	n	R^b	R Mean Comparisons[c]	I, pmoles/mg of Protein	I Mean Comparisons[c]
Control	6	1.005 ± 0.044	α	25.88 ± 2.50	—
1×10^{-6}	8	0.850 ± 0.030	α, β	67.68 ± 9.12	α
5×10^{-6}	7	0.711 ± 0.083	β	74.80 ± 16.24	α
5×10^{-5}	8	0.539 ± 0.068	γ	54.86 ± 3.80	α
1×10^{-4}	7	0.452 ± 0.064	γ	119.51 ± 42.46	α

[a] Values of R and I represent the mean ± SE. Sample size = n. [b] R = postdrug rate/predrug rate. [c] Treatment means that contain a common Greek letter were not significantly different from each other at the 5% level of significance.

Although the I levels gradually increased with increasing concentrations of isoproterenol, only values at 1 × 10^{-5} M were significantly different from values at any other concentration ($p < 0.05$). At this highest concentration, the I level was 66.35 ± 9.42 pmoles/mg of protein, as compared to 25.88 ± 2.50 pmoles/mg of protein for the control value.

Isoproterenol had cardioaccelerator properties in laboratory animals and humans (26). The observed 74% increase in rate (Table III) is close to the 60% increase in heart rate found by Wollenberger (6) in response to β-adrenergic stimulation by epinephrine in isolated rat pacemaker cells. In the organ-cultured mouse heart, isoproterenol promoted an overall increase in rate (11). The same preparation showed concentration-related positive chronotropism in response to 10^{-8}–10^{-6} M epinephrine and levarterenol. These responses can be blocked by propranolol, which implicates β-adrenergic receptors. Concentrations of 10^{-7} and 10^{-6} M isoproterenol also increased heart rate 20 and 50%, respectively, in the cultured fetal mouse heart (27). These values compare favorably with the data in Table III, which show approximately a 34% increase in rate at 5 × 10^{-7} M and a 70% increase at 5 × 10^{-6} M isoproterenol.

Isoproterenol, 10^{-8} M, previously produced approximately a 100% increase in the I level of the electrically driven, isolated perfused adult rat heart (28). As perfusion without drug continued, the level returned to the control value within 4 min. In the same study, 10^{-7} M isoproterenol produced the same degree of increase in I levels. The same effects were shown with epinephrine in isolated rat and rabbit adult perfused hearts (1, 29). Continuous infusion of epinephrine produced a rapid rise in I followed by a decrease to a level approximately three times higher than the control value in adult perfused rat hearts (30).

Table III shows a similar tripling effect in the present system when the fetal rat hearts were incubated for 90 min in the presence of a sufficiently high concentration of isoproterenol. The apparent lack of effect of lower concentrations of isoproterenol seen in this study when compared with the results of Øye and Langslet (28) was related possibly to the observation time after the onset of treatment. These investigators gave isoproterenol as a single dose, and the I levels rapidly returned to the control level. The initial rise caused by a low concentration of isoproterenol in this study perhaps could have disappeared before the 90-min observation time. The I level for 5 × 10^{-6} M isoproterenol was not significantly different from the control value when analysis of variance was employed but was significantly different from the control value at the 5% level of significance when the two means were compared using the Student t test.

The rise in I levels following isoproterenol administration indicates that the β-adrenergic receptor subunit on the adenyl cyclase is present at Day 19. Clark *et al.* (31) found this to be true in the fetal rat heart as early as Day 16, although the glucagon receptor was not present until 28 days postpartum.

Compound II decreased the heart rate significantly from the control value at concentrations of 5 × 10^{-6} M and higher (Table IV). At the highest concentration of 1 × 10^{-4} M, the heart rate was depressed to approximately 45% of the predrug level. The heart rate at 5 × 10^{-6} M was not significantly different from the rate at 1 × 10^{-6} M but was significantly different from the control value and from the rates at higher concentrations. Rates at concentrations of 5 × 10^{-5} and 1 × 10^{-4} M were significantly different from rates at all other concentrations but were not significantly different from each other. At no time during the observation of the effects of II on the heart rate was any evidence of arrhythmias, other than bradycardia, detected. Ventricular tachycardia, fibrillation, and ectopic foci were never present when the fetal rat hearts were treated with II.

Levels of I were significantly elevated above the control level at all concentrations of II. There was no significant difference in the I levels between the drug-treated groups.

Intravenous administration of II to anesthetized adult dogs consis-

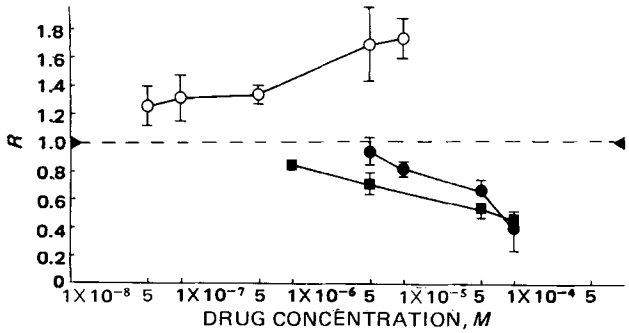

Figure 2—*Effects of quinidine sulfate (●), isoproterenol hydrochloride (○), and II (■) on fetal rat heart rate. The broken line represents the mean control value, and the base of the triangle is equal to the standard error for the control value. Vertical bars represent ± 1* SE.

tently produced a prolongation of the QRS interval (slowing the spread of action potential) and ventricular ectopic beats. These events often terminated in ventricular tachycardia and fibrillation (12). The same effect was shown in the isolated adult rat heart[7]. The fetal rat heart, however, showed only a negative chronotropic response to II. Even at the highest concentration, the fetal rat hearts showed no evidence of tachycardia, ectopic foci, or fibrillation. Cardiac standstill was not observed for any heart treated with II. The variation in the *R* values obtained at various concentrations of II was considerably less than with any other drug treatment.

In contrast, the variation in the fetal heart I levels at a given concentration of II was generally greater than for either quinidine or isoproterenol. Compound II elevated I levels above that of the control at all concentrations. However, the variation in the data was such that no statistically significant difference could be detected between I levels at any drug concentration.

As shown in Figs. 2 and 3, comparison of the effects of isoproterenol (increased rate and increased I concentration), quinidine (decreased rate and no change in I level), and II (decreased rate and increased I level) shows no correlation between changes in the heart rate and the level of I in the entire heart after a 90-min incubation. When the heart rate is altered pharmacologically, certain possibilities exist in which I could still be the mediator of chronotropism. A rapid flux of I could alter some other cellular component, *e.g.*, membrane phosphorylation, and this condition

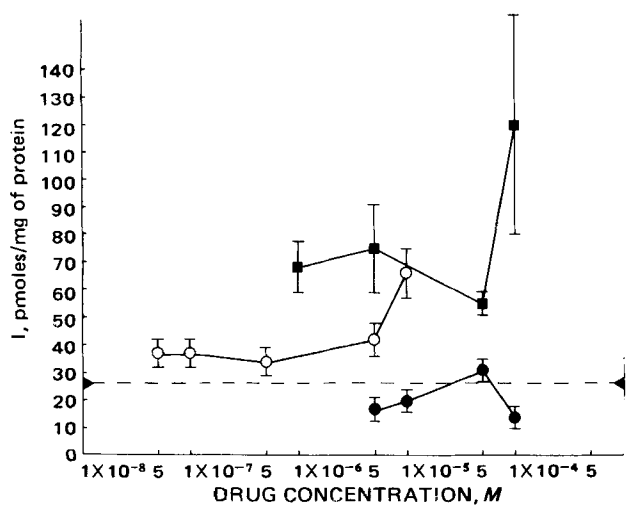

Figure 3—*Effects of isoproterenol hydrochloride (○), quinidine sulfate (●), and II (■) on I levels in the fetal rat heart. The broken line represents the mean control value, and the base of the triangle is equal to the standard error for the control value. Vertical bars represent ± 1* SE.

[7] Unpublished data.

could determine the rate that would still be in effect when the I level had returned to the control value. A separate cellular pool of I responsible for altering the heart rate could be changed without a similar change in the net cellular I level. Epstein *et al.* (2) postulated such separate cellular pools for the regulation of myocardial contractility and glycogenolysis. If changes in I levels were necessary only in pacemaker cells to alter the heart rate, this change could also be masked by the total I concentration of the heart.

REFERENCES

(1) E. W. Sutherland, G. A. Robison, and R. W. Butcher, *Circulation*, **37**, 279 (1968).

(2) S. E. Epstein, G. S. Levey, and C. L. Skelton, *ibid.*, **43**, 437 (1971).

(3) B. G. Benefy, *Br. J. Pharmacol.*, **43**, 757 (1971).

(4) A. Wollenberger and E. G. Krause, *Proc. 5th Int. Congr. Pharmacol.*, **5**, 170 (1972).

(5) A. J. Kaumann and J. R. Blinks, *Fed. Proc.*, **26**, 401 (1967).

(6) A. Wollenberger, *Circ. Res. Suppl.*, **15**, 184 (1964).

(7) E. G. Krause, W. Halle, E. Kallabis, and A. Wollenberger, *J. Mol. Cell. Cardiol.*, **1**, 1 (1970).

(8) K. Wildenthal, *ibid.*, **1**, 101 (1970).

(9) K. Wildenthal, *Am. J. Physiol.*, **221**, 238 (1971).

(10) K. Wildenthal, *J. Clin. Invest.*, **52**, 2250 (1973).

(11) S. R. Armstrong and D. B. Longmore, *Nature*, **243**, 350 (1973).

(12) T. P. Pruss, *Toxicol. Appl. Pharmacol.*, **14**, 1 (1969).

(13) K. Wildenthal, *J. Appl. Physiol.*, **30**, 53 (1971).

(14) H. Wombacher and F. Korber, *Z. Klin. Chem. Klin. Biochem.*, **10**, 206 (1972).

(15) B. L. Brown, J. Abano, R. P. Ekins, A. M. Sgerzi, and W. Tamion, *Biochem. J.*, **121**, 561 (1971).

(16) B. Rabinowitz and J. Katz, *Clin. Chem.*, **19**, 312 (1973).

(17) O. H. Lowry, N. J. Rosebrough, A. L. Farr, and R. J. Randall, *J. Biol. Chem.*, **193**, 265 (1951).

(18) R. G. D. Steel and J. H. Torrie, "Principles and Procedures of Statistics," McGraw-Hill, New York, N.Y., 1960.

(19) J. W. Kebabian, J. F. Kuo, and P. Greengard, in "Advances in Cyclic Nucleotide Research," vol. 2, Raven, New York, N.Y., 1972, p. 131.

(20) M. S. Ebadi, in *ibid.*, p. 89.

(21) B. F. Hoffman and J. T. Bigger, in "Drill's Pharmacology in Medicine," 4th ed., McGraw-Hill, New York, N.Y., 1971, p. 837.

(22) W. Halle, *Naunyn-Schmiedebergs Arch. Pharmakol. Exp. Pathol.*, **256**, 322 (1967).

(23) E. K. Chung, *Postgrad. Med.*, **53**, 107 (1973).

(24) D. H. Namm and S. E. Mayer, *Mol. Pharmacol.*, **4**, 61 (1968).

(25) M. J. Schmidt, D. E. Schmidt, and G. A. Robison, *Science*, **173**, 1142 (1971).

(26) I. R. Innes and M. Nickerson, in "The Pharmacological Basis of Therapeutics," L. S. Goodman and A. Gilman, Eds., Macmillan, New York, N.Y., 1970, p. 499.

(27) K. Wildenthal, *J. Pharmacol. Exp. Ther.*, **190**, 272 (1974).

(28) I. Øye and A. Langslet, *Adv. Cyclic Nucleotide Res.*, **1**, 291 (1972).

(29) G. A. Robison, R. W. Butcher, and E. W. Sutherland, *Mol. Pharmacol.*, **1**, 168 (1965).

(30) J. R. Williamson, *J. Biol. Chem.*, **241**, 5026 (1966).

(31) C. M. Clark, B. Beatty, and D. O. Allen, *J. Clin. Invest.*, **52**, 1018 (1973).

ACKNOWLEDGMENTS AND ADDRESSES

Received November 1, 1976, from the *School of Pharmacy, University of Montana, Missoula, MT 59812.*

Accepted for publication January 6, 1977.

The authors are indebted to McNeil Laboratories for supplying the dysrhythmogenic agent.

* Present address: College of Pharmacy, Washington State University, Pullman, WA 99163.

ˣ To whom inquiries should be directed.

Pharmacokinetics of Mercaptopurine

LAMBROS TTERLIKKIS [x], EDITH ORTEGA, RALPH SOLOMON, and JAMES L. DAY

Abstract □ The anatomical distribution of mercaptopurine was investigated in rats at dose levels of 2.5 and 25 mg/kg iv. The plasma and tissues were analyzed by radioisotopic dilution and spectrofluorometric techniques. The tissue–plasma ratios were: liver–plasma, ≃4.0; kidney–plasma, ≃2.4; spleen–plasma, ≃1.7; muscle–plasma, ≃1.4; gut lumen–plasma, ≃3; and bone marrow–plasma, ≃0.35. Physiologically based pharmacokinetic models were developed to simulate concentrations of mercaptopurine in plasma, kidneys, liver, muscle, spleen, bone marrow, and gut lumen. The agreement between experimental and predicted plasma and tissue profiles was good. Human plasma levels of mercaptopurine were predicted and, when compared with clinical data, demonstrated reasonable agreement.

Keyphrases □ Mercaptopurine—pharmacokinetics in rats □ Pharmacokinetics—mercaptopurine in rats □ Distribution, biological—mercaptopurine in rats □ Antineoplastic agents—mercaptopurine, pharmacokinetics in rats

Recently, the application of physiological pharmacokinetics to cancer chemotherapeutic agents has made possible the quantitative description of the distribution and elimination of methotrexate (1–3), cytarabine (4, 5), and doxorubicin (6). Physiological pharmacokinetics were developed previously (1–3) using a pharmacokinetic model that simultaneously predicts the kinetics of drug distribution in blood, organs, and tissues of pharmacological interest. In contrast, conventional pharmacokinetic models correlate the kinetics of data of drug concentrations in blood by employing one or more exponential terms. Each exponential term represents one compartment. The coefficients and rate constants in pharmacokinetic equations are then determined from curve-fit parameters (7, 8).

Classical pharmacokinetics (conventional) were applied to the study of the clinically useful antineoplastic agent, mercaptopurine (9, 10), in humans. Coffey *et al.* (9) demonstrated that single intravenous doses of mercaptopurine in combination with allopurinol do not alter the plasma mercaptopurine level in humans. Thus, allopurinol appears to have little effect on the pharmacokinetics of large intravenous doses of mercaptopurine in humans. However, lower oral doses of mercaptopurine, which are commonly administered in the clinic concurrently with allopurinol, are significantly potentiated. Thus, the pharmacokinetics of orally and intravenously administered mercaptopurine appear to differ (11).

Donelli *et al.* (12) compared the disposition of mercaptopurine in rats and mice bearing different experimental tumors with the disposition of mercaptopurine in tumor-free animals. The plasma mercaptopurine levels were analyzed by a spectrofluorometric method, and the tissue levels were measured by UV spectroscopy. Substantial mercaptopurine concentrations were observed in peripheral organs, and it was concluded that there was no significant difference between the mercaptopurine concentrations in tissues of normal rats and mice compared to those bearing Walker carcinosarcoma.

Mercaptopurine has been used extensively in the treatment of acute human leukemia (13, 14). In the treatment of acute lymphocytic leukemia, it has been used in combination with prednisone or other agents in three- and four-drug combinations and was an effective remission-inducing therapy. Rapidly multiplying cells are more susceptible to mercaptopurine than are stationary cell populations (15, 16), which is reflected in the toxicity of mercaptopurine toward the proliferating elements of bone marrow, intestine, and spleen.

The present work is an attempt to establish quantitative prediction of mercaptopurine in several tissues of rats and correlation of the predictive values with experimental data.

EXPERIMENTAL

Male Sprague–Dawley rats, 190–210 g, had unrestricted access to food and water before experiments. The concentration of mercaptopurine in various rat tissues was obtained as follows.

8-^{14}C-Mercaptopurine was mixed with nonlabeled mercaptopurine and dissolved in 1 *N* NaOH. The resulting solution was diluted with normal saline. Each animal received 0.5 ml of mercaptopurine (4–10 μCi/kg iv). The mercaptopurine doses ranged from 2.5 to 25 mg/kg.

The animals were decapitated at selected times after mercaptopurine injection, and tissue samples were collected. The entire small intestine minus the expressible contents was homogenized, as were the liver and other tissues. The bone marrow was removed from two femurs by cracking and aspirating the contents into a tared micropipet. The tissue homogenates and plasma were centrifuged at 9000 rpm; radioactivity levels in aliquots of the resulting supernates were determined by scintillation counting. The counts were converted to micrograms of drug per unit of tissue after appropriate correction for quenching, volumes, and tissue weights.

Typically, radioactive contents of bone marrow are determined by counting the products of whole bone marrow combustion. Since a combustion apparatus was unavailable, a biochemical extraction method employing various solubilizing agents was utilized. However, consistent and reliable results could not be obtained.

Plasma mercaptopurine levels also were determined according to the spectrofluorometric method of Finkel (17). The method is based on the conversion of mercaptopurine to purine 6-sulfonate by oxidation with permanganate. The purine 6-sulfonate formed by the reaction is then determined spectrofluorometrically.

Pharmacokinetic Model—Scheme I shows the flow diagram and relevant compartments in the mathematical model. Bischoff *et al.* (18) previously gave a detailed mathematical description. The model is based on mass balance equations for each compartment. A typical mass balance equation is given here for the kidney:

$$V_K \frac{dC}{dt} = Q_K C_P - Q_K \frac{C_K}{R_K} - K_K \frac{C_K}{R_K} \qquad \text{(Eq. 1)}$$

where $V_K\, dC/dt$ is the accumulation of drug in kidney, $Q_K C_P$ is the rate of inflow with blood, $Q_K C_K/R_K$ is the rate of outflow with blood, and $K_K C_K/R_K$ is the clearance by the kidney.

The balance equation for the plasma is:

$$V_P \frac{dCp}{dt} = Mg(t) + \left(Q_K \frac{C_L}{R_L} + Q_K \frac{C_K}{R_K} + Q_{BM} \frac{C_{BM}}{R_{BM}} + Q_{SP} \frac{C_{SP}}{R_{SP}} + Q_M \frac{C_M}{R_M}\right) - (Q_L + Q_K + Q_{BM} + Q_{SP} + Q_M)C_P \qquad \text{(Eq. 2)}$$

where *P, L, K, BM, SP,* and *M* signify plasma, liver, kidney, bone marrow, spleen, and muscle, respectively; *V* is the compartment size (milliliters); *C* is the concentration (micrograms per milliter); *Q* is the blood flow rate to the compartment (milliliters per minute); K_K is the clearance (milli-

Table I—Model Parameters for 200-g Rat and 70-kg Human[a]

Parameter	Compartment						
	Plasma	Muscle	Kidney	Liver	Gut	Spleen	Bone Marrow
Volume, V, ml,	9.0 (2700)	100 (38,000)	1.9 (1100)	8.3 (1700)	11 (3200)	0.54 (200)	4 (1400)
Flow rate, Q, ml/min	—	3.0 (420)	5.0 (700)	6.5 (800)	5.3 (610)	0.25 (110)	0.64 (66)
Linear distribution ratio, R	—	1.4 (1.4)	2.4 (2.4)	4.0 (4.0)	3.0 (3.0)	1.7 (1.7)	0.35 (0.35)
Strong binding constant, a, μg/ml	—	0.0 (0.0)	0.35 (0.35)	0.6 (0.6)	0.1 (0.1)	0.2 (0.2)	0.2 (0.2)
Kidney clearance, K_K, ml/min	—	—	1.2 (315)	—	—	—	—
Bile secretion parameter clearance, k_L/K_L, ml/min	—	—	—	1.2 (500)	—	—	—
Bile transit parameter, $\min_\tau$	—	—	—	1.0 (10)	—	—	—
Gut lumen parameter transit time, min	—	—	—	—	100 (1000)	—	—
$1/k_F$, $\min^{-1}$	—	—	—	—	0.01 (0.001)	—	—
k_G, μg/min	—	—	—	—	20 (1900)	—	—
K_G, μg/ml	—	—	—	—	200 (200)	—	—

[a] Values in parentheses are for the human.

liters per minute); R is the tissue-to-plasma equilibrium distribution ratio; M is the total dose of drug; and $g(t)$ is the injection function, which is a short pulse to simulate an intravenous injection (1, 2):

$$g(t) = 30\lambda(\lambda t)^2(1 - \lambda t)^2 \qquad \text{(Eq. 3)}$$

where λ is the reciprocal of the injection duration.

The mass balance equations are written similarly for the remaining compartments. Fifteen differential equations were solved simultaneously by computer to yield predictions of the mercaptopurine concentration in any compartment as a function of time following an input injection into the plasma compartment.

Physiological Parameters for Rats and Humans—Table I lists the physiological model parameters used in the simulations for rats and humans. Volumes, flow rates, and gut lumen parameters were obtained from previous reports (18, 19) for the rat. The strong and linear binding parameter was obtained from experimental data, with the exception of muscle and bone marrow. The linear binding parameter for muscle was determined by Nelson *et al.* (20).

The binding parameters for bone marrow were estimated from Dedrick *et al.* (19) for the 25-mg/kg dose of methotrexate in the rat. Experimentally obtained strong binding parameters for mercaptopurine in several tissues were observed; these values differed by no more than 50% from those of methotrexate. Also, the bone marrow profile was simulated, varying the strong binding parameter within ±50% of methotrexate (*i.e.*, a = 0.1–0.3). The difference between simulated profiles of a = 0.1–0.3 varied only about 10% below 140 min and roughly less than 25% above 140 min. Therefore, by choosing the strong binding parameter of methotrexate, which falls within a = 0.1–0.3, the simulated variation will be smaller.

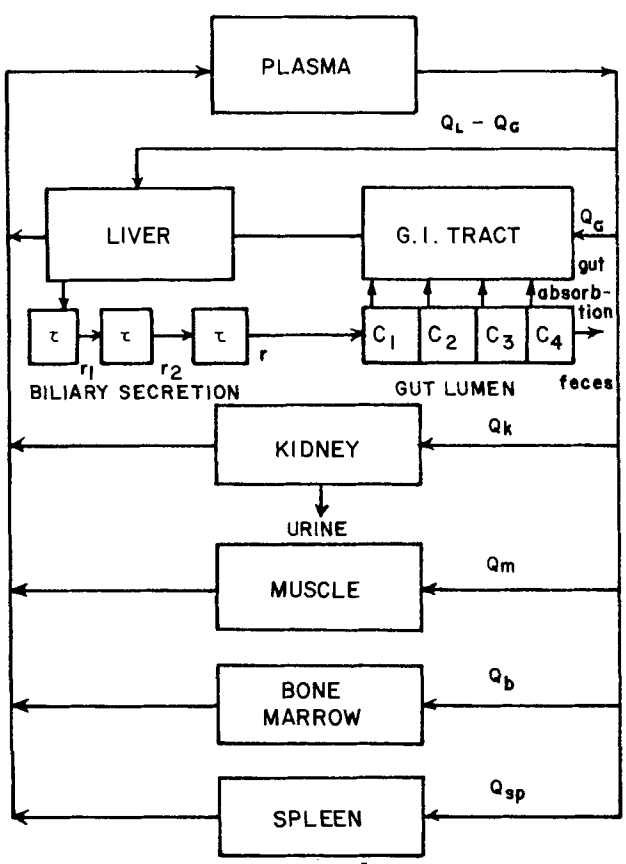

Scheme I

Through simulation of the gut lumen profile and comparison with experimental data, the k_G values varied from 10 to 30 and the K_G values varied from 100 to 300 with various combinations. The comparisons made with all simulations of the gut lumen profiles were almost identical up to 60 min; beyond 60 min, variation at any point in time was less than 15% from that of the methotrexate value. Furthermore, the experimental technique for determination of the absorption parameters is difficult to apply with accuracy. The values for K_G and k_G gave a consistent and uniform fit for virtually all tissues of interest.

The renal clearance was determined using the plasma mercaptopurine level at 10 hr, which was 2.8 μg/ml with a dose of 25 mg/kg iv, and the amount of radioactive mercaptopurine excreted during 20 hr, which amounted to 48% of the administered dose (21). The renal clearance was also evaluated by taking the average of the ratios of $\hat{A}_u{}^T / \int_0^T C_p\, dt$, where $\hat{A}_u{}^T$ is the total amount of radioactive mercaptopurine excreted for 12 hr, and this amount corresponded to 43% of the administered dose. The area under the plasma–time curve was 3700 μg min/ml for a 25-mg/kg dose. Both methods gave approximately the same renal clearance of 0.7 ml/min. The bile secretion parameter gave the best fit for all tissue and plasma profiles.

The values for human tissue, volume, and blood flows used were taken from previous studies. Similarly, in this study, the flow was utilized in the human model for mercaptopurine and a hematocrit volume of 45% was assumed. Reported values were used for human tissue volume and plasma flow (6) and gut lumen parameters (18). The bile secretion parameters were determined by conjecture to create the best fit for the data. The renal clearance was estimated based on 20% mercaptopurine excreted within 4 hr, and the corresponding plasma level at the midpoint was 2.4 μg/ml (9, 22). Then the renal clearance was computed to be 315 ml/min based on a 13-mg/kg dose and a 70-kg body weight.

RESULTS AND DISCUSSION

Figure 1 compares model simulation with experimental values for mercaptopurine levels in several rat tissues following a dose of 25 mg/kg iv. Each point represents an average of four rats. A moderately rapid distribution phase is followed by a slower rate of concentration changes, and the equilibrium between tissues and plasma occurs within 20 min. However, for gut lumen, the equilibrium occurs in about 60 min. The gut lumen has the highest concentration of mercaptopurine, which is due to reabsorption through biliary secretion since a very small amount of mercaptopurine or its metabolites is detected in feces (21). The predictive results are in good agreement with overall tissue profiles.

Figure 2 shows the early phase of the plasma profile using the radioisotope method *versus* the spectrofluorometric method. The simulated plasma curve in Fig. 2 indicates a very rapid drug distribution and a 30-μg/ml drop in value in the first 4 min. The half-life was determined to be 12.15 hr using the β-phase of the plasma profile for 10 hr. These data are not shown in Fig. 2, which illustrates only the first 30 min of the 10-hr period.

The 48-hr renal excretion data previously reported (21) indicated that 56% of the administered radioactivity was recovered in urine. By using these data, the elimination constant was calculated and compared to the

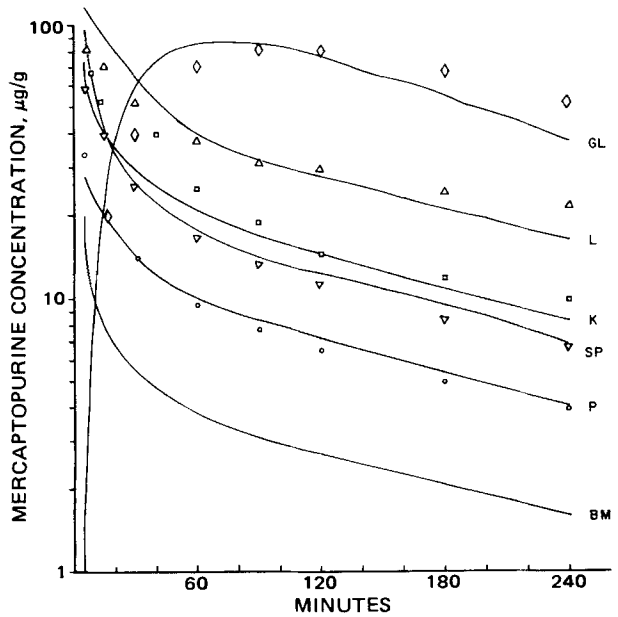

Figure 1—*Model prediction* versus *experimental results in rats given 25 mg/kg iv. Solid lines are model predictions; symbols are experimental data. Key: GL(◊), small intestine; L(△) liver; K(□), kidney; P(○), plasma; SP(▽), spleen; and BM, bone marrow.*

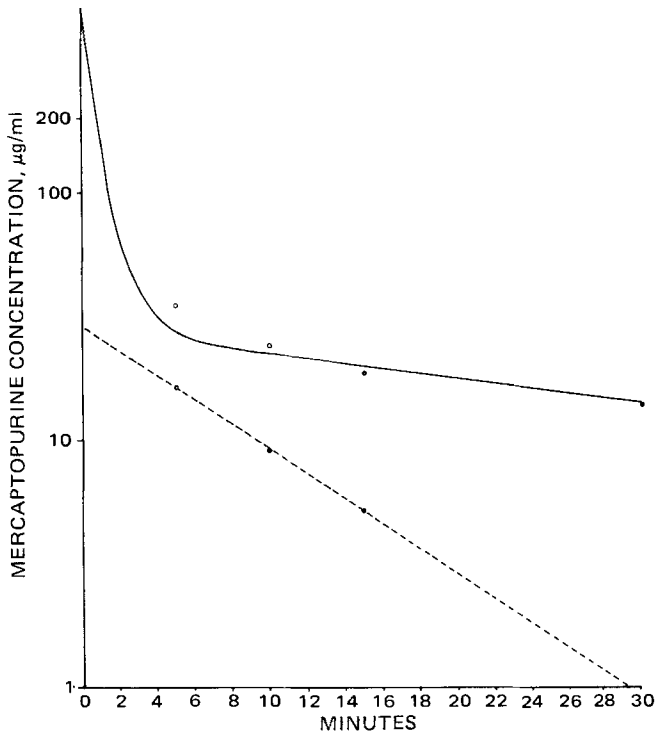

Figure 2—*Solid line is model prediction in rats given 25 mg/kg iv. The open and solid circles are experimental data obtained by the radioactivity and spectrofluorometric methods, respectively.*

constant determined from the plasma values obtained in the experiment. The semilog plot, log $(M_u^\infty - M_t)$ of total radioactive mercaptopurine remaining to be excreted *versus* time, gives a biexponential curve. The M_u^∞ is the amount of dose excreted at infinite time, and M_t represents the amount of dose excreted at any time. From the linear portion of this curve, the slope was estimated and the corresponding half-life was 12.00 hr. Elimination constants from plasma and urinary data correlated very well.

Sarcione and Stutzman (21), using urinary data, found that a significantly large amount of cumulative 6-thiouric acid was excreted during the first 8 hr. In contrast, a relatively small amount of unchanged mercaptopurine was excreted. This result indicates that a large proportion of mercaptopurine undergoes biotransformation *in vivo*. The plasma profile of mercaptopurine obtained spectrofluorometrically follows first-order kinetics and has a half-life of about 6 min. The discrepancy between the two experimental plasma profiles is due to significant biotransformation of mercaptopurine to give 6-thiouric acid, 6-methylsulfinyl-8-hydroxypurine, and some inorganic sulfate (21).

Donelli *et al.* (12) measured the concentration of mercaptopurine in tissues (liver, spleen, and lung) by a spectrophotometric technique and reported that there was a significant accumulation of mercaptopurine in these tissues relative to plasma and that this accumulation persisted for a long time. Also, there was no log–log linear relationship of distribution of mercaptopurine between plasma and tissue concentrations. This result may have been due to the nonspecific nature of the analytical methodology associated with spectrophotometry; many anabolic and catabolic products exist in tissues and may interfere with mercaptopurine determination.

Furthermore, the spectrofluorometric method has a limited sensitivity of about 1 μg/ml in plasma. Within 30 min in the present study, the plasma level approached the sensitivity level of 1 μg/ml for a 25-mg/kg dose, as reported previously (12). This result implies that plasma profiles have not yet reached asymptotic decay. To determine low levels of mercaptopurine in plasma and tissues, one must utilize specific and sensitive assaying techniques, such as mass fragmentography. Experimentally accurate determinations of plasma and tissue profiles are necessary not only for simulation purposes but also for the determination of required parameters such as linear and strong binding and renal clearances. These parameters play a substantial role in pharmacokinetic modeling.

To date, the comparison of analytical methodology has not been investigated in relation to physiological pharmacokinetic modeling. For a comparison of methods on plasma modeling only, previous results (23) with fluorouracil clearly demonstrated the inadequacy of the radioactive method *versus* mass fragmentography. Inasmuch as a specific and sensitive analytical technique was not available for low level determination of mercaptopurine in tissues, it seemed reasonable to use the relatively nonspecific radioisotopic method to evaluate physiological pharmacokinetic modeling in rats.

Figure 3 illustrates a comparison of the model prediction in several tissues with experimental data obtained with a dose of 2.5 mg/kg iv of mercaptopurine in rats. The model was simulated in the same manner and identical parameters were obtained with a 25-mg/kg dose, the only difference being the dose. Overall agreement between model prediction and experimental data was good. The experimentally obtained linear binding parameter for liver tissue for the 25- and 2.5-mg/kg doses showed a 20% variation.

The average linear binding parameter for the liver at 25 mg/kg was 4.4; at 2.5 mg/kg, it was 3.2. Simulations shown in Figs. 1 and 3 were based on a linear binding parameter of 4.0 to minimize variation and still be

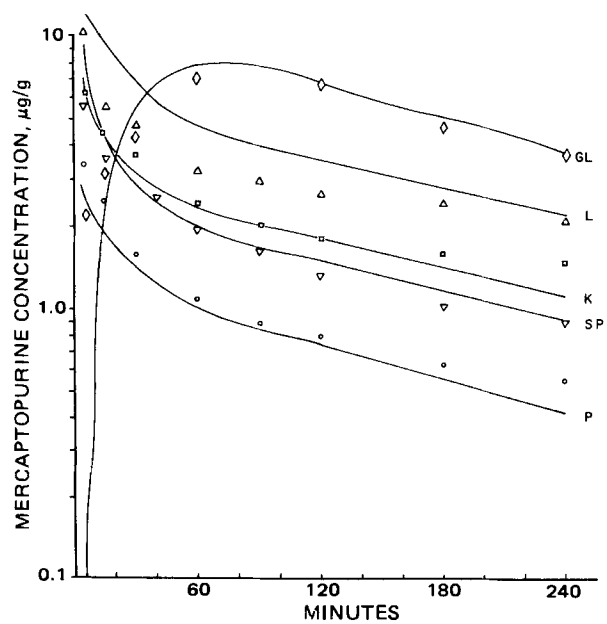

Figure 3—*Model prediction* versus *experimental results in rats given 2.5 mg/kg iv. For other details, see Fig. 1.*

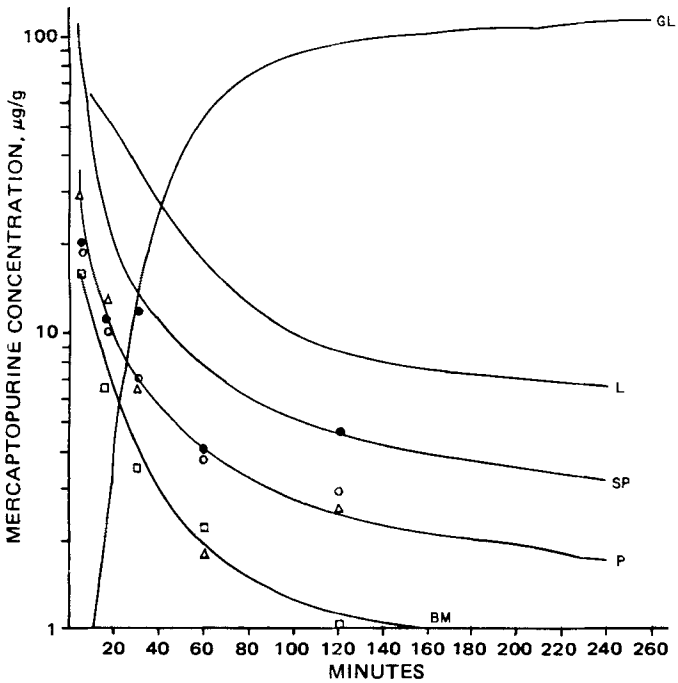

Figure 4—*Comparison between curves predicted by model and observed data of four patients. Key: △, Patient CK; ●, Patient JY; ○, Patient GS; □, Patient CC.*

consistent with the liver profiles at both doses. Had 3.2 been selected for the low dose and 4.4 for the high dose, better agreement for the liver profiles would have been obtained without affecting any other tissue profile. In addition, appropriate manipulation of the biliary excretion rate value did give acceptable liver profiles but induced undesirable variations in profiles for other tissues.

A comparison of the plasma results from several patients with the model predictions is shown in Fig. 4 along with predicted values for the other body regions. The data points are actual values from four different patients obtained previously (9). Patients CK, JY, and GS each received 900 mg iv of mercaptopurine with the exclusion of any other drug therapy. In Patient GS, the plasma level was almost identical with that in the simulated model. For Patient CK, a lower plasma level was observed at 60 min than at 120 min. This type of disagreement might be caused by the lack of analytical specificity and sensitivity or by an artificial effect.

Patient CC, a 73-kg male, was given 12 mg/kg iv of mercaptopurine. This patient also received other drugs during the studies: chloral hydrate, dioctyl sodium sulfosuccinate, morphine, and chlorpromazine hydrochloride. The role of drug interactions in the physiological disposition of mercaptopurine is not well understood. Drugs such as phenobarbital affect drug metabolism (24), but dioctyl sodium sulfosuccinate seems to be without effect. The plasma level of Patient CC was uniformly lower than in the other patients as well as in the model simulations. Although several variables must be accounted for in these studies, the prediction is a reasonable first approximation. It was assumed in the model simulation that binding affinity of human tissue for mercaptopurine is the same as that of binding to rat tissue. To determine more accurately the tissue and plasma levels in humans, the binding affinity of human tissues for mercaptopurine must be investigated.

CONCLUSION

The models predict detailed distribution of mercaptopurine in the tissues for the two different dose levels in rats. Mercaptopurine is metabolically altered so rapidly that a true detailed description of tissue profiles is still uncertain due to nonspecific assaying techniques that might overestimate the concentration for plasma and tissue profiles. Several considerations in the pharmacokinetic modeling of mercaptopurine need further study.

Mercaptopurine, like other thiopurines, must undergo anabolic conversion to nucleotide forms to exert its antineoplastic activity. Thus, it is necessary to incorporate in the pharmacokinetic modeling intracellular reactions and metabolic fate. Morrison *et al.* (5) were able to include intracellular metabolite and enzyme kinetics within those target cells that are the sites of the ultimate cytotoxic and cytostatic effects for cytarabine.

REFERENCES

(1) R. L. Dedrick and K. B. Bischoff, *Chem. Eng. Prog. Symp. Ser.*, **64**, 32 (1968).

(2) K. B. Bischoff and R. L. Dedrick, *J. Pharm. Sci.*, **57**, 1346 (1968).

(3) K. B. Bischoff, R. L. Dedrick, and D. S. Zaharko, *ibid.*, **59**, 149 (1970).

(4) R. L. Dedrick, D. D. Forrester, and D. H. W. Ho, *Biochem. Pharmacol.*, **21**, 1 (1972).

(5) P. F. Morrison, T. L. Lincoln, and J. Aroesty, *Cancer Chemother. Rep.*, **69**, 861 (1975).

(6) P. A. Harris and J. Gross, *ibid.*, **69**, 819 (1975).

(7) J. G. Wagner, "Fundamentals of Clinical Pharmacokinetics," Drug Intelligence Publications, Hamilton, Ill., 1975.

(8) M. Gibaldi and D. Perrier, "Pharmacokinetics," Dekker, New York, N.Y., 1975.

(9) J. J. Coffey, C. A. White, A. B. Lesk, W. I. Rogers, and A. A. Serpick, *Cancer Res.*, **32**, 1283 (1972).

(10) L. Hamilton and G. B. Elion, *Ann. N.Y. Acad. Sci.*, **60**, 304 (1954).

(11) G. B. Elion, *Fed. Proc.*, **26**, 898 (1967).

(12) M. G. Donelli, T. Colombo, A. Forgione, and S. Garattini, *Pharmacology*, **8**, 311 (1972).

(13) E. S. Henderson, *Semin. Hematol.*, **6**, 271 (1969).

(14) A. Goldin, J. S. Sandberg, E. S. Henderson, J. W. Newman, E. Frei, III, and J. F. Holland, *Cancer Chemother. Rep.*, **55**, 309 (1971).

(15) J. A. Montgomery, *Prog. Med. Chem.*, **7**, 69 (1970).

(16) F. M. Schabel, Jr., *Cancer Res.*, **29**, 2384 (1969).

(17) J. M. Finkel, *Anal. Biochem.*, **21**, 362 (1967).

(18) K. B. Bischoff, R. L. Dedrick, D. S. Zaharko, and J. A. Longstreth, *J. Pharm. Sci.*, **60**, 1128 (1971).

(19) R. S. Dedrick, D. S. Zaharko, and R. J. Lutz, *ibid.*, **62**, 882 (1973).

(20) J. A. Nelson, H. F. Cserr, and S. H. Chu, *Cancer Res.*, **34**, 1889 (1974).

(21) E. J. Sarcione and L. Stutzman, *ibid.*, **20**, 387 (1960).

(22) T. L. Loo, J. K. Luce, M. P. Sullivan, and E. Frei, III, *Clin. Pharmacol. Ther.*, **9**, 180 (1968).

(23) C. Finn and W. Saddie, *Cancer Chemother. Rep.*, **59**, 279 (1975).

(24) A. H. Conney, *Pharmacol. Rev.*, **19**, 317 (1967).

ACKNOWLEDGMENTS AND ADDRESSES

Received August 2, 1976, from the *School of Pharmacy, Florida Agricultural and Mechanical University, Tallahassee, FL 32307.*

Accepted for publication January 8, 1977.

Supported in part by Research Grant RR-08111 from the National Institues of Health, Minority Biomedical Support Program, and in part by the National Cancer Institute, Bethesda, MD 20014.

The authors thank Dr. R. W. Trottier and Dr. H. J. Lee of the Florida Agricultural and Mechanical University School of Pharmacy for their assistance in the preliminary phase of this study and Mr. L. Irby for computer programming. In particular, they thank Dr. R. Dedrick.

[x] To whom inquiries should be directed.

Method of Obtaining Drug–Macromolecule Binding Parameters Directly from Dynamic Dialysis Data

PETER VENG PEDERSEN ˣ, **MICHAEL J. CROOKS, and KENNETH F. BROWN**

Abstract □ A new method of treating dynamic dialysis data to obtain binding parameters for drug–macromolecule interactions is presented. This method allows the determination of binding parameters directly from dialysis data according to a theoretical model. It is not necessary to determine the dialysis rate constant accurately in a separate experiment, and bias is not introduced due to differentiation. The proposed method should be applicable where the drug is substantially bound to the dialysis membrane.

Keyphrases □ Drug–macromolecule binding—parameters obtained directly from dynamic dialysis data □ Binding, drug–macromolecule—parameters obtained directly from dynamic dialysis data □ Dialysis data, dynamic—drug–macromolecule binding parameters obtained directly

The dynamic dialysis method for characterizing interactions of small molecules with macromolecules is well established (1–15) and has several advantages compared to equilibrium dialysis and ultrafiltration. A complete binding profile can be obtained rapidly in one experiment, and the method utilizes only a small macromolecule sample. Since the method is based on a dynamic process, an equilibrium state does not need to be defined, and, compared to ultrafiltration, there is no change in the macromolecule concentration.

Meyer and Guttman (3) designed a dynamic dialysis method to characterize drug–protein interactions, but their method has some limitations. The experimental data must be differentiated to evaluate binding parameters, which may introduce substantial errors, particularly if the number of data points is limited. An empirical equation was used to fit dialysis data to obtain instantaneous rates. A recent publication (13) showed that the various empirical equations used can yield substantially different binding parameters.

The technique of Meyer and Guttman (3) requires that the rate constant for dialysis be determined in a separate experiment in the absence of macromolecules. It is assumed that the same rate constant will apply in the presence of macromolecules. This assumption may be unreasonable because the rate constant depends on several factors, such as the physicochemical state of the dialysis membrane (16, 17), that may change between runs.

Several compounds are significantly bound to the membrane material (5, 11). When using previous methods, it has not been possible to determine the dialysis rate constant and to account for the membrane binding in the determination of macromolecule binding parameters of such compounds.

This paper presents a new approach. It rigorously describes the total kinetics of the system in a form that enables binding parameters to be estimated accurately, directly from dialysis data. It eliminates the need to determine an accurate dialysis rate constant separately. The method does not rely on differentiation of experimental data and should be applicable to membrane-bound compounds.

THEORY

Consider an interaction between small molecules and macromolecules that can be described by the general binding expression:

$$\bar{\nu} = \sum_{i=1}^{j} \frac{n_i K_i D_f}{1 + K_i D_f} \qquad \text{(Eq. 1)}$$

where $\bar{\nu}$ is the number of moles of small molecules bound per mole of macromolecule, n_i is the number of binding sites in the ith class of sites, K_i is the association constant for the interaction, and D_f is the molar concentration of unbound small molecules. If a model with two classes ($j = 2$) is assumed, then the total concentration of drug, D_t, in the protein compartment is given by (5):

$$D_t = D_f + P_t D_f \left(\frac{n_1 K_1}{1 + K_1 D_f} + \frac{n_2 K_2}{1 + K_2 D_f}\right) \qquad \text{(Eq. 2)}$$

If sink conditions prevail, the small molecules leave the protein compartment by a first-order process:

$$\frac{dD_t}{dt} = -K_e D_f \qquad \text{(Eq. 3)}$$

where K_e is the dialysis rate constant.

It is convenient to introduce a variable, s, defined as:

$$s = -\frac{dD_t}{dt} \qquad \text{(Eq. 4)}$$

so that $D_f = s/K_e$, and Eq. 2 can be written:

$$D_t = \frac{s}{K_e} + P_t s \left(\frac{n_1 K_1}{K_e + K_1 s} + \frac{n_2 K_2}{K_e + K_2 s}\right) \qquad \text{(Eq. 5)}$$

By taking the differential of this equation, noting $dD_t = -s dt$, it becomes:

$$dt = -\left\{\frac{1}{K_e s} + P_t K_e \left[\frac{n_1 K_1}{s(K_e + K_1 s)^2} + \frac{n_2 K_2}{s(K_e + K_2 s)^2}\right]\right\} ds \qquad \text{(Eq. 6)}$$

which, integrated from $t = 0$ to t, corresponding to $s = s_0$ to s, yields:

$$t = \left|\frac{1}{K_e} \ln s + P_t n_1 K_1 \left[\frac{1}{K_e + K_1 s} + \frac{1}{K_e} \ln\left(\frac{s}{K_e + K_1 s}\right)\right] + P_t n_2 K_2 \left[\frac{1}{K_e + K_2 s} + \frac{1}{K_e} \ln\left(\frac{s}{K_e + K_2 s}\right)\right]\right|_s^{s_0} \qquad \text{(Eq. 7)}$$

If the following function is defined:

$$f(x) = \frac{1}{K_e} \ln x + P_t n_1 K_1 \left[\frac{1}{K_e + K_1 x} + \frac{1}{K_e} \ln\left(\frac{x}{K_e + K_1 x}\right)\right] + P_t n_2 K_2 \left[\frac{1}{K_e + K_2 x} + \frac{1}{K_e} \ln\left(\frac{x}{K_e + K_2 x}\right)\right] \qquad \text{(Eq. 8)}$$

then Eq. 7 can be written more simply as:

$$t = f(s_0) - f(s) \qquad \text{(Eq. 9)}$$

The exact functional relationship describing the change of D_t with t is now described by Eqs. 5 and 9 in parametric form where the variable s is the parameter. With these equations, each value of s defines a unique pair of D_t and t values.

The quantity s_0 is the initial ($t = 0$) value of $-dD_t/dt$ (Eq. 4), which would normally be determined by extrapolation. To avoid the errors and problems of such an extrapolation, it is convenient to define $t = 0$ at the first sampling time. In this way, s_0 is $-dD_t/dt$ at the first sampling.

To determine the binding parameters by nonlinear regression, it is necessary to define the exact functional relationship between D_t and t for any values of n_1, K_1, n_2, K_2, s_0, and K_e, which are changing during the nonlinear fitting procedure. This step can be performed by determining the particular values of s that satisfy Eq. 9. These values are then used to determine the corresponding values of D_t by Eq. 5.

However, Eq. 9 cannot be expressed explicitly in terms of s, so some iterative procedure is needed to solve for s. The Newton–Raphson algorithm is particularly suitable because it is computationally compact and exhibits quadratic convergence. If:

$$\phi(s) = t - f(s_0) + f(s) \qquad \text{(Eq. 10)}$$

then Eq. 9 can be solved by the Newton–Raphson method using the following iteration[1]:

$$s_{i+1} = s_i - \frac{\phi(s_i)}{\phi'(s_i)} \qquad \text{(Eq. 11)}$$

where the functions ϕ and ϕ' are defined by:

$$\phi'(s) = f'(s) = \frac{1}{K_e s} + \frac{P_t K_e}{s}\left[\frac{n_1 K_1}{(K_e + K_1 s)^2} + \frac{n_2 K_2}{(K_e + K_2 s)^2}\right] \qquad \text{(Eq. 12)}$$

and:

$$\phi(s) = t + \frac{1}{K_e}\ln\frac{s}{s_0} + P_t n_1 K_1\left[\frac{K_1(s_0 - s)}{(K_e + K_1 s)(K_e + K_1 s_0)} + \frac{1}{K_e}\ln\frac{s}{s_0}\frac{(K_e + K_1 s_0)}{(K_e + K_1 s)}\right] + P_t n_2 K_2\left[\frac{K_2(s_0 - s)}{(K_e + K_2 s)(K_e + K_2 s_0)} + \frac{1}{K_e}\ln\frac{s}{s_0}\frac{(K_e + K_2 s_0)}{(K_e + K_2 s)}\right] \qquad \text{(Eq. 13)}$$

For the algorithm (Eq. 11) to converge within a given number of iterations, the initial estimates of s must not be too far from the s values for which Eq. 9 is satisfied. These initial estimates can, according to Eq. 4, be obtained as the (positive) values of $-dD_t/dt$ estimated from the observed values of D_t *versus* t. Any simple technique for slope estimation can be used since the actual accuracy of the estimates is of no importance for the final result.

These derivations for two binding classes can easily be extended to any number (j) of classes for which then:

$$D_t = \frac{s}{K_e} + P_t s \sum_{i=1}^{j}\frac{n_i K_i}{K_e + K_i s} \qquad \text{(Eq. 14)}$$

and:

$$t = \left|\frac{1}{K_e}\ln s + P_t\sum_{i=1}^{j} n_i K_i\left[\frac{1}{K_e + K_i s} + \frac{1}{K_e}\ln\left(\frac{s}{K_e + K_i s}\right)\right]\right|_s^{s_0} \qquad \text{(Eq. 15)}$$

and the iteration, Eq. 11, can still be used with:

$$\phi'(s) = \frac{1}{K_e s} + \frac{P_t K_e}{s}\sum_{i=1}^{j}\frac{n_i K_i}{(K_e + K_i s)^2} \qquad \text{(Eq. 16)}$$

and:

$$\phi(s) = t + \frac{1}{K_e}\ln\frac{s}{s_0} + P_t\sum_{i=1}^{j} n_i K_i\left[\frac{K_i(s_0 - s)}{(K_e + K_i s)(K_e + K_i s_0)} + \frac{1}{K_e}\ln\frac{s(K_e + K_i s_0)}{s_0(K_e + K_i s)}\right] \qquad \text{(Eq. 17)}$$

Binding of Small Molecules by Dialysis Membrane—The outlined treatment is based on the assumption that binding occurs only to protein. However, some drugs, particularly those strongly protein bound, can become significantly bound to the dialysis membrane. This fact means that K_e cannot be estimated from plots of $\ln D_t$ *versus* t in the absence of protein using previous techniques because of curvature (Fig. 1).

A special technique is required to estimate the dialysis rate constant, and the membrane binding must be taken into account in the treatment of the dialysis behavior of the small molecule–macromolecule system.

Determination of K_e and Membrane Binding Parameters in Absence of Macromolecules—The binding of small molecules to the membrane can often be considered as a Langmuir-type adsorption phenomenon (5), which is mathematically analogous to binding to a single class of sites, and can be described by:

$$\bar{\nu}^* = \frac{n^* K^* D_f}{1 + K^* D_f} \qquad \text{(Eq. 18)}$$

[1] The function ϕ is not defined for $s \leq 0$. Therefore, it is necessary during the iteration procedure to prevent s from taking a nonpositive value by defining $s_{i+1} = s_i/2$ if $s_{i+1} \leq 0$ since ϕ is a monotone increasing function of s because $\phi' = f' > 0$ ($s > 0$).

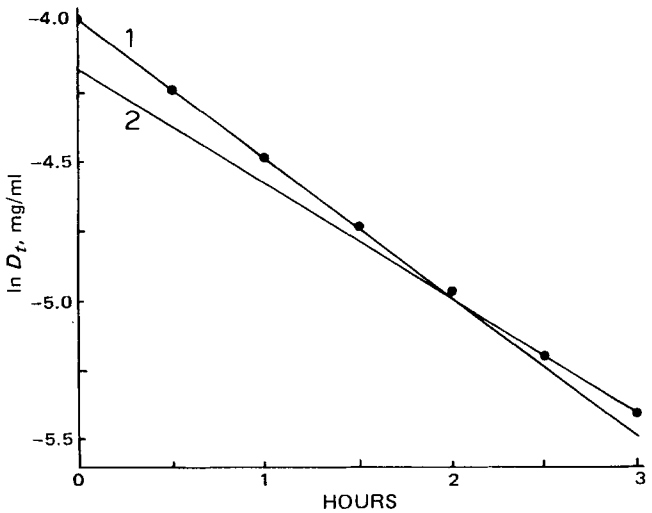

Figure 1—*Dynamic dialysis of glyburide in 0.067* M *phosphate buffer in the absence of macromolecules at pH 7.4 and 37°. The tangents illustrate a difference in the slope at* t = *0 and* t = *3 hr of 15%.*

where $\bar{\nu}^*$ is the amount of small molecules bound per amount of available membrane material, and K^* is the association constant for membrane binding. The quantity n^* does not have the same meaning as n previously defined but is introduced to establish a mathematical analogy leading to the following relationship between D_t and t, similar to Eqs. 14 and 15 ($j = 1$):

$$D_t = \frac{s}{K_e} + \frac{K's}{K_e + K^* s} \qquad \text{(Eq. 19)}$$

and:

$$t = \left|\frac{1}{K_e}\ln s + \frac{K'}{K_e + K^* s} + \frac{K'}{K_e}\ln\frac{s}{K_e + K^* s}\right|_s^{s_0} \qquad \text{(Eq. 20)}$$

where:

$$K' = \frac{Mn^* K^*}{WV} \qquad \text{(Eq. 21)}$$

and M is the amount of membrane material available for binding, W is the molecular weight of the small molecule, and V is the volume of the protein compartment. Equations 19 and 20 can then be used to determine K_e and the membrane binding parameters K^* and K' in the absence of protein using the described technique.

Determination of Drug–Macromolecule Binding Parameters in Presence of Membrane Binding—Once K_e, K', and K^* have been determined using this approach, it is possible to account for membrane binding and to determine parameters for binding to the macromolecule.

Simultaneous binding to the membrane and the macromolecule leads to the following expressions:

$$D_t = \frac{K's}{K_e + K^* s} + \frac{s}{K_e} + P_t s\sum_{i=1}^{j}\frac{n_i K_i}{K_e + K_i s} \qquad \text{(Eq. 22)}$$

$$t = \left|\frac{K'}{K_e + K^* s} + \frac{K'}{K_e}\ln\frac{s}{K_e + K^* s} + \frac{1}{K_e}\ln s + P_t\sum_{i=1}^{j} n_i K_i\left[\frac{1}{K_e + K_i s} + \frac{1}{K_e}\ln\left(\frac{s}{K_e + K_i s}\right)\right]\right|_s^{s_0} \qquad \text{(Eq. 23)}$$

which enables the D_t, t functional relationship to be evaluated using the iterative procedure discussed.

By comparing Eqs. 22 and 23 with Eqs. 14 and 15, it is seen that, in the presence of membrane binding, the dialysis behavior is mathematically analogous to a system where the small molecule is binding to two macromolecular species.

EXPERIMENTAL

The dynamic dialysis technique was described previously (3). To evaluate the new method of data treatment, chlorpropamide was dialyzed from 1% bovine serum albumin in 0.067 *M* phosphate buffer, pH 7.4, at 37° in the presence of a fixed free concentration of warfarin (1.6×10^{-5}

Table I—Chlorpropamide–Bovine Serum Albumin Binding Parameters Obtained in the Presence of 1.6×10^{-5} *M* Free Warfarin by the New Method and Two Derivative Methods

Parameter	New Method	Derivative Method	
		I[a]	II[b]
n_1	2	1.94	5.28
K_1, M^{-1}	2.64×10^4	1.09×10^4	2.92×10^3
n_2	9	9.14	7.77
K_2, M^{-1}	1.94×10^2	1.86×10^2	3.61×10^{-5}
K_e, hr^{-1}	0.714	0.711	0.711
SS[c], mM^2	2.60×10^{-3}	15.0×10^{-3}	5.50×10^{-3}

[a] A fourth-order least-squares polynomial was used to estimate $-dD_t/dt$. The binding parameters were calculated by the method of Hart (19) as used by Crooks and Brown (9). [b] The binding parameters were estimated by nonlinear regression analysis of $\bar{\nu}$ on D_f, obtained by the method of Meyer and Guttman (3) from a three-exponential fitting of D_t *versus* t data. [c] Sum of squared differences (Figs. 3–5) between observed D_t values and exact theoretical values calculated according to Eqs. 5 and 9 for the estimated values of n_1, K_1, n_2, K_2, and K_e.

M) maintained to within ±2% as described previously (12). Although warfarin displaces some chlorpropamide, the latter still appears to bind to two classes of sites (12). This system was selected so that such a model of two classes of sites could be appraised by the new data treatment method.

The starting concentration of chlorpropamide was 3.62×10^{-3} *M*, and the external compartment was sampled at 0.25, 0.5, 1, 1.5, 2, 2.5, 3, 4, 5, 6, and 7 hr. Chlorpropamide and warfarin were estimated by differential UV spectrophotometry at 231 and 310 nm using simultaneous equations. Absorbances of each component were additive at both wavelengths.

Glyburide was dialyzed from 0.067 *M* phosphate buffer, pH 7.4, at 37°. ^{14}C-Labeled material was used and assayed by liquid scintillation counting. All calculations were made to an accuracy of at least eight significant digits using a digital computer.

RESULTS AND DISCUSSION

Data for the dialysis of chlorpropamide from bovine serum albumin in the presence of 1.6×10^{-5} *M* free warfarin were treated according to the proposed method. Binding parameters n_1, K_1, n_2, and K_2 and the dialysis rate constant K_e were estimated using the function relating D_t and t given in Eqs. 5 and 9. This function was evaluated using Eqs. 11–13 and 5, programmed in a subroutine that was executed with the highly interactive time-sharing Fortran program, FUNFIT, written for general nonlinear least-squares regression (18).

The least-squares fit of the model with two classes of binding sites (Fig. 2) agreed well with the experimental data (r = 0.99986). The binding parameters estimated by the method are summarized in Table I. The

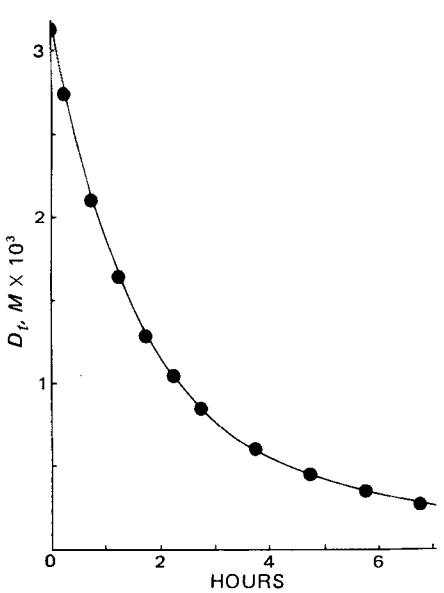

Figure 2—*Dynamic dialysis data for the binding of chlorpropamide to 1% bovine serum albumin at pH 7.4 and 37° in the presence of 1.6 × 10^{-5} M free warfarin. The curve fitted by least squares is the function relating* D_t *and* t *(Eqs. 5 and 9), which provides estimates of* n_1, K_1, n_2, K_2, *and* K_e.

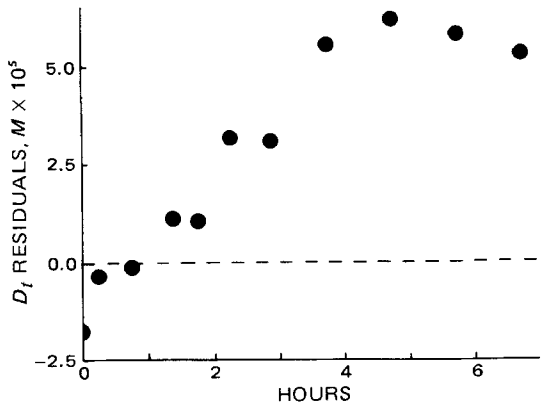

Figure 3—*Differences between observed* D_t *values and exact theoretical values calculated according to Eqs. 5 and 9 for the values of* n_1, K_1, n_2, K_2, *and* K_e *(Table I) estimated by the derivative method of Crooks and Brown (9).*

values for the number of binding sites, n_1 and n_2, were so close to 2 and 9 in a preliminary computation that their values were fixed as integers. Such a model has greater conceptual value, and the slight change in n_1 and n_2 did not substantially alter the values of the other parameters.

Also included in Table I are values for binding parameters estimated by fitting dialysis data to a fourth-order polynomial and then evaluated using a modification of the method of Hart (19) (Method I) as described elsewhere (9). Method II was that of Meyer and Guttman (3), where a three-exponential expression:

$$D_t = \sum_{i=1}^{3} A_i e^{-\alpha_i t} \qquad \text{(Eq. 24)}$$

is used to fit dialysis data. By differentiation at various t values, a $\bar{\nu}$ *versus* D_f profile was constructed; the binding parameters were estimated by a nonlinear regression technique using Eq. 1.

The dialysis rate constant, K_e, used for the derivative methods of data treatment was determined in a separate experiment.

There was good agreement between binding parameters determined using the new method and Method I, particularly for n_1, n_2, K_2, and K_e, although K_1 determined by the new method was somewhat greater. However, entirely different binding parameters were determined by Method II, probably because of the choice of the empirical equation, Eq. 24. The selection of this equation probably was based on a requirement for "smoothness" of the fitted curve and its first derivative. Although this requirement is satisfied, Eq. 24 does not have the same flexibility as a polynomial, which could be just as important. The flexibility of polynomials to approximate arbitrary functions is explained by the well-known Taylor series theorem.

The difference in flexibility is clearly demonstrated by fitting a fourth-order polynomial and Eq. 24 to exact dialysis data generated using the least-squares binding parameter estimates obtained using the new method (Table I)[2]. For the polynomial fitting, the D_t residuals (expressed as percent of calculated values) were 0.286, −0.217, −0.519, −0.0609, 0.466, 0.779, 0.381, −1.49, −1.42, 3.14, and −1.12. For the triexponential fit, the values were 1.73, 1.91, 1.46, 3.38, −1.19, −2.65, −3.91, −4.55, −2.19, 3.10, and 10.7.

These results show that the polynomial is considerably more flexible. The triexponential fitting resulted in significant systematic deviation in residuals, leading to a bias in the slope values and D_t values and, therefore, a bias in the final results. The residual sum of squares (mM^2) were 5.85×10^{-4} and 1.04×10^{-2} for the polynomial and triexponential fittings, respectively.

A further disadvantage of using Eq. 24 is that multiple solutions are possible; this equation is nonlinear (in α) and may result in several sum-of-squares minima. This is not the case with a polynomial, which has a unique least-squares solution.

The fitting of Eq. 24 to the generated exact D_t, t data was repeated several times with different initial estimates for A_i and α_i, but the same solution was obtained each time, suggesting that this fit is the best pos-

[2] The exact theoretical data used were simply the values calculated from the curve using the new method. Any other arbitrary values of the binding parameters could have been used. Theoretical D_t, t data can readily be calculated for given values of $(D_t)_{t=0}$, n_1, K_1, n_2, K_2, P_t, and K_e by first employing Eq. 5 to get s_0 and then using Eqs. 11–13 and 5.

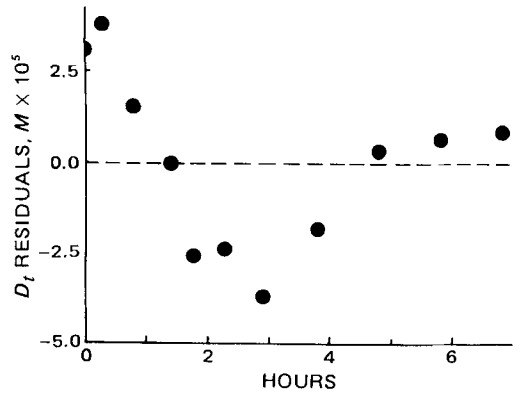

Figure 4—*Differences between observed* D_t *values and exact theoretical values calculated according to Eqs. 5 and 9 for the values of* n_1, K_1, n_2, K_2, *and* K_e *(Table I) estimated by the derivative method of Meyer and Guttman (3).*

sible using the triexponential equation. However, the use of a least-squares polynomial to represent dialysis data is expected to be less suitable than the triexponential when experimental errors are large or significant "gaps" exist between observation points because the ordinary least-squares polynomial fitting completely disregards derivative values. The derivative values are commonly in large error at the first and last observation points and just before or after gaps in the data.

This disadvantage of polynomials can be reduced considerably by imposing constraints on the derivative values by using least-squares spline polynomials. Such polynomials compete favorably with Eq. 24 on data with large errors and gaps, particularly considering the fact that the problem of multiple minima, using Eq. 24, is much larger for large residual problems. However, no matter which empirical equation is used, the results obtained will theoretically never be as exact as those obtained using the true equation as in the proposed method.

To investigate the bias introduced by Methods I and II, the exact D_t, t profile was calculated for the parameter values (Table I) obtained with the two methods. The differences between the observed and calculated D_t values (Figs. 3 and 4) show that the residuals are significantly larger for those methods than for the new method (Fig. 5). The residuals from Method I are particularly biased in a positive direction (Fig. 3), although the pattern resembles that from the new method (Fig. 5). The residuals from Method II (Fig. 4) show an entirely different pattern, consistent with the fact that the binding parameters obtained using Method II represent an entirely different solution.

A final check on the bias introduced by Methods I and II was made by applying them to exact D_t, t data generated from the parameter values (Table I) obtained using the new method. Method I found binding parameters relatively close to the true values, although K_1 seems to be somewhat different (Table II). Method II found an entirely different solution, similar to the one obtained using the real experimental data.

The value for the dialysis rate constant, K_e, estimated by the new method agrees very well with the value determined experimentally (Table I). As stated previously, this result may not always be true since the permeability of the membrane may change between experiments.

Chlorpropamide does not appear to be significantly membrane bound. Figure 1 shows the kinetics of dialysis of glyburide in the absence of bovine serum albumin. The curvature indicates significant membrane

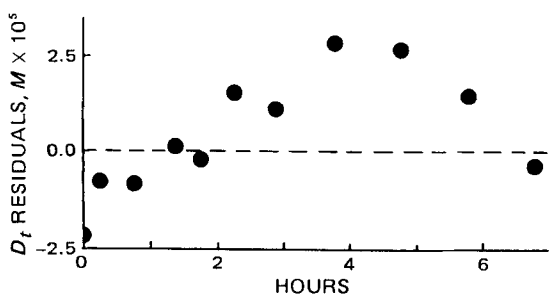

Figure 5—*Differences between observed* D_t *values and exact theoretical values calculated according to Eqs. 5 and 9 for the values of* n_1, K_1, n_2, K_2, *and* K_e *(Table I) estimated by the proposed method.*

Table II—Binding Parameters Obtained from Exact Generated Dialysis Data Using Two Derivative Methods [a]

Parameter	Exact Values	Estimated Values	
		Method I	Method II
n_1	2	1.96	5.02
K_1, M^{-1}	2.64×10^4	1.21×10^4	3.04×10^3
n_2	9	8.78	12.5
K_2, M^{-1}	1.94×10^2	1.74×10^2	3.16×10^{-5}

[a] $K_e = 0.714\ hr^{-1}$, and $P_t = 1.45 \times 10^{-4}\ M$.

binding. For this drug, it would not be possible to determine K_e and the binding parameters using previous approaches. However, they can be determined by the new method in two ways:

1. The membrane binding parameters K' and K^*, the dialysis rate constant K_e, and the drug–macromolecule binding parameters n_i and K_i can all be determined simultaneously and directly from experimental D_t, t data by applying Eqs. 22 and 23.
2. Since many parameters are involved in the first approach, it would be more reliable to determine K_e, K', and K^* in a separate experiment in the absence of the macromolecule and then to use the K_e value as an initial estimate with K' and K^* fixed as constants in the second experiment where n_i and K_i are determined.

As a result of these findings, the question naturally arises as to whether earlier reported binding parameters determined using previous techniques are valid. For certain combinations of binding parameters yielding a D_t *versus* t profile, some previous methods may give sufficiently accurate results. However, an excessively large number of simulation studies would be required to establish for which parameter combinations and sampling times previous methods are deficient. In general, the observer should not be too confident about the accuracy of the results obtained by previous approaches.

Studies on the use of dynamic dialysis for membrane-bound drugs are in progress.

REFERENCES

(1) H. H. Stein, *Anal. Biochem.*, **13**, 605 (1965).
(2) A. Agren, *Acta Pharm. Suec.*, **5**, 37 (1968).
(3) M. C. Meyer and D. E. Guttman, *J. Pharm. Sci.*, **57**, 1627 (1968).
(4) *Ibid.*, **59**, 33 (1970).
(5) *Ibid.*, **59**, 39 (1970).
(6) J. C. Dearden and E. Tomlinson, *J. Pharm. Pharmacol., Suppl.*, **22**, 53S (1970).
(7) S. Goto, T. Ohki, S. Kiryu, and S. Iguchi, *Yakuzaigaka*, **31**, 247 (1971).
(8) K. F. Brown and M. J. Crooks, *Pharm. Acta Helv.*, **48**, 494 (1973).
(9) M. J. Crooks and K. F. Brown, *J. Pharm. Sci.*, **62**, 1904 (1973).
(10) M. J. Crooks and K. F. Brown, *J. Pharm. Pharmacol.*, **26**, 235 (1974).
(11) *Ibid.*, **26**, 304 (1974).
(12) K. F. Brown and M. J. Crooks, *Biochem. Pharmacol.*, in press.
(13) I. Kanfer and D. R. Cooper, *J. Pharm. Pharmacol.*, **28**, 58 (1976).
(14) S. J. A. Kazmi and A. G. Mitchell, *J. Pharm. Sci.*, **62**, 1299 (1973).
(15) F. Bottari, G. Di Colo, E. Nannipieri, M. F. Saettone, and M. F. Serafini, *ibid.*, **64**, 946 (1975).
(16) L. C. Craig, *Adv. Anal. Chem. Instr.*, **4**, 35 (1966).
(17) H. Matsumoto, H. Matsumura, and S. Iguchi, *Chem. Pharm. Bull.*, **14**, 385 (1966).
(18) P. Veng Pedersen, *J. Pharmacokin. Biopharm.*, **5**, 440 (1977).
(19) H. E. Hart, *Bull. Math. Biophys.*, **27**, 87 (1965).

ACKNOWLEDGMENTS AND ADDRESSES

Received April 23, 1976, from the *Department of Pharmacy, University of Sydney, Sydney, N.S.W. 2006, Australia.*

Accepted for publication January 6, 1977.

Supported in part by Grant 7414244 from the National Health and Medical Research Council of Australia.

[x] To whom inquiries should be directed. Present address: Department of Pharmacy, University of California, San Francisco, CA 94143.

Influence of Granulation Liquid Flow Rate on Particle-Size Distribution in Spray-Granulated Products

ASHOK MEHTA, KENNETH ADAMS, M. A. ZOGLIO ˣ, and J. T. CARSTENSEN *

Abstract □ Granulations were made at various air speeds and various rates of addition of granulating liquid in a spray-granulating assembly. The ensuing particle sizes were log-normal, and the data substantiate that the process is of the nature previously described. The mean diameter obtained was approximately proportional to the liquid flow rate squared but was independent of air rate. The standard deviation was independent of both parameters.

Keyphrases □ Granulations, spray—effect of liquid flow rate on particle-size distribution □ Particle-size distribution—spray granulations, effect of liquid flow rate □ Flow rate, liquid—effect on particle-size distribution in spray granulations □ Dosage forms—spray granulations, effect of liquid flow rate on particle-size distribution

The advantage of producing tablets from wet granulations was demonstrated previously (1, 2). Wet granulations are traditionally batch processes (3), although some products are successfully produced by continuous processes (3–7). In general, batch processes lend themselves to better process control than do continuous processes, but this is not the case with wet granulations. The kneading action present in sigma-type mixers (and to some extent in V-type blenders) necessitates close time control, since overkneading produces granules that are denser (less porous) than optimum (8, 9). Granulations formed in a fluid-bed drier (4, 7, 10–12) are not subject to the kneading action, and dried granules are not particularly affected by attrition (13). Therefore, aside from the economic aspects of fluid-bed drying (whether batch or continuous), this process seems to be of great advantage.

Zoglio *et al.* (13) described the dynamics of the fluid-bed drier. The particle-size distributions obtained by wet granulation and subsequent milling also were described (14, 15). Some descriptions were published of distributions from a continuous drier (4, 7). Dimensional and air kinetic parameter effects on several qualities of the spray-granulated product were discussed (16, 17). The purpose of this study was to explain the phenomena leading to experimental particle distributions (18, 19) obtained in a batch fluid-bed granulator.

EXPERIMENTAL

Granulations were made of the following composition: 17.5% sucrose, 69.9% lactose USP, 12.2% starch USP, and 0.4% pregelatinized starch. The powders (500 g) were placed in the basket of a spray granulator[1] and mixed for 5 min by air flow. The granulating liquid (water) was added at various rates, and addition was continued for 5 min. The granulated material was then dried for 8 min.

The temperature of the inlet air was 70° and the temperature of the outlet air was 36–44° for the first 6 min of drying. Drying was continued for 8 min, and the outlet temperature at that point was 44–46°. The moisture content of the granulations was determined by Karl Fischer moisture test and was 6–8% at that point.

[1] Aeromatic spray granulator model STREA-1, Aeromatic AG, Farnsburgerstrasse 6, CH-4132 Muttenz, Switzerland.

Sieve analysis of the granulations was performed, and the percent undersize was calculated. Several samples were discontinued after 2, 4, and 6 min of drying; their particle size was determined and did not differ from that at 8 min (Table I).

The water pressure and the nozzle setting can be changed to give different granulation liquid flow rates; three such flow rates were employed at an air velocity close to the minimum fluidization velocity (48 ft^3/min) and close to the entrainment velocity (58 ft^3/min).

Hardness of granules was tested as described previously (8, 9).

RESULTS AND DISCUSSION

An experiment was run in which the material was wet granulated and the semiwet granulation was dried by a method comparable to that of Bhutani and Bhatia (20). The material was in the first falling rate period, showing that an essential part of the drying (as expected) already was accomplished (3, 9).

Because the dilution of the binder solution has some effect when solutions are added (10–12, 21, 22), it was decided to add water to a mixture containing the binders (sucrose and pregelatinized starch) in the dry powder blend.

Since wrong conclusions could be drawn if the particle-size distributions were to change during the drying step, *i.e.*, after the water addition is complete, this point was checked by stopping the process after 2, 4, 6, and 8 min of drying. The results shown in Table I indicate that the particle-size distribution does not change during the drying step. The hardness (of a 14-mesh fraction) of granules made at a liquid flow rate of 23 ml/min after 2 min of drying was 80 ± 40 g/mg and increased to a plateau level of 230 ± 80 g/mg after 4, 6, and 8 min.

Figures 1 and 2 show the particle-size distributions achieved at the various granulation liquid flow rates at the two different fluidization air rates. All distributions can be characterized as being log-normal. The least-squares fit parameters are shown in Table II; the ordinate in this case is the normal standard deviate (t) corresponding to the cumulative percent over the diameter, and the abscissa (x) is the log of the diameter in micrometers.

The mean diameter, as expected, increased with increasing fluid addition rate; since the liquid was added over a certain time (5 min), a higher fluid rate essentially implies a larger total addition of water. Furthermore, although larger amounts of granulating liquid increased the diameter, the standard deviation of the population (the slopes of the plots in Figs. 1 and 2) remained the same regardless of liquid and air velocities.

These distributions may be explained by the model proposed by Irani and Callis (18); the growth is assumed to be such that the particle size, M, starts as a minimum close to zero, M_0, and grows to a maximum, M_∞. At the end of the process, any agglomerate is characterized by the fact that it has been exposed to growth for a length of time, t, at a unit spray rate, R. There is an average time of growth, $\bar{t}$, and the times are normally distributed around this average; defining the time:

$$\tau = t - \bar{t} \qquad \text{(Eq. 1)}$$

allows expression of time by:

$$f(\tau) = (1/\sqrt{2\pi}) \exp(-\tau^2/2) \qquad \text{(Eq. 2)}$$

where f is the Gaussian frequency function, with unit variance (see *Appendix*).

The conditions of growth are such that (see *Appendix*):

$$dM/dt = \Phi(M) = M/b \qquad \text{(Eq. 3)}$$

or:

$$t = a + b \ln (M/\bar{M}) \qquad \text{(Eq. 4)}$$

Equations 4 and 1 may be combined to read:

$$\tau = b \ln (M/\bar{M}) \qquad \text{(Eq. 5)}$$

Table I—Sieve Analysis of a Granulation at 23 ml/min of Liquid Addition as a Function of Drying Time

Minutes	Percent on Mesh						
	14	20	40	60	80	100	Pan
2	4	15	49	27	4	1	0
4	5	14	48	27	5	1	0
6	4	14	49	28	4	1	0
8	3	14	50	28	4	1	0

where the condition that $\tau = 0$ when $M = \overline{M}$ dictates that:

$$\bar{t} = a \qquad \text{(Eq. 6)}$$

Inserting Eq. 5 into Eq. 2 then yields:

$$f[b \ln (M/\overline{M})] = (1/\sqrt{2\pi}) \exp\{-[b \ln (M/\overline{M})]^2/2\} \qquad \text{(Eq. 7)}$$

which shows[2] that $b(\ln M - \ln \overline{M})$ is normally distributed with mean zero and unit standard deviation; *i.e.*, $\ln M - \ln \overline{M}$ is normally distributed with mean zero and a standard deviation of $\ln \sigma = 1/b$ or $\ln M$ is normally distributed with mean $\ln \overline{M}$ and a standard deviation of $\ln \sigma = 1/b$.

From the development of Eq. 1, increasing the spray rate, R, increases the time elements t and $\bar{t}$ by an (added) constant but leaves τ unaltered. This result is compatible with the fact that b (*e.g.*, in Eqs. 3–5) is a constant. Hence, the standard deviation of the distributions should be independent of the spray rate; examination of Table II shows this to be the case.

The value of $\overline{M}$ must increase with increasing R, and M and $\overline{M}$ must increase in the same fashion (so that $M/\overline{M}$ is rate independent); otherwise, $t - a$ could not remain constant as described. The only way this can be accomplished is by M (and $\overline{M}$) being proportional to R or to a power of R, *i.e.*:

$$\ln \overline{M} = q(\ln R) + p \qquad \text{(Eq. 8)}$$

The data are plotted in this fashion in Fig. 3; the exponent is close to 2 ($2.221 = q$). The correlation is good ($r = 0.96$). Therefore, the spray granulation follows Irani–Callis kinetics in producing log-normal particle distributions, the standard deviation is spray rate independent, and the mean particle diameter is approximately proportional to the square of the spray rate. The mean diameter is not a function of the fluidization air rate (since both sets of data fit the same line).

Some stochastic models are attractive at first sight; their development and the reasons for their rejection are shown in the *Appendix*. This development implies the necessity of employing a kinetic rather than a stochastic model.

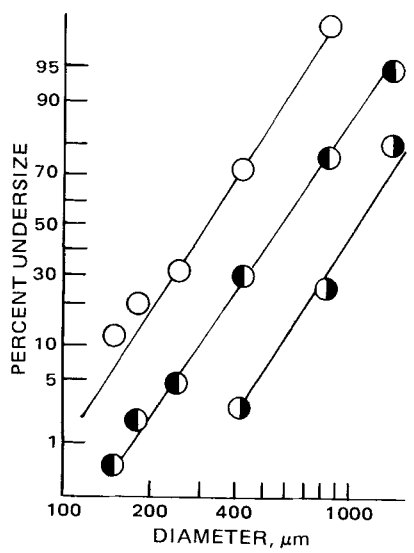

Figure 1—*Particle-size distributions (cumulative undersize) of granulations made at low fluidization air rate. Liquid flow rates are:* ○, *23 ml/min;* ◐, *26 ml/min; and* ◑, *30 ml/min. Least-squares parameters are shown in Table II.*

[2] If d is normally distributed with standard deviation σ' and mean x, then $(d - x)$ is normally distributed with standard deviation σ' and mean zero and $b(d - x)$ is normally distributed with standard deviation $b\sigma'$ and mean zero. In the above, $d = \ln M$ and $x = \ln \overline{M}$, so $b\sigma' = 1$; *i.e.*, $\sigma' = 1/b$. Traditionally, the standard deviation for a log-normal distribution is denoted $\sigma' = \ln \sigma$; *i.e.*, $\ln \sigma = 1/b$.

Table II—Least-Squares Fit Parameters of t^a *versus* $\ln d$ for Six Granulations

Air Flow	Liquid Flow, ml/min	Slope	Intercept	Mean, μm
Low	23	−1.98 ± 0.02	12.52 ± 0.02	557
Low	26	−2.01 ± 0.02	13.22 ± 0.03	718
Low	30	−1.99 ± 0.02	13.24 ± 0.02	775
High	20	−1.90 ± 0.04	10.82 ± 0.06	297
High	26	−1.86 ± 0.10	11.81 ± 0.08	634
High	33	−2.60 ± 0.10	18.02 ± 0.02	1023

[a] Normal standard deviate.

APPENDIX

Distribution of Time of Exposure—To show that the times of exposure of particles to liquid, t, are normally distributed, consider the situation where N particles are exposed to a flow of liquid.

In a time element, δt, a fraction, f, of the solid mass will be wetted and there will be $N(1 - f)$ unwetted particles and Nf wetted particles. After $2\delta t$, there will be $N(1 - f)^2$ unwetted particles and Nf^2 particles that have been wetted twice (*i.e.*, a fraction, f, of the Nf once wetted particles will be wetted again). The amount of once wetted particles will be the original Nf less the Nf^2 that became wetted twice plus the $N(1 - f)f$ particles that were wetted during the second (but not the first) interval. The total is:

$$Nf - Nf^2 + N(1 - f)f = 2N(1 - f)f \qquad \text{(Eq. A1)}$$

A combination of this argument will show that after $n\delta t$ the number of particles that have received i application of liquid will be:

$$N_i = \binom{n}{i} f^i (1 - f)^{n-i} N \qquad \text{(Eq. A2)}$$

Equation A2 is obviously a binomial distribution which, for large n, approaches a normal distribution. The "number of applications" in the discrete sense, δt, is equivalent to the time, t, of exposure on a continuous sense so that the time of exposure is normally distributed.

Growth Rate of Agglomerate—The growth rate of an agglomerate is related to its size, M, in the sense that the larger it is the higher the collisional cross-section, *i.e.*, the higher the probability of growth. If one assumes that:

$$dM/dt = (1/b)M \qquad \text{(Eq. A3)}$$

then:

$$\ln M = (1/b)(t - \bar{t}) + q \qquad \text{(Eq. A4)}$$

where $(1/b)$ is a constant and $q - (\bar{t}/b)$ is an integration constant.

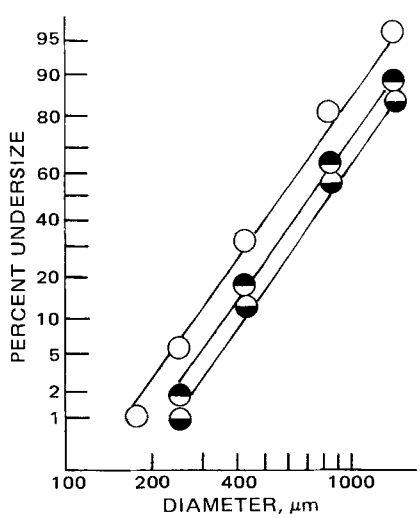

Figure 2—*Particle-size distributions (cumulative undersize) of granulations made at high fluidization air rate. Liquid flow rates are:* ○, *20 ml/min;* ◓, *26 ml/min; and* ◒, *33 ml/min.*

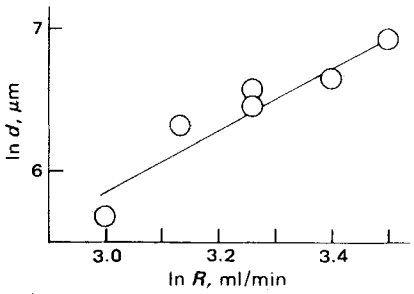

Figure 3—*Plot of the mean diameters from Figs. 1 and 2 plotted* versus *the spray rate in log–log fashion. The least-squares fit equation is ln* $\bar{d} = 2.221 \ln R - 0.8$.

Agglomerates characterized by the average time exposure, $\bar{t}$, will have a size $\overline{M}$ so that:

$$\ln \overline{M} = 0 + q \qquad \text{(Eq. A5)}$$

Inserting Eq. A5 into Eq. A4 gives:

$$\ln (M/\overline{M}) = (1/b)(t - \bar{t}) = \tau/b \qquad \text{(Eq. A6)}$$

which is equivalent to Eq. 5.

It is recalled that $t - \bar{t} = \tau$ is normally distributed with mean zero, so that as $t \to -\infty$, $\ln (M/\overline{M}) \to -\infty$, *i.e.*, $M \to 0$, which is compatible with the process. As $t \to \infty$, $M \to \infty$; but, because of truncation, M will reach a maximal size.

The limit sizes can be introduced formally by expressing Eq. A3 as $dM/dt = (1/b)(M - M_0)$ and imposing boundary conditions if desired.

Other Models—There are other hypothetically feasible models, but they fail to adhere to the experimental data. These models are all based on collision and "sticking" probabilities; the most encompassing of these is exemplified here. If it is assumed that there are ζ collisions per second and a sticking probability of ϵ, then the overall probability of forming a j-mer from a $(j - m)$-mer and an m-mer at time t is:

$$Pr = \gamma C_{j-m}(t) C_m(t) \qquad \text{(Eq. A7)}$$

where $\gamma = \epsilon\zeta$ is the overall reaction probability.

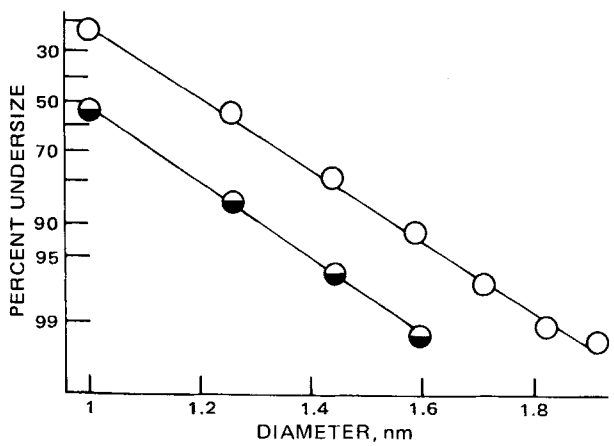

Figure 4—*Distribution of sizes in a particle population initially consisting of 10,000 particles of the same size, calculated according to Eq. A8 with* $\gamma = 0.3$ *after* $\delta t = 3$ (◒) *and* $\delta t = 4$ (○) *time intervals. The diameter is the cube root of the number of particles. Points are calculated, not experimental. Although* $2^4 = 16$*-mers exist after time 4, only 7-mers and lower have significant concentrations.*

If the largest particle is an l-mer, then j's are formed by Eq. A7 in summation of all m's smaller than j, and j-mers are lost in forming $(j + 1)$-mers, $(j + 2)$-mers, and so on up to and including l-mers; *i.e.*, the j-mer population between time t and $t + \delta t$ increases by:

$$\delta C_j(t) = \sum_{m=1}^{j-1} \gamma C_{j-m}(t) C_m(t) - \sum_{q=1}^{l-j} \gamma C_j(t) C_q(t) \qquad \text{(Eq. A8)}$$

Simulated data by this model with a value of $\gamma = 0.3$ and an initial population of $N = 10{,}000$ particles after $\delta t = 3$ and $\delta t = 4$ are shown in Fig. 4; the distribution is *normal* (*i.e.*, not log-normal). The failure of this model to adhere to the data probably lies in assuming that γ is independent of the size of j, q, m, and l. If the probability is a function of the size of the agglomerate, then the best approach is the kinetic one discussed in the body of the paper.

REFERENCES

(1) P. Finholt, in "Dissolution Technology," L. Leeson and J. T. Cartensen, Ed., I. P. T. of the American Pharmaceutical Association, Washington, D.C., 1974, p 106.

(2) W. Erni, W. A. Ritschel, M. R. Scheffler, D. G. Schickling, and W. R. Nadler, "First International Conference on Pharmaceutical Technology," vol. II, 1977, p. 243.

(3) J. T. Carstensen, "Theory of Pharmaceutical Systems," vol. II, Academic, New York, N.Y., 1973, p. 232.

(4) J. T. Carstensen, in "Gas-Fluid Interfaces," J. M. Marchello and A. Gomezplata, Eds., Dekker, New York, N.Y., 1976, chap. VI, p. 6.

(5) C. Pitkin and J. T. Carstensen, *J. Pharm. Sci.*, **62,** 1215 (1973).

(6) M. W. Scott, H. A. Lieberman, A. S. Rankell, and J. V. Battista, *ibid.*, **53,** 314 (1964).

(7) A. S. Rankell, M. W. Scott, H. A. Lieberman, F. S. Chow, and J. V. Battista, *ibid.*, **53,** 320 (1964).

(8) M. A. Zoglio, H. E. Huber, G. Koehne, P. L. Chan, and J. T. Carstensen, *ibid.*, **65,** 1205 (1976).

(9) J. T. Carstensen, T. Lai, D. W. Flickner, H. E. Huber, and M. A. Zoglio, *ibid.*, **65,** 992 (1976).

(10) W. L. Davis and W. T. Gloor, Jr., *ibid.*, **60,** 1869 (1971).

(11) *Ibid.*, **61,** 618 (1972).

(12) *Ibid.*, **62,** 170 (1973).

(13) M. A. Zoglio, W. H. Streng, and J. T. Carstensen, *J. Pharm. Sci.*, **64,** 1869 (1975).

(14) G. Steiner, M. Patel, and J. T. Carstensen, *ibid.*, **63,** 1395 (1974).

(15) J. T. Carstensen and M. Patel, *ibid.*, **63,** 1494 (1974).

(16) U. Thurn, Ph.D. thesis, Eidgenössischen Technischen Hochschule Zürich, 1970, Diss. No. 4511, Juris Druck und Verlag, Zurich, Switzerland.

(17) P. Prioux, D. Lefort des Ylouses, M. Seiller, and D. Duchene, *J. Pharm. Belg.*, **30,** 132 (1975).

(18) R. R. Irani and C. F. Callis, "Particle Size: Measurement, Interpretation and Application," Wiley, New York, N.Y., 1963, p. 39.

(19) P. W. Stern, *J. Pharm. Sci.*, **63,** 1171 (1974).

(20) B. R. Bhutani and V. N. Bhatia, *ibid.*, **64,** 135 (1975).

(21) P. M. Hill, *ibid.*, **65,** 313 (1976).

(22) A. M. Marks and J. J. Sciarra, *ibid.*, **57,** 497 (1968).

ACKNOWLEDGMENTS AND ADDRESSES

Received June 9, 1976, from *Merrell-National Laboratories, Cincinnati, OH 45215.*

Accepted for publication January 5, 1977.

* Present address: School of Pharmacy, University of Wisconsin, Madison, WI 53706.

[x] To whom inquiries should be directed.

Effect of Lipids on Enzymatic Activity of Pig Heart Mitochondrial Malate Dehydrogenase Monomolecular Films

A. W. MALICK * and N. D. WEINER ‡x

Abstract □ The effect of various lipids on the enzymatic activity of pig heart mitochondrial malate dehydrogenase monomolecular films was studied using the subphase exchange technique described previously. Surface pressure–surface area (π–A) curves of mixed films of the enzyme with dipalmitoyllecithin, egg lecithin, cholesterol, and phospholipids extracted from pig hearts showed that the enzyme interacted with all of the lipids and that the enzyme remained in the film at pressures well above the collapse pressure of malate dehydrogenase in the absence of lipid. The surface enzyme activity was dependent on surface pressure for each lipid; in all cases, the lipids greatly broadened the range of surface pressures where surface enzyme activity was observed. The π–A and enzyme activity data showed good correlation. Although the simple model system employed does not simulate the complexity of the biological membrane, it gives some evidence for the role of lipids in the stability of membrane-bound enzymes.

Keyphrases □ Lipids—effect on activity of pig heart mitochondrial malate dehydrogenase monomolecular films □ Enzyme activity—pig heart mitochondrial malate dehydrogenase, monomolecular films, effect of lipids □ Malate dehydrogenase, pig heart mitochondrial—monomolecular films, effect of lipids on activity □ Films, monomolecular—pig heart mitochondrial malate dehydrogenase, effect of lipids on activity

The importance of lipids for the integrity and function of biomembranes is firmly established. New attempts are being made to ascertain more accurately the contribution of lipids to the properties of biological interfaces. Since cellular proteins are mainly situated at interfaces, the association among proteins and lipids at these interfaces is important to understand (1, 2).

Some lipids appear to be crucial for specialized processes, such as enzyme association that affects the orientation and, in turn, the activity of enzyme molecules. Several enzymes associated with membranes and enzymatic reactions at the biological interface are important, and it is of interest to study the catalytic activity of membrane-bound enzymes and complexes of these enzymes with lipids at an interface.

BACKGROUND

Membrane-bound enzymes are believed to interact with membrane lipids, and these interactions may affect the enzyme activity. A lipid requirement for the catalytic activity of a number of enzymes, *e.g.*, some dehydrogenases, was observed (3, 4). Enzyme activity was lost or reduced when the lipid was removed from the enzyme system. Either stimulation or reactivation by lipids of several enzymes was reported (5–11), and the lipid requirement usually exhibited some specificity (3, 4, 12). Both lipid specificity and lipid concentration apparently are involved in the activity of lipid-requiring enzymes. To perform its enzymatic function, an enzyme also must possess the correct conformation.

Film studies at an air–water interface of enzymes and enzyme–lipid complexes can investigate the behavior of membrane-bound enzymes. The principal inducement to the study of such systems is their close analogy to the membrane of normal cells. Therefore, they have been investigated as working models for cell membranes from the point of view of both membrane structure and function (13).

Previously (14), a technique for studying the catalytic activity of enzymes spread as a film at an air–water interface by exchanging the subphase under the film to remove unspread enzyme molecules was reported. In these studies, pig heart mitochondrial malate dehydrogenase, a vital member of the tricarboxylic acid cycle, was used. Mitochondrial malate dehydrogenase was chosen as a model because it is a membrane-bound enzyme that forms stable monolayers at the air–water interface and offers a convenient assay for catalytic activity. Heart muscle has been used as the primary source for the isolation and purification of this enzyme (15).

Mitochondrial malate dehydrogenase is very unstable in aqueous solutions, and this instability has been ascribed to the removal of the enzyme by severe extraction procedures from its bound states, which suggests that the enzyme is firmly bound in the mitochondrion. Phospholipids constitute about 20% of the total weight of the mitochondrion and are present in particulate fractions isolated from pig heart mitochondria (16).

Whole heart micelles, mitochondrial lipids, and fatty acids reportedly increase the stability of the malate dehydrogenase. An increase in activity and stability of this enzyme was reported in the presence of mitochondrial lipids and a series of saturated and unsaturated fatty acids (16). However, at high concentrations of cephalin or egg lecithin, the activity and stability of the enzyme decreased (17). It was reported that lysolecithin stabilized the enzyme, phosphatidylcholine and phosphatidylethanolamine did not significantly alter the enzyme activity, and cardiolipin and phosphatidylserine strongly inhibited the enzyme (18). In all of the studies cited, enzyme activity was determined in the bulk phase.

One study (19) reported that the enzyme adsorbed onto lipid monolayers from a subphase solution and that enzyme adsorption was greater in the case of negatively charged lipids as compared to neutral or positively charged lipids. The catalytic activity of such complexes when removed from the surface was studied, and the surface enzyme activity was only a fraction of that in the bulk (19).

The purpose of this phase of the study was to investigate both the film behavior and the catalytic activity of pig heart mitochondrial malate dehydrogenase–lipid complexes at the air–water interface using both synthetic lipids and lipids of biological origin. An important aspect was to study enzyme activity with lipids at varying film pressures. This aspect is of interest because it allows a change in the conformations, orientations, and interactions of the enzyme molecules.

EXPERIMENTAL

Materials—Malate dehydrogenase[1] (porcine heart) was supplied as a suspension in 70% saturated ammonium sulfate solution. Oxalacetic acid[2] and reduced nicotinamide adenine dinucleotide[1] (NADH), 90%, were used to measure enzyme activity. The lipids egg lecithin[3], dipalmitoyllecithin[2], and cholesterol were chromatographically pure. The mixed pig heart phospholipids were extracted by a procedure outlined by Kates (20).

The inorganic chemicals, all reagent grade, were checked for surface impurities. The water was first deionized by passing distilled water through a mixed resin bed of a demineralizer[4] and then distilled twice from an all-glass still. All buffer solutions were passed through a column of activated charcoal. Organic solvents were spectrograde and were checked for surface impurities.

Apparatus and Monolayer Methods—The apparatus and procedure for subphase exchange and for determining the π–A isotherms for protein monolayers spread at the air–water interface were described previously (1, 14). In mixed films of malate dehydrogenase with lipids, the lipid was spread first; then, after 15 min, the protein was spread by the Trurnit (21) method. After another 25 min, compression of the mixed film was initiated. For lipid films alone, compression was started 40 min after

[1] P. L. Biochemicals, Milwaukee, Wis.
[2] Schwarz/Mann, Orangeburg, N.Y.
[3] Extracted in this laboratory.
[4] Bantam.

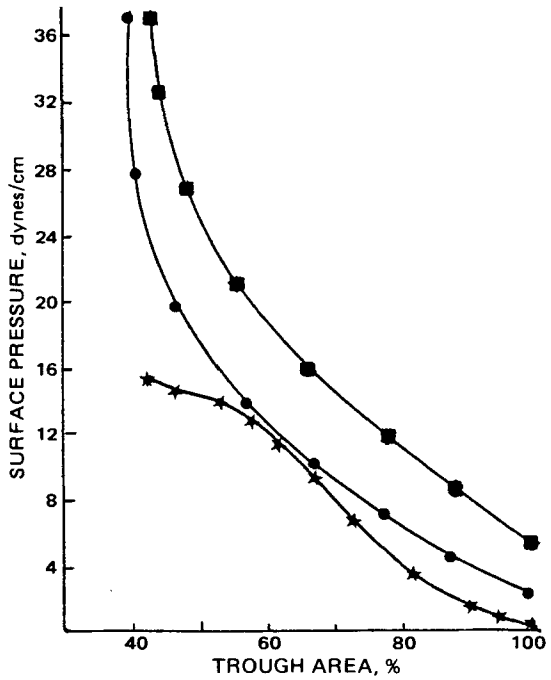

Figure 1—*The π–A curves of films spread on pH 7.4 phosphate buffer. Key: ●, 2.95 × 10^{-2} mg of dipalmitoyllecithin; ■, 8.1 × 10^{-2} mg of malate dehydrogenase and 2.95 × 10^{-2} mg of dipalmitoyllecithin mixed film; and ★, 8.1 × 10^{-2} mg of malate dehydrogenase.*

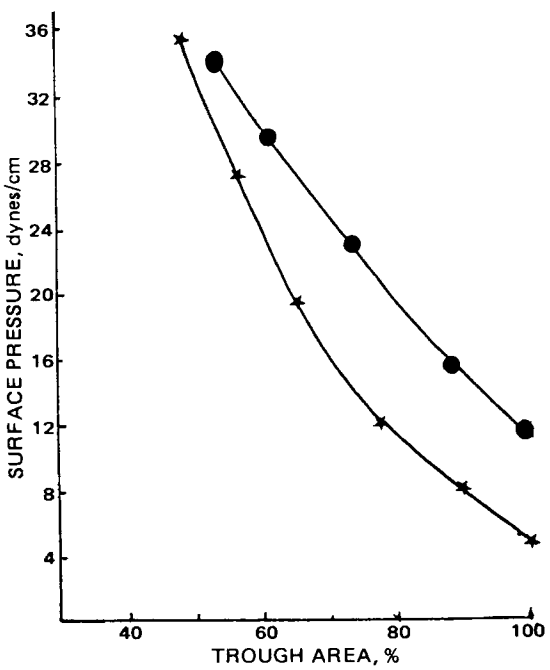

Figure 2—*The π–A curves of films spread on pH 7.4 phosphate buffer. Key: ★, 3.2 × 10^{-2} mg of egg lecithin; and ●, mixed film of 8.1 × 10^{-2} mg of malate dehydrogenase and 3.2 × 10^{-2} mg of egg lecithin.*

spreading. Hexane–ethanol (95:5 v/v) was the solvent used for spreading dipalmitoyllecithin, hexane was used for cholesterol and egg lecithin, and benzene–chloroform (97:3 v/v) was used for pig heart phospholipid extract.

The procedure for determining catalytic activity of the surface-spread enzyme was given previously (14).

To determine the amount of enzyme adsorbed at the air–water interface after subphase exchange, films were removed by negative pressure using a narrow glass tube and then analyzed for protein content by a modification of the Lowry (22) technique.

RESULTS AND DISCUSSION

π–A Behavior of Lipid–Enzyme Mixed Films—The π–A behavior of mixed monolayers of malate dehydrogenase with dipalmitoyllecithin (a saturated phospholipid), egg lecithin (an unsaturated phospholipid), cholesterol, and pig heart phospholipids (a phospholipid of the same source as that of the enzyme) was studied. In all cases, the films were stable and gave reproducible π–A curves.

Penetration and possible interaction between lipids and proteins in monolayers can be detected by an increase in surface pressure if the area is kept constant or by an increase in area if the surface pressure is kept constant. In the presence of a previously spread lipid, the protein can penetrate the film in either a partially unfolded or completely unfolded state, depending on the available space. The protein applied would have its hydrocarbon tails out of the subphase, interacting with the side chains of the lipid, while its polar groups would anchor it to the surface. Thus, protein incorporation into the lipid monolayer indicates the existence of a hydrophobic site capable of association with hydrocarbon chains of the lipid.

Hydrophobic associations of the protein with the phospholipid facilitated by initial electrostatic binding were proposed (23). A similar binding-mediated penetration of cholesterol monolayers by proteins also was proposed (24). It was suggested (25) that the polar portions of the surfactant molecule may interact with their counterparts in the protein film through permanent dipole attraction, dipole-induced dipole interaction, and electrostatic attraction. The nature of this adsorption may disrupt hydrogen bonding, which partially stabilizes the tertiary protein structure and makes the protein molecule more amenable to unfolding.

Adsorption of pig heart mitochondrial malate dehydrogenase from an enzyme subphase solution onto lipid monolayers at high surface pressures was reported (19).

Figure 1 shows the π–A plots of dipalmitoyllecithin, malate dehydrogenase, and dipalmitoyllecithin–malate dehydrogenase mixed films. In all cases, the subphase was exchanged. The dipalmitoyllecithin concentration was chosen so that the interaction of malate dehydrogenase could be studied at low and high surface pressures of the mixed film. The surface pressure of the dipalmitoyllecithin film was about 2 dynes/cm prior to protein addition.

Figure 1 shows that the mixed film was expanded at all areas relative to the dipalmitoyllecithin film alone. The increase in surface pressure at a given surface area is taken as a measure of interaction between the lipid monolayer and the protein. The degree of expansion, $\Delta\pi$, of the mixed film decreased as the surface pressure increased, suggesting that some protein may be squeezed out of the mixed film or may move to a nonarea-determining position at high π values. There is no crossover of the π–A plots of the mixed film and the dipalmitoyllecithin film, and film expansion persisted even beyond the point at which the protein film in the absence of lipid became unstable. An expansion of the mixed film over that of the lipid film at π values below the collapse pressure of the protein can be due to simple adsorption of the protein at the interface. However, if the expansion is observed at higher π values, it suggests penetration of some part of the protein into the hydrocarbon portion of the lipid monolayer (23).

The decrease in $\Delta\pi$ of the mixed film at higher surface pressures suggests that there is no true complex formed. The resultant increase in the area of the dipalmitoyllecithin film after the application of the protein may involve protein penetration, as suggested previously (23, 24, 26, 27), when the polar groups of the protein anchor to the polar head groups of the lipid and the hydrocarbon residues of the enzyme align themselves with the fatty acyl chains of the lipid through van der Waals forces. The possible partial removal of the enzyme at higher surface pressures can be accounted for by differences in chain lengths of the hydrophobic tails of the protein and the lipid. With equal chain lengths, stronger adhesion and less possibility of ejection of the protein molecules would be expected.

Figure 2 shows the π–A plots of egg lecithin and a malate dehydrogenase–egg lecithin mixed film. The molar ratio of lipid to protein was the same as for the dipalmitoyllecithin–enzyme mixed film. The mixed film of the protein and egg lecithin was expanded at all areas relative to the egg lecithin film. The value of $\Delta\pi$ of the mixed film at higher π values decreased, as was the case with the dipalmitoyllecithin–malate dehydrogenase mixed film (Fig. 1). Thus, protein penetration of the lipid film appears to be the interaction mechanism between egg lecithin and malate dehydrogenase.

A comparison of Figs. 1 and 2 shows that the expansion of the lipid

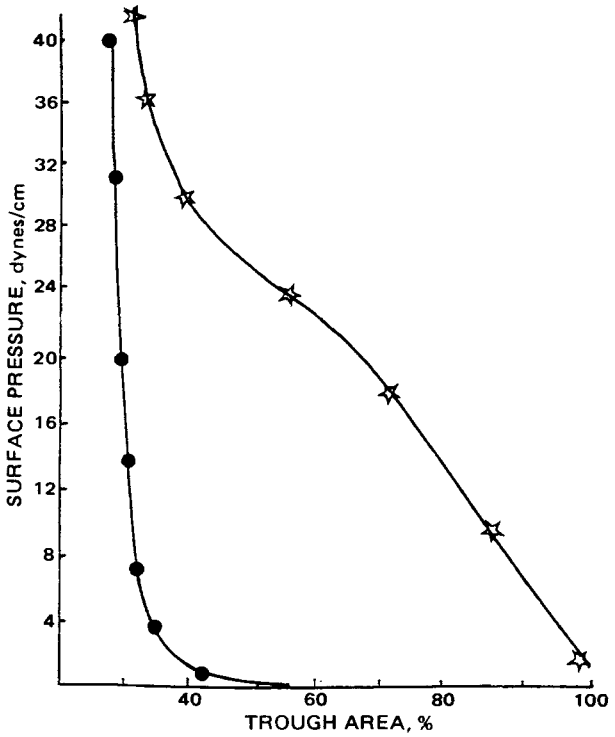

Figure 3—*The π–A curves of films spread on pH 7.4 phosphate buffer. Key: ●, 1.55 × 10^{-2} mg of cholesterol; and ☆, mixed film of 8.1 × 10^{-2} mg of malate dehydrogenase and 1.55 × 10^{-2} mg of cholesterol.*

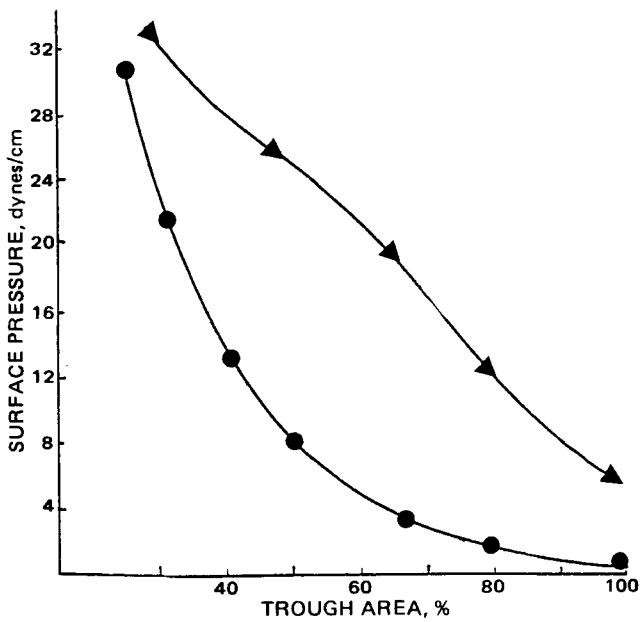

Figure 4—*The π–A curves of films on pH 7.4 phosphate buffer. Key: ●, 2.95 × 10^{-2} mg of pig heart phospholipids; and ▲, mixed film of 8.1 × 10^{-2} mg of malate dehydrogenase and 2.95 × 10^{-2} mg of pig heart phospholipids.*

films by malate dehydrogenase was greater for the egg lecithin film than for the dipalmitoyllecithin film. With the egg lecithin–enzyme mixed film, the expansion seemed to be greatest at intermediate π values.

If the magnitude of expansion of the lipid film by the protein is taken as a criterion of the degree of interaction, these results suggest that malate dehydrogenase interacts more strongly with egg lecithin than dipalmitoyllecithin. The fatty acyl chains of dipalmitoyllecithin are saturated (28), and the molecule of egg lecithin is of the 1-saturated 2-unsaturated type (29). Thus, there is a better packing of molecules in the monomolecular films of dipalmitoyllecithin as compared to egg lecithin, and the greater motional freedom of the acyl side chains of egg lecithin would be expected to result in a greater interaction between the hydrophobic side chains of the protein and the lipid.

Figure 3 shows the π–A plots of cholesterol and a malate dehydrogenase–cholesterol mixed film. The molar ratio of lipid to protein was the same as for the other lipids. The cholesterol film became highly expanded in the presence of malate dehydrogenase, from low π values to about 22 dynes/cm. After this point, an increase in the pressure produced a gradual decrease in the film area. However, beyond 32 dynes/cm, the mixed film became very condensed but not superimposable with the pure cholesterol film.

The large expansion shown suggests a strong interaction of cholesterol and malate dehydrogenase. Reduction of $\Delta\pi$ of the mixed film at higher π values in this case may also be due to the removal of a portion of the enzyme from an area-determining position to a nonarea-determining position or to a portion of the protein being squeezed out of the mixed film.

Colacicco (30) also observed that cholesterol films can pull large quantities of protein into the monolayer. The surface density of anchored protein, as expressed by the $\Delta\pi$ values, is much larger with cholesterol than with the phospholipids studied. How cholesterol interacts with proteins is still quite unclear. Colacicco (30) suggested interspersion of cholesterol within the subunits of protein film. Van Deenen (31) demonstrated that the interaction of the hydrophobic part of the sterol molecule is of critical importance in protein–sterol interactions in monolayers. The presence and orientation of the hydroxyl group in cholesterol also are important for this interaction (30, 31). In mixed monolayers of cholesterol and protein, the hydroxyl group of the cholesterol can interact with the peptide bonds of proteins (32).

Figure 4 shows the π–A plots of films of the total phospholipid extract from the pig heart and the malate dehydrogenase–total phospholipid extract mixed films. On a weight basis, an amount of the total phospholipid extract spread was equivalent to the amount of dipalmitoyllecithin used in the studies of malate dehydrogenase–dipalmitoyllecithin mixed films. The total phospholipid extract from pig heart formed stable films which gave reproducible π–A curves.

Figure 4 shows a large expansion of the total phospholipid extract film by malate dehydrogenase. A comparison of Figs. 1, 2, and 4 shows that the expansion by malate dehydrogenase was greatest for the total phospholipid extract when compared with dipalmitoyllecithin and egg lecithin films. This result suggests a relatively strong interaction between the enzyme and the phospholipids from the same source as the enzyme and could be due to specific interactions between malate dehydrogenase and the phospholipids from the natural source. Penetration of the lipid film, rather than a complex formation between the enzyme and the lipid, seems to be occurring since the degree of expansion is reduced at higher pressures.

Catalytic Activity of Malate Dehydrogenase Films—The catalytic activity of malate dehydrogenase films in the absence of lipids was previously reported (14).

Figure 5 shows the catalytic activity of the enzyme film in the absence of lipid and the catalytic activity of the enzyme film in the presence of dipalmitoyllecithin. The activity of the enzyme–dipalmitoyllecithin film remained relatively constant up to a surface pressure of about 11 dynes/cm. Beyond 11 dynes/cm, catalytic activity decreased with in-

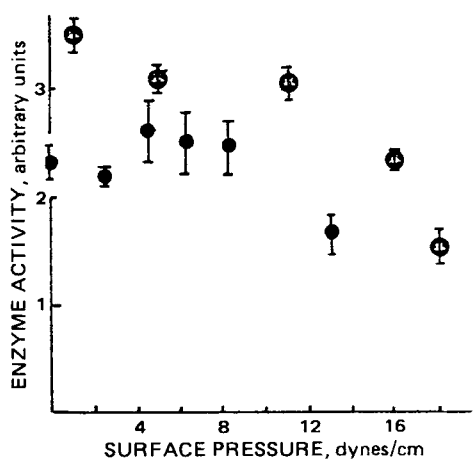

Figure 5—*Catalytic activity of malate dehydrogenase* versus *surface pressure plots. Key: ●, malate dehydrogenase film; and ☆, malate dehydrogenase–dipalmitoyllecithin mixed film.*

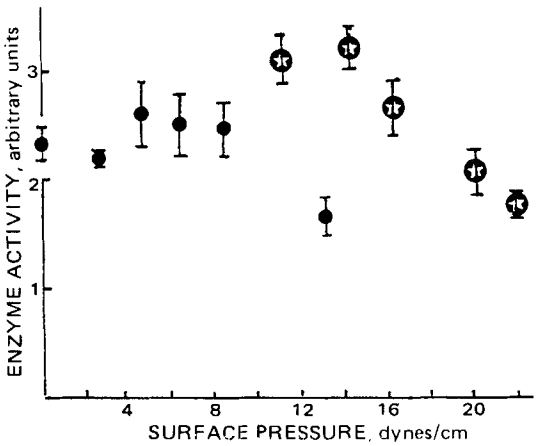

Figure 6—*Catalytic activity of malate dehydrogenase* versus *surface pressure plots. Key:* ●, *malate dehydrogenase film; and* ☆, *malate dehydrogenase–egg lecithin mixed film.*

creasing surface pressures. At high surface pressures, the orientation and conformation of the enzyme–lipid complex must be changing in a way unfavorable for enzyme activity.

Figure 5 shows a stabilizing effect of the lipid, particularly at low surface pressures, where the enzyme activity was significantly increased over that of the enzyme film in the absence of lipid. The stabilizing effect was also apparent at higher surface pressures. At surface pressure values of 16 and 18 dynes/cm, just about all of the surface enzyme activity was lost in malate dehydrogenase films in the absence of dipalmitoyllecithin. Therefore, the dipalmitoyllecithin not only increases the activity of the enzyme but also greatly broadens the pressure range where this activity occurs.

Figure 6 shows the catalytic activity of the enzyme film in the absence of lipid and the catalytic activity of the enzyme film in the presence of egg lecithin. In this mixed film, a dependence of enzyme activity on surface pressure was also observed. At intermediate surface pressures (9–14 dynes/cm), catalytic activity remained relatively constant. Beyond 16 dynes/cm, catalytic activity decreased with increasing surface pressure. Egg lecithin also increased the enzyme activity of malate dehydrogenase and broadened the pressure range over which the enzyme activity was observed as compared to that of the enzyme in the absence of lipid.

A comparison of Figs. 5 and 6 shows that the catalytic activities of the enzyme–dipalmitoyllecithin and the enzyme–egg lecithin films were within the same range of values between surface pressures of 11 and 16 dynes/cm. However, the range of surface pressures over which the enzymatic activity was observed was broader for egg lecithin than for dipalmitoyllecithin. With dipalmitoyllecithin, significant catalytic activity was observed up to a surface pressure of 18 dynes/cm. However, in enzyme–egg lecithin films, catalytic activity was observed up to a surface

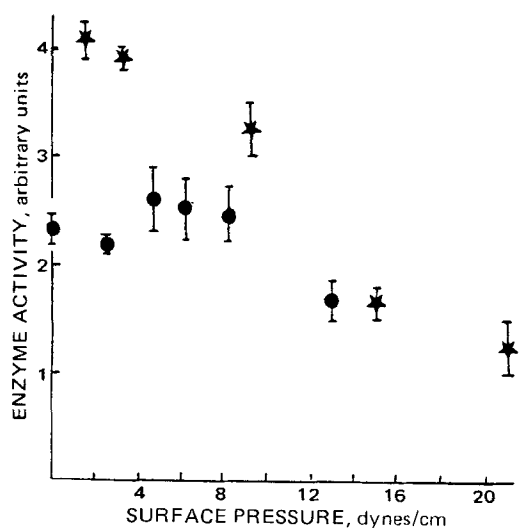

Figure 7—*Catalytic activity of malate dehydrogenase* versus *surface pressure plots. Key:* ●, *malate dehydrogenase film; and* ★, *malate dehydrogenase–cholesterol mixed film.*

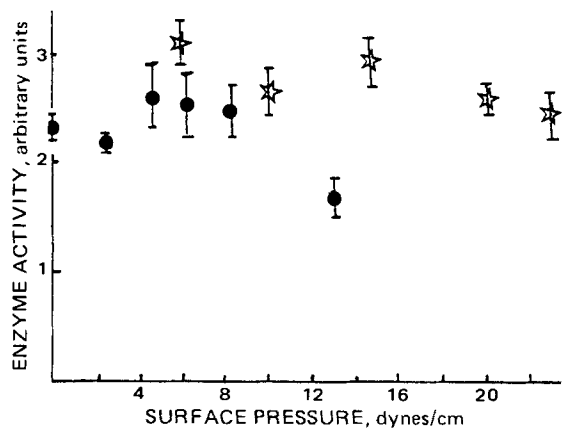

Figure 8—*Catalytic activity of malate dehydrogenase* versus *surface pressure plots. Key:* ●, *malate dehydrogenase film; and* ☆, *malate dehydrogenase–pig heart phospholipids mixed film.*

pressure of about 22 dynes/cm. Therefore, the interaction of the enzyme with the unsaturated phospholipid, egg lecithin, apparently is more favorable for stabilization of the enzyme than the interaction with the saturated phospholipid, dipalmitoyllecithin.

Moreover, the surface area expansion effect was greater with the egg lecithin–enzyme films than with the dipalmitoyllecithin–enzyme films (Figs. 1 and 2), indicating a greater interaction for the former.

Figure 7 shows the catalytic activity of the enzyme film in the absence of lipid and the catalytic activity of the enzyme film in the presence of cholesterol. A comparison of Figs. 5–7 reveals that the maximum catalytic activity observed in any of these systems was with the cholesterol–malate dehydrogenase mixed film at low π values. The maximum activity in arbitrary units observed at any surface pressure was 4.08, 3.5, 3.2, and 2.65 for films of enzyme–cholesterol, enzyme–dipalmitoyllecithin, enzyme–egg lecithin, and enzyme alone, respectively.

Figure 7 shows that catalytic activity of the enzyme–cholesterol film decreased with an increase in surface pressure. Initially, a gradual decrease was observed, but there was a sharp decrease beyond 15 dynes/cm. Comparison with the enzyme activity in the absence of any lipid shows that cholesterol not only stabilized the enzyme film but increased maximum surface enzyme activity significantly at π values up to 9 dynes/cm. Even at a surface pressure as high as 22 dynes/cm, there was significant enzyme activity. A comparison of the surface catalytic activity of enzyme–dipalmitoyllecithin, enzyme–egg lecithin, and enzyme–cholesterol films shows that the activity of the enzyme–cholesterol film was higher at low surface pressure values. The maximum area expansion by the enzyme was observed in the enzyme–cholesterol films.

Figure 8 shows the catalytic activity of the enzyme film in the absence of lipid and the catalytic activity of the enzyme film in the presence of a pig heart phospholipid extract. The enzyme activity of the mixed film was higher at all surface pressures as compared to the film of malate dehydrogenase in the absence of lipids. Considerable enzyme activity was maintained even at pressure as high as 23 dynes/cm. The presence of phospholipid stabilized the enzyme and greatly broadened the surface pressure range over which activity was observed.

A comparison of Figs. 5–7 shows that the activity of the pig heart total phospholipid extract–enzyme mixed film was lower at smaller surface pressure values and greater at higher surface pressure values compared to enzyme–dipalmitoyllecithin, enzyme–egg lecithin, and enzyme–cholesterol mixed films. These results show that the enzyme was stabilized to a greater extent at high surface pressure values by the pig heart phospholipid extract compared to the other lipids studied. This observation is quite meaningful, since the surface pressure exerted by a living membrane is considered to be rather high (33).

Table I—Amount of Protein at the Interface after Subphase Exchange

Film	Found, mg × 10^2
Malate dehydrogenase	2.4
Malate dehydrogenase–cholesterol	2.2
Malate dehydrogenase–dipalmitoyllecithin	2.0
Malate dehydrogenase–egg lecithin	1.9
Malate dehydrogenase–pig heart phospholipids	1.8

It has been suggested that the enzyme may have very specific requirements for optimal stabilization by a phospholipid and that these requirements would be expected to be met by the lipids from the same organ as the enzyme. The greater stabilization of the enzyme at higher surface pressures by the pig heart phospholipid extracts compared to the other lipids studied possibly may result from specific physical interactions between the enzyme and lipid mixture at these higher pressures. An increase in the stability of the enzyme by pig heart lipid micelles also was observed in bulk studies (16).

Amount of Protein Anchored after Subphase Exchange—The results of the protein content analysis for the various malate dehydrogenase films are shown in Table I. The amount of protein remaining at the surface after exchange ranged from 0.018 to 0.024 mg. The amount of protein applied initially to the surface was 0.081 mg. The maximum amount of protein remaining at the interface after subphase exchange occurred with the malate dehydrogenase film in the absence of any lipid. All of the mixed films resulted in a slight reduction in the amount of enzyme remaining at the surface. An obvious explanation for these effects is that protein cannot occupy the same areas of the interface occupied by the lipid molecules and that the area of the interface available to the protein is thereby decreased (34).

Since the amount of protein remaining at the surface in different films studied falls within a narrow range, the differences in enzyme activity of the various enzyme films and the increase in enzyme activity in the presence of the lipids are not results of an increasing amount of enzyme held at the surface but are due to changes in orientation of the enzyme molecules because of surface pressure changes and interaction with lipids.

SUMMARY

The results of this study show that the catalytic activity of the malate dehydrogenase films was dependent both on the lipid present and the surface pressure of the film. The activity of the enzyme was increased in the presence of all of the lipids studied.

Although the simple model system does not simulate the complexity of the biological membrane, it gives some evidence of the lipid requirement for catalytic activity and the role of lipids in the stability of membrane-bound enzymes. Lipids, vis-a-vis membrane-bond enzymes, can be looked upon as serving two functions. First, they restrict and localize the enzyme. Second, they serve a regulatory function, thereby controlling the degree of enzyme activity by changes in the state of compression of the membrane.

REFERENCES

(1) A. W. Malick, A. Felmeister, and N. D. Weiner, *J. Pharm. Sci.*, **62,** 1871 (1973).

(2) L. L. M. van Deenen, in "The Molecular Basis of Membrane Function," D. C. Testeson, Ed., Prentice-Hall, Englewood Cliffs, N.J., 1969, p. 47.

(3) I. Sekuzu, P. Jurtshuk, and D. E. Green, *J. Biol. Chem.*, **238,** 957 (1963).

(4) B. Fleisher, A. Casu, and S. Fleisher, *Biochem. Biophys. Res. Commun.*, **24,** 189 (1966).

(5) H. K. Kimelberg and D. Papahadjopoulos, *Biochim. Biophys. Acta*, **282,** 277 (1972).

(6) G. S. Levey, *Biochem. Biophys. Res. Commun.*, **43,** 108 (1971).

(7) S. Roseman, in "Biomembranes," vol. 2, Plenum, New York, N.Y., 1971, p. 9.

(8) G. S. Gotterer, Ph.D. thesis, Johns Hopkins University, Baltimore, Md., 1964.

(9) P. Cerletti, R. Strom, M. G. Giordano, F. Balestrero, and M. A. Giovenco, *Biochem. Biophys. Res. Commun.*, **14,** 408 (1964).

(10) R. Coleman, *Biochim. Biophys. Acta*, **300,** 1 (1973).

(11) L. Rothfield and D. Romeo, in "Structure and Function of Biological Membranes," L. I. Rothfield, Ed., Academic, New York, N.Y., 1971, p. 252.

(12) M. L. Das and F. L. Crane, *Biochemistry*, **3,** 696 (1964).

(13) J. L. Brash and D. J. Lyman, "The Chemistry of Biosurfaces," vol. I, Dekker, New York, N.Y., 1971, p. 182.

(14) A. W. Malick and N. D. Weiner, *J. Pharm. Sci.*, **66,** 792 (1977).

(15) R. G. Wolfe and J. B. Neiland, *J. Biol. Chem.*, **221,** 61 (1956).

(16) J. W. Callahan and G. W. Kosicki, *Can. J. Biochem.*, **45,** 839 (1967).

(17) S. A. Lodhi, N. D. Weiner, and A. Felmeister, *J. Pharm. Sci.*, **63,** 738 (1974).

(18) G. H. Dodd, *Eur. J. Biochem.*, **33,** 418 (1973).

(19) J. Peters and P. Fromherz, *Biochim. Biophys. Acta*, **394,** 111 (1975).

(20) M. Kates, "Laboratory Techniques in Biochemistry and Molecular Biology," American Elsevier, New York, N.Y., 1972, pp. 349, 350, 394.

(21) H. J. Trurnit, *J. Colloid Sci.*, **15,** 1 (1960).

(22) O. H. Lowry, *J. Biol. Chem.*, **193,** 265 (1951).

(23) D. Papahadjopoulos and H. K. Kimelberg, *Biochim. Biophys. Acta*, **233,** 805 (1971).

(24) G. Colacicco, *Lipids*, **5,** 636 (1970).

(25) M. V. Yudenfreund and P. Becher, in "Monolayers," American Chemical Society Advances in Chemistry Series 144, E. D. Goddard, Ed., American Chemical Society, Washington, D.C., 1975, p. 199.

(26) P. Doty and J. H. Schulman, *Discuss. Faraday Soc.*, **6,** 21 (1949).

(27) R. Matalon and J. H. Schulman, *ibid.*, **6,** 27 (1949).

(28) D. Ghosh, M. A. Williams, and J. Tinoco, *Biochim. Biophys. Acta*, **291,** 351 (1973).

(29) H. Witcoff, "The Phosphatides," Reinhold, New York, N.Y., 1951, pp. 320–322.

(30) G. Colacicco, "Biological Horizons in Surface Sciences," Academic, New York, N.Y., 1973, p. 247.

(31) L. L. M. van Deenen, *Biochim. Biophys. Acta*, **332,** 69 (1974).

(32) D. Papahadjopoulos, M. Cowden, and H. Kimelberg, *ibid.*, **330,** 8 (1973).

(33) J. F. Danielli, "Surface Phenomena in Chemistry and Biology," Pergamon, New York, N.Y., 1959, pp. 246–265.

(34) M. C. Phillips, M. T. A. Evans, and H. Hauser, *Sonderdzuck aus Chemie, Physikalische Chemie und Anwendungstechnik des grenzflachenaktiven Staffe (Zurich)*, **11,** 381 (1972).

ACKNOWLEDGMENTS AND ADDRESSES

Received November 24, 1976, from the *College of Pharmacy and Allied Health Professions, Wayne State University, Detroit, MI 48202, and the ‡College of Pharmacy, University of Michigan, Ann Arbor, MI 48109.

Accepted for publication January 12, 1977.

* To whom inquiries should be directed.

Effect of Sorbitol on Interaction of Phenolic Preservatives with Polysorbate 80

JAMES BLANCHARD ˣ, WILLIAM T. FINK, and JAMES P. DUFFY

Abstract □ The effect of sorbitol on the binding of several commonly used phenolic preservatives (*i.e.*, *p*-hydroxybenzoic acid, methylparaben, ethylparaben, and propylparaben) with the nonionic surfactant polysorbate 80 was investigated using an equilibrium dialysis technique. The binding data were expressed in the form of Scatchard plots utilizing a modified form of the Scatchard equation. The data analysis indicated that all four phenolic preservatives were bound to two distinct loci within the polysorbate micelle; one exhibited a high affinity and a low capacity for the preservative molecules, while the other appeared to have a near-zero affinity but an almost infinite binding capacity. The high affinity site was assumed to be located near the junction of the hydrocarbon core with the polyoxyethylene region of the micelle. The interaction of the preservatives with the second class of sites apparently involved a nonspecific and nonsaturable partitioning of the preservative molecules into the polyoxyethylene region of the micelle. Sorbitol was ineffective in displacing significant amounts of bound preservative from either binding site, presumably because it was too polar to partition into the micelle sufficiently to displace bound preservative.

Keyphrases □ Sorbitol—effect on binding of various phenolic preservatives to polysorbate 80 □ Binding—various phenolic preservatives to polysorbate 80, effect of sorbitol □ Polyols—sorbitol, effect on binding of various phenolic preservatives to polysorbate 80 □ Polysorbate 80—binding to various phenolic preservatives, effect of sorbitol □ Preservatives, phenolic—*p*-hydroxybenzoic acid, methylparaben, ethylparaben, and propylparaben, binding to polysorbate 80, effect of sorbitol □ Surfactants, nonionic—polysorbate 80, binding to various phenolic preservatives, effect of sorbitol

The interference of nonionic surfactants with the preservative activity of parabens was first reported in 1950 by Bolle and Mirimanoff (1). Since that time, several reports confirmed their observations (2–4). It is now generally acknowledged that many preservatives commonly used in pharmaceutical formulations undergo similar complexation reactions and resultant inactivation.

This complexation may be inhibited by certain biologically inactive molecules such as the polyols (5–8). Some polyols, such as sorbitol, are not only compatible with many ingredients common to pharmaceutical formulations but are widely used for their humectant, solubilizing, stabilizing, and anti-cap-lock properties. Thus, a systematic study of the ability of such agents to inhibit the complexation of preservatives by nonionic surfactants seems highly desirable.

In this study, a model system consisting of polysorbate 80, sorbitol, and several phenolic preservatives was utilized to determine the ability of sorbitol to activate complexed paraben molecules.

EXPERIMENTAL

Reagents—The following reagents were used: methylparaben[1] (I), mp 130°; ethylparaben[2] (II), mp 117°; propylparaben[3] (III), mp 96–97°; *p*-hydroxybenzoic acid[4] (IV), mp 214–215°; polysorbate 80[5]; and crystalline sorbitol[6]. Compounds I–IV were recrystallized from distilled water (9, 10) and dried in a desiccator for at least 48 hr prior to use. Polysorbate 80 and sorbitol were used without further purification. All solutions were prepared using double-distilled water from an all-glass apparatus.

Procedures—The dialysis procedures and equipment were similar to those of Patel and Foss (11). Commercially available[7] acrylic plastic dialysis cells were employed. Nylon[8] membranes, previously washed for 1 hr in distilled water heated to 80° to remove any contaminants, proved to be satisfactory. These membranes previously were shown to be impermeable to the polysorbate yet permeable to the parabens, thereby allowing equilibration of the latter (2, 12).

After the cells were assembled, 5 ml of distilled water was added to one cell compartment (the aqueous compartment) and 5 ml of a mixture of varying volume ratios of preservative in 10% (w/v) polysorbate 80 and 10% (w/v) polysorbate 80 was added to the other cell compartment (the surfactant compartment). This procedure was employed to vary the amount of preservative present in the surfactant compartment while maintaining the polysorbate concentration at 10% (w/v). The cells were then placed on a water bath shaker[9] and agitated at 120 oscillations/min for 20 hr at 30° to achieve equilibrium. Preservative samples were removed from both sides of the membrane and assayed spectrophotometrically at 255 nm (2, 11, 13).

Sorbitol was added as a possible competitor to the preservative in 10% (w/v) polysorbate 80 solution so that the molar ratio of sorbitol to paraben was constant in any aliquot. The assay procedure was identical to those in the experiments involving no competitor, since neither polysorbate 80 (2) nor sorbitol interfered with the assay of the preservatives.

RESULTS AND DISCUSSION

Binding phenomena in undersaturated systems, such as those utilized here, can be considered to obey the law of mass action (14). For a macromolecule with n independent and equivalent binding sites, each having an association constant K, the following expression may be written:

$$r = \frac{[DM]}{[M_t]} = \frac{nK[D]}{1 + K[D]} \qquad \text{(Eq. 1)}$$

where r is the number of moles of preservative bound per mole of surfactant; $[DM]$ and $[D]$ are the concentrations of bound and free (unbound) paraben, respectively; and $[M_t]$ is the concentration of macromolecule (surfactant). Theoretically, $[M_t]$ should be the concentration of micelles, n the number of binding sites per micelle, and K the association constant for the reaction with the micelles, since the binding interaction reportedly occurs between the preservative and the surfactant micelles rather than the monomer surfactant molecules (12, 15). From a practical standpoint, however, it is more convenient to express K, n, and M_t in terms of the surfactant concentration, since the micellar molecular weight is not precisely known. Since the critical micelle concentration of polysorbate 80 is very low (15, 16), the monomer concentration may be neglected (12). In analyzing the data, the molecular weight of polysorbate 80 was assumed to be 1470[10].

If there are m classes of independent sites with each class i having n_i sites with an intrinsic association (binding) constant K_i, then Eq. 1 can be generalized to:

$$r = \sum_{i=1}^{m} \frac{n_i K_i [D]}{1 + K_i [D]} \qquad \text{(Eq. 2)}$$

[1] Lot L49260, Ruger Chemical Co., Irvington, NJ 10533.
[2] Eastman Organic Chemicals, Rochester, NY 14650.
[3] Lot C708922, Ruger Chemical Co., Irvington, NJ 10533.
[4] Lot 750543, Calbiochem, La Jolla, CA 92037.
[5] Lot 1546, ICI America Inc., Atlas Chemicals Division, Wilmington, DE 19899.
[6] Lot 7702D, ICI America Inc., Atlas Chemicals Division, Wilmington, DE 19899.
[7] Model 289, Bel-Art Products, Pequannock, NJ 07440.
[8] Capran 77C, 0.6-mil, Allied Chemical Corp., Morristown, NJ 07960.
[9] Model 50, GCA/Precision Scientific, Chicago, IL 60647.
[10] Dr. Paul Becher, ICI America Inc., Wilmington, DE 19897, June 1976, personal communication.

Table I—Binding Parameters for the Interaction of Various Preservatives with Polysorbate 80 at 30° in the Presence of Varying Concentrations of Sorbitol

Preservative	Competitor[a]	n_1, Sites/Molecule	K_1, liters/mole × 10^{-3}	C, liters/mole	$P_{octanol-water}$
p-Hydroxybenzoic acid	None	0.074 ± 0.036[b]	3.01 ± 0.271	69.8 ± 6.3	38.02
	Sorbitol (1:1)	0.078 ± 0.031	3.06 ± 0.264	74.4 ± 5.2	
Methylparaben	None	0.098 ± 0.050	2.64 ± 0.326	84.0 ± 15.1	91.2
	Sorbitol (1:1)	0.123 ± 0.040	2.69 ± 0.205	72.9 ± 8.3	
Ethylparaben	None	0.044 ± 0.011	45.39 ± 1.10	204.2 ± 38.1	295.1
	Sorbitol (50:1)	0.044 ± 0.021	44.30 ± 2.49	179.3 ± 52.8	
Propylparaben	None	0.087 ± 0.016	123.5 ± 11.5	445.6 ± 39.7	1096.5
	Sorbitol (5:1)	0.107 ± 0.015	97.01 ± 5.25	468.0 ± 38.8	

[a] Molar ratio of competitor to preservative shown in parentheses. [b] All parameter uncertainties are expressed as standard deviations.

A Scatchard (17) plot results when $r/[D]$ *versus* r is plotted. By rearranging Eq. 1, it can be seen that such a plot should be linear with a slope of $-K$ and ordinate and abscissa intercepts of nK and n, respectively, when only one class of binding sites is present.

This simplest of binding models is referred to as the "two-parameter model" (18) since only two parameters, n and K, need to be determined to describe the binding process adequately. However, as noted previously (9, 12, 19), Scatchard plots frequently exhibit curvature indicative of the presence of more than one class of binding sites. To describe these more complex binding processes, Eq. 2 may be rewritten as:

$$r = \sum_{i=1}^{m-1} \frac{n_i K_i [D]}{1 + K_i [D]} + n_m K_m [D] \qquad \text{(Eq. 3)}$$

when one association constant becomes very small. The second term on the right-hand side of Eq. 3 is, therefore, indicative of a class of binding sites that possesses an "infinite" (nonsaturable) binding capacity but "zero" affinity, thereby producing a horizontal asymptote on the Scatchard plot.

In analyzing these more complex interactions, the binding data are fitted to a three-, four-, or five-parameter model (18, 20–22). The four-parameter model merely corresponds to a value of $m = 2$ in Eq. 2, whereas the three- and five-parameter models correspond to values of $m = 2$ and 3, respectively, in Eq. 3. In a five-parameter model, the parameters are n_1, n_2, K_1, K_2, and C, where $C = n_m K_m$.

The four-parameter model has been most commonly used to describe binding data in which a nonlinear (curved) Scatchard plot was observed. However, in many cases it appears to have been used inappropriately. Scatchard plots exhibiting a horizontal asymptote (*i.e.*, constant values of $r/[D]$ at high values of r) can best be fitted to a three- or five-parameter model, since, without the inclusion of the $n_m K_m [D]$ term of Eq. 3 to describe the horizontal asymptote (*i.e.*, the nonsaturable binding site), many parameter fitting programs frequently fail to converge as $K_2 \rightarrow 0$ and $n_2 \rightarrow \infty$ (18).

The selection of the most appropriate model to describe the binding data is critical if meaningful estimates of the binding parameters are to be obtained and erroneous inferences avoided (23). An attempt was made to fit the data in this study to three-, four-, and five-parameter models; the data were best described by the three-parameter model, which can be written as:

$$\frac{r}{[D]} = \frac{n_1 K_1}{1 + K_1 [D]} + C \qquad \text{(Eq. 4)}$$

where $C = n_2 K_2$. The best-fit values of the parameters (n_1, K_1, and C) were calculated by means of a nonlinear least-squares procedure (24) executed on a digital computer[11]. These values were then used to construct Scatchard plots for the various binding interactions.

The Scatchard plots depicted in Figs. 1–4 illustrate the interaction between 10% (w/v) polysorbate 80 and IV, I, II, and III, respectively, in the presence and absence of sorbitol. The binding parameters for the interaction of the various preservatives with polysorbate 80 are shown in Table I.

The use of Eq. 4 to fit the binding data seems reasonable in view of the NMR data of Corby and Elworthy (13), who postulated that parabens were solubilized in both the oxyethylene region and the micellar core of the related nonionic surfactant cetomacrogol, which is believed to exhibit binding properties similar to those of polysorbate 80 (25). Several other investigators observed that the interaction of phenolic preservatives with surfactants involves two distinct classes of binding sites (9, 12, 19), but they fitted their data to a four-parameter model in contrast to the three-parameter model used here.

A micelle of polysorbate 80 may be visualized as consisting of a densely

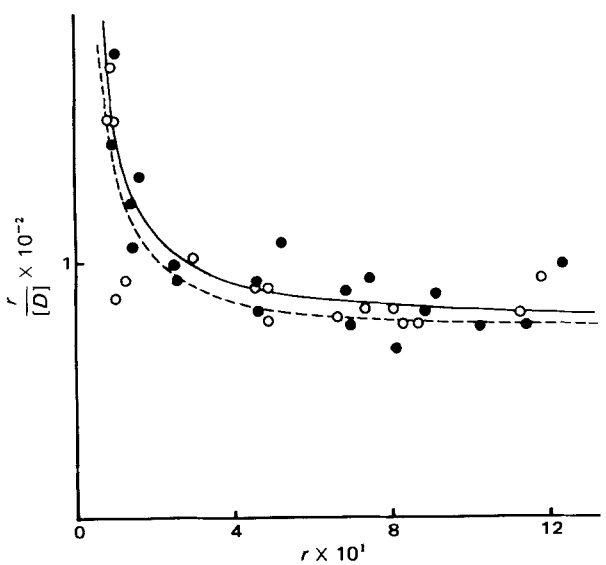

Figure 1—*Influence of sorbitol on the binding of* p-*hydroxybenzoic acid to 10% (w/v) polysorbate 80 at 30°. Key:* ○, p-*hydroxybenzoic acid alone; and* ●, p-*hydroxybenzoic acid plus sorbitol (1:1).*

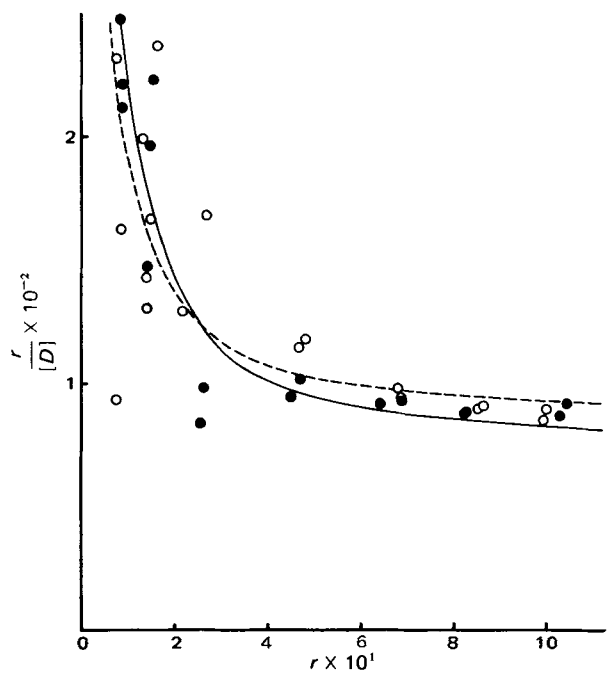

Figure 2—*Influence of sorbitol on the binding of methylparaben to 10% (w/v) polysorbate 80 at 30°. Key:* ○, *methylparaben alone; and* ●, *methylparaben plus sorbitol (1:1).*

[11] Control Data Corp. 6400.

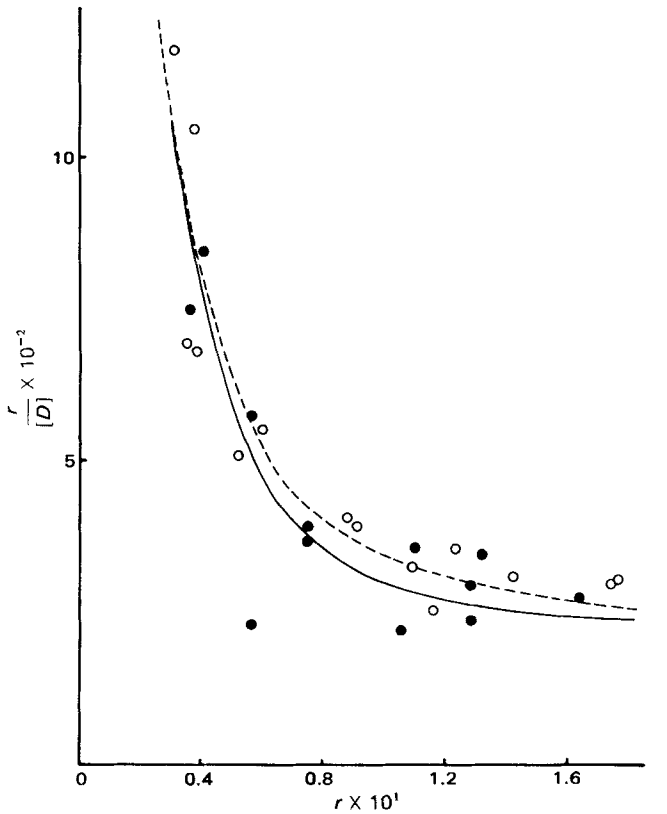

Figure 3—*Influence of sorbitol on the binding of ethylparaben to 10% (w/v) polysorbate 80 at 30°. Key: ○, ethylparaben alone; and ●, ethylparaben plus sorbitol (50:1).*

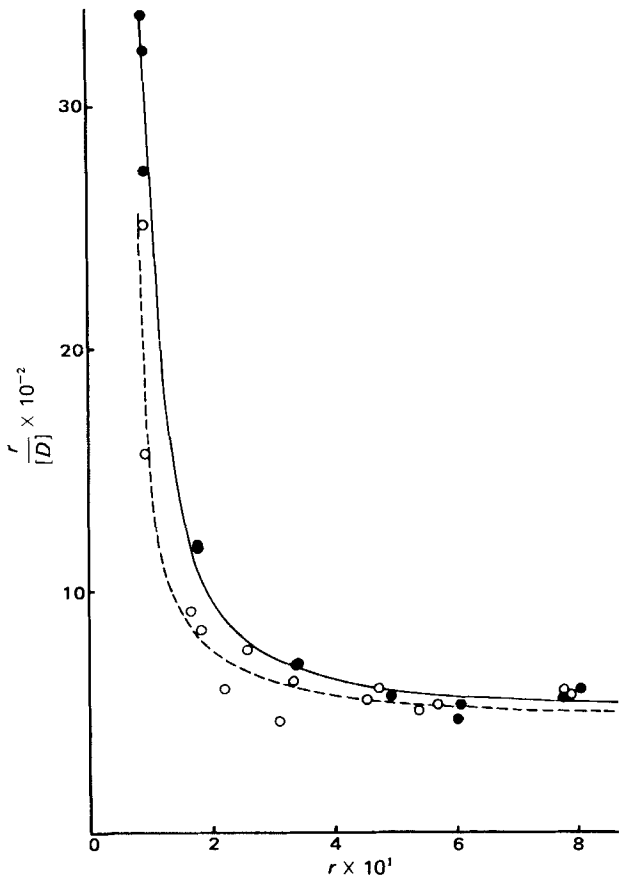

Figure 4—*Influence of sorbitol on the binding of propylparaben to 10% (w/v) polysorbate 80 at 30°. Key: ○, propylparaben alone; and ●, propylparaben plus sorbitol (5:1).*

packed central lipid core of hydrophobically bonded oleate chains surrounded at the periphery by a layer of sorbitan moieties from which emanate the polar polyoxyethylene chains in the form of apically truncated spiral cones (13, 26). Shimamoto and Ogawa (15), utilizing NMR studies, indicated that preservative molecules may reside in one or more of three different loci of a surfactant micelle: (*a*) within the lipid hydrocarbon core, (*b*) within the polyoxyethylene network, and (*c*) at the junction of these two regions.

The horizontal asymptote (C) observed in the Scatchard plots (Figs. 1–4) at high values of r may be interpreted as being indicative of a weak nonspecific (nonsaturable) binding process, analogous to a partitioning of the preservative between the micellar and aqueous phases (18, 22). Therefore, the value of C may be considered to represent a type of partition coefficient describing the distribution of the preservative molecule between the micellar and aqueous phases. This partitioning phenomenon may be envisioned as a process whereby preservative molecules, to lower their free energy, migrate from a thermodynamically less stable aqueous environment in the bulk phase to a more stable (less polar) micellar phase, with the degree of penetration and affinity being proportional to their lipophilicity.

At low r values, the preservative molecules preferentially orient themselves in the vicinity of the high affinity–low capacity sites, which are believed to be located near the junction. When these sites become saturated, the preservative molecules then partition into the somewhat more polar but still relatively stable (in relation to the aqueous phase) class of high capacity–lower affinity sites, which are believed to be located in the polyoxyethylene region of the micelle. A possible explanation for the higher affinity of the junction binding sites relative to those in the polyoxyethylene region may be that it is possible for a molecule situated at the junction to form bonds with several different structures, *i.e.*, apical ethylene oxide units, sorbitan moieties, and the outer surface of the lipid core. The capacity of this class of sites is necessarily low because of the limited number of these structures.

The data in Table I indicate that the C values observed for the various compounds are in good rank order agreement with their reported (27) octanol–water partition coefficients. This finding further substantiates that the binding process described by the C term is a type of partitioning phenomenon. The rank-order agreement between the C value and the degree of lipophilicity of the preservative molecules also substantiates that the binding sites are less polar than the surrounding aqueous environment. Furthermore, the binding parameters shown in Table I are in good inverse rank-order agreement with the relative order in which the preservatives are inactivated by the polysorbate, as measured by their inability to inhibit microbial growth (28).

Crooks and Brown (19) studied the interaction between the polar chloro and dichloro derivatives of xylenol and methylparaben in a cetomacrogol system. The more polar xylenol derivatives were able to displace a portion of the methylparaben from the polyoxyethylene region yet were unable to displace it from the postulated more specific, high affinity site believed to be located near the junction. These findings seem reasonable in view of the relative intramicellar polarity and the polarity of the competitors involved. In light of these and other findings (5–8), certain polar polyols such as sorbitol might be expected to act as competitors for bound preservative in a manner similar to chloroxylenol and dichloroxylenol.

The binding data shown in Figs. 1–4 and Table I illustrate that sorbitol has little influence on the binding of the phenolic preservatives with either class of sites; the plots are virtually superimposable, and the binding parameters in the presence and absence of sorbitol are in close agreement. The sorbitol is probably unable to displace bound phenolic preservatives because it is too polar to partition deeply enough into the micellar phase to displace significant amounts of the bound preservative. The use of other, somewhat less polar molecules that are compatible with various pharmaceutical formulations seems to be a worthwhile area for future research.

REFERENCES

(1) M. A. Bolle and A. Mirimanoff, *J. Pharm. Pharmacol.*, **2**, 685 (1950).

(2) N. K. Patel and H. B. Kostenbauder, *J. Am. Pharm. Assoc., Sci. Ed.*, **47**, 289 (1958).

(3) F. D. Pisano and H. B. Kostenbauder, *ibid.*, **48**, 310 (1959).

(4) M. Barr and L. F. Tice, *ibid.*, **46**, 445 (1957).

(5) P. S. Prickett, H. L. Murray, and N. H. Mercer, *J. Pharm. Sci.*, **50**, 316 (1961).

(6) H. B. Kostenbauder, *Am. Perf. Aromat.*, **75**, 28 (1960).
(7) J. A. Rogers and J. G. Nairn, *Can. J. Pharm. Sci.*, **5**, 96 (1970).
(8) J. Poprzan and M. G. deNavarre, *J. Soc. Cosmet. Chem.*, **12**, 280 (1961).
(9) K. F. Brown and M. J. Crooks, *Pharm. Acta Helv.*, **48**, 494 (1973).
(10) T. C. Corby and P. H. Elworthy, *J. Pharm. Pharmacol., Suppl.*, **23**, 39S (1971).
(11) N. K. Patel and N. E. Foss, *J. Pharm. Sci.*, **53**, 94 (1964).
(12) S. J. A. Kazmi and A. G. Mitchell, *J. Pharm. Pharmacol.*, **23**, 482 (1971).
(13) T. C. Corby and P. H. Elworthy, *J. Pharm. Pharmacol., Suppl.*, **23**, 49S (1971).
(14) E. R. Garrett, *J. Pharm. Pharmacol.*, **18**, 589 (1966).
(15) T. Shimamoto and Y. Ogawa, *Chem. Pharm. Bull.*, **23**, 3088 (1975).
(16) B. Farhadieh, *J. Pharm. Sci.*, **62**, 1685 (1973).
(17) G. F. Scatchard, *Ann. N.Y. Acad. Sci.*, **51**, 660 (1949).
(18) D. Rodbard and H. A. Feldman, in "Methods in Enzymology," vol. 36, B. W. O'Malley and J. G. Hardman, Eds., Academic, New York, N.Y., 1975, pp. 3–16.
(19) M. J. Crooks and K. F. Brown, *J. Pharm. Pharmacol.*, **26**, 235 (1974).
(20) J. P. Raynaud, *Comput. Prog. Biomed.*, **3**, 63 (1973).
(21) D. Rodbard, in "Receptors for Reproductive Hormones," B. W. O'Malley and A. R. Means, Eds., Plenum, New York, N.Y., 1973, pp. 289–326.
(22) J. G. Brand and T. Y. Toribara, *Arch. Biochem. Biophys.*, **167**, 91 (1975).
(23) I. Kanfer and D. R. Cooper, *J. Pharm. Pharmacol.*, **28**, 58 (1976).
(24) D. W. Marquardt, *J. Soc. Ind. Appl. Math.*, **11**, 431 (1963).
(25) S. J. A. Kazmi and A. G. Mitchell, *Can. J. Pharm. Sci.*, **11**, 10 (1976).
(26) J. Schick, S. M. Atlas, and F. R. Eirich, *J. Phys. Chem.*, **66**, 1326 (1962).
(27) A. Leo, C. Hansch, and D. Elkins, *Chem. Rev.*, **71**, 525 (1971).
(28) M. Matsumoto and M. Aoki, *Chem. Pharm. Bull.*, **10**, 251 (1962).

ACKNOWLEDGMENTS AND ADDRESSES

Received October 14, 1976, from the *Department of Pharmaceutical Sciences, College of Pharmacy, University of Arizona, Tucson, AZ 85721.*

Accepted for publication January 11, 1977.

Supported by the University of Arizona Foundation.

The authors thank Mr. Donald Speray, Mathematics Department, University of Arizona, for assistance with the curve-fitting procedures.

[x] To whom inquiries should be directed.

Binding of *N*-Substituted Anthracenecarboxamides to Double-Stranded DNA: An Electronic Spectral Study

STEPHEN G. SCHULMAN [x], W. LARRY PAUL [*], and ROY J. STURGEON [‡]

Abstract □ The electronic absorption and fluorescence spectra of two isomeric anthracenecarboxamides substituted with quaternary alkylammonium groups were studied as a function of solvent polarity, solvent rigidity, and state of protonation. These relatively simple environmental perturbations of the electronic spectra were employed to interpret spectral shifts caused by complexation with the bases or base pairs of DNA. The exocyclic side chains of the compounds studied have some freedom of movement when the spectroscopic probes are bound to double-stranded DNA.

Keyphrases □ Anthracenecarboxamides, *N*-substituted—binding to DNA, electronic absorption and fluorescence spectral study □ Binding—*N*-substituted anthracenecarboxamides to DNA, electronic absorption and fluorescence spectral study □ DNA—binding to *N*-substituted anthracenecarboxamides, electronic absorption and fluorescence spectral study □ Electronic absorption spectrometry—binding of *N*-substituted anthracenecarboxamides to DNA □ Fluorescence spectrometry—binding of *N*-substituted anthracenecarboxamides to DNA

Many drugs active against microorganisms and neoplasms are polycyclic aromatic or heteroaromatic cations, which bind reversibly to the polyanionic nucleic acids *in vitro* and *in vivo* (1). Their modes of action are generally believed to be related, directly or indirectly, to their ability to be bound to DNA, resulting in errors of transcription or replication in the affected organism (1). However, the process of binding to DNA often entails interactions different from, and in addition to, the electrostatic interaction between ions of opposite charge.

Various techniques such as low-shear viscometry, ultracentrifugation, and NMR spectroscopy have yielded information indicating that the aromatic portions of the drugs can become inserted (intercalated) between base pairs of the double helix of DNA. This insertion results in a partial unwinding and linear extension of the double helix to accommodate the intruding drug molecule (2–5).

Several studies of binding believed to result in intercalation of drug or dye molecules with DNA have been carried out, with the binding parameters often estimated absorptiometrically or fluorometrically. However, little has been established concerning the nature of the changes in the electronic absorption or fluorescence spectra of the drug or dye molecules upon such binding. The failure of electronic spectroscopy to deliver useful information about nucleic acid binding has been due in part to the complex structures of the drug and dye molecules involved; the environmental perturbations of these spectra are difficult to interpret.

In the present study, the changes in the electronic absorption and fluorescence spectra of two cationic, *N*-substituted anthracenecarboxamides occurring upon binding to calf thymus DNA were examined. The observed changes were compared to the changes occurring in the spectra of these compounds upon protonation and as a function of solvent rigidity and polarity.

The compounds studied, *N*-(2-anthroyl)-*N'*,*N'*-dimethyl-*N'*-[(3-trimethylammonium)propyl]ethylenediamine dibromide (I) and *N*-(9-anthroyl)-*N'*,*N'*-di-

(6) H. B. Kostenbauder, *Am. Perf. Aromat.*, **75**, 28 (1960).
(7) J. A. Rogers and J. G. Nairn, *Can. J. Pharm. Sci.*, **5**, 96 (1970).
(8) J. Poprzan and M. G. deNavarre, *J. Soc. Cosmet. Chem.*, **12**, 280 (1961).
(9) K. F. Brown and M. J. Crooks, *Pharm. Acta Helv.*, **48**, 494 (1973).
(10) T. C. Corby and P. H. Elworthy, *J. Pharm. Pharmacol., Suppl.*, **23**, 39S (1971).
(11) N. K. Patel and N. E. Foss, *J. Pharm. Sci.*, **53**, 94 (1964).
(12) S. J. A. Kazmi and A. G. Mitchell, *J. Pharm. Pharmacol.*, **23**, 482 (1971).
(13) T. C. Corby and P. H. Elworthy, *J. Pharm. Pharmacol., Suppl.*, **23**, 49S (1971).
(14) E. R. Garrett, *J. Pharm. Pharmacol.*, **18**, 589 (1966).
(15) T. Shimamoto and Y. Ogawa, *Chem. Pharm. Bull.*, **23**, 3088 (1975).
(16) B. Farhadieh, *J. Pharm. Sci.*, **62**, 1685 (1973).
(17) G. F. Scatchard, *Ann. N.Y. Acad. Sci.*, **51**, 660 (1949).
(18) D. Rodbard and H. A. Feldman, in "Methods in Enzymology," vol. 36, B. W. O'Malley and J. G. Hardman, Eds., Academic, New York, N.Y., 1975, pp. 3–16.
(19) M. J. Crooks and K. F. Brown, *J. Pharm. Pharmacol.*, **26**, 235 (1974).
(20) J. P. Raynaud, *Comput. Prog. Biomed.*, **3**, 63 (1973).
(21) D. Rodbard, in "Receptors for Reproductive Hormones," B. W. O'Malley and A. R. Means, Eds., Plenum, New York, N.Y., 1973, pp. 289–326.
(22) J. G. Brand and T. Y. Toribara, *Arch. Biochem. Biophys.*, **167**, 91 (1975).
(23) I. Kanfer and D. R. Cooper, *J. Pharm. Pharmacol.*, **28**, 58 (1976).
(24) D. W. Marquardt, *J. Soc. Ind. Appl. Math.*, **11**, 431 (1963).
(25) S. J. A. Kazmi and A. G. Mitchell, *Can. J. Pharm. Sci.*, **11**, 10 (1976).
(26) J. Schick, S. M. Atlas, and F. R. Eirich, *J. Phys. Chem.*, **66**, 1326 (1962).
(27) A. Leo, C. Hansch, and D. Elkins, *Chem. Rev.*, **71**, 525 (1971).
(28) M. Matsumoto and M. Aoki, *Chem. Pharm. Bull.*, **10**, 251 (1962).

ACKNOWLEDGMENTS AND ADDRESSES

Received October 14, 1976, from the *Department of Pharmaceutical Sciences, College of Pharmacy, University of Arizona, Tucson, AZ 85721.*

Accepted for publication January 11, 1977.

Supported by the University of Arizona Foundation.

The authors thank Mr. Donald Speray, Mathematics Department, University of Arizona, for assistance with the curve-fitting procedures.

[x] To whom inquiries should be directed.

Binding of *N*-Substituted Anthracenecarboxamides to Double-Stranded DNA: An Electronic Spectral Study

STEPHEN G. SCHULMAN [x], W. LARRY PAUL [*], and ROY J. STURGEON [‡]

Abstract □ The electronic absorption and fluorescence spectra of two isomeric anthracenecarboxamides substituted with quaternary alkylammonium groups were studied as a function of solvent polarity, solvent rigidity, and state of protonation. These relatively simple environmental perturbations of the electronic spectra were employed to interpret spectral shifts caused by complexation with the bases or base pairs of DNA. The exocyclic side chains of the compounds studied have some freedom of movement when the spectroscopic probes are bound to double-stranded DNA.

Keyphrases □ Anthracenecarboxamides, *N*-substituted—binding to DNA, electronic absorption and fluorescence spectral study □ Binding—*N*-substituted anthracenecarboxamides to DNA, electronic absorption and fluorescence spectral study □ DNA—binding to *N*-substituted anthracenecarboxamides, electronic absorption and fluorescence spectral study □ Electronic absorption spectrometry—binding of *N*-substituted anthracenecarboxamides to DNA □ Fluorescence spectrometry—binding of *N*-substituted anthracenecarboxamides to DNA

Many drugs active against microorganisms and neoplasms are polycyclic aromatic or heteroaromatic cations, which bind reversibly to the polyanionic nucleic acids *in vitro* and *in vivo* (1). Their modes of action are generally believed to be related, directly or indirectly, to their ability to be bound to DNA, resulting in errors of transcription or replication in the affected organism (1). However, the process of binding to DNA often entails interactions different from, and in addition to, the electrostatic interaction between ions of opposite charge.

Various techniques such as low-shear viscometry, ultracentrifugation, and NMR spectroscopy have yielded information indicating that the aromatic portions of the drugs can become inserted (intercalated) between base pairs of the double helix of DNA. This insertion results in a partial unwinding and linear extension of the double helix to accommodate the intruding drug molecule (2–5).

Several studies of binding believed to result in intercalation of drug or dye molecules with DNA have been carried out, with the binding parameters often estimated absorptiometrically or fluorometrically. However, little has been established concerning the nature of the changes in the electronic absorption or fluorescence spectra of the drug or dye molecules upon such binding. The failure of electronic spectroscopy to deliver useful information about nucleic acid binding has been due in part to the complex structures of the drug and dye molecules involved; the environmental perturbations of these spectra are difficult to interpret.

In the present study, the changes in the electronic absorption and fluorescence spectra of two cationic, *N*-substituted anthracenecarboxamides occurring upon binding to calf thymus DNA were examined. The observed changes were compared to the changes occurring in the spectra of these compounds upon protonation and as a function of solvent rigidity and polarity.

The compounds studied, *N*-(2-anthroyl)-*N'*,*N'*-dimethyl-*N'*-[(3-trimethylammonium)propyl]ethylenediamine dibromide (I) and *N*-(9-anthroyl)-*N'*,*N'*-di-

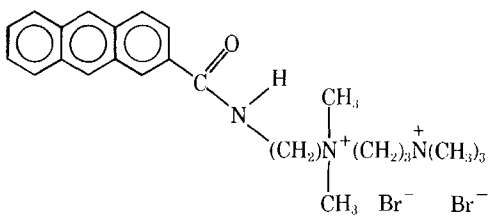

I

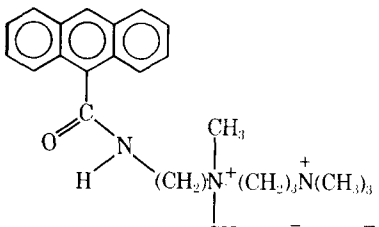

II

methyl-*N'*-[(3 - trimethylammonium)propyl]ethylenediamine dibromide (II), are representatives of a class of doubly charged cations that increase the intrinsic viscosity of solutions of double-stranded DNA upon binding and, therefore, are presumed to intercalate between DNA base pairs (6). These molecules were chosen as probes because they absorb and fluoresce at long wavelengths where the electronic spectra of the purine and pyrimidine bases of DNA do not interfere and because their aromatic systems are functionally simple, each containing a single electron acceptor group (the carboxamido group) that can affect the electronic spectra.

EXPERIMENTAL

Calf thymus DNA[1], supplied as the A grade sodium salt (phosphorus content 8.04% by weight) was dissolved in water containing monobasic and dibasic potassium phosphate as a buffer system (pH 6.9, total potassium-ion concentration of 0.01 *M*) to make a stock solution 1.10×10^{-2} *M* in DNA phosphate. Spectroquality *n*-heptane[2] and analytical reagent grade sulfuric acid[3] also were employed as solvents. Sulfuric acid solutions were prepared by dilution with distilled deionized water. The Hammett acidity scale of Jorgensen and Hartter (7) was employed to calibrate the acid solutions.

Absorption spectra of aqueous buffer and sulfuric acid solutions, $\sim 1 \times 10^{-4}$ *M* in I and II, were taken on a grating spectrophotometer[4]. When the probes were to be complexed by DNA, 200 μl of the DNA stock solution was added to 2 ml of a buffered, aqueous 1×10^{-4} *M* solution of I or II in 1-cm square silica cells. This mixture produced a large ratio (~10) of DNA phosphate to probe concentration, which was necessary to maximize the binding of the probe in the region where intercalation may be expected to predominate ([DNA phosphate] > 4 × [probe]) and to minimize the binding of the probe to the external parts of the DNA double helix. Because of the very low solubility of I and II in *n*-heptane, all spectra in that solvent were taken on solutions saturated with I and II.

Fluorescence spectra were taken on a fluorescence spectrophotometer[5] with a rhodamine-B quantum counter[5]; the monochromators were calibrated against the xenon line emission spectrum, and the spectral output was corrected for a wavelength variable response. Because of the nonlinearity of the fluorescence intensity with varying concentration at high absorbances, the aqueous and acid solutions upon which fluorescence spectra were taken were kept to $\sim 5 \times 10^{-6}$ *M* in I or II. However, the DNA phosphate concentration in the aqueous solutions in which the DNA complexes of I and II were prepared for fluorometric study was identical to that employed in the absorptiometric experiment.

[1] Calbiochem, La Jolla, Calif.
[2] Matheson, Coleman and Bell, East Rutherford, N.J.
[3] Mallinckrodt Chemical Works, St. Louis, Mo.
[4] Model DB-GT, Beckman Instruments, Fullerton, Calif.
[5] Model MPF-2A, Perkin-Elmer, Norwalk, Conn.

Table I—Electronic Absorption (λ_a) Maxima of I and II in Water with and without DNA, in 90% H_2SO_4, and in *n*-Heptane, All at 298 °K

In Water, pH 6.9						
Without DNA		With 1×10^{-3} *M* DNA		In 90% H_2SO_4 without DNA		In *n*-Heptane[a] without DNA,
λ_a, nm	log ε	λ_a, nm	log ε	λ_a, nm	log ε	λ_a, nm
			I			
386	3.36	398	3.29	422	3.43	383
371	3.39	382	3.32	—	—	364
358	3.43	365	3.30	363	3.42	348
340	3.40	346	3.31	347	3.65	338
328	3.25	~330	3.24	330	3.52	~327
			II			
383	3.75	390	3.49	384	3.63	381
364	3.81	371	3.55	363	3.64	362
346	3.64	353	3.43	348	3.47	344
331	3.38	337	3.23	333	3.26	328
318	3.08	~322	3.23	~319	3.15	~313

[a] Absorption spectra in *n*-heptane are only qualitative because of the poor solubilities of I and II in that solvent.

The quantum yields of fluorescence of the free and complexed probes were determined by the comparative method of Parker and Rees (8), using quinine bisulfate in 0.1 *N* H_2SO_4 as a standard. The absorbances of the solutions of I and II and those of the quinine standard solution were less than 0.02 at the wavelength of excitation. This finding circumvented the necessity for corrections to the integrated fluorescence intensity measurements for the nonlinearity at high absorbances (8).

Fluorescence decay times (lifetimes of the lowest excited singlet states) of the free and DNA-bound probes were measured on a pulsed-source fluorometer[6] with an 18-w deuterium lamp[6]. A pulse time of 1.6 nsec and an internal computer[7] were used to resolve the lamp pulse characteristics from the probe decay characteristics. The unit was interfaced with a dual-beam oscilloscope[7] with two 1A2 plug-in amplifiers[7] for visual display of the fluorescence decay characteristics.

RESULTS AND DISCUSSION

The principal absorption and fluorescence features of I and II and their variations with the state of protonation, solvent polarity, and solvent rigidity are listed in Tables I and II. The absorption spectra of I and II in water, concentrated sulfuric acid, and aqueous DNA solutions are shown in Figs. 1 and 2, and their fluorescence spectra are shown in Figs. 3 and 4.

The absorption spectra of substituted anthracenes in the 300–450-nm region are derived from the absorptions from the ground state (^1A) to the two lowest lying excited states (^1L_a and ^1L_b) (9). In anthracene, the $^1L_a \leftarrow {}^1A$ and $^1L_b \leftarrow {}^1A$ transitions, which are short axis and long axis polarized, respectively (9), overlap considerably and give rise to the structured absorption band complex at 300–400 nm. Although the two absorption bands are indistinguishable in anthracene, it is generally believed that the long wavelength edge of the absorption complex belongs to the ^1L_a band (10) and that the ^1L_b band is slightly higher in energy, much less intense than the ^1L_a band, and, therefore, buried under the broad absorption envelope of the latter (11).

Introduction of an electron donor or acceptor substituent to the β-position of anthracene is generally presumed to affect the longitudinally polarized $^1L_b \leftarrow {}^1A$ transition of the anthracene ring to a greater degree than the transversely polarized $^1L_a \leftarrow {}^1A$ transition (9). Therefore, the ^1L_b band of the 2-substituted anthracenes is red shifted, intensified, and blurred to a greater extent than the ^1L_a band (11–14). A strongly interacting substituent in the 2-position may, in theory, cause the ^1L_b band to move to a lower energy than the ^1L_a band of the same compound and, hence, become the longest wavelength absorption band.

The absorption spectra of I demonstrate considerable blurring, especially on the long wavelength side, relative to the absorption spectrum of anthracene. No doubt this blurring results from the intensification and blurring of the $^1L_b \leftarrow {}^1A$ transition. However, whether or not the ^1L_b band lies at a lower energy than the ^1L_a band cannot be established by simple inspection because of substantial overlap. However, when the amide group is protonated in concentrated sulfuric acid, the unstructured band that moves to much longer wavelengths (427 nm) can be assigned

[6] Model 31B, TRW, Inc., El Segundo, Calif.
[7] Model 556, Tektronix, Inc., Beaverton, Ore.

Table II—Fluorescence (λ_f) Maxima of I and II in Water with and without DNA at 298 °K (Fluid) and at 77 °K (Rigid) in 90% H_2SO_4 and in *n*-Heptane at 298 °K along with the Fluorescence Quantum Yields (ϕ_f) and Lifetimes (τ_f) of the Excited Free and DNA-Bound Probes

In Water, pH 6.9, T = 298 °K		In Water, pH 6.9, T = 77 °K		In 90% H_2SO_4, T = 298 °K,	In *n*-heptane, T = 298 °K,
Without DNA	With 1×10^{-3} *M* DNA	Without DNA	With 1×10^{-3} *M* DNA	without DNA	without DNA
			I		
λ_f (nm) = 452 (max) ϕ_f = 0.22 τ_f = 23.1 nsec	λ_f (nm) = 454 (max) ϕ_f = 0.18 τ_f = 16.6 nsec	λ_f (nm) = 415, 437 (max), and 456	λ_f (nm) = 422, 444 (max), and 465	λ_f (nm) = 524 (max)	λ_f (nm) = 390 (max), 414, and 439
			II		
λ_f (nm) = 400 and 417 (max) ϕ_f = 0.03 τ_f = 3.0 nsec	λ_f (nm) = 437 (max) ϕ_f = 0.14 τ_f = 21.5 nsec	λ_f (nm) = 392 (max) and 414	λ_f (nm) = 398 and 419 (max)	λ_f (nm) = 480 (max)	λ_f (nm) = 388 and 424

to the $^1L_b \leftarrow {}^1A$ transition. The highly structured absorption band of the protonated probe is only slightly red shifted relative to the corresponding vibrational features in the unprotonated probe and corresponds to the $^1L_a \leftarrow {}^1A$ transition. A small blue shift of the absorption spectrum of I is observed going from water to *n*-heptane, reflecting the lower polarity of the hydrocarbon solvent, which destabilizes the highly polar excited states involved in absorption relative to the aqueous solvated excited states (15).

The fluorescences of I and its conjugate acid in fluid aqueous solutions are unstructured and occur far downfield from the corresponding absorption spectra (*i.e.*, they are highly Stokes shifted). As in the absorption spectrum, the fluorescence of the protonated form lies at much longer wavelengths than that of I itself. In frozen aqueous media and low dielectric media, the fluorescence spectrum of I blue shifts dramatically and becomes highly structured relative to the fluorescence spectrum in fluid water. By freezing the aqueous solution of I to rigidity, the molecule is "locked" into the equilibrium ground-state geometrical and solvent configurations. As a result of locking the fluorescing molecule into the ground-state geometry and solvent cage, fluorescence originates at a higher potential energy than it would under fluid conditions, causing the blue shift upon freezing. The elimination of thermal motion of the functional group and the solvent cage by freezing results in quantization of the vibrational structure of the ground state and, hence, the highly structured spectrum.

In heptane, the nonpolar solvent interacts very weakly with the ground-state or excited molecule (16), so that the effect of solvent relaxation in the excited state and of thermal motion of the ground-state solvent cage, even in fluid heptane, is small. Therefore, there is a higher energy and a higher degree of vibrational structure in the fluorescence of I in heptane relative to that in water.

In anthracenes substituted in α-positions (1- and 9-positions), the transversely polarized $^1L_a \leftarrow {}^1A$ transition is more affected by substituents and environmental perturbations than is the longitudinally polarized $^1L_b \leftarrow {}^1A$ transition. As a result, the ^1L_a band loses vibrational structure and moves to longer wavelengths relative to its position in anthracene while the ^1L_b band retains structure and is only slightly affected (11–13). However, a qualification must be placed on this general statement.

In 9-substituted anthracenes where the substituent groups are relatively bulky (*e.g.*, COO^-, COOH, COOR, and $CONH_2$), steric hindrance arising from interaction between the bulky substituent in the 9-position and the peri hydrogen atoms in the 1- and 8-positions of the anthracene ring prevents the conjugation (coplanarity) of the exocyclic group in the 9-position with the anthracene ring (17, 18). In this case, the 9-substituent produces a weak perturbation and results in absorption spectra almost identical with those of anthracene: highly structured, shifted slightly to longer wavelengths, and insensitive to changes in the electric field produced by varying the dielectric strength of the solvent or the state of protonation of the exocyclic group (16–19). However, in the ^1L_a state, the charge distribution is more stabilized by conjugation of the exocyclic group with the anthracene ring than in the ground state and the gain of

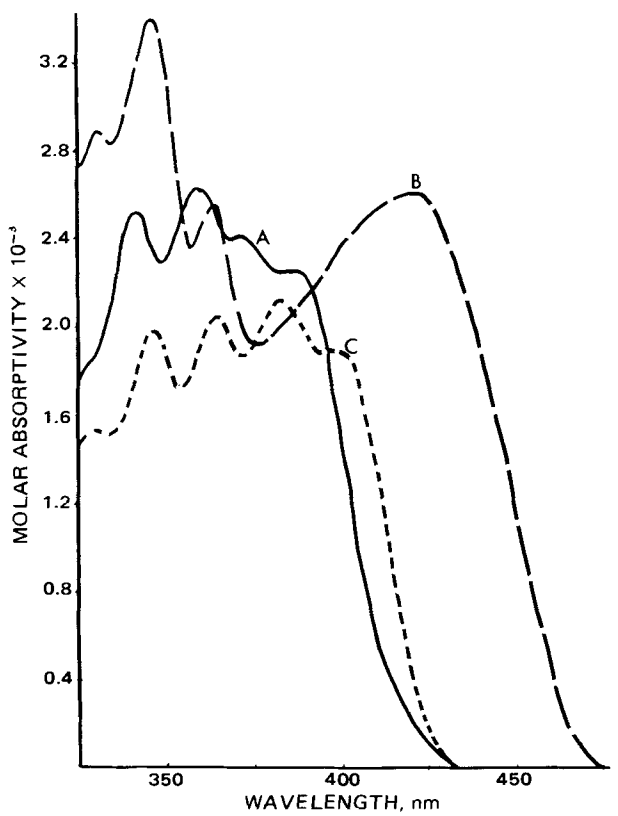

Figure 1—*Electronic absorption spectra of the spectroscopic probe I in aqueous solution (A), in concentrated sulfuric acid (B), and bound to DNA (C). All spectra were taken at 298 °K.*

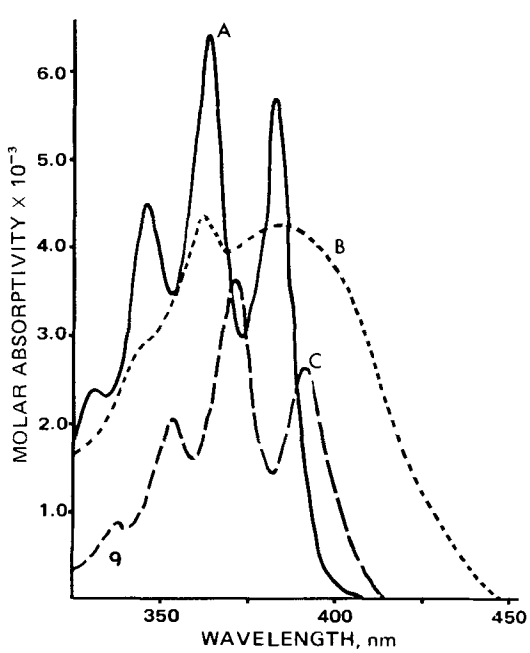

Figure 2—*Electronic absorption spectra of the spectroscopic probe II in aqueous solution (A), in concentrated sulfuric acid (B), and bound to DNA (C). All spectra were taken at 298 °K.*

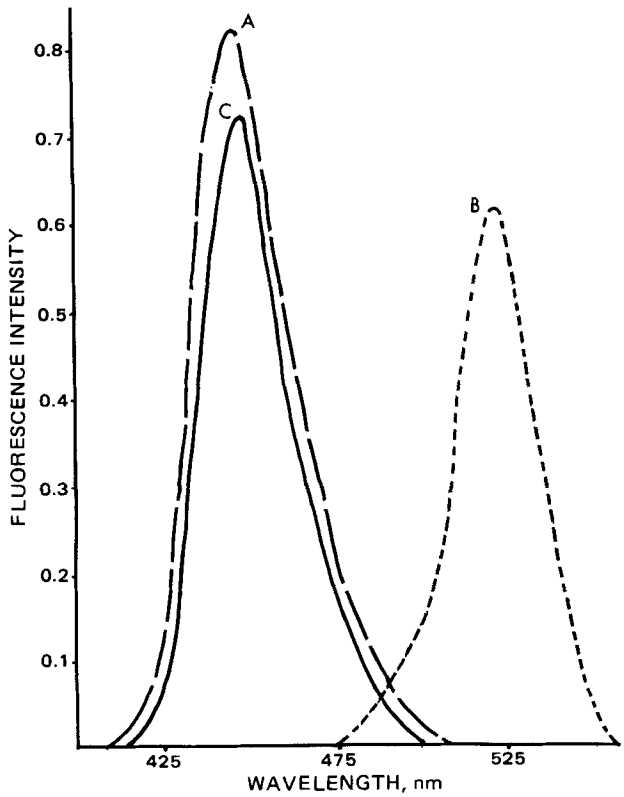

Figure 3—*Fluorescence spectra of the spectroscopic probe I in aqueous solution (A), in concentrated sulfuric acid (B), and bound to DNA (C). All spectra were taken at 298 °K.*

resonance energy attending conjugation may be sufficient to overcome the steric barrier to coplanarity, so that rotation of the 9-substituent into coplanarity with the ring may occur during the lifetime of the excited state.

The fluorescences from these compounds are usually diffuse and shifted to much longer wavelengths than in anthracene (17). Normally, the greater the positive charge on the exocyclic group in the 9-position, the greater is the tendency of electronic charge to be transferred to the exocyclic group and the smaller is the steric barrier to conjugation. Thus, in 9-anthroic acid and its cation, fluorescence is diffuse and lies at much longer wavelengths than in anthracene. However, in the 9-anthroate anion, the fluorescence is anthracene-like in appearance as a result of the failure of the carboxylate group to rotate into coplanarity with the anthracene ring during the lifetime of the ^1L_a state (17).

In amide II, the failure of the bulky substituent in the 9-position to conjugate in the ground state is evident from the highly structured, anthracene-like absorption spectrum of the unprotonated amide. Protonation of II results in a slight red shift of the long wavelength end of the absorption spectrum and some loss of vibrational structure. This result suggests better conjugation of the protonated exocyclic group with the anthracene ring. However, the small change in the absorption spectrum of II upon protonation, relative to that of I upon protonation, suggests that the exocyclic group of protonated II is not quite coplanar with the anthracene ring. The extremely small blue shift of the absorption spectrum of II going from water to heptane is reasonable in light of the low polarity of heptane and the lack of conjugation of the exocyclic group, which is the primary site of solvation, with the anthracene ring.

The blue shiftings of the fluorescence spectrum of II going from fluid water to rigid water or fluid heptane result from the same cause as previously described for I. The smallness of the shifts in this case is due to the fact that II is not well conjugated, even when fluorescence occurs in fluid solution. Therefore, the elimination of thermal relaxation by freezing or low solvent polarity is less pronounced than in the highly conjugated I. Protonation of II does result in a substantial red shift and loss of structure in the fluorescence spectrum, indicating some degree of conjugation between the exocyclic group and the anthracene ring. However, the shift in the fluorescence spectrum of II is much smaller than that occurring in I upon protonation. Even in the fluorescent state, the protonated form of II probably does not have its anthracene ring and its carboxamido group perfectly coplanar.

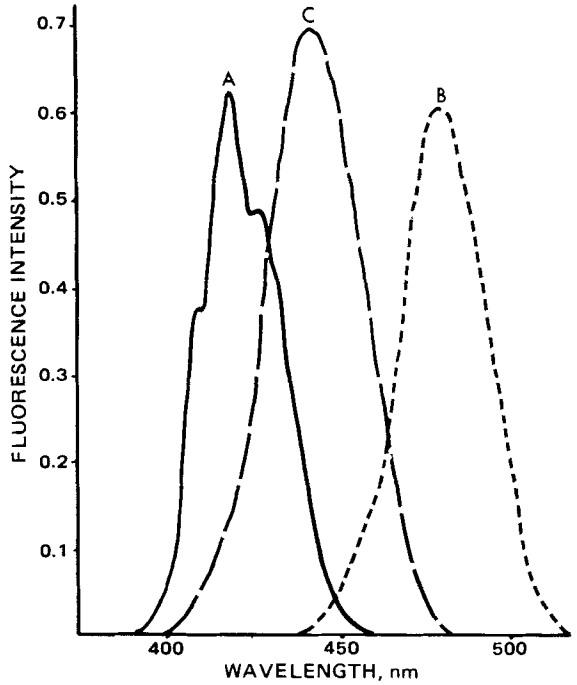

Figure 4—*Fluorescence spectra of the spectroscopic probe II in aqueous solution (A), in concentrated sulfuric acid (B), and bound to DNA (C). All spectra were taken at 298 °K.*

The binding of I and II to DNA results in a shifting of the absorption spectra to lower frequencies (longer wavelengths). In I, the long wavelength end of the absorption spectrum shifts slightly more in frequency than the short wavelength end (Table III), suggesting that the ^1L_b state is somewhat more affected than the ^1L_a state. In II, all vibrational features of the absorption spectrum are shifted in frequency by about the same amount. This result is unlike the spectroscopic effect resulting from transfer from water to a nonpolar solvent, which amounts to a slight blue shift of the absorption spectrum. Nor does it resemble the effect of protonation of the amido groups in which the absorption spectra red shift but also undergo dramatic changes in appearance.

Especially in II, where the exocyclic group is not conjugated with the anthracene ring in the ground state, a DNA-induced displacement of the absorption spectrum as large as that seen in Fig. 2 is not anticipated. It may, therefore, be concluded that the absorption spectral shifts produced by binding result primarily from the interaction of DNA with the π-electrons of the anthracene rings rather than with the carboxamido groups of I and II. If the anthracene rings of I and II are, in fact, intercalated between the base pairs of DNA, the interactions between the polymer and the aromatic portions of the probes could take several forms such as dative π-interaction with the electron-deficient purine and pyrimidine bases and dipole–dipole and dipole-induced dipole attraction. In addition, there would be mutual repulsion between the π-electrons of the anthracene rings and those of the purine and pyrimidine bases of DNA.

The red shifting of the absorption spectra of the probes, upon binding,

Table III—Frequency Shifts ($\Delta\bar{\nu}_a$) of the Discernible Vibronic Features of the Visible Absorption Spectra of I and II upon Binding to DNA in Water at pH 6.9

Without DNA		With DNA		
λ_a, nm	$\bar{\nu}_a$, $cm^{-1} \times 10^{-4}$	λ_a, nm	$\bar{\nu}_a$, $cm^{-1} \times 10^{-4}$	$\Delta\bar{\nu}_a$, $cm^{-1} \times 10^{-4}$
		I		
386	2.59	398	2.51	0.08
371	2.70	382	2.62	0.08
358	2.79	365	2.74	0.05
340	2.94	346	2.89	0.05
328	3.05	330	3.03	0.02
		II		
383	2.61	390	2.56	0.05
364	2.74	371	2.70	0.04
346	2.89	353	2.84	0.05
331	3.02	337	2.97	0.05
318	3.14	322	3.10	0.04

indicates that either the excited states of the bound probes are more stabilized than the ground states by attractive forces or that the ground states are more destabilized by repulsive forces in the bound probes than are the excited states. The fact that the long wavelength side (^1L_b) of the absorption spectrum of I shifts farther to the red than the short wavelength side (^1L_a) indicates that repulsive interaction between the π-systems is dominant in the spectrum. If I intercalates, with the carboxamido group sticking out into the surrounding solution (as it should if the cationic side chain is to be associated with the phosphate backbone of the DNA), the $^1L_b \leftarrow {}^1A$ transition would transfer electronic charge away from the intercalated anthracene ring to the carboxamido group.

The $^1L_a \leftarrow {}^1A$ transition would, however, occur entirely within the intercalated ring. In this case, there would be less interelectronic repulsion in the ^1L_b state than in the ^1L_a state, accounting for the greater red shift of the ^1L_b band as a result of binding to DNA. The observed greater red shift of the ^1L_b band in I cannot be explained in terms of the attractive forces between the anthracene ring and the purine and pyrimidine bases of DNA. With II, the entire *observed* absorption in the 300–400-nm region originates from the $^1L_a \leftarrow {}^1A$ transition (the ^1L_b band is weak and hidden under the ^1L_a band), so that the fact that all vibrational features of the absorption spectrum of II shift equally in frequency is not unexpected.

Since the fluorescence spectra taken in frozen media represent electronic transitions of the fluorophore in the equilibrium ground-state environment, it is not surprising that the DNA-induced fluorescence spectral shifts of I and II in rigid media are similar to those observed for the absorption spectra in fluid media. However, the fluorescence spectra taken in fluid solutions are quite different. The fluorescence spectrum of I when bound to DNA is unstructured and close in position in the electromagnetic spectrum to the fluorescence of free I in fluid solution. The fluorescence of II when bound to DNA in fluid solution has lost its vibrational structure and is shifted to longer wavelengths. This phenomenon strongly suggests that, subsequent to excitation, the anthracene ring and the substituted carboxamido group in the 9-position have moved closer to coplanarity than in the ground state. Both of these observations are indicative of thermal relaxation in the time between absorption and emission.

In I, where the conjugation of the exocyclic group and the aromatic ring is appreciable even in the ground state, thermal relaxation in the excited state is primarily derived from the reorientation of the solvent cage around the carboxamido group. In II, the predominant effect is that the anthracene ring and the 9-carboxamido function come into better conjugation subsequent to absorption and prior to fluorescence. Solvent reorientation alone would not produce much of a change in the fluorescence spectrum of II if the carboxamido group and the anthracene ring were perpendicular (or nearly so) with respect to one another. This means that intercalated II has some freedom of rotation about the bond joining the anthracene ring to the carboxamido group.

It is interesting that II does not become conjugated in the excited state in heptane or water but does when bound to DNA. In a previous study (18), 9-anthracenecarboxamide, a more basic, less hindered precursor of II that does not bind to DNA, became conjugated in the excited state in aprotic solvents but not in water due to steric interference by the aqueous solvent cage around the carboxamido group. The failure of II to become conjugated in the excited state in water or heptane is likely due primarily to the steric restrictions brought about by the bulky side chain substituted onto the basic anthracene structure and the short lifetime of the excited probe. However, the lifetime of the lowest excited singlet state of II increases about sevenfold and its fluorescence efficiency increases about fivefold as a result of binding (Table II).

The reciprocal of the lifetime of the lowest excited singlet state is the sum of the unimolecular rate constants for fluorescence, internal conversion, and singlet–triplet intersystem crossing. For II in fluid aqueous solution, this quantity is 3.3×10^8 sec^{-1}; for II bound to DNA, it is 4.65×10^7 sec^{-1}. Moreover, the ratio of the quantum yield of fluorescence to the lifetime of the lowest excited singlet state is the rate constant for fluorescence alone (*i.e.*, the rate constant for deactivation if fluorescence is the only process deactivating the lowest excited singlet state). For II in fluid aqueous solution, the rate constant for fluorescence is 1.0×10^7 sec^{-1}; for II bound to DNA, it is 6.5×10^6 sec^{-1}.

The sum of the rate constants for radiationless deactivation of II in fluid aqueous solution and bound to DNA are 3.2×10^8 and 4.0×10^7 sec^{-1}, respectively. Since no phosphorescence was observed for any of the species at 77 °K, it may be assumed that radiationless deactivation is mainly limited to internal conversion, *i.e.*, radiationless deactivation due to molecular motion. Since the rate of internal conversion is, in this case, the dominant factor governing the lifetime of the excited state, it is reasonable to surmise that the slower nonradiative deactivation of the singlet state of II resulting from binding to DNA is the result of the decreased freedom of molecular motion. Probably this entails minimization of the random motion of the alkyl side chain by "pinning" to the DNA phosphate backbone and the entrapment of the anthracene ring of II in the helix. The greater lifetime and the restricted motion of the side chain of photoexcited bound II provide a satisfactory explanation for the occurrence of excited-state conjugation in the DNA-bound probe.

REFERENCES

(1) A. Albert, "Selective Toxicity," 5th ed., Chapman and Hall, London, England, 1973, chap. 9.

(2) L. S. Lerman, *J. Mol. Biol.*, **3**, 18 (1961).

(3) L. S. Lerman, *Proc. Natl. Acad. Sci. USA*, **49**, 94 (1963).

(4) L. S. Lerman, *J. Cell. Comp. Physiol., Suppl. 1*, **64**, 1 (1964).

(5) A. R. Peacocke, in "Acridines," 2nd ed., R. M. Acheson, Ed., Wiley–Interscience, New York, N.Y., 1973, chap. 14.

(6) F. Passero, E. J. Gabbay, B. Gaffney, and T. Kurucsev, *Macromolecules*, **3**, 158 (1970).

(7) M. J. Jorgensen and D. R. Hartter, *J. Am. Chem. Soc.*, **85**, 878 (1963).

(8) C. A. Parker and W. T. Rees, *Analyst*, **85**, 587 (1960).

(9) H. B. Klevens and J. R. Platt, *J. Chem. Phys.*, **17**, 470 (1948).

(10) J. W. Sidman, *ibid.*, **25**, 115 (1956).

(11) H. Baba and S. Suzuki, *Bull. Chem. Soc. Jpn.*, **35**, 683 (1962).

(12) T. C. Werner and D. M. Hercules, *J. Phys. Chem.*, **74**, 1030 (1970).

(13) S. G. Schulman, P. J. Kovi, G. Torosian, H. McVeigh, and D. Carter, *J. Pharm. Sci.*, **62**, 1823 (1973).

(14) T. C. Werner, T. Matthews, and B. Soller, *J. Phys. Chem.*, **80**, 533 (1976).

(15) N. S. Bayliss and E. G. McRae, *ibid.*, **58**, 1002 (1954).

(16) B. L. Van Duuren, *J. Org. Chem.*, **26**, 2954 (1961).

(17) T. C. Werner and D. M. Hercules, *J. Phys. Chem.*, **73**, 2005 (1969).

(18) R. J. Sturgeon and S. G. Schulman, *J. Pharm. Sci.*, **65**, 1833 (1976).

(19) S. G. Schulman and I. Pace, *J. Phys. Chem.*, **76**, 1996 (1972).

ACKNOWLEDGMENTS AND ADDRESSES

Received July 19, 1976, from the *College of Pharmacy, University of Florida, Gainesville, FL 32610.*

Accepted for publication January 8, 1977.

The authors are grateful to Dr. E. J. Gabbay of the University of Florida for providing samples of probes I and II and to Mrs. Cindy Jordan for typing the manuscript.

* Present address: Burroughs Wellcome, Inc., Greenville, N.C.

‡ Present address: College of Pharmacy, University of South Carolina, Columbia, S.C.

ˣ To whom inquiries should be directed.

Nature of Acid-Induced Fluorescence of 17α-Methyltestosterone

EFRAIM NJAU

Abstract □ The fluorescence of the 17α-methyltestosterone–trichloroacetic acid reaction product, 1,2,10,15,16,17-hexahydro-10,17,17-trimethylcyclopenta[a]phenanthren-3-one, in strong acid was investigated. Structural requirements for fluorescence were derived from absorption and fluorescence studies of related phenanthrenones and cinnamylidene compounds possessing a similar chromophore. All compounds showed fluorescence intensity that was structure and pH dependent. Fluorescence is attributed to both enol and protonated species.

Keyphrases □ 17α-Methyltestosterone—fluorescence of reaction product with trichloroacetic acid □ Fluorescence—study of reaction product of 17α-methyltestosterone with trichloroacetic acid □ Phenanthrenones, various—structural requirements for fluorescence in strong acid □ Cinnamylidenes, various—structural requirements for fluorescence in strong acid □ Steroids—17α-methyltestosterone, fluorescence of reaction product with trichloroacetic acid

Several fluorometric methods for the determination of steroids and steroidal glycosides devoid of native fluorescence are based on the generation of fluorophores by the action of dehydrating agents on the steroid ring (1–5). The nature and complexity of the reactions remain largely unknown, and the numerous reaction products formed are difficult to isolate (6, 7).

BACKGROUND

Successful development of a fluorometric method with total selectivity for the determination of a particular steroid ideally depends on a reaction taking place on the ring system to form a product with unique photophysical properties. Since this reaction is difficult to achieve, steroid fluorescence analysis has depended largely on chemical transformation of the steroid skeleton using concentrated mineral acids. The use of moderately strong organic acids in steroid analysis has, however, been barely explored (5).

The use of organic acids may reduce the number of reaction products and possibly lead to more specific fluorophores from individual steroids. In an investigation to develop a new fluorometric method for digoxin analysis (8), trichloroacetic acid was highly effective in locating steroidal substances as fluorescent and strongly UV-absorbing products on TLC plates. Of more than 20 steroids subjected to this reagent, the cardiac glycosides and aglycones, 17α-methylandrost-5-ene-3,17-diol (I) and 17α-methyltestosterone (II), reacted most readily (9).

Examination of the trichloroacetic acid reaction with II under controlled conditions (10) showed the major product formed to be 1,2,10,15,16,17 - hexahydro - 10,17,17 - trimethylcyclopenta[a]phenanthren-3-one (III). Other phenanthrenones (IV and V) and cinnamylidene compounds (VI–VIII) with an approximately similar chromophore were synthesized (10–12) and studied to provide information on the structural requirements needed for the fluorescence of III.

EXPERIMENTAL

Apparatus—Absorption measurements were obtained on a recording spectrophotometer[1]. Fluorescence spectra were measured with a spectrophotofluorometer[2] equipped with a 200-w mercury–xenon lamp and an x–y recorder[3]. The following instrumental settings were used for all fluorescence measurements: slit arrangement, 3; photomultiplier shutter, 5 mm; and sensitivity control, 45.

Table I—Absorption and Fluorescence Characteristics of Phenanthrenones and Cinnamylidene Compounds in 80% Phosphoric Acid

Compound	Absorption λ_{max}	Log ε	Excitation λ_{max}	Emission λ_{max}	Quantum Yield
III	480	4.35	465	535	0.0015[a]
IV	463	4.23	465	530	0.33[a]
V	480	4.19	470	550	0.017[a]
VI	430	4.49			
	320	4.07	370	420	0.032[b]
VII	430	4.23	380	430	0.041[b]
VIII	390	4.42	370	420	0.041[b]

[a] Quantum yields (ϕ_f) are relative to fluorescein (ϕ_f = 0.87) in 0.1 *N* NaOH (13). [b] Quantum yields (ϕ_f) are relative to quinine sulfate (ϕ_f = 0.55) with excitation at 366 nm (14).

Reagents—Phenanthrenones (III–V) and cinnamylidene compounds (VI–VIII) were used without further purification. Analytical grade 88% phosphoric acid was diluted with double-distilled absolute ethanol BP to provide solutions of varying acidity for absorptiometric and fluorometric measurements. Analytical grade 60% perchloric acid was prepared similarly. Spectrograde hexane was used for UV studies.

Solutions for Fluorescence Measurements—Fluorescence efficiencies were evaluated by comparing the intensities at the wavelength of maximum emission with respect to the emission intensity of the reference compound (Table I). The sample concentration was adjusted carefully to give the same absorbance as the reference compound at the excitation wavelength chosen. Care was taken to ensure that the concentrations of the samples were well below 10^{-5} *M* to avoid reabsorption

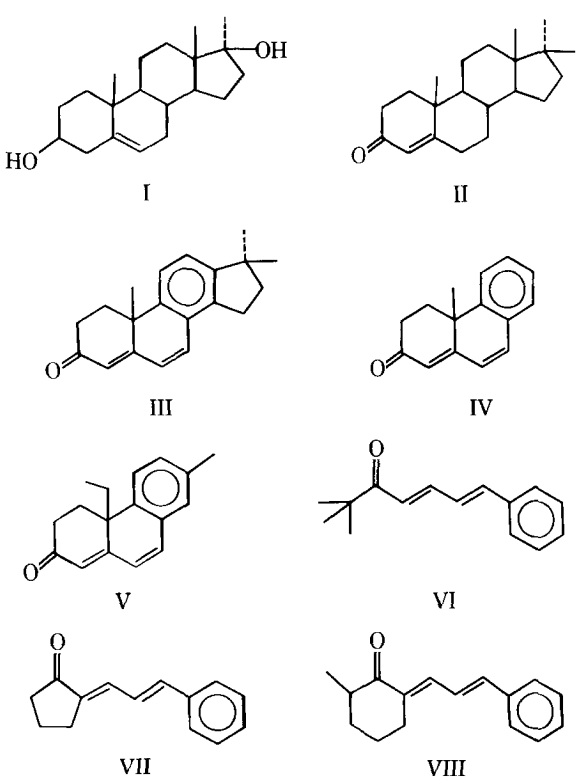

[1] Beckman Acta V.
[2] Aminco-Bowman, American Instrument Co., Silver Spring, Md.
[3] Hewlett-Packard.

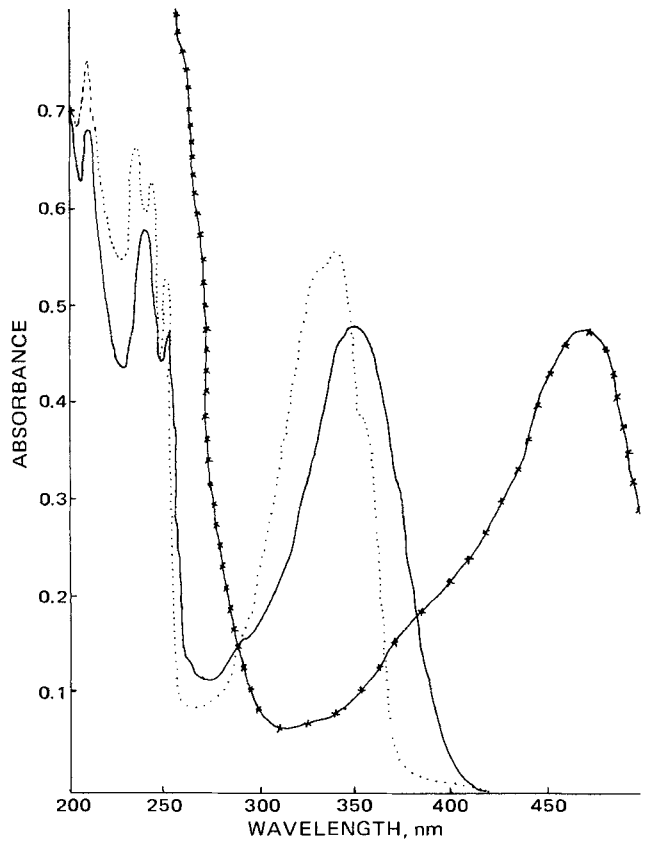

Figure 1—*Absorption characteristics of phenanthrenone IV in ethanol* (——), n-*hexane* (· · ·), *and 88% H_3PO_4* (×—).

of the fluorescence emission (15) in the 1-cm cell at the right-angle illumination viewing geometry.

No differences were observed in intensity on degassing the solutions. No corrections were made for the refractive index of the solutions. The reproducibility of duplicate determinations of the fluorescence quantum yields of the compounds was about ±5%, and the emission spectra were corrected.

RESULTS AND DISCUSSION

The basic phenanthrenone (IV) is essentially identical in structure to III without the cyclopentane side chain and differs slightly from V in substitution. These phenanthrenones have a very similar chromophore to the cinnamylidene compounds (VI–VIII), which are, comparatively, floppy molecules. The compounds studied were chosen to elucidate the

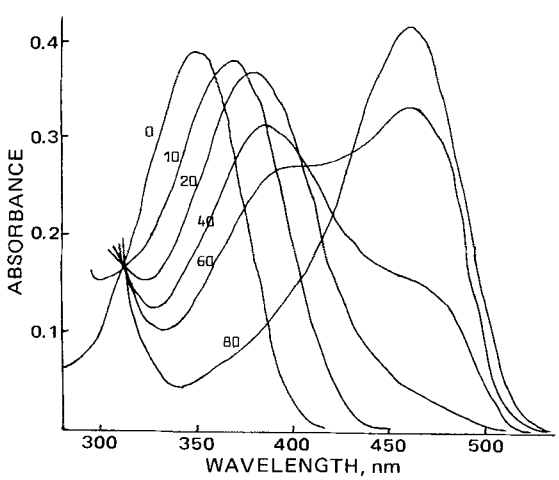

Figure 2—*Enolization of the chromophore of phenanthrenone IV shown as the change in absorption on increasing the phosphoric acid concentration from 0 to 80% in ethanol.*

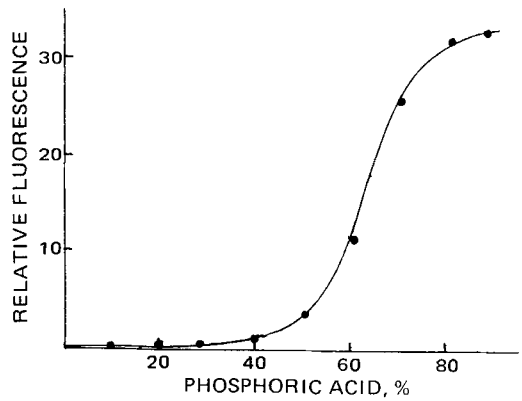

Figure 3—*Relative fluorescence of a 10^{-6} M solution of phenanthrenone IV as a function of phosphoric acid concentration in ethanol.*

structural requirements, if any, and conditions necessary to provide fluorescence emission of the 17α-methyltestosterone–trichloroacetic acid reaction product (III).

The phenanthrenone (IV) in ethanol showed three absorption bands in the UV region (Fig. 1). The intense band at about 350 nm was probably due to $\pi\pi^*$ and $n\pi^*$ absorption of the conjugated chromophore. Of similar intensity was the band at 240 nm, which was interpreted as a $\pi\pi^*$ transition with the character of an intramolecular charge transfer band (16). The most intense band, at about 200 nm, was probably a perturbed local excitation band corresponding to the benzene ^1L_a band.

The $n\pi^*$ transition of this compound was not an isolated band. Its conjugated system was extended enough for the $n\pi^*$ band to be swamped under the more intense $\pi\pi^*$ band (17). On changing to hexane, both the charge transfer and long wavelength absorption bands showed fine structure and were accompanied by solvent shifts of 8 and 13 nm, respectively, toward shorter wavelengths. Phosphoric acid, however, caused a marked change in the chromophore, resulting in the formation of a new absorption band in the visible region (Fig. 1).

TLC evaluation of these ketones revealed that only the phenanthrenones showed appreciable fluorescence; the cinnamylidene compounds were nonfluorescent. In both hexane and ethanol, all compounds (III–VIII) were nonfluorescent. In both perchloric and phosphoric acids, however, they all exhibited intense fluorescence, which was structure and pH dependent.

The effects of pH on the absorption and emission characteristics of IV are summarized in Figs. 2 and 3. It is suggested that in strongly acidic solvents, enolization of the chromophore occurs (Scheme I) and it is the enol form that exhibits fluorescence. This suggestion is consistent with the observed disappearance of fluorescence on neutralization of an acidic solution of the compound followed by ether extraction and subsequent quantitative recovery of the ketonic species. Hence, the fluorescence intensity observed correlated closely with polarity (Fig. 3).

The quantum yields of fluorescence of both phenanthrenones and cinnamylidene compounds (Table I) correlated closely with structure. Compound IV was the most intensely fluorescent in the series since it had the high quantum yield of 0.33. It is likely that the decrease in quantum efficiency observed for both III and V was due to substitution on the aromatic ring. The floppy cinnamylidene compounds fluoresced at shorter wavelengths than the phenanthrenones, and their quantum yields were lower than that of IV by a factor of about 10. Their fluorescence may similarly be attributed to possible enolization of the chromophore under acid conditions.

The *tert*-butyl derivative (VI) is unlikely to enolize in acid. Its fluorescence may be attributed to the $\pi\pi^*$ protonated species since the ketone was recovered on neutralization. Since both excitation and emission of the *tert*-butyl derivative (VI) and the cinnamylidene compound (VIII) occurred at the same wavelengths (Table I), the fluorescence of the ketones (III–VIII) may be attributed, at least in part, to the $\pi\pi^*$ protonated species.

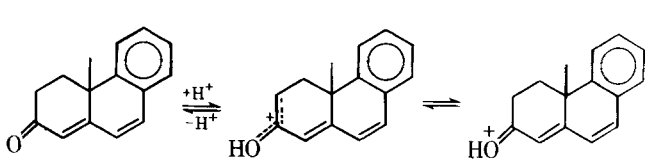

Scheme I

REFERENCES

(1) I. M. Jacovljevick, *Anal. Chem.*, **35**, 1513 (1963).
(2) D. Wells, B. Katzung, and F. H. Meyers, *J. Pharm. Pharmacol.*, **13**, 389 (1961).
(3) R. W. Jelliffe, *J. Chromatogr.*, **27**, 172 (1967).
(4) W. Sadeé, M. Dagcioglu, and S. Riegelman, *J. Pharm. Sci.*, **61**, 1126 (1972).
(5) Y. Kurasawa, A. Takada, and T. Ueda, *Chem. Pharm. Bull.*, **24**, 375 (1976).
(6) M. Kimura, K. Akimaya, and T. Miura, *ibid.*, **20**, 2511 (1972).
(7) M. Kimura, K. Harita, and T. Miura, *ibid.*, **20**, 1829 (1972).
(8) A. Z. Britten and E. Njau, *Anal. Chim. Acta*, **76**, 409 (1975).
(9) E. Njau, *E. Afr. Med. J.*, in press.
(10) A. Z. Britten and E. Njau, *J. Chem. Soc. (Perkin I)*, **1976**, 158.
(11) W. S. Johnson, *J. Am. Chem. Soc.*, **65**, 1317 (1943).
(12) L. Birkofer, S. M. Kim, and H. D. Engels, *Chem. Ber.*, **95**, 1495 (1962).
(13) R. A. Velapoldi, *J. Res. Natl. Bur. Stand.*, **76A** (6), 641 (1972).
(14) W. B. Melhuish, *J. Phys. Chem.*, **64**, 762 (1960). *Ibid.*, **65**, 229 (1961).
(15) I. B. Berlman, "Handbook of Fluorescence Spectra of Aromatic Molecules," Academic, New York, N.Y., 1967.
(16) J. Takana, S. Nagakura, and M. Kobayashi, *J. Chem. Phys.*, **24**, 311 (1956).
(17) H. Suzuki, "Electronic Absorption Spectra and Geometry of Organic Molecules," Academic, New York, N.Y., 1967, chap. 21.

ACKNOWLEDGMENTS AND ADDRESSES

Received July 27, 1976, from the *Faculty of Medicine, Division of Pharmacy, University of Dar Es Salaam, Dar es Salaam, Tanzania.*

Accepted for publication October 12, 1976.

The author acknowledges the Department of Pharmacy, University of Aston, Birmingham, England, for providing facilities for carrying out this work and the Tanzania Government for financial aid.

Contact Angles of Pharmaceutical Powders

C. F. LERK ˣ, M. LAGAS, J. P. BOELSTRA, and P. BROERSMA

Abstract □ Contact angles of pharmaceutical powders were determined by measuring the maximum height of a drop of a saturated solution on a presaturated compact of the material. The results for a series of drugs are presented.

Keyphrases □ Powders, various pharmaceutical—contact angles, densities, and surface tensions □ Contact angles—various pharmaceutical powders □ Densities—various pharmaceutical powders □ Surface tensions—various pharmaceutical powders

The wetting of solid dosage forms is an important initial step in the process of drug dissolution both *in vitro* and *in vivo*. Determination of contact angles of solids gives a measure of their wettability, but problems arise when the solid is finely divided as a powder. Recently (1), a method that consists essentially of measuring the maximum height of a drop of a saturated solution formed on a presaturated compact of the material was used successfully. This report presents the results of contact angle determinations for an additional series of pharmaceutical powders.

EXPERIMENTAL

Materials—The materials and standards are listed in Table I.

Methods—The contact angles were determined using a technique described earlier (1). The densities and surface tensions of the saturated solutions and the densities of the solids were determined with a balance[1], a tensiometer[2], and an air comparison pycnometer[3], respectively. The liquid measurements were carried out at 23°. Saturated solutions were prepared by allowing excess solid to equilibrate with distilled water at a constant temperature of 23°.

RESULTS AND DISCUSSION

Table I lists the contact angles of more than 50 drugs and excipients. The values vary between 21° (ampicillin trihydrate) and 124° (aceto-

[1] Mohr, G. Kern, Ebingen, West Germany.
[2] Du Noüy K 8600 Krüss, Hamburg, West Germany.
[3] Model 930, Beckman Instruments Ned. N.V., Amsterdam, The Netherlands.

Table I—Measured Values of Contact Angles of Pharmaceutical Powders [a]

Material	Standard	Surface Tension, dynes/cm	Density Solid, g/cm³	Contact Angle, θ°
Acetohexamide[b]	—	70.7	1.25	124
Adipic acid[c]	Laboratory grade	58.3	1.38	72
Allobarbital[c]	Ph. Ned. VI	69.4	1.28	61
Aluminum stearate[d]	—	69.4	1.05	120
Aminophylline[e]	—	71.5	1.44	47
Aminophylline (anhydrous)[c]	Ph. Ned. VII	65.5	1.44	40
Aminopyrine[c]	Ph. Ned. VI	57.5	1.19	60
Amobarbital[f]	USP XVII, BP 1973	55.7	1.17	102
Ampicillin (anhydrous)[g]	—	47.9	1.37	35
Ampicillin trihydrate[g]	—	38.6	1.37	21
Aprobarbital[c]	NF XII	57.8	1.28	75
Barbital[c]	Ph. Ned. VI	63.5	1.24	70
Boric acid[c]	Ph. Ned. VI	68.0	1.51	74
Butabarbital[f]	BP 1973	62.0	1.26	82
Butalbital[f]	NF XIII	58.8	1.25	87
Butethal[c]	BP 1968	51.0	1.18	78
Calcium carbonate[c]	Ph. Ned. VI	72.4	2.68	58
Calcium stearate[d]	—	70.7	1.03	115
Calcium sulfate dihydrate[c]	Laboratory grade	44.5	2.32	64
Cyclopentobarbital[f]	—	60.6	1.29	76
Diazepam[h]	BP 1973	64.0	1.37	83
Digoxin[i]	Ph. Eur.	68.1	1.28	49
Ephedrine hydrochloride[c]	Ph. Ned. VI	48.3	1.20	51
Heptobarbital[c]	Ph. Ned. VI	71.3	1.47	74
Hydrochlorothiazide[j]	USP XVIII	72.4	1.69	51
Indomethacin[j]	NF	71.5	1.39	90
Isoniazid[h]	Ph. Ned. VI	61.6	1.42	49
Isoxsuprine hydrochloride[k]	—	66.0	1.28	50
Lithium carbonate[c]	Laboratory grade	71.2	2.08	50
Lithium chloride[d]	Analytical grade	94.7	2.08	51
Mephobarbital[c]	Ph. Ned. VI	68.3	1.38	74
Meprobamate[c]	Ph. Ned. VI	51.9	1.24	83
Nitrofurantoin[h]	USP XVIII	70.6	1.69	69
Oxalic acid[l]	Laboratory grade	70.7	1.66	31

REFERENCES

(1) I. M. Jacovljevick, *Anal. Chem.*, **35**, 1513 (1963).
(2) D. Wells, B. Katzung, and F. H. Meyers, *J. Pharm. Pharmacol.*, **13**, 389 (1961).
(3) R. W. Jelliffe, *J. Chromatogr.*, **27**, 172 (1967).
(4) W. Sadeé, M. Dagcioglu, and S. Riegelman, *J. Pharm. Sci.*, **61**, 1126 (1972).
(5) Y. Kurasawa, A. Takada, and T. Ueda, *Chem. Pharm. Bull.*, **24**, 375 (1976).
(6) M. Kimura, K. Akimaya, and T. Miura, *ibid.*, **20**, 2511 (1972).
(7) M. Kimura, K. Harita, and T. Miura, *ibid.*, **20**, 1829 (1972).
(8) A. Z. Britten and E. Njau, *Anal. Chim. Acta*, **76**, 409 (1975).
(9) E. Njau, *E. Afr. Med. J.*, in press.
(10) A. Z. Britten and E. Njau, *J. Chem. Soc. (Perkin I)*, **1976**, 158.
(11) W. S. Johnson, *J. Am. Chem. Soc.*, **65**, 1317 (1943).
(12) L. Birkofer, S. M. Kim, and H. D. Engels, *Chem. Ber.*, **95**, 1495 (1962).
(13) R. A. Velapoldi, *J. Res. Natl. Bur. Stand.*, **76A** (6), 641 (1972).
(14) W. B. Melhuish, *J. Phys. Chem.*, **64**, 762 (1960). *Ibid.*, **65**, 229 (1961).
(15) I. B. Berlman, "Handbook of Fluorescence Spectra of Aromatic Molecules," Academic, New York, N.Y., 1967.
(16) J. Takana, S. Nagakura, and M. Kobayashi, *J. Chem. Phys.*, **24**, 311 (1956).
(17) H. Suzuki, "Electronic Absorption Spectra and Geometry of Organic Molecules," Academic, New York, N.Y., 1967, chap. 21.

ACKNOWLEDGMENTS AND ADDRESSES

Received July 27, 1976, from the *Faculty of Medicine, Division of Pharmacy, University of Dar Es Salaam, Dar es Salaam, Tanzania.*

Accepted for publication October 12, 1976.

The author acknowledges the Department of Pharmacy, University of Aston, Birmingham, England, for providing facilities for carrying out this work and the Tanzania Government for financial aid.

Contact Angles of Pharmaceutical Powders

C. F. LERK ˣ, M. LAGAS, J. P. BOELSTRA, and P. BROERSMA

Abstract □ Contact angles of pharmaceutical powders were determined by measuring the maximum height of a drop of a saturated solution on a presaturated compact of the material. The results for a series of drugs are presented.

Keyphrases □ Powders, various pharmaceutical—contact angles, densities, and surface tensions □ Contact angles—various pharmaceutical powders □ Densities—various pharmaceutical powders □ Surface tensions—various pharmaceutical powders

The wetting of solid dosage forms is an important initial step in the process of drug dissolution both *in vitro* and *in vivo*. Determination of contact angles of solids gives a measure of their wettability, but problems arise when the solid is finely divided as a powder. Recently (1), a method that consists essentially of measuring the maximum height of a drop of a saturated solution formed on a presaturated compact of the material was used successfully. This report presents the results of contact angle determinations for an additional series of pharmaceutical powders.

EXPERIMENTAL

Materials—The materials and standards are listed in Table I.

Methods—The contact angles were determined using a technique described earlier (1). The densities and surface tensions of the saturated solutions and the densities of the solids were determined with a balance[1], a tensiometer[2], and an air comparison pycnometer[3], respectively. The liquid measurements were carried out at 23°. Saturated solutions were prepared by allowing excess solid to equilibrate with distilled water at a constant temperature of 23°.

RESULTS AND DISCUSSION

Table I lists the contact angles of more than 50 drugs and excipients. The values vary between 21° (ampicillin trihydrate) and 124° (aceto-

[1] Mohr, G. Kern, Ebingen, West Germany.
[2] Du Noüy K 8600 Krüss, Hamburg, West Germany.
[3] Model 930, Beckman Instruments Ned. N.V., Amsterdam, The Netherlands.

Table I—Measured Values of Contact Angles of Pharmaceutical Powders [a]

Material	Standard	Surface Tension, dynes/cm	Density Solid, g/cm³	Contact Angle, θ°
Acetohexamide[b]	—	70.7	1.25	124
Adipic acid[c]	Laboratory grade	58.3	1.38	72
Allobarbital[c]	Ph. Ned. VI	69.4	1.28	61
Aluminum stearate[d]	—	69.4	1.05	120
Aminophylline[e]	—	71.5	1.44	47
Aminophylline (anhydrous)[c]	Ph. Ned. VII	65.5	1.44	40
Aminopyrine[c]	Ph. Ned. VI	57.5	1.19	60
Amobarbital[f]	USP XVII, BP 1973	55.7	1.17	102
Ampicillin (anhydrous)[g]	—	47.9	1.37	35
Ampicillin trihydrate[g]	—	38.6	1.37	21
Aprobarbital[c]	NF XII	57.8	1.28	75
Barbital[c]	Ph. Ned. VI	63.5	1.24	70
Boric acid[c]	Ph. Ned. VI	68.0	1.51	74
Butabarbital[f]	BP 1973	62.0	1.26	82
Butalbital[f]	NF XIII	58.8	1.25	87
Butethal[c]	BP 1968	51.0	1.18	78
Calcium carbonate[c]	Ph. Ned. VI	72.4	2.68	58
Calcium stearate[d]	—	70.7	1.03	115
Calcium sulfate dihydrate[c]	Laboratory grade	44.5	2.32	64
Cyclopentobarbital[f]	—	60.6	1.29	76
Diazepam[h]	BP 1973	64.0	1.37	83
Digoxin[i]	Ph. Eur.	68.1	1.28	49
Ephedrine hydrochloride[c]	Ph. Ned. VI	48.3	1.20	51
Heptobarbital[c]	Ph. Ned. VI	71.3	1.47	74
Hydrochlorothiazide[j]	USP XVIII	72.4	1.69	51
Indomethacin[j]	NF	71.5	1.39	90
Isoniazid[h]	Ph. Ned. VI	61.6	1.42	49
Isoxsuprine hydrochloride[k]	—	66.0	1.28	50
Lithium carbonate[c]	Laboratory grade	71.2	2.08	50
Lithium chloride[d]	Analytical grade	94.7	2.08	51
Mephobarbital[c]	Ph. Ned. VI	68.3	1.38	74
Meprobamate[c]	Ph. Ned. VI	51.9	1.24	83
Nitrofurantoin[h]	USP XVIII	70.6	1.69	69
Oxalic acid[l]	Laboratory grade	70.7	1.66	31

Table I—*(Continued)*

Material	Standard	Surface Tension, dynes/cm	Density Solid, g/cm^3	Contact Angle, θ°
Pentobarbital[c]	Codex Francais	51.5	1.21	86
Phenylbutazone[h]	Ph. Ned. VII	66.2	1.19	109
Phthalylsulfathiazole[m]	—	69.6	1.55	48
Prednisolone[n]	—	68.5	1.30	43
Prednisone[h]	Ph. Ned. VII	65.8	1.41	63
Procaine hydrochloride[c]	Ph. Ned. VI	42.5	1.23	55
Salicylamide[c]	NF XIII	64.0	1.37	70
Secobarbital[c]	USP XVII	48.2	1.19	82
Sodium stearate[c]	—	37.1	1.10	84
Stearic acid[c]	—	62.5	1.01	98
Succinylsulfathiazole[h]	Ph. Ned. VII	71.2	1.55	64
Sulfacetamide[c]	—	68.9	1.37	57
Sulfamerazine[o]	—	69.0	1.32	58
Sulfamethazine[c]	Ph. Ned. VI	71.7	1.44	48
Sulfamethizole[c]	—	69.8	1.52	57
Sulfanilamide[c]	Ph. Ned. VI	66.9	1.46	64
Sulfathiazole[c]	Ph. Ned. VI	69.8	1.61	53
Sulfisoxazole[h]	BP 1973	68.2	1.41	57
Theophylline[c]	Ph. Ned. VI	72.0	1.45	48
Tolbutamide[p]	—	67.9	1.24	72
Vinbarbital[f]	—	60.5	1.25	94
Vinylbital[r]	—	43.3	1.20	71
Chloramphenicol palmitate	β-Form (mp 92–93°)	72.4	1.20	108[q]
Chloramphenicol palmitate	α-Form (mp 87–88°)	72.4	1.20	122[q]

[a] The liquid density of the saturated solutions was 1.00 g/cm^3 except for aminopyrine (1.01), butalbital (1.01), cyclopentobarbital (1.01), aminophylline (Euphyllin) (1.01), amobarbital (1.02), boric acid (1.02), isoniazid (1.03), ephedrine hydrochloride (1.04), oxalic acid (1.05), lithium chloride (1.10), aminophylline anhydrous (1.12), and procaine hydrochloride (1.13 g/cm^3). [b] Lilly Research Centre, Windlesham, Surrey, England. [c] Interpharm, 's-Hertogenbosch, The Netherlands. [d] Merck, Darmstadt, West Germany. [e] Euphyllin, Byk, Zwanenburg, The Netherlands. [f] Siegfried, Zofingen, Switzerland. [g] Gist Brocades, Delft, The Netherlands. [h] Nogepha, Alkmaar, The Netherlands. [i] Boehringer Mannheim, Mannheim, West Germany. [j] Merck Sharp & Dohme, Haarlem, The Netherlands. [k] Philips-Duphar, Weesp, The Netherlands. [l] Brocacef, Maarssen, The Netherlands. [m] Sigma, St. Louis, Mo. [n] Organon, Oss, The Netherlands. [o] A.C.F., Amsterdam, The Netherlands. [p] Hoechst Holland, Amsterdam, The Netherlands. [q] Water contact angle. [r] Byk, Zwanenburg, The Netherlands.

hexamide). The reproducibility of contact angle values was better than 2° for most of the chemicals studied. Chemicals exhibiting poor compressibility (calcium carbonate) or showing swelling and softening of the compact formed (isoniazid and sulfisoxazole) had a reproducibility of contact angle values that was no worse than 4°.

Table I includes all drugs for which a dissolution test for tablets or capsules is required in USP XIX. A great number of these drugs are slightly hydrophobic, including nitrofurantoin, tolbutamide, and meprobamate, or even strongly hydrophobic, such as phenylbutazone and acetohexamide.

A correlation between chemical structure and hydrophobicity is illustrated in Table II for a series of 5,5-substituted barbituric acid derivatives. The results demonstrate the effect of chain length, positional changes in branching, and double bonds on the contact angle of the drugs.

Table II—Chemical Structure and Contact Angle of a Series of Barbiturates

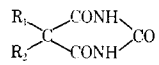

Compound	R_1	R_2	Contact Angle, θ°
Barbital	CH_2CH_3	CH_2CH_3	70
Butethal	CH_2CH_3	$CH_2CH_2CH_2CH_3$	78
Butabarbital	CH_2CH_3	$CH(CH_3)CH_2CH_3$	82
Pentobarbital	CH_2CH_3	$CH(CH_3)CH_2CH_2CH_3$	86
Vinbarbital	CH_2CH_3	$C(CH_3)=CHCH_2CH_3$	94
Amobarbital	CH_2CH_3	$CH_2CH_2CH(CH_3)_2$	102
Aprobarbital	$CH(CH_3)CH_3$	$CH_2CH=CH_2$	75
Butalbital	$CH_2CH(CH_3)CH_3$	$CH_2CH=CH_2$	87
Secobarbital	$CH(CH_3)CH_2CH_2CH_3$	$CH_2CH=CH_2$	82
Vinylbital	$CH(CH_3)CH_2CH_2CH_3$	$CH=CH_2$	71

The wettability of a solid is also affected by its crystallographic structure. This fact is illustrated in Table I for two chloramphenicol palmitate polymorphs. The β-form, mp 92–93°, showed a water contact angle of 108°; the α-form, mp 87–88°, had a water contact angle of 122°. The technique thus provides a sensitive measure of the surface characteristics of chemicals. Variations in contact angle values may be found for different lots from different suppliers of a given chemical, depending on the preparation process. The effect of changes in the wettability of drugs and excipients upon the release from tablets and capsules will be reported later.

REFERENCES

(1) C. F. Lerk, A. J. M. Schoonen, and J. T. Fell, *J. Pharm. Sci.*, **65**, 843 (1976).

ACKNOWLEDGMENTS AND ADDRESSES

Received August 4, 1976, from the *Laboratory for Pharmaceutical Technology, The University, Antonius Deusinglaan 2, Groningen 8004, The Netherlands.*

Accepted for publication November 26, 1976.

The authors thank Boeringer Mannheim, Gist Brocades, Hoechst Holland, Lilly Research, Merck Sharp & Dohme, Nogepha, and Organon for supplying digoxin, ampicillin, tolbutamide, acetohexamide, hydrochlorothiazide, indomethacin, diazepam, and prednisolone.

[x] To whom inquiries should be directed.

Hydroxylation of Three Benzodiazepines *In Vitro*

E. MUSSINI, F. MARCUCCI ˣ, L. AIROLDI, T. FACCHINETTI, and S. GARATTINI

Abstract □ Three structurally related benzodiazepines were studied as substrates for hydroxylation by liver microsomal enzymes of rats and mice. The V_{max} was comparable for dechlorodesmethyldiazepam, desmethyldiazepam, and 2′-chlorodesmethyldiazepam in the two animal species. The apparent K_m decreased from dechlorodesmethyldiazepam to 2′-chlorodesmethyldiazepam for liver microsomal enzymes from both animal species. The hydroxylation of desmethyldiazepam and 2′-chlorodesmethyldiazepam yielded two pharmacologically active metabolites, oxazepam and lorazepam, respectively.

Keyphrases □ Benzodiazepines, various—hydroxylation by rat and mouse liver microsomal enzymes *in vitro* □ Hydroxylation—three benzodiazepines by rat and mouse liver microsomal enzymes *in vitro* □ Metabolism—three benzodiazepines, hydroxylation by rat and mouse liver microsomal enzymes *in vitro* □ Sedatives—three benzodiazepines, hydroxylation by rat and mouse liver microsomal enzymes *in vitro*

Liver microsomal enzymes metabolize 1,4-benzodiazepines *in vitro* (1). Previously, it was shown that diazepam undergoes a process of *N*-1-demethylation and/or C-3-hydroxylation (2), the relative intensity of these pathways depending, among other factors, on animal species (1, 3), age (4), and induction by other treatments (5). This study was designed to investigate how changes in the chemical structure of a benzodiazepine influence its hydroxylation rate. To this end, desmethyldiazepam (I), dechlorodesmethyldiazepam (II), and 2′-chlorodesmethyldiazepam (III) were selected.

EXPERIMENTAL

Chemicals—Compounds I–III and their corresponding 3-hydroxylated metabolites of pharmaceutical grade purity (99%) were used[1].

Animals—Male Charles River rats, 200 ± 10 g, and male CD_1 mice, 22 ± 3 g, were used.

Preparation of Liver Microsomes—Animals were killed, and the livers were immediately removed and homogenized in ice-cold 1.15% KCl (1:4 w/v) with a polytef–glass homogenizer. The homogenate was centrifuged at 9000×*g* for 20 min, and the supernate was centrifuged again at 105,000×*g* for 1 hr[2].

Incubation *In Vitro*—A microsomal suspension in 1.15% KCl containing 8–10 mg of protein/ml was used. Protein determinations were carried out by the Lowry *et al.* (6) method.

Each incubation mixture consisted of 1.5 ml of microsomal suspension equivalent to 0.4 g of liver, NADP (1.5 μmoles), glucose 6-phosphate dehydrogenase (0.5 unit), magnesium chloride (25 μmoles), niacinamide (50 μmoles), 1.4 ml of 0.2 *M* phosphate buffer (pH 7.4), various concentrations of substrates (I–III) ranging from 10^{-4} to 10^{-3} *M*, and 1.15% KCl to obtain a final volume of 5 ml. The substrate concentrations were selected after preliminary experiments.

The mixtures were incubated in a metabolic shaker[3] at 37° under air for 60 min.

At the end of the incubation period, the mixture was extracted twice with 10 ml of ether. The combined extracts were dried, redissolved in a suitable volume of an acetone solution of internal standard (diazepam), and analyzed by GLC.

GLC Determination—A gas chromatograph[4] and a 1-m long glass column (3 mm i.d.) packed with 3% OV-17 on Gas Chrom Q (100–120 mesh) were used. The oven temperatures were 270 and 260° for I–III and their hydroxylated metabolites; the carrier gas flow (nitrogen) was 30 ml/min.

Recovery studies of tested benzodiazepines and their metabolites from water and from microsomal incubation mixtures without cofactors are reported in Table I.

Table I—Recovery Studies

Benzodiazepines[a]	Water, % ± *SE*	Microsomal Incubation Mixture, % ± *SE*
III	95 ± 3	81 ± 1
Lorazepam	95 ± 2	68 ± 0.5
I	95 ± 2	85 ± 2
Oxazepam	95 ± 3	61 ± 3
II	95 ± 1	88 ± 3
Dechlorooxazepam	95 ± 3	65 ± 2

[a] Added amounts ranged from 10 to 50 μg.

RESULTS AND DISCUSSION

The results summarized in Table II show that the three benzodiazepines can be hydroxylated *in vitro* by liver microsomal enzymes obtained from rats or mice. The maximal velocity of hydroxylation, V_{max}, was comparable for the three benzodiazepines with rat liver microsomes, while it was higher for II when mouse liver microsomes were utilized.

The affinity for liver microsomal enzymes, expressed by the value of the apparent K_m, was II < I < III for both rats and mice.

The hydroxylation of 1,4-benzodiazepines may have biological significance, because the hydroxylated products frequently have pharmacological effects[5]. Compound I is, in fact, converted to oxazepam and III is converted to lorazepam, both metabolites being utilized clinically (7–11). It is not known whether the hydroxylated metabolite of II is pharmacologically active, although II was reported (12) to be practically inactive in most experimental tests utilized to screen benzodiazepines.

In mice, lorazepam was more active than oxazepam in antagonizing pentylenetetrazol (13) and the parent compound III was more active than I (12).

The presence of the hydroxylated metabolites in the brain of mice, but not of rats (14), explains the long duration of the effect exerted by I and III in mice but not in rats (12). The facts that both I and III are equally hydroxylated *in vitro* by the liver microsomes of rats and mice but that the hydroxylated metabolites accumulate only in the brain of mice may be due to a rapid metabolism of hydroxylated benzodiazepines in rats (15, 16).

In conclusion, the results indicate that comprehension of the structure–activity relationships of pharmacologically active compounds is tightly bound to studies of drug metabolism and distribution. From a chemical point of view, the presence of a chlorine in positions 7 (ring A) and 2′ (ring C) should influence the energy of the CH bond (ring B) through resonance effects.

The biotransformation of I and III to oxazepam and to chlorooxazepam, respectively, is a stereospecific reaction (17), and the limiting step of this process is the breakdown of the CH bond.

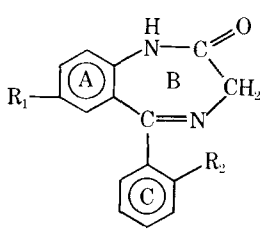

I: R_1 = Cl, R_2 = H
II: R_1 = R_2 = H
III: R_1 = R_2 = Cl

[1] Courtesy of Ravizza, Muggiò, Milan, Italy.
[2] Beckman model L ultracentrifuge with 12.2-m rotor.
[3] Dubnoff.
[4] Model GI, Carlo Erba, Milan, Italy.
[5] S. Garattini, F. Marcucci, and E. Mussini, to be published.

Table II—C-3-Hydroxylation of Benzodiazepines by Liver Microsomal Enzymes of Rats and Mice

Substrates	Rat		Mouse	
	K_m, M	V_{max}, moles/min/mg of Protein	K_m, M	V_{max}, moles/min/mg of Protein
III	4.02×10^{-5} [a]	1.14×10^{-10}	4.52×10^{-4}	6.23×10^{-10}
I	3.30×10^{-4}	1.12×10^{-10}	8.02×10^{-4}	4.58×10^{-10}
II	1.52×10^{-3}	2.35×10^{-10}	1.36×10^{-3}	17.15×10^{-10}

[a] Each figure corresponds to the mean value of four different determinations.

Studies on the distribution of I–III and their metabolites after intravenous administration to rats and mice are in progress. The correlation between *in vitro* and *in vivo* metabolism for both animal species should help explain the species variations in metabolism and pharmacological activity.

REFERENCES

(1) S. Garattini, F. Marcucci, and E. Mussini, *Drug Metab. Rev.*, **1**, 291 (1972).

(2) J. Kvetina, F. Marcucci, and R. Fanelli, *J. Pharm. Pharmacol.*, **20**, 807 (1968).

(3) F. Marcucci, R. Fanelli, E. Mussini, and S. Garattini, *Eur. J. Pharmacol.*, **7**, 307 (1969).

(4) F. Marcucci, E. Mussini, L. Airoldi, A. Guaitani, and S. Garattini, *Biochem. Pharmacol.*, **22**, 3051 (1973).

(5) F. Marcucci, R. Fanelli, E. Mussini, and S. Garattini, *ibid.*, **19**, 1771 (1970).

(6) O. H. Lowry, N. J. Rosebrough, A. L. Farr, and R. J. Randall, *J. Biol. Chem.*, **193**, 265 (1951).

(7) I. Zador, *Dis. Nerv. Syst.*, **30**, 688 (1969).

(8) R. S. Warner, *Psychosomatics*, **6**, 347 (1965).

(9) P. A. Botter, *Curr. Med. Res.*, **1**, 282 (1973).

(10) R. Deberdt, *Curr. Ther. Res.*, **17**, 32 (1975).

(11) J. Venema, *Curr. Med. Res.*, **1**, 285 (1973).

(12) L. De Angelis, U. Traversa, and R. Vertua, *Curr. Ther. Res.*, **16**, 324 (1974).

(13) F. Marcucci, E. Mussini, L. Airoldi, A. Guaitani, and S. Garattini, *J. Pharm. Pharmacol.*, **24**, 63 (1972).

(14) F. Marcucci, E. Mussini, R. Fanelli, and S. Garattini, *Biochem. Pharmacol.*, **19**, 1847 (1970).

(15) P. Bertagni, F. Marcucci, E. Mussini, and S. Garattini, *J. Pharm. Sci.*, **61**, 965 (1972).

(16) S. F. Sisenwine, C. O. Tio, and H. W. Ruelius, *Pharmacologist*, **12**, 272 (1970).

(17) A. Corbella, P. Gariboldi, G. G. Jommi, A. Forgione, F. Marcucci, P. Martelli, and E. Mussini, *J. Chem. Soc. Chem. Commun.*, **1973**, 721.

ACKNOWLEDGMENTS AND ADDRESSES

Received September 28, 1976, from the *Istituto di Ricerche Farmacologiche "Mario Negri," Via Eritrea, 62, 20157 Milano, Italy.*

Accepted for publication December 15, 1976.

[x] To whom inquiries should be directed.

Small Animal Model for Myocardial Infarction

ROBERT J. STAAB, VINCENT de PAUL LYNCH, CESAR LAU-CAM, and MICHAEL BARLETTA [x]

Abstract □ Myocardial infarctions were produced in rats by electrocauterization of the left anterior descending artery, and the extent of myocardial damage was measured by serial serum levels of creatine phosphokinase activity utilizing spectrophotometric analysis. All animals were also evaluated for myocardial damage by electrocardiographic wave alterations. A correlation between myocardial infarct size and serum creatine phosphokinase was demonstrated. Significant arrhythmias and death occurred only in experimental groups where myocardial infarction had been produced. This small animal model offers a quick, inexpensive, and simple method for screening therapeutic agents that alter infarct size.

Keyphrases □ Myocardial infarction—damage correlated with serum creatine phosphokinase levels, rats □ Creatine phosphokinase—serum levels correlated with myocardial damage caused by infarction, rats □ Enzymes—creatine phosphokinase, serum levels correlated with myocardial damage caused by infarction, rats

More than 1,000,000 persons die annually in the United States from cardiovascular disease, the major cause of death in this country. Although a large percentage of deaths resulting from myocardial infarction are associated with cardiac arrhythmias, many patients expire in the coronary care unit due to power failure, especially low output congestive heart failure (1–3). Power failure was suggested to be related to inadequate cardiac output due to necrosis of functional myocardium (4, 5). In power failure, the extent of necrosis, as it is related to the critical mass of functional myocardium, may be used as a determinant of morbidity and mortality in clinical prognosis (6, 7).

BACKGROUND

Several methods have been used to measure the extent of myocardial ischemia, including coronary blood flow, myocardial lactate production, angiography, radioactive scanning, and radioactive potassium tracers (8). Electrocardiographic (ECG) mapping experiments also were used to describe ischemic changes in the myocardium (9, 10). The problem encountered with these methods is that they study the extent of myocardial ischemia without quantitatively ascertaining the infarct size.

The relationship between infarct size and the serum myocardial enzyme levels has been recognized for many years. Myocardial infarct size, measured by excision and weighing of the damaged tissue, correlated closely with the extent of the depletion of myocardial creatine phosphokinase (11). This enzyme offered many advantages over other myocardial enzymes, since it rose first following an infarction and returned to normal levels in approximately 3 days (12). Sequential serum changes of creatine phosphokinase were used to assess damage in the experimentally infarcted dog (13).

A satisfactory quantitative method for the evaluation of myocardial damage would make it possible to determine the effect of therapeutic intervention on limiting the dynamic extension of an infarction. In this study, a simple, inexpensive, small animal model for inducing myocardial infarction, which may prove useful in the preliminary screening of drugs capable of altering infarct size, is presented.

Table II—C-3-Hydroxylation of Benzodiazepines by Liver Microsomal Enzymes of Rats and Mice

Substrates	Rat		Mouse	
	K_m, M	V_{max}, moles/min/mg of Protein	K_m, M	V_{max}, moles/min/mg of Protein
III	4.02×10^{-5} [a]	1.14×10^{-10}	4.52×10^{-4}	6.23×10^{-10}
I	3.30×10^{-4}	1.12×10^{-10}	8.02×10^{-4}	4.58×10^{-10}
II	1.52×10^{-3}	2.35×10^{-10}	1.36×10^{-3}	17.15×10^{-10}

[a] Each figure corresponds to the mean value of four different determinations.

Studies on the distribution of I–III and their metabolites after intravenous administration to rats and mice are in progress. The correlation between *in vitro* and *in vivo* metabolism for both animal species should help explain the species variations in metabolism and pharmacological activity.

REFERENCES

(1) S. Garattini, F. Marcucci, and E. Mussini, *Drug Metab. Rev.*, **1**, 291 (1972).

(2) J. Kvetina, F. Marcucci, and R. Fanelli, *J. Pharm. Pharmacol.*, **20**, 807 (1968).

(3) F. Marcucci, R. Fanelli, E. Mussini, and S. Garattini, *Eur. J. Pharmacol.*, **7**, 307 (1969).

(4) F. Marcucci, E. Mussini, L. Airoldi, A. Guaitani, and S. Garattini, *Biochem. Pharmacol.*, **22**, 3051 (1973).

(5) F. Marcucci, R. Fanelli, E. Mussini, and S. Garattini, *ibid.*, **19**, 1771 (1970).

(6) O. H. Lowry, N. J. Rosebrough, A. L. Farr, and R. J. Randall, *J. Biol. Chem.*, **193**, 265 (1951).

(7) I. Zador, *Dis. Nerv. Syst.*, **30**, 688 (1969).

(8) R. S. Warner, *Psychosomatics*, **6**, 347 (1965).

(9) P. A. Botter, *Curr. Med. Res.*, **1**, 282 (1973).

(10) R. Deberdt, *Curr. Ther. Res.*, **17**, 32 (1975).

(11) J. Venema, *Curr. Med. Res.*, **1**, 285 (1973).

(12) L. De Angelis, U. Traversa, and R. Vertua, *Curr. Ther. Res.*, **16**, 324 (1974).

(13) F. Marcucci, E. Mussini, L. Airoldi, A. Guaitani, and S. Garattini, *J. Pharm. Pharmacol.*, **24**, 63 (1972).

(14) F. Marcucci, E. Mussini, R. Fanelli, and S. Garattini, *Biochem. Pharmacol.*, **19**, 1847 (1970).

(15) P. Bertagni, F. Marcucci, E. Mussini, and S. Garattini, *J. Pharm. Sci.*, **61**, 965 (1972).

(16) S. F. Sisenwine, C. O. Tio, and H. W. Ruelius, *Pharmacologist*, **12**, 272 (1970).

(17) A. Corbella, P. Gariboldi, G. G. Jommi, A. Forgione, F. Marcucci, P. Martelli, and E. Mussini, *J. Chem. Soc. Chem. Commun.*, **1973**, 721.

ACKNOWLEDGMENTS AND ADDRESSES

Received September 28, 1976, from the *Istituto di Ricerche Farmacologiche "Mario Negri," Via Eritrea, 62, 20157 Milano, Italy.*

Accepted for publication December 15, 1976.

[x] To whom inquiries should be directed.

Small Animal Model for Myocardial Infarction

ROBERT J. STAAB, VINCENT de PAUL LYNCH, CESAR LAU-CAM, and MICHAEL BARLETTA [x]

Abstract □ Myocardial infarctions were produced in rats by electrocauterization of the left anterior descending artery, and the extent of myocardial damage was measured by serial serum levels of creatine phosphokinase activity utilizing spectrophotometric analysis. All animals were also evaluated for myocardial damage by electrocardiographic wave alterations. A correlation between myocardial infarct size and serum creatine phosphokinase was demonstrated. Significant arrhythmias and death occurred only in experimental groups where myocardial infarction had been produced. This small animal model offers a quick, inexpensive, and simple method for screening therapeutic agents that alter infarct size.

Keyphrases □ Myocardial infarction—damage correlated with serum creatine phosphokinase levels, rats □ Creatine phosphokinase—serum levels correlated with myocardial damage caused by infarction, rats □ Enzymes—creatine phosphokinase, serum levels correlated with myocardial damage caused by infarction, rats

More than 1,000,000 persons die annually in the United States from cardiovascular disease, the major cause of death in this country. Although a large percentage of deaths resulting from myocardial infarction are associated with cardiac arrhythmias, many patients expire in the coronary care unit due to power failure, especially low output congestive heart failure (1–3). Power failure was suggested to be related to inadequate cardiac output due to necrosis of functional myocardium (4, 5). In power failure, the extent of necrosis, as it is related to the critical mass of functional myocardium, may be used as a determinant of morbidity and mortality in clinical prognosis (6, 7).

BACKGROUND

Several methods have been used to measure the extent of myocardial ischemia, including coronary blood flow, myocardial lactate production, angiography, radioactive scanning, and radioactive potassium tracers (8). Electrocardiographic (ECG) mapping experiments also were used to describe ischemic changes in the myocardium (9, 10). The problem encountered with these methods is that they study the extent of myocardial ischemia without quantitatively ascertaining the infarct size.

The relationship between infarct size and the serum myocardial enzyme levels has been recognized for many years. Myocardial infarct size, measured by excision and weighing of the damaged tissue, correlated closely with the extent of the depletion of myocardial creatine phosphokinase (11). This enzyme offered many advantages over other myocardial enzymes, since it rose first following an infarction and returned to normal levels in approximately 3 days (12). Sequential serum changes of creatine phosphokinase were used to assess damage in the experimentally infarcted dog (13).

A satisfactory quantitative method for the evaluation of myocardial damage would make it possible to determine the effect of therapeutic intervention on limiting the dynamic extension of an infarction. In this study, a simple, inexpensive, small animal model for inducing myocardial infarction, which may prove useful in the preliminary screening of drugs capable of altering infarct size, is presented.

Table I—Experimental Data

Animal Group	Number of Animals	Heart Rate, beats/min ± SE		Incidence of Arrhythmias[a]			Number of Animals with T-Wave Elevations
		Before Surgery	After Surgery	V	VF	VFD	
I	10	350.6 ± 11	328.8 ± 26	0	0	0	0
II	10	353.6 ± 10	335.0 ± 25	0	0	0	0
III	54	354.7 ± 14	322.5 ± 12	13.4[b]	3	14[b]	51

[a] V = ventricular arrhythmias, VF = ventricular fibrillation, and VFD = ventricular fibrillation and death. [b] $p < 0.05$, χ-square analysis.

EXPERIMENTAL

Animals—Seventy-four Sprague–Dawley[1] male rats, 300–400 g, were divided into three groups. Animals in Group I were surgically prepared, but no tissue was infarcted. Group II also served as a control and was handled similarly, except that skeletal muscle was infarcted by cautery. Animals in Group III were prepared surgically, and myocardial tissue was infarcted by cautery. All animals were given food[2] and water *ad libitum*.

Procedure for Inducing Infarction—The surgical preparation was carried out as follows. The animals were anesthesized with pentobarbital sodium[3] (35 mg/kg ip), and the ECG was monitored throughout the surgical procedure. Following depilatation and sterilization with povidone-iodine[4], a 2.54-cm long incision was made through the skin in the left thoracic area to the skeletal muscle. The muscle layers were separated, with minimal damage, using blunt dissection, and a purse string suture was prepared around the incision site.

After the ribs had been spread, the thorax opened, and the heart exposed, a branch of the left anterior descending artery was carefully cauterized[5]. Artificial respiration was not employed, since the procedure involved an open thorax for only 15 sec. The chest was slightly compressed to create a negative intrathoracic pressure, and the purse string suture was closed.

For the measurement of the creatine phosphokinase levels, blood was taken periodically from the tail for 54 hr at intervals of 0, 6, 18, 30, 42, and 54 hr, since creatine phosphokinase activity previously returned to baseline by this time (14–17). After each experiment, the surviving animals were sacrificed, their hearts were removed, and the infarcted tissues were excised carefully. The necrotic tissue was weighed for future correlation with enzyme release data.

Assay of Creatine Phosphokinase—A 0.1-ml volume of serum was used for the assay of creatine phosphokinase levels in a commercial spectrophotometric kit[6].

RESULTS AND DISCUSSION

Significant arrhythmias and deaths occurred in the experimental groups where myocardial infarction had been produced compared to the various control groups (Table I). This finding agrees with previous reports indicating that death associated with an infarct is due to arrhythmias leading to ventricular fibrillation (18). These arrhythmias are believed to be associated with electrically excitable tissue resulting in pacemaker and conduction abnormalities (19).

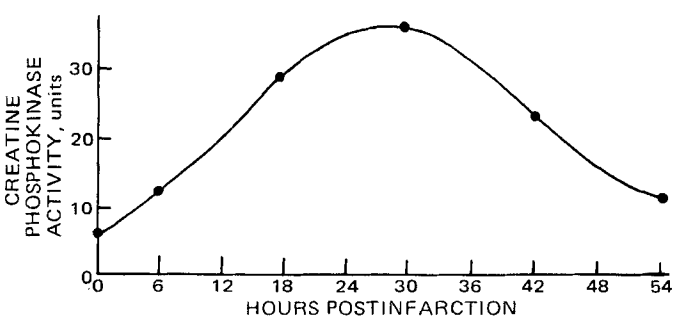

Figure 1—*Variation of serum creatine phosphokinase levels with time in infarcted animals.*

The central zone of an infarct is necrotic tissue that cannot be salvaged and has already released the intracellular enzymes. This zone is believed to be responsible for the early rise in the creatine phosphokinase levels. The intermediate zone consists of ischemic tissue that gradually releases its enzymes. With the incorporation of a proper therapeutic regimen, the conversion of this ischemic zone to necrotic tissue may be precluded (20, 21).

Figure 1 illustrates the mean sequential serum creatine phosphokinase levels[7] for the 54 animals in the experimental group. Since no significant rise in the creatine phosphokinase was observed in control Group II, where the skeletal muscle had been cauterized, it can be concluded that the observed values of creatine phosphokinase in the experimental group are of cardiac origin. The curve is associated with two enzyme pools: a dynamic pool of the enzyme released upon infarction of myocardial tissue and the enzymatic decay associated with the metabolism and excretion. The upslope of the curve (Fig. 1) predominantly represents the release of the enzyme by the myocardium; the apex of the curve represents the

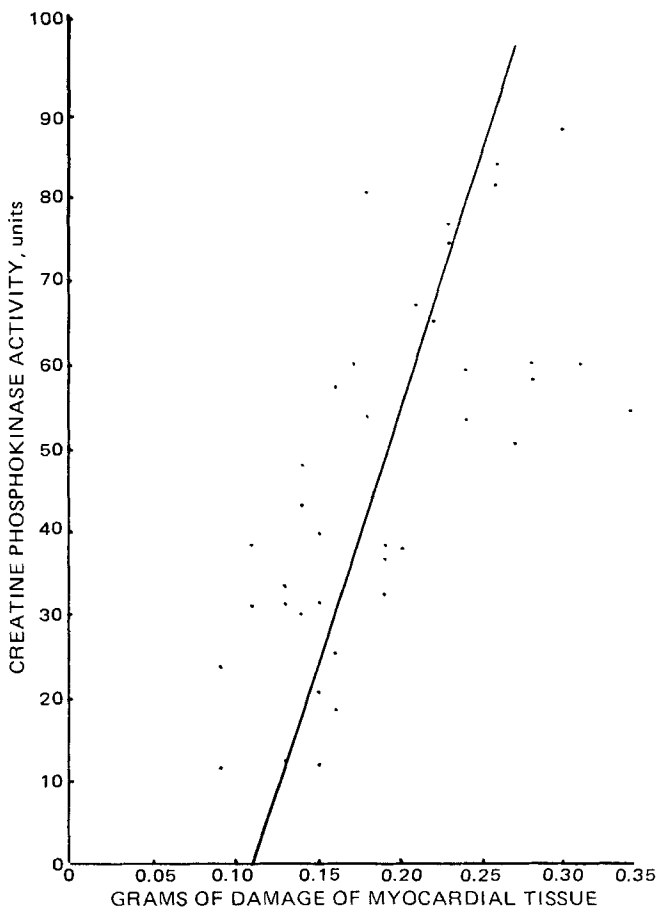

Figure 2—*Creatine phosphokinase activity in terms of the area under the serial creatine phosphokinase curve for each animal in Group III* (n = 54) *plotted* versus *the grams of damage in the excised heart. This linear graph is a result of a standard linear regression analysis. The mean creatine phosphokinase curve area is 50.1975; the mean amount of damage is 0.193 g.*

[1] Taconic Farms, Germantown, N.Y.
[2] Purina Rat Chow, Ralston-Purina, St. Louis, Mo.
[3] Sedasol, Evsco Pharmaceutical Corp., Oceanside, N.Y.
[4] Betadine, Purdue Frederick, Yonkers, N.Y.
[5] Lawton Co., New York, N.Y.
[6] CPK 45-UV, Sigma Chemical Co., St. Louis, Mo.
[7] In Sigma units, Technical Bulletin CPK 45-UV, Sigma Chemical Co., St. Louis, Mo.

equilibrium between myocardial release and decay kinetics. The downslope is predominantly associated with decay phenomena (21).

Animals yielding the upper limits of enzyme release were experiencing serious ventricular arrhythmias and death.

Figure 2 demonstrates the relationship between myocardial damage (in grams) and serum creatine phosphokinase activity. These results agree with a previous conclusion that there is a direct relationship between infarct size and serial enzyme release (22). The pharmacological significance of this model is that it allows study of the dynamic changes of the infarct and also institution of possible therapeutic regimens.

This work also showed that there is a relationship among ECG T-wave elevation, grams of damage, and death in addition to the correlation with enzyme data. Of the 54 experimentally infarcted animals, 51 showed T-wave elevation indicating a hypoxic state. Furthermore, each of the 14 animals experiencing ventricular fibrillation and death was in the group displaying a T-wave elevation. This work demonstrates the sensitivity of enzyme analysis with respect to ECG wave alterations in assessing myocardial infarction.

REFERENCES

(1) "Cardiovascular Diseases in the United States: Facts and Figures," American Heart Association, New York, N.Y., 1965.

(2) D. C. Fluck, E. Olsen, B. L. Pentecost, M. Thomas, S. J. Fillmore, J. P. Shillingford, and J. P. D. Mounsey, *Br. Heart J.*, **29**, 170 (1967).

(3) K. C. Basseter, *Med. Clin. North Am.*, **55**, 435 (1971).

(4) L. C. Page, J. Caulfield, J. Kaston, R. DeSanctis, and C. Sanders, *N. Engl. J. Med.*, **285**, 133 (1971).

(5) C. Hanarayan, M. A. Bennett, B. L. Pentecost, and B. B. Brewer, *Br. Heart J.*, **32**, 728 (1970).

(6) B. E. Sobel and W. E. Shell, *Circulation*, **47**, 215 (1973).

(7) P. R. Maroko, J. K. Kjekshush, B. E. Sobel, T. Watanable, J. W. Covell, J. Ross, and E. Braunwald, *ibid.*, **43**, 67 (1971).

(8) S. Ayres and J. Gregory, "Cardiology," Appleton-Century-Crofts, New York, N.Y., 1971, pp. 144, 145.

(9) P. R. Maroko, P. Libby, J. W. Covell, B. E. Sobel, J. Ross, and E. Braunwald, *Am. J. Cardiol.*, **29**, 223 (1971).

(10) D. S. Reid, L. J. Pelides, and J. P. Shillingford, *Br. Heart J.*, **33**, 370 (1971).

(11) J. K. Kjekshush and B. E. Sobel, *Circ. Res.*, **27**, 403 (1970).

(12) W. Faulkner, J. King, and H. Damm, "Handbook of Clinical Laboratory Data," 2nd ed., Chemical Rubber Co., Cleveland, Ohio, 1968, pp. 259, 260.

(13) W. E. Shell, J. K. Kjekshush, and B. E. Sobel, *J. Clin. Invest.*, **50**, 2614 (1971).

(14) J. W. Hess, R. P. MacDonald, R. J. Frederick, R. Jones, J. Neely, and D. Gross, *Ann. Intern. Med.*, **61**, 1015 (1964).

(15) L. V. Crowley, *Clin. Chem.*, **14**, 1185 (1968).

(16) J. Eschar and H. J. Zimmerman, *Am. J. Med. Sci.*, **253**, 272 (1967).

(17) V. P. Cook, *Am. J. Med. Technol.*, **33**, 275 (1967).

(18) N. B. Low and M. Wolf, *Circulation*, **44**, 130 (1971).

(19) H. J. Levine, "Clinical Cardiovascular Physiology," Grune and Stratton, New York, N.Y., 1976, pp. 309, 310.

(20) J. H. Walton, "The Electrocardiogram in Myocardial Infarction," vol. 20, No. 4, Ciba Clinical Symposia, Summit, N.J., 1968, pp. 22–27.

(21) J. W. Hurst and R. B. Logue, "The Heart," McGraw-Hill, New York, N.Y., 1966, pp. 683, 684.

(22) M. M. Nachlas, *Surgery*, **55**, 700 (1964).

ACKNOWLEDGMENTS AND ADDRESSES

Received September 9, 1976, from the *College of Pharmacy and Allied Health Professions, St. John's University, Jamaica, NY 11439.*

Accepted for publication December 9, 1976.

[x] To whom inquiries should be directed.

Cactus Alkaloids XXXIII: β-Phenethylamines from the Guatemalan Cactus *Pilosocereus maxonii*

S. PUMMANGURA, D. E. NICHOLS, and J. L. McLAUGHLIN [x]

Abstract □ TLC analysis of extracts of *Pilosocereus maxonii* (Rose) Byles and Rowley detected six identifiable alkaloids. Preparative TLC aided in the crystallization of the hydrochlorides of *N*-methyl-3,4-dimethoxyphenethylamine, *N*-methyl-3-methoxytyramine, and *N,N*-dimethyl-3-methoxytyramine. Traces of 3,4-dimethoxyphenethylamine (TLC and mass spectrometry), tyramine (TLC), and *N*-methyltyramine (TLC) were identified. While all of these compounds were isolated and/or detected previously in other cactus species, this study is the first reported crystallization of *N*-methyl- and *N,N*-dimethyl-3-methoxytyramine from a natural source.

Keyphrases □ *Pilosocereus maxonii*—whole plant extract, six alkaloids isolated and identified □ Alkaloids—isolated from whole plant extract of *Pilosocereus maxonii* □ β-Phenethylamines, various—isolated from whole plant extract of *Pilosocereus maxonii*

The cactus genus *Pilosocereus* comprises some 50–60 species, ranging from Florida, the Carribean, and Mexico through Central America into northern South America (1–3). These plants are large, columnar, "giant cacti," and dense wooly hairs or bristles characteristically cover the areoles at the apex of the shoots. Throughout their natural range, species of *Pilosocereus* are used for hedges; a few have edible fruit, but their greatest value in the United States stems from their sale as ornamentals (4, 5). No previous reports have been made regarding the alkaloid content of members of this genus.

In a continuing survey of the Cactaceae for new alkaloid-containing species, extracts of *Pilosocereus maxonii* (Rose) Byles and Rowley were screened. This attractive species is indigenous to Guatemala (3), but propagated plants are available in the United States from commercial cactus dealers. Six β-phenethylamine alkaloids were identified by TLC, and three were successfully crystallized as their hydrochlorides. This paper describes the extraction, isolation, structure elucidation, identification, and synthesis procedures for these alkaloids.

EXPERIMENTAL

Plant Material—Terminal cuttings, both rooted and unrooted, of the plants were received on July 10, 1975, February 5, 1976, and March 5,

equilibrium between myocardial release and decay kinetics. The downslope is predominantly associated with decay phenomena (21).

Animals yielding the upper limits of enzyme release were experiencing serious ventricular arrhythmias and death.

Figure 2 demonstrates the relationship between myocardial damage (in grams) and serum creatine phosphokinase activity. These results agree with a previous conclusion that there is a direct relationship between infarct size and serial enzyme release (22). The pharmacological significance of this model is that it allows study of the dynamic changes of the infarct and also institution of possible therapeutic regimens.

This work also showed that there is a relationship among ECG T-wave elevation, grams of damage, and death in addition to the correlation with enzyme data. Of the 54 experimentally infarcted animals, 51 showed T-wave elevation indicating a hypoxic state. Furthermore, each of the 14 animals experiencing ventricular fibrillation and death was in the group displaying a T-wave elevation. This work demonstrates the sensitivity of enzyme analysis with respect to ECG wave alterations in assessing myocardial infarction.

REFERENCES

(1) "Cardiovascular Diseases in the United States: Facts and Figures," American Heart Association, New York, N.Y., 1965.

(2) D. C. Fluck, E. Olsen, B. L. Pentecost, M. Thomas, S. J. Fillmore, J. P. Shillingford, and J. P. D. Mounsey, *Br. Heart J.*, **29**, 170 (1967).

(3) K. C. Basseter, *Med. Clin. North Am.*, **55**, 435 (1971).

(4) L. C. Page, J. Caulfield, J. Kaston, R. DeSanctis, and C. Sanders, *N. Engl. J. Med.*, **285**, 133 (1971).

(5) C. Hanarayan, M. A. Bennett, B. L. Pentecost, and B. B. Brewer, *Br. Heart J.*, **32**, 728 (1970).

(6) B. E. Sobel and W. E. Shell, *Circulation*, **47**, 215 (1973).

(7) P. R. Maroko, J. K. Kjekshush, B. E. Sobel, T. Watanable, J. W. Covell, J. Ross, and E. Braunwald, *ibid.*, **43**, 67 (1971).

(8) S. Ayres and J. Gregory, "Cardiology," Appleton-Century-Crofts, New York, N.Y., 1971, pp. 144, 145.

(9) P. R. Maroko, P. Libby, J. W. Covell, B. E. Sobel, J. Ross, and E. Braunwald, *Am. J. Cardiol.*, **29**, 223 (1971).

(10) D. S. Reid, L. J. Pelides, and J. P. Shillingford, *Br. Heart J.*, **33**, 370 (1971).

(11) J. K. Kjekshush and B. E. Sobel, *Circ. Res.*, **27**, 403 (1970).

(12) W. Faulkner, J. King, and H. Damm, "Handbook of Clinical Laboratory Data," 2nd ed., Chemical Rubber Co., Cleveland, Ohio, 1968, pp. 259, 260.

(13) W. E. Shell, J. K. Kjekshush, and B. E. Sobel, *J. Clin. Invest.*, **50**, 2614 (1971).

(14) J. W. Hess, R. P. MacDonald, R. J. Frederick, R. Jones, J. Neely, and D. Gross, *Ann. Intern. Med.*, **61**, 1015 (1964).

(15) L. V. Crowley, *Clin. Chem.*, **14**, 1185 (1968).

(16) J. Eschar and H. J. Zimmerman, *Am. J. Med. Sci.*, **253**, 272 (1967).

(17) V. P. Cook, *Am. J. Med. Technol.*, **33**, 275 (1967).

(18) N. B. Low and M. Wolf, *Circulation*, **44**, 130 (1971).

(19) H. J. Levine, "Clinical Cardiovascular Physiology," Grune and Stratton, New York, N.Y., 1976, pp. 309, 310.

(20) J. H. Walton, "The Electrocardiogram in Myocardial Infarction," vol. 20, No. 4, Ciba Clinical Symposia, Summit, N.J., 1968, pp. 22–27.

(21) J. W. Hurst and R. B. Logue, "The Heart," McGraw-Hill, New York, N.Y., 1966, pp. 683, 684.

(22) M. M. Nachlas, *Surgery*, **55**, 700 (1964).

ACKNOWLEDGMENTS AND ADDRESSES

Received September 9, 1976, from the *College of Pharmacy and Allied Health Professions, St. John's University, Jamaica, NY 11439.*

Accepted for publication December 9, 1976.

[x] To whom inquiries should be directed.

Cactus Alkaloids XXXIII: β-Phenethylamines from the Guatemalan Cactus *Pilosocereus maxonii*

S. PUMMANGURA, D. E. NICHOLS, and J. L. McLAUGHLIN [x]

Abstract □ TLC analysis of extracts of *Pilosocereus maxonii* (Rose) Byles and Rowley detected six identifiable alkaloids. Preparative TLC aided in the crystallization of the hydrochlorides of *N*-methyl-3,4-dimethoxyphenethylamine, *N*-methyl-3-methoxytyramine, and *N,N*-dimethyl-3-methoxytyramine. Traces of 3,4-dimethoxyphenethylamine (TLC and mass spectrometry), tyramine (TLC), and *N*-methyltyramine (TLC) were identified. While all of these compounds were isolated and/or detected previously in other cactus species, this study is the first reported crystallization of *N*-methyl- and *N,N*-dimethyl-3-methoxytyramine from a natural source.

Keyphrases □ *Pilosocereus maxonii*—whole plant extract, six alkaloids isolated and identified □ Alkaloids—isolated from whole plant extract of *Pilosocereus maxonii* □ β-Phenethylamines, various—isolated from whole plant extract of *Pilosocereus maxonii*

The cactus genus *Pilosocereus* comprises some 50–60 species, ranging from Florida, the Carribean, and Mexico through Central America into northern South America (1–3). These plants are large, columnar, "giant cacti," and dense wooly hairs or bristles characteristically cover the areoles at the apex of the shoots. Throughout their natural range, species of *Pilosocereus* are used for hedges; a few have edible fruit, but their greatest value in the United States stems from their sale as ornamentals (4, 5). No previous reports have been made regarding the alkaloid content of members of this genus.

In a continuing survey of the Cactaceae for new alkaloid-containing species, extracts of *Pilosocereus maxonii* (Rose) Byles and Rowley were screened. This attractive species is indigenous to Guatemala (3), but propagated plants are available in the United States from commercial cactus dealers. Six β-phenethylamine alkaloids were identified by TLC, and three were successfully crystallized as their hydrochlorides. This paper describes the extraction, isolation, structure elucidation, identification, and synthesis procedures for these alkaloids.

EXPERIMENTAL

Plant Material—Terminal cuttings, both rooted and unrooted, of the plants were received on July 10, 1975, February 5, 1976, and March 5,

1976; rooted commercial stock remains available from the supplier[1]. Reference photographs are on file. The plants conformed to the description of *Cephalocereus maxonii* Rose as described by Britton and Rose (6). The name *Pilosocereus maxonii* (Rose) Byles and Rowley represents the latest taxonomic revision of the species (3); additional names include *Cereus maxonii* Vaupel and *Pilocereus maxonii* (Rose) Knuth (4, 6). The fresh plants were sliced, frozen, freeze dried at temperatures not exceeding 30°, and ground to a powder using a 2-mm sieve in a laboratory mill[2].

Preparation of Crude Alkaloid Fractions—The powdered plant material (500 g) was defatted, basified, and extracted with 16 liters of chloroform *via* percolation (7). The chloroform extract was filtered and condensed to produce a thick syrup, which was extracted with nine successive 300-ml portions of 1 *N* HCl. The filtered aqueous extracts were combined and processed, essentially as previously described (8, 9), to yield crude Fractions A (alkaloids), B (nonalkaloidal materials), and C (water-soluble alkaloids).

Analytical TLC detected an abundance of alkaloids in Fractions A and C, while Fraction B was devoid of alkaloids. Fractions A and C were combined in ethanol and resolved into phenolic and nonphenolic portions using a basic anion-exchange resin as previously reported (10).

TLC—Analytical TLC procedures (8, 9) provided tentative identification of four alkaloids in the extracts. Preparative TLC methods (8, 9) were used to resolve and isolate the major alkaloids in the phenolic and nonphenolic fractions. The TLC systems employed were Solvents A–G as previously described (8, 9); the adsorbants were silica gel plates[3] (analytical) and 1-mm layers of silica gel PF_{254} on 20 × 20-cm plates (preparative). A combination of UV light, fluorescamine[4], dansyl chloride, and tetrazotized benzidine as visualization aids (10, 11) served to distinguish between primary and secondary amines and to provide chromophores distinctive for various structures.

Resolution of Nonphenolic Alkaloids—TLC analysis of this fraction in Solvent E indicated the presence of one major alkaloid (R_f 0.34, secondary amine) and one minor alkaloid (R_f 0.62, primary amine). A 0.30-g portion (from the 2.50-g total) of the nonphenolic alkaloid fraction was resolved *via* preparative TLC (eight plates, one development each) in Solvent E. After detection under UV light (shortwave), the bands were removed and eluted with ethanol followed by methanol.

Identification of Nonphenolic Alkaloids—Synthetic *N*-methyl-3,4-dimethoxyphenethylamine (12) cochromatographed in five TLC solvent systems (A, C, and E–G) with the eluates of the alkaloid having R_f 0.34 in Solvent E. Visualization reactions (dark purple under UV with fluorescamine and a white chromophore with tetrazotized benzidine) were likewise identical with the reference compound. The hydrochloride was prepared as previously described (9) and was crystallized from ethanol–ether. The yield was 56.5 mg (0.094%), mp 135–137° [lit. (12) mp 135–137°], mixed melting point 135–137°; mass spectrum[5]: *m/e* 44 (base peak). The IR[6] spectrum was indistinguishable from the spectrum for reference *N*-methyl-3,4-dimethoxyphenethylamine hydrochloride.

With the same five TLC systems, the alkaloid having R_f 0.62 in Solvent E consistently cochromatographed with reference 3,4-dimethoxyphenethylamine[7]. The visualization reactions (bright yellow under UV with fluorescamine and faint yellow with tetrazotized benzidine) were identical with the reference compound. The trace of alkaloid in the eluate failed to produce a crystalline hydrochloride even after additional preparative TLC. A mass spectral determination of the eluate revealed a molecular ion peak at *m/e* 181 with a base peak at *m/e* 152, consistent with the mass spectrum of reference 3,4-dimethoxyphenethylamine hydrochloride.

Resolution of Phenolic Alkaloids—The phenolic alkaloid fraction (0.88 g) revealed two major alkaloids and two minor alkaloids upon TLC analysis in Solvent G. Preparative TLC (18 plates, three developments each) in Solvent G was used to resolve these compounds into two bands, each containing one major and one minor alkaloid.

The major alkaloid in the lower band gave TLC visualization reactions indicative of a secondary amine (dark purple under UV with fluorescamine and golden under UV after overspraying with dansyl chloride). Tetrazotized benzidine produced a yellow chromophore typical of 4-hydroxyphenethylamines (10). The hydrochloride of the major alkaloid crystallized from methylene chloride–ether (9.5 mg, 0.002% yield).

The major alkaloid in the upper band gave no reaction with fluorescamine, indicating a tertiary amine. Yellow fluorescence under UV after spraying with dansyl chloride confirmed the presence of a phenolic hydroxyl, and a yellow chromophore with tetrazotized benzidine again indicated a 4-hydroxyphenethylamine. The hydrochloride of this major alkaloid also crystallized from methylene chloride–ether (23.4 mg, 0.004% yield).

Crystallizations of the two minor alkaloids from the respective mother liquors of these crystallizations were not attempted.

Identification of *N*-Methyl-3-methoxytyramine—The unknown crystalline hydrochloride from the lower phenolic band gave UV spectra[8] [λ_{max} 228 (ϵ 5510) and 281 (ϵ 2594), 3.2×10^{-5} g/ml in methanol] that were similar to those of 3-methoxytyramine (13). Mass spectral data revealed a molecular ion peak at *m/e* 181 (1.1%, $C_{10}H_{15}NO_2$) with a base peak at *m/e* 44 (100%, C_2H_6N) and another peak at *m/e* 137 (7.4%, $C_8H_9O_2$), indicating β-cleavage of an *N*-methylphenethylamine (9). These data, combined with the TLC visualization reactions, were consistent with the identification of this alkaloid as *N*-methyl-3-methoxytyramine hydrochloride. The observed melting point of 150–153° was close to the literature (14) melting point of 154–155°, and the crystalline compound cochromatographed with a reference sample[9] of *N*-methyl-3-methoxytyramine hydrochloride in five TLC solvents (A, C, and E–G).

Identification of *N,N*-Dimethyl-3-methoxytyramine—The unknown crystalline hydrochloride from the upper phenolic band also gave UV spectra [λ_{max} 228 (ϵ 5590) and 281 (ϵ 2549), 4.0×10^{-5} g/ml in methanol] that were similar to those of 3-methoxytyramine (13). Mass spectral data showed a molecular ion peak at *m/e* 195 (1.2%, $C_{11}H_{17}NO_2$) with a base peak at *m/e* 58 (100%, C_3H_8N) and another peak at *m/e* 137 (3.6%, $C_8H_9O_2$), indicating β-cleavage of an *N,N*-dimethylphenethylamine (15). The data were consistent with the identification of this alkaloid as *N,N*-dimethyl-3-methoxytyramine hydrochloride. The observed melting point of 188–192° was comparable with the literature (14) melting point of 190–191°, and the crystalline alkaloid cochromatographed with a reference sample[10] of *N,N*-dimethyl-3-methoxytyramine hydrochloride in the usual five TLC systems (A, C, and E–G).

Identification of Tyramine and *N*-Methyltyramine—The minor alkaloids in the mother liquors from the upper and lower phenolic bands were identified as tyramine and *N*-methyltyramine, respectively. These compounds consistently cochromatographed (Solvents A, C, and E–G) with reference tyramine hydrochloride[11] and reference *N*-methyltyramine hydrochloride[12], and the TLC visualization reactions were identical with the reference compounds (11).

Synthesis of Reference *N,N*-Dimethyl-3-methoxytyramine Hydrochloride—The method of Cherayil (16) was followed with slight modifications (the suggested chromatographic purification of the product was not necessary). 3-Methoxytyramine hydrochloride[13] (290 mg, 1.5 mmoles) was mixed with sodium bicarbonate (42 mg, 1.5 mmoles), 88% (w/w) formic acid (131 mg, 7.5 mmoles), 37% (w/w) formaldehyde (203 mg, 7.5 mmoles), and 15 ml of dimethylformamide. The mixture was refluxed for 5 hr, cooled, added to a mixture of 15 ml of water and 20 ml of 0.5 *M* pH 10 sodium borate, extracted three times with 50-ml portions of ethyl acetate, and dried over anhydrous sodium sulfate. The extract was then evaporated under reduced pressure to obtain 0.21 g of slightly yellow liquid. The hydrochloride was prepared and crystallized from ethanol–ether to yield white crystals (mp 191–192°, 156 mg, 53.8% yield). Cochromatographic, mixed melting-point, IR, and mass spectral data identified the synthetic and isolated materials as *N,N*-dimethyl-3-methoxytyramine hydrochloride.

Synthesis of Reference *N*-Methyl-3-methoxytyramine Hydrochloride—Nitromethane was condensed with 4-benzyloxy-3-methoxybenzaldehyde[13] (15 g) *via* the method of Gairaud and Lappin (17), using ammonium acetate and acetic acid to yield 4-benzyloxy-3-methoxy-β-nitrostyrene [10.95 g, 73% yield, mp 121–123°, lit. (18) mp 122–123°]. The reduction of this compound (2.85 g) was performed using standard procedures with lithium aluminum hydride in anhydrous ether (19); the ether extract was dried over anhydrous sodium sulfate and saturated with anhydrous hydrogen chloride. The white precipitate of 4-benzyloxy-3-methoxy-β-phenethylamine hydrochloride was recrystallized from ethanol [2.13 g, 75% yield, mp 175–178°, lit. (18) mp 173–175°].

[1] Abbey Garden, Carpinteria, Calif.
[2] Model 4, Thomas-Wiley.
[3] Bakerflex-IB2.
[4] Fluram, Roche.
[5] Hitachi RMU-6 mass spectrometer.
[6] Obtained using potassium bromide pellets and a Beckman IR 33 spectrophotometer.
[7] Calbiochem.
[8] Cary model 17 recording spectrophotometer.
[9] Supplied by Dr. J. Lundström, Astra Pharmaceuticals AB, Sodertalje, Sweden.
[10] Supplied by Dr. G. D. Cherayil, Medical College of Milwaukee, Milwaukee, Wis.
[11] Eastman.
[12] Isolated from *Opuntia clavata* Eng.
[13] Aldrich Chemical Co.

The hydrochloride (1.2 g) was dissolved in 25 ml of water and made alkaline with 1 *N* NaOH. The alkaline solution was extracted three times with equal portions of ether. The ether extracts were dried over anhydrous sodium sulfate and concentrated under reduced pressure to yield the free base as an oily liquid. This oil was dissolved in 50 ml of methyl formate and transferred to a high pressure vessel. The vessel was purged with nitrogen, sealed, and heated for 12 hr on a steam bath. After cooling and removing the solvent under reduced pressure, the *N*-formyl compound was obtained as a yellow oil, which could not be induced to crystallize. The IR spectrum showed expected strong peaks for amide NH and carbonyl. TLC in chloroform–methanol (3:4) and visualization with fluorescamine showed complete absence of the original primary amine.

The entire yield of *N*-formyl-4-benzyloxy-3-methoxy-β-phenethylamine was dissolved in 50 ml of ether and added dropwise into a mixture of 1 g of lithium aluminum hydride and 25 ml of ether. After addition, the mixture was refluxed for 10 hr; the excess reducing agent was destroyed by the careful addition of water and 20% sodium hydroxide. After stirring for 15 min, the ether layer was decanted. The aqueous residue was washed three times with 40-ml portions of ether. After drying over anhydrous sodium sulfate, the combined ether portions were saturated with anhydrous hydrogen chloride. Recrystallization of the precipitate from ethanol yielded *N*-methyl-4-benzyloxy-3-methoxy-β-phenethylamine hydrochloride [580 mg, 50% overall yield, mp 155–156°, lit. (14) mp 154–155°].

Debenzylation of this compound (500 mg) was performed by hydrogenation for 3 hr at 40–50 psi in 20 ml of ethanol over 125 mg of 10% palladium-on-charcoal. The reaction mixture was filtered (diatomaceous earth[14]), and the filtrate was concentrated. Crystallization from ethanol–ether yielded *N*-methyl-3-methoxytyramine hydrochloride [210 mg, 42% yield, mp 152°, lit. (14) mp 154–155°]. Cochromatographic, mixed melting-point, IR, and mass spectral data confirmed the identity of the synthetic product and the isolated alkaloid.

DISCUSSION

By using previously described techniques, an alkaloid extract was obtained from defatted *P. maxonii* and resolved into nonphenolic and phenolic fractions. TLC analyses revealed the presence of one major alkaloid (*N*-methyl-3,4-dimethoxyphenethylamine) and one minor alkaloid (3,4-dimethoxyphenethylamine) in the nonphenolic fraction. Preparative TLC aided in the crystallization of the hydrochloride of the major nonphenolic alkaloid, and comparisons of physical and spectral data (melting point, mixed melting point, and mass and IR spectra) of the isolated alkaloid and reference *N*-methyl-3,4-dimethoxyphenethylamine confirmed the original TLC identification. The trace of 3,4-dimethoxyphenethylamine would not crystallize, but the TLC identification (five solvent systems) was confirmed by mass spectral analysis using concentrated eluates from preparative TLC.

Analysis of the phenolic alkaloid fraction by TLC revealed two major alkaloids (unknowns) and two minor alkaloids (tyramine and *N*-methyltyramine). After preparative TLC, the hydrochlorides of the major alkaloids crystallized and were identified (TLC visualization reactions and UV and mass spectral data) as *N*-methyl-3-methoxytyramine and *N,N*-dimethyl-3-methoxytyramine hydrochlorides. To confirm these identifications, the two compounds were synthesized following established methods; the synthetic compounds were identical in all respects (TLC, melting point, mixed melting point, IR, and mass spectra) to the isolated alkaloids. The mother liquors from the crystallizations of the two major phenolic alkaloids contained traces of tyramine and *N*-methyltyramine, which were identified by TLC (five solvent systems).

[14] Celite.

All six of these alkaloids were detected and/or isolated from other cactus species. Tyramine, *N*-methyltyramine, 3,4-dimethoxyphenethylamine, and *N*-methyl-3,4-dimethoxyphenethylamine are fairly common in alkaloidiferous cacti. However, the two major phenolic alkaloids, *N*-methyl- and *N,N*-dimethyl-3-methoxytyramine, are much less common; this paper is the first report of their crystallization from a natural source. Agurell *et al.* (19) detected *N*-methyl-3-methoxytyramine in *Trichocereus courantii* (K. Sch.) Backb. using TLC, GLC, and GLC–mass spectrometry, and Bruhn and Bruhn (20) used these same methods to detect a trace of *N,N*-dimethyl-3-methoxytyramine in *Ariocarpus agavoides* (Castaneda) E. F. Anderson. Lundström (14) used "trapping experiments" to detect traces of both compounds in peyote, *Lophophora williamsii* (Lem.) Coult. The pharmacological activity and especially the psychoactive effects of these alkaloids remain to be explored.

REFERENCES

(1) C. Backeberg, "Das Kakteenlexikon," 2nd ed., Gustav Fischer, Jena, East Germany, 1970, pp. 362–369.

(2) R. Rawé, "Cacti in Southern Africa," Howard Timmins, Capetown, South Africa, 1966, p. 152.

(3) R. S. Byles and G. D. Rowley, *Cact. Succ. J. G. Br.*, **19,** 67 (1957).

(4) W. T. Marshall and T. M. Bock, "Cactaceae," Abbey Garden Press, Pasadena, Calif., 1941, pp. 72–74.

(5) W. E. Shewell-Cooper and T. C. Rockford, "Cacti as House Plants," Blandford, London, England, 1973, p. 83.

(6) N. L. Britton and J. N. Rose, "The Cactaceae," vol. 2, 2nd ed., Dover, New York, N.Y., 1937, p. 48.

(7) J. M. Neal, P. T. Sato, C. L. Johnson, and J. L. McLaughlin, *J. Pharm. Sci.*, **60,** 477 (1971).

(8) J. J. Dingerdissen and J. L. McLaughlin, *ibid.*, **62,** 1663 (1973).

(9) R. L. Ranieri and J. L. McLaughlin, *J. Org. Chem.*, **41,** 319 (1976).

(10) J. L. McLaughlin and A. G. Paul, *Lloydia*, **29,** 315 (1966).

(11) R. L. Ranieri and J. L. McLaughlin, *J. Chromatogr.*, **111,** 234 (1975).

(12) W. W. Speir, V. Mihranian, and J. L. McLaughlin, *Lloydia*, **33,** 15 (1970).

(13) K. M. Kelley Hornemann, J. M. Neal, and J. L. McLaughlin, *J. Pharm. Sci.*, **61,** 41 (1972).

(14) J. Lundström, *Acta Chem. Scand.*, **25,** 3489 (1971).

(15) R. L. Ranieri and J. L. McLaughlin, *Lloydia*, **40,** 173 (1977).

(16) G. D. Cherayil, *J. Pharm. Sci.*, **62,** 2054 (1973).

(17) C. B. Gairaud and G. R. Lappin, *J. Org. Chem.*, **18,** 1 (1953).

(18) S. Kobayashi, *Sci. Pap. Inst. Phys. Chem. Res. Jpn.*, **6,** 149 (1927); through *Chem. Abstr.*, **22,** 1345 (1928).

(19) S. Agurell, J. G. Bruhn, J. Lundström, and U. Svensson, *Lloydia*, **34,** 183 (1971).

(20) J. G. Bruhn and C. Bruhn, *Econ. Bot.*, **27,** 241 (1973).

ACKNOWLEDGMENTS AND ADDRESSES

Received November 15, 1976, from the *Department of Medicinal Chemistry and Pharmacognosy, School of Pharmacy and Pharmacal Sciences, Purdue University, West Lafayette, IN 47907.*

Accepted for publication December 17, 1976.

Supported by U.S. Public Health Service Research Grant GM-21,211 from the National Institute of General Medical Sciences and by a grant from the Cactus and Succulent Society of America.

The authors acknowledge the valuable advice and assistance of R. Foster, J. E. Bleck, J. G. Bruhn, J. Lundström, G. D. Cherayil, J. W. Clevenger, I. K. Stamos, and I. Jardine.

[x] To whom inquiries should be directed.

Effect of Coadministered Salicylamide on Terbutaline Metabolism in Rats

SAMPAT M. SINGHVI *, WALTER D. CONWAY ×, MILO GIBALDI, and STEPHEN SHAAR ‡

Abstract □ Concomitant oral administration of salicylamide (200 mg/kg) and ^{3}H-terbutaline (1 mg/kg) to rats with ligated bile ducts decreased absorption of terbutaline from the gut from 73 to 56% as measured by urinary excretion of radioactivity in 48 hr. No increase in the fraction of terbutaline excreted unchanged was observed, suggesting that salicylamide does not substantially inhibit the conjugation of terbutaline with glucuronic acid. An increase in the fraction of terbutaline excreted unchanged observed in normal animals may result from enhanced excretion of terbutaline glucuronide into bile rather than from inhibition of conjugation.

Keyphrases □ Salicylamide—effect on absorption and metabolism of terbutaline, rats □ Terbutaline—absorption and metabolism, effect of salicylamide, rats □ Absorption—terbutaline, effect of salicylamide, rats □ Metabolism—terbutaline, effect of salicylamide, rats □ Bronchodilators—terbutaline, absorption and metabolism, effect of salicylamide, rats □ Analgesics—salicylamide, effect on absorption and metabolism of terbutaline, rats

The metabolic fate of the bronchodilator drug terbutaline in rats was reported following administration of 5-mg/kg doses by oral, subcutaneous, intraperitoneal, and intraportal routes (1). Regardless of the route of administration, only one metabolite, a glucuronide conjugate of terbutaline, was excreted in the urine along with unchanged drug. On oral administration, terbutaline was extensively conjugated by the intestinal mucosa during absorption from the gut lumen (1). In fact, the fraction of drug excreted unchanged in the urine was less than 3.5% of the dose at 10 mg/kg or less and rose to only 6.2% at 1000 mg/kg (2). Therefore, it was decided to study the possibility of competitively inhibiting glucuronide conjugation and thereby increasing the transfer of unchanged terbutaline across the intestinal epithelium by concomitant administration of salicylamide, another phenolic drug.

Salicylamide inhibited the glucuronide conjugation of salicylic acid in humans (3) and decreased the formation of acetaminophen sulfate and, to a less extent, acetaminophen glucuronide in humans (4). Salicylamide significantly inhibited the conjugation of isoproterenol in the dog intestine (5). Isoproterenol is structurally similar to terbutaline; on oral administration to dogs, it was extensively metabolized and mainly excreted in urine as a sulfuric acid ester (6, 7). Introduction of 1–2 g of salicylamide into surgically isolated gut loops of dogs prior to isoproterenol administration raised the fraction of radioactivity found in the venous effluent as unchanged isoproterenol to about 74% compared to about 4% in the absence of salicylamide (5).

Since, in rats, terbutaline is excreted in urine mainly as the glucuronide, salicylamide might be expected to inhibit the conjugation. The effect in rats of various doses of salicylamide administered concomitantly with terbutaline on the amounts of free and conjugated drug subsequently excreted in urine is reported in this paper.

EXPERIMENTAL

Aqueous solutions of salicylamide (4–72 mg/ml) were prepared in 1 *N* NaOH, and the pH was adjusted to 10.0 with 1 *N* acetic acid. Appropriate volumes of solutions of nonradioactive and purified ^{3}H-terbutaline were then added to provide solutions containing salicylamide equivalent to doses of 10, 100, and 200 mg/kg and terbutaline base equivalent to a dose of 1 mg/kg in 1 ml. Aliquots of 1 ml of these solutions containing approximately 70 μCi of tritium were administered orally to groups of three male Sprague–Dawley rats weighing approximately 250 g.

Rats in a control group were given 1 ml of a buffered solution (0.15 *M* $NaHCO_3$ adjusted to pH 10 with 1 *N* NaOH) containing 1 mg of terbutaline base/kg and approximately 70 μCi of tritium. All rats were fasted overnight prior to dosing and for 8 hr thereafter. Water was available *ad libitum* before and throughout the experiment. Urine was collected at intervals of 0–8, 8–24, and 24–48 hr postmedication.

An identical experiment was conducted using other groups of rats in which the common bile duct had been ligated with two sutures and then severed between the sutures immediately prior to drug administration.

Aliquots of 10–30 μl of 0–8- and 8–24-hr urine were examined by electrophoresis using the technique of Conway *et al.* (8). Electrophoretic runs were made in pH 3.0 phosphate buffer, which provided adequate separation of all metabolites (1).

The tritium content of urine was analyzed by liquid scintillation counting, and the radioactive zones on electrophoregrams were located and quantitated by scanning in a gas-flow counter as described previously (1, 2).

RESULTS AND DISCUSSION

Following oral administration of ^{3}H-terbutaline in a solution buffered at pH 10 to normal rats, radioactivity was rapidly excreted in urine, accounting for mean values of 31% of the dose in 8 hr and 35% in 24 hr. These results are in good agreement with the reported excretion in urine of 40% of a 1-mg/kg dose of ^{3}H-terbutaline administered in water (2). The excretion of radioactivity decreased with increasing doses of concomitantly administered salicylamide to 18 and 23% in 8 and 24 hr, respectively, with the highest dose (200 mg/kg) of salicylamide administered. Without or with coadministration of salicylamide, little additional radioactivity was excreted in the urine in the 8–24-hr period and a negligible amount was excreted thereafter.

In contrast, groups of rats with ligated bile ducts excreted 49, 70, and 73% of the administered radioactivity in 8-, 24-, and 48-hr periods, respectively; when salicylamide (200 mg/kg) was administered concomitantly, these values decreased to 17, 50, and 56%, respectively.

Ligation of the bile duct resulted in a more prolonged elimination of radioactivity in the urine whether or not salicylamide was administered.

Compositions of the 0–24-hr urines are summarized in Fig. 1. In animals with patent bile ducts, the total radioactivity excreted in urine decreased with increasing doses of salicylamide, although the decrease was significant only at the 200-mg/kg dose. At the same time, the small quantity of free terbutaline excreted increased about twofold in terms of percentage of dose or fourfold in terms of percentage of total radioactivity in urine. In animals with ligated bile ducts, the total radioactivity excreted in urine remained constant for doses of salicylamide up to 100 mg/kg but decreased with the 200-mg/kg dose. Since excretion was essentially complete in 24 hr, these results confirm that coadministration of high doses of salicylamide decreases terbutaline absorption from the gut.

The fraction of terbutaline excreted in unchanged (*i.e.*, free) form remained essentially constant in the bile duct-ligated animals, suggesting

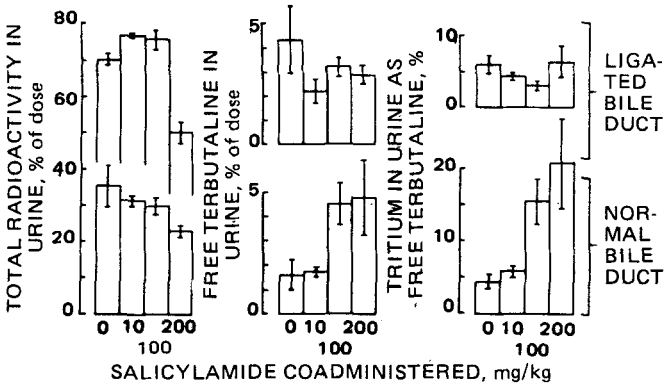

Figure 1—*Excretion of total radioactivity and free terbutaline in the 24-hr urine following oral administration of ^3H-terbutaline (1 mg/kg) coadministered with salicylamide to rats with either patent or ligated bile ducts. Values are the means ±1 SE for groups of three rats.*

that terbutaline in the intestinal wall and in the liver is not appreciably inhibited by coadministered salicylamide. A definitive explanation for the rise in the fraction of terbutaline excreted unchanged when salicylamide was coadministered to normal animals cannot be given. Nevertheless, the observation can be rationalized in terms of the reported finding (2) that unchanged terbutaline passing the gut and subsequently conjugated in the liver is preferentially excreted in the bile while the conjugate previously formed in the intestinal wall is preferentially excreted in urine. The simultaneous presence of salicylamide or its conjugate might influence the partitioning between bile and portal blood of terbutaline glucuronide formed in the liver and thereby influence the observed fraction of terbutaline excreted unchanged in the urine. Such a process would not influence the ratio of metabolites in bile duct-ligated animals since all conjugated drug, regardless of its site of formation, would be excreted in urine.

REFERENCES

(1) W. D. Conway, S. M. Singhvi, M. Gibaldi, and R. N. Boyes, *Xenobiotica*, **3**, 813 (1973).

(2) S. M. Singhvi, W. D. Conway, M. Gibaldi, and R. N. Boyes, *ibid.*, **4**, 563 (1974).

(3) G. Levy and J. A. Procknal, *J. Pharm. Sci.*, **57**, 1330 (1968).

(4) G. Levy and H. Yamada, *ibid.*, **60**, 215 (1971).

(5) C. F. George, E. W. Blackwell, and D. S. Davies, *J. Pharm. Pharmacol.*, **26**, 265 (1974).

(6) M. E. Connolly, D. S. Davies, C. T. Dollery, C. D. Morgan, J. W. Paterson, and M. Sandler, *Br. J. Pharmacol.*, **46**, 458 (1972).

(7) W. D. Conway, H. Minatoya, A. M. Lands, and J. M. Shekosky, *J. Pharm. Sci.*, **57**, 1135 (1968).

(8) W. D. Conway, V. K. Batra, and A. Abramovitz, *ibid.*, **62**, 1810 (1973).

ACKNOWLEDGMENTS AND ADDRESSES

Received October 14, 1976, from the *Department of Pharmaceutics, School of Pharmacy, State University of New York at Buffalo, Amherst, NY 14260.*

Accepted for publication January 8, 1977.

Supported in part by a grant from Astra Pharmaceutical Products, Worcester, Mass., and by General Research Support Grant 5-S01RR-5454-10 from the National Institutes of Health, Bethesda, MD 20014.

* Present address: Drug Metabolism Laboratory, Squibb Institute for Medical Research, New Brunswick, NJ 08903.

‡ Present address: Wyeth Ltd., Toronto, Canada.

ˣ To whom inquiries should be directed.

Dehydrodiisoeugenol: A Naturally Occurring Lignan from *Aristolochia taliscana* (Aristolochiaceae)

F. IONESCU, S. D. JOLAD, and J. R. COLE ˣ

Abstract □ The ethanol–water extract of *Aristolochia taliscana* Hook and Arn (Aristolochiaceae) yielded a compound which was identified as dehydrodiisoeugenol by means of elemental analysis, IR, UV, NMR, and mass spectra, and direct comparison with a synthetic sample.

Keyphrases □ *Aristolochia taliscana*—ethanol–water extract of aboveground parts, dehydrodiisoeugenol isolated and identified □ Dehydrodiisoeugenol—isolated from ethanol–water extract of aboveground parts of *Aristolochia taliscana* □ Lignans—dehydrodiisoeugenol isolated from ethanol–water extract of aboveground parts of *Aristolochia taliscana*

During the search for tumor inhibitory constituents from plants, it was found that the ethanol–water extract of stems, leaves, flowers, and fruits of *Aristolochia taliscana* Hook and Arn (Aristolochiaceae)[1] contained a crystalline substance that did not show tumor inhibition activity against the P-388 lymphocytic leukemia test system[2] (3PS). However, to determine the nature of the potentially active constituents in the ethanol–water extract of this plant, it was decided to characterize the isolated compound. The plant was collected in Nayarit, Mexico, in June 1970.

RESULTS AND DISCUSSION

Elemental analysis and molecular weight determination of the compound, mp 130°, by mass spectrometry indicated the molecular formula $C_{20}H_{22}O_4$. IR, UV, NMR, and mass spectral data revealed that the compound corresponded to dehydrodiisoeugenol (I), an oxidation coupling product of *trans*-isoeugenol (1). This structure was verified by direct comparison of UV and IR spectra, co-TLC, and mixed melting point with a synthetic sample[3].

Dehydrodiisoeugenol, licarin A, was previously isolated for the first time from the trunk wood of *Licaria aritu* Ducke (Lauraceae) and characterized by IR, UV, optical rotatory dispersion, NMR, and mass spectral methods (2). Except for its melting point (114–116°) and optical activity, other data (UV, IR, and NMR) reported for licarin A[4] were identical with the dehydrodiisoeugenol isolated from *A. taliscana*.

[1] Identification was confirmed by Robert Barr, College of Pharmacy, and Dr. Charles Mason, Botany Department, University of Arizona, Tucson, Ariz., where a reference specimen was also deposited.

[2] Data from the Drug Evaluation Branch, Drug Research and Development, Chemotherapy, National Cancer Institute, Bethesda, MD 20014.

[3] Prepared in accordance with the procedure given in Ref. 1.

[4] Courtesy of Dr. O. R. Gottlieb, Laboratoio de Produtos Naturais da Fundacao de Amparo a Pesquisa do Estado de San Paulo, Instituto do Quimica, Universidade do Sao Paulo, Brazil.

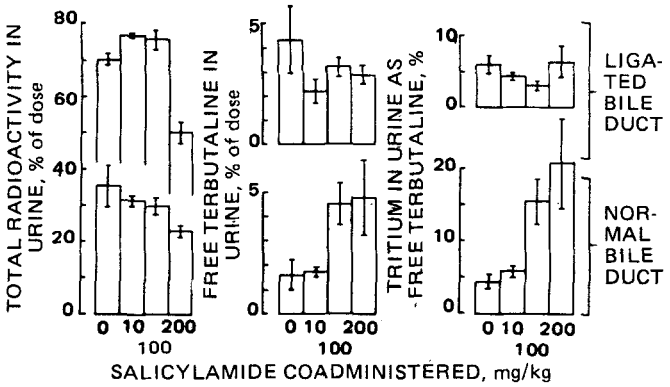

Figure 1—*Excretion of total radioactivity and free terbutaline in the 24-hr urine following oral administration of ^3H-terbutaline (1 mg/kg) coadministered with salicylamide to rats with either patent or ligated bile ducts. Values are the means ±1 SE for groups of three rats.*

that terbutaline in the intestinal wall and in the liver is not appreciably inhibited by coadministered salicylamide. A definitive explanation for the rise in the fraction of terbutaline excreted unchanged when salicylamide was coadministered to normal animals cannot be given. Nevertheless, the observation can be rationalized in terms of the reported finding (2) that unchanged terbutaline passing the gut and subsequently conjugated in the liver is preferentially excreted in the bile while the conjugate previously formed in the intestinal wall is preferentially excreted in urine. The simultaneous presence of salicylamide or its conjugate might influence the partitioning between bile and portal blood of terbutaline glucuronide formed in the liver and thereby influence the observed fraction of terbutaline excreted unchanged in the urine. Such a process would not influence the ratio of metabolites in bile duct-ligated animals since all conjugated drug, regardless of its site of formation, would be excreted in urine.

REFERENCES

(1) W. D. Conway, S. M. Singhvi, M. Gibaldi, and R. N. Boyes, *Xenobiotica*, **3**, 813 (1973).

(2) S. M. Singhvi, W. D. Conway, M. Gibaldi, and R. N. Boyes, *ibid.*, **4**, 563 (1974).

(3) G. Levy and J. A. Procknal, *J. Pharm. Sci.*, **57**, 1330 (1968).

(4) G. Levy and H. Yamada, *ibid.*, **60**, 215 (1971).

(5) C. F. George, E. W. Blackwell, and D. S. Davies, *J. Pharm. Pharmacol.*, **26**, 265 (1974).

(6) M. E. Connolly, D. S. Davies, C. T. Dollery, C. D. Morgan, J. W. Paterson, and M. Sandler, *Br. J. Pharmacol.*, **46**, 458 (1972).

(7) W. D. Conway, H. Minatoya, A. M. Lands, and J. M. Shekosky, *J. Pharm. Sci.*, **57**, 1135 (1968).

(8) W. D. Conway, V. K. Batra, and A. Abramovitz, *ibid.*, **62**, 1810 (1973).

ACKNOWLEDGMENTS AND ADDRESSES

Received October 14, 1976, from the *Department of Pharmaceutics, School of Pharmacy, State University of New York at Buffalo, Amherst, NY 14260.*

Accepted for publication January 8, 1977.

Supported in part by a grant from Astra Pharmaceutical Products, Worcester, Mass., and by General Research Support Grant 5-S01RR-5454-10 from the National Institutes of Health, Bethesda, MD 20014.

* Present address: Drug Metabolism Laboratory, Squibb Institute for Medical Research, New Brunswick, NJ 08903.

‡ Present address: Wyeth Ltd., Toronto, Canada.

ˣ To whom inquiries should be directed.

Dehydrodiisoeugenol: A Naturally Occurring Lignan from *Aristolochia taliscana* (Aristolochiaceae)

F. IONESCU, S. D. JOLAD, and J. R. COLE ˣ

Abstract □ The ethanol–water extract of *Aristolochia taliscana* Hook and Arn (Aristolochiaceae) yielded a compound which was identified as dehydrodiisoeugenol by means of elemental analysis, IR, UV, NMR, and mass spectra, and direct comparison with a synthetic sample.

Keyphrases □ *Aristolochia taliscana*—ethanol–water extract of aboveground parts, dehydrodiisoeugenol isolated and identified □ Dehydrodiisoeugenol—isolated from ethanol–water extract of aboveground parts of *Aristolochia taliscana* □ Lignans—dehydrodiisoeugenol isolated from ethanol–water extract of aboveground parts of *Aristolochia taliscana*

During the search for tumor inhibitory constituents from plants, it was found that the ethanol–water extract of stems, leaves, flowers, and fruits of *Aristolochia taliscana* Hook and Arn (Aristolochiaceae)[1] contained a crystalline substance that did not show tumor inhibition activity against the P-388 lymphocytic leukemia test system[2] (3PS). However, to determine the nature of the potentially active constituents in the ethanol–water extract of this plant, it was decided to characterize the isolated compound. The plant was collected in Nayarit, Mexico, in June 1970.

RESULTS AND DISCUSSION

Elemental analysis and molecular weight determination of the compound, mp 130°, by mass spectrometry indicated the molecular formula $C_{20}H_{22}O_4$. IR, UV, NMR, and mass spectral data revealed that the compound corresponded to dehydrodiisoeugenol (I), an oxidation coupling product of *trans*-isoeugenol (1). This structure was verified by direct comparison of UV and IR spectra, co-TLC, and mixed melting point with a synthetic sample[3].

Dehydrodiisoeugenol, licarin A, was previously isolated for the first time from the trunk wood of *Licaria aritu* Ducke (Lauraceae) and characterized by IR, UV, optical rotatory dispersion, NMR, and mass spectral methods (2). Except for its melting point (114–116°) and optical activity, other data (UV, IR, and NMR) reported for licarin A[4] were identical with the dehydrodiisoeugenol isolated from *A. taliscana*.

[1] Identification was confirmed by Robert Barr, College of Pharmacy, and Dr. Charles Mason, Botany Department, University of Arizona, Tucson, Ariz., where a reference specimen was also deposited.

[2] Data from the Drug Evaluation Branch, Drug Research and Development, Chemotherapy, National Cancer Institute, Bethesda, MD 20014.

[3] Prepared in accordance with the procedure given in Ref. 1.

[4] Courtesy of Dr. O. R. Gottlieb, Laboratoio de Produtos Naturais da Fundacao de Amparo a Pesquisa do Estado de San Paulo, Instituto do Quimica, Universidade do Sao Paulo, Brazil.

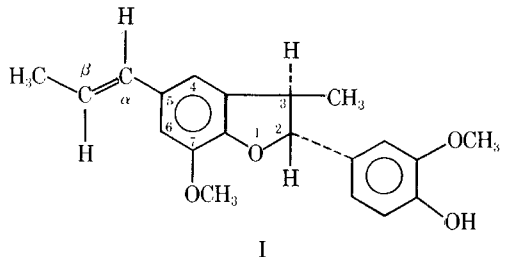

I

EXPERIMENTAL[5]

Air-dried stems, leaves, flowers, and fruits of *A. taliscana* (5.5 kg) were ground in a Wiley mill and macerated with ethanol–water (1:1 v.v). The aqueous ethanol extract was filtered and air dried, and the residue (1 kg) was repeatedly extracted with methanol until the methanol was clear. The combined methanol filtrate was air dried, and the residue was exhaustively extracted with ether. The combined ether extract, after removal of the solvent under vacuum, was subjected to three-funnel partition between benzene–methanol–water (8:5:1 v/v) (each phase was 1600 ml).

The lower phases were combined and air dried, and the residue (28 g) was chromatographed on an aluminum oxide (Grade III; 1 kg) column using hexane with increasing concentrations of acetone (0.1–0.5%) as the eluent. Fifty 250-ml fractions were collected. Based on TLC analysis, fractions 9–34 were combined to give a residue. Treatment with petroleum ether yielded a colorless material, which was filtered and then crystallized from methanol as colorless needles. The melting point, 130°, was undepressed by admixture with a synthetic sample.

The IR (KBr: λ_{max} 3450, 3040, 2970, 2930, 2880, 2850, and 955 cm^{-1}), UV [CH_3OH: λ_{max} 243 (log ϵ 4.55) and 276 (4.35) nm], NMR [$CDCl_3$: δ 1.35 (3H, d), 1.83 (3H, d), 3.12–3.73 (1H, m), 3.38 or 3.85 (3H, s), 3.38 or 3.85 (3H, s), 5.07 (1H, d), 5.67 (1H, s), 6.01–6.27 (1H, m), 6.01–6.27 (1H, m), and 6.73–6.93 (5H, m) ppm], and mass [*m/e* 326 (M^+, base), 311, 283, 202, 189, 163, 151, 149, and 137] spectra are in accord with Structure I. This compound was optically inactive, $[\alpha]_D^{24} \pm 0°$.

Anal.—Calc. for $C_{20}H_{22}O_4$: C, 73.68; H, 6.80; mol. wt., 326. Found: C, 73.70; H, 6.91; *m/e* 326 (M^+).

[5] Carbon and hydrogen analyses were carried out by Chemalytics, Inc., Tempe, Ariz. Melting points were determined on a Kofler hot-stage apparatus and are uncorrected. UV and IR spectra were run on a Beckman KB spectrophotometer and a Beckman IR-33, respectively. NMR and mass spectra were run using a Varian T-60 spectrometer and a Hitachi Perkin-Elmer double-focusing spectrometer (model RMU-6E), respectively. Optical rotations were run in chloroform using a Cary 60 spectropolarimeter.

REFERENCES

(1) B. Leopold, *Acta Chem. Scand.*, **4**, 1531 (1950).

(2) C. J. Aiba, R. G. Campos Correa, and O. R. Gottlieb, *Phytochemistry*, **12**, 1163 (1973).

ACKNOWLEDGMENTS AND ADDRESSES

Received June 24, 1976, from the *Division of Pharmaceutical Chemistry, College of Pharmacy, University of Arizona, Tucson, AZ 85721.*

Accepted for publication December 15, 1976.

Supported in part by Contract N01-CM-3-3750 from the Division of Cancer Treatment, National Cancer Institute, National Institutes of Health, Bethesda, MD 20014, and the Elsa U. Pardee Foundation, Midland, Mich.

[x] To whom inquiries should be directed.

Rapid GLC Determination of Propranolol in Human Plasma Samples

ROBERT E. KATES [x] and CATHERINE L. JONES *

Abstract □ A rapid GLC method for measuring plasma propranolol levels is reported. 4-Methylpropranolol was utilized as an internal standard. Pentafluoropropionate derivatives of propranolol and the internal standard eluted rapidly and gave good sensitivity under the conditions employed. The advantage of this procedure over previously reported methods is the speed of analysis, which is facilitated by rapid elution of contaminant peaks.

Keyphrases □ Propranolol—GLC analysis, human plasma □ GLC—analysis, propranolol in human plasma □ Cardiac depressants—propranolol, GLC analysis in human plasma

Recent studies demonstrated that the effect of propranolol is plasma level related (1, 2). The accurate measurement of plasma propranolol levels has become essential for studies involving the mechanism of action of this agent; in some institutions, the monitoring of plasma propranolol levels is being used to aid patient therapy. Because of the increasing demand for rapid and accurate analysis of propranolol in plasma samples, previously reported procedures are being modified to increase efficiency and new procedures are being offered as improved alternatives.

The fluorometric method for measuring propranolol in biological fluids recently was reported to be limited with respect to both specificity and sensitivity (3). Three GLC procedures were proposed, two utilizing trifluoroacetyl derivatives (4, 5) and one utilizing a difluorobutyrate derivative (6); each employs a different internal standard. These three methods have their subtle differences and each, in order of publication, offers an advantage over the previous method. When analyzing large numbers of samples, however, these methods share one common disadvantage: the slow elution of contaminant peaks, which limits the frequency with which samples can be injected. Because of this limitation, an alternative procedure was developed, affording a greater efficiency by facilitating the more rapid analysis of large numbers of samples.

EXPERIMENTAL

Reagents—Glass-distilled[1] benzene, ethyl acetate, and cyclohexane were used, and 5 *N* NaOH, 0.2 *N* H_2SO_4, and 0.05 *M*, pH 11.5 phosphate buffer were prepared with double-distilled water and extracted twice with benzene. GLC grade pyridine[2] was diluted to 1.5% in ethyl acetate.

[1] Burdick & Jackson Laboratories, Muskegon, Mich.

[2] Pierce Chemical Co., Rockford, Ill.

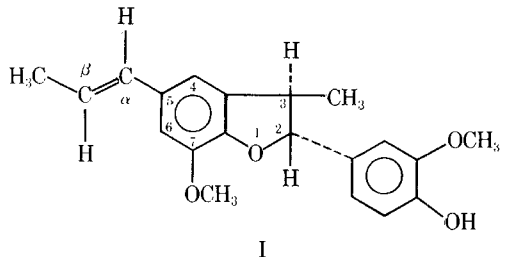

I

EXPERIMENTAL[5]

Air-dried stems, leaves, flowers, and fruits of *A. taliscana* (5.5 kg) were ground in a Wiley mill and macerated with ethanol–water (1:1 v.v). The aqueous ethanol extract was filtered and air dried, and the residue (1 kg) was repeatedly extracted with methanol until the methanol was clear. The combined methanol filtrate was air dried, and the residue was exhaustively extracted with ether. The combined ether extract, after removal of the solvent under vacuum, was subjected to three-funnel partition between benzene–methanol–water (8:5:1 v/v) (each phase was 1600 ml).

The lower phases were combined and air dried, and the residue (28 g) was chromatographed on an aluminum oxide (Grade III; 1 kg) column using hexane with increasing concentrations of acetone (0.1–0.5%) as the eluent. Fifty 250-ml fractions were collected. Based on TLC analysis, fractions 9–34 were combined to give a residue. Treatment with petroleum ether yielded a colorless material, which was filtered and then crystallized from methanol as colorless needles. The melting point, 130°, was undepressed by admixture with a synthetic sample.

The IR (KBr: λ_{max} 3450, 3040, 2970, 2930, 2880, 2850, and 955 cm^{-1}), UV [CH_3OH: λ_{max} 243 (log ϵ 4.55) and 276 (4.35) nm], NMR [$CDCl_3$: δ 1.35 (3H, d), 1.83 (3H, d), 3.12–3.73 (1H, m), 3.38 or 3.85 (3H, s), 3.38 or 3.85 (3H, s), 5.07 (1H, d), 5.67 (1H, s), 6.01–6.27 (1H, m), 6.01–6.27 (1H, m), and 6.73–6.93 (5H, m) ppm], and mass [*m/e* 326 (M^+, base), 311, 283, 202, 189, 163, 151, 149, and 137] spectra are in accord with Structure I. This compound was optically inactive, $[\alpha]_D^{24} \pm 0°$.

Anal.—Calc. for $C_{20}H_{22}O_4$: C, 73.68; H, 6.80; mol. wt., 326. Found: C, 73.70; H, 6.91; *m/e* 326 (M^+).

[5] Carbon and hydrogen analyses were carried out by Chemalytics, Inc., Tempe, Ariz. Melting points were determined on a Kofler hot-stage apparatus and are uncorrected. UV and IR spectra were run on a Beckman KB spectrophotometer and a Beckman IR-33, respectively. NMR and mass spectra were run using a Varian T-60 spectrometer and a Hitachi Perkin-Elmer double-focusing spectrometer (model RMU-6E), respectively. Optical rotations were run in chloroform using a Cary 60 spectropolarimeter.

REFERENCES

(1) B. Leopold, *Acta Chem. Scand.*, **4**, 1531 (1950).

(2) C. J. Aiba, R. G. Campos Correa, and O. R. Gottlieb, *Phytochemistry*, **12**, 1163 (1973).

ACKNOWLEDGMENTS AND ADDRESSES

Received June 24, 1976, from the *Division of Pharmaceutical Chemistry, College of Pharmacy, University of Arizona, Tucson, AZ 85721.*

Accepted for publication December 15, 1976.

Supported in part by Contract N01-CM-3-3750 from the Division of Cancer Treatment, National Cancer Institute, National Institutes of Health, Bethesda, MD 20014, and the Elsa U. Pardee Foundation, Midland, Mich.

[x] To whom inquiries should be directed.

Rapid GLC Determination of Propranolol in Human Plasma Samples

ROBERT E. KATES [x] and CATHERINE L. JONES *

Abstract □ A rapid GLC method for measuring plasma propranolol levels is reported. 4-Methylpropranolol was utilized as an internal standard. Pentafluoropropionate derivatives of propranolol and the internal standard eluted rapidly and gave good sensitivity under the conditions employed. The advantage of this procedure over previously reported methods is the speed of analysis, which is facilitated by rapid elution of contaminant peaks.

Keyphrases □ Propranolol—GLC analysis, human plasma □ GLC—analysis, propranolol in human plasma □ Cardiac depressants—propranolol, GLC analysis in human plasma

Recent studies demonstrated that the effect of propranolol is plasma level related (1, 2). The accurate measurement of plasma propranolol levels has become essential for studies involving the mechanism of action of this agent; in some institutions, the monitoring of plasma propranolol levels is being used to aid patient therapy. Because of the increasing demand for rapid and accurate analysis of propranolol in plasma samples, previously reported procedures are being modified to increase efficiency and new procedures are being offered as improved alternatives.

The fluorometric method for measuring propranolol in biological fluids recently was reported to be limited with respect to both specificity and sensitivity (3). Three GLC procedures were proposed, two utilizing trifluoroacetyl derivatives (4, 5) and one utilizing a difluorobutyrate derivative (6); each employs a different internal standard. These three methods have their subtle differences and each, in order of publication, offers an advantage over the previous method. When analyzing large numbers of samples, however, these methods share one common disadvantage: the slow elution of contaminant peaks, which limits the frequency with which samples can be injected. Because of this limitation, an alternative procedure was developed, affording a greater efficiency by facilitating the more rapid analysis of large numbers of samples.

EXPERIMENTAL

Reagents—Glass-distilled[1] benzene, ethyl acetate, and cyclohexane were used, and 5 *N* NaOH, 0.2 *N* H_2SO_4, and 0.05 *M*, pH 11.5 phosphate buffer were prepared with double-distilled water and extracted twice with benzene. GLC grade pyridine[2] was diluted to 1.5% in ethyl acetate.

[1] Burdick & Jackson Laboratories, Muskegon, Mich.

[2] Pierce Chemical Co., Rockford, Ill.

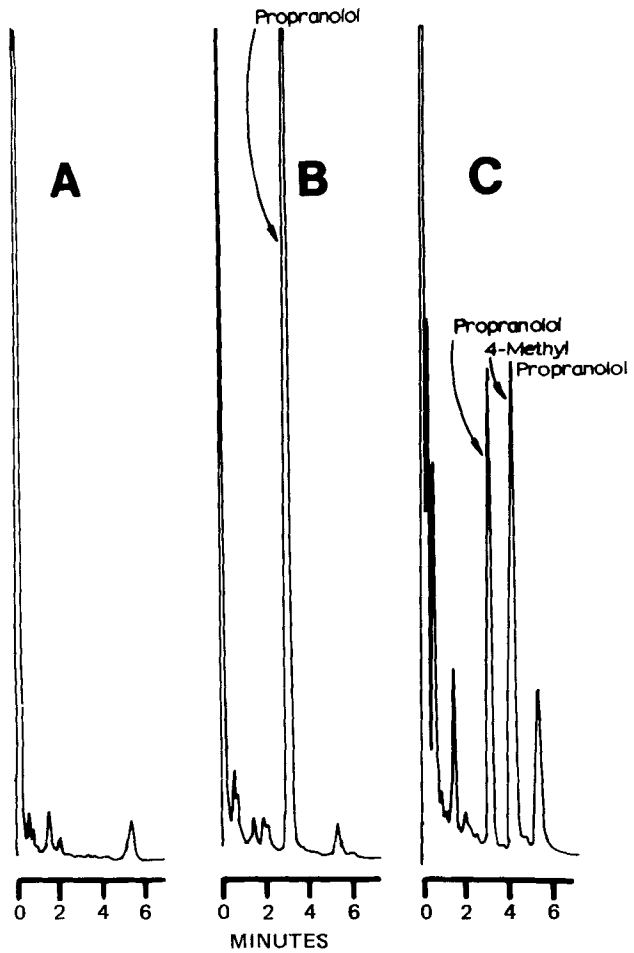

Figure 1—*Chromatograms of blank plasma (A), plasma from a patient taking propranolol (40 mg every 6 hr) (B), and plasma from a patient taking propranolol with 4-methylpropranolol added (C). Each chromatogram was prepared following injection of 3 μl at an attenuation of 256.*

Pentafluoropropionic anhydride[3] was the derivatizing agent, and 4-methylpropranolol[4] was the internal standard. Propranolol[5] was obtained as the hydrochloride salt.

GLC—A gas chromatograph[6] with a ^{63}Ni-electron-capture detector was used. A glass column, 180 cm × 2 mm i.d., was packed with 10% OV-1 on 80–100-mesh Gas Chrom Q[7]. The carrier gas was 5% methane in argon[8], and a flow rate of 20 ml/min was maintained. Analyses were performed under the following conditions: injection port temperature, 250°; column oven temperature, 245°; and detector temperature, 300°. A reporting integrator[9] was used for all data analysis.

Procedure—To 1 ml of plasma were added 200 ng of internal standard (20 μl of an aqueous solution), 3 ml of benzene, and 0.1 ml of 5 *N* NaOH. This mixture was shaken in polytef-coated screw-capped tubes for 5 min and then centrifuged. The benzene layer was transferred to a clean tube containing 1 ml of 0.2 *N* H_2SO_4. This tube was capped and shaken for 2 min and then centrifuged. The benzene layer was removed and discarded.

To the acidic layer was added 3 ml of clean benzene and 0.2 ml of 5 *N* NaOH. The tube was then capped and shaken for 5 min and centrifuged. The benzene was transferred to a clean tube and evaporated to dryness under nitrogen[10]. To the residue was added 0.5 ml of cyclohexane. The tube was then vortexed for 20 sec to redissolve the residue. Aliquots of 25 μl of 1.5% pyridine and pentafluoropropionic anhydride were then added.

[3] P.C.R. Inc., Gainesville, Fla.
[4] ICI 45,749, Imperial Chemical Industries, Macclesfield, England.
[5] Ayerst Laboratories, Rouses Point, N.Y.
[6] Hewlett Packard model 5736A.
[7] Applied Science Laboratories, State College, Pa.
[8] Matheson Gas Products, East Rutherford, N.J.
[9] Hewlett-Packard model 3380A.
[10] N-Evap, Organomation Associates, Shrewsbury, Mass.

Table I—Evaluation of Assay Precision and Accuracy (n = 7)

Concentration of Propranolol Added, ng/ml	Concentration of Propranolol Measured, ng/ml
10	11.2 ± 0.65 (*SD*)
25	27.9 ± 2.7 (*SD*)
50	52.3 ± 5.4 (*SD*)

The tube was capped, vortexed for 10 sec, incubated for 1 min at 70° on a dry bath heater, and then flushed with nitrogen to remove the excess pentafluoropropionic anhydride and to evaporate the cyclohexane. Cyclohexane, 50 μl, was then added, and the tube was vortexed for 10 sec. Phosphate buffer, 1 ml, was added, and the tube was shaken for 5 min and then centrifuged. Aliquots of 1–5 μl of the organic layer were then injected onto the column. All samples were analyzed in duplicate.

RESULTS AND DISCUSSION

Chromatograms of a blank plasma sample (A), a plasma sample from a patient taking propranolol (40 mg every 6 hr) with no internal standard added (B), and a patient plasma sample with internal standard added (C) are shown in Fig. 1. In the chromatogram of the blank plasma, there are no contaminant peaks with retention times near those of propranolol or the internal standard. In chromatogram C, the retention times of propranolol and the internal standard are 3.2 and 4.2 min, respectively. All three chromatograms were made at an attenuation of 256 following injection of a 3-μl sample.

Chromatogram B shows that none of the metabolites of propranolol, which are produced following oral administration of the drug, interferes with the measurement of the internal standard. Of the several propranolol metabolites identified following oral administration to humans (7), 4-hydroxypropranolol is structurally the most similar to propranolol. This metabolite is the most likely one to interfere with an analysis of the parent compound. With a pure sample, a retention time of 3.7 min was identified for the 4-hydroxy metabolite under the conditions employed. However, due either to removal by extraction or decomposition, this metabolite cannot be analyzed by this procedure; no peaks with this retention time were observed in the plasma samples analyzed.

Standard curves were prepared by extracting known drug concentrations and measuring the area under the propranolol and internal standard peaks. The ratio of the propranolol to internal standard areas was then plotted as a function of the concentration added. As a general procedure, a standard curve from 0 to 50 ng of propranolol/ml with 70 ng of internal standard was used for analyzing samples with low propranolol concentrations. For high level samples, a standard curve from 100 to 500 ng of propranolol/ml with 200 ng of internal standard was prepared. This procedure has been used routinely to analyze patient samples with concentrations ranging from below 1 to more than 400 ng/ml.

The standard curves were linear over the two intervals employed. Only a minor daily fluctuation in slope was observed. A mean slope of 0.284 ± 0.012 was found when five different low level standard curves were averaged. All standard curves passed through the origin. The precision and accuracy of this procedure were evaluated by adding measured amounts of propranolol and 70 ng of the internal standard to 21 samples of normal plasma. The samples were then extracted and analyzed (Table I). The percent standard deviation ranged from 6.2% at the low level to 10.3% at the higher level.

The extraction procedure used here is the same as previously published by Walle (4). The derivatization procedure, using pentafluoropropionic anhydride with pyridine as the catalyst, went to completion in less than 1 min under the experimental conditions. Once the samples were derivatized, they were stable for several days, and it was feasible to leave derivatized samples overnight for injection the following morning. However, once the samples were evaporated to dryness prior to derivatization, they had to be derivatized immediately. For unknown reasons, if the residue was left underivatized for any length of time, poor reproducibility occurred.

The final step of shaking the derivatized drugs with pH 11.5 buffer was necessary to hydrolyze contaminant substances. If the tubes were not shaken for this 5-min period, numerous slowly eluting peaks were encountered. The only significant peak eluting after propranolol was apparently due to a contaminant in the pentafluoropropionic anhydride.

This procedure facilitates the analysis of at least twice as many samples per day as with previously tried chromatographic procedures.

REFERENCES

(1) E. L. Alderman, R. O. Davis, J. J. Crowley, M. G. Lopes, J. Z. Brookes, J. P. Friedman, A. F. Graham, H. J. Matlof, and D. C. Harrison, *Circulation*, **51**, 964 (1975).

(2) M. Pine, L. Favrot, S. Smith, K. McDonald, and C. Chidsey, *ibid.*, **52**, 886 (1975).

(3) D. G. Shand, E. M. Nuckolls, and J. A. Oates, *Clin. Pharmacol. Ther.*, **11**, 112 (1970).

(4) T. Walle, *J. Pharm. Sci.*, **63**, 1885 (1974).

(5) E. DiSalle, K. M. Baker, S. R. Bareggi, W. D. Watkins, C. A. Chidsey, A. Frigeris, and P. L. Morselli, *J. Chromatogr.*, **84**, 347 (1973).

(6) P. N. Degen and W. Riess, *ibid.*, **121**, 72 (1976).

(7) T. Walle and T. E. Gaffney, *J. Pharmacol. Exp. Ther.*, **182**, 83 (1972).

ACKNOWLEDGMENTS AND ADDRESSES

Received September 27, 1976, from the *College of Pharmacy, Ohio State University, Columbus, OH 43210.*

Accepted for publication January 7, 1977.

Supported in part by a grant from the Central Ohio Heart Chapter of the American Heart Association.

The authors thank Dr. B. Scales of I.C.I. for supplying 4-methylpropranolol.

* Present address: Department of Bacteriology, University of California, Davis, CA 95616.

ˣ To whom inquiries should be directed.

Alterations Induced in Distribution and *In Vivo* Metabolism of Imipramine by Pregnenolone-16α-carbonitrile

SHELDON BROOKMAN ˣ and PANOS KOUROUNAKIS *

Abstract □ Female rats were given pregnenolone-16α-carbonitrile (I) to investigate its *in vivo* effects on the loss of the righting reflex and the mortality rate induced by imipramine as well as the concentrations of this drug and its metabolite, desipramine, in plasma, brain, liver, lungs, and kidneys. The protective action of I was associated with diminished organ levels of imipramine (catatoxic mechanism), and the relationship between brain and plasma imipramine concentrations remained unaltered. Desipramine–imipramine molar ratios were increased, indicating an elevated rate of *N*-demethylation. The unbound imipramine in plasma was diminished, but the relationship between protein-bound and unbound imipramine levels was not modified.

Keyphrases □ Pregnenolone-16α-carbonitrile—effect on pharmacological activity, distribution, and *in vivo* metabolism of imipramine, rats □ Imipramine—effect of pregnenolone-16α-carbonitrile on pharmacological activity, *in vivo* metabolism, and distribution, rats □ Distribution—imipramine, effect of pregnenolone-16α-carbonitrile, rats □ Metabolism—imipramine, effect of pregnenolone-16α-carbonitrile, rats □ Steroids—pregnenolone-16α-carbonitrile, effect on pharmacological activity, distribution, and *in vivo* metabolism of imipramine, rats □ Antidepressants—imipramine, effect of pregnenolone-16α-carbonitrile on pharmacological activity, distribution, and *in vivo* metabolism, rats

The protection afforded by catatoxic steroids against intoxication of diverse etiology, such as analgesics, carcinogens, and pesticides (1), was associated with induction of liver microsomal enzymes, particularly NADPH-dependent mixed function oxidases (2, 3), as well as with decreased levels of these toxicants in plasma, brain, and other tissues (3–7). Pregnenolone-16α-carbonitrile (I), a well-known hepatic microsomal enzyme inducer devoid of any other hormonal or pharmacological properties, exerts the greatest prophylactic effect *in vivo* (1) of the steroids studied.

At present, imipramine is the most frequently used tricyclic antidepressant. Its main metabolic pathways in the body include *N*-demethylation, *N*-oxidation, hydroxylation, and glucuronidation (8–12). Desipramine, one principal metabolite of imipramine, is pharmacologically active (13–15). Both imipramine and desipramine are lipophilic and pass into the brain, their target organ (16).

In view of the importance of imipramine in therapeutics, it was of interest to determine: (*a*) whether a drug-metabolizing enzyme inducer, *e.g.*, I, would produce characteristic alterations in drug distribution; (*b*) whether the changes in plasma drug concentration would be reflected in the brain as well as in the overall pharmacological effect; and (*c*) whether I would modify the influence of plasma protein binding on drug distribution.

EXPERIMENTAL

Female Charles River rats[1], 160–200 g, were maintained on laboratory chow[2] and tap water *ad libitum*. Compound I[3] was given twice daily for 3 days at a dose level of 68.3 mg/kg po in 0.5 ml of water as a micronized suspension homogenized with a trace of polysorbate 80. For comparative purposes, control animals received water with a trace of polysorbate 80. Imipramine hydrochloride[4], 80 mg/kg ip, was administered to all rats in 1 ml of distilled water once on the 4th day, 18 hr after the last pretreatment, unless otherwise stated.

Tables I and II indicate the various time periods at which blood samples were withdrawn under light ether anesthesia by aorta puncture into a syringe containing 0.2 *M* sodium oxalate. Tissues were removed and frozen until required for analysis. Drug-free plasma and tissues were used for preparing standards and blanks.

GLC—Imipramine and desipramine concentrations were measured by GLC[5]. A 1.5-m × 6.4-mm o.d. glass column packed with 1.5% OV-17 on 80–100-mesh Gas Chrom Q was used. The initial column, injector, and detector temperatures were 240, 300, and 300°, respectively. The column temperature was programmed for increases of 32°/min, starting 1 min after the time of injection. The final column temperature (280°) was maintained until 10 min postinjection. The nitrogen flow rate (as the carrier gas) was 18 ml/min, and hydrogen and compressed air pressures

[1] Canadian Breeding Farms & Laboratories Ltd., St. Constant, Quebec, Canada.

[2] Purina Laboratory Chow.

[3] The Upjohn Co., Kalamazoo, Mich.

[4] Ciba-Geigy (Canada) Ltd., Dorval, Quebec, Canada.

[5] Pye Unicam 104 chromatograph equipped with a flame-ionization detector and a Honeywell Electronik 194 Lab-Test recorder coupled with a disk integrator.

REFERENCES

(1) E. L. Alderman, R. O. Davis, J. J. Crowley, M. G. Lopes, J. Z. Brookes, J. P. Friedman, A. F. Graham, H. J. Matlof, and D. C. Harrison, *Circulation*, **51**, 964 (1975).

(2) M. Pine, L. Favrot, S. Smith, K. McDonald, and C. Chidsey, *ibid.*, **52**, 886 (1975).

(3) D. G. Shand, E. M. Nuckolls, and J. A. Oates, *Clin. Pharmacol. Ther.*, **11**, 112 (1970).

(4) T. Walle, *J. Pharm. Sci.*, **63**, 1885 (1974).

(5) E. DiSalle, K. M. Baker, S. R. Bareggi, W. D. Watkins, C. A. Chidsey, A. Frigeris, and P. L. Morselli, *J. Chromatogr.*, **84**, 347 (1973).

(6) P. N. Degen and W. Riess, *ibid.*, **121**, 72 (1976).

(7) T. Walle and T. E. Gaffney, *J. Pharmacol. Exp. Ther.*, **182**, 83 (1972).

ACKNOWLEDGMENTS AND ADDRESSES

Received September 27, 1976, from the *College of Pharmacy, Ohio State University, Columbus, OH 43210.*

Accepted for publication January 7, 1977.

Supported in part by a grant from the Central Ohio Heart Chapter of the American Heart Association.

The authors thank Dr. B. Scales of I.C.I. for supplying 4-methylpropranolol.

* Present address: Department of Bacteriology, University of California, Davis, CA 95616.

ˣ To whom inquiries should be directed.

Alterations Induced in Distribution and *In Vivo* Metabolism of Imipramine by Pregnenolone-16α-carbonitrile

SHELDON BROOKMAN ˣ and PANOS KOUROUNAKIS *

Abstract □ Female rats were given pregnenolone-16α-carbonitrile (I) to investigate its *in vivo* effects on the loss of the righting reflex and the mortality rate induced by imipramine as well as the concentrations of this drug and its metabolite, desipramine, in plasma, brain, liver, lungs, and kidneys. The protective action of I was associated with diminished organ levels of imipramine (catatoxic mechanism), and the relationship between brain and plasma imipramine concentrations remained unaltered. Desipramine–imipramine molar ratios were increased, indicating an elevated rate of *N*-demethylation. The unbound imipramine in plasma was diminished, but the relationship between protein-bound and unbound imipramine levels was not modified.

Keyphrases □ Pregnenolone-16α-carbonitrile—effect on pharmacological activity, distribution, and *in vivo* metabolism of imipramine, rats □ Imipramine—effect of pregnenolone-16α-carbonitrile on pharmacological activity, *in vivo* metabolism, and distribution, rats □ Distribution—imipramine, effect of pregnenolone-16α-carbonitrile, rats □ Metabolism—imipramine, effect of pregnenolone-16α-carbonitrile, rats □ Steroids—pregnenolone-16α-carbonitrile, effect on pharmacological activity, distribution, and *in vivo* metabolism of imipramine, rats □ Antidepressants—imipramine, effect of pregnenolone-16α-carbonitrile on pharmacological activity, distribution, and *in vivo* metabolism, rats

The protection afforded by catatoxic steroids against intoxication of diverse etiology, such as analgesics, carcinogens, and pesticides (1), was associated with induction of liver microsomal enzymes, particularly NADPH-dependent mixed function oxidases (2, 3), as well as with decreased levels of these toxicants in plasma, brain, and other tissues (3–7). Pregnenolone-16α-carbonitrile (I), a well-known hepatic microsomal enzyme inducer devoid of any other hormonal or pharmacological properties, exerts the greatest prophylactic effect *in vivo* (1) of the steroids studied.

At present, imipramine is the most frequently used tricyclic antidepressant. Its main metabolic pathways in the body include *N*-demethylation, *N*-oxidation, hydroxylation, and glucuronidation (8–12). Desipramine, one principal metabolite of imipramine, is pharmacologically active (13–15). Both imipramine and desipramine are lipophilic and pass into the brain, their target organ (16).

In view of the importance of imipramine in therapeutics, it was of interest to determine: (*a*) whether a drug-metabolizing enzyme inducer, *e.g.*, I, would produce characteristic alterations in drug distribution; (*b*) whether the changes in plasma drug concentration would be reflected in the brain as well as in the overall pharmacological effect; and (*c*) whether I would modify the influence of plasma protein binding on drug distribution.

EXPERIMENTAL

Female Charles River rats[1], 160–200 g, were maintained on laboratory chow[2] and tap water *ad libitum*. Compound I[3] was given twice daily for 3 days at a dose level of 68.3 mg/kg po in 0.5 ml of water as a micronized suspension homogenized with a trace of polysorbate 80. For comparative purposes, control animals received water with a trace of polysorbate 80. Imipramine hydrochloride[4], 80 mg/kg ip, was administered to all rats in 1 ml of distilled water once on the 4th day, 18 hr after the last pretreatment, unless otherwise stated.

Tables I and II indicate the various time periods at which blood samples were withdrawn under light ether anesthesia by aorta puncture into a syringe containing 0.2 *M* sodium oxalate. Tissues were removed and frozen until required for analysis. Drug-free plasma and tissues were used for preparing standards and blanks.

GLC—Imipramine and desipramine concentrations were measured by GLC[5]. A 1.5-m × 6.4-mm o.d. glass column packed with 1.5% OV-17 on 80–100-mesh Gas Chrom Q was used. The initial column, injector, and detector temperatures were 240, 300, and 300°, respectively. The column temperature was programmed for increases of 32°/min, starting 1 min after the time of injection. The final column temperature (280°) was maintained until 10 min postinjection. The nitrogen flow rate (as the carrier gas) was 18 ml/min, and hydrogen and compressed air pressures

[1] Canadian Breeding Farms & Laboratories Ltd., St. Constant, Quebec, Canada.

[2] Purina Laboratory Chow.

[3] The Upjohn Co., Kalamazoo, Mich.

[4] Ciba-Geigy (Canada) Ltd., Dorval, Quebec, Canada.

[5] Pye Unicam 104 chromatograph equipped with a flame-ionization detector and a Honeywell Electronik 194 Lab-Test recorder coupled with a disk integrator.

Table I—Effect of I on Imipramine Distribution in Tissues and Plasma and on the Brain–Plasma Ratios

Parameter	Imipramine Concentration, μg/g				
	15 min	30 min	60 min	120 min	240 min
Liver					
Control	130.0 ± 12.3 (6)[a]	85.2 ± 5.1 (7)	70.6 ± 5.4 (7)	69.0 ± 6.0 (7)	45.3 ± 3.0 (8)
Pretreated	71.7 ± 5.3 (8)[b]	40.8 ± 3.0 (11)[b]	37.0 ± 1.5 (10)[b]	36.5 ± 1.1 (8)[b]	27.7 ± 0.9 (8)[b]
Lungs					
Control	136.1 ± 8.9 (7)	81.1 ± 7.6 (8)	80.8 ± 2.3 (8)	76.5 ± 3.7 (9)	47.4 ± 1.9 (7)
Pretreated	64.3 ± 4.1 (9)[b]	45.1 ± 4.2 (9)[b]	51.7 ± 2.8 (8)[b]	50.2 ± 2.8 (8)[b]	49.7 ± 1.5 (7)[c]
Kidneys					
Control	92.4 ± 5.7 (7)	91.0 ± 4.5 (7)	65.7 ± 3.9 (8)	52.4 ± 2.9 (8)	—
Pretreated	63.1 ± 4.7 (6)[b]	47.8 ± 4.2 (7)[b]	39.9 ± 1.7 (7)[b]	36.4 ± 1.4 (7)[b]	—
Brain					
Control	62.4 ± 4.9 (5)	84.9 ± 8.5 (5)	57.5 ± 4.4 (6)	38.1 ± 1.1 (7)	—
Pretreated	37.7 ± 2.9 (6)[b]	41.2 ± 2.2 (6)[b]	31.8 ± 2.5 (6)[b]	25.9 ± 1.5 (8)[b]	—
Plasma					
Control	2.6 ± 0.2 (8)	2.3 ± 0.3 (5)	1.5 ± 0.1 (7)	0.9 ± 0.1 (9)	—
Pretreated	1.6 ± 0.1 (8)[b]	1.2 ± 0.1 (8)[b]	0.8 ± 0.1 (10)[b]	0.5 ± 0.1 (8)[b]	—
Brain–plasma ratio					
Control	24	37	38	42	—
Pretreated	24	34	40	52	—

[a] Figures in parentheses indicate number of animals. [b] $p < 0.005$. [c] $p > 0.05$.

Table II—Effect of I on Desipramine Distribution in Tissues and Plasma after Imipramine Administration

Parameter	Desipramine Concentration, μg/g				
	15 min	30 min	60 min	120 min	240 min
Liver					
Control	115.0 ± 6.7 (7)[a]	104.0 ± 7.8 (6)	114.5 ± 13.9 (7)	127.5 ± 11.0 (5)	133.7 ± 16.2 (5)
Pretreated	197.0 ± 9.9 (7)[b]	205.0 ± 16.3 (8)[b]	194.8 ± 16.1 (8)[b]	210.2 ± 7.9 (8)[b]	198.6 ± 16.0 (5)[c]
Kidney					
Control	84.2 ± 6.6 (5)	88.8 ± 7.4 (7)	90.5 ± 5.0 (7)	110.5 ± 7.9 (7)	—
Pretreated	89.5 ± 8.2 (7)[d]	121.1 ± 6.1 (7)[b]	117.9 ± 3.0 (7)[b]	105.2 ± 6.3 (7)[d]	—
Lung					
Control	144.0 ± 11.9 (9)	158.1 ± 7.8 (9)	172.6 ± 11.2 (7)	171.0 ± 13.1 (8)	170.1 ± 9.2 (6)
Pretreated	224.0 ± 16.4 (7)[b]	197.1 ± 8.9 (5)[e]	214.5 ± 12.2 (8)[c]	161.0 ± 4.9 (6)[d]	198.8 ± 7.4 (7)[c]
Brain					
Control	—	17.6 ± 1.2 (5)	—	—	17.8 ± 1.3 (7)
Pretreated	—	38.0 ± 1.6 (5)[b]	—	—	15.3 ± 0.4 (8)[d]
Plasma					
Control	—	3.5 ± 0.5 (4)	—	—	—
Pretreated	—	6.6 ± 0.9 (4)[b]	—	—	—

[a] Figures in parentheses indicate number of animals. [b] $p < 0.005$. [c] $p < 0.05$. [d] $p > 0.05$. [e] $p < 0.01$.

were adjusted to maximize the detector response (hydrogen, 1.2 kg/cm^2; and air, 0.95 kg/cm^2).

Plasma Protein Binding—Free and protein-bound imipramine were measured by a modified *in vivo* dialysis method (17, 18). A cellulose sac[6] containing 4 ml of a 6% dextran[7] solution was implanted subcutaneously, under light ether anesthesia and sterile conditions, on the back through a small incision in the sacral region 24 hr prior to imipramine administration (as described). The sac was removed after 30 min; the contents, pooled from three animals, were analyzed for imipramine (corresponding to the level of free drug).

Measurement of Imipramine and Desipramine—In these studies, imipramine and desipramine were extracted from the biological materials as follows. Organs were homogenized in three parts of water. Aliquots of the resulting homogenate or plasma were pipetted into glass-stoppered centrifuge tubes containing 0.1 ml of 2 *N* NaOH and 0.1 ml of internal standard (3 μg of promazine); the total volume was adjusted to 4 ml with distilled water. In the plasma protein binding experiment, 12 ml of 6% dextran solution, 0.1 ml of 2 *N* NaOH, and 0.1 ml of internal standard (2 μg of promazine) were mixed to give a total volume of 12.2 ml. Heptane (10 ml) containing 1% isoamyl alcohol was added, and the whole mixture was shaken for 10 min.

After centrifugation, 9.5 ml of the organic layer was removed, and the procedure was repeated twice using 5 ml of organic solvent. The combined organic phase was transferred to a tube containing 15 ml of 0.1 *N* HCl, and the tube was shaken for 10 min. After centrifugation, 14.5 ml of the acidic phase was adjusted to pH 11 with 2 *N* NaOH. Freshly distilled ether (8 ml) was added, and the tube was shaken for 10 min and then recentrifuged. As much as possible of the ether layer was removed, dried over anhydrous potassium carbonate, and transferred to glass tubes with finely tapered tips. The ether was evaporated in a water bath at 40°. The tubes were stoppered and cooled in an ice bath to give a final volume of ~0.05 ml of ether/vial, of which approximately 5 μl was injected into the gas chromatograph.

The ratio of peak areas of imipramine or desipramine to the internal standard (corrected for attenuation) was then calculated, and the concentration of each sample was obtained by reference to a standard calibration curve constructed of known amounts of imipramine or desipramine and promazine. The peak area ratios of either substrate to that of promazine were plotted against the concentration of imipramine or desipramine in micrograms per milliliter of plasma or micrograms per gram of tissue; a least mean squares linear regression was performed on the points to get the best-fit straight line.

RESULTS AND DISCUSSION

Acute intoxication with imipramine, measured on the basis of the loss of the righting reflex and the mortality rate at 30 min postinjection (120 mg/kg ip), was strikingly diminished by I. The loss of righting reflex values (positive/total) were: control, 15/15; and I, 1/15. The mortality rates (dead/total) were: control, 15/15; and I, 0/15. After reducing the imipramine dose to 80 mg/kg, the mortality rates were: control, 1/15; and I, 0/15. The loss of righting reflex values were then: control, 15/15; and

Table III—Effect of I on the Desipramine–Imipramine Molar Ratio in Plasma, Brain, and Liver after 30 min

Parameter	Desipramine–Imipramine Molar Ratio		Increase, %
	Control	I Pretreated	
Plasma	1.4	5.2	270
Brain	0.2	0.9	350
Liver	1.2	4.8	300

[6] Diameter, 28 mm; pore radius, approximately 26 Å.
[7] Molecular weight 75,000, Abbott Laboratories, Montreal, Quebec, Canada.

I, 2/15. Convulsions were observed in the controls, while ptosis was evident in all animals.

The decreased pharmacological action correlated with reduced drug concentrations in the brain and other tissues (Table I) at 0.25, 0.5, 1, 2, and 4 hr after imipramine treatment. The plasma drug levels of both groups (control and pretreated) were remarkably low in comparison to the tissue values, with most tissues exhibiting the highest concentrations within 15 min after administration. The elevated brain–plasma ratios showed that the nonpolar character of imipramine enhanced its entry through the blood–brain barrier; the brain attained peak concentrations in 30 min. The similarity between the brain–plasma ratios of control and pretreated animals indicates that I did not modify the permeability of the barrier.

At 15 min postinjection, among all concentrations measured, those of the liver and lung were the highest. However, after 30 min, these differences disappeared and all tissues examined had similar drug concentrations. This result could be attributed to a redistribution of the drug with time. Since the liver is the principal site of detoxication, its high drug levels were not unusual. Persistently elevated concentrations in the lung also were observed in fatal intoxications among humans (19).

Table II summarizes the desipramine values in rats after imipramine administration. Like the parent compound, its plasma concentrations were low compared to those of the tissues after 30 min, indicating a rapid tissue uptake. There was no decline of desipramine levels in the various tissues of I-pretreated and control groups at 0.25, 0.5, 1, 2, and 4 hr, with the exception of the brain of I-pretreated animals which showed a significant reduction after 4 hr.

The molar concentration ratios of desipramine and imipramine in plasma, brain, and liver after 30 min were indicative of differences in the biotransformation rate between control and pretreated animals (Table III). The antisedative effects of imipramine vis-à-vis the syndrome evoked by reserpine and certain benzoquinolizines (20, 21) may be mediated through its metabolite, desipramine (19, 22). According to Bickel and Brodie (23), the *N*-demethylation of tertiary amines results in a loss of their sedative properties. Judging from the 350% increase in the desipramine–imipramine molar ratio in I-pretreated rats, this fact may account in part for the diminished loss of the righting reflex.

The plasma free drug concentrations in control and I-pretreated animals were 0.053 ± 0.010 and 0.025 ± 0.000 μg/ml, respectively. These data provide information with respect to imipramine uptake at the site of action, *i.e.*, the brain. The significantly lower concentration of imipramine capable of penetrating the blood–brain barrier is reflected in the diminished pharmacological response. Compound I, on the other hand, was not effective in altering the percentage of free drug: 2.1 *versus* 2.2% for controls.

In conclusion, I pretreatment reduced the toxic manifestations of imipramine in rats because it enhanced the biotransformation of this drug, resulting in lower tissue concentrations.

REFERENCES

(1) H. Selye, "Hormones and Resistance," Springer-Verlag, Heidelberg, Germany, 1971.

(2) E. Horvath, K. Kovacs, J. A. Blascheck, and A. Somogyi, *Virchows Arch. B*, **7**, 348 (1971).

(3) B. Solymoss, S. Varga, and M. Krajny, *Arzneim.-Forsch.*, **21**, 384 (1971).

(4) B. Solymoss, M. Krajny, and S. Varga, *J. Pharm. Sci.*, **59**, 712 (1970).

(5) B. Solymoss, J. Werringloer, and S. Toth, *Steroids*, **17**, 427 (1971).

(6) S. Szabo, H. Selye, P. Kourounakis, and Y. Taché, *Biochem. Pharmacol.*, **23**, 2083 (1974).

(7) P. Kourounakis, S. Szabo, and H. Selye, *J. Pharm. Sci.*, **62**, 1946 (1973).

(8) B. Herrmann, W. Schindler, and R. Pulver, *Med. Exp.*, **1**, 381 (1959).

(9) B. Herrmann and R. Pulver, *Arch. Int. Pharmacodyn. Ther.*, **126**, 454 (1960).

(10) J. Im Obersteg and J. Bäumler, *Arch. Toxicol.*, **19**, 389 (1962).

(11) V. Fishman and H. Goldenberg, *Proc. Soc. Exp. Biol. Med.*, **110**, 187 (1962).

(12) A. H. Beckett and S. Al-Sarraj, *J. Pharm. Pharmacol.*, **25**, 335 (1973).

(13) M. H. Bickel and H. J. Weder, *Arch. Int. Pharmacodyn. Ther.*, **173**, 433 (1968).

(14) M. H. Bickel and M. Baggiolini, *Biochem. Pharmacol.*, **15**, 1155 (1966).

(15) P. L. Gignon and M. H. Bickel, *ibid.*, **20**, 1921 (1971).

(16) J. Christiansen and L. F. Gram, *J. Pharm. Pharmacol.*, **25**, 604 (1973).

(17) E. G. McQueen, *Br. J. Pharmacol.*, **36**, 29 (1969).

(18) S. Szabo, P. Kourounakis, and H. Selye, *Fed. Proc.*, **33**, 532 (1974).

(19) J. V. Dingell, F. Sulser, and J. R. Gillette, *J. Pharmacol. Exp. Ther.*, **143**, 14 (1964).

(20) E. Costa, S. Garattini, and L. Valzelli, *Experientia*, **10**, 461 (1960).

(21) F. Sulser, J. Watts, and B. B. Brodie, *Fed. Proc.*, **20**, 321 (1961).

(22) F. Sulser, J. Watts, and B. B. Brodie, *Ann. N.Y. Acad. Sci.*, **96**, 279 (1962).

(23) M. H. Bickel and B. B. Brodie, *Int. J. Neuropharmacol.*, **3**, 611 (1964).

ACKNOWLEDGMENTS AND ADDRESSES

Received August 3, 1976, from the *Institut de Médecine et de Chirurgie Expérimentales, Université de Montréal, Montreal, Quebec H3C 3J7, Canada.*

Accepted for publication December 21, 1976.

Supported in part by the Medical Research Council of Canada (Block Term Grant MT-1829); the Ministère des Affaires Sociales, Québec, Canada; Succession J. A. DeSève; and the Colonial Research Institute, Freeport, Bahamas.

The authors thank The Upjohn Co. for pregnenolone-16α-carbonitrile and Ciba-Geigy (Canada) Ltd. for the imipramine and desipramine.

* Present address: Laboratory of Pharmaceutical Chemistry, Department of Pharmacy, University of Thessaloniki, Thessaloniki, Greece.

ˣ To whom inquiries should be directed.

Enteric-Coated Pellets: Theoretical Analysis of Effect of Dispersion in the Stomach on Blood Level Profiles

MICHAEL J. STORY

Abstract □ The advantages of encapsulated enteric-coated pellets as dosage forms are discussed theoretically and compared to enteric-coated tablets. An enteric-coated tablet may take from approximately 0.5 to more than 8 hr to pass from the stomach to the duodenum. On the other hand, enteric-coated pellets are subjected to dispersion in the stomach, but they pass through the pyloric sphincter after a mean residence time in the stomach that would not be different from that exhibited by a suspension dosage form. The dispersion effect causes a theoretical reduction in peak blood level over that of an enteric-coated tablet of equivalent potency while maintaining bioavailability. It is hypothesized that enteric-coated pellets will reduce intestinal side effects that may occur with enteric-coated tablet preparations.

Keyphrases □ Pellets, enteric coated—theoretical analysis of effect of dispersion in stomach on blood level profiles □ Enteric-coated pellets—theoretical analysis of effect of dispersion in stomach on blood level profiles □ Dosage forms—enteric-coated pellets, theoretical analysis of effect of dispersion in stomach on blood level profiles

Various drugs, when administered orally, either cause GI problems (*e.g.*, aspirin, indomethacin, and tetracyclines) or are degraded by gastric acid into metabolites leading to poor bioavailability (*e.g.*, erythromycin and penicillin G) or GI side effects (*e.g.*, levodopa). In some cases, these problems have been overcome by the use of enteric-coated tablets. They remain intact during passage through the stomach, the enteric coat not being shed until the tablets pass into the duodenum.

Two outstanding problems are inherent in the administration of enteric-coated tablets:

1. There is a "hit-or-miss" effect; *i.e.*, the tablet may take from about 0.5 to more than 8 hr before it passes into the duodenum, leading to the possibility of two tablets, each from different dosage times, passing through the pyloric sphincter at effectively the same time.
2. Intestinal side effects may result due to a sudden, highly localized dose of drug at one site in the small intestine.

The latter point could account for the significant blood loss reported with enteric-coated aspirin tablets, even though no salicylic acid was detected at any time in the stomach (1). This study illustrates, from a theoretical approach, the advantages of administering drugs, requiring enteric protection, in the form of encapsulated enteric-coated pellets. The model used is based on a simple physical picture of what is envisaged to occur. However, *in vivo* experimental studies to quantify this theoretical analysis probably will show that a more sophisticated analysis is not warranted in view of the large variability of *in vivo* data.

THEORETICAL

Solutions, suspensions, tablets, and capsules, which disintegrate and/or dissolve in the stomach, and enteric-coated pellets all spread (or disperse) throughout the stomach before passing through the pyloric sphincter into the duodenum. The drug particles or molecules do not pass through the pyloric sphincter as a bolus but assume a random distribution. Some drug particles or molecules tend to pass through before the mean passage time, and others pass through at random times greater than the mean passage time. Once the particles or molecules pass through the pyloric sphincter, they are assumed to be no longer subject to dispersion. However, the particles or molecules still in the stomach are subject to dispersion; *i.e.*, the longer they stay in the stomach, the greater the effect of dispersion. The distribution will be skewed.

To illustrate the effect that dispersion has on absorption and, subsequently, on blood levels, it is necessary to assume a simple model for the dispersion effect. The simplest case is provided by considering the stomach as a straight length of pipe of uniform cross-section through which a fluid is passing. The fluid is subjected to a longitudinal mixing or axial dispersion effect, which is superimposed on the mean flow.

The drug is assumed to be chemically inert on passage through the stomach, a property inherent in enteric-coated pellets. The dosage is $n_a{}^0$ mg, and the mean passage is $\bar{t}$ hr from the time of release from a capsule (or from the time of disintegration of a tablet or from the time of administration of a suspension or solution) to the time of passing through the pyloric sphincter.

If the drug can be envisaged to be instantaneously and evenly distributed throughout the stomach at time zero, then the drug passes through the pyloric sphincter at a rate of $n_a{}^0/\bar{t}$ mg/hr if no further dispersion occurs. If the drug dose is administered normally and dispersion does occur, then the amount of drug passing through the pyloric sphincter in time interval Δt is designated $\Delta n_a{}^0$. Thus, from the work of Levenspiel and Smith (2):

$$\frac{\Delta n_a/\Delta t}{n_a{}^0/\bar{t}} = \frac{1}{2\sqrt{\pi\frac{t}{\bar{t}}N_D}} \exp\left[-\frac{\left(1-\frac{t}{\bar{t}}\right)^2}{4\frac{t}{\bar{t}}N_D}\right] \qquad \text{(Eq. 1)}$$

where $\Delta n_a/\Delta t$ is the rate of drug passage through the pyloric sphincter at time t, and N_D, the dispersion number, is equal to D/uL, where D is the longitudinal or axial dispersion coefficient (equivalent to a macroscopic diffusion coefficient), u is the average linear velocity, and L is the length of the "pipe" from the point of drug administration to the pyloric sphincter. In physiological terms, D and u each depend on motility, viscosity of the fluid, and the total volume of fluid in the stomach.

The fraction of the drug dose, $\Delta X_a(t)$, that passes through the pyloric sphincter in time Δt and is available for absorption in the small intestine,

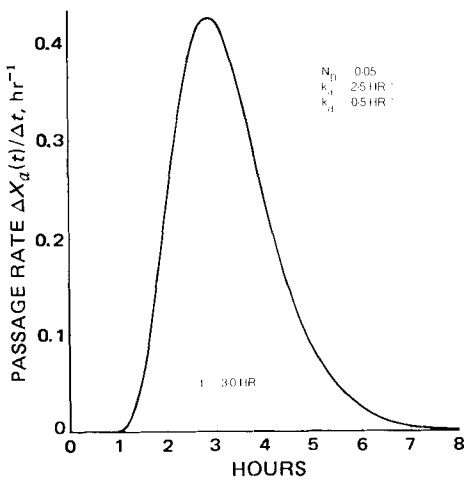

Figure 1—*Rate of passage of drug through pyloric sphincter as a function of time.*

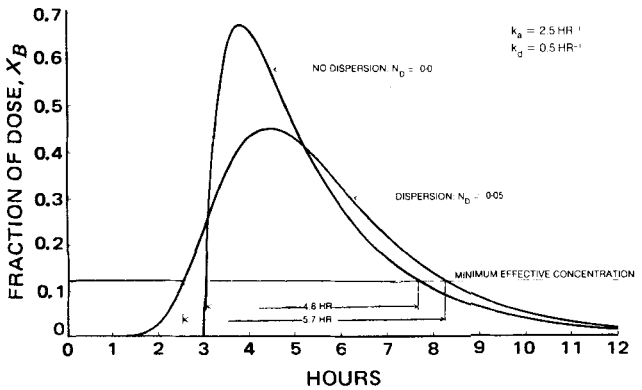

Figure 2—*Fraction of dose in single body compartment as a function of time for the cases of dispersion and no dispersion.*

assuming a rapid dissolution time such that there is negligible deviation in the blood level curve from that for instantaneous dissolution, is given by:

$$\Delta X_a(t) = \frac{\Delta n_a}{n_a{}^0} = \frac{\Delta t}{2\sqrt{\pi t \bar{t} N_D}} \exp\left[-\frac{\left(1-\frac{t}{\bar{t}}\right)^2}{\frac{t}{\bar{t}}N_D}\right] \quad \text{(Eq. 2)}$$

The fraction of the drug in the single body compartment at any time can be calculated for the one-compartment open model with the following working equations:

$$X_A(t) = X_A(t-\Delta t) + \Delta X_A(t) - \frac{k_a}{2}[X_A(t-\Delta t) + X_A(t)]\Delta t \quad \text{(Eq. 3a)}$$

or:

$$X_A(t) = X_A(t-\Delta t)\left[\frac{1-0.5k_a\,\Delta t}{1+0.5k_a\,\Delta t}\right] + \frac{\Delta X_a(t)}{1+0.5k_a\,\Delta t} \quad \text{(Eq. 3b)}$$

and:

$$X_B(t) = X_B(t-\Delta t) + \frac{k_a}{2}[X_a(t-\Delta t) + X_A(t)]\,\Delta t - \frac{k_d}{2}[X_B(t-\Delta t) + X_B(t)]\,\Delta t \quad \text{(Eq. 4a)}$$

or:

$$X_B(t) = X_B(t-\Delta t)\left[\frac{1-0.5k_d\,\Delta t}{1+0.5k_d\,\Delta t}\right] + \frac{k_a[X_A(t-\Delta t) + X_A(t)]\Delta t}{2(1+0.5k_d\,\Delta t)} \quad \text{(Eq. 4b)}$$

where $X_A(t)$ and $X_A(t-\Delta t)$ are the fractions of drug in solution in the small intestine at times t and $t-\Delta t$, respectively; $X_B(t)$ and $X_B(t-\Delta t)$ are the fractions of drug in the single body compartment at times t and $t-\Delta t$, respectively; $\Delta X_a(t)$ is the amount of drug that enters the small intestine and is dissolved between times $t-\Delta t$ and t (see Eq. 2); k_a is the first-order absorption constant; and k_d is the first-order elimination constant, accounting for total metabolism and excretion from the single body compartment.

RESULTS

To demonstrate the effect of dispersion on blood level curves, the following parameters were selected: $\bar{t}$ = 3.0 hr, N_D = 0.05, k_a = 2.5 hr^{-1}, k_d = 0.5 hr^{-1}, and Δt = 0.001 hr.

Figure 1 shows a plot of the rate of passage of the drug through the pyloric sphincter as a function of time, determined from Eq. 2 as $\Delta X_a/\Delta t$. The skewed effect of continued dispersion on the particles remaining in the stomach is observed as time increases beyond the mean time. Figure 2 shows a plot of the fraction of the drug in the single body compartment as a function of time for the case of dispersion in the stomach and zero dispersion. The zero-dispersion case represents, for example, an enteric-coated tablet that takes 3 hr before it releases its coat in the duodenum and is available for absorption in the small intestine.

DISCUSSION

Figure 2 shows that dispersion of the particles or molecules in the stomach leads to a depression of the peak blood level but not at the expense of bioavailability. The value of the use of a large number of enteric-coated pellets in place of a single enteric-coated tablet is indicated by the fact that the blood level exceeds the minimum effective concentration for 5.7 hr in the dispersion case compared to only 4.6 hr in the zero-dispersion example. The use of enteric-coated pellets, therefore, introduces an effective mild sustained-release effect without the reduced bioavailability inherent in the standard sustained-release preparation. Such an effect was noted by Green (3) in studies with enteric-coated aspirin microspheres.

The depression of peak blood level with unimpaired bioavailability may be a distinct advantage with some drugs, because the peak blood level for zero dispersion may be in the toxic region. Aspirin is being marketed as enteric-coated tablets; but despite the fact that no salicylic acid has been detected in the stomach, confirming the effectiveness of the enteric coating, the blood loss is still significantly above that for administration of placebo tablets (1). It is suggested that the blood loss is due to the sudden appearance of a large concentration of aspirin at one location, the total dose moving along the small intestine as a bolus until it is absorbed.

Enteric-coated aspirin pellets would release the drug in the small intestine as small "minidoses"; the drug would be distributed along the small intestine without large concentrations at a particular location at any time. Therefore it is predicted that, for drugs exhibiting GI side effects, the enteric-coated pellet form will obviate intestinal side effects as well as gastric side effects.

REFERENCES

(1) G. D. Champion, A. B. Corrigan, R. O. Day, G. G. Graham, A. Haski, J. Hewson, G. Howe, and P. D. Paull, "The Australian Society of Clinical and Experimental Pharmacologists, 9th Annual Meeting," Melbourne, Australia, 1975, Paper 34.

(2) O. Levenspiel and W. K. Smith, *Chem. Eng. Sci.*, **6**, 227 (1957).

(3) D. M. Green, *J. New Drugs*, **6**, 294 (1966).

ACKNOWLEDGMENTS AND ADDRESSES

Received November 12, 1976, from *F. H. Faulding & Co. Ltd., Adelaide, South Australia 5001.*

Accepted for publication December 15, 1976.

GLC Determination for Ftorafur in Biological Fluids

ELLIOTT B. HILLS ˣ, VIVIANE C. GODEFROI, IRVING A. O'LEARY, MATTHEW BURKE, DENIS ANDRZEJEWSKI, WALTER BRUKWINSKI, and JEROME P. HORWITZ

Abstract □ A GLC analysis for free ftorafur was developed to follow the drug disposition in body fluids of patients. The free drug was extracted from aqueous biological samples with chloroform, derivatized by methylation, and chromatographed on 1% HI-EFF 8BP using flame-ionization detection. The analysis is sensitive (0.25 μg/ml of plasma) and specific for the intact molecule, and it does not interfere with subsequent fluorouracil analysis of the same sample.

Keyphrases □ Ftorafur—GLC analysis, biological fluids □ GLC—analysis, ftorafur in biological fluids □ Antineoplastic agents—ftorafur, GLC analysis in biological fluids

The antitumor agent ftorafur [1-(tetrahydro-2-furanyl)-5-fluorouracil] (I) (1) is a prodrug form of fluorouracil (2, 3). It slowly decomposes *via* aqueous and enzymatic hydrolysis with the release of free fluorouracil. Thus, I has much lower toxicity than fluorouracil (five to seven times less) (4, 5) but possesses similar activity. Additionally, it has a much longer half-life. These properties make I an ideal chemotherapeutic alternative to fluorouracil, which has the attendant difficulties of toxicity and a short half-life (30 min) (6).

Despite substantial clinical work utilizing I (7–9), pharmacokinetic studies have been limited by the lack of a generally available analytical method specific for free intact I. Microbiological assays have been used in disposition studies in animals and humans (10, 11). These methods are indirect in that they measure the amount of fluorouracil resulting from the I decomposition, I itself being essentially inactive, and the results may be high when compared to those obtained by instrumental methods (3). Additionally, the microbiological assay has low sensitivity (0.5 μg/ml) and is time consuming, requiring 24 hr at 5° and 18 hr at 37°. Recently, pharmacokinetic studies of ^{14}C-labeled I were conducted using chromatographic and radiochemical techniques to separate and quantitate the drug and its metabolites (12). The reported half-life for ^{14}C-labeled I was 16.8 hr.

The present work describes an analytical method based on chloroform extraction of I with subsequent derivatization by methylation with a 30% solution of dimethylformamide in dimethylformamide dimethyl acetal (II)[1]. The method is applicable to blood and urine samples and can be performed routinely.

EXPERIMENTAL

Reagents—All chemicals were analytical reagent grade, and all solvents except nanograde chloroform[2] were redistilled. Pyridine was distilled first from *p*-toluenesulfonyl chloride and then from potassium hydroxide. Both pyridine and dimethylformamide were stored over molecular sieves[3]. Compound I[4] and 6-^{3}H-fluorouracil[5] (specific activity of 7.3 Ci/mmole) were used as received. 6-^{3}H-Labeled I was synthesized by sodium tritoxide–tritium oxide exchange[5] (13). Subsequent purification by instant TLC[6], using methanol–chloroform (1:9), yielded 6-^{3}H-I with a specific activity of 0.46 Ci/mmole.

Synthesis of 6-^{2}H-fluorouracil was accomplished by sodium deuteroxide–deuterium oxide exchange (13). Subsequent purification by recrystallization from methanol and ether gave 6-^{2}H-fluorouracil deuterated to the extent of 93% as determined by mass spectral analysis of the trimethylsilyl derivative.

All labeled and nonlabeled standards were prepared in absolute ethanol at concentrations permitting use of 10–20-μl aliquots.

Extraction of Biological Samples—Blood samples were collected in heparinized containers[7] and centrifuged to separate the plasma. The plasma was then frozen until analyzed. Urine samples were collected and frozen directly.

To 1.0 ml of plasma was added 4000 dpm of 6-^{3}H-I and 0.758 μg of 6-^{2}H-fluorouracil to serve as internal standards. After dilution with 1 ml of water, the pH was adjusted to 7.4 with 10 μl of pH 4.7, 0.5 *M* acetate buffer/ml of plasma. The sample was then extracted three times at 0° with 15, 8, and 8 ml of chloroform to remove I. The first two extracts were filtered through cotton, evaporated to dryness under nitrogen, and transferred with chloroform to a 6 × 50-mm test tube[8] for derivatization. The third extraction was included only when levels of I were anticipated to be low. Traces of chloroform were removed from the aqueous phase by bubbling nitrogen through the plasma.

The procedure of Cohen and Brennan (14) was then used to extract fluorouracil. This extract was further purified by instant TLC with methanol–chloroform (6:94) followed by instant TLC with methanol–chloroform (40:60). All elutions and transfers of fluorouracil were with methanol. When sufficient plasma was available, analyses for I and fluorouracil were carried out on separate portions of the same plasma sample.

With only minor variations, urine samples were extracted in the same manner as described, and analyses for I and fluorouracil were performed on separate portions of the same sample. Prior to the chloroform extraction of I, 1.0-ml aliquots were adjusted to pH 7.4 with 1 *N* NaOH or 0.5 *M*, pH 4.7 acetate buffer. Fluorouracil extraction was performed on 0.5-ml urine aliquots. The addition of sodium sulfate was eliminated from the Cohen and Brennan (14) procedure, and the first instant TLC was carried out in methanol–chloroform (3:97).

Derivatization and Measurement of Radioactivity—The evaporated I sample was dissolved in 30 μl of dimethylformamide. Following dissolution of the sample, 70 μl of II was added; the reaction vessel was then sealed in a flame without prior cooling of the solution. The reaction vessel was then cooled to room temperature and totally immersed in an oil bath at 95° for 15 min. After cooling, 10 μl was injected into the gas chromatograph for analysis. An aliquot also was added to toluene phosphor before determining radioactivity in a liquid scintillation spectrometer[9] equipped with automatic external standardization to correct for quenching. The percent extracted was then calculated.

Immediately prior to analysis, the dried fluorouracil sample was reacted with 10 μl of pyridine and 20 μl of *N,O*-bis(trimethylsilyl)trifluoroacetamide containing 1% trimethylchlorosilane (III)[10] for 10 min at room temperature to form the trimethylsilyl derivative.

GLC[11] and Quantitation—The 3-*N*-methyl derivative of I was chromatographed on a glass column, 1.83 m (6 ft) × 0.63 cm (0.25 in.), packed with 1% HI-EFF 8BP on 100–120-mesh Gas Chrom Q[12] and conditioned at 220° for 48 hr. A flame-ionization detector also was used. Nitrogen carrier gas flow was maintained at 40 ml/min. The injection port and detector temperatures were 225 and 250°, respectively.

[1] Aldrich Chemical Co., Milwaukee, Wis.
[2] Mallinckrodt Chemical Works, St. Louis, Mo.
[3] Linde Type 3A, MC & B Manufacturing Chemists, Cincinnati, Ohio.
[4] Microbiological Associates, Washington, D.C.
[5] New England Nuclear, Boston, Mass.
[6] ITLC SA, Gelman Instrument Co., Ann Arbor, Mich.
[7] B-D Vacutainers, Scientific Products, McGaw Park, Ill.
[8] T 1320-1, Scientific Products, McGaw Park, Ill.
[9] Packard Tri-Carb model 3380 and absolute activity analyzer model 554, Packard Instrument Co., Downers Grove, Ill.
[10] Regisil, Regis Chemical Co., Morton Grove, Ill.
[11] Packard Instrument Co., Downers Grove, Ill.
[12] Applied Science Laboratories, State College, Pa.

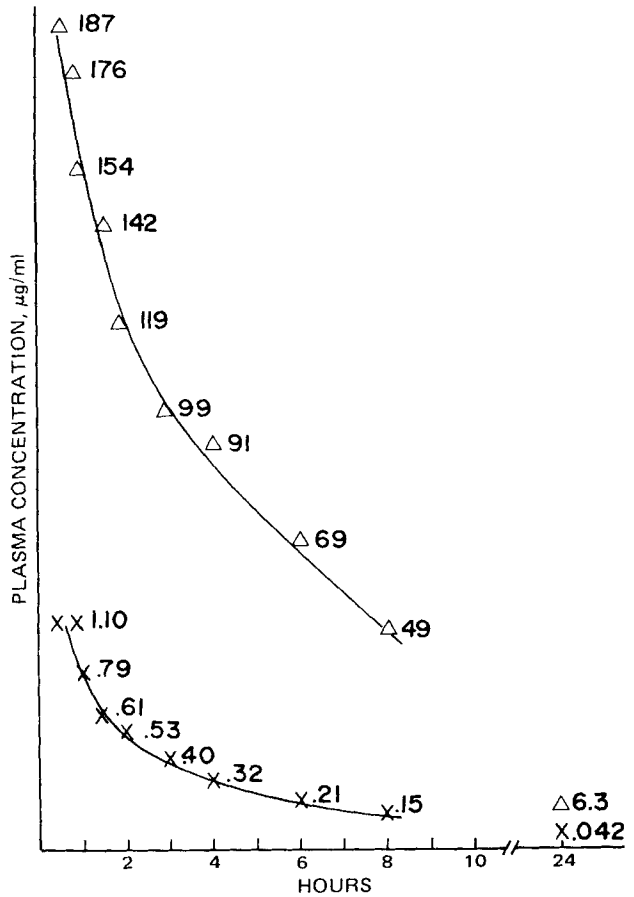

Figure 1—*Plasma concentration of I (△) and fluorouracil (×) in a patient receiving I at 2.25 g/m² iv over 30 min.*

The sample was injected at a column oven temperature of 207°, and the derivative eluted at approximately 7 min. Quantitation was accomplished by prior and subsequent injection of a standard sample of 3-*N*-methyl I and peak height comparison. Blanks were periodically injected to test for any possible sample carryover.

The trimethylsilyl derivative of fluorouracil was chromatographed on a glass column, 1.83 m (6 ft) × 0.63 cm (0.25 in.), packed with 1% SE-30 on 100–120-mesh Gas Chrom Q and conditioned at 300° for 24 hr. The column and injection port temperatures were 85 and 300°, respectively. Helium carrier gas flow was approximately 30 ml/min. The retention time under these conditions was approximately 6.5 min.

Isotope dilution was used to quantitate fluorouracil. Mass spectra[13] from *m/e* 250 to 300 were recorded every 2 sec while the derivative was eluting. The fraction of deuterium in all samples was determined from the average of the abundances of the M − 15 ions and their associated isotope peaks (*m/e* 259, 260, 261, and 262) in the five most intense spectra recorded. Spectral data for both deuterated and nondeuterated standards were recorded at the beginning and end of each day, and these data were used in calculating the fraction of deuterium and the amount of fluorouracil in the plasma samples determined on that day. The variation in the spectral data obtained from the standard samples was small; for example, the average value of 16 measurements of the fraction of deuterium in the deuterated standard made over 45 days was 0.932 ± 0.006 (± 1 *SD*).

RESULTS AND DISCUSSION

The extraction procedure (14) yielded an interference which, upon repeated injection into the gas chromatograph, led to a severe loss of sensitivity. This interference was eliminated by instant TLC using methanol–chloroform (6:94) followed by instant TLC using methanol–chloroform (40:60). The first instant TLC removed most of the interference and all of I; removal of I is crucial since any amount will interfere with subsequent fluorouracil analysis. The second instant TLC further reduced the interference.

[13] Model 01SG-2, Jeol, Cranford, N.J.

Table I—Quantitation of I and Fluorouracil Added to Human Plasma

I		Fluorouracil	
Amount Added, μg/ml	Amount Found, μg/ml[a]	Amount Added, μg/ml	Amount Found, μg/ml
5.0	4.9 ± 0.1	0.100	0.105 ± 0.006[b]
15.0	15.4 ± 0.3	0.153	0.161[c]
50.0	52 ± 2	0.229	0.237[c]
100	105 ± 3	0.382	0.384 ± 0.011[b]
200	201 ± 2	0.764	0.759 ± 0.029[b]
		1.15	1.15[d]
		1.53	1.49[d]

[a] Average of five determinations ± *SD*. [b] Average of four determinations ± *SD*. [c] Average of two determinations. [d] One determination.

Separate control experiments with both ^{3}H-I and 6-^{3}H-fluorouracil showed that the fractionation of the two drugs by chloroform extraction was essentially complete. No detectable amount of fluorouracil was extracted into the chloroform layer, in agreement with previous results (11), while less than 5% of I was picked up in the subsequent fluorouracil extraction.

The thermal instability of I presents special problems in derivatization and instrumental analysis. Attempts to chromatograph free I on various columns (1% SE-30, 3% OV-1, and 3% OV-17) resulted in very low sensitivity. Attempts to form a trimethylsilyl derivative with a 50:50 mixture of III and pyridine were unsuccessful. TLC of the evaporated reaction mixture showed only I, while injection of this reaction mixture onto the gas chromatograph (injection port temperatures of 150, 200, 250, and 300°) resulted in I decomposition with the formation of the trimethylsilyl derivative of fluorouracil to the extent of 10–20%, necessitating the complete removal of I prior to subsequent fluorouracil analysis. The trimethylsilyl derivative of I was not detected. Treatment of the methyl derivative of I in the same manner did not result in the formation of a detectable quantity of 1-trimethylsilyl-3-*N*-methyl-5-fluorouracil, even though such a derivative is formed from 3-*N*-methyl-5-fluorouracil. Thus, the methyl derivative is stable under the GLC conditions.

The methylation reaction is quantitative [>97% complete by TLC on silica gel F-254[14] using methanol–chloroform (1:4 v/v)] with no apparent decomposition of I or its derivative. GLC analysis showed that varying the amount of dimethylformamide from 20 to 40% had no effect on the reaction; however, use of pure II alone gave erratic results. At 90°, the reaction was complete after 15 min; at 95 and 100°, only 5 min was required. Running the reaction at 95 or 100° for 20 min caused no detectable decomposition of the methyl derivative.

The derivative structure was established as 1-(tetrahydro-2-furanyl)-3-*N*-methyl-5-fluorouracil, in agreement with previous results with the same reagent and similar compounds (15). NMR[15] analysis in deuterochloroform showed a doublet at 442 Hz with a relative area of 1 (H_6), a multiplet at 357 Hz with a relative area of 1 (H_1'), a multiplet at 245 Hz with a relative area of 2 (H_4'), a singlet at 200 Hz with a relative area of 3 (NCH_3), and a multiplet at 123 Hz with a relative area of 4 (H_2' and H_3'). The UV spectrum had a maximum at 270 nm (ϵ 7991) and a minimum at 237 nm (ϵ 1854). Characteristic ions in the mass spectrum of the derivative were the molecular ion at *m/e* 214 (13% relative abundance), the base + H and base + 2H at *m/e* 144 (2) and 145 (4), and the tetrahydrofuranyl moiety at *m/e* 71 (100). The corresponding ions occurred in the mass spectrum of I at about the same relative intensities.

Figure 1 shows data obtained from a patient receiving 2.25 g/m² iv of I over 30 min. Its plasma disappearance was biphasic with a β-phase half-life of 5 hr, which differed significantly from the value of 18.6 hr obtained for the median half-life of ^{14}C-labeled I in humans receiving 50 mg/m² (9). Data obtained from seven patients in this laboratory indicate an average half-life of 6.7 hr for I. The plasma fluorouracil level from 2 to 24 hr was similar to levels previously obtained in patients receiving a continuous intravenous infusion of fluorouracil at 1100 mg/m²/24 hr for 72–96 hr[16].

Compound I (90 mg) isolated from 1.5 liters of combined urine from nine patients showed no optical activity, indicating no enzymatic pref-

[14] Brinkmann Instruments, Westbury, N.Y.
[15] Varian A-60, Palo Alto, Calif.
[16] Unpublished data obtained in this laboratory in cooperation with the Milton A. Darling Memorial Center, The Grace Hospital, Detroit, Mich.

erence for either enantiomer. This result is in agreement with results obtained previously with human cell cultures and each pure enantiomer as well as the racemic mixture. No significant difference in the cytotoxic effects or the relative abilities to prevent an increase in cell numbers was observed with the three forms (16).

Control runs with plasma blanks showed no interferences with either the I or fluorouracil procedure. The accuracy and the concentration range over which both methods were tested are indicated in Table I. The correlation coefficients for the amount added *versus* the amount calculated in Table I are 0.999 for both sets of data, indicating that both analyses are linear in the concentration ranges tested. The methods as outlined permit the detection of 0.25 μg of I and 0.025 μg of fluorouracil/ml of plasma and are specific for the intact molecules. The sensitivity and applicability of these analyses indicate that they are suitable for these types of studies, and clinical investigations utilizing these procedures are currently being performed.

REFERENCES[17]

(1) R. A. Earl and L. B. Townsend, *Heterocycl. Chem.*, **9**, 1141 (1972), and references cited therein.

(2) H. Fujita, K. Ogawa, T. Sawabe, and K. Kimura, *Jpn. J. Cancer Clin.*, **18**, 917 (1972).

(3) D. V. Meiren and A. K. Belousova, *Vopr. Med. Khim.*, **18**, 288 (1972).

(4) M. I. Kravchenko, A. Zidermane, and A. Zibere, *Eksp. Klin. Farmakoter.*, **1**, 93 (1970).

(5) S. Germane and A. Kimenis, *ibid.*, **1**, 85 (1970).

(6) K. Lu, T. L. Loo, J. A. Benvenuto, R. S. Benjamin, M. Valdivieso, and E. J. Freireich, *Pharmacologist*, **17**, 202 (1975) (Abstract).

(7) E. K. Vozny and A. M. Garin, *Cancer*, **30**, 390 (1972), and references cited therein.

(8) C. Konda, *Jpn. J. Cancer Clin.*, **19**, 495 (1973), and references cited therein.

(9) A. Valdivieso, G. P. Bodey, J. A. Gottlieb, and E. J. Freireich, *Cancer Res.*, **36**, 1821 (1976).

(10) A. Z. Smolyanskaya and B. A. Tugarinov, *Neoplasma*, **19**, 341 (1972).

(11) H. Fujita, K. Ogawa, T. Sawabe, and K. Kimura, *Gan No Rinsho*, **18**, 911 (1972).

(12) S. W. Hall, R. S. Benjamin, A. C. Griffin, and T. L. Loo, *AACR Abstr.*, **17**, 128 (1976).

(13) J. J. Fox, R. J. Cushley, and S. R. Lipsky, *Tetrahedron Lett.*, **52**, 5393 (1968).

(14) J. L. Cohen and P. B. Brennan, *J. Pharm. Sci.*, **62**, 572 (1973).

(15) J. Žemlička, R. Gasser, J. V. Freisler, and J. P. Horwitz, *J. Am. Chem. Soc.*, **94**, 3213 (1972).

(16) J. P. Horwitz, J. J. McCormick, K. D. Philips, V. M. Maher, J. R. Otto, D. Kessel, and J. Žemlička, *Cancer Res.*, **35**, 1301 (1975).

ACKNOWLEDGMENTS AND ADDRESSES

Received October 21, 1976, from the *Michigan Cancer Foundation, Detroit, MI 48201.*

Accepted for publication January 10, 1977.

Supported in part by U.S. Public Health Service Research Grant CA-07177 and in part by an institutional grant to the Michigan Cancer Foundation from the United Foundation of Greater Detroit.

The authors are indebted to Dr. Laurence Baker for the biological samples. The technical assistance of Ms. Jean Devos is gratefully acknowledged.

[x] To whom inquiries should be directed.

[17] *Note added in proof:* Similar methods for the concurrent determination of I and fluorouracil were reported recently by A. T. Wu, H. J. Schwandt, and W. Sadee, *Res. Commun. Chem. Pathol. Pharmacol.* **14**, 89 (1976).

Estimation of Pharmacokinetic Parameters from Postinfusion Blood Level Data Obtained after Simultaneous Administration of Intravenous Priming and Infusion Doses

SAMPAT M. SINGHVI

Abstract □ Occasionally, it is desirable to attain steady-state blood drug levels rapidly in pharmacokinetic studies as well as in the treatment of certain diseases. In these cases, it is useful to administer an intravenous priming dose in combination with continuous drug infusion. Mathematical relationships are presented for the determination of pharmacokinetic parameters in these situations using postinfusion blood drug level data. The parameters obtained by this method are identical to the parameters obtained after a rapid intravenous injection of a drug.

Keyphrases □ Pharmacokinetic parameters—determined from postinfusion blood level data after simultaneous intravenous priming and infusion doses □ Dosage regimens—simultaneous intravenous priming and infusion doses, pharmacokinetic parameters determined from postinfusion blood level data

Methods for the assessment of pharmacokinetic parameters from postinfusion blood level data obtained after continuous intravenous infusion were presented previously (1). However, in practice, a rapid intravenous priming dose is often given simultaneously with the beginning of a continuous infusion to achieve steady-state blood drug levels rapidly in the body. This paper presents the treatment of postinfusion blood concentration data for the estimation of pharmacokinetic parameters in those instances.

THEORY AND DISCUSSION

Two-Compartment Model—For a drug that exhibits the characteristics of a two-compartment open model (Scheme I), the decay of blood concentration, $C_{p(\text{bolus})}$, with time t, after a rapid intravenous injection (assuming first-order elimination and distribution kinetics) can be expressed as (2):

$$C_{p(\text{bolus})} = \frac{X_0(\alpha - k_{21})}{V_c(\alpha - \beta)} e^{-\alpha t} + \frac{X_0(k_{21} - \beta)}{V_c(\alpha - \beta)} e^{-\beta t} \qquad \text{(Eq. 1)}$$

If:

$$A = \frac{X_0(\alpha - k_{21})}{V_c(\alpha - \beta)} \qquad \text{(Eq. 2)}$$

erence for either enantiomer. This result is in agreement with results obtained previously with human cell cultures and each pure enantiomer as well as the racemic mixture. No significant difference in the cytotoxic effects or the relative abilities to prevent an increase in cell numbers was observed with the three forms (16).

Control runs with plasma blanks showed no interferences with either the I or fluorouracil procedure. The accuracy and the concentration range over which both methods were tested are indicated in Table I. The correlation coefficients for the amount added *versus* the amount calculated in Table I are 0.999 for both sets of data, indicating that both analyses are linear in the concentration ranges tested. The methods as outlined permit the detection of 0.25 μg of I and 0.025 μg of fluorouracil/ml of plasma and are specific for the intact molecules. The sensitivity and applicability of these analyses indicate that they are suitable for these types of studies, and clinical investigations utilizing these procedures are currently being performed.

REFERENCES[17]

(1) R. A. Earl and L. B. Townsend, *Heterocycl. Chem.*, **9**, 1141 (1972), and references cited therein.

(2) H. Fujita, K. Ogawa, T. Sawabe, and K. Kimura, *Jpn. J. Cancer Clin.*, **18**, 917 (1972).

(3) D. V. Meiren and A. K. Belousova, *Vopr. Med. Khim.*, **18**, 288 (1972).

(4) M. I. Kravchenko, A. Zidermane, and A. Zibere, *Eksp. Klin. Farmakoter.*, **1**, 93 (1970).

(5) S. Germane and A. Kimenis, *ibid.*, **1**, 85 (1970).

(6) K. Lu, T. L. Loo, J. A. Benvenuto, R. S. Benjamin, M. Valdivieso, and E. J. Freireich, *Pharmacologist*, **17**, 202 (1975) (Abstract).

(7) E. K. Vozny and A. M. Garin, *Cancer*, **30**, 390 (1972), and references cited therein.

(8) C. Konda, *Jpn. J. Cancer Clin.*, **19**, 495 (1973), and references cited therein.

(9) A. Valdivieso, G. P. Bodey, J. A. Gottlieb, and E. J. Freireich, *Cancer Res.*, **36**, 1821 (1976).

(10) A. Z. Smolyanskaya and B. A. Tugarinov, *Neoplasma*, **19**, 341 (1972).

(11) H. Fujita, K. Ogawa, T. Sawabe, and K. Kimura, *Gan No Rinsho*, **18**, 911 (1972).

(12) S. W. Hall, R. S. Benjamin, A. C. Griffin, and T. L. Loo, *AACR Abstr.*, **17**, 128 (1976).

(13) J. J. Fox, R. J. Cushley, and S. R. Lipsky, *Tetrahedron Lett.*, **52**, 5393 (1968).

(14) J. L. Cohen and P. B. Brennan, *J. Pharm. Sci.*, **62**, 572 (1973).

(15) J. Žemlička, R. Gasser, J. V. Freisler, and J. P. Horwitz, *J. Am. Chem. Soc.*, **94**, 3213 (1972).

(16) J. P. Horwitz, J. J. McCormick, K. D. Philips, V. M. Maher, J. R. Otto, D. Kessel, and J. Žemlička, *Cancer Res.*, **35**, 1301 (1975).

ACKNOWLEDGMENTS AND ADDRESSES

Received October 21, 1976, from the *Michigan Cancer Foundation, Detroit, MI 48201.*

Accepted for publication January 10, 1977.

Supported in part by U.S. Public Health Service Research Grant CA-07177 and in part by an institutional grant to the Michigan Cancer Foundation from the United Foundation of Greater Detroit.

The authors are indebted to Dr. Laurence Baker for the biological samples. The technical assistance of Ms. Jean Devos is gratefully acknowledged.

[x] To whom inquiries should be directed.

[17] *Note added in proof:* Similar methods for the concurrent determination of I and fluorouracil were reported recently by A. T. Wu, H. J. Schwandt, and W. Sadee, *Res. Commun. Chem. Pathol. Pharmacol.* **14**, 89 (1976).

Estimation of Pharmacokinetic Parameters from Postinfusion Blood Level Data Obtained after Simultaneous Administration of Intravenous Priming and Infusion Doses

SAMPAT M. SINGHVI

Abstract □ Occasionally, it is desirable to attain steady-state blood drug levels rapidly in pharmacokinetic studies as well as in the treatment of certain diseases. In these cases, it is useful to administer an intravenous priming dose in combination with continuous drug infusion. Mathematical relationships are presented for the determination of pharmacokinetic parameters in these situations using postinfusion blood drug level data. The parameters obtained by this method are identical to the parameters obtained after a rapid intravenous injection of a drug.

Keyphrases □ Pharmacokinetic parameters—determined from postinfusion blood level data after simultaneous intravenous priming and infusion doses □ Dosage regimens—simultaneous intravenous priming and infusion doses, pharmacokinetic parameters determined from postinfusion blood level data

Methods for the assessment of pharmacokinetic parameters from postinfusion blood level data obtained after continuous intravenous infusion were presented previously (1). However, in practice, a rapid intravenous priming dose is often given simultaneously with the beginning of a continuous infusion to achieve steady-state blood drug levels rapidly in the body. This paper presents the treatment of postinfusion blood concentration data for the estimation of pharmacokinetic parameters in those instances.

THEORY AND DISCUSSION

Two-Compartment Model—For a drug that exhibits the characteristics of a two-compartment open model (Scheme I), the decay of blood concentration, $C_{p(\text{bolus})}$, with time t, after a rapid intravenous injection (assuming first-order elimination and distribution kinetics) can be expressed as (2):

$$C_{p(\text{bolus})} = \frac{X_0(\alpha - k_{21})}{V_c(\alpha - \beta)} e^{-\alpha t} + \frac{X_0(k_{21} - \beta)}{V_c(\alpha - \beta)} e^{-\beta t} \qquad \text{(Eq. 1)}$$

If:

$$A = \frac{X_0(\alpha - k_{21})}{V_c(\alpha - \beta)} \qquad \text{(Eq. 2)}$$

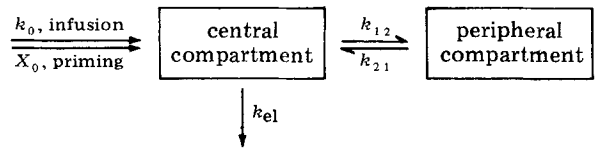

Scheme I

and:

$$B = \frac{X_0(k_{21} - \beta)}{V_c(\alpha - \beta)} \quad \text{(Eq. 3)}$$

then:

$$C_{p(\text{bolus})} = Ae^{-\alpha t} + Be^{-\beta t} \quad \text{(Eq. 4)}$$

where A and B are intercepts at zero time, α and β are disposition rate constants, k_{12} and k_{21} are distribution rate constants, k_{el} is the first-order elimination rate constant from the central compartment, X_0 is the intravenous priming dose, and V_c is the volume of the central compartment.

Similarly, when a drug is administered as a continuous infusion at a constant rate, k_0, the blood levels, $C_{p(\text{inf})}$, at any time t during and after cessation of infusion can be described as (2):

$$C_{p(\text{inf})} = \frac{k_0(k_{21} - \alpha)(1 - e^{\alpha T})}{V_c\alpha(\alpha - \beta)} e^{-\alpha t} + \frac{k_0(\beta - k_{21})(1 - e^{\beta T})}{V_c\beta(\alpha - \beta)} e^{-\beta t} \quad \text{(Eq. 5)}$$

where T is the duration of infusion. The blood drug level after cessation of infusion also can be expressed as:

$$C_{p(\text{inf})} = \frac{k_0(k_{21} - \alpha)(1 - e^{\alpha T})}{V_c\alpha(\alpha - \beta)} e^{-\alpha(T+t')} + \frac{k_0(\beta - k_{21})(1 - e^{\beta T})}{V_c\beta(\alpha - \beta)} e^{-\beta(T+t')} \quad \text{(Eq. 6)}$$

Similarly, the drug concentration at time $(T + t')$ after the bolus dose can be expressed as:

$$C_{p(\text{bolus})} = \frac{X_0(\alpha - k_{21})}{V_c(\alpha - \beta)} e^{-\alpha(T+t')} + \frac{X_0(k_{21} - \beta)}{V_c(\alpha - \beta)} e^{-\beta(T+t')} \quad \text{(Eq. 7)}$$

where t' is the elapsed time after termination of the infusion.

Equations 6 and 7 can be combined to obtain plasma drug levels at the end of an infusion, $C_{p(\text{post})}$, when simultaneous intravenous priming and infusion doses are administered. Combining Eqs. 6 and 7 and simplifying yield:

$$C_{p(\text{post})} = C_{p(\text{bolus})} + C_{p(\text{inf})} = \frac{\alpha - k_{21}}{V_c(\alpha - \beta)} \times \left[X_0 - \frac{k_0}{\alpha}(1 - e^{\alpha T})\right] e^{-\alpha(T+t')} + \frac{k_{21} - \beta}{V_c(\alpha - \beta)} \left[X_0 - \frac{k_0}{\beta}(1 - e^{\beta T})\right] e^{-\beta(T+t')} \quad \text{(Eq. 8)}$$

Combining Eqs. 2, 3, and 8 and rearranging yield:

$$C_{p(\text{post})} = \frac{A}{X_0}\left[X_0 - \frac{k_0}{\alpha}(1 - e^{\alpha T})\right] e^{-\alpha T}e^{-\alpha t'} + \frac{B}{X_0}\left[X_0 - \frac{k_0}{\beta}(1 - e^{\beta T})\right] e^{-\beta T}e^{-\beta t'} \quad \text{(Eq. 9)}$$

or:

$$C_{p(\text{post})} = \frac{A}{X_0}\left[X_0e^{-\alpha T} + \frac{k_0}{\alpha}(1 - e^{-\alpha T})\right] e^{-\alpha t'} + \frac{B}{X_0}\left[X_0e^{-\beta T} + \frac{k_0}{\beta}(1 - e^{-\beta T})\right] e^{-\beta t'} \quad \text{(Eq. 10)}$$

If:

$$\frac{A}{X_0}\left[X_0e^{-\alpha T} + \frac{k_0}{\alpha}(1 - e^{-\alpha T})\right] = A_1 \quad \text{(Eq. 11)}$$

and:

$$\frac{B}{X_0}\left[X_0e^{-\beta T} + \frac{k_0}{\beta}(1 - e^{-\beta T})\right] = B_1 \quad \text{(Eq. 12)}$$

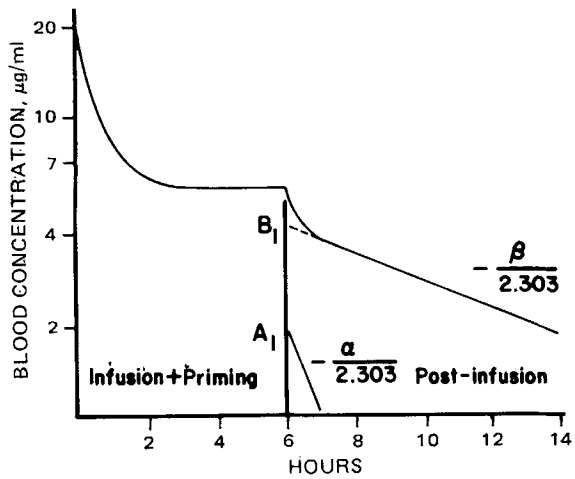

Figure 1—*Simulated blood concentrations after simultaneous administration of intravenous priming and continuous infusion doses of a hypothetical drug.*

then combining Eqs. 10–12 gives:

$$C_{p(\text{post})} = A_1e^{-\alpha t'} + B_1e^{-\beta t'} \quad \text{(Eq. 13)}$$

This equation is equivalent to the biexponential equation defining a rapid intravenous injection blood curve. Thus, when plasma concentrations, $C_{p(\text{post})}$, are plotted semilogarithmically against the postinfusion time, t', a biexponential curve is obtained (Fig. 1).

Parameters A_1, B_1, α, and β can be obtained from these plots, as exemplified in Fig. 1. When these values are known along with X_0, k_0, and T, the intercepts A and B can be computed using Eqs. 11 and 12.

After obtaining A, B, α, and β, various other pharmacokinetic parameters can be calculated by conventional methods (2) as follows:

$$k_{21} = \frac{A\beta + B\alpha}{A + B} \quad \text{(Eq. 14)}$$

$$k_{el} = \frac{\alpha\beta}{k_{21}} \quad \text{(Eq. 15)}$$

$$k_{12} = \alpha + \beta - k_{21} - k_{el} \quad \text{(Eq. 16)}$$

$$AUC = \frac{A}{\alpha} + \frac{B}{\beta} \quad \text{(Eq. 17)}$$

$$V_c = \frac{\text{total dose}}{A + B} \quad \text{(Eq. 18)}$$

$$V_d = \frac{\text{total dose}}{(AUC)\beta} \quad \text{(Eq. 19)}$$

$$Cl_B = V_d\beta \quad \text{(Eq. 20)}$$

where AUC is the area under the plasma level–time curve, V_d is the apparent volume of distribution, Cl_B is the total body clearance, and total dose is the priming plus infusion dose $(X_0 + k_0T)$. All other parameters were defined previously.

Equations 11 and 12 are similar to the corresponding equations (*e.g.*, Eqs. 21 and 22) presented by Loo and Riegelman (1) in their treatment of postinfusion blood level data obtained after an intravenous infusion dose without a simultaneous priming dose:

$$A_1 = \frac{Ak_0(1 - e^{-\alpha T})}{X_0\alpha} \quad \text{(Eq. 21)}$$

and:

$$B_1 = \frac{Bk_0(1 - e^{-\beta T})}{X_0\beta} \quad \text{(Eq. 22)}$$

Three-Compartment Open Model—By using the same treatment for a drug that exhibits the characteristics of a three-compartment open model, the decay of blood levels during the postinfusion period following simultaneous administration of intravenous priming and infusion doses can be expressed as follows:

$$C_{p(\text{post})} = P_1e^{-\pi t'} + A_1e^{-\alpha t'} + B_1e^{-\beta t'} \quad \text{(Eq. 23)}$$

where:

$$P_1 = \frac{P}{X_0}\left[X_0 e^{-\pi T} + \frac{k_0}{\pi}(1 - e^{-\pi T})\right] \quad \text{(Eq. 24)}$$

$$A_1 = \frac{A}{X_0}\left[X_0 e^{-\alpha T} + \frac{k_0}{\alpha}(1 - e^{-\alpha T})\right] \quad \text{(Eq. 25)}$$

$$B_1 = \frac{B}{X_0}\left[X_0 e^{-\beta T} + \frac{k_0}{\beta}(1 - e^{-\beta T})\right] \quad \text{(Eq. 26)}$$

After estimation of P, A, B, π, α, and β, the other pharmacokinetic parameters can be computed using the conventional methods (2) for blood concentration data obtained after a single rapid intravenous injection of the drug.

Occasionally, it is desirable to inject a drug slowly at a constant rate until the desired steady-state blood drug concentration is achieved. However, the time required (about $7 \times t_{1/2\beta}$) to obtain steady-state blood concentrations will be quite long for a drug with a long half-life. It may then be convenient to administer an intravenous priming dose simultaneously with the continuous infusion to obtain steady-state conditions rapidly (3, 4). The relationships derived in this paper are useful for the estimation of pharmacokinetic parameters in these situations.

REFERENCES

(1) J. C. K. Loo and S. Riegelman, *J. Pharm. Sci.*, **59**, 53 (1970).

(2) M. Gibaldi and D. Perrier, in "Pharmacokinetics," J. Swarbrick, Ed., Dekker, New York, N.Y., 1975, chaps. 2 and 3.

(3) P. A. Mitenko and R. I. Oglive, *Clin. Pharmacol. Ther.*, **13**, 329 (1972).

(4) P. D. Thomson, K. L. Melmon, J. A. Richardson, K. Cohen, W. Steinbrunn, R. Cudihee, and M. Rowland, *Ann. Intern. Med.*, **78**, 499 (1973).

ACKNOWLEDGMENTS AND ADDRESSES

Received November 24, 1976, from the *Department of Drug Metabolism, Squibb Institute for Medical Research, New Brunswick, NJ 08903.*

Accepted for publication January 10, 1977.

The author gratefully acknowledges the editorial help of Mr. A. F. Heald and Dr. L. T. DiFazio.

Hydrolysis Mechanism of 7-Acetylacroninium Perchlorate, a Novel Prodrug of Acronine

A. J. REPTA ˣ, J. R. DIMMOCK *, BO KREILGÅRD ‡, and JAMES J. KAMINSKI §

Abstract □ 7-Acetylacroninium perchlorate was hydrolyzed at 25° by both water enriched with ^{18}O-labeled water and by unenriched water. The acronine obtained was examined by mass spectrometry, which indicated the unusual fact that hydrolysis of this ester proceeded by aryl oxygen cleavage to the extent of about 30% under those mild conditions.

Keyphrases □ 7-Acetylacroninium perchlorate—hydrolysis mechanism □ Acronine prodrug—7-acetylacroninium perchlorate, hydrolysis mechanism □ Prodrugs—7-acetylacroninium perchlorate, hydrolysis mechanism □ Hydrolysis—7-acetylacroninium perchlorate, mechanism determined

The alkaloid acronine[1] (I) has activity against a wide range of tumors (1), but a major problem associated with its administration has been its low water solubility, only about 2–3 mg/liter (2).

BACKGROUND

Attempts have been made to increase acronine solubility in water by coprecipitating the drug with povidone (3), using a mixture of an organic solvent and water (4), and complexation with various ligands (4). All of these methods failed to increase the water solubility of acronine to a concentration of 30 mg/100 ml, which was the value desired for intravenous administration.

Another approach was based on the fact that, in the presence of acid, protonation of the 7-oxygen of acronine resulted (II) (4). Thus, in preparing an acronine prodrug, acylation of the 7-hydroxy group of an acroninium salt would be expected to produce a 7-acyloxyacroninium salt with increased water solubility compared to acronine and yet be capable of regenerating acronine *in vivo*. 7-Acetylacroninium perchlorate (III) was prepared and is over 100 times more water soluble than acronine; *in vitro*, it is converted quantitatively to acronine. However, the prodrug suffers from the disadvantage of being hydrolyzed too rapidly [$t_{1/2} \sim 20$ min under ambient temperatures (18–25°) in nonirritating, nontoxic, and water-miscible media] to be of clinical use (5).

The rapid solvolysis of III may be due, in part, to aryl oxygen fission, since modification of the alkyl moiety of the ester group of analogs of III reportedly yielded compounds with nearly identical hydrolysis rates (4). In addition, the reaction of III with both aniline and mercaptide ions resulted in the formation of the corresponding 7-anil and 7-thioketones.

The purpose of this work was to determine whether hydrolysis by aryl oxygen fission would occur to an appreciable extent under mild conditions. Such information is of interest from a general standpoint and might also prove useful in the design of related prodrugs with improved stability properties.

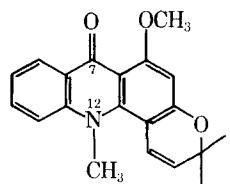

I

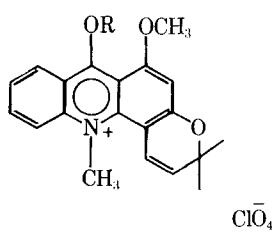

II: R = H
III: R = $COCH_3$

[1] Referred to as acronycine previously.

$$P_1 = \frac{P}{X_0}\left[X_0 e^{-\pi T} + \frac{k_0}{\pi}(1 - e^{-\pi T})\right] \quad \text{(Eq. 24)}$$

$$A_1 = \frac{A}{X_0}\left[X_0 e^{-\alpha T} + \frac{k_0}{\alpha}(1 - e^{-\alpha T})\right] \quad \text{(Eq. 25)}$$

$$B_1 = \frac{B}{X_0}\left[X_0 e^{-\beta T} + \frac{k_0}{\beta}(1 - e^{-\beta T})\right] \quad \text{(Eq. 26)}$$

After estimation of P, A, B, π, α, and β, the other pharmacokinetic parameters can be computed using the conventional methods (2) for blood concentration data obtained after a single rapid intravenous injection of the drug.

Occasionally, it is desirable to inject a drug slowly at a constant rate until the desired steady-state blood drug concentration is achieved. However, the time required (about $7 \times t_{1/2\beta}$) to obtain steady-state blood concentrations will be quite long for a drug with a long half-life. It may then be convenient to administer an intravenous priming dose simultaneously with the continuous infusion to obtain steady-state conditions rapidly (3, 4). The relationships derived in this paper are useful for the estimation of pharmacokinetic parameters in these situations.

REFERENCES

(1) J. C. K. Loo and S. Riegelman, *J. Pharm. Sci.*, **59**, 53 (1970).

(2) M. Gibaldi and D. Perrier, in "Pharmacokinetics," J. Swarbrick, Ed., Dekker, New York, N.Y., 1975, chaps. 2 and 3.

(3) P. A. Mitenko and R. I. Oglive, *Clin. Pharmacol. Ther.*, **13**, 329 (1972).

(4) P. D. Thomson, K. L. Melmon, J. A. Richardson, K. Cohen, W. Steinbrunn, R. Cudihee, and M. Rowland, *Ann. Intern. Med.*, **78**, 499 (1973).

ACKNOWLEDGMENTS AND ADDRESSES

Received November 24, 1976, from the *Department of Drug Metabolism, Squibb Institute for Medical Research, New Brunswick, NJ 08903.*

Accepted for publication January 10, 1977.

The author gratefully acknowledges the editorial help of Mr. A. F. Heald and Dr. L. T. DiFazio.

Hydrolysis Mechanism of 7-Acetylacroninium Perchlorate, a Novel Prodrug of Acronine

A. J. REPTA ˣ, J. R. DIMMOCK *, BO KREILGÅRD ‡, and JAMES J. KAMINSKI §

Abstract □ 7-Acetylacroninium perchlorate was hydrolyzed at 25° by both water enriched with ^{18}O-labeled water and by unenriched water. The acronine obtained was examined by mass spectrometry, which indicated the unusual fact that hydrolysis of this ester proceeded by aryl oxygen cleavage to the extent of about 30% under those mild conditions.

Keyphrases □ 7-Acetylacroninium perchlorate—hydrolysis mechanism □ Acronine prodrug—7-acetylacroninium perchlorate, hydrolysis mechanism □ Prodrugs—7-acetylacroninium perchlorate, hydrolysis mechanism □ Hydrolysis—7-acetylacroninium perchlorate, mechanism determined

The alkaloid acronine[1] (I) has activity against a wide range of tumors (1), but a major problem associated with its administration has been its low water solubility, only about 2–3 mg/liter (2).

BACKGROUND

Attempts have been made to increase acronine solubility in water by coprecipitating the drug with povidone (3), using a mixture of an organic solvent and water (4), and complexation with various ligands (4). All of these methods failed to increase the water solubility of acronine to a concentration of 30 mg/100 ml, which was the value desired for intravenous administration.

Another approach was based on the fact that, in the presence of acid, protonation of the 7-oxygen of acronine resulted (II) (4). Thus, in preparing an acronine prodrug, acylation of the 7-hydroxy group of an acroninium salt would be expected to produce a 7-acyloxyacroninium salt with increased water solubility compared to acronine and yet be capable of regenerating acronine *in vivo*. 7-Acetylacroninium perchlorate (III) was prepared and is over 100 times more water soluble than acronine; *in vitro*, it is converted quantitatively to acronine. However, the prodrug suffers from the disadvantage of being hydrolyzed too rapidly [$t_{1/2} \sim 20$ min under ambient temperatures (18–25°) in nonirritating, nontoxic, and water-miscible media] to be of clinical use (5).

The rapid solvolysis of III may be due, in part, to aryl oxygen fission, since modification of the alkyl moiety of the ester group of analogs of III reportedly yielded compounds with nearly identical hydrolysis rates (4). In addition, the reaction of III with both aniline and mercaptide ions resulted in the formation of the corresponding 7-anil and 7-thioketones.

The purpose of this work was to determine whether hydrolysis by aryl oxygen fission would occur to an appreciable extent under mild conditions. Such information is of interest from a general standpoint and might also prove useful in the design of related prodrugs with improved stability properties.

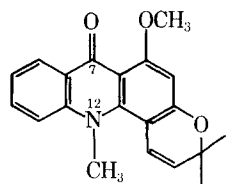

I

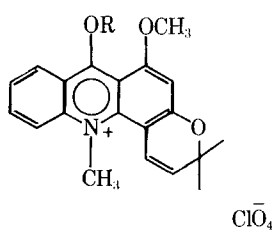

II: R = H
III: R = $COCH_3$

[1] Referred to as acronycine previously.

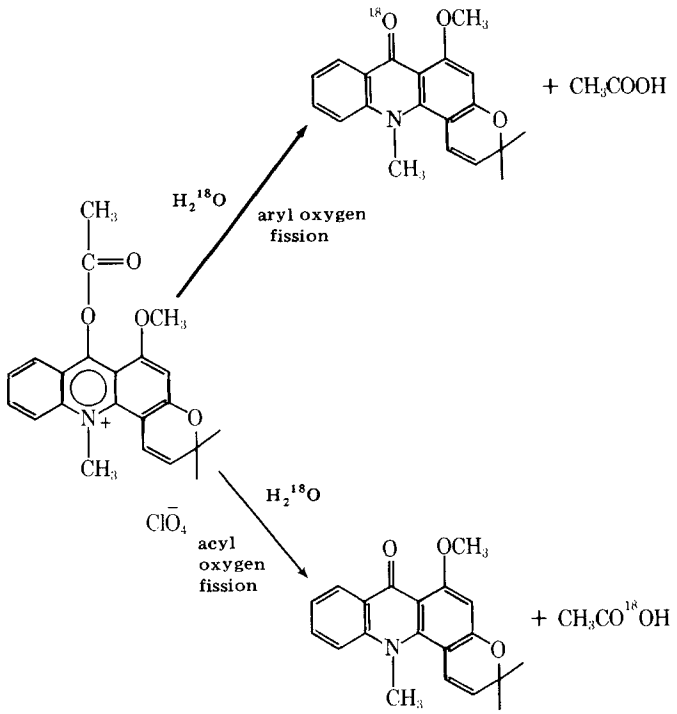

Scheme I

One method of determining the extent to which aryl oxygen cleavage occurs is hydrolysis of the ester in the presence of ^{18}O-labeled water. If acyl oxygen fission solely occurs, the product formed (acronine) will be devoid of any oxygen atoms containing oxygen-18. Alternatively, if aryl oxygen cleavage of the ester occurs, the acronine formed will contain oxygen-18 in the 7-position (Scheme I).

RESULTS AND DISCUSSION

7-Acetylacroninium perchlorate (III) was hydrolyzed in water enriched with 38.0 atom % $H_2{}^{18}O$ and also in unriched water to give products designated A and B, respectively. These products were examined by mass spectrometry. Acronine has a parent ion of *m/e* 321, and acronine containing oxygen-18 in the 7-position has a parent ion of *m/e* 323. Spectra from *m/e* 240 to 324 of both A and B revealed that the intensity of the ion at *m/e* 323 (expressed as a percentage of the total of the ion intensities from *m/e* 240 to 324) was approximately three times greater with A than with B. Since an additional experiment determined that no appreciable exchange between the 7-oxygen of acronine and ^{18}O-labeled water occurred, aryl oxygen cleavage of the ester was indicated.

The question arises as to the extent of aryl ester cleavage during the hydrolysis of III. One solution to this problem is to compare the intensities of pairs of ions representing the same molecular fragment, one of which contains oxygen-16 and the other oxygen-18 in the 7-group. Thus, for A and B, the intensities of the ions at *m/e* 323 and 321 of both spectra were measured; the relative intensity of the *m/e* 323 ion was expressed as a percentage according to the expression $100(M + 2)/[M + (M + 2)]$, where M + 2 and M are the intensities of the ions at *m/e* 323 and 321, respectively. The difference between the figures obtained from the spectra of A and B gives the excess atom percentage of oxygen-18. From this figure, the percentage of aryl oxygen cleavage can be calculated (see *Experimental*).

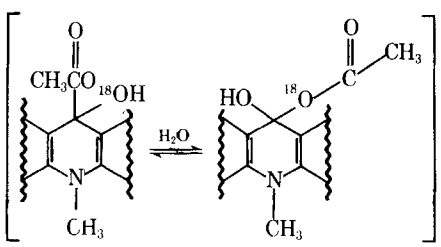

Scheme II

The ions at *m/e* 308 and 306 were also compared, these fragments arising by loss of 15 mass units from the parent ion. Comparison of the ratio of the intensities of the ions *m/e* 323/321 and 308/306 indicated that acyl oxygen cleavage occurred to the extent of nearly 30%.

The fact that only 30% of the III hydrolysis occurred *via* the aryl oxygen route was somewhat surprising in view of previous findings (4) that the hydrolytic rates of more sterically hindered species, such as pivalylacroninium ions, were very similar to those of the acetyl derivative. This finding had suggested that aryl oxygen fission might be a major hydrolytic pathway. With III, a facile nucleophilic attack of aniline and mercaptide ions occurred (which, with aniline, was a quantitative reaction) to yield the corresponding 7-derivative. The results may be due to the greater nucleophilicity of these compounds relative to water.

With several other 7-acyl analogs of III, the hydrolysis rates also were similar to those of III (4). This observation is difficult to rationalize in light of the present results, which imply that acyl oxygen cleavage is the major route for hydrolysis in such a series of esters and that changes in the steric bulk of the acyl component of the ester would be expected to affect hydrolysis rates significantly. One possible contributing factor in this dilemma might be the existence of a tetrahedral intermediate having a sufficient lifetime to permit the exchange of the acyl group between the labeled and unlabeled oxygen atom (Scheme II).

The existence of such an intermediate could reduce the label at the 7-position by a factor of two at most, and this maximum would be achieved only if total equilibration of the sort shown in Scheme II occurred. In that case, half of the ^{18}O-label would be lost as ^{18}O-acetate. Consequently, it is possible that the reaction pathway involving aryl oxygen fission might have occurred to a maximum extent of about 60%, although it seems unlikely that the intermediate would be sufficiently stable to result in statistically complete mixing of the labeled atom. Therefore, an intermediate value between 30 and 60% would be more reasonable.

Nevertheless, the fact that the aryl oxygen fission of the ester linkage occurs to the extent of 30% or more under such mild conditions is unusual and attests to the abnormal properties of the ester linkage of the 7-acylacroninium prodrugs. These results also suggest that utilization of a prodrug approach based on the modification of the ester group is unlikely to increase greatly the prodrug stability since the degradation pathways appear to involve components of both acyl and aryl oxygen fission.

EXPERIMENTAL[2]

A freshly synthesized sample of 7-acetylacroninium perchlorate (III) (0.00556 g) (4, 5), shown by spectrometry (6) to contain 72% of the ester III[3], was added to a tube containing 38.0 atom % $H_2{}^{18}O$ (5.0 ml) and placed in a sonic bath[4] for 18 min. The tube was attached to the spindle of a constant-temperature bath at 25° and agitated by rotating slowly for 19 hr. The contents of the tube were then centrifuged[5] for 25 min, and the precipitate (A) was collected, dried, and weighed (0.00328 g).

The experiment was repeated using III (0.00524 g) and water (5.0 ml) to give a product (B) weighing 0.00355 g. The mass spectra from *m/e* 240 to 324 of products A, B, and acronine were determined using an expanded scale recorder. The intensities of the ions were measured, and peaks shorter than 5 mm were ignored. The abundance of ions was corrected for background intensities.

In the first experiment, the mass spectra of A, B, and acronine were determined at 120° under identical conditions, and the intensity of the *m/e* 323 ion was expressed as a percentage of the sum of the intensities of the ions from *m/e* 240 to 324. Five determinations for A and acronine and four for B were made. The relative intensity of the ion at *m/e* 323 for A, B, and acronine was 1.418% (range of 1.391–1.441%), 0.519% (range of 0.501–0.545%), and 0.513% (range of 0.483–0.552%), respectively.

In another experiment, acronine was placed in 5.0 ml of water containing 38.0 atom % $H_2{}^{18}O$ and rotated for 19 hr at 25° as described previously. The intensity of the ion at *m/e* 323 compared to the intensities of the ions from *m/e* 240 to 324, expressed as a percentage for both the compound suspended in ^{18}O-labeled water for 19 hr and an authentic sample of acronine, was 0.614% (range of 0.583–0.654%) and 0.575% (range

[2] Mass spectra were determined by Mr. R. Drake of the Department of Chemistry, University of Kansas, by direct sample introduction using a Varian CH-5 instrument operating at 70 ev. Water enriched with ^{18}O-labeled water contained 40.0 atom % ^{18}O obtained from Bio-Rad Laboratories, Richmond, CA 94604.

[3] The remaining 28% of the sample consisted of acronine and acroninium perchlorate.

[4] Bransonic model 220.

[5] International clinical model CL.

of 0.523–0.603%), respectively. Five mass spectra for each compound were determined at 120°.

Ten spectra from *m/e* 240 to 324 were then run at 111° for A and B under identical conditions. The intensities of the ions at *m/e* 323 were compared to those at *m/e* 321 for A and B using the formula $[(M + 2)/M + (M + 2)] \times 100\%$, where M + 2 and M were the intensities of the ions at *m/e* 323 and 321, respectively. The values for A and B were 11.3 and 3.4%, respectively. The percentage hydrolysis proceeding *via* aryl oxygen cleavage, 28.9%, was obtained from the expression $[(11.3 - 3.4)/(38 \times 0.72)] \times 100$, 38 and 0.72 being the atom percent of $H_2{}^{18}O$ and the fractional purity of II, respectively. The intensities of the ions at *m/e* 308 and 306 were evaluated similarly, and the percentage of aryl ester cleavage was 28.0%.

REFERENCES

(1) G. H. Svoboda, G. A. Poore, P. J. Simpson, and G. B. Boder, *J. Pharm. Sci.*, **55**, 758 (1966).

(2) C. A. Hewitt, Stanford Research Institute Reports to the National Cancer Institute, Numbers 758 and 770, Palo Alto, Calif., 1968.

(3) G. H. Svoboda, M. J. Sweeney, and W. D. Walkling, *J. Pharm. Sci.*, **60**, 333 (1971).

(4) D. W. A. Bourne, Ph.D. thesis, University of Kansas, Lawrence, Kans., 1974.

(5) D. W. A. Bourne, T. Higuchi, and A. J. Repta, *J. Pharm. Sci.*, **66**, 628 (1977).

(6) C.-H. Huang, B. Kreilgard, and A. J. Repta, *Bull. Parent. Drug Assoc.*, **30**, 1 (1976).

ACKNOWLEDGMENTS AND ADDRESSES

Received September 13, 1976, from the *Department of Pharmaceutical Chemistry, School of Pharmacy, University of Kansas, Lawrence, KS 66044.*

Accepted for publication January 11, 1977.

Presented in part at the Basic Pharmaceutics Section, APhA Academy of Pharmaceutical Sciences, Orlando meeting, November 1976.

Supported in part by Contract N01-CM-23217 from the Division of Cancer Treatment, National Cancer Institute, National Institutes of Health.

The authors acknowledge the technical assistance of Wanda Waugh.

* On sabbatical leave from the College of Pharmacy, University of Saskatchewan, Saskatoon, Saskatchewan, Canada.

‡ On leave from the Royal Danish School of Pharmacy, Copenhagen, Denmark. B. Kreilgård gratefully acknowledges partial financial support from the Danish Medical Research council.

§ Present address: INTERx Research Corp., Lawrence, KS 66044.

ˣ To whom inquiries should be directed.

New Rapid Determination of Pyridoxal Phosphate Using Tyrosine Phenol-lyase

G. G. MEADOWS, L. BOZE, and G. W. ELMER ˣ

Abstract □ A rapid, specific, and precise spectrophotometric assay for the determination of pyridoxal phosphate is described.The assay allows for the determination of the cofactor between 0.1 and 1.0 μg/ml. Its applicability to pyridoxal phosphate in biological fluids was demonstrated by a determination of the plasma half-life in BDF_1 mice. Pyridoxal phosphate is absorbed rapidly from the peritoneal cavity and cleared from the plasma with a half-life of about 15 min.

Keyphrases □ Pyridoxal phosphate—spectrophotometric analysis, biological fluids □ Spectrophotometry—analysis, pyridoxal phosphate in biological fluids □ Enzyme cofactors—pyridoxal phosphate, spectrophotometric analysis in biological fluids

Pyridoxal phosphate is a cofactor for several enzymes that participate in amino acid metabolism (1). Because of this metabolic significance, there is considerable interest in quantitating both suboptimal and elevated plasma pyridoxal phosphate levels. The latter interest stems from the observation that megadoses of pyridoxine have beneficial therapeutic effects in certain vitamin-responsive genetic diseases (2, 3). Increased circulating levels of pyridoxal phosphate may also be of benefit in enhancing the antitumor activity of several pyridoxal phosphate-dependent enzymes such as methioninase (4, 5) and tyrosine phenol-lyase (6).

To elevate pyridoxal phosphate levels in mice in a previous study (6), large amounts of the cofactor were injected. To quantitate and follow the fate of exogenously administered pyridoxal phosphate in mice, a rapid assay utilizing tyrosine phenol-lyase was developed. Although other enzymatic assays specific for pyridoxal phosphate were reported (7–9), they are hampered by the fact that radionuclides and/or extraction of the cofactor are required. These procedures can be both time consuming and costly. The described assay utilizes pyridoxal phosphate-dependent tyrosine phenol-lyase in a coupled reaction with lactate dehydrogenase and NADH. Pyridoxal phosphate levels can be easily and rapidly ascertained by spectrophotometric measurements.

EXPERIMENTAL

Materials—Tyrosine phenol-lyase was purified from *Erwinia herbicola* (ATCC 21434) as described (6). When purified by this method, the enzyme has less than 2% of maximal activity in the absence of pyridoxal phosphate. Pig heart lactate dehydrogenase[1], A grade pyridoxal 5′-phosphate[1], and NADH[1] were used in the coupled assay. All other reagents were analytical grade.

Pyridoxal Phosphate Assay Procedure—Tyrosine phenol-lyase catalyzes tyrosine degradation to pyruvate, phenol, and ammonia. The enzyme activity was determined using the continuous spectrophotometric assay previously reported (6), except that the enzyme was preincubated with the pyridoxal phosphate, lactate dehydrogenase, and NADH for 10 min at 37° prior to addition of tyrosine. The assay measures the formation rate of pyruvate by a coupled reaction using lactate dehydrogenase and NADH. Oxidation of NADH is followed spectrophotometrically. One international unit (IU) of enzyme activity is defined as the amount of enzyme that catalyzes the formation of 1 μmole of product/min.

An adaptation of this assay was used for pyridoxal phosphate. Samples containing pyridoxal phosphate (0.5 ml) were preincubated for 10 min with 0.05 IU of tyrosine phenol-lyase (0.5 ml), 200 μmoles of NADH (0.5 ml), and 1.0 IU of lactate dehydrogenase (0.5 ml). Then 2.5 μmoles of

[1] Calbiochem, Los Angeles, Calif.

of 0.523–0.603%), respectively. Five mass spectra for each compound were determined at 120°.

Ten spectra from *m/e* 240 to 324 were then run at 111° for A and B under identical conditions. The intensities of the ions at *m/e* 323 were compared to those at *m/e* 321 for A and B using the formula $[(M + 2)/M + (M + 2)] \times 100\%$, where M + 2 and M were the intensities of the ions at *m/e* 323 and 321, respectively. The values for A and B were 11.3 and 3.4%, respectively. The percentage hydrolysis proceeding *via* aryl oxygen cleavage, 28.9%, was obtained from the expression $[(11.3 - 3.4)/(38 \times 0.72)] \times 100$, 38 and 0.72 being the atom percent of $H_2{}^{18}O$ and the fractional purity of II, respectively. The intensities of the ions at *m/e* 308 and 306 were evaluated similarly, and the percentage of aryl ester cleavage was 28.0%.

REFERENCES

(1) G. H. Svoboda, G. A. Poore, P. J. Simpson, and G. B. Boder, *J. Pharm. Sci.*, **55**, 758 (1966).

(2) C. A. Hewitt, Stanford Research Institute Reports to the National Cancer Institute, Numbers 758 and 770, Palo Alto, Calif., 1968.

(3) G. H. Svoboda, M. J. Sweeney, and W. D. Walkling, *J. Pharm. Sci.*, **60**, 333 (1971).

(4) D. W. A. Bourne, Ph.D. thesis, University of Kansas, Lawrence, Kans., 1974.

(5) D. W. A. Bourne, T. Higuchi, and A. J. Repta, *J. Pharm. Sci.*, **66**, 628 (1977).

(6) C.-H. Huang, B. Kreilgard, and A. J. Repta, *Bull. Parent. Drug Assoc.*, **30**, 1 (1976).

ACKNOWLEDGMENTS AND ADDRESSES

Received September 13, 1976, from the *Department of Pharmaceutical Chemistry, School of Pharmacy, University of Kansas, Lawrence, KS 66044.*

Accepted for publication January 11, 1977.

Presented in part at the Basic Pharmaceutics Section, APhA Academy of Pharmaceutical Sciences, Orlando meeting, November 1976.

Supported in part by Contract N01-CM-23217 from the Division of Cancer Treatment, National Cancer Institute, National Institutes of Health.

The authors acknowledge the technical assistance of Wanda Waugh.

* On sabbatical leave from the College of Pharmacy, University of Saskatchewan, Saskatoon, Saskatchewan, Canada.

‡ On leave from the Royal Danish School of Pharmacy, Copenhagen, Denmark. B. Kreilgård gratefully acknowledges partial financial support from the Danish Medical Research council.

§ Present address: INTERx Research Corp., Lawrence, KS 66044.

ˣ To whom inquiries should be directed.

New Rapid Determination of Pyridoxal Phosphate Using Tyrosine Phenol-lyase

G. G. MEADOWS, L. BOZE, and G. W. ELMER ˣ

Abstract □ A rapid, specific, and precise spectrophotometric assay for the determination of pyridoxal phosphate is described.The assay allows for the determination of the cofactor between 0.1 and 1.0 μg/ml. Its applicability to pyridoxal phosphate in biological fluids was demonstrated by a determination of the plasma half-life in BDF_1 mice. Pyridoxal phosphate is absorbed rapidly from the peritoneal cavity and cleared from the plasma with a half-life of about 15 min.

Keyphrases □ Pyridoxal phosphate—spectrophotometric analysis, biological fluids □ Spectrophotometry—analysis, pyridoxal phosphate in biological fluids □ Enzyme cofactors—pyridoxal phosphate, spectrophotometric analysis in biological fluids

Pyridoxal phosphate is a cofactor for several enzymes that participate in amino acid metabolism (1). Because of this metabolic significance, there is considerable interest in quantitating both suboptimal and elevated plasma pyridoxal phosphate levels. The latter interest stems from the observation that megadoses of pyridoxine have beneficial therapeutic effects in certain vitamin-responsive genetic diseases (2, 3). Increased circulating levels of pyridoxal phosphate may also be of benefit in enhancing the antitumor activity of several pyridoxal phosphate-dependent enzymes such as methioninase (4, 5) and tyrosine phenol-lyase (6).

To elevate pyridoxal phosphate levels in mice in a previous study (6), large amounts of the cofactor were injected. To quantitate and follow the fate of exogenously administered pyridoxal phosphate in mice, a rapid assay utilizing tyrosine phenol-lyase was developed. Although other enzymatic assays specific for pyridoxal phosphate were reported (7–9), they are hampered by the fact that radionuclides and/or extraction of the cofactor are required. These procedures can be both time consuming and costly. The described assay utilizes pyridoxal phosphate-dependent tyrosine phenol-lyase in a coupled reaction with lactate dehydrogenase and NADH. Pyridoxal phosphate levels can be easily and rapidly ascertained by spectrophotometric measurements.

EXPERIMENTAL

Materials—Tyrosine phenol-lyase was purified from *Erwinia herbicola* (ATCC 21434) as described (6). When purified by this method, the enzyme has less than 2% of maximal activity in the absence of pyridoxal phosphate. Pig heart lactate dehydrogenase[1], A grade pyridoxal 5′-phosphate[1], and NADH[1] were used in the coupled assay. All other reagents were analytical grade.

Pyridoxal Phosphate Assay Procedure—Tyrosine phenol-lyase catalyzes tyrosine degradation to pyruvate, phenol, and ammonia. The enzyme activity was determined using the continuous spectrophotometric assay previously reported (6), except that the enzyme was preincubated with the pyridoxal phosphate, lactate dehydrogenase, and NADH for 10 min at 37° prior to addition of tyrosine. The assay measures the formation rate of pyruvate by a coupled reaction using lactate dehydrogenase and NADH. Oxidation of NADH is followed spectrophotometrically. One international unit (IU) of enzyme activity is defined as the amount of enzyme that catalyzes the formation of 1 μmole of product/min.

An adaptation of this assay was used for pyridoxal phosphate. Samples containing pyridoxal phosphate (0.5 ml) were preincubated for 10 min with 0.05 IU of tyrosine phenol-lyase (0.5 ml), 200 μmoles of NADH (0.5 ml), and 1.0 IU of lactate dehydrogenase (0.5 ml). Then 2.5 μmoles of

[1] Calbiochem, Los Angeles, Calif.

Table I—Comparative Activation of Tyrosine Phenol-lyase by Pyridoxal Phosphate Incubated in Plasma or Buffer

Pyridoxal Phosphate Incubation Time, hr	Ratio of Enzyme Activity in Plasma to Buffer
0.0	1.00
0.5	0.96
1.0	1.00
3.0	0.96
8.0	0.66
12.0	0.45
23.0	0.20

L-tyrosine and 150 μmoles of pH 7.4 potassium phosphate buffer (1 ml) were added to start the reaction, which was run at 37°. The rate of decrease in absorbance of NADH at 340 nm was used to calculate the enzyme activity. All values were corrected for any activity of the tyrosine phenol-lyase obtained in the absence of pyridoxal phosphate (<2% of maximal activity).

Effect of Plasma on Pyridoxal Phosphate Assay—Pyridoxal phosphate (10 μg/ml) was incubated at 37° in mouse plasma and in 0.01 *M* potassium phosphate buffer (pH 7.4) for the indicated time (Table I). Sodium azide (0.025%), which had no effect on enzyme activity, was added to inhibit bacterial growth. The mouse plasma used was obtained from BDF_1[2] female mice by orbital bleeding (10) just prior to use. Aliquots were removed at the indicated times, diluted 1:10 with 0.01 *M* potassium phosphate buffer (pH 7.4), and assayed for pyridoxal phosphate.

Pyridoxal Phosphate Half-Life Determination—BDF_1 female mice, 18–26 g, were housed in metal cages, four mice to a cage. Food[3] and water were available *ad libitum* prior to the pyridoxal phosphate injection, and then only water was available. All mice were injected with 50 mg of pyridoxal phosphate/kg ip in 0.01 *M* potassium phosphate buffer (pH 7.4). The injection volume was about 0.2 ml.

At the indicated times, blood samples from four mice were removed by orbital bleeding (10) and transferred to prechilled heparinized tubes. Each sample was centrifuged at 4° for 10 min, and the plasma was appropriately diluted and assayed for pyridoxal phosphate.

RESULTS AND DISCUSSION

Under these conditions, the enzyme activity was linear over the range of 0.1–1.0 μg of pyridoxal phosphate/ml. The coefficients of variation for triplicate samples of pyridoxal phosphate in 0.01 *M* potassium phosphate buffer (pH 7.4) were 13.3% at 0.1 μg/ml, 8% at 0.2 μg/ml, 6.1% at 0.4 μg/ml, 3.9% at 0.8 μg/ml, and 5.2% at 1.0 μg/ml. The data indicate that this assay provides a precise determination of the cofactor between 0.1 and 1.0 μg/ml. In addition, values can be obtained rapidly with a minimum amount of equipment. A single determination, depending on the pyridoxal phosphate concentration, can be completed within 5–20 min.

To measure the *in vivo* half-life of pyridoxal phosphate in mice, it was necessary to ascertain whether plasma interfered with the assay. Because almost all circulating pyridoxal phosphate is bound to plasma proteins, particularly albumin (11–13), it was necessary to distinguish between removal of the injected cofactor through binding to plasma proteins and removal by metabolism. The results in Table I demonstrate that recovery of cofactor added to plasma is complete provided the plasma pyridoxal phosphate incubation period is within 3 hr. Substantially longer incubation periods resulted in diminished recovery values.

This lower recovery is interpreted as resulting in part from a slow binding of pyridoxal phosphate to plasma proteins and the inability of tyrosine phenol-lyase to utilize protein-bound cofactor completely. Indeed, an albumin–pyridoxal phosphate complex (1:1), when used as a source of cofactor for the enzyme, resulted in a reduction of enzyme activity to 64% of maximal[4]. Masugi *et al.* (14) reported that albumin-bound pyridoxal phosphate was also not as effective as unbound pyridoxal phosphate in activating apoaspartate amino transferase. Pyridoxal phosphate determinations on samples containing substantial amounts of protein-bound cofactor would, therefore, require an extraction step (9) prior to the effective use of the tyrosine phenol-lyase assay procedure.

[2] Charles River Breeding Laboratories, Wilmington, Mass.
[3] Purina Laboratory Chow.
[4] Unpublished results.

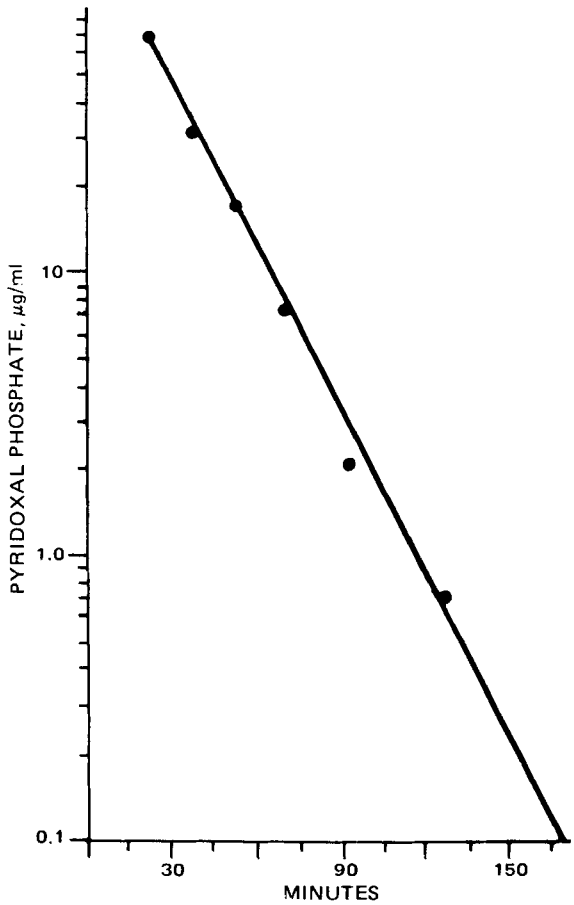

Figure 1—*Plasma clearance of pyridoxal phosphate following administration of 50 mg/kg ip to BDF_1 female mice.*

Plasma pyridoxal phosphate levels following a single injection into BDF_1 mice are shown in Fig. 1. The results demonstrate that the cofactor is absorbed very rapidly when administered by intraperitoneal injection and is cleared from plasma with a half-life of about 15 min. Since all measurements were made within 3 hr, the data reflect true clearance from the plasma rather than binding to plasma proteins. This rapid clearance may be a result of hydrolysis of pyridoxal phosphate to pyridoxal by an alkaline phosphatase (15–17).

The described assay is rapid and convenient for measuring elevated levels of pyridoxal phosphate in laboratory animals and may be useful for monitoring blood levels of this cofactor when megadoses are administered.

REFERENCES

(1) H. E. Sauberlich, in "The Vitamins," vol. 2, W. H. Sebrell and R. S. Harris, Eds., Academic, New York, N.Y., 1968, p. 44.
(2) S. H. Mudd, *Fed. Proc.*, **30**, 970 (1971).
(3) C. R. Scriver, *Metabolism*, **22**, 1319 (1973).
(4) W. Kreis and C. Hession, *Cancer Res.*, **33**, 1862 (1973).
(5) *Ibid.*, **33**, 1866 (1973).
(6) G. G. Meadows, J. DiGiovanni, L. Minor, and G. W. Elmer, *Cancer Res.*, **36**, 167 (1976).
(7) P. R. Sundaresan and D. B. Coursin, in "Methods in Enzymology," vol. XVIII, D. B. McCormick and L. D. Wright, Eds., Academic, New York, N.Y., 1970, p. 509.
(8) K. Okuda, S. Fujii, and M. Wada, in *ibid.*, p. 505.
(9) H. I. Pierce, C. Campbell, E. Moore, and R. S. Hillman, *Biochem. Med.*, **10**, 360 (1974).
(10) V. Riley, *Proc. Soc. Exp. Biol. Med.*, **104**, 751 (1970).
(11) L. Lumeng, R. E. Brashear, and T. Li, *J. Lab. Clin. Med.*, **84**, 334 (1974).
(12) W. B. Dempsey and H. N. Christensen, *J. Biol. Chem.*, **237**, 1113 (1962).
(13) B. B. Anderson, P. A. Newmark, M. Rawlins, and R. Green, *Nature*, **250**, 502 (1974).

(14) F. Masugi, Y. Sumi, S. Shimeyer, and S. Fukui, *J. Nutr. Sci. Vitaminol.*, **19**, 229 (1973).

(15) T. Li, L. Lumeng, and R. L. Veitch, *Biochem. Biophys. Res. Commun.*, **61**, 677 (1974).

(16) J. M. Turner, *Biochem. J.*, **80**, 663 (1961).

(17) L. Lumeng and T. Li, *J. Biol. Chem.*, **250**, 8126 (1975).

ACKNOWLEDGMENTS AND ADDRESSES

Received December 22, 1975, from the *Department of Pharmaceutical Sciences, School of Pharmacy, University of Washington, Seattle, WA 98195.*

Accepted for publication January 12, 1977.

[x] To whom inquiries should be directed.

New Compounds: Organoboron Derivatives of Tetracyclines I: Synthesis of Carboxamido Derivative of Tetracycline with Perhydro-2-phenyl-1,3,6,2-dioxazaborocine

CHARLES W. ROSCOE [x], JOHN W. PHILLIPS [*], and WILLIAM C. GILLCHRIEST [‡]

Abstract □ An organoboron carboxamido derivative of tetracycline, designed for use in the $^{10}_{5}B$-thermal neutron-capture treatment of cancer, was synthesized under the conditions of the Mannich reaction using perhydro-2-phenyl-1,3,6,2-dioxazaborocine as the amine component. Spectral data (UV, IR, and NMR) for the compound and its hydrolytic stability are discussed.

Keyphrases □ Organoboron compounds—carboxamido derivative of tetracycline synthesized, UV, IR, and NMR spectral data and hydrolytic stability evaluated □ Tetracyclines—organoboron carboxamido derivative synthesized, UV, IR, and NMR spectral data and hydrolytic stability evaluated □ Antineoplastic agents, potential—organoboron carboxamido derivative of tetracycline synthesized, UV, IR, and NMR spectral data and hydrolytic stability evaluated

The avidity of the tetracycline antibiotics for various types of neoplastic cells (1–17) suggested their possible use as carrier molecules for selectively localizing the neutron-absorbing isotope of boron, $^{10}_{5}B$, in malignant tumors. The potential therapeutic value of boron thermal neutron capture *in situ* was first discussed by Locher (18) in 1936.

BACKGROUND

Successful use of a boron compound in the neutron-capture treatment of cancer requires its selective uptake by neoplastic cells and its retention for a sufficient period to allow for the clearance of the compound from other body tissues prior to thermal neutron exposure (19–21). Boron was recognized early as an ideal element for this purpose because of the large neutron-capture cross section of its naturally occurring $^{10}_{5}B$-isotope. The energy released from the neutron-capture reaction, $^{10}_{5}B + {}^{1}_{0}n \rightarrow [^{11}_{5}B] \rightarrow {}^{7}_{3}Li + {}^{4}_{2}He + 2.4$ Mev, where $^{1}_{0}n$ represents thermal or slow neutrons having energies of about 0.025 ev, is sufficient to cause localized destruction of boron-containing tumor cells.

Numerous reports on the preparation and evaluation of organoboron compounds for possible use in the neutron-capture treatment of cancer have appeared. With few exceptions, however, the results have been disappointing, primarily because the compounds lacked the necessary specificity to achieve acceptable ratios of tumor to normal tissue boron concentrations.

Because of the specific binding of tetracycline to ribosomes (22–28), tetracycline should be an ideal vehicle for transporting the fissionable element to rapidly proliferating neoplastic cells. Although the precise nature of the interaction between tetracycline and ribosomes remains to be established (24), suitable boronated derivatives might exhibit similar ribosomal binding characteristics. On this basis, the design and syntheses of boron-containing derivatives of the tetracyclines were undertaken. One borocine derivative[1] showed potential in neutron-capture experiments with adenocarcinoma-bearing mice (29), and the results of a human neoplastic cell culture study (30) suggested that the compound might be interacting at the ribosomal level.

The subject of this report is the synthesis of a new borocine Mannich-base derivative of tetracycline, characterized as 4-dimethylamino - 1,4,4a,5,5a,6,11,12a-octahydro-3,6,10,12,12a-pentahydroxy-6-methyl-1,11-dioxo-*N*-[(perhydro-2-phenyl-1,3,6,2-dioxazaborocin -6-yl)methyl]-2-naphthacenecarboxamide (III). The Mannich base was prepared from tetracycline (I), perhydro-2-phenyl-1,3,6,2-dioxazaborocine (II), and paraformaldehyde, $(CH_2O)_n$, using a modification of the methods of Gottstein *et al.* (31) for preparing carboxamido derivatives of I (Scheme I).

EXPERIMENTAL[2]

Perhydro-2-phenyl-1,3,6,2-dioxazaborocine (II)—This compound was prepared according to the method of Musgrave and Park (32) from 2,2′-iminodiethanol and phenylboronic acid, mp 214° [lit. mp 209.5–210° (32) and 214–215° (33)]; IR (KBr): ν_{max} 3100 (NH), 2900, 2850 (CH), 1200 (N → B) (34), 1175 (CO), 920 (N → B) (34), 750, and 705 (Ar) cm^{-1}; NMR (deuteromethanol): δ 2.55–3.17 (m, 4H), 3.47–4.10 (m, 4H), 4.77 (s, 1H), and 7.07–7.67 (m, 5H) ppm.

Compound III—A mixture of 4.32 g (8.68 mmoles) of I, 1.66 g (8.68 mmoles) of II, and 0.312 g (10.4 mmoles) of paraformaldehyde in 200 ml of absolute ethanol was gradually heated to reflux with stirring over 1 hr; nearly all solids dissolved during this time. The hot mixture was filtered, and the filtrate, after standing in the cold overnight, yielded 4.75 g (80%) of III as a water-soluble (~25%), yellow, amorphous solid, mp 300° dec.; $[\alpha]_D^{25}$ −156° (c 0.907, water); UV (methanol): λ 268 (log *a* 4.31) and 366 (4.26) nm.

Anal.—Calc. for $C_{33}H_{38}BN_3O_{10}\cdot 2H_2O$: C, 57.99; H, 6.19; B, 1.58; N, 6.16. Found: C, 58.09; H, 6.16; B, 1.49; N, 5.97. Equivalent weight by titration (perchloric acid in acetic acid) is 340, and water content (Karl Fischer) is 5.5% ($C_{33}H_{38}BN_3O_{10}\cdot 2H_2O$, mol. wt. 683.53, requires 342 and 5.3%, respectively).

[1] The chemical characterization of this compound will be the subject of another report.

[2] Melting points were determined on a Kofler micro hot stage and are uncorrected. Elemental analyses were performed by the Galbraith Laboratories, Knoxville, Tenn. UV and IR spectra were recorded on Hitachi P-E 139 and Beckman IR-5A and IR-10 spectrophotometers. NMR spectra were recorded on Varian A-60 and T-60 instruments with tetramethylsilane as the internal standard. Mass spectra were recorded on an A.E.I. MS9 instrument.

(14) F. Masugi, Y. Sumi, S. Shimeyer, and S. Fukui, *J. Nutr. Sci. Vitaminol.*, **19**, 229 (1973).

(15) T. Li, L. Lumeng, and R. L. Veitch, *Biochem. Biophys. Res. Commun.*, **61**, 677 (1974).

(16) J. M. Turner, *Biochem. J.*, **80**, 663 (1961).

(17) L. Lumeng and T. Li, *J. Biol. Chem.*, **250**, 8126 (1975).

ACKNOWLEDGMENTS AND ADDRESSES

Received December 22, 1975, from the *Department of Pharmaceutical Sciences, School of Pharmacy, University of Washington, Seattle, WA 98195.*

Accepted for publication January 12, 1977.

[x] To whom inquiries should be directed.

New Compounds: Organoboron Derivatives of Tetracyclines I: Synthesis of Carboxamido Derivative of Tetracycline with Perhydro-2-phenyl-1,3,6,2-dioxazaborocine

CHARLES W. ROSCOE [x], JOHN W. PHILLIPS [*], and WILLIAM C. GILLCHRIEST [‡]

Abstract □ An organoboron carboxamido derivative of tetracycline, designed for use in the $^{10}_{5}B$-thermal neutron-capture treatment of cancer, was synthesized under the conditions of the Mannich reaction using perhydro-2-phenyl-1,3,6,2-dioxazaborocine as the amine component. Spectral data (UV, IR, and NMR) for the compound and its hydrolytic stability are discussed.

Keyphrases □ Organoboron compounds—carboxamido derivative of tetracycline synthesized, UV, IR, and NMR spectral data and hydrolytic stability evaluated □ Tetracyclines—organoboron carboxamido derivative synthesized, UV, IR, and NMR spectral data and hydrolytic stability evaluated □ Antineoplastic agents, potential—organoboron carboxamido derivative of tetracycline synthesized, UV, IR, and NMR spectral data and hydrolytic stability evaluated

The avidity of the tetracycline antibiotics for various types of neoplastic cells (1–17) suggested their possible use as carrier molecules for selectively localizing the neutron-absorbing isotope of boron, $^{10}_{5}B$, in malignant tumors. The potential therapeutic value of boron thermal neutron capture *in situ* was first discussed by Locher (18) in 1936.

BACKGROUND

Successful use of a boron compound in the neutron-capture treatment of cancer requires its selective uptake by neoplastic cells and its retention for a sufficient period to allow for the clearance of the compound from other body tissues prior to thermal neutron exposure (19–21). Boron was recognized early as an ideal element for this purpose because of the large neutron-capture cross section of its naturally occurring $^{10}_{5}B$-isotope. The energy released from the neutron-capture reaction, $^{10}_{5}B + {}^{1}_{0}n \rightarrow [^{11}_{5}B] \rightarrow {}^{7}_{3}Li + {}^{4}_{2}He + 2.4$ Mev, where $^{1}_{0}n$ represents thermal or slow neutrons having energies of about 0.025 ev, is sufficient to cause localized destruction of boron-containing tumor cells.

Numerous reports on the preparation and evaluation of organoboron compounds for possible use in the neutron-capture treatment of cancer have appeared. With few exceptions, however, the results have been disappointing, primarily because the compounds lacked the necessary specificity to achieve acceptable ratios of tumor to normal tissue boron concentrations.

Because of the specific binding of tetracycline to ribosomes (22–28), tetracycline should be an ideal vehicle for transporting the fissionable element to rapidly proliferating neoplastic cells. Although the precise nature of the interaction between tetracycline and ribosomes remains to be established (24), suitable boronated derivatives might exhibit similar ribosomal binding characteristics. On this basis, the design and syntheses of boron-containing derivatives of the tetracyclines were undertaken. One borocine derivative[1] showed potential in neutron-capture experiments with adenocarcinoma-bearing mice (29), and the results of a human neoplastic cell culture study (30) suggested that the compound might be interacting at the ribosomal level.

The subject of this report is the synthesis of a new borocine Mannich-base derivative of tetracycline, characterized as 4-dimethylamino - 1,4,4a,5,5a,6,11,12a-octahydro-3,6,10,12,12a-pentahydroxy-6-methyl-1,11-dioxo-*N*-[(perhydro-2-phenyl-1,3,6,2-dioxazaborocin -6-yl)methyl]-2-naphthacenecarboxamide (III). The Mannich base was prepared from tetracycline (I), perhydro-2-phenyl-1,3,6,2-dioxazaborocine (II), and paraformaldehyde, $(CH_2O)_n$, using a modification of the methods of Gottstein *et al.* (31) for preparing carboxamido derivatives of I (Scheme I).

EXPERIMENTAL[2]

Perhydro-2-phenyl-1,3,6,2-dioxazaborocine (II)—This compound was prepared according to the method of Musgrave and Park (32) from 2,2′-iminodiethanol and phenylboronic acid, mp 214° [lit. mp 209.5–210° (32) and 214–215° (33)]; IR (KBr): ν_{max} 3100 (NH), 2900, 2850 (CH), 1200 (N → B) (34), 1175 (CO), 920 (N → B) (34), 750, and 705 (Ar) cm^{-1}; NMR (deuteromethanol): δ 2.55–3.17 (m, 4H), 3.47–4.10 (m, 4H), 4.77 (s, 1H), and 7.07–7.67 (m, 5H) ppm.

Compound III—A mixture of 4.32 g (8.68 mmoles) of I, 1.66 g (8.68 mmoles) of II, and 0.312 g (10.4 mmoles) of paraformaldehyde in 200 ml of absolute ethanol was gradually heated to reflux with stirring over 1 hr; nearly all solids dissolved during this time. The hot mixture was filtered, and the filtrate, after standing in the cold overnight, yielded 4.75 g (80%) of III as a water-soluble (~25%), yellow, amorphous solid, mp 300° dec.; $[\alpha]_D^{25}$ −156° (c 0.907, water); UV (methanol): λ 268 (log *a* 4.31) and 366 (4.26) nm.

Anal.—Calc. for $C_{33}H_{38}BN_3O_{10}\cdot 2H_2O$: C, 57.99; H, 6.19; B, 1.58; N, 6.16. Found: C, 58.09; H, 6.16; B, 1.49; N, 5.97. Equivalent weight by titration (perchloric acid in acetic acid) is 340, and water content (Karl Fischer) is 5.5% ($C_{33}H_{38}BN_3O_{10}\cdot 2H_2O$, mol. wt. 683.53, requires 342 and 5.3%, respectively).

[1] The chemical characterization of this compound will be the subject of another report.

[2] Melting points were determined on a Kofler micro hot stage and are uncorrected. Elemental analyses were performed by the Galbraith Laboratories, Knoxville, Tenn. UV and IR spectra were recorded on Hitachi P-E 139 and Beckman IR-5A and IR-10 spectrophotometers. NMR spectra were recorded on Varian A-60 and T-60 instruments with tetramethylsilane as the internal standard. Mass spectra were recorded on an A.E.I. MS9 instrument.

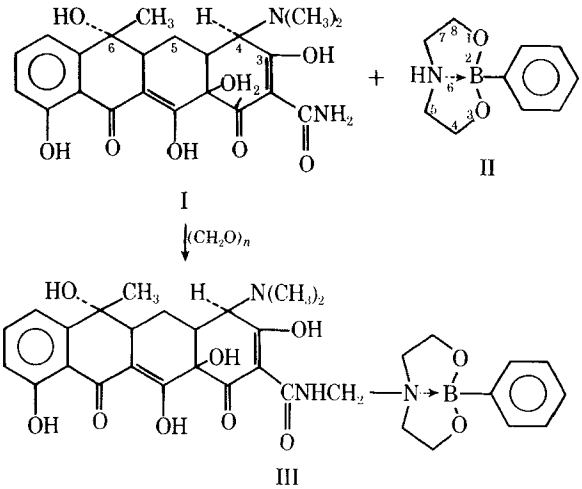

Scheme I

RESULTS AND DISCUSSION

The partial NMR spectra of I and III in deuteropyridine are shown in Fig. 1. The chemical shifts observed for the protons of the C-6 methyl and C-4 dimethylamino groups (δ 1.75 and 2.51) of I were in excellent agreement with previously published values (35). The broad singlet centered at δ 2.54 (6H) and assigned to the methyl protons of the C-4 dimethylamino group of III was partially overlaid by the downfield multiplet due to the C-5 and C-7 methylene protons of the borocine ring of II. The unobstructed broad singlet centered at δ 4.39 (2H) in the spectrum of III was assigned to the methylene protons of the NCH_2N group (calculated value, δ 4.25). This assignment is supported by NMR studies on model Mannich bases[3].

Overlapping of absorption bands in the IR spectrum of III virtually precluded definitive assignments of group frequencies. For example, the expected differences in absorption in the 1700–1500-cm^{-1} region due to the secondary amido group of III as compared to that of the primary amido group of I were obscured by extensive overlapping of bands (Fig. 2). However, with a sample of I in the reference beam, a difference

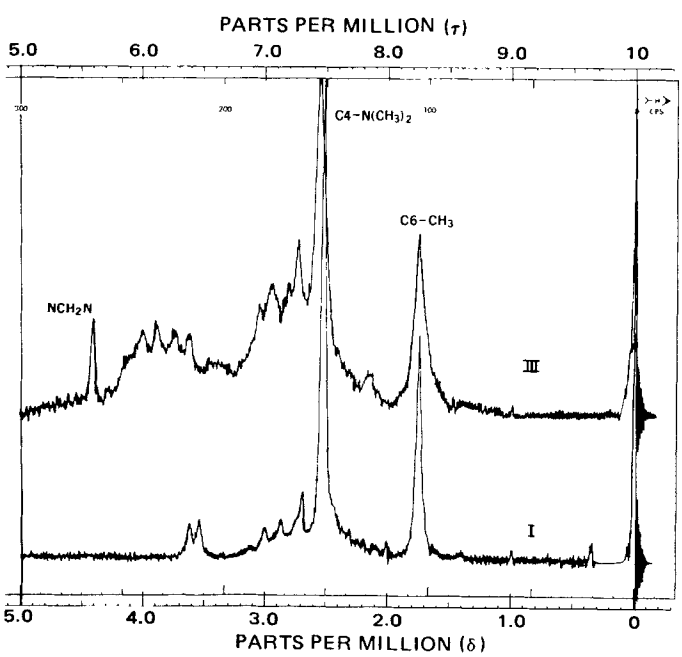

Figure 1—*Partial NMR spectra (deuteropyridine) of I (lower curve) and III (upper curve).*

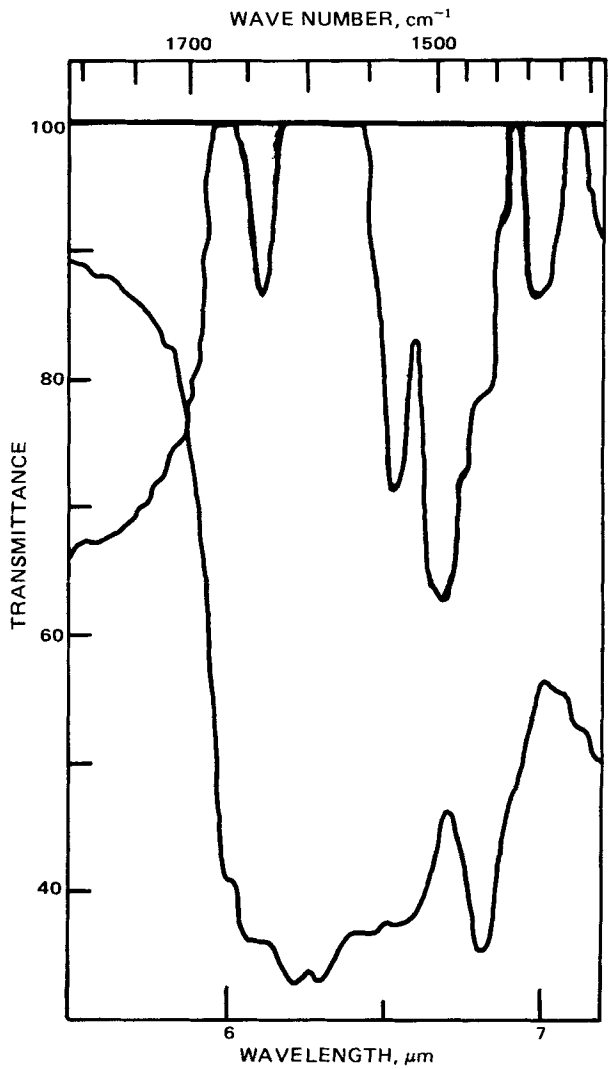

Figure 2—*Partial IR spectrum of III (lower curve) and its difference spectrum (upper curve).*

spectrum (Fig. 2) was obtained that clearly showed maxima at 1640 and 1530 cm^{-1}, to which the amide I and amide II bands, respectively, of the secondary amido group were assigned (36).

Except for slight differences in a_{max} values, the UV spectrum of III is identical to that of I. This finding has been taken as evidence that alkylation of the phenolic D ring of I did not occur as an alternative to alkylation of the amido group, since the former reaction could be expected to cause a detectable bathochromic shift of the aromatic B band.

Aqueous solutions of III changed in color from yellow to reddish-brown on standing at room temperature and unprotected from light for more than a few days. That these changes were preceded by hydrolysis was demonstrated clearly by changes in the NMR spectra of the solutions with time. In the presence of acid, the hydrolysis rate was accelerated greatly. For example, almost complete hydrolysis occurred when an aqueous solution of III (pH ~ 7) was adjusted to pH 2–3 with hydrochloric acid. This pH resulted in the precipitation of phenylboronic acid. Adjustment of the filtrate to pH 6 resulted in the precipitation of pure I. Further adjustment of the filtrate to pH 7 resulted in the precipitation of an additional small amount of I contaminated with III. The identity of recovered I was established by comparison of its melting point and IR, NMR, and mass spectra (70 ev), *m/e* 444 (M^+), with those of an authentic sample. Attempts to obtain a mass spectrum of III, using the direct insertion technique, were unsuccessful.

[3] Unpublished results.

REFERENCES

(1) J. E. Ayre, *Antibiot. Chemother.*, **1**, 339 (1951).
(2) L. E. Bottiger, *ibid.*, **5**, 332 (1955).

(3) D. P. Rall, T. L. Loo, M. Lane, and M. G. Kelly, *J. Natl. Cancer Inst.*, **19,** 79 (1957).
(4) J. F. McLeay, *Am. J. Surg.*, **96,** 415 (1958).
(5) J. W. Phillips, E. G. Cobb, V. Richards, W. D. Rhodes, D. C. Loehrer, and L. J. Ritchie, *ibid.*, **100,** 384 (1960).
(6) P. S. Vossar, A. M. Saunders, and C. F. A. Culling, *Arch. Pathol.*, **69,** 613 (1960).
(7) R. A. Milch, J. E. Tobie, and R. A. Robinson, *J. Histochem. Cytochem.*, **9,** 261 (1961).
(8) J. Klinger and R. Katz, *Gastroenterology*, **41,** 29 (1961).
(9) I. Fusek, *Cesk. Neurol.*, **26,** 321 (1963).
(10) L. H. Riley, Jr., *Bull. Johns Hopkins Hosp.*, **113,** 291 (1963).
(11) N. B. Ackerman and A. S. McFee, *Surgery*, **53,** 247 (1963).
(12) A. Cabrera, J. Jurado, S. de la Pava, and J. Pickren, *N.Y. State J. Med.*, **64,** 981 (1964).
(13) L. Sandlow and N. Heinrich, *J. Am. Med. Assoc.*, **189,** 363 (1964).
(14) J. E. Ayre, J. M. LeGuerrier, and J. Arsenault, *Med. Times*, **93,** 885 (1965).
(15) P. A. Barton and W. J. Cunliffe, *Lancet*, **1,** 1002 (1966).
(16) B. L. Holman, W. D. Kaplan, and M. K. Dewanjee, *Radiology*, **112,** 147 (1974).
(17) K. Breslow, S. Halpern, F. Schwartz, N. Alazraki, and W. Ashburn, *J. Nucl. Med.*, **15,** 987 (1974).
(18) G. L. Locher, *Am. J. Roentgenol.*, **36,** 1 (1936).
(19) A. H. Soloway, in "Progress in Boron Chemistry," A. L. McCloskey and H. Steinberg, Eds., Pergamon, New York, N.Y., 1964, pp. 203–234.
(20) G. L. Brownell, A. H. Soloway, and W. H. Sweet, in "Modern Trends in Radiotherapy," T. J. Deeley and C. A. P. Wood, Eds., Butterworths, London, England, 1967, pp. 132–145.
(21) M. F. Hawthorne, R. J. Wiersema, and M. Takasugi, *J. Med. Chem.*, **15,** 449 (1972).
(22) R. H. Connamacher and H. G. Mandel, *Biochem. Biophys. Res. Commun.*, **20,** 98 (1965).
(23) J. A. Last, K. Izaki, and J. F. Snell, *Biochim. Biophys. Acta*, **103,** 532 (1965).
(24) J. A. Last, *ibid.*, **195,** 506 (1969).
(25) L. E. Day, *J. Bacteriol.*, **91,** 1917 (1966).
(26) *Ibid.*, **92,** 197 (1966).
(27) I. H. Maxwell, *Mol. Pharmacol.*, **4,** 25 (1968).
(28) R. H. Connamacher and H. G. Mandel, *Biochim. Biophys. Acta*, **166,** 475 (1968).
(29) W. C. Gillchriest and D. H. Shaw, *Oncology*, **27,** 97 (1973).
(30) J. M. LeGuerrier, J. E. Ayre, and W. C. Gillchriest, *ibid.*, **25,** 97 (1971).
(31) W. J. Gottstein, W. F. Minor, and L. C. Cheney, *J. Am. Chem. Soc.*, **81,** 1198 (1959).
(32) O. C. Musgrave and T. O. Park, *Chem. Ind.*, **1955,** 1552.
(33) R. L. Letsinger and I. Skoog, *J. Am. Chem. Soc.*, **77,** 2491 (1955).
(34) L. M. Allen and C. W. Roscoe, *J. Pharm. Sci.*, **58,** 368 (1969).
(35) M. Schach von Wittenau and R. K. Blackwood, *J. Org. Chem.*, **31,** 613 (1966).
(36) L. J. Bellamy, "The Infra-red Spectra of Complex Molecules," Wiley, New York, N.Y., 1964, pp. 209–220.

ACKNOWLEDGMENTS AND ADDRESSES

Received September 10, 1976, from the *Division of Pharmaceutical Sciences, School of Pharmacy, University of the Pacific, Stockton, CA 95211.*

Accepted for publication December 1, 1976.

Supported in part by a grant from the International Development Laboratories, Los Angeles, Calif.

The authors are indebted to Dr. Alain C. Huitric, University of Washington, Seattle, Wash., for assistance with the NMR studies and to Dr. Andrew Blair, Harborview Hospital, Seattle, Wash., for the mass spectra. The authors also thank Pfizer Co., New York, N.Y., for a generous supply of tetracycline.

* Present address: El Centro Community Hospital, El Centro, CA 92243.

‡ Present address: 11790 Bellagio Rd., Los Angeles, CA 90049.

ˣ To whom inquiries should be directed.

COMMUNICATIONS

Strain-Gauge Wheatstone Bridge Design for Automatic Capsule-Filling Machine

Keyphrases □ Capsule-filling machine, automatic—strain gauges, explanation of activity □ Instrumentation—automatic capsule-filling machine, explanation of activity of strain gauges

To the Editor:

A recent publication (1) described the application of strain gauges for determining compaction and ejection force in an automated capsule-filling machine. The redesign of the dosator piston for the installation of strain gauges resulted in the sensitive and linear measurement of force applied to the dosator piston. However, the design in which the strain gauges were applied does not provide a pair of passive gauge elements. The two gauge elements mounted perpendicular to the piston axis were described as temperature-compensating gauges and passive arms in the Wheatstone bridge circuit. In fact, these gauge elements in that design are active due to the phenomenon known as the Poisson effect (2). This effect is described in the following example.

When a material undergoes compression resulting in longitudinal compression strain, it also undergoes transverse tension strain (lateral strain). The relationship between the lateral and longitudinal strain is called the Poisson ratio (μ) and, for a given material, is relatively constant within the proportional limits for that material:

$$\mu = \frac{\text{lateral strain}}{\text{longitudinal strain}} \qquad \text{(Eq. 1)}$$

The expected sensitivity for this strain-gauge design can be calculated as follows. Young's modulus (E) for type 304 stainless steel, which is used in the instrumented dosator, is 1.97×10^6 kg cm^{-2} (3). Young's modulus is expressed mathematically as:

$$E = \frac{\sigma}{\epsilon} \qquad \text{(Eq. 2)}$$

(3) D. P. Rall, T. L. Loo, M. Lane, and M. G. Kelly, *J. Natl. Cancer Inst.*, **19,** 79 (1957).
(4) J. F. McLeay, *Am. J. Surg.*, **96,** 415 (1958).
(5) J. W. Phillips, E. G. Cobb, V. Richards, W. D. Rhodes, D. C. Loehrer, and L. J. Ritchie, *ibid.*, **100,** 384 (1960).
(6) P. S. Vossar, A. M. Saunders, and C. F. A. Culling, *Arch. Pathol.*, **69,** 613 (1960).
(7) R. A. Milch, J. E. Tobie, and R. A. Robinson, *J. Histochem. Cytochem.*, **9,** 261 (1961).
(8) J. Klinger and R. Katz, *Gastroenterology*, **41,** 29 (1961).
(9) I. Fusek, *Cesk. Neurol.*, **26,** 321 (1963).
(10) L. H. Riley, Jr., *Bull. Johns Hopkins Hosp.*, **113,** 291 (1963).
(11) N. B. Ackerman and A. S. McFee, *Surgery*, **53,** 247 (1963).
(12) A. Cabrera, J. Jurado, S. de la Pava, and J. Pickren, *N.Y. State J. Med.*, **64,** 981 (1964).
(13) L. Sandlow and N. Heinrich, *J. Am. Med. Assoc.*, **189,** 363 (1964).
(14) J. E. Ayre, J. M. LeGuerrier, and J. Arsenault, *Med. Times*, **93,** 885 (1965).
(15) P. A. Barton and W. J. Cunliffe, *Lancet*, **1,** 1002 (1966).
(16) B. L. Holman, W. D. Kaplan, and M. K. Dewanjee, *Radiology*, **112,** 147 (1974).
(17) K. Breslow, S. Halpern, F. Schwartz, N. Alazraki, and W. Ashburn, *J. Nucl. Med.*, **15,** 987 (1974).
(18) G. L. Locher, *Am. J. Roentgenol.*, **36,** 1 (1936).
(19) A. H. Soloway, in "Progress in Boron Chemistry," A. L. McCloskey and H. Steinberg, Eds., Pergamon, New York, N.Y., 1964, pp. 203–234.
(20) G. L. Brownell, A. H. Soloway, and W. H. Sweet, in "Modern Trends in Radiotherapy," T. J. Deeley and C. A. P. Wood, Eds., Butterworths, London, England, 1967, pp. 132–145.
(21) M. F. Hawthorne, R. J. Wiersema, and M. Takasugi, *J. Med. Chem.*, **15,** 449 (1972).
(22) R. H. Connamacher and H. G. Mandel, *Biochem. Biophys. Res. Commun.*, **20,** 98 (1965).
(23) J. A. Last, K. Izaki, and J. F. Snell, *Biochim. Biophys. Acta*, **103,** 532 (1965).
(24) J. A. Last, *ibid.*, **195,** 506 (1969).
(25) L. E. Day, *J. Bacteriol.*, **91,** 1917 (1966).
(26) *Ibid.*, **92,** 197 (1966).
(27) I. H. Maxwell, *Mol. Pharmacol.*, **4,** 25 (1968).
(28) R. H. Connamacher and H. G. Mandel, *Biochim. Biophys. Acta*, **166,** 475 (1968).
(29) W. C. Gillchriest and D. H. Shaw, *Oncology*, **27,** 97 (1973).
(30) J. M. LeGuerrier, J. E. Ayre, and W. C. Gillchriest, *ibid.*, **25,** 97 (1971).
(31) W. J. Gottstein, W. F. Minor, and L. C. Cheney, *J. Am. Chem. Soc.*, **81,** 1198 (1959).
(32) O. C. Musgrave and T. O. Park, *Chem. Ind.*, **1955,** 1552.
(33) R. L. Letsinger and I. Skoog, *J. Am. Chem. Soc.*, **77,** 2491 (1955).
(34) L. M. Allen and C. W. Roscoe, *J. Pharm. Sci.*, **58,** 368 (1969).
(35) M. Schach von Wittenau and R. K. Blackwood, *J. Org. Chem.*, **31,** 613 (1966).
(36) L. J. Bellamy, "The Infra-red Spectra of Complex Molecules," Wiley, New York, N.Y., 1964, pp. 209–220.

ACKNOWLEDGMENTS AND ADDRESSES

Received September 10, 1976, from the *Division of Pharmaceutical Sciences, School of Pharmacy, University of the Pacific, Stockton, CA 95211.*

Accepted for publication December 1, 1976.

Supported in part by a grant from the International Development Laboratories, Los Angeles, Calif.

The authors are indebted to Dr. Alain C. Huitric, University of Washington, Seattle, Wash., for assistance with the NMR studies and to Dr. Andrew Blair, Harborview Hospital, Seattle, Wash., for the mass spectra. The authors also thank Pfizer Co., New York, N.Y., for a generous supply of tetracycline.

* Present address: El Centro Community Hospital, El Centro, CA 92243.

‡ Present address: 11790 Bellagio Rd., Los Angeles, CA 90049.

ˣ To whom inquiries should be directed.

COMMUNICATIONS

Strain-Gauge Wheatstone Bridge Design for Automatic Capsule-Filling Machine

Keyphrases □ Capsule-filling machine, automatic—strain gauges, explanation of activity □ Instrumentation—automatic capsule-filling machine, explanation of activity of strain gauges

To the Editor:

A recent publication (1) described the application of strain gauges for determining compaction and ejection force in an automated capsule-filling machine. The redesign of the dosator piston for the installation of strain gauges resulted in the sensitive and linear measurement of force applied to the dosator piston. However, the design in which the strain gauges were applied does not provide a pair of passive gauge elements. The two gauge elements mounted perpendicular to the piston axis were described as temperature-compensating gauges and passive arms in the Wheatstone bridge circuit. In fact, these gauge elements in that design are active due to the phenomenon known as the Poisson effect (2). This effect is described in the following example.

When a material undergoes compression resulting in longitudinal compression strain, it also undergoes transverse tension strain (lateral strain). The relationship between the lateral and longitudinal strain is called the Poisson ratio (μ) and, for a given material, is relatively constant within the proportional limits for that material:

$$\mu = \frac{\text{lateral strain}}{\text{longitudinal strain}} \qquad \text{(Eq. 1)}$$

The expected sensitivity for this strain-gauge design can be calculated as follows. Young's modulus (E) for type 304 stainless steel, which is used in the instrumented dosator, is 1.97×10^6 kg cm^{-2} (3). Young's modulus is expressed mathematically as:

$$E = \frac{\sigma}{\epsilon} \qquad \text{(Eq. 2)}$$

where stress (σ) and strain (ϵ) have units of kilograms square centimeters and microstrains $\times 10^{-6}$, respectively. The cross-sectional area (A) of the dosator, where the bonded strain gauges are located, was reported as 0.174 cm^2. Therefore, the expected sensitivity (microstrains per kilogram) from longitudinal compression can be calculated:

$$\text{sensitivity} = (E \times A \times 10^{-6})^{-1} \qquad \text{(Eq. 3)}$$

This value is 2.92 microstrains/kg.

Then, to calculate the contribution to the sensitivity from lateral strain, the Poisson ratio (μ) for steel of 0.3 is used (3). The value for the lateral sensitivity was calculated as 0.88 microstrain/kg. The total sensitivity for this instrumented dosator is the sum of the lateral and longitudinal components, which is 3.80 microstrains/kg. This value compares well with that observed (1), 3.96 microstrains/kg.

The preceding discussion does not invalidate this type of strain-gauge application, but it does clarify and explain the sensitivity obtained.

(1) L. E. Small and L. L. Augsburger, *J. Pharm. Sci.*, **66**, 504 (1977).
(2) K. Arthur, "Transducer Measurements," Tektronix Inc., Beaverton, Ore., 1970, pp. 74–77.
(3) T. Lyman, "Metals Handbook: Properties and Selection of Metals," vol. 1, American Society for Metals, Metals Park, Ohio, 1969, p. 422.

John S. Kent ˣ
Mark T. Yost
Institute of Pharmaceutical Sciences
Syntex Research
Palo Alto, CA 94304

Received May 23, 1977.
Accepted for publication July 8, 1977.
ˣ To whom inquiries should be directed.

Clarification of Nomenclature

Keyphrases □ Capsule-filling machine, automatic—strain gauges, explanation of activity □ Instrumentation—automatic capsule-filling machine, explanation of activity of strain gauges

To the Editor:

Kent and Yost (1) commented on the Wheatstone bridge design for an automatic capsule-filling machine (2). The described position of the gauges on the modified dosator piston to measure the force applied to the dosator piston and to provide temperature compensation is common in experimental stress analysis (3) and pharmaceutical research (4, 5).

Theoretical stress calculations are not required for accurate calibration of the instrumented piston. The calculations offered by Kent and Yost for the net strain, ϵ_{net}, at the strain-gauge bonding site are well known for this bridge application and may be simply expressed as (3):

$$\epsilon_{net} = (1 + \mu)\epsilon_A \qquad \text{(Eq. 1)}$$

where μ is the Poisson ratio and ϵ_A is the axial strain as calculated from Hooke's law.

Kent and Yost agree that this type of calculation does not invalidate the design of the Wheatstone bridge in question nor the validity of the work presented. The issue is the use of the term "passive" to describe the temperature-compensating gauges in Fig. 3 of Ref. 2. Other terms have been applied to these same gauges (4, 6–9). Knoechel *et al.* (4) used the term "dummy" gauges. Arthur (6) stated: "It sometimes happens that it is convenient to use 'dummy' gages for temperature compensation." Neubert (7) mentioned that the dummy gauges "should be mounted in a direction of minimum strain. . . ."

Perhaps the best term for the temperature-compensating gauges in the bridge arrangement in question is *Poisson gauges* (9), in recognition of the fact that these gauges also contribute to the total sensitivity of the piston.

(1) J. S. Kent and M. T. Yost, *J. Pharm. Sci.*, **66**, 1507 (1977).
(2) L. E. Small and L. L. Augsburger, *ibid.*, **66**, 504 (1977).
(3) R. C. Dove and P. H. Adams, "Experimental Stress Analysis and Motion Measurement," Merrill Books, Columbus, Ohio, 1964, pp. 84, 85.
(4) E. L. Knoechel, C. C. Sperry, H. E. Ross, and C. J. Lintner, *J. Pharm. Sci.*, **56**, 109 (1967).
(5) P. E. Wray, J. G. Vincent, F. W. Moller, and G. J. Jackson, paper presented at the Industrial Pharmacy Section, APhA Academy of Pharmaceutical Sciences, Dallas meeting, Apr. 1966.
(6) K. Arthur, "Transducer Measurements," Tektronix Inc., Beaverton, Ore., 1970, p. 140.
(7) H. K. P. Neubert, "Strain Gauges," Macmillan, London, England, 1967, pp. 59, 60.
(8) Tech Note TN-128-2, Micro-measurements, Romulus, Mich., 1976, p. 2.
(9) Tech Note NN-139, Micro-measurements, Romulus, Mich., 1974, p. 2.

L. E. Small
L. L. Augsburger ˣ
Department of Pharmacy (Pharmaceutics)
School of Pharmacy
University of Maryland
Baltimore, MD 21201

Received June 27, 1977.
Accepted for publication August 11, 1977.
ˣ To whom inquiries should be directed.

Effect of Hemodialysis on Cefazolin Protein Binding

Keyphrases □ Cefazolin—protein binding, effect of hemodialysis □ Protein binding—cefazolin, effect of hemodialysis □ Binding, protein—cefazolin, effect of hemodialysis □ Hemodialysis—effect on protein binding of cefazolin □ Antibacterials—cefazolin, protein binding, effect of hemodialysis

To the Editor:

Cefazolin, a semisynthetic derivative of 7-aminocephalosporanic acid, is indicated for use in infections caused by various Gram-positive and Gram-negative bacteria. Cefazolin is very highly bound to serum proteins; over the therapeutic range of 1–200 μg/ml, greater than 80% of the total drug in plasma is in the bound form (1–4). In the presence of renal impairment, the fraction bound

where stress (σ) and strain (ϵ) have units of kilograms square centimeters and microstrains $\times 10^{-6}$, respectively. The cross-sectional area (A) of the dosator, where the bonded strain gauges are located, was reported as 0.174 cm^2. Therefore, the expected sensitivity (microstrains per kilogram) from longitudinal compression can be calculated:

$$\text{sensitivity} = (E \times A \times 10^{-6})^{-1} \qquad \text{(Eq. 3)}$$

This value is 2.92 microstrains/kg.

Then, to calculate the contribution to the sensitivity from lateral strain, the Poisson ratio (μ) for steel of 0.3 is used (3). The value for the lateral sensitivity was calculated as 0.88 microstrain/kg. The total sensitivity for this instrumented dosator is the sum of the lateral and longitudinal components, which is 3.80 microstrains/kg. This value compares well with that observed (1), 3.96 microstrains/kg.

The preceding discussion does not invalidate this type of strain-gauge application, but it does clarify and explain the sensitivity obtained.

(1) L. E. Small and L. L. Augsburger, *J. Pharm. Sci.*, **66**, 504 (1977).
(2) K. Arthur, "Transducer Measurements," Tektronix Inc., Beaverton, Ore., 1970, pp. 74–77.
(3) T. Lyman, "Metals Handbook: Properties and Selection of Metals," vol. 1, American Society for Metals, Metals Park, Ohio, 1969, p. 422.

John S. Kent ˣ
Mark T. Yost
Institute of Pharmaceutical Sciences
Syntex Research
Palo Alto, CA 94304

Received May 23, 1977.
Accepted for publication July 8, 1977.
ˣ To whom inquiries should be directed.

Clarification of Nomenclature

Keyphrases □ Capsule-filling machine, automatic—strain gauges, explanation of activity □ Instrumentation—automatic capsule-filling machine, explanation of activity of strain gauges

To the Editor:

Kent and Yost (1) commented on the Wheatstone bridge design for an automatic capsule-filling machine (2). The described position of the gauges on the modified dosator piston to measure the force applied to the dosator piston and to provide temperature compensation is common in experimental stress analysis (3) and pharmaceutical research (4, 5).

Theoretical stress calculations are not required for accurate calibration of the instrumented piston. The calculations offered by Kent and Yost for the net strain, ϵ_{net}, at the strain-gauge bonding site are well known for this bridge application and may be simply expressed as (3):

$$\epsilon_{net} = (1 + \mu)\epsilon_A \qquad \text{(Eq. 1)}$$

where μ is the Poisson ratio and ϵ_A is the axial strain as calculated from Hooke's law.

Kent and Yost agree that this type of calculation does not invalidate the design of the Wheatstone bridge in question nor the validity of the work presented. The issue is the use of the term "passive" to describe the temperature-compensating gauges in Fig. 3 of Ref. 2. Other terms have been applied to these same gauges (4, 6–9). Knoechel *et al.* (4) used the term "dummy" gauges. Arthur (6) stated: "It sometimes happens that it is convenient to use 'dummy' gages for temperature compensation." Neubert (7) mentioned that the dummy gauges "should be mounted in a direction of minimum strain. . . ."

Perhaps the best term for the temperature-compensating gauges in the bridge arrangement in question is *Poisson gauges* (9), in recognition of the fact that these gauges also contribute to the total sensitivity of the piston.

(1) J. S. Kent and M. T. Yost, *J. Pharm. Sci.*, **66**, 1507 (1977).
(2) L. E. Small and L. L. Augsburger, *ibid.*, **66**, 504 (1977).
(3) R. C. Dove and P. H. Adams, "Experimental Stress Analysis and Motion Measurement," Merrill Books, Columbus, Ohio, 1964, pp. 84, 85.
(4) E. L. Knoechel, C. C. Sperry, H. E. Ross, and C. J. Lintner, *J. Pharm. Sci.*, **56**, 109 (1967).
(5) P. E. Wray, J. G. Vincent, F. W. Moller, and G. J. Jackson, paper presented at the Industrial Pharmacy Section, APhA Academy of Pharmaceutical Sciences, Dallas meeting, Apr. 1966.
(6) K. Arthur, "Transducer Measurements," Tektronix Inc., Beaverton, Ore., 1970, p. 140.
(7) H. K. P. Neubert, "Strain Gauges," Macmillan, London, England, 1967, pp. 59, 60.
(8) Tech Note TN-128-2, Micro-measurements, Romulus, Mich., 1976, p. 2.
(9) Tech Note NN-139, Micro-measurements, Romulus, Mich., 1974, p. 2.

L. E. Small
L. L. Augsburger ˣ
Department of Pharmacy (Pharmaceutics)
School of Pharmacy
University of Maryland
Baltimore, MD 21201

Received June 27, 1977.
Accepted for publication August 11, 1977.
ˣ To whom inquiries should be directed.

Effect of Hemodialysis on Cefazolin Protein Binding

Keyphrases □ Cefazolin—protein binding, effect of hemodialysis □ Protein binding—cefazolin, effect of hemodialysis □ Binding, protein—cefazolin, effect of hemodialysis □ Hemodialysis—effect on protein binding of cefazolin □ Antibacterials—cefazolin, protein binding, effect of hemodialysis

To the Editor:

Cefazolin, a semisynthetic derivative of 7-aminocephalosporanic acid, is indicated for use in infections caused by various Gram-positive and Gram-negative bacteria. Cefazolin is very highly bound to serum proteins; over the therapeutic range of 1–200 μg/ml, greater than 80% of the total drug in plasma is in the bound form (1–4). In the presence of renal impairment, the fraction bound

where stress (σ) and strain (ϵ) have units of kilograms square centimeters and microstrains $\times 10^{-6}$, respectively. The cross-sectional area (A) of the dosator, where the bonded strain gauges are located, was reported as 0.174 cm^2. Therefore, the expected sensitivity (microstrains per kilogram) from longitudinal compression can be calculated:

$$\text{sensitivity} = (E \times A \times 10^{-6})^{-1} \qquad \text{(Eq. 3)}$$

This value is 2.92 microstrains/kg.

Then, to calculate the contribution to the sensitivity from lateral strain, the Poisson ratio (μ) for steel of 0.3 is used (3). The value for the lateral sensitivity was calculated as 0.88 microstrain/kg. The total sensitivity for this instrumented dosator is the sum of the lateral and longitudinal components, which is 3.80 microstrains/kg. This value compares well with that observed (1), 3.96 microstrains/kg.

The preceding discussion does not invalidate this type of strain-gauge application, but it does clarify and explain the sensitivity obtained.

(1) L. E. Small and L. L. Augsburger, *J. Pharm. Sci.*, **66**, 504 (1977).
(2) K. Arthur, "Transducer Measurements," Tektronix Inc., Beaverton, Ore., 1970, pp. 74–77.
(3) T. Lyman, "Metals Handbook: Properties and Selection of Metals," vol. 1, American Society for Metals, Metals Park, Ohio, 1969, p. 422.

John S. Kent ˣ
Mark T. Yost
Institute of Pharmaceutical Sciences
Syntex Research
Palo Alto, CA 94304

Received May 23, 1977.
Accepted for publication July 8, 1977.
ˣ To whom inquiries should be directed.

Clarification of Nomenclature

Keyphrases □ Capsule-filling machine, automatic—strain gauges, explanation of activity □ Instrumentation—automatic capsule-filling machine, explanation of activity of strain gauges

To the Editor:

Kent and Yost (1) commented on the Wheatstone bridge design for an automatic capsule-filling machine (2). The described position of the gauges on the modified dosator piston to measure the force applied to the dosator piston and to provide temperature compensation is common in experimental stress analysis (3) and pharmaceutical research (4, 5).

Theoretical stress calculations are not required for accurate calibration of the instrumented piston. The calculations offered by Kent and Yost for the net strain, ϵ_{net}, at the strain-gauge bonding site are well known for this bridge application and may be simply expressed as (3):

$$\epsilon_{net} = (1 + \mu)\epsilon_A \qquad \text{(Eq. 1)}$$

where μ is the Poisson ratio and ϵ_A is the axial strain as calculated from Hooke's law.

Kent and Yost agree that this type of calculation does not invalidate the design of the Wheatstone bridge in question nor the validity of the work presented. The issue is the use of the term "passive" to describe the temperature-compensating gauges in Fig. 3 of Ref. 2. Other terms have been applied to these same gauges (4, 6–9). Knoechel *et al.* (4) used the term "dummy" gauges. Arthur (6) stated: "It sometimes happens that it is convenient to use 'dummy' gages for temperature compensation." Neubert (7) mentioned that the dummy gauges "should be mounted in a direction of minimum strain. . . ."

Perhaps the best term for the temperature-compensating gauges in the bridge arrangement in question is *Poisson gauges* (9), in recognition of the fact that these gauges also contribute to the total sensitivity of the piston.

(1) J. S. Kent and M. T. Yost, *J. Pharm. Sci.*, **66**, 1507 (1977).
(2) L. E. Small and L. L. Augsburger, *ibid.*, **66**, 504 (1977).
(3) R. C. Dove and P. H. Adams, "Experimental Stress Analysis and Motion Measurement," Merrill Books, Columbus, Ohio, 1964, pp. 84, 85.
(4) E. L. Knoechel, C. C. Sperry, H. E. Ross, and C. J. Lintner, *J. Pharm. Sci.*, **56**, 109 (1967).
(5) P. E. Wray, J. G. Vincent, F. W. Moller, and G. J. Jackson, paper presented at the Industrial Pharmacy Section, APhA Academy of Pharmaceutical Sciences, Dallas meeting, Apr. 1966.
(6) K. Arthur, "Transducer Measurements," Tektronix Inc., Beaverton, Ore., 1970, p. 140.
(7) H. K. P. Neubert, "Strain Gauges," Macmillan, London, England, 1967, pp. 59, 60.
(8) Tech Note TN-128-2, Micro-measurements, Romulus, Mich., 1976, p. 2.
(9) Tech Note NN-139, Micro-measurements, Romulus, Mich., 1974, p. 2.

L. E. Small
L. L. Augsburger ˣ
Department of Pharmacy (Pharmaceutics)
School of Pharmacy
University of Maryland
Baltimore, MD 21201

Received June 27, 1977.
Accepted for publication August 11, 1977.
ˣ To whom inquiries should be directed.

Effect of Hemodialysis on Cefazolin Protein Binding

Keyphrases □ Cefazolin—protein binding, effect of hemodialysis □ Protein binding—cefazolin, effect of hemodialysis □ Binding, protein—cefazolin, effect of hemodialysis □ Hemodialysis—effect on protein binding of cefazolin □ Antibacterials—cefazolin, protein binding, effect of hemodialysis

To the Editor:

Cefazolin, a semisynthetic derivative of 7-aminocephalosporanic acid, is indicated for use in infections caused by various Gram-positive and Gram-negative bacteria. Cefazolin is very highly bound to serum proteins; over the therapeutic range of 1–200 μg/ml, greater than 80% of the total drug in plasma is in the bound form (1–4). In the presence of renal impairment, the fraction bound

has been reported to decrease significantly. In one study, the percent bound decreased from 84% in normal patients to 63% in uremic patients (1). The effect of hemodialysis on the half-life and pharmacokinetics of cefazolin also was studied (5). However, the effects of hemodialysis on protein binding have not been reported.

Craig *et al.* (6) studied serum from uremic patients and reported that treatment with activated charcoal at pH 3 significantly increased the fraction bound for several drugs, *e.g.*, sulfamethoxazole, dicloxacillin, phenytoin, salicylate, and digitoxin. These investigators speculated that the treatment of serum with charcoal removed a protein binding inhibitor present in the serum of uremic patients, thus restoring the binding to near normal levels.

This study was conducted to determine whether the decreased protein binding capacity in uremic serum would be affected by hemodialysis. If hemodialysis removes the protein binding inhibitor present in uremic serum, the binding capacity should return to normal levels.

Twelve patients currently undergoing maintenance hemodialysis[1] were studied. All patients had serum creatinine values above 6.0 mg % (11.5 ± 3.8 mg % *SD*) and blood urea nitrogen values above 32 mg % (90.3 ± 30.9 mg %) before hemodialysis. Serum creatinine and blood urea nitrogen values decreased to 5.2 ± 2.0 and 14.2 ± 18.0 (*SD*) mg %, respectively, after the hemodialysis procedure.

Blood samples were collected both before and after hemodialysis. Hemodialysis was conducted using artificial kidneys[2] in dialysis machines[3] supplied by a central dialysis bath. Dialysis was performed with systemic heparinization for 5–6 hr. Serum was removed from all samples, frozen at −4°, and used within 3 weeks.

Cefazolin was later added to the serum to give a total drug concentration of 92 μg/ml. Seven-milliliter samples of the serum–cefazolin solution were pipetted into an ultrafiltration apparatus[4]. An ultrafiltration membrane[5] with a molecular weight cutoff of 10,000 was used to separate the free drug from the bound drug. Nitrogen gas at a pressure of 15 psi was applied to the ultrafiltration apparatus, and the protein-free ultrafiltrate was collected and frozen until assay.

The drug concentration in the ultrafiltrate samples was determined using the microbial disk diffusion assay of Grove and Randall (7). Twenty microliters of the ultrafiltrate was pipetted onto 6.25-mm disks placed on agar seeded with *Bacillus subtilis* spores. Standards were made in 0.067 *M* phosphate buffer, pH 7.4. All plates were incubated overnight at 37° before the zone sizes were measured. The drug concentration in the ultrafiltrate was determined by interpolation from the standard curve made with phosphate buffer.

The serum protein binding of cefazolin in patients with uremia averaged 72.5 ± 13.4 (*SD*) % prior to dialysis, a significant decrease from the value of 80–90% found in nonuremic patients. All values of protein binding in the uremic patients, except one, were below 86% (Table I). There did not appear to be any significant statistical correlations between the fraction bound and the values of serum creatinine, blood urea nitrogen, calculated creatinine clearance, and serum albumin concentration.

Table I—Protein Binding in Patients with Uremia

Subject	Percent Protein Bound	
	Predialysis	Postdialysis
A	70	5
B	80	15
C	72	2
D	42	6
E	61	42
F	86	30
G	65	20
H	78	26
I	76	26
J	71	0
K	73	22
L	96	75
Mean ± *SD*	72.5 ± 13.4	22.4 ± 20.9

The fraction of cefazolin bound to protein after the patients had undergone dialysis decreased significantly to 22.4 ± 20.9 (*SD*) %. The values ranged from 0 to 75% (Table I). A paired Student *t* test comparing the pre- and postdialysis values for each patient showed a significant difference in the protein binding after hemodialysis ($p < 0.005$). The amount of change in binding did not correlate with the type of artificial kidney, the duration of dialysis, or the amount of heparin used. Therefore, the dialysis procedure apparently does not remove a protein binding inhibitor from the serum; on the contrary, hemodialysis actually introduced, either directly or indirectly, a protein binding inhibitor.

Craig (8) recently demonstrated that the binding of proteins in serum decreased in patients undergoing cardiopulmonary bypass. The decrease in binding was inversely proportional to the increase in the serum free fatty acid levels, which was attributed to the use of heparin during the bypass procedure. The decrease in the binding to serum proteins in each uremic patient after hemodialysis may also possibly be attributed to an increased free fatty acid level due to the administration of heparin during the dialysis procedure.

Drugs in the protein-bound state are neither pharmacologically active (9) nor able to distribute to the tissues (10). Since few infections are located in the circulatory system, the ability of the antimicrobial to leave the circulation and to enter the tissues is critical before the infecting organism can be eradicated. Decreased binding to proteins would increase drug distribution to tissues; thus, the drug may be more effective. The decrease in protein binding also can have certain dangers. Although cefazolin is relatively safe over a wide therapeutic range of concentrations, toxic reactions are more likely with greater tissue concentrations.

Other drugs with a similar decrease in protein binding after dialysis and a narrower therapeutic margin would present a great potential for toxicity due to increased free serum and tissue drug levels. Further studies of the effect of dialysis on the protein binding of other pharmacological agents is necessary to determine whether this phenomenon is common to other highly bound drugs. Adjustment of the dosage regimen after dialysis may be necessary to compensate for the increases in tissue distribution occurring immediately after dialysis.

(1) W. A. Craig, P. G. Welling, T. C. Jackson, and C. M. Kunin, *J.*

[1] Veterans Administration Hospital, Providence, R.I.
[2] Cobe Laboratories, Cranbury, N.J., and Gambro, Inc., Wheeling, Ill.
[3] Milton-Roy, Extracorporal Medical Systems Inc., Pinellas Park, Fla.
[4] Model 8-MC, Amicon, Inc., Lexington, Mass.
[5] PM-10, Amicon, Inc., Lexington, Mass.

Infect. Dis., **128S**, 347 (1973).
(2) C. Regamey, R. C. Gordon, and W. Kirby, *Arch. Intern. Med.*, **133**, 407 (1974).
(3) M. G. Bergeron, J. L. Brusch, M. Barza, and L. Weinstein, *Antimicrob. Agents Chemother.*, **4**, 396 (1973).
(4) W. M. M. Kirby and C. R. Regamey, *J. Infect. Dis.*, **128S**, 341 (1973).
(5) A. W. Czerwinski, J. A. Pederson, and J. P. Barry, *J. Clin. Pharmacol.*, **14**, 560 (1974).
(6) W. A. Craig, M. A. Evenson, K. P. Sarver, and J. P. Wagnild, *J. Lab. Clin. Med.*, **87**, 637 (1976).
(7) D. C. Grove and W. A. Randall, "Assay Methods of Antibiotics: A Laboratory Manual," Medical Encyclopedia, New York, N.Y., 1955, pp. 7–14.
(8) W. A. Craig, *Infection*, **4**, S137 (1976).
(9) C. M. Kunin, *Ann. N.Y. Acad. Sci.*, **145**, 282 (1967).
(10) W. F. Verwey and H. R. Williams, *Antimicrob. Agents Chemother.*, **1962**, 476 (1963).

Douglas S. Greene ˣ
College of Pharmacy
University of Rhode Island
Kingston, RI 02881

Alan D. Tice
Veterans Administration Hospital
Brown University
Providence, RI 02908

Received June 27, 1977.
Accepted for publication August 5, 1977.
The authors thank Victoria Hittinger for assaying the ultrafiltrate samples.
ˣ To whom inquiries should be directed.

Use of Trimethylanilinium Hydroxide–Tetramethylammonium Hydroxide as On-Column Methylating Agent for GLC Analysis of Phenytoin

Keyphrases □ Phenytoin—GLC analysis in plasma □ GLC—analysis, phenytoin in plasma □ Anticonvulsants—phenytoin, GLC analysis in plasma

To the Editor:

Numerous procedures for the GLC analysis of plasma phenytoin have been reported (1–7). One promising procedure was that of Orme *et al.* (7), who were able to analyze phenytoin from 100-μl plasma samples with a lower limit of sensitivity of 0.5 μg/ml. When I attempted to use this procedure, a peak for the on-column methylating agent, trimethylanilinium hydroxide, interfered with the peak for the internal standard, 5-(4-methylphenyl)-5-phenylhydantoin. This interfering peak was not an extracted plasma component or an impurity from the extracting solvent, toluene, since it was seen when just the methanolic trimethylanilinium hydroxide was injected on column as well as when the extractions were performed with water blanks.

Orme *et al.*'s procedure for phenytoin involved the extraction of phenytoin from a 100-μl plasma sample into toluene containing the internal standard. The toluene was then extracted with 25 μl of a 0.5 *M* trimethylanilinium hydroxide–50% (v/v) methanol–water mixture. One microliter of the lower aqueous layer, after aspiration of the upper toluene layer, was injected into a gas chromatograph and analyzed *via* a flame-ionization detector.

Attempts to overcome the peak interference in using Orme *et al.*'s procedure by lowering the trimethylanilinium hydroxide concentration to 0.1 *M* (concentration below 0.1 *M* led to problems with the final extraction step) and altering column conditions proved unsuccessful. The use of commercial as well as fresh batches of trimethylanilinium hydroxide, synthesized by the method of Brochmann–Hanssen and Oke (8) from trimethylanilinium chloride or iodide, was similarly unsuccessful in removing or lessening the interfering peak.

Brochmann–Hanssen and Oke (8) showed that trimethylanilinium hydroxide is a superior methylating agent compared to tetramethylammonium hydroxide and need only be present in reasonable excess to methylate barbiturates, *etc.*, quantitatively. For concentrations of up to 20 μg of phenytoin/ml in 100 μl of plasma and the internal standard used in Orme *et al.*'s procedure, the concentration of trimethylanilinium hydroxide in the final methanol–water mixture needed only to be slightly greater than 0.001 *M; i.e.*, for methylating purposes, the concentration of trimethylanilinium hydroxide of 0.5 *M* appeared to be unnecessary. Of course, the presence of trimethylanilinium hydroxide serves a secondary purpose in that the final methanol–water solution must be sufficiently alkaline to extract phenytoin and the internal standard efficiently from the toluene phase.

In the present study, sufficient alkalinity for the efficient extraction in the final extraction step and quantitative methylation of the extracted phenytoin and internal standard were achieved by the use of 0.1 *M* tetramethylammonium hydroxide–0.01 *M* trimethylanilinium hydroxide and a solvent of 50% (v/v) methanol–water. Tetramethylammonium hydroxide was present as the alkalizing agent and as a secondary methylating agent, while trimethylanilinium hydroxide was primarily present as the methylating agent.

Plasma samples, 100 μl, containing phenytoin were analyzed according to the procedure of Orme *et al.* (7) with the following modifications. To a 100-μl plasma sample was added 100 μl of freshly prepared 10% metaphosphoric acid. This addition was necessary because an interfering amine prodrug of phenytoin of low pKa was present in the plasma samples. Metaphosphoric acid also quenched the conversion of the prodrug to phenytoin. For normal samples, the addition of monobasic sodium phosphate, as suggested by Orme *et al.* (7), is sufficient.

Two milliliters of toluene containing 1.4 μg of 5-(4-methylphenyl)-5-phenylhydantoin was then added to the treated plasma sample, and the sample was vortexed vigorously for 1 min and then centrifuged. Approximately 1.8 ml of the toluene layer was removed by pipet. The toluene was then extracted with 25 μl of 50% (v/v) methanol–water that was 0.1 *M* in tetramethylammonium hydroxide and 0.01 *M* in trimethylanilinium hydroxide. This addition of the 25 μl of methanol–water *to* the toluene while vortexing was crucial for efficient extraction. After vortexing for 1 min and centrifuging, the upper toluene layer was removed by aspiration.

Infect. Dis., **128S**, 347 (1973).
(2) C. Regamey, R. C. Gordon, and W. Kirby, *Arch. Intern. Med.*, **133**, 407 (1974).
(3) M. G. Bergeron, J. L. Brusch, M. Barza, and L. Weinstein, *Antimicrob. Agents Chemother.*, **4**, 396 (1973).
(4) W. M. M. Kirby and C. R. Regamey, *J. Infect. Dis.*, **128S**, 341 (1973).
(5) A. W. Czerwinski, J. A. Pederson, and J. P. Barry, *J. Clin. Pharmacol.*, **14**, 560 (1974).
(6) W. A. Craig, M. A. Evenson, K. P. Sarver, and J. P. Wagnild, *J. Lab. Clin. Med.*, **87**, 637 (1976).
(7) D. C. Grove and W. A. Randall, "Assay Methods of Antibiotics: A Laboratory Manual," Medical Encyclopedia, New York, N.Y., 1955, pp. 7–14.
(8) W. A. Craig, *Infection*, **4**, S137 (1976).
(9) C. M. Kunin, *Ann. N.Y. Acad. Sci.*, **145**, 282 (1967).
(10) W. F. Verwey and H. R. Williams, *Antimicrob. Agents Chemother.*, **1962**, 476 (1963).

Douglas S. Greene ˣ
College of Pharmacy
University of Rhode Island
Kingston, RI 02881

Alan D. Tice
Veterans Administration Hospital
Brown University
Providence, RI 02908

Received June 27, 1977.
Accepted for publication August 5, 1977.
The authors thank Victoria Hittinger for assaying the ultrafiltrate samples.
ˣ To whom inquiries should be directed.

Use of Trimethylanilinium Hydroxide–Tetramethylammonium Hydroxide as On-Column Methylating Agent for GLC Analysis of Phenytoin

Keyphrases □ Phenytoin—GLC analysis in plasma □ GLC—analysis, phenytoin in plasma □ Anticonvulsants—phenytoin, GLC analysis in plasma

To the Editor:

Numerous procedures for the GLC analysis of plasma phenytoin have been reported (1–7). One promising procedure was that of Orme *et al.* (7), who were able to analyze phenytoin from 100-μl plasma samples with a lower limit of sensitivity of 0.5 μg/ml. When I attempted to use this procedure, a peak for the on-column methylating agent, trimethylanilinium hydroxide, interfered with the peak for the internal standard, 5-(4-methylphenyl)-5-phenylhydantoin. This interfering peak was not an extracted plasma component or an impurity from the extracting solvent, toluene, since it was seen when just the methanolic trimethylanilinium hydroxide was injected on column as well as when the extractions were performed with water blanks.

Orme *et al.*'s procedure for phenytoin involved the extraction of phenytoin from a 100-μl plasma sample into toluene containing the internal standard. The toluene was then extracted with 25 μl of a 0.5 *M* trimethylanilinium hydroxide–50% (v/v) methanol–water mixture. One microliter of the lower aqueous layer, after aspiration of the upper toluene layer, was injected into a gas chromatograph and analyzed *via* a flame-ionization detector.

Attempts to overcome the peak interference in using Orme *et al.*'s procedure by lowering the trimethylanilinium hydroxide concentration to 0.1 *M* (concentration below 0.1 *M* led to problems with the final extraction step) and altering column conditions proved unsuccessful. The use of commercial as well as fresh batches of trimethylanilinium hydroxide, synthesized by the method of Brochmann–Hanssen and Oke (8) from trimethylanilinium chloride or iodide, was similarly unsuccessful in removing or lessening the interfering peak.

Brochmann–Hanssen and Oke (8) showed that trimethylanilinium hydroxide is a superior methylating agent compared to tetramethylammonium hydroxide and need only be present in reasonable excess to methylate barbiturates, *etc.*, quantitatively. For concentrations of up to 20 μg of phenytoin/ml in 100 μl of plasma and the internal standard used in Orme *et al.*'s procedure, the concentration of trimethylanilinium hydroxide in the final methanol–water mixture needed only to be slightly greater than 0.001 *M; i.e.*, for methylating purposes, the concentration of trimethylanilinium hydroxide of 0.5 *M* appeared to be unnecessary. Of course, the presence of trimethylanilinium hydroxide serves a secondary purpose in that the final methanol–water solution must be sufficiently alkaline to extract phenytoin and the internal standard efficiently from the toluene phase.

In the present study, sufficient alkalinity for the efficient extraction in the final extraction step and quantitative methylation of the extracted phenytoin and internal standard were achieved by the use of 0.1 *M* tetramethylammonium hydroxide–0.01 *M* trimethylanilinium hydroxide and a solvent of 50% (v/v) methanol–water. Tetramethylammonium hydroxide was present as the alkalizing agent and as a secondary methylating agent, while trimethylanilinium hydroxide was primarily present as the methylating agent.

Plasma samples, 100 μl, containing phenytoin were analyzed according to the procedure of Orme *et al.* (7) with the following modifications. To a 100-μl plasma sample was added 100 μl of freshly prepared 10% metaphosphoric acid. This addition was necessary because an interfering amine prodrug of phenytoin of low pKa was present in the plasma samples. Metaphosphoric acid also quenched the conversion of the prodrug to phenytoin. For normal samples, the addition of monobasic sodium phosphate, as suggested by Orme *et al.* (7), is sufficient.

Two milliliters of toluene containing 1.4 μg of 5-(4-methylphenyl)-5-phenylhydantoin was then added to the treated plasma sample, and the sample was vortexed vigorously for 1 min and then centrifuged. Approximately 1.8 ml of the toluene layer was removed by pipet. The toluene was then extracted with 25 μl of 50% (v/v) methanol–water that was 0.1 *M* in tetramethylammonium hydroxide and 0.01 *M* in trimethylanilinium hydroxide. This addition of the 25 μl of methanol–water *to* the toluene while vortexing was crucial for efficient extraction. After vortexing for 1 min and centrifuging, the upper toluene layer was removed by aspiration.

One microliter of the aqueous methanolic solution was then injected into a gas chromatograph[1] equipped with a flame-ionization detector. A 1.8-m glass column[2] (2 mm i.d.) was packed with 3% OV-17 on 100–120-mesh Gas Chrom Q[3]. The following conditions were used: injector temperature, 260°; column temperature, 210°; detector temperature, 250°; nitrogen flow, 35 ml/min; hydrogen flow, 50 ml/min; and compressed air (19–23% O_2 and 77–81% N_2) flow, 300 ml/min. The retention times for phenytoin and the internal standard were 4.1 and 5.8 min, respectively. With 0.5 *M* trimethylanilinium hydroxide in place of tetramethylammonium hydroxide (0.1 *M*)–trimethylanilinium hydroxide (0.01 *M*) and identical column conditions, the interfering peak had a retention time of 5.6 min.

Peak height ratios were used to prepare standard curves in the 1–20-μg/ml range. The lower limit of sensitivity was 0.5 μg/ml, and repeated injections showed assay reproducibility in the ±0.5-μg/ml range.

With the described procedure, a clean chromatogram that was easily quantitated was obtained. The phenytoin peak at the higher sensitivity settings, *i.e.*, low concentration range, did elute on the solvent front tailing. However, if analysis time is not critical, the column temperature can be lowered slightly, resulting in a slightly longer retention time but a better chromatogram for quantitation purposes.

Use of the mixed methylating agents apparently provides sufficient methylating and alkalizing properties while minimizing peak interferences resulting from high concentrations of trimethylanilinium hydroxide and the relatively poor methylating capability of tetramethylammonium hydroxide.

[1] Varian Aerograph model 2100, Walnut Creek, Calif.
[2] Supelcoport, Supelco, Inc., Supelco Park, Bellefonte, Pa.
[3] Applied Sciences Laboratories, State College, Pa.

(1) J. MacGee, *Anal. Chem.*, **42**, 421 (1970).
(2) R. H. Hammer, B. J. Wilder, R. R. Streiff, and A. Meyersdorf, *J. Pharm. Sci.*, **60**, 327 (1971).
(3) H. J. Kupferberg, *Clin. Chim. Acta*, **29**, 283 (1970).
(4) A. Estes and P. A. Dumont, *J. Chromatogr.*, **82**, 307 (1973).
(5) M. A. Evenson, P. Jones, and B. Darcey, *Clin. Chem.*, **16**, 107 (1970).
(6) K. K. Midha, I. J. McGilveray, and D. L. Wilson, *J. Pharm. Sci.*, **65**, 1240 (1976).
(7) M. Orme, O. Borgå, C. E. Cook, and F. Sjöquist, *Clin. Chem.*, **22**, 246 (1976).
(8) E. Brochmann-Hanssen and T. O. Oke, *J. Pharm. Sci.*, **58**, 370 (1969).

V. J. Stella

Department of Pharmaceutical Chemistry
University of Kansas
Lawrence, KS 66045

Received April 22, 1977.
Accepted for publication August 1, 1977.
Supported by a grant from INTERx Research Corp., Lawrence, KS 66044.
The technical assistance of Mr. Steve Schuller is gratefully acknowledged.

BOOKS

REVIEWS

Textbook of Organic Medicinal and Pharmaceutical Chemistry. 7th ed. Edited by CHARLES O. WILSON, OLE GISVOLD, and ROBERT F. DOERGE. Lippincott, East Washington Square, Philadelphia, PA 19105, 1977. 1085 pp. 18 × 26 cm. Price $33.00.

The seventh edition of this book represents a continued effort of the editors to provide a useful undergraduate pharmacy textbook. The book includes a discussion of all products described in USP XIX, NF XIV, and "Accepted Dental Remedies," as well as other important pharmaceuticals. The introductory material of a few chapters has been completely rewritten, but the overall format remains essentially unchanged.

Three major changes in style represent a departure from the older editions and will considerably improve the practical application of the textbook. One outstanding feature is the extensive use of tables to focus attention upon groups of therapeutic agents in common use (a combination of chemical and pharmacologic classification). The information provided by the tables includes the official title of the drug, proprietary name(s), official dosage forms, usual dose and route of administration, and usual dose range. For the appropriate drugs, the usual pediatric dose is given in terms of body weight and body surface.

A second outstanding feature of this edition is the addition of appendixes. Material relative to pharmaceutic aids and necessities has been extracted from the several chapters of the older editions and placed in one appendix. The title of another appendix, Amine Salts, is misleading, because it actually provides the USAN designations, chemical names, and structural formulas of the anions of the more common organic acids used to form salts with amines. A third appendix provides a referenced list of pKa values of several drugs and reference compounds. A fourth appendix provides an alphabetical list of official titles of chemical entities in the USP and NF. For each title, the Chemical Abstracts Service Index Name and Registry Number, IUPAC name, empirical formula, and molecular weight are given.

A third change from the previous editions is deletion of the material previously discussed in Chapters 4–8, thus reducing the number of chapters to 24. Much of the deleted material has been placed in other appropriate chapters and in an appendix.

All chapters now include literature citations and a selected reading list.

The titles of the remaining 24 chapters are the same as those of the sixth edition. But seven of the chapters were contributed by different authors, thus giving a different slant to the introductory material in each. In the seventh edition, the new authors are Robert F. Doerge, Sulfonamides and Sulfones with Antibacterial Action (Chapter 6) and Adrenergic Agents (Chapter 12); H. Wayne Schultz, Surfactants and Chelating Agents (Chapter 7); Arnold R. Martin, Antibiotics (Chapter 9); Dwight S. Fullerton, Steroids and Therapeutically Related Compounds; and Jaime N. Delgado, Carbohydrates (Chapter 21) and Amino Acids, Proteins, Enzymes, and Hormones with Protein-like Structure (Chapter 22).

The purchaser should be aware of several printing errors that appear in Chapter 20. If the Errata list mailed to schools of pharmacy in January

One microliter of the aqueous methanolic solution was then injected into a gas chromatograph[1] equipped with a flame-ionization detector. A 1.8-m glass column[2] (2 mm i.d.) was packed with 3% OV-17 on 100–120-mesh Gas Chrom Q[3]. The following conditions were used: injector temperature, 260°; column temperature, 210°; detector temperature, 250°; nitrogen flow, 35 ml/min; hydrogen flow, 50 ml/min; and compressed air (19–23% O_2 and 77–81% N_2) flow, 300 ml/min. The retention times for phenytoin and the internal standard were 4.1 and 5.8 min, respectively. With 0.5 *M* trimethylanilinium hydroxide in place of tetramethylammonium hydroxide (0.1 *M*)–trimethylanilinium hydroxide (0.01 *M*) and identical column conditions, the interfering peak had a retention time of 5.6 min.

Peak height ratios were used to prepare standard curves in the 1–20-μg/ml range. The lower limit of sensitivity was 0.5 μg/ml, and repeated injections showed assay reproducibility in the ±0.5-μg/ml range.

With the described procedure, a clean chromatogram that was easily quantitated was obtained. The phenytoin peak at the higher sensitivity settings, *i.e.*, low concentration range, did elute on the solvent front tailing. However, if analysis time is not critical, the column temperature can be lowered slightly, resulting in a slightly longer retention time but a better chromatogram for quantitation purposes.

Use of the mixed methylating agents apparently provides sufficient methylating and alkalizing properties while minimizing peak interferences resulting from high concentrations of trimethylanilinium hydroxide and the relatively poor methylating capability of tetramethylammonium hydroxide.

[1] Varian Aerograph model 2100, Walnut Creek, Calif.
[2] Supelcoport, Supelco, Inc., Supelco Park, Bellefonte, Pa.
[3] Applied Sciences Laboratories, State College, Pa.

(1) J. MacGee, *Anal. Chem.*, **42**, 421 (1970).
(2) R. H. Hammer, B. J. Wilder, R. R. Streiff, and A. Meyersdorf, *J. Pharm. Sci.*, **60**, 327 (1971).
(3) H. J. Kupferberg, *Clin. Chim. Acta*, **29**, 283 (1970).
(4) A. Estes and P. A. Dumont, *J. Chromatogr.*, **82**, 307 (1973).
(5) M. A. Evenson, P. Jones, and B. Darcey, *Clin. Chem.*, **16**, 107 (1970).
(6) K. K. Midha, I. J. McGilveray, and D. L. Wilson, *J. Pharm. Sci.*, **65**, 1240 (1976).
(7) M. Orme, O. Borgå, C. E. Cook, and F. Sjöquist, *Clin. Chem.*, **22**, 246 (1976).
(8) E. Brochmann-Hanssen and T. O. Oke, *J. Pharm. Sci.*, **58**, 370 (1969).

V. J. Stella

Department of Pharmaceutical Chemistry
University of Kansas
Lawrence, KS 66045

Received April 22, 1977.
Accepted for publication August 1, 1977.
Supported by a grant from INTERx Research Corp., Lawrence, KS 66044.
The technical assistance of Mr. Steve Schuller is gratefully acknowledged.

BOOKS

REVIEWS

Textbook of Organic Medicinal and Pharmaceutical Chemistry. 7th ed. Edited by CHARLES O. WILSON, OLE GISVOLD, and ROBERT F. DOERGE. Lippincott, East Washington Square, Philadelphia, PA 19105, 1977. 1085 pp. 18 × 26 cm. Price $33.00.

The seventh edition of this book represents a continued effort of the editors to provide a useful undergraduate pharmacy textbook. The book includes a discussion of all products described in USP XIX, NF XIV, and "Accepted Dental Remedies," as well as other important pharmaceuticals. The introductory material of a few chapters has been completely rewritten, but the overall format remains essentially unchanged.

Three major changes in style represent a departure from the older editions and will considerably improve the practical application of the textbook. One outstanding feature is the extensive use of tables to focus attention upon groups of therapeutic agents in common use (a combination of chemical and pharmacologic classification). The information provided by the tables includes the official title of the drug, proprietary name(s), official dosage forms, usual dose and route of administration, and usual dose range. For the appropriate drugs, the usual pediatric dose is given in terms of body weight and body surface.

A second outstanding feature of this edition is the addition of appendixes. Material relative to pharmaceutic aids and necessities has been extracted from the several chapters of the older editions and placed in one appendix. The title of another appendix, Amine Salts, is misleading, because it actually provides the USAN designations, chemical names, and structural formulas of the anions of the more common organic acids used to form salts with amines. A third appendix provides a referenced list of pKa values of several drugs and reference compounds. A fourth appendix provides an alphabetical list of official titles of chemical entities in the USP and NF. For each title, the Chemical Abstracts Service Index Name and Registry Number, IUPAC name, empirical formula, and molecular weight are given.

A third change from the previous editions is deletion of the material previously discussed in Chapters 4–8, thus reducing the number of chapters to 24. Much of the deleted material has been placed in other appropriate chapters and in an appendix.

All chapters now include literature citations and a selected reading list.

The titles of the remaining 24 chapters are the same as those of the sixth edition. But seven of the chapters were contributed by different authors, thus giving a different slant to the introductory material in each. In the seventh edition, the new authors are Robert F. Doerge, Sulfonamides and Sulfones with Antibacterial Action (Chapter 6) and Adrenergic Agents (Chapter 12); H. Wayne Schultz, Surfactants and Chelating Agents (Chapter 7); Arnold R. Martin, Antibiotics (Chapter 9); Dwight S. Fullerton, Steroids and Therapeutically Related Compounds; and Jaime N. Delgado, Carbohydrates (Chapter 21) and Amino Acids, Proteins, Enzymes, and Hormones with Protein-like Structure (Chapter 22).

The purchaser should be aware of several printing errors that appear in Chapter 20. If the Errata list mailed to schools of pharmacy in January

is not available, a copy can probably be obtained by writing one of the editors. The errors were corrected in the second printing.

A rapid reading revealed surprisingly few misspelled words and only a few errors in the other chapters. Most errors are minor and do not significantly detract from the usefulness of the material.

Errors in structural formulas include carbenicillin indanyl sodium, p. 289; cephalothin sodium, p. 292; cephapirin sodium, cephamycin, and cefoxitin, p. 294; anhydrotetracycline, p. 308; oleandomycin, p. 317; lincomycin, p. 320; nystatin, p. 330; carbachol intermediate, p. 469; and neostigmine, p. 472.

Other minor errors were also noted. On p. 306, a "2" should be replaced by a "3" to read, ". . . protonation of the enol group on carbon atom 3 . . . ." In the "Mechanism of Hydrolysis of AChE," p. 467, a positive charge was omitted and the orientation of a water molecule is misleading. On p. 477, the acid proton is incorrectly placed on pilocarpine hydrochloride. The structural formula number (I) was omitted on p. 555. In the third line on p. 560 "R" should replace "S," which refers to the absolute configuration of bisquaternary species. Since rotoxamine is the levorotatory isomer of carbinoxamine, the following statement should be deleted from pp. 652 and 654: "In compounds that exhibit optical isomerism the dextrorotatory isomer possesses most of the antihistaminic activity." Finally, on p. 665, the acid proton is incorrectly placed on antazoline hydrochloride.

A footnote in the chapter on Analgesic Agents explains that the popular term "analgesic" is used in preference to the etymologically correct term "analgetic." Perhaps it would be appropriate to explain a similar relationship in the usage of the terms "antitubercular" and "antituberculous" either on p. 144 or 331.

In the reviewer's opinion, the seventh edition is an improvement of an already good textbook. It should be well received in the classroom and is highly recommended as a textbook for courses in undergraduate medicinal and pharmaceutical chemistry.

Reviewed by Charles M. Darling
School of Pharmacy
Auburn University
Auburn, AL 36830

Assessing Drug Reactions—Adverse and Beneficial, Vol. 7: Philosophy and Technology of Drug Assessment. Edited by FRANK N. ALLAN. Interdisciplinary Communication Associates, Smithsonian Institute, Washington, DC, 1976. 158 pp. 15 × 23 cm.

This book contains the report of the seventh conference in a series on the Philosophy and Technology of Drug Assessment. This conference dealt with the basic problem of defining, detecting, reporting, and assessing adverse drug reactions. The conference was conducted by the Interdisciplinary Communications Program of the Smithsonian Institution.

The topics discussed in the book include terminology and definition of adverse drug reactions, risk–benefit analysis of adverse drug reactions, and various approaches that can be used in collecting data about adverse drug reactions. The book is written in a narrative style and includes edited statements of conference participants.

The book indicates that there was a lack of agreement among the conference participants regarding the magnitude of the problem, how to assess that magnitude, or who needed the most increased understanding. However, there was a consensus agreement that a national adverse drug reaction monitoring system is needed and that the system should be part of a larger system that includes data collection of the patient's whole response to drug therapy.

The book provides an informative insight into the controversy surrounding the collection and evaluation of adverse drug reaction data. The personal experiences of some conference participants are very enlightening and enable the reader to obtain a better grasp of the problems associated with collecting and evaluating adverse drug reaction data.

Reviewed by Frank Ascione
University of Michigan
Ann Arbor, MI 48104

AMA Drug Evaluations, 3rd Ed. Prepared by the AMA Department of Drugs in cooperation with the American Society for Clinical Pharmacology and Therapeutics. Publishing Sciences Group, 545 Great Rd., Littleton, MA 01460, 1977. 1327 pp. 18 × 26 cm. Price $29.50.

The third edition of this valuable reference source has been completely reorganized, updated, and expanded. The book is divided into 19 sections based on therapeutic category. Each section contains more specific chapters, which begin with a brief introduction and include detailed evaluations for individual drugs and compounds.

The book gives information on dosage, contraindications, and adverse reactions and includes structural formulas for most single-entity drugs. It also lists generic and proprietary names and available dosage forms and sizes. Included are evaluations of over 1300 drugs, information on investigational agents, and extensive listings for normal values of clinical laboratory tests. Also, there is information on drug interactions, labeling, and use of drugs during pregnancy.

This book is essential for those who prescribe, dispense, or administer drugs or who require information on applied therapeutics.

Staff review

Organic Chemistry of Drug Synthesis. By DANIEL LEDNICER and LESTER A. MITSCHER. Wiley, 605 Third Ave., New York, NY 10016, 1977. 471 pp. 16 × 23 cm. Price $22.50.

This book is an attempt to present to synthetic organic and medicinal chemists the synthetic routes used to prepare a great majority of organic compounds used as drugs. The book focuses on compounds that are either used in the clinic or have undergone clinical trial, concentrating on those assigned generic names by the USAN Council. There are 22 chapters, each of which is organized by structural rather than pharmacological classes. The pharmacology involved in the various disease states discussed and the mode of action in selected drug classes are written in terms useful to the chemist with a rudimentary knowledge of biology. A glossary of commonly used pharmacological terms is included.

The book is filled with errors of all types, which the reviewer found to be extremely irritating. In at least three places, the authors refer to substituted ureas as carbamates (structure 10, p. 7). No chapter was error free. Frequently compounds were given wrong numbers in the discussion section. Structure 61 (p. 36) is a piperidyl derivative, not a pyrrolidino derivative as listed. Structure 30 (p. 150) is referred to twice (p. 151) as an allylic halide when it is not one. Alkylation reactions using *N*-(2-chloroethyl)diethylamine are common throughout the book. Only twice is an aziridinium salt mentioned as an intermediate (methadone, p. 79, and promethazine, p. 373). It is quite possible that aziridinium salts play important roles in all such alkylations, not just the two unsymmetrical cases listed by the authors.

The only three groups of compounds with recent references are the benzodiazepines, prostaglandins, and cephalosporins. Only at the end of the chapter on steroids do the authors indicate that drug research in this area has not stopped. This statement can surely be made about all of the other areas covered in the book and should not have been limited to the steroids alone. No mention was made of any drugs for neoplastic diseases, which is certainly another shortcoming of the book.

Short statements related to medicinal chemistry appear throughout the book (rigid analogs, pp. 355 and 387; the role of aromatic rings, pp. 40 and 108; and receptor, p. 218). The statements are often vague, and it would have been helpful if the authors had included an introductory chapter covering the major aspects of medicinal chemistry.

Organic chemists with no background in drugs should find this a useful introduction to the subject. This book provides only a superficial coverage of the subjects included and cannot be recommended as either an introductory text or as a reference source for anyone actively engaged in drug research.

Reviewed by Sharon G. Boots
Medical College of Virginia
Virginia Commonwealth University
Richmond, VA 23298

is not available, a copy can probably be obtained by writing one of the editors. The errors were corrected in the second printing.

A rapid reading revealed surprisingly few misspelled words and only a few errors in the other chapters. Most errors are minor and do not significantly detract from the usefulness of the material.

Errors in structural formulas include carbenicillin indanyl sodium, p. 289; cephalothin sodium, p. 292; cephapirin sodium, cephamycin, and cefoxitin, p. 294; anhydrotetracycline, p. 308; oleandomycin, p. 317; lincomycin, p. 320; nystatin, p. 330; carbachol intermediate, p. 469; and neostigmine, p. 472.

Other minor errors were also noted. On p. 306, a "2" should be replaced by a "3" to read, ". . . protonation of the enol group on carbon atom 3 . . . ." In the "Mechanism of Hydrolysis of AChE," p. 467, a positive charge was omitted and the orientation of a water molecule is misleading. On p. 477, the acid proton is incorrectly placed on pilocarpine hydrochloride. The structural formula number (I) was omitted on p. 555. In the third line on p. 560 "R" should replace "S," which refers to the absolute configuration of bisquaternary species. Since rotoxamine is the levorotatory isomer of carbinoxamine, the following statement should be deleted from pp. 652 and 654: "In compounds that exhibit optical isomerism the dextrorotatory isomer possesses most of the antihistaminic activity." Finally, on p. 665, the acid proton is incorrectly placed on antazoline hydrochloride.

A footnote in the chapter on Analgesic Agents explains that the popular term "analgesic" is used in preference to the etymologically correct term "analgetic." Perhaps it would be appropriate to explain a similar relationship in the usage of the terms "antitubercular" and "antituberculous" either on p. 144 or 331.

In the reviewer's opinion, the seventh edition is an improvement of an already good textbook. It should be well received in the classroom and is highly recommended as a textbook for courses in undergraduate medicinal and pharmaceutical chemistry.

Reviewed by Charles M. Darling
School of Pharmacy
Auburn University
Auburn, AL 36830

Assessing Drug Reactions—Adverse and Beneficial, Vol. 7: Philosophy and Technology of Drug Assessment. Edited by FRANK N. ALLAN. Interdisciplinary Communication Associates, Smithsonian Institute, Washington, DC, 1976. 158 pp. 15 × 23 cm.

This book contains the report of the seventh conference in a series on the Philosophy and Technology of Drug Assessment. This conference dealt with the basic problem of defining, detecting, reporting, and assessing adverse drug reactions. The conference was conducted by the Interdisciplinary Communications Program of the Smithsonian Institution.

The topics discussed in the book include terminology and definition of adverse drug reactions, risk–benefit analysis of adverse drug reactions, and various approaches that can be used in collecting data about adverse drug reactions. The book is written in a narrative style and includes edited statements of conference participants.

The book indicates that there was a lack of agreement among the conference participants regarding the magnitude of the problem, how to assess that magnitude, or who needed the most increased understanding. However, there was a consensus agreement that a national adverse drug reaction monitoring system is needed and that the system should be part of a larger system that includes data collection of the patient's whole response to drug therapy.

The book provides an informative insight into the controversy surrounding the collection and evaluation of adverse drug reaction data. The personal experiences of some conference participants are very enlightening and enable the reader to obtain a better grasp of the problems associated with collecting and evaluating adverse drug reaction data.

Reviewed by Frank Ascione
University of Michigan
Ann Arbor, MI 48104

AMA Drug Evaluations, 3rd Ed. Prepared by the AMA Department of Drugs in cooperation with the American Society for Clinical Pharmacology and Therapeutics. Publishing Sciences Group, 545 Great Rd., Littleton, MA 01460, 1977. 1327 pp. 18 × 26 cm. Price $29.50.

The third edition of this valuable reference source has been completely reorganized, updated, and expanded. The book is divided into 19 sections based on therapeutic category. Each section contains more specific chapters, which begin with a brief introduction and include detailed evaluations for individual drugs and compounds.

The book gives information on dosage, contraindications, and adverse reactions and includes structural formulas for most single-entity drugs. It also lists generic and proprietary names and available dosage forms and sizes. Included are evaluations of over 1300 drugs, information on investigational agents, and extensive listings for normal values of clinical laboratory tests. Also, there is information on drug interactions, labeling, and use of drugs during pregnancy.

This book is essential for those who prescribe, dispense, or administer drugs or who require information on applied therapeutics.

Staff review

Organic Chemistry of Drug Synthesis. By DANIEL LEDNICER and LESTER A. MITSCHER. Wiley, 605 Third Ave., New York, NY 10016, 1977. 471 pp. 16 × 23 cm. Price $22.50.

This book is an attempt to present to synthetic organic and medicinal chemists the synthetic routes used to prepare a great majority of organic compounds used as drugs. The book focuses on compounds that are either used in the clinic or have undergone clinical trial, concentrating on those assigned generic names by the USAN Council. There are 22 chapters, each of which is organized by structural rather than pharmacological classes. The pharmacology involved in the various disease states discussed and the mode of action in selected drug classes are written in terms useful to the chemist with a rudimentary knowledge of biology. A glossary of commonly used pharmacological terms is included.

The book is filled with errors of all types, which the reviewer found to be extremely irritating. In at least three places, the authors refer to substituted ureas as carbamates (structure 10, p. 7). No chapter was error free. Frequently compounds were given wrong numbers in the discussion section. Structure 61 (p. 36) is a piperidyl derivative, not a pyrrolidino derivative as listed. Structure 30 (p. 150) is referred to twice (p. 151) as an allylic halide when it is not one. Alkylation reactions using *N*-(2-chloroethyl)diethylamine are common throughout the book. Only twice is an aziridinium salt mentioned as an intermediate (methadone, p. 79, and promethazine, p. 373). It is quite possible that aziridinium salts play important roles in all such alkylations, not just the two unsymmetrical cases listed by the authors.

The only three groups of compounds with recent references are the benzodiazepines, prostaglandins, and cephalosporins. Only at the end of the chapter on steroids do the authors indicate that drug research in this area has not stopped. This statement can surely be made about all of the other areas covered in the book and should not have been limited to the steroids alone. No mention was made of any drugs for neoplastic diseases, which is certainly another shortcoming of the book.

Short statements related to medicinal chemistry appear throughout the book (rigid analogs, pp. 355 and 387; the role of aromatic rings, pp. 40 and 108; and receptor, p. 218). The statements are often vague, and it would have been helpful if the authors had included an introductory chapter covering the major aspects of medicinal chemistry.

Organic chemists with no background in drugs should find this a useful introduction to the subject. This book provides only a superficial coverage of the subjects included and cannot be recommended as either an introductory text or as a reference source for anyone actively engaged in drug research.

Reviewed by Sharon G. Boots
Medical College of Virginia
Virginia Commonwealth University
Richmond, VA 23298

is not available, a copy can probably be obtained by writing one of the editors. The errors were corrected in the second printing.

A rapid reading revealed surprisingly few misspelled words and only a few errors in the other chapters. Most errors are minor and do not significantly detract from the usefulness of the material.

Errors in structural formulas include carbenicillin indanyl sodium, p. 289; cephalothin sodium, p. 292; cephapirin sodium, cephamycin, and cefoxitin, p. 294; anhydrotetracycline, p. 308; oleandomycin, p. 317; lincomycin, p. 320; nystatin, p. 330; carbachol intermediate, p. 469; and neostigmine, p. 472.

Other minor errors were also noted. On p. 306, a "2" should be replaced by a "3" to read, ". . . protonation of the enol group on carbon atom 3 . . . ." In the "Mechanism of Hydrolysis of AChE," p. 467, a positive charge was omitted and the orientation of a water molecule is misleading. On p. 477, the acid proton is incorrectly placed on pilocarpine hydrochloride. The structural formula number (I) was omitted on p. 555. In the third line on p. 560 "R" should replace "S," which refers to the absolute configuration of bisquaternary species. Since rotoxamine is the levorotatory isomer of carbinoxamine, the following statement should be deleted from pp. 652 and 654: "In compounds that exhibit optical isomerism the dextrorotatory isomer possesses most of the antihistaminic activity." Finally, on p. 665, the acid proton is incorrectly placed on antazoline hydrochloride.

A footnote in the chapter on Analgesic Agents explains that the popular term "analgesic" is used in preference to the etymologically correct term "analgetic." Perhaps it would be appropriate to explain a similar relationship in the usage of the terms "antitubercular" and "antituberculous" either on p. 144 or 331.

In the reviewer's opinion, the seventh edition is an improvement of an already good textbook. It should be well received in the classroom and is highly recommended as a textbook for courses in undergraduate medicinal and pharmaceutical chemistry.

Reviewed by Charles M. Darling
School of Pharmacy
Auburn University
Auburn, AL 36830

Assessing Drug Reactions—Adverse and Beneficial, Vol. 7: Philosophy and Technology of Drug Assessment. Edited by FRANK N. ALLAN. Interdisciplinary Communication Associates, Smithsonian Institute, Washington, DC, 1976. 158 pp. 15 × 23 cm.

This book contains the report of the seventh conference in a series on the Philosophy and Technology of Drug Assessment. This conference dealt with the basic problem of defining, detecting, reporting, and assessing adverse drug reactions. The conference was conducted by the Interdisciplinary Communications Program of the Smithsonian Institution.

The topics discussed in the book include terminology and definition of adverse drug reactions, risk–benefit analysis of adverse drug reactions, and various approaches that can be used in collecting data about adverse drug reactions. The book is written in a narrative style and includes edited statements of conference participants.

The book indicates that there was a lack of agreement among the conference participants regarding the magnitude of the problem, how to assess that magnitude, or who needed the most increased understanding. However, there was a consensus agreement that a national adverse drug reaction monitoring system is needed and that the system should be part of a larger system that includes data collection of the patient's whole response to drug therapy.

The book provides an informative insight into the controversy surrounding the collection and evaluation of adverse drug reaction data. The personal experiences of some conference participants are very enlightening and enable the reader to obtain a better grasp of the problems associated with collecting and evaluating adverse drug reaction data.

Reviewed by Frank Ascione
University of Michigan
Ann Arbor, MI 48104

AMA Drug Evaluations, 3rd Ed. Prepared by the AMA Department of Drugs in cooperation with the American Society for Clinical Pharmacology and Therapeutics. Publishing Sciences Group, 545 Great Rd., Littleton, MA 01460, 1977. 1327 pp. 18 × 26 cm. Price $29.50.

The third edition of this valuable reference source has been completely reorganized, updated, and expanded. The book is divided into 19 sections based on therapeutic category. Each section contains more specific chapters, which begin with a brief introduction and include detailed evaluations for individual drugs and compounds.

The book gives information on dosage, contraindications, and adverse reactions and includes structural formulas for most single-entity drugs. It also lists generic and proprietary names and available dosage forms and sizes. Included are evaluations of over 1300 drugs, information on investigational agents, and extensive listings for normal values of clinical laboratory tests. Also, there is information on drug interactions, labeling, and use of drugs during pregnancy.

This book is essential for those who prescribe, dispense, or administer drugs or who require information on applied therapeutics.

Staff review

Organic Chemistry of Drug Synthesis. By DANIEL LEDNICER and LESTER A. MITSCHER. Wiley, 605 Third Ave., New York, NY 10016, 1977. 471 pp. 16 × 23 cm. Price $22.50.

This book is an attempt to present to synthetic organic and medicinal chemists the synthetic routes used to prepare a great majority of organic compounds used as drugs. The book focuses on compounds that are either used in the clinic or have undergone clinical trial, concentrating on those assigned generic names by the USAN Council. There are 22 chapters, each of which is organized by structural rather than pharmacological classes. The pharmacology involved in the various disease states discussed and the mode of action in selected drug classes are written in terms useful to the chemist with a rudimentary knowledge of biology. A glossary of commonly used pharmacological terms is included.

The book is filled with errors of all types, which the reviewer found to be extremely irritating. In at least three places, the authors refer to substituted ureas as carbamates (structure 10, p. 7). No chapter was error free. Frequently compounds were given wrong numbers in the discussion section. Structure 61 (p. 36) is a piperidyl derivative, not a pyrrolidino derivative as listed. Structure 30 (p. 150) is referred to twice (p. 151) as an allylic halide when it is not one. Alkylation reactions using *N*-(2-chloroethyl)diethylamine are common throughout the book. Only twice is an aziridinium salt mentioned as an intermediate (methadone, p. 79, and promethazine, p. 373). It is quite possible that aziridinium salts play important roles in all such alkylations, not just the two unsymmetrical cases listed by the authors.

The only three groups of compounds with recent references are the benzodiazepines, prostaglandins, and cephalosporins. Only at the end of the chapter on steroids do the authors indicate that drug research in this area has not stopped. This statement can surely be made about all of the other areas covered in the book and should not have been limited to the steroids alone. No mention was made of any drugs for neoplastic diseases, which is certainly another shortcoming of the book.

Short statements related to medicinal chemistry appear throughout the book (rigid analogs, pp. 355 and 387; the role of aromatic rings, pp. 40 and 108; and receptor, p. 218). The statements are often vague, and it would have been helpful if the authors had included an introductory chapter covering the major aspects of medicinal chemistry.

Organic chemists with no background in drugs should find this a useful introduction to the subject. This book provides only a superficial coverage of the subjects included and cannot be recommended as either an introductory text or as a reference source for anyone actively engaged in drug research.

Reviewed by Sharon G. Boots
Medical College of Virginia
Virginia Commonwealth University
Richmond, VA 23298

is not available, a copy can probably be obtained by writing one of the editors. The errors were corrected in the second printing.

A rapid reading revealed surprisingly few misspelled words and only a few errors in the other chapters. Most errors are minor and do not significantly detract from the usefulness of the material.

Errors in structural formulas include carbenicillin indanyl sodium, p. 289; cephalothin sodium, p. 292; cephapirin sodium, cephamycin, and cefoxitin, p. 294; anhydrotetracycline, p. 308; oleandomycin, p. 317; lincomycin, p. 320; nystatin, p. 330; carbachol intermediate, p. 469; and neostigmine, p. 472.

Other minor errors were also noted. On p. 306, a "2" should be replaced by a "3" to read, ". . . protonation of the enol group on carbon atom 3 . . . ." In the "Mechanism of Hydrolysis of AChE," p. 467, a positive charge was omitted and the orientation of a water molecule is misleading. On p. 477, the acid proton is incorrectly placed on pilocarpine hydrochloride. The structural formula number (I) was omitted on p. 555. In the third line on p. 560 "R" should replace "S," which refers to the absolute configuration of bisquaternary species. Since rotoxamine is the levorotatory isomer of carbinoxamine, the following statement should be deleted from pp. 652 and 654: "In compounds that exhibit optical isomerism the dextrorotatory isomer possesses most of the antihistaminic activity." Finally, on p. 665, the acid proton is incorrectly placed on antazoline hydrochloride.

A footnote in the chapter on Analgesic Agents explains that the popular term "analgesic" is used in preference to the etymologically correct term "analgetic." Perhaps it would be appropriate to explain a similar relationship in the usage of the terms "antitubercular" and "antituberculous" either on p. 144 or 331.

In the reviewer's opinion, the seventh edition is an improvement of an already good textbook. It should be well received in the classroom and is highly recommended as a textbook for courses in undergraduate medicinal and pharmaceutical chemistry.

Reviewed by Charles M. Darling
School of Pharmacy
Auburn University
Auburn, AL 36830

Assessing Drug Reactions—Adverse and Beneficial, Vol. 7: Philosophy and Technology of Drug Assessment. Edited by FRANK N. ALLAN. Interdisciplinary Communication Associates, Smithsonian Institute, Washington, DC, 1976. 158 pp. 15 × 23 cm.

This book contains the report of the seventh conference in a series on the Philosophy and Technology of Drug Assessment. This conference dealt with the basic problem of defining, detecting, reporting, and assessing adverse drug reactions. The conference was conducted by the Interdisciplinary Communications Program of the Smithsonian Institution.

The topics discussed in the book include terminology and definition of adverse drug reactions, risk–benefit analysis of adverse drug reactions, and various approaches that can be used in collecting data about adverse drug reactions. The book is written in a narrative style and includes edited statements of conference participants.

The book indicates that there was a lack of agreement among the conference participants regarding the magnitude of the problem, how to assess that magnitude, or who needed the most increased understanding. However, there was a consensus agreement that a national adverse drug reaction monitoring system is needed and that the system should be part of a larger system that includes data collection of the patient's whole response to drug therapy.

The book provides an informative insight into the controversy surrounding the collection and evaluation of adverse drug reaction data. The personal experiences of some conference participants are very enlightening and enable the reader to obtain a better grasp of the problems associated with collecting and evaluating adverse drug reaction data.

Reviewed by Frank Ascione
University of Michigan
Ann Arbor, MI 48104

AMA Drug Evaluations, 3rd Ed. Prepared by the AMA Department of Drugs in cooperation with the American Society for Clinical Pharmacology and Therapeutics. Publishing Sciences Group, 545 Great Rd., Littleton, MA 01460, 1977. 1327 pp. 18 × 26 cm. Price $29.50.

The third edition of this valuable reference source has been completely reorganized, updated, and expanded. The book is divided into 19 sections based on therapeutic category. Each section contains more specific chapters, which begin with a brief introduction and include detailed evaluations for individual drugs and compounds.

The book gives information on dosage, contraindications, and adverse reactions and includes structural formulas for most single-entity drugs. It also lists generic and proprietary names and available dosage forms and sizes. Included are evaluations of over 1300 drugs, information on investigational agents, and extensive listings for normal values of clinical laboratory tests. Also, there is information on drug interactions, labeling, and use of drugs during pregnancy.

This book is essential for those who prescribe, dispense, or administer drugs or who require information on applied therapeutics.

Staff review

Organic Chemistry of Drug Synthesis. By DANIEL LEDNICER and LESTER A. MITSCHER. Wiley, 605 Third Ave., New York, NY 10016, 1977. 471 pp. 16 × 23 cm. Price $22.50.

This book is an attempt to present to synthetic organic and medicinal chemists the synthetic routes used to prepare a great majority of organic compounds used as drugs. The book focuses on compounds that are either used in the clinic or have undergone clinical trial, concentrating on those assigned generic names by the USAN Council. There are 22 chapters, each of which is organized by structural rather than pharmacological classes. The pharmacology involved in the various disease states discussed and the mode of action in selected drug classes are written in terms useful to the chemist with a rudimentary knowledge of biology. A glossary of commonly used pharmacological terms is included.

The book is filled with errors of all types, which the reviewer found to be extremely irritating. In at least three places, the authors refer to substituted ureas as carbamates (structure 10, p. 7). No chapter was error free. Frequently compounds were given wrong numbers in the discussion section. Structure 61 (p. 36) is a piperidyl derivative, not a pyrrolidino derivative as listed. Structure 30 (p. 150) is referred to twice (p. 151) as an allylic halide when it is not one. Alkylation reactions using *N*-(2-chloroethyl)diethylamine are common throughout the book. Only twice is an aziridinium salt mentioned as an intermediate (methadone, p. 79, and promethazine, p. 373). It is quite possible that aziridinium salts play important roles in all such alkylations, not just the two unsymmetrical cases listed by the authors.

The only three groups of compounds with recent references are the benzodiazepines, prostaglandins, and cephalosporins. Only at the end of the chapter on steroids do the authors indicate that drug research in this area has not stopped. This statement can surely be made about all of the other areas covered in the book and should not have been limited to the steroids alone. No mention was made of any drugs for neoplastic diseases, which is certainly another shortcoming of the book.

Short statements related to medicinal chemistry appear throughout the book (rigid analogs, pp. 355 and 387; the role of aromatic rings, pp. 40 and 108; and receptor, p. 218). The statements are often vague, and it would have been helpful if the authors had included an introductory chapter covering the major aspects of medicinal chemistry.

Organic chemists with no background in drugs should find this a useful introduction to the subject. This book provides only a superficial coverage of the subjects included and cannot be recommended as either an introductory text or as a reference source for anyone actively engaged in drug research.

Reviewed by Sharon G. Boots
Medical College of Virginia
Virginia Commonwealth University
Richmond, VA 23298

Pharmaceutics of Solids and Solid Dosage Forms. By JENS T. CARSTENSEN. Wiley, 605 Third Ave., New York, NY 10016, 1977. 256 pp. 16 × 24 cm. Price $18.50.

This book was developed by Dr. Carstensen from the material he uses for a 4th-year pharmacy course. In the Preface, the author quite rightly points out that the "area of pharmaceutical solids constitutes a fascinating field of knowledge." The book covers some of the basic physical chemistry of solid dosage forms and includes a comprehensive treatment of the more common solid dosage forms used in current practice.

At the end of each chapter, there are a short list of relevant references, some problems (calculations), and some questions.

The chapters are logically ordered, and the presentation of concepts is lucid. The numerous figures are well drawn and will greatly assist the student using this text. Furthermore, the book seems commendably free of errors (although a new word, "hepticlation," appears on p. 208), and the index is well prepared.

Of course, it is inevitable that in any book of this type, one can find statements with which one does not agree. Thus, on p. 163 the author states: "A directly compressed tablet (and most often also a slugged tablet) will disintegrate into the particles from which the original blend was made." This is a generalized assertion that this reviewer regards as unjustified. Experimental data clearly suggest that, in direct compression, both particle fracture and cold welding can occur, so the particle-size distribution can be significantly altered by the compaction process.

Some readers may feel that the rather brief chapter (19 pages) titled Biopharmaceutics of Solids might have been omitted, since the topic of Biopharmaceutics justifies a much fuller treatment (*i.e.*, a separate course) and it seems somewhat artificial to separate the biopharmaceutics of solids from other dosage forms.

The last 46 pages of the book are devoted to a description of selected laboratory experiments. Many of these are particularly interesting. This reviewer was intrigued by Carstensen's description of scheduling problems for students; it was good to know that in Wisconsin at least, some students are prepared to attend a laboratory session on Monday evenings!

This book can be recommended as providing a useful basis for those planning an undergraduate pharmacy course on dosage forms. Parts of it may also be very useful for some graduate courses.

Reviewed by Christopher T. Rhodes
Department of Pharmacy
College of Pharmacy
University of Rhode Island
Kingston, RI 02881

Synthetic Methods for Carbohydrates, ACS Symposium Series 39. Edited by HASSAN S. EL KHADEM. American Chemical Society, 1155 Sixteenth St., N. W., Washington DC 20036, 1977. 278 pp. 14 × 23 cm. Price $19.50.

The book consists of 15 separately authored chapters, each of which reviews and reports original research in an important area of carbohydrate chemistry. The invited authors have made internationally notable contributions in the areas they discuss. Some chapters are more important and sophisticated than others. However, the material in each chapter is deftly and authoritatively handled. In each chapter there is much explicit and detailed technical information. In three chapters, the authors appear to have had some problems translating into English. This is a minor flaw in view of the high competence of the authors in the important areas they present.

The advancing sophistication in synthesis of carbohydrates is impressive, as is the expanding knowledge of the biological importance of carbohydrate structure. Also, some of the synthetic procedures employed to affect specific changes in the polyfunctional carbohydrates may find direct application in the synthesis of medicinal agents not directly related to carbohydrates.

The following is a sampling of the contents of the book. Chapter 1 explores the preparation, properties, and range of utility of the *O*-ethylboron protecting group. Chapter 2 examines the use of benzylidine acetals, for example, in the synthesis of 1,2-*trans*-glycosides. Chapter 4 describes the synthesis of oxaprostaglandins and C-nucleosides and the mutational synthesis of aminoglycoside antibiotics. Chapter 5 presents valuable generalizations for predicting the Cotton effect among heterocycles linked to a sugar or hydroxyalkyl moiety. Chapter 6 describes the use of 2-deoxy-2-phthalimido-D-glucopyranosyl halides in the synthesis of 2-amino-2-deoxy-β-D-glucopyranosides.

In Chapter 7, the authors relate their experiences with the chemistry of the unsaturated sugar D-glucal, especially as that chemistry relates to the synthesis of aminoglycoside antibiotics. Chapter 8 furnishes a good review of methods of incorporation of heteroatoms other than oxygen into sugar rings. Chapter 9 describes the facile synthesis and the properties of previously inaccessible 1-*O*-acyl-α-D-glucopyranose derivatives. Chapter 10 reports the synthesis and chemical properties of levoglusenone (1,6-anhydro-3,4-dideoxy-β-D-glycerohex-3-enopyranos-2-ulose), a pyrolysis product of cellulose. Chapter 11 affords answers to longstanding questions about the mechanism of osazone formation.

Chapter 12 reviews the synthesis of polyhydroxyalkyl-substituted furans, pyrroles, 1,5,6,7-tetrahydroindol-4-ones, pyrimidines, imidazolines, and imidazoles *via* reaction of glycosides and aminoglycosides with β-dicarbonyl compounds. In Chapter 13, the authors discuss the reactions between sugars and aromatic hydrocarbons and suggest that similar reactions occur between lignin and carbohydrates when wood converts to coal. Chapter 14 reports the synthesis of Amadori-type sugar derivatives of several biogenic amines (*e.g.*, serotonin) and examines the biological properties of some of these compounds. Chapter 15 reviews the structures of some bioactive glycolipids and details sophisticated reactions leading to their synthesis.

My first impression was that, because of the highly technical nature of much of this work, its appeal would be restricted to those engaged directly in carbohydrate research. After more consideration, I feel that the work should have wide appeal among medicinal chemists. Many of the synthetic procedures are elegant, are accompanied by excellent mechanistic explanations, and appear to have synthetic potential not restricted to carbohydrates. Also, some of the areas discussed, such as glycolipids, have immediate medicinal chemical significance.

Reviewed by Eugene I. Isaacson
College of Pharmacy
Idaho State University
Pocatello, ID 83201

An Introduction to Phytopharmacy. By M. S. F. ROSS and K. R. BRAIN. Pitman Medical, 42 Camden Road, Tunbridge Wells, Kent TN1 2QD, England, 1977. 305 pp. 14 × 22 cm. Price £7.00.

As stated in the introduction (Chapter 1), this book indeed provides an "integrated approach to the consideration of plants and drugs." It has very broad coverage of several aspects relating to the pharmacy disciplines such as botanical, chemical, pharmaceutical, and pharmacological.

The book is divided into two parts. The first part (Chapters 1–5) deals with general principles, and the second (Chapters 6–17) deals with specific pharmacologically active drugs of plant origin.

Chapter 2, Plants and Their Constituents, is an excellent brief account of the fundamental elements of plant biology as well as important groups of biologically active plant constituents such as the alkaloids, the glycosides, and the isoprenoids. This chapter emphasizes that plants are of importance to the pharmacist. Chapter 3, From Plant to Isolate, covers the fundamental principles and methods for the isolation of active components, including extraction and chromatographic separation techniques. Figure 3.7 showing separation of alkaloids and phenolics is neither clear nor adequate. Perhaps a more detailed flow sheet dealing with the separation of certain specific examples of alkaloidal drugs would be more impressive.

Chapter 4, Drug Variability, is concerned with the yield and quality of plant drugs. Chapter 5, The Search for Novel Plant Drugs, is well written and involves discussions of the development of new plant drugs. Chapter 6, Drugs Acting on the Central Nervous System, includes plant constituents used as analgesics, stimulants, and muscle relaxants. However, the traditional structure for tubocurarine as given in Fig. 6.2

Pharmaceutics of Solids and Solid Dosage Forms. By JENS T. CARSTENSEN. Wiley, 605 Third Ave., New York, NY 10016, 1977. 256 pp. 16 × 24 cm. Price $18.50.

This book was developed by Dr. Carstensen from the material he uses for a 4th-year pharmacy course. In the Preface, the author quite rightly points out that the "area of pharmaceutical solids constitutes a fascinating field of knowledge." The book covers some of the basic physical chemistry of solid dosage forms and includes a comprehensive treatment of the more common solid dosage forms used in current practice.

At the end of each chapter, there are a short list of relevant references, some problems (calculations), and some questions.

The chapters are logically ordered, and the presentation of concepts is lucid. The numerous figures are well drawn and will greatly assist the student using this text. Furthermore, the book seems commendably free of errors (although a new word, "hepticlation," appears on p. 208), and the index is well prepared.

Of course, it is inevitable that in any book of this type, one can find statements with which one does not agree. Thus, on p. 163 the author states: "A directly compressed tablet (and most often also a slugged tablet) will disintegrate into the particles from which the original blend was made." This is a generalized assertion that this reviewer regards as unjustified. Experimental data clearly suggest that, in direct compression, both particle fracture and cold welding can occur, so the particle-size distribution can be significantly altered by the compaction process.

Some readers may feel that the rather brief chapter (19 pages) titled Biopharmaceutics of Solids might have been omitted, since the topic of Biopharmaceutics justifies a much fuller treatment (*i.e.*, a separate course) and it seems somewhat artificial to separate the biopharmaceutics of solids from other dosage forms.

The last 46 pages of the book are devoted to a description of selected laboratory experiments. Many of these are particularly interesting. This reviewer was intrigued by Carstensen's description of scheduling problems for students; it was good to know that in Wisconsin at least, some students are prepared to attend a laboratory session on Monday evenings!

This book can be recommended as providing a useful basis for those planning an undergraduate pharmacy course on dosage forms. Parts of it may also be very useful for some graduate courses.

Reviewed by Christopher T. Rhodes
Department of Pharmacy
College of Pharmacy
University of Rhode Island
Kingston, RI 02881

Synthetic Methods for Carbohydrates, ACS Symposium Series 39. Edited by HASSAN S. EL KHADEM. American Chemical Society, 1155 Sixteenth St., N. W., Washington DC 20036, 1977. 278 pp. 14 × 23 cm. Price $19.50.

The book consists of 15 separately authored chapters, each of which reviews and reports original research in an important area of carbohydrate chemistry. The invited authors have made internationally notable contributions in the areas they discuss. Some chapters are more important and sophisticated than others. However, the material in each chapter is deftly and authoritatively handled. In each chapter there is much explicit and detailed technical information. In three chapters, the authors appear to have had some problems translating into English. This is a minor flaw in view of the high competence of the authors in the important areas they present.

The advancing sophistication in synthesis of carbohydrates is impressive, as is the expanding knowledge of the biological importance of carbohydrate structure. Also, some of the synthetic procedures employed to affect specific changes in the polyfunctional carbohydrates may find direct application in the synthesis of medicinal agents not directly related to carbohydrates.

The following is a sampling of the contents of the book. Chapter 1 explores the preparation, properties, and range of utility of the *O*-ethylboron protecting group. Chapter 2 examines the use of benzylidine acetals, for example, in the synthesis of 1,2-*trans*-glycosides. Chapter 4 describes the synthesis of oxaprostaglandins and C-nucleosides and the mutational synthesis of aminoglycoside antibiotics. Chapter 5 presents valuable generalizations for predicting the Cotton effect among heterocycles linked to a sugar or hydroxyalkyl moiety. Chapter 6 describes the use of 2-deoxy-2-phthalimido-D-glucopyranosyl halides in the synthesis of 2-amino-2-deoxy-β-D-glucopyranosides.

In Chapter 7, the authors relate their experiences with the chemistry of the unsaturated sugar D-glucal, especially as that chemistry relates to the synthesis of aminoglycoside antibiotics. Chapter 8 furnishes a good review of methods of incorporation of heteroatoms other than oxygen into sugar rings. Chapter 9 describes the facile synthesis and the properties of previously inaccessible 1-*O*-acyl-α-D-glucopyranose derivatives. Chapter 10 reports the synthesis and chemical properties of levoglusenone (1,6-anhydro-3,4-dideoxy-β-D-glycerohex-3-enopyranos-2-ulose), a pyrolysis product of cellulose. Chapter 11 affords answers to longstanding questions about the mechanism of osazone formation.

Chapter 12 reviews the synthesis of polyhydroxyalkyl-substituted furans, pyrroles, 1,5,6,7-tetrahydroindol-4-ones, pyrimidines, imidazolines, and imidazoles *via* reaction of glycosides and aminoglycosides with β-dicarbonyl compounds. In Chapter 13, the authors discuss the reactions between sugars and aromatic hydrocarbons and suggest that similar reactions occur between lignin and carbohydrates when wood converts to coal. Chapter 14 reports the synthesis of Amadori-type sugar derivatives of several biogenic amines (*e.g.*, serotonin) and examines the biological properties of some of these compounds. Chapter 15 reviews the structures of some bioactive glycolipids and details sophisticated reactions leading to their synthesis.

My first impression was that, because of the highly technical nature of much of this work, its appeal would be restricted to those engaged directly in carbohydrate research. After more consideration, I feel that the work should have wide appeal among medicinal chemists. Many of the synthetic procedures are elegant, are accompanied by excellent mechanistic explanations, and appear to have synthetic potential not restricted to carbohydrates. Also, some of the areas discussed, such as glycolipids, have immediate medicinal chemical significance.

Reviewed by Eugene I. Isaacson
College of Pharmacy
Idaho State University
Pocatello, ID 83201

An Introduction to Phytopharmacy. By M. S. F. ROSS and K. R. BRAIN. Pitman Medical, 42 Camden Road, Tunbridge Wells, Kent TN1 2QD, England, 1977. 305 pp. 14 × 22 cm. Price £7.00.

As stated in the introduction (Chapter 1), this book indeed provides an "integrated approach to the consideration of plants and drugs." It has very broad coverage of several aspects relating to the pharmacy disciplines such as botanical, chemical, pharmaceutical, and pharmacological.

The book is divided into two parts. The first part (Chapters 1–5) deals with general principles, and the second (Chapters 6–17) deals with specific pharmacologically active drugs of plant origin.

Chapter 2, Plants and Their Constituents, is an excellent brief account of the fundamental elements of plant biology as well as important groups of biologically active plant constituents such as the alkaloids, the glycosides, and the isoprenoids. This chapter emphasizes that plants are of importance to the pharmacist. Chapter 3, From Plant to Isolate, covers the fundamental principles and methods for the isolation of active components, including extraction and chromatographic separation techniques. Figure 3.7 showing separation of alkaloids and phenolics is neither clear nor adequate. Perhaps a more detailed flow sheet dealing with the separation of certain specific examples of alkaloidal drugs would be more impressive.

Chapter 4, Drug Variability, is concerned with the yield and quality of plant drugs. Chapter 5, The Search for Novel Plant Drugs, is well written and involves discussions of the development of new plant drugs. Chapter 6, Drugs Acting on the Central Nervous System, includes plant constituents used as analgesics, stimulants, and muscle relaxants. However, the traditional structure for tubocurarine as given in Fig. 6.2

Pharmaceutics of Solids and Solid Dosage Forms. By JENS T. CARSTENSEN. Wiley, 605 Third Ave., New York, NY 10016, 1977. 256 pp. 16 × 24 cm. Price $18.50.

This book was developed by Dr. Carstensen from the material he uses for a 4th-year pharmacy course. In the Preface, the author quite rightly points out that the "area of pharmaceutical solids constitutes a fascinating field of knowledge." The book covers some of the basic physical chemistry of solid dosage forms and includes a comprehensive treatment of the more common solid dosage forms used in current practice.

At the end of each chapter, there are a short list of relevant references, some problems (calculations), and some questions.

The chapters are logically ordered, and the presentation of concepts is lucid. The numerous figures are well drawn and will greatly assist the student using this text. Furthermore, the book seems commendably free of errors (although a new word, "hepticlation," appears on p. 208), and the index is well prepared.

Of course, it is inevitable that in any book of this type, one can find statements with which one does not agree. Thus, on p. 163 the author states: "A directly compressed tablet (and most often also a slugged tablet) will disintegrate into the particles from which the original blend was made." This is a generalized assertion that this reviewer regards as unjustified. Experimental data clearly suggest that, in direct compression, both particle fracture and cold welding can occur, so the particle-size distribution can be significantly altered by the compaction process.

Some readers may feel that the rather brief chapter (19 pages) titled Biopharmaceutics of Solids might have been omitted, since the topic of Biopharmaceutics justifies a much fuller treatment (*i.e.*, a separate course) and it seems somewhat artificial to separate the biopharmaceutics of solids from other dosage forms.

The last 46 pages of the book are devoted to a description of selected laboratory experiments. Many of these are particularly interesting. This reviewer was intrigued by Carstensen's description of scheduling problems for students; it was good to know that in Wisconsin at least, some students are prepared to attend a laboratory session on Monday evenings!

This book can be recommended as providing a useful basis for those planning an undergraduate pharmacy course on dosage forms. Parts of it may also be very useful for some graduate courses.

Reviewed by Christopher T. Rhodes
Department of Pharmacy
College of Pharmacy
University of Rhode Island
Kingston, RI 02881

Synthetic Methods for Carbohydrates, ACS Symposium Series 39. Edited by HASSAN S. EL KHADEM. American Chemical Society, 1155 Sixteenth St., N. W., Washington DC 20036, 1977. 278 pp. 14 × 23 cm. Price $19.50.

The book consists of 15 separately authored chapters, each of which reviews and reports original research in an important area of carbohydrate chemistry. The invited authors have made internationally notable contributions in the areas they discuss. Some chapters are more important and sophisticated than others. However, the material in each chapter is deftly and authoritatively handled. In each chapter there is much explicit and detailed technical information. In three chapters, the authors appear to have had some problems translating into English. This is a minor flaw in view of the high competence of the authors in the important areas they present.

The advancing sophistication in synthesis of carbohydrates is impressive, as is the expanding knowledge of the biological importance of carbohydrate structure. Also, some of the synthetic procedures employed to affect specific changes in the polyfunctional carbohydrates may find direct application in the synthesis of medicinal agents not directly related to carbohydrates.

The following is a sampling of the contents of the book. Chapter 1 explores the preparation, properties, and range of utility of the *O*-ethylboron protecting group. Chapter 2 examines the use of benzylidine acetals, for example, in the synthesis of 1,2-*trans*-glycosides. Chapter 4 describes the synthesis of oxaprostaglandins and C-nucleosides and the mutational synthesis of aminoglycoside antibiotics. Chapter 5 presents valuable generalizations for predicting the Cotton effect among heterocycles linked to a sugar or hydroxyalkyl moiety. Chapter 6 describes the use of 2-deoxy-2-phthalimido-D-glucopyranosyl halides in the synthesis of 2-amino-2-deoxy-β-D-glucopyranosides.

In Chapter 7, the authors relate their experiences with the chemistry of the unsaturated sugar D-glucal, especially as that chemistry relates to the synthesis of aminoglycoside antibiotics. Chapter 8 furnishes a good review of methods of incorporation of heteroatoms other than oxygen into sugar rings. Chapter 9 describes the facile synthesis and the properties of previously inaccessible 1-*O*-acyl-α-D-glucopyranose derivatives. Chapter 10 reports the synthesis and chemical properties of levoglusenone (1,6-anhydro-3,4-dideoxy-β-D-glycerohex-3-enopyranos-2-ulose), a pyrolysis product of cellulose. Chapter 11 affords answers to longstanding questions about the mechanism of osazone formation.

Chapter 12 reviews the synthesis of polyhydroxyalkyl-substituted furans, pyrroles, 1,5,6,7-tetrahydroindol-4-ones, pyrimidines, imidazolines, and imidazoles *via* reaction of glycosides and aminoglycosides with β-dicarbonyl compounds. In Chapter 13, the authors discuss the reactions between sugars and aromatic hydrocarbons and suggest that similar reactions occur between lignin and carbohydrates when wood converts to coal. Chapter 14 reports the synthesis of Amadori-type sugar derivatives of several biogenic amines (*e.g.*, serotonin) and examines the biological properties of some of these compounds. Chapter 15 reviews the structures of some bioactive glycolipids and details sophisticated reactions leading to their synthesis.

My first impression was that, because of the highly technical nature of much of this work, its appeal would be restricted to those engaged directly in carbohydrate research. After more consideration, I feel that the work should have wide appeal among medicinal chemists. Many of the synthetic procedures are elegant, are accompanied by excellent mechanistic explanations, and appear to have synthetic potential not restricted to carbohydrates. Also, some of the areas discussed, such as glycolipids, have immediate medicinal chemical significance.

Reviewed by Eugene I. Isaacson
College of Pharmacy
Idaho State University
Pocatello, ID 83201

An Introduction to Phytopharmacy. By M. S. F. ROSS and K. R. BRAIN. Pitman Medical, 42 Camden Road, Tunbridge Wells, Kent TN1 2QD, England, 1977. 305 pp. 14 × 22 cm. Price £7.00.

As stated in the introduction (Chapter 1), this book indeed provides an "integrated approach to the consideration of plants and drugs." It has very broad coverage of several aspects relating to the pharmacy disciplines such as botanical, chemical, pharmaceutical, and pharmacological.

The book is divided into two parts. The first part (Chapters 1–5) deals with general principles, and the second (Chapters 6–17) deals with specific pharmacologically active drugs of plant origin.

Chapter 2, Plants and Their Constituents, is an excellent brief account of the fundamental elements of plant biology as well as important groups of biologically active plant constituents such as the alkaloids, the glycosides, and the isoprenoids. This chapter emphasizes that plants are of importance to the pharmacist. Chapter 3, From Plant to Isolate, covers the fundamental principles and methods for the isolation of active components, including extraction and chromatographic separation techniques. Figure 3.7 showing separation of alkaloids and phenolics is neither clear nor adequate. Perhaps a more detailed flow sheet dealing with the separation of certain specific examples of alkaloidal drugs would be more impressive.

Chapter 4, Drug Variability, is concerned with the yield and quality of plant drugs. Chapter 5, The Search for Novel Plant Drugs, is well written and involves discussions of the development of new plant drugs. Chapter 6, Drugs Acting on the Central Nervous System, includes plant constituents used as analgesics, stimulants, and muscle relaxants. However, the traditional structure for tubocurarine as given in Fig. 6.2

is incorrect; it is not a bis quaternary but is rather a mono quaternary combined with a tertiary amine moiety.

Chapter 7, Drugs Affecting the Mind, briefly discusses psychotherapeutic drugs, hallucinogenic drugs, and cannabis and is a pleasure to read. Chapter 8, Ophthalmic Drugs, covers tropane, pilocarpine, arecoline, muscarine, cocaine, and related alkaloids, with emphasis on the tropane alkaloids. Chapter 9, Drugs Acting on the Cardiovascular System, discusses cardiac glycosides, hypotensive agents, and anticoagulants. The portion dealing with cardiac glycosides is well written and provides interesting reading. Chapter 10, Steroid Hormones, introduces plant sources for steroidal sapogenins that serve as starting material for the clinically useful semisynthetic steroids. Other chapters (11–17) describe GI agents, drugs affecting respiration, vitamins, antibiosis, natural toxic agents, crop protection agents, and formulation aids. As the names of these chapters imply, the authors have made a great effort to correlate plants and drugs from diversified subjects.

In general, the coverage is good and thorough, despite the fact that the literature survey is in most cases only up to 1973. The text is easy to read, although the stereochemistry of many well-known drugs included in this volume is not indicated.

The book would be a useful addition to undergraduate libraries with interests in drugs of plant origin and would be complementary to advanced undergraduate courses in natural product chemistry.

Reviewed by Kuo-Hsiung Lee
Department of Medicinal Chemistry
School of Pharmacy
University of North Carolina
Chapel Hill, NC 27514

Experimental Pharmaceutics, 4th Ed. By EUGENE L. PARROTT and WITOLD SASKI. Burgess, 7108 Ohms Lane, Minneapolis, MN 55435, 1977. vi + 338 pp. 21 × 28 cm. Price $10.95.

This laboratory manual, composed of 31 chapters and an appendix, is divided into five sections: metrology, solids, solutions, polyphasic systems, and plastic systems.

The authors have presented the material in a manner that relates pharmacy to a mathematical, scientific basis without presupposing a background in calculus or physical chemistry. The manual is different from many in the same field in that pharmaceutical preparations or dosage forms as such are not emphasized. They are, however, considered within their general classification by physical state to point out their relationships and similarities.

Solids can be used as an example of the method of presenting the material. The authors first consider the characteristics of particles and the means of reducing particle size. The blending of solids and some properties of solids are then presented. Methods of combining powdered materials to produce dosage forms of larger size such as granules, tablet triturates, and compressed tablets follow. Experiments on solids include also the coating of tablets and means of evaluating the solid dosage forms by *in vitro* and *in vivo* tests. The *in vivo* test is a urinary recovery test. In this series of experiments with solids, the student is taught techniques and skills in manipulating solids with various types of hand and mechanized equipment, specifications of solid dosage forms, physical testing by *in vitro* procedures, and bioavailability testing and evaluation by *in vivo* procedures.

Students are asked to complete tables and fill in blanks in the manual with information that they have gathered from their experiments and from assigned readings. Adequate space and graphs are provided for these purposes.

"Experimental Pharmaceutics" is not a complete textbook in itself. Use of the manual requires the guidance of an instructor willing to provide or point out references for the student to read. Several lists of references are strategically located in the manual. The publication is flexible in that each section is complete in itself, so that certain sections could be used without using the others. In fact, parts of a section could be utilized to reduce laboratory or discussion time.

The authors have provided, in the appendix, certain valuable data such as dissociation constants, freezing-point depressions, sodium chloride equivalents, ophthalmic buffer systems, and hydrophile–lipophile balance values. The authors have pointed out the importance of presenting data in a clear, concise manner and have included an outline of how to present experimental data.

In this manual, the authors have put together a logical outline of pharmaceutical systems, each supported with an adequate number of pharmaceutical preparations for the student to make and evaluate. The physical science concepts of pharmacy are integrated nicely into the preparation and evaluation of pharmaceutical dosage forms. "Experimental Pharmaceutics" is highly recommended for use as a laboratory manual in beginning courses in pharmaceutics.

Reviewed by Elmer M. Plein
School of Pharmacy
University of Washington
Seattle, WA 98195

Physical Chemistry for the Life Sciences. By JAMES R. BARRANTE. Prentice-Hall, Englewood Cliffs, NJ 07632, 1977. 337 pp. 14 × 22.5 cm. Price $14.95.

The book is designed as a text in basic physical chemistry for students majoring in biochemistry, biology, medicine, and dentistry. It is intended for a one-semester course and includes those areas of physical chemistry important to the life sciences. The level of mathematics is lower than that usually found in a physical chemistry text. At the end of each chapter, under Special Topics, there are on the average three pages of material that require an adequate mathematical background. There are problems and selected answers at the end of each chapter.

The chapters are: Properties of Gases, First Law of Thermodynamics, Second and Third Laws of Thermodynamics, Free Energy and Equilibrium, Solutions, Chemical Equilibrium, Ionic Equilibria, Reaction Kinetics, Electrochemistry, Selected Properties of Macromolecules, and Photochemistry. Although the author states that, when feasible, biological examples are used to illustrate physical–chemical principles, most of the presentation centers about very simple systems for which biological examples are not available.

The book is attractive and is well written for those interested in a concise exposure to the concepts of physical chemistry. For the pharmacy student, the text is too elementary and is not significantly different from other physical chemistry texts written for nonchemistry majors. For the pharmaceutical scientist, the book may serve as a review; however, it probably is not broad enough in scope or great enough in depth to be recommended as an addition to his or her library.

Reviewed by Eugene L. Parrott
Division of Pharmaceutics
College of Pharmacy
University of Iowa
Iowa City, IA 52242

is incorrect; it is not a bis quaternary but is rather a mono quaternary combined with a tertiary amine moiety.

Chapter 7, Drugs Affecting the Mind, briefly discusses psychotherapeutic drugs, hallucinogenic drugs, and cannabis and is a pleasure to read. Chapter 8, Ophthalmic Drugs, covers tropane, pilocarpine, arecoline, muscarine, cocaine, and related alkaloids, with emphasis on the tropane alkaloids. Chapter 9, Drugs Acting on the Cardiovascular System, discusses cardiac glycosides, hypotensive agents, and anticoagulants. The portion dealing with cardiac glycosides is well written and provides interesting reading. Chapter 10, Steroid Hormones, introduces plant sources for steroidal sapogenins that serve as starting material for the clinically useful semisynthetic steroids. Other chapters (11–17) describe GI agents, drugs affecting respiration, vitamins, antibiosis, natural toxic agents, crop protection agents, and formulation aids. As the names of these chapters imply, the authors have made a great effort to correlate plants and drugs from diversified subjects.

In general, the coverage is good and thorough, despite the fact that the literature survey is in most cases only up to 1973. The text is easy to read, although the stereochemistry of many well-known drugs included in this volume is not indicated.

The book would be a useful addition to undergraduate libraries with interests in drugs of plant origin and would be complementary to advanced undergraduate courses in natural product chemistry.

Reviewed by Kuo-Hsiung Lee
Department of Medicinal Chemistry
School of Pharmacy
University of North Carolina
Chapel Hill, NC 27514

Experimental Pharmaceutics, 4th Ed. By EUGENE L. PARROTT and WITOLD SASKI. Burgess, 7108 Ohms Lane, Minneapolis, MN 55435, 1977. vi + 338 pp. 21 × 28 cm. Price $10.95.

This laboratory manual, composed of 31 chapters and an appendix, is divided into five sections: metrology, solids, solutions, polyphasic systems, and plastic systems.

The authors have presented the material in a manner that relates pharmacy to a mathematical, scientific basis without presupposing a background in calculus or physical chemistry. The manual is different from many in the same field in that pharmaceutical preparations or dosage forms as such are not emphasized. They are, however, considered within their general classification by physical state to point out their relationships and similarities.

Solids can be used as an example of the method of presenting the material. The authors first consider the characteristics of particles and the means of reducing particle size. The blending of solids and some properties of solids are then presented. Methods of combining powdered materials to produce dosage forms of larger size such as granules, tablet triturates, and compressed tablets follow. Experiments on solids include also the coating of tablets and means of evaluating the solid dosage forms by *in vitro* and *in vivo* tests. The *in vivo* test is a urinary recovery test. In this series of experiments with solids, the student is taught techniques and skills in manipulating solids with various types of hand and mechanized equipment, specifications of solid dosage forms, physical testing by *in vitro* procedures, and bioavailability testing and evaluation by *in vivo* procedures.

Students are asked to complete tables and fill in blanks in the manual with information that they have gathered from their experiments and from assigned readings. Adequate space and graphs are provided for these purposes.

"Experimental Pharmaceutics" is not a complete textbook in itself. Use of the manual requires the guidance of an instructor willing to provide or point out references for the student to read. Several lists of references are strategically located in the manual. The publication is flexible in that each section is complete in itself, so that certain sections could be used without using the others. In fact, parts of a section could be utilized to reduce laboratory or discussion time.

The authors have provided, in the appendix, certain valuable data such as dissociation constants, freezing-point depressions, sodium chloride equivalents, ophthalmic buffer systems, and hydrophile–lipophile balance values. The authors have pointed out the importance of presenting data in a clear, concise manner and have included an outline of how to present experimental data.

In this manual, the authors have put together a logical outline of pharmaceutical systems, each supported with an adequate number of pharmaceutical preparations for the student to make and evaluate. The physical science concepts of pharmacy are integrated nicely into the preparation and evaluation of pharmaceutical dosage forms. "Experimental Pharmaceutics" is highly recommended for use as a laboratory manual in beginning courses in pharmaceutics.

Reviewed by Elmer M. Plein
School of Pharmacy
University of Washington
Seattle, WA 98195

Physical Chemistry for the Life Sciences. By JAMES R. BARRANTE. Prentice-Hall, Englewood Cliffs, NJ 07632, 1977. 337 pp. 14 × 22.5 cm. Price $14.95.

The book is designed as a text in basic physical chemistry for students majoring in biochemistry, biology, medicine, and dentistry. It is intended for a one-semester course and includes those areas of physical chemistry important to the life sciences. The level of mathematics is lower than that usually found in a physical chemistry text. At the end of each chapter, under Special Topics, there are on the average three pages of material that require an adequate mathematical background. There are problems and selected answers at the end of each chapter.

The chapters are: Properties of Gases, First Law of Thermodynamics, Second and Third Laws of Thermodynamics, Free Energy and Equilibrium, Solutions, Chemical Equilibrium, Ionic Equilibria, Reaction Kinetics, Electrochemistry, Selected Properties of Macromolecules, and Photochemistry. Although the author states that, when feasible, biological examples are used to illustrate physical–chemical principles, most of the presentation centers about very simple systems for which biological examples are not available.

The book is attractive and is well written for those interested in a concise exposure to the concepts of physical chemistry. For the pharmacy student, the text is too elementary and is not significantly different from other physical chemistry texts written for nonchemistry majors. For the pharmaceutical scientist, the book may serve as a review; however, it probably is not broad enough in scope or great enough in depth to be recommended as an addition to his or her library.

Reviewed by Eugene L. Parrott
Division of Pharmaceutics
College of Pharmacy
University of Iowa
Iowa City, IA 52242

is incorrect; it is not a bis quaternary but is rather a mono quaternary combined with a tertiary amine moiety.

Chapter 7, Drugs Affecting the Mind, briefly discusses psychotherapeutic drugs, hallucinogenic drugs, and cannabis and is a pleasure to read. Chapter 8, Ophthalmic Drugs, covers tropane, pilocarpine, arecoline, muscarine, cocaine, and related alkaloids, with emphasis on the tropane alkaloids. Chapter 9, Drugs Acting on the Cardiovascular System, discusses cardiac glycosides, hypotensive agents, and anticoagulants. The portion dealing with cardiac glycosides is well written and provides interesting reading. Chapter 10, Steroid Hormones, introduces plant sources for steroidal sapogenins that serve as starting material for the clinically useful semisynthetic steroids. Other chapters (11–17) describe GI agents, drugs affecting respiration, vitamins, antibiosis, natural toxic agents, crop protection agents, and formulation aids. As the names of these chapters imply, the authors have made a great effort to correlate plants and drugs from diversified subjects.

In general, the coverage is good and thorough, despite the fact that the literature survey is in most cases only up to 1973. The text is easy to read, although the stereochemistry of many well-known drugs included in this volume is not indicated.

The book would be a useful addition to undergraduate libraries with interests in drugs of plant origin and would be complementary to advanced undergraduate courses in natural product chemistry.

Reviewed by Kuo-Hsiung Lee
Department of Medicinal Chemistry
School of Pharmacy
University of North Carolina
Chapel Hill, NC 27514

Experimental Pharmaceutics, 4th Ed. By EUGENE L. PARROTT and WITOLD SASKI. Burgess, 7108 Ohms Lane, Minneapolis, MN 55435, 1977. vi + 338 pp. 21 × 28 cm. Price $10.95.

This laboratory manual, composed of 31 chapters and an appendix, is divided into five sections: metrology, solids, solutions, polyphasic systems, and plastic systems.

The authors have presented the material in a manner that relates pharmacy to a mathematical, scientific basis without presupposing a background in calculus or physical chemistry. The manual is different from many in the same field in that pharmaceutical preparations or dosage forms as such are not emphasized. They are, however, considered within their general classification by physical state to point out their relationships and similarities.

Solids can be used as an example of the method of presenting the material. The authors first consider the characteristics of particles and the means of reducing particle size. The blending of solids and some properties of solids are then presented. Methods of combining powdered materials to produce dosage forms of larger size such as granules, tablet triturates, and compressed tablets follow. Experiments on solids include also the coating of tablets and means of evaluating the solid dosage forms by *in vitro* and *in vivo* tests. The *in vivo* test is a urinary recovery test. In this series of experiments with solids, the student is taught techniques and skills in manipulating solids with various types of hand and mechanized equipment, specifications of solid dosage forms, physical testing by *in vitro* procedures, and bioavailability testing and evaluation by *in vivo* procedures.

Students are asked to complete tables and fill in blanks in the manual with information that they have gathered from their experiments and from assigned readings. Adequate space and graphs are provided for these purposes.

"Experimental Pharmaceutics" is not a complete textbook in itself. Use of the manual requires the guidance of an instructor willing to provide or point out references for the student to read. Several lists of references are strategically located in the manual. The publication is flexible in that each section is complete in itself, so that certain sections could be used without using the others. In fact, parts of a section could be utilized to reduce laboratory or discussion time.

The authors have provided, in the appendix, certain valuable data such as dissociation constants, freezing-point depressions, sodium chloride equivalents, ophthalmic buffer systems, and hydrophile–lipophile balance values. The authors have pointed out the importance of presenting data in a clear, concise manner and have included an outline of how to present experimental data.

In this manual, the authors have put together a logical outline of pharmaceutical systems, each supported with an adequate number of pharmaceutical preparations for the student to make and evaluate. The physical science concepts of pharmacy are integrated nicely into the preparation and evaluation of pharmaceutical dosage forms. "Experimental Pharmaceutics" is highly recommended for use as a laboratory manual in beginning courses in pharmaceutics.

Reviewed by Elmer M. Plein
School of Pharmacy
University of Washington
Seattle, WA 98195

Physical Chemistry for the Life Sciences. By JAMES R. BARRANTE. Prentice-Hall, Englewood Cliffs, NJ 07632, 1977. 337 pp. 14 × 22.5 cm. Price $14.95.

The book is designed as a text in basic physical chemistry for students majoring in biochemistry, biology, medicine, and dentistry. It is intended for a one-semester course and includes those areas of physical chemistry important to the life sciences. The level of mathematics is lower than that usually found in a physical chemistry text. At the end of each chapter, under Special Topics, there are on the average three pages of material that require an adequate mathematical background. There are problems and selected answers at the end of each chapter.

The chapters are: Properties of Gases, First Law of Thermodynamics, Second and Third Laws of Thermodynamics, Free Energy and Equilibrium, Solutions, Chemical Equilibrium, Ionic Equilibria, Reaction Kinetics, Electrochemistry, Selected Properties of Macromolecules, and Photochemistry. Although the author states that, when feasible, biological examples are used to illustrate physical–chemical principles, most of the presentation centers about very simple systems for which biological examples are not available.

The book is attractive and is well written for those interested in a concise exposure to the concepts of physical chemistry. For the pharmacy student, the text is too elementary and is not significantly different from other physical chemistry texts written for nonchemistry majors. For the pharmaceutical scientist, the book may serve as a review; however, it probably is not broad enough in scope or great enough in depth to be recommended as an addition to his or her library.

Reviewed by Eugene L. Parrott
Division of Pharmaceutics
College of Pharmacy
University of Iowa
Iowa City, IA 52242

Journal of Pharmaceutical Sciences

NOVEMBER 1977

VOLUME 66 NUMBER 11

MARY H. FERGUSON
Editor

SHELLY ELLIOTT
Production Editor

JANET D. SHOFF
Copy Editor

EDWARD G. FELDMANN
Contributing Editor

SAMUEL W. GOLDSTEIN
Contributing Editor

DAVID BOHARDT
Director of Publications

L. LUAN CORRIGAN
Assistant Director of Publications

EDITORIAL ADVISORY BOARD

JOHN AUTIAN
NORMAN R. FARNSWORTH
WILLIAM O. FOYE
WILLIAM J. JUSKO
HARRY B. KOSTENBAUDER
HERBERT A. LIEBERMAN
DAVID E. MANN, JR.
GERALD J. PAPARIELLO

The *Journal of Pharmaceutical Sciences* is published monthly by the American Pharmaceutical Association at 2215 Constitution Ave., N.W., Washington, DC 20037. Second-class postage paid at Washington, D.C., and at additional mailing office.

All expressions of opinion and statements of supposed fact appearing in articles or editorials carried in this journal are published on the authority of the writer over whose name they appear and are not to be regarded as necessarily expressing the policies or views of the American Pharmaceutical Association.

Offices—Editorial, Advertising, and Subscription Offices: 2215 Constitution Ave., N.W., Washington, DC 20037. Printing Offices: 20th & Northampton Streets, Easton, PA 18042.

Annual Subscriptions—United States and foreign, industrial and government institutions $50, educational institutions $50, individuals *for personal use only* $30; single copies $5. All foreign subscriptions add $5 for postage. Subscription rates are subject to change without notice. Members of the American Pharmaceutical Association may elect to receive the *Journal of Pharmaceutical Sciences* as a part of their annual $60 (foreign $65) APhA membership dues.

Claims—Missing numbers will not be supplied if dues or subscriptions are in arrears for more than 60 days or if claims are received more than 60 days after the date of the issue, or if loss was due to failure to give notice of change of address. The Association cannot accept responsibility for foreign delivery when its records indicate shipment has been made.

Change of Address—Members and subscribers should notify at once both the Post Office and the American Pharmaceutical Association, 2215 Constitution Ave., N.W., Washington, DC 20037, of any change of address.

Microfilm—Microfilm volumes are available from University Microfilms International, 300 N. Zeeb Road, Ann Arbor, MI 48106.

© Copyright 1977, American Pharmaceutical Association, 2215 Constitution Ave., N.W., Washington, DC 20037; all rights reserved.

FIFTY MORE FDAs?

A great deal has been said and written on the subject of the purported cancer drug, laetrile or amygdalin. The substance has enjoyed an abundant share of both critics and advocates.

The critics have included the majority of what might be characterized as "the health care establishment"; namely, government health agencies, the major societies of practitioners in medicine and pharmacy, the scientific societies in the field of health-related research, and so on.

We, ourselves, commented on the subject in our October 1975 column when we disputed the editorial position of *The New York Times* that the public should not be denied "harmless, but ineffective, remedies." At that time we predicted that a public policy position embodying this concept would return us to the bygone days of nostrums and quack remedies.

The next August, we spoke out on a closely related subject—namely, legislation to overturn the effectiveness or efficacy provision of the 1962 Drug Amendments to the Federal Food, Drug, and Cosmetic Act. If such legislation were enacted, the result would be to permit marketing of unproved drugs without regard to claims made for them. In essence, physicians—if not the general public—would be able to prescribe, to obtain, and to administer "harmless, but ineffective, remedies." In our view, this latter situation would be equally unfortunate from the standpoint of the public health and welfare.

Inasmuch as laetrile has been opposed primarily on the grounds that it is ineffective as a cancer treatment, attention has primarily focused on the repercussions its approval would have on the integrity of the effectiveness requirement as a condition for drug approval and marketing.

However, another problem of potentially major proportions has now surfaced, and it is the purpose of this editorial to bring attention to this aspect.

Laetrile proponents, in failing to obtain permission for laetrile marketing and distribution on the federal level, have turned to the individual state legislatures in an effort to obtain enabling legislation. This strategy would permit manufacture and distribution intrastate—thereby circumventing the federal prohibition which only governs drugs or drug products that move in interstate commerce.

At last count, about a dozen states have already succumbed to the onslaught of lobbying efforts by the laetrile proponents. Various others will probably follow in the next round of state legislative sessions.

What is the effect of this action? Well, for one thing someone has to look after the questions of quality, purity, packaging, and labeling of the laetrile that will be manufactured and marketed within these states.

It is one thing to inject a patient with a costly, but harmless, placebo. It is quite another matter to inject that patient with a costly, contaminated placebo. Hence, comprehensive standards are necessary regarding the purity of the product. Freedom from microbiological contamination, absence of heavy metal impurities, stability of ingredients (which include cyanide precursors), proper labeling, protective packaging, directions for storage, instructions for safe administration, and so on are all the niceties which we take for granted in the case of drugs produced by conventional drug manufacturers and moving through the usual channels of federal Food and Drug Administration scrutiny, approval, and surveillance. But the FDA is inoperative with regard to laetrile; it has no jurisdiction or authority.

Indeed, if a laetrile product were to come before FDA in any manner that would bring it under FDA inspection or monitoring authority, then FDA would be obliged to seize that product because it is illegal under federal law; the statutes prohibit FDA from condoning the existence of such a product in channels of distribution.

The only alternative is for each of these individual states to establish its own mini-FDA. Each state-level mini-FDA would then perform, within the respective states, all of the functions with regard to laetrile that we normally associate with the federal agency for conventional drugs. Already one or more states are moving in this direction. And if anyone believes that once established and operational these state-level agencies will confine themselves to laetrile monitoring, that person is ignoring the clear lessons of history.

In only a short time, we anticipate that we shall have successfully replicated 50 of these mini-FDAs, each contributing its own huge dose of red tape, paperwork, and bureaucratic procedures to a broad spectrum of drugs. Beyond the hassle for the drug industry and the frustration for the health professions, the cost to taxpayers will be enormous.

Whatever the benefits and limitations of the present federal FDA, we suspect that neither its proponents or opponents relish the prospect of such a dual system. Consequently, if this outcome is to be avoided, the potential problem must be recognized, and appropriate action taken to avoid such a development from ensuing.

Edward G. Feldmann

Journal of Pharmaceutical Sciences

NOVEMBER 1977

VOLUME 66 NUMBER 11

MARY H. FERGUSON
Editor

SHELLY ELLIOTT
Production Editor

JANET D. SHOFF
Copy Editor

EDWARD G. FELDMANN
Contributing Editor

SAMUEL W. GOLDSTEIN
Contributing Editor

DAVID BOHARDT
Director of Publications

L. LUAN CORRIGAN
Assistant Director of Publications

EDITORIAL ADVISORY BOARD

JOHN AUTIAN
NORMAN R. FARNSWORTH
WILLIAM O. FOYE
WILLIAM J. JUSKO
HARRY B. KOSTENBAUDER
HERBERT A. LIEBERMAN
DAVID E. MANN, JR.
GERALD J. PAPARIELLO

The *Journal of Pharmaceutical Sciences* is published monthly by the American Pharmaceutical Association at 2215 Constitution Ave., N.W., Washington, DC 20037. Second-class postage paid at Washington, D.C., and at additional mailing office.

All expressions of opinion and statements of supposed fact appearing in articles or editorials carried in this journal are published on the authority of the writer over whose name they appear and are not to be regarded as necessarily expressing the policies or views of the American Pharmaceutical Association.

Offices—Editorial, Advertising, and Subscription Offices: 2215 Constitution Ave., N.W., Washington, DC 20037. Printing Offices: 20th & Northampton Streets, Easton, PA 18042.

Annual Subscriptions—United States and foreign, industrial and government institutions $50, educational institutions $50, individuals *for personal use only* $30; single copies $5. All foreign subscriptions add $5 for postage. Subscription rates are subject to change without notice. Members of the American Pharmaceutical Association may elect to receive the *Journal of Pharmaceutical Sciences* as a part of their annual $60 (foreign $65) APhA membership dues.

Claims—Missing numbers will not be supplied if dues or subscriptions are in arrears for more than 60 days or if claims are received more than 60 days after the date of the issue, or if loss was due to failure to give notice of change of address. The Association cannot accept responsibility for foreign delivery when its records indicate shipment has been made.

Change of Address—Members and subscribers should notify at once both the Post Office and the American Pharmaceutical Association, 2215 Constitution Ave., N.W., Washington, DC 20037, of any change of address.

Microfilm—Microfilm volumes are available from University Microfilms International, 300 N. Zeeb Road, Ann Arbor, MI 48106.

© Copyright 1977, American Pharmaceutical Association, 2215 Constitution Ave., N.W., Washington, DC 20037; all rights reserved.

FIFTY MORE FDAs?

A great deal has been said and written on the subject of the purported cancer drug, laetrile or amygdalin. The substance has enjoyed an abundant share of both critics and advocates.

The critics have included the majority of what might be characterized as "the health care establishment"; namely, government health agencies, the major societies of practitioners in medicine and pharmacy, the scientific societies in the field of health-related research, and so on.

We, ourselves, commented on the subject in our October 1975 column when we disputed the editorial position of *The New York Times* that the public should not be denied "harmless, but ineffective, remedies." At that time we predicted that a public policy position embodying this concept would return us to the bygone days of nostrums and quack remedies.

The next August, we spoke out on a closely related subject—namely, legislation to overturn the effectiveness or efficacy provision of the 1962 Drug Amendments to the Federal Food, Drug, and Cosmetic Act. If such legislation were enacted, the result would be to permit marketing of unproved drugs without regard to claims made for them. In essence, physicians—if not the general public—would be able to prescribe, to obtain, and to administer "harmless, but ineffective, remedies." In our view, this latter situation would be equally unfortunate from the standpoint of the public health and welfare.

Inasmuch as laetrile has been opposed primarily on the grounds that it is ineffective as a cancer treatment, attention has primarily focused on the repercussions its approval would have on the integrity of the effectiveness requirement as a condition for drug approval and marketing.

However, another problem of potentially major proportions has now surfaced, and it is the purpose of this editorial to bring attention to this aspect.

Laetrile proponents, in failing to obtain permission for laetrile marketing and distribution on the federal level, have turned to the individual state legislatures in an effort to obtain enabling legislation. This strategy would permit manufacture and distribution intrastate—thereby circumventing the federal prohibition which only governs drugs or drug products that move in interstate commerce.

At last count, about a dozen states have already succumbed to the onslaught of lobbying efforts by the laetrile proponents. Various others will probably follow in the next round of state legislative sessions.

What is the effect of this action? Well, for one thing someone has to look after the questions of quality, purity, packaging, and labeling of the laetrile that will be manufactured and marketed within these states.

It is one thing to inject a patient with a costly, but harmless, placebo. It is quite another matter to inject that patient with a costly, contaminated placebo. Hence, comprehensive standards are necessary regarding the purity of the product. Freedom from microbiological contamination, absence of heavy metal impurities, stability of ingredients (which include cyanide precursors), proper labeling, protective packaging, directions for storage, instructions for safe administration, and so on are all the niceties which we take for granted in the case of drugs produced by conventional drug manufacturers and moving through the usual channels of federal Food and Drug Administration scrutiny, approval, and surveillance. But the FDA is inoperative with regard to laetrile; it has no jurisdiction or authority.

Indeed, if a laetrile product were to come before FDA in any manner that would bring it under FDA inspection or monitoring authority, then FDA would be obliged to seize that product because it is illegal under federal law; the statutes prohibit FDA from condoning the existence of such a product in channels of distribution.

The only alternative is for each of these individual states to establish its own mini-FDA. Each state-level mini-FDA would then perform, within the respective states, all of the functions with regard to laetrile that we normally associate with the federal agency for conventional drugs. Already one or more states are moving in this direction. And if anyone believes that once established and operational these state-level agencies will confine themselves to laetrile monitoring, that person is ignoring the clear lessons of history.

In only a short time, we anticipate that we shall have successfully replicated 50 of these mini-FDAs, each contributing its own huge dose of red tape, paperwork, and bureaucratic procedures to a broad spectrum of drugs. Beyond the hassle for the drug industry and the frustration for the health professions, the cost to taxpayers will be enormous.

Whatever the benefits and limitations of the present federal FDA, we suspect that neither its proponents or opponents relish the prospect of such a dual system. Consequently, if this outcome is to be avoided, the potential problem must be recognized, and appropriate action taken to avoid such a development from ensuing.

Edward G. Feldmann

Journal of Pharmaceutical Sciences

NOVEMBER 1977
VOLUME 66 NUMBER 11

RESEARCH ARTICLES

Degradation Kinetics of a Novel Antimitogenic and Antiviral Palladium(II) Coordination Compound

ANWAR B. BIKHAZI *x, SARKIS M. AGHAZARIAN *, and HASSAN A. TAYIM ‡

Abstract □ The degradation kinetics of a new organometallic coordination compound, aquadichloro(2,6-diaminopyridine)palladium(II), were studied in acidic and acid halide media. In acidic solutions, the degradation was first order with respect to the complex concentration; *e.g.*, at 77°, the apparent rate constants at pH 1.00, 1.22, and 1.50 were 0.00395, 0.00292, and 0.00225 min^{-1}, respectively. Furthermore, a plot of log (apparent rate constant) *versus* pH gave a straight line with an approximate slope of 0.5, indicating pseudo-first-order catalysis with respect to complex concentration at a specified pH. Activation energies obtained from Arrhenius plots varied from 43 to 57 kcal/deg/mole for pH 1.00 and 1.50, respectively. The pH-independent activation energy was 15 kcal/deg/mole. In acid halide solutions, utilizing the method of initial rates, the degradation was first order with respect to complex concentration. A plot of log (initial rate) *versus* log (chloride-ion concentration) gave a straight line with an apparent slope of 1.0. A plot of log (initial rate) *versus* pH resulted in a straight line with a slope of 0.5. Thus, pseudo-first-order catalysis with respect to complex concentration at a specified pH and pCl occurred. When the method of curve stripping was applied to the data, a plot of log (complex concentration undegraded) *versus* time resulted in a biexponential relationship; *e.g.*, at pH 1.50, 0.10 *M* chloride concentration, and 57°, the biexponential relationship between undegraded complex *versus* time giving the best fit to the data was: complex concentration = $0.237e^{-0.0653t} + 2.213e^{-0.00276t}$. A general mechanistic explanation of the acid- and acid halide-catalyzed degradation of the complex is proposed.

Keyphrases □ Palladium(II) coordination compound—degradation kinetics in acidic and acid halide media □ Aquadichloro(2,6-diaminopyridine)palladium(II)—degradation kinetics in acidic and acid halide media □ Coordination compounds—aquadichloro(2,6-diaminopyridine)palladium(II), degradation kinetics in acidic and acid halide media □ Degradation kinetics—aquadichloro(2,6-diaminopyridine)palladium(II) in acidic and acid halide media □ Stability—aquadichloro(2,6-diaminopyridine)palladium(II) in acidic and acid halide media

The therapeutic significance of organometallic coordination compounds as antiviral, antimitogenic, and antitumor agents gained importance recently (1, 2). Different theories have been proposed for their mode of action (3–5), but none is fully validated. Previous studies on the mechanism of degradation of organometallic coordination compounds were concerned with thermal stability, acid and base catalysis, anation, and other substitution reactions (6–21).

The present paper reports a study of the stability of aquadichloro(2,6-diaminopyridine)palladium(II)[1] in acidic and acid halide media and calculation of rate constants, pseudo-order constants, activation energies, and equilibrium constants. Furthermore, general mechanistic explanations of the catalytic reactions are proposed.

EXPERIMENTAL

Synthesis of Aquadichloro(2,6 - diaminopyridine)palladium(II)—The procedure followed was reported recently (20).

Standard Curves—Appropriate dilutions of the coordination compound and its ligand 2,6-diaminopyridine were prepared in acidic, neutral, and basic media. The UV spectra were recorded on a UV spectrophotometer[2], and the λ_{max} was determined. Standard solutions of the complex and the ligand were then prepared in their corresponding media and assayed spectrophotometrically using appropriate blanks. The molar absorptivities (ϵ^{M}_{1cm}) calculated from the standard curves are reported in Table I.

Analytical Procedures—Solutions of both the ligand and the complex were prepared in various aqueous media at different pH values. Spectral interference between the ligand and the complex were noted for possible use as an analytical assay procedure for the complex and/or the ligand in the presence of one another. At λ_{max} 340 nm, the complex and the ligand did not interfere in basic media (Table I). Therefore, for

[1] Previously referred to in the literature as palladium dichloride (2,6-diaminopyridine)·H_2O.
[2] Model 202, Perkin-Elmer Corp., Norwalk, Conn.

Table I—Estimated λ_{max} Values and Molar Absorptivities ($\epsilon^{M}_{1\,cm}$) of the Ligand and the Complex in Acidic and Basic Media

Compound	Medium	λ_{max}, nm	$\epsilon^{M}_{1\,cm}$
Ligand	Acid, pH 1–2	332	13,550
		243	9,000
	Base, pH 11	240	7,600
		304	7,325
		340	0
Complex	Acid, pH 1–2	Unstable	—
	Base, pH 11	340	4,270
		304[a]	3,590

[a] At $\lambda_{304\,nm}$, complex showed no maximum; $\epsilon_1{}^{M}_{cm}$ at 304 was calculated from absorbance.

stability studies in acidic media, the samples were made basic and read at λ_{max} 340 nm for the undegraded complex. Thus, the following relationship is proposed:

$$\frac{A_{340\,nm}}{\epsilon^{M}_{1\,cm\,(340\,nm)}} = \frac{A_{304\,nm}}{\epsilon^{M}_{1\,cm\,(304\,nm)}} \qquad \text{(Eq. 1)}$$

where A is the absorbance, and $\epsilon^{M}_{1\,cm}$ is the molar absorptivity as reported in Table I. Therefore, it is possible to calculate the absorbance of the complex at 304 nm once $\epsilon^{M}_{1\,cm\,(340\,nm)}$ and $\epsilon^{M}_{1\,cm\,(304\,nm)}$ are known; the value of $A_{340\,nm}$ of the complex is experimentally determined in basic media. This procedure allowed for the analysis of both the ligand and the complex in the presence of one another in any reaction mixture.

Acid Catalysis Procedure—A saturated solution of the complex (7.35×10^{-4} *M*) was prepared in double-distilled water and then diluted in the corresponding acidic medium (30 ml total volume in the reaction flask), with absorbance values ranging between 0.1 and 1.0 at the specific λ_{max}. The reaction flask was preequilibrated at the desired temperature (37–77°) in a thermostatically controlled water bath.

After thermal equilibration was completed, the desired quantity of acid was added to the mixture for the initiation of the reaction. The zero time was immediately recorded, and a 2-ml sample was withdrawn from the reaction flask. The sample was transferred into a precooled test tube in crushed ice for reaction quenching. Samples were similarly withdrawn at different time intervals. At the end of the experiment, 2.0–6.0 ml of 0.1 *N* sodium hydroxide solution was added to the 2.0-ml samples to make the final pH basic. The samples were then spectrophotometrically assayed as discussed under *Analytical Procedures*.

Equilibrium Studies—Acid catalytic reactions were allowed to reach equilibrium as spectrophotometrically observed. The following mathematical relationships were deduced from the reaction mechanism proposed under *Discussion:*

$$K_{eq} = \frac{[Pd(H_2O)_4][LH_2{}^{2+}]}{[Pd(X_2)L]} \qquad \text{(Eq. 2)}$$

where $Pd(X_2)L$ represents the complex, X is chloride, and L is 2,6-diaminopyridine. When $[Pd(H_2O)_4] = [LH_2{}^{2+}]$, then:

$$K_{eq} = \frac{[LH_2{}^{2+}]^2}{[Pd(X_2)L]} \qquad \text{(Eq. 3)}$$

Acid Halide Catalysis Procedure—The halides included chloride and bromide ions. Experiments with iodides and fluorides were not possible because iodides liberated iodine and fluorides liberated hydrogen fluoride gas in acidic media. The procedure for acid halide catalysis was basically the same as that described under *Acid Catalysis Procedure*. However, to assess the effect of the halide ion, perchloric acid was used to acidify the solution; the perchlorate ion has no catalytic effect on the reaction.

Therefore, to the preequilibrated stock solution of the complex in the water bath, a pipetted quantity of a concentrated solution of halide ions was added. The final halide-ion concentration in the reaction mixture varied from 3.3×10^{-3} to 10^{-1} *M*, depending on the experiment. Then, the required amount of concentrated perchloric acid was added, and sampling was exactly the same as described under *Acid Catalysis Procedure*. Both the chloride and bromide ions showed identical effects on the reaction process, so sodium chloride was used as the halide source.

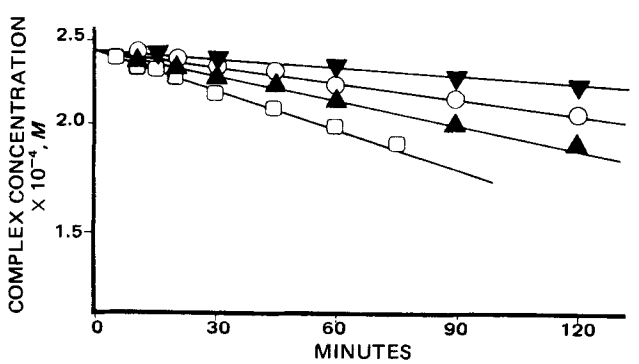

Figure 1—*Semilogarithmic plot of complex concentration undegraded* $\times 10^{-4}$ M versus *time in minutes in acid catalysis experiment at pH 1.0 (thermal stability study). Key:* ▼, *57°;* ○, *67°;* ▲, *72°; and* □, *77°.*

Table II—Calculated Rate Constants in Acid Catalysis of Complex while Varying pH and Temperature and Keeping Complex Concentration Constant

Temperature	pH[a]	Rate Constant, $k_{obs}{}^{b} \times 10^{-3}$, min^{-1}	Rate Constant, $k_H{}^{c} \times 10^{-3}$, liters/mole/min
77°	1.00	3.95	
77°	1.22	2.92	12.7
77°	1.50	2.25	
72°	1.00	2.35	
72°	1.22	1.97	8.0
72°	1.50	1.35	
67°	1.00	1.67	
67°	1.22	1.10	6.25
67°	1.50	0.83	

[a] The pH measurement at the end of the experiment at 25°. [b] Calculated from slope of lines on semilogarithmic plots, and $k_{obs} = k_H[H^+]^{0.5}$. [c] Calculated from slope of lines on rectangular plots when k_{obs} *versus* $[H^+]^{0.5}$ is drawn.

Calculations and Data Treatment—The theory proposed for acid catalysis is based on the following reaction mechanism of the complex:

$$Pd(X_2)L + 4H_2O + 2H^+ \rightleftharpoons Pd(H_2O)_4{}^{2+} + 2X^- + LH_2{}^{2+}$$

Scheme I

The general rate equation for the acid catalytic process is written as:

$$\frac{d[Pd(X_2)L]}{dt} = k_{(H)}[H_2O]^p[H^+]^m[Pd(X_2)L]^n \qquad \text{(Eq. 4)}$$

where $k_{(H)}$ represents the true rate constant for hydrogen-ion catalysis, brackets denote concentration, and the superscripts p, m, and n refer to the order of the reaction with respect to water, hydrogen-ion, and complex concentrations, respectively. It is generally assumed that $[H_2O]$ and $[H^+]$ are constant in the reaction mixture. Thus, Eq. 4 is reduced to the following general pseudo-order rate equation:

$$\frac{d[Pd(X_2)L]}{dt} = k_{obs}[Pd(X_2)L]^n \qquad \text{(Eq. 5)}$$

where:

$$k_{obs} = k_H[H_2O]^p[H^+]^m \qquad \text{(Eq. 6)}$$

Equation 6 can be written as:

$$\log k_{obs} = \log k_H[H_2O]^p - m\text{pH} \qquad \text{(Eq. 7)}$$

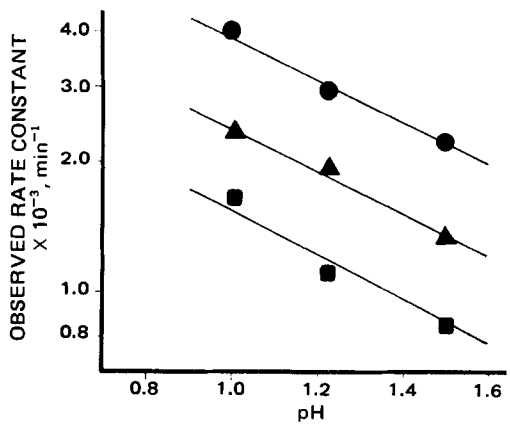

Figure 2—*Semilogarithmic plot of* $k_{obs} \times 10^{-3}$ *in minutes*$^{-1}$ versus *pH in acid catalysis experiment at different temperatures. Key:* ■, *67°;* ▲, *72°; and* ●, *77°.*

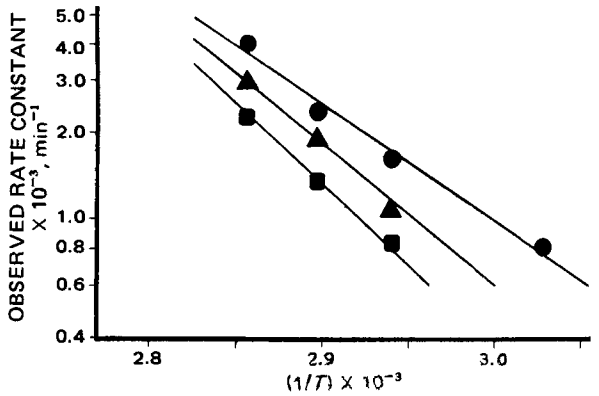

Figure 3—*Arrhenius plot for acid catalysis experiments at different pH values. Key:* ■, *pH 1.50;* ▲, *pH 1.22; and* ●, *pH 1.0.*

The following Arrhenius relationship is used in the thermal stability studies in acidic media of the complex:

$$\log k_{obs} = \log A - \frac{\Delta H}{2.3RT} \qquad \text{(Eq. 8)}$$

where A is the Arrhenius constant, R is the gas constant, ΔH is the activation energy of the reaction, and T is the temperature in absolute degrees.

The reaction mechanism proposed for acid halide catalysis is:

$$Pd(X_2)L + H_2O + 2X^- + 2H^+ \rightarrow Pd(X_4)^{2-} + LH_2^{2+}$$

Scheme II

Therefore, the general rate equation for acid halide catalysis is written as:

$$\frac{d[Pd(X_2)L]}{dt} = k_{(H)(Cl)}[H^+]^{p'}[Cl^-]^{m'}[Pd(X_2)L]^{n'} \qquad \text{(Eq. 9)}$$

where $k_{(H)(Cl)}$ represents the true rate constant for hydrogen-ion–chloride catalysis. The method of initial rate is proposed in the treatment of the data. This method is used by keeping two out of the three variable species in the reaction mixture constant. Then, a plot of log (initial rate of complex degrading) *versus* log (species concentration) results in a straight line with a slope p', m', or n', depending on which species in the reaction is the variable.

Since the data on acid halide catalysis did not fit a zero-, first-, second-, or higher order process, such a complicated mechanism possibly fits a biexponential relationship. This relationship was found to agree with the results when log $[Pd(X_2)L]$ *versus* time was plotted semilogarithmically according to Eq. 10:

$$[Pd(X_2)L] = Ae^{-\alpha t} + Be^{-\beta t} \qquad \text{(Eq. 10)}$$

where A and B represent concentration terms, which at time (t) zero would add up to the initial complex concentration; and α and β stand for the complicated rate constants of the reaction and are possibly functions of chloride- and hydrogen-ion concentrations. The method of curve stripping allows the calculations of both α and β.

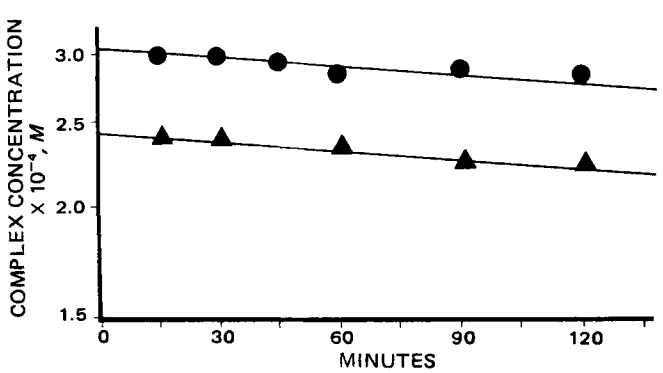

Figure 4—*Semilogarithmic plot of complex concentration undegraded* $\times 10^{-4}$ M versus *time in minutes in acid catalysis experiment at pH 1.0 and 57° while varying the initial complex concentration. Key:* ▲, *2.45* $\times 10^{-4}$ M; *and* ●, *3.06* $\times 10^{-4}$ M.

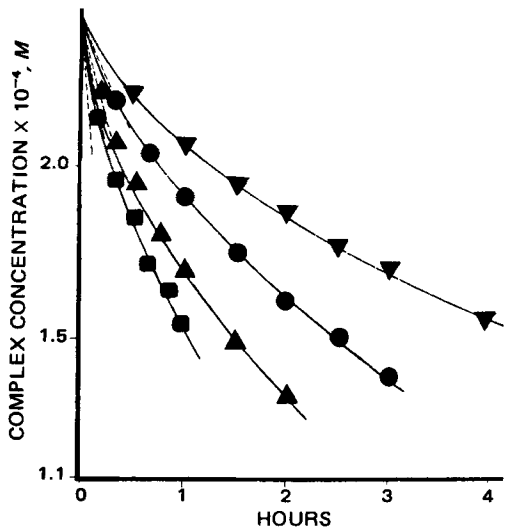

Figure 5—*Plot of complex concentration* $\times 10^{-4}$ M versus *time in hours in acid halide catalysis experiment at chloride-ion concentration of* 10^{-1} M *and 57° while varying the pH. Key:* ▼, *pH 2.20;* ●, *pH 1.50;* ▲, *pH 1.30; and* ■, *pH 1.1.*

RESULTS

Acid Catalysis—The three variables influencing the acid catalytic mechanism of the complex are the complex concentration, pH, and temperature. Therefore, this catalytic mechanism was studied as a function of each variable. For example, Fig. 1 represents a plot of the logarithm of complex concentration remaining in the reaction mixture *versus* time in a system where the initial complex concentration and the pH were constant, the only variable being the temperature. Linearity is observed in the plots for all systems when complex concentration *versus* time is plotted semilogarithmically (Table II).

Figure 2 is a graphical illustration of Eq. 7 for a plot of log k_{obs} *versus* pH of the data as reported in Table II. The average slope of the lines was 0.5 and equal to m in Eq. 7.

Figure 3 is the Arrhenius plot of log k_{obs} *versus* reciprocal temperature (in absolute degrees) of the data presented in Table II. The activation energies calculated from the slopes of the lines were 43 kcal/deg/mole at pH 1.00, 50 kcal/deg/mole at pH 1.22, and 57 kcal/deg/mole at pH 1.50. The variation in the activation energies is explained on the basis that the rate constants are pH dependent. Also, when the data of k_H reported in Table II were plotted as log k_H *versus* reciprocal temperature, a straight line resulted. The slope of this linear plot made it possible to calculate

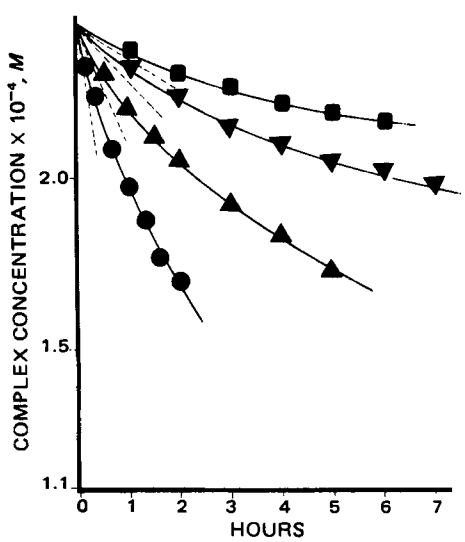

Figure 6—*Plot of complex concentration* $\times 10^{-4}$ M versus *time in hours in acid halide catalysis experiment at pH 1.1 and 47° while varying the chloride-ion concentration. Key:* ■, *3.3* $\times 10^{-3}$ M; ▼, *1* $\times 10^{-2}$ M; ▲, *3.3* $\times 10^{-2}$ M; *and* ●, *1* $\times 10^{-1}$ M.

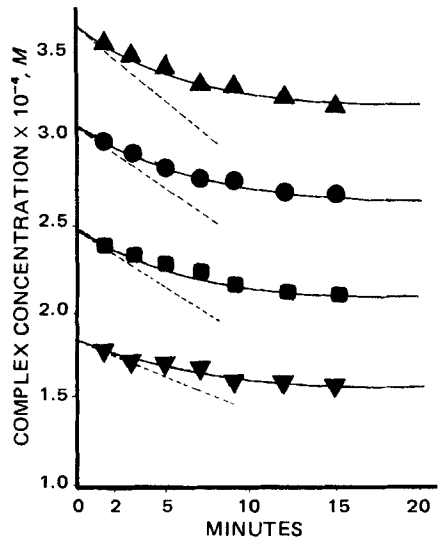

Figure 7—*Plot of complex concentration* × 10^{-4} M versus *time in minutes in acid halide catalysis experiment at pH 1.1, 57°, and a chloride-ion concentration of* 10^{-1} M *while varying the initial complex concentration. Key:* ▼, *1.84* × 10^{-4} M; ■, *2.45* × 10^{-4} M; ●, *3.07* × 10^{-4} M; *and* ▲, *3.7* × 10^{-4} M.

an activation energy of around 15 kcal/deg/mole, which is pH independent.

Figure 4 shows the effect of varying the complex concentration on the reaction mechanism. The semilogarithmic plots are linear and parallel. Thus, the data reported so far supported the fact that the reaction mechanism is hydrogen-ion catalyzed and pseudo-first order with respect to complex concentration. Therefore, Eq. 4 can be written as:

$$\frac{d[Pd(X_2)L]}{dt} = k_{(H)}[H^+]^{0.5}[Pd(X_2)L]^1 \qquad \text{(Eq. 11)}$$

Equilibrium Studies—The calculated K_{eq} values utilizing Eq. 3 were 1.475×10^{-4} at pH 1.10, 0.574×10^{-4} at pH 1.50, and 0.325×10^{-4} at pH 1.70. Thus, the K_{eq} values are dependent on hydrogen-ion concentration. Therefore, a normalized K_{eq} value was calculated by dividing the calculated K_{eq} value by the hydrogen-ion concentration. These normalized values are 1.69×10^{-3} at pH 1.1, 1.77×10^{-3} at pH 1.50, and 1.70×10^{-3} at pH 1.70. The normalized values are almost equal and are independent of the hydrogen-ion concentration.

Acid Halide Catalysis—The results of the acid halide catalysis depended on the following: (*a*) the effect of varying the hydrogen-ion concentration on the degradation mechanism of the complex while keeping the initial complex concentration, chloride-ion concentration, and temperature constant; (*b*) the effect of varying the chloride-ion concentration while keeping the concentration of the other variables constant; and (*c*) the effect of varying the complex concentration while keeping the concentrations of the other two variables constant.

Table III—Estimated Initial Rates of Degradation of Complex in Acid Halide Media while Keeping Temperature, pH, and Complex Concentration Constant

pH	Temperature	Chloride-Ion Concentration, *M*	Initial Rate × 10^{-7}, *M*/min
1.10	47°	0.10	16.2
	47°	0.033	6.57
	47°	0.010	2.43
	57°	0.10	60.0
	57°	0.033	23.2
	57°	0.010	9.08
1.50	57°	0.10	32.5
	57°	0.033	11.5
	57°	0.010	5.18
	67°	0.10	85.0
	67°	0.033	34.3
	67°	0.010	14.0

Table IV—Estimated Initial Rates of Degradation of Complex in Acid Halide Media while Keeping Temperature (57°), Chloride Concentration, and Complex Concentration Constant

pH	Initial Rate × 10^{-7}, *M*/min
1.1	60.00
1.3	43.00
1.5	32.50
2.2	13.40

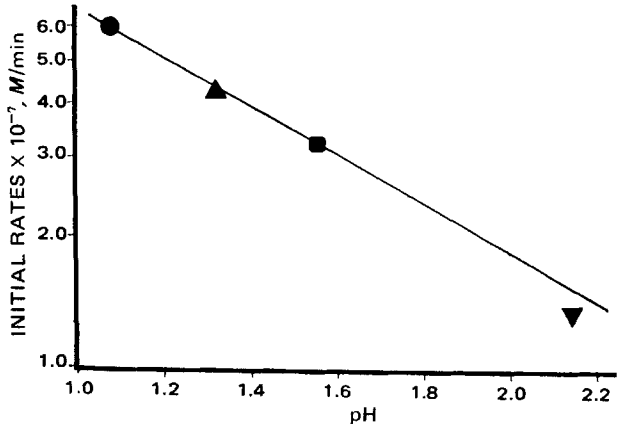

Figure 8—*Semilogarithmic plot of estimated initial rates* × 10^{-7} *in* M/*min* versus *pH in acid halide catalysis experiment at 57° and a chloride-ion concentration of* 10^{-1} M. *Key:* ▼, *pH 2.20;* ■, *pH 1.50;* ▲, *pH 1.30; and* ●, *pH 1.10.*

Figures 5–7 represent these studies when complex concentration is plotted *versus* time on rectangular coordinates. The initial slopes of the plots are calculated and presented in Tables III and IV. Figure 8 represents a plot of log initial rate *versus* pH of the data in Tables III and IV. The slope of the line was 0.5 and equal to p' in Eq. 9. Figure 9 shows the log–log plot of initial rate *versus* chloride concentration at different temperatures as given in Table III. The averaged slope of the lines was around 1.0 and equal to m' in Eq. 9. Similarly, Fig. 10 is a log–log plot of initial rate *versus* complex concentration. The slope of the line was 1.0 and equal to n' in Eq. 9. Therefore, Eq. 9 can be written as:

$$\frac{d[Pd(X_2)L]}{dt} = k_{(H)(Cl)}[H^+]^{0.5}[Cl^-]^1[Pd(X_2)L]^1 \qquad \text{(Eq. 12)}$$

Curve-Stripping Procedure and Residuals—Figure 11 is a semilogarithmic plot of three sets of data for acid halide catalysis. The biexponential shape of the curves is mathematically supported by Eq. 10; therefore, at t large and when $\alpha \gg \beta$, the slope is estimated to be β. The value of α is then obtained by extrapolation of the linear portion of the plot fitting $Be^{-\beta t}$. Therefore, subtracting the subsequent values, at t small, of the extrapolated line from the values of the curved portion of the plot would give residual values. Thus, Eq. 10 is rearranged to give:

$$\text{residual} = [Pd(X_2)L] - Be^{-\beta t} = Ae^{-\alpha t} \qquad \text{(Eq. 13)}$$

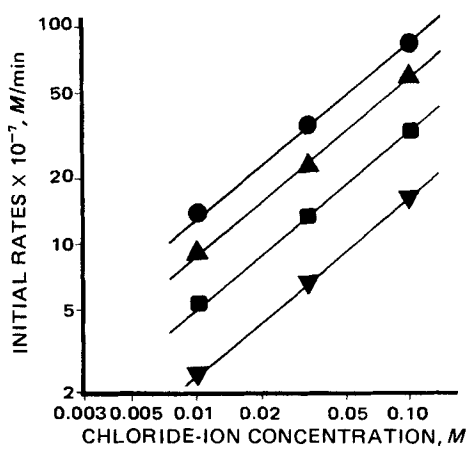

Figure 9—*Log–log plot of estimated initial rates* × 10^{-7} *in* M/*min* versus *chloride-ion concentration in* M *in acid halide catalysis experiment while varying pH and temperature. Key:* ●, *pH 1.1, 47°;* ▲, *pH 1.5, 57°;* ■, *pH 1.1, 57°; and* ▼, *pH 1.5, 67°.*

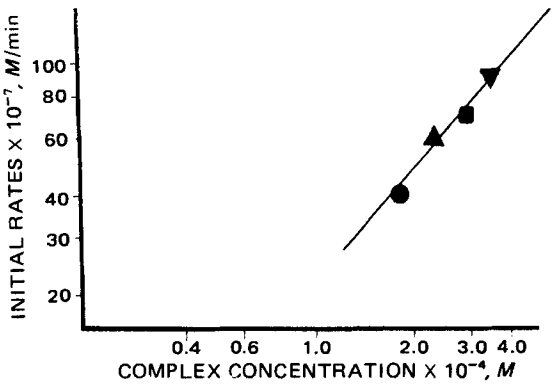

Figure 10—*Log-log plot of estimated initial rates* $\times 10^{-7}$ *in* M/*min* versus *complex concentration* $\times 10^{-4}$ M *in acid halide catalysis experiment at pH 1.1, 57°, and a chloride-ion concentration of* 10^{-1} M *while varying initial complex concentration. Key:* ●, 1.84×10^{-4} M; ▲, 2.45×10^{-4} M; ■, 3.07×10^{-4} M; *and* ▼, 3.7×10^{-4} M.

A semilogarithmic plot of residuals *versus* time, *t*, gave straight lines with slopes equal to α (Fig. 11). Table V gives the values of α, β, *A*, and *B* for the experiments on acid halide catalysis as calculated by the curve-stripping method.

DISCUSSION

The present study explained the mechanism of degradation of aquadichloro(2,6-diaminopyridine)palladium(II) in acidic and acid halide media. For acid catalysis, an overall order of 1.5 with respect to the reacting species in the reaction mixture was observed. The calculated activation energies revealed an extremely sensitive process with acid catalysis. The general reaction mechanism for acid catalysis can be proposed as occurring in two steps, a possible aquation reaction (Scheme III) and acid catalysis (Scheme IV).

The acid halide catalysis process had an overall order of 2.5 with respect to the reacting species. It was also demonstrated by the curve-stripping method that a biexponential relationship easily fit the results. For example, from Table V, when the pH is 1.50, *T* is 57°, chloride concentration is 10^{-1} *M*, and $[Pd(X_2)L]_{t=0}$ is 2.45×10^{-4} *M*, the following relationship

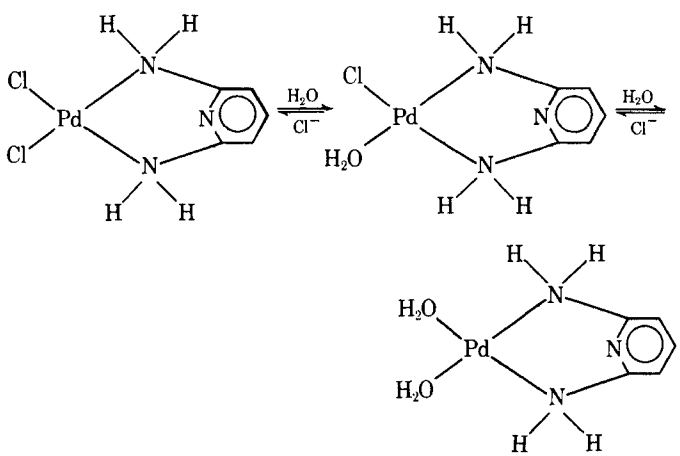

Scheme III

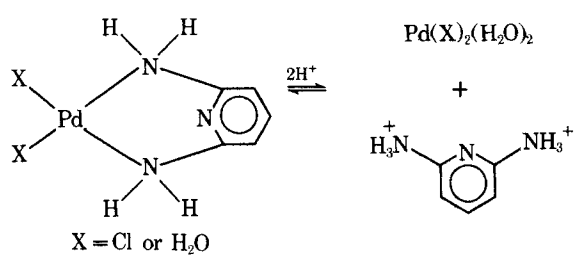

Scheme IV

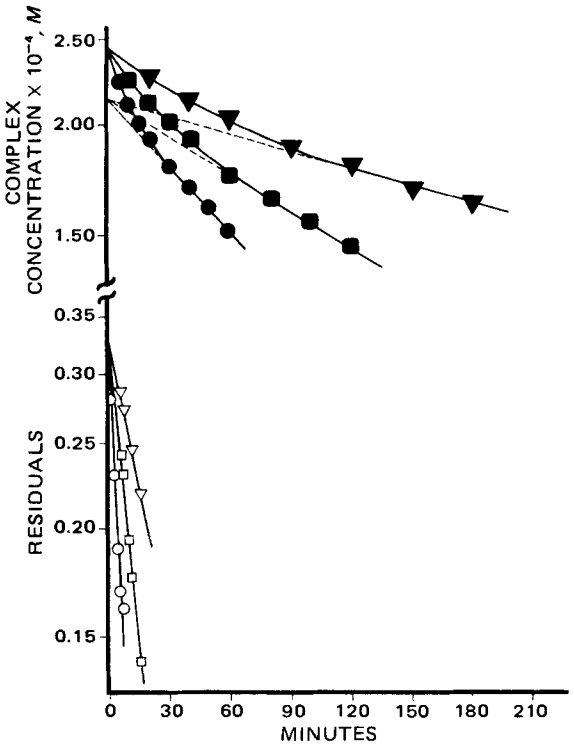

Figure 11—*Top: Semilogarithmic plot of complex concentration* $\times 10^{-4}$ M *undegraded* versus *time in minutes in acid halide catalysis experiment at pH 1.5 and 67° while varying the chloride-ion concentration. Key:* ▼, 1×10^{-2} M; ■, 3.3×10^{-2} M; *and* ●, 1×10^{-1} M. *Bottom: Semilogarithmic plot of residuals* $\times 10^{-4}$ M versus *time in minutes in acid halide catalysis experiment at pH 1.5 and 67° while varying the chloride-ion concentration and utilizing Eq. 10. Key:* ▽, 1×10^{-2} M; □, 3.3×10^{-2} M; *and* ○, 1×10^{-1} M.

applies as the solution to the data:

$$[Pd(X_2)L] = 0.237e^{-0.0653t} + 2.213e^{-0.00276t} \qquad \text{(Eq. 14)}$$

The proposed general reaction mechanism for acid halide catalysis is shown in Scheme V.

The coordination compound was reported to have antimitogenic and antiviral effects (20). Therefore, the chloride ligands are assumed to be displaceable while 2,6-diaminopyridine is a carrier ligand (5). The bidentate *cis*-complex must be employed, since the monodentate *cis*-complex can racemize into the thermodynamically more stable *trans*-configuration. Thus, the *cis*-configuration was postulated as necessary for activity (5), although it may not be stable.

A serious study of the stability of such complexes in the *cis*-configuration form is important for the understanding of their behavior in biological fluids. For example, the rate of chloride release and subsequent hydration of the complex molecule have been reported to be important steps in the mechanism of action. The chloride-ion concentration envi-

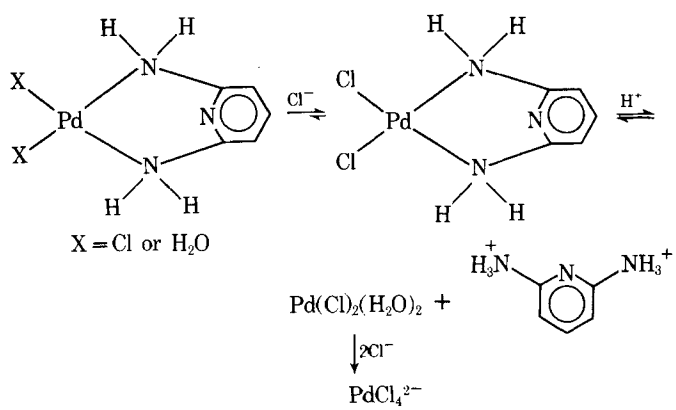

Scheme V

Table V—Calculated Values of A, B, α, and β Utilizing the Curve-Stripping Procedure for Acid Halide Catalysis

pH	Temperature	$[Cl^-]$, M	A, M	B, M	$\alpha \times 10^{-3}$, min^{-1}	$\beta \times 10^{-4}$, min^{-1}
1.10	37°	0.10	0.127	2.323	16.8	9.2
	37°	0.033	0.127	2.323	8.1	3.64
	47°	0.10	0.175	2.275	84.75	24.2
	47°	0.033	0.175	2.275	21.9	8.7
	47°	0.01	0.175	2.275	10.76	3.4
	57°	0.10	0.262	2.188	154.0	58.34
	57°	0.033	0.262	2.188	49.8	21.50
	57°	0.01	0.262	2.188	23.5	9.67
1.50	57°	0.10	0.237	2.213	65.3	27.6
	57°	0.033	0.237	2.213	27.9	13.0
	57°	0.01	0.237	2.213	16.6	5.76
	67°	0.10	0.322	2.128	130.0	50.7
	67°	0.033	0.322	2.128	60.7	31.7
	67°	0.01	0.322	2.128	23.7	14.7

ronment in the extra- and intracellular fluids can be a good justification for the alteration of anionic release and, therefore, activity.

REFERENCES

(1) B. Rosenberg, L. Van Camp, and T. Krigas, *Nature*, **205**, 698 (1965).

(2) B. Rosenberg, L. Van Camp, J. E. Trasko, and V. E. Mansour, *ibid.*, **222**, 385 (1969).

(3) J. A. Howle, G. R. Gale, and A. B. Smith, *Biochem. Pharmacol.*, **21**, 1465 (1972).

(4) A. B. Robins, *Chem.-Biol. Interact.*, **6**, 35 (1973).

(5) D. R. Williams, *Inorg. Chim. Acta Rev.*, **6**, 123 (1972).

(6) J. E. House, Jr., and M. J. Adams, *J. Inorg. Nucl. Chem.*, **32**, 345 (1970).

(7) R. Farrou and J. E. House, Jr., *ibid.*, **34**, 2219 (1972).

(8) L. I. Elding and L. Gustafson, *Inorg. Chim. Acta*, **5**, 643 (1971).

(9) L. I. Elding, *ibid.*, **6**, 647 (1972).

(10) *Ibid.*, **6**, 683 (1972).

(11) *Ibid.*, **7**, 581 (1973).

(12) D. Robb, N. M. De V. Steyn, and H. Kruger, *Inorg. Chim. Acta*, **3**, 383 (1969).

(13) A. J. Poe and D. H. Vaughan, *ibid.*, **1**, 255 (1967).

(14) R. G. Pearson and D. A. Johnson, *J. Am. Chem. Soc.*, **86**, 3983 (1964).

(15) J. S. Coe, J. R. Lyons, and M. D. Hussain, *J. Chem. Soc. A, Part I*, **1970**, 90.

(16) J. S. Coe, M. D. Hussain, and A. A. Malik, *Inorg. Chim. Acta*, **2**, 65 (1968).

(17) R. F. Coley and D. S. Martin, Jr., *ibid.*, **7**, 573 (1973).

(18) J. S. Coe and J. R. Lyons, *J. Chem. Soc. A, Part III*, **1969**, 2669.

(19) C. M. Davidson and R. F. Jameson, *Trans. Faraday Soc.*, **61**, 2462 (1965).

(20) H. A. Tayim, A. H. Malakian, and A. B. Bikhazi, *J. Pharm. Sci.*, **63**, 1469 (1974).

(21) C. E. Skinner and M. M. Jones, *J. Am. Chem. Soc.*, **91**, 1984 (1969).

ACKNOWLEDGMENTS AND ADDRESSES

Received November 24, 1975, from the *School of Pharmacy and the ‡Chemistry Department, American University of Beirut, Beirut, Lebanon.

Accepted for publication December 8, 1976.

Presented at the Basic Pharmaceutics Section, APhA Academy of Pharmaceutical Sciences, Atlanta meeting, November 1975.

Supported in part by a grant from the University Medical Research Fund, American University of Beirut.

ˣ To whom inquiries should be directed.

Microbiological Turbidimetric Methods: Linearization of Antibiotic and Vitamin Standard Curves

F. KAVANAGH

Abstract □ Procedures were devised to linearize the usually curved calibration lines for turbidimetric microbiological assays. Three new equations relating concentration of drug and turbidity are described; two are for antibiotic assays and one for vitamin assays. One equation is for antibiotic assays employing *Klebsiella pneumoniae* as the test organism. The accuracy of interpolation from the three equations was studied by means of appropriate mathematical models based on erythromycin, chlortetracycline (*K. pneumoniae*), and cyanocobalamin assays. The accuracy of the new expressions was significantly superior to those used previously, and they are of general applicability.

Keyphrases □ Microbiological turbidimetry—antibiotic and vitamin assays, procedures devised to linearize curved calibration lines □ Turbidimetry—microbiological antibiotic and vitamin assays, procedures devised to linearize curved calibration lines □ Antibiotics—microbiological turbidimetry assays, procedures devised to linearize curved calibration lines □ Vitamins—microbiological turbidimetry assays, procedures devised to linearize curved calibration lines

Nonlinear standard curves are much more common than straight lines in microbiological turbidimetric assays for growth-promoting substances and antibiotics. The nonlinear calibration line is particularly important in high accuracy assays because of the difficulty of obtaining sample potencies from it with negligible computational error. High accuracy assays are now possible not only from the automated system previously described (1) but also from manual assays. Therefore, the old practice of drawing a "best" straight line through the points of the standard line is no longer appropriate because the line, in reality, is curved. Approximating the slightly curved antibiotic lines by straight-line segments (2, 3) causes a small computational error.

Procedures for straightening both the antibiotic lines and the often more strongly curved vitamin lines are described in this report. Antibiotic lines will be considered separately from vitamin lines because they have different theoretical bases and the procedures have different principles.

Since an equation that truly fits a calibration line is not known, the line can only be approximated. The approximation can be fairly accurate when calibration points are close together. However, if the dose line can be linearized, fewer calibration points are needed to obtain the same accuracy of approximation. The aim of the present study

Table V—Calculated Values of A, B, α, and β Utilizing the Curve-Stripping Procedure for Acid Halide Catalysis

pH	Temperature	$[Cl^-]$, M	A, M	B, M	$\alpha \times 10^{-3}$, min^{-1}	$\beta \times 10^{-4}$, min^{-1}
1.10	37°	0.10	0.127	2.323	16.8	9.2
	37°	0.033	0.127	2.323	8.1	3.64
	47°	0.10	0.175	2.275	84.75	24.2
	47°	0.033	0.175	2.275	21.9	8.7
	47°	0.01	0.175	2.275	10.76	3.4
	57°	0.10	0.262	2.188	154.0	58.34
	57°	0.033	0.262	2.188	49.8	21.50
	57°	0.01	0.262	2.188	23.5	9.67
1.50	57°	0.10	0.237	2.213	65.3	27.6
	57°	0.033	0.237	2.213	27.9	13.0
	57°	0.01	0.237	2.213	16.6	5.76
	67°	0.10	0.322	2.128	130.0	50.7
	67°	0.033	0.322	2.128	60.7	31.7
	67°	0.01	0.322	2.128	23.7	14.7

ronment in the extra- and intracellular fluids can be a good justification for the alteration of anionic release and, therefore, activity.

REFERENCES

(1) B. Rosenberg, L. Van Camp, and T. Krigas, *Nature*, **205**, 698 (1965).

(2) B. Rosenberg, L. Van Camp, J. E. Trasko, and V. E. Mansour, *ibid.*, **222**, 385 (1969).

(3) J. A. Howle, G. R. Gale, and A. B. Smith, *Biochem. Pharmacol.*, **21**, 1465 (1972).

(4) A. B. Robins, *Chem.-Biol. Interact.*, **6**, 35 (1973).

(5) D. R. Williams, *Inorg. Chim. Acta Rev.*, **6**, 123 (1972).

(6) J. E. House, Jr., and M. J. Adams, *J. Inorg. Nucl. Chem.*, **32**, 345 (1970).

(7) R. Farrou and J. E. House, Jr., *ibid.*, **34**, 2219 (1972).

(8) L. I. Elding and L. Gustafson, *Inorg. Chim. Acta*, **5**, 643 (1971).

(9) L. I. Elding, *ibid.*, **6**, 647 (1972).

(10) *Ibid.*, **6**, 683 (1972).

(11) *Ibid.*, **7**, 581 (1973).

(12) D. Robb, N. M. De V. Steyn, and H. Kruger, *Inorg. Chim. Acta*, **3**, 383 (1969).

(13) A. J. Poe and D. H. Vaughan, *ibid.*, **1**, 255 (1967).

(14) R. G. Pearson and D. A. Johnson, *J. Am. Chem. Soc.*, **86**, 3983 (1964).

(15) J. S. Coe, J. R. Lyons, and M. D. Hussain, *J. Chem. Soc. A, Part I*, **1970**, 90.

(16) J. S. Coe, M. D. Hussain, and A. A. Malik, *Inorg. Chim. Acta*, **2**, 65 (1968).

(17) R. F. Coley and D. S. Martin, Jr., *ibid.*, **7**, 573 (1973).

(18) J. S. Coe and J. R. Lyons, *J. Chem. Soc. A, Part III*, **1969**, 2669.

(19) C. M. Davidson and R. F. Jameson, *Trans. Faraday Soc.*, **61**, 2462 (1965).

(20) H. A. Tayim, A. H. Malakian, and A. B. Bikhazi, *J. Pharm. Sci.*, **63**, 1469 (1974).

(21) C. E. Skinner and M. M. Jones, *J. Am. Chem. Soc.*, **91**, 1984 (1969).

ACKNOWLEDGMENTS AND ADDRESSES

Received November 24, 1975, from the *School of Pharmacy and the ‡Chemistry Department, American University of Beirut, Beirut, Lebanon.

Accepted for publication December 8, 1976.

Presented at the Basic Pharmaceutics Section, APhA Academy of Pharmaceutical Sciences, Atlanta meeting, November 1975.

Supported in part by a grant from the University Medical Research Fund, American University of Beirut.

ˣ To whom inquiries should be directed.

Microbiological Turbidimetric Methods: Linearization of Antibiotic and Vitamin Standard Curves

F. KAVANAGH

Abstract □ Procedures were devised to linearize the usually curved calibration lines for turbidimetric microbiological assays. Three new equations relating concentration of drug and turbidity are described; two are for antibiotic assays and one for vitamin assays. One equation is for antibiotic assays employing *Klebsiella pneumoniae* as the test organism. The accuracy of interpolation from the three equations was studied by means of appropriate mathematical models based on erythromycin, chlortetracycline (*K. pneumoniae*), and cyanocobalamin assays. The accuracy of the new expressions was significantly superior to those used previously, and they are of general applicability.

Keyphrases □ Microbiological turbidimetry—antibiotic and vitamin assays, procedures devised to linearize curved calibration lines □ Turbidimetry—microbiological antibiotic and vitamin assays, procedures devised to linearize curved calibration lines □ Antibiotics—microbiological turbidimetry assays, procedures devised to linearize curved calibration lines □ Vitamins—microbiological turbidimetry assays, procedures devised to linearize curved calibration lines

Nonlinear standard curves are much more common than straight lines in microbiological turbidimetric assays for growth-promoting substances and antibiotics. The nonlinear calibration line is particularly important in high accuracy assays because of the difficulty of obtaining sample potencies from it with negligible computational error. High accuracy assays are now possible not only from the automated system previously described (1) but also from manual assays. Therefore, the old practice of drawing a "best" straight line through the points of the standard line is no longer appropriate because the line, in reality, is curved. Approximating the slightly curved antibiotic lines by straight-line segments (2, 3) causes a small computational error.

Procedures for straightening both the antibiotic lines and the often more strongly curved vitamin lines are described in this report. Antibiotic lines will be considered separately from vitamin lines because they have different theoretical bases and the procedures have different principles.

Since an equation that truly fits a calibration line is not known, the line can only be approximated. The approximation can be fairly accurate when calibration points are close together. However, if the dose line can be linearized, fewer calibration points are needed to obtain the same accuracy of approximation. The aim of the present study

Table I—Model of *K. pneumoniae* Automated Antibiotic Assays

Sample Concentration[a]	Standards 1.6, 2, 2.4, 3.2, and 4 with Potencies Interpolated from Best Straight Line: *A versus* log *C*		Standards 1.6, 2.4, 3.2, and 4 with Potencies Interpolated from Point to Point: log $(A + M)$ *versus* C^2	
	0.1[b]	0.15	0.1	0.15
1.8	1.829	1.805	1.799	1.797
2.0	1.939	1.946	1.999	1.997
2.5	2.297	2.384	2.500	2.501
2.8	2.577	2.700	2.801	2.804
3.0	2.796	2.928	3.000	3.003
3.5	3.468	3.538	3.495	3.499
3.6	3.625	3.662	3.595	3.599

[a] Concentration in arbitrary units. [b] Sample volume.

was to achieve a linearization procedure so that interpolation errors are less than 0.25% of potency when the number of standards is five or less. The procedures given here increase the workload of the computer normally used to acquire and process the data by an insignificant amount. If maximum accuracy is needed only occasionally, calculations are practical with desk-top calculators or certain programmable pocket calculators.

Procedures for obtaining potencies with minimum computational errors are needed before naive statistical calculations are undertaken. Biases caused by inappropriate calculations should not become part of an answer or be involved in a validity test of the assays. Statistical procedures designed for both manual and automated assays will be considered in a subsequent publication.

EXPERIMENTAL

Data were obtained from semiautomated assays for cyanocobalamin, erythromycin, and chlortetracycline.

Test Organisms and Media—*Staphylococcus aureus* (ATCC 9144) was used in the erythromycin assay, *Klebsiella pneumoniae* (ATCC 10031) was used in the chlortetracycline assay, and *Lactobacillus leichmannii* (ATCC 7830) was used in the cyanocobalamin assay.

Commercial antibiotic assay broth No. 3 was used for all antibiotic assays. Commercial medium was used for the cyanocobalamin assay.

Assay Procedures—Procedures for erythromycin (4) and chlortetracycline were described previously (5). The cyanocobalamin method was a USP method adapted to the semiautomated system.

The design and operation of the semiautomated turbidimetric assay system were described recently (1–3, 6, 7). The automated diluter produces assay tubes containing about 0.10 or 0.15 ml of sample.

The chlortetracycline assay was essentially that for penicillin (8) modified to employ *K. pneumoniae* (5).

Calibration Lines for Antibiotics—The quality of an assay depends in part upon how well the calibration line describes reality. Ideally, potencies obtained from a dose line should not contain any error attributable to the form of the line. Such error increases bias and complicates conclusions from tests for invalidity. The many dose lines (9) used have different curvatures and, consequently, different errors caused by linear interpolation. The best practical form needs to be found to obtain potencies of test preparations and for validity testing.

The theoretical dose–response line (3) for an antibiotic that reduces the growth rate of the test organism is:

$$N_t = N_0 \exp[k_0 + f(v)k_m - k_aC]t \qquad \text{(Eq. 1)}$$

where N_t is the concentration of bacteria after an incubation period of t, N_0 is the concentration of bacteria in the assay tubes at the beginning of incubation, k_0 is the generation rate constant in the absence of antibiotic, C is the concentration of antibiotic with an inhibitory coefficient k_a, k_m represents the menstruum effect, and $f(v)$ is a function of the volume of sample added to the assay tube.

Equation 1 is used only as a guide to thought because usually N_0, k_0, $f(v)$, k_m, k_a, and t are unknown. In a particular assay, they are constant in all assay tubes; otherwise, the assay is invalid. Therefore, Eq. 1 can be written in an equivalent form as:

$$\log N = G + BC \qquad \text{(Eq. 2)}$$

where G and B are constant in an assay and dependent on details. Conversion of transmittance of the bacterial suspensions into corresponding values of N is by means of a calibration equation.

Since absorbance, A, is much more convenient to use than N in computing potencies in assays, it was used in Eq. 3 to give the absorbance analog of Eq. 2:

$$\log A = E + FC \qquad \text{(Eq. 3)}$$

Equation 3 was modified to straighten the line:

$$\log (A + M) = O + PC \qquad \text{(Eq. 4)}$$

The value and algebraic sign of M were chosen to make the line straight over the region of interest. For *K. pneumoniae* assays, Eq. 4 was modified by substituting C_2 for C:

$$\log (A + M) = R + SC^2 \qquad \text{(Eq. 5)}$$

The value of M in Eqs. 4 and 5 may be zero and the algebraic sign may be + or −. The sign is negative if the log A *versus* C line curves away from the C axis at the higher values of C and is positive if the line curves toward the C axis.

The constant M is introduced to compensate for two sources of curvature: the actual nonlinear relationship between log N and C and the nonlinear response of the photometer. To obtain the least computational error, assay responses should be corrected for photometer response before interpolating from Eqs. 4 and 5. The values of M in these equations are computed to minimize $(\text{error})^2$ for standard responses. Photometer correction is a function of the test organism, wavelength, and instrument (9).

A relationship favored by official bodies and statisticians is a plot of log dose *versus* some response of the photometer (10, 11). Both absorbance and transmittance are used as the response. The absorbance version is given as:

$$A = R + S \log C \qquad \text{(Eq. 6)}$$

and the transmittance version is:

$$T = U + V \log C \qquad \text{(Eq. 7)}$$

Testing the equations by means of a few actual assays was inappropriate because of differences caused by variations in operations. Statistical evaluation of many assays would reveal the preferred dose line. Instead, a mathematical procedure was employed using a model derived from an erythromycin assay.

Model 1 was constructed as follows. Measured absorbances of standards of an automated assay were converted into relative concentration, N, of bacteria by means of a calibration equation (9). These values of N were plotted according to Eq. 2. The lines were curved. Several trials showed that subtracting a constant number from N and plotting the resultant values against concentration gave essentially straight lines. A straight line was drawn through the points corresponding to concentrations 1 and 5, and the coefficients for the lines were calculated.

These equations were used to calculate values of N for each standard concentration and for each of the four "samples" with six-place accuracy. The photometer calibration line was used to find the absorbance corresponding to each N. Transmittances were calculated from the absorbances. These values of N, A, and T represent the values of C with error only in the sixth place, an error too small to be significant in testing forms of response lines.

Six equations were tested to find the one with the least computational

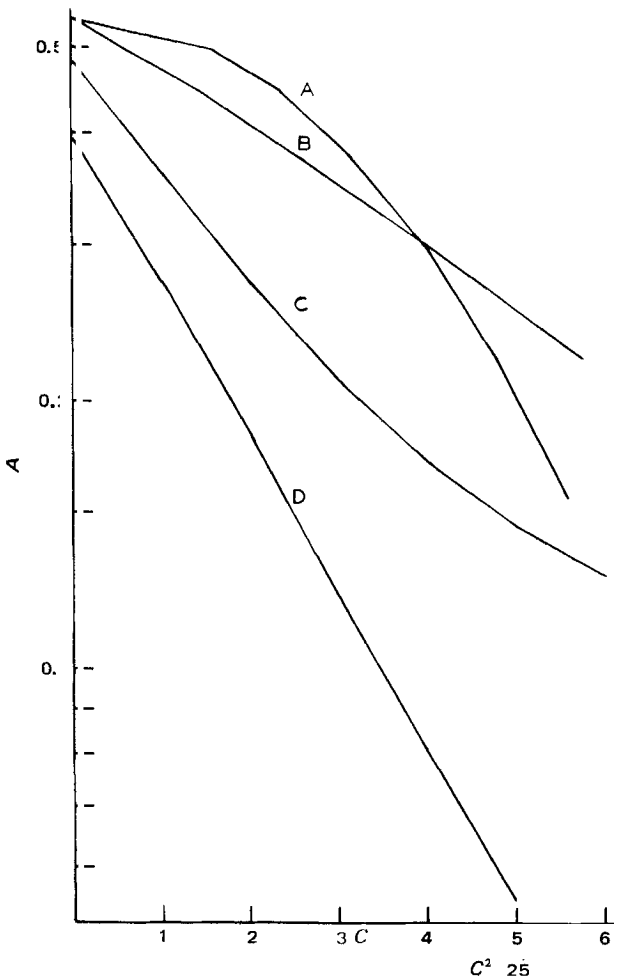

Figure 1—*Standard lines for Models 1 and 2. Key: A, Eq. 3 for Model 2; B, Eq. 5 for Model 2,* M = *0; C, Eq. 3 for Model 1; and D, Eq. 4 for Model 1,* M = *0.09. Responses are given as log* A *or log* (A − M) versus C *or* C^2.

error. Since testing the equations at all points is impossible, they were tested at concentrations midway between calibration points where error may be greatest. Appropriate values of A or T were substituted in them, and concentrations of "samples" were calculated by linear interpolation between bracketing standards or from the best straight lines through the standard responses. Goodness of fit of the several dose lines (Eqs. 2–7) to the true dose line was measured by taking the differences between the interpolated sample potencies and corresponding "potencies" of 1.5, 2.5, 3.5, and 4.5, squaring each difference, and summing to obtain the mean square error.

Because *K. pneumoniae* assays may be strongly curved, a separate model was designed. Model 2, based on a chlortetracycline assay, was constructed in exactly the same way as Model 1 except for substitution of C^2 for C in the equations. Graphs of Eq. 3 in both the C and C^2 versions are given in Fig. 1. Two slightly different designs were tested. One followed FDA practice (10) of spacing five standard concentrations on a logarithmic scale (Eq. 6). The multiplier was about 1.25. The actual concentrations were such that they could be prepared accurately by means of volumetric pipets and flasks. The best straight line through the five points, as required by the official method, was used to obtain "potencies" (Table I). The second set of calculations (Table I) followed a point-to-point version of Eq. 5 using only four standards.

The M in Eqs. 4 and 5 was computed for each three-point segment of the dose line and used for interpolating all potencies falling between end-points.

RESULTS

Since N, A, and T in the model computations were known with six-place accuracy, potencies computed for the samples should be free from error in the fifth place. Therefore, any differences between assigned and

Table II—Model 1 of Automated Antibiotic Assays with Potencies of Samples Interpolated from Three Equations Using Standards of 1, 2, 3, 4, and 5

	Best Straight Line: *A versus* log *C*		Point to Point			
			log *A versus C*		log (*A* + *m*) *versus C*	
Sample[a]	0.1[b]	0.15	0.1	0.15	0.1	0.15
1.5	1.442	1.497	1.509	1.525	1.497	1.498
2.5	2.481	2.707	2.518	2.542	2.503	2.503
3.5	3.573	3.704	3.526	3.558	3.499	3.499
4.5	4.538	4.352	4.534	4.569	4.500	4.501
10^4 (Error)^2	105	1064	22	105	0.2	0.2

[a] Concentration in arbitrary units. [b] Sample volume.

computed potencies represent a lack of fit of the calibration line to the reality of the model. The (error)^2 at the bottom of the table is a measure of the goodness of fit of the dose line to the points and is zero for a perfect fit.

Table II gives potencies computed for samples of Model 1. The results showed Eq. 4 to be better than Eq. 3 or 6. Equation 4 was applied to assays for bacitracin, chlortetracycline, cephaloridine, erythromycin, formaldehyde, furazolidone, hygromycin B, monensin, nitrofurantoin, penicillin G, phenol, tetracycline, thimerosal, and tylosin. The best straight line always gave larger errors than the point-to-point calculations from the same equation.

For Model 2, the results (Fig. 2 and Table I) indicate that the best straight line through the points of the standard (Eq. 6) is a very poor approximation of the true line. The deviations from the true values and the poor agreement between results at the two volumes of sample indicate considerable bias in the computations. Results in Table III show Eq. 5 to be superior to Eqs. 4, 6, and 7. Equation 5 has been applied to assays for chlortetracycline and streptomycin with *K. pneumoniae* as the test organism.

Computations using N in Eqs. 4 (Model 1) and 5 (Model 2) but not the others would have been without error. The (error)^2 shown in Table II for Eq. 4 (Model 1) and in Table III for Eq. 5 (Model 2) result from using uncorrected spectrophotometer responses. Absorbance corrected for the nonlinear response of the spectrophotometer is equivalent to N for calculation purposes. Therefore, to achieve minimum computational error, absorbances should be corrected for spectrophotometer response before substituting in Eq. 4 or 5. Values of M in Eqs. 4 and 5 are selected so that the resulting line is the best straight line through the points.

Computational procedures such as those discussed can be a source of additional errors when applied blindly. The first and last parts of the usual standard line are too flat to permit accurate assays and should be avoided regardless of the procedure. Generally, the usable part of a standard line lies between 20 and 80% of uninhibited growth (0 tube). This portion can be linearized by means of Eqs. 4 and 5. Each assay sys-

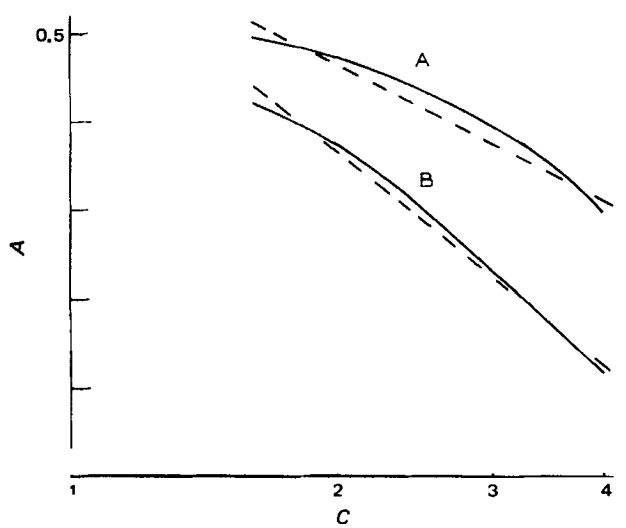

Figure 2—*Standard lines for Eq. 6 representing* K. pneumoniae *assays. Solid lines are smooth curves through the points. Dashed lines are the best straight lines through the five points. Lines A and B are for sample sizes 0.1 and 0.15 ml, respectively. FDA spacing of standards is followed. Responses are given as* A versus *log* C.

Table III—(Error)^2 for Model of *K. pneumoniae* Automated Antibiotic Assays [a]

	Standards 1.6, 2, 2.4, 3.2, 4						Standards 1.6, 2.4, 3.2, 4	
	Best Straight Line				Point to Point:		Using Point to Point:	
	A versus log *C*		*T versus* log *C*		log (*A* + 0.01) *versus C*		log (*A* + *M*) *versus* C^2	
Sample size	0.1	0.15	0.1	0.15	0.1	0.15	0.1	0.15
10^4 (Error)^2	1388	700	2444	1311	36	34	0.5	0.5

[a] Samples are same as those in Table II.

tem should be examined carefully to discover the portion of the standard line to use. The ratio of high to low concentrations may be twofold in some systems and as much as, but rarely more than, fivefold in others.

Calibration Lines for Vitamins—Nonlinear calibration lines are more common than straight lines in vitamin assays. Usually a smooth curve is drawn through the points plotted on graph paper, and sample potency is then interpolated from the curve. Such a procedure is suitable only for a low precision assay because of errors inherent in manual interpolation and in the inability to draw the true line through the points. The more nearly rectilinear is the line, the more accurately it can be drawn and interpolated from by hand or by computer. A nearly straight dose line and interpolation by computer must be used to achieve the potential in high accuracy assays. The assays can be done either manually or by automated systems (1).

Three quite different expressions are used to represent calibration lines in official turbidimetric methods: *T versus C* (11), *T versus* log *C* (12), and log *T versus* log *C* (12). The USP (12) specified that the line nearest to straight is to be used. Others use *A versus C* (13, 14) and *N versus C* (9), where *N* is the concentration of bacteria. The last expression is the dose–response line for growth-promoting substances. Substitution of *A* for *N* increases the curvature of the line because of the nonlinear response of photometers to suspensions (9). These calibration lines are plotted in Figs. 3–5 from the same set of responses for a cyanocobalamin assay.

Of the three forms used in official methods, *T versus* log *C* was the straightest. The line *N versus C*, the one with the theoretical basis, was straight over most of the range. The line *A versus C*, a first approximation to the theoretical one, was slightly curved because of the nonlinear spectrophotometer response.

The theoretical dose–response line for growth-promoting substances is for the limiting case and usually is simpler than reality. It applies when the only factor limiting growth is the one substance being assayed. In practice, a deficient medium, unfavorable growth conditions, and an incubation time too short to achieve limiting growth modify the relationship between *N* and *C* to increase curvature. In general, the *N versus C* dose–response line may be expected to be more strongly curved than the one in Fig. 3. The nonlinear response of the photometer to suspensions also causes curvature. Vitamin assays generally are grown to absorbances of 0.6 or more, and spectrophotometer corrections are relatively large at such absorbances. A large *A* has a proportionally greater correction than a small *A* (9). Therefore, the *A versus C* line curves more than the *N versus C* line.

A disadvantage to the dose–response line is the extra step caused by converting *T* to *N* by means of a calibration line (9). The calibration line for the conversion is a function of the optical properties of the test organism, wavelength of measurement, and geometry of the photometer (9). Since *A* is accurately obtainable from *T*, it is the preferred response metameter to be used in assaying.

Graphs of several assays for different vitamins employing different kinds of photometers had a lower straight portion. Curvature in the *A versus C* lines began at about *a* , 0.2 and then curved toward the *C* axis. The lines could be made essentially rectilinear by the transformation:

$$A' = A + B(A - D)^2 \qquad \text{(Eq. 8)}$$

where *D* is the value of *A* at the beginning of curvature. The calibration line for an assay then becomes:

$$C = E + FA' \qquad \text{(Eq. 9)}$$

However, *A* (not *A'*) is used in Eq. 9 when $A \leq D$.

Model of a Vitamin Assay—Data free from all error were needed to test Eq. 9 and to show the computation errors and biases caused by curved calibration lines. Since such data cannot be obtained from actual assays, they were derived from a model of a cyanocobalamin assay. The model, based on the theoretical dose–response line for growth-promoting substances, is:

$$C = G + HN \qquad \text{(Eq. 10)}$$

where *C* is the concentration of drug, *N* is the concentration of test organism, and *G* and *H* are constants. The line used in constructing this model curves at $N \geq 20$ ($C = 2$) in such a manner that it may be linearized by substituting:

$$N' = N + 0.012(N - 20)^2 \qquad \text{(Eq. 11)}$$

for *N* in Eq. 10 for values of $N > 20$.

A calibration line relating *N* and *A* for a *L. leichmannii* suspension measured at 650 nm is used to obtain *A* from *N*. Then *T* is calculated from *A*. The concentrations, *C*, are assigned values ranging from 0 to 10. The even digits are considered to be standards, and the odd digits are the samples. Values of *A* and *A'* are given in Table IV. The quality of the linearization is tested by comparing *C* computed from *A'* and the true value. Responses as *N*, *A*, and *A'* are given in Fig. 6.

The coefficients *B*, *D*, *E*, and *F* must be found before Eqs. 8 and 9 can be applied. Three responses, A_0, A_i, and A_j, at 0, C_i, and C_j are required; 0, A_0, C_i, and A_i are substituted in Eq. 9, and *E* and *F* are computed. Then A_j is computed for C_j from Eq. 9, and A_j, A_j', and $A_i = D$ are substituted in Eq. 8 to obtain *B*. Then the values of *A* corresponding to measured *A* for $A > D$ are computed from Eq. 8. The C_i is the standard nearest to the upper end of the straight portion of the *C versus A* line. This calculation causes the three points 0, C_i, and C_j to fall on a straight line according to Eq. 9; C_j should be near to the upper limit of the standards.

In the general case, the response line cannot be fitted by an equation

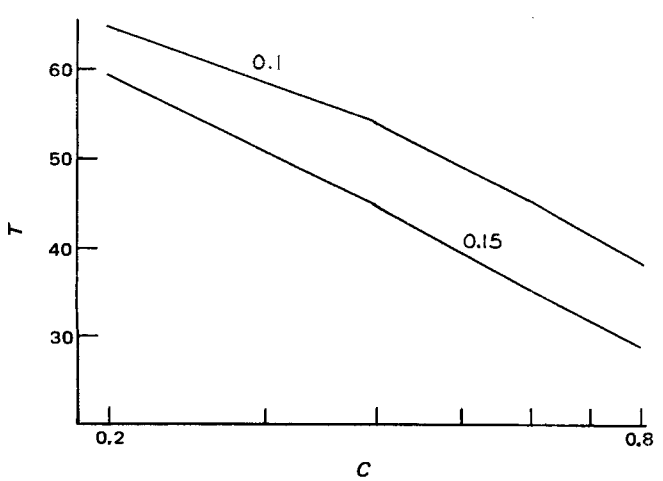

Figure 3—*Responses for a cyanocobalamin assay. Concentration of vitamin is nanograms per milliliter for sample tubes of the automated system. Responses are given as* T versus *log* C.

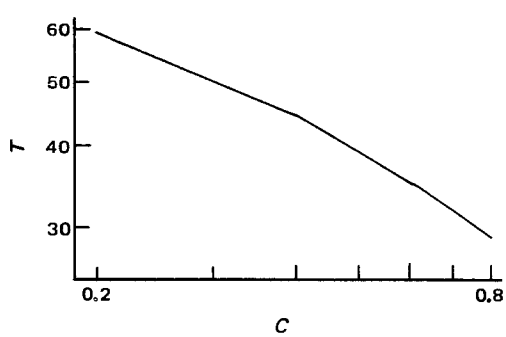

Figure 4—*Responses for a cyanocobalamin assay (same data as in Fig. 3). Responses are given as log* T versus *log* C.

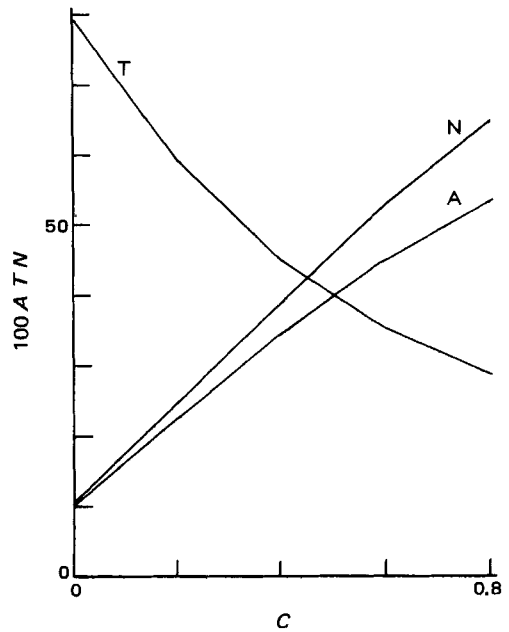

Figure 5—*Responses for cyanocobalamin assay (same data as in Fig. 3). Responses are given as* T versus C, A versus C, *and* N versus C, *where* T *is the percent transmittance,* A *is the absorbance, and* N *is the relative concentration of bacteria.*

as could the lines in Fig. 6, and potency is obtained by interpolation from a point-to-point line bracketing the sample.

The AOAC (11) procedure for vitamins does not indicate the kind of line to be drawn through the points of the standard line of the form *T versus C*. The USP procedure (12) provides the option of drawing either a straight line or a smooth curve through the plotted points of responses of the standards. The assumption was made that a smooth curve was drawn through the points. For interpolation purposes, the smooth curve was assumed to be quadratic in concentration. An equation was fitted to three standards such as 2, 4, and 6, and potency for the 3 and 5 samples was computed from it. Then the equation was fitted to standards 4, 6, 8, *etc.* This approach is a point-to-point procedure applied to a curved line.

Test of Several Calibration Lines—The values of *A* in Table IV after conversion into *T* were used to test dose lines of the forms *A versus C*, *A′ versus C*, *A versus* log *C*, *T versus* log *C*, and *T versus C* for computational error of interpolated potencies (Table V).

The linear *A versus C* relationship was worst followed by the curve *T versus C*. The others would be acceptable for most work at higher concentrations. The *A′ versus C* relationship was the best of the straight lines over the entire concentration range. For most of the range, computational errors were insignificant.

The parabola was no better than the procedure for linearization (Eq. 9) when *A′* was a quadratic function of *C*. However, *A* as a quadratic function of log *C* gave nearly error-free potencies for the samples when the equation was fitted to three contiguous points of the standard line. The quadratic equation was restricted to the curved part of the *A versus C* line. Fitting the equation to more than three standard points of the model increased the interpolation error.

Table IV—Responses in Model Vitamin Assays

C	*A*	*A′*
	Standards	
0	0	0
1	0.0925	0.0925
2	0.1850	0.1850
4	0.3255	0.3731
6	0.4255	0.5649
8	0.5042	0.7498
10	0.5692	0.9251
	Samples	
2	0.1850	0.1850
3	0.2626	0.2771
5	0.3789	0.4695
7	0.4669	0.6584
9	0.5381	0.8387

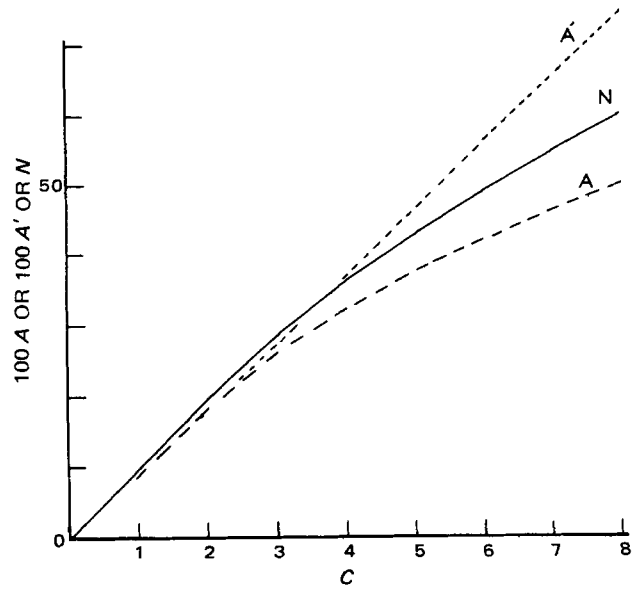

Figure 6—*The* A, N, *and* A′ *responses of the model of a vitamin assay.*

The procedure for straightening calibration lines of growth-promoting substances was applied to lines obtained in turbidimetric assays for thiamine (15), folic acid (16), pyridoxine (17), and cyanocobalamin (18) and to a titrimetric assay for niacin (19). The pyridoxine assay employing *Saccharomyces carlsbergensis* was so strongly curved that the high end correction (Eq. 8) was equal to the observed absorbance. Correction was much smaller for the other assays. The *A versus C* and *A′ versus C* lines for folic acid and pyridoxine standards are shown in Fig. 7.

Graphs of *A versus C* should form a smooth curve. Few graphs of published data were smooth, a not unexpected finding considering that the work was done before highly accurate assays were possible. An occasional rather large error was found such as, for example, a misidentified sample.

Selection of an interpolation formula to be used in an assay depends upon the quality of the assay, the curvature of the standard line, the accuracy needed, and computational facilities. The linear point-to-point versions of *A versus C*, *A′ versus C*, and *T versus* log *C* all are useful. The one giving the straightest line over the part of the standard line to be used in the assay should be selected. A parabola, *A versus* log *C*, fitted to three points may be better than a point-to-point straight line when sample responses fall within the span of three points on the standard line and calculations are done with a programmable calculator. The *N versus C* line is used to evaluate assay design and operations (9).

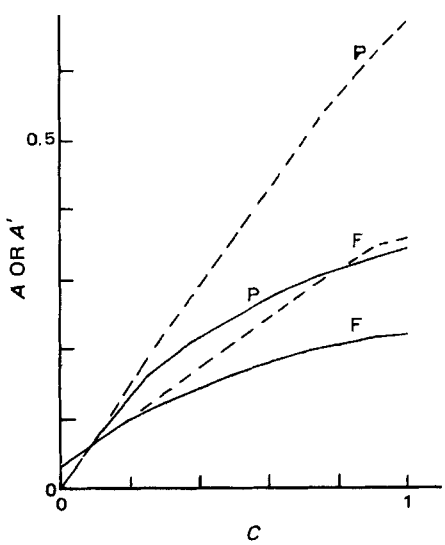

Figure 7—*The* A *and* A′ *lines for folic acid (16) and pyridoxine (17) assays. Solid lines are for* A versus C, *and dashed lines are for* A′ versus C. *The concentration scale is in arbitrary units.*

Table V—Point-to-Point Interpolations from Five Relationships between C and a Response Function for the Vitamin Model

Known C	Linear				Quadratic in C					
	A versus C		A' versus C		A versus log C		T versus C		T versus log C	
	C	Error, %	C	Error, %	C	Error, %	C	Error, %	C	Error, %
3	3.092	3.1	2.991	0.0	3.001	0.0	3.057	1.9	2.986	−0.5
5	5.063	1.2	5.006	0.1	5.000	0.0	4.929	−1.4	5.011	0.2
7	7.050	0.7	7.012	0.2	7.001	0.0	6.963	−0.5	7.005	0.1
9	9.042	0.5	9.015	0.2	9.001	0.0	8.796	−0.3	9.002	0.0

Graphical procedures are adequate when the assay is not of the highest quality or turbidity is measured with low precision and accuracy (±0.5% T). Computational procedures are appropriate for high quality automated assays.

SUMMARY

Common calibration lines for turbidimetric assays are more likely to be curved than straight. Fitting a best straight line to the points or even a point-to-point line causes errors in interpolated potencies. The closer the calibration line is to a straight line, the smaller will be the errors of interpolation.

Three new expressions, two for antibiotic assays and one for vitamin assays, that give straighter lines than those used previously were tested by means of three models based on real assays. The new expressions could be approximated much better by straight-line segments than could the older ones. The relationships used in official methods gave the largest computational errors. One new antibiotic equation was designed for assays employing *K. pneumoniae* as the test organism.

REFERENCES

(1) N. R. Kuzel and F. W. Kavanagh, *J. Pharm. Sci.*, **60**, 767 (1971).

(2) F. Kavanagh, *ibid.*, **60**, 1858 (1971).

(3) *Ibid.*, **64**, 844 (1975).

(4) F. Kavanagh, "Analytical Microbiology," vol. 2, Academic, New York, N.Y., 1972.

(5) H. S. Ragheb and A. M. Cummings, *J. Assoc. Offic. Anal. Chem.*, **57**, 527 (1974).

(6) N. R. Kuzel and F. W. Kavanagh, *J. Pharm. Sci.*, **60**, 764 (1971).

(7) F. W. Kavanagh, *ibid.*, **63**, 1463 (1974).

(8) F. Kavanagh and L. J. Dennin, in "Analytical Microbiology," F. Kavanagh, Ed., Academic, New York, N.Y., 1963, chap. 6.10.

(9) F. Kavanagh, "Analytical Microbiology," vol. 2, Academic, New York, N.Y., 1972, chap. 3.

(10) Code of Federal Regulations, Title 21, Part 436.106, 1974.

(11) "Official Methods of Analysis," 12th ed., Association of Official Analytical Chemists, Washington, D.C., 1975, 43.103.

(12) "The United States Pharmacopeia," 19th rev., Mack Publishing Co., Easton, Pa., 1975.

(13) L. Millbank, R. E. Davis, M. Rawlins, and A. H. Waters, *J. Clin. Pathol.*, **23**, 54 (1970).

(14) R. E. Davis, J. Moulton, and A. Kelly, *ibid.*, **26**, 494 (1973).

(15) E. Hoff-Jorgensen and B. Hansen, *Acta Chem. Scand.*, **9**, 562 (1955).

(16) A. H. Waters and D. L. Mollin, *J. Clin. Pathol.*, **14**, 335 (1961).

(17) W. Hewitt, "Microbiological Assay," Academic, New York, N.Y., 1977, Table 3.1.

(18) C. I. Bliss, *Bacteriol. Rev.*, **20**, 243 (1956).

(19) C. I. Bliss and C. White, in "The Vitamins," vol. VI, P. Gorgy and W. N. Pearson, Eds., Academic, New York, N.Y., 1967, p. 27.

ACKNOWLEDGMENTS AND ADDRESSES

Received October 18, 1976, from *231 Blue Ridge Road, Indianapolis, IN 46208.*

Accepted for publication January 6, 1977.

Skin as an Active Metabolizing Barrier I: Theoretical Analysis of Topical Bioavailability

H. Y. ANDO *, N. F. H. HO, and W. I. HIGUCHI ˣ

Abstract □ A model and explicit equations were developed to be used in the experimental design and data evaluation of situations where simultaneous metabolism and transport of drugs occur in the skin. By treating the skin as a two-ply laminate composed of the stratum corneum and the viable epidermis, which contains most of the catabolic enzymes that might render a drug inactive by metabolism, equations were developed permitting the *in vitro* assessment of factors that may affect topical bioavailability *in vivo*. Two situations were investigated. In the first, the drug was placed on the dermis side of the diffusion cell and did not penetrate the stratum corneum. In the second, the drug, placed on the epidermis side, penetrated the stratum corneum and then passed through the metabolizing epidermis. Expressions for determining the metabolic rate constant from experimental data along with concentration profiles and flux expressions are given both for the drug and its metabolite.

Keyphrases □ Bioavailability, topical—model and equations developed permitting *in vitro* assessment, assuming simultaneous metabolism and drug transport in skin □ Topical bioavailability—model and equations developed permitting *in vitro* assessment, assuming simultaneous metabolism and drug transport in skin □ Metabolism, drug—simultaneous with transport in skin, model and equations developed permitting *in vitro* assessment of bioavailability □ Transport, drug—simultaneous with metabolism in skin, model and equations developed permitting *in vitro* assessment of bioavailability

In the past, the major barrier to the delivery of a topical dosage form to the site of drug action has been considered to be the stratum corneum. The concept of the epidermis as a viable, metabolizing membrane, which can provide a metabolic barrier for drug action, has long been overshadowed by the emphasis on the passive permeability properties of the most superficial skin layer. Topical bioavailability should account for not only skin permeation but also cutaneous drug metabolism.

Studies concerning the passive permeability properties of the skin as a two-ply laminate (stratum corneum and viable epidermis) showed that drugs may enter the epidermis by breaching the stratum corneum and/or by passing through skin follicles, which may be considered

Table V—Point-to-Point Interpolations from Five Relationships between C and a Response Function for the Vitamin Model

Known C	Linear				Quadratic in C					
	A versus C		A' versus C		A versus log C		T versus C		T versus log C	
	C	Error, %	C	Error, %	C	Error, %	C	Error, %	C	Error, %
3	3.092	3.1	2.991	0.0	3.001	0.0	3.057	1.9	2.986	−0.5
5	5.063	1.2	5.006	0.1	5.000	0.0	4.929	−1.4	5.011	0.2
7	7.050	0.7	7.012	0.2	7.001	0.0	6.963	−0.5	7.005	0.1
9	9.042	0.5	9.015	0.2	9.001	0.0	8.796	−0.3	9.002	0.0

Graphical procedures are adequate when the assay is not of the highest quality or turbidity is measured with low precision and accuracy (±0.5% T). Computational procedures are appropriate for high quality automated assays.

SUMMARY

Common calibration lines for turbidimetric assays are more likely to be curved than straight. Fitting a best straight line to the points or even a point-to-point line causes errors in interpolated potencies. The closer the calibration line is to a straight line, the smaller will be the errors of interpolation.

Three new expressions, two for antibiotic assays and one for vitamin assays, that give straighter lines than those used previously were tested by means of three models based on real assays. The new expressions could be approximated much better by straight-line segments than could the older ones. The relationships used in official methods gave the largest computational errors. One new antibiotic equation was designed for assays employing *K. pneumoniae* as the test organism.

REFERENCES

(1) N. R. Kuzel and F. W. Kavanagh, *J. Pharm. Sci.*, **60**, 767 (1971).

(2) F. Kavanagh, *ibid.*, **60**, 1858 (1971).

(3) *Ibid.*, **64**, 844 (1975).

(4) F. Kavanagh, "Analytical Microbiology," vol. 2, Academic, New York, N.Y., 1972.

(5) H. S. Ragheb and A. M. Cummings, *J. Assoc. Offic. Anal. Chem.*, **57**, 527 (1974).

(6) N. R. Kuzel and F. W. Kavanagh, *J. Pharm. Sci.*, **60**, 764 (1971).

(7) F. W. Kavanagh, *ibid.*, **63**, 1463 (1974).

(8) F. Kavanagh and L. J. Dennin, in "Analytical Microbiology," F. Kavanagh, Ed., Academic, New York, N.Y., 1963, chap. 6.10.

(9) F. Kavanagh, "Analytical Microbiology," vol. 2, Academic, New York, N.Y., 1972, chap. 3.

(10) Code of Federal Regulations, Title 21, Part 436.106, 1974.

(11) "Official Methods of Analysis," 12th ed., Association of Official Analytical Chemists, Washington, D.C., 1975, 43.103.

(12) "The United States Pharmacopeia," 19th rev., Mack Publishing Co., Easton, Pa., 1975.

(13) L. Millbank, R. E. Davis, M. Rawlins, and A. H. Waters, *J. Clin. Pathol.*, **23**, 54 (1970).

(14) R. E. Davis, J. Moulton, and A. Kelly, *ibid.*, **26**, 494 (1973).

(15) E. Hoff-Jorgensen and B. Hansen, *Acta Chem. Scand.*, **9**, 562 (1955).

(16) A. H. Waters and D. L. Mollin, *J. Clin. Pathol.*, **14**, 335 (1961).

(17) W. Hewitt, "Microbiological Assay," Academic, New York, N.Y., 1977, Table 3.1.

(18) C. I. Bliss, *Bacteriol. Rev.*, **20**, 243 (1956).

(19) C. I. Bliss and C. White, in "The Vitamins," vol. VI, P. Gorgy and W. N. Pearson, Eds., Academic, New York, N.Y., 1967, p. 27.

ACKNOWLEDGMENTS AND ADDRESSES

Received October 18, 1976, from *231 Blue Ridge Road, Indianapolis, IN 46208.*

Accepted for publication January 6, 1977.

Skin as an Active Metabolizing Barrier I: Theoretical Analysis of Topical Bioavailability

H. Y. ANDO *, N. F. H. HO, and W. I. HIGUCHI ˣ

Abstract □ A model and explicit equations were developed to be used in the experimental design and data evaluation of situations where simultaneous metabolism and transport of drugs occur in the skin. By treating the skin as a two-ply laminate composed of the stratum corneum and the viable epidermis, which contains most of the catabolic enzymes that might render a drug inactive by metabolism, equations were developed permitting the *in vitro* assessment of factors that may affect topical bioavailability *in vivo*. Two situations were investigated. In the first, the drug was placed on the dermis side of the diffusion cell and did not penetrate the stratum corneum. In the second, the drug, placed on the epidermis side, penetrated the stratum corneum and then passed through the metabolizing epidermis. Expressions for determining the metabolic rate constant from experimental data along with concentration profiles and flux expressions are given both for the drug and its metabolite.

Keyphrases □ Bioavailability, topical—model and equations developed permitting *in vitro* assessment, assuming simultaneous metabolism and drug transport in skin □ Topical bioavailability—model and equations developed permitting *in vitro* assessment, assuming simultaneous metabolism and drug transport in skin □ Metabolism, drug—simultaneous with transport in skin, model and equations developed permitting *in vitro* assessment of bioavailability □ Transport, drug—simultaneous with metabolism in skin, model and equations developed permitting *in vitro* assessment of bioavailability

In the past, the major barrier to the delivery of a topical dosage form to the site of drug action has been considered to be the stratum corneum. The concept of the epidermis as a viable, metabolizing membrane, which can provide a metabolic barrier for drug action, has long been overshadowed by the emphasis on the passive permeability properties of the most superficial skin layer. Topical bioavailability should account for not only skin permeation but also cutaneous drug metabolism.

Studies concerning the passive permeability properties of the skin as a two-ply laminate (stratum corneum and viable epidermis) showed that drugs may enter the epidermis by breaching the stratum corneum and/or by passing through skin follicles, which may be considered

essentially lipid- or water-filled pores (1–3). Beneath the stratum corneum (the major passive barrier) is the viable epidermis and the dermis. Of these two layers, the viable epidermis is metabolically the more active. Oxygen consumption was found to be 5.4 times greater in the epidermis than the dermis in the hairless mouse (4); in human skin, the activity of catechol *O*-methyltransferase was 8.3 times higher in the epidermis (5).

The purpose of the present discussion is to increase the understanding of cutaneous metabolism and transport by providing a mathematical basis for designing and evaluating appropriate experiments.

DISCUSSION

Impermeable Stratum Corneum—The preceding evidence indicates that a reasonable mathematical model for the skin might be formulated from a two-ply laminate composed of the stratum corneum and the viable epidermis. The epidermis contains most of the catabolic enzymes that render the drug inactive by metabolism, but it is not clear how the distribution of catabolic enzymes might vary with epidermal depth. Presumably, one would expect a gradual increase in metabolic activity as the basal epithelial layer is approached from the stratum corneum. In this discussion, the epidermis is considered a homogeneous membrane with respect to enzyme activity. Future studies will embody more complicated enzyme distributions and should provide an experimental basis for testing the homogeneous distribution assumption.

It may seem unusual to discuss drug bioavailability when the drug is not able to penetrate the skin. However, this unfortunate clinical situation may be utilized in certain *in vitro* experiments to yield information about the metabolic activity of the epidermis. The problem of stratum corneum permeability possibly may be altered by vehicles used in the dosage form. Such a situation was found for the permeation of vidarabine in hairless mouse skin from saline (6).

Consider the skin in a diffusion cell as illustrated in Fig. 1. In this situation, the drug is placed on the dermal side of the diffusion cell. The stratum corneum side faces the receptor compartment which contains no drug. Let the drug, A, and its major metabolite, X, be impermeable to the stratum corneum ($-s \leq x \leq -m$) but permeable to the metabolizing epidermis ($-m \leq x \leq 0$). The former condition demands that:

$$\frac{dC_A}{dx} = 0 \qquad \text{(Eq. 1)}$$

and that:

$$\frac{dC_X}{dx} = 0 \qquad \text{(Eq. 2)}$$

at $x = -m$, where C_A is the concentration of the drug and C_X is the concentration of the metabolite.

After an initial induction period[1], a steady state will be set up for the diffusing drug into the metabolizing epidermis and for the efflux of the metabolite out of the epidermis. The flux equations at $x = 0$ are:

$$F_A = -D_A \frac{dC_A}{dx} \qquad \text{(Eq. 3)}$$

$$F_A = +P_{aqA}[C_A(h) - C_A(0)] \qquad \text{(Eq. 4)}$$

$$F_X = -D_X \frac{dC_X}{dx} \qquad \text{(Eq. 5)}$$

$$F_X = +P_{aqX}[C_X(0) - C_X(h)] \qquad \text{(Eq. 6)}$$

where F_A and F_X are the steady-state fluxes for A and X, respectively; D_A and D_X are the epidermal membrane diffusion coefficients, respectively; P_{aqA} and P_{aqX} are the aqueous diffusion permeability coefficients for A and X, respectively; and $C_A(h)$ and $C_X(h)$ are the bulk phase concentrations of A and X, respectively, in the donor compartment. Flux is assumed positive when diffusion is from left to right. Within the metabolizing epidermis, it is assumed that the enzyme kinetics are first order so that:

$$D_A \frac{d^2C_A}{dx^2} - k_m C_A = 0 \qquad \text{(Eq. 7)}$$

[1] If both the drug and its metabolite are highly soluble in the epidermis, this induction period may be extended.

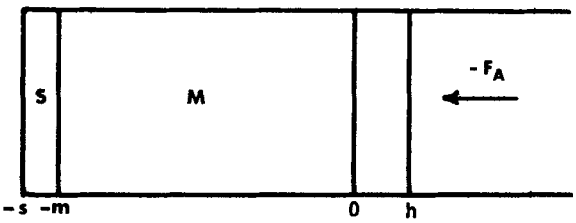

Figure 1—*Impermeable stratum corneum. Drug A moves in negative* x *direction, first penetrating the aqueous diffusion layer* ($0 \leq x \leq h$) *and then the metabolizing epidermis,* M, *located at* $-m \leq x \leq 0$. *The stratum corneum,* S, *at* $-s \leq x \leq -m$, *does not permit passage of A through it. The flux of A is considered negative, moving from right to left.*

and:

$$D_X \frac{d^2C_X}{dx^2} + k_m C_A = 0 \qquad \text{(Eq. 8)}$$

where k_m is the linear enzyme rate constant for metabolism.

Concentration Profiles for C_A *and* C_X—Initially, the drug, A, in the donor compartment diffuses from the bulk into the aqueous diffusion layer ($0 \leq x \leq h$) and penetrates the metabolizing epidermis ($-m \leq x \leq 0$). The drug concentration builds up in the epidermis gradually, consistent with the constraint that it cannot penetrate the stratum corneum ($-s \leq x \leq -m$). The product, X, gradually builds up in the epidermis and effluxes through the aqueous diffusion layer into the bulk phase. It too cannot penetrate the stratum corneum. After a sufficient time, a quasisteady state is assumed to be attained so that the concentration change of A and X at $x = 0$ and $x = h$ is sufficiently slow that Eqs. 4 and 6 are always maintained.

The solution to Eq. 7 has the general form:

$$C_A(x) = P \sinh kx + Q \cosh kx \qquad \text{(Eq. 9)}$$

where:

$$\kappa = \sqrt{k_m/D_A} \qquad \text{(Eq. 10)}$$

When the boundary conditions of Eqs. 1 and 4 are applied to Eq. 9, P and Q can be determined so that:

$$C_A(x) = \frac{\cosh \kappa(x + m)}{\cosh \kappa m + \dfrac{D_A \kappa}{P_{aqA}} \sinh \kappa m} C_A(h) \qquad \text{(Eq. 11)}$$

Integrating Eq. 8, using Eq. 11 for C_A, and evaluating the integration constants for the derivative and the function by using Eqs. 2 and 6, respectively, yield:

$$C_X(x) = C_X(h) - \frac{F_X}{P_{aqX}} \left(\frac{\kappa'}{\kappa}\right)^2 \left[\frac{\cosh \kappa m - \cosh \kappa(x + m)}{\cosh \kappa m + \dfrac{D_A \kappa}{P_{aqA}} \sinh \kappa m}\right] \qquad \text{(Eq. 12)}$$

where:

$$\kappa' = \sqrt{k_m/D_X} \qquad \text{(Eq. 13)}$$

Equations 11 and 12 give the concentration profile for $C_A(x)$ and $C_X(x)$ within the epidermal layer of the skin.

Flux Equations for A *and* X—From Eq. 3, F_A can be determined at $x = 0$. Differentiating Eq. 11 and evaluating the derivative at $x = 0$ yield:

$$F_A = -\frac{C_A(h)}{\dfrac{1}{P_{aqA}} + \dfrac{1}{D_A \kappa \tanh \kappa m}} \qquad \text{(Eq. 14)}$$

Similarly, Eq. 5 gives F_X, so using Eq. 12 yields:

$$F_X = \frac{C_A(h)}{\dfrac{1}{P_{aqA}} + \dfrac{1}{D_A \kappa \tanh \kappa m}} \qquad \text{(Eq. 15)}$$

Thus:

$$F_A + F_X = 0 \qquad \text{(Eq. 16)}$$

or the net flux of A and X is zero during quasisteady state.

Integrating Eq. 7 and using Eq. 3 yield:

$$F_A = k_m \int_0^{-m} C_A(x)\,dx \qquad \text{(Eq. 17)}$$

This equation means that the total drug flux at quasisteady state is due to the metabolism of the drug over the entire concentration profile within the epidermis.

Limits of Low and High Metabolism—Since k_m and κ are directly related by Eqs. 10 and 13, k_m or κ approaches zero in the limit of no metabolism and:

$$C_A(x) = C_A(h) \qquad \text{(Eq. 18)}$$

$$F_A = F_X = 0 \qquad \text{(Eq. 19)}$$

$$C_X(x) = C_X(h) \qquad \text{(Eq. 20)}$$

by taking the limiting values of Eqs. 11, 12, 14, and 15. Equations 18 and 20 show that, in the absence of metabolism, there is no functional dependence of the concentrations of A and X within the epidermis at steady state. Equation 19 is consistent with Eq. 17, since both equations show that there is no flux without metabolism.

In the limit of high metabolism, k_m and κ approach infinity and:

$$C_A(x) = 0 \qquad \text{(Eq. 21)}$$

$$F_A = -P_{aqA}C_A(h) \qquad \text{(Eq. 22)}$$

$$F_X = +P_{aqA}C_A(h) \qquad \text{(Eq. 23)}$$

$$C_X(x) = C_X(h) + \left(\frac{D_A}{D_X}\right)C_A(h) \qquad \text{(Eq. 24)}$$

Equation 21 shows, in the high metabolism limit, that the epidermis at $x = 0$ acts as a perfect sink for the diffusion of A through the diffusion layer.

In the aqueous diffusion layer, the transport of A is aqueous diffusion controlled (see Eq. 22), as is the transport of X, since the sum of A and X is conserved when X is not metabolized.

Calculation of κ—Equations 14 and 15 can be rearranged so that:

$$\frac{1}{\kappa} = C_1 \tanh \kappa m \qquad \text{(Eq. 25)}$$

and:

$$\frac{1}{\kappa} = C_2 \tanh \kappa m \qquad \text{(Eq. 26)}$$

respectively, where:

$$C_1 = D_A\left[\frac{C_A(h)}{-F_A} - \frac{1}{P_{aqA}}\right] \qquad \text{(Eq. 27)}$$

and:

$$C_2 = D_A\left[\frac{C_A(h)}{F_X} - \frac{1}{P_{aqA}}\right] \qquad \text{(Eq. 28)}$$

since $F_A < 0$, for diffusion of A into the epidermis:

$$C_1 = C_2 \qquad \text{(Eq. 29)}$$

if:

$$|F_A| = |F_X| \qquad \text{(Eq. 30)}$$

If Eq. 29 does not hold, then there is probably a significant amount of metabolism of X.

Equations 25 and 26 can be used to determine κ once the diffusion coefficient for A and the thickness of both the aqueous diffusion layer and the epidermis are known. Either a numerical or a graphical solution for κ can be obtained.

Permeable Stratum Corneum—Figure 2 depicts the situation of a permeable stratum corneum. The drug in the donor compartment of a diffusion cell faces the stratum corneum, while the receptor compartment faces the epidermis. The flux of the drug in Fig. 2 is in the opposite direction than in Fig. 1. This physical arrangement is analogous to the application of a topical dosage form. Metabolism is assumed to be only in the epidermis ($-m \le x \le 0$) and not in the stratum corneum ($-s \le x \le -m$). As the drug, A, moves across the stratum corneum, a flux, F_{-mA}, enters the epidermis when quasisteady state is attained. The boundary conditions at $x = -m$ are:

$$F_{-mA} = -D_A \left.\frac{dC_A}{dx}\right|_{x=-m} \qquad \text{(Eq. 31)}$$

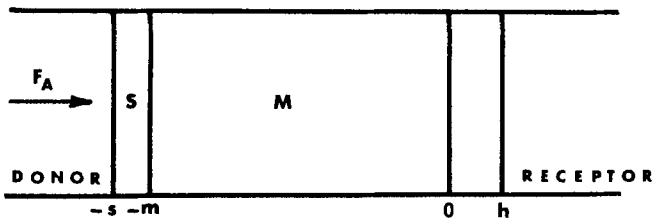

Figure 2—*Permeable stratum corneum. Drug A moves from left to right in the positive flux direction, penetrating first the stratum corneum,* S, *located at* $-s \le x \le -m$, *next the metabolizing epidermis,* M, *at* $-m \le x \le 0$, *and then the aqueous diffusion layer at* $0 \le x \le h$.

$$F_{-mA} = P_{SA}[C_A(-s) - C_A(-m)] \qquad \text{(Eq. 32)}$$

where P_{SA} is the permeability coefficient of the drug in the stratum corneum.

Within the epidermis, linear metabolism is assumed to form the major metabolite, X. At $x = 0$, both A and X diffuse out of the epidermis into the aqueous diffusion layer. The quasisteady-state fluxes of A and X are given by:

$$F_{0A} = -D_A \left.\frac{dC_A}{dx}\right|_{x=0} \qquad \text{(Eq. 33)}$$

$$F_{0A} = P_{aqA}[C_A(0) - C_A(h)] \qquad \text{(Eq. 34)}$$

$$F_{0X} = -D_X \left.\frac{dC_X}{dx}\right|_{x=0} \qquad \text{(Eq. 35)}$$

$$F_{0X} = P_{aqX}[C_X(0) - C_X(h)] \qquad \text{(Eq. 36)}$$

and the differential equations for the concentration profiles for A and X are given by Eqs. 7 and 8.

Concentration Profiles for C_A *and* C_X—The general solution for Eqs. 7 and 8 within the epidermis is given by Eq. 9. By using Eq. 9 in Eqs. 32 and 34, P and Q can be determined so that:

$$C_A(x) = P_{aqA}\frac{[P_{SA}\sinh\kappa(x+m) + D_A\kappa\cosh\kappa(x+m)]C_A(h)}{D_A\kappa(P_{SA}+P_{aqA})\cosh\kappa m + [P_{SA}P_{aqA} + (D_A\kappa)^2]\sinh\kappa m} - \frac{P_{SA}[P_{aqA}\sinh\kappa x - D_A\kappa\cosh\kappa x]C_A(-s)}{D_A\kappa(P_{SA}+P_{aqA})\cosh\kappa m + [P_{SA}P_{aqA} + (D_A\kappa)^2]\sinh\kappa m} \qquad \text{(Eq. 37)}$$

To determine $C_X(x)$, Eq. 8 is integrated twice, and Eqs. 35 and 36 are used to evaluate the constants of integration. Therefore:

$$C_X(x) = C_X(h) - F_{0X}\left[\frac{x}{D_X} - \frac{1}{P_{aqX}}\right] - \left(\frac{\kappa'}{\kappa}\right)^2[P(\sinh\kappa x - \kappa x) - Q(1-\cosh\kappa x)] \qquad \text{(Eq. 38)}$$

where:

$$P = \frac{(P_{SA}\cosh\kappa m + D_A\kappa\sinh\kappa m)P_{aqA}C_A(h) - P_{SA}P_{aqA}C_A(-s)}{D_A\kappa(P_{SA}+P_{aqA})\cosh\kappa m + [P_{SA}P_{aqA} + (D_A\kappa)^2]\sinh\kappa m} \qquad \text{(Eq. 39)}$$

and:

$$Q = \frac{D_A\kappa P_{SA}C_A(-s) + (P_{SA}\sinh\kappa m + D_A\kappa\cosh\kappa m)P_{aqA}C_A(h)}{D_A\kappa(P_{SA}+P_{aqA})\cosh\kappa m + [P_{SA}P_{aqA} + (D_A\kappa)^2]\sinh\kappa m} \qquad \text{(Eq. 40)}$$

Flux Equations for A *and* X—Application of Eqs. 33 and 31 yields:

$$F_{0A} = \frac{\operatorname{sech}\kappa m C_A(-s) - \left[1 + \frac{D_A\kappa}{P_{SA}}\tanh\kappa m\right]C_A(h)}{\frac{1}{P_{SA}} + \frac{1}{P_{aqA}} + \left[1 + \frac{(D_A\kappa)^2}{P_{SA}P_{aqA}}\right]\frac{\tanh\kappa\kappa m}{D_A\kappa}} \qquad \text{(Eq. 41)}$$

and:

$$F_{-mA} = \frac{\left[\frac{D_A\kappa}{P_{aqA}}\tanh\kappa m + 1\right]C_A(-s) - \operatorname{sech}\kappa m C_A(h)}{\frac{1}{P_{SA}} + \frac{1}{P_{aqA}} + \left[1 + \frac{(D_A\kappa)^2}{P_{SA}P_{aqA}}\right]\frac{\tanh\kappa m}{D_A\kappa}} \qquad \text{(Eq. 42)}$$

If Eq. 7 is integrated:

$$F_{-mA} - F_{0A} = k_m \int_{-m}^{0} C_A(x)\,dx \qquad \text{(Eq. 43)}$$

This equation means that the flux difference between the drug that enters the epidermis from the stratum corneum and the drug that leaves the epidermis into the aqueous diffusion layer is due to the total amount of metabolism within the epidermis. The relationship between F_{0X} and F_{-mX} can be found from Eq. 38 to be:

$$F_{-mX} - F_{0X} = \frac{\kappa'^2}{\kappa} D_X[P(\cosh(\kappa m) - 1) - Q\sinh(\kappa m)] \qquad \text{(Eq. 44)}$$

where P and Q are given by Eqs. 39 and 40, respectively. Finally, from Eq. 8:

$$F_{-mX} - F_{0X} = F_{0A} - F_{-mA} \qquad \text{(Eq. 45)}$$

F_{-mX} arises because the stratum corneum is permeable to the metabolite, X, so that X diffuses back into the donor chamber.

Limits of High and Low Metabolism—In the limit of no metabolism when κ tends to zero, Eqs. 37, 38, 41, and 42 become:

$$C_A(x) = \frac{\left[\frac{1}{D_A/(m+x)} + \frac{1}{P_{SA}}\right]C_A(h) - \left[\frac{1}{D_A/x} - \frac{1}{P_{aqA}}\right]C_A(-s)}{\frac{1}{P_{aqA}} + \frac{1}{P_{SA}} + \frac{1}{D_A/m}} \qquad \text{(Eq. 46)}$$

$$C_X(x) = C_X(h) \qquad \text{(Eq. 47)}$$

$$F_{0A} = F_{-mA} \qquad \text{(Eq. 48)}$$

$$F_{0A} = \frac{C_A(-s) - C_A(h)}{\frac{1}{P_{aqA}} + \frac{1}{P_{SA}} + \frac{1}{D_A/m}} \qquad \text{(Eq. 49)}$$

Conversely, in the limit of high metabolism:

$$C_A(s) = 0 \qquad \text{(Eq. 50)}$$

$$C_X(x) = C_X(h) + F_{0X}\left[\frac{1}{P_{aqA}} - \frac{x}{D_X}\right] \qquad \text{(Eq. 51)}$$

$$F_{0A} = -P_{aq}C_A(h) \qquad \text{(Eq. 52)}$$

$$F_{-mA} = P_{SA}C_A(-s) \qquad \text{(Eq. 53)}$$

REFERENCES

(1) R. J. Scheuplein, *J. Invest. Dermatol.*, **45**, 334 (1965).

(2) *Ibid.*, **48**, 79 (1967).

(3) R. J. Scheuplein, I. H. Blank, G. J. Brauner, and D. J. MacFarlane, *J. Invest. Dermatol.*, **52**, 63 (1969).

(4) O. D. Laerum, *ibid.*, **52**, 204 (1969).

(5) J. Bamshad, *ibid.*, **52**, 351 (1969).

(6) H. Y. Ando, N. F. H. Ho, and W. I. Higuchi, *J. Pharm. Sci.*, **66**, 755 (1977).

ACKNOWLEDGMENTS AND ADDRESSES

Received December 18, 1975, from the *College of Pharmacy, University of Michigan, Ann Arbor, MI 48109.*

Accepted for publication January 14, 1977.

Appreciation is expressed to Mr. J. L. Fox for assistance on the mathematical aspects of diffusion and to Ms. Aurora Calvo for editing and proofreading the manuscript.

* Present address: Philadelphia College of Pharmacy and Science, Philadelphia, Pa.

ˣ To whom inquiries should be directed.

pH-Stat Titration of Aluminum Hydroxide Gel

NICHOLAS J. KERKHOF *, ROGER K. VANDERLAAN *, JOE L. WHITE ‡, and STANLEY L. HEM *ˣ

Abstract □ The pH-stat titration of aluminum hydroxide gel was evaluated and was affected by pH, temperature, concentration, and ionic strength. Control of these parameters resulted in a highly sensitive and reproducible *in vitro* antacid test. The utility of the pH-stat test was illustrated by monitoring the aging of several carbonate-containing aluminum hydroxide gels and by comparing the antacid properties as measured by the pH-stat titration, the acid-consuming capacity, the Rossett–Rice test, and the test proposed by the Food and Drug Administration Drug Evaluation Panel. The pH-stat titration also was useful for relatively nonreactive aluminum hydroxide gels. The use of sodium fluoride as the reaction medium extended the capability of the pH-stat titration to monitor the aging of chloride-containing gels. The pH-stat titrigram was interpreted in terms of a previously published polymer model of the structure of a chloride-containing aluminum hydroxide gel. The acid reactivity of relatively nonreactive gels is believed to be due totally to the chemical neutralization of acid, because the milliequivalents of aluminum ion appearing in solution is the same as the milliequivalents of acid neutralized throughout the pH-stat titration.

Keyphrases □ Aluminum hydroxide gel—pH-stat titration evaluated, aging monitored, compared to other tests □ pH-stat titration—evaluated for aluminum hydroxide gel, aging monitored, compared to other tests □ Gels—aluminum hydroxide, pH-stat titration evaluated, aging monitored, compared to other tests □ Aging—aluminum hydroxide gel, monitored with pH-stat titration, compared to other tests □ Antacids—aluminum hydroxide gel, pH-stat titration evaluated, aging monitored, compared to other tests

Available *in vitro* antacid tests may be broadly classified as static or dynamic. The acid-consuming capacity test (1), the most widely used static test, determines the total amount of acid neutralized during 1 hr at 37°. The dynamic methods may measure the pH profile during acid neutralization or determine the acid neutralization rate at a constant pH. The test of Holbert *et al.* (2) and the Rossett–Rice test (3) attempt to simulate the stomach and record the pH profile during acid neutralization. Brody and Bachrach (4) first proposed a test that measures the acid neutralization rate at a constant pH. This test subsequently was automated (5) and recently was correlated with *in vivo* acid neutralization by aluminum hydroxide gel (6).

The Food and Drug Administration (FDA) Drug Evaluation Panel on antacids proposed a test (7) that combines the static approach with the dynamic pH profile.

A sensitive *in vitro* antacid test was needed to study the structure and mechanism of neutralization of aluminum hydroxide gel and to optimize the production of aluminum

If Eq. 7 is integrated:

$$F_{-mA} - F_{0A} = k_m \int_{-m}^{0} C_A(x)\,dx \qquad \text{(Eq. 43)}$$

This equation means that the flux difference between the drug that enters the epidermis from the stratum corneum and the drug that leaves the epidermis into the aqueous diffusion layer is due to the total amount of metabolism within the epidermis. The relationship between F_{0X} and F_{-mX} can be found from Eq. 38 to be:

$$F_{-mX} - F_{0X} = \frac{\kappa'^2}{\kappa} D_X[P(\cosh(\kappa m) - 1) - Q\sinh(\kappa m)] \qquad \text{(Eq. 44)}$$

where P and Q are given by Eqs. 39 and 40, respectively. Finally, from Eq. 8:

$$F_{-mX} - F_{0X} = F_{0A} - F_{-mA} \qquad \text{(Eq. 45)}$$

F_{-mX} arises because the stratum corneum is permeable to the metabolite, X, so that X diffuses back into the donor chamber.

Limits of High and Low Metabolism—In the limit of no metabolism when κ tends to zero, Eqs. 37, 38, 41, and 42 become:

$$C_A(x) = \frac{\left[\frac{1}{D_A/(m+x)} + \frac{1}{P_{SA}}\right]C_A(h) - \left[\frac{1}{D_A/x} - \frac{1}{P_{aqA}}\right]C_A(-s)}{\frac{1}{P_{aqA}} + \frac{1}{P_{SA}} + \frac{1}{D_A/m}} \qquad \text{(Eq. 46)}$$

$$C_X(x) = C_X(h) \qquad \text{(Eq. 47)}$$

$$F_{0A} = F_{-mA} \qquad \text{(Eq. 48)}$$

$$F_{0A} = \frac{C_A(-s) - C_A(h)}{\frac{1}{P_{aqA}} + \frac{1}{P_{SA}} + \frac{1}{D_A/m}} \qquad \text{(Eq. 49)}$$

Conversely, in the limit of high metabolism:

$$C_A(s) = 0 \qquad \text{(Eq. 50)}$$

$$C_X(x) = C_X(h) + F_{0X}\left[\frac{1}{P_{aqA}} - \frac{x}{D_X}\right] \qquad \text{(Eq. 51)}$$

$$F_{0A} = -P_{aq}C_A(h) \qquad \text{(Eq. 52)}$$

$$F_{-mA} = P_{SA}C_A(-s) \qquad \text{(Eq. 53)}$$

REFERENCES

(1) R. J. Scheuplein, *J. Invest. Dermatol.*, **45**, 334 (1965).

(2) *Ibid.*, **48**, 79 (1967).

(3) R. J. Scheuplein, I. H. Blank, G. J. Brauner, and D. J. MacFarlane, *J. Invest. Dermatol.*, **52**, 63 (1969).

(4) O. D. Laerum, *ibid.*, **52**, 204 (1969).

(5) J. Bamshad, *ibid.*, **52**, 351 (1969).

(6) H. Y. Ando, N. F. H. Ho, and W. I. Higuchi, *J. Pharm. Sci.*, **66**, 755 (1977).

ACKNOWLEDGMENTS AND ADDRESSES

Received December 18, 1975, from the *College of Pharmacy, University of Michigan, Ann Arbor, MI 48109.*

Accepted for publication January 14, 1977.

Appreciation is expressed to Mr. J. L. Fox for assistance on the mathematical aspects of diffusion and to Ms. Aurora Calvo for editing and proofreading the manuscript.

* Present address: Philadelphia College of Pharmacy and Science, Philadelphia, Pa.

ˣ To whom inquiries should be directed.

pH-Stat Titration of Aluminum Hydroxide Gel

NICHOLAS J. KERKHOF *, ROGER K. VANDERLAAN *, JOE L. WHITE ‡, and STANLEY L. HEM *ˣ

Abstract □ The pH-stat titration of aluminum hydroxide gel was evaluated and was affected by pH, temperature, concentration, and ionic strength. Control of these parameters resulted in a highly sensitive and reproducible *in vitro* antacid test. The utility of the pH-stat test was illustrated by monitoring the aging of several carbonate-containing aluminum hydroxide gels and by comparing the antacid properties as measured by the pH-stat titration, the acid-consuming capacity, the Rossett–Rice test, and the test proposed by the Food and Drug Administration Drug Evaluation Panel. The pH-stat titration also was useful for relatively nonreactive aluminum hydroxide gels. The use of sodium fluoride as the reaction medium extended the capability of the pH-stat titration to monitor the aging of chloride-containing gels. The pH-stat titrigram was interpreted in terms of a previously published polymer model of the structure of a chloride-containing aluminum hydroxide gel. The acid reactivity of relatively nonreactive gels is believed to be due totally to the chemical neutralization of acid, because the milliequivalents of aluminum ion appearing in solution is the same as the milliequivalents of acid neutralized throughout the pH-stat titration.

Keyphrases □ Aluminum hydroxide gel—pH-stat titration evaluated, aging monitored, compared to other tests □ pH-stat titration—evaluated for aluminum hydroxide gel, aging monitored, compared to other tests □ Gels—aluminum hydroxide, pH-stat titration evaluated, aging monitored, compared to other tests □ Aging—aluminum hydroxide gel, monitored with pH-stat titration, compared to other tests □ Antacids—aluminum hydroxide gel, pH-stat titration evaluated, aging monitored, compared to other tests

Available *in vitro* antacid tests may be broadly classified as static or dynamic. The acid-consuming capacity test (1), the most widely used static test, determines the total amount of acid neutralized during 1 hr at 37°. The dynamic methods may measure the pH profile during acid neutralization or determine the acid neutralization rate at a constant pH. The test of Holbert *et al.* (2) and the Rossett–Rice test (3) attempt to simulate the stomach and record the pH profile during acid neutralization. Brody and Bachrach (4) first proposed a test that measures the acid neutralization rate at a constant pH. This test subsequently was automated (5) and recently was correlated with *in vivo* acid neutralization by aluminum hydroxide gel (6).

The Food and Drug Administration (FDA) Drug Evaluation Panel on antacids proposed a test (7) that combines the static approach with the dynamic pH profile.

A sensitive *in vitro* antacid test was needed to study the structure and mechanism of neutralization of aluminum hydroxide gel and to optimize the production of aluminum

Table I—Effect of Concentration on the pH-Stat Titration of Carbonate-Containing Aluminum Hydroxide Gel[a]

Reaction Volume, ml	k_{II}, mEq/min	k_{III}, mEq/min	Initiation of Phase III, min	T_{50}, min
11	0.32	0.57	1.3	2.2
22	0.29	0.48	1.5	2.6
33	0.26	0.41	1.8	3.0

[a] Contained 38 mg equivalent Al_2O_3 in all cases.

hydroxide gel and the design of aluminum hydroxide gel dosage forms. The present study was undertaken to evaluate critically the test parameters that affect the pH-stat titration, to establish if the test can be used with nonreactive as well as reactive gels, and to determine if the test possesses sufficient sensitivity and precision to be useful in structural studies.

EXPERIMENTAL

Materials—All chemicals used were either official or reagent grade.

Aluminum Hydroxide Gel Preparation—Carbonate-containing aluminum hydroxide gel was prepared by the reaction of aluminum chloride, sodium bicarbonate, and sodium carbonate to a final pH of 6.5 (8). Chloride-containing aluminum hydroxide gels were prepared by the reaction of aluminum chloride and strong ammonia solution to a final pH of 7.0 or 9.2 (8).

Determination of Acid Reactivity by pH-Stat Titration—The acid reactivity was measured using an automated pH-stat technique similar to the method described by Steinberg *et al.* (5). A pH meter, a titrator, an autoburet, a titration assembly, and a recorder[1] were used.

An appropriate volume of water was added to the reaction vessel and adjusted to pH 3.0. A volume of aluminum hydroxide gel containing 38 mg equivalent Al_2O_3 was then added. The volume of water was adjusted for each sample to produce a reaction volume of 22 ml. The instrument was set to maintain pH 3.0 by adding 1.0 *N* HCl from the autoburet and it was activated simultaneously with the sample injection. The recorder plotted milliliters of 1.0 *N* HCl added *versus* time.

The acid reactivity of the chloride-containing aluminum hydroxide gel also was determined using a sodium fluoride solution as the reaction medium. A 25-ml aliquot of 0.5 *N* NaF was added to the reaction vessel and adjusted to pH 6.5 with 1.0 *N* HCl. A gel sample containing 38 mg equivalent Al_2O_3 was added and the instrument was activated to maintain pH 6.5 by the addition of 1.0 *N* HCl from the autoburet.

Variables Affecting pH-Stat Titration—A completely randomized 3^3 factorial study was designed to evaluate the significance of temperature, pH, and stirring speed on the acid reactivity of aluminum hydroxide gel as measured by the pH-stat technique. A freshly precipitated carbonate-containing aluminum hydroxide gel was used. Three levels of each variable were fixed. The temperature levels were 25, 31, and 37°; the pH levels were 2.0, 2.5, and 3.0; and the stirring speeds[2] were 650, 900, and 1400 rpm. The experiment was conducted in 1 day by one operator. Five random replicate trials were determined to estimate the random error.

Three dependent variables, T_{25}, T_{50}, and T_{90}, were determined from the pH-stat reactivity curves; they were the times required to add 25, 50, and 90%, respectively, of the total 1.0 *N* HCl needed to neutralize the aluminum hydroxide gel.

***In Vitro* Antacid Tests**—The official procedure for the acid-consuming capacity test (1) was followed.

The pH profile during the neutralization reaction was followed by the Rossett–Rice test (3). Seventy milliliters of 0.1 *N* HCl and 30 ml of water were added to a 400-ml jacketed reaction vessel. When the temperature reached 37°, a 300-mg equivalent Al_2O_3 sample was added. Simultaneously, a pump calibrated to add 0.1 *N* HCl at a rate of 4 ml/min was activated. A pH meter attached to a recorder provided a record of the time course of the pH during the neutralization reaction. The pH profile is characterized by the lag time, the time to reach pH 3, and the Rossett–Rice time, the time during which the pH is maintained between 3 and 5.

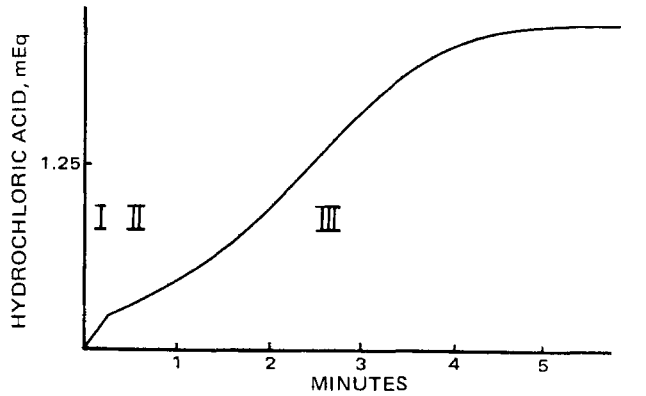

Figure 1—*Characteristic pH-stat titrigram of carbonate-containing aluminum hydroxide gel showing phases I, II, and III.*

The FDA antacid review panel (7) proposed a two-part *in vitro* test for antacids. The preliminary antacid test measures the pH of the neutralization medium after 10 min. If the pH is 3.5 or greater, the acid-neutralizing capacity test is run. This test measures the amount of acid neutralized in the first 15 min.

Analytical Procedures—The equivalent aluminum oxide content of each gel was determined by the ethylenediaminetetraacetic acid titration (1).

The total chloride content of the chloride-containing gels was determined by the Volhard titration (9) after 3 g of gel was dissolved in 15 ml of 6 *N* nitric acid.

The appearance of aluminum ion during the neutralization of chloride-containing aluminum hydroxide gel was monitored by a modified ethylenediaminetetraacetic acid titration. It was assumed that only the aluminum ion in the neutralization reaction mixture would chelate and that aluminum not released from the gel structure by the neutralization reaction would not be detected. The ethylenediaminetetraacetic acid titration (1) was modified by omitting the addition of acid to dissolve the gel and by not heating the sample drawn from the neutralization reaction. These steps would be likely to increase the amount of aluminum ion in solution by accelerating the neutralization reaction. However, these two changes had no effect on the analysis of a standard aluminum chloride solution because both analytical procedures gave the theoretical aluminum concentration.

Ultrafiltration and centrifugation procedures were tried to separate the unreacted solids in the reaction mixture prior to the aluminum assay. These methods were not satisfactory due to the time required for the separation and the rapid aging characteristics of the chloride-containing aluminum hydroxide gel. Thus, the modified ethylenediaminetetraacetic acid titration, which did not require a separation step, was used. Freshly precipitated gel, 20 ml, accurately weighed, was diluted with 20 ml of water, and the pH-stat reactivity was determined at pH 3.0. A 25.0-ml buret was used to deliver 1.0 *N* HCl from the autoburet. During the neutralization reaction, six 2.0-ml samples were withdrawn at various times and analyzed for aluminum ion by the modified ethylenediaminetetraacetic acid titration.

For X-ray analysis, a gel sample was air dried at room temperature and ground to a fine powder with an agate mortar and pestle. Powder specimens were prepared using aluminum McCreery mounts. The diffraction pattern was recorded[3] from 6 to 30° 2θ under the following conditions: CuKα radiation, 40 kv, 20 mamp, 500 Hz full scale, and 2°/min scan speed.

IR spectra[4] were obtained by air drying a 0.10-ml gel sample on a zinc sulfide[5] window. The concentration on the window was 0.3 mg of aluminum oxide/cm^2.

RESULTS AND DISCUSSION

Measurement of Acid Reactivity of Carbonate-Containing Gels—Figure 1 is a characteristic pH-stat neutralization curve of a completely reactive carbonate-containing aluminum hydroxide gel. The neutralization reaction appears to be composed of three phases: an initial rapid phase (I), a slow zero-order period (II), and a more rapid terminal

[1] A pH meter PHM 26, titrator TTT II, autoburet ABU 12 (2.5 ml), titration assembly TTA 3, and recorder SBR 2; Radiometer, Copenhagen, Denmark.
[2] Stirring speed was measured by a stroboscope; Strobotac, General Radio Co., Cambridge, Mass.
[3] Norelco, Phillips Electronic Instruments, Mount Vernon, N.Y.
[4] Model 421, Perkin-Elmer Corp., Norwalk, Conn.
[5] Irtran 2, Eastman Kodak Co., Rochester, N.Y.

Table II—Effect of Ionic Strength of Reaction Medium on pH-Stat Titration of Carbonate-Containing Aluminum Hydroxide Gel

Reaction Medium	Ionic Strength	k_{II}, mEq/min	k_{III}, mEq/min	Initiation of Phase III, min	T_{50}, min
Distilled water	0	0.206	0.367	2.2	3.5
0.2 *M* NaCl	0.20	0.397	0.481	1.7	2.3
0.4 *M* NaCl	0.40	0.543	0.610	1.0	1.8
0.6 *M* NaCl	0.60	0.568	0.657	0.9	1.7
0.8 *M* NaCl	0.80	0.657	0.735	0.8	1.5
1.0 *M* NaCl	1.00	0.694	0.806	0.7	1.4
0.037 *M* $AlCl_3$	0.222	0.357	0.471	1.7	2.2
0.1 *M* $AlCl_3$	0.60	0.555	0.644	0.8	1.6
0.2 *M* $AlCl_3$	1.20	0.610	0.749	0.7	1.4

zero-order phase (III). In Fig. 1, phase II begins at 0.23 min and phase III begins at 1.5 min. The acid neutralization rate during phase I is very rapid and exceeds the capability of the autoburet to add compensating acid. Thus, the total volume of acid neutralized during phase I can be measured, but no rate measurements are possible.

The specially prepared computer program evaluated neutralization rate periods II and III by simple linear regression. The output consisted of the two zero-order rate constants (k_{II} and k_{III}), the linear correlation coefficients, the *F*-test ratio, the percent aluminum oxide based on total acid neutralized, and the time for the initiation of phase III. This time was computed from the intersection of the k_{II} line with the k_{III} line by using simultaneous equations from linear regression analysis of the two neutralization rate periods.

A second approach used to evaluate the pH-stat titrigrams was to determine the time required to add 50% (T_{50}) of the total 1.0 *N* HCl needed to neutralize the aluminum hydroxide gel. This approach is limited to completely reactive aluminum hydroxide gels.

Variables Affecting pH-Stat Titration—Analysis of variance of the 3^3 factorial design experiment, using the three-way interaction as the error term (10), indicated that pH and temperature were significant at the 0.5% level. There was also a significant pH–temperature interaction. Stirring speed was not a significant main effect within the range of stirring speeds available with the titration assembly. The critical factors of pH and temperature can be controlled easily during the titration, resulting in a highly reproducible test. Conditions were standardized using pH 3.0, 25°, and 900 rpm.

The neutralization reaction proceeds faster as the concentration of equivalent aluminum oxide in the sample is increased (Table I). The concentration of the reacting medium was, therefore, standardized at 38 mg equivalent Al_2O_3/22 ml. This concentration was chosen because 2.235 mEq (89.4% of the volume of 1.0 *N* HCl available in the 2.5-ml buret) would be neutralized if the equivalent aluminum oxide reacted stoichiometrically with hydrochloric acid.

The ionic strength of the reaction medium also affects the pH-stat titration. Table II shows that the neutralization reaction proceeds more rapidly as the ionic strength is increased. Distilled water was selected as the reaction medium, although the ions generated during the neutralization reaction caused a slight change in ionic strength during the titration. The complete neutralization of 38 mg of aluminum oxide/22 ml by hydrochloric acid will result in an ionic strength of 0.15. The effect of the continuously changing ionic strength caused by the neutralization reaction could be minimized by using a sodium chloride or aluminum chloride solution as the reaction medium.

Table IV—Effect of pH on Acid Neutralization Rate

pH	T_{50}, min: Aluminum Hydroxide Gel[a]	Sodium Bicarbonate[b]	Calcium Carbonate[c]
2.0	0.5	0.05	0.1
2.5	1.0	—	—
3.0	2.2	0.10	0.1
3.5	3.2	—	—
4.0	7.2	0.10	0.2
4.5	NR[d]	—	—
5.0	NR[e]	0.25	2.9
6.0	NR[e]	0.70	26.2
7.0	NR[e]	4.5	NR[f]

[a] Contained 38 mg of aluminum oxide. [b] Contained 185 mg of sodium bicarbonate. [c] Contained 110 mg of calcium carbonate. [d] Thirty-eight percent reacted in 160 min. [e] No appreciable reaction. [f] Twenty-four percent reacted in 160 min.

The reproducibility of the pH-stat titration of aluminum hydroxide gel under fixed conditions of pH 3.0, 25°, 900 rpm, and 38 mg of aluminum oxide/22 ml of water was determined by 10 replicate pH-stat titrations of a carbonate-containing gel containing 3.52% equivalent aluminum oxide. The mean values for k_{II} and k_{III} were 0.172 and 0.317 mEq/min with standard deviations of 0.005 and 0.017, respectively. The initiation of phase III occurred at 2.4 ± 0.1 min. The T_{50} was 3.9 ± 0.1 min. These results indicate that the parameters affecting the pH-stat titration can be controlled and that it is a sensitive, reliable, and highly reproducible technique for monitoring the acid reactivity of aluminum hydroxide gel.

Comparison of *In Vitro* Antacid Tests—The sensitivity and reproducibility of the pH-stat titration suggest that it may be more useful than present *in vitro* tests in detecting differences in the acid neutralization rate of aluminum hydroxide gel. The *in vitro* tests were compared by monitoring the aging of a laboratory carbonate-containing aluminum hydroxide gel and by examining one laboratory carbonate-containing gel and two commercial gels of different ages.

The data in Table III for Gel 1 indicate that the pH-stat titration is capable of detecting changes in the acid neutralization rate on a daily basis. The time for 50% neutralization increased from 3.7 to 7.2 min over 10 days. The acid-consuming capacity test, the Rossett–Rice time, and the FDA antacid review panel test were insensitive to the changes occurring in the gel structure. The lag time in the Rossett–Rice test did increase from 0.1 to 0.2 min during the 10 days. However, this parameter, although suggesting a structural change, is not capable of monitoring daily changes in acid reactivity of the gel.

The utility of the pH-stat titration also is seen when three aluminum hydroxide gels, ranging in age from 3 to 33 months, are compared. The T_{50} values for Gels 2, 3, and 4 (Table III) were 11.2, 24.8, and 46 min, respectively, and were directly related to age.

The acid-consuming capacity measures the milliliters of 0.1 *N* HCl neutralized by 1 g of gel in 1 hr at 37°. Using this parameter, it is difficult to compare gels of different equivalent aluminum oxide content. The acid

Table III—Comparison of *In Vitro* Antacid Tests

		Acid-Consuming Capacity Test			Rossett–Rice Test[a]		FDA Antacid Review Panel Test[a]		
Gel, % Al_2O_3	Age	0.1 *N* HCl Consumed per Gram of Gel, ml	0.1 *N* HCl Consumed per Gram of Aluminum Oxide, ml	Theoretical Acid-Consuming Capacity, %	Rossett–Rice Time, min	Lag Time, min	pH of Preliminary Antacid Test	Hydrochloric Acid Neutralized in 15 min, mEq	pH-Stat Titration[b] T_{50}, min
1[c], 3.3	1 day	20.34	616.4	104.8	30.0	0.1	4.1	18.5	3.7
1, 3.3	2 days	20.34	616.4	104.8	30.0	0.1	4.1	18.5	3.9
1, 3.3	3 days	20.34	616.4	104.8	30.0	0.1	4.1	18.5	4.4
1, 3.3	6 days	20.34	616.4	104.8	30.0	0.15	4.1	18.5	5.4
1, 3.3	7 days	20.34	616.4	104.8	30.0	0.15	4.1	18.5	5.8
1, 3.3	9 days	20.34	616.4	104.8	30.0	0.2	4.1	18.5	6.6
1, 3.3	10 days	20.34	616.4	104.8	30.0	0.2	4.1	18.5	7.2
2[c], 4.1	3 months	25.65	625.6	106.4	29.2	0.4	4.0	18.5	11.2
3[d], 4.2	21 months	25.22	600.5	102.1	29.0	1.5	3.9	16.9	24.8
4[d], 5.2	33 months	30.99	596.0	101.4	26.3	2.4	3.8	16.9	46.0

[a] Sample contained 300 mg equivalent Al_2O_3. [b] Sample contained 38 mg equivalent Al_2O_3. [c] Laboratory gel. [d] Commercial product.

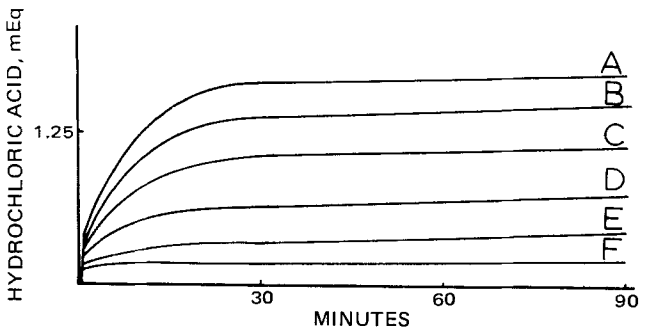

Figure 2—*The pH-stat titrigram of a chloride-containing aluminum hydroxide gel precipitated at pH 9.2 and aged at 25°. Key: A, 15 min; B, 1.5 hr; C, 2.5 hr; D, 4 hr; E, 6.5 hr; and F, 24 hr.*

reactivity of different gels could be compared more accurately if the milliliters of 0.1 *N* HCl that react with 1 g of equivalent aluminum oxide were expressed. Another alternative that would make the acid-consuming capacity test more useful for studying gels of different equivalent aluminum oxide content would be to calculate the percent theoretical acid-consuming capacity assuming that 6 moles of hydrochloric acid react with 1 mole equivalent aluminum oxide. As seen in Table III, the milliliters of hydrochloric acid consumed per gram of gel is confounded by the different equivalent aluminum oxide content of Gels 2, 3, and 4. A comparison is possible using either milliliters of 0.1 *N* HCl consumed per gram of equivalent aluminum oxide or percent theoretical acid-consuming capacity. Both parameters indicate a decrease of 5% in acid-consuming capacity between the 3- and 33-month gels.

The Rossett–Rice data also indicate that a slight difference in acid reactivity existed among Gels 2, 3, and 4 directly related to their ages. The lag time seems to be the most sensitive indicator since it increased from 0.4 to 2.4 min.

The FDA antacid review panel test showed that less than a 10% difference in acid reactivity existed among Gels 2, 3, and 4 and that the 21- and 33-month gels were virtually identical.

It is evident that the pH-stat titration is the most sensitive approach for determining changes in acid reactivity occurring as aluminum hydroxide gel ages as well as the *in vitro* acid reactivity differences between aluminum hydroxide gels. This sensitivity to structural changes in aluminum hydroxide gel makes the pH-stat titration a powerful tool for structural studies and for optimizing the production of aluminum hydroxide gel and the design and manufacture of aluminum hydroxide gel dosage forms.

Effect of pH on Neutralization Rate—The neutralization rate of carbonate-containing aluminum hydroxide gel was inversely related to the pH-stat end-point in the pH range below 4 (Table IV). Aluminum hydroxide gel did not react with acid to any appreciable extent above pH 4.0. It is interesting to compare the behavior of aluminum hydroxide gel to the effect of pH on the neutralization of sodium bicarbonate and calcium carbonate. Sodium bicarbonate reacted very rapidly, even up to pH 7 (Table IV). Calcium carbonate also reacted very rapidly at pH's up to 5. The reaction still proceeded above pH 5 but at a slower rate.

These data suggest that aluminum hydroxide gel will only neutralize acid in the stomach or duodenum where the pH is below 4. In comparison, sodium bicarbonate and calcium carbonate are capable of reacting with acid throughout the GI tract. Since ulcers and hyperacidity problems are localized in the stomach and duodenum, the pH–reactivity pattern of aluminum hydroxide gel seems well suited for antacid therapy.

Table V—Change in pH-Stat Titrigram during Aging at 25° of Chloride-Containing Aluminum Hydroxide Gel Precipitated at pH 9.2

Age	Phase A, %	Phase B, %	Phase C, %	k_B, mEq/min	k_C, mEq/min
15 min	17.4	54.4	28.2	9.73×10^{-2}	1.15×10^{-3}
1.5 hr	14.0	44.9	41.1	9.50×10^{-2}	1.35×10^{-3}
2.5 hr	11.5	35.5	53	8.58×10^{-2}	1.03×10^{-3}
4 hr	8.5	19.5	72	7.25×10^{-2}	1.35×10^{-3}
6.5 hr	7.9	4.1	88	3.15×10^{-2}	1.50×10^{-3}
24 hr	5.7	1.1	93.2	0.45×10^{-2}	1.10×10^{-3}

Table VI—Change in Hydroxyl Exchange during Aging at 25° of Chloride-Containing Aluminum Hydroxide Gel Precipitated at pH 9.2

Age	Phase *a*, %	Phase *b*, %	k_b, mEq/min
4 hr	67.9	32.1	4.57×10^{-3}
8 hr	57.9	42.1	5.07×10^{-3}
1 day	31.0	69.0	4.86×10^{-3}
2 days	18.0	82.0	4.79×10^{-3}
7 days	8.4	91.6	4.77×10^{-3}

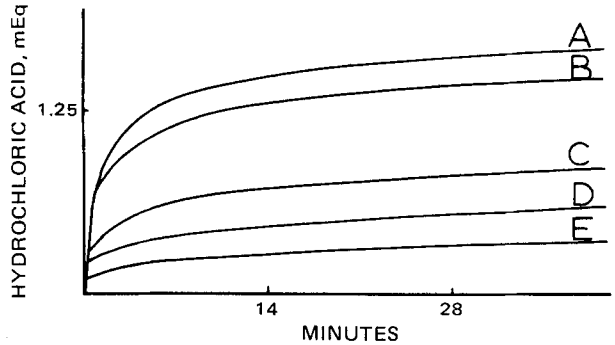

Figure 3—*The pH-stat titrigram of a chloride-containing aluminum hydroxide gel precipitated at pH 9.2 and aged at 25°. Reaction medium was 0.5* N *NaF at pH 6.5. Key: A, 4 hr; B, 8 hr; C, 1 day; D, 2 days; and E, 7 days.*

Measurement of Acid Reactivity of Chloride-Containing Gels—The study of the acid reactivity of chloride-containing aluminum hydroxide gels presents additional problems due to the relatively nonreactive nature of the gel, the rapid change in reactivity during aging, and the possible adsorption of acid by the gel in addition to the chemical neutralization of acid. As seen in Fig. 2, the freshly precipitated chloride-containing gel precipitated at a final pH of 9.2 was still reacting after 1 hr at pH 3.0 and had not reached the theoretical 2.235 mEq of hydrochloric acid required for a 38-mg equivalent Al_2O_3 sample. The neutralization rate decreased rapidly as the gel aged. After 1 day at 25°, the gel was virtually unreactive since only 7% of the theoretical amount of acid was neutralized during 1 hr.

The pH-stat titrigram (Fig. 2) consists of three phases: an initial immediate reaction (A), followed by a slower zero-order phase (B) and a very slow terminal zero-order phase (C). The neutralization curve can be characterized by the fraction represented by each phase obtained by extrapolation of the linear portion of each phase and by k_B and k_C, the zero-order rate constants for phases B and C, respectively. The acid neutralization rate exceeded the speed of the autoburet during phase A. Thus, the total volume of acid neutralized during phase A could be determined but rate measurements for phase A were not possible.

The kinetic parameters for the aging at 25° of the chloride-containing gel precipitated at a final pH of 9.2 are given in Table V. The amounts of phases A and B decreased during aging until both fractions were virtually absent at 24 hr. Phase C increased during aging until it accounted for 93.2% of the gel after 24 hr. The rate of change for each fraction was greatest during the first 4–6 hr following precipitation. The rate constant

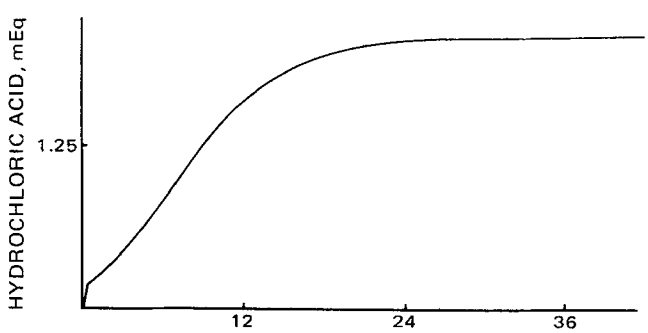

Figure 4—*The pH-stat titrigram of a chloride-containing aluminum hydroxide gel precipitated at pH 7.0 and aged 20 min at 25°.*

Table VII—Change in pH-Stat Titrigram during Aging at 25° of Chloride-Containing Aluminum Hydroxide Gel Precipitated at pH 7.0

Age	Phase 1, %	Phase 2, %	Phase 3, %	Phase 4, %	k_2, mEq/min	k_3, mEq/min	k_4, mEq/min
20 min	7.8	15.4	69.6	7.2	9.13×10^{-2}	14.7×10^{-2}	9.2×10^{-4}
5 days	4.5	11.5	55.9	28.1	2.50×10^{-2}	4.98×10^{-2}	8.8×10^{-4}
12 days	3.0	9.2	41.3	46.5	1.48×10^{-2}	3.38×10^{-2}	10.0×10^{-4}
21 days	2.0	2.9	34.3	60.8	1.00×10^{-2}	1.63×10^{-2}	12.0×10^{-4}
45 days	1.5	0	27.5	71.0	0	0.55×10^{-2}	8.6×10^{-4}
80 days	0	0	7.0	93.0	0	0.43×10^{-2}	10.1×10^{-4}

for phase B decreased with age while k_C remained constant during aging, although the slow zero-order reaction accounted for an increasingly larger portion of the gel.

Based on the changes in the pH-stat titrigram during aging, it was hypothesized that the gel, when initially precipitated, was composed of hydroxyaluminum polymers (11, 12). Free hydroxyls on the surface of the polymers are readily accessible, react immediately with acid, and are seen in the titrigram as phase A. Small polymer units represent phase B and react relatively rapidly with acid. Larger polymers, which form an ordered structure, are responsible for the slow neutralization rate seen in phase C. During aging, the small polymers coalesce to form more highly ordered structures and the surface hydroxyls are incorporated into the gel structure as the polymer grows. This model is consistent with the behavior of the gel studied because phase C increased during aging while phases A and B decreased. After 24 hr of aging, the gel appeared to consist of a small number of accessible hydroxyls and an ordered hydroxyaluminum polymer which reacts with acid at a very slow rate. Thus, the pH-stat titrigram provides information useful in structural studies of aluminum hydroxide gel.

The gel precipitated at pH 9.2 contained 0.067 mole of chloride/mole of aluminum. This low level of chloride had little effect on the stability of the gel or on the neutralization reaction.

Little information concerning further changes in the gel structure is available after 6.5 hr of aging by use of the pH-stat titration. Edge hydroxyls in aluminum hydroxide are quickly replaced by fluoride, and structural hydroxyls are also replaced but at a slow rate (13). The exchange of fluoride for hydroxyl causes a pH increase, which can be monitored by pH-stat titration at pH 6.5.

Figure 3 shows the pH-stat titrigrams of the chloride-containing gel precipitated at a final pH of 9.2 using 0.5 *N* NaF as the reaction medium. The gel appeared to react in two phases: an immediate reaction that exceeded the capability of the autoburet to add compensating acid (*a*) and a slower zero-order reaction (*b*). The kinetic parameters for this series of titrigrams are given in Table VI. The rate of the slow zero-order reaction did not change as the gel aged, although the proportion of structural hydroxyls increased as the gel aged and the amount of edge hydroxyls decreased. X-ray and IR analyses (14) indicate that bayerite initially forms but that gibbsite is the final crystalline phase.

This behavior, when titrated in the presence of fluoride, agrees with the postulated hydroxyaluminum polymer model. The use of sodium fluoride extends the usefulness of the pH-stat titration in the study of the development of order in aged and nonreactive aluminum hydroxide gel.

The chloride-containing aluminum hydroxide gel precipitated at a final pH of 7.0 contained 0.37 mole of chloride/mole of aluminum and aged at a slower rate than the gel precipitated at pH 9.2. In addition, the pH-stat titrigram appeared to be composed of four phases: 1, an immediately reactive fraction; 2, a zero-order phase; 3, a more rapid zero-order phase; and 4, a terminal, very slow zero-order phase. Figure 4 shows the pH-stat titrigram of a freshly precipitated chloride-containing gel at pH 7.0. The kinetic parameters for the aging of this gel are given in Table VII. During aging, phases 1 and 2 disappeared. After 21 days, phase 2 was no longer present. Phase 1 was not present in the 80-day titrigram. At this point, the gel was almost completely composed of the very slow reacting fraction. X-ray and IR analyses (14) indicate that order is developing in the gel which ultimately produces gibbsite. It is interesting that the rate constant for the final slow zero-order phase did not change as the gel aged and had approximately the same value as the rate constant for the slow, terminal phase of the chloride-containing gel precipitated at pH 9.2 (Table V).

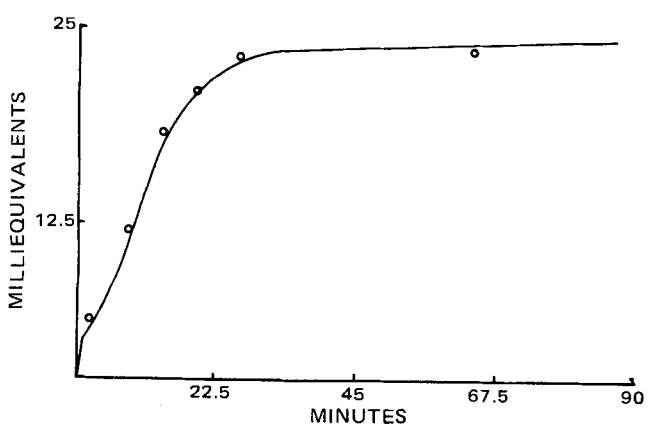

Figure 5—*Appearance of aluminum ions during pH-stat titration of a chloride-containing aluminum hydroxide gel precipitated at pH 7.0. Key: —, H^+ consumed; and O, Al^{3+} released.*

The difference in the aging rate of the chloride-containing gels is believed to be due to the stabilizing effect of chloride ions in inhibiting the development of order. The pH 9.2 gel contained 0.067 mole of chloride/mole of aluminum while the pH 7.0 gel contained 0.37 mole of chloride/mole of aluminum. The initial three phases of the pH-stat titrigram of the pH 7.0 gel are similar to the carbonate-containing gel, except the chloride-containing gel at pH 7.0 appears to contain some highly ordered material (phase 4) not seen in the carbonate-containing gel. Thus, the gel that contained a significant amount of chloride reacted more rapidly and did not lose reactivity as rapidly as the pH 9.2 gel. However, the chloride ion was not as effective as the carbonate ion in stabilizing the gel and facilitating the neutralization reaction.

Adsorption of Acid by Chloride-Containing Gels—The appearance of the aluminum ion in solution during the neutralization of a freshly precipitated pH 7.0 chloride-containing aluminum hydroxide gel was determined. Figure 5 shows the experimentally determined milliequivalents of the aluminum ion produced during neutralization. The solid line is the pH-stat titration curve expressed as milliequivalents of acid added. The mean OH^-/Al^{3+} ratio for six samples analyzed throughout neutralization was 2.63 ± 0.19. This result compares favorably with the previously reported OH^-/Al^{3+} ratio for the gel of 2.55 (11). This behavior suggests that chemical reaction totally accounts for acid neutralization by the slowly reactive aluminum hydroxide gels. If physical adsorption of acid were an important neutralization mechanism, then acid neutralization without a concomitant generation of the aluminum ion would be expected. As shown in Fig. 5, the physical adsorption of acid is insignificant when compared to the amount neutralized following chemical reaction.

REFERENCES

(1) "The United States Pharmacopeia," 19th rev., Mack Publishing Co., Easton, Pa., 1975, p. 21.

(2) J. M. Holbert, N. Noble, and I. W. Grote, *J. Am. Pharm. Assoc., Sci. Ed.*, **37**, 292 (1948).

(3) N. E. Rossett and J. Rice, *Gastroenterology*, **26**, 490 (1954).

(4) M. Brody and W. H. Bachrach, *Am. J. Dig. Dis.*, **4**, 435 (1959).

(5) W. H. Steinberg, W. H. Hastings, H. H. Pick, and J. S. Lazar, *J. Pharm. Sci.*, **54**, 625 (1965).

(6) J. S. Fordtran, S. G. Morawski, and C. T. Richardson, *N. Engl. J. Med.*, **288**, 923 (1973).

(7) *Federal Register*, **39** (108) (June 4, 1974), 19875.

(8) S. L. Hem, E. J. Russo, S. M. Bahal, and R. S. Levi, *J. Pharm. Sci.*, **59**, 317 (1970).

(9) I. M. Kolthoff, E. B. Sandell, E. J. Meehan, and S. Bruckenstein, "Quantitative Analysis," 4th ed., Macmillan, London, England, 1969, p. 799.

(10) C. E. Hicks, "Fundamental Concepts in the Design of Experiments," 2nd ed., Holt, Rinehart, and Winston, New York, N.Y., 1973, p. 163.

(11) S. L. Nail, J. L. White, and S. L. Hem, *J. Pharm. Sci.*, **65**, 1188 (1976).

(12) *Ibid.*, **65**, 1192 (1976).

(13) J. D. Hem and C. E. Roberson, "Form and Stability of Aluminum Hydroxide Complexes in Dilute Solution," Geological Survey Water-Supply Paper 1827-A, U.S. Government Printing Office, Washington, D.C., 1967, p. A45.

(14) S. L. Nail, J. L. White, and S. L. Hem, *J. Pharm. Sci.*, **64**, 1166 (1975).

ACKNOWLEDGMENTS AND ADDRESSES

Received September 15, 1976, from the **Industrial and Physical Pharmacy Department and the ‡Department of Agronomy, Purdue University, West Lafayette, IN 47907.*

Accepted for publication January 17, 1977.

Supported in part by a David Ross Fellowship (to N. J. Kerkhof) and an American Foundation for Pharmaceutical Education Fellowship (to R. K. Vanderlaan).

This report is Journal Paper 6431, Purdue University Agricultural Experiment Station, West Lafayette, IN 47907.

ˣ To whom inquiries should be directed.

Role of Carbonate in Acid Neutralization of Aluminum Hydroxide Gel

NICHOLAS J. KERKHOF *, JOE L. WHITE ‡, and STANLEY L. HEM *ˣ

Abstract □ The role of carbonate in the acid neutralization of a carbonate-containing aluminum hydroxide gel was studied. The pH-stat neutralization reaction was comprised of three phases: an initial, immediately reacting phase; a slow, zero-order phase; and a terminal, fast zero-order phase. The evolution of carbon dioxide and the appearance of aluminum ions were monitored during neutralization. Acid neutralization is believed to occur predominantly at the aluminum–carbonate bond during the slow phase of neutralization. The reaction of structural carbonate disrupts the gel structure and increases the porosity and surface area of the gel. The diffusion of acid into the gel structure is facilitated and accelerates the neutralization rate, as seen in the final phase of the pH-stat titrigrams. This behavior of carbonate is probably responsible for the rapid and complete neutralization of acid generally observed with carbonate-containing aluminum hydroxide gel.

Keyphrases □ Aluminum hydroxide gel—acid neutralization, pH-stat titration, role of carbonate □ Gels—aluminum hydroxide, acid neutralization, pH-stat titration, role of carbonate □ Acid neutralization—aluminum hydroxide gel, pH-stat titration, role of carbonate □ pH-stat titration—aluminum hydroxide gel, acid neutralization, role of carbonate □ Carbonate—role in acid neutralization of aluminum hydroxide gel, pH-stat titration □ Antacids—aluminum hydroxide gel, acid neutralization, pH-stat titration, role of carbonate

Carbonate is an integral part of the aluminum hydroxide gel structure (1). The presence of carbonate in the gel structure contributes to gel stability (2), probably by inhibiting polymerization of the hydroxyaluminum particles and retarding the development of a highly ordered structure. In addition to enhanced stability, carbonate-containing aluminum hydroxide gels usually exhibit a faster acid neutralization rate than is observed in gels stabilized by other anions such as chloride or sulfate (2). The objective of this investigation was to determine the mechanism of acid neutralization in carbonate-containing aluminum hydroxide gels.

EXPERIMENTAL

Materials—All chemicals used were either official or reagent grade.

Aluminum Hydroxide Gel Preparation—Carbonate-containing aluminum hydroxide gel was prepared by the reaction of aluminum chloride, sodium bicarbonate, and sodium carbonate to a final pH of 6.5 (2).

Analytical Procedures—The equivalent aluminum oxide content was determined by the ethylenediaminetetraacetic acid titration (3). The acid reactivity was measured using an automated pH-stat method (4).

The carbonate content of the gels was analyzed by a gasometric displacement technique (5) using a Chittick apparatus[1]. The results are expressed as the ratio of millimoles of carbon dioxide evolved to millimoles of aluminum in the gel.

A specially designed glass reaction vessel, with a polytef head and methyl methacrylate top, was fabricated to study the evolution rate of carbon dioxide from the carbonate-containing aluminum hydroxide gels during neutralization with 1.0 *N* HCl. The reaction assembly consisted of a glass reaction vessel and an airtight head and top, which sealed the system and served as a holder for the electrodes, the titrant delivery tube, and the gas outlet tube connected to the Chittick apparatus.

The glass reaction flask was made of 45-mm o.d. × 100-mm Pyrex glass tubing. The wall thickness was 1.92 mm. The reaction vessel was fabricated with a flat bottom to facilitate the use of a standard 2.54-cm polytef-coated magnetic stirring bar.

The reaction head was fabricated from a 5.08-cm polytef rod (Fig. 1). The bottom side was machined to 41-mm diameter to fit inside the reaction vessel. A groove for a 3.175 × 41.275-mm o.d. O-ring was machined in the circumference of the bottom lip so that a tight press fit was obtained when the reaction vessel was forced over the O-ring.

Appropriately sized holes were drilled through the head to allow the insertion of the electrodes, the titrant delivery tube, and the gas outlet tube. A clear methyl methacrylate top was machined to the same pattern as the head. Eight holes were drilled in the top and threaded in the head to accept binding-head machine screws. The O-rings were fitted over the electrodes, the titrant delivery tube, and the gas outlet and were placed between the top and the head. The openings in the top and head were beveled to compress the O-rings and to seal the head when the machine screws were tightened.

An injection port was included in the reaction head. An appropriately sized hole was machined in the head to accept a high-pressure liquid chromatographic septum.

The reaction vessel, head, and top were combined with the pH-stat titrator and the Chittick apparatus. The sealed reaction vessel replaced the decomposition flask of the Chittick apparatus, and the 25-ml pH-stat autoburet replaced the glass buret.

The following procedure is used to monitor the evolution of carbon dioxide during the neutralization of a sample containing 380 mg equivalent Al_2O_3 by 1.0 *N* HCl at pH 3.0. Transfer an appropriate volume of liquid gel, accurately weighed, into the decomposition reaction vessel. Secure the reaction vessel to the reaction head assembly. With the stopcock open to the atmosphere, adjust the leveling bulb to bring the displacement solution to 20.0 ml above the zero mark. Let the system stand 1–2 min to allow the temperature and pressure within the apparatus to equilibrate to room conditions. Then close the stopcock to the atmosphere. Lower the leveling bulb until the level reads zero on the measuring buret.

Using a glass syringe fitted with a 7.62-cm, 22-gauge needle, insert the needle through the injection port septum and slowly add 20.0 ml of

[1] Sargent-Welch Scientific Co., Skokie, Ill.

(13) J. D. Hem and C. E. Roberson, "Form and Stability of Aluminum Hydroxide Complexes in Dilute Solution," Geological Survey Water-Supply Paper 1827-A, U.S. Government Printing Office, Washington, D.C., 1967, p. A45.

(14) S. L. Nail, J. L. White, and S. L. Hem, *J. Pharm. Sci.*, **64**, 1166 (1975).

ACKNOWLEDGMENTS AND ADDRESSES

Received September 15, 1976, from the **Industrial and Physical Pharmacy Department and the ‡Department of Agronomy, Purdue University, West Lafayette, IN 47907.*

Accepted for publication January 17, 1977.

Supported in part by a David Ross Fellowship (to N. J. Kerkhof) and an American Foundation for Pharmaceutical Education Fellowship (to R. K. Vanderlaan).

This report is Journal Paper 6431, Purdue University Agricultural Experiment Station, West Lafayette, IN 47907.

ˣ To whom inquiries should be directed.

Role of Carbonate in Acid Neutralization of Aluminum Hydroxide Gel

NICHOLAS J. KERKHOF *, JOE L. WHITE ‡, and STANLEY L. HEM *ˣ

Abstract □ The role of carbonate in the acid neutralization of a carbonate-containing aluminum hydroxide gel was studied. The pH-stat neutralization reaction was comprised of three phases: an initial, immediately reacting phase; a slow, zero-order phase; and a terminal, fast zero-order phase. The evolution of carbon dioxide and the appearance of aluminum ions were monitored during neutralization. Acid neutralization is believed to occur predominantly at the aluminum–carbonate bond during the slow phase of neutralization. The reaction of structural carbonate disrupts the gel structure and increases the porosity and surface area of the gel. The diffusion of acid into the gel structure is facilitated and accelerates the neutralization rate, as seen in the final phase of the pH-stat titrigrams. This behavior of carbonate is probably responsible for the rapid and complete neutralization of acid generally observed with carbonate-containing aluminum hydroxide gel.

Keyphrases □ Aluminum hydroxide gel—acid neutralization, pH-stat titration, role of carbonate □ Gels—aluminum hydroxide, acid neutralization, pH-stat titration, role of carbonate □ Acid neutralization—aluminum hydroxide gel, pH-stat titration, role of carbonate □ pH-stat titration—aluminum hydroxide gel, acid neutralization, role of carbonate □ Carbonate—role in acid neutralization of aluminum hydroxide gel, pH-stat titration □ Antacids—aluminum hydroxide gel, acid neutralization, pH-stat titration, role of carbonate

Carbonate is an integral part of the aluminum hydroxide gel structure (1). The presence of carbonate in the gel structure contributes to gel stability (2), probably by inhibiting polymerization of the hydroxyaluminum particles and retarding the development of a highly ordered structure. In addition to enhanced stability, carbonate-containing aluminum hydroxide gels usually exhibit a faster acid neutralization rate than is observed in gels stabilized by other anions such as chloride or sulfate (2). The objective of this investigation was to determine the mechanism of acid neutralization in carbonate-containing aluminum hydroxide gels.

EXPERIMENTAL

Materials—All chemicals used were either official or reagent grade.

Aluminum Hydroxide Gel Preparation—Carbonate-containing aluminum hydroxide gel was prepared by the reaction of aluminum chloride, sodium bicarbonate, and sodium carbonate to a final pH of 6.5 (2).

Analytical Procedures—The equivalent aluminum oxide content was determined by the ethylenediaminetetraacetic acid titration (3). The acid reactivity was measured using an automated pH-stat method (4).

The carbonate content of the gels was analyzed by a gasometric displacement technique (5) using a Chittick apparatus[1]. The results are expressed as the ratio of millimoles of carbon dioxide evolved to millimoles of aluminum in the gel.

A specially designed glass reaction vessel, with a polytef head and methyl methacrylate top, was fabricated to study the evolution rate of carbon dioxide from the carbonate-containing aluminum hydroxide gels during neutralization with 1.0 *N* HCl. The reaction assembly consisted of a glass reaction vessel and an airtight head and top, which sealed the system and served as a holder for the electrodes, the titrant delivery tube, and the gas outlet tube connected to the Chittick apparatus.

The glass reaction flask was made of 45-mm o.d. × 100-mm Pyrex glass tubing. The wall thickness was 1.92 mm. The reaction vessel was fabricated with a flat bottom to facilitate the use of a standard 2.54-cm polytef-coated magnetic stirring bar.

The reaction head was fabricated from a 5.08-cm polytef rod (Fig. 1). The bottom side was machined to 41-mm diameter to fit inside the reaction vessel. A groove for a 3.175 × 41.275-mm o.d. O-ring was machined in the circumference of the bottom lip so that a tight press fit was obtained when the reaction vessel was forced over the O-ring.

Appropriately sized holes were drilled through the head to allow the insertion of the electrodes, the titrant delivery tube, and the gas outlet tube. A clear methyl methacrylate top was machined to the same pattern as the head. Eight holes were drilled in the top and threaded in the head to accept binding-head machine screws. The O-rings were fitted over the electrodes, the titrant delivery tube, and the gas outlet and were placed between the top and the head. The openings in the top and head were beveled to compress the O-rings and to seal the head when the machine screws were tightened.

An injection port was included in the reaction head. An appropriately sized hole was machined in the head to accept a high-pressure liquid chromatographic septum.

The reaction vessel, head, and top were combined with the pH-stat titrator and the Chittick apparatus. The sealed reaction vessel replaced the decomposition flask of the Chittick apparatus, and the 25-ml pH-stat autoburet replaced the glass buret.

The following procedure is used to monitor the evolution of carbon dioxide during the neutralization of a sample containing 380 mg equivalent Al_2O_3 by 1.0 *N* HCl at pH 3.0. Transfer an appropriate volume of liquid gel, accurately weighed, into the decomposition reaction vessel. Secure the reaction vessel to the reaction head assembly. With the stopcock open to the atmosphere, adjust the leveling bulb to bring the displacement solution to 20.0 ml above the zero mark. Let the system stand 1–2 min to allow the temperature and pressure within the apparatus to equilibrate to room conditions. Then close the stopcock to the atmosphere. Lower the leveling bulb until the level reads zero on the measuring buret.

Using a glass syringe fitted with a 7.62-cm, 22-gauge needle, insert the needle through the injection port septum and slowly add 20.0 ml of

[1] Sargent-Welch Scientific Co., Skokie, Ill.

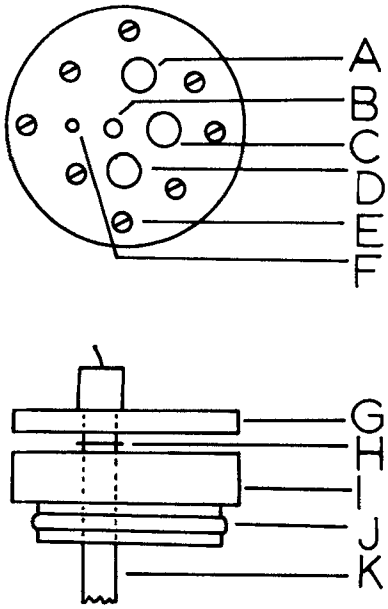

Figure 1—*Top and head for pH-stat carbonate analyzer. Key: A, outlet to Chittick apparatus; B, titrant delivery inlet; C and D, electrode ports; E, machine screw; F, injection port; G, methyl methacrylate top; H, O-ring; I, polytef head; J, O-ring; and K, an electrode.*

double-distilled water maintained at room temperature. Withdraw the needle and check to see that the level of displacement solution in the measuring tube is at the zero mark. Turn on the magnetic stirrer, previously calibrated at 300 rpm, and activate the pH-stat instrument to maintain pH 3.0 by adding 1.0 *N* HCl from the autoburet.

As the reaction proceeds, manually lower the leveling bulb to maintain the level of the measuring buret and leveling bulb at the same level. Record milliliters of carbon dioxide evolved with time from the measuring buret. Note the room temperature and atmospheric pressure and convert the volume displaced to standard conditions.

Anhydrous sodium carbonate, dried at 105° for 4 hr, was used to evaluate the specially designed system to monitor the evolution of carbon dioxide during the pH-stat titration. Weighed samples of sodium carbonate were placed in the reaction vessel and decomposed using 1.0 *N* HCl added by the autoburet. The nine samples analyzed evolved 94.9% of the theoretical amount of carbon dioxide.

The Chittick procedure uses 4 *N* HCl to decompose the sodium carbonate. When 4 *N* HCl was used in the autoburet, five replicate determinations using sodium carbonate evolved 99.8% of the expected amount of carbon dioxide. It was concluded that the use of 1.0 *N* HCl in the pH-stat titration could result in a 5% understatement of the amount of carbon dioxide evolved from the gel. This small error should not interfere with the neutralization study using 1.0 *N* HCl.

The pH-stat apparatus was calibrated with sodium carbonate and 4.0 *N* HCl before and after the experiment. Average values of 99.6 and 99.7% of theory were obtained before and after the experiment, respectively,

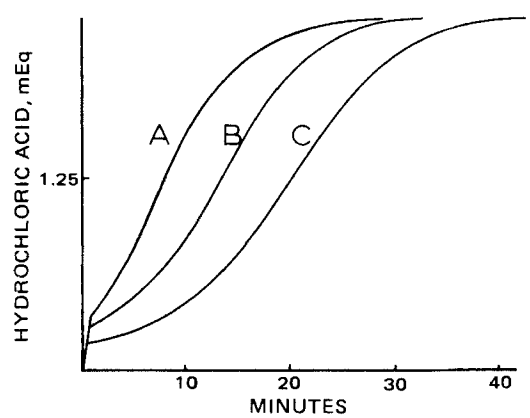

Figure 2—*The pH-stat titrigram of carbonate-containing aluminum hydroxide gels aged at 25°. Key: A, 12 months; B, 19 months; and C, 25 months.*

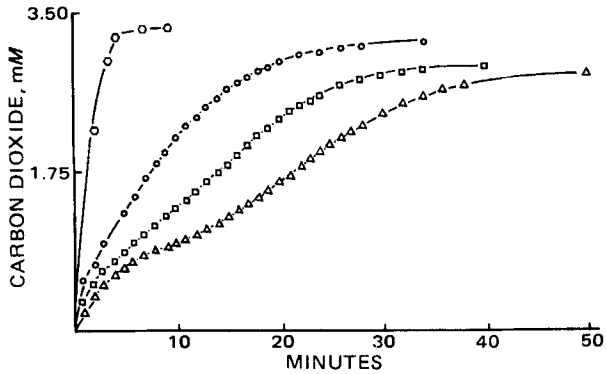

Figure 3—*Evolution of carbon dioxide during pH-stat titration from carbonate-containing aluminum hydroxide gels aged at 25°. Key: ○, sodium carbonate solution; ○, 12 months; □, 19 months; and △, 25 months.*

indicating that the system was functioning properly and had remained sealed during the pH-stat titrations.

IR spectra[2] were obtained by air drying a film of the gel on a zinc sulfide[3] window. The best experimental results were obtained with films containing approximately 0.3 mg of aluminum oxide/cm^2.

IR analysis of partially neutralized aluminum hydroxide gel was obtained by stopping the addition of acid from the autoburet during neutralization. The reacting gel medium was immediately filtered using a 10-ml glass syringe fitted with a filter adapter[4], prefilter, and 0.45-μm-membrane filter. The total elapsed time was 15 sec. An air-dried film of the collected solids on a zinc sulfide window was prepared as previously described.

Atomic absorption spectrophotometry was used to monitor the appearance of aluminum ions in the reaction medium as the aluminum hydroxide gel was neutralized by 1.0 *N* HCl at pH 3.0. The addition of acid from the autoburet was stopped at various points during neutralization. The reaction medium was immediately filtered using the previously described filtration assembly. The filtered medium was appropriately diluted with distilled water, and the aluminum content was determined by atomic absorption analysis. An atomic absorption spectrophotometer[5] equipped with a hollow cathode aluminum lamp[6] was used. The aluminum-ion concentration in the reaction medium was calculated by taking the total reaction volume at the time the reaction was stopped as the sum of the volume of distilled water, the volume of gel, and the volume of 1.0 *N* HCl added to that time as determined from the titrigram.

RESULTS AND DISCUSSION

The aluminum hydroxide gels studied contained carbonate as an integral part of the gel structure, as demonstrated by IR analysis of the gel. The carbonate band that occurs at 1450 cm^{-1} in sodium carbonate split and appeared as two bands at 1525 and 1415 cm^{-1}. This splitting of the carbonate band was due to the coordination of carbonate with aluminum in the gel structure (1).

The acid neutralization of carbonate-containing aluminum hydroxide gel appears to consist of three phases when studied using the pH-stat technique (4): an initial, immediately reacting phase; a slow zero-order phase; and a terminal, fast zero-order phase. This reactivity pattern was somewhat unexpected because, for example, the dissolution rate of a suspension generally decreases as dissolution occurs due to the higher solubility and more rapid dissolution rate of the small particles in the suspension.

To understand the reaction mechanism responsible for the unexpected reactivity pattern, the rates of acid neutralization and carbon dioxide evolution were determined for three carbonate-containing aluminum hydroxide gels aged for 12, 19, and 25 months at 25°. As seen in Fig. 2, the gels all exhibited the same reactivity pattern. As previously reported (4), the effect of aging was to decrease the amount of immediately reacting material and to reduce k_{II} and k_{III}, the zero-order rate constants for the slow phase and the final fast phase, respectively.

[2] Model 421, Perkin-Elmer Corp., Norwalk, Conn.
[3] Irtran 2, Eastman Kodak Co., Rochester, N.Y.
[4] Micro-Syringe holder, Millipore Corp., Bedford, Mass.
[5] Model 290B, Perkin-Elmer Corp., Norwalk, Conn.
[6] Perkin-Elmer Corp., Norwalk, Conn.

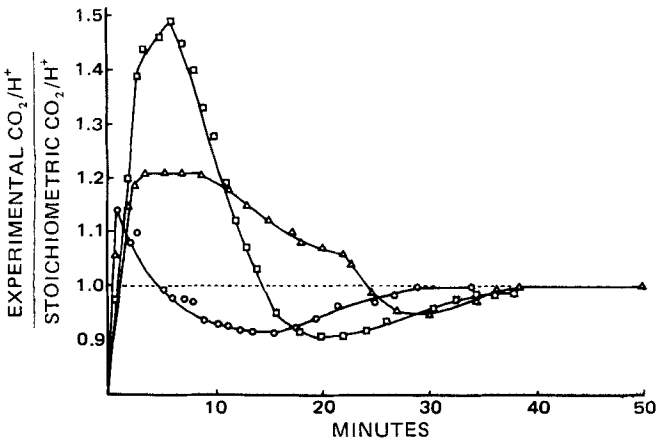

Figure 4—*Experimental ratio of evolved carbon dioxide to acid neutralized compared to the stoichiometric ratio of total carbonate in the gel to total acid neutralized during pH-stat titration of carbonate-containing aluminum hydroxide gels aged at 25°. Key: O, 12 months; □, 19 months; Δ, 25 months; and - - -, expected behavior.*

Carbon dioxide evolution from these gels followed a somewhat different pattern (Fig. 3). The carbon dioxide evolution rate was greatest during the first 10 min, which corresponds to the slow phase of the acid neutralization curve.

Carbon dioxide evolution from a solution of sodium carbonate is shown in Fig. 3. A comparison of the evolution of carbon dioxide from a sodium carbonate solution and from the aluminum hydroxide gels supports the hypothesis that carbonate is part of the gel structure. Carbon dioxide was evolved at a constant, rapid rate from the sodium carbonate solution. Carbonate was released much more slowly from aluminum hydroxide gel and at a rate that varied during neutralization.

The relationship between carbon dioxide evolution and acid neutralization is seen more clearly if the experimental ratio of evolved carbon dioxide to acid neutralized (CO_2/H^+) is compared to the stoichiometric ratio of total carbonate in the gel to the total acid neutralized. The stoichiometric ratio of total carbonate in the gel determined by the Chittick procedure to the total acid neutralized was 0.135 in the 12-month gel, 0.120 in the 19-month gel, and 0.115 in the 25-month gel. The experimental ratio of evolved carbon dioxide to acid neutralized differed from the stoichiometric ratio (Fig. 4). During the first two phases of the neutralization reaction, more carbon dioxide than expected was liberated. Less carbon dioxide was evolved than predicted during the final phase of neutralization.

The role of carbonate in neutralization was further studied by comparing the IR spectra of the gel before neutralization and after partial neutralization. Figure 5 shows that the gel aged 12 months had a split carbonate band, indicating that carbonate was coordinated with aluminum. After the gel was 15% neutralized, the split band was less pronounced. At 50% neutralization, the carbonate band appeared as a single band at 1470 cm^{-1}. A small degree of interaction still existed between carbonate and aluminum at this point since the band was shifted from

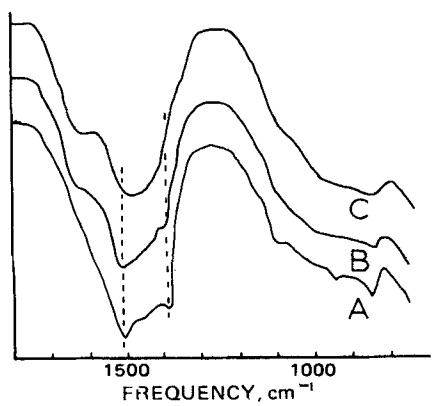

Figure 5—*IR spectrum of a carbonate-containing aluminum hydroxide gel aged 12 months at 25°. Key: A, unreacted, B; after 15% neutralization; and C, after 50% neutralization.*

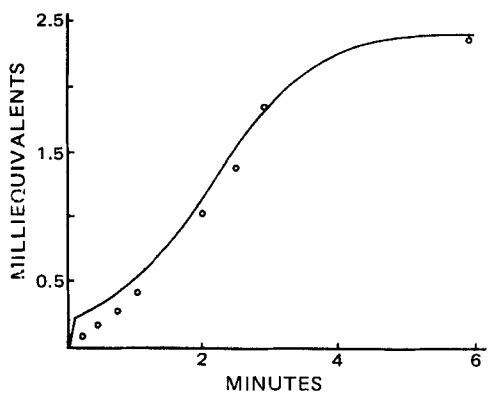

Figure 6—*Appearance of aluminum ion during pH-stat titration of carbonate-containing aluminum hydroxide gel aged 1 day at 25°. Key: —, H^+ consumed; and O, Al^{3+} in solution.*

the normal position at 1445 cm^{-1}. These changes in the IR spectrum during neutralization indicate that the association between carbonate and aluminum is destroyed during the early phases of neutralization. Evidence of coordination with aluminum was virtually gone by the time the gel was 50% neutralized.

The milliequivalents of aluminum ion appearing in solution was less than the milliequivalents of acid neutralized during the first two phases of the pH-stat titration. The result is seen in Fig. 6 for a carbonate-containing aluminum hydroxide gel aged 1 day. Similar behavior was observed after the gel was aged for 40 and 193 days at 25°.

The slow appearance of aluminum ion is consistent with the high ratio of evolved CO_2/H^+ during the early phases of the neutralization reaction. The early acid attack appeared to occur predominantly at the aluminum–carbonate bonds. The appearance of aluminum ions, which were only generated by the complete neutralization of the aluminum hydroxide gel, was delayed. The milliequivalents of aluminum ion in solution was equal to the milliequivalents of acid neutralized during the third phase of the neutralization reaction where the predominant reaction was the attack of aluminum–hydroxyl bonds by protons.

Aluminum hydroxide gel may be considered to have a polymeric structure consisting of aluminum atoms joined by double hydroxide bridges, which may ultimately form a large, ordered structure. Carbonate appears to replace a hydroxyl in the double hydroxide bridges. The carbonate in the gel structure readily reacts with acid during neutralization. The initial acid reaction with carbonate disrupts the gel structure and causes an increased porosity and surface area. This facilitates the diffusion of acid into the gel and causes an accelerated neutralization rate, as seen in the third phase of the pH-stat titrigrams of aluminum hydroxide gel. This unique role of carbonate is probably responsible for the rapid and complete neutralization of acid generally observed with carbonate-containing aluminum hydroxide gel.

REFERENCES

(1) J. L. White and S. L. Hem, *J. Pharm. Sci.*, **64**, 468 (1975).

(2) S. L. Hem, E. J. Russo, S. M. Bahal, and R. S. Levi, *ibid.*, **59**, 317 (1970).

(3) "The United States Pharmacopeia," 19th rev., Mack Publishing Co., Easton, Pa., 1975, p. 21.

(4) N. J. Kerkhof, R. K. Vanderlaan, J. L. White, and S. L. Hem, *J. Pharm. Sci.*, **66**, 1528 (1977).

(5) "Official Methods of Analysis of the Association of Official Analytical Chemists," 11th ed., W. Horwitz, Ed., Association of Official Analytical Chemists, Washington, D.C., 1970, p. 139.

ACKNOWLEDGMENTS AND ADDRESSES

Received September 15, 1976, from the *Industrial and Physical Pharmacy Department and the ‡Department of Agronomy, Purdue University, West Lafayette, IN 47907.

Accepted for publication January 17, 1977.

Supported in part by a David Ross Fellowship (to N. J. Kerkhof).

This report is Journal Paper 6430, Purdue University Agricultural Experiment Station, West Lafayette, IN 47907.

ˣ To whom inquiries should be directed.

Surface Tension Lowering and Dissolution Rate of Hydrocortisone from Solid Solutions of Selected *n*-Acyl Esters of Cholesterol

KWON HO KIM and CHARLES I. JAROWSKI ˣ

Abstract □ The dissolution of hydrocortisone into simulated intestinal fluid from lipid delivery systems followed second-order kinetics. As the ratio of hydrocortisone to lipid was increased from 1:1 to 1:6, the dissolution rate decreased. Solvent deposition of solid solutions of hydrocortisone and lipid on lactose resulted in the enhancement of the dissolution rate. For the 1:1 hydrocortisone–lipid solid solutions, the rank order of the dissolution rate was hydrocortisone–cholesteryl stearate, hydrocortisone, hydrocortisone–cholesterol, hydrocortisone–cholesteryl acetate, hydrocortisone–cholesteryl palmitate, hydrocortisone–cholesteryl *n*-butyrate, hydrocortisone–cholesteryl laurate, and hydrocortisone–cholesteryl *n*-decylate. A direct correlation was found between the dissolution rate of hydrocortisone and the surface tension lowering of simulated intestinal fluid by the corticoid and various lipids.

Keyphrases □ Hydrocortisone—dissolution into simulated intestinal fluid from solid solutions with cholesterol or various esters, effect on surface tension □ Cholesterol and various esters—solid solutions with hydrocortisone, dissolution into simulated intestinal fluid, effect on surface tension □ Dissolution—hydrocortisone into simulated intestinal fluid from solid solutions with cholesterol or various esters □ Surface tension—simulated intestinal fluid, effect of solid solutions of hydrocortisone and cholesterol or various esters □ Solid solutions—hydrocortisone and cholesterol or various esters, dissolution into simulated intestinal fluid, effect on surface tension □ Glucocorticoids—hydrocortisone, dissolution into simulated intestinal fluid from solid solutions of cholesterol or various esters, effect on surface tension □ Lipids—cholesterol and various esters, solid solutions with hydrocortisone, dissolution into simulated intestinal fluid, effect on surface tension

The utility of lipid drug delivery systems has been amply demonstrated. Griseofulvin bioavailability was improved when micronized particles were administered in a corn oil-in-water emulsion (1). Oral progesterone administration gave higher blood levels when the hormone was solvent deposited on lactose as a solid solution with cholesterol or its acetate ester (2). Significant improvement in the *in vitro* stability of the potassium salts of penicillins G and V was achieved when they were coated with cholesterol, its acetate ester, or β-sitosterol (3). The oral administration of such coated penicillins, as well as erythromycin lactobionate, resulted in an increase in the urinary recovery of antibiotic activity (3). The urinary excretion of unchanged salicylate was increased when salicylic acid was given as a solid solution in cholesteryl *n*-decylate (4).

The purpose of this investigation was to study the *in vitro* dissolution rate of hydrocortisone (I) from solid solutions containing cholesterol (II) or one of the following cholesteryl esters: acetate (III), *n*-butyrate (IV), *n*-decylate (V), laurate (VI), palmitate (VII), and stearate (VIII). In addition, the hydrocortisone dissolution rate was determined after solvent deposition of such solid solutions on powdered lactose (IX). The surface tension-lowering effect of selected candidates was measured to ascertain if a direct correlation with the dissolution rate could be made. An additional objective was to treat the accumulated data mathematically to determine the kinetic order followed by hydrocortisone dissolution from such solid solutions.

EXPERIMENTAL

Materials—The following were obtained from commercial sources: hydrocortisone[1], cholesterol[2], cholesteryl acetate[2], cholesteryl butyrate[2], cholesteryl *n*-decylate[2], cholesteryl laurate[2], cholesteryl palmitate[2], cholesteryl stearate[2], lactose powder USP[3], methanol[4], absolute chloroform NF[3], sodium hydroxide[4] (ACS), and monobasic sodium phosphate[5] (laboratory grade).

Equipment—The following equipment was used: a capillary melting-point apparatus[6], a constant-temperature shaker bath[7], a tensiometer[8], a pH meter[9], a dissolution basket stirrer[10], and a spectrophotometer[11].

Hydrocortisone–Lipid Solutions with and without Lactose—Powdered hydrocortisone and the various lipids were weighed in ratios of 1:1, 1:3, and 1:6. The mixture of hydrocortisone and lipid was dissolved in a minimal quantity of 50% (v/v) chloroform in methanol. The solutions were stirred with a magnetic stirrer, and the solvent was evaporated in a stream of air. The residues were completely dried in an oven set at 40° and then ground in a mortar and passed through an 80-mesh screen. After blending to ensure homogeneity, duplicate aliquots were assayed. Only samples containing 100 ± 5% of the theoretical quantity of hydrocortisone were used in the dissolution studies. Assays outside the 5% limits were rare.

Solvent deposition of the various hydrocortisone–lipid combinations on lactose was conducted similarly. Weight ratios of hydrocortisone–lipid–lactose of 1:1:6, 1:3:6, and 1:6:6 were prepared. Again, assays outside the 5% limits were rare.

Dissolution Studies—The hydrocortisone dissolution rate in simulated intestinal fluid USP, without pancreatin, was determined by the Short *et al.* (5) beaker method. Simulated intestinal fluid, 200 ml, was placed in a 300-ml beaker and maintained at 37 ± 0.5° in a constant-temperature water bath. The dissolution medium was stirred with the basket recommended for the USP dissolution test. The stirrer was vertically centered and lowered to a depth of 1 cm above the bottom of the beaker. The stirrer was attached to a synchronous motor set to rotate at 150 rpm.

Accurately weighed samples, equivalent to 60 mg of pure drug, were spread over the surface of the dissolution medium. Any aggregates that formed at this stage were lightly broken up with a microspatula within 10 sec after sample addition. Subsequently, the surface was not disturbed except when 10-ml aliquots were withdrawn at 15, 30, 45, 60, 90, 120, and 150 min. The samples were withdrawn through a sintered-glass filter of medium porosity and filtered again through a membrane filter[12] (0.45 μm). Dissolution medium, 10 ml, was replaced immediately after removal of the aliquot.

The filtrate was diluted to an appropriate concentration in a volumetric flask, and the absorbance was measured at 250 nm. A cumulative correction was made for the previously removed samples in determining the total quantity of hydrocortisone dissolved (6). The data are summarized in Table I, and selected combinations are shown in Fig. 1. Each data point represents the average of at least two determinations. There was no interference from the various lipids or lactose on the hydrocortisone assay by the spectrophotometric procedure.

[1] Pfizer & Co., New York, N.Y.
[2] K and K Laboratories, Plainview, N.Y.
[3] Matheson, Coleman and Bell, Norwood, Ohio.
[4] J.T. Baker Chemical Co., Phillipsburg, N.J.
[5] Fisher Scientific Co., Fair Lawn, N.J.
[6] Thomas–Hoover, Arthur H. Thomas Co., Chicago, Ill.
[7] Model WBR, New Brunswick Scientific Co., New Brunswick, N.J.
[8] Du Nouy, Central Scientific Co., Chicago, Ill.
[9] Zeromatic, Beckman Instruments Co., Fullerton, Calif.
[10] Model 53, Hanson Research Corp., Northridge, Calif.
[11] Coleman Hitachi-124 double-beam model, Coleman Instruments Co., Maywood, Ill.
[12] Millipore Corp., Bedford, Mass.

Table I—Dissolution Rate of Hydrocortisone in Simulated Intestinal Fluid from Hydrocortisone–Lipid and Hydrocortisone–Lipid–Lactose Combinations

Sample	Ratio	Hydrocortisone Dissolved, %						
		15 min	30 min	45 min	60 min	90 min	120 min	150 min
I	—	35.0	51.8	65.1	73.1	78.3	82.6	86.1
I–II	1:1	20.8	35.2	48.1	58.3	66.5	73.1	80.0
	1:3	10.2	16.6	22.7	31.6	40.8	51.6	63.0
	1:6	9.3	14.9	20.2	25.9	34.1	41.0	48.0
I–III	1:1	15.1	22.0	26.4	28.6	29.8	30.9	31.5
	1:3	8.2	12.9	15.7	19.9	22.7	25.8	28.0
	1:6	3.2	3.6	4.0	4.4	5.6	6.2	6.8
I–IV	1:1	11.8	15.6	18.5	20.6	22.3	23.8	25.5
	1:3	4.2	5.4	5.8	6.2	6.8	7.8	8.2
	1:6	0.8	1.0	1.1	1.3	1.5	1.7	1.9
I–V	1:1	5.8	8.7	10.9	12.1	13.0	13.8	14.6
	1:3	2.4	3.6	3.8	4.2	4.5	4.8	5.1
	1:6	0.6	0.8	0.8	0.9	1.0	1.2	1.4
I–VI	1:1	6.0	9.5	12.6	14.5	16.6	17.8	19.4
	1:3	3.0	4.2	5.0	5.8	6.9	7.7	8.3
	1:6	2.0	2.3	2.4	2.6	3.2	3.7	4.3
I–VII	1:1	12.1	15.9	18.8	20.9	22.5	24.6	26.8
	1:3	4.8	7.7	9.1	10.0	11.7	13.1	14.3
	1:6	2.0	2.3	2.5	2.6	3.2	3.7	4.3
I–VIII	1:1	78.3	88.8	90.8	92.3	93.3	93.6	93.8
	1:3	49.7	55.0	62.3	69.8	75.4	82.9	88.2
	1:6	29.2	44.1	50.5	55.1	58.4	61.8	64.1
I–IX	1:6	63.8	79.1	85.6	88.0	92.8	94.0	95.8
I–II–IX	1:1:6	95.5	96.4	97.7	99.0	99.0	99.0	99.0
	1:3:6	72.2	91.7	95.6	97.7	98.3	98.8	99.0
	1:6:6	64.8	81.8	86.0	90.7	92.7	94.1	94.8
I–III–IX	1:1:6	24.8	36.2	44.3	49.8	54.1	60.4	63.9
	1:3:6	16.8	23.2	28.5	32.8	36.5	41.4	45.3
	1:6:6	9.8	11.3	13.8	16.2	19.5	22.9	27.1
I–IV–IX	1:1:6	11.7	16.2	19.0	21.3	23.1	25.1	26.9
	1:3:6	7.0	7.9	8.3	8.7	9.4	9.9	10.3
	1:6:6	3.2	5.4	6.5	7.4	8.9	9.9	10.1
I–V–IX	1:1:6	9.1	12.9	14.0	16.4	17.1	17.8	18.5
	1:3:6	4.7	6.3	7.2	8.1	9.0	9.8	10.6
	1:6:6	3.1	4.0	4.5	5.2	6.2	7.1	7.7
I–VI–IX	1:1:6	14.6	19.8	22.3	24.6	26.1	27.1	28.2
	1:3:6	19.0	22.5	23.2	24.5	25.9	26.9	28.3
	1:6:6	3.2	5.2	6.0	6.2	7.6	9.1	9.3
I–VII–IX	1:1:6	16.1	21.1	25.2	28.4	30.2	31.8	33.7
	1:3:6	19.0	21.6	22.7	23.3	25.9	28.2	30.9
	1:6:6	5.0	8.3	9.1	9.9	11.9	13.5	14.7
I–VIII–IX	1:1:6	85.2	94.9	97.5	99.0	99.0	99.0	99.0
	1:3:6	79.5	89.9	92.3	93.5	94.6	95.5	96.3
	1:6:6	57.0	63.3	66.2	68.9	71.1	73.2	74.5

The addition of the equivalent of 60 mg of hydrocortisone to 200 ml of simulated intestinal fluid ensured that the dissolution test was being conducted under sink conditions. Hydrocortisone solubility in simulated intestinal fluid at 37° was 861 μg/ml. Consequently, approximately 172 mg of hydrocortisone would be required to saturate 200 ml of this medium. Furthermore, saturated solutions of the various lipids in simulated intestinal fluid exerted an insignificant effect on hydrocortisone solubility.

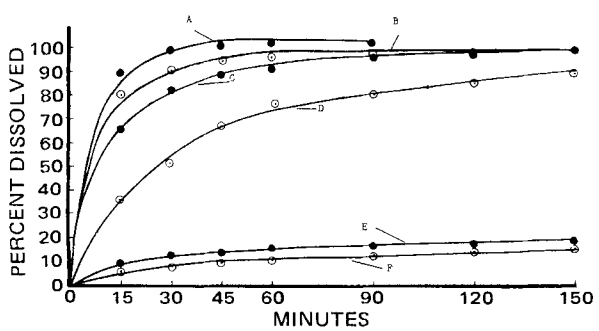

Figure 1—*Dissolution rate of hydrocortisone from selected lipid combinations, with and without lactose, in simulated intestinal fluid at 37°. Key: A, hydrocortisone–cholesteryl stearate–lactose (1:1:6); B, hydrocortisone–cholesteryl stearate (1:1); C, hydrocortisone–lactose (1:6); D, hydrocortisone; E, hydrocortisone–cholesteryl* n*-decylate–lactose (1:1:6); and F, hydrocortisone–cholesteryl* n*-decylate (1:1).*

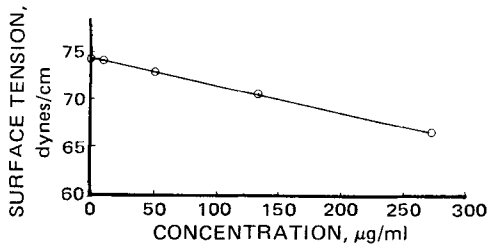

Figure 2—*Surface tension* versus *hydrocortisone concentration in simulated intestinal fluid at 30°. Surface tension = −0.0263C + 73.72.*

Spectrophotometric Absorption, Calibration Curves, and Assay Procedures for Hydrocortisone—A plot of absorbance *versus* wavelength for the hydrocortisone solution in simulated intestinal fluid, without enzymes (20 μg/ml), showed a maximum value at 250 nm. At this wavelength, a linear relationship was found between absorbance and concentration (range of 1–20 μg/ml). A plot of absorbance *versus* wavelength for hydrocortisone in 50% (v/v) chloroform in methanol showed a maximum at 245 nm. At this wavelength, a linear relationship was found between absorbance and concentration (range of 1–20 μg/ml). The slopes for the Beer's plot of the organic and aqueous solutions of hydrocortisone were identical, 4.31×10^{-2} absorbance unit/ml/μg.

Hydrocortisone stability in simulated intestinal fluid at 37° during the 2-hr dissolution study was satisfactory. Even after 48 hr at 37°, only a 0.54% drop in potency occurred. The calibration curve for hydrocortisone in 50% (v/v) chloroform in methanol was of value in the assay of hydrocortisone–lipid and hydrocortisone–lipid–lactose preparations. Thus, an accurately weighed sample was treated with sufficient solvent to dissolve the lipid and the hydrocortisone. Undissolved lactose, in the latter case, was filtered off by passage of the suspension through a 0.45-μm membrane filter. After appropriate dilution with additional solvent, the absorbance of the solution was determined. The pure solvent combination was used as the blank.

Measurement of Surface Tension of Hydrocortisone and Hydrocortisone–Lipid Solutions in Simulated Intestinal Fluid—The surface tension of various concentrations of hydrocortisone in simulated intestinal fluid, without pancreatin, was measured with a tensiometer at 30° using a 4-cm platinum–iridium ring. Correction factors were determined by graphical extrapolation of the values published by Harkins and Jordan (7). The densities of the various solutions were measured with a 10-ml pycnometer. The density values were required in the calculation of the correction factor. The results are summarized in Table II and Fig. 2.

The effect of selected lipids on the surface tension lowering of simulated intestinal fluid was then determined. The powdered hydrocortisone–lipid solid solutions (120 mg) were stirred at 150 rpm in 200 ml of simulated intestinal fluid at 37° for 60 min. The suspensions were filtered through a 0.45-μm filter, and the hydrocortisone concentrations of the filtrates were determined spectrophotometrically. The density of each filtrate was measured for computation of the correction factors (Table III).

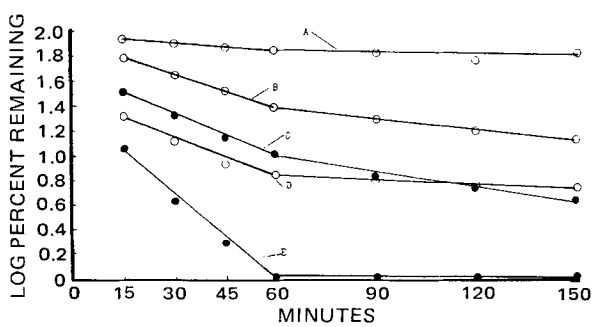

Figure 3—*Dissolution rate of hydrocortisone from selected lipid combinations, with and without lactose, in simulated intestinal fluid at 37° plotted in first-order fashion. Key: A, hydrocortisone–cholesteryl* n*-decylate (1:1); B, hydrocortisone; C, hydrocortisone–lactose (1:6); D, hydrocortisone–cholesteryl stearate (1:1); and E, hydrocortisone–cholesteryl stearate–lactose (1:1:6).*

Table II—Effect of Hydrocortisone Concentration on the Surface Tension of Simulated Intestinal Fluid at 30°

Sample	Hydrocortisone Concentration, μg/ml	Dial Reading[a]	Uncorrected Surface Tension, dynes/cm	Density	R^3/V[b]	Correction Factor	Corrected Surface Tension, dynes/cm
Simulated intestinal fluid	0.0	36.13	75.157	1.0346	0.437	0.981	73.72
Simulated intestinal fluid plus hydrocortisone	13.7	36.07	75.018	1.0346	0.438	0.980	73.50
Simulated intestinal fluid plus hydrocortisone	55.0	35.70	74.258	1.0347	0.442	0.979	72.69
Simulated intestinal fluid plus hydrocortisone	137.0	34.70	72.037	1.0348	0.455	0.976	70.30
Simulated intestinal fluid plus hydrocortisone	275.0	32.90	68.484	1.0349	0.479	0.970	66.42

[a] Average of three readings. Dial scale is 16.64 dynes/dial division. [b] R is the radius of the ring measured from the center of the ring to the center of the wire. The volume of liquid raised above the free surface of the liquid is V.

Table III—Effect of Hydrocortisone plus Lipids on the Surface Tension of Simulated Intestinal Fluid at 30°

Sample[a]	Hydrocortisone Concentration, μg/ml	Percent Dissolved	Dial Reading[b]	Correction Factor	γ_1[c]	γ_2[d]	$\frac{\gamma_2 - \gamma_1}{\gamma_2} \times 100$, %[e]
Hydrocortisone plus cholesterol	208.0	69.3	31.9	0.966	64.15	68.25	6.00
Hydrocortisone plus cholesteryl acetate	80.0	26.6	34.3	0.973	69.41	71.61	3.07
Hydrocortisone plus cholesteryl *n*-decylate	26.0	8.6	34.9	0.976	70.84	73.03	2.99
Hydrocortisone plus cholesteryl stearate	218.0	72.6	31.5	0.965	63.22	67.98	7.00

[a] Hydrocortisone–lipid ratios were 1:1. [b] Average of three readings. [c] Surface tension of the solution containing both hydrocortisone and lipid. [d] Surface tension of the solution containing only hydrocortisone. [e] Percent of surface tension lowering by the lipid.

RESULTS AND DISCUSSION

Several generalizations can be made about the data in Table I. As the ratio of lipid to drug was increased, the hydrocortisone dissolution rate decreased. The only exception to this generalization was hydrocortisone–cholesteryl laurate–lactose in the weight ratio of 1:3:6. Solvent deposition of the hydrocortisone–lipid solid solutions on lactose invariably resulted in more rapid dissolution. This enhancement of the dissolution rate can be attributed to the increased surface attained by such molecular dispersions on lactose.

An unexpected observation was the rapid dissolution of hydrocortisone from hydrocortisone–cholesteryl stearate (1:1). Within 15 min, 78.3% of the hydrocortisone had dissolved, whereas only 35% had dissolved when the pure drug was used. The hydrocortisone dissolution rate from a 1:3 weight ratio of hydrocortisone–cholesteryl stearate was equivalent to that for the pure drug. Unexpectedly, the *n*-decylate ester of cholesterol was the most effective deterrent to the hydrocortisone dissolution.

The rank order in hydrocortisone dissolution was as follows for the 1:1 hydrocortisone–lipid solid solutions: hydrocortisone–cholesteryl stearate, hydrocortisone, hydrocortisone–cholesterol, hydrocortisone–cholesteryl acetate, hydrocortisone–cholesteryl palmitate, hydrocortisone–cholesteryl *n*-butyrate, hydrocortisone–cholesteryl laurate, and, finally, hydrocortisone–cholesteryl *n*-decylate. The solvent deposition of solid solutions on the surface of lactose resulted in improved dissolution rates, whereas increases of 1:3 and 1:6 in drug–lipid ratios resulted in reduced dissolution rates. The superiority of the solid solutions containing the stearate ester of cholesterol was unexpected. It was anticipated that the rapid hydrocortisone release from such solid solutions might be explained by surface tension lowering.

The data in Table II and Fig. 2 show that a linear relationship existed between hydrocortisone concentration in simulated intestinal juice and surface tension lowering. The data in Table III clearly show a direct relationship between the hydrocortisone release rate and surface tension lowering brought about by the lipid. Thus, hydrocortisone–cholesteryl stearate (1:1) released the drug most rapidly. The surface tension of a solution containing both cholesteryl stearate and the corticoid was 7% lower than a solution containing only the corticoid. With hydrocortisone–cholesteryl *n*-decylate (1:1), the surface tension of the aqueous

Table IV—Dissolution Rate Data for Hydrocortisone–Lipid (1:1) and Hydrocortisone–Lipid–Lactose (1:1:6) Expressed as the Parameters of Apparent First-Order Kinetics

Sample	K'[a], $\times 10^{-4}$ min^{-1}	K''[b], $\times 10^{-4}$ min^{-1}	t_{50}[c], min	t_{90}[c], min
I	218.0	73.0	94.9	315.5
I–II	145.7	81.6	84.9	282.0
I–III	38.0	4.6	1506.0	5006.0
I–IV	23.3	7.1	970.0	3225.0
I–V	15.3	3.2	6165.0	7196.0
I–VI	21.0	6.6	1050.0	3489.0
I–VII	23.0	8.6	806.0	2681.0
I–VIII	598.0	24.1	287.5	955.5
I–IX (1:6)	353.0	116.0	59.3	197.3
I–II–IX	884.0	—[d]	7.8	26.0
I–III–IX	89.2	36.2	189.0	629.0
I–IV–IX	23.9	8.2	843.0	2805.0
I–V–IX	16.8	2.8	2440.0	8109.0
I–VI–IX	25.7	5.4	1271.0	4225.0
I–VII–IX	35.7	8.5	817.0	2703.0
I–VIII–IX	767.0	—[d]	9.0	30.0

[a] The apparent first-order rate constant of the first segment of the line (up to 60 min). (See Fig. 3.) [b] The apparent first-order rate constant of the second segment of the line (90–150 min). (See Fig. 3.) [c] Values derived from K''. [d] At the end of 60 min, 99% of the drug had gone into solution.

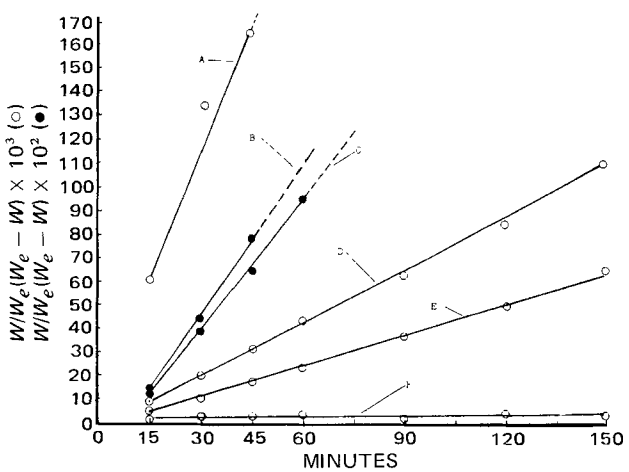

Figure 4—*Dissolution rate of hydrocortisone from selected lipid combinations, with and without lactose, in simulated intestinal fluid at 37° plotted in second-order fashion. Key: A, hydrocortisone–cholesteryl stearate (1:1); B, hydrocortisone–cholesteryl stearate–lactose (1:1:6); C, hydrocortisone–lactose (1:6); D, hydrocortisone; E, hydrocortisone–cholesterol (1:1); and F, hydrocortisone–cholesteryl* n*-decylate (1:1).*

Table V—Dissolution Rate Data for Hydrocortisone–Lipid (1:1) and Hydrocortisone–Lipid–Lactose (1:1:6) Expressed as the Parameters of Apparent Second-Order Kinetics

Sample	K, $\times 10^{-5}$ mg^{-1} min^{-1}	t_{50}, min	t_{90}, min	Initial Dissolution Rate, mg/min
I	68.3	24.3	219.4	2.46
I-II	44.3	37.6	338.0	1.59
I-III	2.9	557.0	5010.0	0.107
I-IV	2.3	705.0	6350.0	0.084
I-V	1.2	1400.0	12600.0	0.042
I-VI	2.0	816.0	7350.0	0.073
I-VII	2.6	645.0	5180.0	0.092
I-VIII	128.6	12.9	117.0	4.63
I-IX (1:6)	250.7	6.6	57.8	9.02
I-II-IX	792.2	2.1	18.9	28.50
I-III-IX	17.1	97.4	877.0	0.61
I-IV-IX	2.6	640.0	5760.0	0.093
I-V-IX	1.3	1300.0	11700.0	0.046
I-VI-IX	2.3	715.0	6430.0	0.083
I-VII-IX	3.5	469.0	4220.0	0.127
I-VIII-IX	1296.9	1.3	11.6	46.40

solution was 2.99% lower than that of an aqueous solution containing only hydrocortisone. Consequently, surface tension lowering is a plausible explanation for the observed rank order in drug dissolution rates for the various drug–lipid combinations.

Apparent First-Order Kinetics—Selected data plotted in first-order fashion are shown in Fig. 3. In Table IV, the hydrocortisone–lipid (1:1) and hydrocortisone–lipid–lactose (1:1:6) preparations are expressed as the parameters of apparent first-order kinetics. The dissolution process followed by these preparations was not simple first order (Fig. 3). From 15 to 60 min, a steeper slope was evident; from 60 to 150 min, the slope changed. Extrapolation of the lines for the bottom three curves to point 2.0 on the ordinate indicates a third slope from 0 to 15 min. Thus, the assumption that the surface area available for dissolution decreases exponentially with time is not true for these drug–lipid delivery systems.

Apparent Second-Order Kinetics—Based on previous studies (8, 9), the *in vitro* dissolution kinetics of the hydrocortisone–lipid and hydrocortisone–lipid–lactose systems could be second order, being functions of the effective surface area and the weight of drug available for dissolution. In Fig. 4, $W/W_e(W_e - W)$ is plotted against time. The parameter W is the weight of drug in solution at time t; W_e is the weight of drug in solution at equilibrium. The slope of each line represents the apparent second-order rate constant, K. The points represent the experimental data, but the lines were drawn from calculated values obtained by regression analysis.

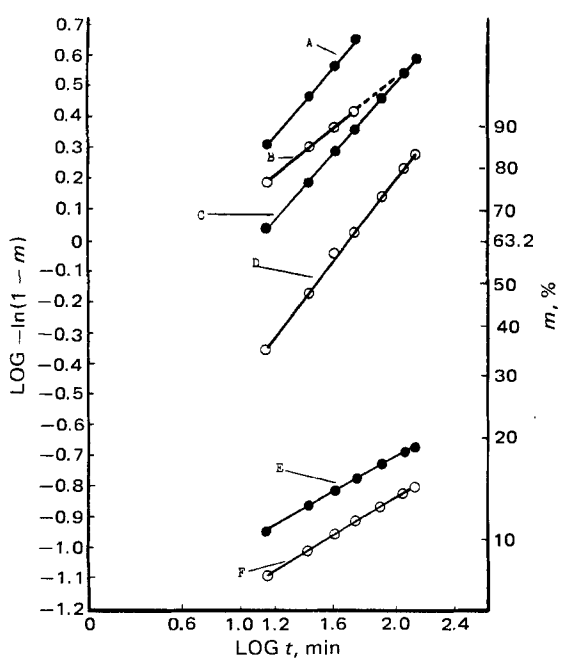

Figure 5—*Dissolution rate of hydrocortisone from selected lipid combinations, with and without lactose, in simulated intestinal fluid at 37° plotted according to the Weibull distribution equation. Key: A, hydrocortisone–cholesteryl stearate–lactose (1:1:6); B, hydrocortisone–cholesteryl stearate (1:1); C, hydrocortisone–lactose (1:6); D, hydrocortisone; E, hydrocortisone–cholesteryl* n*-decylate–lactose (1:1:6); and F, hydrocortisone–cholesteryl* n*-decylate (1:1).*

Table VI—Dissolution Rate Data for Hydrocortisone–Lipid (1:1) and Hydrocortisone–Lipid–Lactose (1:1:6) Expressed as the Parameters of the Weibull Distribution Equation

Sample	Log a[a]	b[b]	T_d[c], min
I	1.10	0.655	47.8
I-II	1.58	0.828	80.7
I-III	1.14	0.351	1.79×10^3
I-IV	1.31	0.346	4.02×10^3
I-V	1.65	0.406	1.16×10^4
I-VI	1.79	0.533	2.31×10^3
I-VII	1.31	0.372	3.36×10^3
I-VIII	0.30	1.100	2.0
I-IX (1:6)	0.51	0.471	12.3
I-II-IX	0.26	0.490	3.1
I-III-IX	1.13	0.529	1.36×10^2
I-IV-IX	1.30	0.371	3.21×10^3
I-V-IX	1.29	0.289	3.00×10^4
I-VI-IX	1.09	0.292	5.63×10^3
I-VII-IX	1.15	0.363	1.52×10^3
I-VIII-IX	0.35	0.577	4.1

[a] The y-intercept of the line, obtained by the least-squares method using a computer. (See Fig. 5.) [b] The slope of the line. [c] The time required to dissolve 63.2% of the hydrocortisone, derived from the Weibull distribution equation (10).

Table V gives the values for K, t_{50}, t_{90}, and the initial dissolution rate for the 1:1 hydrocortisone–lipid and 1:1:6 hydrocortisone–lipid–lactose preparations. The initial dissolution rates, when both t and $W = 0$, are calculated from:

$$\frac{dW}{dt} = kW_e^2 \qquad \text{(Eq. 1)}$$

The most rapid dissolution rate for hydrocortisone was exhibited by the hydrocortisone–cholesteryl stearate–lactose (1:1:6) preparation. The slowest release of the drug occurred from hydrocortisone–cholesteryl n-decylate (1:1).

On the basis of the regression analyses of the dissolution rate data, the assumption of a particular kinetic model is valid if the correlation coefficient, r, approaches unity. Fitting of the experimental data to the second-order kinetic model yielded an average value of $r = 0.955$ for the hydrocortisone–lipid (1:1) preparations. The average value of r for the hydrocortisone–lipid–lactose (1:1:6) preparations was 0.967. Thus, with deviations of only 3.3 and 4.5% from unity, the second-order kinetic model appears to be valid.

Weibull Cumulative Distribution Preparation—Langenbucher (10) reported that a more general function, which might be applied to linearize common types of dissolution curves, is the Weibull distribution equation:

$$\log [-\ln(1 - m)] = b \log (t - T_i) - \log a \qquad \text{(Eq. 2)}$$

where m expresses the accumulated fraction of drug in solution at time t; b is the shape parameter, obtained from the slope of the line; a is the scale parameter estimated from the y-intercept; and T_i is the location parameter, representing the time lag before the onset of dissolution (in this instance $T_i = 0$).

Figure 5 is a log–log plot of $-\ln(1 - m)$ *versus* t for selected 1:1 hydrocortisone–lipid combinations with and without lactose. Table VI lists the log a, b, and T_d values for all 1:1 hydrocortisone–lipid combinations with and without lactose. The T_d value represents the time required to dissolve 63.2% of the drug. The versatility of the log–log plot is evident in Fig. 5; it is possible to calculate the time required for any percentage of the drug to be dissolved by use of the auxiliary ordinate scale shown on the right-hand side. All points on Fig. 5 are experimental; the lines are drawn from the predicted values obtained from the least-squares method using a computer.

The log–log plots (Fig. 5) exhibit the closest fit to the experimental data as compared with the lines generated in Figs. 3 (first order) and 4 (second order). Thus, in Table I, it is apparent that 90.8% of the hydrocortisone had dissolved from the 1:1 hydrocortisone–cholesteryl stearate preparation after 45 min. The t_{90} values from the first-order, second-order, and Weibull distribution curves were 955, 117, and 41 min, respectively. With hydrocortisone–cholesteryl stearate–lactose (1:1:6), 85.2% of the drug

had dissolved after 15 min. The t_{90} values for the first-order, second-order, and Weibull distribution curves were 30, 11.6, and 19 min, respectively. These results support the utility of the Weibull cumulative distribution equation in the linearization of experimental data.

REFERENCES

(1) T. R. Bates and J. A. L. Sequeira, *J. Pharm. Sci.*, **64**, 793 (1975).

(2) H. W. Rudel, U.S. pat. 3,828,106.

(3) S. P. Patel and C. I. Jarowski, *J. Pharm. Sci.*, **64**, 869 (1975).

(4) S. P. Patel and C. I. Jarowski, *Drug Dev. Commun.*, **2**, 465 (1976).

(5) M. P. Short, P. Shakey, and C. T. Rhodes, *J. Pharm. Sci.*, **61**, 1732 (1972).

(6) D. Wurster and P. Taylor, *ibid.*, **54**, 670 (1965).

(7) W. D. Harkins and H. F. Jordan, *J. Am. Chem. Soc.*, **52**, 1751 (1930).

(8) J. C. Cox, Ph.D. dissertation, University of Florida, Gainesville, Fla., 1967.

(9) Y. Raghunathan and C. H. Becker, *J. Pharm. Sci.*, **57**, 1748 (1968).

(10) F. Langenbucher, *J. Pharm. Pharmacol.*, **24**, 979 (1972).

ACKNOWLEDGMENTS AND ADDRESSES

Received July 21, 1976, from the *Department of Allied Health and Industrial Sciences, College of Pharmacy and Allied Health Professions, St. John's University, Jamaica, NY 11439.*

Accepted for publication January 24, 1977.

[x] To whom inquiries should be directed.

Influence of Metoclopramide and Propantheline on GI Absorption of Griseofulvin in Rats

F. JAMALI and J. E. AXELSON [x]

Abstract □ The effect of metoclopramide and propantheline preadministration on the plasma levels of orally administered griseofulvin was studied. Griseofulvin was administered as an aqueous suspension in 0.5% polysorbate 80 or as a 100% polyethylene glycol 600 solution. Metoclopramide preadministration increased the gastric emptying rate, but propantheline retarded it. The effect on griseofulvin absorption induced by metoclopramide and propantheline was sharply dependent upon the dosage form of griseofulvin administered. When griseofulvin was administered as a suspension dosage form following metoclopramide administration, the griseofulvin peak plasma concentration was reduced by 59% while a concurrent 50% reduction in relative bioavailability was observed. Pretreatment with metoclopramide resulted in a shift of the time required for attainment of the peak plasma griseofulvin concentration. In contrast, metoclopramide administration prior to a dose of griseofulvin dissolved in 100% polyethylene glycol 600 sharply increased both the relative bioavailability and the maximum plasma level of griseofulvin by 234 and 145%, respectively. Propantheline administration prior to a single dose of griseofulvin suspension decreased the maximum plasma level by 30% and delayed the time of its attainment from 5.78 to 19.00 hr with a 50% increase in relative availability. When griseofulvin was administered as a 100% polyethylene glycol solution dosage form, propantheline preadministration reduced both the maximum plasma level and the area under the plasma concentration–time curve by 64 and 44%, respectively.

Keyphrases □ Griseofulvin—GI absorption, effect of metoclopramide and propantheline preadministration, rats □ Metoclopramide—effect of preadministration on GI absorption of griseofulvin, rats □ Propantheline—effect of preadministration on GI absorption of griseofulvin, rats □ Absorption, GI—griseofulvin, effect of metoclopramide and propantheline preadministration, rats □ GI absorption—griseofulvin, effect of metoclopramide and propantheline preadministration, rats □ Antifungal agents—griseofulvin, GI absorption, effect of metoclopramide and propantheline preadministration, rats □ Antiemetics—metoclopramide, effect of preadministration on GI absorption of griseofulvin, rats □ Anticholinergic agents—propantheline, effect of preadministration on GI absorption of griseofulvin, rats

Griseofulvin, a chemically neutral systemic antifungal antibiotic, is commonly used in the treatment of dermatophyte infections in humans (1–4) and domestic animals (5). As a result of inherently poor aqueous solubility (approximately 15 mg/liter at 37°), the drug is slowly, erratically, and incompletely absorbed from the human GI tract (6). However, it is an exceptionally effective antifungal agent after oral administration.

Because griseofulvin is poorly absorbed, it has been used as an investigational model to examine various parameters affecting drug absorption. Its slow and erratic absorption characteristics are the direct result of unusually slow dissolution after oral administration as a solid dosage form. Early experimentation with griseofulvin led to classical observations about the effect of particle-size reduction (7), surfactants (8), and dietary lipids (9) on the absorption of a drug with low solubility and poor availability.

The effects of particle-size reduction (7), micellar solubilization (10), molecular dispersion (11), and emulsification (12) on improving the absorption of poorly absorbed drugs are well recognized. However, far less is known about the effect of GI motility on the absorption of poorly absorbed drugs (13–15). Since griseofulvin is a very poorly soluble drug and its absorption takes place largely in the intestine (16), it was desirable to study the effect of gastric emptying and GI motility on its absorption. Metoclopramide (13) and propantheline (13–15) were used successfully as investigational probes in similar absorption studies to increase or decrease GI motility, respectively.

The purpose of this work is to demonstrate the effect of changes in GI motility on the relative availability of griseofulvin after preadministration of motility-modifying agents.

EXPERIMENTAL

Dosage Forms—Micronized griseofulvin[1] (specific surface area of 1.32 m^2/g) was used in the preparation of two dosage forms. The first preparation was an aqueous suspension containing 25 mg of micronized griseofulvin/ml in 0.5% polysorbate 80 in water. The second preparation was a solution of griseofulvin prepared by dissolving 12.5 mg of drug in

[1] Supplied by Dr. Milo Gibaldi, State University of New York at Buffalo, Buffalo, N.Y.

had dissolved after 15 min. The t_{90} values for the first-order, second-order, and Weibull distribution curves were 30, 11.6, and 19 min, respectively. These results support the utility of the Weibull cumulative distribution equation in the linearization of experimental data.

REFERENCES

(1) T. R. Bates and J. A. L. Sequeira, *J. Pharm. Sci.*, **64**, 793 (1975).

(2) H. W. Rudel, U.S. pat. 3,828,106.

(3) S. P. Patel and C. I. Jarowski, *J. Pharm. Sci.*, **64**, 869 (1975).

(4) S. P. Patel and C. I. Jarowski, *Drug Dev. Commun.*, **2**, 465 (1976).

(5) M. P. Short, P. Shakey, and C. T. Rhodes, *J. Pharm. Sci.*, **61**, 1732 (1972).

(6) D. Wurster and P. Taylor, *ibid.*, **54**, 670 (1965).

(7) W. D. Harkins and H. F. Jordan, *J. Am. Chem. Soc.*, **52**, 1751 (1930).

(8) J. C. Cox, Ph.D. dissertation, University of Florida, Gainesville, Fla., 1967.

(9) Y. Raghunathan and C. H. Becker, *J. Pharm. Sci.*, **57**, 1748 (1968).

(10) F. Langenbucher, *J. Pharm. Pharmacol.*, **24**, 979 (1972).

ACKNOWLEDGMENTS AND ADDRESSES

Received July 21, 1976, from the *Department of Allied Health and Industrial Sciences, College of Pharmacy and Allied Health Professions, St. John's University, Jamaica, NY 11439.*

Accepted for publication January 24, 1977.

[x] To whom inquiries should be directed.

Influence of Metoclopramide and Propantheline on GI Absorption of Griseofulvin in Rats

F. JAMALI and J. E. AXELSON [x]

Abstract □ The effect of metoclopramide and propantheline preadministration on the plasma levels of orally administered griseofulvin was studied. Griseofulvin was administered as an aqueous suspension in 0.5% polysorbate 80 or as a 100% polyethylene glycol 600 solution. Metoclopramide preadministration increased the gastric emptying rate, but propantheline retarded it. The effect on griseofulvin absorption induced by metoclopramide and propantheline was sharply dependent upon the dosage form of griseofulvin administered. When griseofulvin was administered as a suspension dosage form following metoclopramide administration, the griseofulvin peak plasma concentration was reduced by 59% while a concurrent 50% reduction in relative bioavailability was observed. Pretreatment with metoclopramide resulted in a shift of the time required for attainment of the peak plasma griseofulvin concentration. In contrast, metoclopramide administration prior to a dose of griseofulvin dissolved in 100% polyethylene glycol 600 sharply increased both the relative bioavailability and the maximum plasma level of griseofulvin by 234 and 145%, respectively. Propantheline administration prior to a single dose of griseofulvin suspension decreased the maximum plasma level by 30% and delayed the time of its attainment from 5.78 to 19.00 hr with a 50% increase in relative availability. When griseofulvin was administered as a 100% polyethylene glycol solution dosage form, propantheline preadministration reduced both the maximum plasma level and the area under the plasma concentration–time curve by 64 and 44%, respectively.

Keyphrases □ Griseofulvin—GI absorption, effect of metoclopramide and propantheline preadministration, rats □ Metoclopramide—effect of preadministration on GI absorption of griseofulvin, rats □ Propantheline—effect of preadministration on GI absorption of griseofulvin, rats □ Absorption, GI—griseofulvin, effect of metoclopramide and propantheline preadministration, rats □ GI absorption—griseofulvin, effect of metoclopramide and propantheline preadministration, rats □ Antifungal agents—griseofulvin, GI absorption, effect of metoclopramide and propantheline preadministration, rats □ Antiemetics—metoclopramide, effect of preadministration on GI absorption of griseofulvin, rats □ Anticholinergic agents—propantheline, effect of preadministration on GI absorption of griseofulvin, rats

Griseofulvin, a chemically neutral systemic antifungal antibiotic, is commonly used in the treatment of dermatophyte infections in humans (1–4) and domestic animals (5). As a result of inherently poor aqueous solubility (approximately 15 mg/liter at 37°), the drug is slowly, erratically, and incompletely absorbed from the human GI tract (6). However, it is an exceptionally effective antifungal agent after oral administration.

Because griseofulvin is poorly absorbed, it has been used as an investigational model to examine various parameters affecting drug absorption. Its slow and erratic absorption characteristics are the direct result of unusually slow dissolution after oral administration as a solid dosage form. Early experimentation with griseofulvin led to classical observations about the effect of particle-size reduction (7), surfactants (8), and dietary lipids (9) on the absorption of a drug with low solubility and poor availability.

The effects of particle-size reduction (7), micellar solubilization (10), molecular dispersion (11), and emulsification (12) on improving the absorption of poorly absorbed drugs are well recognized. However, far less is known about the effect of GI motility on the absorption of poorly absorbed drugs (13–15). Since griseofulvin is a very poorly soluble drug and its absorption takes place largely in the intestine (16), it was desirable to study the effect of gastric emptying and GI motility on its absorption. Metoclopramide (13) and propantheline (13–15) were used successfully as investigational probes in similar absorption studies to increase or decrease GI motility, respectively.

The purpose of this work is to demonstrate the effect of changes in GI motility on the relative availability of griseofulvin after preadministration of motility-modifying agents.

EXPERIMENTAL

Dosage Forms—Micronized griseofulvin[1] (specific surface area of 1.32 m^2/g) was used in the preparation of two dosage forms. The first preparation was an aqueous suspension containing 25 mg of micronized griseofulvin/ml in 0.5% polysorbate 80 in water. The second preparation was a solution of griseofulvin prepared by dissolving 12.5 mg of drug in

[1] Supplied by Dr. Milo Gibaldi, State University of New York at Buffalo, Buffalo, N.Y.

Table I—Peak Plasma Levels, C_{max} (Micrograms per Milliliter), Time of Occurrence, T_{max} (Hours), and the Area under Plasma Concentration–Time Curves, *AUC* (Micrograms Hour per Milliliter), following Oral Administration of a Micronized Griseofulvin Suspension (100 mg/kg), with Metoclopramide (10 mg/kg) or Propantheline (5 mg/kg) Given Intraperitoneally to the Test Animals 2 hr prior to Griseofulvin Administration

	Control			Metoclopramide Pretreated			Propantheline Pretreated		
	AUC	C_{max}	T_{max}	*AUC*	C_{max}	T_{max}	*AUC*	C_{max}	T_{max}
	37.5	7.35	6	24.9	3.12	4	50.4	3.37	23
	53.0	7.68	5	30.9	4.01	4	41.6	1.78	20
	37.3	6.92	6	19.9	2.50	4	42.3	7.62	23
	37.8	7.02	6	10.5	1.31	2	76.0	1.83	6
	52.9	6.02	6	15.8	2.63	2	42.8	5.42	23
	50.6	6.05	6	27.2	1.90	4	85.7	6.28	20
	45.8	6.60	6	23.5	3.82	2	73.2	4.78	14
	34.1	6.24	6	—	—	—	65.9	6.63	23
	40.4	6.32	5	—	—	—	105.7	—	—
Mean	43.3	6.69	5.78	21.8	2.75	3.14	65.1	4.71	19.00
SE	2.46	0.20	0.15	2.62	0.37	0.40	7.64	0.78	2.15
CV, %	17.1	8.9	7.8	32.0	35.6	33.7	35.3	46.6	32.1
Significance[a]				s	s	s	s	s	s

[a] Determined by Student *t* test; $\alpha = 0.05$ (two tailed), and s = significant.

1 ml of polyethylene glycol 600. A solution containing the same dose as the suspension dosage form could not be prepared due to the limited solubility of griseofulvin in polyethylene glycol 600.

Aqueous solutions of metoclopramide hydrochloride[2] (2.5 mg/ml) and propantheline bromide[3] (1.25 mg/ml) were prepared for intraperitoneal administration. All administered dosage forms were used immediately after preparation.

Plasma Level Studies—Adult male Wistar rats, average weight of 250 g, were fasted for 24 hr prior to and during the experiments. All animals were allowed water *ad libitum* throughout the experiments. Griseofulvin was administered by gastric intubation at constant dose levels of 100 mg/kg (25 mg/250-g rat) with the suspension and of 50 mg/kg (12.5 mg/250-g rat) with the solution.

Different groups of rats were separately injected with either 10 mg of metoclopramide hydrochloride/kg ip or 5 mg of propantheline bromide/kg ip 2 hr prior to oral griseofulvin administration. Control animals received only the respective griseofulvin dosage forms and were included in all experiments.

Blood samples were taken in heparinized tubes from the tail artery of anesthetized rats at suitable time intervals up to 48 hr postdosing. The blood samples were then centrifuged, and the plasma was frozen until assayed.

Gastric Emptying Studies—To evaluate the effect of metoclopramide and propantheline on the gastric emptying rate, single doses of a polyethylene glycol 600 solution or 0.5% polysorbate 80 suspension of griseofulvin were administered orally to the appropriately pretreated rats. Different animals were ether anesthetized at 0, 1, 2, 4, 6, and 11 hr after receiving griseofulvin, the stomach was clamped at the cardiac and pyloric sphincters, and the animal was sacrificed. During the suspension study, a cardiac blood sample was taken immediately prior to sacrifice.

Subsequent to sacrifice, the stomach was excised and homogenized and the homogenate was diluted with distilled water. The amount of griseofulvin in the organ homogenate and, where appropriate, plasma was determined using the procedure utilized for the plasma level studies.

Assay Procedure—A literature method (17) was employed with some modification to determine griseofulvin in biological samples. A 0.01–0.1-ml aliquot of the plasma sample was transferred accurately into a 45-ml polytef-stoppered centrifuge tube containing 5 ml of 0.1 *N* HCl. Anhydrous ether[4], 10 ml, was added to each tube, and the tubes were shaken for 30 min. Then 5 ml of the ether layer was transferred to a 10-ml volumetric flask containing 1 ml of 17.2 μg of diazepam/100 ml of benzene.

The solvent was evaporated to dryness under nitrogen, 1 ml of pesticide grade benzene[5] was added, and 5 μl of the resulting solution was injected into a gas chromatograph[6] equipped with a ^{63}Ni-electron-capture detector. The following conditions were used: glass column, 1.83 m long and 2 mm i.d. packed with 3% OV-25 on 80–100-mesh Chromosorb W; column oven temperature, 285°; injection port temperature, 250°; detector temperature, 350°; and carrier gas (95% argon and 5% methane) flow, 40 ml/min. The injection port configuration permitted on-column injection.

The peak height ratio (griseofulvin–diazepam) method was used to construct a standard curve and to quantitate griseofulvin.

RESULTS AND DISCUSSION

It was reported previously that preadministration of either metoclopramide or propantheline altered the absorption of griseofulvin administered as a suspension in 0.5% polysorbate 80 and as a solution in 100% polyethylene glycol 600 (18, 19). The results of these studies are summarized in Tables I–IV.

Plasma Levels after Oral Suspension of Griseofulvin—Figure 1 depicts representative plasma griseofulvin level–time plots obtained following a single dose of a 100-mg of griseofulvin/kg suspension in control, metoclopramide-predosed, and propantheline-predosed animals.

Pretreatment with metoclopramide, an agent capable of stimulating the gastric emptying reflex and GI motility (13, 18–22), decreased the maximum plasma concentration (C_{max}) by 59% (Table I) while at the same time decreasing the time for attainment of the peak level (T_{max}) by 2.7 hr. The area under the plasma griseofulvin level–time curve (*AUC*) was reduced by 50% (Table I) from controls as a result of metoclopramide preadministration. The observed reduction in the *AUC* for griseofulvin after metoclopramide preadministration is consistent with a 50% reduction in the relative availability of the poorly absorbed antifungal agent.

Alternatively, predosing with propantheline delayed the time for attainment of the maximum plasma griseofulvin level from 5.8 to 19 hr while at the same time increasing the *AUC* by 50% (Table I). These alterations were accompanied by a 30% reduction in the C_{max} for griseofulvin in plasma (Table I).

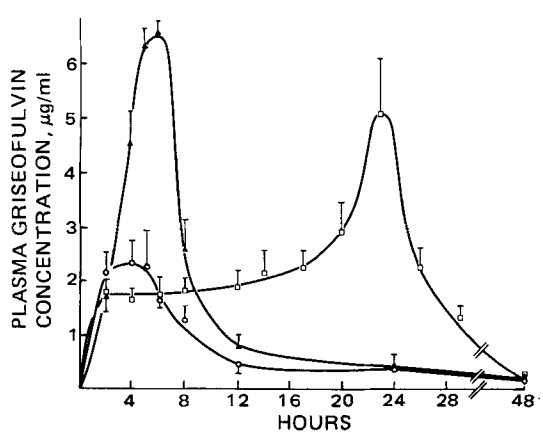

Figure 1—*Plasma griseofulvin concentrations as a function of time following the oral administration of a 100-mg/kg dose of micronized griseofulvin suspension in 0.5% polysorbate 80 to nine control rats* (▲), *seven rats predosed with 10 mg of metoclopramide hydrochloride/kg* (○), *and nine rats predosed with 5 mg of propantheline bromide/kg* (□). *Error bars represent the standard error of the mean.*

[2] Lot L-593-865-01F06, supplied by Merck Sharp and Dohme, West Point, Pa.
[3] Lot 239, supplied by Novopharm Ltd., Toronto, Ontario, Canada.
[4] Analytical reagent grade.
[5] Nanograde, Mallinckrodt.
[6] Hewlett-Packard model 5713A, Avondale, Pa.

Table II—Area under Plasma Concentration–Time Curves, *AUC* (Micrograms Hour per Milliliter), and the Peak Plasma Concentrations, C_{max} (Micrograms per Milliliter), following Oral Administration of Griseofulvin (50 mg/kg) in 100% Polyethylene Glycol 600, with Metoclopramide (10 mg/kg) or Propantheline (5 mg/kg) Given Intraperitoneally to the Test Animals 2 hr prior to Griseofulvin Administration

	Control		Metoclopramide Pretreated		Propantheline Pretreated	
	AUC	C_{max}	*AUC*	C_{max}	*AUC*	C_{max}
	37.6	15.32	126.6	20.34	37.4	5.83
	38.8	13.10	138.6	25.42	27.5	3.87
	55.5	12.01	84.6	22.03	16.4	3.51
	30.1	6.09	142.4	34.81	28.2	3.40
	37.9	11.68	115.0	33.03	17.8	3.40
	41.3	12.33	126.4	25.25	22.6	—
	28.9	8.12	119.4	17.60	13.5	—
	32.6	9.23	158.2	37.20	6.1	—
Mean	37.8	10.98	126.4	26.96	21.2	4.00
SE	2.96	1.05	7.73	2.55	3.46	0.48
CV, %	22.1	27.1	17.3	26.8	46.3	27.0
Significance[a]			s	s	s	s

[a] Determination by Student *t* test; $\alpha = 0.05$ (two tailed), and s = significant.

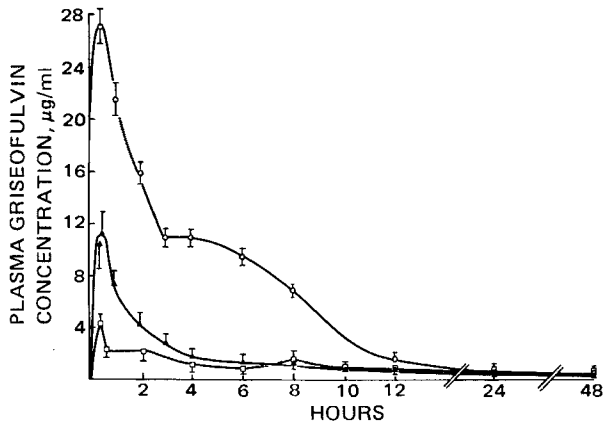

Figure 2—*Plasma griseofulvin concentrations as a function of time following the oral administration of a 50-mg/kg dose of griseofulvin in polyethylene glycol 600 to eight control rats (▲), eight rats predosed with 10 mg of metoclopramide hydrochloride/kg (○), and seven rats predosed with 5 mg of propantheline bromide/kg (□). Error bars represent the standard error of the mean.*

These observations are consistent with the previously observed influences of GI motility modifiers on drug absorption. Metoclopramide was shown to decrease effectively the time for attainment of peak plasma levels of acetaminophen (22) while only slightly influencing the total absorption of this drug. With griseofulvin, a dramatically different situation is encountered since the absorption of this drug is erratic and incomplete (6). Metoclopramide, through its stimulatory influence on the GI tract, decreased the residence time of griseofulvin in the small intestine, resulting in a substantial decrease in total absorption from the less readily available dosage form.

When propantheline was preadministered to rats, the findings were in sharp contrast with the observations after metoclopramide preadministration. Propantheline preadministration markedly increased the relative availability of griseofulvin suspension from controls, presumably through a mechanism similar to that reported with digoxin tablets (13); *i.e.*, an increased residence time in the GI tract allowed additional time for dissolution and subsequent absorption. This observation is consistent with the findings of Bates and Sequeira (15), where propantheline preadministration in humans caused a 1.53-fold increase in the absorption of the antifungal agent administered as an oral suspension.

Plasma Levels after Polyethylene Glycol 600 Solution of Griseofulvin—During the attempt to clarify the effect of motility on griseofulvin absorption, an interesting contrasting interaction between the motility modifiers and griseofulvin was observed when the antifungal agent was administered in polyethylene glycol 600. Figure 2 represents mean plasma griseofulvin level–time plots measured after oral administration of griseofulvin dissolved in 100% polyethylene glycol 600 in control and test rats. Griseofulvin absorption in all cases was rapid, and maximum plasma levels were attained in 20–30 min. With the control rats, the availability of the administered dose after the solution dosage form was nearly twice that observed after the suspension dosage form [(*AUC*) suspension (100 mg/kg) was 43.3 μg hr/ml as opposed to (*AUC*) solution (50 mg/kg) which was 37.8 μg hr/ml] (Tables I and II).

Figure 2 shows the plasma level–time curves of griseofulvin obtained following metoclopramide preadministration to animals receiving griseofulvin dissolved in polyethylene glycol 600. Metoclopramide increased the C_{max} by 145% and the *AUC* by 234% (Table II). Since metoclopramide shortens gastric emptying time and stimulates GI motility (13, 18–22), the absorption of the readily available dissolved drug is enhanced by a more rapid exposure to the proximal small intestine.

In sharp contrast to the observations after metoclopramide preadministration, propantheline reduced the relative availability of griseofulvin administered in solution by 44% (Table II) and decreased the mean peak plasma level by 64% (Fig. 2). This observation was not unexpected since propantheline pretreatment induces a longer residence time of the drug in the stomach where griseofulvin absorption is limited. This delayed drug release to the absorption site may result in either precipitation of the drug or degradation of griseofulvin.

Davis *et al.* (23) noticed a continuous disappearance of griseofulvin from the rat alimentary canal corresponding with the fall in blood level. They attributed this observation to griseofulvin destruction in the gut. However, in this work, addition of 1 ml of distilled water to griseofulvin dissolved in 1 ml of polyethylene glycol 600 caused the drug to precipitate gradually in fine crystals. This observation, coupled with the fact that a large percent of unchanged griseofulvin was recovered from the stomach of the propantheline-pretreated rats 11 hr after griseofulvin administration (Table III), suggests that precipitation rather than destruction may be responsible for the poor relative bioavailability.

In contrast to the observed effect of propantheline on griseofulvin solution, Manninen *et al.* (13) noticed that the absorption properties of digoxin, when given in solution form, were unaffected by treatment with the anticholinergic drug. This difference can perhaps be explained by the different solubility properties of these two drugs; *i.e.*, following administration, with a longer residence time in the stomach, griseofulvin

Table III—Percent Griseofulvin Remaining in Stomach and Corresponding Plasma Levels in the Rat following Oral Administration of Single Doses of 100 mg of Griseofulvin/kg in 0.5% Polysorbate 80 with Test Rats Given Single Doses of Either 10 mg of Metoclopramide Hydrochloride/kg or 5 mg of Propantheline Bromide/kg 2 hr prior to Griseofulvin Administration

Hour Postdosing	Control		Metoclopramide Pretreated		Propantheline Pretreated	
	% in Stomach	Plasma Level, μg/ml	% in Stomach	Plasma Level, μg/ml	% in Stomach	Plasma Level, μg/ml
0	98.4	—	99.3	—	96.0	—
	96.8	—	100.4	—	98.1	—
1	74.2	1.02	20.1	2.74	84.4	0.73
	77.7	1.02	27.7	3.85	89.2	0.83
2	69.6	1.61	32.7	1.44	60.9	1.93
	57.7	0.83	16.4	3.13	89.7	0.99
4	18.7	2.85	7.8	2.07	32.1	4.85
	31.1	3.11	1.6	3.91	31.9	0.89
6	1.9	5.75	0.9	1.01	4.3	0.94
	9.2	2.78	0.5	2.18	28.0	0.75
11	0.2	0.08	0.5	0.01	25.2	2.12
	1.8	0.04	1.4	0.02	47.6	0.21

Table IV—Percent Griseofulvin Remaining in Stomach following Oral Administration of Single Doses of 50 mg of Griseofulvin/kg in Polyethylene Glycol 600 to the Control, Metoclopramide Hydrochloride-Pretreated Rats (10 mg/kg), and Propantheline Bromide-Pretreated Rats (5 mg/kg)

Hour Postdosing	Percent Remaining in Stomach		
	Control	Metoclopramide Pretreated	Propantheline Pretreated
0	98.1	96.5	103.3
	101.3	95.9	96.4
1	86.3	46.7	96.1
	87.8	88.6	97.1
	77.6	50.9	—
2	89.4	44.8	104.3
	65.6	49.0	81.5
	82.9	30.8	96.4
4	56.5	37.5	102.4
	46.9	7.3	74.6
	49.7	41.7	73.0
6	31.4	5.5	68.7
	—	2.6	52.1
	24.6	22.6	—
11	0.0	0.4	49.4
	—	—	54.4
	2.3	1.4	35.1

may precipitate and yield a lower relative availability while digoxin may remain in solution and subsequently be absorbed.

Gastric Emptying—The determination of the amount of griseofulvin remaining in the stomach at different time intervals in control, metoclopramide-predosed, and propantheline-predosed animals lends credence to the speculated effects of the motility modifiers on the gastric emptying pattern obtained after oral griseofulvin administration. The accelerated emptying rate induced by metoclopramide is clearly illustrated by the findings at 1 hr after administration of the griseofulvin suspension; 76% of the suspension dosage form remained in the stomach of control animals while only 24% remained after metoclopramide preadministration (Table III). A somewhat similar finding was seen with animals receiving griseofulvin in a 100% polyethylene glycol 600 solution dosage form. In animals receiving the solubilized griseofulvin, the controls retained 84% of the dose at 1 hr postdosing while the test animals retained 62%.

As anticipated, propantheline influenced the gastric emptying process by reducing its rate. Even at 11 hr after griseofulvin administration, 36% of the suspension (Table III) and 46% of the solution (Table IV) could be found in the stomach.

Table III also contains the plasma griseofulvin levels at the time of determination of the gastric contents. These plasma levels are in good agreement with those observed in the suspension dosage form plasma level studies (Fig. 1).

The gastric emptying rate in all three groups of rats (controls, metoclopramide pretreated, and propantheline pretreated) was lower when the drug was administered in polyethylene glycol 600 as compared to the suspension (Tables III and IV). However, large intersubject variations and the limited number of experimental data do not permit a definitive evaluation. Griseofulvin administration in polyethylene glycol 600 also caused a noticeable change in the appearance of the gut along with an apparent tendency to retain water.

SUMMARY

The observed plasma level data and gastric emptying experiments suggest that the absorption of the griseofulvin suspension may be limited by two major factors, the gastric emptying rate and the dissolution process. The shorter onset of absorption of the griseofulvin suspension following metoclopramide predosing was probably due to the higher gastric emptying rate, and the lower relative availability was due to the slow dissolution rate when the suspension was forced out of the absorption site prior to complete absorption. On the other hand, propantheline pretreatment resulted in a delayed T_{max}, perhaps due to a very low gastric emptying rate; the undissolved drug traveled through the GI tract very slowly, permitting more drug dissolution and subsequent absorption.

The oral solution studies and gastric emptying experiments support the preceding explanation. With an oral solution of griseofulvin, the drug is readily available and a dissolution process is not involved; the absorption is more rapid and begins from the moment that the dosage form contacts the absorption site. Metoclopramide pretreatment markedly increased the bioavailability of the solution because the transit time in the GI tract was shortened; since there was no dissolution process to delay absorption, the drug was quickly exposed to the proximal small intestine where absorption was rapid.

Finally, propantheline preadministration prior to a solution dosage form of griseofulvin adversely influences the availability of the poorly absorbed antifungal agent through a mechanism not completely understood. Nevertheless, the noted interaction of the motility modifiers with griseofulvin is of particular interest since the results are dependent upon the formulation of griseofulvin administered.

REFERENCES

(1) G. Riehl, *Klin. Med.*, **3**, 131 (1959).

(2) D. I. Williams, R. H. Marten, and I. Sarkany, *Lancet*, **2**, 1216 (1958).

(3) H. Blank and F. J. Roth, *Arch. Dermatol.*, **79**, 259 (1959).

(4) H. Blank, *Am. J. Med.*, **39**, 831 (1965).

(5) I. M. Lauder and J. G. O'Sullivan, *Vet. Rec.*, **70**, 949 (1958).

(6) C. Bedford, D. Busfield, K. J. Child, I. MacGregor, P. Sutherland, and E. G. Tomich, *Arch. Dermatol.*, **81**, 735 (1960).

(7) M. Kraml, J. Dubuc, and D. Beall, *Can. J. Biochem. Physiol.*, **40**, 1449 (1962).

(8) W. A. Duncan, G. Macdonald, and M. J. Thornton, *J. Pharm. Pharmacol.*, **14**, 217 (1962).

(9) R. G. Crounse, *J. Invest. Dermatol.*, **37**, 529 (1961).

(10) T. R. Bates, M. Gibaldi, and J. L. Kanig, *J. Pharm. Sci.*, **55**, 191 (1966).

(11) W. L. Chiou and S. Riegelman, *ibid.*, **59**, 937 (1970).

(12) P. J. Carrigan and T. R. Bates, *ibid.*, **62**, 1476 (1973).

(13) V. Manninen, A. Apajalahti, J. Melin, and M. Karesoja, *Lancet*, **1**, 398 (1973).

(14) G. Levy, M. Gibaldi, and J. A. Procknal, *J. Pharm. Sci.*, **61**, 798 (1972).

(15) T. R. Bates and J. A. Sequeira, *ibid.*, **64**, 793 (1975).

(16) W. L. Chiou and S. Riegelman, *ibid.*, **60**, 1376 (1971).

(17) V. P. Shah, S. Riegelman, and W. L. Epstein, *ibid.*, **61**, 634 (1972).

(18) J. E. Axelson and F. Jamali, "Abstracts of the Research Symposium and Research Conference of the Association of Faculties of Pharmacy," Ottawa, Canada, May 1974, paper 15.

(19) F. Jamali and J. E. Axelson, "Abstracts of the APhA Academy of Pharmaceutical Sciences," vol. 5, American Pharmaceutical Association, Washington, D.C., 1975, p. 132.

(20) J. Nimmo, *Postgrad Med. J., Suppl.*, **July**, 25 (1973).

(21) G. Gothoni, P. Pentikainen, H. I. Vapaatalo, R. Hackman, and K. Af Bjorksten, *Ann. Clin. Res.*, **4**, 228 (1972).

(22) J. Nimo, R. C. Heading, P. Tothill, and L. F. Prescott, *Br. Med. J.*, **1**, 587 (1973).

(23) B. Davis, K. J. Child, and E. G. Tomich, *J. Pharm. Pharmacol.*, **13**, 166 (1961).

ACKNOWLEDGMENTS AND ADDRESSES

Received October 12, 1976, from the *Faculty of Pharmaceutical Sciences, University of British Columbia, Vancouver, British Columbia V6T 1W5, Canada.*

Accepted for publication January 12, 1977.

Presented in part at the Research Symposium and Research Conference of the Association of Faculties of Pharmacy of Canada, Ottawa, Canada, May 1974, and at the Basic Pharmaceutics Section, APhA Academy of Pharmaceutical Sciences, San Francisco meeting, April 1975.

Supported by M.R.C. Grant Ma-5358.

The analytical support by Mr. W. Campbell, Jr., of Hewlett-Packard, Ltd., is gratefully acknowledged.

[x] To whom inquiries should be directed.

Competitive Binding between Cocaine and Various Drugs to Synthetic Levodopa Melanin

R. BAWEJA, T. D. SOKOLOSKI, and P. N. PATIL ˣ

Abstract □ The interaction of 15 drugs with synthetic levodopa melanin was studied by measuring their relative tendency to compete with ^{14}C-cocaine for sites on the polymer. The binding of cocaine to melanin followed a Type I Langmuir adsorption isotherm in the absence of added drugs. Cocaine in the presence of a ninefold greater concentration of (+)-norepinephrine, levarterenol, dextroamphetamine, levamfetamine, (−)-ephedrine, dopamine, cyclopentolate, tropicamide, and, perhaps, desipramine conformed to a Type I adsorption relationship modified to account for competitive binding. Reciprocal plots for the binding of cocaine in the presence of these drugs permit a comparison of their relative affinities to melanin. Chlorpromazine, promazine, fluphenazine, thioridazine, imipramine, and chloroquine in ratios of 9:1 (drug–cocaine) gave results that are not explainable by a model based on competitive inhibition of cocaine binding. However, studies at ratios of 1:1 for promazine and of 0.25:1 and 1:1 for chloroquine showed conformity with the competitive inhibition model, so affinities could be compared. The behavior of cocaine in the presence of thioridazine even at a 1:1 ratio cannot be judged as competitive inhibition. The overall results showed that the relative binding found was: some phenothiazines ≈ chloroquine > cyclopentolate > tropicamide > sympathomimetic amines.

Keyphrases □ Cocaine—competitive binding with various drugs to synthetic levodopa melanin □ Binding, competitive—cocaine and various drugs to synthetic levodopa melanin □ Levodopa melanin, synthetic—competitive binding with cocaine and various drugs □ Melanin, synthetic levodopa—competitive binding with cocaine and various drugs □ Narcotic anesthetics, topical—cocaine, competitive binding with various drugs to synthetic levodopa melanin □ Pigments—synthetic levodopa melanin, competitive binding with cocaine and various drugs

Many drugs are accumulated and retained by pigmented tissue (1–9). Since nonpigmented tissue accumulates only small amounts of drug, retention is assumed to be dependent on pigment cells and their constituents. The melanin of the pigment granules in these cells has been implicated as the intracellular material responsible for drug binding (1, 4–6).

An earlier study (10) attempted to quantify the drug interactions with synthetic melanin by assuming that the process involved was analogous to adsorption on a solid, permitting a calculation of affinity and capacity constants to characterize binding. It was observed (10) that (±)-cocaine hydrochloride had an affinity for melanin of a magnitude and reproducibility that suggested it might be used to study the binding of various drugs; the approach suggested was the measurement of the tendency of drugs to compete with labeled cocaine for melanin sites.

The present study reports the relative ability of several drugs to bind to melanin by measuring their competitive displacement of labeled cocaine. Cyclopentolate and tropicamide were selected because they are extensively used in ophthalmology (11) and, like cocaine, are less effective in pigmented iris (4). The phenothiazines, chlorpromazine, fluphenazine, promazine, and thioridazine, were studied to see if structural differences affected binding. Desipramine and imipramine were studied because of their structural similarity to phenothiazines. Chloroquine, like chlorpromazine, was used because it is reported to produce retinopathy and is known to bind to melanin (12). Dextroamphetamine [(+)-amphetamine] and levamfetamine [(−)-amphetamine], (+)-norepinephrine and levarterenol [(−)-norepinephrine], and dopamine were studied to determine if there was a stereospecific component to binding. The remaining sympathomimetic amine used, (−)-ephedrine, is known to be retained by the pigmented iris (5, 6).

EXPERIMENTAL

Preparation of Levodopa Melanin—The melanin was prepared as reported previously (10). The yield resulting was 4.38 g using exactly the same amounts and procedures. This yield is approximately three times more than was obtained earlier for unknown reasons. The resulting material, as well as that obtained earlier, showed that a free radical is present, as evidenced by its characteristic electron spin resonance signal[1] similar to that of melanin found in nature.

Materials—^{14}C-Methoxy-labeled-(±)-cocaine hydrochloride[2] (specific activity of 3.12 mCi/mmole) was found to be pure using TLC. The unlabeled drugs used without further purification were: fluphenazine[3], promazine hydrochloride[4], chloroquine diphosphate[5], imipramine hydrochloride[6], thioridazine hydrochloride[7], desipramine hydrochloride[8], dextroamphetamine [(+)-amphetamine] sulfate[9], levamfetamine [(−)-amphetamine] sulfate[9], (+)-norepinephrine (+)-bitartrate[5], levarterenol[10] [(−)-norepinephrine], dopamine hydrochloride[11], (−)-ephedrine hydrochloride[12], cyclopentolate hydrochloride[13], tropicamide[13], and (±)-cocaine hydrochloride[14]. All other chemicals were reagent grade.

Methodology for Binding Studies—Portions of 2, 4, 6, 8, and 10 mg of synthetic melanin were placed in separate 25-ml flasks. Nonlabeled drug was added to 5 ml of 0.1 *M* phosphate buffer, pH 7.4, to give a concentration normally nine times (5.24×10^{-5} *M*) that of labeled cocaine. The suspension was shaken at 37° for 1 hr in a thermostated water bath. Then labeled (±)-cocaine hydrochloride (0.15 ml of a stock solution) was added, resulting in a concentration of 5.83×10^{-6} *M* (5.8 nCi/ml), and shaking was continued for another hour.

The suspension was then centrifuged[15] at 19,000 rpm for 30 min at −2°. The supernate, 1 ml, was placed in a counting vial, and 1 ml of water and 12 ml of a liquid scintillation cocktail[16] were added. All samples were then counted[17] for 10 min. The counting efficiency for the instrument was 86–87%. In a few cases where results showed that the 9:1 ratio (unlabeled–labeled) was too high, a 1:1 or 0.25:1 study was performed.

In another study, saturation of melanin by cocaine was carried out using a constant amount of melanin (2 mg). Unlabeled cocaine was added to the labeled compound whose concentration was fixed at 5.83×10^{-6} *M* (5.8 nCi/ml). Ratios (unlabeled–labeled) of between 5:1 and 750:1 were used, and the systems were analyzed for free and bound drug as outlined previously (10).

All experiments were repeated five times. The concentration of cocaine bound (as free base) was calculated by taking the difference between the amount initially added and the amount remaining in the supernate after

[1] The spectrum was obtained through the courtesy of Dr. Louis Malspeis, College of Pharmacy, Ohio State University.
[2] Mallinckrodt Nuclear, St. Louis, Mo.
[3] Schering Corp., Bloomfield, N.J.
[4] Wyeth Laboratories, Philadelphia, Pa.
[5] Sterling-Winthrop Research Institute, Rensselaer, N.Y.
[6] Ciba Pharmaceutical Co., Summit, N.J.
[7] Sandoz Pharmaceuticals, Hanover, N.J.
[8] USV Pharmaceuticals Corp., Tuckahoe, N.Y.
[9] Smith Kline & French Laboratories, Philadelphia, Pa.
[10] Regis Chemicals, Chicago, Ill.
[11] General Biochemicals, Chagrin Falls, Ohio.
[12] Mallinckrodt, St. Louis, Mo.
[13] Alcon Laboratories, Fort Worth, Tex.
[14] Merck Sharp & Dohme Research Laboratories, West Point, Pa.
[15] Sorvall RC-2B centrifuge.
[16] Aquasol, New England Nuclear, Boston, Mass.
[17] Packard liquid scintillation spectrometer.

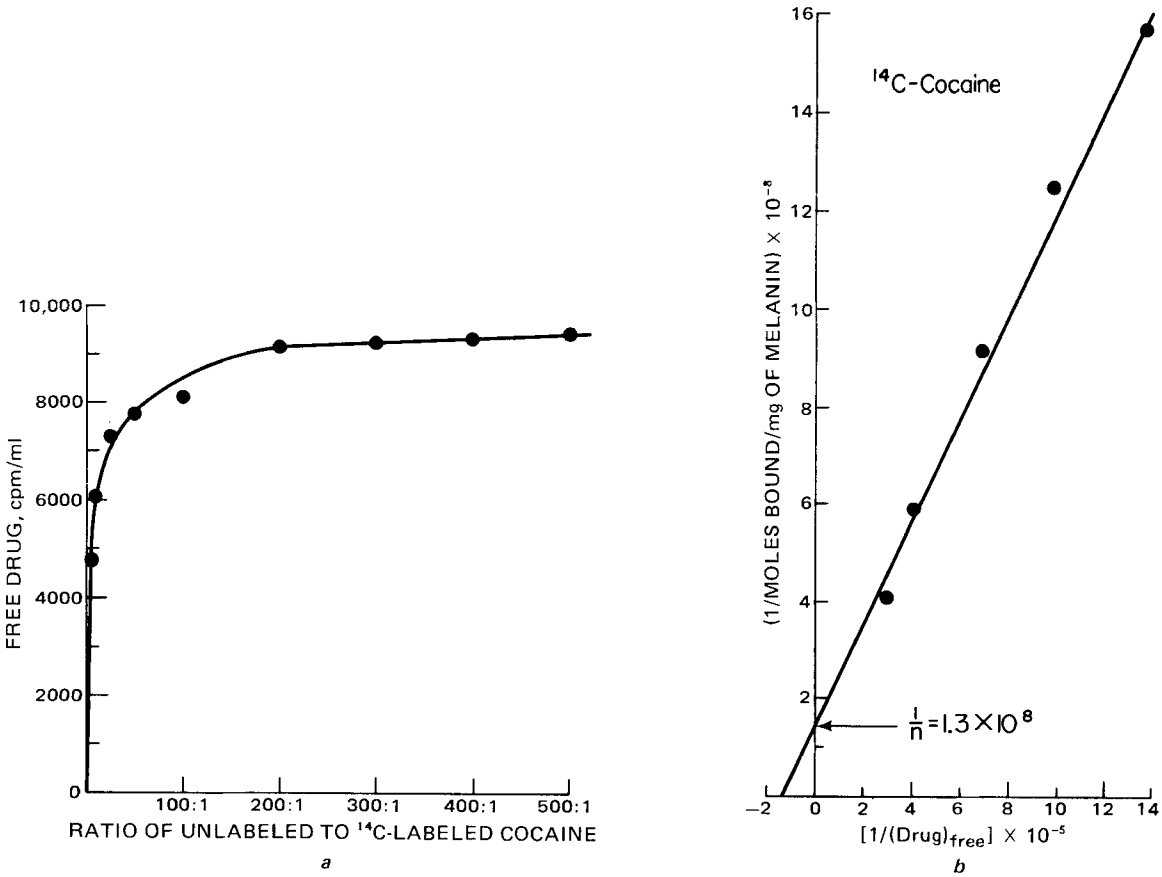

Figure 1—(a) *Free drug concentration as measured by counts per minute per milliliter for cocaine as a function of the cocaine concentrations where various proportions of unlabeled to labeled cocaine were used.* (b) *Reciprocal of the moles of cocaine bound per milligram of melanin as a function of the reciprocal of the free cocaine concentration. The affinity constant* K = 1.203×10^5 M^{-1}, *and the capacity* n = 7.69×10^{-9} *mole/mg.*

centrifugation. The average of the five determinations (standard error of mean between 1 and 5%) was used for data analysis.

Treatment of Binding Data—Cocaine binding to melanin was assumed to follow a Type I Langmuir adsorption isotherm according to:

$$r = \frac{nK[c]_{free}}{1 + K[c]_{free}} \quad \text{(Eq. 1)}$$

where r is the number of moles of cocaine bound per milligram of melanin, $[c]_{free}$ is the concentration of free cocaine, n is the maximum number of moles of cocaine that can be bound per milligram of melanin, and K is proportional to the affinity constant for cocaine binding under the experimental conditions. Equation 1 is modified when cocaine binding is studied in the presence of a drug that competes for cocaine binding sites. In the case of reversible inhibition by the added drug, Eq. 1 becomes:

$$r = \frac{nK[c]_{free}}{1 + K[c]_{free} + K'[D]_{free}} \quad \text{(Eq. 2)}$$

where K' is the constant related to the affinity of the drug and $[D]_{free}$ is the free inhibitor concentration. Defining the term K_{app} as:

$$K_{app} = \frac{K}{1 + K'[D]_{free}} \quad \text{(Eq. 3)}$$

and substituting into Eq. 2 gives the following equation upon rearrangement:

$$\frac{1}{r} = \frac{1}{n} + \frac{1}{nK_{app}} \frac{1}{[c]_{free}} \quad \text{(Eq. 4)}$$

Thus, a plot of the reciprocal of the amount of cocaine bound per milligram of melanin as a function of the reciprocal of the free cocaine concentration should be linear in the presence of a constant concentration of inhibitor. In competitive inhibition of cocaine binding, the y-axis intercept should be the same as that found in the absence of inhibitor but the slope should be greater since K_{app} must be less than K. The greater the slope at a constant inhibitor concentration, the greater is the affinity, K', of the inhibitor for melanin. If the added drug is an irreversible inhibitor of cocaine binding, both the slope and y-axis intercept should increase. However, the value for K, the x-axis intercept, remains the same in the presence and absence of drug inhibitor.

RESULTS

When cocaine binding to melanin was studied using a constant weight of melanin (2 mg) and increasing amounts of cocaine (ratios of unlabeled to labeled drug increased from 5:1 to 750:1), the relation between the counts per minute per milliliter and the increasing ratio reached a plateau above ratios of about 200:1 (Fig. 1*a*). Since an increase in counts per minute per milliliter reflected displacement of bound labeled cocaine, saturation of 2 mg of melanin in 5.15 ml of buffer occurred at concentrations of about 1.17×10^{-3} M. This result showed that the subsequent studies involving cocaine binding to melanin in the presence and absence of inhibitors were conducted at levels well below cocaine saturation.

In studies using a constant concentration of labeled cocaine (5.83×10^{-6} M) with varying amounts of melanin added (2–10 mg/5.15 ml), a plot of the reciprocal of the experimentally measured amount bound per milligram of melanin as a function of the reciprocal of the free cocaine concentration was linear (Fig. 1*b*). The result conforms with that predicted by Eq. 1, where the n and K values found (7.7×10^{-9} mole/mg and 1.20×10^5 M^{-1}, respectively) are of the same order of magnitude as those reported earlier (7) where $n = 2.4 \times 10^{-9}$ mole/mg and $K = 8.9 \times 10^5$ M^{-1}. The values are not expected to be exactly the same because of the error involved in getting the constants (Table I) and because different batches of synthetic melanin were used where the physical characteristics (external surface area) affecting binding may have been quite different. Thus, in spite of different melanins used, the values for cocaine can be considered approximately equal within the limits of experimental error. The relationship found for cocaine alone (Fig. 1*b*) was used as the reference for all subsequent drug comparison studies.

Competition for binding sites between cocaine and drugs of several pharmacological classes was characterized by plotting the reciprocal of the amount of cocaine bound as a function of the reciprocal of the free cocaine concentration. Linear relationships were always obtained where slopes in plots for cocaine in the presence of another drug were always greater than the slope found for cocaine alone (Table I). The amine salts, (+)-norepinephrine, levarterenol, dextroamphetamine, levamfetamine, (−)-ephedrine, and dopamine, studied at a ratio of 9:1 (amine–cocaine) gave good linear double-reciprocal plots as typified by those for (+)-

Table I—Linear Regression Parameters for the Langmuir Treatment of the Binding of ^{14}C-Cocaine to Melanin in the Presence of Several Drugs

Drug	Ratio, Drug–Cocaine	Slope, mg/liter × 10^{-3} (Lower/Upper Limit)[a]	Intercept, mg/mole × 10^{-8} (Lower/Upper Limit)[a]
(+)-Norepinephrine	9:1	1.9 (1.4/2.3)	4.1 (1.1/7.1)
Levarterenol	9:1	1.7 (1.3/2.0)	2.9 (1.7/4.2)
Dextroamphetamine	9:1	2.2 (1.7/2.7)	2.0 (0.5/3.5)
Levamfetamine	9:1	2.3 (1.8/2.8)	2.1 (0.5/3.8)
(−)-Ephedrine	9:1	2.1 (1.5/2.6)	3.1 (0.9/5.4)
Dopamine	9:1	2.3 (1.4/3.1)	3.3 (0.6/5.9)
Cyclopentolate	9:1	3.1 (2.6/3.6)	2.2 (−0.4/4.8)
Tropicamide	9:1	2.5 (2.2/2.8)	0.8 (−0.7/2.3)
Chlorpromazine	9:1	2.0 (1.2/2.8)	10.4 (5.9/14.8)
Fluphenazine	9:1	2.2 (1.7/2.6)	9.4 (5.5/13.2)
Promazine	9:1	2.0 (1.5/2.6)	14.4 (11.7/17.1)
	1:1	2.4 (1.8/3.0)	1.7 (−2.4/5.8)
Thioridazine	1:1	1.6 (1.4/1.9)	8.1 (6.0/10.2)
Imipramine	9:1	2.2 (1.8/2.8)	6.1 (3.4/8.9)
Desipramine	9:1	2.2 (1.9/2.6)	4.0 (2.0/6.0)
Chloroquine	9:1	1.9 (1.4/2.4)	17.4 (13.4/21.4)
	1:1	2.0 (1.3/2.7)	7.6 (0.6/14.7)
	0.25:1	2.1 (1.4/2.9)	5.8 (−1.8/13.4)
(±)-^{14}C-Cocaine	Control	1.1 (0.9/1.3)	1.3 (−0.2/2.8)

[a] Parentheses contain 95% confidence intervals calculated at $p = 0.05$.

norepinephrine and levarterenol (Fig. 2). The slopes for all six compounds were greater than the slope for cocaine alone, and their intercepts do not appear to be statistically different from the intercept of cocaine (Table I).

Cyclopentolate and tropicamide gave slopes larger than those found for amine salts (Table I). In comparing the two drugs, cyclopentolate gave a slightly larger slope (Fig. 3).

Studies at ratios of 9:1 (drug–cocaine) using the tranquilizers promazine, chlorpromazine, fluphenazine, thioridazine, imipramine, and desipramine and the retinotoxic drug chloroquine gave reciprocal plots with slopes greater than those for cocaine alone (Table I). Except for desipramine, the y-axis intercepts were greater and statistically different from those for cocaine alone, as represented in Fig. 4*a* for chloroquine. Desipramine showed a y-axis intercept (Fig. 4*c*) with its lower 95% confidence limit falling within the range for cocaine (Table I). Table I shows that the intercept limits for fluphenazine, imipramine, chlorpromazine, promazine, and chloroquine were outside the error limit for cocaine. For

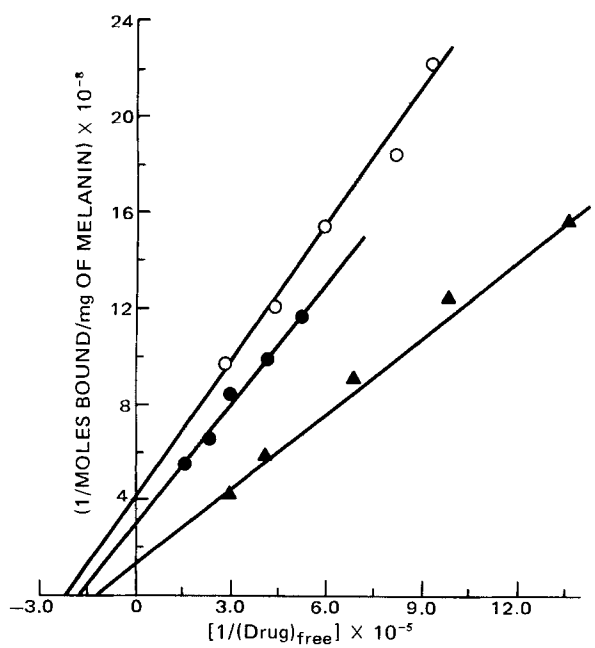

Figure 2—*Reciprocal of the moles of cocaine bound per milligram of melanin as a function of the reciprocal of the free cocaine concentration. Key: ▲, cocaine alone; ●, cocaine in the presence of levarterenol (1:9); and ○, cocaine in the presence of (+)-norepinephrine (1:9).*

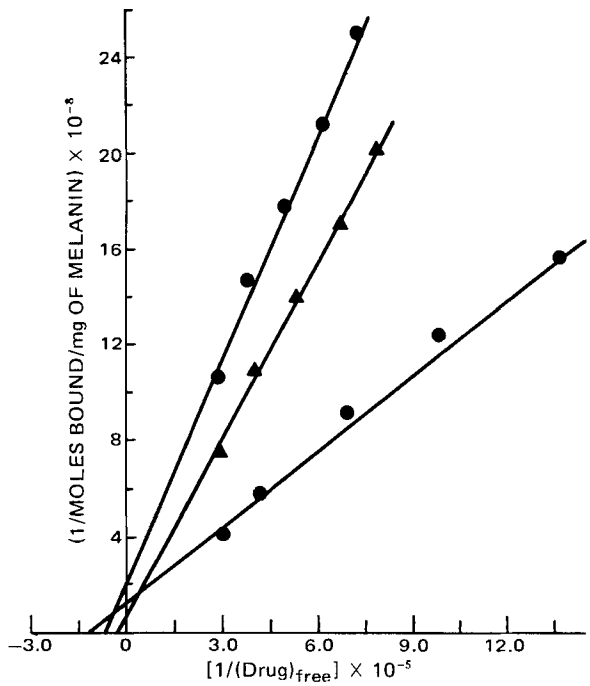

Figure 3—*Reciprocal of the moles of cocaine bound per milligram of melanin as a function of the reciprocal of the free cocaine concentration. Key: ●, cocaine alone; ▲, cocaine in the presence of tropicamide (1:9); and ○, cocaine in the presence of cyclopentolate (1:9).*

an unexplained reason, thioridazine at a 9:1 ratio gave results that were not analyzable.

With the assumption that the findings obtained were a result of high affinities of the several drugs (except desipramine) for melanin, which effectively displaced cocaine from binding sites with a concomitant introduction of large errors in the calculation of bound cocaine, studies were made using chloroquine at ratios of 1:1 and 0.25:1 (drug–cocaine) and promazine and thioridazine at ratios of 1:1. At the 1:1 ratio, analyzable results were obtained for thioridazine. The result for chloroquine at the 1:1 ratio is presented in Fig. 4*b*. The other compounds gave similar results. The slopes of the reciprocal plots obtained in these studies were greater than those of cocaine alone and the intercepts, except for thioridazine, were not statistically different from those found for cocaine alone (Table I).

DISCUSSION

The linear relationship obtained in the reciprocal plots for the six amine salts in the presence of cocaine at ratios of 9:1, for desipramine at the same ratio, for chloroquine at ratios of 1:1 and 0.25:1, and for promazine at a ratio of 1:1, where the y-axis intercepts were not significantly different from the intercept for cocaine studied alone, strongly suggests compliance with Eq. 3. The equation assumes that a drug reversibly competes with cocaine for binding sites on melanin where the concentration of free inhibitor is relatively constant. Compliance by the several drugs suggests that a comparison of the slopes obtained for cocaine in the presence of drugs with the slope obtained for cocaine alone can be used to compare the relative affinities of the several drugs for melanin. Thioridazine is the only drug that does not comply with Eq. 3 at a 1:1 ratio.

With the amine salts, an increase in the slope of the reciprocal plots occurred at ratios of 9:1; therefore, among the compounds studied, the amine salts showed the weakest binding to melanin. Furthermore, dextroamphetamine and levamfetamine had similar slopes, as did (+)-norepinephrine and levarterenol. This result indicates that competitive binding is nonstereoselective. The observations with the stereoisomers of amphetamine are consistent with the previous studies where the binding of each labeled isomer was investigated (10).

Cyclopentolate and tropicamide showed a greater slope and, hence, a greater affinity for melanin than the amine salts at similar ratios of drug to labeled cocaine. Cyclopentolate reflected a slightly greater inhibitory effect and presumably has a greater affinity for melanin than tropicamide, which may be a result of their differing chemical structures.

For most phenothiazines at a 9:1 ratio, it was not possible to charac-

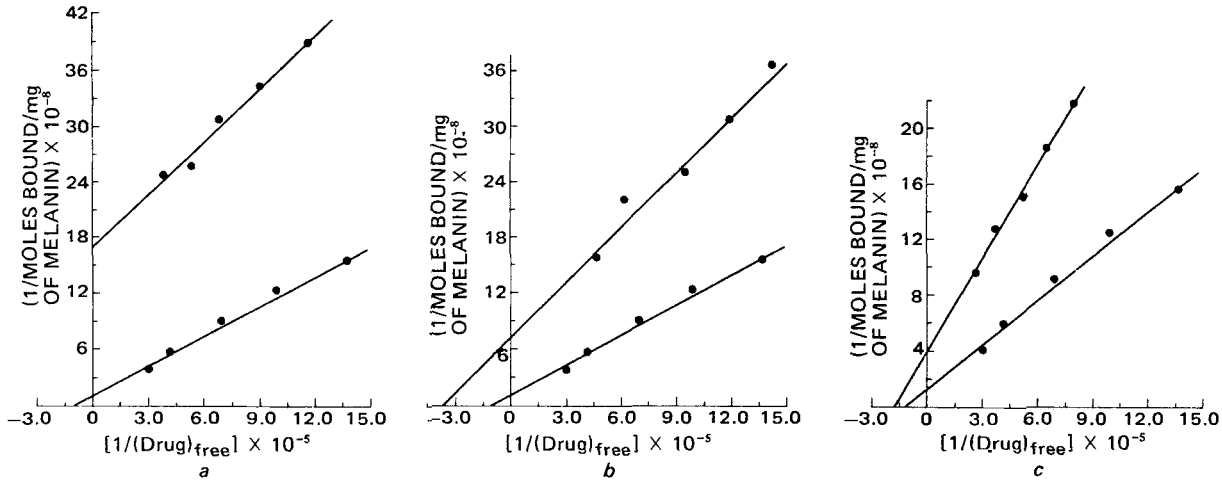

Figure 4—*Reciprocal of the moles of cocaine bound per milligram of melanin as a function of the reciprocal of the free cocaine concentration in the presence and absence of (upper curves) chloroquine (9:1) (a), chloroquine (1:1) (b), and desipramine (9:1) (c). The lower curves are ^{14}C-cocaine alone.*

terize the exact nature of the inhibitory effect since the isotherms obtained were not typical of the Type I adsorption. This result probably is a consequence of both the amount of phenothiazine present and the strength of the interaction. Desipramine is apparently a much weaker inhibitor than other phenothiazines studied since its behavior at a 9:1 ratio was similar to that of other phenothiazines studied at a 1:1 ratio. Chloroquine at a 9:1 ratio behaved similarly to most of the phenothiazines (not desipramine) at the same ratio. Just as with the phenothiazines, this behavior is probably related to its concentration and affinity for melanin.

The phenothiazines displaced cocaine at a 1:1 ratio, analogous to the amine salts at a 9:1 ratio, which indicates that phenothiazine affinity is greater than amine salt affinity. Chloroquine at ratios of 1:1 and 0.25:1 showed competitive effects similar to the amine salts at 9:1; it probably has a melanin affinity greater than the amine salts. Cyclopentolate and tropicamide, both at a 9:1 ratio, exhibited greater inhibitory effects than the amine salts at a similar ratio. When the anomalous behavior of phenothiazines at a 9:1 ratio is compared with the behavior of cyclopentolate and tropicamide at the same ratio, the phenothiazines show a greater affinity for melanin than these drugs.

The significance of these studies is that there is a difference among drugs in their affinity for melanin: some phenothiazines ≈ chloroquine > cyclopentolate > tropicamide > sympathomimetic amines. It has been suggested that binding occurs with melanin *via* interaction of unshared electrons on drugs with the free radical of melanin (13). Further study is necessary to clarify the mechanism of drug binding to melanins.

Because of the binding, regardless of its mechanism, it is possible that a drug may localize in the vicinity of melanin in melanin-containing tissue. It is easy to visualize such a phenomenon occurring, for example, in the eye where a localized high total concentration could remain over a long period (8, 9). Such a situation might foster toxicity. Chloroquine and chlorpromazine are known to produce ocular toxicity (12), and indeed they are among the strongest binders to melanin. Thus, it is tempting to suggest that there is a relationship between melanin affinity and toxicity.

The pharmacological and toxicological significance of the interaction of certain drugs with melanins is well recognized (1–6, 8, 9). Since many other drugs also interact and bind with melanins, the pharmacological and toxicological significance of these interactions is perhaps underestimated.

REFERENCES

(1) A. Potts, *Invest. Ophthalmol.*, **1**, 522 (1962).

(2) *Ibid.*, **3**, 405 (1964).

(3) N. G. Lindquist, *Acta Radiol., Suppl.*, **1973**, 325.

(4) P. N. Patil, *Invest. Ophthalmol.*, **11**, 739 (1972a).

(5) P. N. Patil and D. Jacobowitz, *Am. J. Ophthalmol.*, **78**, 470 (1974).

(6) P. N. Patil, K. Shimada, D. R. Feller, and L. Malspeis, *J. Pharmacol. Exp. Ther.*, **188**, 342 (1974).

(7) W. H. Harrison, R. M. Gray, and L. M. Soloman, *Br. J. Dermatol.*, **91**, 415 (1974).

(8) M. Salazar, R. G. Rahwan, and P. N. Patil, *Eur. J. Pharmacol.*, **38**, 233 (1976).

(9) M. Salazar, K. Shimada, and P. N. Patil, *J. Pharmacol. Exp. Ther.*, **197**, 79 (1976).

(10) K. Shimada, R. Baweja, T. Sokoloski, and P. N. Patil, *J. Pharm. Sci.*, **65**, 1057 (1976).

(11) W. H. Havener, "Ocular Pharmacology," 3rd ed., Mosby, St. Louis, Mo., 1974.

(12) H. N. Bernstein, *Surv. Ophthalmol.*, **12**, 415 (1967).

(13) G. Karreman, I. Isenberg, and A. Szent-Gyorgyi, *Science*, **130**, 1191 (1959).

ACKNOWLEDGMENTS AND ADDRESSES

Received October 26, 1976, from the *Divisions of Pharmaceutics and Pharmacology, College of Pharmacy, Ohio State University, Columbus, OH 43210.*

Accepted for publication January 17, 1977.

Supported in part by the National Eye Institute, U.S. Public Health Service Grant EY-01308, and in part by Alcon Laboratories, Fort Worth, Tex.

[x] To whom inquiries should be directed.

Relationship between Zero Point of Charge and Solubility Product for Hydroxides of Polyvalent Cations

HANS SCHOTT

Abstract □ The zero point of charge (ZPC) of slightly soluble compounds is the pH at which their particles suspended in water have zero charge. The ZPC values of slightly soluble hydroxides were compared with their solubility product in the form of its negative logarithm, pK_{SP}, and with the pH of their suspensions in pure water, pH_{SP}, which is a function of pK_{SP}. The ZPC–pK_{SP} relation was nonlinear while the ZPC–pH_{SP} relation was linear. Either equation can be used to estimate the ZPC value of a hydroxide from its solubility product. The ZPC of a given hydroxide was higher than its pH_{SP} because polyvalent cations are more extensively adsorbed and less extensively desorbed from the particle surface than the monovalent hydroxide ion. At the pH_{SP}, there are equivalent amounts of the cation and of the hydroxide anion in solution, but the surface layer of the hydroxide particle contains an excess cation on an equivalent basis. This imbalance confers a positive charge to the particle. The solubility product of aluminum hydroxide, redetermined at 25° by means of pH measurements, was 8×10^{-33}. Its ZPC, redetermined by microelectrophoresis, was 8.5 ± 0.1.

Keyphrases □ Zero point of charge—slightly soluble hydroxides, related to solubility product □ Solubility product—slightly soluble hydroxides, related to zero point of charge □ Hydroxides, slightly soluble—zero point of charge related to solubility product □ Aluminum hydroxide—zero point of charge related to solubility product

A slightly soluble hydroxide, $M^{z+}(OH)_z^-$, of cation M of valence z has a surface layer of composition $[M^{z+}(OH)_n]^{z-n}$, which depends on the pH of the solution. The surface charge of the particle is negative at high pH values where $z < n$ and positive at low pH values where $z > n$. At an intermediate pH value where $z = n$, the surface layer has the same composition as the bulk of the hydroxide particle, and the net charge is zero. This pH value, called the zero point of charge (ZPC) (1–3), is analogous to the isoelectric point of proteins.

The net surface charges at other pH values arise from one of two effects:

1. Frequently, the amphoteric dissociation of surface hydroxide groups produces such a surface charge. For aluminum hydroxide, $Al(OH)_2^+$ or $Al(OH)_2OH_2^+$ surface groups confer a positive charge to the particle at pH values below the ZPC while $Al(OH)_4^-$ surface groups confer a negative charge to the particle at pH values above the ZPC (2, 3).

2. The adsorption from solution of metal hydroxo complexes produced by hydrolysis of material dissolved from the precipitated hydroxide may confer a charge to the particle surface. For aluminum, such complexes include $[Al_8(OH)_{20}]^{4+}$ (4).

BACKGROUND

The ZPC is an important property of the hydroxides. It is equal to the pH value at which their suspensions are most highly flocculated, as shown by maxima in the sedimentation volume, the rate of sedimentation, and the viscosity (2, 5, 6). Since the ζ-potential of the particles at the ZPC is zero, there is no electrostatic repulsion to oppose the interparticle attraction due to London–van der Waals forces. Hence, the most extensive aggregation occurs at the ZPC. An implication of pharmaceutical interest is that caking in aluminum hydroxide and magnesium hydroxide suspensions is least extensive at the ZPC.

The methods used for measuring the ZPC are lengthy and require special experimental precautions (1, 2). In electrokinetic measurements, for instance, supporting electrolytes are used to adjust the ionic strength. These must be indifferent; *i.e.*, the added counterions should display no specific adsorption or interaction with the precipitated hydroxides. If any anions or cations introduced *via* the reagents used in precipitating the hydroxides are adsorbed by the particles, they should be removed. This removal may be difficult because the gelatinous precipitates exhibit pronounced sorptive properties due to their large specific surface areas. Moreover, impurities that may have been incorporated in the bulk of the particles *via* coprecipitation are known to affect the ZPC. These experimental difficulties are reflected by the lack of agreement frequently found among ZPC values reported for a single compound (1).

Solubility products of slightly soluble hydroxides are relatively easy to determine, and an extensive tabulation has been published (7). Values reported for the solubility product of a single compound at a given temperature are generally in good agreement, except for some values published before the late 1930's when reliable techniques for measuring hydrogen-ion activity and concentrations of trace amounts of metals were not available.

Among the published solubility product values, only the value of aluminum hydroxide has some uncertainty attached to it. Reference 7 lists 14 values measured at room temperature; 10 are in the range of 10^{-32}–10^{-30} while the earliest four values, determined in 1924 and 1933, vary between 10^{-17} and 10^{-13}. However, the most recent edition of a widely used handbook lists the following three values: 4×10^{-13} at 15°, 1.1×10^{-15} at 18°, and 3.7×10^{-15} at 25° (8).

In addition to being at variance with the recent values of Ref. 7, this set also seems to be internally inconsistent. When the three values are used to calculate the pH of an aluminum hydroxide suspension at the three temperatures, using the appropriate values for the ionization product of water, the results are 11.37, 10.62, and 10.51, respectively. It is unlikely that the 3° temperature increase from 15 to 18° lowered the pH by 0.75 unit while the 7° increase from 18 to 25° lowered it by only 0.11 unit.

The purpose of this study was to investigate the existence of a correlation between the ZPC of polyvalent hydroxides and the solubility product or the pH value calculated from the solubility product, pH_{SP}. The latter is the pH of a suspension or saturated solution of the hydroxide in pure water. It equals the ZPC only if the surface layer has the same composition as the bulk of the hydroxide particle, *e.g.*, $Al(OH)_3$ in the case of aluminum hydroxide. This condition precludes the adsorption of dissolved hydroxo complexes as well as the amphoteric dissociation of surface groups.

The only measurements made to supplement the published data were redeterminations of the solubility product and of the zero point of charge of aluminum hydroxide for the following reasons. Aluminum hydroxide suspensions are widely used as antacids and as adsorbents for vaccines and toxoids. There are discrepancies in the published values of its solubility product. The published ZPC values differ somewhat among each other and from the values calculated by Eqs. 2 and 3. The redetermined ZPC value of aluminum hydroxide would serve as a verification of these equations.

EXPERIMENTAL

All chemicals were ACS reagent grade. To determine the solubility product of aluminum hydroxide, aluminum sulfate octadecahydrate was recrystallized three times from water. A 0.01 *M* solution was treated with the stoichiometric amount of sodium hydroxide at the boiling point. The precipitate was immediately purified by washing, electrodialysis, and electrodecantation. It was resuspended in freshly redistilled conductivity water under careful exclusion of carbon dioxide.

The pH of the suspension was measured at 25.0 ± 0.1° at regular intervals, using three different types of pH meters equipped with glass electrode systems. The electrodes were immersed in the upper portion

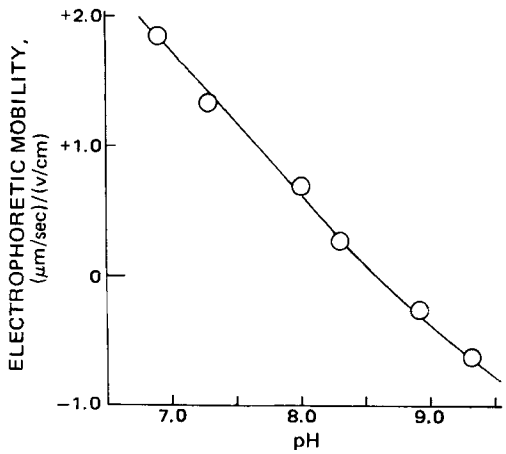

Figure 1—*Effect of pH on electrophoretic mobility of aluminum hydroxide at constant ionic strength.*

of a suspension, and measurements were made after the flocs had settled at least 2 cm below the electrode tips. Between measurements, the flocs were maintained in suspension with gentle magnetic stirring.

The maximum age of the preparations after a constant pH had been reached was 11 hr. These short times were designed to prevent extensive oxolation of the precipitated hydroxide and the formation of dissolved polynuclear hydroxo complexes by leaching.

For the determination of the ZPC by electrophoresis, aluminum nitrate nonahydrate was recrystallized twice from water. Aluminum hydroxide was precipitated by dropwise addition of ammonia to a stirred 0.01 *M* solution of aluminum nitrate heated to 80–90°. After cooling, it was washed repeatedly by centrifugation and further purified by electrodialysis. The aluminum hydroxide dispersions were diluted with equal volumes of sodium nitrate solutions containing various amounts of sodium hydroxide or nitric acid. Carbon dioxide was excluded by means of a nitrogen blanket. The ionic strength of the diluted dispersions was maintained constant at 0.010 *M*. Nitrate ions had been found to be indifferent counterions for ferric and aluminum oxides (2).

The dispersions were stirred gently for 48 hr prior to electrophoresis to permit the leaching of any formed hydroxo complexes and their adsorption on the hydroxide particles. Aging for an additional 5 days did not produce significantly different mobility values for the two dispersions tested. The maximum time elapsed between precipitation and electrophoresis was 2 weeks. Such short aging periods at room temperature did not produce significant crystallization of aluminum hydroxide (9).

Electrophoretic mobilities were measured with the commercial microelectrophoresis apparatus described previously (10), using the glass cell with a molybdenum cylinder as the anode and a platinum–iridium strip as the cathode. The temperature of the dispersions during the measurements varied from 22 to 25°, a variation unlikely to produce measurable changes in the electrophoretic mobility (11). The pH of the dispersions was measured before and after electrophoresis. The differences were 0.2 pH unit or less, except for two electrophoresis runs that were excluded from Fig. 1.

RESULTS

The observed pH_{SP} values of aluminum hydroxide fell in the 5.95–6.25 range with a mean of 6.10, in agreement with the majority of values reported in Ref. 7. This result corresponds to a pK_{SP} range of 32.7–31.5 and a mean of 32.08. Each point in Fig. 1 represents the average of eight electrophoresis measurements. Negative mobility values indicate that the particles are negatively charged and migrate to the anode. Interpolation of the plot of Fig. 1 to zero mobility places the ZPC of aluminum hydroxide at 8.52. The preferred value is 8.5 ± 0.2.

The new value for the solubility product of aluminum hydroxide, other values from Ref. 7, and ZPC values from Ref. 1 are listed in Table I, where pK_{SP} represents the logarithm of the reciprocal of the solubility product. For the equilibrium:

$$M(OH)_z(s) \rightleftharpoons M^{z+} + zOH^-$$

Scheme I

the following equation is readily derived for 24–25°, at which temperature the product of the concentrations of hydrogen and hydroxide ions of water is equal to 1.00×10^{-14}:

$$pH_{SP} = 14.00 + \frac{\log z - pK_{SP}}{z + 1} \qquad \text{(Eq. 1)}$$

Table I—ZPC, Solubility Product, and Derived pH Value for Sparingly Soluble Metal Hydroxides

Cation	ZPC	pK_{SP}[a]	pH_{SP}[b]
Zirconium	6.7	50.8	3.96
Cerium(IV)	6.75	50.6	4.00
Chromium(III)	7.0	30.2	6.57
Mercury(II)	7.3	25.5	5.60
Iron(III)	8.6	37.5	4.75
Tin(II)	8.7	25.8	5.50
Yttrium	9.0	22.9	8.40
Aluminum	9.1 (8.5)	32.1	6.10
Zinc	9.3	16.4	8.63
Copper(II)	9.4	19.5	7.60
Beryllium	10.2	21.3	7.00
Lanthanum	10.4	19.8	9.17
Lead(II)	10.5	15.1	9.07
Cadmium	10.5	13.8	9.50
Nickel(II)	11.1	15.2	9.03
Cobalt(II)	11.4	14.8	9.17
Iron(II)	12.0	14.4	9.30
Magnesium	12.0	10.8	10.50
Manganese(II)	12.4	12.8	9.83

[a] The negative logarithm of the solubility product. [b] Defined by Eq. 1.

Regression analysis of the data in Table I produced the following two correlations. The nonlinear relationship between the ZPC and pK_{SP} can be represented by the equation:

$$ZPC = 15.41 - 0.355pK_{SP} + 0.00371pK_{SP}^2 \qquad \text{(Eq. 2)}$$

The values of *F*, of the coefficient of multiple correlation, and of the standard error of the estimate were 29.42, 0.917, and 0.869, respectively. The inclusion of a cubic term in Eq. 2 improved the precision only marginally.

The linear relationship between the ZPC and pH_{SP} is shown in Fig. 2 and can be represented by the equation:

$$ZPC = 3.82 + 0.764pH_{SP} \qquad \text{(Eq. 3)}$$

The values of *F* and of the correlation coefficient are 56.6 and 0.877, respectively. When the experimental difficulties in determining the ZPC and the lack of agreement among reported ZPC values for a single compound are considered, the scatter of data points about Eqs. 2 and 3 is not too serious.

The redetermined ZPC value of aluminum hydroxide, 8.5, is identical with the value of 8.48 calculated by Eq. 3. It is somewhat lower than the value of 9.1 given in Ref. 1 and higher than the value of 7.85 calculated by Eq. 2. The ZPC values for nickel and cobalt hydroxides were recently

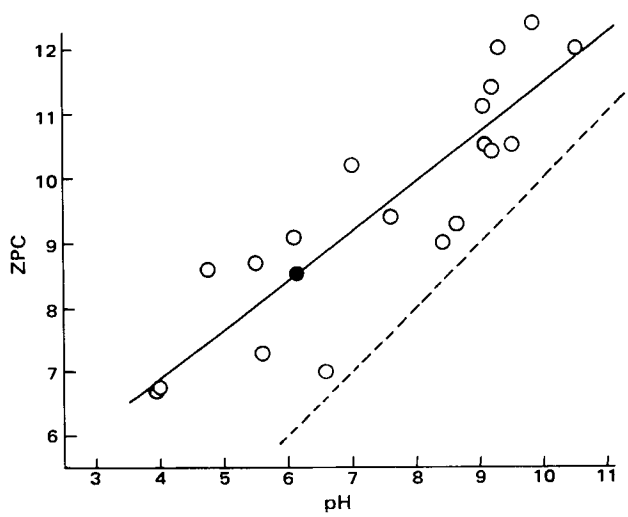

Figure 2—*The ZPC–pH_{SP} relation for slightly soluble hydroxides. The solid line represents the linear regression (Eq. 3); the broken line has a 45° or unit slope. The solid circle refers to the ZPC and pH_{SP} values of aluminum hydroxide determined in the present work.*

redetermined on thoroughly analyzed samples (11). The value found for nickel hydroxide, 11.1 ± 0.1, is identical with the value of Ref. 1 and close to the values of 10.88 and 10.72 calculated by Eqs. 2 and 3, respectively. Likewise, the ZPC value determined for cobaltous hydroxide, 11.5 ± 0.1, is nearly identical with the 11.4 value of Ref. 1 and in reasonable agreement with the values calculated by Eqs. 2 and 3, 10.97 and 10.83, respectively.

It is, therefore, possible to estimate the ZPC of an inorganic hydroxide from its solubility product or, more specifically, from the pK_{SP} or pH_{SP} value by means of Eq. 2 or 3, respectively.

DISCUSSION

The cations listed in Table I were arranged in order of increasing ZPC values which, according to Eq. 3, also corresponds to increasing pH_{SP} values. The ZPC and pH_{SP} values of the hydroxides generally increase as the valence of the cations decreases. The two tetravalent cations are at the top of the table, having the lowest ZPC and pH_{SP} values. All but two of the eight lowest ZPC values belong to tetravalent or trivalent cations, and 10 of the 11 highest ZPC values belong to divalent cations.

The ZPC of the hydroxide is always higher than its pH_{SP}. This result is shown in Fig. 2 by the fact that the straight line based on experimental data lies above the 45° or unit-slope line representing ZPC = pH_{SP}. For aluminum hydroxide, as an example, the ZPC value of 8.5 or 9.1 is 2.4 or 3.0 pH units higher than the pH_{SP} value of 6.1. At pH 6.1, the surface layer contains less hydroxide and more aluminum than the stoichiometric 3:1 ratio, while the solution contains these two ions in the exact 3:1 ratio.

There are two equivalent explanations to account for the difference between the ZPC and pH_{SP} or for the difference in the composition of the surface layer and the bulk of a hydroxide particle. Again, aluminum hydroxide is used for illustration. According to the first viewpoint, the trivalent aluminum ion is held more strongly in the aluminum hydroxide lattice than the monovalent hydroxide ion because of its higher valence. Hence, when the concentration of the two ions in solution is in the ratio of 1:3 (which occurs at pH_{SP} = 6.1), the negative hydroxide ions escape more readily from the surface layer, conferring a positive charge to the particle (12).

From an alternative viewpoint (13), a suspension of aluminum hydroxide contains the following potential-determining ions in solution: hydrated aluminum, possibly a polynuclear hydroxo complex of higher positive charge (*e.g.*, 4+), and hydroxide ions. At pH 6.1, the former two are more extensively adsorbed from solution onto an aluminum hydroxide particle than the latter, based on the number of equivalents, because of their higher charge. The greater adsorption of cationic equivalents confers a positive charge to the particle. There is a continuous dynamic adsorption–desorption equilibrium between ions in solution and ions in the surface and the Stern layer of the hydroxide particles. According to both explanations, their higher charge is responsible for the greater retention or adsorption of the cations by the surface of the hydroxide particles when compared to the hydroxide anion, based on the number of equivalents.

As more hydroxide ions are added to the solution, the concentration of dissolved aluminum ions diminishes correspondingly to maintain the solubility product constant, and the adsorption of these two ions onto the particle surface approaches the stoichiometric 3:1 ratio. When the concentration of hydroxide ions is increased from pOH = 14.0 − 6.1 = 7.9 to pOH = 14.0 − 8.5 = 5.5, equivalent amounts of hydroxide and aluminum ions are adsorbed, rendering the particle surface neutral and reducing the charge of the particle to zero. At still higher hydroxide-ion concentrations, the particle becomes negatively charged because an excess of hydroxide ions chemisorbed in the surface layer produces aluminate ions in that layer, with a 4:1 ratio of hydroxide to aluminum ions (3).

Comparison of the slopes of the least-squares line of Fig. 2 represented by Eq. 3 and of the 45° line by means of the t test (14, 15) revealed that the value of the former, namely, 0.764, differs significantly from 1.000 despite the scatter of the experimental points. Since their two intercepts are also significantly different, the two straight lines are not parallel but will converge at a very high value of pH_{SP}.

In view of the variability of the ZPC values for different batches of a single hydroxide, the following two observations are presented to document the usefulness of knowing the ζ-potential of the pure hydroxide as a function of pH and its ZPC. In manufacturing hydroxide suspensions, it is important to achieve uniformity and to minimize batch-to-batch variations in the sedimentation volume, the viscosity, the tendency to cake, and, hence, in the surface charge density or ζ-potential at the pH of the suspension and in the ZPC.

It is known from practical experience (16) that the pH values for various batches of a given hydroxide differ little or not at all from the pH_{SP} of the pure hydroxide. The ζ-potentials of these batches at the pH_{SP}, on the other hand, often differ significantly from the ζ-potential of the pure hydroxide because of frequent deviations in their ZPC values from the value of the pure hydroxide by as much as 1 pH unit or more. Greater deviations in ζ-potential at the suspension pH and in ZPC from the corresponding values of the pure hydroxide frequently cause increased batch-to-batch variability in suspension properties and commensurately larger drifts of these properties with time.

Furthermore, the sign and magnitude of the deviation of the ZPC value of a batch from that of the pure hydroxide (or the sign and magnitude of the difference between their ζ-potentials at pH_{SP}) often indicate the cause of such a deviation. For instance, the large variation among the ZPC values reported for aluminum hydroxide (1) is probably due to its tendency to form soluble complexes of high positive valence (4, 17) which are leached from the precipitate and subsequently adsorbed on its surface.

REFERENCES

(1) G. A. Parks, *Chem. Rev.*, **65,** 177 (1965).

(2) J. A. Yopps and D. W. Fuerstenau, *J. Colloid Sci.*, **19,** 61 (1964).

(3) L. A. Reber and H. Schott, in "Remington's Pharmaceutical Sciences," 15th ed., Mack Publishing Co., Easton, Pa., 1975, chap. 21.

(4) E. Matijevic, K. G. Mathai, R. H. Ottewill, and M. Kerker, *J. Phys. Chem.*, **65,** 826 (1961).

(5) E. K. Fischer, "Colloidal Dispersions," Wiley, New York, N.Y., 1950, chaps. 4 and 5.

(6) K. J. Mysels, "Introduction to Colloid Chemistry," Wiley–Interscience, New York, N.Y., 1959, chap. 4.

(7) L. G. Sillén and A. E. Martell, "Stability Constants of Metal-Ion Complexes," Special Publication No. 17, The Chemical Society, London, England, 1964.

(8) "Handbook of Chemistry and Physics," 56th ed., R. C. Weast, Ed., CRC Press, Cleveland, Ohio, 1975, p. B236.

(9) S. L. Nail, J. L. White, and S. L. Hem, *J. Pharm. Sci.*, **65,** 231 (1976).

(10) H. Schott and C. Y. Young, *ibid.*, **61,** 182 (1972).

(11) P. H. Tewari and A. B. Campbell, *J. Colloid Interface Sci.*, **55,** 531 (1976).

(12) K. J. Mysels, "Introduction to Colloid Chemistry," Wiley–Interscience, New York, N.Y., 1959, chap. 17.

(13) I. M. Kolthoff and J. J. Lingane, *J. Am. Chem. Soc.*, **58,** 1528 (1936).

(14) W. W. Cleland, in "Advances in Enzymology," vol. 29, F. F. Nord, Ed., Wiley–Interscience, New York, N.Y., 1967, p. 20.

(15) A. Goldstein, "Biostatistics, an Introductory Text," Macmillan, New York, N.Y., 1964, p. 144.

(16) H. Schott and I. J. Kazella, *J. Am. Oil Chem. Soc.*, **44,** 416 (1967).

(17) L. G. Sillén, *Pure Appl. Chem.*, **17,** 55 (1968).

ACKNOWLEDGMENTS AND ADDRESSES

Received June 9, 1976, from the *School of Pharmacy, Temple University, Philadelphia, PA 19140.*

Accepted for publication January 12, 1977.

Presented at the Basic Pharmaceutics Section, APhA Academy of Pharmaceutical Sciences, Orlando meeting, November 1976.

Polyethylene Glycol as a Binder for Tablets

R. C. SHAH ˣ, P. V. RAMAN, and P. V. SHETH

Abstract □ Polyethylene glycol 6000 was evaluated as a binder for the direct compression of 11 tablet formulations. Six formulations compressed quite well, and the resulting tablets were satisfactory in all respects. To evaluate stability, actual shelflife studies were considered more appropriate than the accelerated studies. After a shelflife of 3 years, five of the six formulations were stable. The ascorbic acid formulation was stable for up to 18 months.

Keyphrases □ Polyethylene glycol—as binder for direct compression of tablets, various drugs, stability evaluated □ Tablets—various drugs, polyethylene glycol as binder for direct compression, stability evaluated □ Stability—tablets of various drugs using polyethylene glycol as binder □ Binders—polyethylene glycol in direct compression of tablets, various drugs, stability evaluated □ Dosage forms—tablets, various drugs, polyethylene glycol as binder for direct compression, stability evaluated

Most therapeutic agents lack compression and flow characteristics required for direct compression and must be processed prior to tableting. The most widely used method of tablet preparation is wet granulation (1). This process is obviously unsuitable for heat- and solvent-labile substances. In such cases, the precompression or slugging method is applicable (1). At present, one promising alternative to granulation is direct compression. It offers several advantages, *e.g.*, ease, economy, and increased product stability and dissolution.

BACKGROUND

Few drugs possess a crystalline structure suitable (1) for direct compression. For tablets where the drug constitutes a major portion of the total weight, direct compression should not be used. Direct compression is feasible when the drug makes up only a small percentage of the total tablet. The drug is formulated with a suitable agent like pregranulated calcium phosphate (1), a mixture of sucrose powder and invert sugar[1] (1), spray-dried mannitol (1), spray-dried lactose USP[2] (2), a special form of dextrose[3] (2), lactose USP (beadlets[4]) (3), dextrose corn syrup solids[5] (3), directly compressible starch[6] (4), and microcrystalline cellulose[7] (5).

The discoloration on standing that occurs with directly compressible sugars and the moisture absorption and poor flow properties of microcrystalline cellulose and directly compressible starch are their main drawbacks.

Recently, polyethylene glycols or polyglycols, which have the basic formula of $HO(CH_2CH_2O)_nH$, have become very useful and versatile in pharmaceutical formulation due to their chemical stability, physiological inertness, and water solubility. The lower molecular weight liquids are useful solvents; the higher molecular weight solids, having a waxy appearance and various melting ranges, are ideally suited to preparing ointment and suppository bases (6).

Polyethylene glycol 6000 has been used to prepare solid dispersions of poorly water-soluble or water-insoluble drugs such as griseofulvin (7), hydrocortisone acetate (8), methyltestosterone (8), prednisolone acetate (8), and digitoxin (8) to increase dissolution, absorption, and total availability. Five poorly water-soluble liquids (9), benzonatate, clofibrate, methyl salicylate, benzyl benzoate, and *dl*-alpha-tocopheryl acetate, were converted into convenient solid dosage forms by dispersing them in polyethylene glycol 6000 as a carrier by the melting method. Solid polyethylene glycols[8] of higher molecular weights are potentially strong binders and have been used as wet granulating agents (10) and coating materials (11). Acid-neutralizing rates of the conventional antacids can be tailored by incorporation of polyethylene glycol 6000 (12).

This study was initiated to investigate the use of polyethylene glycol 6000 as a tablet binder for direct compression. When the bulk of the tablet consists of the potent drug, the process is highly economical in restricting the size and weight of the tablet to the minimum without impairing pharmaceutical elegance, hardness, weight uniformity, friability, disintegration, and dissolution.

EXPERIMENTAL

Materials and Equipment—Polyethylene glycol 6000[9] in the form of flakes, mp 60–63°, was used.

The tablets were compressed on a rotary tableting machine[10], using punches and dies ranging from 8.5 to 13.5 mm.

Tablet hardness was determined on a hardness tester[11], and disintegration times[12] were measured by the BP method using distilled water at room temperature. The tablet disintegration unit[12], using No. 50 mesh sieves for the baskets, was employed to study the dissolution patterns.

An air oven with a thermostatic control (±5°) was used to heat the formulations after pulverization through a comminuting mill[13]. The active ingredients, excipients, and magnesium stearate in the formulations complied with USP requirements. Phenprobamate[14] and glucuronolactone[15] were tested according to the specifications of their manufacturers, and clefamide[16] was tested according to the BPC.

Methods—The active ingredient with the required excipients was uniformly mixed with 8–17% of polyethylene glycol 6000. The mixture was passed through the pulverizer using a No. 20 mesh sieve. The powdered mixture was heated at 80–85° in an air oven for 3 hr. Then the heated mass was cooled and screened through a No. 12 mesh sieve by hand and blended with magnesium stearate, if necessary. For sulfisomidine tablets, a mixture of sulfisomidine and polyethylene glycol 6000 was pulverized, heated, cooled, passed through a No. 12 mesh sieve by hand, and then mixed with the excipients. About 5000 tablets were compressed at a rate of 300 tablets/min after correct adjustments of weight and pressure. The first 500 and the last 500 tablets were rejected. Eleven formulations of the tablets were evaluated.

The compressed tablets were evaluated for weight variation, hardness, content uniformity, disintegration time, and 50% dissolution time. A 2-ml aliquot of the 1 liter of dissolution medium (distilled water) was sampled every 5 min with a filter pipet for 30 min. The withdrawn samples were assayed for the active ingredients, and percent dissolved–time plots were drawn. The time for 50% dissolution of the active ingredient was determined from the respective plot. Friabilities for fresh samples were determined in a Roche-type friabilator. The tablets of each type were weighed, subjected to rotation for 20 min at 25 rpm, and then reweighed after careful dusting. The percentage of weight loss was then calculated.

Each sample was packed in 100-ml amber glass bottles having child-proof seals and subjected to a shelflife study for 3 years. Every year the samples were examined for physical appearance, hardness, disintegration time, and 50% dissolution time. Active ingredients in the formulations at the time of preparation and at the end of 3 years were determined by the official methods.

RESULTS AND DISCUSSION

Out of the 11 formulations evaluated, five formulations failed to give satisfactory tablets. The 250-mg iodochlorhydroxyquin tablets and the

[1] Dry-Tab, Nulomoline Division, Sucrest Corp., New York, NY 10005.
[2] Foremost Dairies Inc., Appleton, Wis.
[3] Cerelose, Corn Products Co., New York, N.Y.
[4] Foremost Dairies Inc., San Francisco, Calif.
[5] Catalog No. PAF-2011, Celutab, Penic and Ford Ltd., Cedar Rapids, Iowa.
[6] Sta-Rx 1500, A. E. Staley Manufacturing Co., Decatur, Ill.
[7] Avicel, F.M.C. Corp., New York, N.Y.
[8] Polyox WSR-35, WSR-205, and WSR-301, Carbon and Carbide Chemicals Co.
[9] Carbowax 6000, Union Carbide Chemicals Co., New York, NY 10017.
[10] Manesty model D3A.
[11] Monsanto, distributed by F. J. Stokes Co.
[12] Thermonic tablet disintegration machine, B. P. Standard, Campbell Electronics, Bombay-28, India.
[13] Fitzmill model D, 5000 rpm, W. T. Fitzpatric Co., Chicago, Ill.
[14] Gamaquil, Siegfried Ltd., Zofingen, Switzerland.
[15] Chugai Pharmaceuticals Ltd., Tokyo 101, Japan.
[16] Mebinol, Carlo Erba Sp.A., Milan, Italy.

Table I—Weight Variation and Friability of the Tablets at the Time of Preparation and Hardness Data of the Tablets for 3 Years

Tablet	Weight Variation[a] Mean Weight, mg	*SD*	Hardness[b], kg 0	1	2	3	Friability[c], %
Ascorbic acid	602	2.3	4	5.3	7.1	7.3	0.33
Diethylcarbamazine citrate	203	1.4	3.2	3.5	3.3	3.1	0.17
B complex	147.3	1.5	2.4	2.3	2.7	2.5	0.15
Chloramphenicol[d] (film coated)	302 (cores)	1.9	6.1	6.3	6.2	6.5	—
Tetracycline[d] (film coated)	268 (cores)	1.8	7.1	6.8	6.7	7	—
Sulfisomidine	631	3	4	3.8	4.1	4.2	0.37

[a] Average of 20 tablets. [b] Average of 10 readings taken at: 0, the time of preparation; 1, the end of the 1st year; 2, the end of the 2nd year; and 3, the end of the 3rd year. [c] Average of two readings. [d] Friability data are not given because both tablets are film coated.

400-mg phenprobamate tablets had satisfactory compressibility and hardness but very high disintegration time. The 100-mg isoniazid and 37.5-mg thiacetazone tablets showed appreciable capping. The 250-mg clefamide tablets displayed sticking to the punches and die even when 2% magnesium stearate was used. The 150-mg glucuronolactone tablets discolored on heating, resulting in mottled tablets.

The following six formulations gave satisfactory tablets:

1. Ascorbic acid tablets containing 500 mg of ascorbic acid and 100 mg of polyethylene glycol 6000.
2. Diethylcarbamazine citrate tablets containing 50 mg of diethylcarbamazine citrate, 20 mg of starch, 104 mg of lactose, 25.4 mg of polyethylene glycol 6000, and 0.6 mg of magnesium stearate.
3. B complex tablets containing 6 mg of thiamine mononitrate, 2 mg of riboflavin, 0.5 mg of pyridoxine hydrochloride, 1.5 mg of calcium pantothenate, 0.55 mg of folic acid, 25 mg of niacinamide, 50 mg of lactose, 40 mg of starch, and 24.45 mg of polyethylene glycol 6000.
4. Chloramphenicol tablets containing 250 mg of chloramphenicol, 30 mg of starch, and 30 mg of polyethylene glycol 6000.
5. Tetracycline hydrochloride tablets containing 250 mg of tetracycline hydrochloride and 20 mg of polyethylene glycol 6000.
6. Sulfisomidine tablets containing 500 mg of sulfisomidine, 37 mg of starch, 12 mg of talc, 70 mg of polyethylene glycol 6000, and 6 mg of magnesium stearate.

The granules of all satisfactory formulations were uniform and free flowing. The flow of sulfisomidine granules was not satisfactory, and it was necessary to use talc as a glidant.

The data for weight variation and friability of the fresh samples and for hardness of the fresh as well as the aged samples of the six satisfactory formulations are given in Table I. Disintegration times and 50% dissolution times for the fresh as well as the aged samples are given in Table II. From these tables, it is evident that the weight variation, hardness, friability, disintegration time, and 50% dissolution time of all fresh samples fell within the prescribed limits.

There was no significant change in hardness, disintegration time, and 50% dissolution time during the shelflife period of 3 years with diethylcarbamazine citrate, B complex, chloramphenicol (film-coated green), tetracycline hydrochloride (film-coated orange), and sulfisomidine tablets. With ascorbic acid tablets, there was a stepwise increase in hardness, disintegration time, and 50% dissolution time. The content uniformity of diethylcarbamazine citrate and B complex tablets was well within the limits prescribed in NF XIV.

Diethylcarbamazine citrate and sulfisomidine tablets maintained their original whiteness throughout the 3 years. The coatings of chloramphenicol (film-coated green) and tetracycline hydrochloride (film-coated orange) maintained their original color and gloss and remained intact without any cracks during this period. The inside cores of chloramphenicol and tetracycline hydrochloride tablets did not show any sign of discoloration. These two cores were subjected to TLC, and decomposition products were totally absent at the end of 3 years.

B complex tablets, which usually need a protective coating to prevent decomposition and development of unpleasant odor, maintained freshness throughout the 3 years. A slight deepening of the yellow color of B complex tablets at the end of 3 years was not significant. With ascorbic acid tablets, there was a progressive discoloration; the tablets were light brown at the end of 3 years.

The complete analytical data for the fresh and aged samples are given in Table III. The ascorbic acid formulation decomposed to an extent of 17% in 3 years. The other five formulations were reasonably stable for 3 years.

Table II—Disintegration and Dissolution Data of the Tablets for 3 Years

Tablet	Disintegration Time[a], sec 0	1	2	3	Time for 50% Dissolution[a], sec 0	1	2	3
Ascorbic acid	510	630	1260	1530	180	330	420	420
Diethylcarbamazine citrate	270	270	330	300	60	90	90	60
B complex	300	270	360	330	120	150	120	120
Chloramphenicol (film coated)	510	450	420	450	300	330	300	390
Tetracycline (film coated)	720	840	810	930	480	450	510	390
Sulfisomidine[b]	420	510	390	450	—	—	—	—

[a] Average of five readings taken at: 0, the time of preparation; 1, the end of the 1st year; 2, the end of the 2nd year; and 3, the end of the 3rd year. [b] It was not possible to get dissolution data for sulfisomidine tablets because a perfect sink condition could not be attained.

Table III—Assay[a] of Active Ingredients

Tablet	At Time of Preparation, %	After 3 Years, %
Ascorbic acid	107	90
Diethylcarbamazine citrate	103	105
B complex	—	—
Thiamine mononitrate	98	90
Riboflavin	97	94.5
Folic acid	103	105
Pyridoxine hydrochloride	98	103
Calcium pantothenate	105	103
Niacinamide	95	98
Chloramphenicol (film coated)	97.5	95
Tetracycline (film coated)	105.5	108
Sulfisomidine	95	96.5

[a] Average of two readings.

REFERENCES

(1) "Remington's Pharmaceutical Sciences," 15th ed., Mack Publishing Co., Easton, Pa., 1975, pp. 1583–1587.

(2) R. N. Duvall, K. T. Koshy, and R. E. Dashiell, *J. Pharm. Sci.*, **54**, 1196 (1965).

(3) N. L. Handerson and A. J. Bruno, *ibid.*, **59**, 1336 (1970).

(4) K. S. Manudhane, A. M. Contractor, H. V. Kim, and R. F. Shangraw, *ibid.*, **58**, 616 (1969).

(5) M. A. Shah and R. G. Wilson, *ibid.*, **57**, 181 (1968).

(6) "Dispensing of Medication," 7th ed., E. W. Martin, Ed., Mack Publishing Co., Easton, Pa., 1971, p. 831.

(7) W. L. Chiou and S. Riegelman, *J. Pharm. Sci.*, **58**, 1505 (1969).

(8) *Ibid.*, **60**, 1569 (1971).

(9) W. L. Chiou and L. D. Smith, *J. Pharm. Sci.*, **60**, 125 (1971).

(10) C. R. Willis, Jr., G. S. Banker, and H. G. DeKay, *ibid.*, **54**, 366 (1965).

(11) E. H. Gans and L. Chavkin, *J. Am. Pharm. Assoc., Sci. Ed.*, **43**, 483 (1954).

(12) R. G. H. Persson and J. A. Sjogren, German pat. 1,467,767 (1961); through *Chem. Abstr.*, **73**, 18480Y (1970).

ACKNOWLEDGMENTS AND ADDRESSES

Received September 22, 1976, from the *Research and Development Department, Mac Laboratories (P) Ltd., Vidyavihar, Bombay 400086, India.*

Accepted for publication January 18, 1977.

[x] To whom inquiries should be directed.

Determination of Diphenoxylate Hydrochloride and Atropine Sulfate in Solutions and Tablets

RAY L. BALLBACH, DANIEL J. BROWN, and STEPHEN M. WALTERS ×

Abstract □ Methods for the determination of diphenoxylate hydrochloride and atropine sulfate combinations in solutions and powdered tablet composites are presented. A semiautomated assay for diphenoxylate hydrochloride in individual tablets (content uniformity) also is presented. The USP XIX assays for these products are cumbersome and, in the case of solutions, inaccurate due to spectral interferences; the proposed methods offer substantial improvements in sensitivity, specificity, and speed. Results obtained by the USP and proposed methods are compared for several lots of commercial products. The accuracy and precision of the proposed methods are shown by standard recovery studies.

Keyphrases □ Diphenoxylate hydrochloride—spectrophotometric analysis in solutions and tablets containing atropine sulfate □ Atropine sulfate—GLC analysis in solutions and tablets containing diphenoxylate hydrochloride □ Spectrophotometry—analysis, diphenoxylate hydrochloride in solutions and tablets containing atropine sulfate □ GLC—analysis, atropine sulfate in solutions and tablets containing diphenoxylate hydrochloride □ Antiperistaltic agents—diphenoxylate hydrochloride, spectrophotometric analysis in solutions and tablets containing atropine sulfate □ Anticholinergic agents—atropine sulfate, GLC analysis in solutions and tablets containing diphenoxylate hydrochloride

The official USP assays (1) for diphenoxylate hydrochloride and atropine sulfate combinations in tablets and solutions have several disadvantages. The titrimetric assay for diphenoxylate hydrochloride requires the extraction of a large sample portion, which presents troublesome emulsion problems. The colorimetric assay for atropine sulfate in solution gave inaccurately high results when applied to commercial products because of appreciable background interference. The procedures are also time consuming since separate sample portions must be weighed or measured and extracted for each component.

The USP assay for diphenoxylate hydrochloride is an application of the commonly used nitrogenous organic base determination by nonaqueous titration with perchloric acid. Alternative analytical methods for this drug have not been found in literature reviews.

The *p*-dimethylaminobenzaldehyde reaction in the USP colorimetric assay for atropine sulfate also was used for the determination of tropic acid (2) and other tropane alkaloids (3). Various other reagents were reported for the colorimetric determination of atropine and related alkaloids (4–7). IR (8) and fluorometric (9) methods also were developed.

The USP methods for atropine sulfate in single-ingredient dosage forms (10) are a result of the collaborative study of a GLC method (11). Since this approach offered the sensitivity and specificity desired, its adaptation to the assay of atropine sulfate in diphenoxylate hydrochloride–atropine sulfate combination dosage forms was investigated and found suitable.

A UV spectrophotometric determination is used in the USP content uniformity analysis for diphenoxylate hydrochloride in tablets. When combined with a preliminary column chromatographic separation, this procedure was suitable for the assay of diphenoxylate hydrochloride in composited diphenoxylate hydrochloride–atropine sulfate tablets. However, UV spectrophotometry was unsuitable for the assay of diphenoxylate hydrochloride in commercial solutions. The relatively low absorptivity of the drug necessitated the extraction of a volume of solution too large for practical column chromatography. Separator extraction resulted in the coextraction of UV-absorbing interferences.

Sensitive methods for tertiary amines based on dye complex formation with various sulfonphthalein dyes were reported (12–15). This approach was subsequently investigated for the determination of diphenoxylate hydrochloride in commercial solutions. Bromphenol blue was investigated and provided good sensitivity. Reagent blanks showed baseline absorbance relative to the dye complex extraction solvent. This dye also was suitable for use in a semiautomated system for the content uniformity analysis of diphenoxylate hydrochloride in tablets.

EXPERIMENTAL

Bromphenol Blue Dye Solution—Dissolve 400 mg of bromphenol blue in 20.0 ml of 0.1 *N* NaOH in a 1-liter volumetric flask. Add 800 ml of water and 10.0 g of potassium acid phthalate. Mix to dissolve. Add 125 ml of 0.1 *N* HCl, dilute to volume with water, and mix. Prepare fresh daily.

Diphenoxylate Hydrochloride Standard Solution—Dissolve about 50 mg of USP diphenoxylate hydrochloride reference standard, accurately weighed, in chloroform contained in a 100-ml volumetric flask. Dilute to volume with chloroform and mix.

Atropine Sulfate Standard Solution—Dissolve about 15 mg of USP atropine sulfate reference standard, accurately weighed, in 0.05 *N* HCl contained in a 100-ml volumetric flask. Dilute to volume with 0.05 *N* HCl and mix.

Homatropine Hydrobromide GLC Internal Standard Solution—Dissolve about 20 mg of USP homatropine hydrobromide reference standard, accurately weighed, in 0.05 *N* HCl contained in a 100-ml volumetric flask. Dilute to volume with 0.05 *N* HCl and mix.

Solutions—*Determination of Diphenoxylate Hydrochloride*—Transfer an accurately measured volume of solution, equivalent to about 25 mg of diphenoxylate hydrochloride, to a 250-ml separator. Add sufficient water to give a total volume of 100 ml; then add exactly 1.0 ml of homatropine hydrobromide standard solution and 5 ml of 1 *N* HCl. Extract with seven 30-ml portions of chloroform. After each extraction, transfer the chloroform layer to a second separator containing 10 ml of water and reextract.

Use the same separator and 10 ml of water for each reextraction. Transfer the reextracted chloroform solutions to a 250-ml volumetric flask and dilute to volume with chloroform. Combine the aqueous wash with the original sample solution and save it for the atropine determination.

Transfer 10.0 ml of the chloroform extract, 2.0 ml of diphenoxylate hydrochloride standard solution plus 8 ml of chloroform, and 10 ml of chloroform (to serve as a blank) to three separate 125-ml separators. Add 30.0 ml of dye solution to each separator and shake vigorously for 1 min. Let the solutions stand for 5 min and then transfer the chloroform layers to separate 100-ml volumetric flasks. Reextract the aqueous layers with 10-ml portions of chloroform, adding the extracts to the respective volumetric flasks. Continue extractions until no yellow color is apparent in chloroform and then extract with one additional 10-ml portion of chloroform.

Dilute combined extracts in separate flasks to volume with chloroform. Concomitantly determine the absorbances of the solutions in 1-cm cells, at the wavelength of maximum absorbance at about 410 nm, with a suitable spectrophotometer, using chloroform as the blank. Calculate

Table I—Comparison of Results Obtained by USP and Proposed Assay Procedures for Commercial Solutions Labeled to Contain 2.5 mg of Diphenoxylate Hydrochloride (I) and 25 μg of Atropine Sulfate (II)/5 ml

Sample (Lot)	Component	Percent of Label Declaration	
		USP	Proposed
1	I	99.2	—
	II	126	102.8
2	I	100.4	—
	II	128	105.0
3	I	101.8	99.1, 101.3, 100.5 (ave. = 100.3)
	II	115.6	96.4
4	I	97.4	97.2, 97.9, 97.9 (ave. = 97.7)
	II	—	101.2, 99.6 (ave. = 99.9)

the milligrams of diphenoxylate hydrochloride in the volume of solution taken as follows: milligrams = $50C(A_u/A_s)$, where C is the concentration, in milligrams per milliliter, of the diphenoxylate hydrochloride standard solution; and A_u and A_s are the absorbances of the final sample and standard solutions, respectively, both being corrected for the reagent blank absorbance.

Determination of Atropine Sulfate—Make the aqueous solution saved from the diphenoxylate determination alkaline with 6 *N* NH_4OH. Extract with six 10-ml portions of chloroform, filtering each extract through a single 5-g portion of anhydrous sodium sulfate supported by a small pledget of glass wool in a funnel. Evaporate the solution to about 0.3 ml using a suitable evaporation device[1]. (If evaporated from an open container using positive pressure, a current of dry nitrogen is recommended to aid the evaporation.)

Pipet 1-, 2-, and 3-ml aliquots of atropine sulfate standard solution into three separate 250-ml separators. Add 100 ml of water and exactly 1.0 ml of homatropine hydrobromide standard solution to each separator, make alkaline with 6 *N* NH_4OH, and proceed as directed for the sample assay preparation beginning with: "Extract with six 10-ml portions of chloroform . . . ." Inject the solutions into a GLC system[2] as described in the USP XIX monograph for atropine sulfate injection and plot a standard curve as specified in the monograph. Read from the standard curve the quantity of atropine sulfate in the volume of solution taken.

Tablets—*Determination of Diphenoxylate Hydrochloride*—Insert a small pledget of glass wool above the stem constriction of a 20 × 2.5-cm chromatographic tube and uniformly pack with a mixture of about 2 g of chromatographic siliceous earth[3] and 1 ml of 0.05 *N* HCl. To an accurately weighed quantity of finely ground powdered tablets, equivalent to about 30 mg of diphenoxylate hydrochloride, add 0.5 ml of dimethyl sulfoxide and mix to a uniform paste. Add about 3 g of chromatographic siliceous earth, exactly 1.0 ml of homatropine hydrobromide standard solution, and 1 ml of 0.05 *N* HCl. Mix and add to the column.

Scrub the sample container with about 1 g of chromatographic siliceous earth and add the latter to the column. Place a pledget of glass wool on top and uniformly pack the sample mixture onto the column. Elute the diphenoxylate hydrochloride with 200 ml of water-saturated chloroform, added in several portions, into a 200-ml volumetric flask[4]. Then dilute to volume with chloroform. Pipet 50 ml of this solution and 15 ml of diphenoxylate hydrochloride standard solution into separate glass-stoppered erlenmeyer flasks and evaporate the solutions to dryness on a steam bath.

Dissolve each residue in 15 ml of a 1:100 solution of hydrochloric acid in methanol and concomitantly determine the absorbances of the solutions in 1-cm cells at the wavelength of maximum absorbance (about 257 nm) and at 280 nm (background absorbance) with a suitable spectrophotometer[5], using a 1:100 solution of hydrochloric acid in methanol as the blank. Calculate the milligrams of diphenoxylate hydrochloride in the quantity of tablets taken as follows: milligrams = $60C[A_u(257) - A_u(280)/A_s(257) - A_s(280)]$, where C is the concentration, in milligrams per milliliter, of the diphenoxylate hydrochloride standard solution; and $A_u(257)$, $A_u(280)$, $A_s(257)$, and $A_s(280)$ are the absorbances of the final sample (A_u) and standard (A_s) solutions at 257 and 280 nm, respectively.

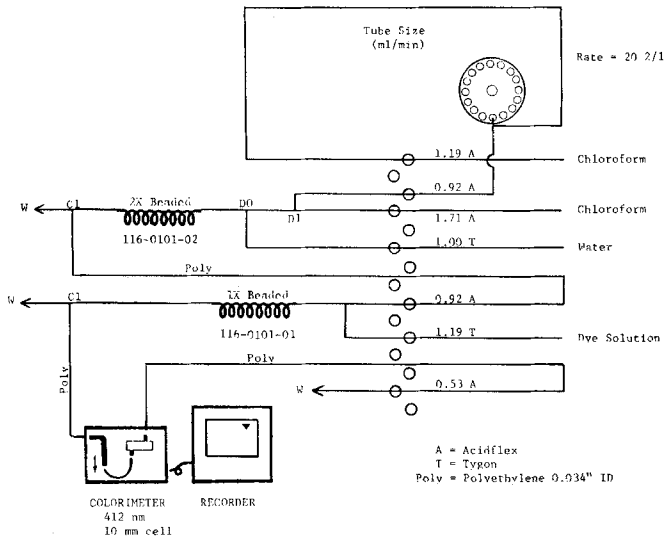

Figure 1—*Flow diagram for automated colorimetric determination of diphenoxylate hydrochloride in tablets. Both C1 fittings are silanized and oriented as shown.*

Determination of Atropine Sulfate—Insert a small pledget of glass wool above the stem constriction of a 20 × 2.5-cm chromatographic tube and place 10 g of anhydrous sodium sulfate in the tube. Place the tube under the column prepared for the determination of diphenoxylate hydrochloride tablets. Then elute atropine from the column and through the sodium sulfate with 50 ml of ammonia-saturated chloroform (prepared by mixing 4 volumes of chloroform with 1 volume of ammonium hydroxide in a separator), followed by 50 ml of water-saturated chloroform. Evaporate the combined eluates using a suitable evaporation device and proceed with the GLC determination as directed in the *Determination of Atropine Sulfate* under *Solutions*. Read from the standard curve the amount of atropine sulfate in the quantity of tablets taken.

Tablet Content Uniformity: Semiautomated Determination of Diphenoxylate Hydrochloride in Single Tablets—To each tablet and 2.50 mg of USP diphenoxylate hydrochloride reference standard contained in glass-stoppered erlenmeyer flasks, add 0.5 ml of water and disperse by placing the flasks in an ultrasonic bath. Then add 50.0 ml of chloroform and shake vigorously to dissolve the drug. Add 5 g of anhydrous sodium sulfate granules and shake. Allow the solutions to stand until the chloroform is clear, decant about 3 ml of each solution into 4-ml polyethylene sample cups, and overlay each with 10 drops of water to prevent evaporation.

The automated system[6] is assembled as shown in Fig. 1. The tablet and standard solutions are sampled at a rate of 20 cups/hr with a sample-to-wash ratio of 2:1. A sampling pattern of two standards, five samples, one standard . . . five samples, one standard is used. The first standard peak is ignored in the calculations.

The sample stream is diluted with chloroform and washed with water. The chloroform layer is resampled and mixed with the aqueous bromphenol blue dye solution. The chloroform layer, containing the diphenoxylate–dye complex, is pumped through a flowcell where the intensity of the color is measured at 412 nm[7]. The tablet content is calculated from the absorbance values.

Identification Tests—IR identification of diphenoxylate hydrochloride in solutions and tablets was done as follows. A portion of the chloroform extract prepared for the assay, equivalent to about 2.5 mg of diphenoxylate hydrochloride, was evaporated to dryness. The residue was crystallized by adding several drops of hydrochloric acid-saturated ether and again evaporated to dryness. A potassium bromide disk was prepared from a mixture of the crystalline residue with 200 mg of potassium bromide, and the IR spectrum was then compared with a reference standard prepared similarly. This technique was preferred to the USP XIX identification test since less drug was required, which eliminated the need for additional sample extraction, and the spectra obtained were of better quality.

[1] Kuderna Danish evaporative concentrator, catalog No. K-570000 (125-ml size), with graduated concentrator tube, catalog No. K-570050 (1-ml capacity), Kontes Glass Co., Vineland, NJ 08360.

[2] Perkin-Elmer model 3920.

[3] See USP XIX, p. 750.

[4] At this point, it is preferable to proceed with the elution of atropine from the column as described under *Determination of Atropine Sulfate*.

[5] Cary model 118.

[6] Technicon AutoAnalyzer system with sampler II and proportioning pump I.

[7] Beckman DB-GT spectrophotometer equipped with a 1-cm flowcell.

Table II—Comparison of Results Obtained by USP and Proposed Manual and Semiautomated Procedures for Composites of Commercial Tablets Labeled to Contain 2.5 mg of Diphenoxylate Hydrochloride (I) and 25 μg of Atropine Sulfate (II)/Tablet

Sample (Lot)	Component	Percent of Label Declaration		
		USP	Proposed Manual	Proposed Semiautomated
1	I	100.8	98.8	101.3
	II	—	110.8, 109.6 (ave. = 110.2)	—
2	I	—	100.0	100.0
	II	96.0, 99.2 (ave. = 97.6)	103.2, 102.8 (ave. = 103.0)	—
3	I	92.0	96.8	99.9
	II	—	100.8	—
4	I	—	100.4	99.1, 100.9, 102.4 (ave. = 100.8)
	II	107.2	116.0, 116.4 (ave. = 116.2)	—
5	I	99.2	94.8	95.7
	II	109.2	105.6	—
6	I	101.2	99.6	101.5
	II	—	106.4, 103.2 (ave. = 104.8)	—

Atropine was identified in the samples by comparison of the GLC retention time with that of the standard.

RESULTS AND DISCUSSION

Solution Assay Results—A comparison of results obtained using the USP and proposed assay procedures for several lots of commercial diphenoxylate hydrochloride and atropine sulfate solutions is shown in Table I. Due to obvious background interference in the spectra of the sample solutions, the USP results for atropine sulfate were considerably higher than the proposed procedure results. Samples 1 and 2 exceeded the USP upper potency limit on the basis of the USP assays.

The results for diphenoxylate hydrochloride in solutions show close agreement between the two procedures. However, the sensitivity of the proposed procedure required 1 mg of the drug for the determinative step as compared with the 100 mg required for the USP determination.

Repetitive assay results obtained for Samples 3 and 4 suggest that good precision can be expected with the proposed procedure.

Tablet Assay Results—A comparison of the results obtained for several lots of commercial tablets using the USP and proposed manual and semiautomated assays is shown in Table II. (Semiautomated assays were done on portions of powdered composites equivalent to single tablets.) The results of the proposed manual and semiautomated assays for diphenoxylate hydrochloride were in close agreement. The USP results for both diphenoxylate hydrochloride and atropine sulfate differed in some cases, primarily because of an apparent loss of the drugs as a result of emulsion problems. The lack of sensitivity of the USP titrimetric method for diphenoxylate hydrochloride is also likely to introduce error.

The semiautomated method permits rapid, unattended, multiple-tablet analysis. The proposed manual procedures require less sample and less time and are less painstaking than the USP procedures.

Table III—Recoveries from Fortified Commercial Solutions[a]

Drug	Fortified Sample		Recovery of Added Drug, %
Diphenoxylate hydrochloride, 12.5 mg added	1		101.3
	2		100.5
	3		99.8
	4		98.1
	5		100.2
		Average	100.0
		SD	1.186
Atropine sulfate, 0.1 mg added	1		98.8
	2		100.6
	3		99.3
	4		97.4
	5		103.3
		Average	99.9
		SD	2.229

[a] The amount of solution taken for fortification was one-half the amount specified in the procedure so as not to exceed the optimum detection levels of the procedure.

Standard Recovery Results—Recovery studies, using the respective proposed procedures, were made on fortified samples of commercial solutions (Table III) and on simulated mixtures of the drugs with tablet excipients based on manufacturing formulations (Table IV). Essentially 100% recoveries were achieved in all cases.

Extraction of Drugs from Commercial Products—The extraction of atropine from samples of commercial diphenoxylate hydrochloride and atropine sulfate solutions was initially attempted as in the USP assay of atropine sulfate injection (10); that is, a single separator extraction was made of each standard and sample solution. However, extraction of the drug from sample solutions was apparently suppressed by the sample matrix, resulting in considerable loss relative to the amounts extracted from standard solution. Therefore, it was necessary to conduct multiple shakeouts to assure complete and uniform extraction of the drug from all solutions.

Drying the chloroform extracts containing atropine by eluting through anhydrous sodium sulfate, prior to concentration and GLC analysis, was essential; elimination of this step resulted in low recoveries of atropine. While not thoroughly investigated, it was theorized that hydrolysis of the drug could occur while concentrating the undried chloroform extracts with heat.

The column chromatographic extraction of the drugs from commercial tablets was initially attempted without the addition of dimethyl sulfoxide to the powdered tablet samples. The results of diphenoxylate hydrochloride assays thus performed were consistently lower than the results obtained by the semiautomated method. Investigation revealed a "tailing" retention of the drug on the column, resulting in incomplete elution using a practical volume of solvent. Since this problem was not evident when eluting diphenoxylate hydrochloride standard material from the column, it was assumed that the tablet matrix was retaining the drug through interactive "binding." Preliminary trituration of the tablet material with dimethyl sulfoxide, which has been used fairly extensively as a drug solubilizing agent, eliminated this problem.

Addition of a small volume of water to individual tablets and subse-

Table IV—Analysis of Simulated Tablet Mixtures

Drug	Simulated Mixture		Recovery, %	
			Proposed Manual	Proposed Semi-automated
Diphenoxylate hydrochloride	1		99.1	101.1
	2		98.9	100.4
	3		99.9	103.1
	4		100.3	100.8
	5		100.4	99.7
		Average	99.7	101.1
		SD	0.687	1.276
Atropine sulfate	1		97.0	—
	2		99.5	—
	3		103.0	—
	4		99.3	—
	5		101.0	—
		Average	100.0	
		SD	2.221	

quent ultrasonication were necessary to effect complete dissolution of diphenoxylate hydrochloride in chloroform prior to automated analysis. In addition to hastening tablet dispersion, the water retains atropine sulfate and water-soluble excipients, which are subsequently separated from the chloroform solution.

Bromphenol Blue Dye Solution—The pH of the dye solution prepared as specified is approximately 3.4. The effect of the pH of the dye solution on the color intensity of the resultant diphenoxylate–dye complex was investigated. The intensity was fairly constant between pH 2 and 4, with a maximum at pH 3–3.5. Above pH 4, the intensity decreased rapidly.

The concentration of the dye required in the solution was similarly determined by incrementing the weight ratio of dye to diphenoxylate hydrochloride until a constant color intensity was attained for the resultant complex. The amount of dye specified in the solution prepared for the assays is an excess of about twice that needed to react completely with the anticipated concentration of drug.

GLC—The collaborative study of the GLC method for atropine (11) cited references to reports of injection site decomposition. However, the authors of the collaborative study did not observe decomposition, which they attributed to the use of commercial silanized glass wool. GLC decomposition of the atropine was observed in the present study, even when using silanized glass wool, if an excessive amount of wool was placed in the injection site end of the column. The decomposition was evidenced by the appearance of one or more small peaks preceding the atropine and homatropine peaks. By using very little glass wool or none at all, the decomposition problem can be avoided.

Linearity Studies—The standard curve prepared for the GLC determination of atropine was linear over the range of standard concentrations specified.

Conformity to Beer's law was observed when concentrations of diphenoxylate hydrochloride introduced into the automated system were varied from 70 to 150% of the tablet dosage level. The manual dye complexation procedure also provided linear absorbance readings when the drug concentrations were varied from 50 to 150% of the level anticipated in solution sample extracts.

REFERENCES

(1) "The United States Pharmacopeia," 19th rev., Mack Publishing Co., Easton, Pa., 1975, p. 158.

(2) K. R. Gottleib, *Dan. Tidsskr. Farm.*, **24,** 40 (1950).

(3) O. A. Akopyan, *Aptechn. Delo,* **7** (2), 19 (1958); *cf., ibid.*, **4,** 431 (1955).

(4) V. D. Gupta and N. M. Ferguson, *Am. J. Hosp. Pharm.*, **26,** 168 (1969).

(5) S. El-Masry and S. A. H. Khalil, *J. Pharm. Sci.*, **62,** 1332 (1973).

(6) J. Levine and J. E. Roe, *J. Assoc. Offic. Agr. Chem.*, **42,** 693 (1959).

(7) J. A. Feldman and B. J. Robb, *J. Pharm. Sci.*, **59,** 1647 (1970).

(8) "Official Methods of Analysis of the Association of Official Agricultural Chemists," 10th ed., Association of Official Agricultural Chemists, Philadelphia, Pa., 1965, p. 540 (32.035–32.036).

(9) L. A. Roberts, *J. Pharm. Sci.*, **58,** 1015 (1969).

(10) "The United States Pharmacopeia," 19th rev., Mack Publishing Co., Easton, Pa., 1975, pp. 40, 41.

(11) L. T. Grady and R. O. Zimmerer, *J. Pharm. Sci.*, **59,** 1324 (1970).

(12) B. B. Brodie and S. Udenfriend, *J. Biol. Chem.*, **158,** 705 (1945).

(13) G. Cronheim and P. A. Ware, *J. Pharmacol. Exp. Ther.*, **92,** 98 (1948).

(14) R. A. Lehman and T. Aitken, *J. Lab. Clin. Med.*, **28,** 787 (1943).

(15) N. R. Kuzel, *J. Pharm. Sci.*, **57,** 852 (1968).

ACKNOWLEDGMENTS AND ADDRESSES

Received November 22, 1976, from the *Detroit District, Public Health Service, Food and Drug Administration, Detroit, MI 48207.*

Accepted for publication January 25, 1977.

[x] To whom inquiries should be directed.

Synthesis and Anticancer Activity of Novel Cyclic *N*-Hydroxyureas

J. T. CHOU, W. T. BECK [*], T. KHWAJA [‡], K. MAYER, and E. J. LIEN [x]

Abstract □ To overcome the disadvantages of hydroxyurea in anticancer therapy such as fast biotransformation and low potency, five cyclic *N*-hydroxyureas were synthesized. A new reaction was developed to prepare the desired products from the appropriate alkyl ω-haloalkylcarbamates with hydroxylamine. This reaction probably involves a two-step mechanism: nucleophilic substitution and intramolecular cyclization. The anticancer screening tests of these compounds were done both *in vitro* using tissue culture and *in vivo*. One compound, 1-hydroxy-1,3-diazacyclohexan-2-one, had anticancer activity comparable to hydroxyurea both *in vivo* and *in vitro*.

Keyphrases □ *N*-Hydroxyureas, cyclic—various derivatives synthesized, anticancer activity evaluated □ Anticancer activity—various cyclic *N*-hydroxyureas evaluated □ Structure-activity relationships—various cyclic *N*-hydroxyureas evaluated for anticancer activity

Hydroxyurea (I) was first synthesized in 1869 (1). Although hydroxyurea was reported not to be active against sarcoma 180 (2) and RC mouse mammary carcinoma (3) in mice, it demonstrated antitumor activities against cancers such as L-1210, Walker carcinoma, P-388 leukemia, and B16 melanoma in mice (4–6). Clinically, hydroxyurea is a simple organic compound currently used as a cancer chemotherapeutic agent in the treatment of chronic myeloid leukemia and in the management of malignant melanoma, head and neck cancers, and brain tumors concomitantly with X-ray therapy (7, 8).

Hydroxyurea immediately inhibits DNA synthesis (S phase) in various systems without any or with slight effect on the synthesis and metabolism of RNA and protein (9, 10). Hydroxyurea-induced inhibition of DNA synthesis is due primarily to interference with the biosynthetic reduction of ribonucleotides to deoxyribonucleotides by inhibition of the enzyme ribonucleotide reductase (11). This inhibition blocks the formation of deoxyribonucleotides required for *de novo* DNA synthesis.

Hydroxyurea has some advantages and disadvantages

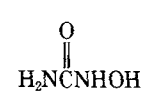

I

quent ultrasonication were necessary to effect complete dissolution of diphenoxylate hydrochloride in chloroform prior to automated analysis. In addition to hastening tablet dispersion, the water retains atropine sulfate and water-soluble excipients, which are subsequently separated from the chloroform solution.

Bromphenol Blue Dye Solution—The pH of the dye solution prepared as specified is approximately 3.4. The effect of the pH of the dye solution on the color intensity of the resultant diphenoxylate–dye complex was investigated. The intensity was fairly constant between pH 2 and 4, with a maximum at pH 3–3.5. Above pH 4, the intensity decreased rapidly.

The concentration of the dye required in the solution was similarly determined by incrementing the weight ratio of dye to diphenoxylate hydrochloride until a constant color intensity was attained for the resultant complex. The amount of dye specified in the solution prepared for the assays is an excess of about twice that needed to react completely with the anticipated concentration of drug.

GLC—The collaborative study of the GLC method for atropine (11) cited references to reports of injection site decomposition. However, the authors of the collaborative study did not observe decomposition, which they attributed to the use of commercial silanized glass wool. GLC decomposition of the atropine was observed in the present study, even when using silanized glass wool, if an excessive amount of wool was placed in the injection site end of the column. The decomposition was evidenced by the appearance of one or more small peaks preceding the atropine and homatropine peaks. By using very little glass wool or none at all, the decomposition problem can be avoided.

Linearity Studies—The standard curve prepared for the GLC determination of atropine was linear over the range of standard concentrations specified.

Conformity to Beer's law was observed when concentrations of diphenoxylate hydrochloride introduced into the automated system were varied from 70 to 150% of the tablet dosage level. The manual dye complexation procedure also provided linear absorbance readings when the drug concentrations were varied from 50 to 150% of the level anticipated in solution sample extracts.

REFERENCES

(1) "The United States Pharmacopeia," 19th rev., Mack Publishing Co., Easton, Pa., 1975, p. 158.

(2) K. R. Gottleib, *Dan. Tidsskr. Farm.*, **24,** 40 (1950).

(3) O. A. Akopyan, *Aptechn. Delo,* **7** (2), 19 (1958); *cf., ibid.*, **4,** 431 (1955).

(4) V. D. Gupta and N. M. Ferguson, *Am. J. Hosp. Pharm.*, **26,** 168 (1969).

(5) S. El-Masry and S. A. H. Khalil, *J. Pharm. Sci.*, **62,** 1332 (1973).

(6) J. Levine and J. E. Roe, *J. Assoc. Offic. Agr. Chem.*, **42,** 693 (1959).

(7) J. A. Feldman and B. J. Robb, *J. Pharm. Sci.*, **59,** 1647 (1970).

(8) "Official Methods of Analysis of the Association of Official Agricultural Chemists," 10th ed., Association of Official Agricultural Chemists, Philadelphia, Pa., 1965, p. 540 (32.035–32.036).

(9) L. A. Roberts, *J. Pharm. Sci.*, **58,** 1015 (1969).

(10) "The United States Pharmacopeia," 19th rev., Mack Publishing Co., Easton, Pa., 1975, pp. 40, 41.

(11) L. T. Grady and R. O. Zimmerer, *J. Pharm. Sci.*, **59,** 1324 (1970).

(12) B. B. Brodie and S. Udenfriend, *J. Biol. Chem.*, **158,** 705 (1945).

(13) G. Cronheim and P. A. Ware, *J. Pharmacol. Exp. Ther.*, **92,** 98 (1948).

(14) R. A. Lehman and T. Aitken, *J. Lab. Clin. Med.*, **28,** 787 (1943).

(15) N. R. Kuzel, *J. Pharm. Sci.*, **57,** 852 (1968).

ACKNOWLEDGMENTS AND ADDRESSES

Received November 22, 1976, from the *Detroit District, Public Health Service, Food and Drug Administration, Detroit, MI 48207.*

Accepted for publication January 25, 1977.

[x] To whom inquiries should be directed.

Synthesis and Anticancer Activity of Novel Cyclic *N*-Hydroxyureas

J. T. CHOU, W. T. BECK [*], T. KHWAJA [‡], K. MAYER, and E. J. LIEN [x]

Abstract □ To overcome the disadvantages of hydroxyurea in anticancer therapy such as fast biotransformation and low potency, five cyclic *N*-hydroxyureas were synthesized. A new reaction was developed to prepare the desired products from the appropriate alkyl ω-haloalkylcarbamates with hydroxylamine. This reaction probably involves a two-step mechanism: nucleophilic substitution and intramolecular cyclization. The anticancer screening tests of these compounds were done both *in vitro* using tissue culture and *in vivo*. One compound, 1-hydroxy-1,3-diazacyclohexan-2-one, had anticancer activity comparable to hydroxyurea both *in vivo* and *in vitro*.

Keyphrases □ *N*-Hydroxyureas, cyclic—various derivatives synthesized, anticancer activity evaluated □ Anticancer activity—various cyclic *N*-hydroxyureas evaluated □ Structure-activity relationships—various cyclic *N*-hydroxyureas evaluated for anticancer activity

Hydroxyurea (I) was first synthesized in 1869 (1). Although hydroxyurea was reported not to be active against sarcoma 180 (2) and RC mouse mammary carcinoma (3) in mice, it demonstrated antitumor activities against cancers such as L-1210, Walker carcinoma, P-388 leukemia, and B16 melanoma in mice (4–6). Clinically, hydroxyurea is a simple organic compound currently used as a cancer chemotherapeutic agent in the treatment of chronic myeloid leukemia and in the management of malignant melanoma, head and neck cancers, and brain tumors concomitantly with X-ray therapy (7, 8).

Hydroxyurea immediately inhibits DNA synthesis (S phase) in various systems without any or with slight effect on the synthesis and metabolism of RNA and protein (9, 10). Hydroxyurea-induced inhibition of DNA synthesis is due primarily to interference with the biosynthetic reduction of ribonucleotides to deoxyribonucleotides by inhibition of the enzyme ribonucleotide reductase (11). This inhibition blocks the formation of deoxyribonucleotides required for *de novo* DNA synthesis.

Hydroxyurea has some advantages and disadvantages

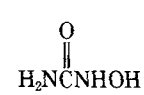

I

Table I—Physical Properties of Cyclic *N*-Hydroxyureas

Compound	Formula	Melting Point[a] (Corrected)	Yield[b], %	Analysis, %[c] Calc.	Found
V*a*	$C_4H_8N_2O_2$	176.0–177.5°	18.5	C 41.37	41.98
				H 6.95	6.94
				N 24.02	24.12
V*b*	$C_5H_{10}N_2O_2$	115.0–117.0°	10.1	C 46.14	46.47
				H 7.75	7.52
				N 21.52	21.83
V*c*	$C_6H_{12}N_2O_2$	69.0–71.0°	<2	C 49.98	50.26
				H 8.39	8.67
				N 19.43	19.21
VI	$C_4H_7N_3O_3$	95.0–97.0° dec.	45.7	C 33.10	32.87
				H 5.53	4.86
				N 28.96	29.14
VII	$C_5H_9NO_2$	42–44°	16.5	C 52.16	50.71
				H 7.88	7.89
				N 12.17	11.91

[a] Melting points were determined using a Thomas-Hoover capillary melting-point apparatus, Arthur H. Thomas Co., Philadelphia, Pa. [b] The percentage yield of the final step. [c] Performed by C. F. Geiger, Ontario, Calif.

as an anticancer drug. It has low toxicity (12), and no carcinogenicity or mutagenicity has been reported[1] (13–18). The disadvantages of hydroxyurea are that frequent relatively high doses are needed and rapid biotransformation occurs. The rapid elimination from the body and short half-life (19–22) are due to its high polarity (water solubility) and rapid hydrolysis. Some side effects such as GI disturbance and bone marrow depression were observed (4, 21).

Since medium size cyclic compounds (five- to seven-membered rings) are usually more resistant to hydrolysis than open-chain compounds because of the blockade of nucleophilic attack and since cyclic *N*-hydroxyureas should be more lipophilic than hydroxyurea itself, the cyclic *N*-hydroxyureas possessing the essential pharmacophore [C(=O)NOH] (23) may have higher intrinsic activity and a longer duration of action than hydroxyurea. This paper reports the results of such an investigation.

EXPERIMENTAL

Synthesis—The synthesis of six-membered cyclic *N*-hydroxyureas involved a multiple-step reaction (Scheme I). The primary amines (II, X = chloro or bromo) were obtained commercially, but the required secondary amines (III) were prepared from the corresponding primary amines (24, 25). The intermediate carbamates (IV, R_2 = methyl or ethyl) were prepared by the method of Hartman and Brethen (26).

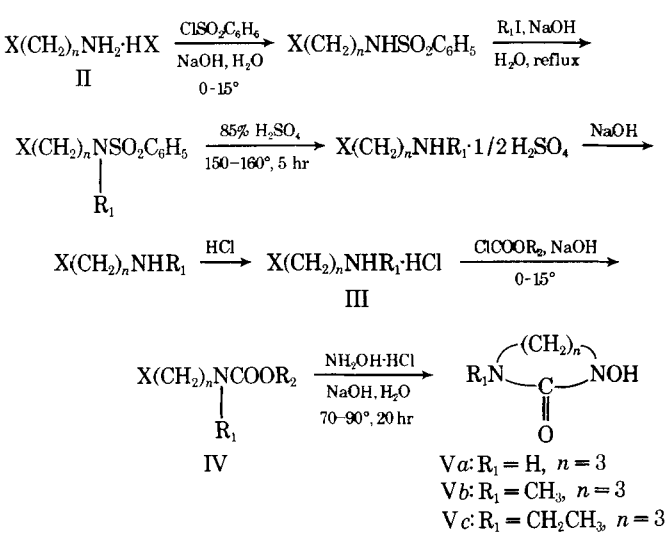

Scheme I

Six-membered cyclic *N'*-nitroso-*N*-hydroxyurea (VI) was synthesized by the nitrosation of the parent compound (V*a*) (27, 28) (Scheme II). The *N*-hydroxylactam, 1-hydroxy-5-methyl-2-pyrrolidinone (VII), was prepared by the reductive cyclization (29) from methyl 4-nitropentanoate (Scheme III). The identities of the desired products were unequivocally established by IR, NMR, and elemental analyses (Table I).

General Procedure for Carbamates (IV)—Fifty grams (0.38 mole) of 3-chloropropylamine hydrochloride was dissolved in 120 ml of distilled water in a 500-ml, three-necked, round-bottom flask equipped with a magnetic stirrer. The solution was cooled to 0° in an ice bath with stirring. Sodium hydroxide, 30.7 g (0.68 mole), was dissolved in 30 ml of distilled water and cooled to 0°. The base solution was added to the amine solution slowly, and the temperature was kept at around 5°. Then 41.6 g (0.38 mole) of ethyl chloroformate was added slowly to maintain the reaction mixture between 5 and 15° over 45 min.

Stirring was continued for 2 hr at the ice-bath temperature and then for 2 hr at room temperature. Two layers separated upon standing. The organic layer (upper layer) was separated from the aqueous phase. The aqueous phase was extracted with 50 ml of chloroform three times. These chloroform extracts were combined and evaporated to dryness under reduced pressure, and the residue was combined with the organic phase. Ethyl *N*-3-chloropropylcarbamate was purified by fractional vacuum distillation.

Other intermediate carbamates also were prepared by the same procedure.

1-Hydroxy-1,3-diazacyclohexan-2-one (V*a*)—Fifty-seven grams (0.82 mole) of hydroxylamine hydrochloride was dissolved in 100 ml of distilled water in a 1-liter, three-necked, round-bottom flask equipped with a magnetic stirrer, and the solution was cooled to 0°. The sodium hydroxide solution was added to the hydroxylamine hydrochloride solution slowly to keep the temperature at around 5°. Then 83.4 g (0.55 mole) of methyl *N*-3-chloropropylcarbamate was added with vigorous stirring. The reaction mixture was kept at 0° for 2 hr, heated to 70°

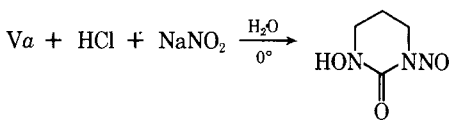

Scheme II

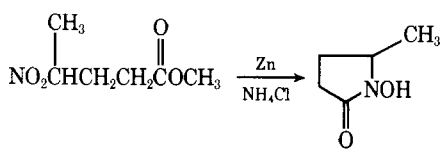

Scheme III

[1] W. F. Benedict, Childrens Hospital, Los Angeles, Calif., personal communication.

Table II—Effect of V$_a$ against Lymphoid Leukemia L-1210 in BDF$_1$ Female Mice[a]

Treatment (Intraperitoneal)	Mean Survival (days), Treated/Control	Survival Range, days	Weight Change on Day 5, g	T/C
V*a*				
1000 mg/kg, qd (1–9)	13.17/8.40	13–14	−0.17	1.57
1500 mg/kg, qd (1–9)	13.50/8.40	13–15	−1.00	1.61
3000 mg/kg, qd (1–3)	14.50/9.67	14–15	−5.50	1.50[b]
I				
1000 mg/kg, qd (1–9)	15.17/8.40	15–16	−0.50	1.81
3000 mg/kg, qd (1–3)	14.00/9.67	14[c]	−5.50	1.45[b]

[a] Work performed at the Animal Tumor Research Facility of the LAC–USC Cancer Center. Groups of six animals were given 10^5 cells each intraperitoneally on Day 0. Drug treatment was started 24 hr after the transplants. Controls (10) received only isotonic sterile saline. [b] Two animals per treated group and six animals per control group were used because of the limited amount of V*a* available. [c] One animal died on Day 3 postinjection.

continuously for 18 hr over a water bath, and then cooled to 0°; the pH was adjusted to 4–5 by using concentrated hydrochloric acid.

For the removal of inorganic salts, the reaction mixture was poured into 1.5 liters of absolute ethanol at 60° and kept at this temperature for 15 min. This mixture was left in the refrigerator overnight and filtered. The filtrate was evaporated to dryness *in vacuo*, and a viscous liquid was obtained. Dry column chromatography (30) was used to isolate the desired product. The syrupy liquid was dissolved in a minimum amount of absolute ethanol and passed through a column packed with silica gel[2]. The gradient elution technique was used from pure chloroform to 40% ethanol in chloroform.

Silica gel thin-layer plates[3] were used for the detection of the content of each fraction. The desired product was obtained from a 10% ethanol in chloroform elution after the solvent was evaporated. Slightly pink-colored crystals were obtained and recrystallized from absolute ethanol.

1-Hydroxy-3-methyl-1,3-diazacyclohexan-2-one (V*b*)—This compound was prepared by the same procedure as V*a*, except that it was obtained from dry column chromatography using 5% ethanol–chloroform for elution. It was also recrystallized from absolute ethanol.

1-Hydroxy-3-ethyl-1,3-diazacyclohexan-2-one (V*c*)—This compound was prepared by the same procedure as V*a*, except that the desired product was obtained after passage through three columns. It eluted with pure chloroform from the first silica gel column. It also eluted with pure chloroform from the second alumina column. Finally, it eluted from the third silica gel column when 60% chloroform in hexane was used. It was analytically pure without further recrystallization.

1-Hydroxy-3-nitroso-1,3-diazacyclohexan-2-one (VI)—To a solution of 1-hydroxy-1,3-diazacyclohexan-2-one (7 g, 60 mmoles) in dilute hydrochloric acid at 0° was added a solution of sodium nitrite (4.4 g, 63 mmoles) slowly, with stirring, for 2 hr. The mixture was then left in a freezer for 2 hr. The solid residue was filtered and washed with cold water. The yellow residue was collected and dried *in vacuo* at 60° for 4 hr.

1-Hydroxy-5-methyl-2-pyrrolidinone (VII)—In a 150-ml round-bottom flask, 10.2 g (63.3 mmoles) of methyl 4-nitropentanoate and 3.4 g (63.3 mmoles) of ammonium chloride were dissolved in 80 ml of 50% ethanol. Zinc dust, 15.9 g (242.7 mmoles), was added slowly to this mixture over 20 min with stirring. The mixture was cooled in an ice bath for 30 min with continuous stirring and then heated over a water bath at 40° for 4 hr. It was then filtered, and the filtrate was evaporated to a viscous liquid under reduced pressure. This syrupy mixture was dissolved in 30 ml of 2 *N* HCl and then extracted with 50 ml of chloroform three times.

The extract was evaporated to dryness using a rotary evaporator. The residue was dissolved in a small amount of chloroform and passed through a silica gel column. Chloroform was used as an eluent. All ferric chloride-positive fractions were chromatographed on silica gel TLC plates. All TLC-identical fractions were combined and extracted with chloroform; the solvent was evaporated under reduced pressure. The residue was further purified by the sublimation technique.

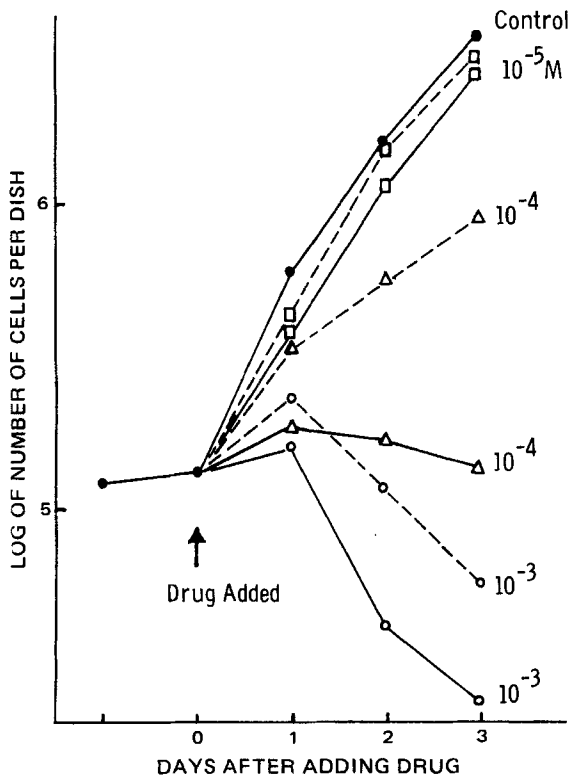

Figure 1—*Growth curve of 3T3 cells with and without drugs. The dead cells did not adhere to the plate and were washed out before counting. Key: ——, I; and - - -, V*a.

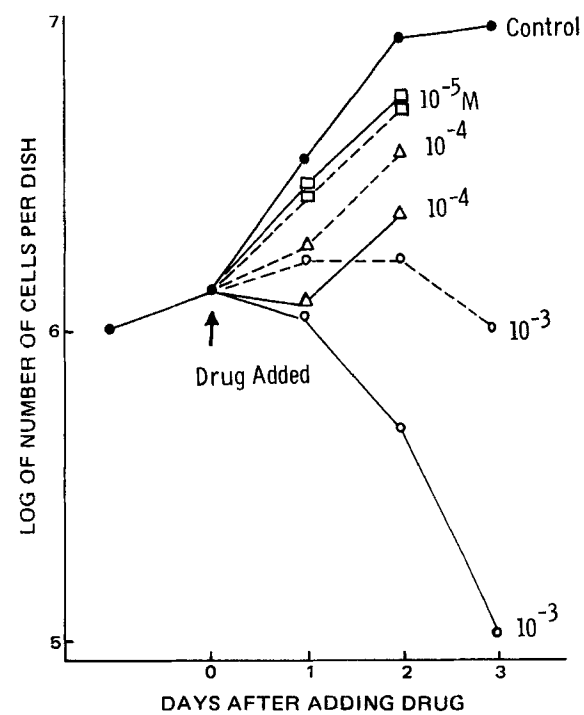

Figure 2—*Growth curve of H-35 cells with and without drugs. The dead cells were washed out and not counted. Key: ——, I; and - - -, V*a.

[2] Woelm dry-column chromatography, ICN.
[3] Eastman Kodak.

Table III—Effect of Cyclic *N*-Hydroxyureas against Lymphoid Leukemia L-1210 (Intraperitoneal) in CDF_1 Female Mice[a]

Treatment (Intraperitoneal)	Mean Survival (days), Treated/ Control	Weight Change on Day 5, g	T/C
V*a*			
400 mg/kg, q4d (1, 5, 9)	9.3/8.3	−1.4	1.12
200 mg/kg, q4d (1, 5, 9)	8.3/8.3	−0.4	1.00
100 mg/kg, q4d (1, 5, 9)	8.7/8.3	−0.2	1.04
V*b*			
600 mg/kg, qd (1–7)	9.0/9.0	−1.1	1.00
300 mg/kg, qd (1–7)	9.0/9.0	−0.5	1.00
150 mg/kg, qd (1–7)	8.5/9.0	−0.3	0.94
75 mg/kg, qd (1–7)	8.3/9.0	−0.2	0.92
37.5 mg/kg, qd (1–7)	8.3/9.0	−0.3	0.94

[a] National Cancer Institute supplied data.

***In Vitro* Anticancer Screening Tests**[4]—The inhibition of cell growth of one fibroblastic and two tumor cell lines in tissue culture was used for *in vitro* tests. The cell lines were BALB/c 3T3 mouse embryo fibroblasts clone 42, Reuber H-35 rat hepatoma, and human Wilms' tumor cells.

BALB/c 3T3 mouse fibroblasts were grown in Dulbecco's modified minimal essential medium (MEM) supplemented with 10% calf serum. The H-35 cells were grown in Eagle's minimal essential medium supplemented with sodium pyruvate, fourfold amino acids, vitamins, and 13% heat-inactivated fetal calf serum. Human Wilms' tumor cells (TuWi) were grown in medium 199 supplemented with 5% calf serum and 5% heat-inactivated fetal calf serum.

All cells were grown in 60- × 15-mm plastic dishes in a humidified incubator in an atmosphere of 95% air–5% CO_2 at 37°. Drug solutions were added to the cells at the beginning or in the middle of the logarithmic growth phase. Following a saline wash and mild trypsinization, the total cells per dish were counted with a hemocytometer under the microscope each day during the experimental period (Figs. 1–3).

Calculation of pI_{50}—The I_{50} is the molar concentration of the drug that inhibits 50% of normal cell growth. The I_{50}'s were calculated from the best-fit regression equations derived *via* the method of least squares using the probit-log of the concentration method (31). The value of pI_{50} is equal to $-\log I_{50}$. The larger the pI_{50} is, the more potent the drug is.

***In Vivo* Anticancer Screening Tests**—For *in vivo* studies, animals were obtained commercially[5]. The L-1210 leukemia[6] was maintained by serial transplants in DBA/2 mice. The *in vivo* anticancer screening tests were performed according to the National Cancer Institute screening protocol (32) (Tables II and III).

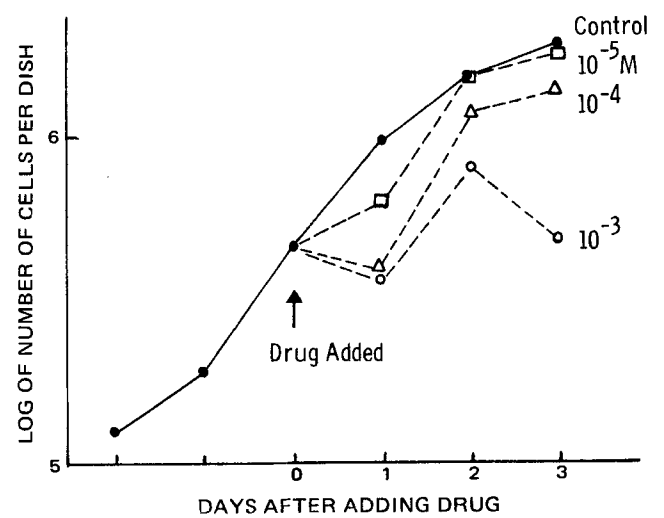

Figure 3—*Growth curve of Wilms' human tumor cells with (- - -) and without (—) the drug (Va).*

[4] All growth media were purchased from Grand Island Biological Co., Santa Clara, Calif.

[5] Simenson Laboratories, Gilroy, Calif.

[6] From Dr. G. R. Laster, Jr., Southern Research Institute, Birmingham, Ala.

Table IV—*In Vitro* Inhibition of BALB 3T3 Fibroblast Cell Growth by I and V*a*

Day	$pI_{50} \pm SE$ I	$pI_{50} \pm SE$ V*a*
1	4.61 ± 0.82	3.66 ± 0.85
2	4.70 ± 0.37	4.01 ± 0.29
3	4.72 ± 0.25	4.31 ± 0.29
ΔpI_{50} (Day 3 − Day 2)	0.02	0.30

RESULTS AND DISCUSSION

After many unsuccessful trials, the desired products were finally obtained by a new reaction. This reaction may involve a two-step mechanism (29, 33): (*a*) nucleophilic substitution (Scheme IV) and (*b*) intramolecular cyclization (Scheme V). The yield decreases as the alkyl group becomes bulkier, primarily due to the steric hindrance that decreases or prevents the cyclization (Table I).

Compound VII was synthesized by reductive cyclization, *i.e.*, reduction of NO_2 to NHOH, followed by intramolecular cyclization (Scheme VI).

The growth curves of three cell lines with or without the drug are shown in Figs. 1–3. The pI_{50}'s for hydroxyurea and cyclic *N*-hydroxyureas are shown in Tables IV–VII. Morphologically, there is no difference between control cells and drug-treated cells in these three cell lines examined under the microscope.

These drugs were added to the logarithmic growth phase (Figs. 1–3) either at the beginning or the middle of this phase. However, if the cells in the plateau or other nondividing phase are used, the accuracy in assessment of antitumor activity becomes difficult (34). In the present experiments, the cell number declined 2 or 3 days after the drug solutions were added to the cells, indicating drug cytotoxicity. Hydroxyurea and the cyclic *N*-hydroxyureas were more cytotoxic toward fast growing cells such as H-35 and 3T3 cells than toward slower growing cells such as the Wilms' tumor line, as indicated by the lower pI_{50} against TuWi cells.

Compound V*a* was comparable to hydroxyurea in cytotoxicity on H-35 and 3T3 cells, as indicated by the close pI_{50} values. From Tables VI and VII, one can see a more favorable ΔpI_{50} value, reflecting greater stability or persistence of cytoxicity of the cyclic compounds.

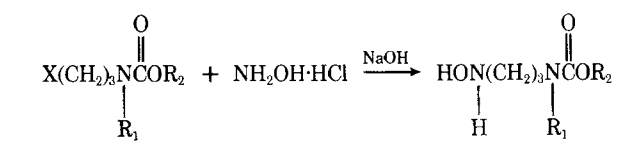

Scheme IV

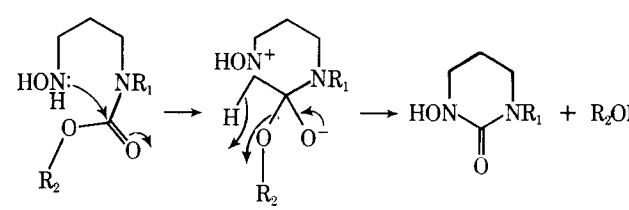

Scheme V

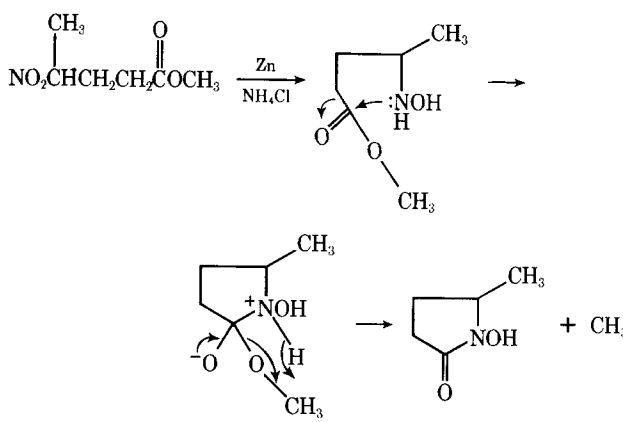

Scheme VI

Table V—*In Vitro* Inhibition of Rat H-35 Hepatoma Cell Growth by Hydroxyurea and Cyclic *N*-Hydroxyureas[a]

Compound	pI_{50} Day 1[b]	pI_{50} Day 2[b]	pI_{50} Day 3[b]
I	≃3	3.97 ± 0.32[c]	4.56 ± 0.32[c]
V*a*	≃3	3.33 ± 0.36	4.05 ± 0.35
V*b*	<3	3.29 ± 0.49	3.89 ± 0.39
V*c*	<3	2.96 ± 0.86	3.14 ± 0.63
VI	<3	3.35 ± 0.52	3.61 ± 0.43
VII	<3	2.43 ± 0.71	3.18 ± 0.58

[a] The pI_{50} values were obtained from the same experiment. [b] Days after adding the drugs. [c] Standard error.

Two cyclic compounds, V*a* and V*b*, tested by the National Cancer Institute, were not active against L-1210 at dose levels up to 400 and 600 mg/kg, respectively. Nevertheless, in this study V*a* at a dosage of 1000–3000 mg/kg (Table II) showed a highly significant activity against leukemia L-1210; this activity was comparable to hydroxyurea used as a positive control. Even though hydroxyurea itself was reported to be very active against L-1210 *in vivo* (5), it is known that the effectiveness of hydroxyurea is highly schedule dependent (35). Perhaps these new cyclic *N*-hydroxyureas (V*a* and V*b*) are also schedule dependent. The dose regimen used by the National Cancer Institute might not be frequent enough to show a definite anticancer activity.

Compound V*a* had comparable cytotoxicity *in vitro* and similar anticancer activity *in vivo* as compared to hydroxyurea. However, the negative results found by the National Cancer Institute appear to be due to the use of a suboptimal dose regimen. The other cyclic *N*-hydroxyureas apparently are less cytotoxic than either hydroxyurea or V*a*. Hydroxyurea always showed a lower ΔpI_{50} (Day 3 − Day 2) than the cyclic compounds (Tables IV, VI, and VII), reflecting the better persistence of the cyclic compounds under the testing conditions used.

A positive correlation between the log of molecular weight (mol. wt.) and the potency of several series of clinically used drugs, including anticancer drugs, was shown recently (35). The best-fit regression line for 15 different anticancer drugs was derived by using simple regression analysis. The equation is:

$$\log 1/C = 3.411 \log \text{mol. wt.} - 2.559$$

$$n = 15, r = 0.786, s = 0.837 \qquad \text{(Eq. 1)}$$

That is, the higher the molecular weight, the more potent the drug will be if the molecule fits into the receptor site and if the drug is active.

The optimal lipophilicity, as expressed by the logarithm of the 1-octanol–water partition coefficient (log *P*) of some anticancer drugs in an animal study, lies between 1 and −1 and the optimal log *P*'s for different series of anticancer drugs are different (36, 37). The parent compound (V*a*) of cyclic *N*-hydroxyurea is more cytotoxic than the *N'*-methylated derivative (V*b*), and V*b* is more cytotoxic than the *N'*-ethylated derivative (V*c*). These findings reflect a negative dependence on the lipophilicity and may indicate that hydrophilic character is necessary to have higher cytotoxicity for this series of compounds. In other words, the benefit derived from the greater stability of the cyclic structure may be offset by the undesired higher lipophilicity. Alternatively, there may be a very restricted bulk tolerance on the *N'*-substituent.

From this limited amount of information and previous findings (35), it appears that the *N*-hydroxyurea derivatives with substantially higher molecular weights and polar functional groups to maintain low lipophilicity (log *P*) may be worth pursuing.

Table VI—*In Vitro* Inhibition of Hepatoma H-35 Cell Growth by I and V*a*[a]

Day	pI_{50}[b] ± *SE* V*a*	pI_{50}[b] ± *SE* I
1	3.51 ± 0.59	3.80 ± 0.52
	2.87 ± 2.28	—
	3.23 ± 0.46	—
2	4.52 ± 0.68	4.63 ± 0.43
	3.43 ± 0.61	—
	3.51 ± 0.35	4.24 ± 0.35
3	—	—
	4.14 ± 0.52	—
	3.80 ± 0.34	4.06 ± 0.27
ΔpI_{50} (Day 3 − Day 2)[c]	+0.29	−0.18[c]

[a] Different experiments from Table V. [b] The pI_{50} values were obtained from three different experiments. [c] Calculated from only one experiment.

Table VII—*In Vitro* Inhibition of Wilms' Human Tumor Cell Growth by Hydroxyurea and Cyclic *N*-Hydroxyureas

Compound	pI_{50} Day 1[a]	pI_{50} Day 2[a]	pI_{50} Day 3[a]	ΔpI_{50} (Day 3 − Day 2)
I[b]	<3	4.29 ± 0.88	3.77 ± 0.38	−0.52
V*b*[b]	<3	2.48 ± 3.32	2.52 ± 1.12	0.04
VI[b]	<3	3.01 ± 1.13	3.70 ± 0.84	0.69
V*a*[c]	<3	<3	≃3.00	—

[a] Days after adding the drug. [b] The pI_{50} value of these compounds were obtained from the same experiment. [c] The pI_{50} value was obtained from a different experiment.

REFERENCES

(1) W. F. C. Dresler and R. Stein, *Justus Liebigs Ann. Chem.*, **150,** 242 (1869).

(2) C. C. Stock, D. A. Clarke, F. S. Philips, R. K. Barclay, and S. A. Myron, *Cancer Res.*, **20** (5), part 2, 270 (1960).

(3) G. S. Tarnowski and C. C. Stock, *Cancer Res.*, **18** (8), part 2, 45 (1958).

(4) W. G. Thurman, C. Bloedow, C. D. Howe, W. C. Levin, P. Davis, M. Lane, M. P. Sullivan, and K. M. Friffith, *Cancer Chemother. Rep.*, **29,** 103 (1963).

(5) B. Stearns, K. A. Losee, and J. Bernstein, *J. Med. Chem.*, **6,** 201 (1963).

(6) A. Goldin and K. Carter, in "Cancer Medicine," J. F. Holland and E. Frei, III, Eds., Lea & Febiger, Philadelphia, Pa., 1973, p. 620.

(7) E. S. Greenwald, "Cancer Chemotherapy," 2nd ed., Medical Examination Publishing Co., New York, N.Y., 1973, pp. 250–252.

(8) H. Lipshutz and H. J. Lerner, *Am. Surg.* **126,** 519 (1973).

(9) C. W. Young and S. Hodas, *Science,* **146,** 1172 (1964).

(10) C. W. Young, G. Schochetman, and D. A. Karnofsky, *Cancer Res.*, **27,** 526 (1967).

(11) J. C. Theiss and G. A. Fischer, *Biochem. Pharmacol.*, **25,** 73 (1976).

(12) G. R. Gale, *J. Natl. Cancer Inst.*, **38,** 51 (1967).

(13) R. S. Yamamoto, E. K. Weisberger, and J. Korzis, *Proc. Soc. Exp. Biol. Med.*, **124,** 1217 (1967).

(14) S. S. Mirvisch, L. Chen, N. Haran-Ghera, and I. Berenblum, *Int. J. Cancer,* **4,** 318 (1969).

(15) I. Muranyi-Kovacs and G. Rudali, *Rev. Eur. Etudes Clin. Biol.*, **17,** 93 (1972).

(16) H. Huberman and C. Heidelberger, *Mutation Res.*, **14,** 130 (1972).

(17) S. S. Epstein and H. Shafner, *Nature,* **219,** 385 (1968).

(18) S. S. Epstein, E. Arnold, J. Andrea, W. Bass, and Y. Bishop, *Toxicol. Appl. Pharmacol.*, **23,** 288 (1972).

(19) J. D. Davidson and T. S. Winter, *Cancer Chemother. Rep.*, **27,** 97 (1963).

(20) E. Fabricus and M. F. Rajewsky, *Rev. Eur. Etudes Clin. Biol.*, **16,** 679 (1971).

(21) R. H. Adamson, S. L. Ague, S. M. Hess, and J. D. Davidson, *J. Pharmacol. Exp. Ther.*, **150,** 322 (1965).

(22) G. L. Beckloff, *Clin. Trial. J.*, **4,** 873 (1967).

(23) C. W. Young, G. Schochetman, S. Hodas, and M. E. Balis, *Cancer Res.*, **27,** part 1, 535 (1967).

(24) W. H. Carothers, C. F. Brickford, and G. J. Hurwitz, *J. Am. Chem. Soc.*, **49,** 2908 (1927).

(25) D. Klamann and G. Hofbauer, *Monatsh. Chem.*, **84,** 62 (1953).

(26) W. W. Hartman and M. R. Brethen, "Organic Synthesis," coll. vol. II, Wiley, New York, N.Y., 1943, p. 278.

(27) T. P. Johnston, G. S. McClaeb, and J. A. Montgomery, *J. Med. Chem.*, **6,** 669 (1963).

(28) J. G. Michels, *J. Org. Chem.*, **25,** 2246 (1960).

(29) R. Bonnett, R. F. C. Brown, V. M. Clark, I. O. Sutherland, and A. Todd, *J. Chem. Soc.*, **1959,** 2100.

(30) B. Loev and M. M. Goodman, *Intrasci. Chem. Rep.*, **4,** 283 (1970).

(31) L. C. Miller and M. L. Tainter, *Proc. Soc. Exp. Biol. Med.*, **57,** 261 (1944).

(32) R. I. Geran, N. H. Greenberg, M. M. MacDonald, A. M. Schu-

macher, and B. J. Abbott, *Cancer Chemother. Rep.*, **3** (2), part 3, 1 (1972).
(33) P. Frankhauser and M. Brenner, *Helv. Chim. Acta*, **53**, 2298 (1970).
(34) T. A. Connors and B. J. Phillips, *Biochem. Pharmacol.*, **24**, 2217 (1975).
(35) E. J. Lien, paper presented at the APhA Academy of Pharmaceutical Sciences, Orlando meeting, Nov. 1976.
(36) C. Hansch, N. Smith, R. Engle, and H. Wood, *Cancer Chemother. Rep.*, **56**, part 1, 443 (1972).
(37) V. A. Levin and P. Kabra, *ibid.*, **58**, part 1, 787 (1974).

ACKNOWLEDGMENTS AND ADDRESSES

Received November 16, 1976, from the *School of Pharmacy and LAC-USC Cancer Center, University of Southern California, Los Angeles, CA 90033.*
Accepted for publication February 10, 1977.
Presented in part at the APhA Academy of Pharmaceutical Sciences, New Orleans meeting, April 1976.
Abstracted in part from the dissertation submitted by J. T. Chou to the University of Southern California in partial fulfillment of the Doctor of Philosophy degree requirements.
Supported in part by LAC-USC Cancer Center Grant CA 14089 from the National Cancer Institute and pilot project Grant ACS IN-21 from the American Cancer Society.
The authors thank Dr. Harry B. Wood, Jr., of the National Cancer Institute for part of the *in vivo* data and Mr. Ahmed EidAwad for his initial assistance in the tissue culture study. They also thank Ms. J. Varven for excellent technical assistance in animal model studies. E. J. Lien acknowledges the Lederle Pharmacy Faculty Award (1976).
* Present address: St. Jude Children's Research Hospital, Memphis, TN 38101.
‡ Present address: Department of Pathology and LAC-USC Cancer Center, School of Medicine, University of Southern California, Los Angeles, CA 90033.
ˣ To whom inquiries should be directed.

In Vitro Photodecomposition of Uric Acid in Presence of Riboflavin II

JEROLD NEWBURGER ˣ, ALAN B. COMBS, and TING-FENG HSU

Abstract □ *In vitro* studies on the photodecomposition of uric acid in the presence of the monosodium salt of riboflavin 5′-phosphate in buffers at various pH values, in methanol, and in human plasma are reported. The decomposition rate increased with increasing pH and was independent of solvent or buffer species. The mechanism appears to be an energy transfer process involving triplet riboflavin and singlet oxygen. Riboflavin-enhanced photodecomposition of uric acid occurred *in vitro* in hyperuricemic human plasma.

Keyphrases □ Uric acid—*in vitro* photodecomposition in presence of riboflavin, effect of pH and solvent □ Riboflavin—effect on *in vitro* photodecomposition of uric acid, various pH's and solvents □ Photodecomposition—uric acid in presence of riboflavin, effect of pH and solvent □ Vitamins—riboflavin, effect on *in vitro* photodecomposition of uric acid, various pH's and solvents

The successful phototherapy of psoriasis was reported using methoxsalen and longwave UV light (1), and phototherapy alone was used to treat neonatal hyperbilirubinemia (2–4). Riboflavin was reported to enhance bilirubin photocatabolism in rats (5).

Recently, an *in vitro* photodecomposition of uric acid was observed in the presence of the monosodium salt of riboflavin 5′-phosphate (I) and visible light in aqueous solutions (6). Increasing the I concentration appeared to increase the disappearance rate of uric acid. The addition of potassium iodide (10^{-3} *M*) to the reaction mixture retarded photodecomposition.

Because of the potential clinical importance of this observation (treatment of hyperuricemia), experiments were undertaken to characterize the pH dependence of the reaction and to determine if the reaction would proceed in a nonaqueous solvent, if the reaction was oxygen dependent, and if photodecomposition would occur *in vitro* in human plasma.

EXPERIMENTAL

The irradiation light box used standardized test tubes distributed radially at equal distances (approximately 26 cm) measured from the center of the test tubes to the center of a vertically positioned, unfiltered 15-w fluorescent bulb[1] emitting visible light. The inside of the apparatus was painted flat black to reduce any internally reflected light, and the outside was draped with black cloth to eliminate external light. The light intensity was monitored using a light meter placed underneath a test tube and was held constant using a transformer[2].

The light intensity was approximately 40 foot-candles for all experiments, except the plasma study performed at approximately 50 foot-candles. Test tubes used for the irradiation[3] were standardized (±2%) by measuring[4] the absorbance of a 9.7×10^{-6} *M* aqueous I solution at 450 nm.

All solutions were prepared using deionized water, except for the methanol studies, and stock solutions of uric acid and riboflavin were prepared fresh daily. Irradiation, spectrophotometric analysis[5], and all sample preparation were performed in a darkened laboratory. Plasma samples, analyzed by high-pressure liquid chromatography (HPLC), were kept in light-resistant containers from which samples were withdrawn.

Reagents—Uric acid[6], lithium carbonate[6], and the monosodium salt of I[7] were used as received. All other solvents and reagents were reagent grade.

HPLC System and Conditions—HPLC analysis[8] was performed at a fixed wavelength of 280 nm, using a stainless steel column (0.61 m × 2 mm i.d.) packed with an anion-exchange material[9] (7). A Sorenson phosphate buffer, pH 5.9, was the eluting solution.

Buffers—Sorenson phosphate buffers of approximately pH 5, 6, 7, and 8 and a Delory and King carbonate buffer of approximately pH 9 were

[1] Sylvania F15T8-CW.
[2] Powerstat type 3PN11688, Superior Electric Co., Bristol, Conn.
[3] Pyrex No. 9800.
[4] Coleman Jr. II spectrophotometer.
[5] Beckman model 25 recording spectrophotometer.
[6] J. T. Baker Chemical Co., Phillipsburg, N.J.
[7] Nutritional Biochemical Co., Cleveland, Ohio.
[8] Waters Associates liquid chromatograph model 6000 with Soltec recorder.
[9] VYDAK AM, Catalog No. 301, The Separations Group, Hesperia, Calif.

macher, and B. J. Abbott, *Cancer Chemother. Rep.*, **3** (2), part 3, 1 (1972).
(33) P. Frankhauser and M. Brenner, *Helv. Chim. Acta*, **53**, 2298 (1970).
(34) T. A. Connors and B. J. Phillips, *Biochem. Pharmacol.*, **24**, 2217 (1975).
(35) E. J. Lien, paper presented at the APhA Academy of Pharmaceutical Sciences, Orlando meeting, Nov. 1976.
(36) C. Hansch, N. Smith, R. Engle, and H. Wood, *Cancer Chemother. Rep.*, **56**, part 1, 443 (1972).
(37) V. A. Levin and P. Kabra, *ibid.*, **58**, part 1, 787 (1974).

ACKNOWLEDGMENTS AND ADDRESSES

Received November 16, 1976, from the *School of Pharmacy and LAC-USC Cancer Center, University of Southern California, Los Angeles, CA 90033.*
Accepted for publication February 10, 1977.
Presented in part at the APhA Academy of Pharmaceutical Sciences, New Orleans meeting, April 1976.
Abstracted in part from the dissertation submitted by J. T. Chou to the University of Southern California in partial fulfillment of the Doctor of Philosophy degree requirements.
Supported in part by LAC-USC Cancer Center Grant CA 14089 from the National Cancer Institute and pilot project Grant ACS IN-21 from the American Cancer Society.
The authors thank Dr. Harry B. Wood, Jr., of the National Cancer Institute for part of the *in vivo* data and Mr. Ahmed EidAwad for his initial assistance in the tissue culture study. They also thank Ms. J. Varven for excellent technical assistance in animal model studies. E. J. Lien acknowledges the Lederle Pharmacy Faculty Award (1976).
* Present address: St. Jude Children's Research Hospital, Memphis, TN 38101.
‡ Present address: Department of Pathology and LAC-USC Cancer Center, School of Medicine, University of Southern California, Los Angeles, CA 90033.
ˣ To whom inquiries should be directed.

In Vitro Photodecomposition of Uric Acid in Presence of Riboflavin II

JEROLD NEWBURGER ˣ, ALAN B. COMBS, and TING-FENG HSU

Abstract □ *In vitro* studies on the photodecomposition of uric acid in the presence of the monosodium salt of riboflavin 5′-phosphate in buffers at various pH values, in methanol, and in human plasma are reported. The decomposition rate increased with increasing pH and was independent of solvent or buffer species. The mechanism appears to be an energy transfer process involving triplet riboflavin and singlet oxygen. Riboflavin-enhanced photodecomposition of uric acid occurred *in vitro* in hyperuricemic human plasma.

Keyphrases □ Uric acid—*in vitro* photodecomposition in presence of riboflavin, effect of pH and solvent □ Riboflavin—effect on *in vitro* photodecomposition of uric acid, various pH's and solvents □ Photodecomposition—uric acid in presence of riboflavin, effect of pH and solvent □ Vitamins—riboflavin, effect on *in vitro* photodecomposition of uric acid, various pH's and solvents

The successful phototherapy of psoriasis was reported using methoxsalen and longwave UV light (1), and phototherapy alone was used to treat neonatal hyperbilirubinemia (2–4). Riboflavin was reported to enhance bilirubin photocatabolism in rats (5).

Recently, an *in vitro* photodecomposition of uric acid was observed in the presence of the monosodium salt of riboflavin 5′-phosphate (I) and visible light in aqueous solutions (6). Increasing the I concentration appeared to increase the disappearance rate of uric acid. The addition of potassium iodide (10^{-3} *M*) to the reaction mixture retarded photodecomposition.

Because of the potential clinical importance of this observation (treatment of hyperuricemia), experiments were undertaken to characterize the pH dependence of the reaction and to determine if the reaction would proceed in a nonaqueous solvent, if the reaction was oxygen dependent, and if photodecomposition would occur *in vitro* in human plasma.

EXPERIMENTAL

The irradiation light box used standardized test tubes distributed radially at equal distances (approximately 26 cm) measured from the center of the test tubes to the center of a vertically positioned, unfiltered 15-w fluorescent bulb[1] emitting visible light. The inside of the apparatus was painted flat black to reduce any internally reflected light, and the outside was draped with black cloth to eliminate external light. The light intensity was monitored using a light meter placed underneath a test tube and was held constant using a transformer[2].

The light intensity was approximately 40 foot-candles for all experiments, except the plasma study performed at approximately 50 foot-candles. Test tubes used for the irradiation[3] were standardized (±2%) by measuring[4] the absorbance of a 9.7×10^{-6} *M* aqueous I solution at 450 nm.

All solutions were prepared using deionized water, except for the methanol studies, and stock solutions of uric acid and riboflavin were prepared fresh daily. Irradiation, spectrophotometric analysis[5], and all sample preparation were performed in a darkened laboratory. Plasma samples, analyzed by high-pressure liquid chromatography (HPLC), were kept in light-resistant containers from which samples were withdrawn.

Reagents—Uric acid[6], lithium carbonate[6], and the monosodium salt of I[7] were used as received. All other solvents and reagents were reagent grade.

HPLC System and Conditions—HPLC analysis[8] was performed at a fixed wavelength of 280 nm, using a stainless steel column (0.61 m × 2 mm i.d.) packed with an anion-exchange material[9] (7). A Sorenson phosphate buffer, pH 5.9, was the eluting solution.

Buffers—Sorenson phosphate buffers of approximately pH 5, 6, 7, and 8 and a Delory and King carbonate buffer of approximately pH 9 were

[1] Sylvania F15T8-CW.
[2] Powerstat type 3PN11688, Superior Electric Co., Bristol, Conn.
[3] Pyrex No. 9800.
[4] Coleman Jr. II spectrophotometer.
[5] Beckman model 25 recording spectrophotometer.
[6] J. T. Baker Chemical Co., Phillipsburg, N.J.
[7] Nutritional Biochemical Co., Cleveland, Ohio.
[8] Waters Associates liquid chromatograph model 6000 with Soltec recorder.
[9] VYDAK AM, Catalog No. 301, The Separations Group, Hesperia, Calif.

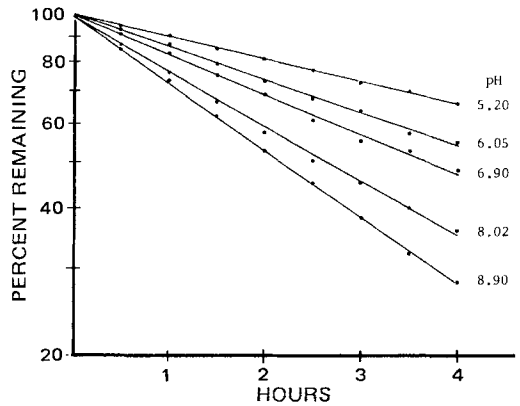

Figure 1—*Apparent first-order photodecomposition of uric acid (1.19 × 10^{-4} M) in the presence of riboflavin (3.88 × 10^{-5} M) in various phosphate buffers. Each point represents the average of four separate experiments performed in triplicate.*

prepared. In addition, a phosphate buffer of approximately pH 9 was prepared by adjusting the pH of 0.067 *M* dibasic sodium phosphate solution with 1 *M* NaOH. All buffers were boiled for 10 min after preparation, cooled, oxygenated for 5 min, and stored in the refrigerator. Before use, the buffers were removed from the refrigerator and allowed to reach room temperature.

Stock Solutions—Stock solutions of I (1.94 × 10^{-3} *M*) and uric acid (5.96 × 10^{-3} *M*) were prepared. The uric acid stock solution was prepared by solubilizing 10.0 mg of uric acid in 2.5 ml of 5.41 × 10^{-2} *M* lithium carbonate solution in a 10-ml volumetric flask and bringing the solution to volume with deionized water.

Test Solutions—Test solutions containing I (3.88 × 10^{-5} *M*) plus uric acid (1.19 × 10^{-4} *M*) and blanks containing I alone (3.88 × 10^{-5} *M*) were prepared from the stock solutions, the various buffers, and methanol. Test solutions of human plasma[10] were prepared containing uric acid (2.98 × 10^{-4} *M*) plus I (3.88 × 10^{-5} *M*) or uric acid alone (2.98 × 10^{-4} *M*) from the stock solutions. The uric acid concentrations in the plasma samples were elevated to simulate the levels in hyperuricemic patients.

pH Studies[11]—The standardized test tubes, each containing 10 ml of test solution or blank, were placed in the irradiation apparatus for light exposure. Other samples were kept in the dark. A stopwatch was used to measure sampling times, and tubes were removed randomly at each time interval. The pH of each solution was recorded before and after irradiation. The decrease in uric acid peak height was recorded using similarly irradiated I solutions as blanks. The wavelength for maximum absorption of the uric acid exhibited a bathochromic shift with increased pH (277 nm at pH 5.2 and 287 nm at pH 8.9).

Methanol Studies—These studies were performed in the same manner as the pH studies, except that methanol was used as the solvent and pH values were not recorded. Spectrophotometric analysis was performed at 293 nm using irradiated I solutions as blanks.

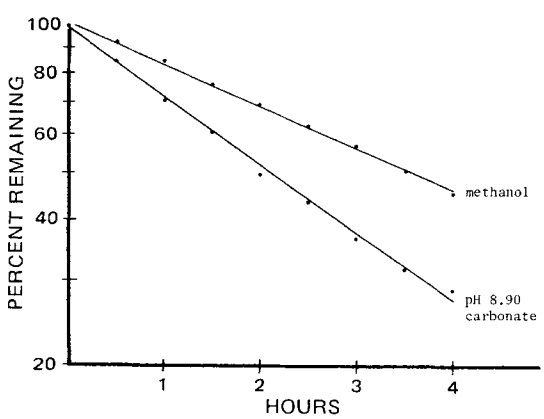

Figure 2—*Apparent first-order photodecomposition of uric acid (1.19 × 10^{-4} M) in the presence of riboflavin (3.88 × 10^{-5} M) in methanol and in a carbonate buffer. Each point is the average of four separate experiments performed in triplicate.*

[10] Outdated plasma, obtained from the Travis County Blood Bank, Austin, Tex.

[11] Model 5 pH meter, Corning Scientific Instruments.

Table I—Observed Rate Constants for Uric Acid Photodecomposition in the Presence of Riboflavin

Solvent	pH	K_{obs}, hr^{-1}
Phosphate buffer	5.20	0.102
Phosphate buffer	6.05	0.152
Phosphate buffer	6.90	0.185
Phosphate buffer	8.02	0.255
Phosphate buffer	8.90	0.317
Carbonate buffer	8.90	0.320
Methanol	—	0.198

Plasma Studies—Samples of 15 ml of plasma containing either uric acid plus I or uric acid alone were irradiated as already described. After irradiation, all samples were transferred to light-resistant containers and frozen until analyzed. The unfrozen samples were subjected to ultrafiltration[12] under darkened laboratory conditions prior to analysis, and the filtrate was collected in light-protected containers. Triplicate 20-μl aliquots of each filtrate were analyzed by HPLC.

A standard curve was prepared using filtered plasma solutions that were first spiked with uric acid plus I or uric acid alone. Analyses also were performed on samples of the original plasma to determine endogenous uric acid levels.

Anaerobic Studies—A 1000-ml volumetric flask containing approximately 900 ml of deionized water and a 500-ml volumetric flask containing 10.0 mg of uric acid dissolved in 2.5 ml of lithium carbonate (5.41 × 10^{-2} *M*) and brought to approximately 400 ml with deionized water were each boiled for 0.5 hr. After the heat was removed, nitrogen was bubbled through both solutions for 15 min. Then both solutions were capped and cooled. A 100-ml flask and 16 test tubes were flushed with nitrogen and placed in a glove bag[13] under a continuous nitrogen flow. A test tube rack and previously weighed packets of I (2.0 and 10.0 mg) were also placed in the bag, which was then sealed with clamps.

The laboratory lights were extinguished, and solutions of uric acid (1.19 × 10^{-4} *M*) plus I (3.88 × 10^{-5} *M*) and I alone (3.88 × 10^{-5} *M*) were prepared in the glove bag. Four blanks and 12 test solutions were placed in the test tubes, and the tubes were capped with waxed paper[14]-covered corks. The test tubes were removed from the bag, wiped clean, and placed in the light box. The glove bag was then placed over the light box to provide a nitrogen blanket during the experimental run. Spectrophotometric analysis was performed as previously described.

RESULTS AND DISCUSSION

Figures 1 and 2 show the pH dependence of the observed first-order disappearance of uric acid in the presence of visible light and riboflavin. There was no measurable decrease in uric acid when uric acid alone was exposed to light or when uric acid plus riboflavin was maintained in the

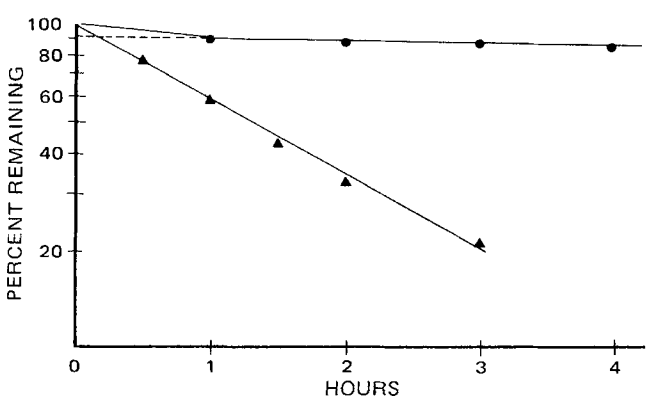

Figure 3—*Effect of oxygen on the photodecomposition of uric acid (1.19 × 10^{-4} M) in the presence of riboflavin (3.88 × 10^{-5} M). Key: ●, deoxygenated solutions; and ▲, nondeoxygenated solutions (6). Each point represents the average of three separate experiments performed in triplicate.*

[12] Millipore 47-mm stirred ultrafiltration cell XX42 047 10 with Pellicon membrane (PT Series, 10K).

[13] Model X-37-37, Instruments for Research and Industry, Cheltenham, Pa.

[14] Parafilm.

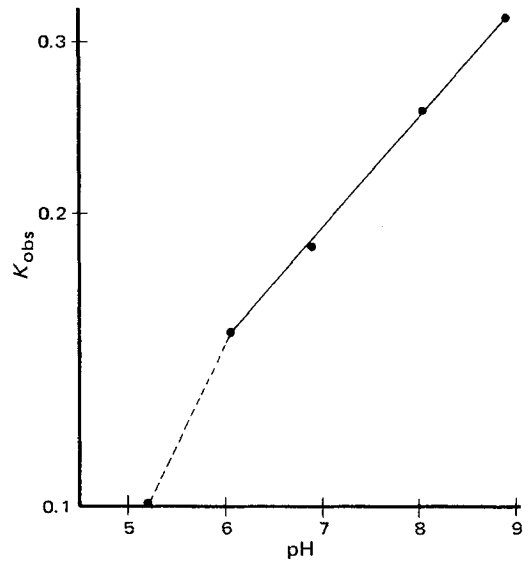

Figure 4—*Semilogarithmic plot of the observed rate constant* versus *pH in phosphate buffer.*

dark. The pH of the buffered solutions showed no significant change during the experiments. Figure 2 also shows that the photodecomposition occurred in methanol, indicating that the reaction is not solvent dependent.

Table I lists the observed first-order rate constants calculated for each buffer solution and methanol. The rate constants at pH 8.9 for both the phosphate and carbonate buffers are in good agreement, indicating that the process is dependent on pH and not the buffer species.

As shown in Fig. 3, the absence of oxygen inhibits the photodecomposition of uric acid in the presence of riboflavin and light. The approximate 10% loss of uric acid during the 1st hr plus the 5% decrease over the next 3 hr is considerably less than the almost 80% decrease previously shown to occur aerobically under the same conditions (6). The occurrence of some photodecomposition may be attributed to residual oxygen not removed during the deoxygenation procedures. Hartley and Kilby (8) showed a similar fast initial hydrolysis of *p*-nitrophenyl acetate in the presence of chymotrypsin followed by a slower steady-state release of product.

Many photooxidation reactions proceed *via* singlet oxygen. It was proposed that the photooxidation of bilirubin alone proceeds by singlet oxygen (9). An increase in singlet oxygen production was found with an increase in pH of aqueous solutions containing a photosensitizer (10). Figure 4 shows that the observed rate constant increased with an increase in pH; this increase seems to involve singlet oxygen in the uric acid photodecomposition.

Flavin triplet also seems to be implicated in the process. Previous work (6) showed that potassium iodide inhibited the reaction. Potassium iodide is known to be an effective quencher of the riboflavin triplet state (11, 12). Digenis *et al.* (13) proposed that riboflavin triplet is involved in the anaerobic photodecomposition of 2-chloro-9-(3-dimethylaminopropyl)acridan phosphate to its acridine derivative through an energy transfer process.

Riboflavin triplet is capable of generating singlet oxygen (14, 15). It was proposed that both riboflavin triplet and singlet oxygen are involved in bilirubin photodecomposition in the presence of riboflavin (16). Therefore, the following mechanism (Scheme I) is proposed to account for uric acid photodecomposition in the presence of riboflavin. Light absorption by ground-state riboflavin, Rb^0, produces riboflavin singlet, Rb^1. A radiationless transition of riboflavin singlet produces riboflavin triplet, Rb^3, which, upon collision with ground-state oxygen, $O_2{}^3$, generates singlet oxygen, $O_2{}^1$, *via* energy transfer. The singlet oxygen reacting with uric acid gives the decomposition products.

Figure 5 shows the effect of light on the 450-nm peak of riboflavin in both the absence and presence of uric acid. This peak showed a decrease

$$Rb^0 + h\nu \rightarrow Rb^1 \text{ (riboflavin singlet)}$$
$$Rb^1 \rightarrow Rb^3 \text{ (riboflavin triplet)}$$
$$Rb^3 + O_2{}^3 \rightarrow Rb^0 + O_2{}^1 \text{ (singlet oxygen)}$$
$$O_2{}^1 + \text{uric acid} \rightarrow \text{products}$$

Scheme I

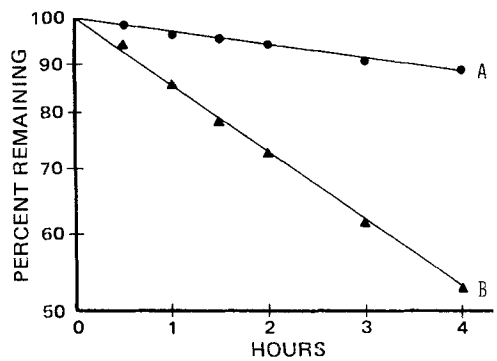

Figure 5—*Effect of light on the 450-nm peak of riboflavin. Key: A, riboflavin alone (3.88 × 10^{-5} M); and B, riboflavin (3.88 × 10^{-5} M) plus uric acid (1.19 × 10^{-4} M). Each point represents the average of three experiments performed in triplicate.*

of 12% in the absence of uric acid and a 47% decrease in the presence of uric acid. On a molar basis, uric acid disappearance was approximately 10 times greater than was the riboflavin loss, as evidenced by the decrease in the 450-nm peak. Thus, uric acid photodecomposition is not a coupled oxidation–reduction involving reduced flavin.

There was no spectral evidence for complex formation between the substrate and riboflavin. The spectra for mixtures of riboflavin plus uric acid exhibited the expected additivity of the spectra for both uric acid and riboflavin alone (Fig. 6).

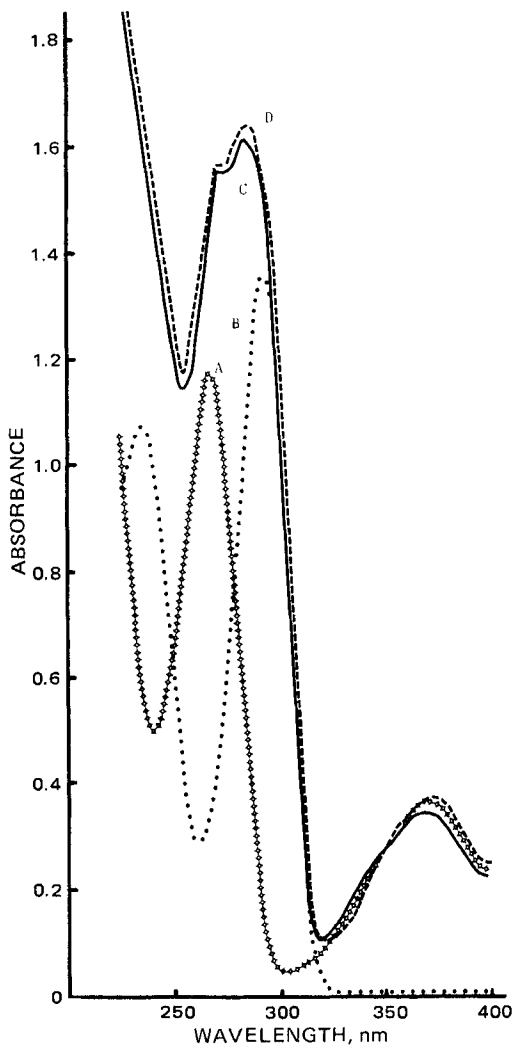

Figure 6—*UV spectra of riboflavin (3.88 × 10^{-5} M) (A), uric acid (1.19 × 10^{-4} M) (B), and a mixture of riboflavin (3.88 × 10^{-5} M) and uric acid (1.19 × 10^{-4} M) (C). The theoretical summation of the mixture is shown by curve D.*

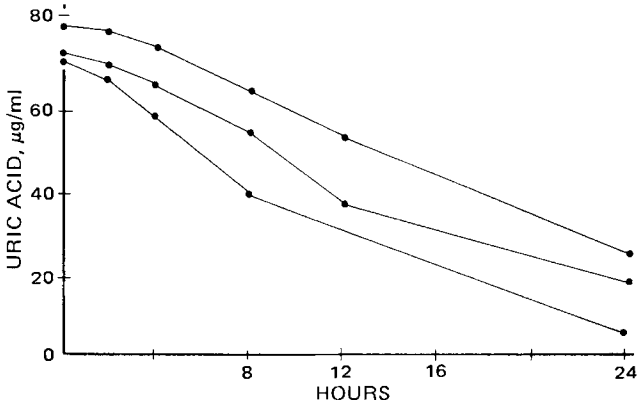

Figure 7—*Photodecomposition of uric acid in the presence of riboflavin in human plasma. Each line represents a different human plasma. Each point represents the average of triplicate determinations.*

The plasma curves (Fig. 7) indicate that the photodecomposition occurred in plasma *in vitro*. Uric acid levels at the termination of each experiment were lower than endogenous levels. Plasma containing uric acid in the absence of riboflavin showed no significant loss of uric acid after exposure to light for 24 hr. During HPLC analysis, the uric acid peak appeared 2.75 min after sample injection. A minor peak, which was not present in the aqueous solutions, was observed 1.75 min after sample injection and may be attributed to a lower molecular weight compound which was not retained by the membrane filter. The nonlinearity of the plasma curves may be due to the settling out of less translucent plasma components during irradiation. Also, a more complex reaction may occur in plasma than in the aqueous solutions.

REFERENCES

(1) J. S. Parrish, T. B. Fitzpatrick, L. Tannenbaum, and M. A. Pathak, *N. Engl. J. Med.*, **281**, 1207 (1974).

(2) R. J. Cremer, P. W. Perryman, and D. H. Richards, *Lancet*, **274**, 1094 (1958).

(3) A. W. Franklin, *ibid.*, **274**, 1227 (1958).

(4) J. Lucey, M. Ferreiro, and J. Hewitt, *Pediatrics*, **41**, 1047 (1968).

(5) H. B. Kostenbauder and D. R. Sanvordeker, *Experientia*, **29**, 282 (1973).

(6) J. Newburger and A. B. Combs, *Life Sci.*, **17**, 443 (1975).

(7) W. D. Slaunwhite, L. A. Pachala, D. C. Wenke, and P. T. Kissinger, *Clin. Chem.*, **21**, 1427 (1975).

(8) B. S. Hartley and B. A. Kilby, *Biochem. J.*, **56**, 288 (1954).

(9) A. F. McDonagh, *Biochem. Biophys. Res. Commun.*, **44**, 1306 (1971).

(10) R. Pottier, R. Bonneau, and J. Joussot-Dubien, *Photochem. Photobiol.*, **22**, 59 (1975).

(11) G. Oster and A. H. Adelman, *J. Am. Chem. Soc.*, **78**, 913 (1956).

(12) H. B. Kostenbauder, P. P. DeLuca, and C. R. Kowarski, *J. Pharm. Sci.*, **54**, 1243 (1965).

(13) G. A. Digenis, S. Shakhshir, M. A. Miyamoto, and H. B. Kostenbauder, *ibid.*, **65**, 247 (1976).

(14) C. S. Foote, *Acc. Chem. Res.*, **1**, 104 (1968).

(15) D. R. Kearns, *Chem. Rev.*, **71**, 395 (1971).

(16) D. R. Sanvordeker and H. B. Kostenbauder, *J. Pharm. Sci.*, **63**, 404 (1974).

ACKNOWLEDGMENTS AND ADDRESSES

Received July 7, 1976, from the *College of Pharmacy, University of Texas at Austin, Austin, TX 78712.*

Accepted for publication January 19, 1977.

Supported by Biomedical Sciences Support Grant 26-16994-0650 from the University of Texas at Austin.

The authors express their appreciation to Mr. James A. Smith for technical assistance.

[x] To whom inquiries should be directed.

ac Polarography for Tetracycline Analysis

CEDRIC J. OLLIFF [*] and LESLIE G. CHATTEN [‡x]

Abstract □ The electrode processes for the reduction of several tetracyclines by ac polarography were examined. In pH 4.0 Walpole acetic acid–acetate buffer, two main waves occurred; the first was quasireversible and the second was reversible. Results showed that the first wave can readily be used for quantitative work. The second wave would also be suitable provided that there was no interference from other electroreducible substances.

Keyphrases □ Tetracyclines, various—ac polarographic analysis, electrode processes identified □ Polarography, ac—analysis, various tetracyclines, electrode processes identified □ Antibacterials—various tetracyclines, ac polarographic analysis, electrode processes identified

Many methods have been reported for the quantitative analysis of the tetracycline antibacterials (1), including a range of electroanalytical methods (2). One method utilized ac polarography for the assay of tetracycline, chlortetracycline, and oxytetracycline with a mercury pool reference electrode (3). This method also was used to analyze doxycycline capsules (4). Studies on minocycline, lymecycline, and demeclocycline have not been reported. Therefore, it was of interest to see whether these antibiotics behaved similarly and to extend the examination, using phase-sensitive ac polarography, to some pharmaceutical preparations on the British market.

Previous workers (3, 4) who investigated the application of ac polarography to tetracycline analysis made no attempt to determine whether the wave was the result of a reversible, a quasireversible, or an irreversible electrode process. Bond (5) stated that a knowledge of the reversibility of the electrode reaction involved is very important when using ac polarography for quantitative analysis but that the analytical use of quasireversible ac electrode processes can be extremely unreliable. Moreover, irreversible electrode processes may be a source of interference (5).

EXPERIMENTAL

Apparatus—All polarograms were obtained on a polarograph[1] equipped with a saturated calomel electrode (SCE), a dropping mercury electrode (DME), a mercury pool counter electrode, and a drop timer.

[1] Cambridge polarographic analyzer model 82P.

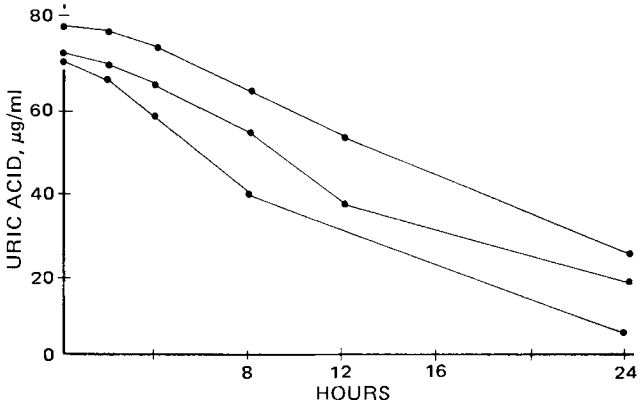

Figure 7—*Photodecomposition of uric acid in the presence of riboflavin in human plasma. Each line represents a different human plasma. Each point represents the average of triplicate determinations.*

The plasma curves (Fig. 7) indicate that the photodecomposition occurred in plasma *in vitro*. Uric acid levels at the termination of each experiment were lower than endogenous levels. Plasma containing uric acid in the absence of riboflavin showed no significant loss of uric acid after exposure to light for 24 hr. During HPLC analysis, the uric acid peak appeared 2.75 min after sample injection. A minor peak, which was not present in the aqueous solutions, was observed 1.75 min after sample injection and may be attributed to a lower molecular weight compound which was not retained by the membrane filter. The nonlinearity of the plasma curves may be due to the settling out of less translucent plasma components during irradiation. Also, a more complex reaction may occur in plasma than in the aqueous solutions.

REFERENCES

(1) J. S. Parrish, T. B. Fitzpatrick, L. Tannenbaum, and M. A. Pathak, *N. Engl. J. Med.*, **281**, 1207 (1974).

(2) R. J. Cremer, P. W. Perryman, and D. H. Richards, *Lancet*, **274**, 1094 (1958).

(3) A. W. Franklin, *ibid.*, **274**, 1227 (1958).

(4) J. Lucey, M. Ferreiro, and J. Hewitt, *Pediatrics*, **41**, 1047 (1968).

(5) H. B. Kostenbauder and D. R. Sanvordeker, *Experientia*, **29**, 282 (1973).

(6) J. Newburger and A. B. Combs, *Life Sci.*, **17**, 443 (1975).

(7) W. D. Slaunwhite, L. A. Pachala, D. C. Wenke, and P. T. Kissinger, *Clin. Chem.*, **21**, 1427 (1975).

(8) B. S. Hartley and B. A. Kilby, *Biochem. J.*, **56**, 288 (1954).

(9) A. F. McDonagh, *Biochem. Biophys. Res. Commun.*, **44**, 1306 (1971).

(10) R. Pottier, R. Bonneau, and J. Joussot-Dubien, *Photochem. Photobiol.*, **22**, 59 (1975).

(11) G. Oster and A. H. Adelman, *J. Am. Chem. Soc.*, **78**, 913 (1956).

(12) H. B. Kostenbauder, P. P. DeLuca, and C. R. Kowarski, *J. Pharm. Sci.*, **54**, 1243 (1965).

(13) G. A. Digenis, S. Shakhshir, M. A. Miyamoto, and H. B. Kostenbauder, *ibid.*, **65**, 247 (1976).

(14) C. S. Foote, *Acc. Chem. Res.*, **1**, 104 (1968).

(15) D. R. Kearns, *Chem. Rev.*, **71**, 395 (1971).

(16) D. R. Sanvordeker and H. B. Kostenbauder, *J. Pharm. Sci.*, **63**, 404 (1974).

ACKNOWLEDGMENTS AND ADDRESSES

Received July 7, 1976, from the *College of Pharmacy, University of Texas at Austin, Austin, TX 78712.*

Accepted for publication January 19, 1977.

Supported by Biomedical Sciences Support Grant 26-16994-0650 from the University of Texas at Austin.

The authors express their appreciation to Mr. James A. Smith for technical assistance.

[x] To whom inquiries should be directed.

ac Polarography for Tetracycline Analysis

CEDRIC J. OLLIFF [*] and LESLIE G. CHATTEN [‡x]

Abstract □ The electrode processes for the reduction of several tetracyclines by ac polarography were examined. In pH 4.0 Walpole acetic acid–acetate buffer, two main waves occurred; the first was quasireversible and the second was reversible. Results showed that the first wave can readily be used for quantitative work. The second wave would also be suitable provided that there was no interference from other electroreducible substances.

Keyphrases □ Tetracyclines, various—ac polarographic analysis, electrode processes identified □ Polarography, ac—analysis, various tetracyclines, electrode processes identified □ Antibacterials—various tetracyclines, ac polarographic analysis, electrode processes identified

Many methods have been reported for the quantitative analysis of the tetracycline antibacterials (1), including a range of electroanalytical methods (2). One method utilized ac polarography for the assay of tetracycline, chlortetracycline, and oxytetracycline with a mercury pool reference electrode (3). This method also was used to analyze doxycycline capsules (4). Studies on minocycline, lymecycline, and demeclocycline have not been reported. Therefore, it was of interest to see whether these antibiotics behaved similarly and to extend the examination, using phase-sensitive ac polarography, to some pharmaceutical preparations on the British market.

Previous workers (3, 4) who investigated the application of ac polarography to tetracycline analysis made no attempt to determine whether the wave was the result of a reversible, a quasireversible, or an irreversible electrode process. Bond (5) stated that a knowledge of the reversibility of the electrode reaction involved is very important when using ac polarography for quantitative analysis but that the analytical use of quasireversible ac electrode processes can be extremely unreliable. Moreover, irreversible electrode processes may be a source of interference (5).

EXPERIMENTAL

Apparatus—All polarograms were obtained on a polarograph[1] equipped with a saturated calomel electrode (SCE), a dropping mercury electrode (DME), a mercury pool counter electrode, and a drop timer.

[1] Cambridge polarographic analyzer model 82P.

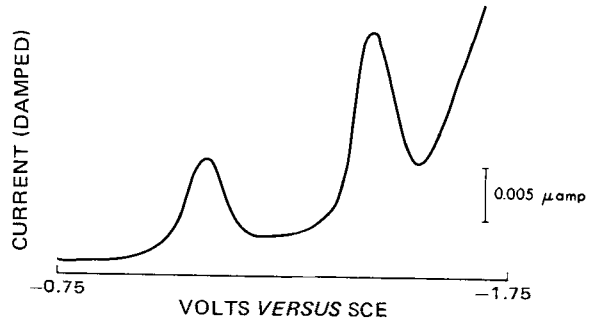

Figure 1—*The ac polarogram for 5 × 10⁻⁵ M tetracycline hydrochloride in pH 4.0 acetate buffer.*

A recorder[2] was attached to the polarograph. A pH meter[3] was fitted with a glass–calomel electrode system.

Reagents and Solutions—All chemicals were reagent grade. The tetracyclines were used as received. The potency of the reference tetracyclines was taken as the value provided by the manufacturer's microbiological assay. This value was employed in calculating the weight of material required to prepare 10^{-3} *M* stock solutions in pH 4.0 Walpole acetic acid–acetate buffer (6).

The concentration range (1×10^{-6}–5×10^{-4} *M*), the pH range of the buffer (3.7–5.8), the drop time, and the damping were varied as required to determine the relationship between these variables and the ac waves. The linearity range for six tetracyclines was determined using the given concentration range and the acetate buffer, scanning over a voltage range of from −0.75 to −1.75 v *versus* a saturated calomel electrode with a scan time of 200 sec, a drop time of 0.5 sec, a damping of 6, and an applied ac voltage of 10 mv, root mean square (rms) at 38 Hz.

Working standards contained either 5×10^{-4} *M* or 25 mg of tetracycline/100 ml in the pH 4 acetate buffer.

Tablets—Depending upon the number available, either 10 or 20 tablets were weighed and finely ground. According to the weight per tablet and the labeled potency, suitable samples were weighed to give 100 ml of solution in the pH 4.0 acetate buffer of theoretically either 5×10^{-4} *M* or 25 mg of the tetracycline salt. This solution was filtered, and 1 ml was diluted to 10 ml with the same buffer to give a theoretical concentration of 5×10^{-5} *M* or 2.5 mg/100 ml. Five samples were prepared from each batch of tablets.

Capsules—The contents of 10 capsules were emptied and weighed, and a suitable sample was taken as for the tablets. In certain cases, 3 min of sonication[4] of the solution was necessary.

Syrups—Appropriately sized samples were weighed and diluted with buffer to give a theoretical 5×10^{-4} *M* solution after determination of the density of the syrup. The rest of the procedure was identical to that for tablets.

Polarographic Analysis of Samples—All solutions were deoxygenated with oxygen-free nitrogen for 10 min. In all instances, the polarographic analyzer was set with the same conditions as for the linearity range experiments and with a suitable current sensitivity. Working standards were run alternately with the samples. Triplicate runs were carried out on each sample solution. All assays were performed at room temperature.

The standard addition technique also was used. In these instances, four 10-ml samples containing a theoretical tetracycline content of 1.25 mg were measured. Three samples received an accurately measured aliquot of the standard solution, *i.e.*, 0.5, 1, or 1.5 ml. The usual calculations were performed to compensate for dilution of the sample and the standard.

RESULTS AND DISCUSSION

Two well-defined ac polarographic waves resulted at pH 4 for all tetracyclines studied when a damping of 6 was used (Fig. 1). With zero damping, other waves became apparent (Fig. 2), the number and position depending upon the solution pH. The half-widths for the two main waves for tetracycline are given in Table I. The logarithmic analysis of the first of these waves at pH 4 gave two intersecting lines with slopes of 60 ± 4 and 108 ± 3 mv; the second main wave gave a value of 120 ± 2 mv. Variation in the drop time had no effect on the peak potential, E_p, of the second wave, but an increased drop time caused a cathodic shift in the first wave. Concentration changes appeared to have no effect on the E_p values of either main wave. At pH 4 and damping 6, the values for the first and second waves were −1.11 and −1.42 v, respectively.

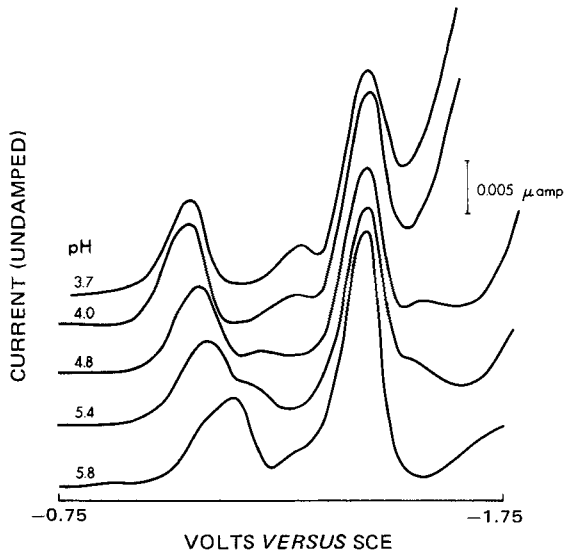

Figure 2—*Effect of pH on ac polarogram of tetracycline hydrochloride, 5×10^{-5} M in acetate buffer.*

On the basis of the logarithmic analysis, the variation of E_p with drop time, and its asymmetry, the first main wave would appear to be complex, involving quasireversible or irreversible electrode processes. The second wave had a slope of 120 mv for the logarithmic analysis and a half-width of 90 mv. These parameters indicate that it is the result of a one-electron reversible process (5). Both waves gave linear relationships over the range from 2×10^{-6} to 1×10^{-4} *M* for all tetracyclines tested including methacycline. The correlation coefficients for all plots were greater than 0.9997 for the first wave and 0.998 for the second wave. Deviations from linearity occurred with both waves when the concentration of the solutions exceeded 1×10^{-4} *M*.

With controlled conditions, the first wave was reproducible, as indicated by the correlation coefficient and the results in Table II. In the present investigation, conditions were established so that only one buffer system was required for all seven tetracyclines. With the acetate buffer, a pH of 4 was suitable for the first wave in all instances. For the second wave, no single pH value was suitable for all tetracyclines. As shown in Fig. 2, the curved baseline demonstrates the influence of the background current for the second wave at pH 4.0. This curvature could account for the slightly lower correlation coefficient (0.998) obtained with the second wave compared to that for the first wave (0.9997).

The results obtained using the ac polarographic procedure for the analysis of tablets, capsules, and a syrup, together with the microbiological assay results supplied by the manufacturers, are summarized in Table II. The first wave was employed in all instances, and generally good agreement was obtained between the values obtained by the proposed method and those supplied by the manufacturers. In most instances, the calibration method gave answers similar to those obtained with the standard addition technique.

For the first four products in Table II, however, the standard addition method gave results that agreed well with those of manufacturer but the calibration method did not. The significant differences between the values obtained by the proposed method and those of the manufacturer for the last entry in Table II can be explained on the basis of the rather lengthy lapse between the time of manufacture and its analysis in this investigation. Where appreciable differences occurred between the two techniques, the standard addition method gave a nonlinear relationship between peak current, I_p, and the concentrations of tetracycline added.

Table I—Half-Width Values for the Two Main ac Waves for a 5 × 10^{-5} *M* Tetracycline Solution at Various pH Values

	pH					
Wave	3.7	4.0	4.8	5.2	5.4	5.8
First, mv ± 2	75	80	88	98	100	103
Second, mv ± 2	88	90	87	91	88	86

[2] Telsec model 700.
[3] Vibret.
[4] Elliott Accoustica ESC520.

Table II—Results for Tetracycline Content of Commercial Preparations Using the First ac Polarographic Wave

Antibiotic	Dosage Form	Mean of Stated Potency ± *SD*, %		Manufacturer's Results
		Calibration Method	Standard Addition Method	
Tetracycline hydrochloride	250-mg capsule	98.1 ± 1.0	102.8 ± 2.8	104.1[a]
	250-mg capsule	101.1 ± 0.3	108.4 ± 2.2	106[b]
	250-mg tablet	98.8 ± 0.5	106.4 ± 3.0	108[b]
	250-mg tablet	102.1 ± 0.4	109.2 ± 2.5	109[b]
	250-mg tablet	100.1 ± 0.6	105.2 ± 3.1	101.4[b]
	100-mg tablet	100.9 ± 0.8	102.1 ± 2.3	104[b]
	250-mg tablet	97.9 ± 0.3	99.5 ± 2.0	98.8[b]
Chlortetracycline hydrochloride	250-mg capsule	99.2 ± 0.6	98.9 ± 1.9	101.1[b]
Oxytetracycline hydrochloride	250-mg tablet	98.9 ± 0.7	100.3 ± 2.5	102.1[b]
Demeclocycline hydrochloride	300-mg tablet	103.8 ± 0.8	102.6 ± 1.8	101.8[b]
	150-mg capsule	100.5 ± 0.6	101.9 ± 2.1	101.0[b]
Minocycline hydrochloride	100-mg tablet	107.8 ± 0.4 103.3 ± 0.4	110.2 ± 2.3 103.9 ± 2.5	106.3[b] 102.0[b]
Lymecycline	204-mg capsule	104.9 ± 0.4	105.5 ± 2.0	103.8[b]
Doxycycline hyclate	100-mg capsule	100.6 ± 0.3	106.4 ± 2.9	101.5[b] 104[a]
	10 mg/ml syrup	99.2 ± 1.2	98.8 ± 3.2	110[b] 115.4[a]

[a] UV absorption method of manufacturer. [b] Microbiological assay (BP 1973).

This deviation could be due to adsorbable species (5) such as methylcellulose, polysorbate, gelatin, and povidone, which may be present in pharmaceutical preparations.

Where nonlinearity occurs in the assay of dosage forms and there is linearity between log I_p and log concentration for the pure drug, the method of Beukelman and Lord (7) may be applicable for determining the tetracycline concentration in pharmaceutical products. The results obtained by this method gave reasonable agreement between the values calculated from the three additions. The standard deviation was approximately ±2.5%. Although a filtration step was always carried out, in many instances this step was unnecessary because the solution contained no undissolved material.

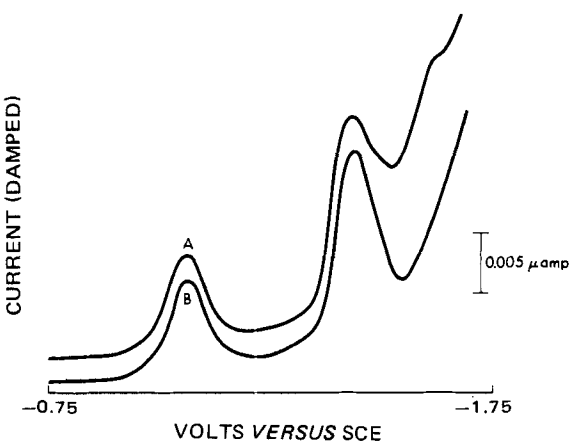

Figure 3—*Effect of nystatin, 10 mg/ml, on the ac polarogram of tetracycline hydrochloride, 5 × 10⁻⁵ M, in pH 4 acetate buffer. Key: A, tetracycline hydrochloride plus nystatin; and B, tetracycline hydrochloride.*

In some instances, erratic results occurred; they were attributed to incomplete dissolution of the tetracycline, even after continuous shaking for several hours. A few minutes of sonication overcame this problem. If the sonication was prolonged for 10 min or more, however, low results occurred for which no satisfactory explanation can be offered.

The assay exhibits a high degree of precision and accuracy if standard addition techniques do not have to be employed. It is also rapid when compared to many chemical methods, and the sensitivity is sufficiently high to permit single tablet or capsule assays.

The second wave is reversible and appears to be ideal for use in analytical ac polarography (5). At pH 4, however, the precision, as shown by the correlation coefficient for the second wave, is less than that for the first wave. Linear relationships were also obtained at pH 5.8 for tetracycline over the concentration range of 2×10^{-6}–1×10^{-4} *M* with the first wave and of 5×10^{-7}–1×10^{-4} *M* with the second wave. The correlation coefficients were 0.996 and 0.999, respectively. The baseline for the second wave was almost parallel to the axis at pH 5.8 (Fig. 2), which may account for the increased sensitivity when compared with the results at pH 4.

An assay carried out at pH 5.8 for a batch of 250-mg tetracycline hydrochloride capsules by the standard addition technique gave a mean percentage of the stated potency of 102.0 ± 3.2 and 103.9 ± 1.0% for the first and second waves, respectively. These values compared favorably with the manufacturer's value of 104.1%. Thus, for tetracycline, it may be preferable to use pH 5.8, provided no other substance in the preparation is electroreducible at a potential of −1.42 v *versus* SCE. This value is considerably more negative than that of the first wave (E_p = −1.22 v *versus* SCE); therefore, there is an increased possibility of interfering reductions overlapping with the second wave. For example, nystatin at a concentration greater than 1 mg/ml in the final solution will interfere with the results obtained with the second wave but have no effect on the first wave (Fig. 3). Substances such as amphotericin and common excipients such as lactose and magnesium stearate have no effect on tetracycline reduction at either the first or second wave. Thus, for certain tetracyclines, a pH value other than 4 may be preferred and, in some instances, it may be advantageous to use the second wave.

More detailed studies are being carried out on the mechanism of the electrode processes.

REFERENCES

(1) D. W. Hughes and W. L. Wilson, *Can. J. Pharm. Sci.*, **8**, 67 (1973).

(2) H. W. Unterman and S. Weissbuch, *Pharmazie*, **29**, 762 (1974).

(3) M. E. Caplis, H. S. Ragheb, and E. D. Schall, *J. Pharm. Sci.*, **54**, 694 (1965).

(4) S. Silvestri, *Pharm. Acta Helv.*, **47**, 209 (1972).

(5) A. M. Bond, *Anal. Chem.*, **44**, 315 (1972).

(6) "Documenta Geigy, Scientific Tables," 7th ed., Geigy Pharmaceuticals, Ardsley, N.Y., 1970, p. 281.

(7) T. E. Beukelman and S. S. Lord, Jr., *Appl. Spectrosc.*, **14**, 12 (1960).

ACKNOWLEDGMENTS AND ADDRESSES

Received February 11, 1976, from the *Department of Pharmacy, Brighton Polytechnic, Brighton, England, and the ‡Faculty of Pharmacy and Pharmaceutical Sciences, University of Alberta, Edmonton, Alberta, Canada.

Accepted for publication January 18, 1977.

L. G. Chatten thanks Smith Kline and French Canada Ltd. for the award of a travel grant and the School of Pharmacy, Brighton Polytechnic, Brighton, England, for providing research facilities.

The Cambridge polarograph was purchased partly by funds provided by the Medical Research Council of Canada.

Grateful acknowledgment is made to the following drug manufacturers for supplying samples: Armour Pharmaceuticals Co. Ltd., Berk Pharmaceutical Ltd., Carlo Erba, Cyanamid of Great Britain Ltd., I.C.I. Pharmaceuticals Division, Pfizer Ltd., and E. R. Squibb and Sons Ltd.

x To whom inquiries should be directed.

Evaluation of Drug Formulations Using LD_{50} Testing in Mice

P. R. SHETH ˣ, N. H. SHAH, and W. POOL

Abstract □ The LD_{50} values were utilized to assess the relative rate of absorption of two very poorly soluble drugs. Formulations of these drugs were studied by micronization; addition of surfactant, alkaline or buffering agents, and/or bile salts; coprecipitation; melt or fusion techniques; or granulation with hydrophilic agents. Differences in toxicities were demonstrated from formulations compared to pure drugs by the LD_{50} method. This study shows that the LD_{50} is a practical, rapid method of achieving comparative evaluations of drug formulations.

Keyphrases □ Absorption, relative rate—poorly soluble drugs, various formulations evaluated using LD_{50} testing, mice □ Toxicity—poorly soluble drugs, various formulations evaluated using LD_{50} testing, mice □ LD_{50} testing—relative absorption rate and toxicity of various formulations of poorly soluble drugs evaluated, mice

The rate and extent of absorption of a drug are dependent on its solubility and transfer characteristics in the GI tract. Improvement of either the intrinsic solubility or the solubility rate of a poorly soluble drug invariably has a beneficial effect on GI absorption (1).

BACKGROUND

Enhancement of absorption by adjuvants and formulation parameters has been the topic of many previous investigations (2–5). In addition, the techniques in designing drug delivery systems can affect the absorption profile. At the early stages of drug development, the physical and chemical factors of the drug and the design of the dosage form should be evaluated carefully for enhancement of bioavailability to yield the desired pharmacological response.

The following steps are considered important for a new compound with very poor solubility (6): (*a*) improve the intrinsic solubility and/or solubility rate by physical or chemical means, (*b*) develop a drug delivery system, (*c*) design and study methods for the *in vitro* evaluation of the drug delivery system, (*d*) select the most efficient drug delivery system in terms of chemical and physical stability and the future manufacturing procedure, (*e*) evaluate the stability of the drug in GI fluid, (*f*) test the drug delivery system *in vivo* for drug bioavailability, and (*g*) correlate *in vitro* and *in vivo* data.

Steps *a* and *b* are important in the early stages of development. The relative *in vivo* efficiency of absorption of the various drug delivery systems can be measured by blood level or urinary excretion studies. However, these studies are expensive, time consuming, and frequently involve complicated analytical procedures. Several investigators reported that drug absorption may be assessed indirectly by determining quantitatively the oral toxicity of the drug (7–9). This method is based on the assumption that the toxicity of an orally administered drug is directly proportional to the amount of the drug in the body or its blood level, which, in turn, is directly proportional to its absorption rate from the GI tract (10). The two parameters most commonly employed to reflect the toxicity of a drug are its oral LD_{50} (mean lethal dose) and LT_{50} (median lethal time).

Several formulations were screened for their absorption rates by determining their LD_{50} values. This procedure is relatively rapid and inexpensive. Such toxicity studies are particularly useful when a limited amount of new drug is available.

Table I—Solubilities of Drugs A and B in Various Solvents

Solvent	Solubility, mg/ml Drug A	Drug B
Water	0.17	0.3
Ethanol	5.1	66
Propylene glycol	2.8	35
0.1 *N* HCl	0.05	0.82
Intestinal fluid	0.13	0.88
0.1 *N* NaOH	2.9	—
Chloroform	>150	>50

Table II—Design and Rationale for Different Formulations of Drug A

Excipient	Ratio, Drug–Excipient	Type of Preparation
—	—	Drug *per se*
Poloxamer 188	1:9	Surfactant addition
Polysorbate 80	1:1	Suspension of drug in surfactant solution
Meglumine	1:3.5	Inclusion of alkaline material
Dibasic potassium phosphate–monobasic potassium phosphate	1:2:1	Buffering agent
Sodium glycocholate	1:4	Addition of bile salt
Sodium glycocholate	1:4	Coprecipitate with bile salt
Povidone	1:4	Coprecipitate with hydrophilic polymer
Urea	1:4	Melt in soluble carrier
Methylcellulose–dibasic calcium phosphate–corn starch	1:0.3:9:1.5	Granulation by dispersing agent

EXPERIMENTAL

Materials—Drugs A[1] and B[1], povidone[2], polysorbate 80[3], mannitol[3], meglumine[4], monobasic potassium phosphate[5], dibasic potassium phosphate[5], poloxamer 188[6], sodium glycocholate[7], sodium taurocholate[7], urea[8], methylcellulose[9], dibasic calcium phosphate[10], corn starch[11], sodium lauryl sulfate[12], and polyethylene glycol 6000[13] were used as received.

Solubility of Drugs A and B—The solubility studies of Drugs A and B were performed in various solvents using the method described in the USP (11) (Table I).

Preparation of Test Systems—The test preparations were made by one of the following methods.

Control—Drug *per se* was passed through a 100-mesh stainless steel screen.

Micronization—Drug was micronized[14] to approximate an average particle size of 3 μm.

Physical Mixture—The drug and the carrier (*e.g.*, surfactants, buffers, and/or bile salts) in the required amounts were geometrically mixed in a mortar with a pestle. No frictional pressure was applied that could significantly reduce size. The mixture was passed through a 100-mesh screen.

Coprecipitation—Requisite amounts of drug and soluble carrier were dissolved in a suitable solvent and evaporated to yield the coprecipitates. The coprecipitates were dried and passed through a 100-mesh screen.

Melts—Appropriate quantities of the drug and a carrier were mixed and heated to give a clear solution. The solution was chilled, and the resulting mass was reduced to fine particles by passing through a 100-mesh screen.

[1] Roche research compounds with very low solubility.
[2] General Aniline & Film Co., Linden, N.J.
[3] ICI America Inc., Wilmington, Del.
[4] Matheson, Coleman & Bell Co., East Rutherford, N.J.
[5] Mallinckrodt Chemical Works, St. Louis, Mo.
[6] Pluronic F68, BASF Wyandotte Corp., Wyandotte, Mich.
[7] National Biochemical Inc., Cleveland, Ohio.
[8] J. T. Baker Chemical Co., Phillipsburg, N.J.
[9] Dow Chemical, Midland, Mich.
[10] Stauffer Chemical Co., New York, N.Y.
[11] National Starch & Chemical, New York, N.Y.
[12] E. I. du Pont de Nemours, Wilmington, Del.
[13] Union Carbide Corp., New York, N.Y.
[14] Spex Industries, Metuchen, N.J.

Table III—Design and Rationale for Different Formulations of Drug B

Excipient	Ratio, Drug–Excipient	Type of Preparation
—	—	Drug *per se* nonmicronized
—	—	Micronized drug
Sodium lauryl sulfate	1:10	Surfactant addition
Sodium taurocholate	1:4	Bile salt addition
Sodium glycocholate	1:4	Coprecipitate with bile salt
Sodium glycocholate	1:4	Admixture of bile salt
Polyethylene glycol 6000–sodium glycocholate	1:5:4	Effect of soluble polymer and bile salt
Polyethylene glycol 6000–sodium glycocholate	1:5:4	Coprecipitate of soluble polymer and bile salt
Polyethylene glycol 6000	1:9	Melt with water-soluble polymer
Mannitol	1:9	Melt with water-soluble carrier
Povidone	1:9	Coprecipitate with water-soluble polymer
Urea	1:9	Melt in water-soluble carrier

Suspension/Solution—The requisite amount of nonmicronized drug was dispersed or dissolved in an aqueous polysorbate 80 solution. The particle-size ranges of suspended drug were 1–37.0 μm for Drug A, with more than 80% below 5 μm, and 10–150 μm for Drug B, with more than 80% below 50 μm.

Granulation—The drug and carriers were uniformly mixed in a mortar with a pestle. The mixture was granulated with water or an aqueous solution of polymer and dried overnight at 120°F. The dried mixture was passed through a 40-mesh screen.

LD_{50} Studies—*Drug A*—Charles River DCl mice, 17–25 g, were used. The powder mixtures were suspended in gum acacia solution as a 4% concentration of the active ingredient. The preparations were administered orally by intubation to six to 16 mice per dose level. Dosed animals were observed for 5 days, and the total mortality was reported. The LD_{50} values were calculated using a computer program based on the method of Finney (12).

Drug B—CF 1S mice, 17–25 g, were used. Six to 10 mice were used per dose level, and the dosed animals were observed for 5 days for mortality. All preparations were administered orally as a 5% concentration of the active ingredient in gum acacia solution. The LD_{50} values were calculated by the method of Finney (12) or Miller and Tainter (13).

Oral Toxicity of Excipients—The excipients added to the formulations were evaluated in the same manner as the drug.

RESULTS AND DISCUSSION

Tables II and III show the design of different formulations for an evaluation of the absorption rate of Drugs A and B, respectively. Tables IV and V show the resulting LD_{50} values. Drug A had an average particle size of about 4 μm as measured by a microscopic method. The LD_{50} values were considered as an index of relative absorption rates.

Three formulations, each containing an additive (*e.g.*, meglumine, sodium glycocholate, or urea), showed a decrease in the LD_{50} with an assumed increase in the *in vivo* absorption rate. The solubility data for Drug A (Table I) showed that the solubility was pH dependent; absolute drug solubility was increased considerably from 0.05 mg/ml in 0.1 *N* HCl to 0.17 mg/ml in water and to 2.9 mg/ml in 0.1 *N* NaOH. This result clearly explains why the compositions containing alkaline materials showed the highest toxicity.

Formulations containing povidone coprecipitate, polysorbate 80, and monobasic and dibasic potassium phosphates showed a considerable increase in toxicity when evaluated by the LD_{50} test. The fine dispersion of the drug may be the possible explanation (14, 15). The granulation technique employed with methylcellulose as a wet binder, dibasic calcium phosphate as the filler, and corn starch as the disintegrant may lower LD_{50} values due to the increased hydrophilicity of the drug.

The use of meglumine, sodium glycocholate, or urea was restricted because of instability in the alkaline environment. This finding might explain why the admixture of the drug and sodium glycocholate gave a

Table IV—Acute Toxicity (in Mice) of Drug A

Formulation	Dose, mg/kg po	Number Dead/ Number Dosed	$LD_{50} \pm SE$, mg/kg po	Relative Potency[a]
100% active (control)	800	2/10	1271 ± 111	1.0
	1000	4/16		
	1250	2/6		
	1600	8/10		
	2000	5/6		
Drug and poloxamer 188	600	0/6	934 ± 59	1.17
	800	1/6		
	1000	4/6		
Drug and polysorbate 80	300	0/10	497 ± 39[b]	2.53
	400	3/10		
	600	7/10		
	1000	10/10		
Admixture of drug and meglumine	100	0/10	351 ± 56[b]	3.65
	200	2/10		
	300	6/10		
	600	7/10		
	1000	9/10		
Admixture of drug with monobasic potassium phosphate and dibasic potassium phosphate	300	2/10	707 ± 137[c]	1.91
	600	2/10		
	1000	8/10		
Admixture of drug and sodium glycocholate	300	1/10	454 ± 42[b]	2.93
	500	8/10		
	600	6/10		
	1000	10/10		
Drug and sodium glycocholate (coprecipitate)	600	2/10	1033 ± 172	1.27
	1000	5/10		
	1250	6/10		
Coprecipitates of drug and povidone	300	0/10	660 ± 77[b]	1.95
	600	5/10		
	1000	8/10		
Drug in urea	100	0/6	423 ± 104[b]	3.24
	200	1/6		
	300	2/6		
	600	4/6		
Drug granulation with methylcellulose, dibasic calcium phosphate, and corn starch	300	0/6	518 ± 62[b]	2.48
	400	1/6		
	600	6/6		
	1000	5/6		

[a] Compared to Drug A alone. [b] The *t* test *versus* controls, $p < 0.01$. [c] The *t* test *versus* control, $p < 0.05$.

Table V—Acute Toxicity in Mice of Drug B

Preparation	Dose, mg/kg	Number Dead/ Number Dosed	$LD_{50} \pm SE$, mg/kg	Relative Potency[a]
Nonmicronized (control)	2000	4/10	2150 ± 196	—
	2500	7/10		
	3200	9/10		
Micronized	1250	0/6	1600 ± 126	1.34
	1600	3/6		
	2000	6/6		
Drug and sodium lauryl sulfate	1250	0/6	1550	1.39
	1400	2/6		
	1600	6/6		
	2000	6/6		
Drug and sodium taurocholate (coprecipitate)	800	5/6	700[b]	3.07
	1250	4/6		
	2000	6/6		
Drug and sodium glycocholate (coprecipitate)	200	0/6	310 ± 26[b]	7.0
	320	4/6		
	400	5/6		
Admixture of drug and sodium glycocholate	500	0/6	615 ± 2[b]	3.49
	560	2/6		
	630	3/6		
	700	5/6		
	800	6/6		
Drug and polyethylene glycol 6000 and sodium glycocholate (coprecipitate)	100	0/6	425 ± 101[b]	5.07
	400	3/6		
	800	5/6		
Drug in polyethylene glycol 6000	2000	1/6	2250 ± 86	1.0
	2250	0/3		
	2500	6/6		
Drug in mannitol	1250	0/6	1615 ± 129	1.33
	1400	2/4		
	1600	4/6		
	2000	4/6		
Coprecipitate of drug with povidone	1250	1/6	1490	1.44
	1600	2/2		
	2000	6/6		
Drug in urea	1250	0/6	1440 ● 47[b]	1.49
	1400	3/6		
	1600	5/6		
	2000	6/6		

[a] Compared to Drug B alone. [b] The t test *versus* controls, $p < 0.01$.

lower LD_{50} value than a coprecipitate of the same combination. In the preparation of the coprecipitate, the solvent and heat might have accelerated the degradation of Drug A in the alkaline environment. The formulation containing the povidone coprecipitate was completely stable.

Drug A with polysorbate 80, even though stable and having a low LD_{50} value, was not a formulation of choice because of encapsulation and tableting problems generally associated with the high amounts of polysorbate 80 in the formula. Thus, formulations containing a povidone coprecipitate or the granulation with methylcellulose were considered formulations of choice for future drug delivery systems.

The value of this LD_{50} procedure can be appreciated readily if one considers a hydrophobic drug like Drug A, where passive absorption was limited by the rate at which solution was effected in the GI fluids. In this type of absorption pattern, any change in the rate of solution of drug in the GI fluids produces a corresponding change in its absorption rate. Due to the intricate assay procedure, the dissolution rates of the formulations were not determined. However, enhanced aqueous solubility with an increasing pH suggests that the higher solubility of Drug A in an alkaline environment can account for the lower LD_{50} values with meglumine, sodium glycocholate, and urea formulations.

Micronization has been known to improve absorption of poorly soluble drugs. Nonmicronized Drug B had an average particle size of approximately 50 μm by microscopic examination, which was reduced to an average of approximately 3 μm by micronization. Drug B in micronized form, as urea or mannitol melts, and as a povidone coprecipitate exhibited LD_{50} values in the same approximate range and considerably lower than the control nonmicronized drug. The results are in agreement with previously published reports (2, 3, 8).

The polyethylene glycol melt of Drug B surprisingly did not show any change from the control. This result may be due to interaction of the drug with polyethylene glycol. Polyethylene glycols are known to form insoluble complexes with drug moieties, thereby impeding drug absorption (16). In other instances, improvement in dissolution and absorption rates may be obtained when polyethylene glycol is used as a carrier to form glass solutions (5).

Table VI—Acute Toxicity of Excipients Used in Drug A Formulations

Formulation Excipient	Dose, mg/kg		Number Dead/Number Dosed	
	Drug A	Excipients[a]	Excipient and Drug A	Excipient Alone
Poloxamer 188	1000	4000	4/6	0/10
Polysorbate 80	1000	1000	10/10	1/10
Meglumine	1000	3500	9/10	0/10
Monobasic potassium phosphate and dibasic potassium phosphate	— + 1000	2000 + 1000	8/10	1/10
Sodium glycocholate	1000	4000	16/20	0/10
Povidone	1000	4000	8/10	0/10
Urea	1000	4000	4/6	0/10
Methylcellulose plus dibasic calcium phosphate and corn starch	1000	300 + 9000 + 1500	5/6	0/10

[a] Quantity of excipients contained in each formulation when 1000 mg/kg of Drug A was administered (ratio of excipients to Drug A is the same as in Table II).

The coprecipitates of Drug B with the salt of cholic acid increased toxicity, while coprecipitates with sodium glycocholate were the most toxic. Cholic acid and its salts may have increased the drug solubility by micellar effects and thus showed better absorption. This type of effect is well documented (17).

For Drug B, which was stable in alkaline medium, the coprecipitate with sodium glycocholate was more toxic than the physical admixture. This result indicates that a molecular dispersion was obtained and was absorbed more readily than the physical admixture. Thus, the coprecipitate formulation containing sodium glycocholate would be considered a formula of choice for further development work.

The excipients used in the formulations of both drugs administered individually had little effect on the LD_{50} values in the maximum amount used in the formulation and, therefore, did not contribute to the toxicity (Table VI).

CONCLUSION

The LD_{50} procedure can estimate relative absorption rate differences between formulations of drugs with very low solubility. The most pharmaceutically acceptable formulations in this study were the povidone coprecipitate with Drug A and the sodium glycocholate coprecipitate with Drug B.

In the design of future drug delivery systems, a formulation with an optimum availability rate would be necessary for an acceptable pharmaceutical product. The relatively inexpensive LD_{50} studies can be a practical rapid method of achieving comparative ratings of drug formulations.

REFERENCES

(1) M. Gibaldi, "Introduction to Biopharmaceutics," Lea & Febiger, Philadelphia, Pa., 1971, pp. 6–8.

(2) G. Levy, *Am. J. Pharm.*, **135**, 78 (1963).

(3) G. Levy, *J. Mod. Pharm.*, **10**, 237 (1967).

(4) A. H. Goldberg, M. Gibaldi, and J. L. Kanig, *J. Pharm. Sci.*, **54**, 1145 (1965).

(5) W. L. Chiou and S. Riegelman, *ibid.*, **58**, 1505 (1969).

(6) J. Swarbrick, "Current Concepts in Pharmaceutical Sciences, Dosage Form Design and Bioavailability," Lea & Febiger, Philadelphia, Pa., 1973, pp. 1, 31, 181.

(7) T. R. Bates and M. Gibaldi, in "Current Concepts in the Pharmaceutical Sciences, Biopharmaceutics," J. Swarbrick, Ed., Lea & Febiger, Philadelphia, Pa., 1970, p. 95.

(8) E. Stupak and T. Bates, *J. Pharm. Sci.*, **62**, 1806 (1973).

(9) W. F. White and O. Grisvold, *J. Am. Pharm. Assoc., Sci. Ed.*, **41**, 42 (1952).

(10) L. W. Dittert, H. J. Adams, F. Alexander, C. W. Chong, T. Ellison, and J. Swintosky, *J. Pharm. Sci.*, **57**, 1146 (1968).

(11) "The United States Pharmacopeia," 18th rev., Mack Publishing Co., Easton, Pa., 1970, p. 942.

(12) D. J. Finney, "Probit Analysis," Cambridge University Press, Cambridge, England, 1971.

(13) L. C. Miller and M. L. Tainter, *Proc. Soc. Exp. Biol. Med.*, **57**, 261 (1944).

(14) M. Gibaldi and T. Bates, *J. Pharm. Sci.*, **57**, 708 (1968).

(15) D. E. Wurster and P. Taylor, *ibid.*, **54**, 1654 (1965).

(16) P. Singh, S. Guillory, T. Sokolosky, L. Benet, and V. Bhatia, *ibid.*, **55**, 63 (1966).

(17) R. Stoll, T. Bates, K. Nieforth, and J. Swarbrick, *ibid.*, **58**, 1457 (1969).

ACKNOWLEDGMENTS AND ADDRESSES

Received May 26, 1976, from *Product Development, Hoffmann-La Roche, Inc., Nutley, NJ 07110.*

Accepted for publication January 27, 1977.

[x] To whom inquiries should be directed.

Bunolol Metabolism by Dogs: Identification of Basic Metabolites and Their Conjugates

FRANZ-JOSEF LEINWEBER [*§], R. CLIVE GREENOUGH [‡¶], and FREDERICK J. DI CARLO [*x]

Abstract □ Female beagles dosed once with encapsulated ^{14}C-bunolol (10 mg/kg) excreted 61% of the isotope in urine in 24 hr. The pooled urine contained a minimum of 18 labeled compounds. Two previously unknown metabolites were purified and were identified by UV and mass spectral data; they were hydroxybunolol (10.1% of urinary radioactivity) and hydroxydihydrobunolol (9.8%). The urine also contained bunolol (0.7% of urinary carbon-14), dihydrobunolol (0.5%), conjugated dihydrobunolol (2.8%), β-(5-oxytetralonyl)lactic acid (16.3%), and (5-oxytetralonyl)acetic acid (7.1%).

Keyphrases □ Bunolol—metabolites and conjugates identified, dog urine □ Metabolism—bunolol in dogs, metabolites and conjugates identified in urine □ Antiadrenergic agents—bunolol, metabolism in dogs, metabolites and conjugates identified in urine

Bunolol [*dl*-5-[3-(*tert*-butylamino)-2-hydroxypropoxy]-3,4-dihydro-1(2*H*)-naphthalenone hydrochloride] (I) is a potent β-adrenoceptor blocking agent (1–3). Previous studies showed that I was absorbed rapidly by dogs (4) and biotransformed extensively to acidic metabolites (5). Additionally, I was reduced to a secondary alcohol by human cadaver liver (6), human and rat erythrocytes, and liver and extrahepatic tissues (7).

The secondary alcohol, dihydrobunolol (II), is an interesting metabolite because it is a β-adrenergic blocking agent with approximately the same potency as I (6). The present report describes the identification and quantification of II and previously unidentified basic metabolites in the urine of dogs dosed with ^{14}C-labeled bunolol.

EXPERIMENTAL

^{14}C-Labeled Bunolol—Bunolol labeled on the 1-carbonyl was synthesized (8). The preparation was 99.0% pure, both chemically and radiochemically, as judged by TLC; it had a specific activity of 4.90 mCi/g.

Radioactivity Counting—Quantitative assays for carbon-14 were performed using a liquid scintillation spectrometer[1]. The external standardization method was used for quench corrections.

TLC—Chromatograms for analytical purposes were run on 5 × 20-cm glass plates coated with 250 μm of silica gel G bound with calcium sulfate[2]. For preparative efforts, 20 × 20-cm plates were used; they were prewashed by one development in methanol, dried in air, and heated for 1 hr at 100°.

[1] Packard Tri-Carb model 3320.

[2] Analtech.

The coprecipitates of Drug B with the salt of cholic acid increased toxicity, while coprecipitates with sodium glycocholate were the most toxic. Cholic acid and its salts may have increased the drug solubility by micellar effects and thus showed better absorption. This type of effect is well documented (17).

For Drug B, which was stable in alkaline medium, the coprecipitate with sodium glycocholate was more toxic than the physical admixture. This result indicates that a molecular dispersion was obtained and was absorbed more readily than the physical admixture. Thus, the coprecipitate formulation containing sodium glycocholate would be considered a formula of choice for further development work.

The excipients used in the formulations of both drugs administered individually had little effect on the LD_{50} values in the maximum amount used in the formulation and, therefore, did not contribute to the toxicity (Table VI).

CONCLUSION

The LD_{50} procedure can estimate relative absorption rate differences between formulations of drugs with very low solubility. The most pharmaceutically acceptable formulations in this study were the povidone coprecipitate with Drug A and the sodium glycocholate coprecipitate with Drug B.

In the design of future drug delivery systems, a formulation with an optimum availability rate would be necessary for an acceptable pharmaceutical product. The relatively inexpensive LD_{50} studies can be a practical rapid method of achieving comparative ratings of drug formulations.

REFERENCES

(1) M. Gibaldi, "Introduction to Biopharmaceutics," Lea & Febiger, Philadelphia, Pa., 1971, pp. 6–8.

(2) G. Levy, *Am. J. Pharm.*, **135**, 78 (1963).

(3) G. Levy, *J. Mod. Pharm.*, **10**, 237 (1967).

(4) A. H. Goldberg, M. Gibaldi, and J. L. Kanig, *J. Pharm. Sci.*, **54**, 1145 (1965).

(5) W. L. Chiou and S. Riegelman, *ibid.*, **58**, 1505 (1969).

(6) J. Swarbrick, "Current Concepts in Pharmaceutical Sciences, Dosage Form Design and Bioavailability," Lea & Febiger, Philadelphia, Pa., 1973, pp. 1, 31, 181.

(7) T. R. Bates and M. Gibaldi, in "Current Concepts in the Pharmaceutical Sciences, Biopharmaceutics," J. Swarbrick, Ed., Lea & Febiger, Philadelphia, Pa., 1970, p. 95.

(8) E. Stupak and T. Bates, *J. Pharm. Sci.*, **62**, 1806 (1973).

(9) W. F. White and O. Grisvold, *J. Am. Pharm. Assoc., Sci. Ed.*, **41**, 42 (1952).

(10) L. W. Dittert, H. J. Adams, F. Alexander, C. W. Chong, T. Ellison, and J. Swintosky, *J. Pharm. Sci.*, **57**, 1146 (1968).

(11) "The United States Pharmacopeia," 18th rev., Mack Publishing Co., Easton, Pa., 1970, p. 942.

(12) D. J. Finney, "Probit Analysis," Cambridge University Press, Cambridge, England, 1971.

(13) L. C. Miller and M. L. Tainter, *Proc. Soc. Exp. Biol. Med.*, **57**, 261 (1944).

(14) M. Gibaldi and T. Bates, *J. Pharm. Sci.*, **57**, 708 (1968).

(15) D. E. Wurster and P. Taylor, *ibid.*, **54**, 1654 (1965).

(16) P. Singh, S. Guillory, T. Sokolosky, L. Benet, and V. Bhatia, *ibid.*, **55**, 63 (1966).

(17) R. Stoll, T. Bates, K. Nieforth, and J. Swarbrick, *ibid.*, **58**, 1457 (1969).

ACKNOWLEDGMENTS AND ADDRESSES

Received May 26, 1976, from *Product Development, Hoffmann-La Roche, Inc., Nutley, NJ 07110.*

Accepted for publication January 27, 1977.

[x] To whom inquiries should be directed.

Bunolol Metabolism by Dogs: Identification of Basic Metabolites and Their Conjugates

FRANZ-JOSEF LEINWEBER [*§], R. CLIVE GREENOUGH [‡¶], and FREDERICK J. DI CARLO [*x]

Abstract □ Female beagles dosed once with encapsulated ^{14}C-bunolol (10 mg/kg) excreted 61% of the isotope in urine in 24 hr. The pooled urine contained a minimum of 18 labeled compounds. Two previously unknown metabolites were purified and were identified by UV and mass spectral data; they were hydroxybunolol (10.1% of urinary radioactivity) and hydroxydihydrobunolol (9.8%). The urine also contained bunolol (0.7% of urinary carbon-14), dihydrobunolol (0.5%), conjugated dihydrobunolol (2.8%), β-(5-oxytetralonyl)lactic acid (16.3%), and (5-oxytetralonyl)acetic acid (7.1%).

Keyphrases □ Bunolol—metabolites and conjugates identified, dog urine □ Metabolism—bunolol in dogs, metabolites and conjugates identified in urine □ Antiadrenergic agents—bunolol, metabolism in dogs, metabolites and conjugates identified in urine

Bunolol [*dl*-5-[3-(*tert*-butylamino)-2-hydroxypropoxy]-3,4-dihydro-1(2*H*)-naphthalenone hydrochloride] (I) is a potent β-adrenoceptor blocking agent (1–3). Previous studies showed that I was absorbed rapidly by dogs (4) and biotransformed extensively to acidic metabolites (5). Additionally, I was reduced to a secondary alcohol by human cadaver liver (6), human and rat erythrocytes, and liver and extrahepatic tissues (7).

The secondary alcohol, dihydrobunolol (II), is an interesting metabolite because it is a β-adrenergic blocking agent with approximately the same potency as I (6). The present report describes the identification and quantification of II and previously unidentified basic metabolites in the urine of dogs dosed with ^{14}C-labeled bunolol.

EXPERIMENTAL

^{14}C-Labeled Bunolol—Bunolol labeled on the 1-carbonyl was synthesized (8). The preparation was 99.0% pure, both chemically and radiochemically, as judged by TLC; it had a specific activity of 4.90 mCi/g.

Radioactivity Counting—Quantitative assays for carbon-14 were performed using a liquid scintillation spectrometer[1]. The external standardization method was used for quench corrections.

TLC—Chromatograms for analytical purposes were run on 5 × 20-cm glass plates coated with 250 μm of silica gel G bound with calcium sulfate[2]. For preparative efforts, 20 × 20-cm plates were used; they were prewashed by one development in methanol, dried in air, and heated for 1 hr at 100°.

[1] Packard Tri-Carb model 3320.

[2] Analtech.

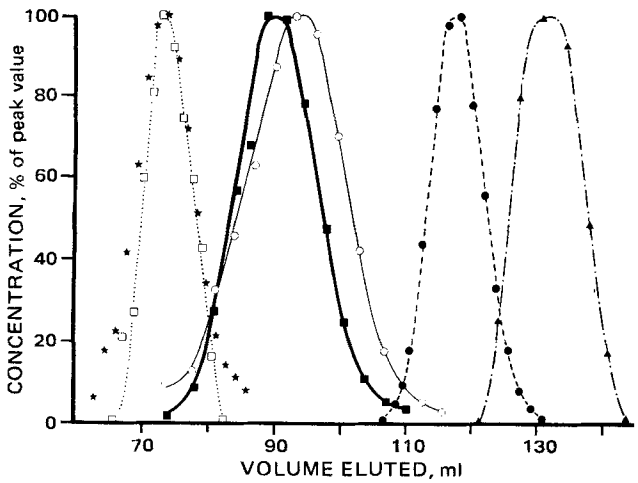

Figure 1—*Separation of bunolol and its metabolites and analogs on a dextran column (1.5 × 83 cm). Separate runs were made using the following amounts: 3 μmoles each of I (●), II (■), and V (▲); 3.6 μmoles of ^{14}C-labeled III (○); 1 μmole of ^{14}C-labeled IV from unconjugated fraction (□); and 2.3 μmoles of ^{14}C-labeled IV from conjugated fraction (★). The peak at 73 ml was drawn only for the values of unconjugated IV.*

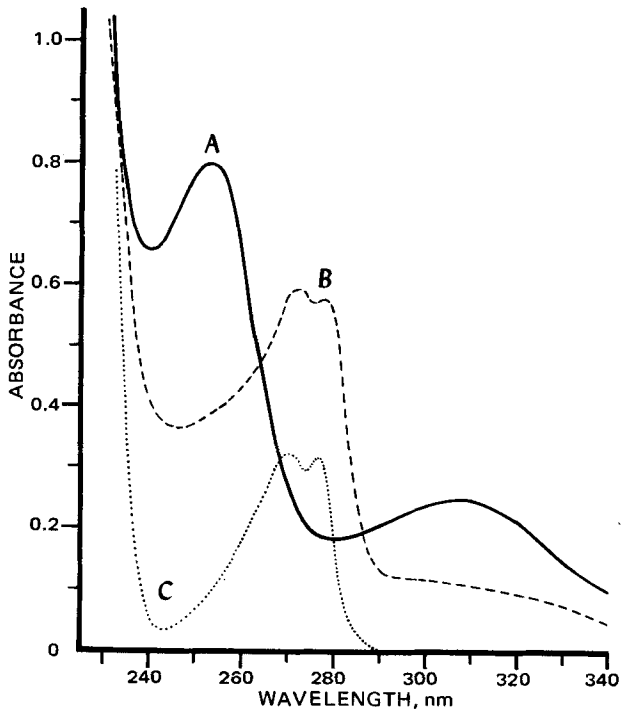

Figure 2—*UV absorption spectra of urinary III (A, 108 μM), urinary IV (B, 348 μM), and nadolol (C, 300 μM). Each compound was dissolved in methanol.*

The solvent systems used were: A, ethanol–15 *N* ammonium hydroxide–distilled water (12:1:7); B, 1-butanol–15 *N* ammonium hydroxide–distilled water (4:1:3, upper phase); C, 1-butanol–acetic acid–ether–distilled water (9:6:3:1); D, 1-butanol–acetic acid–ether–distilled water (6:3:9:1); E, chloroform–acetic acid–methanol (15:1:4); and F, ethyl acetate–15 *N* ammonium hydroxide–ethanol–distilled water (4:1:1:2, upper phase).

One-dimensional chromatograms were scanned for radioactivity with a radiochromatogram scanner[3]. The area under each peak was determined with a compensating polar planimeter[4]. In this manner, R_f values and relative amounts of each metabolite were determined. Radioactivity on preparative chromatograms was located with a two-dimensional scanner fitted with a dot printer[5]. Radioactive bands were scraped from the plates, and the metabolites were eluted with methanol. The estimation of the quantities of metabolites isolated is based on a calculated value of 1813 dpm/μg of administered ^{14}C-bunolol.

Phenolic compounds were detected on TLC plates by spraying with ferricyanide–ferric chloride solution (9); this test permits detection of 0.1 μg of 8-hydroxybunolol.

Mass and UV Spectrometry—Mass spectra were obtained with a double-focusing mass spectrometer using a heated direct insertion probe[6]. The accelerating potential was 8 kv, the ionizing voltage was 60 v, and the trap current was 100 μamp. Hydroxybunolol (III) was run at a probe temperature of 75°; 120° was used for hydroxydihydrobunolol (IV). Exact mass determination was done by the peak matching technique using perfluorokerosene as a reference. UV spectra were recorded[7]. The solvent for all compounds was methanol.

Protocol—Twenty-milligram portions of ^{14}C-bunolol were weighed into gelatin capsules, and enough carrier bunolol was added to provide 10-mg/kg doses. The capsules were administered to female beagles weighing 11.5 (Dog 1), 11.5 (Dog 2), 13.0 (Dog 3), and 10.0 (Dog 4) kg. The dogs had free access to food and water. Urine collected from 0 to 24 hr from each dog was kept frozen until needed. The 0–24-hr urine samples from Dogs 1–3 were pooled before investigation and were identical with those used to determine the extent of bunolol excretion (4).

Dog 4 was given two additional identical doses of ^{14}C-bunolol 8 and 15 days after the first dose. Urine was collected for 24 hr following each dose. The three urine collections contained 47.6, 58.7, and 59.4% of the radioactivity of the respective doses. These urine collections, totaling 1050 ml, were pooled and stored frozen.

Recovery of Reference I–IV from Urine of Untreated Dogs—To determine the stability of bunolol and its basic metabolites during isolation, 50 μg of each radioactive compound in 50 μl of methanol was added to a separate 10-ml portion of urine from an untreated dog. After adding 1 ml of ether to each solution, air was passed over the surface for 4 hr to simulate the operation designed to free urine of residual ether.

Each urine specimen was extracted six times with ether, and the extracts were concentrated. Comparative TLC in Solvent E was performed on the ether concentrates and on solutions of the four reference compounds. Radiochromatogram scanning showed that no decomposition resulted from exposure to air under these experimental conditions.

Fractionation of Unconjugated Labeled Bases—The pooled urine (1050 ml) from Dog 4, containing 165-mg equivalents of bunolol, was adjusted to pH 2 and extracted 10 times with 500-ml volumes of ether. The pH of the aqueous phase was brought to 10, and 12 extractions with 500 ml each of ether were performed. The pooled ether extract obtained at pH 10 contained 30-mg equivalents of bunolol.

After the volume was reduced to 2 ml, the solution was chromatographed on a 1.5 × 83-cm dextran column[8], prepared and operated in 20 m*M* sodium phosphate buffer at pH 7.0. [The column had been precalibrated by separate successive applications of 3 μmoles each of I hydrochloride, II oxalate, and 8-hydroxybunolol (V) hydrochloride and by monitoring the effluent at 255 nm for I and V and at 272 nm for II.] The urine extract of unconjugated bases yielded two radioactive fractions. One was the column effluent from 65 to 80 ml, and the other was the effluent from 80 to 105 ml.

Isolation of Unconjugated IV—The fraction eluted from the dextran column from 65 to 80 ml was lyophilized, and the residue was extracted with methanol. The extracts were reduced to 0.2 ml, and the concentrate was streaked onto two 20 × 20-cm TLC plates. After development in Solvent E, the plates were air dried and the radioactivity was located by two-dimensional scanning. A single radioactive band at R_f 0.37 was scraped from the plates and eluted with methanol. The volume of the methanol extract was reduced to 0.2 ml, and the concentrate was streaked onto a 20 × 20-cm plate. After development in Solvent B, two-dimensional scanning revealed a single radioactive band at R_f 0.65.

The plate was cut 46 mm above the origin, and the lower section of the plate was discarded. The upper section now contained the radioactive band 25 mm above the lower edge. This section was developed a second time in Solvent B, with the solvent front moving in the same direction as during the first development. The second development improved the separation of the radioactivity from a nonradioactive band visible under UV light. A band containing radioactive material (22 mm wide) was lo-

[3] Packard model 7201.
[4] Keuffel and Esser.
[5] Varian-Berthold.
[6] AEI Scientific MS902C.
[7] Beckman DU spectrophotometer.
[8] Sephadex G-10.

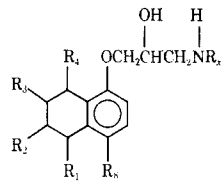

Table I—Structures[a] and R_f Values of Bunolol and Its Urinary Metabolites and Analogs[b]

Compound	R_1	R_2	R_3	R_4	R_8	R_x	R_f Values in Solvent[c] A	B	C	D	E	F
I	=O	H	H	H	H	$C(CH_3)_3$	0.78	0.71	0.31	0.38	0.53	0.43
^{14}C-III[d]	=O	H	H	OH[e]	H	$C(CH_3)_3$	0.75	0.67	0.27	0.24	0.40	0.34
^{14}C-IV[d]	OH	H	H	OH[e]	H	$C(CH_3)_3$	0.75	0.64	0.30	0.24	0.33	0.21
^{14}C-II[d]	OH	H	H	H	H	$C(CH_3)_3$	0.80	0.73	0.40	0.33	0.46	0.41
II[f]	OH	H	H	H	H	$C(CH_3)_3$	0.80	0.74	0.39	0.32	0.45	0.40
V[f]	=O	H	H	H	OH	$C(CH_3)_3$	0.79	0.70	0.31	0.37	0.53	0.43
VI[f]	=O	H	H	H	H	H	0.76	0.46	0.28	0.24	0.20	0.16
Nadolol	H	OH	OH	H	H	$C(CH_3)_3$	0.70	0.57	0.27	0.20	0.25	0.16

[a] Subscripts for substituents are numbered according to the system for the carbon atoms in the tetralone ring system. [b] Approximately 10 μg of each compound was applied to each TLC plate. [c] Unwashed plates were used. Some R_f values were changed by prewashing with methanol. [d] Pure isolate from the unconjugated basic fraction. [e] The hydroxyl group probably is in this position, but conclusive structural proof is lacking. [f] Synthetic.

cated 65 mm above the cut lower edge of the plate. Following scraping, the radioactivity was eluted with methanol.

The eluate was concentrated to 0.2 ml, and the concentrate was purified by preparative TLC in Solvent F. The metabolite was obtained from a 12-mm wide band at R_f 0.27 by scraping and eluting with methanol. The methanol solution was concentrated to 0.2 ml, and 2 ml of chloroform was added. The metabolite solution was purified by passage over a 4 × 6-mm column of diatomaceous earth[9]. After removal of the solvent, the sample weighed 3.8 mg; the calculated weight based on the radioactivity of bunolol was 2.1 mg.

Isolation of Unconjugated III—The fraction eluted from the dextran column from 80 to 105 ml was lyophilized, and the residue was extracted with methanol. The extracts were concentrated to approximately 0.3 ml. The concentrate containing 11-mg equivalents of bunolol was chromatographed in Solvent E using seven prewashed 20 × 20-cm TLC plates. The major radioactive peak at R_f 0.48 was scraped and eluted with methanol. The volume of the methanol extract was reduced to approximately 0.2 ml, and the concentrate was chromatographed in Solvent D on four 20 × 20-cm TLC plates.

A radioactive band at R_f 0.29 represented 74% of the radioactivity on the plate; the balance of the isotope was at R_f 0.41. For further purification, the radioactive band at R_f 0.29 was scraped from the plates and eluted with methanol. The methanol was concentrated to 0.5 ml and then passed over a 1 × 54-cm dextran column[10] equilibrated with methanol. A radioactive peak emerged from 29 to 31.6 ml. After evaporation of the methanol, the residue weighed 3.4 mg; the calculated weight based on the radioactivity of bunolol was 2.4 mg.

Isolation of Unconjugated II—The radioactive band at R_f 0.41 was eluted with methanol. Solvent evaporation left a residue weighing 30 mg, whereas the carbon-14 content corresponded to only 1.3 mg of bunolol. The material was purified by rechromatography in Solvent B and elution of the band at R_f 0.71 with methanol. After solvent removal, the residue weighed 1.7 mg; its radioactivity corresponded to 0.83 mg of bunolol.

Isolation of II and IV after Enzymic Hydrolysis—A 368-ml aliquot of pooled urine from Dogs 1–3, containing 55-mg equivalents of bunolol, was extracted repeatedly at pH 1.8 and 10.5 with ether to remove unconjugated bunolol metabolites. The pH was brought to 6.5, and air was blown over the solution for 4 hr to remove residual ether. For each 100 ml of urine, 0.2 ml of a preparation of aryl sulfatase–β-glucuronidase[11] was added. The amounts corresponded to 0.6 international unit of aryl sulfatase and 1.2 international units of β-glucuronidase.

After incubation at 37° for 15 hr, another 0.2 ml of enzyme solution was added and incubation was resumed for 7 hr. Then deconjugated acids were removed by three extractions at pH 1.8 with ether. Bases were collected by four ether extractions at pH 10.5; radioactivity counting showed the presence of 8.6-mg equivalents of bunolol. The solution of bases was taken almost to dryness and chromatographed in Solvent E on 10 TLC plates. The two radioactive bands were eluted repeatedly with 10-ml portions of methanol.

The eluate of the slower moving material was purified further by preparative TLC in Solvent B on 12 TLC plates. The radioactive bands were eluted and contained carbon-14 equivalent to 1.3 mg of bunolol. This fraction represented IV. The fraction obtained by elution of the faster moving band was rechromatographed on nine plates in Solvent B, and elution yielded 1.3-mg equivalents of II.

Determination of Quantities of Metabolites in Urine—All quantification experiments were conducted with urine pooled from Dogs 1–3. The amounts of metabolites in pooled urine were estimated by a sequence of fractionation steps. Conjugated bases were enzymatically hydrolyzed after ether extraction of the unconjugated bases. Following separation in Solvent E, the radioactive bands were collected by scraping the silica gel containing the radioactive metabolites off the plate, extracting the scrapings four or five times with 1- or 2-ml portions of methanol, and concentrating the pooled methanol fractions to 0.1 or 0.2 ml. After detection of the major peak by radioscanning, its relative quantities were determined by planimetry. The amount of each urinary metabolite was calculated by multiplying the percentage of the dose in the urine by the

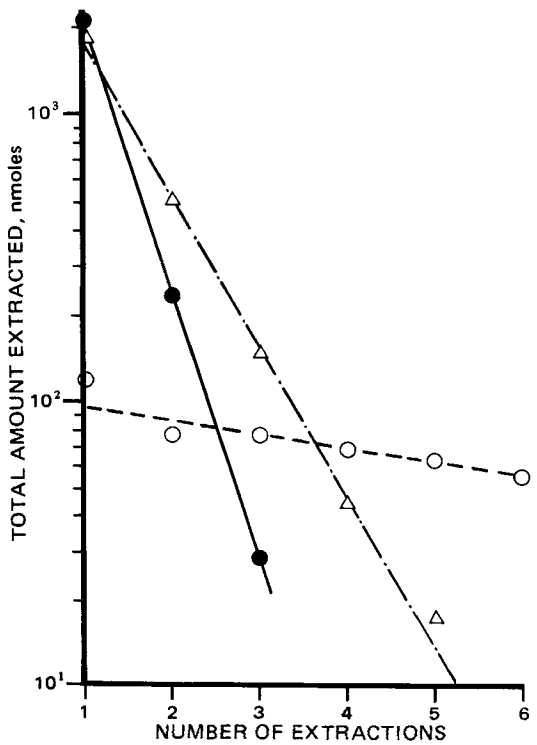

Figure 3—*Ether extraction of I (●), 2.7 μmoles; II (△), 2.0 μmoles; and IV (○), 2.3 μmoles, from aqueous solution. Each aqueous solution (16 ml) was extracted at pH 10 each time with 8 ml of ether.*

[9] Hyflo Supercel Celite.
[10] Sephadex LH-20.
[11] Calbiochem.

Table II—UV Absorption Maxima and Molar Absorptivities of Synthetic Bunolol, Nadolol, and Unconjugated and Deconjugated Basic Bunolol Metabolites

Compound	UV Absorption Peak, nm	Molar Absorptivity[a]
I	253	9000
	310	2400
V	260	8210
Nadolol	270	1080
	277	1060
III	253	8800
	308	2740
II	271	2450
	279	2380
II (deconjugated)	271	2210
	279	2080
IV	272	1810
	278	1760
IV[b]	272	2550
	278	2490

[a] The absorption coefficients of I, V, and nadolol were determined from weighed samples. Coefficients for the other compounds were estimated from the carbon-14 content of solutions. [b] From deconjugated fraction.

percentage of the dose in the ether fraction and by the percentages of the metabolite found on each successive TLC plate.

Unconjugated III and IV were assayed in the same urine aliquot (32 ml of the total pool of 805 ml). The specimens were extracted five times at pH 1.8 with two volumes of ether. The aqueous phase pH was brought to 10.5, and the solution was extracted with ether to collect the unconjugated bases. The latter ether extract was reduced to ~0.2 ml and chromatographed on 20 × 20-cm plates in Solvent E. The radioactivity at R_f 0.43 represented III, and the radioactivity at R_f 0.33 represented IV. Compound III was collected, eluted, and chromatographed successively in Solvents C and B. Compound IV was assayed independently by successive TLC in Solvents B and C.

Unconjugated II was assayed similarly using a 22-ml aliquot of the pooled urine. Since synthetic II was available, it was chromatographed in parallel with the urinary metabolite and located in TLC plates by exposure to iodine vapor. The sequence of developing solvents employed was E, C, and B.

Table III—Recovery of Bunolol Metabolites at Major Stages of Purification from Pooled 0–24-hr Urine of Dogs Dosed with ^{14}C-Bunolol (10 mg/kg po)

Metabolite	Purification Step	Percent of Preceding Step
II	Unfractionated urine	61.2[a]
	Ether extract, pH 10	24.6
	Eluate at R_f 0.57 from TLC, Solvent E	52.4
	Eluate at R_f 0.54 from TLC, Solvent C	4.7
	Eluate at R_f 0.73 from TLC, Solvent B	81.6
III	Unfractionated urine	61.2[a]
	Ether extract, pH 10	24.6
	Eluate at R_f 0.43 from TLC, Solvent E	60.7
	Eluate at R_f 0.29 from TLC, Solvent C	83.5
	Eluate at R_f 0.65 from TLC, Solvent B	81.0
IV	Unfractionated urine	61.2[a]
	Ether extract, pH 10	24.6
	Eluate at R_f 0.22 from TLC, Solvent E	29.6
	Eluate at R_f 0.50 from TLC, Solvent B	88.2
	Eluate at R_f 0.32 from TLC, Solvent C	98.0
II (deconjugated)	Unfractionated urine	61.2[a]
	Ether extract, pH 10[b]	7.8
	Eluate at R_f 0.43 from TLC, Solvent E	45.6
	Eluate at R_f 0.53 from TLC, Solvent C	77.6
	Eluate at R_f 0.83 from TLC, Solvent A	100
IV[c]	Unfractionated urine	61.2[a]
	Ether extract, pH 10[b]	7.8
	Eluate at R_f 0.23 from TLC, Solvent E	50.8
	Eluate at R_f 0.35 from TLC, Solvent C	94.1
	Eluate at R_f 0.78 from TLC, Solvent A	92.0
VI	Unfractionated urine	61.2[a]
	Ether extract, pH 10	26.6
	Eluate at R_f 0.16 from TLC, Solvent E	0.46
	Eluate at R_f 0.28 from TLC, Solvent C	24.1
	Eluate at R_f 0.40 from TLC, Solvent B	11.0

[a] Percent of total dose excreted. [b] Preceded by aryl sulfatase–glucuronidase treatment. [c] From deconjugated fraction.

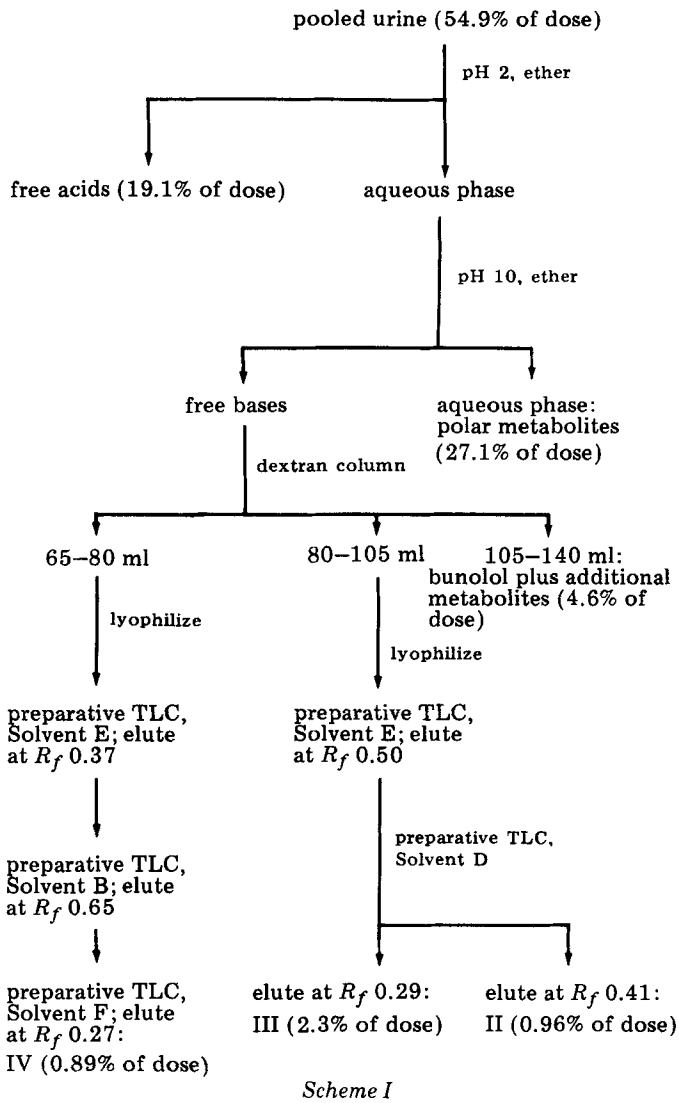

Scheme I

The quantities of basic metabolites extracted after enzyme hydrolysis were determined from a 100-ml aliquot of urine. After extracting unconjugated acids and bases at pH 1.8 and 10.5 with ether and evaporating residual solvent, the pH was adjusted to 6.6 for incubation with aryl sulfatase–β-glucuronidase as described. An ether extract containing both deconjugated bases was chromatographed in Solvent E. The slower moving radioactive band contained IV, which was eluted and rechromatographed sequentially in Solvents C and A. The faster moving band contained II, which was eluted and also rechromatographed in Solvents C and A.

Attempt to Identify Des-*tert*-butylbunolol (VI) in Urine—A 68-ml aliquot of pooled urine was extracted thoroughly with ether to remove acids at pH 1.8 and bases at pH 10.5. The extract of bases was concentrated to 0.3 ml and then streaked onto several 20 × 20-cm TLC plates. Synthetic VI was spotted on both sides of the urine extract, and the plates were developed in Solvent E.

Each plate had three major bands of radioactivity; none corresponded to the synthetic amine. The small quantity of radioactivity at the R_f value of the reference compound was scraped from the plates, eluted, and rechromatographed in Solvent C in parallel with the authentic compound. The process was repeated with Solvent B.

RESULTS

Figure 1 shows that I, II, IV, and V are separable by adsorption chromatography using a dextran[10] column. Scheme I shows how this resolution capability was employed to isolate II–IV from the urine of Dog 4 (which received three doses of ^{14}C-bunolol). Scheme II shows the mass

spectral fragmentation patterns of III and IV, metabolites previously discussed (4) and now identified for the first time. The UV spectra of these metabolites are compared with the nadolol spectrum in Fig. 2. The positional isomers, nadolol and IV (Table I), have similar spectra (Table II), a finding that supports the identification of the metabolite by interpreting mass spectral data. The spectrum of III is very similar to that of bunolol (Table II).

Table I presents the structures and R_f values in six solvents of the reference compounds used in this study and of purified bunolol metabolites from dog urine. Table II lists the UV absorption maxima and the molar absorption coefficients of bunolol, nadolol, and unconjugated and deconjugated basic bunolol metabolites isolated from dog urine.

Table III is a condensation of quantitative estimates at the major steps involved in the purification of unconjugated II–IV and of II and IV after enzyme hydrolysis. Table III also shows that the total urinary excretion of the label in 24 hr was 61.2% of the administered dose and that VI could not be isolated from dog urine.

The fractionation and chromatography studies showed that the pooled urine of Dogs 1–3 contained at least 18 isotopically labeled compounds. The major fractions were four unconjugated acids that accounted for 22.5% of the dose, three unconjugated bases (14.7% of dose), and an unknown number of unclassified polar metabolites (14.2% of dose). The minor fractions consisted of six conjugated acids (2.8% of dose) and four conjugated bases (7.0% of dose).

Table IV further illustrates the extensive biotransformation of bunolol in the dog. Seven compounds represented 47% of the urinary radioactivity, and two acidic metabolites, β-(5-oxytetralonyl)lactic acid (VII) and (5-oxytetralonyl)acetic acid (VIII), accounted for almost half of the material identified. The balance consisted of unconjugated and conjugated bases. Compounds I–IV were found in unconjugated form, and conjugated II was also present. Although IV was extracted after enzyme hydrolysis (Table III), this material was assigned to the unconjugated base. This assignment was based upon an extraction study that indicated that IV, collected after enzyme treatment, represented carryover from the unconjugated fraction. Briefly, the extraction experiments with pure

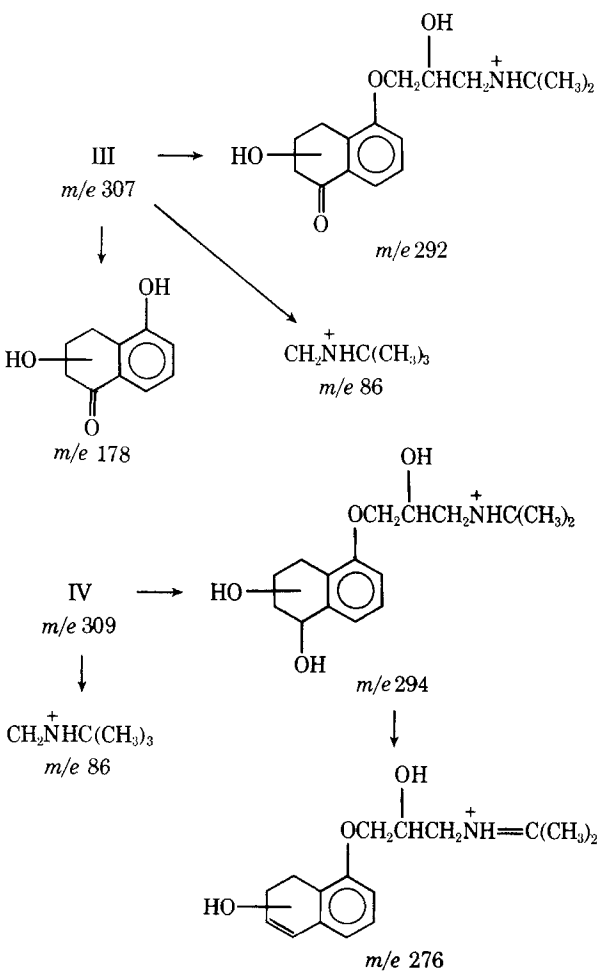

Scheme II

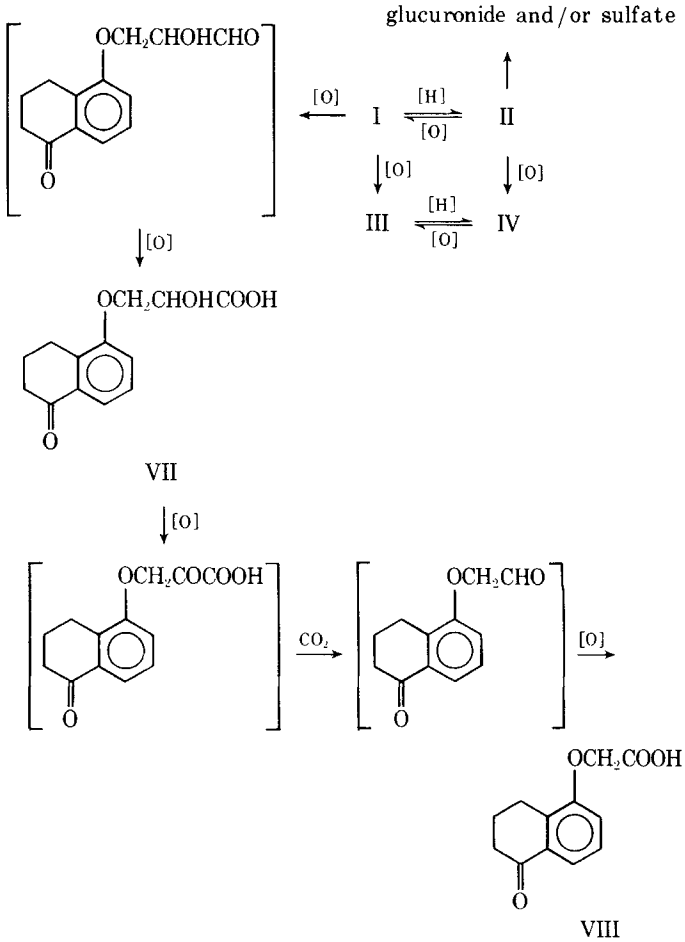

Scheme III

compounds in aqueous solutions at pH 10 showed that six ether extractions removed only 20% of IV whereas only three extractions removed at least 96% of I and II (Fig. 3).

DISCUSSION

The pathways proposed for bunolol biotransformation in the dog are illustrated in Scheme III. Reductive as well as oxidative reactions are involved. The acidic metabolites were described earlier (5). The present study supports the depicted oxidation of the side chain to yield *tert*-butylamine rather than desalkylbunolol because the latter compound could not be detected in dog urine. This experimental observation and interpretation are consistent with the literature showing that the *tert*-butyl group is refractory to *N*-dealkylation (10, 11).

The presence of II in dog urine was mentioned previously (6), but its extensive conjugation was unknown. Compound III is a newly identified metabolite. Although synthetic work is needed for assignment of the position of the hydroxyl group, it is clear that the radical is in the saturated ring because the metabolite did not respond to the phenol spray test (9) whereas reference compound 8-hydroxybunolol (V) gave a strong color reaction. The hydroxylated metabolite was also readily distin-

Table IV—Quantities of Identified Labeled Compounds in Pooled Urine in Dogs 1–3

Compound	Percent of Dose	Percent of Urinary Carbon-14
I[a]	0.4	0.7
III[a]	6.2	10.1
II	0.3	0.5
II (conjugated)	1.7	2.8
IV	6.0	9.8
VII[a]	10.0	16.3
VIII[a]	4.3	7.1
Total	28.9	47.3

[a] No conjugate detected.

guishable from the synthetic hydroxyl compound by dextran adsorption chromatography (Fig. 1) and by migration in Solvents D–F (Table I). Compound V could not be detected as a metabolite.

Another newly identified metabolite is unconjugated IV. It is assumed tentatively that the second ring hydroxyl group is in the same position as in III and that the diol metabolite may be formed from this intermediate and from II.

One cannot be certain about the oxidation of II or IV *in vivo*. Nevertheless, these conversions are postulated in Scheme III because II was oxidized readily *in vitro* by human and rat erythrocytes (7). In view of the β-adrenoceptor blocking activity of both I and II (6), it seems reasonable to speculate that III and IV are active metabolites and, therefore, to consider that I is not only an active compound but a prodrug which is converted to three active metabolites.

REFERENCES

(1) C. F. Schwender, S. Farber, C. Blaum, and J. Shavel, Jr., *J. Med. Chem.*, **13**, 684 (1970).

(2) R. D. Robson and H. R. Kaplan, *J. Pharmacol. Exp. Ther.*, **175**, 157 (1970).

(3) H. R. Kaplan and R. D. Robson, *ibid.*, **175**, 168 (1970).

(4) F.-J. Leinweber, L. J. Haynes, M. C. Crew, and F. J. Di Carlo, *J. Pharm. Sci.*, **60**, 1512 (1971).

(5) F.-J. Leinweber, R. C. Greenough, C. F. Schwender, L. J. Haynes, and F. J. Di Carlo, *ibid.*, **60**, 1516 (1971).

(6) F.-J. Leinweber, R. C. Greenough, C. F. Schwender, H. R. Kaplan, and F. J. Di Carlo, *Xenobiotica*, **2**, 191 (1972).

(7) F.-J. Leinweber and F. J. Di Carlo, *J. Pharmacol. Exp. Ther.*, **189**, 271 (1974).

(8) E. J. Merrill, *J. Pharm. Sci.*, **60**, 1589 (1971).

(9) H. Gänshirt, in "Thin-Layer Chromatography," E. Stahl, Ed., Springer-Verlag, New York, N.Y., 1969, p. 540.

(10) L. Lemberger, *J. Pharm. Sci.*, **61**, 1690 (1972).

(11) B. Testa and P. Jenner, "Drug Metabolism: Chemical and Biochemical Aspects," Dekker, New York, N.Y., 1976, p. 86.

ACKNOWLEDGMENTS AND ADDRESSES

Received November 1, 1976, from the *Departments of Drug Metabolism and †Analytical/Physical Chemistry, Warner-Lambert Research Institute, Morris Plains, NJ 07950.

Accepted for publication February 14, 1977.

The authors thank Mr. Edward J. Merrill for furnishing ^{14}C-bunolol and Dr. Charles F. Schwender for synthesizing V and VI. They also appreciate the sample of nadolol supplied by Dr. S. J. Lucania, Squibb Institute for Medical Research, Princeton, N.J.

§ Present address: Department of Biochemistry and Drug Metabolism, Hoffmann-La Roche Inc., Nutley, NJ 07710.

¶ Present address: Uniroyal Inc., Middlebury, CT 06749.

x To whom inquiries should be directed. Present address: Office of Toxic Substances (WH-557), U.S. Environmental Protection Agency, Washington, DC 20460.

Effects of Adenine Nucleotides on Oxidation of Phenothiazine Tranquilizers

IRA BLEI

Abstract □ The effects of adenosine diphosphate and triphosphate on the periodic acid oxidation of the phenothiazine tranquilizing drugs were studied. The principal effect was a marked reduction in the rate of formation and decay of the drug free radical. The oxidation rates of the nucleotide free drugs seemed to be most strongly influenced by the inductive effects of substituents at the 2-position of the phenothiazine nucleus. However, the oxidation rates of the drugs in the presence of nucleotide were most strongly influenced by the substituents at the 10-position. Variations of the structure of substituents at the 10-position have only a modest effect on the electronic state of the phenothiazine nucleus. Therefore, the marked effect of structural variation in the 10-substituents in the presence of nucleotide on the periodate oxidation rate most likely is an expression of steric effects related to an interaction between drug and nucleotide.

Keyphrases □ Adenosine diphosphate and triphosphate—effect on periodic acid oxidation of various phenothiazines □ Phenothiazines, various—periodic acid oxidation, effect of adenosine diphosphate and triphosphate □ Oxidation—various phenothiazines by periodic acid, effect of adenosine diphosphate and triphosphate □ Nucleotides—adenosine diphosphate and triphosphate, effect on periodic acid oxidation of various phenothiazines □ Tranquilizers—various phenothiazines, periodic acid oxidation, effect of adenosine diphosphate and triphosphate

This study was based on an effect observed during a fluorescence quenching study of chlorpromazine (I)–adenosine triphosphate (II) complex formation, previously studied by surface chemical methods (1) and later verified by spectroscopic techniques (2). In the presence of nucleotides, the phenothiazine drug oxidation rates caused by UV irradiation were markedly reduced compared with nucleotide free drug systems. It was felt that a study of this effect might reveal useful details regarding the nucleotide–drug interaction. The general objective of this work was not to obtain absolute rate constants or other kinetic parameters but rather to obtain relative reaction rates from oxidation systems identical with respect to all variables except for structural variations of a group of phenothiazine tranquilizing drugs.

EXPERIMENTAL

Qualitative and quantitative analyses for phenothiazine free radicals were performed principally by spectrophotometry. The identity of the free radical was verified by parallel electron spin resonance measurements (3). The products of oxidation were characterized by TLC, spot tests (4), and UV–visible spectrophotometry (5).

To use spectrophotometry for quantitative analysis, the initial drug concentration had to be about 1×10^{-3} *M*. The system then had to be poised with respect to both nucleotide and oxidant concentrations. The nucleotide concentration was made high enough to assure maximal free radical formation. The periodic acid concentration was not too low so that too small a fraction of drug would be converted to semiquinone nor too high so that the reaction would proceed too rapidly for adequate quantitation. A typical final reaction mixture was: drug, 1×10^{-3} *M*; II, 1×10^{-2} *M*, tromethamine (III)–hydrochloride buffer, pH 7.0, 2×10^{-2} *M*; and periodic acid, 1×10^{-2} *M*.

A typical experiment was performed as follows. Drug, nucleotide, and buffer were added to a volumetric flask and diluted to a precalibrated mark with distilled water. An aliquot of periodic acid stock solution was then added to begin the reaction, followed by final adjustment of volume. Under these conditions, the final pH ranged from 3.0 to 4.0.

Molar absorptivities were determined by periodic acid oxidation of

guishable from the synthetic hydroxyl compound by dextran adsorption chromatography (Fig. 1) and by migration in Solvents D–F (Table I). Compound V could not be detected as a metabolite.

Another newly identified metabolite is unconjugated IV. It is assumed tentatively that the second ring hydroxyl group is in the same position as in III and that the diol metabolite may be formed from this intermediate and from II.

One cannot be certain about the oxidation of II or IV *in vivo*. Nevertheless, these conversions are postulated in Scheme III because II was oxidized readily *in vitro* by human and rat erythrocytes (7). In view of the β-adrenoceptor blocking activity of both I and II (6), it seems reasonable to speculate that III and IV are active metabolites and, therefore, to consider that I is not only an active compound but a prodrug which is converted to three active metabolites.

REFERENCES

(1) C. F. Schwender, S. Farber, C. Blaum, and J. Shavel, Jr., *J. Med. Chem.*, **13**, 684 (1970).

(2) R. D. Robson and H. R. Kaplan, *J. Pharmacol. Exp. Ther.*, **175**, 157 (1970).

(3) H. R. Kaplan and R. D. Robson, *ibid.*, **175**, 168 (1970).

(4) F.-J. Leinweber, L. J. Haynes, M. C. Crew, and F. J. Di Carlo, *J. Pharm. Sci.*, **60**, 1512 (1971).

(5) F.-J. Leinweber, R. C. Greenough, C. F. Schwender, L. J. Haynes, and F. J. Di Carlo, *ibid.*, **60**, 1516 (1971).

(6) F.-J. Leinweber, R. C. Greenough, C. F. Schwender, H. R. Kaplan, and F. J. Di Carlo, *Xenobiotica*, **2**, 191 (1972).

(7) F.-J. Leinweber and F. J. Di Carlo, *J. Pharmacol. Exp. Ther.*, **189**, 271 (1974).

(8) E. J. Merrill, *J. Pharm. Sci.*, **60**, 1589 (1971).

(9) H. Gänshirt, in "Thin-Layer Chromatography," E. Stahl, Ed., Springer-Verlag, New York, N.Y., 1969, p. 540.

(10) L. Lemberger, *J. Pharm. Sci.*, **61**, 1690 (1972).

(11) B. Testa and P. Jenner, "Drug Metabolism: Chemical and Biochemical Aspects," Dekker, New York, N.Y., 1976, p. 86.

ACKNOWLEDGMENTS AND ADDRESSES

Received November 1, 1976, from the *Departments of Drug Metabolism and †Analytical/Physical Chemistry, Warner-Lambert Research Institute, Morris Plains, NJ 07950.

Accepted for publication February 14, 1977.

The authors thank Mr. Edward J. Merrill for furnishing ^{14}C-bunolol and Dr. Charles F. Schwender for synthesizing V and VI. They also appreciate the sample of nadolol supplied by Dr. S. J. Lucania, Squibb Institute for Medical Research, Princeton, N.J.

§ Present address: Department of Biochemistry and Drug Metabolism, Hoffmann-La Roche Inc., Nutley, NJ 07710.

¶ Present address: Uniroyal Inc., Middlebury, CT 06749.

x To whom inquiries should be directed. Present address: Office of Toxic Substances (WH-557), U.S. Environmental Protection Agency, Washington, DC 20460.

Effects of Adenine Nucleotides on Oxidation of Phenothiazine Tranquilizers

IRA BLEI

Abstract □ The effects of adenosine diphosphate and triphosphate on the periodic acid oxidation of the phenothiazine tranquilizing drugs were studied. The principal effect was a marked reduction in the rate of formation and decay of the drug free radical. The oxidation rates of the nucleotide free drugs seemed to be most strongly influenced by the inductive effects of substituents at the 2-position of the phenothiazine nucleus. However, the oxidation rates of the drugs in the presence of nucleotide were most strongly influenced by the substituents at the 10-position. Variations of the structure of substituents at the 10-position have only a modest effect on the electronic state of the phenothiazine nucleus. Therefore, the marked effect of structural variation in the 10-substituents in the presence of nucleotide on the periodate oxidation rate most likely is an expression of steric effects related to an interaction between drug and nucleotide.

Keyphrases □ Adenosine diphosphate and triphosphate—effect on periodic acid oxidation of various phenothiazines □ Phenothiazines, various—periodic acid oxidation, effect of adenosine diphosphate and triphosphate □ Oxidation—various phenothiazines by periodic acid, effect of adenosine diphosphate and triphosphate □ Nucleotides—adenosine diphosphate and triphosphate, effect on periodic acid oxidation of various phenothiazines □ Tranquilizers—various phenothiazines, periodic acid oxidation, effect of adenosine diphosphate and triphosphate

This study was based on an effect observed during a fluorescence quenching study of chlorpromazine (I)–adenosine triphosphate (II) complex formation, previously studied by surface chemical methods (1) and later verified by spectroscopic techniques (2). In the presence of nucleotides, the phenothiazine drug oxidation rates caused by UV irradiation were markedly reduced compared with nucleotide free drug systems. It was felt that a study of this effect might reveal useful details regarding the nucleotide–drug interaction. The general objective of this work was not to obtain absolute rate constants or other kinetic parameters but rather to obtain relative reaction rates from oxidation systems identical with respect to all variables except for structural variations of a group of phenothiazine tranquilizing drugs.

EXPERIMENTAL

Qualitative and quantitative analyses for phenothiazine free radicals were performed principally by spectrophotometry. The identity of the free radical was verified by parallel electron spin resonance measurements (3). The products of oxidation were characterized by TLC, spot tests (4), and UV–visible spectrophotometry (5).

To use spectrophotometry for quantitative analysis, the initial drug concentration had to be about 1×10^{-3} *M*. The system then had to be poised with respect to both nucleotide and oxidant concentrations. The nucleotide concentration was made high enough to assure maximal free radical formation. The periodic acid concentration was not too low so that too small a fraction of drug would be converted to semiquinone nor too high so that the reaction would proceed too rapidly for adequate quantitation. A typical final reaction mixture was: drug, 1×10^{-3} *M*; II, 1×10^{-2} *M*, tromethamine (III)–hydrochloride buffer, pH 7.0, 2×10^{-2} *M*; and periodic acid, 1×10^{-2} *M*.

A typical experiment was performed as follows. Drug, nucleotide, and buffer were added to a volumetric flask and diluted to a precalibrated mark with distilled water. An aliquot of periodic acid stock solution was then added to begin the reaction, followed by final adjustment of volume. Under these conditions, the final pH ranged from 3.0 to 4.0.

Molar absorptivities were determined by periodic acid oxidation of

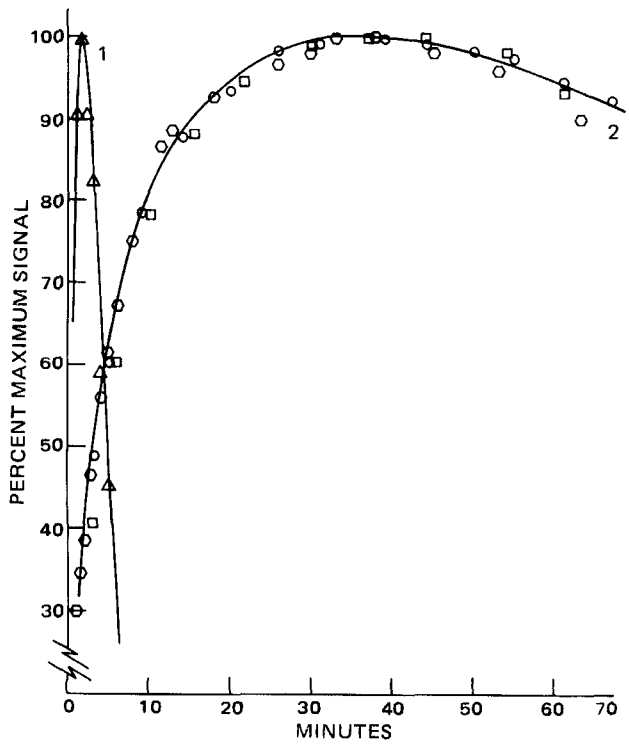

Figure 1—*Time course of periodic acid oxidation of chlorpromazine with and without adenosine triphosphate. The reaction mixture contained: drug, 1 × 10^{-3} M; periodic acid, 1 × 10^{-2} M; pH 7.0 buffer, 2 × 10^{-2} M; and II, 1 × 10^{-2} M. Key: △, absorbance at 525 nm, drug alone; ○, absorbance at 525 nm, drug plus II; and ○, □, electron spin resonance signals, drug plus II.*

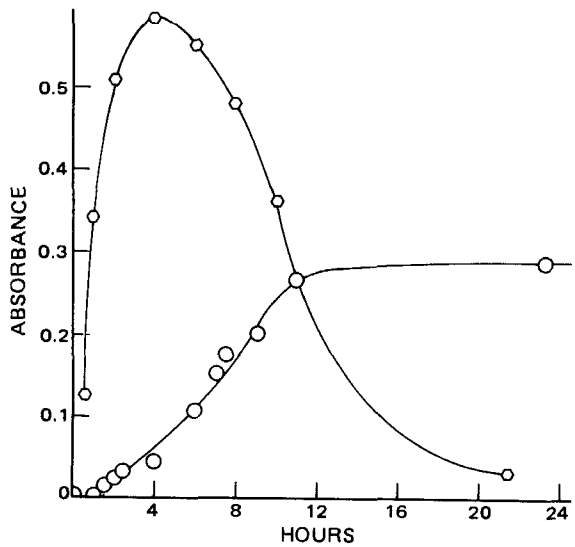

Figure 2—*Time course of promazine oxidation by periodic acid in the presence of II. The reaction mixture contained: promazine, 1 × 10^{-3} M; periodic acid, 5 × 10^{-3} M; II, 1 × 10^{-2} M; and pH 7.0 buffer, 2 × 10^{-2} M. Key: ○, absorbance of the drug free radical at 510 nm; and ○, twice the absorbance of iodine at 515 nm in carbon tetrachloride. Iodine was extracted from reaction mixtures by shaking an aliquot of reaction mixture with an equal volume of carbon tetrachloride.*

the drugs in 2 *M* H_2SO_4 (3). The log of absorbance varied linearly with time. Furthermore, different concentrations of periodic acid resulted in lines with correspondingly different slopes, all converging on the same absorbance value when extrapolated back to zero time. The zero-time absorbance values were used to compute the molar absorptivities. The value of the I free radical obtained in this way compares well with previously published data (6). The absolute values of absorptivities for the drug free radicals were not critical for comparison of initial reaction rates. This comparison required only that the values were correct relative to each other, and the approach described was sufficient to that end.

The drugs in this study were chlorpromazine[1], promazine[1], trifluoperazine[1], fluphenazine[2], triflupromazine[2], and thioridazine[3]. Nucleotides II and adenosine diphosphate (IV)[4] were used without purification. All other materials were reagent grade. Spectrophotometric measurements[5] and electron spin resonance spectra[6] were taken at room temperature.

RESULTS AND DISCUSSION

Phenothiazine oxidation is considered to proceed in acid media through two consecutive steps (7):

$$H^+ + R = S^+ + e \qquad \text{(Eq. 1)}$$

$$S^+ = T^+ + e \qquad \text{(Eq. 2)}$$

where R represents the totally reduced form of the drug, S^+ is the free radical or semiquinone, and T^+ is the totally oxidized phenazathionium cation. Depending upon pH and concentration, T^+ can react with water to form either sulfoxide or aromatic hydroxylated derivatives.

Over a wide range of experimental conditions and types of drugs and nucleotides, the initial stage of the oxidation process resulted only in the formation of semiquinone. The second stage of oxidation, semiquinone decay in the presence of nucleotide, resulted in complex mixtures of iodine and dehalogenated, demethylated, and variably hydroxylated phenothiazine derivatives. The work therefore focused on the initial reaction of the oxidation process—*viz.*, semiquinone formation, for two reasons. First, that approach minimized analytical and kinetic complexities. Second, since the effects of nucleotide on both free radical formation and decay probably reflected the same underlying molecular mechanism, little information would be lost by not studying the decay process.

The likelihood of complexation was presumed to be maximized in the pH range from 2.0 to 7.0, where the drug was cationic and the nucleotide was anionic. It would have been most desirable to poise the system as close to pH 7.0 as possible. However, at about that pH, several complicating phenomena occur: formation of neutral (insoluble) drug base, formation of drug micelles dependent upon salt type and concentration, and formation of insoluble periodic acid salts. By employing the described conditions, the system was optimized with respect to the electrostatic state of the drug and nucleotide and solution homogeneity.

The reaction of periodate with the phenothiazines is illustrated by two types of experiments in Fig. 1. Curve 1 represents the periodic acid oxidation of I measured spectrophotometrically; curve 2 represents the same system, with II added, measured both spectrophotometrically and by electron spin resonance spectroscopy. In all cases, the data are presented as percent of maximum signal of the free radical and absorbance:

$$\% \text{ maximum signal} = \left(\frac{\text{observed signal}}{\text{maximum signal}}\right) 100 \qquad \text{(Eq. 3)}$$

The assumption was that both the absorbance and intensity of the electron spin resonance signal were linearly related to free radical concentrations at the drug concentration used. The periodic acid oxidation of drug in nucleotide-free systems, as illustrated by curve 1 of Fig. 1, was typically biphasic, with the rapid appearance of the free radical followed by its equally rapid decay. Under these conditions, the oxidation appeared to be complete within about 10 min. The presence of II dramatically altered the rates of formation and decay of the free radical, as illustrated by curve 2 of Fig. 1. The absorbance and electron spin resonance data fell on the same curve, satisfying the assumptions concerning the relationship of the free radical concentration to both absorbance and the electron spin resonance signal and also permitting the legitimate use of absorbance as a measure of the free radical concentration in these systems. The addition of II had a marked stabilizing effect on the I free radical. Similar effects were observed when IV replaced II.

As the reaction proceeded, other striking differences were observed between the pure drug and nucleotide-containing systems (Fig. 2). The free radical-stabilizing effects of II were best illustrated by the oxidizing system employing promazine, since this drug was the least stable phe-

[1] Smith Kline and French.
[2] E. R. Squibb.
[3] Sandoz.
[4] Sigma Chemical Co.
[5] Hitachi-Coleman model 124 double-beam spectrophotometer.
[6] Varian E3 ESR spectrometer.

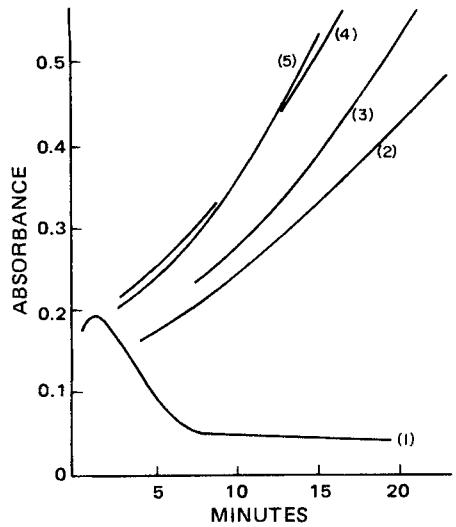

Figure 3—*Time course of oxidation of chlorpromazine in the presence of varying quantities of II. The reaction mixture contained: drug, 1 × 10^{-3} M; periodic acid, 5 × 10^{-3} M; pH 7.0 buffer, 2 × 10^{-2} M; and no II (curve 1), 5 × 10^{-5} M II (curve 2), 1 × 10^{-4} M II (curve 3), 2 × 10^{-4} M II (curve 4), or 3 × 10^{-4} M II (curve 5).*

nothiazine. The upper biphasic curve represents the appearance and decay of the promazine free radical in the presence of II. The periodate concentration was half that of the system illustrated in Fig. 1. The maximum concentration of the free radical occurred after ~4 hr. Under the same conditions without II, the maximum free radical concentration was reached in about 5 min and totally decayed in about 20 min.

The lower curve traces the appearance of iodine. For ease of visualization, the iodine concentrations are presented as double their actual values. Only in the drug–nucleotide systems is iodine a product of the drug–periodate reaction. In nucleotide-free, drug–periodate systems, the oxidant is reduced to iodate and no iodine is formed. The time course of iodine generation is typical for that of the final product of a two-step consecutive reaction system, here probably two consecutive oxidation steps. Furthermore, although detailed analyses of the drug oxidation products were not undertaken, spot tests and TLC indicated the presence of demethylated, dehalogenated, and aromatic hydroxylated products in the systems containing nucleotides. However, only the sulfoxide was produced in the nucleotide-free systems.

Control experiments showed that the nucleotide had no effect on the

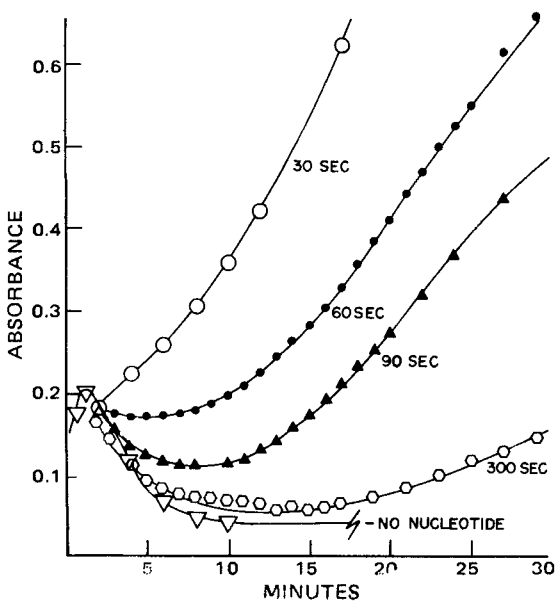

Figure 4—*Time course of oxidation of 1 × 10^{-3} M promazine by 1 × 10^{-2} M periodic acid in 2 × 10^{-2} M pH 7.0 buffer. Curves are labeled to represent elapsed times of reaction prior to addition of II sufficient to bring the solutions to 1 × 10^{-2} M with respect to nucleotide.*

Table I—Initial Rates of Drug Free Radical Formation *versus* Drug Potency [a]

Drug	Rate of Formation × 5 ± 0.5 × 10^7, moles/liter/min With IV	Rate of Formation × 5 ± 0.5 × 10^7, moles/liter/min Without IV	$E_m \pm 0.1\ E_m$, liters/mole cm	Average Antipsychotic Dosage (9), mg
Promazine	875	7000	1 × 10^4 (510 nm)	750
Chlorpromazine	250	1750	1 × 10^4 (525 nm)	550
Thioridazine	65	4850	1.5 × 10^4 (625 nm)	300
Triflupromazine	40	—	5 × 10^3 (500 nm)	200
Trifluoperazine	17	630	9.5 × 10^3 (500 nm)	9
Fluphenazine	6	1320	5 × 10^3 (510 nm)	6

[a] A typical reaction mixture contained: drug, 1 × 10^{-3} *M*; adenosine diphosphate (IV), 1 × 10^{-2} *M*; III–hydrochloride pH 7.0 buffer, 2 × 10^{-2} *M*; and periodic acid, 1 × 10^{-2} *M*.

periodic acid oxidation of sodium metabisulfite, sodium sulfite, aniline, and *o*-phenylenediamine. Furthermore, exposure of II to 0.1 *M* periodic acid for 24 hr had no effect on the nucleotide's ability to stabilize the drug free radical. The effects of II concentration on the initial rate of periodate oxidation of chlorpromazine are illustrated in Fig. 3. Curve 1 represents a nucleotide-free system in which free radical rapidly forms and decays. Curves 2–5 represent similar systems with increasing II concentrations.

These differences in oxidation rates and the nature of products between systems with and without nucleotide are best explained as consequences of nucleotide–drug complex formation. In an earlier study, intercalation or complexation also seemed to provide the basis for the ability of deoxyribonucleic acid to stabilize the I free radical (8). This finding posed the next question: if a complex was formed, was the complex oxidized directly or did the free drug arise from complex dissociation.

This question was probed by the following experiments (Fig. 4). Compound II was added as dry powder to buffered promazine–periodic acid systems at 30, 60, 90, and 300 sec after the oxidation was begun. For reference purposes, the lowest curve is a system without nucleotide; the free radical concentration rose to a maximum in about 1 min and then began to decay. From the data in Fig. 4, it is clear that the sooner nucleotide is added to the drug–oxidant system, the greater is the extent of stable free radical formation. An alternative view is that the extent of stable free radical formation and/or accumulation depends upon the concentration of unoxidized drug. The first oxidation step in the drug–nucleotide systems therefore appears to be subsequent to a process requiring both the presence of nucleotide and unoxidized drug—*viz.*, complex formation.

It seemed desirable to attempt to correlate the effects of nucleotide on drug oxidation with some pertinent biological data. The specific approach was to obtain initial oxidation rates of drug–nucleotide systems under identical experimental conditions, varying only the nature of the drug. The goal was to determine whether or not a reasonable relationship between these oxidation rates and the "clinical effectiveness," *i.e.*, human drug dosage for a specific behavioral end-point, could be established. Although the specific values for drug dosage (9) may be controversial, the relative values of dose *versus* drug type seem well established. Therefore, it was considered satisfactory to use these values to explore the relationship between the oxidation rate of the drug–nucleotide complex and drug structure. Accordingly, the results of experiments designed to obtain these data along with experimental conditions are presented in Table I and Fig. 5. Reference to Fig. 5 indicates an apparent correlation of initial oxidation rates of drug–nucleotide systems with clinical dosages. There appears to be no correlation of initial oxidation rates of nucleotide-free drug systems with drug dosages (Table I).

The differences in oxidation rates among the different drug–nucleotide systems may be viewed as reflecting differences in the degree of steric hindrance to oxidation as a result of complex formation. Figure 6 illustrates the manner in which nucleotide and drug might interact to form a complex.

In Fig. 6A, space-filling models of II and chlorpromazine are poised in a relationship allowing an approach favoring complexation. In Fig. 6B, the approach is complete and shows a close complementary fit. There appears to be ample opportunity for salt formation between phosphate groups of II and the quaternized terminal nitrogen of the drug's pendant 3-(*N,N*-dimethylamino)propyl group. As a result of this apposition, the hydrophobic moieties approach in such a way as virtually to "bury" the

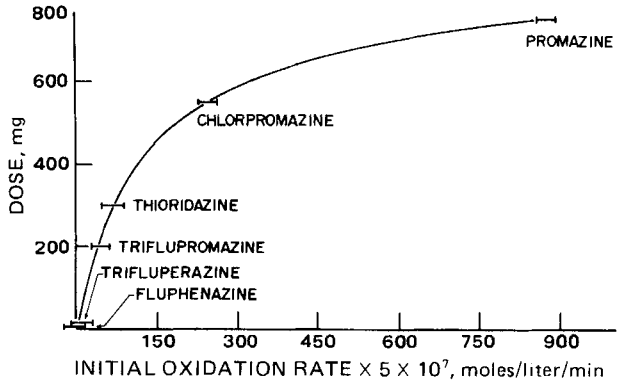

Figure 5—*Initial rates of phenothiazine drug free radical formation in the presence of IV as a function of drug potency. The rates were arbitrarily scaled for convenient comparison of values. Experimental details may be found in Table I.*

sulfide sulfur within the domain of the complex (see arrows) and to hinder severely the approach of an oxidant, particularly one as bulky as periodate. Complexation should also reduce the electrostatic attraction between the drug cation and the oxidant anion.

Reference to Fig. 6 shows that the plane of the phenothiazine nucleus is normal to the plane formed by the purine and ribose–phosphate moieties of the nucleotide. The substituent at the 2-position is removed from the area of contact between the two molecules. Therefore, it should have only an electronic inductive effect on the oxidation rate rather than a steric effect.

Promazine and chlorpromazine differ in structure only at the 2-position. Reference to Table I indicates a significant effect on the rates of drug oxidation by the nucleotide. However, the ratios of promazine oxidation rate to that of chlorpromazine in the presence and absence of nucleotide are the same to within ±7%. This result indicates that the inductive effects on the oxidation rate caused by substituents at the 2-position continue to operate, apparently unmodified by complexation, along with the superposition of steric effects caused by substituents at the 10-position.

Substituents at the 10-position are intimately involved in the proposed complex, and differences there should be reflected in the extent to which oxidation rates are modified. Fluphenazine, trifluoperazine, and triflupromazine have identical substituents at the 2-position but differ in structure at the 10-position. They demonstrated significant differences in drug oxidation rates in the presence of nucleotide, not related simply to their oxidation rates in nucleotide-free systems (Table I). However, the extent of oxidation rate reduction for these three drugs in the presence of nucleotide did seem to be related to the dimensions of the substituents at the 10-position; the larger the dimensions, the greater was the reduction in the oxidation rate. These facts are consistent with the proposal that drugs and nucleotide interact to form a sterically hindered reductant.

The experimental systems described required drug concentrations much higher than would ever be encountered in an *in vivo* situation. Even so, the general relationships demonstrated with this model system would not be significantly altered by decreasing drug concentrations to those comparable to the *in vivo* situation where nucleotide concentrations may be orders of magnitude greater than those of the drugs.

The relationship described in Fig. 5 is consistent with the view that, within a family of similarly acting drugs, differences in effectiveness are

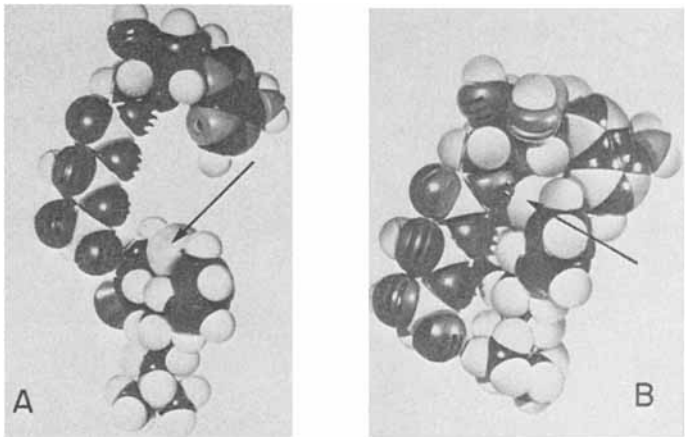

Figure 6—*Photographs of space-filling models. Key: A, II and chlorpromazine as they might approach in solution; and B, view of a possible model of the resulting complex. The arrows point to the ring sulfur atoms for reference.*

related to differences in absorption rates, distributions, and metabolic fates. In this particular case, the data indicate that the differences may be principally related to metabolic fate: oxidation. Furthermore, the clinical or apparent effectiveness of the phenothiazine tranquilizers did not correlate with the oxidation rate of free drug but rather of a drug–nucleotide complex. Implicit in this finding is the possibility that the drugs may exist within the cell to a significant extent in the form of drug–nucleotide complexes. The data presented here support the probability of the *in vitro* existence of such complexes.

REFERENCES

(1) I. Blei, *Arch. Biochem. Biophys.*, **109,** 321 (1965).

(2) I. Moriguchi, S. Fushimi, R. Umehara, and N. Kaneniwa, *Chem. Pharm. Bull.*, **20,** 834 (1972).

(3) T. N. Tozer and L. D. Tuck, *J. Pharm. Sci.*, **54,** 1169 (1965).

(4) E. Usdin, *Psychopharm. Bull.*, **6,** 44 (1970).

(5) R. J. Warren, I. B. Eisdorfer, W. E. Thompson, and J. E. Zarembo, *J. Pharm. Sci.*, **55,** 144 (1966).

(6) T. Akera and T. M. Brody, *Mol. Pharmacol.*, **4,** 600 (1968).

(7) L. Michaelis, M. P. Schubert, and S. J. Granick, *J. Am. Chem. Soc.*, **62,** 204 (1940).

(8) S. Ohnishi and H. McConnell, *ibid.*, **87,** 2293 (1965).

(9) "The Pharmacological Basis of Therapeutics," 3rd ed., L. S. Goodman and A. Gilman, Eds., Macmillan, New York, N.Y., 1965, p. 164.

ACKNOWLEDGMENTS AND ADDRESSES

Received July 14, 1976, from the *Division of Pure and Applied Sciences, College of Staten Island, Staten Island, NY 10301.*

Accepted for publication January 31, 1977.

Supported in part by Grant 1R01 MH 16479-01 from the National Institute of Mental Health and by Grant 1150 from the City University of New York.

The author thanks Professor N.-L. Yang for the electron spin resonance analyses.

Quantitative Analysis of Methadone in Biological Fluids Using Deuterium-Labeled Methadone and GLC–Chemical-Ionization Mass Spectrometry

D. L. HACHEY *x, M. J. KREEK ‡, and D. H. MATTSON *

Abstract □ The (+)-, (−)-, and (±)-$^2H_5$-methadones, which contained five deuterium atoms in one aromatic ring, were synthesized for use in clinical pharmacological studies and as internal standards. GLC–chemical-ionization mass spectrometry was used to determine plasma and urinary methadone levels by an inverse isotope dilution assay. Plasma drug levels could be determined to 10 pmoles/ml, and urine levels could be measured to 5 pmoles/ml. Plasma methadone levels were examined in several patients undergoing methadone maintenance therapy. These levels generally ranged between 100 and 400 ng/ml (320–1300 pmoles/ml) after an average oral dose of 1 mg/kg/day. The methadone half-life was 28.8 ± 4.8 hr.

Keyphrases □ Methadone—GLC–chemical-ionization mass spectrometric analysis in plasma and urine, deuterium-labeled enantiomers and racemate synthesized □ GLC–chemical-ionization mass spectrometry—analysis, methadone in plasma and urine □ Deuterium-labeled compounds—(+)-, (−)-, and (±)-$^2H_5$-methadones synthesized □ Stereoisomers—(+)-, (−)-, and (±)-$^2H_5$-methadones synthesized □ Narcotic analgesics—methadone, GLC–chemical-ionization mass spectrometric analysis in plasma and urine, deuterium-labeled enantiomers and racemate synthesized

Low level quantitation of methadone in biological samples is most commonly done by GLC using the internal standard technique (1). This method, however, cannot detect quantities less than 10 ng/ml reliably and with high precision. Stable isotope-labeled compounds have recently proved useful as internal standards for quantitation of drugs and drug metabolites in biological fluids (2, 3). The technique, which involves adding a large excess of labeled compound directly to the biological sample, was first utilized to study the metabolism of nortriptyline (4). Recently, chemical-ionization mass spectrometry and deuterium-labeled morphine were used to monitor the possible abuse of narcotics by methadone maintenance patients (5).

1-$^2H_3$-Methadone and a methadone homolog were used to measure plasma levels and turnover rates of methadone simultaneously in human subjects (6). In this technique, ion intensities were measured by electron-ionization mass spectrometry, using the ion resulting from loss of a methyl group (M − 15). Quantitative data were obtained by comparing peak heights of methadone and 1-$^2H_3$-methadone to the internal standard, 2-dimethylamino-4,4-diphenyl-5-octanone. Since the chemical properties of deuterated drugs are virtually identical with those of the parent compound, this procedure overcomes problems caused by incomplete extraction and derivatization and also minimizes absorptive losses encountered on GLC. Chemical-ionization mass spectrometry offers a significant advantage in determining isotope ratios on compounds obtained from biological sources by improving the uniqueness of a particular ion and thus minimizing interferences from ions due to natural biological contaminants (7).

The present paper reports synthesis of deuterium-labeled methadone and its use in measuring picomolar quantities of methadone in biological fluids by GLC–chemical-ionization mass spectrometry. In addition, the synthesis of (+)-$^2H_5$-methadone and (−)-$^2H_5$-methadone also is described. These two compounds will be useful in studies of the pharmacological behavior of individual methadone enantiomers.

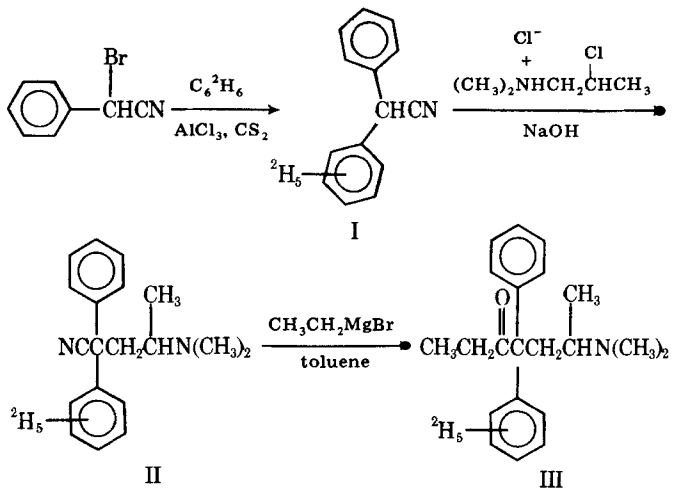

Scheme I

EXPERIMENTAL

Melting points were determined using standard techniques, and the uncorrected values are reported unless noted differently. Proton NMR spectra were obtained in deuterochloroform at 220 MHz[1]. The data are presented in parts per million (ppm) relative to tetramethylsilane. Optical rotations were measured using a polarimeter[2]. GLC analyses were carried out using a 1.83-m × 1-mm i.d. glass column packed with 10% W-98 on 80-100-mesh Gas Chrom Q[3].

Electron-impact mass spectra were run at a source temperature of 150° using an ionization potential of 30 ev[4]. Chemical-ionization mass spectra were obtained at a source pressure of 0.4 torr methane or isobutane and a source temperature of 150°[5]. Isotope ratios were measured using the stable isotope ratiometer–multiple-ion detection system described elsewhere (8).

Synthesis—2-Phenyl-2-($^2H_5$-phenyl)acetonitrile (I) was prepared by alkylation of $^2H_6$-benzene with α-bromophenylacetonitrile according to a procedure described by Schultz *et al.* (9) and suitably modified by using carbon disulfide as the solvent for the Friedel–Crafts reaction (Scheme I). Thus, from 50 g (0.595 mole) of $^2H_6$-benzene[6], 42 g (0.212 mole, 36% yield) of I was obtained as pale-yellow crystals. The product was pure by GLC analysis.

(±)-, (+)-, and (−)-4-Dimethylamino-2-phenyl-2-($^2H_5$-phenyl)-valeronitriles (II)—Compound I, 42.0 g (0.212 mole), and 47.5 g (0.300

[1] Model HR-220, Varian Analytical Instruments Division, Palo Alto, CA 94303.
[2] Model M4 QIII, Carl Zeiss, West Germany.
[3] Model 1440 gas chromatograph, Varian Aerograph, Walnut Creek, CA 94598.
[4] Model 270 mass spectrometer, Perkin-Elmer, Norwalk, CT 06852.
[5] Biospect quadrupole chemical-ionization mass spectrometer, Scientific Research Instruments, Baltimore, MD 21207.
[6] Containing 99 atom % ^2H, Aldrich, Milwaukee, WI 53233.

mole) of 1-dimethylamino-2-chloropropane hydrochloride were combined in 30 ml of water containing 24 g (0.0600 mole) of sodium hydroxide (10) (Scheme I). The reaction mixture was stirred at 88° for 6 hr and then cooled, and the product was isolated in ether. The ethereal solution was washed with 0.1 *N* NaOH, and the labeled product was extracted into 3 *N* HCl. The aqueous solution was washed twice with ether to remove neutral products.

The free base was obtained by adjusting the pH to 12 with sodium hydroxide, extraction into ether, and drying over magnesium sulfate. The ethereal solution was clarified with activated charcoal, filtered, and then evaporated to dryness. The oily product was crystallized three times from hexane to give 23.8 g (0.084 mole, 40% yield) of (±)-II. The racemic product was resolved into pure enantiomers by crystallization of the tartrate salt as described by Pohland *et al.* (11). For this reaction, 23.8 g (0.084 mole) of (±)-II and 6.65 g (0.045 mole) of (+)-tartaric acid were combined in acetone and refluxed. Sufficient water was added to dissolve the reagents. Crystallization was induced by evaporating the solvent in the cold and allowing the product to crystallize at −10° overnight. The (−)-II bitartrate salt was recrystallized once more from acetone.

The free base, obtained after neutralization with hydroxide, was crystallized twice from hexane. The yield was 8.02 g (0.028 mole, 67% yield) of white prisms, mp 97.5–99.0° [lit. (12) mp 99–101°]. The specific rotation of the product was $[\alpha]_D^{23.7}$ −50.9° (1-dm cell, 1.0205 g/ml) [lit. (11) $[\alpha]_D^{25}$ −50.0°]. The mother liquors obtained from the resolution were combined, and the free base [primarily the (+)-enantiomer] was recovered. Resolution of the (+)-enantiomer was attempted by treatment of the base with (−)-tartaric acid in the manner just described, but crystallization could not be induced. The free base was recovered and crystallized twice from hexane to give 11.6 g of (+)-II, mp 87.5–90.0° (corrected) [lit. (9) mp 97–100°].

The specific rotation was determined in ethanol, $[\alpha]_D^{24.0}$ +31.3° (1-dm cell, 1.087 g/ml) [lit. (11) $[\alpha]_D^{25}$ +50.0°]. This specific rotation represents an 81% enantiomeric purity. The electron-impact mass spectrum (30 ev) showed a base peak at *m/e* 72 [$M^+ - \cdot CH_2C(C_6H_5)(C_6{}^2H_5)CN$], a weak molecular ion at *m/e* 283 (M^+), and a characteristic ion at *m/e* 197 [$M^+ - \cdot CH_2CH(CH_2)N(CH_3)_2$]. The material was pure by GLC analysis.

(±), (+)-, and (−)-$^2H_5$-Methadones (III)—Compound (−)-II, 8.021 g (0.028 mole), was dissolved in 100 ml of anhydrous toluene and treated with ethylmagnesium bromide (0.060 mole) at reflux temperature under nitrogen. The intermediate imine was hydrolyzed with 3 *N* HCl at reflux temperature for 1 hr. Following isolation in ether, (−)-III was recrystallized twice from methanol to give 7.064 g (0.022 mole, 79%) of white prisms, mp 96.5–97.0° (corrected) [lit. (12) mp 98.7–99.0°]. The product was analyzed by GLC on a 1.83-m × 1-mm i.d. glass column packed with 3% W-98 on 80–100-mesh Gas Chrom Q at 190° and exhibited a single peak at 288 sec (the nitrile had a retention time of 232 sec under these conditions).

The electron-impact mass spectrum (30 ev) showed a base peak at *m/e* 72 [$M^+ - \cdot CH_2C(C_6H_5)(C_6{}^2H_5)COCH_2CH_3$], a weak molecular ion at *m/e* 314 (M^+, 0.4%), and several low intensity ions of diagnostic importance. These ions are *m/e* 172 [$M^+ - CH_2CHCO - CH_2CH(CH_3)N(CH_3)_2$], 228 [$M^+ - \cdot CH_2CH(CH_3)N(CH_3)_2$], and 299 [$M^+ - \cdot CH_3$]. The chemical-ionization mass spectrum (0.4 torr methane, source temperature 130°) exhibited an intense pseudomolecular ion at *m/e* 315 (MH^+), a base peak at *m/e* 72 [$MH^+ - CH_2C(C_6H_5)COCH_2CH_3$], and a minor ion at *m/e* 270 [$MH^+ - HN(CH_3)_2$].

The NMR spectrum (0.1 *M* in deuterochloroform) showed proton resonance signals at δ 0.47 (d, J = 6.5 Hz, C_7 methyl), 0.83 (t, J = 7 Hz, C_1 methyl), 2.10 (s, *N*-methyl protons), 2.32 (m, C_2 methylene and C_6 methine protons), and 7.15–7.40 (m, aromatic protons) ppm. The NMR spectrum was identical with the published spectrum (13). Integration of the aromatic proton signal indicated a 50% deuterium content. The isotope composition was determined by methane chemical-ionization mass spectrometry on a probe sample using the protonated molecular ion and contained 1.2% $^2H_0$, 1.6% $^2H_1$, 2.9% $^2H_2$, 8.9% $^2H_3$, 16.8% $^2H_4$, and 68.6% $^2H_5$ species. Since the long-term stability of methadone is poor, it was converted to the hydrochloride salt in ethanolic hydrochloric acid. The hydrochloride was recovered in 97% yield after two crystallizations from ethanol.

Compound (+)-III was prepared from 6.013 g (0.021 mole) of the corresponding nitrile [(±)-II] in 64% yield. The crystalline product, mp 95–96° (corrected) [lit. (12) mp 98.7–99.0°], was pure by GLC and exhibited mass spectra identical with those obtained for the (−)-enantiomer. The free base, 3.389 g (0.0107 mole), was converted to the hydrochloride salt in 98% yield. Racemic methadone, (±)-III, was obtained by combining equimolar amounts of (+)- and (−)-III.

Standard Solutions—Methadone hydrochloride and $^2H_5$-methadone hydrochloride were dissolved in water to give a nominal concentration of 1 mg/ml. In these studies, either the racemate or one enantiomer was used. Stock solutions of urine and plasma, obtained from healthy, drug-free adult donors, were made by serial dilution of a 1-ml aliquot of the aqueous methadone hydrochloride stock solution with urine or plasma. Concentrations of these solutions ranged from 0.3 pmole to 289 nmoles/ml of unlabeled methadone. An aqueous solution of $^2H_5$-methadone hydrochloride (3.074 nmoles/ml) was prepared for use in adding the labeled internal standard to the biological samples.

Table I—Linear Regression Analysis Data for Urine and Plasma Dilution Curves[a]

Curve	Slope ± *SD*	Intercept ± *SD*	*r*
Urine[b]	0.9986 ± 0.0091	0.2221 ± 0.0129	0.9999
Urine	0.9975 ± 0.0211	0.2364 ± 0.0302	0.9982
Plasma	1.0107 ± 0.0153	0.1793 ± 0.0221	0.9992
Plasma	1.0352 ± 0.0140	0.2040 ± 0.0200	0.9993

[a] Regression data were calculated using the log of the difference in the isotope ratio between dilution standards and blank values *versus* the log of the molar ratio of methadone present in the sample to the internal standard added to the sample. [b] Determined using 3.85 nmoles of internal standard. All other curves were prepared using 1.54 nmoles of internal standard.

Sample Preparation—Plasma or urine, 1 ml, was treated with the appropriate amount of internal standard and allowed to equilibrate at room temperature for 1.5 hr. The sample was adjusted to pH 9 with 2 ml of 0.5% ammonium hydroxide, and the solution was extracted with 5 ml of ethyl acetate. The aqueous layer was discarded, the organic phase was extracted a second time with 0.5% ammonium hydroxide, and the aqueous phase was discarded. Then the methadone was back-extracted into 2 ml of 0.05 *N* HCl, and the organic phase was discarded.

The aqueous phase was adjusted to pH 9 and extracted with 5 ml of ethyl acetate. The ethyl acetate extract was dried over sodium sulfate and evaporated under nitrogen. The samples were dissolved in 20 μl of ethyl acetate to give a nominal concentration of 25 ng of methadone/μl. A 5-μl aliquot was analyzed by GLC–chemical-ionization mass spectrometry.

Mass Spectrometric Analysis—Methadone samples were analyzed using isobutane chemical-ionization mass spectrometry (0.5 torr source pressure and 160° source temperature). Samples (about 50–100 ng each) were introduced through the GLC inlet system and were analyzed on a 1.8-m × 1-mm i.d. glass column packed with 10% W-98 on 80-100-mesh Gas Chrom Q at a temperature of 180° and a helium flow rate of 9.2 ml/min. Under these conditions, methadone had a retention time of 7.3 min and the pyrrolidine metabolite had a retention time of 4.3 min. Isotope ratios were measured using the stable isotope radiometer–multiple-ion detection system described by Klein *et al.* (8).

Standard Dilution Curves—Urine dilution curves were routinely prepared by treating 1 ml of urine stock solutions with 1.75–3.85 nmoles of $^2H_5$-methadone hydrochloride. Plasma dilution curves were prepared by treating 1 ml of plasma stock solutions with 1.75 nmoles of $^2H_5$-methadone hydrochloride. In all cases, a plasma or urine blank value also was determined.

Isotope ratios were obtained using isobutane chemical ionization and by monitoring the protonated molecular ions at *m/e* 310 and 315 for methadone and $^2H_5$-methadone, respectively. Dilution curves were constructed by plotting the log of the difference in the isotope ratio between the dilution standard and the plasma or urine blank against the log of the mole ratio of methadone to the internal standard.

RESULTS AND DISCUSSION

The most attractive position for labeling methadone with deuterium is on one of the aromatic rings. These positions are chemically inert and offer the advantage that several deuterium atoms may be introduced into the molecule from an inexpensive precursor ($^2H_6$-benzene). Although methadone and its pyrrolidine and pyrroline metabolites may be hydroxylated in the aromatic ring, this metabolic pathway is minor and does not interfere with the use of III for quantitative purposes.

To relate the observed isotope ratio to the mole composition of an isotopic mixture, standard isotope dilution curves were routinely prepared for both plasma and urine methadone standards by adding a known amount of internal standard (typically 2–4 nmoles) to each sample. The samples were allowed to stand at 4° for 1.5 hr to permit equilibration of protein-bound methadone with the internal standard. Samples were then extracted and analyzed. In both cases, plasma and urine blank values also were determined.

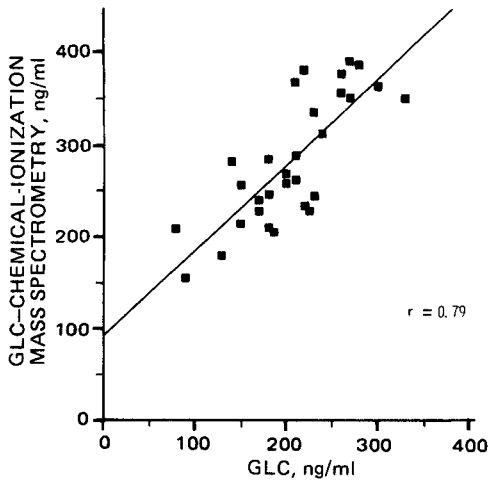

Figure 1—*Comparison of plasma methadone levels by GLC and by GLC–chemical-ionization mass spectrometry* (r = *0.79 and slope = 0.93*). *These data were obtained over 6 months from several individuals undergoing maintenance therapy.*

The protonated molecular ions observed at *m/e* 310 and 315 in the isobutane chemical-ionization mass spectra for methadone and $^2H_5$-methadone, respectively, were used to measure the isotope ratios. Standard isotope dilution curves were used to relate the observed integrated ion intensity ratio of methadone to $^2H_5$-methadone (I_{310}/I_{315}) present in a sample to the mole ratios of methadone to $^2H_5$-methadone (M_{2H_0}/M_{2H_5}) in that sample. The logarithm of the difference in the isotope ratio between the dilution sample and the plasma or urine blank (log *D*):

$$\log D = \log [(I_{310}/I_{315})_{\text{sample}} - (I_{310}/I_{315})_{\text{blank}}] \qquad \text{(Eq. 1)}$$

was plotted on the ordinate.

The logarithm of the mole ratio of methadone, M_{2H_0}, present in a sample to the amount of internal standard, M_{2H_5}, added to the sample (log *M*):

$$\log M = \log \left[\frac{M_{2H_0}}{M_{2H_5}}\right] \qquad \text{(Eq. 2)}$$

was plotted on the abscissa.

The technique of using the difference in isotope ratios between the standard and the unknown yields more reproducible data by minimizing small daily variations in mass spectrometer performance. Plasma and urine methadone isotope dilution curves were prepared for concentrations ranging from 0.3 pmole to 289 nmoles/ml. Both curves covered a useful linear range of 5 pmoles/ml to 289 nmoles/ml. These concentrations are typical of those encountered in samples obtained from patients receiving methadone maintenance therapy at doses of 40–100 mg/day. Occasionally, there was interference in the plasma methadone assay from a component in blood that obscured both the GLC peak and the ion at *m/e* 310. This contaminant was difficult to remove completely, and it interfered with the plasma assay below 10–15 pmoles/ml. Back-extraction of methadone into dilute hydrochloric acid, as described, partially eliminated this interference.

To preserve the accuracy of isotope ratio measurements throughout the calculations (the coefficient of variation is typically 5% at an isotope ratio of 100:1), the data were treated as logarithms. Slopes and intercepts were calculated using standard linear regression techniques (14). The linear regression data (Table I) were obtained over 6 months and show excellent long-term reproducibility. The slight difference observed in the slopes and intercepts between plasma and urine curves was not statistically significant. The correlation coefficients indicate a tight fit of the data to the regression line.

The GLC–chemical-ionization mass spectrometric method presented was used to determine urinary methadone levels in a sample obtained immediately *postpartum* from an infant whose mother was maintained on methadone during pregnancy. Two samples (500 and 100 μl) were analyzed. The samples contained 19.0 ± 1.1 and 19.6 ± 1.1 μg/ml (22.6 μg/ml by GLC), respectively, for the runs, indicating that the determination was independent of sample size.

Plasma methadone levels in several individuals receiving a daily oral maintenance dose (1 mg/kg) of methadone were examined by a GLC method (15) and by the described procedure. Figure 1 shows the correlation between plasma drug levels measured by these two methods. Linear regression analysis of these data gives a slope of 0.93 (r = 0.79 and n = 30) and an intercept of 90 ng/ml. These data suggest that the difference from zero of the intercept may be due either to overestimation by the GLC–chemical-ionization mass spectrometric procedure or to underestimation by the GLC procedure. In the former case, the presence of a background ion at *m/e* 310 would raise the estimated mole ratio and give inflated values for methadone present in the sample. Since this effect did not occur in those direct recovery studies conducted on aqueous, urinary, and plasma standards, this contaminant possibility is not the cause.

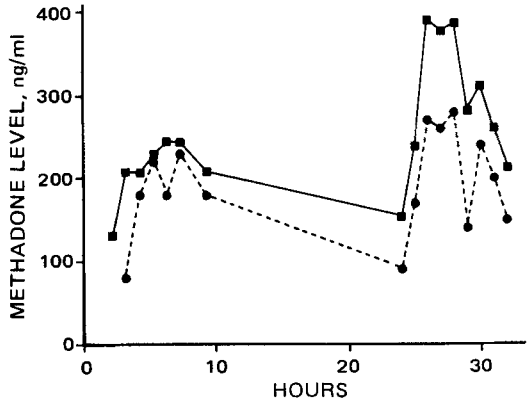

Figure 2—*Plasma methadone levels observed in an individual receiving 80 mg/day (1 mg/kg/day) of methadone. Levels were measured by GLC* (●) *and GLC–chemical-ionization mass spectrometry* (■).

Methadone is extensively bound to both albumin and globulin fractions of plasma proteins (16). Presumably, solvent extraction of a drug causes denaturation of plasma proteins and allows equilibration of free and bound methadone. However, using ethyl acetate, the extent of protein denaturation is not known and may be incomplete. Methadone may also be occluded in the denatured protein matrix that occurs at the interface between the organic and aqueous phases and may not be completely extracted. Quantitative studies of plasma methadone levels by GLC involve adding a small mass (~1–5 ng) of ^3H-methadone to the sample to serve as a recovery marker in the extraction of methadone from plasma[7]. It is assumed that the radiotracer is fully equilibrated with the 100–400 ng of methadone present and bound to plasma proteins and that all

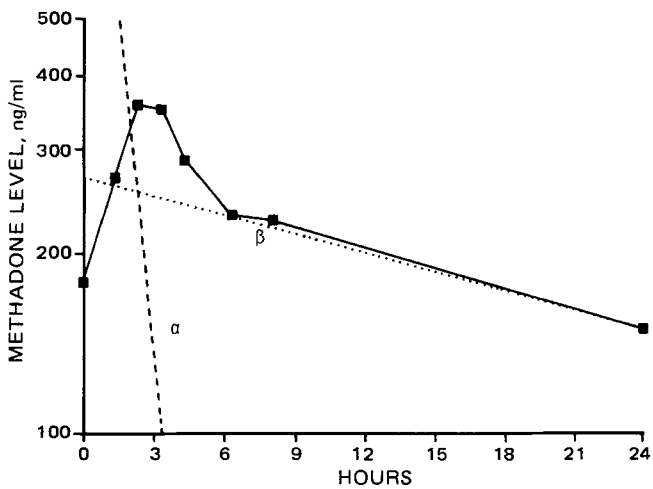

Figure 3—*Pharmacokinetic analysis of plasma methadone levels in an individual receiving 100 mg of methadone/day po. Methadone levels were measured by GLC–chemical-ionization mass spectrometry. The rapidly changing curve* (- - -) *represents the distribution phase* (α) *of the plasma methadone level–time profile* ($T_{1/2\alpha}$ = *0.79 hr*). *The slowly changing curve* (· · ·) *represents the elimination phase* (β) *of the drug* ($T_{1/2\beta}$ = *28.8 hr*).

[7] Recovery of radiolabeled methadone through the extraction and back-extraction procedure described ranges from approximately 55 to 65% for plasma and from approximately 85 to 90% for urine (M. J. Kreek, C. L. Gutjahr, J. W. Garfield, D. V. Bowen, and F. H. Field, *Ann. N.Y. Acad. Sci.*, in press). The remainder of the radioactivity is left in the aqueous, protein-containing fraction.

binding sites are equivalent, which may not be the case (17). Incomplete equilibration of the small mass of radiolabeled methadone with various protein-bound fractions of methadone may result in an artificially high estimate of drug recovery based on recovery of the radioactive marker. If this were true, the apparent dilution would respond to changes in the specific activity of the radioactive marker. These studies are currently in progress.

Data presented in Fig. 2 show the plasma methadone levels in an individual maintained on 80 mg of methadone/day. Plasma methadone levels were measured for 2 successive days following administration of the maintenance dose at 0 and 24 hr. Plasma drug levels generally ranged between 100 and 400 ng/ml and were consistent with those obtained previously (18, 19). The GLC curve showed consistently lower plasma levels than the GLC–chemical-ionization mass spectrometric curve, even though the profiles of the plasma disappearance curves were very similar.

Data obtained using the GLC–chemical-ionization mass spectrometric procedure are sufficiently accurate and reproducible to permit pharmacokinetic studies in human subjects. Figure 3 shows the plasma methadone disappearance curve for a study conducted in a patient receiving 100 mg of methadone/day. These data were fitted to a two-component exponential function [$y = 1876 \exp(-0.87t) + 268 \exp(-0.024t)$] by a weighted nonlinear, least-squares computer program. The half-life for the elimination phase (β) of the plasma disappearance curve was 28.8 ± 4.8 hr. Methadone clearance, defined as the sum of all hepatic and renal excretory routes and biotransformation pathways (20), was 125 ml/min in this patient[8].

The described procedure has a lower detection limit of about 5 pmoles/ml in urine and about 10 pmoles/ml in plasma. Since the required sample volume is only 1 ml, the assay is actually about five times more sensitive than the procedure described by Sullivan *et al.* (6), which requires 4 ml of plasma. The limiting factor in their procedure is the low abundance of the ion [m/e 294 $(M - 15)^+$] used for quantitative ion ratio measurements. The procedure described here uses one of the most intense ions in chemical-ionization mass spectrum of methadone [m/e 310, $(MH)^+$].

The sensitivity of the present method is also about a factor of 15–20 better than GLC procedures (19, 21), which require a larger volume of plasma. This method will permit more accurate measurement of low methadone levels present in adolescent heroin addicts on methadone maintenance therapy who are receiving lower dosages (5–40 mg/day) and in newborn infants whose mothers are maintained on methadone. This method will also permit studies in animal models in which plasma methadone levels are lower and turnover rates are much faster than in humans.

REFERENCES

(1) H. R. Sullivan and D. A. Blake, *Res. Commun. Chem. Pathol. Pharmacol.*, **3,** 467 (1972).

(2) D. J. Jenden and A. K. Cho, *Annu. Rev. Pharmacol.*, **13,** 371 (1972).

(3) E. Costa and B. Holmstedt, in "Advances in Biochemical Psychopharmacology," vol. 7, Raven, New York, N.Y., 1973, pp. 57, 83, 135.

(4) T. E. Gaffney, C. G. Hammar, B. Holmstedt, and R. E. McMahon, *Anal. Chem.*, **43,** 307 (1971).

(5) P. A. Clarke and R. L. Foltz, *Clin. Chem.*, **4,** 465 (1974).

(6) H. R. Sullivan, F. J. Marshall, R. E. McMahon, E. Anggard, L.-M. Gunne, and J. H. Holmstrand, *Biomed. Mass Spectrom.*, **2,** 197 (1975).

(7) E. C. Horning, in "Advances in Biochemical Psychopharmacology," vol. 7, Raven, New York, N.Y., 1973, p. 15.

(8) P. D. Klein, J. R. Haumann, and D. L. Hachey, *Clin. Chem.*, **21,** 1253 (1975).

(9) E. M. Schultz, C. M. Robb, and J. M. Sprague, *J. Am. Chem. Soc.*, **69,** 2454 (1947).

(10) J. W. Cusic, *ibid.*, **71,** 3546 (1949).

(11) A. Pohland, F. J. Marshall, and T. P. Curney, *ibid.*, **71,** 460 (1949).

(12) W. R. Brode and M. W. Hill, *J. Org. Chem.*, **13,** 191 (1948).

(13) L. L. Smith, *J. Pharm. Sci.*, **55,** 101 (1966).

(14) O. L. Davies, "Statistical Methods in Research and Production," 3rd ed., Hofner, New York, N.Y., 1967, pp. 150–207.

(15) M. J. Kreek, A. Schecter, and C. L. Gutjahr, *Am. J. Drug Alcohol Abuse,* **1,** 409 (1974).

(16) G. D. Olsen, *Clin. Pharmacol. Ther.*, **14,** 338 (1973).

(17) R. F. Mais, S. Keresztes-Nagy, J. F. Zarolinski, and Y. T. Oester, *J. Pharm. Sci.*, **63,** 1423 (1974).

(18) C. E. Inturrisi and K. Verebely, *Clin. Pharmacol. Ther.*, **13,** 633 (1972).

(19) M. J. Kreek, *N.Y. State J. Med.*, **73,** 2773 (1973).

(20) D. J. Greenblatt and J. Koch-Weser, *N. Engl. J. Med.*, **293,** 702 (1975).

(21) C. E. Inturrisi and K. Verebely, *J. Chromatogr.*, **65,** 361 (1972).

ACKNOWLEDGMENTS AND ADDRESSES

Received August 1, 1975, from the *Division of Biological and Medical Research, Argonne National Laboratory, Argonne, IL 60439,* and the ‡*Department of Biology of Addictive Diseases, Rockefeller University, New York, NY 10021.*

Accepted for publication January 31, 1977.

Supported by the U.S. Energy Research and Development Administration and by a grant to M. J. Kreek from the U.S. Public Health Service, Grant DA 01138 from the National Institute of Drug Abuse, and a grant from the New York State Narcotic Addiction Control Commission. M. J. Kreek is the recipient of a Career Scientist Award from the Health Research Council of the City of New York.

The authors thank Dr. P. D. Klein for advice and encouragement and Searle Analytics for providing the chemical-ionization mass spectrometer.

ˣ To whom inquiries should be directed.

[8] *In vivo* metabolic tracer studies with deuterium-labeled methadone [M. J. Kreek and D. L. Hachey, *Clin. Res.*, **23,** 571A (1975)] indicate the drug half-life for the elimination phase of the plasma disappearance curve was 31.5 ± 2.9 hr. A more detailed report of methadone pharmacokinetics will be presented elsewhere.

Piperidine Derivatives: Synthesis of Potential Analgesics in 3-Substituted 4-Phenylpiperidine Series

RANA ABBAS, ROBERT E. WILLETTE *, and J. MICHAEL EDWARDS ˣ

Abstract □ The syntheses of 1-methyl-3-(3-hydroxy-3-phenylpropyl)-4-phenyl-4-piperidinol and 1-methyl-3-(3-hydroxy-3-phenylpropyl)-4-phenyl-4-propanoyloxypiperidine are described. Preliminary pharmacological testing showed these compounds to be weakly active in the writhing test.

Keyphrases □ Piperidine derivatives—synthesized, pharmacological activity evaluated □ Analgesic activity, potential—piperidine derivatives synthesized and evaluated □ Structure–activity relationships—piperidine derivatives, pharmacological activity evaluated

Various compounds based on the morphinan nucleus and its fragments were synthesized, and several correlations of structure–analgesic activity relationships were made (1, 2). However, relatively few, if any, definitive studies were reported on remote peripheral areas that are not in the proximity of the active or essential binding area of the molecule, *e.g.*, the polycyclic moiety of the benzomorphans. A series of morphine derivatives (I) was synthesized (3) with remarkably high analgesic activities (in some cases 10,000 times morphine), and additional binding sites believed to be located away from the periphery of the polycyclic nucleus were postulated (4).

Substitutions at the 3-position in the 4-phenylpiperidines produced compounds with significant analgesic activity, *e.g.*, the 3-methyl (II*a*), 3-ethyl (II*b*), and 3-allyl (II*c*) analogs in the "reversed ester" series of the 4-phenylpiperidines (1).

The purpose of this investigation was to synthesize compounds based on the 4-phenylpiperidine unit of the morphine derivative (shown by solid lines in Structure I) in an attempt to illustrate the significance of the alcoholic group and to determine a possible site of attachment in the periphery of the analgesic receptor. This report discusses the synthetic work involved in the preparation of 1-methyl-3-(3-hydroxy-3-phenylpropyl)-4-phenyl-4-piperidinol (VIII) and 1-methyl-3-(3-hydroxy-3-phenylpropyl)-4-phenyl-4-propanoyloxypiperidine (IX).

EXPERIMENTAL[1]

1-Methyl-3-cyanoethyl-4-piperidone (V)—A solution of 1-methyl-4-piperidone (33.9 g, 0.3 mole), pyrrolidine (42.6 g, 0.6 mole), and *p*-toluenesulfonic acid (10 mg) in 250 ml of dry toluene was refluxed overnight (~10 hr), and the water formed (7 ml) was removed using a Dean–Stark trap (Scheme I). The solvent and excess pyrrolidine were removed under reduced pressure; the residue, upon distillation, gave 43.7 g (87.8%) of the pyrrolidine enamine of 1-methyl-4-piperidone (III), bp 80–80.5°/0.05 mm. The IR spectrum (liquid film) showed strong absorption for enamine at 1650 cm^{-1}; NMR: δ 2.28 (s, 3H, NCH_3) and 4.15 (t, 1H, CH=C) ppm.

To a solution of 43.7 g (0.26 mole) of III in 150 ml of dry dioxane was added acrylonitrile (14.8 g, 0.28 mole) dropwise. The contents were heated cautiously and allowed to reflux overnight. The reaction mixture was cooled, and evaporation of the solvent yielded a residual oil, which was

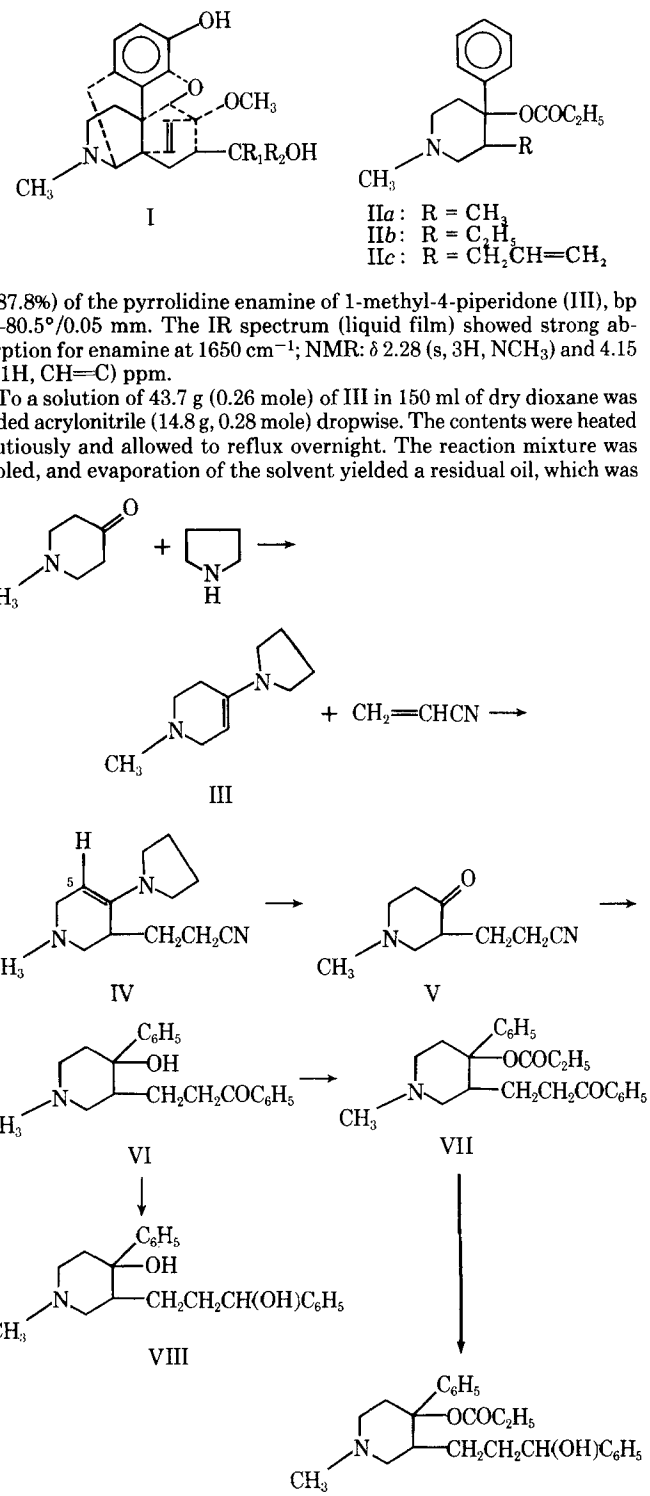

Scheme I

[1] Melting points were determined in a Thomas-Hoover melting-point apparatus and are uncorrected. IR spectra were determined on a Beckman Acculab 3. NMR spectra were determined on a Hitachi Perkin-Elmer R-24. If not otherwise stated, the spectra were recorded in chloroform-*d* using tetramethylsilane as the internal standard. Mass spectra were obtained on an A.E.I. MS-902 spectrometer. Elemental analyses were performed by Baron Consulting Co., Orange, Conn. TLC was carried out on silica gel GF_{254} plates. The solvent systems used were: A, ammonium hydroxide-saturated benzene–methanol (4:1); and B, ammonium hydroxide-saturated chloroform–acetone (2:1). Dragendorff spray reagent was used to visualize products on TLC plates.

subjected to fractional distillation *in vacuo*. The fractions boiling between 130 and 141°/0.32–0.33 mm were combined to give 18.2 g (31.6%) of IV; IR (liquid film): 1645 (strong, enamine) and 2250 (medium, nitrile) cm^{-1}; NMR: δ 2.28 (s, 3H, NCH_3), 4.27, and 4.35 (dd, 1H, CH=C, J = ~3 Hz) ppm.

To 18.2 g of IV were added 60 ml of water and 80 ml of dioxane, and the mixture was heated at reflux temperature for 1.75 hr. Excess pyrrolidine and water were removed under reduced pressure; the residue was dissolved in chloroform, dried over anhydrous potassium carbonate, and filtered. Evaporation of solvent gave a residual oil which, upon distillation, yielded 10.4 g (75%) of 1-methyl-3-cyanoethyl-4-piperidone (V), bp 100–108°/0.20–0.27 mm; IR (liquid film): 1710 (strong, carbonyl) and 2245 (medium, nitrile) cm^{-1}; NMR: δ 2.28 (s, 3H, NCH_3) ppm.

An analytical sample of V was obtained by column chromatography (silica gel, 60–200 mesh, 80 g). Five grams of V was dissolved in a minimum amount of petroleum ether and chromatographed. Fractions of 15 ml were collected, and the column was eluted with solvents of increasing polarity [petroleum ether (bp 30–60°)–benzene (3:2), 1.5 liters, and (2:3) 1.5 liters; benzene, 2 liters; and benzene–ethanol (19:1), 1.5 liters]. Fractions 371–652 gave the desired product V (4.2 g, 84%), R_f 0.51 (System A). An analytical sample of V was obtained from fractions 643–650.

Anal.—Calc. for $C_9H_{14}N_2O$: C, 65.02; H, 8.49; N, 16.86. Found: C, 64.93; H, 8.46; N, 16.70.

1-Methyl -3- (3-phenyl-3-oxopropyl) -4- phenyl-4-piperidinol (VI)—Under a nitrogen atmosphere, a solution of phenyllithium was freshly prepared by allowing 23.5 g of bromobenzene and 2.13 g of lithium wire to react in 200 ml of anhydrous ether (Scheme I). The flask and its contents were immersed in an ice bath during the addition of 5 g (0.03 mole) of V. After the reaction mixture was stirred at 0–5° for 45 min and for 5 additional hr at room temperature, it was hydrolyzed by the slow addition of 100 ml of 10% sulfuric acid solution, during which time the flask and its contents were kept cool in an ice bath.

After stirring at room temperature for 14 hr, 50 ml of water was added and the contents were refluxed for 45 min. The flask was cooled, and the insoluble solid (13.5 g) was obtained by filtration. The solid was dissolved in water (with gentle warming), made basic with ammonium hydroxide solution, and extracted with chloroform (7 × 100 ml). The combined chloroform extracts were dried over anhydrous potassium carbonate and filtered. Evaporation of solvent gave an oil, 8.9 g (91.5%) of VI.

The oil was crystallized with 20 ml of ether to yield 6.5 g (66.8%) of piperidinol VI, mp 110–112° (with previous softening) after recrystallization from benzene. TLC showed VI to be a mixture, R_f 0.51 and 0.57 (System A). Attempts to separate the two compounds by repeated crystallizations were not successful; IR (potassium bromide): 3470 (OH) and 1675 (carbonyl) cm^{-1}; NMR: δ 7.09–7.80 (m, 10H, ArH) and 2.29 (s, 3H, NCH_3) ppm. The mass spectrum showed M^+ at m/e 323.

Anal.—Calc. for $C_{21}H_{25}NO_2$: C, 77.97; H, 7.79; N, 4.33. Found: C, 76.31, 75.99, 76.40; H, 7.94, 8.01, 7.70; N, 4.25, 4.22, 4.26.

Repeated recrystallizations did not improve the analysis. The picrate had a melting point of 207–211° after recrystallization from benzene–ethanol.

Anal.—Calc. for $C_{21}H_{25}NO_2 \cdot C_6H_3N_3O_7$: C, 58.67; H, 5.11; N, 10.14. Found: C, 58.66; H, 5.13; N, 10.26.

1-Methyl-3-(3-phenyl-3-oxopropyl)-4-phenyl-4-propanoyloxypiperidine (VII)—To a solution of 2 g (0.006 mole) of VI and 2 ml of triethylamine (redistilled) in 25 ml of dry toluene was added 3.5 g of propanoyl chloride in 5 ml of dry toluene dropwise, with refluxing, over 15 min (Scheme I). The reaction mixture was heated under reflux temperature for an additional 1.5 hr. The flask was cooled, the contents were transferred with chloroform (50 ml) and water (20 ml) to a separator, and the layers separated.

The aqueous layer was extracted once with a 25-ml portion of chloroform. The combined chloroform extracts were dried over anhydrous potassium carbonate and filtered. Evaporation of the solvent gave a residue characterized as a hydrochloride by its IR spectrum (broad, 2500 cm^{-1}). The residue was made basic with 100 ml of saturated solution of sodium bicarbonate and then extracted with five 50-ml portions of ether. The combined ether extracts were dried over anhydrous potassium carbonate and filtered.

Evaporation of the solvent gave an oil, 2.2 g (93.6%) of ester VII; IR (liquid film): 1735 (strong, ester), 1680 (strong, carbonyl), 760, and 700 (aromatic hydrogens) cm^{-1}. Unsuccessful attempts were made to effect crystallization of this oil using common solvents. The hydrochloride was prepared by passing anhydrous hydrogen chloride through an ethereal solution of the oil, mp 167–169° (after recrystallization from ethyl acetate–petroleum ether); NMR [deuterium oxide with sodium 3-(trimethylsilyl)propanesulfonate as internal standard]: 7.3–8.05 (m, 10H, ArH), 3.26 (s, 3H, NCH_3), and 1.25 (t, 3H, $OCOCH_2CH_3$, J = ~7 Hz) ppm. The hydrochloride was converted into a free base, and TLC showed it to be a mixture, R_f 0.73 and 0.84 (System A); the mass spectrum showed M^+ at m/e 379. An analytical sample of the hydrochloride was obtained after recrystallization from ethyl acetate–ethanol, mp 183–185°.

Anal.—Calc. for $C_{24}H_{30}ClNO_3$: C, 69.28; H, 7.27; N, 3.36. Found: C, 69.30; H, 6.98; N, 3.61.

The picrate had a melting point of 209.5–211° after recrystallization from benzene–ethanol.

Anal.—Calc. for $C_{24}H_{29}NO_3 \cdot C_6H_3N_3O_7$: C, 59.19; H, 5.30; N, 9.20. Found: C, 59.49; H, 5.34; N, 9.10.

1-Methyl-3-(3-hydroxy-3-phenylpropyl) -4-phenyl-4-propanoyloxypiperidine (IX)—To a solution of 5.07 g (0.013 mole) of VII and sodium hydroxide (0.25 g) in 10 ml of methanol was added a solution of sodium borohydride (1.28 g) and sodium hydroxide (0.25 g) in 15 ml of methanol dropwise, with stirring, at 0° (Scheme I). The funnel was washed with 5 ml of methanol, and the contents were allowed to stir at 0° for 6 hr and at room temperature for an additional 18 hr. At this point, 10 ml of water was added and stirring was continued for 15 min.

Most of the methanol was evaporated under reduced pressure, and the residue was extracted with chloroform (4 × 25 ml). The combined chloroform extracts were dried over anhydrous potassium carbonate and filtered. Evaporation of solvent gave 4.4 g of an oil. This material was dissolved in a minimum amount of benzene and was subjected to column chromatography (silica gel, 60–200 mesh, 80 g). The column was eluted with 6.1 liters of benzene–ethanol (16:1), and 15-ml fractions were collected.

Fractions 116–230, on evaporation, gave a solid, 0.70 g (13.8%) of IX, mp 153–155° (after recrystallization from benzene–heptane), R_f 0.45 (System A) and 0.77 and 0.66 (System B). The mass spectrum showed M^+ at m/e 381; IR (potassium bromide): 3400 (broad, not clear, OH), 1735 (strong, ester), 754, and 700 (aromatic hydrogens) cm^{-1}; NMR: δ 6.95–7.39 (m, 10H, ArH), 2.19 (s, 3H, NCH_3), 1.16 (t, 3H, $OCOCH_2CH_3$, J = ~7 Hz), and 4.34 (t, 1H, $CHOH$, J = ~6 Hz) ppm.

Anal.—Calc. for $C_{24}H_{31}NO_3$: C, 75.55; H, 8.19; N, 3.67; O, 12.59. Found: C, 75.31; H, 8.09; N, 3.89; O, 12.97.

1-Methyl-3-(3-hydroxy-3-phenylpropyl)-4-phenyl-4-piperidinol (VIII)—A solution of 2 g (0.006 mole) of VI, 2.56 g of sodium hydroxide, and 2.84 g of sodium borohydride in 160 ml of methanol was stirred for 48 hr at room temperature (Scheme I). At this point, 50 ml of water was added and the contents were allowed to stir for an additional 75 min at room temperature. Most of the methanol was removed under reduced pressure, and the aqueous phase was extracted with chloroform (5 × 50 ml). The combined chloroform extracts were dried over anhydrous potassium carbonate and filtered.

Evaporation of solvent yielded 1.6 g (79.5%) of VIII, mp 61–64° (after sublimation at 0.15 mm), R_f 0.49 and 0.55 (System A). The mass spectrum showed M^+ at m/e 325; IR (potassium bromide): 3390 (broad, OH), 754, and 700 (aromatic hydrogens) cm^{-1}; NMR: δ 7.22, 7.34 (two s, 10H, ArH), 2.22 (s, 3H, NCH_3), and 4.36 (t, 1H, $CHOH$, J = ~6 Hz) ppm.

Anal.—Calc. for $C_{21}H_{27}NO_2$: C, 77.49; H, 8.37; N, 4.31. Found: C, 77.67; H, 8.37; N, 4.59.

1-Methyl-3-(3-hydroxy-3,3-diphenylpropyl)-4-phenyl-4-piperidinol (X)—In a 500-ml flask, a solution of phenyllithium was freshly prepared by allowing 31.5 g of bromobenzene and 3.24 g of lithium wire to react in 90 ml of anhydrous ether under nitrogen for 2 hr at room temperature. The flask and its contents were immersed in an ice bath, and a solution of 2 g (0.006 mole) of VI in 10 ml of dry tetrahydrofuran was added dropwise. The reaction mixture was allowed to stir at room temperature for 15 hr and was subsequently hydrolyzed by the slow addition of water (20 ml), during which time the flask and its contents were kept cool in an ice bath. After stirring for 1.5 hr at room temperature, the contents were poured into a separator and the layers separated.

The aqueous phase was extracted with ether (4 × 50 ml). The combined ether extracts were dried over anhydrous potassium carbonate and filtered. Removal of ether under reduced pressure gave 1.5 g (60.5%) of X, mp 171–172° (after two recrystallizations from heptane–carbon tetrachloride). The mass spectrum showed M^+ at m/e 401; IR (potassium bromide): 3425 (broad, OH), 758, and 700 (aromatic hydrogens) cm^{-1}; NMR: δ 7.14–7.32 (m, 15H, ArH) and 2.3 (s, 3H, NCH_3) ppm.

Anal.—Calc. for $C_{27}H_{31}NO_2$: C, 80.75; H, 7.79; N, 3.49. Found: C, 80.54; H, 7.95; N, 3.38.

RESULTS AND DISCUSSION

Chemistry—Reaction of the enamine III with acrylonitrile in dry dioxane gave IV. The conclusion that the product consisted of the tri-

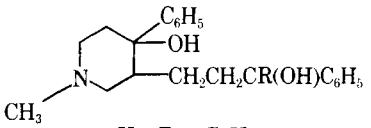

X: R = C_6H_5
XI: R = CH_3

substituted isomer IV was based on NMR spectral evidence. The olefinic proton at C-5 appeared as two doublets centered at δ 4.27 and 4.35 ppm. The formation of the tetrasubstituted isomer was not expected on steric grounds, but analogous results were reported previously for the pyrrolidine enamines of 2-methylcyclohexanone and 2-phenylcyclohexanone (5). The presence of absorption bands at 1645 (enamine) and 2250 (nitrile) cm^{-1} in the IR spectrum further confirmed the structure. Hydrolysis of IV afforded the monoalkylated ketonitrile V.

The ketoalcohol VI was obtained by the reaction of V with phenyllithium. TLC indicated VI to be a mixture. Attempts to obtain the major diastereomer in high purity by repeated crystallizations proved unsuccessful. Satisfactory elemental analysis[2] for VI could not be obtained. Treatment of VI with propanoyl chloride in the presence of triethylamine in refluxing toluene afforded the desired compound VII as an oil. Compound VII was further characterized as a hydrochloride and picrate.

Selective reduction of ketones and aldehydes in the presence of other functional groups such as esters, amides, and alkylhalides is generally possible using sodium borohydride as a reducing agent (6). Thus, IX was prepared by the reaction of VII with sodium borohydride. Isolation of IX was achieved by column chromatography. Similarly, VIII was obtained in 79.5% yield by the treatment of VI with sodium borohydride.

Reaction of VI and VII with methylmagnesium bromide or iodide failed to give the desired compound XI. Treatment of VI with methyllithium or ethyllithium also failed. Enolization of VI possibly may hinder the desired addition by these reagents. However, addition at the aryl carbonyl was successfully achieved using phenyllithium. Compound X was obtained using this reagent.

The reaction of 3-substituted 4-piperidiones with aryl lithium could give a mixture of diastereomeric alcohols [XII (β-*cis*-R_1–R_3) and XIII (α-*trans*-R_1–R_3)]. Based upon the stereochemical course of addition to ketones (6), the formation of the *trans*-diastereomer (XIII) should be favored. Thus, by analogy with the results previously reported for the prodinols XII*b* and XIII*b* and the 3-allyl derivatives XII*c* and XIII*c* in which XIII*b* and XIII*c* were 60 and 91%, respectively, of the diastereomeric mixture (7, 8), it could be assumed that the major diastereomer would correspond to XIII*a* in the treatment of V with phenyllithium.

In the NMR spectrum (chloroform-*d*) of VI[3], a complex aromatic pattern was observed at δ 7.09–7.80 ppm (W_H = 15 Hz; Fig. 1A). Comparatively broader and more complex NMR signals were reported for the aromatic protons of *trans*-XIII*b* than for the corresponding *cis*-compound (9); furthermore, the band width at half-weight of the aromatic proton signals appeared to be considerably greater for the α-diastereomer (14 Hz) than for the β-diastereomer (5 Hz). Similar differences also were observed in the spectra of the 3-allyl derivatives XIII*c* (14 Hz) and XII*c* (4.5 Hz) (8). The *N*-methyl signal of VI appeared as a singlet (with the

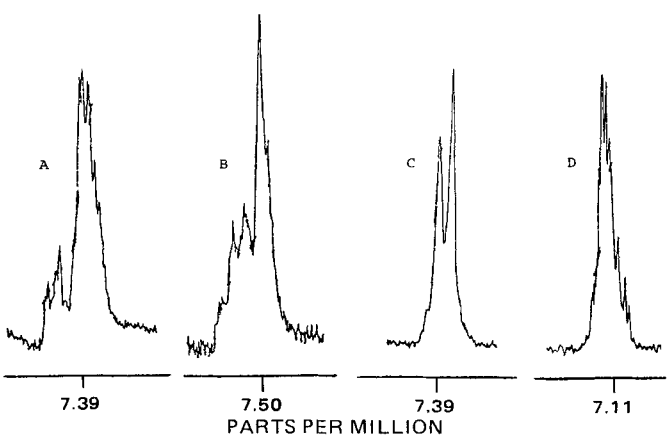

Figure 1—*Aromatic NMR signals of VI (A), VII (B), VIII (C), and IX (D).*

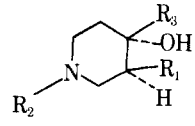

XII*a*–XII*e*

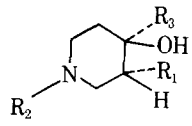

XIII*a*–XIII*e*

XII*a* and XIII*a*: R_1 = $CH_2CH_2COC_6H_5$, R_2 = CH_3, R_3 = C_6H_5
XII*b* and XIII*b*: R_1 = R_2 = CH_3, R_3 = C_6H_5
XII*c* and XIII*c*: R_1 = $CH_2CH{=}CH_2$, R_2 = CH_3, R_3 = C_6H_5
XII*d* and XIII*d*: R_1 = CH_3, R_2 = C_2H_5, R_3 = *o*-$CH_3C_6H_4$
XII*e* and XIII*e*: R_1 = CH_3, R_2 = $CH_2C_6H_5$, R_3 = *o*-$CH_3C_6H_4$

slight trace of the *N*-methyl signal of the other diastereomer) at δ 2.29 ppm.

A complex aromatic absorption was also seen in the NMR spectrum of VII[4] at δ 7.3–8.05 ppm (W_H = ~8 Hz; Fig. 1B). The *N*-methyl protons appeared as a 3H singlet at δ 3.26 ppm, and the methyl of the propanoyloxy ester was a triplet at δ 1.25 (J = ~7 Hz) ppm. However, the aromatic pattern of VIII[5] appeared as two sharp singlets at δ 7.22 and 7.34 ppm. The *N*-methyl signal appeared as a 3H singlet (W_H = ~6 Hz) at δ 2.22, and the benzylic proton appeared as a near 1:2:1 triplet at δ 4.36 (J = ~6 Hz) ppm.

In the NMR spectrum of IX[5], the aromatic pattern did not show a hump downfield and appeared less complex compared to the patterns of VI and VII. Perhaps the aromatic signal patterns of VIII and IX were being obscured to a greater extent by the C_6H_5CHOH signal than the VI and VII patterns were being obscured by the C_6H_5CO signal, assuming of course that the compound with the α-configuration in these diastereomeric mixtures was the predominant diastereomer. A similar example, in which the presence of another aromatic group in the molecule influences the aromatic pattern, is seen with XIII*d* and XIII*e* (10). The methyl signal of the propanoyloxy ester group in the NMR spectrum of IX was a triplet at δ 1.16 (J = ~7 Hz) ppm, and the benzylic proton appeared as a near 1:2:1 triplet (J = ~6 Hz) at δ 4.34 ppm.

Pharmacology—In preliminary pharmacological testing, VIII (NIH 9082) showed no activity in the hot-plate test (inactive up to 100 mg/kg) and in the tail-flick test (inactive up to 30 mg/kg); however, in the writhing test it had an ED_{50} value of 80.5 mg/kg in mice. Similarly, IX (NIH 9083) appeared inactive in the hot-plate test (inactive up to 50 mg/kg) and in the tail-flick test (inactive up to 30 mg/kg) but had an ED_{50} value of 32 mg/kg in the writhing test.

REFERENCES

(1) "Analgetics," vol. 5, G. deStevens, Ed., Academic, New York, N.Y., 1965.

(2) P. S. Portoghese, *J. Pharm. Sci.*, **55**, 865 (1966).

(3) K. W. Bentley, D. G. Hardy, H. P. Crocker, D. I. Haddlesey, and P. A. Mayor, *J. Am. Chem. Soc.*, **89**, 3312 (1967), and preceding papers.

(4) J. W. Lewis, K. W. Bentley, and A. Cowan, *Ann. Rev. Pharmacol.*, **12**, 241 (1971).

(5) "Enamines: Synthesis, Structure, and Reactions," A. G. Cook, Ed., Dekker, New York, N.Y., 1969.

(6) H. O. House, "Modern Synthetic Reactions," Benjamin, Menlo Park, Calif., 1972.

(7) A. H. Beckett, A. F. Casy, and G. Kirk, *J. Med. Pharm. Chem.*, **1**, 37 (1959).

(8) K. H. Bell and P. S. Portoghese, *J. Med. Chem.*, **16**, 203 (1973).

(9) A. F. Casy, *Tetrahedron*, **22**, 2711 (1966).

(10) M. A. Iorio and A. F. Casy, *J. Chem. Soc. C*, **1970**, 135.

ACKNOWLEDGMENTS AND ADDRESSES

Received December 6, 1976, from the *School of Pharmacy, University of Connecticut, Storrs, CT 06268.*

Accepted for publication February 2, 1977.

The authors thank Dr. Everette L. May of the National Institute of Arthritis, Metabolism, and Digestive Diseases for the pharmacological testing.

* Present address: National Institute on Drug Abuse, Rockville, MD 20852.

ˣ To whom inquiries should be directed.

[2] Microanalyses of the picrate of VI were, however, within 0.3% of theory.

[3] Assumed to be a diastereomeric mixture based upon stereochemical grounds and as indicated by its TLC (see *Experimental*).

[4] Hydrochloride salt in deuterium oxide with sodium 3-(trimethylsilyl)propanesulfonate as the internal standard. TLC indicated it to be a mixture.

[5] In chloroform-*d*. TLC indicated it to be a mixture.

Inhibitors of Polyamine Biosynthesis V: *In Vivo* Effects of α-Methyl-(±)-ornithine and α-Methyl-(±)-ornithine *tert*-Butyl Ester

CHARLES E. WEEKS * and MAHMOUD M. ABDEL-MONEM ˣ

Abstract □ The effects of α-methyl-(±)-ornithine and its *tert*-butyl ester on the survival time and the levels of polyamines in spleen tissue of mice inoculated intraperitoneally with L-1210 lymphoid leukemic cells were studied *in vivo*. These compounds were administered at doses of 100–300 mg/kg from Day 1 of tumor inoculation until death. This treatment neither significantly increased survival time nor altered the increases in polyamine levels normally observed during tumor growth. A method was developed to determine polyamine levels in spleen tissue. The polyamines in the tissue extracts were converted to their 5-(dimethylamino)-1-naphthalenesulfonyl derivatives, and these derivatives were separated by TLC followed by high-pressure liquid chromatography on a bonded phase microparticle column. The *in vivo* metabolism of 1-^{14}C-α-methyl-(±)-ornithine was studied and compared to that of 1-^{14}C-(±)-ornithine. 1-^{14}C-α-Methyl-(±)-ornithine was rapidly excreted after administration to mice inoculated with L-1210 leukemic cells. Within 24 hr after injection, over 70% of the radioactive dose was found in the urine, primarily as the unchanged compound. Less than 0.1% of the administered dose appeared as ^{14}C-labeled carbon dioxide during the 24 hr following injection. In contrast, 34% of the administered dose of 1-^{14}C-(±)-ornithine was metabolized to labeled carbon dioxide and 28% was excreted in urine during the 24 hr following injection.

Keyphrases □ Polyamines—effects of α-methyl-(±)-ornithine and its *tert*-butyl ester on biosynthesis in leukemic mice, TLC–high-pressure liquid chromatographic analysis of tissue extracts □ α-Methyl-(±)-ornithine—radiochemical study of metabolism in mice, effects on polyamine biosynthesis in leukemic mice, *tert*-butyl ester synthesized □ TLC–high-pressure liquid chromatography—analysis, polyamines in tissue extracts, mice □ Radiochemistry—study of metabolism of α-methyl-(±)-ornithine in mice

In spite of the many biological roles attributed to the polyamines, their exact physiological function is still not known. The multitude of effects elicited by the polyamines in cell free systems complicates definition of their true physiological function. However, recent evidence strongly implies that their primary function is the regulation of growth processes (1).

Previously, the synthesis and evaluation of inhibitors of polyamine biosynthesis were described (2–5). In particular, inhibitors of ornithine decarboxylase were studied because this enzyme appears to catalyze the rate-limiting step in the overall polyamine biosynthetic pathway. α-Alkyl- and aralkyl-(±)-ornithine and (±)-5-amino-2-hydrazino-2-methylpentanoic acid were synthesized and were potent reversible inhibitors of mammalian ornithine decarboxylase *in vitro*. It was also shown that α-methyl-(±)-ornithine (I) did not produce its inhibitory effects by acting as an alternative substrate for ornithine decarboxylase *in vitro* (3). A recent study found that I decreased the cellular levels of putrescine and spermidine in L-1210 leukemic cells of mice grown in culture. This inhibition of polyamine biosynthesis was not accompanied by inhibition of growth of these cells (5).

To elucidate the function of the polyamines, a study of the effects of I on the survival time and polyamine levels in mice inoculated with L-1210 lymphoid leukemia cells in *vivo* was undertaken. The results are reported in the present paper. The synthesis and *in vivo* evaluation of α-methyl-(±)-ornithine *tert*-butyl ester (V) also are described. This compound was prepared in an attempt to provide an inhibitor with prolonged *in vivo* activity. Furthermore, a method for the determination of polyamines in tissue is described, and preliminary studies of the metabolic fate of I in mice are discussed.

EXPERIMENTAL[1]

Melting points were determined in open capillary tubes and are uncorrected. NMR spectra were taken in deuterochloroform or deuterium oxide with tetramethylsilane or sodium 2,2-dimethyl-2-silapentane-5-sulfonate as the internal standard, respectively. Mass spectral analyses were performed at 70 ev with a 200° chamber temperature.

Metabolic studies with radiolabeled compounds were performed using enclosed environment glass metabolic cages[2]. Autoradiographic data were obtained using medical X-ray film[3] developed by a rapid process developer[4]. TLC plates for the separation of biological samples were silica gel GF and Avicel F[5], 250 μm, 20 × 20 cm. High-pressure liquid chromatography (HPLC) was performed on a bonded phase column[6]. Eluted compounds were detected by monitoring absorbance at 254 nm.

(±) - N^2,N^5-Bis(benzyloxycarbonyl)-2,5-diamino-2-methylpentanoic Acid (III)—The procedure was a modification of the method of Synge (6). To a solution of I monohydrochloride monohydrate (4.387 g, 0.02 mole) in 2 *N* NaOH (30 ml) at 0° were added alternately four portions of 2 *N* NaOH (20 ml) and benzyl chloroformate (II) (5 ml) (Scheme I). Each addition pair was stirred for 5–10 min, and the final reaction mixture was stirred for 0.5 hr. Concentrated hydrochloric acid (25 ml) was then added, and the resulting oily mixture was extracted with ether (3 × 50 ml).

The ether layer was then extracted with 7% sodium bicarbonate (4 × 200 ml), and the aqueous layer was acidified with concentrated hydrochloric acid (110 ml) and extracted with ether containing 10% ethyl acetate (3 × 250 ml). The organic layer was dried (anhydrous calcium sulfate) and then evaporated to dryness. Crystallization from toluene–petroleum ether (bp 60–70°) gave III (5.15 g, 41% yield), mp 112–114°; IR (KBr): 3370, 3320, 1715, 1680, 1520, 1250, 740, and 685 cm^{-1}; NMR (deuterochloroform): δ 1.41 (broad m, 2H), 1.56 (s, 3H), 1.90 (broad m, 2H), 3.1 (t, 2H), 5.08 (s, 4H), and 7.32 (s, 10H) ppm.

Anal.—Calc. for $C_{22}H_{26}N_2O_6$: C, 63.76; H, 6.32; N, 6.76. Found C, 63.79; H, 6.32; N, 6.57.

(±) -N^2,N^5-Bis(benzyloxycarbonyl)-2,5-diamino-2-methylpentanoic Acid *tert*-Butyl Ester (IV)—Preparation of IV was accomplished by modifications of the method by Pandit[7]. To a suspension of III (3.70 g, 0.0089 mole) in methylene chloride (250 ml) containing 0.5 ml of sulfuric acid was added isobutylene gas (about 40–50 ml) until no further volume change occurred (Scheme I). The reaction mixture was capped and stirred for 72 hr at room temperature. Then ammonia gas was added to bring the pH to 8, and excess isobutylene was removed with a nitrogen stream.

[1] Instruments used were: a Thomas-Hoover melting-point apparatus; a Perkin-Elmer 237 or Beckman IR-9 IR spectrophotometer; a Varian A-60 D NMR spectrometer; an AEI MS-30 mass spectrometer; a Beckman LS-150 liquid scintillation counter; a model U6K injector and a model 6000 solvent delivery system, Waters Associates, Bedford, Mass.; an LDC UV-monitor, model 1285; and a Hewlett-Packard 9100A calculator. Elemental analysis was performed by MHW Laboratories, Garden City, Mich., and Galbraith Laboratories, Knoxville, Tenn.

[2] Colman-Delmar, Newark, Del.

[3] Kodak RP/R-54.

[4] Kodak X-OMAT.

[5] Analtech, Newark, Del.

[6] Micropak CN-10 (25 cm × 2.2 mm i.d.), Varian Aerograph.

[7] Dr. U. Pandit, Laboratorium Voor Organische Scheikunde Der Universitat Van Amsterdam, Amsterdam, The Netherlands, personal communication.

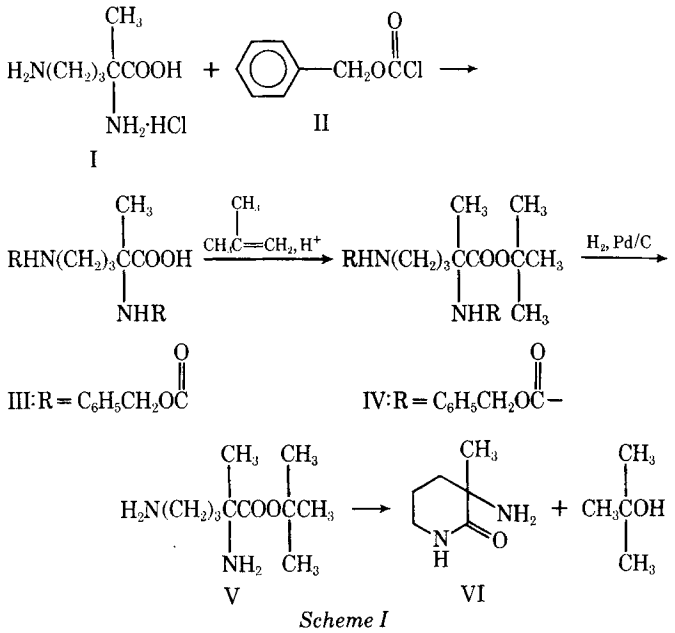

Scheme I

The reaction mixture was washed with water, dried over anhydrous calcium sulfate, and evaporated to provide crude IV as an oil (3.59 g, 86% yield); IR (neat): 3420, 3350, 2975, 2940, 1720, 1520, 1500, 1450, 1365, 1250, 735, and 690 cm^{-1}; NMR (deuterochloroform): δ 1.43 (s, 9H), 1.51 (s, 3H), 1.86 (broad m, 4H), 3.17 (t, 2H), 5.08 (d, 4H), and 7.33 (s, 10H) ppm.

Anal.—Calc. for $C_{26}H_{34}N_2O_6$: C, 66.36; H, 7.28; N, 5.95. Found: C, 66.23; H, 7.30; N, 5.81.

After prolonged storage at 0°, the oil crystallized from ethanol–water, mp 85–86.5°. All spectral data established identity of the solid with the oil (IV).

(±)-2,5-Diamino-2-methylpentanoic Acid *tert*-Butyl Ester Dihydrochloride (V Dihydrochloride)—Palladium catalyst (10% on carbon, 100 mg) was added to a solution of IV (3.59 g, 0.0076 mole) in ethanol (75 ml), and the reaction mixture was hydrogenolyzed with 2.2 kg/cm^2 of hydrogen for 24 hr at room temperature (Scheme I). The slurry was then filtered through a diatomaceous earth[8] bed, rinsed with ethanol, and carefully evaporated to dryness. The oil was quickly dissolved in cold absolute ethanol, and then ether saturated with hydrogen chloride was added slowly, with stirring, to the chilled solution.

The precipitated solid was filtered and crystallized from ethanol–ether to give V dihydrochloride (1.69 g, 81% yield), mp >90° dec.; IR (KBr): 2000, 1730, 1595, 1515, 1365, 1250, 1150, 830, and 735 cm^{-1}; NMR (deuterium oxide): δ 1.55 (s, 9H), 1.58 (s, 3H), 1.91 (m, 4H), and 3.04 (t, 2H) ppm.

Anal.—Calc. for $C_{10}H_{24}Cl_2N_2O_2$: C, 43.66; H, 8.79; N, 10.18. Found: C, 43.67; H, 8.70; N, 9.87.

Anal.—Calc. for $C_{20}H_{50}Cl_4N_4O_5$: C, 42.26; H, 8.87; N, 9.86. Found: C, 42.26; H, 8.83; N, 10.04.

Animals—Adult male DBA/2 mice[9], 15–20 g, and adult male BDF_1 mice[10], 18–20 g, were allowed food[11] and water *ad libitum*.

Materials and Solutions—^{14}C-Toluene (4.0×10^5 dpm/ml), 1-^{14}C-DL-ornithine (specific activity 7.66 mCi/mmole), and sodium ^{14}C-bicarbonate (specific activity 8.4 mCi/mmole) were obtained commercially[12]. 1-^{14}C-Compound I (specific activity 0.53 mCi/mmole) was synthesized as described previously (3). The counting cocktail was either 5.5 g of fluor[13] dissolved in 1 liter of toluene–methanol (1:2) or 5.5 g of fluor dissolved in 1 liter of nonionic surfactant[14]–toluene (1:2). Liquid chromatographic grade solvents[15] were used.

Tumor Inoculation—The L-1210 lymphoid leukemia was obtained as a frozen cell suspension. The tumor was carried in DBA/2 male mice by weekly intraperitoneal passages. A 0.1-ml volume of a suspension (in Eagle's 1-X balanced media) containing $1.0–2.0 \times 10^6$ L-1210 ascites leukemic cells/ml, which were obtained on Day 7 from DBA/2 mice, was inoculated intraperitoneally into each recipient BDF_1 test mouse. Each test group was inoculated with cells obtained from the same DBA/2 mouse.

Drug Regimen—A daily intraperitoneal injection of 0.1 ml of the test compounds, from Day 1 until death, was given to leukemic BDF_1 mice inoculated on Day 0 with tumor cells as described. All test compounds were dissolved in sterile 0.9% NaCl solution, and the solutions were prepared on Days 1 and 5 of tumor growth. A 0.1-ml volume of a 0.9% NaCl solution was injected into each control group. Compounds I at 300 and 100 mg/kg and V at 100 mg/kg were used in the survival time study and in the polyamine metabolism study. 1-^{14}C-Compound I was administered at 300 mg/kg once on Day 3 of tumor growth to study I metabolism.

Survival Time Test—Protocol 1.100 (7) of the National Cancer Institute was followed. Eight mice were used in each test group, and 18 mice were used in the control group. A suspension of 1.2×10^5 L-1210 cells was inoculated into each BDF_1 mouse on Day 0.

Preparation of Spleen Extracts for Polyamine Determination—Two animals from each test group and two animals from the control group were sacrificed by cervical dislocation on Days 0 (control only), 3, 6, and 8 after tumor inoculation. The spleens were removed quickly, excised from surrounding fatty tissue, rinsed in 0.9% NaCl, blotted dry, and frozen immediately in a liquid fluorocarbon[16]. The spleens were weighed and then quickly homogenized in 10 volumes of chilled 0.4 *N* perchloric acid homogenization solution. The homogenate was centrifuged at 5000 rpm for 20 min, and the supernate was removed and stored at −70° until analysis.

Determination of Polyamines in Spleen Extracts—Spleen extracts were dansylated according to the method of Seiler and Wiechmann (8), but the following modifications were necessary to obtain optimal conditions. A 100-μl portion of the spleen tissue extract was shaken overnight in a stoppered tube in a reaction mixture containing 600 μl of a solution of 1-dimethylaminonaphthalene-5-sulfonyl (dansyl) chloride (12 mg/ml) in acetone, 200 μl of a saturated sodium carbonate solution, and 50 μl of 80.0 μM 1,3-propanediamine in water. Duplicate samples were analyzed. In a similar fashion, polyamine standard solutions were dansylated. Volumes of 10, 25, 50, 75, and 100 μl of an aqueous solution containing 0.0454 m*M* putrescine, 0.333 m*M* spermidine, and 0.320 m*M* spermine were reacted. A 100-μl portion of 0.4 *N* perchloric acid was added to the standards along with 50 μl of the 1,3-propanediamine solution. Standards were run in duplicate or triplicate.

After a 16-hr reaction period, 300 μl of an aqueous proline solution (300 m*M*) was added to each sample and the mixtures were shaken for 2 hr to eliminate excess dansyl chloride. Acetone in the reaction mixture was evaporated at 40° under a nitrogen stream. Water (0.5 ml) was added to the evaporated mixture, and the dansylated polyamines were extracted into benzene (5 ml). The benzene layer was evaporated to dryness at 40° under a nitrogen stream, and the resulting residue was dissolved in a small portion of chloroform. The chloroform solution was applied to silica gel GF TLC plates, and the plates were developed for 15 cm with cyclohexane–ether (1:9).

The dansylated polyamine standards were developed concurrently with the tissue extracts; areas corresponding to the polyamines and to 1,3-propanediamine (UV visualization) were scraped, using a glass recovery tube[17], and eluted with 5 ml of triethylamine–2-propanol (1:1). The eluant was evaporated to dryness at 40° under a nitrogen stream. The residue was dissolved in methylene chloride (50 or 100 μl), and 5–10-μl aliquots were used for separation by HPLC. The solvent system used for the HPLC separation was cyclohexane–methylene chloride–2-propanol (88.5:7.5:4) at a flow rate of 1.0 ml/min.

Monitoring of the eluted dansylated polyamines was accomplished by a UV detector at 254 nm. Baseline separation of all amines was achieved, and the total time per sample was under 25 min (Fig. 1). To ensure chromatographic purity, the eluants from the HPLC column corresponding to each amine were collected separately during two individual separations, evaporated to dryness, and then rechromatographed two dimensionally (15 cm each direction) on silica gel GF TLC plates, first with chloroform–triethylamine (10:1) and then with cyclohexane–ethyl acetate (1:1).

Each chromatogram yielded only one fluorescent spot that coincided exactly to the respective dansylated polyamine standard. The ratio of the area under the peaks of the polyamines to that of 1,3-propanediamine

[8] Celite.
[9] Jackson Laboratories, Bar Harbor, Me.
[10] ARS Sprague-Dawley, Madison, Wis.
[11] Purina chow.
[12] New England Nuclear, Boston, Mass.
[13] Permablend III, Packard Instruments, Downers Grove, Ill.
[14] Triton X-100, Packard Instruments, Downers Grove, Ill.
[15] Burdick and Jackson Laboratories, Muskegon, Mich.
[16] Freon.
[17] Chromaflex recovery tube, Kontes Glass Co., Vineland, N.J.

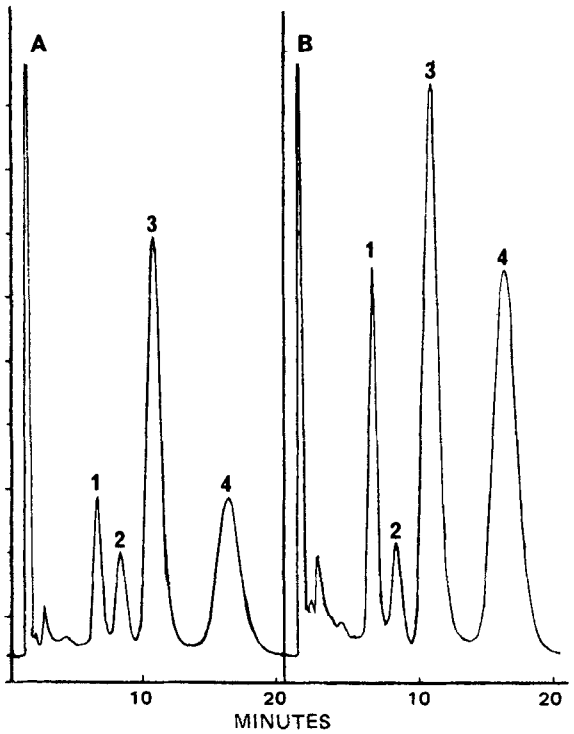

Figure 1—*HPLC separation of a standard solution of the dansyl derivatives of the polyamines (A) and of the dansyl derivatives of the polyamines obtained from the spleens of mice inoculated with L-1210 leukemic cells (B). The compounds tested were the dansyl derivatives of 1,3-propanediamine (internal standard) (1), putrescine (2), spermidine (3), and spermine (4).*

was calculated from the HPLC charts by the triangulation method. Standard curves for each amine were obtained by linear regression analysis of area ratios. Values of the polyamine content in spleen tissue were obtained from each standard curve.

Determination of 1-^{14}C-I Metabolism—Two adult male BDF_1 mice, 19–20 g, were inoculated with a suspension of 1.7×10^5 L-1210 leukemic ascites cells on Day 0. On Day 3 of tumor growth, each mouse was injected with 0.1 ml (0.1035 g) of a solution containing 0.0392 g (0.195 mmole) of 1-^{14}C-I and 0.0797 g of unlabeled I dissolved in 2.00 ml of 0.9% NaCl. The animals were then placed into a glass-enclosed environment metabolism cage, designed to separate the urine and feces and to allow carbon dioxide collection.

Air was pulled through the cage at the rate of 150–200 cm^3/min. The air entry tube contained granulated sodium hydroxide[18], which removed all atmospheric carbon dioxide. Expired carbon dioxide was collected at 4 hr and from 4 to 24 hr in separate traps containing 75 ml of 10 *N* NaOH. A backup trap of 10 *N* NaOH (200 ml) was used during the entire experiment. The urine was collected at 4 hr and from 4 to 24 hr, and the metabolic cage was rinsed carefully with water at each period. The diluted urine solutions were filtered through sintered-glass funnels and then frozen until analysis.

Previously, a standard curve was prepared to determine the quenching effect of urine on the counting efficiency. Various dilutions of urine obtained from male BDF_1 mice and a constant amount of 1-^{14}C-I were mixed in water to a final volume of 1.0 ml. Then the toluene–nonionic surfactant cocktail (10 ml) was added to each sample, and the counts per minute of the samples were measured. Examination of the standard quench curve showed that urine diluted between 1:10 and 1:100 had no effect on the counting efficiency in the scintillation system used.

^{14}C-Toluene and 1-^{14}C-DL-ornithine standards were used to determine the cocktail counting efficiency, which was calculated to be 86.7%. Triplicate samples of each urine collection were analyzed. For each sample, a 1.0-ml volume of the diluted urine solution was added to 10.0 ml of the cocktail. The percent of the administered dose of 1-^{14}C-I found in the urine was calculated by converting all values obtained by liquid scintillation counting to disintegrations per minute.

[18] Ascarite.

Table I—Effects of I and V on the Survival Time of Male BDF_1 Mice Inoculated Intraperitoneally with L-1210 Leukemic Cells of Mice

Group	Test Compound	Dose, mg/kg	Number of Animals	Mean Survival Time, days[a]
1	I hydrochloride	100	8	7.7
2	I hydrochloride	300	8	7.4
3	V dihydrochloride	100	8	8.1
4	Control (0.9% NaCl)	—	18	7.4 (±0.55)

[a] Mean survival time was calculated according to Protocol 11 in Ref. 7.

The ^{14}C-labeled carbon dioxide collected during the metabolism study was measured as follows. Duplicate samples of 1.0, 2.0, and 5.0 ml of each collection time period were pipetted into separate 25-ml conical flasks. The flasks were sealed with a rubber stopper, which held a polypropylene center well containing 200 μl of ethanolamine. The labeled carbon dioxide was liberated by the injection of similar volumes of concentrated hydrochloric acid into the reaction flasks. The flasks stood for 20–24 hr to ensure complete absorption of the carbon dioxide by the ethanolamine. Then the polypropylene cups were carefully cut and placed into a counting vial containing 10.0 ml of methanol–toluene cocktail.

The efficiency of the carbon dioxide collection was determined by comparison of values obtained from a standard sodium ^{14}C-bicarbonate solution using the described method to values obtained by a direct count of an identical volume (0.01 ml) of the sodium ^{14}C-bicarbonate solution in the cocktail. Collection efficiency was calculated to be 93.2 ± 0.8%. The counting efficiency of the cocktail, determined by use of ^{14}C-toluene and 1-^{14}C-DL-ornithine, was calculated to be 73%. All final cocktail mixtures contained 10.0 ml of the methanol–toluene cocktail, 0.2 ml of ethanolamine, and 0.01 ml of water.

Portions of the urine samples were freeze dried and then applied to cellulose TLC plates. The plates were developed two dimensionally (15 cm in each direction) by combinations of the following systems: A, methanol–pyridine–1.2 *N* HCl (8:1:2); B, methanol–pyridine–water–acetic acid (6:6:4:1); and C, 1-butanol–water–acetic acid (3:1:1). Each developed chromatogram was coated with a saturated solution of anthracene (in benzene), dried, placed into a metal cassette containing X-ray film, and then exposed for 48 hr in a dry ice chamber. The autoradiogram was developed and fixed.

Authentic I (2–3 mg) was added to the freeze-dried solutions prior to the TLC application. The same TLC plates that were used for autoradiography were afterward sprayed with ninhydrin (1% in ethanol) and then heated. The ninhydrin-positive spots that appeared were correlated to the autoradiograms. Authentic 1-^{14}C-I was run separately in each TLC system, autoradiographed, and visualized with ninhydrin as described. Results were correlated to urine samples.

1-^{14}C-DL-Ornithine was diluted appropriately, and 0.1 ml of this solution (0.0993 g) was injected on Day 3 into two BDF_1 male mice; these mice had been inoculated on Day 0 with 1.02×10^5 L-1210 cells. The mice were housed in the metabolism cages, and the urine and ^{14}C-labeled carbon dioxide were collected and measured as described. The specific activity of the stock 1-^{14}C-DL-ornithine solution was determined using a toluene–nonionic surfactant cocktail.

The animals were not fed throughout both metabolic studies, but water was given *ad libitum*.

RESULTS AND DISCUSSION

The synthesis of I and ^{14}C-I were reported previously (2, 3). Compound V was very susceptible to intramolecular ring closure and gave the lactam VI and *tert*-butanol (Scheme I). The dihydrochloride salt of V was not susceptible to this decomposition. However, V dihydrochloride must be prepared with ice-cold dilute ethereal hydrogen chloride to prevent the acid hydrolysis of the *tert*-butyl ester moiety. Compound V dihydrochloride was very hygroscopic and formed a stable hemihydrate upon exposure to air. Periodic proton magnetic resonance examination of dried samples of V dihydrochloride stored at 0° under vacuum showed that no formation of *tert*-butanol had occurred.

Compound V was prepared to act as a prodrug that may have better *in vivo* transport and distribution characteristics than I. *In vivo*, V would hydrolyze to liberate the active decarboxylase inhibitor I.

Compounds I and V produced no increase in the survival time of mice (Table I). Russell (9) reported similar results using I (10); however, no details of dosage regimen or test conditions were given.

The effects of I and V on the changes in the polyamine levels during

Table II—Effects of I on the Polyamine Levels in Spleen of BDF_1 Mice Inoculated with L-1210 Leukemic Cells of Mice

Polyamine	Day[a]	Levels, μmoles/g (Range)[b] Group 1[c]	Group 2[c]	Group 3[c]	Group 4[c]
Putrescine	3	0.19 (0.16–0.22)	0.11 (0.10–0.12)	0.19 (0.13–0.26)	0.18 (0.14–0.21)
	6	0.31 (0.29–0.34)	0.28 (0.35–0.32)	0.29 (0.22–0.36)	0.32 (0.30–0.33)
	8	0.30	0.23	0.38	0.26
Spermidine	3	1.64 (1.30–1.97)	1.21 (1.13–1.28)	1.70 (1.46–1.96)	1.59 (1.18–2.01)
	6	2.14 (2.09–2.19)	2.00 (1.95–2.05)	2.05 (1.72–2.38)	2.06 (1.66–2.45)
	8	1.99	1.82	2.10	1.70
Spermine	3	1.06 (0.92–1.20)	0.84 (0.77–0.90)	1.00 (0.86–1.14)	1.00 (0.79–1.21)
	6	1.15 (1.03–1.27)	1.02 (0.99–1.05)	1.05 (0.86–1.23)	1.02 (0.95–1.09)
	8	0.77	0.78	0.84	0.72

[a] Days after inoculation of mice with 1.2×10^5 L-1210 ascites tumor cells. [b] Ranges between animals within each test group. [c] Compounds were administered by intraperitoneal injection from Days 1 through 7 to the mice in the following groups: Group 1, 100 mg/kg of I hydrochloride monohydrate; Group 2, 300 mg/kg of I hydrochloride monohydrate; Group 3, 100 mg/kg of V dihydrochloride; and Group 4, 0.9% NaCl.

tumor growth were studied using spleen tissue obtained from BDF_1 mice inoculated with L-1210 leukemic cells. The basal polyamine levels on Day 0 were 0.17, 1.5, and 0.9 μmoles/g of tissue for putrescine, spermidine, and spermine, respectively. These levels progressively increased to the maxima on Day 6. Although the animals were of the same age, weight, and sex, the levels of each polyamine varied widely from animal to animal within each test group. In general, the mean values for the accumulation of the polyamines during L-1210 tumor growth were consistent in magnitude with values reported by others (11, 12). One notable exception was that the putrescine levels were slightly higher than those reported previously (11). Daily injections of I at doses of 100 and 300 mg/kg or V at a dose of 100 mg/kg had no significant effect on the polyamine level changes occurring during L-1210 tumor growth (Table II).

Standard solutions of each polyamine were used to obtain standard curves. A linear relationship between the amount of amine added and the ratio of the area of its peak to that of the internal standard was observed. The correlation coefficients, calculated by regression analysis, were 0.995 for putrescine, 0.996 for spermidine, and 0.996 for spermine. The polyamine concentrations in the spleen extracts were obtained by entering the ratio of the peak areas of the polyamine to that of 1,3-propanediamine onto the standard curve. Duplicate samples from each spleen extract were within ±10%.

To delineate the factors that may have contributed to the lack of *in vivo* activity of I, the fate of the 1-^{14}C-labeled compound was studied in mice. The fate of (±)-ornithine (VII) was also studied to monitor the metabolic changes of the substrate L-ornithine. Less than 0.1% of the injected dose of I was recovered as ^{14}C-labeled carbon dioxide during 24 hr (Table III). This value correlated well with results obtained by others with α-methyl-substituted amino acid analogs that inhibit decarboxylase enzymes (13–15). It is also in agreement with results of studies on the decarboxylation of I *in vitro* (3). Compound I was eliminated relatively rapidly in urine. Four hours after injection, 38% of the injected dose of I was recovered in the urine. During the 4–24-hr period, another 32% of the dose was excreted in urine. The rapid elimination of I *via* the kidney after intraperitoneal injection may be responsible for the lack of *in vivo* activity.

During a 24-hr period, 34% of the administered dose of ^{14}C-VII was metabolized to ^{14}C-labeled carbon dioxide and 28% was excreted in urine. The pattern of the major elimination pathway changed dramatically over the 24 hr. During the 0–4-hr interval after administration, decarboxylation occurred to the extent of 28% while urinary excretion accounted for only 0.1% of the injected dose. It is assumed that only the L-form of the injected ^{14}C-VII was decarboxylated. Thus, over 50% of the natural substrate was rapidly decarboxylated. From 4 to 24 hr, metabolism *via* labeled carbon dioxide loss amounted to only 6% whereas urinary excretion represented 28% of the injected dose. The radioactivity excreted in the urine was probably due solely to the D-enantiomer since this enantiomer cannot be decarboxylated (16) and probably cannot be reabsorbed by kidney tubules.

The urine samples collected after intraperitoneal injection of 1-^{14}C-I were examined for possible metabolites. In all chromatographic systems examined, the radioactivity was located entirely in ninhydrin-positive areas and these spots were coincident with authentic 1-^{14}C-I. These results indicate that I was excreted in urine primarily unchanged.

Table III—Elimination of ^{14}C-I and ^{14}C-VII after Intraperitoneal Injection in Mice

Compound[a]	Hours[b]	Percent of Dose Excreted in Urine	Percent of Dose Excreted as Labeled Carbon Dioxide
^{14}C-I	0–4	38.20	0.04
	4–24	32.43	0.03
^{14}C-VII	0–4	0.10	27.50
	4–24	28.01	6.00

[a] Compounds were injected intraperitoneally in BDF_1 mice on Day 3 after inoculation with 1.71×10^5 L-1210 cells. [b] Hours after intraperitoneal injection of the test compounds.

REFERENCES

(1) U. Bachrach, "Function of Naturally Occurring Polyamines," Academic, New York, N.Y., 1973, pp. 47–95.

(2) M. M. Abdel-Monem, N. E. Newton, and C. E. Weeks, *J. Med. Chem.*, **17**, 447 (1974).

(3) M. M. Abdel-Monem, N. E. Newton, B. C. Ho, and C. E. Weeks, *ibid.*, **18**, 600 (1975).

(4) M. M. Abdel-Monem, N. E. Newton, and C. E. Weeks, *ibid.*, **18**, 945 (1975).

(5) N. E. Newton and M. M. Abdel-Monem, *ibid.*, **20**, 249 (1977).

(6) R. Synge, *Biochem. J.*, **42**, 99 (1948).

(7) R. I. Geran, N. H. Greenberg, M. M. MacDonald, A. M. Schumacher, and B. J. Abbott, *Cancer Chemother. Rep. Part 3*, **3** (2), 7 (1972).

(8) N. Seiler and M. Wiechmann, *Z. Physiol. Chem.*, **348**, 1285 (1967).

(9) D. H. Russell, in "Polyamine in Normal and Neoplastic Growth," D. H. Russell, Ed., Raven, New York, N.Y., 1973, p. 5.

(10) I. Horniberg and J. Ellington, *J. Org. Chem.*, **39**, 104 (1974).

(11) D. Russell and O. Heby, *Cancer Res.*, **33**, 159 (1973).

(12) O. Heby and D. Russell, *ibid.*, **34**, 886 (1974).

(13) C. Porter, L. Watson, D. Titus, J. Totaro, and S. Byer, *Biochem. Pharmacol.*, **11**, 1067 (1962).

(14) S. Udenfriend, H. Weissbach, and W. Lovenberg, *Biochem. Biophys. Res. Commun.*, **3**, 225 (1960).

(15) C. Voltattorni, A. Minelli, and C. Turano, *FEBS Lett.*, **17**, 231 (1971).

(16) A. Pegg, *Ann. N.Y. Acad. Sci.*, **171**, 977 (1970).

ACKNOWLEDGMENTS AND ADDRESSES

Received September 8, 1976, from the *College of Pharmacy, University of Minnesota, Minneapolis, MN 55455.*

Accepted for publication February 4, 1977.

Supported by Research Grant CA 14239 and Training Grant GM 02064 from the National Institutes of Health.

The authors thank H. T. Nagasawa and his staff at the Veterans Administration Hospital, Minneapolis, Minn., for the use of their equipment.

* Present address: National Center for Toxicological Research, Jefferson, AR 72209.

[x] To whom inquiries should be directed.

Stability of Prostaglandin E_1 and Dinoprostone (Prostaglandin E_2) under Strongly Acidic and Basic Conditions

R. G. STEHLE ˣ and T. O. OESTERLING *

Abstract □ The stability of prostaglandin E_1 and dinoprostone was investigated at the extremes of the pH range (≤ 3 and ≥ 10) in the sequence prostaglandin E → prostaglandin A → prostaglandin B. The degradation rate is first order with hydrogen-ion and hydroxide-ion concentrations. Separation and analysis of the E prostaglandins were accomplished by TLC and UV spectrophotometry. At the lowest pH values and at elevated or low temperatures, significant amounts of 15-epiprostaglandin E were present. Apparent activation energies for the total dinoprostone loss, calculated from elevated temperature data, were 21 kcal/mole in the strongly acidic region and about 18 kcal/mole at pH 3. Corresponding studies in the alkaline region led to a derived Arrhenius activation energy of 15 kcal/mole with the appearance of significant amounts of 8-iso-prostaglandin E. This difference in activation energies may reflect the different mechanisms operant at high and low pH values.

Keyphrases □ Prostaglandins—E_1 and dinoprostone, stability at pH extremes □ Dinoprostone—stability at pH extremes □ Stability—prostaglandin E_1 and dinoprostone at pH extremes □ Degradation—prostaglandin E_1 and dinoprostone at pH extremes □ Oxytocic agents—prostaglandin E_1 and dinoprostone, stability at pH extremes

The biological aspects of prostaglandins dominate the literature on these substances. Prostaglandins appear to be widely involved in the body's biochemistry, with potential applications in such areas as labor induction, contraception, control of ulcers, asthma, and blood pressure regulation. The ready availability from certain forms of *Plexaura homomalla* of A prostaglandin derivatives, which have been converted to E and F prostaglandins (1, 2), has facilitated research on these long chain fatty acids.

BACKGROUND

The E prostaglandins, those containing the β-hydroxycyclopentanone ring such as dinoprostone[1] (I) ($\lambda_{max} \sim 170$ nm), are important clinically. This β-hydroxy ketone system is unstable and readily undergoes dehydration (3–5) under acidic or basic conditions to A-type prostaglandins, those containing a cyclopentenone ring such as prostaglandin A_2 (III) ($\lambda_{max} \sim 220$ nm). Under basic conditions, the A prostaglandins can isomerize further to B prostaglandins (3) such as prostaglandin B_2 (IV) ($\lambda_{max} \sim 280$ nm).

In addition to this main reaction pathway, the formation of epimers

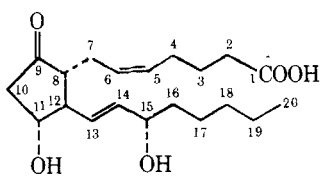

I

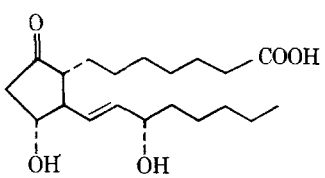

II

[1] Code designation prostaglandin E_2.

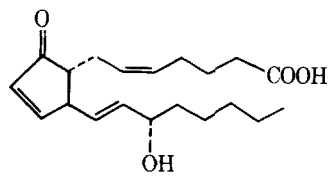

III

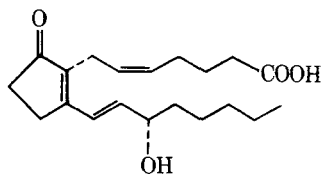

IV

at C-15 may occur under strongly acidic conditions (6) (Scheme I). In mildly to strongly basic media, the E prostaglandin can form an equilibrium mixture with its C-8 isomer (7) (Scheme II). The 13,15-allylic rearrangement product of A prostaglandins was found in acidic reaction mixtures (8), and it was implied that E prostaglandins can also undergo 13,15-rearrangement under similar conditions to small amounts of, for example, V. Other limited evidence (8) indicates that the 13,15-prostaglandin A rearrangement product also can dehydrate to give "minor elimination products."

A kinetic study of the prostaglandin E → prostaglandin A → prostaglandin B reaction as a function of pH and temperature was reported recently (9), in which the total amounts of E, A, and B prostaglandins present were followed by UV spectrophotometry. This procedure did not, however, account for the concentrations of epimers and other prostaglandin derivatives with the same or similar absorption properties. At low pH values (<~2.5), the dehydration rate was directly proportional

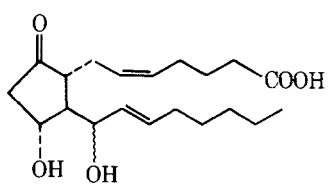

V

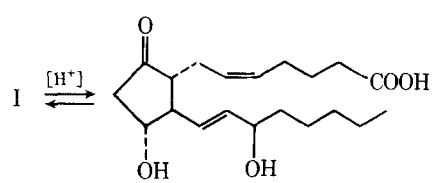

VIII

Scheme I

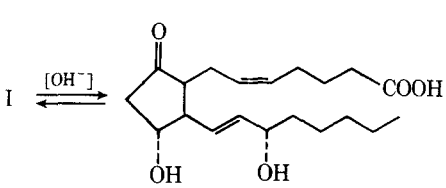

VII

Scheme II

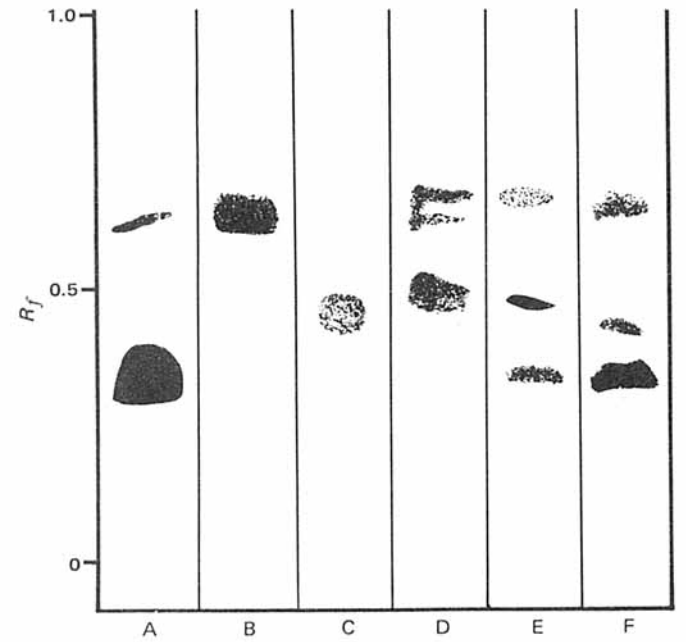

Figure 1—*Thin-layer chromatograms (on silica gel) of prostaglandins developed in ethyl acetate–ethanol–acetic acid (100:1:1). The heavily spotted I sample shows a small amount of III. Isomers found in acidic and basic degradation mixtures are clearly different. The acidic solution was a 12-hr, 37°, pH 1.1 sample; the basic solution was from 0.01 N KOH, approximately 10 min at 37°. Prostaglandins of the 1 and 2 series are not resolved in this TLC system. Key: A, I; B, III; C, VII; D, VIII (impure); E, acidic solution; and F, basic solution.*

to the hydrogen-ion concentration. The calculated activation energy, E_a, values for the dehydration process were 18 kcal/mole at low pH values and 24 kcal/mole at intermediate (neutral) pH values. The E_a for the prostaglandin A → prostaglandin B process was 20 kcal/mole, and there was a difference in the dehydration rate constants for prostaglandin E_1 (II) and I in the pH 3–10 range.

In another study (10), a total rate equation for I decomposition was developed. The high temperature data were consistent with literature data (9). The room temperature studies, however, led to a more thorough interpretation of the kinetic data in the pH 4–9 range.

In previous work (11), the prostaglandin E → prostaglandin A → prostaglandin B reaction was studied in dilute sodium hydroxide solutions. Isomerization (prostaglandin A → prostaglandin B) constants were measured by: (*a*) monitoring the development of the B prostaglandin peak at 283 nm when starting with alkaline solutions of the corresponding A prostaglandin, and (*b*) reacting E prostaglandins under conditions identical to those used for the A prostaglandins and again measuring the appearance of the prostaglandin B peak at 283 nm. Estimation of dehydration (prostaglandin E → prostaglandin A) and isomerization (prostaglandin A → prostaglandin B) rate constants involved the fitting of product–time data to the rate equations with an iterative nonlinear least-squares computer program.

In those studies (11), the apparent dehydration rate constants were approximately six times the values of the corresponding prostaglandin A → prostaglandin B rate constants. For prostaglandin A_1 → prostaglandin B_1 and prostaglandin A_2 → prostaglandin B_2, the respective Arrhenius activation energies were 15.5 ± 1.2 and 13.4 ± 0.8 kcal/mole.

This report focuses mainly on the kinetics of the total degradation of I and II as a function of temperature and pH and attempts to evaluate the relative contribution of the various isomerization reactions.

EXPERIMENTAL

White crystalline II[2], mp 113–115°, and I[2], mp 65–68°, were used. The estimated purity in each case was ≥98% by TLC. White, crystalline 8-isoprostaglandin E_1[2] (VI), mp 73–75°, and 8-isoprostaglandin E_2[2] (VII), mp 107–108°, showed one spot by TLC.

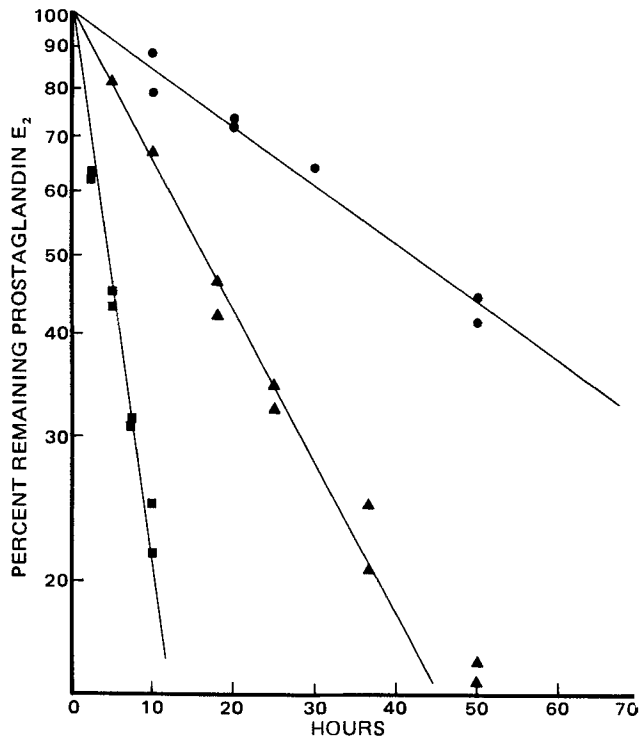

Figure 2—*Kinetic data for total disappearance of I from aqueous solution, pH 2.05. Key:* ●, *47°;* ▲, *57°; and* ■, *70°.*

Low pH Studies—The total loss of I from solutions of low pH was measured by assaying the remaining I as a function of time. A 0.25-ml volume of ethanolic I, 50 mg/ml, was slowly added, with vigorous agitation, to 25 ml of the aqueous solutions (0.1 *N* HCl, pH 1.10; 0.01 *N* HCl, pH 2.05; and 0.1 *M* citrate buffer, pH 2.99) at the reaction temperatures. The resulting 0.5-mg/ml solutions were well within the room temperature solubility of I in solutions below pH 4 (12).

Samples of 2 ml were withdrawn from the 0.5-mg/ml I solution at zero time and at appropriate time intervals. Each sample was extracted twice with water-saturated ethyl acetate; the organic phase was removed after vigorous shaking and centrifugation. The cumulative extract was evaporated to dryness under nitrogen and vacuum, and ethanol was added to make 100 μl. Samples of 10 μl of the concentrate were analyzed by TLC.

High pH Studies—Studies at pH > 10 were carried out in various concentrations of sodium or potassium hydroxide. The system was adjusted to an ionic strength of 0.4 with potassium chloride. Runs were performed at two initial prostaglandin concentrations to verify that the overall loss followed first-order kinetics.

Solutions of 0.1 mg of I or II/ml were prepared in 25-ml stoppered erlenmeyer flasks with aqueous sodium hydroxide (0.002–0.010 *N*) containing sufficient potassium chloride to adjust the ionic strength to 0.4. Acidified 10-ml aliquots, removed at various times, were quantitatively extracted with three 10-ml portions of methylene chloride or water-saturated ethyl acetate. The cumulative organic phase was dried under vacuum with a nitrogen stream, concentrated, and treated as described under TLC.

Rate constants for the total disappearance of I from alkaline solutions between pH 10.3 and 11.5 were obtained by dissolving I at a concentration of 0.5 mg/ml (1.42×10^{-3} *M*) in 0.0025–0.010 *N* KOH and adjusting to ionic strength 0.4 with potassium chloride. The pH of the solution was then read to within ±0.02 unit[3] at the reaction temperature since the II concentration was not negligible compared to the hydroxide-ion concentration. Samples of 2 ml were withdrawn at suitable times after the initial mixing, acidified to pH 3 with dilute hydrochloric acid, and prepared for quantitative TLC as already described. Three 3-ml volumes of ethyl acetate were sufficient for quantitative extraction. The pH was read again after the final sample was withdrawn.

TLC—Andersen (13) evaluated the ability of many solvent systems to separate A and B prostaglandins and epimers of E prostaglandins from

[2] Supplied by research laboratories at The Upjohn Co.

[3] Fisher Accumet, model 310, Fisher Scientific Co., Pittsburgh, PA 15219.

Table I—Rate Constants for Total Loss of I from Acidic Media

pH	Temperature	K, $sec^{-1} \times 10^6$	E_a, kcal/mole
1.10	17°	1.51, 1.50	20.7 ± 0.1
	37°	13.9, 14.6	
	47°	41.9, 42.2, 44.7	
	56°	94.7, 96.9	
	70°	344, 351	
2.05	37°	1.73, 1.75	21.2 ± 0.2
	47°	4.92, 4.28	
	57°	12.5, 11.9	
	70°	42.8, 42.5	
2.99	37°	1.25	18.4 ± 0.3
	49°	3.64	
	57°	7.19	
	70°	22.1	

the natural E prostaglandins. It was decided that quantitative TLC would provide a reliable and accurate method of analysis and separation of I or II from all degradation products. Alcoholic concentrates of reaction mixtures were spotted onto prescored silica gel plates[4], which were then developed in ethyl acetate–acetic acid–ethanol (100:1:1) (13). This system provided adequate separation of E prostaglandins and their isomers, particularly 15-epiprostaglandin E_2 (VIII) and VII (Fig. 1).

Since high laboratory humidity (>50%) resulted in a significant loss in resolution, the plates were activated by heating overnight at 70° and stored and spotted in a constant (15–20%) humidity room. After development, one end of the prescored plate, reserved as a marker to locate the E prostaglandin in the developed kinetic samples, was broken off, sprayed with 15% ammonium sulfate, and charred on a hot plate. Once located, an unknown sample was scraped into a sintered- glass funnel and eluted with methanol into a 10-ml volumetric flask. A "plate blank" served to subtract out any background absorbance due to plate binders and/or colloidal silica gel particles.

Each flask was treated with 1 ml of 5 *N* KOH, virtually instantaneously converting the E prostaglandin to the corresponding B prostaglandin, and diluted to volume with methanol. After 10 min, the samples were scanned from 350 to 250 nm against a potassium hydroxide–methanol blank on a recording spectrophotometer[5]; results were compared to a standard curve (λ_{max} 278 nm) for E prostaglandin converted to B prostaglandin in aqueous methanolic potassium hydroxide.

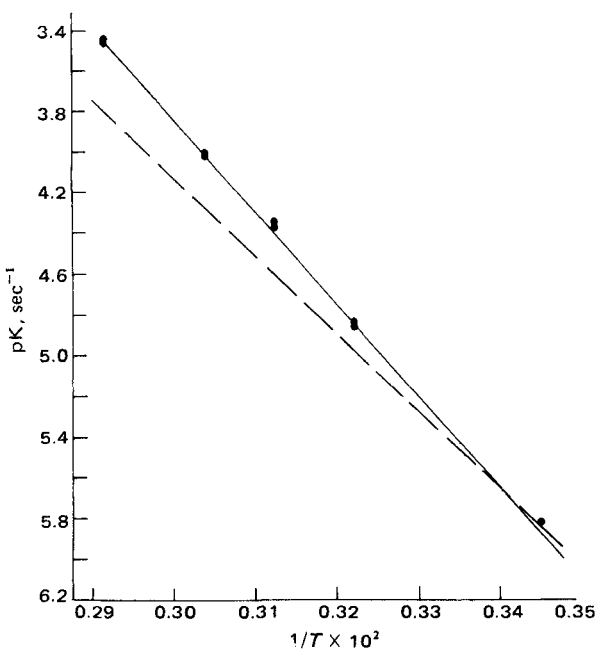

Figure 3—*Arrhenius plot of I degradation at pH 1.10. Data of Monkhouse* et al. *(9), pH 1.2, are included for comparison (dashed line); K refers to overall apparent first-order rate constant.*

[4] Silica gel GF, 250 μm, Analtech, Newark, DE 19711.
[5] Zeiss DMR 21, Carl Zeiss, Oberkochen, West Germany.

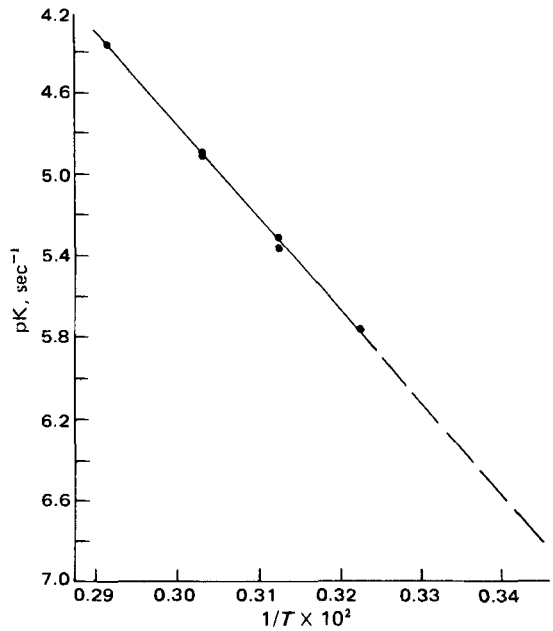

Figure 4—*Arrhenius plot of I degradation at pH 2.05.*

RESULTS

Figure 2 shows typical first-order time data for the total disappearance of I from solution at pH 2.05. Data were plotted as percent of the initial assay. No significant change in pH occurred during a run in acid media. Table I lists the low pH degradation data for I. These data are also summarized in Figs. 3–5.

The pH 1.2 dehydration rate data of Monkhouse *et al.* (9) were included for comparison in Fig. 3. The present E_a values at the lower pH values, where appreciable epimerization and possible rearrangement products were observed, are essentially identical, and higher than the 18-kcal/mole value previously found (9). The E_a observed at pH 2.99, however, where negligible epimerization, *etc.*, was seen, agreed with that reported (9) for dehydration alone.

The rate of total loss of I was proportional to the hydrogen-ion concentration in the pH 1–2 region but not around pH 3. Above about pH 2.5, specific hydrogen-ion catalysis decreases in relative importance, a significant part of the total loss of E prostaglandin being due to water or buffer catalysis. Under the most severe conditions encountered in the oral administration of an E prostaglandin (37°, pH 1–1.5), roughly 5% of the prostaglandin would be lost per hour from nonenzymatic causes.

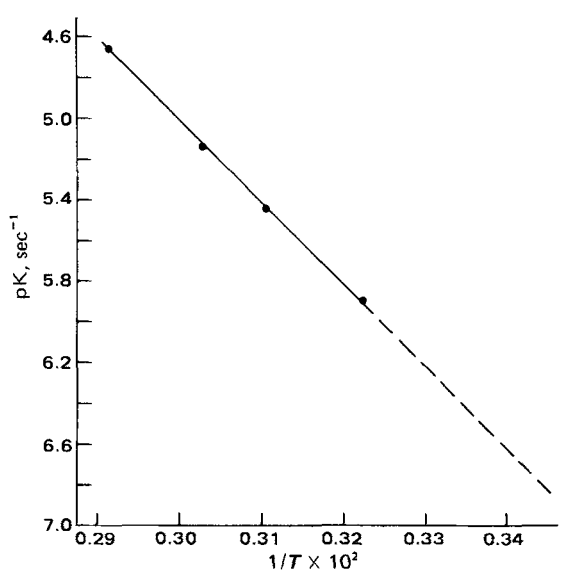

Figure 5—*Arrhenius plot of I degradation at pH 2.99.*

Table II—Effect of pH and Temperature on Apparent First-Order Rate Constants of Alkaline Dehydration of I and II and Their 8-Isomers at 0.1 mg/ml

Prostaglandin	Temperature	Sodium Hydroxide Concentration, *N*	pOH	*K*, sec^{-1} × 10^4
II	37°	0.002	2.70	4.40
II	37°	0.004	2.40	7.21
II	37°	0.006	2.22	10.0
II	37°	0.008	2.10	17.3
II	37°	0.010	2.00	19.3
VI	37°	0.004	2.40	8.07
I	37°	0.002	2.70	4.09
I	37°	0.004	2.40	9.30
I	37°	0.006	2.22	11.8
I	37°	0.008	2.10	16.9
I	37°	0.010	2.00	18.2
II	27°	0.004	2.40	3.36
II	47°	0.004	2.40	15.4
II	57°	0.004	2.40	35.2
VII	37°	0.004	2.40	8.26
I	27°	0.004	2.40	3.17
I	47°	0.004	2.40	16.6
I	57°	0.004	2.40	29.1

Table II lists first-order data for the loss of I and II from alkaline solutions made with sodium hydroxide. There is little difference between the rate constants measured for an 8-iso-E prostaglandin and the E prostaglandin itself. Moreover, no significant difference is seen between I and II. This result is consistent with the previous data (9) where the I and II curves appeared to be converging at pH 10.

Figure 6 shows the rate dependence of the overall loss of E prostaglandin on temperature in 0.004 *N* NaOH. Arrhenius activation energies from these data are 15.4 ± 0.5 kcal/mole for II and 14.3 ± 1.5 kcal/mole for I where the ± figure is the least-squares standard deviation. The lower E_a values at alkaline pH's may reflect the different mechanisms operant at low and high pH values. At high pH, the mechanism is probably the abstraction of an activated hydrogen alpha to the carbonyl group or from the enol form of the prostaglandin; in strongly acid solutions, attack of a suitable site, such as C-11, by a proton forming a good leaving group (HOH) can be the first step in the elimination process.

Table III presents results obtained in I stability studies in potassium hydroxide solution at 0.5 mg/ml. Figure 7 summarizes the 37° data contained in Tables II and III; net hydroxide-ion concentrations were estimated as initial hydroxide-ion concentrations for the 0.1-mg/ml prostaglandin solutions, and as $[OH^-] = [OH^-]_0 - [I]_0 = [OH^-]_0 - 1.42 \times 10^{-3}$ in the 0.5-mg/ml runs in potassium hydroxide, where the subscript indicates initial values.

The least-squares slope is 0.95 for the II data and 0.94 for I when sodium hydroxide is the alkaline medium. The corresponding slope for the I solutions in potassium hydroxide is 1.17. When more accurately plotted against the average pH during the run (Fig. 8), the dependence of the rate constant in potassium hydroxide becomes 0.93. Therefore, the overall loss rate constant is directly proportional to the hydroxide-ion concentration in the pH 10.3–11.5 range. The data in Fig. 7 suggest that the process is first order with respect to the prostaglandin E concentration in the 0.1–0.5-mg/ml range.

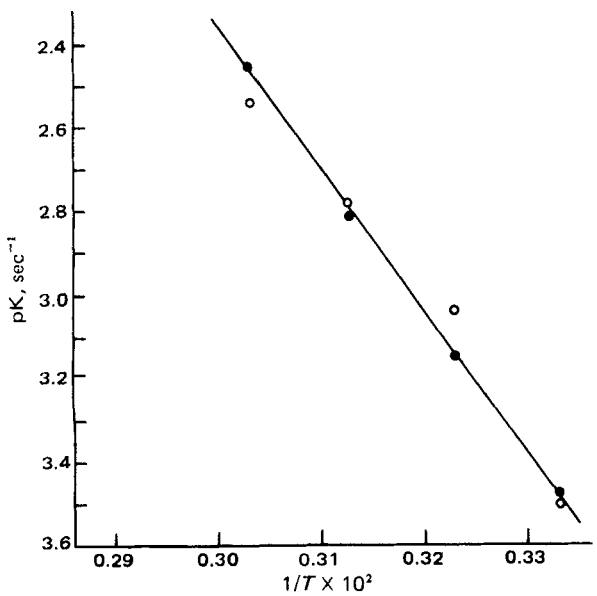

Figure 6—*Effect of temperature on II (●) and I (○) degradation in sodium hydroxide solutions.*

Table III—Rate Data for I in Alkaline Media (Potassium Hydroxide) at 37°; $[I]_0 = 1.42 \times 10^{-3}$ *M*

Potassium Hydroxide Concentration, *N*	Initial pH	Final pH	Average pH	*K* sec^{-1} × 10^4	pK
0.0025	10.47	10.23	10.35	1.85	3.73
0.0025	10.47	10.23	10.35	1.81	3.74
0.0030	10.66	10.37	10.52	3.25	3.49
0.0035	10.90	10.63	10.77	3.98	3.40
0.0035	10.90	10.63	10.77	3.94	3.40
0.0040	10.90	10.70	10.80	5.43	3.27
	10.90	10.70	10.80	5.28	3.28
0.0050	11.19	10.92	11.06	9.31	3.03
	11.19	10.92	11.06	9.07	3.04
0.0060	11.31	11.04	11.18	11.2	2.95
	11.31	11.04	11.18	10.9	2.96
0.0075	11.46	11.22	11.34	18.0	2.75
	11.46	11.22	11.34	17.6	2.75
0.010	11.54	11.42	11.48	19.6	2.71
	11.54	11.42	11.48	19.6	2.72

DISCUSSION

Thin-layer chromatograms of extracts from acidic reaction mixtures show spots other than those attributable to prostaglandins E, A, and B and 15-epiprostaglandin E. This result is particularly true of the most acidic mixtures (pH 1.10) at the higher reaction temperatures (60 and 70°). One spot, which appeared just above the 15-epiprostaglandin E on the TLC plate, probably represents the 13,15-rearrangement product; it never appeared to be more than a few percent of the total material present.

Scans of these solutions in the UV range showed a peak at 283 nm, implicating formation of B prostaglandins in acidic media. Occasionally, two spots appeared above the A/B prostaglandin spot. One apparently was the 15-epiprostaglandin A/B spot; the other was a degradation product with a λ_{max} of ~325 nm and was observed in various kinetic studies[6] (9). This spot may be the 13,15-dehydration product of prostaglandin A containing a highly conjugated trienone system (IX).

Schematic Model for Reaction Products—With these considerations in mind, a model illustrating the various pathways involved in the total loss of E prostaglandins from aqueous solution may be constructed to aid in the interpretation of experimental data. Although this paper deals with the total loss of the E prostaglandin by whatever paths exist, analogous routes for losses of A and B prostaglandins from acidic solutions may also be proposed as in Scheme III. Scheme IV shows the similar possibilities in strongly basic media.

For the prostaglandin E (E), 15-epiprostaglandin E (15E), and 13,15-rearrangement product (E*) compartments (in the case of acid solutions), which are assumed isolated from the remaining scheme by irreversible reactions, the differential equations for the system, with the assumption that all processes are first order, are:

$$\frac{d[E]}{dt} = (-k_1 - k_5 - k_8)[E] + k_{-5}[15E] \quad \text{(Eq. 1)}$$

$$\frac{d[15E]}{dt} = k_5[E] + (-k_3 - k_{-5} - k_9)[15E] \quad \text{(Eq. 2)}$$

$$\frac{d[E^*]}{dt} = k_8[E] + k_9[15E] - k_{14}[E^*] \quad \text{(Eq. 3)}$$

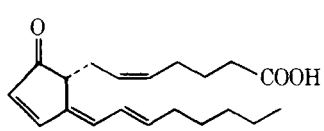

IX

[6] T. O. Oesterling, unpublished observations.

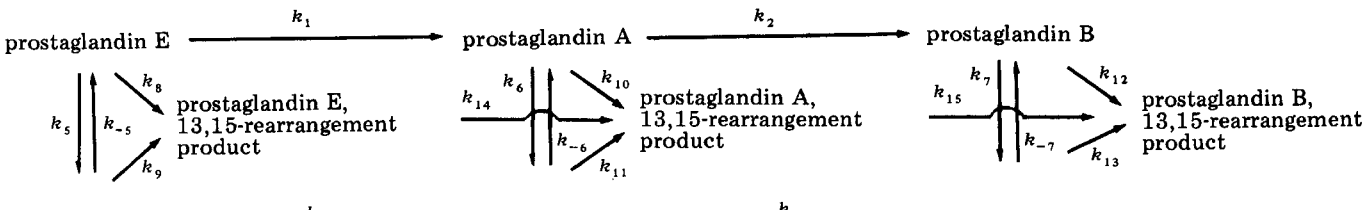

Scheme III

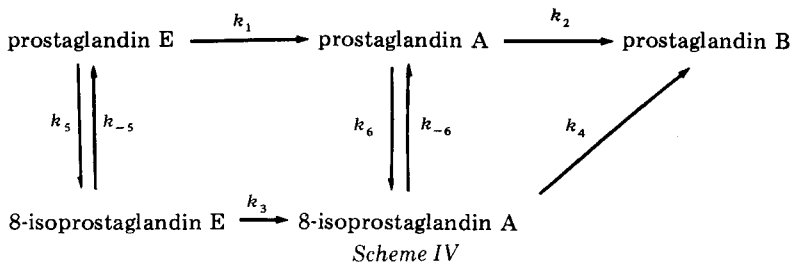

Scheme IV

All k's are, in reality, pseudo-first-order rate constants, containing factors accounting for specific hydrogen-ion, water, and buffer catalyses, and remain constant in any given experiment. Because of the assumption of irreversibility (k_8 and k_9), Eqs. 1 and 2 may be solved as a separate system by using the Laplace transform method, as recently applied to pharmacokinetic systems (14). When assuming that the starting material is pure prostaglandin E at concentration E_0, the total solution is:

$$E(t) = E_0\left[\frac{(k_3 + k_{-5} + k_9 - \alpha)e^{-\alpha t}}{\beta - \alpha} + \frac{(k_3 + k_{-5} + k_9 - \beta)e^{-\beta t}}{\alpha - \beta}\right] \quad \text{(Eq. 4)}$$

$$15E(t) = \frac{k_5 E_0}{\alpha - \beta}(-e^{-\alpha t} + e^{-\beta t}) \quad \text{(Eq. 5)}$$

where:

$$\alpha = \frac{(k_1 + k_3 + k_5 + k_8 + k_{-5} + k_9) + \sqrt{(k_1 + k_3 + k_5 + k_8 + k_{-5} + k_9)^2 - 4(k_1k_{-5} + k_1k_9 + k_5k_9 + k_8k_{-5} + k_8k_9 + k_1k_3 + k_3k_5 + k_3k_8)}}{2} \quad \text{(Eq. 6)}$$

$$\beta = \frac{(k_1 + k_3 + k_5 + k_8 + k_{-5} + k_9) - \sqrt{(k_1 + k_3 + k_5 + k_8 + k_{-5} + k_9)^2 - 4(k_1k_{-5} + k_1k_9 + k_5k_9 + k_8k_{-5} + k_8k_9 + k_1k_3 + k_3k_5 + k_3k_8)}}{2} \quad \text{(Eq. 7)}$$

In all cases, the data for the total disappearance of E from solution suggested that:

$$E(t) = E_0e^{-Kt} \quad \text{(Eq. 8)}$$

where K is some composite of the individual rate constants. If this assumption is made, solution of Eq. 2 gives the biexponential expression:

$$15E(t) = \frac{k_5E_0}{-K + k_{-5} + k_9 + k_3}[e^{-Kt} - e^{-(k_{-5}+k_9+k_3)t}] \quad \text{(Eq. 9)}$$

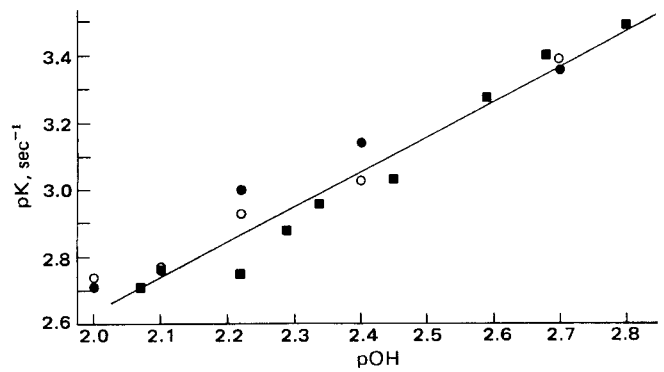

Figure 7—*Effect of OH^- concentration on degradation of II in sodium hydroxide (●), I in sodium hydroxide (○), both 0.1 mg/ml, and I in potassium hydroxide solution (■), 0.5 mg/ml.*

Comparison with Eq. 5 reveals that $\alpha - \beta = -K + k_{-5} + k_9 + k_3$, $\beta = K$, and $\alpha = k_{-5} + k_9 + k_3$. Therefore, the expression for $E(t)$ becomes:

$$E(t) = E_0e^{-\beta t} \quad \text{(Eq. 10)}$$

The apparent first-order total disappearance of I or II is, therefore, a composite of all individual rate constants in the system. The overall rate constant will, depending on the amount of epimerization, *etc.*, be greater than k_1, the dehydration rate constant. This result explains why the E_a values at pH 1–2 were greater than those seen previously (9) in the same pH region. Furthermore, in a 4° run with I in 0.1 *N* HCl (not included in Fig. 3 or Table I), a significant portion of the total loss was in the form of the 15-epimer. The epimerization rate was, therefore, more comparable to the dehydration rate to III. This could show up as a changed slope on the log K *versus* $1/T$ plot, particularly if the activation energy for epimerization is significantly less than that for dehydration. In the extreme case, where the dehydration is negligible compared to epimerization, the E prostaglandin would form an equilibrium mixture with its 15-epimer. At pH 3, however, the amount of epimer and 13,15-rearrangement product appeared to be negligible, *e.g.*, k_5 and k_8 approached zero. Equation 10 then becomes:

$$\lim_{k_5,k_8 \to 0} E(t) = E_0e^{-t/2}[(k_1 + k_3 + k_{-5} + k_9) - \sqrt{(k_1 + k_3 + k_{-5} + k_9)^2 - 4(k_1k_{-5} + k_1k_9 + k_1k_3)}] \quad \text{(Eq. 11a)}$$

$$E(t) = E_0e^{-k_1t} \quad \text{(Eq. 11b)}$$

The total loss of the E prostaglandin should, therefore, be dependent only on k_1, the dehydration rate constant around pH 3. Similar predictions would apply to strongly alkaline reaction mixtures, with 8-isoprostaglandin E replacing 15-epiprostaglandin E and with k_8–$k_{15} = 0$. In the present experiments, no more than 5–10% 8-isoprostaglandin E was formed under any conditions (Fig. 1). The reaction environment necessary to produce enough isomer to show a significant discrepancy between k_{obs} and ($k_{dehydration} = k_1$) would produce an overall rate too rapid to be measured accurately by the present experimental technique.

Comparisons with thin-layer chromatograms of standard methyl and ethyl esters of E prostaglandins showed that negligible esterification occurs in the presence of the small amount of alcohol vehicle in which the free acid prostaglandin is introduced to the aqueous buffer system. The methyl or ethyl ester of an E prostaglandin has a slightly greater R_f than the respective 15-epimer.

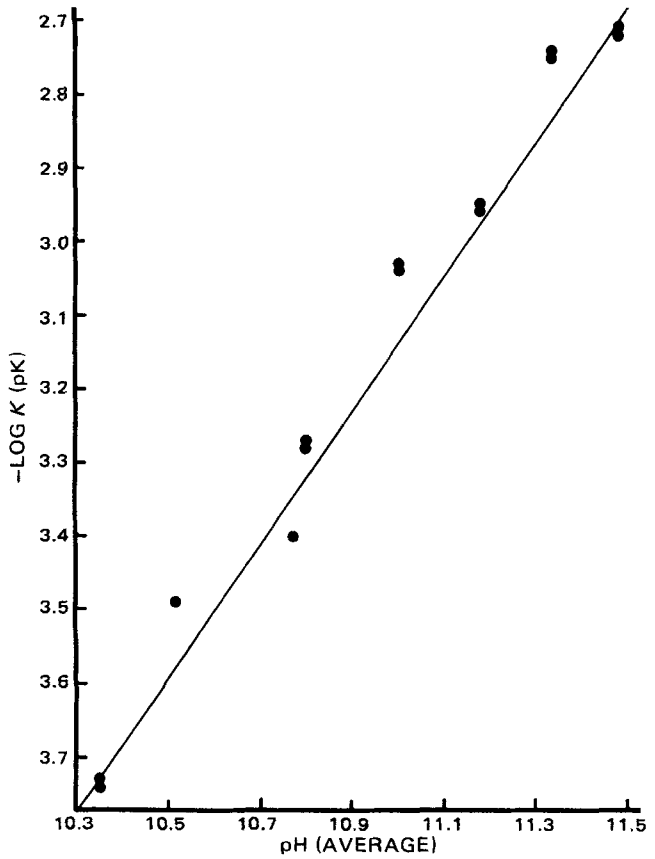

Figure 8—*Degradation rate of I in potassium hydroxide solutions as a function of the average pH during the individual kinetic run (0.5 mg/ml).*

Proposed Experimental Testing of Model—A primary requisite for testing the model depicted in Schemes III and IV is the development of a rapid, sensitive assay to measure the amounts of the various minor degradation products as a function of time. Recent work in high-performance liquid chromatography (HPLC) of prostaglandins (15, 16) closely related in structure revealed a promising technique for analysis of minor prostaglandin components in solution, provided appropriate standards are available. Given a workable HPLC assay, key experiments with E prostaglandins may be run to measure simultaneously the individual reaction products in the scheme on both relative and absolute bases.

Furthermore, if one can assume independence of the various reactions (*e.g.*, 15-epimerization and dehydration), the degradation of prostaglandins, in which one or more of these reactions is blocked through lack of a necessary group, may be studied. For example, the 15-oxo derivative of I (X), a primary metabolite (17–19), could not epimerize at C-15 or rearrange at C-13–C-15; therefore, pure dehydration rate constants could be obtained. Prostaglandin $F_{1\alpha}$ or dinoprost[7] (XI) has hydroxyl groups at C-9 and C-11, obviating consideration of the dehydration rate which is so rapid in E prostaglandins as to hamper measurement of the other slower, but probably more comparable, reaction rates.

Of particular interest is the epimerization equilibrium described by the relative values of k_5 and k_{-5}, which become appreciable only at very low pH values. Studies with XI and its 15-epimer could, therefore, lead to reasonable estimates of values of k_5, k_{-5}, and, possibly, k_8 and k_9. Values of all derived rate constants could then be inserted appropriately in Eq. 10 for the E prostaglandin, and the calculated value of K, the overall rate constant, could be compared to the observed value.

If the model is found to be seriously in error, changes in Scheme III would be necessary. For example, if formation of the 13,15-rearrangement product proved to be an equilibrium process, additional rate constants would be required. The modified forms of Eqs. 1–3 would then be resolved as a unit.

One criticism of the present model is that it does not assign formation

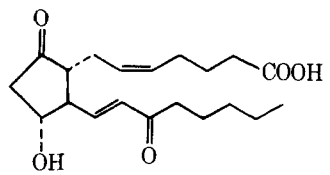

X

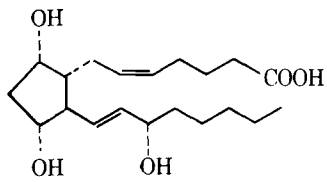

XI

mechanisms for the various products, as did Thompson *et al.* (10). The problem is the consideration of more than one reaction and product. The rationale for avoiding the detailed consideration of reaction mechanisms here is that specific acid (H^+) and base (OH^-) catalyses are probably responsible for virtually all reactions observed at these extremes of pH. In acidic solutions, the relative contributions of the different possible mechanisms change appreciably only when the pH rises to ~3, leading to a different product balance and apparent energy of activation. The same situation holds true for low temperature studies (*e.g.*, 4° at pH 1.1).

REFERENCES

(1) A. J. Weinheimer and R. L. Spraggins, *Tetrahedron Lett.*, **1969**, 5185.

(2) W. P. Schneider, R. D. Hamilton, and L. E. Rhuland, *J. Am. Chem. Soc.*, **94**, 2122 (1972).

(3) S. Bergström, in "Prostaglandins," Nobel Symposium 2, S. Bergström and B. Samuelsson, Eds., Interscience, New York, N.Y., 1967, p. 21.

(4) S. M. M. Karim, J. Devlin, and K. Hillier, *Eur. J. Pharmacol.*, **4**, 416 (1968).

(5) N. H. Andersen, *J. Lipid Res.*, **10**, 320 (1969).

(6) J. E. Pike, F. H. Lincoln, and W. P. Schneider, *J. Org. Chem.*, **34**, 3552 (1969).

(7) E. G. Daniels, W. C. Krueger, F. P. Kupiecki, J. E. Pike, and W. P. Schneider, *J. Am. Chem. Soc.*, **90**, 5894 (1968).

(8) R. L. Spraggins, *Tetrahedron Lett.*, **1972**, 4343.

(9) D. C. Monkhouse, L. VanCampen, and A. J. Aguiar, *J. Pharm. Sci.*, **62**, 576 (1973).

(10) G. F. Thompson, J. M. Collins, and L. M. Schmalzried, *ibid.*, **62**, 1738 (1973).

(11) T. O. Oesterling, paper presented at the Basic Pharmaceutics Section, APhA Academy of Pharmaceutical Sciences, Washington meeting, 1970.

(12) T. J. Roseman, B. Sims, and R. G. Stehle, *Am. J. Hosp. Pharm.*, **30**, 236 (1973).

(13) N. H. Andersen, *J. Lipid Res.*, **10**, 316 (1969).

(14) L. Z. Benet and J. S. Turi, *J. Pharm. Sci.*, **60**, 1593 (1971).

(15) W. Morozowich and S. L. Douglas, *Prostaglandins*, **10**, 19 (1975).

(16) T. J. Roseman, S. S. Butler, and S. L. Douglas, *J. Pharm. Sci.*, **65**, 673 (1976).

(17) E. Änggård and C. Larsson, *Eur. J. Pharmacol.*, **14**, 66 (1971).

(18) M. Hamberg and B. Samuelsson, *J. Biol. Chem.*, **246**, 6713 (1971).

(19) A. Raz, *FEBS Lett.*, **27**, 245 (1972).

ACKNOWLEDGMENTS AND ADDRESSES

Received April 1, 1974, from *Pharmacy Research, The Upjohn Company, Kalamazoo, MI 49001.*

Accepted for publication February 4, 1977.

The assistance of Dr. J. S. Turi in the theoretical discussions was very helpful. The technical assistance of J. W. Woltersom, G. R. Munting, and R. W. Smith is also greatly appreciated.

* Present address: Johnson and Johnson Research, New Brunswick, NJ 08903.

x To whom inquiries should be directed.

[7] Code designation prostaglandin $F_{2\alpha}$.

Identification of Urinary Catechol and Methylated Catechol Metabolites of Phenytoin in Humans, Monkeys, and Dogs by GLC and GLC–Mass Spectrometry

K. K. MIDHA *x, K. W. HINDMARSH ‡, I. J. McGILVERAY *, and J. K. COOPER *

Abstract □ A catechol metabolite, 5-(3,4-dihydroxyphenyl)-5-phenylhydantoin, and a methylated catechol metabolite, 5-(3-methoxy-4-hydroxyphenyl)-5-phenylhydantoin, were identified as urinary metabolites in humans, monkeys, and dogs following the administration of phenytoin. These metabolites were separated from each other and from other known metabolites of phenytoin as *n*-butyl derivatives by GLC and positively identified by combined GLC–mass spectrometry.

Keyphrases □ Phenytoin metabolites—GLC and GLC–mass spectrometric analyses and identification, human, monkey, and dog urine □ Catechol and methylcatechol metabolites—of phenytoin, GLC and GLC–mass spectrometric analyses and identification, human, monkey, and dog urine □ GLC and GLC–mass spectrometry—analyses and identification of phenytoin metabolites in human, monkey, and dog urine □ Anticonvulsants—phenytoin, GLC and GLC–mass spectrometric analyses and identification of catechol and methylcatechol metabolites in human, monkey, and dog urine

Phenytoin (I) is a commonly prescribed anticonvulsant (1). The metabolism of I was reviewed recently (2–4). The presence of a catechol metabolite, 5-(3,4-dihydroxyphenyl)-5-phenylhydantoin (II), in rat urine was suggested (5) and later confirmed (6). This metabolite and the methylated catechol 5-(3-methoxy-4-hydroxyphenyl)-5-phenylhydantoin (III) (7) also were identified in the bile from isolated perfused rat liver (8).

Borga *et al.* (9) reported the identification of II in the urine of both rats and humans. However, an on-column methylation technique was used and, under these conditions, II and III would be converted to the same tetramethyl derivative 1,3-dimethyl-5-(3,4-dimethoxyphenyl)-5-phenylhydantoin. Therefore, the structure of the metabolite is tentative and may be II as suggested, III, or a mixture of both.

This report describes the positive identification of these two metabolites (II and III) in the urine of humans, monkeys, and dogs. These metabolites were separated from each other and from other known metabolites of I as their respective *n*-butyl derivatives by GLC and identified by combined GLC–mass spectrometry.

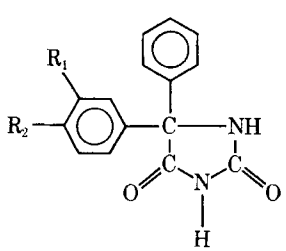

I: $R_1 = R_2 = H$
II: $R_1 = R_2 = OH$
III: $R_1 = OCH_3$, $R_2 = OH$
IV: $R_1 = H$, $R_2 = OH$
V: $R_1 = OH$, $R_2 = H$

EXPERIMENTAL

Ether[1] and methylene chloride[2] were distilled in glass prior to use. The hydrolytic enzyme used was β-glucuronidase[3]. Methanolic trimethylanilinium hydroxide (0.4 *M*) was synthesized according to the method of Barret (10). Tetraethylammonium hydroxide (0.62 *M*) and tetra-*n*-butylammonium hydroxide (0.4 *M*) were synthesized from their respective substituted ammonium iodides and silver oxide following the procedure described by Barret (10).

A gas chromatograph[4] equipped with a metal sleeve injection port and flame-ionization detector was employed. The column was coiled glass tubing[5], 1.8 m × 2.0 mm i.d., packed with 5% methyl phenyl silicone containing 75% phenyl silicone[6] coated on acid-washed, dimethyldichlorosilane-treated, 100–120-mesh, high-performance flux-calcined diatomite support[7]. The column was conditioned at 290° for 18 hr with a low nitrogen flow.

The operating temperatures were: injection port, 350°; column, 260° (for methyl and ethyl derivatives) and 280° (for butyl derivatives); and detector, 310°. The flow rate of the carrier gas (nitrogen) was 65 ml/min. Hydrogen and compressed air flow rates were adjusted to give maximum response.

GLC–Mass Spectrometry—GLC–mass spectrometry was carried out on a gas chromatograph[8] attached through a jet separator interface to a single-focusing mass spectrometer[9]. The ionization potential was 70 ev. The GLC column and conditions were the same as for direct GLC.

Human Studies—A 300-mg dose of phenytoin (3 × 100-mg capsules[10]) was administered orally to a healthy 80-kg male volunteer. All urine was collected for the first 72 hr and either used immediately or stored at −15° for later analysis. Urine samples were also collected from a 60-kg patient receiving 300 mg of phenytoin/day (3 × 100-mg capsules[10]).

Monkey Studies—A 125-mg dose of phenytoin suspension[11] (5 ml) was administered orally (30 mg/kg) to two healthy male Rhesus monkeys (*Macaca mulatta*), 4.74 and 3.76 kg, by stomach intubation. The animals were placed in metabolism cages, and total urine was collected for the 0–24- and 24–48-hr periods. The urine was stored at −15° prior to extraction.

Dog Studies—Phenytoin sodium was administered orally in a gelatin capsule to each of two healthy male Labrador dogs, 37.3 and 27.3 kg, at 20 mg/kg. The dogs were placed in metabolism cages, and urine collections were taken as described for the monkey studies.

Extraction of Urine—Aliquots of accumulated urine from humans, monkeys, or dogs (300 ml), after adjustment to pH 5.0 with 0.2 *M* sodium acetate–acetic acid buffer, were hydrolyzed at 37° for 20 hr following the addition of 1 ml of β-glucuronidase. The hydrolyzed urine samples were then extracted on a urine extraction apparatus[12] with 500 ml of methylene chloride–ether (11:14) for 24 hr. Extracts were concentrated under vacuum on a rotary evaporator[13] to approximately 20 ml using a 40° water bath temperature.

Each concentrated extract was divided into two equal portions in polytef-lined screw-capped tubes (15 ml) and evaporated[14] to dryness

[1] Mallinckrodt Chemical Works Ltd., Montreal, Quebec, Canada.
[2] Caledon Laboratories Ltd., Georgetown, Ontario, Canada.
[3] No. G-0876, Sigma Chemical Co., St. Louis, Mo.
[4] Model 3920, Perkin-Elmer, Montreal, Quebec, Canada.
[5] Chromatographic Specialities, Brockville, Ontario, Canada.
[6] OV-25, Chromatographic Specialities, Brockville, Ontario, Canada.
[7] Chromosorb W, Chromatographic Specialities, Brockville, Ontario, Canada.
[8] Model 990, Perkin-Elmer, Montreal, Quebec, Canada.
[9] Model RMU-6L, Hitachi Perkin-Elmer.
[10] Dilantin Kapseals, 100 mg, Parke, Davis and Co., Montreal, Quebec, Canada.
[11] Dilantin-125 suspension, Parke, Davis and Co., Montreal, Quebec, Canada.
[12] Kontes Glass Co., Vineland, N.J.
[13] Buchler Instruments, Fort Lee, N.J.
[14] Thermolyne Dri-Bath, Fisher Scientific Co., Ottawa, Ontario, Canada.

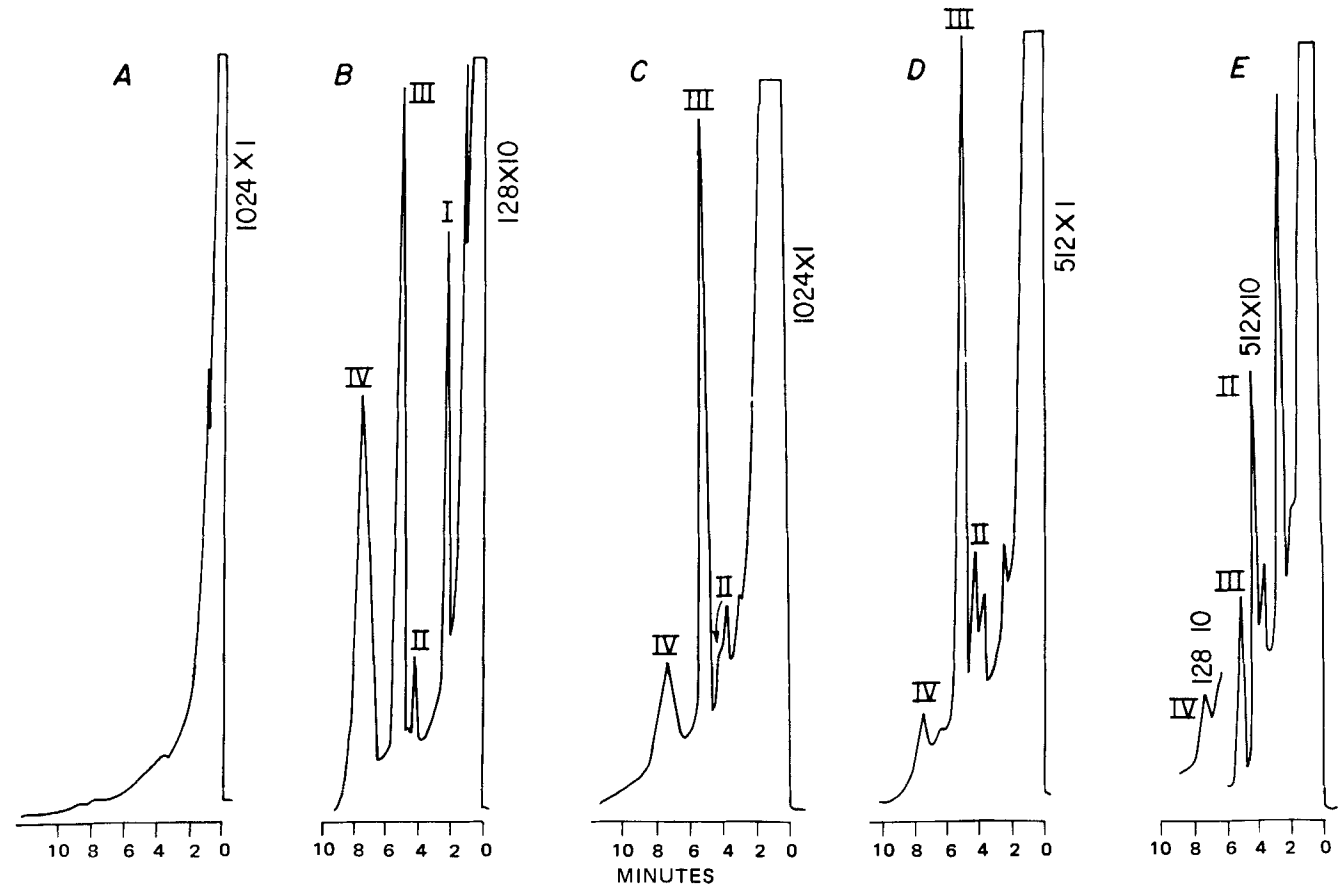

Figure 1—*Gas chromatograms of flash-heater methylated extracts of urine. Key: A, blank human urine; B, blank human urine spiked with I–V; C, urine from a patient receiving I; D, urine from a monkey dosed with I; E, urine from a dog dosed with I; peak I, methylated I; peak II, methylated V; and peak III, methylated IV.*

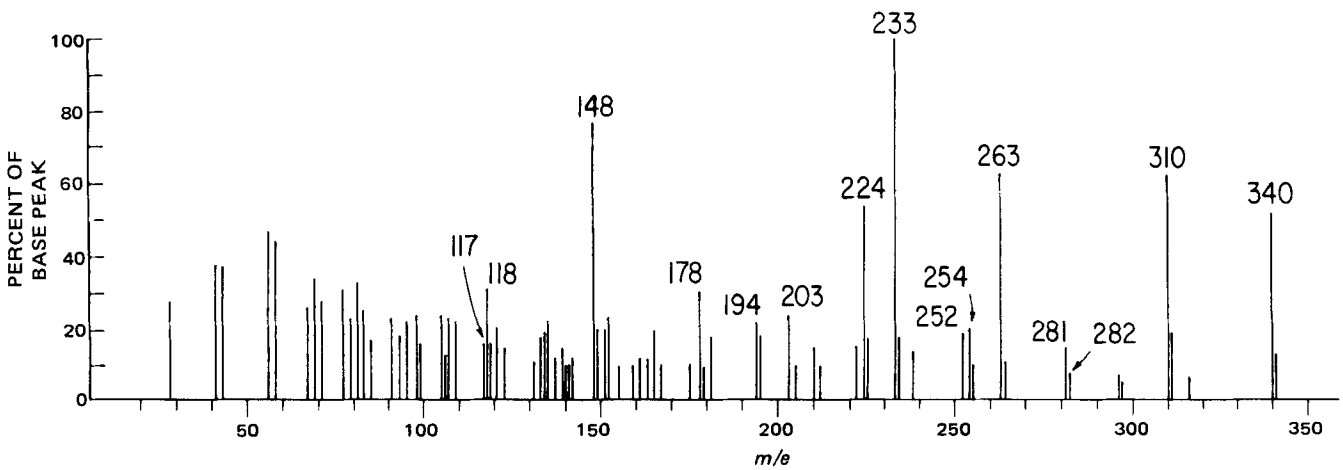

Figure 2—*Normalized electron-impact mass spectrum of the compound giving rise to peak IV (Fig. 1).*

under dry filtered nitrogen. Trimethylanilinium hydroxide (1 ml) was added to the first tube, and tetra-*n*-butylammonium hydroxide (1 ml) was added to the second tube. The contents were dissolved by swirling on a mixer[15] before injecting 1–2 μl into the gas chromatograph.

Aliquots of urine (300 ml) were also hydrolyzed with concentrated hydrochloric acid (300 ml) in a boiling water bath for 1 hr. The acid-hydrolyzed urine was adjusted to pH 5 with 6 *N* NaOH and then treated in a similar manner to that described for enzyme-hydrolyzed urine. Aliquots of urine (100 ml) were extracted similarly at pH 5.0 without prior enzymatic or acidic hydrolysis.

Control urine specimens (200 ml) collected prior to phenytoin administration were hydrolyzed with acid and β-glucuronidase and treated in parallel to the conditions described.

[15] Vortex Genie, Fisher Scientific Co., Montreal, Quebec, Canada.

RESULTS AND DISCUSSION

Flash-heater methylation, with trimethylanilinium hydroxide, of enzymatically hydrolyzed human urine, obtained following phenytoin administration, showed three peaks on GLC (Fig. 1C) that were not present in the control urine (Fig. 1A). Previously (11, 12), phenytoin (I) and its metabolite 5-(*p*-hydroxyphenyl)-5-phenylhydantoin (IV) were separated from each other using this methylation technique.

Peak II (Fig. 1C) had the same GLC retention time (4 min) as the methylated synthetic sample of 5-(*m*-hydroxyphenyl)-5-phenylhydantoin (V, Fig. 1B, peak II). Peak III (Fig. 1C) had the same retention time (4.8 min) as the methylated product of synthetic IV (Fig. 1B, peak III). GLC–mass spectrometric analysis of these two peaks indicated that they were the trimethylated derivatives with the structures 1,3-dimethyl-5-(*m*-methoxyphenyl)-5-phenylhydantoin and 1,3-dimethyl-5-(*p*-

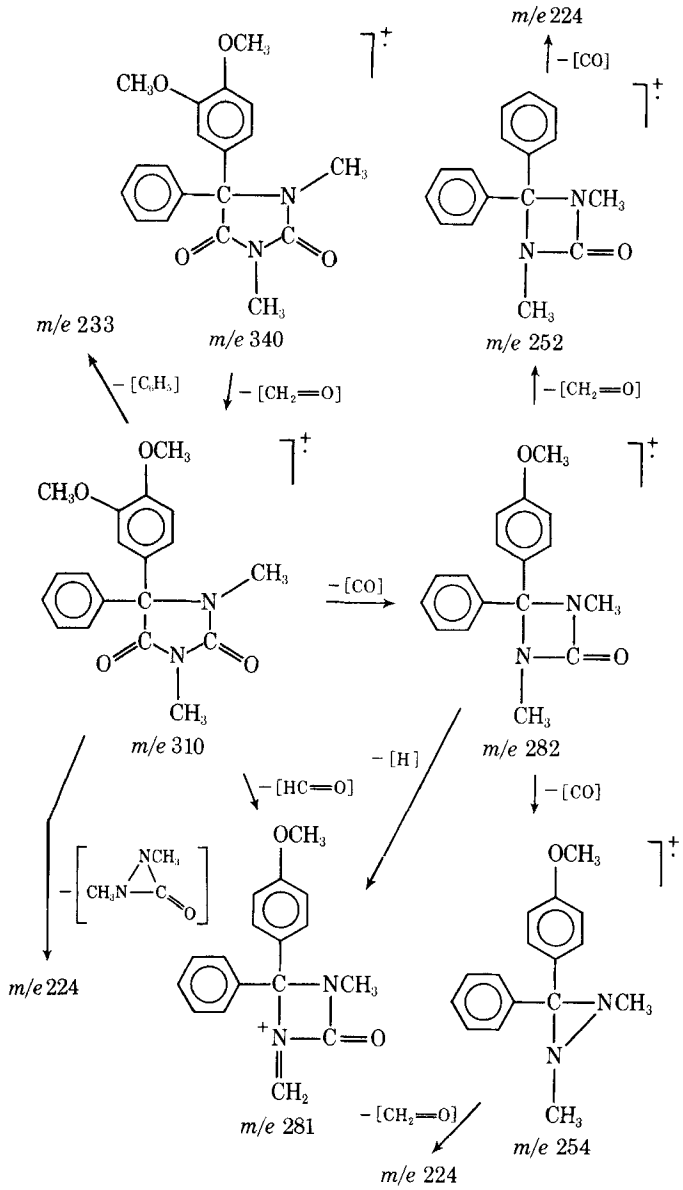

Scheme I

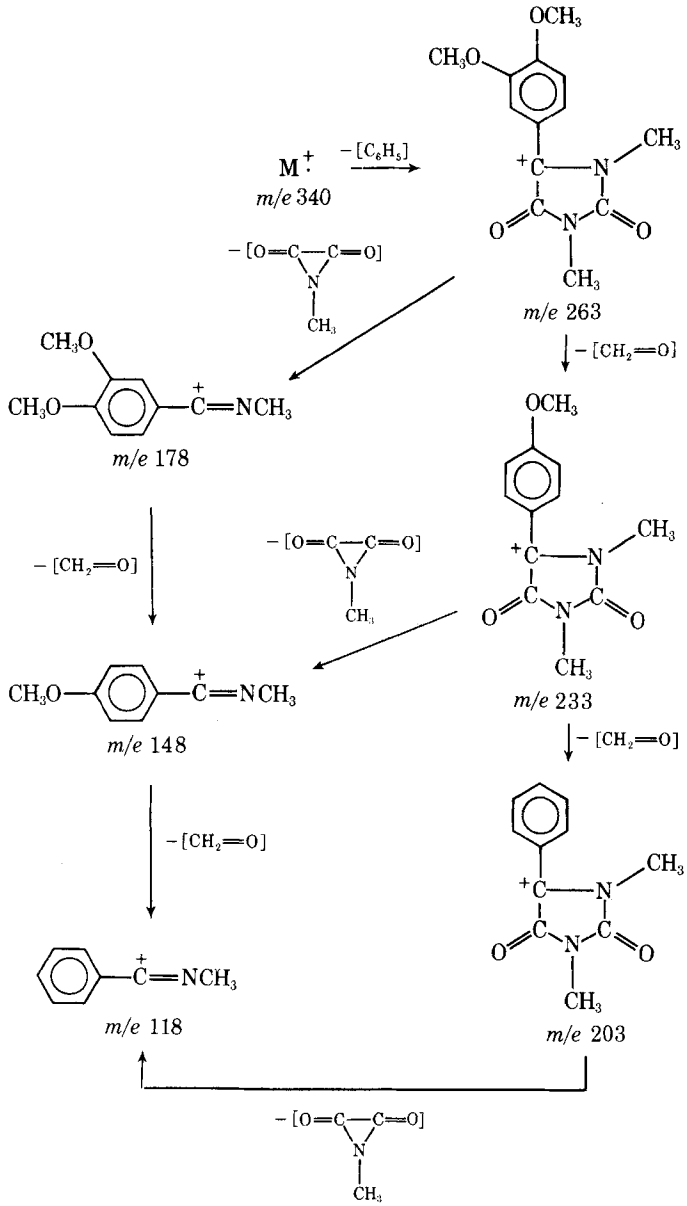

Scheme II

methoxyphenyl)-5-phenylhydantoin. A molecular ion at *m/e* 310 and characteristic ions at *m/e* 280, 233, 224, 148, and 118 are in agreement with two trimethylated structures reported earlier (11–13).

Peak IV (Fig. 1C, R_t 7.2 min) had the same retention time as the flash-heater methylated product of synthetic II and III (Fig. 1B, peak IV). GLC–mass spectrometric analysis of this peak indicated that it was a tetramethylated derivative, 1,3-dimethyl-5-(3,4-dimethoxyphenyl)-5-phenylhydantoin. The normalized spectrum (Fig. 2) reveals the presence of a molecular ion at *m/e* 340 and other characteristic ions at *m/e* 310, 282, 281, 263, 254, 252, 233, 224, 203, 194, 178, 148, 118, and 117. Formation of these ions is postulated in Schemes I–III.

Scheme I depicts the formation of the diagnostic ions *m/e* 310, 282, 281, 254, 252, 233, and 224. Scheme II indicates that the ion at *m/e* 263 is formed by the loss of a phenyl radical from the molecular ion. The formation of this ion suggests that the two methoxy groups are on the same benzene ring. Formation of the ion at *m/e* 178 (Scheme II) appears to be the result of cleavage of the imidazolidine ring of the ion at *m/e* 263. Other characteristic ions at *m/e* 233, 203, 148, and 118 are rationalized in Scheme II.

An alternative pathway for the formation of ions at *m/e* 254 and 224 is shown in Scheme III. The ion at *m/e* 224 in Scheme III further fragments, by the loss of formaldehyde, to give an ion at *m/e* 194 which, in turn, loses a phenyl radical to give the ion at *m/e* 117.

The GLC analysis of the enzyme-hydrolyzed extracts of monkey and dog urine (Figs. 1D and 1E) showed peaks for methylated V and IV and

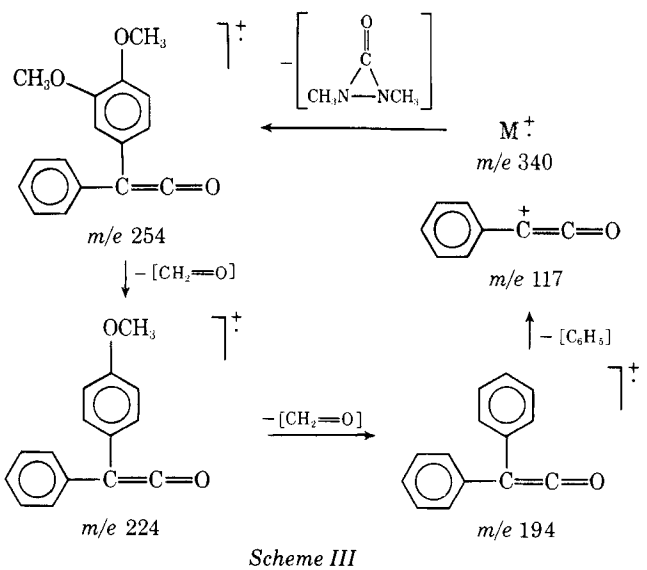

Scheme III

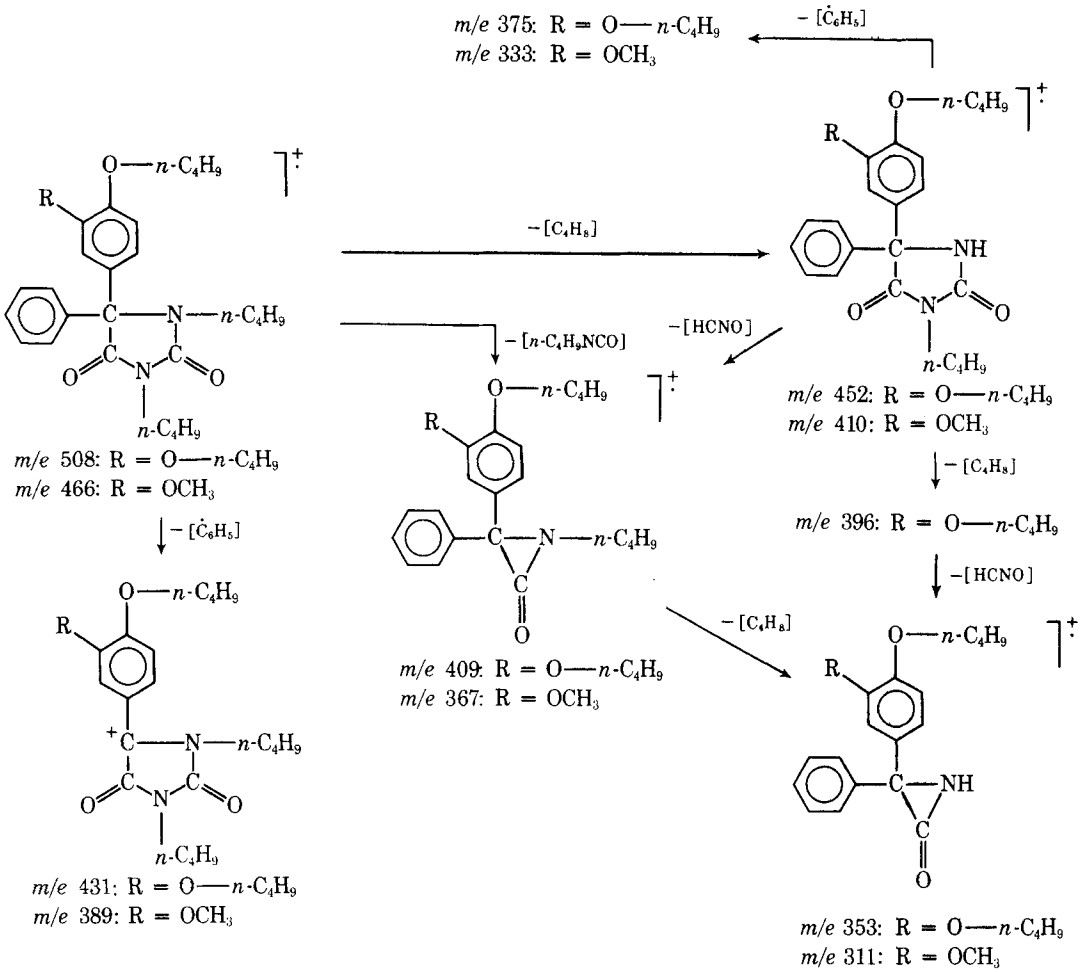

Scheme IV

the catechol metabolites (Peak IV). In the dog, V was the major metabolite, in agreement with previously reported findings (12).

Similar peaks were obtained on GLC analysis of the acid-hydrolyzed urine of humans, monkeys, and dogs. However, the amounts of the methylated derivatives of V and IV had increased. This increase may be due to the decomposition of the 5-(3,4-dihydroxy-1,5-cyclohexadien-1-yl)-5-phenylhydantoin, as observed by Chang and Glazko (4).

To determine whether peak IV (Figs. 1C–1E) was due to II or III or a combination of both, synthetic samples of these metabolites were flash-heater butylated on GLC with tetrabutylammonium hydroxide.

Flash-heater butylation of synthetic II and III, under the experimental conditions described, gave two peaks on GLC in each case. Figure 3B shows the separation of these peaks. Peak V (R_t 7 min) was shown by GLC–mass spectrometric analysis to be the tributyl monomethylated derivative, 1,3-di-*n*-butyl-5-(3-methoxy-4-*n*-butoxyphenyl)-5-phenylhydantoin. Peak VI was due to a dibutyl monomethylated derivative.

It appeared from the mass spectrum that either the N-1 or N-3 position of the imidazolidine ring was not butylated. Peak VII was the tetrabutyl derivative, 1,3-di-*n*-butyl-5-(3,4-di-*n*-butoxyphenyl)-5-phenylhydantoin. Peak VIII was a tributylated derivative of II. Several different conditions, such as increasing the injection port temperature of the chromatograph and adding excess butylating agent, did not result in complete butylation.

Figure 3A shows the chromatogram of the flash-heater butylated urine extract obtained after enzymatic hydrolysis from a patient receiving I. Comparison of GLC retention times and GLC–mass spectra with those of the synthetic butylated metabolites (V, IV, II, and III) indicated that peak I (R_t 4.5 min) was 1,3-di-*n*-butyl-5-(3-*n*-butoxyphenyl)-5-phenylhydantoin. Peak II (R_t 4.9 min) was shown to be the incompletely butylated product of V. Peak III was identified as 1,3-di-*n*-butyl-5-(4-*n*-butoxyphenyl)-5-phenylhydantoin, and peak IV was due to the incomplete butylation of IV.

The shoulder indicated that peaks V and VI had the same retention times as the completely and incompletely butylated derivatives, respectively, of III (Fig. 3B). Peaks V and VI (Fig. 3A) were collected at their respective retention times on a methyl phenyl silicone column[6] from the detector end, after extinguishing the flame and rechromatographing on columns packed with phenyl methyldimethyl silicone[16] and cyanopropylmethyl phenyl methyl silicone[17], respectively. The retention times of the two peaks on these columns corresponded to those of synthetic III when flash-heater butylated. Similarly, the shoulder shown as peaks VII and VIII had retention times corresponding with those of the completely and incompletely butylated derivatives, respectively, of II.

Figures 4 and 5 show the normalized mass spectra of peaks V and VII, respectively (Fig. 3A). The mass spectra of these peaks show molecular ions at *m/e* 466 and 508, respectively. Formation of most of the diagnostic ions for both derivatized metabolites is proposed in Schemes IV–VII.

These mass spectra (Figs. 4 and 5) were virtually identical to the spectra of completely butylated derivatives of synthetic III and II, respectively. The molecular ions for both compounds lose C_4H_8 to give ions at *m/e* 410 and 452. The loss of the C_4H_8 unit can be rationalized either by a McLafferty rearrangement or by a 1,4-shift, as shown for ions at *m/e* 235 and 193 in Scheme VII.

Ions at *m/e* 410 and 452 (Scheme IV) can lose HNCO, as a neutral molecule, to give ions at *m/e* 367 and 409, respectively. The ions at *m/e* 367 and 409 may also be formed from the molecular ions by the loss of C_4H_9NCO as a neutral molecule. The ions at *m/e* 311 and 353 (Scheme IV) are the result of the loss of C_4H_8 from ions at *m/e* 367 and 409, respectively. Alternatively, the ion at *m/e* 452 may lose C_4H_8 to give an ion at *m/e* 396 and then, by the loss of HNCO, may go to *m/e* 353.

Ions at *m/e* 389 and 431 (Scheme V) can be formed from their respective molecular ions by the loss of a phenyl radical, (*cf.*, ion at *m/e* 263, Scheme II). The occurrence of these and subsequent ions at *m/e* 333, 375, 277, and 319 are indicative of the presence of both substituents on one

[16] OV-7, Chromatographic Specialities, Brockville, Ontario, Canada.
[17] OV-225, Chromatographic Specialities, Brockville, Ontario, Canada.

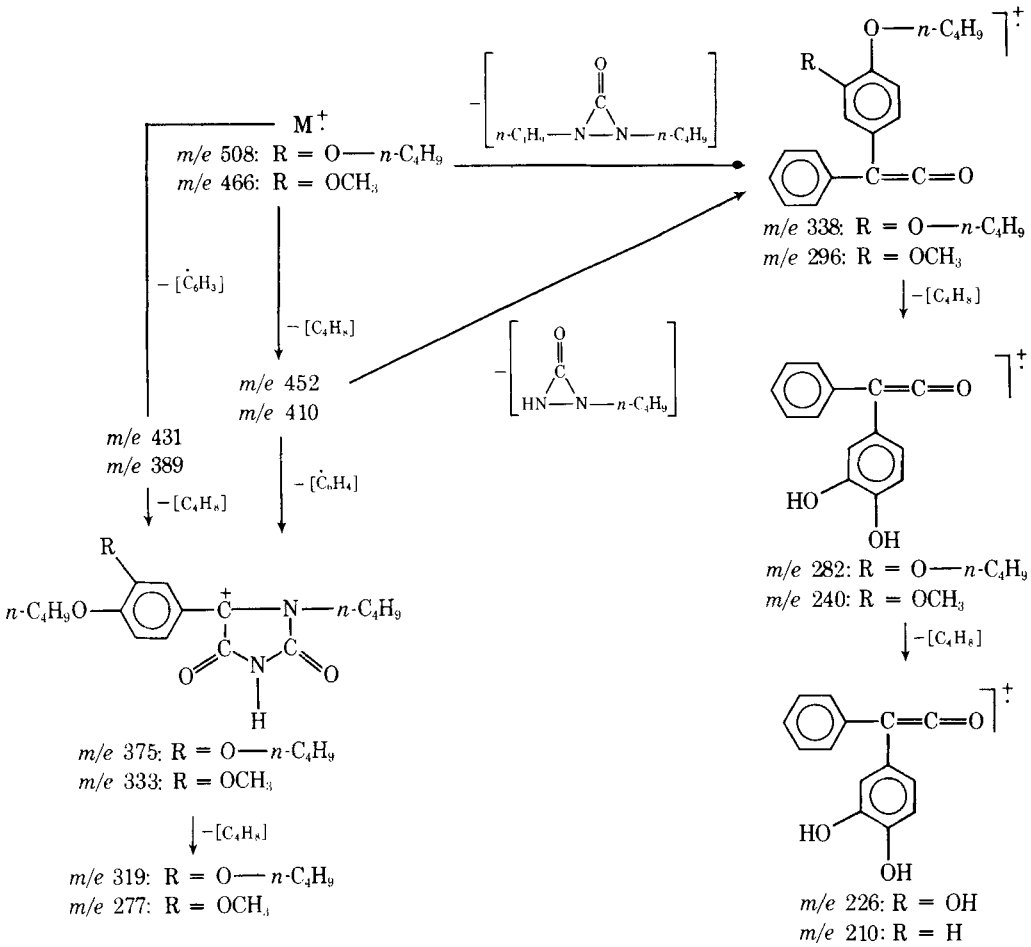

Scheme V

aromatic ring. Ions at *m/e* 333 and 375 seem to give rise to ions at *m/e* 193 and 235, respectively, by a rearrangement. A rationale for this rearrangement is suggested in Scheme VI.

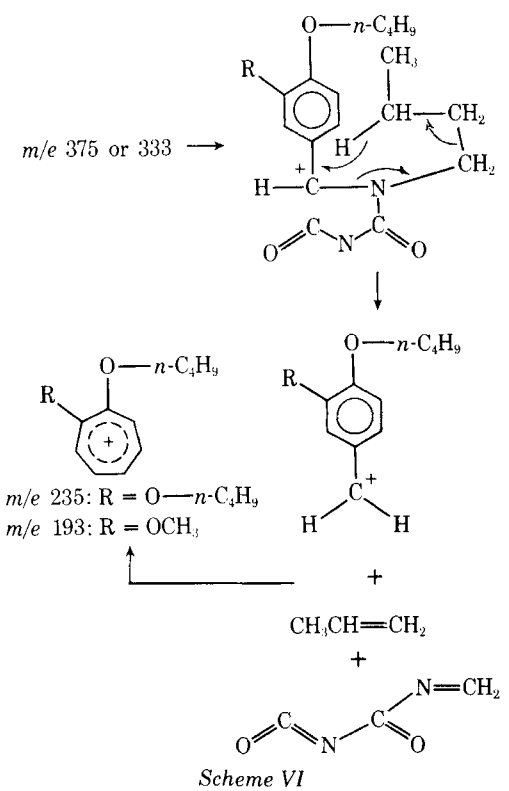

Scheme VI

Scheme VII presents a postulation of the formation of ions at *m/e* 179 and 123 observed in the spectrum of the tetrabutylated catechol metabolite (II). Ions at *m/e* 179 and 123 further demonstrate that the two hydroxyl groups are on the same ring. Similarly, the ion at *m/e* 137 observed in the spectrum of the tributylated derivative of the 3-*O*-methylcatechol metabolite (III) suggests that the methoxy and hydroxy sub-

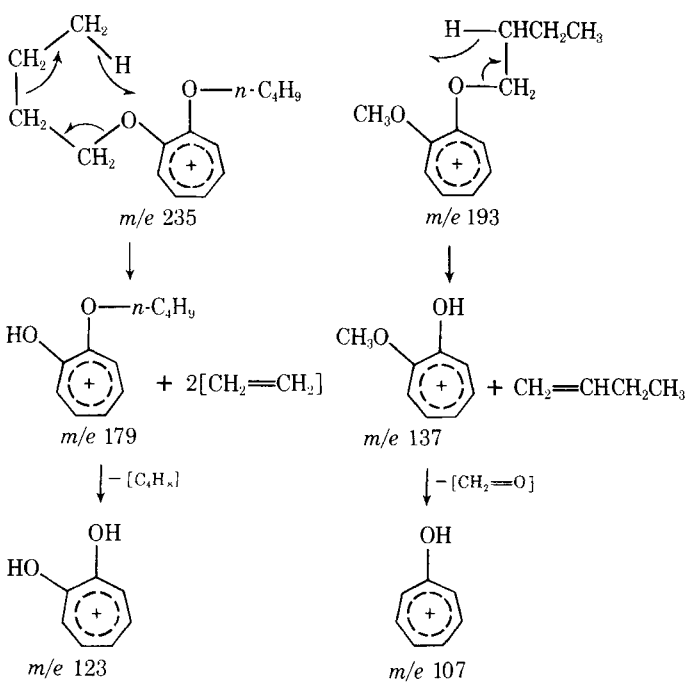

Scheme VII

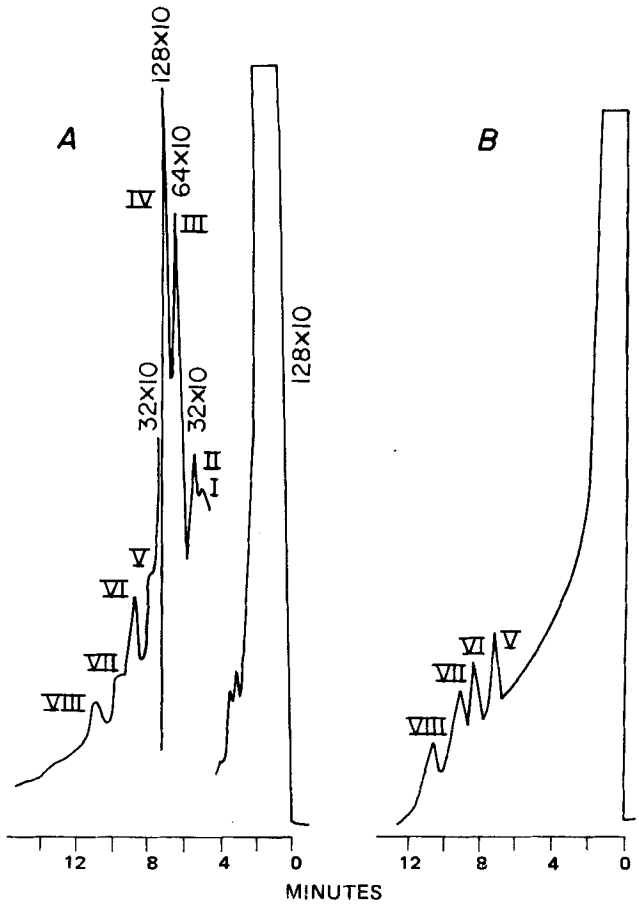

Figure 3—*Gas chromatograms of a flash-heater butylated extract of urine from a patient receiving I (A) and that of synthetic catechol II and methylated catechol III (B). Key: peak V, tributylated monomethylated III; peak VI, dibutylated monomethylated III; peak VII, tetrabutylated II; and peak VIII, tributylated II.*

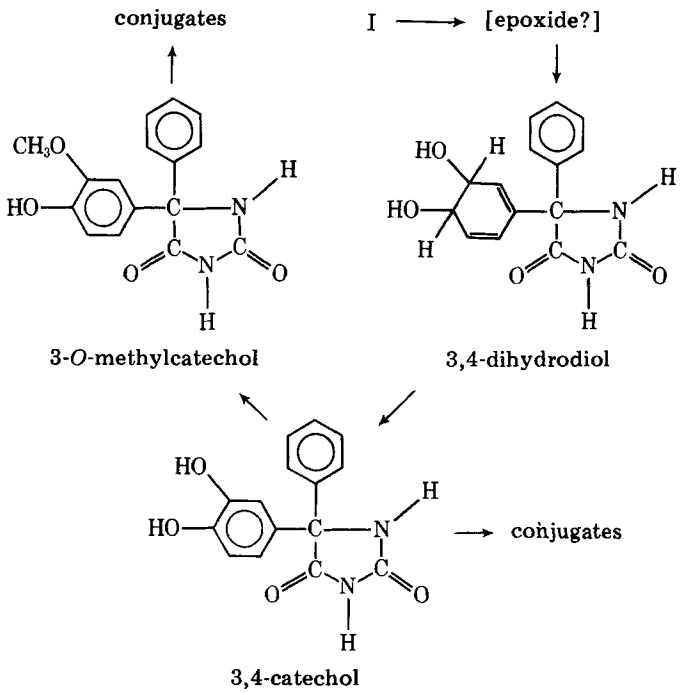

Scheme VIII

stituents are attached to the same ring. Comparison of the retention times and mass spectra with those of the authentic butylated metabolites demonstrates that peak V was due to the butylated derivative of III and peak VII was due to the butylated derivative of II.

Minute amounts of both of these metabolites were observed in the unhydrolyzed urine from humans, monkeys, and dogs. However, the amount of each metabolite increased on hydrolysis. Quantitative determination of II and III is under investigation.

The possible biotransformation pathway for the formation of these metabolites (II and III) in humans, monkeys, and dogs is shown in Scheme VIII and is in agreement with that suggested by Glazko (2). The

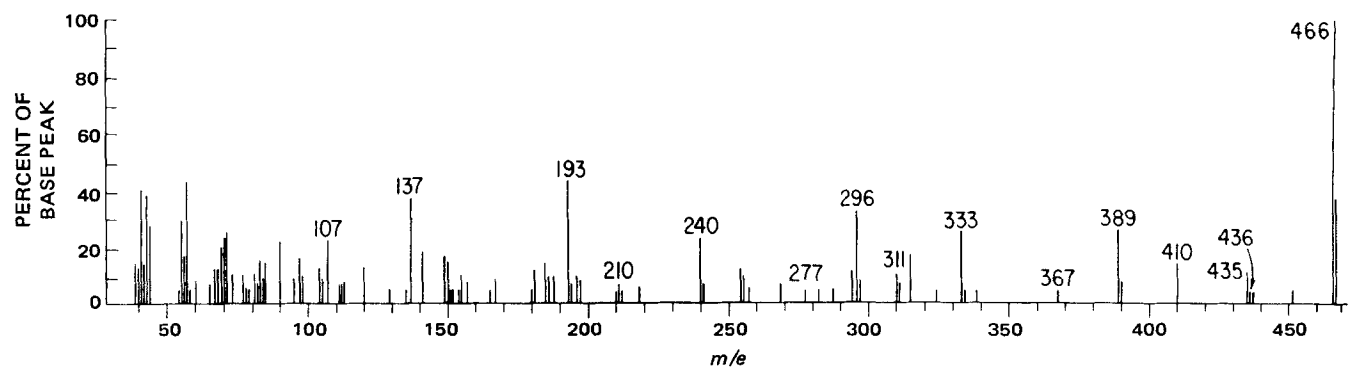

Figure 4—*Normalized electron-impact mass spectrum of the compound giving rise to peak V (Fig. 3).*

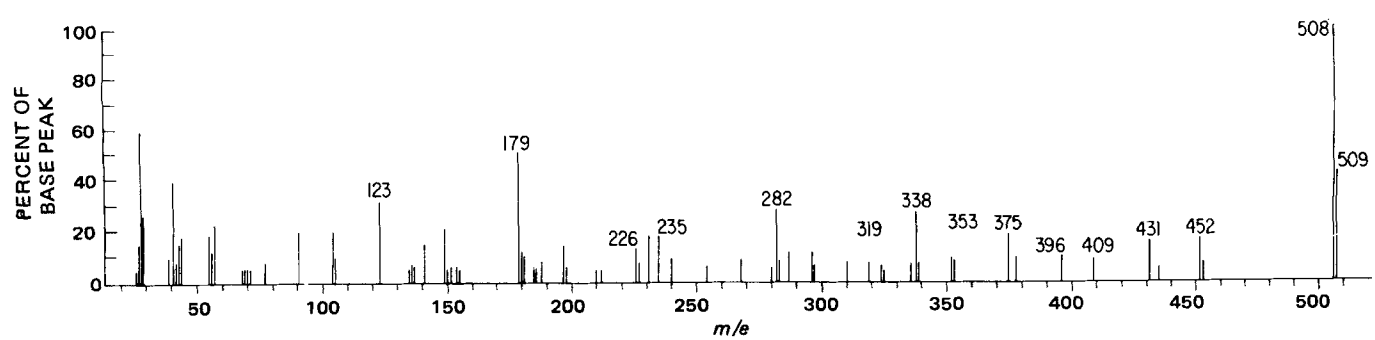

Figure 5—*Normalized electron-impact mass spectrum of the compound giving rise to peak VII (Fig. 3).*

dehydrogenation of dihydrodiols to catechols was observed previously (14–16). The formation of the methylated catechol from 3,4-catechol may be due to the enzyme, catechol O-methyltransferase, since other catechols are known to be methylated *via* this enzyme (8, 17, 18).

In conclusion, it was demonstrated that the catechol metabolite in humans, reported by Borga *et al.* (9), is a mixture of the catechol Metabolite II and the methylated catechol Metabolite III. These metabolites are also formed in minor amounts in other species such as the monkey and dog.

REFERENCES

(1) W. S. Parker and R. J. Gumnit, *J. Neurol.*, **24**, 1178 (1974).

(2) A. J. Glazko, *Epilepsia*, **16**, 367 (1975).

(3) A. J. Glazko, *Drug Metab. Dispos.*, **1**, 711 (1973).

(4) T. Chang and A. J. Glazko, in "Antiepileptic Drugs," D. M. Woodbury, J. K. Perry, and R. P. Schmidt, Eds., Raven, New York, N.Y., 1959, p. 149.

(5) D. M. Woodbury, *Epilepsia*, **10**, 121 (1969).

(6) T. Chang, R. A. Okerholm, and A. J. Glazko, *Anal. Lett.*, **5**, 195 (1972).

(7) T. Chang, R. A. Okerholm, and A. J. Glazko, *Res. Commun. Chem. Pathol. Pharmacol.*, **4**, 13 (1972).

(8) N. Gerber, R. A. Seibert, and R. M. Thompson, *ibid.*, **6**, 499 (1973).

(9) O. Borga, M. Garle, and M. Gutova, *Pharmacologist*, **7**, 129 (1972).

(10) M. J. Barret, *Clin. Chem. Newslett.*, **3**, 16 (1971).

(11) K. K. Midha, I. J. McGilveray, and D. L. Wilson, *J. Pharm. Sci.*, **65**, 1240 (1976).

(12) A. J. Atkinson, J. MacGee, J. Strong, D. Garteiz, and T. E. Gaffney, *Biochem. Pharmacol.*, **19**, 2483 (1970).

(13) R. H. Hammer, B. J. Wilder, R. E. Streiff, and A. J. Mayersdorf, *J. Pharm. Sci.*, **60**, 327 (1971).

(14) P. K. Ayengar, O. Hayaishi, M. Nakajima, and I. Tomida, *Biochim. Biophys. Acta*, **33**, 111 (1959).

(15) E. Boyland and P. Sims, *Biochem. J.*, **84**, 583 (1962).

(16) D. V. Parke, in "The Biochemistry of Foreign Compounds," Pergamon, Elmsford, N.Y., 1968, p. 121.

(17) J. Axelrod and R. J. Tomchik, *Biol. Chem.*, **233**, 702 (1958).

(18) J. K. Inscoe, J. Daly, and J. Axelrod, *Biochem. Pharmacol.*, **14**, 1257 (1965).

ACKNOWLEDGMENTS AND ADDRESSES

Received November 29, 1976, from the *Drug Research Laboratories, Health and Welfare Canada, Ottawa, Ontario, Canada, and the ‡College of Pharmacy, University of Saskatchewan, Saskatoon, Saskatchewan, Canada.

Accepted for publication February 11, 1977.

The authors express their appreciation to Dr. T. Chang for supplying the synthetic metabolites, Dr. A. By and Mr. J.-C. Ethier for running the mass spectra, and Mr. A. Trottier for drafting. Appreciation is extended to the University of Saskatchewan (Saskatoon) for a study leave to K. W. Hindmarsh. Dr. J. W. Hubbard, University of Manitoba, Winnipeg, Manitoba, Canada, is gratefully acknowledged for his helpful discussions.

ˣ To whom inquiries should be directed.

Synthesis and Structure–Activity Relationships of Selected Isomeric Oxime *O*-Ethers as Anticholinergic Agents

WILLIAM G. HANEY, ROBERT G. BROWN, EUGENE I. ISAACSON *, and JAIME N. DELGADO ˣ

Abstract □ A series of isomeric (*Z*)- and (*E*)-oxime *O*-β-dimethylaminoethyl ether methylhalide derivatives was synthesized, and their (*Z*)- and (*E*)-assignments were made on the basis of chemical and spectral data. The respective (*Z*)- and (*E*)-isomers were evaluated as anticholinergic agents on the rat ileum. The antimuscarinic potencies of the respective (*Z*)- and (*E*)-isomers were compared to determine the effect upon potency of this type of geometric isomerism. Three general structure–activity relationships are discernible among the synthesized compounds: (*a*) among oxime *O*-ethers derived from aromatic aldehydes, the higher potency consistently resides in the isomer where the aryl substituent is (*E*) to the ammonium ether substituent; (*b*) among oxime *O*-ethers derived from diaryl ketones, the (*Z*)- and (*E*)-isomers are approximately equipotent; and (*c*) oxime *O*-ethers derived from diaryl ketones are the most potent of the synthesized compounds.

Keyphrases □ Oxime *O*-ethers, various—isomers synthesized, anticholinergic activity of methylhalide salts evaluated on rat ileum □ *O*-Dimethylaminoethyl oxime ethers, various—isomers synthesized, anticholinergic activity of methylhalide salts evaluated on rat ileum □ Anticholinergic activity—evaluated on rat ileum for isomers of various oxime *O*-dimethylaminoethyl ethers □ Structure–activity relationships—isomers of various oxime *O*-dimethylaminoethyl ethers evaluated for anticholinergic activity on rat ileum

The parasympathetic postganglionic cholinergic receptor site is of considerable interest. In particular, among anticholinergics the muscarinic receptor exhibits stereospecificity toward optical isomers, and this stereospecificity contributes to a knowledge of the receptor (1). The relationship between anticholinergic potency and geometric isomerism also may be informative, but it has not been investigated extensively. Therefore, such an investigation was undertaken to determine whether or not the receptor was stereospecific toward geometric isomers and to yield further information about the receptor.

Oxime *O*-ethers were selected for study since they possess anticholinergic activity (2, 3) and the oxyimino moiety allows the preparation of geometric isomers.

DISCUSSION

The ketone oximes were prepared by the method of Lachman and Noller (4) (Table I). The method involves the generation of hydroxylamine from the hydrochloride salt with excess base in the presence of the ketone, with water as the solvent for low molecular weight ketones and with alcohol for higher molecular weight ketones. The isomer ratios produced are easily predicted qualitatively based on the general rule that the more nearly equal they are in bulk the more nearly equal will be the isomer ratio (5). Thus, the ratio is 89:11 (*E*)–(*Z*) for acetophenone oxime. As can be expected for the diaryl compounds, the isomer ratio is not great.

Separation by fractional crystallization was successful for only one of the 3,4-dimethylbenzophenone oxime isomers. Differences in chelating

dehydrogenation of dihydrodiols to catechols was observed previously (14–16). The formation of the methylated catechol from 3,4-catechol may be due to the enzyme, catechol O-methyltransferase, since other catechols are known to be methylated *via* this enzyme (8, 17, 18).

In conclusion, it was demonstrated that the catechol metabolite in humans, reported by Borga *et al.* (9), is a mixture of the catechol Metabolite II and the methylated catechol Metabolite III. These metabolites are also formed in minor amounts in other species such as the monkey and dog.

REFERENCES

(1) W. S. Parker and R. J. Gumnit, *J. Neurol.*, **24**, 1178 (1974).

(2) A. J. Glazko, *Epilepsia*, **16**, 367 (1975).

(3) A. J. Glazko, *Drug Metab. Dispos.*, **1**, 711 (1973).

(4) T. Chang and A. J. Glazko, in "Antiepileptic Drugs," D. M. Woodbury, J. K. Perry, and R. P. Schmidt, Eds., Raven, New York, N.Y., 1959, p. 149.

(5) D. M. Woodbury, *Epilepsia*, **10**, 121 (1969).

(6) T. Chang, R. A. Okerholm, and A. J. Glazko, *Anal. Lett.*, **5**, 195 (1972).

(7) T. Chang, R. A. Okerholm, and A. J. Glazko, *Res. Commun. Chem. Pathol. Pharmacol.*, **4**, 13 (1972).

(8) N. Gerber, R. A. Seibert, and R. M. Thompson, *ibid.*, **6**, 499 (1973).

(9) O. Borga, M. Garle, and M. Gutova, *Pharmacologist*, **7**, 129 (1972).

(10) M. J. Barret, *Clin. Chem. Newslett.*, **3**, 16 (1971).

(11) K. K. Midha, I. J. McGilveray, and D. L. Wilson, *J. Pharm. Sci.*, **65**, 1240 (1976).

(12) A. J. Atkinson, J. MacGee, J. Strong, D. Garteiz, and T. E. Gaffney, *Biochem. Pharmacol.*, **19**, 2483 (1970).

(13) R. H. Hammer, B. J. Wilder, R. E. Streiff, and A. J. Mayersdorf, *J. Pharm. Sci.*, **60**, 327 (1971).

(14) P. K. Ayengar, O. Hayaishi, M. Nakajima, and I. Tomida, *Biochim. Biophys. Acta*, **33**, 111 (1959).

(15) E. Boyland and P. Sims, *Biochem. J.*, **84**, 583 (1962).

(16) D. V. Parke, in "The Biochemistry of Foreign Compounds," Pergamon, Elmsford, N.Y., 1968, p. 121.

(17) J. Axelrod and R. J. Tomchik, *Biol. Chem.*, **233**, 702 (1958).

(18) J. K. Inscoe, J. Daly, and J. Axelrod, *Biochem. Pharmacol.*, **14**, 1257 (1965).

ACKNOWLEDGMENTS AND ADDRESSES

Received November 29, 1976, from the *Drug Research Laboratories, Health and Welfare Canada, Ottawa, Ontario, Canada, and the ‡College of Pharmacy, University of Saskatchewan, Saskatoon, Saskatchewan, Canada.

Accepted for publication February 11, 1977.

The authors express their appreciation to Dr. T. Chang for supplying the synthetic metabolites, Dr. A. By and Mr. J.-C. Ethier for running the mass spectra, and Mr. A. Trottier for drafting. Appreciation is extended to the University of Saskatchewan (Saskatoon) for a study leave to K. W. Hindmarsh. Dr. J. W. Hubbard, University of Manitoba, Winnipeg, Manitoba, Canada, is gratefully acknowledged for his helpful discussions.

ˣ To whom inquiries should be directed.

Synthesis and Structure–Activity Relationships of Selected Isomeric Oxime *O*-Ethers as Anticholinergic Agents

WILLIAM G. HANEY, ROBERT G. BROWN, EUGENE I. ISAACSON *, and JAIME N. DELGADO ˣ

Abstract □ A series of isomeric (*Z*)- and (*E*)-oxime *O*-β-dimethylaminoethyl ether methylhalide derivatives was synthesized, and their (*Z*)- and (*E*)-assignments were made on the basis of chemical and spectral data. The respective (*Z*)- and (*E*)-isomers were evaluated as anticholinergic agents on the rat ileum. The antimuscarinic potencies of the respective (*Z*)- and (*E*)-isomers were compared to determine the effect upon potency of this type of geometric isomerism. Three general structure–activity relationships are discernible among the synthesized compounds: (*a*) among oxime *O*-ethers derived from aromatic aldehydes, the higher potency consistently resides in the isomer where the aryl substituent is (*E*) to the ammonium ether substituent; (*b*) among oxime *O*-ethers derived from diaryl ketones, the (*Z*)- and (*E*)-isomers are approximately equipotent; and (*c*) oxime *O*-ethers derived from diaryl ketones are the most potent of the synthesized compounds.

Keyphrases □ Oxime *O*-ethers, various—isomers synthesized, anticholinergic activity of methylhalide salts evaluated on rat ileum □ *O*-Dimethylaminoethyl oxime ethers, various—isomers synthesized, anticholinergic activity of methylhalide salts evaluated on rat ileum □ Anticholinergic activity—evaluated on rat ileum for isomers of various oxime *O*-dimethylaminoethyl ethers □ Structure–activity relationships—isomers of various oxime *O*-dimethylaminoethyl ethers evaluated for anticholinergic activity on rat ileum

The parasympathetic postganglionic cholinergic receptor site is of considerable interest. In particular, among anticholinergics the muscarinic receptor exhibits stereospecificity toward optical isomers, and this stereospecificity contributes to a knowledge of the receptor (1). The relationship between anticholinergic potency and geometric isomerism also may be informative, but it has not been investigated extensively. Therefore, such an investigation was undertaken to determine whether or not the receptor was stereospecific toward geometric isomers and to yield further information about the receptor.

Oxime *O*-ethers were selected for study since they possess anticholinergic activity (2, 3) and the oxyimino moiety allows the preparation of geometric isomers.

DISCUSSION

The ketone oximes were prepared by the method of Lachman and Noller (4) (Table I). The method involves the generation of hydroxylamine from the hydrochloride salt with excess base in the presence of the ketone, with water as the solvent for low molecular weight ketones and with alcohol for higher molecular weight ketones. The isomer ratios produced are easily predicted qualitatively based on the general rule that the more nearly equal they are in bulk the more nearly equal will be the isomer ratio (5). Thus, the ratio is 89:11 (*E*)–(*Z*) for acetophenone oxime. As can be expected for the diaryl compounds, the isomer ratio is not great.

Separation by fractional crystallization was successful for only one of the 3,4-dimethylbenzophenone oxime isomers. Differences in chelating

Table I—Elemental Analysis for the Synthesized Compounds

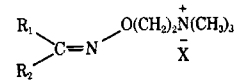

Compound[a]	R_1	R_2	Recrystallization Solvent	Melting Point	Analysis, % Calc.	Found
I*a*	H		Ethanol	180–182°	C 50.1 H 6.6	50.26 6.89
I*b*		H	2-Propanol	212–214°	C 43.32 H 5.78	43.47 5.83
II*a*	H	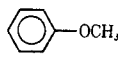	2-Propanol	146–147°	C 42.86 H 5.76	42.72 5.70
II*b*	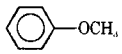	H	2-Propanol	239–240°	C 42.86 H 5.76	43.14 5.87
III*a*	H	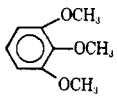	Ethanol	185–186°	C 42.48 H 5.89	42.66 6.04
III*b*	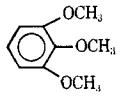	H	2-Propanol	199–200°	C 42.48 H 5.89	42.63 6.00
IV*a*	H		2-Propanol	164–166°	C 35.27 H 5.00	35.20 4.94
IV*b*		H	2-Propanol	258–259°	C 35.27 H 5.00	35.14 4.96
V*a*	CH_3		2-Propanol	182–183°	C 44.83 H 6.10	44.57 6.09
V*b*		CH_3	2-Propanol–ethanol	182–183°	C 44.83 H 6.10	45.03 6.18
VI*a*	CH_3	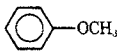	2-Propanol	185–186°	C 42.48 H 5.89	42.63 6.00
VI*b*	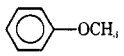	CH_3	2-Propanol	199–200°	C 42.48 H 5.89	42.66 6.04
VII*a*			2-Propanol	189–190°	C 56.00 H 6.04	55.96 5.94
VII*b*			2-Propanol–ethanol	196–198°	C 56.00 H 6.04	55.98 6.16
VIII*a*		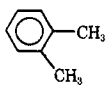	Hexane–2-propanol	165–166°	C 53.70 H 6.35	53.76 6.45
VIII*b*	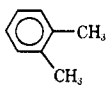		Isopropyl ether–2-propanol	184–186°	C 53.70 H 6.35	53.20 6.20

[a] The methiodide derivative of the ether was characterized, with the exception of I*a*, VII*a*, and VII*b*, in which the methobromide derivative was characterized. [b] NMR analysis revealed about 10% of the opposite isomer.

ability of the phenyl-2-pyridyl isomers were used to effect a separation. The other oximes were etherified as mixtures, and the isomeric ethers were separated *via* fractional distillation.

For the aldehyde oximes, the same method (4) was employed for (*Z*)-isomers. Because the rule for the production of isomers applies, the method is not applicable for the (*E*)-isomers. Initially, an adaption of Vogel's method (6) was employed, *e.g.*, passing hydrogen bromide gas through a refluxing methylene chloride solution of the oxime and neutralizing the resulting hydrobromide salt at low temperatures. The method was not highly successful, and the more stable isomer was usually obtained. An adaptation of the Schoenewaldt *et al.* method (7), which employs a higher boiling solvent (benzene), gave better yields and was used thereafter.

The oximes were converted to the corresponding ethers by treatment of their anions with 2-dimethylaminoethyl chloride. Acetophenone and *p*-methoxyacetophenone oximes were etherified as a mixture, and the ethers were separated *via* fractional distillation. The (*E*)- and (*Z*)-3,4-dimethylbenzophenone oximes were etherified as a mixture, but only the (*E*)-isomer was obtained on multiple distillation. The pure (*Z*)-oxime isomer was used to obtain the (*Z*)-oxime ether.

Alkylation of the (*Z*)-aldehyde oximes proceeded satisfactorily with the cited method. With the (*E*)-oximes, 50–70% etherification occurred. However, isomerization occurred, and the yield of the (*E*)-oxime ether fell in the range of 8–14% based on the aldehyde. The isomerization appeared to be unidirectional since no (*E*)-oxime derivative was obtained from procedures beginning with the (*Z*)-oxime. This result might be expected from a consideration of the relative stability of the two oximes. Because isomerization occurred during etherification, it was necessary to separate the oxime ethers derived from the (*E*)-oximes. This separation was done by vacuum distillation and, for the (*E*)-*p*-methoxybenzaldehyde and (*E*)-3,4,5-trimethoxybenzaldehyde *O*-oxime ethers, by chromatography on silica.

Isomeric identity of the oxime *O*-ethers was established primarily on the basis of magnetic resonance values of protons of the *O*-alkyl substituent. The isomeric differences in the resonance values depend on the position of the substituent relative to the aromatic ring of the ether. In the benzaldehyde oxime ethers, for example, the OCH_2 resonance occurs at τ 5.8 ppm in the (*e*)-isomer and at τ 6.0 ppm in the (*Z*)-isomer. The NCH_2 absorption occurs at τ 7.4 ppm in the latter. Since diamagnetic anisotropic effects decrease rapidly with distance, the anisotropic effects are strongest in the (*Z*)-isomer.

The diamagnetic field of the aromatic substituent, which may shield or deshield proximate protons depending on their position relative to the field (8), shields the OCH_2 protons. However, since the preferred con-

formation of protons of the aromatic substituent is skew (9), the NCH_2 protons are deshielded because the field of the aromatic substituent is different in this area. This rationalization is supported by the fact that the OCH_2 absorption is more strongly affected, indicating that the effect is strongly distance dependent.

For aryl aldehyde oxime derivatives, the NMR isomeric assignments were supported by UV spectral data. Assignments were based on the convention (10) that the isomer with the highest λ_{max} and molar absorptivity is the (*E*)-isomer.

Structural assignments based upon the Beckmann rearrangement were used only for oximes (VIII*a* and VIII*b*) with similar substituents since isomerization may precede rearrangement where the migratory propensity of the two substituents is greatly different. The rearrangement was conducted with the oxime prior to etherification, and subsequent spectral data confirmed that isomerization had not taken place in the ether derivative.

EXPERIMENTAL[1]

Synthesis of Oximes—*Method 1* (*4*): (Z)-*Benzaldehyde Oxime*—Freshly distilled benzaldehyde (106 g, 1.0 mole) was mixed with a solution of sodium hydroxide (95 g) in water (175 ml) and cooled to room temperature. Hydroxylamine hydrochloride (146 g, 2.0 moles) was added in one portion to the reaction mixture, and the clear solution was heated to boiling. The solution was cooled to room temperature and acidified by means of a carbon dioxide generator. The separated oil was extracted with ether (two 100-ml portions), and the combined extracts were dried over sodium sulfate. The solvent was removed under reduced pressure, and the remaining mass was recrystallized from benzene. The yield was 96 g (80%), mp 28–29°. NMR analysis (11) showed the presence of only one oxime.

Method 2 (*6*): (E)-*Benzaldehyde Oxime*—The (*Z*)-oxime was dissolved in methylene chloride (300 ml), and hydrogen bromide gas was passed through the system. Following partial solvent evaporation, the resulting precipitate was neutralized with aqueous sodium hydroxide solution (10%). The product was recrystallized from hexane, and the yield was 5 g (44%), mp 127–129° [lit. (6) mp 130°].

Method 3 (*7*): (E)-*Benzaldehyde Oxime*—(*Z*)-Benzaldehyde oxime (40 g, 0.32 mole) was placed in dry benzene (600 ml), and the solution was heated to boiling. While the solution was heated and vigorously stirred, hydrogen bromide gas was forced through the system. This treatment was maintained until the temperature dropped to 50°. Then the solution was cooled to room temperature, and the oxime salt was removed by filtration. An aqueous solution of sodium hydroxide (80 g in 150 ml) was cooled to 10°. The salt was dropped into the solution, and the mixture was stirred until complete dissolution occurred. Excess ammonium chloride was dropped into the mixture, and the mixture then was extracted with ether (two 100-ml portions). The combined ether extracts were dried over sodium sulfate, and the ether was removed under reduced pressure. The yield was 36 g (88%), mp 124–126°.

Synthesis of Oxime Precursors Using Method 1—Method 1 also was used for the synthesis of the oxime precursors of II*a*, III*a*, IV*a*, IV*b*, V*a*, V*b*, VI*a*, VI*b*, VII*a*, VII*b*, VIII*a*, and VIII*b*. The yields were never lower than 44%. No separation was made of the oxime precursors of IV*a* and IV*b*, V*a* and V*b*, and VI*a* and VI*b*. Separation of the (*E*)- and (*Z*)-isomers was made after etherification. The isomeric oxime precursors of VII were separated and identified on the basis of their chelating ability (adopted from Ref. 12).

The mixture of oxime isomers was used for the synthesis of the ether VIII*a*. Both ethers probably were formed, but fractional distillations were repeated until only pure VIII*a* was isolated. The oxime precursor to VIII*b* was obtained *via* repeated fractional crystallizations of the mixture of oxime isomers and used for the synthesis of that ether. Since VIII*b* was deduced from Beckmann rearrangement data to be the (*Z*)-isomer, it may be considered that VIII*a* is the (*E*)-isomer.

Synthesis of Other Oximes—The following summarizes the results of Method 1 applied to oximes other than (*Z*)-benzaldehyde oxime.

(Z)-p-*Methoxybenzaldehyde Oxime*—Freshly redistilled *p*-methoxybenzaldehyde (68.07 g, 0.5 mole) gave, after refluxing for 2 hr and recrystallizing from heptane, 65 g (87%) of the oxime precursor to II*a*, mp 62–64°.

(Z)-*3,4,5-Trimethoxybenzaldehyde Oxime*—3,4,5-Trimethoxybenzaldehyde (25 g, 0.125 mole) dissolved in ethanol (200 ml) was treated according to Method 1 with potassium hydroxide replacing sodium hydroxide (reflux time of 2 hr). The oxime precursor to III*a* crystallized from the reaction mixture in a yield of 21.3 g (85%), mp 99–101°.

(E)- *and* (Z)-*2-Thienylaldehyde Oximes*—Freshly distilled 2-thienylaldehyde (reflux time of 0.5 hr) gave 24.6 g (75%) of the (*E*)- and (*Z*)-oxime precursors to IV*a* and IV*b*.

(E)- *and* (Z)-*Acetophenone Oximes*—Acetophenone (20 g, 0.166 mole) was treated according to Method 1 (reflux time of 2 hr). The oxime precursors to VI*a* and VI*b* were recrystallized from heptane, 18.5 g (82%), mp 52–55°.

(E)- *and* (Z)-*2-Pyridophenone Oximes*—An adaptation of the procedure of Huntress and Walter (12) gave the isomeric oximes. The ketone (110 g, 0.6 mole), dissolved in ethanol (180 ml) and treated according to Method 1, gave the oximes, 121 g (100%), mp 117–131°. This mixture was placed in dry chloroform (210 ml) and refluxed 20 min. Then the solution was cooled to room temperature and filtered. The residue was washed with dry chloroform (30 ml) and recrystallized (ethanol), giving 54 g (90%) of the (*E*)-isomer, mp 150–152°.

The combined filtrates and washings from recrystallization were evaporated under reduced pressure, and the residue (24 g) was solubilized with aqueous hydrochloric acid (20%, 80 ml). Copper sulfate solution (20 g in 100 ml of water) was added, and the mixture was allowed to stand overnight. The mixture was filtered, washed with water (30 ml), and dried. The combined filtrate and washings were purged with hydrogen sulfide. After removal of the black precipitate, the solution was titrated to pH 3.8 with 1 *N* ammonium hydroxide. The precipitate that formed was removed, and titration was continued to neutrality. The yield was 8.5 g (14%) of the (*Z*)-oxime, mp 165–167°.

(E)- *and* (Z)-*3,4-Dimethylbenzophenone Oximes*—The oxime precursors to VII*a* and VII*b* were obtained from the ketone (21 g, 0.1 mole) dissolved in ethanol (250 ml) and treated according to Method 1 (reflux time of 0.5 hr). The yield was 22 g (88%), mp 124–127°. A portion of the mixture was subsequently used in the etherification procedure. Repeated distillation thereafter gave only the amino ether which, in turn, gave the salt VIII*a*. Additionally, a portion of the mixture was recrystallized repeatedly from 2-propanol–water to give one oxime isomer, mp 154–155°, in a 6% yield. Beckmann rearrangement data on this oxime, described under the structural determination of isomer set VIII*a* and VIII*b*, indicated this compound to be the (*Z*)-oxime.

Synthesis of Oxime Precursors Using Method 3—Since Method 3 gave better yields than Method 2, it was used exclusively for the conversion of (*Z*)- to (*E*)-forms. The (*E*)-forms resulting from Method 3 were used for the synthesis of I*b*, II*b*, and III*b*. The following summarizes the results of Method 3 as used for the synthesis of the oxime precursors to II*b* and III*b*.

(E)-p-*Methoxybenzaldehyde Oxime*—(*Z*)-*p*-Methoxybenzaldehyde oxime (50 g, 0.311 mole) was dissolved in anhydrous benzene (700 ml). The solution was heated to boiling with stirring, and 60 ml of the solution was distilled. External heating was discontinued, and hydrogen chloride gas was passed through the solution, the heat of reaction maintaining the solution at reflux. Passage was continued until the temperature fell to 50°, and the mixture was cooled to 10° and filtered. The oxime hydrochloride was dissolved in a solution of sodium hydroxide (50 g) in water (250 ml). Excess ammonium chloride was added, and the resulting precipitate was extracted with ether (two 100-ml portions). The ether extracts were dried, and the ether was removed under reduced pressure to give the (*E*)-oxime, 46.5 g (93%), mp 131–133°.

(E)-*3,4,5-Trimethoxybenzaldehyde Oxime*—The compound, mp 157–158°, was obtained in a yield of 8.8 g (82%) from 12.0 g (0.057 mole) of the (*Z*)-oxime dissolved in dry benzene (750 ml). The solution was brought to reflux, and 100 ml of benzene was distilled out. Treatment thereafter was as described previously, except that the (*E*)-oxime was precipitated by the addition of ammonium phosphate, removed by filtration, and dried at 75° overnight.

Synthesis of Oxime *O*-Ethers—(Z)-*Benzaldehyde Oxime* O-*Dimethylaminoethyl Ether and Methobromide* (*Ia*)—The oxime (20 g, 0.16 mole) was dissolved in ethanol (200 ml). Sodium hydride (24 g of a 51.2% mineral oil dispersion, 0.48 mole) was added with caution to the stirred solution. 2-Dimethylaminoethyl chloride hydrochloride (23 g, 0.16 mole) was dissolved in ethanol (150 ml) and dropped into the reaction mixture over 30 min. The stirred reaction mixture was maintained at reflux for 24 hr. Then the solvent was evaporated under reduced pressure, the residue was dissolved in isopropyl ether, and the solids were filtered off.

[1] Melting points were determined on a Thomas–Hoover Mel-Temp apparatus and are uncorrected. IR spectra for all final compounds and intermediates were determined on a Beckman IR-8 and are in accord with the assigned structures. NMR data were obtained for all compounds in a Varian A-60 and are in accordance with the assigned structures. Noteworthy NMR data used to distinguish between isomers are given in Table II. UV data were obtained on a Beckman DB with ethanol as solvent. Elemental analyses were performed by Schwarzkopf Microanalytical Laboratories, Woodside, N.Y.

Table II—Physical Constants of the Amines Synthesized

Amino Precursor to Compound	Yield, %	Boiling Point and Pressure (mm Hg) of Amine	NMR Data[a], ppm			UV Data	
			OCH_2	NCH_2	$N(CH_3)_2$	λ_{max}, nm	ξ_{max}
I*a*	51.3	62–70°/0.1–0.05	5.70	7.36	7.75	246	19,770
I*b*	18.2	112°/1.25	6.07	7.20	7.83	236	17,500
II*a*	92.0	88–90°/0.015	5.82	7.42	7.78	248	19,900
II*b*[b]	32.5	69–70°/0.05	6.16	7.21	7.86	237	17,700
III*a*	76.6	126–130°/0.02	5.94	7.56	7.85	256	24,600
III*b*[b,c]	14.2		6.38	7.30	7.92	247	19,750
IV*a*	22.9	84–86°/0.015	5.80	7.42	7.80		
IV*b*	40.0	118–20°/0.01	5.92	7.09	7.70		
V*a*	78.7	82.5–85°/0.20	5.70	7.38	7.79		
V*b*	7.5	104–106°/0.20	6.17	7.20	7.92		
VI*a*	83.0	110–113°/0.05	5.78	7.38	7.79		
VI*b*[b]	4.4	134–137°/0.05	6.18	7.10	7.96		
VII*a*	24.3	147–154°/0.09	5.73	7.43	7.82		
VII*b*	19.0	143–144°/0.40	5.81	7.36	7.86		
VIII*a*	16.4	139–141°/0.05	5.84	7.56	7.91		
VIII*b*[b]	12.2		5.70	7.48	7.96		

[a] Values were obtained on a Varian A-60 [25% (v/v) $DCCl_3$] and are expressed as τ. [b] Chromatographed on silica. [c] NMR analysis indicated about 10% of the (*Z*)-isomer.

The rest of the solvent was removed under reduced pressure, and the remaining liquid was distilled.

The major distillation fraction (bp 65–69°/0.08 mm, 13.83 g, 45%) was subjected to NMR and UV analysis and found to be the (*Z*)-oxime ether. The yield and physical constants are summarized in Table II. The methobromide (I*a*) was prepared by dissolving the amine in isopropyl ether and treating with excess methyl bromide. The analytically pure methobromide was obtained after repeated recrystallization. The recrystallization solvent, melting piont, and analytical data are given in Table I.

The described procedure was applied to the synthesis of the following compounds with exceptions and variations in quantities of reactants as noted. Yields and physical constants for the amino ethers are given in Table II. Recrystallization solvents, melting points, and elemental analytical data for the quaternary derivatives are given in Table I.

(E)-*Benzaldehyde Oxime* O-*Dimethylaminoethyl Ether*—The (*E*)-oxime (20 g, 0.16 mole) was dissolved in ethanol (500 ml), and sodium hydride–mineral oil dispersion (16 g, 0.27 mole) was added. 2-Dimethylaminoethyl chloride hydrochloride (23 g, 0.16 mole) in ethanol (400 ml) then was added over 1 hr. The methiodide (I*b*) was prepared in hexane.

(Z)-p-*Methoxybenzaldehyde Oxime* O-*Dimethylaminoethyl Ether*—The oxime (8.8 g, 0.06 mole) was dissolved in ethanol (250 ml). The sodium hydride dispersion (6.2 g, 0.13 mole) and then the alkylating agent (9.1 g, 0.06 mole) in ethanol (100 ml) were added.

(E)-p-*Methoxybenzaldehyde Oxime* O-*Dimethylaminoethyl Ether*—To the oxime (10 g, 0.066 mole) in ethanol (200 ml) was added the sodium hydride dispersion (6.2 g, 0.13 mole). The alkylating agent (10.1 g, 0.07 mole) in ethanol (150 ml) then was added. The reflux time was 18 hr. Workup gave an oil which was distilled. Data for the first fraction are given in Table II. NMR revealed a contaminant with triplets at τ 7.4 and 6.3 ppm. A short column was packed with silica gel in a slurry form with pentane. The oil was dissolved in the minimum amount of isopropyl ether. The column was developed with pentane–ether mixtures (1:0, 1:25, 1:0.5, 1:1, 0.5:1, and 0:1). Eluates were reduced in volume and treated with iodomethane to determine the presence of the (*E*)-amino ether. The methiodide (II*b*) was prepared in heptane.

A second fraction (bp 101–103°/0.05 mm Hg, 2.4 g, 17%) was shown by NMR analysis to be the (*Z*)-ether.

(Z)-*3,4,5-Trimethoxybenzaldehyde Oxime* O-*Dimethylaminoethyl Ether*—The oxime (6.4 g, 0.03 mole) was added to the sodium hydride dispersion (4 g, 0.08 mole) in ethanol (175 ml). 2-Dimethylaminoethyl chloride hydrochloride (7.2 g, 0.05 mole) then was added slowly to the solution. The methiodide (III*a*) also was prepared.

(E)-*3,4,5-Trimethoxybenzaldehyde Oxime* O-*Dimethylaminoethyl Ether*—The oxime (6.4 g, 0.03 mole) was dissolved in ethanol (200 ml). The sodium hydride dispersion (3.8 g, 0.08 mole) was added, and then the alkylating agent (7.2 g, 0.05 mole) was added slowly. After an attempted distillation, the oil was placed on a silica gel column packed with a hexane slurry. Isopropyl ether was passed through the column until all colored material was eluted; then the column was eluted with ethanol. Evaporation of the ethanol gave a colorless oil. NMR analysis indicated that the oil was the (*E*)-isomer with about 10% of the (*Z*)-isomer. The methiodide (III*b*) also was prepared.

(Z)- *and* (E)-*2-Thienylaldehyde Oxime* O-*Dimethylaminoethyl Ethers*—The oxime mixture (8.6 g, 0.07 mole) was dissolved in ethanol (200 ml), and the sodium hydride dispersion (7.2 g, 0.15 mole) was added. Then the alkylating agent (11.52 g, 0.08 mole) was added. The reflux time was 48 hr. Workup and fractional distillation gave the (*E*)- and (*Z*)-ethers. The methiodides (IV*a* and IV*b*) were prepared in heptane.

(Z)- *and* (E)-*Acetophenone Oxime* O-*Dimethylaminoethyl Ethers*—The oxime mixture (13.5 g, 0.1 mole) was dissolved in ethanol (200 ml). The sodium hydride dispersion (9.6 g, 0.2 mole) and then the alkylating agent (14.4 g, 0.1 mole) were added. The reflux time was 48 hr. Workup and fractional distillation gave the (*E*)- and (*Z*)-isomers. The methiodes (V*a* and V*b*) were prepared in heptane.

(Z)- *and* (E)-p-*Methoxyacetophenone Oxime* O-*Dimethylaminoethyl Ethers*—To the oxime mixture (11.0 g, 0.07 mole) in ethanol was added the sodium hydride dispersion (7.2 g, 0.15 mole) and then the alkylating agent (11.52 g, 0.08 mole). The reflux time was 27 hr. Workup and fractional distillation gave the two compounds. The methiodides (VI*a* and VI*b*) also were prepared.

(E)-*2-Pyridophenone Oxime* O-*Dimethylaminoethyl Ether*—The (*E*)-oxime (11 g, 0.56 mole) was dissolved in ethanol (200 ml). The sodium hydride dispersion (7.2 g, 0.15 mole) and then the alkylating agent (14.4 g, 0.1 mole) in ethanol (110 ml) were added. The methiodide (VII*a*) also was prepared.

(Z)-*2-Pyridophenone Oxime* O-*Dimethylaminoethyl Ether*—The oxime (11 g, 0.056 mole) was mixed with a solution of the sodium hydride dispersion (9.0 g, 0.18 mole) in ethanol (200 ml), and the alkylating agent (14.4 g, 0.1 mole) was added. The reflux time was 16 hr. The methobromide (VII*b*) also was prepared.

(E)-*3,4-Dimethylbenzophenone Oxime* O-*Dimethylaminoethyl Ether*—The oxime mixture (11.2 g, 0.1 mole) was added to the sodium hydride dispersion (4.8 g, 0.1 mole) in ethanol (200 ml), and then the alkylating agent (7.2 g, 0.1 mole) in ethanol (150 ml) was added. The reflux time was 36 hr. Workup and distillation gave a fraction (bp 134–138°/0.05 mm Hg, 9.4 g) which, on NMR analysis, proved to be a mixture of the (*E*)- and (*Z*)-ethers. A second distillation gave a fraction (bp 135–137°/0.05 mm Hg, 8.0 g) which had an increased concentration of the (*E*)-isomer according to NMR analysis. A third distillation gave the pure isomer. The methiodide (VIII*a*) was prepared in hexane.

(Z)-*3,4-Dimethylbenzophenone Oxime* O-*Dimethylaminoethyl Ether*—To the oxime (0.50 g, 0.0024 mole) in ethanol (50 ml) was added the sodium hydride dispersion (0.3 g, 0.006 mole) and the alkylating agent (0.43 g, 0.003 mole). Workup gave an oil, which was chromatographed on silica in the manner described for the amine precursor to III*b*. The methiodide (VIII*b*) was prepared in hexane.

Structural determination for the isomer set VIII*a* and VIII*b* was accomplished in the following manner. The recrystallized oxime (0.225 g, 0.0011 mole) was dissolved in chloroform (10 ml), and the solution was heated to reflux. Excess phosphorus pentachloride was added to the mixture, and an exothermic reaction occurred. Following a period of standing, the solvent was evaporated under reduced pressure. The remaining yellow semisolid was dissolved in concentrated hydrochloric acid (30 ml) and stirred at reflux for 3 hr.

The resultant mixture was cooled to 10° and extracted with two 50-ml portions of ether. The extracts were dried, and the solvent was removed

under reduced pressure. The yield was 0.147 g of the acid, mp 140–143°. NMR data confirmed that only 3,4-dimethylbenzoic acid was present. Subsequent etherification of the oxime derivable from recrystallization gave a product whose NMR spectrum was superimposable on the spectrum of the isomer that disappeared during multiple distillation.

Pharmacology—The anticholinergic potency of these compounds was determined by the classic Magnus method with quantitative procedures devised by Ariens (13). The method involves the measurement of spasmogen-induced intestinal contractions in the presence of the spasmolytic agent. The test tissue consisted of smooth muscle from the rat ileum. The dose–effect curves for spasmogens were determined alone, in the presence of the test compound, and in the presence of the standard spasmolytic agent.

The dose of the spasmogen required to contract the muscle to a maximal level was determined, and the data were plotted using percent response on a probability scale *versus* dose of spasmogen (log millimolar). In this manner, it was possible to determine the dose of spasmogen necessary to induce 50% contraction in the test tissue under the various conditions. This estimation then allowed the comparison of the relative activity of the compounds.

Test samples of the methylhalide derivatives in water were prepared. The spasmogen (bethanechol chloride) was prepared in aqueous solution in dilutions of greatly different concentrations. Since the solutions were potentially susceptible to degradation, no solution was utilized more than 2 hr after preparation.

A glass cylinder of 80-ml capacity, with an inlet for the introduction of the bathing solution and for drainage, was assembled in a constant-temperature bath. A mechanism was devised for the constant aeration of the muscle in the chamber. The bathing solution was composed of 9 g of sodium chloride, 0.4 g of potassium chloride, 0.12 g of calcium chloride, and 0.3 g of sodium bicarbonate in 1 liter of distilled water.

Strips of ileum of uniform length were taken from an unanesthetized male albino rat which had been recently sacrificed. The strip was suspended in the muscle bath chamber, and the bathing solution was added to constant volume (70 ml). The temperature was held constant at 37°. Records of the muscle contractions were recorded using a physiograph with a myograph attachment.

The method for determining dose–response curves uses successive geometric additions of the spasmogen without washing between dose increments. The spasmogen was added to the aerated bath at regular intervals until maximum response was obtained. This constituted the control curve for the spasmogen. The muscle bath was then rinsed repeatedly with the bathing solution (previously heated to 37°). After the muscle resumed spontaneous contractions, the unknown drug was added to the muscle bath. Again, the spasmogen was added in increasing amounts until maximum response was obtained. The muscle was repeatedly washed, then the opposite isomer was added to the bath, and a similar sequence of treatments was used. Following repeated washing, the initial spasmogen–response curve was duplicated to ensure the muscle's responsiveness. The data are summarized in Table III.

Table III—Summary of the Pharmacological Data

Compound	Dose of Test Compound, m*M*/70 ml	Dose of Spasmogen, m*M*/70 ml at 50% Contraction	Ratio *a*/*b*[a]
I*a*	3.0×10^{-2}	$29.33 (\pm 1.40) \times 10^{-2}$	3.25
I*b*	3.0×10^{-2}	$9.03 (\pm 0.73) \times 10^{-2}$	
II*a*	1.09×10^{-2}	$19.4 (\pm 0.09) \times 10^{-2}$	2.66
II*b*	1.09×10^{-2}	$7.3 (\pm 0.34) \times 10^{-2}$	
III*a*	1.17×10^{-2}	$26.00 (\pm 0.27) \times 10^{-2}$	4.40
III*b*	1.17×10^{-2}	$5.90 (\pm 0.18) \times 10^{-2}$	
IV*a*	6.17×10^{-3}	$17.8 (\pm 0.43) \times 10^{-2}$	3.17
IV*b*	6.17×10^{-3}	$5.6 (\pm 0.31) \times 10^{-2}$	3.17
V*a*	5.70×10^{-3}	$28.05 (\pm 0.46) \times 10^{-2}$	4.75
V*b*	5.70×10^{-3}	$6.00 (\pm 0.42) \times 10^{-2}$	
VI*a*	7.33×10^{-3}	$32.68 (\pm 0.79) \times 10^{-2}$	4.39
VI*b*	7.33×10^{-3}	$7.44 (\pm 0.32) \times 10^{-2}$	
VII*a*	1.0×10^{-5}	$22.0 (\pm 0.26) \times 10^{-2}$	1.01
VII*b*	1.0×10^{-5}	$21.45 (\pm 0.30) \times 10^{-2}$	
VIII*a*	1.8×10^{-5}	$17.33 (\pm 0.36) \times 10^{-2}$	0.98
VIII*b*	1.8×10^{-5}	$17.50 (\pm 0.40) \times 10^{-2}$	

[a] Values are the means of at least six separate determinations. The differences between the ED_{50}'s for I–VI are significant at the 0.01 level.

RESULTS

Certain general activity patterns emerge. Compounds I*a*, II*a*, III*a*, IV*a*, V*a*, and VI*a* were uniformly more active than their (*Z*)-counterparts. It is apparent that the muscarinic receptor is stereospecific toward this series of geometric isomers. From this finding, it might be conjectured that the receptor is most nonpolar in the portion complementary to the (*E*)-aryl group.

A second activity pattern is that the isomers are approximately equipotent among the diaryl oxime ethers (VII*a*, VII*b*, VIII*a*, and VIII*b*). A third general activity pattern is that the diaryl compounds are all more active than the monoaryl compounds. The higher activity of the diaryl compounds is in accord with the general structure–activity relationships among anticholinergics. The higher activity of diaryl compounds and the equipotency between diaryl isomers may be explained if the nonpolar portion in this area of the receptor is fairly extensive. Also, the auxiliary polar group often noted for the muscarinic receptor, which may be in this portion of the receptor, is possibly very small and would not interfere with the binding of a second aryl group.

REFERENCES

(1) E. J. Ariens, "Advances in Drug Research," vol. 3, Academic, New York, N.Y., 1966, p. 271.

(2) M. M. Kochhar, R. G. Brown, and J. N. Delgado, *J. Pharm. Sci.*, **54**, 393 (1965).

(3) S. K. Gomer, E. I. Isaacson, R. G. Brown, and J. N. Delgado, *ibid.*, **57**, 1586 (1968).

(4) A. Lachman and C. R. Noller, in "Organic Syntheses," coll. vol. II, A. H. Blatt, Ed., Wiley, New York, N.Y., 1943, p. 70.

(5) W. E. Bachmann and M. X. Barton, *J. Org. Chem.*, **3**, 300 (1938).

(6) A. I. Vogel, "A Textbook of Practical Organic Chemistry," Longmans, Green, London, England, 1948, pp. 683, 684.

(7) E. F. Schoenewaldt, R. B. Kinnel, and P. Davis, *J. Org. Chem.*, **33**, 4270 (1968).

(8) D. J. Pasto and C. R. Johnson, "Organic Structure Determination," Prentice-Hall, Englewood Cliffs, N.J., 1969, pp. 171–174.

(9) E. L. Eliel, "Stereochemistry of Carbon Compounds," McGraw-Hill, New York, N.Y., 1962, p. 134.

(10) L. Lang, G. Horvath, L. Vargha, and G. Ocskay, *Bull. Soc. Chim. Fr.*, **1965**, 2724.

(11) W. D. Phillips, *Ann. N.Y. Acad. Sci.*, **70**, 817 (1958).

(12) E. H. Huntress and H. C. Walter, *J. Am. Chem. Soc.*, **70**, 3702 (1948).

(13) E. J. Ariens, paper presented at the APhA Academy of Pharmaceutical Sciences, Detroit meeting, Apr. 1965.

ACKNOWLEDGMENTS AND ADDRESSES

Received February 19, 1976, from the *College of Pharmacy, University of Texas at Austin, Austin, TX 78712.*

Accepted for publication February 7, 1977.

The authors thank Dr. James F. Stubbins for helpful comments and suggestions.

* Present address: College of Pharmacy, Idaho State University, Pocatello, ID 83209.

[x] To whom inquiries should be directed.

N-Glucopyranosyl-5-aralkylidenerhodanines: Synthesis and Antibacterial and Antiviral Activities

WILLIAM O. FOYE ˣ and PHICHAI TOVIVICH *

Abstract □ A series of *N*-(2,3,4,6-tetra-*O*-acetyl-β-D-glucopyranosyl)-5-aralkylidenerhodanines was synthesized, and the acetyl groups were removed to give *N*-β-D-glucopyranosyl-5-aralkylidenerhodanines without cleavage of the rhodanine ring by means of acid hydrolysis. Alkaline hydrolysis with ammonia in methanol resulted in cleavage to *N*-glucosylthiourea, providing evidence for *N*-glycoside formation. A number of the rhodanine derivatives, especially those with nitro or chloro groups in the aromatic ring, showed antibacterial activity. *N*-β-D-Glucopyranosyl-5-(4-nitrobenzylidene)rhodanine showed antiviral activity by inhibition of viral RNA synthesis. Some effect on blood sugar levels also was observed with several rhodanines.

Keyphrases □ Rhodanine derivatives, various—synthesized, evaluated for antibacterial and antiviral activities □ Antibacterial activity—evaluated in various rhodanine derivatives □ Antiviral activity—evaluated in various rhodanine derivatives □ Structure–activity relationships—various rhodanine derivatives evaluated for antibacterial and antiviral activities

Rhodanine (2-thioxo-4-thiazolidinone) has shown some antiviral properties, specifically in echovirus 12 as a result of the inhibition of the synthesis of the viral protein coat (1). In various other viruses, hydrolysis products of rhodanine derivatives (α-mercaptoacrylic acids and their disulfides) act as inhibitors of neuraminidases (2), enzymes involved with the entry and release of virus particles in host cells (3). Rhodanine and its derivatives also have the ability to complex iron and other metals (4). This ability enables the rhodanines to inhibit the ribonucleoside diphosphate reductase enzyme system, which requires iron as a cofactor, and thereby inhibit the synthesis of DNA (5).

In addition to these possibilities as a basis for antiviral action, rhodanines possibly may act as analogs of purine bases in nucleic acid synthesis. In this event, glycosylated derivatives should be more effective inhibitors. The presence of a sugar moiety attached to the rhodanine ring may also provide rhodanines with less toxicity. This reduction in toxicity by formation of sugar derivatives was observed with some antitubercular agents (6).

Rhodanine and its derivatives also have exhibited antibacterial (7), antitubercular (8), antimalarial (9), antifungal (10), insecticidal (11), pesticidal (11), and antiparasitic (12) activities. Nitrodan [3-methyl-5-[(*p*-nitrophenyl)azo]rhodanine] has been used as an anthelmintic agent (13). No glycosylated derivative of rhodanine or its derivatives has been screened for antiviral activity or for any of the biological activities listed. The only mention in the literature of previous glycosylated rhodanines was made by Bognar and Wieniawski (14), who prepared the *N*-tetraacetylglucosyl derivatives of the 5-isopropylidene, 5-benzylidene, and 5-anisylidene derivatives of rhodanine. They were unable to remove the acetyl groups without decomposition, but they showed that the sugar moiety was attached to the nitrogen of the rhodanine ring.

Accordingly, a series of *N*-tetraacetyl-D-glucosyl derivatives of 5-ylidenerhodanines, prepared from both aldehydes and ketones, was prepared for screening for antiviral and other biological activities. The *N*-tetraacetyl-D-glucosylrhodanines were obtained from reaction of the 5-ylidenerhodanines with acetobromo-D-glucose, and it was possible to remove the acetyl groups by acid hydrolysis without cleavage of the rhodanine ring. The compounds prepared can be represented by Structure I, where R_1 is tetraacetyl-D-glucosyl or D-glucosyl and R_2 is H or CH_3.

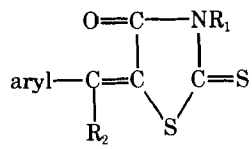

I

EXPERIMENTAL[1]

The following procedures are representative.

Condensation of Rhodanine with Aldehydes and Methyl Ketones—*Method A*—2,6-Dichlorobenzaldehyde (8.75 g, 0.05 mole) was added to a solution of rhodanine (6.66 g, 0.05 mole) in 75 ml of acetic acid, followed by the addition of 12.5 g of anhydrous sodium acetate. The reaction mixture was refluxed on a water bath for 1 hr, cooled to room temperature, and poured into 500 ml of water. After refrigeration, it was filtered; the precipitate was washed with water and dried *in vacuo* to give 11.8 g (81% yield) of crude product. Recrystallization from methanol gave yellow needles, mp 184–186°; IR (KBr): ν 3190 (NH), 1705 (C=O), and 1230 (C=S) cm^{-1}.

Anal.—Calc. for $C_{10}H_5Cl_2NOS_2$: C, 41.39; H, 1.74; N, 4.83; S, 22.10. Found: C, 41.50; H, 2.06; N, 4.93; S, 21.64.

Method B—2-Acetylthiophene (12.13 g, 0.096 mole) was added to rhodanine (12.8 g, 0.096 mole) in 100 ml of ethanol containing 7.5 ml of concentrated ammonium hydroxide and ammonium chloride (7.5 g in 15 ml of water). The mixture was refluxed for 1.5 hr and refrigerated overnight. Yellow crystals were isolated, washed with water, and dried in a vacuum oven. A second crop was obtained by adding the filtrate to 500 ml of water and chilling; the crude yellow product was recrystallized from acetone. The total yield was 6.5 g (28%), mp 230–233° [lit. (15) mp 218–221.5° dec.].

Condensation of 5-Arylalkylidenerhodanines with 2,3,4,6-Tetra-*O*-acetyl-β-D-glucose: *N*-(2,3,4,6-Tetra-*O*-acetyl-β-D-glucopyranosyl)-5-(*p*-dimethylaminobenzylidene)rhodanine—5-*p*-Dimethylaminobenzylidenerhodanine (5.28 g, 0.02 mole) was dissolved in 1250 ml of acetone and 250 ml of tetrahydrofuran with heating. The solution was cooled to room temperature, and 8.22 g (0.02 mole) of acetobromo-α-D-glucose was added followed by 8 ml of 10% sodium hydroxide solution. The mixture was stirred at room temperature for 68 hr and filtered. The filtrate was evaporated in a rotary evaporator at 30° under reduced pressure. A red syrup was obtained, which crystallized from methanol to give 7.8 g (66% yield) of orange solid, mp 197–201°; IR (KBr): ν 1750

[1] Melting points were determined in capillaries with a Mel-Temp melting-point block and are uncorrected. IR absorption spectra were obtained with a Perkin-Elmer model 137B or model 457A grating spectrophotometer. NMR spectra were determined with a Varian T60 spectrometer using tetramethylsilane as the internal standard. Optical rotations were obtained with a Carl Zeiss polarimeter. Elemental analyses were done by Dr. F. B. Strauss, Oxford, England, or by Dr. Carol K. Fitz, Carlisle, Mass. TLC was carried out using silica gel, and products were detected by exposure to iodine vapor.

The rhodanine, aldehydes, and methyl ketones were supplied by Aldrich Chemical Co., and D-glucose and common solvents were obtained from the Fisher Scientific Co. Acetobromo-D-glucose, obtained from Sigma Chemical Co., contained 1% $CaCO_3$ as a stabilizer. It was recrystallized from ether before use.

Table I—*N*-(2,3,4,6-Tetra-*O*-acetyl-β-D-glucopyranosyl)-5-arylalkylidenerhodanines

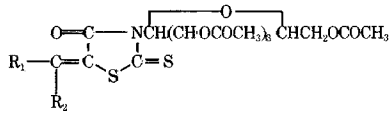

R_1	R_2	Formula	Melting Point	Yield, %	$[\alpha]_D^{20}$ (Solvent)	IR (KBr), cm^{-1}	Analysis, %	
							Calc.	Found
C_6H_5	H	$C_{24}H_{25}NO_{10}S_2$	192–194°[a]	79	−169.0° (pyridine)	1750, 1225, 910	—	—
4-$NO_2C_6H_4$	H	$C_{24}H_{24}N_2O_{12}S_2$	222–224°	30	−195.0° (pyridine)	1750, 1240, 910	C 48.32	48.39
							H 4.06	4.10
							N 4.70	4.78
							S 10.75	10.49
2-$NO_2C_6H_4$	H	$C_{24}H_{24}N_2O_{12}S_2$	185–187°	65	—	1750, 1235, 900	C 48.32	48.26
							H 4.06	4.30
							N 4.70	4.57
							S 10.75	10.43
4-$(CH_3)_2NC_6H_4$	H	$C_{26}H_{30}N_2O_{10}S_2$	197–201°	66	−104.0° (tetrahydrofuran)	1750, 1225, 900	C 52.52	52.74
							H 5.08	5.08
							N 4.71	4.75
							S 10.78	10.91
3,4-$[CH_2(O)_2]C_6H_3$	H	$C_{25}H_{25}NO_{12}S_2$	195–196°	78	−159.3° (pyridine)	1750, 1225, 900	C 50.42	50.76
							H 4.23	4.35
							N 2.35	2.53
							S 10.77	10.96
3,4-$(CH_3O)_2C_6H_3$	H	$C_{26}H_{29}NO_{12}S_2$	186–189°	57	−273.0° (tetrahydrofuran)	1750, 1225, 900	C 51.06	50.95
							H 4.75	4.99
							N 2.29	2.31
							S 10.47	10.16
2,5-$(CH_3O)_2C_6H_3$	H	$C_{26}H_{29}NO_{12}S_2$	207–211°	64	−137.7° (tetrahydrofuran)	1750, 1225, 900	C 51.06	50.79
							H 4.75	4.78
							N 2.29	2.31
							S 10.47	10.22
2-$CH_3OC_6H_4$	H	$C_{25}H_{27}NO_{11}S_2$	189–190°	30	−150.0° (pyridine)	1750, 1230, 900	C 51.62	51.67
							H 4.68	4.90
							N 2.41	2.35
							S 11.03	11.16
2,6-$Cl_2C_6H_3$	H	$C_{24}H_{23}Cl_2NO_{10}S_2$	78–81°	65	−52.0° (pyridine)	1750, 1230, 900	C 46.56	46.43
							H 3.74	4.00
							N 2.26	1.99
							S 10.34	10.03
4-ClC_6H_4	H	$C_{24}H_{24}ClNO_{10}S_2$	226–228°	85	−170.0° (pyridine)	1740, 1225, 900	C 49.19	49.56
							H 4.13	4.23
							N 2.39	2.27
							S 10.94	11.20
2-ClC_6H_4	H	$C_{24}H_{24}ClNO_{10}S_2$	200–202°	61	−146.3° (pyridine)	1750, 1225, 908	C 49.19	49.24
							H 4.13	4.47
							N 2.39	2.42
							S 10.94	10.89
	H	$C_{22}H_{23}NO_{11}S_2$	189–193°	—	−200.0° (pyridine)	1750, 1225, 900	C 48.79	48.39
							H 4.28	4.62
							N 2.59	2.72
							S 11.84	12.03
	CH_3	$C_{23}H_{25}NO_{11}S_2$	118–122°	56	−173.5° (tetrahydrofuran)	1750, 1225, 910	C 49.72	49.30
							H 4.54	4.74
							N 2.52	2.54
							S 11.54	11.25
	H	$C_{22}H_{23}NO_{10}S_3$	217–220°	60	−175.5° (pyridine)	1750, 1240, 908	C 47.39	46.95
							H 4.16	4.46
							N 2.51	2.58
							S 17.25	16.93
	CH_3	$C_{23}H_{25}NO_{10}S_3$	187–190°	54	−78.0° (pyridine)	1750, 1225, 900	C 48.33	48.38
							H 4.41	4.70
							N 2.45	2.42
							S 16.83	16.31
	H	$C_{23}H_{25}NO_{10}S_3$	192–193°	91	−210.0° (pyridine)	1750, 1225, 900	C 48.34	48.50
							H 4.38	4.61
							N 2.45	2.39
							S 16.81	16.36
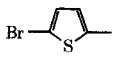	H	$C_{22}H_{22}BrNO_{10}S_3$	182–187°	94	−130.0° (pyridine)	1730, 1215, 900	C 41.51	41.62
							H 3.46	3.30
							N 2.21	2.24
							S 15.09	14.90
	H	$C_{23}H_{24}N_2O_{10}S_2$	177–181°	78	−180.0° (pyridine)	1748, 1230, 903	C 50.00	50.06
							H 4.35	4.46
							N 5.01	5.14
							S 11.59	11.47
	CH_3	$C_{24}H_{26}N_2O_{10}S_2$	184–187°	72	−143.0° (tetrahydrofuran)	1750, 1225, 902	C 50.87	50.50
							H 4.62	4.72
							N 4.95	5.23
							S 11.32	11.52
	H	$C_{23}H_{24}N_2O_{10}S_2$	191–193°	54	−195.0° (tetrahydrofuran)	1748, 1223, 902	C 50.00	49.61
							H 4.35	4.42
							N 5.01	5.24
							S 11.59	11.35

Table I—(*Continued*)

R_1	R_2	Formula	Melting Point	Yield, %	$[\alpha]_D^{20}$ (Solvent)	IR (KBr), cm^{-1}	Analysis, % Calc.	Found
	CH_3	$C_{24}H_{26}N_2O_{10}S_2$	183–187°	37	−84.0° (dimethylformamide)	1750, 1235, 900	C 50.87 H 4.62 N 4.95 S 11.32	51.05 4.89 5.09 10.97
	H	$C_{23}H_{24}N_2O_{10}S_2$	228–231°	19	−161.8° (pyridine)	1750, 1225, 900	C 50.00 H 4.35 N 5.01 S 11.59	49.67 4.11 5.00 11.22
	CH_3	$C_{24}H_{26}N_2O_{10}S_2$	227–229°	41	−170.0° (pyridine)	1750, 1225, 910	C 50.87 H 4.62 N 4.95 S 11.32	50.55 4.67 4.97 11.08
	H	$C_{28}H_{27}NO_{10}S_2$	215–216°	30	−182.0° (tetrahydrofuran)	1750, 1210, 890	C 55.91 H 4.49 N 2.33 S 10.65	55.92 4.64 2.45 10.38
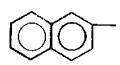	H	$C_{28}H_{27}NO_{10}S_2$	229–230°	66	−60.8° (pyridine)	1750, 1230, 895	C 55.91 H 4.49 N 2.33 S 10.65	55.83 4.51 2.42 10.44
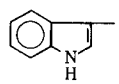	H	$C_{26}H_{26}N_2O_{10}S_2$	251–253°	96	−80.0° (pyridine)	1750, 1230, 902	C 52.88 H 4.41 N 4.74 S 10.85	52.65 4.50 4.56 10.80

[a] Lit. (16) mp 193–194°.

(C=O), 1225 (C=S), and 900 (β-form) cm^{-1}; $[\alpha]_D^{20}$ −104.0° (c = 3.1, tetrahydrofuran).

Hydrolysis of *N*-(2,3,4,6-Tetra-*O*-acetyl-β-D-glucopyranosyl)-5 - arylalkylidenerhodanines—N-β-D-*Glucopyranosyl-5-benzylidenerhodanine*—*N*-(2,3,4,6 - Tetra-*O*-acetyl-β-D-glucopyranosyl)-5-benzylidenerhodanine (2.56 g, 0.0046 mole) was suspended in 700 ml of methanol, and 10.5 ml of 1.9 *M* HCl was added. The reaction mixture was stirred in a stoppered flask at room temperature for 4 days, and the resulting solution was filtered. The filtrate was evaporated under reduced pressure in a rotary evaporator at a temperature below 30°, and a yellow-brown semisolid was obtained and then dissolved in ethanol. The ethanolic solution was added to water until cloudiness first appeared, and the solution was refrigerated overnight. Yellow crystals were filtered and dried in a vacuum oven, yielding 1.7 g (96%), mp 104–110°; IR (KBr): ν 3500–3300 (OH), 1715 (C=O), 1230 (C=S), and 890 (β-form) cm^{-1}; $[\alpha]_D^{20}$ −78.0° (c = 0.8, pyridine).

N-β-D - *Glucopyranosylthiourea*—*N*-(2,3,4,6-Tetra-*O*-acetyl-β-D-glucopyranosyl)-5-benzylidenerhodanine (2.0 g, 0.0036 mole) was added to a solution of methanol saturated with ammonia at 0° in a pressure bottle. The bottle was stoppered, and the mixture was shaken at room temperature for 20 hr. Then the mixture was filtered, and the filtrate was evaporated under reduced pressure in a rotary evaporator at a temperature below 30°. The resulting white powder was washed with anhydrous acetone and recrystallized from methanol, yielding 0.6 g (70%) of hygroscopic white crystals, mp 211–212° [lit. (16) mp 210°]; IR (KBr): ν 3500 (OH), 3400 (NH_2), 3220 (NH), 1650 (NH_2), 1030 (C=S), and 910 (β-form) cm^{-1}; $[\alpha]_D^{20}$ +33.5° (c = 3.0, H_2O).

Anal.—Calc. for $C_7H_{14}N_2O_5S$: C, 35.29; H, 5.88; N, 11.78; S, 13.44. Found: C, 35.60; H, 6.01; N, 11.58; S, 13.26.

An identical product was obtained when *N*-(2,3,4,6-tetra-*O*-acetyl-β-D-glucopyranosyl)-5-(3,4-dimethoxybenzylidene)rhodanine was subjected to the same conditions.

Antibacterial Activity—Tests for antibacterial activity were first done by the agar plate method, using 20–30 mg of each compound and measuring the zones of inhibition. The organisms used included *Staphylococcus aureus* (ATCC 6538), *Escherichia coli* (ATCC 15221), *Aspergillus niger* (ATCC 16404), and *Candida albicans* (ATCC 10231). Plates inoculated with *S. aureus* and *E. coli* were incubated at 37° for 24–48 hr, and those inoculated with *A. niger* and *C. albicans* were incubated at 25° for 48–72 hr.

Compounds showing activity by the agar plate method were screened by the *in vitro* serial tube dilution procedure. Trypticase soy broth was used for growing *S. aureus* and *E. coli*, and the preparation was sterilized for 15 min at 172 × 10^4 dynes/cm^2 at 120°. Stock solutions (0.1 *M*) of compounds to be tested were made in acetone and sterilized by membrane filtration.

Five colonies of each organism were inoculated into 5.0 ml of the broth preparation and incubated at 37° for 18–24 hr. Serial dilutions of the test compounds were made from the 0.1 *M* stock solutions, and to each dilution was added 0.1 ml of the broth culture. Tubes were incubated for 24–48 hr at 37° and were then examined for growth.

Antiviral Activity—The rate of viral and host cell RNA synthesis was measured in the presence of various drug concentrations and compared to normal viral and host cell RNA synthesis. Measurements were made using vesicular stomatitis virus growth in Chinese hamster ovary cell suspension culture. ^{14}C-Uridine was used as a marker to measure RNA synthesis. Viral RNA synthesis was measured by adding 5 μg/ml of dactinomycin to inhibit host cell RNA synthesis.

RESULTS AND DISCUSSION

Chemistry—The 5-aralkylidenerhodanines were readily obtained from reaction of rhodanine with aromatic aldehydes and ketones, using either acetic acid–sodium acetate or ammonium hydroxide–ammonium chloride as the reaction medium. Essentially all of these compounds are known, and they are not tabulated here. The *N*-tetra-*O*-acetyl-D-glucosyl derivatives (Table I) were prepared essentially by the procedure of Michael (17), which utilized acetobromo-α-D-glucose in acetone with sodium hydroxide. Yields of product varied from 30 to 96%.

Proof that the *N*-glycoside was obtained was given by hydrolysis to *N*-glucosylthiourea (II) (Scheme I), previously synthesized by Fischer (16), from the 5-benzylidene- and 5-(3,4-dimethoxybenzylidene)rhodanine tetraacetyl-D-glucosyl derivatives using ammonia in methanol. The IR spectra of the products also indicated *N*-glycosylation. The doublet characteristic of NH stretching between 3100 and 3400 cm^{-1} was changed to a weak singlet after glycosylation, and no change was observed in the thionyl and carbonyl absorptions at 1200–1250 and 1700–1760 cm^{-1}, respectively. Furthermore, the NMR spectra for rhodanine and 5-substituted derivatives showed a broad peak at 11.7 ppm for one proton, which was exchangeable with deuterium, characteristic of an imino proton. This peak disappeared after glycosylation, providing further evidence of *N*-glycosylation.

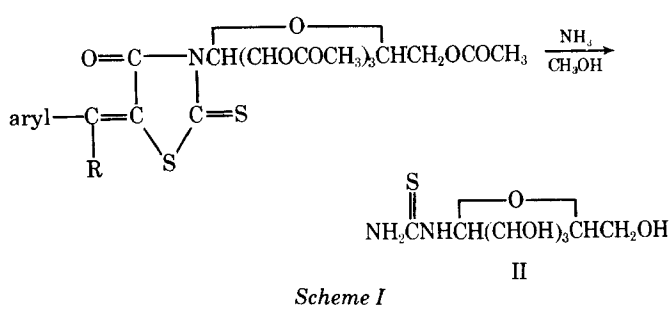

Scheme I

Table II—*N*-β-D-Glucopyranosyl-5-arylalkylidenerhodanines

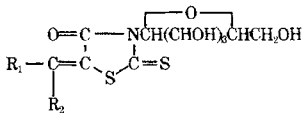

R_1	R_2	Formula	Melting Point	Yield, %	$[\alpha]_D^{20}$ (Solvent)	IR (KBr), cm^{-1}	Analysis, % Calc.	Found
C_6H_5	H	$C_{16}H_{17}NO_6S_2$	104–110°	96	−78.0° (pyridine)	3400 (br), 1715, 1230, 890	C 50.11 H 4.47 N 3.66 S 16.72	49.80 4.62 3.49 16.97
4-$NO_2C_6H_4$	H	$C_{16}H_{16}N_2O_8S_2$	130–135°	93	−131.8° (tetrahydrofuran)	3400 (br), 1720, 1230, 900	C 44.85 H 3.76 N 6.54	44.80 4.03 6.35
	H	$C_{14}H_{15}NO_7S_2 \cdot 1/2H_2O$	150–155°	72	−74.4° (tetrahydrofuran)	3400 (br), 1710, 1225, 885	C 43.99 H 4.19 N 3.66	44.12 4.06 3.67
	CH_3	$C_{15}H_{17}NO_7S_2 \cdot H_2O$	135–140°	95	−104.0° (methanol)	3400 (br), 1700, 1225, 882	C 44.44 H 4.69 N 3.45	44.48 4.58 3.60
	H	$C_{14}H_{15}NO_6S_3 \cdot H_2O$	130–135°	74	−108.8° (methanol)	3400 (br), 1710, 1225, 910	C 41.28 H 4.17 N 3.44	41.10 4.15 3.35
	H	$C_{15}H_{16}N_2O_6S_2$	130–135°	78	−104.0° (pyridine)	3400 (br), 1720, 1225, 900	C 46.90 H 4.17 N 7.29	47.12 3.74 6.93

Whether the *N*-glycosylated derivatives were the α- or β-forms was determined by the IR spectra. Glycoside formation, using acetobromo-α-D-glucose, invariably proceeds with Walden inversion at C-1 (18), yielding the β-glycoside from the α-halide. In addition, α-D-glucopyranose structures show absorption between 833 and 855 cm^{-1}, whereas the β-structures absorb in the 876–905-cm^{-1} region (19). All of the *N*-tetraacetylglucosylrhodanines were found to be β-glucosides by their absorption between 882 and 910 cm^{-1}.

Deacetylation of the tetraacetylglucosyl derivatives was complicated by the sensitivity of the rhodanine ring to alkaline hydrolysis. A mild hydrolytic method, ammonia in methanol, resulted in cleavage to give *N*-glucosylthiourea. Direct condensation between the 5-substituted rhodanines and glucose also failed. A successful method for deacetylation was the use of 2 *N* HCl in methanol. Yields of deacetylated glucosides were generally better than 90% by this method. The compounds prepared are listed in Table II.

Biology—A cell culture test for antiviral activity was carried out on *N*-glucosyl-5-*p*-nitrobenzylidenerhodanine[2]. When using vesicular stomatitis virus growth in Chinese hamster ovary cell suspension culture, rhodanine itself (150 μg/ml) had no effect on either Chinese hamster ovary cells or vesicular stomatitis viral RNA synthesis. This result supports the previous observation of Eggers *et al.* (1). *N*-Glucosyl-5-*p*-nitrobenzylidenerhodanine, however, at the same concentration, inhibited RNA synthesis of both host cells and virus to a similar extent. At concentrations of 50 and 100 μg/ml, the rhodanine derivative inhibited 10% of cellular RNA synthesis but 40% of viral RNA synthesis. This difference in inhibition of RNA synthesis is sufficient to state that the rhodanine derivative has definite antiviral activity.

Antibacterial activities were observed by the agar plate screening method using *S. aureus*, *E. coli*, *A. niger*, and *C. albicans*. These organisms represent a Gram-positive and a Gram-negative bacterium, a mold, and a yeast, respectively. None of the rhodanines showed inhibitory activity against *A. niger* and *C. albicans*. Compounds showing inhibitory activity against the bacteria were then measured by the serial tube dilution method.

Only rhodanine and *o*-nitrobenzylidenerhodanine showed activity against *E. coli*. Many of the 5-substituted rhodanine derivatives were active against *S. aureus*, but in general the tetraacetylglucosyl derivatives were not. Exceptions were found with the tetraacetyl derivatives of 5-(5-bromothienylmethylene)rhodanine and 5-(1-naphthylidene)rhodanine. With the benzylidene derivatives, electron-withdrawing substituents increased activity, whereas electron-releasing substituents decreased activity. Methyl substitution at the methylene side chain either decreased or removed inhibitory activity.

[2] By Dr. A. Huang and Dr. P. Sinarachatanant, Department of Microbiology and Molecular Genetics, Harvard Medical School.

Results of this study confirm previous findings that either 3- or 5-substituted rhodanines are active antimicrobials and that the 3,5-disubstituted rhodanines are not (10), with the exception of *N*-phenyl-5-(5-nitrofurylidene)rhodanine (20). The presence of a nitro group seems to be essential for high activity against bacteria, protozoa, and schistosomes but has little effect toward other helminths than schistosomes and fungi (21). Antimicrobial testing results by serial tube dilution are listed in Table III.

Table III—Antibacterial Activities

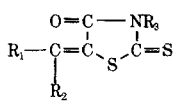

R_1	R_2	R_3	Minimum Inhibitory Concentration, 1/*M* *S. aureus*	*E. coli*
C_6H_5	H	H	<1,000	—
4-$NO_2C_6H_4$	H	H	<10,000	—
2-$NO_2C_6H_4$	H	H	<100,000	<1000
2,6-$Cl_2C_6H_3$	H	H	<10,000	—
2-ClC_6H_4	H	H	<1,000	—
	H	H	<1,000	—
	CH_3	H	<100	—
	H	H	<10,000	—
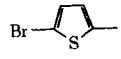	H	$C_6H_7(OCOCH_3)_4$	<1,000	—
	H	H	<1,000	—
	H	$C_6H_7(OCOCH_3)_4$	<1,000	—
C_6H_5	H	$C_6H_{11}O_5$	<1,000	—
Rhodanine	—	—	<1,000	<1000

Effects on blood sugar levels in Charles River rats were observed for several of the rhodanine derivatives[3]. 5-(2-Pyrrolylmethylene)rhodanine (22) (150 mg/kg) increased blood glucose significantly at 1, 2, and 4 hr after oral dosing, and 5-(2-thienylmethylene)rhodanine (150 mg/kg) increased blood glucose at 4 hr after oral dosing. No effect on blood glucose was observed for 5-(4-pyridylmethylene)rhodanine (150 mg/kg) or for 5-(2-pyridylethylidene)rhodanine (150 mg/kg). Increases in blood glucose at 4 hr after oral administration were also found for 2,2′-dithiobis[3-(2-furyl)acrylic acid] (22) (100 mg/kg) and 2,2′-dithiobis-(3-phenylacrylic acid) (23) (75 mg/kg). Significant effects on blood glucose levels may be caused either by suitable 5-substituted rhodanines or their hydrolysis products, the dithioacrylic acids.

REFERENCES

(1) H. J. Eggers, M. A. Koch, A. Furst, G. D. Daves, Jr., J. J. Wilczynski, and K. Folkers, *Science*, **167**, 294 (1970).

(2) T. H. Haskell, F. E. Peterson, D. Watson, N. R. Plessas, and T. Culbertson, *J. Med. Chem.*, **13**, 697 (1970).

(3) A. P. Grollman and S. B. Horwitz, in "Drug Design," vol. II, E. J. Ariens, Ed., Academic, New York, N.Y., 1971, p. 261.

(4) F. G. Moers, J. W. M. Goossens, and J. P. M. Langhout, *J. Inorg. Nucl. Chem.*, **35**, 855 (1973).

(5) R. W. Brockman, R. W. Sidwell, G. Arnett, and S. Shaddix, *Proc. Soc. Exp. Biol. Med.*, **133**, 609 (1970).

(6) W. O. Foye and E. G. Feldmann, *J. Am. Pharm. Assoc., Sci. Ed.*, **45**, 30 (1956). W. O. Foye, W. E. Lange, and E. G. Feldmann, *ibid.*, **47**, 831 (1958).

(7) T. Zsolnai, *Arzneim.-Forsch.*, **19**, 558 (1969).

(8) H. Taniyama, S. Takemura, B. Yasui, and H. Uchida, *J. Pharm. Soc. Jpn.*, **74**, 113 (1954).

(9) L. M. Werbel, N. Headen, and E. F. Elslager, *J. Med. Chem.*, **11**, 364 (1968).

(10) F. C. Brown, C. K. Bradsher, S. M. Bond, and R. J. Granthan, *Ind. Eng. Chem.*, **46**, 1508 (1954). G. Matolcsy, B. Bordas, and M. Hamran, *Acta Phytopathol.*, **4**, 345 (1969).

(11) T. Takematsu, M. Furushima, Y. Hasegawa, M. Morioka, and T. Tsuchiyama, Japanese pat. 7,243,812 (1972). M. Mousseron, S. African pat. 6,803,535 (1969).

(12) A. Mackie and G. M. Stewart, *Arch. Int. Pharmacodyn. Ther.*, **102**, 476 (1955).

(13) W. C. McGuire, C. O. O'Neill, and G. Brody, *J. Parasitol.*, **52**, 528 (1966).

(14) R. Bognar and W. Wieniawski, *Acta Chim. Acad. Sci. Hung.*, **33**, 415 (1962).

(15) F. C. Brown, C. K. Bradsher, S. G. McCallum, and M. Potter, *J. Org. Chem.*, **15**, 174 (1950).

(16) E. Fischer, *Chem. Ber.*, **47**, 1377 (1914).

(17) A. Michael, *Am. Chem. J.*, **6**, 336 (1885).

(18) J. Conchie, G. A. Levvy, and C. A. Martin, *Adv. Carbohydr. Chem.*, **12**, 157 (1957). J. Stanek, M. Cerny, J. Kocourek, and J. Pacak, "The Monosaccharides," Academic, New York, N.Y., 1963.

(19) H. Spedding, in "Methods in Carbohydrate Chemistry," vol. I, R. L. Whistler and M. L. Wolfrom, Eds., Academic, New York, N.Y., 1962, p. 548.

(20) S. K. Mallick and A. R. Martin, *J. Med. Chem.*, **14**, 528 (1971).

(21) E. Grunberg and E. H. Titsworth, *Ann. Rev. Microbiol.*, **27**, 317 (1973).

(22) P. Tovivich, M.S. thesis, Massachusetts College of Pharmacy, Boston, Mass., 1972.

(23) E. Campaigne and R. E. Cline, *J. Org. Chem.*, **21**, 32 (1956).

ACKNOWLEDGMENTS AND ADDRESSES

Received December 20, 1976, from the *Samuel M. Best Research Laboratory, Massachusetts College of Pharmacy, Boston, MA 02115.*

Accepted for publication February 10, 1977.

Abstracted from a thesis submitted by P. Tovivich to the Massachusetts College of Pharmacy in partial fulfillment of the Doctor of Philosophy degree requirements.

The authors are indebted to Dr. J. W. Wilson of Smith Kline and French Laboratories, Philadelphia, Pa., for the results of the blood glucose determinations, and to Dr. A. Huang and Dr. P. Sinarachatanant of Harvard Medical School, Boston, Mass., for the results of the antiviral testing.

* Present address: Faculty of Science, Chulalongkorn University, Bangkok 5, Thailand.

[x] To whom inquiries should be directed.

[3] Results were made available through the courtesy of Dr. J. W. Wilson, Smith Kline & French Laboratories.

Effects of Polyelectrolytes on Drug Transport II: Permeation

K. F. FARNG * and K. G. NELSON [x]

Abstract □ The permeation rate of salicylate across a dialysis membrane was studied in the presence of various types of carboxymethylcellulose. The presence of the polymer in the salicylate solution increased the permeation rate of salicylate. The data were analyzed with a diffusional model in which the viscosity and charge effects were evaluated separately.

Keyphrases □ Salicylate—permeation rate across a dialysis membrane in presence of various types of carboxymethylcellulose □ Permeation rate—salicylate across a dialysis membrane in presence of various types of carboxymethylcellulose □ Drug transport—permeation rate of salicylate across a dialysis membrane in presence of various types of carboxymethylcellulose □ Carboxymethylcellulose, various types—effect on permeation rate of salicylate across a dialysis membrane □ Polyelectrolytes—various types of carboxymethylcellulose, effect on permeation rate of salicylate across a dialysis membrane

Previously (1), it was observed that the presence of the polyelectrolyte carboxymethylcellulose decreased the aqueous diffusivity of a small solute (salicylate) only moderately and that salicylate, which was present as a co-ion of the polymer, was transported out of the polymer solution and into an aqueous environment more rapidly than if the polymer were not present. This report describes further studies on this enhanced transport phenomenon involving an *in vitro* permeation apparatus.

EXPERIMENTAL

Permeation Cell—A permeation cell was constructed from plastic[1] and consisted of two symmetrical parts clamped together with a dialysis membrane at the plane of symmetry. The diffusion cell was described previously (2). Each compartment holds about 125 ml of liquid, and the area of the membrane available for permeation is 16.8 cm^2. The cell was immersed in a water bath for temperature control, and each compartment was stirred with a stirring rod tipped with flattened rubber tubing and rotated at 2000 rpm.

[1] Lucite, Rohm & Haas, Philadelphia, Pa.

Effects on blood sugar levels in Charles River rats were observed for several of the rhodanine derivatives[3]. 5-(2-Pyrrolylmethylene)rhodanine (22) (150 mg/kg) increased blood glucose significantly at 1, 2, and 4 hr after oral dosing, and 5-(2-thienylmethylene)rhodanine (150 mg/kg) increased blood glucose at 4 hr after oral dosing. No effect on blood glucose was observed for 5-(4-pyridylmethylene)rhodanine (150 mg/kg) or for 5-(2-pyridylethylidene)rhodanine (150 mg/kg). Increases in blood glucose at 4 hr after oral administration were also found for 2,2′-dithiobis[3-(2-furyl)acrylic acid] (22) (100 mg/kg) and 2,2′-dithiobis-(3-phenylacrylic acid) (23) (75 mg/kg). Significant effects on blood glucose levels may be caused either by suitable 5-substituted rhodanines or their hydrolysis products, the dithioacrylic acids.

REFERENCES

(1) H. J. Eggers, M. A. Koch, A. Furst, G. D. Daves, Jr., J. J. Wilczynski, and K. Folkers, *Science*, **167**, 294 (1970).

(2) T. H. Haskell, F. E. Peterson, D. Watson, N. R. Plessas, and T. Culbertson, *J. Med. Chem.*, **13**, 697 (1970).

(3) A. P. Grollman and S. B. Horwitz, in "Drug Design," vol. II, E. J. Ariens, Ed., Academic, New York, N.Y., 1971, p. 261.

(4) F. G. Moers, J. W. M. Goossens, and J. P. M. Langhout, *J. Inorg. Nucl. Chem.*, **35**, 855 (1973).

(5) R. W. Brockman, R. W. Sidwell, G. Arnett, and S. Shaddix, *Proc. Soc. Exp. Biol. Med.*, **133**, 609 (1970).

(6) W. O. Foye and E. G. Feldmann, *J. Am. Pharm. Assoc., Sci. Ed.*, **45**, 30 (1956). W. O. Foye, W. E. Lange, and E. G. Feldmann, *ibid.*, **47**, 831 (1958).

(7) T. Zsolnai, *Arzneim.-Forsch.*, **19**, 558 (1969).

(8) H. Taniyama, S. Takemura, B. Yasui, and H. Uchida, *J. Pharm. Soc. Jpn.*, **74**, 113 (1954).

(9) L. M. Werbel, N. Headen, and E. F. Elslager, *J. Med. Chem.*, **11**, 364 (1968).

(10) F. C. Brown, C. K. Bradsher, S. M. Bond, and R. J. Granthan, *Ind. Eng. Chem.*, **46**, 1508 (1954). G. Matolcsy, B. Bordas, and M. Hamran, *Acta Phytopathol.*, **4**, 345 (1969).

(11) T. Takematsu, M. Furushima, Y. Hasegawa, M. Morioka, and T. Tsuchiyama, Japanese pat. 7,243,812 (1972). M. Mousseron, S. African pat. 6,803,535 (1969).

(12) A. Mackie and G. M. Stewart, *Arch. Int. Pharmacodyn. Ther.*, **102**, 476 (1955).

(13) W. C. McGuire, C. O. O'Neill, and G. Brody, *J. Parasitol.*, **52**, 528 (1966).

(14) R. Bognar and W. Wieniawski, *Acta Chim. Acad. Sci. Hung.*, **33**, 415 (1962).

(15) F. C. Brown, C. K. Bradsher, S. G. McCallum, and M. Potter, *J. Org. Chem.*, **15**, 174 (1950).

(16) E. Fischer, *Chem. Ber.*, **47**, 1377 (1914).

(17) A. Michael, *Am. Chem. J.*, **6**, 336 (1885).

(18) J. Conchie, G. A. Levvy, and C. A. Martin, *Adv. Carbohydr. Chem.*, **12**, 157 (1957). J. Stanek, M. Cerny, J. Kocourek, and J. Pacak, "The Monosaccharides," Academic, New York, N.Y., 1963.

(19) H. Spedding, in "Methods in Carbohydrate Chemistry," vol. I, R. L. Whistler and M. L. Wolfrom, Eds., Academic, New York, N.Y., 1962, p. 548.

(20) S. K. Mallick and A. R. Martin, *J. Med. Chem.*, **14**, 528 (1971).

(21) E. Grunberg and E. H. Titsworth, *Ann. Rev. Microbiol.*, **27**, 317 (1973).

(22) P. Tovivich, M.S. thesis, Massachusetts College of Pharmacy, Boston, Mass., 1972.

(23) E. Campaigne and R. E. Cline, *J. Org. Chem.*, **21**, 32 (1956).

ACKNOWLEDGMENTS AND ADDRESSES

Received December 20, 1976, from the *Samuel M. Best Research Laboratory, Massachusetts College of Pharmacy, Boston, MA 02115.*

Accepted for publication February 10, 1977.

Abstracted from a thesis submitted by P. Tovivich to the Massachusetts College of Pharmacy in partial fulfillment of the Doctor of Philosophy degree requirements.

The authors are indebted to Dr. J. W. Wilson of Smith Kline and French Laboratories, Philadelphia, Pa., for the results of the blood glucose determinations, and to Dr. A. Huang and Dr. P. Sinarachatanant of Harvard Medical School, Boston, Mass., for the results of the antiviral testing.

* Present address: Faculty of Science, Chulalongkorn University, Bangkok 5, Thailand.

[x] To whom inquiries should be directed.

[3] Results were made available through the courtesy of Dr. J. W. Wilson, Smith Kline & French Laboratories.

Effects of Polyelectrolytes on Drug Transport II: Permeation

K. F. FARNG * and K. G. NELSON [x]

Abstract □ The permeation rate of salicylate across a dialysis membrane was studied in the presence of various types of carboxymethylcellulose. The presence of the polymer in the salicylate solution increased the permeation rate of salicylate. The data were analyzed with a diffusional model in which the viscosity and charge effects were evaluated separately.

Keyphrases □ Salicylate—permeation rate across a dialysis membrane in presence of various types of carboxymethylcellulose □ Permeation rate—salicylate across a dialysis membrane in presence of various types of carboxymethylcellulose □ Drug transport—permeation rate of salicylate across a dialysis membrane in presence of various types of carboxymethylcellulose □ Carboxymethylcellulose, various types—effect on permeation rate of salicylate across a dialysis membrane □ Polyelectrolytes—various types of carboxymethylcellulose, effect on permeation rate of salicylate across a dialysis membrane

Previously (1), it was observed that the presence of the polyelectrolyte carboxymethylcellulose decreased the aqueous diffusivity of a small solute (salicylate) only moderately and that salicylate, which was present as a co-ion of the polymer, was transported out of the polymer solution and into an aqueous environment more rapidly than if the polymer were not present. This report describes further studies on this enhanced transport phenomenon involving an *in vitro* permeation apparatus.

EXPERIMENTAL

Permeation Cell—A permeation cell was constructed from plastic[1] and consisted of two symmetrical parts clamped together with a dialysis membrane at the plane of symmetry. The diffusion cell was described previously (2). Each compartment holds about 125 ml of liquid, and the area of the membrane available for permeation is 16.8 cm^2. The cell was immersed in a water bath for temperature control, and each compartment was stirred with a stirring rod tipped with flattened rubber tubing and rotated at 2000 rpm.

[1] Lucite, Rohm & Haas, Philadelphia, Pa.

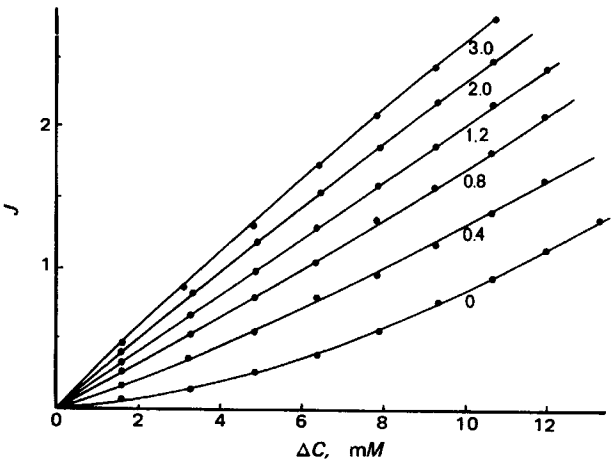

Figure 1—*Permeation flux (nanomoles per square centimeter per second) of salicylate* versus *salicylate concentration difference. Numbers adjacent to curves represent percent (w/v) carboxymethylcellulose sodium (V).*

The cellulose membrane, cut from dialysis tubing[2], was soaked at least 2 days in water containing a preservative (1% sodium azide) under refrigeration. It was then washed with distilled water and kept wet during the assembling of the apparatus. The thickness of the wet membrane was 46.6 μm as measured with a micrometer. With this thickness, the lag time to reach steady-state flux was short and could not be detected.

The water content of the wet membrane was determined by the weight difference between a membrane dried with filter paper and a membrane dried under vacuum. The weight fraction of water in a wet membrane was 0.568, which corresponds to a volume fraction of water of 0.667. The figures agree with reported values (3, 4).

Materials—Various types of pharmaceutical grade carboxymethylcellulose sodium[3] were used as obtained without further purification. Two types with a 1.2 degree of substitution were used; one[4] was a medium high viscosity grade (I) and the other[5] was a medium grade (II). Three types had a degree of substitution of 0.7; the first[6] was a medium high viscosity grade (III), the second[7] was a medium grade (IV), and the third[8] was a low grade (V). Hydroxyethylcellulose[9] (VI) was used as the nonionic polymer. The physical properties of these polymers have been reported (1) or are available from the manufacturer (5). Reagent grade sodium salicylate[10] was used as supplied.

Procedures—The permeation cell and the solutions were equilibrated with the water bath (37°) prior to an experiment. To start an experiment, 125 ml of the solution containing sodium salicylate (1.6 m*M*) and the polymer was transferred to one side of the cell (Compartment 1). In most cases, the other side (Compartment 2) was filled with 125 ml of distilled water. The appearance of salicylate in Compartment 2 was monitored by a flow system consisting of a peristaltic pump[11], polyethylene tubing, and a flowcell. The latter had a 1-mm light path and was mounted in a recording spectrophotometer[12] (202 nm). Data obtained in this manner indicated a linear relationship between absorbance and time, and such experiments were carried out for about 3–7 min.

After this initial phase of the experiment, 4 ml of solution was removed from Compartment 1 and replaced with 4 ml of 50 m*M* sodium salicylate solution containing the same concentration of polymer as the original solution. Again, the absorbance increase with time was measured. By continuing in this manner, the concentration difference of salicylate across the membrane could be increased stepwise from 1.6 to 12 m*M* without changing the solutions. The salicylate concentration in Compartment 2 increased, of course, but it never achieved a concentration of over 0.2 m*M*.

[2] Visking dialysis membrane, Union Carbide Corp., Chicago, Ill.
[3] Cellulose Gum, Hercules, Inc., Wilmington, Del.
[4] Type 12M31P.
[5] Type 12M8P.
[6] Type 7M27SF.
[7] Type 7MXF.
[8] Type 7LXF.
[9] Type KR.
[10] Mallinckrodt Chemical Works, St. Louis, Mo.
[11] Proportioning pump model I, Technicon Instrument Co.
[12] Cary 15, Cary Instruments, Monrovia, Calif.

Table I—Permeability and Apparent Partition Coefficient for Transport of Salicylate across Cellophane Membrane from Polymer Solutions to Water (37°)

Polymer	Percent (w/v)	$P \pm SE$ × 10^4, cm/sec	K
I	0.4	1.89 ± 0.02	1.23
	0.8	1.98 ± 0.03	1.49
	1.2	2.06 ± 0.04	1.89
	1.6	2.18 ± 0.03	2.63
	2.0	2.06 ± 0.01	2.98
II	0.2	1.76 ± 0.03	1.03
	0.5	1.86 ± 0.03	1.16
	1.0	2.07 ± 0.03	1.52
	1.5	2.19 ± 0.02	1.98
III	0.4	1.83 ± 0.02	1.18
	0.8	2.03 ± 0.01	1.55
	1.2	2.22 ± 0.02	2.18
	1.6	2.13 ± 0.03	2.50
	2.0	1.96 ± 0.13	2.59
IV	0.3	1.72 ± 0.03	1.02
	0.6	1.91 ± 0.02	1.23
	1.0	1.90 ± 0.01	1.35
	1.5	2.14 ± 0.02	1.90
	2.0	2.34 ± 0.04	2.84
V	0.4	1.68 ± 0.05	0.98
	0.8	1.81 ± 0.02	1.12
	1.2	2.07 ± 0.01	1.39
	2.0	2.32 ± 0.02	1.83
	3.0	2.59 ± 0.03	2.62
VI	0.42	1.65 ± 0.02	—[a]
	0.84	1.54 ± 0.04	—
	1.26	1.30 ± 0.02	—
	1.68	1.25 ± 0.05	—

[a] With K assumed to be unity.

RESULTS AND DISCUSSION

Permeability—The absorbance–time charts obtained as described were read by a digitizer, and the data were transferred directly into a calculator[13]. Because the absorbance is linearly proportional to the concentration in the range studied, the flux per unit area, J, could be readily calculated from the least-squares slopes of the absorbance–time data and the absorptivity together with the following relationship:

$$J = \frac{V_2}{A}\frac{dC_2}{dt} \qquad \text{(Eq. 1)}$$

where V_2 and C_2 are the volume and concentration, respectively, in Compartment 2; A is the area of the membrane; and t is the time. Since each flux determination required only about 5 min and the absorbance–time data were linear, the fluxes obtained may be considered to be initial transport rates. The mass balance and sequential additions also were programmed in the calculator so that flux–concentration difference lines were constructed by the calculator plotter directly. Typical data are shown in Fig. 1.

The experimental permeability, P, defined as:

$$P = \frac{J}{\Delta C} \qquad \text{(Eq. 2)}$$

where ΔC is the concentration difference across the membrane, was determined directly from the slope of the linear region on the flux–concentration difference plots. Although a more extensive analysis can be carried out utilizing the phenomenological equations of Kedem and Katchalsky (6, 7), the use of the more simple form of transport expression, Eq. 2, results in not more than 2% error, which is in the range of the experimental precision (2). The curvature at lower ionic concentrations due to either salicylate or polyelectrolyte is apparently the result of residual carboxyl groups on the membrane (4). The permeability of salicylate at various concentrations of polymer was obtained as the least-squares slope of the linear portion ($r > 0.99$) of the flux–concentration difference curves to exclude this residual charge effect. Permeabilities obtained in this manner along with the standard errors are given in Table I. The salicylate permeability without polymer was 1.77×10^{-4} cm/sec.

Salicylate permeability across the dialysis membrane was increased when carboxymethylcellulose sodium was in Compartment 1. Since any effect of the charged membrane was eliminated by using only the linear regions of the flux–concentration difference curves, the results were

[13] HP9100, Hewlett-Packard Co., Palo Alto, Calif.

Table II—Permeability of Salicylate under Various Polyelectrolyte Gradient Conditions

Compartment 1	Compartment 2	Polymer, % w/v	$P \pm SE \times 10^4$, cm/sec
I	Water	0.4	1.89 ± 0.02
I	I	0.4	1.70 ± 0.02
Water	I	0.4	1.52 ± 0.03
III	Water	0.4	1.83 ± 0.02
III	III	0.4	1.56 ± 0.02
Water	III	0.4	1.55 ± 0.03
IV	Water	0.3	1.72 ± 0.03
IV	IV	0.3	1.56 ± 0.05
IV	Water	0.6	1.91 ± 0.02
IV	IV	0.6	1.47 ± 0.02
IV	Water	1.0	1.90 ± 0.01
IV	IV	1.0	1.37 ± 0.08

probably due, at least in part, to the interaction of the charges between the co-ion and the polyelectrolyte (1). The polyelectrolyte concentration gradient at the interface of Compartment 1 and the membrane gives rise to an electrical field, which creates a driving force for the transport of ions in this vicinity. This effect would be in addition to the normal diffusional movement.

To explore this charge effect further, three types of experiments were performed: (*a*) polyelectrolyte was added to Compartment 2, *i.e.*, it is present in both compartments; (*b*) a nonionic polymer was used in place of the polyelectrolyte in Compartment 1; and (*c*) a swamping electrolyte was added to nullify the charge interaction.

The experimental results for the case where polyelectrolyte was present on both sides of the membrane are given in Table II. Salicylate permeability decreased when the concentration of carboxymethylcellulose in Compartment 2 was the same as in Compartment 1. Although this type of experiment effectively eliminates the net polyelectrolyte gradient that should reduce the permeation rate, it also may increase the diffusional resistance at the interface between the membrane and Compartment 2. The further reduction in permeability when salicylate diffuses against the polyelectrolyte gradient, *i.e.*, with water in Compartment 1, suggests that this latter effect is only of secondary importance.

When the nonionic polymer hydroxyethylcellulose was used in Compartment 1 in place of the polyelectrolyte, the permeability decreased with an increase in the polymer concentration. These results are shown as the last entries in Table I. Because there is no possibility for charge interaction under these conditions, the effect is due to the increase in diffusional resistance, which will be discussed later.

When a "swamping" electrolyte (0.2 *N* NaF) was added to the solutions in both compartments, the permeability decreased as the polyelectrolyte concentration increased (Fig. 2). This high ionic strength effectively eliminated the ionic interactions between salicylate and the polymer. At zero polymer concentration, the permeabilities do not coincide in Fig. 2 because of the widely differing ionic strength.

Permeation Model—Where the polyelectrolyte gradient exists, the enhancement of salicylate transport can be interpreted in terms of an apparent partition coefficient. Based on the stagnant or unstirred liquid diffusion layer hypothesis, the model shown in Fig. 3 was used for data analysis. The h is the thickness of the diffusion barrier; D is the diffusivity; subscripts 1, 2, and m distinguish the properties in the two compartments and the membrane; and K is the apparent partition coefficient of salicylate between the solution in Compartment 1 and the water in the membrane.

From the application of Fick's first law to the case of three barriers in series, as shown in the model of Fig. 3, with an apparent partition coefficient between the first and second layers only, the following relationship can be derived:

$$\frac{1}{P} = \frac{h_1}{D_1} + \left[\frac{h_m}{\psi_m D_m} + \frac{h_2}{D_2}\right]\frac{1}{K} \qquad \text{(Eq. 3)}$$

where ψ_m is the volume fraction of water in the membrane and D_m is an apparent diffusivity because it includes any tortuosity effects in the membrane.

To calculate K from experimental permeation data, the values for D_m and the h's must first be determined as follows. For salicylate transport with only water in the two compartments, D_m can be determined as a function of h_w (=h_1, h_2), where the subscript w indicates water only, from Eq. 3 with $K = 1$. Similarly, with hydroxyethylcellulose in Compartment 1, h_1 can be calculated as a function of h_w (=h_2). For this calculation, it is necessary to know D_1, the diffusion coefficient of salicylate in the

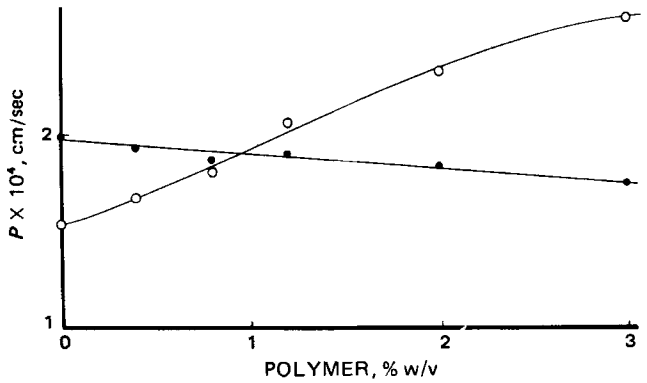

Figure 2—*Effect of strong electrolyte on permeability of salicylate (centimeters per second) as a function of carboxymethylcellulose sodium (V) concentration. Key: ●, 0.2 N NaF in both compartments; and ○, no sodium fluoride.*

polymer solution. Experimentally, it was found (1, 2) that it is described by the linear relationship:

$$D_1 = D_0(1 - 3.8V_p) \qquad \text{(Eq. 4)}$$

where D_0 is the diffusivity in pure water and V_p is the volume fraction of polymer. Assuming a value for h_w, one can calculate h_1 as the viscosity of solution in Compartment 1 changes. The simplest relationship between h_1 and viscosity η experimentally was:

$$\ln h_1 = a + b \ln \eta \qquad \text{(Eq. 5)}$$

where a and b are constants (Fig. 4). If the assumed value of h_w is correct, the value of h_1 in Eq. 5 extrapolated to $\eta = 1$ cps (viscosity of water) should be equal to the assumed h_w. A value of h_w near 82 μm satisfied this criterion. This value corresponds to $a = -4.800 \pm 0.086$ (*SE*) and $b = 0.189 \pm 0.016$, with a correlation coefficient of 0.993. From Eq. 3, a calculated value for D_m of 1.69×10^{-6} cm²/sec corresponds to this h_w.

To check the validity of this value for h_w, a similar computation was carried out for salicylate transport in the presence of a polyelectrolyte gradient but with a swamping electrolyte of 0.2 *M* NaF on both sides of the membrane to nullify the charge effect. A value of 81.9 μm was obtained. A plot of data according to Eq. 5 is given in Fig. 4.

Knowing D_m, h_w, η, the constants in Eq. 5, and D_1 from Eq. 4, one can calculate the apparent partition coefficient K from Eq. 3. The values of K calculated in this manner are included in Table I and shown in Fig. 5.

The presence of carboxymethylcellulose sodium in Compartment 1 facilitates the salicylate transport across the membrane by providing a driving force in addition to diffusion. This driving force arises from the electrical interaction between the charge of the co-ion and the electrical

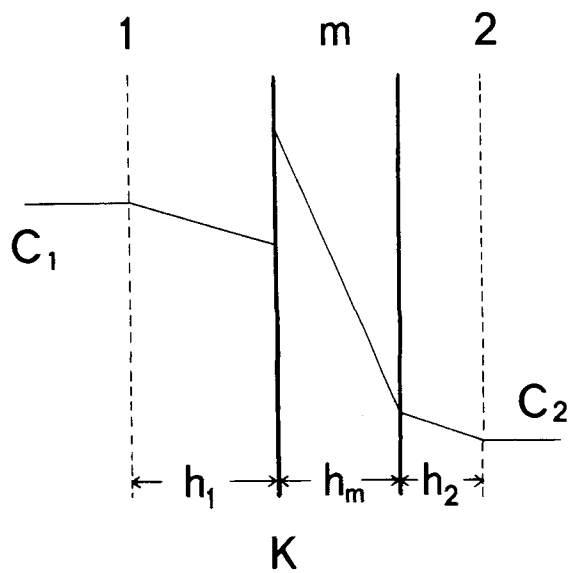

Figure 3—*Diffusion layer model.*

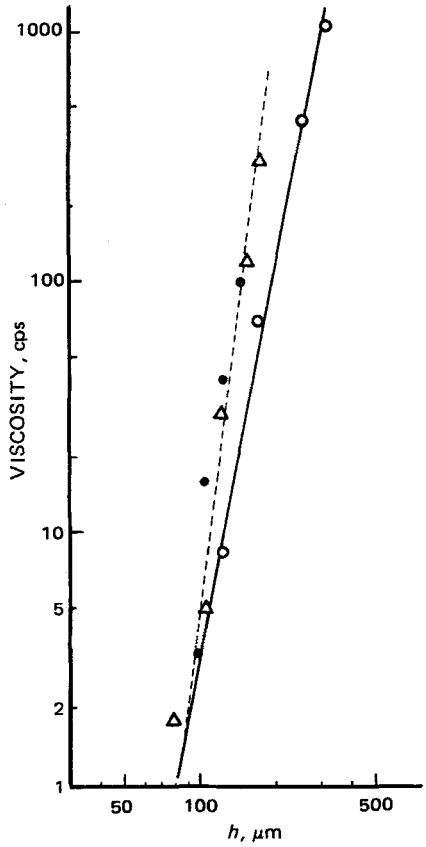

Figure 4—*Relationship between viscosity and hypothetical diffusion layer thickness. Key:* ○, *hydroxyethylcellulose (VI);* ●, *carboxymethylcellulose sodium (V); and* △, *carboxymethylcellulose sodium (IV).*

field of the polyelectrolyte gradient. While perhaps not reflecting the most fundamental parameter involved, *i.e.*, the force exerted on the co-ion, the use of Eq. 3 to evaluate the experimental data results in a measure of this co-ion enhancement in terms of an apparent partition coefficient of the permeant as a function of polyelectrolyte concentration.

When carboxymethylcellulose sodium was present in Compartment 1, the salicylate permeation rate was increased. If this increase arose from the co-ionic charge interaction, one would expect the chain length and the degree of substitution to affect this permeation enhancement. The calculated apparent partition coefficients are plotted in Fig. 5 as a function of polymer concentration for various polyelectrolytes. The longer

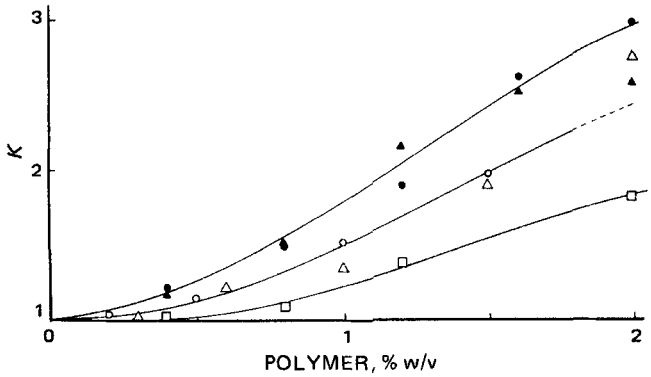

Figure 5—*Apparent partition coefficient* versus *concentration of carboxymethylcellulose sodium. Key (types):* ●, *I;* ○, *II;* ▲, *III;* △, *IV; and* □, *V.*

the chain length (higher viscosity grades), the greater is the charge effect between the co-ion and the polyelectrolyte, which may be summarized for the various grades as III > IV > V and I > II. Regarding the degree of substitution, however, no conclusion could be reached because the curves involving polymers having about the same chain length but different degrees of substitution on the carboxymethylcellulose are rather close to each other, *e.g.*, II and IV and I and III; therefore, only two lines are included on Fig. 5 for these data.

REFERENCES

(1) K. F. Farng and K. G. Nelson, *J. Pharm. Sci.*, **62,** 1435 (1973).

(2) K. F. Farng, Ph.D. thesis, University of Minnesota, Minneapolis, Minn., 1973.

(3) B. G. Ginburg and A. Katchalsky, *J. Gen. Physiol.*, **47,** 403 (1963).

(4) C. K. Colton, A. K. Smith, E. W. Merrill, and P. C. Farrell, *J. Biomed. Mater. Res.*, **5,** 459 (1971).

(5) "Cellulose Gum," Hercules, Inc., Wilmington, Del., 1969.

(6) O. Kedem and A. Katchalsky, *Biochim. Biophys. Acta*, **17,** 229 (1958).

(7) O. Kedem and A. Katchalsky, *J. Gen. Physiol.*, **45,** 143 (1961).

ACKNOWLEDGMENTS AND ADDRESSES

Received January 22, 1976, from the *College of Pharmacy, University of Minnesota, Minneapolis, MN 55455.*

Accepted for publication February 11, 1977.

* Present address: Johnson and Johnson, New Brunswick, N.J.

ˣ To whom inquiries should be directed.

Metoclopramide Metabolism and Determination by High-Pressure Liquid Chromatography

LINA TENG ˣ, ROBERT B. BRUCE, and L. KAY DUNNING

Abstract □ A high-pressure liquid chromatographic method suitable for determining plasma metoclopramide levels at normal (10–20 mg) doses is described. Eight metabolites as well as metoclopramide were isolated and identified in rat, dog, and human urine. The only common metabolite in these species is 2-[(4-amino-5-chloro-2-methoxybenzoyl)-amino]acetic acid. *N*-Deethylation is a major pathway for metoclopramide metabolism in the lower animals but not in humans. Metoclopramide is excreted mainly unchanged or as its conjugates by humans.

Keyphrases □ Metoclopramide—high-pressure liquid chromatographic analysis, various metabolites isolated and identified, rat, dog, and human urine □ Metabolites, various—of metoclopramide, isolated and identified, high-pressure liquid chromatographic analyses, rat, dog, and human urine □ High-pressure liquid chromatography—analyses, metoclopramide and various metabolites in rat, dog, and human urine □ Antiemetic agents—metoclopramide and various metabolites, high-pressure liquid chromatographic analyses in rat, dog, and human urine

Metoclopramide is an antiemetic and antispasmodic agent presently undergoing clinical testing in the United States. Results previously were reported on its metabolism in lower animals (1–3). Plasma levels were followed in lower animals (2) after relatively large doses by use of a colorimetric procedure and TLC–colorimetry. However, human plasma levels following normal (10–20 mg) doses have not been reported.

This study confirms some metabolites found in lower animals and reports additional metabolites not previously found in animals and humans following usual clinical doses. An analytical method suitable for determining plasma levels at clinical doses is also reported.

EXPERIMENTAL

Animals—Three female Sprague–Dawley rats[1], 200–225 g, were given metoclopramide solution orally at 100 mg/kg. Each rat received 20.16 mg (12.5 μCi). One male beagle dog[2], 10.8 kg, received metoclopramide solution orally at 20 mg/kg. The dog received 215.7 mg in 50.0 ml of water (21.3 μCi). The animals were housed in individual metal metabolism cages with free access to food and water.

Blood samples from the dog were collected in oxalate-containing tubes and analyzed immediately for radioactivity. The urinary and fecal excrements were collected at 24-hr intervals for 3 or 4 days. The urine samples were frozen until analysis, and the fecal samples were freeze dried.

Human Subjects—Two healthy male volunteers who had given informed written consent each received an oral capsule containing ^{14}C-metoclopramide (10.0 mg, 45.0 μCi). Blood, urine, and feces were collected at intervals and kept frozen until analysis.

Materials—Metoclopramide[3] was used as received. The radiochemical purity of carbonyl-labeled ^{14}C-metoclopramide[4] (4.5 μCi/mg) was higher than 98% as determined by TLC in three solvent systems.

Enzyme[5] was used as purchased. The resin[6] was washed with methanol, acetone, and water before use.

Identification of Metabolites—The metabolites were purified by preparative TLC, and the purified metabolites were identified by mass spectrometry. Comparisons of IR and NMR spectra were used when enough material was available. The mass spectra[7] were taken with a direct probe method. NMR spectrometry[8] was carried out in chloroform-*d* solution. IR[9] spectra were run as thin films or potassium bromide pellets.

TLC—Aliquots or extracts of urine were spotted on precoated silica gel GF plates[10] and developed with the following solvent systems: A, chloroform–methanol–concentrated ammonium hydroxide (70:30:1); B, 2 *N* ammonium hydroxide–ethanol–ethyl acetate (3:3:8); C, ethyl acetate–acetic acid–water–ethanol (25:12:8:5); D, chloroform–methanol–concentrated ammonium hydroxide (70:30:2); E, chloroform–methanol–concentrated ammonium hydroxide (90:10:1); and F, 1-butanol–ethyl acetate–acetic acid–water (1:1:1:1).

Radioassay—Aliquots of solution were put in glass liquid scintillation counting vials and counted in a liquid scintillation spectrometer[11] using KTT phosphor. The freeze-dried fecal samples were combusted[12] and counted in a scintillation spectrometer. KTT phosphor was prepared by mixing 2,5-diphenyloxazole (8.25 g), 1,4-bis[2-(4-methyl-5-phenyloxazolyl)]benzene (0.25 g), isooctylphenoxypolyethoxyethanol (500 ml), and toluene (1000 ml).

Column Chromatography—Raw urine samples were put through a resin[6] column (bed volume = one-half of the sample volume) and washed with water (two times bed volume); the drug-related compounds were eluted with methanol (three times bed volume).

Enzyme Hydrolysis—Raw urine was adjusted to pH 5.0 with acetic acid. The methanol eluate from column chromatography was evaporated to dryness, and the residue was taken up in 0.2 *M* acetate buffer (pH 5.0). The buffered solution was incubated with enzyme at 37° overnight[13].

Analysis of Plasma—The analysis method developed for the study of metoclopramide pharmacokinetics is based on HPLC with a UV detector at 280 nm. Since the UV spectrum of metoclopramide in water indicates a minimum of absorbance at 250 nm with maxima at 272 and 308 nm, the usual detector employed at 254 nm is not suitable and the 280-nm wavelength was used.

The following liquid chromatographic parameters were used: column, 15 cm × 0.5 mm silica gel M131; flow rate, 2.0 ml/min; temperature, ambient; and solvent, methanol–chloroform–concentrated ammonium hydroxide (30:70:0.5).

Procedure—A 5.0-ml sample of plasma (whole blood and urine also were analyzed) was mixed with 9.0 ml of water and 1.0 ml of 500 ng/ml of internal standard. Concentrated ammonium hydroxide, 2 ml, was added, and the mixture was extracted twice with 10.0-ml portions of chloroform. Layers were separated by centrifugation, and the chloroform extracts were combined.

The chloroform phase was extracted with 5 ml of 0.5 *N* HCl, and the organic phase was discarded after centrifugation. The aqueous layer was made alkaline, and the metoclopramide was extracted back into 5.0 ml of chloroform. Then the chloroform layer was transferred to another tube, evaporated under nitrogen to dryness, and dissolved in 100 μl of chloroform; 25 μl was injected into the liquid chromatograph[14].

The internal standard was prepared by the reaction of 4-amino-5-chloro-2-methoxy-*N*-(aminoethyl)benzamide with *n*-propyl bromide by refluxing overnight in ethanol. The ethanol was evaporated, and the residue was taken up in water, made basic, and extracted with chloroform. On evaporation, an oily residue crystallized. This residue was recrystallized from benzene to give 4-amino-5-chloro-*N*-[2-(propylamino)ethyl]-

[1] Charles River Animal Laboratory, Wilmington, Mass.
[2] Hazelton Research Laboratory, Cumberland County, Va.
[3] Laboratories Delagrange, Paris Cedex 07, France.
[4] A gift from Merck Sharp and Dohme, Rahway, N.J.
[5] Glusulase, Endo Laboratories, Garden City, N.Y.
[6] XAD-2, Rohm & Haas, Philadelphia, Pa.
[7] Hitachi RMU-6H mass spectrometer, Perkin-Elmer, Norwalk, Conn.
[8] Varian A60 NMR spectrometer, Varian, Palo Alto, Calif.
[9] Model 621 IR spectrometer, Perkin-Elmer, Norwalk, Conn.
[10] Analtech, Inc., Newark, Del.
[11] Tri-Carb model 3385, Packard Instrument Co., Downers Grove, Ill.
[12] Model 305 sample oxidizer. Packard Instrument Co., Downers Grove, Ill.
[13] Thelco model 83 incubator, Precision Scientific Co., Chicago, Ill.
[14] Model 3500 liquid chromatograph with model 225 dual-channel UV absorbance detector, Spectra-Physics, Santa Clara, Calif.

Table I—Excretion of ^{14}C-Metoclopramide (Percent) in Rats, Dogs, and Humans

	Rat[a]		Dog		Human[b]	
Hours	Urine	Feces	Urine	Feces	Urine	Feces
0–24	71.9	5.7	65.3	—	77.8	2.0
24–48	8.5	4.4	6.9	18.3	5.7	1.0
48–72	1.0	1.7	1.0	1.0	0.8	1.6
72–96	N.C.[c]	N.C.	N.C.	N.C.	—	0.7
Subtotal	81.4	11.8	73.2	19.3	84.3	5.3
	93.2		92.5		89.6	

[a] Average of three rats. [b] Average of two human subjects. [c] N.C. = not collected.

2-methoxybenzamide. This compound shows the same solubility properties as metoclopramide and is well separated from both metoclopramide and the monodeethylated metabolite on chromatography, acting as an ideal internal standard. The retention times of metoclopramide and the internal standard were 2.8 and 4.5 min, respectively. The monodeethylated compound appeared at 7.5 min, and the dideethylated metabolite appeared at 5.7 min.

RESULTS

Excretion—Table I shows the radioactivity recovery from rats, dogs, and humans. The majority of the radioactivity was eliminated in the urine in the first 24 hr after dosing.

Metabolites in Rat Urine—The methanol eluate from column chromatography showed three major radioactive zones. There was no qualitative or quantitative difference in the raw urine and enzyme-hydrolyzed urine. The metabolites identified in the 0–24-hr rat urine accounted for over 60% of the total dose. The metabolites are listed according to descending R_f values.

Zone RA—The radioactivity in this zone accounted for 1–2% of the dose. Rechromatography with System E resolved this zone into several minor zones, two of which were identified.

Zone RA1—Mass spectrum of this metabolite showed a molecular ion at 200, indicating an even number of nitrogen atoms in the molecule. The base peak at *m/e* 184 indicated that there was no change on the ring substituents. This compound was assigned as 4-amino-5-chloro-2-methoxybenzamide (II).

Zone RA2—Two metabolites were in this zone, and one showed a molecular ion at *m/e* 244. The even molecular weight indicated an even number of nitrogen atoms. The base peak was at 184, indicating no change on the ring. Acetylation of this metabolite with acetic anhydride and pyridine gave a derivative of M + 328 with the base peak shifted to *m/e* 226. The metabolite picked up two acetyl groupings, one on the ring amino group and the other on the side chain. Another significant peak of the acetyl derivative at 268 was probably due to the loss of acetic acid. From these mass spectral data, Structure III, 4-amino-5-chloro-*N*-(2-hydroxyethyl)-2-methoxybenzamide, was assigned to this metabolite. The second component, M + 285, was not identified until the same metabolite was found later in dog urine.

Zone RB—IR, NMR, and mass spectra of this compound matched those of metoclopramide. Recrystallization of the compound twice from benzene gave a crystalline powder, mp 142–144° [lit. (1) mp 146.5°]. Therefore, this component was unchanged metoclopramide (I). Metoclopramide did not show a molecular ion under the present experimental

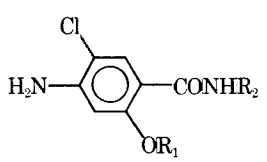

I: $R_1 = CH_3$, $R_2 = CH_2CH_2N(C_2H_5)_2$
II: $R_1 = CH_3$, $R_2 = H$
III: $R_1 = CH_3$, $R_2 = CH_2CH_2OH$
IV: $R_1 = H$, $R_2 = CH_2CH_2N(C_2H_5)_2$
V: $R_1 = CH_3$, $R_2 = CH_2CH_2NHC_2H_5$
VI*a*: $R_1 = CH_3$, $R_2 = CH_2COOH$
VI*b*: $R_1 = CH_3$, $R_2 = CH_2COOCH_3$
VI*c*: $R_1 = CH_3$, $R_2 = CH_2COOC_2H_5$
VII: $R_1 = CH_3$, $R_2 = CH{=}CH_2$
VIII: $R_1 = CH_3$, $R_2 = CH_2CH_2NH(COCH_3)$
IX: $R_1 = H$, $R_2 = CH_2CH_2NHC_2H_5$

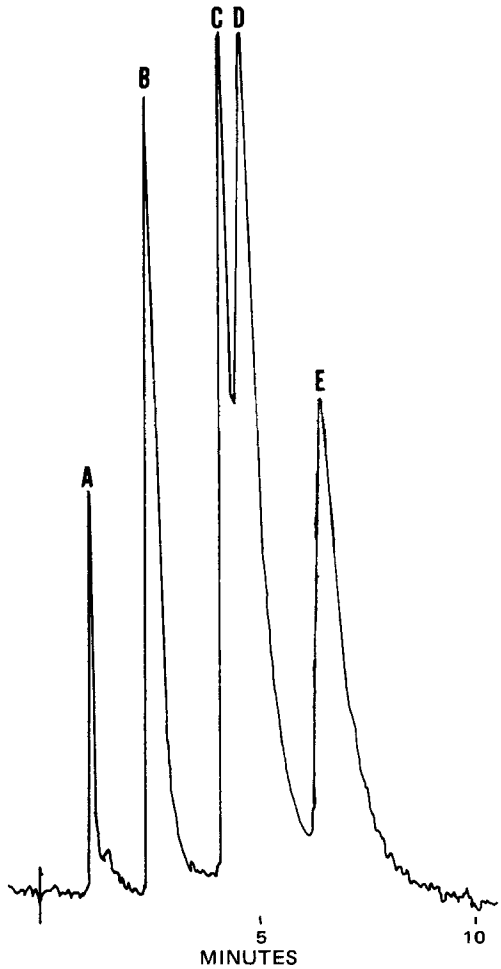

Figure 1—*Chromatogram of metoclopramide (B), internal standard (C), dideethylated metoclopramide (D), and monodeethylated metoclopramide (E). Peak A is the solvent.*

conditions. The base peak for this compound was 86 with strong peaks at 227, 201, 184, and 99.

Zone RC—On rechromatography with System E, this zone resolved into two components; one had a molecular weight of 285 by mass spectrometry. The base peak at 86 along with a strong peak at 99 suggested the existence of a $CH_2CH_2N(CH_2CH_3)_2$ grouping. The presence of a peak at 170 and the absence of a 184 peak suggested demethylation of the methoxy group on the ring. Not enough sample was available for derivatization. Structure IV, 4-amino-5-chloro-*N*-(2-hydroxy)-*N*-[2-(diethylamino)ethyl]benzamide, was assigned for this metabolite. The second metabolite in this zone was not identified.

Zone RD—On rechromatography with System F, this zone resolved into two compounds; one was identified as 4-amino-5-chloro-*N*-[2-(ethylamino)ethyl]-2-methoxybenzamide (V) by the following findings. The metabolite did not show a molecular ion. The base peak at *m/e* 58 along with other peaks at 213, 201, 184, and 71 was identical to the mass spectrum of the authentic sample. Comparison of the IR spectra of the metabolite and the authentic compound confirmed the identity further. The second metabolite was not identified.

Zone RE—Only one metabolite was found, and its mass spectrum showed only two peaks at *m/e* 184 and 44. The peak at *m/e* 44 (CO_2) indicated that the metabolite was probably an acid. The peak at *m/e* 184 indicated no change on ring substituents. Methylation of the metabolite with ethereal diazomethane gave a compound with a molecular weight of 272 and a strong peak at *m/e* 184. Ethylation of the metabolite with ethanol and hydrogen chloride gas gave an ethyl ester with a molecular weight of 286. This compound was assigned as 2-[(4-amino-5-chloro-2-methoxybenzoyl)amino]acetic acid (VI*a*). Its methyl and ethyl esters are VI*b* and VI*c*, respectively.

Metabolites in Dog Urine—TLC of the methanol eluate from the column revealed only two major radioactive zones. The metabolites were identified by TLC and mass spectrometry. The following metabolites

Table II—Results of Recovery of Known Amounts of Metoclopramide Added to Control Plasma (n = 6)

Metoclopramide, ng/ml		
Added	Found (Mean)	*SD*
10	9.6	±1.77
20	21.1	±1.89
60	61.3	±2.71
100	93.3	±5.93

were found in the 0–24-hr urine and amounted to about 60% of the dose.

Zone DA—This zone resolved into several minor zones with System E.

Zone DA1—This zone had a molecular ion at *m/e* 272. The metabolite had the same chromatographic behavior as 2-[(4-amino-5-chloro-2-methoxybenzoyl)amino]acetic acid methyl ester (VI*b*). This compound is possibly an artifact formed by the reaction of methanol and the acidic metabolite of Zone DF during workup.

Zone DA2—The molecular weight of this metabolite was established as 226 by mass spectrometry. Two other significant peaks were at *m/e* 200 and 184; unfortunately, not enough material was available for derivatization. This metabolite was tentatively assigned as 4-amino-5-chloro-*N*-ethenyl-2-methoxybenzamide (VII).

Zone DA3—This zone was identical to Zone RA1 in rat urine.

Zone DA4—The molecular weight of this metabolite was determined as 285 by mass spectrometry, indicating an odd number of nitrogen atoms. The base peak at *m/e* 184 indicated no change on the ring substituents. Acetylation of the metabolite gave a derivative M + 327, 42 mass units higher than the metabolite. The base peak shifted to *m/e* 226 from 184, indicating the only acetylation site to be NH_2 on the ring. The other nitrogen atoms were probably amide nitrogen or tertiary amine nitrogen. The mass spectrum of this acetylated metabolite was identical to that of the acetyl derivative of 4-amino-*N*-(2-aminoethyl)-5-chloro-2-methoxybenzamide. It was concluded that this metabolite was *N*-[2-(acetylamino)ethyl]-4-amino-5-chloro-2-methoxybenzamide (VIII).

Zone DA5—This metabolite was identical to the metabolite of Zone RA2 in rat urine.

Zone DB—This zone contained unchanged metoclopramide as shown by mass spectrometry and TLC.

Zone DD—This zone contained only one drug-related compound. The mass spectrum and TLC were identical to those of V.

Zone DE—This zone resolved into two drug-related compounds; one showed a weak molecular ion at *m/e* 257. The base peak at *m/e* 58 and another peak at *m/e* 71 suggested *N*-deethylation on the side chain. A strong peak at *m/e* 170 and others at *m/e* 200, 199, and 187 strongly indicated demethylation on the ring. From these data, 4-amino-5-chloro-*N*-[2-(ethylamino)ethyl]-2-hydroxybenzamide (IX) was proposed for this metabolite.

Zone DF—The only metabolite in this zone was identical to the metabolite of Zone RE in rat urine. Structure VI was proposed for it.

Metabolites in Human Urine—There were three significant radioactive spots in human urine. These three metabolites, found in the 0–24-hr urine, amounted to 60% of the dose.

Zone HA—This radioactive zone was shown to be unchanged metoclopramide by mass spectrometry and TLC comparisons in several solvent systems.

Zone HB—Due to large amounts of impurity, no meaningful spectral data were obtained initially for this metabolite. After treatment with diazomethane, a single radioactive derivative was isolated in the pure state. The methylated compound had M + 272 and the base peak was at *m/e* 184. This methyl ester was identical to the methyl ester of Zone RE in rat urine and Zone DF in dog urine. Therefore, the metabolite was VI*a*.

Zone HC—The intensity of this zone differed markedly before and after enzyme hydrolysis of the urine. This spot accounted for about 50% of the urinary radioactivity before enzyme hydrolysis, about 18% after hydrolysis, and practically none after acid hydrolysis. Hydrolysis of this spot gave unchanged metoclopramide. This zone was concluded to be the glucuronide and/or sulfate of metoclopramide.

HPLC Method—This method is sensitive to the determination of as little as 10 ng of metoclopramide/ml of plasma or blood when 5-ml samples are used. This sensitivity is sufficient for following kinetics of 10- or 20-mg doses. The method also appears to be specific under the conditions described, and I is well separated from expected metabolites (Fig. 1). However, no metabolite was detected in plasma or blood. The accuracy and precision of the procedure are indicated by the results shown in Table II. These results were obtained by analyzing samples of control plasma containing known quantities of added metoclopramide.

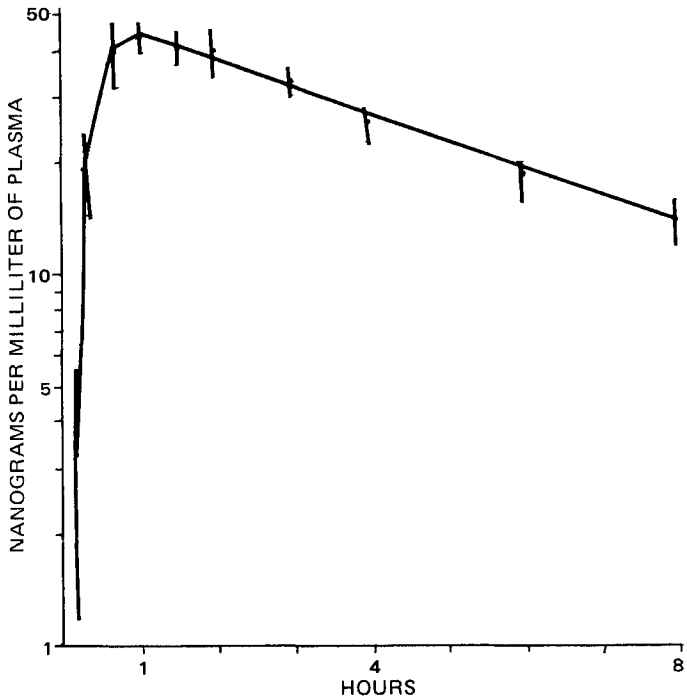

Figure 2—*Average blood levels of six normal male subjects who received oral doses of 10 mg of metoclopramide in solution. Vertical lines denote standard errors.*

A preliminary study was conducted with two normal male subjects to determine whether the method was sufficiently sensitive to determine blood levels of metoclopramide at an oral dose of 20 mg. The results are shown in Table III for the 8 hr during which the samples were taken. These results indicate that the necessary sensitivity was obtained. The results of a second study in which an oral dose of 10 mg was administered to each of six subjects as a liquid also indicated that sufficient sensitivity is obtained by this method (Fig. 2).

Blood levels were also obtained in the radioactive metoclopramide studies with humans. Both the total radioactivity of blood and unchanged metoclopramide levels are shown in Fig. 3. The levels were considerably higher as determined by radioactivity, even in the initial samples, indicating rapid drug metabolism.

DISCUSSION

Earlier investigators (1–4) showed that the major urinary metabolite of metoclopramide in rabbits, dogs, and rats is monodeethylated metoclopramide (V). This finding was confirmed in the present studies. There was no indication of the presence of a dideethylated drug in the urine of the three species studied (3). Neither the mono- nor dideethylated derivative could be detected in human urine.

Rabbits, according to Arita *et al.* (1), excrete metoclopramide in part as sulfate and glucuronide conjugates. This has also been found to be true in humans but not in dogs or rats. In humans, about one-half of the total radioactivity excreted was as a metoclopramide conjugate, indicating that this is a major route of excretion. The other metabolite found in humans

Table III—Plasma Metoclopramide Levels for Two Male Subjects who Received a 20-mg Oral Dose

Hours after Dose	Metoclopramide, ng/ml	
	Subject 1	Subject 2
0.25	0	0
0.50	63.0	28.6
1.0	72.1	87.2
1.5	71.1	81.0
2.0	66.7	81.1
3.0	53.0	76.8
4.0	42.1	58.0
6.0	33.3	35.0
8.0	20.3	22.6

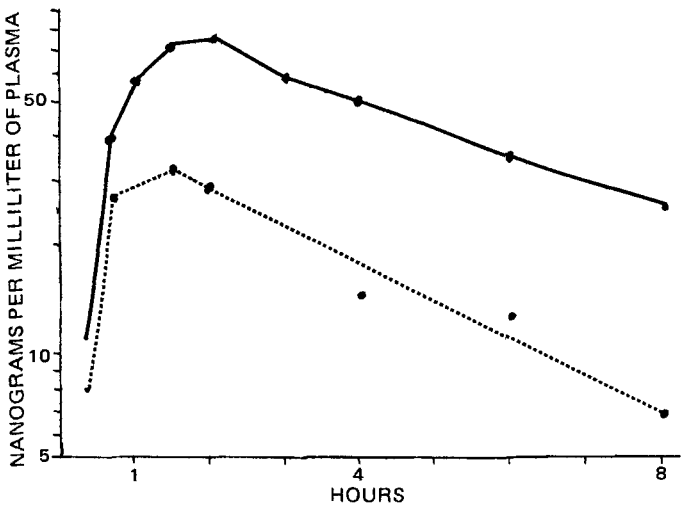

Figure 3—*Average plasma levels of total radioactivity, calculated as unchanged drug, and unchanged metoclopramide (by HPLC) of two subjects who received 10 mg of ^{14}C-metoclopramide. Key: —, radioactivity; and - - -, unchanged drug.*

(VI) also was observed in dog and rat urine, but it had not been observed previously.

A number of other metabolites were isolated and identifed from the urine of dogs and rats. An *O*-demethylated metabolite was earlier identified in rat urine by Hucker *et al.* (5). Two metabolites, IV and IX, were identified in the present study. No evidence of the aromatic amine oxidation could be found in these studies, as was noted by Arita *et al.* (1) for rabbits.

Previous studies showed that metoclopramide is rapidly and well absorbed in lower animals. The results in these studies indicate that this is also true in humans. About 78% was excreted in the urine (Table I) in the first 24 hr. Maximum blood levels following oral doses were found within the first 2 hr. The half-life of the drug for the 3–8-hr period following dosing was 4.00 hr (*SEM* 0.23) for the six subjects who received 10-mg doses (Fig. 2). The maximum concentration in the blood for these subjects was approximately 40 ng/ml; subjects that received 20 mg in the preliminary study gave twofold higher blood levels (Table III), indicating that the blood level is proportional to dose in this range. Further information concerning pharmacokinetics will appear in another report.

A comparison of the curves in Fig. 3 shows that a considerable amount of the radioactive material in the blood cannot be accounted for as unchanged metoclopramide. Because such a large portion of the drug was excreted as conjugates, samples were analyzed both before and following enzyme[5] hydrolysis of plasma samples from one subject. However, the results indicated that such conjugates were not present in appreciable concentrations. This difference must, therefore, be due to some unidentified metabolite.

REFERENCES

(1) T. Arita, R. Hori, K. Ito, K. Ichikawa, and T. Uesugi, *Chem. Pharm. Bull.*, **18**, 1663 (1970).

(2) O. M. Bakke and J. Segura, *J. Pharm. Pharmacol.*, **28**, 32 (1976).

(3) A. H. Beckett and G. Huizing, *ibid.*, **27**, 42P (1975).

(4) L. Sorrentino, M. DiRossa, and G. De Ruggiero, *Atti Acad. Sci.*, **123**, 52 (1969).

(5) H. B. Hucker, A. Hochberg, E. A. Hoffman, and J. K. Miller, *Pharmacologist*, **8**, 274 (1966).

ACKNOWLEDGMENTS AND ADDRESSES

Received November 17, 1976, from *A. H. Robins Research Laboratories, Richmond, VA 23220.*

Accepted for publication February 8, 1977.

The authors express their appreciation to Dr. A. N. Chremos, Clinical Pharmacology, A. H. Robins, for the clinical studies.

[x] To whom inquiries should be directed.

High-Speed Liquid Chromatographic Analysis of Dapsone and Related Compounds

C. A. MANNAN, G. J. KROL [x], and B. T. KHO

Abstract □ A nonaqueous solvent absorptive support system and an aqueous solvent reversed-phase support liquid chromatographic system for analysis of dapsone and related compounds were investigated. The absorptive support system was more suitable for analysis of dapsone in raw materials, formulations, and tissue residues. The suitability was judged by the relative selectivity, efficiency, precision, and sensitivity of the systems. The adsorptive support system was used for the analysis of trace amounts of raw material impurities and dapsone metabolites. Coupling fluorometric detection to the chromatographic system yielded a 10-pg on-column detection limit for dapsone; the UV detection limit was 250 pg.

Keyphrases □ Dapsone and related compounds—high-speed liquid chromatographic analyses, bulk drug, pharmaceutical formulations, and biological fluids □ High-speed liquid chromatography—analyses, dapsone and related compounds, bulk drug, pharmaceutical formulations, and biological fluids □ Leprostatic antibacterials—dapsone and related compounds, high-speed liquid chromatographic analyses, bulk drug, pharmaceutical formulations, and biological fluids

Dapsone (4,4′-sulfonylbisbenzeneamine) (I), a potent antileprotic drug (1–3), has been commercially available since 1949. Various analytical techniques have been investigated for its analysis in pharmaceutical preparations and biological fluids.

Colorimetry and titrimetry, the first techniques to be used, were reviewed previously (4). Although these methods are sufficiently sensitive for the analysis of pharmaceutical preparations, they are not sufficiently selective for the determination of chemical stability or for metabolite studies. The current USP method for the analysis of dapsone in tablet formulations is a sodium nitrite titration (5). This method is not specific for dapsone, however, since other arylamino sulfones present as decomposition products and synthetic impurities (4) interfere.

Later, fluorometric methods were developed; they are more sensitive and specific and, thus, are especially suitable for biological fluid metabolite studies (4, 6). However, these methods are not very accurate because of quenching and other complications, and they also involve complicated extraction and cleanup steps.

These limitations led to the development of TLC (7),

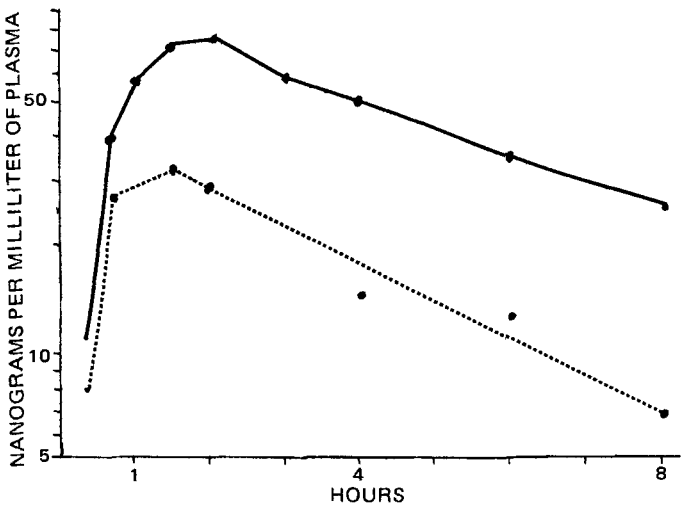

Figure 3—*Average plasma levels of total radioactivity, calculated as unchanged drug, and unchanged metoclopramide (by HPLC) of two subjects who received 10 mg of ^{14}C-metoclopramide. Key: —, radioactivity; and - - -, unchanged drug.*

(VI) also was observed in dog and rat urine, but it had not been observed previously.

A number of other metabolites were isolated and identifed from the urine of dogs and rats. An *O*-demethylated metabolite was earlier identified in rat urine by Hucker *et al.* (5). Two metabolites, IV and IX, were identified in the present study. No evidence of the aromatic amine oxidation could be found in these studies, as was noted by Arita *et al.* (1) for rabbits.

Previous studies showed that metoclopramide is rapidly and well absorbed in lower animals. The results in these studies indicate that this is also true in humans. About 78% was excreted in the urine (Table I) in the first 24 hr. Maximum blood levels following oral doses were found within the first 2 hr. The half-life of the drug for the 3–8-hr period following dosing was 4.00 hr (*SEM* 0.23) for the six subjects who received 10-mg doses (Fig. 2). The maximum concentration in the blood for these subjects was approximately 40 ng/ml; subjects that received 20 mg in the preliminary study gave twofold higher blood levels (Table III), indicating that the blood level is proportional to dose in this range. Further information concerning pharmacokinetics will appear in another report.

A comparison of the curves in Fig. 3 shows that a considerable amount of the radioactive material in the blood cannot be accounted for as unchanged metoclopramide. Because such a large portion of the drug was excreted as conjugates, samples were analyzed both before and following enzyme[5] hydrolysis of plasma samples from one subject. However, the results indicated that such conjugates were not present in appreciable concentrations. This difference must, therefore, be due to some unidentified metabolite.

REFERENCES

(1) T. Arita, R. Hori, K. Ito, K. Ichikawa, and T. Uesugi, *Chem. Pharm. Bull.*, **18**, 1663 (1970).

(2) O. M. Bakke and J. Segura, *J. Pharm. Pharmacol.*, **28**, 32 (1976).

(3) A. H. Beckett and G. Huizing, *ibid.*, **27**, 42P (1975).

(4) L. Sorrentino, M. DiRossa, and G. De Ruggiero, *Atti Acad. Sci.*, **123**, 52 (1969).

(5) H. B. Hucker, A. Hochberg, E. A. Hoffman, and J. K. Miller, *Pharmacologist*, **8**, 274 (1966).

ACKNOWLEDGMENTS AND ADDRESSES

Received November 17, 1976, from *A. H. Robins Research Laboratories, Richmond, VA 23220.*

Accepted for publication February 8, 1977.

The authors express their appreciation to Dr. A. N. Chremos, Clinical Pharmacology, A. H. Robins, for the clinical studies.

[x] To whom inquiries should be directed.

High-Speed Liquid Chromatographic Analysis of Dapsone and Related Compounds

C. A. MANNAN, G. J. KROL [x], and B. T. KHO

Abstract □ A nonaqueous solvent absorptive support system and an aqueous solvent reversed-phase support liquid chromatographic system for analysis of dapsone and related compounds were investigated. The absorptive support system was more suitable for analysis of dapsone in raw materials, formulations, and tissue residues. The suitability was judged by the relative selectivity, efficiency, precision, and sensitivity of the systems. The adsorptive support system was used for the analysis of trace amounts of raw material impurities and dapsone metabolites. Coupling fluorometric detection to the chromatographic system yielded a 10-pg on-column detection limit for dapsone; the UV detection limit was 250 pg.

Keyphrases □ Dapsone and related compounds—high-speed liquid chromatographic analyses, bulk drug, pharmaceutical formulations, and biological fluids □ High-speed liquid chromatography—analyses, dapsone and related compounds, bulk drug, pharmaceutical formulations, and biological fluids □ Leprostatic antibacterials—dapsone and related compounds, high-speed liquid chromatographic analyses, bulk drug, pharmaceutical formulations, and biological fluids

Dapsone (4,4′-sulfonylbisbenzeneamine) (I), a potent antileprotic drug (1–3), has been commercially available since 1949. Various analytical techniques have been investigated for its analysis in pharmaceutical preparations and biological fluids.

Colorimetry and titrimetry, the first techniques to be used, were reviewed previously (4). Although these methods are sufficiently sensitive for the analysis of pharmaceutical preparations, they are not sufficiently selective for the determination of chemical stability or for metabolite studies. The current USP method for the analysis of dapsone in tablet formulations is a sodium nitrite titration (5). This method is not specific for dapsone, however, since other arylamino sulfones present as decomposition products and synthetic impurities (4) interfere.

Later, fluorometric methods were developed; they are more sensitive and specific and, thus, are especially suitable for biological fluid metabolite studies (4, 6). However, these methods are not very accurate because of quenching and other complications, and they also involve complicated extraction and cleanup steps.

These limitations led to the development of TLC (7),

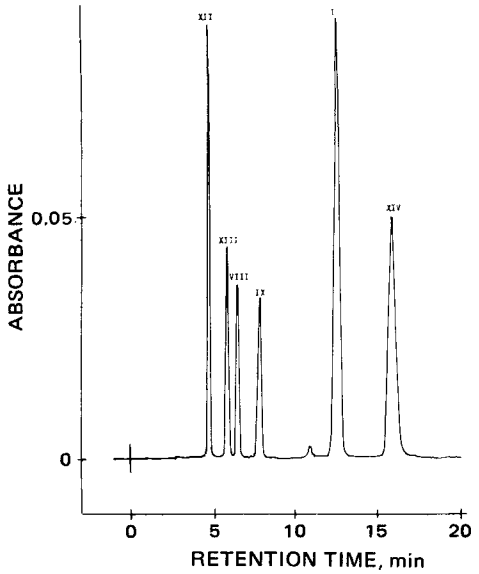

Figure 1—*System 1 chromatogram of dapsone and related compounds. The flow rate was 1.0 ml/min. Detection was in the UV at 295 nm, 0.1 absorbance unit full-scale (aufs).*

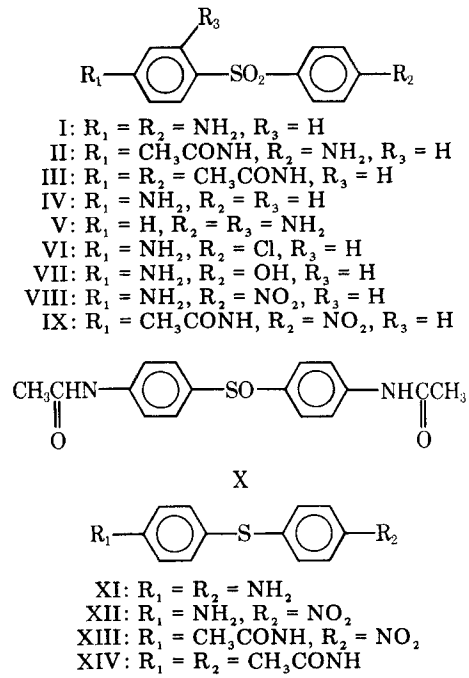

paper chromatographic (8), and GLC (9, 10) methods for dapsone analysis. However, in view of its relative simplicity and accuracy, current emphasis is on the use of liquid chromatography for the analysis of dapsone and its metabolites. Initially, Gordon and Peters (11) applied microbore silica gel-packed column chromatography to the separation of dapsone from 4-aminophenyl 4-acetamidophenyl sulfone (II) and bis(4-acetamidophenyl) sulfone (III). This procedure was later applied to the quantitation of dapsone tablet preparations in the presence of small amounts of the possible raw material impurities: 4-aminophenyl phenyl sulfone (IV), 2-aminophenyl 4-aminophenyl sulfone (V), and 4-aminophenyl 4-chlorophenyl sulfone (VI) (12). Subsequently, this system was modified to incorporate fluorometric detection (13, 14), which decreased the detection limit of dapsone to about 100 pg.

The objective of this work was to develop a fast, sensitive, and selective liquid chromatographic system suitable for the quantitation of dapsone in pure drugs, pharmaceutical formulations, and biological fluids. Comparison of the relative selectivity and efficiency of a reversed-phase system and a microparticle adsorptive system led to selection of the adsorptive support and a low viscosity nonaqueous solvent system. Both UV and fluorometric detection methods were investigated.

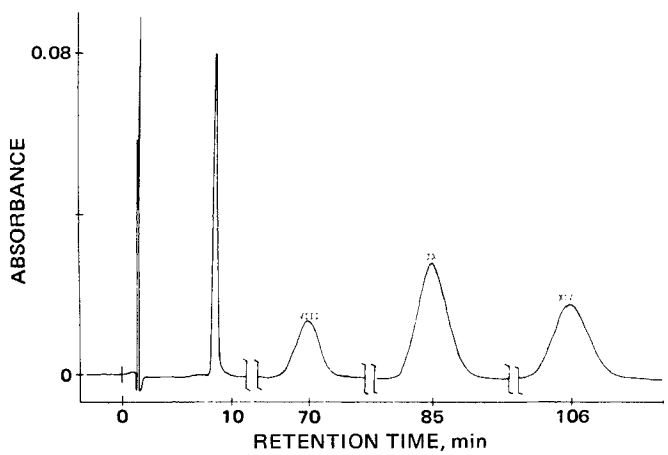

Figure 2—*System 2 chromatogram of dapsone and related compounds. The flow rate was 1.2 ml/min. Detection was in the UV at 295 nm.*

EXPERIMENTAL

Reagents and Chemicals—All reagents were spectrograde distilled-in-glass solvents[1]. USP dapsone reference standard was used as received[2]. Compounds II, III, and VII–XIV were prepared in this laboratory[3]. Compounds IV–VI were used as received[4].

Chromatographic Systems—*System 1*—The mobile phase, consisting of isopropyl alcohol–ethyl acetate–acetonitrile–*n*-pentane (1:1:1:7 v/v), was pumped through a 30-cm × 4-mm i.d. stainless steel column packed with 10-μm silica microparticles[5]. The pump was a constant-flow rate screw-driven syringe[6].

System 2—The mobile phase was water–acetonitrile (84:16 v/v). A 15-cm × 4-mm i.d. stainless steel column was packed with a 5-μm non-

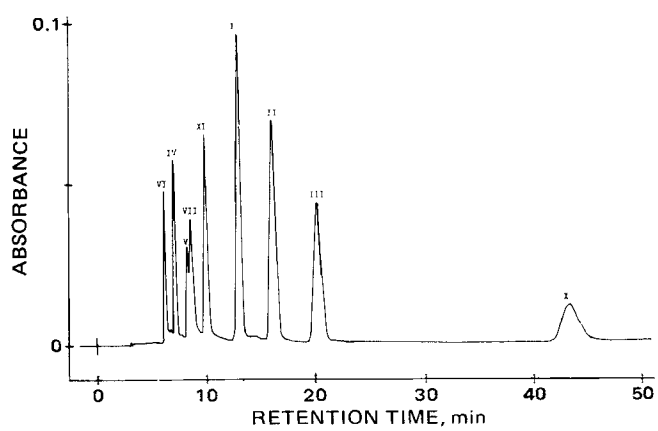

Figure 3—*System 1 chromatogram of dapsone and related compounds. The flow rate was 1.0 ml/min. Detection was in the UV at 295 nm.*

[1] Burdick and Jackson Laboratories, Muskegon, Mich.
[2] Lot 0371-F-3.
[3] By C. E. Orzech and F. Gemmill, Jr.
[4] Provided by G. R. Gordon, Stanford Research Institute, Menlo Park, Calif.
[5] μPorasil, Waters Associates, Milford, Mass.
[6] Model 314 metering pump, Instrumentation Specialties Co., Lincoln, Neb.

Table I—Comparison of Chromatographic Parameters[a] for Systems 1 and 2

Compound	System 1			System 2		
	RT^b	α^c	R^d	RT	α^c	R^d
I	1.00	—	—	1.00	—	—
II	1.21	1.2	2.2	1.43	1.5	4.5
III	1.54	1.7	5.7	2.07	2.3	7.7
IV	0.52	2.7	8.6	>20	—	—
V	0.62	2.0	2.2	>20	—	—
VI	0.46	3.1	10.4	>20	—	—
VIII	0.51	2.7	12.4	8.40	9.4	11.5
IX	0.62	2.0	9.0	10.45	11.7	14.2
XII	0.36	5.1	15.6	>20	—	—
XIII	0.45	3.2	12.9	>20	—	—
XIV	1.27	1.4	4.5	12.80	14.5	16.0

[a] All parameters are relative to dapsone. [b] Relative retention time. [c] Selectivity parameter. [d] Resolution parameter.

spherical octadecyltrichlorosilane bonded support[7]. A dual-piston reciprocating constant-flow rate pump[8] was used.

Sample Preparation—Compounds to be chromatographed were first prepared as 1-mg/ml stock solutions in chloroform or methanol. The solutions were diluted to the appropriate concentration with chromatographic solvent before chromatography. Samples were injected with a high-pressure six-port rotary valve with a 10-μl external loop[9].

Detection—The column eluate was monitored in the UV at 254[10] or 295[11] nm and by fluorometry[12] with excitation at 285 nm and emission above 340 nm.

Recording and Integration—Chromatographic peaks were recorded on a 25.4-cm strip-chart recorder[13]. Quantitation was based on either mechanical disk[14] or electronic integration[15].

Temperature Protection—To reduce detector noise due to ambient temperature fluctuations at the high detector sensitivity setting, the column, flowcell housing, monochromator, and light source for System 1 were kept in a constant-temperature box[16] at 25°.

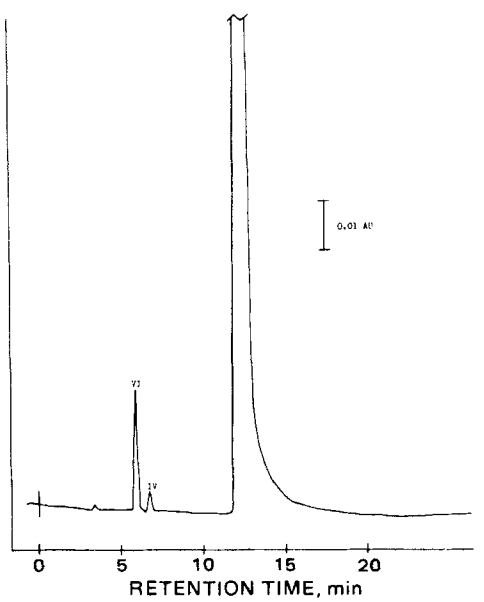

Figure 4—*System 1 chromatogram of USP dapsone reference standard. The flow rate was 1.0 ml/min. Detection was in the UV at 295 nm.*

[7] Merck Lichrosorb RP 18, EM Laboratories, Elmsford, N.Y.
[8] Spectra-Physics model 740, Spectra-Physics Inc., Santa Clara, Calif.
[9] Model CV-UHPA-C-20, Valco Instruments Co., Houston, Tex.
[10] Chromatronix model 220 UV absorbance monitor, Spectra-Physics Inc., Santa Clara, Calif.
[11] Model SF-770 variable spectroflow monitor, Schoeffel Instruments Corp., Westwood, N.J.
[12] Model FS-970, LC fluorescence detector, Schoeffel Instruments Corp., Westwood, N.J.
[13] Model 282 (10 in.), Linear Instruments Corp., Irvine, Calif.
[14] Series 200 Disc integrator, Disc Instruments, Santa Ana, Calif.
[15] Autolab System I computing integrator, Spectra-Physics Inc., Santa Clara, Calif.
[16] A 71 × 51 × 30-cm (28 × 20 × 15-in.) stainless steel cork-lined box, held at constant temperature with a Yellow Springs Instruments Co. model 74 temperature controller powering Watlow model 7424 250-w heating strips.

Precision and Accuracy for Tablet Formulations—The tablets[17] (25 and 100 mg) were assayed over 1 month. The precision was established as follows. Twenty tablets were ground to powder. The equivalent of one tablet was weighed from the bulk, and dapsone was extracted with 200 ml of methanol in an ultrasonic bath. The mixture was centrifuged, and an aliquot was diluted to approximately 25 μg/ml for analysis.

The instrument was standardized at a 1.2-ml/min flow rate with two to four separate injections of a USP reference standard solution of known concentration. The sample solution was injected a minimum of two times. The average area of the sample peaks was then compared to the average area of the standard peaks[18].

Assay accuracy was determined by spiking blank tablet material with known amounts of dapsone. Subsequently, the spiked sample was extracted, chromatographed, and quantitated as described.

Tablet Uniformity Analysis—Dapsone tablets (10 single 25 mg) were extracted by adding 0.5 ml of water to each tablet in a 200-ml volumetric flask. The flask was placed in an ultrasonic bath briefly to disintegrate the tablet. Methanol was then added to volume, and the flask was again placed in the ultrasonic bath for about 10 min. After centrifugation and dilution, an aliquot of the sample was chromatographed at a flow rate of 3.0 ml/min for fast sample turnover.

RESULTS AND DISCUSSION

Selection of Chromatographic System—Separation of dapsone from possible synthetic impurities and related compounds was studied using an adsorptive system and a reversed-phase system. The adsorptive system consisted of a microparticulate silica support and a nonaqueous solvent mobile phase. The reversed-phase system consisted of octadecyltrichlorosilane bonded to a microparticulate silica support and an aqueous solvent mobile phase.

The complete separation of dapsone from VIII, IX, and XII–XIV using

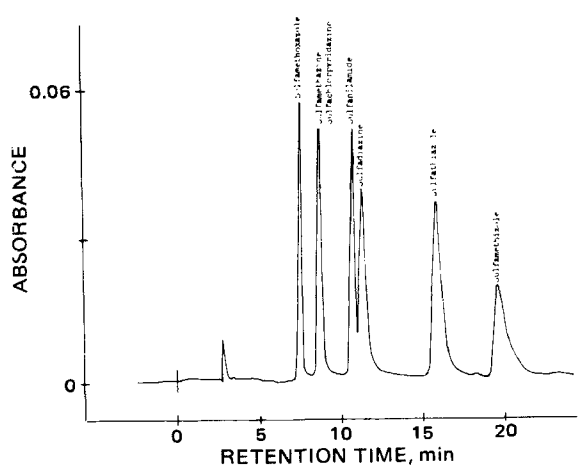

Figure 5—*System 1 chromatogram of sulfa drugs. The flow rate was 1.0 ml/min. Detection was in the UV at 254 nm.*

[17] Avlosulfon tablets, Ayerst Laboratories.
[18] These data were obtained with a Chromatronix model 3100 liquid chromatograph monitored at 254 nm and disk integration.

Table II—Chromatographic Efficiency *versus* Flow Rate Dependence Observed with Related Compounds

Compound	Plate Count at Decreasing Linear Velocity[a]			
	0.54	0.36	0.18	0.09
XII	5250	7130	9640	12,310
XIII	5300	6920	8860	11,640
VIII	5370	7300	9860	12,710
IX	3890	5460	8220	10,720
Dapsone	4710	5960	8660	11,730
XIV	3220	4550	6320	8,350

[a] Linear velocity in centimeters per second; 1 cm/sec = 5.56 ml/min.

the adsorptive system is shown in Fig. 1. Chromatography of some of these compounds with the reversed-phase system is shown in Fig. 2; XII and XIII were not eluted from the column. Table I lists the retention time, resolution, and selectivity of the adsorptive and reversed-phase systems. The differences in retention time are reflected by the selectivity values (α) relative to dapsone.

Compound XIV had a longer retention time than dapsone with the adsorptive system and would be expected to precede dapsone using the reversed-phase system. Instead, it was retained by the reversed-phase column considerably longer than dapsone. A similar observation applied to II and III.

The apparent lack of correlation between the observed order of elution on the adsorptive and reversed-phase supports may be attributed to the fact that the two systems use different solvents as well as supports. Since the aqueous solvent used with the reversed-phase support can influence the relative polarity of the solute by induction of dipoles and ionization, the relative polarity of a molecule in a nonaqueous solvent may be different from its relative polarity in an aqueous solvent. The effect of pH on the relative retention times of ionizable molecules chromatographed on a reversed-phase support was reported previously (15).

Although the elution pattern obtained with the reversed-phase system showed greater selectivity than that obtained with the adsorptive support system, the adsorptive support system was selected for routine analysis to minimize the time necessary to separate and quantitate dapsone and several related compounds. The reversed-phase system exhibited excessive elution times for possible impurities and metabolites of dapsone. Furthermore, since possible impurities in dapsone raw material (IV–VI) are not eluted on the reversed-phase support unless dapsone elutes at the solvent front or a gradient solvent system is utilized, the reversed-phase system is not suitable for simultaneous analysis of dapsone and its impurities. In contrast, the nonaqueous solvent–adsorptive support system yields adequate separation and short retention times for dapsone

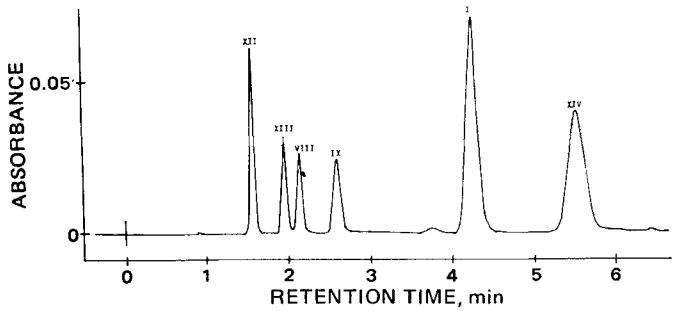

Figure 7—*System 1 chromatogram of dapsone and possible raw material impurities. The flow rate was 3.0 ml/min. Detection was in the UV at 295 nm, 0.1 aufs.*

impurities and, hence, sharp impurity peaks (Figs. 1 and 3) that can be quantitated accurately even at trace amount levels. Figure 4 illustrates a chromatogram obtained with USP dapsone reference standard. The observed impurities, IV and VI, were present at 0.4 and 0.08%, respectively.

The selectivity and efficiency of the adsorptive support system are also reflected by the observed resolution of dapsone from a known dapsone metabolite (II), a dapsone prodrug derivative (III), three previously identified impurities (IV–VI), and three structurally related compounds (VII, X, and XI). Figure 3 illustrates the separation obtained. Excluding X, all compounds were resolved within 22 min.

The adsorptive support system also was applied to the separation of several sulfa drugs. Although this system was not optimized for the separation of sulfa compounds, only sulfamethazine and sulfachlorpyridazine were unresolved (Fig. 5). However, the adsorptive support system does not appear to be as suitable for the separation of sulfa compounds as it is for the separation of dapsone and its analogs.

Efficiency of Nonaqueous Solvent–Adsorptive Support System—The selection of pentane as the major component of the nonaqueous solvent was based primarily on its low viscosity. The relationship between solvent viscosity and chromatographic efficiency was investigated previously (16).

As expected, an increased flow rate decreased column efficiency (Table II and Fig. 6). With few exceptions, essentially linear relationships between the flow rate and the width of the theoretical plate were observed. However, the slope of the plate width *versus* the flow rate line was dependent on the structure of the molecule. Thus, the chromatographic efficiency of the more polar molecule (*e.g.*, XIV, Fig. 6) decreased more

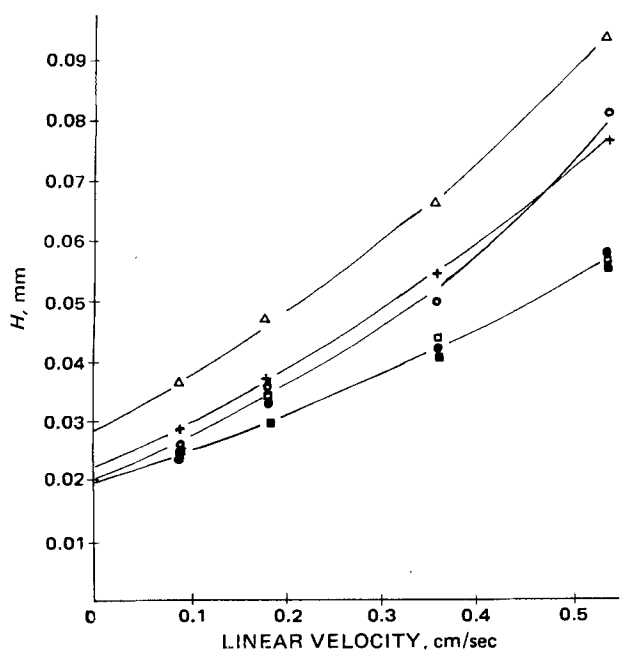

Figure 6—*VanDeemter plot based on System 1 chromatograms. Key:* ○, *I;* ●, *XII;* □, *XIII;* ■, *VIII;* +, *IX; and* △, *XIV;* H = *HETP (height equivalent to a theoretical plate).*

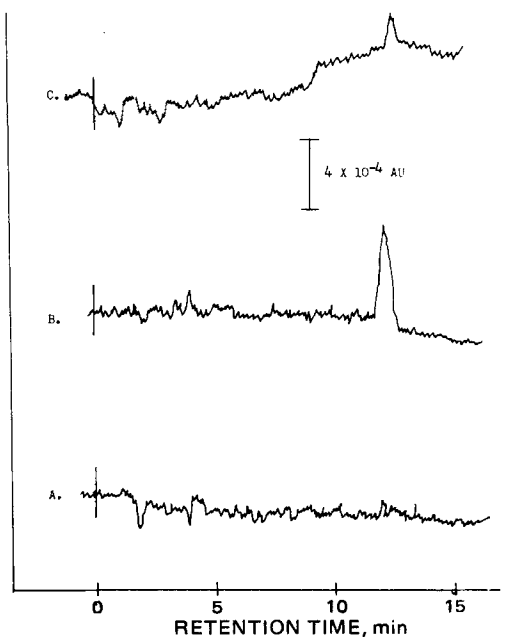

Figure 8—*System 1 chromatograms at high UV and fluorescence detector sensitivity settings. Key: A, 50 pg of dapsone, UV detector, 295 nm; B, 50 pg of dapsone, fluorescence detector; and C, 250 pg of dapsone, UV detector, 295 nm.*

Table III—Accuracy and Precision Data for Dapsone Tablets

Run	Date	25-mg Tablets		100-mg Tablets	
		Precision[a], mg/Tablet	Accuracy[b], %	Precision[a], mg/Tablet	Accuracy[b], %
1	Feb. 10, 1976	24.6	101.9	100.6	100.8
2	Feb. 11, 1976	24.3	98.3	99.2	100.9
3	Feb. 12, 1976	24.5	99.3	98.3	97.1
4	Feb. 13, 1976	24.5	99.0	97.5	99.7
5	Feb. 18, 1976	24.7	100.6	99.8	101.3
6	Feb. 19, 1976	23.0	100.9	97.6	98.5
7	Feb. 20, 1976	—	—	100.2	103.6
8	Feb. 20, 1976	—	—	99.3	97.5
9	Feb. 25, 1976	24.8	98.1	100.6	100.2
10	Mar. 1, 1976	24.1	97.2	99.8	100.8
11	Mar. 2, 1976	24.4	97.6	96.2	99.2
12	Mar. 3, 1976	23.8	101.7	102.4	99.4
$\bar{X}$		24.3	99.5	99.3	99.9
S		0.5	1.7	1.7	1.8
CV, %		2.2	1.7	1.7	1.8

[a] Twenty tablets were used for each run. [b] A ground placebo was spiked with a known amount of sample corresponding to claim. Number presented in table represents percent recovered.

with the flow rate than the chromatographic efficiency of a less polar molecule (*e.g.*, XII, Fig. 6). This trend may be attributed to the fact that the relative contribution of the mass transfer term to the overall column efficiency increased with the flow rate. Since the mass transfer process involves mobile and stationary phase interactions, the structure of the molecules chromatographed will influence the kinetics of mass transfer.

The relatively high efficiency of the nonaqueous chromatographic solvent, even at high flow rates, makes possible an accurate and specific analysis within a relatively short time. This possibility is an important consideration in uniformity and dissolution assays of tablets where the analysis of numerous samples is involved. Thus, dapsone was completely resolved from five related compounds even at a 3-ml/min flow rate (Fig. 7).

Detection—Although the quantitation of dapsone and related compounds with the aid of a variable wavelength UV detector is applicable to the analysis of pure drug and pharmaceutical formulations, fluorometric detection is more sensitive and, thus, more suitable for the analysis of tissue residue samples. This study utilized a novel spectrofluorometric liquid chromatographic detector. The unique design of the spectrofluorometric detector flowcell and optics made possible the detection of subnanogram amounts of dapsone and related compounds. Figure 8*b* illustrates a chromatogram of dapsone close to the fluorometric detection limit, approximately 10 pg. In contrast, 50 pg cannot be detected by UV (Fig. 8*a*); the detection limit of the UV detector is about 250 pg (Fig. 8*c*).

Figure 9 illustrates a chromatogram of dapsone and related compounds,

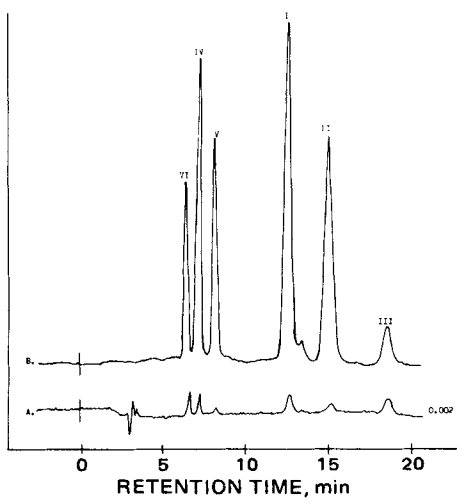

Figure 9—*System 1 chromatograms of dapsone and related compounds monitored by UV (at 295 nm) (A) and fluorescence (B) detectors. Amounts of samples injected were: IV and VI, 0.08 ng; V, 0.05 ng; I and II, 2.5 ng; and III, 4.0 ng. The UV detector setting was 0.02 aufs.*

obtained with UV and fluorometric detectors connected in series to monitor the same chromatographic elution. The patterns indicate that the UV and fluorometric detection limits vary with the compound. However, except for dapsone, no attempt was made to select the optimum cutoff filters for each compound. Therefore, the fluorometric detection limits of compounds other than dapsone are uncertain.

Precision and Accuracy—The accuracy and precision of the adsorptive support system are presented in Table III. Since the tablet formulations were analyzed on different days, the observed results include the day-to-day contribution to assay variability. Since individual tablet content uniformity assay involves a relatively high volume of samples, the procedure for the determination of tablet potency was modified. The flow rate was increased to yield less than a 6-min retention for dapsone with marginal sacrifice of assay accuracy, selectivity, and precision.

REFERENCES

(1) C. C. Shepard, *Ann. Rev. Pharmacol.*, **9**, 37 (1969).

(2) R. L. Degowin, R. B. Eppes, P. E. Carson, and R. D. Powell, *Bull. WHO*, **34**, 671 (1966).

(3) D. Willerson, Jr., K. H. Rickmann, L. Kass, P. E. Carson, H. Frischer, and J. E. Bowman, *Am. J. Trop. Med. Hyg.*, **21**, 138 (1972).

(4) C. E. Orzech, N. G. Nash, and R. D. Daley, in "Analytical Profiles of Drug Substances," vol. 5, K. Florey, Ed., Academic, New York, N.Y., 1976, pp. 88–114.

(5) "The United States Pharmacopeia," 19th rev., Mack Publishing Co., Easton, Pa., 1975, pp. 118, 119.

(6) A. J. Glazko, W. A. Dill, J. Baukema, and P. E. Thompson, *Int. J. Lepr.*, **36**, 511 (1968).

(7) L. M. S. Armasecu and M. Manda, *Farmacia (Bucharest)*, **22**, 165 (1974).

(8) S. Tsutsumi, *Chem. Pharm. Bull.*, **9**, 432 (1961).

(9) H. P. Burchfield, E. E. Storrs, R. J. Wheeler, V. K. Bhat, and L. L. Green, *Anal. Chem.*, **45**, 916 (1973).

(10) E. Sawicki, H. Johnson, and K. Kosinski, *Microchem. J.*, **10**, 72 (1966).

(11) G. R. Gordon and J. H. Peters, *J. Chromatogr.*, **47**, 269 (1970).

(12) G. R. Gordon, D. C. Ghaul, and J. H. Peters, *J. Pharm. Sci.*, **64**, 1205 (1975).

(13) J. F. Murray, Jr., G. R. Gordon, and J. H. Peters, *J. Lab. Clin. Med.*, **78**, 464 (1971).

(14) J. F. Murray, Jr., G. R. Gordon, C. C. Gulledge, and J. H. Peters, *J. Chromatogr.*, **107**, 67 (1975).

(15) P. J. Twitchett and A. C. Moffat, *ibid.*, **111**, 149 (1975).

(16) G. J. Krol, C. A. Mannan, F. Q. Gemmill, Jr., G. E. Hicks, and B. T. Kho, *ibid.*, **74**, 43 (1972).

ACKNOWLEDGMENTS AND ADDRESSES

Received November 18, 1976, from the *Analytical Research and Development Department, Ayerst Laboratories, Inc., Rouses Point, NY 12979.*

Accepted for publication February 11, 1977.
Presented at the Pharmaceutical Analysis Section, APhA Academy of Pharmaceutical Sciences, Orlando meeting, November 1976.
The authors gratefully acknowledge preparation of several dapsone analogs by Dr. C. Orzech and F. Gemmill, Jr., preparation of the octadecyltrichlorosilane column by Dr. D. Amato, determination of assay accuracy and precision by K. Roberts, and review of the manuscript by R. Daley. The authors also thank Dr. G. R. Gordon, Stanford Research Institute, for three analogs of dapsone and Schoeffel Instrument Corp. for the loan of the FS-970 liquid chromatographic fluorescence detector.
[x] To whom inquiries should be directed.

NOTES

Preparation and Skin-Photosensitizing Activity of Substituted Psoralens

MOHAMMED A. LOUTFY [x] and HAMED A. ABU-SHADY [*]

Abstract □ 8-Monosubstituted and 5,8-disubstituted psoralen derivatives were prepared, and their skin-photosensitizing activity was evaluated. The results were correlated in terms of molecular configuration, and 8-allyloxypsoralen can be considered as a new agent of potent photodynamic activity.

Keyphrases □ Psoralens, substituted—synthesized, evaluated for skin-photosensitizing activity □ Photosensitizing activity, skin—various substituted psoralens evaluated □ Structure–activity relationships—various substituted psoralens evaluated for skin-photosensitizing activity

In a continuation of previous studies (1–5), this report describes the preparation and skin-photosensitizing activity of substituted psoralens. The synthesis and photosensitizing activity of many psoralen (I) derivatives have been investigated extensively (6, 7), but little has been published concerning the 5,8-disubstituted psoralens. For example, while 5-methylpsoralen and 8-methylpsoralen are potent skin photosensitizers (8), nothing has been reported about 5,8-dimethylpsoralen. Furthermore, it was observed (9) that allyloxycoumarins have weak, but definite, photodynamic activity. Nevertheless, the effect on the photodynamic activity of introducing allyl, allyloxy, or dimethylallyl substituents in the psoralen molecule has not been studied.

On the other hand, the structure–activity relationships in the furocoumarin series demonstrated clearly the following. 2-Thiopsoralen derivatives and oxazolocoumarins do not exhibit any photodynamic activity (6). There is great variation in the potency of the skin-photosensitizing activity of the derivatives, determined by the number and the position of methyl groups (8). Methyl substitution at the 5′-carbon of psoralen does not alter the activity, but methyl substitution at the 4′-position results in a considerable loss of activity (9). Substitution with a methoxy group at the 5- or 8-carbon results in decreased activity, while nitro or amino group substitution renders the compound completely inactive (9). The fact that 2,6,8-trimethylbenzodifuran (10) and some other coumarin derivatives (9) do elicit photosensitized responses suggests that the furocoumarin structure is not essential for photosensitizing activity.

Further investigation is needed to reveal definite points in the structure–activity relationship in the furocoumarin series.

DISCUSSION

Previously, the isolation of xanthotoxin (II) and imperatorin (III) from the fruits of the umbellifer *Ammi majus* (L.)[1] was reported (1). These compounds were readily transformed into xanthotoxol (IV) according to a reported (4) procedure. The identity of xanthotoxin, imperatorin, and xanthotoxol was established through mixed melting-point, UV, IR, and NMR spectral comparisons with authentic samples[1]. For the preparation of derivatives V–VII, the procedure followed was essentially the same as that described previously (3).

It was reported (11) that imperatorin underwent Claisen rearrangement to afford alloimperatorin (IX) by heating in a vacuum. In the present work, to induce the allyl ethers to undergo Claisen rearrangement, the ethers were heated under reflux for 6 hr in ethylene glycol. In this way, 5-allyl-8-hydroxypsoralen (VIII) and IX were obtained in low yields (65%). Better results or even quantitative yields were obtained by refluxing the allyl ethers in *N*,*N*-diethylaniline for 1 hr. In the latter method, Claisen rearrangement products were of higher purity; 1 hr of refluxing was sufficient.

Methylation, acetylation, and allylation reactions were carried out according to the general method of etherification and esterification (3). However, allylation of VIII ended in failure. The identity of the new psoralen derivatives was ascertained by spectral (IR and NMR) analysis.

Compounds V–XIV (Table I) were prepared and screened as dermal photosensitizing agents. Two tests were performed with albino guinea pig skin. The preliminary test, employing very strong conditions (high amount of substance and high amount of radiation), was used for selecting the active compounds, even if weakly active, from the inactive ones. In a second test, only the active compounds were tested in very mild conditions and their photosensitizing activities were compared with that of psoralen.

The relative activity was evaluated by comparing the erythema re-

[1] Provided by Memphis Chemical Co., Cairo, Egypt.

Accepted for publication February 11, 1977.
Presented at the Pharmaceutical Analysis Section, APhA Academy of Pharmaceutical Sciences, Orlando meeting, November 1976.
The authors gratefully acknowledge preparation of several dapsone analogs by Dr. C. Orzech and F. Gemmill, Jr., preparation of the octadecyltrichlorosilane column by Dr. D. Amato, determination of assay accuracy and precision by K. Roberts, and review of the manuscript by R. Daley. The authors also thank Dr. G. R. Gordon, Stanford Research Institute, for three analogs of dapsone and Schoeffel Instrument Corp. for the loan of the FS-970 liquid chromatographic fluorescence detector.
[x] To whom inquiries should be directed.

NOTES

Preparation and Skin-Photosensitizing Activity of Substituted Psoralens

MOHAMMED A. LOUTFY [x] and HAMED A. ABU-SHADY [*]

Abstract □ 8-Monosubstituted and 5,8-disubstituted psoralen derivatives were prepared, and their skin-photosensitizing activity was evaluated. The results were correlated in terms of molecular configuration, and 8-allyloxypsoralen can be considered as a new agent of potent photodynamic activity.

Keyphrases □ Psoralens, substituted—synthesized, evaluated for skin-photosensitizing activity □ Photosensitizing activity, skin—various substituted psoralens evaluated □ Structure–activity relationships—various substituted psoralens evaluated for skin-photosensitizing activity

In a continuation of previous studies (1–5), this report describes the preparation and skin-photosensitizing activity of substituted psoralens. The synthesis and photosensitizing activity of many psoralen (I) derivatives have been investigated extensively (6, 7), but little has been published concerning the 5,8-disubstituted psoralens. For example, while 5-methylpsoralen and 8-methylpsoralen are potent skin photosensitizers (8), nothing has been reported about 5,8-dimethylpsoralen. Furthermore, it was observed (9) that allyloxycoumarins have weak, but definite, photodynamic activity. Nevertheless, the effect on the photodynamic activity of introducing allyl, allyloxy, or dimethylallyl substituents in the psoralen molecule has not been studied.

On the other hand, the structure–activity relationships in the furocoumarin series demonstrated clearly the following. 2-Thiopsoralen derivatives and oxazolocoumarins do not exhibit any photodynamic activity (6). There is great variation in the potency of the skin-photosensitizing activity of the derivatives, determined by the number and the position of methyl groups (8). Methyl substitution at the 5′-carbon of psoralen does not alter the activity, but methyl substitution at the 4′-position results in a considerable loss of activity (9). Substitution with a methoxy group at the 5- or 8-carbon results in decreased activity, while nitro or amino group substitution renders the compound completely inactive (9). The fact that 2,6,8-trimethylbenzodifuran (10) and some other coumarin derivatives (9) do elicit photosensitized responses suggests that the furocoumarin structure is not essential for photosensitizing activity.

Further investigation is needed to reveal definite points in the structure–activity relationship in the furocoumarin series.

DISCUSSION

Previously, the isolation of xanthotoxin (II) and imperatorin (III) from the fruits of the umbellifer *Ammi majus* (L.)[1] was reported (1). These compounds were readily transformed into xanthotoxol (IV) according to a reported (4) procedure. The identity of xanthotoxin, imperatorin, and xanthotoxol was established through mixed melting-point, UV, IR, and NMR spectral comparisons with authentic samples[1]. For the preparation of derivatives V–VII, the procedure followed was essentially the same as that described previously (3).

It was reported (11) that imperatorin underwent Claisen rearrangement to afford alloimperatorin (IX) by heating in a vacuum. In the present work, to induce the allyl ethers to undergo Claisen rearrangement, the ethers were heated under reflux for 6 hr in ethylene glycol. In this way, 5-allyl-8-hydroxypsoralen (VIII) and IX were obtained in low yields (65%). Better results or even quantitative yields were obtained by refluxing the allyl ethers in *N*,*N*-diethylaniline for 1 hr. In the latter method, Claisen rearrangement products were of higher purity; 1 hr of refluxing was sufficient.

Methylation, acetylation, and allylation reactions were carried out according to the general method of etherification and esterification (3). However, allylation of VIII ended in failure. The identity of the new psoralen derivatives was ascertained by spectral (IR and NMR) analysis.

Compounds V–XIV (Table I) were prepared and screened as dermal photosensitizing agents. Two tests were performed with albino guinea pig skin. The preliminary test, employing very strong conditions (high amount of substance and high amount of radiation), was used for selecting the active compounds, even if weakly active, from the inactive ones. In a second test, only the active compounds were tested in very mild conditions and their photosensitizing activities were compared with that of psoralen.

The relative activity was evaluated by comparing the erythema re-

[1] Provided by Memphis Chemical Co., Cairo, Egypt.

Table I—Data for 8-Monosubstituted and 5,8-Disubstituted Psoralens[a]

Compound	Melting Point	Yield, %	Empirical Formula	Analysis, % Calc.	Found
V	68–70°	95	$C_{14}H_{10}O_4$	C 69.42	69.39
				H 4.13	4.24
VI	175–177°[b]	95	$C_{13}H_8O_5$	C 63.93	63.91
				H 3.28	3.40
VII	194–196°	90	$C_{18}H_{10}O_5$	C 70.59	70.77
				H 3.27	3.44
VIII	203–205°	65[c], 98[d]	$C_{14}H_{10}O_4$	C 69.4	69.24
				H 4.13	4.10
IX	228–230°[e]	63[c], 97[d]	$C_{16}H_{14}O_4$	C 71.11	70.79
				H 5.11	5.08
X	98–100°	90	$C_{15}H_{12}O_4$	C 70.31	69.96
				H 4.70	4.61
XI	158–160°	80	$C_{16}H_{12}O_5$	C 67.61	67.42
				H 4.23	4.32
XII	109–111°[f]	90	$C_{17}H_{16}O_4$	C 71.83	71.88
				H 5.63	5.67
XIII	106–108°	87	$C_{18}H_{16}O_5$	C 69.23	68.98
				H 5.13	5.17
XIV	71–73°	85	$C_{19}H_{18}O_4$	C 73.55	73.88
				H 5.81	5.87

[a] The crystallization solvent was ethanol except for VII for which benzene was used. [b] Lit. (7) mp 178°. [c] Method I. [d] Method II. [e] Lit. (11) mp 233°. [f] Lit. (7) mp 113°.

sponse as observed by visible intensity grading. Introduction of hydroxy (VIII and IX), acetoxy (VI, XI, and XIII), or benzoyloxy (VII) substituents at the 8-position in the psoralen molecule resulted in a marked loss of the photodynamic effect. However, 5,8-disubstituted psoralens (X, XII, and XIV) did not show significant activity. Experimental evidence has now been obtained to confirm that the activity of psoralens is markedly reduced or eliminated upon blocking the 5- and 8-positions, which are the active centers in the psoralen molecule. Moreover, methylation of the hydroxyl group (X and XII) partially restores the photosensitizing activity of psoralen derivatives. Such results are analogous to previous findings (9).

Surprisingly, 8-allyloxypsoralen (V) proved very active; it was only slightly less active than psoralen itself. This result appears to be in contradiction with other reported (6, 9) studies. Accordingly, these data, coupled with the previously mentioned observations, served to confirm that it is desirable to explore the precise structure–activity relationship fully.

EXPERIMENTAL[2]

Claisen Rearrangement—*Method I*—A solution of 5 g of the allyloxypsoralen derivative in 25 ml of ethylene glycol was refluxed for 6 hr. The solution was cooled, and the solid product was filtered and recrystallized from a suitable solvent.

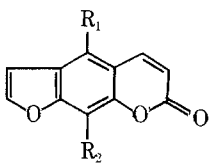

I: $R_1 = R_2 = H$
II: $R_1 = H$, $R_2 = OCH_3$
III: $R_1 = H$, $R_2 = OCH_2CH{=}C(CH_3)_2$
IV: $R_1 = H$, $R_2 = OH$
V: $R_1 = H$, $R_2 = OCH_2CH{=}CH_2$
VI: $R_1 = H$, $R_2 = OCOCH_3$
VII: $R_1 = H$, $R_2 = OCOC_6H_5$
VIII: $R_1 = CH_2CH{=}CH_2$, $R_2 = OH$
IX: $R_1 = CH_2CH{=}C(CH_3)_2$, $R_2 = OH$
X: $R_1 = CH_2CH{=}CH_2$, $R_2 = OCH_3$
XI: $R_1 = CH_2CH{=}CH_2$, $R_2 = OCOCH_3$
XII: $R_1 = CH_2CH{=}C(CH_3)_2$, $R_2 = OCH_3$
XIII: $R_1 = CH_2CH{=}C(CH_3)_2$, $R_2 = OCOCH_3$
XIV: $R_1 = CH_2CH{=}C(CH_3)_2$, $R_2 = OCH_2CH{=}CH_2$

Method II—A solution of the allyl ether in about 25 ml of *N,N*-diethylaniline was refluxed for 1 hr. The precipitated product was collected and purified.

Methylation—A mixture of 2 g of the corresponding crude Claisen rearranged product (VIII or IX), 20 g of anhydrous potassium carbonate, 20 ml of methyl iodide, and 250 ml of dry acetone was refluxed and stirred for 24 hr. The acetone filtrate and washings were evaporated to dryness; the residue, after washing with water, was recrystallized from alcohol.

Acetylation—A mixture of 2 g of VIII or IX and a few crystals of fused sodium acetate in 20 ml of acetic anhydride was heated under reflux for 3 hr and then stirred with water until excess acetic anhydride had decomposed. The insoluble product was filtered and recrystallized from alcohol.

Allylation—A mixture of 2 g of the 8-hydroxypsoralen derivative (VIII or IX), 10 g of anhydrous potassium carbonate, 10 ml of allyl bromide, and 250 ml of dry acetone was stirred and refluxed for 20 hr. Evaporation of the acetone filtrate under reduced pressure left a residue, which was washed thoroughly with water, dried, and washed once with petroleum ether (bp 30–60°) to remove excess allyl bromide. The residue was then dried and recrystallized from the appropriate solvent.

Table I lists the psoralens (V–XIV) with their physical constants. Their identity was established by UV, IR, and NMR spectral properties.

Skin-Photosensitizing Activity—*Animals*—Common guinea pigs were used; the hair was removed from the abdomen with scissors. Exact amounts of an acetone solution of the compound to be tested were then placed on 4 cm^2 (2 × 2 cm) of nonpigmented skin, and rapid evaporation of the acetone was accomplished.

Irradiation—A 500-w solar lamp[3] was used; it emitted strongly at 365 nm and in the visible region.

Preliminary Pharmacological Test—A concentration of 50 $\mu g/cm^2$ of a compound was tested with the lamp at a distance of 25 cm, an irradiation time of 60 min, and observation after 24 hr. Compounds VI–IX, XI, and XIII were inactive. Compounds X, XII, and XIV were slightly active. In contrast, V was very active.

Comparative Screening with Psoralen—Only V, X, XII, and XIV were tested at 2.5 $\mu g/cm^2$ with the lamp at 45-cm distance, irradiation for 60 min, and observation of erythema after 24 hr. In these pharmacological tests, the compounds were placed on square areas of the abdomen of the same animal. The tests were repeated on five different animals with the same results. Compared to I, which was very active (3+ erythema), V was also very active (2+ ± erythema), X and XII were weakly active (1+ erythema), and XIV was very weak (± erythema).

REFERENCES

(1) M. A. Loutfy, M. A. Hassan, and H. A. Abu-Shady, *Pharmazie*, **30**, 748 (1975).

[2] Melting points were determined in capillary tubes heated in a Mel-Temp apparatus and are uncorrected. IR spectra were recorded with a Perkin-Elmer model 621 spectrophotometer from samples in potassium bromide disks. UV absorption spectra were measured with a Perkin-Elmer 124 double-beam spectrophotometer. NMR spectra were determined with a Varian model A-60A spectrometer. All IR and NMR spectra of the new compounds were in agreement with assigned structures. Elemental analyses were performed by Dr. F. B. Strauss, Oxford, England.

[3] Osram HWA.

(2) M. A. Loutfy and H. A. Abu-Shady, *ibid.*, **31**, 573 (1976).
(3) M. A. Loutfy, M. A. Hassan, A. I. Jado, and H. A. Abu-Shady, *ibid.*, **31**, 819 (1976).
(4) M. A. Loutfy, Ph.D. thesis, University of Riyadh, Riyadh, Saudi Arabia, 1976.
(5) M. A. Loutfy and H. A. Abu-Shady, *Pharmazie*, **32**, 240 (1977).
(6) L. Musajo and G. Rodighiero, "Photophysiology," vol. VII, A. C. Giese, Ed., Academic, New York, N.Y., 1972, p. 115.
(7) A. Mustafa, "Furopyrans and Furopyrones," Interscience, London, England, 1967, p. 14.
(8) F. Dall'Acqua, S. Marciani, D. Vedaldi, and G. Rodighiero, *Biochim. Biophys. Acta*, **353**, 267 (1974).
(9) M. A. Pathak, J. H. Fellman, and K. D. Kaufman, *J. Invest. Dermatol.*, **35**, 165 (1960).
(10) L. R. Worden, A. W. Bergstahler, K. D. Kaufman, J. A. Weis, and T. K. Schaaf, *J. Heterocycl. Chem.*, **6**, 191 (1969).
(11) A. Schonberg and A. Sina, *J. Am. Chem. Soc.*, **72**, 4827 (1950).

ACKNOWLEDGMENTS AND ADDRESSES

Received October 12, 1976, from the *Pharmaceutical Chemistry Research Laboratory, Pharmaceutical Chemistry Department, College of Pharmacy, University of Riyadh, Riyadh, Saudi Arabia.*

Accepted for publication January 11, 1977.

The authors gratefully acknowledge the assistance of Dr. G. Rodighiero and Dr. F. R. Baccichetti, Pharmaceutical Chemistry Institute, University of Padova, Padova, Italy, in securing the pharmacological data and for help and advice. The authors are also indebted to Dr. G. Schwenker, College of Pharmacy, University of Heidelberg, Heidelberg, West Germany, for carrying out some spectral analyses.

* Present address: Department of Pharmaceutical Chemistry, University of Cairo, Cairo, Egypt.

ˣ To whom inquiries should be directed.

High-Speed Liquid Chromatographic Determination of Pilocarpine in Pharmaceutical Dosage Forms

S. K. WAHBA KHALIL

Abstract □ A specific method for the direct determination of pilocarpine in aqueous pharmaceuticals in the presence of decomposition products, methylcellulose, and other ingredients usually present in pharmaceuticals is described. The method involves separation by high-speed liquid chromatography using, in series, octadecylsilane bonded to silica and cyanopropylsilane bonded to silica columns and a tetrahydrofuran–pH 9.2 borate buffer (3:7) eluant. Quantitation is achieved by monitoring the absorbance of the effluent at 254 nm and using a pyridine internal standard and a calibration curve prepared from known concentrations of pilocarpine nitrate. The reproducibility of the retention time and peak area was better than 2.0%.

Keyphrases □ Pilocarpine—high-speed liquid chromatographic analysis, pharmaceutical preparations □ High-speed liquid chromatography—analysis, pilocarpine in pharmaceutical preparations □ Ophthalmic cholinergics—pilocarpine, high-speed liquid chromatographic analysis, pharmaceutical preparations

Many methods for estimating pilocarpine and its salts are available. Several are based on the titration of the extracted base with standard acid, with bromphenol blue (1–3), methyl red (4, 5), methyl orange (6), or dimethyl yellow (7) as the indicator. Several gravimetric (8–10), colorimetric (11), and iodometric (12) methods were developed. Recently, a GLC method using electron-capture detection was employed (13).

The USP XIX monographs for pilocarpine hydrochloride (14) and pilocarpine nitrate (15) incorporate a nonaqueous titration. However, the monographs on pilocarpine hydrochloride ophthalmic solution (15) and pilocarpine nitrate ophthalmic solution (16) require an extraction procedure, followed by colorimetric determination. Most of these methods lack the specificity and simplicity desired in routine analysis, especially in the presence of degradation products and/or other ingredients. In addition, the extraction of pilocarpine base from pharmaceuticals followed by colorimetric determination leads to erroneous results[1].

Recently, high-speed liquid chromatography (HSLC) was used to analyze alkaloids (17, 18). This paper describes an HSLC method that permits the quantitative determination of pilocarpine in the presence of its degradation products and other chemicals commonly included with pilocarpine salts in pharmaceutical products.

Table I—Calibration Data[a] for HSLC Pilocarpine Analysis

Concentration Added, mg/ml	Peak Area of Pilocarpine / Peak Area of Standard
5	0.141 ± 0.0065[b]
10	0.286 ± 0.0104
20	0.562 ± 0.0084
30	0.830 ± 0.0080

[a] Average of 10 replicate injections. [b] Standard deviation.

EXPERIMENTAL

Apparatus—A high-speed liquid chromatograph[2] equipped with a pump[3], a single-wavelength UV monitor (254 nm), and a liquid chromatograph injector[4] was used.

Columns—An octadecylsilane bonded to silica[5] column and a cyanopropylsilane[6] column were used in series. Both columns were 300-mm long × 4-mm i.d. stainless steel tubes.

Reagents—Sodium borate, tetrahydrofuran, and pyridine were reagent grades. Pilocarpine nitrate USP was used without further purification.

[1] U.S. Pharmacopeia, Drug Standards Division, personal communication.
[2] Model 202, Waters Associates.
[3] M-6000.
[4] U6K Universal.
[5] μBondapak C_{18}, Waters Associates.
[6] μBondapak CN, Waters Associates.

(2) M. A. Loutfy and H. A. Abu-Shady, *ibid.*, **31**, 573 (1976).
(3) M. A. Loutfy, M. A. Hassan, A. I. Jado, and H. A. Abu-Shady, *ibid.*, **31**, 819 (1976).
(4) M. A. Loutfy, Ph.D. thesis, University of Riyadh, Riyadh, Saudi Arabia, 1976.
(5) M. A. Loutfy and H. A. Abu-Shady, *Pharmazie*, **32**, 240 (1977).
(6) L. Musajo and G. Rodighiero, "Photophysiology," vol. VII, A. C. Giese, Ed., Academic, New York, N.Y., 1972, p. 115.
(7) A. Mustafa, "Furopyrans and Furopyrones," Interscience, London, England, 1967, p. 14.
(8) F. Dall'Acqua, S. Marciani, D. Vedaldi, and G. Rodighiero, *Biochim. Biophys. Acta*, **353**, 267 (1974).
(9) M. A. Pathak, J. H. Fellman, and K. D. Kaufman, *J. Invest. Dermatol.*, **35**, 165 (1960).
(10) L. R. Worden, A. W. Bergstahler, K. D. Kaufman, J. A. Weis, and T. K. Schaaf, *J. Heterocycl. Chem.*, **6**, 191 (1969).
(11) A. Schonberg and A. Sina, *J. Am. Chem. Soc.*, **72**, 4827 (1950).

ACKNOWLEDGMENTS AND ADDRESSES

Received October 12, 1976, from the *Pharmaceutical Chemistry Research Laboratory, Pharmaceutical Chemistry Department, College of Pharmacy, University of Riyadh, Riyadh, Saudi Arabia.*

Accepted for publication January 11, 1977.

The authors gratefully acknowledge the assistance of Dr. G. Rodighiero and Dr. F. R. Baccichetti, Pharmaceutical Chemistry Institute, University of Padova, Padova, Italy, in securing the pharmacological data and for help and advice. The authors are also indebted to Dr. G. Schwenker, College of Pharmacy, University of Heidelberg, Heidelberg, West Germany, for carrying out some spectral analyses.

* Present address: Department of Pharmaceutical Chemistry, University of Cairo, Cairo, Egypt.

ˣ To whom inquiries should be directed.

High-Speed Liquid Chromatographic Determination of Pilocarpine in Pharmaceutical Dosage Forms

S. K. WAHBA KHALIL

Abstract □ A specific method for the direct determination of pilocarpine in aqueous pharmaceuticals in the presence of decomposition products, methylcellulose, and other ingredients usually present in pharmaceuticals is described. The method involves separation by high-speed liquid chromatography using, in series, octadecylsilane bonded to silica and cyanopropylsilane bonded to silica columns and a tetrahydrofuran–pH 9.2 borate buffer (3:7) eluant. Quantitation is achieved by monitoring the absorbance of the effluent at 254 nm and using a pyridine internal standard and a calibration curve prepared from known concentrations of pilocarpine nitrate. The reproducibility of the retention time and peak area was better than 2.0%.

Keyphrases □ Pilocarpine—high-speed liquid chromatographic analysis, pharmaceutical preparations □ High-speed liquid chromatography—analysis, pilocarpine in pharmaceutical preparations □ Ophthalmic cholinergics—pilocarpine, high-speed liquid chromatographic analysis, pharmaceutical preparations

Many methods for estimating pilocarpine and its salts are available. Several are based on the titration of the extracted base with standard acid, with bromphenol blue (1–3), methyl red (4, 5), methyl orange (6), or dimethyl yellow (7) as the indicator. Several gravimetric (8–10), colorimetric (11), and iodometric (12) methods were developed. Recently, a GLC method using electron-capture detection was employed (13).

The USP XIX monographs for pilocarpine hydrochloride (14) and pilocarpine nitrate (15) incorporate a nonaqueous titration. However, the monographs on pilocarpine hydrochloride ophthalmic solution (15) and pilocarpine nitrate ophthalmic solution (16) require an extraction procedure, followed by colorimetric determination. Most of these methods lack the specificity and simplicity desired in routine analysis, especially in the presence of degradation products and/or other ingredients. In addition, the extraction of pilocarpine base from pharmaceuticals followed by colorimetric determination leads to erroneous results[1].

Recently, high-speed liquid chromatography (HSLC) was used to analyze alkaloids (17, 18). This paper describes an HSLC method that permits the quantitative determination of pilocarpine in the presence of its degradation products and other chemicals commonly included with pilocarpine salts in pharmaceutical products.

Table I—Calibration Data[a] for HSLC Pilocarpine Analysis

Concentration Added, mg/ml	Peak Area of Pilocarpine / Peak Area of Standard
5	0.141 ± 0.0065[b]
10	0.286 ± 0.0104
20	0.562 ± 0.0084
30	0.830 ± 0.0080

[a] Average of 10 replicate injections. [b] Standard deviation.

EXPERIMENTAL

Apparatus—A high-speed liquid chromatograph[2] equipped with a pump[3], a single-wavelength UV monitor (254 nm), and a liquid chromatograph injector[4] was used.

Columns—An octadecylsilane bonded to silica[5] column and a cyanopropylsilane[6] column were used in series. Both columns were 300-mm long × 4-mm i.d. stainless steel tubes.

Reagents—Sodium borate, tetrahydrofuran, and pyridine were reagent grades. Pilocarpine nitrate USP was used without further purification.

[1] U.S. Pharmacopeia, Drug Standards Division, personal communication.
[2] Model 202, Waters Associates.
[3] M-6000.
[4] U6K Universal.
[5] μBondapak C_{18}, Waters Associates.
[6] μBondapak CN, Waters Associates.

Table II—Analysis and Recovery of Pilocarpine from Pharmaceutical Preparations by HSLC

Preparation	Labeled Amount, mg/ml	Amount Added, mg/ml	Amount Found, mg/ml: Before Addition	Amount Found, mg/ml: After Addition	Recovery, %
Ophthalmic buffered solution	20	20	19.6	39.4	99.0 ± 1.0[a]
Ophthalmic solution containing pilocarpine hydrochloride and hydroxypropyl methylcellulose	10	20	10.3	20.2	99.5 ± 0.5
Ophthalmic solution containing pilocarpine hydrochloride and methylcellulose	100	50	97.5	148.2	101.4 ± 1.4
Ophthalmic solution containing pilocarpine nitrate, polyvinyl alcohol, chlorobutanol, and volatile oil constituents	10	10	10.1	20.1	100.0 ± 0.0

[a] Standard deviation.

Mobile Phase—The mobile phase, consisting of 30% tetrahydrofuran and 70% pH 9.2 borate buffer, was degassed by applying a water aspirator vacuum for 1 hr.

Internal Standard Solution—Pyridine, 50 μl/100 ml of water, was used.

Standard Pilocarpine Nitrate Solution—A 10-g/100 ml pilocarpine nitrate aqueous solution was used.

Conditions for Chromatographic Analysis—The degassed mobile phase was pumped through the columns at 1.0 ml/min (3000–3500 psi) at ambient temperature until a stable baseline was obtained.

Preparation of Standard Curve—Replicate 10-, 15-, and 20-μl injections of pyridine–pilocarpine nitrate (1:4) solutions were made using a 25-μl syringe[7]. The chromatograms were recorded[8] at a chart speed of 5 mm/min. The output from the UV monitor at 0.04 absorbance unit was fed into an electronic integrator[9] where the peak areas were integrated.

Interferences—The possible interferences from hydroxypropyl methylcellulose and benzalkonium chloride were studied by adding different amounts to a standard pilocarpine nitrate solution and performing the analysis.

The interference of decomposition products was studied also by rendering a sample of pilocarpine nitrate solution strongly alkaline with sodium hydroxide solution and refluxing for 30 min; the pH was adjusted to 7.0, the solution was diluted to volume, and the analysis was performed.

[7] Precision Sampling Corp., Baton Rouge, La.
[8] Perkin-Elmer model 56.
[9] Hewlett-Packard model 3370 B with digital printout.

Sample Preparation and Analysis—An aliquot of the pilocarpine preparation containing 0.5–1.0 g of pilocarpine as the free base was measured into a 10-ml volumetric flask, and 2 ml of the standard pyridine solution was added. Then 20 μl of the mixture was injected, and the amount of pilocarpine was calculated by comparison with a standard or the standard curve.

RESULTS AND DISCUSSION

The utilization of a mobile phase consisting of 30% tetrahydrofuran and 70% pH 9.2 borate buffer gave well-resolved, sharp peaks for pilocarpine and pyridine, with retention times of 5.0 and 9.3 min, respectively. The use of the columns in series afforded a better separation, especially between pilocarpine and hydroxypropyl methylcellulose. The ratio of the area of the pilocarpine peak to the area of the internal standard (pyridine) was calculated (Table I). The data show excellent linearity and reproducibility.

The method was applied to four pharmaceutical preparations containing pilocarpine salts to determine its suitability. These preparations were analyzed before and after the addition of known quantities of standard pilocarpine nitrate solution (Table II).

The proposed method allows for direct sampling from aqueous solutions of pilocarpine salts and eliminates the disadvantages of extraction. Hence, the method is suited for the routine quality control of pilocarpine salts in ophthalmic solutions.

REFERENCES

(1) J. M. Kolthoff, *Biochem. Z.*, **162,** 289 (1925).
(2) H. Wales, *Ind. Eng. Chem.*, **18,** 390 (1926).
(3) F. Reimers, K. R. Gottlieb, and V. A. Christensen, *J. Pharm. Pharmacol.*, **20,** 99 (1947).
(4) I. S. Shupe, *J. Assoc. Offic. Agr. Chem.*, **24,** 757 (1941).
(5) G. R. Lynch and 12 collaborators, *Analyst*, **73,** 311 (1948).
(6) V. Wurtzen, *Dan. Tidsskr. Farm.*, **13,** 160 (1939).
(7) J. M. Kolthoff, *Biochem. Z.*, **162,** 289 (1925).
(8) H. Matthes and O. Rammstedt, *Arch. Pharm.*, **245,** 131 (1907).
(9) G. Heikel, *Chem. Centr.*, **80,** 949 (1909).
(10) M. Mascre and J. Loiseau, *Bull. Sci. Pharmacol.*, **48,** 272 (1941).
(11) I. S. Gibbs and M. M. Tuckerman, *J. Pharm. Sci.*, **59,** 395 (1970).
(12) G. N. Thomis and D. Jatrides, *J. Pharm. Chem.*, **21,** 585 (1935).
(13) S. W. Dziedzic, S. E. Gitlow, and D. L. Krohn, *J. Pharm. Sci.*, **65,** 1262 (1976).
(14) "The United States Pharmacopeia," 19th rev., Mack Publishing Co., Easton, Pa., 1975, p. 384.
(15) *Ibid.*, p. 385.
(16) *Ibid.*, p. 386.
(17) C.-Y. Wu and S. Sigga, *Anal. Chem.*, **44,** 1499 (1972).
(18) J. N. Done, J. H. Knox, and J. Loheac, "Applications of High-Speed Liquid Chromatography," Wiley, London, England, 1974, p. 164.

ACKNOWLEDGMENTS AND ADDRESSES

Received November 26, 1976, from the *College of Pharmacy, North Dakota State University, Fargo, ND 58102.*

Accepted for publication January 11, 1977.

Alkaloids of *Nelumbo lutea* (Willd.) pers. (Nymphaeaceae)

STEVEN G. ZELENSKI

Abstract □ A phytochemical investigation of an alcoholic extract of the petioles of *Nelumbo lutea* resulted in the identification of the alkaloids *N*-methylasimilobine, anonaine, and roemerine. The alkaloids nuciferine, armepavine, *N*-nornuciferine, and *N*-norarmepavine, previously reported in the whole plant, were also identified.

Keyphrases □ *Nelumbo lutea*—alcoholic extract of petioles, various alkaloids identified □ Alkaloids, various—identified in alcoholic extract of petioles of *Nelumbo lutea*

Nelumbo lutea (Willd.) pers. (Nymphaeaceae), or American lotus, is widely distributed in the United States and can be found from Louisiana north to Wisconsin. In previous phytochemical investigations, the alkaloids nuciferine, armepavine, *N*-nornuciferine, and *N*-norarmepavine were isolated from leaves and stems of this species (1).

A 2-propanol extract of the petioles was fractionated to yield an alkaloid fraction. Chromatography of this fraction was followed by combined GLC–mass spectrometry of the alkaloids. Analysis of the spectra and comparison with standard materials resulted in the identification of the benzylisoquinoline alkaloids *N*-methylasimilobine (I), anonaine (II), and roemerine (III).

The previously reported alkaloids (nuciferine, armepavine, *N*-nornuciferine, and *N*-norarmepavine) also were identified in this extract. Since only trace amounts of each alkaloid were isolated by semipreparative GLC (2) for melting-point determinations or derivatization, no information is available on their stereochemistry. All of these alkaloids previously were isolated from the Asiatic lotus, *N. nucifera* Gaertn. (Nymphaeaceae) (3). The alkaloid nuciferine has been shown to possess an inhibitory action toward acetylcholine in rat Renshaw cells (4).

EXPERIMENTAL

Plant Material—The petioles of *N. lutea* were collected in July 1975[1].

Extraction—Fresh plant material of *N. lutea* (18 kg) was homogenized in a large blender at 5° with 10 liters of 2-propanol. The extract was filtered, and the marc was allowed to macerate with another 20 liters of 2-propanol. The combined filtrates were evaporated *in vacuo* at 37° to leave a dark-green syrupy extract (1.2 kg).

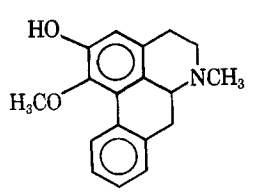

I

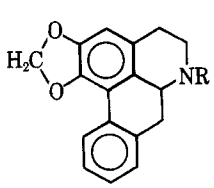

II: R = H
III: R = CH_3

Fractionation—This extract was acidified with 2 liters of 10% acetic acid and extracted with 400 ml each of ether, ethyl acetate, and chloroform. The acidic aqueous layer was made basic with 28% NH_4OH and extracted with 2 × 500 ml of chloroform. The chloroform residue was evaporated *in vacuo* to yield a tan crystalline solid (225 mg). This material was further purified by silica gel[2] column chromatography (140 g, 2 × 65 cm) and elution with increasing concentrations of methanol in chloroform to which 1% pyridine had been added.

Procedures—*Methylation of* N-*Nornuciferine and* N-*Norarmepavine*—Isolated *N*-nornuciferine and *N*-norarmepavine were methylated with formaldehyde–formic acid (5) to yield nuciferine and armepavine, respectively.

Combined GLC–Mass Spectrometry—The fractions from silica gel chromatography were injected directly into a 2-m × 2-mm i.d. glass column containing 1.5% OV-17–1.95% QF-1 on Varaport 30. The column temperature was programmed from 160 to 260° at 2°/min. The injection temperature was 230°. The carrier gas was helium at 28 ml/min. The effluent from the column entered the mass spectrometer through a glass jet separator maintained at 220°, and the ion source temperature was maintained at 220°. The ionizing voltage was 70 ev, and the accelerating voltage was 12,600 to 900 ev. Spectra were recorded every 10 sec on a low-resolution mass spectrometer interfaced with a data reduction system[3].

Identification of I—The GLC retention time was 800 sec (standard 800 sec). The mass spectrum showed ions at M^+ *m/e* 281 (87%), 280 (100), 266 (77), 250 (48), 178 (57), 165 (40), and 152 (25) [standard M^+ *m/e* 281 (85%), 280 (100), 266 (70), 250 (52), 178 (57), 165 (37), and 152 (25)]. The melting point was 194–195° [lit. (6) mp 195–196°].

Identification of II—The GLC retention time was 1040 sec (standard 1033 sec). The mass spectrum showed ions at M^+ *m/e* 265 (15%), 264 (82), 176 (9), 151 (49), 102 (100), and 88 (60) [standard M^+ *m/e* 265 (10%), 264 (84), 176 (11), 151 (51), 102 (100), and 88 (57)]. The melting point was 120–121° [lit. (3) mp 118–121°].

Identification of III—The GLC retention time was 900 sec (standard 903 sec). The mass spectrum showed ions at M^+ *m/e* 279 (24%), 278 (100), 262 (13), 236 (9), 204 (5), 178 (67), and 165 (24) [standard M^+ *m/e* 279 (20%), 278 (100), 262 (11), 236 (11), 204 (5), 178 (69), and 165 (25)]. The melting point was 100–101° [lit. (6) mp 100–101°].

Identification of Nuciferine—The GLC retention time was 1430 sec (standard 1410 sec). The mass spectrum showed ions at M^+ *m/e* 295 (100%), 294 (56), 280 (38), 265 (38), 252 (23), and 139 (11) [standard M^+ *m/e* 295 (100%), 294 (55), 280 (35), 265 (35), 252 (23), and 139 (10)]. The melting point was 164–165° [lit. (6) mp 162–163°].

Identification of Armepavine—The GLC retention time was 1028 sec (standard 1030 sec). The mass spectrum showed ions at M^+ *m/e* 313 (0.09%), 206 (49), 190 (10), 177 (6), 132 (50), 118 (18), 107 (77), and 91 (43) [standard M^+ *m/e* 313 (0.08%), 206 (48), 190 (11), 177 (6), 132 (52), 118 (18), 107 (75), and 91 (45)]. The melting point was 167–168° [lit. (1) mp 166–167°].

Identification of *N*-Nornuciferine—The GLC retention time was 930 sec. The mass spectrum showed ions at M^+ *m/e* 281 (49%), 280 (78), 266 (20), 264 (60), 251 (17), 221 (23), 207 (27), 194 (52), and 165 (100). Methylation of this compound yielded a compound whose mass spectrum was identical with nuciferine.

Identification of *N*-Norarmepavine—The GLC retention time was 1150 sec. The mass spectrum showed ions at M^+ *m/e* 299 (0.15%), 192 (93), 176 (100), 159 (22), 148 (68), 146 (21), and 131 (35). Methylation of this compound yielded a compound whose mass spectrum was identical with armepavine.

[1] The plant material was identified as *N. lutea* (Willd.) pers. (Nymphaeaceae) by Dr. Dale Thomas, Department of Botany, Northeast Louisiana University. A voucher specimen (SZ-03:069) is available for inspection at the Herbarium of the Department of Pharmacy, Northeast Louisiana University.

[2] Hi-Flosil, 60–200 mesh, Applied Science Laboratories.

[3] Du Pont 321 Dimespec and 320 data system.

REFERENCES

(1) S. M. Kupchan, B. Dasgupta, E. Jujita, and M. L. King, *Tetrahedron*, **19**, 227 (1963).

(2) S. G. Zelenski, Ph.D. thesis, University of Rhode Island, Kingston, R.I., 1973.

(3) J. Kunitomo, Y. Nagai, Y. Okamoto, and H. Furukawa, *J. Pharm. Soc. Jpn.*, **90** (9), 165 (1970).

(4) A. W. Duggan, D. Lodge, T. J. Bixcoe, and P. M. Headley, *Arch. Int. Pharmacodyn. Ther.*, **204** (1), 147 (1973).

(5) R. N. Icke and B. B. Wisegarver, "Organic Synthesis," coll. vol. III, Wiley, New York, N.Y., 1955, p. 723.

(6) M. Tomita, Y. Watanabe, M. Tomita, and H. Furukawa, *J. Pharm. Soc. Jpn.*, **81**, 469 (1961).

ACKNOWLEDGMENTS AND ADDRESSES

Received August 25, 1976, from the *School of Pharmacy, Northeast Louisiana University, Monroe, LA 71203.*

Accepted for publication January 31, 1977.

The author thanks Dr. Jun-ichi Kunitomo for samples of roemerine, *O*-nornuciferine, anonaine, nuciferine, and armepavine.

GLC Microanalyses of Phenacetin and Acetaminophen Plasma Levels

M. A. EVANS and R. D. HARBISON ˣ

Abstract □ A GLC method utilizing a flame-ionization detector is described for the simultaneous analysis of acetaminophen and phenacetin in plasma. *p*-Bromoacetanilide is used as an internal standard. The drugs are extracted with ether from plasma diluted with 1 *M* phosphate buffer (pH 7.4). The ether extract is evaporated to dryness under nitrogen, and the residue is dissolved in 300 μl of ethyl acetate. The ethyl acetate is transferred to a microcentrifuge tube (0.4 ml), and the sample is evaporated in a vacuum centrifuge. Then the residue is redissolved in 0.2 *M* trimethylanilinium hydroxide in methanol for GLC analysis. Extraction efficiency of added phenacetin and acetaminophen in plasma at concentrations of 1–10 μg/ml was complete, and the limit of detection in plasma was less than 0.1 μg.

Keyphrases □ Phenacetin—GLC analysis in presence of acetaminophen, plasma □ Acetaminophen—GLC analysis in presence of phenacetin, plasma □ GLC—simultaneous analyses, phenacetin and acetaminophen in plasma □ Analgesics—phenacetin and acetaminophen, simultaneous GLC analyses in plasma

Acetaminophen (I) and phenacetin (II) are commonly used analgesics available without prescription. Acute overdose with either compound can produce a dose-dependent, potentially fatal hepatic necrosis (1). Renal tubular necrosis and hypoglycemic coma also can occur (2). Chronic overdosage of I or II has been reported to produce blood dyscrasia including methemoglobinemia, hemolytic anemia, and thrombocytopenia (3). Thus, toxicity coupled with widespread use necessitates specific and rapid detection of the compounds in biological specimens.

A sensitive and specific method for the estimations of I and II in plasma and urine by a GLC technique using trimethylsilyl derivatives was reported recently (4). However, it has a significant time requisite and absolute dryness is required to achieve effective silylating reactions. Furthermore, the continued use of silylating agents leads to rapid detector contamination. A GLC method for I based on sequential alkylation, followed by on-column derivatization with trimethylanilinium hydroxide, also was demonstrated (5). This method is time consuming and specific only for I (5).

Other reported methods for the estimation of I or II in biological specimens are nonspecific, lack sensitivity, or require a large sample volume (6–9). Therefore, a GLC method was developed for the rapid analysis of small amounts of I and II in plasma using an internal standard for quantitation. The sensitivity of this method was greater than 0.1 μg/ml of plasma for both compounds, and no interference was observed with peak identification.

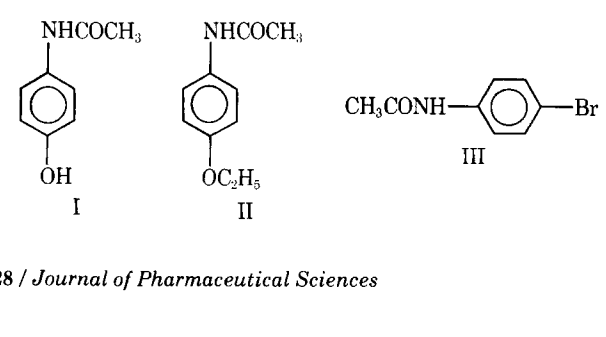

I II III

EXPERIMENTAL

Apparatus—A gas chromatograph[1] equipped with a flame-ionization detector was maintained with gas flows of 5, 30, and 150 ml/min for nitrogen, hydrogen, and air, respectively. A column oven temperature of 165° was used; the injection port and detector were maintained at 300°.

Column—A glass column, 2 m × 2 mm, was packed with 3% SP 2250 on 80–100-mesh Chromosorb W, AW/DMCS[2]. Before packing, the column was rinsed with methanol and acetone, dried, and conditioned 6 hr with a 10% solution of dimethyldichlorosilane[3] in toluene to silylate reactive sites. Following silylation, the column was again rinsed with acetone and dried.

Analytical Procedures—Plasma, 0.1–0.5 ml, was transferred to a 13-ml glass-stoppered centrifuge tube, mixed with the internal standard *p*-bromoacetanilide[4] (III) (10 μg/ml), and diluted with an equal volume of 1 *M* phosphate buffer (pH 7.4). The plasma was extracted with reagent grade ether (7 ml) by stirring on a vortex mixer (30 sec). The ether was transferred by disposable pipet to a dry, clean, 12-ml centrifuge tube and evaporated to dryness in a water bath (45°) using a nitrogen flow. Then the residue was dissolved in 300 μl of spectrophotometric grade ethyl acetate[5] and transferred to a microcentrifuge tube[6] (0.4 ml).

The sample was taken to dryness under vacuum in a rotary vacuum centrifuge[7] and redissolved in 4–8 μl of trimethylanilinium hydroxide (0.2 *M* in methanol)[8]. Samples of 1–3 μl were injected into the gas chro-

[1] Varian model 2100.
[2] Supelco, Bellefonte, Pa.
[3] Applied Science Laboratories, State College, Pa.
[4] Aldrich Chemicals, Atlanta, Ga.
[5] Mallinckrodt Chemicals, St. Louis, Mo.
[6] Brinkmann Instruments, Westbury, N.Y.
[7] Speed Vac concentrator, Savant Instruments, Hicksville, N.Y.
[8] Methulate, Pierce Chemicals, Rockford, Ill.

REFERENCES

(1) S. M. Kupchan, B. Dasgupta, E. Jujita, and M. L. King, *Tetrahedron*, **19**, 227 (1963).

(2) S. G. Zelenski, Ph.D. thesis, University of Rhode Island, Kingston, R.I., 1973.

(3) J. Kunitomo, Y. Nagai, Y. Okamoto, and H. Furukawa, *J. Pharm. Soc. Jpn.*, **90** (9), 165 (1970).

(4) A. W. Duggan, D. Lodge, T. J. Bixcoe, and P. M. Headley, *Arch. Int. Pharmacodyn. Ther.*, **204** (1), 147 (1973).

(5) R. N. Icke and B. B. Wisegarver, "Organic Synthesis," coll. vol. III, Wiley, New York, N.Y., 1955, p. 723.

(6) M. Tomita, Y. Watanabe, M. Tomita, and H. Furukawa, *J. Pharm. Soc. Jpn.*, **81**, 469 (1961).

ACKNOWLEDGMENTS AND ADDRESSES

Received August 25, 1976, from the *School of Pharmacy, Northeast Louisiana University, Monroe, LA 71203.*

Accepted for publication January 31, 1977.

The author thanks Dr. Jun-ichi Kunitomo for samples of roemerine, *O*-nornuciferine, anonaine, nuciferine, and armepavine.

GLC Microanalyses of Phenacetin and Acetaminophen Plasma Levels

M. A. EVANS and R. D. HARBISON ˣ

Abstract □ A GLC method utilizing a flame-ionization detector is described for the simultaneous analysis of acetaminophen and phenacetin in plasma. *p*-Bromoacetanilide is used as an internal standard. The drugs are extracted with ether from plasma diluted with 1 *M* phosphate buffer (pH 7.4). The ether extract is evaporated to dryness under nitrogen, and the residue is dissolved in 300 μl of ethyl acetate. The ethyl acetate is transferred to a microcentrifuge tube (0.4 ml), and the sample is evaporated in a vacuum centrifuge. Then the residue is redissolved in 0.2 *M* trimethylanilinium hydroxide in methanol for GLC analysis. Extraction efficiency of added phenacetin and acetaminophen in plasma at concentrations of 1–10 μg/ml was complete, and the limit of detection in plasma was less than 0.1 μg.

Keyphrases □ Phenacetin—GLC analysis in presence of acetaminophen, plasma □ Acetaminophen—GLC analysis in presence of phenacetin, plasma □ GLC—simultaneous analyses, phenacetin and acetaminophen in plasma □ Analgesics—phenacetin and acetaminophen, simultaneous GLC analyses in plasma

Acetaminophen (I) and phenacetin (II) are commonly used analgesics available without prescription. Acute overdose with either compound can produce a dose-dependent, potentially fatal hepatic necrosis (1). Renal tubular necrosis and hypoglycemic coma also can occur (2). Chronic overdosage of I or II has been reported to produce blood dyscrasia including methemoglobinemia, hemolytic anemia, and thrombocytopenia (3). Thus, toxicity coupled with widespread use necessitates specific and rapid detection of the compounds in biological specimens.

A sensitive and specific method for the estimations of I and II in plasma and urine by a GLC technique using trimethylsilyl derivatives was reported recently (4). However, it has a significant time requisite and absolute dryness is required to achieve effective silylating reactions. Furthermore, the continued use of silylating agents leads to rapid detector contamination. A GLC method for I based on sequential alkylation, followed by on-column derivatization with trimethylanilinium hydroxide, also was demonstrated (5). This method is time consuming and specific only for I (5).

Other reported methods for the estimation of I or II in biological specimens are nonspecific, lack sensitivity, or require a large sample volume (6–9). Therefore, a GLC method was developed for the rapid analysis of small amounts of I and II in plasma using an internal standard for quantitation. The sensitivity of this method was greater than 0.1 μg/ml of plasma for both compounds, and no interference was observed with peak identification.

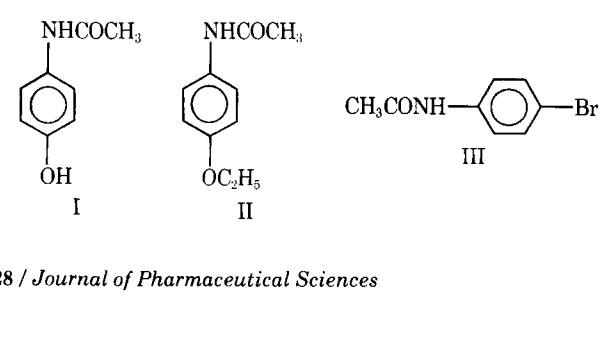

I II III

EXPERIMENTAL

Apparatus—A gas chromatograph[1] equipped with a flame-ionization detector was maintained with gas flows of 5, 30, and 150 ml/min for nitrogen, hydrogen, and air, respectively. A column oven temperature of 165° was used; the injection port and detector were maintained at 300°.

Column—A glass column, 2 m × 2 mm, was packed with 3% SP 2250 on 80–100-mesh Chromosorb W, AW/DMCS[2]. Before packing, the column was rinsed with methanol and acetone, dried, and conditioned 6 hr with a 10% solution of dimethyldichlorosilane[3] in toluene to silylate reactive sites. Following silylation, the column was again rinsed with acetone and dried.

Analytical Procedures—Plasma, 0.1–0.5 ml, was transferred to a 13-ml glass-stoppered centrifuge tube, mixed with the internal standard *p*-bromoacetanilide[4] (III) (10 μg/ml), and diluted with an equal volume of 1 *M* phosphate buffer (pH 7.4). The plasma was extracted with reagent grade ether (7 ml) by stirring on a vortex mixer (30 sec). The ether was transferred by disposable pipet to a dry, clean, 12-ml centrifuge tube and evaporated to dryness in a water bath (45°) using a nitrogen flow. Then the residue was dissolved in 300 μl of spectrophotometric grade ethyl acetate[5] and transferred to a microcentrifuge tube[6] (0.4 ml).

The sample was taken to dryness under vacuum in a rotary vacuum centrifuge[7] and redissolved in 4–8 μl of trimethylanilinium hydroxide (0.2 *M* in methanol)[8]. Samples of 1–3 μl were injected into the gas chro-

[1] Varian model 2100.
[2] Supelco, Bellefonte, Pa.
[3] Applied Science Laboratories, State College, Pa.
[4] Aldrich Chemicals, Atlanta, Ga.
[5] Mallinckrodt Chemicals, St. Louis, Mo.
[6] Brinkmann Instruments, Westbury, N.Y.
[7] Speed Vac concentrator, Savant Instruments, Hicksville, N.Y.
[8] Methulate, Pierce Chemicals, Rockford, Ill.

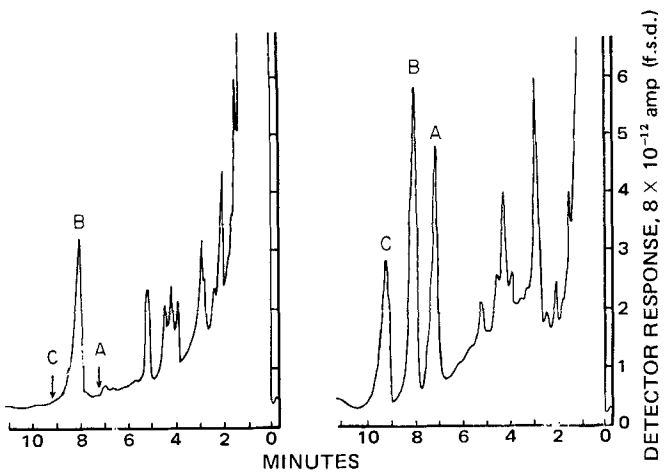

Figure 1—*Gas chromatograms of human plasma (0.5 ml). Key: left, control plasma containing 5 μg of internal standard (peak B); and right, plasma containing 2.5 μg of I (peak A) and II (peak C) with 5 μg of III. Compounds I–III were chromatographed as methylated derivatives.*

matograph for analysis. A total of 30 samples was analyzed for the determination of the standard curve. Extraction efficiency was determined by GLC peak height comparison of plasma extracts and standards prepared in ethyl acetate.

RESULTS AND DISCUSSION

The GLC retention times for the *N,O*-dimethyl derivative of I, the *N*-methyl derivative of III, and the *N*-methyl derivative of II were about 7.0, 8.0, and 9.0 min, respectively. A gas chromatogram from a control human plasma (0.5 ml) containing 10 μg of III/ml and plasma (0.5 ml) containing 5 μg of I–III/ml is shown in Fig. 1. Peaks for all three agents were symmetrical, so quantitation was made by comparison of peak heights. The detector response and calibration curve were linear for all three compounds over the 0.1–10-μg range. Blanks were prepared from plasma of drug-free subjects, and no peaks were observed that would interfere with the measurements of the compounds.

Linear regression analysis of the individual data points from the standards plotted as the ratio of peak height drug/peak height internal standard *versus* plasma drug level gave computed slopes of 0.274/μg of I and 0.172/μg of II. The correlation coefficient for I based on analysis of 30 samples was 0.990; for II, it was 0.998. The intercept for both compounds within the regression analysis was less than 0.02.

The extraction of both drugs from plasma was essentially complete within the 0.1–10-μg/ml range, and the reproducibility of the assay was good down to concentrations of less than 0.1 μg/ml of plasma. The mean recovery from 10 samples containing 0.1–10 μg of both compounds/ml was 97.8% (*SE* 4.2). No interference in peak height measurements was noted from plasma samples spiked with aspirin, caffeine, codeine, or barbiturates, all of which are likely to be in taken combination with I and II.

The use of the rotary vacuum centrifuge allows the efficient concentration of the sample. Previous use of this instrument was primarily restricted to a radioenzymatic assay for neurotransmitters where sample size was necessarily limited (10). Application to routine drug analysis by GLC allowed up to a 20-fold increase in sensitivity of the assay. Furthermore, the instrument is designed for routine, multisample use, and the total assay time from plasma extraction to GLC was less than 1.5 hr.

GLC analysis of I was reported previously (11), but in the present studies the drug could not be chromatographed directly in low concentrations without peak tailing and absorption losses. Flash heater methylation with trimethylanilinium hydroxide gave a complete reaction for the internal standard and both drugs under the described conditions without degradation peaks. On-column methylation to a less polar derivative results in a much more volatile compound suitable for quantitative GLC analysis in the submicrogram range (12). The use of trimethylanilinium hydroxide as a derivatizing agent also allows for rapid analysis without excessive detector contamination.

Maximum plasma concentrations for six normal adults following ingestion of 1 g of I ranged from 5.7 to 13.3 μg/ml. Acute ingestion of toxic amounts of I can produce a blood concentration above 100 μg/ml of plasma (13). Chronic intoxication with I and II, however, can produce intermediate plasma concentrations, necessitating specific quantitative analysis. Additionally, in the normal individual, 75–80% of administered II is rapidly metabolized to I, with peak plasma concentration of unchanged II occurring in about 1 hr and that of I occurring in 1–2 hr (1). This rapid method of analysis may be useful in correlating plasma levels with the prognosis of cases of intoxication and may be applied to the study of dosage regimens for both I and II.

REFERENCES

(1) "The Pharmacological Basis of Therapeutics," 5th ed., L. S. Goodman and A. Gilman, Eds., Macmillan, New York, N.Y., 1975, p. 345.

(2) G. E. Schreiner, *Ann. Intern. Med.*, **57**, 1047 (1902).

(3) C. H. Thienes and T. J. Hardy, "Clinical Toxicology," 5th ed., Lea and Febiger, Philadelphia, Pa., 1972, p. 80.

(4) L. F. Prescott, *J. Pharm. Pharmacol.*, **23**, 111 (1971).

(5) W. A. Dechliaruk, G. F. Johnson, and H. M. Soloman, *Clin. Chem.*, **22**, 879 (1976).

(6) H. Buch, K. Pflegel, and W. Rudigel, *Z. Klin. Chem.*, **5**, 110 (1967).

(7) A. J. Cummings, M. L. King, and B. K. Martin, *Br. J. Pharmacol. Chemother.*, **29**, 150 (1967).

(8) J. E. Wallace, J. D. Biggs, H. E. Hamilton, L. L. Foster, and K. Blum, *J. Pharm. Sci.*, **62**, 599 (1973).

(9) J. I. Routh, N. A. Shane, E. G. Arredongo, and W. D. Paul, *Clin. Chem.*, **14**, 882 (1968).

(10) B. P. Abramson, M. W. McCaman, and R. E. McCaman, *Anal. Biochem.*, **57**, (1974).

(11) A. Klutch and M. Bordun, *J. Pharm. Sci.*, **57**, 524 (1968).

(12) E. Brochmann-Hanssen and T. O. Oke, *ibid.*, **58**, 370 (1969).

(13) J. Grove, *J. Chromatogr.*, **58**, 289 (1971).

ACKNOWLEDGMENTS AND ADDRESSES

Received August 2, 1976, from the *Department of Pharmacology, Vanderbilt Medical Center, Nashville, TN 37232.*

Accepted for publication January 19, 1977.

Supported in part by U.S. Public Health Service Grants ES00267 and DA00141. M. A. Evans was supported by Research Development Award NS00346.

[x] To whom inquiries should be directed.

Molecular Connectivity and Retention Indexes

Y. MICHOTTE and D. L. MASSART ˣ

Abstract □ The molecular connectivity indexes, χ, of some alcohols, ethers, esters, and ketones did not correlate very well with their retention volumes in some GLC systems. It was concluded that the utility of χ for the prediction of biological activities could prove rather limited.

Keyphrases □ Molecular connectivity indexes—attempted correlation with GLC retention indexes of various alcohols, ethers, esters, and ketones □ GLC retention indexes—attempted correlation with molecular connectivity indexes of various alcohols, ethers, esters, and ketones □ Topological indexes—molecular connectivity indexes correlated with GLC retention indexes of various alcohols, ethers, esters, and ketones

Recently, the molecular connectivity index, χ, was used to predict several parameters related to biological activities of drugs (1). One of these parameters was log P, the partition coefficient between octanol and water, which is one of the three principal parameters in the Hansch equations (2) that are used to predict (or rationalize) biological activities of drugs. The authors concluded (1) that direct correlation of molecular connectivity to biological activity is possible.

If the biological activity of a substance is to be predicted from χ, then this property must be correlated with the magnitude of the diverse physicochemical interactions the substance is subjected to from resorption to receptor. These interactions are often very specific in nature. Even log P is a rather complex quantity, since it is determined by interactions with two different phases. Therefore, if χ is to have some general value, it should be sufficiently correlated with interactions of diverse natures.

To have a more precise idea of the potential value of χ, it was of interest to study interactions with some simpler systems. Since large compilations of GLC data exist (3) and since GLC retention is the result of a relatively simple equilibrium between a liquid phase and a gas, the correlation of χ with retention indexes (R.I.) was investigated.

EXPERIMENTAL

The connectivity index, χ, is calculated in the following way (1). The chemical formula is written down in the skeletal form, and each atom is assigned a number corresponding to the number of atoms attached. Hydrogen atoms are suppressed. For carbon atoms, the number equals 1, 2, 3, or 4. An ether oxygen is assigned the number 2; the N-atoms of the amines RNH and R_2N are assigned the numbers 2 and 3, respectively. The product of the numbers associated with the two atoms of one bond is then found. The sum of the reciprocal square root of these products is calculated to give a number, called the connectivity index.

For example, for 2-methyl-2-pentanol (I):

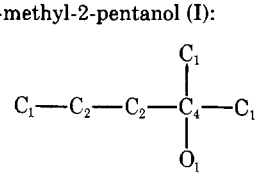

I

$$\chi = \frac{1}{\sqrt{2}} + \frac{1}{\sqrt{4}} + \frac{1}{\sqrt{8}} + \frac{1}{\sqrt{4}} + \frac{1}{\sqrt{4}} + \frac{1}{\sqrt{4}} = 3.061 \quad \text{(Eq. 1)}$$

Retention indexes are the logarithms of the adjusted retention volume (log V_R') relative to those of normal paraffins. Correlations between χ and the retention index were obtained for four stationary phases, namely the apolar squalane, the polar diethylene glycol succinate and polyethylene glycol 300, and one rather special phase[1] (II), which has unique properties (4, 5) and interacts strongly with ketones.

Table I—Correlation Coefficients between the Retention Index and χ

Compound Family	Squalane	Diethylene Glycol Succinate	Polyethylene Glycol 300	II
Alcohols	0.95	0.76	0.78	0.92
Esters	0.99	0.91	0.96	0.98
Ketones	0.99	0.94	0.96	0.98
Ethers	0.97	0.71	0.82	0.71
All compounds	0.91	0.55	0.56	0.73

Four groups of substances were studied. The first included methanol, ethanol, 1-propanol, 1-butanol, 1-pentanol, 3-pentanol, 1-hexanol, 2-hexanol, 3-hexanol, 1-heptanol, 1-octanol, 2-methyl-2-butanol, 3-methyl-2-butanol, 2,2-dimethyl-1-propanol, 2-methyl-2-pentanol, 3-methyl-2-pentanol, 4-methyl-2-pentanol, 2-methyl-3-pentanol, 3-methyl-3-pentanol, 2,4-dimethyl-3-pentanol, 3-ethyl-3-pentanol, and cyclohexanol.

The second group included acetone, 2-butanone, 2-pentanone, 3-pentanone, 3-methyl-2-butanone, 2-hexanone, 3-hexanone, 3-methyl-2-pentanone, 4-methyl-2-pentanone, 2-heptanone, 3-heptanone, 2,4-dimethyl-3-pentanone, 2-nonanone, and 5-nonanone.

The third group consisted of ether, methyl butyl ether, methyl propyl ether, isobutyl methyl ether, *tert*-butyl methyl ether, dipropyl ether, and isopropyl propyl ether. And the fourth group included ethyl formate, propyl formate, methyl acetate, ethyl acetate, propyl acetate, isopropyl acetate, butyl acetate, *sec*-butyl acetate, methyl propanoate, ethyl propanoate, methyl butanoate, ethyl butanoate, and pentyl acetate.

The χ values for these substances were taken from Murray *et al.* (1), and the retention index values were taken from the data of McReynolds (3).

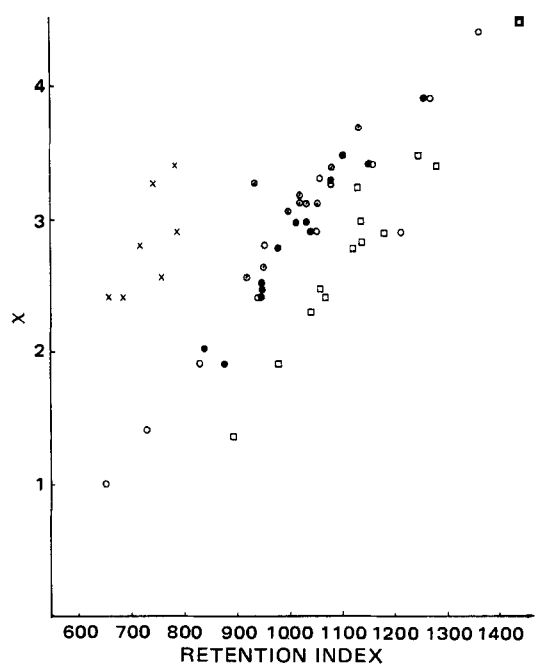

Figure 1—*Plot of* χ versus *retention indexes obtained using II as the stationary phase. Key:* ○, *straight chain alcohols;* ⊙, *branched chain alcohols;* ●, *esters;* □, *ketones; and* ×, *ethers.*

[1] Zonyl E7.

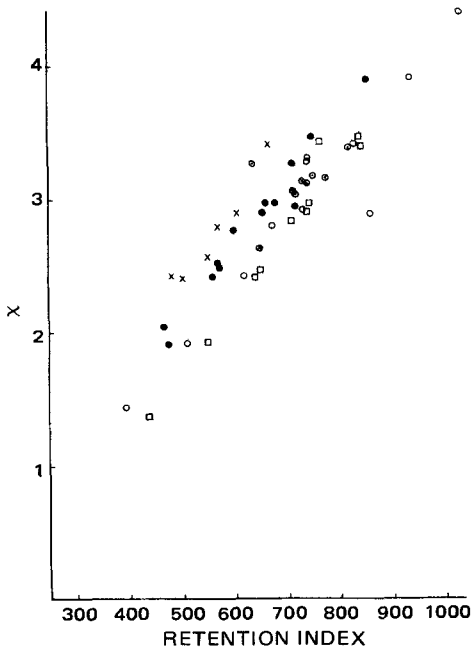

Figure 2—*Plot of* χ versus *retention indexes obtained using squalane as the stationary phase. Key:* ○, *straight chain alcohols;* ⊙, *branched chain alcohols;* ●, *esters;* □, *ketones; and* ×, *ethers.*

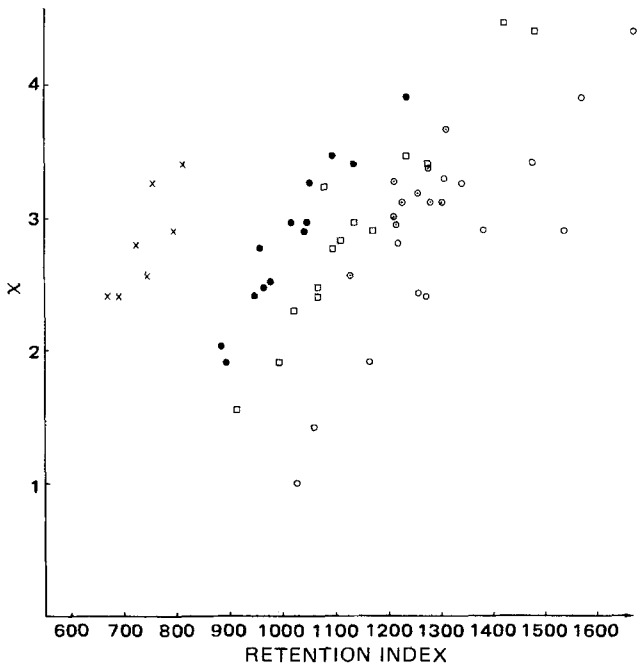

Figure 4—*Plot of* χ versus *retention indexes obtained using polyethylene glycol 300 as the stationary phase. Key:* ○, *straight chain alcohols;* ⊙, *branched chain alcohols;* ●, *esters;* □, *ketones; and* ×, *ethers.*

DISCUSSION

The correlation coefficients are given in Table I, and the results are shown in Figs. 1–4. While some correlations are good, many correlation coefficients are lower than 0.976, the lowest correlation found between χ and log P for a class of compounds (the ether family) by Murray *et al.* (1).

Of particular interest is the behavior of the alcohols. The retention index values of the straight chain alcohols are perfectly correlated with χ. This result was, of course, to be expected since the retention index values of these substances plotted as a function of the number of carbon atoms fall on a straight line and since χ is also a linear function of the number of carbon atoms. On the two polar phases, however, the branched chain alcohols do not fall on this straight line; cyclohexanol is a point by itself, apparently unrelated to the other alcohols.

The ethers, esters, and ketones fall on other lines rather distant from that of the straight chain alcohols. This result leads to correlation coefficients for all compounds on the two polar phases of 0.5–0.6.

The interactions on the two polar phases may be unrepresentative of what happens in biological systems; but if the molecular connectivity is a fundamental property, as advocated by Murray *et al.* (1), a better correlation should be expected. From the results obtained with the two polar phases, one can anticipate that rather bad results will be obtained, at least in some cases, for the prediction of biological activities.

The correlation on squalane is better but less than would be expected from the performance of χ for the parameters studied previously (1). Squalane is a hydrocarbon, and its interactions resemble those of octanol or the lipid phase for which the latter is representative in the Hansch equations. Here again, the clear segregation of the four families of compounds results in a correlation coefficient of 0.91. This segregation points out that the primary defect of χ is that the role of functional groups such as hydroxyl and carbonyl is not sufficiently taken into account. This fact is demonstrated by the results with II. Where, on other phases, the ketone line is found before (at a lower retention index) or at about the same retention index as the alcohol line, it lags rather considerably behind on II. As stated before, II is known to interact with ketones.

The object of this report is not to say that χ is useless. It is a topological quantity which, as shown conclusively (1), allows prediction or rationalization of some interesting parameters. However, it may be of more limited use than can be expected from the previous conclusion (1) and, in any case, the results obtained should be used with caution, particularly when there is reason to believe that functional groups play a determining role in the biological activity.

Kier and coworkers altered the way of calculating the molecular connectivity index[2]. They developed extended connectivity functions, which encode additional information about multiple paths in a molecule. They also developed nonempirical self-consistent parameters, which can be used to treat heteroatoms of interest in biology. The improved connectivity calculations might allow a better prediction of retention indexes than was obtained here with the simple χ parameter.

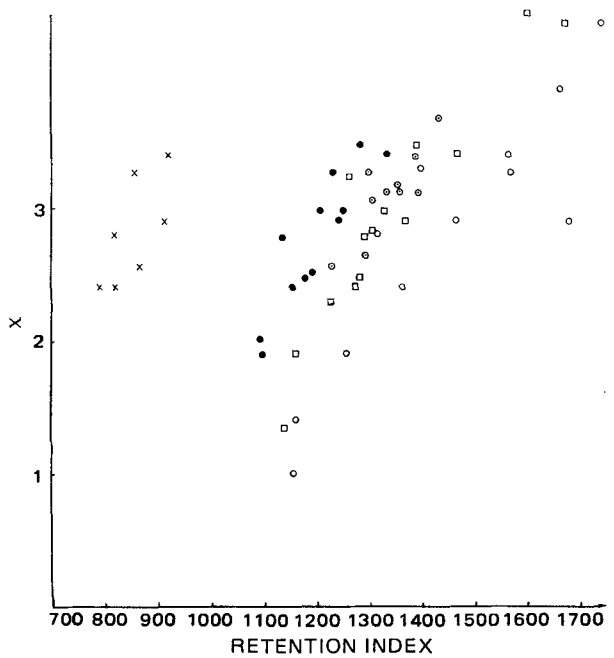

Figure 3—*Plot of* χ versus *retention indexes obtained using diethylene glycol succinate as the stationary phase. Key:* ○, *straight chain alcohols;* ⊙, *branched chain alcohols;* ●, *esters;* □, *ketones; and* ×, *ethers.*

REFERENCES

(1) W. J. Murray, L. H. Hall, and L. B. Kier, *J. Pharm. Sci.*, **64**, 1978 (1975).

[2] Personal communication.

(2) C. Hansch, J. E. Quinlan, and G. L. Lawrence *J. Org. Chem.*, **33**, 347 (1968).
(3) W. O. M. McReynolds, "Gas Chromatographic Retention Data," Preston Technical Abstracts Co., Evanston, Ill., 1964.
(4) S. Wold and K. Andersson, *J. Chromatogr.*, **80**, 43 (1973).
(5) D. L. Massart, P. Lenders, and M. Lauwereys, *J. Chromatogr. Sci.*, **12**, 617 (1974).

ACKNOWLEDGMENTS AND ADDRESSES

Received October 28, 1976, from the *Farmaceutisch Instituut, Vrije Universiteit Brussel, Paardenstraat 67, B-1640 Sint Genesius Rhode, Belgium.*

Accepted for publication January 27, 1977.

[x] To whom inquiries should be directed.

Fluorometric Determination of Methyldopa in Biological Fluids

BONG K. KIM and ROBERT T. KODA [x]

Abstract □ A fluorometric method for the analysis of methyldopa, based on the formation of a fluorophore after oxidation and rearrangement, is described. The drug is isolated from biological fluids by adsorption on alumina and elution with an organic solvent. Fluorescence is linear from 0.1 to 1.5 μg of methyldopa/ml. The assay has a lower limit of sensitivity of 100 ng/ml and is suitable for pharmacokinetic studies following therapeutic doses in animals and humans.

Keyphrases □ Methyldopa—fluorometric analysis, biological fluids □ Fluorometry—analysis, methyldopa in biological fluids □ Antihypertensive agents—methyldopa, fluorometric analysis in biological fluids

Methyldopa is a widely used antihypertensive agent with sedative and aromatic L-aminodecarboxylase-inhibiting properties (1–7). Methods to analyze the drug in pharmaceutical preparations and biological fluids have utilized visible spectrophotometry (8, 9), GLC (10), high-pressure liquid chromatography (11), and fluorometry (12, 13). In addition, tracer methodology has been used for metabolic and disposition studies (14, 15).

Fluorometric methods have been primarily based on the production of a fluorescent indole derivative (lutin) by oxidation and subsequent rearrangement. This technique has also been applied to estimate catecholamines and related compounds (16). Existing fluorometric methods appear to be insufficiently sensitive for the determination of drug levels in biological fluids.

This paper describes an improved analytical method in which methyldopa is adsorbed on alumina, eluted with an organic solvent, and then oxidized to form the fluorophore, dihydroxyindole. The establishment of optimal conditions for maximal fluorescence resulted in an increased sensitivity for estimating methyldopa in biological fluids. The method has provided increased sensitivity, consistency, and reproducibility.

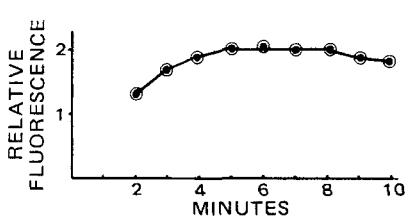

Figure 1—*Stability of methyldopa oxidation product.*

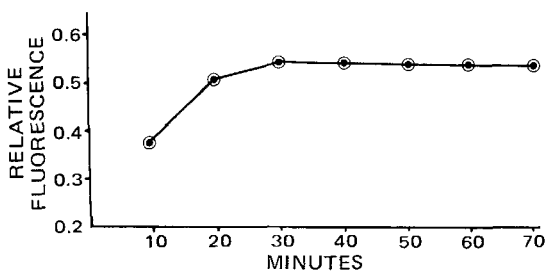

Figure 2—*Stability of fluorophore of methyldopa following oxidation and rearrangement.*

EXPERIMENTAL

Apparatus—All fluorescence measurements were made using a spectrophotofluorometer[1]. Microphotometer sensitivity was set at 30 with multiplier positions ranging from 0.01 to 0.1.

Reagents—All chemicals and solvents were analytical reagent grades, and freshly distilled water was used. All glassware was rinsed with 10% nitric acid and distilled water. Alumina[2] was reactivated by refluxing in 2 *N* HCl, washing with distilled water until the pH was 3.5–4, and drying at 250–300°. Methyldopa was used as received[3].

The phosphate buffer was prepared by adding 0.1 *M* dibasic sodium phosphate containing 0.1% edetate sodium to 0.1 *M* monobasic sodium phosphate containing 0.1% edetate sodium.

Analytical Procedure—Blood samples were collected in heparinized tubes containing 15 mg of sodium metabisulfite. The blood was centrifuged immediately, and the plasma was separated and frozen until assayed. Aliquots of biological fluids (0.1–1.0 ml) were placed in screw-capped test tubes, and 4–5 ml of 0.4 *N* perchloric acid was added. After shaking for 5 min, the precipitated protein was separated by centrifugation.

A specific volume (1–5 ml) of the supernate was transferred to a screw-capped test tube containing 0.5 g of activated alumina and 0.25 g of edetate sodium. The mixture was adjusted to pH 8.5–8.6 with 1 *N* sodium carbonate with constant stirring, and shaking was continued for an additional 5 min. The alumina was allowed to settle, and then the supernate was aspirated and discarded. The alumina was washed twice with 5 ml of distilled water, and the washings were discarded. The adsorbed methyldopa was eluted by vigorously shaking the washed alumina for 15 min with 6 ml of acetone–formic acid (85:15).

The alumina suspension was centrifuged, and 5.0 ml of the supernate was transferred to a test tube and evaporated under a nitrogen stream at 40°. The dried residue was dissolved in 1 ml of pH 6.5 phosphate buffer. Then 0.1 ml of ethanol, 0.05 ml of 0.2% zinc sulfate, and 0.05 ml of 0.1%

[1] Aminco-Bowman, American Instrument Co.
[2] Woelm Neutral Activity Grade 1.
[3] Courtesy of Merck Sharp & Dohme Laboratories.

(2) C. Hansch, J. E. Quinlan, and G. L. Lawrence *J. Org. Chem.*, **33**, 347 (1968).
(3) W. O. M. McReynolds, "Gas Chromatographic Retention Data," Preston Technical Abstracts Co., Evanston, Ill., 1964.
(4) S. Wold and K. Andersson, *J. Chromatogr.*, **80**, 43 (1973).
(5) D. L. Massart, P. Lenders, and M. Lauwereys, *J. Chromatogr. Sci.*, **12**, 617 (1974).

ACKNOWLEDGMENTS AND ADDRESSES

Received October 28, 1976, from the *Farmaceutisch Instituut, Vrije Universiteit Brussel, Paardenstraat 67, B-1640 Sint Genesius Rhode, Belgium.*

Accepted for publication January 27, 1977.

[x] To whom inquiries should be directed.

Fluorometric Determination of Methyldopa in Biological Fluids

BONG K. KIM and ROBERT T. KODA [x]

Abstract □ A fluorometric method for the analysis of methyldopa, based on the formation of a fluorophore after oxidation and rearrangement, is described. The drug is isolated from biological fluids by adsorption on alumina and elution with an organic solvent. Fluorescence is linear from 0.1 to 1.5 μg of methyldopa/ml. The assay has a lower limit of sensitivity of 100 ng/ml and is suitable for pharmacokinetic studies following therapeutic doses in animals and humans.

Keyphrases □ Methyldopa—fluorometric analysis, biological fluids □ Fluorometry—analysis, methyldopa in biological fluids □ Antihypertensive agents—methyldopa, fluorometric analysis in biological fluids

Methyldopa is a widely used antihypertensive agent with sedative and aromatic L-aminodecarboxylase-inhibiting properties (1–7). Methods to analyze the drug in pharmaceutical preparations and biological fluids have utilized visible spectrophotometry (8, 9), GLC (10), high-pressure liquid chromatography (11), and fluorometry (12, 13). In addition, tracer methodology has been used for metabolic and disposition studies (14, 15).

Fluorometric methods have been primarily based on the production of a fluorescent indole derivative (lutin) by oxidation and subsequent rearrangement. This technique has also been applied to estimate catecholamines and related compounds (16). Existing fluorometric methods appear to be insufficiently sensitive for the determination of drug levels in biological fluids.

This paper describes an improved analytical method in which methyldopa is adsorbed on alumina, eluted with an organic solvent, and then oxidized to form the fluorophore, dihydroxyindole. The establishment of optimal conditions for maximal fluorescence resulted in an increased sensitivity for estimating methyldopa in biological fluids. The method has provided increased sensitivity, consistency, and reproducibility.

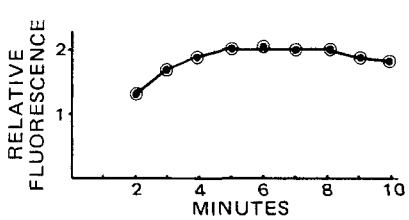

Figure 1—*Stability of methyldopa oxidation product.*

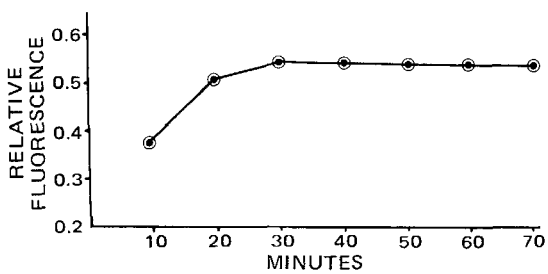

Figure 2—*Stability of fluorophore of methyldopa following oxidation and rearrangement.*

EXPERIMENTAL

Apparatus—All fluorescence measurements were made using a spectrophotofluorometer[1]. Microphotometer sensitivity was set at 30 with multiplier positions ranging from 0.01 to 0.1.

Reagents—All chemicals and solvents were analytical reagent grades, and freshly distilled water was used. All glassware was rinsed with 10% nitric acid and distilled water. Alumina[2] was reactivated by refluxing in 2 *N* HCl, washing with distilled water until the pH was 3.5–4, and drying at 250–300°. Methyldopa was used as received[3].

The phosphate buffer was prepared by adding 0.1 *M* dibasic sodium phosphate containing 0.1% edetate sodium to 0.1 *M* monobasic sodium phosphate containing 0.1% edetate sodium.

Analytical Procedure—Blood samples were collected in heparinized tubes containing 15 mg of sodium metabisulfite. The blood was centrifuged immediately, and the plasma was separated and frozen until assayed. Aliquots of biological fluids (0.1–1.0 ml) were placed in screw-capped test tubes, and 4–5 ml of 0.4 *N* perchloric acid was added. After shaking for 5 min, the precipitated protein was separated by centrifugation.

A specific volume (1–5 ml) of the supernate was transferred to a screw-capped test tube containing 0.5 g of activated alumina and 0.25 g of edetate sodium. The mixture was adjusted to pH 8.5–8.6 with 1 *N* sodium carbonate with constant stirring, and shaking was continued for an additional 5 min. The alumina was allowed to settle, and then the supernate was aspirated and discarded. The alumina was washed twice with 5 ml of distilled water, and the washings were discarded. The adsorbed methyldopa was eluted by vigorously shaking the washed alumina for 15 min with 6 ml of acetone–formic acid (85:15).

The alumina suspension was centrifuged, and 5.0 ml of the supernate was transferred to a test tube and evaporated under a nitrogen stream at 40°. The dried residue was dissolved in 1 ml of pH 6.5 phosphate buffer. Then 0.1 ml of ethanol, 0.05 ml of 0.2% zinc sulfate, and 0.05 ml of 0.1%

[1] Aminco-Bowman, American Instrument Co.
[2] Woelm Neutral Activity Grade 1.
[3] Courtesy of Merck Sharp & Dohme Laboratories.

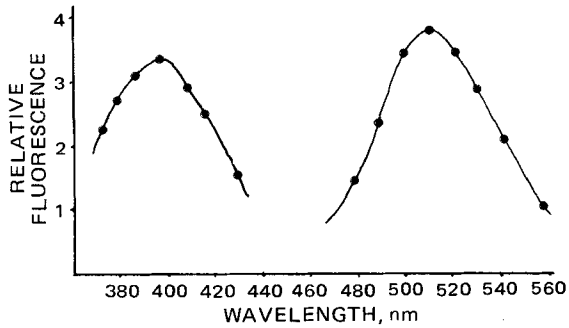

Figure 3—*Wavelength maxima for excitation (left) and emission (right) of methyldopa fluorophore.*

potassium ferricyanide were added, and the mixture, after shaking, was allowed to stand for 6 min at room temperature. After the reaction, 0.5 ml of 5.0 *N* NaOH–1% ascorbic acid (9:1) was added, and the solution was allowed to stand at room temperature for an additional 40 min. The fluorescence was measured at an excitation wavelength of 400 nm and an emission wavelength of 510 nm.

Plasma samples with added known amounts of methyldopa were analyzed, and a standard curve of fluorescence *versus* concentration was determined. Control plasma and urine samples were analyzed to assess background fluorescence arising from fluorescent materials in biological fluids. Other commonly used antihypertensive agents such as guanethidine, hydralazine, propranolol, polythiazide, and reserpine were added to methyldopa samples to determine interference.

RESULTS AND DISCUSSION

Methyldopa is selectively adsorbed on activated alumina and is eluted under acidic conditions. Catecholamines have similar characteristics, but the methyldopa concentration under therapeutic conditions was usually many hundredfold greater than the endogenous catecholamine levels. The major metabolites of methyldopa, 3-*O*-methylmethyldopa and methyldopa *O*-sulfate, were not adsorbed on alumina at pH 8.5–8.6 and thus were separable from the parent compound (17, 18).

Anton and Sayre (19) studied factors affecting alumina adsorption of trihydroxyindole for the analysis of catecholamines and reported that pH adjustment of sample solutions containing alumina and edetate sodium and the pH of the eluting solvent were critical variables. In previously reported catecholamine assays, sodium hydroxide and potassium carbonate solutions were used for the adjustment of sample solution pH (19, 20). Methyldopa is rapidly destroyed in solutions of high pH, and the recovery is poor when using sodium hydroxide. Potassium carbonate precipitates perchloric acid from solution as potassium perchlorate, with some drug coprecipitating. Sodium carbonate solution gave improved results.

Previously reported methods used 0.01 *N* $HClO_4$ and 0.5 *N* acetic acid to elute the adsorbed methyldopa from alumina (19, 21, 22). The method reported here, with an acetone–formic acid (85:15) mixture, gave improved recovery of adsorbed drug. Plasma samples spiked with 0.1, 0.5, and 1.0 μg of methyldopa gave average recoveries (five determinations) of 83.3 ± 2.7, 86.0 ± 1.6, and 91.6 ± 1.4%, respectively.

The oxidation of methyldopa to a chromophoric species was accomplished using potassium ferricyanide at pH 6.5. This oxidation was further improved by the addition of 0.1 ml of ethanol and 0.05 ml of 0.2% zinc sulfate.

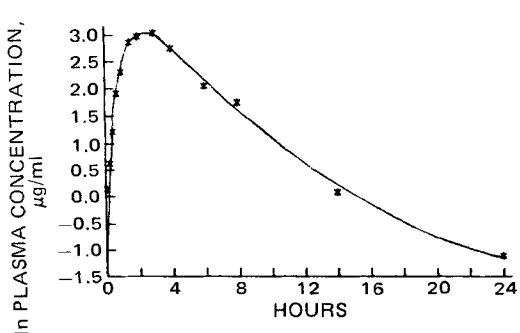

Figure 4—*Computer-drawn (SPEAKEZ) plasma level–time profile following a 300-mg oral dose of methyldopa in a rabbit.*

Table I—Analysis of Methyldopa in the Presence of Other Antihypertensive Drugs

Mixture[a]	Fluorescence[b], Arbitrary Units
Methyldopa	6.2 ± 0.3
Methyldopa–guanethidine sulfate	6.3 ± 0.2
Methyldopa–hydralazine	6.1 ± 0.4
Methyldopa–propranolol	6.0 ± 0.3
Methyldopa–polythiazide–reserpine	6.1 ± 0.2

[a] Methyldopa, 5 μg, and 20 mg of other drugs except 2 μg of polythiazide and 0.25 μg of reserpine. [b] Mean of four assays ± *SD*.

The oxidation reaction was completed within 5 min, and the product was stable up to 8 min (Fig. 1). In the reported method, 6 min was chosen as the oxidation reaction time. The formation of the fluorophore was completed within 40 min after the addition of ascorbic acid–sodium hydroxide and was stable up to 70 min (Fig. 2). The wavelength maxima of excitation and emission were 400 and 510 nm, respectively (Fig. 3). The standard curve of relative fluorescence *versus* concentration was linear over the concentration range of 0.1–1.5 μg/ml. The lower limit of sensitivity was 100 ng/ml. At this concentration, the sample fluorescence was at least twice that of the background. Below this concentration, the reproducibility of the analytical method was variable.

The applicability of the assay to clinical studies was demonstrated by determining the plasma concentration–time curve of methyldopa in a fasted rabbit after a single oral dose of 300 mg of methyldopa. The results were treated by a SPEAKEZ nonlinear computer program (Fig. 4). Urine samples were collected for 24 hr and assayed; 91.2 mg of free drug (30%) was excreted in 24 hr.

Experiments in which methyldopa was not separated from plasma or urine showed significant interference. Other widely used antihypertensive agents (*e.g.*, guanethidine sulfate, hydralazine, propranolol, polythiazide, and reserpine) did not interfere in this assay (Table I). This fluorescence method is rapid and simple for the determination of methyldopa in biological fluids and is applicable for pharmacokinetic studies in animals and humans.

REFERENCES

(1) J. A. Oates, L. Gillespie, S. Udenfriend, and A. Sjoerdsma, *Science*, **131**, 1890 (1960).

(2) C. T. Dollery and M. Harington, *Lancet*, **1**, 759 (1962).

(3) P. J. Cannon, R. T. Whitlock, C. R. Morris, M. Angers, and J. H. Laragh, *J. Am. Med. Assoc.*, **179**, 673 (1962).

(4) L. Gillespie, J. A. Oates, J. R. Crout, and A. Sjoerdsma, *Circulation*, **25**, 281 (1962).

(5) R. O. H. Irvine, K. P. O'Brien, and J. D. K. North, *Lancet*, **1**, 300 (1962).

(6) H. Smirk, *Br. Med. J.*, **1**, 146 (1963).

(7) N. Nikos, C. Victor, and F. A. Finnerty, *Am. J. Cardiol.*, **13**, 489 (1964).

(8) "The United States Pharmacopeia," 19th rev., Mack Publishing Co., Easton, Pa., 1975, pp. 319, 320.

(9) S. K. Wahba Khalil and R. B. Salama, *J. Pharm. Pharmacol.*, **26**, 972 (1974).

(10) J. R. Watson and R. C. Lawrence, *J. Chromatogr.*, **103**, 63 (1975).

(11) P. D. Walson, K. S. Marshall, R. P. Forsyth, R. Rapoport, K. L. Melmon, and N. Castagoli, Jr., *J. Pharmacol. Exp. Ther.*, **195**, 1 (1975).

(12) T. L. Sourkes, G. F. Murphy, and B. C. Lara, *Br. J. Med. Pharm. Chem.*, **5**, 204 (1962).

(13) A. Sjoerdsma, A. Vendsalu, and K. Engelman, *Circulation*, **28**, 492 (1963).

(14) R. P. Buhs, J. L. Beck, O. C. Speth, J. L. Smith, N. R. Trenner, P. J. Cannon, and J. H. Laragh, *J. Pharmacol. Exp. Ther.*, **143**, 205 (1964).

(15) L. F. Prescott, R. P. Buhs, J. O. Beattie, O. C. Speth, N. R. Trenner, and L. Lasagna, *Circulation*, **34**, 308 (1966).

(16) R. Laverty and K. M. Taylor, *Anal. Biochem.*, **22**, 269 (1968).

(17) J. R. Bianchine, L. R. Calimlim, J. P. Morgan, C. A. Dujuvne, and L. Lasagna, *Ann. N.Y. Acad. Sci.*, **179**, 126 (1975).

(18) R. D. Hoeldtke and J. W. Sloan, *J. Lab. Clin. Med.*, **75**, 159 (1970).

(19) A. H. Anton and D. F. Sayre, *J. Pharmacol.*, **138**, 360 (1962).
(20) A. Bertler, A. Carlsson, and E. Rosengren, *Acta Physiol. Scand.*, **44**, 273 (1958).
(21) A. H. Anton and D. F. Sayre, *J. Pharmacol.*, **145**, 326 (1964).
(22) T. L. Sourkes and G. F. Murphy, "Methods in Medicinal Research," vol. IX, Medical Publisher, Chicago, Ill., 1961, pp. 147–152.

ACKNOWLEDGMENTS AND ADDRESSES

Received November 22, 1976, from the *School of Pharmacy, University of Southern California, Los Angeles, CA 90033.*
Accepted for publication January 18, 1977.
[x] To whom inquiries should be directed.

GLC Determination of *N,N*-Dimethylaniline in Penicillins

MICHEL MARGOSIS

Abstract □ A reliable GLC procedure was developed for the determination of residual *N,N*-dimethylaniline as a contaminant in ampicillin commercial samples from various sources. This procedure was similarly applied to other penicillins and cephalosporins. The method involves dissolution of the sample in aqueous alkali, extraction of the organic base with cyclohexane containing naphthalene as an internal standard, and injection into a gas chromatograph with a phenyl methyl silicone column. Levels of 0.1 ppm of dimethylaniline were easily measured with a coefficient of variation less than 10%, and recoveries from spiked samples exceeded 99%.

Keyphrases □ *N,N*-Dimethylaniline—GLC analysis in various penicillins and cephalosporins, commercial samples □ Penicillins, various—GLC analysis of *N,N*-dimethylaniline as contaminant in commercial samples □ Cephalosporins, various—GLC analysis of *N,N*-dimethylaniline as contaminant in commercial samples □ GLC—analysis, *N,N*-dimethylaniline in various penicillins and cephalosporins, commercial samples □ Contaminants—*N,N*-dimethylaniline, GLC analysis in various penicillins and cephalosporins, commercial samples □ Antibacterials—various penicillins and cephalosporins, GLC analysis of *N,N*-dimethylaniline as contaminant in commercial samples

The premarketing certification process assures that each bulk and dosage form batch of antibiotics intended for human use complies with the specifications of proposed and established standards for identity, potency, quality, and purity.

The Code of Federal Regulations provides for Good Manufacturing Practices (GMP) in the production of pharmaceuticals. The direction to "... minimize contamination of products by extraneous adulterants ..." (1) applies also to residual reagents that may exhibit undesirable properties such as toxicity or carcinogenicity during antibiotic therapy and/or possible accumulation from other drugs.

Ampicillin, a semisynthetic penicillin, has been synthesized through diverse routes (2) by using 6-aminopenicillanic acid (II) as an intermediate and an organic base such as *N,N*-dimethylaniline (I) to abstract generated hydrogen chloride, the presence of which inhibits the synthesis.

Although gross contaminations can normally be detected by the general analytical techniques employed in certification, trace impurities are often too elusive. As the Food and Drug Administration became increasingly aware of the adventitious presence of residual dimethylaniline in ampicillin, the GLC method was developed to ascertain the extent of the problem. The pharmacological properties of dimethylaniline have not been fully elucidated, but it seemed advisable to limit its presence because of its dubious nature and possible carcinogenicity.

This report presents and discusses a GLC method[1] for the analysis of residual dimethylaniline in ampicillin and its applicability to survey-related antibiotics.

EXPERIMENTAL

Apparatus—A gas chromatograph[2] was fitted with an inlet system modified to accommodate a one-piece glass column directly from the site of injection, as described previously (3), and with a flame-ionization detector. It was used together with a 1-mv range strip-chart recorder. The instrument was also equipped with individual controls, allowing for separate heating of the inlet, column, and outlet. Peak area measurements were made with a digital electronic integrator[3].

A glass column, 1.9 m (6 ft) × 2 mm i.d., was packed with 3% of a 50% phenyl-substituted methyl silicone on silanized, acid-washed, flux calcined diatomite[4].

Typical Conditions—The gases were hydrogen at 1.55 kg/cm^2 (22 psi) and air at 2.11 kg/cm^2 (30 psi) adjusted to obtain maximum response and helium at 3.52 kg/cm^2 (50 psi) with a flow rate of about 30 ml/min. The temperatures were column, 60°; and injector and detector, about 150°. The column temperature and carrier flow rates were adjusted to obtain the first peak preferably within 5 min and complete resolution of the peaks. The current was 2×10^{-11} amp full-scale deflection (fsd) or was adjusted to obtain peak heights greater than 50% fsd, depending on peak sharpness.

Standard Solution—Weigh accurately about 25 mg of *N,N*-dimethylaniline base in a 25-ml volumetric flask. Add 1 ml of concentrated hydrochloric acid and about 10 ml of water. Shake to dissolve into one phase and dilute to volume. Use this solution to make standard solutions of varying concentrations ranging from 1.5 to 1500 μg/ml.

Internal Standard Solution—Dissolve about 5 mg of naphthalene in 100 ml of cyclohexane.

Sample Preparation—Weigh accurately about 1 g of bulk sample into a conical 15-ml centrifuge tube. Add 5 ml of 5% NaOH and stir on a mixer until dissolved. For the recovery study, add 1.00 ml of a standard dimethylaniline solution, mix thoroughly into a suspension, and then add 4 ml of 5% NaOH to dissolve.

Procedure—Add 1.00 ml of the cyclohexane solution, shake vigorously for about 1 min, and allow the phases to separate, centrifuging if necessary. Carefully draw a 1-μl sample from the upper cyclohexane phase and inject it into the chromatograph. For greater accuracy, make comparisons with standards having concentrations of the same order of magnitude

[1] Although this method was developed independently, it is similar in principle to those subsequently submitted in confidence from several manufacturers; it differs in details, however.
[2] Perkin-Elmer model 900.
[3] Infotronics CRS-100.
[4] OV-17 on 100–120-mesh Gas Chrom Q.

(19) A. H. Anton and D. F. Sayre, *J. Pharmacol.*, **138**, 360 (1962).
(20) A. Bertler, A. Carlsson, and E. Rosengren, *Acta Physiol. Scand.*, **44**, 273 (1958).
(21) A. H. Anton and D. F. Sayre, *J. Pharmacol.*, **145**, 326 (1964).
(22) T. L. Sourkes and G. F. Murphy, "Methods in Medicinal Research," vol. IX, Medical Publisher, Chicago, Ill., 1961, pp. 147–152.

ACKNOWLEDGMENTS AND ADDRESSES

Received November 22, 1976, from the *School of Pharmacy, University of Southern California, Los Angeles, CA 90033.*
Accepted for publication January 18, 1977.
[x] To whom inquiries should be directed.

GLC Determination of *N,N*-Dimethylaniline in Penicillins

MICHEL MARGOSIS

Abstract □ A reliable GLC procedure was developed for the determination of residual *N,N*-dimethylaniline as a contaminant in ampicillin commercial samples from various sources. This procedure was similarly applied to other penicillins and cephalosporins. The method involves dissolution of the sample in aqueous alkali, extraction of the organic base with cyclohexane containing naphthalene as an internal standard, and injection into a gas chromatograph with a phenyl methyl silicone column. Levels of 0.1 ppm of dimethylaniline were easily measured with a coefficient of variation less than 10%, and recoveries from spiked samples exceeded 99%.

Keyphrases □ *N,N*-Dimethylaniline—GLC analysis in various penicillins and cephalosporins, commercial samples □ Penicillins, various—GLC analysis of *N,N*-dimethylaniline as contaminant in commercial samples □ Cephalosporins, various—GLC analysis of *N,N*-dimethylaniline as contaminant in commercial samples □ GLC—analysis, *N,N*-dimethylaniline in various penicillins and cephalosporins, commercial samples □ Contaminants—*N,N*-dimethylaniline, GLC analysis in various penicillins and cephalosporins, commercial samples □ Antibacterials—various penicillins and cephalosporins, GLC analysis of *N,N*-dimethylaniline as contaminant in commercial samples

The premarketing certification process assures that each bulk and dosage form batch of antibiotics intended for human use complies with the specifications of proposed and established standards for identity, potency, quality, and purity.

The Code of Federal Regulations provides for Good Manufacturing Practices (GMP) in the production of pharmaceuticals. The direction to "... minimize contamination of products by extraneous adulterants ..." (1) applies also to residual reagents that may exhibit undesirable properties such as toxicity or carcinogenicity during antibiotic therapy and/or possible accumulation from other drugs.

Ampicillin, a semisynthetic penicillin, has been synthesized through diverse routes (2) by using 6-aminopenicillanic acid (II) as an intermediate and an organic base such as *N,N*-dimethylaniline (I) to abstract generated hydrogen chloride, the presence of which inhibits the synthesis.

Although gross contaminations can normally be detected by the general analytical techniques employed in certification, trace impurities are often too elusive. As the Food and Drug Administration became increasingly aware of the adventitious presence of residual dimethylaniline in ampicillin, the GLC method was developed to ascertain the extent of the problem. The pharmacological properties of dimethylaniline have not been fully elucidated, but it seemed advisable to limit its presence because of its dubious nature and possible carcinogenicity.

This report presents and discusses a GLC method[1] for the analysis of residual dimethylaniline in ampicillin and its applicability to survey-related antibiotics.

EXPERIMENTAL

Apparatus—A gas chromatograph[2] was fitted with an inlet system modified to accommodate a one-piece glass column directly from the site of injection, as described previously (3), and with a flame-ionization detector. It was used together with a 1-mv range strip-chart recorder. The instrument was also equipped with individual controls, allowing for separate heating of the inlet, column, and outlet. Peak area measurements were made with a digital electronic integrator[3].

A glass column, 1.9 m (6 ft) × 2 mm i.d., was packed with 3% of a 50% phenyl-substituted methyl silicone on silanized, acid-washed, flux calcined diatomite[4].

Typical Conditions—The gases were hydrogen at 1.55 kg/cm^2 (22 psi) and air at 2.11 kg/cm^2 (30 psi) adjusted to obtain maximum response and helium at 3.52 kg/cm^2 (50 psi) with a flow rate of about 30 ml/min. The temperatures were column, 60°; and injector and detector, about 150°. The column temperature and carrier flow rates were adjusted to obtain the first peak preferably within 5 min and complete resolution of the peaks. The current was 2×10^{-11} amp full-scale deflection (fsd) or was adjusted to obtain peak heights greater than 50% fsd, depending on peak sharpness.

Standard Solution—Weigh accurately about 25 mg of *N,N*-dimethylaniline base in a 25-ml volumetric flask. Add 1 ml of concentrated hydrochloric acid and about 10 ml of water. Shake to dissolve into one phase and dilute to volume. Use this solution to make standard solutions of varying concentrations ranging from 1.5 to 1500 μg/ml.

Internal Standard Solution—Dissolve about 5 mg of naphthalene in 100 ml of cyclohexane.

Sample Preparation—Weigh accurately about 1 g of bulk sample into a conical 15-ml centrifuge tube. Add 5 ml of 5% NaOH and stir on a mixer until dissolved. For the recovery study, add 1.00 ml of a standard dimethylaniline solution, mix thoroughly into a suspension, and then add 4 ml of 5% NaOH to dissolve.

Procedure—Add 1.00 ml of the cyclohexane solution, shake vigorously for about 1 min, and allow the phases to separate, centrifuging if necessary. Carefully draw a 1-μl sample from the upper cyclohexane phase and inject it into the chromatograph. For greater accuracy, make comparisons with standards having concentrations of the same order of magnitude

[1] Although this method was developed independently, it is similar in principle to those subsequently submitted in confidence from several manufacturers; it differs in details, however.
[2] Perkin-Elmer model 900.
[3] Infotronics CRS-100.
[4] OV-17 on 100–120-mesh Gas Chrom Q.

Table I—Dimethylaniline in Various Penicillins and Cephalosporins[a]

Sample[b]	Manufacturer	Type[c]	Size	I, ppm[d]
II	1	b	2	340, 433
II	2	b	2	60, 330
II	3	b	2	339, 512
II	4	b	2	280, 774
III	1	b	3	3–5
III	1	b	3	10–28
III	1	b	8	500–800
III	1	b	12	800–1000
III	1	b	6	1000–1500
III	2	b	5	200–300
III	2	b	1	700
III	3	b	8	5–8
III	4	b	7	<1.5
III	5	b	7	<1.5
III	6	b	4	1–4
III	7	b	3	<1
III	8	b	4	0–6
III	9	b	2	1250–1310
III	10	b	2	<1
III	11	b	3	<1.5
III	12	b	4	4.5–8
III sodium	13	b	1	<1.5
III sodium	14	b	1	1
III	15	c	2	4
III	16	c	1	2
III	17	c	2	230, 300
III	18	c	2	305, 325
III	19	c	1	250
III	20	s	1	<0.5
IV	1	b	1	8
V	1	b	3	<0.5
V	2	b	5	<0.5
V	3	b	3	<0.5
V	4	b	3	0.1–5
V	3	c	1	0.1
V	5	s	1	<0.05
V	6	c	2	<0.05
VI	1	b	2	7, 10
VI	2	b	3	39–51
VI	3	b	2	<0.3
VI	3	c	1	4
VI	3	c	2	<0.1
VII	1	b	1	0.5
VII	1	s	1	0.2

[a] No dimethylaniline was detected (<0.15 ppm) in samples of cephradine, cephaloglycin, cefazolin, penicillamine, penicillin G procaine, penicillin G potassium, penicillin V, oxacillin, cloxacillin, dicloxacillin, and carbenicillin. [b] Compound III is ampicillin, IV is hetacillin, V is amoxicillin, VI is cephalexin, and VII is cephapirin. [c] b = bulk, c = capsule (per capsule), and s = oral suspension. [d] "Less than" indicates that dimethylaniline was not detected, but an upper limit of detectability was calculated based on the instrument conditions.

as that contained in the sample. The elution sequence is such that dimethylaniline emerges first and naphthalene follows.

Calculations—The area of each peak is measured by a suitable technique such as electronic integration. Then:

$$\text{wt. \% I} = (R_x \times W_{std})/(R_{std} \times W_u) \times 100 \qquad \text{(Eq. 1)}$$

where R is the ratio of the area of the I peak to the area of the internal standard peak, and W is the weight of the standard (std) or sample (u).

Identity—The relative retention time (sample–internal standard) of the unknown sample is identical to that of the working standard under identical operating conditions.

RESULTS AND DISCUSSION

Results of the determination of dimethylaniline in various commercial penicillins and cephalosporins are summarized in Table I. The samples accumulated over the past 4 years were selected at random and, therefore, do not necessarily reflect the current market. As expected, all samples of 6-aminopenicillanic acid contained significant amounts of dimethylaniline. However, subsequent processing to produce the semisynthetic penicillins ostensibly rendered the final bulk product relatively free of this contaminant. The amount of residual dimethylaniline found in a few batches of ampicillins was significant, but this situation has been largely

Figure 1—*Chromatograms of 1.66 μg (A) and 41.6 μg (B) of dimethylaniline.*

rectified by improved cleanup or by substitution with other more innocuous organic bases.

The protocol of analysis includes the identical curing and conditioning treatment cited in the collaborative GLC studies of chloramphenicol (4) and griseofulvin (5, 6). This protocol includes calculations for the different parameters that characterize column performance. In this study, an efficiency of 1265 plates/m for dimethylaniline and of 1560 plates/m for naphthalene, a resolution factor of 7.3, and a tailing factor of 1.29 were calculated. In actual assays, a coefficient of variation of less than 2% can easily be obtained, but it normally increases as the concentration of the components to be determined decreases. This effect results mainly from a worsening baseline geometry (Fig. 1) with an accompanying decrease in the reliability of the electronic integrator. Thus, at the 1.66-ppm level, a coefficient of variation no greater than 7.9% was readily obtained.

The column requires injection of a silyl reagent at a higher temperature (275°) prior to sample conditioning at the operating temperature. This reagent is also injected several times at the end of the day with the column temperature reset to 275° to flush out the system. This treatment may also be necessary during the day to obtain a satisfactory baseline. Di-

Table II—Comparison of Quantitative Tests

Sample	Potency	Amine	Acid	I, μEq	Cl, μEq
1	98.2	106.7	94.9	8.2	203
2	98.8	97.0	99.3	5.8	121
3	97.2	98.0	100.0	0.008	7.6
4	100.6	99.7	98.7	0.012	2.9
5	102.1	99.4	97.4	2.4	85
6	100.8	98.3	96.4	1.7	101
7	101.9	99.3	97.5	2.4	89
8	102.2	99.0	102.2	2.4	93
9	99.6	98.3	103.0	2.4	92
10	102.4	105.2	96.1	0.041	72
11	102.2	96.4	100.3	0.012	62
12	101.6	95.6	99.2	0.046	118

methylaniline is relatively nonpolar because of the alkyl shielding and need not be derivatized to show good chromatographic properties except during separation from other intractable anilines (7). The standard is prepared as an aqueous solution to minimize evaporation of the solvent and solute as well as to simulate actual conditions.

Linearity of response was tested by injecting standard solutions of varying concentrations of dimethylaniline containing a fixed amount of the internal standard. A linear regression analysis of seven points in the concentration range of 3–200 ppm yielded a statistically significant squared multiple correlation coefficient of 0.9998 ($p > 0.01$). To improve the precision and reliability of electronic integration, the use of a standard approximating the concentration of the analyte in the unknown while maintaining identical instrument parameters is recommended. Method reliability was verified by spiking samples of ostensibly dimethylaniline-free ampicillin with different amounts of standards. Recoveries in excess of 99% were obtained, although residual dimethylaniline was occasionally detected at low concentrations (*e.g.*, <25 ppm).

Chromatography was performed at a low temperature, which is capable of detecting but is limited to relatively nonpolar substances of low molecular weights. Confirmation of identity by the relative retention times of the peaks attributed to dimethylaniline and naphthalene was obtained by combination GLC and electron-impact mass spectrometry applied to several bulk materials. However, conditions were inadequate to characterize the occasional foreign peaks.

Several samples were extracted directly with cyclohexane but did not manifest the presence of dimethylaniline until alkali was added. The logical presumption is that dimethylaniline was bound as a hydrochloride salt. Thus, a measure of total chlorine might correlate with the dimethylaniline content and with other quantitative tests as well. However, the results listed in Table II clearly show that the total chloride content obtained by neutron activation analysis (8), which ranges up to 7.3 mg/g, is far greater than the equivalent amount of dimethylaniline, indicating that other contaminants are present. In this context, the amount of dimethylaniline found in ampicillin has not demonstrated any correlation with the potency or concordance results obtained as prescribed in the regulations (9).

REFERENCES

(1) "Code of Federal Regulations," Title 21, part 211 (1975).

(2) "Analytical Profiles of Drug Substances," vol. 2, K. Florey, Ed., Academic, New York, N.Y., 1973.

(3) M. Margosis and K. Tsuji, *J. Pharm. Sci.*, **62**, 1836 (1973).

(4) M. Margosis, *ibid.*, **63**, 435 (1974).

(5) M. Margosis, *J. Chromatogr.*, **70**, 73 (1972).

(6) M. Margosis, *J. Pharm. Sci.*, **64**, 1020 (1975).

(7) R. A. Dove, *Anal. Chem.*, **39**, 1188 (1967).

(8) M. Margosis, J. T. Tanner, and J. P. F. Lambert, *J. Pharm. Sci.*, **60**, 1550 (1971).

(9) "Code of Federal Regulations," Title 21, part 440.5 (1975).

ACKNOWLEDGMENTS AND ADDRESSES

Received August 4, 1976, from the *National Center for Antibiotic Analysis, Food and Drug Administration, U.S. Department of Health, Education, and Welfare, Washington, DC 20204.*

Accepted for publication January 21, 1977.

Presented at the American Chemical Society, San Francisco, Calif., August 1976.

The author thanks Robert P. Barron, Division of Drug Chemistry, Food and Drug Administration, for mass spectral analyses.

Aging of Tablets Made with Dibasic Calcium Phosphate Dihydrate as Matrix

J. M. LAUSIER, CHIA-WHEI CHIANG, H. A. ZOMPA, and C. T. RHODES ˣ

Abstract □ The aging of direct compression tablets made using dibasic calcium phosphate dihydrate as the tablet matrix was investigated over 16 weeks. The formula included 6% amaranth as a dye tracer. Two sets of stress storage conditions were used: 25° and 50% relative humidity and 45° and 75% relative humidity. Tablets were evaluated periodically by visual inspection; determination of the weight of 10 separate tablets, the size of 10 tablets measured by a micrometer screw gauge, and the hardness of 10 tablets as indicated by a Strong–Cobb hardness tester; the USP disintegration time test; and the USP dissolution test. Tablets stored at 25° and 50% relative humidity showed an approximately linear increase in disintegration and dissolution time over 16 weeks with no other significant changes. Storage at 45° and 75% relative humidity resulted in significant changes in most measured parameters; tablets showed blotching, substantial weight loss, and complex changes in disintegration and dissolution. The changes at elevated temperatures are related to loss of water of hydration; changes at 25° must be due to other causes.

Keyphrases □ Calcium phosphate, dibasic—direct compression tablets, aging, effect of temperature and humidity □ Tablets, direct compression—dibasic calcium phosphate, aging, effect of temperature and humidity □ Aging—direct compression dibasic calcium phosphate tablets, effect of temperature and humidity □ Dosage forms—direct compression tablets, dibasic calcium phosphate, aging, effect of temperature and humidity

Recently, the physical aging of compressed tablets was studied, and it was found that complex changes of hardness and dissolution may occur over a relatively short period (1). However, because of the limited preliminary nature of that study, no hypothesis was proposed to rationalize these changes. The present report concerns a more detailed investigation of the aging of a directly compressed tablet formulation. In addition to dissolution and hardness measurements, diameter, thickness, disintegration, and tablet weight were evaluated over 16 weeks.

EXPERIMENTAL

The tablets were prepared by direct compression on a single-punch press[1] as described previously (1). The following formulation was used:

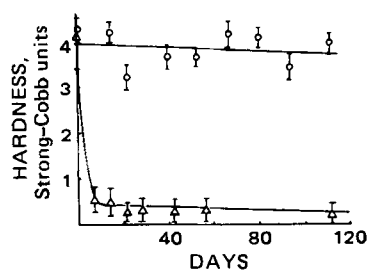

Figure 1—*Plot of hardness data over 16 weeks for dibasic calcium phosphate dihydrate tablets at 25° and 50% relative humidity (○) and at 45° and 75% relative humidity (△).*

[1] Stokes model F, Warminster, Pa.

methylaniline is relatively nonpolar because of the alkyl shielding and need not be derivatized to show good chromatographic properties except during separation from other intractable anilines (7). The standard is prepared as an aqueous solution to minimize evaporation of the solvent and solute as well as to simulate actual conditions.

Linearity of response was tested by injecting standard solutions of varying concentrations of dimethylaniline containing a fixed amount of the internal standard. A linear regression analysis of seven points in the concentration range of 3–200 ppm yielded a statistically significant squared multiple correlation coefficient of 0.9998 ($p > 0.01$). To improve the precision and reliability of electronic integration, the use of a standard approximating the concentration of the analyte in the unknown while maintaining identical instrument parameters is recommended. Method reliability was verified by spiking samples of ostensibly dimethylaniline-free ampicillin with different amounts of standards. Recoveries in excess of 99% were obtained, although residual dimethylaniline was occasionally detected at low concentrations (*e.g.*, <25 ppm).

Chromatography was performed at a low temperature, which is capable of detecting but is limited to relatively nonpolar substances of low molecular weights. Confirmation of identity by the relative retention times of the peaks attributed to dimethylaniline and naphthalene was obtained by combination GLC and electron-impact mass spectrometry applied to several bulk materials. However, conditions were inadequate to characterize the occasional foreign peaks.

Several samples were extracted directly with cyclohexane but did not manifest the presence of dimethylaniline until alkali was added. The logical presumption is that dimethylaniline was bound as a hydrochloride salt. Thus, a measure of total chlorine might correlate with the dimethylaniline content and with other quantitative tests as well. However, the results listed in Table II clearly show that the total chloride content obtained by neutron activation analysis (8), which ranges up to 7.3 mg/g, is far greater than the equivalent amount of dimethylaniline, indicating that other contaminants are present. In this context, the amount of dimethylaniline found in ampicillin has not demonstrated any correlation with the potency or concordance results obtained as prescribed in the regulations (9).

REFERENCES

(1) "Code of Federal Regulations," Title 21, part 211 (1975).

(2) "Analytical Profiles of Drug Substances," vol. 2, K. Florey, Ed., Academic, New York, N.Y., 1973.

(3) M. Margosis and K. Tsuji, *J. Pharm. Sci.*, **62**, 1836 (1973).

(4) M. Margosis, *ibid.*, **63**, 435 (1974).

(5) M. Margosis, *J. Chromatogr.*, **70**, 73 (1972).

(6) M. Margosis, *J. Pharm. Sci.*, **64**, 1020 (1975).

(7) R. A. Dove, *Anal. Chem.*, **39**, 1188 (1967).

(8) M. Margosis, J. T. Tanner, and J. P. F. Lambert, *J. Pharm. Sci.*, **60**, 1550 (1971).

(9) "Code of Federal Regulations," Title 21, part 440.5 (1975).

ACKNOWLEDGMENTS AND ADDRESSES

Received August 4, 1976, from the *National Center for Antibiotic Analysis, Food and Drug Administration, U.S. Department of Health, Education, and Welfare, Washington, DC 20204.*

Accepted for publication January 21, 1977.

Presented at the American Chemical Society, San Francisco, Calif., August 1976.

The author thanks Robert P. Barron, Division of Drug Chemistry, Food and Drug Administration, for mass spectral analyses.

Aging of Tablets Made with Dibasic Calcium Phosphate Dihydrate as Matrix

J. M. LAUSIER, CHIA-WHEI CHIANG, H. A. ZOMPA, and C. T. RHODES ˣ

Abstract □ The aging of direct compression tablets made using dibasic calcium phosphate dihydrate as the tablet matrix was investigated over 16 weeks. The formula included 6% amaranth as a dye tracer. Two sets of stress storage conditions were used: 25° and 50% relative humidity and 45° and 75% relative humidity. Tablets were evaluated periodically by visual inspection; determination of the weight of 10 separate tablets, the size of 10 tablets measured by a micrometer screw gauge, and the hardness of 10 tablets as indicated by a Strong–Cobb hardness tester; the USP disintegration time test; and the USP dissolution test. Tablets stored at 25° and 50% relative humidity showed an approximately linear increase in disintegration and dissolution time over 16 weeks with no other significant changes. Storage at 45° and 75% relative humidity resulted in significant changes in most measured parameters; tablets showed blotching, substantial weight loss, and complex changes in disintegration and dissolution. The changes at elevated temperatures are related to loss of water of hydration; changes at 25° must be due to other causes.

Keyphrases □ Calcium phosphate, dibasic—direct compression tablets, aging, effect of temperature and humidity □ Tablets, direct compression—dibasic calcium phosphate, aging, effect of temperature and humidity □ Aging—direct compression dibasic calcium phosphate tablets, effect of temperature and humidity □ Dosage forms—direct compression tablets, dibasic calcium phosphate, aging, effect of temperature and humidity

Recently, the physical aging of compressed tablets was studied, and it was found that complex changes of hardness and dissolution may occur over a relatively short period (1). However, because of the limited preliminary nature of that study, no hypothesis was proposed to rationalize these changes. The present report concerns a more detailed investigation of the aging of a directly compressed tablet formulation. In addition to dissolution and hardness measurements, diameter, thickness, disintegration, and tablet weight were evaluated over 16 weeks.

EXPERIMENTAL

The tablets were prepared by direct compression on a single-punch press[1] as described previously (1). The following formulation was used:

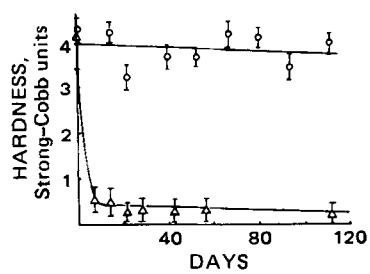

Figure 1—*Plot of hardness data over 16 weeks for dibasic calcium phosphate dihydrate tablets at 25° and 50% relative humidity (○) and at 45° and 75% relative humidity (△).*

[1] Stokes model F, Warminster, Pa.

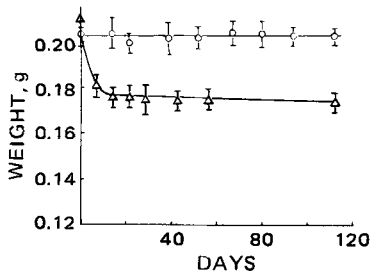

Figure 2—*Plot of weight variation over 16 weeks for dibasic calcium phosphate dihydrate tablets at 25° and 50% relative humidity (○) and at 45° and 75% relative humidity (△).*

6.0% (w/w) amaranth as the dye tracer, 0.5% (w/w) magnesium stearate as the lubricant, 2.5% (w/w) sodium alginate as the disintegrant, and 91.0% (w/w) dibasic calcium phosphate dihydrate as the matrix.

All tablet samples were obtained from a single batch of the formulation and had an average weight of 200 mg. Tablets were placed under two sets of stress storage conditions: 25° and 50% relative humidity and 45° and 75% relative humidity. Temperature was controlled ±3°, and relative humidity remained ±5%. Techniques for temperature and humidity control were as previously described (1).

Representative samples were removed and evaluated over 16 weeks by the following parameters: visual inspection, size measurements using micrometer screw gauge, individual weights of 10 tablets, hardness of 10 tablets made with pneumatic Strong-Cobb hardness tester, USP disintegration time of six tablets, and USP dissolution test. Dissolution tests were performed as previously described (1).

RESULTS AND DISCUSSION

Storage conditions of 45° and 75% relative humidity produced significant changes in most measured parameters. During the first 6 weeks, the tablets were blotchy, indicating that appreciable moisture was collecting on the tablet surface. This phenomenon disappeared by the 8th week.

While tablet size did not change appreciably under this storage condition, tablet hardness decreased dramatically during the 1st week (from 4.0 to 0.5). The hardness then became invariant (Fig. 1). Although hardness did not change during the later part of the study, both disintegration and dissolution continued to change. This result supports the previous finding that hardness and disintegration changes are not always related.

Similar effects were observed in tablet weight evaluations. An initial weight of 200 mg decreased to an average value of 174 mg after the 2nd week (Fig. 2). Calculations of formula weight of the tablet matrix suggest that the loss in weight was approximately equivalent to the water of hydration in the matrix, thus indicating a release of this substance from the matrix material. This fact would explain the blotching observed on the tablet surface in the first few weeks.

The similarity of results in hardness and weight evaluations at this storage condition indicates that the loss of water of hydration from the tablet matrix affected the integrity of the dosage form in direct relation

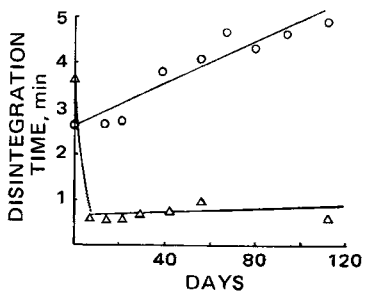

Figure 3—*Plot of disintegration times over 16 weeks for dibasic calcium phosphate dihydrate tablets at 25° and 50% relative humidity (○) and at 45° and 75% (△).*

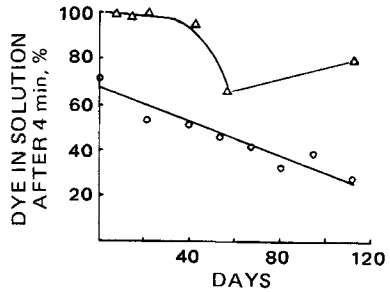

Figure 4—*Plot of release rate of dye over 16 weeks from dibasic calcium phosphate dihydrate tablets at 25° and 50% relative humidity (○) and at 45° and 75% relative humidity.*

to the amount of water lost. An initial sharp decrease in both weight and hardness suggests that most of the water loss occurred during the first 2 weeks of stress.

Figure 3 shows the effect of increased storage temperature and relative humidity on disintegration time. At 45° and 75% relative humidity, the disintegration time decreased substantially after 1 week (from 3.5 to 0.5 min) and remained constant thereafter. Since the hardness evaluation showed parallel decreases, this result was not unexpected.

Dissolution data (expressed as percentage of dye in solution after 4 min) showed a complex change over the test period (Fig. 4). There was no substantial change in the rate until the 8th week, at which time the amount of dye in solution decreased significantly (from 98 to 65%), and then the rate increased to 80% by the end of the study. These results suggest that loss of water of hydration from the matrix alters the dissolution characteristics of the tablet in a presently unpredictable manner. However, other aging factors are probably occurring simultaneously, making the evaluation process complex.

Tablets stored at 25° and 50% relative humidity were sampled at appropriate intervals over 16 weeks. There were no significant changes in size or physical appearance. Hardness and weight data, as represented by Figs. 1 and 2, respectively, indicate that loss of water of hydration did not occur under these storage conditions and would not be a factor in the interpretation of disintegration and dissolution data.

Disintegration time under these storage conditions increased in an approximately linear fashion (Fig. 3) from an initial value of 2.5 to 5.0 min at 16 weeks. The release rate of dye (Fig. 4) showed a corresponding linear decrease (from 75 to 25%) over the same period, which would be expected in light of the disintegration data.

A comparison of test results shows that a multifaceted evaluation must be performed in aging studies. At an elevated temperature of 45° and 75% relative humidity, the loss of water of hydration not only affected the disintegration and dissolution characteristics of the tablets but also significantly altered their weight and hardness. Since this phenomenon did not occur at 25° and 50% relative humidity, other factors, such as case hardening, must play an important role in the aging process.

Results of this study support the previous finding (1) that evaluation of tablet hardness is not a reliable measure of physical aging of tablets. In the present study, some significant changes occurred when hardness was not changing to any appreciable extent. Of course, this study and the previous report (1) dealt only with one type of tablet matrix. It will be useful to study other systems, but the results presented here indicate that tablet aging is a complex problem, the causes of which are not fully understood.

REFERENCE

(1) S. T. Horhota, J. Burgio, L. Lonski, and C. T. Rhodes, *J. Pharm. Sci.*, **65**, 1746 (1976).

ACKNOWLEDGMENTS AND ADDRESSES

Received July 21, 1976, from the *Department of Pharmacy, College of Pharmacy, University of Rhode Island, Kingston, RI 02881.*

Accepted for publication January 27, 1977.

Supported by Edward Mendell, Inc.

ˣ To whom inquiries should be directed.

Plasma Concentrations and Bioavailability of Clofibric Acid from Its Calcium Salt in Humans

T. TAYLOR [x] and L. F. CHASSEAUD

Abstract □ The bioavailability of clofibric acid from formulations containing calcium clofibrate alone and mixed with calcium carbonate (1:1 w/w) was compared to that from a standard clofibrate formulation in a crossover study in 12 human subjects. The 95% confidence intervals of bioavailability differences were such that they were unlikely to be detected in clinical practice; all three formulations may be considered bioequivalent, although the bioavailability rate was probably greater from the formulation containing calcium clofibrate alone. Peaks of mean concentrations of 80 ± 13, 67 ± 16, and 64 ± 18 μg/ml ± *SD* occurred after administration of 853 mg of clofibric acid calcium salt alone, 809 mg of clofibric acid calcium salt mixed with calcium carbonate, and 885 mg of clofibrate, respectively; mean concentrations declined from peak levels with half-lives of 15–17 hr.

Keyphrases □ Clofibric acid—bioavailability from various formulations compared, humans □ Bioavailability—clofibric acid, various formulations compared, humans □ Antihyperlipidemic agents—clofibric acid, bioavailability from various formulations compared, humans

Clofibrate [ethyl 2-(4-chlorophenoxy)-2-methylpropanoate], which is hydrolyzed either during or after absorption to the active form, clofibric acid [2-(4-chlorophenoxy)-2-methylpropanoic acid] (1), is an antihyperlipidemic agent effective in the treatment of hyperlipoproteinemias primarily of Fredrickson Types III, IV, and V. Clofibrate also produces an antilipemic effect, mainly by reducing triglyceride levels, in patients with hyperlipoproteinemia of Type IIb (2–4).

Calcium also exerts an antilipemic action by forming insoluble complexes with bile salts and fatty acids within the intestinal lumen. Calcium lowered plasma cholesterol levels and, to some extent, triglyceride levels in patients with hyperlipoproteinemias of Types II and IV (5).

To obtain the benefit of the antilipemic actions of both clofibrate and calcium in patients with the most commonly occurring hyperlipoproteinemias, Types II and IV, a product containing calcium clofibrate and calcium carbonate, in approximately equal proportions, was formulated. In addition to broadening the antilipemic action, this combination provides a convenient solid dosage form as an alternative to the currently available liquid-filled capsule of clofibrate. However, the presence of calcium carbonate in the formulation may change the pH of the gut contents after oral administration (6–8) and affect clofibrate bioavailability. Therefore, plasma levels of the active metabolite, clofibric acid, were measured following administration of capsules containing similar doses of this test formulation, a formulation containing calcium clofibrate alone, and the reference agent, clofibrate.

EXPERIMENTAL

Drug Administration—Twelve healthy subjects, six males and six females, 19–52 years old and 52–87 kg, participated after being informed of the aim of the study and the nature of the drug. Before and after the study, each subject was given a complete physical examination, including routine laboratory screening tests. During the study, the subjects remained under medical supervision.

Each of the three drug formulations was administered with 100 ml of water in a crossover Latin-square design wherein the subjects were grouped by sex. There was a 1-week washout period between doses. Before dosing, the subjects fasted for 12 hr; afterwards, they did not eat or rest for 3 hr. Each subject received doses of 885 mg of clofibric acid as clofibrate (the reference[1] Formulation A), 853 mg as calcium clofibrate alone (Formulation B), and 809 mg as the calcium clofibrate–carbonate combination (1:1 w/w, Formulation C).

Blood samples (5 ml) were collected in tubes containing heparin just before dosing and at 1, 2, 3, 4, 6, 8, 12, 24, 32, and 48 hr after dosing. Plasma was separated and kept frozen until analysis.

Measurement of Plasma Clofibric Acid Levels—Clofibric acid was measured spectrophotometrically at 226 nm after extraction from acidified plasma by isooctane (9). The extraction efficiency (recovery) was 72% in the 10–100-μg/ml concentration range. Plasma clofibric acid levels were calculated by reference to a standard curve constructed by adding known amounts of clofibric acid to untreated human plasma. New standard curves were constructed for each batch of plasma analyzed.

The absorbance of extracts of the predose plasma was subtracted from the absorbance of postdose samples before calculation of clofibric acid concentrations. The precision of the method was such that, with 95% confidence, clofibric acid could be measured within ±6% of the mean of 10 replicate analyses.

Data Processing—Apparent half-lives of drug elimination were calculated by least-squares regression analysis of log concentration against time from measurements during the terminal linear phase of the log concentration–time curves. Areas under the plasma concentration–time curves (scaled to equal doses of 885 mg of clofibric acid) to 48 hr were calculated by the trapezoidal rule. Although areas beyond 48 hr contributed approximately 10% of the total area to infinite time, plasma concentrations at the last sampling time were close to the limit of sensitivity of the analytical method. Areas to 48 hr were linearly related to the total areas ($r = 0.95$), and bioavailability was estimated from the areas to 48 hr. Estimates from the total areas were similar.

Areas, peak plasma concentrations (scaled to equal doses of 885 mg) and times of occurrence, and apparent half-lives of elimination were analyzed by an analysis of variance for crossover designs. The total variance was separated into that due to sex, subjects, day of administration, formulation, and residual.

Table I—Mean Plasma Clofibric Acid Concentrations (Micrograms per Milliliter) after Administration of the Three Formulations

Hours	Clofibrate[a]	Calcium Clofibrate	Calcium Clofibrate–Carbonate Combination
1	19.7 (81.4)[b]	48.4 (49.1)	27.6 (82.5)
2	44.3 (50.8)	69.0 (30.0)	46.9 (41.2)
3	53.8 (43.6)	80.4 (16.8)	58.5 (32.5)
4	62.8 (39.2)	78.2 (13.7)	67.1 (23.8)
6	64.1 (28.9)	72.2 (19.0)	63.6 (25.4)
8	62.7 (18.9)	63.9 (17.7)	59.9 (23.6)
12	54.1 (9.4)	50.5 (18.6)	52.6 (20.4)
24	35.1 (21.1)	29.6 (16.4)	39.9 (20.8)
32	25.3 (18.9)	19.7 (38.9)	26.4 (27.5)
48	9.0 (61.4)	8.3 (57.3)	9.2 (73.4)

[a] Reference formulation. [b] Coefficients of variation (percent) in parentheses.

RESULTS

Plasma Clofibric Acid Levels—Mean concentrations of clofibric acid in plasma after administration of slightly different doses in the three

[1] Atromid-S capsules manufactured by ICI Pharmaceuticals, Macclesfield, England, and marketed in the United States by Ayerst Laboratories, Division of American Home Products Corp., New York, N.Y.

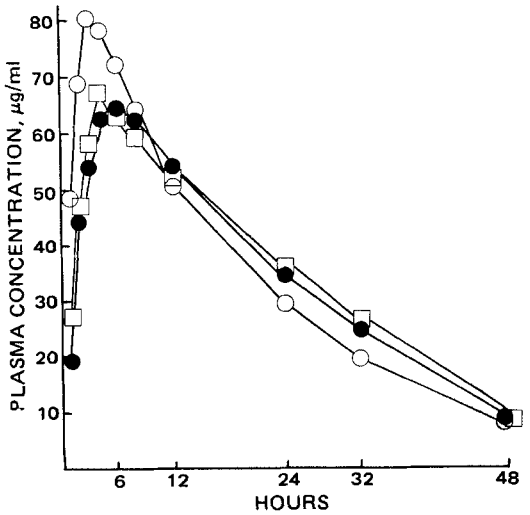

Figure 1—*Plasma clofibric acid concentrations after administration of clofibrate (●), calcium clofibrate (○), and the calcium clofibrate–carbonate combination (■).*

formulations are shown in Table I and Fig. 1. Mean concentrations were similar after administration of Formulation C and the reference Formulation A. Mean concentrations were higher after administration of Formulation B. Peak plasma levels in individual subjects were similar after administration of Formulations A (mean of 71 μg/ml ± 17 *SD*) and C (mean of 73 μg/ml ± 15 *SD*) and higher after Formulation B (mean of 85 μg/ml ● 13 *SD*). Plasma clofibric acid levels were slightly higher than those reported previously (10).

The mean half-life of clofibric acid in plasma after administration of Formulation B (15.4 hr ± 3.0 *SD*) was slightly shorter but not significantly different (Tables II and III) from those after administration of Formulations A and C (17.2 ± 2.0 and 16.9 ± 3.0 hr ± *SD*, respectively). Similar half-lives of 19 and 15–17 hr were reported previously (11, 12).

Bioavailability Parameters—The mean ratio of areas showed that the bioavailability of clofibric acid from Formulations B and C was 101 and 110%, respectively, of that from Formulation A. An analysis of variance of areas showed that formulation-related differences were not significant (Table III). However, subject-related effects were significant ($p < 0.01$), and two male subjects provided consistently higher areas regardless of the formulation administered.

The 95% confidence limits (13, 14) of differences between the mean areas after administration of Formulations B and C were from −10.7 to +13.4 and from +1.2 to +22.9%, respectively, of the mean for Formulation A. Significant formulation-related differences were found for peak plasma concentrations (scaled for equal doses) and their times of occurrence (Tables II and III).

DISCUSSION

Differences in the extent of bioavailability of clofibric acid between formulations containing clofibrate, calcium clofibrate, or the calcium clofibrate–carbonate combination were not statistically significant ($p > 0.05$). Clinical usage is unlikely to detect differences of the orders found, and all three formulations may be regarded as bioequivalent. However, higher plasma clofibric acid levels at earlier times were provided by single doses of calcium clofibrate alone, and the bioavailability rate was probably greatest after administration of this formulation. Differences in bioavailability rates are of less importance with drugs, such as clofibric acid, that are administered chronically to achieve a steady-state plasma level.

The 95% confidence limits of differences in areas under the concentration–time curves indicated that formulation as the calcium salt of clofibric acid had little effect on the extent of drug bioavailability. Clofibrate is almost completely absorbed, 98% of a daily dose of 2 g being excreted in the urine as the free and conjugated acid (12). The *in vivo* performance of the formulations of calcium clofibrate compared favorably with that reported for the basic aluminum salt of the acid, which gave significantly lower plasma levels at all times of sampling after 500-mg doses when tested against four other preparations of clofibrate (11).

Table II—Mean Bioavailability Parameters of Clofibric Acid from the Three Formulations

Parameter	Clofibrate[a]	Calcium Clofibrate	Calcium Clofibrate–Carbonate Combination
Area[b], μg hr/ml	1683 (12)[c]	1706 (18)	1866 (17)
Peak concentrations[b] in individuals, μg/ml	71 (24)	88 (15)	80 (21)
Time of peak concentration, hr	6.3 (48)	3.6 (40)	4.6 (57)
Half-life, hr	17.2 (12)	15.4 (20)	16.9 (18)

[a] Reference formulation. [b] Scaled to equal doses of 885 mg. [c] Coefficients of variation (percent) in parentheses.

Table III—Levels of Significance of Sources of Variation in the Analyses of Bioavailability Parameters

Source of Variation	Parameter: Area	Peak Concentration	Peak Time	Half-Life
Sex	NS[a]	$p < 0.01$	NS	NS
Subjects	$p < 0.05$	NS	NS	NS
Day of administration	NS	NS	NS	NS
Formulation	NS	$p < 0.01$[b]	$p < 0.05$[b]	NS

[a] NS = not significant ($p > 0.05$). [b] The reference Formulation A (clofibrate) was significantly different from B (calcium clofibrate) but not from C (clofibrate–carbonate combination). Formulations B and C were not significantly different.

REFERENCES

(1) J. M. Thorp, *Lancet*, **1**, 1323 (1962).

(2) D. S. Fredrickson, R. I. Levy, and R. S. Lees, *N. Engl. J. Med.*, **276**, 34, 94, 148, 215, 273 (1967).

(3) D. B. Hunninghake, D. R. Tucker, and D. L. Azarnoff, *Circulation*, **39**, 675 (1969).

(4) S. M. Grundy, E. H. Ahrens, G. Salen, P. H. Schreibman, and P. J. Nestal, *J. Lipid Res.*, **13**, 531 (1972).

(5) M. L. Bierenbaum, A. I. Fleischman, and R. I. Raichelson, *Lipids*, **7**, 202 (1972).

(6) L. F. Chasseaud and T. Taylor, *Ann. Rev. Pharmacol.*, **14**, 35 (1974).

(7) W. H. Barr, *Drug Inform. Bull.*, **3**, 27 (1969).

(8) W. A. Ritschel, *Drug Intel. Clin. Pharm.*, **6**, 246 (1972).

(9) A. M. Barrett and J. M. Thorp, *Br. J. Pharmacol.*, **14**, 35 (1968).

(10) L. F. Chasseaud, A. J. Cooper, and V. H. Saggers, *J. Clin. Pharmacol.*, **14**, 382 (1974).

(11) P. T. Männistö, J. Tuomisto, A. Jounela, and O. Penttilä, *Acta Pharmacol. Toxicol.*, **36**, 353 (1975).

(12) A. Sedaghat and E. H. Ahrens, Jr., *Eur. J. Clin. Invest.*, **5**, 177 (1975).

(13) C. Metzler, *Biometrics*, **30**, 309 (1974).

(14) E. Shirley, *J. Pharm. Pharmacol.*, **28**, 312 (1976).

ACKNOWLEDGMENTS AND ADDRESSES

Received November 2, 1976, from the *Department of Metabolism and Pharmacokinetics, Huntingdon Research Centre, Huntingdon, PE18 6ES, England.*

Accepted for publication January 12, 1977.

The authors express their gratitude to Dr. P. Gooding of the Bristol-Myers Co. International Division, New York, N.Y., for advice and interest. They also thank Dr. C. White for medical supervision of the subjects and Mr. D. Assinder for technical assistance.

[x] To whom inquiries should be directed.

Comparative Drug Adsorption by Activated Charcoal

E. M. SELLERS *x, V. KHOUW *, and L. DOLMAN ‡

Abstract □ Comparative *in vitro* studies were carried out to determine the adsorption characteristics of 12 drugs on activated charcoal. At pH 1.3 and 37°, the adsorption capacity of activated charcoal (milligrams per gram of charcoal) was: aspirin, 262; glutethimide, 252; methaqualone, 179; chlordiazepoxide, 157; propoxyphene napsylate, 137; diazepam, 136; amitriptyline, 133; propoxyphene hydrochloride, 127; secobarbital, 124; pentobarbital, 103; phenobarbital, 70; and amobarbital, 51. The adsorption of the weak acids was most markedly decreased at pH 10.8. In patients, actual drug adsorption probably is lower than these maxima because of the presence of mucus, bile salts, and other drugs. In patients ingesting large amounts of poorly adsorbed drugs, activated charcoal would not be helpful.

Keyphrases □ Charcoal, activated—adsorption of various drugs *in vitro*, effect of pH □ Adsorption—various drugs to activated charcoal *in vitro*, effect of pH □ Analgesics—aspirin and propoxyphene, adsorption to activated charcoal *in vitro*, effect of pH □ Sedatives—glutethimide, methaqualone, diazepam, secobarbital, pentobarbital, phenobarbital, and amobarbital, adsorption to activated charcoal, effect of pH □ Tranquilizers—chlordiazepoxide, adsorption to activated charcoal *in vitro*, effect of pH □ Antidepressants—amitriptyline, adsorption to activated charcoal *in vitro*, effect of pH

Activated charcoal is frequently given to patients after acute drug ingestion (drug overdose) in an attempt to adsorb some ingested drug and thereby decrease the duration of the coma and/or the incidence of drug-induced morbidity. The efficacy of instilling activated charcoal down the lavage tube after lavage is not proven in adults (1).

The binding of psychoactive drugs to activated charcoal has been studied extensively. With rare exceptions, these studies are at nonphysiologic pH, in nonphysiologic solutions, at temperatures less than 37°, conducted in nonprimates, and seldom of a wide spectrum of chemical substances in the same study. Studies in humans are frequently anecdotal in nature and often pertain to children.

In *in vivo* animal studies, activated charcoal reduced GI absorption of phenobarbital (2), secobarbital (3), pentobarbital (2), glutethimide (3), propoxyphene (4–6), and aspirin (7, 8). Activated charcoal also significantly reduced GI absorption of drugs in humans (8–11).

As a prelude to efficacy studies of charcoal and other adsorbents in humans, the adsorption characteristics of various drugs on activated charcoal were determined.

EXPERIMENTAL

In vitro charcoal adsorption studies were carried out by dissolving psychoactive drugs in solutions at pH 1.3 and 10.8. Each liter of pH 1.3 solution contained: Na^+, 40 mEq; K^+, 10 mEq; and Cl^-, 95 mEq. Each liter of pH 10.8 solution contained: Na^+, 157 mEq; K^+, 10 mEq; Cl^-, 114 mEq; and HCO_3^{2-}, 106 mEq. Maximum adsorption wavelengths were determined[1] for each drug, and standard adsorption–concentration curves were prepared for each drug.

Twenty milliliters of solution containing 10–25 mg of drug was placed in a 50-ml centrifuge tube and incubated at 37° in a metabolic shaker. Various amounts of activated charcoal[2] (0.04–0.64 g) were then added to the tube carefully. The charcoal–drug solution was mixed, and incubation with shaking was continued for 15 min. The charcoal was allowed to settle for 5 min, and the supernate was then immediately filtered through a filter syringe[3]. The drug concentration in the simulated physiologic solution was determined spectrophotometrically after suitable dilution with 0.2 *M* carbonate buffer (pH 10).

RESULTS AND DISCUSSION

Experimental results on the adsorption of psychoactive drugs at pH 1.3 by activated charcoal are shown in Figs. 1 and 2. These data are plotted according to the Langmuir equation:

$$\frac{C_{eq}}{x/m} = \frac{C_{eq}}{k_2} + \frac{1}{k_1 k_2} \qquad \text{(Eq. 1)}$$

where C_{eq} is the free drug concentration in solution at equilibrium, x/m is the amount of drug adsorbed by the quantity of charcoal used, and k_2 and k_1k_2 are constants. The best straight line through these experimental data was calculated by the method of least squares, and the values of k_2 and k_1k_2 were evaluated from the reciprocals of the respective isotherm slope and intercept values of the regression equation.

Langmuir constants k_2 and k_1k_2 are summarized in Table I. The k_1k_2 values are relatively similar, presumably reflecting similar adsorption affinities between activated charcoal and the various drugs tested. However, since these values were calculated from the reciprocal of the intercept values of the Langmuir equation, k_1k_2 values are potentially subject to some error (12).

Aspirin was the most extensively bound (262 mg/g). A maximum binding capacity of 283 mg/g of charcoal at pH 1.0 was reported previously (11). Because large volumes of activated charcoal slurry may precipitate vomiting, one practice is to standardize the amount of charcoal by giving 1 g of activated charcoal/kg (13). Preferably, the dose of activated charcoal should be on the basis of the amount of drug ingested, but this information is seldom available. Therefore, the therapeutic need is to ensure that an excess of charcoal is given with minimal risk of vomiting. The present findings suggest that a dose of 1 g of activated charcoal/kg would adsorb 18.34 g of aspirin (*i.e.*, 58 300-mg tablets).

Whether propoxyphene is the napsylate or hydrochloride salt makes no difference to the adsorption of drug on charcoal. The benzodiazepines chlordiazepoxide and diazepam were adsorbed with intermediate capacity. Tablet equivalents of adsorption are: chlordiazepoxide, 400 25-mg tablets; and diazepam, 1904 5-mg tablets.

Figures 1 and 2 show the binding isotherms for the various drugs at pH 1.3, and Table I summarizes the results at both pH values. For sufficiently

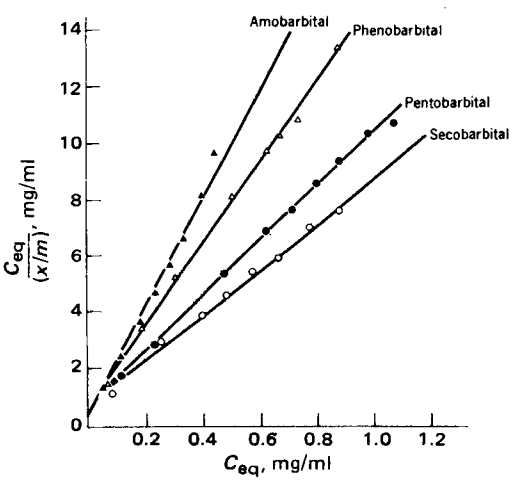

Figure 1—*Langmuir plots for barbiturate adsorption on activated charcoal at pH 1.3.*

[1] Beckman DBG UV spectrophotometer.
[2] Norit A, Fisher Scientific.
[3] Millipore Corp., Bedford, Mass.

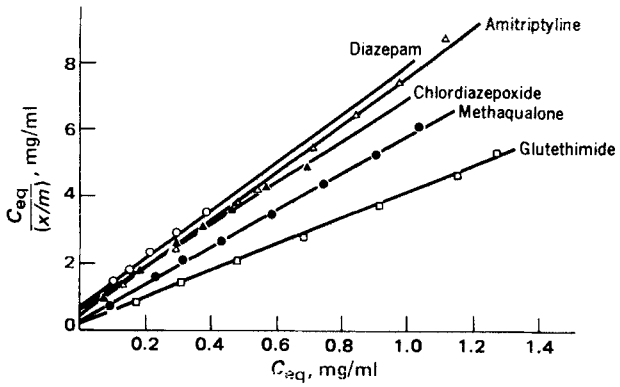

Figure 2—*Langmuir plots for adsorption of diazepam, amitriptyline, chlordiazepoxide, methaqualone, and glutethimide on activated charcoal at pH 1.3.*

soluble drugs, adsorption was less at the higher pH. The decrease in binding was greatest for aspirin (pKa 3.5). These results raise the possibility that aspirin adsorbed in the stomach may be transported adsorbed to charcoal into the small intestine where desorption occurs, with the consequent release of drug for absorption into the bloodstream.

Since patients may well ingest more drug than the charcoal's adsorption capacity, charcoal should not be used alone but be combined with emesis or lavage. Allowance should be made for giving larger amounts of charcoal to some patients, since the results of these *in vitro* studies probably represent maximum binding capacities. The capacities will likely be less in the presence of mucus, bile salts, blood, food, or alcohol, which more realistically represent the upper GI tract milieu in the overdose patient.

Table I—Values of Langmuir Constants Expressing Adsorption of Various Psychoactive Drugs by Activated Charcoal at pH 1.3 and 10.8, 37°

Drug	Charcoal Adsorbent (pH 1.3)		Charcoal Adsorbent (pH 10.8)	
	k_2[a]	k_1k_2	k_2[b]	k_1k_2
Amobarbital	51	3.44	47	1.20
Aspirin	262	3.08	141	1.23
Amitriptyline	133	3.72	—	—
Chlordiazepoxide	157	1.53	—	—
Diazepam	136	1.39	—	—
Methaqualone	179	3.51	—	—
Glutethimide	252	6.35	—	—
Pentobarbital	103	1.45	95	1.09
Phenobarbital	70	1.32	56	1.34
Propoxyphene hydrochloride	127	3.60	—	—
Propoxyphene napsylate	137	5.72	—	—
Secobarbital	124	1.53	85	2.19

[a] Milligrams of drug per gram of charcoal at 37°. [b] For seven drugs, solubility was insufficient to determine the adsorption isotherm accurately.

An additional complication is that frequently small amounts of a number of drugs are taken together, so competition for adsorption may occur. A dose of 100 g of activated charcoal would usually provide sufficient adsorption capacity. The current practice of lavaging patients before administering charcoal may not be optimal, and it might be possible to increase the efficiency of lavage by instilling the adsorbing substance *before* lavage as well as after.

Clinical studies in adults to determine the *in vivo* adsorption of drugs and the clinical efficacy of activated charcoal or other adsorbent materials such as ion-exchange resins are needed, since drug overdose seems to be increasing in incidence.

REFERENCES

(1) S. M. MacLeod, E. M. Sellers, H. Kaplan, and C. S. Stapleton, *Ann. Roy. Coll. Phys. Surg.*, **9**, 57 (1976).

(2) J. P. Atkinson and D. L. Azarnoff, *Clin. Toxicol.*, **4**, 31 (1971).

(3) W. J. Decker and D. G. Corby, *ibid.*, **3**, 1 (1970).

(4) D. G. Corby and W. J. Decker, *J. Am. Med. Assoc.*, **205**, 750 (1968).

(5) S. M. Chernish, R. L. Wolen, and B. E. Rodda, *Clin. Toxicol.*, **5**, 317 (1972).

(6) D. G. Corby and W. J. Decker, *J. Am. Med. Assoc.*, **203**, 1074 (1968).

(7) S. V. Phansalker and L. E. Holt, Jr., *J. Pediat.*, **72**, 683 (1968).

(8) W. J. Decker, D. G. Corby, and J. D. Ibanez, Jr., *Lancet*, **1**, 754 (1968).

(9) G. Levy and T. Tsuchiya, *Clin. Pharmacol. Ther.*, **13**, 317 (1972).

(10) W. J. Decker, R. A. Shpall, D. G. Corby, H. F. Combs, and C. E. Payne, *ibid.*, **10**, 710 (1969).

(11) T. Tsuchiya and G. Levy, *J. Pharm. Sci.*, **61**, 586 (1972).

(12) J. B. Milne and G. L. Chatten, *J. Pharm. Pharmacol.*, **9**, 686 (1959).

(13) R. E. Rangno, in, "Clinical Pharmacology of Psychoactive Drugs," E. M. Sellers, Ed., Alcoholism and Drug Addiction Research Foundation, Toronto, Canada, 1975, pp. 43–54.

ACKNOWLEDGMENTS AND ADDRESSES

Received August 13, 1976, from the **Division of Clinical Pharmacology, Clinical Institute, Addiction Research Foundation and Toronto Western Hospital, Toronto, Ontario, M5S 2S1, Canada,* and the ‡*Departments of Medicine and Pharmacology, Faculty of Medicine, University of Toronto, Toronto, Ontario, Canada.*

Accepted for publication January 31, 1977.

The authors thank Dr. S. Cooper, Clinical Pharmacology Laboratory, Addiction Research Foundation, Toronto, Canada, for suggestions. They also thank Dr. R. S. Dolman, Medical Director, Eli Lilly Co., Toronto, Canada, for supplying propoxyphene napsylate and Dr. J. Weyman, Medical Director, Hoffmann–La Roche Ltd., Vaudreuil, Quebec, Canada, for supplying the benzodiazepines.

L. Dolman was supported by a RODA summer scholarship, Non-Medical Use of Drug Directorate, Health Protection Branch, Ottawa, Canada.

ˣ To whom inquiries should be directed.

Tetrazole Analogs of Phenylalanine Derivatives as Tyrosine Hydroxylase Inhibitors

H. R. McNEIL *, B. B. WILLIAMS, Jr., and C. M. DARLING ˣ

Abstract □ Eight new tetrazole analogs of phenylalanine derivatives in which the carboxyl group was replaced by a tetrazole ring were synthesized. At a concentration of 2.5×10^{-5} *M*, each compound exhibited greater than 50% inhibition of tyrosine hydroxylase activity.

Keyphrases □ Tetrazole analogs of phenylalanine derivatives—synthesized, effect on tyrosine hydroxylase activity □ Phenylalanine derivatives—various tetrazole analogs synthesized, effect on tyrosine hydroxylase activity □ Tyrosine hydroxylase activity—effect of various tetrazole analogs of phenylalanine derivatives □ Enzymes—tyrosine hydroxylase activity, effect of various tetrazole analogs of phenylalanine derivatives □ Structure–activity relationships—various tetrazole analogs of phenylalanine derivatives, effect on tyrosine hydroxylase activity

Because it catalyzes the rate-determining step in catecholamine biosynthesis (1), tyrosine hydroxylase has been the target for the synthesis of numerous agents. The majority of these agents may be considered derivatives of phenylalanine and tyrosine, with attention focused on the aromatic portion of the structure.

BACKGROUND

With an intact amino acid side chain, derivatives of phenylalanine and tyrosine potentially can be metabolized to catecholamines, which may modify the overall pharmacological action. The α-methylated analog, α-methyltyrosine, a potent competitive inhibitor of tyrosine hydroxylase (2), is metabolized to methyldopa, α-methyldopamine, and α-methylnorepinephrine (3). These metabolites exhibit weak sympathomimetic action, which led to the false transmitter hypothesis for the antihypertensive action of methyldopa (4). However, if the carboxyl group is replaced by a tetrazole ring, the derivatives are not likely to be metabolized to catecholamines.

The chemically similar tetrazole ring system (5) has been used to replace a carboxyl group. Elwood *et al.* (6) reported weak inhibition of glutamic acid dehydrogenase by tetrazole analogs of glutamic acid. They suggested that the low degree of binding of the tetrazole analogs to the receptor was not due to poor steric fit or the degree of ionization but to the much greater area available within the tetrazole ring for the distribution of charge in the ionized form. The preparation of tetrazole analogs of other amino acids was reported (7).

The purpose of this study was to determine whether tetrazole analogs of phenylalanine derivatives would inhibit tyrosine hydroxylase. Several analogs in which the carboxyl group was replaced by a tetrazole ring were evaluated.

The aryl-substituted tetrazole analogs of phenylalanine were synthesized by the route outlined in Scheme I.

EXPERIMENTAL[1]

Aryl-Substituted Ethyl 2-Acetamido-2-cyano-3-phenylpropanoates (I–IX)—Intermediates I–IX were prepared by a modification of the method of Matsumoto (8). A mixture of ethyl acetamidocyanoacetate (68.0 g, 0.40 mole), sodium iodide (1.0 g), and anhydrous potassium carbonate (30.0 g, 0.22 mole) in dry acetone (300 ml) was heated at reflux while the appropriately substituted benzyl halide (0.30 mole) was added dropwise during 15 min. After heating at reflux for 7 hr, the mixture was poured over ice and filtered. The residue was recrystallized from the appropriate solvent (Table I) and activated charcoal.

NMR data agreed with the proposed structures. The NMR spectra (dimethyl sulfoxide-d_6, tetramethylsilane internal standard) showed the following common absorption peaks: δ 1.10 (t, 3H, CCH_3), 1.99 (s, 3H, $COCH_3$), 3.35 (s, 2H, Ar-CH_2C), and 4.10 (q, 2H, OCH_2C) ppm. Depending on the ring substituents, the absorption in the aromatic region ranged from δ 7.10 to 7.90 ppm and the pattern varied from singlet to multiplet. Each spectrum integrated for the correct number of protons. The NMR spectrum of VII showed an absorption peak at δ 2.25 ppm while that of VIII showed one at δ 2.30 ppm, each of which integrated for three protons corresponding to an aromatic methyl substituent.

Aryl-Substituted Ethyl 1-Acetamido-1-tetrazol-5-yl-2-phenylpropanoates (X–XIV)—These compounds were synthesized by a modification of the method of Finnegan *et al.* (9), which is exemplified by the procedure for X.

A mixture of II (14.5 g, 0.052 mole), sodium azide (6.8 g, 0.104 mole), and ammonium chloride (5.5 g, 0.104 mole) in dry dimethylformamide (125 ml) was heated at 88–95° for 28 hr. The hot mixture was filtered, and the filtrate was concentrated *in vacuo*. The residue was dissolved in distilled water, and the solution was adjusted to pH 2 with dilute hydrochloric acid. The resulting precipitate was washed with cold water and recrystallized twice from distilled water and activated charcoal, 8.4 g (50.3%), mp 147–149°. Table II contains physical and chemical data for X–XIV.

NMR data agreed with the proposed structures. Assignments of the common absorption peaks are (dimethyl sulfoxide-d_6): δ 1.10–1.15 (t, 3H, CCH_3), 1.90–1.99 (s, 3H, $COCH_3$), 3.65–3.75 (s, 2H, Ar-CH_2C), 4.10–4.15 (q, 2H, CH_2C), and 6.85–7.25 (m, 3H or 4H, aromatic) ppm. There was an additional absorption peak for XIII at δ 2.20 (s, 3H, Ar-CH_3) ppm and for XIV at δ 2.25 (s, 3H, Ar-CH_3) ppm.

Aryl-Substituted 5-(1-Amino-2-phenylethyl)tetrazoles (XV–XXIII)—These compounds were prepared by two different methods (Table III).

Method A—The procedure is a modification of the method of McManus and Herbst (7). Typically, a mixture of the appropriately substituted cyano ester (I, III, IV, or IX) (0.10 mole), sodium azide (19.5 g, 0.30 mole), and anhydrous aluminum chloride (13.3 g, 0.10 mole) in dry tetrahydrofuran (250 ml) was heated at reflux for 24 hr. After cooling, the solvent was displaced with an equal volume of water on a continuous flow flash evaporator. The solids were filtered and air dried.

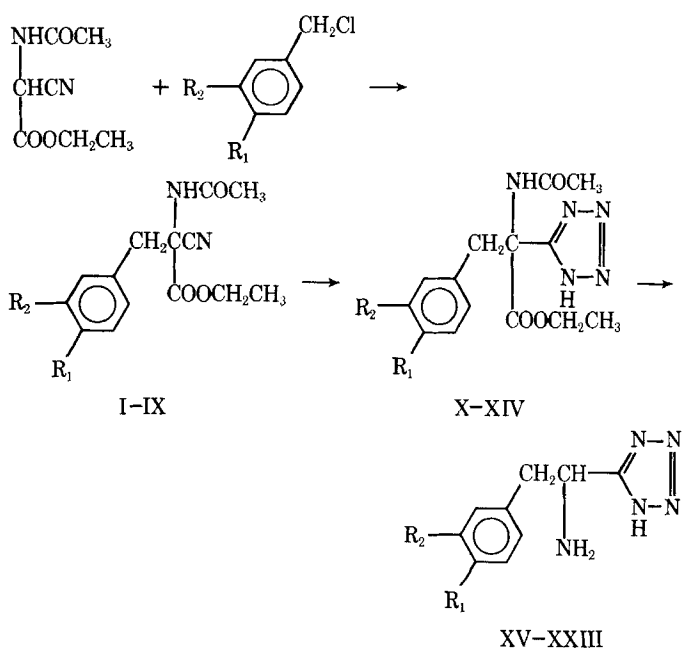

Scheme I

[1] Elemental analyses were performed by Atlantic Microlab, Inc., Atlanta, Ga. NMR data were recorded on a Varian Associates T-60A spectrophotometer.

Table I—Aryl-Substituted Ethyl 2-Acetamido-2-cyano-3-phenylpropanoates

Compound	R_1	R_2	Melting Point[a]	Crude Yield, %	Recrystallization[b] Solvent	Formula	Analysis, % Calc.	Found
I	H	H	130–132°[c]	92	A	—	—	—
II	H	F	88–90°	90	B	$C_{14}H_{15}FN_2O_3$	C 60.43	60.42
							H 5.43	5.50
							N 10.07	9.92
III	F	H	162–163°[d]	90	B	—	—	—
IV	H	Cl	80–82°	95	A	$C_{14}H_{15}ClN_2O_3$	C 57.05	57.12
							H 5.13	5.17
							N 9.50	9.57
V	Cl	H	161–163°[e]	96	B	—	—	—
VI	Cl	Cl	119–121°	71	A	$C_{14}H_{14}Cl_2N_2O_3$	C 51.08	51.25
							H 4.29	4.32
							N 8.51	8.33
VII	H	CH_3	84–86°	90	A	$C_{15}H_{18}N_2O_3$	C 65.68	65.63
							H 6.61	6.71
							N 10.21	10.29
VIII	CH_3	H	152–154°	92	A	$C_{15}H_{18}N_2O_3$	C 65.68	65.42
							H 6.61	6.69
							N 10.21	10.28
IX	NO_2	H	183–185°[f]	98	A	—	—	—

[a] Melting points were taken in open capillary tubes and are uncorrected. [b] A = 50% ethanol; B = toluene. [c] Lit. (8) mp 132–134°. [d] Lit. (8) mp 162–163°. [e] Lit. (8) mp 163–164°. [f] Lit. (8) mp 185–186°.

Table II—Aryl-Substituted Ethyl 1-Acetamido-1-tetrazol-5-yl-2-phenylpropanoates

Compound	R_1	R_2	Melting Point[a]	Yield, %	Formula	Analysis, % Calc.	Found
X	H	F	147–149°	50.3	$C_{14}H_{16}FN_5O_3$	C 52.33	52.44
						H 5.02	5.02
						N 21.80	21.86
XI	Cl	H	138–140°	17.2	$C_{14}H_{16}ClN_5O_3$	C 49.78	49.37
						H 4.77	4.88
						N 20.73	20.87
XII	Cl	Cl	183–185°	45.1	$C_{14}H_{15}Cl_2N_5O_3$	C 45.18	45.29
						H 4.06	4.11
						N 18.82	18.69
XIII	H	CH_3	130–132°	23.8	$C_{15}H_{19}N_5O_3$	C 56.77	56.80
						H 6.03	6.06
						N 22.07	22.11
XIV	CH_3	H	101–105°	43.2	$C_{15}H_{19}N_5O_3 \cdot H_2O$	C 53.72	53.72
						H 6.31	6.33
						N 20.88	20.97

[a] Melting points were taken in open capillary tubes and are uncorrected.

The dried residue was suspended in concentrated hydrochloric acid (300 ml), and the mixture was heated at reflux for 3 hr. The mixture was concentrated *in vacuo*, and the residue was added to a solution of pyridine (30 ml) and 95% ethanol (250 ml). After refrigeration, the product was filtered and recrystallized from water–activated charcoal. Table III lists physical and chemical data for XV–XXIII.

Method B—The tetrazole ester (from Table II) (0.05 mole) was added to concentrated hydrochloric acid (100 ml) and heated at reflux overnight. After the mixture was concentrated *in vacuo*, the residue was dissolved in distilled water and the solution was adjusted to pH 8 with ammonium hydroxide solution. After decanting, the gummy residue was recrystallized from water and activated charcoal. Table III lists physical and chemical data for XV–XXIII.

NMR data agreed with the proposed structures. Assignments of the common absorption peaks are (10% sodium deuteroxide): δ 2.90–2.95 (m, 2H, Ar-CH_2), 4.25–4.35 (m, 1H, CCH), and 6.75–6.90 (m, 3H or 4H, aromatic) ppm. There was an additional absorption peak for XXI at δ 2.00 (s, 3H, Ar-CH_3) ppm and for XXII at δ 1.93 (s, 3H, Ar-CH_3) ppm.

Tyrosine Hydroxylase Inhibition—Tyrosine hydroxylase was isolated from beef adrenals[2] by the method of Nagatsu *et al.* (10). Active enzyme was precipitated by the addition of ammonium sulfate, resuspended in 10^{-3} *M* mercaptoethanol, and stored at −20°. Tetrazole derivatives, dissolved in dilute hydrochloric acid and measured at final concentrations of 2.5×10^{-5} *M*, were incubated at 37° for 15 min with shaking in the following medium: 200 μmoles of 1 *M* acetate buffer (pH 6.0), 0.1 μmole of *l*-tyrosine, 1.5–2.5 × 10^5 cpm of 3,5-ditritiotyrosine, 1.0 μmole of 2-amino-4-hydroxy-6,7-dimethyltetrahydropteridin in 0.1 ml of 0.1 *M* phosphate buffer (pH 7.4), 100 μmoles of mercaptoethanol, 0.5 μmole of ferrous sulfate, 0.2 ml of enzyme preparation, and water to a total volume of 1.0 ml. The medium alone was used as the control.

The reaction was stopped by the addition of 0.05 ml of acetic acid. The mixture was centrifuged, and the supernate was placed on an ion-exchange column[3] and washed once with 1.0 ml of water. The original supernate and washing were collected in a liquid scintillation vial, scintillation fluid[4] was added, and the solution was counted[5]. Data as nanomoles of tyrosine oxidized were calculated by measuring tritiated water released following the conversion of 3,5-ditritiotyrosine to 5-tritiodihydroxyphenylalanine. Enzyme activity in the presence of tetrazoles is presented in Table III.

RESULTS AND DISCUSSION

These preliminary results (Table III) indicate that replacement of the carboxyl group of phenylalanine derivatives with a tetrazole ring does not abolish the inhibitory properties of the respective parent compounds. Although no statistically significant differences (Duncan multiple range test) (11) in percent inhibition were found among the tetrazoles, statistical analysis by Dunnett's test (12) did reveal that all tetrazole analogs induced significant reduction ($p < 0.01$) of tyrosine hydroxylase activity compared to control enzyme activity.

Counsell *et al.* (13) reported 0, 35, 26, and 30% inhibition of tyrosine hydroxylase activity for 3-fluoro-, 4-fluoro-, 3-chloro-, and 4-chlorophenylalanine, respectively, at a concentration of 2×10^{-4} *M*. This result may be compared to the greater percent inhibition at a lower concentration by the corresponding tetrazole analogs, XVI, XVII, XVIII, and XIX (Table III).

[2] Meats Laboratory, Auburn University.

[3] Dowex 5 H^+.

[4] Riafluor, New England Nuclear, Boston, Mass.

[5] Beckman LS-150 liquid scintillation system.

Table III—Tetrazole Analogs of Phenylalanine and Their Inhibition of Tyrosine Hydroxylase

Compound[a]	R_1	R_2	Melting Point[b]	Method	Yield, %[c]	Formula	Analysis, % Calc.	Analysis, % Found	Enzyme Activity[d]	Inhibition, % ± *SEM*
Control									18.29 (10)	
XV	H	H	273°[e]	A	19	$C_9H_{11}N_5$	—	—	9.27 (6)	49.3 ± 5.2
XVI	H	F	288°	B	69.2	$C_9H_{10}FN_5$	C 52.17	52.14	7.84 (5)	57.1 ± 4.8
							H 4.86	4.70		
							N 33.80	34.12		
XVII	F	H	283°	A	17	$C_9H_{10}FN_5$	C 52.17	52.04	6.61 (7)	63.6 ± 5.7
							H 4.86	4.82		
							N 33.80	33.76		
XVIII	H	Cl	274°	A	11	$C_9H_{10}ClN_5$	C 48.33	48.26	8.51 (7)	53.6 ± 4.3
							H 4.51	4.49		
							N 31.31	31.26		
XIX	Cl	H	286°	B	50.1	$C_9H_{10}ClN_5$	C 48.33	48.18	7.57 (7)	58.7 ± 8.6
							H 4.51	4.54		
							N 31.31	31.20		
XX	Cl	Cl	282°	B	43.5	$C_9H_9Cl_2N_5$	C 41.88	41.79	6.87 (8)	62.5 ± 4.9
							H 3.51	3.55		
							N 27.13	27.17		
XXI	H	CH_3	284°	B	70.5	$C_{10}H_{13}N_5$	C 59.10	59.06	5.73 (6)	68.6 ± 1.4
							H 6.45	6.20		
							N 34.46	34.65		
XXII	CH_3	H	288°	B	44.2	$C_{10}H_{13}N_5$	C 59.10	58.96	6.09 (8)	66.9 ± 1.3
							H 6.45	6.26		
							N 34.46	34.61		
XXIII	NO_2	H	256°	A	17	$C_9H_{10}N_6O_2$	C 46.15	46.26	6.63 (6)	63.8 ± 2.8
							H 4.30	3.89		
							N 35.88	36.07		

[a] All racemates. [b] All compounds melted with decomposition. Melting points were taken in open capillary tubes and are uncorrected. [c] Yields in Method A are calculated from the cyano derivative; in Method B, they are calculated from the tetrazole ester. [d] Nanomoles of *l*-tyrosine oxidized in presence of inhibitor (2.5×10^{-5} *M*). Parentheses indicate the number of replicates. [e] Lit. (7) mp 270.5–271.5°.

This preliminary study indicates that tetrazole analogs of phenylalanine derivatives inhibit tyrosine hydroxylase *in vitro*. This study is being utilized as the basis for the design of additional compounds and more detailed pharmacological studies.

REFERENCES

(1) S. Udenfriend, *Pharmacol. Rev.*, **18**, 43(1966).

(2) S. Udenfriend, P. Zaltsman-Nirenberg, and T. Nagatsu, *Biochem. Pharmacol.*, **14**, 837(1965).

(3) K. Engelman, E. Jequier, S. Udenfriend, and A. Sjoerdsma, *J. Clin. Invest.*, **47**, 568(1968).

(4) L. Maitre, P. R. Hedwall, and P. C. Waldmeier, in "Aromatic Amino Acids in the Brain," Ciba Foundation Symposium, Associated Scientific Publishers, New York, N.Y., 1974, p. 335.

(5) F. R. Benson, *Chem. Rev.*, **41**, 1(1947).

(6) J. K. Elwood, R. M. Herbst, and G. L. Kilgour, *J. Biol. Chem.*, **240**, 2073(1965).

(7) J. M. McManus and R. M. Herbst, *J. Org. Chem.*, **24**, 1643(1959).

(8) I. Matsumoto, *Chem. Pharm. Bull.*, **15**, 1990(1967).

(9) W. G. Finnegan, R. A. Henry, and R. Lofquist, *J. Am. Chem. Soc.*, **80**, 3908(1958).

(10) T. Nagatsu, M. Levitt, and S. Udenfriend, *J. Biol. Chem.*, **239**, 2910(1964).

(11) D. B. Duncan, *Biometrics*, **11**, 1(1955).

(12) C. W. Dunnett, *ibid.*, **3**, 1(1964).

(13) R. E. Counsell, P. Desai, T. D. Smith, P. S. Chan, P. A. Weinhold, V. B. Rethy, and D. Burke, *J. Med. Chem.*, **13**, 1040(1970).

ACKNOWLEDGMENTS AND ADDRESSES

Received December 22, 1976, from the *School of Pharmacy, Auburn University, Auburn, AL 36830.*

Accepted for publication February 10, 1977.

Adapted in part from a thesis submitted by H. R. McNeil to Auburn University in partial fulfillment of the Master of Science degree requirements.

The authors thank Mrs. Pamela Pryor for technical assistance.

* Present address: Patterson Coleman Laboratories, Tampa, FL 33603.

[x] To whom inquiries should be directed.

Determination of Anthranilic Acid in Plasma

J. F. DOUGLAS ˣ and Y. PHILOPOULOUS

Abstract □ A simple, specific GLC method was developed for the determination of anthranilic acid in plasma. This method is based on extraction from a carefully controlled buffer followed by removal of solvent, silylation, and detection in the gas chromatograph. The procedure is quantitative in the 2–10-μg/ml range.

Keyphrases □ Anthranilic acid—GLC analysis in plasma □ GLC—analysis, anthranilic acid in plasma □ Ascaricides, veterinary—anthranilic acid, GLC analysis in plasma

Anthranilic acid has been used to treat roundworm infestation in animals. Recently, it was identified in the blood of animals receiving the new analgesic 2,3-dihydro-9*H*-isoxazolo[3,2-*b*]quinazolin-9-one[1] (1, 2). Although anthranilic acid also is a naturally occurring body constituent, a sensitive, specific analytical method for its determination in biological fluids has not been described. It has been identified in urine by chromatography (3) and diazotization (4, 5). A nondetailed GC procedure for its detection as the methyl ester has also been cited (6).

This report describes a sensitive, specific quantitative method for the determination of anthranilic acid in plasma.

EXPERIMENTAL

GLC—A dual-column gas chromatograph[2] equipped with a hydrogen flame-ionization detector and a 1-mv recorder[3] was employed. The chromatographic columns used were 2-m × 3-mm i.d. glass tubes packed with 3% XE-60 on 100–120-mesh Gas Chrom Q[4]. The instrument settings were: column temperature, 140°; injection port temperature, 200°; and detector block temperature, 195°. Gas flow rates were: hydrogen, 29 ml/min; and helium (carrier gas), 60 ml/min. Sensitivity settings were: range, 10; and attenuation factor, 8×. The retention times under these conditions were 1.2 min for anthranilic acid and 2.2 min for 4-bromobiphenyl (Fig. 1).

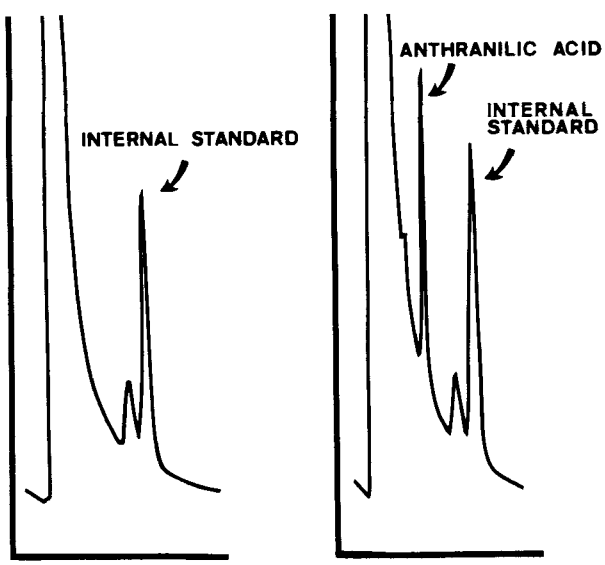

Figure 1—*Gas chromatograms of plasma treated as described. Key: left, chromatogram from normal plasma; and right, chromatogram from normal plasma with anthranilic acid added.*

[1] W2429.
[2] F and M model 402.
[3] Minneapolis-Honeywell.
[4] Applied Science.

Table I—Anthranilic Acid Recovered from Dog Plasma at pH 4.75 by Extraction with Ethyl Acetate

Anthranilic Acid Added to Dog Plasma, μg/ml	Anthranilic Acid Found[a], μg/ml	Anthranilic Acid Extracted[a], %
2.0	2.0	100
5.0	5.0	100
7.0	7.1	102
10.0	10.6	106

[a] Average of duplicates.

Reagents—The reagents were redistilled chloroform, peroxide-free ethyl acetate, 4-bromobiphenyl[5], and bis(trimethylsilyl)acetamide[4].

Procedure—Dog plasma, 1.0 ml, was adjusted to pH 4.75 with 0.3 ml of 2 *M* acetic acid–sodium acetate buffer, pH 4.75. Ethyl acetate, 3 ml, was added, and the mixture was agitated on a mixer for 2 min. After centrifugation for 10 min, 2.0 ml of the organic phase was removed, placed in a 5-ml glass tube, and evaporated to dryness under a nitrogen stream at room temperature.

Chloroform, 0.2 ml, containing 18 μg of 4-bromobiphenyl/ml and 9% bis(trimethylsilyl)acetamide was added to the residue, and it was stirred on a mixer for a few seconds. A 2-μl aliquot of this solution was injected into the gas chromatograph. The concentration of anthranilic acid was determined by the relative peak height method, using 4-bromobiphenyl as the internal standard.

RESULTS AND DISCUSSION

The relative peak heights (±*SE*) for 2, 5, 7, and 10 μg of anthranilic acid/ml were 0.37 ± 0.0053, 0.96 ± 0.0091, 1.34 ± 0.0008, and 2.00 ± 0.0102, respectively. The reproducibility of the procedure is indicated by the standard error of quadruplicate determinations.

The extraction technique effectively separates anthranilic acid from normally interfering plasma constituents since determinations with normal plasma give little or no blank (Fig. 1). The pH of the ethyl acetate

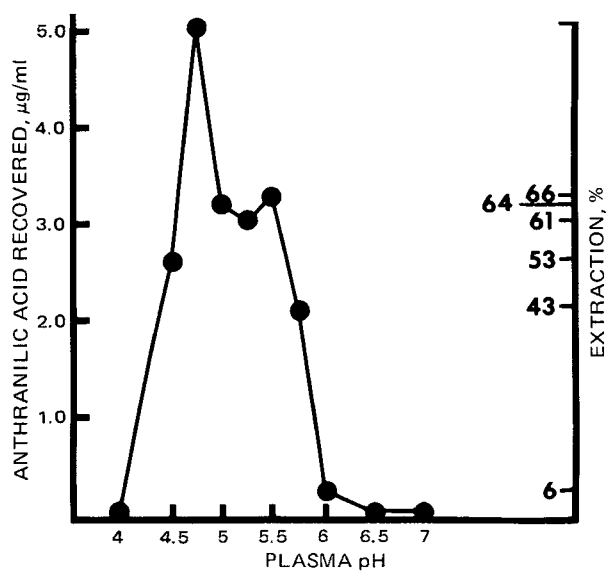

Figure 2—*Effect of pH on the extraction of 5.0 μg/ml of anthranilic acid from plasma.*

[5] Eastman Chemical Co.

extraction is critical. Recovery studies at pH 4.75 showed complete extraction of anthranilic acid over the effective assay range of 2–10 μg/ml (Table I); but at a slightly higher pH level of 5.0 or at a slightly lower level of 4.5, only about one-half of the anthranilic acid was extracted (Fig. 2).

REFERENCES

(1) R. D. Sofia, W. Diamantis, B. J. Ludwig, and R. Gordon, *Arzneim.-Forsch.*, **27**, 770 (1977).

(2) J. Edelson, J. F. Douglas, and B. J. Ludwig, *ibid.*, **27**, 789 (1977).

(3) L. T. Tenconi, *Boll. Soc. Hol. Sper.*, **29**, 504 (1953); through *Chem. Abstr.*, **49**, 7670i.

(4) R. R. Brow and J. M. Price, *J. Biol. Chem.*, **219**, 985 (1956).

(5) S. L. Tompsett, *Clin. Chim. Acta*, **4**, 411 (1959).

(6) C. S. W. Brooks and E. C. Horning, *Anal. Chem.*, **36**, 1540 (1964).

ACKNOWLEDGMENTS AND ADDRESSES

Received October 7, 1976, from *Wallace Laboratories, Cranbury, NJ 08512.*

Accepted for publication January 25, 1977.

[x] To whom inquiries should be directed. Present address: National Cancer Institute, National Institutes of Health, Bethesda, MD 20014.

Detection of Penicillin G and Ampicillin as Contaminants in Tetracyclines and Penicillamine

DORIS HERBST

Abstract □ A method was developed to detect residual levels of ampicillin and penicillin G in various tetracyclines and penicillamine. Residues are detected by reversed-phase TLC followed by bioautography. The directness of the techniques makes this method a good means of detecting residual contaminants in drugs.

Keyphrases □ Penicillin G—TLC–bioautographic analysis as contaminant in various tetracyclines and penicillamine □ Ampicillin—TLC–bioautographic analysis as contaminant in various tetracyclines and penicillamine □ TLC–bioautography—analysis, penicillin G and ampicillin as contaminants in various tetracyclines and penicillamine □ Tetracyclines, various—TLC–bioautographic analysis of penicillin G and ampicillin as contaminants □ Penicillamine—TLC–bioautographic analysis of penicillin G and ampicillin as contaminants □ Antibacterials—TLC–bioautographic analysis of penicillin G and ampicillin as contaminants in various tetracyclines and penicillamine

The problem of penicillin contamination in nonpenicillin products was recognized as early as 1964. An ad hoc Advisory Committee on Penicillin Contamination composed of experts in the fields of allergy and penicillin therapy (1) was convened by the Commissioner of Food and Drugs to evaluate the potential public health problems. The potential danger of allergic reactions, ranging from minor symptoms to fatal anaphylaxis, and the possibility of sensitizing individuals by repeated trace doses were considered.

Based on the data then available, limits on the amount of penicillin allowable in nonpenicillin drugs were recommended. These limits were less than 0.05 unit/maximum single dose for parenteral drugs and less than 0.5 unit/maximum single dose for oral drugs. Methods to detect penicillin G were specified by the Food and Drug Administration (2).

BACKGROUND

In 1974, a screening study (3) was conducted to ascertain which, if any, of the other penicillins could be detected in erythromycin and tetracycline by existing methods. That study showed that the current methods were less sensitive to residual levels of phenethicillin, methicillin, nafcillin, oxacillin, and cephalothin and were completely incapable of detecting residual ampicillin.

This 1974 evaluation indicated the need for new methods to detect residual ampicillin. Investigations conducted in 1974 resulted in a new bioautographic method (4) to separate and detect as little as 1 ppm of ampicillin from tetracycline hydrochloride bulk powder.

In 1975, new procedures (5) were described for the detection of ampicillin and penicillin G contaminants in demeclocycline and chlortetracycline. Although analytical capabilities had been expanded, additional methods were needed to detect ampicillin and penicillin G in doxycycline, oxytetracycline, and methacycline. Biagi *et al.* (6) described a reversed-phase TLC method to determine partition data for the penicillins. Using various concentrations of acetone in the mobile phase (6) of this system, they varied the R_f values of 11 penicillins and concluded: "The most hydrophilic compounds are the first to reach a maximum R_f value. On the other hand, at 0% acetone in the mobile phase the most lipophilic compounds remained close to the origin" (6).

The possibility that this type of system might be applied to residual contamination of other antibiotics seemed feasible. The techniques described by Biagi *et al.* (6) were applied to the detection of residual ampicillin and penicillin G in the tetracyclines and residual penicillin G in penicillamine.

EXPERIMENTAL

Preparation of TLC Plates—TLC plates[1], 20 × 20 cm, precoated with silica gel GF[2], were impregnated with silicone[3] by developing the plates in 200 ml of silicone–ether[4] (5:95 v/v) in a covered developing chamber. After overnight development, the plates were removed from the chamber and allowed to air dry at room temperature.

Sample Preparation—With glass-stoppered volumetric flasks to prevent evaporation of the solvent, standard solutions of ampicillin were prepared in acetone[5] to contain 0.1, 0.05, 0.025, 0.0125, and 0.00625 μg/ml. A similar set of penicillin G standards was prepared. Portions of 25 mg of chlortetracycline (I), demeclocycline (II), methacycline (III), minocycline (IV), oxytetracycline (V), tetracycline (VI), and doxycycline hyclate (VII) were placed in small (7 ml) glass-stoppered weighing vials. One milliliter of each standard solution was added to the vials containing the tetracyclines; then the vials were stoppered and gently shaken for a few seconds to form a suspension of the drugs.

This same procedure was followed for a second set of samples using the penicillin G standards. In addition, 250-mg portions of penicillamine

[1] Analtech, Inc., Blue Hen Industrial Park, Newark, DE 19711.

[2] Brinkmann Instruments, Westbury, NY 11590.

[3] Silicone DC 200 (350 centistokes), Applied Science Laboratories, State College, PA 16801.

[4] Burdick & Jackson Laboratories, Muskegon, MI 49442.

[5] Fisher Scientific, Fair Lawn, N.J.

extraction is critical. Recovery studies at pH 4.75 showed complete extraction of anthranilic acid over the effective assay range of 2–10 μg/ml (Table I); but at a slightly higher pH level of 5.0 or at a slightly lower level of 4.5, only about one-half of the anthranilic acid was extracted (Fig. 2).

REFERENCES

(1) R. D. Sofia, W. Diamantis, B. J. Ludwig, and R. Gordon, *Arzneim.-Forsch.*, **27**, 770 (1977).

(2) J. Edelson, J. F. Douglas, and B. J. Ludwig, *ibid.*, **27**, 789 (1977).

(3) L. T. Tenconi, *Boll. Soc. Hol. Sper.*, **29**, 504 (1953); through *Chem. Abstr.*, **49**, 7670i.

(4) R. R. Brow and J. M. Price, *J. Biol. Chem.*, **219**, 985 (1956).

(5) S. L. Tompsett, *Clin. Chim. Acta*, **4**, 411 (1959).

(6) C. S. W. Brooks and E. C. Horning, *Anal. Chem.*, **36**, 1540 (1964).

ACKNOWLEDGMENTS AND ADDRESSES

Received October 7, 1976, from *Wallace Laboratories, Cranbury, NJ 08512.*

Accepted for publication January 25, 1977.

[x] To whom inquiries should be directed. Present address: National Cancer Institute, National Institutes of Health, Bethesda, MD 20014.

Detection of Penicillin G and Ampicillin as Contaminants in Tetracyclines and Penicillamine

DORIS HERBST

Abstract □ A method was developed to detect residual levels of ampicillin and penicillin G in various tetracyclines and penicillamine. Residues are detected by reversed-phase TLC followed by bioautography. The directness of the techniques makes this method a good means of detecting residual contaminants in drugs.

Keyphrases □ Penicillin G—TLC–bioautographic analysis as contaminant in various tetracyclines and penicillamine □ Ampicillin—TLC–bioautographic analysis as contaminant in various tetracyclines and penicillamine □ TLC–bioautography—analysis, penicillin G and ampicillin as contaminants in various tetracyclines and penicillamine □ Tetracyclines, various—TLC–bioautographic analysis of penicillin G and ampicillin as contaminants □ Penicillamine—TLC–bioautographic analysis of penicillin G and ampicillin as contaminants □ Antibacterials—TLC–bioautographic analysis of penicillin G and ampicillin as contaminants in various tetracyclines and penicillamine

The problem of penicillin contamination in nonpenicillin products was recognized as early as 1964. An ad hoc Advisory Committee on Penicillin Contamination composed of experts in the fields of allergy and penicillin therapy (1) was convened by the Commissioner of Food and Drugs to evaluate the potential public health problems. The potential danger of allergic reactions, ranging from minor symptoms to fatal anaphylaxis, and the possibility of sensitizing individuals by repeated trace doses were considered.

Based on the data then available, limits on the amount of penicillin allowable in nonpenicillin drugs were recommended. These limits were less than 0.05 unit/maximum single dose for parenteral drugs and less than 0.5 unit/maximum single dose for oral drugs. Methods to detect penicillin G were specified by the Food and Drug Administration (2).

BACKGROUND

In 1974, a screening study (3) was conducted to ascertain which, if any, of the other penicillins could be detected in erythromycin and tetracycline by existing methods. That study showed that the current methods were less sensitive to residual levels of phenethicillin, methicillin, nafcillin, oxacillin, and cephalothin and were completely incapable of detecting residual ampicillin.

This 1974 evaluation indicated the need for new methods to detect residual ampicillin. Investigations conducted in 1974 resulted in a new bioautographic method (4) to separate and detect as little as 1 ppm of ampicillin from tetracycline hydrochloride bulk powder.

In 1975, new procedures (5) were described for the detection of ampicillin and penicillin G contaminants in demeclocycline and chlortetracycline. Although analytical capabilities had been expanded, additional methods were needed to detect ampicillin and penicillin G in doxycycline, oxytetracycline, and methacycline. Biagi *et al.* (6) described a reversed-phase TLC method to determine partition data for the penicillins. Using various concentrations of acetone in the mobile phase (6) of this system, they varied the R_f values of 11 penicillins and concluded: "The most hydrophilic compounds are the first to reach a maximum R_f value. On the other hand, at 0% acetone in the mobile phase the most lipophilic compounds remained close to the origin" (6).

The possibility that this type of system might be applied to residual contamination of other antibiotics seemed feasible. The techniques described by Biagi *et al.* (6) were applied to the detection of residual ampicillin and penicillin G in the tetracyclines and residual penicillin G in penicillamine.

EXPERIMENTAL

Preparation of TLC Plates—TLC plates[1], 20 × 20 cm, precoated with silica gel GF[2], were impregnated with silicone[3] by developing the plates in 200 ml of silicone–ether[4] (5:95 v/v) in a covered developing chamber. After overnight development, the plates were removed from the chamber and allowed to air dry at room temperature.

Sample Preparation—With glass-stoppered volumetric flasks to prevent evaporation of the solvent, standard solutions of ampicillin were prepared in acetone[5] to contain 0.1, 0.05, 0.025, 0.0125, and 0.00625 μg/ml. A similar set of penicillin G standards was prepared. Portions of 25 mg of chlortetracycline (I), demeclocycline (II), methacycline (III), minocycline (IV), oxytetracycline (V), tetracycline (VI), and doxycycline hyclate (VII) were placed in small (7 ml) glass-stoppered weighing vials. One milliliter of each standard solution was added to the vials containing the tetracyclines; then the vials were stoppered and gently shaken for a few seconds to form a suspension of the drugs.

This same procedure was followed for a second set of samples using the penicillin G standards. In addition, 250-mg portions of penicillamine

[1] Analtech, Inc., Blue Hen Industrial Park, Newark, DE 19711.

[2] Brinkmann Instruments, Westbury, NY 11590.

[3] Silicone DC 200 (350 centistokes), Applied Science Laboratories, State College, PA 16801.

[4] Burdick & Jackson Laboratories, Muskegon, MI 49442.

[5] Fisher Scientific, Fair Lawn, N.J.

Table I—Maximum Volume Spotted and Lower Limits of Detection of Penicillin Residues in Tetracyclines and Penicillamine[a]

Antibiotic	Volume Spotted, μl	Total Units of Suspensions, μg/ml	Lower Detection Limits, ng
Tetracycline	50	0.025	0.75
Methacycline	50	0.025	0.75
Doxycycline	50	0.025	0.75
Demeclocycline	50	0.025	0.75
Minocycline	50	0.025	0.75
Oxytetracycline	20	0.05	0.60
Chlortetracycline	50	0.025	0.75
Penicillamine	60	0.0125	0.45

[a] Suspensions were made by adding 1 ml of acetone containing the levels of penicillin listed above to 25 mg of each tetracycline. A solution was made by adding 10 ml of acetone containing 0.0125 unit of penicillin/ml to the contents of one 250-mg penicillamine capsule. The maximum amount of these samples that exhibited acceptable separation and the lower limits of detection are listed.

capsules were placed in screw-capped glass test tubes (16 × 125 mm) and spiked with 10 ml of each standard solution of penicillin G.

Chromatographic Procedure—The silicone-impregnated plates were marked with a finish line horizontally about 1 cm from the top of the plate. With a 10-μl tip and holder, aliquots of 10–100 μl were spotted on a line 2 cm from the bottom of the plates. Various aliquots were used to determine the maximum amount that could be spotted and still maintain sufficient separation of the contaminant from the antibiotic. These aliquots were delivered 10 μl at a time and dried with a gentle air flow to keep the spots as small as possible.

An aqueous buffer was prepared by placing 19.4 g of sodium acetate[6] (crystal) in 1 liter of distilled water and lowering the pH to 7.4 by adding small amounts of barbital[5] while stirring. This buffer was then filtered through analytical filter paper[7] to remove any undissolved barbital. The impregnated plates were then placed in an unsaturated tank containing 100 ml of barbital acetate buffer–acetone (94:6 v/v). The solvent front was allowed to move to the finish line, and the plates were removed and air dried at room temperature. The drying process was hastened by incubating the plates at 54° for approximately 10 min.

Bioautographic Procedure—The dried chromatographic plates were placed in plastic bioassay trays[8] (23 × 23 cm, with lids) and secured to the bottom of the plastic trays with double-sided tape to prevent the plates from floating when the liquid agar medium was added. Each plate was flooded with 100 ml of antibiotic medium No. 4 (yeast beef agar),

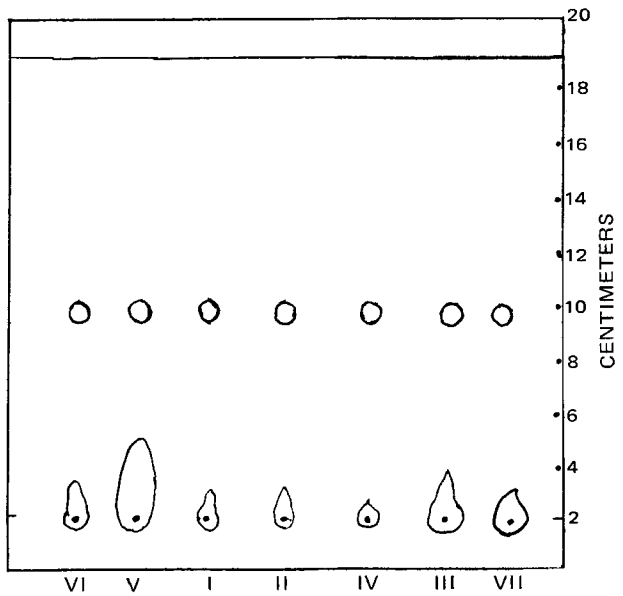

Figure 1—*Sketch of typical plate. Key: circular zones, ampicillin; and bearded zones, various tetracyclines.*

[6] J. T. Baker Chemical Co., Phillipsburg, NJ 08865.
[7] No. 588, Schleicher & Schuell, Keene, NH 03431.
[8] Vanguard International Inc., Red Bank, NJ 07701.

Table II—Maximum Volume Spotted and Lower Limits of Detection of Ampicillin Residues in Tetracyclines[a]

Antibiotic	Volume Spotted, μl	Total Units of Suspensions, μg/ml	Lower Detection Limits, ng
Tetracycline	30	0.025	0.75
Methacycline	30	0.025	0.75
Doxycycline	30	0.025	0.75
Demeclocycline	30	0.025	0.75
Minocycline	30	0.025	0.75
Oxytetracycline	20	0.025	0.5
Chlortetracycline	30	0.025	0.75

[a] Suspensions were made by adding 1 ml of acetone containing 0.025 μg of ampicillin/ml to 25 mg of each tetracycline. The maximum amounts of these suspensions spotted that exhibited acceptable separation and the lower limits of detection are listed.

which had been inoculated with 0.02 ml of a suspension of *Sarcina lutea* (ATCC 9431[9]).

When the agar had set (about 20 min), the bioassay trays were covered, placed in a plastic bag with a piece of damp paper, sealed, and refrigerated for approximately 1 hr. The trays were then incubated with the sealed bag intact at 30° overnight. After 16–18 hr of incubation, the areas of inhibition were visualized by spraying the plates with a solution of 2% 2,3,5-triphenyltetrazolium chloride[5] plus 2% dextrose[10] in 50% methanol[5].

RESULTS AND DISCUSSION

The bioautographic plates exhibited clear areas of inhibition in the presence of the drugs in contrast to a dark-purple background. The tetracyclines tended to produce areas of inhibition that remained at the starting line but bearded upward. Ampicillin migrated an average distance of 8 cm; its R_f value was 0.47 (Fig. 1). Penicillin residues, when separated from the tetracyclines, presented a picture similar to that shown in Fig. 1 but had migrated a distance of 5 cm for an R_f value of 0.29.

To determine the maximum amount of the spiked antibiotic suspensions that could be spotted and still maintain adequate separation of the two drugs, suspensions at levels of 0.2, 0.1, 0.05, 0.025, and 0.0125 μg of ampicillin/ml and unit of penicillin G/ml were spotted in varying amounts (10–100 μl). The amounts spotted and the sensitivities of this system to penicillin G and ampicillin in the various drugs used are shown in Tables I and II.

Penicillamine (250 mg) was spiked with penicillin G (10 ml) at levels of 0.2, 0.1, 0.05, 0.025, and 0.0125 unit/ml, and 60 μl of each solution was spotted. Good separation was effected, the penicillin G migrated 6.5 cm, and an R_f value of 0.38 was obtained.

Although an extensive stability study of the spiked sample suspensions was not conducted, spot checks indicated that penicillin G activity had not diminished appreciably in 6 days when suspensions were stored in stoppered vials at room temperature. Tetracycline, methacycline, and chlortetracycline in suspension with penicillin G solutions, as well as a standard solution of penicillin G, were tested and responded similarly to the original assays.

In conclusion, this method has the capability of screening large numbers of samples for contamination in a relatively short time. Seven samples and one control can be run on each plate. The directness of the procedures and the minimum amount of handling involved substantially reduced the risk of cross-contamination.

Further application of these procedures, now in progress, will be the subject of a future paper.

REFERENCES

(1) *Fed. Regist.*, Title 21, Subchapter C, Part 133, Jan. 29, 1965.

(2) "Procedures for Detecting and Measuring Penicillin Contamination in Drugs," Division of Antibiotic and Insulin Certification, Food and Drug Administration, Washington, DC 20204, Oct. 1965.

(3) D. V. Herbst, H. Bryant, B. Anderson, and P. Weiss, *FDA By-*

[9] American Type Culture Collection, Rockville, MD 20841.
[10] Mallinckrodt Chemical Works, St. Louis, MO 63160.

Lines, **5** (3), 111 (1974).
(4) D. V. Herbst, *ibid.*, **5**(3), 114 (1974).
(5) *Ibid.*, **6**(1), 1 (1975).
(6) G. L. Biagi, A. M. Barbaro, M. F. Gamba, and M. C. Guerra, *J. Chromatogr.*, **41**, 371 (1969).

ACKNOWLEDGMENTS AND ADDRESSES

Received October 12, 1976, from the *National Center for Antibiotic Analysis, Food and Drug Administration, Washington, DC 20204.*
Accepted for publication January 26, 1977.

Kinetics of Concomitant Degradation of Tetracycline to Epitetracycline, Anhydrotetracycline, and Epianhydrotetracycline in Acid Phosphate Solution

P. H. YUEN and T. D. SOKOLOSKI ˣ

Abstract □ The concentrations of tetracycline, epitetracycline, anhydrotetracycline, and epianhydrotetracycline in pH 1.5 phosphate solution were followed as a function of time at four temperatures. Separation and quantification of all four species were accomplished using high-pressure liquid chromatography. Through nonlinear regression analysis, rate constants for the reversible first-order epimerization of tetracycline and anhydrotetracycline and for the first-order dehydration of tetracycline and epitetracycline were obtained. Solutions to the differential equations obtained through Laplace transforms successfully predict concentrations found experimentally. The energy of activation for each reaction step was calculated and ranged from 15 to 27 kcal/mole. The rate constants for tetracycline and epitetracycline dehydration conform with those of earlier studies that used different experimental methods. The study shows that epimerization of tetracycline and anhydrotetracycline can take place at a low pH.

Keyphrases □ Tetracycline—kinetics of degradation at pH 1.5, effect of temperature □ Degradation kinetics—tetracycline at pH 1.5, effect of temperature □ Antibacterials—tetracycline, kinetics of degradation at pH 1.5, effect of temperature

Tetracycline degradation to toxic epianhydrotetracycline can take place through tetracycline epimerization to epitetracycline (1, 2) followed by dehydration to epianhydrotetracycline (3) or by dehydration of tetracycline to anhydrotetracycline (4) followed by epimerization to epianhydrotetracycline (5). The kinetics of each individual step have been studied separately under conditions where it was assumed that only the reaction of interest was operative. No reported studies followed all potential reactions simultaneously under the same experimental conditions. The use of high-pressure liquid chromatography (HPLC), which separates all four compounds (tetracycline, epitetracycline, anhydrotetracycline, and epianhydrotetracycline), permits such a study (5). This paper presents the results for the solution degradation of tetracycline at pH 1.5 together with the rate expressions defining these results.

EXPERIMENTAL

Materials—Tetracycline hydrochloride[1] (I), 4-epitetracycline ammonium salt[2] (II), anhydrotetracycline hydrochloride[3] (III), and 4-epianhydrotetracycline[4] (IV) were used as obtained. All other chemicals were reagent grade, and double-distilled deionized water was used to make all solutions.

Apparatus—A high-pressure liquid chromatograph[5] with a multiwavelength detector[6] was used with a 1-m × 2.1-mm strong cation-exchange column[7].

Separation and Quantification—The mobile phase employed in the HPLC separation consisted of 0.07 *M* phosphate–0.0075 *M* ethylenediaminetetraacetic acid adjusted to pH 7.0. To improve the separation for tetracycline and its degradation products, the operating procedure was a slight modification of a previously reported method (5). Specifically, the elution was carried out at a column temperature of 36° and a flow rate of 0.55 ml/min (575 psi). The eluent was monitored at 254 nm at 0.08 absorbance unit full scale (aufs).

Areas under the individual peaks were measured with a polar compensating planimeter[8]. Known injected amounts of I–IV in 0.03 *N* HCl were correlated with the areas under the chromatograms obtained. The slopes of the linear relationship between moles added and area were 2.625×10^{-10}, 2.681×10^{-10}, 1.154×10^{-10}, and 1.377×10^{-10} mole/cm^2 for I, II, III, and IV, respectively.

Kinetic Method—A phosphoric acid stock solution (1 *M*) was adjusted to pH 1.5 with a concentrated potassium hydroxide solution. The solution was scrubbed with nitrogen and allowed to equilibrate at the temperature desired. Appropriate amounts of I were weighed into volumetric flasks and dissolved in the phosphate solution. The pH did not change during the study. The reaction flasks, sealed with a rubber septum, were immediately placed in a water bath[9] that also protected the solution from light.

At appropriate time intervals, samples were withdrawn, placed in vials, and immersed in ice to stop the reaction. A fixed volume of this sample was assayed chromatographically by equating areas found with concentration through a standard curve. The reactions were followed until all I was lost.

RESULTS AND DISCUSSION

A modification of a previously reported HPLC assay for tetracycline and its degradation products (5) results in less overlap between I and its epimer (Fig. 1). The retention times for IV, III, II, and I were 5.5, 8.25, 22.75, and 30.25 min, respectively.

The relationship between the concentration of each of the four species in the reaction as a function of time gave results as shown in Fig. 2 (obtained at 75°). Four temperatures were used (60–80°), and duplicate kinetic experiments were run at each temperature. Studies made at higher temperatures yielded results involving large errors, making data analysis tenuous.

The concentration–time profile found at each temperature was assumed to be a consequence of the reaction illustrated in Scheme I.

[1] Lot 2K030-71 EA, Pfizer.
[2] Batch 430, British Pharmacopoeia Commission.
[3] Batch 428, British Pharmacopoeia Commission.
[4] Lot 3339-99-1, GS-6659, Pfizer.
[5] DuPont model 830.
[6] DuPont model 835.
[7] DuPont Zipax SCX.
[8] Model 62005, Keuffel and Esser Co.
[9] Haake model FS2.

Lines, **5** (3), 111 (1974).
(4) D. V. Herbst, *ibid.*, **5**(3), 114 (1974).
(5) *Ibid.*, **6**(1), 1 (1975).
(6) G. L. Biagi, A. M. Barbaro, M. F. Gamba, and M. C. Guerra, *J. Chromatogr.*, **41**, 371 (1969).

ACKNOWLEDGMENTS AND ADDRESSES

Received October 12, 1976, from the *National Center for Antibiotic Analysis, Food and Drug Administration, Washington, DC 20204.*
Accepted for publication January 26, 1977.

Kinetics of Concomitant Degradation of Tetracycline to Epitetracycline, Anhydrotetracycline, and Epianhydrotetracycline in Acid Phosphate Solution

P. H. YUEN and T. D. SOKOLOSKI ˣ

Abstract □ The concentrations of tetracycline, epitetracycline, anhydrotetracycline, and epianhydrotetracycline in pH 1.5 phosphate solution were followed as a function of time at four temperatures. Separation and quantification of all four species were accomplished using high-pressure liquid chromatography. Through nonlinear regression analysis, rate constants for the reversible first-order epimerization of tetracycline and anhydrotetracycline and for the first-order dehydration of tetracycline and epitetracycline were obtained. Solutions to the differential equations obtained through Laplace transforms successfully predict concentrations found experimentally. The energy of activation for each reaction step was calculated and ranged from 15 to 27 kcal/mole. The rate constants for tetracycline and epitetracycline dehydration conform with those of earlier studies that used different experimental methods. The study shows that epimerization of tetracycline and anhydrotetracycline can take place at a low pH.

Keyphrases □ Tetracycline—kinetics of degradation at pH 1.5, effect of temperature □ Degradation kinetics—tetracycline at pH 1.5, effect of temperature □ Antibacterials—tetracycline, kinetics of degradation at pH 1.5, effect of temperature

Tetracycline degradation to toxic epianhydrotetracycline can take place through tetracycline epimerization to epitetracycline (1, 2) followed by dehydration to epianhydrotetracycline (3) or by dehydration of tetracycline to anhydrotetracycline (4) followed by epimerization to epianhydrotetracycline (5). The kinetics of each individual step have been studied separately under conditions where it was assumed that only the reaction of interest was operative. No reported studies followed all potential reactions simultaneously under the same experimental conditions. The use of high-pressure liquid chromatography (HPLC), which separates all four compounds (tetracycline, epitetracycline, anhydrotetracycline, and epianhydrotetracycline), permits such a study (5). This paper presents the results for the solution degradation of tetracycline at pH 1.5 together with the rate expressions defining these results.

EXPERIMENTAL

Materials—Tetracycline hydrochloride[1] (I), 4-epitetracycline ammonium salt[2] (II), anhydrotetracycline hydrochloride[3] (III), and 4-epianhydrotetracycline[4] (IV) were used as obtained. All other chemicals were reagent grade, and double-distilled deionized water was used to make all solutions.

Apparatus—A high-pressure liquid chromatograph[5] with a multiwavelength detector[6] was used with a 1-m × 2.1-mm strong cation-exchange column[7].

Separation and Quantification—The mobile phase employed in the HPLC separation consisted of 0.07 *M* phosphate–0.0075 *M* ethylenediaminetetraacetic acid adjusted to pH 7.0. To improve the separation for tetracycline and its degradation products, the operating procedure was a slight modification of a previously reported method (5). Specifically, the elution was carried out at a column temperature of 36° and a flow rate of 0.55 ml/min (575 psi). The eluent was monitored at 254 nm at 0.08 absorbance unit full scale (aufs).

Areas under the individual peaks were measured with a polar compensating planimeter[8]. Known injected amounts of I–IV in 0.03 *N* HCl were correlated with the areas under the chromatograms obtained. The slopes of the linear relationship between moles added and area were 2.625×10^{-10}, 2.681×10^{-10}, 1.154×10^{-10}, and 1.377×10^{-10} mole/cm^2 for I, II, III, and IV, respectively.

Kinetic Method—A phosphoric acid stock solution (1 *M*) was adjusted to pH 1.5 with a concentrated potassium hydroxide solution. The solution was scrubbed with nitrogen and allowed to equilibrate at the temperature desired. Appropriate amounts of I were weighed into volumetric flasks and dissolved in the phosphate solution. The pH did not change during the study. The reaction flasks, sealed with a rubber septum, were immediately placed in a water bath[9] that also protected the solution from light.

At appropriate time intervals, samples were withdrawn, placed in vials, and immersed in ice to stop the reaction. A fixed volume of this sample was assayed chromatographically by equating areas found with concentration through a standard curve. The reactions were followed until all I was lost.

RESULTS AND DISCUSSION

A modification of a previously reported HPLC assay for tetracycline and its degradation products (5) results in less overlap between I and its epimer (Fig. 1). The retention times for IV, III, II, and I were 5.5, 8.25, 22.75, and 30.25 min, respectively.

The relationship between the concentration of each of the four species in the reaction as a function of time gave results as shown in Fig. 2 (obtained at 75°). Four temperatures were used (60–80°), and duplicate kinetic experiments were run at each temperature. Studies made at higher temperatures yielded results involving large errors, making data analysis tenuous.

The concentration–time profile found at each temperature was assumed to be a consequence of the reaction illustrated in Scheme I.

[1] Lot 2K030-71 EA, Pfizer.
[2] Batch 430, British Pharmacopoeia Commission.
[3] Batch 428, British Pharmacopoeia Commission.
[4] Lot 3339-99-1, GS-6659, Pfizer.
[5] DuPont model 830.
[6] DuPont model 835.
[7] DuPont Zipax SCX.
[8] Model 62005, Keuffel and Esser Co.
[9] Haake model FS2.

$$\begin{array}{ccc} \text{tetracycline} & \underset{k_{-1}}{\overset{k_1}{\rightleftharpoons}} & \text{epitetracycline} \\ \downarrow k_3 & & \downarrow k_4 \\ \text{anhydrotetracycline} & \underset{k_{-2}}{\overset{k_2}{\rightleftharpoons}} & \text{epianhydrotetracycline} \end{array}$$

Scheme I

The rate constants for the individual reaction steps can be obtained from differential equations defined by the model. The equations are:

$$\frac{d[\mathrm{I}]}{dt} = k_{-1}[\mathrm{II}] - (k_1 + k_3)[\mathrm{I}] \quad \text{(Eq. 1)}$$

$$\frac{d[\mathrm{II}]}{dt} = k_1[\mathrm{I}] - (k_{-1} + k_4)[\mathrm{II}] \quad \text{(Eq. 2)}$$

$$\frac{d[\mathrm{III}]}{dt} = k_3[\mathrm{I}] + k_{-2}[\mathrm{IV}] - k_2[\mathrm{III}] \quad \text{(Eq. 3)}$$

$$\frac{d[\mathrm{IV}]}{dt} = k_2[\mathrm{III}] + k_4[\mathrm{II}] - k_{-2}[\mathrm{IV}] \quad \text{(Eq. 4)}$$

where the rate constants conform to the designation in Scheme I.

The differential equations for I and II (Eqs. 1 and 2) can be solved using Laplace transforms without considering the III and IV reactions since the dehydration process is irreversible first order for both I and II. The solutions to Eqs. 1 and 2 are:

$$[\mathrm{I}]_t = \frac{[\mathrm{I}]_0(k_{-1} + k_4 - a)}{(b - a)} e^{-at} + \frac{[\mathrm{I}]_0(k_{-1} + k_4 - b)}{(a - b)} e^{-bt} \quad \text{(Eq. 5)}$$

$$[\mathrm{II}]_t = \frac{[\mathrm{I}]_0 k_1}{(b - a)} e^{-at} + \frac{[\mathrm{I}]_0 k_1}{(a - b)} e^{-bt} \quad \text{(Eq. 6)}$$

where the subscripts to the concentration terms indicate any time, t, and initial, 0, concentrations and where a and b are complex constants used in the Laplace transforms. They are comprised of the reaction rate constants given in Scheme I and are partly defined in Eqs. 9–11.

When Eqs. 5 and 6 are substituted into Eqs. 3 and 4, the resulting differential equations for III and IV can be solved using Laplace transforms. The integrated equations resulting are:

$$[\mathrm{III}]_t = \frac{k_{-2}k_4k_1[\mathrm{I}]_0 + k_{-2}k_3(k_{-1} + k_4)[\mathrm{I}]_0}{abc} + \frac{k_{-2}k_4k_1[\mathrm{I}]_0 + (k_{-2} - a)(k_{-1} + k_4 - a)k_3[\mathrm{I}]_0}{(-a)(b - a)(c - a)} e^{-at} + \frac{k_{-2}k_4k_1[\mathrm{I}]_0 + (k_{-2} - b)(k_{-1} + k_4 - b)k_3[\mathrm{I}]_0}{(-b)(a - b)(c - b)} e^{-bt} + \frac{k_{-2}k_4k_1[\mathrm{I}]_0 + (k_{-2} - c)(k_{-1} + k_4 - c)k_3[\mathrm{I}]_0}{(-c)(a - c)(b - c)} e^{-ct} \quad \text{(Eq. 7)}$$

and:

$$[\mathrm{IV}]_t = \frac{k_2k_4k_1[\mathrm{I}]_0 + k_2k_3(k_{-1} + k_4)[\mathrm{I}]_0}{abc} + \frac{(k_2 - a)k_4k_1[\mathrm{I}]_0 + k_2k_3(k_{-1} + k_4 - a)[\mathrm{I}]_0}{(-a)(b - a)(c - a)} e^{-at} + \frac{(k_2 - b)k_4k_1[\mathrm{I}]_0 + k_2k_3(k_{-1} + k_4 - b)[\mathrm{I}]_0}{(-b)(a - b)(c - b)} e^{-bt} + \frac{(k_2 - c)k_4k_1[\mathrm{I}]_0 + k_2k_3(k_{-1} + k_4 - c)[\mathrm{I}]_0}{(-c)(a - c)(b - c)} e^{-ct} \quad \text{(Eq. 8)}$$

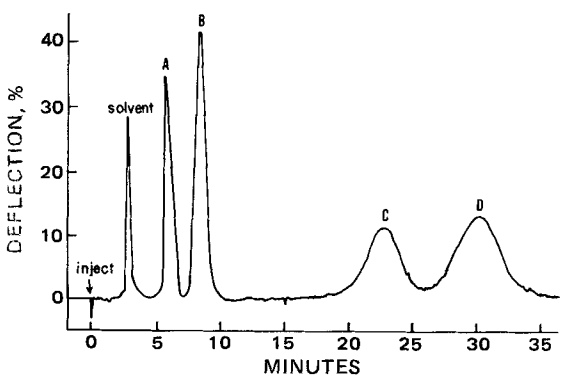

Figure 1—*Relationship between detector response and time in the HPLC separation of IV (A), III (B), II (C), and I (D).*

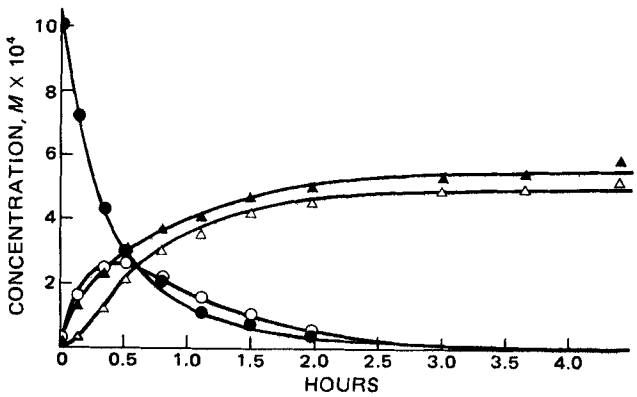

Figure 2—*Relationship between concentration and time for I (●), II (○), III (▲), and IV (△) in pH 1.5 phosphate solution and 75° The solid lines are the least-squares fit (NONLIN) of the experimental data shown.*

where:

$$a + b = k_1 + k_{-1} + k_3 + k_4 \quad \text{(Eq. 9)}$$

$$ab = k_1k_4 + k_{-1}k_3 + k_3k_4 \quad \text{(Eq. 10)}$$

$$c = k_{-2} + k_2 \quad \text{(Eq. 11)}$$

The experimental data, typified in Fig. 2, were fitted using both the differential (Eqs. 1–4) and integrated (Eqs. 5–8) forms of the equations through nonlinear regression analysis (NONLIN program[10]). To use this program, initial estimates of the six rate constants are required. The values of these initial estimates appear to be quite critical to the outcome of the NONLIN program when using the differential equations (Eqs. 1–4).

A computerized Runge–Kutta method was used to obtain the six initial estimates (6). Trial and error values for the six rate constants defined in Scheme I were used until the Runge–Kutta estimation of the concentrations of I–IV at any time approximately agreed with the concentrations found experimentally. With these Runge–Kutta estimates as initial estimates, the rate constants generated by the NONLIN program were determined (Table I). The largest errors obtained were in the constants for the epimerization of III (k_2 and k_{-2}).

The use of the integrated forms of the equations in the NONLIN program yielded rate constants that were relatively insensitive to the initial estimates. The rate constants generated and their accompanying standard deviations were virtually identical to those found using the differential forms (Table I). For example, when the integrated equations (Eqs. 5–8) were used with the data obtained in Trial 1 at 80°, where the largest errors were found, the rate constants generated (standard deviations in parentheses) were 2.08 (0.153), 0.937 (0.279), 1.87 (0.654), 2.19 (0.729), 1.56 (0.0897), and 2.38 (0.172) for k_1, k_{-1}, k_2, k_{-2}, k_3, and k_4, respectively.

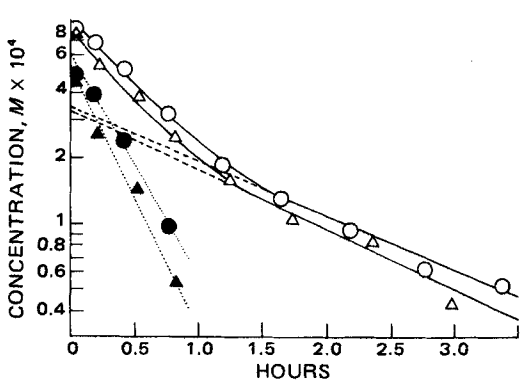

Figure 3—*Relationship between the logarithm of I concentration and time for two trials (○ and △) at 70°. Broken lines (- - -) indicate terminal slope and dotted lines (· · ·) indicate feathered initial data for Trial 1 (●) and Trial 2 (▲).*

[10] Unit 7292, The Upjohn Co.

Table I—Computer-Generated Rate Constants in Hours^{-1} for the Degradation of I in pH 1.5 Phosphate Solution at Several Temperatures

Temperature ± 0.5°	k_1[a]	k_{-1}	k_2	k_{-2}	k_3	k_4
60°[b]	0.414 (0.0274)[c]	0.373 (0.0531)	0.659 (0.162)	0.665 (0.166)	0.323 (0.0207)	0.206 (0.0344)
	0.392 (0.0192)	0.296 (0.0375)	0.585 (0.130)	0.607 (0.135)	0.302 (0.0156)	0.231 (0.0252)
70°	1.03 (0.0978)	0.661 (0.178)	1.31 (0.715)	1.46 (0.780)	0.687 (0.0714)	0.732 (0.118)
	0.982 (0.0504)	0.655 (0.0966)	1.33 (0.300)	1.46 (0.325)	0.743 (0.0369)	0.662 (0.0613)
75°	1.65 (0.0901)	1.43 (0.184)	1.88 (0.422)	2.07 (0.466)	1.28 (0.0677)	0.921 (0.123)
	1.53 (0.0800)	1.05 (0.159)	1.92 (0.436)	2.15 (0.483)	1.23 (0.0601)	1.11 (0.108)
80°	2.08 (0.153)	0.941 (0.282)	1.87 (0.673)	2.19 (0.750)	1.56 (0.0905)	2.37 (0.176)
	2.27 (0.208)	1.58 (0.405)	1.80 (0.909)	2.03 (0.996)	1.60 (0.128)	2.17 (0.251)

[a] Rate constant designation conforms to that of Scheme I. [b] The results of duplicate trials run at each temperature are listed. [c] Parentheses contain the NONLIN-generated standard deviations.

Table II—Values for Constants *a* and *b* Determined Experimentally at Four Temperatures and a Comparison of Their Sum with that Calculated from Rate Constants Generated by Nonlinear Regression Analysis

Temperature	Trial	a, hr^{-1}	b, hr^{-1}	$a+b$ Experimental	$a+b$ Calculated[a]	Ratio of Sums, Calc./Exp.
60°	1	0.91	0.22	1.13	1.32	1.17
	2	1.1	0.22	1.32	1.22	0.92
70°	1	2.4	0.59	2.99	3.11	1.04
	2	2.7	0.63	3.33	3.04	0.91
75°	1	3.8	0.99	4.79	4.81	1.00
	2	3.1	1.0	4.10	4.92	1.20
80°	1[b]	6.4[c]	2.1	8.5	7.8	0.92
	2[d]	6.4	2.1	8.5	7.6	0.89

[a] Using the data from Table I and Eq. 9. [b] Only six data points were available. [c] The 80° data for Trials 1 and 2 were used as one set in the semilogarithmic plots. [d] Only five data points were available.

The constants a and b in Eqs. 5 and 6 also can be obtained from semilogarithmic plots of concentration *versus* time using either I or II data, with the terminal slope reflecting b and the slope of the feathered initial data reflecting a. With the concentration–time data for I, semilogarithmic plots were constructed as represented by those in Fig. 3 for the two trials made at 70°. The a and b values obtained from such plots are given in Table II.

A comparison of the sum of the experimentally obtained a and b constants was made with the sum calculated according to Eq. 9 using the constants (Table I) generated by nonlinear regression analysis. These sums, together with their ratio (calculated to experimental), are given in Table II. The data at 80° are subject to considerable error since the number of data points available to estimate initial and terminal slopes was small due to the fast reaction rates. The agreement between the calculated and experimental sums of a and b is quite good. The average of the ratios (calculated to experimental) is 1.01.

Experimental confirmation of the constant c (Eq. 11) is difficult because it is necessary to construct a plot of the logarithm of the difference in equilibrium and time t concentrations as a function of time (Eq. 7 or 8). The difference in concentrations at long times is subject to large errors, making estimates of the terminal log-linear slope (constant c) highly inaccurate.

An Arrhenius plot of the average rate constant for each reaction step was made using the results obtained at four temperatures (Table I). Estimates of the activation energies for all six reactions are summarized in Table III. The epimerization reaction of the anhydro compounds appears to require less energy than the other steps, but the error involved in the determination of these energies is large, making any conclusion regarding energy effect tenuous.

In an earlier study (3), the rate constant for the dehydration of II, determined by following spectral changes, was 0.618 hr^{-1} at 71° and pH 1.53 (hydrochloric acid at 0.1 M ionic strength). The average value in the present study at 70° was 0.697 hr^{-1}, which is in reasonable agreement with the earlier value found under slightly different conditions. Schlecht and Frank (4) studied I dehydration at various temperatures and hydrogen-ion concentrations. By using their activation energy value (4) of 25.1 kcal/mole (ionic strength of 1 M), it is possible to calculate the rate constant at 60° if it is assumed that the hydrogen-ion concentration is reasonably close to the present hydrogen-ion activity (0.0361 M). Based on their rate constant at 50° (4), the rate constant calculated at 60° is about 0.44 hr^{-1}, which is of the same order of magnitude as the constants found in the present study, 0.323 and 0.302 hr^{-1}, again under different conditions.

In earlier studies on II (3) and I (4) dehydration, it was validly assumed that no epimerization was taking place at pH < 2. However, the present study shows that epimerization of both I and II can occur at pH 1.5, but the system used was different from that of both earlier studies. The present study used a 1 M phosphate solution adjusted to pH 1.5, which should contain significant amounts of monobasic phosphate, a species known to catalyze epimerization (1, 5). The significance of this result is that if a catalytic species is present in sufficient amounts, significant epimerization can occur even if the pH is less than 3.

Table III—Activation Energy for Each Step in I Degradation in pH 1.5 Phosphate Solution

Reaction as Indicated by Rate Constant	Activation Energy, kcal/mole
k_1	20.5 (19.0–21.7)[a]
k_{-1}	18.7 (10.2–27.0)
k_2	14.1 (3.84–24.4)
k_{-2}	15.3 (4.33–26.2)
k_3	19.4)12.8–25.8)
k_4	26.6 (17.3–36.0)

[a] Parentheses contain the upper and lower 95% confidence limits obtained from linear regression analysis.

REFERENCES

(1) E. G. Remmers, G. M. Sieger, and A. P. Doershuk, *J. Pharm. Sci.*, **52,** 752 (1963).

(2) D. A. Hussar, P. J. Niebergall, E. T. Sugita, and J. T. Doluisio, *J. Pharm. Pharmacol.*, **20,** 259 (1968).

(3) B. Hoener, T. D. Sokoloski, L. A. Mitscher, and L. Malspeis, *J. Pharm. Sci.*, **63,** 1901 (1974).

(4) K. D. Schlecht and C. W. Frank, *ibid.*, **64,** 352 (1975).

(5) T. D. Sokoloski, L. A. Mitscher, P. H. Yuen, J. V. Juvarkar, and B. Hoener, *ibid.*, **66,** 1159 (1977).

(6) C. F. Gerald, "Applied Numerical Analysis," Addison-Wesley, Reading, Mass., 1970, chap. 6.

ACKNOWLEDGMENTS AND ADDRESSES

Received December 9, 1976, from the *College of Pharmacy, Ohio State University, Columbus, OH 43210.*

Accepted for publication February 10, 1977.

Presented at the APhA Academy of Pharmaceutical Sciences, New York meeting, May 1977, under a Lederle Pharmacy Faculty Award.

Supported by Research Grant 5R01-FD-00689-03 from the Food and Drug Administration, U.S. Department of Health, Education, and Welfare, and by Pfizer, Inc., Groton, CT 06340.

[x] To whom inquiries should be directed.

Interactions of Indomethacin with Lysosomes and Proteins

D. A. LEWIS ˣ and HELEN E. KRYGIER

Abstract □ The stabilizing action of indomethacin on lysosomes and protein *in vitro* was studied. The magnitude of the stabilizing action on lysosomes was greater than that of aspirin or oxyphenbutazone, similar to that of phenylbutazone, but less than that of prednisolone. The stabilizing action of indomethacin on lysosomes possibly may contribute to its anti-inflammatory properties.

Keyphrases □ Indomethacin—effect on lysosome and protein stability *in vitro*, compared to other drugs □ Lysosomes—stability, effect of indomethacin *in vitro*, compared to other drugs □ Protein—stability, egg albumin, effect of indomethacin *in vitro*, compared to other drugs □ Anti-inflammatory agents—indomethacin, effect on lysosome and protein stability *in vitro*, compared to other drugs □ Stability—lysosome and protein *in vitro*, effect of indomethacin, compared to other drugs

It was reported (1) that indomethacin has little action on lysosomes but stabilizes canine and human erythrocytes from heat-induced and hypotonic rupture (2). It was suggested (2) that the stabilizing action of the drug was due to its stabilizing action on membrane proteins and that erythrocyte and lysosomal membranes have certain common properties.

Variations in experimental procedures can lead to different results in lysosome stabilization experiments (3). This study compared the action of indomethacin on lysosomes with that of other drugs under identical conditions and over a wide concentration range. The action of indomethacin on protein stability also was studied.

EXPERIMENTAL

Action of Indomethacin on Lysosomes—Lysosomes were isolated, as previously described (4), from freshly excised rat liver homogenates in 0.05 *M* tromethamine–acetate-buffered sucrose (0.25 *M*) (pH 7.4). The homogenate was subjected to differential centrifugation[1] at 4° and the lysosomes were isolated in the fraction sedimenting at 10,000×*g* after 20 min of centrifugation. Then the lysosomes were suspended in tromethamine–acetate-buffered isotonic sucrose (pH 7.4) to a final protein concentration of 5 mg/ml. The drugs were dissolved in dimethyl sulfoxide, and portions (0.1 ml) were added to 5 ml of the lysosome suspension (5 mg of protein/ml) in tromethamine–acetate-buffered isotonic sucrose (pH 7.4).

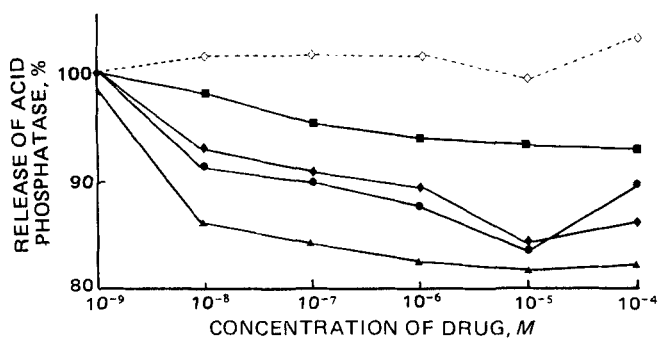

Figure 1—*Action of indomethacin and other drugs on lysosomes. Values below 100% (control values) represent a stabilizing action by the drug. Values greater than 100% represent a lytic action by the drug. Each point represents the mean of four determinations for each concentration. Key: ◊, aspirin; ■, oxyphenbutazone; ●, phenylbutazone; ♦, indomethacin; and ▲, prednisolone.*

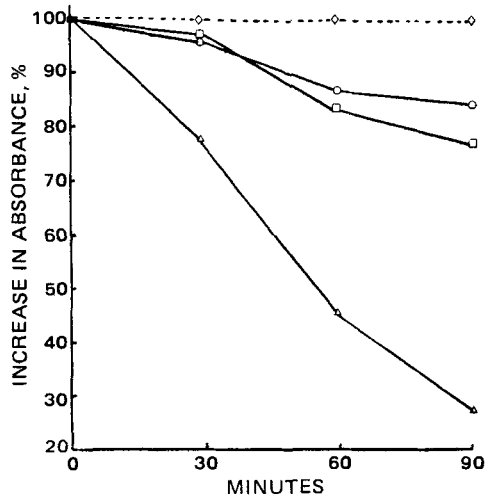

Figure 2—*Effect of indomethacin on protein stabilization. The control values represent a mean of nine determinations, and the test results represent a mean of three determinations for each concentration. The control values were adjusted to 100% at each reading, and the experimental values were calculated as a percent of that figure. Values below 100% represent a stabilizing action by the drug on the protein. Key: □, 10^{-2} M; ○, 10^{-7} M; △, 10^{-5} M; and ◊, controls.*

The suspensions were incubated for 90 min at 37° in a shaking reaction incubator and then centrifuged at 20,000×*g* for 20 min. The acid phosphatase activity was determined by incubating 0.1 ml of the supernate with 0.05 ml of *p*-nitrophenyl phosphate[2] (0.015 *M*) and 0.5 ml of 0.09 *M* citrate buffer (pH 4.8) for 30 min at 37°. The reaction was stopped by the addition of 0.1 *M* NaOH, and the liberated *p*-nitrophenol was determined at 410 nm. Drugs were omitted from the controls.

Action of Indomethacin on Proteins—Portions (0.1 ml) of the drug in dimethyl sulfoxide were incubated with 5 ml of egg albumin solution (pH 7.4) at 65° in a water bath, and the absorbance was measured periodically at 420 nm (4). The drug was omitted from the controls.

RESULTS

Action of Indomethacin on Lysosomes—The results (Fig. 1) show that indomethacin stabilized the lysosomes over a wide concentration range. The effect was greater than that of aspirin (which did not stabilize the lysosomes) and oxyphenbutazone, similar to that of phenylbutazone, but less than that of prednisolone.

Action of Indomethacin on Proteins—Indomethacin stabilized the protein against thermal denaturation, with maximum values at 10^{-5} *M* (Fig. 2). The fall off in stabilization at 10^{-2} *M* may be a consequence of solubility of the drug–protein complexes at this high concentration since immediate precipitation of the complex occurred at concentrations above this value ($10^{-1.3}$ and 10^{-1} *M*). This result is in agreement with previous findings that many nonsteroidal drugs stabilize proteins (5, 6).

REFERENCES

(1) K. Tanaka and Y. Iisuka, *Biochem. Pharmacol.*, **17**, 2023 (1968).

[1] M.S.E. Superspeed 50.

[2] Sigma.

(2) A. D. Inglot and E. Wolna, *ibid.*, **17**, 269 (1968).
(3) L. J. Ignarro, *ibid.*, **20**, 2841 (1971).
(4) D. A. Lewis, A. M. Symons, and R. J. Ancill, *J. Pharm. Pharmacol.*, **22**, 902 (1970).
(5) D. A. Lewis, *ibid.*, **22**, 909 (1970).
(6) Y. Mizushima and H. Suzuki, *Arch. Int. Pharmacodyn. Ther.*, **157**, 115 (1965).

ACKNOWLEDGMENTS AND ADDRESSES

Received September 9, 1976, from the *Pharmacological Laboratories, Department of Pharmacy, University of Aston in Birmingham, Birmingham B4 7ET, England.*

Accepted for publication February 8, 1977.

[x] To whom inquiries should be directed.

Effect of Pentazocine on Pressor Responses of Epinephrine and Levarterenol

G. D. RUSSI [x] and F. GENE MARTIN

Abstract □ In rats anesthetized with pentobarbital, pentazocine potentiated the pressor response of two exogenous amines, epinephrine and levarterenol. Although the mechanism for the pentazocine-induced potentiation of the pressor amines has not been proven, it is speculated that pentazocine may increase the blood pressure response of certain amines by interacting with the sympathetic nervous system.

Keyphrases □ Pentazocine—effect on pressor responses of epinephrine and levarterenol, rats □ Epinephrine—pressor responses, effect of pentazocine, rats □ Levarterenol—pressor responses, effect of pentazocine, rats □ Pressor responses—epinephrine and levarterenol, effect of pentazocine, rats □ Analgesics—pentazocine, effect on pressor responses of epinephrine and levarterenol, rats □ Adrenergic agents—epinephrine and levarterenol, pressor responses, effect of pentazocine, rats

Pentazocine, a weak narcotic antagonist of the benzomorphan series, was first synthesized by Archer *et al.* (1). It is an effective analgesic in humans (2) with a low incidence of adverse effects (3).

Whereas the cardiovascular effects of morphine are hypotension and bradycardia, pentazocine produces a rise in systemic arterial blood pressure and heart rate (2). Therefore, Hobler *et al.* (4) suggested that pentazocine might be a useful analgesic and less dangerous than morphine in hypotensive patients.

The present study concerned the possibility that pentazocine might increase blood pressure and heart rate by altering the responses to transmitter amines. This paper reports the effects of pentazocine on the pressor responses to exogenous epinephrine (I) and levarterenol (II).

EXPERIMENTAL

Male Sprague–Dawley rats were anesthetized with pentobarbital sodium, 40 mg/kg ip, combined with atropine sulfate, 1 mg/kg. Animals were artificially respired throughout the experiment with a rodent respirator[1]. The right carotid or femoral artery was cannulated with polyethylene tubing filled with heparin in saline to facilitate pressure measurements using a pressure transducer[2]. The right femoral vein was cannulated for intravenous injections of drugs.

Pressure changes were analyzed by planimetric measurement of the area, in square centimeters, under the dose–mean blood pressure response curve and by measurement of the time, in seconds, for the mean blood pressure response to return half-way to the control value. Statistical analysis was performed by using the analysis of variance combined with Duncan's new multiple range test (5). Levarterenol bitartrate[3] and epinephrine bitartrate[3] solutions were prepared from stock solutions on the day of use. Pentazocine[4] was dissolved in acidic aqueous solutions prior to use. All doses are reported as the salt.

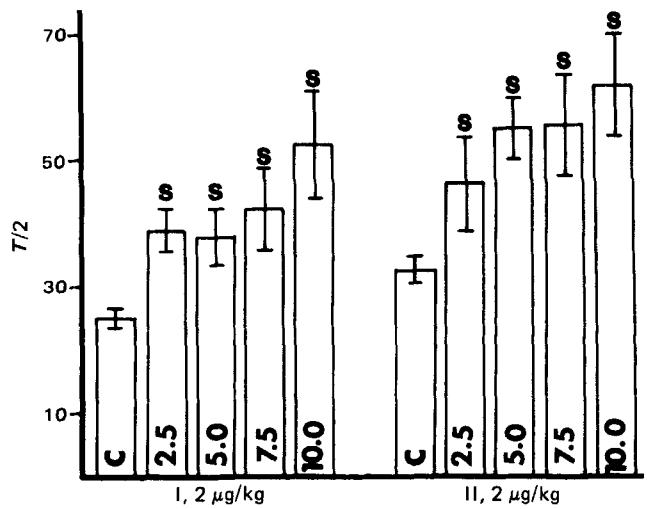

Figure 1—*Effect of intravenous pentazocine (milligrams per kilogram shown in the bars) on the duration (T/2, in seconds) of the pressor responses to I and II. All doses of pentazocine significantly (S) potentiated the duration of the pressor responses to I and II when compared to the control (C) at* $p < 0.05$.

RESULTS AND DISCUSSION

Epinephrine, 2 μg/kg, and levarterenol, 2 μg/kg, were given intravenously to rats to determine control blood pressure responses. Pentazocine was given in 2.5-mg/kg increments intravenously until a total dose of 10 mg/kg had been administered. The intravenous administration of pentazocine routinely depressed the blood pressure, but the depression was transient and the blood pressure was allowed to return to control levels before the agonists were given.

After each dose of pentazocine, the agonists were again administered and the responses were measured and compared to control responses. All doses of pentazocine significantly increased the duration of the pressor responses to epinephrine and levarterenol (Fig. 1), while the area under the dose–response curve of these two amines was significantly increased only after a 10-mg/kg dose (Fig. 2).

Since these experiments involved a long period and several injections per animal, a study was conducted to evaluate the possibility that the responses to epinephrine and levarterenol might be increased by some sort of autopotentiation instead of an action by pentazocine. Blood pressure responses to four doses of epinephrine were obtained several

[1] Harvard Apparatus Co. model 680.
[2] Statham P23AC.
[3] Sigma Chemical Co., St. Louis, Mo.
[4] Talwin, Sterling-Winthrop Research Institute.

(2) A. D. Inglot and E. Wolna, *ibid.*, **17**, 269 (1968).
(3) L. J. Ignarro, *ibid.*, **20**, 2841 (1971).
(4) D. A. Lewis, A. M. Symons, and R. J. Ancill, *J. Pharm. Pharmacol.*, **22**, 902 (1970).
(5) D. A. Lewis, *ibid.*, **22**, 909 (1970).
(6) Y. Mizushima and H. Suzuki, *Arch. Int. Pharmacodyn. Ther.*, **157**, 115 (1965).

ACKNOWLEDGMENTS AND ADDRESSES

Received September 9, 1976, from the *Pharmacological Laboratories, Department of Pharmacy, University of Aston in Birmingham, Birmingham B4 7ET, England.*

Accepted for publication February 8, 1977.

[x] To whom inquiries should be directed.

Effect of Pentazocine on Pressor Responses of Epinephrine and Levarterenol

G. D. RUSSI [x] and F. GENE MARTIN

Abstract □ In rats anesthetized with pentobarbital, pentazocine potentiated the pressor response of two exogenous amines, epinephrine and levarterenol. Although the mechanism for the pentazocine-induced potentiation of the pressor amines has not been proven, it is speculated that pentazocine may increase the blood pressure response of certain amines by interacting with the sympathetic nervous system.

Keyphrases □ Pentazocine—effect on pressor responses of epinephrine and levarterenol, rats □ Epinephrine—pressor responses, effect of pentazocine, rats □ Levarterenol—pressor responses, effect of pentazocine, rats □ Pressor responses—epinephrine and levarterenol, effect of pentazocine, rats □ Analgesics—pentazocine, effect on pressor responses of epinephrine and levarterenol, rats □ Adrenergic agents—epinephrine and levarterenol, pressor responses, effect of pentazocine, rats

Pentazocine, a weak narcotic antagonist of the benzomorphan series, was first synthesized by Archer *et al.* (1). It is an effective analgesic in humans (2) with a low incidence of adverse effects (3).

Whereas the cardiovascular effects of morphine are hypotension and bradycardia, pentazocine produces a rise in systemic arterial blood pressure and heart rate (2). Therefore, Hobler *et al.* (4) suggested that pentazocine might be a useful analgesic and less dangerous than morphine in hypotensive patients.

The present study concerned the possibility that pentazocine might increase blood pressure and heart rate by altering the responses to transmitter amines. This paper reports the effects of pentazocine on the pressor responses to exogenous epinephrine (I) and levarterenol (II).

EXPERIMENTAL

Male Sprague–Dawley rats were anesthetized with pentobarbital sodium, 40 mg/kg ip, combined with atropine sulfate, 1 mg/kg. Animals were artificially respired throughout the experiment with a rodent respirator[1]. The right carotid or femoral artery was cannulated with polyethylene tubing filled with heparin in saline to facilitate pressure measurements using a pressure transducer[2]. The right femoral vein was cannulated for intravenous injections of drugs.

Pressure changes were analyzed by planimetric measurement of the area, in square centimeters, under the dose–mean blood pressure response curve and by measurement of the time, in seconds, for the mean blood pressure response to return half-way to the control value. Statistical analysis was performed by using the analysis of variance combined with Duncan's new multiple range test (5). Levarterenol bitartrate[3] and epinephrine bitartrate[3] solutions were prepared from stock solutions on the day of use. Pentazocine[4] was dissolved in acidic aqueous solutions prior to use. All doses are reported as the salt.

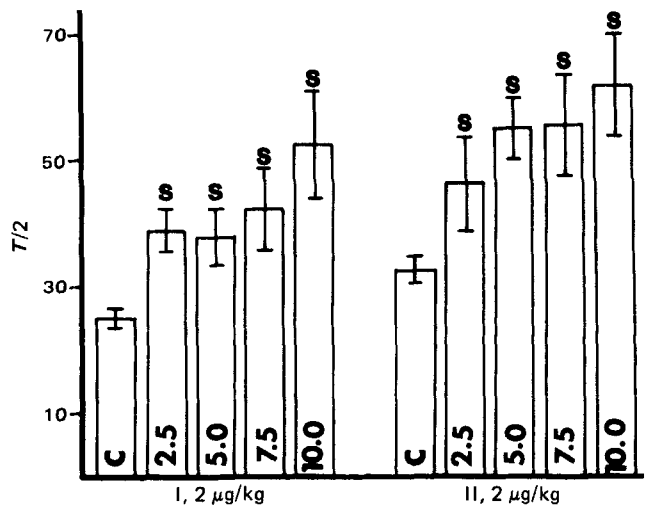

Figure 1—*Effect of intravenous pentazocine (milligrams per kilogram shown in the bars) on the duration (T/2, in seconds) of the pressor responses to I and II. All doses of pentazocine significantly (S) potentiated the duration of the pressor responses to I and II when compared to the control (C) at* $p < 0.05$.

RESULTS AND DISCUSSION

Epinephrine, 2 μg/kg, and levarterenol, 2 μg/kg, were given intravenously to rats to determine control blood pressure responses. Pentazocine was given in 2.5-mg/kg increments intravenously until a total dose of 10 mg/kg had been administered. The intravenous administration of pentazocine routinely depressed the blood pressure, but the depression was transient and the blood pressure was allowed to return to control levels before the agonists were given.

After each dose of pentazocine, the agonists were again administered and the responses were measured and compared to control responses. All doses of pentazocine significantly increased the duration of the pressor responses to epinephrine and levarterenol (Fig. 1), while the area under the dose–response curve of these two amines was significantly increased only after a 10-mg/kg dose (Fig. 2).

Since these experiments involved a long period and several injections per animal, a study was conducted to evaluate the possibility that the responses to epinephrine and levarterenol might be increased by some sort of autopotentiation instead of an action by pentazocine. Blood pressure responses to four doses of epinephrine were obtained several

[1] Harvard Apparatus Co. model 680.
[2] Statham P23AC.
[3] Sigma Chemical Co., St. Louis, Mo.
[4] Talwin, Sterling-Winthrop Research Institute.

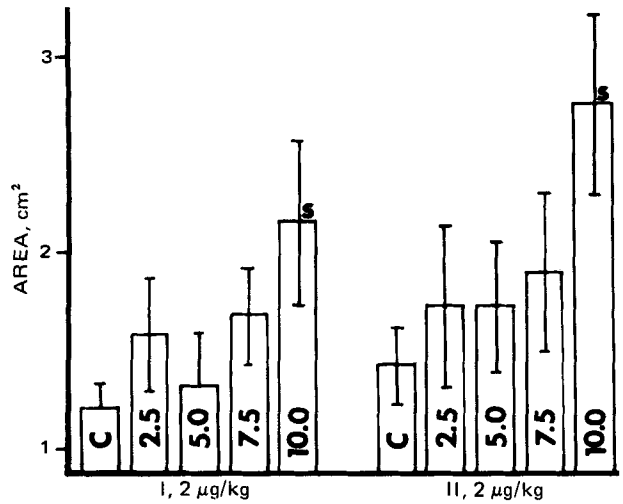

Figure 2—*Effect of intravenous pentazocine (milligrams per kilogram shown in the bars) on the pressor responses to I and II. At a dose of 10 mg/kg, pentazocine significantly (S) potentiated the pressor response to I and II when compared to the control (C) at* $p < 0.05$.

times. No autopotentiation was found; in fact, the responses tended to decrease after the agonist had been administered several times[5].

Tammisto *et al.* (6) reported a marked increase in plasma catecholamine levels after an intravenous injection of pentazocine, 1.2 mg/kg, in humans. The rise in plasma catecholamine levels was concomitant with the rise in blood pressure and heart rate in the same patients. It was concluded that the rise in circulating catecholamines was due to peripheral release of epinephrine and levarterenol caused by central sympathetic stimulation by pentazocine. These investigators also suggested that the pentazocine-induced increase in plasma catecholamines was not due to an inhibition of reuptake or of enzymatic degradation of the catecholamines since pentazocine did not potentiate the pressor responses of exogenous epinephrine or levarterenol.

The results presented in this study do not agree with those of Tammisto *et al.* (6). Pentazocine potentiated the pressor responses of exogenous amines. It is tempting to suggest that one possible explanation for the pentazocine–pressor amine interaction would be a pentazocine-induced alteration of the physiological disposition of the neurotransmitters by interaction with the sympathetic nervous system.

Investigations into the actions of pentazocine on neural function in the central nervous system support the hypothesis that pentazocine may alter adrenergic function.

Holtzman and Jewett (7) demonstrated that pentazocine, at a wide range of doses, significantly lowered rat brain norepinephrine and theorized that the drop in brain norepinephrine content might be related to a pentazocine-induced release of the adrenergic transmitter. Likewise, Paalzow *et al.* (8) reported a drop in rat brain norepinephrine after pentazocine treatment. They also showed that pentazocine accelerated the depletion of the adrenergic neurotransmitter in the brain after tyrosine hydroxylase or dopamine β-hydroxylase was inhibited, thereby indicating that the turnover of norepinephrine was increased.

[5] Unpublished results.

REFERENCES

(1) S. Archer, N. F. Albertson, L. S. Harris, A. K. Pierson, J. G. Bird, A. S. Keats, J. Telford, and D. N. Papdopoulos, *Science*, **137**, 541 (1962).

(2) A. S. Keats and J. Telford, *J. Pharmacol, Exp. Ther.*, **143**, 157 (1964).

(3) W. T. Beaver, S. L. Wallenstein, R. W. Houde, and A. Rogers, *Clin. Pharmacol. Ther.*, **9**, 582 (1968).

(4) K. E. Hobler, A. R. Borja, and C. O. Sahler, *Am. J. Med. Sci.*, **190**, 57 (1966).

(5) R. G. D. Steel and J. H. Torrie, "Principles and Procedures of Statistics," McGraw-Hill, New York, N.Y., 1960, pp. 132–134.

(6) J. Tammisto, A. Jaatela, P. Nikki, and S. Takki, *Ann. Clin. Res.*, **3**, 22 (1971).

(7) S. G. Holtzman and R. E. Jewett, *J. Pharmacol. Exp. Ther.*, **181**, 346 (1972).

(8) G. Paalzow, L. Paalzow, and B. Stalby, *Eur. J. Pharmacol.*, **27**, 78 (1974).

ACKNOWLEDGMENTS AND ADDRESSES

Received June 21, 1976, from the *Department of Pharmacology and Toxicology, School of Pharmacy, University of Kansas, Lawrence, KS 66044.*

Accepted for publication February 2, 1977.

Supported in part by a grant from the University of Kansas and by Public Health Service General Research Support Grant 5-S01-RR05606-05.

[x] To whom inquiries should be directed. Present address: Department of Pharmacology, College of Pharmacy, Drake University, Des Moines, IA 50311.

Synthesis and Hydrolysis of Fluorene-9-spiro-2′-(*N*-aryl-3′,3′-dichloroaziridines)

MAGID ABOU-GHARBIA and MADELEINE M. JOULLIÉ [x]

Abstract □ The synthesis of eight fluorene-9-spiro-2′-(*N*-aryl-3′,3′-dichloroaziridines) was achieved *via* the reaction of dichlorocarbene with the appropriately substituted *N*-fluorenylideneanilines. Hydrolysis of the spirofluorenes afforded the corresponding 9-chlorofluorene-9-carboxanilides in excellent yields.

Keyphrases □ Fluorene-9-spiro-2′-aziridines, various—synthesized, hydrolyzed to 9-chlorofluorene-9-carboxanilides □ Aziridines, fluorene-9-spiro—synthesized, hydrolyzed to 9-chlorofluorene-9-carboxanilides □ Hydrolysis—various fluorene-9-spiro-2′-aziridines to 9-chlorofluorene-9-carboxanilides □ Spiro compounds—various fluorene-9-spiro-2′-aziridines synthesized, hydrolyzed to 9-chlorofluorene-9-carboxanilides

The synthesis of aziridines from imines has been accomplished either by the reactions of imines with dimethylsulfoxonium methylide in dimethyl sulfoxide (1) or by the insertion of carbenes in the carbon–nitrogen double bond of imines (2, 3).

The reaction of *N*-fluorenylideneanilines (I) with dimethylsulfoxonium methylide afforded a mixture of the starting imine and fluorenone instead of the expected spiroaziridines. However, the reactions of I with dichlorocarbene, generated by the reaction of chloroform with

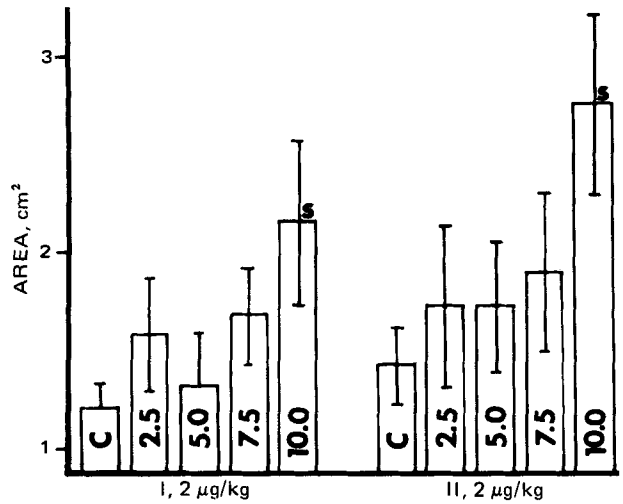

Figure 2—*Effect of intravenous pentazocine (milligrams per kilogram shown in the bars) on the pressor responses to I and II. At a dose of 10 mg/kg, pentazocine significantly (S) potentiated the pressor response to I and II when compared to the control (C) at* $p < 0.05$.

times. No autopotentiation was found; in fact, the responses tended to decrease after the agonist had been administered several times[5].

Tammisto *et al.* (6) reported a marked increase in plasma catecholamine levels after an intravenous injection of pentazocine, 1.2 mg/kg, in humans. The rise in plasma catecholamine levels was concomitant with the rise in blood pressure and heart rate in the same patients. It was concluded that the rise in circulating catecholamines was due to peripheral release of epinephrine and levarterenol caused by central sympathetic stimulation by pentazocine. These investigators also suggested that the pentazocine-induced increase in plasma catecholamines was not due to an inhibition of reuptake or of enzymatic degradation of the catecholamines since pentazocine did not potentiate the pressor responses of exogenous epinephrine or levarterenol.

The results presented in this study do not agree with those of Tammisto *et al.* (6). Pentazocine potentiated the pressor responses of exogenous amines. It is tempting to suggest that one possible explanation for the pentazocine–pressor amine interaction would be a pentazocine-induced alteration of the physiological disposition of the neurotransmitters by interaction with the sympathetic nervous system.

Investigations into the actions of pentazocine on neural function in the central nervous system support the hypothesis that pentazocine may alter adrenergic function.

Holtzman and Jewett (7) demonstrated that pentazocine, at a wide range of doses, significantly lowered rat brain norepinephrine and theorized that the drop in brain norepinephrine content might be related to a pentazocine-induced release of the adrenergic transmitter. Likewise, Paalzow *et al.* (8) reported a drop in rat brain norepinephrine after pentazocine treatment. They also showed that pentazocine accelerated the depletion of the adrenergic neurotransmitter in the brain after tyrosine hydroxylase or dopamine β-hydroxylase was inhibited, thereby indicating that the turnover of norepinephrine was increased.

[5] Unpublished results.

REFERENCES

(1) S. Archer, N. F. Albertson, L. S. Harris, A. K. Pierson, J. G. Bird, A. S. Keats, J. Telford, and D. N. Papdopoulos, *Science*, **137**, 541 (1962).

(2) A. S. Keats and J. Telford, *J. Pharmacol, Exp. Ther.*, **143**, 157 (1964).

(3) W. T. Beaver, S. L. Wallenstein, R. W. Houde, and A. Rogers, *Clin. Pharmacol. Ther.*, **9**, 582 (1968).

(4) K. E. Hobler, A. R. Borja, and C. O. Sahler, *Am. J. Med. Sci.*, **190**, 57 (1966).

(5) R. G. D. Steel and J. H. Torrie, "Principles and Procedures of Statistics," McGraw-Hill, New York, N.Y., 1960, pp. 132–134.

(6) J. Tammisto, A. Jaatela, P. Nikki, and S. Takki, *Ann. Clin. Res.*, **3**, 22 (1971).

(7) S. G. Holtzman and R. E. Jewett, *J. Pharmacol. Exp. Ther.*, **181**, 346 (1972).

(8) G. Paalzow, L. Paalzow, and B. Stalby, *Eur. J. Pharmacol.*, **27**, 78 (1974).

ACKNOWLEDGMENTS AND ADDRESSES

Received June 21, 1976, from the *Department of Pharmacology and Toxicology, School of Pharmacy, University of Kansas, Lawrence, KS 66044.*

Accepted for publication February 2, 1977.

Supported in part by a grant from the University of Kansas and by Public Health Service General Research Support Grant 5-S01-RR05606-05.

[x] To whom inquiries should be directed. Present address: Department of Pharmacology, College of Pharmacy, Drake University, Des Moines, IA 50311.

Synthesis and Hydrolysis of Fluorene-9-spiro-2′-(*N*-aryl-3′,3′-dichloroaziridines)

MAGID ABOU-GHARBIA and MADELEINE M. JOULLIÉ [x]

Abstract □ The synthesis of eight fluorene-9-spiro-2′-(*N*-aryl-3′,3′-dichloroaziridines) was achieved *via* the reaction of dichlorocarbene with the appropriately substituted *N*-fluorenylideneanilines. Hydrolysis of the spirofluorenes afforded the corresponding 9-chlorofluorene-9-carboxanilides in excellent yields.

Keyphrases □ Fluorene-9-spiro-2′-aziridines, various—synthesized, hydrolyzed to 9-chlorofluorene-9-carboxanilides □ Aziridines, fluorene-9-spiro—synthesized, hydrolyzed to 9-chlorofluorene-9-carboxanilides □ Hydrolysis—various fluorene-9-spiro-2′-aziridines to 9-chlorofluorene-9-carboxanilides □ Spiro compounds—various fluorene-9-spiro-2′-aziridines synthesized, hydrolyzed to 9-chlorofluorene-9-carboxanilides

The synthesis of aziridines from imines has been accomplished either by the reactions of imines with dimethylsulfoxonium methylide in dimethyl sulfoxide (1) or by the insertion of carbenes in the carbon–nitrogen double bond of imines (2, 3).

The reaction of *N*-fluorenylideneanilines (I) with dimethylsulfoxonium methylide afforded a mixture of the starting imine and fluorenone instead of the expected spiroaziridines. However, the reactions of I with dichlorocarbene, generated by the reaction of chloroform with

Table I—*N*-Fluorenylideneanilines

Compound[a]	R	Yield, %	Melting Point	Molecular Formula		Analysis, % Calc.	Found	IR Spectra, cm^{-1} (C=N)
Id[b]	C_2H_5	80	88–89°	$C_{21}H_{17}N$	C	89.00	89.21	1640
					H	6.04	5.86	
					N	4.94	5.15	
Ig	Br	100	140–141°	$C_{19}H_{12}BrN$	C	68.27	68.36	1650
					H	3.62	3.58	
					Br	23.91	24.13	
					N	4.19	4.15	
Ih	I	100	133–135°	$C_{19}H_{12}IN$	C	59.85	54.89	1635
					H	3.17	3.13	
					I	33.29	32.99	
					N	3.67	3.64	

[a] All compounds were recrystallized from ethanol–chloroform. [b] NMR: δ 1.15–1.45 (t, 3H), 2.55–2.95 (q, 2H), and 6.6–8.0 (m, 12H) ppm.

Table II—Fluorene-9-spiro-2′-(*N*-aryl-3′,3′-dichloroaziridines)

Compound	Yield, %	Melting Point	Molecular Formula		Analysis, % Calc.	Found
IIa	81	98–99°	$C_{20}H_{13}Cl_2N$	C	71.01	71.29
				H	3.87	3.95
				Cl	20.96	21.28
				N	4.14	4.09
IIb[a]	88	135–136°	$C_{21}H_{15}Cl_2N$	C	71.60	71.50
				H	4.29	4.26
				Cl	20.13	19.92
				N	3.97	3.76
IIc[b]	83	108–109°	$C_{21}H_{15}Cl_2NO$	C	68.48	68.62
				H	4.10	4.09
				Cl	19.25	19.25
				N	3.80	3.81
IId[c]	86[d]	82–84°	$C_{22}H_{17}Cl_2N$	C	72.13	72.94
				H	4.67	4.95
				N	3.82	3.87
IIe	80	111–112°	$C_{20}H_{12}Cl_2FN$	C	67.43	67.53
				H	3.39	3.35
				Cl	19.90	20.10
				F	5.33	5.33
				N	3.93	3.96
IIf	80	134–135°	$C_{20}H_{12}Cl_3N$	C	64.45	64.69
				H	3.24	3.29
				Cl	28.54	28.26
				N	3.75	3.79
IIg	89	145–147°	$C_{20}H_{12}BrCl_2N$	C	57.58	57.60
				H	2.90	2.90
				Br	16.99	17.10
				Cl	19.15	19.34
				N	3.35	3.30
IIh	75	113–115°	$C_{20}H_{12}Cl_2IN$	C	51.75	51.47
				H	2.60	2.87
				Cl	15.27	15.34
				I	27.34	27.20
				N	3.01	3.07

[a] NMR: δ 2.29 (s, 3H) and 6.85–7.85 (m, 12H) ppm. Mass spectrum: M^+ 353. [b] NMR: δ 3.8 (s, 3H) and 6.95–7.9 (m, 12H) ppm. [c] NMR: δ 1.1–1.35 (t, 3H), 2.4–2.8 (q, 2H), and 6.85–7.85 (m, 12H) ppm. [d] Only 45% of this material could be isolated as a crystalline solid since it becomes an oil on standing.

potassium *tert*-butoxide, afforded the corresponding spirodichloroaziridines (IIa–IIh) in 75–90% yields (Scheme I).

The hydrolysis of IIa–IIh occurred rapidly in boiling water to afford 9-chlorofluorene-9-carboxanilides (IIIa–IIIh) in excellent yields (Scheme II).

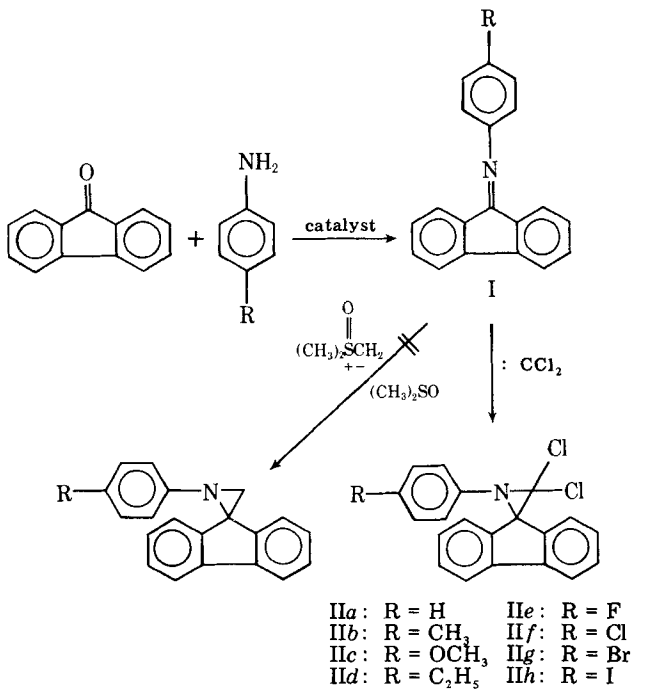

Scheme I

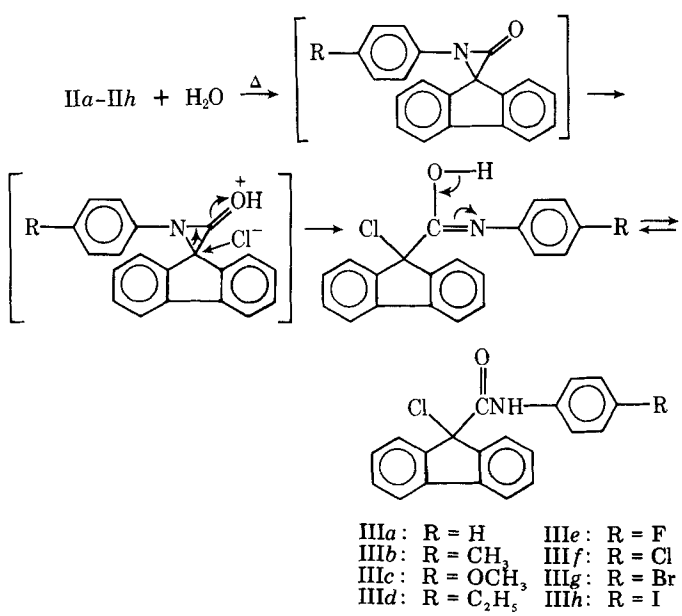

Scheme II

EXPERIMENTAL[1]

***N*-Fluorenylideneanilines (I)**—These imines were prepared by the

[1] Melting points are uncorrected. IR spectra were recorded on a Perkin-Elmer model 137B spectrophotometer calibrated with polystyrene. Samples were determined as potassium bromide disks. NMR spectra were determined on a Varian A-60 spectrometer using tetramethylsilane as an internal standard. Samples were dissolved in deuterochloroform unless otherwise noted. Elemental analyses were performed by Midwest Microlab, Indianapolis, IN 46226. Mass spectra were obtained on a Finnigan model F-3300 with a data system 6000 mass spectrometer, with an ionizing potential of 30 ev.

Table III—9-Chlorofluorene-9-carboxanilides

Compound	Yield, %	Melting Point	Molecular Formula		Analysis, % Calc.	Found	IR Spectra, cm^{-1} (NH and C=O)
III*a*	100	164–165°	$C_{19}H_{14}ClNO$	C	75.11	75.00	3300
				H	4.41	5.00	1675
				Cl	11.08	10.83	
				N	4.38	4.41	
III*b*[a]	100	282–284°	$C_{21}H_{16}ClNO$	C	75.55	75.47	3200
				H	4.83	4.77	1660
				Cl	10.62	10.50	
				N	4.19	4.08	
III*c*[b]	88	134–135°	$C_{21}H_{16}ClNO_2$	C	72.10	72.43	3310
				H	4.61	4.77	1670
				Cl	10.13	9.98	
				N	4.00	4.03	
III*d*[c]	93	123–124°	$C_{22}H_{18}ClNO$	C	75.96	75.98	3250
				H	5.21	5.13	1655
				Cl	10.19	10.37	
				N	4.02	3.94	
III*e*	80	157–159°	$C_{20}H_{13}ClFNO$	C	71.11	71.16	3200
				H	3.87	3.85	1650
				Cl	10.49	10.60	
				F	5.62	5.73	
				N	4.14	4.03	
III*f*	95	199–201°	$C_{20}H_{13}Cl_2NO$	C	67.81	67.64	3280
				H	3.64	3.76	1660
				Cl	20.01	19.86	
				N	3.95	3.96	
III*g*	89	208–210°	$C_{20}H_{13}BrClNO$	C	60.24	60.34	3280
				H	3.28	3.26	1660
				Br	20.04	19.79	
				Cl	8.89	8.73	
				N	3.51	3.43	
III*h*	88	202–204°	$C_{20}H_{13}ClINO$	C	53.89	54.15	3230
				H	2.93	2.99	1660
				Cl	7.95	7.98	
				I	28.47	28.75	
				N	3.14	3.07	

[a] NMR (dimethyl sulfoxide): δ 2.29 (s, 3H) and 7.15–7.9 (m, 13H) ppm. Mass spectrum: M^+ 333. [b] NMR: δ 3.85 (s, 3H) and 6.75–7.8 (m, 13H) ppm. [c] NMR: δ 1.05–1.35 (t, 3H), 2.4–2.8 (q, 2H), and 7–7.9 (m, 13H) ppm.

reaction of fluorenone with the appropriate substituted anilines in the presence of either zinc chloride (4) or boron trifluoride etherate (5) as the catalyst. All compounds shown in Table I were prepared using boron trifluoride etherate.

Fluorene-9-spiro-2′-(*N*-aryl-3′,3′-dichloroaziridines) (II*a*–II*h*)—Dry chloroform (47.8 g, 0.4 mole) was added slowly to a stirred slurry of 0.1 mole of the *N*-fluorenylideneaniline derivative, 60 g (0.5 mole) of potassium *tert*-butoxide, and 250 ml of hexane. The reaction was stirred at room temperature for 16 hr. The mixture was filtered, and the residue was collected and washed three times with hot hexane. The combined filtrates were concentrated *in vacuo* to afford a crystalline product. The aziridine derivatives were recrystallized from hexane (Table II).

9-Chlorofluorene-9-carboxanilides (III*a*–III*h*)—These compounds were obtained in excellent yields by allowing the spirodichloroaziridine derivatives to remain in contact with excess water at 25° for 24 hr. Compounds III*a*–III*h* were recrystallized from aqueous ethanol (Table III).

REFERENCES

(1) E. J. Corey and M. Chaykovsky, *J. Am. Chem. Soc.*, **87**, 1353 (1965).

(2) A. G. Cook and E. K. Fields, *J. Org. Chem.*, **27**, 3686 (1962).

(3) D. Seyferth and W. Tronich, *J. Organomet. Chem.*, **21**, P3 (1970).

(4) M. E. Taylor and T. L. Fletcher, *J. Org. Chem.*, **21**, 523 (1956).

(5) *Ibid.*, **26**, 940 (1961).

ACKNOWLEDGMENTS AND ADDRESSES

Received December 17, 1976, from the *Department of Chemistry, University of Pennsylvania, Philadelphia, PA 19104.*

Accepted for publication February 8, 1977.

[x] To whom inquiries should be directed.

TLC Sensitivity of Six Modifications of Dragendorff's Reagent

LINDA B. RUBIA and RALPH GOMEZ ˣ

Abstract □ The relative sensitivities of six modifications of Dragendorff's reagent were measured on TLC plates by spectrodensitometry, using compounds containing specific functional groups. A correlation between the structures of the compounds reactive to Dragendorff's reagents and the sensitivities of the reagents was made. Explanations for the variations in sensitivities between different modifications of Dragendorff's reagent are given.

Keyphrases □ Dragendorff's reagent—several modifications, effect on relative TLC sensitivities of compounds containing various functional groups □ TLC—effect of modifications of Dragendorff's reagent on relative sensitivities of compounds containing various functional groups □ Structure–activity relationships—compounds containing various functional groups, effect of modification of Dragendorff's reagent on relative TLC sensitivities

Dragendorff's reagent is a commonly used spray reagent for the detection of nitrogen-containing compounds in the TLC analysis of pharmaceutical products (1–3). Its sensitivity of detection of different compounds, relative ease of preparation, and stability are some reasons for its extensive use. Dragendorff's reagent has been known for over a century (4) and has been used as a TLC reagent for over 25 years.

Many modifications have been suggested to increase its sensitivity, specificity, and stability (5–8). The purpose of this investigation was to determine whether any modification offered advantages over the others and whether one could be used as a general spray reagent for the detection of nitrogen-containing active pharmaceuticals.

The sensitivities of six modifications of Dragendorff's reagent were measured on TLC plates by spectrodensitometry, using compounds containing specific basic functional groups. The sensitivities of the modifications were determined, and their reactivity to the functional groups was studied. The reactions that explain the differences in sensitivities between the reagents are discussed.

EXPERIMENTAL

Equipment—A spectrodensitometer[1] equipped with a monochromator was used. The wavelength was 500 nm, and the signal was fed into a properly attenuated recorder.

Materials and Reagents—*Plates*—Silica gel G was slurried with water and coated on 20 × 20-cm glass plates using a mechanically operated TLC coating apparatus[2]. The plates were dried at 40° overnight; the average layer thickness was 0.25 mm.

Solutions—The following solutions were prepared: 1% (w/v) aqueous sodium nitrite, 40% (w/v) aqueous potassium iodide, 1.7% (w/v) bismuth nitrate in 20% (v/v) acetic acid, and 10% (w/v) aqueous sulfuric acid.

Acid-Modified Dragendorff's Reagent (Reagent A)—Potassium iodide solution, 100 ml, was added to 100 ml of bismuth nitrate solution, and the mixture was diluted to 1 liter with 10% (w/v) sulfuric acid.

Peroxide–Acid-Modified Dragendorff's Reagent (Reagent B)—To 300 ml of Reagent A, 0.6 ml of 30% hydrogen peroxide was added.

Iodine–Acid-Modified Dragendorff's Reagent (Reagent C)—To 300 ml of Reagent A, 6 g of iodine crystals was added. Then the mixture was shaken for 30 min.

[1] Schoeffel model SD 3000.
[2] Camag model 21-602.

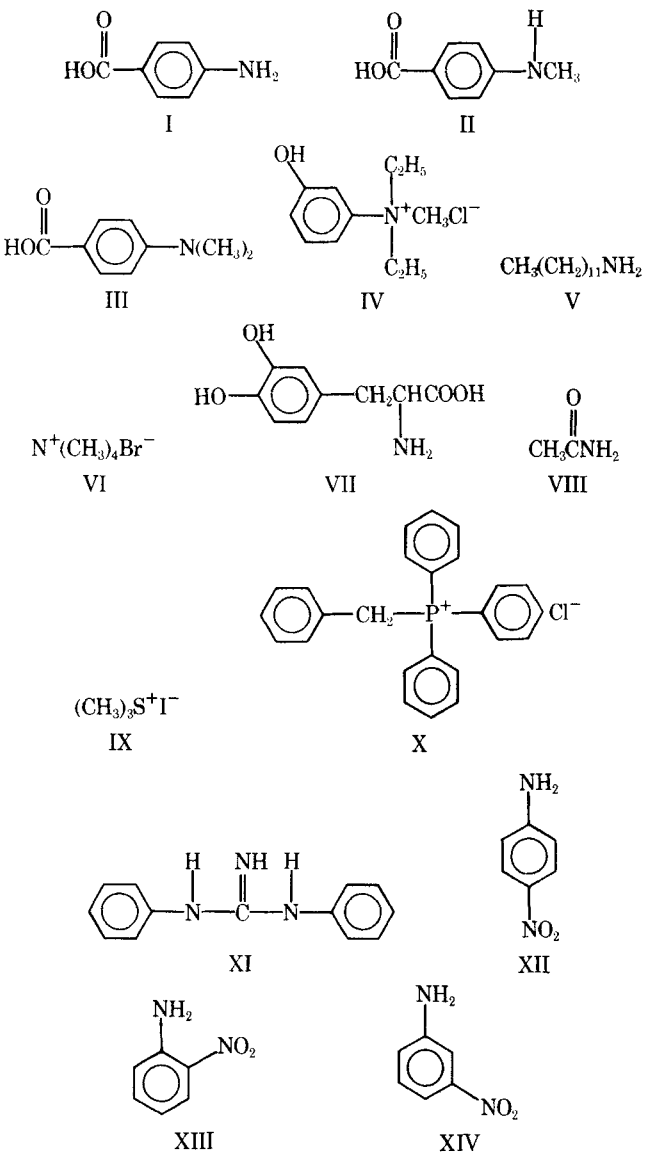

Acid-Modified Dragendorff's Reagent Oversprayed with Sodium Nitrite (Reagent D)—After spraying the TLC plate with Reagent A, the plate was lightly sprayed with sodium nitrite solution.

Peroxide–Acid-Modified Dragendorff's Reagent Oversprayed with Sodium Nitrite (Reagent E)—After spraying the TLC plate with Reagent B, the plate was lightly sprayed with sodium nitrite solution.

Iodine–Acid-Modified Dragendorff's Reagent Oversprayed with Sodium Nitrite (Reagent F)—After spraying the TLC plate with Reagent C, the plate was lightly sprayed with sodium nitrite solution.

Iodine Solution—To 10 ml of 40% potassium iodide solution, 2 g of iodine crystals was added. The mixture was diluted to 100 ml with 10% (w/v) sulfuric acid and mixed well.

Samples and Standard—The compounds studied were: 4-aminobenzoic acid (I), 4-(*N*-methylamino)benzoic acid (II), 4-(*N*,*N*-dimethylamino)benzoic acid (III), edrophonium chloride (IV), dodecylamine (V), tetramethylammonium bromide (VI), levodopa (VII), acetamide (VIII), trimethylsulfonium iodide (IX), benzyltriphenylphosphonium chloride (X), diphenylguanidine (XI), 4-nitroaniline (XII), 2-nitroaniline

Table I—Relative Response to Dragendorff's Reagents

Compound	Reagent A	Reagent B	Reagent C	Reagent D	Reagent E	Reagent F
I	0.2	0.7	0.9	1.0	0.8	1.0
II	0.2	0.9	1.6	1.2	1.2	1.6
III	0.4	1.4	2.8	2.4	2.5	2.9
IV	0.9	2.8	3.8	3.9	3.9	4.4
V	0.6	1.0	1.2	1.4	1.3	2.6
VI	1.7	3.7	4.2	3.8	3.6	4.4
VII	0.0	0.0	0.0	0.0	0.0	0.0
VIII	0.0	0.0	0.0	0.0	0.0	0.0
IX	0.9	2.7	3.4	3.5	4.3	4.1
X	1.4	3.5	4.7	4.5	4 8	5.1
XI	0.5	2.1	2.9	3.1	4.1	4.9
XII	0.2	0.9	1.2	0.9	1.6	1.8
XIII	0.4	0.5	0.7	0.4	0.8	0.5
XIV	0.1	0.2	0.7	0.2	0.6	0.8

(XIII), and 3-nitroaniline (XIV). Solutions of the compounds were prepared in either chloroform or chloroform–methanol (92:8) at a concentration of 0.6 mg/ml. The standard was 1% (w/v) methanolic thymol blue (thymolsulfonphthalein sodium salt).

Procedure—A 20 × 20-cm TLC plate was scored into 20 parallel 1-cm lanes. With a syringe, alternate lanes were spotted with 5 μl of sample solution. The spots were thoroughly dried, and the plates were sprayed evenly with 10 ml of Dragendorff's reagent. Then the plates were immediately covered with a 20 × 20-cm piece of clear glass and scanned. Five determinations on five separate plates were performed for each sample. On each plate, 2 μl of thymol blue solution was spotted. The areas of all spots were measured relative to the area of the thymol blue spot.

RESULTS AND DISCUSSION

The relative sensitivities of 14 compounds sprayed with six modifications of Dragendorff's reagent are summarized in Table I. In most cases, Reagent F proved to be the most sensitive, followed by Reagent C. Reagents A and B had the lowest sensitivities, while Reagents D and E had intermediate sensitivities.

An explanation for the observed order of sensitivities may be found in the preparation of the reagents since the relative sensitivity of each reagent can be roughly correlated to the amount of available iodine. To illustrate this correlation, IV–VI and IX–XI were spotted on TLC plates, sprayed with a solution of iodine of an equal concentration, and prepared in the same solvent as Dragendorff's reagent. The relative responses for IV, V, VI, IX, X, and XI were 4.0, 1.7, 4.1, 3.3, 5.3, and 3.9, respectively. These results show that the relative areas were similar to those obtained for Reagents C and F and greater than those obtained for Reagents A and B, which do not contain added iodine, and indicate that the high sensitivity of Reagents C and F is due largely to their iodine content.

The contribution of sodium nitrite to the total sensitivity of the reagent can be seen from the data in Table I. Comparison of the data for Reagents A and D shows that the latter was more sensitive. Similar results are seen when Reagents B and E and C and F are compared. The difference between reagents in each pair is that Reagents E and F are oversprayed with sodium nitrite solution while B and C are not. This increase in sensitivity, therefore, is attributed to sodium nitrite overspraying. As Fike (9) proposed, sodium nitrite releases iodine from the excess iodide in the reagents, which enhances the sensitivity.

A possible reaction that explains the role of sodium nitrite in the reagent is shown in Scheme I (10).

$$2NO_2^- + 2I^- + 4H^+ \rightarrow I_2 + 2NO + 2H_2O$$

Scheme I

The contribution of hydrogen peroxide to the sensitivity of the reagent can be seen by inspecting Table I, which shows that Reagent B was more reactive than Reagent A. The only difference in the two is that Reagent B has added hydrogen peroxide. Hydrogen peroxide reacts with excess iodide in the reagent to liberate iodine, similar to sodium nitrite.

A possible reaction is shown in Scheme II (10).

$$H_2O_2 + 2H^+ + 2I^- \rightarrow I_2 + 2H_2O$$

Scheme II

Reagent 3 cannot be expected to be as sensitive as the other reagents containing iodine or oversprayed with sodium nitrite, since the amount of hydrogen peroxide added is small and, therefore, the amount of iodine that can form and be available for reaction is small.

The data show that addition of crystalline iodine or formation of iodine by reaction with sodium nitrite or hydrogen peroxide increased the sensitivity of each reagent over its noniodine-containing counterpart.

Table I shows that IV, VI, IX, and X were the most reactive with Dragendorff's reagents, while III and XI were close behind in reactivity. These reactive compounds are quaternary nitrogen and phosphorus salts and tertiary sulfur salts. Compounds III and XI are tertiary amines, which can be easily converted to quaternary amine salts by reaction with the excess sulfuric acid in the reagents. Presumably, reaction with the reagent then proceeds by the same mechanism as with the salts.

Compounds I, V, XII, XIII, and XIV, all primary amines, had a relatively low reactivity with the reagents, although V, the aliphatic primary amine, had a higher sensitivity than the other four compounds.

Compounds VII and VIII, an amino acid and amide, respectively, did not react with any of the six modifications of the reagent.

For a homologous series, I–III, reactivity increased from primary to secondary to tertiary amine; with *ortho*-, *para*- and *meta*-substituted nitroanilines, reactivity was generally poor and the order of reactivity varied with the reagent.

The role of light and air on the stability of plates sprayed with Reagent C was investigated. Duplicate plates were spotted with 3 μg of IV, sprayed with Reagent C, and immediately covered with a 20 × 20-cm piece of plain glass. The sides were sealed with tape. One plate was left exposed to room light, and the second was kept in the dark. Both plates were periodically scanned on the densitometer. After 5 hr, the relative areas of the spots were fairly constant for both plates.

The experiment was repeated. This time the plates were left uncovered. After several hours, the spots had faded a great deal. However, the decrease was approximately the same for the plate exposed to light and the plate kept in the dark. This result indicates that the spot on the plate is not light sensitive but appears to be sensitive to air.

Since Dragendorff's reagent is used extensively in the pharmaceutical industry for the detection of nitrogen-containing drug substances on TLC plates, these results should aid in improving the detection limits of these active drug substances and their degradation products on TLC plates.

REFERENCES

(1) "Thin-Layer Chromatography," 2nd ed., E. Stahl, Ed., Academic, New York, N.Y., 1969, p. 873.

(2) J. G. Kirchner, "Thin-Layer Chromatography," Interscience, New York, N.Y., 1967, p. 160.

(3) K. Randerath, "Thin-Layer Chromatography," Academic, New York, N.Y., 1964, p. 74.

(4) G. Dragendorff, *Russ. J. Pharm.*, **5**, 85 (1866). *Ibid.*, **6**, 663 (1867).

(5) H. M. Bregoff, E. Roberts, and C. C. Deliveche, *J. Biol. Chem.*, **205**, 565 (1953).

(6) R. Munier and M. Machebouf, *Bull. Soc. Chem. Biol.*, **31**, 1144 (1949). *Ibid.*, **33**, 846 (1951).

(7) R. Munier, *Bull. Soc. Chem. Biol.*, **35**, 1225 (1953).

(8) H. Thies and F. W. Reuther, *Naturwissenschaften*, **41**, 230 (1954).

(9) W. W. Fike, *Anal. Chem.*, **38**, 1697 (1966).

(10) G. H. Ayres, "Quantitative Chemical Analysis," Harper, New York, N.Y., 1958, p. 471.

ACKNOWLEDGMENTS AND ADDRESSES

Received January 3, 1977, from the *Research Products Section, Quality Control Department, Hoffmann-La Roche Inc., Nutley, NJ 07110.*

Accepted for publication January 31, 1977.

The authors acknowledge the assistance of the Scientific Literature Department of Hoffmann-La Roche Inc.

[x] To whom inquiries should be directed.

Sodium Nitroprusside-Induced Hypothermia in Mice

DAVID H. BURKE ˣ and GERALD P. O'HARA

Abstract □ The hypothermic response following sublethal doses (1.25, 2.5, and 5 mg/kg) of sodium nitroprusside was investigated in mice. The magnitude and duration of rectal temperature depression were shown to be dose related. Oral administration of nitroprusside (5 mg/kg) failed to alter rectal temperature significantly; subcutaneous, intraperitoneal, intravenous, and intracerebral injections at the same dosage level caused respective drops of 3.61, 3.65, 6.44, and 3.48°. The degree of rectal temperature depression following nitroprusside (5 mg/kg ip) was dependent upon the ambient temperature. The time course of the effect of nitroprusside (5 mg/kg ip) on tail temperature was noted. A transient rise in tail temperature, which coincided with the onset of rectal temperature depression, was attributed to the vasodilatory effect of the drug. Tail temperature depression occurred at the peak and throughout the remainder of the rectal temperature response, suggesting that nitroprusside may decrease heat production. Body temperature depression *via* intracerebral administration, as well as pronounced sedation following nitroprusside injection, suggests a central component to the thermolytic response.

Keyphrases □ Sodium nitroprusside—effect on body temperature, various routes of administration, various ambient temperatures, mice □ Temperature, body—effect of sodium nitroprusside, various routes of administration, various ambient temperatures, mice □ Hypothermia—induced by sodium nitroprusside, effect of various routes of administration and various ambient temperatures, mice □ Antihypertensive agents—sodium nitroprusside, effect on body temperature, various routes of administration, various ambient temperatures, mice

In previous experiments (1), sodium nitroprusside (sodium nitroferricyanide) produced marked hypothermia in mice. Rectal temperature depression averaging approximately 3.5° was noted 15 min following sublethal doses (5 mg/kg ip) of this potent hypotensive agent. Although the mechanism of this response has not been established, nitroprusside apparently is devoid of action on central and peripheral cholinoceptive sites.

To provide insight into the mechanism of nitroprusside-elicited hypothermia, this study investigated in greater detail the temperature response to sodium nitroprusside.

EXPERIMENTAL

Adult male Swiss albino mice, 20–25 g, were housed in groups of 25 with *ad libitum* access to laboratory food[1] and water for several days prior to experimentation. For 24 hr prior to and including the time of the experiment, the mice were kept in a room free from drafts at a constant environmental temperature of 23 ± 1° unless otherwise noted.

Solutions of sodium nitroprusside were freshly prepared with distilled water in concentrations (calculated as the salt) such that a volume of 0.01 ml/g was delivered. Intracerebral injections, however, were administered in a fixed volume of 0.01 ml/mouse.

A thermistor thermometer[2] was used for obtaining rectal and tail temperatures. Rectal temperatures were recorded with a thermistor probe inserted to a distance of 2.5 cm and held in position until constant readings were attained. Tail temperatures were obtained by placement of a disk probe on the base of the tail. A small amount of electrode paste was applied to the surface of the disk probe.

Intracerebral injections were accomplished according to the method of Haley and McCormick (2). Sodium nitroprusside or water (warmed to 38°) was administered at a point lateral to the midline joining the anterior bases of the ears. A 22-gauge needle attached to a microliter syringe[3] was inserted through the skull to a depth of 3 mm. The prior injection of several animals with a solution of methylene blue (0.5%) resulted in localization of the dye in the third and fourth ventricles.

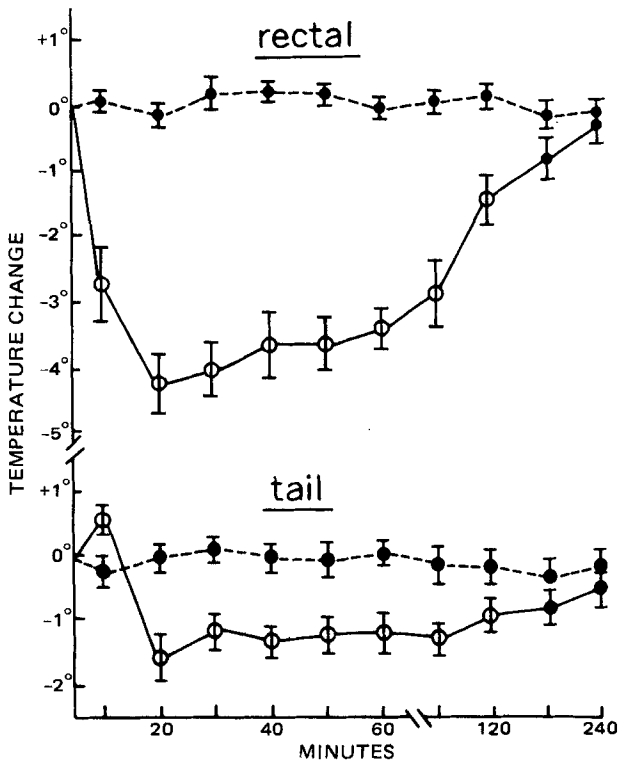

Figure 1—*Time course of the effect of distilled water (0.01 ml/g ip) (---●---) and sodium nitroprusside (5 mg/kg ip) (—●—) on rectal and tail temperature in mice. Water or nitroprusside was administered at zero time. Open symbols denote a significant difference ($p < 0.05$) from the water treatment at the corresponding time interval. Each point represents the average of 12 determinations. Vertical bars represent standard errors.*

At the start of each day's testing, the mice were placed singly in circular wire-mesh cages and individual weights were obtained with a triple-beam balance[4]. Immediately following weight determination, initial temperatures were recorded and treatment administration was accomplished. Temperatures were recorded again at various intervals. Unless otherwise stated, all treatments were given by the intraperitoneal route. Animals that served as controls received distilled water (0.01 ml/g).

In the comparison of mean temperature changes (*i.e.*, the difference between temperature immediately prior to and at the appropriate interval following treatment), statistical significance was determined by the use of the Student *t* test. Temperature differences were considered to be significant at the probability level of 5% or less.

RESULTS AND DISCUSSION

The effect of sodium nitroprusside (1.25, 2.5, and 5 mg/kg ip) on the body temperature of mice was determined at various intervals over 4 hr (Table I). At the lower dosage level (1.25 mg/kg), nitroprusside produced a body temperature depression lasting approximately 30 min. The intensity and duration of the hypothermic response were increased with higher doses. At all dosage levels investigated, maximal hypothermia was evident within 15–30 min. Decreased locomotor activity and muscle

[1] Purina chow.
[2] YSI model 46 Tele-Thermometer, Yellow Springs Instrument Co., Yellow Springs, Ohio.
[3] Hamilton.
[4] Ohaus.

Table I—Effect of Intraperitoneal Administration of Sodium Nitroprusside at Various Dosage Levels on the Body Temperature of Mice

Minutes	Temperature Change (Mean ± *SE*)[a]			
	Water	Sodium Nitroprusside		
		1.25 mg/kg	2.5 mg/kg	5 mg/kg
15	+0.28 ± 0.18°	−1.35 ± 0.25°[b]	−2.43 ± 0.27°[b]	−4.08 ± 0.53°[b]
30	+0.35 ± 0.16°	−0.79 ± 0.19°[b]	−1.45 ± 0.21°[b]	−4.11 ± 0.51°[b]
60	+0.23 ± 0.24°	−0.15 ± 0.09°	−0.93 ± 0.25°[b]	−3.48 ± 0.43°[b]
90	+0.16 ± 0.21°	−0.07 ± 0.19°	−0.73 ± 0.23°[b]	−2.82 ± 0.52°[b]
120	+0.28 ± 0.15°	+0.02 ± 0.20°	+0.18 ± 0.14°	−1.56 ± 0.43°[b]
180	+0.13 ± 0.16°	−0.03 ± 0.18°	+0.19 ± 0.17°	−0.53 ± 0.37°[b]
240	+0.22 ± 0.17°	+0.10 ± 0.14°	+0.24 ± 0.16°	−0.13 ± 0.31°

[a] Temperature changes represent the difference between body temperature recorded initially and that obtained at the designated interval following water or nitroprusside treatment in groups of 12 mice. [b] Compared to water at the corresponding time interval, $p < 0.05$.

Table II—Mean Changes in Body Temperature 30 min following Sodium Nitroprusside Administration by Various Routes in Mice

Route	Water		Sodium Nitroprusside (5 mg/kg)	
	Initial Temperature	Temperature Change (Mean ± *SE*)[a]	Initial Temperature	Temperature Change (Mean ± *SE*)[a]
Oral	37.52°	−0.12 ± 0.16°	37.16°	−0.21 ± 0.29°
Subcutaneous	37.41°	−0.15 ± 0.11°	37.61°	−3.61 ± 0.33°[b]
Intraperitoneal	37.29°	0.00 ± 0.12°	37.45°	−3.65 ± 0.46°[b]
Intravenous	37.46°	+0.24 ± 0.25°	37.60°	−6.44 ± 0.52°[b]
Intracerebral	37.61°	−0.48 ± 0.33°	37.75°	−3.48 ± 0.34°[b]

[a] Temperature changes represent the difference between body temperature recorded initially and that obtained 30 min following water or nitroprusside treatment in groups of 12 mice. [b] Compared to water by the corresponding route, $p < 0.05$.

Table III—Body Temperature Changes 30 min after Intraperitoneal Injection of Sodium Nitroprusside to Mice at Various Ambient Temperatures

Ambient Temperature	Water		Sodium Nitroprusside (5 mg/kg)	
	Initial Temperature	Temperature Change (Mean ± *SE*)[a]	Initial Temperature	Temperature Change (Mean ± *SE*)[a]
18°	36.95°	+0.06 ± 0.09°	37.11°	−6.53 ± 0.46°[b,c]
23°	37.33°	+0.06 ± 0.16°	37.52°	−4.44 ± 0.44°[b]
28°	38.06°	−0.01 ± 0.10°	38.24°	−1.75 ± 0.14°[b,c]

[a] Temperature changes represent the difference between body temperature recorded initially and that obtained 30 min following water or nitroprusside treatment in groups of 12 mice. [b] Compared to water at the corresponding ambient temperature, $p < 0.05$. [c] Compared to sodium nitroprusside at 23°, $p < 0.05$.

weakness developed approximately 10 min after administration and were present throughout the entire body temperature response. Visible shivering and increased muscle tone were unapparent during and upon recovery from hypothermia.

Sodium nitroprusside (5 mg/kg) was administered to groups of 12 mice by the oral, subcutaneous, intraperitoneal, intravenous, and intracerebral routes, and the effect on body temperature at 30 min was noted (Table II). The compound was inactive when given by oral intubation. This observation supports the work of Page *et al.* (3), who noted that sodium nitroprusside produced minimal hypotension by this route in various species. Significant hypothermia occurred following injection by the subcutaneous, intraperitoneal, intravenous, and intracerebral routes. Greatest activity was seen with the intravenous route; rectal temperatures averaged 6–7° lower than the values obtained prior to treatment.

Symptoms were depressant in nature, except in the case of the intracerebral route where the animals exhibited profound clonic and tonic convulsant activity after a latent period of approximately 30 min. During this latency, however, symptoms were characteristically depressant. All animals injected by this route died between 60 and 90 min following treatment. Intracerebral injection with lower doses of nitroprusside (0.025 mg/kg) caused a lesser degree of hypothermia (0.81°) and no incidence of lethality (data not included).

The influence of ambient temperature upon the thermal response of mice to sodium nitroprusside (5 mg/kg ip) is illustrated in Table III. Animals exposed to an environmental temperature of 18° exhibited rectal temperature depression amounting to 6.53°, while mice exposed to 23 and 28° gave drops of 4.44 and 1.75°, respectively. These values were significantly different from one another.

Figure 1 depicts the time course of changes in rectal and tail temperatures after sodium nitroprusside (5 mg/kg) administration. Prior to the intraperitoneal injection, rectal and tail temperatures averaged 37.50 and 25.12°, respectively. The rectal temperature response was similar to that shown in Table I. Tail temperature was elevated (+0.54°) 10 min after nitroprusside injection, followed by a sharp decline lasting approximately 3 hr.

These results support the earlier report (1) that sodium nitroprusside induces a pronounced fall in the body temperature of mice, dependent upon the dose and route of administration.

The ambient temperature had a pronounced effect on the intensity of body temperature depression by nitroprusside. Since the metabolism rate is temperature dependent, it is important to regulate the hypothermic response while measuring other pharmacological parameters. Such information may be useful in future studies on the mechanism of action of this compound.

During the rapid fall in rectal temperature, tail temperature was transiently elevated (Fig. 1). Presumably, this elevation was due to the well-known vasodilator action of the drug. Vasodilation and, thus, increased peripheral heat loss apparently contribute early in the production of hypothermia. However, from 20 min onward, tail temperature depression paralleled the rectal temperature response. This observation suggests that a mechanism (or mechanisms) other than vasodilation contributes to the thermolytic response. Tail temperature depression throughout most of the rectal temperature response suggests that decreased heat production, rather than increased heat dissipation, plays a major role in nitroprusside-induced hypothermia. The vasodilatory action of the drug may, in fact, play only a minor transient role in body temperature depression.

Thus far, no data support an effect of nitroprusside on the central nervous system (CNS), nor is there any evidence that its effects are mediated through this system. Certain observations during this investigation suggest a possible central component of the hypothermic activity of nitroprusside. The decrease in body temperature produced by intracerebral administration and the pronounced sedation produced by doses that

significantly depress body temperature suggest that nitroprusside causes hypothermia, in part, through an action on the CNS. Conceivably, the drug may cause nonspecific depression of thermoregulatory control centrally. This action could explain the absence of compensatory shivering and increased muscle tone, although nitroprusside interference at the effector level could account for these absences.

REFERENCES

(1) D. H. Burke and D. E. Mann, Jr., *J. Pharm. Sci.*, **59**, 1814 (1970).

(2) T. Haley and W. McCormick, *Br. J. Pharmacol.*, **12**, 12 (1957).

(3) I. H. Page, A. C. Corcoran, H. P. Dustan, and T. Koppanyi, *Circulation*, **11**, 188 (1955).

ACKNOWLEDGMENTS AND ADDRESSES

Received September 1, 1976, from the *Division of Pharmacology, School of Dentistry, Marquette University, Milwaukee, WI 53233.*

Accepted for publication February 7, 1977.

The authors are indebted to Bobbi Stewart, Steven Payson, and Mary Williamson for their capable assistance and to David E. Mann, Jr., for his helpful suggestions.

[x] To whom inquiries should be directed.

Application of ^{13}C-NMR Spectroscopy to *In Vitro* Analysis of Enzyme Kinetics

H. L. JOHNSON [x], D. W. THOMAS, M. ELLIS, L. CARY, and J. I. DeGRAW

Abstract □ The conversion of D,L-α-^{13}C-histidine to similarly labeled α-^{13}C-histamine by bacterial and mammalian histidine decarboxylase was studied by ^{13}C-NMR spectroscopy and GLC–mass spectrometry. The results obtained with the partially purified bacterial enzyme were in essentially perfect agreement with results obtained simultaneously with a standard radioisotopic method using carboxyl-labeled-^{14}C-L-histidine. For a crude tissue preparation of the mammalian enzyme, the radioisotopic method indicated an activity three times that based on ^{13}C-NMR measurement of α-^{13}C-histamine. The difference in results was accountable in terms of additional ^{13}C-NMR signals attributable to products other than histamine due in part to enzymatic degradation of the latter.

Keyphrases □ D,L-α-^{13}C-Histidine—conversion to histamine by histidine decarboxylase, ^{13}C-NMR and GLC–mass spectral study □ D,L-α-^{13}C-Histamine—conversion from histidine by histidine decarboxylase, ^{13}C-NMR and GLC–mass spectral study □ Enzyme activity—histidine decarboxylase, conversion of D,L-α-^{13}C-histidine to histamine, ^{13}C-NMR and GLC–mass spectral study □ ^{13}C-NMR spectroscopy—study of conversion of D,L-α-^{13}C-histidine to histamine by histidine decarboxylase □ GLC–mass spectrometry—study of conversion of D,L-α-^{13}C-histidine to histamine by histidine decarboxylase

Many *in vitro* assays of enzyme activity are relatively inconvenient, time consuming, or indirect in that measurements are based on cofactors or coproducts rather than the major product. Furthermore, compounds are frequently assayed for inhibitory activity using crude tissue preparations where the primary product may be exposed to further enzymatic transformations that may or may not be affected by the test compound. An example is the assay of specific histidine decarboxylase (EC 4.1.1.22) in minced tissue or crude extracts of mammalian tissues (1). One method of assay measures the ^{14}C-carbon dioxide evolved from carboxyl-labeled ^{14}C-histidine (2), and other methods are based on the measurement of the histamine produced (1).

The increasing availability of stable isotopic intermediates suggested exploration of NMR spectra using synthetic isotopic-enriched substrates as a convenient means of quantitatively and directly determining the kinetics of formation of multiple products in a crude enzyme assay. For initial exploration, ^{13}C-enriched histidine (3) was used; ^{13}C-NMR results were compared with a standard radioisotopic method (2) using histidine decarboxylase of both bacterial and mammalian origin. With the bacterial enzyme, mass spectrometry served as an additional comparison.

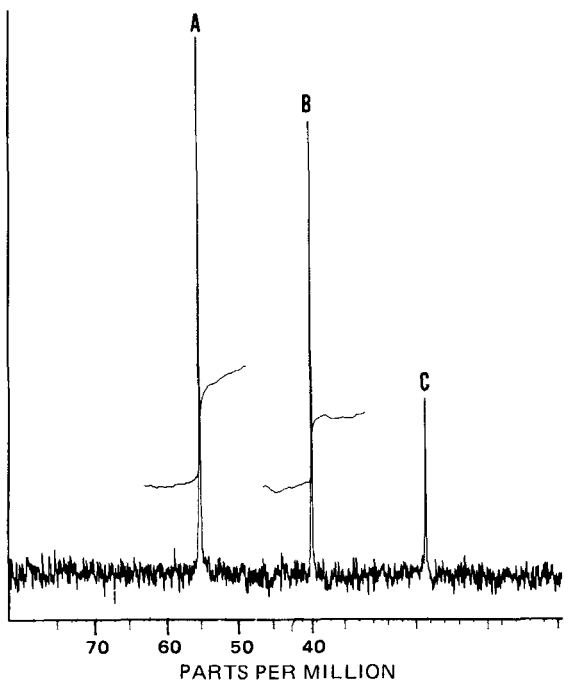

Figure 1—*^{13}C-NMR spectrum of bacterial histidine decarboxylase reaction mixture [conversion of D,L-α-^{13}C-histidine (M + 4) to α-^{13}C-histamine (M + 4)]. Protein was removed by heat precipitation. Key: A, α-^{13}C-histidine; B, α-^{13}C-histamine; and C, reference ^{13}C-acetate.*

EXPERIMENTAL

Carboxyl-labeled-^{14}C-L-histidine (13 mCi/mmole) was obtained commercially[1]. Nonradioactive isotopic D,L-histidine (2,5-^{2}H,3-^{15}N,α-^{13}C-labeled) was synthesized with 80% enrichment in M + 4 and 20% M

[1] New England Nuclear Corp., Boston, Mass.

significantly depress body temperature suggest that nitroprusside causes hypothermia, in part, through an action on the CNS. Conceivably, the drug may cause nonspecific depression of thermoregulatory control centrally. This action could explain the absence of compensatory shivering and increased muscle tone, although nitroprusside interference at the effector level could account for these absences.

REFERENCES

(1) D. H. Burke and D. E. Mann, Jr., *J. Pharm. Sci.*, **59**, 1814 (1970).

(2) T. Haley and W. McCormick, *Br. J. Pharmacol.*, **12**, 12 (1957).

(3) I. H. Page, A. C. Corcoran, H. P. Dustan, and T. Koppanyi, *Circulation*, **11**, 188 (1955).

ACKNOWLEDGMENTS AND ADDRESSES

Received September 1, 1976, from the *Division of Pharmacology, School of Dentistry, Marquette University, Milwaukee, WI 53233.*

Accepted for publication February 7, 1977.

The authors are indebted to Bobbi Stewart, Steven Payson, and Mary Williamson for their capable assistance and to David E. Mann, Jr., for his helpful suggestions.

[x] To whom inquiries should be directed.

Application of ^{13}C-NMR Spectroscopy to *In Vitro* Analysis of Enzyme Kinetics

H. L. JOHNSON [x], D. W. THOMAS, M. ELLIS, L. CARY, and J. I. DeGRAW

Abstract □ The conversion of D,L-α-^{13}C-histidine to similarly labeled α-^{13}C-histamine by bacterial and mammalian histidine decarboxylase was studied by ^{13}C-NMR spectroscopy and GLC–mass spectrometry. The results obtained with the partially purified bacterial enzyme were in essentially perfect agreement with results obtained simultaneously with a standard radioisotopic method using carboxyl-labeled-^{14}C-L-histidine. For a crude tissue preparation of the mammalian enzyme, the radioisotopic method indicated an activity three times that based on ^{13}C-NMR measurement of α-^{13}C-histamine. The difference in results was accountable in terms of additional ^{13}C-NMR signals attributable to products other than histamine due in part to enzymatic degradation of the latter.

Keyphrases □ D,L-α-^{13}C-Histidine—conversion to histamine by histidine decarboxylase, ^{13}C-NMR and GLC–mass spectral study □ D,L-α-^{13}C-Histamine—conversion from histidine by histidine decarboxylase, ^{13}C-NMR and GLC–mass spectral study □ Enzyme activity—histidine decarboxylase, conversion of D,L-α-^{13}C-histidine to histamine, ^{13}C-NMR and GLC–mass spectral study □ ^{13}C-NMR spectroscopy—study of conversion of D,L-α-^{13}C-histidine to histamine by histidine decarboxylase □ GLC–mass spectrometry—study of conversion of D,L-α-^{13}C-histidine to histamine by histidine decarboxylase

Many *in vitro* assays of enzyme activity are relatively inconvenient, time consuming, or indirect in that measurements are based on cofactors or coproducts rather than the major product. Furthermore, compounds are frequently assayed for inhibitory activity using crude tissue preparations where the primary product may be exposed to further enzymatic transformations that may or may not be affected by the test compound. An example is the assay of specific histidine decarboxylase (EC 4.1.1.22) in minced tissue or crude extracts of mammalian tissues (1). One method of assay measures the ^{14}C-carbon dioxide evolved from carboxyl-labeled ^{14}C-histidine (2), and other methods are based on the measurement of the histamine produced (1).

The increasing availability of stable isotopic intermediates suggested exploration of NMR spectra using synthetic isotopic-enriched substrates as a convenient means of quantitatively and directly determining the kinetics of formation of multiple products in a crude enzyme assay. For initial exploration, ^{13}C-enriched histidine (3) was used; ^{13}C-NMR results were compared with a standard radioisotopic method (2) using histidine decarboxylase of both bacterial and mammalian origin. With the bacterial enzyme, mass spectrometry served as an additional comparison.

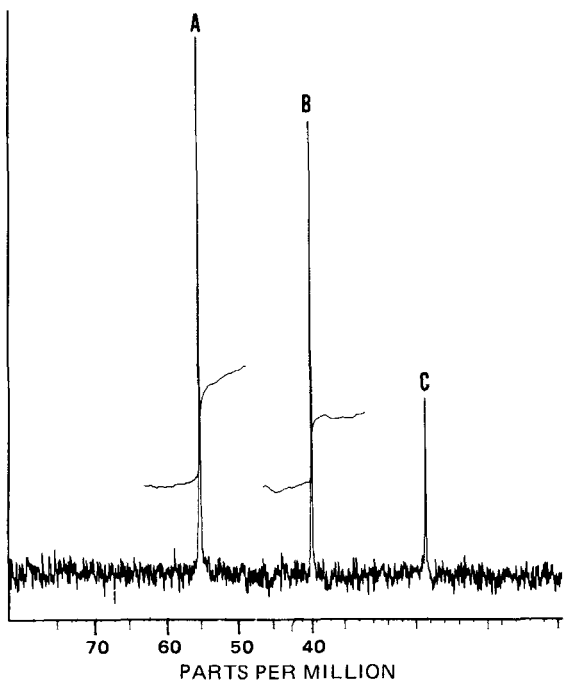

Figure 1—*^{13}C-NMR spectrum of bacterial histidine decarboxylase reaction mixture [conversion of D,L-α-^{13}C-histidine (M + 4) to α-^{13}C-histamine (M + 4)]. Protein was removed by heat precipitation. Key: A, α-^{13}C-histidine; B, α-^{13}C-histamine; and C, reference ^{13}C-acetate.*

EXPERIMENTAL

Carboxyl-labeled-^{14}C-L-histidine (13 mCi/mmole) was obtained commercially[1]. Nonradioactive isotopic D,L-histidine (2,5-^{2}H,3-^{15}N,α-^{13}C-labeled) was synthesized with 80% enrichment in M + 4 and 20% M

[1] New England Nuclear Corp., Boston, Mass.

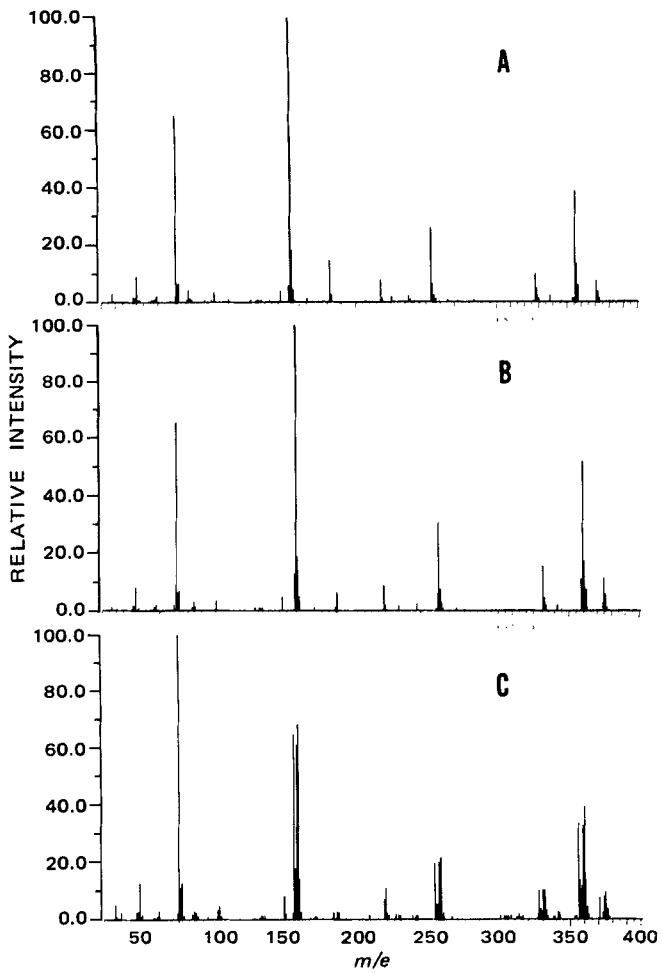

Figure 2—*Mass spectra of trimethylsilyl-derivatized histidine. Key: A, reference histidine (M); B, M + 4 histidine; and C, M and M + 4 histidine from the decarboxylase reaction mixture of Fig. 1.*

+ 3 (3). Bacterial histidine decarboxylase (*Clostridium welchii*) was obtained as the acetone powder (Type I[2], 0.015 unit/mg), which was used as a lightly homogenized suspension (2 mg/ml) in 0.2 *M* ammonium acetate buffer (pH 4.8). Mammalian histidine decarboxylase was obtained as a crude pyloric stomach extract (clear supernate) from male Sprague–Dawley rats [1:2.5 homogenization in 0.05 *M* phosphate buffer (pH 7.2) centrifuged at 5000×*g* for 30 min at 0°].

The bacterial enzyme was incubated at 37° with ^{14}C-L-histidine (0.033 μCi/ml) and D,L-α-^{13}C-histidine (M + 4) (0.33 mg/ml) at pH 4.8 (4). The mammalian enzyme was incubated under nitrogen at 37° (for 1.5 and 3 hr) with L-^{14}C-histidine (0.038 μCi/ml), D,L-α-^{13}C-histidine (M + 4) (0.2 mg/ml), streptomycin sulfate (0.05 mg/ml), and pyridoxal 5-phosphate (2×10^{-5} *M*; 10-min preincubation before addition of substrate) at pH 7.2 (5). The radioisotopic assay (^{14}C-carbon dioxide) was a modification of the Levine and Watts (2) method, with termination of the reaction by citric acid addition. ^{14}C-Carbon dioxide was absorbed on 10 × 20-mm folded strips of filter paper[3] dipped in quaternary ammonium hydroxide[4] and allowed to drip dry.

For ^{13}C-NMR and mass spectrometry, the reaction was stopped by heat treatment (100° for 10 min). Protein was removed by centrifugation prior to analysis. Samples (10.0 ml) were lyophilized and reconstituted in 2.0 ml of water containing 10% D_2O prior to NMR analysis of mammalian enzyme activity. A 2-ml aliquot of the bacterial enzyme samples was analyzed directly by NMR spectroscopy after addition of 10% D_2O. For mass spectrometry, nonisotopic histidine and histamine were added as standards, and samples were evaporated to dryness before treatment with trimethylsilyl chloride.

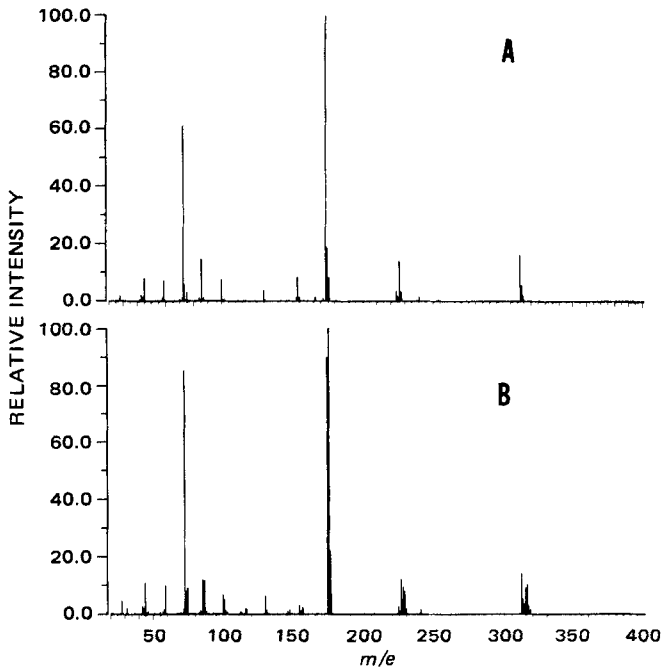

Figure 3—*Mass spectra of trimethylsilyl-derivatized histamine. Key: A, reference histamine (M); and B, M and M + 4 histamine from the decarboxylase reaction mixture of Fig. 1.*

Mass spectral analysis was performed on a combination gas chromatograph–mass spectrometer[5] using an OV-17 column and multiple ion detection. Measurements by ^{13}C-NMR spectroscopy utilized a Fourier transform spectrometer[6] (50,000 transients) with wide band proton decoupling (12-mm tube). Adequate signal-to-noise ratios were obtained. Radioisotopic assays used a scintillation spectrometer[7] with a counting efficiency of 93% (*p*-bis[2-(5-phenyloxazolyl)]benzene and 2,5-diphenyloxazole) in toluene with 1.0 ml of ethanol.

RESULTS AND DISCUSSION

Bacterial enzyme was used for establishing the accuracies and repro-

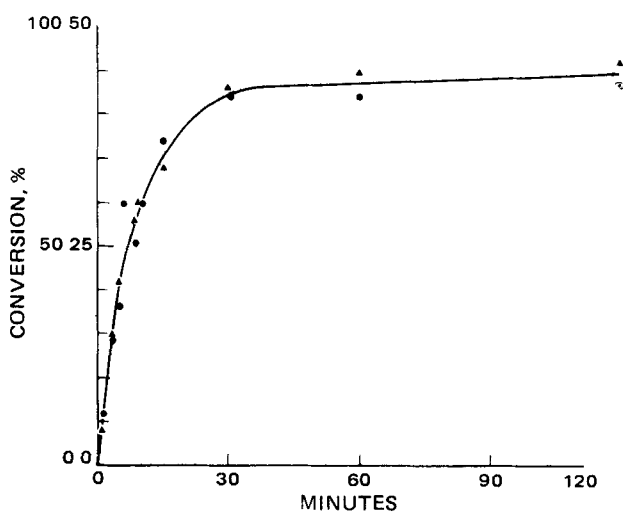

Figure 4—*Conversion by bacterial histidine decarboxylase of* L-^{14}C-*histidine to histamine plus* ^{14}C-*carbon dioxide (●) (0–100% scale) versus conversion of* D,L-α-^{13}C,3-^{15}N,2,5-^{2}H-*histidine (M + 4) to* α-^{13}C,3-^{15}N,2,5-^{2}H-*histamine (M + 4) (0–50% scale) as measured by* ^{13}C-*NMR (▲) and GLC–mass spectrometry (□).*

[2] Sigma Chemical Co., St. Louis, Mo.
[3] Whatman 3MM.
[4] Hyamine.

[5] LKB 9000, LKB Instruments, Rockville, Md.
[6] XL-100, Varian Instrument Division, Palo Alto, Calif.
[7] Mark III, Searle Analytic, Des Plaines, Ill.

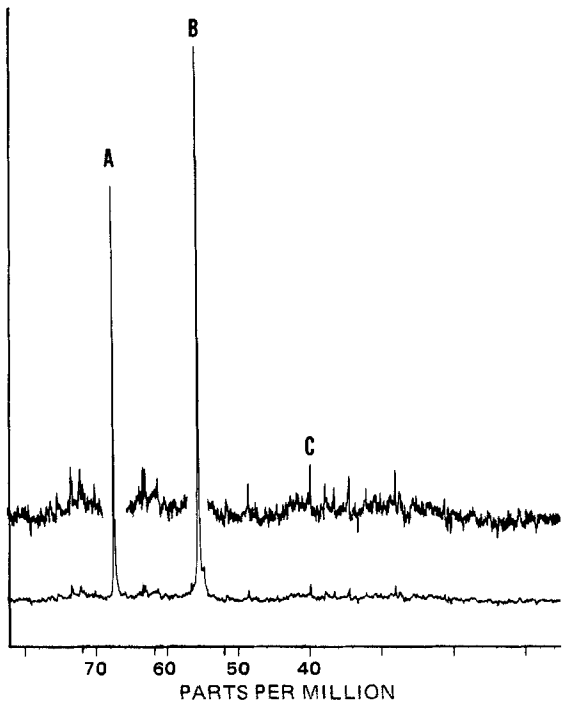

Figure 5—*^{13}C-NMR spectrum of mammalian histidine decarboxylase reaction mixture [rat pyloric stomach extract; conversion of D,L-α-^{13}C-histidine (M + 4) to α-^{13}C-histamine (M + 4)]. Protein was removed by heat precipitation. Key: A, reference dioxane; B, α-^{13}C-histidine; and C, α-^{13}C-histamine.*

ducibilities of the methods. A typical NMR spectrum is illustrated in Fig. 1 (bacterial enzyme sample, 2 hr), showing 43% α-^{13}C-histamine and 57% α-^{13}C-histidine. The maximum theoretical conversion was 50% because of the use of D,L-α-^{13}C-histidine. Added α-^{13}C-acetate served as an additional quantitation standard.

Typical mass spectra for histidine, M + 4 histidine, and the mixture of the two obtained from the 2-hr bacterial enzyme sample are shown in Fig. 2. Similarly, Fig. 3 shows the mass spectra of histamine and the mixture of histamine and M + 4 histamine obtained from the enzyme sample. Based on the amounts of histidine and histamine added to the sample before analysis, M + 4 histamine was 46% and M + 4 histidine was 54%. Included in the measurements are the M + 3 and M + 2 peaks of isotopic histidine. These were increased in the enzyme sample at the expense of the M + 4 peak because of some exchange loss of deuterium during enzymatic conversion (Fig. 2).

Typical radioisotopic results for the bacterial enzyme (^{14}C-carbon dioxide counts as a percent of initial ^{14}C-histidine counts) are plotted as a function of incubation time in Fig. 4. A common curve could be drawn through these data points and those obtained by ^{13}C-NMR spectroscopy and GLC–mass spectrometry. Radioisotopic results were based on a theoretical maximum conversion of 100% of L-^{14}C-histidine.

Typical results obtained with the mammalian enzyme preparation are shown in Fig. 5. In addition to the small amount of α-^{13}C-histamine formed (~3.3%), other ^{13}C-signals of comparable intensity are evident. One of these was tentatively identified as methylhistamine, formed by the enzymatic methylation of histamine on imidazole nitrogen (6); others are presumably direct metabolites of histidine and other metabolites of histamine. Results of the radioisotopic assay indicated 10% decarboxylation of α-^{13}C-histidine.

The radioisotopic carbon dioxide method is presumed to provide a reliable estimate of decarboxylase activity but gives no information concerning further metabolism. Methods based on measurement of product histamine may yield erroneously low estimates of activity due to such metabolism (1). These points are well illustrated by the present results, confirming the accuracy and reliability of the radioisotopic carbon dioxide method.

Crude enzyme preparations can be useful for purposes of *in vitro* drug screening where actions on various enzymes concerned with synthesis and metabolism of a given substrate are of interest. The increasing sensitivity of NMR instrumentation provides the potential for conveniently assessing such drug effects simultaneously in a single assay on a routine basis. Appropriate nonradioactive isotopic labeling of substrates introduces the additional advantage of further quantitative identification of metabolites by GLC–mass spectrometry through the simple expedient of using nonlabeled samples of presumed or suspected metabolites as carrier-standards.

Assays involving TLC frequently leave doubt because of superimposed spots. The NMR methodology, particularly when coupled with GLC–mass spectrometry, eliminates the need for extensive separation procedures and simplifies product identification when adequate UV, fluorometric, or other quantitative characterization techniques are not available.

REFERENCES

(1) R. W. Schayer, in "Handbook of Experimental Pharmacology," vol. 18, part 1, M. Rocha e Silva, Ed., Springer-Verlag, Berlin, Germany 1966, pp. 688–725.

(2) R. J. Levine and D. E. Watts, *Biochem. Pharmacol.*, **15**, 841 (1966).

(3) C. SooHoo, J. L. Lawson, and J. I. DeGraw, *J. Labelled Compd.*, **13**, 97 (1977).

(4) "Methods in Enzymology," vol. XVIIB, H. Tabor and C. W. Tabor, Eds., Academic, New York, N.Y., 1971, p. 663.

(5) *Ibid.*, p. 667.

(6) C. Maslinski, *Agents Actions*, **5**, 183 (1975).

ACKNOWLEDGMENTS AND ADDRESSES

Received November 15, 1976, from the *Life Sciences Division, Stanford Research Institute, Menlo Park, CA 94025.*

Accepted for publication February 25, 1977.

Supported by Grants AM 14763 (National Institute of Arthritis, Metabolism, and Digestive Diseases) and NS 11053 (National Institute of Neurological and Communicative Disorders and Stroke), Department of Health, Education, and Welfare.

[x] To whom inquiries should be directed.

Binding Rate of Antibacterials to Serum Proteins

Keyphrases □ Cefazolin—rate and extent of binding to serum protein, dogs □ Protein binding, serum—cefazolin, rate and extent, dogs □ Binding, serum protein—cefazolin, rate and extent, dogs □ Antibacterials—cefazolin, rate and extent of binding to serum protein, dogs

To the Editor:

It is generally accepted that the equilibrium between protein and drug occurs instantaneously, *i.e.*, within a fraction of a second (1). Measurement of the time necessary for the equilibrium between levothyroxine and serum protein showed that equilibrium was reached within 150 msec (2). Other reports confirmed the rapidity of this binding reaction (3, 4).

Contrary to previously published reports, Waterman *et al.* (5) reported that up to 50 min was required to attain the equilibrium between dog serum and several cephalosporin antibacterials. Cefazolin was approximately 20% protein bound to dog serum at 10 min after mixing and 80% bound after 50 min. This reported (5) value for the maximum binding of cefazolin (80%) to canine serum proteins was vastly different from that reported by Nishida *et al.* (6). They found 20% 1 hr after mixing of the drug–protein solution, but they did not measure binding as a function of time.

If these results are truly representative of the time necessary for the attainment of the protein-binding equilibrium, the effect of this lag time on drug distribution and elimination would be extremely complex. The cephalosporin antibacterials have a distributive phase with a half-life of 10 min (7). If it takes 50 min to reach the protein-binding equilibrium, then the drug will have distributed before maximum binding is attained. This result would have a drastic effect on the tissue availability of unbound drugs. Due to the pharmacokinetic and possible clinical implications involved with prolonged rates of attainment of the protein-binding equilibrium, we decided to investigate the rate and extent of the binding of cefazolin to serum protein.

Five milliliters of a 200-μg/ml solution of cefazolin in canine serum was added to 45 ml of canine serum at 37° to yield a serum cefazolin concentration of 20 μg/ml. Time zero was defined as the time the cefazolin was introduced into the flask containing the serum. The solution was stirred by a magnetic stirrer. At selected times during the hour after mixing, 7-ml samples of the cefazolin–serum solution were removed from the stirred flask and placed in the ultrafiltration apparatus[1] having an ultrafiltration membrane with a molecular weight cutoff of 10,000[2].

Nitrogen gas (12 psi) was applied to the system, and the protein-free filtrate was collected. The first 0.4 ml of filtrate samples was discarded since this portion was required to saturate all drug binding sites on the membrane. The next 0.6 ml was collected, and the time of collection was noted. All filtrates were frozen until assayed microbiologically using a disk diffusion assay with *Bacillus subtilis* as the test organism (8).

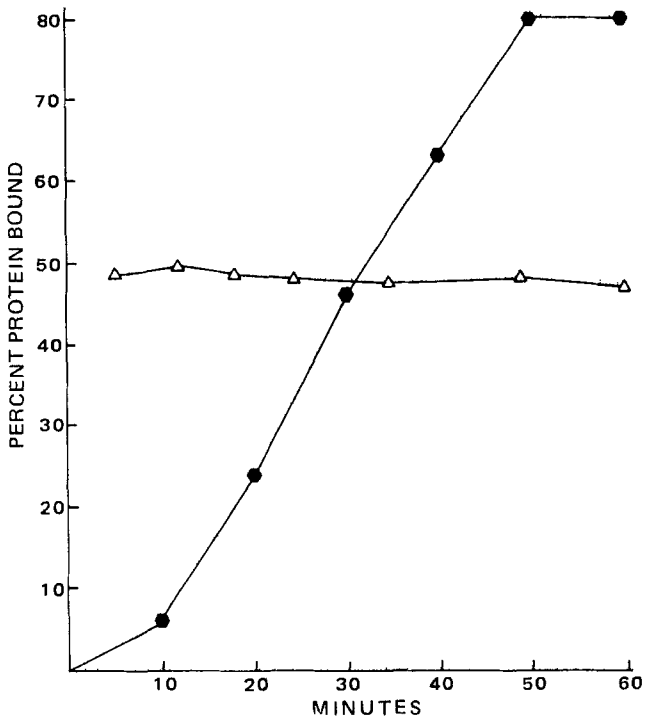

Figure 1—*Cefazolin binding to canine serum. Samples were taken as a function of time after mixing of serum and cefazolin. Total cefazolin concentration was 20 μg/ml. Key: △, data from the present study; and ●, data from Ref. 5.*

All experiments showed that the binding equilibrium was attained within 3–5 min, the shortest possible measurement time with the ultrafiltration apparatus. Approximately 48% of the total drug was in the protein-bound form throughout the hour interval of the experiment (Fig. 1), which is higher than the previously reported value for the binding of cefazolin to canine serum (6) but significantly lower than the value reported by Waterman *et al.* (5). No changes in binding were found with canine serum as a function of time. The previously reported (5) prolonged time to reach the protein-binding equilibrium was probably artifactual due to a technical problem with ultrafiltration.

Since a considerable species difference exists between the binding capacity of dog serum (48%) *versus* human serum (80%) (7), caution is advised in extrapolating experiments with a dog model to the human situation unless it has been previously established that the degree and extent of protein binding to serum protein are similar. This is especially true of comparative studies involving tissue or interstitial fluid distribution of drugs that are highly protein bound. For example, a comparison of cephaloridine, cephradine, or cephalexin (all poorly bound) to cefazolin might show equivalent distribution patterns in the interstitial fluid of dogs (9) but vastly different pat-

[1] Amicon MMC, Lexington, Mass.
[2] Amicon PM-10, Lexington, Mass.

terns in humans. Although other animal species represent convenient models for studying interstitial fluid distribution patterns of antibacterials, we feel that a significant potential for misinterpretation of the data exists unless the protein-binding characteristics of the antibacterial in the animal species are similar to those of humans.

(1) M. C. Meyer and D. E. Guttman, *J. Pharm. Sci.*, **57**, 895 (1968).
(2) J. Robbins, J. E. Rall, and M. Berman, in *Proc. Int. Thyroid Conf.*, Rome, 1965, M. Adriole, Ed., p. 635.
(3) I. M. Klotz, *Ann. N. Y. Acad. Sci.*, **256**, 10 (1972).
(4) J. H. Baldo, S. E. Halford, S. L. Patt, and B. D. Sykes, *Biochemistry*, **14**, 1893 (1975).
(5) N. G. Waterman, L. Scharfenberger, and M. J. Raff, *Antimicrob. Agents Chemother.*, **5**, 294 (1974).
(6) M. Nishida, T. Matsubara, T. Murakawa, Y. Mine, and Y. Yokata, *J. Antibiot. (Tokyo)*, **23**, 284 (1970).
(7) C. H. Nightingale, D. S. Greene, and R. Quintiliani, *J. Pharm. Sci.*, **64**, 1899 (1975).
(8) H. P. Bassaris, R. Quintiliani, E. G. Maderazo, R. C. Tilton, and C. H. Nightingale, *Curr. Ther. Res.*, **19**, 1 (1976).
(9) N. G. Waterman, M. J. Raff, L. Scharfenberger, and P. A. Barnwell, *J. Infect. Dis.*, **133**, 642 (1976).

D. S. Greene *
R. Quintiliani
C. H. Nightingale ˣ
School of Pharmacy
University of Connecticut
Storrs, CT 06268
and
Department of Medicine
Hartford Hospital
Hartford, CT 06115

Received February 11, 1977.
Accepted for publication August 12, 1977.
* Present address: College of Pharmacy, University of Rhode Island, Kingston, RI 02881.
ˣ To whom inquiries should be directed. Present address: School of Pharmacy, State University of New York at Buffalo, Amherst, NY 14260.

BOOKS

REVIEWS

Drug Fate and Metabolism: Methods and Techniques, Vol. 1. Edited by EDWARD R. GARRETT and JEAN L. HIRTZ. Dekker, 270 Madison Ave., New York, NY 10016, 1977. 313 pp. 15 × 23 cm. Price $35.00.

This volume is the first of a proposed series of texts on drug fate and metabolism. As indicated by the editors, the intent of this volume and future volumes is "to review all the techniques, physical, chemical, biological, medical, and mathematical, which can be applied to the study of drug fate in the organism. It is addressed primarily to the research scientist and is devoted to *methods*, with only the minimal theory given for perspective, appreciation, and proper evaluation of results." Volume I meets these goals, with the major emphasis being placed on the use of analytical methods.

Chapters I and II deal with autoradiography and autoradiography in cytopharmacology. Both chapters were written by experts in their area of speciality and are of particular importance to a novice in autoradiography. Chapters III and IV explore the use of electrophoresis and ion-pair extraction and chromatography. Chapter V reviews protein binding, and Chapter VI briefly looks at atomic absorption spectroscopy. The use of a fairly recent analytical method, spin immunoassay, is discussed in Chapter VII. The last chapter describes facilities and other pertinent information needed in animal care.

The editors state that "it was deemed proper to include chapters on methods that would not be modern methods of choice but are of historical importance in evaluating the significance and limitations of the earlier studies in these fields." The selection of these methods is one notable weakness that occurs in Volume I. All of the volumes in this series apparently will be required if an individual desires to have the methods most frequently used in drug metabolism. Another weakness is that the chapters have no rhyme or reason to their order. It would be more sensible to have the chapter on animal care at the beginning of the book since metabolism studies are based on the use of animals as a testing source.

One strong feature of this text, in addition to its being well written, is a list of the source of supplies and equipment included in Chapters I and III. This list is particularly important in saving time that would otherwise be spent in looking for this material. The reviewer recommends this volume for the researcher in the area of drug metabolism, especially the analytical chemist, pharmacologist, and toxicologist.

Reviewed by Gerald W. Slywka
School of Pharmacy
Ferris State College
Big Rapids, MI 49307

Martindale: The Extra Pharmacopoeia. 27th Ed. Edited by AINLEY WADE and JAMES E. F. REYNOLDS. The Pharmaceutical Press, 1 Lambeth High Street, London, SE1 7JN, England, 1977. 19 × 25.4 cm. 2077 pp. Price $60. Available from Rittenhouse Book Distributors, 251 S. 24th St., Philadelphia, PA 19103.

The 27th edition of "Martindale" is the largest ever published. It has been revised thoroughly and updated and extended in coverage. The book is divided into six main sections. Part 1, the largest, contains monographs on more than 3100 drugs and ancillary substances in current use throughout the world. Drugs having similar uses or actions are grouped together. Part 2, Supplementary Drugs and Ancillary Substances, describes 1040 new drugs that are too recently introduced or of insufficient importance to be included in Part 1. Also in Part 2 are monographs on obsolescent drugs about which information may still be required.

Part 3 gives the composition and source of more than 1450 over-the-counter medicines marketed in Great Britain. Part 4 is a Directory of Manufacturers, listing full names and addresses of over 1400 manufacturers throughout the world. The Index to Clinical Uses, Part 5, is a guide to drug usage presented in alphabetical order of diseases.

The final section, the General Index, has more than 43,000 entries. Substances are indexed by generic names, proprietary names, chemical names, and synonyms.

This book represents the most comprehensive reference source of information on drugs used throughout the world. Pharmacists as well as professionals and students in all health-related and scientific fields will find this book most valuable. It is a necessity in every pharmacy and medical library.

Staff review

terns in humans. Although other animal species represent convenient models for studying interstitial fluid distribution patterns of antibacterials, we feel that a significant potential for misinterpretation of the data exists unless the protein-binding characteristics of the antibacterial in the animal species are similar to those of humans.

(1) M. C. Meyer and D. E. Guttman, *J. Pharm. Sci.*, **57**, 895 (1968).
(2) J. Robbins, J. E. Rall, and M. Berman, in *Proc. Int. Thyroid Conf.*, Rome, 1965, M. Adriole, Ed., p. 635.
(3) I. M. Klotz, *Ann. N. Y. Acad. Sci.*, **256**, 10 (1972).
(4) J. H. Baldo, S. E. Halford, S. L. Patt, and B. D. Sykes, *Biochemistry*, **14**, 1893 (1975).
(5) N. G. Waterman, L. Scharfenberger, and M. J. Raff, *Antimicrob. Agents Chemother.*, **5**, 294 (1974).
(6) M. Nishida, T. Matsubara, T. Murakawa, Y. Mine, and Y. Yokata, *J. Antibiot. (Tokyo)*, **23**, 284 (1970).
(7) C. H. Nightingale, D. S. Greene, and R. Quintiliani, *J. Pharm. Sci.*, **64**, 1899 (1975).
(8) H. P. Bassaris, R. Quintiliani, E. G. Maderazo, R. C. Tilton, and C. H. Nightingale, *Curr. Ther. Res.*, **19**, 1 (1976).
(9) N. G. Waterman, M. J. Raff, L. Scharfenberger, and P. A. Barnwell, *J. Infect. Dis.*, **133**, 642 (1976).

D. S. Greene *
R. Quintiliani
C. H. Nightingale ˣ
School of Pharmacy
University of Connecticut
Storrs, CT 06268
and
Department of Medicine
Hartford Hospital
Hartford, CT 06115

Received February 11, 1977.
Accepted for publication August 12, 1977.
* Present address: College of Pharmacy, University of Rhode Island, Kingston, RI 02881.
ˣ To whom inquiries should be directed. Present address: School of Pharmacy, State University of New York at Buffalo, Amherst, NY 14260.

BOOKS

REVIEWS

Drug Fate and Metabolism: Methods and Techniques, Vol. 1. Edited by EDWARD R. GARRETT and JEAN L. HIRTZ. Dekker, 270 Madison Ave., New York, NY 10016, 1977. 313 pp. 15 × 23 cm. Price $35.00.

This volume is the first of a proposed series of texts on drug fate and metabolism. As indicated by the editors, the intent of this volume and future volumes is "to review all the techniques, physical, chemical, biological, medical, and mathematical, which can be applied to the study of drug fate in the organism. It is addressed primarily to the research scientist and is devoted to *methods*, with only the minimal theory given for perspective, appreciation, and proper evaluation of results." Volume I meets these goals, with the major emphasis being placed on the use of analytical methods.

Chapters I and II deal with autoradiography and autoradiography in cytopharmacology. Both chapters were written by experts in their area of speciality and are of particular importance to a novice in autoradiography. Chapters III and IV explore the use of electrophoresis and ion-pair extraction and chromatography. Chapter V reviews protein binding, and Chapter VI briefly looks at atomic absorption spectroscopy. The use of a fairly recent analytical method, spin immunoassay, is discussed in Chapter VII. The last chapter describes facilities and other pertinent information needed in animal care.

The editors state that "it was deemed proper to include chapters on methods that would not be modern methods of choice but are of historical importance in evaluating the significance and limitations of the earlier studies in these fields." The selection of these methods is one notable weakness that occurs in Volume I. All of the volumes in this series apparently will be required if an individual desires to have the methods most frequently used in drug metabolism. Another weakness is that the chapters have no rhyme or reason to their order. It would be more sensible to have the chapter on animal care at the beginning of the book since metabolism studies are based on the use of animals as a testing source.

One strong feature of this text, in addition to its being well written, is a list of the source of supplies and equipment included in Chapters I and III. This list is particularly important in saving time that would otherwise be spent in looking for this material. The reviewer recommends this volume for the researcher in the area of drug metabolism, especially the analytical chemist, pharmacologist, and toxicologist.

Reviewed by Gerald W. Slywka
School of Pharmacy
Ferris State College
Big Rapids, MI 49307

Martindale: The Extra Pharmacopoeia. 27th Ed. Edited by AINLEY WADE and JAMES E. F. REYNOLDS. The Pharmaceutical Press, 1 Lambeth High Street, London, SE1 7JN, England, 1977. 19 × 25.4 cm. 2077 pp. Price $60. Available from Rittenhouse Book Distributors, 251 S. 24th St., Philadelphia, PA 19103.

The 27th edition of "Martindale" is the largest ever published. It has been revised thoroughly and updated and extended in coverage. The book is divided into six main sections. Part 1, the largest, contains monographs on more than 3100 drugs and ancillary substances in current use throughout the world. Drugs having similar uses or actions are grouped together. Part 2, Supplementary Drugs and Ancillary Substances, describes 1040 new drugs that are too recently introduced or of insufficient importance to be included in Part 1. Also in Part 2 are monographs on obsolescent drugs about which information may still be required.

Part 3 gives the composition and source of more than 1450 over-the-counter medicines marketed in Great Britain. Part 4 is a Directory of Manufacturers, listing full names and addresses of over 1400 manufacturers throughout the world. The Index to Clinical Uses, Part 5, is a guide to drug usage presented in alphabetical order of diseases.

The final section, the General Index, has more than 43,000 entries. Substances are indexed by generic names, proprietary names, chemical names, and synonyms.

This book represents the most comprehensive reference source of information on drugs used throughout the world. Pharmacists as well as professionals and students in all health-related and scientific fields will find this book most valuable. It is a necessity in every pharmacy and medical library.

Staff review

terns in humans. Although other animal species represent convenient models for studying interstitial fluid distribution patterns of antibacterials, we feel that a significant potential for misinterpretation of the data exists unless the protein-binding characteristics of the antibacterial in the animal species are similar to those of humans.

(1) M. C. Meyer and D. E. Guttman, *J. Pharm. Sci.*, **57**, 895 (1968).
(2) J. Robbins, J. E. Rall, and M. Berman, in *Proc. Int. Thyroid Conf.*, Rome, 1965, M. Adriole, Ed., p. 635.
(3) I. M. Klotz, *Ann. N. Y. Acad. Sci.*, **256**, 10 (1972).
(4) J. H. Baldo, S. E. Halford, S. L. Patt, and B. D. Sykes, *Biochemistry*, **14**, 1893 (1975).
(5) N. G. Waterman, L. Scharfenberger, and M. J. Raff, *Antimicrob. Agents Chemother.*, **5**, 294 (1974).
(6) M. Nishida, T. Matsubara, T. Murakawa, Y. Mine, and Y. Yokata, *J. Antibiot. (Tokyo)*, **23**, 284 (1970).
(7) C. H. Nightingale, D. S. Greene, and R. Quintiliani, *J. Pharm. Sci.*, **64**, 1899 (1975).
(8) H. P. Bassaris, R. Quintiliani, E. G. Maderazo, R. C. Tilton, and C. H. Nightingale, *Curr. Ther. Res.*, **19**, 1 (1976).
(9) N. G. Waterman, M. J. Raff, L. Scharfenberger, and P. A. Barnwell, *J. Infect. Dis.*, **133**, 642 (1976).

D. S. Greene *
R. Quintiliani
C. H. Nightingale ˣ
School of Pharmacy
University of Connecticut
Storrs, CT 06268
and
Department of Medicine
Hartford Hospital
Hartford, CT 06115

Received February 11, 1977.
Accepted for publication August 12, 1977.
* Present address: College of Pharmacy, University of Rhode Island, Kingston, RI 02881.
ˣ To whom inquiries should be directed. Present address: School of Pharmacy, State University of New York at Buffalo, Amherst, NY 14260.

BOOKS

REVIEWS

Drug Fate and Metabolism: Methods and Techniques, Vol. 1. Edited by EDWARD R. GARRETT and JEAN L. HIRTZ. Dekker, 270 Madison Ave., New York, NY 10016, 1977. 313 pp. 15 × 23 cm. Price $35.00.

This volume is the first of a proposed series of texts on drug fate and metabolism. As indicated by the editors, the intent of this volume and future volumes is "to review all the techniques, physical, chemical, biological, medical, and mathematical, which can be applied to the study of drug fate in the organism. It is addressed primarily to the research scientist and is devoted to *methods*, with only the minimal theory given for perspective, appreciation, and proper evaluation of results." Volume I meets these goals, with the major emphasis being placed on the use of analytical methods.

Chapters I and II deal with autoradiography and autoradiography in cytopharmacology. Both chapters were written by experts in their area of speciality and are of particular importance to a novice in autoradiography. Chapters III and IV explore the use of electrophoresis and ion-pair extraction and chromatography. Chapter V reviews protein binding, and Chapter VI briefly looks at atomic absorption spectroscopy. The use of a fairly recent analytical method, spin immunoassay, is discussed in Chapter VII. The last chapter describes facilities and other pertinent information needed in animal care.

The editors state that "it was deemed proper to include chapters on methods that would not be modern methods of choice but are of historical importance in evaluating the significance and limitations of the earlier studies in these fields." The selection of these methods is one notable weakness that occurs in Volume I. All of the volumes in this series apparently will be required if an individual desires to have the methods most frequently used in drug metabolism. Another weakness is that the chapters have no rhyme or reason to their order. It would be more sensible to have the chapter on animal care at the beginning of the book since metabolism studies are based on the use of animals as a testing source.

One strong feature of this text, in addition to its being well written, is a list of the source of supplies and equipment included in Chapters I and III. This list is particularly important in saving time that would otherwise be spent in looking for this material. The reviewer recommends this volume for the researcher in the area of drug metabolism, especially the analytical chemist, pharmacologist, and toxicologist.

Reviewed by Gerald W. Slywka
School of Pharmacy
Ferris State College
Big Rapids, MI 49307

Martindale: The Extra Pharmacopoeia. 27th Ed. Edited by AINLEY WADE and JAMES E. F. REYNOLDS. The Pharmaceutical Press, 1 Lambeth High Street, London, SE1 7JN, England, 1977. 19 × 25.4 cm. 2077 pp. Price $60. Available from Rittenhouse Book Distributors, 251 S. 24th St., Philadelphia, PA 19103.

The 27th edition of "Martindale" is the largest ever published. It has been revised thoroughly and updated and extended in coverage. The book is divided into six main sections. Part 1, the largest, contains monographs on more than 3100 drugs and ancillary substances in current use throughout the world. Drugs having similar uses or actions are grouped together. Part 2, Supplementary Drugs and Ancillary Substances, describes 1040 new drugs that are too recently introduced or of insufficient importance to be included in Part 1. Also in Part 2 are monographs on obsolescent drugs about which information may still be required.

Part 3 gives the composition and source of more than 1450 over-the-counter medicines marketed in Great Britain. Part 4 is a Directory of Manufacturers, listing full names and addresses of over 1400 manufacturers throughout the world. The Index to Clinical Uses, Part 5, is a guide to drug usage presented in alphabetical order of diseases.

The final section, the General Index, has more than 43,000 entries. Substances are indexed by generic names, proprietary names, chemical names, and synonyms.

This book represents the most comprehensive reference source of information on drugs used throughout the world. Pharmacists as well as professionals and students in all health-related and scientific fields will find this book most valuable. It is a necessity in every pharmacy and medical library.

Staff review

Journal of Pharmaceutical Sciences

DECEMBER 1977

VOLUME 66 NUMBER 12

MARY H. FERGUSON
Editor

SHELLY ELLIOTT
Production Editor

JANET D. SHOFF
Copy Editor

EDWARD G. FELDMANN
Contributing Editor

SAMUEL W. GOLDSTEIN
Contributing Editor

DAVID BOHARDT
Director of Publications

L. LUAN CORRIGAN
Assistant Director of Publications

EDITORIAL ADVISORY BOARD

JOHN AUTIAN	HARRY B. KOSTENBAUDER
NORMAN R. FARNSWORTH	HERBERT A. LIEBERMAN
WILLIAM O. FOYE	DAVID E. MANN, JR.
WILLIAM J. JUSKO	GERALD J. PAPARIELLO

The *Journal of Pharmaceutical Sciences* is published monthly by the American Pharmaceutical Association at 2215 Constitution Ave., N.W., Washington, DC 20037. Second-class postage paid at Washington, D.C., and at additional mailing office.

All expressions of opinion and statements of supposed fact appearing in articles or editorials carried in this journal are published on the authority of the writer over whose name they appear and are not to be regarded as necessarily expressing the policies or views of the American Pharmaceutical Association.

Offices—Editorial, Advertising, and Subscription Offices: 2215 Constitution Ave., N.W., Washington, DC 20037. Printing Offices: 20th & Northampton Streets, Easton, PA 18042.

Annual Subscriptions—United States and foreign, industrial and government institutions $50, educational institutions $50, individuals *for personal use only* $30; single copies $5. All foreign subscriptions add $5 for postage. Subscription rates are subject to change without notice. Members of the American Pharmaceutical Association may elect to receive the *Journal of Pharmaceutical Sciences* as a part of their annual $70 (foreign $75) APhA membership dues.

Claims—Missing numbers will not be supplied if dues or subscriptions are in arrears for more than 60 days or if claims are received more than 60 days after the date of the issue, or if loss was due to failure to give notice of change of address. The Association cannot accept responsibility for foreign delivery when its records indicate shipment has been made.

Change of Address—Members and subscribers should notify at once both the Post Office and the American Pharmaceutical Association, 2215 Constitution Ave., N.W., Washington, DC 20037, of any change of address.

Microfilm—Microfilm volumes are available from University Microfilms International, 300 N. Zeeb Road, Ann Arbor, MI 48106.

© Copyright 1977, American Pharmaceutical Association, 2215 Constitution Ave., N.W., Washington, DC 20037; all rights reserved.

PREDICTION: NEW DRUG LAW COMING

Washington, as the focal point of the federal government operation, has often been characterized as a "three-ring circus." That's probably a fair characterization, and it would be equally fair to say that, in recent years at least, one of those three rings has been devoted exclusively to health care-related issues. Moreover, from our own particular point of interest, it is difficult to recall very many of these issues that didn't involve drugs and pharmaceuticals partially, if not exclusively.

Not surprisingly, therefore, various bills have been introduced each year both in the House and the Senate calling for some revision of the principal law that deals with pharmaceuticals—namely, the Federal Food, Drug, and Cosmetic Act. But of the hundreds of such bills sponsored, only a few relatively minor ones have been enacted.

Historically, the present law was passed in 1938, and it represented the first and only major overhaul of federal drug legislation since the original Pure Food and Drugs Act became law in 1906. Furthermore, the Drug Amendments of 1962—which, among other things, added the concept of efficacy as a condition of new drug approval—constituted the last major change in the 1938 Act.

Virtually all bills subsequently put into the legislative hopper have gone nowhere, although some of them enjoyed serious consideration to the point that congressional hearings were conducted with APhA witnesses and others trooping dutifully to Capitol Hill to present views and testimony on the particular proposal at hand. In the words of one cynical association spokesman, "Senator X snaps his fingers, and like so many trained show dogs we all go through our routine, knowing full well nothing will come of it, but fearful that if we don't we'll appear to be asleep for not voicing our views on the subject!"

Well, it now looks to us and to at least some other long time "Washington-watchers" that the preliminaries are about to end and 1978 may well be the year that we see a top-to-bottom new drug law go on the books. Congress has become increasingly restless, involved, and concerned. Public controversy has been stirred by issues such as the proposed saccharin ban, the efforts to keep laetrile off the market, the purported drug lag, the allegations of disgruntled FDA employees, and a barrage of lawsuits filed against the FDA and its parent department by diverse groups ranging from consumers to professional societies to the drug industry.

In the case of many issues that get into the congressional mill, there is some division along party, philosophical, or interest lines as to a group seeking new legislation and a group wishing to thwart new legislation. However, regarding drug legislation, the situation in the past few years is reminiscent of comedian Jimmy Durante's famous line: "Everybody wants to get into the act!" Liberals and conservatives, Republicans and Democrats, urban representatives and rural representatives, have all sponsored various proposals for major changes in the current drug laws.

If this were not indication enough that something might be going to happen this time around, the odds became enormously greater with a minor bombshell announcement this past October.

HEW Secretary Joseph A. Califano, Jr., unexpectedly came out with a call for "a top-to-bottom, thorough overhaul" of the nation's drug regulatory laws. And in the year that Mr. Califano has been on the job, Washingtonians have come to know that when this cabinet officer speaks, he means business. Consequently, not only is there philosophic support from the Carter administration for drug reform legislation, but it most likely will benefit from the push of one of the most activist people in the current administration.

Mr. Califano's statement was greeted warmly by a broad spectrum of interested parties. These ranged from consumer organizations to drug industry trade groups. The public press reported that "top staff members for Sen. Edward M. Kennedy and Rep. Paul Rogers, said that the two chairmen of the key health committees in the Senate and House were enthusiastic about the proposed changes outlined by Califano." Other congressional figures were also identified as voicing their concurrence.

Collectively, these developments lead us to the prediction in the headline of this column. A member of Senator Kennedy's staff speculated that Califano's position meant that a bill would pass the Senate by mid-1978; he added, "The key point is that this is the first time since 1962 that all the major actors are in agreement." Or as the astrologists would put it: "The stars are right!"

Edward G. Feldmann

Journal of Pharmaceutical Sciences

DECEMBER 1977

VOLUME 66 NUMBER 12

MARY H. FERGUSON
Editor

SHELLY ELLIOTT
Production Editor

JANET D. SHOFF
Copy Editor

EDWARD G. FELDMANN
Contributing Editor

SAMUEL W. GOLDSTEIN
Contributing Editor

DAVID BOHARDT
Director of Publications

L. LUAN CORRIGAN
Assistant Director of Publications

EDITORIAL ADVISORY BOARD

JOHN AUTIAN	HARRY B. KOSTENBAUDER
NORMAN R. FARNSWORTH	HERBERT A. LIEBERMAN
WILLIAM O. FOYE	DAVID E. MANN, JR.
WILLIAM J. JUSKO	GERALD J. PAPARIELLO

The *Journal of Pharmaceutical Sciences* is published monthly by the American Pharmaceutical Association at 2215 Constitution Ave., N.W., Washington, DC 20037. Second-class postage paid at Washington, D.C., and at additional mailing office.

All expressions of opinion and statements of supposed fact appearing in articles or editorials carried in this journal are published on the authority of the writer over whose name they appear and are not to be regarded as necessarily expressing the policies or views of the American Pharmaceutical Association.

Offices—Editorial, Advertising, and Subscription Offices: 2215 Constitution Ave., N.W., Washington, DC 20037. Printing Offices: 20th & Northampton Streets, Easton, PA 18042.

Annual Subscriptions—United States and foreign, industrial and government institutions $50, educational institutions $50, individuals *for personal use only* $30; single copies $5. All foreign subscriptions add $5 for postage. Subscription rates are subject to change without notice. Members of the American Pharmaceutical Association may elect to receive the *Journal of Pharmaceutical Sciences* as a part of their annual $70 (foreign $75) APhA membership dues.

Claims—Missing numbers will not be supplied if dues or subscriptions are in arrears for more than 60 days or if claims are received more than 60 days after the date of the issue, or if loss was due to failure to give notice of change of address. The Association cannot accept responsibility for foreign delivery when its records indicate shipment has been made.

Change of Address—Members and subscribers should notify at once both the Post Office and the American Pharmaceutical Association, 2215 Constitution Ave., N.W., Washington, DC 20037, of any change of address.

Microfilm—Microfilm volumes are available from University Microfilms International, 300 N. Zeeb Road, Ann Arbor, MI 48106.

© Copyright 1977, American Pharmaceutical Association, 2215 Constitution Ave., N.W., Washington, DC 20037; all rights reserved.

PREDICTION: NEW DRUG LAW COMING

Washington, as the focal point of the federal government operation, has often been characterized as a "three-ring circus." That's probably a fair characterization, and it would be equally fair to say that, in recent years at least, one of those three rings has been devoted exclusively to health care-related issues. Moreover, from our own particular point of interest, it is difficult to recall very many of these issues that didn't involve drugs and pharmaceuticals partially, if not exclusively.

Not surprisingly, therefore, various bills have been introduced each year both in the House and the Senate calling for some revision of the principal law that deals with pharmaceuticals—namely, the Federal Food, Drug, and Cosmetic Act. But of the hundreds of such bills sponsored, only a few relatively minor ones have been enacted.

Historically, the present law was passed in 1938, and it represented the first and only major overhaul of federal drug legislation since the original Pure Food and Drugs Act became law in 1906. Furthermore, the Drug Amendments of 1962—which, among other things, added the concept of efficacy as a condition of new drug approval—constituted the last major change in the 1938 Act.

Virtually all bills subsequently put into the legislative hopper have gone nowhere, although some of them enjoyed serious consideration to the point that congressional hearings were conducted with APhA witnesses and others trooping dutifully to Capitol Hill to present views and testimony on the particular proposal at hand. In the words of one cynical association spokesman, "Senator X snaps his fingers, and like so many trained show dogs we all go through our routine, knowing full well nothing will come of it, but fearful that if we don't we'll appear to be asleep for not voicing our views on the subject!"

Well, it now looks to us and to at least some other long time "Washington-watchers" that the preliminaries are about to end and 1978 may well be the year that we see a top-to-bottom new drug law go on the books. Congress has become increasingly restless, involved, and concerned. Public controversy has been stirred by issues such as the proposed saccharin ban, the efforts to keep laetrile off the market, the purported drug lag, the allegations of disgruntled FDA employees, and a barrage of lawsuits filed against the FDA and its parent department by diverse groups ranging from consumers to professional societies to the drug industry.

In the case of many issues that get into the congressional mill, there is some division along party, philosophical, or interest lines as to a group seeking new legislation and a group wishing to thwart new legislation. However, regarding drug legislation, the situation in the past few years is reminiscent of comedian Jimmy Durante's famous line: "Everybody wants to get into the act!" Liberals and conservatives, Republicans and Democrats, urban representatives and rural representatives, have all sponsored various proposals for major changes in the current drug laws.

If this were not indication enough that something might be going to happen this time around, the odds became enormously greater with a minor bombshell announcement this past October.

HEW Secretary Joseph A. Califano, Jr., unexpectedly came out with a call for "a top-to-bottom, thorough overhaul" of the nation's drug regulatory laws. And in the year that Mr. Califano has been on the job, Washingtonians have come to know that when this cabinet officer speaks, he means business. Consequently, not only is there philosophic support from the Carter administration for drug reform legislation, but it most likely will benefit from the push of one of the most activist people in the current administration.

Mr. Califano's statement was greeted warmly by a broad spectrum of interested parties. These ranged from consumer organizations to drug industry trade groups. The public press reported that "top staff members for Sen. Edward M. Kennedy and Rep. Paul Rogers, said that the two chairmen of the key health committees in the Senate and House were enthusiastic about the proposed changes outlined by Califano." Other congressional figures were also identified as voicing their concurrence.

Collectively, these developments lead us to the prediction in the headline of this column. A member of Senator Kennedy's staff speculated that Califano's position meant that a bill would pass the Senate by mid-1978; he added, "The key point is that this is the first time since 1962 that all the major actors are in agreement." Or as the astrologists would put it: "The stars are right!"

Edward G. Feldmann

Journal of Pharmaceutical Sciences

DECEMBER 1977
VOLUME 66 NUMBER 12

RESEARCH ARTICLES

Design and Evaluation of an Automated System for *In Vitro* Dissolution Testing Utilizing a High-Pressure Liquid Chromatographic Multiport Switching Valve

JOHN S. KENT ˣ, PAUL P. WONG, and G. P. HEGDE

Abstract □ An automated system for the simultaneous dissolution testing of six samples was developed consisting of four basic units: dissolution vessels and stirring unit, a peristaltic pump, a rotary stream multiport switching valve and programmer, and a UV spectrophotometer with recorder. Among the major advantages of such a system are: (*a*) paddle or basket stirring with variable speed is used, (*b*) the tablet or capsule (wire coil required) locates reproducibly at the bottom of a round-bottom reaction flask when utilizing paddle-type stirring, (*c*) a USP basket for tablet or capsule dissolution testing can be used, (*d*) continuous or intermittent sampling is possible, (*e*) the flow system readily adapts to UV–visible detector or fluorescence spectroscopy, (*f*) the system readily adapts to automated determination of the intrinsic dissolution of a material, and (*g*) the cost is low because of the multiport switching valve and inexpensive UV monitor required. Studies were performed using this apparatus to demonstrate the response characteristics of the system, its reproducibility, potential problems, and precautions required. This dissolution system was used to determine the dissolution characteristics of a new steroid tablet formulation, including a formulation and lot demonstrated to be bioavailable.

Keyphrases □ Dissolution testing—six samples simultaneously, automated system designed and evaluated □ Automated systems—dissolution testing of six samples simultaneously, system designed and evaluated

Dissolution rate testing is an important aspect (1, 2) of dosage form development. It can provide a means for the prediction of drug bioavailability. It is an important test during the optimization of a tablet or capsule formulation as well as a control test on the final product. Numerous dissolution rate testing methods have been employed, all having the following essential features: a dissolution container, a device for agitating the dissolution fluid, a method for sampling or transporting the dissolution fluid, and an analytical technique for measuring the dissolved drug.

To make the procedure more efficient, multiple dissolution systems with automated sampling and analysis have been designed and tested (3–13). The systems differ in the type of dissolution vessel and stirring used but generally employ one of two sampling designs. Most systems (3–5, 8–13) use a pumping arrangement that causes flow from the dissolution vessel to a spectrometer and back to the dissolution vessel. With multiple dissolution vessels, the spectrometer must be capable of switching cells at preprogrammed intervals to accommodate the multiple samples. Alternatively, the switching of cells at the spectrometer can be replaced by a stream switching valve. One commercially available system (7) utilizes this technique, and another application of this configuration was reported recently (6).

The objective of this research was to determine if a satisfactory and economical dissolution system could be constructed using a standard dissolution vessel and stirring apparatus in conjunction with a peristaltic pump, high-pressure liquid chromatographic (HPLC) multiport stream switching valve, and UV spectrometer. This report discusses the construction and testing of such a system and its application to tablet and capsule dissolution testing; the advantages and disadvantages are described.

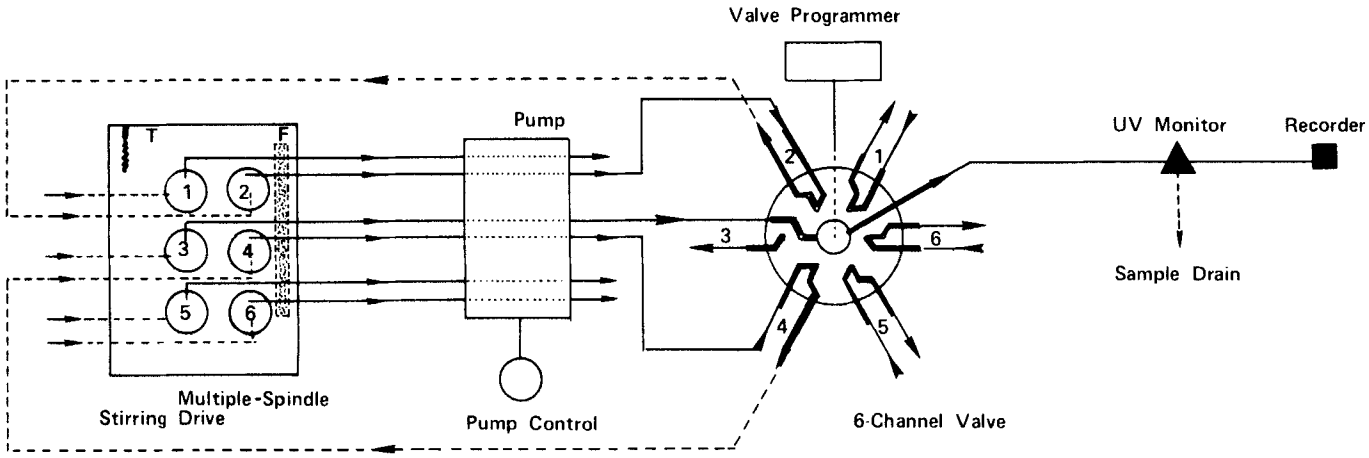

Figure 1—*Schematic diagram of automated dissolution apparatus. Key: T, thermostat; and F, sintered-glass or Millipore filter.*

EXPERIMENTAL

Automated Dissolution System—The automated dissolution system is shown in Fig. 1, and the instruments used are described as follows.

Multiple-Spindle Stirring Drive with Variable Speed Drive Control[1]—This unit has the capacity for six dissolution vessels. The stirring can be accomplished by paddles or L-shaped stirrers (14) or the USP basket. This assortment allows the versatility for performing tablet or capsule dissolution testing as well as intrinsic dissolution rate determination.

Dissolution Vessel—A closeup of the dissolution vessel, a 1-liter round-bottom reaction kettle[2], is shown in Fig. 2. This particular stirring propeller[3] is polyethylene. Figure 3 pictures the two types of sampling devices used. The filter device consists of an 18-gauge needle[4] (i) joined to a connector[4] (ii), which is connected to a filter holder[5] (iii). The remaining adaptor[4] (iv) connects the filter to the tubing.

The second type of sampling device (Fig. 3*b*) was a modified sintered-glass filter. The cup of a sintered-glass filter[6] was cut off at the glass frit. The stem was then replaced with a capillary tube (0.8 mm i.d. × 4.1 mm o.d.; 14-cm length), with 1.5 cm of the end ground to a smaller diameter (approximately 3.0 mm) to accept the silicone rubber tubing. The filter holder sampling device requires filter replacement after each use, and the sintered-glass filter requires cleaning between samples. Under these conditions, no filter clogging was observed with the formulations and products tested.

The sintered-glass filter has been acceptable for tablets and capsules other than the cloprednol tablets and capsules tested, including certain commercially available prednisone and prednisolone tablets and capsules and tablets of three new nonhormonal anti-inflammatory drugs. The acceptability of either filter depends on the tablet or capsule formulation undergoing dissolution testing.

Pump—A peristaltic tubing pump[7] with six pump heads was used. The tubing between the dissolution vessel and the valve was silicone rubber (0.8 mm i.d.; 4.13 mm o.d.). The connection of this tubing to the switching valve was accomplished as indicated in Fig. 4.

Two sizes of polytef tubing were used to make the connector. The one[8] that formed the sleeve was 1.5 mm i.d. × 3.0 mm o.d.; the other[8] was 0.8 mm i.d. × 1.5 mm o.d. The return tubing from the valve to the dissolution vessel was also polytef[9], 0.8 mm i.d. × 1.5 mm o.d., as was the tubing connection between the switching valve and the UV flowcell.

Six-Channel Stream Selection Valve for HPLC and Sequential Valve Programmer—The stream selection valve[10] is designed for the selection of one stream to send to the analyzer (UV monitor in this case) and for the continuous return of all other streams. The valve is of rotary design and advances *via* an air solenoid. The valve is controlled by a special programmer[10] that allows the switching between streams to occur at a preset time interval. The available intervals are 0–99 sec and 0–9.9 and 0–99 min.

UV Monitor and Recorder—The UV monitor[8] monitors the effluent from the HPLC column. The unit allows multiple-frequency monitoring by use of interchangeable filters. The absorbance ranges from 0.05 to 2.0 absorbance units full scale. The instrument utilizes a 1-cm 100-μl bubble-free flowcell. Other cells with shorter path lengths also are available.

The absorbance readings were recorded on a 25.4-cm laboratory chart recorder[11].

Volume in Tubing System and Lag Time—The tubing sections of the dissolution systems were designed to contain a small volume. This volume allows the utilization of the small bore switching valve and prevents a large dissolution fluid loss after it passes through the detector. This procedure generally does not require concentration corrections for the small volume loss from the dissolution vessel. The pump speed of 50 rpm delivers 2.4 ml/min, which is 80% of the theoretical rate for that size pump head. The difference can be assigned to the flow resistances in the system.

With a total volume in the system from the vessel to the detector (filter stick configuration design) of only 0.90 ml, there is a lag time of approximately 0.375 min between the vessel and the detector. The observed lag time from the switching valve to the detector is 0.09 min, which compares favorably with that calculated for a volume of 0.2 ml and a flow rate of 2.4 ml/min. Additional time is required for the true absorbance level to be reached because of the mixing that occurs as the fluid flows through the tubing and flowcell. The minimum switching interval that can then be used is 1 min. The time values reported here are not corrected for the instrument lag time.

Intrinsic Dissolution Studies—The intrinsic dissolution studies were performed using a static disk, a variation of that described previously (15, 16). The die was constructed of stainless steel (diameter 3.81 cm, thickness 0.953 cm, and diameter of hole 1.27 cm). Cloprednol[12] (6-chloro-11β,17α,21-trihydroxypregna-1,4,6-triene-3,20-dione) was compressed in the die using a hydraulic press[13] at 1134 kg. The pure steroid tablet was positioned at the die surface, and the unit was placed at the bottom of the dissolution vessel. The polyethylene propeller was positioned 2.5 cm above the bottom of the vessel and revolved at 100 rpm; 0.5 liter of deaerated, distilled water was used.

Tablet Dissolution Studies—Tablet dissolution studies were performed using deaerated, distilled water. The polyethylene propeller was used as described previously, or the USP basket (40 mesh) was located 2.5 cm from the bottom of the dissolution flask. With the propeller stirrer, the tablet was added to the dissolution vessel and then descended to the bottom of the vessel.

The polyethylene propeller stirrer was used because: (*a*) it provided equivalent or better mixing characteristics than other commercially

[1] Model 72R115, Hanson Research Corp., Northridge, CA 91324.
[2] Kimax 33700-S1, Owens-Illinois, Toledo, OH 43666.
[3] No. S-76680, Sargent-Welch, Anaheim, CA 92803.
[4] Needle 1293 (T462 LNR), connector 3114 (MLL/MLL), and adaptor 3084 (L 1609), Becton-Dickinson & Co., Rutherford, NJ 07070.
[5] Swinnex (13 mm), Millipore Corp., Bedford, MA 01730.
[6] Kimble 28400, Scientific Products, Menlo Park, CA 94025.
[7] Variable speed Masterflex 7545-13 with pump heads No. 7013 and tubing 6411-41, Cole-Parmer, Chicago, IL 60648.
[8] Sleeve tubing No. 200-32, inner tubing No. 200-31, and Biochemical UV monitor model 150, Altex Scientific, Inc., Berkeley, CA 94710.
[9] No. 3114-030, Glenco Scientific Inc., Houston, TX 77007.
[10] Valve ASF-6-HPa-HC and programmer VSP-216R, Valco Instruments Co., Houston, TX 77024.
[11] Model 261, Linear Instruments Corp., Irvine, CA 92705.
[12] Syntex Corp., Palo Alto, CA 94304.
[13] Fred S. Carver Co., Summit, N.J.

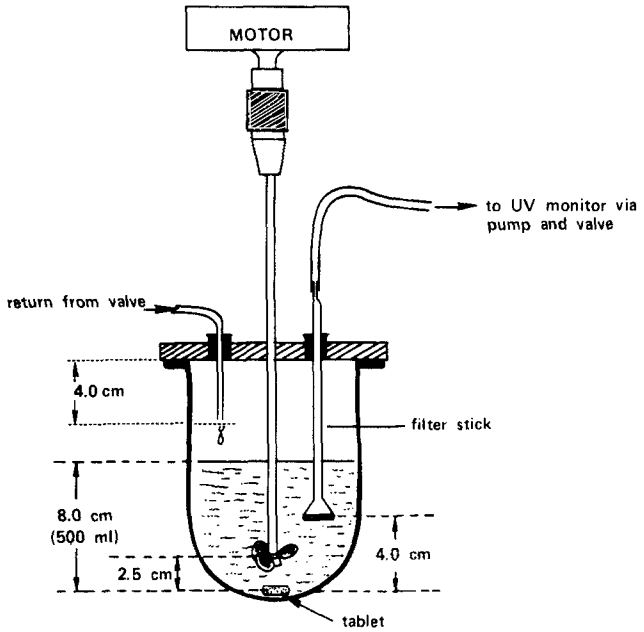

Figure 2—*Dissolution vessel as set for tablet dissolution.*

available stirrers, (*b*) it was in a fixed position on the shaft so it was not subject to a shift in position, (*c*) it was essentially unbreakable, and (*d*) it was readily available commercially.

RESULTS AND DISCUSSION

Intrinsic Dissolution as a Test for System Reproducibility—A measure of the reproducibility of the dissolution system was determined by comparing the intrinsic dissolution rate of cloprednol. Three of the six dissolution vessels were randomly chosen to be representative of the dissolution system; the results from these determinations are given in Table I. To determine if the dissolution rate (slope) of each run was equivalent, the Student *t* test (17) was performed on each pair of results. From the calculated values (Table I), the dissolution rates were equivalent at the 95% level of significance.

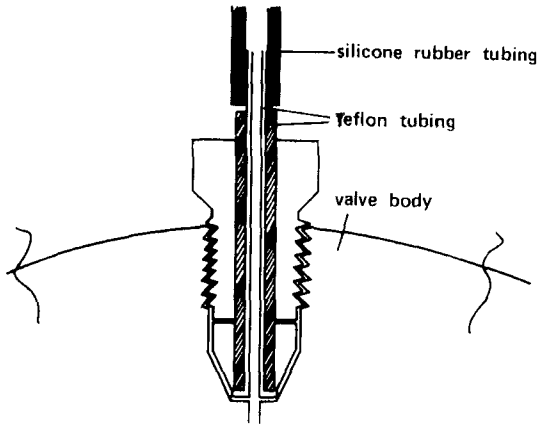

Figure 4—*Diagram of silicone tubing connection to inlet of switching valve.*

Effect of Stirring Rate on Cloprednol Tablet Dissolution—The described tablet dissolution apparatus was used employing a polyethylene stirrer and sintered-glass filter. The effect of stirring on cloprednol tablet dissolution is demonstrated in Fig. 5. The tablet batch was representative of those produced during the later stages of development. The results indicated an increase in dissolution rate with an increase in stirring, as expected. Although an increased stirring rate may be used to produce an increased dissolution rate, the risk exists that important differences in dissolution of tablets of different lots and/or formulation composition may be masked. A slow stirring rate, however, may produce a tablet dissolution condition that is too sensitive; *i.e.*, differences in the dissolution

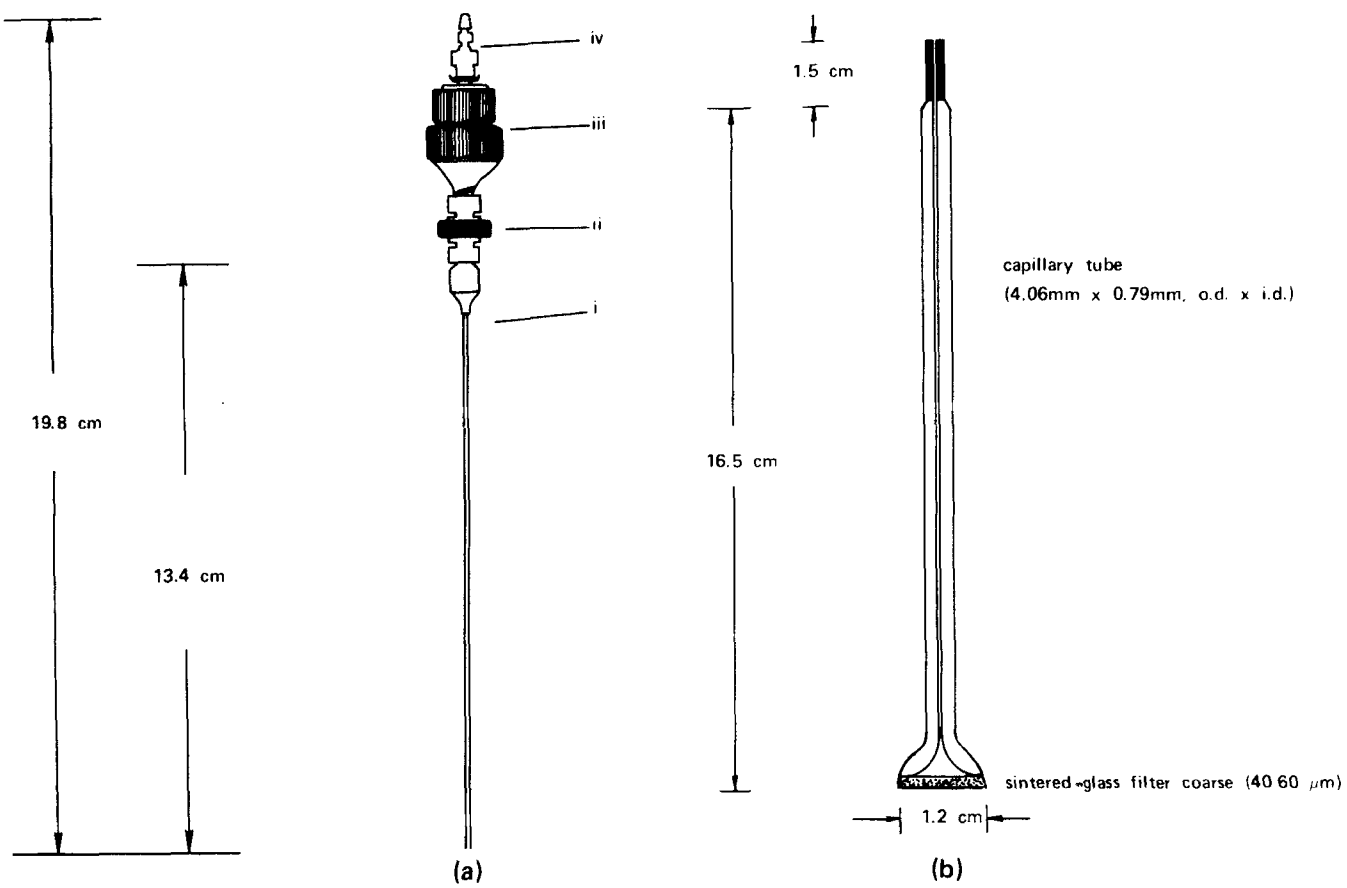

Figure 3—*Dissolution sampling devices. Key: a, filter device; and b, filter stick.*

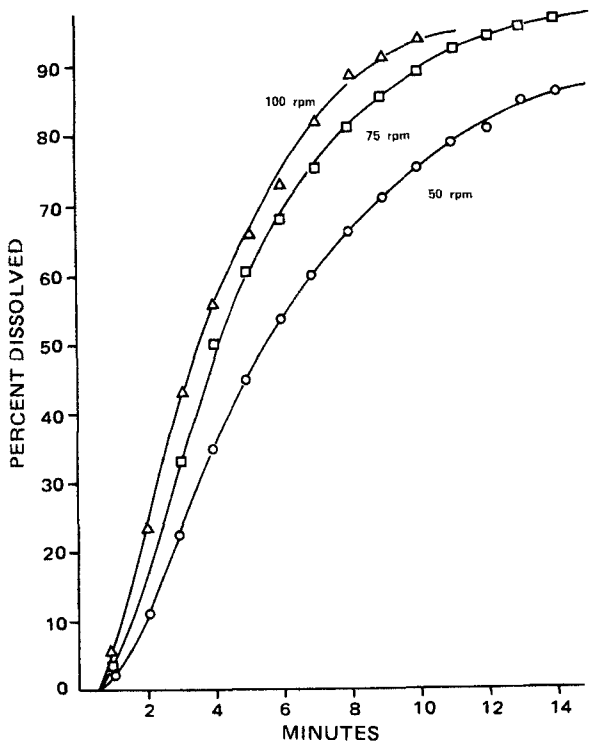

Figure 5—*Effect of stirring rate on the dissolution rate of 2.5-mg cloprednol tablets at a pump speed of 50 rpm and 37°.*

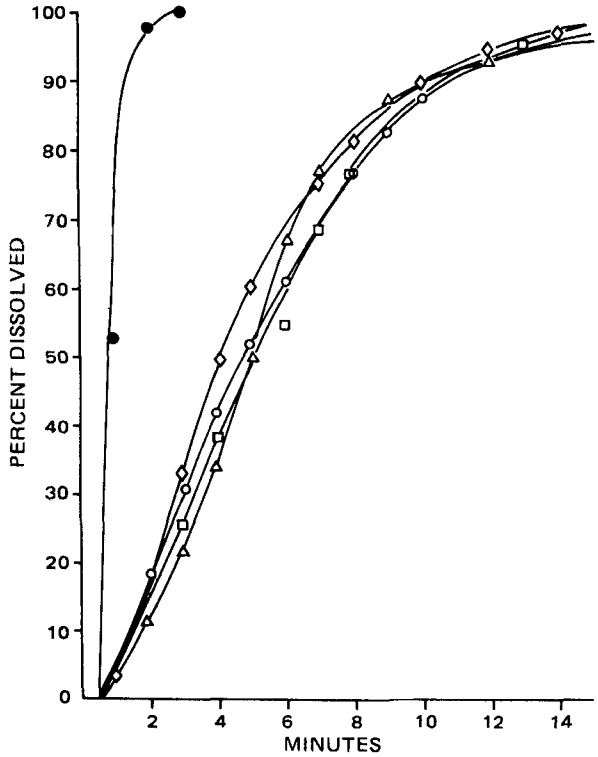

Figure 6—In vitro *dissolution of four representative 2.5-mg cloprednol tablet batches [Lots S (○), U (△), T (□), and W (◇)] and one experimental batch [Lot Z (●)]. The pump speed was 50 rpm, the propeller speed was 75 rpm, and the temperature was 37°. The automated dissolution apparatus with a coarse sintered-glass filter was used.*

rate of tablet lots and/or formulations may be observed that have no relevance to *in vivo* bioavailability or absorption rate.

Ideally, a stirring rate should be chosen to correlate with bioavailability. The choice of stirring rate was discussed previously (1); short of having a bioavailability correlation, the stirring rate should distinguish formulation differences and correspond to that reported in the pertinent literature. The stirring rate of 75 rpm in the studies on cloprednol tablet dissolution was chosen in that manner.

Dissolution Profiles of Representative Cloprednol Tablet Batches—The dissolution profiles of four representative batches (S, U, T, and W) of cloprednol tablets were determined (Fig. 6). The dissolution procedure was described previously. The tablet hardness values of these batches (Table II) were within the hardness specification for cloprednol tablets. As shown in Fig. 7, the dissolution profiles and the percent dissolved at 10 min were very similar.

Preliminary Examination of Effect of Cloprednol Particle Size on Tablet Dissolution—The dissolution results presented thus far have been for tablets prepared by a wet granulation process. The particle size of cloprednol for Batches S, U, T, and W was monitored, and most particles prior to granulation were 100–250 μm. The dissolution from tablets made with cloprednol of this particle size was rapid and complete, as discussed previously. It was judged important to determine whether a reduction in particle size of the cloprednol would further improve its dissolution from tablets.

Accordingly, micronized cloprednol (particle size ≤ 10 μm) was incorporated into a direct compression tablet formulation. The dissolution profile of this lot (Z) indicated improved dissolution characteristics (Fig. 6). Some improvement, besides greater surface area due to micronization, may result from: (*a*) softer tablets (Table II) or (*b*) the difference between the direct compression and granulation formulations. These possibilities are currently being explored. The importance of the increased tablet dissolution rate with the micronized material may be considered limited after study of the following results on bioavailability and dissolution.

***In Vitro* Dissolution Results from a Tablet Lot and Two Capsule Lots Used in a Bioavailability Study**—The *in vitro* dissolution of tablets may become a meaningful test upon establishing its relationship with bioavailability. During cloprednol tablet development, many dissolution profiles were obtained on formulation modifications, tablet hardness, *etc.*, some of which have been presented here. To provide a tablet lot for *in vivo* bioavailability testing, the following rationale was used.

The tablet formulation had certain ranges for the levels of excipients used, which allowed formula changes (within the designated range) during scale-up development. If the "poorest" formula was chosen, that being the one with excipients adjusted within their ranges to provide a tablet with a reduced dissolution rate, a base level could be established for a dissolution test, provided it exhibited satisfactory bioavailability. A tablet (C) such as this was manufactured and used in a bioavailability study. Also included were two capsule lots previously used in clinical studies and an oral solution.

The results of this study were reported previously (18) and indicated that the two capsules and tablet were equivalently bioavailable. The *in vitro* dissolution data obtained for these solid oral dosage forms are presented in Fig. 7. The difference between the two capsule formulations

Table I—Cloprednol Intrinsic Dissolution Results as a Measure of the Reproducibility of the Dissolution System

Minutes	Absorbance of Run[a]		
	a	*b*	*c*
14	0.033	0.032	0.034
26	0.062	0.059	0.062
38	0.086	0.082	0.084
50	0.110	0.104	0.106
62	0.132	0.126	0.128
74	0.148	0.144	0.144
Least-squares calculation for slope, absorbance unit/min	0.00192	0.00186	0.00183

[a] Calculated t values: *a versus b* = 0.505, *b versus c* = 0.313, and *a versus c* = 0.679; $t_{0.95}$ (df = 8) = 1.86.

Table II—Cloprednol Tablet Hardness and *In Vitro* Dissolution Data

Tablet Batch	Hardness (Strong–Cobb) ± *SD*	Percent Dissolved in 10 min ± *SD*
Z	6.22 ± 0.50	100.00 ± 0.00
S	7.57 ± 0.83	87.95 ± 8.90
U	9.11 ± 0.48	89.08 ± 4.30
T	9.09 ± 0.49	89.28 ± 4.07
W	9.62 ± 0.68	89.48 ± 5.09

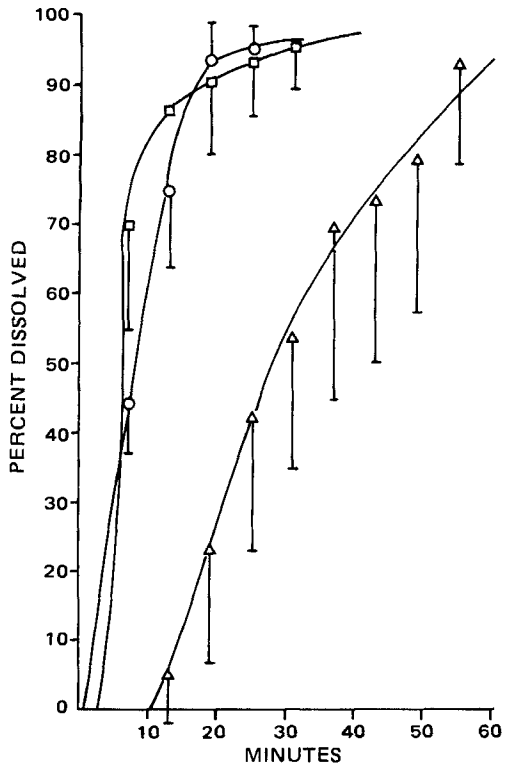

Figure 7—In vitro *dissolution of two 1.25-mg capsule lots [A (□) and B (△)] and one 2.50-mg tablet lot [C (○)], all shown to be bioequivalent and bioavailable. The pump speed was 50 rpm, the propeller speed was 75 rpm, and the temperature was 37°. The automated dissolution apparatus with a coarse sintered-glass filter was used.*

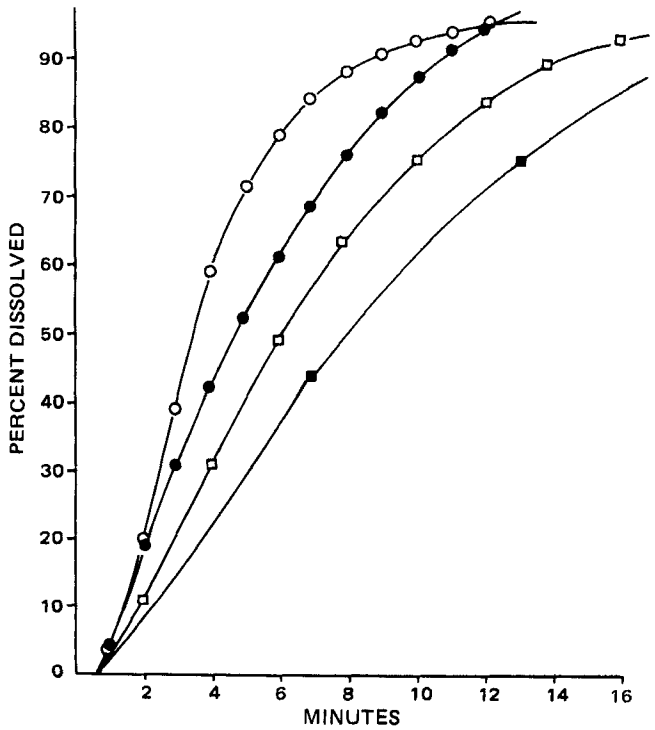

Figure 8—In vitro *dissolution of two formulations of cloprednol tablets comparing the USP basket and propeller method. Key: ○, Lot S, USP basket method, 50 rpm; ●, Lot S, propeller method, 75 rpm; □, Lot C, USP basket method, 50 rpm; and ■, Lot C, propeller method, 75 rpm. The pump speed was 50 rpm, and the temperature was 37°. The automated dissolution apparatus with a coarse sintered-glass filter was used.*

was that Tablet B, with the slower dissolution, contained lubricant (magnesium stearate) and Tablet A did not. These differences in dissolution were observed as a twofold difference in plasma levels at 0.25 hr in the bioavailability study (18). These differences were not significant and disappeared at 0.5 hr.

Therefore, for all subsequent tablet batches to be considered completely bioavailable, their *in vitro* dissolution rate must be comparable to or better than the *in vitro* dissolution rate of the tablets demonstrated to be bioavailable. The major risk of such a requirement is that the *in vitro* dissolution test may be too rigorous, since an *in vitro* dissolution profile has not been established for a cloprednol tablet that was poorly bioavailable.

Comparison to USP Basket Dissolution Procedure—One further measure of the discriminatory nature of this *in vitro* dissolution test is to compare it to the USP basket dissolution procedure. The USP requires dissolution testing of prednisolone and prednisone tablets, both steroids similar in their physical properties to cloprednol. The USP test for these two steroids designates a basket rotation of 100 rpm and 60% dissolution in 20 min.

With a rotation of 100 rpm, the cloprednol tablets dissolved extremely rapidly; therefore, the results reported (Fig. 8) are at 50 rpm. Even at this rate, the dissolution rates with the USP basket are faster than those observed with the propeller method. The cloprednol tablet dissolution results under these conditions were more than adequate to pass the USP requirements for the steroid tablets of prednisone and prednisolone, indicating that the propeller dissolution method has greater sensitivity than the USP basket dissolution test for prednisone and prednisolone tablets. As discussed previously, this result may indicate that the propeller dissolution method for cloprednol tablets can distinguish differences in tablet batches or formulation changes that are not distinguished *in vivo*.

This finding points to a particular difficulty in choosing an *in vitro* dissolution procedure that will show dissolution differences corresponding to differences *in vivo*. It is expected that the *in vitro* procedure will detect some dissolution differences not detected *in vivo*, as was adequately shown by Sullivan *et al.* (19). Obviously, a highly sensitive dissolution procedure provides a safety margin during the early product life of a new drug entity. The dissolution procedure may then be refined as more data become available.

REFERENCES

(1) L. J. Leeson and J. T. Carstensen, "Dissolution Technology," APhA Academy of Pharmaceutical Sciences, Washington, D.C., 1974, p. 163.

(2) J. Swarbrick, "Current Concepts in the Pharmaceutical Sciences: Biopharmaceutics," Lea & Febiger, Philadelphia, Pa., 1970, p. 265.

(3) W. F. Beyer and E. W. Smith, *J. Pharm. Sci.*, **60**, 1556 (1971).

(4) C. Cakiryildiz, P. J. Mehta, W. Rahmen, and D. Schoenleber, *ibid.*, **64**, 1692 (1975).

(5) R. W. Castello, G. Jellinek, J. M. Konieczny, K. C. Kwan, and R. O. Toberman, *ibid.*, **57**, 485 (1968).

(6) P. J. Cioffi, H. M. Abdou, and A. T. Warren, *ibid.*, **65**, 1234 (1976).

(7) "Dissograph Technical Information," Hanson Research Corp., Northridge, Calif.

(8) R. Fatton, D. Fielding, S. C. Khanna, and A. Richter, *Pharm. Acta Helv.*, **47**, 487 (1972).

(9) A. Ferrari and A. J. Khoury, *Ann. N.Y. Acad. Sci.*, **130**, 661 (1965).

(10) J. B. Johnson, P. G. Kennedy, and S. H. Rubin, *J. Pharm. Sci.*, **63**, 1931 (1974).

(11) J. W. Poole, *Drug Inf. Bull.*, **3**, 8 (1969).

(12) A. C. Shah, C. B. Peot, and J. F. Ochs, *J. Pharm. Sci.*, **62**, 671 (1973).

(13) A. C. Shah and J. F. Ochs, *ibid.*, **63**, 110 (1974).

(14) G. Haringer, B. J. Poulsen, and R. N. Havemeyer, *ibid.*, **62**, 130 (1973).

(15) G. Milosovich, *ibid.*, **53**, 484 (1964).

(16) A. P. Simonelli, S. C. Mehta, and W. I. Higuchi, *ibid.*, **58**, 538 (1969).

(17) W. J. Dixon and F. J. Massey, Jr., "Introduction to Statistical Analysis," 3rd ed., McGraw-Hill, New York, N.Y., 1969, p. 207.

(18) E. J. Mroszczak, R. Runkel, A. Fratis, and J. Strand, presented at the APhA Academy of Pharmaceutical Sciences, Orlando meeting, Nov. 1976.

(19) T. J. Sullivan, E. Sakmar, and J. G. Wagner, *J. Pharmacokinet. Biopharm.*, **4**, 173 (1976).

ACKNOWLEDGMENTS AND ADDRESSES

Received November 8, 1976, from the *Institute of Pharmaceutical Sciences, Syntex Research, Division of Syntex Corporation, Palo Alto, CA 94304.*

Accepted for publication March 2, 1977.

Presented at the Basic Pharmaceutics Section, APhA Academy of Pharmaceutical Sciences, Orlando meeting, November 1976.

[x] To whom inquiries should be directed.

Iodipamide Kinetics: Capacity-Limited Biliary Excretion with Simultaneous Pseudo-First-Order Renal Excretion

SHENG K. LIN [*], ALBERT A. MOSS [‡], and SIDNEY RIEGELMAN [*x]

Abstract □ Iodipamide was infused into three dogs with bile fistulas to achieve various steady-state blood levels. When using ultracentrifugation techniques, iodipamide was found to be highly bound to plasma protein. The total blood clearance was low relative to hepatic blood flow. For either the whole blood concentration or the unbound concentration of iodipamide, the biliary excretion was shown to be capacity limited with a transport maximum, T_m, of approximately 1.0 μmole/kg/min. The steady-state renal excretion rate, plotted against the whole blood concentration of iodipamide, resulted in a concave ascending curve, which could lead to the false conclusion that iodipamide was undergoing active renal tubular reabsorption. However, when corrected for plasma protein binding, a linear relationship was obtained, suggesting that the renal excretion of iodipamide is a pseudo-first-order process. The Michaelis–Menten parameters for the extrarenal elimination, when calculated using the whole blood concentration of iodipamide, led to a similar discrepancy compared to the parameter estimates obtained from biliary excretion rate data. This discrepancy can be eliminated when one uses the unbound concentration of iodipamide in the parameter estimates.

Keyphrases □ Iodipamide—capacity-limited excretion kinetics, dogs □ Excretion kinetics, capacity limited—iodipamide in dogs □ Pharmacokinetics—excretion of iodipamide in dogs □ Radiopaque media—iodipamide, capacity-limited excretion kinetics, dogs

Iodipamide, 3,3′-(adipoyldiimino)bis[2,4,6-triiodobenzoic acid], is the most commonly used intravenous cholangiographic agent in the United States. Clinically, a dose of 166 or 233 mg/kg is recommended for intravenous administration over 3–10 min or the same dose is administered by a slow infusion over 2 hr (1). Nausea, vomiting, hypotension, and occasional kidney damage have been reported with these administration methods. Conflicting opinions exist concerning the appropriate dose and administration route of iodipamide to produce maximal radiological opacification of the biliary tree (1–3) with negligible side effects.

Following intravenous administration, iodipamide is taken up by the liver and excreted unchanged into the bile. Biliary excretion was demonstrated to be capacity limited with a transport maximum, T_m (4, 5). Therefore, plasma levels in excess of those necessary to saturate the biliary excretion offer little or no advantages in opacification of the biliary tree. Increased doses lead to increased drug concentrations in other body organs and add stress on the kidney excretory process. Iodipamide exists in the blood as the unchanged drug and is excreted unchanged in the urine. The percentage of the dose excreted in the urine increases with an increasing dose (6). Therefore, iodipamide offers a good opportunity to investigate the capacity-limited hepatic uptake or biliary excretion in the presence of renal excretion.

A steady-state approach was utilized in the pharmacokinetic studies of iodipamide in dogs to gain a better understanding of the capacity-limited hepatic elimination with simultaneous renal excretion. It is hoped that through this understanding, an optimal dosage and route of administration can be developed to provide maximal visualization of the biliary tree and the least toxic effects.

THEORETICAL

When a drug is infused into the animal for a sufficiently long time to establish steady-state blood concentration, the elimination rate by all routes should equal the infusion rate. For a drug such as iodipamide, which is eliminated by the kidney and other organs, the elimination rate from the blood is the sum of renal excretion and extrarenal elimination. Therefore, if the renal excretion rate at steady state is determined, the difference between the infusion rate and the steady-state renal excretion should equal the extrarenal elimination rate; *i.e.*:

$$R' = R^0 - \frac{dAu}{dt} \qquad \text{(Eq. 1)}$$

where R^0 is the zero-order infusion rate, R' is the steady-state extrarenal elimination rate, and dAu/dt is the steady-state renal excretion rate.

If one assumes that the extrarenal elimination is capacity limited, it can be described by the Michaelis–Menten equation:

$$R' = \frac{V_m C_{ss}}{K_m + C_{ss}} \qquad \text{(Eq. 2)}$$

where V_m is the maximal rate of extrarenal elimination and K_m is the apparent Michaelis–Menten constant. For a drug that has high blood clearance, C_{ss} will be the whole blood concentration at a steady state; for a drug with low clearance, C_{ss} should be referred to the unbound concentration. If the unbound drug concentration shows a constant proportionality to the whole blood concentration, the use of the steady-state whole blood concentration should theoretically yield the same value of V_m and an apparent value of K_m as when the unbound concentration is used. However, this is not the case with iodipamide, which has a relatively low clearance, probably because the unbound fraction varies with concentration.

The term V_m is used to denote the maximal rate of capacity-limited extrarenal elimination, as defined in Eq. 2, and T_m is used to denote the maximal rate of capacity-limited biliary excretion since it is not known whether these two referred to the same or different capacity-limited

(19) T. J. Sullivan, E. Sakmar, and J. G. Wagner, *J. Pharmacokinet. Biopharm.*, **4**, 173 (1976).

ACKNOWLEDGMENTS AND ADDRESSES

Received November 8, 1976, from the *Institute of Pharmaceutical Sciences, Syntex Research, Division of Syntex Corporation, Palo Alto, CA 94304.*

Accepted for publication March 2, 1977.

Presented at the Basic Pharmaceutics Section, APhA Academy of Pharmaceutical Sciences, Orlando meeting, November 1976.

[x] To whom inquiries should be directed.

Iodipamide Kinetics: Capacity-Limited Biliary Excretion with Simultaneous Pseudo-First-Order Renal Excretion

SHENG K. LIN [*], ALBERT A. MOSS [‡], and SIDNEY RIEGELMAN [*x]

Abstract □ Iodipamide was infused into three dogs with bile fistulas to achieve various steady-state blood levels. When using ultracentrifugation techniques, iodipamide was found to be highly bound to plasma protein. The total blood clearance was low relative to hepatic blood flow. For either the whole blood concentration or the unbound concentration of iodipamide, the biliary excretion was shown to be capacity limited with a transport maximum, T_m, of approximately 1.0 μmole/kg/min. The steady-state renal excretion rate, plotted against the whole blood concentration of iodipamide, resulted in a concave ascending curve, which could lead to the false conclusion that iodipamide was undergoing active renal tubular reabsorption. However, when corrected for plasma protein binding, a linear relationship was obtained, suggesting that the renal excretion of iodipamide is a pseudo-first-order process. The Michaelis–Menten parameters for the extrarenal elimination, when calculated using the whole blood concentration of iodipamide, led to a similar discrepancy compared to the parameter estimates obtained from biliary excretion rate data. This discrepancy can be eliminated when one uses the unbound concentration of iodipamide in the parameter estimates.

Keyphrases □ Iodipamide—capacity-limited excretion kinetics, dogs □ Excretion kinetics, capacity limited—iodipamide in dogs □ Pharmacokinetics—excretion of iodipamide in dogs □ Radiopaque media—iodipamide, capacity-limited excretion kinetics, dogs

Iodipamide, 3,3′-(adipoyldiimino)bis[2,4,6-triiodobenzoic acid], is the most commonly used intravenous cholangiographic agent in the United States. Clinically, a dose of 166 or 233 mg/kg is recommended for intravenous administration over 3–10 min or the same dose is administered by a slow infusion over 2 hr (1). Nausea, vomiting, hypotension, and occasional kidney damage have been reported with these administration methods. Conflicting opinions exist concerning the appropriate dose and administration route of iodipamide to produce maximal radiological opacification of the biliary tree (1–3) with negligible side effects.

Following intravenous administration, iodipamide is taken up by the liver and excreted unchanged into the bile. Biliary excretion was demonstrated to be capacity limited with a transport maximum, T_m (4, 5). Therefore, plasma levels in excess of those necessary to saturate the biliary excretion offer little or no advantages in opacification of the biliary tree. Increased doses lead to increased drug concentrations in other body organs and add stress on the kidney excretory process. Iodipamide exists in the blood as the unchanged drug and is excreted unchanged in the urine. The percentage of the dose excreted in the urine increases with an increasing dose (6). Therefore, iodipamide offers a good opportunity to investigate the capacity-limited hepatic uptake or biliary excretion in the presence of renal excretion.

A steady-state approach was utilized in the pharmacokinetic studies of iodipamide in dogs to gain a better understanding of the capacity-limited hepatic elimination with simultaneous renal excretion. It is hoped that through this understanding, an optimal dosage and route of administration can be developed to provide maximal visualization of the biliary tree and the least toxic effects.

THEORETICAL

When a drug is infused into the animal for a sufficiently long time to establish steady-state blood concentration, the elimination rate by all routes should equal the infusion rate. For a drug such as iodipamide, which is eliminated by the kidney and other organs, the elimination rate from the blood is the sum of renal excretion and extrarenal elimination. Therefore, if the renal excretion rate at steady state is determined, the difference between the infusion rate and the steady-state renal excretion should equal the extrarenal elimination rate; *i.e.*:

$$R' = R^0 - \frac{dAu}{dt} \qquad \text{(Eq. 1)}$$

where R^0 is the zero-order infusion rate, R' is the steady-state extrarenal elimination rate, and dAu/dt is the steady-state renal excretion rate.

If one assumes that the extrarenal elimination is capacity limited, it can be described by the Michaelis–Menten equation:

$$R' = \frac{V_m C_{ss}}{K_m + C_{ss}} \qquad \text{(Eq. 2)}$$

where V_m is the maximal rate of extrarenal elimination and K_m is the apparent Michaelis–Menten constant. For a drug that has high blood clearance, C_{ss} will be the whole blood concentration at a steady state; for a drug with low clearance, C_{ss} should be referred to the unbound concentration. If the unbound drug concentration shows a constant proportionality to the whole blood concentration, the use of the steady-state whole blood concentration should theoretically yield the same value of V_m and an apparent value of K_m as when the unbound concentration is used. However, this is not the case with iodipamide, which has a relatively low clearance, probably because the unbound fraction varies with concentration.

The term V_m is used to denote the maximal rate of capacity-limited extrarenal elimination, as defined in Eq. 2, and T_m is used to denote the maximal rate of capacity-limited biliary excretion since it is not known whether these two referred to the same or different capacity-limited

processes. The Michaelis–Menten equation can be linearized in the following manner:

$$\frac{R'}{C_{ss}} = \frac{V_m}{K_m} - \frac{1}{K_m} R' \qquad \text{(Eq. 3)}$$

$$\frac{C_{ss}}{R'} = \frac{K_m}{V_m} + \frac{1}{V_m} C_{ss} \qquad \text{(Eq. 4)}$$

Therefore, from the intercept and the slope of the R'/C_{ss} *versus* R' plot or C_{ss}/R' *versus* C_{ss} plot, initial estimates of V_m and K_m can be obtained and used for the computer fitting of the data.

However, if two capacity-limited processes are involved in the extrarenal elimination, one must fit the extrarenal elimination data to the following equation:

$$R' = \frac{V_{m_1} C_{ss}}{K_{m_1} + C_{ss}} + \frac{V_{m_2} C_{ss}}{K_{m_2} + C_{ss}} \qquad \text{(Eq. 5)}$$

where V_{m_1} and V_{m_2} represent the maximal elimination rates for Processes one and two, respectively, whereas K_{m_1} and K_{m_2} represent the Michaelis–Menten constants for these two elimination processes, respectively. Furthermore, if R'/C_{ss} *versus* R' is plotted, a curvilinear relationship results; it can be resolved into two straight lines with intercepts of V_{m_1} and V_{m_2} on the abscissa and slopes of $1/-K_{m_1}$ and $1/-K_{m_2}$, respectively, for the two processes.

EXPERIMENTAL

Materials—The infusion solution of iodipamide was prepared by diluting commercially available iodipamide meglumine[1,2] with normal saline to concentrations of 21.3 and 55.5 μM. Sodium taurocholate[3] was prepared as a 1% solution in normal saline. Chronic bile fistulas were implanted in dogs by cholecystectomy, ligation of the accessory pancreatic duct, and insertion of a modified Thomas cannula (7) in the duodenum opposite the opening of the ampulla of Vater.

Chronic Infusion Studies—Chronic infusion studies were performed on three unanesthetized, adult labrador dogs (23.4–25.8 kg) with bile fistulas. The dogs were fasted 24 hr prior to each study. The common bile duct was catheterized through the duodenal fistula with a polyethylene tubing (No. 100). Bile was collected by gravity siphoning into graduated cylinders such that the volume could be measured to the nearest 0.1 ml. Superficial leg veins were catheterized with polyethylene tubings for the infusion of iodipamide and sodium taurocholate and for the collection of blood samples.

Sodium taurocholate was infused at rates varying from 7.4 to 10.0 μmoles/min to maintain, insofar as possible, a constant bile flow rate and to replace the loss of the bile salts during the experiment (8). The bladders were catheterized with polyethylene tubing (No. 240) for urine collection.

Throughout each experiment, blood samples were taken at 20-min intervals; bile and urine samples were taken at 30-min intervals. The iodipamide concentration in each sample was determined according to its iodine content by fluorescent excitation analysis (9). Fluorescent excitation analysis assays the iodine concentration in the biological samples in the range of 0.002–40.0 mg of iodine/ml with a ±2% error.

Following appropriate loading doses, iodipamide was infused at rates varying from 0.35 to 4.20 μmoles/kg/min for a minimum of 2 hr at each rate to achieve various steady-state blood concentrations. At least three steady-state blood concentrations were achieved in one experiment.

Acute Infusion Studies in Anesthetized Dogs—Infusion studies were performed in two adult mongrel dogs (21.0 and 27.2 kg) under pentobarbital sodium anesthesia. The visceral organs were exposed through a midline incision, the cystic duct was ligated, and the common bile duct was catheterized with polyethylene tubing (No. 100) for bile collection. Femoral veins were catheterized for the infusion of iodipamide and sodium taurocholate and for the collection of blood samples. The bladder was catheterized, and the total urine output was collected. Timed blood, bile, and urine samples were obtained as in the chronic infusion studies.

After the appropriate loading dose, iodipamide was infused for 3–5 hr at 4.25 and 5.50 μmoles/kg/min, doses that were in excess of the rate reported to saturate the biliary excretory mechanisms (4). The dogs were then sacrificed by anesthetic overdose. The liver, kidneys, heart, and intestines were isolated, drained, weighed, and homogenized. The iodipamide concentration in the blood, bile, urine, and isolated organs was determined by fluorescent excitation analysis (9).

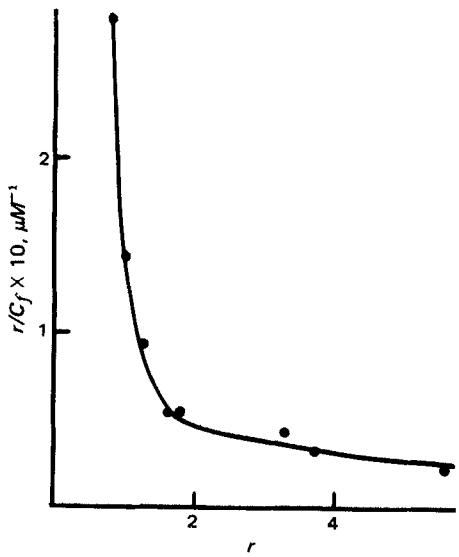

Figure 1—*Scatchard plot of iodipamide binding to plasma albumin in Dog C. An attempt to calculate the binding constants was unsuccessful due to insufficient data in the low* r *region.*

Plasma Protein Binding Studies—On separate occasions, appropriate amounts of the iodipamide were added to the blood taken from the dogs with bile fistulas used in the chronic infusion experiments to achieve blood iodipamide concentrations varying from 113 to 1295 μM. These samples were allowed to equilibrate for 2 hr at 37°. The plasma was then separated from blood cells by centrifugation, and the plasma iodipamide concentration was determined by fluorescent excitation analysis. From the hematocrit and the ratio of plasma iodipamide concentration over blood iodipamide concentration, the fraction of iodipamide in the red blood cells was calculated.

The plasma samples were then centrifuged at 60,000 rpm (average force of 369,000×g, maximal force of 485,000×g) in a preparative ultracentrifuge[4], using a swinging bucket rotor[5], for 18 hr at 37°. The iodipamide concentration in the upper 0.2 fraction of the supernate was determined, and the fraction unbound to plasma protein was calculated.

Creatinine Clearance Determination—Endogenous creatinine clearance was determined for two dogs with bile fistulas used in the chronic infusion studies. Twenty-four-hour urine collections were made. A blood sample was taken at the midpoint of the urine collection period. The creatinine concentration in the urine and serum samples was determined by the alkaline picrate method. The creatinine clearance was then calculated by dividing the amount of endogenous creatinine excreted over 24 hr by the serum creatinine concentration at the midpoint time.

In the third dog with a bile fistula used in the chronic infusion studies, the exogenous creatinine clearance was determined by infusing creatinine throughout one infusion experiment along with iodipamide. The creatinine concentration in the timed serum and urine samples was determined. The exogenous creatinine clearance was calculated as already described.

RESULTS AND DISCUSSION

Iodipamide was highly bound to plasma protein (Fig. 1 and Table I). The percentage unbound varied from 1 to 12% as the blood iodipamide level increased from 113 to 1295 μM. The iodipamide fraction in the red blood cells varied from less than 1 to 9%; therefore, iodipamide binding to red blood cells should not be a significant factor in iodipamide elimination. Lang and Lasser (10) showed that iodipamide binds to plasma albumin but not to γ-globulin. The plasma level of albumin was determined to be 2.4%, and a molecular weight of 69,000 was used for albumin in the calculation of r in the Scatchard plot (Fig. 1).

The total blood clearance, calculated by dividing the infusion rates by

[1] E. R. Squibb & Sons, Princeton, NJ 08540.
[2] Cholografin meglumine.
[3] ICN Pharmaceuticals, Cleveland, OH 44128.
[4] Beckman model L2-65B.
[5] Beckman SW60 Ti rotor.

Table I—Plasma Protein Binding of Iodipamide in the Dog

Dog	Concentration				Fraction Unbound	Hematocrit	Fraction[b] in Red Blood Cells
	Blood[a]	Plasma[a]	Blood / Plasma	Unbound[a]			
A	113	—[c]	—[c]	2	—[c]	—[c]	—[c]
	294	610	0.48	38	0.062	0.50	0.00
	546	920	0.59	66	0.071	0.42	0.02
	886	1492	0.59	111	0.074	0.46	0.09
B	133	228	0.58	3	0.014	0.41	0.01
	491	839	0.59	55	0.066	0.41	0.01
	942	1495	0.63	157	0.105	0.42	0.08
C	168	302	0.57	3	0.010	0.41	0.00
	215	361	0.60	7	0.020	0.45	0.08
	264	458	0.58	14	0.030	0.45	0.05
	336	602	0.59	31	0.051	0.45	0.02
	394	665	0.59	33	0.050	0.41	0.06
	693	1231	0.56	77	0.063	0.41	0.00
	864	1409	0.61	115	0.081	0.43	0.07
	1295	2228	0.58	255	0.116	0.42	0.01

[a] Expressed in units of micromolarity of iodipamide. [b] Calculated from the equation $F = 1 - (1/\lambda)(1 - H)$, where F is the fraction in the red blood cells, λ is the ratio of the blood concentration divided by the plasma concentration, and H is hematocrit. [c] Not determined.

Table II[a]—Relationships among the Rate of Infusion (R^0), the Steady-State Blood Concentration (C_b), the Total Blood Clearance[b] (Cl_b), the Renal Clearance Based on Blood Concentration[b] (Cl_r), and the Renal Clearance Based on the Unbound Concentration[b] of Iodipamide (Cl_{rf})

Dog	R^0, μmoles/kg/min	C_b, μM	Cl_b, ml/kg/min	Cl_r, ml/kg/min	Cl_{rf}, ml/kg/min
A	0.40	129 ± 0.0	3.1 ± 0.000	0.2 ± 0.012	6.8 ± 0.42
	1.40	399 ± 8.3	3.5 ± 0.076	0.8 ± 0.015	9.4 ± 1.20
	2.51	690 ± 11.4	3.6 ± 0.059	1.3 ± 0.022	9.3 ± 0.06
	4.20	1089 ± 1.9	3.9 ± 0.006	1.9 ± 0.003	8.4 ± 0.35
B	0.35	122 ± 1.5	2.8 ± 0.035	0.1 ± 0.002	6.5 ± 0.12
	0.69	193 ± 1.5	3.6 ± 0.074	0.4 ± 0.009	12.2 ± 0.50
	2.08	562 ± 7.7	3.7 ± 0.051	1.4 ± 0.019	12.9 ± 0.45
	3.50	945 ± 7.1	3.7 ± 0.028	2.1 ± 0.015	11.4 ± 0.14
C	0.73	267 ± 5.5	2.7 ± 0.057	0.5 ± 0.010	10.2 ± 1.08
	1.60	539 ± 8.0	3.0 ± 0.045	1.1 ± 0.017	12.1 ± 1.36
	2.00	752 ± 3.7	2.7 ± 0.014	1.5 ± 0.005	12.0 ± 0.07
	3.33	1079 ± 0.9	3.1 ± 0.003	1.6 ± 0.003	8.6 ± 1.20

[a] All data, except the infusion rate, are expressed as the mean steady-state values following each infusion ± *SD*. [b] Total blood clearance was obtained by dividing the infusion rate by the corresponding blood concentration of iodipamide at steady state. Renal clearance based on blood iodipamide concentration was obtained by dividing the steady-state renal excretion rate by the corresponding blood iodipamide concentration. Renal clearance based on the unbound iodipamide concentration was obtained by dividing the steady-state renal excretion rate by the corresponding unbound iodipamide concentration.

the steady-state blood iodipamide concentrations, was low, varying from 2.7 to 3.9 ml/kg/min (Table II). The low total blood clearance and the high degree of plasma protein binding of iodipamide make it likely that the unbound fraction is the major determinant in iodipamide elimination. The data analysis was made using both the whole blood and the unbound concentration of iodipamide.

Pooled data from a series of chronic infusion experiments in the dogs with bile fistulas are reported here. Different symbols in each figure represent data from each experiment in the same dog. In two dogs, the biliary excretion rate reached a maximal value of 0.9 and 1.0 μmole/kg/min, respectively, with increasing blood levels, indicating a saturation phenomenon with a transport maximum, T_m (Fig. 2).

Transport maxima of 1.07 (%CV = 14%) and 1.10 (%CV = 8%) μmoles/kg/min were obtained when the data of the biliary excretion rate and blood iodipamide levels were fitted to the Michaelis–Menten equation using a nonlinear least-squares computer program[6] and a digital computer[7] (Fig. 2). When the same data were fitted to the unbound iodipamide concentration, transport maxima of 0.88 (%CV = 7%) and 0.94 (%CV = 3%) μmole/kg/min were obtained (Fig. 3). The estimated T_m values were statistically different at the $p = 0.05$ level when compared with T_m values obtained using blood iodipamide levels. Theoretically, the T_m values would not change if the degree of plasma protein binding remained constant. However, the percent iodipamide unbound varied up to 10-fold (Table I) in the concentration range studied.

While the renal excretion rate of iodipamide remained essentially constant once steady-state blood iodipamide concentrations had been achieved, the steady-state renal excretion rate increased disproportionately with an increasing blood iodipamide concentration (Table II). Plotting the relationship between steady-state renal excretion rates and the blood iodipamide levels yielded a concave ascending curve from which one might conclude that active tubular reabsorption was occurring (Fig. 4) with an apparent threshold blood concentration of approximately 130 μM. This conclusion, of course, neglects the effect of plasma protein binding on the renal excretion.

When the steady-state renal excretion rates were plotted against the unbound iodipamide concentrations, the data appeared to fit a linear relationship with a zero intercept (Fig. 5). This result indicates that the renal clearance remains relatively constant and that the renal excretion can be treated as a pseudo-first-order process (in the concentration range studied) when one corrects for the effect of plasma protein binding. The renal clearance of unbound iodipamide estimated from the slope of this plot (Fig. 5) was 10.4 ml/kg/min for Dog A. Creatinine clearance for this dog was 2.4 ml/kg/min. Similar ratios were found in other dogs.

This fourfold difference indicated the existence of an active secretion process of iodipamide occurring in the renal tubule. Usually one presumes active tubular secretion to be saturable. The fact that renal clearance of unbound iodipamide remained constant over the iodipamide concentration range studied might lead to the conclusion that the Michaelis–Menten constant for the active secretion process was significantly greater than the unbound iodipamide concentrations achieved.

When the extrarenal elimination rate data were plotted against blood iodipamide concentrations according to one linearized Michaelis–Menten equation (Eq. 3), estimated values of 5.67 μmoles/kg/min and 1529 μM were obtained for V_m and K_m, respectively, for Dog A (Fig. 6A). These estimates were then used as the initial estimates for the computer fitting[7] of the data to the hyperbolic function of the Michaelis–Menten equation using a nonlinear least-squares program[6]. Values of 3.77 (%CV = 13%) μmoles/kg/min and 833 (%CV = 23%) μM were obtained for V_m and K_m, respectively.

Comparison of the V_m value to the biliary excretory T_m reported indicates an approximately fourfold difference. This difference suggests that if the liver is the only eliminating organ besides the kidney, it should

[6] BMDO7RT.
[7] IBM 360-50.

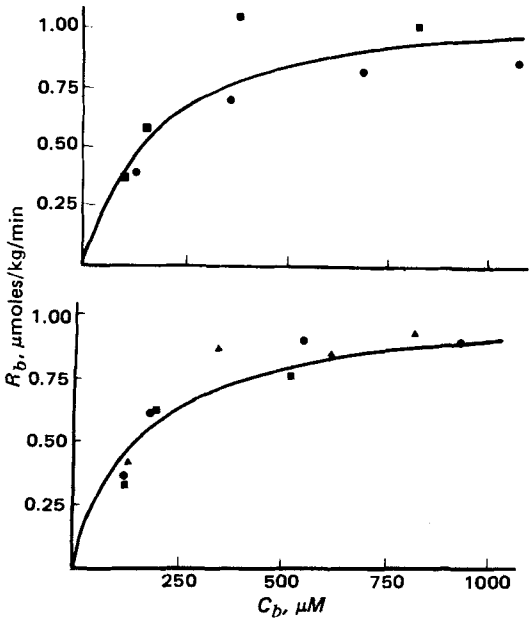

Figure 2—*Relationship between the steady-state biliary excretion rate* (R_b) *and the steady-state blood concentration* (C_b) *of iodipamide in Dogs A (upper curve) and B (lower curve).*

have a larger capacity to take up iodipamide than to excrete it into the bile. Under these conditions, if iodipamide is infused into the dog at the rate greater than that needed to saturate the biliary excretory mechanism, iodipamide must accumulate in the liver.

The V_m value for the hepatic uptake has been reported to be greater than the T_m value for biliary excretion for sulfobromophthalein sodium (11), indocyanine green (12), and taurocholate (13). These results led various investigators to propose that these compounds accumulate within the liver when they are infused at rates greater than those needed to saturate the biliary excretory mechanisms (12, 14). When iodipamide was infused into anethesized dogs at rates greater than those needed to saturate the biliary excretion, the data shown in Table III were obtained. These results clearly showed no accumulation of iodipamide in the liver. This discrepancy can partly be explained when one calculates the Michaelis–Menten parameters using the unbound iodipamide concentration.

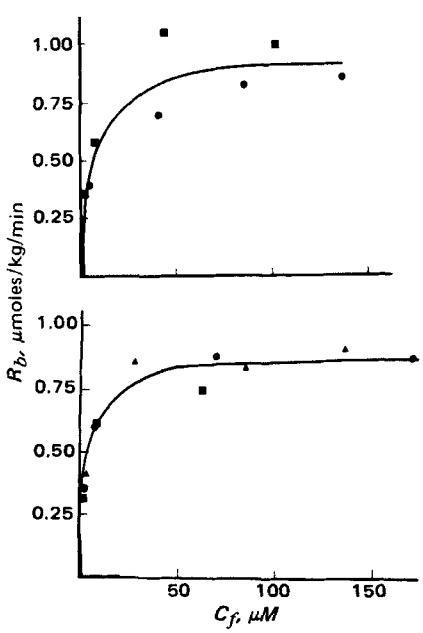

Figure 3—*Relationship between the steady-state biliary excretion rate* (R_b) *and the steady-state unbound concentration* (C_f) *of iodipamide in Dogs A (upper curve) and B (lower curve).*

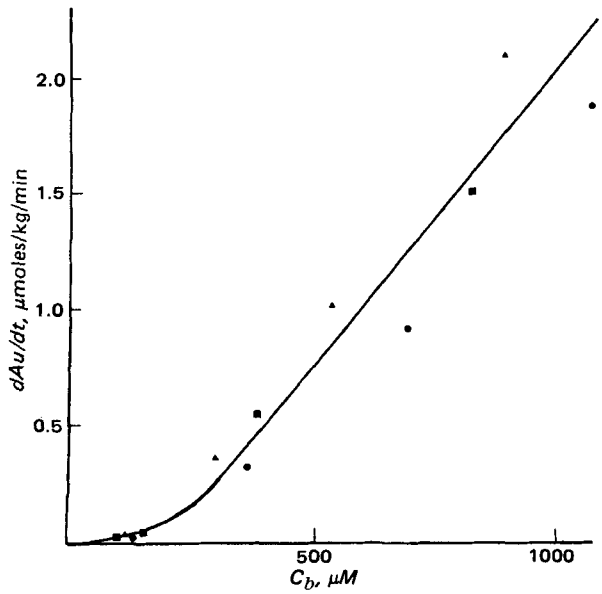

Figure 4—*Relationship between the steady-state renal excretion rate* (dAu/dt) *and the steady-state blood concentration* (C_b) *of iodipamide in Dog A.*

When the extrarenal elimination rate data were plotted against the unbound iodipamide concentration according to one linearized Michaelis–Menten equation (Eq. 3), a curvilinear relationship was obtained (Fig. 6B); it can be interpreted as indicating the existence of more than one capacity-limited elimination process. By presuming that two capacity-limited processes are occurring, the initial estimates of V_m and K_m for these two processes were obtained from this plot. These initial estimates were then used for the computer fitting[7] of the data using a nonlinear least-squares program[6] according to Eq. 5.

A V_m value of 0.86 (%CV = 45%) μmole/kg/min was obtained, which was comparable to the experimentally determined T_m of 1.01 μmoles/

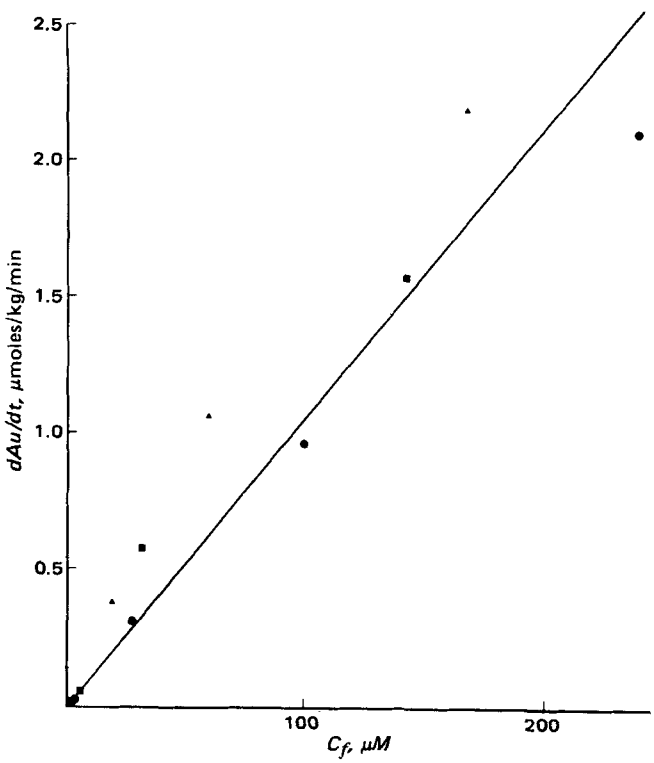

Figure 5—*Relationship between the steady-state renal excretion rate* (dAu/dt) *and the steady-state unbound concentration* (C_f) *of iodipamide in Dog A.*

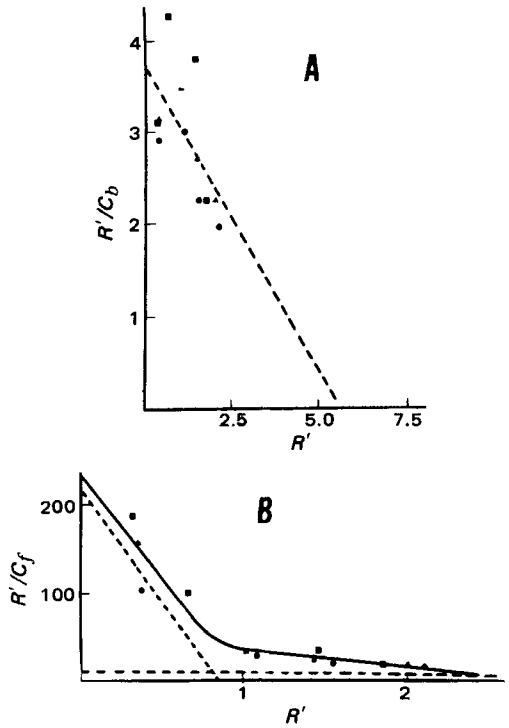

Figure 6—*A: Relationship between the steady-state extrarenal elimination rate (R′ in micromoles per kilogram per minute) and the steady-state blood concentration (C_b in micromolar) of iodipamide in Dog A shown as* R'/C_b versus R′. *The broken line is the unweighted linear regression. B: Relationship between the steady-state extrarenal elimination rate (R′ in micromoles per kilogram per minute) and the steady-state unbound concentration (C_f in micromolar) of iodipamide shown as* R'/C_f versus R′. *Key: —, computer-fitted line; and - - -, computer-resolved linear component.*

kg/min for biliary excretion. The V_{m_2} was evaluated to be 10.77 (%CV = 443%) μmoles/kg/min, indicating the presence of another elimination process with a higher capacity to take up iodipamide than the biliary excretion route. However, since it is more difficult to ascertain that steady states were achieved following the higher iodipamide infusion rates, the value of V_{m_2} should be considered only as an approximate estimate.

Present data analysis, therefore, supports the contention that the unbound drug concentration should be used in the calculation of the parameters of elimination for drugs such as iodipamide with a high degree of plasma protein binding and low blood clearance.

Iodipamide, sulfobromophthalein sodium, and indocyanine green share common hepatic uptake binding sites (15, 16). It is particularly important to compare iodipamide and indocyanine green, since both are excreted in the bile unchanged. However, iodipamide is eliminated to a varying degree (depending on the dose) by the kidney, while indocyanine green apparently is only eliminated by the liver. While iodipamide has a low hepatic extraction ratio (<10%), indocyanine green has a high hepatic extraction ratio (>80%) (based on plasma clearance). Klassen and Plaa (17) administered indocyanine green to dogs by both intravenous bolus and infusion and obtained a T_m value of approximately 20 nmoles/kg/min. In contrast, a T_m for iodipamide in dogs of about 1.0 nmole/kg/min was obtained in the present study, about a 50-fold greater value.

Paumgartner (12) showed the V_m for indocyanine green in the rat to be 3200 μmoles/kg/min while the T_m for the biliary excretion was 240 μmoles/kg/min. Paumgartner also measured the liver concentration of indocyanine green in rats and verified that indocyanine green accumulated in the liver at the rate equivalent to the V_m (12). This result is in remarkable contrast to the results obtained in the present study on iodipamide in dogs using the steady-state infusion method wherein no accumulation of iodipamide was found in the liver. It is possible that these two compounds are handled by different mechanisms in the biliary excretion.

Table III—Distribution of Iodipamide following an Acute Infusion to Anesthetized Dogs

Amount of Iodipamide, μmoles	Dog 19018	Dog 19213
Administered	29,181	46,761
Excreted in bile and urine	11,853	12,828
In liver	639	903
In kidneys	—[a]	812
In heart	—[a]	118
In intestines	—[a]	1,988
In blood	2,887	2,556
Not accounted for	13,802	27,555

[a] Not determined.

REFERENCES

(1) A. A. Moss, J. A. Nelson, and J. R. Amberg, *Am. J. Roentgenol. Radium Ther. Nucl. Med.*, **117**, 406 (1973).

(2) R. E. Wise and F. J. Scholz, *Gastroenterology*, **65**, 967 (1973).

(3) B. Whitney and G. D. Bell, *Br. J. Radiol.*, **45**, 891 (1972).

(4) G. Rosati and P. Schiantarelli, *Invest. Radiol.*, **5**, 232 (1970).

(5) P. M. Loeb, R. N. Berk, G. K. Feld, and H. O. Wheeler, *Gastroenterology*, **68**, 554 (1975).

(6) H. W. Fischer, *Radiology*, **84**, 483 (1965).

(7) R. S. Jones, T. K. Yee, and C. E. Michielsen, *J. Appl. Physiol.*, **30**, 427 (1971).

(8) A. A. Moss, J. R. Amberg, and R. S. Jones, *Invest. Radiol.*, **7**, 11 (1972).

(9) A. A. Moss, L. Kaufman, and J. A. Nelson, *ibid.*, **7**, 335 (1972).

(10) J. H. Lang and E. C. Lasser, *ibid.*, **2**, 396 (1967).

(11) C. A. Goresky, *Am. J. Physiol.*, **207**, 13 (1964).

(12) G. Paumgartner, *Suppl. Schweiz. Med. Wochenschr.*, **105**, 1 (1975).

(13) J. Reichen and G. Paumgartner, *Gastroenterology*, **68**, 132 (1975).

(14) N. G. Javitt, in "Progress in Liver Diseases," vol. 3, H. Popper and F. Schaffner, Eds., Grune and Stratton, New York, N.Y., 1970, p. 110.

(15) A. J. Levi, Z. Gatmaitain, and I. M. Arias, *J. Clin. Invest.*, **48**, 2156 (1969).

(16) C. E. Cornelius, J. Ben-Ezzer, and I. M. Arias, *Proc. Soc. Exp. Biol. Med.*, **124**, 665 (1967).

(17) C. D. Klassen and G. L. Plaa, *Toxicol. Appl. Pharmacol.*, **15**, 374 (1969).

ACKNOWLEDGMENTS AND ADDRESSES

Received October 12, 1976, from the *Department of Pharmacy, School of Pharmacy, and the ‡Department of Radiology, School of Medicine, University of California, San Francisco, CA 94143.

Accepted for publication March 7, 1977.

Supported in part by U.S. Public Health Service Grants NIGMS 16496-08 and GM 00728.

The authors are grateful to Dr. Thomas N. Tozer and Dr. Sylvia M. Wallace for valuable suggestions.

* To whom inquiries should be directed.

Physicochemical Properties of β-Lactam Antibiotics: Oil–Water Distribution

AKIRA TSUJI, OSAMU KUBO, ETSUKO MIYAMOTO, and TSUKINAKA YAMANA ˣ

Abstract □ Apparent partition coefficients, P_{app}, of β-lactam antibiotics were determined in octanol–water and 2-methylpropanol–water systems at various pH values. The pKa values also were determined by potentiometry under the conditions of partition experiments. The intrinsic partition coefficients for the unionized form, P_u, and the ionized form, P_i, of β-lactam antibiotics were calculated from the equation $P_{app} = P_u[a_{H^+}/(K_a + a_{H^+})] + P_i[K_a/(K_a + a_{H^+})]$. The correlation between P_u and P_i values and lipophilic parameters of penicillins measured in other systems was examined.

Keyphrases □ Partition coefficients, apparent—various β-lactam antibiotics in octanol–water and 2-methylpropanol–water at various pH values □ pKa—various β-lactam antibiotics □ β-Lactam antibiotics—apparent partition coefficients in octanol–water and 2-methylpropanol–water at various pH values □ Antibiotics, various—apparent partition coefficients in octanol–water and 2-methylpropanol–water at various pH values

In biopharmaceutical studies of β-lactam antibiotics, the partition coefficient between two immiscible phases is an important physicochemical property for correlating their structure with their absorption, tissue distribution, renal reabsorption, and other membrane transport. Previously (1), the partition coefficient, k', determined by high-pressure liquid chromatography (HPLC) was reported for β-lactam antibiotics, and their log k' values were correlated with other reported partition properties such as log P (2) in octanol–water and R_m (2–4) determined by TLC.

Previously reported log P values for penicillins were determined either at only a single pH by a convenient flask-shaking method (5–7) or at one or two pH values by a pH-stat technique (2). Somewhat different partition properties from the previous data, however, were noted for several penicillins in this laboratory when particular attention was paid to the pKa, pH conditions, and their chemical instabilities.

This study investigated a series of β-lactam antibiotics; the results of pKa measurement, the apparent partition coefficient as a function of pH for determining the intrinsic P values for unionized and ionized species in octanol–water and 2-methylpropanol–water, and quantitative correlations among partition coefficients are discussed.

EXPERIMENTAL

Materials—All β-lactam antibiotics except methicillin and carbenicillin indanyl sodium (I) were described previously (1). Compound I[1] (704 μg/mg, containing 0.84% 5-indanol, 0.6% carbenicillin, and 1.4% penicillin G) and methicillin sodium[2] (853 μg/mg) were used as supplied. All other chemicals were analytical grade and were used without further purification, except that octanol was purified according to the literature (8) and 2-methylpropanol was used after a single distillation.

Determination of pKa—The apparent dissociation constant, K_a, for each penicillin was determined at 37° by a potentiometric titration (9). Twenty milliliters of 1.0×10^{-2} M solution of the sodium or potassium salt of penicillin, adjusted with potassium chloride to a constant ionic strength of 0.15, was titrated with 0.1 N HCl ($\mu = 0.15$ with potassium chloride) until precipitation of the penicillin free acid occurred.

The titrant was added in 0.2-ml portions from a buret[3], and the pH changes during titration were measured[4]. For acid-unstable penicillins such as penicillin G and methicillin, titrations were carried out as rapidly as possible to avoid the β-lactam cleavage. The apparent pKa values of penicillins were computed by the equation of Albert and Serjeant (9).

Determination of Apparent Partition Coefficient—For distribution experiments in octanol–water, the aqueous phase was prepared by dissolving an exactly weighed quantity of the sodium or potassium salt of the antibiotics to make a final concentration of 1×10^{-3} M and a calculated amount of potassium chloride to maintain a constant ionic strength of 0.15 in an appropriate buffer solution. To minimize the volume change due to mutual miscibility, the aqueous and organic phases were saturated previously with each solvent.

Exactly 10 ml of each solution (50 ml of organic phase was used for penicillin G, methicillin, and cephalothin) was transferred to a glass-stoppered flask and shaken for 2 hr (30 min for penicillin G and methicillin) to achieve complete equilibrium at 37 ± 0.1°. The two phases separated on standing for 1 hr, and the aqueous phase was centrifuged at 3000 rpm for 10 min. If necessary, after appropriate dilution with distilled water, the concentration of the antibiotics was determined by spectrophotometry[5] at 260 nm and/or by the imidazole method reported by Bundgaard and Ilver (10).

For the distribution study in 2-methylpropanol–water, each aqueous phase was prepared to make a constant Na^+ concentration of 0.1 M by the addition of a calculated amount of sodium chloride in buffer. Other procedures were the same as for the octanol–water system. Acetate, phosphate, and borate buffers were used in the distribution studies.

The apparent partition coefficient, P_{app}, was calculated from:

$$P_{app} = \frac{C_o V_w}{C_w V_o} \qquad \text{(Eq. 1a)}$$

$$P_{app} = \left(\frac{C_i - C_w}{C_w}\right)\frac{V_w}{V_o} \qquad \text{(Eq. 1b)}$$

where C and V represent the concentration and volume of the aqueous (subscript w) and organic (subscript o) phases, respectively, and C_i indicates the initial concentration of an antibiotic, which was determined by a simultaneous incubation of the antibiotic in the same buffer solution and for the same time as were used in the distribution experiment. In most cases, the suitable ratio, V_w/V_o, was used to maintain the condition of $1 < (C_i - C_w)/C_w < 10$.

RESULTS AND DISCUSSION

Dissociation Constants of Penicillins—Table I gives the apparent pKa values obtained as the average of a set of pKa values calculated at each pH measured during the titration, corresponding in most cases to 25–75% neutralization. In all cases, results from two or three titrations never deviated more than ±0.03 pKa unit.

Table I also lists similar results determined for some penicillins from titration in ethanol–water at 37°. For penicillin V and oxacillin, the pKa values extrapolated to 0% ethanol concentration in plots of the apparent pKa against the ethanol concentration [percent (weight per volume)] were in good agreement with the value determined directly in water. Therefore, the pKa values corresponding to those in water were obtained by extrapolation to 0% ethanol for the antibiotics unsuited to the usual de-

[1] Taito-Pfizer Co., Tokyo, Japan.
[2] Banyu Pharmaceutical Co., Tokyo.
[3] ABU12b autoburet, Radiometer, Copenhagen, Denmark.
[4] PHM26 pH meter, Radiometer, Copenhagen, Denmark.
[5] UV-200S double-beam spectrophotometer, Shimadzu, Kyoto, Japan.

Table I—Apparent Dissociation Constants of Penicillins in Water and Ethanol–Water Mixtures

Penicillin	pKa (This Research)[a] Temperature	Ethanol Concentration, w/v % 0.0	0.0[c]	16.0	32.8	41.9	51.4	pKa (Literature)[b] Temperature	Reported	Reference
I Carbenicillin indanyl sodium	37°	—	2.94	—	3.73	3.95	4.16	—		
II Carbenicillin phenyl sodium	37°	—	2.91	—	3.70	3.92	4.15	—		
III Dicloxacillin	37°	—	2.76	—	3.55	3.77	3.98	25°	2.67[c]	17
IV Floxacillin	37°	—	2.76	—	3.55	3.77	3.98	—		
V Cloxacillin	37°	—	2.78	3.11	3.57	3.79	4.01	25°	2.70, 2.73	11
								35°	2.68[d]	18
VI Oxacillin	37°	2.73	2.72	3.09	3.57	3.81	4.03	—		
VII Propicillin	37°	2.76	—	—	—	—	—	25°	2.72	11
VIII Phenethicillin	37°	2.80	—	—	—	—	—	25°	2.72, 2.74	11
								35°	2.9[d]	19
IX Penicillin V	37°	2.79	2.78	3.15	3.61	3.85	4.06	25°	2.73, 2.74	11
X Penicillin G	37°	2.75	—	—	—	—	—	25°	2.71, 2.73	11
								60°	2.78[d]	20
XI Methicillin	37°	2.77	—	—	—	—	—	25°	2.76, 2.78	11
								25°	2.74[d]	21

[a] The values were determined potentiometrically at $\mu = 0.15$. These values were computed from the equation of Albert and Serjeant (9) for the data corresponding to 25–75% of neutralization and averaged from at least three experiments, never deviating more than ±0.03 pKa unit. [b] The values were determined potentiometrically. [c] The pKa values were obtained by extrapolation to 0% (w/v) ethanol. [d] The values were determined at $\mu = 0.5$.

termination of the pKa in water because of their low solubility in aqueous acidic solution.

The pKa values in water determined directly or extrapolated at 37° and $\mu = 0.15$ were about 0.04 pKa unit higher than those determined at 25° by Rapson and Bird (11) for the corresponding penicillins (Table I). This difference may be due to different experimental conditions, temperature, and ionic strength, and it may be reasonable for the dissociation behavior of many carboxylic acids (9).

pH-Dependent Oil–Water Partition Behavior—If it is assumed that a certain β-lactam antibiotic, which is in the free acid and anionic forms at the dissociation equilibrium in water, is distributed between the oil and water phases as shown in Scheme I, then the apparent partition coefficient, P_{app}, can be expressed as:

$$P_{app} = \frac{(HA)_o + (A^-)_o}{(HA)_w + (A^-)_w} \quad \text{(Eq. 2)}$$

where (HA) and (A^-) represent the activities of the unionized and ionized forms, respectively, and the subscripts w and o indicate the water and oil phases, respectively. The true partition coefficient for unionized, P_u, and ionized, P_i, forms of an antibiotic and the dissociation constant, K_a, are given by Eqs. 3–5, respectively:

$$P_u = \frac{(HA)_o}{(HA)_w} \quad \text{(Eq. 3)}$$

$$P_i = \frac{(A^-)_o}{(A^-)_w} \quad \text{(Eq. 4)}$$

$$K_a = \frac{(A^-)_w a_{H^+}}{(HA)_w} \quad \text{(Eq. 5)}$$

Therefore, Eq. 6 can be derived from Eqs. 2–5:

$$P_{app} = P_u\left(\frac{a_{H^+}}{K_a + a_{H^+}}\right) + P_i\left(\frac{K_a}{K_a + a_{H^+}}\right) \quad \text{(Eq. 6)}$$

where a_{H^+} is the hydrogen-ion activity. In these equations, the activity of the species in each phase is assumed to be approximately the same as its concentration. Rearrangement of Eq. 6 gives:

$$P_{app}\left(\frac{a_{H^+}}{K_a} + 1\right) = P_u\frac{a_{H^+}}{K_a} + P_i \quad \text{(Eq. 7)}$$

Equation 7 predicts that a plot of P_{app} ($a_{H^+}/K_a + 1$) against a_{H^+}/K_a should give a straight line with a slope of P_u and intercept of P_i.

Octanol–Water Distribution—The experimental results are summarized in Table II. All experimental conditions were selected for each antibiotic so that sufficient solubility in the aqueous phase could be achieved and that the β-lactam degradation was within 2% when the distribution equilibrium was attained. The degradation was checked in every case by simultaneous incubation of the antibiotic in the same buffer solution as that used for the distribution study.

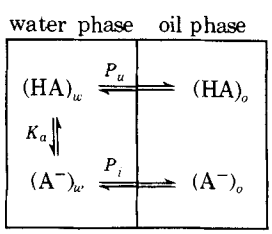

Scheme I

Apparent partition coefficients of penicillin V were measured with various concentrations (5×10^{-4}–5×10^{-3} M) at a constant pH. No significant changes in P_{app} were observed (Table II), suggesting that no appreciable association between the molecules occurred in each phase. This result may be expected for other β-lactam antibiotics.

Figures 1 and 2 show the plots of $P_{app}(a_{H^+}/K_a + 1)$ *versus* a_{H^+}/K_a according to Eq. 7 for the data listed in Table II, where the K_a values used were those determined directly in water or extrapolated to 0% ethanol under the identical experimental conditions of 37° and $\mu = 0.15$ (Table I). For cephalothin, a pKa of 2.22, determined previously (12) at 35° and $\mu = 0.5$, was employed. The plots yielded straight lines for all β-lactam antibiotics studied and provided appreciable P_i values from the intercept only for antibiotics having log P_u values larger than about 2. These results suggest that the anionic species of β-lactam antibiotics also can be distributed depending on their side-chain lipophilicity.

Table III summarizes the log P_u and log P_i values for the octanol–water distribution. For comparison, previously reported values of log P_u for penicillins are listed in Table III. There are some close agreements and

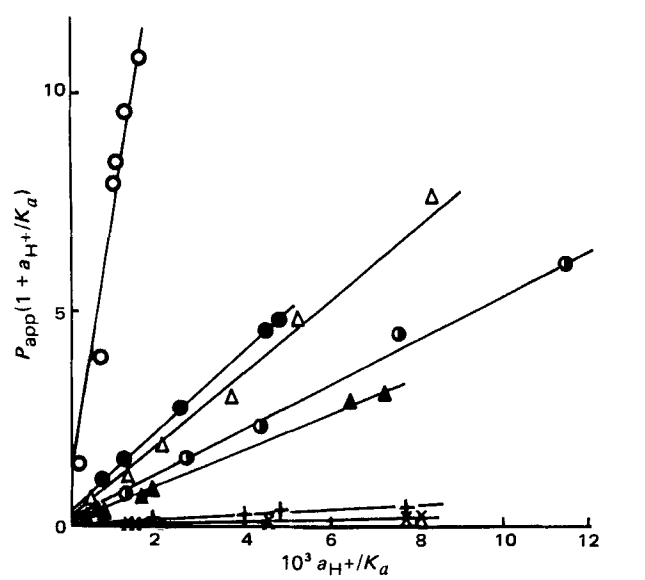

Figure 1—*Plots of* $P_{app}(1 + a_{H^+}/K_a)$ *against* a_{H^+}/K_a *for β-lactam antibiotics in octanol–water at 37° and* $\mu = 0.15$. *The compounds are numbered as in Table I. Key:* ○, *I;* ●, *II;* △, *III;* ▲, *IV;* ◑, *VII;* +, *X; and* ×, *XI.*

Table II—Apparent Partition Coefficient, P_{app}, of β-Lactam Antibiotics between Octanol and Water as a Function of the Aqueous Phase at 37° and $\mu = 0.15$

Compound	pH[a]	P_{app}[b]
I	5.73	10.80
	5.84	9.55
	5.92	8.39
	5.94	7.93
	6.55	3.89
	7.75	1.43
II	5.23	4.73
	5.26	4.47
	5.51	2.74
	5.84	1.54
	6.07	1.09
III	5.04	4.77
	5.19	2.96
	5.44	1.88
	5.65	1.17
	6.13	0.67
IV	4.90	3.07
	4.95	2.87
	5.49	0.87
	5.55	0.76
	5.90	0.41
	5.96	0.41
	6.22	0.27
V	4.26	8.08
	4.44	5.68
	4.77	3.04
	4.89	2.49
VI	4.15	7.21
	4.39	5.00
	4.83	2.13
VII	4.70	6.00
	4.88	4.39
	5.12	2.24
	5.35	1.55
	5.66	0.76
VIII	3.98	9.79
	4.06	7.88
	4.10	7.47
	5.21	0.76
IX	3.71	9.20
	4.05	4.56
	4.50	1.88
	4.93	0.66
	3.90	7.22[c]
	3.90	7.09
	3.91	6.77[d]
X	4.86	0.37
	5.07	0.32
	5.15	0.23
	5.47	0.15
XI	4.86	0.18
	4.88	0.14
	5.11	0.09
	5.61	0.02
	5.63	0.01
Cephalothin (XII)	3.13	0.97
	3.32	0.70
	3.55	0.39
	3.75	0.28
	3.77	0.27
	4.06	0.15
	4.40	0.08

[a] At equilibrium. [b] Initial concentration = 1×10^{-3} M. [c] Initial concentration = 5×10^{-4} M. [d] Initial concentration = 5×10^{-3} M.

some differences between the present values and those reported by Bird and Marshall (2), which were determined by the pH-stat titration method at pH 3 and 4 or only at pH 4. Unfortunately, since in that study there was no mention of the results available for recalculation and the temperature at which the partition coefficients were measured, it is difficult to evaluate the correlations between their values and the present ones.

2-Methylpropanol–Water Distribution—The apparent partition coefficients of several penicillins and cephalothin between 2-methylpropanol and aqueous buffer with a constant Na^+ concentration (0.1 M) are depicted in Fig. 3. The P_{app} values depended on the lipophilicity of the side chain for the penicillin series but were independent of pH above pH 6 for all β-lactam antibiotics, indicating the major contribution of the anionic forms for the P_{app} value. The average log P_i values are listed in Table III. In the pH–P_{app} profiles for penicillin V and propicillin, the increasing P_{app} with decreasing pH is undoubtedly attributed to the distribution of unionized forms.

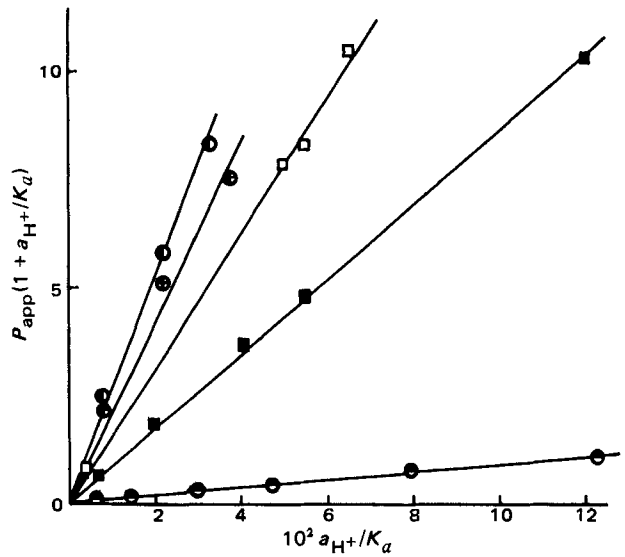

Figure 2—*Plots of* $P_{app}(1 + a_{H^+}/K_a)$ *against* a_{H^+}/K_a *for β-lactam antibiotics in octanol–water at 37° and* $\mu = 0.15$. *The compounds are numbered as in Table I. Key:* ◐, *V;* ⊕, *VI;* □, *VIII;* ■, *IX; and* ⊖, *XII.*

Scholtan (13) determined P_{app} values of penicillins in 2-methylpropanol–pH 7.4 phosphate buffer, and those values were 1.5–2 times larger than those in this work. Since Scholtan made no mention of experimental temperature conditions and the total buffer concentration, this large difference cannot be clarified. However, the partition coefficients of the penicillin anion in the present 2-methylpropanol–water system largely depend on the total Na^+ or K^+ concentration used for the buffer, and these phenomena also were observed in octanol–water (Table IV). Such behavior should be the result of a salting-out effect and/or ion-pair extraction of the penicillin anion with a buffer cation as suggested by Bird and Marshall (2).

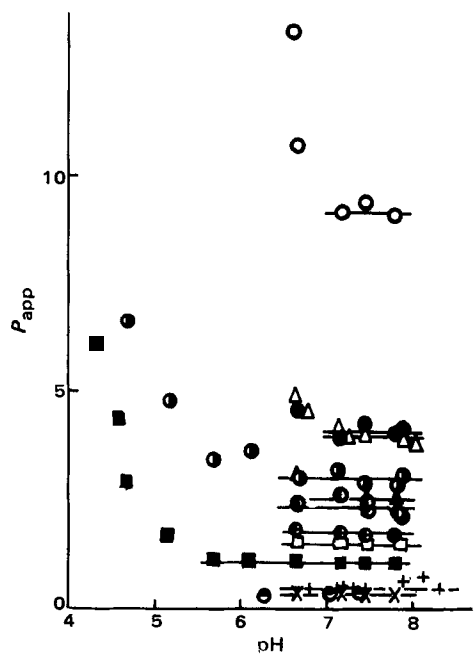

Figure 3—*Plots of* $P_{app}(1 + a_{H^+}/K_a)$ *against* a_{H^+}/K_a *for β-lactam antibiotics in 2-methylpropanol–water at 37° and constant* Na^+ *concentration (0.1 M). The compounds are numbered as in Table I. Key:* ○, *I;* ●, *II;* △, *III;* ▲, *IV;* ◐, *V;* ⊕, *VI;* ◑, *VII;* □, *VIII;* ■, *IX;* +, *X;* ×, *XI; and* ⊖, *XII.*

Table III—Partition Coefficients of β-Lactam Antibiotics

Compound	Octanol						Silicone			2-Methyl-propanol,	
	log P_u	log P_i	log P^a	log P^b	$R_m{}^a$ (pH 3)	$R_m{}^a$ (pH 4)	$R_m{}^c$ (pH 7.4)	$R_m{}^d$ (pH 2.6)	$R_m{}^d$ (pH 9.4)	log P_i	log k'^e
I	3.77	0.18	—	—	—	—	—	—	—	0.96	—
II	2.96	−0.52	—	—	—	—	—	—	—	0.62	2.68
III	2.91	−0.60	2.83	3.24	1.18	0.44	1.62	1.76	1.43	0.61	2.30
IV	2.61	−0.82	—	—	—	—	1.41[f]	—	—	0.41	2.14
V	2.43	—	2.44	2.49	0.71	0.01	1.34	1.67	1.21	0.38	2.04
VI	2.31	—	2.34	2.38	0.57	−0.15	1.05	1.39	0.96	0.25	—
VII	2.70	−0.70	2.58	—	0.97	0.21	—	—	—	0.48	—
VIII	2.20	—	2.19	2.20	0.50	−0.23	1.03	1.35	0.91	0.19	1.80
IX	1.95	−1.65[g]	2.01	2.03	0.34	−0.37	0.89	1.17	0.89	0.04	1.62
X	1.70	—	1.76	1.72	0.09	−0.66	0.55	0.84	0.45	−0.30	1.30
XI	1.30	—	1.13	1.06	−0.60	−1.34	0.47	0.78	0.41	−0.44	—
XII	0.95	—	—	—	—	—	—	—	—	—	—

[a] Reference 2. [b] Reference 7. [c] Reference 3. [d] Reference 15. [e] Reference 1. [f] Reference 14. [g] Evaluated from the data in Table IV.

Therefore, in the present experiment with 2-methylpropanol–water, the total Na^+ concentration was kept constant at 0.1 *M*. Thus, this effect would probably account for the greater discrepancy between the present data and those of Scholtan (13).

Linear Free Energy Relationship for Distribution Equilibrium of Penicillins in Various Systems—Since the partition coefficient is an equilibrium constant, there should be a linear free energy relationship between distribution values in different systems such as log *P* and R_m from the TLC method and log *k'* from the HPLC technique. The regression equations between two partition coefficients for penicillins determined in this study and available from the literature (1–6, 13–15) are given by Eqs. 8–21, where *n*, *r*, and *s* are the number of data, the correlation coefficient, and the standard deviation, respectively:

	n	*r*	*s*	
log P_u(octanol) = 0.994 log P_i(octanol) + 3.498	6	0.990	0.082	(Eq. 8)
log P_i(2-methylpropanol) = 0.598 log P_u(octanol) − 1.168	11	0.983	0.077	(Eq. 9)
log P_i(2-methylpropanol) = 0.510 log P_i(octanol) − 0.869	6	0.994	0.033	(Eq. 10)
R_m(octanol, pH 3.0) = 1.034 log P_u(octanol) − 1.791	8	0.984	0.080	(Eq. 11)
R_m(octanol, pH 4.0) = 1.034 log P_u(octanol) − 2.522	8	0.985	0.095	(Eq. 12)
R_m(silicone, pH 2.6) = 0.695 log P_u(octanol) − 0.190	7	0.963	0.102	(Eq. 13)
R_m(silicone, pH 7.4) = 0.775 log P_u(octanol) − 0.640	8	0.979	0.084	(Eq. 14)
R_m(silicone, pH 7.4) = 0.683 log P_i(octanol) + 2.009	3	0.996	0.036	(Eq. 15)
R_m(silicone, pH 7.4) = 1.116 log P_i(2-methylpropanol) + 0.887	8	0.985	0.071	(Eq. 16)
R_m(silicone, pH 9.4) = 0.682 log P_u(octanol) − 0.549	7	0.963	0.099	(Eq. 17)
R_m(silicone, pH 9.4) = 0.986 log P_i(2-methylpropanol) + 0.791	7	0.986	0.062	(Eq. 18)

Table IV—Effect of Na^+ or K^+ Concentration on Apparent Partition Coefficient (P_{app}) of Penicillin V in Octanol–Water and 2-Methylpropanol–Water Systems at 37°

Ionic Strength, *M*	Octanol–Water, with K^+	2-Methylpropanol–Water	
		K^+	Na^+
0.09	0.015	1.03	1.00
0.28	0.045	1.69	1.50
0.56	0.042	2.21	2.29

log *k'*(pH 7.4) = 0.936 log P_u(octanol) − 0.259	7	0.975	0.103	(Eq. 19)
log *k'*(pH 7.4) = 0.800 log P_i(octanol) + 2.903	4	0.942	0.146	(Eq. 20)
log *k'*(pH 7.4) = 1.327 log P_i(2-methylpropanol) + 1.163	7	0.961	0.125	(Eq. 21)

In the system with octanol as the organic phase, the slopes of these lines (Eqs. 8, 11, and 12) were close to 1.0, consistent with the theoretical expectation. The regression slope between log *P*(octanol) and log *k'* was near 1.0. This result probably means that the distribution process between the aqueous and stationary phases, octadecylsilane, is almost the same as that between water and octanol (16). A slope less than unity in the regression line was observed for the correlation between the octanol and 2-methylpropanol systems. The decreased lipophilic character of the nonaqueous phase decreases the energy required to transfer a distributing solute from the nonaqueous to the aqueous phase, which would result in a decrease of the slope going from octanol to 2-methylpropanol.

A good correlation between the partition coefficient for the unionized species and that of the ionized species of penicillin molecules was obtained in every partitioning system, indicating that the lipophilic character of the side chain of unionized penicillins is reflected in the lipoid solubility of the ionized forms. The present results suggest that the ionized form as well as the undissociated form of β-lactam antibiotics may be able to act in various processes *in vivo*, such as GI absorption, tissue distribution, serum binding, renal reabsorption, and cell wall permeability. Since penicillins and cephalosporins are almost all ionized at physiological pH, knowledge of the predominant species and the mechanism in these *in vivo* processes is important in the design of suitable β-lactam antibiotics and their dosage forms.

REFERENCES

(1) T. Yamana, A. Tsuji, E. Miyamoto, and O. Kubo, *J. Pharm. Sci.*, **66**, 747 (1977).

(2) A. E. Bird and A. C. Marshall, *J. Chromatogr.*, **63**, 313 (1971).

(3) G. L. Biagi, A. M. Barbaro, M. F. Gamba, and M. C. Guerra, *ibid.*, **41**, 371 (1969).

(4) *Ibid.*, **44**, 195 (1969).

(5) A. E. Bird and A. C. Marshall, *Biochem. Pharmacol.*, **16**, 2275 (1967).

(6) A. E. Bird and J. H. C. Nayler, in "Drug Design," vol. II, E. J. Ariens, Ed., Academic, New York, N.Y., 1971, chap. 8.

(7) A. Ryrfeldt, *J. Pharm. Pharmacol.*, **23**, 463 (1971).

(8) T. Fujita, J. Iwasa, and C. Hansch, *J. Am. Chem. Soc.*, **86**, 5175 (1964).

(9) A. Albert and E. P. Serjeant, "The Determination of Ionization Constants," Chapman and Hall, London, England, 1971.

(10) H. Bundgaard and K. Ilver, *J. Pharm. Pharmacol.*, **24**, 790 (1972).

(11) H. D. C. Rapson and A. E. Bird, *ibid.*, **15**, 222T (1963).

(12) T. Yamana and A. Tsuji, *J. Pharm. Sci.*, **65**, 1563 (1976).

(13) W. Scholtan, *Arzneim.-Forsch.*, **18**, 505 (1968).

(14) G. L. Biagi, M. C. Guerra, A. M. Barbaro, G. Cantelli-Forti, and T. Rossi, *Boll. Soc. Ital. Biol. Sper.*, **51**, 403 (1975).

(15) G. L. Biagi, A. M. Barbaro, and M. C. Guerra, *J. Chromatogr.*, **51**, 548 (1970).
(16) A. Leo, C. Hansch, and D. Elkins, *Chem. Rev.*, **71**, 525 (1971).
(17) J. P. Hou and J. W. Poole, *J. Pharm. Sci.*, **58**, 1510 (1969).
(18) H. Bundgaard and K. Ilver, *Dan. Tidsskr. Farm.*, **44**, 365 (1970).
(19) M. A. Schwartz, A. P. Granatek, and F. H. Buckwalter, *J. Pharm. Sci.*, **51**, 523 (1962).
(20) P. Finholt, G. Jurgensen, and H. Kristiansen, *ibid.*, **54**, 387 (1965).
(21) M. A. Schwartz, E. Bara, I. Rubycz, and A. P. Granatek, *ibid.*, **54**, 149 (1965).

ACKNOWLEDGMENTS AND ADDRESSES

Received December 14, 1976, from the *Faculty of Pharmaceutical Sciences, Kanazawa University, Takara-machi, Kanazawa 920, Japan.*

Accepted for publication March 4, 1977.

Supported in part by a grant-in-aid for Scientific Research from the Ministry of Education, Science, and Culture, Japan.

The authors thank Mr. I. Kagami for technical assistance. They are also grateful to Meiji Seika Kaisha, Fujisawa Pharmaceutical Co., Banyu Pharmaceutical Co., Takeda Chemical Industries, Shionogi & Co., and Taito-Pfizer Co. for the gifts of penicillins and cephalothin.

[x] To whom inquiries should be directed.

Physiologically Based Pharmacokinetic Model for Digoxin Disposition in Dogs and Its Preliminary Application to Humans

LESTER I. HARRISON [*] and MILO GIBALDI [x]

Abstract □ A physiologically based pharmacokinetic model for digoxin disposition developed in the rat was modified to account for the interspecies differences in tissue-to-plasma digoxin concentration ratios and applied to the dog. The model provided a quantitative assessment of the time course of digoxin concentrations in dog plasma, various tissues, and urine. It also predicted the effect of renal failure on digoxin pharmacokinetics in the dog. An attempt to scale the dog model to humans by simply considering differences in organ volumes, organ flow rates, and digoxin clearances was partially successful. Good predictions of plasma digoxin concentration and urinary digoxin excretion after a single dose and of steady-state plasma, heart, and skeletal muscle digoxin concentrations were obtained. However, the model predicted considerably higher kidney digoxin concentrations than are actually found. Although the model adequately characterized the time course of digoxin concentrations in patients with moderate renal impairment, it provided a relatively poor fit to that observed in anuric patients.

Keyphrases □ Digoxin—pharmacokinetic model for disposition in dog developed, applied to humans □ Pharmacokinetics—digoxin, model for disposition in dog developed, applied to humans □ Models, pharmacokinetic—for digoxin disposition in dog, developed, applied to humans □ Cardiotonic agents—digoxin, pharmacokinetic model for disposition in dog developed, applied to humans

Two- and three-compartment open models based on curve fits of plasma concentration–time data are commonly used to describe digoxin pharmacokinetics in humans and other species (1–4). Although these models are useful for clinical application, the basic information that they provide regarding distribution and elimination is intrinsically limited. Transfer rate constants calculated from such models have a high degree of uncertainty (5). Moreover, compartment volumes and transfer rate constants derived from these models have no anatomical or physiological reality. Neither the drug concentrations nor the time course of drug concentrations in particular target tissues other than the plasma can be predicted.

Recently, there has been an interest in the development of physiologically realistic pharmacokinetic models for drug disposition based on organ volumes and blood perfusion rates. In principle, these models permit the prediction of drug concentrations in any tissue at any time and may provide considerable insight to drug dynamics. Another useful feature of these models is that drug disposition in certain pathophysiological conditions may be simulated by altering estimates of organ blood flow (6, 7), drug clearance (8), or drug binding to tissues. Furthermore, under certain conditions, physiologically based models can be scaled to apply to more than one species (9). Therefore, for certain drugs, the large data base needed to develop a physiological pharmacokinetic model may be acquired in a laboratory animal and scaled to apply to humans. This approach has been used with several drugs (6, 10–13).

A detailed physiological model (Scheme I) recently was developed to describe digoxin pharmacokinetics in the rat

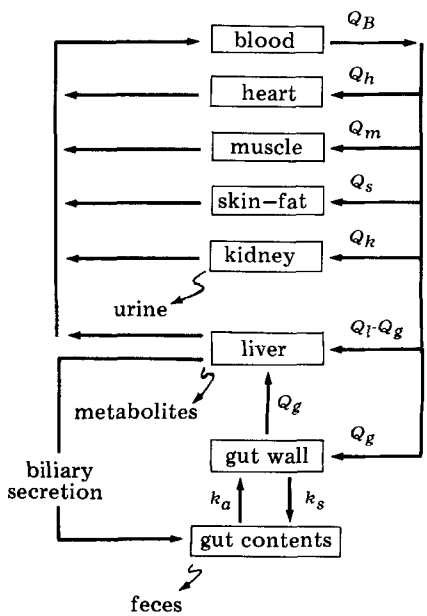

Scheme I

(15) G. L. Biagi, A. M. Barbaro, and M. C. Guerra, *J. Chromatogr.*, **51**, 548 (1970).
(16) A. Leo, C. Hansch, and D. Elkins, *Chem. Rev.*, **71**, 525 (1971).
(17) J. P. Hou and J. W. Poole, *J. Pharm. Sci.*, **58**, 1510 (1969).
(18) H. Bundgaard and K. Ilver, *Dan. Tidsskr. Farm.*, **44**, 365 (1970).
(19) M. A. Schwartz, A. P. Granatek, and F. H. Buckwalter, *J. Pharm. Sci.*, **51**, 523 (1962).
(20) P. Finholt, G. Jurgensen, and H. Kristiansen, *ibid.*, **54**, 387 (1965).
(21) M. A. Schwartz, E. Bara, I. Rubycz, and A. P. Granatek, *ibid.*, **54**, 149 (1965).

ACKNOWLEDGMENTS AND ADDRESSES

Received December 14, 1976, from the *Faculty of Pharmaceutical Sciences, Kanazawa University, Takara-machi, Kanazawa 920, Japan.*

Accepted for publication March 4, 1977.

Supported in part by a grant-in-aid for Scientific Research from the Ministry of Education, Science, and Culture, Japan.

The authors thank Mr. I. Kagami for technical assistance. They are also grateful to Meiji Seika Kaisha, Fujisawa Pharmaceutical Co., Banyu Pharmaceutical Co., Takeda Chemical Industries, Shionogi & Co., and Taito-Pfizer Co. for the gifts of penicillins and cephalothin.

[x] To whom inquiries should be directed.

Physiologically Based Pharmacokinetic Model for Digoxin Disposition in Dogs and Its Preliminary Application to Humans

LESTER I. HARRISON [*] and MILO GIBALDI [x]

Abstract □ A physiologically based pharmacokinetic model for digoxin disposition developed in the rat was modified to account for the interspecies differences in tissue-to-plasma digoxin concentration ratios and applied to the dog. The model provided a quantitative assessment of the time course of digoxin concentrations in dog plasma, various tissues, and urine. It also predicted the effect of renal failure on digoxin pharmacokinetics in the dog. An attempt to scale the dog model to humans by simply considering differences in organ volumes, organ flow rates, and digoxin clearances was partially successful. Good predictions of plasma digoxin concentration and urinary digoxin excretion after a single dose and of steady-state plasma, heart, and skeletal muscle digoxin concentrations were obtained. However, the model predicted considerably higher kidney digoxin concentrations than are actually found. Although the model adequately characterized the time course of digoxin concentrations in patients with moderate renal impairment, it provided a relatively poor fit to that observed in anuric patients.

Keyphrases □ Digoxin—pharmacokinetic model for disposition in dog developed, applied to humans □ Pharmacokinetics—digoxin, model for disposition in dog developed, applied to humans □ Models, pharmacokinetic—for digoxin disposition in dog, developed, applied to humans □ Cardiotonic agents—digoxin, pharmacokinetic model for disposition in dog developed, applied to humans

Two- and three-compartment open models based on curve fits of plasma concentration–time data are commonly used to describe digoxin pharmacokinetics in humans and other species (1–4). Although these models are useful for clinical application, the basic information that they provide regarding distribution and elimination is intrinsically limited. Transfer rate constants calculated from such models have a high degree of uncertainty (5). Moreover, compartment volumes and transfer rate constants derived from these models have no anatomical or physiological reality. Neither the drug concentrations nor the time course of drug concentrations in particular target tissues other than the plasma can be predicted.

Recently, there has been an interest in the development of physiologically realistic pharmacokinetic models for drug disposition based on organ volumes and blood perfusion rates. In principle, these models permit the prediction of drug concentrations in any tissue at any time and may provide considerable insight to drug dynamics. Another useful feature of these models is that drug disposition in certain pathophysiological conditions may be simulated by altering estimates of organ blood flow (6, 7), drug clearance (8), or drug binding to tissues. Furthermore, under certain conditions, physiologically based models can be scaled to apply to more than one species (9). Therefore, for certain drugs, the large data base needed to develop a physiological pharmacokinetic model may be acquired in a laboratory animal and scaled to apply to humans. This approach has been used with several drugs (6, 10–13).

A detailed physiological model (Scheme I) recently was developed to describe digoxin pharmacokinetics in the rat

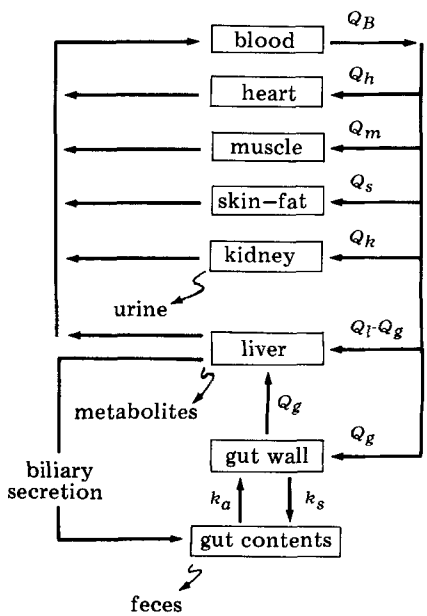

Scheme I

Table I—Physiological and Experimental Constants for Digoxin Distribution

Tissue	Volume[a], liters		Blood Flow, liters/hr		R_i[d]
	Dog	Human	Dog[b]	Human[c]	
Blood	0.5	5.4	—	—	—
Heart	0.05	0.3	3	15	40
Skeletal muscle	5.0	30.0	12	75	9
Skin, fat, *etc.*[e]	3.5	30.0	12	75	9
Kidney	0.05	0.3	12	80	200
Liver	0.25	1.5	24	100	15
GI tissues	0.24	1.0	18	70	30
GI contents	0.42	1.7	—	—	—

[a] Values for a 10-kg dog and a 70-kg human (11, 29, 40). [b] Total blood flow = 63 liters/hr (41, 42). [c] Total blood flow = 345 liters/hr (6, 40). [d] Tissue-to-plasma digoxin concentration ratios; values estimated in the dog (17, 18). [e] Lump compartment incorporating all other body regions.

(8). This model describes the time course of plasma and tissue digoxin concentrations in normal rats as well as the time course of plasma digoxin concentrations in rats with ligated bile ducts or ligated ureters. The model also predicts successfully the time course of urinary digoxin excretion in normal and bile duct-ligated rats.

Although the pharmacokinetic model is a qualitatively accurate representation of digoxin disposition not only in the rat but also in other species, including humans, direct quantitative scale-up was not possible because of substantial differences in tissue-to-plasma digoxin concentration ratios between rats and humans (8). For example, rat kidneys and heart show little ability to concentrate digoxin whereas kidney-to-plasma and heart-to-plasma digoxin concentration ratios in humans exceed 30 (14). The present report concerns efforts to develop a physiological pharmacokinetic model for digoxin disposition in the dog, a species in which digoxin distribution appears similar to that observed in humans, and to extend this model to humans.

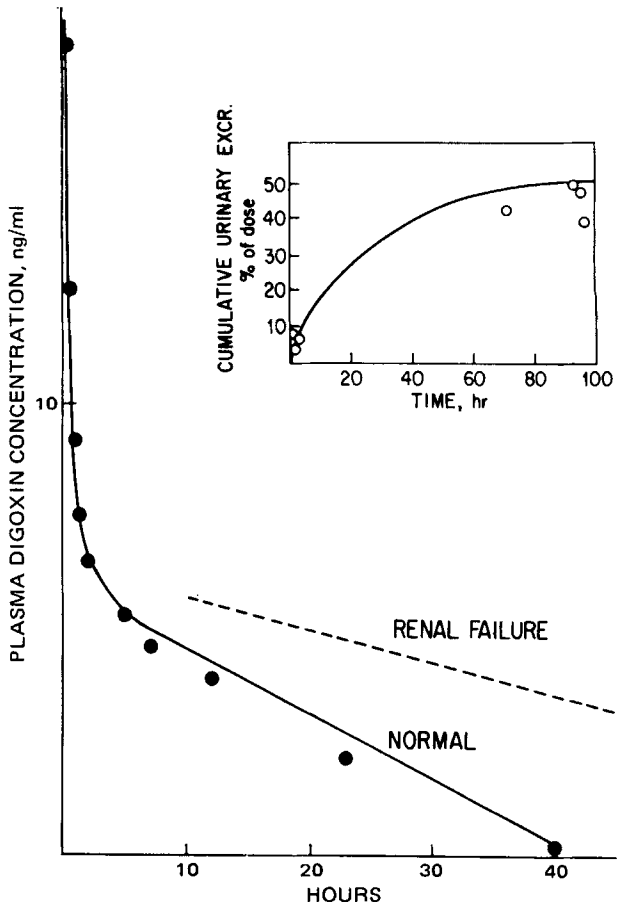

Figure 1—*Predicted plasma digoxin concentrations in normal (—) and ureter-ligated (- - -) dogs after a 50-μg/kg iv dose. The closed circles are data from dogs given the same dose (from Ref. 17). The inset shows the predicted (—) and observed (○) cumulative urinary excretion in the dog after a single dose. Experimental data were taken from Refs. 46–48.*

EXPERIMENTAL

The model shown in Scheme I adequately describes the pharmacokinetics of digoxin disposition in the rat. *A priori,* the same model seemed to be a reasonable choice for the dog and human. This model assumes that each tissue acts as a well-stirred compartment, that drug distribution is blood flow rate limited, that tissue-to-plasma digoxin concentration ratios are independent of drug concentration, and that all rate processes are linear.

A mathematical description of the model is given in the *Appendix*. The concentration of a drug in a tissue, C_i, depends on the volume of the tissue, V_i, the blood flow through the tissue, Q_i, the drug concentration in the blood, C_B, the binding of the drug in the tissue relative to its binding in the blood, R_i, and the tissue's ability to eliminate or clear the drug irreversibly, K_i, *i.e.*:

$$V_i(dC_i/dt) = Q_i[C_B - (C_i/R_i)] - K_iC_i/R_i \qquad \text{(Eq. 1)}$$

Organ volumes and blood flow rates for a 10-kg dog and for a 70-kg human are given in Table I. Since digoxin has little effect on cardiac output (15, 16), blood flow rate values are those estimated in normal individuals. Also listed in Table I are tissue-to-plasma digoxin concentration ratios determined during steady-state studies in dogs (17, 18).

Table II—Clearance and Rate Constants for Digoxin Disposition

Parameter	Estimate	
	Dog	Human
Renal clearance	2.4 liters/hr	7.5 liters/hr
Hepatic clearance	0.8 liter/hr	2.5 liters/hr
Biliary clearance	0.5 liter/hr	1.5 liters/hr
GI clearance	0.04 liter/hr	0.05 liter/hr
Absorption rate constant	0.22 hr^{-1}	0.22 hr^{-1}
Secretion rate constant	0.44 hr^{-1}	0.44 hr^{-1}

Estimates of the required clearance parameters and rate constants are listed in Table II. Renal clearance of digoxin was assumed to be equal to the glomerular filtration rate (19, 20); the net contribution of tubular secretion (21) and reabsorption (22) was considered negligible. The total body clearance of digoxin in each species was estimated from plasma or serum digoxin concentration data after intravenous injection (2, 3, 17, 21). Metabolic clearance was assumed to be the difference between total body clearance and renal clearance. Biliary clearance was estimated from literature data (18, 23).

Initial estimates of fecal clearance of digoxin for dogs and humans were about 0.02 and 0.05 liter/hr, respectively. These values were calculated by assuming a 20-hr half-life for gut transit for both species (24, 25). For the dog, however, simulations based on this estimate resulted in higher digoxin concentration in the plasma and in higher urinary excretion rates than those observed in various studies. After testing several estimates, a value of 0.04 liter/hr was selected. The need for a higher estimate of fecal clearance suggests that digoxin transit from the absorption site(s) is faster than the average transit of fluid through the gut or that other processes, such as gut or bacterial metabolism, contribute to the elimination of digoxin from the GI tract.

The absorption half-life for digoxin was assumed to be 1 hr for both species (26). The rate constant for GI secretion was set equal to twice the absorption rate constant based on previous studies in the rat (8).

The mass balance equations described in the *Appendix* and the constants listed in Tables I and II served as input for a digital computer analog simulation program (27) to calculate digoxin concentrations in the various model compartments. Predicted digoxin concentrations in blood were assumed equal to those in plasma since the blood/plasma digoxin concentration ratio is about unity in both dogs and humans (28). Steady-state digoxin levels were simulated by incorporating a zero-order

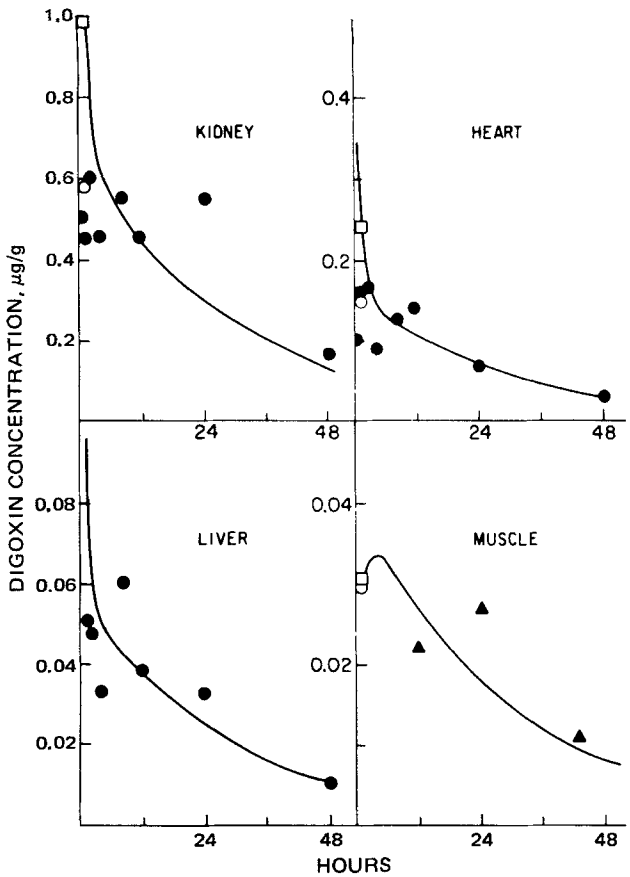

Figure 2—*Predicted (—) and observed digoxin concentrations in different tissues after a 50-μg/kg iv dose to normal dogs. Experimental data were taken from Refs. 17 (●), 47 (▲), 31 (○), and 48 (□).*

input function into the appropriate equations listed in the *Appendix*.

Literature values for plasma and tissue digoxin concentrations in the dog were based on total tritium assays. Most literature references for plasma and tissue digoxin levels in humans utilized either radioimmunoassay or ^{86}Rb-uptake measurements. Reported values in Refs. 1, 18, 19, and 29–31 were based on total tritium analyses. In all cases in which

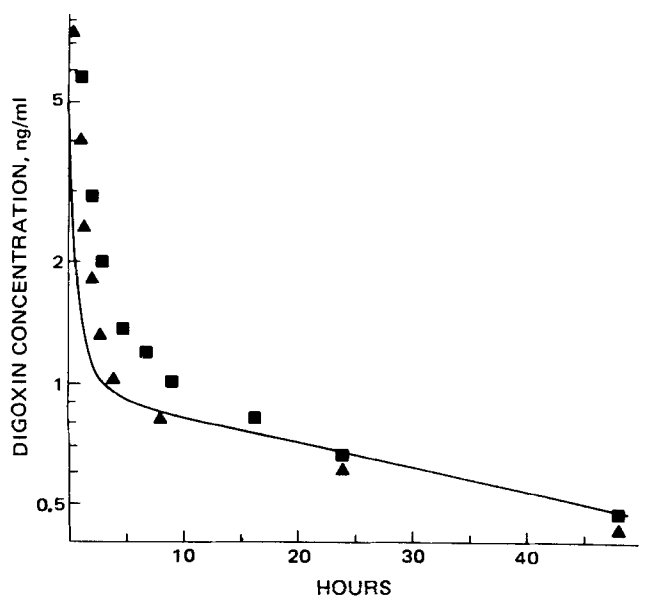

Figure 3—*Predicted (—) and observed plasma digoxin concentrations in adults given a 0.75-mg iv dose. Experimental data were taken from Refs. 34 (▲) and 36 (■).*

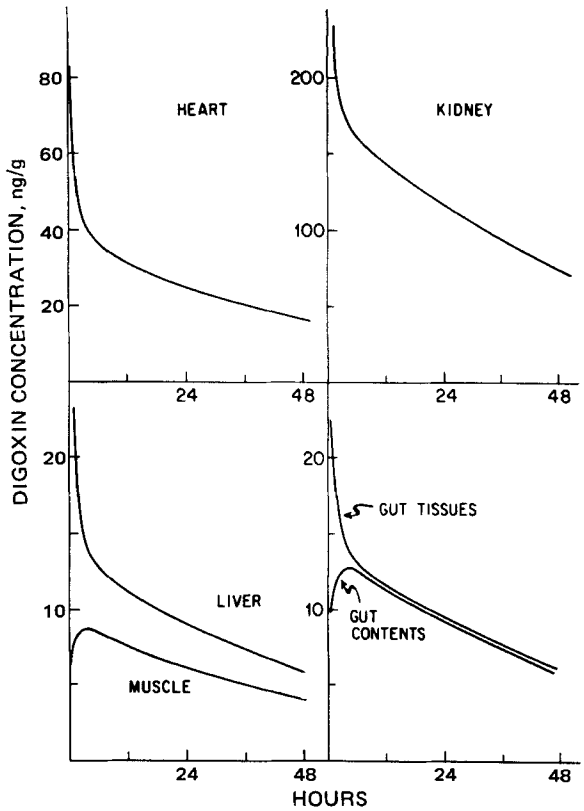

Figure 4—*Predicted tissue digoxin concentrations in adults given a single 0.75-mg iv dose.*

renal function was normal, the values probably closely reflect unchanged digoxin concentrations.

RESULTS AND DISCUSSION

Predicted digoxin concentrations in the plasma and in certain tissues of the dog after a 50-μg/kg iv dose are compared to observed values in Figs. 1 and 2. In general, good agreement is noted. The model also provided a reasonably good prediction of the urinary excretion of digoxin in the dog (inset in Fig. 1).

A pharmacokinetic model for digoxin disposition in dogs with renal failure was developed by setting renal clearance equal to zero but maintaining all other parameters constant. The postdistributive plasma digoxin concentrations after a single intravenous dose, as predicted by the

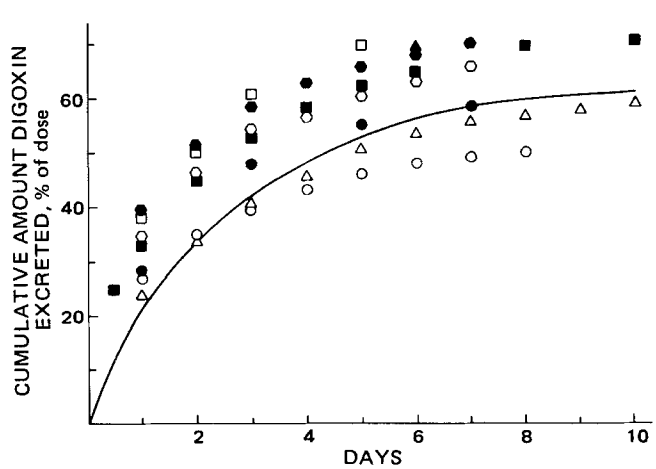

Figure 5—*Predicted (—) and observed cumulative urinary excretion of digoxin in adults after an intravenous dose. Experimental data were taken from Refs. 19 (●), 1 (□), 29 (●), 34 (▲), 35 (△), 36 (■), 30 (○), and 38 (○).*

Table III—Observed and Predicted Steady-State Digoxin Concentrations[a] (Nanograms per Gram) in Various Tissues of Patients Receiving Digoxin Maintenance Therapy

Number of Patients	Plasma Digoxin Concentration, ng/ml	Heart[b]	Skeletal Muscle	Liver	Kidneys	Reference
		Observed				
3	1.3–2.3	LV = 58 ± 18 RV = 47 ± 13 LA = 19 ± 7	8 ± 2	33 ± 6	94 ± 54	33
12	0.9–1.9	V = 133 ± 16 A = 65 ± 9	30 ± 4	72 ± 13	128 ± 20	14
4	1.0–2.5	95 ± 30	9 ± 2	—	—	43
12	1.0–2.3	86 ± 41	—	—	—	32
10	0.9–2.4	31 ± 13	—	—	—	44
8	1.0–2.2	107 ± 33	—	—	—	45
		Predicted				
—	0.9–2.5	36–100	8–23	14–38	180–500	—

[a] Concentration ± *SD*. [b] LV = left ventricle, RV = right ventricle, LA = left atrium, V = ventricle, and A = atrium.

modified model, are shown in Fig. 1. The pharmacokinetic model indicates that both plasma and tissue digoxin concentrations are elevated in the anuric dog compared to those in the dog with normal renal function. These findings are consistent with experimental observations in dogs with ligated ureters (18).

The physiologically based pharmacokinetic model developed for the dog was scaled to apply to humans by adjusting only organ blood flow rates, organ volumes, and clearance parameters (Tables I and II). Predicted and observed plasma digoxin concentrations in adults given a 0.75-mg iv dose are compared in Fig. 3. Although the model predictions underestimate the early digoxin concentrations, good agreement is seen after 10 hr. Many reasons are possible for the initially poor predictions. Estimates of average blood flows and tissue-to-plasma concentration ratios (Table I) or of average biliary clearance (Table II) may be too high to reflect accurately the situation in these patients. Alternatively, diffusion of drug to the intracellular space may play a more important role than is assumed by a blood flow rate-limited distribution model.

The predicted tissue digoxin concentrations in humans after a single intravenous dose, based on tissue-to-plasma digoxin concentration ratios estimated in the dog, are shown in Fig. 4. Unfortunately, there are little published data to compare with these values. However, postmortem measurements of tissue digoxin levels in patients who had been receiving digoxin maintenance therapy and who had plasma digoxin concentrations of 0.9–1.9 ng/ml (14, 32, 33) are in good agreement with predicted steady-state digoxin levels in plasma, heart, and skeletal muscle (Table III). Postmortem digoxin concentrations in the liver are about 1.5–2 times greater than those predicted. A larger difference was noted between observed and predicted digoxin concentrations in the kidney; predicted digoxin levels are two to three times higher than those found.

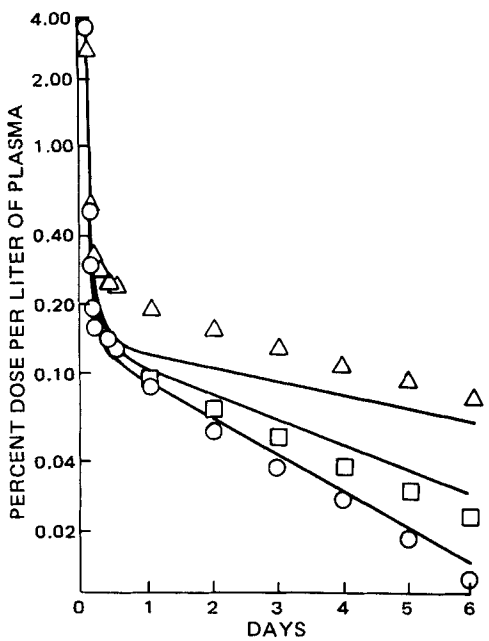

Figure 6—*Predicted (—) and observed plasma digoxin concentrations in patients with normal renal function (○), in patients with moderate renal impairment (□), and in patients with severe renal failure (△). Experimental data were taken from Ref. 19.*

A wide range of results has been reported for the urinary digoxin excretion in patients with normal renal function (1, 19, 29–31, 34–36). The predicted urinary excretion rate of digoxin is consistent with these data (Fig. 5).

An effort to simulate plasma digoxin concentrations in patients with impaired renal function by simply reducing the renal clearance parameter of the model was only partially successful. Figure 6 shows predicted and observed plasma digoxin levels after a single intravenous dose to patients with different degrees of renal function. Reasonably good predictions of plasma digoxin concentrations are seen for patients with normal renal function and with moderate renal impairment, *i.e.*, renal function about 50% of normal. However, the predicted plasma digoxin levels of anephric patients consistently underestimate the observed values. This discrepancy may be related in part to the fact that uremia also decreases the binding of digoxin to myocardial tissue (37) as well as its apparent volume of distribution (3, 38). More importantly, it undoubtedly reflects the use of a nonspecific assay that measures digoxin as well as all its metabolites that accumulate in the absence of renal function, thus overestimating digoxin concentration.

In conclusion, the present pharmacokinetic model requires significant modification before it can be used to describe the average time course of digoxin in humans. It is also evident, at least with digoxin, that it is not reasonable to assume that tissue-to-plasma drug concentration ratios are similar in different species. Scaling of physiological models must routinely consider such differences.

APPENDIX

The following mass balance–blood flow equations describe the concentrations in each compartment of the pharmacokinetic model shown in Scheme I:

$$V_B(dC_B/dt) = (Q_hC_h/R_h) + (Q_mC_m/R_m) + (Q_sC_s/R_s) + (Q_kC_k/R_k) + (Q_lC_l/R_l) - Q_BC_B \quad \text{(Eq. A1)}$$

$$V_h(dC_h/dt) = Q_h[C_B - (C_h/R_h)] \quad \text{(Eq. A2)}$$

$$V_m(dC_m/dt) = Q_m[C_B - (C_m/R_m)] \quad \text{(Eq. A3)}$$

$$V_s(dC_s/dt) = Q_s[C_B - (C_s/R_s)] \quad \text{(Eq. A4)}$$

$$V_k(dC_k/dt) = Q_k[C_B - (C_k/R_k)] - (K_kC_k/R_k) \quad \text{(Eq. A5)}$$

$$V_l(dC_l/dt) = (Q_l - Q_g)C_B + (Q_gC_g/R_g) - (Q_lC_l/R_l) - (K_lC_l/R_l) - (K_bC_l/R_l) \quad \text{(Eq. A6)}$$

$$V_g(dC_g/dt) = Q_g[C_B - (C_g/R_g)] + k_aV_cC_c - k_sV_gC_g \quad \text{(Eq. A7)}$$

$$V_c(dC_c/dt) = k_sV_gC_g + (K_bC_l/R_l) - k_aV_cC_c - K_gC_c \quad \text{(Eq. A8)}$$

where K_k, K_l, K_b, and K_g represent renal, metabolic, biliary, and GI clearances, respectively; and k_a and k_s represent first-order rate constants for GI absorption and secretion, respectively. The terms V_i, C_i, Q_i, and R_i represent tissue volumes, drug concentrations, blood flow rates, and tissue-to-blood partition coefficients, respectively. The subscripts of these terms are as follows: B = blood; h = heart; m = skeletal muscle; s = skin, fat, *etc.*; k = kidney; l = liver; g = GI tissues; and c = GI contents.

REFERENCES

(1) J. E. Doherty and W. H. Perkins, *Am. Heart J.*, **63,** 528 (1962).

(2) L. Nyberg, K.-E. Andersson, and Å. Bertler, *Acta Pharm. Suec.*, **11,** 459 (1974).

(3) R. H. Reuning, R. A. Sams, and R. E. Notari, *J. Clin. Pharmacol.*, **13,** 127 (1973).

(4) D. J. Sumner, A. J. Russell, and B. Whiting, *Br. J. Clin. Pharmacol.*, **3,** 221 (1976).

(5) W. J. Westlake, *J. Pharm. Sci.*, **60,** 882 (1971).

(6) N. Benowitz, R. P. Forsyth, K. L. Melmon, and M. Rowland, *Clin. Pharmacol. Ther.*, **16,** 87 (1974).

(7) *Ibid.*, **16,** 99 (1974).

(8) L. I. Harrison and M. Gibaldi, *J. Pharm. Sci.*, **66,** 1138 (1977).

(9) R. L. Dedrick, *J. Pharmacokinet. Biopharm.*, **1,** 435 (1973).

(10) K. B. Bischoff and R. L. Dedrick, *J. Pharm. Sci.*, **57,** 1346 (1968).

(11) K. B. Bischoff, R. L. Dedrick, D. S. Zaharko, and J. A. Longstreth, *ibid.*, **60,** 1128 (1971).

(12) R. L. Dedrick, D. D. Forrester, J. N. Cannon, S. M. El Dareer, and L. M. Mellett, *Biochem. Pharmacol.*, **22,** 2405 (1973).

(13) B. Montandon, R. J. Roberts, and L. J. Fisher, *J. Pharmacokinet. Biopharm.*, **3,** 277 (1975).

(14) K.-E. Andersson, Å. Bertler, and G. Wettrell, *Acta Ped. Scand.*, **64,** 497 (1975).

(15) C. E. Harrison and K. G. Waken, *Circ. Res.*, **24,** 263 (1969).

(16) T. W. Smith and E. Haber, *N. Engl. J. Med.*, **289,** 1010 (1973).

(17) J. E. Doherty and W. H. Perkins, *Am. J. Cardiol.*, **17,** 47 (1966).

(18) F. I. Marcus, A. Peterson, A. Salel, J. Scully, and G. G. Kapadia, *J. Pharmacol. Exp. Ther.*, **152,** 373 (1966).

(19) P. M. Bloom, W. B. Nelp, and S. H. Tuell, *Am. J. Med. Sci.*, **251,** 133 (1966).

(20) T. W. Smith and E. Haber, *N. Engl. J. Med.*, **289,** 1063 (1973).

(21) J. R. Koup, D. J. Greenblatt, W. J. Jusko, T. W. Smith, and J. Koch-Weser, *J. Pharmacokinet. Biopharm.*, **3,** 181 (1975).

(22) H. Halkin, K. B. Sheiner, C. C. Peck, and K. L. Melmon, *Clin. Pharmacol. Ther.*, **17,** 385 (1975).

(23) J. Q. Russell and C. D. Klaassen, *J. Pharmacol. Exp. Ther.*, **186,** 455 (1973).

(24) S. R. Bernard and R. L. Hayes, in "Medical Radionuclides: Radiation Dose and Effects," R. J. Cloutier, C. L. Edwards, and W. D. Snyder, Eds., U.S. Atomic Energy Commission, Division of Technical Information Extension, Oak Ridge, Tenn., 1970, pp. 295–314.

(25) I. S. Eve, *Health Phys.*, **12,** 131 (1966).

(26) K.-E. Andersson, L. Nyberg, H. Denker, and J. Göthlin, *Eur. J. Clin. Pharmacol.*, **9,** 39 (1975).

(27) "MIMED, State University of New York at Buffalo Computer Center Adaptation of MIMIC," Publication 44610400, Control Data Corp., St. Paul, Minn., 1968.

(28) U. Abshagen, H. Kewitz, and N. Rietbrock, *Naunyn-Schmiedebergs Arch. Pharmakol.*, **270,** 105 (1971).

(29) J. E. Doherty, W. J. Flannigan, M. L. Murphy, R. T. Bullock, G. L. Dalyrymple, O. W. Beard, and W. H. Perkins, *Circulation*, **42,** 867 (1970).

(30) F. I. Marcus, G. J. Kapadia, and G. G. Kapadia, *J. Pharmacol. Exp. Ther.*, **145,** 203 (1964).

(31) F. I. Marcus, J. Pavlovich, M. Lullin, and G. Kapadia, *ibid.*, **159,** 314 (1968).

(32) P. R. Carroll, A. Gelbort, M. F. O'Rourke, and J. Shortus, *Aust. N.Z. J. Med.*, **3,** 400 (1973).

(33) J. Karjalainen, K. Ojala, and P. Reissell, *Acta Pharmacol. Toxicol.*, **34,** 385 (1974).

(34) D. J. Greenblatt, D. W. Duhme, J. Koch-Weser, and T. W. Smith, *Clin. Pharmacol. Ther.*, **15,** 510 (1974).

(35) D. H. Huffman and D. L. Azarnoff, *J. Am. Med. Assoc.*, **222,** 957 (1972).

(36) B. F. Johnson and C. Bye, *Br. Heart J.*, **37,** 203 (1975).

(37) W. J. Jusko and M. Weintraub, *Clin. Pharmacol. Ther.*, **16,** 449 (1974).

(38) J. R. Koup, W. J. Jusko, C. M. Elwood, and R. K. Kohli, *ibid.*, **18,** 9 (1975).

(39) E. F. Adolf, *Science*, **109,** 579 (1949).

(40) W. W. Mapleson, *J. Appl. Physiol.*, **18,** 197 (1963).

(41) G. Bounos, L. G. Hampson, and F. N. Gurd, *Arch. Surg.*, **87,** 340 (1963).

(42) S. Kaihara, R. D. Rutherford, E. P. Schwentker, and H. N. Wagner, *J. Appl. Physiol.*, **27,** 218 (1969).

(43) J. Coltart, M. Howard, and D. Chamberlain, *Br. Med. J.*, **2,** 318 (1972).

(44) H.-G. Gullner, E. B. Stinson, D. C. Harrison, and S. M. Kalman, *Circulation*, **50,** 653 (1974).

(45) G. Härtel, K. Kyllönen, E. Merikallio, K. Ojala, V. Manninen, and P. Reissel, *Clin. Pharmacol. Ther.*, **19,** 153 (1976).

(46) L. F. Gonzalez and E. C. Layne, *J. Clin. Invest.*, **39,** 1578 (1960).

(47) C. E. Harrison, R. O. Brandenburg, P. A. Ongley, A. L. Orvis, and C. A. Owen, *J. Lab. Clin. Med.*, **67,** 764 (1966).

(48) F. I. Marcus, L. Nimmo, G. G. Kapadia, and C. Goldsmith, *J. Pharmacol. Exp. Ther.*, **178,** 271 (1971).

ACKNOWLEDGMENTS AND ADDRESSES

Received November 2, 1976, from the *Department of Pharmaceutics, School of Pharmacy, State University of New York at Buffalo, Amherst, NY 14260.*

Accepted for publication February 15, 1977.

Supported in part by Grant GM-20852 from the National Institutes of Health.

* Present address: Drug Metabolism, Riker Laboratories, 3M Center, St. Paul, MN 55101.

ˣ To whom inquiries should be directed.

Fluorescence Studies of Oxygen Binding in *Limulus* Hemocyanin

JOSEPH K. H. MA *x, LOUIS A. LUZZI *, JANE Y. C. MA ‡, and NORMAN C. LI ‡

Abstract □ *Limulus* hemocyanin, a weakly fluorescent copper protein when oxygenated, is highly fluorescent in the deoxygenated forms. A large enhancement of the fluorescence yield, 8.8-fold at neutral pH, was observed on complete deoxygenation, and a 9.4-fold increase was observed on removal of copper from oxyhemocyanin. The weak fluorescence of oxyhemocyanin is attributed to radiationless energy transfer from the tryptophan residues to the Cu···O group. The average distance between these two moieties was 21.4 Å. In oxyhemocyanin, the active site containing copper and oxygen is strongly hydrophobic, and a change in oxygen binding may profoundly alter the hydrophobic structure of the protein. This alteration is indicated by the binding of tetracycline to the protein where the distance between tryptophans and the tetracycline binding site is significantly increased when the protein is deoxygenated or when copper is removed. From the fluorescence results, it was found that the Cu···O group in *Limulus*, an arthropod hemocyanin, is nearer and interacts more strongly with the tryptophan residues than these groups in the mollusk (*Leventina hierosolima* and *Murex trunculus*) hemocyanins. Deoxygenation of oxyhemocyanin by sodium sulfite was catalyzed by trace amounts of certain metal ions. The reaction rate was increased significantly by Co(II), Cu(II), and Mn(II), in decreasing order, but not by Zn(II).

Keyphrases □ *Limulus* hemocyanin—oxygen binding, energy transfer, fluorometric study □ Hemocyanin, *Limulus*—oxygen binding, energy transfer, fluorometric study □ Oxygen binding—*Limulus* hemocyanin, fluorometric study □ Energy transfer—*Limulus* hemocyanin, fluorometric study □ Fluorometry—study of *Limulus* hemocyanin oxygen binding and energy transfer

Hemocyanin is a nonheme, oxygen-carrying copper protein found in many mollusks and arthropods. The protein, a deep-blue color when oxygenated, becomes colorless when deoxygenated. One oxygen molecule binds to two copper atoms in the protein (1). All hemocyanins reversibly bind oxygen and, in most cases, appear to play a physiological role analogous to that of hemoglobin in higher animals, *i.e.*, the transport of oxygen to tissues.

BACKGROUND

While the oxygen binding phenomenon of hemocyanin has been known for some time, the binding mechanism and the nature of the binding site are still not clear. Spectrophotometric studies showed that the absorption spectrum of a deoxyhemocyanin is, in general, a typical protein spectrum. Upon binding oxygen, hemocyanin exhibits a profound change in its absorption spectrum. In addition to the absorption at 280 nm, strong bands in the 340–350- and 400–800-nm regions have been observed. Oxygen binding also results in profound changes in the fluorescence spectrum of the protein.

Shaklai and Daniel (2), in studying the fluorescence of mollusk *Levantina hierosolima* hemocyanin, reported that when the protein was deoxygenated or when copper was removed, the fluorescence yield at pH 6.6 increased fourfold in each case. The fluorescence change was traced to radiationless energy transfer from the tryptophan residues to the Cu···O groups with the average distance between the two units reported to be about 25 Å. Bannister and coworkers (3, 4) reported that for *Murex trunculus*, another mollusk hemocyanin, the fluorescence was attributable to tryptophan and that the fluorescence was enhanced 513% when copper was removed from the protein.

Fluorescence spectroscopy is a useful tool for energy transfer studies. In a protein, the fluorescent tryptophan residue may transfer its electronic energy to a bound ligand if, among other conditions, the two units are closely located on the macromolecule. The energy transfer data permit calculation of the distance between the energy donor and acceptor and, thus, provide useful information about the nature of the binding site. In this investigation, the energy transfer studies on *Limulus* hemocyanin, an arthropod protein that has been extensively investigated for rapid endotoxin assay (5), were carried out using the fluorescence technique. The reasons for this investigation were:

1. There are significant differences between hemocyanins from mollusks and arthropods, including differences in molecular architecture as revealed by electron microscopy, circular dichroism, and subunit dissociation properties (6). Fluorescence studies have been reported only on mollusk hemocyanin.
2. The equations used previously (2) for the energy transfer calculations need to be modified.

To provide additional insight into the oxygen binding of hemocyanin, the effect of metal ions on the deoxygenation of *Limulus* hemocyanin and the effect of oxygen binding on protein interaction with small molecules also were studied. The latter is demonstrated by the binding and energy transfer studies of tetracycline with oxy-, deoxy-, and apohemocyanins.

EXPERIMENTAL

Materials—*Limulus* hemocyanin hemolymph[1] was purified as follows (7, 8). The hemolymph was centrifuged[2] in the cold (4°) at 120,000×*g*. The pellet was dissolved with a small amount of water, dialyzed against water at 4° for 2 days, and ultracentrifuged again; the resulting pellet was dissolved in water. The purified protein was stored at 4°.

Dilutions of the protein solutions were made using 0.05 *M* tromethamine hydrochloride buffer, pH 7. The protein concentration was determined from the absorbance at 280 nm ($E^{1\%}_{1cm}$ = 15.71), using a value of 74,900 for the molecular weight carrying one oxygen binding site in hemocyanin (7, 8). The purified protein did not display a detectable Cu(II) electron spin resonance signal measured at 77° K with a spectrometer[3] operating at 9.06 GHz.

Apohemocyanin was prepared by dialyzing a 3% solution of the purified oxyhemocyanin against 0.1 *M* phosphate buffer containing 0.1 *M* KCN and 0.05 *M* $MgCl_2$ at pH 7.8 for 2 days. Excess cyanide was removed by dialyzing against water for 2 days. The apohemocyanin thus prepared showed no absorption at 340 nm.

Tetracycline hydrochloride[4] and bovine serum albumin[5] were obtained commercially. All other chemicals were reagent grade.

Instruments and Methods—Fluorescence measurements were made with a spectrophotofluorometer[6] equipped with a 150-w xenon lamp, a 1P21 photomultiplier tube, and an *x-y* spectral recorder[7]. The absorption spectra were recorded with a spectrophotometer[8] using a matched set of 1-cm cells. Unless otherwise mentioned, all experiments were carried out in pH 7 tromethamine at 25 ± 0.5°. Fluorescence quenching titrations, in which the fluorescence of the protein was recorded after each addition of a small amount of tetracycline (2 μl of a 0.01 or 0.001 *M* stock solution), were performed manually with microsyringes.

Binding Studies—The binding of tetracycline to hemocyanin was determined using the Scatchard equation:

$$\overline{V}/D_f = nK - \overline{V}K \qquad \text{(Eq. 1)}$$

where $\overline{V}$ is the number of moles of bound tetracycline (D_b) per mole of

[1] Marine Biological Laboratory, Woods Hole, Mass.
[2] Spinco model L ultracentrifuge.
[3] Model E-4, Varian Instrument Division, Palo Alto, Calif.
[4] Lot 73F503, Bristol Laboratories, Syracuse, N.Y.
[5] Lot 1662, Nutritional Biochemicals Corp.
[6] Aminco-Bowman, American Instrument Co., Silver Spring, Md.
[7] Omnigraphic, Houston Instrument, Bellaire, Tex.
[8] Cary 118, model C, Varian Instrument Division, Palo Alto, Calif.

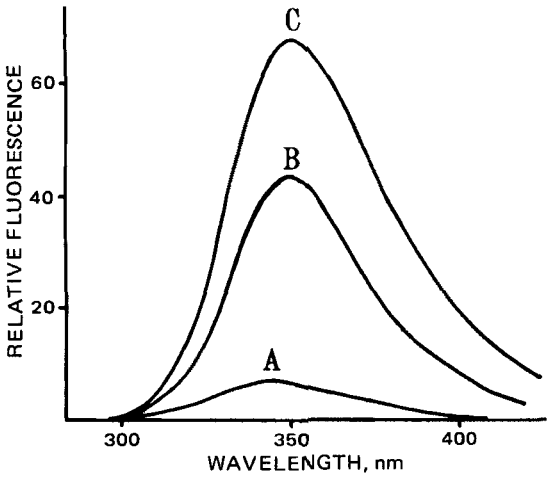

Figure 1—*Fluorescence spectra of* Limulus *hemocyanin in pH 7 tromethamine (excited at 280 nm). Key: A, 1.36 × 10⁻⁶ M oxyhemocyanin; B, 1.36 × 10⁻⁶ M oxyhemocyanin with 0.003 M sodium sulfite (the spectrum was taken after the sample was stored in the covered cell compartment for 25 min); and C, 1.36 × 10⁻⁶ M apohemocyanin.*

protein, D_f is the concentration of unbound tetracycline, n is the number of binding sites, and K is the binding constant. To calculate D_b, from which the values of $\overline{V}$ and D_f were obtained, fluorescence quenching titrations were made over a range of protein concentrations. The fluorescence intensities, expressed as percentages of the initial fluorescence of the protein, were then plotted as a function of the tetracycline–protein concentration ratio. Above a certain critical protein concentration, the titration curves were superimposable since all tetracycline molecules were bound. The concentration of bound tetracycline for a solution of lower protein concentration was then calculated by (9):

$$D_b = (D_t)(R_h)/(R_l) \qquad \text{(Eq. 2)}$$

where D_t is the total tetracycline concentration, and R_h and R_l are the tetracycline–protein ratios at the same intensity for high and low protein solutions, respectively. In this study, tetracycline binding to 1.36×10^{-6} M oxy- and apohemocyanins was determined using 3.4×10^{-5} M as the high protein concentration.

Energy Transfer Theory—The quenching of the fluorescence of deoxyhemocyanin by oxygen binding is due to the energy transfer from excited-state tryptophan residues (energy donor) to the Cu···O groups (energy acceptors). The energy transfer information allows calculation of the mean distances, R, between the donor and acceptor by (10):

$$X/(1 - X) = (R_0/R)^6 \qquad \text{(Eq. 3)}$$

where X is the fraction of the absorbed photons transferred and R_0 is the characteristic distance at which the probability of energy transfer is equal to the probability of fluorescence. The fraction of energy transfer read may be calculated from the percent quenching of the protein fluorescence.

According to Forster's theory (11):

$$R_0 = (1.69 \times 10^{-33} \tau J_v / n^2 \overline{v}_0^2)^{1/6} \text{ cm} \qquad \text{(Eq. 4)}$$

where τ is the fluorescence lifetime of the donor in the absence of transfer, n is the refractive index of the solvent, $\overline{v}_0$ is the mean of the wave numbers of the maximum absorption of the acceptor and the emission of the donor, and J_v is the overlap integral. To determine J_v and $\overline{v}_0$, Eq. 5 may be used:

$$J_v = \int_0^\infty E(v)F(v)dv \qquad \text{(Eq. 5)}$$

where $E(v)$ is the molar absorption coefficient of the acceptor and $F(v)$ is the molar emission coefficient of the donor. The molar emission function, $F(v)$, represents the photospectral distribution of the fluorescence in the unit set by the equality that $F(v)$ at maximum emission equals the molar absorption coefficient of the donor. The values of J_v and $\overline{v}_0$ can be determined graphically. A simplified approach to the determination of J_v was introduced by Weber (12) using Gaussian approximations. By letting:

$$E(v) = E_1 \exp - [(v - v_a)/\sigma_a]^2 \qquad \text{(Eq. 6)}$$

$$F(v) = E_2 \exp - [(v - v_e)/\sigma_e]^2 \qquad \text{(Eq. 7)}$$

the overlap integral was obtained as:

$$J_v = E_1 E_2 \frac{\sqrt{\pi}}{\sqrt{\frac{1}{\sigma_a^2} + \frac{1}{\sigma_e^2}}} \exp - [(v_a - v_e)^2/(\sigma_a^2 + \sigma_e^2)] \qquad \text{(Eq. 8)}$$

where E_1 and E_2 are the maximum molar absorption coefficients for the acceptor and donor, respectively; v_a is the wave number of maximum absorption of the acceptor with standard deviation σ_a; and v_e is the wave number of maximum emission of the donor with standard deviation σ_e. Equation 8 was used in the energy transfer studies of *L. hierosolima* hemocyanin (2). However, the equation is subject to modification since Eqs. 6 and 7 do not represent the Gaussian distribution. To represent the Gaussian curves, where 1 SD = ~68% of the total curve area, Eqs. 6 and 7 should be rewritten as:

$$E(v) = E_1 \exp - \tfrac{1}{2}[(v - v_a)/\sigma_a]^2 \qquad \text{(Eq. 9)}$$

$$F(v) = E_2 \exp - \tfrac{1}{2}[(v - v_e)/\sigma_e]^2 \qquad \text{(Eq. 10)}$$

By using Eqs. 9 and 10, the integration of Eq. 5 gives:

$$J_v = E_1 E_2 \frac{\sqrt{2\pi}}{\sqrt{\frac{1}{\sigma_a^2} + \frac{1}{\sigma_e^2}}} \exp - \tfrac{1}{2}[(v_a - v_e)^2/(\sigma_a^2 + \sigma_e^2)] \qquad \text{(Eq. 11)}$$

The maximum of the overlap function, $\overline{v}_0$, can be calculated from the following equation:

$$\overline{v}_0 = (\sigma_e^2 v_a + \sigma_a^2 v_e)/(\sigma_a^2 + \sigma_e^2) \qquad \text{(Eq. 12)}$$

The result calculated from Eq. 11 is significantly different from that calculated from Eq. 8, especially in a system where the absorption maximum of the acceptor and the emission of the donor are largely separated.

RESULTS AND DISCUSSION

The fluorescence spectra of 1.36×10^{-6} M oxyhemocyanin and apohemocyanin from *Limulus*, measured in pH 7 tromethamine, are shown in Fig. 1. The excitation and emission maxima for oxyhemocyanin were 280 and 345 nm, respectively. Apohemocyanin, the copper-free protein, showed an enhanced fluorescence, 10-fold in intensity as compared to oxyhemocyanin at 350 nm (curve C). Curve B shows the effect of sodium sulfite (0.003 M) on oxyhemocyanin fluorescence. The spectrum was taken after the sample was stored in the covered cell compartment for 25 min when the intensity had ceased to increase. Deoxygenation was indicated by the sixfold increase of fluorescence intensity accompanied by a shift of the emission maximum from 345 to 350 nm. The shift indicates a change of the hydrophobic environment of the tryptophan residues in the protein upon oxygen binding.

Hemocyanin denaturation in low pH solutions resulted in protein precipitation. At pH < 3, the solution became clear and colorless. The relationship of pH and fluorescence of oxyhemocyanin and of the amino acid tryptophan is shown in Fig. 2. For tryptophan, which is primarily

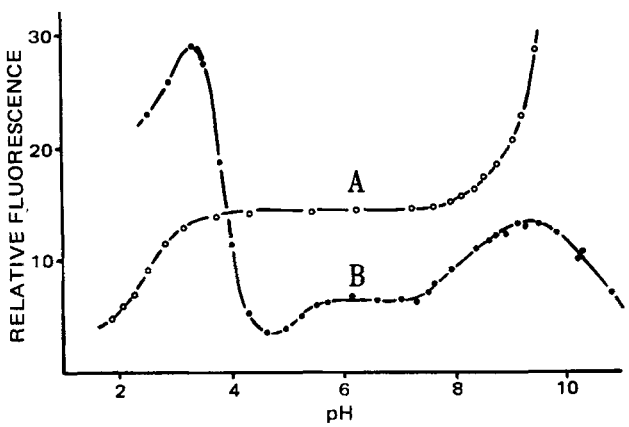

Figure 2—*The pH effect on the fluorescence of oxyhemocyanin and tryptophan in pH 7 tromethamine. Key: A, 5 × 10⁻⁶ M tryptophan; and B, 6.2 × 10⁻⁶ M oxyhemocyanin.*

Table I—Fluorescence Data of *Limulus* Hemocyanin in pH 7 Tromethamine

Type	Emission Maximum, nm	Quantum Yield, %	Fluorescence Lifetime, nsec
Oxyhemocyanin	345	1.2	0.15
Deoxyhemocyanin	350	10.5	1.26
Apohemocyanin	350	11.3	1.36

responsible for the fluorescence of the protein, a pH titration curve was obtained where the pH of the inflection points corresponded to pK_1 (2.3) and pK_2 (9.38) (13). White (14) reported similar pH titration curves for the fluorescence of tryptophan, tryptophan methyl ester, and *N*-acetyltryptophan.

For oxyhemocyanin, a sharp increase in fluorescence occurred at low pH values, indicating the dissociation of oxygen from hemocyanin upon denaturation in acid solution. In the pH 6.0–9.5 range, oxyhemocyanin fluorescence increased with increasing pH, indicating a reverse Bohr effect, where the oxygen binding affinity decreases with increasing pH. Most hemocyanins have a positive Bohr effect, but reverse Bohr effects have been reported for *Limulus* and several other gastropod mollusks (15, 16). The presence of a reverse Bohr effect has been proposed to have physiological significance. *Limulus* hemolymph often has low oxygen and carbon dioxide concentrations, as for example, when the animal burrows in mud or is exposed in air during egg laying. Oxygen binding and pH studies (6) showed that the biological significance of a reverse Bohr effect is to ensure a constant supply of oxygen to the tissues. When oxygen is less available, the blood pH normally drops because of an increase in the carbon dioxide concentration. The increased Bohr effect thus compensates for the lowered oxygen pressure.

Similar to the pH effect, the addition of Cu(II) ion to hemocyanin also produced a cloudy suspension. The absorption spectrum of the copper-treated hemocyanin was similar to that of aged hemocyanin, which had partly lost its oxygen binding capacity. The addition of small amounts of Co(II) and Mn(II) ions did not affect the fluorescence or absorption of oxyhemocyanin; only Cu(II) ion quenched the fluorescence of the protein. The latter effect may be explained as follows. Tryptophan has two excited single states from which fluorescence can occur and a triplet state from which phosphorescence can take place. Since the Cu(II) ion can facilitate singlet–triplet conversion (3), the addition of a small amount of Cu(II) quenches the protein fluorescence.

Oxyhemocyanin is slowly deoxygenated by sodium sulfite. Complete deoxygenation, however, can be achieved rapidly by adding traces of certain metal ions. In a solution containing 4.4×10^{-6} *M* oxyhemocyanin and 0.005 *M* sodium sulfite, the addition of 1×10^{-4} *M* Co(II), Cu(II), or Mn(II) resulted in an immediate diminution of the copper absorption band at 340 nm as well as a large enhancement of protein fluorescence. In the absence of these metal ions, the fluorescence or absorption bands did not change during the measuring time. On the other hand, the Zn(II) ion did not affect the fluorescence or absorption spectrum of the sulfite-treated protein.

Veprek-Siska and Lunka (17) discussed the role of the copper ion in

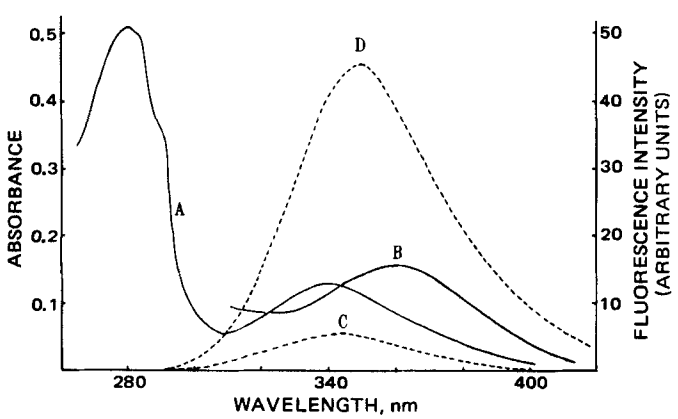

Figure 3—*Fluorescence and absorption spectra of* Limulus *hemocyanin and tetracycline. Key: A, absorption spectrum of* 4.21×10^{-6} M *oxyhemocyanin; B, absorption spectrum of* 1×10^{-5} M *tetracycline; C, fluorescence spectrum of* 4.21×10^{-6} M *oxyhemocyanin; and D, fluorescence spectrum of* 4.21×10^{-6} M *deoxyhemocyanin.*

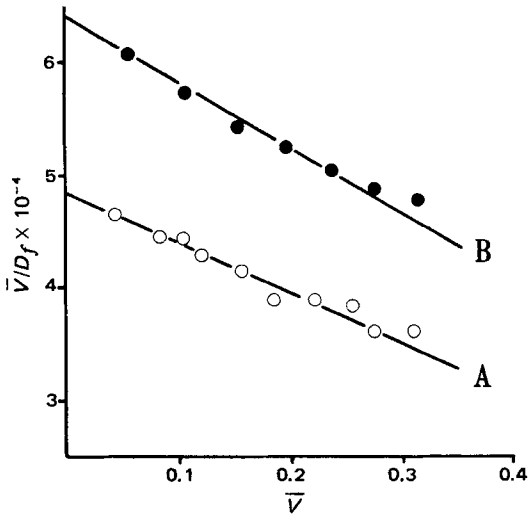

Figure 4—*Scatchard plots for the binding of tetracycline to oxyhemocyanin (A) and apohemocyanin (B).*

copper-catalyzed oxidation of sulfite and proposed the formation of a sulfito–cuprous complex $Cu(SO_3)_n^{-2n+1}$. Oxygen would react with the sulfito–cuprous complex to form intermediate products of the type $O_2Cu(SO_3)_n^{-2n+1}$. It may well be that the same mechanism holds for the copper-catalyzed reaction of sulfite with hemocyanin in the formation of deoxyhemocyanin.

Table I summarizes the fluorescence data of *Limulus* oxy-, deoxy-, and apohemocyanins (all at 4.21×10^{-6} *M*) at neutral pH. The fluorescence yield was calculated by comparing the area under the emission peak with that of a bovine serum albumin solution of equal absorbance at 280 nm and taking 15.2% for the quantum yield of bovine serum albumin (18). Complete deoxygenation of oxyhemocyanin, obtained by treating the oxygenated protein with 0.005 *M* sodium sulfite and 1×10^{-5} *M* $CuCl_2$, resulted in an 8.8-fold increase of the fluorescence yield, significantly greater than the increases reported for the mollusk *L. hierosolima* (fourfold) and *M. trunculus* (fivefold) hemocyanins (2, 3). The fluorescence lifetime data shown in Table I were calculated from the natural lifetime of tryptophan, which was taken to be 12 nsec (19), and the fluorescence yield of hemocyanins.

The fluorescence change of hemocyanin on oxygen binding is due to the energy transfer from the tryptophan residues to the Cu···O groups. The conditions necessary for energy transfer are: (*a*) the absorption spectrum of the acceptor must overlap the emission spectrum of the donor, (*b*) the relative orientations of the oscillators must permit strong interaction, and (*c*) the donor and acceptor must be within a certain distance for a given efficiency of energy transfer (20).

Figure 3 shows that the protein fluorescence band strongly overlaps the Cu···O absorption band at 340 nm. The fact that the fluorescence of hemocyanin is a function of oxygenation (2, 3) also suggests that the fluorescence change is due to the energy transfer process. When using Eqs. 4 and 11 and the following values: $E_1 = 2.996 \times 10^4$ cm²/mmole (molar absorption of the Cu···O group at 340 nm, calculated from the value of $E^{1\%}_{1\,cm} = 4.0$ and using a value of 74,900 for the molecular weight carrying one oxygen binding site), $E_2 = 0.59 \times 10^4$ cm²/mmole (molar absorption of tryptophan at 280 nm), $\upsilon_a = 29{,}410$ cm^{-1}, $\upsilon_e = 28{,}570$ cm^{-1}, $\sigma_a = 1850$ cm^{-1}, $\sigma_e = 1710$ cm^{-1}, $\bar{\upsilon}_0 = 2.9 \times 10^4$ cm^{-1}, $n = 1.33$, and $\tau = 1.26$ nsec, the energy transfer parameters were calculated as follows: $J_\upsilon = 5.26 \times 10^{11}$ cm³/mmole² and $R_0 = 30.2$ Å.

The average distance R between the tryptophan residues and the Cu···O group was calculated, based on the quantum yield data given in Table I and Eq. 3, to be 21.4 Å. The calculated R value represents a random distribution of the Cu···O group with respect to all tryptophan residues in the protein subunit. It is conceivable that the fluorescence of certain tryptophans may be 100% quenched upon oxygen binding while that of other residues is quenched to a lesser degree. Nevertheless, the results do suggest an interrelationship between the tryptophan residues and the Cu···O group.

By using the same equations and the data reported by Shaklai and Daniel (2), the values of R_0 and R for the mollusk *L. hierosolima* hemocyanin at pH 6.6 were calculated to be 29.4 and 24.5 Å, respectively. The Cu···O group in the arthropod *Limulus* hemocyanin is closer to the

Table II—Energy Transfer Parameters in *Limulus* Hemocyanin

Donor	Acceptor	J_v, cm³/mmole²	R_0, Å	R, Å
Deoxyhemocyanin tryptophans	Cu···O group	5.26×10^{11}	30.2	21.4
Oxyhemocyanin tryptophans	Tetracycline	2.74×10^{11}	19.0	11.6
Deoxyhemocyanin tryptophans	Tetracycline	2.87×10^{11}	27.5	16.8
Apohemocyanin tryptophans	Tetracycline	2.99×10^{11}	28.1	17.2

tryptophan residues, in line with the more pronounced fluorescence change found in *Limulus* in going from the oxy to deoxy form as compared to the mollusk hemocyanins. In oxyhemocyanin, the active site containing copper and oxygen is in a hydrophobic region. The tyrosine and tryptophan residues may be located near the hemocyanin copper ions, stabilizing the hydrophobic oxygen site (2, 4, 21).

To show the effect of oxygen binding on the interaction of hemocyanin with small molecules, binding and energy transfer studies of tetracycline to *Limulus* hemocyanin were performed. The use of tetracycline is interesting, since it is capable of receiving energy from tryptophan and has been reported to bind close to the tryptophan residues of plasma protein (22). Figure 4 shows the Scatchard plots for the binding of tetracycline to oxy- and apohemocyanins. Tetracycline binds to the proteins in a ratio of one molecule per protein unit carrying one oxygen binding site. The binding affinity in apohemocyanin ($K = 5.9 \times 10^4\ M^{-1}$) is slightly higher than that in oxyhemocyanin ($K = 4.5 \times 10^4\ M^{-1}$).

The R_0 values for the binding of tetracycline to the proteins are shown in Table II. These values were calculated by Eqs. 4 and 11, using the following data: $E_1 = 1.56 \times 10^4$ cm²/mmole (molar absorption of tetracycline at 360 nm; the spectrum is shown in Fig. 3); $E_2 = 0.59 \times 10^4$ cm²/mmole; $\upsilon_a = 27{,}780$ cm^{-1}; $\upsilon_e = 28{,}990$ cm^{-1} for oxyhemocyanin and 28,570 cm^{-1} for deoxy- and apohemocyanins; $\sigma_a = 2000$ cm^{-1}; $\sigma_e = 1750$ cm^{-1} for oxyhemocyanin, 1710 cm^{-1} for deoxyhemocyanin, and 1840 cm^{-1} for apohemocyanin; $\bar{\upsilon}_0 = 28{,}500$ cm^{-1} for oxyhemocyanin, 28,240 cm^{-1} for deoxyhemocyanin, and 28,210 cm^{-1} for apohemocyanin; $n = 1.33$; and $\tau = 0.15$ nsec for oxyhemocyanin, 1.26 nsec for deoxyhemocyanin, and 1.36 nsec for apohemocyanin.

Tetracycline strongly quenched the fluorescence of hemocyanin. In a solution of $3.4 \times 10^{-5}\ M$ oxy-, deoxy-, or apohemocyanin, the fluorescence titration with tetracycline, in each case, resulted in about 95% quenching of the protein fluorescence. Based on 95% quenching, values of R were calculated using Eq. 3 (Table II). The results indicate that the energy transfer distance between hemocyanin tryptophan and bound tetracycline is the same in deoxy- and apohemocyanins but that the distance is significantly smaller in oxyhemocyanin.

Schoot-Uiterkamp *et al.* (23) reported a Cu–Cu distance of 6 Å in *N,O*-hemocyanin. Since the copper in this hemocyanin and in deoxyhemocyanin is cuprous, Freedman *et al.* (24) took 6 Å as the Cu–Cu distance in deoxyhemocyanin and compared this value with the 3.5–5-Å distance calculated for oxyhemocyanin, where both coppers are cupric and the oxygen is peroxide ion (O_2^{2-}). Considerable movement of the copper ions away from each other must have occurred when the oxyhemocyanin was deoxygenated. This finding is in line with the increase in the hemocyanin tryptophan-bound tetracycline distance when the oxyhemocyanin was deoxygenated.

REFERENCES

(1) A. C. Redfield, T. Coolidge, and H. Montgomery, *J. Biol. Chem.*, **76,** 197 (1928).

(2) N. Shaklai and E. Daniel, *Biochemistry,* **9,** 564 (1970).

(3) W. H. Bannister and E. J. Wood, *Comp. Biochem. Physiol.,* **40B,** 7 (1971).

(4) W. H. Bannister, P. Camilleri, and E. N. Chantler, *ibid.,* **45B,** 325 (1973).

(5) J. D. Sullivan, Jr., and S. W. Watson, *Appl. Microbiol.,* **28,** 1023 (1975).

(6) B. Sullivan, J. Bonaventura, and C. Bonaventura, *Proc. Natl. Acad. Sci. USA,* **71,** 2558 (1974).

(7) A. Ghiretti-Magaldi, C. Nuzzolo, and F. Ghiretti, *Biochemistry,* **5,** 1943 (1966).

(8) C. H. Ke, J. Schubert, C. I. Lin, and M. C. Li, *J. Am. Chem. Soc.,* **95,** 3375 (1973).

(9) C. F. Chignell, in "Methods in Pharmacology," vol. 2, Appleton-Century-Crofts, New York, N.Y., 1972, pp. 57, 58.

(10) T. Forster, *Discuss. Faraday Soc.,* **27,** 7 (1959).

(11) T. Forster, *Ann. Phys. (Leipzig),* **2,** 55 (1947).

(12) G. Weber, *Biochem. J.,* **75,** 335 (1960).

(13) S. V. Konev, in "Fluorescence and Phosphorescence of Proteins and Nucleic Acids" (translated from Russian), S. Udenfriend, Translation Ed., Plenum, New York, N.Y., 1967, pp. 22, 23.

(14) A. White, *Biochem. J.,* **71,** 217 (1959).

(15) J. L. Lanimar and A. G. Riggs, *Comp. Biochem. Physiol.,* **13,** 35 (1964).

(16) R. VanDriel, *Biochemistry,* **12,** 2696 (1973).

(17) J. Veprek-Siska and S. Lunka, *Z. Naturforsh.,* **29B,** 689 (1974).

(18) W. J. Teale, *Biochem. J.,* **76,** 381 (1960).

(19) G. Weber, in "Light and Life," W. D. McElroy and B. Glass, Eds., Johns Hopkins, Baltimore, Md., 1961, p. 82.

(20) I. Z. Steinberg, *Ann. Rev. Biochem.,* **40,** 83 (1971).

(21) B. Salvato, A. Ghiretti-Magaldi, and F. Ghiretti, *Biochemistry,* **13,** 4778 (1974).

(22) J. K. H. Ma, H. W. Jun, and L. A. Luzzi, *J. Pharm. Sci.,* **62,** 1261 (1973).

(23) A. J. M. Schoot-Uiterkamp, H. Van der Deen, H. J. C. Berendsen, and J. F. Boas, *Biochim. Biophys. Acta,* **372,** 407 (1974).

(24) T. B. Freedman, J. S. Loehr, and T. M. Loehr, *J. Am. Chem. Soc.,* **98,** 2809 (1976).

ACKNOWLEDGMENTS AND ADDRESSES

Received December 27, 1976, from the [*]*School of Pharmacy, West Virginia University, Morgantown, WV 26506,* and the [†]*Department of Chemistry, Duquesne University, Pittsburgh, Pa.*

Accepted for publication February 10, 1977.

Supported at Duquesne University by National Science Foundation Grant PCM 76-11744.

The authors thank Mrs. Irene Fu for her assistance in the preparation of purified oxy- and apohemocyanins. They are indebted to Professor R. Lontie for helpful discussions.

[x] To whom inquiries should be directed.

Kinetic Parameter Estimation by Numerical Algorithms and Multiple Linear Regression: Theoretical

KUANG C. YEH

Abstract □ A new method is presented for the determination of kinetic parameters based on a functional relationship among experimental data derived from the postulated model. The data, even though containing errors, are manifestations of this relationship, which should be satisfied by parameters fitted to the system. The procedure involves the use of numerical integration and/or differentiation of the data, followed by multiple linear regression. It does not require initial estimates or repetitive iteration for linear systems and can be applied to nonlinear models. The accuracy of the estimated parameter depends on the goodness of the particular numerical approximation method used.

Keyphrases □ Kinetic parameters—estimated by numerical algorithms and multiple linear regression □ Models, mathematical—kinetic parameters estimated by numerical algorithms and multiple linear regression

The estimation of parameter values is essential in the analysis of many chemical kinetic, biochemical kinetic, and pharmacokinetic processes. The procedure involves the initial development of a model with the corresponding mathematical equations. The latter are then fitted, in a least-squares sense, to the experimental data by adjusting the parameter values.

Computer programs were developed (1, 2) using nonlinear regression procedures with modified Gauss–Newton methods (3, 4). The subject of nonlinear optimization methods was reviewed previously (5) and will not be elaborated here. Because of inherent difficulties associated with the nonlinear fitting procedure, such as the requirement of good initial estimates and lengthy computations, other alternative methods were developed. A method was described (6) in which the differential (rate) equations are approximated by Picard's polynomials, while the experimental data are approximated by least-squares orthogonal polynomials. The parameters are then computed by equating the matching coefficients of the corresponding series. In this method, the computation time is greatly reduced by sacrificing some accuracy of the parameter estimates.

A new procedure involves numerical differentiation by fitting smoothed least-squares polynomials to the data (7). The parameters are calculated algebraically from rate equations and then further improved by a nonlinear optimization method. Because of the inherent difficulty in obtaining reliable derivatives, occasional divergence of the results occurs. The method is applicable to models where all dependent variables are experimentally measured. Other special methods include one for a biexponential equation where data points are equally spaced (8).

The present paper describes a new general alternative method using linear regression analysis. The method is sufficiently flexible and applicable to many linear and nonlinear systems.

THEORETICAL

The principle of the method lies in the fact that experimental observations, if error free, are not random outcomes. They are functionally related and are themselves manifestations of this relationship. This relationship is dictated by the empirical equations proposed to be consistent with the data.

In reality, experimental data inevitably contain measurement errors, so manifestations of the relationships may be distorted or completely obscured. However, if errors are within some arbitrary tolerable limits, the relationships may still be discernible in the observed data and should be describable by parameters fitted to the system.

The mathematical procedures include the use of numerical integration and/or differentiation of the experimental data as well as algebraic substitution of entities not observed. The use of numerical approximation methods is an attempt to reconstruct complete time profiles based on available information since most kinetic data are often obtained and presented as discrete data points. These manipulations are linear, and the resultant solution can be expressed as a linear function of a new set of independent variables generated by data transformation. Because of this linearity, they become amenable to the method of multiple linear regression for parameter optimization. The following examples illustrate the principle and procedures of the proposed method.

Case I—In the reaction system shown in Scheme I:

$$B + C \underset{k_2}{\overset{k_1}{\rightleftharpoons}} D \xrightarrow{k_3} E$$

Scheme I

reactants B and C form a reversible intermediate D, which is then converted into product E. The rate equations are:

$$\dot{B} = \dot{C} = -k_1BC + k_2D \quad \text{(Eq. 1)}$$

$$\dot{D} = k_1BC - (k_2 + k_3)D \quad \text{(Eq. 2)}$$

$$\dot{E} = k_3D \quad \text{(Eq. 3)}$$

with the initial values and mass balance constraints of:

$$B(0) = B_0 \quad \text{(Eq. 4}a\text{)}$$

$$C(0) = C_0 \quad \text{(Eq. 4}b\text{)}$$

$$D(0) = E(0) = 0 \quad \text{(Eq. 4}c\text{)}$$

$$B(0) = B + D + E \quad \text{(Eq. 5}a\text{)}$$

$$C(0) = C + D + E \quad \text{(Eq. 5}b\text{)}$$

where B, C, D, and E are functions of time t and the dot accent denotes a first-time derivative.

Mathematically, Eqs. 1–3 represent a linear transformation from $[BC, D]'$ into $[\dot{B}, \dot{C}, \dot{D}, \dot{E}]'$ as follows:

$$\begin{bmatrix} \dot{B} \\ \dot{C} \\ \dot{D} \\ \dot{E} \end{bmatrix} = \begin{bmatrix} -k_1 & k_2 \\ -k_1 & k_2 \\ k_1 & -(k_2 + k_3) \\ 0 & k_3 \end{bmatrix} \begin{bmatrix} BC \\ D \end{bmatrix} \quad \text{(Eq. 6)}$$

If B and C are assumed to be experimental observations, the unknown variable D in Eq. 1 can be eliminated by using Eqs. 3 and 5a (or 5b):

$$\dot{B} = (k_2 + k_3)[B(0) - B] - k_1BC - k_1k_3 \int_0^t BC\,dt \quad \text{(Eq. 7)}$$

Upon integration, Eq. 7 gives:

$$B = B(0) + (k_2 + k_3)\left[B(0)t - \int_0^t B\,dt\right] - k_1 \int_0^t BC\,dt - k_1k_3 \int_0^t \int_0^t BC\,dt\,dt \quad \text{(Eq. 8)}$$

In regression form, Eq. 8 may be written as:

$$B = A_0 + A_1X_1 + A_2X_2 + A_3X_3 \qquad \text{(Eq. 9)}$$

where A_j's are regression coefficients, X_j's are independent variables[1], and:

$$A_0 = B(0) \qquad \text{(Eq. 10}a\text{)}$$

$$A_1 = k_2 + k_3 \qquad \text{(Eq. 10}b\text{)}$$

$$A_2 = -k_1 \qquad \text{(Eq. 10}c\text{)}$$

$$A_3 = -k_1k_3 \qquad \text{(Eq. 10}d\text{)}$$

$$X_1 = B(0)t - \int_0^t B\,dt \qquad \text{(Eq. 11}a\text{)}$$

$$X_2 = \int_0^t BC\,dt \qquad \text{(Eq. 11}b\text{)}$$

$$X_3 = \int_0^t \int_0^t BC\,dt\,dt \qquad \text{(Eq. 11}c\text{)}$$

Equation 9 shows that the dependent variable B can be expressed as a linear function of the three independent variables, which can be estimated from observations B and C by any suitable numerical integration method. When appropriate weighting factors are assigned to the data points, the intercept and the three coefficients can be obtained by multiple linear regression. The intercept represents the fitted initial value, and the three coefficients can be used to compute the three model parameters.

Equation 8 indicates that the experimental observations are not functions of time alone but are also the cumulative behavior of all previous events. Therefore, it is important that the experimental data points be strategically located to minimize errors in numerical approximation. The variable C can be further eliminated by substitution if it is not an experimental observation.

The present method does not consider each model parameter as a separate entity. The parameters are grouped together to form hybrid regression coefficients. When partial derivatives of the weighted sum of residuals with respect to coefficients are taken, the resultant normal equations are linear in the coefficients, yielding a unique set of coefficient values. By appropriate data transformation, the number of coefficients can be adjusted to equal the number of model parameters so that the resultant parameter values are also unique to the system.

An important task in the present method is to obtain reliable numerical estimates of the independent variables. The trapezoidal method tends to produce systematic errors due to the nature of linear data interpolation. Polynomial interpolation has been successfully implemented in these laboratories using spline functions (9). Specifically, local data are fitted with serial cubic polynominal functions for sections of data that are theoretically differentiable. Other methods, including the Lagrange method, are available (10, 11).

Case II—For some systems, the procedure may involve direct scanning of parameters that are not linearly related. Consider the reaction shown in Scheme II:

$$G \underset{k_5}{\overset{k_4}{\rightleftharpoons}} F \xrightarrow{V_m,K_m} H$$

Scheme II

in which the reactant F forms the product H *via* Michaelis–Menten-type kinetics. Concurrently, the formation of intermediate G is reversible and first order. The reaction may be written as:

$$\dot{F} = -k_4F + k_5G - \frac{V_mF}{K_m + F} \qquad \text{(Eq. 12)}$$

$$\dot{G} = k_4F - k_5G \qquad \text{(Eq. 13)}$$

$$\dot{H} = \frac{V_mF}{K_m + F} \qquad \text{(Eq. 14)}$$

where V_m is the maximum rate; K_m, the nonlinear parameter of the system, is the Michaelis constant having the same dimensions as F.

With the following initial values and the mass balance constraints:

$$F(0) = F_0 \qquad \text{(Eq. 15}a\text{)}$$

$$G(0) = H(0) = 0 \qquad \text{(Eq. 15}b\text{)}$$

$$F(0) = F + G + H \qquad \text{(Eq. 16)}$$

Eq. 12 can be transformed into:

$$F = \frac{k_5F(0)}{(k_4 + k_5)} - \left[\frac{1}{(k_4 + k_5)}\right]\dot{F} - \left[\frac{V_m}{(k_4 + k_5)}\right]\left[\frac{F}{(K_m + F)}\right] - \frac{V_mk_5}{(k_4 + k_5)}\int_0^t \frac{F\,dt}{(K_m + F)} \qquad \text{(Eq. 17)}$$

or, in regression form:

$$F = A_0 + A_1X_1 + A_2X_2 + A_3X_3 \qquad \text{(Eq. 18)}$$

where:

$$A_0 = \frac{k_5F(0)}{(k_4 + k_5)} \qquad \text{(Eq. 19}a\text{)}$$

$$A_1 = \frac{-1}{(k_4 + k_5)} \qquad \text{(Eq. 19}b\text{)}$$

$$A_2 = \frac{-V_m}{(k_4 + k_5)} \qquad \text{(Eq. 19}c\text{)}$$

$$A_3 = \frac{-V_mk_5}{(k_4 + k_5)} \qquad \text{(Eq. 19}d\text{)}$$

$$X_1 = \dot{F} \qquad \text{(Eq. 20}a\text{)}$$

$$X_2 = \frac{F}{(K_m + F)} \qquad \text{(Eq. 20}b\text{)}$$

$$X_3 = \int_0^t \frac{F}{(K_m + F)}\,dt \qquad \text{(Eq. 20}c\text{)}$$

Values for X_1 can be obtained by numerical differentiation of the local data using spline interpolation or the polynomial smoothing technique (7). Numerical differentiation is a difficult procedure and requires great care to obtain reliable results. Values for X_2 can be computed at each data point by assigning an arbitrary constant value to K_m. Values for X_3 can be then estimated by numerical integration of X_2. Thus, for each assumed K_m value, the coefficients in Eq. 18 can be obtained by regression analysis after appropriate weights are assigned to the data.

The corresponding F_0 and the unknown constants k_4, k_5, and V_m can be computed from Eqs. 19a–19d. By using this set of parameters, including K_m, the theoretical values of F can be generated by any suitable means such as the Runge–Kutta method. The goodness of the fit can be measured by computing the weighted sum of the squares of residuals, SS, and scanning the SS values as a function of K_m. Such a plot represents a projection of the SS surface on the K_m coordinate and has a unique minimum; it yields a corresponding set of best fit parameter values.

Case III—For a large body of kinetic data described by a nonspecific multiexponential equation of the form:

$$Y = \sum_{i=1}^{n} a_i \exp(-\lambda_i t) \qquad \text{(Eq. 21)}$$

the intercept parameter a_i and the exponent parameter λ_i can be similarly estimated by using multiple integrals of t and Y (also see *Appendix*). This result is due to the special properties of the equation in that its derivatives and integrals are again multiexponential equations. For example, if $n = 3$, there are six undetermined constants and the regression equation takes the form:

$$Y = \sum_{j=1}^{6} A_jX_j \qquad \text{(Eq. 22)}$$

where:

$$A_1 = a_1 + a_2 + a_3 \qquad \text{(Eq. 23}a\text{)}$$

$$A_2 = -q_1A_5 + q_2A_6 \qquad \text{(Eq. 23}b\text{)}$$

$$A_3 = -q_1A_6 \qquad \text{(Eq. 23}c\text{)}$$

$$A_4 = -(\lambda_1 + \lambda_2 + \lambda_3) \qquad \text{(Eq. 24}a\text{)}$$

$$A_5 = -(\lambda_1\lambda_2 + \lambda_2\lambda_3 + \lambda_3\lambda_1) \qquad \text{(Eq. 24}b\text{)}$$

$$A_6 = -(\lambda_1\lambda_2\lambda_3) \qquad \text{(Eq. 24}c\text{)}$$

$$X_1 = 1.0 \qquad \text{(Eq. 25}a\text{)}$$

$$X_2 = t \qquad \text{(Eq. 25}b\text{)}$$

[1] Although X_j's are obtained by data transformation, they are considered independent variables so long as they are not linearly dependent.

$$X_3 = \frac{1}{2!}t^2 \qquad \text{(Eq. 25c)}$$

$$X_4 = \int_0^t Y\,dt \qquad \text{(Eq. 25d)}$$

$$X_5 = \int_0^t \int_0^t Y\,dt\,dt \qquad \text{(Eq. 25e)}$$

$$X_6 = \int_0^t \int_0^t \int_0^t Y\,dt\,dt\,dt \qquad \text{(Eq. 25f)}$$

$$q_1 = (a_1/\lambda_1) + (a_2/\lambda_2) + (a_3/\lambda_3) \qquad \text{(Eq. 26a)}$$

$$q_2 = (a_1/\lambda_1^2) + (a_2/\lambda_2^2) + (a_3/\lambda_3^2) \qquad \text{(Eq. 26b)}$$

The three exponent parameters can be calculated from coefficients A_4, A_5, and A_6, as shown in Eqs. 24a–24c, by finding the roots of the cubic equation:

$$x^3 + A_4x^2 - A_5x + A_6 = 0 \qquad \text{(Eq. 27)}$$

General methods of finding roots of nth-degree polynomial equations can be found in many text books (10, 12). Computer subroutines are also available (13). A cubic equation can also be solved by using the trigonometric method (14). The three intercept parameters can be obtained by solving Eqs. 23a, 26a, and 26b, which represent a system of three simultaneous equations in three unknowns where q_1 and q_2 can be computed from Eqs. 23b and 23c.

DISCUSSION

The goodness of the estimated parameters depends on the accuracy of the calculated X_j values. For a given set of X_j values, the proposed method yields a unique set of parameter values. For this reason, it is important to choose a reliable empirical function that can best numerically approximate the true, but unknown, function. Of the several numerical approximation methods, such as least-squares polynomials (7), the Akima method (11), spline functions (15, 16), or modified splines (17), spline functions have been tested and found to be a convenient procedure (16).

Splines are ideal in the estimation of areas because the errors they generate are usually small and less biased and the effects of fluctuation in input data are usually dampened by numerical integration. However, since some X_j values are obtained by data transformation, they are not error free. The errors are related to those of the input data. Currently, the statistical aspect of the present method is under investigation.

While integration is a smoothing operation, numerical differentiation is a rather hard and undesirable one. It tends to magnify even small noises in the data. Thus, when it is used to obtain X_1 values of Eq. 17, large errors should be anticipated. The least-squares polynomials (7) are usually more satisfactory but do not completely eliminate the problem. Because of the unreliability, application of numerical differentiation should be monitored carefully or avoided whenever possible. For example, the $\dot{F}$ in Eq. 17 may be eliminated by further integration to yield a new regression equation after rearrangement. In any event, the estimated parameters may be refined further by using a nonlinear regression procedure.

In nonlinear regression, parameters are often searched by iteration in confined parameter spaces to prevent meaningless results. On the other hand, no constraints are imposed on parameters in the present method. Thus, unexpected solutions, such as negative rate constants, may occur, but this result does not imply that the method is inadequate. Rather, it may suggest that the model is inadequate for the data or that large and/or systematic errors have been introduced in some calculated X_j values. In cases such as multiexponential equations, such inconsistencies may lead to the formation of λ_i parameters in conjugated complex form.

Implicit in the application of the proposed method is that each data point should be single valued so that the corresponding X_j values are also single valued after numerical integration or differentiation. For replicate observations, the data should be fitted with smoothing least-squares polynomials (7) or least-squares splines as described by Wold (15). The fitted curve can be used to calculate the required X_j values.

In essence, the present method is predicated on the recognition that, for a given kinetic system, there is one unique functional relationship among all experimental data. The data are conceptually tied together to form one or more continuous strings and then utilized in one regression step to obtain the best fit parameters. Therefore, the algorithm is greatly simplified, resulting in high efficiency in data processing. The estimated parameters are also comparable to those obtained by other more complicated methods. A recent report (18) indicated that parameters obtained by the present method agreed well with those obtained by Pfeffer (19), using the spectinomycin pharmacokinetic data of Wagner *et al.* (20).

Another advantage is that solutions to many linear systems, which may be difficult to obtain, are not required. For nonlinear systems where explicit solutions are not available, the use of the Runge–Kutta procedure does not represent a new complicating factor in the present method since it is a well-established technique.

APPENDIX

This section describes the derivation of the regression equation discussed in Case III. The procedure is general and can be applied to any multiexponential equations.

In connection with Eq. 21, which simplifies to:

$$Y = \Sigma a_i \exp(-\lambda_i t) \qquad \text{(Eq. A1)}$$

the following notations are defined:

$$q_1 = \Sigma(a_i/\lambda_i) \qquad \text{(Eq. A2)}$$

$$q_2 = \Sigma(a_i/\lambda_i^2) \qquad \text{(Eq. A3)}$$

$$q_3 = \Sigma(a_i/\lambda_i^3) \qquad \text{(Eq. A4)}$$

$$\vdots$$

$$q_n = \Sigma(a_i/\lambda_i^n) \qquad \text{(Eq. A5)}$$

$$s_1 = \Sigma\lambda_i \qquad \text{(Eq. A6)}$$

$$s_2 = \sum_{i \neq k} \lambda_i\lambda_k = \text{sum of product of } \lambda_i \text{ taken two at a time} \qquad \text{(Eq. A7)}$$

$$s_3 = \text{sum of product of } \lambda_i \text{ taken three at a time} \qquad \text{(Eq. A8)}$$

$$\vdots$$

$$s_n = \Pi\lambda_i \qquad \text{(Eq. A9)}$$

$$Q_1 = \Sigma(a_i/\lambda_i)\exp(-\lambda_i t) \qquad \text{(Eq. A10)}$$

$$Q_2 = \Sigma(a_i/\lambda_i^2)\exp(-\lambda_i t) \qquad \text{(Eq. A11)}$$

$$Q_3 = \Sigma(a_i/\lambda_i^3)\exp(-\lambda_i t) \qquad \text{(Eq. A12)}$$

$$\vdots$$

$$Q_n = \Sigma(a_i/\lambda_i^n)\exp(-\lambda_i t) \qquad \text{(Eq. A13)}$$

$$R_1 = \int_0^t Y\,dt \qquad \text{(Eq. A14)}$$

$$R_2 = \int_0^t R_1\,dt \qquad \text{(Eq. A15)}$$

$$R_3 = \int_0^t R_2\,dt \qquad \text{(Eq. A16)}$$

$$\vdots$$

$$R_n = \int_0^t R_{n-1}\,dt \qquad \text{(Eq. A17)}$$

As can be seen, both q_i's and s_i's are time-independent constants while R_i's and Q_i's are functions of time t. In addition, R_i's are obtained by successive integration and are related to Q_i's as follows:

$$R_1 = q_1 - Q_1 \qquad \text{(Eq. A18)}$$

$$R_2 = q_1t - q_2 + Q_2 \qquad \text{(Eq. A19)}$$

$$R_3 = \tfrac{1}{2}q_1t^2 - q_2t + q_3 - Q_3 \qquad \text{(Eq. A20)}$$

$$R_n = \frac{1}{(n-1)!}q_1t^{n-1} - \frac{1}{(n-2)!}q_2t^{n-2} + \cdots + (-1)^{n-1}q_n + (-1)^nQ_n \qquad \text{(Eq. A21)}$$

In the case of $n = 2$, Eqs. A6–A9 yield:

$$S_1 = \lambda_1 + \lambda_2 \qquad \text{(Eq. A22)}$$

$$S_2 = \lambda_1\lambda_2 \qquad \text{(Eq. A23)}$$

Multiplying both sides of Eq. A18 by $(1/\lambda_1 + 1/\lambda_2)$ yields:

$$R_1\left(\frac{1}{\lambda_1}+\frac{1}{\lambda_2}\right) = q_1\left(\frac{1}{\lambda_1}+\frac{1}{\lambda_2}\right) - Q_1\left(\frac{1}{\lambda_1}+\frac{1}{\lambda_2}\right) \quad \text{(Eq. A24)}$$

$$R_1(\lambda_1 + \lambda_2)/(\lambda_1\lambda_2) = q_2 + (a_1 + a_2)/(\lambda_1\lambda_2) - (R_2 - q_1 t + q_2) - Y/(\lambda_1\lambda_2) \quad \text{(Eq. A25)}$$

or:

$$Y = (a_1 + a_2) + (\lambda_1\lambda_2)q_1 t - (\lambda_1 + \lambda_2)R_1 - (\lambda_1\lambda_2)R_2 \quad \text{(Eq. A26)}$$

In regression form, Eq. 26 may be written as:

$$Y = \sum_{j=1}^{4} A_j X_j \quad \text{(Eq. A27)}$$

where $A_1 = a_1 + a_2$, $A_2 = -q_1 A_4$, $A_3 = -(\lambda_1 + \lambda_2)$, $A_4 = -(\lambda_1\lambda_2)$, $X_1 = 1.0$, $X_2 = t$, $X_3 = \int_0^t Y\,dt$, and $X_4 = \int_0^t X_3\,dt$.

This procedure may be applied to other cases. For example, if $n = 3$, then:

$$s_1 = \lambda_1 + \lambda_2 + \lambda_3 \quad \text{(Eq. A28)}$$

$$s_2 = \lambda_1\lambda_2 + \lambda_2\lambda_3 + \lambda_3\lambda_1 \quad \text{(Eq. A29)}$$

and:

$$s_3 = \lambda_1\lambda_2\lambda_3 \quad \text{(Eq. A30)}$$

Multiplying Eq. A19 by $(1/\lambda_1 + 1/\lambda_2 + 1/\lambda_3)$ yields:

$$R_2\left(\frac{1}{\lambda_1}+\frac{1}{\lambda_2}+\frac{1}{\lambda_3}\right) = (q_1 t - q_2)\left(\frac{1}{\lambda_1}+\frac{1}{\lambda_2}+\frac{1}{\lambda_3}\right) + Q_2\left(\frac{1}{\lambda_1}+\frac{1}{\lambda_2}+\frac{1}{\lambda_3}\right) \quad \text{(Eq. A31)}$$

which, when expanded, gives:

$$\frac{S_2R_2}{S_3} = \frac{S_2}{S_3}(q_1 t - q_2) - (R_3 - \tfrac{1}{2} q_1 t^2 + q_2 t - q_3) + \left(\frac{1}{\lambda_2}+\frac{1}{\lambda_3}\right)(a_1/\lambda_1^2)\exp(-\lambda_1 t) + \left(\frac{1}{\lambda_1}+\frac{1}{\lambda_3}\right)(a_2/\lambda_2^2)\exp(-\lambda_2 t) + \left(\frac{1}{\lambda_1}+\frac{1}{\lambda_2}\right)(a_3/\lambda_3^2)\exp(-\lambda_3 t) \quad \text{(Eq. A32)}$$

Equation A32 is simplified, yielding:

$$s_2R_2 = s_2(q_1 t - q_2) - s_3(R_3 - \tfrac{1}{2} q_1 t^2 + q_2 t - q_3) + s_1(q_1 - R_1) - Y \quad \text{(Eq. A33)}$$

or:

$$Y = (a_1 + a_2 + a_3) + (s_2 q_1 - s_3 q_2)t + \tfrac{1}{2} s_3 q_1 t^2 - s_1 R_1 - s_2 R_2 - s_3 R_3 \quad \text{(Eq. A34)}$$

Equation A34 can be written in the following regression form:

$$Y = \sum_{j=1}^{6} A_j X_j \quad \text{(Eq. A35)}$$

where $A_1 = a_1 + a_2 + a_3$, $A_2 = -A_5 q_1 + A_6 q_2$, $A_3 = -A_6 q_1$, $A_4 = -(\lambda_1 + \lambda_2 + \lambda_3)$, $A_5 = -(\lambda_1\lambda_2 + \lambda_2\lambda_3 + \lambda_3\lambda_1)$, $A_6 = -(\lambda_1\lambda_2\lambda_3)$, $X_1 = 1.0$, $X_2 = t$, $X_3 = \tfrac{1}{2} t^2$, $X_4 = \int_0^t Y\,dt$, $X_5 = \int_0^t X_4\,dt$, and $X_6 = \int_0^t X_5\,dt$.

Thus, Eq. A35 is identical to Eq. 22 in the text. By induction, the regression equation can be proved to take the following general form:

$$Y = \sum_{j=1}^{2n} A_j X_j \quad \text{(Eq. A36)}$$

where:

$$A_1 = \Sigma a_i$$
$$A_2 = -q_1 A_{n+2} + \cdots + (-1)^{n-1} q_{n-1} A_{2n}$$
$$A_3 = -q_1 A_{n+3} + \cdots + (-1)^{n-2} q_{n-2} A_{2n}$$
$$\vdots$$
$$A_n = -q_1 A_{2n}$$
$$A_{n+1} = -s_1$$
$$A_{n+2} = -s_2$$
$$\vdots$$
$$A_{2n} = -s_n$$
$$X_1 = 1.0$$
$$X_2 = t$$
$$X_3 = t^2/2!$$
$$\vdots$$
$$X_n = t^{n-1}/(n-1)!$$
$$X_{n+1} = \int_0^t Y\,dt$$
$$X_{n+2} = \int_0^t X_{n+1}\,dt$$
$$\vdots$$
$$X_{2n} = \int_0^t X_{2n-1}\,dt$$

Equation A36 has some distinct properties. First, there are two series in X_j: consecutive integrals of t and those of Y. Analogously, A_j can also be separated into two series: (a) functions of both the intercept parameters a_i and exponent parameters λ_i, and (b) strictly functions of λ_i only. Finally, the first term A_1X_1 in Eq. A36 can be viewed as the intercept of the fitted curve. In a special situation where the multiexponential function is constrained to pass through zero, the regression equation contains only $2n - 1$ terms rather than $2n$ terms. This is due to the disappearance of the A_1X_1 term since A_1 is forced to be identically zero, and there are only $2n - 1$ unknown parameters in the original multiexponential equation.

REFERENCES

(1) M. Berman and M. F. Weiss, "Users Manual for SAAM," National Institutes of Health, Bethesda, Md., 1971.

(2) C. M. Metzler, G. L. Elfring, and A. J. McEwen, "A Users Manual for NONLIN and Associated Programs," Upjohn Co., Kalamazoo, Mich., 1974.

(3) H. O. Hartley, *Technometrics*, **3**, 269 (1961).

(4) N. R. Draper and H. Smith, "Applied Regression Analysis," Wiley, New York, N.Y., 1966.

(5) W. H. Swann, *FEBS Lett., Suppl.*, **2**, S39 (1969).

(6) R. Tanner, *Ind. Eng. Chem. Fundam.*, **11**, 1 (1972).

(7) J. Swartz and H. Bremermann, *J. Math. Biol.*, **1**, 241 (1975).

(8) B. K. Shah, *J. Pharm. Sci.*, **62**, 1208 (1973).

(9) J. H. Ahlberg, E. N. Nilson, and J. E. Walsh, "The Theory of Splines and Their Applications," Academic, New York, N.Y., 1967.

(10) B. Carnahan, H. A. Luther, and J. O. Wilkes, "Applied Numerical Methods," Wiley, New York, N.Y., 1969.

(11) J. Fried and S. Zietz, *Phys. Med. Biol.*, **18**, 550 (1973).

(12) F. Scheid, "Schaum's Outline of Theory and Problems of Numerical Analysis," McGraw-Hill, New York, N.Y., 1968.

(13) "User's Guide. Numerical Analysis Routines," General Electric, Bethesda, Md., 1971, p. 132.

(14) M. S. Samuel, "Standard Mathematical Tables," 20th ed., Chemical Rubber Co., Cleveland, Ohio, 1972, p. 104.

(15) S. Wold, *Technometrics*, **16**, 1 (1974).

(16) K. C. Yeh and K. C. Kwan, *J. Pharmacokinet. Biopharm.*, in press.

(17) A. K. Cline, *Commun. ACM*, **17**, 218 (1974).

(18) K. C. Yeh and K. C. Kwan, paper presented at the APhA Academy of Pharmaceutical Sciences, New Orleans meeting, Apr. 1976.

(19) M. Pfeffer, *J. Pharmacokinet. Biopharm.*, **1**, 137 (1973).

(20) J. G. Wagner, E. Novak, L. G. Leslie, and C. M. Metzler, *Int. J. Clin. Pharmacol.*, **1**, 261 (1968).

ACKNOWLEDGMENTS AND ADDRESSES

Received March 25, 1976, from *Merck Sharp & Dohme Research Laboratories, West Point, PA 19486.*

Accepted for publication February 16, 1977.

The author thanks Dr. K. C. Kwan for many valuable suggestions.

Indolizine Derivatives with Biological Activity III: 3-(3-Aminopropyl)-2-methylindolizine, 3-(3-Aminopropyl)-2-methyl-5,6,7,8-tetrahydroindolizine, and Their *N*-Alkyl Derivatives

IPPOLITO ANTONINI, MARIO CARDELLINI ˣ, FRANCESCO CLAUDI, PALMARISA FRANCHETTI, UGO GULINI, GIUSEPPE De CARO *, and FABRIZIO VENTURI *

Abstract □ The syntheses and a preliminary pharmacological evaluation of some aminopropylindolizines and aminopropyltetrahydroindolizines are reported. All compounds showed anti-5-hydroxytryptamine, antihistamine, and antiacetylcholine activities. Some also exhibited weak CNS activity.

Keyphrases □ Indolizines, substituted—series synthesized, evaluated for pharmacological activity □ Anti-5-hydroxytryptamine activity—evaluated in series of substituted indolizines □ Antihistaminic activity—evaluated in series of substituted indolizines □ Antiacetylcholine activity—evaluated in series of substituted indolizines □ Structure–activity relationships—series of substituted indolizines evaluated for pharmacological activity

Among the biologically active compounds with an indole structure, various indolylalkylamines are of particular importance. Interest in such substances suggested the synthesis and the study of their isosteres with indan, indene, benzisoxazole, benzofuran, and benzothiophene systems and other structures.

Investigations on derivatives related to gramine showed that the replacement of the indole by the benzothiophene system reduced the agonistic activity in various types of smooth musculature and led to the appearance of variable, nonspecific, antagonistic properties toward 5-hydroxytryptamine, acetylcholine, and histamine (1). Comparative studies on tryptamines and analogs with a benzothiophene and indene structure suggested the hypothesis that the NH group of the indolylalkylamines does not react significantly with the receptors. In fact, the activity [contractile on the rat stomach (2) and stimulating on the central nervous system (CNS) (3)] of the compounds examined did not generally undergo appreciable variations in comparison with the indole isosteres.

In investigations on compounds with an indolizine structure (4), some indolizinylalkylamine analogs of the well-known indolylalkylamines were synthesized and their pharmacological activities were tested. Few alkylaminoalkylindolizines have been prepared (5–9). Some revealed CNS activity; however, it is not possible at the moment to indicate any correlation between structure and activity.

The present paper reports the syntheses and a preliminary pharmacological screening of a series of 3-(3-alkylaminopropyl)-2-methylindolizines and their tetrahydro derivatives. These compounds were synthesized in view of the pharmacological activities of aminopropyl analogs such as 3-(3-aminopropyl)indole (2, 10), 3-(3-aminopropyl)indene (2), and 1-(3-dimethylaminopropyl)-2-phenylindolizine (5). The presence of a methyl group at the 2-position of indolizine derivatives suggests a favorable influence. In fact, various studies on derivatives related to tryptamine (11) or other substituted indoles (12) indicated that the anti-5-hydroxytryptamine activity is potentiated by the introduction of a methyl group at the 2-position.

EXPERIMENTAL

Chemistry—The 3-(3-alkylaminopropyl)indolizine derivatives (Table I) were prepared as shown in Scheme I.

2-Methyl-3-indolizinepropionitrile (II) was obtained by reaction of 2-methylindolizine (I) with acrylonitrile. The structure of II was established on the basis of the NMR spectrum, which showed a singlet at δ 6.13 (1-H) ppm and signals at δ 7.63–7.33 (m, 5-H), 7.26–6.97 (m, 8-H), and 6.6–6.26 (m, 7- and 6-H) ppm.

Reduction of II with lithium aluminum hydride gave 3-(3-aminopropyl)-2-methylindolizine (III). Treatment of III with ethyl chloroformate, followed by reduction of the 3-ethoxycarbonylaminopropyl derivative (IV), afforded the 3-(3-methylaminopropyl)-2-methylindolizine (V).

Compound V was converted into the dimethyl derivative (VII) by the same system. Again, acetylation of III gave the *N*-acetyl derivative (VIII), which was converted by reduction into 3-(3-ethylaminopropyl)-2-methylindolizine (IX). Compound IX, again by acetylation followed by reduction, yielded 3-(3-diethylaminopropyl)-2-methylindolizine (XI).

The 5,6,7,8-tetrahydroindolizines (XII–XVI, Table II) were prepared by catalytic hydrogenation of the corresponding indolizines (III, V, VII, IX, and XI) in the presence of palladium-on-charcoal. All of the NMR spectra showed the signal of the 1-proton as a singlet whose position varied, depending on the compound, between δ 5.26 and 5.60 ppm. However, the typical signals of the pyridine moiety protons, between δ 7.9 and 5.8 ppm in the unreduced products, had disappeared. All amines were transformed into maleates.

Syntheses[1]—*2-Methyl-3-indolizinepropionitrile (II)*—A solution of 0.152 mole of I (13), 0.60 mole of acrylonitrile, and 0.237 mole of acetic acid was stirred for 20 hr at room temperature. It was then made alkaline with 2 *N* NaOH and extracted with ether. The extracts were dried over anhydrous calcium sulfate. Evaporation of the ethereal solution gave a dark oily residue from which a solid product was precipitated by the addition of ethanol. The nitrile crystallized from ethanol, mp 70–72°; IR: ν_{max} (mineral oil) 2240 (C≡N) cm^{-1}; NMR (CCl_4): δ 7.63–7.33 (m, 1H, 5-H), 7.26–6.97 (m, 1H, 8-H), 6.6–6.26 (m, 2H, 6,7-H), 6.13 (s, 1H, 1-H), 3.16 (t, 2H, CH_2CN), 2.46 (t, 2H, $ArCH_2$), and 2.26 (s, 3H, 2-CH_3) ppm.

Anal.—Calc. for $C_{12}H_{12}N_2$: C, 78.25; H, 6.57; N, 15.2. Found: C, 78.16; H, 6.42; N, 15.47.

3-(3-Aminopropyl)-2-methylindolizine (III)—Slowly, with stirring, a solution of 0.054 mole of II in 200 ml of anhydrous ether was added to a suspension of 0.105 mole of lithium aluminum hydride in 50 ml of anhydrous ether. The mixture then was stirred at room temperature for 15 hr. Excess lithium aluminum hydride was destroyed with aqueous ethanol, and 30 ml of 2 *N* NaOH was added. The solid formed was filtered off, and the ethereal solution was dried over anhydrous sodium sulfate. Evaporation of the solvent gave an oil which was distilled; IR: ν_{max} (liquid film) 3270 and 3245 (NH_2) cm^{-1}; NMR (CCl_4); δ 7.8–7.47 (m, 1H, 5-H), 7.23–6.9 (m, 1H, 8-H), 6.52–6.13 (m, 2H, 6,7-H), 6.03 (s, 1H, 1-H),

[1] Boiling points are uncorrected. Melting points were determined on a Büchi melting-point apparatus and are uncorrected. IR spectra were obtained with a Perkin-Elmer 257 spectrophotometer. NMR spectra were recorded on a Jeol C 60 HL instrument.

Table I—Characteristics of 3-(3-Aminopropyl)-2-methylindolizines

Compound	Boiling Point/mm	Yield, %	Maleate Melting Point	Recrystallization Solvent	Formula	Analysis, % Calc.	Analysis, % Found	Maleate Analysis, % Calc.	Maleate Analysis, % Found
III	98°/0.05	78	141–142°[a,b]	Ethanol–ether	$C_{12}H_{16}N_2$	C 76.55 H 8.57 N 14.88	76.71 8.43 14.62	C 63.14 H 16.62 N 9.21	63.41 6.71 9.04
IV	115°/0.05	73	—	—	$C_{15}H_{20}N_2O_2$	C 69.20 H 7.74 N 10.76	69.31 7.69 10.85	—	—
V	105°/0.05	73	115–116°[b]	Ethanol–ether	$C_{13}H_{18}N_2$	C 77.18 H 8.97 N 13.85	77.24 9.03 13.65	C 64.13 H 6.97 N 8.80	64.21 7.22 8.67
VI	131°/0.1	90	—	—	$C_{16}H_{22}N_2O_2$	C 70.04 H 8.08 N 10.21	69.96 8.1 10.26	—	—
VII	95°/0.05	31	94–96°[b]	Ethanol–ether	$C_{14}H_{20}N_2$	C 77.73 H 9.32 N 12.95	77.84 9.21 13.06	C 65.04 H 7.28 N 8.43	64.84 7.59 8.19
VIII	142°/0.05	87	—	—	$C_{14}H_{18}N_2O$	C 73.01 H 7.88 N 12.17	73.18 8.03 12.24	—	—
IX	104°/0.1	92	112–113°[b]	Ethanol–ether	$C_{14}H_{20}N_2$	C 77.73 H 9.32 N 12.95	77.54 9.36 12.88	C 65.04 H 7.28 N 8.43	65.26 7.24 8.69
X	125°/0.05	80	—	—	$C_{16}H_{22}N_2O$	C 74.38 H 8.58 N 10.84	74.25 8.42 10.96	—	—
XI	104°/0.05	—	—[c]	—	$C_{16}H_{22}N_2$	C 78.63 H 9.90 N 10.84	78.45 9.86 10.96	C 63.47[d] H 7.99 N 7.40	63.25 7.73 7.54

[a] Picrate: mp 193–194°. Recrystallization solvent: ethanol. Formula: $C_{18}H_{19}N_5O_6$. Calc.: C, 53.86; H, 4.77; N, 17.46. Found: C, 54.12; H, 4.85, N, 17.21. [b] Anhydrous solvents. [c] This maleate decomposed when heated in solution and is highly hygroscopic. [d] With 1 mole of water.

2.91–2.44 (m, 4H, CH_2CCH_2), 2.19 (s, 3H, 2-CH_3), 1.56 (q, 2H, CCH_2C), and 0.79 (s, 2H, NH_2) ppm.

3-(3-Ethoxycarbonylaminopropyl)-2-methylindolizine (IV) and 3-(N - Ethoxycarbonyl -3- methylaminopropyl)-2-methylindolizine (VI)—With stirring, a solution of 0.064 mole of ethyl chloroformate in 30 ml of chloroform was added slowly to an ice-cooled solution of 0.053 mole of III or V and 0.053 mole of pyridine in 200 ml of chloroform. After 2.5 hr, 50 ml of water was added; stirring was continued for 3 hr. The chloroform layer was recovered, washed with 2 *N* NaOH, and dried over anhydrous calcium sulfate. Evaporation of the solvent gave an oil, which was distilled.

3-(3-Methylaminopropyl)-2-methylindolizine (V) and 3-(3-Dimethylaminopropyl)-2-methylindolizine (VII)—To a suspension of 0.014 mole of lithium aluminum hydride in 50 ml of anhydrous ether was slowly added 0.067 mole of IV or VI in 300 ml of anhydrous ether. The mixture was heated under reflux for 10 hr and then stirred at room temperature for 5 hr. Aqueous ethanol was added to destroy excess lithium aluminum hydride, and then 30 ml of 2 *N* NaOH was added. The ethereal solution was filtered and dried over anhydrous calcium sulfate. Evaporation of the solvent gave an oil, which was distilled.

3-(3-Acetylaminopropyl)-2-methylindolizine (VIII) and 3-(N-Acetyl-3-ethylaminopropyl)-2-methylindolizine (X)—With stirring, 0.011 mole of acetyl chloride in 10 ml of anhydrous ether was slowly added to a solution of 0.011 mole of III or IX and 0.011 mole of triethylamine

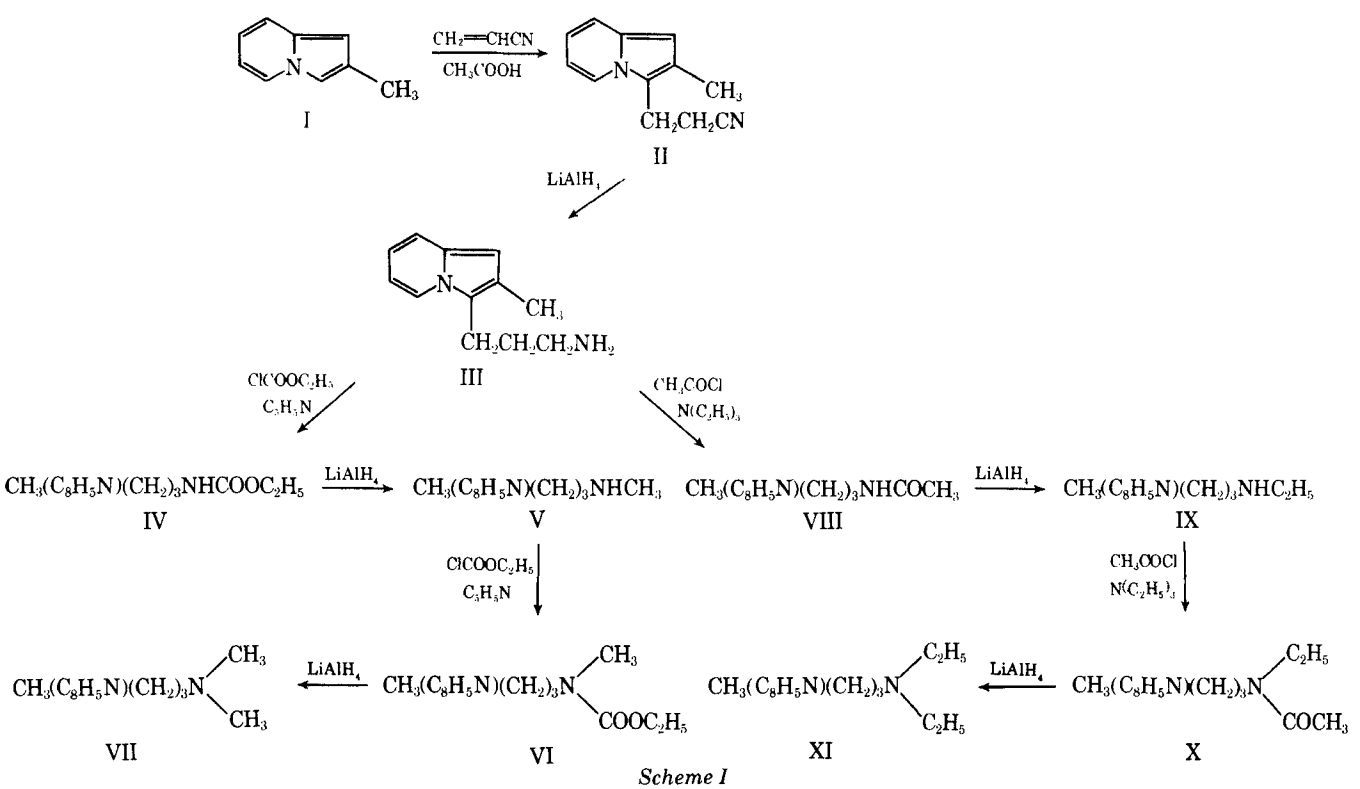

Scheme I

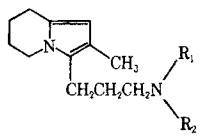

Table II—Characteristics of 3-(3-Aminopropyl)-2-methyl-5,6,7,8-tetrahydroindolizines

Compound	R_1	R_2	Boiling Point/mm	Yield, %	Maleate Melting Point	Recrystallization Solvent	Formula	Analysis, % Calc.	Analysis, % Found	Maleate Analysis, % Calc.	Maleate Analysis, % Found
XII	H	H	76°/0.05	81	128–130°	Ethyl acetate	$C_{12}H_{20}N_2$	C 74.95	74.88	C 62.31	62.62[b]
								H 10.48	10.52	H 7.85	7.76
								N 14.57	14.63	N 9.09	9.15
XIII	H	C_2H_5	78°/0.05	67	93–95°	Ethyl acetate	$C_{14}H_{24}N_2$	C 76.31	76.47	C 60.99	60.78[b]
								H 10.98	10.87	H 8.53	8.34
								N 12.71	12.83	N 7.90	8.15
XIV	H	CH_3	82°/0.05	65	—[a]	—	$C_{13}H_{22}N_2$	C 75.67	75.51	C 59.98	59.73[b]
								H 10.75	10.69	H 8.29	8.17
								N 13.58	13.64	N 8.23	8.31
XV	C_2H_5	C_2H_5	75°/0.05	69	78–79°	Anhydrous ether	$C_{16}H_{28}N_2$	C 77.36	77.24	C 62.80	62.59[b]
								H 11.36	11.23	H 8.96	8.85
								N 11.28	11.13	N 7.32	7.35
XVI	CH_3	CH_3	81°/0.05	43	—[a]	—	$C_{14}H_{24}N_2$	C 76.31	76.45	C 60.99	60.85[b]
								H 10.98	10.86	H 8.53	8.41
								N 12.71	12.84	N 7.90	7.84

[a] The maleate decomposed when heated in solution and is highly hygroscopic. [b] With 1 mole of water.

Table III—*In Vitro* ID_{50} Values on Different Smooth Muscle Preparations[a]

Compound	Guinea Pig Ileum, Acetylcholine	Guinea Pig Ileum, Histamine	Rat Uterus, 5-Hydroxytryptamine
Atropine	0.025 (7.9)	—	—
Metergoline	—	—	7×10^{-7} (24.2×10^3)
Diphenhydramine	—	0.00578 (2.75)	—
Tryptamine	23.7 (0.0084)	8.69 (0.0018)	—[b]
III	3.86 (0.05)	6.18 (0.0025)	1.23 (0.014)
V	1.3 (0.153)	1.27 (0.0125)	0.31 (0.055)
VII	8.64 (0.023)	0.0354 (0.44)	0.195 (0.088)
IX	2.68 (0.074)	2.14 (0.0074)	0.32 (0.054)
XI	11.23 (0.017)	0.186 (0.085)	—[c]
XII	10.35 (0.019)	—[d]	3.1 (0.0055)
XIII	2.7 (0.074)	34.91 (0.0004)	2.62 (0.0066)
XV	72.59 (0.0027)	2.64 (0.006)	13.62 (0.0012)
XVI	21.77 (0.0091)	0.108 (0.146)	6.54 (0.0026)

[a] All concentrations (micrograms per milliliter) refer to the free base. The numbers in parentheses are the antagonistic activity rates (agonist concentration/antagonist concentration ratio). [b] Doses up to 3.3 μg/ml stimulated the uterus contraction. [c] Doses of 2.7 μg/ml yielded inhibition; 4 μg/ml sensitized the rat uterus toward 5-hydroxytryptamine. [d] Doses of 16.6 μg/ml showed an inhibition of 15%. Increasing doses (progression factor = 2) yielded the same response.

in 20 ml of anhydrous ether at 0°. The mixture was stirred for 15 min, water (20 ml) was added, and the ether was separated off. The aqueous solution was again extracted with ether. The extracts were dried with anhydrous sodium sulfate, and the solvent was driven off. The liquid obtained was distilled.

3-(3-Ethylaminopropyl)-2-methylindolizine (IX) and 3-(3-Diethylaminopropyl)-2-methylindolizine (XI)—A solution of 0.025 mole of VIII or X in 50 ml of anhydrous ether was slowly added to a suspension of 0.052 mole of lithium aluminum hydride in 50 ml of ether. The mixture was stirred at room temperature for 18 hr; then aqueous ethanol and 30 ml of 2 *N* NaOH were added. After filtration, the ethereal solution was dried over calcium sulfate, and the solvent was driven off. The liquid obtained was distilled.

Table IV-Acute Toxicity[a]

Compound	LD_{50} (Confidence Limits), mg/kg
Intravenous Administration	
III	24.76 (18.37–33.38)
VII	26.26 (24.24–28.46)
Intraperitoneal Administration	
Tryptamine	223.2 (208.2–260.13)
V	106.10 (90.67–124.14)
IX	102.11 (94.38–110.5)
XI	126.32 (107.91–147.92)
XII	52.97 (47.76–58.48)
XIII	28.89 (24.73–33.89)
XV	62.54 (55.7–70.14)
XVI	19.44 (17.38–21.74)

[a] All values refer to the free base.

3-(3-Aminopropyl)-2-methyl-5,6,7,8-tetrahydroindolizine (XII) and N-Alkyl Derivatives (XIII–XVI)—A mixture of 0.023 mole of the suitable indolizine III, V, VII, IX, or XI in 100 ml of absolute ethanol, 1 g of 5% palladium-on-charcoal, and a few drops of acetic acid was hydrogenated at room temperature at a pressure of 0.027 atm. Hydrogenation was stopped when 2 moles of hydrogen/mole of the compound had been absorbed (7 days). The catalyst was filtered off, and the solution was made alkaline with 2 *N* NaOH and extracted with ether. The ethereal extract, dried over anhydrous sodium sulfate, was evaporated. The liquid obtained was distilled.

For Compound XII, the IR spectrum showed ν_{max} (liquid film) 3350 and 3280 (NH_2) cm^{-1}; NMR (CCl_4): δ 5.26 (s, 1H, 1-H), 3.6 (t, 2H, 5-CH_2), 2.92–2.23 (m, 6H, 8-CH_2, CH_2CCH_2), 2–1.9 (m, 2-CH_3, 7-CH_2, 6-CH_2, CCH_2C); and 0.89 (s, 2H, NH_2) ppm.

Maleates of Indolizines III, V, VII, IX, and XI–XVI—The suitable base in anhydrous ether was added slowly to a stirred equimolar solution of maleic acid in anhydrous ether. The maleate precipitated and was then filtered off and recrystallized. The maleates of bases XI and XIV–XVI are highly hygroscopic, and it was not possible to crystallize them; they were used in the pharmacological tests after drying in vacuum. The other maleates and the indolizines synthesized, with the exception of the nitrile, are unstable to light and air but can be kept for several months in an inert atmosphere in a refrigerator.

Biological Activities—The following properties of the synthesized compounds were studied: (*a*) *in vitro*, the anti-5-hydroxytryptamine action, using the uterus of the rat in estrus, and the antihistamine and antiacetylcholine activities, using the isolated terminal guinea pig ileum; and (*b*) *in vivo*, the effects on the CNS. In addition, the LD_{50} after administration of a single drug dose was determined.

Uterus of Estrous Rat—The technique described by Erspamer (14)

Table V—Effects on the CNS[a]

Compound	Dose[b], mg/kg	Grip Strength[c]	Grooming[d]	Behavior in Open Field[e]	Barbiturate Narcosis Potentiation[f]
		Intravenous Administration			
Controls		221.1 ± 9.3	51.8 ± 19.7	9.5 ± 2.1	0
III	8.03	178 ± 7	76.1 ± 18.3	4.3 ± 1.3	0
VII	8.45	207 ± 17.2	82.8 ± 19.4	5.4 ± 1	0
		Intraperitoneal Administration			
Controls		169 ± 12.4	17.8 ± 4.3	17.4 ± 1.8	0
Tryptamine	76.6	140.19 ± 10.59	128.9 ± 15.46	1.3 ± 0.44	90
V	34.92	150.73 ± 11.33	51.8 ± 21.4	8.84 ± 2	20
IX	32.5	198.39 ± 13.1	33.1 ± 22.2	3.39 ± 2	30
XI	41.97	137 ± 7.75	133.9 ± 18.9	2.81 ± 0.93	20
XII	17.44	133.9 ± 13	108.38 ± 21.42	17.69 ± 4.6	40
XIII	9.82	121.77 ± 13.5	61.94 ± 17.29	8.7 ± 2.35	0
XV	20.43	152 ± 6.2	135.5 ± 18.9	4.33 ± 0.24	0
XVI	6.54	183 ± 7	68.3 ± 17.8	11.42 ± 1.75	0

[a] Figures are the mean ± *SE* of the results obtained on 10–15 mice. [b] All values refer to the free base. [c] Arbitrary units. [d] Latency time of the reflex. [e] Rearing reaction (during a 3-min period of observation). [f] Percentage of mice that lost the righting reflex.

was followed. The organ was suspended in 15 ml of Tyrode nutrient solution (15) oxygenated by bubbling air and kept at 32°.

Guinea Pig Ileum—A segment of terminal guinea pig ileum was immersed in 15 ml of Krebs liquid (16), aerated, and kept at 32°. The technique described by Zamboni and Vitali was followed (17).

Determination of Antagonistic Activity—The dose of drug capable of reducing by 50% the response evoked by a standard dose of 5-hydroxytryptamine (0.017 μg/ml), histamine (0.016 μg/ml), and acetylcholine (0.2 μg/ml) was determined. The time of contact of the antagonists with the organ was always 2 min for the guinea pig ileum and 4 min for the rat uterus (Table III).

As comparison standards, tryptamine hydrochloride[2] and specific inhibitors of 5-hydroxytryptamine (metergoline maleate[3]), histamine (diphenhydramine[4]), and acetylcholine (atropine sulfate[5]) were used. In addition, the following agonists were used: 5-hydroxytryptamine creatinine sulfate[5], histamine dihydrochloride[6], and acetylcholine chloride[7].

The products synthesized were used as maleates. Compound XIV was not tested because of its rapid decomposition in solution.

In Vivo *Tests*—The experiments were performed on 25–35-g Swiss male albino mice. The drugs were dissolved in distilled water and injected in a fixed volume of 1 ml/100 g ip. Compounds III and VII, available only in very small amounts, were injected intravenously.

The LD_{50} was determined by Weil's method (18), evaluating the effect of the drugs 14 days after administration (Table IV). The effects on the CNS were studied by the following tests on groups of at least 10 animals: grip strength (19), grooming (20), exploratory activity in an open field (rearing reaction) (21), and potentiation of the hypnotic action of barbiturates (22). In these experiments, the drugs were always injected at a concentration of one-third of the LD_{50} (Table V).

A control test was performed on groups of animals to which pure distilled water was administered under the same conditions. As the comparison standard, tryptamine hydrochloride was used.

RESULTS AND DISCUSSION

Since the scope of this work was to investigate whether the replacement of the indole by the indolizine system led to particular variations in pharmacological activity, tryptamine as a reference indole derivative was included. As can be seen from Table III, all compounds showed *in vitro* inhibitory action toward 5-hydroxytryptamine, histamine, and acetylcholine.

The action was always more pronounced in the indolizine derivatives than in the corresponding tetrahydroindolizine derivatives. The degree of alkylation of the nitrogen atom of the chain had some influence on the magnitude of the pharmacological activity. Thus, the antihistamine activity decreased in the following sequence: dialkyl, monoalkyl, and unalkylated amines; the antiacetylcholine activity decreased in the sequence: monosubstituted, unsubstituted, and disubstituted amines.

The anti-5-hydroxytryptamine activity was most marked in the dimethylated product among the indolizine derivatives and in the monoethylated product among the tetrahydroindolizine derivatives. In the tests on the guinea pig ileum, the activity of 3-(3-aminopropyl)-2-methylindolizine and its derivatives was always greater than that of tryptamine. On the other hand, some reduced products appeared more active and some less active than tryptamine.

All compounds showed weaker activity than that of the specific antagonists such as metergoline, atropine, and diphenhydramine. The products proved to be moderate depressors of the CNS, as shown by reduction in the exploratory activity in the open field and by potentiation of the hypnotic activity of barbiturates (Table V). The reflexes were not appreciably changed; muscular force and motor coordination were not affected. On the whole, the activity of the compounds in the various trials was less than that shown by tryptamine under the same conditions.

The acute toxicity was always greater than that of tryptamine, except for XI (Table IV).

In conclusion, this preliminary investigation showed that the type of activity found in tryptamine persists on the whole, particularly in *in vitro* experiments with the terminal guinea pig ileum. In fact, in this test, all compounds showed a pronounced inhibitory action toward both acetylcholine and histamine. Furthermore, the ratios between the concentrations of agonist to indolizine derivatives were always higher than concentration ratios of agonist to tryptamine.

The tests on the rat uterus showed a stimulating action for tryptamine, as reported in the literature (23). Among the new compounds, a similar activity was found in XI; a clear anti-5-hydroxytryptamine activity was shown by all other compounds, particularly by the *N,N*-dimethyl derivative (VII). Similarly, in a study on tryptamine analogs, the most active compounds as antagonists of 5-hydroxytryptamine were those with a dimethyl group in the side chain (23).

These first results appear to confirm that the NH group of indole is not indispensable for pharmacological activity. Hence, the indolizine system may be considered as a basis for biologically active compounds. Investigation will be extended to other series of analogous compounds.

[2] Fluka.
[3] Farmitalia, Milan, Italy.
[4] Parke-Davis.
[5] Merck.
[6] Ibis, Florence, Italy.
[7] Roche, Milan, Italy.

REFERENCES

(1) J. J. Lewis, M. Martin-Smith, T. C. Muir, S. N. Nanjappa, and S. T. Reid, *J. Med. Chem.*, **6**, 711 (1963).

(2) J. C. Winter, P. K. Gessner, and D. D. Godse, *ibid.*, **10**, 856 (1967).

(3) E. Campaigne, E. S. Neiss, C. C. Pfeifer, and R. A. Beck, *ibid.*, **11**, 1049 (1968).

(4) M. Cardellini, F. Claudi, M. Grifantini, U. Gulini, and S. Martelli, *J. Pharm. Sci.*, **66**, 259 (1977).

(5) L. A. Walter and P. Margolis, *J. Med. Chem.*, **10**, 498 (1967).

(6) W. B. Harrel and R. F. Doerge, *J. Pharm. Sci.*, **56**, 225 (1967).

(7) *Ibid.*, **56**, 1200 (1967).

(8) *Ibid.*, **57**, 1989 (1968).

(9) W. B. Harrel, *J. Pharm. Sci.*, **59**, 275 (1970).

(10) J. R. Vane, *Br. J. Pharmacol.*, **14**, 87 (1959).

(11) J. H. Gaddum, K. A. Hameed, D. E. Hathway, and F. F. Stephens,

Q. J. Exp. Physiol., **40**, 49 (1955).
(12) D. W. Woolley and E. Shaw, *J. Biol. Chem.*, **203**, 69 (1953).
(13) D. O. Holland and J. H. C. Nayler, *J. Chem. Soc.*, **1955**, 1657.
(14) V. Erspamer, *Arch. Exp. Pathol. Pharmakol.*, **196**, 343 (1940).
(15) M. V. Tyrode, *Arch. Int. Pharmacodyn. Ther.*, **20**, 205 (1910).
(16) M. Krebs, *Biochim. Biophys. Acta*, **4**, 249 (1910).
(17) P. Zamboni and T. Vitali, *Arch. Ital. Sci. Pharmacol.*, **8**, 128 (1938).
(18) C. S. Weil, *Biometrics*, **8**, 249 (1952).
(19) H. Van Riezen and L. Boersma, *Eur. J. Pharmacol.*, **6**, 353 (1969).
(20) M. G. Hansen and I. Q. Whishaw, *Psychopharmacologia*, **29**, 33 (1973).
(21) D. F. Smith and H. B. Smith, *ibid.*, **30**, 83 (1973).
(22) K. Morita, I. Yamamoto, and H. Iwata, *Biochem. Pharmacol.*, **22**, 1115 (1973).
(23) R. B. Barlow and I. Khan, *Br. J. Pharmacol.*, **14**, 99 (1959).

ACKNOWLEDGMENTS AND ADDRESSES

Received November 12, 1976, from the *Istituto di Chimica Farmaceutica e di Chimica Organica, Università di Camerino, 62032 Camerino (MC), Italy.*

Accepted for publication February 16, 1977.

Supported by a grant from the Consiglio Nazionale delle Ricerche, Rome.

* Istituto di Farmacologia, Farmacognosia e Tecnica Farmaceutica dell'Università di Camerino.

[x] To whom inquiries should be directed.

Dissolution Kinetics of Soluble Nondisintegrating Disks

C. J. de BLAEY [x] and H. van der GRAAFF

Abstract □ An equation describing the isotropical dissolution of soluble nondisintegrating disks was developed. It was equivalent to the cube root law only if the height and diameter of the disk were equal. The dissolution kinetics of sodium chloride disks were examined, using a beaker equipped with a centrifugal stirrer as the dissolution chamber. The fit of the experimental data to the cube root law had a coefficient of variation of about 4–5%. It was demonstrated statistically that a fit to a square root of mass *versus* time relation was significantly better. With increasing porosity, the dissolution process proceeded faster than predicted on the basis of the diffusion–convection model. An explanation is proposed by assuming an increased effective dissolution surface.

Keyphrases □ Dissolution kinetics—soluble nondisintegrating disks, equation developed, related to cube root law □ Kinetics, dissolution—soluble nondisintegrating disks, equation developed, related to cube root law

Dissolution kinetics have been studied mainly by applying film theory. Recently, the subject was reviewed for monodisperse particles (1) and polydisperse particle systems (2). Larger bodies such as tablets, which have received little attention so far, have had a constant surface exposed to the dissolution fluid when studied (3). Completely exposed 1-cm sodium chloride cubes were studied (4), as were benzoic acid spheres (5).

The present article discusses the validity of the cube root law for completely exposed water-soluble bodies; the role of tablet porosity was investigated.

THEORETICAL

In the derivation of the cube root law (6), the changing surface during dissolution is expressed in terms of mass change. This approach is possible only for symmetrical bodies; disks do not lend themselves to treatment requiring a fixed ratio between surface and mass. Such treatment requires the inversion of the third-order expression: mass = $2\pi\rho r^3 + a\pi\rho r^2$, in which ρ is the tablet density, r is the radius, and a is a constant equal to height (H) minus $2r$.

The root $r = f(M)$ is such that no procedure for the integration of dM/dt is available. Therefore, another approach was followed based on the zero-order decrease rate of linear dimensions of isotropically dissolving particles. In this way, an equation was derived (7) that describes the dissolution kinetics of small spheres and one arrives at the cube root law.

If a flat cylindrical disk is assumed, the following expressions for isotropical dissolution ensue:

$$\text{mass } M = \pi\rho r_t^2 H_t \qquad \text{(Eq. 1)}$$

$$dr/dt = b \qquad \text{(Eq. 2)}$$

$$dH/dt = 2b \qquad \text{(Eq. 3)}$$

$$r_t = r_0 - bt \qquad \text{(Eq. 4)}$$

$$H_t = H_0 - 2bt \qquad \text{(Eq. 5)}$$

where subscripts 0 and t stand for time zero and t, respectively, and b is a constant. Therefore:

$$dM/dt = \pi\rho\, d(r_t^2 H_t)/dt \qquad \text{(Eq. 6a)}$$

$$dM/dt = \pi\rho r_t^2\, dH/dt + \pi\rho H_t\, dr_t^2/dt \qquad \text{(Eq. 6b)}$$

$$dM/dt = \pi\rho r_t^2\, dH/dt + 2\pi\rho H_t r_t\, dr/dt \qquad \text{(Eq. 6c)}$$

Substitution of Eqs. 2–5 in Eq. 6c gives:

$$dM/dt = 2\pi\rho b(r_0 - bt)^2 + 2\pi\rho b(H_0 - 2bt)(r_0 - bt) \qquad \text{(Eq. 7)}$$

which can be rewritten as:

$$dM/dt = C_1 + C_2 t + C_3 t^2 \qquad \text{(Eq. 8)}$$

with $C_1 = 2\pi\rho b r_0(H_0 + r_0)$, $C_2 = -2\pi\rho b^2(H_0 + 4r_0)$, and $C_3 = 6\pi\rho b^3$. Integration of Eq. 8 results in:

$$M_t = C_1 t + 0.5C_2 t^2 + 0.33C_3 t^3 + M_0 \qquad \text{(Eq. 9a)}$$

or:

$$M_t/M_0 = 1 + C_4 t + C_5 t^2 + C_6 t^3 \qquad \text{(Eq. 9b)}$$

Equation 9b describes the dissolution of flat nondisintegrating disks; it is equivalent to the Hixson–Crowell cube root law if a cube root of Eq. 9b can be found. Thus, if its coefficients are related as in $(x + y)^3$, then $(C_4)^3 = 27C_6$ and $(C_4)^2 = -3C_5$. Writing $C_4 = C_1/M_0$ and then substituting C_1 (Eq. 8) and M_0 (Eq. 1) give:

$$C_4 = \frac{2(bH_0 + br_0)}{r_0^2 H_0} \qquad \text{(Eq. 10)}$$

Similarly, C_5 and C_6 can be elaborated. This approach shows that the

Q. J. Exp. Physiol., **40**, 49 (1955).
(12) D. W. Woolley and E. Shaw, *J. Biol. Chem.*, **203**, 69 (1953).
(13) D. O. Holland and J. H. C. Nayler, *J. Chem. Soc.*, **1955**, 1657.
(14) V. Erspamer, *Arch. Exp. Pathol. Pharmakol.*, **196**, 343 (1940).
(15) M. V. Tyrode, *Arch. Int. Pharmacodyn. Ther.*, **20**, 205 (1910).
(16) M. Krebs, *Biochim. Biophys. Acta*, **4**, 249 (1910).
(17) P. Zamboni and T. Vitali, *Arch. Ital. Sci. Pharmacol.*, **8**, 128 (1938).
(18) C. S. Weil, *Biometrics*, **8**, 249 (1952).
(19) H. Van Riezen and L. Boersma, *Eur. J. Pharmacol.*, **6**, 353 (1969).
(20) M. G. Hansen and I. Q. Whishaw, *Psychopharmacologia*, **29**, 33 (1973).
(21) D. F. Smith and H. B. Smith, *ibid.*, **30**, 83 (1973).
(22) K. Morita, I. Yamamoto, and H. Iwata, *Biochem. Pharmacol.*, **22**, 1115 (1973).
(23) R. B. Barlow and I. Khan, *Br. J. Pharmacol.*, **14**, 99 (1959).

ACKNOWLEDGMENTS AND ADDRESSES

Received November 12, 1976, from the *Istituto di Chimica Farmaceutica e di Chimica Organica, Università di Camerino, 62032 Camerino (MC), Italy.*

Accepted for publication February 16, 1977.

Supported by a grant from the Consiglio Nazionale delle Ricerche, Rome.

* Istituto di Farmacologia, Farmacognosia e Tecnica Farmaceutica dell'Università di Camerino.

[x] To whom inquiries should be directed.

Dissolution Kinetics of Soluble Nondisintegrating Disks

C. J. de BLAEY [x] and H. van der GRAAFF

Abstract □ An equation describing the isotropical dissolution of soluble nondisintegrating disks was developed. It was equivalent to the cube root law only if the height and diameter of the disk were equal. The dissolution kinetics of sodium chloride disks were examined, using a beaker equipped with a centrifugal stirrer as the dissolution chamber. The fit of the experimental data to the cube root law had a coefficient of variation of about 4–5%. It was demonstrated statistically that a fit to a square root of mass *versus* time relation was significantly better. With increasing porosity, the dissolution process proceeded faster than predicted on the basis of the diffusion–convection model. An explanation is proposed by assuming an increased effective dissolution surface.

Keyphrases □ Dissolution kinetics—soluble nondisintegrating disks, equation developed, related to cube root law □ Kinetics, dissolution—soluble nondisintegrating disks, equation developed, related to cube root law

Dissolution kinetics have been studied mainly by applying film theory. Recently, the subject was reviewed for monodisperse particles (1) and polydisperse particle systems (2). Larger bodies such as tablets, which have received little attention so far, have had a constant surface exposed to the dissolution fluid when studied (3). Completely exposed 1-cm sodium chloride cubes were studied (4), as were benzoic acid spheres (5).

The present article discusses the validity of the cube root law for completely exposed water-soluble bodies; the role of tablet porosity was investigated.

THEORETICAL

In the derivation of the cube root law (6), the changing surface during dissolution is expressed in terms of mass change. This approach is possible only for symmetrical bodies; disks do not lend themselves to treatment requiring a fixed ratio between surface and mass. Such treatment requires the inversion of the third-order expression: mass = $2\pi\rho r^3 + a\pi\rho r^2$, in which ρ is the tablet density, r is the radius, and a is a constant equal to height (H) minus $2r$.

The root $r = f(M)$ is such that no procedure for the integration of dM/dt is available. Therefore, another approach was followed based on the zero-order decrease rate of linear dimensions of isotropically dissolving particles. In this way, an equation was derived (7) that describes the dissolution kinetics of small spheres and one arrives at the cube root law.

If a flat cylindrical disk is assumed, the following expressions for isotropical dissolution ensue:

$$\text{mass } M = \pi\rho r_t^2 H_t \qquad \text{(Eq. 1)}$$

$$dr/dt = b \qquad \text{(Eq. 2)}$$

$$dH/dt = 2b \qquad \text{(Eq. 3)}$$

$$r_t = r_0 - bt \qquad \text{(Eq. 4)}$$

$$H_t = H_0 - 2bt \qquad \text{(Eq. 5)}$$

where subscripts 0 and t stand for time zero and t, respectively, and b is a constant. Therefore:

$$dM/dt = \pi\rho\, d(r_t^2 H_t)/dt \qquad \text{(Eq. 6a)}$$

$$dM/dt = \pi\rho r_t^2\, dH/dt + \pi\rho H_t\, dr_t^2/dt \qquad \text{(Eq. 6b)}$$

$$dM/dt = \pi\rho r_t^2\, dH/dt + 2\pi\rho H_t r_t\, dr/dt \qquad \text{(Eq. 6c)}$$

Substitution of Eqs. 2–5 in Eq. 6c gives:

$$dM/dt = 2\pi\rho b(r_0 - bt)^2 + 2\pi\rho b(H_0 - 2bt)(r_0 - bt) \qquad \text{(Eq. 7)}$$

which can be rewritten as:

$$dM/dt = C_1 + C_2 t + C_3 t^2 \qquad \text{(Eq. 8)}$$

with $C_1 = 2\pi\rho b r_0(H_0 + r_0)$, $C_2 = -2\pi\rho b^2(H_0 + 4r_0)$, and $C_3 = 6\pi\rho b^3$. Integration of Eq. 8 results in:

$$M_t = C_1 t + 0.5C_2 t^2 + 0.33C_3 t^3 + M_0 \qquad \text{(Eq. 9a)}$$

or:

$$M_t/M_0 = 1 + C_4 t + C_5 t^2 + C_6 t^3 \qquad \text{(Eq. 9b)}$$

Equation 9b describes the dissolution of flat nondisintegrating disks; it is equivalent to the Hixson–Crowell cube root law if a cube root of Eq. 9b can be found. Thus, if its coefficients are related as in $(x + y)^3$, then $(C_4)^3 = 27C_6$ and $(C_4)^2 = -3C_5$. Writing $C_4 = C_1/M_0$ and then substituting C_1 (Eq. 8) and M_0 (Eq. 1) give:

$$C_4 = \frac{2(bH_0 + br_0)}{r_0^2 H_0} \qquad \text{(Eq. 10)}$$

Similarly, C_5 and C_6 can be elaborated. This approach shows that the

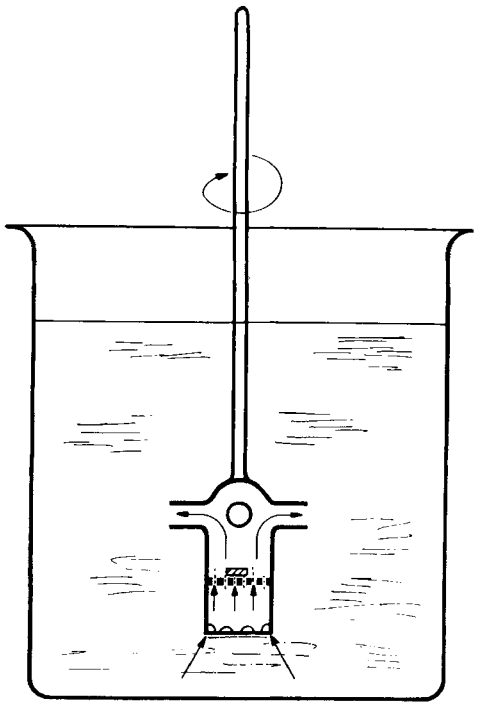

Figure 1—*Centrifugal stirrer dissolution assembly.*

cube root law applies to the dissolution of nondisintegrating flat disks only if height equals diameter.

The zero-order rate decrease, $b = DC_s/h\rho$, follows directly from the Noyes–Whitney equation, being a function of the experimental conditions (diffusion layer thickness h), the compound involved (diffusion coefficient D and solubility C_s), and the tablet structure (density ρ).

EXPERIMENTAL

Sodium chloride particles (200–500 μm) were compressed into two series of flat cylindrical disks of 7.0-mm diameter and of constant volume, constant height of 7.00 ± 0.05 mm (I), or constant weight of 505–520 mg (II). By varying the weight in Series I and the compaction pressure in II, different porosities were obtained. The porosity was calculated as the percent void space from the densities of sodium chloride and the tablet.

Dissolution experiments were followed conductometrically (Fig. 1). They were carried out in water at 25° in a 250-ml beaker equipped with a centrifugal stirrer; this beaker also served as the dissolution chamber. It combines the versatility of a beaker method with the flow conditions of a column method and is similar to the rotating compartmentalized disk described by Simmons *et al.* (8).

RESULTS AND DISCUSSION

Dissolution Equipment—The centrifugal stirrer assembly was tested for reproducibility of t_{30}, t_{60}, and t_{90} with tablets of Series I at 65 and 135 rpm. The reproducibility of t_{60} is given in Table I as the coefficient of variation of five runs. The reproducibility of t_{30} and t_{90} was comparable to that observed for t_{60}. For example, at 65 rpm, it varied from 0 to 13.7% (t_{30}) and from 2.2 to 5.8% (t_{90}). At 135 rpm, these values were 4.2–11.9% and 4.0–9.9%. Similar results were obtained with Series II.

Comparison of these figures with literature data and experiences with the USP, Levy, and column methods shows that this method performs well as to reproducibility and versatility.

Dissolution Model—The derivation of Eq. 9*b* assumes isotropical dissolution under sink conditions. This assumption was checked by photographing the dissolution process of a 500-mg disk of 7.0-mm height and diameter at various times during dissolution. The porosity of this disk was 14%. The shape of the disk was retained, and no disintegration was observed.

Since the height to diameter ratio was virtually constant throughout the study, isotropical dissolution was assumed; visually, disintegration was absent in all tests performed. A group of identical disks was dissolved

Table I—Reproducibility of Dissolution Rate of Sodium Chloride Disks in a Centrifugal Stirrer Assembly (n = 5)

Weight, mg	Porosity, %	65 rpm Average t_{60}, min	65 rpm CV, %	135 rpm Average t_{60}, min	135 rpm CV, %
562	3.4	3.43	5.3	2.23	5.7
549	5.6	3.34	2.8	2.20	5.4
527	9.4	3.15	0.1	2.05	3.6
508	12.7	3.02	2.9	1.96	4.1
461	20.7	2.52	2.7	1.32	8.9
419	28.0	1.80	3.6	0.70	10.1

at different stirring speeds to check whether their dissolution rate was diffusion controlled. The data were transformed (see *Dissolution Kinetics*) according to $1 - (M_t/M_0)^{0.5} = t/T$, and the rate $DC_s/h\rho$ was calculated, giving a value for the diffusion layer thickness. This parameter was plotted *versus* the reciprocal of the stirring rate$^{0.5}$ (Fig. 2). According to Levich's equation, this should give a linear relation under diffusion-controlled dissolution:

$$h = 0.643D^{0.33}\nu^{0.17}W^{-0.5} \qquad \text{(Eq. 11)}$$

where $D_{NaCl} = 1.484 \times 10^{-5}$ cm^2/sec in water at 25°, ν is the kinematic viscosity of water = 0.0092 cm^2/sec at 25°, and W is the stirring rate (second^{-1}). From independent estimates of D and ν, the slope of the curve would be 0.0072 cm sec$^{-0.5}$; the experimental data have a slope of 0.0049 cm sec$^{-0.5}$, implying that the dissolution was faster than predicted. This finding is consistent with the fact that for a highly water-soluble substance, like sodium chloride, not only a solute gradient but also an appreciable solvent, *i.e.*, water, gradient exists, resulting in an additional bulk solution flow and a faster dissolution process than through diffusion alone (9). The graph, being linear, supports the assumption of a diffusion-controlled process.

Dissolution Kinetics—The validity of the theoretical prediction (Eq. 9*b*) for the dissolution of nondisintegrating, completely exposed, sodium chloride disks was investigated. The best fit obtainable is not given by Eq. 9*b* but by a polynomial of the $(n - 1)$th degree for n data points. To permit evaluation of the fit, the data were transformed to a linear relation of the form $1 - (M_t/M_0)^p = t/T$ for p = 1, 0.5, and 0.33. The p = 0.33 stands for the cube root law, which should hold if height and diameter are equal; p = 1 and 0.5 are not based on a physical model and were chosen to permit statistical evaluation of the fit.

Therefore, M_t/M_0 values of 1, 0.9, 0.8, 0.7, 0.6, 0.5, 0.4, 0.3, 0.2, 0.15, 0.1, and 0.05, representing t_0, t_{10}, *etc.*, up to and including t_{95}, were used. Experimental values for t_0, t_{10}, *etc.*, were then used to calculate the linear regression line by the least-squares method. Five dissolution runs were averaged. The deviation of the data points from the regression line, calculated as the standard deviation, served as a criterion for the quality of the fit. The fits were compared with an F test at a 95% confidence level (Tables II and III).

The fits are given in the tables for different portions of the dissolution curves, *i.e.*, t_0–t_{50}, t_0–t_{80}, and t_0–t_{95}, to note possible trends in the model. The best of every three fits (p = 1, 0.5, and 0.33) is underlined. Up to t_{50}, no discrimination was observed (all three were underlined), while p =

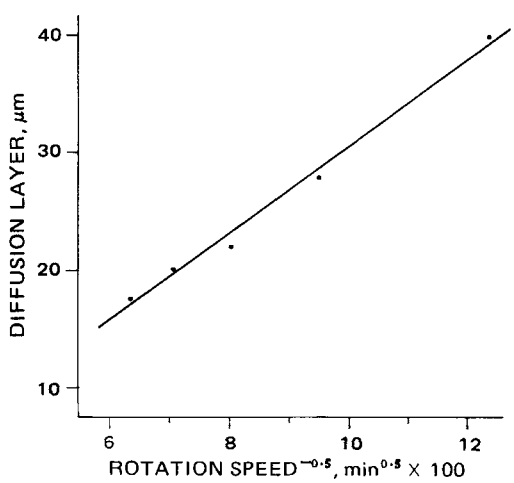

Figure 2—*Diffusion layer thickness* versus *stirring rate for sodium chloride disks using a centrifugal stirrer assembly.*

Table II—Standard Deviation of the Fit [a] of Dissolution Kinetics (Averaged over Five Runs at 65 rpm) of Sodium Chloride Disks (Height and Diameter 7.0 mm)

Weight, mg	Porosity, %	Average t_{50}, min	t_0–t_{50}			t_0–t_{80}			t_0–t_{95}		
			$p = 1$	$p = 0.5$	$p = 0.33$	$p = 1$	$p = 0.5$	$p = 0.33$	$p = 1$	$p = 0.5$	$p = 0.33$
562	3.4	2.77	0.035	0.040	0.052	0.204	0.061	0.082	0.400	0.241	0.163
549	5.6	2.71	0.078	0.057	0.056	0.156	0.049	0.097	0.394	0.053	0.136
527	9.4	2.52	0.022	0.032	0.044	0.180	0.040	0.066	0.436	0.073	0.088
508	12.7	2.44	0.026	0.037	0.046	0.162	0.046	0.077	0.401	0.068	0.099
461	20.7	1.97	0.029	0.022	0.026	0.151	0.023	0.042	0.333	0.041	0.079
419	28.0	1.43	0.029	0.035	0.038	0.122	0.032	0.029	0.248	0.038	0.056

[a] Best fits are underlined ($\alpha = 0.05$).

Table III—Standard Deviation of the Fit [a] of Dissolution Kinetics (Averaged over Five Runs at 135 rpm) of Sodium Chloride Disks (Height and Diameter 7.0 mm)

Weight, mg	Porosity, %	Average t_{50}, min	t_0–t_{50}			t_0–t_{80}			t_0–t_{95}		
			$p = 1$	$p = 0.5$	$p = 0.33$	$p = 1$	$p = 0.5$	$p = 0.33$	$p = 1$	$p = 0.5$	$p = 0.33$
562	3.4	1.78	0.086	0.080	0.082	0.112	0.074	0.100	0.180	0.063	0.123
549	5.6	1.75	0.027	0.006	0.017	0.104	0.019	0.059	0.218	0.032	0.036
527	9.4	1.64	0.022	0.005	0.008	0.101	0.014	0.051	0.222	0.017	0.103
508	12.7	1.56	0.023	0.014	0.021	0.107	0.014	0.041	0.246	0.043	0.075
461	20.7	1.04	0.027	0.009	0.006	0.094	0.020	0.011	0.363	0.052	0.020
419	28.0	0.56	0.013	0.006	0.006	0.035	0.007	0.018	0.088	0.021	0.028

[a] Best fits are underlined ($\alpha = 0.05$).

0.5 provided the best result, at t_{80} and t_{95} (*e.g.*, for a 461-mg tablet at 65 rpm). Generally, $p = 0.5$ gave the best fits, but $p = 0.33$ was still usually acceptable, with a coefficient of variation (relative to t_{50}) of about 4–5%. Nevertheless, the derived expression (Eq. 9*b*) is not supported by the experiments where $p = 0.5$ has to be preferred. Only a comparative statistical evaluation revealed this finding.

The stirrer speed influence for $p = 0.5$ showed a tendency for a better fit up to t_{50} for 135 rpm and up to t_{80} and t_{95} for 65 rpm. Both rates can be used in this type of experiment.

Again for $p = 0.5$, it was checked whether the fit changed during dissolution. At 65 rpm, the fit was always better up to t_{50} and t_{80} compared with t_{95}. At 135 rpm, the best fit was found up to t_{50}. The best fit was still given by $p = 0.5$ in most cases. Especially toward the end of the process, deviations became larger, suggesting more deviation from the conditions under which the model applies.

Little can be said about the influence of porosity on the fit, except that it seems to improve somewhat at higher porosities.

Predicted *versus* Experimental Dissolution Rate—The data for the disks of equal height and diameter were further investigated to compare the experimentally determined dissolution rate with the rate predicted from the diffusion model, *i.e.*, $b = DC_s/h\rho$. Values for D (1.484×10^{-5} cm^2/sec) and C_s (1 g in 2.8 ml) were taken from the literature. Values for h were taken from Fig. 1, and ρ was calculated for the tablet involved, yielding the predicted rate. The experimental rate coefficient was estimated from the t_{50} at which 3.50 mm of the original 7.00-mm tablet height had dissolved. Table IV shows the results.

The usual diffusion–convection models, including Nernst and Levich theory, predict a linear relation with the reciprocal of density. Parrott *et al.* (5) found such a relation for benzoic acid spheres, showing that an equal weight dissolves per unit of surface area in a unit of time. However, their rate value, $DC_s/h\rho$, was much smaller than predicted.

The present results do not confirm these findings; the rate is not equal to the predicted one, although it is substantially closer than in their case. The higher experimental rate may be explained by the presence of a solvent gradient as well as a solute gradient in the dissolution of very soluble substances, as pointed out by Desai *et al.* (9). This, however, would not explain the failure of the relation between rate and the reciprocal of density. This relation holds reasonably well down to a density of 1.89. Tablets of higher porosity, however, deviate substantially.

Table IV—Comparison of Predicted (PR) and Experimental (EXP) Dissolution Rate Constants (Centimeters per Second × 10^3) for Sodium Chloride Disks of Equal Height and Diameter Dissolved at 65 and 135 rpm

ρ [a]	65 rpm			135 rpm		
	PR	EXP	EXP ρ	PR	EXP	EXP ρ
2.09	0.633	1.05	2.10	1.02	1.64	3.42
2.04	0.648	1.08	2.19	1.04	1.66	3.38
1.96	0.676	1.16	2.26	1.08	1.78	3.49
1.89	0.701	1.20	2.25	1.12	1.87	3.53
1.71	0.771	1.48	2.53	1.24	2.80	4.80
1.57	0.843	2.04	3.20	1.35	5.21	8.17

[a] ρ is tablet density (grams per cubic centimeter).

To explain this phenomenon, disintegration was disregarded, being visually absent throughout; t_{50} can thus be regarded as practically not influenced by this process. Similarly, the diffusion layer is unlikely to vary between different porosity disks since stirring conditions and disk size are equal. This leaves the influence of the porosity itself, which should then be translated into pore dimensions. Since all disks of varying porosity (Tables II and III) had the same dimensions, the porosity was varied by introducing different numbers of particles. Therefore, high porosity disks contain fewer particles and have larger voids than do low porosity disks.

Without an exact knowledge of the pore size distribution, it is a matter of speculation whether the pores are just smaller or whether particle breaking, owing to higher compression forces necessary to produce low porosity disks, also results in a certain number of larger pores. It seems justified to assume smaller pores in low porosity tablets and larger pores in high porosity tablets. The consequence for the dissolution rate could be as follows. Pores smaller than the diffusion layer fill up rapidly with a saturated solution. The effective dissolution surface then equals the outside dimensions of the tablet, and t_{50} is directly proportional to (1 − porosity).

When larger pores are present, discharge of dissolved material may be faster than saturation of pores, leaving these pores undersaturated. Assuming the same diffusion layer thickness as before would, at least partly, increase the effective diffusion pathlength and thus increase the dissolution time less than expected from the relation with (1 − porosity). In the present experiments, the reverse is true, indicating that other factors are also effective here. A possible explanation might be that the diffusion layer surface becomes larger than the outer surface of the disk by curving inside the pores when they are large enough. A definite conclusion could be reached with a better knowledge of the pore dimensions and the particular hydrodynamics involved.

Diffusion Kinetics for Height Not Equal to Diameter—Experiments were also performed with disks of varying porosity that did not meet the requirements under which the cube root law applies (Tables V and VI). These results indicate that, at both rotation speeds, the dissolution is described fairly well by a square root or cube root expression. Coefficients of variation, relative to t_{50}, were usually smaller than 5%. There seemed to be a preference for a fit based on a $p = 0.5$ transformation, but it was less general than before. In the height range studied, 6.2–8.8 mm, the deviation from the condition $H = 2r$ seemed to have no great consequence. The fits were quite comparable with the ones for the tablets meeting this condition. The dissolution rate again increased with porosity somewhat faster than predicted, *i.e.*, 0.252 cm^4/g min at the low porosity range and 0.722 cm^4/g min in the high porosity range.

The difference from the rates given cannot be explained as yet. On the basis of these findings, earlier results (10) on dissolution of 1% potassium sulfate from sucrose lozenges (13 mm, 640 mg, height 3.40 mm, porosity

Table V—Standard Deviation of the Fit [a] of Dissolution Kinetics (Averaged over Five Runs at 65 rpm) of 500-mg Sodium Chloride Disks of 7.0-mm Diameter and Variable Height

Height, mm	Porosity, %	Average t_{50}, min	t_0–t_{50}			t_0–t_{80}			t_0–t_{95}		
			$p = 1$	$p = 0.5$	$p = 0.33$	$p = 1$	$p = 0.5$	$p = 0.33$	$p = 1$	$p = 0.5$	$p = 0.33$
6.50	7.9	2.58	0.035	0.040	0.052	0.155	0.036	0.083	0.407	0.056	0.113
6.97	14.1	2.38	0.078	0.057	0.056	0.182	0.047	0.065	0.359	0.040	0.134
7.43	19.4	2.17	0.022	0.032	0.044	0.192	0.083	0.080	0.332	0.080	0.142
7.92	24.4	1.86	0.026	0.037	0.046	0.133	0.031	0.050	0.308	0.051	0.079
8.38	28.5	1.42	0.029	0.022	0.028	0.124	0.031	0.023	0.345	0.124	0.049
8.79	31.9	0.90	0.029	0.035	0.038	0.089	0.038	0.031	0.204	0.063	0.027

[a] Best fits are underlined ($\alpha = 0.05$).

Table VI—Standard Deviation of the Fit [a] of Dissolution Kinetics (Averaged over Five Runs at 135 rpm) of 500-mg Sodium Chloride Disks of 7.0-mm Diameter and Variable Height

Height, mm	Porosity, %	Average t_{50}, min	t_0–t_{50}			t_0–t_{80}			t_0–t_{95}		
			$p = 1$	$p = 0.5$	$p = 0.33$	$p = 1$	$p = 0.5$	$p = 0.33$	$p = 1$	$p = 0.5$	$p = 0.33$
6.21	3.5	1.85	0.028	0.009	0.020	0.147	0.026	0.033	0.261	0.038	0.059
6.50	7.9	1.75	0.024	0.011	0.021	0.108	0.019	0.052	0.269	0.031	0.079
6.97	14.1	1.95	0.022	0.036	0.047	0.141	0.036	0.053	0.379	0.096	0.049
7.43	19.4	1.33	0.039	0.014	0.006	0.111	0.018	0.022	0.225	0.026	0.061
7.92	24.4	0.75	0.028	0.014	0.010	0.082	0.025	0.011	0.177	0.053	0.017
8.38	28.5	0.52	0.018	0.009	0.006	0.068	0.048	0.045	0.134	0.060	0.043
8.79	31.9	0.34	0.008	0.008	0.009	0.033	0.011	0.007	0.128	0.066	0.029

[a] Best fits are underlined ($\alpha = 0.05$).

~12%) were reinvestigated. The dissolution was carried out using a column method with a relatively small dissolution compartment. Similar to our findings on sodium chloride disks, the results could be fitted to either a square or a cube root expression, with a slight preference for the square root. This finding suggests a wider occurrence of the square root fit.

CONCLUSIONS

1. Theoretically, dissolution of disks (flat tablets) may be described by the cube root law only if height equals diameter.

2. Experimentally, the dissolution of sodium chloride disks of equal height and diameter is described adequately by the cube root law (CV = ~4–5%). Statistically, a square root expression is better, however.

3. Disk porosity influence on dissolution rate deviates from expectations on the basis of diffusion–convection models. The rate is higher than predicted at low porosities. This result might be explained by assuming an increased effective surface area owing to distortion of the stagnant diffusion layer.

4. Dissolution kinetics of disks with unequal height and diameter are satisfactorily fitted by a square root or a cube root expression, the former sometimes being preferred.

REFERENCES

(1) J. T. Carstensen, in "Dissolution Technology," L. J. Leeson and J. T. Carstensen, Eds., American Pharmaceutical Association, Washington, D.C., 1974, p. 1.

(2) L. Z. Benet, in *ibid.*, p. 29.

(3) J. V. Fee, D. J. W. Grant, and J. M. Newton, *J. Pharm. Sci.*, **65**, 48, 182 (1976).

(4) J. R. Withey, *J. Pharm. Pharmacol.*, **23**, 573 (1971).

(5) E. L. Parrott, D. E. Wurster, and T. Higuchi, *J. Am. Pharm. Assoc., Sci. Ed.*, **44**, 269 (1955).

(6) A. W. Hixson and J. H. Crowell, *Ind. Eng. Chem.*, **23**, 923 (1931).

(7) J. Cobby, M. Mayersohn, and B. Farlinger, *Can. J. Pharm. Sci.*, **9**, 91 (1974).

(8) D. L. Simmons, M. Freckette, R. J. Ranz, W. S. Chen, and N. K. Patel, *ibid.*, **7**, 62 (1972).

(9) S. J. Desai, P. Singh, A. P. Simonelli, and W. I. Higuchi, *J. Pharm. Sci.*, **55**, 1224 (1966).

(10) C. P. de Haseth, Research Report, Department of Pharmaceutics, University of Leiden, Leiden, The Netherlands, 1973.

ACKNOWLEDGMENTS AND ADDRESSES

Received October 29,,1976, from the *Department of Pharmaceutics, Subfaculty of Pharmacy, Gorlaeus Laboratories, University of Leiden, Wassenaarseweg 76, Leiden, The Netherlands.*

Accepted for publication February 24, 1977.

Presented as a research communication, F.I.P. Congress, Dublin, Ireland, 1975.

[x] To whom inquiries should be directed.

Determination of an Anti-Inflammatory Methanesulfonanilide in Plasma by High-Speed Liquid Chromatography

SHAW F. CHANG ˣ, ALDORA M. MILLER, and ROBERT E. OBER

Abstract □ A sensitive and chemically specific high-speed liquid chromatographic method was developed for the determination of 4-nitro-2-phenoxymethanesulfonanilide in plasma. The method includes selective extraction of the anti-inflammatory drug and an internal standard, 2-(4′-chlorophenoxy)-4-nitromethanesulfonanilide, into benzene from acidified plasma followed by reextraction into 0.2 *N* NaOH. The aqueous layer is acidified, and the drug is reextracted into benzene. The benzene is evaporated, and the residue is dissolved in a small volume of acetonitrile. A 10-μl aliquot is analyzed on a reversed-phase column. The mean overall extraction recovery, after correction for aliquot factors, is 99%. The accuracy, expressed as the relative error, is 4, 0.3, and −3% at 0.60, 1.50, and 3.00 μg/ml, respectively. Repeated analysis of reference standards indicates that the precision, expressed as the relative standard deviation, is 3% or less. The lower sensitivity limit is 0.2 μg/ml with a 2-ml plasma sample. The method was applied successfully to the determination of plasma levels of 4-nitro-2-phenoxymethanesulfonanilide in humans and rats in metabolic experiments at pharmacological doses.

Keyphrases □ 4-Nitro-2-phenoxymethanesulfonanilide—high-speed liquid chromatographic analysis, plasma □ High-speed liquid chromatography—analysis, 4-nitro-2-phenoxymethanesulfonanilide in plasma □ Anti-inflammatory agents—4-nitro-2-phenoxymethanesulfonanilide, high-speed liquid chromatographic analysis in plasma

The anti-inflammatory properties of methanesulfonanilides in animal screening models (1–3) led to the synthesis of various compounds containing the methanesulfonanilide group (4). 4-Nitro-2-phenoxymethanesulfonanilide (I) has anti-inflammatory activity in animals (3).

Since the pharmacologically effective dose for animals and the therapeutic dose projected for humans are relatively low, a sensitive and specific plasma level method is needed to follow the pharmacokinetics of I. An electron-capture GLC method was developed and used; however, the procedure was quite time consuming and sometimes erratic. Recent advances in high-speed liquid chromatography (HSLC) and many examples of the determination of drugs in biological fluids by this technique (5–10) prompted the development of a sensitive and specific HSLC method using a reversed-phase column, capable of quantitating the plasma I levels in rats and humans following a single, oral, pharmacological dose. This method was applied successfully to the measurement of plasma pharmacokinetic parameters and used in dosage form comparison studies.

EXPERIMENTAL

Reagents—All solvents were nanograde or pesticide grade, and all reagents were analytical grade. The following aqueous solutions were made in distilled water: 1 *N* HCl, 0.2 *N* NaOH, and 2 *N* HCl.

Blank Plasma—Human plasma was obtained from volunteers who had fasted overnight and had not taken any medication for the previous week. Blank rat plasma samples were obtained from male Holtzman rats *via* cardiac puncture.

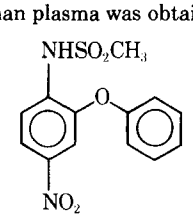

I

HSLC—A liquid chromatograph[1] equipped with a constant-flow pump, a fixed-wavelength UV detector (254 nm), and a septumless injector[2] was used. A 0.64 × 30-cm reversed-phase column[3] was preconditioned with the elution solvent, 50% (v/v) acetonitrile in distilled water, at a flow rate of 2.7 ml/min. The solvent was degassed by stirring for 2 min under slight vacuum prior to use.

The liquid chromatograph was operated at room temperature. The range was set at 0.02 absorption unit full scale. Less sensitive settings were used, if necessary, to contain the peak on scale. The chart speed was 1.27 cm/min.

Standard Solutions—All stock solutions of I and the internal standard were made in methanol. Standard solutions containing 20, 10, 5, 1, and 0.2 μg of I/0.1 ml were made by diluting a 1-mg/ml primary standard solution. The concentrated stock solution of 2-(4′-chlorophenoxy)-4-nitromethanesulfonanilide was diluted 20-fold to give an internal standard solution of 5 μg/0.1 ml.

Extraction of I from Plasma—To a 15 × 125-mm culture tube with a screw cap, add 2 ml of plasma and 0.1 ml of methanol. Along with the samples, prepare six standards in blank plasma by adding 0, 0.2, 1, 5, 10, and 20 μg of I in 0.1 ml of methanol to 2 ml of blank plasma (for the 0.2-μg standard, I was added in 0.2 ml of methanol). Add 0.1 ml of internal standard solution, 0.4 ml of 1 *N* HCl, and 4 ml of benzene to all tubes. Shake the tubes on a equipoise shaker[4] for 30 min and centrifuge at 1000×*g* for 5 min.

Transfer 3.5 ml of the benzene layer into a tube containing 2 ml of 0.2 *N* NaOH, shake for 15 min, and centrifuge for 5 min. Then transfer 1.8 ml of the aqueous phase into a tube containing 0.5 ml of 2 *N* HCl. Add 2 ml of benzene, shake for 15 min, and centrifuge for 5 min. Evaporate the benzene layer (1.7 ml) to dryness at 60° with a nitrogen stream, redissolve the residue in 40–100 μl of acetonitrile, and mix with a mixer[5] for 60 sec. Then inject a 10-μl aliquot into the liquid chromatograph.

Calculation—Peak height ratios between I standards and the internal standard were plotted against I concentration. A straight line was fitted by the least-squares method, and its slope and intercept at the peak height ratio axis were determined. A mathematical expression of the standard curve is:

$$\text{peak height ratio} = A(\text{I concentration}) + B \qquad \text{(Eq. 1)}$$

where A is the slope of the line, and B is the intercept of the line at the peak height ratio axis.

Unknown samples are calculated from the following equation:

$$\text{I concentration in unknown sample} = \frac{\text{peak height ratio} - B}{A} \qquad \text{(Eq. 2)}$$

RESULTS

Separation—Baseline separation between I and the internal standard was achieved, and there was practically no interference with I or the internal standard by endogenous materials from human plasma or by metabolites of I (Fig. 1). Under the experimental conditions indicated, the elution volumes for I and the internal standard were 12.4 ml (4.6 min) and 15.7 ml (5.8 min), respectively. The 2.5-min peak was due to a metabolite of I.

Similar results were obtained from rat plasma (Fig. 2), but there was minor interference from endogenous material in the vicinity of the I peak. This small interference represented 0.02 μg/ml and was routinely subtracted from the calculation of I concentrations in the rat samples.

[1] Model 202, Waters Associates.
[2] Model U6K, Waters Associates.
[3] μBondapak C_{18}, Waters Associates.
[4] Precision Scientific Co.
[5] Deluxe mixer model S8220, Scientific Products.

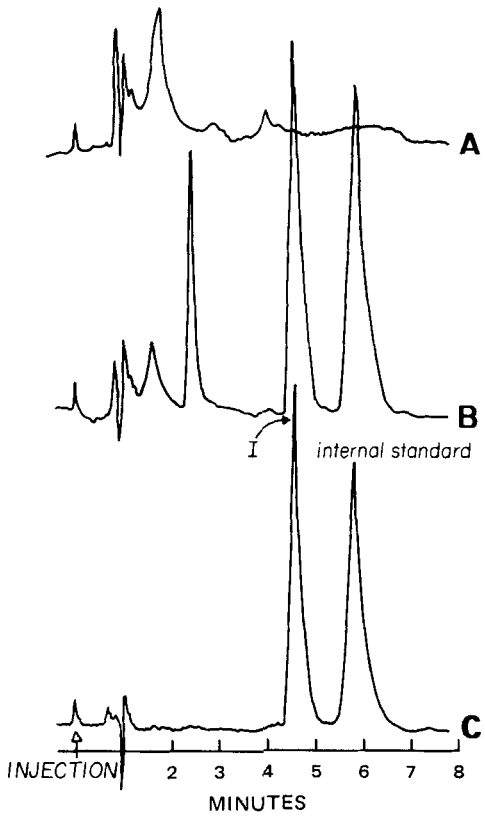

Figure 1—*Chromatogram from human plasma. Key: A, blank plasma; B, plasma of human dosed with I with the internal standard added; and C, mixture of authentic I and the internal standard.*

Extraction Recovery Check—The extraction recovery of I from plasma was determined by a slightly modified extraction procedure in which the internal standard was added after the extraction was completed. The standard curve for this particular experiment was obtained by directly analyzing various mixtures of I and the internal standard without extraction. The extraction recovery check from human plasma was made in duplicate at five concentrations: 0.2, 0.5, 2.5, 5.0, and 10.0 μg/ml. Excellent recovery (Table I) was obtained over this concentration range.

All samples, after correcting for aliquot factors, demonstrated 95% or better recovery except one sample each at 0.2 and 0.5 μg/ml, which gave recoveries of 89.5 and 93.8%, respectively. Their duplicate samples gave excellent recoveries (96.0 and 101.4%, respectively). Thus, the relatively poor recovery for one of the 0.2- and 0.5-μg/ml duplicates is likely a random error rather than a concentration-related effect.

The overall mean extraction recovery was 98.8 ± 4.5%. These overall results indicate that quantitative extraction from human plasma is achieved over a concentration range of 0.2–10 μg/ml, which covers the concentrations found in most biological samples obtained from metabolic studies of I.

Accuracy and Precision—The accuracy of this method was checked by carrying samples at three concentration levels, 0.6, 1.5, and 3.0 μg/ml, in replicates of five through the entire method; the detected concentration was calculated from a pooled standard curve. The precision of this method was examined similarly by comparing the results between these five replicate samples at each concentration level (Table II).

The mean detected concentrations were 0.63, 1.50, and 2.91 μg/ml for the 0.60-, 1.50-, and 3.00-μg/ml samples, respectively. The standard deviations were 0.02, 0.04, and 0.05 μg/ml, respectively, and the relative

Table I—Extraction Recovery of I from Human Plasma

Added, μg/ml	Detected[a], μg/ml	Recovery, %
0.2	0.19	96.0
0.2	0.18	89.5
0.5	0.51	101.4
0.5	0.47	93.8
2.5	2.55	102.1
2.5	2.56	102.4
5.0	5.20	104.0
5.0	5.04	100.7
10.0	9.91	99.1
10.0	9.86	98.6
		Mean ± *SD* = 98.8 ± 4.5

[a] After correction for aliquot factors (×1.494).

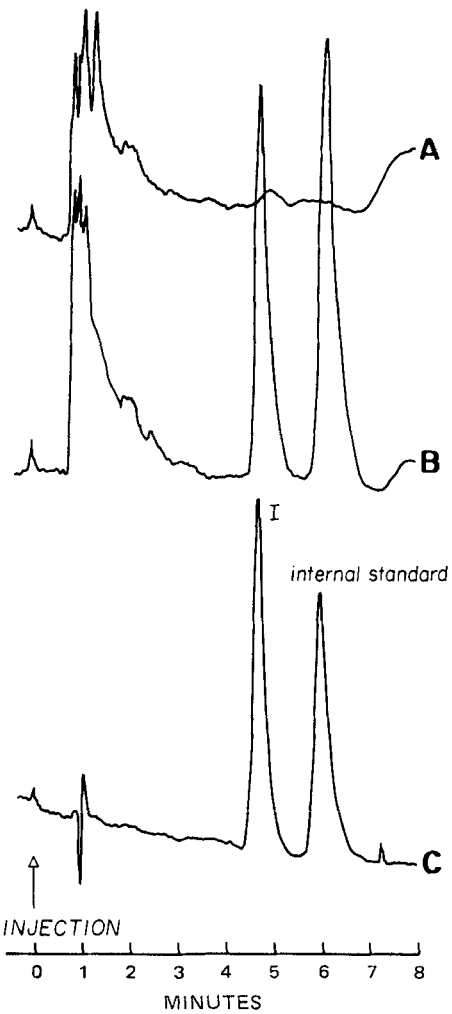

Figure 2—*Chromatogram from rat plasma. Key: A, blank plasma; B, plasma of rat dosed with I with the internal standard added; and C, mixture of authentic I and the internal standard.*

Table II—Accuracy and Precision of I Analysis in Human Plasma by HSLC

I Added to Human Plasma, μg/ml	I Detected, μg/ml	Difference, μg/ml
0.60	0.63	+0.03
0.60	0.64	+0.04
0.60	0.60	0.00
0.60	0.64	+0.04
0.60	0.60	+0.02
	Mean ± *SD* 0.63 ± 0.02	Mean error +0.026
	RSD 3%	Relative error +4%
1.50	1.48	−0.02
1.50	1.48	−0.02
1.50	1.54	+0.04
1.50	1.46	−0.04
1.50	1.56	+0.06
	Mean ± *SD* 1.50 ± 0.04	Mean error +0.004
	RSD 3%	Relative error +0.3%
3.00	2.98	−0.02
3.00	2.90	−0.10
3.00	2.93	−0.07
3.00	2.84	−0.16
3.00	2.90	−0.10
	Mean ± *SD* 2.91 ± 0.05	Mean error −0.09
	RSD 2%	Relative error 3%

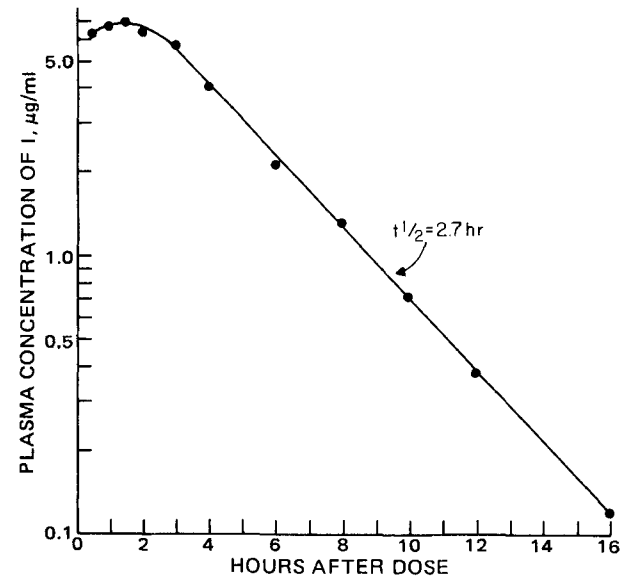

Figure 3—*Plasma I levels in a human subject following a single oral 200-mg dose of I in aqueous suspension.*

standard deviation was 3% or less at all three levels. Thus, excellent precision was demonstrated. The accuracy of this method is indicated by the small mean error between the detected and theoretical values. The mean errors were 0.026, 0.004, and −0.090 μg/ml for the 0.60-, 1.50-, and 3.00-μg/ml samples, respectively. Their corresponding relative errors were 4, 0.3, and −3%.

Specificity—In a metabolic study in humans, the HSLC fraction of I from plasma was collected and purified by repeated chromatography under the analytical conditions described. The purified material (~200 μg) was analyzed by NMR, IR, and high-resolution mass spectrometry in comparison with authentic I. The results unequivocally prove that the HSLC fraction from plasma corresponding to I is in fact I.

Human Plasma Standard Curves—Twenty-two standard curves (0.2–10 μg/ml) were constructed with the same I standard solutions by two analysts over 2 months. The response ratios, I/internal standard for each concentration standard, were pooled, and the mean and standard deviation were calculated. The relative standard deviations were 9, 8, 5, 6, and 5% for the 0.2-, 0.5-, 2.5-, 5.0-, and 10.0-μg/ml standards, respectively. The small relative standard deviations again indicate the precision of this method.

A pooled standard curve of mean response ratios *versus* their corresponding concentrations was constructed by linear regression fitting. The mathematical expression of the pooled standard curve based on all data is $y = 0.540x - 0.016$ (where y = response ratios and x = plasma I concentration in micrograms per milliliter). A correlation coefficient (r) of 0.99991 was obtained, and the excellent linear fit is indicated by the coefficient of determination (r^2) of 0.99982.

The minimum concentration that can be quantitatively determined by this method is 0.2 μg/ml with a 2-ml plasma sample. Lower concentrations can be detected, but quantitation is less accurate.

Rat Plasma Standard Curves—Five standard curves (0.2–10 μg/ml) from blank rat plasma were pooled and treated similarly to those from human plasma. The relative standard deviations were 9, 5, 3, 2, and 1% of their corresponding mean response ratios for the 0.2-, 0.5-, 2.5-, 5.0-, and 10.0-μg/ml standards, respectively. The good precision is indicated by the small relative standard deviation. A straight line was fitted through the mean response ratios and their corresponding concentration standards by linear regression. The mathematical expression of the standard curve based on all data is $y = 0.512x + 0.012$. The correlation coefficient was 0.99999, and the coefficient of determination was 0.99998.

Application to I Analysis in Human and Rat Plasma—A normal human volunteer was given a single, oral, 200-mg dose of I in aqueous suspension in a comparative absorption study. Heparinized blood samples were taken before medication and at 0.5, 1, 1.5, 2, 3, 4, 6, 8, 10, 12, 16, and 24 hr. The plasma I levels determined by this HSLC method are plotted on a log–linear scale in Fig. 3. Following an oral 200-mg dose in this human subject, a peak plasma level of 7 μg/ml was reached at 1.5 hr; the decrease in plasma level followed a monoexponential decline with an estimated plasma I $t_{1/2}$ of 2.7 hr. These results indicate that the method is more than adequate to determine plasma I concentrations in humans at this and lower dose levels.

Ten rats were sacrificed at each of the several time periods following a single oral 1.5-mg/kg dose of I. Heparinized blood samples were collected, and the concentration of I in plasma was determined by the HSLC method. The mean plasma concentrations at various sampling times are plotted on a log–linear scale in Fig. 4. The first sample, 3 hr after the dose, had the highest concentration, 3 μg/ml; the decrease in plasma concentrations between 6 and 12 hr followed a monoexponential decline with an estimated plasma $t_{1/2}$ of 4 hr. These results indicate that the method is capable of monitoring plasma I levels in the rat at low doses.

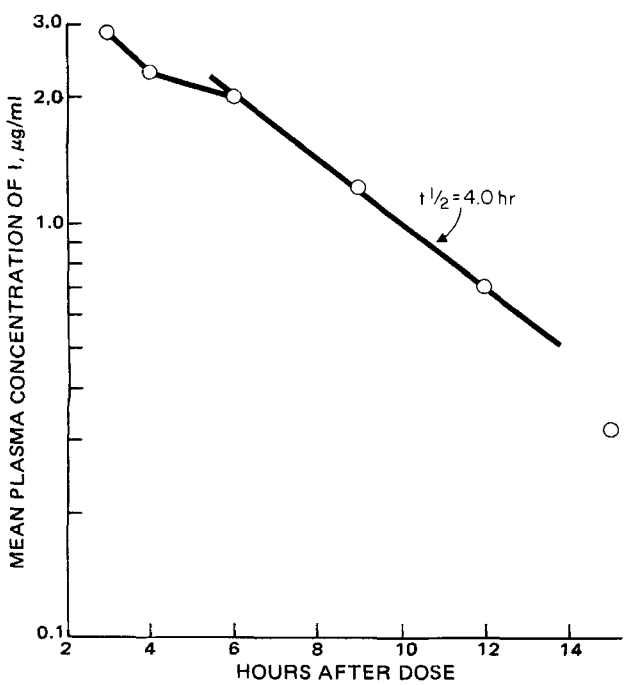

Figure 4—*Mean plasma I levels in 10 rats following a single oral 1.5-mg/kg dose of I in 4% gum acacia.*

DISCUSSION

The results demonstrate that the reversed-phase column is effective in the determination of I, a highly lipophilic compound, in human and rat plasma. The lipophilicity of I provides the strong affinity for the liquid phase, and the drug is eluted with a large elution volume. Most of the endogenous material or metabolites of I carried over in the extraction are relatively less lipophilic than I, so a clean separation is obtained. A minor interference from rat plasma extract (equivalent to 0.02 μg/ml) was present and was routinely corrected.

The low limit of sensitivity is 0.2 μg/ml with a 2-ml plasma sample; if needed, the sensitivity can be improved by measuring I at 300 nm instead of 254 nm. At 300 nm, the response of I is 130% of that at 254 nm. In the present procedure, the residue from the extraction of low concentration samples is dissolved in 40 μl of acetonitrile, and only 10 μl is injected into the chromatograph. Injecting a larger aliquot of the sample should improve the sensitivity.

Both the accuracy and precision of this method are very good. The precision, expressed by the relative standard deviation, is 3% or less at 0.6, 1.5, and 3.0 μg/ml; at the same concentration levels, the accuracy, expressed by the relative error, is 4, 0.3, and −3%, respectively. The precision is further documented by the small relative standard deviation at various concentration levels from the pooled standard curves in humans and rats. Since this analytical method is intended for samples from biological experiments, these levels of precision and accuracy are more than adequate.

For 30 samples, including six standards, the total extraction and analysis time was 10 hr. About 1000 human and rat plasma samples were analyzed by this method over 6 months. About 10% of these samples were subjected to replicate analysis, and duplicate analyses were rarely different by more than 10%.

REFERENCES

(1) K. F. Swingle, R. R. Hamilton, J. K. Harrington, and D. C. Kvam, *Arch. Int. Pharmacodyn. Ther.*, **189**, 129 (1971).

(2) K. F. Swingle, J. K. Harrington, R. R. Hamilton, and D. C. Kvam, *ibid.*, **192**, 16 (1971).

(3) T. J. Grant, G. G. I. Moore, and K. F. Swingle, *Fed. Proc.*, **34**, 759 (1975).

(4) G. G. I. Moore, in "Antiinflammatory Agents," R. A. Scherrer and M. W. Whitehouse, Eds., Academic, New York, N.Y., 1974, pp. 160–176.

(5) L. Shargel, R. F. Koss, A. V. R. Crain, and V. J. Boyle, *J. Pharm. Sci.*, **62**, 1452 (1973).

(6) W. Dunges, G. Naundorf, and N. Seiler, *J. Chromatogr. Sci.*, **12**, 655 (1974).

(7) B. D. Nahlovsky and J. H. Lang, *J. Chromatogr.*, **101**, 225 (1974).

(8) C. V. Marion, D. W. Shoeman, and D. I. Azarnoff, *ibid.*, **101**, 169 (1974).

(9) B. Lindstrom, *ibid.*, **100**, 189 (1974).

(10) R. P. Bush, T. E. Maxim, N. Allen, T. A. Jacob, and F. J. Wolf, *ibid.*, **99**, 609 (1974).

ACKNOWLEDGMENTS AND ADDRESSES

Received November 9, 1976, from the *Drug Metabolism Group, Riker Laboratories, Inc., Subsidiary of 3M Co., 3M Center, St. Paul, MN 55101.*

Accepted for publication February 17, 1977.

Presented in part at the APhA Academy of Pharmaceutical Sciences, Atlanta meeting, November 1975.

The authors thank Dr. K. F. Swingle for collaboration in the rat experiment; Dr. R. Newmark, Dr. R. C. Williams, and Mr. G. J. Lillquist for NMR, IR, and mass spectral analyses; and Dr. H. Miller for collaboration in the clinical study.

[x] To whom inquiries should be directed.

Equilibrium Reaction of Pyrazolodiazepinones in Aqueous Solution

W. H. HONG, C. JOHNSTON, and D. SZULCZEWSKI [x]

Abstract □ This study of the behavior of some pyrazolodiazepinones in aqueous solution at near ambient temperature indicated that they form stable equilibrium mixtures consisting of ring and opened forms. Under isothermal conditions, mixtures are produced whose composition is dependent on pH and may vary from that corresponding to essentially complete ring opening to complete closure. Ring closure equilibrium constants were calculated, and the influence of methyl substitution was determined. Substitution of a methyl group for an amido hydrogen in the open form results in a fivefold increase in this constant. Methylation of the terminal amino group, however, did not cause a corresponding increase and may not significantly affect equilibrium.

Keyphrases □ Pyrazolodiazepinones, various—equilibrium reaction in aqueous solution, effect of pH and methyl substitution □ Equilibrium—various pyrazolodiazepinones in aqueous solution, effect of pH and methyl substitution □ Structure–activity relationships—various pyrazolodiazepinones, equilibrium reaction in aqueous solution, effect of pH and methyl substitution

1-Ethyl - 4,6 - dihydro-3-methyl-8-phenylpyrazolo[4,3-*e*][1,4]diazepin-5(1*H*)-one (I*a*) (ripazepam) is an investigational new drug of the diazepinone class being evaluated for clinical utility (1–3). This pyrazolodiazepinone, in contrast to 1,4-benzodiazepinones, is easily hydrolyzed to yield the open chain compound 4-(2-aminoacetamido)-5-benzoyl-1-ethyl-3-methylpyrazole (II*a*) (1).

Reports concerning hydrolysis or stability of benzodiazepinones (4–8) indicate that the open form in this series is usually unstable under the conditions required to hydrolyze the diazepinone ring, so it does not permanently accumulate. In addition to the ease of hydrolysis, other characteristics associated with the reaction of the pyrazolodiazepinones in aqueous solution are sufficiently different from those of the benzodiazepinones to warrant further study.

EXPERIMENTAL

Reagents—All chemicals used to prepare 0.1 and 0.05 *M* acetate, citrate, phosphate, and borate buffers of known pH values were reagent grade and were used without further purification. Hydrochloric acid solutions were prepared from prestandardized volumetric solutions[1]. The solvents for equilibrium studies, including hydrochloric acid solutions and various buffers, were adjusted to an ionic strength of 0.3 with potassium chloride.

Compound I*a* was from an experimental batch[2] with a purity of 99.75% *via* differential scanning calorimetric analysis. 4-(2-Aminoacetamido)-5-benzoyl-1-ethyl-3-methylpyrazole (II*a*) dihydrochloride and 1-ethyl-4,6- dihydro -3,4- dimethyl-8-phenylpyrazolo[4,3-*e*][1,4]diazepin-5(1*H*)-one (V*a*) were used as received[3].

Synthesis of 4-[2-(Methylamino)acetamido]-5-benzoyl-1-ethyl-3-methylpyrazole Hydrochloride (VII*c*)—To a solution of I*a*, 10 g in 100 ml of dichloromethane, 8 g of methyl fluorosulfonate was added dropwise over 5 min with stirring. The reaction mixture was allowed to stir for another 2 hr and was then poured into 1 liter of ether with stirring. The yellow precipitate was collected, rinsed with ether, and dissolved in 160 ml of water. The resulting solution was washed with 3 × 30-ml portions of chloroform, and the washings were discarded. The aqueous layer was adjusted to pH 8 to obtain optimal turbidity with sodium hydroxide solution and subsequently extracted with 5 × 30-ml portions of chloroform.

The combined chloroform extract was dried over anhydrous sodium sulfate and filtered. Then dried hydrochloric acid gas was introduced into the chloroform solution until the turbidity was no longer increased. The solvent was removed *in vacuo* using a flash evaporator. The residue thus obtained was recrystallized several times from acetonitrile to afford fine white needles, mp 187–188° dec., in a yield of 6.8 g (54%); UV (methanol): $\epsilon_{258.5} = 1.23 \times 10^4$.

Anal.—Calc. for $C_{16}H_{21}ClN_4O_2$: C, 57.05; H, 6.28; Cl, 10.53; N, 16.64. Found: C, 57.27; H, 6.21; Cl, 10.57; N, 16.65.

Determination of Methylation Site in VII*a*—One gram of VIIc in

[1] Acculute standard volumetric solution, Anachemia Chemicals Ltd.
[2] RxX Lot 41201.
[3] Dr. H. DeWald, Chemistry Department, Parke, Davis & Co.

REFERENCES

(1) K. F. Swingle, R. R. Hamilton, J. K. Harrington, and D. C. Kvam, *Arch. Int. Pharmacodyn. Ther.*, **189**, 129 (1971).

(2) K. F. Swingle, J. K. Harrington, R. R. Hamilton, and D. C. Kvam, *ibid.*, **192**, 16 (1971).

(3) T. J. Grant, G. G. I. Moore, and K. F. Swingle, *Fed. Proc.*, **34**, 759 (1975).

(4) G. G. I. Moore, in "Antiinflammatory Agents," R. A. Scherrer and M. W. Whitehouse, Eds., Academic, New York, N.Y., 1974, pp. 160–176.

(5) L. Shargel, R. F. Koss, A. V. R. Crain, and V. J. Boyle, *J. Pharm. Sci.*, **62**, 1452 (1973).

(6) W. Dunges, G. Naundorf, and N. Seiler, *J. Chromatogr. Sci.*, **12**, 655 (1974).

(7) B. D. Nahlovsky and J. H. Lang, *J. Chromatogr.*, **101**, 225 (1974).

(8) C. V. Marion, D. W. Shoeman, and D. I. Azarnoff, *ibid.*, **101**, 169 (1974).

(9) B. Lindstrom, *ibid.*, **100**, 189 (1974).

(10) R. P. Bush, T. E. Maxim, N. Allen, T. A. Jacob, and F. J. Wolf, *ibid.*, **99**, 609 (1974).

ACKNOWLEDGMENTS AND ADDRESSES

Received November 9, 1976, from the *Drug Metabolism Group, Riker Laboratories, Inc., Subsidiary of 3M Co., 3M Center, St. Paul, MN 55101.*

Accepted for publication February 17, 1977.

Presented in part at the APhA Academy of Pharmaceutical Sciences, Atlanta meeting, November 1975.

The authors thank Dr. K. F. Swingle for collaboration in the rat experiment; Dr. R. Newmark, Dr. R. C. Williams, and Mr. G. J. Lillquist for NMR, IR, and mass spectral analyses; and Dr. H. Miller for collaboration in the clinical study.

[x] To whom inquiries should be directed.

Equilibrium Reaction of Pyrazolodiazepinones in Aqueous Solution

W. H. HONG, C. JOHNSTON, and D. SZULCZEWSKI [x]

Abstract □ This study of the behavior of some pyrazolodiazepinones in aqueous solution at near ambient temperature indicated that they form stable equilibrium mixtures consisting of ring and opened forms. Under isothermal conditions, mixtures are produced whose composition is dependent on pH and may vary from that corresponding to essentially complete ring opening to complete closure. Ring closure equilibrium constants were calculated, and the influence of methyl substitution was determined. Substitution of a methyl group for an amido hydrogen in the open form results in a fivefold increase in this constant. Methylation of the terminal amino group, however, did not cause a corresponding increase and may not significantly affect equilibrium.

Keyphrases □ Pyrazolodiazepinones, various—equilibrium reaction in aqueous solution, effect of pH and methyl substitution □ Equilibrium—various pyrazolodiazepinones in aqueous solution, effect of pH and methyl substitution □ Structure–activity relationships—various pyrazolodiazepinones, equilibrium reaction in aqueous solution, effect of pH and methyl substitution

1-Ethyl - 4,6 - dihydro-3-methyl-8-phenylpyrazolo[4,3-*e*][1,4]diazepin-5(1*H*)-one (I*a*) (ripazepam) is an investigational new drug of the diazepinone class being evaluated for clinical utility (1–3). This pyrazolodiazepinone, in contrast to 1,4-benzodiazepinones, is easily hydrolyzed to yield the open chain compound 4-(2-aminoacetamido)-5-benzoyl-1-ethyl-3-methylpyrazole (II*a*) (1).

Reports concerning hydrolysis or stability of benzodiazepinones (4–8) indicate that the open form in this series is usually unstable under the conditions required to hydrolyze the diazepinone ring, so it does not permanently accumulate. In addition to the ease of hydrolysis, other characteristics associated with the reaction of the pyrazolodiazepinones in aqueous solution are sufficiently different from those of the benzodiazepinones to warrant further study.

EXPERIMENTAL

Reagents—All chemicals used to prepare 0.1 and 0.05 *M* acetate, citrate, phosphate, and borate buffers of known pH values were reagent grade and were used without further purification. Hydrochloric acid solutions were prepared from prestandardized volumetric solutions[1]. The solvents for equilibrium studies, including hydrochloric acid solutions and various buffers, were adjusted to an ionic strength of 0.3 with potassium chloride.

Compound I*a* was from an experimental batch[2] with a purity of 99.75% *via* differential scanning calorimetric analysis. 4-(2-Aminoacetamido)-5-benzoyl-1-ethyl-3-methylpyrazole (II*a*) dihydrochloride and 1-ethyl-4,6- dihydro -3,4- dimethyl-8-phenylpyrazolo[4,3-*e*][1,4]diazepin-5(1*H*)-one (V*a*) were used as received[3].

Synthesis of 4-[2-(Methylamino)acetamido]-5-benzoyl-1-ethyl-3-methylpyrazole Hydrochloride (VII*c*)—To a solution of I*a*, 10 g in 100 ml of dichloromethane, 8 g of methyl fluorosulfonate was added dropwise over 5 min with stirring. The reaction mixture was allowed to stir for another 2 hr and was then poured into 1 liter of ether with stirring. The yellow precipitate was collected, rinsed with ether, and dissolved in 160 ml of water. The resulting solution was washed with 3 × 30-ml portions of chloroform, and the washings were discarded. The aqueous layer was adjusted to pH 8 to obtain optimal turbidity with sodium hydroxide solution and subsequently extracted with 5 × 30-ml portions of chloroform.

The combined chloroform extract was dried over anhydrous sodium sulfate and filtered. Then dried hydrochloric acid gas was introduced into the chloroform solution until the turbidity was no longer increased. The solvent was removed *in vacuo* using a flash evaporator. The residue thus obtained was recrystallized several times from acetonitrile to afford fine white needles, mp 187–188° dec., in a yield of 6.8 g (54%); UV (methanol): $\epsilon_{258.5} = 1.23 \times 10^4$.

Anal.—Calc. for $C_{16}H_{21}ClN_4O_2$: C, 57.05; H, 6.28; Cl, 10.53; N, 16.64. Found: C, 57.27; H, 6.21; Cl, 10.57; N, 16.65.

Determination of Methylation Site in VII*a*—One gram of VIIc in

[1] Acculute standard volumetric solution, Anachemia Chemicals Ltd.
[2] RxX Lot 41201.
[3] Dr. H. DeWald, Chemistry Department, Parke, Davis & Co.

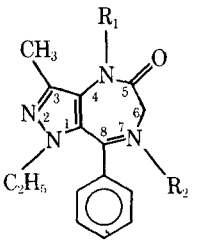

Ia: R_1 = H, no R_2
Ib: R_1 = R_2 = H, charge = + 1
Va: R_1 = CH_3, no R_2
Vb: R_1 = CH_3, R_2 = H, charge = +1
VIII: R_1 = H, R_2 = CH_3, charge = +1
IX: R_1 = R_2 = CH_3, charge = +1

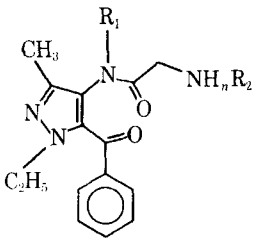

IIa: R_1 = R_2 = H, n = 1
IIb: R_1 = R_2 = H, n = 2, charge = +1
IIc: dihydrochloride
VIa: R_1 = CH_3, R_2 = H, n = 1
VIb: R_1 = CH_3, R_2 = H, n = 2, charge = +1
VIIa: R_1 = H, R_2 = CH_3, n = 1
VIIb: R_1 = H, R_2 = CH_3, n = 2, charge = +1
VIIc: hydrochloride

25 ml of 0.4 *N* HCl was sealed in a 50-ml glass ampul and heated in a steam bath for 3 days. After cooling, the hydrolysis mixture was quantitatively transferred into a 250-ml separator with 20 ml of water. The resulting yellow solution was washed with 3 × 30-ml portions of chloroform, and the washings were discarded. The aqueous layer was then made alkaline (pH >12) and washed with 3 × 30-ml portions of chloroform, and the washings were discarded again. The aqueous layer was neutralized with 2 *N* HCl and evaporated to dryness *in vacuo* at 35° using a flash evaporator.

The white solid thus obtained was repetitively treated with hot methanol, yielding an off-white powder. This compound showed only one TLC spot, which had the same characteristics as those of sarcosine when the sample was spotted on a silica gel plate[4], developed in 2-propanol–water (70:30) and 2-propanol–concentrated ammonia (70:30), and detected by ninhydrin reagent.

Synthesis of 1-Ethyl-1,4,5,6-tetrahydro-3,4,7-trimethyl-5-oxo-8-phenylpyrazolo[4,3-*e*][1,4]diazepinium Iodide (IX)—Compound IX was prepared as follows. To a solution of Va (0.5 g in 4 ml of acetonitrile) in a 50-ml glass ampul, a solution of methyl iodide (0.31 g in 1 ml of acetonitrile) was added dropwise over 2 min with shaking. The ampul was then sealed and heated in a steam bath for 3 hr. After cooling, the mixture was poured into 500 ml of ether with stirring. The yellow precipitate was filtered, rinsed with ether, and recrystallized from the acetonitrile–ether mixture, giving a yellow crystalline powder, mp 230° dec., in a yield of 0.59 g (79%); UV (acetonitrile): $\epsilon_{381} = 4.50 \times 10^3$ and $\epsilon_{301} = 1.12 \times 10^4$.

Anal.—Calc. for $C_{17}H_{21}IN_4O$: C, 48.12; H, 4.99; I, 29.91; N, 13.21. Found: C, 47.92; H, 4.79; I, 29.50; N, 13.08.

Determination of Methylation Site in IX—Compound IX, 0.45 g, in 20 ml of 0.4 *N* HCl was sealed in a 50-ml glass ampul and heated in a steam bath for 2 days. After cooling, the hydrolysis mixture was filtered, and the yellow filtrate was quantitatively transferred into a 60-ml separator with 10 ml of water. The yellow solution was washed with 3 × 20-ml portions of chloroform, and the washings were discarded. The aqueous layer was then made alkaline (pH >12) and washed with 3 × 20-ml portions of chloroform, and the washings were discarded again. The aqueous layer was neutralized with 2 *N* HCl and evaporated to dryness *in vacuo* at 35° using a flash evaporator.

[4] Q1-F, Quantum Industries.

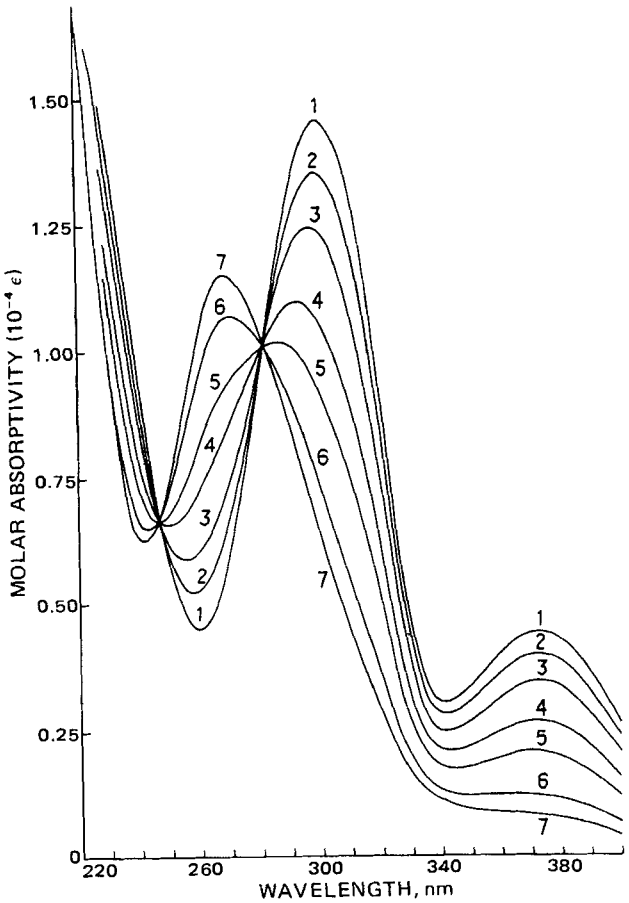

Figure 1—*Sequential UV spectra in 1.0* N *HCl accompanying equilibration of Ia. Reaction solution was 0.1 M citrate buffer, pH 4.0, μ = 0.3. Spectra were obtained at the following times: 1, 2 min; 2, 10 min; 3, 20 min; 4, 40 min; 5, 1 hr; 6, 2 hr; and 7, 72 hr.*

The yellowish-white solid thus obtained was repetitively treated with hot methanol, yielding an off-white powder. This compound showed one TLC spot, which had the same chromatographic characteristics as those of sarcosine when the sample was spotted on a silica gel plate[4], developed in 2-propanol–water (70:30) and 2-propanol–concentrated ammonia (70:30), and detected by ninhydrin reagent.

Instrumentation—The pH measurements were made using direct reading, digital pH meters[5,6]. UV spectra were obtained using a recording UV spectrophotometer[7].

pKa Determination of IIa—Portions, 107 mg, of IIa dihydrochloride were accurately weighed and quantitatively transferred to each of 10 20-ml beakers. Distilled water, 15 ml, was added to a beaker, the compound was allowed to dissolve, and a known volume of 0.5 *N* NaOH (0–1.60 ml in 0.2-ml increments) was added. The pH of the resulting solution was recorded immediately after preparation (2 min) and periodically thereafter for 7 min. This process was then repeated for each different volume of 0.5 *N* NaOH added.

The initial pH was determined by extrapolation of the pH *versus* time curves obtained to zero time. A plot was then made of initial pH *versus* alkali added, and the pKa was calculated as described by Albert and Serjeant (9).

Spectrophotometric pKa Determination of Ia and Va—A stock solution of Ia or Va in water, 1.8×10^{-3} *M*, containing 10% methanol was freshly prepared. Aliquots of 2 ml were diluted to 25 ml with hydrochloric acid solution, 0.01 *M* acetate buffer, and 0.01 *M* phosphate buffer, separately, to cover the pH range of 1.3–7.3. The resulting solutions were then scanned from 400 to 220 nm *versus* the respective solvents. The pKa's were then calculated from the absorbances at 300 nm as described by Albert and Serjeant (10).

Equilibrium Studies—Approximately 0.08 mEq of Ia or IIc was ac-

[5] Model 701, Orion digital pH meter.
[6] Model DR, Sargent digital pH meter.
[7] Cary model 11 or 14.

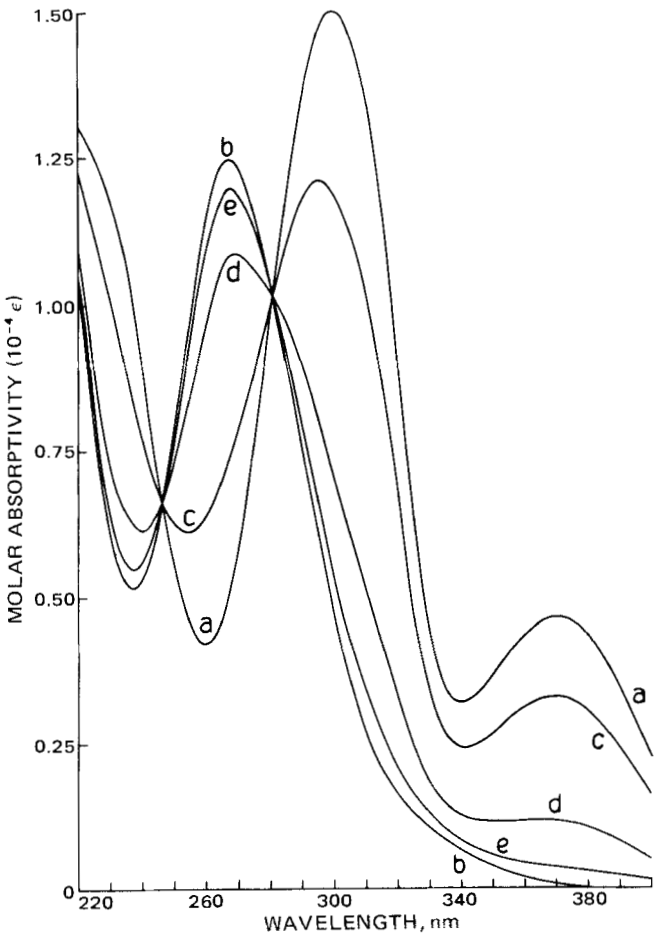

Figure 2—*UV spectra in 1.0* N *HCl of* Ia (*a*), *IIa* (*b*), *and equilibrium mixtures as produced at pH 5.0* (*c*), *4.0* (*d*), *and 2.0* (*e*).

curately weighed and quantitatively transferred into a 50-ml volumetric flask. Then 1 ml of methanol was added to dissolve the compound. The reaction was initiated by bringing to volume with an adequate solvent or buffer of known pH and constant ionic strength (27°, $\mu = 0.3$). At appropriate intervals, a 2-ml aliquot was withdrawn and diluted to 25 ml with 1 *N* HCl. The resulting solution was immediately scanned from 400 to 220 nm *versus* 1 *N* HCl using 1-cm silica cells. Spectra were obtained until they became redundant. Hydrochloric acid (1.0 *N*) was used as the solvent for spectral measurement to avoid changes in spectra resulting from varying degrees of protonation and because it effectively quenched the reaction.

Determination of Composition of Equilibrium Mixtures—The composition of equilibrium mixtures was calculated from the redundant spectra as follows:

$$\%\,\mathrm{I} = \frac{a_{\lambda 371}}{4.76 \times 10^3\, C} \frac{1}{} 100 \qquad \text{(Eq. 1)}$$

$$\%\,\mathrm{II} = 100 - \%\,\mathrm{I} \qquad \text{(Eq. 2)}$$

where $a_{\lambda 371}$ is the absorbance of the final dilution of the reaction solution, C is the initial molar concentration of Ia or IIc, 4.76×10^3 is the molar absorptivity of Ia in 1 *N* HCl at 371 nm, [I] = [I*a*] + [I*b*], and [II] = [II*a*] + [II*b*].

RESULTS AND DISCUSSION

A preliminary study indicated that the UV spectrum of Ia, as determined in aqueous buffers having a pH of 6 or less, changed quite rapidly. Although the rate at which the spectrum changed depended on the pH in a complex manner, the difference between initial and final spectra was regular and became greater as the pH diminished.

Sequential spectra were obtained from reaction solutions of Ia maintained at 27° in buffers of known but varying pH (Fig. 1). Absorption at 371 and 300 nm decreased whereas absorption at 266 nm increased concurrently until the spectra became redundant with time. The shape of the redundant spectra varied with the pH of the reaction solution (Fig. 2).

Table I—Composition of Equilibrium Mixtures (27°)

Equilibration of Ia		Equilibration of Va	
pH	f_{II}[a]	pH	f_{VI}
1.18	0.95	1.44	0.71
2.10	0.95		
3.11	0.92	2.24	0.69
3.76	0.89	3.04	0.62
4.19	0.83	3.98	0.34
4.80	0.55	5.05	0.07
5.40	0.23		
5.80	0.12		
6.35	0.06		
7.20	0.02		

[a] Results at pH 1.18 and 2.10 were obtained by polarographic analysis. All other results were obtained spectrophotometrically.

Solutions of Ia at pH 1–6 were prepared and allowed to equilibrate until spectral redundancy was attained. The remaining portion of these solutions, after adjusting to pH 8.0, generated the spectrum of Ia. These results, together with information from previous studies (1), indicate that Ia undergoes a reversible reaction involving conversion of Ia to equilibrium mixtures containing I and II.

Additional evidence in this regard was obtained by studying the behavior of IIc after exposure to the same conditions used to study Ia. As seen from Fig. 2, the spectrum of IIc closely resembled the terminal spectra obtained when Ia was allowed to equilibrate at pH 2.5 or less. Some difference, however, existed between these spectra. The terminal spectra had greater absorption in the 371-nm region and somewhat less absorption at the 266-nm maximum of IIa than would be expected if Ia were completely converted to II. Furthermore, when IIc was allowed to equilibrate at pH 2.5–1.0, its spectrum changed slightly, and spectra identical to those obtained by equilibrating Ia at the same acidic pH values were produced.

Reaction solutions of IIc having pH 2.5 or greater produced redundant spectra which differed from those of IIa to an increasing degree as the pH increased. At pH 7.0 or higher, spectra consistent with equimolar conversion of IIa to Ia were obtained. The same set of isosbestic points existed in the sets of spectra obtained from equilibration starting with

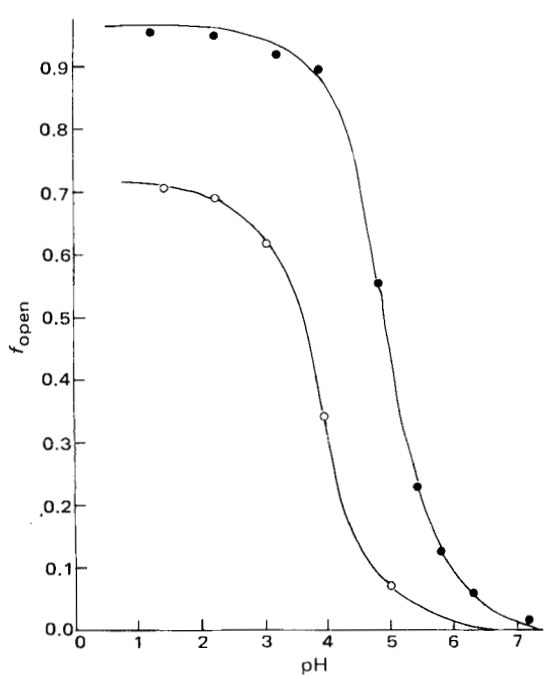

Figure 3—*Plot of the composition of equilibrium mixtures* versus *pH* (27°). *Key:* ●, *experimentally determined values for the I–II system; and* ○, *experimentally determined values for the V–VI system. The solid lines are values calculated using Eq. 5 with* $K^*_{II} = 1.13 \times 10^6\ M^{-1}$ *and* $K^*_{V\text{-}VI} = 6.1 \times 10^6\ M^{-1}$.

Ia (Fig. 1) as in the sets of spectra obtained from equilibration starting with IIc.

The shape of the redundant spectra produced upon equilibration was pH dependent. Since UV properties of both Ia and IIa are known, the composition of equilibrium mixtures corresponding to these spectra can be calculated. Analysis of the redundant spectra produced at various pH values gave the results in Table I and Fig. 3. The fraction of total open and closed species present as open species at equilibrium, f_{II} (see *Appendix*), increased in a sigmoidal fashion as pH decreased until, at pH values less than approximately 2.5, it became independent of pH but was not unity.

Results obtained thus far may be explained on the basis of Scheme I, representing the simultaneous occurrence of three equilibrium reactions.

$$IIb \overset{K_{a2}^{IIb}}{\rightleftharpoons} IIa + H^+ \overset{K^*}{\rightleftharpoons} Ib + H_2O \overset{K_{a1}^{Ib}}{\rightleftharpoons} Ia + H^+$$

Scheme I

The reaction accommodates intermediate carbinolamine formation from the free base form of IIa and the protonated form of Ia (Ib) in accord with established mechanistic principles (11). The reaction is probably more complicated than is indicated by Scheme I and likely involves (11) the equilibria shown in Scheme II.

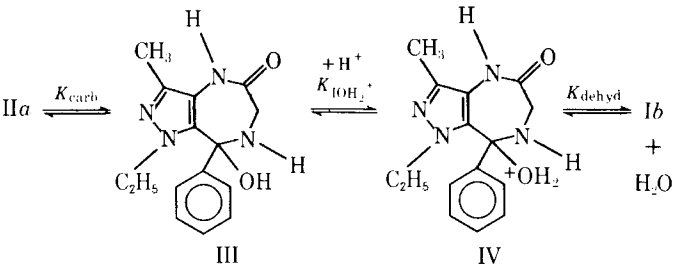

Scheme II

Intermediate compounds (III and IV), however, were never present in detectable concentrations. The sets of isosbestic points observed in the complete conversion of II to I or virtually complete conversion of I to II (Fig. 1) were the same and explicable on the basis of a binary system consisting of only I and II. Furthermore, the spectra of Ia in less reactive nonaqueous solvents such as acidified acetonitrile or methanol emulated those initially observed in water (Table II).

The net reaction resulting from the three reactions involving carbinolamine formation and dehydration is given as Scheme III.

$$IIa + H^+ \overset{K^*}{\rightleftharpoons} Ib + H_2O$$

Scheme III

The ring closure equilibrium constant, $K^{*\prime}$, is then defined by:

$$K^* = \frac{[Ib][H_2O]}{[IIa][H^+]} \qquad \text{(Eq. 3)}$$

$$K^{*\prime} = \frac{[Ib]}{[IIa][H^+]} \qquad \text{(Eq. 4)}$$

The equilibrium constant, $K^{*\prime}$, which governs ring closure is actually a composite, being equal to the product $K_{carb}K_{IOH_2}K_{dehyd}$.

Consideration of the equilibria involved in Scheme I leads to the following expression[8], which relates the composition of equilibrium mixtures to the hydrogen-ion concentration:

$$f_{II} = \frac{K_{a2}^{IIb} + [H^+]}{K_{a2}^{IIb} + [H^+] + K_{a2}^{IIb}K^{*\prime}\{K_{a1}^{Ib} + [H^+]\}} \qquad \text{(Eq. 5)}$$

The limiting forms of Eq. 5 are:

$$\lim f_{II}^{H^+ \to \infty} = \frac{1}{1 + K_{a2}^{IIb}K^{*\prime}} \qquad \text{(Eq. 6)}$$

$$\lim f_{II}^{H^+ \to 0} = \frac{1}{1 + K_{a1}^{Ib}K^{*\prime}} \qquad \text{(Eq. 7)}$$

Equations 6 and 7 are consistent with results obtained thus far in that they indicate that two regions of pH independence can exist, that the limiting values of f_{II} need not be unity, and that the limiting value of f_{II} reached at more acidic pH values should be greater than the limiting value reached at less acidic pH's[9]. Since Eq. 5 is in qualitative agreement with results obtained, it will be accepted as valid and tested further.

The value of $K^{*\prime}$, *i.e.*, the net equilibrium constant for the equilibrium reaction between open and closed forms, can be calculated from Eq. 5 and the experimental results. At pH 5.5 or less, the hydrogen-ion concentration is much greater than the value of K_{a2}^{IIb}, so Eq. 5 reduces to:

$$\frac{1}{f_{II}} = (1 + K^{*\prime}K_{a2}^{IIb}) + K^{*\prime}K_{a2}^{IIb}K_{a1}^{Ib}\frac{1}{[H^+]} \qquad \text{(Eq. 8)}$$

Equation 8 indicates that a plot of $1/f_{II}$ *versus* $1/[H^+]$ should be a straight line whose slope is $K^{*\prime}K_{a2}^{IIb}K_{a1}^{Ib}$. Since the two ionization constants are known, $K^{*\prime}$ can be calculated (Fig. 4). This method of calculating $K^{*\prime}$ uses data obtained at pH values at which the spectral measurement of f_{II} is most accurate and avoids the analytical difficulty encountered when the redundant spectra, representing equilibration, are similar to those of IIa.

When the value of $K^{*\prime}$ (= 1.13×10^6) as previously determined is substituted in Eq. 5, together with corresponding dissociation constants (*Appendix*) and values of f_{II} calculated by mathematically changing the hydrogen-ion concentration, the curve shown as the solid line in Fig. 3 is generated. As seen, this curve closely approximates experimentally determined results[10].

The preceding considerations developed for the II–I system are general and can be applied to other diazepinone systems to interpret results and to compare corresponding equilibria. The utility of this approach to determine the influence of structural modification on the ring closure equilibrium constant, $K^{*\prime}$, is illustrated by the following examples.

The 4-*N*-methyl derivative of Ia, Va, behaves as does Ia in kind but not degree (Fig. 3 and Table I). The values of f_{VI}, when plotted *versus* pH, "break" at a lower pH, and the limiting value of f_{VI} attained at lower pH values is less than that for the system involving II. Since the pKa of the open form of Va, VIa, is similar to that of IIa, Eqs. 9 and 10 are valid:

$$K^{*\prime}\,(\text{VI–V system}) = \left\{\frac{1 - \lim f_{VI}^{H^+ \to \infty}}{\lim f_{VI}^{H^+ \to \infty}} \cdot \frac{\lim f_{II}^{H^+ \to \infty}}{1 - \lim f_{II}^{H^+ \to \infty}}\right\} K^{*\prime}\,(\text{I–II system}) \qquad \text{(Eq. 9)}$$

$$K^{*\prime}\,(\text{VI–V system}) = 5.4K^{*\prime}\,(\text{II–I system}) \qquad \text{(Eq. 10)}$$

This result indicates that substitution of a methyl group for an amido hydrogen results in approximately a fivefold increase in the value of the equilibrium constant governing ring formation.

Table II—UV Spectral Properties of Various Compounds or Ions

Compound or Ion	Solvent	λ_{max} (log ϵ)
Ia	0.1 *M*, pH 7 phosphate buffer (aqueous)	305 s (3.55)
Ib	0.1 *N* HCl (aqueous)	300 (4.18), 371 (3.67)
Ib	1.0 *N* HCl (aqueous)	300 (4.18), 371 (3.67)
Ib	Methanol, 0.1 *N* H_2SO_4	298 (4.14), 377 (3.67)
Ib	98% Acetonitrile–2% 5 *N* HCl (aqueous)	300 (4.17), 377 (3.68)
I^-	0.1 *N* NaOH (aqueous)	346 (3.62)
IIb	0.01 *N* HCl (aqueous)	266 (3.997)
IIb	0.1 *N* HCl (aqueous)	266 (3.996)
IIb	1.0 *N* HCl (aqueous)	266 (3.998)
IIb	2.0 *N* HCl (aqueous)	269 (3.980)
IIb	5.0 *N* HCl (aqueous)	272 (3.979)
Va	0.1 *M*, pH 7 phosphate buffer (aqueous)	251 s (4.04), 305 s (3.52)
Vb	0.1 *N* HCl (aqueous)	300 (4.17), 373 (3.66)
Vb	1.0 *N* HCl (aqueous)	300 (4.14), 372 (3.64)
VIIb	0.1 *N* HCl (aqueous)	266 (4.001)
IX	98% Acetonitrile–2% water	301 (4.05), 381 (3.65)

[8] See *Appendix* for derivation and definitions.

[9] Some caution must be exercised in applying this conclusion since if both $K_a^{open}K^{*\prime}$ and $K_a^{closed}K^{*\prime}$ are either very large or very small as compared to unity, there would be no observable difference between the limits as attained at more or less acidic pH values.

[10] Polarographic analysis of the composition of equilibrium mixtures produced at more acidic pH values indicate $\lim f_{II}^{H^+ \to \infty} = 0.95$ rather than 0.93 as determined by UV measurement.

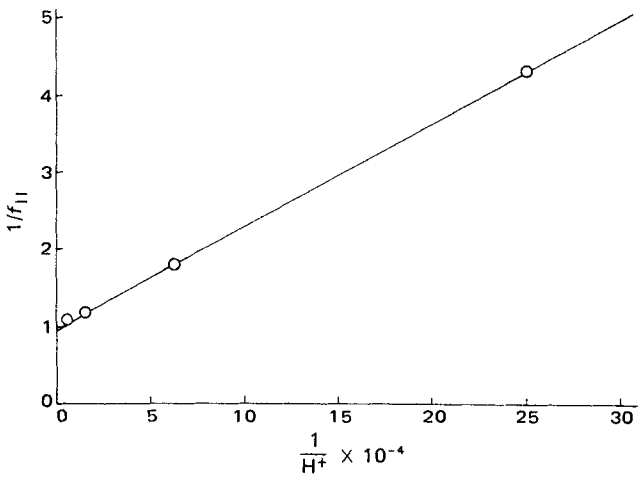

Figure 4—*Plot of* $1/f_{II}$ versus $1/a_{H^+}$. *Slope of straight line obtained is* 4.6×10^2. *The* $K^{*'}_{II-I}$, *as calculated from this value, equals* 1.13×10^6 M^{-1}.

The effect of replacing an amino hydrogen with a methyl group was likewise determined. To this end, VII*a* was prepared, and preparation of VIII was attempted. Attempts to isolate VIII as a pure compound were unsuccessful, the end-product being contaminated with VII*a* and other impurities. Nevertheless, studies done as before, using impure material, indicated that VIII was rapidly and completely hydrolyzed in aqueous solution, irrespective of pH. Corresponding studies with VII*a*, which was isolable as a pure compound, confirmed these observations in that no significant ring formation was observed.

The situation in this case is somewhat different than the general case because free base and protonated forms for the diazepinone no longer exist in equilibrium. The reaction involved can be represented by Scheme IV.

$$\text{VII}b \overset{K_a^{\text{VII}b}}{\rightleftharpoons} \text{VII}a + H^+ \overset{K^{*'}_{\text{VII-VIII}}}{\rightleftharpoons} \text{VIII} + H_2O$$

Scheme IV

The following equation, derived as was Eq. 5, would then relate $f_{\text{VII}a}$ to hydrogen-ion activity:

$$f_{\text{VII}} = \frac{K_a^{\text{VII}b} + [H^+]}{K_a^{\text{VII}b} + [H^+](1 + K_a^{\text{VII}b} K^{*'}_{\text{VII-VIII}})} \qquad \text{(Eq. 11)}$$

Equation 11 has the following limiting forms:

$$\lim f_{\text{VII}}^{H^+ \to \infty} = \frac{1}{1 + K_a^{\text{VII}b} K^{*'}_{\text{VII-VIII}}} \qquad \text{(Eq. 12)}$$

$$\lim f_{\text{VII}}^{H^+ \to 0} = 1 \qquad \text{(Eq. 13)}$$

As seen by examination of Eq. 12, for measurable coexistence of both open

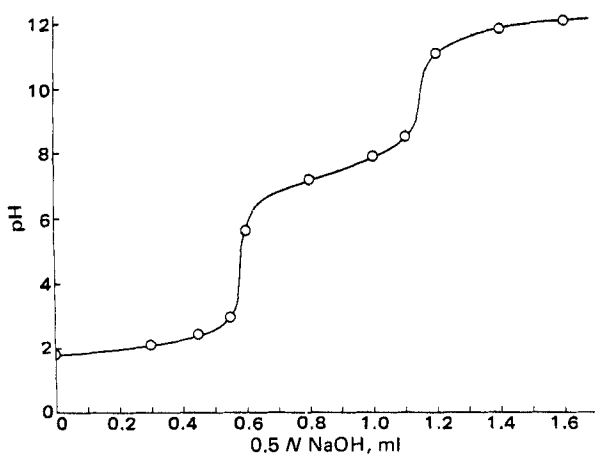

Figure 5—*Plot of initial pH values obtained by extrapolation for partially neutralized solutions of II*c.

Table III—Dissociation Constants (27°)

Compound	pKa_1	K_{a_1}	pKa_2	K_{a_2}
I*b*[a]	3.54 ± 0.03	2.89×10^{-4}	11.4 ± 0.05	3.98×10^{-12}
II*b*[b]	Very low	Very high	7.39 ± 0.06	4.07×10^{-8}
V*b*[a]	3.42 ± 0.05	3.80×10^{-4}	—	—
VII*b*[b]	Very low	Very high	7.74 ± 0.05	1.82×10^{-8}

[a] Determined spectrophotometrically. [b] Determined titrimetrically.

and closed forms to occur, the term $K_a^{\text{VII}b} K^{*'}_{\text{VII-VIII}}$ must be significant compared with 1. The value of $K_a^{\text{VII}b}$ (Table III) is somewhat less than the value of $K_{a2}^{\text{II}b}$. If $K^{*'}_{\text{I-II}}$ were equal to $K^{*'}_{\text{VII-VIII}}$, this decrease in K_a would account for an increase in the value of the limit in very acidic solution from 0.96 (as it is for the II–I system) to 0.98. It is apparent then that the values of $K^{*'}_{\text{II-I}}$ and $K^{*'}_{\text{VII-VIII}}$ need not be different, despite the fact that f_{VII} is independent of pH and near unity. Certainly, no increase in the value of the ring closure equilibrium constant occurs. The primary reason for the observed difference in behavior between the II–I and VII–VIII systems is that no storage of an unreactive form of the pyrazolodiazepinone can occur in the VII–VIII system whereas storage in the form of unprotonated I is allowed in the II–I system.

CONCLUSIONS

At near ambient temperatures, I*a* and its 4-*N*-methyl derivative (V*a*) undergo facile reversible hydrolysis in aqueous solvents of pH 7.0 or less. Under these conditions, equilibrium mixtures consisting of the unhydrolyzed diazepinones and corresponding open forms II and VI are produced. The composition of equilibrium mixtures depends on the pH of the reaction solution and has been shown to be related to the hydrogen-ion concentration according to:

$$f_{\text{open}} = \frac{K_a^{\text{open}} + [H^+]}{K_a^{\text{open}} + [H^+] + K_a^{\text{open}} K^{*'} (K_a^{\text{closed}} + [H^+])} \qquad \text{(Eq. 14)}$$

The values of $K^{*'}$, the intrinsic closure constants for II*a* and VI*a*, were calculated to be 1.13×10^6 and 6.1×10^6, respectively. Methylation of the amido nitrogen of II*a* caused a significant increase in the value of the ring closure equilibrium constant. Methylation of the terminal amino group caused no corresponding increase and may not significantly influence equilibrium.

APPENDIX

Dissociation Constants and Sites of Protonation—Other properties associated with I and II relate to this study and require determination. Among these are dissociation constants and protonation sites. This information is pertinent to this equilibrium study as well as to a kinetic investigation to be reported later. In regard to the open form, II, the determination of dissociation constant(s) is complicated by its instability. As has been established, II converts to I or equilibrium mixtures containing I in aqueous solution at 27°. To cope with this situation, the initial pH resulting from partial neutralization of the dihydrochloride salt of II*a* was determined by extrapolation (see *Experimental*). The pKa of II*a* (Table III) was then calculated using pH values defined by the smooth curve (Fig. 5) drawn through these extrapolated pH values.

As seen from Fig. 5, II*c* has two well-separated pKa values. The pH's observed during addition of up to 1 mole of sodium hydroxide/mole of the II*a* dihydrochloride salt were the same as those obtained when an equimolar solution of hydrochloric acid was similarly titrated. The UV spectra of II*a*, determined in hydrochloric acid solutions, showed no significant difference in cases where the concentration of hydrochloric acid was 1.0 *N* or less (Table II). The pKa of 1,3-dimethylpyrazole was reported to be 3.11 (12). Since the 1,3-dialkylpyrazole ring present in II*a* contains the benzoyl substituent, its pKa would be expected to be lower than that of 1,3-dimethylpyrazole. The presence of a positive charge would cause a further diminution of the pKa. These considerations indicate that the first dissociation of diprotonated II*a* involves proton loss from pyrazole nitrogens. The pKa associated with this process is very low and has a value less than zero.

The second pKa, $pKa_2^{\text{II}b}$, is much greater, indicating that a stronger basic site is involved. Since the pyrazole nitrogens have been excluded, this dissociation must involve the primary amino group of the acetamido chain. This conclusion is consistent with pKa values of C-carbamoyl-C-aminomethane compounds whose pKa's are reported to be 8.3–8.8 (13). The pKa of the model carbamoylaminomethane derivatives would be modified by substitution as present in II*a*.

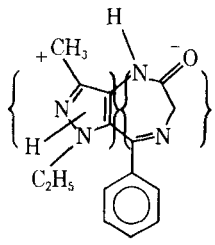

Ic

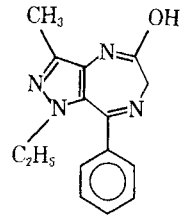

Id

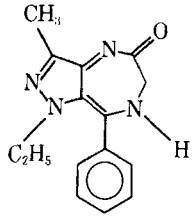

Ie

Dissociation constants of Ia were determined spectrophotometrically. This procedure is preferred since the spectra of charged and neutral forms are significantly different (Table IV) and the time required for spectrophotometric measurement (with precautions) is short compared with the time required for significant hydrolysis (Table III). The possibility that Ia might behave as a polyfunctional base was considered. Nonaqueous titration of Ia, using acetic acid as solvent and perchloric acid as titrant, indicated that only 1 mole of hydrogen ion was neutralized per mole of compound, so it could not behave as a polyfunctional base in aqueous solution over the pH region of interest. Compound Ia is, however, amphoteric. The second dissociation of Ib involves deprotonation from the diazepinone nitrogen in the 4-position since the 4-*N*-methyl derivative of Ia, Va, does not dissociate accordingly.

Several tautomeric structures can be written to represent other species of Ia with no net charge that might exist in aqueous solution. Significant concentration of forms Ic–Ie, however, cannot exist because the UV properties of Va (for which these tautomers could not exist) and Ia are very similar (Table II).

Evidence for the site of protonation of Ib is also available from comparison of its UV spectrum and that obtained from suitably methylated derivatives. The spectrum of Ib was significantly different from that of Ia and was characterized by absorption at near 300 and 371 nm (Table II). Compound IX (see *Experimental*), which contains methyl groups on both 4- and 7-nitrogens, was prepared and had a UV spectrum with essentially the same shape as Ib with maxima at nearly the same wavelengths (Table II). This result indicates that protonated Ia has the structure shown as Ib. Apparently, Ia behaves as do other benzodiazepinones in regard to proton addition (14).

Derivation of f_{II}—Let:

$$T = [IIa] + [IIb] + [Ia] + [Ib] \qquad \text{(Eq. A1)}$$

Then:

$$f_{II} = \frac{[IIa] + [IIb]}{T} \qquad \text{(Eq. A2)}$$

$$f_{II} = \frac{1 + \dfrac{[IIb]}{[IIa]}}{1 + \dfrac{[IIb]}{[IIa]} + \dfrac{[Ia]}{[IIa]} + \dfrac{[Ib]}{[IIa]}} \qquad \text{(Eq. A3)}$$

$$f_{II} = \frac{1 + \dfrac{[H^+]}{K_{a2}^{IIb}}}{1 + \dfrac{[H^+]}{K_{a2}^{IIb}} + K_{a1}^{Ib}K^{*\prime} + K^{*\prime}[H^+]} \qquad \text{(Eq. A4)}$$

$$f_{II} = \frac{K_{a2}^{IIb} + [H^+]}{K_{a2}^{IIb} + [H^+] + K^{*\prime}K_{a2}^{IIb}K_{a1}^{Ib} + K_{a2}^{IIb}K^{*\prime}[H^+]} \qquad \text{(Eq. A5)}$$

$$f_{II} = \frac{K_{a2}^{IIb} + [H^+]}{K_{a2}^{IIb} + [H^+] + K_{a2}^{IIb}K^{*\prime}(K_{a1}^{Ib} + [H^+])} \qquad \text{(Eq. A6)}$$

REFERENCES

(1) H. DeWald, I. Nordin, Y. L'Italien, and R. Parcell, *J. Med. Chem.*, **16**, 1346 (1973).

(2) B. Poschel, D. McCarthy, G. Chen, and C. Ensor, *Psychopharmacologia*, **35**, 257 (1974).

(3) R. Santos, C. Bowling, L. Mudgil, and J. Nodine, *Pharmacologist*, **13**, 205 (1971).

(4) G. Archer and L. Steinbach, *Chem. Rev.*, **68**, 751 (1969).

(5) J. Carstensen, K. Su, P. Maddrell, J. Johnson, and H. Newmark, *Bull. Parent. Drug. Assoc.*, **25**, 193 (1971).

(6) H. Maulding, J. P. Nazarero, J. E. Pearson, and A. F. Michaelis, *J. Pharm. Sci.*, **64**, 278 (1975).

(7) W. W. Han, D. D. Maress, and G. J. Yakatan, "Abstracts of Papers," APhA Academy of Pharmaceutical Sciences, American Pharmaceutical Association, Washington, D.C., Apr. 1975, Abstract 30.

(8) T. L. Lemke and A. R. Hanze, *J. Heterocycl. Chem.*, **8**, 127 (1971).

(9) A. Albert and E. Serjeant, "Ionization Constants of Acids and Bases," Wiley, New York, N.Y., 1962, pp. 16–42.

(10) *Ibid.*, pp. 69–92.

(11) W. P. Jencks, "Catalysis in Chemistry and Enzymology," McGraw-Hill, New York, N.Y., 1969, p. 491.

(12) D. D. Perrin, "Dissociation Constants of Organic Bases in Aqueous Solution," Page, Washington, D.C., 1965, p. 206.

(13) *Ibid.*, p. 14.

(14) J. Barrett, W. Smith, and I. E. Davidson, *J. Pharm. Pharmacol.*, **25**, 387 (1973).

ACKNOWLEDGMENTS AND ADDRESSES

Received April 7, 1976, from the *Pharmaceutical Research and Development Department, Parke, Davis & Co., Detroit, MI 48232.*

Accepted for publication January 17, 1977.

The authors are indebted to Dr. H. DeWald and Dr. C. Kulier for the synthesis of most compounds, to Dr. A. Kinkel who carried out computerized calculations, to Dr. F. Eng for polarographic analysis, and to Dr. L. M. Wheeler for encouragement and support.

[x] To whom inquiries should be directed.

Urinary Excretion of Hydromorphone and Metabolites in Humans, Rats, Dogs, Guinea Pigs, and Rabbits

E. J. CONE ˣ, B. A. PHELPS, and C. W. GORODETZKY

Abstract □ Hydromorphone was administered as a single dose to humans, rats, dogs, guinea pigs, and rabbits, and timed urinary collections were made. GLC–mass spectrometric and GLC analyses of the samples revealed the presence of the parent compound and both 6-hydroxy epimers as metabolites in the urine of all species. Free or conjugated parent drug predominated, while levels of free or conjugated 6β-hydroxy metabolite were higher than or equal to those of the 6α-form. The time courses of excretion of drug and metabolites were similar for all species, with the major portion being excreted in the first 24 hr. Generally, free and conjugated drug were undetectable in human urine after 8 and 48 hr, respectively.

Keyphrases □ Hydromorphone and metabolites—urinary excretion in humans, rats, dogs, guinea pigs, and rabbits □ Excretion, urinary—hydromorphone and metabolites, humans, rats, dogs, guinea pigs, and rabbits □ Metabolites—hydromorphone, urinary excretion in humans, rats, dogs, guinea pigs, and rabbits □ Narcotic analgesics—hydromorphone and metabolites, urinary excretion in humans, rats, dogs, guinea pigs, and rabbits

Hydromorphone (I) (dihydromorphinone) is a potent narcotic analgesic widely used for pain relief orally and parenterally. Its metabolism in rabbits is by conjugation and reduction to dihydromorphine (1). However, little is known regarding its metabolism and excretion in humans and other mammalian species.

Since hydromorphone is structurally related to the narcotic antagonists naltrexone (II) and naloxone (III) whose metabolic profiles include C-6 reduction to both α- and/or β-hydroxy metabolites, depending on species, it was of interest to determine if analogous pathways existed for hydromorphone. This report describes the determination of free and conjugated hydromorphone and the 6-hydroxy metabolites dihydromorphine (Iα) and dihydroisomorphine (Iβ) in the urine of humans, rats, dogs, guinea pigs, and rabbits given single doses of hydromorphone.

EXPERIMENTAL

Reagents and Chemicals—Reagent grade chloroform, 2-propanol, and methanol were used as received. Ethyl acetate was dried over calcium hydride. Compounds I[1], Iα[2], and Iβ[2] were used as received. The drug purity was determined prior to the study by TLC, GLC, and GLC–mass spectrometry (2).

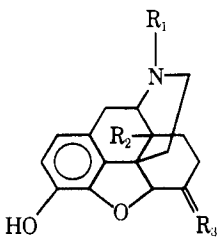

I: $R_1 = CH_3$, $R_2 = H$, $R_3 = O$

II: $R_1 = CH_2$—cyclopropyl, $R_2 = OH$, $R_3 = O$

III: $R_1 = CH_2CH{=}CH_2$, $R_2 = OH$, $R_3 = O$

Iα: $R_1 = CH_3$, $R_2 = H$, $R_3 = $

Iβ: $R_1 = CH_3$, $R_2 = H$, $R_3 = $

Table I—Protocol for Animal Experiments

Species	*n*	Average Weight	Dose of I Hydrochloride, mg
Guinea pig	6	998 g	5
Rat	5	462 g	5
Dog	2	7.75 kg	10
Rabbit	4	4.15 kg	5

GLC—A gas chromatograph[3], equipped with a flame-ionization detector, was used with a 1.83-m × 2-mm glass column packed with 3% OV-225 on 100–120-mesh Gas Chrom Q. The injector, detector, and column oven were maintained at 250, 260, and 215°, respectively. The air, hydrogen, and nitrogen carrier gas flows were 300, 30, and 26 ml/min, respectively. The retention times (in minutes) of the trifluoro derivatives were 2.60 for I, 2.94 for Iα, 2.13 for Iβ, and 3.56 for the internal standard, morphine.

GLC–Mass Spectrometry—Chemical-ionization mass spectral data were obtained on a quadrupole gas chromatograph–mass spectrometer[4] equipped with a glass column (1.52 m × 2 mm) packed with 3% OV-225 on 100–120-mesh Gas Chrom Q. The gas chromatograph was coupled to the mass spectrometer by a 0.31-cm glass-lined stainless steel tube and a venting valve. The electron energy was 80 ev. Methane, with a flow rate giving an ion source pressure of 1000 μm, was used as the carrier and reagent gas.

The temperatures of the injector, column, and ion source were 230, 215, and 100°, respectively. After sample injection, the venting valve was opened for 20 sec, allowing solvent and highly volatile substances to escape without entering the ion source. Selected ion recording was performed while focusing on *m/e* 480, 478, and 366 using a 1.8-kv multiplier setting.

TLC—Compounds I, Iα, and Iβ were applied to glass fiber sheets[5] and eluted in a saturation-type chamber containing chloroform saturated with aqueous ammonia. Conditions in the chamber were allowed to equilibrate for approximately 10 min prior to elution. The R_f values for I, Iα, and Iβ were 0.26, 0.08, and 0.04, respectively.

Sample Collections—The animals were housed individually in stainless steel metabolic cages equipped with urine collectors. Predrug control urine was collected the day before drug administration. A single dose of I hydrochloride was administered subcutaneously, and the urine was collected in 24-hr aliquots for 2 days. At the end of each collection period, the cages were rinsed with water, which was then added to the urine collection. Feces remained separated from the urine during collection and were discarded. The samples were centrifuged, decanted, and frozen until analyzed. The animal species, number in each experiment (*n*), average weight, and dose used are summarized in Table I.

The human subjects were healthy, adult male, federal prisoners from whom informed consent was obtained. Their ages ranged from 25 to 46 years. All were former narcotic addicts incarcerated at the National Institute on Drug Abuse Addiction Research Center. The subjects were drug free. Control urine from five subjects was collected for 24 hr before drug administration. Compound I hydrochloride (4 mg po) was administered, and all urine was collected for 144 hr, with collection periods ending at 2, 4, 8, 12, 24, 48, 72, 96, 120, and 144 hr after drug administration.

All samples for each individual were pooled for each collection period.

[1] Knoll Pharmaceutical Co., Whippany, N.Y.
[2] Drug Addiction Laboratory, University of Virginia.
[3] Varian model 2700.
[4] Finnigan model 3300 equipped with a Finnigan model 6000 interactive data system.
[5] Gelman I.T.L.C. type SG, Gelman Instrument Co., Ann Arbor, Mich.

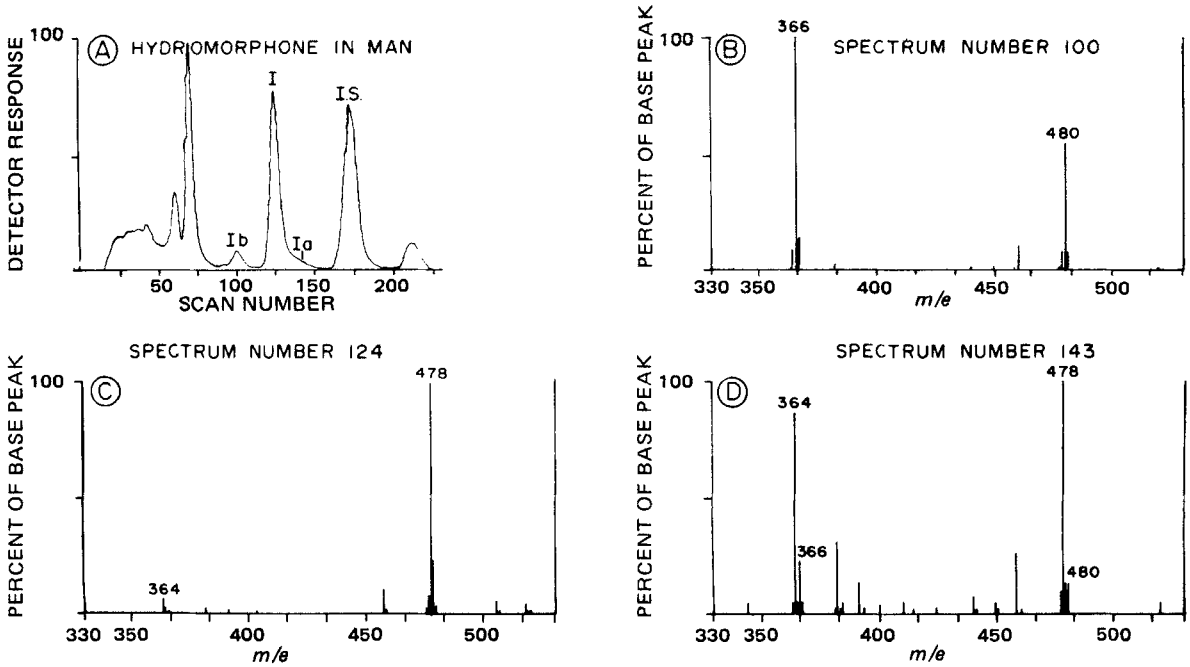

Figure 1—*GLC–chemical-ionization mass spectral (methane) analysis of drug in human urine. Key: A, integrated total ion current chromatogram of urine extract derivatized with trifluoroacetic anhydride; IS, internal standard (morphine); B, spectrum 100 identified as the 6β-hydroxy metabolite of I; C, spectrum 124 identified as I; and D, spectrum 143 identified as mixture of I and Ia.*

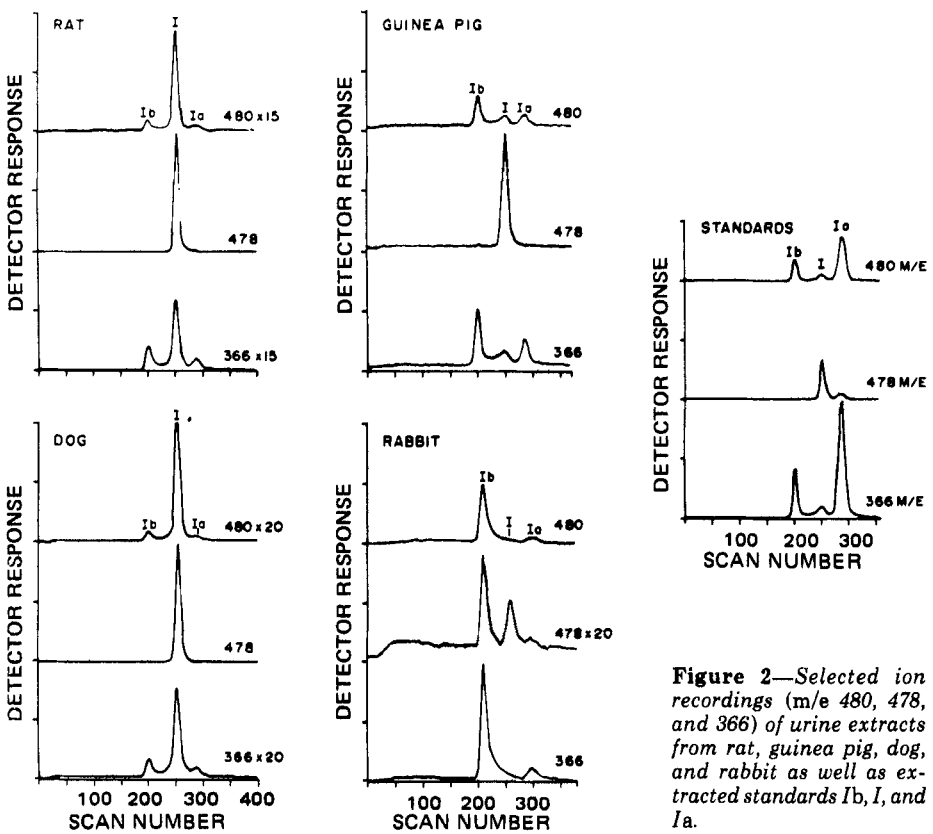

Figure 2—*Selected ion recordings (m/e 480, 478, and 366) of urine extracts from rat, guinea pig, dog, and rabbit as well as extracted standards Ib, I, and Ia.*

During the first two collection intervals (postdrug), the subjects were requested to drink at least 240 ml of liquid to ensure adequate urine volume. No special food or water intake conditions were maintained thereafter. The urine volume was measured, and the samples were frozen until assayed.

Extraction of Samples—Urine samples were acid hydrolyzed for 30 min in 10% HCl in an autoclave at 1.27 kg/cm^2 in a manner similar to that reported (3) for the acid hydrolysis of morphine. The free and acid-hydrolyzed samples were extracted as previously described for the analysis of II (4), with chloroform–2-propanol (9:1) substituted for the extracting solvent. The sample pH during extraction was maintained at 10.0 ± 0.02.

The extract was evaporated to dryness in an acylation tube[6], and 100 μl of trifluoroacetic anhydride[7] was added. The tube was sealed and

[6] Regis Chemical Co., Morton Grove, Ill.
[7] Aldrich Chemical Co., Milwaukee, Wis.

Table II—Recovery of Drug and 6-Hydroxy Metabolites from Urine of Animals Given Hydromorphone[a]

	I				Ib				Ia					
	Free		Conjugated		Free		Conjugated		Free		Conjugated		Total	
Species (n)	Day 1	Day 2	Day 1	Day 2	Day 1	Day 2	Day 1	Day 2	Day 1	Day 2	Day 1	Day 2	Day 1	Day 2
Guinea pig (6)	33.2	0.8	10.7	0.6	18.7	0.4	0	0.2	8.1	0.2	0	0	70.7	2.2
Rat (5)	8.4	0.7	17.0	2.4	0.6	0.1	0.8	0.3	0.7	0.4	0.2	0.3	27.7	4.2
Dog (2)	10.5	0.7	46.6	3.9	0.9	0.2	1.0	0	0.5	0.1	1.0	0	60.5	4.9
Rabbit (4)	6.0	1.6	9.1	3.9	2.0	0.2	3.8	0.9	0.2	0.1	0.7	0.1	21.8	6.8
Human (5)	5.6	0	29.9	6.9	—[b]	—[b]	1.0[c]	0[c]	0	0	0.1[d]	0	36.6	6.9

[a] Values represent the means of triplicate determinations and are expressed as the percent of the administered dose. Levels of conjugated drug and metabolites were determined by subtraction of free from total concentrations after acid hydrolysis. [b] Not determined. [c] Value is based on one subject. [d] Estimated by GLC–mass spectral determination.

heated in an oil bath at 90–95° for 1–2 hr. After heating, the tube was cooled under tap water, and the mixture was evaporated to dryness under dry nitrogen at room temperature. Ethyl acetate (50 μl), dried over calcium hydride, was added; then the tube was resealed, shaken, and analyzed by GLC or GLC–mass spectrometry immediately. Each sample was worked up just prior to analysis to prevent sample hydrolysis.

pH Study—The effect of pH in the 8–12 range on the extraction of I, Ia, and Ib was determined by extracting triplicate samples of each drug with chloroform and adding the internal standard in the final step prior to analysis. A pH range of 9.5–10.5 was optimum.

Extraction Efficiency Study—The efficiency of chloroform *versus* chloroform–2 propanol (9:1) for extraction of I, Ia, and Ib at pH 10.0 was determined in a manner similar to that for the pH study. Peak height ratios of the extracted sample were compared to those of the unextracted substances. Percent recoveries ± SE (n = 6) for chloroform and chloroform–2-propanol were 64.1 ± 20.7 and 49.2 ± 6.8 for I, 39.3 ± 11.8 and 64.0 ±10.7 for Ia, and 25.8 ± 8.2 and 66.8 ± 8.1 for Ib, respectively.

GLC Quantitation—Standard curves for I, Ia, and Ib were prepared by adding known amounts (0–50 μg of I and Ib and 0–12.5 μg of Ia as the free base) to predrug control urine containing morphine (40 μg) added as the internal standard. The samples were extracted with or without acid hydrolysis, derivatized, and analyzed by GLC. Linear relationships of peak height ratios of I, Ia, and Ib were observed for this concentration range. The standard curves for I, Ia, and Ib can be described by $R = 0.0374C - 0.0420$, $R = 0.0399C - 0.0032$, and $R = 0.0541C + 0.0017$, respectively, where R is the peak height ratio of drug to internal standard and C is the concentration.

Prediction limits were constructed from these data as generally described (5). Day-to-day variability of the analysis procedure was monitored by inclusion of standard control samples. Analyses in which the standard control samples fell outside the 95% prediction intervals were rejected. The samples from the untreated and acid-hydrolyzed urine were analyzed on the same curve since the standard controls taken through the hydrolysis and extraction procedures were within the prediction intervals. The reported values represent the mean of at least three determinations.

RESULTS AND DISCUSSION

Qualitative identification of hydromorphone (I) and the 6-hydroxy-metabolites in the urine of humans and animals was made by a series of GLC–mass spectral studies. Figure 1 contains a typical GLC–chemical-ionization mass spectral (methane) chromatogram and associated spectra obtained for a human urine extract. Compounds I (spectrum 124) and Ib (spectrum 100) were identified by comparison of their retention times and chemical-ionization spectra with analytical standards. Small amounts of Ia (spectrum 143) also could be detected.

Table III—Order of Urinary Excretion of Hydromorphone and Metabolites within Species

Species	Relative Amount in Urine
Guinea pig	I > Ib > conjugated I > Ia ≫ conjugated Ib
Rat	Conjugated I > I ≫ conjugated Ib = Ia > Ib > conjugated Ia
Dog	Conjugated I ≫ I ≫ Ib ≥ conjugated Ib = conjugated Ia > Ia
Rabbit	Conjugated I > I > conjugated Ib > Ib > conjugated Ia > Ia
Human	Conjugated I ≫ I ≫ conjugated Ib > conjugated Ia

Screening of the animal urines (Fig. 2) for these metabolites was achieved by selected ion recordings of m/e 480 (M + 1 ion of Ia and Ib), 478 (M + 1 ion of I), and 366 (M + 1 ion − CF_3COOH of Ia and Ib). A detector response at these settings at scan numbers 200 (3.40 min), 250 (4.23 min), and 285 (4.84 min) was characteristic of Ib, I, and Ia, respectively. Both Ib and Ia as well as I were present in the urine of all species.

Quantitative studies on the urinary excretion of these compounds were performed using GLC. Figure 3 shows a sample chromatogram for a guinea pig urine extract, demonstrating the separation of I and the epimeric 6-hydroxy metabolites (Ia and Ib). By using the GLC method described, near baseline resolution was achieved for each component on the relatively polar OV-225 liquid phase. This method was used for the quantitative determination of these substances in urine as free and acid-hydrolyzable conjugates of I, Ia, and Ib in several animal species.

Resolution problems were encountered only in human samples, where caffeine presented serious interference in the determination of the small amounts of Ib present. For these samples, prior elimination of the interfering peak was necessary and was accomplished by elution of the sample extract on glass fiber TLC with chloroform saturated with

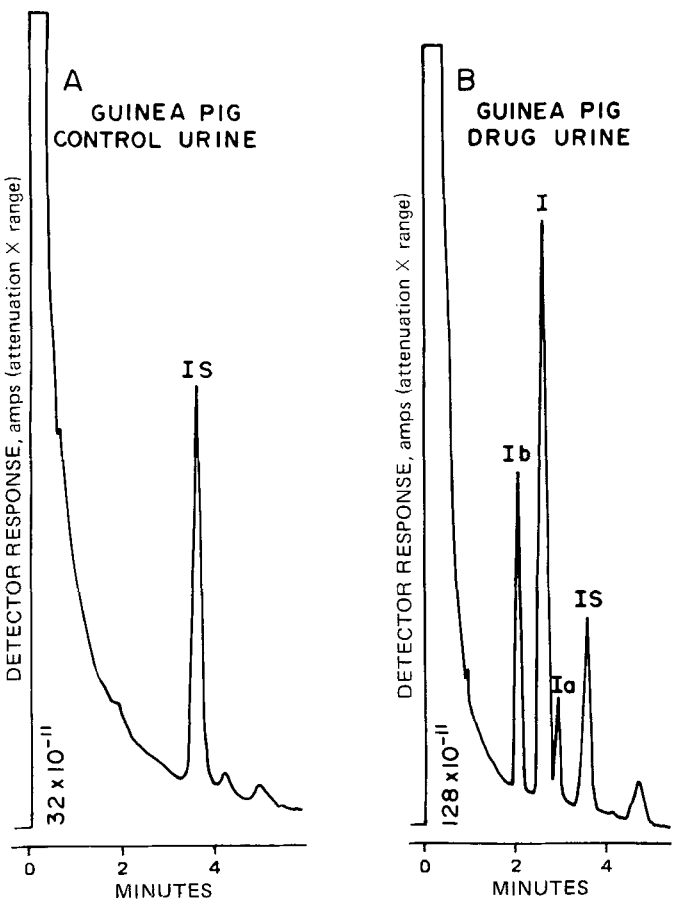

Figure 3—*Gas chromatograms of unhydrolyzed guinea pig urinary extracts derivatized with trifluoroacetic anhydride (IS is the internal standard morphine.)*

Table IV—Timed Urinary Excretion of Free and Conjugated Hydromorphone in Five Human Subjects[a]

	Subject J		Subject W		Subject I		Subject M		Subject D	
Hours	Free	Conjugated	Free	Conjugated	Free	Conjugated	Free	Conjugated	Free	Conjugated
2	1.7	6.7	—[b]	—	—	—	0.5	3.2	4.6	4.5
4	—	—	2.2	17.7	6.3	11.9	0.8	4.6	5.7	4.8
8	2.1	16.8	2.1	6.3	1.0	4.4	0	8.1	0	10.9
12	0	3.3	0	4.2	—	—	0	1.8	0.7	0.8
24	0	6.0	0	3.5	0	19.7	0	7.4	2.2	1.0
48	0	8.4	0	11.0	0	15.1	0	0	0	0
72	0	0	0	0	0	0	0	0	0	0
Total	3.8	41.2	4.3	42.7	7.3	51.1	1.3	25.1	13.2	22.0

[a] Values represent the means of triplicate determinations and are expressed as the percent of the administered dose. Levels of conjugated drug and metabolite were determined by subtraction of free from total concentrations after acid hydrolysis. [b] Sample was not produced.

aqueous ammonia. The zone containing I*b* (R_f 0–0.1) was removed and extracted with methanol. Evaporation followed by derivatization and injection of the extract produced a chromatogram of I*b* free of interferences. No interferences were encountered in the determination of I and I*a*.

Solvent and pH effects on the extractability of the drug and metabolites were determined prior to the metabolic study. Optimal extraction efficiency was found for a chloroform–2-propanol mixture (9:1) where about 50 and 65% recoveries were observed for I and the 6-hydroxy metabolites, respectively. The optimal pH for extraction was 9.5–10.5.

The results of the urinary excretion study of single doses of I in animals and humans are shown in Table II. Both free and conjugated I and the 6-hydroxy metabolites I*a* and I*b* were detected in the urine of all species. As shown in Fig. 4, I was excreted predominantly as an acid-hydrolyzable conjugate (presumably glucuronide); in the guinea pig, however, free I (34.0%) was highest in amount followed by free I*b* (19.1%) and conjugated I (11.3%). The order of excretion of drug and metabolites is illustrated in Table III.

Levels of free or conjugated I*b* were generally higher than or equal to those of the epimeric I*a* for all species. This result was reversed only for the rat, where levels of free I*a* exceeded those of I*b* in the Day 1 and 2 samples (Table II). Apparently, the reduction pathway leading to formation of 6-hydroxy metabolites of hydromorphone is relatively minor for the rat, dog, and human. Greater amounts of free and conjugated I*b* were encountered for the rabbit (2.2 and 4.7%) and guinea pig (19.1 and 0.2%). Levels of I*a* were also highest for the guinea pig (8.3%). Overall total recoveries of drug and metabolite from urine ranged from lows of 28.6 and 31.9% for the rabbit and rat to 65.4 and 72.9% for the dog and guinea pig. Total recovery of drug from humans was intermediate at 43.5%.

The time course of urinary excretion of drug and metabolite was similar for all species, with the major portion being excreted in the first 24 hr. Levels of drug and metabolite in the Day 2 samples were generally lower, ranging from 10 to 50% of the levels in Day 1 samples. The rat was an exception; levels of conjugated I*a*, unlike I*b*, increased in the Day 2 sample. The apparent longer half-life of I*a* *versus* I*b* in the rat might be a result of enterohepatic recirculation of I*a*.

Excretion of free and conjugated I in human subjects was examined at timed intervals during Day 1 through Day 5. Table IV contains the excretion data for free and conjugated I for five subjects. Considerable intersubject variability existed. The initial urine sample of all subjects contained the highest drug concentration. Levels dropped rapidly, and I was undetectable in the free form after 8 hr for four of five subjects. The remaining subject had free I through 24 hr. Conjugated I was detectable in Day 2 samples for three of five subjects.

With TLC for the elimination of the interfering substance, I*b* was quantitatively determined for one subject. Only 1.0% of the administered dose was found. GLC–mass spectral screening of the human samples indicated that both I*a* and I*b* were present in all Day 1 pooled urine samples. The levels of I*a* were consistently below the lower limits of sensitivity of the GLC method (Fig. 1) and were estimated to represent approximately 0.1% of the administered dose.

The relatively small amounts of I*a* and I*b* (Fig. 4) found in rat, dog, rabbit, and human urine suggest that the contribution to pharmacological activity from these active metabolites would be minimal (I*a* and I*b* are approximately two-thirds and one-fifth as potent as I in producing analgesia) (6). However, the amounts of free I*b* and I*a* in the guinea pig were considerably higher, and some pharmacological contribution by these metabolites is likely. This study demonstrated that the species studied

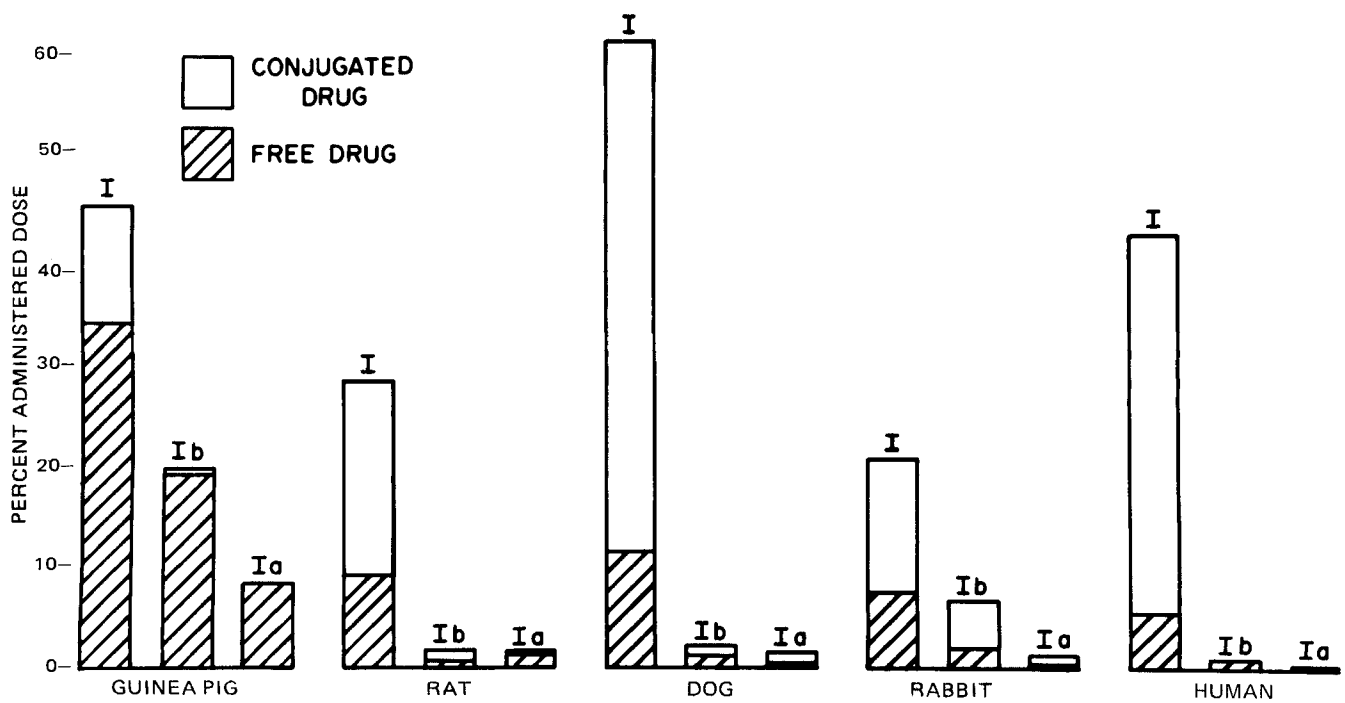

Figure 4—*Overall mean urinary excretion levels of free and conjugated hydromorphone and 6-hydroxy metabolites in humans and animals.*

have the capability of metabolic reduction of I to both epimeric 6-hydroxy metabolites. However, considerable stereospecificity by the drug-metabolizing enzyme(s) favoring formation of the 6β-hydroxy metabolite was observed for all species. This result is consistent with metabolic data reported for other 6-oxo compounds containing the hydromorphone structure (2, 4).

REFERENCES

(1) S. Roerig, J. M. Fujimoto, and R. I. H. Wang, *Proc. Soc. Exp. Biol. Med.*, **143**, 230 (1973).

(2) E. J. Cone, *J. Chromatogr.*, **129**, 355 (1976).

(3) S. Y. Yeh and L. A. Woods, *J. Pharm. Sci.*, **59**, 380 (1970).

(4) E. J. Cone, C. W. Gorodetzky, and S. Y. Yeh, *Drug. Metab. Dispos.*, **2**, 506 (1974).

(5) G. W. Snedecor, "Statistical Methods," Iowa State University Press, Ames, Iowa, 1956, p. 138.

(6) L. F. Small, N. B. Eddy, E. Mosettig, and C. K. Himmelsbach, "Studies on Drug Addiction," Public Health Reports Suppl. 138, U.S. Government Printing Office, Washington, D.C., 1938.

ACKNOWLEDGMENTS AND ADDRESSES

Received November 1, 1976, from the *National Institute on Drug Abuse, Division of Research, Addiction Research Center, Lexington, KY 40511.*

Accepted for publication February 22, 1977.

[x] To whom inquiries should be directed.

Generic Propoxyphene: Need for Clinical Bioavailability Evaluation

K. A. DeSANTE [x], R. G. STOLL [*], D. G. KAISER, and A. R. DiSANTO

Abstract □ Plasma level data on two investigational capsule formulations of propoxyphene with similar physicochemical parameters demonstrate that the formulations have different *in vivo* bioavailabilities. The potential for bioavailability problems with water-soluble drugs and the lack of correlation of *in vitro* and *in vivo* parameters for equivalent drug formulations are discussed.

Keyphrases □ Propoxyphene hydrochloride—different formulations, bioavailability compared □ Bioavailability—propoxyphene hydrochloride, different formulations compared □ Analgesics—propoxyphene hydrochloride, different formulations, bioavailability compared

With the recent expiration of the propoxyphene hydrochloride patent, several pharmaceutical manufacturers have marketed a generic formulation of this drug. These manufacturers were required to assess *in vitro* parameters such as drug content and dissolution rate to assure equivalence to the innovator's product. To date, no *in vitro* dissolution rate standard that has been shown to correlate with *in vivo* bioavailability has been developed.

However, with digoxin, for which *in vitro* standards were used to assure product equivalence (through batch certification), the Food and Drug Administration (FDA) clearly recognized that *in vitro* testing alone often does not ensure bioequivalence (1). This knowledge recently resulted in written bioavailability requirements for marketed digoxin products by the FDA (2).

Propoxyphene hydrochloride is a readily soluble drug. A simple capsule formulation of this drug would generally be considered as having a very low potential for bioavailability problems. Usually, only drugs with low water solubility are considered potential problems in formulating a readily available dosage form (3–5). The converse of this hypothesis (*i.e.*, soluble drugs have low potential for bioavailability problems) has not been investigated adequately. To ascertain possible bioavailability problems of drugs with high risk potential, the low risk potential drugs are rarely studied (6).

Although propoxyphene hydrochloride is a very soluble drug, comparative bioavailability data should be obtained prior to marketing any new formulation. Even the finding of equivalent *in vitro* parameters should not be sufficient justification for assuming bioequivalence of two different formulations of the same parent drug without *in vivo* data.

This paper reports the results of two bioequivalence studies in which two proposed marketed formulations with nearly identical *in vitro* parameters of potency and dissolution rate were compared to the recognized standard propoxyphene product.

EXPERIMENTAL

Bioavailability Studies—The design for both studies was identical. In Study 1, 21 healty adult volunteers[1] (14 males and seven females), averaging 23 years of age (range of 22–33 years) and weighing 68.6 kg (range of 52.2–86.4 kg), were selected. In Study 2, 24 healthy adult male volunteers, averaging 24.5 years (range of 19–51 years) and weighing 77.5 kg (range of 61.4–89.1 kg), were selected.

All subjects had normal screening vital signs (blood pressure, pulse, respiration, and temperature) and laboratory parameters (complete blood count, urinalysis, blood urea nitrogen, serum alkaline phosphatase, serum glutamic–oxaloacetic transaminase, serum bilirubin, and glucose). No subject received any barbiturates or other enzyme-inducing drugs for 30 days, or any other medication for 7 days, preceding the start of the study. All subjects received only the medication prescribed in the protocol for the duration of the study.

At zero time of each treatment period, each subject received single oral doses of medication[2] as follows: Treatment A, one 65-mg hard-filled capsule of propoxyphene hydrochloride (test formulation); or Treatment

[1] Study was initiated with 22 subjects, but one subject was dropped before completion of the clinical phase.

[2] Identity of products is available from authors upon request.

have the capability of metabolic reduction of I to both epimeric 6-hydroxy metabolites. However, considerable stereospecificity by the drug-metabolizing enzyme(s) favoring formation of the 6β-hydroxy metabolite was observed for all species. This result is consistent with metabolic data reported for other 6-oxo compounds containing the hydromorphone structure (2, 4).

REFERENCES

(1) S. Roerig, J. M. Fujimoto, and R. I. H. Wang, *Proc. Soc. Exp. Biol. Med.*, **143**, 230 (1973).

(2) E. J. Cone, *J. Chromatogr.*, **129**, 355 (1976).

(3) S. Y. Yeh and L. A. Woods, *J. Pharm. Sci.*, **59**, 380 (1970).

(4) E. J. Cone, C. W. Gorodetzky, and S. Y. Yeh, *Drug. Metab. Dispos.*, **2**, 506 (1974).

(5) G. W. Snedecor, "Statistical Methods," Iowa State University Press, Ames, Iowa, 1956, p. 138.

(6) L. F. Small, N. B. Eddy, E. Mosettig, and C. K. Himmelsbach, "Studies on Drug Addiction," Public Health Reports Suppl. 138, U.S. Government Printing Office, Washington, D.C., 1938.

ACKNOWLEDGMENTS AND ADDRESSES

Received November 1, 1976, from the *National Institute on Drug Abuse, Division of Research, Addiction Research Center, Lexington, KY 40511.*

Accepted for publication February 22, 1977.

[x] To whom inquiries should be directed.

Generic Propoxyphene: Need for Clinical Bioavailability Evaluation

K. A. DeSANTE [x], R. G. STOLL [*], D. G. KAISER, and A. R. DiSANTO

Abstract □ Plasma level data on two investigational capsule formulations of propoxyphene with similar physicochemical parameters demonstrate that the formulations have different *in vivo* bioavailabilities. The potential for bioavailability problems with water-soluble drugs and the lack of correlation of *in vitro* and *in vivo* parameters for equivalent drug formulations are discussed.

Keyphrases □ Propoxyphene hydrochloride—different formulations, bioavailability compared □ Bioavailability—propoxyphene hydrochloride, different formulations compared □ Analgesics—propoxyphene hydrochloride, different formulations, bioavailability compared

With the recent expiration of the propoxyphene hydrochloride patent, several pharmaceutical manufacturers have marketed a generic formulation of this drug. These manufacturers were required to assess *in vitro* parameters such as drug content and dissolution rate to assure equivalence to the innovator's product. To date, no *in vitro* dissolution rate standard that has been shown to correlate with *in vivo* bioavailability has been developed.

However, with digoxin, for which *in vitro* standards were used to assure product equivalence (through batch certification), the Food and Drug Administration (FDA) clearly recognized that *in vitro* testing alone often does not ensure bioequivalence (1). This knowledge recently resulted in written bioavailability requirements for marketed digoxin products by the FDA (2).

Propoxyphene hydrochloride is a readily soluble drug. A simple capsule formulation of this drug would generally be considered as having a very low potential for bioavailability problems. Usually, only drugs with low water solubility are considered potential problems in formulating a readily available dosage form (3–5). The converse of this hypothesis (*i.e.*, soluble drugs have low potential for bioavailability problems) has not been investigated adequately. To ascertain possible bioavailability problems of drugs with high risk potential, the low risk potential drugs are rarely studied (6).

Although propoxyphene hydrochloride is a very soluble drug, comparative bioavailability data should be obtained prior to marketing any new formulation. Even the finding of equivalent *in vitro* parameters should not be sufficient justification for assuming bioequivalence of two different formulations of the same parent drug without *in vivo* data.

This paper reports the results of two bioequivalence studies in which two proposed marketed formulations with nearly identical *in vitro* parameters of potency and dissolution rate were compared to the recognized standard propoxyphene product.

EXPERIMENTAL

Bioavailability Studies—The design for both studies was identical. In Study 1, 21 healty adult volunteers[1] (14 males and seven females), averaging 23 years of age (range of 22–33 years) and weighing 68.6 kg (range of 52.2–86.4 kg), were selected. In Study 2, 24 healthy adult male volunteers, averaging 24.5 years (range of 19–51 years) and weighing 77.5 kg (range of 61.4–89.1 kg), were selected.

All subjects had normal screening vital signs (blood pressure, pulse, respiration, and temperature) and laboratory parameters (complete blood count, urinalysis, blood urea nitrogen, serum alkaline phosphatase, serum glutamic–oxaloacetic transaminase, serum bilirubin, and glucose). No subject received any barbiturates or other enzyme-inducing drugs for 30 days, or any other medication for 7 days, preceding the start of the study. All subjects received only the medication prescribed in the protocol for the duration of the study.

At zero time of each treatment period, each subject received single oral doses of medication[2] as follows: Treatment A, one 65-mg hard-filled capsule of propoxyphene hydrochloride (test formulation); or Treatment

[1] Study was initiated with 22 subjects, but one subject was dropped before completion of the clinical phase.

[2] Identity of products is available from authors upon request.

Table I—Physicochemical Parameters Obtained for the Different 65-mg Propoxyphene Hydrochloride Capsule Formulations

Property	Study 1		Study 2	
	Treatment A Formulation I	Treatment B Recognized Standard I	Treatment A Formulation II	Treatment B Recognized Standard II
Assay potency[a]	63.7 ± 0.85 mg	62.9 ± 1.4 mg	68.2 ± 1.7 mg	65.1 ± 0.6 mg
Dissolution rate[b] at 10 min, %	96.5 ± 8.9	89.9 ± 1.3	99.80 ± 1.0	99.68 ± 3.1

[a] Assay 10 capsules and report average of three or more assays for each lot. [b] Mean ± *SD* for six capsules. Unpublished assay procedure.

Table II—Average Plasma Propoxyphene Concentrations and Related Parameters Obtained from 21 Normal Volunteers after Receiving Single Oral Doses (65 mg) of Two Propoxyphene Formulations

Hours	Average Plasma Propoxyphene Level, ng/ml		Significance
	Treatment A	Treatment B	
0.0	0.20 (0.20)[a]	0.0 (0)[a]	N.S.
0.5	10.12 (2.40)	6.29 (2.43)	N.S.
1.0	32.11 (4.45)	48.84 (12.45)	N.S.
2.0	44.09 (4.51)	53.05 (3.84)	$p < 0.025$
3.0	40.75 (5.01)	44.52 (4.23)	N.S.
5.0	17.87 (1.61)	24.88 (2.47)	$p < 0.001$
7.0	12.98 (1.47)	20.84 (3.43)	$p < 0.05$
9.0	8.85 (1.02)	13.25 (2.10)	$p < 0.025$
12.0	5.77 (1.02)	8.46 (1.19)	$p < 0.005$
Average of individual peak plasma concentrations, ng/ml	51.58 (4.99)	69.81 (11.46)	N.S.
Average *AUC*, ng hr/ml (0–12 hr)	226.9 (19.95)	296.87 (25.39)	$0.001 < p < 0.005$
Average of individual peak times, hr	1.95 (0.21)	2.14 (0.28)	N.S.

[a] The ( ) represents the standard error of the mean.

B, one 65-mg hard-filled capsule of propoxyphene hydrochloride (recognized standard). Individual subjects were assigned treatments according to a randomized two-way crossover design. The studies were separated by 7 days.

Subjects were required to fast overnight and for 4 hr immediately after the medication was administered. The medication was taken at zero time with 180 ml of water. No beverages (except water) were permitted during the fasting period. The subjects were not permitted to engage in any strenuous or athletic activities during the days of drug administration.

Blood, 20 ml, was taken from each subject at zero time, *i.e.*, just before dosing with each medication and at 0.5, 1.0, 2.0, 3.0, 5.0, 7.0, 9.0, and 12 hr. In Study 2, a 16-hr postadministration sample also was drawn. Plasma was harvested from all samples as soon after drawing as possible and immediately frozen.

Assay Methodology—All plasma specimens were extracted using the procedure described by Wolen and Gruber (7). The extract residues were reconstituted in carbon disulfide for GLC analysis. All samples were chromatographed on U-shaped glass columns (0.31 m × 3 mm i.d.) of 3% (w/w) Apiezon-L and 2% (w/w) potassium hydroxide on 80–100-mesh Gas Chrom Q[3]. All newly prepared columns were preconditioned at 225° for 6 hr without carrier gas flow and for 16 hr with carrier gas flow of 10 ml/min.

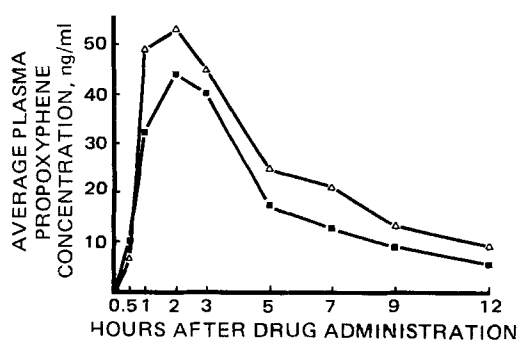

Figure 1—*Average plasma propoxyphene concentrations obtained from 21 normal volunteers after receiving a single 65-mg oral dose of propoxyphene. Key:* ■, *Treatment A; and* △, *Treatment B.*

[3] Applied Science Laboratories, State College, Pa.

During analysis, the column, injection port, and flame-ionization detector were maintained at 170, 175, and 205°, respectively. Helium, hydrogen, and air flow rates were 40, 50, and 350 ml/min, respectively. The retention times for propoxyphene, pyrroliphene, and norproxypheneamide were 3.2, 7.4, and 12 min, respectively.

Physical and Chemical Characteristics of Medication—The physical and chemical characteristics of the two formulations are presented in Table I. The test formulations and recognized standards were nearly identical in potency and dissolution rates.

Statistical Analysis—In both studies, the plasma data were submitted to a computer[4] programmed with an analysis of variance (ANOVA) program for crossover design. The variance components due to subjects, subjects per group (equal or unequal groups), time period, and treatments were estimated. The results of these estimations for plasma concentrations and the related parameters of peak concentration, peak time, and area under the plasma concentration–time curve are reported in Tables II and III.

RESULTS AND DISCUSSION

With any product, the rate and extent parameters of drug delivery to the general circulation are important in obtaining the desired pharmacologic or therapeutic response. If the drug is "absorbed" from two formulations at the same rate and to the same extent, the bioequivalence of these formulations is assured. The peak concentration, time of peak concentration, and area under the blood (plasma or serum) concentration–time curve are three parameters that allow estimation of the rate and extent of bioavailability.

Study 1—As shown in Fig. 1, both the test[5] and reference[6] formulations had measurable plasma levels at the 0.5-hr sampling time, with the average plasma propoxyphene curves peaking at 2 hr. Throughout the 12-hr sampling period, plasma levels of the test formulation were below those of the reference product. The statistical analysis from Table II indicates that the test formulation plasma levels were significantly lower than the recognized standard plasma levels at the 2-, 5-, 7-, 9-, and 12-hr sampling times.

The averages of the individual peak plasma concentrations for the test and reference products were 51.58 and 69.81 ng/ml, respectively, a 26% difference in peak concentration. The times of peak concentration were 1.95 hr for the test formulation and 2.14 hr for the recognized standard.

[4] IBM 360-50.
[5] Research lot 17,015-4.
[6] Lot 5HR70A.

Table III—Average Plasma Propoxyphene Concentrations and Related Parameters Obtained from 24 Normal Volunteers after Receiving Single Oral Doses of Two Different Propoxyphene Formulations

Hours	Average Plasma Propoxyphene Level, ng/ml		Significance
	Treatment A	Treatment B	
0.0	0.00 (0)[a]	0.00 (0)[a]	N.S.
0.5	2.22 (1.25)	0.32 (0.32)	N.S.
1.0	44.65 (4.44)	43.24 (5.23)	N.S.
2.0	64.36 (5.24)	64.59 (4.63)	N.S.
3.0	57.32 (4.39)	52.81 (3.99)	N.S.
5.0	35.58 (3.02)	34.73 (3.41)	N.S.
7.0	24.69 (2.98)	22.06 (3.03)	N.S.
9.0	17.22 (2.24)	14.75 (2.66)	N.S.
12.0	10.33 (1.84)	4.88 (1.47)	$p = 0.001$
16.0	5.52 (1.72)	2.29 (1.30)	$p = 0.01$
Average of individual peak plasma concentrations, ng/ml	69.03 (5.11)	68.67 (5.03)	N.S.
Average *AUC*, ng hr/ml, 0–12 hr	364.02 (30.8)	334.17 (32.8)	$p < 0.05$
0–16 hr	395.73 (33.9)	348.51 (35.28)	$p < 0.05$
Average of individual peak times, hr	1.96 (0.15)	2.04 (0.11)	N.S.

[a] The ( ) represents the standard error of the mean.

Neither the peak nor peak time differences were statistically significant.

The average areas under the plasma concentration–time curve (*AUC*) were 226.9 ng hr/ml for the test formulation and 296.87 ng hr/ml for the reference standard; this 24% difference was statistically significant ($p < 0.005$). A difference in this parameter indicates that the test formulation has approximately 76% the extent of availability of the reference standard. As previously noted, the *in vitro* parameters of assay potency and dissolution rate were quite similar for the test and reference formulations and did not detect the observed difference in bioavailability.

For the recognized standard, the plasma propoxyphene levels, peak concentration, peak time, and *AUC* for Studies 1 and 2 were quite similar to reported data (8, 9).

Study 2—As a result of the bioavailability findings of the first test formulation, the product was reformulated and tested for bioequivalence. As shown in Fig. 2 and Table III, test Formulation[7] II produced plasma levels essentially identical to a second lot of the recognized standard[8].

The averages of the individual peak plasma concentrations for the test and reference products were 69.03 and 68.67 ng/ml, respectively, while the averages of the individual peak times were 1.96 and 2.04 hr, respectively. The average *AUC* values (0–16 hr) were 395.73 ng hr/ml for the test formulation and 348.51 ng hr/ml for the recognized standard. This 12% difference in the *AUC* means tested statistically significant, but the formulations were judged equivalent.

The finding of statistically significant differences in the means of bioavailability parameters does not necessarily demand the declaration of bioinequivalence, nor does the lack of statistical significance imply bioequivalence. In many instances, small differences in mean values test statistically significant or large differences do not test statistically different. This result, of course, is related to the coefficient of variation (*CV*) observed in the individual studies and the power of the statistical analysis. In the first study, the test formulation produced plasma levels consistently lower than those of the recognized standard (as seen in the mean plasma levels of Fig. 1). This result was reflected in significant *AUC* differences despite high coefficients of variation for plasma level means and peak concentration.

In Study 2, the plasma level and bioavailability parameter coefficients of variation were generally lower than those of Study 1, and a much smaller (12 *versus* 24%) difference tested significant. The plasma levels in Study 2 were practically identical for test and standard formulations. The *AUC* differences were due to plasma level differences at the extreme tail-points of the serum level curve. It is very doubtful that these differences would have any clinical meaning.

Current federal regulations (10) for capsule formulations of propoxyphene hydrochloride require submission of an abbreviated NDA and proof of biological availability. However, the biological availability requirements were deferred for capsule formulations of propoxyphene hydrochloride when not in combination with aspirin or aspirin, phenacetin, and caffeine (11). Both the test formulations and the recognized standards were practically identical in the *in vitro* specifications of assay potency and dissolution rate. Although the lack of predictability of the *in vitro* parameters was unexpected, this point must be considered in the overall evaluation of propoxyphene formulations. Clearly, *in vitro* product equivalence does not assure *in vivo* bioequivalence. Thus, *in vitro* test parameters should not be used as the sole criterion in determining product bioequivalence. Confirmatory *in vivo* bioavailability testing should not be deferred for single-entity propoxyphene capsules in light of the data presented.

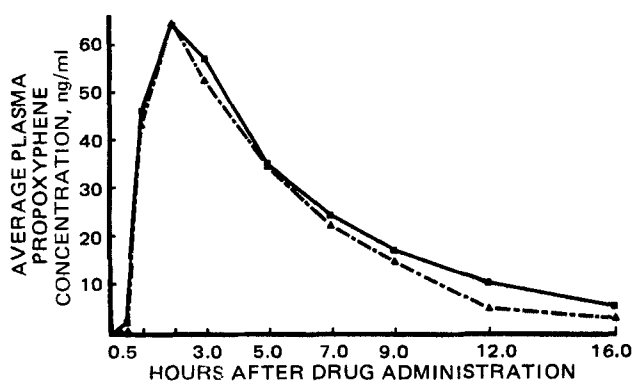

Figure 2—*Average plasma propoxyphene concentrations obtained from 24 normal volunteers after receiving a single 65-mg oral dose of propoxyphene hydrochloride. Key:* ■, *Treatment A; and* ▲, *Treatment B.*

[7] Research lot 17,320-1.
[8] Lot 5KL89C.

REFERENCES

(1) J. P. Skelley and S. Knapp, *J. Am. Med. Assoc.*, **224**, 243 (1973).

(2) *Fed. Regist.*, **39**, 2471 (Jan. 22, 1974), Title 21, subchapter C, part 130.

(3) "Current Concepts in the Pharmaceutical Sciences: Biopharmaceutics," J. Swarbrick, Ed., Lea & Febiger, Philadelphia, Pa., 1970, chap. 6.

(4) "Biopharmaceutics and Drug Interaction," D. E. Cadwallader, Ed., Roche Monograph, Hoffmann-La Roche, Nutley, N.J., chap. 7.

(5) "Considerations in Drug Product Selection by Pharmacists," a slide presentation prepared by the Committee on Drug Product Equivalence, APhA Academy of Pharmaceutical Sciences, Washington, D.C., Feb. 1972.

(6) "Bioavailability of Drug Products—The APhA Bioavailability Pilot Project," American Pharmaceutical Association, Washington, D.C., 1973.

(7) R. L. Wolen, and C. M. Gruber, Jr., *Anal. Chem.*, **40**, 1243 (1968).

(8) J. G. Wagner, P. G. Welling, S. B. Roth, E. Sakmar, K. P. Lee, and J. E. Walker, *Int. J. Clin. Pharmacol.*, **5**, 371 (1972).

(9) J. G. Wagner, P. G. Welling, and A. J. Sedman, *ibid.*, **5**, 381 (1972).

(10) *Fed. Regist.*, **34**, 66 (Apr. 8, 1969).
(11) *Ibid.*, **37**, 240 (Dec. 13, 1972).

ACKNOWLEDGMENTS AND ADDRESSES

Received February 20, 1976, from the *Medical Bioavailability Unit and the Physical and Analytical Chemistry Research Unit, The Upjohn Company, Kalamazoo, MI 49001.*

Accepted for publication February 21, 1977.

The authors thank R. S. Martin, Upjohn, for assistance in assaying the propoxyphene plasma samples and R. E. Monovich, Upjohn, for assistance in coordinating the clinical study and data analysis.

* Present address: Arnar-Stone Laboratories, Mt. Prospect, IL 60056.

[x] To whom inquiries should be directed.

Thebaine Content of Selections of *Papaver bracteatum* Lindl. at Different Ages

P. G. VINCENT [x], C. E. BARE, and W. A. GENTNER

Abstract □ Approximately 200 accessions of *Papaver* species were evaluated for identification as *P. bracteatum* Lindl. and for thebaine content. Fifteen authentic *P. bracteatum* accessions were selected on the basis of chromosome count. Statistical analyses of variation in alkaloid content were made for these accessions. Four of the 15 warranted further study based on the vigor of the plant and the total thebaine present in the tissue. Significant variability in thebaine content was found in wild strains of *P. bracteatum*, thus requiring genetic selection studies. The data showed that total yield potential of thebaine should be considered in selecting *P. bracteatum* strains for commercial growth rather than concentrating on strains that produce the highest thebaine concentrations. A method for the quantitative estimation of thebaine from *P. bracteatum* is presented.

Keyphrases □ Thebaine—GLC analysis, root and aboveground portions of various strains of *Papaver bracteatum* □ *Papaver bracteatum*—various strains, root and aboveground portions, GLC analysis of thebaine □ GLC—analysis, thebaine in root and aboveground portions of various strains of *Papaver bracteatum* □ Alkaloids—thebaine, GLC analysis in root and aboveground portions of various strains of *Papaver bracteatum* □ Narcotics—thebaine, GLC analysis in root and aboveground portions of various strains of *Papaver bracteatum*

Plants in the family Papaveraceae have been analyzed for alkaloids for more than a century. The genus *Papaver* and specifically *P. somniferum*, the opium poppy that produces thebaine, codeine, morphine, and other alkaloids, has received the most attention (1).

With the growing shortage of medically useful codeine, an alternative source has been sought. *P. bracteatum*, a potential source of thebaine, reportedly contains as much as 3.5% of this alkaloid in mature capsules at a purity of 95% or greater (2, 3). Treating thebaine with hydrogen bromide results in a 76% yield of codeinone. Codeinone is reduced to codeine by the Meerwein–Pondorff process or by sodium borohydride in commercial preparations (4).

Extraction from *P. bracteatum* of reliable supplies of thebaine and chemical transformation to codeine and related derivatives for legitimate medical needs might reduce dependency on morphine. Morphine from opium now supplies about 95% of the codeine used in the United States (5) as well as 100% of the heroin, the most abused illicit drug in the United States[1].

[1] Dr. Quentin Jones, Staff Scientist in charge of Narcotics Program, National Program Staff, Agricultural Research Service, U.S. Department of Agriculture, personal communication.

EXPERIMENTAL

Plant Source—The origin of collections and chromosome numbers of the 15 accessions of *P. bracteatum* used are shown in Table I. The initial genetic stock of the *Papaver* species consisted of about 200 accessions from the Middle East and were reduced to the 15 accessions on the basis of chromosome counts of root tip cells, floral characteristics, and alkaloid profile. The remaining accessions (~185) were found not to be *P. bracteatum*. Chromosome counts were made[2] on immature plants to separate three closely related species found in the same geographic area where the seeds were collected from stands with no apparent prior cultivation, *i.e.*, *P. orientale* (2n = 28), *P. pseudo-orientale* (2n = 42), and *P. bracteatum* (2n = 14).

Plant Culture—Seeds from accessions were planted in 7.6-cm peat pots[3] in the greenhouse in composted potting soil with about 4.2% organic matter and 33% pit washed sand; the pH was 6.2–6.5. Greenhouse conditions were: illumination, ambient (September–November); temperature, 20–25°; fertilizer, none; and insecticides (applied once each month), (5-benzyl-3-furyl)methyl *cis-trans*-(+)-2,2-dimethyl-3-(2-methylpropenyl)cyclopropanecarboxylate for white fly control and tricyclohexylhydroxystannane for spider mite control.

Seedlings were successively thinned to five, three, and one per pot. Plants were sampled for thebaine content at 5, 7, and 11 months of growth. In September, after 11 months, the plants were transferred to the field; field soil was Elkton silt loam (typic ochraquult), pH 5.8. Soil analysis showed: magnesium, 143 kg/hectare; phosphate, 280 kg/hectare; and potash, 77 kg/hectare. Fertilizer amendments were: limestone, 840 kg/hectare, ammonium nitrate (34% N), 84 kg/hectare; phosphate (46% P_2O_5), 90 kg/hectare; and potash (60% K_2O in KCl), 269 kg/hectare.

Immature plants were analyzed for the thebaine content, fresh and dry weight yields of roots, and aboveground parts at time of harvest. The leaf, stem, capsule, and sometimes root tissue of mature plants were analyzed on a fresh and dry weight basis the following May, 2 weeks after petal fall. Approximately 80–90% of plants transferred to the field flowered. All plant harvesting was done at the same time of day to eliminate effects of diurnal variation on alkaloid concentrations.

Analytical—Analysis of variance was made of 11-month-old immature plants.

Thebaine yields from root, aboveground part, stem, and capsule tissues oven dried at 60° or freeze dried were compared. All tissues were ground to pass a 40-mesh sieve. Three 100-mg samples of each tissue dried by each method were taken. One sample was oven dried at 110° overnight for the determination of residual water content; the second was extracted in 50 ml of methanol–ammonium hydroxide (98:2 v/v) by rotation for 1 hr at 120 rpm; the third was extracted with 5% aqueous acetic acid, the reference extraction solvent, and purified as recommended by the United Nations (6). Routine analyses were from samples extracted in metha-

[2] M. L. Stiff, U.S. Department of Agriculture.

[3] Jiffy pots. (Mention of a trademark or proprietary product does not constitute a guarantee or warranty of the product by the U.S. Department of Agriculture and does not imply its approval to the exclusion of other products that may also be suitable.)

(10) *Fed. Regist.*, **34**, 66 (Apr. 8, 1969).
(11) *Ibid.*, **37**, 240 (Dec. 13, 1972).

ACKNOWLEDGMENTS AND ADDRESSES

Received February 20, 1976, from the *Medical Bioavailability Unit and the Physical and Analytical Chemistry Research Unit, The Upjohn Company, Kalamazoo, MI 49001.*

Accepted for publication February 21, 1977.

The authors thank R. S. Martin, Upjohn, for assistance in assaying the propoxyphene plasma samples and R. E. Monovich, Upjohn, for assistance in coordinating the clinical study and data analysis.

* Present address: Arnar-Stone Laboratories, Mt. Prospect, IL 60056.

[x] To whom inquiries should be directed.

Thebaine Content of Selections of *Papaver bracteatum* Lindl. at Different Ages

P. G. VINCENT [x], C. E. BARE, and W. A. GENTNER

Abstract □ Approximately 200 accessions of *Papaver* species were evaluated for identification as *P. bracteatum* Lindl. and for thebaine content. Fifteen authentic *P. bracteatum* accessions were selected on the basis of chromosome count. Statistical analyses of variation in alkaloid content were made for these accessions. Four of the 15 warranted further study based on the vigor of the plant and the total thebaine present in the tissue. Significant variability in thebaine content was found in wild strains of *P. bracteatum*, thus requiring genetic selection studies. The data showed that total yield potential of thebaine should be considered in selecting *P. bracteatum* strains for commercial growth rather than concentrating on strains that produce the highest thebaine concentrations. A method for the quantitative estimation of thebaine from *P. bracteatum* is presented.

Keyphrases □ Thebaine—GLC analysis, root and aboveground portions of various strains of *Papaver bracteatum* □ *Papaver bracteatum*—various strains, root and aboveground portions, GLC analysis of thebaine □ GLC—analysis, thebaine in root and aboveground portions of various strains of *Papaver bracteatum* □ Alkaloids—thebaine, GLC analysis in root and aboveground portions of various strains of *Papaver bracteatum* □ Narcotics—thebaine, GLC analysis in root and aboveground portions of various strains of *Papaver bracteatum*

Plants in the family Papaveraceae have been analyzed for alkaloids for more than a century. The genus *Papaver* and specifically *P. somniferum*, the opium poppy that produces thebaine, codeine, morphine, and other alkaloids, has received the most attention (1).

With the growing shortage of medically useful codeine, an alternative source has been sought. *P. bracteatum*, a potential source of thebaine, reportedly contains as much as 3.5% of this alkaloid in mature capsules at a purity of 95% or greater (2, 3). Treating thebaine with hydrogen bromide results in a 76% yield of codeinone. Codeinone is reduced to codeine by the Meerwein–Pondorff process or by sodium borohydride in commercial preparations (4).

Extraction from *P. bracteatum* of reliable supplies of thebaine and chemical transformation to codeine and related derivatives for legitimate medical needs might reduce dependency on morphine. Morphine from opium now supplies about 95% of the codeine used in the United States (5) as well as 100% of the heroin, the most abused illicit drug in the United States[1].

[1] Dr. Quentin Jones, Staff Scientist in charge of Narcotics Program, National Program Staff, Agricultural Research Service, U.S. Department of Agriculture, personal communication.

EXPERIMENTAL

Plant Source—The origin of collections and chromosome numbers of the 15 accessions of *P. bracteatum* used are shown in Table I. The initial genetic stock of the *Papaver* species consisted of about 200 accessions from the Middle East and were reduced to the 15 accessions on the basis of chromosome counts of root tip cells, floral characteristics, and alkaloid profile. The remaining accessions (~185) were found not to be *P. bracteatum*. Chromosome counts were made[2] on immature plants to separate three closely related species found in the same geographic area where the seeds were collected from stands with no apparent prior cultivation, *i.e.*, *P. orientale* (2n = 28), *P. pseudo-orientale* (2n = 42), and *P. bracteatum* (2n = 14).

Plant Culture—Seeds from accessions were planted in 7.6-cm peat pots[3] in the greenhouse in composted potting soil with about 4.2% organic matter and 33% pit washed sand; the pH was 6.2–6.5. Greenhouse conditions were: illumination, ambient (September–November); temperature, 20–25°; fertilizer, none; and insecticides (applied once each month), (5-benzyl-3-furyl)methyl *cis-trans*-(+)-2,2-dimethyl-3-(2-methylpropenyl)cyclopropanecarboxylate for white fly control and tricyclohexylhydroxystannane for spider mite control.

Seedlings were successively thinned to five, three, and one per pot. Plants were sampled for thebaine content at 5, 7, and 11 months of growth. In September, after 11 months, the plants were transferred to the field; field soil was Elkton silt loam (typic ochraquult), pH 5.8. Soil analysis showed: magnesium, 143 kg/hectare; phosphate, 280 kg/hectare; and potash, 77 kg/hectare. Fertilizer amendments were: limestone, 840 kg/hectare, ammonium nitrate (34% N), 84 kg/hectare; phosphate (46% P_2O_5), 90 kg/hectare; and potash (60% K_2O in KCl), 269 kg/hectare.

Immature plants were analyzed for the thebaine content, fresh and dry weight yields of roots, and aboveground parts at time of harvest. The leaf, stem, capsule, and sometimes root tissue of mature plants were analyzed on a fresh and dry weight basis the following May, 2 weeks after petal fall. Approximately 80–90% of plants transferred to the field flowered. All plant harvesting was done at the same time of day to eliminate effects of diurnal variation on alkaloid concentrations.

Analytical—Analysis of variance was made of 11-month-old immature plants.

Thebaine yields from root, aboveground part, stem, and capsule tissues oven dried at 60° or freeze dried were compared. All tissues were ground to pass a 40-mesh sieve. Three 100-mg samples of each tissue dried by each method were taken. One sample was oven dried at 110° overnight for the determination of residual water content; the second was extracted in 50 ml of methanol–ammonium hydroxide (98:2 v/v) by rotation for 1 hr at 120 rpm; the third was extracted with 5% aqueous acetic acid, the reference extraction solvent, and purified as recommended by the United Nations (6). Routine analyses were from samples extracted in metha-

[2] M. L. Stiff, U.S. Department of Agriculture.

[3] Jiffy pots. (Mention of a trademark or proprietary product does not constitute a guarantee or warranty of the product by the U.S. Department of Agriculture and does not imply its approval to the exclusion of other products that may also be suitable.)

Table I—Sources and Chromosome Numbers of *P. bracteatum*[a]

P.I.[b] or Other Designation	Seed Source	Location	SAT[c]	2n[d]
383211 (Arya II)	United Nations	Iran	2	14
383309 (Arya I)	United Nations	Iran	2	14
UNB-4	United Nations	Iran	2	14
378554	Abraham	Iran	1, 1	14, 21[e]
378555	Abraham	Iran	1	14
378556	Abraham	Iran	1	14
378581	Abraham	Iran	1	14
381600	Goldblatt	Mahabad, Iran	2	14
381601	Goldblatt	Pol-e-zanguleb, Iran	0	14
381602	Goldblatt	Damauand, Iran	2	14
381603	Goldblatt	Damauand, Iran	2	14
381604	Goldblatt	Marivan, Iran	1	14
381605	Goldblatt	51 Km. N. Marivan, Iran	2	14
381606	Goldblatt	81 Km. N. Marivan, Iran	1	14
381607	Goldblatt	Banch Road, Iran	0	14

[a] Data from M. L. Stiff. [b] Plant introduction number (U. S. Department of Agriculture). [c] Number of satellite chromosomes. [d] Diploid chromosome number. [e] Triploids and aneuploids not previously reported in these species.

nol–ammonium hydroxide (98:2 v/v). Other solvent systems and the stability of thebaine were evaluated and discussed elsewhere (7).

Thebaine was quantitated by GLC and by spectrophotometry at 285 nm. A dual-column chromatograph[4] was used. The U-shaped glass columns, 1.5 m × 4 mm i.d., previously treated with trimethylchlorosilane, were packed with 2% OV-17 on 100–120-mesh Gas Chrom Q. Packed columns were conditioned until stable at 300° in a forced stream of nitrogen. The hydrogen-flame detector was used with a sensitivity of 1×10^{-11} amp. The gases and pressures used were: air, 1.2 kg/cm^2; hydrogen, 2.5 kg/cm^2; and nitrogen, 1.2 kg/cm^2. Head pressure at the injection port was 2.5 kg/cm^2. Operating temperatures were: injection port, 280°; column, 270°; and detector, 300°.

Cholesterol acetate was the internal standard. Retention times, detector responses, and column efficiencies were calibrated with authentic thebaine, codeine, and morphine. Morphine was calibrated as its *N,O*-bis(trimethylsilyl)acetamide derivative because morphine partially adsorbs on the column. Data were reduced with a digital computing integrator[5]. The integrator, calibrated with different weights of alkaloids and a constant weight of cholesterol acetate in ethanol, was accurate to 0.02%. Standards used for daily calibration of the chromatograph and integrator were codeine (0.2 μg/μl), thebaine (0.2 μg/μl), isothebaine (0.2 μg/μl), morphine (0.4 μg/μl), and cholesterol acetate (1 μg/μl).

One milliliter of absolute ethanol containing cholesterol acetate (1 μg/μl) was added to the dried plant extracts prior to analyses. Sample size was about 1.5 μl. Standards and extractants were analyzed in triplicate. Stock solutions of thebaine standards were monitored by spectrophotometry at 285 nm in accordance with the recommendations proposed by the United Nations Working Group on *P. bracteatum* (6).

TLC of extracted alkaloids of plants corroborated the GLC data. Silica gel C was used as the adsorbent on 20 × 20-cm glass plates. The solvent system was toluene–acetone–ethanol–6 *N* ammonium hydroxide (20:20:3:1 v/v) (8, 9). Plates were activated at 105° for 2 hr and allowed to develop beyond 10 cm. For visualization of alkaloids, the developed plates were sprayed with Dragendorff's reagent (10) and potassium iodoplatinate reagent (11, 12).

Data in Table II show the range, mean $R_f \times 100$, R_x, and standard deviation values for nine *Papaver* alkaloids.

RESULTS AND DISCUSSION

In all tissues examined, 13–17% less thebaine was extracted from 60° oven-dried tissues than from freeze-dried tissues. Residual water content of freeze-dried tissue was ~5% after atmospheric equilibration compared to 110° oven-dried tissue.

Table III shows means, standard deviations, ranges, and coefficients of variation for 11-month-old plants. All accessions were tested since differentiation or identification of *P. bracteatum* beyond the species level was based on the area of geographic origin of seed. The total thebaine in root tissue varied from 75 to 22,015 μg, a difference between values of 99.7% of the highest value. For all variables evaluated, the coefficient of variation ranged from 22% (thebaine yield from roots per 100 mg of dry weight) to 55% (thebaine yield from shoots per total dry weight). These data show that the characteristics of *P. bracteatum* vary among accessions.

Table II—TLC Values for Opium Alkaloids[a]

Alkaloid	Range ($R_f \times 100$)	Mean[b] ($R_f \times 100$)	R_x[c]
Narceine	0	0	0
Morphine	8–18	11 ± 3	0.3
Codeine	13–19	15 ± 2	0.3
Oripavine	30–40	35 ± 2	0.8
Thebaine	39–50	45 ± 3	1.0
Orientalidine	49–60	55 ± 3	1.2
Isothebaine	52–63	57 ± 3	1.3
Papaverine	53–65	59 ± 5	1.3
Alpinigenine	60–75	67 ± 4	1.5

[a] Results of no less than 60 TLC runs. The solvent system was toluene–acetone–ethanol–ammonium hydroxide (20:20:3:1). [b] Mean of 60 determinations ± *SD*. [c] Retention relative to thebaine.

Table IV shows the mean thebaine in micrograms per 100 mg of dry weight of *P. bracteatum* after 11 months of growth. The highest thebaine concentration (micrograms per 100 mg of plant dry weight) was found in roots of Arya II plants. Although this concentration was not significantly higher than that of Arya I plants, it was significantly higher than that of all other accessions. However, thebaine content per plant (aboveground, roots, and total) was highest for Arya I (Table V), but it was not significantly higher than the content in P.I. 381607, for aboveground parts. Thus, when dry weights were evaluated (Tables IV and V), it was apparent that although accession Arya II may have slightly more thebaine on a per unit weight basis (although not significantly so) than Arya I, accession Arya I does have significantly more thebaine yield per plant (dry weight).

The magnitude of the difference by which Arya I exceeded Arya II in thebaine per plant could be attributed to differences in vigor of plants grown at Beltsville but, nevertheless, indicates the need for determining thebaine content in plants on a total dry weight basis rather than by concentration (*i.e.*, percent) when evaluating new germ plasm sources for alkaloid content. Most reports of thebaine content in *P. bracteatum* have been made as a percent of unit weight. Among mature field-grown plants, total dry weight was greater for Arya I than for Arya II.

Characteristics of two promising high thebaine-yielding accessions of *P. bracteatum*, Arya I and Arya II, appear in Table VI. The total thebaine variation in dried plants of Arya I and Arya II was 52 and 45%, respectively. The difference between the high and low values for total thebaine was 98% of the highest value for Arya I and 82% of the highest value for Arya II, which suggested that Arya II plants vary less than do Arya I plants. For all variables, the coefficient of variation was lower for Arya II than for Arya I.

The mean dry weight of roots of Arya II was 64% that of Arya I. The mean fresh weight of Arya II was 68% that of Arya I. Although Arya II plants contained a higher concentration of thebaine (micrograms per 100 mg of plant dry weight) in the roots (2% more than Arya I plants), the total thebaine yield was higher for Arya I roots, shoots, and whole plants by 55, 85, and 60%, respectively.

Differences in thebaine content in root tissue per unit weight among 14 of the 15 accessions at 5, 7, and 11 months were significant. The combined values for the thebaine content of 14 accessions declined about 20% between 7 and 11 months, indicating that maximum thebaine synthesis occurs prior to 7 months in immature plants.

Data showed that thebaine content varied among and within accessions. In root tissue from 20 plants of Arya I (data not shown), thebaine content ranged from 502 to 22,016 μg and averaged 11,153 μg with a standard deviation of 5955. The extent of variation in thebaine content on comparison of one germ plasm source to another may be seen by calculating the difference in total thebaine dry weight per plant needed between adjacent values in the array for significance with plants for each accession (the least significant difference). Thus, if 20 plants are evaluated for thebaine content, the thebaine content must exceed 2525 μg between plants to be significant.

The Third Working Group for study of *P. bracteatum*, sponsored by the United Nations, at Beltsville, Md., (5) reported "... that Arya II

[4] Searle-Analytic.
[5] Spectra-Physics.

Table III—Average Values for a *P. bracteatum* Plant[a]

Variable	Mean	*SD*	Low	High	CV, %
Dry weight of root, g	1.00	0.38	0.21	3.97	38.0
Fresh weight of root, g	5.21	1.95	0.47	19.91	37.4
Thebaine concentration in root, μg per 100 mg of dry weight	595.04	131.67	61.24	1,615.98	22.1
Dry weight of shoots[b], g	0.57	0.15	0.10	1.80	26.3
Fresh weight of shoots, g	3.57	1.08	0.91	12.48	30.3
Thebaine concentration in shoots, μg per 100 mg of dry weight	293.93	108.23	5.43	947.75	36.8
Total thebaine yield from root, μg	5950.40	2,337.98	74.85	22,015.89	39.3
Total thebaine yield from shoots, μg	1367.60	740.26	32.00	11,278.23	54.1
Total thebaine yield from plant, μg	7318.00	2,909.56	174.90	26,077.01	39.8

[a] Average of 300 observations; 20 values each of 15 accessions for 11-month-old plants. [b] Aboveground parts.

Table IV—Mean Thebaine in Micrograms per 100 mg of Dry Weight of Different Accessions of *P. bracteatum* after 11 Months of Growth in a Greenhouse[a]

Accession[b]	Aboveground Parts	Roots
383211 (Ayra II)	298.5 b–d[c]	839.7 a
383309 (Arya I)	331.2 bc	825.9 ab
UNB-4	305.7 b–d	673.9 cd
378554	197.9 f	533.1 d–g
378555	206.6 ef	451.3 fg
378556	409.4 a	697.8 bc
378581	82.5 g	497.6 e–g
381600	279.8 c–e	603.0 c–e
381601	98.5 g	399.4 g
381602	92.2 g	581.8 c–f
381603	83.2 g	453.4 fg
381604	287.9 g	521.8 e–g
381605	309.2 b–d	680.1 c
381606	248.1 d–f	522.7 e–g
381607	368.0 ab	643.8 c–e

[a] Means of 20 immature plants of each accession. [b] Where appropriate, numbers refer to U.S. Department of Agriculture plant introduction numbers. [c] Means within columns followed by a common letter are not significantly different at the 5% level by the new Duncan's multiple range test.

material gave consistently higher and more uniform values for the thebaine content in the various plants parts." Arya I and other plants had previously been evaluated by the Working Group by using concentrations of thebaine content as the criteria for selecting germ plasm.

The thebaine content was determined in this laboratory for mature plants of Arya I (four plants) and Arya II (five plants) 2 weeks after petal fall; root, leaf, stem, and capsule tissues were evaluated (Table VII). The mean thebaine content for all tissues was 161,150 μg of total dry weight for Arya I and 97,540 μg for Arya II, a difference of 63,610 μg. Means of the four plants of Arya I showed that thebaine was distributed as follows: root, 60%; leaf, 13%; stem, 12%; and capsule, 15%. For the five plants of Arya II, the values were: root, 47%; leaf, 14%; stem, 13%; and capsule, 26%.

Thebaine was also determined in Arya I (11 plants) and Arya II (12 plants) for leaf, stem, capsule, and total but not for root tissue (Table VII). Plants were harvested 5 cm from ground level so that roots could remain for future studies. For plants grown at Beltsville, these data showed that Arya I had nearly twice the thebaine content of Arya II and followed the trend for immature 11-month-old plants shown in Table V for thebaine content in root and aboveground tissue. Distributions of total thebaine yield in Arya I were: leaves, 16%; stems, 30%; and capsules, 54%. In Arya II, the distributions were: leaves, 32%; stem, 28%; and capsules, 40% (Table VII).

In the study in which roots were analyzed, the mean dry weights (data not shown) for Arya I root, leaf, stem, capsule, and total tissues were 13.78, 9.35, 6.03, 2.79, and 31.95 g, respectively. The corresponding values for Arya II were 7.11, 7.38, 3.76, 1.54, and 19.79 g. When the mean total micrograms of thebaine for each accession was divided by its total mean dry weight, the thebaine per unit weight for Arya I and Arya II was 5044 and 4929 μg, respectively. The capsules of Arya I and II plants contained about equal amounts of thebaine (~25,000 μg), and plants sampled from each accession had one capsule per plant. The percent distribution of thebaine in the aboveground parts for Arya I and II capsules was 39 and 49%, respectively.

In the second study in which roots were not harvested, the capsules of Arya I and II plants contained ~77,000 and 32,000 μg of total thebaine, respectively; some plants sampled from Arya I plots had multiple capsules per plant, whereas all plants sampled from Arya II plots had one capsule per plant. The percent distribution of thebaine in the aboveground parts for Arya I and II capsules was 54 and 40%, respectively, in the second study. A projected yield for 100,000 plants, assuming harvest of all aboveground parts 2 weeks after petal fall, would be 14.2 kg of thebaine for Arya I and 7.9 kg of thebaine for Arya II. A similar projection based on harvest of capsules alone would be 5.1 kg of thebaine for Arya I and 2.8 kg for Arya II.

Thebaine content varies significantly among the accessions of *P. bracteatum*, and yield potential should be considered in selecting accessions for cultivation. *P. bracteatum*, although a wild and variable species, contains thebaine at relatively high concentrations (2.5–3.5%) when compared to closely related species containing this alkaloid such as *P. somniferum*, *P. pseudo-orientale*, and *P. orientale*. Another advantage in cultivating *P. bracteatum* is the purity in which thebaine occurs; 95% of the total alkaloid content occurs as thebaine and thus may permit commercial extraction with minimal purification. As a source of thebaine and, hence, codeine, *P. bracteatum* cultivation offers a significant potential answer to the world shortage of legitimate narcotics and may reduce dependence on the cultivation of *P. somniferum*.

Table V—Mean Thebaine in Micrograms per Plant (Total Dry Weight) of 15 Accessions of *P. bracteatum* Grown in a Greenhouse for 11 Months[a]

Accession[b]	Aboveground Parts	Roots	Total
383211 (Ayra II)	1,418.5 cd[c]	7,194.0 b–d	8,612.5 bc
383309 (Arya I)	2,695.4 a	11,152.0 a	13,847.4 a
UNB-4	1,881.7 bc	5,687.6 d–f	7,569.3 b
378554	1,451.7 cd	9,177.0 ab	10,628.7 b
378555	1,546.1 cd	6,778.3 c–e	8,324.4 bc
378556	2,330.2 ab	8,030.8 bc	10,361.0 b
378581	625.1 ef	4,472.3 eh	5,097.4 d–f
381600	963.3 d–f	5,351.2 d–g	6,314.5 c–e
381601	502.6 ef	4,545.7 e–h	5,048.3 d–f
381602	352.5 f	5,215.3 d–h	5,567.8 d–f
381603	501.1 ef	2,894.4 h	3,395.5 f
381604	1,482.0 cd	3,725.5 f–h	5,207.5 d–f
381605	997.9 d–f	3,541.5 f–h	4,539.4 ef
381606	1,085.0 de	3,269.5 gh	4,354.5 ef
381607	2,465.6 ab	6,482.9 c–e	8,948.5 bc

[a] Twenty immature plants of each accession were used in analysis. [b] Where appropriate, numbers refer to U.S. Department of Agriculture plant introduction numbers. [c] Means within columns followed by a common letter are not significantly different at the 5% level by the new Duncan's multiple range test.

Table VI—Average Value for *P. bracteatum* Accessions Arya I (P.I. 383309) (I) and Arya II (P.I. 383211) (II) Plants at 11 Months of Age[a]

Variable	Arya	Mean	*SD*	Low	High	*CV*, %
Dry weight of root, g	I	1.32	0.53	0.58	2.48	40.2
	II	0.84	0.28	0.41	1.39	33.3
Fresh weight of root, g	I	7.07	2.45	3.40	13.65	34.7
	II	4.80	1.18	2.71	7.19	24.6
Thebaine concentration in roots, μg per 100 mg of dry weight	I	825.91	349.64	61.24	1,615.98	42.3
	II	839.70	255.10	399.59	1,325.03	30.4
Dry weight of shoots[b], g	I	0.80	0.27	0.41	1.37	33.8
	II	0.48	0.16	0.21	0.85	33.3
Fresh weight of shoots, g	I	5.19	1.81	2.71	10.29	34.9
	II	3.02	0.95	1.61	4.84	31.5
Thebaine concentration in shoots, μg per 100 mg of dry weight	I	331.19	215.16	5.43	947.75	65.0
	II	298.49	139.95	100.09	635.14	46.9
Total thebaine yield from root, μg	I	10,902.01	5954.88	502.17	22,015.89	54.6
	II	7,053.48	3296.58	2277.66	13,825.44	46.7
Total thebaine yield from shoots, μg	I	2,649.52	2324.42	32.04	11,278.23	87.7
	II	1,432.75	907.24	500.45	3,857.98	63.3
Total thebaine yield from plant, μg	I	13,551.53	7177.42	534.11	26,077.01	53.0
	II	8,486.23	3860.69	2846.04	15,720.95	45.5

[a] Each item represents the mean of 20 plants. [b] Aboveground parts.

Table VII—Distribution of Thebaine in Various Mature Plant Tissues of Accessions Arya I (P.I. 383309) and Arya II (P.I. 383211)

	Thebaine Yield, μg					
Accession	Root	Leaf	Stem	Capsule		Total
Arya I	94,810[a]	4,193	9,583	16,896		125,482
	131,063	44,935	35,449	32,900		244,347
	102,476	18,974	20,748	32,616		174,814
	56,739	15,590	9,387	18,242		99,958
	$\bar{x}$ 96,272	20,923	18,792	25,164	$\Delta\bar{x}_1$	161,150
	—[b]	3,671	9,070	15,934		28,675
	—	62,575	69,785	86,840		219,200
	—	1,288	24,390	45,881		71,559
	—	8,340	30,917	34,482		73,739
	—	69,563	77,920	150,062		297,545
	—	29,450	47,376	59,530		136,356
	—	18,834	64,956	88,697		172,487
	—	19,492	47,297	122,028		188,817
	—	5,873	29,466	99,775		135,114
	—	15,008	24,248	29,675		68,931
	—	13,787	48,200	111,111		173,098
	$\bar{x}$	22,535	43,057	76,729	$\Delta\bar{x}_2$	142,320
Arya II	57,483	17,818	12,512	27,593		115,406
	63,142	4,693	23,565	31,974		123,374
	28,796	5,726	10,067	8,239		52,828
	37,044	36,692	8,169	48,010		129,915
	44,320	2,366	9,697	9,796		66,179
	$\bar{x}$ 46,157	13,459	12,802	25,122	$\Delta\bar{x}_3$	97,540
	—	44,636	9,937	21,339		75,912
	—	13,120	20,921	25,839		59,880
	—	20,280	28,963	41,367		90,610
	—	6,749	16,865	12,242		35,856
	—	49,117	28,165	31,059		108,341
	—	22,866	50,382	29,948		103,196
	—	6,332	6,621	12,003		24,956
	—	43,572	19,531	37,298		100,401
	—	47,114	30,204	43,609		120,927
	—	9,052	16,365	23,742		49,159
	—	23,841	22,288	90,400		136,529
	—	10,402	15,295	11,618		37,315
	$\bar{x}$	24,757	22,128	31,705	$\Delta\bar{x}_4$	78,590

[a] Each entry represents an individual plant. All values are rounded to whole numbers. [b] Plant root tissue not taken.

REFERENCES

(1) J. A. Duke, C. R. Gunn, E. E. Leppik, C. F. Reed, M. L. Solt, and E. E. Terrell, U.S. Department of Agriculture Publication ARS-NE 28, 1973.

(2) N. Sharghi and I. Lalezari, *Nature*, **213**, 1244 (1967).

(3) I. Lalezari, P. Nasseri, and R. Asgharian, *J. Pharm. Sci.*, **63**, 1331 (1974).

(4) French pat. 1,290,174 and French pat. 1,282,642.

(5) United Nations Document, MNAR/9, 1976.

(6) United Nations Document, ST/SOA/SER.J/15, 1974.

(7) P. G. Vincent and W. A. Gentner, United Nations Document, ST/SOA/SER.J/9, 1974.

(8) V. E. Stahl, H. Jork, E. Dumont, H. Bohrman, and H. Vollman, *Arzneim.-Forsch.*, **19**, 194 (1969).

(9) N. Y. Mary and E. Brochmann-Hanssen, *Lloydia*, **26**, 223 (1963).

(10) R. Munier, *Bull. Soc. Chim. Biol.*, **35**, 1225 (1953).

(11) D. Waldi, K. Schnackerz, and F. Munter, Jr., *Chromatography*, **6**, 61 (1961).

(12) E. Schlittler and J. Hohl, *Helv. Chim. Acta*, **35**, 29 (1952).

ACKNOWLEDGMENTS AND ADDRESSES

Received August 16, 1976, from the *U.S. Department of Agriculture, Agricultural Research Service, Beltsville, MD 20705.*

Accepted for publication February 24, 1977.

[x] To whom inquiries should be directed.

Digoxin Bioavailability: Evaluation of a Generic Tablet and Proposed FDA Guidelines

WILLIAM G. KRAMER *, ALBERT J. KOLIBASH, MOHINDER S. BATHALA ‡, JAMES A. VISCONTI, RICHARD P. LEWIS, and RICHARD H. REUNING x

Abstract □ The relative bioavailability of a generic digoxin tablet formulation was investigated according to proposed FDA guidelines. After administration of digoxin in three different oral formulations on separate occasions to 12 subjects, multiple serum samples were obtained over the first 5 hr and assayed for digoxin by radioimmunoassay. The average 0–5-hr area under the serum digoxin concentration–time curve (*AUC*) for the generic tablet was 99.6% of the combined mean of the average *AUC* values for the reference tablet and a solution. In addition, the average peak heights, peak times, and *AUC* values for the two tablet formulations were not significantly different. The currently proposed FDA method of data analysis utilizes a combination of the means of three experimental measurements and provides no measure of the variability of the relative bioavailability estimate. Three other methods of data analysis that do provide variance estimates were evaluated: (*a*) the FDA method on an individual subject basis followed by averaging, (*b*) a logarithmic transformation of the *AUC* values, and (*c*) comparison of the *AUC* values of the generic and reference tablets using a paired *t*-test. A consideration of the experimental design required by the FDA and the statistics involved indicated that the last method may be the most appropriate for examination of the bioavailability of digoxin tablets relative to a market standard. It is also suggested that the proposed regulations be amended to make the standard a solution rather than a specific manufacturer's product.

Keyphrases □ Digoxin—bioavailability, various formulations compared, proposed guidelines evaluated, humans □ Bioavailability—digoxin, various formulations compared, proposed guidelines evaluated, humans □ Cardiotonic agents—digoxin, bioavailability of various formulations compared, proposed guidelines evaluated, humans

The lack of equivalent bioavailability among various digoxin tablets has been the subject of numerous publications (1–12). When tested against the current market standard[1], several digoxin tablets have been shown to be absorbed to a lesser extent. This type of evidence, along with clinical reports of a lack of pharmacological response to several generic brands of digoxin tablets, led the Food and Drug Administration (FDA) to propose bioavailability standards for digoxin tablets (13). These standards indicate that the extent of drug absorption is to be measured by the area under the 0–5-hr serum digoxin concentration–time curve (*AUC*) and that the "bioavailability of the test product shall be demonstrated if a mean absorption of at least 75 percent of the combined mean of the two reference standards is observed"[2]. The reference standards are a tablet supplied by the FDA[1] and an aqueous digoxin solution, and all treatments are at a dose of 0.5 mg. The suggested protocol requires the use of 12 normal subjects in a three-way crossover study and 11 serum samples during the 5-hr period.

The obvious objective of such a regulation is to assure that all marketed digoxin tablets are not appreciably different from a bioavailability standpoint and that, regardless of the brand dispensed to the patient, there are only inconsequential differences in the amount of drug absorbed. Therefore, the method used to evaluate bioavailability should permit measurement of the precision of the bioavailability estimate so that the data may be interpreted correctly. This paper reports the results of a bioavailability study of a generic digoxin tablet[3] conducted according to the protocol outlined by the FDA[4]. The method employed is then examined with respect to permitting a valid estimate of precision and the detection of unsuitable tablet formulations.

EXPERIMENTAL

The three treatments discussed in this paper were part of a larger study in which digoxin was administered in two doses and four dosage forms to 12 healthy male volunteers in a seven-way crossover study. Each subject was given a physical examination with appropriate laboratory tests prior to entering the study. Blood chemistry and hematological values were within normal limits. Subjects were informed of the nature and hazards of the study and gave written consent.

Subjects fasted for 12 hr before and 4 hr after drug administration. The tablet treatments (two 0.25-mg tablets) were administered with 250 ml of water, and the solution (0.5 mg/200 ml) was given with a 50-ml rinse. A minimum of 2 weeks separated consecutive treatments to allow for the complete elimination of the previous dose. The two commercial digoxin tablet preparations were tested and found to meet compendial standards.

A 10-ml blood sample was drawn before each treatment to provide the blank and the diluent for standards used in the assay of samples from that treatment. Blood samples (5 ml) were withdrawn from a forearm vein at 10, 20, 30, 45, 60, and 90 min and at 2, 3, 4, and 5 hr after drug administration. Samples taken during the initial 3–4 hr were withdrawn through a 19-gauge infusion set kept open by a normal saline drip; remaining samples were withdrawn by venipuncture.

All samples were centrifuged, and the serum was kept frozen until assay. Serum samples were assayed using a ^{125}I-radioimmunoassay[5], modified slightly from the kit instructions to increase accuracy and precision (14).

Serum digoxin concentrations at each experimental time for each treatment in each subject were determined and plotted against time. The area under each curve from 0 to 5 hr was calculated using the trapezoidal method.

RESULTS AND DISCUSSION

The averaged serum digoxin concentration–time data from the 12 subjects for the three treatments are plotted in Fig. 1. The average peak heights and peak times are summarized in Table I. Table II contains the areas under the curve from 0 to 5 hr for each treatment in each subject and the relative bioavailability of the generic tablet calculated according to the FDA procedure but on an individual subject basis.

The generic digoxin tablet met the proposed FDA bioavailability requirements, yielding a mean absorption (ratio of the mean area for the test tablet to the combined mean area for the standards) of 99.6%. The bioequivalence of the two tablet formulations is further substantiated by Fig. 1; the serum digoxin concentration–time curves for the two tablet

[1] Lanoxin (Lot 022-1, Burroughs Wellcome and Co.) was used in this study.

[2] The complete text of this section of the proposed bioavailability standards is given in the *Appendix*.

[3] Lot 7161B3, Philips Roxane Laboratories, Columbus, Ohio (a new formulation not previously tested for bioavailability).

[4] The complete protocol used in this study was approved by the FDA prior to the start of the study.

[5] Catalog No. 0750-06, Schwarz/Mann.

Table I—Summary of Peak Heights and Peak Times for the Three Treatments

Treatment	Peak Height[a], ng/ml	Peak Time[a], min
Generic tablet	2.62 (0.87)	65 (29)
Reference tablet	1.89 (1.16)	94 (77)
Aqueous solution	3.39 (0.85)	41 (9)

[a] Mean with standard deviation in parentheses.

preparations are similar. In addition, the peak heights and peak times (Table I) and areas under the curve (0–5 hr) for the two tablet treatments were not significantly different (paired t test, $p > 0.05$). Therefore, it may be concluded that, under the conditions of this study and based upon both the criteria proposed by the FDA and the lack of significant differences between peak heights, peak times, and areas under the curve, the generic digoxin tablet is bioequivalent to the market standard.

As stated previously, the purpose of the proposed bioavailability standards is to detect batches of tablets that are not as well absorbed as current market standards. This conclusion should be based on establishing the existence or lack of statistically significant differences. Therefore, in addition to providing an estimate of relative bioavailability, any test must also provide a measure of the variability of that estimate, which the FDA method of combining means obviously does not. Using the FDA method but calculating relative bioavailability for each subject and *then* averaging yields an estimate of 106% with 95% confidence limits of 79.1–133%. The standard error (12.2%) is large relative to the mean (percent coefficient of variation of 11.5%) and indicates that the sensitivity of this technique for detecting unsuitable formulations is low.

If this variability is typical of other studies, tablet formulations with a "true" relative bioavailability of considerably less than the minimum 75% could still, purely by random chance, appear to meet the requirements. If one assumes that the standard error of the mean is equal to 11.5% of the mean and that there are 11 degrees of freedom, the data in Table III can be calculated and indicate that a formulation must have a true relative bioavailability of 64% or less before the probability of obtaining an experimental value ≥75% decreases below even 10%; a more acceptable level of 5% requires a true relative bioavailability ≤62%.

This apparent lack of sensitivity may be due to the method of data analysis since three different experimental measurements, each with its own error distribution, are included in the relative bioavailability ratio. A logical and statistical basis for using three measurements is not readily apparent to the authors, regardless of whether the means are used to estimate the ratio (as recommended by the FDA) or whether the ratio is calculated for each subject and these ratios are then averaged. The FDA states in the *Federal Register* (13) that the method used should "be capable of detecting the difference between the reference tablet and the reference oral solution." This requirement is fine as a test of the experimental design, methodology, and precision of measurement, but it is not justification for the use of the average of two reference treatments as a basis for a relative bioavailability calculation. Therefore, the authors propose alternative methods of data analysis which are more correct statistically, thus allowing for a greater probability of the regulations performing their intended task.

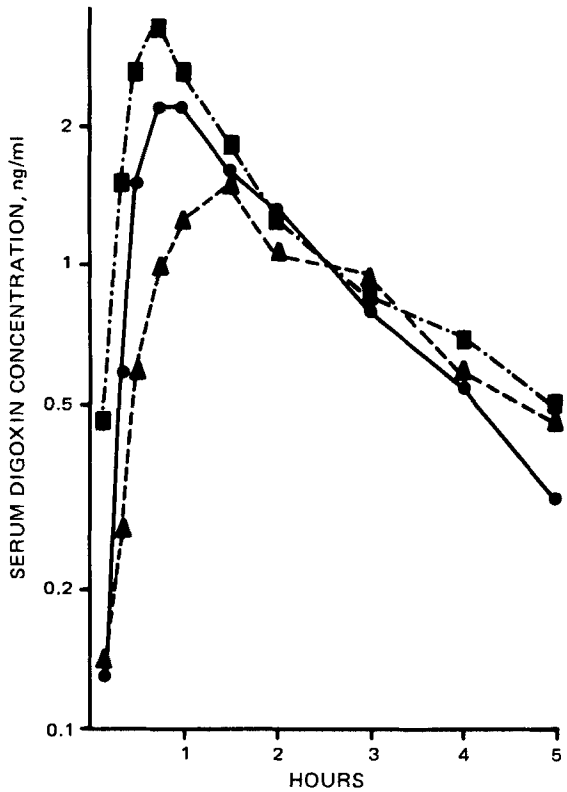

Figure 1—*Semilogarithmic plot of the averaged serum digoxin concentration–time data for the three treatments. Key:* ●, *generic digoxin tablet;* ▲, *current market standard tablet; and* ■, *aqueous solution.*

If all three of the treatments suggested by the FDA must be used in the estimation of one relative bioavailability number, then a method suggested by Finney (15) for estimating relative potency in biological assays (which can include bioavailability studies) utilizing a logarithmic transformation may be applied. Let the average area under the curve (0–5 hr) for the test tablet and the average mean reference (Table II, columns 2 and 5) be the two experimental means whose ratio is to be calculated. Each individual measurement is converted to its common logarithm, and the logarithms are averaged. The average logarithms are then subtracted to give the ratio, and a pooled estimate of the standard deviation of the ratio is calculated. This estimate is then used to calculate fiducial limits (similar to confidence limits) for the potency ratio.

This method gives a ratio of 101% with 95% fiducial limits of 84–122%. Although the result is similar, *i.e.*, the mean absorption of the test tablet is >75% of the mean absorption of the standards, there is now some measure of precision and, in this case, some certainty that the probability of the relative bioavailability actually being <75% is extremely low. There

Table II—Areas under the Serum Digoxin Concentration–Time Curves (in Nanogram Hours per Milliliter) from 0 to 5 hr[a] and the Relative Bioavailability[b] of the Test Tablet

Subject	Test Tablet	Reference Tablet	Reference Solution	Mean Reference[c]	Relative Bioavailability
M.G.	4.23	3.15	6.21	4.68	90.4
R.R.	4.85	6.81	7.54	7.18	67.5
P.H.	5.59	3.22	6.08	4.65	120.
C.N.	4.52	4.03	7.55	5.79	78.1
H.P.	4.21	4.43	6.05	5.24	80.3
D.S.	7.36	0.81	5.60	3.21	229.
R.S.	6.07	5.20	7.67	6.44	94.3
J.M.	5.55	4.08	7.07	5.58	99.5
S.R.	5.82	3.39	6.99	5.19	112.
H.B.	3.90	2.91	5.11	4.01	97.3
W.W.	6.40	9.20	6.32	7.76	82.5
R.M.	5.39	3.37	5.31	4.34	124.
Mean	5.32	4.22[d]	6.46	5.34	106.
SD	1.03	2.12	0.89	1.31	42.3

[a] Areas were calculated using the trapezoidal rule. [b] Relative bioavailability is defined according to the proposed FDA regulations as the ratio of the area under the curve (0–5 hr) for the test tablet to the mean of the areas under the curve for the reference tablet and solution. [c] Mean of the reference tablet and reference solution. [d] Significantly different from reference solution (paired t test, $p < 0.05$).

Table III—Probability of Obtaining a Mean Relative Bioavailability Estimate[a] of 75% or Greater

True Relative Bioavailability	*SEM*[b]	Calculated[c] *t* Value	Probability[d], %
74	8.51	0.12	45.4
73	8.40	0.24	40.8
72	8.28	0.36	36.2
71	8.16	0.49	31.7
70	8.05	0.62	27.4
69	7.93	0.76	23.3
68	7.82	0.90	19.5
67	7.70	1.04	16.1
66	7.59	1.19	13.0
65	7.47	1.34	10.4
64	7.36	1.49	8.16
63	7.24	1.66	6.29
62	7.13	1.82	4.78
61	7.01	2.00	3.57
60	6.90	2.17	2.62

[a] Defined as in Table II. [b] Equal to 11.5% of the mean or true relative bioavailability. [c] Calculated according to: $t = (75 - \bar{X})/s$, where $\bar{X}$ = true relative bioavailability and s = standard error of the mean. [d] Probability of obtaining t greater than the calculated value (equal to the area under the t distribution curve from the calculated t to infinity) due to random error or chance.

are, however, two drawbacks to this method. First, it still utilizes three experimental measurements in the relative bioavailability calculation. Second, even though the studies are done in a crossover manner, the influence of subject-to-subject variability is not minimized because of the utilization of only the means and standard deviation estimates. Thus, the advantage of a crossover study, *i.e.*, being able to look at differences independent of intersubject variation, is ignored. But if one *must* utilize the FDA method as currently written, then this type of data analysis may be preferred.

The authors believe the intent of the FDA at the present time is to guarantee that all digoxin tablets are as good as the market standard. Consequently, the most direct method would be to do a two-way crossover study with the test and reference tablets or to do the FDA three-way crossover study, comparing the reference tablet and solution *only* as a means of testing the methodology and then calculating relative bioavailability using only the test and reference tablets. Since the same subjects are to be used in all treatments, a comparison of the data using the paired t test may be done, thus minimizing the influence of subject-to-subject variability, and a determination of whether the products are significantly different can be made. When using this method (data in Table II, columns 2 and 3), the average difference was 1.11 units with 95% confidence limits of from −0.386 to 2.61, not significantly different from zero ($p > 0.05$).

The last method probably provides as good an estimate as any of the bioavailability of a test tablet relative to the current market standard under the conditions of the FDA protocol. However, it does require that the regulations utilize a specific manufacturer's product as a standard. It may be better to utilize as a standard the oral solution and to require that *all* manufacturers, including the manufacturer of the market standard, demonstrate that the absorption of their tablets is greater than some minimum percent of the absorption of the solution. This requirement would allow for future changes in the regulations to increase the bioavailability of digoxin from tablets to more closely approximate that of the solution.

The FDA has taken a major step forward by suggesting bioavailability requirements for digoxin tablets. However, these standards need to be reevaluated and some changes made before final regulations are enacted.

APPENDIX

Regulation 130.51, part (d), from Ref. 13 reads as follows:

The protocol for the in vivo bioavailability tests required in paragraphs (a) and (c) of this section shall employ a three-way crossover design using the digoxin test product; a reference digoxin tablet supplied, on request, by the Food and Drug Administration; and bulk digoxin USP in an oral solution. Appropriate venous blood and urinary samples are to be collected and analyzed. This method shall be capable of detecting the difference between the reference tablet and the reference oral solution. Bioavailability of the test product shall be demonstrated if a mean absorption of at least 75 percent of the combined mean of the two reference standards is observed. Assistance in developing a protocol for a particular dosage formulation may be obtained by contacting the Food and Drug Administration, Bureau of Drugs (HFD-220), 5600 Fishers Lane, Rockville, MD 20852.

REFERENCES

(1) E. J. Fraser, R. H. Leach, J. W. Poston, A. M. Bold, L. S. Culank, and A. B. Lipede, *J. Pharm. Pharmacol.*, **25,** 968 (1973).

(2) D. J. Greenblatt, D. W. Duhme, J. Koch-Weser, and T. W. Smith, *N. Engl. J. Med.*, **289,** 651 (1973).

(3) D. J. Greenblatt, D. W. Duhme, J. Koch-Weser, and T. W. Smith, *J. Am. Med. Assoc.*, **229,** 1774 (1974).

(4) D. H. Huffman and D. L. Azarnoff, *ibid.*, **222,** 957 (1972).

(5) D. H. Huffman, C. V. Manion, and D. L. Azarnoff, *Clin. Pharmacol. Ther.*, **16,** 310 (1974).

(6) D. H. Huffman, C. V. Manion, and D. L. Azarnoff, *J. Pharm. Sci.*, **64,** 433 (1975).

(7) A. J. Jounela, P. J. Pentikainen, and A. Sothmann, *Eur. J. Clin. Pharmacol.*, **8,** 365 (1975).

(8) J. Lindenbaum, *Pharmacol. Rev.*, **25,** 229 (1973).

(9) J. Lindenbaum, *Clin. Pharmacol. Ther.*, **17,** 296 (1975).

(10) J. Lindenbaum, *N. Engl. J. Med.*, **285,** 1344 (1971).

(11) E. Steiness, V. Christensen, and H. Johansen, *Clin. Pharmacol. Ther.*, **14,** 949 (1973).

(12) J. G. Wagner, M. Christensen, E. Sakmar, D. Blair, J. D. Yates, P. W. Willis, III, and A. J. Sedman, *J. Am. Med. Assoc.*, **224,** 199 (1973).

(13) *Fed. Regist.*, **39,** 2471 (1974).

(14) W. G. Kramer, Ph.D. dissertation, College of Pharmacy, Ohio State University, Columbus, Ohio, 1976.

(15) D. J. Finney, "Statistical Methods in Biological Assay," 2nd ed., Hafner, New York, N.Y., 1964, p. 41.

ACKNOWLEDGMENTS AND ADDRESSES

Received November 4, 1976, from the *Colleges of Pharmacy and Medicine, Ohio State University, and the Drug Information Center, Ohio State University Hospitals, Columbus, OH 43210.*

Accepted for publication February 23, 1977.

Abstracted in part from a dissertation submitted by W. G. Kramer to Ohio State University in partial fulfillment of the Doctor of Philosophy degree requirements.

Supported in part by Philips Roxane Laboratories, Columbus, Ohio, by Medicinal Chemistry Training Grant GM-1949 (National Institutes of Health) for W. G. Kramer, and by the Center Ohio Heart Chapter of the American Heart Association and the National Heart and Lung Institute Training Grant 5-T01-HL05968 for A. J. Kolibash.

The authors are indebted to Mr. Wilbur F. Forester, Jr., for assistance on statistical aspects of the study.

* Present address: Department of Pharmaceutics, College of Pharmacy, University of Houston, Houston, TX 77004.

‡ Present address: Cooper Laboratories, Cedar Knolls, N.J.

ˣ To whom inquiries should be directed (at the Division of Pharmaceutics and Pharmaceutical Chemistry, College of Pharmacy, Ohio State University, Columbus, OH 43210).

Contaminants in Commercial Dapsone

ANDREW P. CHEUNG and PETER LIM ˣ

Abstract □ Three contaminants commonly found in commercial dapsone were identified as 2,4′-sulfonylbis(benzeneamine), 4-(phenylsulfonyl)benzeneamine, and 4-(4′-chlorophenylsulfonyl)benzeneamine. The identities were based on the spectral analysis and unambiguous synthesis of each compound. Solvent-free, pure dapsone was prepared by recrystallization from chloroform.

Keyphrases □ Dapsone—commercial samples, contaminants identified □ Contaminants—identified in commercial samples of dapsone □ Antibacterial agents—dapsone, contaminants identified in commercial samples

Dapsone, 4,4′-sulfonylbis(benzeneamine), has long been used in chemotherapy. Its activity against streptococci (1), *Mycobacterium avium* (2), and *M. tuberculosis* (3) was first observed in the late 1930's. Since 1942, dapsone has been used primarily in the treatment of human leprosy (4), but it is also useful in the treatment of mycetoma (*Nocardia brasiliensis*) (5), actinomycosis (6), dermatitis herpetiformis (Duhring's disease) (7), and pyoderma gangrenosum (8).

DISCUSSION

Although the antimalarial activity of dapsone was demonstrated in 1941 (9), it was not used in the treatment of malaria for the next 20 years because chloroquine was more effective. However, with the emergence of malaria strains resistant to chloroquine and other commonly used antimalarial drugs (10, 11), interest in dapsone as an antimalarial agent was revived (12, 13). Until recently, dapsone has been used as a daily prophylactic against falciparum malaria (14).

Considering the current interest in drug purity, commercial dapsone samples were examined by TLC; three contaminants[1] were consistently present. They were identified as 2,4′-sulfonylbis(benzeneamine) (I, R_f 0.62), 4-(phenylsulfonyl)benzeneamine (II, R_f 0.73), and 4-(4′-chlorophenylsulfonyl)benzeneamine (III, R_f 0.77). (The R_f of dapsone was 0.42.) As estimated by TLC, these contaminants constituted 2–9% of the samples. This paper describes the isolation and identification of these contaminants.

Recrystallization of commercial dapsone samples from chloroform enriched the subject contaminants in the mother liquor; through chromatography on silica gel, the various contaminants were separated. The isolated individual contaminants shared certain common chemical and spectral characteristics that are also common to dapsone. All four compounds responded positively to yield a similar color when sprayed with a diazotization reagent[2], suggesting the presence of an anilino group.

The IR spectra showed strong bands near 7.8 and 8.8 μm, indicative of a sulfone group in each molecule. The PMR spectra showed resonances only in the aryl region, apart from those due to exchangeable protons (*i.e.*, OH and NH_2) (Figs. 1–4). The spectra for I, II, and III (Figs. 2, 3, and 4, respectively) clearly showed a pair of doublets near δ 6.6 and 7.6 ppm with coupling constants of 8.8 ± 0.1 Hz. These characteristics are similar to those found in the spectrum for dapsone (Fig. 1) and are indicative of a 4-aminobenzenesulfonyl group, which is common to all four compounds.

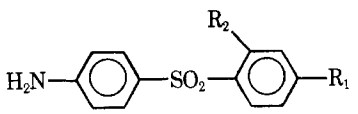

I: R_1 = H, R_2 = NH_2
II: R_1 = R_2 = H
III: R_1 = Cl, R_2 = H

On the basis of mass spectral and elemental data, the molecular weight of I is 248, consistent with the empirical formula $C_{12}H_{12}N_2O_2S$. In addition to signals assigned the 4-aminobenzenesulfonyl group, the PMR spectrum of I (Fig. 2) showed four other protons in the aryl region. Analysis of the coupling constants (J = 1.8, 7.0, and 8.3 Hz) for the one-proton multiplet centered at δ 7.23 ppm suggested that this proton is coupled to two *ortho*- and one *meta*-protons. This arrangement is a 1,2-disubstituted benzene, which is substantiated by analysis of the three remaining aryl protons. The PMR spectrum of I also showed two broad overlapping singlets at δ 6.00 and 6.06 ppm, each representing two protons with both singlets exchangeable with deuterium oxide. These characteristics are consistent with those of two primary amino groups. Based on this evidence, I probably is 2,4′-sulfonylbis(benzeneamine).

According to the mass spectral and elemental results, the molecular weight of II is 233, which is in agreement with the empirical formula $C_{12}H_{11}N_2O_2S$. The PMR spectrum of II showed a broad singlet of two exchangeable protons at δ 6.14 ppm, a doublet of two protons at δ 6.63 (J = 8.9 Hz) ppm, a multiplet of five protons centered near δ 7.55 ppm, and a multiplet of two protons centered near δ 7.84 ppm. After subtraction of the 4-aminobenzenesulfonyl doublet from the δ 7.55-ppm multiplet that is complementary to the δ 6.63-ppm doublet, the remaining three protons in the δ 7.55-ppm group and the two protons in the δ 7.84-ppm group closely resemble the pattern of a benzenesulfonyl. This observation suggests that II is 4-(phenylsulfonyl)benzeneamine.

The elemental and mass spectral data for III are consistent with a molecular weight of 267 and the empirical formula $C_{12}H_{10}ClN_2O_2S$. The PMR spectrum for III (Fig. 4) showed only two exchangeable protons, appearing as a broad singlet at δ 6.20 ppm, and four doublets in the aryl region in agreement with two 1,4-disubstituted benzenes. Data gathered for III are consistent with those for 4-(4′-chlorophenylsulfonyl)benzeneamine.

For validation of the structures proposed for I–III, these three compounds were prepared by unambiguous syntheses. Compound I was prepared by treating 4-acetamidobenzenesulfinic acid with 2-bromonitrobenzene (15) to give 4-(2′-nitrophenylsulfonyl)benzeneacetamide (IV). Reduction (16, 17) of IV gave 4-(2′-aminophenylsulfonyl)benzeneacetamide (V), which, upon hydrolysis, yielded I.

Compound II was prepared in high yield by diazotization of I with sodium nitrite and sulfuric acid followed by heating (18). Compound III was prepared by the method of Richter and Frey (19), in which 4-acetamidobenzenesulfonyl chloride was treated with chlorobenzene in a

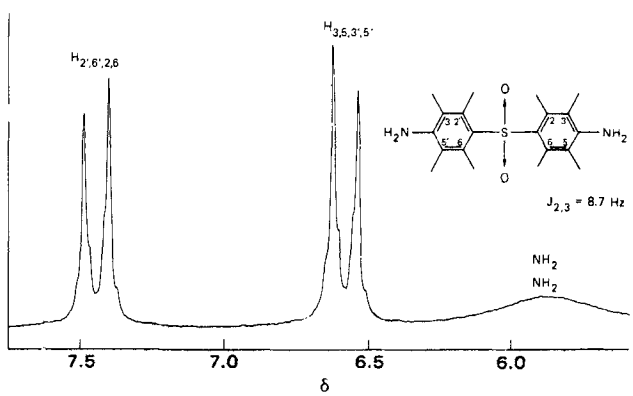

Figure 1—*PMR spectrum of dapsone.*

[1] Usually two trace impurities were found in addition to these three contaminants. Because of their very low concentrations—estimated at ≪0.1%—the trace impurities were not isolated and characterized. Dr. Robert Lofberg (personal communication), Walter Reed Army Institute of Research, identified one impurity as 4-(4′-hydroxyphenylsulfonyl)benzeneamine.

[2] The three contaminants and dapsone were separated on a silica plate. When sprayed with 1 *N* HCl, 2% $NaNO_2$, 3% sulfamic acid (all aqueous solutions), and 1% *N*-(1-naphthyl)ethylenediamine dihydrochloride in propylene glycol–water (1:2 v/v) in the order given, all four compounds responded positively to give pink spots.

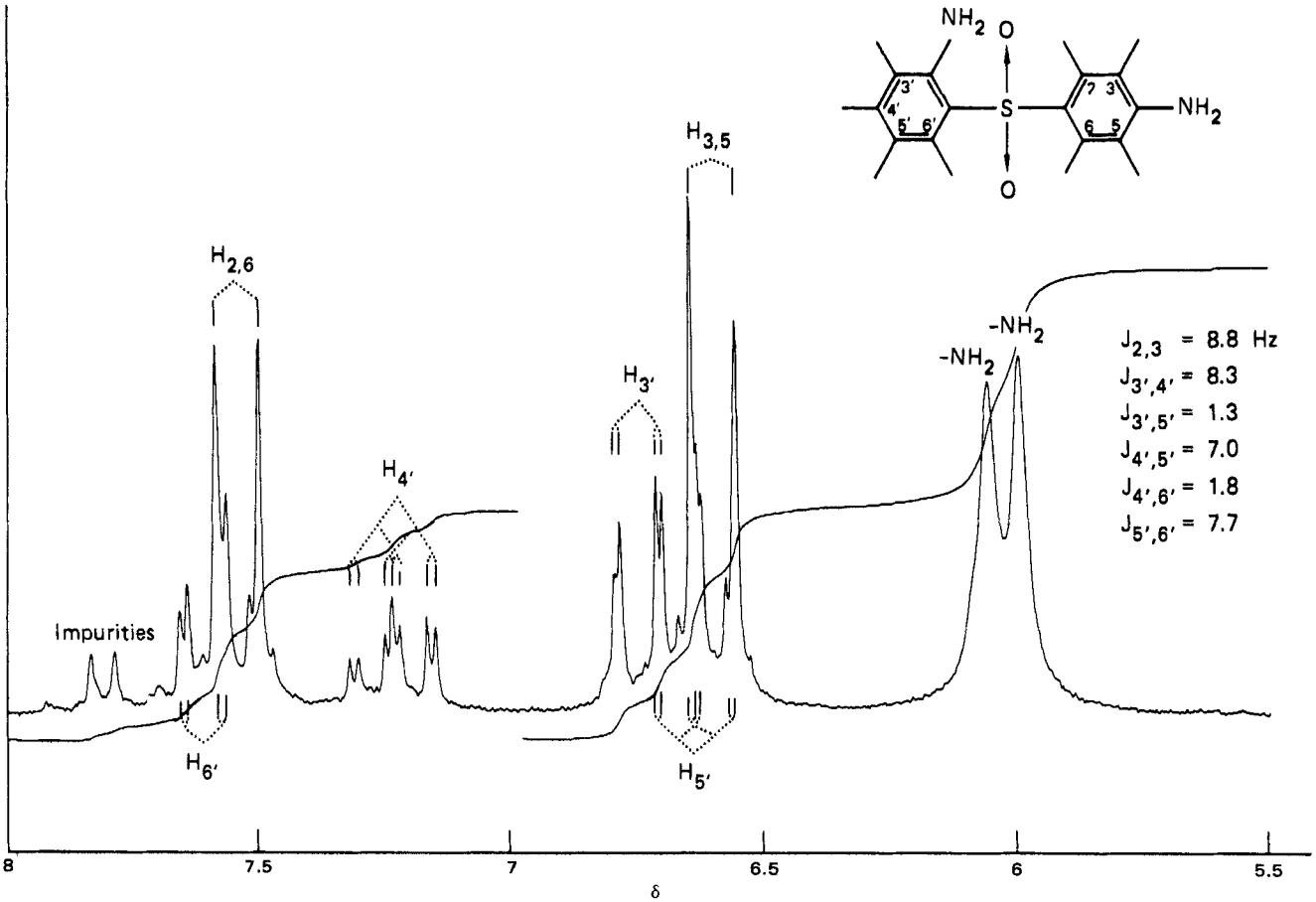

Figure 2—*PMR spectrum of contaminant I.*

Friedel–Crafts sulfonation followed by hydrolysis of the acetyl group.

Equivalence of the unambiguously synthesized materials to those isolated from commercial dapsone samples was established by IR, UV, PMR, TLC, GLC, and mixed melting-point comparisons.

The appearance of these impurities in the dapsone samples probably resulted from contaminations in the starting material. An established method for preparing dapsone is the coupling of 4-chloronitrobenzene with sodium 4-acetamidobenzenesulfonate, followed by reduction of the nitro group to the amine and hydrolysis of the acetamido group (20). The presence of 2-chloronitrobenzene, chlorobenzene, and 1,4-dichlorobenzene in the 4-chloronitrobenzene would have resulted in I, II, and III, respectively.

EXPERIMENTAL

IR spectra were determined as mineral oil mulls on a commercial spectrometer[3]. PMR spectra were recorded as dimethyl sulfoxide-d_6 solutions on a 100-MHz spectrometer[4]; chemical shifts were reported on a δ scale using an internal tetramethylsilane reference (δ 0.00 ppm). UV spectra were scanned as solutions in 95% ethanol on a recording spectrometer[5]. Melting points were obtained on a commercial apparatus[6]. TLC utilized silica plates developed with chloroform–ether–methanol (7:2:1 v/v).

GLC data were obtained for the trifluoroacetyl derivatives[7] on a gas chromatograph equipped with a flame-ionization detector. A 1.9-m × 2-mm i.d. glass column packed with 3% ultraphase SE-30 coated on 80–100-mesh Chromosorb W (HP)[8] was used. Temperatures were 250° (inlet), 200° (column), and 300° (detector); the carrier gas was nitrogen at 40 ml/min. All chemicals were reagent grade or the best quality available.

Recrystallization of Commercial Dapsone—Two grams of commercial dapsone[9] was dissolved in 500 ml of chloroform with reflux. The solution was filtered hot, and the filtrate was allowed to evaporate slowly to 200 ml on a steam bath. Then the solution was carefully set aside to allow crystal formation. The needles that formed were collected, washed with cold chloroform, and dried. From this material, 1.6 g of solvent-free dapsone was obtained. This material was chromatographically homogeneous, mp 177–178° [lit. (21) mp 175–176°][10].

The mother liquor from this recrystallization was evaporated to dryness, and the residue was used for isolation of the contaminants.

Isolation of I–III—The residue from the recrystallization mother liquor was redissolved in 10 ml of chloroform. The solution was applied onto 1-mm thick silica gel plates, which were developed in chloroform–ether–methanol (7:2:1 v/v). The resolved bands were located by 254-nm UV light and scraped from the plates. The respective bands from numerous plates were combined and extracted with methanol.

The respective methanol solutions were reduced to minimum volumes on a steam bath under a nitrogen stream, and the chromatographic-isolation procedure was repeated until all three contaminants isolated were chromatographically homogeneous. At this stage of purity, each contaminant was crystallized from hexane–methanol (10:1).

Compound I—mp 114–116° [lit. (22) mp 117°]; TLC R_f 0.62; GLC retention time, 3.0 min; *m/e* 248.

Anal.—Calc. for $C_{12}H_{12}N_2O_2S$: C, 58.04; H, 4.87; N, 11.28; S, 12.91. Found: C, 57.93; H, 4.94; N, 10.98; S, 12.71.

[3] Perkin-Elmer model 137.
[4] Varian HA-100.
[5] Cary model 15.
[6] Mel-Temp.
[7] Approximately 1 mg of each compound was treated with 0.3 ml of trifluoroacetic anhydride. The mixture was heated until a complete solution resulted, and excess trifluoroacetic anhydride and trifluoroacetic acid were evaporated with a stream of dried nitrogen. The residue was redissolved in 0.4 ml of benzene plus 1 drop of trifluoroacetic acid and then injected into the gas chromatograph (Micro-Tek 220).
[8] Johns-Manville, Celite Division, New York, N.Y.
[9] Lot 8L-2223 (typical of many Sterling Winthrop lots analyzed), Sterling Winthrop Research Institute, Rensselaer, N.Y.
[10] In this study, material recrystallized several times from 95% ethanol still contained the subject impurities.

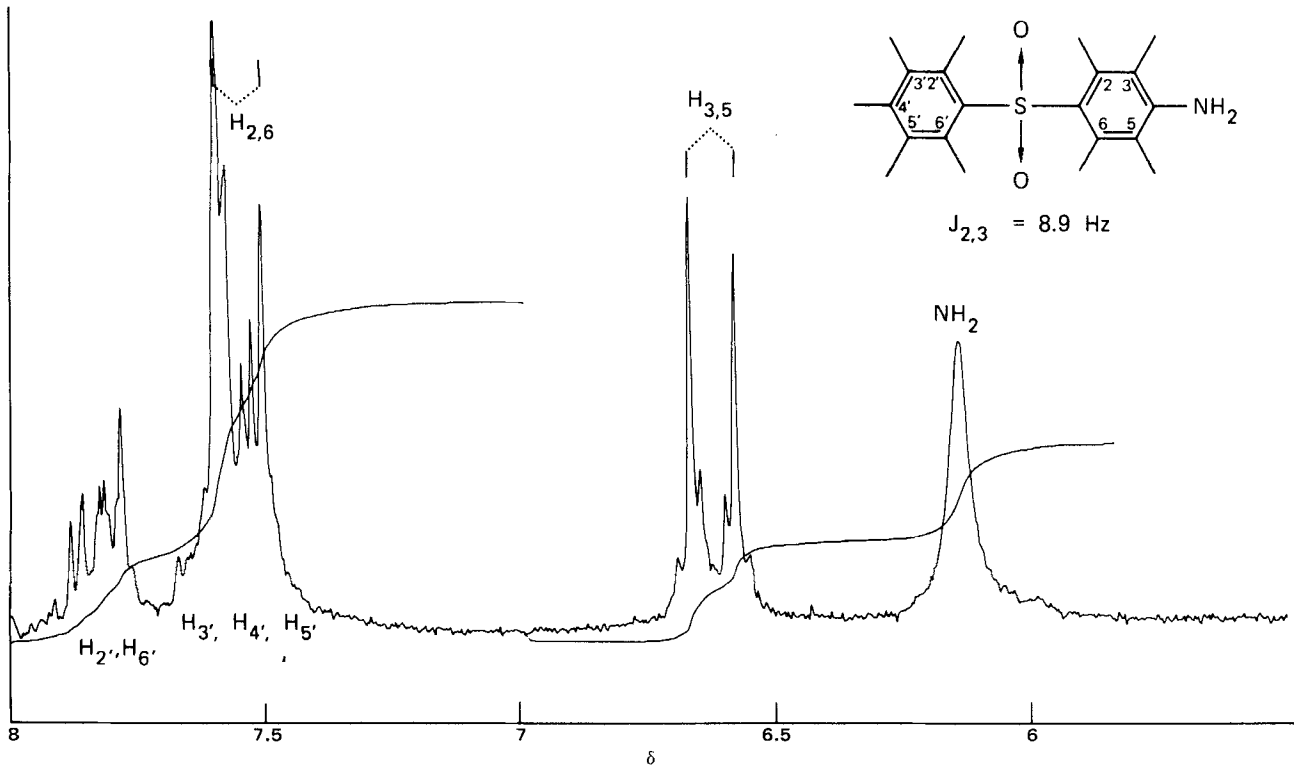

Figure 3—*PMR spectrum of contaminant II.*

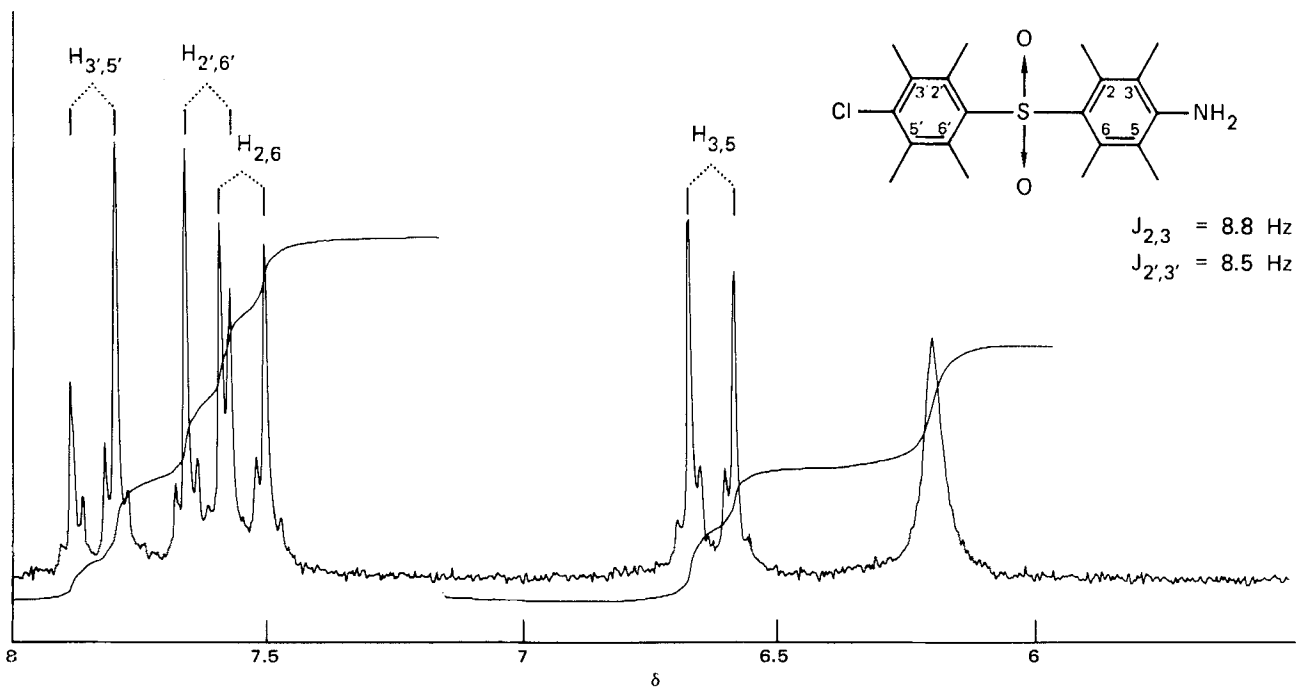

Figure 4—*PMR spectrum of contaminant III.*

Compound II—mp 167–170° [lit. (23) mp 172–173°]; TLC R_f 0.73; GLC retention time, 2.5 min; *m/e* 233.

Anal.—Calc. for $C_{12}H_{11}NO_2S$: C, 61.78; H, 4.75; N, 6.00; S, 13.72. Found: C, 61.50; H, 4.70; N, 5.97; S, 13.40.

Compound III—mp 186–188° [lit. (24) mp 187.8–188.4°]; TLC R_f 0.77; GLC retention time, 4.0 min; *m/e* 257.

Anal.—Calc. for $C_{12}H_{10}ClNO_2S$: C, 53.83; H, 3.76; Cl, 13.24; N, 5.23; S, 11.98. Found: C, 54.00; H, 3.80; Cl, 13.49; N, 5.36; S, 12.10.

Preparation of V—4-Acetamidobenzenesulfinic acid (2.6 g) was dissolved in 12 ml of methanol containing 1 g of sodium hydroxide. To this solution was added 20 ml of dimethylformamide containing 3.8 g of 2-bromonitrobenzene, and the resulting solution was refluxed (108°) for 1.5 hr. The methanol was distilled, and the remaining solution was refluxed (164°) for an additional 2.5 hr. After cooling, water was added to the dimethylformamide solution until precipitation was complete.

The precipitate was collected, washed with warm water followed by methanol, and air dried. The dried material consisted of 3.6 g of IV, mp 244–246°. Compound IV (2.0 g) was added to 60 ml of 6 *N* acetic acid (aqueous), and the mixture was heated to reflux. During the 1st hr of reflux, iron filings (1 g) were slowly added to the refluxing solution; after a total reflux time of 3 hr, the mixture was allowed to cool. After the insoluble material was removed by filtration, the filtrate was evaporated

to dryness, and the residue was extracted several times with a total of 300 ml of methanolic 0.1 *N* NaOH.

The insoluble matter was removed by filtration, and the filtrate was again evaporated to dryness. The residue was triturated several times with a total of 400 ml of water. The insoluble material was collected by filtration and redissolved in 30 ml of methanol, and the solution was filtered. The clear filtrate was diluted with 150 ml of water to cause the complete precipitation of V. The white precipitate was collected and dried; the material weighed 1.9 g (80% yield, mp 97–99°).

Compound I—Compound V (500 mg) and 100 ml of ethanol–concentrated hydrochloric acid (4:1 v/v) were refluxed for 2 hr. The mixture was filtered, and the pH of the filtrate was adjusted to ~7.0 with dilute sodium hydroxide. The ethanol was removed by evaporation, and the precipitate that resulted was collected and dried. The material weighed 440 mg (88% yield, mp 115–117°).

Anal.—Calc. for $C_{12}H_{12}N_2O_2S$: C, 58.04; H, 4.87; N, 11.28; S, 12.91. Found: C, 58.14; H, 4.87; N, 11.25; S, 12.88.

Compound II—Compound I (500 mg) was dissolved in 100 ml of ethanol–benzene (4:1 v/v) by warming on a steam bath. To this solution was added 0.5 ml of concentrated sulfuric acid, followed by 350 mg of sodium nitrite—in portions—as rapidly as the violent reaction would permit. After the reaction moderated, the solution was heated to reflux for 2 hr. The reaction was allowed to cool, and then the insoluble matter was removed by filtration.

The filtrate was neutralized with sodium hydroxide and evaporated to dryness. The residue was triturated twice with a total of 200 ml of water, and the insoluble matter was collected by filtration. The solid matter was exhaustively extracted with 20 ml of ethanol; the insolubles were removed by filtration. The ethanol filtrate was diluted with 80 ml of water to cause the complete precipitation of II, which was collected by filtration and dried. The material weighed 320 mg (64% yield, mp 169–172°).

Anal.—Calc. for $C_{12}H_{11}NO_2S$: C, 61.78; H, 4.75; N, 6.00; S, 13.72. Found: C, 62.04; H, 4.76; N, 5.81; S, 13.48.

Compound III—4-Acetamidobenzenesulfonyl chloride (1 g) and aluminum chloride (3 g) in 25 ml of chlorobenzene were stirred for 2 hr at 140°. The mixture was filtered, and the filtrate was evaporated to dryness. The residue was dissolved in 50 ml of methanol; the insolubles were removed by filtration. Concentrated hydrochloric acid (10 ml) was added to the filtrate, and the resulting solution was refluxed for 2 hr.

The mixture was allowed to cool, and then the solution was filtered. The filtrate was neutralized with dilute sodium hydroxide and evaporated to dryness. The residue was triturated twice with a total volume of 20 ml of water. The water-insoluble matter was recrystallized from aqueous methanol to yield III, mp 187–189°.

Anal.—Calc. for $C_{12}H_{10}ClNO_2S$: C, 53.83; H, 3.76; Cl, 13.24; N, 5.23; S, 11.98. Found: C, 53.69; H, 3.83; Cl, 13.54; N, 5.32; S, 12.18.

REFERENCES

(1) G. A. H. Buttle, D. Stephenson, S. Smith, T. Dowing, and G. E. Foster, *Lancet*, **232**, 1331 (1937).

(2) N. Rist, *C. R. Soc. Biol.*, **130**, 972 (1939).

(3) W. H. Feldman, H. C. Hinshaw, and H. E. Moses, *Proc. Mayo Clin.*, **15**, 695 (1940).

(4) C. C. Shepard, *Ann. Rev. Pharmacol.*, **9**, 37 (1969).

(5) A. Gonzalez Ochoa, J. Shiels, and P. Vasquez, *Gac. Med. Mex.*, **82**, 345 (1952).

(6) J. L. Pipkin, in "Current Therapy," H. E. Conn, Ed., Saunders, Philadelphia, Pa., 1967, p. 514.

(7) D. R. Weakley, in *ibid.*, p. 495.

(8) J. Altman and C. Mopper, *Minn. Med.*, **49**, 22 (1966).

(9) L. T. Coggeshall, J. Maier, and C. A. Best, *J. Am. Med. Assoc.*, **117**, 1007 (1941).

(10) E. D. Bix, Q. T. Box, and M. D. Yound, *Am. J. Trop. Med.*, **12**, 300 (1963).

(11) L. J. Legters, D. K. Wallace, R. D. Powell, and S. Pollack, *Mil. Med.*, **130**, 168 (1965).

(12) D. L. Leiker, *Leprosy Rev.*, **27**, 66 (1956).

(13) H. M. Archibald and C. M. Ross, *J. Trop. Med. Hyg.*, **63**, 25 (1960).

(14) A. J. Ognibene, *Ann. Intern. Med.*, **72**, 521 (1970).

(15) H. Dorn and G. Hilgetag, East German pat. 33094 (1965); through *Chem. Abstr.*, **64**, 650g (1966).

(16) C. B. Torsi, *Gazz. Chim. Ital.*, **90**, 1658 (1960).

(17) E. Wertheim, in "Organic Syntheses," coll. vol. II, A. H. Blatt, Ed., Wiley, New York, N.Y., 1943, p. 471.

(18) G. H. Coleman and W. F. Talbot, in *ibid.*, p. 592.

(19) C. Richter and W. Frey, Swiss pat. 278,939 (1952); through *Chem. Abstr.*, **48**, 718h (1954).

(20) C. W. Ferry, J. S. Bick, and R. Baltzly, in "Organic Syntheses," coll. vol. III, A. J. Blatt, Ed., Wiley, New York, N.Y., 1955, p. 239.

(21) "The Merck Index," 8th ed., Merck & Co., Rahway, N.J., 1968, p. 321.

(22) R. O. Robbin, Jr., J. H. Williams, and G. W. Anderson, *J. Am. Chem. Soc.*, **63**, 1930 (1941).

(23) H. Nozaki, T. Okada, R. Noyori, and M. Kawanisi, *Tetrahedron*, **22**, 2177 (1966).

(24) H. Heymann and L. F. Fieser, *J. Am. Chem. Soc.*, **67**, 1979 (1945).

ACKNOWLEDGMENTS AND ADDRESSES

Received May 28, 1974, from *Stanford Research Institute, Life Sciences Division, Menlo Park, CA 94025.*

Accepted for publication February 25, 1977.

Supported by the U.S. Army Medical Research and Development Command, Office of the Surgeon General, under Contract DA-49-193-MD-2753.

This report is Contribution 1239 to the Army Research Program on Malaria.

[x] To whom inquiries should be directed.

Evaluation of Teratogenic Potential of Codeine Sulfate in CF-1 Mice

JOHN E. ZELLERS and RONALD F. GAUTIERI ˣ

Abstract □ The most prominent defect of codeine sulfate, 100 mg/kg sc, was delayed ossification of the supraoccipital bone, paws, xiphoid, and sternebrae as well as other sternebral defects such as checkerboard sternebrae and polysternebrae. Although these anomalies were similar to the minor defects seen in the fetuses of morphine sulfate-treated mice, the major anomalies such as exencephaly, cryptorchid testes, and rib and vertebral fusions produced by morphine were not present in the fetuses of mice challenged with codeine. Thus, codeine sulfate appears to be less teratogenic than morphine sulfate. A review of the incidences of the various defects in mice treated on a single day with codeine showed that there was a range of days on which the mouse fetus was susceptible to codeine's teratogenic effects, with the most critical days of gestation being Days 8–10. Furthermore, a comparison of the defects that occurred in those treated on both Days 8 and 9 with the defects that occurred in those treated on a single day of gestation reveals an additive or cumulative teratogenic response to codeine.

Keyphrases □ Codeine sulfate—teratogenic activity evaluated, mice □ Teratogenicity—codeine sulfate evaluated, mice □ Narcotic analgesics—codeine sulfate, teratogenic activity evaluated, mice

In 1968, Harpel and Gautieri (1), noting the lack of teratogenic studies involving narcotic analgesics, demonstrated that high subcutaneous doses of morphine sulfate administered to nontolerant CF-1 albino mice on the 8th or 9th day of gestation were capable of inducing various fetal malformations. The most prominent defect observed with drug challenge on Day 8 was exencephaly, while axial skeletal fusion was the most conspicuous malformation occurring with drug insult on Day 9 of gestation. In mice, exencephaly and axial skeletal fusions have been reported after many types of treatment, including the administration of insulin (2), galactoflavin (3), vitamins (4), and urethan (5), as well as with riboflavin deficiency (3), X-ray exposure (3), and anoxia (6).

Due to its close structural relationship to morphine, codeine was suspected of having teratogenic potential. Because the literature is devoid of studies concerning the effects of codeine on developing fetuses, the purposes of this study were: (*a*) to test the hypothesis that codeine is a potential teratogen and (*b*) to determine the day or range of days of gestation on which the fetus is most susceptible to any of its teratogenic effects.

EXPERIMENTAL

CF-1 albino mice[1], 25–30 g, were used. Females were placed in aggregate cages, each holding 25 mice. No attempt was made to breed these mice for at least 2 weeks following their arrival and unless they maintained a minimum weight of 25 g. Male mice were placed in individual metal cages, 12.5 × 15 × 10 cm, with a wire mesh front and bottom. All animals were maintained on laboratory food[2] and tap water *ad libitum*.

To produce timed pregnancies, two females were placed into the cage of a male at 4:00 pm and permitted to remain there until 8:00 am the following morning. At this time, the females were removed and examined for the presence of a vaginal plug. Females exhibiting this plug were regarded as being gravid, and the day on which the plug appeared was considered to be Day 0 of gestation. Pregnant mice were weighed to the nearest 0.1 g, and this weight was designated as the maternal starting weight. Gravid females were placed into individual cages, identical to those occupied by the males, and allowed to remain undisturbed until the morning of the 7th day of gestation, when they were weighed for a second time. A weight gain of 2 g or more at this time was accepted as a confirmation of pregnancy.

The confirmed pregnant females were assigned at random to one of eight experimental categories: six groups injected with 100 mg of codeine sulfate[3]/kg on a single day of gestation from Day 7 through Day 12, one group injected with 100 mg of codeine sulfate/kg on both Days 8 and 9 of gestation, and one group of untreated control mice which was examined to establish norms.

Since single saline injections administered subcutaneously on either Day 8 or 9 of gestation produced no significant change in the occurrence of fetal abnormalities compared to untreated controls in previous studies (7, 8), all treatment groups in this study were compared to one group of untreated controls. Arcuri and Gautieri (8) injected gravid CF-1 mice subcutaneously with 60 mg of sodium sulfate/kg on Day 9 of gestation and found no significant change in the number of fetal abnormalities. Because sodium sulfate contains approximately 68% sulfate or 40.8 mg/kg in the 60-mg/kg dose used in the latter study, while codeine sulfate contains only approximately 14% sulfate or 14.0 mg/kg in the 100-mg/kg dose used in the present study, sulfate-ion controls were not included.

An injectable solution of codeine sulfate[4], 3% (30.0 mg/ml), was prepared fresh weekly by dissolving the drug in triple-distilled water. All injections were made subcutaneously in the upper left abdomen using 1-ml tuberculin syringes equipped with 1.27-cm 26-gauge needles.

Following treatment, each mouse was permitted to proceed to Day 18, 1 day short of term in the gestation of the CF-1 mouse. The pregnant animal was weighed, and this weight was referred to as the terminal maternal weight. The animal was then sacrificed, and the abdominal wall was opened to expose the entire peritoneal cavity. Prior to actual opening, the uterine horns were examined grossly for fetal swellings and resorption sites, as indicated by the presence of small dark nodules (the metrial glands), which were counted and recorded.

The uterine horns were incised individually, and the exposed fetuses were removed by blunt dissection, blotted dry, and weighed to the nearest 0.01 g on a torsion balance. Each fetus was examined grossly for any externally visible soft tissue defects and determination of sex. Fetal viability was determined by reflex movement of the limbs in response to mechanical stimulus with a blunt probe.

Every second fetus was placed in either bone-staining solution or Bouin's fixative and processed for skeletal or soft tissue examination, respectively. Fetuses destined to be examined for soft tissue defects were fixed and decalcified in Bouin's fixative for a minimum of 2 weeks. These fetuses were reexamined for external defects under a low power binocular dissecting microscope and sectioned according to the method of Wilson and Warkany (9). Those fetuses designated from each litter for skeletal examinations were processed according to the method of Staples and Schnell (10).

The significance of observed variations among the experimental groups was determined by using the Student t test (11) and the uncorrected χ^2 test for binomial populations (11).

RESULTS AND DISCUSSION

The observations support the hypothesis that codeine is a potential teratogen. It is closely related structurally to morphine (12), which is known to produce soft tissue and skeletal anomalies in the fetuses of CF-1 mice when administered in high doses on Day 8 or 9 of gestation (1, 7, 8).

[1] Carworth Farms, New City, N.Y.
[2] Teklad rat and mouse diet (6% fat), Teklad Mills, Winfield, Iowa.
[3] Highest dose, as determined in a pilot study, where no maternal death or excessive excitement was observed.
[4] USP quality, Control No. 63375, Merck & Co., Rahway, N.J.

Table I—Mean Values of the Test Groups

Treatment[a]	Maternal Weight Ratio, S/T[b]	Fetal Ratio, Right Horn/ Left Horn	Resorption Ratio, Right Horn/ Left Horn	$\bar{X}$ Fetal Weight, g	Sex Ratio, M/F	Soft Tissue Abnormalities	Skeletal Abnormalities
Control (untreated)	25.3/50.2	5.4/5.5	0.5/0.5	1.38	5.3/5.6	0.75	1.63
Codeine on Day 7	26.1/50.3	6.3/4.7	1.1/0.6	1.26[c]	5.1/5.9	0.57	5.86[c]
Codeine on Day 8	25.4/48.3	6.9[c]/4.0	0.6/0.4	1.23[c]	5.6/5.3	0.13	6.00[c]
Codeine on Day 9	25.7/47.4	5.0/5.4	0.1/0.3	1.20[c]	6.1/4.3[c]	1.14	7.71[c]
Codeine on Day 10	26.4/55.1[c]	8.0[c]/6.0	0.2/0.2	1.18[c]	8.0/6.0	0.50	9.33[c]
Codeine on Day 11	26.7/50.1	4.3/5.2	0.3/0.2	1.32	4.7/4.8	1.00	6.33[c]
Codeine on Day 12	24.6/49.2	5.0/5.0	0.7/1.5	1.37	5.0/5.0	0.33	3.17
Codeine on Days 8 and 9	26.7/48.8	5.6/5.8	0.2/0.6	0.98[c]	5.4/6.0	0.80	15.60[c]

[a] The dose of codeine was 100 mg/kg sc in all cases. [b] S = starting weight and T = terminal weight. [c] Statistically significant in comparison with untreated control, $p < 0.05$

Table II—Occurrence of Delayed Ossification of the Supraoccipital Bone

Treatment[a]	Litters Absent	Litters Present	Normal Fetuses	Abnormal Fetuses
Control (untreated)	7	1	40	1
Codeine on Day 7	5	2	35	2
Codeine on Day 8	4	4	32	8[b]
Codeine on Day 9	3	4[b]	26	9[b]
Codeine on Day 10	2	4[b]	33	9[b]
Codeine on Day 11	3	3	18	9[b]
Codeine on Day 12	5	1	27	1
Codeine on Days 8 and 9	0	5[b]	7	22[b]

[a] The dose of codeine was 100 mg/kg sc in all cases. [b] Significance is indicated in p values of 0.05 or less when compared to control.

Although the teratogenic effects of codeine sulfate were similar to those of morphine sulfate, many distinct differences between the effects of codeine and morphine on gravid mice and their fetuses also were observed.

One paradoxical variation was the difference in the gross maternal effects of codeine sulfate and morphine sulfate. Although codeine is at least twice as toxic as morphine (13–15) when injected subcutaneously or intraperitoneally in mice, the maternal effects of 100 mg of codeine sulfate/kg sc were minimal compared to the stimulation followed by depression with a hyperactive recovery period with doses of 100–500 mg of morphine sulfate/kg sc (1). Slight excitation occurred in a few mice after 100 mg of the codeine sulfate solution/kg sc. However, a similar excitation also occurred in some untreated control mice from general handling and moving. A few mice seemed quiescent when returned to their cages postinjection, but most resumed the same level of activity as that prior to injection. None of the mice went through a period of great excitation followed by severe depression, which is typical with doses of codeine sulfate above 100 mg/kg. Furthermore, there was no variation in the maternal response of mice injected on a 2nd day with 100 mg of codeine sulfate/kg.

Another major variation between the effects of codeine sulfate and morphine sulfate on CF-1 mouse fetuses was in the production of soft tissue anomalies. While morphine sulfate shows a tendency to produce exencephaly and cryptorchid testes, especially when administered on Day 8 of gestation (1, 7), these defects were rare in the fetuses of codeine-treated mice. The only soft tissue defect that occurred with any frequency in the fetuses of codeine-treated mice was a small extra digit on the outside of one or both forepaws, but the incidence of this defect was not statistically significant. The one fetus of the codeine-treated mice that did have exencephaly was from the litter of a gravid mouse treated on Day 8 of gestation with 100 mg of codeine sulfate/kg.

Skeletal defects in the fetuses of codeine-treated mice were both similar and different from the defects seen in the fetuses of morphine-treated mice. Both morphine- and codeine-induced skeletal anomalies appear to be related to a reduction in the mean fetal weight (8). Mean fetal weights were decreased significantly in the groups of mice treated with

Table III—Occurrence of Sternebrae Defects

Treatment[a]	Litters Absent	Litters Present	Normal Fetuses	Abnormal Fetuses
Control (untreated)	5	3	34	7
Codeine on Day 7	0	7[b]	11	26[b]
Codeine on Day 8	2	6	25	15[b]
Codeine on Day 9	1	6[b]	17	18[b]
Codeine on Day 10	0	6[b]	18	24[b]
Codeine on Day 11	0	6[b]	14	13[b]
Codeine on Day 12	1	5	18	10
Codeine on Days 8 and 9	0	5[b]	8	21[b]

[a] The dose of codeine was 100 mg/kg sc in all cases. [b] Significance is indcated in p values of 0.05 or less when compared to control.

Table IV—Occurrence of Delayed Ossification of the Xiphoid

Treatment[a]	Litters Absent	Litters Present	Normal Fetuses	Abnormal Fetuses
Control (untreated)	8	0	41	0
Codeine on Day 7	7	0	37	0
Codeine on Day 8	8	0	40	0
Codeine on Day 9	4	3[b]	29	6[b]
Codeine on Day 10	5	1	41	1
Codeine on Day 11	6	0	27	0
Codeine on Day 12	5	1	27	1
Codeine on Days 8 and 9	0	5[b]	16	13[b]

[a] The dose of codeine was 100 mg/kg sc in all cases. [b] Significance is indicated in p values of 0.05 or less when compared to control.

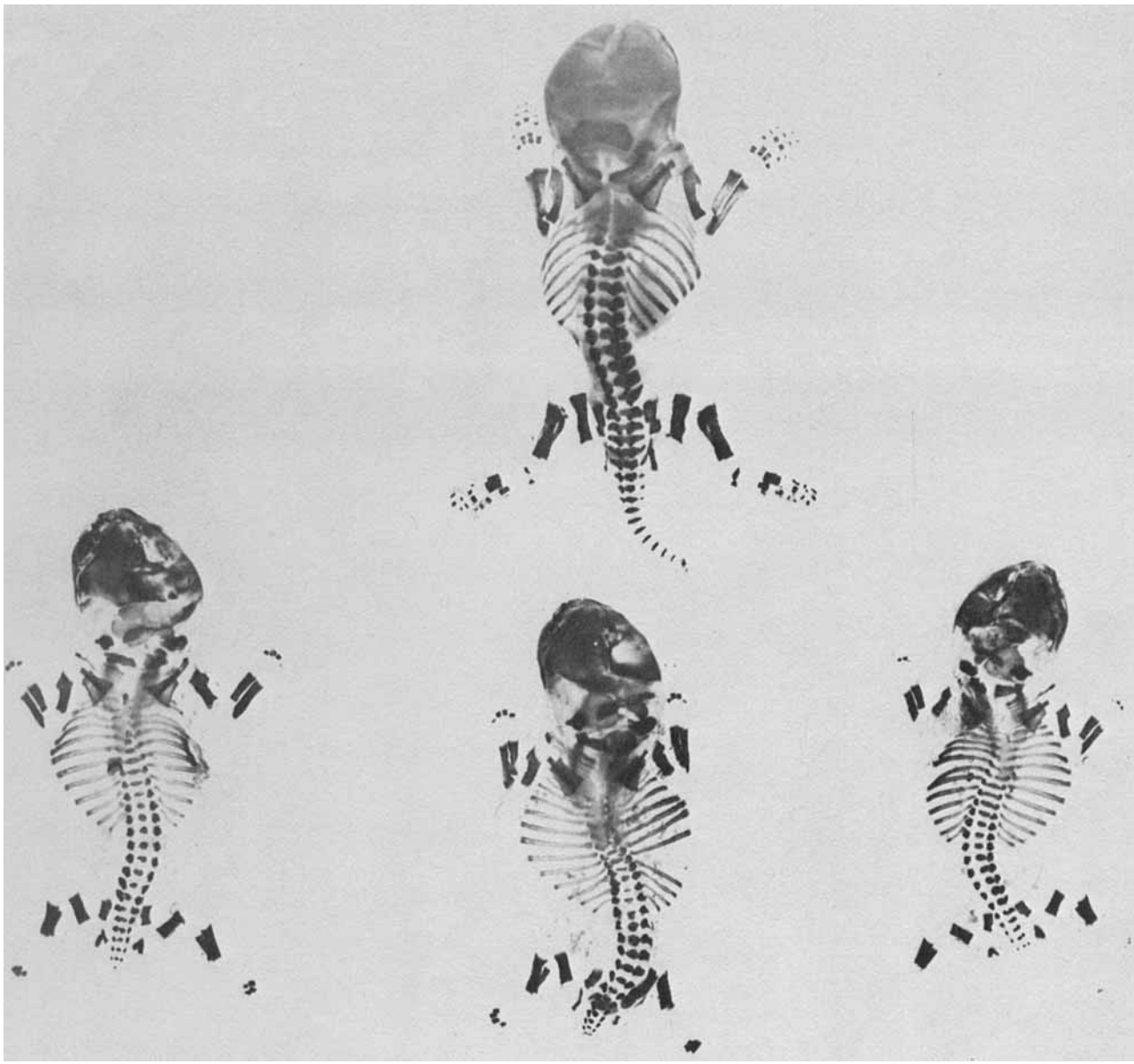

Figure 1—*Alizarin red S stained skeletal specimens of 18-day-old mouse fetuses, showing normal and delayed ossification of the supraoccipital bone and paws. Top: fetus of untreated control mouse with normal supraoccipital bone and paws. Bottom: fetuses of mice treated with 100 mg of codeine sulfate/kg on both Days 8 and 9 of gestation, showing delayed ossification of the supraoccipital bone and paws.*

100 mg of codeine sulfate/kg on Day 7, 8, 9, 10, or 11 or on both Days 8 and 9 of gestation. The most significant decrease occurred in the group treated on both Days 8 and 9 (Table I). Not only was the mean fetal weight lowest and the mean number of skeletal defects highest in this group, but the severity of the defects in this group was also greater than in any other codeine-treated group, suggesting an additive or cumulative effect of the drug and a range of days of gestation on which the fetus is susceptible to the effects of codeine sulfate.

Skeletal defects consisted of delayed ossification of the supraoccipital bone, split supraoccipital bone, missing supraoccipital bone, delayed ossification of the sternebrae, split sternebrae, checkerboard sternebrae, polysternebrae, missing sternebrae, delayed ossification of the xiphoid, split xiphoid, and delayed ossification of the paws (Figs. 1 and 2). When these defects were summarized into four categories (delayed ossification of the supraoccipital bone, sternebrae defects, delayed ossification of the xiphoid, and delayed ossification of the paws) and compared to the control group on a litter and fetal basis (Tables II–V), the range of days on which the fetus is susceptible and the additive or cumulative effect of codeine sulfate can again be seen.

One common defect occurring from treatment with codeine was delayed ossification of the paws. To set a standard for the determination of this defect, eight litters of alizarin red S bone stained fetuses from untreated mice were examined. The forepaws had 12 ossification sites each, while the hindpaws had 14 ossification sites each (excluding the toenails). In the forepaws, the ossification sites were arranged in three rows containing four sites each. The ossification sites in the hindpaws were also arranged in three rows, except that the first and second rows each contained five sites, counting from the metatarsals toward the toenails. Also, each hindpaw had two ossification sites in the lower ankle or heel. Thus, the total number of ossification sites in the forepaws and hindpaws, excluding the toenails, was 56.

However, due to the lateness of the ossification of the paws in gestation and minor variations in the exact time of conception, the third set of ossification sites nearest the toes was often missing, even in the fetuses of untreated mice. Therefore, eliminating the latter set of sites from the overall count of ossification sites in the four paws left 40 sites present in normally developing fetuses at Day 18 of gestation. Thus, any fetus having 40 or more ossification sites in its four paws, excluding the toenails, was considered to have normal ossification of the paws; any fetus having less was considered to have delayed ossification of the paws.

On this basis, there was a significant increase in the litter incidence of delayed ossification of the paws in all treated groups of gravid mice except the group treated with 100 mg of codeine sulfate/kg on Day 12 of gestation (Table V). The fetal incidence of this defect was significantly

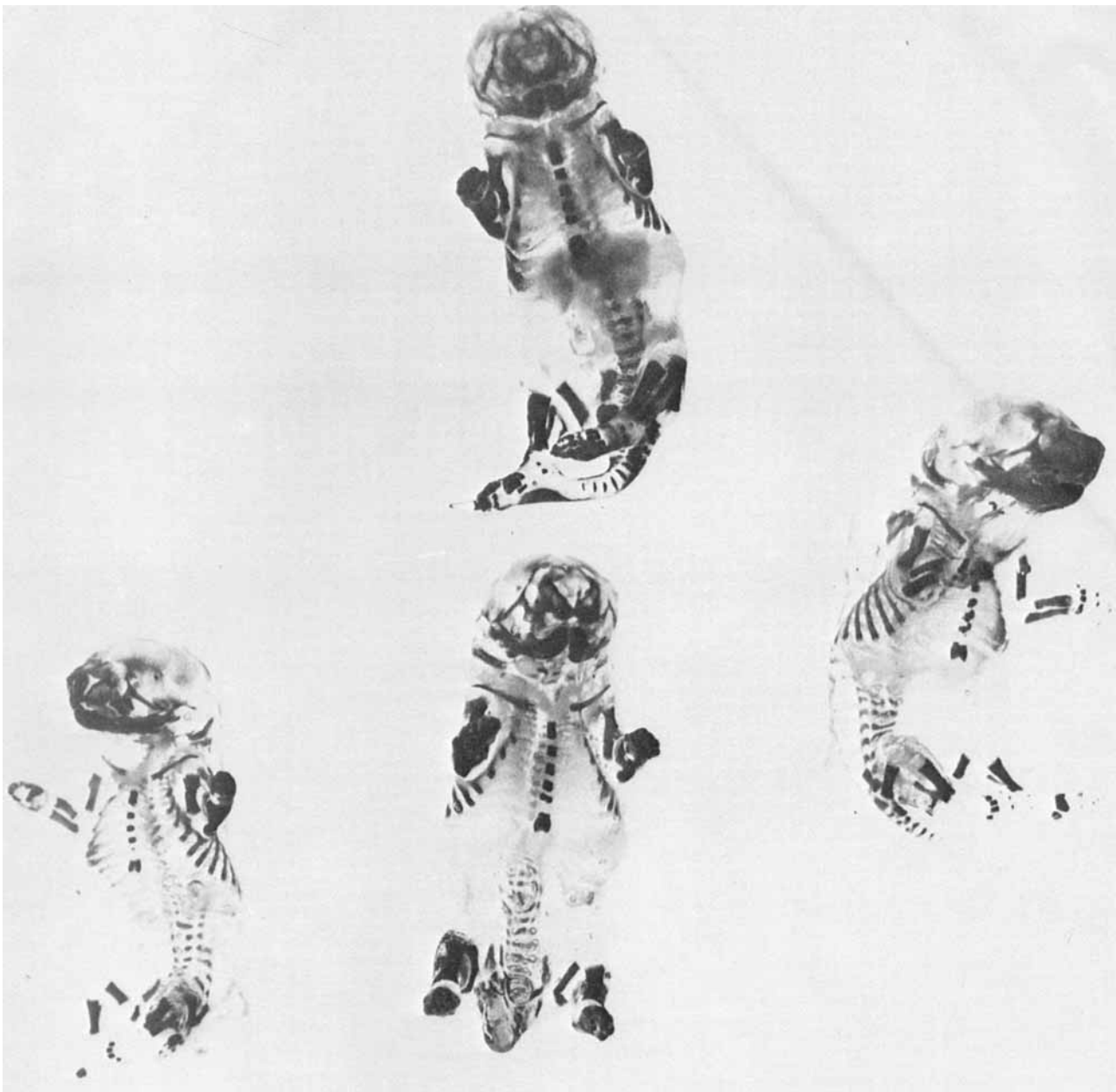

Figure 2—*Alizarin red S stained skeletal specimens of 18-day-old mouse fetuses, showing normal and abnormal sternebrae and xiphoids. Top: fetus of untreated control mouse, showing normal sternebrae and xiphoid. Bottom (left to right): fetuses of mice treated with 100 mg of codeine sulfate/kg on both Days 8 and 9 of gestation, showing delayed ossification of the sternebrae and split xiphoid, misaligned fifth sternebra, slightly delayed ossification of the xiphoid (note butterfly shape), checkerboard sternebrae, and split xiphoid.*

higher than the control group in all treated groups. The least-significant increase occurred in the group treated with a single dose of codeine on Day 12 of gestation, and the most significant increase occurred in the group treated with codeine on both Days 8 and 9 of gestation (Table V). With a single dose of codeine on a specific day of gestation from Days 7 to 12, the most significant increases in the incidence of delayed ossification of the paws on both a litter and fetal basis occurred with treatment on Day 8, 9, or 10, suggesting that these are the days of gestation on which the fetus is most susceptible to this effect of codeine (Table V).

Similarly, the highest incidence of sternebrae defects on a fetal basis, as well as the most severe defects such as split or missing sternebrae, occurred with injection of 100 mg of codeine sulfate/kg on both Days 8 and 9 of gestation. Significant increases in the incidences of sternebrae defects occurred in all treated groups except the group treated on Day 12 of gestation (Table III). On a litter basis, significant increases in the incidence of sternebrae defects occurred in the groups treated with a single dose of codeine on Day 7, 9, 10, or 11 of gestation as well as in the group treated on both Days 8 and 9 of gestation (Table III). Thus, much like the defect of delayed ossification of the paws, the most critical days for the production of sternebrae defects by codeine sulfate appear to be centered around Days 8–10 of gestation.

Another defect showing the most significant increase in incidence on both a fetal and litter basis with treatment on both Days 8 and 9 of gestation with 100 mg of codeine sulfate/kg was delayed ossification of the supraoccipital bone (Table II). Moreover, the degree of delayed ossification of the supraoccipital bone varied throughout the affected groups but was most severe in the fetuses of gravid mice treated on both Days 8 and 9 of gestation, often resulting in a split or missing supraoccipital bone. However, the range of days of gestation on which the mouse fetus was susceptible to the production of this defect by codeine was slightly smaller than the ranges for sternebrae defects and delayed ossification of the paws (Tables III and V). On a fetal basis, significant increases in the incidence of delayed ossification of the supraoccipital bone occurred with treatment on Day 8, 9, 10, or 11 of gestation; on a litter basis, only treatment on either Day 9 or 10 caused a significant increase in the incidence of this defect (Table II). Thus, the most susceptible period of

Table V—Occurrence of Delayed Ossification of the Paws

Treatment[a]	Litters Absent	Litters Present	Normal Fetuses	Abnormal Fetuses
Control (untreated)	7	1	40	1
Codeine on Day 7	3	4[b]	27	10[b]
Codeine on Day 8	0	8[b]	17	23[b]
Codeine on Day 9	1	6[b]	17	18[b]
Codeine on Day 10	0	6[b]	23	19[b]
Codeine on Day 11	1	5[b]	17	10[b]
Codeine on Day 12	4	2	22	6[b]
Codeine on Days 8 and 9	0	5[b]	7	22[b]

[a] The dose of codeine was 100 mg/kg sc in all cases. [b] Significance is indicated in p values of 0.05 or less when compared to control.

gestation of the CF-1 mouse fetus to the effects of codeine sulfate in the production of delayed ossification of the supraoccipital bone centers around Days 9 and 10.

The least frequent of the defects that increased significantly in a treated group was delayed ossification of the xiphoid. The most significant increase in the incidence of this defect on a litter and fetal basis occurred with treatment on both Days 8 and 9 of gestation (Table IV). However, with a single 100-mg/kg dose of codeine sulfate on a single day of gestation from Days 7 through 12, the only day of treatment showing a significant increase in the incidence of delayed ossification of the xiphoid on either a litter or fetal basis was Day 9 of gestation (Table IV). Although treatment on Day 7, 8, 10, 11, or 12 of gestation did not significantly increase the incidence of delayed ossification of the xiphoid and, in fact, treatment on Day 8 caused no incidence of delayed ossification of the xiphoid, treatment on both Days 8 and 9 of gestation with 100 mg of codeine sulfate/kg more significantly increased the incidence of this defect than treatment on Day 9 alone (Table IV). Thus, this finding again suggests that there is an additive or cumulative effect of the drug in the tissues that accounts for the increase in the teratogenic response.

In conclusion, the effects of codeine sulfate on the development of the CF-1 mouse fetus parallel the effects of morphine sulfate with regard to mean fetal weight reduction and the production of skeletal defects such as delayed ossification of the supraoccipital bone, sternebrae, and paws. However, the gross soft tissue defects, such as exencephaly and cryptorchid testes, and the gross skeletal defects, such as vertebral and rib fusions, present in the fetuses of mice treated on Day 8 or 9 of gestation with morphine sulfate (1, 7, 8) were not present in the fetuses of codeine-treated mice.

The major defects caused by codeine sulfate appear to parallel closely the minor defects caused by morphine sulfate. Consequently, the effects of codeine sulfate on fetuses of CF-1 mice appear to be those of a weakened morphine, which is not unexpected since about 10% of a dose of codeine is metabolized to morphine (16). Therefore, although the toxicity of codeine in mice when injected subcutaneously is at least twice that of morphine (13), the teratogenic potential of codeine sulfate in pregnant mice apparently is much lower than that of morphine sulfate. On the other hand, considering the additive or cumulative effect of codeine in regard to the teratogenicity demonstrated in this study and the known potentiation of the teratogenic effects of morphine by antihistamines and anticholinergics (7, 8), one cannot rule out the possibility of an enhanced teratogenic response to codeine when given in combination with either or both of the latter types of agents during early pregnancy.

REFERENCES

(1) H. S. Harpel and R. F. Gautieri, *J. Pharm. Sci.*, **57**, 1590 (1968).

(2) M. Smithberg and M. N. Runner, *Am. J. Anat.*, **113**, 479 (1963).

(3) H. Kalter and J. Warkany, *Physiol. Rev.*, **39**, 69 (1959).

(4) H. Kalter and J. Warkany, *Am. J. Pathol.*, **38**, 1 (1961).

(5) J. G. Sinclair, *Tex. Rep. Biol. Med.*, **8**, 623 (1950).

(6) T. H. Ingalls and F. J. C. Curley, *N. Engl. J. Med.*, **257**, 1121 (1957).

(7) J. D. Iuliucci and R. F. Gautieri, *J. Pharm. Sci.*, **60**, 420 (1971).

(8) P. A. Arcuri and R. F. Gautieri, *ibid.*, **62**, 1626 (1973).

(9) J. G. Wilson and J. Warkany, "Teratology Principles and Techniques," University of Chicago Press, Chicago, Ill., 1965, p. 267.

(10) R. E. Staples and V. L. Schnell, *Stain Technol.*, **39**, 61 (1964).

(11) G. G. Simpson, A. Roe, and R. C. Lewontin, "Quantitative Zoology," Harcourt, Brace, New York, N.Y., 1960, pp. 176, 186.

(12) "Codeine and Certain Other Analgesics and Antitussives—A Review," Merck & Co., Rahway, N.J., 1970, p. 1.

(13) C. D. Barnes and L. G. Eltherington, "Drug Dosage in Laboratory Animals," University of California Press, Berkeley, Calif., 1965, pp. 72, 155.

(14) N. B. Eddy, *J. Pharmacol. Exp. Ther.*, **45**, 361 (1932)

(15) D. H. Burke and D. E. Mann, *J. Pharm. Sci.*, **63**, 452 (1974).

(16) E. L. Way and T. K. Adler, *Bull. WHO*, **26**, 51 (1962).

ACKNOWLEDGMENTS AND ADDRESSES

Received November 29, 1976, from the *Department of Pharmacology, School of Pharmacy, Temple University, Philadelphia, PA 19140.*

Accepted for publication March 16, 1977.

Abstracted from a thesis submitted by J. E. Zellers to Temple University in partial fulfillment of the Master of Science degree requirements.

[x] To whom inquiries should be directed.

GLC Determination of Urinary Chlorthalidone Levels

HERSCHEL LI [x], MARTHA M. JOHNSTON, and DANIEL MUFSON

Abstract □ A sensitive and specific GLC method for the determination of urinary chlorthalidone levels was developed using on-column methylation. Chlorthalidone is converted to a tetramethylated derivative with trimethylanilinium hydroxide in methanol. This method, which permits the determination of as little as 0.1 μg of chlorthalidone/ml of dog urine, should be adequate for use with human subjects receiving a clinical dose.

Keyphrases □ Chlorthalidone—GLC analysis in urine □ GLC—analysis, chlorthalidone in urine □ Diuretics—chlorthalidone, GLC analysis in urine

Chlorthalidone[1] (I), 2-chloro-5-(1-hydroxy-3-oxo-1-isoindolinyl)benzenesulfonamide, is an oral diuretic agent for the treatment of edema and hypertension. The need to study the pharmacokinetics and bioequivalence of chlorthalidone formulations led to the development of two analytical methods: an enzymatic method based on the inhibition of carbonic anhydrase[2] and a GLC method, which is described in this paper.

One method (1) that used ^{14}C-chlorthalidone was not specific for chlorthalidone since the total radioactivity of the unchanged drug and the metabolites was measured. A spectrophotometric method was reported, based on the conversion of chlorthalidone to 2-(3′-sulfonamido-4′-chlorobenzoyl)benzoic acid (2, 3). This method also was not sufficiently specific or sensitive to determine chlorthalidone levels after a clinical dose.

GLC has been used widely in the quantification of substances isolated from biological materials when both sensitivity and specificity are required. However, underivatized chlorthalidone is not suitable for GLC because of polar active groups. In one GLC method (4), a suitable tetramethylated derivative of chlorthalidone was prepared successfully by extractive alkylation. However, the key reagent for the preparation, tetrahexylammonium hydrogen sulfate, is not commercially available. Attempts in this laboratory to use other quaternary ammonium reagents such as tetrabutylammonium hydroxide and tetrahexylammonium benzoate resulted in a low yield of the derivative. Other approaches to chlorthalidone derivatization such as silylation and acetylation also were explored but were not feasible.

Suitable methylated derivatives of barbiturates, phenolic alkaloids, and xanthine bases were prepared by on-column methylation (5). The procedure was simple and gave quantitative yields. This report describes the application of this technique to chlorthalidone analysis. On-column methylation of chlorthalidone under optimized conditions produced only one derivative peak as compared to the chromatogram obtained by injecting the methylating agent alone. This method is sensitive enough to detect 0.1 μg of chlorthalidone/ml in urine. Based on the reported (3) urinary chlorthalidone concentrations, the present method should be adequate for the determination of urinary chlorthalidone from human subjects after a 100-mg oral dose.

EXPERIMENTAL

Apparatus—A gas chromatograph[3] equipped with a flame-ionization detector was used. A 1.8-m × 0.63-cm i.d. glass column was packed with 3% JXR on 100–120-mesh Gas Chrom Q[4]. The injector and manifold were set at 300°. The column temperature was 190° initially and was programmed at 4°/min to 260°. For some experiments, an isothermal mode at 260° also was employed. The carrier gas was helium with a flow rate of 40 ml/min.

Reagents—Trimethylanilinium hydroxide[5] (0.2 *M*) in methanol was used as a methylating agent. Stock solutions of the following compounds[6] were made in acetone[7]: chlorthalidone, isopropyl 2-(3′-sulfonamido-4′-chlorobenzoyl)benzoate (II), 2-hydroxymethylphenyl-3′-sulfonamido-4′-chlorophenylcarbinol (III), and 3-isobutyloxy-3-(3′-sulfonamido-4′-chlorophenyl)phthalimidine (IV).

Procedure—A series of control human urine samples (5.0 ml) in 15-ml polytef-lined screw-capped tubes was spiked with 5, 10, 20, 30, 40, or 50 μl of chlorthalidone stock solution (1.03 μg/10 μl in acetone). These samples were used to generate a standard curve from which the chlorthalidone concentrations in unknown samples were calculated. Aliquots (5.0 ml) of the unknown urine samples were pipetted into similar tubes. Excess sodium bicarbonate was added to each tube, and saturation was obtained by vortexing. Five milliliters of ether[7] with 30 μl of *n*-docosane[4] (40 ng/μl in chloroform[7]) as an internal standard was added.

The samples were extracted for 10 min in a horizontal shaker[8]. After centrifugation at 5°, the ether phase was transferred to a conical tube. The extraction was repeated similarly for a second time with the omission of the internal standard, and the pooled ether phase was then evaporated to dryness by a gentle nitrogen stream. The residue was redissolved in 50 μl of 0.2 *M* trimethylanilinium hydroxide in methanol by vigorous vortexing. An aliquot (2.0 μl) was then injected into the gas chromatograph.

RESULTS AND DISCUSSION

Injector Temperature and Injector Geometry—The function of the injector was to act as a flash vaporizer and a reaction chamber. Initial studies showed that its effectiveness depended on the appropriate injector temperature and the integrity of the injector geometry. At an injector temperature of 250°, no methylated chlorthalidone peak was observed. However, at 300°, methylation took place instantaneously. A further increase in the injector temperature to 350° did not affect the reaction.

Experience in this laboratory also indicated that the injector geometry of some gas chromatographs gave more dependable results for the direct methylation of chlorthalidone. With a gas chromatograph[3] equipped with a removable glass injector liner in a heated injector assembly, reproducible derivatization was observed. However, with a different gas chromatograph[9] that employed an extension of the glass column proper as the injector instead of a removable glass injector liner, care had to be exercised to exclude any column packing materials in the heated zone of the injector. This precaution was critical for reproducible chlorthalidone derivatization.

Molar Ratio—Studies on the extent of chlorthalidone methylation showed that the products were dependent upon the methylating agent concentration (Table I). When the molar ratio of chlorthalidone to

[1] Hygroton, USV Pharmaceutical Corp., Tuckahoe, N.Y.

[2] Paper presented at the APhA Academy of Pharmaceutical Sciences, Atlanta meeting, November 1975.

[3] Model 900, Perkin-Elmer Corp., Norwalk, Conn.

[4] Applied Science Laboratories, State College, Pa.

[5] Pierce Chemical Co., Rockford, Ill.

[6] The Pilot Plant and Analytical Research & Development Department, USV Pharmaceutical Corp., Tuckahoe, N.Y.

[7] Mallinckrodt Chemical Works, St. Louis, Mo.

[8] Eberbach Corp., Ann Arbor, Mich.

[9] Model MT-550, Tracor Inc., Austin, Tex.

Table I—Qualitative Relationships between Molar Ratio of Chlorthalidone to Trimethylanilinium Hydroxide and Methylation of Chlorthalidone

Molar Ratio	Peak A (15.3 min)	Peak B (15.4–15.6 min)	Peak C (16.7–16.9 min)	Peak D (17.7 min)
1:20 or above	Very large	—	—	—
1:10	Large	Small	—	—
1:4	Medium	Small	Small	—
Chlorthalidone in excess[a]	—	Very small	Small	Large

[a] A saturated solution of chlorthalidone in 0.2 *M* trimethylanilinium hydroxide in methanol.

methylating agent was 1:20, one peak at the retention time of 15.3 min (*i.e.*, peak A) was observed. Further increases of the molar ratio did not cause any change. However, when the molar ratio was reduced stepwise, two or three additional peaks with tailing at higher retention times (*i.e.*, peaks B, C, and D) were observed. In the absence of the methylating agent, no derivative peak was observed.

The shorter retention time of peak A indicates that peak A has a higher degree of methylation than peaks B, C, and D. Furthermore, the absence of tailing in peak A as compared to the progressive severity of tailing in peaks B, C, and D suggests the total conversion of the active hydrogen atoms to methyl groups. Therefore, these results indicate that the derivative is tetramethylated chlorthalidone.

GLC–Mass Spectrometry—Further structure elucidation of the postulated tetramethylated chlorthalidone was studied by GLC–mass spectrometry[10]. The optimized derivatization conditions and GLC conditions described were employed. The single derivative peak obtained was examined by electron-ionization and chemical-ionization mass spectrometry.

The molecular weight of tetramethylated chlorthalidone ($C_{18}H_{19}ClN_2O_4S$) is 394. With electron ionization, the expected molecular ion, M^+, was not observed at *m/e* 394, probably due to its low intensity. However, when chemical ionization with isobutane as the reactant gas was employed, an intense quasimolecular ion at *m/e* 395 and the corresponding chlorine isotope ion at 397 were observed. The intensity of these two peaks bore a ratio of 3:1, in accordance with the characteristic abundance of ^{35}Cl to ^{37}Cl.

The electron-ionization spectrum also showed strong fragment ions at *m/e* 363 and 365 with an intensity ratio of 3:1. These ions were probably formed by the loss of a methoxy radical. Furthermore, a similar doublet of the same intensity ratio at *m/e* 287 and 289 was observed. These peaks were probably due to the loss of a dimethylsulfonamide group. Based on these studies, the structure of the derivative formed by on-column methylation was assigned as 2-chloro-5-(2-methyl-1-methoxy-3-oxo-isoindolinyl)benzene-*N,N*-dimethylsulfonamide.

Standard Curves—With the temperature program mode as specified under *Apparatus*, the retention time and temperature of the *n*-docosane peak were 5.3 min and 211°; for the tetramethylated chlorthalidone peak, they were 15.3 min and 251°. The relative retention time of the tetramethylated chlorthalidone peak with respect to the *n*-docosane peak was, therefore, 2.9. Extracts of control urine samples from eight human subjects gave no interference with either the tetramethylated chlorthalidone or *n*-docosane peak.

The composite standard curves for the extracted and unextracted chlorthalidone for the range of 0.5–5 μg/5 ml of urine were obtained from two experiments. The values for chlorthalidone-spiked urine after extraction were compared with a similar series of unextracted reference standard solutions of chlorthalidone. The standard curves of the relative peak areas *versus* concentrations in micrograms per 5 ml of urine were determined by regression analysis. The equation for the extracted chlorthalidone was ($n_1 = 23$, $r_1 = 0.9740$) $y_1 = 0.0521 + 0.2040x_1$; that for the reference standard of chlorthalidone was ($n_2 = 9$, $r_2 = 0.9869$) $y_2 = 0.0271 + 0.2040x_2$. The standard curves for both the extracted and unextracted chlorthalidone were linear, as reflected by the values of the correlation coefficient.

Internal Standard—An ideal internal standard for GLC has similar chromatographic properties to the compound under investigation and can be quantitatively extracted under identical conditions from biological samples. Such an internal standard can be added to biological samples at the initial step of the procedure and is then subjected to the same extraction, derivatization, and chromatographic conditions as the compound of interest.

Initial testing for a suitable internal standard was carried out with chlorthalidone analogs. Among these, II and III showed both desirable retention times with reference to chlorthalidone and linear relative area–concentration relationships. However, these compounds were not quantitatively coextracted with chlorthalidone under the specified conditions. For this reason, *n*-docosane was used as an internal standard for the initial study.

Subsequent studies revealed that IV was a suitable internal standard and satisfied the aforementioned criteria. To establish the recovery after solvent extraction and the linearity of the standard curves using IV as an internal standard, a series of control human urine samples was spiked with different concentrations of IV and chlorthalidone. The concentration ratio between IV and chlorthalidone was 1.5. Extraction and sample analysis were performed as described under *Procedure*. For comparison, a similar series of unextracted reference standard solutions of chlorthalidone and IV also was determined.

The GLC analysis was performed on a similar model gas chromatograph[9] with a glass column (1.8 m × 0.63 cm i.d.) of 3% SP-2100 on 100–120-mesh Supelcoport[11]. At a column temperature of 260°, the retention times for the methylated chlorthalidone and IV were 4.8 and 6.3 min, respectively (Fig. 1). With the temperature programmed at 5°/min from 190 to 260°, the baseline disturbance was minimized and, therefore, was more suitable for the determination of low concentration samples.

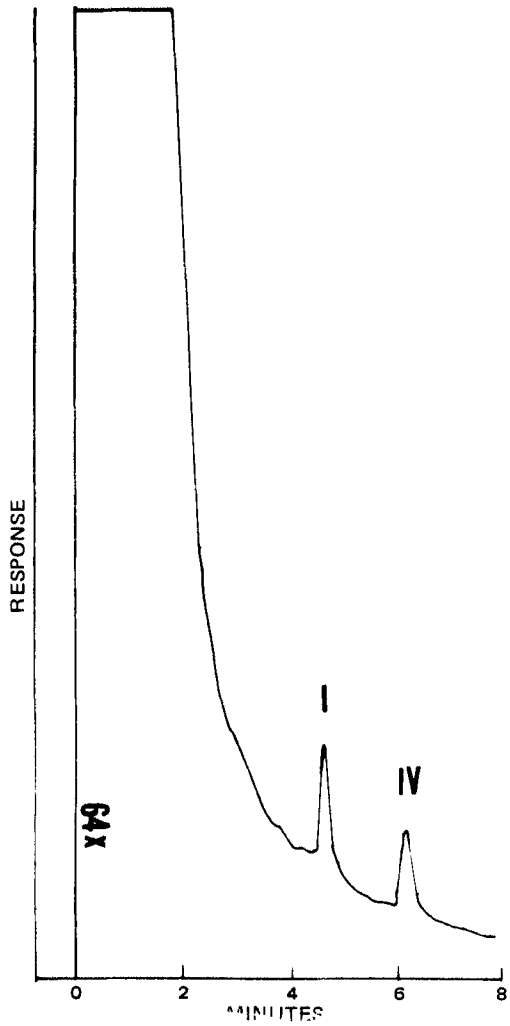

Figure 1—*Gas chromatogram showing the separation of chlorthalidone (I) and IV after on-column methylation. Compounds I and IV were coextracted after a control human urine sample was spiked with the compounds.*

[10] DuPont 492 gas chromatograph–mass spectrometer interfaced to an A.E.I. data processing system.

[11] Supelco Inc., Bellefonte, Pa.

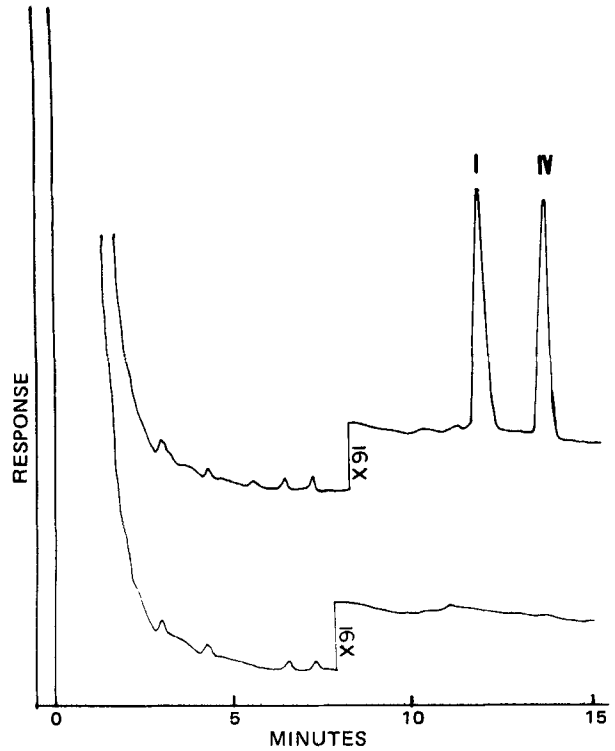

Figure 2—*Gas chromatogram from an extract of a control human urine sample spiked with I and IV. The peaks represent 67 ng of I and 100 ng of IV (upper tracing). The chromatogram of the corresponding blank urine extract is shown in the lower tracing.*

The retention times of the methylated chlorthalidone and IV were 12 and 13.8 min, respectively. The upper tracing in Fig. 2 was obtained from an extract of a control human urine sample spiked with the drug and the internal standard. The lower tracing represents the extract of the same urine sample without spiking and shows no interfering peaks with either chlorthalidone or IV.

With the temperature program mode, the regression equation for the unextracted samples ($n = 16, r = 0.9922$) was $y_3 = 0.1245 + 1.3440x_3$; that for the unextracted samples ($n = 16, r = 0.9927$) was $y_4 = 0.0993 + 1.2931x_4$. These results demonstrated good agreement and linearity of the standard curves for the extracted and unextracted chlorthalidone when IV was used as an internal standard.

The recovery of chlorthalidone from urine by solvent extraction is shown in Table II. As compared to a similar series of unextracted reference standards of chlorthalidone samples, the average recovery was 96% for the range of 0.6–5.8 μg/5 ml of urine. Therefore, these results showed that IV was coextracted with chlorthalidone under the same conditions and demonstrated similar reactivity in the derivatization and chromatographic conditions. For these reasons, IV can be added to the urine samples as an internal standard at the initial step of the procedure and is recommended for use in future studies.

Determination of Chlorthalidone in Dog Urine Samples—The suitability of this method for the determination of urinary chlorthalidone was tested with urine from a male 18-kg mongrel dog. A 200-mg oral dose of chlorthalidone dissolved in 2 ml of polyethylene glycol 200 was given to the dog, and the urine was collected in a metabolic cage. The results (Table III) indicated rather rapid chlorthalidone excretion; 62% of the administered dose was found in the urine after 30 hr.

Conclusions—The present procedure is simple to use as compared to the extractive alkylation employed by Ervik and Gustavii (4). Furthermore, the feasibility of using an electron-capture detector in conjunction with on-column methylation was demonstrated by VandenHeuvel *et al.* (6) in the determination of hydrochlorothiazide. Since the same derivative of chlorthalidone was formed in both the extractive alkylation and the on-column methylation, the use of an electron-capture detector would increase the sensitivity limit of the present method.

Table II—Coextraction of Chlorthalidone and IV (Internal Standard) from Urine as Compared to the Unextracted Reference Standards

Chlorthalidone Concentration, μg/5 ml of Urine	Corrected Relative Area[a]		Recovery, %
	Unextracted	Extracted	
5.82	7.693 ± 0.002	7.542 ± 0.147	98
4.99	7.010 ± 0.383	6.432 ± 0.397	92
4.16	5.489 ± 0.017	5.529 ± 0.390	101
3.33	4.959 ± 0.195	4.560 ± 0.204	92
2.50	3.576 ± 0.331	3.453 ± 0.286	97
1.66	2.501 ± 0.158	2.406 ± 0.006	96
0.83	1.226 ± 0.014	1.192 ± 0.030	97
0.62	0.660 ± 0.009	0.614 ± 0.045	93

[a] Corrected relative area = (peak area of chlorthalidone/peak area of IV) × μg of IV. Each value represents the mean of duplicate determinations.

Table III—Urinary Excretion of Chlorthalidone from a Dog[a]

Sample, hr	Chlorthalidone Excretion, mg	Cumulative Excretion, % of Dose	Excretion Rate, mg/hr
4	48	24	12
6	31	40	15.5
23.5	37	58	2.1
30	7	62	1.1

[a] Oral dose: 200 mg of chlorthalidone dissolved in 2 ml of polyethylene glycol 200.

REFERENCES

(1) G. Beizenherz, F. W. Koss, L. Klatt, and B. Binder, *Arch. Int. Pharmacodyn. Ther.*, **161**, 76 (1966).

(2) R. Pulver, H. Wirz, and E. G. Stenger, *Schweiz. Med. Wochenschr.*, **89**, 1130 (1959).

(3) M. G. Tweeddale and R. I. Ogilvie, *J. Pharm. Sci.*, **63**, 1065 (1974).

(4) M. Ervik and K. Gustavii, *Anal. Chem.*, **46**, 39 (1974).

(5) E. Brochmann-Hanssen and T. O. Oke, *J. Pharm. Sci.*, **58**, 370 (1969).

(6) W. J. A. VandenHeuvel, V. F. Gruber, R. W. Walker, and F. J. Wolf, *ibid.*, **64**, 1309 (1975).

ACKNOWLEDGMENTS AND ADDRESSES

Received December 23, 1976, from the *Department of Biochemistry and Drug Disposition, USV Pharmaceutical Corp., Tuckahoe, NY 10707.*

Accepted for publication March 9, 1977.

Presented in part at the 10th Middle Atlantic Regional Meeting, American Chemical Society, February 1976.

The authors thank the Mass Spectrometry Center, Rockefeller University, for the GLC–mass spectral analysis. The spectrometric analysis was supported in part by Grant RR00862, Division of Research Resources, National Institutes of Health. The authors also thank Dr. M. J. O'Hare of the Analytical Research and Development Department, USV Pharmaceutical Corp., for assistance in the interpretation of the GLC–mass spectral data.

[x] To whom inquiries should be directed.

Chlorthalidone Analysis Using Carbonic Anhydrase Inhibition

MARTHA M. JOHNSTON ˣ, HERSCHEL LI, and DANIEL MUFSON

Abstract □ Chlorthalidone was analyzed in the concentration range of 0.1–3.0 μg/ml with a precision of ±0.05 μg/ml. Chlorthalidone inhibition of the enzymatic hydrolysis rate of *p*-nitrophenyl acetate by bovine erythrocyte carbonic anhydrase was used as a basis for the determination. The amount of *p*-nitrophenol formed was measured by monitoring the absorbance at 400 nm, and its formation rate was proportional to the chlorthalidone concentration. The mixing of the enzyme, substrate, and sample, the incubation of the reaction mixture, and the recording of the absorbance were automated. A survey of urine samples from 26 normal human subjects did not reveal any endogenous substances that interfered with the assay. Analyses of urine samples from six subjects after oral administration of 100 mg of chlorthalidone indicated rapid absorption and a biphasic elimination. The α-phase half-life was 1.5 hr, and the β-phase half-life was 35 hr.

Keyphrases □ Chlorthalidone—spectrophotometric analysis based on inhibition of carbonic anhydrase, urine □ Spectrophotometry—analysis, chlorthalidone, based on inhibition of carbonic anhydrase, urine □ Carbonic anhydrase—inhibition by chlorthalidone, spectrophotometric analysis, urine □ Diuretics—chlorthalidone, spectrophotometric analysis based on inhibition of carbonic anhydrase, urine □ Enzymes—carbonic anhydrase, inhibition by chlorthalidone, spectrophotometric analysis, urine

Two methods were reported for chlorthalidone analysis in biological fluids. One method involved the conversion of chlorthalidone to 2-(3′-sulfonamido-4′-chlorobenzoyl)benzoic acid and the measurement of the resulting change in UV absorption (1); the other method used GLC (2). The UV spectrophotometric method was not sensitive enough to detect the chlorthalidone levels in urine after a therapeutic dose of 50 or 100 mg, and the GLC method could not be reproduced since one reagent was not available commercially. Because of these difficulties, an alternative method of analysis was needed. Developmental work yielded two methods concurrently: one method was a GLC analysis utilizing on-column methylation (3), and the second was the enzymatic method described in this report.

Chlorthalidone inhibits carbonic anhydrase (EC 4.2.1.1) by decreasing the production rate of the product from the substrate by the catalytic action of the enzyme (4). Since the decrease in the catalytic rate is proportional to the chlorthalidone concentration, measurement of this decrease can be used to determine the chlorthalidone level in unknown samples. This principle was utilized previously for the assay of acetazolamide (5, 6) and furosemide (7). Carbonic anhydrase catalyzes the hydration of carbon dioxide, and the activity of the enzyme toward the physiological substrate, carbon dioxide, is usually measured by determining the rate of increase that the enzyme causes in pH during bubbling of carbon dioxide through a slightly alkaline buffer (5).

However, the enzyme also has estrolytic activity toward nonphysiological substrates (8). One substrate, *p*-nitrophenyl acetate, is hydrolyzed to *p*-nitrophenol; the hydrolysis rate is proportional to the change in absorbance at 400 nm. With this substrate, an automated analysis was developed for solutions containing 0.1–3.0 μg of chlorthalidone/ml.

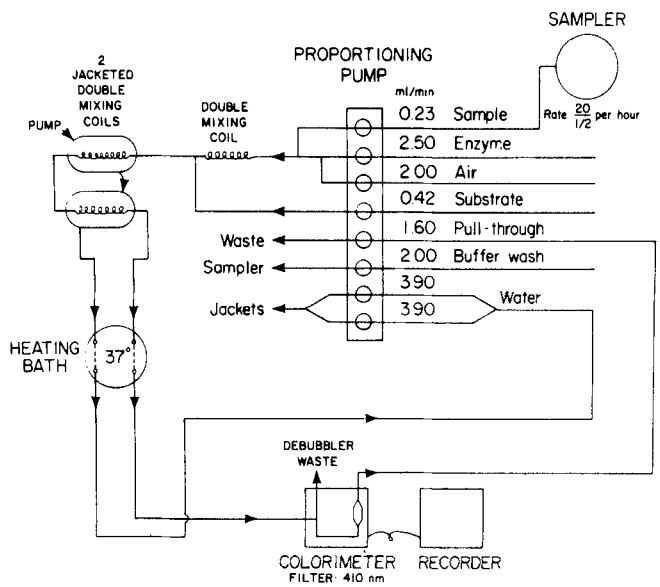

Figure 1—*Diagram of automated analysis system. For the substrate line, a silicone pump tube connected to polyethylene tubing was used. All other pump tubes and other tubing were polyvinyl chloride. Either 400- or 410-nm filters may be used for the colorimeter.*

The drug in urine can be analyzed by this method either directly or after chlorthalidone has been extracted selectively. The direct assay yields only an estimate of chlorthalidone since it is influenced by the yellow pigments in the urine and the urine pH. However, an estimate is useful, particularly for samples with a high chlorthalidone concentration, so that the the urine can be diluted appropriately before the extraction.

Scheme I shows a flowchart for the analysis of chlorthalidone in urine samples. First, the sample is assayed directly; then it is diluted and reassayed until the inhibition is less than that caused by 2 μg of chlorthalidone/ml. With the use of this information, the urine sample is diluted, extracted, and assayed. The methods for the direct assay, the extraction, and the assay of the extracts are described here.

EXPERIMENTAL

Reagents for Automated Analysis System[1]—The buffer was 0.1 *M* tromethamine[2], pH 7.5, plus 0.1% surfactant[3]. The enzyme solution contained 30 mg of bovine erythrocyte carbonic anhydrase[4]/liter of buffer. The substrate solution contained 1.0 m*M* *p*-nitrophenyl acetate[5] in polyethylene glycol 400[6].

[1] AutoAnalyzer I, Technicon Industrial Systems, Tarrytown, N.Y.
[2] Nutritional Biochemical Corp., Cleveland, Ohio.
[3] Triton X-405, Rohm and Haas Co., Philadelphia, Pa.
[4] Sigma Chemical Co., St. Louis, Mo.
[5] Schwarz/Mann, Orangeberg, N.Y.
[6] J. T. Baker Chemical Co., Phillipsburg, N.J.

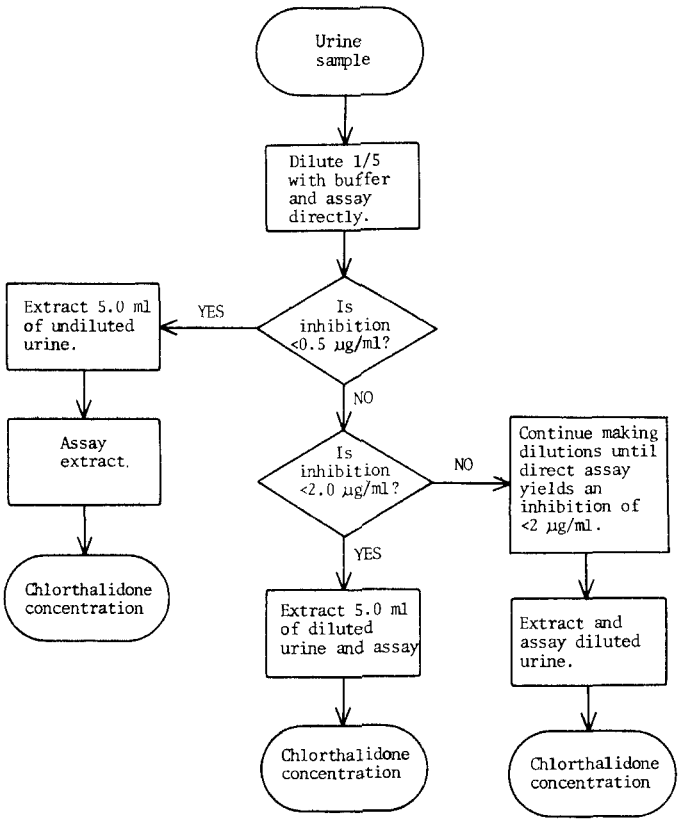

Scheme I

Chlorthalidone Standards—To prepare a stock solution, 10 mg of chlorthalidone[7] was dissolved in 10 ml of dioxane[8] and diluted to 100 ml with 0.1 *M* tromethamine, pH 7.5. For the direct assay method, chlorthalidone standards of 0.5, 1.0, 2.0, 3.0, and 4.0 μg/ml were made by dilution of the stock solution with buffer. For the assay of extracted urine samples, chlorthalidone standards were prepared by adding 2.5, 5.0, 7.5, 10.0, 12.5, 15.0, and 20.0 μg of chlorthalidone to 4.0-ml aliquots of normal human urine. Sufficient water was added to bring the sample volumes to 5.0 ml. These standards were extracted with the unknown urine samples.

Automated Procedure—Figure 1 is a diagram of the automated analysis system. The colorimeter was calibrated by adjusting the absorbance to zero, with buffer being pumped through the enzyme and sample lines and substrate being pumped through the substrate line. This baseline corrected for the nonenzymatic hydrolysis of the substrate during the reaction. The enzyme pump line was then switched from the buffer solution to the enzyme solution, which caused the increase in absorbance, A_0, shown in Fig. 2. This increase represents the uninhibited enzymatic velocity. Five minutes later, the samples were introduced, and the degree of inhibition of carbonic anhydrase by chlorthalidone was reflected by the reduction in absorbance, ΔA.

Standards were reassayed repeatedly during the automated procedure, with no more than 15 unknowns between each set of standards. The chlorthalidone concentrations of each set of unknowns were calculated by using a standard curve of ΔA *versus* chlorthalidone concentration values from the sets of standards run immediately before and after the unknowns.

Direct Assay Procedure—The urine samples were diluted 1:5 with buffer, as indicated in Scheme I, and assayed automatically. To correct for the effect of the yellow urine pigments, the samples were run through the automated system using buffer instead of enzyme. The differences in absorbance caused by the urine samples were subtracted from the ΔA values obtained when the enzyme was introduced. The chlorthalidone concentration was calculated from this corrected ΔA value. Unextracted chlorthalidone standards were used for the standard curve.

Extraction Procedure—The results of the direct assay were used to estimate the amount of dilution necessary to bring the chlorthalidone concentration of the sample to between 1.0 and 2.0 μg/ml. The urine dilutions were made with water, and 5.0 ml of the diluted sample was placed in a polytef-lined screw-capped culture tube. Sodium bicarbonate (0.6–1.0 g) was added to saturate each sample, 5.0 ml of anhydrous ether[8] also was added, and the tubes were shaken for 10 min at 140 oscillations/min and centrifuged for 5 min at 500×*g* and 5° to separate the phases. Then the ethereal layer was transferred to conical sample cups[9].

A second portion of 5.0 ml of ether was added to the aqueous phase, the extraction was repeated, and the second ether extract was added to the first. The samples were dried under nitrogen at 40°, and the residues were dissolved in 0.5 ml of polyethylene glycol 400. The samples were diluted with 4.5 ml of buffer and assayed.

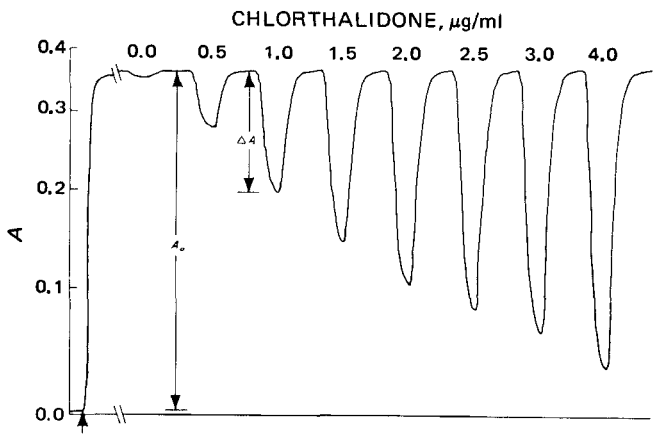

Figure 2—*Typical recording obtained using chlorthalidone standards extracted from urine. The initial portion of the tracing shows the baseline obtained when only substrate and buffer were pumped through the system. The arrow indicates the addition of enzyme, and* A_0 *represents the velocity of the uninhibited enzymatic reaction. The inhibition of the enzyme by the samples caused the decreases in absorbance,* ΔA. *The samples were prepared by adding chlorthalidone to normal human urine and extracting as described in the text.*

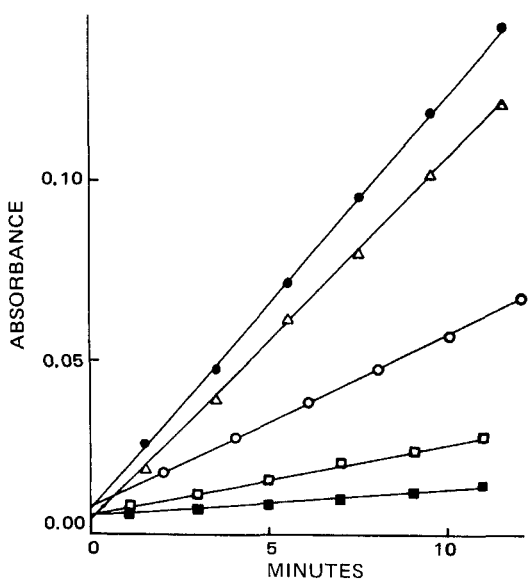

Figure 3—*Inhibition of carbonic anhydrase by chlorthalidone. The reaction mixtures contained 0.09 mg of carbonic anhydrase and 1.0 μg (□), 0.5 μg (○), 0.1 μg (△), or no (●) chlorthalidone in 2.7 ml of 0.05* M *tromethamine, pH 7.5. The reaction was started at zero time by adding the substrate, 0.3 ml of 1.0 m*M *p-nitrophenyl acetate in acetonitrile. The absorbance was measured at 400 nm at the times indicated. The rate of nonenzymatic hydrolysis of* p*-nitrophenyl acetate was measured in an acetonitrile–tromethamine control (■).*

[7] USV Pharmaceutical Corp., Tuckahoe, N.Y.
[8] Mallinckrodt, St. Louis, Mo.
[9] Brinkmann Instruments, Westbury, N.Y.

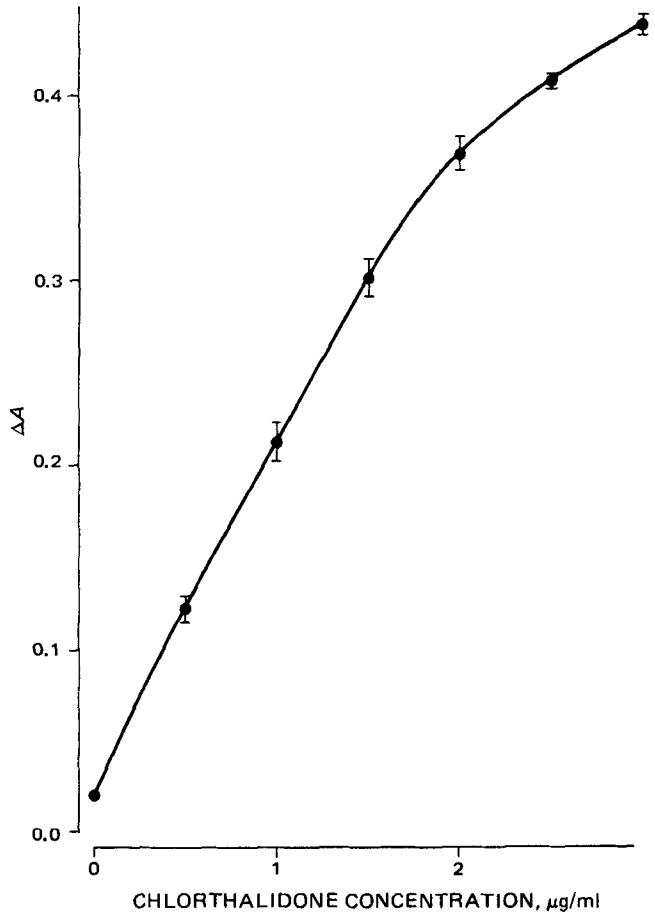

Figure 4—*Typical standard curve for chlorthalidone extracted from urine. Standards of chlorthalidone in normal human urine were prepared, and three or four samples of each standard were extracted and analyzed. The error bars represent the standard error of the* ΔA *values obtained at each concentration.*

RESULTS

Initial Development—The feasibility of the assay was first determined using a spectrophotometer[10] to measure the absorbance changes. Figure 3 shows the rate of enzymatic hydrolysis, the rate of nonenzymatic hydrolysis, the slight inhibition by 0.03 μg of chlorthalidone/ml, and the nearly complete inhibition by 0.33 μg of chlorthalidone/ml. The small variations in the y-intercepts were due to variations in the elapsed time for the manual addition and mixing of the substrate before the initial absorbance reading was made. However, the slope, which is proportional to the enzymatic velocity, was constant for repetitive samples. The amount of product formed in 12 min by enzymatic hydrolysis was 10% of the available substrate.

Since some inhibitors of carbonic anhydrase cause a time-dependent inhibition (9), chlorthalidone was preincubated with the enzyme for various time intervals before substrate addition. The percent of inhibition did not depend on the preincubation time for intervals between 1 and 120 min.

Assay Automation—Figure 1 is a diagram of the manifold designed for the assay. The transit time of the first mixing coil was greater than 1 min, eliminating any possible effect due to time dependency of the chlorthalidone–enzyme interaction. Acetonitrile, used as a solvent for p-nitrophenyl acetate in the manual procedure, was changed to polyethylene glycol 400 to avoid degradation of the tubing.

Figure 2 is a typical recording of the chlorthalidone standards extracted from urine. The small ΔA value obtained with the urine without chlorthalidone was due to the polyethylene glycol 400 used to reconstitute the sample. The system was sensitive to small changes in chlorthalidone concentration between 0.5 and 3.0 μg/ml, indicating the useful range of the automated system. Above 3.0 μg/ml, there was little change in the amount of inhibition as the drug concentration was increased. Thus, samples with a high drug concentration were diluted before analysis. Some batches of the commercial carbonic anhydrase exhibited different sensitivities to chlorthalidone inhibition than the batch used for the data in Fig. 2. This variation in sensitivity may have been due to the purity of the enzyme preparation.

To test the variability of the automated analysis system, solutions containing 1.0–4.0 μg of chlorthalidone/ml in buffer were assayed six times each, and ΔA was calculated. The standard deviation at each chlorthalidone concentration was ±0.003.

Sensitivity of Direct Assay—Control urine samples from 26 normal human males were diluted fivefold with buffer and assayed directly. For 25 subjects, the range of apparent chlorthalidone values was from −0.03 to +0.57 μg/ml. The value of the 26th subject was 7.8 μg/ml. Additional control samples taken at a later time from the same subjects were also assayed. The apparent chlorthalidone values ranged from −0.08 to +0.71 μg/ml. The value of the sample from the 26th subject was zero.

Some samples were assayed after diluting 10-fold with buffer, and the apparent chlorthalidone values were the same as those obtained with a fivefold dilution, indicating that the positive values were not due to the buffering capacity of the urine. The positive values are possibly due to inhibition of the carbonic anhydrase by anions, a phenomenon reported previously (8).

Sensitivity of Assay after Extraction—The urine samples from the 26 normal subjects that were assayed directly were also assayed after extraction. The range of the apparent chlorthalidone values after extraction was from −0.07 to +0.09 μg/ml, indicating that the sensitivity limit of the assay was approximately 0.1 μg/ml.

Standard Curve—Figure 4 shows a standard curve obtained after the extraction of normal human urine spiked with known amounts of chlorthalidone. The variation in the ΔA values indicates that chlorthalidone concentrations can be determined with a precision of ±0.05 μg/ml. The curvature in the standard curve at the higher chlorthalidone concentrations could be reduced by plotting log $(A_0/A_0 - \Delta A)$ *versus* chlorthalidone concentration, but a reverse curvature became evident at the lower levels. If dilutions are made before extraction, as indicated in Scheme I, then the values of unknown samples should be <2 μg/ml and thus be in the most linear portion of the standard curve.

The slope of the standard curve varied slightly from day to day because of small variations in the concentration of the enzyme solution, which was made fresh daily. Use of a different batch of enzyme from the supplier would sometimes cause a change in the slope. The standard curve was not dependent on the composition of the aqueous phase from which the chlorthalidone was extracted since the extraction efficiency was the same for various normal urine samples and buffer. The data in Fig. 4 are a composite of standard chlorthalidone samples extracted from two different normal human urines.

Selectivity—Although these results indicate that endogenous urinary substances have little or no effect on the assay, particularly after extraction, other drugs that contain an unsubstituted aryl sulfonamide group do inhibit carbonic anhydrase (9). Aqueous solutions of several such drugs were tested in the automated analysis system, and the drug concentration necessary to cause the same inhibition as 1.0 μg of chlorthalidone/ml was determined. The results were (per milliliter) 0.5 μg of acetazolamide[4], 1.1 μg of benzthiazide[11], 3.5 μg of trichlormethiazide[12], 10 μg of sulfanilamide[4], 11 μg of hydrochlorothiazide[13], 12 μg of polythiazide[14], 14 μg of methyclothiazide[15], 18 μg of cyclothiazide[16], 36 μg of bendroflumethiazide[17], and 58 μg of hydroflumethiazide[18]. The substituted aryl sulfonamides, sulfisoxazole[4], sulfacetamide[4], and sulfadiazine[4], did not inhibit the carbonic anhydrase at concentrations up to 100 μg/ml.

Since the only urinary metabolite reported for chlorthalidone is an acid (10), it would not be extracted into the ether at pH 8.3 and would not affect the chlorthalidone assay.

Extraction Efficiency—The extraction efficiencies from normal human urine at various concentrations of chlorthalidone are shown in Table I. The trend toward lower efficiency at higher concentrations meant that samples had to be diluted into an assayable range before extraction to be compared accurately to the extracted standards. Thus, the process

[10] DU spectrophotometer, Beckman Instruments, Fullerton, Calif.

[11] A. H. Robins Co., Richmond, Va.
[12] Schering Corp., Kenilworth, N.J.
[13] Merck Sharp & Dohme, Rahway, N.J.
[14] Pfizer Inc., Brooklyn, N.Y.
[15] Abbott Laboratories, North Chicago, Ill.
[16] Eli Lilly and Co., Indianapolis, Ind.
[17] E. R. Squibb & Sons, Princeton, N.J.
[18] Bristol Laboratories, Syracuse, N.Y.

Table I—Extraction Efficiency for Chlorthalidone from Urine

Chlorthalidone Concentration, μg/ml	Recovery[a], %
0.5	99
1.0	88
1.5	89
2.0	89
2.5	84
3.0	83
4.0	84
10.0	74
50.0	42

[a] Average of duplicates.

for handling unknown samples shown in Scheme I was developed. The decrease in extraction efficiency may be due to the limited chlorthalidone solubility in ether, since increasing the number of ether extractions from two to four yielded a greater extraction efficiency.

Stability—There was no detectable loss of chlorthalidone from urine samples during 16 weeks of frozen storage. In addition, no substances were produced in the urine that interfered with the assay. After extraction and reconstitution, chlorthalidone samples were stable for 24 hr at room temperature or at least 3 weeks at −15°. The polystyrene sample cups used for the automated system were inert to the solution containing polyethylene glycol 400, which was used to reconstitute the extracted samples.

Human Urinary Excretion—Six male subjects each received a 100-mg chlorthalidone tablet, and urine samples were collected for 72 hr. Figure 5 shows the mean excretion rate *versus* time. The peak excretion rate occurred between 2 and 3 hr after drug administration, indicating rapid absorption. After absorption, the elimination was biexponential, indicating a pharmacokinetic model with a minimum of two compartments. The half-life values obtained by the method of residuals were 1.5 hr for the α-phase and 35 hr for the β-phase. Analysis of urine samples from a subject given orally 100 mg of chlorthalidone as a solution showed that the chlorthalidone concentration could be determined up to 11 days after drug administration.

DISCUSSION

The described method is sensitive enough to determine urinary levels after the administration of therapeutic doses of chlorthalidone to humans. The only compounds that would interfere with the analysis of urinary extracts would be other drugs containing unsubstituted aryl sulfonamide groups. In a controlled clinical trial, these drugs would not be present.

The two-compartment pharmacokinetic model for chlorthalidone indicated in Fig. 5 is consistent with previous studies on its pharmacokinetics. Two studies (10, 11) used ^{14}C-chlorthalidone, and a third study in a single subject (12) used a GLC assay. The α-phase shown by the urinary data may reflect the distribution rate of chlorthalidone from the plasma to the erythrocytes since the half-life of this phase is consistent with the report that it takes several hours for the distribution of ^{14}C-chlorthalidone between the plasma and the erythrocytes to reach a steady state (10).

Assay automation is a major advantage for analysis of a large number of samples. However, this method can be performed manually with a colorimeter or spectrophotometer, as shown in Fig. 3, if an automated system is not available.

The underlying principle of this assay for chlorthalidone is that the drug inhibits the catalytic activity of the carbonic anhydrase. Because of the catalytic nature of the enzyme, a low concentration of carbonic anhydrase can catalyze the formation of a large amount of product in a short time. Chlorthalidone, present at a low concentration, can interact directly with the enzyme, inhibiting the catalytic rate of product formation. The effect of the drug is determined by measuring the difference in the amount of product formed during the transit time in the automated analysis system before and after addition of the sample. Because of the catalytic nature of the product formation, the effect of a low concentration of chlorthalidone in the reaction mixture (about 0.2 μg/ml) is magnified so that the difference in the concentration of product formed (about 2 μg of *p*-nitrophenol/ml) is large enough to be easily measured spectrophotometrically.

This principle could be applied to the analysis of other drugs. Carbonic anhydrase and the automated system described could be used for other drugs containing unsubstituted aryl sulfonamides such as hydrochlorothiazide. Methods could be developed for inhibitors or activators of other enzymes. Because of the magnification effect of the enzymatic catalysis, these methods, which could be spectrophotometric, would have sensitivity limits similar to fluorometric assays or to GLC assays using a flame-ionization detector. In addition, the enzymatic assays would be amenable to automation.

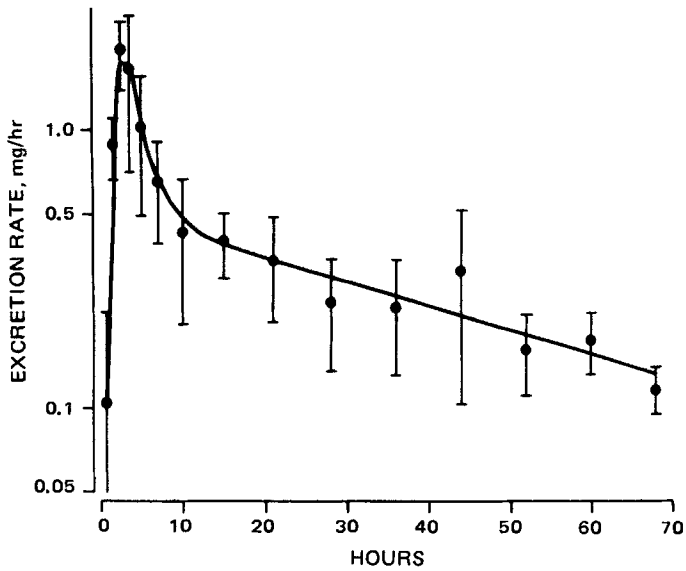

Figure 5—*Urinary excretion rate of chlorthalidone by normal human subjects. Six male subjects, 19–30 years old, each received a 100-mg chlorthalidone tablet. The mean excretion rate and standard error for the six subjects during each collection period were calculated.*

REFERENCES

(1) M. G. Tweeddale and R. I. Ogilvie, *J. Pharm. Sci.*, **63**, 1065 (1974).

(2) M. Ervik and K. Gustavii, *Anal. Chem.*, **46**, 39 (1974).

(3) H. Li, M. M. Johnston, and D. Mufson, *J. Pharm. Sci.*, **66**, 1732 (1977).

(4) R. E. Tashian and Y. L. Yu, *Adv. Exp. Med. Biol.*, **28**, 209 (1972).

(5) T. H. Maren, V. I. Ash, and E. M. Bailey, *Bull. Johns Hopkins Hosp.*, **95**, 244 (1954).

(6) G. J. Yakatan, C. A. Martin, and R. V. Smith, *Anal. Chim. Acta*, **84**, 173 (1976).

(7) G. Navon, J. Shani, R. Panigel, and S. Schoenberg, *J. Med. Chem.*, **18**, 1152 (1975).

(8) Y. Pocker and J. T. Stone, *Biochemistry*, **6**, 668 (1967).

(9) T. Mann and D. Keilen, *Nature*, 146, 164 (1940).

(10) B. Beermann, K. Hellström, B. Lindström, and A. Rosen, *Clin. Pharm. Ther.*, **17**, 424 (1975).

(11) P. Collste, M. Garle, M. D. Rawlins, and F. Sjöqvist, *Eur. J. Clin. Pharmacol.*, **9**, 319 (1976).

(12) H. L. J. M. Fleuren and J. M. Van Rossum, *Pharm. Weekbl.*, **110**, 1262 (1975).

ACKNOWLEDGMENTS AND ADDRESSES

Received December 2, 1976, from the *Biochemistry and Drug Disposition Department, USV Pharmaceutical Corp., Tuckahoe, NY 10707.*

Accepted for publication March 16, 1977.

Presented in part at the Pharmaceutical Analysis and Control Section, APhA Academy of Pharmaceutical Sciences, Atlanta meeting, November 1975.

The authors thank Mr. D. Sweeney, Mr. M. Rosenberg, and Ms. P. Espiritu for excellent technical assistance.

[x] To whom inquiries should be directed.

Comparative Pharmacokinetics of Coumarin Anticoagulants XXX: Relationship between Total Clearance and Serum Protein Binding of Dicumarol in Rats

CHII-MING LAI and GERHARD LEVY ˣ

Abstract □ The effect of serum protein binding on the elimination kinetics of dicumarol was studied. The serum free fraction of dicumarol was essentially independent of concentration over a wide concentration range and ranged from 0.00015 to 0.00079 in 10 adult rats. The total clearance of dicumarol in these animals ranged from 3.93 to 14.5 ml/kg/hr. As in previous studies, there was an excellent linear correlation between the elimination rate constant for dicumarol and the fraction of dicumarol in the liver (*i.e.*, the amount of drug in the liver divided by the amount of drug in the body). Consistent with theoretical considerations, there was a positive and apparently linear relationship between the total clearance and the serum free fraction of dicumarol. The individual serum free fraction and the fraction in liver values for dicumarol were strongly correlated. The pharmacokinetic model based on a proportional relationship between the apparent elimination rate constant and the fraction in the liver applies to dicumarol but not to warfarin and has limited utility. On the other hand, the model relating total clearance to the serum free fraction has been found to apply to dicumarol, warfarin, and other extensively plasma protein-bound drugs and can be utilized under clinical conditions.

Keyphrases □ Dicumarol—effect of serum protein binding on elimination kinetics, rats □ Protein binding, serum—dicumarol, effect on elimination kinetics, rats □ Binding, serum protein—dicumarol, effect on elimination kinetics, rats □ Elimination kinetics—dicumarol, effect of serum protein binding, rats □ Coumarin anticoagulants—dicumarol, effect of serum protein binding on elimination kinetics, rats □ Anticoagulants, coumarin—dicumarol, effect of serum protein binding on elimination kinetics, rats

There are pronounced intersubject differences in the elimination kinetics and in the serum protein binding of dicumarol in rats (1). The apparent first-order elimination rate constant for dicumarol in rats is proportional to the fraction of dicumarol in the liver, *i.e.*, to the amount of dicumarol in the liver divided by the amount of the drug in the entire body (2, 3). This proportionality is consistent with results of experiments with isolated perfused rat livers and with theoretical considerations that indicate that the biotransformation rate of dicumarol should be proportional to the amount of drug in the drug-metabolizing compartment, *i.e.*, the liver (4–6). However, subsequent studies with another coumarin anticoagulant, warfarin, failed to show any significant correlation between the elimination rate constant of that drug and its fraction in the liver (7).

Based on the results of the warfarin study, a theoretical model was developed which predicts a linear relationship between the total clearance and the serum free fraction of warfarin[1] (8). This model has been found to apply to warfarin in rats (7, 8) and humans (9), to bilirubin in rats (10), and to phenytoin in humans (11). Accordingly, this study was initiated to determine the relationship between the total clearance and the serum free fraction of dicumarol in rats.

[1] The serum free fraction is defined as the concentration of unbound drug divided by the concentration of total (free and bound) drug in serum.

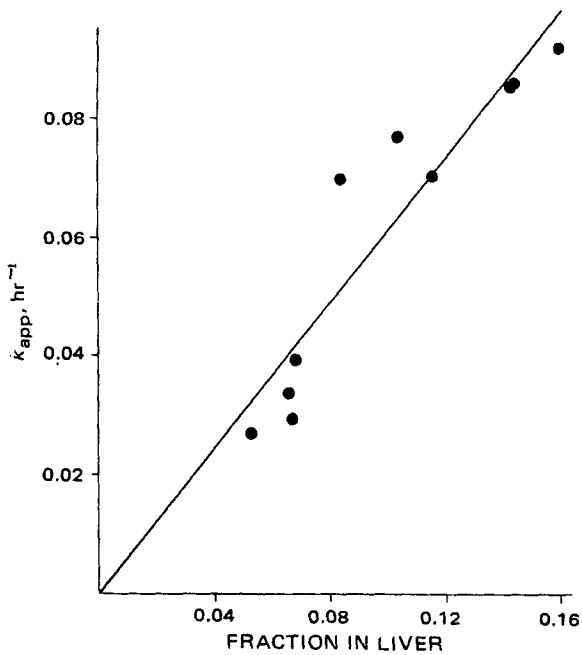

Figure 1—*Relationship between the apparent first-order elimination rate constant and the fraction of dicumarol in the liver (r = 0.931, p < 0.001).*

EXPERIMENTAL

Blood samples were obtained from 40 adult male Sprague–Dawley rats, and the serum was separated. ^{14}C-Dicumarol, 20 μg/ml, was added, and the serum free fraction was determined by equilibrium dialysis at 37° (1). Based on the results of this screening experiment, 10 rats with a wide and relatively even distribution of free fraction values were selected for further study. These animals, weighing 337–419 g, received a single 8-mg/kg iv dose of ^{14}C-dicumarol (specific activity, 61.7 μCi/mg).

Blood samples (0.22 ml) were obtained at 4–10-hr intervals (depending on the biological half-life) until the plasma dicumarol concentration had declined to about 8 μg/ml, at which time the animals were sacrificed by removing as much blood as possible from the aorta under ether anesthesia. The liver was then removed, blotted under slight pressure, and weighed. Dicumarol concentrations in plasma and liver were determined after selective extraction as previously described (12). The blood obtained when the animals were sacrificed was permitted to clot, and ^{14}C-dicumarol, 20 μg/ml, was added to the serum. The free fraction of dicumarol in these serum samples was determined by equilibrium dialysis (1). Pharmacokinetic analysis of the data was carried out as previously described (2).

Serum from five adult male Sprague–Dawley rats (who had not received dicumarol) was pooled to determine the relationship between the serum free fraction and the dicumarol concentration. ^{14}C-Dicumarol was added to yield serum samples with 10 different concentrations, ranging from about 9 to about 90 μg/ml. The serum free fraction of dicumarol in these samples was then determined in duplicate by equilibrium dialysis.

RESULTS

Results of the pharmacokinetic study are summarized in Table I. There were pronounced intersubject differences in the biological half-life, total

Table I—Pharmacokinetic Constants for Dicumarol in Adult Male Sprague–Dawley Rats

Rat	Half-Life, hr	Volume of Distribution, ml/kg	Total Clearance, ml/kg/hr	Free Fraction in Serum × 10^4	Fraction in Liver[a]	Liver/Serum Concentration Ratio[a]
1	25.8	149	4.00	1.50	0.0528	0.303
2	23.5	150	4.42	3.39	0.0670	0.341
3	20.6	179	6.02	2.13	0.0658	0.355
4	17.5	233	9.23	3.72	0.0679	0.481
5	9.80	128	9.05	6.25	0.115	0.427
6	9.90	162	11.3	3.79	0.0829	0.380
7	8.97	151	11.7	7.79	0.103	0.444
8	8.04	174	15.0	7.90	0.142	0.661
9	8.02	171	14.8	5.94	0.143	0.737
10	7.51	163	15.0	7.30	0.159	0.714

[a] At a plasma dicumarol concentration of about 8 μg/ml.

Table II—Relationship between Concentration and Free Fraction of Dicumarol in Pooled Serum from Five Untreated Rats[a]

Concentration, μg/ml	Free Fraction × 10^4
8.69	1.87
17.3	1.91
24.8	2.10
32.2	2.57
42.8	1.67
54.4	1.99
60.6	1.79
68.9	2.13
77.3	2.12
89.3	2.23

[a] Mean of two dialysis experiments for each concentration.

clearance, serum free fraction, and liver fraction of dicumarol and smaller differences in the apparent volume of distribution. Unlike warfarin (7), dicumarol had liver/serum concentration ratios less than unity under the experimental conditions. The free fraction of dicumarol in serum ranged from 0.00015 to 0.00079, indicating that the drug was 99.921–99.985% serum protein bound. The serum free fraction of dicumarol was independent of concentration over a wide concentration range (Table II). The coefficient of variation for the free fraction data summarized in Table II is 12.5%; the difference between duplicate samples was 14 ± 13.5% (mean ± *SD*), reflecting the technical difficulties of determining the serum protein binding of a very extensively bound drug.

As in previous studies (2, 3), there was a strong and apparently linear correlation between the apparent first-order elimination rate constant and the fraction of dicumarol in the liver (Fig. 1). However, this study also revealed a strong and apparent linear relationship between the total clearance and the free fraction of dicumarol in the serum (Fig. 2). There was a significant positive correlation between fraction in liver and serum free fraction values for dicumarol in individual animals ($r = 0.867$, $p < 0.003$, $n = 10$). No such correlation was found for warfarin (7).

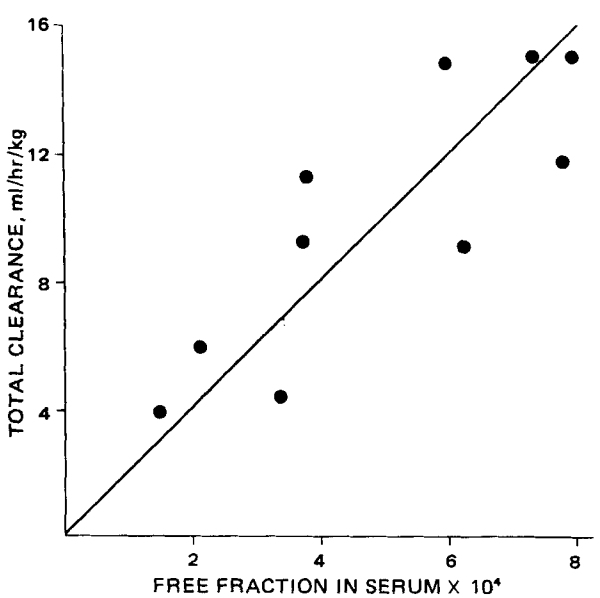

Figure 2—*Relationship between the total clearance and the serum free fraction of dicumarol* (r = 0.831, p < 0.005).

DISCUSSION

There is a strong theoretical basis and increasing experimental evidence for the concept that the total clearance of drugs subject to elimination by apparently linear biotransformation processes is proportional to their free fraction in serum unless clearance is so high as to be limited or affected by organ blood flow (13). Dicumarol is not subject to such limitation by blood flow through the liver (3, 14). The results of this study demonstrate that the total clearance of this very extensively serum protein-bound anticoagulant is proportional to its free fraction in serum and that serum protein binding is the major determinant of interindividual differences in the elimination of dicumarol by rats.

It is likely that such is the case also in humans, based on the following indirect evidence. There is a strong correlation between the total clearances of dicumarol and warfarin in individual rats (1). There is a similar strong correlation between individual serum free fraction values for dicumarol and warfarin in rats (1). Finally, the total clearance of warfarin in humans is proportional to the free fraction of the drug in serum (9). These observations, taken together, suggest that the total clearance of dicumarol in humans is likely to be proportional to its serum free fraction. Unlike the relationship between the apparent first-order elimination rate constant and the fraction of drug in the liver, the relationship between total clearance and the serum free fraction can be determined in humans under clinical conditions.

REFERENCES

(1) A. Yacobi, C.-M. Lai, and G. Levy, *J. Pharm. Sci.*, **64**, 1995 (1975).

(2) E. Jähnchen and G. Levy, *J. Pharmacol. Exp. Ther.*, **188**, 293 (1974).

(3) C.-M. Lai, A. Yacobi, and G. Levy, *ibid.*, **199**, 74 (1976).

(4) R. Nagashima, G. Levy, and E. J. Sarcione, *J. Pharm. Sci.*, **57**, 1881 (1968).

(5) G. Levy and R. Nagashima, *ibid.*, **58**, 1001 (1969).

(6) G. Levy, *Proc. 4th Int. Congr. Pharmacol.*, **4**, 134 (1970).

(7) A. Yacobi and G. Levy, *J. Pharm. Sci.*, **64**, 1660 (1975).

(8) G. Levy and A. Yacobi, *ibid.*, **63**, 805 (1974).

(9) A. Yacobi, J. A. Udall, and G. Levy, *Clin. Pharmacol. Ther.*, **19**, 552 (1976).

(10) S. Øie and G. Levy, *J. Pharm. Sci.*, **64**, 1433 (1975).

(11) R. Gugler and D. L. Azarnoff, *Clin. Pharmacokinet.*, **1**, 25 (1976).

(12) E. Jähnchen, L. B. Wingard, Jr., and G. Levy, *J. Pharmacol. Exp. Ther.*, **187**, 176 (1973).

(13) G. Levy, in "The Effect of Disease States on Drug Pharmacokinetics," L. Z. Benet, Ed., American Pharmaceutical Association, Washington, D.C., 1976, chap. 9.

(14) R. Nagashima and G. Levy, *J. Pharm. Sci.*, **57**, 1991 (1968).

ACKNOWLEDGMENTS AND ADDRESSES

Received December 8, 1976, from the *Department of Pharmaceutics, School of Pharmacy, State University of New York at Buffalo, Amherst, NY 14260.*

Accepted for publication February 17, 1977.
Supported in part by Grant GM 20852 from the National Institute of General Medical Sciences, National Institutes of Health.

Previous paper in this series: A. Yacobi and G. Levy, *J. Pharm. Sci.*, **66**, 1275 (1977).

[x] To whom inquiries should be directed.

Comparative Pharmacokinetics of Coumarin Anticoagulants XXXI: Effect of Plasma Protein Binding on Distribution Kinetics of Dicumarol in Rats

AVRAHAM YACOBI, CHII-MING LAI, and GERHARD LEVY [x]

Abstract □ The purpose of this investigation was to determine, with respect to dicumarol, the effect of plasma protein binding on the pharmacokinetic parameters used conventionally to describe the distribution kinetics of a drug on the basis of the time course of its plasma concentration. After rapid intravenous injection, plasma dicumarol concentrations in adult male Sprague–Dawley rats declined triexponentially, with the terminal exponential phase starting at about 4 hr. The free fraction, f, of dicumarol in the serum of individual animals ranged from 0.000150 to 0.000790. The parameters of the equation $C_t = Pe^{-\pi t} + Ae^{-\alpha t} + Be^{-\beta t}$ for plasma concentration C_t at time t were obtained by nonlinear least-squares computer fitting of the experimental data and varied appreciably between animals. Of these parameters, only β showed a significant correlation with f. These observations indicate that the distribution kinetics of this very extensively plasma protein-bound drug, as reflected by the time course of its plasma concentration after intravenous injection, are apparently not affected by intersubject differences in plasma protein binding. There is a remarkable similarity in the values of P, A, B, π, and α for dicumarol and warfarin, even though the serum free fraction of these drugs differs considerably.

Keyphrases □ Dicumarol—distribution kinetics, effect of plasma protein binding, rats □ Distribution kinetics—dicumarol, effect of plasma protein binding, rats □ Pharmacokinetics—distribution of dicumarol, effect of plasma protein binding, rats □ Protein binding, plasma—effect on distribution kinetics of dicumarol, rats □ Binding, plasma protein—effect on distribution kinetics of dicumarol, rats □ Anticoagulants—dicumarol, distribution kinetics, effect of plasma protein binding, rats

Serum (or plasma) protein binding can have a pronounced effect on the kinetics of drug elimination (1, 2). This effect is particularly striking with respect to the elimination of the extensively serum protein-bound anticoagulants warfarin and dicumarol by rats since the serum free fraction of these drugs varies over a wide range in these animals (3, 4). Consistent with theoretical considerations (5), the total clearance of warfarin and dicumarol is directly proportional to the serum free fraction of these drugs.

While the role of serum protein binding in drug elimination is beginning to be understood (1, 2), its effect on the kinetics of drug distribution from the blood to extravascular sites has not yet been elucidated. In a detailed study of the effect of serum protein binding on the distribution kinetics of warfarin in rats, no apparent relationship was found between the serum free fraction of warfarin and the pharmacokinetic parameters conventionally used to describe the distribution kinetics of a drug on the basis of a multiexponential decline of plasma drug concentrations after rapid intravenous injection (6). A similar study was initiated with dicumarol since its free fraction in rat serum is only about one-fiftieth that of warfarin (7). The results of this study and a comparison of the data obtained with dicumarol and warfarin are presented here.

EXPERIMENTAL

Single 3-ml blood samples were obtained from 40 adult male Sprague–Dawley rats, and the serum was separated. ^{14}C-Dicumarol was added to yield a concentration of 20 μg/ml, and the serum free fraction of dicumarol was determined by equilibrium dialysis (7). Ten animals with widely differing free fraction values were selected for further study. Two to 3 weeks later, a two-piece cannula of silicone rubber and polyethylene was implanted in their right jugular veins under light ether anesthesia (8, 9).

One or 2 days after cannulation, the rats were placed in individual metabolism cages with food and water freely available. A single dose of ^{14}C-dicumarol (specific activity of 61.7 μCi/mg), 8 mg/kg, was injected rapidly through the cannula. Blood samples (about 0.22 ml) were obtained at 5, 10, 20, 40, 60, and 120 min and then at less frequent intervals for a period equivalent to about three times the biological half-life of the drug in the particular animal. The blood samples were transferred immediately to heparinized micro blood collecting tubes[1], and the plasma was separated by centrifugation. The plasma dicumarol concentration was determined after selective extraction (10).

At the end of the experiment, a larger quantity of blood was obtained for the determination of the free fraction of dicumarol in serum. For this purpose, ^{14}C-dicumarol, 20 μg/ml, was added to the serum to yield a total concentration of 25–30 μg/ml and two or three serum samples from each rat were subjected to equilibrium dialysis (7).

The plasma dicumarol concentration data for individual animals were fitted to the triexponential equation $C_t = Pe^{-\pi t} + Ae^{-\alpha t} + Be^{-\beta t}$ for plasma concentration C_t at time t by nonlinear least-squares regression (11). Convergence was defined as a relative change in the residual sum of squares $<10^{-4}$. Data in all functions were weighted numerically equal. Volume and clearance values were determined from the constants of the triexponential equation (12).

RESULTS

Plasma dicumarol concentrations declined exponentially with time after injection following an initial distribution phase. Data for the animals with the shortest and longest biological half-lives of dicumarol observed in this study are shown in Fig. 1. Data of similar quality were obtained from the other animals. A triexponential equation was required to describe the data; a biexponential equation was not adequate for this purpose.

The mean and range of the individual parameter values are listed in Table I. The intersubject distribution of the parameter values is shown in Fig. 2. The relatively widest range of values was observed with respect to A, π, and α; the least intersubject variation was found for B. However,

[1] Scientific Products, Evanston, Ill.

Accepted for publication February 17, 1977.
Supported in part by Grant GM 20852 from the National Institute of General Medical Sciences, National Institutes of Health.

Previous paper in this series: A. Yacobi and G. Levy, *J. Pharm. Sci.*, **66**, 1275 (1977).

[x] To whom inquiries should be directed.

Comparative Pharmacokinetics of Coumarin Anticoagulants XXXI: Effect of Plasma Protein Binding on Distribution Kinetics of Dicumarol in Rats

AVRAHAM YACOBI, CHII-MING LAI, and GERHARD LEVY [x]

Abstract □ The purpose of this investigation was to determine, with respect to dicumarol, the effect of plasma protein binding on the pharmacokinetic parameters used conventionally to describe the distribution kinetics of a drug on the basis of the time course of its plasma concentration. After rapid intravenous injection, plasma dicumarol concentrations in adult male Sprague–Dawley rats declined triexponentially, with the terminal exponential phase starting at about 4 hr. The free fraction, f, of dicumarol in the serum of individual animals ranged from 0.000150 to 0.000790. The parameters of the equation $C_t = Pe^{-\pi t} + Ae^{-\alpha t} + Be^{-\beta t}$ for plasma concentration C_t at time t were obtained by nonlinear least-squares computer fitting of the experimental data and varied appreciably between animals. Of these parameters, only β showed a significant correlation with f. These observations indicate that the distribution kinetics of this very extensively plasma protein-bound drug, as reflected by the time course of its plasma concentration after intravenous injection, are apparently not affected by intersubject differences in plasma protein binding. There is a remarkable similarity in the values of P, A, B, π, and α for dicumarol and warfarin, even though the serum free fraction of these drugs differs considerably.

Keyphrases □ Dicumarol—distribution kinetics, effect of plasma protein binding, rats □ Distribution kinetics—dicumarol, effect of plasma protein binding, rats □ Pharmacokinetics—distribution of dicumarol, effect of plasma protein binding, rats □ Protein binding, plasma—effect on distribution kinetics of dicumarol, rats □ Binding, plasma protein—effect on distribution kinetics of dicumarol, rats □ Anticoagulants—dicumarol, distribution kinetics, effect of plasma protein binding, rats

Serum (or plasma) protein binding can have a pronounced effect on the kinetics of drug elimination (1, 2). This effect is particularly striking with respect to the elimination of the extensively serum protein-bound anticoagulants warfarin and dicumarol by rats since the serum free fraction of these drugs varies over a wide range in these animals (3, 4). Consistent with theoretical considerations (5), the total clearance of warfarin and dicumarol is directly proportional to the serum free fraction of these drugs.

While the role of serum protein binding in drug elimination is beginning to be understood (1, 2), its effect on the kinetics of drug distribution from the blood to extravascular sites has not yet been elucidated. In a detailed study of the effect of serum protein binding on the distribution kinetics of warfarin in rats, no apparent relationship was found between the serum free fraction of warfarin and the pharmacokinetic parameters conventionally used to describe the distribution kinetics of a drug on the basis of a multiexponential decline of plasma drug concentrations after rapid intravenous injection (6). A similar study was initiated with dicumarol since its free fraction in rat serum is only about one-fiftieth that of warfarin (7). The results of this study and a comparison of the data obtained with dicumarol and warfarin are presented here.

EXPERIMENTAL

Single 3-ml blood samples were obtained from 40 adult male Sprague–Dawley rats, and the serum was separated. ^{14}C-Dicumarol was added to yield a concentration of 20 μg/ml, and the serum free fraction of dicumarol was determined by equilibrium dialysis (7). Ten animals with widely differing free fraction values were selected for further study. Two to 3 weeks later, a two-piece cannula of silicone rubber and polyethylene was implanted in their right jugular veins under light ether anesthesia (8, 9).

One or 2 days after cannulation, the rats were placed in individual metabolism cages with food and water freely available. A single dose of ^{14}C-dicumarol (specific activity of 61.7 μCi/mg), 8 mg/kg, was injected rapidly through the cannula. Blood samples (about 0.22 ml) were obtained at 5, 10, 20, 40, 60, and 120 min and then at less frequent intervals for a period equivalent to about three times the biological half-life of the drug in the particular animal. The blood samples were transferred immediately to heparinized micro blood collecting tubes[1], and the plasma was separated by centrifugation. The plasma dicumarol concentration was determined after selective extraction (10).

At the end of the experiment, a larger quantity of blood was obtained for the determination of the free fraction of dicumarol in serum. For this purpose, ^{14}C-dicumarol, 20 μg/ml, was added to the serum to yield a total concentration of 25–30 μg/ml and two or three serum samples from each rat were subjected to equilibrium dialysis (7).

The plasma dicumarol concentration data for individual animals were fitted to the triexponential equation $C_t = Pe^{-\pi t} + Ae^{-\alpha t} + Be^{-\beta t}$ for plasma concentration C_t at time t by nonlinear least-squares regression (11). Convergence was defined as a relative change in the residual sum of squares $<10^{-4}$. Data in all functions were weighted numerically equal. Volume and clearance values were determined from the constants of the triexponential equation (12).

RESULTS

Plasma dicumarol concentrations declined exponentially with time after injection following an initial distribution phase. Data for the animals with the shortest and longest biological half-lives of dicumarol observed in this study are shown in Fig. 1. Data of similar quality were obtained from the other animals. A triexponential equation was required to describe the data; a biexponential equation was not adequate for this purpose.

The mean and range of the individual parameter values are listed in Table I. The intersubject distribution of the parameter values is shown in Fig. 2. The relatively widest range of values was observed with respect to A, π, and α; the least intersubject variation was found for B. However,

[1] Scientific Products, Evanston, Ill.

Table I—Dicumarol Kinetics in 10 Adult Male Sprague–Dawley Rats

Parameter	Mean	Range	*CV* of Individual Parameter Estimate[b]
P, μg/ml[a]	47.3	31.4–74.4	62.1 ± 59.3
A, μg/ml[a]	29.2	12.3–49.4	47.8 ± 46.0
B, μg/ml[a]	49.3	34.4–62.8	4.66 ± 1.86
π, hr^{-1}	10.0	3.38–18.8	80.8 ± 61.6
α, hr^{-1}	1.2	0.333–2.16	56.6 ± 44.8
β, hr^{-1}	0.0612	0.0269–0.0923	4.95 ± 1.66
V_c, ml/kg	65.2	45.2–83.7	
V_{area}, ml/kg	159	125–217	
$V_{intercept}$, ml/kg	166	128–233	
Total clearance, ml/hr kg	9.64	3.93–14.5	

[a] For an 8-mg/kg dose. [b] Mean ± *SD* of coefficient values for individual animals.

the estimated values for A, P, α, and π also had very large coefficients of variation (Table I). The drug has practically one-compartment characteristics if judged on the basis of the similarity of V_{area} and $V_{intercept}$.

The serum free fraction values for dicumarol ranged from 0.000150 to 0.000790. The relationship between serum free fraction and various pharmacokinetic constants is summarized in Table II. There is no apparent correlation between the serum free fraction of dicumarol and those constants that are thought to reflect (at least in part) the distribution kinetics of the drug: P, A, π, and α. As reported previously (4) and consistent with theoretical considerations (5), the free fraction values are strongly correlated with the total clearance of dicumarol. There is also a strong correlation between the free fraction and β.

Serum protein binding, as reflected by the serum free fraction values, had no apparent effect on the apparent volume of distribution of the hypothetical central compartment, V_c, for the drug (Table II and Fig. 3). This result is not an artifact of the data-fitting procedure since the earliest (5 min) plasma concentrations also showed no apparent relationship with the serum free fraction values (Fig. 3). This result is of interest since a strong, positive correlation between V_c and serum free fraction was found for warfarin in a previous study in which the protocol and methodology were almost identical to those of this investigation (6). Figure 4 shows the strong negative correlation between the warfarin concentrations 5 min after injection and the serum free fraction values of warfarin in 14 rats used in the previous study (6).

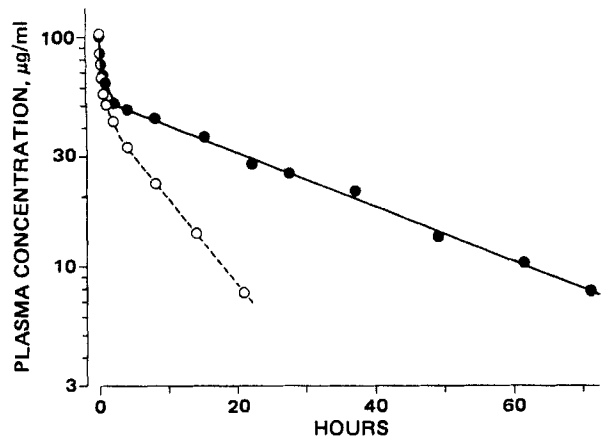

Figure 1—*Plasma dicumarol concentrations of two rats after 8 mg/kg iv of ^{14}C-dicumarol. The curves were fitted to the data by a nonlinear least-squares computer program.*

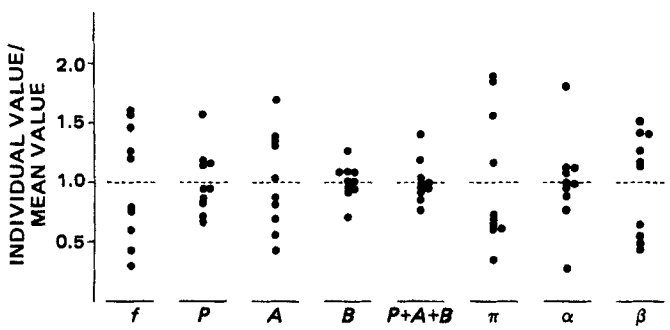

Figure 2—*Intersubject distribution of values for the parameters of the triexponential equation that describes the time course of plasma dicumarol concentrations and of values for the free fraction, f, of dicumarol in the serum of 10 rats.*

DISCUSSION

The results of this investigation show that serum protein binding, as reflected by the serum free fraction values, has no apparent effect on the pharmacokinetic parameters of dicumarol conventionally associated with the distribution kinetics of a drug: P, A, π, and α for the drug whose plasma concentrations decline triexponentially after intravenous injection. This conclusion must be viewed in the context that these parameters also have the greatest quantitative uncertainty, as reflected by the large coefficients of variation.

Dicumarol differs from warfarin in that serum protein binding has no apparent effect on the V_c of the former. The reason for this difference is not known. As discussed previously (6), there is no point in converting the directly determined pharmacokinetic constants of the triexponential equation to compartmental rate constants. Although this exercise was carried out as a matter of routine in the data analysis, the results provide no significant additional information and are not presented here.

The free fraction of warfarin is about 50 times larger than that of dicumarol when determined in the same serum samples (7). For both drugs, the free fraction value is essentially independent of concentration over a wide range (3, 4). It is informative, therefore, to compare the magnitude of the pharmacokinetic constants for the two drugs in rats. The mean

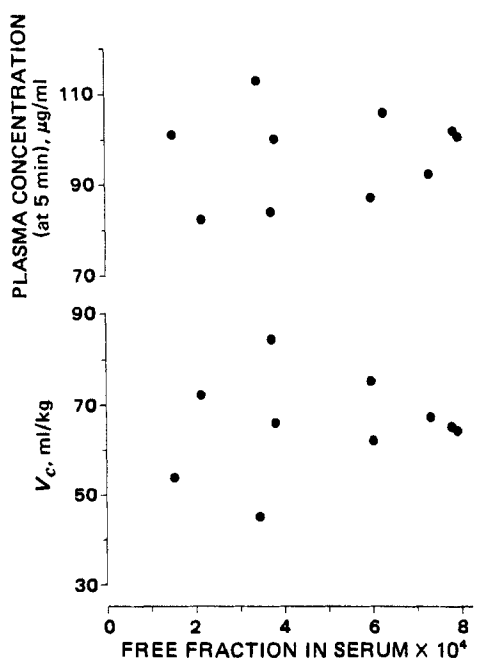

Figure 3—*Relationship between the serum free fraction of dicumarol and (a) plasma dicumarol concentration 5 min after intravenous injection (upper panel) and (b) the apparent volume of the hypothetical central compartment for dicumarol (lower panel) in 10 rats.*

Table II—Correlation between Pharmacokinetic Parameters for Dicumarol and the Serum Free Fraction of Dicumarol in 10 Rats

Parameter	r	Statistical Significance
P	0.187	N.S.
A	0.395	N.S.
B	0.162	N.S.
π	−0.615	N.S. ($p > 0.1$)
α	0.132	N.S.
β	0.892	$p < 0.001$
V_c	0.172	N.S.
V_{area}	0.242	N.S.
$V_{intercept}$	0.171	N.S.
Total clearance	0.831	$p < 0.005$

values of these constants are listed in Table III. Such a comparison cannot be rigorous since these data were obtained from different groups of animals (note, for example, that the free fraction ratio is about 25 rather than 50, which would be the expected ratio had the studies been performed in the same or in well-matched animals). Despite these limitations and the pronounced intersubject differences, the similarity in the mean values of all pharmacokinetic parameters[2] except β is striking. It may be that the distribution rate of both drugs from the blood to extravascular sites is limited by blood flow or diffusion, but this remains to be determined. Studies are now in progress with a drug much less extensively bound to serum proteins to determine if its distribution kinetics are different from those of dicumarol and warfarin.

Although dicumarol and warfarin have similar pharmacokinetic "distribution" parameter values (as shown in this study), almost identical total clearance values when determined in the same rats (7), and similar equieffective free plasma concentrations in terms of anticoagulant activity

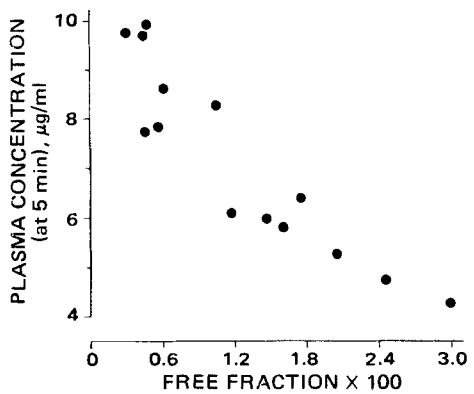

Figure 4—*Relationship between the serum free fraction of warfarin and plasma warfarin concentration of 14 rats 5 min after intravenous injection of warfarin, 0.51 mg/kg* (r = −0.913, p < 0.001).

[2] The serum free fraction value is not considered to be a "pharmacokinetic parameter" in the context of this discussion. The molecular weights of dicumarol and warfarin are similar so that P, A, and B need not be normalized on a molecular weight basis.

Table III—Comparison of Mean Values of Pharmacokinetic Parameters for Dicumarol and Warfarin in Rats

Parameter	Dicumarol[a]	Warfarin[b]
P, μg/ml[c]	5.91	9.16
A, μg/ml[c]	3.65	3.45
B, μg/ml[c]	6.16	6.04
π, hr^{-1}	10.0	6.98
α, hr^{-1}	1.20	1.03
β, hr^{-1}	0.0612	0.0310
Free fraction in serum × 10^4	4.97	123

[a] Results of this study, $n = 10$. [b] Results of a previous study (6), $n = 14$. [c] For a 1-mg/kg dose.

(7), these two drugs differ considerably in the extent of serum protein binding (7). Because of that difference and the similarity of their total clearance values, the intrinsic clearance (5) of dicumarol is much higher than that of warfarin. These comparisons are based on the "average" results of pharmacokinetic studies with racemic warfarin. While there are some quantitative differences in elimination kinetics and anticoagulant activity of (*R*)-(+)- and (*S*)-(−)-warfarin, respectively (13), these conclusions apply also when the intrinsic clearance of dicumarol is compared to that of the individual enantiomers of warfarin.

REFERENCES

(1) G. Levy, in "The Effect of Disease States on Drug Pharmacokinetics," L. Z. Benet, Ed., American Pharmaceutical Association, Washington, D.C., 1976, chap. 9.

(2) G. Wilkinson and D. G. Shand, *Clin. Pharmacol. Ther.*, **18**, 377 (1975).

(3) A. Yacobi and G. Levy, *J. Pharm. Sci.*, **64**, 1660 (1975).

(4) C.-M. Lai and G. Levy, *ibid.*, **66**, 1739 (1977).

(5) G. Levy and A. Yacobi, *ibid.*, **63**, 805 (1974).

(6) A. Yacobi and G. Levy, *ibid.*, **66**, 567 (1977).

(7) A. Yacobi, C.-M. Lai, and G. Levy, *ibid.*, **64**, 1995 (1975).

(8) J. R. Weeks and J. D. Davis, *J. Appl. Physiol.*, **19**, 540 (1964).

(9) J. J. Ashley and G. Levy, *Res. Commun. Chem. Pathol. Pharmacol.*, **4**, 297 (1972).

(10) L. B. Wingard, Jr., and G. Levy, *J. Pharmacol. Exp. Ther.*, **184**, 253 (1973).

(11) C. M. Metzler, "NONLIN, a Computer Program for Parameter Estimation in Nonlinear Situations," The Upjohn Co., Kalamazoo, Mich., 1969.

(12) M. Gibaldi and D. Perrier, "Pharmacokinetics," Dekker, New York, N.Y., 1975.

(13) A. Yacobi and G. Levy, *J. Pharmacokinet. Biopharm.*, **2**, 239 (1974).

ACKNOWLEDGMENTS AND ADDRESSES

Received December 7, 1976, from the *Department of Pharmaceutics, School of Pharmacy, State University of New York at Buffalo, Amherst, NY 14260.*

Accepted for publication March 1, 1977.

Supported in part by Grant GM 20852 from the National Institute of General Medical Sciences, National Institutes of Health.

[x] To whom inquiries should be directed.

Progesterone Retention by Rat Uterus I: Pharmacokinetics after Uterine Intraluminal Instillation

SEN M. FANG ˣ, CHING S. LIN, and VICKY LYON

Abstract □ Tritium-labeled progesterone was administered to mature female rats in the proestrous stage by three different routes, gastric intubation, subcutaneous injection, and uterine intraluminal instillation, to study the kinetics involved in the uptake and retention of radioactivity by the uterus and various other tissues. Progesterone was retained at a much higher level and for a more prolonged period in the rat uterus after uterine intraluminal instillation. Progesterone bioavailability to the uterus was 45 times higher by uterine intraluminal instillation than by either gastric intubation or subcutaneous injection. Progesterone absorption by the rat endometrium was extremely fast. The observed biphasic decrease of radioactivity from the uterine tissue was explained adequately by a pharmacokinetic model in which progesterone is assumed to be present in two compartments within the uterine tissue. The pharmacokinetic parameters showed that the progesterone biological half-life in the uterine tissue during the α-phase was about 6.5 min while that in the β-phase was about 230 min.

Keyphrases □ Progesterone—tissue distribution, different routes of administration compared □ Distribution, tissue—progesterone, different routes of administration compared □ Pharmacokinetics—progesterone, tissue distribution, different routes of administration compared □ Administration routes—uterine intraluminal instillation compared to gastric intubation and subcutaneous injection, progesterone tissue distribution □ Progestins—progesterone, tissue distribution, different routes of administration compared

The effectiveness of progestins as contraceptives, with or without the addition of estrogens, is well known, as witnessed by the successful application of "the pill" and "the minipill" in fertility control. The pill, which contains combinations of an estrogen and a progestin, exerts its effect through ovulation inhibition. With the minipill, which contains only progestin and in smaller amounts, the exact mechanism involved in the prevention of conception is still not clear but does not necessarily require the concomitant inhibition of ovulation. Evidence suggests that the site of action is probably the uterus, cervix, or fallopian tubes (1). Therefore, progestin may act directly on end target tissue to produce a contraceptive effect without the necessary participation of, or mediation by, the ovary or pituitary glands. If this is the case, the local administration of contraceptive progestins to the uterus logically should be the route of choice. This route would deliver the drug directly to the target tissue, require a much smaller dose than oral tablets, and, consequently, minimize undesirable feedback controls that are inevitable in systemic administrations.

Contraceptive progestins have been impregnated in intrauterine devices to form a sustained-release drug delivery system (2–12). The device[1], also called the "Uterine Progesterone System," releases a constant amount of progesterone at a controlled rate for many months upon placement in the uterine intraluminal cavity.

The present study was designed to investigate the pharmacokinetics involved in the uterine absorption and retention of progesterone administered by direct uterine intraluminal instillation as well as the relative bioavailability of progesterone to the rat uterine tissue upon three different routes of administration: oral intubation, subcutaneous injection, and uterine intraluminal instillation.

EXPERIMENTAL

Reagents and Chemicals—1,2-^{3}H-Progesterone[2] (56 Ci/mmole) was purified by TLC before use. Other chemicals were reagent grade.

Administration of ^{3}H-Progesterone—Mature female Sprague–Dawley rats, 180–250 g, were acclimated in an animal room with a 12-hr day–12-hr night lighting schedule until their estrous cycles had stabilized and resumed regular 4–5-day cycles as determined by vaginal smear cell typing. Tritium-labeled progesterone was administered to separate groups of female rats in proestrous stages by gastric intubation, subcutaneous injection, or direct uterine intraluminal instillation.

In oral administration, the rats were fasted overnight for 16 hr and ^{3}H-progesterone (0.15 μg = 5.26 × 10^6 dpm) in 1 ml of 5% ethanol was administered by gastric intubation. The same amount of ^{3}H-progesterone in 1 ml of 5% ethanol was used in subcutaneous injection. For the uterine intraluminal instillation, ^{3}H-progesterone (either 0.015 or 0.15 μg = 8.26 × 10^6 dpm) was dissolved in 40 μl of 5% ethanol and one-half of the solution (20 μl) was instilled into the luminal cavity of each uterine horn through the vaginal route or laparotomy. The solution was placed approximately at the midpoint of the uterine horn. Earlier tests with the dye solution showed no observable discharge of the injected solution through the uterine cervix using this route. Each experimental point was obtained from the pooled data of three or four rats.

Quantification of Radioactivity in Various Tissues—The rats were killed by cervical dislocation at selected times from 5 min to 16 hr after tritium-labeled progesterone administration. Uterus and other tissues, *i.e.*, liver, brain, diaphragm, muscle, lung, plasma, vaginal wall, and fat, were excised, rinsed with Ringer's solution, and minced with scissors. The minced tissue (0.1–0.5 g) was digested with 2 ml of tissue solubilizer[3] at 55° for 16 hr. After digestion, 0.5 ml of benzoyl peroxide solution (15% in toluene) was added and the mixture was further incubated at 55° for another 30 min.

With the exception of the uterine preparation, aliquots of the digested tissue solution (0.3–1.5 ml) were taken for the measurement of radioactivity. For the uterine tissue, 5 ml of scintillation fluor cocktail was added following the treatment with benzoyl peroxide solution to dissolve the resulting white precipitates. The mixture was shaken, and 1 ml of the solution was taken for the estimation of radioactivity.

To the sample to be counted was added 12 ml of toluene-based scintillation fluor cocktail containing 0.4% (w/v) diphenyloxazole, 0.005% (w/v) 1,4-bis[2-(5-phenyloxazolyl)]benzene, 25% (v/v) nonionic surfactant[4], and 5% (v/v) water. This mixture was then maintained at 4° for at least 16 hr in the dark before it was counted in a liquid scintillation spectrometer[5]. The quenching effect was estimated by means of a preconstructed calibration curve plotted using the external standard channel ratio *versus* counting efficiency.

RESULTS AND DISCUSSION

Distribution of Radioactivity in Various Tissues—After the oral administration of 0.15 μg of tritium-labeled progesterone, most radioactivity was found in the liver throughout the study (Fig. 1). As much as 40% of the radioactivity administered was in the liver 4 hr after admin-

[1] Progestasert, Alza Corp.

[2] New England Nuclear, Boston, Mass.

[3] Protosol, New England Nuclear.

[4] Triton X-100.

[5] Packard model 3385 Tri-Carb liquid scintillation spectrometer.

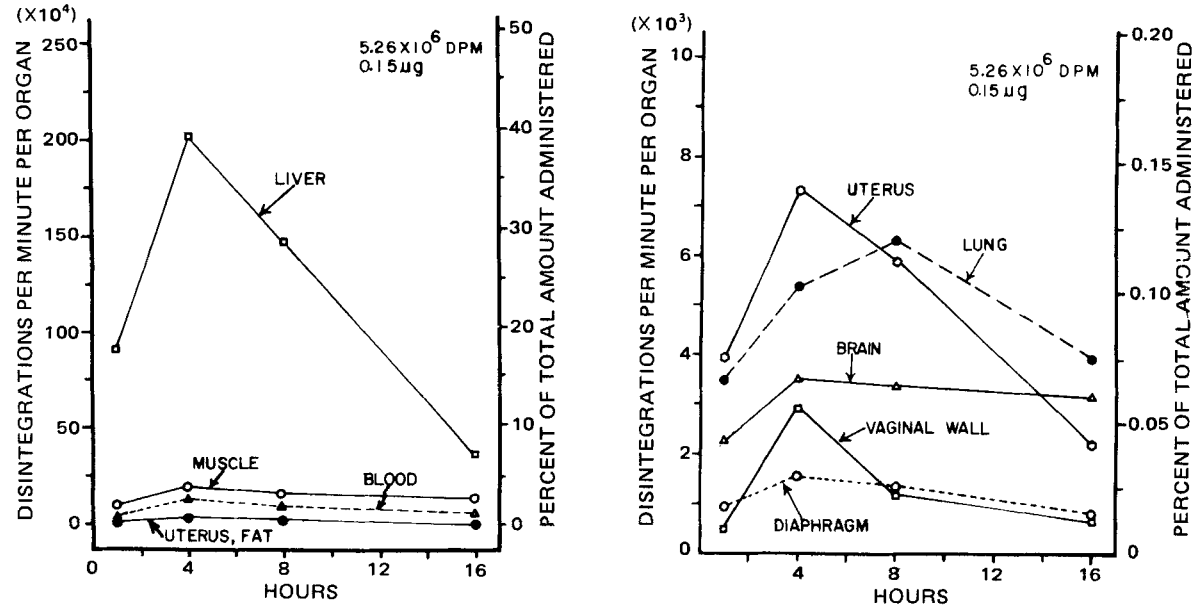

Figure 1—*Retention of radioactivity by various tissues after the gastric intubation of ^3H-progesterone.*

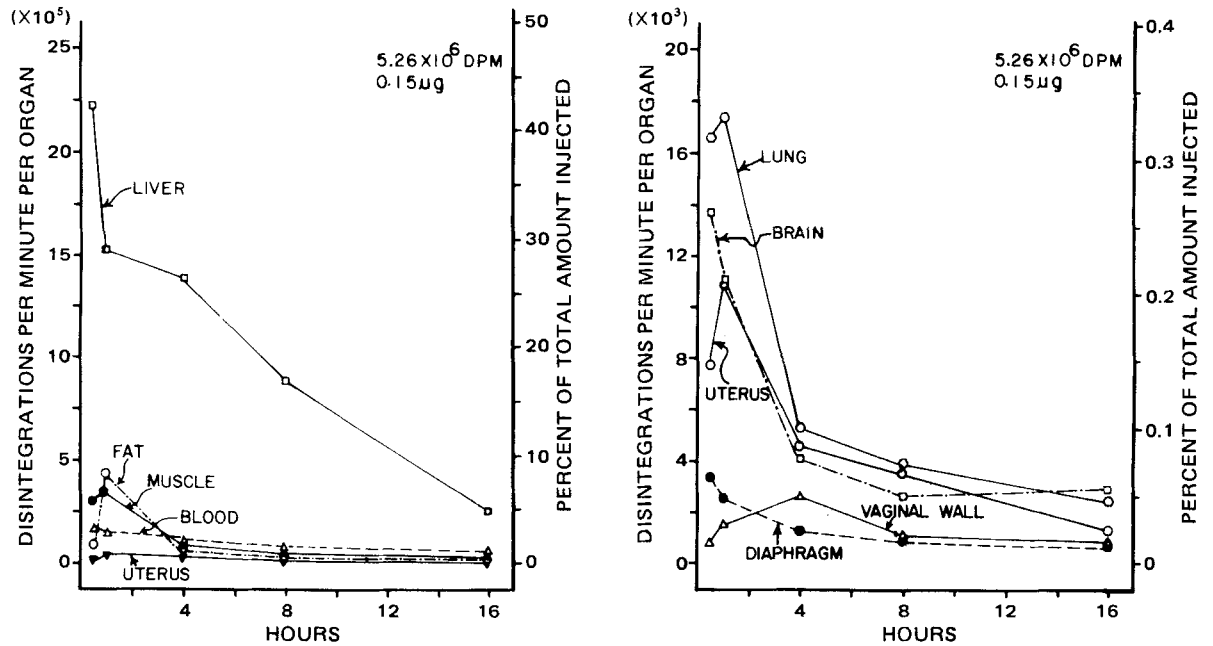

Figure 2—*Retention of radioactivity by various tissues after the subcutaneous injection of ^3H-progesterone.*

istration. In comparison, other organs or tissues, such as the uterus, muscle, blood, fat, lung, brain, diaphragm, and vaginal wall, retained only a fraction of a percent of the administered radioactivity. For instance, a maximum of only 0.15% of the total radioactivity administered was in the uterus tissue 4 hr after gastric intubation.

On a concentration basis expressed as disintegrations per minute per gram of tissue, however, uterus and vaginal wall tissues retained high concentrations of radioactivity for a prolonged period, typical of progesterone target tissues (Table I). The liver, however, retained the highest concentration of radioactivity expressed on a disintegrations per minute per gram of tissue basis. The radioactivity concentration in the liver was about 20 times that of the uterus up to 8 hr after administration.

Table I—Radioactivity Distribution in Rat Tissues after Gastric Intubation of ^3H-Progesterone

	Radioactivity[a], dpm/g of Tissue								
Hours	Uterus	Vaginal Wall	Brain	Liver	Lung	Diaphragm	Thigh Muscle	Fat	Blood
1	5937 ± 1312	2652 ± 375	1446 ± 79	107,063 ± 28,997	3388 ± 416	1774 ± 369	1139 ± 221	725 ± 90	3630 ± 901
4	11,762 ± 1729	19,405 ± 2705	2223 ± 255	255,913 ± 55,401	5227 ± 769	3132 ± 875	2257 ± 727	2057 ± 308	9000 ± 2385
8	10,158 ± 1327	7430 ± 1884	2113 ± 201	181,916 ± 50,085	6148 ± 960	2699 ± 533	2029 ± 351	2265 ± 302	6753 ± 329
16	6387 ± 727	3644 ± 994	2042 ± 227	51,499 ± 6458	3804 ± 575	1656 ± 246	1954 ± 289	1724 ± 361	4460 ± 364

[a] Total ^3H-progesterone administered = 0.15 µg = 5.26 × 10^6 dpm in 1 ml of 5% ethanol. The data pooled from either three or four rats were expressed as mean ± *SD*.

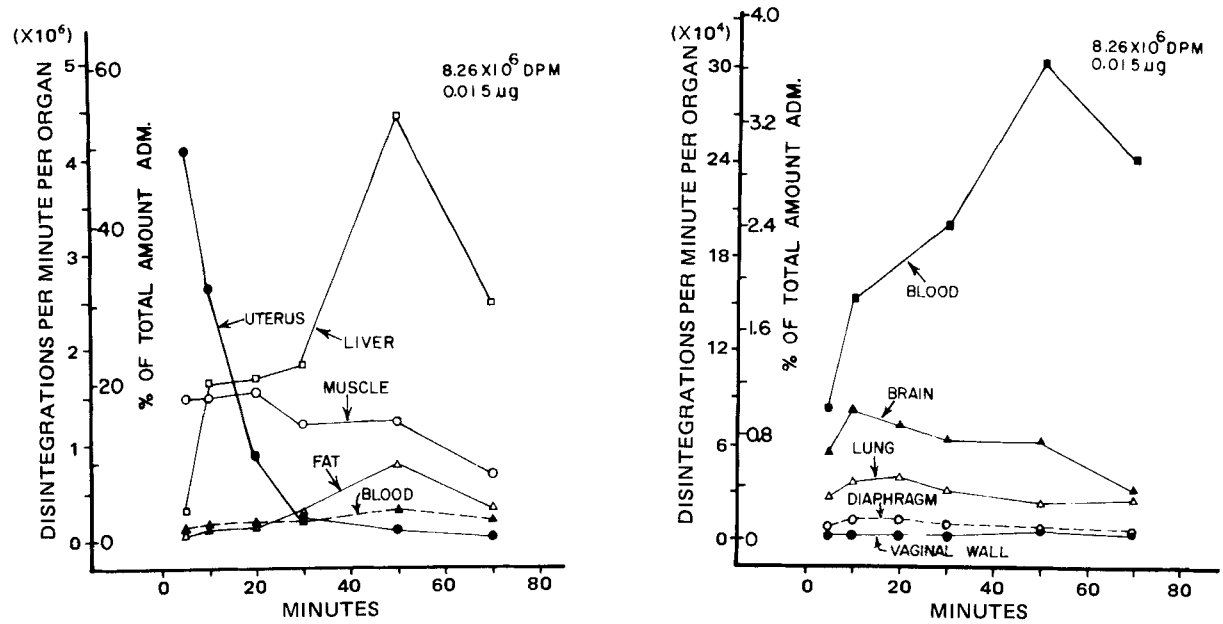

Figure 3—*Retention of radioactivity by various tissues after the uterine intraluminal instillation of ^3H-progesterone.*

A similar pattern and level of radioactivity distribution in various rat tissues were observed when the tritium-labeled progesterone (0.15 μg) was administered by subcutaneous injection (Fig. 2 and Table II). Most radioactivity again was found in the liver. Although as much as 7% of the total dose was in fat tissues 60 min after administration, only a fraction of a percent of the total dose was in other organs and tissues.

Tritium-labeled progesterone (0.15 μg) was also administered by direct instillation into the luminal cavity of rat uterine horns through laparotomy. In an earlier attempt, progesterone solution was introduced into the uterine luminal cavity by the vaginal route according to the method reported by Stone and Martin (13). However, uncertainties always arose with this route regarding the definitive placement of the solutions in two separate uterine horns of a rat and not twice in the same horn. Furthermore, the exact point of placement of the solution along the length of the uterine horn was also rather difficult to ascertain. Therefore, direct injection of the progesterone solution into the luminal cavity of the uterine horn after laparotomy was preferred.

As expected, large amounts of radioactivity were initially found in the uterine tissue after uterine intraluminal instillation (Figs. 3 and 4). The decrease in uterine radioactivity followed a typical biphasic exponential curve: an initial phase of rapid decrease, which lasted for about 30 min, followed by a second phase with a much slower rate of decrease. The decrease in uterine radioactivity coincided with the increases in liver and blood uptake (Fig. 3). The maximum amount of radioactivity in the liver, about 55% of the total dose, was reached 50 min after instillation.

In oral administration, the liver uptake of progesterone did not peak until 4 hr after administration. This result indicates that progesterone absorption is definitely much faster in the uterus than in the GI tract. Although direct comparisons with subcutaneous injection is difficult because the studies were done on different time courses, the rate of systemic availability of progesterone administered by uterine intraluminal instillation is probably faster than that after subcutaneous injection.

As with the other two modes of administration, only a small fraction of administered progesterone reached various other tissues after uterine

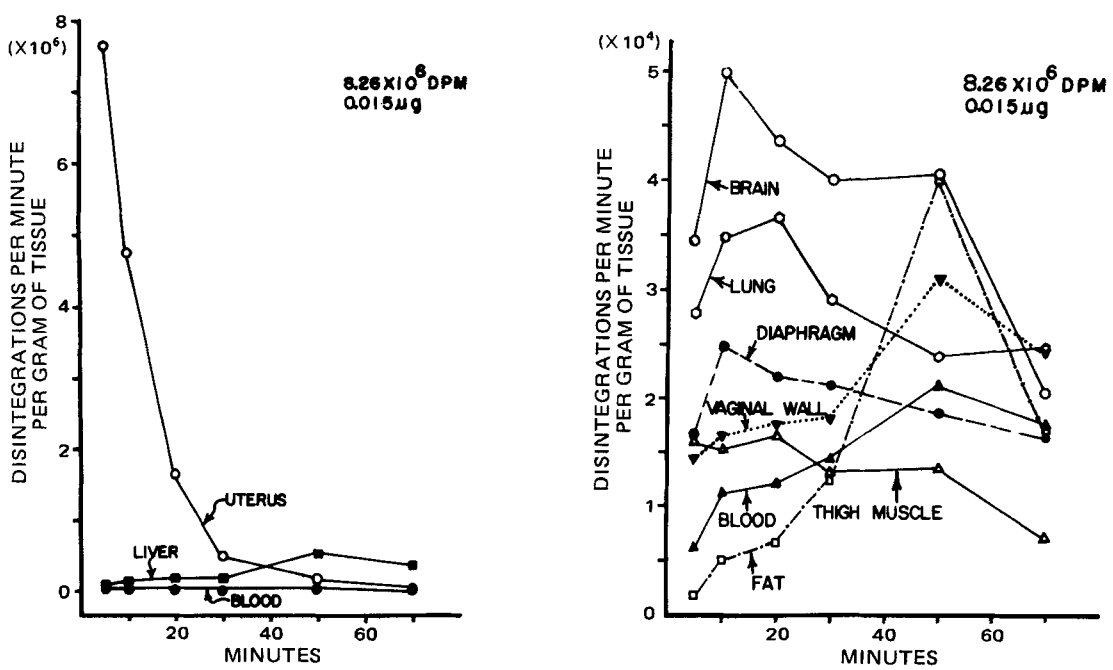

Figure 4—*Radioactivity concentrations in various tissues after the uterine intraluminal instillation of ^3H-progesterone.*

Table II—Radioactivity Distribution in Rat Tissues after Subcutaneous Administration of ^{3}H-Progesterone

	Radioactivity[a], dpm/g of tissue								
Hours	Uterus	Vaginal Wall	Brain	Liver	Lung	Diaphragm	Thigh Muscle	Fat	Blood
0.5	15,646 ± 4386	5738 ± 688	8684 ± 333	283,431 ± 53,826	16,105 ± 3064	6773 ± 912	2774 ± 60	5533 ± 848	11,837 ± 3050
1	20,455 ± 4627	7973 ± 2161	7107 ± 751	187,986 ± 13,686	16,845 ± 2696	5011 ± 502	2836 ± 896	18,900 ± 3128	9337 ± 1510
4	7539 ± 776	17,920 ± 1248	2585 ± 154	179,073 ± 3830	5111 ± 434	2383 ± 176	1588 ± 35	7619 ± 647	8547 ± 2184
8	5591 ± 756	3339 ± 158	1648 ± 196	109,179 ± 16,957	3719 ± 361	1581 ± 153	1545 ± 181	4584 ± 1026	3753 ± 1067
16	3787 ± 707	3877 ± 1318	1850 ± 284	41,951 ± 9443	2367 ± 1128	1424 ± 10	1314 ± 163	2070 ± 71	3877 ± 329

[a] Total ^{3}H-progesterone administered = 0.15 μg = 5.26 × 10^6 dpm in 1 ml of 5% ethanol. The data pooled from either three or four rats were expressed as mean ± *SD*.

intraluminal instillation (Figs. 3 and 4). Substantially higher concentrations of progesterone, however, were detected in most tissues studied with this mode of administration than those obtained by the other two routes of administration (Tables I and II and Fig. 4). Uterine tissue, as expected, retained a high concentration of radioactivity for a rather long time. Progesterone bioavailability in the uterus, estimated from the area under the radioactivity–time curve, was about 45 times higher by uterine intraluminal instillation than that obtained by either gastric intubation or subcutaneous injection (Figs. 1–3).

Uterine Absorption of Progesterone Administered by Direct Uterine Intraluminal Instillation—The absorption rate of progesterone by uterine tissue was estimated by measuring the radioactivity remaining in the luminal cavity at various times after instillation. Uterine endometrium absorbed progesterone with great rapidity. At a dose of 0.15 μg (in 40 μl of 5% ethanol solution), essentially all radioactivity (95%) was absorbed by the uterine tissue 5 min after instillation. Similar results were obtained with a 0.015-μg dose. Therefore, the rat uterine endometrium is an extremely efficient tissue for progesterone absorption. Similar results in spayed mice were reported (14).

Pharmacokinetic Analysis of Uterine Retention of Progesterone Administered by Uterine Intraluminal Instillation—The amount of radioactivity retained by uterine tissue was determined at different intervals after the instillation of tritium-labeled progesterone into the luminal cavity of the uterus. The radioactivity in the uterine tissue following rapid absorption from the luminal cavity was eliminated in a kinetic pattern closely resembling a biphasic exponential curve (Fig. 5). A plausible pharmacokinetic model to describe this phenomenon is shown in Scheme I, where [*A*] is the progesterone in compartment *A* of the uterus, [*B*] is the progesterone in compartment *B* of the uterus, [*C*] is the amount of progesterone excreted out of the uterus, k_{12} is the rate constant for $A \rightarrow B$, k_{21} is the rate constant for $B \rightarrow A$, and k_{el} is the elimination rate constant.

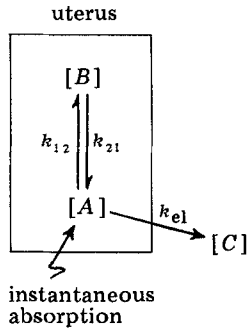

Scheme I

The derivation of the pertinent pharmacokinetic parameters is given as follows. Let *D* equal the total amount of progesterone administered and V_d equal the apparent volume of distribution. Then:

$$\frac{dA}{dt} = k_{21}B - (k_{12} + k_{el})A \quad \text{(Eq. 1)}$$

$$\frac{dB}{dt} = k_{12}A - k_{21}B \quad \text{(Eq. 2)}$$

$$\frac{dC}{dt} = k_{el}A \quad \text{(Eq. 3)}$$

Solving for *A* and *B* from Eqs. 1–3 yields:

$$A = \frac{D}{\alpha - \beta}[(\alpha - k_{21})e^{-\alpha t} + (k_{21} - \beta)e^{-\beta t}] \quad \text{(Eq. 4)}$$

$$B = \frac{Dk_{12}}{\alpha - \beta}(e^{-\beta t} - e^{-\alpha t}) \quad \text{(Eq. 5)}$$

where:

$$\alpha = \tfrac{1}{2}[(k_{12} + k_{21} + k_{el}) + \sqrt{(k_{12} + k_{21} + k_{el})^2 - 4k_{21}k_{el}}] \quad \text{(Eq. 6)}$$

$$\beta = \tfrac{1}{2}[(k_{12} + k_{21} + k_{el}) - \sqrt{(k_{12} + k_{21} + k_{el})^2 - 4k_{21}k_{el}}] \quad \text{(Eq. 7)}$$

$$A + B = \frac{D}{\alpha - \beta}[(k_{el} - \beta)e^{-\alpha t} + (\alpha - k_{el})e^{-\beta t}] \quad \text{(Eq. 8)}$$

The total concentration of radioactivity in the uterus, C_{ut}, is:

$$C_{ut} = \frac{A + B}{V_d} = \frac{D}{V_d(\alpha - \beta)}[(k_{el} - \beta)e^{-\alpha t} + (\alpha - k_{el})e^{-\beta t}] \quad \text{(Eq. 9)}$$

Let:

$$m_1 = \frac{D(k_{el} - \beta)}{V_d(\alpha - \beta)} \quad \text{(Eq. 10)}$$

and:

$$m_2 = \frac{D(\alpha - k_{el})}{V_d(\alpha - \beta)} \quad \text{(Eq. 11)}$$

Then:

$$C_{ut} = m_1e^{-\alpha t} + m_2e^{-\beta t} \quad \text{(Eq. 12)}$$

where m_1, m_2, α, and β are obtained from graphical analysis of experimental data plotted as log C_{ut} *versus* *t* and:

$$k_{el} = \frac{\alpha m_1 + \beta m_2}{m_1 + m_2} \quad \text{(Eq. 13)}$$

$$k_{21} = \frac{\alpha\beta}{k_{el}} \quad \text{(Eq. 14)}$$

$$k_{12} = \alpha + \beta - k_{21} - k_{el} \quad \text{(Eq. 15)}$$

This particular model is established with the following assumptions and/or approximations:

1. Progesterone is absorbed so rapidly by uterine tissue upon intraluminal instillation that absorption is assumed, for practical purposes, as instantaneous.

2. Upon reaching uterine tissue, progesterone is quickly redistributed into other parts of the body in a first-order kinetic rate with a rate constant of k_{el}, while a simultaneous process also takes place within uterine tissue where progesterone molecules diffuse to a deep compartment within the uterine cell. Progesterone redistribution within the uterine tissue is a reversible process with a forward rate constant of k_{12} and a reverse rate constant of k_{21}.

3. The nonpolar and conjugated metabolites of progesterone in the uterus are all treated as progesterone in this model. This treatment is based on the fact that most nonpolar metabolites are also known progestins, while the conjugates, since they form a reversible equilibration with nonconjugated moieties within the uterine tissue, should be considered equally active physiologically. Since progesterone is proposed to act directly on uterine tissue to cause contraception, for the collective quantitative assessment of the steroid action in uterine tissue, one should pool all these metabolites to achieve a better approximation.

4. Since progesterone is eliminated out of the body not directly *via* the uterus, the reversible influx of progesterone from blood to the uterus is likely to be insignificant. Therefore, the process was omitted for simplification.

The values for β, m_1, α, and m_2 were obtained by feathering analysis of the plot of log disintegrations per minute per gram of tissue *versus* time. The values for k_{el}, k_{12}, and k_{21} are 0.110, 8.27 × 10^{-4}, and 3.09 ×

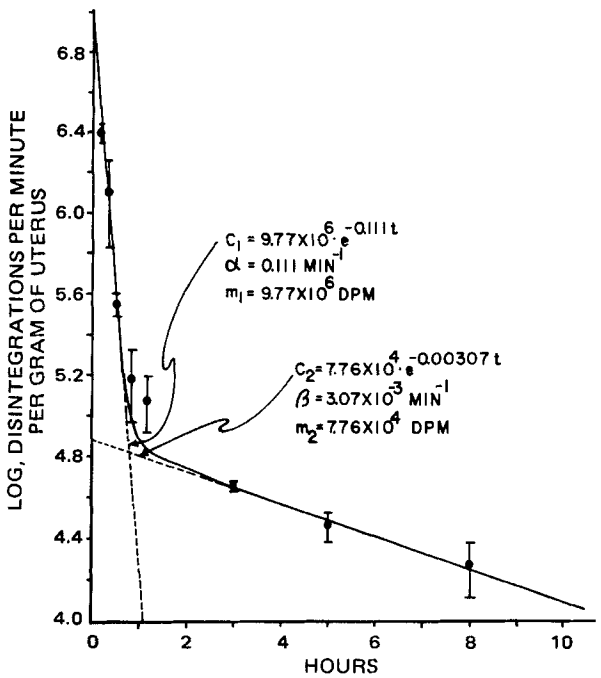

Figure 5—*Pharmacokinetic analysis of the uterine retention of radioactivity after the uterine intraluminal instillation of ^3H-progesterone (0.15 μg = 8.26 × 10^6 dpm). Key: C_2, straight line obtained from the β-phase decay; C_1, straight line obtained by "feathering method"; and solid biphasic line, computer-predicted value for C_{ut} (Eq. 12) based on the obtained pharmacokinetic parameters. The experimental values are presented as mean ± SD.*

10^{-3} min^{-1}, respectively. The computer plot of Eq. 12 is shown in Fig. 5. Except for a few points in the inflection area, the experimental values fit reasonably well with the computer-predicted values derived from the proposed pharmacokinetic model. This model is definitely oversimplified and should not be used to argue the definitive mechanisms involved in the uterine retention of progesterone. The constant obtained from k_{12}/k_{21} is a complex value probably contributed by various mixed factors such as progesterone binding to various subcellular components or the heterogeneous distribution of progesterone between the intracellular and interstitial fluids of the uterine tissue.

Based on these kinetic model analyses, the slope in the α-phase approximates k_{el} while the slope in the β-phase approximates the dissociation constant k_{21}. This result connotes a different physiological significance than the two-compartment open model analysis commonly used in describing drug disappearance from blood where the slope in the β-phase approximates the k_{el} value. Based on the values of k_{el} and k_{21}, the progesterone biological half-life in the uterine tissue was calculated to be 6.5 min in the α-phase and 230 min in the β-phase. In comparison, the progesterone biological half-life in rat peripheral serum was reported to be 18 min in the β-phase (15), which is much shorter than that in the uterus. This result further substantiates the earlier hypothesis that the reverse influx of progesterone from blood to uterus is likely to be insignificant in uterine intraluminal instillation.

To investigate the consequences of the application of a "Uterine Progesterone System," further studies should simulate constant uterine administration of progesterone until a steady state is reached. Progesterone distribution in uterus and various other tissues should then be assessed to compare the relative amount of progesterone that may exist in the uterus against other parts of the body. Since progesterone is likely to exert the contraceptive effect locally on uterine tissue, the ideal steady state after drug administration should exhibit a large amount of drug in the uterus and negligible amounts in other parts of the body. Furthermore, the extent of the uterine retention of progesterone in the steady state assessed by the actual experimental measurement should be compared to the predicted value based on the pharmacokinetic parameters obtained in this study. These and other studies pertinent to the use of the "Uterine Progesterone System" will be published in subsequent papers.

REFERENCES

(1) J. M. Morris, *Am. J. Obstet. Gynecol.*, **117**, 167 (1973).

(2) L. L. Doyle and T. Clewe, *ibid.*, **101**, 564 (1968).

(3) A. Scommegna, G. N. Pandya, M. Christ, A. W. Lee, and M. K. Cohen, *Fertil. Steril.*, **21**, 201 (1970).

(4) D. R. Mishell, Jr., M. Talas, A. F. Parlow, and D. L. Moyer, *Am. J. Obstet. Gynecol.*, **107**, 100 (1970).

(5) M. R. Henzl, D. R. Mishell, Jr., J. G. Velazquez, and W. E. Leitch, *ibid.*, **117**, 101 (1973).

(6) U. Leone, *Int. J. Fertil.*, **19**, 17 (1974).

(7) A. Zaffaroni, *Acta Endocrinol., Suppl. 185*, **75**, 423 (1974).

(8) S. A. Tillson, M. Marian, R. Hudson, P. Wong, B. B. Pharriss, R. Aznar, and J. Martinez-Manatou, *Contraception*, **11**, 179 (1975).

(9) J. Martinez-Manatou, *J. Steroid Biochem.*, **6**, 889 (1975).

(10) K. Hagenfeldt and B. Landgren, *ibid.*, **6**, 895 (1975).

(11) G. Gyözö, *Am. J. Obstet. Gynecol.*, **124**, 214 (1976).

(12) G. Zador, B. A. Nilsson, B. Nilsson, N. O. Sjöberg, L. Weström, and J. Wiese, *Contraception*, **13**, 559 (1976).

(13) G. M. Stone and L. Martin, *Steroids*, **3**, 699 (1964).

(14) B. F. Clark, *J. Endocrinol.*, **58**, 555 (1973).

(15) G. J. Pepe and I. Rothchild, *Endocrinology*, **93**, 1200 (1973).

ACKNOWLEDGMENTS AND ADDRESSES

Received November 10, 1976, from the *Department of Applied Pharmaceutical Sciences and Biopharmaceutical Sciences, College of Pharmacy, University of Utah, Salt Lake City, UT 84112.*

Accepted for publication March 1, 1977.

Supported by Grant HD-09420 from the National Institutes of Health.

[x] To whom inquiries should be directed.

High-Performance Liquid Chromatographic Analysis of Methadone Hydrochloride Oral Solution

THOMAS H. BEASLEY, Sr., and HOWARD W. ZIEGLER ˣ

Abstract □ A direct and rapid high-performance liquid chromatographic assay for methadone hydrochloride in a flavored oral solution dosage form is described. A syrup sample, one part diluted with three parts of water, is introduced onto a column packed with octadecylsilane bonded on 10-μm porous silica gel (reversed phase). A formic acid–ammonium formate-buffered mobile phase is linear programmed with acetonitrile. The absorbance is monitored continuously at 280 or 254 nm, using a flow-through, UV, double-beam photometer. An aqueous methadone hydrochloride solution is used for external standardization. The relative standard deviation was not more than 1.0%. Drug recovery from a syrup base was better than 99.8%.

Keyphrases □ Methadone hydrochloride—high-performance liquid chromatographic analysis, liquid pharmaceutical preparation □ High-performance liquid chromatography—analysis, methadone hydrochloride in liquid pharmaceutical preparation □ Narcotic analgesics—methadone hydrochloride, high-performance liquid chromatographic analysis in liquid pharmaceutical preparation

Methadone hydrochloride is used widely in drug maintenance treatment programs. Although tablet and injection formulas are available, the preferred dosage form is a flavored oral solution. A rapid and simple analysis of methadone hydrochloride in a proprietary dosage form[1] was sought. The USP GLC method for methadone hydrochloride injection and tablets (1) is cumbersome and lengthy and often lacks precision. Also, the GLC column can become overloaded with thermal decomposition products readily.

The British Pharmacopoeia specifies an extraction–acid titration procedure for methadone injection and tablets (2). A simplified gravimetric method for methadone hydrochloride in flavored syrup formulations was described (3). The alkaloid was precipitated as the phosphomolybdate complex and weighed. Choulis and Papadopoulous (4) developed a GLC assay of methadone in sustained-release tablets after dissolving the drug with dissolution fluids used for *in vitro* evaluation. Most methadone hydrochloride assays are trace methods after extraction of the drug from human urine, blood, or serum.

Some advantages of reversed-phase high-performance liquid chromatography (HPLC) are: (*a*) aqueous samples can be diluted and chromatographed without extraction, concentration, or derivatization; (*b*) samples can be run at ambient temperature; (*c*) analyses can be completed in about 20 min; and (*d*) a formulation can be analyzed for preservative, flavor, or another drug if present.

EXPERIMENTAL

Apparatus—A modular liquid chromatograph equipped with 280- and 254-nm UV detectors[2] was used along with a 10-mv recorder, a piston pump[3], suitable pulse dampening, a stainless steel sampling valve[4], a pressure gauge, valves, tubing, and fittings necessary to complete a closed system.

The stainless steel column was 3.2 × 250 mm, slurry packed with octadecylsilane bonded on 10-μm porous silica gel[5]. A stainless steel precolumn, 3.2 × 75 mm, containing porous silica coated with a monomolecular layer of octadecylsilane[6] (37 μm, nominal particle size) was placed in the HPLC system ahead of the sample injection valve.

The gradient elution cell consisted of a 25-ml glass bulb with fittings compatible with the instrument. The gradient cell and valving were described previously (5).

Reagents—*Mobile Phase A*—Distilled formic acid, 100 ml, and 1000 ml of water were transferred to a 2-liter flask or vessel and mixed. After 2.5 ml of concentrated ammonium hydroxide was added, the solution was diluted to 2000 ml with water and mixed.

Mobile Phase B—Spectrophotometric grade acetonitrile[7], which shows little or no absorbance in the UV from 220 to 350 nm, was used.

Gradient Elution—A programmed linear gradient elution from 100% Mobile Phase A to 80% Mobile Phase B in Mobile Phase A in about 20 min was used.

Chromatographic Conditions—The column temperature was ambient. The electrometer was set at 0.32 absorbance unit full scale (aufs) with a recorder chart speed of 5.08 mm/min. The flow rate was 2 ml/min, and column pressure was about 1500 psi. The volume of the sample and standard sample introduced onto the column was 50 μl. Water, pumped through the system, was used to rinse the sugars, *etc.*, from the column. Mobile Phase A can be stored in the system.

Methadone Hydrochloride Standard Solutions—*Stock*—Methadone hydrochloride USP[8] was used as the working standard. Approximately 1.0 g of the standard was accurately weighed, transferred to a 100-ml volumetric flask, and dissolved in and diluted to volume with water.

Diluted—A 25.0-ml aliquot of stock methadone hydrochloride standard solution was transferred to a 100-ml volumetric flask and diluted to volume with water. This solution contained 2.5 mg/ml of standard.

Both solutions were freshly prepared.

Sample Preparation—Water, 75 ml, was transferred to a dry 100-ml volumetric flask. The sample syrup formulation, delivered from a 30-ml syringe fitted with a long needle, was used to dilute to the mark. Then the solution was mixed thoroughly.

Analysis—Aliquots of 50 μl of diluted sample solution were injected into a prepared chromatograph operated at the designated flow rate of Mobile Phase A. The gradient system and recorder were started; the run was 20 min. Reequilibration to Mobile Phase A required about 10 min. Diluted standard solution, 50 μl, was injected under the same conditions used for the sample. Replicate sample and standard solutions were generally run to test for system stability.

Table I—Replicate Assay Results from a Production Lot of a Proprietary Methadone Hydrochloride Oral Solution

	Methadone Hydrochloride, mg/ml		
Sample[a]	1	2	3
A	10.01	10.14	10.07
B	10.05	10.23	10.15
C	10.14	10.10	10.06
D	10.12	10.14	10.07
E	10.20	10.09	10.09

[a] Statistically sampled from the lot. Each individual sample run using triplicate sample injections.

[1] Methadose, Mallinckrodt, St. Louis, Mo.
[2] Model 151, Altex, Berkeley, Calif.
[3] Model 3366-460, Glenco, Houston, Tex.
[4] Valco CV6-UHPa-N60, 7000 psi, Glenco, Houston, Tex.
[5] LiChrosorb S160, reversed phase, 10 μm, Altex (5-μm material may also be used).
[6] C_{18} reversed phase, Waters Associates, Milford, Mass.
[7] SpectrAR, Mallinckrodt, St. Louis, Mo.
[8] Mallinckrodt, St. Louis, Mo.

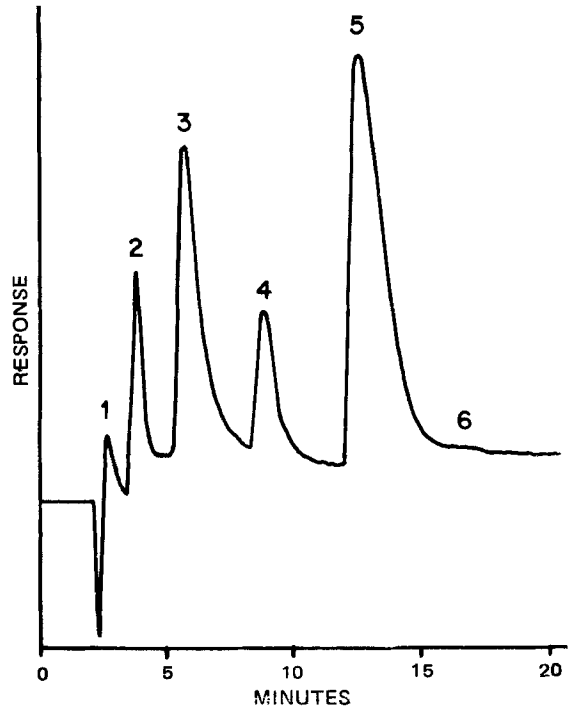

Figure 1—*Typical chromatogram of a proprietary methadone hydrochloride oral solution. Key: 1, solvent front; 2, preservative (sodium benzoate); 3 and 4, flavor components; 5, methadone hydrochloride; and 6, dye.*

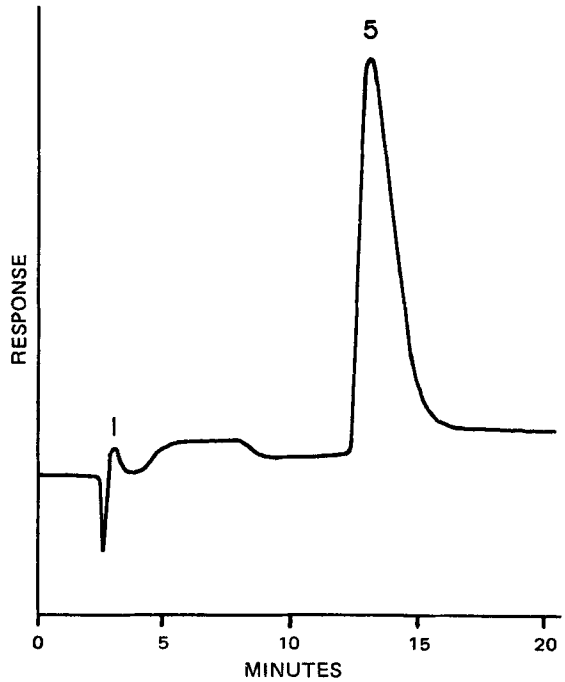

Figure 2—*Chromatogram of an aqueous methadone hydrochloride reference material solution (50 μl of a 2.5-mg/ml solution). Key: 1, solvent front; and, 5, methadone hydrochloride.*

Calculations—Peak areas were measured by electronic methods, and peak heights were measured manually. The methadone hydrochloride concentration was calculated using:

$$\frac{(A_1 \text{ or } H_1)(4C)}{A_2 \text{ or } H_2} = \text{mg/ml} \qquad \text{(Eq. 1)}$$

where A_1 is the average area of peaks from the diluted sample solution, A_2 is the average area of peaks from the diluted standard solution, H_1 is the average height of peaks from the diluted sample solution, H_2 is the average height of peaks from the diluted standard solution, C is the concentration in milligrams per milliliter of methadone hydrochloride in the diluted standard solution, and 4 is the dilution factor.

RESULTS AND DISCUSSION

A typical chromatogram of a diluted sample of a proprietary methadone hydrochloride oral solution is shown in Fig. 1. Diluted methadone hydrochloride standard solution is displayed in the chromatogram in Fig. 2. The standard solution is unstable and must be freshly prepared and diluted for each analysis. About 1 mg of sodium benzoate/ml can be added to the solutions to stabilize the standards for at least 1 month if it is necessary to retain them.

No chromatographic interference is encountered with the preservative. Some laboratory distilled water contains trace impurities that display varying chromatographic baselines. For this reason, both the sample syrup and stock standard solution aliquots should be diluted with identical amounts of the same water before chromatographic analysis. The rather unconventional reverse technique of using sample syrup as the volumetric diluent was selected because the formulation is very viscous. More precise sample measurements were made using this procedure.

HPLC results of replicate analyses are displayed in Table I. The relative standard deviation was not more than 1.0%. Recovery data of weighed amounts of methadone hydrochloride added to laboratory prepared formulation base are shown in Table II. The average recovery was not less than 99.8%. In no case could it be proven statistically, at the 95% confidence level, that the recovery was different from 100%. All data were calculated by an on-line computer[9] that calculates from integrated areas. With the computer interface, chromatographic analysis time can be cut in half. The procedure recommended allows for manual computations using either peak area or peak height.

HPLC parameters require that methadone hydrochloride be chromatographed as the protonated amine in an acid system. Methadone hydrochloride in an acidified mobile phase attacks some types of stainless steel, necessitating the use of chloride-resistant types. Stainless steel No. 304 or 316 cannot be used.

The formic acid used for Mobile Phase A had to be distilled to remove UV absorbers, which are apparently leached from the plastic containers in which the acid is supplied.

The method described is a unique application of *direct* chromatography of a sample with little or no sample preparation, extraction, or derivatization. The technique may be applicable to other aqueous dosage forms such as cough–cold preparations.

Table II—Recovery of Methadone Hydrochloride from Synthetic Formulation Syrup Base

Methadone Hydrochloride Added, mg/ml					
4.96		9.78		14.96	
Recovered, mg	Recovered, %	Recovered, mg	Recovered, %	Recovered, mg	Recovered, %
5.16	104.0	9.85	100.7	14.93	99.8
5.01	101.0	9.82	100.4	14.98	100.1
5.05	101.8	9.77	99.9	14.90	99.6
4.98	100.4	9.67	98.9	14.97	100.1
—	—	9.68	99.0	14.96	100.0
—	—	9.78	100.0	14.91	99.7
—	—	9.76	99.8	—	—

REFERENCES

(1) "The United States Pharmacopeia," 19th rev., Mack Publishing Co., Easton, Pa., 1975, pp. 310, 311.

(2) "The British Pharmacopoeia," Her Majesty's Stationery Office, Cambridge, England, 1973, pp. 294, 295.

(3) S. P. Loucas, R. L. Feinberg, P. A. Gunning, F. F. Hartman, and B. Mehl, *Am. J. Hosp. Pharm.*, **31**, 1193 (1974).

(4) N. H. Choulis and H. Papadopoulous, *J. Chromatogr.*, **106**, 180 (1975).

(5) H. W. Ziegler, T. H. Beasley, Sr., and D. W. Smith, *J. Assoc. Offic.*

[9] Model 3354 Lab Data System, Hewlett-Packard.

Anal. Chem., 58, 888 (1975).

ACKNOWLEDGMENTS AND ADDRESSES

Received December 27, 1976, from the *Corporate Analytical Services Laboratory, Mallinckrodt, Inc., St. Louis, MO 63147.*

Accepted for publication February 24, 1977.

The authors appreciate the technical assistance of Elmer Kemmery.

[x] To whom inquiries should be directed.

Prednisolone Bioavailability in the Dog

FRANCIS L. S. TSE and PETER G. WELLING [x]

Abstract □ With a fasted dog as an animal model, the bioavailability and pharmacokinetics of prednisolone were studied following rapid intravenous injection and oral dosing of a prednisolone sodium phosphate solution and also following oral doses of prednisolone as tablets and a slurry. Hydrolysis of the phosphate ester to prednisolone in the body is extremely rapid and complete, thus permitting accurate calculation of the distribution volume of prednisolone. Enteral absorption of prednisolone from a slurry is superior to that from prednisolone tablets and from a prednisolone sodium phosphate solution. Reduced absorption from tablets, compared to the slurry, is probably due to tablet disintegration characteristics; reduced absorption from the solution is probably due to poor membrane permeability of the ionized drug. Information obtained from a single animal may indicate the need for expanded studies in humans.

Keyphrases □ Prednisolone—bioavailability and pharmacokinetics, various dosage forms compared, dogs □ Bioavailability—prednisolone, various dosage forms compared, dogs □ Pharmacokinetics—prednisolone, various dosage forms compared, dogs □ Glucocorticoids—prednisolone, bioavailability and pharmacokinetics, various dosage forms compared, dogs

Prednisolone is used primarily for its anti-inflammatory activity in several diseases. It is cleared from the body predominantly by hepatic metabolism; only about 10% of orally dosed compound is excreted unchanged in urine (1).

Peak serum prednisolone concentrations of 160 ng/ml at 0.5 hr and 298 ng/ml at 1 hr were reported following 2.5- and 5.0-mg oral doses of prednisolone, respectively, to male beagle dogs (2). Studies in humans yielded peak serum prednisolone levels at 1–2 hr following oral doses and a serum half-life of about 3 hr (3–8).

Although the influence of *in vitro* disintegration and dissolution characteristics on prednisolone pharmacokinetics was reported (5–8), no information is available on the effect of the dosage form on bioavailability characteristics.

With the beagle dog as a model system, the present study was undertaken to compare the bioavailability and pharmacokinetics of prednisolone from two different doses of a commercial tablet, a slurry, and a solution of a water-soluble prednisolone salt.

EXPERIMENTAL

A 3-year-old male beagle dog, 17.5 kg, was given 30- and 60-mg doses of prednisolone tablets[1] (oral), oral prednisolone slurry[1], and oral and intravenous prednisolone sodium phosphate solution[2] in separate experiments. All experiments were done in duplicate.

Food was withheld at least 12 hr before and throughout each experiment. During an experiment, the dog was placed in a restraining apparatus so that it could stand normally but could not disturb indwelling catheters.

In the intravenous dosing experiments, an infusion set was positioned in each front leg. Each set consisted of a 19-gauge needle with 30 cm of flexible plastic tubing with a total volume of 0.6 ml. Clotting of blood in infusion sets was prevented by infusing 2 ml of saline-diluted heparin sodium solution (10 units/ml) into the set each hour it was in position. Prednisolone sodium phosphate was administered *via* one infusion set, with injection being completed in about 30 sec. The set was flushed with 10 ml of normal saline solution and was then removed.

Blood samples (8 ml) were collected through the other infusion set shortly before dosing and at 5, 15, and 30 min and 1, 2, 4, and 6 hr after dosing. Before each sample was taken, 5 ml of residual fluid was withdrawn to remove the heparin solution in the infusion set. The blood sample was then drawn, and the volume was replaced by an 8-ml injection of normal saline. The residual fluid was reinjected followed by 2 ml of heparin solution.

Tablets were administered by placing them on the posterior portion of the tongue so that they were not fractured or chewed before being swallowed; then 50 ml of water was immediately given. The slurry was prepared by triturating prednisolone tablets to a powder and dispersing this powder in 50 ml of water. The slurry was administered directly into the dog's stomach by means of a 120-cm × 3-mm (i.d.) stomach tube. Water, 25 ml, was used to flush residual drug from the syringe and stomach tube into the stomach. The oral solution was administered directly into the stomach in identical fashion to the slurry. With all oral dosing experiments, blood samples were collected *via* an infusion set as in the intravenous case.

Blood samples were placed in heparinized tubes[3] and centrifuged at 2300 rpm for 10 min. Plasma was removed and frozen until analyzed, usually within 1 week.

Experiments were performed 3 weeks apart to avoid changes in drug pharmacokinetic parameters due to prior exposure and to ensure complete drug washout from a previous dose.

Assay of Plasma Samples—The assay used to measure prednisolone in plasma was a modification of the GLC method described by Bacon and Kokenakes (9). In the purification step by column chromatography, the volume of the first eluting solvent [benzene–acetone (9:1)] was reduced from 70 to 30 ml and the volume of the second eluting solvent [benzene–acetone (1:3)] was increased from 20 to 30 ml. This change improved separation of prednisolone from other plasma components[4].

A solution containing the silylating agent[5] was prepared by combining 0.3 ml of pyridine, 37 μl of dotriacontane (as the internal standard) in carbon tetrachloride (0.95 μg/μl), and 0.5 ml of the silylating agent. A 20-μl aliquot of this solution was added to the extracted and purified prednisolone sample in a 1-ml vial[6]. This vial was immediately sealed with a polytef-lined cap, agitated on a vortex-type mixer, and allowed to stand at room temperature for 18 hr before assay.

GLC was carried out on an instrument[7] fitted with dual flame-ionization detectors. The column was a 1.8-m × 2-mm (i.d.) U-shaped glass

[1] Meticortelone, Schering Corp., Bloomfield, N.J.

[2] Hydeltrasol, Merck Sharp and Dohme, West Point, Pa.

[3] Vacutainer, Becton-Dickinson, Rutherford, N.J.

[4] G. E. Bacon, University of Michigan Medical Center, Ann Arbor, Mich., personal communication.

[5] Tri-Sil TBT, Pierce Chemical Co., Rockford, Ill.

[6] Reacti-vial, Pierce Chemical Co., Rockford, Ill.

[7] Nuclear Chicago Selecta System model 5000, Searle, Des Plaines, Ill.

Anal. Chem., 58, 888 (1975).

ACKNOWLEDGMENTS AND ADDRESSES

Received December 27, 1976, from the *Corporate Analytical Services Laboratory, Mallinckrodt, Inc., St. Louis, MO 63147.*

Accepted for publication February 24, 1977.

The authors appreciate the technical assistance of Elmer Kemmery.

[x] To whom inquiries should be directed.

Prednisolone Bioavailability in the Dog

FRANCIS L. S. TSE and PETER G. WELLING [x]

Abstract □ With a fasted dog as an animal model, the bioavailability and pharmacokinetics of prednisolone were studied following rapid intravenous injection and oral dosing of a prednisolone sodium phosphate solution and also following oral doses of prednisolone as tablets and a slurry. Hydrolysis of the phosphate ester to prednisolone in the body is extremely rapid and complete, thus permitting accurate calculation of the distribution volume of prednisolone. Enteral absorption of prednisolone from a slurry is superior to that from prednisolone tablets and from a prednisolone sodium phosphate solution. Reduced absorption from tablets, compared to the slurry, is probably due to tablet disintegration characteristics; reduced absorption from the solution is probably due to poor membrane permeability of the ionized drug. Information obtained from a single animal may indicate the need for expanded studies in humans.

Keyphrases □ Prednisolone—bioavailability and pharmacokinetics, various dosage forms compared, dogs □ Bioavailability—prednisolone, various dosage forms compared, dogs □ Pharmacokinetics—prednisolone, various dosage forms compared, dogs □ Glucocorticoids—prednisolone, bioavailability and pharmacokinetics, various dosage forms compared, dogs

Prednisolone is used primarily for its anti-inflammatory activity in several diseases. It is cleared from the body predominantly by hepatic metabolism; only about 10% of orally dosed compound is excreted unchanged in urine (1).

Peak serum prednisolone concentrations of 160 ng/ml at 0.5 hr and 298 ng/ml at 1 hr were reported following 2.5- and 5.0-mg oral doses of prednisolone, respectively, to male beagle dogs (2). Studies in humans yielded peak serum prednisolone levels at 1–2 hr following oral doses and a serum half-life of about 3 hr (3–8).

Although the influence of *in vitro* disintegration and dissolution characteristics on prednisolone pharmacokinetics was reported (5–8), no information is available on the effect of the dosage form on bioavailability characteristics.

With the beagle dog as a model system, the present study was undertaken to compare the bioavailability and pharmacokinetics of prednisolone from two different doses of a commercial tablet, a slurry, and a solution of a water-soluble prednisolone salt.

EXPERIMENTAL

A 3-year-old male beagle dog, 17.5 kg, was given 30- and 60-mg doses of prednisolone tablets[1] (oral), oral prednisolone slurry[1], and oral and intravenous prednisolone sodium phosphate solution[2] in separate experiments. All experiments were done in duplicate.

Food was withheld at least 12 hr before and throughout each experiment. During an experiment, the dog was placed in a restraining apparatus so that it could stand normally but could not disturb indwelling catheters.

In the intravenous dosing experiments, an infusion set was positioned in each front leg. Each set consisted of a 19-gauge needle with 30 cm of flexible plastic tubing with a total volume of 0.6 ml. Clotting of blood in infusion sets was prevented by infusing 2 ml of saline-diluted heparin sodium solution (10 units/ml) into the set each hour it was in position. Prednisolone sodium phosphate was administered *via* one infusion set, with injection being completed in about 30 sec. The set was flushed with 10 ml of normal saline solution and was then removed.

Blood samples (8 ml) were collected through the other infusion set shortly before dosing and at 5, 15, and 30 min and 1, 2, 4, and 6 hr after dosing. Before each sample was taken, 5 ml of residual fluid was withdrawn to remove the heparin solution in the infusion set. The blood sample was then drawn, and the volume was replaced by an 8-ml injection of normal saline. The residual fluid was reinjected followed by 2 ml of heparin solution.

Tablets were administered by placing them on the posterior portion of the tongue so that they were not fractured or chewed before being swallowed; then 50 ml of water was immediately given. The slurry was prepared by triturating prednisolone tablets to a powder and dispersing this powder in 50 ml of water. The slurry was administered directly into the dog's stomach by means of a 120-cm × 3-mm (i.d.) stomach tube. Water, 25 ml, was used to flush residual drug from the syringe and stomach tube into the stomach. The oral solution was administered directly into the stomach in identical fashion to the slurry. With all oral dosing experiments, blood samples were collected *via* an infusion set as in the intravenous case.

Blood samples were placed in heparinized tubes[3] and centrifuged at 2300 rpm for 10 min. Plasma was removed and frozen until analyzed, usually within 1 week.

Experiments were performed 3 weeks apart to avoid changes in drug pharmacokinetic parameters due to prior exposure and to ensure complete drug washout from a previous dose.

Assay of Plasma Samples—The assay used to measure prednisolone in plasma was a modification of the GLC method described by Bacon and Kokenakes (9). In the purification step by column chromatography, the volume of the first eluting solvent [benzene–acetone (9:1)] was reduced from 70 to 30 ml and the volume of the second eluting solvent [benzene–acetone (1:3)] was increased from 20 to 30 ml. This change improved separation of prednisolone from other plasma components[4].

A solution containing the silylating agent[5] was prepared by combining 0.3 ml of pyridine, 37 μl of dotriacontane (as the internal standard) in carbon tetrachloride (0.95 μg/μl), and 0.5 ml of the silylating agent. A 20-μl aliquot of this solution was added to the extracted and purified prednisolone sample in a 1-ml vial[6]. This vial was immediately sealed with a polytef-lined cap, agitated on a vortex-type mixer, and allowed to stand at room temperature for 18 hr before assay.

GLC was carried out on an instrument[7] fitted with dual flame-ionization detectors. The column was a 1.8-m × 2-mm (i.d.) U-shaped glass

[1] Meticortelone, Schering Corp., Bloomfield, N.J.

[2] Hydeltrasol, Merck Sharp and Dohme, West Point, Pa.

[3] Vacutainer, Becton-Dickinson, Rutherford, N.J.

[4] G. E. Bacon, University of Michigan Medical Center, Ann Arbor, Mich., personal communication.

[5] Tri-Sil TBT, Pierce Chemical Co., Rockford, Ill.

[6] Reacti-vial, Pierce Chemical Co., Rockford, Ill.

[7] Nuclear Chicago Selecta System model 5000, Searle, Des Plaines, Ill.

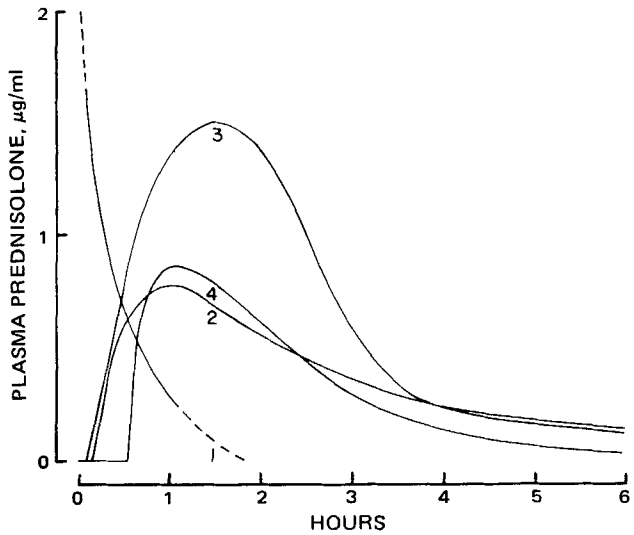

Figure 1—*Plasma prednisolone levels after doses of 30-mg prednisolone tablets (curve 4) and slurry (curve 3) and 24.7 mg of prednisolone as a prednisolone sodium phosphate oral (curve 2) and intravenous (curve 1) solution.*

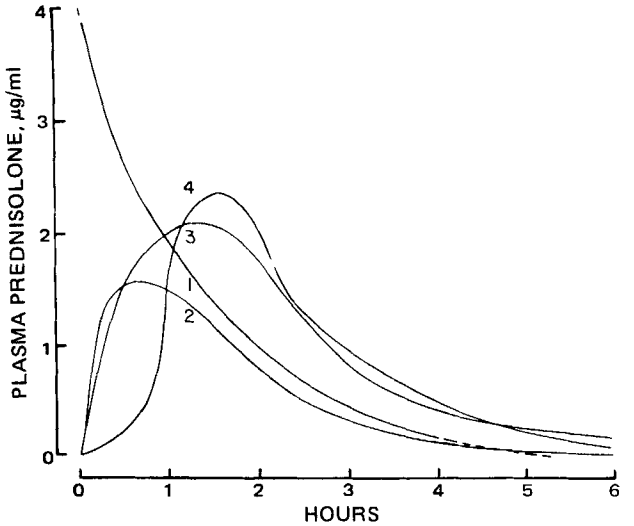

Figure 2—*Plasma prednisolone levels after doses of 60-mg prednisolone tablets (curve 4) and slurry (curve 3) and 49.3 mg of prednisolone as a prednisolone sodium phosphate oral (curve 2) and intravenous (curve 1) solution.*

tube packed with 3% OV-1 on 60–80-mesh Gas Chrom Q. The column was conditioned at 275° initially for 48 hr and then overnight after each day of sample analysis. The electrometer was set at a range of 10^{-12} amp, and the attenuator was set at 32 to give full-scale recorder deflection from an input signal of 3.2×10^{-11} amp.

Gas flow rates were 20, 25, and 200 ml/min for nitrogen, hydrogen, and air, respectively. The chromatograph was operated in the single-column mode at an isothermal column temperature of 245° with the detector bath at 300° and the injector port at 275°. Aliquots of 1 μl of solution were injected. Retention times were 341 sec for dotriacontane and 412 sec for prednisolone trimethylsilyl derivative.

Recovery of prednisolone from plasma was 68.8 ± 2.2 (*SD*) % (n = 20). A linear regression of peak area ratios of the prednisolone trimethylsilyl derivative to dotriacontane *versus* plasma prednisolone levels of 0.3–4.0 μg/ml was described by the equation $y = 1.67x - 0.01$ with $r = 1.00$.

Interpretation of Data—Semilogarithmic plots of prednisolone plasma concentrations *versus* time after intravenous doses were linear throughout the sampling period. It was, therefore, considered appropriate to analyze all data in terms of the pharmacokinetic one-compartment open model with first-order absorption and elimination. Prednisolone previously was shown to obey these types of kinetics following oral doses of prednisone tablets in humans (7).

Intravenous data were analyzed by linear regression, and oral data were analyzed on a digital computer following graphical analysis. The equation and symbolism pertaining to the one-compartment model and the method of computer analysis were described previously (10).

Pharmacokinetic parameters obtained from the three oral dosage forms were compared using the Student t test.

RESULTS

Average plasma prednisolone levels for the 30- and 60-mg doses are shown in Figs. 1 and 2. Results of pharmacokinetic and statistical analyses are presented in Tables I–III.

Individual plasma level–time curves making up the pair from each treatment were very similar, as indicated by the values of the pharmacokinetic parameters in the tables. Peak plasma prednisolone levels were obtained immediately following intravenous doses of prednisolone sodium phosphate, indicating rapid hydrolysis of the phosphate ester to prednisolone. The prednisolone elimination rate after the 60-mg injection was slower than after the 30-mg injection but was similar to that observed following oral doses (Tables I and II). The rapid elimination observed following the 30-mg doses is not clearly understood but was reproducible.

The primary objective of the intravenous doses was to obtain an accurate description of the prednisolone distribution space in the body;

Table I—Prednisolone Pharmacokinetic Parameters after a 30-mg[a] Dose to a Dog

Parameter	Intravenous Solution		Oral Solution		Slurry		Tablet	
	Run 1	Run 2	Run 1	Run 2	Run 1	Run 2	Run 1[b]	Run 2
k, hr^{-1}	—[c]	—	4.1 (2.6–5.5)[d]	4.2 (2.8–5.6)	1.8 (1.6–2.1)	1.7 (0.74–2.6)	3.2	4.5 (4.5–4.6)
$t_{1/2}$ (absorbance), hr	—	—	0.17	0.16	0.38	0.42	0.22	0.15
K, hr^{-1}	2.7	2.0	0.41 (0.32–0.50)	0.37 (0.30–0.45)	0.62 (0.56–0.69)	0.73[e]	0.63	0.85 (0.84–0.85)
$t_{1/2}$ (elimination), hr	0.26	0.34	1.7	1.9	1.1	0.95	1.1	0.82
FD/V^f, μg/ml	2.0	2.1	1.0 (0.92–1.2)	1.0 (0.91–1.1)	2.2 (2.0–2.4)	2.9 (2.4–3.4)	1.4	1.2 (1.21–1.23)
V, liter	12.58	12.03	—	—	—	—	—	—
t_0, hr	—	—	0.18 (0.15–0.21)	0.18 (0.15–0.21)	0.39 (0.38–0.40)	0.15 (0.05–0.26)	0.75	1.0
r^2	—	—	0.998	0.998	0.999	0.985	—	1.00
r	—	—	0.996	0.997	0.999	0.978	—	1.00
F^g	1	1	0.51	0.48	0.87	1.16	0.58	0.49
Total body clearance (VK), ml/min	560	409	82	74	124	146	126	169
Area (FD/VK), μg hr/ml	0.73	1.0	2.5(3.1)[h]	2.7(3.3)	3.5	4.0	2.3	1.5
Area (trapezoidal), μg hr/ml	—	—	2.6(3.2)	2.7(3.3)	3.4	3.8	1.6	1.5
C_{max}[i], μg/ml	—	—	0.80(0.97)	0.79(0.96)	1.3	1.5	—	0.83
t_{max}[j], hr	—	—	0.81	0.81	1.3	1.0	—	1.5

[a] For intravenous and oral solutions, 30 mg of prednisolone sodium phosphate is equivalent to 24.66 mg of prednisolone. [b] Initial graphical estimates. [c] Not relevant. [d] The 95% confidence interval. [e] Parameter fixed during computer analysis. [f] For intravenous study, $F = 1$. [g] Based on $V = 12$ liters from intravenous data. [h] Equivalent value after a 30-mg dose of prednisolone, obtained by (calculated value × 30/24.66). [i] $C_{max} = (FD/V)(k/K)^{K/(K-k)}$. [j] $t_{max} = \ln (k/K)/(k - K) + t_0$.

Table II—Prednisolone Pharmacokinetic Parameters after a 60-mg[a] Dose to a Dog

Parameter	Intravenous Solution		Oral Solution		Slurry		Tablet	
	Run 1	Run 2	Run 1	Run 2	Run 1	Run 2	Run 1[b]	Run 2[b]
k, hr^{-1}	—	—	5.5 (−7.9–19)	2.4 (1.2–3.6)	1.1 (0.7–1.5)	1.7 (1.2–2.1)	1.5	0.90
$t_{1/2}$ (absorbance), hr	—	—	0.13	0.29	0.62	0.42	0.47	0.77
K, hr^{-1}	0.79	0.89	0.71 (0.37–1.05)	0.72 (0.50–0.93)	0.56[c]	0.73[c]	0.66	0.82
$t_{1/2}$ (elimination), hr	0.88	0.78	0.98	0.96	1.2	1.0	1.1	0.85
FD/V, μg/ml	4.1	4.4	2.3 (1.1–3.4)	2.7 (2.0–3.3)	3.8 (3.4–4.3)	4.4 (4.0–4.8)	3.3	0.89
V, liters	12.09	11.29	—	—	—	—	—	—
t_0, hr	—	—	0.00 (−0.49–0.49)	0.03 (−0.05–0.11)	0.02 (−0.10–0.13)	0.07 (−0.10–0.16)	0.67	0.00
r^2	—	—	0.997	0.999	0.996	0.993	—	—
r	—	—	0.997	0.999	0.992	0.989	—	—
F	1	1	0.55	0.67	0.77	0.88	0.66	0.18
Total body clearance (VK), ml/min	159	167	142	144	112	146	132	164
Area (FD/VK), μg hr/ml	5.2	4.9	3.2(3.9)[d]	3.8(4.6)	6.8	6.0	5.0	1.1
Area (trapezoidal), μg hr/ml	—	—	3.1(3.8)	3.8(4.7)	6.5	5.9	3.8	4.6
C_{max}, μg/ml	—	—	1.7(2.0)	1.6(2.0)	1.9	2.3	—	—
t_{max}, hr	—	—	0.43	0.75	1.3	0.95	—	—

[a] For intravenous and oral solutions, 60 mg of prednisolone sodium phosphate is equivalent to 49.33 mg of prednisolone. [b] Initial graphical estimates. [c] Parameter fixed during computer analysis. [d] Equivalent value after a 60-mg dose of prednisolone obtained by (calculated value × 60/49.33).

volumes calculated from the zero-time intercepts of semilogarithmic plasma level–time plots were virtually identical for the four doses. The mean distribution volume was 12 liters, or 69% of total body volume, and was approximately equal to total body water. This volume was used to calculate the absolute prednisolone bioavailability in the oral experiments.

Average plasma level–time curves from oral doses showed that the slurry produced higher plasma prednisolone levels than other dosage forms following the 30-mg dose while both the slurry and tablets produced higher prednisolone levels than the solution following the 60-mg dose. The solution, however, tended to yield peak prednisolone levels somewhat earlier than the slurry and tablet doses.

In three slurry dosing experiments, computer pharmacokinetic analysis was unsatisfactory when initial graphical parameter estimates of the first-order absorption and elimination rate constants, k and K, respectively, and FD/V were allowed to float during the nonlinear fitting process. In each case, the computer generated similar values for K and k. This result can be explained in terms of the nature of the equation for the one-compartment open model:

$$C = \frac{FD}{V}\left(\frac{k}{k-K}\right)(e^{-Kt} - e^{-kt}) \qquad \text{(Eq. 1)}$$

When K and k approach a common value, $(FD/V)[k/(k-K)]$ becomes a large number while $(e^{-Kt} - e^{-kt})$ attains a diminishing value. Owing to the long word length used by the digital computer, the product of these two expressions becomes a very flexible term for fitting the plasma level–time data. However, meaningless values of k and K are generated in the process.

A similar phenomenon during two-compartment model analysis was reported previously (11, 12). To avoid this artifact, the elimination rate constant, K, was fixed at its graphically estimated value during the computer fitting. This step may be justified by the high dependability of this rate constant, compared to k and FD/V, during graphical analysis.

In three out of four plasma data sets from tablet doses, the computer prolonged the absorption lag time, t_0, and increased k to an unrealistically high value to fit the data to the model. Consequently, it was necessary to use initial graphical estimates of pharmacokinetic values instead of computer estimates in these cases. Because of the uncertainty of the kinetics associated with the absorption phase of these data, C_{max} and t_{max} were not calculated. In experiments where computer fitting was successful, r^2 and r values approached +1.0, indicating excellent agreement between the data and the proposed model.

Comparisons between Dose Levels—There were no apparent differences between k values from 30- and 60-mg doses in the solution and slurry experiments. Dose dependency of this rate constant was observed in the tablet experiments, but this result may have been due to poor description of the data by the model. Similarly, although the K values obtained from the oral solution experiments appeared higher for the 60- than for the 30-mg dose, they were almost identical for the two dose levels in the slurry and tablet experiments. This result is also true for the total body clearance, VK, since a constant distribution volume (12 liters) was used to calculate this parameter. In addition, F values for the two dose levels were virtually identical for each dosage form.

With the exception of one 60-mg tablet experiment, all areas under plasma level–time curves calculated from FD/VK were similar to those obtained using the trapezoidal rule. With the tablet and slurry doses, area values from the 60-mg dose were approximately double those from the 30-mg dose. With the solution doses, however, the 60 to 30-mg area ratios were somewhat less than 2.

The value of C_{max}, where calculated, was approximately twice as high from 60-mg doses than from 30-mg doses.

Comparisons between Dosage Forms—Since similar pharmacokinetic parameter values were obtained from the two dose levels (with the exception of K values from solution doses), parameters from the four experiments of each dosage form were combined for statistical comparison. The results (Table III) show that, of the three dosage forms studied, greatest absorption efficiency was obtained from the slurry. Areas under plasma level–time curves, normalized by dividing by the dose in prednisolone equivalents, were also larger from the slurry compared to the other treatments, but differences were significant only between the slurry and tablet treatments. No significant differences were observed in

Table III—Average Values and Results of Statistical Analysis of Pharmacokinetic Parameters for Oral Prednisolone Doses in the Dog

Parameter	Average Value[a]			t Test[b]
	Solution (1)	Slurry (2)	Tablet (3)	
F	0.55 ± 0.08[c]	0.92 ± 0.17	0.48 ± 0.21	2 > 1,3
k, hr^{-1}	4.1 ± 1.3	1.6 ± 0.3	2.5 ± 1.7	1 > 2
K, hr^{-1}	0.55 ± 0.19	0.66 ± 0.08	0.74 ± 0.11	NSD[d]
VK, ml/min	111 ± 38	132 ± 17	148 ± 22	NSD
t_{max}, hr	0.70 ± 0.18	1.13 ± 0.17	—	2 > 1
t_0, hr	0.10 ± 0.10	10.16 ± 0.16	0.61 ± 0.43	NSD
Normalized area[e] (F/VK), hr/liter	0.09 ± 0.02	0.12 ± 0.01	0.06 ± 0.03	2 > 3
Normalized area[e] (trapezoidal), hr/liter	0.09 ± 0.02	0.11 ± 0.13	0.06 ± 0.01	2 > 3

[a] $n = 4$. [b] Differences are considered significant when $p < 0.05$. [c] Standard deviation. [d] No significant differences. [e] Area divided by dose.

elimination rate constants or clearance values between treatments. The elimination half-lives were similar to those reported previously in beagle dogs (13).

DISCUSSION

Prednisolone sodium phosphate is known to produce its pharmacological action after being converted to prednisolone in the body (14). Kitagawa *et al.* (15) showed that phosphate ester hydrolysis is extremely rapid in rats, rabbits, and dogs, with peak plasma free steroid levels occurring almost immediately following intravenous injection of the ester. The monoexponential decline in plasma prednisolone levels following intravenous doses and the close similarity between the intravenous elimination rate constants and those obtained following oral doses of prednisolone indicate that the ester is rapidly and quantitatively hydrolyzed as soon as it enters the body. Any delayed hydrolysis would decrease the observed elimination rate constant. Thus, the prednisolone distribution volume of 68% total body volume, obtained following intravenous prednisolone sodium phosphate, is probably an accurate estimate of free prednisolone distribution.

Although prednisolone sodium phosphate is rapidly converted to free prednisolone *in vivo*, plasma levels following oral doses of a solution of this drug form tended to be lower than those from the slurry and tablets. Differences between solution plasma levels and those obtained from solid dosage forms were significant even when values were normalized for the slightly different doses (Table III). This result may be rationalized in terms of the ability of dissolved drug to permeate the GI membrane. Prednisolone sodium phosphate exists in solution in Forms I–III (Scheme I), depending on the solution pH.

$$\underset{\text{I}}{RH_2PO_4} \overset{K_1}{\rightleftharpoons} \underset{\text{II}}{RHPO_4^-} \overset{K_2}{\rightleftharpoons} \underset{\text{III}}{RPO_4^{2-}}$$

Scheme I

By analogy with 2-glycerolphosphoric acid, which has a pK_1 of 1.34 and a pK_2 of 6.65 (16), the pK_1 of prednisolone phosphoric acid is estimated to be ~1.5. Hence, in the stomach, with a pH range of 1–3, drug administered as III would exist mainly as either I or II. Based on a pK_1 of 1.5, the ratio of II to I species in the gastric pH range would be 0.32 at pH 1, 3.2 at pH 2, and 32.0 at pH 3. Therefore, a considerable proportion of the drug would be in the ionized form in the stomach. Since the GI epithelium is preferentially permeable to the unionized, lipid-soluble forms of most drugs (17), prednisolone sodium phosphate absorption might be expected to be hampered. Even where the pH of the stomach is as low as 1 and the drug is largely undissociated, its high water solubility and low fat solubility, compared to prednisolone, would still hinder membrane penetration. Recent studies (18) suggested that the site of prednisolone absorption is probably in the upper jejunum where the pH is close to 6. In this case, a greater percentage of drug would be in an ionized form at the absorption site, resulting in poor absorption.

The results in Tables I–III indicate that absorption of orally dosed prednisolone is somewhat reduced and delayed from tablets compared to a slurry. This result suggests, for the formulations used in this study at least, that prednisolone absorption from compressed tablets may be disintegration rate as well as dissolution rate (5) controlled. For any patient on corticosteroid therapy with demonstrated malabsorption, improved absorption from oral doses would probably be obtained by administering pulverized tablets as a slurry but not by administering a solution of a water-soluble form of the drug.

The Food and Drug Administration recommended that animal models be developed to correlate bioavailability studies in animals and humans (19). Although these results were obtained in a single animal, sufficient information has been generated to warrant expanded studies of these aspects of prednisolone bioavailability in humans.

REFERENCES

(1) T. Uete and N. Shimano, *Clin. Chem.*, **17**, 161 (1971).

(2) W. A. Colburn and R. H. Buller, *Steroids*, **21**, 833 (1973).

(3) P. F. D'Arcy, J. P. Griffin, J. S. Jenkins, W. F. Kirk, and A. W. Peacock, *J. Pharm. Sci.*, **60**, 1028 (1971).

(4) R. Leclercq and G. Copinschi, *J. Pharmacokinet. Biopharm.*, **2**, 175 (1974).

(5) T. J. Sullivan, R. G. Stoll, E. Sakmar, D. C. Blair, and J. G. Wagner, *ibid.*, **2**, 29 (1974).

(6) A. R. DiSanto and K. A. DeSante, *Clin. Pharmacol. Ther.*, **14**, 134 (1973).

(7) A. R. DiSanto and K. A. DeSante, *J. Pharm. Sci.*, **64**, 109 (1975).

(8) T. J. Sullivan, E. Sakmar, K. S. Albert, D. C. Blair, and J. G. Wagner, *ibid.*, **64**, 1723 (1975).

(9) G. E. Bacon and S. Kokenakes, *J. Lab. Clin. Med.*, **73**, 1030 (1969).

(10) P. G. Welling, L. L. Lyons, W. A. Craig, and G. A. Trochta, *Clin. Pharmacol. Ther.*, **17**, 475 (1975).

(11) W. J. Westlake, *J. Pharm. Sci.*, **60**, 882 (1971).

(12) L. Saunders and T. Natunen, presented at the British Pharmaceutical Conference, London, England, Sept. 1973.

(13) W. A. Colburn, C. R. Sibley, and R. H. Buller, *J. Pharm. Sci.*, **65**, 997 (1976).

(14) "Remington's Pharmaceutical Sciences," 15th ed., Mack Publishing Co., Easton, Pa., 1975, p. 896.

(15) H. G. Kitagawa, T. Mohri, and M. Kitagawa, *Arzneim.-Forsch.*, **22**, 402 (1972).

(16) J. T. Edsall and J. Wyman, "Biophysical Chemistry," vol. 1, Academic, New York, N.Y., 1958, p. 452.

(17) P. A. Shore, B. B. Brodie, and C. A. M. Hogben, *J. Pharmacol. Exp. Ther.*, **119**, 361 (1957).

(18) B. Hulme, V. H. T. James, and R. Rault, *Br. J. Clin. Pharmacol.*, **2**, 317 (1975).

(19) B. Cabana, presented at the Food and Drug Administration Workshop on Antibiotic Availability, Washington, D.C., June 1974.

ACKNOWLEDGMENTS AND ADDRESSES

Received November 11, 1976, from the *Center for Health Sciences, School of Pharmacy, University of Wisconsin, Madison, WI 53706.*

Accepted for publication March 18, 1977.

Adapted in part from a thesis submitted by F. L. S. Tse to the University of Wisconsin in partial fulfillment of the Master of Science degree requirements.

[x] To whom inquiries should be directed.

Teratogenicity of Zinc Chloride, 1,10-Phenanthroline, and a Zinc–1,10-Phenanthroline Complex in Mice

CHI-HSIUNG CHANG *, DAVID E. MANN, Jr. ˣ, and RONALD F. GAUTIERI

Abstract □ Zinc chloride, in single doses of 12.5, 20.5, and 25 mg/kg ip on Day 8, 9, 10, or 11 of gestation in CF-1 albino mice, produced skeletal anomalies without accompanying soft tissue defects. Ripple ribs, the most unusual anomaly, first appeared when the zinc salt was given on Day 9 of gestation in a dose of 20.5 mg/kg, becoming more prevalent when 25 mg/kg of the drug was administered on Day 11. 1,10-Phenanthroline, in single doses of 30 mg/kg ip on Day 8, 9, 10, or 11 of gestation, elicited skeletal defects comparable to those caused by zinc chloride as well as soft tissue anomalies, but a significant incidence of the former occurred with this agent only following its injection on Day 8 of gestation. A zinc–1,10-phenanthroline complex in single doses of 50 mg/kg on Day 8, 9, 10, or 11 of gestation yielded significant incidences of skeletal and soft tissue anomalies only when the complex was administered on Day 8 or 9 of gestation. This dosage level was toxic to both the mother and fetus when given on Day 10 of gestation. However, when the complex was given on Day 8, 9, 10, or 11 in a dose of 25 mg/kg, neither toxic nor teratogenic effects were observed in the mother or fetus, respectively.

Keyphrases □ Zinc chloride—alone and complexed with 1,10-phenanthroline, teratogenic effects evaluated in mice □ 1,10-Phenanthroline—alone and complexed with zinc, teratogenic effects evaluated in mice □ Teratogenicity—zinc chloride and 1,10-phenanthroline, alone and complexed, mice □ Metals—zinc as chloride, alone and complexed with 1,10-phenanthroline, teratogenic effects evaluated in mice □ Chelating agents—1,10-phenanthroline, alone and complexed with zinc, teratogenic effects evaluated in mice

The importance of zinc for biological (botanical) growth was first recognized by Raulin (1), who discovered that it was essential for the development of *Aspergillus niger*. Lutz (2), after finding traces of the element in every organ of the cat, rat, and human, concluded that zinc was indispensable for zoological growth as well. Presently, the role of zinc in human nutrition has not been elucidated completely, although evidence has accumulated that it is necessary for nucleic acid synthesis and cell division (3–7).

Recent studies (8, 9) revealed that zinc is a limiting nutrient among members of village populations; in its absence, growth retardation and hypogonadism occur. Few reports pertain to the teratogenic effects arising from zinc supplementation and deprivation in mammals. Dietary studies in lower species have, however, shed some light on the results of zinc deprivation on fetal development. Hurley and Swenerton (10), after feeding a purified diet lacking zinc to pregnant rats, observed that all of the full-term fetuses had a wide variety of gross skeletal and soft tissue defects. Utilizing a different approach to determine the consequences of zinc deficiency in rodents, these investigators administered a chelating agent (edetic acid) to pregnant rats and succeeded in impairing reproduction and inducing congenital malformations (11). When this agent was fed to gravid rats on Days 6–21 of gestation, all full-term fetuses developed gross deformities, the recurrence of which was prevented in a later study identical to the first except for the supplementation of 1000 ppm of dietary zinc.

From these studies, it was assumed that zinc deficiency is a major etiologic factor in the occurrence of fetal anomalies in rodents. It was recently demonstrated (12) that zinc challenge also can cause congenital malformations in rodents; the injection of 2 mg of zinc sulfate/kg iv in pregnant golden hamsters resulted in teratogenic responses in the offspring.

Because of these results and the prevalence of malnutrition throughout the world along with the threat of widespread environmental pollution, this study attempted to verify the effects of deprivation and excessive challenge of zinc in another rodent species (mouse) by using a different chelating agent (1,10-phenanthroline) and a different zinc salt (the chloride). Affirmative results would stress the urgency to perform comparable studies in higher mammals (primates) whose teratogenic responsiveness is more relevant to that of humans.

EXPERIMENTAL

CF-1 albino mice[1] were employed. The females were placed in groups of 25–30 in aggregate cages and were not mated until they weighed at least 24 g. Males were placed in individual metal cages[2], 12.5 × 15 × 10 cm, with a wire mesh front and floor. Excreta pans were elevated to the cage floor to permit coprophagy[3]. The animals were maintained on laboratory food[4] and tap water *ad libitum*.

To produce timed pregnancies, two female mice were placed in the cage of a fertile male at 4:00 pm. The following morning, at 8:00 am, the females were removed and inspected for the presence of a vaginal plug, which represents the last part of an ejaculate. Animals exhibiting this sign were considered to be gravid, and the morning of the appearance of the plug was designated as the start of gestation or Day 0. The gravid animals were then weighed and placed in individual cages, similar to those of the males, where they remained undisturbed until the morning of Day 7 when they were reweighed. Pregnancy was confirmed by a weight gain of 2 g or more.

Following the respective treatments, the mice were allowed to continue their gestation periods uninterrupted until Day 18, which was 1 day prior to the time of expected delivery. On this day, each pregnant mouse was sacrificed by cervical dislocation and its weight was recorded. The abdominal cavity was opened to expose the uterine horns. The number of fetuses and resorption sites (metrial glands) was determined and recorded. The exposed fetuses were removed by blunt dissection, blotted dry, and weighed to the nearest 0.01 g on a torsion balance. Each fetus was then examined for external defects and sexed.

Viability was ascertained by reflex movement of the limbs in response to mechanical stimulation with a blunt probe after removal of the fetus from the uterus. Every second fetus was processed for skeletal examination according to the method of Staples and Schnell (13). The remaining fetuses were fixed and decalcified in Bouin's fixative. After 2 weeks, the fixative was replaced by 70% ethyl alcohol in which the spec-

[1] Carworth Farms, New City, N.Y.
[2] Norwich Wire Works, Norwich, N.Y.
[3] To prevent skin lesions.
[4] Purina.

Table I—Skeletal Anomalies Induced by Zinc Chloride, I, and II on Days 8–11 of Gestation in CF-1 Albino Mice

Drug	Day of Gestation	Total Number of Fetuses	Number of Fetuses with Respective Defects	Total Number of Fetuses with Defects[a] / Total Number of Fetuses
Water	8	47	4, delayed ossification and fused sternebrae 2, supernumerary ribs 1, delayed ossification of xiphoid process	5/47 (10.6%)
Zinc chloride, 20.5 mg/kg	8	34	26, delayed ossification and fused sternebrae; crankshaft sternebrae 1, supernumerary ribs 13, delayed ossification of xiphoid 5, delayed ossification of hindpaws 2, delayed ossification of forepaws	26/34[b] (76.4%)
I, 30 mg/kg	8	53	14, delayed ossification and fused sternebrae; crankshaft sternebrae 2, supernumerary ribs 1, delayed ossification of xiphoid 1, delayed ossification of phalanges of hindpaws 1, delayed ossification of forepaws	16/53[b] (30.1%)
II, 50 mg/kg	8	20	15, delayed ossification and fused sternebrae; crankshaft sternebrae 3, supernumerary ribs 6, delayed ossification of xiphoid 2, delayed ossification of hindpaws 2, exencephaly	17/20[b] (85.0%)
Water	9	53	9, delayed ossification and fused sternebrae; crankshaft sternebrae 2, delayed ossification of xiphoid 2, delayed ossification of phalanges of hindpaws 2, delayed ossification of phalanges of forepaws 1, exencephaly	9/53 (16.9%)
Zinc chloride, 20.5 mg/kg	9	48	16, delayed ossification and fused sternebrae; supernumerary and crankshaft sternebrae 10, supernumerary and ripple ribs 6, ripple ribs 12, delayed ossification of xiphoid 6, delayed ossification of phalanges of hindpaws 6, delayed ossification of phalanges of forepaws	19/48[b] (39.5%)
II, 50 mg/kg	9	19	17, fused vertebrae 7, delayed ossification and crankshaft sternebrae 10, fused or missing ribs 6, delayed ossification of xiphoid 1, delayed ossification of phalanges of hindpaws 2, delayed ossification of phalanges of forepaws	18/19[b] (94.7%)
Water	10	38	2, fused and crankshaft sternebrae 4, supernumerary ribs 1, delayed ossification of xiphoid 1, delayed ossification of phalanges of hindpaws 1, delayed ossification of phalanges of forepaws	6/38 (15.7%)
Zinc chloride, 20.5 mg/kg	10	30	8, delayed ossification of sternebrae 5, supernumerary and ripple ribs 4, ripple ribs 8, delayed ossification of xiphoid 7, delayed ossification of phalanges of hindpaws 10, delayed ossification of phalanges of forepaws	11/30[b] (36.6%)
Water	11	87	6, crankshaft and fused sternebrae; supernumerary ribs	7/87 (8.0%)
Zinc chloride, 20.5 mg/kg	11	79	23, crankshaft sternebrae 26, supernumerary and ripple ribs and missing ribs 21, ripple ribs 2, delayed ossification of phalanges of hindpaws 2, delayed ossification of phalanges of forepaws 1, exencephaly	38/79[b] (48.1%)
Zinc chloride, 25 mg/kg	11	39	12, delayed ossification of sternebrae 26, supernumerary and ripple ribs 24, ripple ribs 8, delayed ossification of xiphoid 18, delayed ossification of phalanges of hindpaws 5, delayed ossification of phalanges of forepaws	30/39[b] (76.9%)
II, 50 mg/kg	11	15	3, supernumerary and ripple ribs 2, ripple ribs 3, delayed ossification of phalanges of hindpaws	5/15[b] (33.3%)

[a] Total number of defects refers to total number of fetuses with skeletal anomalies. [b] Statistically different at level of $p < 0.05$ (compared to respective water-treated group).

imens were stored until freehand sections were made with a double-edged, stainless steel razor blade[5] according to the technique of Wilson (14).

Statistical Methods and Analysis—The statistical significance of variations among the experimental groups was estimated by the Student t test for continuous variates and the unadjusted χ-square or Yates' corrected χ-square for binomial proportions (15). Probabilities, p, less than 0.05 were considered to represent significant differences.

[5] Durham Duplex, Durham Enders Co., Mystic, Conn.

Treatment Regimen—Animals were divided into seven groups and received the following treatment regimens: zinc chloride, 12.5, 20.5, and 25 mg/kg (three groups); 1,10-phenanthroline (I), 30 mg/kg (one group); a zinc–1,10-phenanthroline complex (II), 25 and 50 mg/kg (two groups), and distilled water (one group). The number of litters ranged from six to 10 for each group. All injections were given intraperitoneally, utilizing aqueous preparations of each drug whose volume never exceeded 0.45 ml. The complex was prepared by mixing zinc chloride (2.045 mg/0.5 ml of distilled water) with 1,10-phenanthroline (3 mg/ml of distilled water).

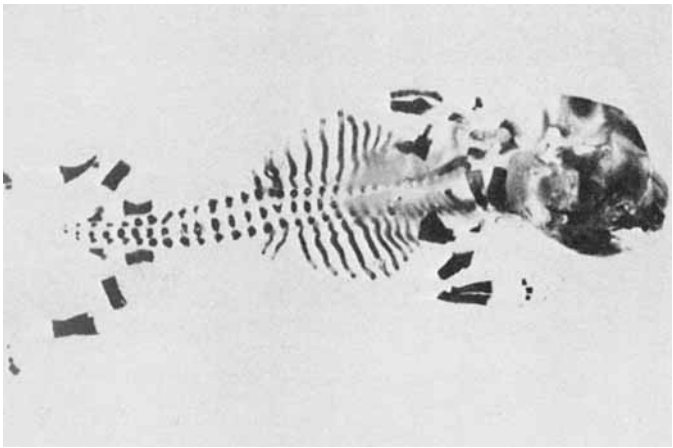

Figure 1—*Alizarin skeletal preparation of near-term mouse fetus from a female treated on Day 9 of gestation with 20.5 mg of zinc chloride/kg, showing ripple ribs.*

RESULTS

Zinc Chloride-Induced Teratogenesis—Zinc chloride, in a dose of 20.5 mg/kg on Day 8 of gestation, produced a 76.4% incidence of skeletal anomalies (Table I). Two out of seven gravid mice resorbed all of their fetuses. This dosage, when administered on Day 9 of gestation, yielded a 39.5% incidence of skeletal anomalies including the ripple rib, a thickening of the midportion of the rib with a peculiar undulation (Fig. 1). The ripple rib anomaly, which first appeared on Day 9 of gestation with a 12.5% occurrence in response to zinc chloride challenge, was accompanied by other skeletal defects similar to those caused by the zinc salt on Day 8.

When zinc chloride was given on Day 10 or 11 of gestation in a dose of 20.5 mg/kg, incidences of skeletal defects of 36.6 and 48.1%, respectively, were produced that were comparable to those appearing in response to the challenge by the zinc salt on Day 9 with respect to morphological alteration. This dose was most toxic when given on Day 10 of gestation; four out of 10 gravid mice died several days after having received single injections. The incidence of skeletal anomalies caused by zinc chloride on Days 8–11 of gestation was significantly higher than that of the water-treated group, but the occurrence of soft tissue anomalies in response to this dose of the zinc salt during the same period was not significant as compared to that of the water-treated group.

Zinc chloride, 25 mg/kg on Day 11 of gestation, produced an incidence of 76.9% of skeletal deformities, including a 61.5% occurrence of ripple ribs (Table I). The difference between the percent incidence of skeletal anomalies caused by this dose of the zinc salt and that of the water-treated group was significant. This dose of zinc chloride elicited the greatest incidence of maternal deaths; five out of 15 gravid mice died when the injection was made on Day 11 of gestation.

Zinc chloride, 12.5 mg/kg on Day 11 of gestation, induced nonsignificant incidences of both skeletal and soft tissue defects as compared to those of the water-treated group. No deaths were observed in the gravid animals, and no ripple ribs were noted in the fetuses.

Compound I-Induced Teratogenesis—Compound I, 30 mg/kg, produced a 30.1% incidence of skeletal defects (Table I) when administered on Day 8 of gestation and a 13.0% incidence of soft tissue anomalies (Table II) when given on Day 9. Both percent incidences were significantly different from those of the water-treated group.

No significant differences in the incidence of skeletal and soft tissue anomalies were noted between the I and water-treated groups when administrations were given on Days 10 and 11. Four fetuses out of 10 litters and 13 fetuses out of seven litters were resorbed when this dose of I was given on Days 10 and 11, respectively. No maternal deaths occurred following the administration of I on Days 8–11 of gestation.

Complex II-Induced Teratogenesis—Complex II, 50 mg/kg on Day 8, produced an incidence of skeletal anomalies of 85.0%. This dose of the complex, when given on Day 9 of gestation, produced a 94.7% incidence of skeletal defects, including fused vertebrae. The latter malformation was initially observed when the complex was injected on Day 9 at this dosage level. Interestingly, neither the zinc salt nor I elicited the anomaly, regardless of the day of injection.

A number of soft tissue defects, including extra thumbs and missing digits and tail, were caused by the complex. Both the incidences of skeletal anomalies (94.7%) and soft tissue defects (23.5%) were significantly higher than those of the water-treated group that received injections on Day 9 (Tables I and II). A high incidence of maternal deaths was observed a few days after II was administered. Seven out of 14 gravid animals died, and two out of 14 gravid mice resorbed all of their fetuses. Twenty-one fetal resorptions in seven litters occurred after the injection of the complex on Day 9.

Table II—Soft Tissue Anomalies Induced by I and II on Day 8 or 9 of Gestation in CF-1 Albino Mice[a]

Drug	Day of Gestation	Total Number of Fetuses	Number of Fetuses with Respective Defects	Total Number of Fetuses with Defects[b] / Total Number of Fetuses
Water	8	43	3, sixth digit[c] 1, cleft palate	4/43 (9.3%)
II, 50 mg/kg	8	18	1, sixth digit 2, exencephaly 1, cleft palate 3, cryptorchidism	7/18 (38.9%)[d]
Water	9	46	1, cryptorchidism	1/46 (2.2%)
I, 30 mg/kg	9	46	3, sixth digit 1, cleft palate 1, talipes 1, cryptorchidism	6/46 (13.0%)[d]
II, 50 mg/kg	9	17	4, two thumbs; four digits 1, tail absent	4/17 (23.5%)[d]

[a] No significant defects of soft tissues were noted on Days 10 and 11 of gestation when zinc chloride, I, or half as much II was administered individually to mice. Neither the injection of zinc chloride nor half as much II on Day 8 or 9 of gestation produced a significant incidence of soft tissue anomalies. [b] Total number of defects refers to total number of fetuses with soft tissue anomalies. [c] Actually is a protuberance adjacent to fifth digit of forepaw. [d] Statistically different at level of $p < 0.05$ (compared to water-treated group).

The administration of II on Day 10 of gestation, in a dose of 50 mg/kg, proved to be highly toxic to both the mother and fetus. Five of 14 gravid animals succumbed, and eight of 14 mice resorbed all of their fetuses. Nine fetuses in nine litters were resorbed. Obviously, these conditions preempted the study of skeletal and soft tissue defects.

Complex II, 50 mg/kg on Day 11 of gestation, produced a 33.3% incidence of skeletal anomalies (Table I), including ripple ribs which had not been noted when the complex was injected on earlier gestation days at this dosage level. The incidence of skeletal defects (33.3%) was significantly higher than that observed in the water-treated group. Only one in eight gravid mice resorbed all of her fetuses, but the maternal death rate was high (50%). Fourteen fetuses in four litters were resorbed.

The single administration of II, in a dose of 25 mg/kg on Days 9–11, yielded nonsignificant incidences of skeletal and soft tissue defects as compared to those of the water-treated groups. Maternal deaths and total fetal resorptions were not elicited by this dose of the complex.

DISCUSSION

Zinc chloride, when administered intraperitoneally to CF-1 albino mice in doses of 20.5 and 25 mg/kg, produced significant incidences of skeletal defects as compared to those observed in the water-treated group on Day 11. However, the zinc salt failed to produce a significant incidence of soft tissue anomalies with this treatment regimen. As the dosage of the zinc salt was reduced, maternal and fetal toxicity, relative fetal weights, and the incidence of skeletal anomalies were correspondingly decreased. The principal site for the teratogenicity of the zinc salt apparently is the skeletal system and, with increased doses, the majority of the defects produced involve the rib cage (*i.e.*, ripple ribs).

Zinc chloride, 20.5 mg/kg, exerted greater toxic effects on the mother and fetuses when administered on Day 10 of gestation than on any other day. Ripple ribs (Fig. 1) caused by the zinc salt first appeared when the drug was given on Day 9 of gestation and became more frequent and pronounced after the injection on Day 11.

Compound I, in a dose of 30 mg/kg, produced a significant incidence of skeletal defects on Day 8 and soft tissue anomalies on Day 9. Maternal deaths were not observed when the chelating agent was injected on Days 8–11. Only one in 10 gravid mice resorbed all of her fetuses when I was given on Day 10. At this dose, the chelator exerted relatively little toxicity since the teratogenic effects occurred only when I was given on Day 8 or 9. If the majority of the defects arising from I injections were due to

chelation with endogenous zinc in a bound or free state, it could then be assumed that the metal requirements of fetuses on Days 8 and 9 of gestation are considerably higher or more important than the demands for the metal after Day 9.

Complex II, in a dose of 25 mg/kg, failed to elicit significant skeletal and soft tissue anomalies when injected on Days 8–11, suggesting that any lower dose would be unlikely to cause teratogenesis and toxicity in fetuses and maternal animals, respectively. A dose of 50 mg/kg of the complex did produce significant incidences of skeletal and soft tissue defects when given on Day 8 or 9. When the complex was administered in this dose on Day 10, increased toxicity to both gravid mice and fetuses overshadowed its teratogenic actions. Yet, when the complex was given on Day 11, skeletal instead of soft tissue anomalies appeared in significant incidences. Furthermore, although the zinc is bound with 1,10-phenanthroline when injected as a complex, sufficient amounts of the metal apparently are available to elicit teratogenic effects in a manner comparable to that achieved by free zinc since ripple ribs occurred only when large doses of the complex were given and in an incidence considerably lower than that induced by the intermediate dose (20.5 mg/kg) of the zinc salt on Days 11 and 9.

CONCLUSION

On the basis of these results utilizing lower species, it is recommended that similar studies be carried out in higher mammals to determine more precisely the relevancy of deprivation and excessive challenge of zinc as etiologic factors in the development of human teratogenesis.

REFERENCES

(1) J. Raulin, *Ann. Sci. Nat. Bot. Biol. Veg.*, 11, 93 (1869).

(2) R. E. Lutz, *J. Ind. Hyg.*, 8, 177 (1926).

(3) B. J. Poiesz, N. Battula, and L. A. Loeb, *Biochem. Biophys. Res. Commun.*, **56**, 959 (1974).

(4) M. C. Scrutton, C. W. Wu, and D. A. Goldthwait, *Proc. Natl. Acad. Sci. USA*, **68**, 2497 (1971).

(5) J. P. Slater, A. S. Mildvan, and L. A. Loeb, *Biochem. Biophys. Res. Commun.*, **44**, 37 (1971).

(6) C. F. Springate, A. S. Mildvan, R. Abramson, J. L. Engle, and L. A. Loeb, *J. Biol. Chem.*, **248**, 5987 (1973).

(7) B. L. Vallee, in "Advances in Protein Chemistry," M. L. Anson, V. Bailey, and J. T. Edsall, Eds., Academic, New York, N.Y., 1955, p. 317.

(8) A. S. Prasad, A. Miale, Jr., Z. Farid, H. H. Sandstead, and A. R. Schulert, *J. Lab. Clin. Med.*, **61**, 537 (1963).

(9) H. H. Sandstead, A. S. Prasad, A. R. Schulert, Z. Farid, A. Miale, Jr., S. Bassily, and W. J. Darby, *Am. J. Clin. Nutr.*, **20**, 422 (1967).

(10) L. S. Hurley and H. Swenerton, *Proc. Soc. Exp. Biol. Med.*, **123**, 692 (1966).

(11) H. Swenerton and L. S. Hurley, *Science*, **173**, 62 (1971).

(12) V. H. Ferm and S. J. Carpenter, *Nature*, **216**, 1123 (1967).

(13) R. E. Staples and V. L. Schnell, *Stain Technol.*, **39**, 61 (1964).

(14) J. G. Wilson, in "Teratology Principles and Techniques," J. G. Wilson and J. Warkany, Eds., University of Chicago Press, Chicago, Ill., 1965, p. 267.

(15) G. G. Simpson, A. Roe, and R. C. Lewontin, "Quantitative Zoology," Harcourt, Brace, New York, N.Y., 1960, pp. 186–195.

ACKNOWLEDGMENTS AND ADDRESSES

Received November 29, 1976, from the *Department of Pharmacology, School of Pharmacy, Temple University, Philadelphia, PA 19140.*

Accepted for publication March 11, 1977.

The authors thank Peter Lemke and Ray Brooke for technical assistance.

* Present address: Cancer Drug Center, Roswell Park Memorial Institute, Buffalo, NY 14203.

[x] To whom inquiries should be directed.

Determination of Time Course of Tablet Disintegration I: Numerical Method

K. G. NELSON [x] and L. Y. WANG

Abstract □ A method is described for determining the time course of tablet disintegration. It involves a numerical analysis of the experimental dissolution profile of a tablet and the dissolution characteristics of the primary drug particles in the tablet. The disintegration profile is determined for an acetaminophen tablet to demonstrate the application of the method. Tablet dissolution is simulated with the disintegration–dissolution model, and the interrelationship between the two fundamental processes is studied theoretically by varying the parameters describing the two processes.

Keyphrases □ Disintegration—tablets, time course determined using numerical analysis of dissolution profile □ Dissolution profile—numerical analysis used to determine time course of tablet disintegration □ Tablets—time course of disintegration determined using numerical analysis of dissolution profile

The release of an active ingredient from a tablet involves two distinct processes: disintegration of the tablet and dissolution of the active ingredient. Although both processes commence when the tablet encounters an aqueous environment, the bulk of the active ingredient cannot dissolve until disintegration has occurred. The two processes are thus sequential and occur simultaneously until the tablet has disintegrated completely.

Studies on the temporal aspect of disintegration have largely involved only one time point, the disintegration time. The disintegration time is a subjective measure involving the time it takes the tablet to disintegrate and pass through a screen of arbitrary size in a standard apparatus (1). Attempts at determining the time course of disintegration have been reported (2, 3), but generally research in this area has involved the study of parameters that affect disintegration such as disintegrant type, compression force, and binders, and the results have been monitored by the official disintegration test (4).

Dissolution processes for powders and nondisintegrating tablets have been studied rather extensively. Several reports discuss dissolution theory and provide mathematical models (5–8) which serve as a means to evaluate dissolution rate data and dissolution test systems. A dissolution theory for disintegrating tablets, however, has not been developed, although equations with adjustable parameters have described the process (9, 10).

This paper describes a method for processing dissolution rate data to determine a quantitative description of the disintegration process as a function of time. The method was applied to experimental dissolution rate data from a tablet having a rather idealized formulation to demon-

chelation with endogenous zinc in a bound or free state, it could then be assumed that the metal requirements of fetuses on Days 8 and 9 of gestation are considerably higher or more important than the demands for the metal after Day 9.

Complex II, in a dose of 25 mg/kg, failed to elicit significant skeletal and soft tissue anomalies when injected on Days 8–11, suggesting that any lower dose would be unlikely to cause teratogenesis and toxicity in fetuses and maternal animals, respectively. A dose of 50 mg/kg of the complex did produce significant incidences of skeletal and soft tissue defects when given on Day 8 or 9. When the complex was administered in this dose on Day 10, increased toxicity to both gravid mice and fetuses overshadowed its teratogenic actions. Yet, when the complex was given on Day 11, skeletal instead of soft tissue anomalies appeared in significant incidences. Furthermore, although the zinc is bound with 1,10-phenanthroline when injected as a complex, sufficient amounts of the metal apparently are available to elicit teratogenic effects in a manner comparable to that achieved by free zinc since ripple ribs occurred only when large doses of the complex were given and in an incidence considerably lower than that induced by the intermediate dose (20.5 mg/kg) of the zinc salt on Days 11 and 9.

CONCLUSION

On the basis of these results utilizing lower species, it is recommended that similar studies be carried out in higher mammals to determine more precisely the relevancy of deprivation and excessive challenge of zinc as etiologic factors in the development of human teratogenesis.

REFERENCES

(1) J. Raulin, *Ann. Sci. Nat. Bot. Biol. Veg.*, 11, 93 (1869).

(2) R. E. Lutz, *J. Ind. Hyg.*, 8, 177 (1926).

(3) B. J. Poiesz, N. Battula, and L. A. Loeb, *Biochem. Biophys. Res. Commun.*, **56**, 959 (1974).

(4) M. C. Scrutton, C. W. Wu, and D. A. Goldthwait, *Proc. Natl. Acad. Sci. USA*, **68**, 2497 (1971).

(5) J. P. Slater, A. S. Mildvan, and L. A. Loeb, *Biochem. Biophys. Res. Commun.*, **44**, 37 (1971).

(6) C. F. Springate, A. S. Mildvan, R. Abramson, J. L. Engle, and L. A. Loeb, *J. Biol. Chem.*, **248**, 5987 (1973).

(7) B. L. Vallee, in "Advances in Protein Chemistry," M. L. Anson, V. Bailey, and J. T. Edsall, Eds., Academic, New York, N.Y., 1955, p. 317.

(8) A. S. Prasad, A. Miale, Jr., Z. Farid, H. H. Sandstead, and A. R. Schulert, *J. Lab. Clin. Med.*, **61**, 537 (1963).

(9) H. H. Sandstead, A. S. Prasad, A. R. Schulert, Z. Farid, A. Miale, Jr., S. Bassily, and W. J. Darby, *Am. J. Clin. Nutr.*, **20**, 422 (1967).

(10) L. S. Hurley and H. Swenerton, *Proc. Soc. Exp. Biol. Med.*, **123**, 692 (1966).

(11) H. Swenerton and L. S. Hurley, *Science*, **173**, 62 (1971).

(12) V. H. Ferm and S. J. Carpenter, *Nature*, **216**, 1123 (1967).

(13) R. E. Staples and V. L. Schnell, *Stain Technol.*, **39**, 61 (1964).

(14) J. G. Wilson, in "Teratology Principles and Techniques," J. G. Wilson and J. Warkany, Eds., University of Chicago Press, Chicago, Ill., 1965, p. 267.

(15) G. G. Simpson, A. Roe, and R. C. Lewontin, "Quantitative Zoology," Harcourt, Brace, New York, N.Y., 1960, pp. 186–195.

ACKNOWLEDGMENTS AND ADDRESSES

Received November 29, 1976, from the *Department of Pharmacology, School of Pharmacy, Temple University, Philadelphia, PA 19140.*

Accepted for publication March 11, 1977.

The authors thank Peter Lemke and Ray Brooke for technical assistance.

* Present address: Cancer Drug Center, Roswell Park Memorial Institute, Buffalo, NY 14203.

[x] To whom inquiries should be directed.

Determination of Time Course of Tablet Disintegration I: Numerical Method

K. G. NELSON [x] and L. Y. WANG

Abstract □ A method is described for determining the time course of tablet disintegration. It involves a numerical analysis of the experimental dissolution profile of a tablet and the dissolution characteristics of the primary drug particles in the tablet. The disintegration profile is determined for an acetaminophen tablet to demonstrate the application of the method. Tablet dissolution is simulated with the disintegration–dissolution model, and the interrelationship between the two fundamental processes is studied theoretically by varying the parameters describing the two processes.

Keyphrases □ Disintegration—tablets, time course determined using numerical analysis of dissolution profile □ Dissolution profile—numerical analysis used to determine time course of tablet disintegration □ Tablets—time course of disintegration determined using numerical analysis of dissolution profile

The release of an active ingredient from a tablet involves two distinct processes: disintegration of the tablet and dissolution of the active ingredient. Although both processes commence when the tablet encounters an aqueous environment, the bulk of the active ingredient cannot dissolve until disintegration has occurred. The two processes are thus sequential and occur simultaneously until the tablet has disintegrated completely.

Studies on the temporal aspect of disintegration have largely involved only one time point, the disintegration time. The disintegration time is a subjective measure involving the time it takes the tablet to disintegrate and pass through a screen of arbitrary size in a standard apparatus (1). Attempts at determining the time course of disintegration have been reported (2, 3), but generally research in this area has involved the study of parameters that affect disintegration such as disintegrant type, compression force, and binders, and the results have been monitored by the official disintegration test (4).

Dissolution processes for powders and nondisintegrating tablets have been studied rather extensively. Several reports discuss dissolution theory and provide mathematical models (5–8) which serve as a means to evaluate dissolution rate data and dissolution test systems. A dissolution theory for disintegrating tablets, however, has not been developed, although equations with adjustable parameters have described the process (9, 10).

This paper describes a method for processing dissolution rate data to determine a quantitative description of the disintegration process as a function of time. The method was applied to experimental dissolution rate data from a tablet having a rather idealized formulation to demon-

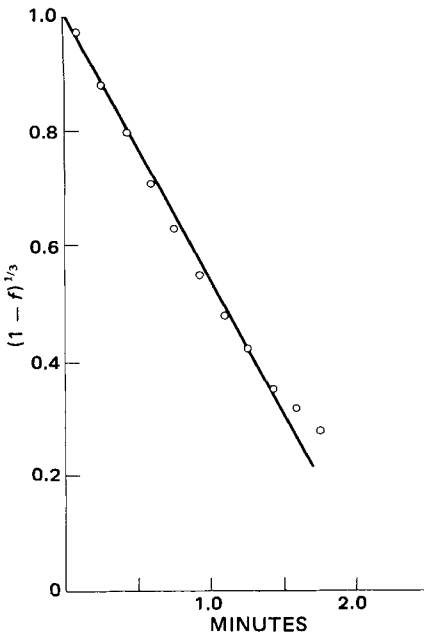

Figure 1—*Powder dissolution data plotted according to the cube-root equation.*

strate the principles of the method. This disintegration–dissolution analysis should provide the framework for a quantitative model for tablet dissolution.

THEORETICAL

Disintegration may be considered to be the process whereby the individual solid drug particles are released from the tablet to the aqueous medium so that they may undergo dissolution. A quantitative description of this process would involve the amount or fraction of the drug in a tablet that has disintegrated as a function of time. Once an individual drug particle is exposed to the aqueous environment, a mathematical expression exists to describe its time course of dissolution, *e.g.*, the Hixson–Crowell equation (5).

The dissolution profile that results from a dissolution test on a tablet in a dissolution apparatus is a composite of the disintegration and dissolution functions. The principle of the method outlined later is the application of a numerical analysis technique to the dissolution profile along with the known dissolution rate function to generate the disintegration function.

A rearrangement of the Hixson–Crowell cube-root equation (5) describes the dissolution of a powder:

$$f = 1 - (1 - Kt)^3 \qquad \text{(Eq. 1)}$$

where f is the fraction dissolved, t is the time, and K is an experimentally determined constant, which depends upon the initial particle size and the solubility of the drug among other things. Of course, f cannot exceed 1, so f is defined equal to 1 when t gets greater than the time for complete dissolution.

If the time course of tablet disintegration is considered in terms of many discrete steps, then the fraction of drug in the tablet that has dissolved after the first small time interval may be obtained by applying Eq. 1:

$$M_1 = w_0[1 - (1 - Kt_1)^3] \qquad \text{(Eq. 2)}$$

where M_1 is the fraction of drug in the tablet that has dissolved at time t_1, and w_0 is the fraction of the drug in the tablet that was disintegrated at the beginning of the time interval, *i.e.*, t_0 (=0). For the second time interval:

$$M_2 = w_0[1 - (1 - Kt_2)^3] + w_1\{1 - [1 - K(t_2 - t_1)]^3\} \qquad \text{(Eq. 3)}$$

where the first term on the right is analogous to Eq. 2 but at t_2, and the second term now accounts for the fraction of drug dissolved during the second time interval that arises from the fraction of drug disintegrated, w_1, at the beginning of the second interval (at t_1). In general:

$$M_n = \sum_{i=0}^{n} w_i\{1 - [1 - K(t_n - t_i)]^3\} \qquad \text{(Eq. 4)}$$

where M_n is the fraction of drug in the tablet that has dissolved after n time intervals, corresponding to time t_n. As before, the term in braces that arises from Eq. 1 should be defined as 1 once it attains that value.

The cumulative fraction of drug disintegrated, W_n, up to time t_n then is:

$$W_n = \sum_{i=0}^{n} w_i \qquad \text{(Eq. 5)}$$

Thus, the disintegration profile can be constructed from Eq. 5.

To determine the w_i values, the experimental dissolution profile of a tablet is divided into many small intervals, *e.g.*, 30, and the fractional amount dissolved is determined at each interval. The intervals are numbered and, considering that M_n is the fraction dissolved at the nth interval, Eq. 4 is written out for each interval. If K is known, then the set of Eq. 4 for all intervals gives a system of linear equations with the same number of unknowns, *i.e.*, the w_i values, which can then be solved.

Once the system is solved for the w_i values, the disintegration profile can be obtained by applying Eq. 5 for each time interval.

EXPERIMENTAL

Tablet Preparation—Tablets (500.0 mg) were prepared from 25.0 mg of acetaminophen[1], 15.0 mg of sodium carboxymethyl starch[2], 75.0 mg of microcrystalline cellulose[3], 382.5 mg of lactose (spray dried)[4], and 2.5 mg of magnesium stearate[5]. The acetaminophen crystals were ground in a mortar and separated into a 70–80-mesh fraction with a U.S. Standard sieve series[6] and a sieve shaker[7]. All other ingredients were passed through a 60-mesh sieve, and the formulation was well mixed. The 500-mg tablets were compressed individually with a laboratory press[8], using a 1.27-cm (0.5-in.) die and flat-faced punches. The compressional force was increased slowly to 1360 kg (3000 lb) and retained for 30 sec before release.

Dissolution Rate—The tablet dissolution profile was determined in water using a rotating-filter–stationary basket dissolution test apparatus[9] (11) at 37° and 400 rpm. The amount of drug dissolved with time was monitored by circulating (flow rate of 71 ml/min) the filtered dissolution fluid through a flowcell in a recording spectrophotometer[10] and returning it to the vessel. After accounting for the holdup volume, a chart of the absorbance of acetaminophen (at 243 nm) *versus* time thus represented the dissolution profile of the tablet, and the fractional amount released at any time could be readily determined by dividing the absorbance at that time by the absorbance after complete dissolution.

The dissolution profile for the pure acetaminophen powder (70–80 mesh) was obtained by introducing the powder directly into the vessel with all of the other conditions the same as for the tablets.

RESULTS AND DISCUSSION

The value for the dissolution rate constant, K, was determined by monitoring the dissolution of the 70–80-mesh acetaminophen powder in the dissolution test apparatus. In accordance with Eq. 1, the data were plotted as $(1 - f)^{1/3}$ *versus* time (Fig. 1) and K was obtained directly from the slope. The linearity of this plot was excellent ($r^2 = 0.997$) over the experimental range of f from 0 to 0.96. The least-squares slope in this range yielded $K = 0.465$. The positive curvature at times corresponding to the last 4% of the powder dissolution probably resulted because the powder was not strictly monodisperse.

The experimental dissolution profile for the acetaminophen tablet, as obtained from the spectrophotometer recording, was divided into 36 equal time intervals of 10 sec each for the numerical analysis. The points in Fig. 2 show the dissolution profile thus obtained and represent the required data, along with the value for K, to generate the set of 36 linear equations from Eq. 4. A digital computer[11] was programmed to solve this

[1] Rhodia, Inc., New York, N.Y.
[2] Primojel, Edward Mandell Co., Carmel, N.Y.
[3] Avicel PH-101, Avicel Department, FMC Corp., Philadelphia, Pa.
[4] Fast Flo Lactose, Foremost Foods Co., Foremost-McKesson, Inc., San Francisco, Calif.
[5] Fisher Scientific Co., Fair Lawn, N.J.
[6] W. S. Tyler Co., Cleveland, Ohio.
[7] Ro-Tap shaker, W. S. Tyler Co., Cleveland, Ohio.
[8] Model C, Fred S. Carver, Menomonee Falls, Wis.
[9] Coffman Industries, Kansas City, Kans.
[10] Cary 14, Cary Instruments, Monrovia, Calif.
[11] CDC 3300, Health Computer Sciences, University of Minnesota.

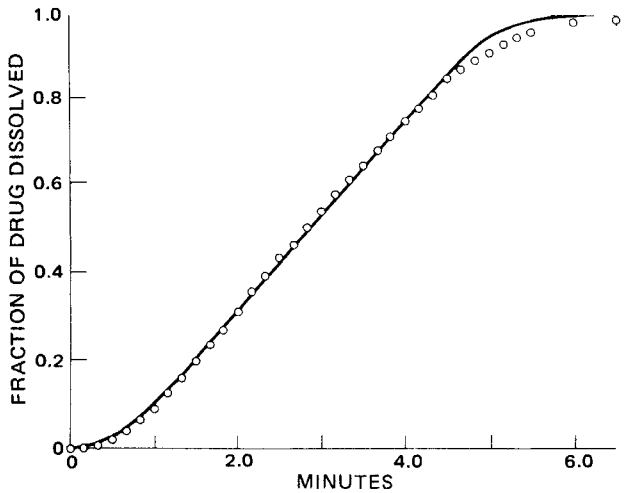

Figure 2—*Tablet dissolution profile (points) and model-simulated curve.*

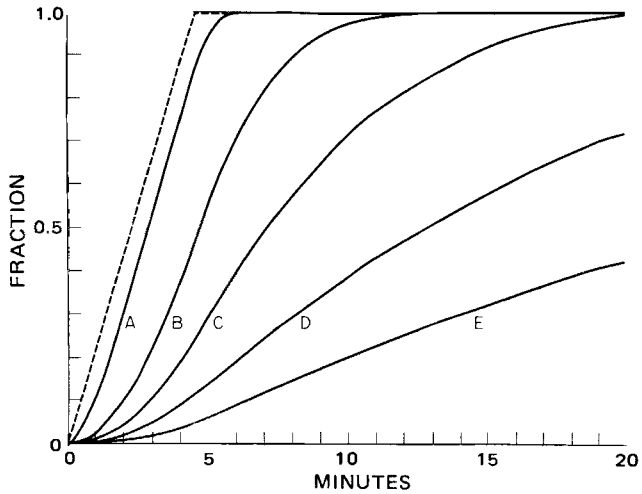

Figure 4—*Disintegration profile (dashed line) and simulated dissolution curves (solid lines) for* $k_0 = 0.219$. *Key: A,* K = *0.465; B,* K = *0.1; C,* K = *0.0465; D,* K = *0.02; and E,* K = *0.01.*

set of equations for the w_i values, and the disintegration profile was then generated by repetitive application of Eq. 5. The disintegration profile obtained in this manner is shown as the points in Fig. 3. At 4.25 min, the tablet had disintegrated such that it passed entirely through the wire mesh basket. This time would be analogous to the USP disintegration time (1).

Figure 3 shows that the disintegration profile is quite linear for this formulation. A linear regression of the data up to t = 4.17 min gives:

$$W = 0.007 + 0.219t \qquad \text{(Eq. 6)}$$

with a coefficient of determination of 0.995. Because of the good linearity, the coefficient of t can be considered to be an apparent zero-order disintegration rate constant, k_0. To test the self-consistency of the method, Eq. 6 can be used to calculate the w_i values for Eq. 4, which, together with the value for K, can be used to simulate the tablet dissolution profile. The dissolution profile generated in this way is shown as the curve in Fig. 2. It is apparent that the simulation is quite good, except for some moderate deviation at large times. This result may be expected, however, because in this region the dissolution would be influenced by the disintegration function when disintegration is nearing completion. Hence, the variation at large times results from the deviation of Eq. 6 from the determined disintegration profile, as is apparent in Fig. 3, as well as the experimental problem regarding Eq. 1 at high fractions dissolved.

To explore theoretically the interaction between the disintegration and dissolution processes and the resultant drug release pattern, the values for K and k_0 can be systematically varied. Shown as the dashed line in Fig. 4 is the disintegration profile drawn according to Eq. 6; curve A is the generated dissolution function. Because these functions are parallel for the greater part of the dissolution curve, the drug release from this particular acetaminophen formulation is largely controlled by the disintegration rate. If K is now decreased in value stepwise from 0.465 to 0.1, 0.0465, 0.02, and 0.01, then the four dissolution profiles can be generated from Eq. 4 (curves B, C, D, and E, respectively, in Fig. 4). For the case with a relatively small K (curve E), the calculated time for complete dissolution is about 100 min, which is considerably larger than the disintegration time. Thus, curve E represents the case where drug release is controlled by the dissolution rate.

Curve C in Fig. 4 represents an example of the intermediate case where both disintegration and dissolution influence drug release. Up to the time of complete disintegration, the dissolution curve has positive curvature because additional solid drug is released to the medium at a rate faster than it can dissolve. At the disintegration time, the dissolution curve goes through an inflection point because the drug release subsequently occurs by dissolution of the suspended particles, which is analogous to powder dissolution.

The effect of changing k_0 while holding K constant can also be simulated. In Fig. 5, curves C represent the disintegration and dissolution determined for the tablet as before. Decreasing k_0 by 50% results in curves D, which show a disintegration-controlled release. Increasing k_0 to 0.439 (curves B) demonstrates a case where the disintegration control is shorter; with k_0 = 4.39 (curves A), which corresponds to a disintegration time of 13 sec, the large region of negative curvature on the dissolution profile indicates that the drug release is largely dissolution rate controlled.

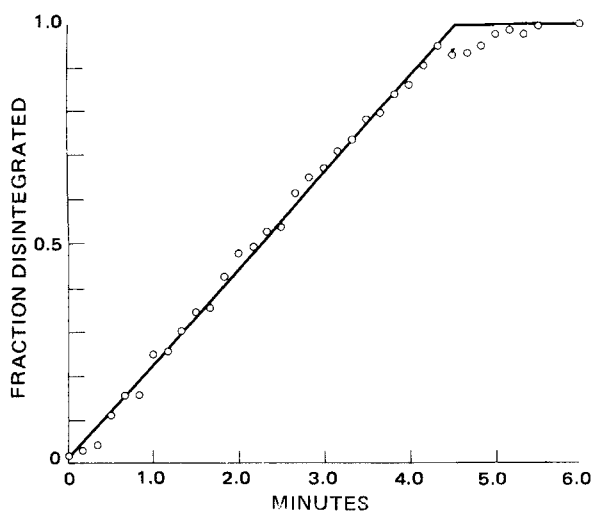

Figure 3—*Disintegration profile determined by numerical analysis of dissolution data. The line represents linear regression up to* t = *4.17 min.*

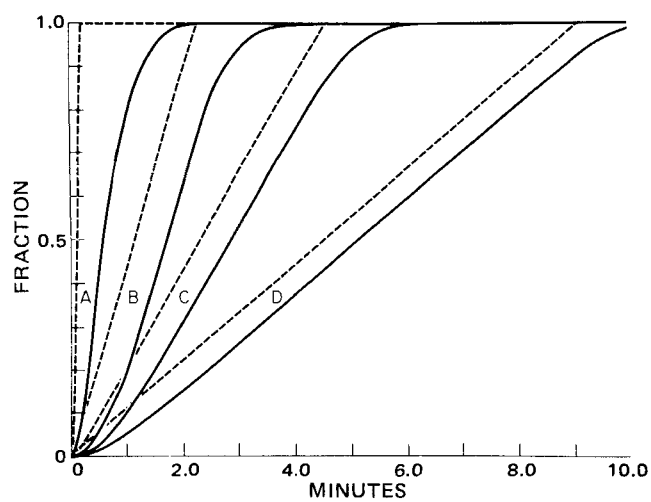

Figure 5—*Simulated disintegration (dashed lines) and associated dissolution (solid lines) profiles for* K = *0.465. Key: A,* k_0 = *4.39; B,* k_0 = *0.439; C,* k_0 = *0.219; and D,* k_0 = *0.109.*

The described concept of the disintegration-dissolution analysis can be rather general, but several restrictions were employed to study a simple system and to demonstrate the use of the method. First, the tablet was prepared by direct compaction, which permits disintegration directly into primary particles. A granulation may introduce a more complex disintegration pattern and may also modify somewhat the primary particles. Second, the Hixson–Crowell equation (5) was employed. Alternative theories for powder dissolution exist, but the resulting mathematical equations do not describe the experimental dissolution process as well as the cube-root law (12).

Third, the drug powder was of a uniform particle size. If a powder with a wide size distribution were used, an additional feature would have to be included to account for the change in size distribution over time for each fraction disintegrated. Fourth, it was assumed that the compression force did not alter the primary particles, *i.e.*, that K for the pure powder represented K for the disintegrated powder. Although compression can fracture particles, the relatively low force used apparently did not have a significant effect because the experimentally observed disintegration time was in close agreement with the time for complete disintegration on the disintegration profile determined by Eqs. 4 and 5.

Finally, because the disintegration profile for the acetaminophen tablet was zero order, the discussion regarding the linearity of the dissolution profile vis-á-vis the disintegration-controlled release and the significance of the inflection points are restricted to this case. As further studies indicate other disintegration profiles, *e.g.*, with negative curvature or sigmoidal, model simulations can be employed to explore these effects.

The described method for determining the time course of disintegration can provide a means to study tablet disintegration under idealized conditions. Work is being continued to extend the model so that regular tablet formulations, *i.e.*, not idealized, can be evaluated.

REFERENCES

(1) "The United States Pharmacopeia," 19th rev., Mack Publishing Co., Easton, Pa., 1975, p. 650.

(2) H. Nogami, J. Hasegawa, and Y. Nakai, *Chem. Pharm. Bull.*, **7**, 331 (1959).

(3) M. H. Rubinstein, J. I. Wells, and C. A. Holland, *J. Pharm. Pharmacol. Suppl.*, **27**, 54 (1975).

(4) W. Lowenthal, *J. Pharm. Sci.*, **61**, 1695 (1972).

(5) A. Hixson and J. Crowell, *Ind. Eng. Chem.*, **23**, 923 (1931).

(6) W. I. Higuchi and E. N. Hiestand, *J. Pharm. Sci.*, **52**, 67 (1963).

(7) K. G. Nelson and A. C. Shah, *ibid.*, **64**, 610 (1975).

(8) L. J. Leeson and J. T. Carstensen, "Dissolution Technology," Academy of Pharmaceutical Sciences, American Pharmaceutical Association, Washington, D.C., 1974.

(9) J. G. Wagner, *J. Pharm. Sci.*, **58**, 1253 (1969).

(10) F. Langenbucher, *J. Pharm. Pharmacol.*, **24**, 979 (1972).

(11) A. C. Shah, C. B. Poet, and J. F. Ochs, *J. Pharm Sci.*, **62**, 671 (1973).

(12) P. V. Pedersen and K. F. Brown, *ibid.*, **65**, 1442 (1976).

ACKNOWLEDGMENTS AND ADDRESSES

Received November 22, 1976, from the *College of Pharmacy, University of Minnesota, Minneapolis, MN 55455.*

Accepted for publication March 11, 1977.

Supported by a grant from the Pharmacy Research Unit, The Upjohn Co., Kalamazoo, Mich.

[x] To whom inquiries should be directed.

Bioavailability of Three Isoniazid Formulations

S. SVED [x], I. J. McGILVERAY, and N. BEAUDOIN

Abstract □ The bioavailability of three isoniazid formulations was assessed using a procedure specific for the free drug. Nine human volunteers, all slow acetylators, were each given 4 × 100 mg of isoniazid of three different tablet formulations at weekly intervals; the plasma drug levels were measured at different times during the first 24 hr. No significant differences ($p > 0.05$) were detected among the three products as to relative bioavailability, peak plasma concentrations, C_{max}, and the time of C_{max}, t_{max}. Analysis of variance of the pharmacokinetic parameters obtained according to a one-compartment open model did not demonstrate any significant formulation or time effect but revealed a significant intersubject variation in all parameters involved.

Keyphrases □ Isoniazid—bioavailability of three commercial formulations compared □ Bioavailability—isoniazid, three commercial formulations compared □ Tuberculostatic antibacterials—isoniazid, bioavailability of three commercial formulations compared

Isoniazid has been used since the early 1950's for the treatment of tuberculosis and has been largely responsible for the virtual eradication of this disease in certain parts of the world. It is widely used in preventive therapy in the United States and Canada. Its clinical efficacy and bioavailability assessment are complicated by methodological and metabolic problems. First, the presence of slow and fast acetylator genotypes in the population has been demonstrated (1–5), and the inclusion of both types in a study could lead to increased variability and difficulties in design. Second, isoniazid tends to form relatively stable, probably less active, hydrazones with either physiological (sugars and pyruvate) or excipient (lactose and glucose) aldehydes and ketones (6–9), thus necessitating an assay that can distinguish between the free drug and its hydrazones.

Earlier studies (10) on isoniazid bioavailability did not demonstrate any difference between six commercial preparations available in the United States. The method used, however, could not distinguish between free isoniazid and its hydrazones. This study was initiated to compare the bioavailability of three Canadian isoniazid preparations using a homogeneous group and an assay that measures only free isoniazid in the plasma.

EXPERIMENTAL

Materials—Isoniazid tablets, 100 mg, were supplied[1] from current production lots. Evacuated heparinized blood collection tubes were obtained locally[2]. Extractions were done in glass tubes with polytef-lined screw caps[3]. 2,4-Pentanedione (practical), diethanolamine, ethylene glycol, potassium carbonate, zinc acetate (all reagent grade)[4], methyl

[1] See "Quad Review 4," Health Protection Branch, Health and Welfare Canada, Ottawa, Canada, 1975, p. 44.

[2] Vacutainers, Becton-Dickinson; obtained through Canlab, Ottawa, Canada.

[3] Catalog No. T 1356-1, Canlab, Ottawa, Canada.

[4] Baker; obtained through Canlab, Ottawa, Canada.

The described concept of the disintegration-dissolution analysis can be rather general, but several restrictions were employed to study a simple system and to demonstrate the use of the method. First, the tablet was prepared by direct compaction, which permits disintegration directly into primary particles. A granulation may introduce a more complex disintegration pattern and may also modify somewhat the primary particles. Second, the Hixson–Crowell equation (5) was employed. Alternative theories for powder dissolution exist, but the resulting mathematical equations do not describe the experimental dissolution process as well as the cube-root law (12).

Third, the drug powder was of a uniform particle size. If a powder with a wide size distribution were used, an additional feature would have to be included to account for the change in size distribution over time for each fraction disintegrated. Fourth, it was assumed that the compression force did not alter the primary particles, *i.e.*, that K for the pure powder represented K for the disintegrated powder. Although compression can fracture particles, the relatively low force used apparently did not have a significant effect because the experimentally observed disintegration time was in close agreement with the time for complete disintegration on the disintegration profile determined by Eqs. 4 and 5.

Finally, because the disintegration profile for the acetaminophen tablet was zero order, the discussion regarding the linearity of the dissolution profile vis-á-vis the disintegration-controlled release and the significance of the inflection points are restricted to this case. As further studies indicate other disintegration profiles, *e.g.*, with negative curvature or sigmoidal, model simulations can be employed to explore these effects.

The described method for determining the time course of disintegration can provide a means to study tablet disintegration under idealized conditions. Work is being continued to extend the model so that regular tablet formulations, *i.e.*, not idealized, can be evaluated.

REFERENCES

(1) "The United States Pharmacopeia," 19th rev., Mack Publishing Co., Easton, Pa., 1975, p. 650.

(2) H. Nogami, J. Hasegawa, and Y. Nakai, *Chem. Pharm. Bull.*, **7**, 331 (1959).

(3) M. H. Rubinstein, J. I. Wells, and C. A. Holland, *J. Pharm. Pharmacol. Suppl.*, **27**, 54 (1975).

(4) W. Lowenthal, *J. Pharm. Sci.*, **61**, 1695 (1972).

(5) A. Hixson and J. Crowell, *Ind. Eng. Chem.*, **23**, 923 (1931).

(6) W. I. Higuchi and E. N. Hiestand, *J. Pharm. Sci.*, **52**, 67 (1963).

(7) K. G. Nelson and A. C. Shah, *ibid.*, **64**, 610 (1975).

(8) L. J. Leeson and J. T. Carstensen, "Dissolution Technology," Academy of Pharmaceutical Sciences, American Pharmaceutical Association, Washington, D.C., 1974.

(9) J. G. Wagner, *J. Pharm. Sci.*, **58**, 1253 (1969).

(10) F. Langenbucher, *J. Pharm. Pharmacol.*, **24**, 979 (1972).

(11) A. C. Shah, C. B. Poet, and J. F. Ochs, *J. Pharm Sci.*, **62**, 671 (1973).

(12) P. V. Pedersen and K. F. Brown, *ibid.*, **65**, 1442 (1976).

ACKNOWLEDGMENTS AND ADDRESSES

Received November 22, 1976, from the *College of Pharmacy, University of Minnesota, Minneapolis, MN 55455.*

Accepted for publication March 11, 1977.

Supported by a grant from the Pharmacy Research Unit, The Upjohn Co., Kalamazoo, Mich.

[x] To whom inquiries should be directed.

Bioavailability of Three Isoniazid Formulations

S. SVED [x], I. J. McGILVERAY, and N. BEAUDOIN

Abstract □ The bioavailability of three isoniazid formulations was assessed using a procedure specific for the free drug. Nine human volunteers, all slow acetylators, were each given 4 × 100 mg of isoniazid of three different tablet formulations at weekly intervals; the plasma drug levels were measured at different times during the first 24 hr. No significant differences ($p > 0.05$) were detected among the three products as to relative bioavailability, peak plasma concentrations, C_{max}, and the time of C_{max}, t_{max}. Analysis of variance of the pharmacokinetic parameters obtained according to a one-compartment open model did not demonstrate any significant formulation or time effect but revealed a significant intersubject variation in all parameters involved.

Keyphrases □ Isoniazid—bioavailability of three commercial formulations compared □ Bioavailability—isoniazid, three commercial formulations compared □ Tuberculostatic antibacterials—isoniazid, bioavailability of three commercial formulations compared

Isoniazid has been used since the early 1950's for the treatment of tuberculosis and has been largely responsible for the virtual eradication of this disease in certain parts of the world. It is widely used in preventive therapy in the United States and Canada. Its clinical efficacy and bioavailability assessment are complicated by methodological and metabolic problems. First, the presence of slow and fast acetylator genotypes in the population has been demonstrated (1–5), and the inclusion of both types in a study could lead to increased variability and difficulties in design. Second, isoniazid tends to form relatively stable, probably less active, hydrazones with either physiological (sugars and pyruvate) or excipient (lactose and glucose) aldehydes and ketones (6–9), thus necessitating an assay that can distinguish between the free drug and its hydrazones.

Earlier studies (10) on isoniazid bioavailability did not demonstrate any difference between six commercial preparations available in the United States. The method used, however, could not distinguish between free isoniazid and its hydrazones. This study was initiated to compare the bioavailability of three Canadian isoniazid preparations using a homogeneous group and an assay that measures only free isoniazid in the plasma.

EXPERIMENTAL

Materials—Isoniazid tablets, 100 mg, were supplied[1] from current production lots. Evacuated heparinized blood collection tubes were obtained locally[2]. Extractions were done in glass tubes with polytef-lined screw caps[3]. 2,4-Pentanedione (practical), diethanolamine, ethylene glycol, potassium carbonate, zinc acetate (all reagent grade)[4], methyl

[1] See "Quad Review 4," Health Protection Branch, Health and Welfare Canada, Ottawa, Canada, 1975, p. 44.

[2] Vacutainers, Becton-Dickinson; obtained through Canlab, Ottawa, Canada.

[3] Catalog No. T 1356-1, Canlab, Ottawa, Canada.

[4] Baker; obtained through Canlab, Ottawa, Canada.

Table I—Specificity of Assay Used for Isoniazid

Substance	Amount Added, nmoles	Amount Found[a], nmoles	Recovery, %
Isoniazid	72.9	74.4	102
I	55.5	0	0
II	48.3	2.9	6
III	37.7	1.5	4

[a] Estimated by the method of Lever (13) as described under *Experimental*. (Means of duplicate determinations.)

isobutyl ketone[5], and chloramine-T[6] were used without further purification. Ether[7] was freshly distilled before use.

Solutions—Acetylisoniazid (I) and isoniazid hydrazones of pyruvate (II) and α-ketoglutarate (III)[8] were dissolved in water containing excess sodium bicarbonate to keep the solution pH above 7.

***In Vitro* Testing**—Potency, content uniformity, and disintegration time were tested according to the USP XVIII (11) requirements for isoniazid tablets. Dissolution time, $\bar{t}_{60}$, was measured using the USP rotating-basket method (11) with 900 ml of distilled water at 37° as the dissolution medium. The basket was rotated at 100 rpm, and the dissolved drug was measured by following the absorbance of the filtered dissolution medium at 262 nm in a suitable spectrophotometric system[9].

Subjects—Nine normal, healthy, male volunteers, all slow acetylators, 26–44 years old and 66–86 kg, were selected on the basis of a complete medical and biochemical examination. Isoniazid acetylator phenotype was determined according to the test described by Hodgkin *et al.* (12).

Bioavailability Trial—The three isoniazid preparations were administered to each subject at a dose of 400 mg (4 × 100-mg tablets), at intervals of 1 week, according to a design incorporating three replicate 3 × 3 Latin squares. The subjects, having fasted overnight, ingested the drug with 50 ml of water (0 time), took a light, xanthine-free beverage at 1.5 hr, and had food and water *ad libitum* from 3 hr on. Blood was obtained by venipuncture using heparinized collection tubes[2] at 0, 0.25, 0.5, 1.0, 1.5, 2, 3, 4, 7.5, and 24 hr; the plasma was separated by centrifugation and kept frozen at −20° for not more than 5 days before analysis.

Assay—Plasma isoniazid was estimated by a minor modification of the fluorometric procedure of Lever (13). Plasma, 1 ml, was incubated in a polytef-lined screw-capped tube[3] with 0.6 ml of 7% 2,4-pentanedione in 1 *M* Na_2HPO_4 for 20 min at 45°. After the addition of 0.4 ml of 5 *M* K_2CO_3 and 5 ml of methyl isobutyl ketone, the mixture was extracted[10]

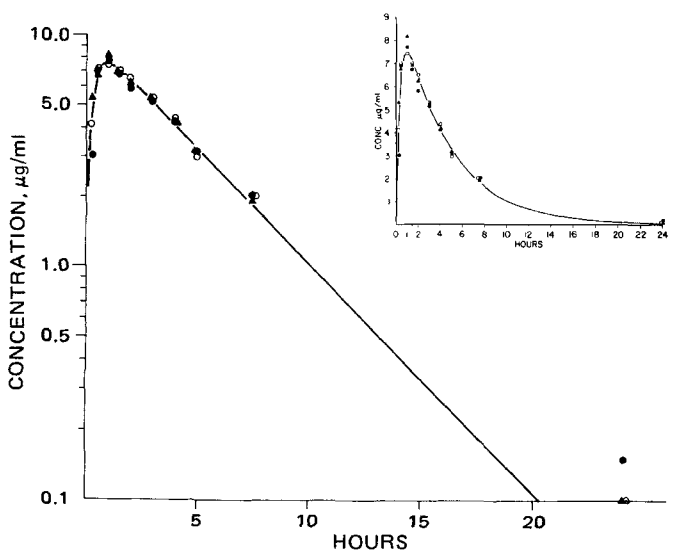

Figure 1—*Plasma profile of isoniazid following the administration of 400 mg to human volunteers. The points represent the mean plasma isoniazid concentration for each formulation. Key: ●, Formulation R; ▲, Formulation 1; and ○, Formulation 2. The solid line is the curve fitted to the overall means of concentrations. The inset is the linear plot.*

[5] Certified, Fisher Scientific, Ottawa, Canada.
[6] Eastman; obtained through Fisher Scientific.
[7] Anhydrous, Mallinckrodt Chemicals, Montreal, Canada.
[8] Gift of Dr. L. Eidus, Ottawa, Canada.
[9] Beckman DB-GT, Beckman Instruments, Fullerton, Calif.
[10] Roto Rack, Fisher Scientific, Ottawa, Canada.

Table II—*In Vitro* Test Results of the Isoniazid Formulations[a]

Formulation	Potency[b], mg/Tablet	Content Uniformity[c]	Disintegration Time[d], min	Dissolution Time[e], min
R	103.7	Pass	—	3
1	101.1	—	0.5	1
2	99.3	Pass	5.5	11

[a] Specifications according to USP XVIII (11). [b] From 93 to 107% of label claim. [c] Minimum of nine tablets out of 10 within 15% of label claim. [d] A 30-min maximum. [e] Test not required by the USP XVIII.

for 15 min and centrifuged for 10 min. The organic phase (4 ml) was extracted as already described with 1.2 ml of a solution of 2.5 *M* diethanolamine and 2 *M* zinc acetate in ethylene glycol and centrifuged.

The ethylene glycol layer was washed with 1 ml of ether and placed under vacuum for 10 min to remove the dissolved ether, and its fluorescence was measured on a fluorometer[11] using as excitation the mercury line at 436 nm and an emission wavelength of 540 nm. Readings were made against blanks prepared identically using pooled plasma of normal blood donors. All 0-hr samples of the bioavailability trial gave consistently zero readings within instrumental error.

Calculations—The areas under the plasma isoniazid concentration–time curve, *AUC*, were estimated by the trapezoidal method; the analyses of variance on the *AUC* and on the maximum observed plasma concentration, C_{max}, were done using the logarithmic transform of the raw data adjusted for potency. The pharmacokinetic parameters for each individual treatment were obtained by a nonlinear regression program[12] according to:

$$C_p = C_0 \frac{k_a}{k_a - k_e} (e^{-k_e t} - e^{-k_a t}) \qquad \text{(Eq. 1)}$$

where C_p is the plasma concentration at time t, C_0 is the dose absorbed divided by the volume of distribution, and k_a and k_e are the rate constants for absorption and elimination, respectively. The starting parameters for the program were obtained using the graphic method of Rescigno and Segré (14).

RESULTS AND DISCUSSION

Isoniazid Assay—Two problems were encountered when evaluating suitable procedures for plasma isoniazid: the specificity of the procedure and the stability of the drug in plasma stored in the frozen state. Specificity has been a problem since isoniazid therapy was introduced, as witnessed by the plethora of published procedures (*cf.*, 15, also 13, 16–19). The ease with which isoniazid forms derivatives with ketones and aldehydes and the controversy as to the therapeutic efficacy of the resulting hydrazones were described previously (6–9). Observations in this laboratory with rabbits suggest that at least some hydrazones of isoniazid remain intact and are rapidly eliminated when injected. The method selected was, therefore, chosen without acid treatment during extraction or deproteinization to avoid possible hydrolysis of any isoniazid hydrazones present.

The second problem, loss of isoniazid during frozen storage of plasma, has been reviewed (20). It appears to be minimal when the chromogenic reaction is performed in the presence of plasma proteins within a few days of storage, as in the present study.

To verify the specificity of the method, isoniazid and I–III were added to plasma and assayed for isoniazid. Table I shows the recoveries as isoniazid. Physiological hydrazones did not interfere to any appreciable extent when the temperature was kept below 50°, although considerable interference was noted at higher temperatures (up to 80% at 100°). The final ether wash and drying were found advisable to avoid development of turbidity, caused by residual methyl isobutyl ketone, on cooling of the final solution.

***In Vitro* Tests**—The results of the test performed on the isoniazid formulations are summarized in Table II. All parameters studied were within the specifications of USP XVIII (11). Two of the three formulations contained lactose as excipient, but the amount of isoniazid bound as hydrazone was too small (4.2% or less[13]) to vitiate the estimation of bioavailability.

Bioavailability—The plasma isoniazid concentrations following the

[11] Aminco-Bowman SPF-125, American Instrument Co., Silver Spring, Md.
[12] The program used was a modification of the Bio-medical Statistical Program, BMD-X-85 package.
[13] Dr. K. McErlane of these Laboratories, personal communication.

Table III—Plasma Profiles for Isoniazid (Formulation Means)

Formulation	*AUC*, μg hr/ml	Plasma Concentration[a], μg/ml, at 0.25 hr	0.5 hr	1 hr	1.5 hr	2 hr	3 hr	4 hr	5 hr	7.5 hr	24 hr
R	50.29	3.03	6.92	7.72	6.75	5.82	5.16	4.15	3.12	2.03	0.15
(*CV*)	(14.53)	(69.14)	(38.33)	(26.89)	(16.72)	(14.69)	(16.36)	(17.18)	(14.92)	(17.92)	(50.31)
1	49.87	5.32	6.76	8.20	6.93	6.22	5.27	4.18	3.08	1.91	0.10
(*CV*)	(16.59)	(78.53)	(39.77)	(19.17)	(17.29)	(18.93)	(19.81)	(18.28)	(23.12)	(19.49)	(62.45)
2	50.63	4.14	7.00	7.44	6.99	6.50	5.31	4.38	2.97	2.02	0.10
(*CV*)	(17.20)	(74.49)	(52.63)	(33.36)	(22.27)	(20.28)	(12.53)	(16.40)	(15.73)	(22.02)	(42.13)

[a] Arithmetic means, $n = 9$ for each formulation.

Table IV—Bioavailability Parameters of Isoniazid Formulations

Formulation	Potency[a], %	*AUC*[b], μg hr/ml	RBA[c], %	C_{max}, μg/ml	T_{max}, hr
R	103.7	50.3	100	7.86	0.83
1	99.3	49.9	101.4	9.15	0.75
2	101.1	50.6	105.0	8.27	1.03
CV	—	—	11	17.5	60

[a] Percent of label claim. [b] Area under the 0–24-hr plasma concentration–time curve (arithmetic means of uncorrected data). [c] Relative bioavailability: *AUC* relative to the reference formulation (*R*) (geometric mean of data corrected for potency).

ingestion of 400 mg each of three different formulations are given in Table III. The *AUC* and mean plasma concentrations at each time were very similar to each other, and the coefficient of variation (*CV*) between 1.5 and 7.5 hr was 22% or less. The high values for the coefficient of variation at 24 hr were probably due to the very low concentrations, which were near the detection limit, while those during the first 30–60 min (up to 78% at 0.25 hr) may have been indicative of person-dependent irregularities in absorption. However, since this time interval represented a small fraction of the total area (typically ~15%; *cf.*, Fig 1, inset), it had only a minor effect on the overall variability of the area under the curve (*CV* = 14–17%). In fast acetylators, where the elimination phase is several times shorter (1), irregularities during absorption would probably be more marked.

The results of the analysis of variance are summarized in Table IV. The bioavailabilities of Formulations 1 and 2 relative to the reference formulation (*R*) were 101.4 and 105%, respectively (values corrected for potency), and the coefficient of variation was 11%. None of these values was significantly different from the others at the 95% confidence level. These results are similar to those obtained by Gelber *et al.* (10) who found no differences in the bioavailability of six different isoniazid formulations.

Table IV also gives the geometric means for maximum plasma concentrations, C_{max}, observed with the formulations. These ranged from 7.86 to 9.15 μg/ml, with an overall coefficient of variation of 17.5%, and gave no significant difference ($p > 0.05$). The times, t_{max}, at which C_{max} was observed ranged from 0.25 to 2 hr (arithmetic means of 0.75–1.03, $CV = 60\%$). An apparent rank correlation between t_{max} and dissolution time could not be considered significant with the small number of formulations tested.

Pharmacokinetic Considerations—The mean plasma concentrations obtained for each formulation are compared in Fig. 1 with the theoretical curve fitted by a nonlinear regression to the overall means. The parameters obtained in fitting this curve gave half-lives of absorption and elimination of 0.25 and 3.01 hr, respectively. The C_{max}, 7.5 μg/ml, occurred at 0.98 hr ("mean fit," Table V). All points were close to the theoretical curve, except the 24-hr values which were near the lower limit of the assay method used and appeared to fit poorly on the semilogarithmic plot. However, this discrepancy had a minor effect on the *AUC* (Fig. 1, inset).

The trapezoidal method appeared to overestimate the 0–24-hr *AUC* by about 20% compared to the theoretical value. The major part of this error was due to the lack of points between 7.5 and 24 hr. However, similar relative bioavailabilities were obtained by using either the theoretical 0–∞ *AUC* (C^0/k_e) or the truncated 0–7.5- or 0–24-hr *AUC*, in agreement with findings of Lovering *et al.* (21).

To examine the pharmacokinetic behavior of isoniazid, data points from each individual treatment were used to fit individual theoretical curves by means of the nonlinear regression program. The data for 19 out of the total 27 treatments, as well as the mean data, demonstrated a good fit to the theoretical equation. The remaining eight treatments (mostly with 0.25-hr values in the upper or lower extremes) did not fit the equation and could not be used.

The pharmacokinetic parameters derived are summarized in Table V. The overall mean of the parameters gave a C_0 of 9.94 μg/ml, an ab-

Table V—Formulation Means of Parameters Derived from the Fitting of Plasma Isoniazid Concentration Data to a One-Compartment Open Model

Formulation	Number of Observations	C_0	k_a	k_e	Theoretical C_{max}	Theoretical[a] T_{max}
1	5	10.35	2.35	0.26	7.66	1.13
2	6	10.10	2.98	0.26	7.78	1.00
R	8	9.40	3.30	0.24	7.60	0.88
All combined	19	9.94	2.85	0.25	7.58	1.00
CV, %		10.02	30.6	12.0	9.4	20.6
Mean fit[b]	27	9.37	2.78	0.23	7.50	0.98

[a] Means for theoretical T_{max} are arithmetic; all others are geometric means. [b] Parameters of the curve fitted to the arithmetic means of all observed plasma concentrations ($n = 27$ for each point, $r^2 = 0.998$).

Table VI—Analysis of Variance of All Parameters Derived from the Fitting of Plasma Isoniazid Concentration Data to a One-Compartment Open Model[a]

Parameter	Factor: Subject, Value of *F* Test	Subject, Significance[b]	Period, Value of *F* Test	Period, Significance	Formulation, Value of *F* Test	Formulation, Significance
C_0	7.44	*	0.12	n.s.	1.29	n.s.
K_a	7.32	*	1.08	n.s.	1.23	n.s.
K_e	4.59	*	0.80	n.s.	1.61	n.s.
C_{max}	6.75	*	1.18	n.s.	0.09	n.s.
T_{max}	5.95	*	2.11	n.s.	1.58	n.s.
Degrees of freedom	8,6		2,6		2,6	

[a] Only values of the *F* test and its significance and the degrees of freedom are given for each factor for each parameter. [b] * = significant at $\alpha = 0.05$; n.s. = not significant at $\alpha = 0.05$.

sorption rate constant of 2.85 hr^{-1}, and an elimination rate constant of 0.25 hr^{-1} (half-life ~3 hr). The theoretical C_{max}, reached at 1 hr, was 7.58 μg/ml. A similar set of parameters was obtained when the equation was applied to the means of all 27 treatments, which gave an excellent fit (r^2 = 0.998).

The results of an analysis of variance of the parameters are shown in Table VI. Of the three parameters, as well as C_{max} and t_{max}, none showed any significant formulation or time effect. However, analysis of variance revealed a statistically significant between-subject variation ($p < 0.05$) for all parameters studied, including k_e. Since all subjects were of the slow inactivator phenotype, the finding with this small sample lends support to the proposed existence of additional minor genes involved in the elimination of isoniazid (2), although other mechanisms, *e.g.*, multiphasic absorption, cannot be ruled out entirely.

In conclusion, no significant differences in the relative rate or extent of bioavailability could be demonstrated in three Canadian isoniazid formulations. In slow acetylator subjects, the drug was absorbed rapidly from the gut and was eliminated with a half-life of approximately 3 hr.

REFERENCES

(1) J. H. Peters, *Am. Rev. Resp. Dis.*, **81**, 485 (1960).

(2) D. A. Price Evans, *Ann. N.Y. Acad. Sci.*, **151** (Art. 2), 723 (1968).

(3) L. Eidus, M. M. Hodgkin, and A. H. E. Hsu, *Int. J. Clin. Pharmacol.*, **8**, 154 (1973).

(4) C. W. L. Jeanes, O. Schaefer, and L. Eidus, *Can. Med. Assoc. J.*, **109**, 483 (1973).

(5) G. Raghupati Sarma, S. Kailasam, D. A. Mitchison, N. G. K. Nair, S. Radhakrishna, and S. P. Tripathy, *Tubercle*, **56**, 314 (1975).

(6) J. H. Peters and V. E. Hayes, *Arch. Int. Pharmacodyn. Ther.*, **159**, 328 (1966).

(7) K. Kakemi, T. Arita, H. Sezaki, and N. Takasugi, *Chem. Pharm. Bull.*, **13**, 551 (1965).

(8) K. V. N. Rao, S. Kailasam, N. K. Menon, and S. Radhakrishna, *Indian J. Med. Res.*, **59**, 1343 (1971).

(9) W.-H. Wu, T.-F. Chin, and J. L. Lach, *J. Pharm. Sci.*, **59**, 1234 (1970).

(10) R. Gelber, P. Jacobsen, and L. Levy, *Clin. Pharmacol. Ther.*, **10**, 841 (1969).

(11) "The United States Pharmacopeia," 18th rev., Mack Publishing Co, Easton, Pa., 1970.

(12) M. M. Hodgkin, A. H. E. Hsu, P. Varughese, and L. Eidus, *Int. J. Clin. Pharmacol.*, **7**, 355 (1973).

(13) M. Lever, *Biochem. Med.*, **6**, 65 (1972).

(14) A. Rescigno and G. Segré, in "Drug Tracer Kinetics," Blaisdell, Waltham, Mass., 1966, p. 20.

(15) J. N. Miceli, W. A. Olson, and W. W. Weber, *Biochem. Med.*, **12**, 348 (1975).

(16) H. Bartels and P. Spring, *Chemotherapy*, **21**, 1 (1975).

(17) J. T. Stewart and D. A. Settle, *J. Pharm. Sci.*, **64**, 1403 (1975).

(18) J. T. Stewart, I. L. Honigberg, J. P. Brant, W. A. Murray, J. L. Webb, and J. B. Smith, "Abstracts of the 19th National Meeting of the APhA Academy of Pharmaceutical Sciences," vol. 5, American Pharmaceutical Association, Washington, D.C., 1975, p. 163.

(19) D. W. Russell, *Clin. Chim. Acta*, **41**, 163 (1972).

(20) T. O. O'Barr, D. J. Keith, and E. B. Blair, *Am. Rev. Resp. Dis.*, **107**, 472 (1973).

(21) E. G. Lovering, I. J. McGilveray, I. McMillan, and W. Tostowaryk, *J. Pharm. Sci.*, **64**, 1521 (1975).

ACKNOWLEDGMENTS AND ADDRESSES

Received October 14, 1976, from the *Drug Research Laboratories, Health Protection Branch, Ottawa, Ontario, K1A 0L2, Canada.*

Accepted for publication March 11, 1977.

The authors thank Dr. L. Eidus for valuable discussions, Dr. W. Tostowaryk for the statistical analyses of the results, and Dr. J. C. K. Loo and Mr. P. Fitzsimmons for setting up the computer program.

[x] To whom inquiries should be directed.

NOTES

Influence of Human Skin Surface Lipids on Protection Time of Topical Mosquito Repellent

W. A. SKINNER [x], H. C. TONG, H. JOHNSON, R. M. PARKHURST, D. THOMAS, T. SPENCER [*], W. AKERS [*], D. SKIDMORE [‡], and H. MAIBACH [‡]

Abstract □ Skin surface lipids were extracted from volunteers who had been ranked according to the duration of protection from mosquitoes by diethyltoluamide. These lipids were analyzed by GLC–mass spectrometry for their fatty acid contents. Correlations were found between total skin lipid content and protection time of diethyltoluamide and between certain fatty acid concentrations in the skin lipids and the protection time of diethyltoluamide.

Keyphrases □ Lipids, skin surface—effect on protection time of diethyltoluamide, humans □ Diethyltoluamide—protection time, effect of skin surface lipids, humans □ Repellents, insect—diethyltoluamide, protection time, effect of skin surface lipids, humans

Topical mosquito repellents protect some individuals longer than others. In studies of repellents applied to forearms, the repellency duration with diethyltoluamide (I) against female *Aedes aegypti* (yellow fever) mosquitoes varied in a reproducible way among the volunteers[1]. This report investigated the role of skin surface lipids in affecting the protection time of I toward mosquitoes.

Surface lipids contain certain components that are repellent to *A. aegypti* mosquitoes when evaluated in a dual-port olfactometer (1, 2). The primary repellency of these lipids is derived from the volatile fatty acids, whereas the hydrocarbon fraction exhibits a degree of repellency, primarily due to the unsaturated components present (3).

[1] W. Akers, unpublished data.

sorption rate constant of 2.85 hr^{-1}, and an elimination rate constant of 0.25 hr^{-1} (half-life ~3 hr). The theoretical C_{max}, reached at 1 hr, was 7.58 μg/ml. A similar set of parameters was obtained when the equation was applied to the means of all 27 treatments, which gave an excellent fit (r^2 = 0.998).

The results of an analysis of variance of the parameters are shown in Table VI. Of the three parameters, as well as C_{max} and t_{max}, none showed any significant formulation or time effect. However, analysis of variance revealed a statistically significant between-subject variation ($p < 0.05$) for all parameters studied, including k_e. Since all subjects were of the slow inactivator phenotype, the finding with this small sample lends support to the proposed existence of additional minor genes involved in the elimination of isoniazid (2), although other mechanisms, *e.g.*, multiphasic absorption, cannot be ruled out entirely.

In conclusion, no significant differences in the relative rate or extent of bioavailability could be demonstrated in three Canadian isoniazid formulations. In slow acetylator subjects, the drug was absorbed rapidly from the gut and was eliminated with a half-life of approximately 3 hr.

REFERENCES

(1) J. H. Peters, *Am. Rev. Resp. Dis.*, **81**, 485 (1960).

(2) D. A. Price Evans, *Ann. N.Y. Acad. Sci.*, **151** (Art. 2), 723 (1968).

(3) L. Eidus, M. M. Hodgkin, and A. H. E. Hsu, *Int. J. Clin. Pharmacol.*, **8**, 154 (1973).

(4) C. W. L. Jeanes, O. Schaefer, and L. Eidus, *Can. Med. Assoc. J.*, **109**, 483 (1973).

(5) G. Raghupati Sarma, S. Kailasam, D. A. Mitchison, N. G. K. Nair, S. Radhakrishna, and S. P. Tripathy, *Tubercle*, **56**, 314 (1975).

(6) J. H. Peters and V. E. Hayes, *Arch. Int. Pharmacodyn. Ther.*, **159**, 328 (1966).

(7) K. Kakemi, T. Arita, H. Sezaki, and N. Takasugi, *Chem. Pharm. Bull.*, **13**, 551 (1965).

(8) K. V. N. Rao, S. Kailasam, N. K. Menon, and S. Radhakrishna, *Indian J. Med. Res.*, **59**, 1343 (1971).

(9) W.-H. Wu, T.-F. Chin, and J. L. Lach, *J. Pharm. Sci.*, **59**, 1234 (1970).

(10) R. Gelber, P. Jacobsen, and L. Levy, *Clin. Pharmacol. Ther.*, **10**, 841 (1969).

(11) "The United States Pharmacopeia," 18th rev., Mack Publishing Co, Easton, Pa., 1970.

(12) M. M. Hodgkin, A. H. E. Hsu, P. Varughese, and L. Eidus, *Int. J. Clin. Pharmacol.*, **7**, 355 (1973).

(13) M. Lever, *Biochem. Med.*, **6**, 65 (1972).

(14) A. Rescigno and G. Segré, in "Drug Tracer Kinetics," Blaisdell, Waltham, Mass., 1966, p. 20.

(15) J. N. Miceli, W. A. Olson, and W. W. Weber, *Biochem. Med.*, **12**, 348 (1975).

(16) H. Bartels and P. Spring, *Chemotherapy*, **21**, 1 (1975).

(17) J. T. Stewart and D. A. Settle, *J. Pharm. Sci.*, **64**, 1403 (1975).

(18) J. T. Stewart, I. L. Honigberg, J. P. Brant, W. A. Murray, J. L. Webb, and J. B. Smith, "Abstracts of the 19th National Meeting of the APhA Academy of Pharmaceutical Sciences," vol. 5, American Pharmaceutical Association, Washington, D.C., 1975, p. 163.

(19) D. W. Russell, *Clin. Chim. Acta*, **41**, 163 (1972).

(20) T. O. O'Barr, D. J. Keith, and E. B. Blair, *Am. Rev. Resp. Dis.*, **107**, 472 (1973).

(21) E. G. Lovering, I. J. McGilveray, I. McMillan, and W. Tostowaryk, *J. Pharm. Sci.*, **64**, 1521 (1975).

ACKNOWLEDGMENTS AND ADDRESSES

Received October 14, 1976, from the *Drug Research Laboratories, Health Protection Branch, Ottawa, Ontario, K1A 0L2, Canada.*

Accepted for publication March 11, 1977.

The authors thank Dr. L. Eidus for valuable discussions, Dr. W. Tostowaryk for the statistical analyses of the results, and Dr. J. C. K. Loo and Mr. P. Fitzsimmons for setting up the computer program.

[x] To whom inquiries should be directed.

NOTES

Influence of Human Skin Surface Lipids on Protection Time of Topical Mosquito Repellent

W. A. SKINNER [x], H. C. TONG, H. JOHNSON, R. M. PARKHURST, D. THOMAS, T. SPENCER [*], W. AKERS [*], D. SKIDMORE [‡], and H. MAIBACH [‡]

Abstract □ Skin surface lipids were extracted from volunteers who had been ranked according to the duration of protection from mosquitoes by diethyltoluamide. These lipids were analyzed by GLC–mass spectrometry for their fatty acid contents. Correlations were found between total skin lipid content and protection time of diethyltoluamide and between certain fatty acid concentrations in the skin lipids and the protection time of diethyltoluamide.

Keyphrases □ Lipids, skin surface—effect on protection time of diethyltoluamide, humans □ Diethyltoluamide—protection time, effect of skin surface lipids, humans □ Repellents, insect—diethyltoluamide, protection time, effect of skin surface lipids, humans

Topical mosquito repellents protect some individuals longer than others. In studies of repellents applied to forearms, the repellency duration with diethyltoluamide (I) against female *Aedes aegypti* (yellow fever) mosquitoes varied in a reproducible way among the volunteers[1]. This report investigated the role of skin surface lipids in affecting the protection time of I toward mosquitoes.

Surface lipids contain certain components that are repellent to *A. aegypti* mosquitoes when evaluated in a dual-port olfactometer (1, 2). The primary repellency of these lipids is derived from the volatile fatty acids, whereas the hydrocarbon fraction exhibits a degree of repellency, primarily due to the unsaturated components present (3).

[1] W. Akers, unpublished data.

Table I—Ranking of Volunteers Based on Descending Order of Duration of Protection of I toward Biting of Female *A. aegypti* Mosquitoes

Volunteer	Average Protection Time, hr, for 0.32 mg of I/cm^2 ± *SD*[a]
P	10.0 (2) ± 2.12
S	9.7 (8) ± 2.24
B	9.2 (3) ± 0.58
A	8.5 (4) ± 2.16
D	8.3 (4) ± 0.50
R	6.5 (5) ± 0.71
LT	6.2 (3) ± 1.53
L	5.6 (8) ± 1.13
M	5.3 (5) ± 1.10
T	5.0 (6) ± 0.55
C	4.5 (5) ± 0.71

[a] Number in parentheses is the number of replicates.

Skin surface lipids have been studied for their chemical composition (4–9), and considerable information concerning their composition has been developed using GLC and mass spectrometric techniques.

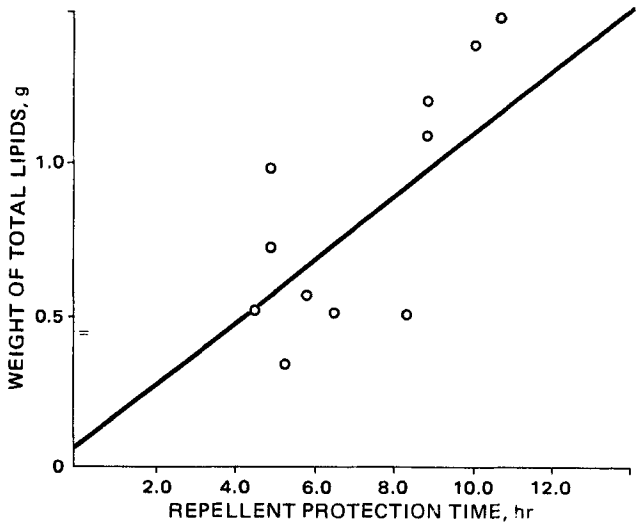

Figure 1—*Repellent protection time of I on individuals as a function of the total skin surface lipid weight.*

EXPERIMENTAL

Attractancy and Repellency—Relative individual attractiveness to mosquitoes was determined using a probing test. Each subject had a 9 × 12-cm foam pad with a 7 × 10-cm hole in the center placed on his or her ventral forearm. The participating volunteer placed this forearm under a 5 × 8-cm screen-covered hole in the center of the bottom of a standard test cage containing 250 avid female mosquitoes. The foam pad prevented cage contamination by the individual's forearm. The number of mosquitoes landing and probing in a 1-min period was recorded.

Each volunteer exposed his or her arm under each of six test cages in a random order with at least a 1-min rest between exposures. All subjects were tested over a 4-hr period on the same day. The average number of mosquitoes probing in 1 min was taken as a measure of the individual's attractiveness to mosquitoes.

Duration of repellent protection time against mosquitoes was determined by application of 0.32 mg of I/cm^2 to a 7 × 10-cm test site on the ventral forearm. Once each hour, the forearm was covered by a plastic sleeve with a 5 × 8-cm hole corresponding to the repellent-treated area. The forearm was inserted into a cage containing 250 avid female *A. aegypti* mosquitoes for a 3-min exposure. The test exposure was repeated hourly until two bites were received on the treated site; that time was recorded as the protection time. The protection times reported are averages over 18 months of testing for each individual (Table I).

Lipid Collection—For the lipid analysis, six subjects consistently exhibiting a longer duration of repellent protection than the average were selected from a volunteer population of 22 along with five additional individuals who consistently exhibited a shorter duration of protection than the average. Acetone extractions were made on each subject three times weekly for 4 weeks as follows. The subject held his or her elbow over a glass funnel assigned exclusively to that individual. Analytical grade acetone, 50 ml, was used to rinse the elbow in each extraction, and acetone extractions were stored in polyethylene bottles in a freezer during the 4 weeks of collection. Subjects used only plain soap[2] and no perfumes for 1 week prior to and during the 4 collection weeks.

GLC–Mass Spectral Analysis of Fatty Acids—Standard amounts (500 μg) of *cis*-13-docosenoic acid were added to the total lipid sample from each volunteer. After derivatization with bis(trimethylsilyl)trifluoroacetamide, the sample was submitted to analysis. An SE-30 column was used for GLC separations. The results are shown in Table II for each volunteer.

Multiple Regression Analysis—The relative effect of each fatty acid on mosquitoes is influenced by two factors in addition to the molar quantity: the intrinsic repellency of the fatty acid molecule to mosquitoes and the relative volatility of the fatty acid. Both factors were included in the relative intrinsic repellency determined (10) in olfactometer testing against mosquitoes. The molar concentration of each fatty acid (Table II) was multiplied by the relative intrinsic repellency (10) to obtain a factor suitable for correlation with the individual attractiveness to mosquitoes and the individual protection times afforded each subject by the repellent.

A multiple regression from the literature (11) was run on the fatty acid intrinsic repellency product as a function of first the protection time and then the attractiveness to mosquitoes. The hierarchial regressional analysis was performed stepwise so that the covariant factors with the highest correlations were introduced into the regression equation first. Saturated fatty acid fractions C_{13} and C_{15} and unsaturated fatty acid fractions C_{14}, C_{15}, C_{16}, and C_{17} were found to be multicollinear with the C_{17} saturated fatty acid fraction (Table III); the six fractions were omitted from the regressional analysis, using the approximation that the partial correlation coefficient for C_{17} would describe their effect on the dependent variable.

The multiple regression analysis equation of dry protection time *versus* the relative fatty acid repellency factor (*RF*) is:

$$\text{dry protection time} = 8.5\,(\text{m}M\ C_{17} \times RF_{C17}) + 50.1\,(\text{m}M\ C_{11} \times RF_{C11}) - 36.1\,(\text{m}M\ C_7 \times RF_{C7}) - 7.9\,(\text{m}M\ C_{16} \times RF_{C16}) + 3.3\,(\text{m}M\ C_{18} \times RF_{C18}) - 0.1\,(\text{m}M\ C_{12} \times RF_{C12}) + 3.5 \quad \text{(Eq. 1)}$$

The significance = 0.042. The repellency factors from Skinner *et al.* (10) are: RF_{C17}, 23; RF_{C11}, 52; RF_{C7}, 61; RF_{C16}, 4; RF_{C18}, 9; and RF_{C12}, 35. The coefficients for the attractiveness correlation are different from those for the protection time correlation. One exception is the coefficient C_{11}, which has the opposite sign in the attractiveness compared to the protection time correlation; that is, negative attractiveness is positive repellency or duration of protection.

The multiple regression analysis equation of attractiveness (Att) *versus* the relative fatty acid repellency factor is:

$$\text{Att} = -44.7\,(\text{m}M\ C_{14} \times RF_{C14}) - 85.9\,(\text{m}M\ C_{11} \times RF_{C11}) + 54.0\,(\text{m}M\ C_{15U} \times RF_{C15U}) + 32.71 \quad \text{(Eq. 2)}$$

The significance = 0.049. The repellency factors from Skinner *et al.* (10) are: RF_{C14}, −2; RF_{C11}, 52; and RF_{C15U}, 17.

DISCUSSION

The duration of repellent protection has a significantly positive correlation ($\alpha < 0.05$) with the amount of lipid recovered from the skin (Fig. 1). Disregarding for the moment the repellent nature of the fatty acids, the correlation can be explained in terms of the film-forming nature of lipids on the skin. One might surmise that the lipids and repellent form a mixture, suppressing the evaporation rate from the skin surface. Gabel *et al.* (12) demonstrated that a lower evaporation rate increases the duration of repellent protection; moreover, musks, vanillin, and vanillin derivatives mixed with I increase repellent persistence when applied to the skin by suppressing repellent evaporation (13). Nicolaides (9) noted the possibility of free fatty acids and mono- and diacylglycerols forming films to reduce evaporative losses of water from the skin. Therefore, the fatty acids may influence repellent protection time by a physical mech-

[2] Ivory.

Table II—Fatty Acid Composition of Skin Surface Lipids from Volunteers

Subject	Fatty Acid Saturated, mg												Fatty Acid Unsaturated, mg					Total Lipid Extract, g
	C_7	C_8	C_9	C_{10}	C_{11}	C_{12}	C_{13}	C_{14}	C_{15}	C_{16}	C_{17}	C_{18}	C_{14}	C_{15}	C_{16}	C_{17}	C_{18}	
P	0.1	0.3	0.7	1.7	0.3	6.9	3.2	68.7	43.5	133.4	12.2	38.3	5.8	4.3	47.6	10.7	64.6	1.39
S	0.0	0.2	0.4	1.0	0.1	28.0	2.1	71.0	34.4	139.5	7.3	52.4	3.3	3.1	27.7	6.9	85.1	1.21
B	0.2	0.1	0.2	0.5	0.2	8.4	2.0	50.6	29.9	12.9	7.0	35.1	2.4	3.4	27.2	7.1	58.7	1.10
A	0.2	0.4	0.6	1.9	0.4	15.1	0.6	42.4	11.7	116.3	4.9	42.4	1.4	1.5	25.4	3.2	84.2	0.77
D	0.0	0.1	0.5	0.5	0.2	3.3	0.4	16.4	9.1	64.0	2.4	18.4	0.6	1.0	13.0	1.8	33.0	0.51
R	0.0	0.1	0.3	0.5	0.1	5.1	0.3	15.1	4.9	37.4	2.1	18.1	0.5	0.4	5.9	1.6	31.1	0.52
LT	0.2	0.2	0.5	0.6	0.2	6.4	1.3	42.1	19.4	108.2	4.1	34.6	1.9	2.1	26.6	5.6	83.3	0.99
L	0.0	0.1	0.2	0.5	0.2	6.4	1.0	27.8	15.4	57.9	3.2	16.9	1.5	1.1	14.2	3.7	38.3	0.57
M	0.1	0.3	0.2	1.3	0.1	22.6	0.2	23.7	5.0	51.1	2.1	20.0	0.8	0.3	8.2	1.4	43.7	0.35
T	0.0	0.4	0.3	1.6	0.0	30.4	0.2	35.4	14.1	118.0	4.9	38.9	1.7	1.5	23.0	5.0	66.5	0.73
C	0.1	0.1	0.2	0.4	0.5	3.4	0.1	13.1	4.8	50.3	1.8	18.3	0.6	0.3	9.9	1.5	49.5	0.53

anism in addition to their repellent effects.

Since the fatty acids exhibit repellency to mosquitoes, the effect of fatty acids on individual attractiveness to mosquitoes was considered. Nicholaides (9) indicated that lipases from microbial sources on the skin hydrolyze triacylglycerols to yield fatty acids and that the amount of hydrolysis increases the longer the lipids remain on the skin. Regression analysis of the total weight of extract from each individual produced a significant negative regression coefficient ($\alpha < 0.05$). Therefore, fatty acids in total appear to exhibit a negative attractiveness or positive repellency.

When multiple regression analysis was employed to ascertain the relative effects of fatty acid fractions on individual attractiveness to mosquitoes, C_{14} and C_{11} saturated fatty acids exhibited the highest degree of correlation with negative attractiveness. These fatty acids have a higher volatility than the longer chain fatty acids constituting the bulk of the lipid extract. A higher volatility might indicate more repellent effect against mosquitoes in the air above the skin.

In the second multiple regression analysis, the relation between repellent protection time and the fatty acid fractions was considered. The long chain fatty acids, including those multicollinear with C_{17} (Table III), dominate the regressional coefficients, indicating a positive correlation between the fatty acid fractions and repellent protection time. It cannot be determined whether or not the dominance of the long chain fatty acids in this correlation is a result of film-forming action with the repellent or of an actual repellent effect of these low volatility fatty acids; however, the second coefficient (C_{11}) indicates that a relatively volatile fatty acid, from the mosquito repellency consideration, does exhibit a positive correlation with repellent duration of protection.

With the current data, the multiple regression analysis gives only inferential coefficients so that the precise identification of the fatty acid components affecting attractiveness or protection time is tenuous. The low volatility, long chain fatty acids probably affect repellent persistence by a film-forming mechanism, which slows the evaporative (and possible penetrative) loss of repellent from the skin surface.

Further studies of these factors are needed. Understanding how these factors influence the protection time of repellents should help in the development of more effective repellents.

Table III—Correlation Coefficients Exhibiting a High Degree of Collinearity

C_{13}	0.919					
C_{15}	0.947	0.947				
C_{14U}	0.961	0.941	0.948			
C_{15U}	0.936	0.955	0.985	0.915		
C_{16U}	0.953	0.900	0.937	0.949	0.941	
C_{17U}	0.937	0.930	0.967	0.955	0.970	0.970
	C_{17}	C_{13}	C_{15}	C_{14U}	C_{15U}	C_{16U}

REFERENCES

(1) W. A. Skinner, H. Tong, H. Maibach, A. A. Khan, and T. Pearson, *Science*, **149**, 305 (1965).

(2) H. I. Maibach, W. A. Skinner, W. E. Strauss, and A. A. Khan, *J. Am. Med. Assoc.*, **196**, 263 (1966).

(3) W. A. Skinner, H. C. Tong, T. R. Pearson, and H. I. Maibach, *J. Econ. Entomol.*, **60**, 927 (1967).

(4) E. Haahti, *Scand. J. Clin. Lab. Invest., Suppl. 59*, **13**, 11 (1961).

(5) N. Nicolaides and S. Rothman, *Invest. Dermatol.*, **21**, 9 (1953).

(6) N. Nicolaides, *J. Oil Chem. Soc.*, **42** (8), 691 (1965).

(7) C. A. Lewis, B. J. Hayward, and R. M. B. MacKenna, *Br. J. Dermatol.*, **77** (6), 303 (1965).

(8) T. Shinohara, *J. Biochem.*, **68**, 125 (1970).

(9) N. Nicolaides, *Science*, **186**, 19 (1974).

(10) W. A. Skinner, H. C. Tong, H. I. Maibach, and D. Skidmore, *Experientia*, **26**, 728 (1970).

(11) N. H. Nie, C. H. Hull, J. G. Jenkins, K. Steinbrenner, and D. H. Brent, "Statistical Package for the Social Sciences," 2nd ed., McGraw-Hill, New York, N.Y., 1975.

(12) M. L. Gabel, T. S. Spencer, and W. A. Akers, *Mosquito News*, **36**, 141 (1976).

(13) A. A. Khan, H. I. Maibach, and D. L. Skidmore, *ibid.*, **35**, 332 (1975).

ACKNOWLEDGMENTS AND ADDRESSES

Received January 3, 1977, from the *Life Sciences Research Division, Stanford Research Institute, Menlo Park, CA 94025.*

Accepted for publication March 9, 1977.

Supported by U.S. Army Medical Research and Development Command Contracts DADA-170-70-C-0112 and DADA-170-70-C-0109.

The authors thank Kathy L. Zeller, Steven F. Bayles, and Ronald K. Shimmin for assistance.

* Present address: LAIR, Presidio, San Francisco, CA 94129.

‡ Present address: Department of Dermatology, University of California Medical Center, San Francisco, CA 94025.

ˣ To whom inquiries should be directed.

Preparation, Identification, and Quantitative NMR Determination of Silyl Derivatives of 6-Aminopenicillanic Acid, 7-Amino-3-methyl-Δ^3-cephem-4-carboxylic Acid, and 7-Amino-3-acetoxymethyl-Δ^3-cephem-4-carboxylic Acid

FULVIO BORTESI, SILVANO CAVALLI, and ALBERTO MANGIA ˣ

Abstract □ A rapid and accurate method for the quantitative determination of the extent and ratio of amino and carboxyl group trimethylsilylation of 6-aminopenicillanic acid, 7-amino-3-methyl-Δ^3-cephem-4-carboxylic acid, and 7-amino-3-acetoxymethyl-Δ^3-cephem-4-carboxylic acid is presented. The method utilizes NMR spectroscopy and is based on the difference in chemical shifts between *N*-trimethylsilyl and *O*-trimethylsilyl groups or, in cephalosporin derivatives, between the methyl group in the 3-position and free amino resonances. The spectra of the *N,O*-bis(trimethylsilyl) derivatives are discussed.

Keyphrases □ 6-Aminopenicillanic acid—silyl derivative, preparation and NMR analysis □ Cephemcarboxylic acids, substituted—silyl derivatives, preparation and NMR analyses □ NMR—analyses, silyl derivatives of 6-aminopenicillanic and substituted cephemcarboxylic acids □ Silyl derivatives—6-aminopenicillanic and substituted cephemcarboxylic acids, prepared, NMR analyses □ Antibacterial intermediates—6-aminopenicillanic and substituted cephemcarboxylic acids, silyl derivatives prepared, NMR analyses

Silylation (1) has a wide range of applications in analytical chemistry (2) and organic synthesis (1, 3) as a useful means of altering the solubility of materials, increasing their stability, and blocking reactive sites, allowing a successive, easy removal of the silyl group. All these advantages are present in the silylation of amino acids (4) using different silylating agents such as hexamethyldisilazane (I) (5), trimethylchlorosilane (II) (6), *N*-trimethylsilyldialkylamines (7), and *N,O*-bis(trimethylsilyl)acetamide (III) (8). Elemental analyses, refractive indexes, or IR spectra were the physical means used to determine the structure of *O*-mono- or *N,O*-disilylated products.

The silylation of 6-aminopenicillanic acid (IV), 7-amino-3-methyl-Δ^3-cephem-4-carboxylic acid (V), or 7-amino-3-acetoxymethyl-Δ^3-cephem-4-carboxylic acid (VI), prepared (9, 10) from naturally occurring penicillins and cephalosporins, is important in the commercial synthesis of semisynthetic β-lactam antibacterials (11, 12). Although there are several patents in this field, no analytical or physical data have been reported on these silylated β-lactam amino acids except monosilylated IV (13).

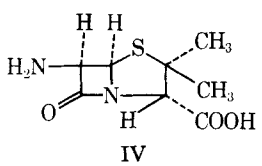

IV

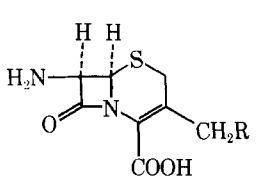

V: R = H
VI: R = $OCOCH_3$

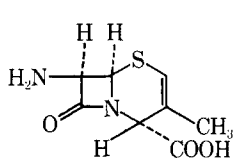

VII

Table I—NMR Quantitative Data

Experimental Condition[a]	Substrate	Silylation, %[b] $100 \times \frac{I_N}{I_O}$	Silylation, %[b] $100 \times \left(1 - \frac{I_A}{2} \times \frac{3}{I_M}\right)$	Solvent[c]
A	IV	15	—	VII
A	V	22	25	VIII
A	VI	16	18	VIII
2A	V	34	30	VIII
B	IV	42	—	VII
B	V	44	41	VIII
B	VI	40	42	VIII
2B	IV	92	—	VII
2B	V	95	—[d]	VIII
2B	VI	88	—[d]	VIII

[a] See *Experimental*. [b] Experiments were carried out at least three times, and the results are reproducible within ±5%. The values represent the percentage of silylation of the amino against the carboxyl group. In the first column, I_N = integration value of $(CH_3)_3SiN$ peak, and I_O = integration value of $(CH_3)_3SiO$ peak. In the second column, I_A = integration value of free amino group, and I_M = integration value of methyl resonance in position 3 for cephalosporin derivatives. [c] VII = deuterochloroform, and VIII = tetrachloroethylene. [d] The amino signal is broadened and the integration is difficult to evaluate due to its small value.

The described NMR method is a rapid and accurate tool to determine quantitatively the extent and ratio of amino and carboxyl group silylation directly in solution, avoiding handling of products sensitive to hydrolysis.

EXPERIMENTAL

Materials—Compounds IV–VI were laboratory reference grade. Deuterochloroform[1] and tetrachloroethylene[2] were dried over phosphorus pentoxide (water content <0.01%); I[3] and II[3] were used without purification.

NMR Measurements—A 60-MHz spectrometer[4] was used at 33°, with benzene as the internal reference (δ 7.37 ppm from tetramethylsilane) to avoid overlapping between tetramethylsilane and trimethylsilyl groups. The NMR spectrum was run at a 500-Hz sweep width and a 250-sec scan time for identification purposes.

For quantitative measurements, the spectrum was run at 50-Hz sweep width in the 0–50-Hz region or at 100-Hz sweep width in the 80–180-Hz region (for methods of calculation, see Table I). These regions were integrated carefully five times. The spectra of disilylated compounds were also run at 100-Hz sweep width in the β-lactam region both at 60 and 100 MHz[5].

Sample Preparations—In a flask protected from moisture by a calcium chloride tube, I (1 mmole, 0.217 ml) (Condition A), a mixture (14) of I (0.66 mmole, 0.145 ml) and II (0.66 mmole, 0.084 ml) (Condition B),

[1] Ciba.
[2] C. Erba.
[3] Dow Corning.
[4] Varian model T 60 A.
[5] Varian model HA-100.

Table II—60-MHz Signals[a] of Monosilyl[b] Derivative Protons (δ)

Substrate	Solvent[c]	NH_2	C-7	C-6	C-5	C-3	C-2		$OSi(CH_3)_3$	$OCOCH_3$
IV	VII	1.83 bs	—	4.38 d[d]	5.48 d[d]	4.47	1.68	1.77	0.5	—
V	VIII	1.68 bs	4.6 d[e]	4.87 d[e]	—	2.16	3.1 d[f]	3.53 d[f]	0.5	—
VI	VIII	1.76 bs	4.66 d[e]	4.88 d[e]	—	4.9 d[g] 5.33 d[g]	3.3 d[f]	3.68 d[f]	0.55	2.15

[a] Singlet if not stated; bs = broad singlet; d = doublet. [b] Condition A; $NSi(CH_3)_3$, as partial resonance at 0.3 δ. [c] VII = deuterochloroform, and VIII = tetrachloroethylene. [d] J = 4.3 Hz. [e] J = 4.5 Hz. [f] J = 18 Hz. [g] J = 13.4 Hz.

or twice these quantities (Condition 2A or 2B) was added to a suspension of IV, V, or VI (1 mmole) in the chosen solvent (2 ml) at room temperature under magnetic stirring.

The mixture was heated at about 64° for IV (with deuterochloroform as the solvent) and at 120° (tetrachloroethylene) for V and VI until a complete solution was attained and then for an additional 0.5 hr (60–90 min total). After cooling to room temperature, a 1-ml sample was put in the NMR tube in a dry box. Alternatively, the solvent was removed *in vacuo* in a rotary evaporator, carefully protected from moisture, to eliminate the last traces of the silylating agents and the solution was remade with fresh dry solvent.

Isomerization of V—Triethylamine (2 mmoles, 0.28 ml) and trimethylchlorosilane (2 mmoles, 0.254 ml) were added to a suspension of V (1 mmole, 0.214 g) in tetrachloroethylene (4 ml) at room temperature under magnetic stirring. The suspension was refluxed for 2 hr. After cooling to room temperature, a 1-ml sample was analyzed by NMR spectroscopy. Besides other peaks, the spectrum showed a doublet (J = 1 Hz) at δ 2.08 ppm and a singlet at δ 2.26 ppm for methyl resonances on a Δ^2- and Δ^3-cephem moiety, respectively (15). By integration of these two peaks, 32.5% of the Δ^2-derivative (VII) was obtained. The same ratio was obtained in a larger scale preparation in methylene chloride. After hydrolysis and filtration, the recovery was practically quantitative[6]; NMR (D_2O + DCl): δ 1.93 (dd, CH_3), 5.0 (m, H_4), 6.08 (m, H_2), 5.0 (d, H_7, J = 4.5 Hz), and 5.3 (d, H_6, J = 4.5 Hz) ppm for VII *versus* 2.25 (s, CH_3), 3.56 (s, CH_2), 5.08 (d, H_7, J = 4.5 hz), and 5.23 (d, H_6, J = 4.5 Hz) ppm for V; [α] + 230° (c = 1, 0.5 *M* HCl).

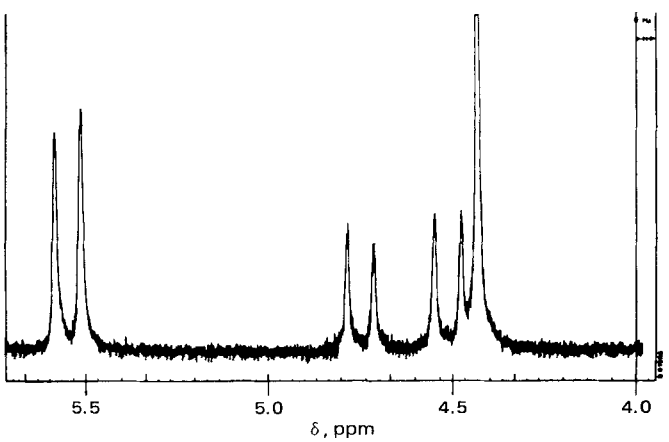

Figure 1—*The 60-MHz NMR spectrum of the β-lactam region of disilylated IV; singlet is the resonance for the 3-proton.*

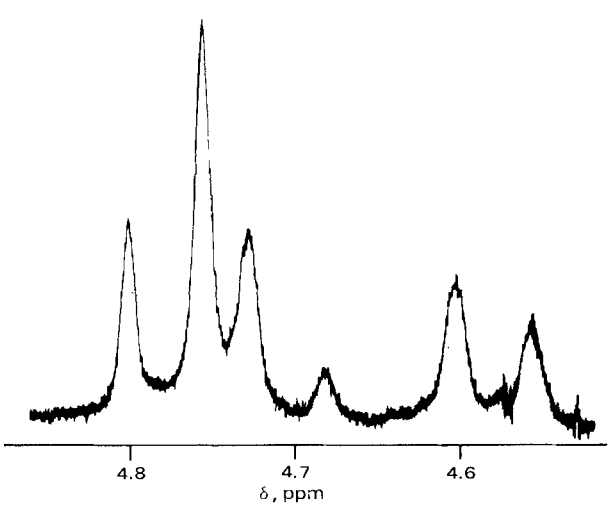

Figure 2—*The 100-MHz spectrum of the β-lactam region of disilylated V.*

RESULTS AND DISCUSSION

Compound I alone or I and II in an equimolar mixture were chosen as the silylating reagents because their low cost and availability in bulk amounts would allow the process to be extended to the industrial stage. In comparison with the β-lactam radicals, their quantity was varied from stoichiometric (Condition A or B) to twice as much (Condition 2A or 2B) to ascertain if further silylation of the amino group was possible. In preliminary experiments on V, the trimethylchlorosilane–triethylamine mixture (11) was discarded because of the ready formation of the Δ^2-cephem derivative (see *Experimental*).

The silylation of the amino against the carboxylic group may be determined quantitatively by the ratio of integrations over *N*- and *O*-trimethylsilyl peaks (δ 0.28–0.30 *versus* δ 0.5–0.55 ppm)[7] after the preliminary removal of I, II, and hexamethyldisiloxane whose signals (δ 0.17, 0.46, and 0.2 ppm, respectively, in deuterochloroform) interfere with the preceding peaks.

With cephalosporin derivatives, however, because there is complete agreement between integrations of the *O*-trimethylsilyl group and the methyl groups in the 3-position (indicating a quantitative silylation of the carboxyl group), the silylation of the amino group can also be calculated through the integrations over resonances of methyl groups and the free amino group (δ 2.16 *versus* about δ 1.66 ppm) without manipulation of the solution. Both methods of calculation gave similar results (Table I). The latter method is not applicable for IV because of the overlapping of free amino and methyl signals.

The three substrates behaved similarly on silylation. While a complete reaction on the carboxyl group was attained in all conditions, the amino group was silylated 15–25% with Condition A[8] and 90% with the more drastic operative conditions (2B), giving rise almost completely to disilylated compounds.

While the NMR signals of the protons of the monosilylated products (Table II) were similar to those of the corresponding amino acids (16, 17) and of their esters (18, 19), the pattern of the peaks for the two β-lactam protons of disilyl[9] derivatives appeared to be anomalous. For IV (Fig. 1), the 5-proton gave a normal doublet at δ 5.54 ppm (J = 5.5 Hz) whereas the 6-proton gave two doublets of equal intensity centered at δ 4.74 and 4.51 ppm (J = 5.5 Hz for both); irradiation of the resonance at δ 5.54 ppm led to the collapse of the doublets to two singlets.

The β-lactam peaks for disilylated V and VI were partially overlapped, being much closer together (also with the signals of the exocyclic methylene protons in VI). Two doublets centered at δ 4.56 and 4.83 ppm (J = 4.8 Hz) and a sharp singlet at δ 4.81 ppm were present in both their spectra at 60 MHz. This anomaly was resolved for V by the 100-MHz spectrum (Fig. 2), showing a doublet for the 6-proton (4.78 ppm) and two doublets of equal intensity (4.71 and 4.58 ppm) for the 7-proton, with a pattern similar to that of disilylated IV (J = 4.7 Hz for all doublets).

The splitting of the proton alpha to the trimethylsilylamino group in two doublets of like intensity might be explained by a HCNH proton–proton coupling (12.6–14 Hz) that is, however, roughly 50% as large as

[6] Analogously, the recovery of mono- and disilylated derivatives was quantitative, giving NMR spectra superimposable with the starting ones.

[7] The assignments of these resonances were made by comparison with the respective ones of 2,2,2-trichloroethyl-7-trimethylsilylamino-3-methyl-Δ^3-cephem-4-carboxylate and trimethylsilyl-7-phenylacetamido-3-methyl-Δ^3-cephem-4-carboxylate silylated with III or I, respectively.

[8] The present results agree with Glombitza's data (13) for IV.

[9] The peaks of the other protons had the same chemical shifts as monosilyl derivatives.

other values reported (16). Its increase is similar to that observed in *N*-trimethylsilylcyclohexylamine (20) between the proton on nitrogen and the cyclohexyl α-proton, indicative perhaps, in the same way, of a probable *trans*-coplanar arrangement of $H_\alpha C$ and NH bonds in these β-lactam derivatives.

REFERENCES

(1) L. Birkofer and A. Ritter, *Angew. Chem. Int. Ed. Engl.*, **4**, 417 (1965).
(2) A. E. Pierce, "Silylation of Organic Compounds," Pierce Chemical Co., Rockford, Ill., 1968.
(3) C. A. Roth, *Ind. Eng. Chem. Prod. Res. Dev.*, **11**, 134 (1972).
(4) A. E. Pierce, "Silylation of Organic Compounds," Pierce Chemical Co., Rockford, Ill., 1968, pp. 218–221.
(5) L. Birkofer and A. Ritter, *Chem. Ber.*, **93**, 424 (1960).
(6) K. Rühlmann, *J. Prakt. Chem.*, **9**, 86 (1959).
(7) K. Rühlmann, *Chem. Ber.*, **94**, 1876 (1961).
(8) J. F. Klebe, H. Finkbeiner, and D. M. White, *J. Am. Chem. Soc.*, **88**, 3390 (1966).
(9) H. W. O. Weissenburger and M. G. Van Der Hoeven, *Rec. Trav. Chim. Pays-Bas*, **89**, 1081 (1970).
(10) H. W. O. Weissenburger and M. G. Van Der Hoeven, U.S. pat. 3,499,909 (1970).
(11) American Home Products Corp., British pat. 1,201,542 (1970).
(12) Eli Lilly and Co., U.S. pat. 3,694,437 (1972).
(13) K. W. Glombitza, *Ann. Chem.*, **673**, 166 (1964).
(14) S. H. Langer, S. Connell, and I. Wender, *J. Org. Chem.*, **23**, 50 (1958).
(15) E. Van Heyningen and L. K. Ahern, *J. Med. Chem.*, **11**, 933 (1968).
(16) G. F. H. Green, J. E. Page, and S. E. Staniforth, *J. Chem. Soc.*, **1965**, 1595.
(17) R. A. Archer and B. S. Kitchell, *J. Org. Chem.*, **31**, 3409 (1966).
(18) R. W. Ratcliffe and B. G. Christensen, *Tetrahedron Lett.*, **1973**, 4649.
(19) T. Jen, J. Frazee, and J. R. E. Hoover, *J. Org. Chem.*, **38**, 2857 (1973).
(20) J. P. Hardy and W. D. Cumming, *J. Am. Chem. Soc.*, **93**, 928 (1971).

ACKNOWLEDGMENTS AND ADDRESSES

Received October 22, 1976, from *Pierrel S.p.A., Research and Development Laboratories, Via Degli Artigianelli 10, 20159 Milan, Italy.*
Accepted for publication January 18, 1977.
[x] To whom inquiries should be directed.

GLC Determination of 6-Aminopenicillanic Acid and 7-Amino-3-methyl-Δ^3-cephem-4-carboxylic Acid

SILVESTRO SILINGARDI, MAURO Di BITETTO, and ALBERTO MANGIA [x]

Abstract □ A quantitative GLC determination of 6-aminopenicillanic acid and 7-amino-3-methyl-Δ^3-cephem-4-carboxylic acid is presented. The results obtained are in good agreement with those of known chemical procedures. The method is free from interference by related substances.

Keyphrases □ 6-Aminopenicillanic acid—GLC analysis, prepared samples □ Cephemcarboxylic acid, substituted—GLC analysis, prepared samples □ GLC—analyses, 6-aminopenicillanic acid and 7-amino-3-methyl-Δ^3-cephem-4-carboxylic acid, prepared samples □ Antibacterial intermediates—6-aminopenicillanic acid and 7-amino-3-methyl-Δ^3-cephem-4-carboxylic acid, GLC analyses, prepared samples

6-Aminopenicillanic acid (I), 7-amino-3-methyl-Δ^3-cephem-4-carboxylic acid (II), and 7-amino-3-acetoxymethyl-Δ^3-cephem-4-carboxylic acid (III) are the key intermediates in the preparation of several semisynthetic β-lactam antibacterials (1). Their characterization can be made from IR (2) and UV (3, 4) spectra or by TLC procedures (5–7), and chemical methods are known for their quantitative analysis (8, 9).

GLC determinations of some penicillins were reported (10, 11), but no procedure on cephalosporin antibiotics has been published. This paper reports the separation and quantitative determination of I and II[1] by GLC after silylation.

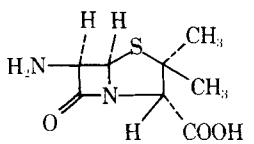

I

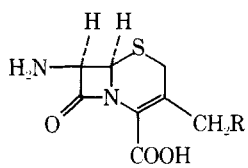

II: R = H
III: R = $OCOCH_3$

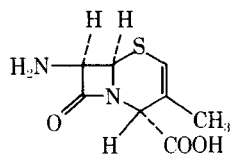

IV

EXPERIMENTAL

Apparatus—A gas chromatograph[2] equipped with a flame-ionization detector, maintained at 200°, was used with gas flow rates of 40 ml/min for hydrogen and 300 ml/min for air. The areas of the peaks were calculated by an electronic integrator[3]. A column oven temperature of 180° with the injector at 220° and nitrogen flow rates of 40 ml/min was used for the analysis of I. For the analysis of II, the column oven temperature was programmed from 160 to 210° with an increase of 6°/min, the injector was at 220°, and nitrogen flow rates were 57 ml/min.

Glass columns, 2 mm i.d. × 2.0 m for the analysis of I or 2 mm i.d. × 0.5 m for II, were packed with 4% OV-17[4] on 80–100-mesh HP Chromosorb

[1] In spite of several trials, III was partially decomposed in the operative conditions.

[2] Perkin-Elmer model 900.
[3] Perkin-Elmer model SIP 1.
[4] Applied Science Laboratories, State College, Pa.

other values reported (16). Its increase is similar to that observed in *N*-trimethylsilylcyclohexylamine (20) between the proton on nitrogen and the cyclohexyl α-proton, indicative perhaps, in the same way, of a probable *trans*-coplanar arrangement of $H_\alpha C$ and NH bonds in these β-lactam derivatives.

REFERENCES

(1) L. Birkofer and A. Ritter, *Angew. Chem. Int. Ed. Engl.*, **4**, 417 (1965).
(2) A. E. Pierce, "Silylation of Organic Compounds," Pierce Chemical Co., Rockford, Ill., 1968.
(3) C. A. Roth, *Ind. Eng. Chem. Prod. Res. Dev.*, **11**, 134 (1972).
(4) A. E. Pierce, "Silylation of Organic Compounds," Pierce Chemical Co., Rockford, Ill., 1968, pp. 218–221.
(5) L. Birkofer and A. Ritter, *Chem. Ber.*, **93**, 424 (1960).
(6) K. Rühlmann, *J. Prakt. Chem.*, **9**, 86 (1959).
(7) K. Rühlmann, *Chem. Ber.*, **94**, 1876 (1961).
(8) J. F. Klebe, H. Finkbeiner, and D. M. White, *J. Am. Chem. Soc.*, **88**, 3390 (1966).
(9) H. W. O. Weissenburger and M. G. Van Der Hoeven, *Rec. Trav. Chim. Pays-Bas*, **89**, 1081 (1970).
(10) H. W. O. Weissenburger and M. G. Van Der Hoeven, U.S. pat. 3,499,909 (1970).
(11) American Home Products Corp., British pat. 1,201,542 (1970).
(12) Eli Lilly and Co., U.S. pat. 3,694,437 (1972).
(13) K. W. Glombitza, *Ann. Chem.*, **673**, 166 (1964).
(14) S. H. Langer, S. Connell, and I. Wender, *J. Org. Chem.*, **23**, 50 (1958).
(15) E. Van Heyningen and L. K. Ahern, *J. Med. Chem.*, **11**, 933 (1968).
(16) G. F. H. Green, J. E. Page, and S. E. Staniforth, *J. Chem. Soc.*, **1965**, 1595.
(17) R. A. Archer and B. S. Kitchell, *J. Org. Chem.*, **31**, 3409 (1966).
(18) R. W. Ratcliffe and B. G. Christensen, *Tetrahedron Lett.*, **1973**, 4649.
(19) T. Jen, J. Frazee, and J. R. E. Hoover, *J. Org. Chem.*, **38**, 2857 (1973).
(20) J. P. Hardy and W. D. Cumming, *J. Am. Chem. Soc.*, **93**, 928 (1971).

ACKNOWLEDGMENTS AND ADDRESSES

Received October 22, 1976, from *Pierrel S.p.A., Research and Development Laboratories, Via Degli Artigianelli 10, 20159 Milan, Italy.*
Accepted for publication January 18, 1977.
[x] To whom inquiries should be directed.

GLC Determination of 6-Aminopenicillanic Acid and 7-Amino-3-methyl-Δ^3-cephem-4-carboxylic Acid

SILVESTRO SILINGARDI, MAURO Di BITETTO, and ALBERTO MANGIA [x]

Abstract □ A quantitative GLC determination of 6-aminopenicillanic acid and 7-amino-3-methyl-Δ^3-cephem-4-carboxylic acid is presented. The results obtained are in good agreement with those of known chemical procedures. The method is free from interference by related substances.

Keyphrases □ 6-Aminopenicillanic acid—GLC analysis, prepared samples □ Cephemcarboxylic acid, substituted—GLC analysis, prepared samples □ GLC—analyses, 6-aminopenicillanic acid and 7-amino-3-methyl-Δ^3-cephem-4-carboxylic acid, prepared samples □ Antibacterial intermediates—6-aminopenicillanic acid and 7-amino-3-methyl-Δ^3-cephem-4-carboxylic acid, GLC analyses, prepared samples

6-Aminopenicillanic acid (I), 7-amino-3-methyl-Δ^3-cephem-4-carboxylic acid (II), and 7-amino-3-acetoxymethyl-Δ^3-cephem-4-carboxylic acid (III) are the key intermediates in the preparation of several semisynthetic β-lactam antibacterials (1). Their characterization can be made from IR (2) and UV (3, 4) spectra or by TLC procedures (5–7), and chemical methods are known for their quantitative analysis (8, 9).

GLC determinations of some penicillins were reported (10, 11), but no procedure on cephalosporin antibiotics has been published. This paper reports the separation and quantitative determination of I and II[1] by GLC after silylation.

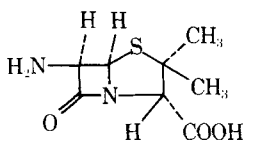

I

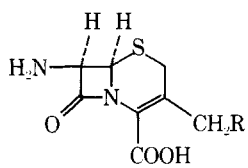

II: R = H
III: R = $OCOCH_3$

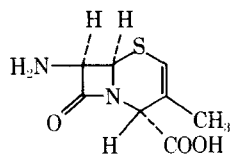

IV

EXPERIMENTAL

Apparatus—A gas chromatograph[2] equipped with a flame-ionization detector, maintained at 200°, was used with gas flow rates of 40 ml/min for hydrogen and 300 ml/min for air. The areas of the peaks were calculated by an electronic integrator[3]. A column oven temperature of 180° with the injector at 220° and nitrogen flow rates of 40 ml/min was used for the analysis of I. For the analysis of II, the column oven temperature was programmed from 160 to 210° with an increase of 6°/min, the injector was at 220°, and nitrogen flow rates were 57 ml/min.

Glass columns, 2 mm i.d. × 2.0 m for the analysis of I or 2 mm i.d. × 0.5 m for II, were packed with 4% OV-17[4] on 80–100-mesh HP Chromosorb

[1] In spite of several trials, III was partially decomposed in the operative conditions.

[2] Perkin-Elmer model 900.
[3] Perkin-Elmer model SIP 1.
[4] Applied Science Laboratories, State College, Pa.

Table I—GLC Data

Compound	Relative Retention Time[a] 2-m Column	2-m Column[b]	0.5-m Column	Relative Response Factor	*RSD* of Response Factor, %[c]
Phenanthrene	1.0 (4.2 min)	1.0 (2.3 min)	1.0 (1.3 min)	1.0	—
I	1.29	—	—	1.51	1.78
IV	—	1.92	2.42	1.62[d]	—
II	—	3.24	3.52	1.62	2.07

[a] For column conditions, see *Experimental.* [b] Oven temperature was 200°. [c] Relative standard deviations of response factors were obtained from eight separate preparations of reference standard for I and from six for II. [d] Estimated in a similar manner as II.

W[5]. The column packing was prepared by the standard slurry–filtration method. The columns were conditioned overnight at 300° in nitrogen flow and treated with repeated 10-μl injections of a column conditioner[6].

Reference Standards—Compounds I–III were obtained commercially[7]. 7-Amino-3-methyl-Δ^2-cephem-4-carboxylic acid (IV) was prepared by a known procedure (12).

Silylating Reagents and Silylation Procedures—*6-Aminopenicillanic Acid*—A 50% (v/v) solution of *N,O*-bis(trimethylsilyl)acetamide (V) in pyridine containing 0.82 mg of phenanthrene[8]/ml was prepared. The sample of I was carefully weighed (about 10 mg), and 2 ml of the silylating solution was added to each vial. After sealing, the vials were heated at 60° for 1 hr and allowed to stand at room temperature for 1 additional hr.

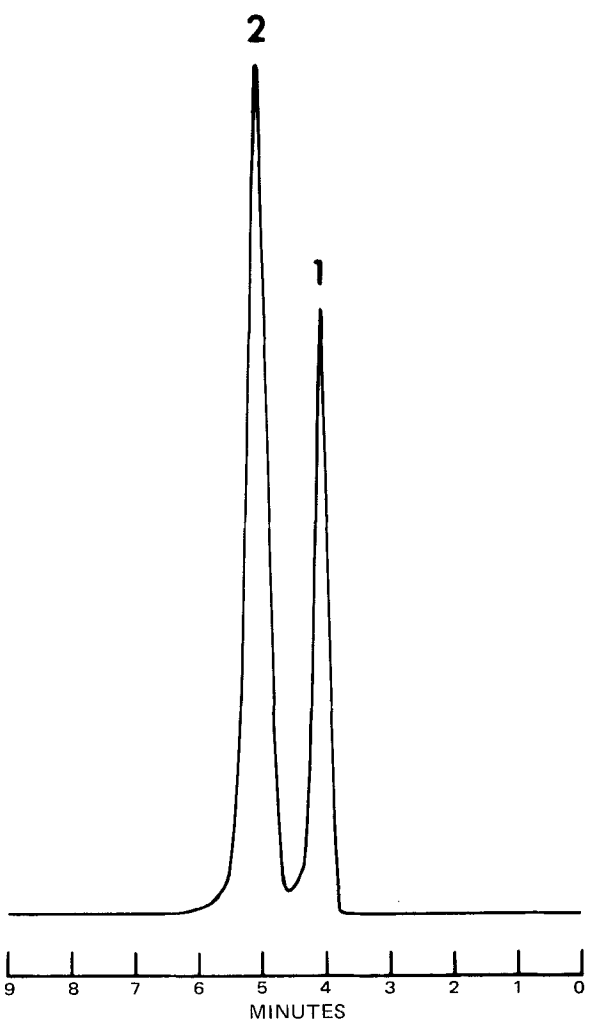

Figure 1—*Chromatogram of I. Key: 1, phenanthrene; and 2, I.*

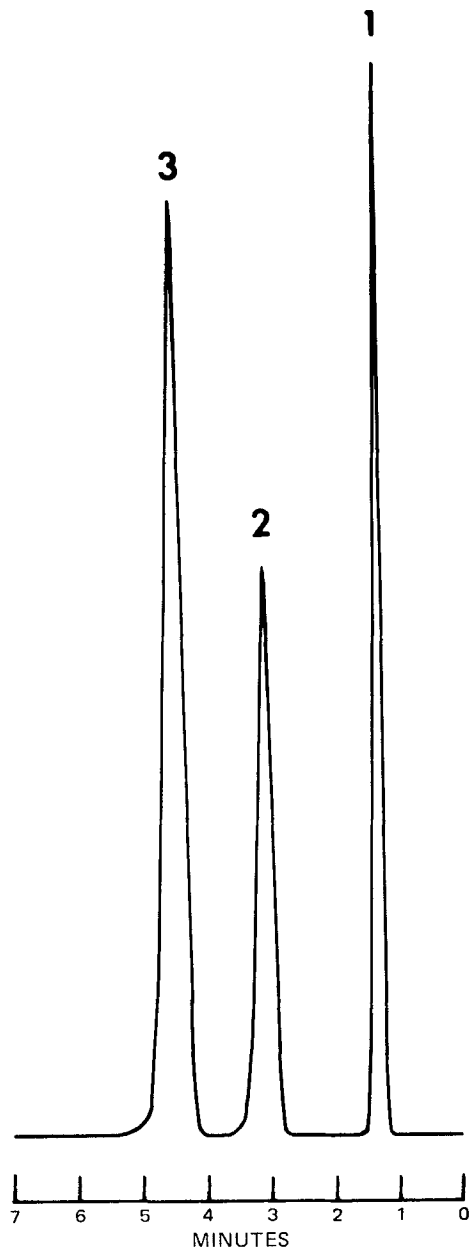

Figure 2—*Chromatogram of II (Sample 8; see Table II). Key: 1, phenanthrene; 2, IV; and 3, II.*

7-Amino-3-methyl-Δ^3-cephem-4-carboxylic Acid—The sample of II was accurately weighed (about 10 mg), and *sym*-dichloroethane (2 ml) containing phenanthrene (1.0 mg/ml), trimethylchlorosilane (328 mg = 0.38 ml), and hexamethyldisilazane (161 mg = 0.21 ml) were added to a 10-ml flask equipped with a reflux condenser. The mixture was stirred with refluxing for 1 hr (complete solution was attained within 20 min) and then cooled to room temperature; V was then added (203 mg = 0.245 ml) with additional stirring for 1 hr. Aliquots of 2 μl of the respective solutions were injected.

RESULTS AND DISCUSSION

Compound V is the best reagent to disilylate amino acids (13) using mild conditions. Derivatization for I was complete at room temperature in about 20 hr in chloroform or pyridine; shorter silylation times were obtained at 60°.

The silylation of II for quantitative purposes was much more difficult because of the ready formation of the Δ^2-compound (IV) (about 8–10%) with the reported conditions and at room temperature or with other

[5] Johns-Manville, New York, N.Y.
[6] Silyl 8, Pierce Chemical Co., Rockford, Ill.
[7] Pierrel Analytical Laboratories.
[8] Schuchardt, München, Germany.

Table II—Comparison of Analytical Data[a] (Percent Purity)

Sample	GLC Procedure	Colorimetric Assay[b]	Iodometric Assay[c]
Compound I			
1	98.7	100.3	98.5
2	99.3	99.5	98.6
3	95.2	96.7	97.5
Compound II			
4	95.2	94.6	90.0
5	88.2	87.7	88.7
6	96.6	93.6	93.3
7	99.7	97.4	94.6
8	57.8[d]	81.5	86.5
9	93.3	93.4	89.3

[a] Standard deviations of known procedures are calculated on our results (average of at least two determinations). [b] For I samples, $\sigma = \pm 1.30\%$. For II samples, $\sigma = \pm 0.96\%$. [c] For I samples, $\sigma = \pm 1.25\%$. For II samples, $\sigma = \pm 3.04\%$. [d] The sample has a content of 29.3% of IV. The ratio of II to IV was 2.08 as determined by NMR spectroscopy *versus* 1.97 as calculated by GLC.

strong silylating agents such as *N,O*-bis(trimethylsilyl)formamide (about 30% of IV), *N*-trimethylsilylimidazole (60% of IV), and *N*-trimethylsilylacetamide (about 10% of IV). In the last two trials, incomplete silylation was obtained.

Hexamethyldisilazane alone or with trimethylchlorosilane[9] does not form IV during derivatization of II (12), which is, however, incomplete. Quantitative silylation on the amino group, which is much more difficult (14) to react than the carboxylic group, was attained in a second step by adding V at room temperature. This procedure leaves the double bond of the dihydrothiazinyl ring unaltered. Furthermore, a shorter column was finally chosen to minimize previously observed decomposition phenomena. The analytical data are reported in Table I.

The analytical results of samples of I and II obtained by GLC (Figs. 1 and 2), compared with the colorimetric determination of Marrelli (9) and with the iodometric assay of Alicino (8), are reported in Table II. The GLC determinations of these substrates are independent of related substances such as IV, which interfere in the chemical methods (see Sample 8, Table II). Furthermore, IV as an impurity can be detected accurately up to 0.5% in samples of II by this GLC method.

The good agreement between the data reported in Table II supports the use of the GLC procedure and indicates that it might supplement the chemical methods.

[9] The 1:3 molar ratio of these two silylating reagents was found to be the most suitable after preliminary experiments.

REFERENCES

(1) E. H. Flynn, "Cephalosporins and Penicillins, Chemistry and Biology," Academic, New York, N.Y., 1972.

(2) B. Casu and P. Ventura, *J. Pharm. Sci.*, **63**, 211 (1974).

(3) R. J. Stedman, K. Swered, and J. R. E. Hoover, *J. Med. Chem.*, **7**, 117 (1964).

(4) Eli Lilly and Co., British pat. 948858 (Feb. 5, 1964).

(5) E. J. Vandamme and J. P. Voets, *J. Chromatogr.*, **71**, 141 (1972).

(6) C. J. Budd, *ibid.*, **76**, 509 (1973).

(7) M. Pokorny, N. Vitezic, M. Japely, and U. Valcavi, *Farmaco, Ed. Prat.*, **31**, 23 (1976).

(8) J. F. Alicino, *Anal. Chem.*, **33**, 648 (1961).

(9) L. P. Marrelli, *J. Pharm. Sci.*, **57**, 2172 (1968).

(10) E. Evrard, M. Claesen, and H. Vanderhaeghe, *Nature*, **201**, 1124 (1964).

(11) C. Hishta, D. L. Mays, and M. Garofalo, *Anal. Chem.*, **43**, 1530 (1971).

(12) F. Bortesi, S. Cavalli, and A. Mangia, *J. Pharm. Sci.*, **66**, 1767 (1977).

(13) J. F. Klebe, H. Finkbeiner, and D. M. White, *J. Am. Chem. Soc.*, **88**, 3390 (1966).

(14) C. A. Roth, *Ind. Eng. Chem. Prod. Res. Dev.*, **11**, 134 (1972).

ACKNOWLEDGMENTS AND ADDRESSES

Received October 22, 1976, from *Pierrel S.p.A., Research and Development Laboratories, Via Degli Artigianelli 10, 20159 Milan, Italy.*

Accepted for publication January 19, 1977.

The authors thank Professor M. Riva and Dr. C. Pistoja for their encouragement.

[x] To whom inquiries should be directed.

Fluorescence Properties of Glafenine

W. BAEYENS [x] and P. DE MOERLOOSE

Abstract □ The fluorescence properties of glafenine are partly caused by the anthranilic acid nucleus of the molecule. Correlations are made between fluorescence capacities and UV absorbance. Analytical determinations can be carried out in different solvents, *e.g.*, ether, benzene, and ethanol. Linearity of the emission intensity with the concentration, limiting detectable sample concentrations, and Stokes shifts are reported.

Keyphrases □ Glafenine—fluorescence characteristics in various solvents, effect of pH □ Fluorescence characteristics—glafenine in various solvents, effect of pH □ Analgesics—glafenine, fluorescence characteristics in various solvents, effect of pH

Glafenine[1] (I), 2-[(7-chloro-4-quinolinyl)amino]benzoic acid 2,3-dihydroxypropyl ester, is used frequently for its analgesic properties. It is a pale-yellow powder, mp 165°, and is nearly insoluble in water, slightly soluble in organic solvents, and soluble in aqueous acid solutions. Since this substance contains the anthranilic acid nucleus, the following report is concerned with the question of whether this molecule possesses native fluorescence characteristics.

Anthranilic acid, *o*-aminobenzoic acid, exhibits a strong native fluorescence (λ_{exc} = 300 nm and λ_{em} = 405 nm at pH 7) (1), for which pH dependence (2), decay time (3), and assay in human urine (4) have been reported.

Solutions of glafenine in diluted mineral acids show an intense yellow color but do not fluoresce. In neutral and

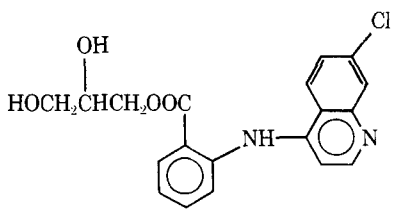

I

[1] Glifanan, 200-mg tablets, Roussel-Labunis, France.

Table II—Comparison of Analytical Data[a] (Percent Purity)

Sample	GLC Procedure	Colorimetric Assay[b]	Iodometric Assay[c]
Compound I			
1	98.7	100.3	98.5
2	99.3	99.5	98.6
3	95.2	96.7	97.5
Compound II			
4	95.2	94.6	90.0
5	88.2	87.7	88.7
6	96.6	93.6	93.3
7	99.7	97.4	94.6
8	57.8[d]	81.5	86.5
9	93.3	93.4	89.3

[a] Standard deviations of known procedures are calculated on our results (average of at least two determinations). [b] For I samples, $\sigma = \pm 1.30\%$. For II samples, $\sigma = \pm 0.96\%$. [c] For I samples, $\sigma = \pm 1.25\%$. For II samples, $\sigma = \pm 3.04\%$. [d] The sample has a content of 29.3% of IV. The ratio of II to IV was 2.08 as determined by NMR spectroscopy *versus* 1.97 as calculated by GLC.

strong silylating agents such as *N,O*-bis(trimethylsilyl)formamide (about 30% of IV), *N*-trimethylsilylimidazole (60% of IV), and *N*-trimethylsilylacetamide (about 10% of IV). In the last two trials, incomplete silylation was obtained.

Hexamethyldisilazane alone or with trimethylchlorosilane[9] does not form IV during derivatization of II (12), which is, however, incomplete. Quantitative silylation on the amino group, which is much more difficult (14) to react than the carboxylic group, was attained in a second step by adding V at room temperature. This procedure leaves the double bond of the dihydrothiazinyl ring unaltered. Furthermore, a shorter column was finally chosen to minimize previously observed decomposition phenomena. The analytical data are reported in Table I.

The analytical results of samples of I and II obtained by GLC (Figs. 1 and 2), compared with the colorimetric determination of Marrelli (9) and with the iodometric assay of Alicino (8), are reported in Table II. The GLC determinations of these substrates are independent of related substances such as IV, which interfere in the chemical methods (see Sample 8, Table II). Furthermore, IV as an impurity can be detected accurately up to 0.5% in samples of II by this GLC method.

The good agreement between the data reported in Table II supports the use of the GLC procedure and indicates that it might supplement the chemical methods.

[9] The 1:3 molar ratio of these two silylating reagents was found to be the most suitable after preliminary experiments.

REFERENCES

(1) E. H. Flynn, "Cephalosporins and Penicillins, Chemistry and Biology," Academic, New York, N.Y., 1972.

(2) B. Casu and P. Ventura, *J. Pharm. Sci.*, **63**, 211 (1974).

(3) R. J. Stedman, K. Swered, and J. R. E. Hoover, *J. Med. Chem.*, **7**, 117 (1964).

(4) Eli Lilly and Co., British pat. 948858 (Feb. 5, 1964).

(5) E. J. Vandamme and J. P. Voets, *J. Chromatogr.*, **71**, 141 (1972).

(6) C. J. Budd, *ibid.*, **76**, 509 (1973).

(7) M. Pokorny, N. Vitezic, M. Japely, and U. Valcavi, *Farmaco, Ed. Prat.*, **31**, 23 (1976).

(8) J. F. Alicino, *Anal. Chem.*, **33**, 648 (1961).

(9) L. P. Marrelli, *J. Pharm. Sci.*, **57**, 2172 (1968).

(10) E. Evrard, M. Claesen, and H. Vanderhaeghe, *Nature*, **201**, 1124 (1964).

(11) C. Hishta, D. L. Mays, and M. Garofalo, *Anal. Chem.*, **43**, 1530 (1971).

(12) F. Bortesi, S. Cavalli, and A. Mangia, *J. Pharm. Sci.*, **66**, 1767 (1977).

(13) J. F. Klebe, H. Finkbeiner, and D. M. White, *J. Am. Chem. Soc.*, **88**, 3390 (1966).

(14) C. A. Roth, *Ind. Eng. Chem. Prod. Res. Dev.*, **11**, 134 (1972).

ACKNOWLEDGMENTS AND ADDRESSES

Received October 22, 1976, from *Pierrel S.p.A., Research and Development Laboratories, Via Degli Artigianelli 10, 20159 Milan, Italy.*

Accepted for publication January 19, 1977.

The authors thank Professor M. Riva and Dr. C. Pistoja for their encouragement.

[x] To whom inquiries should be directed.

Fluorescence Properties of Glafenine

W. BAEYENS [x] and P. DE MOERLOOSE

Abstract □ The fluorescence properties of glafenine are partly caused by the anthranilic acid nucleus of the molecule. Correlations are made between fluorescence capacities and UV absorbance. Analytical determinations can be carried out in different solvents, *e.g.*, ether, benzene, and ethanol. Linearity of the emission intensity with the concentration, limiting detectable sample concentrations, and Stokes shifts are reported.

Keyphrases □ Glafenine—fluorescence characteristics in various solvents, effect of pH □ Fluorescence characteristics—glafenine in various solvents, effect of pH □ Analgesics—glafenine, fluorescence characteristics in various solvents, effect of pH

Glafenine[1] (I), 2-[(7-chloro-4-quinolinyl)amino]benzoic acid 2,3-dihydroxypropyl ester, is used frequently for its analgesic properties. It is a pale-yellow powder, mp 165°, and is nearly insoluble in water, slightly soluble in organic solvents, and soluble in aqueous acid solutions. Since this substance contains the anthranilic acid nucleus, the following report is concerned with the question of whether this molecule possesses native fluorescence characteristics.

Anthranilic acid, *o*-aminobenzoic acid, exhibits a strong native fluorescence (λ_{exc} = 300 nm and λ_{em} = 405 nm at pH 7) (1), for which pH dependence (2), decay time (3), and assay in human urine (4) have been reported.

Solutions of glafenine in diluted mineral acids show an intense yellow color but do not fluoresce. In neutral and

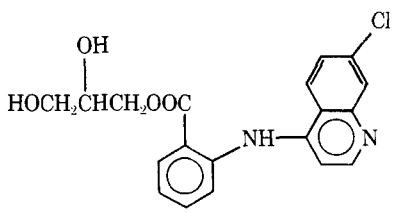

I

[1] Glifanan, 200-mg tablets, Roussel-Labunis, France.

Table I—Fluorescence Characteristics of Glafenine in Various Solvents (5 μg/ml)

Solvent	λ_{exc}, nm	λ_{em}, nm	Intensity[a]	Stokes Shift, cm^{-1} (5, 6)
Benzene	330	392	20	4790
Ether	250[b], 327	400	17	5580
Chloroform	250[b], 340	436	10	6480
2-Propanol–10% (v/v) buffer, pH 9[c] (0.1 *N* glycine–sodium hydroxide)	340	410	6	5020
2-Propanol–10% (v/v) buffer, pH 4 (0.1 *N* citrate–hydrochloric acid)	265[b], 355	450	2	5950
2-Propanol–10% (v/v) buffer, pH 1 (0.2 *N* potassium chloride–hydrochloric acid)	300	407	0.5	8760
Ethanol	245[b], 336	439	6	6980
Methanol	245[b], 336	425	2	6230
Methanol–10% (v/v) ammonia[c] (28% w/w)	273[b], 365	455	0.5	5420
Acetone	330	430	0.5	7050
Sulfuric acid (10–0.005 *N*)	—	—	No signal	—

[a] Referred to a solution of quinine sulfate in a concentration of 1 μg/ml in 0.5 *N* sulfuric acid, of which the relative fluorescence intensity is 100, measured simultaneously. [b] Secondary excitation value with much less intensity. [c] Care should be taken for possible precipitation in the alkaline medium.

alkaline media, however, a remarkable blue fluorescence is observed on irradiation at 350 nm.

DISCUSSION

Since the fluorescence phenomenon basically is preceded by the light absorption of the molecule, the visible and UV spectra of this compound were checked in various solvents to correlate them with the activation spectra. The following absorption maxima can be assigned: ethanol, 355 (ε 19,600) and 255 (ε 17,000) nm; acetone, 355 (ε 18,700) and 255 (ε 5600) nm; chloroform, 360 (ε 22,900) and 255 (ε 18,100) nm; ether, 351 (ε 19,300) and 255 (ε 19,000) nm; and benzene, 360 (ε 14,900) and 255 (ε 4100) nm.

Activation and fluorescence spectra were taken in various solvents at different pH values. No fluorescence emission occurred in the lower pH range; from pH 4 to more alkaline media, fluorescence occurred with a maximum at pH 9–10.

Table I illustrates excitation and emission maxima in order of decreasing intensity. The Stokes shift, a measure of the energy dissipated during the lifetime of the excited state before return to the ground state, increased with increasing solvent polarity, and the compound behaved as an organic base (Table I).

When comparing wavelength maxima of light absorption and those corresponding with the activation maxima, it can be noticed that fluorescence emission occurred most intensely after illumination at 320–360 nm, the wavelengths of highest molar absorptivities, considering instrumental artifacts of wavelength calibration. However, the energetically most favorable 245–265-nm wavelengths of absorption distinctly were of inferior value in the fluorescence process. When ε was low (<6000), no secondary excitation maximum could be assigned in the fluorescence process.

Figure 1 illustrates the dual excitation pattern and the emission spectrum of glafenine dissolved in ether. The relation between the relative emission intensity and the analytical concentration is shown in Fig. 2. The signal was linear up to 8 μg/ml, followed by the self-absorption effect, causing a negative curvature from 15 to 20 μg/ml. The limiting detectable sample concentration estimated graphically (7) is 8×10^{-2} μg/ml. Analogous results were obtained from benzene: λ_{exc} = 330 nm, λ_{em} = 392 nm, linearity up to 8 μg/ml, negative curve at 25 μg/ml, and limiting detectable sample concentration 5×10^{-2} μg/ml. For ethanol, the results were: λ_{exc} = 336 nm, λ_{em} = 439 nm, linearity up to 8 μg/ml, negative curve at 15–20 μg/ml, and limiting detectable sample concentration 1×10^{-1} μg/ml.

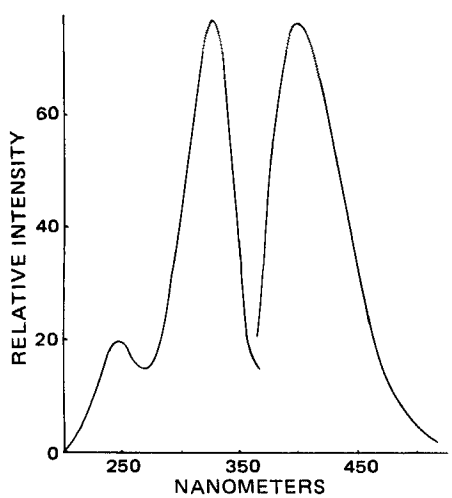

Figure 1—*Excitation and emission spectra of glafenine in ether (10 μg/ml); λ_{exc} = (250, secondary value with much less intensity) 327 nm and λ_{em} = 400 nm.*

The absence of any clear fluorescence signal of the glafenine molecule in the aqueous acid medium illustrates that the native fluorescence capacities belong to the undissociated free base, in which the chlorine atom causes a decrease of the fluorescence quantum efficiency.

The native fluorescence of glafenine in ether was used for determining this compound directly in tablets after extraction with ether. Samples were diluted to a concentration of 5 μg/ml and measured at the appropriate excitation and emission wavelengths. The time period of extraction of the tablets depends on the room temperature and on the particle size of the powdered tablets. In the present experiments, magnetic stirring periods for extraction varied between 1 and 2 hr.

A relative standard deviation of 1.7% was obtained.

EXPERIMENTAL[2]

Apparatus—A recording spectrophotofluorometer was used for determining excitation and emission spectra and for measuring fluorescence intensities. Spectra were not corrected for variations in lamp intensity or photomultiplier sensitivity.

Chemicals—All chemicals[3] were analytical grade.

Preparation of Solutions for Fluorescence Measurement—All

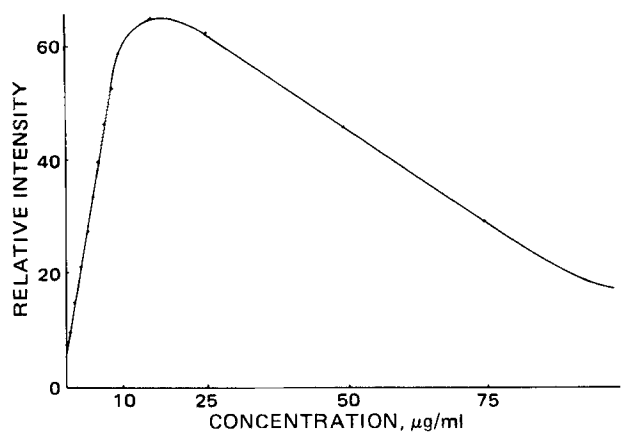

Figure 2—*Analytical curve of glafenine in ether.*

[2] The instruments used were: an Aminco-Bowman spectrofluorometer, Catalog No. 4-8203 DE, American Instrument Co., Silver Spring, Md.; a Hanovia 150-w xenon arc lamp; two grating monochromators; 1 × 1-cm quartz cells; photomultiplier R 446 S with high voltage of 0.7 kv and slits varying between 0.5 and 2 mm; a Zeiss DMR 21 spectrophotometer; and a Camag TL 900 Universal UV lamp at 254 and 350 nm.

[3] E. Merck, Darmstadt, Germany.

solutions measured fluorometrically contained 1×10^{-2}–100 μg of glafenine/ml of solvent. All glassware should be free of fluorescent contaminants and, therefore, frequently rinsed with distilled water; quartz sample cells are preferably cleaned with nitric acid followed by distilled water.

Determination of Glafenine in Tablets—Ten tablets were weighed accurately, and the average weight was calculated. They were brought to a homogeneous fine powder in a mortar, and a quantity equivalent to 25 mg of glafenine was transferred into a 500-ml conical flask. About 450 ml of ether was added, and the mixture was stirred with a magnetic stirrer for 2 hr. After filtration on a paper filter, the filtrate was diluted to 500 ml with ether. Then 10 ml of this solution was diluted to 100 ml with ether.

An analogous standard solution was prepared by dissolving 25 mg of glafenine in 500 ml of ether; 10 ml of this solution was diluted to 100 ml with ether.

It is advisable to extract the tablets simultaneously with the preparation of the standard solution or during at least the same period to avoid incomplete extraction.

Pure ether was used as a blank solution. Fluorometric measurement was performed at 327-nm excitation and 400-nm emission.

REFERENCES

(1) D. E. Duggan, R. L. Bowman, B. B. Brodie, and S. Udenfriend, *Arch. Biochem. Biophys.*, **68**, 1 (1957).

(2) F. Kavanagh and R. O. Goodwin, *Arch. Biochem.*, **20**, 315 (1949).

(3) R. F. Chen, G. G. Vurek, and N. Alexander, *Science*, **156**, 949 (1967).

(4) K. F. Nakken, *Scand. J. Clin. Lab. Invest., Suppl. 76*, **15**, 78 (1963).

(5) S. Udenfriend, "Fluorescence Assay in Biology and Medicine," vol. II, Academic, New York, N.Y., 1969, pp. 7–10.

(6) H. G. Leeman, K. Stich, and M. Thomas, in "Progress in Drug Research," vol. 6, E. Jucker, Ed., Birkhäuser, Basel, Switzerland, 1963, p. 152.

(7) S. Udenfriend, "Fluorescence Assay in Biology and Medicine," vol. II, Academic, New York, N.Y., 1969, p. 97.

ACKNOWLEDGMENTS AND ADDRESSES

Received July 2, 1976, from the *State University of Ghent, Faculty of Pharmacy, Laboratory of Drug Analysis, De Pintelaan 135, 9000 Gent, Belgium.*

Accepted for publication April 13, 1977.

The authors thank Roussel-Labunis Ltd. for the gift of pure glafenine base and of Glifanan tablets.

[x] To whom inquiries should be directed.

Gonadotropin-Inhibitory Contaminants in Partially Purified Pharmaceutical Preparations of Human Chorionic Gonadotropin

MARÍA LUISA FORCELLEDO and MANUEL de la LASTRA [x]

Abstract □ Various commercial preparations of partially purified human chorionic gonadotropin, inactivated by heating, inhibited the uterine growth induced in immature mice with the same active gonadotropins as well as spontaneous uterine growth. The more purified preparations of chorionic gonadotropin failed to produce these effects after inactivation by boiling, suggesting that the inhibitory activity is not generated from gonadotropin by the procedure but may be related to some contaminant similar to the gonadotropin-inhibitory substance previously found in human urine.

Keyphrases □ Gonadotropin, human chorionic—various commercial preparations, presence of inhibitory contaminants □ Contaminants, inhibitory—presence in various commercial preparations of human chorionic gonadotropin □ Inhibitory contaminants—presence in various commercial preparations of human chorionic gonadotropin

Human chorionic gonadotropin (I) for clinical purposes is a concentrate of the urine of pregnant women containing several hundred to 1000 international units (IU)/mg. It is obtained by a procedure that may also extract the gonadotropin-inhibitory substance (II) reported previously (1–3). In the present work, the occurrence of II was studied in various commercially available brands of I and in highly purified preparations. Preliminary results were reported previously (4).

EXPERIMENTAL

Five preparations of human chorionic gonadotropin were studied: partially purified preparations Ia[1], Ib[2], and Ic[3] and highly purified preparations Id[4] and Ie[5], with an activity of 13,000 and 10,000 IU/mg, respectively. These materials were dissolved in distilled water (500 IU/ml), pH 5–6, and boiled under reflux in a water bath for 1 hr to inactivate the gonadotropin activity (3). The final volume was adjusted to the desired concentration by adding water.

Biological assays were done in immature mice, 7.5–10.0 g, of the Balb-c strain. Different doses of boiled I preparations were injected, alone or with unboiled I, at different sites or mixed in the same syringe. The total dose of boiled and unboiled I was given in five subcutaneous injections, 0.2 ml each, for 3 days. Necropsy was performed on the 4th day, 24 hr after the last injection.

The mice were killed with ether. The uteri were dissected clean of surrounding tissue, dried by blotting on filter paper, and weighed on a precision balance to the nearest hundredth of a milligram. The Student *t* test was used to compare the mean weights of the uteri obtained from the different experimental groups.

RESULTS AND DISCUSSION

The less pure preparations of I, with 1000 IU/mg, inactivated by boiling, inhibited the vaginal opening and uterine growth induced with unboiled I in immature mice (Table I). This effect appeared when both preparations were injected together or separately in different subcutaneous sites. No signs of toxicity were evidenced, and the growth of the treated and untreated mice was similar. The heat-inactivated I also in-

[1] Apoidine, Parke-Davis.
[2] APL, Ayerst Laboratories.
[3] Profasi, Serono, Italy.
[4] Lot E 231 TEBZ, Serono, Italy.
[5] Donated by Professor C. H. Li.

solutions measured fluorometrically contained 1×10^{-2}–100 μg of glafenine/ml of solvent. All glassware should be free of fluorescent contaminants and, therefore, frequently rinsed with distilled water; quartz sample cells are preferably cleaned with nitric acid followed by distilled water.

Determination of Glafenine in Tablets—Ten tablets were weighed accurately, and the average weight was calculated. They were brought to a homogeneous fine powder in a mortar, and a quantity equivalent to 25 mg of glafenine was transferred into a 500-ml conical flask. About 450 ml of ether was added, and the mixture was stirred with a magnetic stirrer for 2 hr. After filtration on a paper filter, the filtrate was diluted to 500 ml with ether. Then 10 ml of this solution was diluted to 100 ml with ether.

An analogous standard solution was prepared by dissolving 25 mg of glafenine in 500 ml of ether; 10 ml of this solution was diluted to 100 ml with ether.

It is advisable to extract the tablets simultaneously with the preparation of the standard solution or during at least the same period to avoid incomplete extraction.

Pure ether was used as a blank solution. Fluorometric measurement was performed at 327-nm excitation and 400-nm emission.

REFERENCES

(1) D. E. Duggan, R. L. Bowman, B. B. Brodie, and S. Udenfriend, *Arch. Biochem. Biophys.*, **68**, 1 (1957).

(2) F. Kavanagh and R. O. Goodwin, *Arch. Biochem.*, **20**, 315 (1949).

(3) R. F. Chen, G. G. Vurek, and N. Alexander, *Science*, **156**, 949 (1967).

(4) K. F. Nakken, *Scand. J. Clin. Lab. Invest., Suppl. 76*, **15**, 78 (1963).

(5) S. Udenfriend, "Fluorescence Assay in Biology and Medicine," vol. II, Academic, New York, N.Y., 1969, pp. 7–10.

(6) H. G. Leeman, K. Stich, and M. Thomas, in "Progress in Drug Research," vol. 6, E. Jucker, Ed., Birkhäuser, Basel, Switzerland, 1963, p. 152.

(7) S. Udenfriend, "Fluorescence Assay in Biology and Medicine," vol. II, Academic, New York, N.Y., 1969, p. 97.

ACKNOWLEDGMENTS AND ADDRESSES

Received July 2, 1976, from the *State University of Ghent, Faculty of Pharmacy, Laboratory of Drug Analysis, De Pintelaan 135, 9000 Gent, Belgium.*

Accepted for publication April 13, 1977.

The authors thank Roussel-Labunis Ltd. for the gift of pure glafenine base and of Glifanan tablets.

[x] To whom inquiries should be directed.

Gonadotropin-Inhibitory Contaminants in Partially Purified Pharmaceutical Preparations of Human Chorionic Gonadotropin

MARÍA LUISA FORCELLEDO and MANUEL de la LASTRA [x]

Abstract □ Various commercial preparations of partially purified human chorionic gonadotropin, inactivated by heating, inhibited the uterine growth induced in immature mice with the same active gonadotropins as well as spontaneous uterine growth. The more purified preparations of chorionic gonadotropin failed to produce these effects after inactivation by boiling, suggesting that the inhibitory activity is not generated from gonadotropin by the procedure but may be related to some contaminant similar to the gonadotropin-inhibitory substance previously found in human urine.

Keyphrases □ Gonadotropin, human chorionic—various commercial preparations, presence of inhibitory contaminants □ Contaminants, inhibitory—presence in various commercial preparations of human chorionic gonadotropin □ Inhibitory contaminants—presence in various commercial preparations of human chorionic gonadotropin

Human chorionic gonadotropin (I) for clinical purposes is a concentrate of the urine of pregnant women containing several hundred to 1000 international units (IU)/mg. It is obtained by a procedure that may also extract the gonadotropin-inhibitory substance (II) reported previously (1–3). In the present work, the occurrence of II was studied in various commercially available brands of I and in highly purified preparations. Preliminary results were reported previously (4).

EXPERIMENTAL

Five preparations of human chorionic gonadotropin were studied: partially purified preparations Ia[1], Ib[2], and Ic[3] and highly purified preparations Id[4] and Ie[5], with an activity of 13,000 and 10,000 IU/mg, respectively. These materials were dissolved in distilled water (500 IU/ml), pH 5–6, and boiled under reflux in a water bath for 1 hr to inactivate the gonadotropin activity (3). The final volume was adjusted to the desired concentration by adding water.

Biological assays were done in immature mice, 7.5–10.0 g, of the Balb-c strain. Different doses of boiled I preparations were injected, alone or with unboiled I, at different sites or mixed in the same syringe. The total dose of boiled and unboiled I was given in five subcutaneous injections, 0.2 ml each, for 3 days. Necropsy was performed on the 4th day, 24 hr after the last injection.

The mice were killed with ether. The uteri were dissected clean of surrounding tissue, dried by blotting on filter paper, and weighed on a precision balance to the nearest hundredth of a milligram. The Student *t* test was used to compare the mean weights of the uteri obtained from the different experimental groups.

RESULTS AND DISCUSSION

The less pure preparations of I, with 1000 IU/mg, inactivated by boiling, inhibited the vaginal opening and uterine growth induced with unboiled I in immature mice (Table I). This effect appeared when both preparations were injected together or separately in different subcutaneous sites. No signs of toxicity were evidenced, and the growth of the treated and untreated mice was similar. The heat-inactivated I also in-

[1] Apoidine, Parke-Davis.
[2] APL, Ayerst Laboratories.
[3] Profasi, Serono, Italy.
[4] Lot E 231 TEBZ, Serono, Italy.
[5] Donated by Professor C. H. Li.

Table I—Antagonism between Boiled and Unboiled I on Uterine Growth in Immature Mice

Treatment	Open Vagina, %	Uterine Weight, Mean ± *SE*, mg	*n*	*p*
Unboiled I*a*, 0.125 I	100	19.05 ± 1.69	7	NS[a]
Unboiled I*a*, 0.125 IU, plus boiled I*a*, 0.125 IU	83	17.40 ± 2.34	6	
Unboiled I*a*, 0.25 I	100	26.67 ± 2.45	12	= 0.01
Unboiled I*a*, 0.25 IU, plus boiled I*a*, 0.25 IU	55	15.11 ± 2.28	9	
Unboiled I*a*, 0.50 I	100	41.50 ± 1.61	8	<0.01
Unboiled I*a*, 0.50 IU, plus boiled I*a*, 0.50 IU	50	22.50 ± 4.12	6	

[a] NS = not significant.

hibited spontaneous uterine growth (Table II). The more purified preparations of I, with 10,000 and 13,000 IU/mg, failed to produce this inhibition after inactivation by boiling.

According to these results, various preparations of I for clinical purposes contain a gonadotropin-inhibitory substance, apparently similar to that found in human urine previously (1–3). Previous investigators also reported an inhibition of the exogenous hormonal stimulation. In the present experiments, the material contained in different preparations of I also inhibited spontaneous sexual maturation, as shown by a delay in uterine growth.

The possibility that this gonadotropin-inhibitory substance might be generated from gonadotropin by the inactivation procedure was disproved by the fact that the more purified preparations showed no inhibitory activity after inactivation by heating. It seems more possible to relate II to some of the molecules contaminating I in the partially purified commercial preparations (5). One study (6) supported this contention. The urine of a patient with choriocarcinoma was concentrated by pressure dialysis, and a fourfold increase in the total amount of human chorionic gonadotropin activity of the sample was obtained, suggesting that the dialysis procedure eliminated an inhibitory contaminant of I.

The effect of II in humans is still unknown, but it may account for the variability of the biological activity of human chorionic gonadotropin preparations. Knowledge of an inhibiting impurity contaminating preparations of I might be an incentive to produce purer preparations.

Table II—Inhibitory Effect of Boiled Preparations of I on Uterine Growth in Immature Mice

Treatment, IU of Boiled I	Uterine Weight, Mean ± *SE*, mg	*n*	*p versus* Saline
Saline	6.03 ± 0.28	12	
I*a*, 0.125	5.42 ± 0.18	9	NS[a]
I*a*, 0.250	4.42 ± 0.25	8	<0.001
I*a*, 0.500	3.10 ± 0.43	8	<0.001
Saline	8.64 ± 0.98	19	
I*b*, 1.0	7.37 ± 0.55	12	NS
I*b*, 2.0	6.54 ± 0.94	6	NS
I*b*, 5.0	5.75 ± 0.47	6	<0.01
Saline	8.60 ± 0.53	6	
I*c*, 1.0	7.17 ± 0.49	7	NS
I*c*, 2.0	5.91 ± 0.44	7	<0.01
Saline	7.45 ± 0.40	10	
I*d*, 1.0	7.18 ± 0.94	5	NS
I*d*, 2.0	7.91 ± 0.90	5	NS
I*d*, 10.0	7.93 ± 0.94	6	NS
Saline	9.44 ± 0.90	10	
I*e*, 1.0	8.56 ± 0.66	6	NS
I*e*, 2.0	7.50 ± 0.53	6	NS
I*e*, 10.0	8.30 ± 0.58	6	NS

[a] NS = not significant.

REFERENCES

(1) B. Landau, H. S. Schwartz, and L. J. Soffer, *Metabolism*, **9**, 85 (1960).

(2) L. J. Soffer, W. Futterweit, and J. Salvaneschi, *J. Clin. Endocrinol. Metab.*, **21**, 1267 (1961).

(3) L. J. Soffer, J. Salvaneschi, and W. Futterweit, *ibid.*, **22**, 532 (1962).

(4) M. de la Lastra, M. L. Forcelledo, and L. Barnafi, V Reunión de la Asociación Latinoamericana de Investigaciones en Reproduccion Humana, Buenos Aires, Argentina, 1972, p. 160.

(5) B. Lunenfeld and A. Eshkol, *Vitam. Horm.*, **25**, 137 (1967).

(6) M. L. Taymor, R. Todd, and W. F. Blatt, *J. Endocrinol.*, **36**, 417 (1966).

ACKNOWLEDGMENTS AND ADDRESSES

Received September 10, 1976, from the *Laboratorio de Endocrinología, Departamento de Fisiología y Embrinología, Instituto de Ciencias Biológicas, Universidad Católica de Chile, Casilla 114-D, Santiago, Chile.*

Accepted for publication March 7, 1977.

Supported by Ford Foundation Grant 720-0384 and Fondo de Investigación Científica, Universidad Católica de Chile, Grant 61/74.

The authors are indebted to Miss Gladys Suárez for technical assistance.

[x] To whom inquiries should be directed.

Precautionary Note for Use of Bisulfite in Pharmaceutical Formulations

JAMES W. MUNSON ˣ, ANWAR HUSSAIN, and ROMAN BILOUS *

Abstract □ The effect of sodium bisulfite on aspirin hydrolysis was studied at 40° in the pH range of 6.5–7.5. Significant catalytic activity by the sulfite ion was observed. Second-order rate constants were calculated for this catalysis and compared to other buffer species. The sulfite ion was a much more efficient catalyst than acetate, phosphate, or carbonate.

Keyphrases □ Sodium bisulfite—effect on aspirin hydrolysis, various pH values □ Aspirin—hydrolysis, effect of sodium bisulfite, various pH values □ Hydrolysis—aspirin, effect of sodium bisulfite, various pH values □ Antioxidants—sodium bisulfite, effect on aspirin hydrolysis, various pH values

Sodium bisulfite, a widely used antioxidant, is known to react reversibly or irreversibly with various functional groups in drug molecules such as aldehyde, ketone, and alkene (1, 2). The inactivation of epinephrine and other drug molecules by bisulfite (3, 4) and the addition of bisulfite to a carbon–carbon double bond in uracil-type molecules (5) also were reported.

However, the catalytic effect of bisulfite on ester hydrolysis has not been recognized fully. Since many pharmaceutical preparations that employ bisulfite as an antioxidant may also contain esters as active ingredients or preservatives, the catalytic effect of bisulfite, if any, on ester hydrolysis should be examined.

Aspirin was chosen as the model ester because its rate and mechanism of hydrolysis have been investigated thoroughly.

EXPERIMENTAL

Materials—All reagents were either analytical reagent grade or USP and were used without further purification. All water was double distilled in glass. All sodium bisulfite solutions were prepared fresh in double-distilled water saturated with nitrogen. Nitrogen was passed through a series of gas washing bottles containing vanadous oxychloride to remove trace amounts of oxygen.

Methods—All pH measurements were made at 40.0° using a research pH meter[1] and a combination electrode with a silver–silver chloride reference electrode. Standard pH buffers were prepared according to Bates (6). All spectral measurements[2] were made at 296 nm using distilled water as the blank. Temperature control was maintained to ±0.1° using circulating water baths[3].

Determination of pKa for Sodium Bisulfite—The pKa for the dissociation was determined potentiometrically. A stock solution of sodium bisulfite was prepared in nitrogen-saturated distilled water. Sufficient sodium chloride was added to produce an ionic strength of 1.0 in the region where the bisulfite was half-neutralized. A potentiometric titration was then performed at 40° under nitrogen atmosphere using 0.1 *M* NaOH containing 1 *M* NaCl. The pKa was calculated using the titration data near the half-neutralization point.

Determination of Rate Constants for Aspirin Hydrolysis—Aliquots of stock solutions of sodium bisulfite, sodium chloride, and ethylenediaminetetraacetic acid (I) were mixed such that the final ionic strength at 40° and at the pH given would be 1.0 *M*. The bisulfite concentrations varied from 0.1 to 0.4 *M*. The final concentration of I was 0.0001 *M* in all cases. Compound I was added to suppress heavy metal-catalyzed oxidation of bisulfite. The volume of this mixture was adjusted to approximately 90 ml with nitrogen-saturated water.

The pH of this mixture was adjusted to the desired value under a nitrogen atmosphere. The mixture was then brought to volume, and final pH adjustments were made at 40° under nitrogen. Aliquots of 1 ml of the aspirin stock solution (acetonitrile) were added to this mixture and stirred. Samples were removed as a function of time, and the absorbance was measured immediately at 296 nm. A nitrogen atmosphere was maintained at all times. The pH of the reaction mixtures was measured at the end of the reaction. If the pH changed more than 0.05 unit during the reaction, the data were discarded.

Pseudo-first-order rate constants were determined from plots of $A_\infty - A_t$ *versus* time, where A_∞ is the absorbance at 296 nm at the end of the reaction and A_t is the absorbance at a given time t. The actual rate constants were evaluated by an exponential least-squares fit[4]. Only reactions that gave a correlation coefficient greater than 0.995 were used in the final calculations.

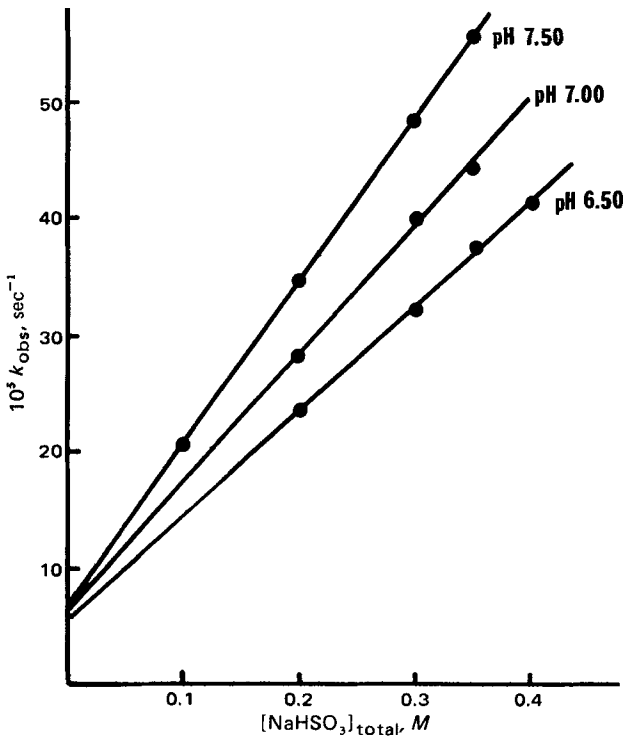

Figure 1—*Plot of first-order rate constants for the hydrolysis of aspirin as a function of total sodium bisulfite concentration.*

RESULTS AND DISCUSSION

The pKa for the dissociation of bisulfite to sulfite was 6.36 ($K_a = 4.29 \times 10^{-7}$ *M*) at 40° and an ionic strength of 1.0 *M*. This value was used to calculate ionic strength adjustments for the kinetic analysis and in the calculation of the second-order rate constants. The increase in the hydrolysis rate with increasing pH and increasing total bisulfite concentration suggested that both bisulfite and sulfite catalyses play an important role.

[1] Beckman.
[2] Gilford model 240 spectrophotometer.
[3] Haake F2 and Sargent ST. thermometers carried an American Society of Testing Materials certificate of calibration.
[4] Wang 600 programmable calculator.

Table I—Linear Regression Analysis Data for Plots of k_{obs} *versus* $[NaHSO_3]_{total}$

pH	Slope, liter mole^{-1} sec^{-1}	Intercept, sec^{-1}	Correlation Coefficient	*SE* of Estimate (S_{xy})
6.5	9.09×10^{-4}	5.30×10^{-5}	0.998	3.87×10^{-6}
7.0	11.08×10^{-4}	6.26×10^{-5}	0.995	7.09×10^{-6}
7.5	13.98×10^{-4}	6.59×10^{-5}	0.999	1.48×10^{-6}

The rate equation that describes catalysis by both species is:

$$k_{obs} = k_0 + k_1[HSO_3^-] + k_2[SO_3^{2-}] \quad \text{(Eq. 1)}$$

where k_0 is the rate constant for the uncatalyzed hydrolysis, k_1 is the rate constant for the bisulfite-catalyzed hydrolysis, and k_2 is the rate constant for the sulfite-catalyzed hydrolysis. This equation can be written as:

$$k_{obs} = k_0 + (k_1F_{HSO_3^-} + k_2F_{SO_3^{2-}})[NaHSO_3]_{total} \quad \text{(Eq. 2)}$$

where $F_{HSO_3^-}$ is the fraction of the total concentration that exists as the bisulfite ion and $F_{SO_3^{2-}}$ is the fraction that exists as the sulfite ion. In solving the appropriate simultaneous equations derived from the data, the value for k_1 sometimes appears as a negative number. Furthermore, the values for k_2 differ by as much as 25%. These findings suggest that the bisulfite ion does not play a significant role in the catalysis of aspirin hydrolysis.

The rate equation that describes only sulfite catalysis is:

$$k_{obs} = k_1 + k_2[SO_3^{2-}] \quad \text{(Eq. 3)}$$

where k_1 is the rate constant for uncatalyzed aspirin hydrolysis and k_2 is the rate constant for sulfite-catalyzed aspirin hydrolysis. This equation can be written as a function of total bisulfite concentration:

$$k_{obs} = k_1 + k_2F_{SO_3^{2-}}[NaHSO_3]_{total} \quad \text{(Eq. 4)}$$

The values for $F_{SO_3^{2-}}$ are 0.576 (pH 6.50), 0.88 (pH 7.00), and 0.931 (pH 7.50). Therefore, the slope of a plot of k_{obs} *versus* total bisulfite concentration, at a given pH, is equal to the fraction existing as the sulfite ion times the second-order rate constant, k_2. The intercept of this plot corresponds to the rate constant for the uncatalyzed reaction, k_1. The slopes and intercepts for the lines shown in Fig. 1 are given in Table I. The rate constants derived from these data are presented in Table II. The average values for the rate constants are: k_1, 6.05×10^{-5} sec^{-1} ($SD \pm 6.70 \times 10^{-6}$); and k_2, 1.48×10^{-3} liter mole^{-1} sec^{-1} ($SD \pm 1.07 \times 10^{-4}$).

Table II—Rate Constants at 40°, $\mu = 1.0$

pH	$10^5 k_1$, sec^{-1}	$10^3 k_2$, liter mole^{-1} sec^{-1}
6.5	5.30	1.57
7.0	6.26	1.36
7.5	6.59	1.50

Table III—Second-Order Rate Constant for Aspirin Hydrolysis by Different Species at 40°

Species	$k \times 10^5 M^{-1}$ min^{-1}
Sulfite	8800.0
Acetate	7.4
Phosphate	69.0
Carbonate	291.0

To compare the catalytic effect of sulfite to other catalytic species commonly employed in pharmaceutical formulations, the data of Fersht and Kirby (7) for the hydrolysis of aspirin catalyzed by acetate, phosphate, and carbonate have been included in Table III. As can be seen from these data, sulfite is 1200 times more effective than acetate and 120 times more effective than phosphate.

The significance of these findings with regard to the mechanism of aspirin hydrolysis as well as the catalytic effect of sulfite on the hydrolysis of other esters employed in pharmacuetical products is being studied in this laboratory. In conclusion, these results suggest that the possibility of sulfite-catalyzed ester hydrolysis should be considered carefully in formulations.

REFERENCES

(1) C. M. Suter, "The Organic Chemistry of Sulfur," Wiley, New York, N.Y., 1944, pp. 98, 101, 126.

(2) M. S. Kharasch, E. M. May, and F. B. Mayo, *J. Org. Chem.*, **3**, 175 (1938).

(3) T. Higuchi and L. Schroeter, *J. Am. Pharm. Assoc., Sci. Ed.*, **48**, 535 (1959).

(4) T. Higuchi and L. Schroeter, *J. Am. Chem. Soc.*, **82**, 1904 (1960).

(5) G. C. Rork and I. H. Pitman, *ibid.*, **97**, 5559 (1975).

(6) R. G. Bates, *J. Res. Natl. Bur. Stand.*, **66A**, 179 (1962).

(7) A. R. Fersht and A. J. Kirby, *J. Am. Chem. Soc.*, **89**, 4857 (1967).

ACKNOWLEDGMENTS AND ADDRESSES

Received August 23, 1976, from the *College of Pharmacy, University of Kentucky, Lexington, KY 40506.*

Accepted for publication February 28, 1977.

The authors thank Mr. Kenneth Pearce and Dr. Hassan Abdine for assistance.

* Present address: Faculty of Pharmacy, University of Manitoba, Winnipeg, Manitoba, Canada.

[x] To whom inquiries should be directed.

In Vitro Evaluation of an Anticholinergic Agent in a Timed-Release Solid Dosage Formulation

ROBERT H. GUMTOW ˣ, HEATHER BEECHER, DIANNE HARTNETT, and DIANE GLOGOWSKI

Abstract □ Determinations of intact drug content and *in vitro* dissolution tests were carried out on a commercially available brand of the anticholinergic drug propantheline in 15-mg single-dose and 30-mg sustained-release tablets. These tests were made following a report of unsatisfactory therapeutic response in human subjects after ingestion of the 30-mg sustained-release dosage form. A chemical assay, specific for intact drug, showed that all tablets contained essentially the labeled amount of active drug species (±4%). However, the slow dissolution of the first 15 mg of drug (a usual single dose) from the 30-mg dosage form, as observed in acidic solution (0.1 *N* HCl), was unexpected based on manufacturer claims. Older and fresher lots of the 30-mg formulation, both of which fell within a recently revised 2-year expiration period at the time of testing, released only 6.0 ± 1.4 mg of active ingredient during the 1st hr compared to 14.5 ± 0.7 mg from regular 15-mg tablets. Of the 30-mg tablets, the fresher lot released consistently more drug with time; the difference reached a statistically significant level of $p < 0.01$ at 2 hr. The dissolution rates of all tablets were enhanced in more alkaline media, and little difference ($p > 0.2$) was evident between the older and fresher sustained-release lots at any time during 4-hr dissolution trials when the medium had been adjusted to pH 6.38 or above at 1 hr. *In vitro* dissolution test results correlated well with *in vivo* findings and showed that rapid dissolution of the initial 15 mg of propantheline from solid dosage forms in acidic gastric juices is critical to its therapeutic effectiveness. It was concluded that reformulation of the 30-mg sustained-release dosage form to promote more rapid release of the first 15 mg of drug or full reliance on single-dose tablets is necessary to ensure therapeutic efficacy.

Keyphrases □ Propantheline—quantitative analysis and *in vitro* dissolution, regular and sustained-release tablets compared □ Tablets—propantheline, regular and sustained release, quantitative analysis and *in vitro* dissolution □ Dosage forms—regular and sustained-release tablets of propantheline, quantitative analysis and *in vitro* dissolution □ Dissolution, *in vitro*—propantheline regular and sustained-release tablets compared □ Anticholinergic agents—propantheline, quantitative analysis and *in vitro* dissolution, regular and sustained-release tablets compared

Propantheline is an anticholinergic drug extensively used in the treatment of peptic ulcers. Gibaldi and Grundhofer (1) followed salivary flow reduction as an index of drug activity. These data permitted comparison of the time of onset, intensity, and duration of effect derived from 15-mg regular and 30-mg sustained-release tablets and showed the 15-mg tablets to be superior in every respect. This discovery was unanticipated since the 30-mg tablets are reportedly designed to release a single 15-mg dose rapidly followed by relatively slow release of another 15 mg of active ingredient to sustain the desired therapeutic response. These investigators concluded that commercially available prolonged-acting tablets[1], containing 30 mg of propantheline bromide in timed-release (2) beads, apparently did not release 15 mg of intact drug during the 1st hr as claimed (3).

This investigation determined whether or not the failure of the 30-mg dosage form to produce a consistent anticholinergic effect might be attributed to a dissolution and/or chemical stability problem.

[1] Pro-Banthine P.A. tablets, Searle & Co., San Juan, PR 00936.

EXPERIMENTAL

Dissolution Apparatus—The dissolution apparatus was similar to that of Levy and Hayes (4). However, a 400-ml jacketed Pyrex beaker was employed, through which heated water was circulated to maintain the beaker contents at 37 ± 0.1°.

General Dissolution Procedure—Dissolution medium, 300 ml, was placed in the beaker and allowed to equilibrate to 37°. The stirrer paddle was immersed to a depth of 27 mm in the medium and adjusted to rotate at 50 rpm[2]. Tablets were introduced at time zero by sliding them down the inside of the beaker and carefully releasing them just below the surface.

Cotton-filtered 5-ml samples of solution were removed at the times shown in Fig. 1. Aliquots of 5 ml of the appropriate replacement medium were added to the dissolution beaker immediately after the withdrawal of each sample.

Dissolution Media—Acidic media included 0.1 (pH 1.09 ± 0.01) and 0.001 (pH 3.15 ± 0.01) *N* HCl. Measured portions of phosphate buffer (0.5 *M*) were used to raise the pH of the 0.1 *N* HCl medium to 6.38 or 7.38 ± 0.01.

Conversion of Media—Change of media was accomplished by adding 5 ml of 5 *N* NaOH to 300 ml of 0.1 *N* HCl, mixing well, removing 55 ml of the resulting solution, and finally incorporating 50 ml of the appropriate buffer to restore the original 300-ml volume.

The 30-mg prolonged-acting tablets were subjected to the change of medium procedure at 60 min *in situ* to simulate passage of the residual dosage form from the stomach into the upper small intestine.

Assays—Propantheline powder[3], standardized according to the USP (6), was utilized to prepare standard curves for Assays A and B. Assay B was developed for use with relatively basic media because Assay A was sensitive only to intact drug[4]. Propantheline hydrolyzes in solution above pH 5 to xanthinecarboxylic acid (7).

Ion-Pair Extraction Assay (A)—The calibration curve preparation for the propantheline assay *via* an organic dye salt partition technique, followed by spectrophotometric measurement of complex color intensity, was described previously (8).

UV Spectrophotometric Assay (B)—A series of drug solutions, prepared from propantheline powder in 0.1 *N* HCl, ranged from 0.0016 to 0.16 g/liter. Each solution was treated as described under *Conversion of Media*. Five-milliliter samples were then hydrolyzed with 5 ml of 1 *N* NaOH. After 10 min, 10 ml of 1 *N* HCl was added to acidify hydrolysates, which were diluted to 50 ml with 0.1 *N* HCl. Absorbances of the resulting solutions were read in a spectrophotometer[5] at 220 nm against a blank prepared without drug.

Corrections were made for all dilutions encountered during the change of medium, hydrolysis, and acidification steps. A reproducible Beer's curve, characterized by an absorptivity of 41.6 liters/g, was obtained. Identical absorptivity was found for standard curves prepared from drug in acidic media (0.001 and 0.1 *N* HCl). However, with the acidic media the conversion of media procedure was omitted and samples were processed by adding 1 ml of 1 *N* NaOH, waiting 10 min, acidifying with 1.5 ml of 1 *N* HCl, and finally diluting to 50 ml with 0.1 *N* HCl.

Effect of Tablet Excipients on Assays A and B—Three tablets of each lot[6] studied were crushed thoroughly and dissolved in both 0.1 *N* HCl

[2] Levy *et al.* (5) demonstrated reasonable *in vitro–in vivo* correlations between markedly different solid dosage forms at this degree of agitation in a similar apparatus.

[3] Lot 046A, Searle & Co., San Juan, PR 00936.

[4] When a solution of propantheline in 0.1 *N* HCl was hydrolyzed by the addition of sodium hydroxide and then reacidified and subjected to Assay A, zero absorbance was observed.

[5] Coleman model 101 Hitachi, Coleman Instruments Corp., Maywood, IL 60154.

[6] Lots 1074-461 (the "older" lot, which was manufactured in October 1974 and has an original expiration date of October 1979) and 875-503 (the "fresher" lot, manufactured in August 1975 with a revised 2-year expiration date of July 1977) of 30-mg Pro-Banthine P.A. tablets plus the same 15-mg Pro-Banthine tablets referred to in Ref. 1 (lot number unknown).

Table I—Dissolution Experiments Conducted

Experiment	Number of Tablets Tested[a]	Tablet Strength, mg	Duration, min/pH	Assay
1	5	15	60/1.09	A[b]
2	5	30[c]	60/1.09, 180/6.38	B[b]
3	5	30[d]	60/1.09, 180/6.38	B[b]
4	2	30[c]	60/1.09, 180/7.38	B
5	5	30[c]	240/1.09	B[b]
6	5	30[d]	240/1.09	B[b]
7	2	15	5/7.12	B
8	2	30[d]	60/7.12	B

[a] Each tablet represents a separate dissolution test. [b] Results depicted in Fig. 1. [c] Older lot of tablets. [d] Fresher lot of tablets.

and phosphate buffer (pH 6.38) with ample shaking. Cotton-filtered samples from each solution were assayed by Assay B, while only the acidic filtrates were analyzed by Assay A. No detectable influence on either assay by tablet excipients was observed since all lots yielded within ± 4% of the labeled amount of drug.

Dissolution Experiments—Specifications for all dissolution tests performed in this study are summarized in Table I.

RESULTS AND DISCUSSION

Dissolution curves generated from the 15-mg tablets and the two lots of 30-mg prolonged-acting propantheline tablets under different pH conditions are shown in Fig. 1. The markedly slower drug release from the prolonged-acting formulations in acidic media during the 1st hr parallels the comparatively poor *in vivo* response observed previously (1). Relatively slow release of drug from the prolonged-acting tablets during the initial stages of dissolution was surprising since the manufacturer claimed that: "on ingestion about half of the drug is released within an hour and the remainder continuously as earlier increments are metabolized" (3).

Both types of tablet could be expected to exhibit similar dissolution profiles early in the dissolution process provided that the sustained-release formulation was functioning as claimed. Suppression of salivary secretion following administration of 15-mg tablets to three human subjects was pronounced whereas that from the 30-mg preparations was either less than satisfactory or nil. When Subject 3 of Ref. 1 ingested two of the older 30-mg propantheline tablets, no detectable depression of salivary secretion occurred. The other subjects experienced only about 12% of the anticholinergic response produced by one 15-mg tablet when they took one of the older 30-mg tablets. When Subject 3 took two of the fresher 30-mg tablets, an area under the salivary flow *versus* time curve comparable to two 15-mg tablets was measured. That is, the subject experienced an effect equivalent to about half the dose contained in the fresher prolonged-acting preparation. However, the onset of action associated with the fresher 30-mg dosage form was delayed approximately 1.5 hr. Hence, although the fresher lot of 30-mg tablets exhibited better availability, improvement represented a less than satisfactory level of performance.

Accountability for the labeled amount of drug in all lots of 30-mg prolonged-acting tablets *via* Assay A precludes the possibility that inadequate therapeutic effect was due to chemical instability of drug in the solid dosage form.

No significant difference in dissolution patterns could be discerned between the older and fresher 30-mg tablets over 4 hr when they were subjected to the conversion of media procedure at 1 hr ($p > 0.2$). This result presumably is due to the natural leveling effect of enhanced dissolution on 30-mg tablets by basic media. (Results of Experiments 7 and 8 in Table I showed that drug dissolved about twice as rapidly from both dosage forms when the pH of the medium was raised from 1 to 7.) However, when dissolution in 0.1 *N* HCl was continued beyond the 1st hr[7], the difference in drug released from the older and fresher lots of 30-mg tablets steadily increased and became statistically significant between the 1st ($p > 0.3$) and 2nd ($p < 0.01$) hr and thereafter.

Apparently, the improvement in *in vivo* effectiveness derived from the fresher 30-mg product may be interpreted on the basis of dissolution dissimilarity in an acidic milieu. This experimental finding is consistent with literature reports indicating that the rate and extent of propantheline release from solid dosage forms, during residence in the gastric fluids, should be critical to its bioavailability and, hence, to the onset, intensity, and duration of the anticholinergic effect manifested. One report (7) indicated that almost no absorption of ^{14}C-propantheline occurs from the stomach and that extensive decomposition takes place in the small intestine. Turnheim and Lauterbach (9) pointed out the main site of propantheline absorption is likely the upper small intestine where active uptake of other quaternary compounds has been postulated. Möller and Rosén (10) discovered that an oral dose of propantheline must be about 10 times as large as the usual parenteral dose to achieve similar pharmacological effect.

It follows that propantheline not in solution ready for absorption as it enters the upper small gut from the stomach cavity could be expected to exhibit low systemic availability and, consequently, reduced activity. The propantheline case is further complicated by the fact that anticholinergic drugs retard gastric emptying, making the dissolution rate process of drug from a solid dosage form in gastric fluids an extremely critical determinant of propantheline bioavailability.

Under these limitations, even careful optimization of the 30-mg prolonged-acting formulation may be insufficient to render it effective. Reformulation of the 30-mg sustained-release dosage form to promote more rapid release of the first 15 mg of drug or full reliance on regular tablets is necessary to ensure therapeutic efficacy.

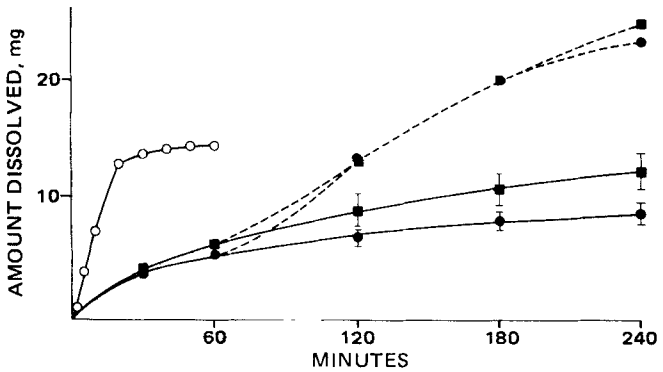

Figure 1—*Amount of propantheline dissolved as a function of time from 15-mg tablets (○) and older (●) and fresher (■) 30-mg prolonged-acting tablets in 0.1 N HCl (—) and pH 6.38 phosphate buffer (---) at 37°. Each data point represents the average of five separate trials. Vertical bars indicate ± 1 SD. The difference in amount of drug released from older and fresher 30-mg prolonged-acting tablets in 0.1 N HCl was statistically significant at 120 min and beyond ($p < 0.01$).*

REFERENCES

(1) M. Gibaldi and B. Grundhofer, *Clin. Pharmacol. Ther.*, **18**, 457 (1975).

(2) "The National Formulary," 14th ed., Mack Publishing Co., Easton, Pa., 1975, pp. 985, 986.

(3) "Physicians Desk Reference," 30th ed., Medical Economics Co., Oradell, N.J., 1976, p. 1415.

(4) G. Levy and B. A. Hayes, *N. Engl. J. Med.*, **262**, 1053 (1960).

(5) G. Levy, J. R. Leonards, and J. A. Procknal, *J. Pharm. Sci.*, **54**, 1719 (1965).

(6) "The United States Pharmacopeia," 19th rev., Mack Publishing Co., Easton, Pa., 1975, p. 418.

(7) B. Beermann, K. Hellström, and A. Rosén, *Clin. Pharmacol. Ther.*, **13**, 212 (1971).

(8) L. G. Chatten and K. O. Okamura, *J. Pharm. Sci.*, **62**, 1328 (1973).

(9) K. Turnheim and F. Lauterbach, "Abstracts of Volunteer Papers, 5th International Congress on Pharmacology," San Francisco, Calif., 1972, p. 136; from D. M. Chaput de Saintonge and A. Herxheimer, *Eur. J. Clin. Pharmacol.*, **5**, 239 (1973).

(10) J. Möller and A. Rosén, *Acta Med. Scand.*, **184**, 201 (1968).

ACKNOWLEDGMENTS AND ADDRESSES

Received November 2, 1976, from the *Department of Pharmaceutics,*

[7] Long-term dissolution runs in acidic media were considered realistic since the prolonged-acting tablets disintegrated slowly (hence, stand a greater chance of being retained in the stomach longer) and the anticholinergic effect of the drug could be expected to retard stomach emptying.

School of Pharmacy, State University of New York at Buffalo, Buffalo, NY 14214.

Accepted for publication March 2, 1977.

Supported in part by an award from the University Allocations Committee, State University of New York at Buffalo, Buffalo, NY 14214.

The authors thank Dr. Milo Gibaldi for his helpful review of the manuscript.

[x] To whom inquiries should be directed.

Viscosity and Surface Tension of Dilute Salicylic Acid–Cetrimide Systems

LUCY S. C. WAN

Abstract □ The viscosity and surface tension of systems containing small amounts of salicylic acid in aqueous solutions of cetrimide were determined. An abrupt increase in viscosity was observed, and the molar ratio of salicylic acid to cetrimide at which this viscosity increase occurred was 1:2. The surface tension of these systems also increased sharply after an initial lowering. The salicylic acid concentration at which this behavior was demonstrated was almost the same as that at maximum solubility in the surfactant solution.

Keyphrases □ Salicylic acid–cetrimide—aqueous solutions, viscosity and surface tension □ Cetrimide–salicylic acid—aqueous solutions, viscosity and surface tension □ Viscosity—aqueous solutions of salicylic acid and cetrimide □ Surface tension—aqueous solutions of salicylic acid and cetrimide

Salicylic acid previously was found to interact with cetrimide in aqueous solutions, leading to a rise in viscosity (1). This interaction was attributed to the formation of macromolecules, and the interaction was shown to be highly specific. It is restricted to the *ortho*-hydroxy-substituted benzoic acid and does not apply to the amino, chloro, or nitro derivatives.

Determination of viscosity in previous studies involved the use of a viscometer that limited the lower range of viscosity measurements that could be made. Dilute concentrations of salicylic acid in cetrimide solutions produce much less viscous systems, and their viscosity can be determined using a U-tube viscometer. The purpose of this investigation was to determine whether the viscosity behavior observed in the salicylic acid–cetrimide systems studied earlier (1) also occurs in similar, but much more dilute, systems. Since the surface activity of these systems is likely to be affected by the interaction between salicylic acid and cetrimide, surface tension measurements made at the same temperature also are included.

EXPERIMENTAL

The recrystallized salicylic acid, mp 158–159°, and cetrimide[1] BP used were the same as described previously (2). The viscosity was measured using a U-tube viscometer, equilibrated in a thermostatically controlled water bath at 25 ± 0.5°. The drop-weight method, employing a micrometer syringe[2], was used to determine the surface tension at the same temperature.

RESULTS AND DISCUSSION

An abrupt increase in viscosity occurred in surfactant solutions of varying concentrations when the salicylic acid content was increased (Fig. 1). The sudden viscosity increase indicated that interaction took place and that macromolecules were formed. At concentrations less than 0.0149 *M* cetrimide in the presence of different amounts of salicylic acid, no such rise in viscosity was produced. This result may have been due to the fact that the quantities of the acid and surfactant used were small and not adequate to demonstrate this pattern of behavior. The degree of interaction produced under such conditions may be inappreciable.

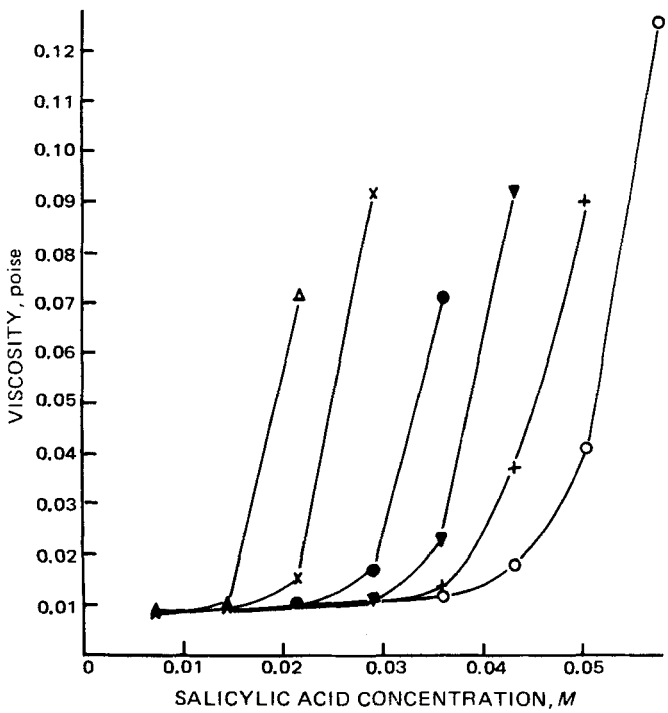

Figure 1—*Viscosity change in cetrimide solutions containing salicylic acid at 25°. Key [cetrimide concentration (M)]: △, 0.0149; ×, 0.0298; ●, 0.0446; ▼, 0.0595; +, 0.0744; and ○, 0.0893.*

Aqueous solutions of cetrimide gave rise to this viscosity change only when certain quantities of salicylic acid were present. The acid needed for this purpose increased proportionately with cetrimide concentration (Fig. 2). The molar ratio of salicylic acid to cetrimide needed for this viscosity change to occur was 1:2, as calculated from the slope of the graph in Fig. 2. In addition, as the cetrimide concentration approached zero, the corresponding concentration of salicylic acid required to cause the viscosity increase approached that of its solubility in water, *i.e.*, 0.0156 *M*, as determined by taking the mean between a clear aqueous solution and one in which excess salicylic acid was present.

This water solubility value was in good agreement with literature values (3–8), suggesting that the minimum amount of salicylic acid necessary to bring about an increase in viscosity must exceed that required to saturate the aqueous phase. The minimum amount of cetrimide required for the same purpose has to be greater than 0.0149 *M*. This surfactant

[1] Glovers Chemicals Ltd., Leeds 12, England.

[2] Agla, Burroughs Wellcome and Co., London, England.

School of Pharmacy, State University of New York at Buffalo, Buffalo, NY 14214.

Accepted for publication March 2, 1977.

Supported in part by an award from the University Allocations Committee, State University of New York at Buffalo, Buffalo, NY 14214.

The authors thank Dr. Milo Gibaldi for his helpful review of the manuscript.

[x] To whom inquiries should be directed.

Viscosity and Surface Tension of Dilute Salicylic Acid–Cetrimide Systems

LUCY S. C. WAN

Abstract □ The viscosity and surface tension of systems containing small amounts of salicylic acid in aqueous solutions of cetrimide were determined. An abrupt increase in viscosity was observed, and the molar ratio of salicylic acid to cetrimide at which this viscosity increase occurred was 1:2. The surface tension of these systems also increased sharply after an initial lowering. The salicylic acid concentration at which this behavior was demonstrated was almost the same as that at maximum solubility in the surfactant solution.

Keyphrases □ Salicylic acid–cetrimide—aqueous solutions, viscosity and surface tension □ Cetrimide–salicylic acid—aqueous solutions, viscosity and surface tension □ Viscosity—aqueous solutions of salicylic acid and cetrimide □ Surface tension—aqueous solutions of salicylic acid and cetrimide

Salicylic acid previously was found to interact with cetrimide in aqueous solutions, leading to a rise in viscosity (1). This interaction was attributed to the formation of macromolecules, and the interaction was shown to be highly specific. It is restricted to the *ortho*-hydroxy-substituted benzoic acid and does not apply to the amino, chloro, or nitro derivatives.

Determination of viscosity in previous studies involved the use of a viscometer that limited the lower range of viscosity measurements that could be made. Dilute concentrations of salicylic acid in cetrimide solutions produce much less viscous systems, and their viscosity can be determined using a U-tube viscometer. The purpose of this investigation was to determine whether the viscosity behavior observed in the salicylic acid–cetrimide systems studied earlier (1) also occurs in similar, but much more dilute, systems. Since the surface activity of these systems is likely to be affected by the interaction between salicylic acid and cetrimide, surface tension measurements made at the same temperature also are included.

EXPERIMENTAL

The recrystallized salicylic acid, mp 158–159°, and cetrimide[1] BP used were the same as described previously (2). The viscosity was measured using a U-tube viscometer, equilibrated in a thermostatically controlled water bath at 25 ± 0.5°. The drop-weight method, employing a micrometer syringe[2], was used to determine the surface tension at the same temperature.

RESULTS AND DISCUSSION

An abrupt increase in viscosity occurred in surfactant solutions of varying concentrations when the salicylic acid content was increased (Fig. 1). The sudden viscosity increase indicated that interaction took place and that macromolecules were formed. At concentrations less than 0.0149 *M* cetrimide in the presence of different amounts of salicylic acid, no such rise in viscosity was produced. This result may have been due to the fact that the quantities of the acid and surfactant used were small and not adequate to demonstrate this pattern of behavior. The degree of interaction produced under such conditions may be inappreciable.

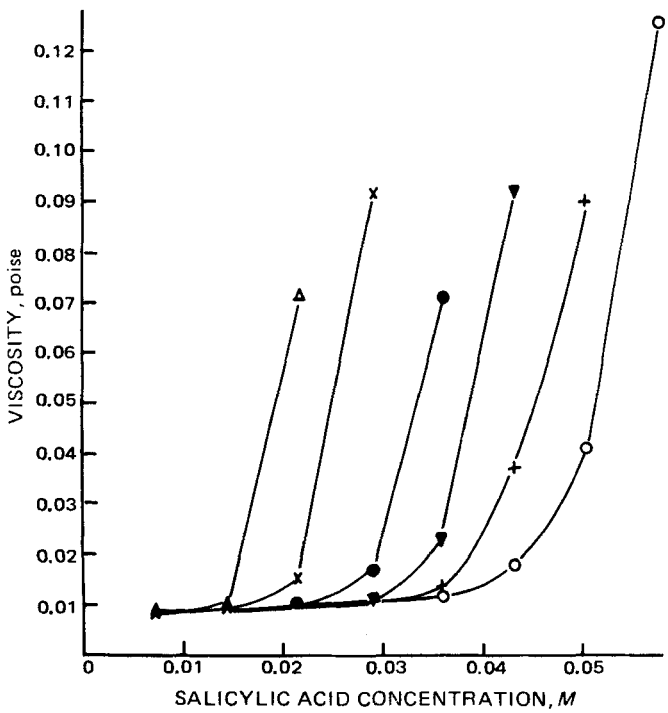

Figure 1—*Viscosity change in cetrimide solutions containing salicylic acid at 25°. Key [cetrimide concentration (M)]: △, 0.0149; ×, 0.0298; ●, 0.0446; ▼, 0.0595; +, 0.0744; and ○, 0.0893.*

Aqueous solutions of cetrimide gave rise to this viscosity change only when certain quantities of salicylic acid were present. The acid needed for this purpose increased proportionately with cetrimide concentration (Fig. 2). The molar ratio of salicylic acid to cetrimide needed for this viscosity change to occur was 1:2, as calculated from the slope of the graph in Fig. 2. In addition, as the cetrimide concentration approached zero, the corresponding concentration of salicylic acid required to cause the viscosity increase approached that of its solubility in water, *i.e.*, 0.0156 *M*, as determined by taking the mean between a clear aqueous solution and one in which excess salicylic acid was present.

This water solubility value was in good agreement with literature values (3–8), suggesting that the minimum amount of salicylic acid necessary to bring about an increase in viscosity must exceed that required to saturate the aqueous phase. The minimum amount of cetrimide required for the same purpose has to be greater than 0.0149 *M*. This surfactant

[1] Glovers Chemicals Ltd., Leeds 12, England.

[2] Agla, Burroughs Wellcome and Co., London, England.

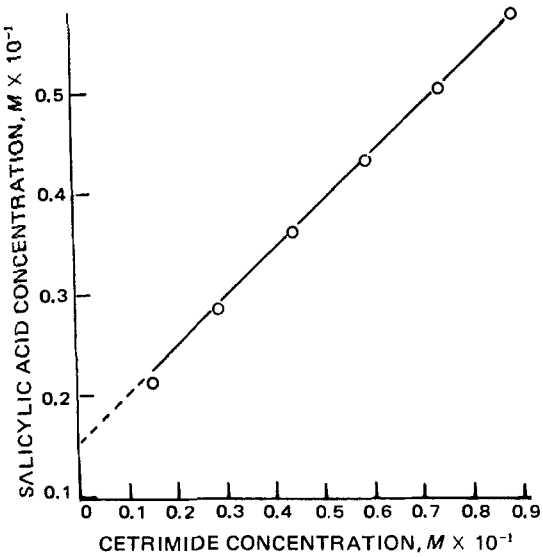

Figure 2—*Relationship between salicylic acid concentration and cetrimide concentration at which a marked increase in viscosity occurs at 25°.*

concentration is well above the critical micelle concentration (CMC), which was 0.0015 *M* at 25°, using the Du Nouy tensiometer[3]. Therefore, the interaction takes place in the presence of micelles. The molar ratio of 1:2 for salicylic acid–cetrimide suggests that twice as many of the larger size cetrimide molecules are probably involved in the interaction with one smaller size salicylic acid molecule. This effect could be associated with the two OH^- groups in the acid molecule. The proximity of the OH^- group to the $COOH^-$ group is essential for interaction (1).

The viscosity of the salicylic acid–cetrimide systems continued to increase after the marked viscosity change occurred until the surfactant solutions became saturated with the acid. The saturated dispersions were allowed to stand to separate the excess acid, which otherwise would interfere with the viscosity measurement, and the viscosity of the clear solution thus obtained was determined. The viscosity tended to decrease. A similar reduction in viscosity was also observed in systems containing higher concentrations of salicylic acid and cetrimide (1), except that the reduced viscosity referred to the viscosity of the saturated system (1). It was not necessary to remove the excess acid since it did not interfere with the rotation of the viscometer cylinders.

When a solution changes to a dispersion, its viscosity generally increases, particularly if the dispersed particles are mainly responsible for the viscous nature of the system. However, this generalization apparently does not apply to these saturated salicylic acid–cetrimide systems. The mesh-like network formed by the macromolecules, which result from the interaction between salicylic acid and cetrimide, is probably easily disrupted. The presence of excess salicylic acid may weaken the links and lead to a structural breakdown, so the viscosity decreases.

From the data plotted (Fig. 3), it is seen that the surface tension was initially depressed and then tended to become constant before rising. The amount of salicylic acid giving this sharp rise in surface tension was slightly greater than that causing the viscosity rise in corresponding systems. The particular acid concentrations responsible for this effect

[3] Cambridge Instrument Co., England.

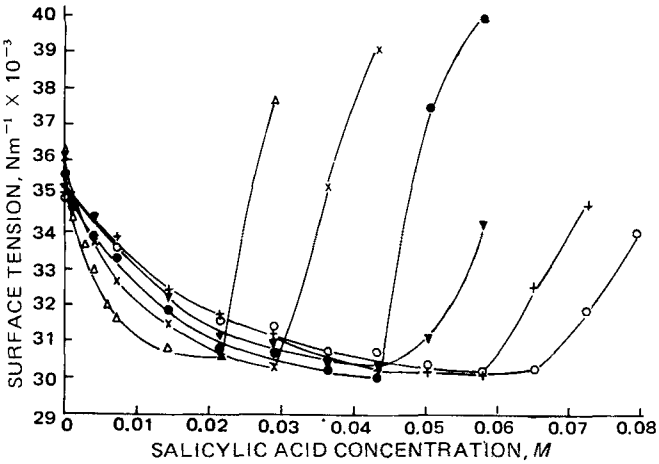

Figure 3—*Change in surface tension of cetrimide solutions containing varying amounts of salicylic acid at 25°. Key [cetrimide concentration (M)]: △, 0.0149; ×, 0.0298; ●, 0.0446; ▼, 0.0595; +, 0.0744; and ○, 0.0893.*

were about the same as the concentration of salicylic acid at maximum solubility in the respective surfactant solution. With cetrimide concentrations lower than 0.0149 *M* and in the presence of different quantities of salicylic acid, this pattern of surface tension changes was not obvious, indicating that the surface activity of the system is only affected if there is an appreciable degree of interaction.

The fall in surface tension at a low salicylic acid concentration may be brought about by the salicylic acid interacting with the cetrimide molecules adsorbed at the interface in preference to those in the bulk of the system, thereby affecting the interfacial packing. As the concentration of salicylic acid is increased, fewer interfacially adsorbed cetrimide molecules are available for the interaction and the surface tension reduction becomes more gradual. With further additions of salicylic acid, the interaction probably involves mainly the cetrimide molecules in the bulk of the system. Eventually, as the degree of interaction approaches its maximum, *i.e.*, most of the surfactant molecules have interacted with the acid, the surface activity of the system appears to reach its highest level and, thereafter, the surface tension increases.

REFERENCES

(1) L. S. C. Wan, *J. Pharm. Sci.*, **55**, 1395 (1966).

(2) *Ibid.*, **60**, 939 (1971).

(3) E. Larsson, *Z. Phys. Chem.*, **127**, 233 (1927).

(4) W. Herz and F. Hiebenthal, *Z. Anorg. Chem.*, **177**, 363, 368 (1928–29).

(5) E. Cohen and H. Goldhart, *Proc. Acad. Sci. (Amst.)*, **34**, 1 (1931).

(6) E. Cohen and L. Thonessen, *ibid.*, **35**, 798 (1932).

(7) A. Oslo and M. Kilpatrick, *J. Am. Chem. Soc.*, **55**, 4440 (1933).

(8) "The Merck Index," 8th ed., Merck and Co., Rahway, N.J., 1968, p. 930.

ACKNOWLEDGMENTS AND ADDRESSES

Received September 16, 1976, from the *Department of Pharmacy, University of Singapore, Sepoy Lines, Singapore 3.*

Accepted for publication March 14, 1977.

Absence of Mutagenicity of Coralyne and Related Antileukemic Agents: Structural Comparison with the Potent Carcinogen 7,12-Dimethylbenz[*a*]anthracene

C. C. CHENG*x, ROBERT R. ENGLE ‡, JOHN R. HODGSON *, ROBERT B. ING ‡, HARRY B. WOOD, Jr. ‡, SHOU-JEN YAN *, and ROBERT K. Y. ZEE-CHENG *

Abstract □ The structural similarity between the antileukemic alkaloid coralyne and the carcinogenic and antineoplastic hydrocarbon 7,12-dimethylbenz[*a*]anthracene, as well as the similarity between the antileukemic alkaloid nitidine and the carcinogenic hydrocarbon 5-methylchrysene, prompted a mutagenicity evaluation of coralyne sulfoacetate, nitidine chloride, the 8-ethyl homolog of coralyne, nitidine methosulfate, and the tetramethoxy analog of nitidine by the Ames method against the histidine-auxotroph strains of *Salmonella typhimurium* TA-1537, TA-1538, TA-98, and TA-100; 7,12-dimethylbenz[*a*]anthracene was used as a reference standard. The mutagenicity of these antileukemic compounds was either completely eliminated or drastically reduced, but the mutagenic response was generally high for 7,12-dimethylbenz[*a*]anthracene. The results suggest that the presence of a quaternary nitrogen atom and alkoxy groups could be important in alleviating the mutagenicity of the parent mutagenic and carcinogenic hydrocarbons.

Keyphrases □ Coralyne and related compounds—mutagenicity evaluated, compared to 7,12-dimethylbenz[*a*]anthracene □ 7,12-Dimethylbenz[*a*]anthracene—mutagenicity compared to coralyne and related compounds □ Mutagenicity—evaluated in coralyne and related compounds, compared to 7,12-dimethylbenz[*a*]anthracene □ Antileukemic agents—coralyne and related compounds, mutagenicity evaluated, compared to 7,12-dimethylbenz[*a*]anthracene □ Carcinogenic agents—7,12-dimethylbenz[*a*]anthracene, mutagenicity compared to coralyne and related compounds □ Structure-activity relationships—coralyne and related compounds, mutagenicity evaluated and compared to 7,12-dimethylbenz[*a*]anthracene

Among numerous polycyclic hydrocarbons studied, the carcinogenic activity of benzo[*a*]pyrene (I) is well documented. While two structurally related hydrocarbons, benz[*a*]anthracene (II*a*) and chrysene (III*a*), are relatively noncarcinogenic, several of their methylated derivatives, such as 7-methylbenz[*a*]anthracene (II*b*), 7,12-dimethylbenz[*a*]anthracene (II*c*), 5-methylchrysene (III*b*), and 5,6-dimethylchrysene (III*c*), exhibited strong carcinogenicity and some were no less potent than benzo[*a*]pyrene (1–6).

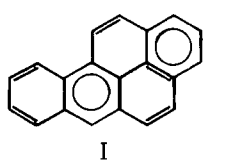

I

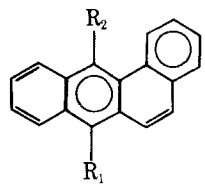

II*a*: $R_1 = R_2 = H$
II*b*: $R_1 = CH_3$, $R_2 = H$
II*c*: $R_1 = R_2 = CH_3$

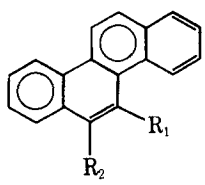

III*a*: $R_1 = R_2 = H$
III*b*: $R_1 = CH_3$, $R_2 = H$
III*c*: $R_1 = R_2 = CH_3$

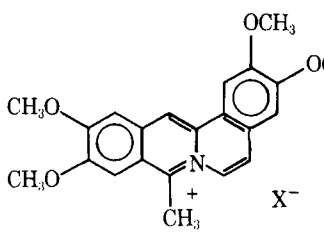

IV

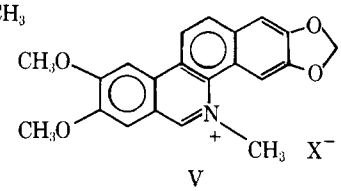

V

DISCUSSION

Carcinogenesis of compounds of this type has been interpreted and correlated by electronic and geometric structures of these polycyclic ring systems (7–10), resulting in the postulation of K, L, and M regions at different parts of polynuclear structures as areas possibly involved in carcinogenic metabolism, noncarcinogenic metabolism, and metabolic epoxidation–perhydroxylation, respectively (2, 11). These regional assignments are by no means decisive for the explanation and prediction of carcinogenicity of polycyclic hydrocarbons, and certain aspects of the original postulation may be obsolete and may have to be modified or correlated with other factors (12–17). Nevertheless, the concept is still being used in structure-activity studies of carcinogenesis (18–23).

The antileukemic activity of coralyne (IV), nitidine (V), and related structural and positional isomers against the P-388 lymphocytic leukemia system in mice was reported (24–27). The basic structural skeleton of IV bears a striking resemblance to that of II, and the ring structure of V is similar to that of III. Furthermore, the methyl group of IV and the 7-methyl group of II occupy the same position when one structure is superimposed on the other. In a similar manner, it can be readily visualized that the methyl group of V matches the position of the methyl group of the carcinogenic III*b*.

Some carcinogenic agents also inhibit tumor growth (28, 34). (The antitumor activity of the potent carcinogen II*c*, NSC-408823, is illustrated in Table I.) Conversely, many antineoplastic agents were reported to be carcinogenic (35, 36). The remarkable structural similarity between the aforementioned antileukemic alkaloids and the carcinogenic methylated polycyclic hydrocarbons naturally led to a concern that these alkaloids and related compounds may possess the undesired oncogenic action.

A comparison of the structures of IV and V with those of the methylated benzanthracenes II*a*–II*c* and chrysenes III*a*–III*c* revealed that, although both alkaloids contain the methyl groups at positions corresponding to the polycyclic hydrocarbon sites that manifest carcinogenicity, the presence of the quaternized nitrogen atom of coralyne and nitidine close to the K and L regions of the corresponding polynuclear ring systems may drastically modify the chemical reactivity of the original molecule, which may alleviate the biological action toward carcinogenesis. In addition, the alkoxy groups of both alkaloids are situated at the corresponding M region, which may also interfere with the oncogenic *in vivo* epoxidation–perhydroxylation process.

Introduction of nitrogen atoms into carcinogenic polycyclic ring compounds, depending upon the nature of ring systems and the position of nitrogen atoms, may either produce compounds with increased carcinogenicity (37–42), decreased carcinogenicity (43), similar biological activity (44), or carcinolytic activity (45). There is, as yet, little information concerning the relationship between quaternized nitrogen het-

Table I—Antitumor Activity of 7,12-Dimethylbenz[*a*]-anthracene[a]

Test System	Dose[b], mg/kg	Survivors[c]	Animal Weight Difference, T − C[d]	T/C[e], %
Ca-755	38	58/60	−0.2	32
	19	18/20	0.2	32
	9	9/10	0.3	44
S-180	94	18/24	−1.1	37
	71	4/6	−0.9	69
	50	6/6	−0.2	37
L-1210	200	6/6	−5.2	165
	100	6/6	−4.2	143
	50	6/6	−4.6	147
	37.5	6/6	−1.4	145
	25	12/12	−1.8	139
	16.5	6/6	−1.7	141
	12.5	6/6	−1.2	126
	6.25	6/6	0.1	123
P-388	13	6/6	−2.4	172
	12.5	6/6	−3.0	175
	6.25	6/6	−2.2	180
	6	6/6	−1.5	168
	4	12/12	−2.7	170
	2.6	6/6	−1.7	163
	1.7	6/6	−2.0	172

[a] For general screening procedure and data interpretation, see R. I. Geran, N. H. Greenberg, M. M. MacDonald, A. M. Schumacher, and B. J. Abbott, *Cancer Chemother. Rep.*, **3** (2), 1 (1972), and Instruction Booklet 14, "Screening Data Summary Interpretation and Outline of Current Screen," Drug Evaluation Branch, Drug Research and Development, Division of Drug Treatment, National Cancer Institute, Bethesda, Md., 1974. [b] Single dose daily. [c] Ratio of number of animals alive on day of evaluation to number of animals used at the beginning of the evaluation. [d] Average weight change of test group minus average weight change of control animals in grams measured at the end of the evaluation. [e] Ratio of test evaluation to control evaluation. For Ca-755 and S-180 (tumor inhibition systems), the criterion for minimum activity is T/C ≤ 42%. For L-1210 and P-388 (survival tumor systems), the criterion for minimum activity is T/C ≥ 125%.

erocycles and carcinogenicity. As an initial step to test the postulation that quaternized nitrogen atoms close to the known "oncogenic area" may alleviate carcinogenicity, coralyne sulfoacetate (IV, X = $C_2H_3SO_5$, NSC-154890), nitidine chloride (V, X = Cl, NSC-146397), nitidine methosulfate (V, X = CH_3SO_4, NSC-160842), the 8-ethyl homolog of coralyne (VI, homocoralyne, NSC-156625), and the tetramethoxy analog of nitidine (VII, *O*-methylfagaronine, NSC-166720), together with IIc as a standard, were subjected to the Ames method for mutagenicity evaluation (46–49). The relationship of mutagenicity and carcinogenicity was discussed previously (46–55).

Mutagenicity tests were carried out according to the specific procedure developed by Ames *et al.* (47) using the histidine–auxotroph strains of *Salmonella typhimurium* TA-1537, TA-1538, TA-98, and TA-100. In this system, petri dishes containing minimal agar were overlayed with a soft agar containing 9000×*g* liver supernate from phenobarbital-induced rats, an NADPH-generating system, bacteria, and various concentrations of test chemical or reference standard. The cultures were incubated at 37° for 72 hr, after which the number of histidine-revertant colonies per plate was determined.

Table II shows the mutagenic effect of IIc and the five test compounds on the *Salmonella* indicator organisms. Compound IIc was mutagenic in all strains. The mutagenic response was high for IIc in TA-1537, TA-1538, TA-98, and TA-100, averaging a three- to 10-fold increase in the number of revertants. With the exception of TA-100, a very sensitive strain, the mutagenic response was absent with all five coralyne and nitidine compounds tested. Even with TA-100, *O*-methylfagaronine methosulfate and coralyne sulfoacetate were nonmutagenic. The dose-response curve for Strain TA-100 is shown in Fig. 1. Similar curves were obtained for all positive strains.

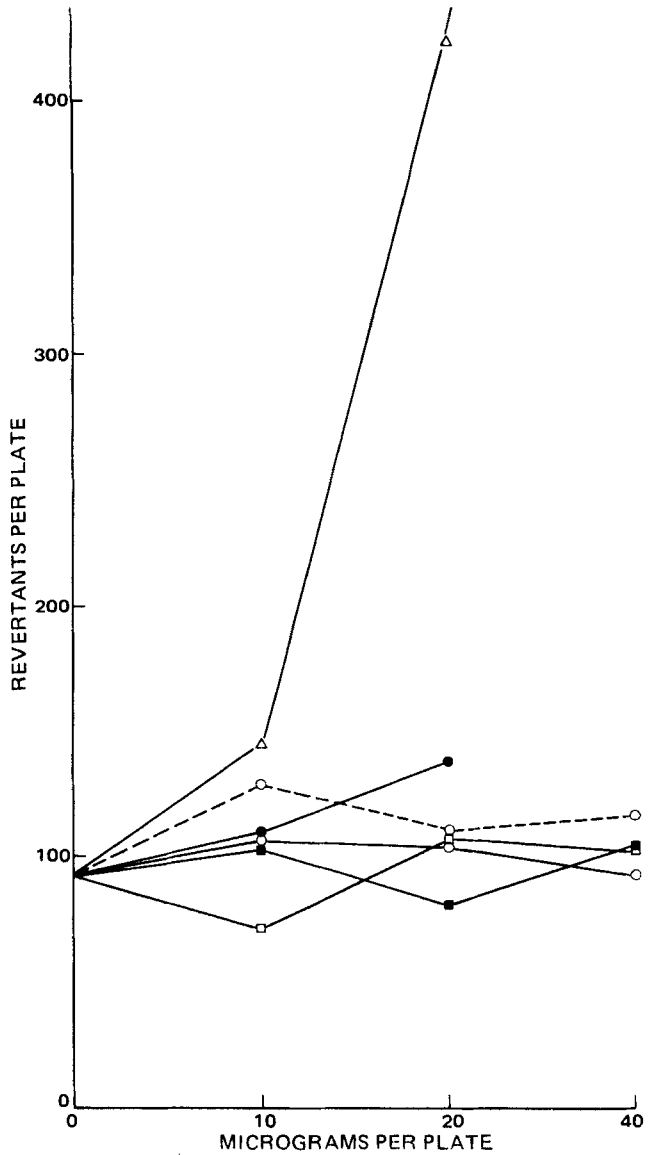

Figure 1—*Mutagenic dose–response relationship of IIc, coralyne, nitidine, and related compounds* versus S. typhimurium *TA-100. Key:* △, *IIc;* ●, *nitidine chloride;* - - - ○ - - -, *nitidine methosulfate;* —○—, *coralyne sulfoacetate;* ■, *O-methylfagaronine; and* □, *homocoralyne sulfopropionate.*

These results indicate that the presence of a quaternary nitrogen atom and alkoxy groups at strategic positions may be important in alleviating mutagenicity of the parent mutagenic and carcinogenic hydrocarbons.

Table II—Mutagenicity Evaluation of 7,12-Dimethylbenz[*a*]anthracene, Coralyne, Nitidine, and Related Compounds

Compounds Tested (40 μg/plate)	Number of Histidine Revertants (Histidine Revertants per Nanomole)[a]			
	TA-1537	TA-1538	TA-98	TA-100
IIc	30 (0.18[c])	22 (0.10[c])	94 (0.47[c])	425 (2.13[c])
Nitidine chloride[b]	5 (0.03)	10 (0.04)	30 (0.10)	117 (0.25[c])
O-Methylfagaronine	6 (0.04)	4 (0)	25 (0.06)	95 (0.02)
Homocoralyne sulfopropionate	2 (0)	4 (0)	20 (0)	103 (0.14[c,d])
Coralyne sulfoacetate	4 (0.02)	8 (0.02)	20 (0)	94 (0.01)
Nitidine methosulfate	3 (0.01)	6 (0)	22 (0.02)	117 (0.29[c])
Control	2	6	20	93

[a] Number of revertants (R) per nanomole = $(R_t - R_c)/(C/mw)$, where R_t is the number of revertants in the treated dish, R_c is the number of revertants in the control dish, C is the concentration of test compound in nanograms, and mw is the molecular weight of the test compound. [b] Due to the insolubility of this compound, only 20 μg was used. [c] Classified to be mutagenic by Ames' criteria (48), *i.e.*, > 0.1 revertant/nmole. [d] Not significantly different from the control value. The reproducibility of the test is ±15%.

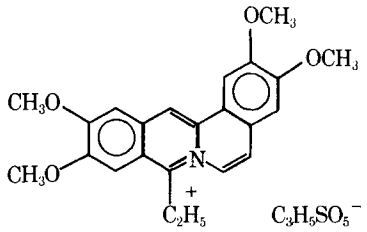

VI

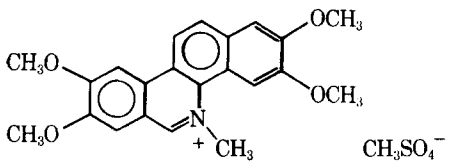

VII

While the relationship between mutagenicity and carcinogenicity of biologically active compounds cannot be fully correlated, its closeness has been recognized. Therefore, the results can be regarded as *suggestive* of the absence of carcinogenicity of coralyne and related antileukemic agents.

REFERENCES

(1) C. E. Dunlap and S. Warren, *Cancer Res.*, **3,** 606 (1943).
(2) A. Pullman and B. Pullman, *Adv. Cancer Res.*, **3,** 117 (1955).
(3) W. F. Dunning and M. R. Curtis, *J. Natl. Cancer Inst.*, **25,** 387 (1960).
(4) A. Lacassagne, F. Zajdela, N. P. Buu-Hoï, and O. Chalvet, *Bull. Cancer*, **49,** 312 (1962).
(5) D. Hoffmann, W. E. Bondinell, and E. L. Wynder, *Science*, **183,** 215 (1974).
(6) M. M. Coombs, T. S. Bhatt, M. Hall, and C. J. Croft, *Cancer Res.*, **34,** 1315 (1974).
(7) F. Bergmann, *ibid.*, **2,** 660 (1942).
(8) A. Pullman and B. Pullman, *Acta Unio. Int. Cancrum*, **6,** 57 (1948).
(9) J. E. Lovelock, A. Zlatkis, and R. S. Becker, *Nature*, **193,** 540 (1962).
(10) Y. Valladares, *Acta Oncol.*, **8,** 3 (1969).
(11) A. Pullman and B. Pullman, *Nature*, **196,** 228 (1962).
(12) J. A. Miller and E. C. Miller, *Cancer Res.*, **23,** 229 (1963).
(13) W. Lijinsky, H. Garcia, and U. Saffiotti, *J. Natl. Cancer Inst.*, **44,** 641 (1970).
(14) J. W. Daly, D. M. Jerina, and B. Witkop, *Experientia*, **28,** 1129 (1972).
(15) N. Kinoshita, B. Shears, and H. V. Gelboin, *Cancer Res.*, **33,** 1937
(16) P. B. Hulbert, *Nature*, **256,** 146 (1975).
(17) P. L. Grover, P. Sims, B. C. V. Mitchley, and F. J. C. Roe, *Br. J. Cancer*, **31,** 182 (1975).
(18) W. C. Herndon, *Trans. N.Y. Acad. Sci.* [*II*], **36,** 200 (1974).
(19) D. M. Jerina and J. W. Daly, *Science*, **185,** 573 (1974).
(20) A. Flaks and P. Sims, *Br. J. Cancer*, **32,** 604 (1975).
(21) P. Y. Bruice, T. C. Bruice, P. M. Dansette, H. G. Selander, H. Yagi, and D. M. Jerina, *J. Am. Chem. Soc.*, **98,** 2965 (1976).
(22) H. Marquardt, P. L. Grover, and P. Sims, *Cancer Res.*, **36,** 2059 (1976).
(23) F. A. Beland and R. G. Harvey, *J. Am. Chem. Soc.*, **98,** 4963 (1976).
(24) K. Y. Zee-Cheng and C. C. Cheng, *J. Pharm. Sci.*, **61,** 969 (1972).
(25) K. Y. Zee-Cheng, K. D. Paull, and C. C. Cheng, *J. Med. Chem.*, **17,** 347 (1974).
(26) R. K. Y. Zee-Cheng and C. C. Cheng, *ibid.*, **18,** 66 (1975).
(27) *Ibid.*, **19,** 882 (1976).
(28) A. Haddow and A. M. Robinson, *Proc. Roy. Soc. B*, **122,** 442 (1937).
(29) A. Haddow, *J. Pathol. Bacteriol.*, **47,** 567, 581 (1938).
(30) G. M. Badger and J. W. Cook, *J. Chem. Soc.*, **1940,** 409.
(31) T. B. Sorokina, *Vopr. Khim. Zlok. Opukh.*, **11,** 152 (1960); through *Cancer Chemother. Abstr.*, **3,** 62 (1962).
(32) V. Armaghan, *J. Natl. Cancer Inst.*, **25,** 125 (1960).
(33) V. Armaghan, *Cancer Chemother. Rep.*, **14,** 117 (1961).
(34) N. P. Buu-Hoï, *Med. Exp.*, **8,** 209 (1963).
(35) J. A. Miller, *Cancer Res.*, **30,** 559 (1970).
(36) C. C. Harris, *Cancer*, **37,** 1014 (1976), and references cited therein.
(37) E. Boyland and A. M. Brues, *Proc. Roy. Soc. B*, **122,** 429 (1937).
(38) E. Boyland and E. H. Manson, *Biochem. J.*, **32,** 1640 (1938).
(39) C. Hackmann, *Z. Krebforsch.*, **58,** 56 (1951).
(40) A. Lacassagne, N. P. Buu-Hoï, F. Zajdela, and N. D. Xuong, *Bull. Cancer*, **42,** 3 (1955).
(41) A. Lacassagne, N. P. Buu-Hoï, R. Daudel, and F. Zajdela, *Adv. Cancer Res.*, **4,** 315 (1956).
(42) A. Lacassagne, N. P. Buu-Hoï, F. Zajdela, F. Périn, and P. Jacquignon, *Nature*, **191,** 1005 (1961).
(43) M. J. Shear and J. Leiter, *J. Natl. Cancer Inst.*, **2,** 99 (1941).
(44) P. Markovits, J. Coppey, D. Papadopoulo, A. Mazabraud, and M. Hubert-Habart, *Int. J. Cancer*, **14,** 215 (1974).
(45) J. Moszew and B. Adamczyk, *Bull. Acad. Polon. Sci. Ser. Sci. Chim.*, **13,** 383 (1965).
(46) B. N. Ames, in "Chemical Mutagens," vol. 1, H. Hollander, Ed., Plenum, New York, N.Y., 1971, p. 267.
(47) B. N. Ames, J. McCann, and E. Yamasaki, *Mutation Res.*, **31,** 347 (1975).
(48) J. McCann, E. Choi, E. Yamasaki, and B. N. Ames, *Proc. Natl. Acad. Sci. USA*, **72,** 5135 (1975).
(49) J. McCann and B. N. Ames, *ibid.*, **73,** 950 (1976).
(50) G. Obe, K. Sperling, and H. J. Belitz, *Angew. Chem.*, **83,** 301 (1971).
(51) J. P. Seiler, *Chimia*, **29,** 8 (1975).
(52) E. Huberman and L. Sachs, *Proc. Natl. Acad. Sci. USA*, **73,** 188 (1976).
(53) E. Huberman, L. Sachs, S. K. Yang, and H. V. Gelboin, *ibid.*, **73,** 607 (1976).
(54) B. A. Bridges, *Nature*, **261,** 195 (1976).
(55) J. McCann, *Chem. Technol.*, **1976,** 682.

ACKNOWLEDGMENTS AND ADDRESSES

Received December 13, 1976, from the *Midwest Research Institute, Kansas City, MO 64110, and the ‡National Cancer Institute, Bethesda, MD 20014.

Accepted for publication February 16, 1977.

Supported by Contract N01-CM-33743 from the Division of Cancer Treatment, National Cancer Institute, National Institutes of Health.

The authors thank Mary Kowalski and Tonya Olmstead for technical assistance in the mutagenesis testing.

ˣ To whom inquiries should be directed.

Multiple Sulfa Compounds: High-Pressure Liquid Chromatographic Assay and Mobile Phase Correlation

E. C. JENNINGS and W. C. LANDGRAF ˣ

Abstract □ A mixture of sulfacetamide, sulfathiazole, and sulfabenzamide was used to develop a rapid high-pressure liquid chromatographic assay. In addition, this study provided a means to develop concepts relating solvent molar polarization parameters and retention times. A linear correlation between molar polarization and retention time was observed and will permit reasonably rapid predictions about the dependent variable.

Keyphrases □ Sulfacetamide—high-pressure liquid chromatographic analysis in mixtures with sulfathiazole and sulfabenzamide □ Sulfathiazole—high-pressure liquid chromatographic analysis in mixtures with sulfacetamide and sulfabenzamide □ Sulfabenzamide—high-pressure liquid chromatographic analysis in mixtures with sulfacetamide and sulfathiazole □ High-pressure liquid chromatography—analyses, sulfacetamide, sulfathiazole, and sulfabenzamide in mixtures □ Antibacterials—sulfacetamide, sulfathiazole, and sulfabenzamide, high-pressure liquid chromatographic analyses of mixtures

The fundamental concepts of adsorption and partition chromatography are sufficiently well developed that their application or extension to high-pressure liquid chromatography (HPLC) are, in general, quite straightforward (1). Perhaps the most difficult challenge in this area lies in the ability of the scientist to provide information of a predictive nature. Several researchers tried rational approaches to the use of liquid chromatography (1). Perhaps more to the point would be a better understanding of the behavior of chromatographic mobile phase systems based on relationships providing predictive insight for the selection of mobile phase systems.

A concept based on readily calculable values of polarizability, directly obtainable from the physical properties of the solvent system, is developed and discussed. This approach is similar to that of Snyder (2), but it is unique in that it does not relate to an elutropic series of solvents.

EXPERIMENTAL

Analytical Development—The primary purpose was to develop an analytical procedure for the rapid determination of three sulfa compounds: sulfacetamide, sulfabenzamide, and sulfathiazole. A convenient commercially available substrate, 10-μm silica gel[1], was filled into a 2-mm stainless steel tube, 50 cm long, using the usual neutral density filling techniques (3).

In the initial selection process for the mobile phase, trimethylpentane–chloroform (8:1) was used since it provided good UV transparency of the 254-nm detector[2]. The polar phase of the system, acetonitrile–isopropyl alcohol (1:1), was added in small increments until there was no further improvement in the resolution of the sulfa compounds on this silica gel column with the operating conditions. A small quantity of acetic acid (0.8%) was added *via* the polar phase to minimize the amount of tailing of such polar compounds. This addition permitted the mobile phase to produce clearly Gaussian shaped lines (Fig. 1). The final composition of this mobile phase was: trimethylpentane, 80%; chloroform, 9.8%; isopropyl alcohol, 4.7%; acetonitrile, 4.7%; and acetic acid, 0.8%.

The usual operating conditions chosen for such a determination were 1.75 ml/min for the flow rate, 80° for the operating temperature, and 1500 psi as the pressure. The use of a high-pressure injection port[3] for sample introduction permitted about 4 μg of each compound to be introduced into the system *via* a 10-μl injection slot without special sample preparation. Table I details the precision results obtained. The data collected from the commercial instruments during analysis were delivered to a fixed-purpose calculating integrator[4] where the digital integration and the determination of resolution (4) were performed. This HPLC unit was capable of both high temperature operation and solvent programming.

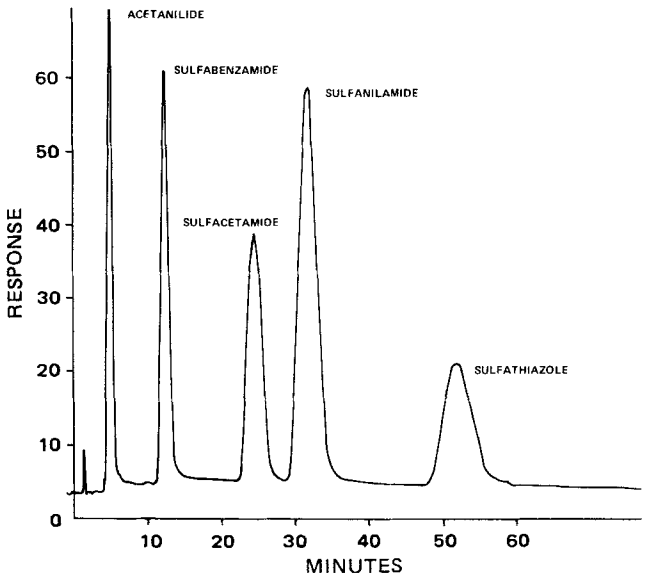

Figure 1—*Chromatogram of mixed sulfa compounds. Operating conditions were: 2.50-ml/mm flow rate, 1210 psi, 78.5°, 0.1 × 2 aufs, and* $\Sigma(X_i P\mu) = 9.9$.

Mobile Phase Aspect of Separation—To extend the knowledge and utility of mobile phase systems, attention was focused on their colligative properties. Therefore, molar polarization contributions from each solvent were calculated (5) and summed together to yield a final value called total molar polarization, $P\mu$, for the solvent system (2, 5). A plot of $P\mu$ *versus* the reciprocal of the retention times of the current solutes is presented in Fig. 2.

RESULTS AND DISCUSSION

This HPLC method for the rapid analysis of sulfa compounds in a complex mixture permits the automation of data collection and reduction. Statistical analysis (Table I) reveals an acceptable 95% confidence limit. This method employs a unique, nonaqueous, multiple-component, mobile phase system. Its choice permits a wider range of operating conditions for chromatographic separations relative to other combinations of mobile phases and substrates (6). It will, because of its nonaqueous composition, permit longer silica gel column lifetimes (up to 6 months); furthermore, it is a simplified procedure for similar compounds.

However, to understand this mobile phase system better, it is important to consider the polarizability effects of such solvents and to examine how they might influence chromatographic solutes on supports such as silica gel. This adsorption–desorption phenomenon for such sulfa compounds from silica gel should be influenced by nondispersive, specific solvent interactions (4).

[1] LiChrosorb S160, E. M. Laboratories.
[2] Model 7000, Micromeritics Instrument Corp.
[3] Model 706L, Disc Instruments.
[4] Auto Lab IV, Spectra Physics Corp.

Table I—Precision Data for Sulfa Compounds *via* HPLC

Peak Areas[a], $S = 0.05 \times 2$				Peak Ratios		
Acetanilide (I), 0.10 mg/ml	Sulfabenzamide (II), 0.20 mg/ml	Sulfacetamide (III), 0.20 mg/ml	Sulfathiazole (IV), 0.20 mg/ml	$\left(\frac{II}{I}\right)$	$\left(\frac{III}{I}\right)$	$\left(\frac{IV}{I}\right)$
352,365	400,398	486,907	702,742	1.136	1.382	1.994
371,023	429,121	492,524	766,862	1.157	1.327	2.067
373,953	430,055	495,171	697,044	1.150	1.324	1.864
354,977	402,077	475,428	694,111	1.133	1.339	1.955
383,246	404,375	487,215	709,354	1.055	1.271	1.851
345,554	382,822	448,458	678,537	1.108	1.298	1.964
			Mean $\bar{x}$	1.123	1.324	1.949
			SD S	0.037	0.038	0.081
			95% *CL*	±0.039	±0.040	±0.085
				±3.5%	±3.0%	±4.4%

[a] Area counts.

For nonpolar molecules, such as pentane, the amount of molecular deformation resulting from a polarizing dc field is called the induced molar polarization: $P\alpha = \frac{4}{3}\pi N\alpha$, where N is Avogadro's number and the magnitude, α, reflects the amount of polarizability that the molecule experiences in that dc field. Furthermore, a dipole in a molecule experiences a similar, but induced, polarization. As a result, it moves itself relative to the dc field to minimize the action of that field. The condition that results in added polarization is referred to as permanent molar polarization and is expressed as $P\mu = \frac{4}{3}\pi N[\mu^2/3KT]$, where μ is the dipole moment and K is the Boltzman constant. The net observed polarization, $P = [P\alpha + P\mu]$, and its thermal coefficient yield the dipole moment. Rearranging terms, one can state that $P = \frac{4}{3}\pi N[\alpha + \mu^2/3KT]$ (7).

For relatively dilute solutions of dipolar molecules in nonpolar solvents, the Clausius–Mossotti equation is valid (8) and leads to the expression $P = [(\epsilon - 1)/(\epsilon + 2)]M/\rho$, where ϵ is the dielectric constant, M is the molecular weight, and ρ is the solvent density. To obtain the value for the total molar polarization, the value for $P\alpha$ must be computed. From Maxwell's relationship of $\epsilon = \eta^2$, where η is the refractive index, it follows that $P\alpha = [(\eta^2 - 1)/(\eta^2 + 2)]M/\rho$, and this expression is referred to as the Lorentz–Lorentz equation (8, 9).

To calculate the net total molar polarization of the solvent system, each

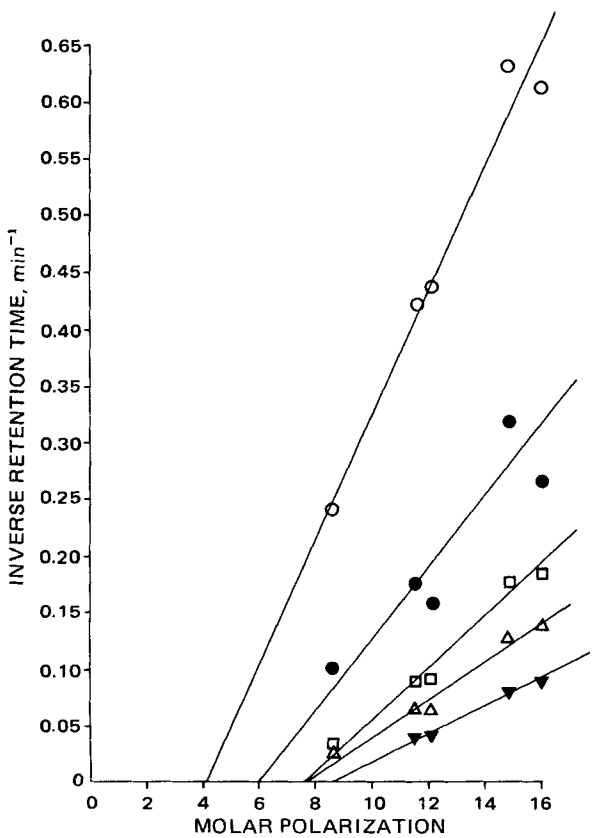

Figure 2—*Plot of inverse retention time* versus *molar polarization*, Pμ. *Key:* ○, *acetanilide;* ●, *sulfabenzamide;* □, *sulfacetamide;* △, *sulfanilamide; and* ▼, *sulfathiazole.*

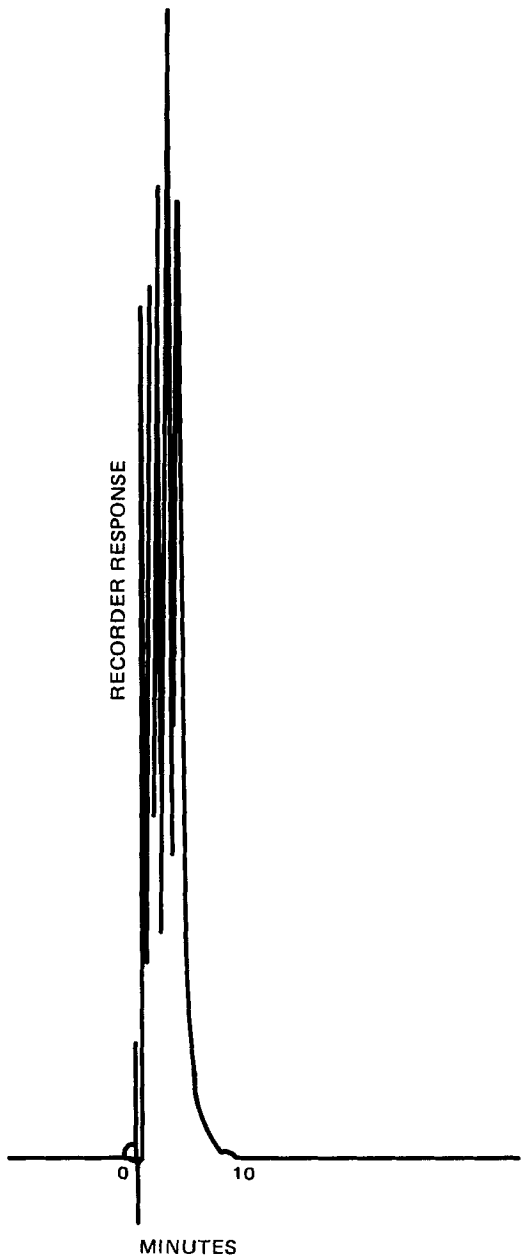

Figure 3—*Chromatogram of mixed sulfa compounds. Operating conditions were: 2.50-ml/mm flow rate, 1200 psi, 78.5°, 0.1 × 2 aufs, and* $\Sigma(X_i P\mu) = 2.0$.

Table II—Total Molar Polarization of Typical Solvent Systems

	Solvent					
	Trimethylpentane	Chloroform	Acetonitrile	Isopropyl Alcohol	Acetic Acid	$\Sigma P\mu$
MW/ρ	165	80.18	52.86	76.91	57.20	—
ϵ	1.94	4.806	37.5	19.92	6.15	—
η	1.404	1.443	1.344	1.38	1.372	—
$P\mu$	−0.95	23.58	37.34	47.47	23.14	—
System						
A: % (v/v)	80	9.8	4.4	5.0	0.8	100%
X_i	0.627	0.158	0.074	0.123	0.018	1.000
$P\mu_i$	−0.596	3.726	2.763	5.839	0.417	12.15
B: % (v/v)	80	12.3	4.4	2.5	0.8	100%
X_i	0.641	0.203	0.075	0.063	0.018	1.000
$P\mu_i$	−0.609	4.787	2.801	2.991	0.417	11.61
C: % (v/v)	80	14.8	4.4	ϕ	0.8	100%
X_i	0.655	0.250	0.076	ϕ	0.019	1.000
$P\mu_i$	−0.622	5.895	2.838	ϕ	0.440	8.55
D: % (v/v)	80	12.0	2.2	5.0	0.8	100%
X_i	0.556	0.286	0.033	0.109	0.016	1.000
$P\mu_i$	−0.528	6.794	1.232	5.174	0.370	12.99
F: % (v/v)	76.6	9.0	4.4	9.5	0.7	100%
X_i	0.562	0.136	0.067	0.220	0.015	1.000
$P\mu_i$	−0.534	3.207	2.502	10.44	0.347	15.97
G: % (v/v)	69.8	20.0	4.4	5.0	0.8	100%
X_i	0.505	0.297	0.068	0.113	0.017	1.000
$P\mu_i$	0.480	7.003	2.539	5.364	0.393	14.82

solvent's contribution based on its mole fraction is added and, by rearranging terms, the following equation results:

$$P\mu = \sum_{1}^{N} [X_i(P - P\alpha)_i] \quad \text{(Eq. 1)}$$

Further substitution yields:

$$P\mu = \sum_{1}^{N} X_i \{[(\epsilon - 1)/(\epsilon + 2)] - [(\eta^2 - 1)(\eta^2 + 2)]\}M/\rho \quad \text{(Eq. 2)}$$

which readily yields $P\mu$ (total molar polarization) (Table II).

When the retention time, t_r, is examined and plotted *versus* $P\mu$, a linear relationship is evident. These two parameters are shown in Fig. 2; the second variable can be predicted easily by knowing the first when using such a plot. Alternatively, the values of $P\mu$ and t_r can be plotted rectalinearly with respect to each other, and a hyperbolic function is observed. With three data points and the use of numerical methods (10, 11), one can solve for the expression using Cramer's determinates. Such an approach yields the constants for this function. In addition, a program written in BASIC permits quick and convenient calculation of new values for either $P\mu$ or t_r by merely inserting several data points into the program without additional plotting. This approach permits the analyst to go from one set of chromatographic conditions to another very quickly and to predict either parameter accurately. This comparison is rather evident through a comparison of Figs. 1 and 3 where the changes in retention times were very simple using these concepts (see Table III for derived constants).

Table III—Hyperbolic Constants from HPLC Data

Compound	Derived Constants			
	A	*B*	*C*	*K*
Acetanilide	−1.05	−0.125	−0.14	0.55
Sulfabenzamide	−20.11	0.50	−0.19	6.20
Sulfanilamide	80.31	−5.77	−0.68	8.29
Sulfacetamide	144.7	−9.91	−0.48	2.27
Sulfathiazole	−21.59	+0.32	−0.12	12.34

REFERENCES

(1) P. Scott and P. Kureca, *Anal. Chem.*, **45**, 749 (1973).

(2) L. R. Snyder, "Principles of Adsorption Chromatography," Dekker, New York, N.Y., 1968, chap. 8.

(3) J. Kirkland, *J. Chromatogr. Sci.*, **8**, 618 (1970).

(4) L. R. Snyder and J. J. Kirkland, "Modern Liquid Chromatography," American Chemical Society, Washington, D.C., 1973, p. 97.

(5) "Conformational Analysis," E. L. Eliel, Ed., Wiley–Interscience, New York, N.Y., 1976, p. 156.

(6) J. Kirkland, "Modern Practice of Liquid Chromatography," Wiley–Interscience, New York, N.Y., 1970, chaps. 10 and 11.

(7) W. J. Moore, "Physical Chemistry," 2nd ed., Prentice-Hall, Englewood Cliffs, N.J., 1954, p. 314.

(8) *Ibid.*, p. 321.

(9) C. P. Smith, "Techniques of Organic Chemistry," 3rd ed., vol. I, part III, Interscience, New York, N.Y., 1960, p. 2599.

(10) E. C. Hohmann and F. J. Lockhart, *Chem. Tech.*, **2**, 614 (1972).

(11) E. Johnson, *Chem. Eng.*, Aug. 11, 1969.

ACKNOWLEDGMENTS AND ADDRESSES

Received January 14, 1976, from the *Applications Research Department, Quality Control Division, Syntex Laboratories, Inc., Palo Alto, CA 94304.*

Accepted for publication March 4, 1977.

[x] To whom inquiries should be directed.

Fluorescence Characteristics of Azaperone and of an Azaperone Mononitrogen Oxide

W. BAEYENS ˣ, P. DE MOERLOOSE, and L. DE TAEYE

Abstract □ The structure elucidation of the compound isolated after peroxide treatment of azaperone is described. A mononitrogen oxide was formed at the piperazine N_1 atom after reaction with excess hydrogen peroxide. The fluorescence characteristics of the derivative were examined and compared with the native fluorescence capacities of the azaperone base; both were identical, depending on the solvent nature. The phenomenon is explained by the fact that the fluorescent properties of the azaperone molecule are principally produced by its *ortho*-nitrogen-substituted pyridine nucleus.

Keyphrases □ Azaperone and oxide—fluorescence characteristics, effect of pH □ Fluorescence characteristics—azaperone and oxide, effect of pH □ Tranquilizers—azaperone and oxide, fluorescence characteristics, effect of pH

Azaperone (I), 1-(4-fluorophenyl)-4-[4-(2-pyridinyl)-1-piperazinyl]-1-butanone, is a butyrophenone neuroleptic. Butyrophenones can be considered as 4-aminobutyric acid derivatives, a prototype of which, haloperidol, is frequently used as an antipsychotic and antiemetic agent. Pharmacologically, the butyrophenones resemble the neuroleptic phenothiazines (1–3). Azaperone is commonly used in veterinary medicine. It occurs as an almost white to slightly yellowish amorphous or crystalline powder, is nearly insoluble in water, and is soluble in dilute acids and organic solvents.

During the spectrofluorometric investigation of some therapeutically used butyrophenones (4), the remarkable fluorescence characteristics of the azaperone molecule were noted and shown to be caused by the heterocyclic substituent of the γ-aminobutyric acid chain.

The purpose of this investigation was to determine whether nitrogen oxidation of the azaperone molecule would affect its native fluorescence characteristics. These experiments were performed simultaneously with spectrofluorometric analyses of some mono- and diaminopyridine isomers before and after peroxide treatment because of the general shortage of literature references concerning fluorometric data of aminopyridines, which frequently occur as molecular fractions in various drugs.

The present paper reports the preparation and structure elucidation of the compound resulting from the reaction of azaperone with concentrated hydrogen peroxide.

EXPERIMENTAL[1]

Apparatus—A recording spectrophotofluorometer was used for recording excitation and emission spectra and for measuring fluorescence intensities. Spectra were not corrected for variations in lamp intensity or photomultiplier sensitivity.

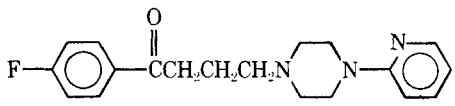

I

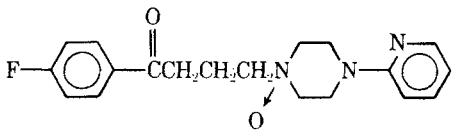

II

Chemicals—All chemicals[2] were analytical grade.

Preparation of Solutions for Fluorescence Measurement—All solutions measured fluorometrically contained 0.5–10 μg of azaperone or derivative/ml. All glassware should be free of fluorescent contaminants and, therefore, frequently rinsed with distilled water; quartz sample cells are preferably cleaned with nitric acid followed by distilled water.

Preparation of Azaperone Peroxide Derivative (II)—Azaperone (9.16 mmoles, 3 g) was dissolved in methanol (100 ml); hydrogen peroxide (490 mmoles, 50 ml of 30% w/w) was added, and the reaction mixture was placed in a boiling water bath for 1 hr with frequent stirring. The solution was allowed to cool at room temperature and was subsequently cooled in ice. If no crystallization occurred, further evaporation was required.

A white precipitate appeared along with a yellow, oily phase. Scratching the sides of the glass vessel with a glass rod finally provided a homogeneous white crystalline product. After filtration, the residue was recrystallized a few times from 50% (v/v) methanol–water and finally dried at 30–40°. An 80% yield was obtained.

A stoichiometrically similar hydrogen peroxide treatment of the two molecular fractions of azaperone was performed. 1-(4-Fluorophenyl)-1-butanone[3] apparently was not attacked in these circumstances. 1-(2-Pyridyl)piperazine[3], however, was converted into a mixture in which at least 10 components could be distinguished by TLC but none of which could be crystallized.

RESULTS

The isolated II appeared as a white crystalline powder, mp 138° (azaperone mp 90°), and was stable on storage at room temperature in the dark. It is very soluble in water and methanol, soluble in chloroform, and less soluble in acetone and ether. The compound can release iodine from an aqueous acid solution of potassium iodide at room temperature.

The UV maxima of II were: (methanol) 244 (ε 25,400)[4] and 298 (ε 2500) nm and (chloroform) 247 (ε 30,400) and 298 (ε 3800) nm. The UV maxima of azaperone were: (methanol) 247 (ε 28,400) and 304 (ε 4100) nm and (chloroform) 248 (22,900) and 305 (ε 2100) nm.

Excitation and fluorescence spectra were obtained from azaperone, II, and 1-(2-pyridyl)piperazine dissolved in various solvents in a concentration of 0.5 μg/ml. In each case, identical results were obtained for the three compounds. For example, in 0.1 *N* sulfuric acid, λ_{exc} = 315 nm and λ_{em} = 405 nm. In 20% (v/v) methanol–water, λ_{exc} = (245)[5] 300 nm and λ_{em} = 375 nm. In 0.1 *N* sulfuric acid in 20% (v/v) methanol–water, λ_{exc} = (245) 315 nm and λ_{em} = 405 nm. Variation of the acid strength up to 20% (w/v) yielded identical spectra. When pure organic solvents (*e.g.*, methanol, ethanol, 2-propanol, 2-methoxyethanol, ethyl acetate, and

[1] The instruments used were: an Aminco-Bowman spectrofluorometer, Catalog No. 4-8203 DE, American Instrument Co., Silver Spring, Md.; a Hanovia 150-w xenon arc lamp; two grating monochromators; 1 × 1-cm quartz cells; photomultiplier R 446 S with high voltage of 0.7 kv and slits varying between 0.5 and 2 mm; a Zeiss DMR 21 spectrophotometer; a Beckman IR 7 spectrometer; an L.K.B. 9000 S mass spectrometer; and a Varian HA-100 NMR spectrometer, Varian Associates, with a permanent frequency of 100 MHz. Melting points were taken on a Büchi apparatus. TLC plates were visualized with a Camag TL 900 Universal UV lamp at 254 and 350 nm.

[2] E. Merck, Darmstadt, West Germany.

[3] Aldrich Chemicals, Beerse, Belgium.

[4] Approximate molar absorptivities were calculated using 327.4 as the molecular weight of azaperone and 343.4 for II, as will be shown from the mass spectral data.

[5] Numbers in parentheses refer to a secondary excitation value of much less intensity.

chloroform) were used, similar results were obtained, with the maxima depending on the polarity of the solvent. The detection limit of both compounds determined fluorometrically in 0.1 *N* sulfuric acid was 1×10^{-2} μg/ml.

IR absorption spectra were taken by dissolving 1 mg in methanol and mixing it with 300 mg of potassium bromide (spectroscopic grade) until complete evaporation occurred. The mixture was then compressed into a tablet. Azaperone absorption bands were: 3100–3000 (aromatic =CH), 3000–2700 (CH_2), 1680 (aryl ketone C=O), 1593–1503–1475 (aromatic C=C), 1590–1500 (C=N), 1228 (CF), 1200–1100–1000 and 730–650 (CH deformations, pyridine nucleus ring vibrations), 825 (CH out of plane: 1,4-aromatic substituents), and 772 (CH out of plane: 1,2-aromatic substituents, piperazine ring vibrations) cm^{-1}. The Compound II spectrum was similar to the azaperone spectrum with minute changes in the fingerprint region: 1400–1350, 1350–1210, 1200–1100, and 875–725 cm^{-1}; strong absorption at 933 (>N → O nonaromatic) cm^{-1}.

Mass spectral data (70 ev) of azaperone differed from the reported fragmentation paths of butyrophenones (5–9) because of the pyridine nitrogen involved in the fragmentation process (Structure III):

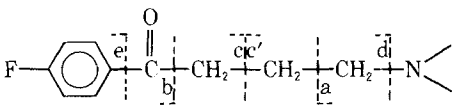

III

m/e (relative intensity) 327 (6) ($M^{+\cdot}$), 309 (4) ($M^{+\cdot} - H_2O$) (m* at 292), 189 (8) (c′, Mc Lafferty), 176 (9) (a, usually base peak in other butyrophenones), 165 (21) (d), 133 (10) ($C_8H_9N_2$, piperazine fragmentation), 123 (30) (b, *p*-fluorobenzoyl ion), 107 (100) (base peak $C_6H_7N_2$), 95 (27) (e, *p*-fluorophenyl ion from *m/e* 123 − CO), and 79 (25)–78 (22) (pyridine fragmentations).

The mass spectrum for II (70 ev) was similar to the azaperone spectrum: *m/e* 343 (3) ($M^{+\cdot}$ azaperone + 16), 327 (3) ($M^{+\cdot} - O$), 326 (4) ($M^{+\cdot} - OH$), 325 (12) ($M^{+\cdot} - H_2O$) in order of increasing intensity (10), 309 (3) ($M^{+\cdot} - H_2O$), 165 (12) (d), 162 (57) (pyridylpiperazine$^+$ after loss of oxygen), 133 (24) ($C_8H_9N_2$), 123 (100) (base peak *p*-fluorobenzoyl nucleus), 107 (63) (base peak azaperone), 95 (45) (*p*-fluorophenyl ion), and 79 (17)–78 (23) (pyridine fragment ions).

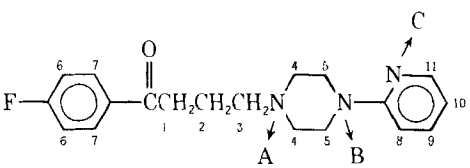

IV

NMR[6] of azaperone (Structure IV) (deuterochloroform, 1% tetramethylsilane) showed: δ 1.97 (2 × t, 2, $J_{2,1}$ = 7 Hz, $J_{2,3}$ = 7.5 Hz, H-2), 2.44 (t, 2, $J_{3,2}$ = 7.5 Hz, H-3), 2.52 (t, 4, $J_{4,5}$ = 5 Hz, H-4), 2.98 (t, 2, $J_{1,2}$ = 7 Hz, H-1), 3.47 (t, 4, $J_{5,4}$ = 5 Hz, H-5), 6.56 (2 × d, 1, $J_{10,9}$ = 7 Hz, $J_{10,11}$ = 5 Hz, $J_{10,8}$ = 2.3 Hz, H-10), 6.60 (d, 1, $J_{8,9}$ = 7.5 Hz, $J_{8,10}$ = 2.3 Hz, H-8), 7.09 (t, 2, $J_{6,7}$ = 8.5 Hz, $J_{6,F}$ = 8.5 Hz, H-6), 7.47 (2 × d, 1, $J_{9,8}$ = 7.5 Hz, $J_{9,10}$ = 7 Hz, $J_{9,11}$ = 2 Hz, H-9), 7.94 (2 × d, 2, $J_{7,6}$ = 8.5 Hz, $J_{7,F}$ = 5.5 Hz, H-7), and 8.14 (d, 1, $J_{11,10}$ = 5 Hz, $J_{11,9}$ = 2 Hz, H-11) ppm.

NMR of Compound II (methanol-d_4, 1% tetramethylsilane) showed: δ 2.29 (m, 2, H-2), 3.30–3.80 (m, 12, H-1, 3, 4, and 5), 6.68 (2 × d, 1, $J_{10,9}$ = 7 Hz, $J_{10,11}$ = 5 Hz, H-10), 6.72 (d, 1, $J_{8,9}$ = 8.5 Hz, $J_{8,10}$ = 1 Hz, H-8), 7.19 (t, 2, $J_{6,7}$ = 8 Hz, $J_{6,F}$ = 8 Hz, H-6), 7.58 (2 × d, 1, $J_{9,8}$ = 8.5 Hz, $J_{9,10}$ = 7 Hz, $J_{9,11}$ = 2 Hz, H-9), 8.07 (2 × d, 2, $J_{7,6}$ = 8 Hz, $J_{7,F}$ = 5 Hz, H-7), and 8.10 (m, 1, H-11) ppm.

Anal.—Calc. for $C_{19}H_{22}FN_3O_2$: C, 66.46; H, 6.46; F, 5.53; N, 12.24. Found: C, 66.43; H, 6.51; F, 5.55; N, 12.22.

DISCUSSION

Since no data were available concerning the formation of nitrogen oxides of the butyrophenone derivatives, an attempt was made to work out a suitable reaction scheme starting from some general rules (11).

Methanolic solutions of azaperone were treated with aqueous solutions of hydrogen peroxide of different strengths at varying pH values and times of reaction. The described method for converting the azaperone base into a mononitrogen derivative using a large excess of hydrogen peroxide originally produced a mixture containing at least three components; one occurred in relatively large amounts, as checked by TLC. It was this component that was purified in the recrystallization process and that fluoresced blue on chromatographic plates in an acid medium on UV exposure. The other substances did not show this phenomenon.

Some of the TLC systems tested to control the purity and stability of synthesized II are shown in Table I. As the azaperone base, its peroxide derivative showed a weak blue native fluorescence on thin layers that was remarkably intensified on contact with acids. In Solvent System 4, for example, both substances were very distinctly recognizable as blue spots on irradiation at 350 nm. Treatment with ammonia vapors largely inhibited the fluorescense emission.

The UV absorption spectra of azaperone and II only demonstrated small differences, as expected. The peroxide derivative showed a slight hypsochromic shift. Absorption in the 300-nm range was mainly caused by the 1-(2-pyridyl)piperazine fraction in the molecule. Absorption in the 240-nm area was due to this fraction as well as to the 1-(*p*-fluorophenyl)-1-butanone substituent, as was noticed after registration of the spectra of these pure compounds in identical conditions.

The azaperone molecule possessed intense fluorescent properties in various solvents because of the heterocyclic pyridylpiperazine substitution of the γ-aminobutyric acid chain. These properties were strongly influenced by the acidity of the medium. Table II illustrates the qualitative effect of pH on the native fluorescence of azaperone. Between the extreme excitation maxima, there was an area of 20 nm; between the two extreme emission maxima, the difference was 42 nm.

Analogous results were obtained with methanol, 2-propanol, propylene glycol, 2-methoxyethanol, and dimethylformamide. Measurements were made on two volumes of azaperone (50 μg/ml of solvent) mixed with one volume of buffer solution. Care should be taken to avoid possible precipitation in the alkaline medium. The compositions of the buffer solutions were: 0.2 *M* potassium chloride–0.2 *N* hydrochloric acid (pH 1.0 and 2.0), 0.1 *M* potassium biphthalate–0.1 *N* hydrochloric acid (pH 3.0 and 4.0), 0.1 *M* potassium biphthalate–0.1 *N* sodium hydroxide (pH 5.0), 0.1 *M* monobasic potassium phosphate–0.1 *N* sodium hydroxide (pH 6.0, 7.0, and 8.0), 0.1 *M* boric acid in 0.1 *M* potassium chloride–0.1 *N* sodium hydroxide (pH 9.0 and 10.0), and 0.1 *M* glycine in 0.1 *M* sodium chloride–0.1 *N* sodium hydroxide (pH 11.0 and 12.0).

Azaperone fluoresced most intensely in an acid medium with an optimum at pH 2. These fluorescent properties at low pH values as well as in pure organic solvents or in aqueous solutions were worked out quantitatively (4). Figure 1 illustrates the excitation and emission spectra of azaperone and II in an acid medium. Both compounds showed identical fluorescent properties, qualitatively and quantitatively. Pure 1-(2-pyridyl)piperazine also yielded analogous spectra. 1-(4-Fluorophenyl)-1-

Table I—TLC R_f Values[a] of I and II

Solvent System	I	II
1. Chloroform	0.02	0.00
2. Chloroform–methanol (90:10 v/v)	0.69	0.12
3. Methanol–28% (w/w) ammonia (100:1.5 v/v)	0.72	0.58
4. Benzene–methanol–acetic acid (80:15:5 v/v)	0.42	0.47
5. Benzene–acetone–petroleum ether (bp 25–70°) –28% (w/w) ammonia (35:35:35:1 v/v)	0.80	0.00
6. Acetone	0.53	0.00

[a] Five micrograms of each compound was spotted on a silica gel 60 F_{254} 0.25-mm plate (Merck). Visualization at 254 nm.

Table II—Influence of Acidity on Fluorescence Characteristics of Azaperone in Ethanol

pH	λ_{exc}, nm	λ_{em}, nm
1	325	403
2	322	398
3	314	365
4	313	361
5	312	367
6	305	367
7	308	373
8	316	370
9	310	375
10	309	376
11	309	378
12	310	378

[6] In NMR descriptions, s = singlet, d = doublet, 2 × d = doublet of doublets, t = triplet, and m = multiplet.

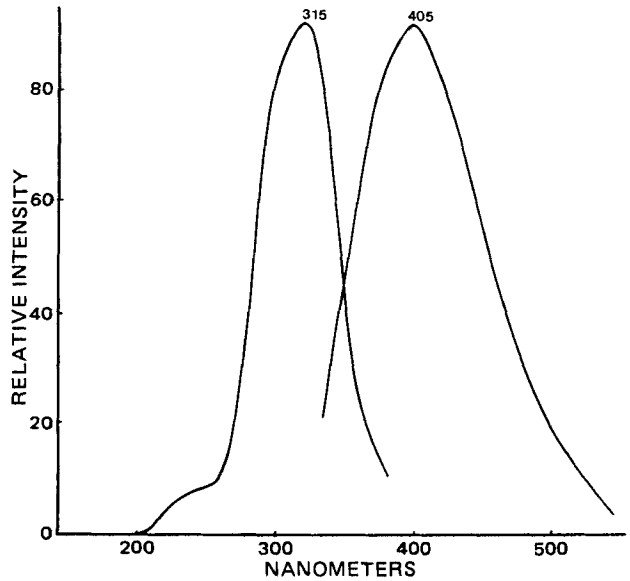

Figure 1—*Activation and emission spectra of azaperone and its peroxide derivatve in 0.1* N *sulfuric acid, 0.5 μg/ml;* λ_{exc} *= 315 nm and* λ_{em} *= 405 nm.*

butanone, dissolved in an organic solvent such as methanol, showed no fluorescent properties at all, as expected.

The NMR spectrometric data show that oxidation apparently occurred at nitrogen atom A of the piperazine ring system. Only this selective oxidation can explain the considerable downfield shift of protons 1, 2, 3, and 4. *N*-Oxidation at nitrogen atom B would merely cause a significant downshift at protons 4 and 5; for nitrogen C, the shift would occur at protons 8, 9, 10, and 11. Integration of the protons of azaperone and II yielded 22 protons for both compounds. This result and the elemental analysis results and mass spectral data suggest that the isolated azaperone peroxide derivative has Structure II.

Compound II possessed identical fluorescent properties as the azaperone molecule in different solvents.

The absence of any influence of *N*-oxidation on the native fluorescence characteristics of the azaperone molecule confirms the localization of the amine oxide formation. The nucleus of the electronic transitions leading to fluorescence emission is situated in the aromatic aminopyridine substituent. Modification of this ring or of the *ortho*-nitrogen substituent certainly would result in an alteration of the fluorescent properties of the molecule by directly influencing the π-electrons of the aromatic system.

REFERENCES

(1) T. Ban, "Psychopharmacology," Williams & Wilkins, Baltimore, Md., 1969, p. 238.

(2) "The Pharmacological Basis of Therapeutics," 3rd ed., L. S. Goodman and A. Gilman, Eds., Macmillan, New York, N.Y., 1966, p. 182.

(3) P. A. J. Janssen, in "Structure–Activity Relationships," C. J. Cavallito, Ed., vol. 1, Pergamon, New York, N.Y., 1973, chap. 2, p. 37.

(4) W. Baeyens, Ph.D. thesis, State University of Ghent, Ghent, Belgium, Jan. 1976.

(5) F. Marcucci, E. Mussini, L. Airoldi, R. Fanelli, A. Frigerio, F. De Nadai, A. Bizzi, M. Rizzo, P. L. Morselli, and S. Garattini, *Clin. Chim. Acta*, **34**, 321 (1971).

(6) B. Blessington, *Org. Mass Spectrom.*, **5**, 1113 (1971).

(7) A. Frigerio and C. Rovere, *ibid.*, **6**, 1051 (1972).

(8) A. Frigerio, A. Forgione, P. Martelli, and R. Fanelli, *Atti Convegno di Ispra–Euratom*, **Sept. 1971**, 401.

(9) H. Budzikiewicz, C. Djerassi, and D. H. Williams, "Mass Spectrometry of Organic Compounds," Holden-Day, San Francisco, Calif., 1967, p. 155.

(10) W. Benz, "Massaspektrometrie Organischer Verbindungen," Academy Verlagsgesellschaft, Frankfurt, Germany, 1969, p. 192.

(11) P. Lebeau and M.-M. Janot, "Traité de Pharmacie Chimique," Tome IV, Masson et Cie, Paris, France, 1955–56, p. 2705.

ACKNOWLEDGMENTS AND ADDRESSES

Received June 10, 1976, from the *Laboratoria voor Farmaceutische Chemie en voor Ontleding van Geneesmiddelen, Farmaceutisch Instituut, A.Z., De Pintelaan 135, 9000-Gent, Belgium.*

Accepted for publication March 14, 1977.

The authors thank Professor Dr. M. Verzele, Department of Organic Chemistry, State University of Ghent, Ghent, Belgium, for the collaboration concerning the NMR spectral data; Mr. P. Demoen, Development Coordinator of Janssen Pharmaceutica, Beerse, Belgium, for the generous gifts of pure butyrophenone compounds; and F.G.W.O. for support through Grant 20210.

[x] To whom inquiries should be directed.

Comparative Pharmacokinetics of Coumarin Anticoagulants XXXVI: Predicted Steady-State Patterns of Prothrombin Complex Activity Produced by Equieffective Doses of (*R*)-(+)- and (*S*)-(−)-Warfarin in Humans

Keyphrases □ Warfarin—(*R*)-(+)- and (*S*)-(−)-enantiomers, steady-state anticoagulant activity compared □ Coumarin anticoagulants—warfarin, (*R*)-(+)- and (*S*)-(−)-enantiomers, steady-state anticoagulant activity compared □ Pharmacokinetics—(*R*)-(+)- and (*S*)-(−)-warfarin, steady-state anticoagulant activity compared □ Anticoagulants—(*R*)-(+)- and (*S*)-(−)-warfarin, activity at steady state compared

To the Editor:

The biological half-life of (*S*)-(−)-warfarin is considerably shorter than that of (*R*)-(+)-warfarin in humans (1). However, the slope of the regression line relating anticoagulant effect and log plasma concentration for (*R*)-(+)-warfarin is considerably steeper than that for (*S*)-(−)-warfarin (2). It is of interest to compare the maximum and minimum anticoagulant activity during a dosing interval at the steady state produced by equieffective doses of the two enantiomers.

To assure adequate anticoagulation and to facilitate clinical monitoring of prothrombin complex activity, it is desirable to minimize the fluctuation of prothrombin complex activity during a dosing interval. Thus, if all else is equal, the enantiomer producing the least fluctuation of prothrombin complex activity during a dosing interval may be preferred therapeutically. Using average pharmacokinetic and pharmacodynamic parameters obtained in a study of 10 healthy men who received single doses of (*R*)-(+)- and (*S*)-(−)-warfarin on separate occasions (1, 2), we calculated the steady-state time course of prothrombin complex activity for each enantiomer during the usual dosing interval of 24 hr.

The calculations were performed in the following manner. The time course of plasma concentrations, C_t, for a one-compartment type drug administered in equal doses, D, at constant intervals, τ, in a manner resulting in essentially instantaneous absorption is:

$$C_t = \frac{D}{V}\left[\frac{1 - e^{-nk\tau}}{1 - e^{-k\tau}}\right]e^{-kt} \qquad \text{(Eq. 1)}$$

where V is the apparent volume of distribution, n is the number of doses administered, t is the time elapsed since dose n was administered, and k is the apparent first-order elimination rate constant (3). The right side of Eq. 1 was substituted for C_p in Eq. 1A of Nagashima *et al.* (4). When solved in the manner described by these investigators but with P^0 defined as the prothrombin complex activity (PCA) at the beginning of each dosing interval (so that P^0 changes with successive doses until a steady state is reached), the following relationship is obtained:

$$\text{PCA} = P^0 e^{-k_d t} + [1 - e^{-k_d t}] \times \left[\frac{R^0_{syn}}{k_d} - W \log \frac{C^0}{C_{p\,min}} - \frac{WZ}{k_d}\right] + WZt \qquad \text{(Eq. 2)}$$

where k_d is the apparent first-order degradation rate constant of prothrombin complex activity, C^0 is the drug concentration at $t = 0$ (calculated from Eq. 1), $Z = k/2.303$, and $W = m/k_d$. The parameters R^0_{syn} and R_{syn} are the synthesis rates of prothrombin complex activity before and during warfarin administration, respectively; m is the slope of a plot of R_{syn} *versus* the logarithm of the plasma warfarin concentration; and $C_{p\,min}$ is the intercept at R^0_{syn} of the extrapolated regression line of a plot of R_{syn} *versus* log plasma warfarin concentration (4).

The following parameter values were used in the calculations of prothrombin complex activity for (*R*)-(+)- and (*S*)-(−)-warfarin (listed in that order): k, 0.0129 and 0.0221 hr^{-1}; V, 99.2 and 95.4 ml/kg; m, −140 and −89%/day; and $C_{p\,min}$, 1.70 and 0.194 μg/ml. The k_d was 1.31 day^{-1}, P^0 before the first dose was 100% of normal, and τ was 24 hr. By successive trial calculations, a daily dose of (*R*)-(+)-warfarin suitable to produce a therapeutic range of prothrombin complex activity (≃30–35% of normal) was found to be 0.225 mg/kg; that of (*S*)-(−)-warfarin was 0.100 mg/kg. The calculations were carried out with a digital computer for $n = 24$.

The results of the simulations are shown in Fig. 1. The prothrombin complex activity *versus* time patterns for the two enantiomers were practically identical. In terms of clotting time, the difference between the maximum and minimum prothrombin complex activities is less than 1 sec. Thus, the greater fluctuation of (*S*)-(−)-enantiomer concentrations in plasma (due to its shorter half-life) is compensated by its more shallow effect–log concentration relationship. It appears, therefore, that there is no significant difference between the two enantiomers with respect to the constancy of prothrombin complex activity during a dosing interval. However, (*R*)-(+)-warfarin may be less subject to interactions with other drugs and may be the preferred form for that reason (5).

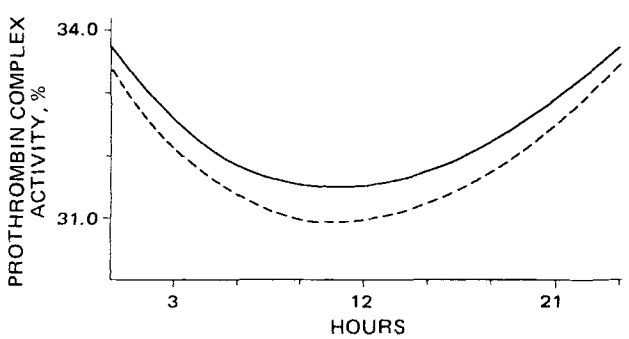

Figure 1—*Predicted time course of prothrombin complex activity in humans during a 24-hr dosing interval at the steady state during administration of essentially equieffective doses of* (R)-(+)-*warfarin* (——) *and* (S)-(−)-*warfarin* (- - - -).

(1) R. A. O'Reilly, *Clin. Pharmacol. Ther.*, 16, 348 (1974).

(2) L. B. Wingard, Jr., R. A. O'Reilly, and G. Levy, *Clin. Pharmacol. Ther.*, in press.

(3) M. Gibaldi and D. Perrier, "Pharmacokinetics," Dekker, New York,

N.Y., 1975, p. 101.
(4) R. Nagashima, R. A. O'Reilly, and G. Levy, *Clin. Pharmacol. Ther.*, **10**, 22 (1969).
(5) R. A. O'Reilly, *N. Engl. J. Med.*, **295**, 354 (1976).

Lemuel B. Wingard, Jr.
Department of Pharmacology
University of Pittsburgh
Pittsburgh, PA 15261

Gerhard Levy [x]
Department of Pharmaceutics
State University of New York
at Buffalo
Amherst, NY 14260

Received August 22, 1977.
Accepted for publication September 20, 1977.
Supported in part by Grant GM 20852 and by use of the Prophet Computer System from the National Institutes of Health.
[x] To whom inquiries should be directed.

BOOKS

REVIEWS

Special Topics in Heterocyclic Chemistry. Vol. 30 of The Chemistry of Heterocyclic Compounds. Edited by ARNOLD WEISSBERGER and EDWARD C. TAYLOR. Wiley, 605 Third Ave., New York, NY 10016, 1977. 601 pp. 15 × 24 cm. Price $57.50.

Although this book is the 30th volume of a 25-year series of monographs on heterocyclic compounds, it is the first to contain treatments of various topics not necessarily related to each other or to a specific ring system. This volume, therefore, represents the editors' desire to discuss limited topics not requiring separate monographs.

The first four chapters share in common discussions of various bridgehead nitrogen heterocycles. Chapter I, 5,5-Systems with a Bridgehead Nitrogen Atom, by John P. Paolini, covers these conjugated 10π-electron heterocycles and their polycyclic derivatives but excludes cyclazines. Chapter II, Indolizine and Aza Derivatives with Additional Nitrogen in the 5-Membered Ring, by H. L. Blewitt, discusses indolizine and 1-, 2-, and 3-azaindolizines; the third chapter by Georges Maury covers azaindolizine systems having more than one nitrogen atom in the six-membered ring. Chapter III also includes azaindolizines containing diazines, triazines, and tetrazines together with pyrrolo-, imidazo-, *s*-triazolo-, and *v*-triazolo ring systems. Chapter IV, The Chemistry of Cyclazines, by Alfred Taurins,includes cycl[3.2.2]azines, cycl[3.3.2]azines, cycl[3.3.3]azines, 1-, 5-, 6-azacycl[3.2.2]azines, 1,4-diazacycl[3.2.2]azines, 8-azacycl[2.2.2]azines, and the 1,3,6-triaza-, 1,3,6,7-tetraza-, and 1,3,4,7-tetrazacycl[3.3.3]azines.

These four chapters are well coordinated, each covering synthetic methods, chemical properties, and physical properties including spectral properties and quantum chemical calculations. References following each chapter average 300 citations for the first three chapters. Chapters II and III include short sections relating to biological properties and uses. Very liberal usage of structural formulas in all but Chapter III makes it easy for the reader to follow the synthetic approaches to these systems.

Chapter V, Dithiole and Dithiolium Systems, by R. D. Hamilton and E. Campaigne, includes interesting discussions of the chemical reactivity of 1,2- and 1,3-dithiolium salts, illustrating their potential synthetic utility. Coverage of dithioles such as the thiothiophthene "no-bond" resonance system, dithiafulvalenes, and mesoionic systems does not proceed beyond the 1972 literature.

In a more up-to-date fashion (including references to the 1976 literature), heteropentalenes are reviewed in Chapter VI by Kevin T. Potts. Of the many possible heteropentalenes, this chapter is devoted to those heteropentalenes with ylidic characteristics, being 10π-electron systems representable by only charge-separated structures (dicoordinate, tetravalent sulfur-containing structures are included). The synthesis, physical properties, and chemical characteristics of these heteropentalenes containing heteroatoms at bridgehead or nonbridgehead positions and in one or both rings are presented in a clear and concise manner.

Chapter VII, Borazaromatic Compounds, by Albert J. Fritsch, treats heterocycles derived from benzenoid-type aromatic or heteroaromatic ring systems by replacement of a pair of carbon atoms by one atom each of boron and nitrogen. These include 2,1-borazarobenzene, 2,1-borazaronaphthalene, 10,9-borazaronaphthalene, 10,9-borazarophenanthrene, several five-membered borazaromatic compounds, and borazaromatic compounds containing another heteroatom in a six-membered ring. In addition to a section on spectral and theoretical considerations that undoubtedly provided initial stimulation in this area, an interesting section is devoted to the comparison of properties such as acidity, localization energies, and aromaticity of borazaromatic compounds.

The final and longest chapter (146 pages) is Syntheses and Properties of Cyanine and Related Dyes by David M. Sturmer. This review concentrates on dyes used as photographic spectral sensitizers and as desensitizers as opposed to those used in color imaging or antihalation and filtering. Sections on historical perspective and generic concepts serve to orientate the newcomer to this field rapidly. Of particular interest are the extended discussions of ground-state physical properties, electronic structure, substituent effects, and color shifts produced by isomerism and environment.

The inclusion of an appreciable amount of tabulated data throughout this volume enhances its value beyond its function of updating the reader in these specific areas.

Reviewed by Robert A. Coburn
Department of Medicinal Chemistry
School of Pharmacy
State University of New York at Buffalo
Buffalo, NY 14260

Narcotic Antagonists: The Search for Long-Acting Preparations, NIDA Research Monograph Series 4. Edited by ROBERT WILLETTE. National Institute on Drug Abuse, 11400 Rockville Pike, Rockville, MD 20852, 1977. 45 pp. 20 × 27 cm. Price $1.10.

Many pharmacologists and behavioral scientists believe that compulsive drug abuse is related to the reinforcing or satisfying properties of dependence-producing drugs. Since narcotic antagonists such as naloxone and naltrexone can entirely block the effects of ordinary doses of opioids, use of these drugs in the treatment of opiate addiction frequently has been advocated. However, in practice the narcotic antagonists have met with limited success, primarily because of their relatively short duration of action and the attendant problems of patient compliance.

The National Institute on Drug Abuse (NIDA), through its contractors, is attempting to develop a long-acting narcotic antagonist drug delivery system or a sustained-release preparation that can be used in the treatment of opiate addiction. This monograph contains abstracts and concise progress reports from seven NIDA supported projects. Six of the reports deal with the development of novel delivery systems. The approaches are quite varied and include the use of coated injectable microcapsules, sustained-release zinc and aluminum tannate complexes, and implantable polypeptide tubes filled with narcotic antagonist. One particularly interesting approach uses a dispersion of naltrexone in a bioerodable polymeric matrix to release drug at a predetermined, continuous, and substantially constant rate.

A seventh report describes the *in vivo* drug release characteristics and pharmacological activity of several delivery systems and also includes results of studies on the metabolic disposition and pharmacokinetics of naltrexone. Nearly all of the experimental data contained in the monograph are preliminary and preclinical. Only three reports list references.

Because of its very narrow scope, the monograph probably will be of major interest only to scientists presently engaged in research directly related to the development of long-acting pharmaceutical dosage forms. However, those persons who wish to keep abreast of current trends in the pharmacological control of compulsive opioid use also may find the monograph a source of useful, up-to-date information.

Reviewed by Louis Diamond
College of Pharmacy
University of Kentucky
Lexington, KY 40506

N.Y., 1975, p. 101.
(4) R. Nagashima, R. A. O'Reilly, and G. Levy, *Clin. Pharmacol. Ther.*, **10**, 22 (1969).
(5) R. A. O'Reilly, *N. Engl. J. Med.*, **295**, 354 (1976).

Lemuel B. Wingard, Jr.
Department of Pharmacology
University of Pittsburgh
Pittsburgh, PA 15261

Gerhard Levy [x]
Department of Pharmaceutics
State University of New York
at Buffalo
Amherst, NY 14260

Received August 22, 1977.
Accepted for publication September 20, 1977.
Supported in part by Grant GM 20852 and by use of the Prophet Computer System from the National Institutes of Health.
[x] To whom inquiries should be directed.

BOOKS

REVIEWS

Special Topics in Heterocyclic Chemistry. Vol. 30 of The Chemistry of Heterocyclic Compounds. Edited by ARNOLD WEISSBERGER and EDWARD C. TAYLOR. Wiley, 605 Third Ave., New York, NY 10016, 1977. 601 pp. 15 × 24 cm. Price $57.50.

Although this book is the 30th volume of a 25-year series of monographs on heterocyclic compounds, it is the first to contain treatments of various topics not necessarily related to each other or to a specific ring system. This volume, therefore, represents the editors' desire to discuss limited topics not requiring separate monographs.

The first four chapters share in common discussions of various bridgehead nitrogen heterocycles. Chapter I, 5,5-Systems with a Bridgehead Nitrogen Atom, by John P. Paolini, covers these conjugated 10π-electron heterocycles and their polycyclic derivatives but excludes cyclazines. Chapter II, Indolizine and Aza Derivatives with Additional Nitrogen in the 5-Membered Ring, by H. L. Blewitt, discusses indolizine and 1-, 2-, and 3-azaindolizines; the third chapter by Georges Maury covers azaindolizine systems having more than one nitrogen atom in the six-membered ring. Chapter III also includes azaindolizines containing diazines, triazines, and tetrazines together with pyrrolo-, imidazo-, *s*-triazolo-, and *v*-triazolo ring systems. Chapter IV, The Chemistry of Cyclazines, by Alfred Taurins,includes cycl[3.2.2]azines, cycl[3.3.2]azines, cycl[3.3.3]azines, 1-, 5-, 6-azacycl[3.2.2]azines, 1,4-diazacycl[3.2.2]azines, 8-azacycl[2.2.2]azines, and the 1,3,6-triaza-, 1,3,6,7-tetraza-, and 1,3,4,7-tetrazacycl[3.3.3]azines.

These four chapters are well coordinated, each covering synthetic methods, chemical properties, and physical properties including spectral properties and quantum chemical calculations. References following each chapter average 300 citations for the first three chapters. Chapters II and III include short sections relating to biological properties and uses. Very liberal usage of structural formulas in all but Chapter III makes it easy for the reader to follow the synthetic approaches to these systems.

Chapter V, Dithiole and Dithiolium Systems, by R. D. Hamilton and E. Campaigne, includes interesting discussions of the chemical reactivity of 1,2- and 1,3-dithiolium salts, illustrating their potential synthetic utility. Coverage of dithioles such as the thiothiophthene "no-bond" resonance system, dithiafulvalenes, and mesoionic systems does not proceed beyond the 1972 literature.

In a more up-to-date fashion (including references to the 1976 literature), heteropentalenes are reviewed in Chapter VI by Kevin T. Potts. Of the many possible heteropentalenes, this chapter is devoted to those heteropentalenes with ylidic characteristics, being 10π-electron systems representable by only charge-separated structures (dicoordinate, tetravalent sulfur-containing structures are included). The synthesis, physical properties, and chemical characteristics of these heteropentalenes containing heteroatoms at bridgehead or nonbridgehead positions and in one or both rings are presented in a clear and concise manner.

Chapter VII, Borazaromatic Compounds, by Albert J. Fritsch, treats heterocycles derived from benzenoid-type aromatic or heteroaromatic ring systems by replacement of a pair of carbon atoms by one atom each of boron and nitrogen. These include 2,1-borazarobenzene, 2,1-borazaronaphthalene, 10,9-borazaronaphthalene, 10,9-borazarophenanthrene, several five-membered borazaromatic compounds, and borazaromatic compounds containing another heteroatom in a six-membered ring. In addition to a section on spectral and theoretical considerations that undoubtedly provided initial stimulation in this area, an interesting section is devoted to the comparison of properties such as acidity, localization energies, and aromaticity of borazaromatic compounds.

The final and longest chapter (146 pages) is Syntheses and Properties of Cyanine and Related Dyes by David M. Sturmer. This review concentrates on dyes used as photographic spectral sensitizers and as desensitizers as opposed to those used in color imaging or antihalation and filtering. Sections on historical perspective and generic concepts serve to orientate the newcomer to this field rapidly. Of particular interest are the extended discussions of ground-state physical properties, electronic structure, substituent effects, and color shifts produced by isomerism and environment.

The inclusion of an appreciable amount of tabulated data throughout this volume enhances its value beyond its function of updating the reader in these specific areas.

Reviewed by Robert A. Coburn
Department of Medicinal Chemistry
School of Pharmacy
State University of New York at Buffalo
Buffalo, NY 14260

Narcotic Antagonists: The Search for Long-Acting Preparations, NIDA Research Monograph Series 4. Edited by ROBERT WILLETTE. National Institute on Drug Abuse, 11400 Rockville Pike, Rockville, MD 20852, 1977. 45 pp. 20 × 27 cm. Price $1.10.

Many pharmacologists and behavioral scientists believe that compulsive drug abuse is related to the reinforcing or satisfying properties of dependence-producing drugs. Since narcotic antagonists such as naloxone and naltrexone can entirely block the effects of ordinary doses of opioids, use of these drugs in the treatment of opiate addiction frequently has been advocated. However, in practice the narcotic antagonists have met with limited success, primarily because of their relatively short duration of action and the attendant problems of patient compliance.

The National Institute on Drug Abuse (NIDA), through its contractors, is attempting to develop a long-acting narcotic antagonist drug delivery system or a sustained-release preparation that can be used in the treatment of opiate addiction. This monograph contains abstracts and concise progress reports from seven NIDA supported projects. Six of the reports deal with the development of novel delivery systems. The approaches are quite varied and include the use of coated injectable microcapsules, sustained-release zinc and aluminum tannate complexes, and implantable polypeptide tubes filled with narcotic antagonist. One particularly interesting approach uses a dispersion of naltrexone in a bioerodable polymeric matrix to release drug at a predetermined, continuous, and substantially constant rate.

A seventh report describes the *in vivo* drug release characteristics and pharmacological activity of several delivery systems and also includes results of studies on the metabolic disposition and pharmacokinetics of naltrexone. Nearly all of the experimental data contained in the monograph are preliminary and preclinical. Only three reports list references.

Because of its very narrow scope, the monograph probably will be of major interest only to scientists presently engaged in research directly related to the development of long-acting pharmaceutical dosage forms. However, those persons who wish to keep abreast of current trends in the pharmacological control of compulsive opioid use also may find the monograph a source of useful, up-to-date information.

Reviewed by Louis Diamond
College of Pharmacy
University of Kentucky
Lexington, KY 40506

N.Y., 1975, p. 101.
(4) R. Nagashima, R. A. O'Reilly, and G. Levy, *Clin. Pharmacol. Ther.*, **10**, 22 (1969).
(5) R. A. O'Reilly, *N. Engl. J. Med.*, **295**, 354 (1976).

Lemuel B. Wingard, Jr.
Department of Pharmacology
University of Pittsburgh
Pittsburgh, PA 15261

Gerhard Levy [x]
Department of Pharmaceutics
State University of New York
at Buffalo
Amherst, NY 14260

Received August 22, 1977.
Accepted for publication September 20, 1977.
Supported in part by Grant GM 20852 and by use of the Prophet Computer System from the National Institutes of Health.
[x] To whom inquiries should be directed.

BOOKS

REVIEWS

Special Topics in Heterocyclic Chemistry. Vol. 30 of The Chemistry of Heterocyclic Compounds. Edited by ARNOLD WEISSBERGER and EDWARD C. TAYLOR. Wiley, 605 Third Ave., New York, NY 10016, 1977. 601 pp. 15 × 24 cm. Price $57.50.

Although this book is the 30th volume of a 25-year series of monographs on heterocyclic compounds, it is the first to contain treatments of various topics not necessarily related to each other or to a specific ring system. This volume, therefore, represents the editors' desire to discuss limited topics not requiring separate monographs.

The first four chapters share in common discussions of various bridgehead nitrogen heterocycles. Chapter I, 5,5-Systems with a Bridgehead Nitrogen Atom, by John P. Paolini, covers these conjugated 10π-electron heterocycles and their polycyclic derivatives but excludes cyclazines. Chapter II, Indolizine and Aza Derivatives with Additional Nitrogen in the 5-Membered Ring, by H. L. Blewitt, discusses indolizine and 1-, 2-, and 3-azaindolizines; the third chapter by Georges Maury covers azaindolizine systems having more than one nitrogen atom in the six-membered ring. Chapter III also includes azaindolizines containing diazines, triazines, and tetrazines together with pyrrolo-, imidazo-, *s*-triazolo-, and *v*-triazolo ring systems. Chapter IV, The Chemistry of Cyclazines, by Alfred Taurins,includes cycl[3.2.2]azines, cycl[3.3.2]azines, cycl[3.3.3]azines, 1-, 5-, 6-azacycl[3.2.2]azines, 1,4-diazacycl[3.2.2]azines, 8-azacycl[2.2.2]azines, and the 1,3,6-triaza-, 1,3,6,7-tetraza-, and 1,3,4,7-tetrazacycl[3.3.3]azines.

These four chapters are well coordinated, each covering synthetic methods, chemical properties, and physical properties including spectral properties and quantum chemical calculations. References following each chapter average 300 citations for the first three chapters. Chapters II and III include short sections relating to biological properties and uses. Very liberal usage of structural formulas in all but Chapter III makes it easy for the reader to follow the synthetic approaches to these systems.

Chapter V, Dithiole and Dithiolium Systems, by R. D. Hamilton and E. Campaigne, includes interesting discussions of the chemical reactivity of 1,2- and 1,3-dithiolium salts, illustrating their potential synthetic utility. Coverage of dithioles such as the thiothiophthene "no-bond" resonance system, dithiafulvalenes, and mesoionic systems does not proceed beyond the 1972 literature.

In a more up-to-date fashion (including references to the 1976 literature), heteropentalenes are reviewed in Chapter VI by Kevin T. Potts. Of the many possible heteropentalenes, this chapter is devoted to those heteropentalenes with ylidic characteristics, being 10π-electron systems representable by only charge-separated structures (dicoordinate, tetravalent sulfur-containing structures are included). The synthesis, physical properties, and chemical characteristics of these heteropentalenes containing heteroatoms at bridgehead or nonbridgehead positions and in one or both rings are presented in a clear and concise manner.

Chapter VII, Borazaromatic Compounds, by Albert J. Fritsch, treats heterocycles derived from benzenoid-type aromatic or heteroaromatic ring systems by replacement of a pair of carbon atoms by one atom each of boron and nitrogen. These include 2,1-borazarobenzene, 2,1-borazaronaphthalene, 10,9-borazaronaphthalene, 10,9-borazarophenanthrene, several five-membered borazaromatic compounds, and borazaromatic compounds containing another heteroatom in a six-membered ring. In addition to a section on spectral and theoretical considerations that undoubtedly provided initial stimulation in this area, an interesting section is devoted to the comparison of properties such as acidity, localization energies, and aromaticity of borazaromatic compounds.

The final and longest chapter (146 pages) is Syntheses and Properties of Cyanine and Related Dyes by David M. Sturmer. This review concentrates on dyes used as photographic spectral sensitizers and as desensitizers as opposed to those used in color imaging or antihalation and filtering. Sections on historical perspective and generic concepts serve to orientate the newcomer to this field rapidly. Of particular interest are the extended discussions of ground-state physical properties, electronic structure, substituent effects, and color shifts produced by isomerism and environment.

The inclusion of an appreciable amount of tabulated data throughout this volume enhances its value beyond its function of updating the reader in these specific areas.

Reviewed by Robert A. Coburn
Department of Medicinal Chemistry
School of Pharmacy
State University of New York at Buffalo
Buffalo, NY 14260

Narcotic Antagonists: The Search for Long-Acting Preparations, NIDA Research Monograph Series 4. Edited by ROBERT WILLETTE. National Institute on Drug Abuse, 11400 Rockville Pike, Rockville, MD 20852, 1977. 45 pp. 20 × 27 cm. Price $1.10.

Many pharmacologists and behavioral scientists believe that compulsive drug abuse is related to the reinforcing or satisfying properties of dependence-producing drugs. Since narcotic antagonists such as naloxone and naltrexone can entirely block the effects of ordinary doses of opioids, use of these drugs in the treatment of opiate addiction frequently has been advocated. However, in practice the narcotic antagonists have met with limited success, primarily because of their relatively short duration of action and the attendant problems of patient compliance.

The National Institute on Drug Abuse (NIDA), through its contractors, is attempting to develop a long-acting narcotic antagonist drug delivery system or a sustained-release preparation that can be used in the treatment of opiate addiction. This monograph contains abstracts and concise progress reports from seven NIDA supported projects. Six of the reports deal with the development of novel delivery systems. The approaches are quite varied and include the use of coated injectable microcapsules, sustained-release zinc and aluminum tannate complexes, and implantable polypeptide tubes filled with narcotic antagonist. One particularly interesting approach uses a dispersion of naltrexone in a bioerodable polymeric matrix to release drug at a predetermined, continuous, and substantially constant rate.

A seventh report describes the *in vivo* drug release characteristics and pharmacological activity of several delivery systems and also includes results of studies on the metabolic disposition and pharmacokinetics of naltrexone. Nearly all of the experimental data contained in the monograph are preliminary and preclinical. Only three reports list references.

Because of its very narrow scope, the monograph probably will be of major interest only to scientists presently engaged in research directly related to the development of long-acting pharmaceutical dosage forms. However, those persons who wish to keep abreast of current trends in the pharmacological control of compulsive opioid use also may find the monograph a source of useful, up-to-date information.

Reviewed by Louis Diamond
College of Pharmacy
University of Kentucky
Lexington, KY 40506

Drug Interactions. Edited by D. G. GRAHAME-SMITH. University Park Press, Chamber of Commerce Bldg., Baltimore, MD 21202, 1977. viii + 310 pp. 15 × 23 cm. Price $44.50.

This volume, consisting of five major sections, presents the proceedings of a symposium held in London in March 1975. The book contains information particularly useful for clinical pharmacologists and toxicologists. Unfortunately, the practicing clinician will find the material too esoteric to be of much value in the care of patients. Primarily, this may not be a fault of the book but rather the recognition that our knowledge of this area is still scanty, especially when applied to the clinical setting, as opposed to studying drug interactions *in vitro*.

The first two sections (10 chapters) are devoted to fundamental aspects of drug interactions, but basic principles are also scattered throughout the remaining 13 chapters, which deal with Drug Interactions in Psychopharmacology, Influence of Disease on Drug Effects and Interactions, and Specific Drug Interaction Problems.

Hershel Jick defines drug interaction as "a pharmacological response which cannot be explained by the action of a single drug but is due to two or more drugs acting simultaneously." C. T. Dollery points out that "the main importance of drug-disease interactions . . . lies in their unpredictability, or the fact that, even when predictable, they are often not predicted."

M. D. Rawlins underscores the complexity of the entire field for pharmacodynamic interactions alone. He envisions four types: (*a*) enhanced effects produced by two drugs acting at the same site, (*b*) increased effects produced by two drugs acting at different receptor sites, (*c*) enhanced effects of a drug by one that is devoid of action itself, and (*d*) antagonism of the effect of one drug by another. J. W. Bridges highlights the further complexity of the field by indicating that, for complete predictability, all receptor sites for each drug must be identified, the physiological consequences recognized, and the concentrations and persistence of the drugs at the receptor sites determined. Obviously, we are far from having begun to attain this goal.

"Drug Interactions" is well referenced but not casually read. This thrifty reviewer considers the book to be excessively priced.

Reviewed by Jacques Dreyfuss
The Squibb Institute for Medical Research
New Brunswick, NJ 08903

Advances in Mass Spectrometry in Biochemistry and Medicine, Vol. II. Edited by ALBERTO FRIGERIO. Halsted, 605 Third Ave., New York, NY 10016, 1977. 609 pp. 15 × 23 cm. Price $48.50.

The book is a report on the proceedings of the Third International Symposium on Mass Spectrometry in Biochemistry and Medicine, Mario Negri Institute for Pharmacological Research in Milan, Italy, in June 1975. Volume II follows the same basic format established in Volume I, which detailed the proceedings of the 1974 Symposium.

It contains a cross-section of mass spectral applications being implemented by the authors in various laboratories for the solution of biomedical problems. Forty-eight separate entries on individual topics, ranging from Automated Multicomponent Analysis of Biological Mixtures by Gas Chromatography–Mass Spectrometry to Peptide Fragmentation Mechanisms have been contributed by specialists in the field. The articles are of varying quality and importance. They cover a wide range of interest areas and should appeal to a large segment of the scientific community. One of the book's strong points is the excellent use of diagrams and illustrations, which complete most presentations. Also, all entries are followed by thorough bibliographies.

In particular, the major topics include detection and identification of low levels of drug metabolites and other biomedical applications. Uses of mass spectrometry for the study of such medically important compounds as steroids, prostaglandins, peptides, and catecholamines are given. Although gas chromatography–mass spectrometry is the principal means of separation and identification of compounds, several other examples of isolation and separation are discussed. Some of the major topics covered include mass fragmentography, gas chromatography–mass spectrometry using stable isotopes, derivatization, electro-optical ion detection, electron impact, chemical ionization, field ionization, field desorption, high-resolution mass measurements, and data acquisition and processing.

Due to the nature of this book, a single review is a virtual impossibility. The scientific merit, the method of presentation, the writing style, and the readability differ with each article. After taking into consideration the highs and lows, an overall view of these presentations is very positive. This book will have definite value to many chemists, biochemists, pharmacologists, and medical researchers as well as mass spectrometrists.

Reviewed by Charles Kuhlman
Wyeth Laboratories
Research Division
Radnor, PA 19087

NOTICES

The Plasma Membrane: Models for Structure and Function. By B. D. GOMPERTS. Academic, 111 Fifth Ave., New York, NY 10003, 1977. 224 pp. 15 × 23 cm. Price $22.25.

Reviews of Physiology, Biochemistry and Pharmacology, Vol. 77. Contains: Regulation of Noradrenaline Release by Presynaptic Receptor Systems, by K. STARKE; Biology of Leukotaxis, by P. A. WARD and E. L. BECKER; and Capillary Structures and O_2 Supply to Tissue, by W. A. GRUNEWALD and W. SOWA. Springer-Verlag, 175 Fifth Ave., New York, NY 10010, 1977. 236 pp. 16 × 24 cm. Price $52.80.

Yeasts and Yeast-Like Microorganisms In Medical Science. Edited by KAZUO IWATA. University of Tokyo Press, Distributor: ISBS, PO Box 555, Forest Grove, OR 97116, 1977. 346 pp. 18 × 26 cm. Price $24.50.

Receptors and Mechanism of Action of Steroid Hormones, Part II. Edited by JORGE R. PASQUALINI. Dekker, 270 Madison Ave., New York, NY 10016, 1977. 440 pp. 15 × 23 cm. Price $39.75.

The Lymphocyte: Structure and Function, Part 1. Edited by JOHN J. MARCHALONIS. Dekker, 270 Madison Ave., New York, NY 10016, 1977. 384 pp. 14 × 23 cm. Price $37.50.

Foams. Edited by R. J. AKERS. Academic (London), 24–28 Oval Rd., London NW1 7DX, England, 1977. 301 pp. 15 × 23 cm. Price $23.50.

Inhibition and Inactivation of Vegetative Microbes. Edited by F. A. SKINNER and W. B. HUGO. Academic (London), 24–28 Oval Rd., London, NW1 7DX, England, 1977. 378 pp. 15 × 23 cm. Price $26.25.

Actualités Pharmacologiques. Edited by RENE HAZARD. Masson, 120 Coulevard, Saint-Germain, 75280 Paris Cedex 06, France, 1977. 206 pp. 16 × 24 cm. Price 140 Fr.

Reviews of Physiology, Biochemistry and Pharmacology, Vol. 78. Contains: Properties and Structural Basis of Simple Diffusion Pathways in the Erythrocyte Membrane, by B. DEUTICKE; and The Gradient Hypothesis and Other Models of Carrier-Mediated Active Transport, by R. K. CRANE. Springer-Verlag, 175 Fifth Ave., New York, NY 10010, 1977. 183 pp. 17 × 25 cm. Price $42.70.

Hazards in the Chemical Laboratory, 2nd Ed. Edited by G. D. MUIR. The Chemical Society, Burlington House, London, WIV OBN, England, 1977. 473 pp. 15 × 23 cm. Price $14.00.

Chemical Pharmacology of the Synapse. By D. J. TRIGGLE and C. R. TRIGGLE. Academic (London), 24-28 Oval Rd., London, NW1 7DX, England, 1977. 654 pp. 15 × 23 cm. Price $43.75.

Toxicology of Trace Elements: Advances in Modern Toxicology, Vol. 2. Edited by ROBERT A. GOYER and MYRON A. MEHLMAN. Halsted, 605 Third Ave., New York, NY 10016, 1977. 303 pp. 14 × 23 cm. Price $24.50.

Radiotracer Techniques and Applications, Vol. 1. Edited by E. ANTHONY EVANS and MITSUO MURAMATSU. Dekker, 270 Madison Ave., New York, NY 10016, 1977. 704 pp. 16 × 24 cm. Price $65.00.

Disinfection, Sterilization, and Preservation, 2nd Ed. Edited by SEYMOUR S. BLOCK. Lea & Febiger, 600 Washington Square, Philadelphia, PA 19106, 1977. 1049 pp. 18 × 26 cm. Price $48.50.

Newburger's Manual of Cosmetic Analysis, 2nd Ed. Edited by ALAN J. SENZEL. The Association of Official Analytical Chemists, PO Box 540, Benjamin Franklin Station, Washington, DC 20044, 1977. 150 pp. 17 × 26 cm. Price $10.50.

Dermatotoxicology and Pharmacology: Advances in Modern Toxicology, Vol. 4. Edited by FRANCIS N. MARZULLI and HOWARD I. MAIBACH. Halsted, 605 Third Ave., New York, NY 10016, 1977. 567 pp. 16 × 24 cm. Price $37.50.

Drug Interactions. Edited by D. G. GRAHAME-SMITH. University Park Press, Chamber of Commerce Bldg., Baltimore, MD 21202, 1977. viii + 310 pp. 15 × 23 cm. Price $44.50.

This volume, consisting of five major sections, presents the proceedings of a symposium held in London in March 1975. The book contains information particularly useful for clinical pharmacologists and toxicologists. Unfortunately, the practicing clinician will find the material too esoteric to be of much value in the care of patients. Primarily, this may not be a fault of the book but rather the recognition that our knowledge of this area is still scanty, especially when applied to the clinical setting, as opposed to studying drug interactions *in vitro*.

The first two sections (10 chapters) are devoted to fundamental aspects of drug interactions, but basic principles are also scattered throughout the remaining 13 chapters, which deal with Drug Interactions in Psychopharmacology, Influence of Disease on Drug Effects and Interactions, and Specific Drug Interaction Problems.

Hershel Jick defines drug interaction as "a pharmacological response which cannot be explained by the action of a single drug but is due to two or more drugs acting simultaneously." C. T. Dollery points out that "the main importance of drug-disease interactions . . . lies in their unpredictability, or the fact that, even when predictable, they are often not predicted."

M. D. Rawlins underscores the complexity of the entire field for pharmacodynamic interactions alone. He envisions four types: (*a*) enhanced effects produced by two drugs acting at the same site, (*b*) increased effects produced by two drugs acting at different receptor sites, (*c*) enhanced effects of a drug by one that is devoid of action itself, and (*d*) antagonism of the effect of one drug by another. J. W. Bridges highlights the further complexity of the field by indicating that, for complete predictability, all receptor sites for each drug must be identified, the physiological consequences recognized, and the concentrations and persistence of the drugs at the receptor sites determined. Obviously, we are far from having begun to attain this goal.

"Drug Interactions" is well referenced but not casually read. This thrifty reviewer considers the book to be excessively priced.

Reviewed by Jacques Dreyfuss
The Squibb Institute for Medical Research
New Brunswick, NJ 08903

Advances in Mass Spectrometry in Biochemistry and Medicine, Vol. II. Edited by ALBERTO FRIGERIO. Halsted, 605 Third Ave., New York, NY 10016, 1977. 609 pp. 15 × 23 cm. Price $48.50.

The book is a report on the proceedings of the Third International Symposium on Mass Spectrometry in Biochemistry and Medicine, Mario Negri Institute for Pharmacological Research in Milan, Italy, in June 1975. Volume II follows the same basic format established in Volume I, which detailed the proceedings of the 1974 Symposium.

It contains a cross-section of mass spectral applications being implemented by the authors in various laboratories for the solution of biomedical problems. Forty-eight separate entries on individual topics, ranging from Automated Multicomponent Analysis of Biological Mixtures by Gas Chromatography–Mass Spectrometry to Peptide Fragmentation Mechanisms have been contributed by specialists in the field. The articles are of varying quality and importance. They cover a wide range of interest areas and should appeal to a large segment of the scientific community. One of the book's strong points is the excellent use of diagrams and illustrations, which complete most presentations. Also, all entries are followed by thorough bibliographies.

In particular, the major topics include detection and identification of low levels of drug metabolites and other biomedical applications. Uses of mass spectrometry for the study of such medically important compounds as steroids, prostaglandins, peptides, and catecholamines are given. Although gas chromatography–mass spectrometry is the principal means of separation and identification of compounds, several other examples of isolation and separation are discussed. Some of the major topics covered include mass fragmentography, gas chromatography–mass spectrometry using stable isotopes, derivatization, electro-optical ion detection, electron impact, chemical ionization, field ionization, field desorption, high-resolution mass measurements, and data acquisition and processing.

Due to the nature of this book, a single review is a virtual impossibility. The scientific merit, the method of presentation, the writing style, and the readability differ with each article. After taking into consideration the highs and lows, an overall view of these presentations is very positive. This book will have definite value to many chemists, biochemists, pharmacologists, and medical researchers as well as mass spectrometrists.

Reviewed by Charles Kuhlman
Wyeth Laboratories
Research Division
Radnor, PA 19087

NOTICES

The Plasma Membrane: Models for Structure and Function. By B. D. GOMPERTS. Academic, 111 Fifth Ave., New York, NY 10003, 1977. 224 pp. 15 × 23 cm. Price $22.25.

Reviews of Physiology, Biochemistry and Pharmacology, Vol. 77. Contains: Regulation of Noradrenaline Release by Presynaptic Receptor Systems, by K. STARKE; Biology of Leukotaxis, by P. A. WARD and E. L. BECKER; and Capillary Structures and O_2 Supply to Tissue, by W. A. GRUNEWALD and W. SOWA. Springer-Verlag, 175 Fifth Ave., New York, NY 10010, 1977. 236 pp. 16 × 24 cm. Price $52.80.

Yeasts and Yeast-Like Microorganisms In Medical Science. Edited by KAZUO IWATA. University of Tokyo Press, Distributor: ISBS, PO Box 555, Forest Grove, OR 97116, 1977. 346 pp. 18 × 26 cm. Price $24.50.

Receptors and Mechanism of Action of Steroid Hormones, Part II. Edited by JORGE R. PASQUALINI. Dekker, 270 Madison Ave., New York, NY 10016, 1977. 440 pp. 15 × 23 cm. Price $39.75.

The Lymphocyte: Structure and Function, Part 1. Edited by JOHN J. MARCHALONIS. Dekker, 270 Madison Ave., New York, NY 10016, 1977. 384 pp. 14 × 23 cm. Price $37.50.

Foams. Edited by R. J. AKERS. Academic (London), 24–28 Oval Rd., London NW1 7DX, England, 1977. 301 pp. 15 × 23 cm. Price $23.50.

Inhibition and Inactivation of Vegetative Microbes. Edited by F. A. SKINNER and W. B. HUGO. Academic (London), 24–28 Oval Rd., London, NW1 7DX, England, 1977. 378 pp. 15 × 23 cm. Price $26.25.

Actualités Pharmacologiques. Edited by RENE HAZARD. Masson, 120 Coulevard, Saint-Germain, 75280 Paris Cedex 06, France, 1977. 206 pp. 16 × 24 cm. Price 140 Fr.

Reviews of Physiology, Biochemistry and Pharmacology, Vol. 78. Contains: Properties and Structural Basis of Simple Diffusion Pathways in the Erythrocyte Membrane, by B. DEUTICKE; and The Gradient Hypothesis and Other Models of Carrier-Mediated Active Transport, by R. K. CRANE. Springer-Verlag, 175 Fifth Ave., New York, NY 10010, 1977. 183 pp. 17 × 25 cm. Price $42.70.

Hazards in the Chemical Laboratory, 2nd Ed. Edited by G. D. MUIR. The Chemical Society, Burlington House, London, WIV OBN, England, 1977. 473 pp. 15 × 23 cm. Price $14.00.

Chemical Pharmacology of the Synapse. By D. J. TRIGGLE and C. R. TRIGGLE. Academic (London), 24-28 Oval Rd., London, NW1 7DX, England, 1977. 654 pp. 15 × 23 cm. Price $43.75.

Toxicology of Trace Elements: Advances in Modern Toxicology, Vol. 2. Edited by ROBERT A. GOYER and MYRON A. MEHLMAN. Halsted, 605 Third Ave., New York, NY 10016, 1977. 303 pp. 14 × 23 cm. Price $24.50.

Radiotracer Techniques and Applications, Vol. 1. Edited by E. ANTHONY EVANS and MITSUO MURAMATSU. Dekker, 270 Madison Ave., New York, NY 10016, 1977. 704 pp. 16 × 24 cm. Price $65.00.

Disinfection, Sterilization, and Preservation, 2nd Ed. Edited by SEYMOUR S. BLOCK. Lea & Febiger, 600 Washington Square, Philadelphia, PA 19106, 1977. 1049 pp. 18 × 26 cm. Price $48.50.

Newburger's Manual of Cosmetic Analysis, 2nd Ed. Edited by ALAN J. SENZEL. The Association of Official Analytical Chemists, PO Box 540, Benjamin Franklin Station, Washington, DC 20044, 1977. 150 pp. 17 × 26 cm. Price $10.50.

Dermatotoxicology and Pharmacology: Advances in Modern Toxicology, Vol. 4. Edited by FRANCIS N. MARZULLI and HOWARD I. MAIBACH. Halsted, 605 Third Ave., New York, NY 10016, 1977. 567 pp. 16 × 24 cm. Price $37.50.

Drug Interactions. Edited by D. G. GRAHAME-SMITH. University Park Press, Chamber of Commerce Bldg., Baltimore, MD 21202, 1977. viii + 310 pp. 15 × 23 cm. Price $44.50.

This volume, consisting of five major sections, presents the proceedings of a symposium held in London in March 1975. The book contains information particularly useful for clinical pharmacologists and toxicologists. Unfortunately, the practicing clinician will find the material too esoteric to be of much value in the care of patients. Primarily, this may not be a fault of the book but rather the recognition that our knowledge of this area is still scanty, especially when applied to the clinical setting, as opposed to studying drug interactions *in vitro*.

The first two sections (10 chapters) are devoted to fundamental aspects of drug interactions, but basic principles are also scattered throughout the remaining 13 chapters, which deal with Drug Interactions in Psychopharmacology, Influence of Disease on Drug Effects and Interactions, and Specific Drug Interaction Problems.

Hershel Jick defines drug interaction as "a pharmacological response which cannot be explained by the action of a single drug but is due to two or more drugs acting simultaneously." C. T. Dollery points out that "the main importance of drug-disease interactions . . . lies in their unpredictability, or the fact that, even when predictable, they are often not predicted."

M. D. Rawlins underscores the complexity of the entire field for pharmacodynamic interactions alone. He envisions four types: (*a*) enhanced effects produced by two drugs acting at the same site, (*b*) increased effects produced by two drugs acting at different receptor sites, (*c*) enhanced effects of a drug by one that is devoid of action itself, and (*d*) antagonism of the effect of one drug by another. J. W. Bridges highlights the further complexity of the field by indicating that, for complete predictability, all receptor sites for each drug must be identified, the physiological consequences recognized, and the concentrations and persistence of the drugs at the receptor sites determined. Obviously, we are far from having begun to attain this goal.

"Drug Interactions" is well referenced but not casually read. This thrifty reviewer considers the book to be excessively priced.

Reviewed by Jacques Dreyfuss
The Squibb Institute for Medical Research
New Brunswick, NJ 08903

Advances in Mass Spectrometry in Biochemistry and Medicine, Vol. II. Edited by ALBERTO FRIGERIO. Halsted, 605 Third Ave., New York, NY 10016, 1977. 609 pp. 15 × 23 cm. Price $48.50.

The book is a report on the proceedings of the Third International Symposium on Mass Spectrometry in Biochemistry and Medicine, Mario Negri Institute for Pharmacological Research in Milan, Italy, in June 1975. Volume II follows the same basic format established in Volume I, which detailed the proceedings of the 1974 Symposium.

It contains a cross-section of mass spectral applications being implemented by the authors in various laboratories for the solution of biomedical problems. Forty-eight separate entries on individual topics, ranging from Automated Multicomponent Analysis of Biological Mixtures by Gas Chromatography–Mass Spectrometry to Peptide Fragmentation Mechanisms have been contributed by specialists in the field. The articles are of varying quality and importance. They cover a wide range of interest areas and should appeal to a large segment of the scientific community. One of the book's strong points is the excellent use of diagrams and illustrations, which complete most presentations. Also, all entries are followed by thorough bibliographies.

In particular, the major topics include detection and identification of low levels of drug metabolites and other biomedical applications. Uses of mass spectrometry for the study of such medically important compounds as steroids, prostaglandins, peptides, and catecholamines are given. Although gas chromatography–mass spectrometry is the principal means of separation and identification of compounds, several other examples of isolation and separation are discussed. Some of the major topics covered include mass fragmentography, gas chromatography–mass spectrometry using stable isotopes, derivatization, electro-optical ion detection, electron impact, chemical ionization, field ionization, field desorption, high-resolution mass measurements, and data acquisition and processing.

Due to the nature of this book, a single review is a virtual impossibility. The scientific merit, the method of presentation, the writing style, and the readability differ with each article. After taking into consideration the highs and lows, an overall view of these presentations is very positive. This book will have definite value to many chemists, biochemists, pharmacologists, and medical researchers as well as mass spectrometrists.

Reviewed by Charles Kuhlman
Wyeth Laboratories
Research Division
Radnor, PA 19087

NOTICES

The Plasma Membrane: Models for Structure and Function. By B. D. GOMPERTS. Academic, 111 Fifth Ave., New York, NY 10003, 1977. 224 pp. 15 × 23 cm. Price $22.25.

Reviews of Physiology, Biochemistry and Pharmacology, Vol. 77. Contains: Regulation of Noradrenaline Release by Presynaptic Receptor Systems, by K. STARKE; Biology of Leukotaxis, by P. A. WARD and E. L. BECKER; and Capillary Structures and O_2 Supply to Tissue, by W. A. GRUNEWALD and W. SOWA. Springer-Verlag, 175 Fifth Ave., New York, NY 10010, 1977. 236 pp. 16 × 24 cm. Price $52.80.

Yeasts and Yeast-Like Microorganisms In Medical Science. Edited by KAZUO IWATA. University of Tokyo Press, Distributor: ISBS, PO Box 555, Forest Grove, OR 97116, 1977. 346 pp. 18 × 26 cm. Price $24.50.

Receptors and Mechanism of Action of Steroid Hormones, Part II. Edited by JORGE R. PASQUALINI. Dekker, 270 Madison Ave., New York, NY 10016, 1977. 440 pp. 15 × 23 cm. Price $39.75.

The Lymphocyte: Structure and Function, Part 1. Edited by JOHN J. MARCHALONIS. Dekker, 270 Madison Ave., New York, NY 10016, 1977. 384 pp. 14 × 23 cm. Price $37.50.

Foams. Edited by R. J. AKERS. Academic (London), 24–28 Oval Rd., London NW1 7DX, England, 1977. 301 pp. 15 × 23 cm. Price $23.50.

Inhibition and Inactivation of Vegetative Microbes. Edited by F. A. SKINNER and W. B. HUGO. Academic (London), 24–28 Oval Rd., London, NW1 7DX, England, 1977. 378 pp. 15 × 23 cm. Price $26.25.

Actualités Pharmacologiques. Edited by RENE HAZARD. Masson, 120 Coulevard, Saint-Germain, 75280 Paris Cedex 06, France, 1977. 206 pp. 16 × 24 cm. Price 140 Fr.

Reviews of Physiology, Biochemistry and Pharmacology, Vol. 78. Contains: Properties and Structural Basis of Simple Diffusion Pathways in the Erythrocyte Membrane, by B. DEUTICKE; and The Gradient Hypothesis and Other Models of Carrier-Mediated Active Transport, by R. K. CRANE. Springer-Verlag, 175 Fifth Ave., New York, NY 10010, 1977. 183 pp. 17 × 25 cm. Price $42.70.

Hazards in the Chemical Laboratory, 2nd Ed. Edited by G. D. MUIR. The Chemical Society, Burlington House, London, WIV OBN, England, 1977. 473 pp. 15 × 23 cm. Price $14.00.

Chemical Pharmacology of the Synapse. By D. J. TRIGGLE and C. R. TRIGGLE. Academic (London), 24-28 Oval Rd., London, NW1 7DX, England, 1977. 654 pp. 15 × 23 cm. Price $43.75.

Toxicology of Trace Elements: Advances in Modern Toxicology, Vol. 2. Edited by ROBERT A. GOYER and MYRON A. MEHLMAN. Halsted, 605 Third Ave., New York, NY 10016, 1977. 303 pp. 14 × 23 cm. Price $24.50.

Radiotracer Techniques and Applications, Vol. 1. Edited by E. ANTHONY EVANS and MITSUO MURAMATSU. Dekker, 270 Madison Ave., New York, NY 10016, 1977. 704 pp. 16 × 24 cm. Price $65.00.

Disinfection, Sterilization, and Preservation, 2nd Ed. Edited by SEYMOUR S. BLOCK. Lea & Febiger, 600 Washington Square, Philadelphia, PA 19106, 1977. 1049 pp. 18 × 26 cm. Price $48.50.

Newburger's Manual of Cosmetic Analysis, 2nd Ed. Edited by ALAN J. SENZEL. The Association of Official Analytical Chemists, PO Box 540, Benjamin Franklin Station, Washington, DC 20044, 1977. 150 pp. 17 × 26 cm. Price $10.50.

Dermatotoxicology and Pharmacology: Advances in Modern Toxicology, Vol. 4. Edited by FRANCIS N. MARZULLI and HOWARD I. MAIBACH. Halsted, 605 Third Ave., New York, NY 10016, 1977. 567 pp. 16 × 24 cm. Price $37.50.

ERRATA

In the article titled "Possible Antineoplastic Agents I" (1), the following corrections should be made:

On page 265, Table IV, the Melting Point column should read:

258–260°
150–152°
148–150°
130–132°
136–138°
100–102°
70–72°
262–264° dec.
278–280° dec.

The Boiling Point column should be deleted. A footnote should be added for Compounds II*b*–II*g* that reads:

"Purified by crystallization from water or dilute ethanol with charcoal treatment."

(1) A. U. De and D. Pal, *J. Pharm. Sci.*, **64**, 262 (1975).

In the article titled "Effect of Micellization on Rate of Cupric-Ion-Promoted Hydrolysis of Dicarboxylic Acid Hemiesters" (1), the following correction should be made:

On page 1713, column 2, Structure I should be:

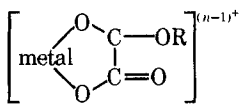

(1) J. T. H. Ong and H. B. Kostenbauder, *J. Pharm. Sci.*, **65**, 1713 (1976).

In the article titled "Steric Inhibition of Conjugation in Lowest Excited Singlet State of 9-Anthramide by Hydrogen Bond Donor Solvents: Role of Solvent in Chemical Structure" (1), the following corrections should be made:

On page 1834, Table I should read:

Table I—Absorption (Abs) and Fluorescence (Fl) of the Neutral and Cationic Species Derived from 9-Anthramide

Cation	λ, Abs, nm	λ, Fl^{max}, nm	Neutral	λ, Abs, nm	λ, Fl^{max}, nm
Aqueous sulfuric acid (H_0 − 4)	405	470	Water	385	407
Ethanol + 2% trifluoroacetic acid	—	442	Ethanol	385	404
—	—	—	Dioxane	384	440
—	—	—	Acetonitrile	382	448
Heptane + 2% trifluoroacetic acid	—	462	Heptane	380	451
—	—	—	Chloroform	384	461

On page 1834, column 1, the second line under *Experimental* should read "from chloroform" instead of "from absolute ethanol."

(1) R. J. Sturgeon and S. G. Schulman, *J. Pharm. Sci.*, **65**, 1833 (1976).

In the article titled "NMR Determination of Trimethoprim and Sulfamethoxazole in Tablets and Powders" (1), the following corrections should be made:

On page 121, column 2, Figure 1, the second line of the legend should read "b, benzylic protons" instead of "b, aromatic protons."

On page 122, column 1, line 6, "the aromatic protons of I" should read "the benzylic protons of I."

On page 122, column 1, Figure 3, the second and third lines of the legend should read "c, benzylic protons of I" instead of "c, aromatic protons of I."

(1) M. R. Rodriguez, M. T. Pizzorno, and S. M. Albonico, *J. Pharm. Sci.*, **66**, 121 (1977).

In the article titled "IR Spectrophotometric Assay of Carbachol Solutions" (1), the following correction should be made:

On page 439, column 1, the last sentence of the second paragraph under *Experimental* should read "Determine the corrected absorbance by subtracting the absorbance at the baseline from the absorbance at the maximum, where absorbance $A = \log 1/T$."

(1) J. Frank and L. Chafetz, *J. Pharm. Sci.*, **66**, 439 (1977).

In the article titled "Anthelmintic 2-Arylhydrazino- and 2-Arylazo-2-thiazolines" (1), the following correction should be made:

On page 1152, Table III, the R column entry for Compound XXXII should read "3-$CH_3C_6H_4$."

(1) M. T. Wu, F. S. Waksmunski, D. R. Hoff, M. H. Fisher, J. R. Egerton, and A. A. Patchett, *J. Pharm. Sci.*, **66**, 1150 (1977).

In the article titled "Kinetics and Mechanism of Blue Tetrazolium Reaction with Corticosteroids" (1), the following correction should be made:

On page 1386, column 1, the last sentence of the first complete paragraph should read: "A free radical mechanism was proposed for tetrazolium reactions with nonketol compounds (21) but was found not to apply to tetrazolium reduction by corticosteroids (19).

(1) R. M. Oteiza, R. S. Wooten, C. T. Kenner, R. E. Graham, and E. R. Biehl, *J. Pharm. Sci.*, **66**, 1385 (1977).